VOLUME 28
1990
ACC. NOS. N90-10001 TO N90-30170

STAR
AN ABSTRACT JOURNAL

Scientific and Technical Aerospace Reports

Annual Index 1990

Part One
SUBJECT

PRODUCED BY THE
SCIENTIFIC AND TECHNICAL
INFORMATION
DIVISION

NASA



NATIONAL AERONAUTICS AND SPACE ADMINISTRATION

WHAT YOU CAN DO FOR *STAR*

All users of this abstract service are urged to forward reports to be considered for announcement in *STAR*. This will aid NASA in its efforts to provide the fullest possible coverage of all scientific and technical publications that might support aeronautics and space research and development. If you have prepared relevant reports (other than those that you will transmit to NASA, DOD, or DOE through the usual contract- or grant-reporting channels), please send them for consideration to the NASA Scientific and Technical Information Facility, P.O. Box 8757, BWI Airport, MD 21240.

Reprints of journal articles, book chapters, and conference papers are also welcome. These will be considered for announcement in *STAR's* companion journal, *International Aerospace Abstracts*.

You may specify a particular source to be included in a report announcement if you wish; otherwise the report will be placed on public sale at the National Technical Information Service. Copyrighted publications will be announced but not distributed or sold.

PURCHASE OF *STAR*

The semimonthly issues are available to registered users on annual subscription from the NASA Scientific and Technical Information Facility, ATTN: Registration Services, P.O. Box 8757, BWI Airport, MD 21240. *STAR* is publicly available on annual subscription from the Superintendent of Documents, U.S. Government Printing Office, Washington, DC 20402.

PUBLISHED BY:

UNITED STATES GOVERNMENT
NATIONAL AERONAUTICS AND SPACE ADMINISTRATION
SCIENTIFIC AND TECHNICAL INFORMATION DIVISION
Scientific and Technical Aerospace Reports, Volume 28, is prepared by the NASA Scientific and Technical Information Facility operated for the National Aeronautics and Space Administration by RMS Associates.

The Administrator of the National Aeronautics and Space Administration has determined that the publication of this periodical is necessary in the transaction of the public business required by law of this agency. Use of funds for printing this periodical has been approved by the Director of the Office of Management and Budget through March 22, 1991.

US ISSN 0036-8741

SPECIAL NOTICE

The abstract sections of the semimonthly *STAR* journals can be bound separately. Individual abstracts can be located readily by means of the page numbers given at each entry, e.g., p 2213. To assist the user in binding *STAR* Volume 28, four (4) title pages are included in the back of Part 1 of the Annual Index.

For sale by the Superintendent of Documents, U.S. Government Printing Office Washington, D.C. 20402

VOLUME 28 NUMBERS 1-24

Scientific and Technical Aerospace Reports

Annual Index (Part I) January - December 1990

TABLE OF CONTENTS

Page

PART I

Introduction iii
Subject Index A-1

PART II

Introduction iii
Personal Author Index B-1
Corporate Source Index C-1
Contract Number Index D-1
Report/Accession Number Index E-1

INTRODUCTION

WHAT STAR ANNUAL INDEXES ARE

This Annual Index is an edited consolidation of the indexes to the individual issues of *Scientific and Technical Aerospace Reports (STAR)* for the calendar year 1990 (Volume 28 Numbers 1 through 24). For the convenience of the user, it is divided into two parts, each bound separately. Part I contains the Subject Index. Part II contains the Personal Author Index, Corporate Source Index, Contract Number Index, and Report/Accession Number Index. The Annual Index supersedes the semimonthly indexes previously issued during 1990.

Each entry in this index includes a group of identifying numbers in the following form: 16 p 2213 N90-22625. The first two digits (16) identify the issue in which the document was announced. The "p" and the four digits that follow (2213) refer to the page number, in the designated issue, on which the abstract of the document appears. The next group of numbers (N90-22625) is the NASA Accession Number, a unique identification number assigned by NASA to each document that was acquired, indexed, and announced in *STAR* during the year.

In addition to these identifying numbers each entry in the Subject Index contains a title, or title and title extension. Each entry in the Personal Author and Corporate Source Indexes contains the title.

At the beginning of each index in this cumulation, a typical listing is illustrated with each of its elements identified to assist the reader in using the different types of index entries.

HOW TO USE THE SUBJECT INDEX

Subject terms in this cumulative index are arranged alphabetically, and are supplemented with cross-references which are intended to serve as directions that will enable the user to modify, enlarge, or narrow his search in accordance with his specific interest. The subject headings have been selected from the latest revision of the *NASA Thesaurus*. Two types of cross-references are used:

1. Use (U) references direct the user to alternate headings under which materials on the subject may be found. For example:

   ANNULAR JETS
   U ANNULAR FLOW
   U JET FLOW
   COLUMBIUM
   U NIOBIUM

2. Narrower Term (NT) references refer the user to more specific headings in the same subject area, under which additional material on the subjects may be found. For example:

   EMISSION
   NT ELECTRON EMISSION
   NT NEUTRON EMISSION
   NT THERMAL EMISSION

Finally, a searcher should use the titles and title extensions in the index to narrow further his quest for particular items. This is because subject terms can readily refer to more than one class of document. For example:

CATHODES
Cesium plasma cathodes as sources of high intensity electron beams
Cathode material testing in electrochemical half cells

This illustrates a case where two references on different topics are listed under the same subject term.

HOW TO USE THE PERSONAL AUTHOR INDEX

All personal authors identified in the abstract-section citations in the individual *STAR* issues appear in this index. Differences in transliteration schemes may require multiple searching of the index for variants of an author's name. For example:

EMELIANOV, M. D.
YEMELYANOV, M. D.

HOW TO USE THE CORPORATE SOURCE INDEX

The corporate source index entries are abridged versions of the corporate sources used in the abstract-section citations in the individual issue supplements. The corporate source supplementary (organizational component) does not appear in the index. For example:

PRINCETON UNIV., N.J. DEPT. OF CHEMICAL ENGINEERING.
(Corporate source at citation)
PRINCETON UNIV., N.J.
(Corporate source index entry)

HOW TO USE THE CONTRACT NUMBER INDEX

All contract numbers that are identified in the abstract-section citations in the individual *STAR* issues appear in this index. Changes by agencies in the style in which contract numbers are presented may require multiple searching for variants. For example:

AF 33(615)-67-C-1758
F33615-67-C-1758

HOW TO USE THE REPORT/ACCESSION NUMBER INDEX

All report numbers that have been assigned by the corporate source, monitoring activity, or cataloging activity appear in this index. Variations in initial input may result in different report number series. For example:

TP-924
ONERA-TP-924

A COMPREHENSIVE INFORMATION SERVICE

The National Aeronautics and Space Administration makes the results of worldwide research and development activities in aeronautics, space, and supporting disciplines promptly available to participants in its program. NASA's scientific and technical information system now contains over three million documents, which are abstracted, indexed, and obtained through retrieval and dissemination services. These services which include the abstract journal, *Scientific and Technical Aerospace Reports (STAR),* are described fully in a bulletin, *The NASA Scientific and Technical Information System... and How to Use It,* available at no charge from the NASA Scientific and Technical Information Facility, P.O. Box 8757, BWI Airport, MD 21240.

AVAILABILITY OF DOCUMENTS

Information concerning the availability of documents announced in the *STAR* issues covered in this index is found in the introduction to the most currently issued semimonthly issue.

PUBLIC COLLECTIONS OF NASA DOCUMENTS

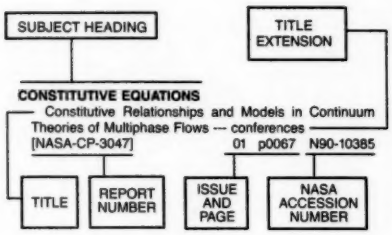
DOMESTIC: NASA and NASA-sponsored documents and a large number of aerospace publications are available to the public for reference purposes at the library maintained by the American Institute of Aeronautics and Astronautics, Technical Information Service, 555 West 57th Street, 12th Floor, New York, NY 10019.

EUROPEAN: An extensive collection of NASA and NASA-sponsored publications is maintained by the British Library Lending Division, Boston Spa, Wetherby, Yorkshire, England for public access. The British Library Lending Division also has available many of the non-NASA publications cited in *STAR*. European requesters may purchase facsimile copy or microfiche of NASA and NASA-sponsored documents, those identified by both the symbols # and * from ESA – Information Retrieval Service European Space Agency, 8-10 rue Mario-Nikis, 75738 CEDEX 15, France.

FEDERAL DEPOSITORY LIBRARY PROGRAM

In order to provide the general public with greater access to U.S. Government publications, Congress established the Federal Depository Library Program under the Government Printing Office (GPO), with 51 regional depositories responsible for permanent retention of material, inter-library loan, and reference services. At least one copy of nearly every NASA and NASA-sponsored publication, either in printed or microfiche format, is received and retained by the 51 regional depositories. A list of the regional GPO libraries, arranged alphabetically by state, appears on the inside back cover. These libraries are *not* sales outlets. A local library can contact a Regional Depository to help locate specific reports, or direct contact may be made by an individual.

Typical Subject Index Listing



The subject heading is a key to the subject content of the document. Titles, issues, page numbers, report numbers, and accession numbers of pertinent documents are provided under each subject heading. When the title is insufficiently descriptive of the document content, a title extension has been added, separated from the title by three hyphens. The report number helps to indicate the type of document cited (e.g., NASA report, NASA translation, NASA contractor report). The issue and page identify the *STAR* issue in which the document was announced and the page number on which the citation appears. The NASA accession number denotes the number by which the citation is identified on that page. The titles, with title extensions if present, are arranged under each subject heading in ascending accession number order. The subject headings have been selected from the latest revision of the *NASA Thesaurus* (NASA SP-7064).

A

A STARS
As observational and theoretical investigation of stellar flares 06 p0862 N90-15012
Perturbation methods for the calculation of gravitational waves from slightly non-spherical spacetimes with applications to stellar core collapse 06 p0863 N90-15015
A theoretical study of circumstellar dust around Ae/Be stars 14 p2040 N90-21700

A-300 AIRCRAFT
Comparison of the results of tests on A300 aircraft in the RAE 5 metre and ONERA F1 wind tunnels
[RAE-TM-AERO-2130] 03 p0311 N90-11768
Simulation of transport aeroplanes
[MBB-UT-007/89-PUB] 19 p2651 N90-25089
Study of the flow around the prototype of A300: Results of the third test campaign at F2 and comparison with calculations
[CERT-33/5025-29-DERAT] 22 p3109 N90-27663

A-310 AIRCRAFT
Simulation of transport aeroplanes
[MBB-UT-007/89-PUB] 19 p2651 N90-25089

A-320 AIRCRAFT
A320 flight tests: Particularities and innovations 02 p0151 N90-10864
Determination of the ground effect on the characteristics of the A320 aircraft 23 p3275 N90-28534

ABEL FUNCTION
Scaling in a non Abelian string network
[ROM1F-89-676] 05 p0695 N90-14066
Non Abelian string correlations and galaxies formation
[ROM1F-89-678] 05 p0714 N90-14171
Abelian gauge theory in topologically non-trivial space
[DE90-710100] 07 p1007 N90-15830
Anyons and Chern-Simons theory on compact spaces of finite genus
[DE90-627216] 23 p3391 N90-29157

ABERRATION
Deferred electronic heterodyne moire deflectometry: A method for transient density fields measurement
[NASA-CR-182982] 06 p0843 N90-14907
Isoplanatic systems in mesooptics
[DE90-009785] 17 p2406 N90-23705
One way imaging and amplification through an aberrator
[AD-A221640] 21 p3009 N90-27106

ABILITIES
SINCGARS (Single-Channel Ground/Airborne Radio System) operator performance decay
[AD-A210716] 01 p0057 N90-10326
Comprehension processes in mechanical reasoning
[AD-A210459] 02 p0255 N90-11442
Stimulus-response compatibility in spatial precuing and symbolic identification: Effects of coding practice, retention, and transfer
[AD-A210745] 02 p0255 N90-11443
Effects of the advanced map interpretation and terrain analysis course on contour-level navigation performance
[AD-A212163] 03 p0304 N90-11723
Numerical facility: Convergence of cognitive and factor analytic models
[AD-A213627] 07 p0983 N90-15680
Expertise, stress, and pilot judgment 09 p1255 N90-17284
Feedback effects in computer-based skill learning
[AD-A214560] 09 p1258 N90-17298
Measuring learning ability by dynamic testing
[AD-A215273] 09 p1259 N90-17304
Learning events in the acquisition of three skills
[AD-A219038] 16 p2264 N90-22905
Ability distributions pattern probabilities and quasidensities
[AD-A218471] 16 p2308 N90-23153
The incremental validity of spatial and perceptual-psychomotor tests relative to the armed services vocational aptitude battery
[AD-A220903] 18 p2585 N90-24719
The integration of complex information from auditory and visual channels under stress
[AD-A222686] 21 p3033 N90-27245
Predicting F/A-18 fleet replacement squadron performance using an automated battery of performance-based tests
[AD-A223899] 23 p3277 N90-28543
Neurophysiological correlates of information processing abilities during divided attention situations in air traffic controllers 23 p3360 N90-28989
Ability and metacognitive determinants of skill acquisition and transfer
[AD-A224569] 24 p3499 N90-29776

ABLATION
Modifications to the aerotherm charring material thermal response and ablation program (CMA) for carbon ablation analysis
[AD-A211069] 02 p0195 N90-11115
Studies of neutral and ion transport during laser ablation of 1:2:3 superconductors by optical absorption spectroscopy
[DE90-001968] 06 p0790 N90-14604
Laser-induced surface ablation and optical damage of ZnS crystals caused by single- and multiple-pulse laser-irradiation
[DE90-003807] 07 p0936 N90-15419
Investigation of ablation phenomena using IR thermography in a hypersonic wind tunnel 08 p1081 N90-16258
The effect of loading on the laser ablation of graphite/epoxy composite material
[AD-A216209] 10 p1349 N90-17826
In situ growth of epitaxial superconducting YBa2Cu3O(7-x) films on insulating semiconducting and ferroelectric K(Ta, Nb)O3 by pulsed laser ablation
[DE90-006568] 11 p1571 N90-19043
In situ growth of high quality epitaxial YBa2Cu3O(7-x) thin films at moderate temperatures by pulsed laser ablation
[DE90-006629] 11 p1571 N90-19045
Laser mass spectrometric studies of high temperature superconductor ablation
[DE90-006518] 12 p1668 N90-19585
Laser-matter interaction at intensities of 10(sup 12) W/cm(sup 2) and below
[DE90-007536] 12 p1669 N90-19590
Characterization of ground state neutral and ion transport during laser ablation of 1:2:3 superconductors by transient optical absorption spectroscopy
[DE90-006623] 12 p1720 N90-19878
Y1Ba2Cu3O(7-x) laser-ablation plume dynamics measurement by nanosecond response ion probe: Comparison with optical measurements
[DE90-007658] 13 p1807 N90-20375
Growth and patterning of laser ablated superconducting YBa2Cu3O7 films on LaAlO3 substrates
[NASA-TM-102436] 15 p2173 N90-22421
Control of surface melting and ablation in electromagnetic launchers via the magnetic vapor shielding mechanism
[AD-A219035] 16 p2204 N90-22578
SiC film deposited by pulsed excimer laser ablation
[DE90-010634] 18 p2622 N90-24938
Preparation and properties of superconducting thin films by excimer laser ablation
[DE90-011929] 18 p2626 N90-24967
Superconductivity in nonsymmetric epitaxial YBa2Cu3O(sub 7-delta)-PrBa2Cu3O(sub 7-delta) superlattices grown by pulsed laser ablation
[DE90-011637] 19 p2761 N90-25687
Microstructures of superconducting YBa2Cu3O(7-x) thin films
[DE90-011976] 19 p2761 N90-25688
Ellipsometric study of YBa2Cu3O(7-x) laser ablated and co-evaporated films
[NASA-TM-103223] 20 p2932 N90-26682
Laser ablated high T(sub c) superconducting thin YBa2Cu3O(7-x) films on substrates suitable for microwave applications 22 p3139 N90-27808

ABLATIVE MATERIALS
High temperature insulators
[AD-D014193] 04 p0479 N90-12751
Technique for evaluating the erosive properties of ablative internal insulation materials 11 p1471 N90-18466
Nonequilibrium radiation and chemistry models for aerocapture vehicle flowfields
[NASA-CR-186728] 22 p3169 N90-27973

ABLATIVE NOSE CONES
A difference scheme with autocontrol artificial viscosity to predict ablated nosetip shape
[AD-A216625] 11 p1468 N90-18452
Ablative cooling of aerodynamically heated radomes
[AD-D014426] 14 p1971 N90-21293

ABM
U APOGEE BOOST MOTORS

ABNORMALITIES
Review of component defects, their relationship to manufacturing process, and their effect on materials behaviour (for critical rotating parts) 11 p1458 N90-18399
Techniques for studying the effects of microgravity on model particle/cell systems 12 p1640 N90-19424
Decompression sickness affecting the temporomandibular joint
[AD-A220959] 18 p2584 N90-24715

ABRASION
The response of isotropic brittle materials to abrasive processes
[DE89-016637] 01 p0045 N90-10251
Evaluation of copper slag blast media for railcar maintenance
[NASA-CR-183744] 05 p0630 N90-13681
Abrasion resistant coatings on plastics 18 p2529 N90-24428
Aeolian removal of dust from radiator surfaces on Mars
[NASA-TM-103205] 20 p2824 N90-26068
Mechanical properties testing of diamond and diamond-like films by ultra-low load indentation
[DE90-014456] 23 p3337 N90-28861

ABRASION RESISTANCE
Quality evaluation of coatings by automatic scratch testing
[AD-A219331] 17 p2379 N90-23548
Evaluation of abrasion-resistant metallized coatings for civil works applications
[AD-A221078] 18 p2530 N90-24438
Cryogenic anti-friction bearing with inner race
[NASA-CASE-MFS-28384-1] 21 p3010 N90-27112

ABRASIVES
Evaluation of copper slag blast media for railcar maintenance
[NASA-CR-183744] 05 p0630 N90-13681
Erosion mechanisms in composite materials and ripple formation mechanism in erosion
[IAR-89-4-PT-2] 20 p2825 N90-26079

ABRIKOSOV THEORY
Elliptical flux vortices in polycrystalline YBa2Cu3O7
22 p3136 N90-27795
Nonlogarithmic magnetization relaxation at the initial time intervals and magnetic field dependence of the flux creep rate in Bi2Sr2Ca(sub I)Cu2Ox single crystals
22 p3137 N90-27801
Measurement of H(sub c1) in a single crystal of YBa2Cu3O7 with low pinning 22 p3151 N90-27864

ABSORBERS (EQUIPMENT)
Analysis and realization of integrated optical polarizers and absorbers on LiNbO3
[ETN-90-96504] 18 p2623 N90-24949

ABSORBERS (MATERIALS)
NT RADAR ABSORBERS
Analysis of catalytically enhanced solar absorption chemical reactors: 1 - numerical model description
[DE89-014742] 07 p0951 N90-15505
A summary of measurements of permittivities and permeabilities of some microwave absorbing materials
[AD-A223221] 21 p2995 N90-27026
Parametric studies of acoustic duct attenuation ofperforated-plate-on-honeycomb absorber
[NAL-TM-603] 24 p3542 N90-30030

ABSORPTION
Non-linear optical studies of adsorbates: Spectroscopy and dynamics
[DE90-001543] 06 p0741 N90-14312

ABSORPTION BANDS
U ABSORPTION SPECTRA

ABSORPTION COEFFICIENT
U ABSORPTIVITY

ABSORPTION COOLING
Intermittent Solar Ammonia Absorption Cycle (ISAAC) refrigeration for lesser developed countries
[DE90-006700] 11 p1496 N90-18810
Numerical and experimental analysis of a thin liquid film on a rotating disk related to development of a spacecraft absorption cooling system
[NASA-CR-183457] 12 p1657 N90-19523
A theoretical and experimental investigation of an absorption refrigeration system for application with solar energy units 16 p2226 N90-22697
A cost-effective realization of environmental temperature control
[DE90-011651] 24 p3458 N90-29532

ABSORPTION CROSS SECTIONS
Investigations into the influence of the state functions on the cross sections of the direct p,gamma reactions at energies in the 100 keV range, and project of a cascade accelerator for the measurement of the p,gamma capture cross sections
[ETN-89-94662] 02 p0273 N90-11561
Ultraviolet absorption cross-sections of bromoform in the temperature range 295-240 K
[AERONOMICA-ACTA-A-348-1989]
05 p0622 N90-13630
New calculations of photodissociation cross-sections in the O2 Schumann-Runge system
05 p0657 N90-13834
Absorption experiments on electron-beam pumped rare gases
[DE90-008504] 11 p1515 N90-18722
A ground state depleted laser in neodymium doped yttrium orthosilicate
[DE90-006773] 12 p1668 N90-19586
Measurement of cross sections: New needs and possibilities
[DE90-007248] 12 p1711 N90-19829
Photodissociation of O2 in the stratosphere and mesosphere: A general parametrization of the Schumman-Runge Bands 20 p2887 N90-26427
Absolute vacuum ultraviolet photoabsorption cross section studies of atomic and molecular species: Techniques and observational data
20 p2944 N90-26754
High resolution, low temperature photoabsorption cross-section of C2H2 with application to Saturn's atmosphere 20 p2945 N90-26757

ABSORPTION SPECTRA
NT FRAUNHOFER LINES
Spectropolarimetry, variability, and the taxonomy of active galactic nuclei 02 p0292 N90-11687
Small grains in reflection nebulae: A study of diffuse interstellar bands, elemental depletions and infrared flux
02 p0293 N90-11672
A nonlinear-optical method for combining high power laser beams
[AD-A211730] 03 p0354 N90-12022
The low-ion QSO absorption-line systems
05 p0712 N90-14162
Archival research on absorption lines in violently star-forming galaxies
[NASA-CR-185960] 05 p0712 N90-14163
Anomalous absorption by atmospheric water vapor and stabilized water fogs in the infrared and CM-wave regions
[AD-A214202] 07 p0964 N90-15572
X ray absorption studies of YBa2Cu3O(6+x), La(2-x)Sr(x)CuO4, and Nd(2-x)Ce(x)CuO4
[DE90-003640] 07 p1002 N90-15797
Auger and x ray absorption studies of solid molecular oxygen
[DE90-003966] 07 p1006 N90-15825
Theoretical study of the Townes-Merritt effect in level crossing experiments
[AD-A214909] 09 p1191 N90-16900
Radiometric observations at 20.6, 31.65, and 90.0 GHz: Continuing studies 10 p1373 N90-17958
Temperature dependence of photon-gated persistent spectral hole-burning for the meso-tetra-p-tolyl Zn-tetrabenzoporphyrin/chloroform system in poly(methylmethacrylate)
[AD-A216086] 11 p1482 N90-18531
Millimeter-wave propagation in the mesosphere
[PB90-119868] 11 p1496 N90-18612
Persistant spectral hole-burning: Photon-gating and fundamental statistical limits
[AD-A216084] 11 p1501 N90-18640
An almost total disjunction between emission and absorption dust features: What does it tell us?
11 p1581 N90-19106
A coal model for the carriers of the unidentified IR bands 11 p1581 N90-19110
Spectroscopy and physico-chemistry of CO:H2O and CO2:H2O ices 11 p1581 N90-19111
Infrared line emission from high-velocity outflows in star-forming regions 11 p1582 N90-19116
Zones of feasibility for retrieval of surface pressure from observations of absorption in the A band of oxygen
[DAR-TP-19] 14 p2006 N90-21495
Near field curvature at parallel phase objects: Model examination with microwaves
[ETN-90-96499] 18 p2545 N90-24525
Space station contamination study: Assessment of contaminant spectral brightness
[NASA-CR-186173] 19 p2666 N90-25169
Soft x ray resist characterization: Studies with a laser plasma x ray source
[DE90-013493] 20 p2928 N90-26661
Wear metal analysis in engine oil by microwave digestion and atomic absorption spectroscopy
[AD-A223070] 21 p2985 N90-26964
Spectral absorption of marine stratocumulus clouds derived from in situ cloud radiation measurements
22 p3215 N90-28238
The 27-28 October 1986 FIRE IFO cirrus case study: Comparison of satellite and aircraft derived particle size
22 p3224 N90-28285
Remote sounding through semi-transparent cirrus cloud 22 p3226 N90-28296
Strong associated C 4 absorption in low redshift quasars
[NASA-CR-186936] 22 p3262 N90-28469
Spectroscopic study of combustion diagnostics on hydroxyl radicals
[NASA-CR-186998] 23 p3305 N90-28694
Zonal winds between 25 and 120 km retrieved from solar occultation spectra 24 p3489 N90-29718

ABSORPTION SPECTROSCOPY
NT OPTOGALVANIC SPECTROSCOPY
Study of high frequency water vapor absorption parameters
[AD-A210676] 02 p0194 N90-11108
The low-ion QSO absorption-line systems
05 p0712 N90-14162
Mapping of upper electronic reaction surfaces by tuned laser photolysis and by absorption and emission spectroscopies
[DE90-000125] 06 p0741 N90-14314
Measurement of the high density zone of a plasma target by absorption spectroscopy 06 p0784 N90-14560
Studies of neutral and ion transport during laser ablation of 1:2:3 superconductors by optical absorption spectroscopy
[DE90-001968] 06 p0790 N90-14604
Spectral studies of solid propellant combustion. 2: Emission and absorption results for M-30 and HMX1 propellants
[AD-A213857] 07 p0915 N90-15292
Study of chemical systems in static and time resolved mode by x ray absorption spectroscopy
[AD-A215383] 09 p1191 N90-16904
Ultrasensitive laser spectroscopy in solids: Single-molecule detection
[AD-A216085] 11 p1514 N90-18716
Characterization of ground state neutral and ion transport during laser ablation of 1:2:3 superconductors by transient optical absorption spectroscopy
[DE90-006623] 12 p1720 N90-19878
Study of new technique of solid combustible materials to determination of volatile elements by flame atomic absorption spectrophotometry
[DE90-612907] 14 p1947 N90-21147
Infrared absorption spectroscopy and chemical kinetics of free radicals
[DE90-009469] 15 p2067 N90-21837
Saturated fluorescence measurements of the hydroxyl radical in laminar high-pressure flames
[NASA-CR-185218] 15 p2101 N90-22022
Measurement of HCl by near-infrared diode laser absorption 16 p2209 N90-22601
IR transition moments and collisional dynamics of vibrationally excited OH radicals via time-resolved laser absorption spectroscopy
[AD-A221005] 18 p2580 N90-24696
Temperature and OH concentrations in a solid propellant flame using absorption techniques
[AD-A222591] 20 p2830 N90-26100
Intracavity Dye-Laser Absorption Spectroscopy (IDLAS) for application to planetary molecules
20 p2945 N90-26761
Methane overtone absorption by intracavity laser spectroscopy 20 p2946 N90-26762
The influence of IMF on the lower ionosphere plasma in high and middle latitudes 22 p3208 N90-28200

ABSORPTIVE INDEX
U ABSORPTIVITY

ABSORPTIVITY
Theoretical and experimental investigation of nonlinear optoacoustics in liquids
[AD-A210427] 01 p0124 N90-10708
Laboratory measurements of microwave and millimeter-wave properties of planetary atmospheric constituents
[NASA-CR-185914] 01 p0141 N90-10815
A SAW Slanted Array Correlator (SAC) with separate amplitude compensation channel
[AD-D014174] 03 p0336 N90-11914
Photodissociation of XeF2 (xenon difluoride) at 193 nm
[AD-A211663] 04 p0506 N90-12916
The average ion model. Computation of the absorption and emission coefficients in hot plasmas
06 p0785 N90-14569
Laboratory evaluation and application of microwave absorption properties under simulated conditions for planetary atmospheres
[NASA-CR-185916] 06 p0865 N90-15025
Kinetic studies following state-selective laser excitation
[DE90-003232] 07 p0935 N90-15415
Absorption fluids data survey: 1989 update
[DE90-003985] 08 p1096 N90-16346
Multi-dimensional discrete ordinates solutions to combined mode radiation heat transfer problems and their application to a free-falling particle, direct absorption solar receiver
[DE90-004987] 09 p1300 N90-17531
Background studies in gas ionizing x ray detectors
12 p1636 N90-19399
Full wave computation of electromagnetic wave excitation, propagation, and absorption at the ion cyclotron frequency in fusion experiments
[DE90-009399] 14 p2030 N90-21642
Measurement of HCl by near-infrared diode laser absorption 16 p2209 N90-22601
Laboratory measurements of microwave and millimeter-wave properties of planetary constituents
20 p2943 N90-26745
Laboratory measurements and modeling of microwave absorption by ammonia in gas mixtures applicable to giant planet atmospheres 20 p2944 N90-26750
Radiative properties of cirrus clouds inferred from broadband measurements during FIRE
22 p3226 N90-28295

Physically-based general circulation model parameterization of clouds and their radiative interaction
22 p3228 N90-28306
XANES and EXAFS study of Au-substituted YBa2Cu3O(7-delta)
[NASA-TM-103291] 23 p3401 N90-29219

ABSTRACTS
Publications of the National Institute of Standards and Technology, 1988 catalog
[PB89-218382] 04 p0563 N90-13279
AFOSR technical report summaries
[AD-A213148] 05 p0707 N90-14142
Advances in techniques and technologies for air vehicle navigation and guidance
[AGARD-AR-276] 08 p1020 N90-15899
Reports of planetary astronomy, 1986
[NASA-TM-100776] 08 p1138 N90-16596
Noise and sonic boom impact technology. Effects of aircraft noise and sonic booms on structures: An assessment of the current state-of-knowledge
[AD-A213919] 09 p1278 N90-17409
Proceedings of a contractors meeting on Combustion Rocket Propulsion Diagnostics of Reacting Flow
[AD-A216445] 12 p1617 N90-19297
Topical Conference on the Origin of the Earth
[NASA-CR-185061] 15 p2128 N90-22166
Atlas/data abstract for the United States and selected areas, fiscal year 1989
[AD-A219289] 16 p2327 N90-23270
Proceedings of the 12th Symposium on Signal and Image Processing English-Language Abstracts
[AD-A218606] 17 p2388 N90-23598
The biogeochemistry of metal cycling
[NASA-CR-4295] 17 p2439 N90-23897
Conference on the Science and Technology of Thin-Film Superconductors
[DE90-000326] 18 p2620 N90-24926
Proceedings of the Second Symposium on GPS Applications in space, volume 1
[AD-A219978] 20 p2806 N90-25962
Proceedings of the Second Symposium on GPS Applications in Space, volume 2
[AD-A219979] 20 p2806 N90-25963
Press abstracts of the 21st Lunar and Planetary Science Conference
[NASA-CR-186874] 20 p2941 N90-26738
Abstracts of 1989 Japan Solar Energy Society and Japan Wind Energy Association Joint Conference
[DE90-503616] 21 p3019 N90-27168
Scientific and technical information management
22 p3257 N90-28444
FAA Rotorcraft Research, Engineering, and Development Bibliography 1962-1989
[AD-A224256] 24 p3417 N90-29299
Proceedings of the 45th Ohio State University Symposium on Molecular Spectroscopy
[AD-A224349] 24 p3445 N90-29457
JPRS report: Science and technology. USSR: Earth sciences
[JPRS-UES-90-004] 24 p3483 N90-29688
JPRS report: Science and technology. USSR: Earth sciences
[JPRS-UES-90-003] 24 p3483 N90-29689
JPRS Report: Science and technology. USSR: Life sciences
[JPRS-ULS-90-007] 24 p3497 N90-29762
JPRS report: Science and technology. USSR: Life sciences
[JPRS-ULS-90-004] 24 p3497 N90-29763
Book of abstracts of the 1st Benelux-Japan Workshop on Information and Communication Theory
[PB90-191446] 24 p3556 N90-30124

ABUNDANCE
Carbon isotope ratios and lithium abundances in open cluster giants 02 p0292 N90-11664
Research in cosmic and gamma ray astrophysics
[NASA-CR-185451] 04 p0589 N90-13316
Trace element abundance determinations by Synchrotron X Ray Fluorescence (SXRF) on returned comet nucleus mineral grains 08 p1142 N90-16619
Prompt Gamma Activation Analysis (PGAA): Technique of choice for nondestructive bulk analysis of returned comet samples 08 p1144 N90-16633
Solar nebula condensates and the composition of comets 08 p1144 N90-16634
The excess flux in the cosmic submillimeter background radiation and the primordial deuterium abundance
[NASA-CR-186312] 08 p1154 N90-16683
Infrared lines as probes of galactic structure
11 p1585 N90-19139
Photometric analyses of abundances in dwarf spheroidal galaxies and globular clusters 12 p1736 N90-19978
Evolutionary effects in B stars
14 p2041 N90-21704
A balloon measurement of the isotopic composition of galactic cosmic ray iron 14 p2043 N90-21717
Abundance differences among G and K giants
17 p2484 N90-24208
Upper limits on Co-57 abundance in SN1987A according to the Kvant data 19 p2769 N90-25735
Line identification studies using traditional techniques and wavelength coincidence statistics
[NASA-CR-186901] 22 p3261 N90-28467
The ionization structure of planetary nebulae 10: NGC 2392
[NASA-CR-186960] 23 p3411 N90-29274
PW Vul: A classical nova with nearly solar abundances
[NASA-CR-185080] 23 p3411 N90-29275
Carbon monoxide isotopes and clumping in giant molecular clouds 24 p3562 N90-30151

AC (CURRENT)
U ALTERNATING CURRENT

AC GENERATORS
Automation in the Space Station module power management and distribution Breadboard
19 p2728 N90-25509

ACCELERATED LIFE TESTS
Predictive aging of polymers
[NASA-CASE-NPO-17524-1-CU]
01 p0046 N90-10261
Accelerated aging of metal matrix composites
02 p0190 N90-11085
Accelerated aging embrittlement of cast duplex stainless steel: Activation energy for extrapolation
[DE90-001773] 07 p0903 N90-15221
Status and results of ANL life evaluation of valve-regulated lead-acid load-leveling batteries
[DE90-001918] 07 p0921 N90-15329
Life evaluation of valve-regulated lead-acid batteries for load-leveling applications
[DE90-002188] 07 p0922 N90-15336
Fast algorithms for estimating mixture parameters
[AD-A213869] 07 p0976 N90-15636
Statistical theory of reliability
[AD-A215320] 09 p1234 N90-17161
Life test programme of ERS-1 AMI-high power amplifier 10 p1330 N90-17684
Fuel-elastomer compatibility studies: Results of 80 C/14-day exposure experiments
[AD-A216015] 10 p1361 N90-17893
Durable heat diaphragm from ordered polymer films
[AD-A220794] 17 p2381 N90-23559
Diffusion in the thermal degradation of NC base propellants
[AD-A219831] 17 p2383 N90-23572
T4A thruster starting sequences and the design of an electromagnetic sequencer for cyclic life tests
[RAE-TR-77042] 19 p2669 N90-25179
Method and apparatus for assessing distillate fuel stability by oxygen overpressure
[AD-D014499] 19 p2679 N90-25237
Life evaluation of valve regulated lead-acid batteries for cycling applications
[DE90-013649] 21 p2999 N90-27044
Component behaviour and life management: The need for common AGARD approaches and actions
22 p3118 N90-27710
Metallurgical analysis of leaking tray packs
[AD-A223157] 22 p3157 N90-27899

ACCELERATION (PHYSICS)
NT ANGULAR ACCELERATION
NT DECELERATION
NT ELECTRON ACCELERATION
NT HIGH ACCELERATION
NT IMPACT ACCELERATION
NT PARTICLE ACCELERATION
NT PLASMA ACCELERATION
NT TRANSVERSE ACCELERATION
VIBRAFUGE: A combined environment testing facility-vibration testing on a centrifuge
[DE89-015120] 01 p0080 N90-10458
Acceleration of metal plates
[DE89-016816] 02 p0209 N90-11197
Interferometry and high speed photography of laser-driven flyer plates
[DE89-016990] 02 p0225 N90-11290
Computational aspects of sensitivity calculations in linear transient structural analysis 02 p0231 N90-11327
Vibration isolation technology: Sensitivity of selected classes of space experiments to residual accelerations
[NASA-CR-185443] 04 p0482 N90-12768
Acceleration sets of planar manipulators. Part 1: Theory
[AD-A213162] 04 p0510 N90-12945
Acceleration sets of planar manipulators. Part 2: Applications and experiments
[AD-A213336] 05 p0650 N90-13791
Definition, determination and characterization of acceleration sets for spatial manipulators
[AD-A213366] 05 p0651 N90-13793
Acceleration of small, light projectiles (including hydrogen isotopes) to high speeds using a two-stage light gas gun
[DE90-002479] 06 p0729 N90-14253
Methodology for the calibration of and data acquisition with a six-degree-of-freedom acceleration measurement device
[PB89-233597] 06 p0779 N90-14531
Physics with ultra-low energy antiprotons
[DE90-002397] 06 p0840 N90-14888
VIBRAFUGE: Combined vibration and centrifuge testing
[DE90-001091] 07 p0884 N90-15114
Research in knowledge-based vision techniques for the Autonomous Land Vehicle Program
[AD-A213440] 07 p0942 N90-15453
Use of lower body negative pressure as a countermeasure to negative Gz acceleration
[AD-A213927] 07 p0967 N90-15583
The use of hypervelocity launchers to explore previously inaccessible states of matter
[DE90-004088] 08 p1034 N90-15973
An introduction to shaker shock simulations
[DE90-003057] 08 p1088 N90-16298
Progress with small, high-magnetic-field spheromaks in CTX
[DE90-003395] 08 p1127 N90-16527
Micro-miniature roll rate sensor
[AD-A214778] 09 p1225 N90-17107
Relationship of fragment size to normalized spall strength for materials
[DE90-004165] 09 p1231 N90-17140
Guidelines for safe human exposure to impact acceleration, update A
[AD-A215287] 09 p1253 N90-17268
Hypervelocity acceleration and impact experiments with the LLNL electric gun
[DE90-006924] 10 p1326 N90-17664
The effect of the virtual mass force term on the stability of transient two-phase flow analysis
[DE90-733142] 10 p1384 N90-18010
Theory for high gain, high power free electron lasers
[DE90-005546] 11 p1514 N90-18714
Visual processing of object velocity and acceleration
[AD-A216509] 11 p1539 N90-18858
Nonlinear system vibration: The appearance of chaos
[DE90-007546] 12 p1708 N90-19810
Resolved motion rate and resolved acceleration servo-control of wheeled mobile robots
[DE90-002585] 13 p1811 N90-20399
Collective ion acceleration in high current relativistic electron beams
[DE90-008328] 13 p1886 N90-20821
The vibro-acoustic mapping of low gravity trajectories on a Learjet aircraft
[NASA-TM-103103] 15 p2045 N90-21723
Active primary lithium thionyl chloride battery for artillery applications
[DE90-009511] 15 p2089 N90-21955
Severe shock and vibration environments for electronic components
[DE90-007686] 15 p2117 N90-22113
Engagement analysis study
[DE90-009529] 15 p2163 N90-22359
Brain stem evoked responses in altered G environments
[AD-A220097] 17 p2435 N90-23874
Short time Force and moment measurement System for shock tubes (SFS) for measuring times less than 10 ms 18 p2490 N90-24233
Prevalence of G-induced cervical injury in US Air Force pilots 19 p2717 N90-25460
Vibration test procedures for orbiter sidewall-mounted payloads, phase 2
[AD-A220774] 20 p2818 N90-26038
Viking data analysis
[AD-A222609] 20 p2823 N90-26062
DURIP: Instrumentation for laser switched power LINAC
[AD-A222629] 20 p2868 N90-26318
Absolute measurements of gravity
[AD-A222731] 20 p2922 N90-26629
Development of a sealed bipolar Li-alloy/FeS2 battery for electric vehicles
[DE90-013650] 21 p2999 N90-27045
Collision forces for compliant projectiles
[NASA-TM-4203] 22 p3192 N90-28111
Measurement of gravitational acceleration of antimatter
[DE90-627464] 23 p3403 N90-29233
Application of a rechargeable, small caliber railgun power supply
[AD-A224207] 24 p3438 N90-29418
Prospects for nuclear astrophysics with intense radioactive ion beams
[DE90-015616] 24 p3544 N90-30044

ACCELERATION STRESSES (PHYSIOLOGY)
Parachute opening shocks during high speed ejections: Normalization 13 p1751 N90-20056
Space adaptation syndrome induced by a long duration +3Gx centrifuge run
[AD-A218248] 14 p2010 N90-21518
Mobility of the head and load effects: Experimental approach in a centrifuge 19 p2720 N90-25473
Risk of cervical injury in real and simulated accidents 19 p2721 N90-25475
Biofidelity of a dummy's neck during automobile collision testing 19 p2721 N90-25477
Influence of gravito-inertial force on vestibular nystagmus in man
[IZF-1989-24] 22 p3231 N90-28325

ACCELERATION TOLERANCE
Use of lower body negative pressure as a countermeasure to negative Gz acceleration
[AD-A213927] 07 p0967 N90-15583
Guidelines for safe human exposure to impact acceleration, update A
[AD-A215287] 09 p1253 N90-17268
Development of acceleration exposure limits for advanced escape systems 13 p1751 N90-20055
Parachute opening shocks during high speed ejections: Normalization 13 p1751 N90-20056
The +Gz protection in the future: Review of scientific literature
[AD-A217887] 13 p1851 N90-20623
The effects of linear acceleration on perception and nystagmus 15 p2136 N90-22209
Rheoencephalography in simulated aviation environmental stress
[AD-A221150] 18 p2584 N90-24716

ACCELEROMETERS
In service life monitoring system using g-meter readings and mass configuration control
[ETN-89-95218] 03 p0356 N90-12035
Methodology for the calibration of and data acquisition with a six-degree-of-freedom acceleration measurement device
[PB89-233597] 06 p0779 N90-14531
Evaluation of shock isolation techniques for a piezoresistive accelerometer
[DE89-014496] 06 p0780 N90-14535
Superconducting gravity gradiometer mission. Volume 1: Study team executive summary
[NASA-TM-4091-VOL-1] 07 p0959 N90-15545
Micro-miniature roll rate sensor
[AD-A214778] 09 p1225 N90-17107
Development of a superconducting six-axis accelerometer
[AD-A215948] 10 p1319 N90-17625
Development and polarization of ferroelectric polymer gauges, for dynamical acceleration experiments, as those in ballistics shocks
[ISL-R-119/88] 11 p1511 N90-18703
Test component attachment effects on resonant plate pyrotechnic shock simulation
[DE90-006478] 12 p1662 N90-19551
Software to characterize tuning fork resonators used in the Quartz Digital Accelerometer
[DE90-007913] 14 p1963 N90-21363
Special test and evaluation methods used for a nine-axis accelerometer
[PB90-209578] 23 p3329 N90-28822

ACCEPTABILITY
Simulation of synthetic aperture radar 3: Evaluation of prototype digital feature analysis data
[AD-A216750] 11 p1498 N90-18620
En route noise of turboprop aircraft and their acceptability: Report of tests 18 p2609 N90-24858
SONA: A measurement system for the determination of the end-of-flight burst behaviour of projectiles equipped with proximity fuses
[FEL-89-A293] 24 p3459 N90-29536

ACCEPTANCE
U ACCEPTABILITY

ACCEPTOR MATERIALS
Electrically conducting organic materials: Design, synthesis and characterization
[AD-A212214] 04 p0471 N90-12700
Strong-inversion model of threshold voltage in modulation doped field effect transistors: The role of unintentional acceptors
[AD-A212750] 04 p0498 N90-12870

ACCESS CONTHOL
Performance analysis of hybrid ARQ protocols in a slotted code division multiple-access network
[AD-A211078] 02 p0213 N90-11219
A security model and its implementation
[RSRE-MEMO-4222] 03 p0385 N90-12190
Long-range plan for management and use of the radio spectrum by agencies and establishments of the Federal Government
[PB89-232367] 05 p0633 N90-13693
On the privacy problems involved in allowing access to computers via the public telephone system
[RSRE-88006] 07 p0917 N90-15303
Reconfigurable N-dimensional computer memory
[AD-D014309] 07 p0971 N90-15607
Sequential rapid communication visual displays
[AD-D014282] 08 p1056 N90-16106
CHIMERA 2: A real-time UNIX-compatible multiprocessor operating system for sensor-based control applications
[AD-A215958] 10 p1392 N90-18051
The contour model architecture and assembly language
[AD-A217114] 13 p1865 N90-20697
CSMA/RN: A universal protocol for gigabit networks 15 p2150 N90-22280
Access to supercomputers 16 p2277 N90-22979
Results of the REALAN project: Replacing the Ethernet access mechanism by the real-time access mechanism of Twentenet
[MEMO-INF-89-55] 18 p2595 N90-24788
Privacy-enhanced electronic mail
[PCS-TR90-150-REV-1] 19 p2683 N90-25261
Computer access security code system
[NASA-CASE-NPO-17525-1-CU] 19 p2742 N90-25583
Theft of information in the take-grant protection model
[NASA-CR-186638] 19 p2763 N90-25702
Multiple-access techniques for communication over dispersive radio channels 20 p2848 N90-26196
Packet radio network concepts for the Norwegian field army 20 p2850 N90-26206
Parallel architectures and algorithms for image understanding
[AD-A223479] 24 p3526 N90-29940

ACCESS TIME
Temporal, processor, and spatial locality in multiprocessor memory references
[AD-A213790] 07 p0969 N90-15598
The implementation of a coherent memory abstraction on a NUMA (Non-Uniform Memory Access) multiprocessor: Experiences with PLATINUM (Platform for Investigating Non-Uniform Memory)
[AD-A213909] 07 p0970 N90-15600
Memory management for large-scale NUMA (Non-Uniform Memory Access) multiprocessors
[AD-A213910] 07 p0970 N90-15601
An overview of PLATINUM: A Platform for Investiga ting Non-Uniform Memory (preliminary version)
[AD-A213911] 07 p0970 N90-15602
Evolution of an operating system for large-scale shared-memory multiprocessors
[AD-A213912] 07 p0970 N90-15603
Reconfigurable N-dimensional computer memory
[AD-D014309] 07 p0971 N90-15607
New optimization techniques in database access and maintenance 08 p1137 N90-16586
A carrier sensed multiple access protocol for high data base rate ring networks 15 p2151 N90-22288
The semantics of TRIDL
[TR-89-17] 17 p2450 N90-23973

ACCIDENT INVESTIGATION
NT AIRCRAFT ACCIDENT INVESTIGATION
Investigation and characteristics of major fire-related accidents in civil air transports over the past ten years 10 p1311 N90-17582
General purpose heat source radioisotope thermoelectric generator program. Book 1: Accident analysis
[REPT-90SDS4202-BK-1] 15 p2165 N90-22379
General purpose heat source radioisotope thermoelectric generator. Book 2: Accident analysis, appendices
[REPT-90SDS4202-BK-2] 15 p2166 N90-22380

ACCIDENT PREVENTION
UK airmisses involving commercial air transport
[CAA-2/88] 03 p0303 N90-11718
Field evaluation of a Nissan laser collision avoidance system
[PB90-105602] 06 p0722 N90-14215
Improved lighting of taxiway/taxiway intersections for instrument Flight Rules (IFR) operations
[DOT/FAA/CT-TN89/64] 07 p0878 N90-15089
Security calculations of rip reached construction elements by means of probabilistic breaking mechanics and a Markov process
[ETN-90-95890] 12 p1678 N90-19624
Results of TCAS-2 simulations in reconstructed dangerous encounters (Jul. 1988 to Jun. 1989)
[ETN-90-96474] 17 p2349 N90-23375

ACCIDENTS
NT BIRD-AIRCRAFT COLLISIONS
NT LOSS OF COOLANT
Space nuclear safety program
[DE90-006435] 11 p1565 N90-19007
Safety analysis for the Galileo light-weight radioisotope heater unit
[DE90-007147] 11 p1566 N90-19009
Safety Status Report for the Ulysses mission. Book 1: Risk analysis. General purpose heat source radioisotope thermoelectric generator program
[DE90-006826] 12 p1614 N90-19282
Safety status report for the Ulysses mission. Book 2: Risk analysis. General purpose heat source radioisotope thermoelectric generator program
[DE90-006827] 12 p1614 N90-19283
Safety Status Report for the Ulysses mission: Summary. General purpose heat source radioisotope thermoelectric generator program
[DE90-006828] 12 p1614 N90-19284
Safety Status Report for the Ulysses mission. Book 2: Accident analysis-appendices. General purpose heat source radioisotope thermoelectric generator program
[DE90-006830] 12 p1614 N90-19286
A guide to performing and documenting safety analyses
[DE90-008687] 13 p1788 N90-20260
Final safety analysis report for the Ulysses Mission. Volume 2: Accident model document-appendices
[DE90-008695] 14 p1940 N90-21104
Final safety analysis report for the Ulysses Mission
[DE90-008690] 14 p1940 N90-21106
Final safety analysis report for the Ulysses mission. Volume 1: Reference design document
[DE90-008693] 14 p1940 N90-21107
Final (Tier 1) environmental impact statement for the Galileo and Ulysses Missions
[NASA-TM-102917] 15 p2056 N90-21779
Final environmental impact statement for the Galileo Mission (Tier 2)
[NASA-TM-102925] 15 p2124 N90-22147
General purpose heat source radioisotope thermoelectric generator program. Book 1: Accident analysis
[REPT-90SDS4202-BK-1] 15 p2166 N90-22379
Peacetime replacement and crash damage factors for army aircraft
[AD-A218544] 17 p2348 N90-23372
GPHS-RTG response to Challenger type accident 19 p2665 N90-25163
Arctic cold weather medicine and accidental hypothermia
[AD-A223090] 20 p2899 N90-26487
Helicopter aircrew helmets and head injury: A protective effect
[AD-A223024] 23 p3377 N90-29080

ACCLIMATIZATION
NT COLD ACCLIMATIZATION
NT HEAT ACCLIMATIZATION
Adaptation and resistance of ecosystems to stress
[AD-A212999] 05 p0665 N90-13889

ACCRETION
U DEPOSITION

ACCRETION DISKS
Electromagnetic jets in pulsar magnetospheres and near magnetized accretion disks 02 p0294 N90-11675
Ice grains in the dust disk of the bipolar nebula M 1-92 11 p1584 N90-19127
Nearly simultaneous optical, ultraviolet, and x ray observations of three PG quasars
[NASA-CR-186355] 12 p1728 N90-19932
The inter-outburst behavior of cataclysmic variables
[NASA-CR-186374] 13 p1902 N90-20914
Relativistic processes in active galactic nuclei 14 p2040 N90-21698
Does mass accretion lead to field decay in neutron stars
[CAL-394] 15 p2182 N90-22470
Synthetic spectra of accretion disks in DQ Her binaries
[NASA-CR-186837] 18 p2638 N90-25029
Iron K-shell lines from relativistic accretion disks 19 p2766 N90-25714
Accretion disks in low-mass X ray binaries 19 p2768 N90-25726
Studies of the possible X ray triple 4U1915-05 19 p2768 N90-25727
Superhumps in accretion disks 19 p2768 N90-25728
A unified model of accretion flows and X ray emission in low mass X ray binary systems 19 p2770 N90-25742
Three dimensional accretion disk simulation with external magnetic field 19 p2772 N90-25754
A search for radio pulsars in globular clusters and transient X ray sources 19 p2772 N90-25755
X ray nova GS 2000+25 = Nova Vul 1988: X ray and optical light curves, spectra, and model 19 p2772 N90-25757
Turbulization of shear flows in astrophysics 19 p2773 N90-25763

Coronae and winds around accretion discs
19 p2774 N90-25771
On the viscosity in accretion disks
19 p2774 N90-25775
Nonlinear phenomena in accretion disks: Possibility for observational verification 19 p2775 N90-25779
Simulation of the boundary layer in accretion disks with the SPH method 19 p2779 N90-25807
Ginga observations of dipping low mass X ray binaries
19 p2781 N90-25821
X ray burster spectra in the state of the persistent flux level. Two temperature models of the neutron star atmosphere 19 p2782 N90-25824
Astrophysical importance of the slim accretion disks
19 p2782 N90-25827
IUE observations of Cyg X-2 and Sco X-1: Accretion disks and the z-shaped curve 19 p2783 N90-25832
The 23rd ESLAB Symposium on Two Topics in X Ray Astronomy. Volume 2: AGN and the X Ray Background [ESA-SP-296-VOL-2] 19 p2784 N90-25841
The optical characteristics of a sample of soft X ray selected active galactic nuclei 19 p2784 N90-25843
The spectra (2 to 10 keV) of high luminosity quasars
19 p2786 N90-25852
X ray AGN variability with hour to month timescales
19 p2788 N90-25869
Extended line emission in AGN: Looking at the central engine 19 p2788 N90-25870
The EUV spectral shape of the big-bump in HS1700+6416 and F9: A genuine difference between Seyfert's and QSO's 19 p2789 N90-25878
The accretion disk in the galactic center: An independent indication for a massive central object
19 p2790 N90-25881
Iron lines from X ray illuminated accretion discs in AGN 19 p2790 N90-25884
Thermal comptonization in accretion disks
19 p2791 N90-25890
X ray polarization of the reprocessed emission from accretion disk in Seyfert galaxies
19 p2792 N90-25892
Spherical accretion with thermal pair production as models of AGN 19 p2793 N90-25897
The X ray spectrum of MCG-6-30-15
19 p2793 N90-25898
Variability of the continuum emission of GQ Comae
19 p2793 N90-25903

ACCUMULATIONS
Time-weighted accumulations ap(tau) and Kp(tau)
[RAE-TR-88050] 03 p0421 N90-12422
Mechanical properties of fluffy agglomerates consisting of core-mantle-particles 12 p1743 N90-20019
Interaction of electromagnetic fields with chondrocytes in gel culture
[AD-A223397] 24 p3497 N90-29765

ACCUMULATORS
NT ACCUMULATORS (COMPUTERS)
NT DUST COLLECTORS
NT SOLAR COLLECTORS
Laser velocimeter seed particle sizing by the whisker particle collector and laser aerosol spectrometer methods
[PB90-111287] 09 p1224 N90-17103
Beam collector and output window for a 35 GHz 100 kW gyrotron
[INPE-4958-RPE/603] 11 p1511 N90-18699
The effect of carbon type and processing on high rate thionyl chloride cathode collectors
[AD-A219823] 18 p2546 N90-24532
Spent-beam refocusing analysis and multistage depressed collector design for a 75-W, 59- to 64-GHz coupled-cavity traveling-wave tube
[NASA-TP-3039] 22 p3167 N90-27965
Heavy Nucleus Collector (HNC) project for the NASA Long Duration Exposure Facility (LDEF)
[NASA-CR-182094] 24 p3544 N90-30045

ACCUMULATORS (COMPUTERS)
Area-time efficient adders
[MEMO-INF-89-61] 17 p2440 N90-23905

ACCURACY
NT GEODETIC ACCURACY
Assessing the accuracy of vulnerability models by comparison with vulnerability experiments
[AD-A210871] 01 p0116 N90-10669
High accuracy coordinate determination using the global positioning system 02 p0150 N90-10658
Adaptive structures to meet future requirements for large precision structures 02 p0178 N90-11001
Simulation of synthetic aperture radar 1: Feature density and accuracy requirements
[AD-A211019] 02 p0213 N90-11218
Error allocation and accuracy assessment
05 p0603 N90-13501
Accuracy and characteristics of the Hipparcos catalog
05 p0611 N90-13566
A mixed finite element solution of the linear acoustic equations
[ECL-89-006] 05 p0697 N90-14075
A statistical study of the surface accuracy of a planar truss beam
[NASA-TM-4161] 09 p1235 N90-17171
Application of Bayesian reliability concepts to cruise missile electronic components
[AD-A216208] 10 p1394 N90-18059
An improved airborne wind measurement technique for the NAE (National Aeronautical Establishment) Twin Otter
[AD-A217978] 13 p1842 N90-20575
Foundations of measurement and instrumentation
[NASA-RP-1222] 14 p1981 N90-21351
Error correction of the DEA (Digital Electronic Automation) coordinate measuring machines at LLNL
[DE90-008913] 14 p1983 N90-21365
Wind forecasting for utility operations
[DE90-009466] 15 p2133 N90-22193
Characterization and calibration of coordinate measuring machines
[DE90-009320] 16 p2242 N90-22791
On the calibration of an autocollimator-comparator guide of a vertical target levelling rod differing from the ABBE's principle
[ISBN-951-754-887-7] 19 p2694 N90-25331
NASA project status reports: Congressional requirements can be met, but reliability must be ensured
[GAO/NSIAD-90-40] 20 p2843 N90-26169
Earth Radiation Budget Experiment (ERBE) validation
[NASA-TM-103481] 20 p2888 N90-26433
Accuracy analysis of the space shuttle solid rocket motor profile measuring device
[NASA-TM-101131] 21 p2968 N90-26871
Experiences with modern absolute instruments
21 p3022 N90-27183
Institut de Physique du Globe de Paris automatic magnetic observatory 21 p3022 N90-27184
Effects of basis set contraction in relativistic calculations on neon, argon, and germanium
[AD-A223357] 24 p3446 N90-29460

ACEE PROGRAM
Energy Efficient Engine high pressure turbine component test performance report
[NASA-CR-168289] 23 p3278 N90-28553
Energy Efficient Engine combustor test hardware detailed design report
[NASA-CR-168301] 23 p3279 N90-28554
Energy Efficient Engine acoustic supporting technology report
[NASA-CR-174834] 23 p3279 N90-28557
Energy Efficient Engine: Flight propulsion system final design and analysis
[NASA-CR-168219] 23 p3279 N90-28558
Energy Efficient Engine core design and performance report
[NASA-CR-168069] 23 p3279 N90-28559
Energy Efficient Engine integrated core/low spool design and performance report
[NASA-CR-168211] 23 p3280 N90-28561
Energy Efficient Engine: Control system component performance report
[NASA-CR-174851] 23 p3280 N90-28562
NASA/GE Energy Efficient Engine low pressure turbine scaled test vehicle performance report
[NASA-CR-168290] 23 p3280 N90-28563
Energy efficient engine program technology benefit/cost study. Volume 1: Executive summary
[NASA-CR-174766-VOL-1] 23 p3280 N90-28564
Energy efficient engine program technology benefit/cost study, volume 2
[NASA-CR-174766-VOL-2] 23 p3280 N90-28565
Energy efficient engine pin fin and ceramic composite segmented liner combustor sector rig test report
[NASA-CR-179534] 23 p3281 N90-28567
Energy Efficient Engine: Combustor component performance program
[NASA-CR-179533] 23 p3281 N90-28568
Energy Efficient Engine: High-pressure compressor test hardware detailed design report
[NASA-CR-180850] 23 p3281 N90-28570

ACETALS
Polyarylacetylene resin composites
[AD-A221507] 21 p2972 N90-26890

ACETATES
Single particle friction tests with cellulose acetate sphere samples
[DE89-017537] 06 p0793 N90-14622
An evaluation of ethylene-vinyl acetate copolymers as desensitizers for RDX in insensitive booster compositions prepared by slurry coating technology
[MRL-TR-89-33] 12 p1633 N90-19385
Preparation, characterisation and cookoff behaviour of booster compositions prepared from RDX and acrylic or ethylene-vinyl acetate dispersions
[MRL-TR-89-44] 14 p1957 N90-21203

ACETIC ACID
Contribution to the electrochemical study of corrosion in the low conductivity media: Application to the study of the behavior of austenitic stainless steels in concentrated solutions of acetic acid
[ISAL-89-0014] 05 p0625 N90-13648

ACETONITRILE
Electrochemistry in near-critical and supercritical fluids. 8: Methyl viologen, decamethylferrocene, Os(bpy)3(sup 2+) and ferrocene in acetonitrile and the effect of pressure on diffusion coefficients under supercritical conditions
[AD-A213407] 07 p0895 N90-15172

ACETYL COMPOUNDS
Heterogeneous transformation of peroxyacetylnitrate
20 p2887 N90-26430

ACETYLENE
Investigation of fuel additive effects on sooting flames
[AD-A212925] 04 p0473 N90-12709
Review of polyarylacetylene matrices for thin-walled composites
[AD-A214921] 09 p1186 N90-16872
On the vapour phase deposition mechanism of carbon-boron-nitrogen compounds between 800 and 1000 C
[REPT-892-430-101] 16 p2214 N90-22632
Acetylene terminated aspartimides and resins therefrom
[NASA-CASE-LAR-14188-1] 17 p2379 N90-23545
Thermal analysis of Acetylene Terminated Sulfone (ATS) resin
[AD-A220775] 17 p2381 N90-23558
Laboratory studies, analysis, and interpretation of the spectra of hydrocarbons present in planetary atmospheres including cyanoacetylene, acetylene, propane, and ethane 20 p2943 N90-26748
High resolution, low temperature photoabsorption cross-section of C2H2 with application to Saturn's atmosphere 20 p2945 N90-26757
Laboratory studies of photodissociation processes relevant to the formation of cometary radicals
20 p2947 N90-26772
Vapor pressures of acetylene at low temperatures
20 p2949 N90-26777
Polyarylacetylene resin composites
[AD-A221507] 21 p2972 N90-26890
An ionic mechanism of carbon formation in flames
21 p3093 N90-27582
Structure and radiation properties of turbulent diffusion flames
[PB90-218777] 22 p3155 N90-27887

ACHONDRITES
Meteoritic basalts
[NASA-CR-185949] 06 p0861 N90-15004

ACID BASE EQUILIBRIUM
Effects of high altitude hypoxia on lung and chest wall function during exercise
[AD-A219814] 17 p2434 N90-23869

ACID RAIN
Characterization and evaluation of acid rain in East Central Florida from 1978 to 1987: Ten year summary report
[NASA-TM-102149] 01 p0084 N90-10478
Spatial characterization of acid rain stress in Canadian Shield Lakes
[NASA-CR-183446] 01 p0084 N90-10479
Development of an inventory of materials potentially sensitive to ambient atmospheric acidity in the South Coast Air Basin
[PB89-224604] 04 p0516 N90-12982
Mesoscale acid deposition modeling studies
[NASA-CR-4262] 04 p0554 N90-13228
Computational solution of chemistry problems
[NASA-CR-186000] 05 p0620 N90-13618
An evaluation of trend detection techniques for use in water quality monitoring programs
[PB89-100058] 06 p0808 N90-14702
Steady state model to determine lake resources at risk to acid deposition in the Sierra Nevada, California
[PB89-103995] 06 p0809 N90-14705
Application of surface analysis methods to studies of atmospheric deposition in forests
[DE90-000562] 06 p0810 N90-14714
Analysis of acid rain and associated phenomena
[DE90-002555] 06 p0812 N90-14725
Nitrogen deposition to forest trees
[DE90-003285] 06 p0812 N90-14726
Long-term worldwide environmental effects caused by acid rain from fossil fuels
[DE90-001534] 07 p0956 N90-15533
Acid rain research
[DE90-003283] 07 p0957 N90-15537

Assessment of the importance of acidic fogwater and cloudwater in affecting terrestrial vegetation: Some important case studies
[DE90-002216] 08 p1098 N90-16361
Dispelling the North American acid rain clouds: Developing a framework for political consensus through the identification of elite viewpoints, volumes 1 and 2
09 p1243 N90-17213
A collaborative effort to model plant response to acidic rain
[DE90-003002] 09 p1244 N90-17215
NAPAP (National Acid Precipitation Assessment Program) emissions inventory: Overview of allocation factors, 1985
[PB90-126012] 12 p1685 N90-19679
The EURAD Model: Structure and First Results
[REPT-61] 12 p1686 N90-19680
Development and status of the EURAD project
12 p1686 N90-19681
Cloud parameterization in EURAD and its future development 12 p1687 N90-19692
Initialization of EURAD. Part 1: Utilization of ECMWF analysis data 12 p1688 N90-19695
Initialization of EURAD, part 2
12 p1688 N90-19696
Modelization of dry deposition in the Chemical Transport Model (CTM) of EURAD 12 p1688 N90-19698
Estimation of the distribution of SO2 and NOX emission in Europe 12 p1688 N90-19699
Emission data for the EURAD project
12 p1688 N90-19700
The EURAD model in EUROTRAC
12 p1689 N90-19701
A study of mesoscale acid deposition in the lower Ohio River Valley 16 p2253 N90-22848
Evaluation of the role of ozone, acid deposition, and other airborne pollutants in the forests of eastern North America
[PB90-164896] 22 p3197 N90-28140
Investigation of the effects of acid deposition on materials
[PB90-156973] 22 p3197 N90-28143
Quality assurance support for the National Atmospheric Deposition Program and national trends network monitoring activities: 1987-1990
[PB90-187162] 22 p3198 N90-28149
Role of grid-based, reactive air quality modeling in policy analysis: Perspectives and implications, as drawn from a case study
[PB90-187204] 22 p3198 N90-28150
Analysis of acid precipitation samples collected by state agencies: January to December 1988
[PB90-191784] 22 p3198 N90-28151
Laboratory and field evaluations of extrasensitive sulfur dioxide and nitrogen dioxide analyzers for acid deposition monitoring
[PB90-201062] 22 p3199 N90-28153
Acid deposition in Maryland: Summary of results through 1989
[PB90-229782] 22 p3200 N90-28160
Preliminary exposure study to determine the effects of acid deposition on coated steel substrates
[PB90-201799] 23 p3309 N90-28715
Acid deposition: No such thing as a free launch
[DE90-015085] 23 p3348 N90-28920

ACIDITY
Effects of Air Pollution on Western Forests
[PB90-131111] 14 p2003 N90-21481
Cloud chemistry and occurrence in the western United States: A synopsis of current information
[PB90-134248] 15 p2131 N90-22182
The effects of acid fog and dew on materials
[PB90-157496] 19 p2712 N90-25436
Experimental and kinetic modeling of acid/base redox reactions over metal oxide catalysts
[DE90-013835] 22 p3156 N90-27893
Prediction of episodic acidification in Maryland coastal plain streams
[PB90-194978] 22 p3199 N90-28152
Estimating the spatial variability of trace gas deposition velocities
[PB90-208570] 23 p3349 N90-28928

ACIDS
NT ACETIC ACID
NT ACRYLIC ACID
NT ALANINE
NT AMINO ACIDS
NT BORIC ACIDS
NT CARBOXYLIC ACIDS
NT DEOXYRIBONUCLEIC ACID
NT FORMIC ACID
NT GLYCINE
NT HYDROCHLORIC ACID
NT HYDROCYANIC ACID
NT HYDROFLUORIC ACID
NT NICOTINIC ACID
NT NITRIC ACID
NT OXIDASE
NT PHENYLALANINE
NT PHOSPHORIC ACID
NT RIBONUCLEIC ACIDS
NT SULFONIC ACID
NT SULFURIC ACID
NT TRYPTOPHAN
NT TYROSINE
Infrared and X ray photoelectron spectroscopy studies of the polyimide/metal interface
[AD-A218249] 13 p1773 N90-20179

ACOUSTIC ATTENUATION
NT SHOCK WAVE ATTENUATION
Investigation of materials and bonding using the scanning laser acoustic microscope
[KCP-613-4033] 01 p0048 N90-10270
Calculation of sound transmission through a cylindrical shell using ASKA acoustics 02 p0179 N90-11009
A SAW Slanted Array Correlator (SAC) with separate amplitude compensation channel
[AD-D014174] 03 p0336 N90-11914
Application of active noise reduction for hearing protection and speech intelligibility improvement
[IZF-1988-21] 04 p0527 N90-13042
Localization of ultrasound in thick composites
[AD-A212994] 05 p0618 N90-13602
Sound attenuation apparatus
[NASA-CASE-LAR-13968-1] 07 p0988 N90-15710
Study of active noise control in ducts
[DE89-772353] 10 p1425 N90-18224
Comparison between design and installed acoustic characteristics of NASA Lewis 9- by 15-foot low-speed wind tunnel acoustic treatment
[NASA-TP-2996] 12 p1606 N90-19242
Evidence for self-refraction in a convergence zone: NPE (Nonlinear progressive wave equation) model results
[AD-A218546] 16 p2259 N90-22879
Numerical studies of the active control of sound transmission through double partitions
[ISVR-TR-183] 16 p2313 N90-23181
Normal-mode and phase-integral methods for determining phase and group velocities in simple underwater acoustic ducts
[AD-A221393] 18 p2612 N90-24877
A preliminary study of the masking of wind turbine noise by ambient sound
[FFA-TN-1990-01] 20 p2923 N90-26636
Parametric studies of acoustic duct attenuation ofperforated-plate-on-honeycomb absorber
[NAL-TM-603] 24 p3542 N90-30030

ACOUSTIC COMBUSTION
U COMBUSTION STABILITY

ACOUSTIC COUPLING
Combustion instability coupling with feed system acoustics 23 p3293 N90-28629

ACOUSTIC DUCTS
Normal-mode and phase-integral methods for determining phase and group velocities in simple underwater acoustic ducts
[AD-A221393] 18 p2612 N90-24877
Canonical eigenvalues. Part 1: General theory
[AD-A222812] 20 p2920 N90-26617
Parametric studies of acoustic duct attenuation ofperforated-plate-on-honeycomb absorber
[NAL-TM-603] 24 p3542 N90-30030

ACOUSTIC EMISSION
Characterization of electron-beam weld processes in uranium by acoustic emission monitoring
[DE89-016044] 01 p0078 N90-10444
A counter gating circuit for acoustic emission monitoring of structures cracking under repetitive alternating loads
[ARL-MAT-TM-398] 05 p0653 N90-13808
Acoustic emission during intergranular stress corrosion cracking
[DE90-002894] 06 p0749 N90-14355
Cavitation-controlled ultrasonic agitator
[DE90-002773] 06 p0838 N90-14871
A computational and experimental study of steady and transient acoustic energy flow from a complex mechanical structure 08 p1119 N90-16478
Acoustic radiation of cylindrical shells, with stiffening finishing and coated with masking materials
[ISAL-89-0035] 10 p1426 N90-18227
Optimization of Gaussian beam widths in acoustic propagation
[AD-A215893] 10 p1427 N90-18231
Damage assessment in composites by acousto-ultrasonic technique
[AD-A216590] 11 p1479 N90-18510
Acoustic emission diagnostic techniques for high-field high current-density super inducting poles
[DE90-007400] 11 p1562 N90-19000
Mechanical disturbances in high-performance superconducting dipoles
[DE90-006237] 11 p1570 N90-19040
Spallation of oxide scales from 20 percent Cr/25 percent Ni/Nb stainless steel
[AERE-R-13464] 13 p1775 N90-20189
Acoustic characterisation of an aluminium silicon carbide metal matrix composite
[AERE-R-13273] 14 p1943 N90-21121
Impact tolerant material
[NASA-CASE-LAR-12887-3] 15 p2064 N90-21822
Propagation environments, effects, and decision aids
15 p2081 N90-21918
Combining acoustic emission locations and a microcrack damage model to study development of damage in brittle materials
[DE90-005195] 15 p2117 N90-22111
Polarization coupling in the acousto-optic interaction of surface waves 15 p2164 N90-22365
Impact damage in graphite/epoxy laminates: Damage characterization, acoustic emission, and finite element simulation, volumes 1 and 2 16 p2211 N90-22610
Characterization of particle impact by quantitative acoustic emission
[AERE-R-13028] 16 p2246 N90-22810
Characterisation of fatigue of aluminium alloys by acoustic emission. Part 1: Identification of source mechanism
[AERE-R-13302-PT-1] 17 p2375 N90-23522
Characterisation of fatigue of aluminium alloys by acoustic emission. Part 2: Discrimination between primary and other emissions
[AERE-R-13303-PT-2] 17 p2375 N90-23523
AECM3: Acoustic Emission Conditions for failure prediction of winding carbon structures
[REPT-892-430-115] 18 p2517 N90-24374
Applications of an acoustic-emission data-acquisition workstation: 2
[DE90-010941] 18 p2612 N90-24880
Study on failure modes of boron fiber reinforced aluminum composite materials by AE method, part 2
[DE90-505522] 20 p2828 N90-26086
Application and extension of an analytical model of the confined acoustic beam generated by a transducer
[AD-A222994] 20 p2924 N90-26639
Study on failure modes of SiC fiber reinforced aluminum composite materials by AE method
[DE90-505518] 21 p2971 N90-26884
Acoustic emission detection of crack presence and crack advance during flight 22 p3186 N90-28082
Acoustic emission from a growing crack
22 p3188 N90-28089
Study of failure processes in fiber reinforced composites using acoustic emission techniques
22 p3188 N90-28090
Use of acoustic emission for continuous surveillance of aircraft structures 22 p3188 N90-28092

ACOUSTIC EXCITATION
Materials characterization using holographic mapping of transient lamb waves
[AD-A211414] 03 p0358 N90-12050
Bulk acoustic waves resonators made of amorphous materials
[NOTE-TECHNIQUE-1989-4] 04 p0550 N90-13199
Mobility power flow analysis of an L-shaped plate structure subjected to acoustic excitation
[NASA-CR-186130] 05 p0655 N90-13817
Double valve mechanism for an acoustic modulator
[AD-D014401] 14 p1987 N90-21386
Destabilization of supersonic free shear layers by parametric excitation using Mach waves generated by a wavy wall
[AD-A219655] 17 p2345 N90-23352
Investigation of a heat driven thermoacoustic prime mover
[AD-A223928] 24 p3484 N90-29694

ACOUSTIC FREQUENCIES
NT AUDIO FREQUENCIES
Low ppb level detection of toxic compounds with a fully automated CO2 laser photoacoustic detector
02 p0206 N90-11181
A computational and experimental study of steady and transient acoustic energy flow from a complex mechanical structure 08 p1119 N90-16478
Study of active noise control in ducts
[DE89-772353] 10 p1425 N90-18224
The radiation of sound from a propeller at angle of attack
[NASA-CR-4264] 14 p2023 N90-21602
Percussive sound analysis using an autoregressive model. Application of modified covariance
[TELECOM-PARIS-89-D-016] 18 p2612 N90-24879
The effects of acoustic orientation cues on instrument flight performance in a flight simulator
23 p3359 N90-28985

ACOUSTIC GENERATORS
U SOUND GENERATORS

ACOUSTIC IMPEDANCE
An investigation of the diffraction of an acoustic plane wave by a curved surface of finite impedance
[NASA-CR-186069] 04 p0550 N90-13204
Localization of ultrasound in thick composites
[AD-A212994] 05 p0618 N90-13602
The optical measurement of acoustic velocity fields
14 p2023 N90-21601
Impact tolerant material
[NASA-CASE-LAR-12887-3] 15 p2064 N90-21822
Apparatus to determine the complex mass of a viscous fluid contained in a rigid porous solid from acoustic pressure measurements
[AD-A223709] 24 p3472 N90-29619
ACOUSTIC INSTABILITY
The physics of double layers and their role in astrophysics
[TRITA-EPP-89-03] 03 p0421 N90-12421
Spatial evolution of nonlinear acoustic mode instabilities on hypersonic boundary layers
[NASA-TM-102431] 06 p0777 N90-14517
ACOUSTIC LEVITATION
Acoustic controlled rotation and orientation
[NASA-CASE-NPO-16995-1-CU]
03 p0400 N90-12289
Non-contact temperature measurement requirements
10 p1363 N90-17898
Non-Contact Temperature Requirements (NCTM) for drop and bubble physics 10 p1366 N90-17918
ACOUSTIC MEASUREMENT
NT NOISE MEASUREMENT
Acoustic test and analysis of a counterrotating prop-fan model
[NASA-CR-179590] 01 p0119 N90-10683
Tower wake/blade interaction noise of a wind turbine
[NAL-TR-945] 02 p0236 N90-11344
A frequency domain technique for improving sound field reproduction
[RAE-TM-MM-10] 04 p0551 N90-13205
Test procedures for the evaluation of helmet and headset mounted active noise reduction systems
[AD-A212991] 05 p0676 N90-13937
Propagation of sound in vibrationally excited nitrogen and hydrogen gas mixtures
[AD-A213002] 05 p0696 N90-14073
Pulsed EMAT (Electromagnetic Acoustic Transducer) acoustic measurements on a horizontal continuous caster for internal temperature determination
[DE90-002735] 07 p0968 N90-15709
Wind speed dependence of acoustic ambient vertical directional spectra at high frequency
[AD-A214293] 07 p0989 N90-15712
Evaluation of two objective measures of effective auditory stimulus level
[AD-A214669] 09 p1250 N90-17255
Speech synthesis: From segmental synthesis to acoustic rules, using temporal decomposition
[TELECOM-88-E-019] 10 p1375 N90-17972
An analysis of diurnal wind variability in the Santa Barbara Channel from SODAR measurements
[AD-A215769] 10 p1408 N90-18121
Observations of fine-scale vertical shear and strain in the upper ocean
[AD-A214476] 10 p1410 N90-18130
Comparison between design and installed acoustic characteristics of NASA Lewis 9- by 15-foot low-speed wind tunnel acoustic treatment
[NASA-TP-2996] 12 p1606 N90-19242
Sandia National Laboratories' new high level acoustic test facility
[DE90-006810] 12 p1710 N90-19820
High-resolution Brillouin gain spectroscopy in solids
[DE90-009475] 14 p1949 N90-21155
The optical measurement of acoustic velocity fields
14 p2023 N90-21601
Applications of laser ultrasound
[AERE-R-13106] 16 p2239 N90-22777
Temporal attributes of the ambient seismo-acoustic environment: La Junta, Colorado
[AD-A219369] 16 p2249 N90-22825
Helicopter Airborne Laser Positioning System (HALPS)
[NASA-TM-102814] 17 p2354 N90-23399
Voice measures of workload in the advanced flight deck: Additional studies
[NASA-CR-4258] 17 p2437 N90-23887
Environmental measurements and analysis: Arctic acoustics experiments in the marginal ice zone
[AD-A220509] 18 p2582 N90-24708
Preliminary thoughts on an acoustic metric for the wilderness aircraft overflight study
18 p2609 N90-24862
Problems of internal acoustics in two and three dimensional cavities with deformable walls using the MSC/Nastran code
[DLC/STR-INT-TN-004] 18 p2612 N90-24876
Percussive sound analysis using an autoregressive model. Application of modified covariance
[TELECOM-PARIS-89-D-016] 18 p2612 N90-24879
Gradient microphone for measurement of the vectorial sound velocity
[MBB-Z-0259/89-PUB] 19 p2650 N90-25080
Experimental validation study of an analytical model of discrete frequency sound propagation in closed-test-section wind tunnels
[NASA-TM-102801] 19 p2754 N90-25647
The acoustic results of a United Technologies scale model helicopter rotor tested at DNW
[NASA-TM-101879] 21 p3073 N90-27471
Acoustic qualification of an anechoic chamber
[RAE-TM-MAT/STR-1136] 22 p3245 N90-28400
Wind tunnel investigation of periodic vortex separation from rough surface circular cylinders by means of acoustic measurements
[ESA-TT-1092] 23 p3268 N90-28499
Measuring the vertical directional spectra caused by sea surface sound
[AD-A223883] 23 p3354 N90-28957
Large hydrodynamic tunnel: Calculation of the acoustic transparency of the jet stream
[REPT-89/115] 23 p3393 N90-29167
Large aperture acoustic arrays in support of reverberation studies
[AD-A224002] 23 p3393 N90-29168
SONA: A measurement system for the determination of the end-of-flight burst behaviour of projectiles equipped with proximity fuses
[FEL-89-A293] 24 p3459 N90-29536
Apparatus to determine the complex mass of a viscous fluid contained in a rigid porous solid from acoustic pressure measurements
[AD-A223709] 24 p3472 N90-29619
ACOUSTIC MICROSCOPES
Investigation of materials and bonding using the scanning laser acoustic microscope
[KCP-613-4033] 01 p0048 N90-10270
An air coupled transmission mode acoustic microscope for on-line non-destructive evaluation
[AD-A211416] 04 p0511 N90-12947
Utilization of focused acoustic beams to inspect composite materials
[ETN-90-96084] 09 p1188 N90-16880
Foundations of millimeter-wave frequency acoustic microscopy 12 p1709 N90-19816
Nondestructive testing of ceramics by acoustic microscopy
[AERE-R-13350] 13 p1813 N90-20411
Nonlinear acoustic interactions in superfluid helium
15 p2164 N90-22367
Crack detection in silicon nitride by acoustic microscopy
[AERE-R-13196] 16 p2245 N90-22803
ACOUSTIC PROPAGATION
Investigation of materials and bonding using the scanning laser acoustic microscope
[KCP-613-4033] 01 p0048 N90-10270
Non-linear wave-equations for low-frequency acoustic gravity waves 02 p0240 N90-11365
Medium scale structure of the F-region
02 p0241 N90-11372
Transport composite fuselage technology: Impact dynamics and acoustic transmission
[NASA-CR-4035] 03 p0321 N90-11821
Wind effect on sound wave propagation at ground vicinity
[CSTB-2-87-008] 04 p0550 N90-13201
Localization of ultrasound in thick composites
[AD-A212994] 05 p0618 N90-13602
Optimization of Gaussian beam widths in acoustic propagation
[AD-A215893] 10 p1427 N90-18231
Propagation of transient acoustic waves in porous media
[ETN-90-96401] 15 p2099 N90-22015
An investigation of the generation and radiation of aerodynamic noise in real piping systems
15 p2164 N90-22368
A range-dependent analysis of acoustic transmission across a cold filament in the California current
[AD-A220175] 18 p2583 N90-24709
Study of a variable step network and comparison between the radii method and the parabolic equations, applied to the acoustic propagation in the atmosphere
[ONERA-RF-12/3641-PY] 22 p3245 N90-28401
ACOUSTIC PROPERTIES
NT ACOUSTIC IMPEDANCE
NT ACOUSTIC INSTABILITY
NT ACOUSTIC SCATTERING
NT ACOUSTIC VELOCITY
NT REVERBERATION
NT SOUND INTENSITY
NT ZERO SOUND
IFD (Implicit Finite Difference): Interfaced with Harvard open ocean model forecasts
[AD-A210521] 01 p0090 N90-10517
The dynamics of circular plates with patch damping: A numerical and experimental study
02 p0232 N90-11329
Acoustic studies of new materials: Quasicrystals, low-loss glasses and high Tc superconductors
[AD-A211281] 02 p0272 N90-11551
Problems in nonlinear acoustics: Scattering of sound by sound, parametric receiving arrays, nonlinear effects in asymmetric sound beams and pulsed finite amplitude sound beams
[AD-A211756] 04 p0550 N90-13200
ULF/VLF (0.001 to 50 Hz) Seismo-Acoustic Noise in the Ocean
[AD-A212942] 05 p0671 N90-13913
Annual summary of basic research in thermoacoustic heat transport
[AD-A214185] 07 p1007 N90-15834
Observations of fine-scale vertical shear and strain in the upper ocean
[AD-A214476] 10 p1410 N90-18130
A note on an acoustic response during an engine nacelle flight experiment
[NASA-TM-102585] 12 p1710 N90-19821
Localization and delocalization in periodic one-dimensional dynamic systems
[AD-A217939] 13 p1882 N90-20797
Air Force Boom Event Analyzer Recorder (BEAR): Sysstem description
[AD-A218048] 13 p1882 N90-20800
Relating flow between counter-rotating propellers to aerodynamic interaction noise 14 p1909 N90-20944
Acoustic characterisation of an aluminium silicon carbide metal matrix composite
[AERE-R-13273] 14 p1943 N90-21121
Low-sidelobe phased array antenna characteristics using the planar near-field Scanning technique: Theory and experiment
[AD-A220611] 17 p2390 N90-23613
Experimental validation study of an analytical model of discrete frequency sound propagation in closed-test-section wind tunnels
[NASA-TM-102801] 19 p2754 N90-25647
Aerodynamic loads and blade vortex interaction noise prediction
[ISL-PU-310/89] 20 p2802 N90-25942
Asymptotic modal analysis and statistical energy analysis
[NASA-CR-186732] 20 p2923 N90-26634
The speech signal 21 p2992 N90-27008
Measuring the vertical directional spectra caused by sea surface sound
[AD-A223883] 23 p3354 N90-28957
Electron acoustic and magnetoacoustic modes in a magnetized beam plasma system
[DE90-627473] 23 p3398 N90-29199
ACOUSTIC RADIATION
U SOUND WAVES
ACOUSTIC SCATTERING
NT REVERBERATION
Nonlinear acoustics: Reflection and refraction, propagation in a periodic waveguide, scattering of sound by sound and ellipsoidal focusing
[AD-A211224] 02 p0271 N90-11550
Numerical solution of acoustic-structure interaction problems
[AD-A211505] 03 p0400 N90-12293
Problems in nonlinear acoustics: Scattering of sound by sound, parametric receiving arrays, nonlinear effects in asymmetric sound beams and pulsed finite amplitude sound beams
[AD-A211756] 04 p0550 N90-13200
Numerical analysis of scattering by interface flaws
[AD-A212996] 05 p0654 N90-13810
Research on acoustical scattering, diffraction catastrophes, optics of bubbles, acoustical phase conjugation, and wake of an oscillating circular cylinder
[AD-A214168] 07 p0989 N90-15711
Underwater acoustic scattering from spherical particulates and bubbles
[AD-A214827] 09 p1279 N90-17414
Numerical simulation of acoustic scatter from subsurface bubble clouds
[AD-A217068] 12 p1710 N90-19822
Generalized Herglotz functions and inverse scattering problem in a finite depth ocean
[PB90-150996] 15 p2134 N90-22197
The effects of caustics in acoustic inverse scattering experiments
[AD-A218454] 16 p2313 N90-23185
Contributions of individual structural modes to the scattered acoustic field
[AD-A219128] 16 p2314 N90-23187

Application of frequency interpolation to acoustic-structure interaction problems
[AD-A219330] 17 p2469 N90-24113
Laboratory studies of acoustic scattering from the underside of sea ice
[AD-A221333] 19 p2753 N90-25644
A preliminary analysis of threshold signal detection in ambient and signal-dependent noise environments
[AD-A222089] 21 p2996 N90-27030
Separable coordinate systems for PDE
[AD-A223052] 21 p3063 N90-27415
Acoustic confinement in the large hydrodynamic tunnel: Identification of the acoustic charateristics with a one-directional source
[REPT-8228-88] 22 p3244 N90-28399

ACOUSTIC SIMULATION
Acoustic response analysis in the low frequency domain 02 p0179 N90-11010
The large European Acoustic Facility at ESTEC 02 p0187 N90-11067
Acoustic-thermal environment for USB flap structure. Report 1: Ground simulation test results
[NAL-TM-567] 03 p0300 N90-11697
Simulation of transport aeroplanes
[MBB-UT-007/89-PUB] 19 p2651 N90-25089
The simulation of localized sounds for improved situational awareness 23 p3359 N90-28984

ACOUSTIC SOUNDING
Acoustic recording systems for use in military aircraft
[RAE-TM-MM-11] 04 p0551 N90-13207
Preliminary comparison of temperature soundings obtained from simultaneous radiometric, radio-acoustic, and rawinsonde measurements
[PB90-119835] 11 p1535 N90-18838

ACOUSTIC STABILITY
U FREQUENCY STABILITY

ACOUSTIC STREAMING
Microgravity acoustic mixing for particle cloud combustors
[NASA-CR-185159] 14 p2023 N90-21600
The optical measurement of acoustic velocity fields 14 p2023 N90-21601

ACOUSTIC VELOCITY
IFD (Implicit Finite Difference): Interfaced with Harvard open ocean model forecasts
[AD-A210521] 01 p0090 N90-10517
Comparison of two Navy environmental database models: Generalized Digital Environmental Model and Podeszwa sound speed profile model
[AD-A215848] 11 p1544 N90-18889
Elastic properties of silica xerogels
[AD-A216528] 12 p1630 N90-19366
Geometric scale of interaction between moving shock and stationary thermal layer
[AD-A217769] 13 p1802 N90-20344
The optical measurement of acoustic velocity fields 14 p2023 N90-21601
The effects of caustics in acoustic inverse scattering experiments
[AD-A218454] 16 p2313 N90-23185
A range-dependent analysis of acoustic transmission across a cold filament in the California current
[AD-A220175] 18 p2583 N90-24709
Summary of sonic boom rise times observed during FAA community response studies over a 6-month period in the Oklahoma City area
[NASA-CR-4277] 18 p2608 N90-24852
Normal-mode and phase-integral methods for determining phase and group velocities in simple underwater acoustic ducts
[AD-A221393] 18 p2612 N90-24877
Gradient microphone for measurement of the vectorial sound velocity
[MBB-Z-0259/89-PUB] 19 p2650 N90-25080
Dynamic properties of porous B4C
[AD-A222650] 21 p2985 N90-26960
Thermophysical properties of Helium-4 from 0.8 to 1500 K with pressures to 2000 MPa
[NASA-CR-186992] 23 p3303 N90-28681
Measuring the vertical directional spectra caused by sea surface sound
[AD-A223683] 23 p3354 N90-28957
Nondestructive material characterization
[DE90-015176] 24 p3477 N90-29652
Numerical pulse propagation studies using two classical ocean waveguide models
[AD-A224118] 24 p3542 N90-30033

ACOUSTIC VIBRATIONS
U SOUND WAVES

ACOUSTICAL HOLOGRAPHY
The investigation of the fundamental limits of heterodyne holographic interferometry with the application of imaging laser generated lamb waves
[AD-A211048] 02 p0224 N90-11285
Full field visualization of surface and bulk acoustic waves using heterodyne holographic interferometry
[AD-A214353] 10 p1387 N90-18023
Improved processes for ultrasonic object recognition in robotics
[ETN-90-95362] 12 p1672 N90-19504
High-resolution acoustical imaging 13 p1881 N90-20793

ACOUSTICS
NT AEROACOUSTICS
NT ELECTROACOUSTICS
NT GEOMETRICAL ACOUSTICS
NT MAGNETOACOUSTICS
NT PSYCHOACOUSTICS
NT UNDERWATER ACOUSTICS
The theory and application of quadratic minimization in the active reduction of sound and vibration 01 p0119 N90-10682
Development of the electroacoustic dewatering (EAD) process for fine/ultrafine coal
[DE89-015883] 01 p0122 N90-10700
Development of a thermoacoustic test facility 02 p0183 N90-11041
Analysis of two-pass Modified Hough Transform (MHT) technique for the detection of wake like signals
[AD-A211982] 03 p0338 N90-11924
NDE (Non-Destructive Evaluation) publications, 1985
[PB89-229025] 03 p0356 N90-12036
Computation of generalized modal loads in an acoustic field define by a distribution of correlated pressures
[NASA-CR-186041] 03 p0358 N90-12047
Acoustical effects of a large ridge on low-frequency sound propagation in stationary and moving atmospheres
[NASA-CR-186001] 03 p0400 N90-12290
Bulk acoustic waves resonators made of amorphous materials
[NOTE-TECHNIQUE-1989-4] 04 p0550 N90-13199
Problems in nonlinear acoustics: Scattering of sound by sound, parametric receiving arrays, nonlinear effects in asymmetric sound beams and pulsed finite amplitude sound beams
[AD-A211756] 04 p0550 N90-13200
A mixed finite element solution of the linear acoustic equations
[ECL-89-006] 05 p0697 N90-14075
NRL (Naval Research Laboratory) Review
[AD-A212886] 05 p0716 N90-14182
Acoustic-vortical-combustion interaction in a solid fuel ramjet simulator 06 p0726 N90-14234
Boundary element analysis of single and multidomain problems in acoustics 06 p0837 N90-14867
Effective utilization of acoustic wave sensor responses: Simultaneous measurement of velocity and attenuation
[DE90-002580] 06 p0838 N90-14872
Sound attenuation apparatus
[NASA-CASE-LAR-13968-1] 07 p0988 N90-15710
SAW (Surface Acoustic Wave) transducer with improved bus-bar design
[AD-D014250] 08 p1060 N90-16125
Measurement of reflection and impedance in a beam by the structural intensity technique
[DE90-728212] 08 p1088 N90-16299
NASA/ASEE Summer Faculty Fellowship Program
[NASA-CR-166837] 08 p1154 N90-16686
Modeling the near acoustic field of a rocket during launch 08 p1156 N90-16694
Proceedings of the 79th SEGJ Conference
[DE89-760006] 08 p1157 N90-16704
Physical models for supersonic turbulent boundary layer structure
[AD-A215284] 09 p1160 N90-16716
Phase space and path integral methods applied to direct and inverse ocean seismo-acoustic modeling
[AD-A214777] 09 p1249 N90-17247
Surface acoustic wave sensors and piezoelectric actuators for investigations of transitional and turbulent flows
[AD-A214889] 09 p1279 N90-17415
Non-Contact Temperature Requirements (NCTM) for drop and bubble physics 10 p1366 N90-17918
Acetylcholinesterase inhibition and information processing in the auditory cortex
[AD-A216092] 10 p1411 N90-18139
An approximate model for the performance and acoustic predictions of counterrotating propeller configurations
[NASA-CR-180667] 10 p1426 N90-18228
Measuring Day-Night Noise Levels (DNL) using the metrosonics db-310 sound level analyzer (Dosimeter)
[AD-A215757] 10 p1427 N90-18230
A linear systems theory approach to the range-independent acoustic channel
[AD-A216551] 12 p1710 N90-19817
Modeling and classification of acoustic transients by speech recognition techniques
[AD-A218070] 13 p1791 N90-20277
VAPEPS user's reference manual, version 5.0
[NASA-CR-180781] 13 p1868 N90-20713
Acoustic convective system
[NASA-CASE-NPO-17278-1-CU] 14 p1959 N90-21215
Double valve mechanism for an acoustic modulator
[AD-D014401] 14 p1987 N90-21386
The Shock and Vibration Digest, volume 22, no. 2 14 p2022 N90-21596
State of the art of acoustics of active and passive mufflers 14 p2023 N90-21597
The optical measurement of acoustic velocity fields 14 p2023 N90-21601
The vibro-acoustic mapping of low gravity trajectories on a Learjet aircraft
[NASA-TM-103103] 15 p2045 N90-21723
JPRS report: Science and technology. USSR: Physics and mathematics
[JPRS-UPM-89-001] 16 p2310 N90-23162
Acoustoelectronic interaction of surface waves in GaAs-InGaAs superlattices 16 p2310 N90-23163
Learning environment for neural networks and transient acoustics
[AD-A219000] 16 p2314 N90-23186
Simulation and analysis of a MFQPSK signal transmitted through an acoustic medium
[AD-A220345] 17 p2393 N90-23833
Acousto-ultrasonic nondestructive evaluation of materials using laser beam generation and detection
[NASA-CR-186694] 17 p2398 N90-23664
Finite element formulations for coupled fluid/structure eigenvalue analysis
[AD-A220793] 17 p2416 N90-23766
Analyses of the predictability of noise-induced sleep disturbance
[AD-A220156] 17 p2435 N90-23876
Mental lapses and event-related potentials
[AD-A219454] 17 p2436 N90-23878
Cumulative reports and publications through December 31, 1989
[NASA-CR-182041] 17 p2439 N90-23898
Integral and series representation of infinitely divisible processes with applications to their prediction and to their sample path, statistical, and structural properties
[AD-A219625] 17 p2456 N90-24017
Activities report in technical-physical research
[ETN-90-96771] 17 p2487 N90-24223
Fluid dynamic and acoustic experiments on turbomachine rotors subject to variable flow conditions
[AD-A220298] 18 p2552 N90-24565
Random vibration analysis of space flight hardware using NASTRAN 18 p2570 N90-24645
Coupled BE/FE/BE approach for scattering from fluid-filled structures 18 p2570 N90-24649
Direct conversion technology
[NASA-CR-186795] 18 p2576 N90-24675
Normal-mode and phase-integral methods for determining phase and group velocities in simple underwater acoustic ducts
[AD-A221393] 18 p2612 N90-24877
Millimeter-wave acoustic transducers
[AD-A221402] 18 p2612 N90-24878
Creating a VAPEPS database: A VAPEPS tutorial
[NASA-CR-186629] 20 p2936 N90-26705
Aspects of acoustic noise generation by a laser-propelled vehicle
[DE90-012087] 21 p2964 N90-26851
Phase-sensitive optical detection of ballistic phonon pulses using frequency-modulation spectroscopy and persistent spectral holes
[AD-A221521] 21 p2979 N90-26930
The speech signal 21 p2992 N90-27008
Speech recognition based on pattern recognition techniques 21 p2993 N90-27011
A preliminary analysis of threshold signal detection in ambient and signal-dependent noise environments
[AD-A222089] 21 p2996 N90-27030
Method and apparatus for applying a mechanical force to surface
[NASA-CASE-LAR-14009-1] 21 p3011 N90-27115
Interaction of acoustic waves generated by coupled plate
[NASA-CR-186873] 21 p3072 N90-27464
The validation and application of a rotor acoustic prediction computer program
[NASA-TM-101794] 21 p3072 N90-27465
Air Force procedure for predicting aircraft noise around airbases: Noise Exposure Model (NOISEMAP). User's manual
[AD-A223162] 21 p3072 N90-27467
Noise from tip vortex and bubble cavitation
[AD-A221962] 21 p3072 N90-27468
Aviation acoustical noise measurement
[AD-A222014] 21 p3073 N90-27469

Temporal response of coupled one-dimensional dynamic systems
[AD-A222375] 21 p3073 N90-27470
The acoustic results of a United Technologies scale model helicopter rotor tested at DNW
[NASA-TM-101879] 21 p3073 N90-27471
Entropy wave instability in compact ramjets
22 p3162 N90-27932
Improved compact optical RF spectrum analyzer
[AD-D014481] 22 p3177 N90-28026
Energy Efficient Engine acoustic supporting technology report
[NASA-CR-174834] 23 p3279 N90-28557
Liquid Rocket Booster (LRB) for the Space Transportation System (STS) systems study. Appendix B: Liquid rocket booster acoustic and thermal environments
[NASA-CR-183788-APP-B] 23 p3288 N90-28602
Methods for detecting low-frequency signals in the presence of strong winds
[AD-A223980] 23 p3320 N90-28769
SuperCHIEF: A modified CHIEF (Combined Helmholz Integral Equation Formulation) method
[DE90-014744] 23 p3387 N90-29123
Large aperture acoustic arrays in support of reverberation studies
[AD-A224002] 23 p3393 N90-29168
Proceedings of a Workshop on the Geoelectric and Geomagnetic Environment of Continental Margins
[AD-A223743] 24 p3493 N90-29739
Activities report of the Institute of Sound and Vibration Research
[ETN-90-97604] 24 p3565 N90-30170

ACOUSTO-OPTICS
Theoretical and experimental investigation of nonlinear optoacoustics in liquids
[AD-A210427] 01 p0124 N90-10708
A remote sensor to monitor combustion products using a tunable acousto-optic filter 02 p0223 N90-11275
Acoustic studies of new materials: Quasicrystals, low-loss glasses and high Tc superconductors
[AD-A211281] 02 p0272 N90-11551
An imaging vector magnetograph for the next solar maximum 03 p0435 N90-12489
An air coupled transmission mode acoustic microscope for on-line non-destructive evaluation
[AD-A211416] 04 p0511 N90-12947
Sound Localization by Human Observers symposium proceedings
[AD-A212877] 04 p0524 N90-13026
Spectrometer technology recommendations
05 p0597 N90-13468
Laser glass (1989)
[DE90-002754] 07 p0909 N90-15257
Optical acoustic sensor using optical fiber
[DE89-901267] 07 p0992 N90-15730
Design of a large angular aperture TeO2 acousto-optic tunable filter
[AD-A213999] 07 p0993 N90-15738
Classification of acousto-optic correlation signatures of spread spectrum signals using artificial neural networks
[AD-A215045] 09 p1206 N90-16992
Damage assessment in composites by acousto-ultrasonic technique
[AD-A216590] 11 p1479 N90-18510
Applications of acousto-optical correlation devices in radar signal processing
[AD-A216624] 11 p1497 N90-18616
Modeling and realization of plane acousto-optic unilateral band modulators
[ETN-90-95824] 12 p1710 N90-19818
An acousto-optic image correlator with a throughput rate of 1000 templates per second
[DE90-009323] 15 p2144 N90-22249
Polarization coupling in the acousto-optic interaction of surface waves 15 p2164 N90-22365
Optical excisor modeling
[AD-A219338] 16 p2230 N90-22722
Proceedings of the 12th Symposium on Signal and Image Processing English-Language Abstracts
[AD-A218806] 17 p2388 N90-23598
Optical fiber for acoustic sensor applications
[AD-A219323] 17 p2472 N90-24130
Optical signal processing
[AD-A220332] 18 p2615 N90-24897
Interstellar HCN, HNC and HCO+: Stability experiments with acoustooptic spectrometers
[ETN-90-96495] 18 p2638 N90-25028
Acousto-optical localization of speed maneuvering flight targets
[FB-11-89] 19 p2758 N90-25676
Acousto-optic signature analysis for inspection of the orbiter thermal protection tile bonds
[DE90-013089] 20 p2819 N90-26043
A compact real-time acousto-optic image correlator
[DE90-015564] 24 p3546 N90-30054

ACQUISITION
NT DATA ACQUISITION
NT TARGET ACQUISITION
Rosetta/CNSR, ESA's planetary cornerstone mission
12 p1738 N90-19990
Design and development activities on the candidate sample acquisition system for the Rosetta mission
12 p1738 N90-19993
A dictionary of acquisition and contracting terms
[AD-A221681] 21 p3088 N90-27560

ACRYLATES
Negative-working electron beam resist based on poly(methyl methacrylate)
[AD-A207834] 01 p0128 N90-10733
Dynamics of bulk and surface-adsorbed polyacrylates
[AD-A221046] 18 p2530 N90-24437
Mass spectrometry of poly(methyl methacrylate)s of low molecular weight 20 p2829 N90-26091

ACRYLIC ACID
Shear-resistant drag reduction polymers. Part 1: Molecular investigations of polymer drag reduction and the development of laboratory screening methods
[AD-A223353] 24 p3454 N90-29508

ACRYLIC RESINS
UV-curable polyurethane-methacrylate co-networks and interpenetrating networks
[AD-A210445] 01 p0050 N90-10285
Synthesis and interfacial properties of new generation polyurethane systems
[AD-A210446] 01 p0050 N90-10286
Crazing and degradation of flexure strength in acrylic plates as a function of time
[AD-A212835] 06 p0749 N90-14357
Crosslinked, flexible, low-molecular-weight polyacrylamide gels for mobility control
[DE90-000202] 07 p0913 N90-15280
Surface-enhanced Raman scattering from model acrylic adhesive systems
[AD-A216117] 10 p1359 N90-17883
Investigation into the mechanism of polymer thread drag reduction
[AD-A217492] 13 p1800 N90-20329
Preparation, characterisation and cookoff behaviour of booster compositions prepared from RDX and acrylic or ethylene-vinyl acetate dispersions
[MRL-TR-89-44] 14 p1957 N90-21203
Thermomechanical properties of polymeric materials and related stresses
[NASA-TM-100758] 15 p2071 N90-21864
Solubility characteristics of a methacrylate copolymer
[AD-A222938] 21 p2985 N90-26962
Non-destructive characterization of polymer/metal interphases using surface-enhanced Raman scattering
[AD-A222490] 21 p2988 N90-26980
Aqueous solution properties of ampholytic ionomers
[AD-A222152] 22 p3156 N90-27890
Precursor structure-fiber property relationships in polyacrylonitrile-based carbon fibers
[AD-A224246] 24 p3454 N90-29503

ACRYLONITRILES
NT POLYACRYLONITRILE
Toughening of SAN copolymers by an SAN emulsion grafted rubber
[AD-A224213] 24 p3453 N90-29502

ACTINIDE SERIES
NT AMERICIUM
NT CURIUM
NT PLUTONIUM
NT URANIUM
NT URANIUM ISOTOPES

ACTINIDE SERIES COMPOUNDS
NT PLUTONIUM COMPOUNDS
NT PLUTONIUM OXIDES
NT THORIUM COMPOUNDS
NT URANIUM COMPOUNDS
NT URANIUM OXIDES
Luminescence of lanthanides and actinides implanted into binary III-V semiconductors and AlGaAs
[AD-A215759] 11 p1569 N90-19031

ACTINOMETERS
NT ADVANCED VERY HIGH RESOLUTION RADIOMETER
NT INFRARED DETECTORS
NT INFRARED RADIOMETERS
NT INFRARED SCANNERS
NT INFRARED SPECTROMETERS
NT MICROWAVE RADIOMETERS
NT PYRANOMETERS
NT RADIOMETERS
NT SOLAR SPECTROMETERS
NT SPECTROPHOTOMETERS
NT SPECTRORADIOMETERS
NT TOTAL OZONE MAPPING SPECTROMETER
NT ULTRAVIOLET DETECTORS
NT ULTRAVIOLET SPECTROMETERS

ACTIVATION
Scientific and technical report voice activated gun turrent control
[AD-A210350] 01 p0110 N90-10623
Mechanism of electrochemical activation of carbon electrodes: Role of graphite lattice defects
[AD-A211644] 03 p0325 N90-11845
Synaptic plasticity and memory formation
[AD-A211368] 03 p0379 N90-12158
A room-temperature, laser diode-pumped, Q-switched, 2 micron, thulium-doped, solid state laser
[AD-D014527] 19 p2695 N90-25334

ACTIVATION (BIOLOGY)
Activation: Positive and negative effects of the alarm system in the brain 09 p1257 N90-17290
Dynamical solvent effects on electron-transfer processes: Recent progress and perspectives
[AD-A222603] 20 p2830 N90-26101

ACTIVATION ANALYSIS
NT NEUTRON ACTIVATION ANALYSIS
Proof of the feasibility of coherent and incoherent schemes for pumping a gamma-ray laser
[AD-A212315] 04 p0506 N90-12921
Semiconductor measurement technology: Database for and statistical analysis of the interlaboratory determination of the conversion coefficient for the measurement of the interstitial oxygen content of silicon by infrared absorption
[PB89-221170] 04 p0558 N90-13253
Prompt Gamma Activation Analysis (PGAA): Technique of choice for nondestructive bulk analysis of returned comet samples 08 p1144 N90-16633

ACTIVATION ENERGY
Two photon absorption characterization
[AD-A210508] 01 p0121 N90-10694
Quasi-diffusion between phonon and roton gases in two- and three-dimensional liquid helium
[AD-A210565] 02 p0192 N90-11096
Asymptotic analyses of the structures and characteristics of flames 04 p0468 N90-12683
Embrittlement of laboratory- and reactor-aged CF-3, CF-8, and CF-8M duplex stainless steels
[DE90-002777] 06 p0748 N90-14354
Accelerated aging embrittlement of cast duplex stainless steel: Activation energy for extrapolation
[DE90-001773] 07 p0903 N90-15221
Effects of non-linearity in the variation of pinning potential with current-density on magnetic flux creep in high and low T(sub c) superconductors
[DE90-003952] 07 p1005 N90-15822
Kinetics of boron hydride interconversion reactions
[AD-A215386] 09 p1192 N90-16906
Chemical activation of molecules by metals: Experimental studies of electron distributions and bonding
[DE90-005371] 10 p1428 N90-18238
Supercooling and germ formation
13 p1784 N90-20242
Metal alkoxides: Models for metal oxides. Alkoxide ligands in early transition metal organometallic chemistry
[DE90-007523] 13 p1894 N90-20869
Testing carbon fabric for oxidation mass loss
15 p2063 N90-21819
Stress versus temperature dependent activation energies in creep
[NASA-TM-103192] 17 p2417 N90-23773
Structure and dynamic properties of combined polymeric main-chain/side-chain liquid crystals
[ETN-90-97299] 22 p3160 N90-27921
Double layer effects on the enthalpy of activation of heterogeneous electron transfer reactions
[AD-A221934] 22 p3245 N90-28404

ACTIVE CONTROL
Control law synthesis and optimization software for large order aeroservoelastic systems
01 p0022 N90-10111
Combustion instabilities in liquid-fueled propulsion systems: An overview 01 p0035 N90-10192
Attenuation of reheat buzz by active control
01 p0036 N90-10201
Application of formal optimization techniques in thermal/structural design of a heat-pipe-cooled panel for a hypersonic vehicle
[NASA-TM-89131] 01 p0071 N90-10409
The active control of an unstable canard aircraft
02 p0156 N90-10894
Independent Orbiter Assessment (IOA): CIL issues resolution report, volume 1
[NASA-CR-185524-VOL-1] 02 p0169 N90-10954
Independent Orbiter Assessment (IOA): Assessment of the active thermal control system
[NASA-CR-185573] 02 p0174 N90-10979
Active control of unsteady and separated flow structures
[AD-A212109] 03 p0301 N90-11707

Independent Orbiter Assessment (IOA): Analysis of the active thermal control subsystem
[NASA-CR-185553] 03 p0314 N90-11782
Active control of the forced and transient response of a finite beam 03 p0357 N90-12040
Effect of control surface mass unbalance on the stability of a closed-loop active control system
[NASA-TP-2952] 03 p0357 N90-12042
Application of sound and temperature to control boundary-layer transition 04 p0443 N90-12537
An approach to optical structures control 05 p0595 N90-13456
Segment alignment control system 05 p0595 N90-13457
Control of optical systems 05 p0600 N90-13484
PACOSS program 05 p0601 N90-13487
LDR structural technology activities at JPL 05 p0601 N90-13488
Payload thermal control 05 p0604 N90-13511
Spacecraft thermal control 05 p0604 N90-13513
Active control system for gust load allevation and structural damping 07 p0871 N90-15056
Numerical investigation of transition control of a flat plate boundary layer 07 p0926 N90-15361
Cooperative control of two active spacecraft during proximity operations
[NASA-CR-185596] 09 p1172 N90-16778
Feedback control of combustion instabilities: A case study in active adaptive control of complex physical systems
[AD-A215385] 09 p1192 N90-16905
Active control of a flexible structure using a modal positive position feedback controller
[NASA-CR-186336] 09 p1272 N90-17371
The 59th Shock and Vibration Symposium, volume 3
[AD-A214580] 10 p1395 N90-18066
Baseline experiment for active control of structural vibrations
[AD-A216194] 10 p1397 N90-18076
Study of active noise control in ducts
[DE89-772353] 10 p1425 N90-18224
Active stabilization of aeromechanical systems
[AD-A216629] 11 p1506 N90-18672
Modified independent modal space control of flexible structures 12 p1671 N90-19597
The application of active controls technology to a generic hypersonic aircraft configuration
[NASA-TM-101689] 13 p1754 N90-20071
Active control of the forced and transient response of a finite beam
[NASA-CR-181957] 13 p1816 N90-20430
PACOSS program status and results 14 p1933 N90-21065
A distributed finite-element modeling and control approach for large flexible structures 14 p1934 N90-21071
Controller reduction for effective interdisciplinary design of active structures 14 p1935 N90-21077
A survey of experiments and experimental facilities for active control of flexible structures 14 p1936 N90-21079
Experimental evaluation of active-member control of precision structures 14 p1936 N90-21084
In-house experiments in large space structures at the Air Force Wright Aeronautical Laboratories Flight Dynamics Laboratory 14 p1938 N90-21092
Attitude control modes for the MECB remote sensing satellites
[INPE-4755-PRE/1427] 14 p1938 N90-21094
Active control of multi-dimensional random sound in ducts
[NASA-TM-102653] 14 p2024 N90-21603
Advances in optimal active control techniques for aerospace systems; application to aircraft active landing gear 15 p2054 N90-21769
Bi-directional thruster development and test report
[NASA-CR-182013] 15 p2058 N90-21785
Modern developments in shear flow control with swirl
[NASA-CR-186586] 15 p2097 N90-22000
The Shock and Vibration Digest, volume 21, no. 1 15 p2109 N90-22061
Recent advances in structural control 15 p2109 N90-22062
Active control of bearing preload using piezoelectric translators 15 p2115 N90-22098
The Shock and Vibration Digest, volume 21, no. 6 15 p2163 N90-22363
Noise transmission into propeller-driven airplanes 15 p2163 N90-22364
Elements of active vibration control for rotating machinery
[NASA-TM-102368] 16 p2227 N90-22703
Control of a flexible planar truss using proof mass actuators 16 p2288 N90-23035
Distributed neural control of a hexapod walking vehicle 16 p2293 N90-23061
Autonomous power expert system
[NASA-CR-185263] 19 p2670 N90-25187
Robot vibration control using inertial damping forces
[NASA-CR-186808] 19 p2698 N90-25352
Design and implementation of robust decentralized control laws for the ACES structure at Marshall Space Flight Center
[NASA-CR-4310] 20 p2820 N90-26046
Active control of aerothermoelastic effects for a conceptual hypersonic aircraft
[NASA-TM-102713] 22 p3122 N90-27725
A new method for a tethered system aided space station assembly 22 p3130 N90-27765
Magnetic forces in high-T(sub c) superconducting bearings 22 p3137 N90-27799
Active control of flexible structures 23 p3282 N90-28575
The KALI multi-arm robot programming and control environment 23 p3373 N90-29060
Distributed control architecture for CNI preprocessors 24 p3426 N90-29356
A digital controller for active aeroelastic controls
[NAL-TR-1014] 24 p3435 N90-29402
Suspension systems for ground testing large space structures
[NASA-CR-4325] 24 p3439 N90-29424
Redundancy in sensors, control and planning of a robotic system for space telerobotics 24 p3511 N90-29847
Real-time cartesian force feedback control of a teleoperated robot 24 p3513 N90-29857
A distributed control and monitor system used in laser fusion research
[DE90-011483] 24 p3549 N90-30078

ACTIVE GALACTIC NUCLEI
Analysis of nearly simultaneous X-ray and optical observations of active galactic nuclei 01 p0139 N90-10806
The softest Einstein AGN (Active Galactic Nuclei)
[DE89-009389] 06 p0864 N90-15020
Ion-heated thermal Comptonization models and x ray spectral correlations in active galactic nuclei
[DE90-003597] 08 p1151 N90-16667
EXOSAT observations of Seyfert type galaxies 13 p1901 N90-20910
Relativistic processes in active galactic nuclei 14 p2040 N90-21698
Spectrum formation in active galactic nuclei and Type 2 supernovae 15 p2187 N90-22490
Gamma rays from active galactic nuclei 16 p2337 N90-23316
Spectral evolution of active galactic nuclei Penrose Compton scattering processes and gamma ray emission from Seyfert galaxies 16 p2337 N90-23317
The high energy source 3C 273 16 p2337 N90-23318
COMPTEL observations of active galactic nuclei 16 p2337 N90-23319
OSSE observations of active galactic nuclei 16 p2337 N90-23320
Black holes in X ray binaries: X ray properties of the galactic black hole candidates 19 p2765 N90-25712
A model for 1/f-type variability in active galactic nuclei 19 p2778 N90-25799
Astrophysical importance of the slim accretion disks 19 p2782 N90-25827
The 23rd ESLAB Symposium on Two Topics in X Ray Astronomy. Volume 2: AGN and the X Ray Background
[ESA-SP-296-VOL-2] 19 p2784 N90-25841
Theories of the X ray background 19 p2784 N90-25842
The optical characteristics of a sample of soft X ray selected active galactic nuclei 19 p2784 N90-25843
Population properties of AGN in the soft X-ray band 19 p2784 N90-25844
Contributions of discrete sources to the X ray background 19 p2785 N90-25847
BL Lacs from the EMSS: Number-counts and implications for the luminosity function 19 p2785 N90-25849
The X ray spectra of emission line AGN 19 p2785 N90-25850
Very low luminosity AGN 19 p2786 N90-25851
The spectra (2 to 10 keV) of high luminosity quasars 19 p2786 N90-25852
The environmental impact of the X ray flux from active galactic nuclei 19 p2786 N90-25853
Ginga observations of the X ray spectra of AGN 19 p2786 N90-25854
The complex X ray spectra of AGN 19 p2786 N90-25855
Is AGN spectral evolution needed for the CXB 19 p2786 N90-25856
AGNs and the spectrum of the X ray background 19 p2787 N90-25858
Reacceleration of pairs in compact sources 19 p2787 N90-25859
Complex X ray spectra and thick matter in Seyfert 1 galaxies 19 p2787 N90-25860
Ultrasoft components in X ray-selected AGN 19 p2787 N90-25864
Properties of sources that may contribute the other half of the cosmic X ray background 19 p2788 N90-25866
Signposts to the future 19 p2788 N90-25867
Long timescale X ray variability in AGN 19 p2788 N90-25868
X ray AGN variability with hour to month timescales 19 p2788 N90-25869
Extended line emission in AGN: Looking at the central engine 19 p2788 N90-25870
Quantum effects in pair cascade models of AGN spectra 19 p2789 N90-25873
The dependence of the soft X ray spectral slope with radio property, luminosity, and redshift, for a large sample of AGN from the Einstein IPC data base 19 p2789 N90-25876
Ion-heated thermal comptonization models and X ray spectral correlations in active galactic nuclei 19 p2790 N90-25880
Pure luminosity evolution and the AGN contribution to the X ray background 19 p2790 N90-25883
Iron lines from X ray illuminated accretion discs in AGN 19 p2790 N90-25884
Simulations of high-resolution X ray spectra of AGNs 19 p2791 N90-25885
Hard X ray observations of AGN 19 p2791 N90-25889
Thermal comptonization in accretion disks 19 p2791 N90-25890
X ray emission from relativistic jets in AGNs and statistical implications 19 p2792 N90-25893
Constraints on the high energy properties of active galactic nuclei 19 p2792 N90-25894
Spherical accretion with thermal pair production as models of AGN 19 p2793 N90-25897
Comparing measurements of AGN X ray spectra with the shape of the diffuse X ray background spectrum 19 p2793 N90-25902
A magnetic flare model for X ray variability in AGN 19 p2794 N90-25907
Neutral column density and soft excesses in active galactic nuclei 19 p2794 N90-25908
Spectroscopy of AGNs with Xspect/Sodart in 1993 19 p2794 N90-25909
The soft X ray excess in Einstein quasar spectra 19 p2794 N90-25910
The origin of the continuum of AGN and the X ray background 19 p2795 N90-25912
X ray variability of active galactic nuclei 19 p2795 N90-25914

ACTIVE GALAXIES
NT RADIO GALAXIES
NT SEYFERT GALAXIES
Spectropolarimetry, variability, and the taxonomy of active galactic nuclei 02 p0292 N90-11667
Near infrared spectroscopy of active galaxies 11 p1586 N90-19143
A search for the CO feature in active galactic nuclei 11 p1587 N90-19151
Far infrared fine structure lines in active galaxies 11 p1588 N90-19157
Nuclear activity, morphology, and far infrared properties of spiral galaxies
[ETN-90-95373] 12 p1744 N90-20024
Active star-forming galaxies in the X ray foreground 19 p2785 N90-25848

ACTIVE GLACIERS
U GLACIERS

ACTIVE SATELLITES
NT SYNCOM SATELLITES

ACTIVE VOLCANOES
U VOLCANOES

ACTIVITY (BIOLOGY)
Activation: Positive and negative effects of the alarm system in the brain 09 p1257 N90-17290
Ceramic oxide thin film formation utilizing biological processes
[DE90-008599] 13 p1781 N90-20225

ACTIVITY CYCLES (BIOLOGY)
Effects of solar ultraviolet radiation on biogeochemical dynamics in aquatic environments
[AD-A221119] 18 p2578 N90-24687

ACTS
Pattern recognition techniques applied to the NASA-ACTS order-wire problem 06 p0764 N90-14446
Proceedings of the Thirteenth NASA Propagation Experimenters Meeting (NAPEX 13)
[NASA-CR-186062] 10 p1371 N90-17945
ACTS propagation concerns, issues, and plans 10 p1374 N90-17963

NASA's Advanced Communications Technology Satellite (ACTS): Will it benefit commercial/military satellites
[AD-A217710] 14 p1939 N90-21100
The Advanced Communications Technology Satellite (ACTS) capabilities for serving science
[NASA-CR-186584] 15 p2059 N90-21789

ACTUATION
Battery actuation of NITINOL at sub-zero temperatures
[AD-A211254] 02 p0216 N90-11237

ACTUATORS
Independent Orbiter Assessment (IOA): Analysis of the elevon subsystem
[NASA-CR-185576] 02 p0166 N90-10935
Independent Orbiter Assessment (IOA): Analysis of the mechanical actuation subsystem
[NASA-CR-185525] 02 p0168 N90-10944
Independent Orbiter Assessment (IOA): Assessment of the mechanical actuation subsystem, volume 1
[NASA-CR-185527-VOL-1] 02 p0169 N90-10952
Independent Orbiter Assessment (IOA): Assessment of the mechanical actuation subsystem, volume 2
[NASA-CR-185527-VOL-2] 02 p0169 N90-10953
Independent Orbiter Assessment (IOA): Assessment of the ascent thrust vector control actuator subsystem FMEA/CIL
[NASA-CR-185590] 02 p0170 N90-10959
Independent Orbiter Assessment (IOA): Assessment of the elevon actuator subsystem FMEA/CIL
[NASA-CR-185578] 02 p0173 N90-10970
Solid-State Sensor and Actuator
[AD-A211427] 03 p0344 N90-11961
Advanced actuation systems development, volume 1
[AD-A213334] 04 p0458 N90-12624
Acceleration sets of planar manipulators. Part 1: Theory
[AD-A213162] 04 p0510 N90-12945
Advanced actuation systems development, volume 2
[AD-A213378] 05 p0583 N90-13398
Evaluation of selected computer models for modeling pyrotechnic and propellant devices
[AD-A213003] 05 p0629 N90-13671
Acceleration sets of planar manipulators. Part 2: Applications and experiments
[AD-A213336] 05 p0650 N90-13791
A versatile stepping motor controller for systems with many motors
[DE90-001556] 07 p0921 N90-15327
Single element magnetic suspension actuator
[NASA-CASE-LAR-13981-1] 07 p0940 N90-15442
Screening actuator locations for static shape control
[NASA-CR-181970] 09 p1182 N90-16851
Permanent magnet flux-biased magnetic actuator with flux feedback
[NASA-CASE-LAR-13785-1] 09 p1277 N90-17403
Surface acoustic wave sensors and piezoelectric actuators for investigations of transitional and turbulent flows
[AD-A214889] 09 p1279 N90-17415
Flexible heat pipe cold plate
[AD-A216053] 11 p1464 N90-18433
Optimization of sensors and actuators positioning aimed at obtaining reduced models for the synthesis of optimal control regulators of flexible structures
[INPE-4760-TDL/348] 11 p1468 N90-18450
Development and test of power amplifiers for the driving of low-voltage piezo-actuators in multistable interferometers
[DLR-MITT-89-19] 11 p1504 N90-18662
Advanced topics in structural dynamics: The maneuver of flexible spacecraft, and on-off decentralized control of flexible structures 12 p1612 N90-19274
Dynamics and control of robot manipulators with closed-kinematic chain mechanism 12 p1671 N90-19598
Aerospace induction motor actuators driven from a 20-kHz power link
[NASA-TM-102482] 13 p1756 N90-20085
Sensor and actuator selection for fault-tolerant control of flexible structures
[AD-A217384] 13 p1817 N90-20433
Advanced Launch System (ALS): Electrical actuation and power systems improve operability and cost picture
[NASA-TM-102547] 14 p1968 N90-21271
Electromechanical actuation for thrust vector control applications
[NASA-TM-102548] 14 p1968 N90-21272
Civil air transport: A fresh look at power-by-wire and fly-by-light
[NASA-TM-102574] 14 p1969 N90-21283
Application of optimization in design and motion control of robot manipulators 14 p1988 N90-21393
Bi-directional thruster development and test report
[NASA-CR-182013] 15 p2058 N90-21785
The 24th Aerospace Mechanisms Symposium
[NASA-CP-3062] 15 p2112 N90-22079
Development of shape memory metal as the actuator of a fail safe mechanism 15 p2112 N90-22081
A soft actuation system for segmented reflector articulation and isolation 15 p2113 N90-22084
Active control of bearing preload using piezoelectric translators 15 p2115 N90-22098
Elements of active vibration control for rotating machinery
[NASA-TM-102368] 16 p2227 N90-22703
Field oriented control of induction motors
[NASA-TM-103154] 16 p2231 N90-22731
Control of a flexible planar truss using proof mass actuators 16 p2288 N90-23035
Electromagnetic machines which utilize microgeometry field structures
[AD-A219828] 17 p2398 N90-23660
Shape memory alloys for robot grippers and mechanical hands 18 p2536 N90-24466
Precision pointing and locking capabilities combined by a linear actuator 18 p2537 N90-24475
Some remarks on a hinge actuator for large spot antenna arm deployers 18 p2539 N90-24495
The large wheel actuator LDR 100-0: Development status and test results 18 p2539 N90-24487
Adaptive control of visually guided grasping in neural networks
[AD-A221387] 18 p2597 N90-24780
Robot vibration control using inertial damping forces
[NASA-CR-186808] 19 p2698 N90-25352
Trajectory planning and control of a 6 DOF manipulator with Stewart platform-based mechanism
[NASA-CR-186813] 19 p2747 N90-25610
Simulated dynamic response of a servovalve controlled hydraulic actuator
[NASA-TM-101644] 20 p2842 N90-26167
Fluid-loop reaction system
[NASA-CASE-NPO-17204-1-CU] 20 p2864 N90-26292
Method and apparatus for applying a mechanical force to surface
[NASA-CASE-LAR-14009-1] 21 p3011 N90-27115
Integrated structural/control design via multiobjective optimization
[AD-A223088] 21 p3071 N90-27459
Active control of flexible structures 23 p3282 N90-28575
Liquid Rocket Booster (LRB) for the Space Transportation System (STS) systems study. Appendix C: Battery report for the liquid rocket booster TVC actuators
[NASA-CR-183789-APP-C] 23 p3288 N90-28603
Preliminary study of a serial-parallel redundant manipulator 23 p3371 N90-29048
Preliminary results on noncollocated torque control of space robot actuators 23 p3373 N90-29057
Portable Dextrous Force Feedback Master for robot telemanipulation (PDMFF) 23 p3373 N90-29058
Procedure for calibrating fly-by-wire control chains of the flying testbed ATTAS
[DLR-MITT-90-02] 24 p3435 N90-29401
Time optimal movement of cooperating robots 24 p3505 N90-29815

ACUITY
NT VISUAL ACUITY
Development of microcomputer-based mental acuity tests for repeated-measures studies
[NASA-CR-185607] 14 p2010 N90-21521

ADA (PROGRAMMING LANGUAGE)
Ada (trademark) projects at NASA. Runtime environment issues and recommendations
[NASA-CR-183435] 01 p0103 N90-10583
Research, development, training and education using the Ada programming language
[AD-A210760] 02 p0259 N90-11466
A mapping for converting Mascot designs to Ada programs
[RSRE-MEMO-4244] 04 p0531 N90-13070
The development of a program analysis environment for Ada
[NASA-CR-185860] 05 p0681 N90-13962
Software engineering and Ada (Trademark) training: An implementation model for NASA
[NASA-CR-186071] 05 p0681 N90-13966
Ada task scheduling: A focused Ada investigation
[NASA-CR-186072] 05 p0682 N90-13967
Ada programming guidelines for deterministic storage management
[NASA-CR-181308] 05 p0684 N90-13982
Transferring data objects: A focused Ada investigation
[NASA-CR-186065] 06 p0823 N90-14786
QUEST/Ada: Query utility environment for software testing of Ada
[NASA-CR-186121] 06 p0823 N90-14787
Classic-Ada(TM) 06 p0824 N90-14793
Reuse research plans at Langley Research Center 06 p0825 N90-14797
SSFP approach to software reuse 06 p0826 N90-14799
An SSE approach to reusability 06 p0826 N90-14801
Initial Ada components evaluation 06 p0826 N90-14803
Advanced Software Development Workstation Project 06 p0827 N90-14807
The development of an Ada programming support environment database: SEAD (Software Engineering and Ada Database), user's manual
[NASA-CR-181219] 06 p0828 N90-14811
A graphically oriented specification language for automatic code generation. GRASP/Ada: A Graphical Representation of Algorithms, Structure, and Processes for Ada, phase 1
[NASA-CR-183212] 06 p0828 N90-14813
Ada 9X project report. Revision request report
[AD-A213503] 07 p0975 N90-15629
Basic mathematical function libraries for scientific computation
[NASA-TM-102256] 08 p1110 N90-16423
The performance implications of Ada in a MASCOT 3 design
[YM-5748-M304/2] 09 p1263 N90-17324
Proceedings of the 4th Annual Ada Software Engineering Education and Training Symposium
[AD-A214663] 10 p1417 N90-18162
KAPSE Interface Team (KIT) public report, volume 7
[AD-A215838] 10 p1418 N90-18176
KAPSE Interface Team (KIT) public report, volume 8, part 1
[AD-A215839] 10 p1418 N90-18177
Structured analysis tool interface to the strategic defense initiative architecture dataflow modeling technique
[AD-A216281] 10 p1424 N90-18218
Guidelines for the use of the SAME
[AD-A215846] 11 p1544 N90-18888
Determination of the underlying task scheduling algorithm for and Ada runtime system
[AD-A215880] 11 p1544 N90-18890
Ada-Linda preliminary report: Motivation, informal description, and examples
[AD-A216004] 11 p1545 N90-18892
Development of an Ada programming support environment database SEAD (Software Engineering and Ada Database) administration manual
[NASA-CR-186064] 12 p1699 N90-19757
Object Oriented Programming Systems (OOPS) and frame representations: An investigation of programming paradigms
[NASA-CR-186084] 12 p1699 N90-19758
Lessons learned in the transition to ADA from FORTRAN at NASA/Goddard
[NASA-CR-186458] 12 p1701 N90-19765
Lessons learned in the transition to Ada from FORTRAN at NASA/Goddard
[NASA-TM-103311] 14 p2014 N90-21538
Evolution of Ada technology in the flight dynamics area: Implementation/testing phase analysis
[NASA-TM-103310] 14 p2014 N90-21539
System testing of a production Ada (trademark) project: The GRODY study
[NASA-TM-103308] 14 p2014 N90-21541
Evolution of Ada technology in the flight dynamics area: Design phase analysis
[NASA-TM-103307] 14 p2014 N90-21542
Implementation of a production Ada project: The GRODY study
[NASA-TM-103305] 14 p2015 N90-21544
DARK (Distributed Ada Real-Time Kernel) porting and extension guide Kernel version 3.0
[AD-A219291] 16 p2301 N90-23112
Explanation generation in expert systems (a literature review and implementation)
[AD-A218741] 16 p2327 N90-23268
Hartstone: Synthetic benchmark requirements for hard real-time applications
[AD-A219326] 17 p2442 N90-23917
Testing of elementary functions in Ada
[CWI-NM-R8909] 17 p2446 N90-23941
National Airspace System (NAS) software life cycle management study
[AD-A221180] 19 p2657 N90-25122
Application of artificial intelligence to the architectural synthesis of VLSI integrated circuits
[ETN-90-97253] 20 p2916 N90-26589
An application generator for rapid prototyping of Ada real-time control software 21 p3046 N90-27316
Compiling knowledge-based systems from KEE to Ada 21 p3049 N90-27334
SDI satellite autonomy using AI and Ada 21 p3050 N90-27336

Ada as an implementation language for knowledge based systems 21 p3050 N90-27337
An Ada evaluation report for the Verdix Corp. VADS version 5.5 release h compiler
[NPL-DITC-145/89] 22 p3235 N90-28342
Storage allocation in Ada
[NPL-DITC-156/90] 22 p3235 N90-28343
Improving software reusability by program specialization: A case study
[REPT-90-011] 22 p3240 N90-28374
Issues in expanding the software base management system supporting the Computer Aided Prototyping System (CAPS)
[AD-A224344] 24 p3525 N90-29933
The effect of software reusability on information theory based software metrics
[AD-A224472] 24 p3526 N90-29936
An Ada-based marine radar simulator for collision avoidance training
[ETN-90-97611] 24 p3531 N90-29970

ADAPTATION
NT ACCLIMATIZATION
NT COLD ACCLIMATIZATION
NT DARK ADAPTATION
NT HEAT ACCLIMATIZATION
NT LIGHT ADAPTATION
USSR Space Life Sciences Digest, issue 22
[NASA-CR-3922(26)] 03 p0378 N90-12153
USSR Space Life Sciences Digest, issue 23
[NASA-CR-3922(27)] 03 p0378 N90-12154
Studies on predicting the resynchronization of the circadian system after transmedian flights
[DFVLR-FB-89-10] 03 p0382 N90-12172
A simplified self-adaptive grid method, SAGE
[NASA-TM-102198] 03 p0388 N90-12211
Performance analysis of large adaptive sidelobe canceller arrays with reused elements
[AD-A212888] 04 p0494 N90-12841
Advanced actuation systems development, volume 2
[AD-A213378] 05 p0583 N90-13398
The relationship between subjective and objective measures of simulator-induced ataxia
[AD-A213095] 05 p0673 N90-13922
The role of attention in visual processing
[AD-A214158] 07 p0967 N90-15588
Young Investigator's Award and distributed self-adaptive databases
[AD-A214194] 07 p1010 N90-15854
Implementation of adaptive arrays in the block oriented systems simulator
[AD-A215545] 09 p1171 N90-16774
Multiple model adaptive estimation techniques for adaptive model-based robot control
[AD-A215742] 09 p1231 N90-17146
Residual interference and wind tunnel wall adaption 10 p1324 N90-17655
Psychophysiological correlates of human adaptation in antarctica
[AD-A216679] 10 p1412 N90-18142
On categorizing sounds
[AD-A216417] 10 p1427 N90-18232
Active phase and amplitude modulator
[AD-D014318] 12 p1650 N90-19480
Adaptive Resonance Theory 1
[AD-A219044] 16 p2304 N90-23126
Computational aspects of adaptive dimensional reduction for nonlinear boundary value problems
[AD-A219869] 17 p2461 N90-24052
Development of a hybrid adaptive beamformer
[AD-A219652] 17 p2471 N90-24128
Nonlinear modeling of time series using Multivariate Adaptive Regression Splines (MARS)
[AD-A222710] 20 p2921 N90-26623
High productivity testing 21 p2962 N90-26843
Adaptation for unsteady flow 21 p2963 N90-26845
Noise adaptation and correlated maneuver gating of an extended Kalman filter
[AD-A221713] 21 p3001 N90-27060

ADAPTERS
NT MULTIPLE DOCKING ADAPTERS
The connector space reduction mechanism 15 p2114 N90-22092
Igniter adapter-to-igniter chamber deflection test
[NASA-CR-184002] 22 p3133 N90-27780

ADAPTIVE CONTROL
NT ACTIVE CONTROL
NT MACHINE LEARNING
NT MODEL REFERENCE ADAPTIVE CONTROL
NT SELF ADAPTIVE CONTROL SYSTEMS
Adaptive machine vision
[AD-A208130] 01 p0076 N90-10436
An adaptive controller for enhancing operator performance during teleoperation
[NASA-CR-183445] 01 p0077 N90-10438
Adaptive robust control 01 p0109 N90-10620
Performance and robustness of adaptive controllers for linear stochastic systems 02 p0261 N90-11485
Adaptive control law design for model uncertainty compensation
[AD-A211712] 03 p0309 N90-11758
Adaptive information processing in auditory cortex
[AD-A211294] 03 p0380 N90-12168
Adaptive feedback linearization: Stability and robustness
[PB89-219497] 03 p0390 N90-12220
A hybrid optimisation strategy for adaptive feed-forward layered networks
[RSRE-MEMO-4193] 03 p0391 N90-12226
Expert systems for adaptive control of large space structures 05 p0595 N90-13452
A practical approach for minimum time control of the Spacecraft Control Laboratory Experiment (SCOLE), appendix A
[NASA-CR-186008] 05 p0602 N90-13495
Adaptive strategies for controls of flexible arms
[NASA-CR-185868] 05 p0649 N90-13783
A new approach to control single-link flexible arms. Part 3: Adaptive control of the tip position with payload changes
[AD-A213337] 05 p0650 N90-13792
Non-linear vibrations, stability, and dynamics of structures and mechanisms
[AD-A212152] 06 p0796 N90-14839
Survey of adaptive control theory and its applications
[DE89-901270] 06 p0833 N90-14840
Adaptive control of helicopter vibrations via the impulse response method
[AD-A213728] 07 p0883 N90-15113
Gaze controls with interactions and delays
[AD-A214286] 07 p0981 N90-15667
Mathematical model for adaptive control system of ASEA robot at Kennedy Space Center 08 p1157 N90-16701
Robustness of a moving-bank multiple model adaptive controller for a large space structure
[AD-A215670] 09 p1183 N90-16859
Multiple model adaptive estimation techniques for adaptive model-based robot control
[AD-A215742] 09 p1231 N90-17146
Payload invariant control via neural networks: Development and experimental evaluation
[AD-A215740] 09 p1260 N90-17306
A new approach to active vibration isolation for microgravity space experiments
[NASA-TM-102470] 10 p1368 N90-17929
Adaptive vibration control of vibration isolation mounts, using an LMS-based control algorithm
[AD-A214386] 10 p1394 N90-18061
Stochastic adaptive control and estimation enhancement
[AD-A215486] 10 p1420 N90-18187
Discrete proportional Plus Integral (PI) multivariable control laws for the Control Reconfigurable Combat Aircraft (CRCA)
[AD-A215664] 11 p1464 N90-18431
Appropriateness measurement for computerized adaptive tests
[AD-A216121] 11 p1541 N90-18870
A rule-based paradigm for intelligent adaptive flight control 12 p1605 N90-19238
Multi-dimensional LADAR tracking and adaptive grasping for spaceborne assembly of SDI (Strategic Defense Initiative) platforms
[AD-A218236] 13 p1791 N90-20279
A learning regulator for the plane longitudinal movement
[ETN-90-95381] 13 p1864 N90-20695
Robust adaptive nonlinear conirol under extended matching conditions
[AD-A217684] 13 p1874 N90-20744
Rule-based mechaniams of learning for intelligent adaptive flight control 14 p1908 N90-20939
Design of a helicopter automatic flight control system using adaptive control 14 p1928 N90-21040
CSI technology validation on an LSS ground experiment facility 14 p1937 N90-21089
Adaptive learning fuzzy control of a mobile robot
[DE90-759898] 14 p2018 N90-21562
An adaptive human response mechanism controlling the V/STOL aircraft. Appendix 3: The adaptive control model of a pilot in V/STOL aircraft control loops
[NASA-CR-186599] 15 p2056 N90-21777
Three-dimensional adaptive grids with limited skewness 15 p2095 N90-21987
Nonlinear stability analysis and control of dynamical robotic systems 15 p2104 N90-22037
A methodology for knowledge-based restructurable control to accommodate system failures 15 p2109 N90-22058
Adaptive control of a flexible manipulator with unknown changing loads 15 p2152 N90-22293
The role of input weighting and bounding in the characteristic GPC method
[OUEL-1762/89] 15 p2158 N90-22328
A robust stability result for generalised predictive control
[OUEL-1773/89] 15 p2158 N90-22330
Bicausal representations and multivariable generalized predictive control
[OUEL-1781/89] 15 p2159 N90-22331
Computational issue in the analysis of adaptive control systems 16 p2281 N90-23001
Experimental adaptive control of a hydraulic robot 16 p2303 N90-23121
Robust adaptive control: Stability and asymptotic performance
[AD-A219259] 16 p2304 N90-23127
Adaptive control of a system with periodic dynamics: Application of an impulse response method to the helicopter vibration problem 17 p2453 N90-23990
Real time adaptive control of an Autonomous Underwater Vehicle (AUV)
[AD-A219544] 17 p2454 N90-23996
Adaptive filtering and control
[AD-A219556] 17 p2454 N90-23998
Stochastic adaptive control and estimation enhancement
[AD-A219629] 17 p2454 N90-24001
Neuromorphic learning of continuous-valued mappings from noise-corrupted data. Application to real-time adaptive control
[NASA-TM-4176] 19 p2747 N90-25607
Adaptive tracking for complex systems using reduced-order models
[NASA-CR-183464] 19 p2747 N90-25609
Adaptive robot control using artificial neural networks: An application in the theory of cognition
[RR-374] 19 p2748 N90-25618
Beam rider for an Articulated Robot Manipulator (ARM) accurate positioning of long flexible manipulators
[NASA-CR-185151] 20 p2914 N90-26581
Temperature and melt solid interface control during crystal growth
[NASA-CR-186731] 20 p2929 N90-26664
Robust adaptive control: Handling the excitation problem 22 p3241 N90-28382
An expert system to perform on-line controller restructuring for abrupt model changes
[NASA-TM-103609] 23 p3385 N90-29121
Adaptive control of an arc welding process
[AD-A223626] 24 p3476 N90-29645
An improved adaptive control for repetitive motion of robots 24 p3508 N90-29831
Direct adaptive control of a PUMA 560 industrial robot 24 p3508 N90-29832
On discrete control of nonlinear systems with applications to robotics 24 p3519 N90-29893
MUSE: A systolic array for adaptive nulling with 64 degrees of freedom, using Givens transformations and wafer scale integration
[AD-A223812] 24 p3529 N90-29953
Optimal control law phenomena in certain adaptive second-order observation systems
[AD-A224274] 24 p3534 N90-29986

ADAPTIVE CONTROL SYSTEMS
U ADAPTIVE CONTROL

ADAPTIVE FILTERS
Adaptive tracking of maneuvering targets based on IR image data 02 p0149 N90-10853
Improving the quality of a spread-spectrum radiomobile link 06 p0761 N90-14426
Adaptive clutter rejection filters for airborne Doppler weather radar applied to the detection of low altitude windshear
[NASA-CR-186211] 06 p0766 N90-14453
Adaptive canceller limitations caused by I,Q mismatch errors
[AD-A214287] 07 p0919 N90-15318
An analysis of the time variation of the frequency response of the LMS adaptive line enhancer
[ISVR-TR-175] 08 p1058 N90-16115
Orbit determination of artificial Earth satellites through estmation techniques combined with state smoothing techniques
[INPE-4959-TDL/388] 11 p1465 N90-18440
A simple algebraic grid adaptation scheme with applications to two- and three-dimensional flow problems
[NASA-TM-102446] 11 p1505 N90-18667
Adaptive state estimation and sampling rate analysis for invariant linear dynamic systems in time
[INPE-4960-TDL/389] 11 p1554 N90-18951
General multidimensional scanning ratio transformation and its utilization for norm transformation of television signals
[ETN-90-96058] 12 p1648 N90-19470

Evaluation of an adaptive unstructured remeshing technique for integrated fluid-thermal-structural analysis
[NASA-TM-102611] 13 p1815 N90-20426
UD filtering and smoothing applied to orbit determination
[INPE-4966-PRE/1535] 15 p2189 N90-22501
Model order determination methods for autoregressive radio direction finding techniques
[AD-A220707] 17 p2350 N90-23384
Adaptive filtering and control
[AD-A219556] 17 p2454 N90-23998

ADAPTIVE OPTICS
Adaptive gigabit fiber optics local area network
[AD-A210794] 02 p0275 N90-11571
Enhanced performance IR focal plane arrays using adaptive subtraction
[RSRE-MEMO-4286] 08 p1123 N90-16502
Develop techniques for ion implantation of PLZT for adaptive optics
[AD-A216005] 10 p1431 N90-18253
Design and performance analysis of adaptive optical telescopes using laser guide stars
[AD-A218025] 13 p1902 N90-20913
Atmospheric turbulence measurements in support of adaptive optics technology
[AD-A220445] 17 p2423 N90-23805
Optical wavefront computer for stabilizing large space structures
[AD-A221707] 21 p2967 N90-26866
Adaptive optics correction in real-time for dynamic wavefront errors
[AD-A221588] 21 p3077 N90-27495
High resolution optical imaging through the atmosphere
[AD-A221913] 21 p3097 N90-27599

ADDERS (CIRCUITS)
U ADDING CIRCUITS

ADDING CIRCUITS
Area-time efficient adders
[MEMO-INF-89-61] 17 p2440 N90-23905

ADDITION
Minimizing sums of addition chains
[RUU-CS-89-15] 18 p2635 N90-25013

ADDITION RESINS
NT ACRYLIC RESINS
NT VINYL COPOLYMERS
Condensation polyimides
[NASA-TM-103467] 20 p2836 N90-26129
Autoclavable addition polyimides for 371 C composite applications
[NASA-TM-103233] 22 p3153 N90-27874

ADDITIVES
NT ANTIICING ADDITIVES
NT PLASTICIZERS
NT PROPELLANT ADDITIVES
NT PROPELLANT BINDERS
Influence of grain refining on the casting, physical, mechanical, and electrochemical properties of technical aluminum
[ETN-89-94661] 02 p0199 N90-11135
Spectroscopic ellipsometry characterization of CVD deposition and doping of polysilicon multilayer structures
[RSRE-MEMO-4258] 04 p0466 N90-12671
Novel carbamates, their production and their use as fuels additives
[EP-PATENT-0-298-636-A-1] 05 p0629 N90-13676
CRC (Coordinating Research Council) octane number requirement survey 1988
[AD-A214845] 09 p1200 N90-16954
Improvement of impulse breakdown strength of an XLPE cable by modifing semiconducting layer
[DE90-734942] 09 p1287 N90-17463
Development of fuel wear tests using the Cameron-Plint high-frequency reciprocating machine
[AD-A216003] 10 p1361 N90-17892
Chemistry of the doping mechanism in Ba(1-x)K(x)BiO3 and La2CuO(sub 4 + delta) oxide superconductors
[DE90-005640] 10 p1437 N90-18293
Materials processing of diamond: Etching, doping by ion implantation and contact formation
[AD-A216530] 10 p1438 N90-18301
Crystallization behavior and properties of BaO-Al2O3-2SiO2 glass matrices
[NASA-CR-185209] 12 p1631 N90-19374
Annealing group III-V compound doped silicon-germanium alloy for improved thermo-electric conversion efficiency
[NASA-CASE-NPO-17259-1-CU] 12 p1721 N90-19884
The preparation and properties of iron doped II-VI chalcogenides
[AD-A217569] 12 p1724 N90-19903
Infrared absorption study of zinc-doped silicon
[DE90-007779] 13 p1771 N90-20164
Non-noble electrocatalysts for alkaline fuel cells 13 p1824 N90-20470
Process for lowering the dielectric constant of polyimides using diamic acid additives
[NASA-CASE-LAR-13902-1] 17 p2379 N90-23546
Tin doping of InSb grown by MOCVD using tetraethyltin
[DE90-009727] 18 p2620 N90-24929
Micro separometer and ball-on-cylinder lubricity evaluator tests or corrosion inhibitor/lubricity improver additives
[AD-A221339] 19 p2678 N90-25228

ADDRESSING
Evaluating local indirect addressing in SIMD proc essors
[NASA-CR-181845] 01 p0103 N90-10581
Parallel memory addressing using coincident optical pulses
[AD-A216302] 11 p1501 N90-18641
A scalable multiprocessor architecture using Cartesian network: Relative addressing
[AD-A216580] 11 p1542 N90-18878
Architectures for optical computing
[AD-A221435] 21 p3054 N90-27364

ADENOSINE TRIPHOSPHATE
Conservation of body calcium by increased dietary intake of potassium: A potential measure to reduce the osteoporosis process during prolonged exposure to microgravity 18 p2631 N90-24993
Experiment K-6-10. Effects of zero gravity on myofibril protein content and isomyosin distribution in rodent skeletal muscle 20 p2894 N90-26464

ADENOSINES
NT ADENOSINE TRIPHOSPHATE

ADHEROMETERS
U ADHESION TESTS

ADHESION
Adhesion of encapsulating elastomer to polyolefin sleeve
[BDX-613-3985] 01 p0048 N90-10271
Fundamental tribological properties of ion-beam-deposited boron nitride films
[NASA-TM-102088] 03 p0331 N90-11881
Implementation and analysis of adhesion in multimaterials of the type Al(Si)-ZrO2 and graphite, metal or ceramics
[ECL-89-004] 05 p0628 N90-13667
Characterization and in situ testing of diamond films
[DE90-003155] 07 p0911 N90-15265
Benefits from combining electroplating and physical vapor deposition technologies
[DE90-002700] 07 p0917 N90-15301
The effect of primer age on adhesion of polysulphide sealant 08 p1022 N90-15909
Improved performance polysulfide based sealant 08 p1022 N90-15910
Fuel resistant coatings for metal and composite fuel tanks 08 p1022 N90-15911
Study of adherent oxide scales
[AD-A215189] 09 p1198 N90-16940
Adhesion of silver films to ion-bombarded alumina
[DE90-005642] 09 p1199 N90-16947
Interfacial chemistry of MoS2 films on Si
[AD-A216527] 11 p1482 N90-18532
The improved adhesion of organic polymers to silica and to aluminum metal with zirconium Schiff-base block copolymer coatings
[AD-A216669] 11 p1490 N90-18575
Oxygen concentrations on surfaces of carbon fibers
[AD-A217724] 13 p1769 N90-20152
Determination of flow-regime boundaries for cohesive particles
[DE90-007425] 13 p1800 N90-20332
High gloss corrosion-resistant coatings
[AD-D014403] 14 p1954 N90-21184
Combination primer/topcoat coating
[AD-D014445] 14 p1954 N90-21189
Energy beam treatment for improved adhesion of coatings to surfaces
[AD-D014449] 14 p1954 N90-21190
Development of planar geometry solid oxide fuel cell technology, phase 2
[PB90-131293] 14 p2001 N90-21467
Interfacial studies in fiber-reinforced thermoplastic-matrix composites 15 p2062 N90-21814
Effect of surface oxygen on adhesion of carbon fiber-reinforced composites
[AD-A220777] 17 p2369 N90-23486
Effects of microstructure and adhesion on performance of sputter-deposited MoS2 solid lubricant coatings
[AD-A220900] 18 p2530 N90-24434
Effect of film adhesion on tribological properties of silver-coated alumina
[DE90-010090] 18 p2564 N90-24632
Method of insetting predesigned disbond areas into composite laminates
[NASA-CASE-LAR-13225-1] 19 p2672 N90-25197
Model studies of the effect of surface roughness and mechanical interlocking on adhesion
[AD-A222402] 21 p2987 N90-26977
Development of a mathematical model for the thermal decomposition of aviation fuels
[AD-A221673] 21 p2990 N90-26994
Microscopic modeling of tribological phenomena
[AD-A222049] 21 p3011 N90-27117
Factors influencing the mode I interlaminar fracture resistance of toughened matrix composites 23 p3300 N90-28668
Scale adherence effects in oxidation and sulfidation 23 p3307 N90-28703
Adhesion of silver films to ion-bombarded zirconia
[DE90-010088] 24 p3456 N90-29517

ADHESION TESTS
Adhesion of encapsulating elastomer to polyolefin sleeve
[BDX-613-3985] 01 p0048 N90-10271
Behavior of the adhesive A2 submitted to mechanical traction
[CETIM-105290] 04 p0479 N90-12748
Nondestructive analysis of aileron fatigue and aging in a Mirage F1
[REPT-M6-594000] 05 p0580 N90-13378
Contamination removal using various solvents and methodologies
[NASA-CR-183747] 05 p0626 N90-13652
Effects of tacky mat contamination on bond degradation for Chemlok/liner and NBR/liner bonds
[NASA-CR-183742] 05 p0626 N90-13653
Evaluation of a metering, mixing, and dispensing system for mixing polysulfide adhesive
[NASA-CR-183749] 05 p0626 N90-13654
Interfacial studies in fiber-reinforced thermoplastic-matrix composites 15 p2062 N90-21814
Criteria for coal tar seal coats on airport pavements. Volume 2: Laboratory and field studies
[AD-A220167] 18 p2498 N90-24277
The interface chemistry of phenolic and epoxy adhesives with a model aluminium surface
[MBB-Z-0288-89-PUB] 18 p2531 N90-24441
Resistivity, adhesive strength, and residual stress measurements of thin film metallizations on single crystal quartz
[DE90-011902] 20 p2837 N90-26135
Renewed aging control of adhesion of inhibitor on the gas generator charges for RB 24
[FOA-C-20780-2.1] 20 p2840 N90-26153
M-52 spray booth qualification test
[NASA-CR-184003] 22 p3122 N90-27727
Evaluation of EA-934NA with 2.5 percent Cab-O-Sil
[NASA-CR-184005] 22 p3158 N90-27909

ADHESIVE BONDING
Adhesion of encapsulating elastomer to polyolefin sleeve.
[BDX-613-3985] 01 p0048 N90-10271
Design of glued joints, elastoplastic adhesives
[DRIC-T-8168] 03 p0333 N90-11894
Behavior of the adhesive A2 submitted to mechanical traction
[CETIM-105290] 04 p0479 N90-12748
Structure and properties of polymer interphases
[AD-A212796] 04 p0481 N90-12763
RSRM nozzle fixed housing cooldown test
[NASA-CR-183741] 05 p0614 N90-13587
The adhesive bonding of thermoplastic composites
[AD-A213358] 05 p0618 N90-13605
Effects of tacky mat contamination on bond degradation for Chemlok/liner and NBR/liner bonds
[NASA-CR-183742] 05 p0626 N90-13653
Evaluation of a metering, mixing, and dispensing system for mixing polysulfide adhesive
[NASA-CR-183749] 05 p0626 N90-13654
Bonding aerogels with polyurethanes
[DE90-003050] 07 p0910 N90-15258
Adhesive for composite bonding
[DE90-005683] 09 p1188 N90-16885
Simple shear tests of the FMI 23.5.06 adhesive cured at low pressure (12 PSI)
[INFORME-I-298/88] 10 p1357 N90-17871
Test data of flow field of shuttle SRM nozzle joint with bond defects, using unheated air 11 p1470 N90-18464
Viscoelastic adherend effects in adhesively bonded composite-to-composite joints 12 p1670 N90-19594
Crack stoppers and ARALL laminates
[PB90-166588] 14 p1947 N90-21142
On the design and development of a miniature ceramic gimbal bearing 15 p2115 N90-22100
Evaluation of joints bonded with elastoplastic adhesives
[REPT-892-430-120] 16 p2247 N90-22816

An investigation of the chemistry of silane coupling agents for adhesive bonding of aluminum
[AD-A220797] 17 p2381 N90-23560
Simplified design procedures for fiber composite structural components/joints
[NASA-TM-103113] 18 p2519 N90-24384
The interface chemistry of phenolic and epoxy adhesives with a model aluminium surface
[MBB-Z-0288-89-PUB] 18 p2531 N90-24441
Static and fatigue strength of an adhesive bonded CFRP butt-strap joint: The effects of stacking sequence and temperature
[NLR-TR-88036-U] 20 p2877 N90-26370
Model studies of the effect of surface roughness and mechanical interlocking on adhesion
[AD-A222402] 21 p2987 N90-26977
An interdisciplinary approach to the predictive modeling of structural adhesive bonding
[AD-A221703] 21 p2988 N90-26982
Evaluation of EA-934NA with 2.5 percent Cab-O-Sil
[NASA-CR-184005] 22 p3158 N90-27909
Nondestructive evaluation of adhesively-bonded joints
22 p3185 N90-28074
Aircraft battle damage repair of transparencies
[AD-A224168] 24 p3432 N90-29387

ADHESIVES
NT GLUES
NT PASTES
Behavior of the adhesive A2 submitted to mechanical traction
[CETIM-.05290] 04 p0479 N90-12748
The adhesive bonding of thermoplastic composites
[AD-A213358] 05 p0618 N90-13805
Evaluation of a metering, mixing, and dispensing system for mixing polysulfide adhesive
[NASA-CR-183749] 05 p0626 N90-13654
Adhesive for composite bonding
[DE90-005683] 09 p1188 N90-16885
LARC-IA: A flexible backbone polyimide
[NASA-TM-102586] 09 p1196 N90-16926
Surface-enhanced Raman scattering from model acrylic adhesive systems
[AD-A216117] 10 p1359 N90-17883
Viscoelastic adherend effects in adhesively bonded composite-to-composite joints 12 p1670 N90-19594
The controlled-damage concept in design of laminated composites 15 p2065 N90-21830
An alternate interconnect method for joining flexible circuits using conductive adhesives
[DE90-008194] 16 p2222 N90-22674
An investigation of the chemistry of silane coupling agents for adhesive bonding of aluminum
[AD-A220797] 17 p2381 N90-23560
Tensile and shear strength of adhesives
18 p2515 N90-24366
Molecular structure of interphases between DGEBA/BTDA adhesives and silver substances using surface-enhanced Raman scattering
[AD-A222750] 20 p2841 N90-26157
Evaluation of EA-934NA with 2.5 percent Cab-O-Sil
[NASA-CR-184005] 22 p3158 N90-27909

ADI METHODS
U ALTERNATING DIRECTION IMPLICIT METHODS

ADIABATIC CONDITIONS
Global distribution of moisture, evaporation-precipitation, and diabatic heating rates
03 p0362 N90-12069
A 100 micro Kelvin bolometer system for SIRTF
14 p1976 N90-21317
Methods for evaluation of thermally induced reactions in liquid propellants
[AD-A218750] 16 p2225 N90-22694
Effect of constitutive modeling on the dynamic development of shear bands in viscoplastic materials
[AD-A220443] 17 p2416 N90-23765
Stability projections for high temperature superconductors
[AD-A218945] 18 p2618 N90-24913
The sensitivity of several explosives to ignition in the launch environment
[AD-A221581] 21 p2990 N90-26993

ADIABATIC DEMAGNETIZATION COOLING
A progress report on using bolometers cooled by adiabatic demagnetization refrigeration
14 p1976 N90-21318

ADIABATIC EQUATIONS
Convergence of hyperspherical adiabatic expansion for helium-like systems
[DE90-620526] 16 p2214 N90-22631
Approximate analysis for the formation of adiabatic shear bands
[AD-A218751] 16 p2221 N90-22670
Adiabatic invariance and transient resonance in very slowly varying oscillatory Hamiltonian systems
[DE90-016118] 24 p3538 N90-30007

ADIABATIC FLOW
Experimental and analytical investigation of adiabatic critical water air two phase flow in small diameter tubes
[TB-88/1] 12 p1660 N90-19540

ADIPOSE TISSUES
Measurement of body fat by neutron inelastic scattering: Comments on installation, operation, and error analysis
[DE90-006765] 11 p1540 N90-18868

ADJOINTS
Global linear representations of nonlinear systems and the adjoint map
[RR-347] 03 p0394 N90-12247
Hahn-Banach type theorems for dual semigroups
[CWI-AM-R8903] 04 p0543 N90-13149
The algebraic basis of mathematical morphology. Part 1: Dilations and erosions
[CWI-AM-R8807] 05 p0695 N90-14065
Automated sensitivity analysis with the Gradient Enhanced Software System (GRESS)
[DE90-011291] 20 p2906 N90-26529
Variational formulation and finite element implementation of Pagano's theory of laminated plates
24 p3442 N90-29437

ADJUSTING
Geodetic network adjustment using GPS triple difference observations and a priori stochastic information
[TR-1-1987] 05 p0577 N90-13367
A study on the sensitivity and simultaneous adjustment of a hoop-column antenna surface
[NASA-TM-101538] 05 p0653 N90-13807
Adjustable choke for fluids nozzle
[NASA-CASE-NPO-17625-1-CU]
21 p3003 N90-27070
Adjustable speed drive applications guidebook
[DE90-014151] 23 p3321 N90-28780

ADJUSTMENT
U ADJUSTING

ADMINISTRATION
U MANAGEMENT

ADMITTANCE
U ELECTRICAL IMPEDANCE

ADRENAL GLAND
The effects of high intensity cycle exercise on sympatho-adrenal-medullary response patterns
[AD-A217962] 13 p1852 N90-20628

ADRENALINE
U EPINEPHRINE

ADRENERGICS
Analysis of neural systems involved in modulation of memory storage
[AD-A220230] 18 p2584 N90-24714

ADSORBENTS
An experimental investigation of the thermal conductivity of porous adsorbents
[AD-A217854] 13 p1899 N90-20899

ADSORPTION
NT CHEMISORPTION
Multiple internal reflection Fourier transform infrared spectroscopy studies of thiocyanate adsorption on silver and gold
[AD-A210245] 01 p0041 N90-10223
The structure determination of molecular adsorbates with large unit cells or lattice-gas disorder on metal surfaces
[AD-A210926] 01 p0042 N90-10230
Interfacial adsorption and crystallization of polycarbonate in carbon fiber composites
[AD-A211230] 02 p0191 N90-11090
Modeling of hydrazine surface interactions in environmental reaction chambers
02 p0203 N90-11162
A diffuse reflectance infrared Fourier transform spectroscopic study of adsorbed hydrazines
02 p0205 N90-11170
Photolysis of spacecraft contaminants
[AD-A211715] 03 p0317 N90-11801
Thermal stability of the carbon-carbon bond in ethylene adsorbed on Si(100): An isotopic mixing study
[AD-A211591] 04 p0470 N90-12691
Studies of the adsorption/desorption behavior of explosive-like molecules
[DE90-001867] 07 p0913 N90-15283
Non-destructive characterization of epoxy/dicyandiamide interphases using surface-enhanced Raman scattering
[AD-A215894] 10 p1353 N90-17846
Scuffing modelling and experiments for heavily loaded elastohydrodynamic lubrication contacts
10 p1391 N90-18047
Multicomponent glass surfaces structure and adsorption
[DE90-007179] 11 p1493 N90-18596
Direct absorption receiver
[DE90-000311] 12 p1683 N90-19867
Tunneling microscopy of submonolayer adsorbates on Si3
[AD-A216985] 12 p1719 N90-19876
Modes of attachment of pyridine to gold surfaces
[AD-A219519] 17 p2372 N90-23504
An examination of the relationship between SERS intensities and surface concentration for pyridine adsorbed at the gold/aqueous solution interface
[AD-A219520] 17 p2372 N90-23505
Density profile of terminally adsorbed polymers
[AD-A220897] 18 p2529 N90-24433
Dynamics of bulk and surface-adsorbed polyacrylates
[AD-A221046] 18 p2530 N90-24437
ISS and TPD study of the adsorption and interaction of CO and H2 on polycrystalline Pt
18 p2559 N90-24602
Surface defects and chemistry on the SnO2(110) surface 18 p2559 N90-24603
Review of model sensor studies on Pd/SnO2(110) surfaces 18 p2559 N90-24604
The application of HREELS to model catalysts: CO and C2H4 adsorption on Pt/Al2O3
[AD-A222744] 20 p2831 N90-26103
Exact results for the structured liquid-solid interface
[AD-A222762] 20 p2922 N90-26630
Field-induced surface chemistry of NO
[AD-A223007] 21 p2977 N90-26915
Ni impurity effects on hydrogen surface chemistry and etching of Si(111)
[AD-A222083] 21 p2977 N90-26921
The adsorption and thermal decomposition of PH3 on Si(111)-(7x7)
[AD-A222417] 21 p2978 N90-26927
Interfacial viscosity measurements of adsorbed monolayers on metal surfaces
[AD-A221689] 21 p2979 N90-26931
Characterization of model polyimide/silver interphases using surface-enhanced Raman scattering
[AD-A222488] 21 p2988 N90-26979
An interdisciplinary approach to the predictive modeling of structural adhesive bonding
[AD-A221703] 21 p2988 N90-26982
Hyperthermal atomic oxygen generator
[NASA-CR-186573] 22 p3155 N90-27889
Infrared reflection-adsorption spectroscopy of the electrode/electrolyte solution interface: Optical considerations
[AD-A221935] 22 p3246 N90-28409

ADVANCED COMMUNICATIONS TECHNOLOGY SAT
U ACTS

ADVANCED LAUNCH SYSTEM (STS)
The joint DOD/NASA Advanced Launch System (ALS) programme 09 p1179 N90-16832
Low-energy impact resistance of graphite-epoxy plates and ALS honeycomb sandwich panels
12 p1637 N90-19405
Aerospace induction motor actuators driven from a 20-kHz power link
[NASA-TM-102482] 13 p1756 N90-20085
Advanced Launch System (ALS): Electrical actuation and power systems improve operability and cost picture
[NASA-TM-102547] 14 p1968 N90-21271
Electromechanical actuation for thrust vector control applications
[NASA-TM-102548] 14 p1968 N90-21272
Trajectory optimization for an asymmetric launch vehicle
[NASA-CR-185630] 20 p2817 N90-26033
Multimegawatt space nuclear power supply, phase 1. Volume 2: Phase 2 plan D180-30619-6
[DE90-012431] 20 p2925 N90-26645
Liquid Rocket Booster (LRB) for the Space Transportation System (STS) systems study. Volume 1: Executive summary
[NASA-CR-183822] 23 p3288 N90-28599
Liquid Rocket Booster (LRB) for the Space Transportation System (STS) systems study, volume 2
[NASA-CR-183786] 23 p3288 N90-28600
Liquid Rocket Booster (LRB) for the Space Transportation System (STS) systems study. Appendix F: Performance and trajectory for ALS/LRB launch vehicles
[NASA-CR-183792-APP-F] 23 p3289 N90-28606

ADVANCED SOLID ROCKET MOTOR (STS)
Review of the Aerospace Safety Advisory Panel report for NASA fiscal year 1990 authorization
[GPO-24-234] 06 p0722 N90-14213

ADVANCED VERY HIGH RESOLUTION RADIOMETER
Senegalese land surface change analysis and biophysical parameter estimation using NOAA AVHRR spectral data
[NASA-CR-186120] 05 p0664 N90-13883
Determination of optical porperties of clouds from NOAA-AVHRR data using Apollo
08 p1092 N90-16321

Recognition and distinction of clouds, snow, and ice using AVHRR data 08 p1092 N90-16322
Correlation of AVHRR imagery with sub-surface features in California current
[AD-A218184] 13 p1848 N90-20607
The analysis of polar clouds from AVHRR satellite data using pattern recognition techniques
[NASA-CR-183300] 16 p2257 N90-22868
Implementation of reflectance models in operational AVHRR radiation budget processing
[NOAA-TR-NESDIS-49] 18 p2578 N90-24688
Reflection indicatrices of natural surfaces for AVHRR channels 1 and 2
[ESA-TT-1192] 19 p2709 N90-25417
Observed cloud reflectivities and liquid water paths: An update 22 p3215 N90-28237

ADVANCED X RAY ASTROPHYSICS FACILITY
U X RAY ASTROPHYSICS FACILITY

ADVANCING GLACIERS
U GLACIERS

ADVECTION
Composited local area forecast techniques
[AD-A210802] 02 p0253 N90-11432
Synoptic/planetary-scale interactions and blocking over the North Atlantic Ocean 03 p0360 N90-12061
Inverted surface troughs accompanying Rocky Mountain lee-side cyclogenesis 06 p0816 N90-14746
Some numerical experiments concerning the equation of state algorithm for multi-material cells in HULL
[DE89-008240] 06 p0830 N90-14827
Potential vorticity in extratropical cyclones 07 p0962 N90-15564
Numerical methods for parabolic equations and inequalities in very high dimensions
[AD-A214102] 07 p0985 N90-15690
Triangle based TVD schemes for hyperbolic conservation laws
[NASA-CR-181984] 08 p1106 N90-16401
Effects of heating/cooling on changes in sea surface temperature: Consequences for computation of surface advection from satellite images
[AD-A214125] 10 p1409 N90-18129
A sub-cloud layer vorticity budget analysis for two microburst-producing storms from jaws dual-Doppler data
[AD-A218180] 13 p1847 N90-20599
A case study of a quasi-stationary tropical convective line
[AD-A218325] 13 p1847 N90-20604
Rigorous upper bounds for turbulent transport in bounded systems: Passive advection and reversed-field pinches 15 p2168 N90-22390
An interactive method for estimating hailstone size and convectively-driven wind gusts from forecast soundings
[AD-A218499] 16 p2258 N90-22871
A case study of explosive cyclogenesis in the eastern Pacific Ocean 14 to 17 December 1987
[AD-A219543] 17 p2426 N90-23824
Barotropic vortex adjustment to asymmetric forcing with application to tropical cyclone motion
[AD-A219883] 17 p2427 N90-23831
Distribution and movement of smokes from forest fires that occurred along the boundary of the People's Republic of China and the USSR on April-May 1987 21 p3028 N90-27216
A nonhydrostatic numerical model in sigma-coordinates and simulations of mesoscale phenomena 23 p3350 N90-28932
A parallel least squares collocation conjugate gradient approach for the advection diffusion equation
[DE90-015965] 24 p3530 N90-29961

AEOLIAN TONES
Aeolian processes on Venus 03 p0425 N90-12436
Saltation thresholds and entrainment of fine particles at Earth and Martian pressures
[NASA-TM-102193] 06 p0860 N90-14997
Wind tunnel investigation of periodic vortex separation from rough surface circular cylinders by means of acoustic measurements
[ESA-TT-1092] 23 p3268 N90-28499

AERIAL EXPLOSIONS
Minutes of the 23rd Eplosives Safety Seminar, volume 2
[AD-A218265] 14 p1959 N90-21214

AERIAL IMAGERY
U AERIAL PHOTOGRAPHY

AERIAL PHOTOGRAPHY
Ice runways near the South Pole
[AD-A211606] 03 p0335 N90-11908
Visualization of high-resolution digital terrain
[AD-A212149] 04 p0515 N90-12971
Vision in dynamic environments
[AD-A213434] 07 p0967 N90-15587
Use of remote sensing data for land and building statistics 08 p1094 N90-16335
The use of photographs for identification and analysis of urban residential sectors, with planning views
[INPE-4788-PRE/1448] 10 p1399 N90-18087
Remote sensing in agriculture: Basic concepts, methodology and applications
[INPE-4806-MD/39] 10 p1399 N90-18088
Aerial photographs to support the fiscalization process of agriculture loans in the Irece-BA region
[INPE-4839-PRE/1468] 10 p1400 N90-18092
Development of the agricultural information system. Characteristics and results of the Distrito Federal model
[INPE-4940-PRE/1430] 11 p1524 N90-18773
Introduction of aerial photography in agricultural research
[BCRS-89-14] 11 p1526 N90-18784
Possible applications of remote sensing in the preparatory phase of a land management project
[BCRS-88-19] 12 p1679 N90-19642
Technical and administrative feasibility of microlight remote sensing applications for river boards
[BCRS-89-01] 12 p1679 N90-19643
Project CANASATE: Remote sensing applied to sugar cane crop survey
[INPE-4902-PRE/1503] 14 p1997 N90-21446
Aerial photography as an aid for agricultural credit control
[INPE-5019-RPE/613] 14 p1999 N90-21455
Evaluation of classification performance and proportion estimate of the sugar cane crop through PROCEDURE-INPE utilizing LANDSAT data
[INPE-4899-PRE/1500] 14 p1999 N90-21458
The accuracy of the monitoring of pioneer vegetation in the Oostvaardersplassen, Netherlands
[ETN-90-96692] 17 p2419 N90-23783
The application of remote sensing techniques for regional planning, environmental studies, and environment maintenance
[BCRS-89-16] 18 p2574 N90-24667
Automatic line network extraction from aerial imagery of urban areas through knowledge based image analysis
[AD-A222675] 20 p2880 N90-26385
National mapping program. Fact sheet: Black and white photographs. NHAP (National High Altitude Photography Program)
[PB90-185042] 21 p3015 N90-27139
Integration of multispectral SPOT imagery and panchromatic aerial photography for study in urban land use
[INPE-4967-PRE/1536] 22 p3194 N90-28125
The above-inversion moisture structure observed during FIRE 22 p3215 N90-28235
FIRE aircraft observations of horizontal and vertical transport in marine stratocumulus 22 p3220 N90-28261
The October 27-28, 1986, FIRE cirrus case study: Cloud microstructure 22 p3224 N90-28283

AERIAL RECONNAISSANCE
NT AIRBORNE INTEGRATED RECONNAISSANCE SYSTEM
Airborne FLIR detection of surface targets 06 p0759 N90-14416
Evaluation of the pasture potential in the dry areas of Kenya using combined Earth reconnaissance 08 p1093 N90-16327
Position fixing by detection of roads and rivers 09 p1163 N90-16733
Proposition for an airborne remote sensing system
[INPE-4872-PRE/1483] 10 p1399 N90-18090
Activities report in DLR research field communication engineering and reconnaissance
[ISSN-0173-0118] 11 p1525 N90-18781
Cockpit display of hazardous wind shear information 14 p1905 N90-20924
Remote sensing of the ocean surface with C- and Ku-band airborne scatterometers 22 p3195 N90-28129
Large-scale variability in marine stratocumulus clouds defined from simultaneous aircraft and satellite measurements 22 p3213 N90-28226
July 16, 1987 revisited: Lessons for modelers 22 p3214 N90-28232
Airborne target detection, acquisition, and tracking devices
[AD-A223852] 24 p3462 N90-29555
Proceedings of a Workshop on the Geoelectric and Geomagnetic Environment of Continental Margins
[AD-A223743] 24 p3493 N90-29739

AERIAL RUDDERS
Independent Orbiter Assessment (IOA): Assessment of the rudder/speed brake subsystem FMEA/CIL
[NASA-CR-185558] 02 p0174 N90-10975
Stability characteristics of a combat aircraft with control surface failure
[AD-A216196] 10 p1323 N90-17646
Flutter investigations on a Transavia PL12/T-400 aircraft
[AD-A219108] 16 p2203 N90-22570

AEROACOUSTICS
Large-scale Advanced Prop-fan (LAP) technology assessment report
[NASA-CR-182142] 01 p0010 N90-10046
Measurement resolution of noise directivity patterns from acoustic flight tests
[NASA-TM-4134] 01 p0118 N90-10679
An investigation of counterrotating tip vortex interaction
[NASA-CR-185135] 02 p0271 N90-11549
Review and analysis of the DNW/Model 360 rotor acoustic data base
[NASA-TM-102253] 03 p0299 N90-11692
Effects of acoustic sources 04 p0446 N90-12553
Acoustic design considerations: Review of rotor acoustic sources 04 p0451 N90-12585
An experimental and theoretical study of the aeroacoustics of external-Coanda gas flares 06 p0773 N90-14495
NASA aerodynamics program
[NASA-TM-4175] 09 p1247 N90-17235
Predicted and measured boundary layer refraction for advanced turboprop propeller noise
[NASA-TM-102365] 09 p1279 N90-17413
Experimental performance and acoustic investigation of modern, counterrotating blade concepts
[NASA-CR-185158] 17 p2352 N90-23393
PTA en route noise measurements 18 p2608 N90-24855
Aero-acoustic investigations of the magnetic train Transrapid 06
[MBB-UW-0009/89-PUB] 19 p2654 N90-25104
A review of instability and noise propagation in supersonic flows
[NASA-CR-186800] 19 p2655 N90-25112
Data of aero acoustic measurements on ultra-light aircraft propellers
[ESA-TT-1147] 19 p2754 N90-25648
Aeroacoustics of advanced propellers
[NASA-TM-103137] 20 p2923 N90-26635
The acoustic results of a United Technologies scale model helicopter rotor tested at DNW
[NASA-TM-101879] 21 p3073 N90-27471
Development of a linearized unsteady aerodynamic analysis for cascade gust response predictions
[NASA-CR-4308] 22 p3108 N90-27655
Cavity aeroacoustics
[AD-A223853] 24 p3418 N90-29307
Generalized Advanced Propeller Analysis System (GAPAS). Volume 2: Computer program user manual
[NASA-CR-185277] 24 p3434 N90-29394

AEROASSIST
The controllability of the aeroassist flight experiment atmospheric skip trajectory 05 p0591 N90-13438
Measured and predicted aerodynamic coefficients and shock shapes for Aeroassist Flight Experiment (AFE) configuration
[NASA-TP-2956] 06 p0717 N90-14185
Optimal control of aero-assisted orbit transfer vehicles 06 p0727 N90-14241
Guidance and Control strategies for aerospace vehicles
[NASA-CR-186195] 06 p0727 N90-14243
Optimal trajectories for the aeroassisted flight experiment
[NASA-CR-186133] 06 p0729 N90-14250
Project Argo: The design and analysis of an all-propulsive and an aeroassisted version of a manned space transportation vehicle
[NASA-CR-186047] 06 p0732 N90-14266
Aerobraking characteristics for several potential manned Mars entry vehicles
[NASA-TM-101669] 06 p0733 N90-14272
Singular perturbation analysis of AOTV-related trajectory optimization problems
[NASA-CR-186202] 08 p1027 N90-15936
Preliminary investigation of parameter sensitivities for atmospheric entry and aerobraking at Mars
[NASA-TM-101607] 10 p1327 N90-17667
Optimal trajectories for the aeroassisted flight experiment. Part 3: Formulation, results, and analysis
[NASA-CR-186165] 14 p1930 N90-21051
Optimal trajectories for the aeroassisted flight experiment. Part 4: Data, tables, and graphs
[NASA-CR-186164] 15 p2056 N90-21780
Approximate optimal guidance schemes for atmospheric orbital maneuvering 16 p2206 N90-22585
AFE dynamic effects in inhomogeneous plasmas 18 p2643 N90-25053
Guidance and control strategies for aerospace vehicles
[NASA-CR-186878] 20 p2814 N90-26013

Project SPARC: Space-based aeroassisted reusable craft
[NASA-CR-186816] 20 p2821 N90-26051
Noncoplanar orbit transfer optimization for an aeroassisted sortie vehicle 22 p3128 N90-27752
Flowfield computation of entry vehicles
[NASA-CR-186946] 22 p3171 N90-27986
Theoretical investigation of non-equilibrium chemistry and optical radiation in hypersonic flow fields
[NASA-CR-186335] 24 p3417 N90-29300
Optimal trajectories for hypervelocity flight 24 p3430 N90-29378
Design and evaluation of candidate pressure distribution and air data system tile penetration for the aeroassist flight experiment
[NASA-CR-4312] 24 p3471 N90-29615

AEROBRAKING
Preliminary design of a large tetrahedral truss/hexagonal heatshield panel aerobrake
[NASA-TM-101612] 01 p0025 N90-10127
Aerobraking characteristics for several potential manned Mars entry vehicles
[NASA-TM-101669] 06 p0733 N90-14272
Preliminary investigation of parameter sensitivities for atmospheric entry and aerobraking at Mars
[NASA-TM-101607] 10 p1327 N90-17667
Use of random Martian atmosphere to evaluate potential entry guidance schemes
[NASA-TM-102606] 13 p1764 N90-20122
Mechanistic model for catalytic recombination during aerobraking maneuvers
[NASA-CR-185611] 14 p1932 N90-21059
Heavily loaded joints for assembling aerobrake support trusses
[NASA-CR-181992] 14 p1939 N90-21099
Equilibrium radiative heating tables for Earth entry
[NASA-TM-102652] 17 p2401 N90-23675
Equilibrium radiative heating tables for aerobraking in the Martian atmosphere
[NASA-TM-102659] 19 p2688 N90-25290
Guidance and control strategies for aerospace vehicles
[NASA-CR-186678] 20 p2814 N90-26013
The effect of interplanetary trajectory options on a manned Mars aerobrake configuration
[NASA-TP-3019] 20 p2818 N90-26036
Project SPARC: Space-based aeroassisted reusable craft
[NASA-CR-186816] 20 p2821 N90-26051
The aerobraking space transfer vehicle
[NASA-CR-186819] 20 p2821 N90-26053

AEROCAPTURE
Preliminary investigation of parameter sensitivities for atmospheric entry and aerobraking at Mars
[NASA-TM-101607] 10 p1327 N90-17667
Nonequilibrium radiation and chemistry models for aerocapture vehicle flowfields
[NASA-CR-186728] 22 p3169 N90-27973
Nonequilibrium radiation and chemistry models for aerocapture vehicle flowfields
[NASA-CR-186379] 23 p3267 N90-28490

AERODYNAMIC AXIS
U AERODYNAMIC BALANCE

AERODYNAMIC BALANCE
Development of a three-axis trim program
[AD-A212883] 06 p0726 N90-14237
Stability characteristics of a combat aircraft with control surface failure
[AD-A216196] 10 p1323 N90-17646
Influence of forebody geometry on aerodynamic characteristics and a design guide for defining departure/spin resistant forebody configurations
[AD-A216714] 11 p1456 N90-18388
Coupled rotor-body equations of motion hover flight
[NASA-CR-186710] 19 p2655 N90-25111

AERODYNAMIC BRAKES
NT DRAG CHUTES
NT LEADING EDGE FLAPS
Tribomaterial factors in space mechanism brake performance 15 p2114 N90-22095
Preliminary subsystem designs for the Assured Crew Return Vehicle (ACRV), volume 1
[NASA-CR-186677-VOL-1] 20 p2818 N90-26039

AERODYNAMIC BUZZ
U FLUTTER

AERODYNAMIC CENTER
U AERODYNAMIC BALANCE

AERODYNAMIC CHARACTERISTICS
NT AERODYNAMIC BALANCE
NT AERODYNAMIC DRAG
NT AERODYNAMIC STABILITY
NT INTERFERENCE DRAG
NT LIFT
NT STATIC AERODYNAMIC CHARACTERISTICS
NT SUPERSONIC DRAG
NT ZERO LIFT

Development of a flight test methodology for a US Navy half-scale unmanned air vehicle
[AD-A210563] 01 p0005 N90-10029
Stability and Control of Tactical Missile Systems
[AGARD-CP-451] 01 p0011 N90-10050
The present status and the future of missile aerodynamics 01 p0012 N90-10051
Wind tunnel tests: The role of the model 01 p0013 N90-10064
High temperature VSCF (Variable Speed Constant Frequency) generator system
[AD-A210823] 01 p0061 N90-10351
Low-speed, high-lift aerodynamic characteristics of slender, hypersonic accelerator-type configurations
[NASA-TP-2945] 02 p0145 N90-10830
An experimental investigation of the aerodynamic characteristics of slanted base ogive cylinders using magnetic suspension technology
[NASA-CR-181708] 02 p0146 N90-10834
P-180 AVANTI: Project and flight test program comprehensive overview 02 p0151 N90-10863
The determination of the aerodynamic characteristics of an ogive-cylinder body in subsonic, curved, incompressible flow, and an assessment of the effect of flow curvature
[REPT-87-13] 03 p0302 N90-11712
Nacelle aerodynamic performance 04 p0446 N90-12552
Aerodynamic test and analysis of a slender generic missile configuration
[AD-A212522] 04 p0448 N90-12567
The development of a high response aerodynamic wedge probe and use on a high-speed research compressor
[PNR90598] 04 p0456 N90-12613
Large-scale Advanced Prop-fan (LAP) static rotor test report
[NASA-CR-180848] 04 p0457 N90-12617
Analysis of experimental data for CAST 10-2/DOA 2 supercritical airfoil at low Reynolds numbers and application to high Reynolds number flow
[AD-A211654] 05 p0571 N90-13326
Efficient methods for integrated structural-aerodynamic wing optimum design 05 p0579 N90-13376
Measured and predicted aerodynamic coefficients and shock shapes for Aeroassist Flight Experiment (AFE) configuration
[NASA-TP-2956] 06 p0717 N90-14185
An in-flight investigation of ground effect on a forward-swept wing airplane
[NASA-TM-101708] 06 p0720 N90-14202
Effect of unshielded and shielded horn balances on hinge moment coefficients for controls at low speeds
[ESDU-89003-A] 06 p0726 N90-14238
Concurrent processing adaptation of aeroplastic analysis of propfans
[NASA-TM-102455] 06 p0799 N90-14656
Flight and wind tunnel investigation of aerodynamic effects of aircraft ground deicing/antiicing fluids 07 p0873 N90-15064
Serrated trailing edges for improving lift and drag characteristics of lifting surfaces
[NASA-CASE-LAR-13870-1] 07 p0879 N90-15094
The US National Transonic Facility, NTF 08 p1028 N90-15942
NASA supercritical airfoils: A matrix of family-related airfoils
[NASA-TP-2969] 09 p1159 N90-16710
A survey of missile aerodynamics 10 p1303 N90-17541
The role of computational fluid dynamics in missile aerodynamics 10 p1304 N90-17547
Supersonic aerodynamic characteristics of a proposed Assured Crew Return Capability (ACRC) lifting-body configuration
[NASA-TM-4136] 10 p1307 N90-17560
Analysis and numerical solution of flow over airfoil with control flap 10 p1307 N90-17564
Hypersonic nozzle/afterbody performance at low Mach numbers
[AD-A216223] 10 p1309 N90-17575
CAST-10-2/DOA 2 Airfoil Studies Workshop Results
[NASA-CP-3052] 10 p1323 N90-17647
High Reynolds number tests of the CAST-10-2/DOA 2 transonic airfoil at ambient and cryogenic temperature conditions 10 p1324 N90-17650
Main results of CAST-10 airfoil tested in T2 cryogenic wind tunnel 10 p1324 N90-17652
Investigation of CAST-10-2/DOA 2 airfoil in NAE high Reynolds number two-dimensional test facility 10 p1324 N90-17654
Generating optimally evasive MaRV trajectories
[DE90-004495] 10 p1328 N90-17671
Modeling the wake as a continuous vortex sheet in a potential-flow solution using vortex panels
[AD-A216220] 10 p1385 N90-18016

Static and rotational aerodynamic data from 0 deg to 90 deg angle of attack for a series of basic and altered forebody shapes
[AD-A216582] 11 p1451 N90-18361
Aerodynamic testing of a rotating wind turbine blade
[DE90-000312] 11 p1451 N90-18362
Prediction of rotor blade-vortex interaction noise from 2-D aerodynamic calculations and measurements
[ISL-CO-243/88] 11 p1451 N90-18365
The effects of wind tunnel data uncertainty on aircraft point performance predictions
[AD-A216091] 11 p1456 N90-18387
Computation of hypersonic unsteady viscous flow over a cylinder 12 p1597 N90-19194
Performance of an optimized rotor blade at off-design flight conditions
[NASA-CR-4288] 12 p1603 N90-19226
Low-speed wind-tunnel investigation of the flight dynamic characteristics of an advanced turboprop business/commuter aircraft configuration
[NASA-TP-2982] 12 p1606 N90-19239
Output model-following control synthesis for an oblique-wing aircraft
[NASA-TM-100454] 12 p1606 N90-19241
Experimental and theoretical aerodynamic characteristics of a high-lift semispan wing model
[NASA-TP-2990] 13 p1749 N90-20046
Unsteady free-wake viscous aerodynamic analysis of helicopter rotors
[AD-A217166] 13 p1750 N90-20048
Windblast protection for advanced ejection seats 13 p1752 N90-20063
Measurement and prediction of propeller blade surface pressure distributions 14 p1912 N90-20961
Computational Methods for Aerodynamic Design (Inverse) and Optimization
[AGARD-CP-463] 14 p1916 N90-20976
Aerodynamic design techniques at DLR Institute for Design Aerodynamics 14 p1916 N90-20979
Aerodynamic design by optimization 14 p1920 N90-20996
Aerodynamic design via control theory 14 p1920 N90-20998
Optimization of aerodynamic designs using computational fluid dynamics 14 p1920 N90-20999
Prediction of forces and moments for flight vehicle control effectors. Part 1: Validation of methods for predicting hypersonic vehicle controls forces and moments
[NASA-CR-186571] 15 p2047 N90-21734
On the way to an integrated mesh generation system for industrial applications 15 p2095 N90-21989
Application of the TRANAIR rectangular grid approach to the aerodynamic analysis of complex configurations 15 p2096 N90-21996
Aerodynamics of a full-scale, non rotating wind turbine blade under natural wind conditions
[RISOE-M-2768] 15 p2123 N90-22144
Dynamic ground-effect measurements on the F-15 STOL and Maneuver Technology Demonstrator (S/MTD) configuration
[NASA-TP-3000] 16 p2195 N90-22531
The aerodynamic characteristics of power-law bodies in continuum and transitional hypersonic flow
[RAE-TM-AERO-2164] 16 p2196 N90-22537
Destabilization of supersonic free shear layers by parametric excitation using Mach waves generated by a wavy wall
[AD-A219655] 17 p2345 N90-23352
A new stress routine for the Projectile Design Analysis System (PRODAS)
[AD-A220564] 17 p2346 N90-23357
A computer code for the prediction of aerodynamic characteristics of lifting airfoils at transonic speed
[DLC-EST-TN-030] 17 p2346 N90-23359
Experimental performance and acoustic investigation of modern, counterrotating blade concepts
[NASA-CR-185158] 17 p2352 N90-23393
AVION: A detailed report on the preliminary design of a 79-passenger, high-efficiency, commercial transport aircraft
[NASA-CR-186663] 17 p2353 N90-23395
Lateral-directional stability and control characteristics of the Quiet Short-Haul Research Aircraft (QSRA)
[NASA-TM-102250] 17 p2356 N90-23413
Fluid dynamic mechanisms and interactions within separated flows
[AD-A219628] 17 p2403 N90-23689
Missile aerodynamics
[ISBN-0-9620629-0-1] 18 p2490 N90-24236
Aerodynamic performance of a 0.27-scale model of an AH-64 helicopter with baseline and alternate rotor blade sets
[NASA-TM-4201] 18 p2491 N90-24237

Aerodynamic characteristics of two rotorcraft airfoils designed for application to the inboard region of a main rotor blade
[NASA-TP-3009] 18 p2491 N90-24239
Subsonic sting interference on the aerodynamic characteristics of a family of slanted-base ogive-cylinders
[NASA-CR-4299] 18 p2492 N90-24242
Wind tunnel tests of a 20-gore disk-gap-band parachute
[AD-A221326] 18 p2493 N90-24251
New transonic test sections for the NAE 5 ft x 5 ft trisonic wind tunnel
[AD-A220933] 18 p2499 N90-24278
An analytic study of nonsteady two-phase laminar boundary layer around an airfoil
18 p2643 N90-25051
Design of a low cost short takeoff-vertical landing export fighter/attack aircraft
[NASA-CR-186658] 19 p2659 N90-25132
A computational efficient modelling of laminar separation bubbles
[NASA-CR-186729] 19 p2688 N90-25291
Prediction methodologies for nonlinear aerodynamic characteristics of control surfaces
[NIAR-90-17] 20 p2801 N90-25937
Effect of tail size reductions on longitudinal aerodynamic characteristics of a three surface F-15 model with nonaxisymmetric nozzles
[NASA-TP-3036] 20 p2802 N90-25938
Identification of aerodynamic models for maneuvering aircraft
[NASA-CR-186630] 20 p2802 N90-25943
Technical evaluation report on the Fluid Dynamics Panel Symposium on Computational Methods for Aerodynamic Design (Inverse) and Optimization
[AGARD-AR-267] 20 p2803 N90-25947
Computation of viscous aerodynamic characteristics of 2-D airfoils for helicopter applications
[NLR-MP-88052-U] 20 p2804 N90-25951
The role of computational fluids dynamics in missile aerodynamics
[NLR-MP-88072-U] 20 p2804 N90-25952
Effect of vortex generators on the aerodynamic wing characteristics and body of revolution
[AD-A222813] 20 p2804 N90-25955
Transatmospheric vehicle research
[NASA-CR-186705] 20 p2807 N90-25970
Turbulent reacting flows and supersonic combustion
[AD-A221793] 21 p2979 N90-26933
The acoustic results of a United Technologies scale model helicopter rotor tested at DNW
[NASA-TM-101879] 21 p3073 N90-27471
Development of a linearized unsteady aerodynamic analysis for cascade gust response predictions
[NASA-CR-4308] 22 p3108 N90-27655
Study of missiles in flight
[ETN-90-97457] 22 p3109 N90-27662
Active control of aerothermoelastic effects for a conceptual hypersonic aircraft
[NASA-TM-102713] 22 p3122 N90-27725
Tests of an ultra-light tunnel in the anechoic wind tunnel facility CEPRA 19
[ONERA-RF-20/7294-PH] 22 p3122 N90-27729
Advanced launch vehicle configurations and performance trades 22 p3126 N90-27744
Prediction of subsonic vortex shedding from forebodies with chines
[NASA-CR-4323] 23 p3268 N90-28494
Projectile supersonic drag characteristics
[AD-A224217] 23 p3270 N90-28506
Aerodynamics of Combat Aircraft Controls and of Ground Effects
[AGARD-CP-465] 23 p3271 N90-28513
Effects of canard position on the aerodynamic characteristics of a close-coupled canard configuration at low speed 23 p3272 N90-28519
The steady and time-dependent aerodynamic characteristics of a combat aircraft with a delta or swept canard 23 p3274 N90-28526
Study of ground effects on flying scaled models
23 p3275 N90-28532
An in-flight investigation of ground effect on a forward-swept wing airplane 23 p3275 N90-28533
Determination of the ground effect on the characteristics of the A320 aircraft 23 p3275 N90-28534
Aerodynamic parameters of High-Angle-of attack Research Vehicle (HARV) estimated from flight data
[NASA-TM-102692] 23 p3283 N90-28578
Transonic 3-D Euler analysis of flows around fanjet engine and TPS (Turbine Powered Simulator). Comparison with wind tunnel experiment, evaluation of TPS testing method and 3-D flow
[NAL-TR-1045] 24 p3421 N90-29327
The DELTA MONSTER: An RPV designed to investigate the aerodynamics of a delta wing platform
[NASA-CR-186226] 24 p3431 N90-29381
Fighter agility metrics
[NASA-CR-187289] 24 p3432 N90-29389
Generalized Advanced Propeller Analysis System (GAPAS). Volume 2: Computer program user manual
[NASA-CR-185277] 24 p3434 N90-29394
Numerical simulations of the structure of supersonic shear layers
[AD-A224164] 24 p3467 N90-29587
The experimental investigation of flow in the core of a vortex structure
[BR114893] 24 p3468 N90-29597

AERODYNAMIC CHORDS
U AIRFOIL PROFILES

AERODYNAMIC COEFFICIENTS
Independent Orbiter Assessment (IOA): Assessment of the Orbiter Experiment (OEX) subsystem
[NASA-CR-185587] 02 p0171 N90-10962
Independent Orbiter Assessment (IOA): Analysis of the Orbiter Experiment (OEX) subsystem
[NASA-CR-185586] 02 p0171 N90-10963
On transonic flow over segmented slotted wind tunnel wall with mass transfer 02 p0294 N90-11676
Design and test of a natural laminar flow/large Reynolds number airfoil with a high design cruise lift coefficient
04 p0444 N90-12543
Effects of acoustic sources 04 p0446 N90-12553
Powered-lift aircraft technology
[NASA-SP-501] 04 p0452 N90-12589
Measured and predicted aerodynamic coefficients and shock shapes for Aeroassist Flight Experiment (AFE) configuration
[NASA-TP-2956] 06 p0717 N90-14185
The maximum lift coefficient of plain wings at subsonic speeds
[ESDU-89034] 07 p0876 N90-15082
Inclusion of nonlinear aerodynamics in the FLAP code
[DE89-009507] 07 p0954 N90-15519
Measurement of the aerodynamical coefficients related to square section models defined by resemblance to the normalized models AGARD HB1 and HB2 in supersonic flow. Part 2: Incidence up to 25 deg
[ISL-R-108/88-PT-2] 09 p1161 N90-16718
Main results of CAST-10 airfoil tested in T2 cryogenic wind tunnel 10 p1324 N90-17652
Comparison of NAE porous wall and NASA adaptive wall test results using the NAE CAST-10 airfoil model
10 p1325 N90-17656
On the evaluation of aerodynamic influence coefficients
[NLR-MP-87019-U] 12 p1597 N90-19191
An aerodynamic tradeoff study of the scissor wing configuration
[NASA-CR-186576] 14 p1913 N90-20965
Slotted-wall research with disk and parachute models in a low-speed wind tunnel
[DE90-002989] 15 p2048 N90-21737
Six-degree-of-freedom aircraft simulation with mixed-data structure using the applied dynamics simulation language, ADSIM 16 p2294 N90-23067
Aerodynamic characteristics of two rotorcraft airfoils designed for application to the inboard region of a main rotor blade
[NASA-TP-3009] 18 p2491 N90-24239
An interactive boundary-layer method for unsteady airfoil flows. Part 1: Quasi-steady-state model
[AD-A221220] 18 p2493 N90-24250
DRAG-n-FLY: A proposal in response to a low Reynolds number station keeping mission
[NASA-CR-186668] 19 p2658 N90-25130
Projectile supersonic drag characteristics
[AD-A224217] 23 p3270 N90-28506
A flight dynamic model of aircraft spinning
[AR-005-600] 23 p3283 N90-28576
Aerodynamic parameters of High-Angle-of attack Research Vehicle (HARV) estimated from flight data
[NASA-TM-102692] 23 p3283 N90-28578
Aerodynamic forces acting on a finite rectangular slender body
[NAL-TR-1035] 24 p3421 N90-29329

AERODYNAMIC CONFIGURATIONS
NT WAVERIDERS
Prediction of stability derivatives for missiles using the HISSS panel code 01 p0012 N90-10053
Experience gained in the improvement of the Aspide aerodynamic configuration for the surface to air role
01 p0015 N90-10072
Analysis of flight data from a High-Incidence Research Model by system identification methods
[NASA-TP-2940] 01 p0015 N90-10074
US Navy principal site testing concept and the F-18
02 p0151 N90-10861
P-180 AVANTI: Project and flight test program comprehensive overview 02 p0151 N90-10863
Study of the integration of wind tunnel and computational methods for aerodynamic configurations
[NASA-TM-102196] 05 p0572 N90-13332
Reduction of profile drag by modifying the structure next to the wake area
[IMFL-88/35] 05 p0576 N90-13356
A model suitable for predicting the noise associated with the ducted tail rotor of a helicopter
[ECL-88-09] 05 p0697 N90-14074
Measured and predicted aerodynamic coefficients and shock shapes for Aeroassist Flight Experiment (AFE) configuration
[NASA-TP-2956] 06 p0717 N90-14185
Program VSAERO theory document: A computer program for calculating nonlinear aerodynamic characteristics of arbitrary configurations
[NASA-CR-4023] 06 p0720 N90-14200
Aerobraking characteristics for several potential manned Mars entry vehicles
[NASA-TM-101669] 06 p0733 N90-14272
Application of the joined wing to tiltrotor aircraft
[NASA-CR-177543] 07 p0879 N90-15093
Models for cryogenic wind tunnels
08 p1031 N90-15956
Preliminary design of a family of three close air support aircraft
[NASA-CR-186070] 09 p1166 N90-16751
The use of lateral jet control at Aerospatiale
10 p1305 N90-17551
An approximate model for the performance and acoustic predictions of counterrotating propeller configurations
[NASA-CR-180667] 10 p1426 N90-18228
Static and rotational aerodynamic data from 0 deg to 90 deg angle of attack for a series of basic and altered forebody shapes
[AD-A216582] 11 p1451 N90-18361
A difference scheme with autocontrol artificial viscosity to predict ablated nosetip shape
[AD-A216625] 11 p1468 N90-18452
Implementation of a finite element process for the Euler equations of the gas dynamics
[PREPRINT-500] 12 p1661 N90-19545
Experimental and theoretical aerodynamic characteristics of a high-lift semispan wing model
[NASA-TP-2990] 13 p1749 N90-20046
An aerodynamic tradeoff study of the scissor wing configuration
[NASA-CR-186576] 14 p1913 N90-20965
An intensive procedure for the design of pressure-specified three-dimensional configurations at subsonic and supersonic speeds by means of a higher-order panel method 14 p1917 N90-20982
Numerical optimization of wings in transonic flow
14 p1920 N90-20997
Prediction of forces and moments for flight vehicle control effectors. Part 1: Validation of methods for predicting hypersonic vehicle controls forces and moments
[NASA-CR-186571] 15 p2047 N90-21734
Geometry and grids of complex configurations for aerodynamic calculation 15 p2093 N90-21980
A new stress routine for the Projectile Design Analysis System (PRODAS)
[AD-A220564] 17 p2346 N90-23357
Actuated forebody strakes
[NASA-CASE-LAR-13983-1] 17 p2352 N90-23390
Activities report in aerospace and aerodynamics
[ETN-90-96774] 17 p2487 N90-24224
Static wind-tunnel and radio-controlled flight test investigation of a remotely piloted vehicle having a delta wing planform
[NASA-TM-4200] 18 p2491 N90-24238
Overview on the Hermes in-orbit control system
[MBB-UK-0056/89-PUB] 19 p2652 N90-25094
AM-X high incidence trials, development and results
[ETN-90-97277] 20 p2814 N90-26016
Ramjet and ramrocket propulsion systems for missiles
21 p2973 N90-26897
Numerical interactive grid generation for 3-D flow calculations
[NLR-MP-88055-U] 21 p3003 N90-27069
Combat aircraft control requirements for agility
23 p3272 N90-28517
Energy Efficient Engine high pressure turbine component test performance report
[NASA-CR-168289] 23 p3278 N90-28553
Energy Efficient Engine program advanced turbofan nacelle definition study
[NASA-CR-174942] 23 p3280 N90-28560
The space transportation main engine phase A' study
[NASA-CR-179399] 23 p3290 N90-28610
Dynamic separation: Search for the cause of dynamic stall and search for its control
[AD-A223412] 24 p3418 N90-29305

Chemical kinetic and aerodynamic structures of flames
[AD-A224281] 24 p3445 N90-29455

AERODYNAMIC DRAG
NT SUPERSONIC DRAG
Atmospheric drag model calibrations for spacecraft lifetime prediction 05 p0591 N90-13439
Serrated trailing edges for improving lift and drag characteristics of lifting surfaces
[NASA-CASE-LAR-13870-1] 07 p0879 N90-15094
Effect of riblets on flow separation from a cylinder and an airfoil in subsonic flow
[AD-A216197] 10 p1309 N90-17574
An investigation of long term orbits about the planet Mars using a dynamic atmosphere model
[AD-A216111] 10 p1447 N90-18351
Optimum spanwise camber for minimum induced drag
[BU-403] 11 p1452 N90-18369
Flight test investigation of certification issues pertaining to general-aviation-type aircraft with natural laminar flow
[NASA-CR-181967] 14 p1911 N90-20952
Constrained spanload optimization for minimum drag of multi-lifting-surface configurations 14 p1919 N90-20992
Exhaust nozzles for propulsion systems with emphasis on supersonic cruise aircraft
[NASA-RP-1235] 14 p1927 N90-21037
On the use of external burning to reduce aerospace vehicle transonic drag
[NASA-TM-103107] 15 p2052 N90-21762
Proceedings of Workshop on Atmospheric Density and Aerodynamic Drag Models for Air Force Operations, volume 1
[AD-A220381] 17 p2345 N90-23355
Proceedings of Workshop on Atmospheric Density and Aerodynamic Drag Models for Air Force Operations, volume 2
[AD-A220382] 17 p2345 N90-23356
Preliminary airworthiness evaluation of the RC-12K
[AD-A219545] 17 p2351 N90-23387
Extrapolation of missile flight lines
[ETN-90-96494] 18 p2508 N90-24336
Aero-acoustic investigations of the magnetic train Transrapid 06
[MBB-UW-0009/89-PUB] 19 p2654 N90-25104
Application of laminar flow control to supersonic transport configurations
[NASA-CR-181917] 20 p2803 N90-25944
A method for the reduction of aerodynamic drag of road vehicles
[NASA-TM-102589] 22 p3108 N90-27656
Study of the structure of the vortices created by the drag of a notched edge by thermal tracing
[IMFL-89-26] 22 p3109 N90-27660
Study of the compressibility effects on the turbulence of supersonic drags
[ETN-90-97448] 22 p3109 N90-27661
Study of the flow around the prototype of A300: Results of the third test campaign at F2 and comparison with calculations
[CERT-33/5025-29-DERAT] 22 p3109 N90-27663
Sting-support interference on afterbody drag at transonic speeds
[NAL-TM-EA-8902] 23 p3267 N90-28492
Theoretical investigation of non-equilibrium chemistry and optical radiation in hypersonic flow fields
[NASA-CR-186335] 24 p3417 N90-29300

AERODYNAMIC FORCES
NT AERODYNAMIC DRAG
NT AERODYNAMIC INTERFERENCE
NT AERODYNAMIC LOADS
NT BLAST LOADS
NT GUST LOADS
NT HYPERSONIC FORCES
NT LIFT
NT SUPERSONIC DRAG
NT WING LOADING
NT ZERO LIFT
An integrated CFD/experimental analysis of aerodynamic forces and moments
[NASA-TM-102195] 01 p0002 N90-10006
A scalar/vector potential solution for aerodynamic coefficients in wind shear 02 p0147 N90-10838
Normal-force-curve and pitching-moment-curve slopes of forebody-cylinder combinations at zero angle of attack for Mach numbers up to 5
[ESDU-89008] 03 p0301 N90-11709
In-plane forces and moments on installed inclined propellers at low forward speeds
[ESDU-89047] 09 p1161 N90-16720
Windblast protection for advanced ejection seats 13 p1752 N90-20063
Application of a dynamic stall model to rotor trim and aeroelastic response 16 p2200 N90-22556
Approximate optimal guidance schemes for atmospheric orbital maneuvering 16 p2206 N90-22585
STARS: An integrated general-purpose finite element structural, aeroelastic, and aeroservoelastic analysis computer program
[NASA-TM-101709] 17 p2416 N90-23768
Reduced order models for nonlinear aerodynamics 18 p2492 N90-24244
Short time-dynamometer system for shock wave channels
[MBB-UT-115/89-PUB] 19 p2651 N90-25084
Aerodynamic interferences of in-flight thrust reversers in ground effect 23 p3274 N90-28529
Turbomachinery rotor forces
[NASA-CR-183779] 23 p3334 N90-28852
Aerodynamic forces acting on a finite rectangular slender body
[NAL-TR-1035] 24 p3421 N90-29329
Windshear estimation along the trajectory of an aircraft 24 p3494 N90-29745

AERODYNAMIC HEAT TRANSFER
Heat transfer measurements from a NACA 0012 airfoil in flight and in the NASA Lewis icing research tunnel
[NASA-CR-4278] 12 p1599 N90-19203
Supersonic/hypersonic aerodynamics and heat transfer for projectile design using viscous-inviscid interaction
[AD-A224354] 24 p3418 N90-29303

AERODYNAMIC HEATING
NT SHOCK HEATING
Optimum shape of a blunt forebody in hypersonic flow
[NASA-CR-181955] 05 p0575 N90-13351
Thermal/structural analyses of several hydrogen-cooled leading-edge concepts for hypersonic flight vehicles
[NASA-TM-102391] 06 p0775 N90-14511
Numerical investigation of transition control of a flat plate boundary layer 07 p0926 N90-15361
Resultant forces and moments in completely restrained plates subjected to a recovery temperature varying linearly with time
[ESDU-89024] 07 p0947 N90-15480
Thermal stresses in unrestrained plates subjected to a recovery temperature varying linearly with time
[ESDU-89025] 07 p0947 N90-15481
Temperatures in plates subjected to a recovery temperature varying linearly with time
[ESDU-89023] 07 p1007 N90-15831
A review of high-speed, convective, heat-transfer computation methods 10 p1305 N90-17548
A difference scheme with autocontrol artificial viscosity to predict ablated nosetip shape
[AD-A216625] 11 p1468 N90-18452
Heat transfer definitions and equations
[ESDU-89022] 12 p1657 N90-19522
Information on the use of data items on hot structures
[ESDU-89021] 12 p1674 N90-19611
Temperatures in plates subjected to a sudden increase in recovery temperature
[ESDU-89026] 12 p1724 N90-19904
Analysis of flow-, thermal-, and structural-interaction of hypersonic structures subjected to severe aerodynamic heating
[AD-A217882] 13 p1750 N90-20053
The application of active controls technology to a generic hypersonic aircraft configuration
[NASA-TM-101689] 13 p1754 N90-20071
Ablative cooling of aerodynamically heated radomes
[AD-D014426] 14 p1971 N90-21293
A brief review of some mechanisms causing boundary layer transition at high speeds
[NASA-TM-102834] 20 p2803 N90-25945
Space plane model for visual measurement of aerodynamic heating
[DE90-505514] 20 p2803 N90-25949
A computational study of the effectiveness of coating materials for KE projectile fins subjected to the combined effects of inbore and aerodynamic heating
[AD-A222595] 20 p2840 N90-26155
Real-time aerodynamic heating and surface temperature calculations for hypersonic flight simulation
[NASA-TM-4222] 23 p3327 N90-28815

AERODYNAMIC INTERFERENCE
Wind tunnel support system effects on a fighter aircraft model at Mach numbers from 0.6 to 2.0
[AD-A210614] 01 p0002 N90-10010
Transonic Euler solutions on mutually interfering finned bodies
[AD-A213395] 05 p0572 N90-13331
A wall interference assessment/correction interface measurement system for the NASA/ARC 12-ft PWT
[NASA-CR-185474] 05 p0584 N90-13401
A two-dimensional adaptive-wall test section with ventilated walls in the Ames 2- by 2-foot transonic wind tunnel
[NASA-TM-102207] 05 p0585 N90-13407
An experimental investigation of wall-interference effects for parachutes in closed wind tunnels
[DE90-001802] 07 p0875 N90-15076
Installed tailplane lift-curve slope at subsonic speeds
[ESDU-89029] 07 p0876 N90-15081
Wind tunnel investigations on the configuration of the international vortex flow experiment 08 p1068 N90-16181
Prediction methods for store separation 10 p1305 N90-17549
CAST-10-2/DOA 2 Airfoil Studies Workshop Results
[NASA-CP-3052] 10 p1323 N90-17647
Nonlinear transonic Wall-Interference Assessment/Correction (WIAC) procedures and application to cast-10 airfoil results from the NASA 0.3-m TCT 8- by 24-inch Slotted Wall Test Section (SWTS) 10 p1323 N90-17648
Comparison of conventional and adaptive wall wind tunnel results with regard to Reynolds number effects 10 p1323 N90-17649
High Reynolds number tests of the CAST-10-2/DOA 2 transonic airfoil at ambient and cryogenic temper ature conditions 10 p1324 N90-17650
Investigation of CAST-10-2/DOA 2 airfoil in NAE high Reynolds number two-dimensional test facility 10 p1324 N90-17654
Residual interference and wind tunnel wall adaption 10 p1324 N90-17655
Comparison of NAE porous wall and NASA adaptive wall test results using the NAE CAST-10 airfoil model 10 p1325 N90-17656
Experience with some repeat tests on the 9 inch chord CAST-10-2/DOA 2 airfoil model in the Langley 0.3-m TCT adaptive wall test section 10 p1325 N90-17657
Comparison of two- and three-dimensional Navier-Stokes solutions with NASA experimental data for CAST-10 airfoil 10 p1325 N90-17658
The MANTA: An RPV design to investigate forces and moments on a lifting surface
[NASA-CR-186227] 14 p1915 N90-20971
An experimental investigation of support strut interference on a three-percent fighter model at high angles of attack
[AD-A219793] 17 p2345 N90-23353
A contribution to the improvement of the accuracy in the parameter identification of nonlinear processes, by example of the aircraft motion
[ETN-90-96961] 20 p2808 N90-25974
Limits of adaptation, residual interferences 21 p2963 N90-26844
Adaptation for unsteady flow 21 p2963 N90-26845
Sting-support interference on afterbody drag at transonic speeds
[NAL-TM-EA-8902] 23 p3267 N90-28492
Unsteady aerodynamics of controls 23 p3273 N90-28525
Aerodynamic interferences of in-flight thrust reversers in ground effect 23 p3274 N90-28529
Three-dimensional model testing in the transonic self-streamlining wind tunnel 23 p3284 N90-28583
Microgravitation experiments in space: Compatibility with interfering dynamic influences 23 p3392 N90-29162

AERODYNAMIC LIFT
U LIFT

AERODYNAMIC LOADS
NT BLAST LOADS
NT GUST LOADS
Rotor blade structural design 04 p0451 N90-12584
Correlation of Puma airloads: Lifting-line and wake calculation
[NASA-TM-102212] 05 p0572 N90-13327
Description of atmospheric turbulence 07 p0869 N90-15043
The interference of flightmechanical control laws with those of load alleviation and its influence on structural design 07 p0871 N90-15054
An examination of helicopter rotor load calculations
[AD-A214295] 07 p0880 N90-15098
A survey of nonuniform inflow models for rotorcraft flight dynamics and control applications
[NASA-TM-102219] 08 p1028 N90-15938
Cryogenic balances for the US NTF 08 p1031 N90-15959
The response of helicopter rotors to vibratory airload
[AD-A215678] 09 p1167 N90-16756
Design guidance to minimize unsteady forces in turbomachines 11 p1460 N90-18411
Unsteady blade loads due to wake influence 11 p1460 N90-18413
Active stabilization of aeromechanical systems
[AD-A216629] 11 p1506 N90-18672
Calculation of flight vibration levels of the AH-1G helicopter and correlation with existing flight vibration measurements
[NASA-CR-181923] 11 p1518 N90-18743
X-29A aircraft structural loads flight testing
[NASA-TM-101715] 12 p1603 N90-19225

Aeroelastic characteristics of aircraft with circulation control wings 13 p1754 N90-20070
Parametric resonance in horizontal axis wind turbines 14 p1912 N90-20962
The MANTA: An RPV design to investigate forces and moments on a lifting surface
[NASA-CR-186227] 14 p1915 N90-20971
A computational design method for shock free transonic cascades and airfoils 14 p1918 N90-20986
The radiation of sound from a propeller at angle of attack
[NASA-CR-4264] 14 p2023 N90-21602
Airloads, wakes, and aeroelasticity
[NASA-CR-177551] 15 p2048 N90-21738
Aeroelastic simulation of higher harmonic control 15 p2054 N90-21768
Nonaxisymmetric body, supersonic, inviscid dynamic derivative prediction
[AD-A220839] 17 p2346 N90-23358
Aerodynamic pressure and heating-rate distributions in tile gaps around chine regions with pressure gradients at a Mach number of 6.6
[NASA-TP 2988] 17 p2400 N90-23670
Aerodynamic pressure measurements on a rotating wind turbine blade
[DE90-000327] 18 p2494 N90-24256
Aerodynamic loads and blade vortex interaction noise prediction
[ISL-PU-310/89] 20 p2802 N90-25942
Identification of aerodynamic models for maneuvering aircraft
[NASA-CR-186630] 20 p2802 N90-25943
Formation of design envelope criterion in terms of deterministic spectral procedure
[RAE-TM-SS-9] 20 p2804 N90-25953
An in-flight interaction of the X-29A canard and flight control system
[NASA-TM-101718] 20 p2807 N90-25973
New inflight experiments to measure aerodynamics loads
[ETN-90-97276] 21 p2961 N90-26834
NASA/GE Energy Efficient Engine low pressure turbine scaled test vehicle performance report
[NASA-CR-168290] 23 p3280 N90-28563
The Second ARO Workshop on Rotorcraft Interactional Aerodynamics
[AD-A223310] 24 p3418 N90-29304
Analysis of dynamic transient response and postflutter behavior of super-maneuvering airplane
[AD-A224126] 24 p3432 N90-29386

AERODYNAMIC MOMENTS
U STABILITY DERIVATIVES

AERODYNAMIC NOISE
NT BLADE SLAP NOISE
NT PROPELLER NOISE
Acoustic design considerations: Review of rotor acoustic sources 04 p0451 N90-12585
An experimental and theoretical study of the aeroacoustics of external-Coanda gas flares 06 p0773 N90-14495
Estimation of subsonic far-field jet-mixing noise from single-stream circular nozzles
[ESDU-89041] 09 p1161 N90-16721
Direct numerical simulation of aerodynamic noise
[AD-A214122] 10 p1426 N90-18225
Air Force Boom Event Analyzer Recorder (BEAR): Sysstem description
[AD-A218048] 13 p1882 N90-20800
Relating flow between counter-rotating propellers to aerodynamic interaction noise 14 p1909 N90-20944
An investigation of the generation and radiation of aerodynamic noise in real piping systems 15 p2164 N90-22368
Summary of sonic boom rise times observed during FAA community response studies over a 6-month period in the Oklahoma City area
[NASA-CR-4277] 18 p2608 N90-24852
A preliminary study of the masking of wind turbine noise by ambient sound
[FFA-TN-1990-01] 20 p2923 N90-26636

AERODYNAMIC STABILITY
Airworthiness and flight characteristics test of the UH-60A Black Hawk helicopter equipped with the XM-139 multiple mine dispensing system (VOLCANO)
[AD-A210271] 01 p0006 N90-10025
Prediction of the aerodynamic stability of missiles 01 p0012 N90-10052
Analysis of flight data from a High-Incidence Research Model by system identification methods
[NASA-TP-2940] 01 p0015 N90-10074
Unsteady aerodynamics with applications to flight mechanics
[AD-A211944] 03 p0301 N90-11706
Active control of unsteady and separated flow structures
[AD-A212109] 03 p0301 N90-11707
Stability and control derivatives of the De Havilland DHC-2 BEAVER aircraft
[PB89-217525] 03 p0309 N90-11754
Effect of control surface mass unbalance on the stability of a closed-loop active control system
[NASA-TP-2952] 03 p0357 N90-12042
Rotor blade dynamic design 04 p0451 N90-12583
Airframe design considerations: Overview — rotor design optimization 04 p0451 N90-12586
Stability of a supersonic boundary layer on a sharp cone at a small angle of attack 06 p0775 N90-14510
Applications of modern control theory synthesis to a super-augmented aircraft
[AD-A215431] 09 p1167 N90-16753
Stability characteristics of a combat aircraft with control surface failure
[AD-A216196] 10 p1323 N90-17646
The application of active controls technology to a generic hypersonic aircraft configuration
[NASA-TM-101689] 13 p1754 N90-20071
Prediction of forces and moments for flight vehicle control effectors. Part 2: An analysis of delta wing aerodynamic control effectiveness in ground effect
[NASA-CR-186572] 15 p2047 N90-21735
Actuated forebody strakes
[NASA-CASE-LAR-13983-1] 17 p2352 N90-23390
Prediction methods of launcher aeroelastic stability. Application to the Ariane 5/Hermes vehicle. Comparison with test results
[REPT-892-422-107] 17 p2362 N90-23451
Rotorcraft aeromechanical stability-methodology assessment. Phase 2: Workshop
[NASA-TM-102272] 21 p2955 N90-26800
The SKY SHARK: An RPV designed to investigate the pressure distribution on a lifting surface
[NASA-CR-186222] 21 p2959 N90-26824
The role of C(sub n beta,dyn) in the aircraft stability at high angles of attack
[AD-A221586] 21 p2961 N90-26833
Inflight thrust vectoring: A further degree of freedom in the aerodynamic/flight mechanical design of modern fighter aircraft 23 p3274 N90-28528

AERODYNAMIC STALLING
Stall/spin/flight simulation
[DOT/FAA/CT-88/28] 03 p0310 N90-11765
Some observations on transitory stall in conical diffusers
[NASA-TM-102387] 04 p0447 N90-12561
Stall/spin aerodynamic data project
[DOT/FAA/CT-88/29] 06 p0723 N90-14222
Schleicher ASK-21 glider (TG-9) stall and spin
[AD-A213513] 07 p0879 N90-15096
Aircraft performance enhancement with active compressor stabilization
[AD-A213652] 07 p0879 N90-15097
Dynamic derivatives of missiles and fighter-type configurations at high angles of attack 10 p1306 N90-17554
Measurement of velocity profiles and Reynolds stresses on an oscillating airfoil 11 p1463 N90-18427
Stall and recovery in multistage axial flow compressors 11 p1464 N90-18429
Active stabilization of aeromechanical systems
[AD-A216629] 11 p1506 N90-18672
Application of a dynamic stall model to rotor trim and aeroelastic response 16 p2200 N90-22556
Flow visualization of dynamic stall on an oscillating airfoil
[AD-A222202] 21 p2954 N90-26797
Control research in the NASA high-alpha technology program 23 p3272 N90-28516
Dynamic separation: Search for the cause of dynamic stall and search for its control
[AD-A223412] 24 p3418 N90-29305

AERODYNAMICS
NT AEROTHERMODYNAMICS
NT HYPERSONICS
NT ROTOR AERODYNAMICS
NT SUPERSONICS
NT UNSTEADY AERODYNAMICS
The application of TSIM software to act design and analysis on flexible aircraft 01 p0018 N90-10086
The spinning of aircraft: A discussion of spin prediction techniques including a chronological bibliography
[ARL-AERO-R-177] 02 p0155 N90-10888
Analytical study of mistuning/friction/aerodynamics interaction in a bladed disk assembly
[AD-A211139] 02 p0156 N90-10893
Aeronautical engineering: A continuing bibliography with indexes (supplement 243)
[NASA-SP-7037(243)] 03 p0299 N90-11693
Aeronautical engineering: A continuing bibliography with indexes (supplement 244)
[NASA-SP-7037(244)] 03 p0299 N90-11694
Computer simulation of aircraft aerodynamics
[NASA-TM-102221] 03 p0300 N90-11699
Effect of control surface mass unbalance on the stability of a closed-loop active control system
[NASA-TP-2952] 03 p0357 N90-12042
Aeronautical engineering: A continuing bibliography with indexes (supplement 245)
[NASA-SP-7037(245)] 04 p0437 N90-12497
Development of a VSAERO (Vortex Separation Aerodynamics) model of the F/A-18
[AD-A212442] 04 p0448 N90-12566
Chordwise loading and camber for two-dimensional thin sections
[AD-A213318] 04 p0448 N90-12568
Vortex dynamics
[AD-A212119] 04 p0499 N90-12877
Research and Technology annual report, 1988
[NASA-TM-101070] 04 p0569 N90-13319
Block-structured solution of three-dimensional transonic flows using parallel processing
[AD-A212851] 05 p0572 N90-13330
An Introduction to Hypersonic Aerodynamics
[VKI-LS-1989-01] 05 p0573 N90-13334
Hypersonic aerodynamics 05 p0573 N90-13335
Measurement Techniques in Aerodynamics
[VKI-LS-1989-05] 05 p0575 N90-13339
A technique for the prediction of aerodynamics and aeroelasticity of rotor blades 05 p0579 N90-13377
Multigrid and defect correction for the steady Navier-Stokes equations: Applications to aerodynamics
[ETN-90-96011] 05 p0639 N90-13727
Control of the variable speed generator on the Sandia 34-metre vertical axis wind turbine
[DE90-000803] 06 p0803 N90-14674
Aeronautical engineering: A continuing bibliography with indexes (supplement 246)
[NASA-SP-7037(246)] 07 p0874 N90-15068
An alternative derivation for an integral equation for linearized subsonic flow over a wing
[AD-A214140] 07 p0876 N90-15079
Aerodynamic design and initial performance measurements for the SANDIA 34-metre diameter vertical-axis wind turbine
[DE90-002574] 07 p0955 N90-15523
Weapon aerodynamics overview
[RAE-TM-AERO-2150] 08 p1018 N90-15888
Aerodynamic and heat transfer measurements on blading for a high rim-speed transonic turbine
[RAE-TM-P-1151] 08 p1024 N90-15920
High frequency pulsed diode lasers and phase-coupled diode arrays for aerodynamics 08 p1078 N90-16238
Research and technology, 1989: Langley Research Center
[NASA-TM-4150] 08 p1157 N90-16703
Aerodynamic and structural design challenges of a reusable single stage to orbit air-breathing launch vehicle 09 p1177 N90-16814
Aeronautical engineering: A continuing bibliography with indexes (supplement 247)
[NASA-SP-7037(247)] 10 p1303 N90-17537
Missile Aerodynamics: NEAR Conference on Missile Aerodynamics
[ISBN-0-9620629-1-X] 10 p1303 N90-17540
A survey of missile aerodynamics 10 p1303 N90-17541
Missile dynamics: A critical assessment of prediction capabilities 10 p1304 N90-17543
Use of semiempirical aerodynamic methods for preliminary design 10 p1304 N90-17546
The use of lateral jet control at Aerospatiale 10 p1305 N90-17551
VLA missile development and high angle of attack behavior 10 p1305 N90-17553
A wind tunnel study of a sting-mounted circulation control wing
[AD-A216248] 10 p1310 N90-17577
Experimental investigation to suppress flow-induced pressure oscillations in open cavities
[AD-A216285] 10 p1310 N90-17578
Stability characteristics of a combat aircraft with control surface failure
[AD-A216196] 10 p1323 N90-17646
Preliminary collection 891 of lectures/papers in Symposium by Society of Automotive Engineers of Japan
[DE90-710449] 10 p1391 N90-18045
Static and rotational aerodynamic data from 0 deg to 90 deg angle of attack for a series of basic and altered forebody shapes
[AD-A216582] 11 p1451 N90-18361
Aerodynamic testing of a rotating wind turbine blade
[DE90-000312] 11 p1451 N90-18362
Vertical axis wind turbine turbulent response model. Part 2: Response of Sandia National laboratories' 34-meter VAWT with aeroelastic effects
[DE90-005721] 11 p1529 N90-18804

Measurements of surface pressures on an operating vertical-axis wind turbine
[DE90-005722] 11 p1529 N90-18805
Aeronautical engineering: A continuing bibliography with indexes (supplement 249)
[NASA-SP-7037(249)] 12 p1597 N90-19190
Three-dimensional structural analyses of reentry vehicles
[DE90-006278] 12 p1615 N90-19291
Nonlinear mechanics of unstable plasmas as related to high altitude aerodynamics
[AD-A215126] 12 p1716 N90-19852
Unsteady free-wake viscous aerodynamic analysis of helicopter rotors
[AD-A217166] 13 p1750 N90-20048
Aerodynamic analysis of a US Navy and Marine Corps unmanned air vehicle
[AD-A218282] 13 p1755 N90-20077
ETO (Earth-To-Orbit): A trajectory program for aerospace vehicles
[AD-A218157] 13 p1760 N90-20103
Aerodynamic and kinetic processes in flames
[AD-A217796] 13 p1773 N90-20176
Analysis of small-scale rotor hover performance data
[NASA-TM-102271] 13 p1799 N90-20325
A comparison of two-and three-dimensional S809 airfoil properties for rough and smooth HAWT (Horizontal-Axis Wind Tunnel) rotor operation
[DE89-009512] 13 p1827 N90-20492
Operational computer graphics in the flight dynamics environment 13 p1859 N90-20668
Progress in inverse design and optimization in aerodynamics 14 p1916 N90-20977
LACE flight dynamics experiment 14 p1937 N90-21086
Small business innovation research. Abstracts of 1988 phase 1 awards
[NASA-TM-102991] 14 p2036 N90-21680
Small business innovation research. Abstracts of completed 1987 phase 1 projects
[NASA-TM-101797] 14 p2036 N90-21681
Aeronautical engineering: A continuing bibliography with indexes (supplement 250)
[NASA-SP-7037(250)] 15 p2045 N90-21722
Prediction of forces and moments for flight vehicle control effectors. Part 2: An analysis of delta wing aerodynamic control effectiveness in ground effect
[NASA-CR-186572] 15 p2047 N90-21735
Modeling of vortex-induced oscillations based on indicial response approach
[NASA-CR-186560] 15 p2047 N90-21736
Aerodynamics of a full-scale, non rotating wind turbine blade under natural wind conditions
[RISOE-M-2768] 15 p2123 N90-22144
Water-tunnel study results of a TF/A-18 and F/A-18 canopy flow visualization
[NASA-TM-101705] 16 p2195 N90-22532
Methods of jet calculation
[REPT-892-422-102] 16 p2209 N90-22603
Side moment exerted by a spinning, coning, highly viscous liquid payload
[AD-A218746] 16 p2237 N90-22763
Aeronautical engineering: A continuing bibliography with indexes (supplement 251)
[NASA-SP-7037(251)] 17 p2343 N90-23344
Aeronautical engineering: A continuing bibliography with indexes (supplement 252)
[NASA-SP-7037(252)] 17 p2343 N90-23345
A study of supermanuever aerodynamics
[AD-A218378] 17 p2344 N90-23349
Flowfield measurements in the wake of a missile at high angle of attack
[AD-A219645] 17 p2345 N90-23351
Hypersonic aerodynamics of spacecraft
[DLC-EST-TD-032] 17 p2346 N90-23361
Aerodynamic development perspective for traffic aeroplanes
[DGLR-89-141] 18 p2495 N90-24260
Aerodynamics and flight mechanics of formation flight
[ETN-90-96497] 18 p2497 N90-24269
Aeronautical engineering: A cumulative index to a continuing bibliography (supplement 248)
[NASA-SP-7037(248)] 19 p2649 N90-25072
Convex models of malfunction diagnosis in high performance aircraft
[AD-A218514] 19 p2649 N90-25073
Aeronautical engineering: A continuing bibliography with indexes (supplement 253)
[NASA-SP-7037(253)] 19 p2654 N90-25105
On the receptivity problem for Goertler vortices: Vortex motions induced by wall roughness
[NASA-CR-182036] 19 p2654 N90-25109
The Penguin: A low Reynolds number powered glider for station keeping missions
[NASA-CR-186667] 19 p2658 N90-25129
Wind energy program summary. Volume 2: Research summaries
[DE89-009480] 19 p2710 N90-25423
An unsteady lifting surface method for single rotation propellers
[NASA-CR-4302] 20 p2802 N90-25940
Identification of aerodynamic models for maneuvering aircraft
[NASA-CR-186630] 20 p2802 N90-25943
Computational fluid dynamics for missiles
[RAE-TM-AERO-2171] 20 p2863 N90-26288
Computational methods for problems in aerodynamics using parallel and vector architecture
[AD-A221979] 21 p2954 N90-26795
Special essays for the 40th anniversary of the revolution: The chief designer discusses the F-8 2 and future fighter planes
[AD-A221587] 21 p2960 N90-26829
Parallel numerical simulations of axisymmetric projectile flows using zonal-overlapped grids
[AD-A221711] 21 p3005 N90-27082
Aeronautical engineering: A continuing bibliography with indexes (supplement 254)
[NASA-SP-7037(254)] 22 p3107 N90-27647
Aeronautical engineering: A continuing bibliography with indexes (supplement 255)
[NASA-SP-7037(255)] 22 p3107 N90-27648
Advanced recovery systems wind tunnel test report
[NASA-CR-177563] 22 p3108 N90-27653
Aerodynamics of a linear oscillating cascade
[NASA-TM-103250] 22 p3108 N90-27657
Hypersonic Arbitrary-Body Aerodynamics (HABA) for conceptual design
[DE90-014750] 23 p3268 N90-28495
Aerodynamics of bodies in shear flow 23 p3268 N90-28496
Aerodynamic and propulsive control development of the STOL and maneuver technology demonstrator 23 p3271 N90-28514
Aerodynamic control design: Experience and results at Vermacchi 23 p3272 N90-28518
Control of vortex aerodynamics at high angles of attack 23 p3273 N90-28523
Study of the ground effects in the CEAT aerohydrodynamic tunnel: Using the results 23 p3274 N90-28530
Parallelization of a software relating to aerodynamics on MIMD type computers
[ONERA-RT-31/3479-CY] 23 p3384 N90-29114
Scientific Colloquium in Honor of Prof. Dr. Rer. Nat. Hermann L. Jordan
[ESA-TT-1101] 23 p3391 N90-29159
Numeric fluid mechanics 23 p3392 N90-29161
Comparison of wind tunnel airfoil performance data with wind turbine blade data
[DE90-000343] 24 p3418 N90-29308
Investigation of ATP blades, part 2. Validation of two-dimensional viscous flow simulation codes around thin airfoils
[NAL-TR-1046] 24 p3421 N90-29326
Some topics in computational transonic aerodynamics: Revision
[NAL-TR-1018T] 24 p3422 N90-29332
The DELTA MONSTER: An RPV designed to investigate the aerodynamics of a delta wing platform
[NASA-CR-186226] 24 p3431 N90-29381
Real-time concentration monitoring of large aerodynamic diameter fiber aerosols using the geometric optic inversion technique
[AD-A224167] 24 p3545 N90-30048

AEROELASTICITY
NT AEROTHERMOELASTICITY
Static aeroelastic analysis for generic configuration aircraft
[NASA-TM-89423] 01 p0009 N90-10042
Large-scale Advanced Prop-fan (LAP) technology assessment report
[NASA-CR-182142] 01 p0010 N90-10046
Aeroelastic tailoring procedure for controlling fin hinge moments 01 p0013 N90-10058
Aeroelastic analysis of missile control surfaces with structural non-linearity 01 p0015 N90-10071
The application of TSIM software to act design and analysis on flexible aircraft 01 p0018 N90-10086
Modifying high-order aeroelastic math model of a jet transport using maximum likelihood estimation 01 p0021 N90-10106
Control law synthesis and optimization software for large order aeroservoelastic systems 01 p0022 N90-10111
Flexible aircraft dynamic modeling for dynamic analysis and control synthesis 01 p0022 N90-10112
The active flexible wing aeroservoelastic wind-tunnel test program 01 p0024 N90-10119
Numerical simulation of unsteady rotational flow over propfan configurations
[NASA-CR-186037] 04 p0438 N90-12500
Application of an efficient hybrid scheme for aeroelastic analysis of advanced propellers
[NASA-TM-102428] 05 p0576 N90-13355
A technique for the prediction of aerodynamics and aeroelasticity of rotor blades 05 p0579 N90-13377
Aeroelastic control of composite lifting surfaces: Integrated aeroelastic control optimization 05 p0583 N90-13396
Dynamic testing techniques and applications for an aeroelastic rotor test facility 05 p0584 N90-13406
Concurrent processing adaptation of aeroplastic analysis of propfans
[NASA-TM-102455] 06 p0799 N90-14656
Nonlinear phenomena in computational transonic aeroelasticity 07 p0874 N90-15070
Current status of the application of conventional aluminium-lithium alloys and the potential for future developments 07 p0900 N90-15203
Solution of potential flow past an elastic body using the boundary element technique
[AD-A213843] 07 p0931 N90-15390
Structural dynamics division research and technology accomplishments for FY 1989 and plans for FY 1990
[NASA-TM-101683] 08 p1019 N90-15894
Wind-excited behavior of structures, 5 09 p1235 N90-17189
An iterative solution to aeroelastic effects in potential flow
[AD-A216291] 10 p1310 N90-17580
A fractional calculus model of aeroelasticity
[AD-A216244] 10 p1423 N90-18212
Aeroservoelasticity
[NASA-TM-102620] 12 p1603 N90-19227
An experimental study of the aeroelastic behaviour of two parallel interfering circular cylinders 12 p1673 N90-19609
Using transonic small disturbance theory for predicting the aeroelastic stability of a flexible wind-tunnel model
[NASA-TM-102617] 13 p1749 N90-20047
Aeroelastic characteristics of aircraft with circulation control wings 13 p1754 N90-20070
Static aeroelastic analysis of a three-dimensional generic wing
[NASA-TM-102231] 13 p1757 N90-20087
Performance data from a wind-tunnel test of two main-rotor blade designs for a utility-class helicopter
[NASA-TM-4183] 14 p1916 N90-20974
Experimental aeroelasticity history, status and future in brief
[NASA-TM-102651] 14 p1930 N90-21047
Airloads, wakes, and aeroelasticity
[NASA-CR-177551] 15 p2048 N90-21738
Identification of XV-15 aeroelastic modes using frequency-domain methods
[NASA-TM-101021] 15 p2051 N90-21756
Aeroelastic simulation of higher harmonic control 15 p2054 N90-21768
Application of a dynamic stall model to rotor trim and aeroelastic response 16 p2200 N90-22558
Flutter investigations on a Transavia PL12/T-400 aircraft
[AD-A219108] 16 p2203 N90-22570
Prediction methods of launcher aeroelastic stability. Application to the Ariane 5/Hermes vehicle. Comparison with test results
[REPT-892-422-107] 17 p2362 N90-23451
STARS: An integrated general-purpose finite element structural, aeroelastic, and aeroservoelastic analysis computer program
[NASA-TM-101709] 17 p2416 N90-23768
Aeroelastic and stability behaviour of the WTS 3 Maglarp wind turbine. Calculations and comparisons with tests
[FFA-TN-1989-23] 17 p2420 N90-23792
Calculation of the aeroelastic blade stabilization with linearized process
[MITT-87-01] 18 p2497 N90-24272
Integral-equation methods in steady and unsteady subsonic, transonic and supersonic aerodynamics for interdisciplinary design
[NASA-TM-102677] 19 p2655 N90-25110
Modeling flexible aircraft for flight control design
[AD-A219123] 19 p2660 N90-25140
Structural dynamics branch research and accomplishments
[NASA-TM-102488] 20 p2878 N90-26373
Adaptation for unsteady flow 21 p2963 N90-26845
Development and testing of methodology for evaluating the performance of multi-input/multi-output digital control systems
[NASA-TM-102704] 22 p3115 N90-27699

Effects of spoiler surfaces on the aeroelastic behavior of a low-aspect-ratio rectangular wing
[NASA-TM-102622] 22 p3115 N90-27700

Active control of aerothermoelastic effects for a conceptual hypersonic aircraft
[NASA-TM-102713] 22 p3122 N90-27725

Multi-disciplinary optimization of aeroservoelastic systems
[NASA-CR-185931] 24 p3432 N90-29385

A digital controller for active aeroelastic controls
[NAL-TR-1014] 24 p3435 N90-29402

AEROLOGY

Meeting Review: Workshop on Airborne Instrumentation
[PB89-174775] 01 p0007 N90-10032

AEROMAGNETO FLUTTER

U FLUTTER

AEROMANEUVERING

Optimal trajectories for the aeroassisted flight experiment, 1988-89
[NASA-CR-186132] 05 p0592 N90-13443

Optimal trajectories for the aeroassisted flight experiment. Part 3: Formulation, results, and analysis
[NASA-CR-186165] 14 p1930 N90-21051

AERONAUTICAL ENGINEERING

A review of Australian and New Zealand investigations on aeronautical fatigue during the period April 1987 to March 1989
[AD-A210373] 01 p0006 N90-10026

Technical communications in aeronautics: Results of an exploratory study. An analysis of managers' and nonmanagers' responses
[NASA-TM-101625] 02 p0288 N90-11647

Aeronautical engineering: A continuing bibliography with indexes (supplement 243)
[NASA-SP-7037(243)] 03 p0299 N90-11693

Aeronautical engineering: A continuing bibliography with indexes (supplement 244)
[NASA-SP-7037(244)] 03 p0299 N90-11694

AFRAPT (Air Force Research in Aero Propulsion Technology) Trainee Program
[AD-A211540] 03 p0307 N90-11744

Aeronautical engineering: A continuing bibliography with indexes (supplement 245)
[NASA-SP-7037(245)] 04 p0437 N90-12497

California air transportation study: A transportation system for the California Corridor of the year 2010
[NASA-CR-186219] 06 p0722 N90-14212

Aeronautical engineering: A continuing bibliography with indexes (supplement 246)
[NASA-SP-7037(246)] 07 p0874 N90-15068

Bibliography of Lewis Research Center technical publications announced in 1988
[NASA-TM-102034] 07 p1009 N90-15846

Research and technology, 1989: Langley Research Center
[NASA-TM-4150] 08 p1157 N90-16703

Profiles-aeronautical/astronautical engineering: Human resources and funding
[PB90-103888] 09 p1203 N90-16969

Aeronautical engineering: A continuing bibliography with indexes (supplement 247)
[NASA-SP-7037(247)] 10 p1303 N90-17537

Aeronautical engineering: A continuing bibliography with indexes (supplement 249)
[NASA-SP-7037(249)] 12 p1597 N90-19190

In-house experiments in large space structures at the Air Force Wright Aeronautical Laboratories Flight Dynamics Laboratory 14 p1938 N90-21092

Small business innovation research. Abstracts of 1988 phase 1 awards
[NASA-TM-102991] 14 p2036 N90-21680

Research programs in aeronautical engineering, solid state physics, and materials science at Technion-Israel Institute of Technology, Haifa, Israel
[EOARD-LR-89-068] 14 p2044 N90-21720

Aeronautical engineering: A continuing bibliography with indexes (supplement 250)
[NASA-SP-7037(250)] 15 p2045 N90-21722

Aeronautics and space report of the President: 1987 activities 15 p2181 N90-22462

Supercomputer and Technology
[NLR-PUB-8801] 16 p2277 N90-22974

Aeronautical engineering: A continuing bibliography with indexes (supplement 251)
[NASA-SP-7037(251)] 17 p2343 N90-23344

Aeronautical engineering: A continuing bibliography with indexes (supplement 252)
[NASA-SP-7037(252)] 17 p2343 N90-23345

Evaluating Statistical Process Control (SPC) techniques and computing the uncertainty of force calibrations 18 p2631 N90-24992

NASA/American Society for Engineering Education (ASEE) Summer Faculty Fellowship Program 1989
[NASA-CR-181894] 18 p2639 N90-25034

Aeronautical engineering: A cumulative index to a continuing bibliography (supplement 248)
[NASA-SP-7037(248)] 19 p2649 N90-25072

Aeronautical engineering: A continuing bibliography with indexes (supplement 253)
[NASA-SP-7037(253)] 19 p2654 N90-25105

The environmental control and life support system advanced automation project. Phase 1: Application evaluation 19 p2730 N90-25523

Astronautics and Aeronautics, 1979-1984: A chronology
[NASA-SP-4024] 19 p2800 N90-25928

Combustion in the gas turbine. Part 1: Combustor types and design
[CIT/SME/VKI/RS/1] 20 p2810 N90-25986

The integration of complex information from auditory and visual channels under stress
[AD-A222686] 21 p3033 N90-27245

The role of the US government technical report in aeronautics: An exploratory study
[NASA-TM-893470] 21 p3087 N90-27553

Aeronautical engineering: A continuing bibliography with indexes (supplement 254)
[NASA-SP-7037(254)] 22 p3107 N90-27647

Aeronautical engineering: A continuing bibliography with indexes (supplement 255)
[NASA-SP-7037(255)] 22 p3107 N90-27648

Calculation of the combustion distribution in a liquid-fuel ramjet 22 p3162 N90-27931

AERONAUTICAL SATELLITES

An aeronautical mobile satellite experiment
[NASA-CR-186971] 23 p3287 N90-28593

AERONAUTICS

Technical communications in aeronautics: Results of an exploratory study. An analysis of profit managers' and nonprofit managers' responses
[NASA-TM-101626] 07 p1009 N90-15848

AGARD index of publications, 1986-1988
[AGARD-INDEX-86-88] 08 p1136 N90-16585

FY 1989 scientific and technical reports, articles, papers, and presentations
[NASA-TM-100384] 12 p1725 N90-19916

Research and Technology Objectives and Plans Summary (RTOPS)
[NASA-TM-89662] 15 p2194 N90-22528

Research and development: Technical and scientific publications 1989
[ISSN-0931-9751] 19 p2649 N90-25075

AERONOMY

Studies of cubic ice crystals
[AD-A216574] 11 p1534 N90-18832

Research and technology 1989
[NASA-TM-100369] 17 p2486 N90-24219

A model of the perturbed spinning motion of the San Marco 5th spacecraft 22 p3129 N90-27755

AEROPHYSICS

U ATMOSPHERIC PHYSICS

AEROSOLS

NT FOG

Real-time observations of aerosol composition changes
[DE89-012382] 01 p0073 N90-10422

Paper 1. Impact of volcanic aerosols on stratospheric chemistry. Paper 2. O2 (1 sigma g +) and O2 (1 delta g) in the H + O2 reaction system. Paper 3. Barotropic instability of zonal jets on Mars, Earth and Venus 01 p0084 N90-10477

International Conference on Aerosols and Background Pollution Abstracts
[AD-A210970] 01 p0085 N90-10483

Geophysical monitoring for climatic change number 16
[PB89-159628] 01 p0087 N90-10494

Analysis of forest fire smoke using satellite imagery
[AD-A210657] 02 p0236 N90-11339

Lidar observations of the stratospheric aerosol: Boulder, Colorado, 1985 to 1987
[PB89-203871] 02 p0251 N90-11425

Atmospheric aerosol size distributions and optical properties found in the marine boundary layer over the Atlantic Ocean
[AD-A210800] 02 p0252 N90-11431

Aerosol in the Pacific troposphere 03 p0363 N90-12078

Aerosol backscatter studies supporting LAWS 03 p0363 N90-12079

Global backscatter assessment 03 p0364 N90-12080

Measurements of aerosol properties needed to infer backscatter characteristics in support of the NASA Doppler Lidar program 03 p0364 N90-12082

Airborne profiles taken near San Nicolas Island, California, during Operation FIRE (First ISCCP (International Satellite Cloud Climatology Project) regional experiment) (1987): Aerosol size distributions, air and surface temperatures, cloud top temperatures, and relative humidities
[AD-A211664] 03 p0374 N90-12136

Small particle scattering and absorption
[AD-A213168] 04 p0473 N90-12711

Infrared spectrometry of aerosols
[AD-A213303] 04 p0473 N90-12713

Comments on the use of LOWTRAN in transmission calculations for sites with the ground elevated relative to sea level
[AD-A212724] 04 p0519 N90-12995

Transport phenomena and interfacial kinetics in multiphase combustion systems
[AD-A212932] 05 p0621 N90-13620

Recovery of particle size distribution of ultrafine aerosols from diffusional decay measurements
[AD-A213006] 05 p0621 N90-13621

Pilot investigation of indoor-outdoor and personal PM10 (thoracic) and associated ionic compounds and mutagenic activity
[PB89-222723] 05 p0673 N90-13920

Remote sensing of the aerosol scattering coefficient with a multi-field-of view lidar 06 p0763 N90-14437

Physical models for aerosol in the marine mixed-layer 06 p0763 N90-14438

Aerosol heating and vaporization of high-flux laser beams
[DE90-003471] 07 p0937 N90-15428

Evaluate and characterize mechanisms controlling transport, fate, and effects of army smokes in the aerosol wind tunnel: Transport, transformations, fate, and terrestrial ecological effects of hexachloroethane obscurant smokes
[DE90-002923] 07 p0957 N90-15536

HCl monitor, phase 2
[AD-A213572] 07 p0958 N90-15542

Vertical distribution of pollutants in the presence of convective storms
[DE90-002590] 07 p0960 N90-15549

The middle Martian atmosphere 07 p1014 N90-15874

Lidar technique for adjusting aerosol model number densities to existing conditions
[AD-A213846] 08 p1101 N90-16374

Short-term bioassays may be useful in evaluating fiber/whisker hazards
[DE90-003707] 08 p1104 N90-16393

Laser velocimeter seed particle sizing by the whisker particle collector and laser aerosol spectrometer methods
[PB90-111287] 09 p1224 N90-17103

Chamber investigations of the fate of diesel emissions in the atmosphere, volume 1, task 3
[PB90-114422] 10 p1405 N90-18103

Chamber investigations of the fate of diesel emissions in the atmosphere. Volume 2: AMES assay and GCMS final data reports and gas phase projections
[PB90-114430] 10 p1405 N90-18104

Effect of marine atmosphere on performance of electrooptical systems
[AD-A215947] 10 p1430 N90-18252

Perspectives on aerosol deposition to natural surfaces
[DE90-003398] 11 p1532 N90-18819

Transport of atmospheric aerosols above the Sierra Nevada slopes
[PB90-120288] 12 p1685 N90-19675

Atmospheric thermal blooming and beam clearing by aerosol vaporization
[DE90-006271] 12 p1690 N90-19711

Numerical modeling of atmospheric growth processes
[REPT-70] 12 p1693 N90-19726

Multiple versus single scattering of terrestrial infrared longwave radiation in an aerosol-laden planetary boundary layer
[AD-A217709] 13 p1790 N90-20272

The receiving system of a dual dye lidar to study molecular and aerosol densities at the base of the stratosphere
[AD-A218286] 13 p1843 N90-20581

A survey of the maritime-aerosol data collected at South Uist and the implications for the LOWTRAN maritime aerosol model 15 p2079 N90-21908

The Mediterranean marine environment and its effects on aerosols and infrared transmission 15 p2079 N90-21909

Models of aerosols, clouds, and precipitation for atmospheric propagation studies 15 p2081 N90-21919

Interpreting meteorological data reports for LOWTRAN Navy aerosol model extinction calculations 15 p2082 N90-21920

The naval oceanic vertical aerosol model
15 p2082 N90-21921
Inclusion of clouds and rain in atmospheric slant path calculations
15 p2083 N90-21925
Cirrus cloud optical properties measured with the University of Wisconsin high spectral resolution and volume imaging lidars
15 p2084 N90-21932
Technique for selecting an aerosol model useful for infrared atmospheric transmittance calculations
15 p2085 N90-21934
Aerosol separator for use in aircraft
[PB90-142217] 15 p2125 N90-22155
The sources and chemistry of late winter Arctic tropospheric aerosols
[PB90-131988] 15 p2126 N90-22158
Estimation of extra drag force on a circular cylinder due to the presence of solid particles in subsonic compressible flow
[AD-A218635] 16 p2197 N90-22542
HCl Vapor Characterization and Detection. JANNAF Safety and Environmental Protection Subcommittee Workshop
[AD-A216252] 16 p2208 N90-22596
The HCl/aerosol problem
16 p2208 N90-22597
Sticking coefficient of HCl on aerosols
16 p2208 N90-22598
HCl monitor
16 p2209 N90-22599
Nonlinear interaction between laser radiation and aerosols
[FOA-C-20768-2.3] 16 p2563 N90-24623
The effects of urban air pollution on solar radiation
[DE89-009455] 19 p2712 N90-25438
Atmospheric correction of thematic mapping measurements about seabeds of the German Bay
[GKSS-89/E/47] 20 p2816 N90-26029
Characterization of biogenic aerosol particles from the Amazon Basin during dry and wet season
20 p2886 N90-26418
Development of eye-safe lidar for aerosol measurements
[NASA-CR-186905] 20 p2901 N90-26503
Aureole lidar: Ground based measurement
[AD-A223207] 21 p3008 N90-27101
A LOWTRAN7 sensitivity study in the 8-12 and 3-5 micron bands: Includes comparison with LOWTRAN6 results
[AD-A222094] 21 p3031 N90-27231
Scattering of CO2-laser radiation by water droplets
[FOA-C-20776-2.3] 22 p3181 N90-28049
Aircraft measurements of pollution species near Bermuda and the east coast of the United States during CASE-WATOX
[PB90-159450] 22 p3197 N90-28141
Lidar observations of stratospheric aerosols in 1988
[PB90-180670] 22 p3198 N90-28145
Front range lidar, aircraft, and balloon experiment
[PB90-225301] 22 p3212 N90-28218
The influence of continental sources of aerosols on the marine stratocumulus during FIRE IFO-1
22 p3218 N90-28250
Optical properties of marine stratocumulus clouds modified by ship track effluents
22 p3218 N90-28253
Verification of the naval oceanic vertical aerosol model during FIRE
22 p3219 N90-28257
The affect of gravity on particle collection in inertial impactors
[DE90-013372] 23 p3393 N90-29173
Real-time concentration monitoring of large aerodynamic diameter fiber aerosols using the geometric optic inversion technique
[AD-A224167] 24 p3545 N90-30048
Submicron particle analyzer
[AD-A223558] 24 p3545 N90-30050

AEROSPACE ENGINEERING
NT AERONAUTICAL ENGINEERING
Technology for large space systems: A bibliography with indexes (supplement 21)
[NASA-SP-7046(21)] 01 p0026 N90-10130
The Environmental Test Centre at ESTEC (an overview)
02 p0187 N90-11064
Evolution of flight commands in Aeritalia design
[ETN-89-95211] 03 p0309 N90-11759
Choice and characterization of new materials for aerospace applications
[ETN-89-95219] 03 p0320 N90-11819
The evolution of light alloys in the aerospace industry
[ETN-89-95216] 03 p0329 N90-11872
Requirements for multidisciplinary design of aerospace vehicles on high performance computers
[NASA-CR-181915] 03 p0384 N90-12183
On the occasion of the 100th birthday of Ernst Heinkel
[MBB/LW/3015/S/PUB/321] 03 p0436 N90-12494
Project, implementation, and utilization of composite structures
[ETN-89-95209] 04 p0466 N90-12665
Research and Technology annual report, 1988
[NASA-TM-101070] 04 p0569 N90-13319
Space Station Engineering Design Issues
[NASA-CR-185978] 05 p0601 N90-13492
The evaluation of a metered mixer for RTV silicone for RSRM nozzle backfill operations
[NASA-CR-183831] 05 p0645 N90-13763
The space station tethered elevator system
[NASA-CR-186051] 06 p0732 N90-14265
CIS-lunar space infrastructure lunar technologies: Executive summary
[NASA-CR-186220] 06 p0865 N90-15029
Manned spacecraft
[AD-A214218] 07 p0887 N90-15129
Al-Li alloy developed by Pechiney
07 p0897 N90-15186
The microstructure and properties of aluminum-lithium alloys
07 p0897 N90-15187
Current status of the application of conventional aluminium-lithium alloys and the potential for future developments
07 p0900 N90-15203
Magnesium alloy technology for aerospace applications
07 p0901 N90-15209
Bibliography of Lewis Research Center technical publications announced in 1988
[NASA-TM-102034] 07 p1009 N90-15846
NASA Patent Abstracts Bibliography: A continuing bibliography. Section 1: Abstracts (supplement 36)
[NASA-SP-7039(36)-SECT-1] 07 p1010 N90-15851
A foundation for the design of an astronautics specification system based on dynamic motivation analysis
[ILR-MITT-220] 08 p1033 N90-15969
AGARD index of publications, 1986-1988
[AGARD-INDEX-86-88] 08 p1136 N90-16585
JSC document index
[NASA-TM-102923] 08 p1137 N90-16589
Catalogue of ESA publications in 1987
[ESA-SP-1067] 08 p1137 N90-16590
The international space transportation market: A European perspective
09 p1173 N90-16785
Compression testing of carbon fibers
[AD-A215296] 09 p1187 N90-16877
NASA Patent Abstracts Bibliography: A continuing bibliography. Section 2: Indexes (supplement 36)
[NASA-SP-7039(36)-SECT-2] 10 p1441 N90-18317
Impact of composites in the aerospace industry
[ETN-90-96231] 11 p1481 N90-18527
The manufacturing procedures for composite materials, automation, and robotization
[ETN-90-96232] 11 p1482 N90-18528
Comparison of circulation obtained through the trajectory of a drifting buoy tracked by satellite and hydrographic data in the Bransfield Strait
[INPE-4946-TDL/387] 11 p1537 N90-18850
Purchase of technology
11 p1576 N90-19072
Remote Attitude Measurement Sensor (RAMS)
12 p1611 N90-19271
Research Reports: 1989 NASA/ASEE Summer Faculty Fellowship Program
[NASA-CR-183837] 12 p1634 N90-19390
FY 1989 scientific and technical reports, articles, papers, and presentations
[NASA-TM-100384] 12 p1725 N90-19916
Power conditioning techniques
[NASA-TM-102577] 13 p1795 N90-20301
Numerical simulation methods of incompressible flows and an application to the space shuttle main engine
[NASA-TM-100038] 13 p1800 N90-20333
Bearing and gear steels for aerospace applications
[NASA-TM-102529] 13 p1809 N90-20391
Engineering visualization utilizing advanced animation
13 p1859 N90-20664
USSR Space Life Sciences Digest, Issue 26
[NASA-CR-3922(31)] 14 p2009 N90-21513
The 24th Aerospace Mechanisms Symposium
[NASA-CP-3062] 15 p2112 N90-22079
Aeronautics and space report of the President: 1987 activities
15 p2181 N90-22462
Research and Technology Objectives and Plans Summary (RTOPS)
[NASA-TM-89662] 15 p2194 N90-22528
An expert system for the study of high duty bonded joints in aerospace structures
[REPT-892-430-110] 17 p2414 N90-23753
Strategic implementation plan
[NASA-TM-102907] 17 p2433 N90-23861
Langley aerospace test highlights, 1989
[NASA-TM-102631] 17 p2487 N90-24221
Optical techniques for determination of normal shock position in supersonic flows for aerospace applications
[NASA-TM-103201] 19 p2693 N90-25323
Center for Space Microelectronics Technology 1988-1989 technical report
[NASA-CR-186849] 19 p2753 N90-25642
NASA Patent Abstracts Bibliography: A continuing bibliography. Section 1: Abstracts (supplement 37)
[NASA-SP-7039(37)-SECT-1] 19 p2763 N90-25698
NASA's experience in the international exchange of scientific and technical information in the aerospace field
[NASA-TM-103093] 19 p2764 N90-25704
Astronautics and Aeronautics, 1979-1984: A chronology
[NASA-SP-4024] 19 p2800 N90-25928
Materials and structures for 2000 and beyond: An attempted forecast by the DLR Materials and Structures Department
[ESA-TT-1154-REV] 20 p2843 N90-26173
NASA Patent Abstracts Bibliography: A continuing bibliography. Section 2: Indexes (supplement 37)
[NASA-SP-7039(37)-SECT-2] 20 p2935 N90-26700
Stochastic structural dynamics for aerospace applications
[AD-A221517] 21 p3013 N90-27133
Radars in space
21 p3015 N90-27144
Space Vehicle Flight Mechanics
[AGARD-CP-489] 22 p3126 N90-27741
Introduction to National Aeronautics and Space Administration's scientific and technical information programs
22 p3257 N90-28441
Technology utilization: Managing the transfer of NASA aerospace technology to other industries
22 p3257 N90-28446
NASA's educational programs
22 p3258 N90-28447
Fabrication of spherical pressure vessels from composite materials
[INPE-4598-RPE/570] 23 p3302 N90-28675
Proceedings of the NASA Conference on Space Telerobotics, volume 2
[NASA-CR-186857] 23 p3370 N90-29044
Control and estimation for aerospace applications with system time delays
24 p3428 N90-29367
Workshop on Low Level Flight Training
[AGARD-AR-288] 24 p3436 N90-29404
Development of dual fiber reinforced glass matrix composites for structural space based applications
[AD-A223801] 24 p3444 N90-29446
Lubrication characteristics of rolling bearings lubricated by self-lubricating composite retainers. Part 1: Selection of bearings for Earth sensors
[NAL-TR-1019] 24 p3477 N90-29651
Proceedings of damping '89. Volume 1: Pages AAB-1 through DCD-11
[AD-A223431] 24 p3479 N90-29664
Proceedings of Damping '89. Volume 3: Pages ICA-1 through KDC-15
[AD-A223433] 24 p3479 N90-29666
Proceedings of the 17th Annual Gravity Gradiometer Conference
[AD-A223568] 24 p3492 N90-29735
NASA authorization, 1991, volume 2
[GPO-32-196] 24 p3559 N90-30138

AEROSPACE ENVIRONMENTS
NT CISLUNAR SPACE
NT DEEP SPACE
NT EARTH ORBITAL ENVIRONMENTS
NT INTERPLANETARY SPACE
NT INTERSTELLAR SPACE
Biology in microgravity: A guide for experimenters
[ESA-TM-02] 04 p0482 N90-12769
Development of a shuttle plume radiation heating indicator
[NASA-CR-183679] 05 p0614 N90-13584
Optical properties monitor: Experiment definition phase
[NASA-CR-183836] 05 p0699 N90-14092
Particle simulations in magnetospheric plasmas
[NASA-CR-186238] 06 p0848 N90-14934
Intrinsic properties of high voltage wires that may cause sporadic discharges in space vacuum
10 p1338 N90-17743
Development and use of data analysis procedures for the CRRES (Combined Release and Radiation Effects Satellite) payloads AFGL-701-2/Dosimeter and AFGL-701-4/Fluxmeter and application of the data analysis results to improve the static and dynamic models of the Earth's radiation belts
[AD-A215953] 10 p1447 N90-18348
Radiation-hard high-efficiency InP space solar cell development
[AD-A216857] 11 p1528 N90-18800
Large antenna measurement and compensation techniques
12 p1610 N90-19263
Reflector surface distortion analysis techniques (thermal distortion analysis of antennas in space)
12 p1611 N90-19267

Efficient utilization of graphics technology for space animation 13 p1859 N90-20663
Proceedings of the 13th International Congress on Instrumentation in Aerospace Simulation Facilities [EOARD-LR-89-069] 14 p1929 N90-21048
United States Air Force Academy get-away-special flexible beam experiment 14 p1937 N90-21088
Experience with synthetic fluorinated fluid lubricants 15 p2114 N90-22095
Lunar rated fasteners [NASA-CR-182856] 17 p2411 N90-23737
Interdigitated back contact silicon solar cell analysis and design recommendations for space use [AD-A220414] 17 p2420 N90-23790
Radiation-hard-high-efficiency InP space solar cell development [AD-A220500] 17 p2420 N90-23791
Optical properties monitor: Experiment definition phase [NASA-CR-4293] 19 p2666 N90-25170
A noncontacting motion monitoring system for an astronaut translation aid [NASA-TM-102640] 19 p2693 N90-25325
Third Annual Workshop on Space Operations Automation and Robotics (SOAR 1989) [NASA-CP-3059] 19 p2727 N90-25503
Space environments and their effects on space automation and robotics 19 p2735 N90-25543
Photovoltaic array space power plus diagnostics experiment 19 p2737 N90-25559
Comparison of currents predicted by NASCAP/LEO model simulations with elementary Langmuir-type bare probe models for an insulated cable containing a single pinhole [NASA-TM-102486] 20 p2821 N90-26054
Experiment K-6-09. Morphological and biochemical investigation of microgravity-induced nerve and muscle breakdown. Part 1: Investigation of nerve and muscle breakdown during spaceflight; Part 2: Biochemical analysis of EDL and PLT muscles 20 p2893 N90-26463
Automation of closed environments in space for human comfort and safety [NASA-CR-186834] 20 p2901 N90-26500
Surface reactions in the space environment [AD-A221767] 21 p2979 N90-26932
The near-Earth orbital environment coupling to its energy sources [AD-A222435] 21 p3026 N90-27206
Final design for a comprehensive orbital debris management program [NASA-CR-186674] 22 p3126 N90-27739
Utilization of space station, part 3 [NAL-TM-597-PT-3] 24 p3439 N90-29422
Effects of energy, momentum and particle transport in the near-earth solar terrestrial system [AD-A224393] 24 p3490 N90-29726
Re-analysis of data on the space radiation environment above southeast Asia [AD-A224155] 24 p3564 N90-30162

AEROSPACE INDUSTRY
NT AIRCRAFT INDUSTRY
On the occasion of the 100th birthday of Ernst Heinkel [MBB/LW/3015/S/PUB/321] 03 p0436 N90-12494
Issues in NASA program and project management [NASA-SP-6101(02)] 04 p0562 N90-13277
Design and demonstration of heat pipe cooling for NASP and evaluation of heating methods at high heating rates [DE89-016995] 06 p0724 N90-14227
Reuse at the Software Productivity Consortium 06 p0825 N90-14798
Technical communications in aeronautics: Results of an exploratory study. An analysis of profit managers' and nonprofit managers' responses [NASA-TM-101626] 07 p1009 N90-15848
Structural characterization of Spacelab [ETN-90-95214] 08 p1087 N90-16289
An investigation into the effects which aerospace industry offset trade agreements have on United States Air Force mission performance [AD-A215093] 09 p1294 N90-17502
Impact of composites in the aerospace industry [ETN-90-96231] 11 p1481 N90-18527
The manufacturing procedures for composite materials, automation, and robotization [ETN-90-96232] 11 p1482 N90-18528
French approach to space technology transfer 11 p1576 N90-19074
NASA airframe structural integrity program [NASA-TM-102637] 14 p1993 N90-21422
Electronic Transfer of Information and its Impact on Aerospace and Defence Research and Development [AGARD-CP-466] 15 p2177 N90-22440
Nondestructive x ray methods for characterization of advanced aerospace materials [DE90-011751] 19 p2699 N90-25356
A model for a knowledge-based system's life cycle 19 p2739 N90-25569
NASA's experience in the international exchange of scientific and technical information in the aerospace field [NASA-TM-103093] 19 p2764 N90-25704
Winged cargo return vehicle. Volume 1: Conceptual design [NASA-CR-186823] 20 p2821 N90-26050
Technology utilization: Managing the transfer of NASA aerospace technology to other industries 22 p3257 N90-28446
A package for 3-D unstructured grid generation, finite-element flow solution and flow field visualization [NASA-CR-182090] 24 p3419 N90-29309

AEROSPACE MEDICINE
NT AVIATION PSYCHOLOGY
Aerospace medicine and biology: A continuing bibliography with indexes (supplement 328) [NASA-SP-7011(328)] 01 p0092 N90-10524
USSR Space Life Sciences Digest, issue 24 [NASA-CR-3922(28)] 03 p0378 N90-12152
USSR Space Life Sciences Digest, issue 22 [NASA-CR-3922(26)] 03 p0378 N90-12153
USSR Space Life Sciences Digest, issue 23 [NASA-CR-3922(27)] 03 p0378 N90-12154
Aerospace medicine and biology: A continuing bibliography with indexes (supplement 329) [NASA-SP-7011(329)] 03 p0382 N90-12173
Biochemical and physiological changes in glider pilots during multihour flights [DLR-FB-89-29] 04 p0523 N90-13018
Aerospace medicine and biology: A continuing bibliography with indexes (supplement 330) [NASA-SP-7011(330)] 05 p0674 N90-13925
Preliminary study of pharmacological control of space disease [ETN-90-95015] 05 p0674 N90-13927
USSR Space Life Sciences Digest. Index to issues 21-25 [NASA-CR-3922(30)] 06 p0819 N90-14763
Exploring the living universe: A strategy for space life sciences [NASA-TM-101891] 06 p0822 N90-14778
Assessment of visual function in aerospace medicine [BMVG-FBWM-89-5] 08 p1105 N90-16397
Environmental quality and occupational health Special Emphasis Area Plan (SEAP) [AD-A214738] 09 p1251 N90-17259
The research program at the Civil Aeromedical Institute concerning protective breathing equipment for use by crew and passengers in an aviation smoke/fume environment 10 p1317 N90-17616
Aerospace medicine and biology: A continuing bibliography with indexes (supplement 333) [NASA-SP-7011(333)] 10 p1411 N90-18136
Aerospace medicine and biology: A continuing bibliography with indexes (supplement 331) [NASA-SP-7011(331)] 10 p1411 N90-18137
Activities in aerospace medicine [ETN-90-95468] 12 p1696 N90-19739
Ejection seat training of jet pilots and weapon system officers at the German Air Force School of Aviation Medicine 13 p1752 N90-20061
The United States Air Force School of Aerospace Medicine: Special report [AD-A217740] 13 p1851 N90-20822
Human centrifuge controller [NAL-TM-SE-8901] 14 p1929 N90-21043
USSR Space Life Sciences Digest, issue 26 [NASA-CR-3922(31)] 14 p2009 N90-21513
USSR Space Life Sciences Digest, issue 25 [NASA-CR-3922(29)] 15 p2135 N90-22203
Aerospace medicine and biology: A continuing bibliography with indexes (supplement 334) [NASA-SP-7011(334)] 15 p2136 N90-22207
Aerospace medicine and biology: A continuing bibliography with indexes (supplement 335) [NASA-SP-7011(335)] 15 p2136 N90-22208
Strategic implementation plan [NASA-TM-102907] 17 p2433 N90-23861
Aerospace medicine and biology: A continuing bibliography with indexes (supplement 336) [NASA-SP-7011(336)] 17 p2436 N90-23877
National Aeronautics and Space Administration (NASA)/American Society for Engineering Education (ASEE) Summer Faculty Fellowship Program-1989, volume 1 [NASA-CR-185601-VOL-1] 18 p2627 N90-24972
Index of FAA office of aviation medicine reports: 1961 through 1989 [AD-A221414] 18 p2635 N90-25011
USSR space life sciences digest, issue 27 [NASA-CR-3922(32)] 19 p2717 N90-25457
A survey of cervical pain in pilots of a Belgian F-16 Air Defence Wing 19 p2718 N90-25462
Aerospace medicine and biology: A cumulative index to a continuing bibliography (supplement 332) [NASA-SP-7011(332)] 19 p2722 N90-25480
Aerospace medicine and biology: A continuing bibliography with indexes (supplement 337) [NASA-SP-7011(337)] 19 p2722 N90-25481
Aerospace medicine and biology: A continuing bibliography with indexes (supplement 338) [NASA-SP-7011(338)] 19 p2722 N90-25482
Aerospace medicine and biology: A continuing bibliography with indexes (supplement 339) [NASA-SP-7011(339)] 22 p3232 N90-28327
Aerospace medicine and biology: A continuing bibliography with indexes (supplement 340) [NASA-SP-7011(340)] 23 p3355 N90-28963

AEROSPACE PLANES
NT HOTOL LAUNCH VEHICLE
Low-speed, high-lift aerodynamic characteristics of slender, hypersonic accelerator-type configurations [NASA-TP-2945] 02 p0145 N90-10830
Trajectory optimization and guidance for an aerospace plane [NASA-CR-185884] 05 p0578 N90-13369
Slush Hydrogen (SLH2) technology development for application to the National Aerospace Plane (NASP) [NASA-TM-102315] 06 p0732 N90-14268
Hypersonic nozzle design [NASA-CR-186261] 07 p0876 N90-15077
The German hypersonic technology programme 09 p1174 N90-16790
Progress in Saenger space transportation system definition 09 p1175 N90-16799
HOTOL: A future launcher for Europe 09 p1175 N90-16800
National aero-spaceplane status and plans 09 p1175 N90-16801
Cost optimisation of reusable aerospaceplane transportation systems 09 p1175 N90-16803
A computational model for thickening boundary layers with mass addition for hypersonic engine inlet testing [AD-A216246] 10 p1310 N90-17576
Structures and materials technology for hypersonic aerospacecraft [NASA-TM-102583] 11 p1519 N90-18752
Rapid near-optimal trajectory generation and guidance law development for single-stage-to-orbit airbreathing vehicles [NASA-CR-186299] 12 p1612 N90-19275
HOTOL structures and materials at British Aerospace, Warton, UK [EOARD-LR-90-001] 14 p1921 N90-21001
Performance of an aero-space plane propulsion nozzle 14 p1926 N90-21034
Numerical simulation of hypersonic flow around a space plane. Part 2: Application to high angles of attack flow [NAL-TR-1011T] 15 p2045 N90-21726
Space plane model for visual measurement of aerodynamic heating [DE90-505514] 20 p2803 N90-25949
Background, current status, and prognosis of the ongoing slush hydrogen technology development program for the NASP [NASA-TM-103220] 20 p2822 N90-26055
Prediction of the ullage gas thermal stratification in a NASP vehicle propellant tank experimental simulation using FLOW-3D [NASA-TM-103217] 20 p2841 N90-26160
Flight control issues of the next generation space transportation launch vehicles 22 p3126 N90-27742
National aero-space plane: Flight mechanics 22 p3129 N90-27759
Optimal trajectories for hypervelocity flight 24 p3430 N90-29378
Utilization of space station, part 3 [NAL-TM-597-PT-3] 24 p3439 N90-29422
A collision avoidance system for a spaceplane manipulator arm 24 p3521 N90-29903

AEROSPACE SAFETY
Liquid rocket booster study. Volume 2, book 2, appendix 1: Trades studies [NASA-CR-183601] 01 p0027 N90-10136
Evaluation of tests and design factors 02 p0176 N90-10987
Active rendezvous between a low-earth orbit user spacecraft and the Space Transportation System (STS) shuttle 05 p0590 N90-13436
Hermes space vehicle: Safety considerations 09 p1178 N90-16825
Fire safety applications for spacecraft 10 p1314 N90-17595
Space nuclear safety program [DE90-006436] 11 p1565 N90-19007
Safety Status Report for the Ulysses mission. Book 1: Accident analysis. General purpose heat source radioisotope thermoelectric generator program [DE90-006829] 12 p1614 N90-19285

Aerospace Safety Advisory Panel
[NASA-TM-101748] 12 p1634 N90-19389
Requirements for protective pressure suits for the Hermes spacecrew 13 p1753 N90-20065
Space Propulsion Hazards Analysis Manual (SPHAM), volume 1
[AD-A219607] 21 p2969 N90-26874
Multi-sensor analysis techniques for SSME safety monitoring
[NASA-CR-185260] 22 p3124 N90-27732

AEROSPACE SCIENCES
NASA scientific and technical publications: A catalog of special publications, reference publications, conference publications, and technical papers, 1988
[NASA-SP-7063(03)] 01 p0135 N90-10782
The French balloon program and related space research 05 p0656 N90-13828
JSC document index
[NASA-TM-102923] 08 p1137 N90-16589
Catalogue of ESA publications in 1987
[ESA-SP-1087] 08 p1137 N90-16590
FY 1989 scientific and technical reports, articles, papers, and presentations
[NASA-TM-100384] 12 p1725 N90-19916
Science and technology report and outlook, 1985-1988
[PB90-115270] 12 p1727 N90-19926
NASA Thesaurus supplement: A four part cumulative supplement to the 1988 edition of the NASA Thesaurus (supplement 3)
[NASA-SP-7064-SUPPL-3] 15 p2177 N90-22438
Research and Technology Objectives and Plans Summary (RTOPS)
[NASA-TM-89662] 15 p2194 N90-22528
Activities report of the Netherlands Space Research Organization
[ETN-90-96927] 18 p2636 N90-25021
Activities report of the Space Science Department
[ESA-SP-1126] 24 p3560 N90-30142

AEROSPACE SYSTEMS
Supersonic flow computations over aerospace configurations using an Euler marching solver
[NASA-CR-4085] 01 p0003 N90-10012
Conference on Aerospace Transparent Materials and Enclosures (15th) 16-20 January 1989. Volume 2: Sessions 6-9
[AD-A210201] 01 p0006 N90-10024
Proceedings of the Workshop on Computational Aspects in the Control of Flexible Systems, part 1
[NASA-TM-101578-PT-1] 01 p0017 N90-10080
Computational controls for aerospace systems 01 p0017 N90-10082
A comparison of software for the modeling and control of flexible systems 01 p0019 N90-10092
Proceedings of the Workshop on Computational Aspects in the Control of Flexible Systems, part 2
[NASA-TM-101578-PT-2] 01 p0021 N90-10103
Aerospace system unified life cycle engineering producibility measurement issues
[AD-A210937] 01 p0106 N90-10807
AFRAPT (Air Force Research in Aero Propulsion Technology) Trainee Program
[AD-A211540] 03 p0307 N90-11744
Airborne/spaceborne pulsed power source
[AD-A211762] 04 p0495 N90-12850
Project ORION microcomputer management system
[AD-A212945] 05 p0680 N90-13959
NRL (Naval Research Laboratory) Review
[AD-A212866] 05 p0716 N90-14182
Recent developments in TERPROM
09 p1163 N90-16732
An assessment of potential markets for small satellites
[NASA-TM-101943] 09 p1181 N90-16848
Sensitivity of space system availability predictions to underlying component reliability estimates
[AD-A215535] 09 p1183 N90-16858
Use of hypermedia as a user interface for an artificial intelligence-based problem solver
[AD-A215551] 09 p1271 N90-17370
Investigation of applications of diamond film
[AD-A216104] 10 p1368 N90-17931
Orbital servicing: Issue or answer
[AD-A217284] 12 p1616 N90-19295
Trajectory optimization in the presence of constraints
[AD-A218271] 13 p1760 N90-20104
Measurements of the interaction of high-voltage biassed conductors with the ionosphere
[AD-A218285] 13 p1843 N90-20580
Space in warfare
[AD-A217527] 13 p1879 N90-20782
PACOSS program status and results
14 p1933 N90-21065
Initial operational capability of the ASTREX large space structures test bed 14 p1938 N90-21091
Curvature continuity of cubic Bezier curves in the solid modeling aerospace research tools design software
[NASA-CR-186583] 14 p2016 N90-21554
Research and Technology
[NASA-TM-102161] 14 p2044 N90-21721
Advances in optimal active control techniques for aerospace systems; application to aircraft active landing gear 15 p2054 N90-21769
Large space systems antenna technology
15 p2060 N90-21798
Performance analysis of CCSDS path service
[NASA-CR-180699] 17 p2364 N90-23457
Qualitative models for space system engineering
[NASA-CR-180682] 17 p2385 N90-23585
Research and technology 1989
[NASA-TM-100369] 17 p2486 N90-24219
Spacecraft contamination programs within the Air Force Systems Command Laboratories
19 p2727 N90-25507
StarPlan: A model-based diagnostic system for spacecraft 19 p2728 N90-25511
Smart built-in test 19 p2728 N90-25512
Monitoring and control of spacecraft systems using procedural reasoning 19 p2731 N90-25524
Knowledge representation to support reasoning based on multiple models 19 p2731 N90-25525
Space environments and their effects on space automation and robotics 19 p2735 N90-25543
Discharge transient coupling in large space power systems 19 p2735 N90-25544
Low-gravity fluid physics: A program overview
[NASA-TM-103215] 20 p2861 N90-26273
Bidirectional drive and brake mechanism
[NASA-CASE-MSC-21540-1] 20 p2872 N90-26342
NASA aerospace flight battery systems program
[NASA-TM-103237] 20 p2882 N90-26397
Pilot interaction with automated airborne decision making systems
[NASA-CR-186730] 20 p2899 N90-26492
Preliminary designs for 25 kWe advanced Stirling conversion systems for dish electric applications
[NASA-TM-103188] 20 p2940 N90-26729
Polyarylacetylene resin composites
[AD-A221507] 21 p2972 N90-26890
Stochastic structural dynamics for aerospace applications
[AD-A221517] 21 p3013 N90-27133
An automated tool for the design and assessment of space systems 21 p3042 N90-27269
VIP: A knowledge-based design aid for the engineering of space systems 21 p3048 N90-27327
Tactical Applications of Space Systems
[AGARD-CP-460] 21 p3067 N90-27438
Tactical oceanography from space: The next decade
21 p3068 N90-27442
Block 6: The future DMSP space systems
21 p3068 N90-27443
Tactical uses of the DSCS 3 communications system
21 p3069 N90-27450
Testing DoD space systems: The challenge
22 p3132 N90-27771
Advanced onboard propulsion benefits and status
[NASA-TM-103174] 22 p3134 N90-27786
Situational Awareness in Aerospace Operations
[AGARD-CP-478] 23 p3357 N90-28972
Automation and robotics technology for intelligent mining systems 23 p3366 N90-29018
Causal simulation and sensor planning in predictive monitoring 23 p3369 N90-29037
Proceedings of the NASA Conference on Space Telerobotics, volume 2
[NASA-CR-186857] 23 p3370 N90-29044
External information sources and aerospace R/D: The use and importance of technical reports by US Aerospace engineers and scientists
[NASA-TM-101232] 24 p3558 N90-30132

AEROSPACE TECHNOLOGY TRANSFER
NASA technology applications
[GPO-99-412] 04 p0564 N90-13290
Research and technology, 1989: Langley Research Center
[NASA-TM-4150] 08 p1157 N90-16703
An exploration of benefits from NASA Spinoff
10 p1443 N90-18325
Promotion of European Space Technology Transfer
[ESA-SP-1122] 11 p1575 N90-19068
ESA project to promote and assist technology transfer by industry 11 p1576 N90-19069
Space technology transfers in Europe
11 p1576 N90-19070
DTE and space technology transfer
11 p1576 N90-19071
Purchase of technology 11 p1576 N90-19072
The bringing to market of the RF alert (a case study in technology transfer) 11 p1576 N90-19073
French approach to space technology transfer
11 p1576 N90-19074
Introductory remarks for the panel discussions on technology transfer 11 p1576 N90-19075
Methodology panel 11 p1576 N90-19076
Problems on transfer of space technology to non-space areas and solutions: Legal aspects
11 p1577 N90-19077
Identification of and response to market demand
11 p1577 N90-19078
The improvement of technology transfer from space to industry 11 p1577 N90-19079
Internal technology transfer 11 p1577 N90-19080
Magnetic suspension railway systems based on space technology 11 p1577 N90-19081
An example of technology transfer by Aerospatiale: Fire protection materials 11 p1577 N90-19082
Government Information Quarterly. Volume 7, no. 2: National Aeronautics and Space Administration Scientific and Technical Information Programs. Special issue
[ISSN-0740-624X] 22 p3257 N90-28440
Enhancing US competitiveness through Federal scientific and technical information: Issues and opportunities 22 p3258 N90-28450

AEROSPACE VEHICLES
NT AEROSPACE PLANES
NT FLEXIBLE SPACECRAFT
NT HOTOL LAUNCH VEHICLE
Hierarchical damage tolerant controllers for smart structures
[AD-A209422] 01 p0005 N90-10022
Requirements for multidisciplinary design of aerospace vehicles on high performance computers
[NASA-CR-181915] 03 p0384 N90-12183
Guidance and Control strategies for aerospace vehicles
[NASA-CR-186195] 08 p0727 N90-14243
Aerobraking characteristics for several potential manned Mars entry vehicles
[NASA-TM-101669] 06 p0733 N90-14272
Effects of lightning on operations of aerospace vehicles 07 p0873 N90-15065
A Mars/Phobos transportation system
[NASA-CR-186217] 09 p1230 N90-17135
Fire safety applications for spacecraft
10 p1314 N90-17595
Analytical formulation for the interaction problem of dynamic reentry, and effects due to flexibility and vibration in an aerospace vehicle
[INPE-4963-TDL/392] 11 p1487 N90-18448
Structures and materials technology for hypersonic aerospacecraft
[NASA-TM-102583] 11 p1519 N90-18752
Development of acceleration exposure limits for advanced escape systems 13 p1751 N90-20055
On the use of external burning to reduce aerospace vehicle transonic drag
[NASA-TM-103107] 15 p2052 N90-21762
Approximate optimal guidance schemes for atmospheric orbital maneuvering 16 p2206 N90-22585
Conceptual design for aerospace vehicles
16 p2641 N90-25043
PDWAP: A preliminary design and weights analysis program for aerospace vehicles
[AD-A222614] 20 p2808 N90-25979
Guidance and control strategies for aerospace vehicles
[NASA-CR-186878] 20 p2814 N90-26013
Model designation of military aerospace vehicles
[PB90-206301] 22 p3107 N90-27646
Nonequilibrium radiation and chemistry models for aerocapture vehicle flowfields
[NASA-CR-186728] 22 p3169 N90-27973
Flowfield computation of entry vehicles
[NASA-CR-186946] 22 p3171 N90-27986
Thermal structures: Four decades of progress
[NASA-CR-186898] 22 p3191 N90-28105
Nonequilibrium radiation and chemistry models for aerocapture vehicle flowfields
[NASA-CR-186379] 23 p3267 N90-28490

AEROSTATS
U AIRSHIPS

AEROTHERMOCHEMISTRY
Modifications to the aerotherm charring material thermal response and ablation program (CMA) for carbon ablation analysis
[AD-A211069] 02 p0195 N90-11115
Results from the IVL TOR Station at Roervik, Sweden. A contribution to the EURATRAC subproject TOR
20 p2885 N90-26415

AEROTHERMODYNAMICS
Boost-phase discrimination research activities
[NASA-TM-101889] 01 p0032 N90-10176
Development of a thermoacoustic test facility
02 p0183 N90-11041

Wake interaction effects on the transition process on turbine blades
[AD-A214492] 09 p1168 N90-16759
Verification of aerothermodynamic codes by means of a winged experimental re-entry vehicle
09 p1180 N90-16842
NASA aerodynamics program
[NASA-TM-4175] 09 p1247 N90-17235
Shock-shock boundary layer interactions
10 p1308 N90-17569
Activities report in German aerospace
[ISSN-0070-3966] 11 p1595 N90-19189
Heat transfer measurements from a NACA 0012 airfoil in flight and in the NASA Lewis icing research tunnel
[NASA-CR-4278] 12 p1599 N90-19203
Evaluation of an adaptive unstructured remeshing technique for integrated fluid-thermal-structural analysis
[NASA-TM-102611] 13 p1815 N90-20426
Probabilistic modeling for simulation of aerodynamic uncertainties in propulsion systems
[NASA-TM-102472] 14 p1927 N90-21036
Navier-Stokes analysis of turbine blade heat transfer
[NASA-TM-102496] 14 p1972 N90-21300
Infrared thermography at hypersonic channel H2K
18 p2490 N90-24235
AFE dynamic effects in inhomogeneous plasmas
18 p2643 N90-25053
Experimental aerothermodynamic research of hypersonic aircraft
[NASA-CR-186903] 20 p2804 N90-25954
Structural Mechanics Division research and technology plans for FY 1990 and accomplishments for FY 1989
[NASA-TM-102654] 20 p2876 N90-26361
Computer modeling and data processing methods: An essential part of jet engine condition monitoring and fault diagnosis 22 p3104 N90-27626
Reentry trajectory optimization and control
22 p3127 N90-27746
Flight mechanics applications for tethers in space: Cooperative Italian-US programs
22 p3131 N90-27770
Thermal structures: Four decades of progress
[NASA-CR-186898] 22 p3191 N90-28105
Supersonic/hypersonic aerodynamics and heat transfer for projectile design using viscous-inviscid interaction
[AD-A224354] 24 p3418 N90-29303
Numerical simulation of hypersonic viscous flow for the design of H-2 orbiting plane (HOPE)
[NAL-TR-1028] 24 p3422 N90-29330

AEROTHERMOELASTICITY
The application of active controls technology to a generic hypersonic aircraft configuration
[NASA-TM-101689] 13 p1754 N90-20071
Active control of aerothermoelastic effects for a conceptual hypersonic aircraft
[NASA-TM-102713] 22 p3122 N90-27725

AFC (CONTROL)
U AUTOMATIC FREQUENCY CONTROL

AFCS (CONTROL SYSTEM)
U AUTOMATIC FLIGHT CONTROL

AFFINITY
NT ELECTRON AFFINITY
NT NEGATIVE ELECTRON AFFINITY

AFRICA
Rainfall estimation over Africa using satellite data
06 p0815 N90-14742
US Navy regional climatic study of southern African waters
[AD-A218792] 16 p2258 N90-22874
US Navy regional climatic study of the Mozambique channel and adjacent waters
[AD-A218793] 16 p2258 N90-22875
Multisensor monitoring of deforestation in the Guinea Highlands of West Africa
[NASA-CR-186709] 19 p2706 N90-25396
Dust clouds from African dust storms in 1986-1987 as observed by Meteosat 21 p3029 N90-27222

AFTERBODIES
Hypersonic nozzle/afterbody performance at low Mach numbers
[AD-A216223] 10 p1309 N90-17575
Study of the turbulent boundary layer on an afterbody
[TM-EA-8901] 12 p1601 N90-19212
The interaction between a plane shock wave and a cylindrical afterbody 15 p2046 N90-21728
The 3-D composite velocity solutions for subsonic/transonic flow over forebodies and afterbodies
[AD-A220370] 17 p2345 N90-23354
Sting-support interference on afterbody drag at transonic speeds
[NAL-TM-EA-8902] 23 p3267 N90-28492

AFTERBURNERS
U AFTERBURNING

AFTERBURNING
Characteristics of combustion driven pressure oscillations in advanced turbo-fan engines with afterburner 01 p0035 N90-10194
Reheat buzz: An acoustically coupled combustion instability 01 p0036 N90-10200
Attenuation of reheat buzz by active control
01 p0036 N90-10201
Measurement effects on the calculation of in-flight thrust for an F404 turbofan engine
[NASA-TM-4140] 03 p0307 N90-11741
Relativistic klystron afterburner simulation techniques
[DE90-008539] 13 p1796 N90-20305
Exhaust environment measurements of a turbofan engine equipped with an afterburner and 2D nozzle
[NASA-CR-4289] 15 p2052 N90-21760
High-temperature test facility at the NASA Lewis engine components research laboratory
[NASA-TM-103143] 19 p2662 N90-25151

AFTERGLOWS
Ion and electron interactions at thermal and suprathermal energies
[AD-A216905] 12 p1622 N90-19323

AGB STARS
U ASYMPTOTIC GIANT BRANCH STARS

AGC (CONTROL)
U AUTOMATIC GAIN CONTROL

AGE DETERMINATION
U CHRONOLOGY

AGE FACTOR
Age-related changes in human posture control: Motor coordination tests
[NASA-CR-185855] 03 p0383 N90-12178

AGE HARDENING
U PRECIPITATION HARDENING

AGGLOMERATION
Agglomeration of ceramic powders
09 p1223 N90-17098
Mechanical properties of fluffy agglomerates consisting of core-mantle-particles 12 p1743 N90-20019
Model-based Gaussian and non-Gaussian clustering
[AD-A222097] 21 p3066 N90-27430

AGGREGATES
Laser light scattering as a probe of fractal colloid aggregates 09 p1223 N90-17097
Development and testing of rapid repair methods for war damaged runways
[AD-A223970] 23 p3285 N90-28586

AGING
Physical ageing and short term creep in amorphous and semicrystalline polymers
[NPL-DMA(A)-185] 04 p0479 N90-12745

AGING (BIOLOGY)
Microgravity effects on insect development and aging
19 p2680 N90-25243
Program review: The lifetime effects of space radiation in rhesus monkeys
[AD-A221127] 19 p2716 N90-25454

AGING (MATERIALS)
NT AGING (METALLURGY)
Predictive aging of polymers
[NASA-CASE-NPO-17524-1-CU]
01 p0046 N90-10261
Space environment effects on carbon/epoxy materials
02 p0185 N90-11056
Aging of CFRP due to longterm storage in heated air
[ESA-TT-1124] 03 p0333 N90-11893
A model for long-term creep and the effects of physical ageing in poly (butylene terephthalate)
[NPL-DMA(A)-182] 03 p0333 N90-11895
Nondestructive analysis of aileron fatigue and aging in a Mirage F1
[REPT-M6-594000] 05 p0580 N90-13378
Mechanical property characterization of VascoMax T-300
[AD-A212950] 05 p0623 N90-13637
The mechanisms of dispersion strengthening and fracture in Al-based XD (TM) alloys
[NASA-CR-4276] 09 p1187 N90-16879
Experimental results of aging and thermal effects in high-power laser diodes
[DE90-005955] 12 p1666 N90-19573
Hydrogen, thermal ageing and the role of carbides in fatigue of a high strength steel
[AERE-R-13599] 13 p1774 N90-20183
Ageing effects in welded cast CF3 stainless steel
[AERE-R-13559] 13 p1775 N90-20188
The ageing effect of the matrix-reinforcement interface on the ageing response of an aluminium 6061 alloy reinforced with 20vol percent SiC particulates
[AERE-R-13361] 13 p1776 N90-20193
Positron annihilation spectroscopy: A nondestructive, submicroscopic characterization technique for structural polymers
[AD-A217748] 13 p1782 N90-20226
Nine-year aging behavior of the ceramic flatpack resonator
[DE90-008044] 13 p1813 N90-20412
Theory system reliability demonstration and burn-in design
[AD-A217775] 13 p1814 N90-20416
Aging and compatibility of TNF-doped Mylar
[DE90-008508] 14 p1954 N90-21186
Grain boundary intermetallic phases in alloy 718
[DE90-009812] 15 p2173 N90-22417
Diffusion in the thermal degradation of NC base propellants
[AD-A219831] 17 p2383 N90-23572
Second Annual International Conference on Aging Aircraft
[AD-A222715] 20 p2805 N90-25961
Effect of casting procedures and diesel engine environment on the behavior of aluminum titanate
[AD-A223079] 20 p2835 N90-26126
Renewed aging control of adhesion of inhibitor on the gas generator charges for RB 24
[FOA-C-20780-2.1] 20 p2840 N90-26153
Applications of digital image processing in testing and evaluation of composite materials
[AD-A222939] 21 p2971 N90-26887
Molecular dynamics of physical aging processes in polymer glasses (experiment and theory)
[AD-A222848] 21 p2984 N90-26959
Development of testing and analysis methodology to assess the long term durability of polymeric composites at high temperatures
[NASA-TM-102714] 23 p3339 N90-28871

AGING (METALLURGY)
Strain aging in tungsten-heavy alloys
[AD-A211166] 01 p0046 N90-10259
Accelerated aging of metal matrix composites
02 p0190 N90-11085
The effect of composition and aging treatment on the microstructure and mechanical properties of aluminum-lithium-titanium alloys
[AD-A213144] 05 p0624 N90-13640
Embrittlement of laboratory- and reactor-aged CF-3, CF-8, and CF-8M duplex stainless steels
[DE90-002777] 06 p0748 N90-14354
BES welding science contractors summary report, 1988 to 1989
[DE90-001004] 06 p0793 N90-14619
Accelerated aging embrittlement of cast duplex stainless steel: Activation energy for extrapolation
[DE90-001773] 07 p0903 N90-15221
Cast stainless steel aging: Mechanisms and predictions
[DE90-003772] 07 p0907 N90-15241
Heat treatment study of the SiC/Ti-15-3 composite system
[NASA-TP-2970] 12 p1618 N90-19302
The effect of aging at 343 C on type 308 stainless steel weldments
[DE90-009232] 15 p2069 N90-21853

AGITATION
NT ULTRASONIC AGITATION

AGREEMENTS
Effects of stress on judgment and decision making in dynamic tasks
[AD-A210605] 01 p0135 N90-10781
Prospects for space arms control
[DE90-003392] 07 p0987 N90-15700
An investigation into the effects which aerospace industry offset trade agreements have on United States Air Force mission performance
[AD-A215093] 09 p1294 N90-17502
Polar prospects: A minerals treaty for Antarctica
[OTA-O-428] 17 p2480 N90-24185
Technology transfer: Implementation status of the Federal Technology Transfer Act of 1986. Report to Congressional requesters
[GAO/RCED-89-154] 19 p2764 N90-25707
The International Space Station: The legal framework
20 p2938 N90-26716
The partnership concept and international management 20 p2938 N90-26717
The International Space Station: Conditions of access and use 20 p2938 N90-26718
The manned national space station: International legal considerations 20 p2938 N90-26720
Crossborder movements: Goods, personnel and technologies 20 p2939 N90-26722
Space law put to the test by the International Space Station 20 p2939 N90-26727
Department of Energy Strategic Defense Initiative programs: Potential programmatic and facility impacts due to a prospective defense and space treaty
[DE90-012717] 21 p3067 N90-27437

AGRICULTURE
Computer-aided boundary delineation of agricultural lands
[NASA-TM-102243] 08 p1091 N90-16313
Use of remote sensing in operational inventory and monitoring agricultural and forestry tasks
08 p1094 N90-16335
Remote sensing in agriculture: Basic concepts, methodology and applications
[INPE-4806-MD/39] 10 p1399 N90-18086
LANDSAT-TM and agrometeorological data in the wheat crop yield estimation at the farm level
[INPE-4842-PRE/1471] 10 p1400 N90-18091
Aerial photographs to support the fiscalization process of agriculture loans in the Irece-BA region
[INPE-4839-PRE/1468] 10 p1400 N90-18092
Evaluation of two methods for acquisition of training statistics for digital analysis of areas prepared for plowing
[INPE-4901-PRE/1502] 11 p1522 N90-18763
Radiometric study of wheat and bean crops in three types of latossolo
[INPE-4843-PRE/1472] 11 p1523 N90-18767
Relationships between spectral parameters and agronomics of wheat and beam crops
[INPE-4791-RPE/584] 11 p1523 N90-18768
Development of the agricultural information system. Characteristics and results of the Distrito Federal model
[INPE-4940-PRE/1430] 11 p1524 N90-18773
Spectral response of wheat and its relationship with agronomical prameters
[INPE-4950-RPE/599] 11 p1524 N90-18774
Introduction of aerial photography in agricultural research
[BCRS-89-14] 11 p1526 N90-18784
Effects of global climate change on agroecosystems: Scope of work
[PB90-120023] 11 p1531 N90-18813
Mechanics of aeolian processes: Soil erosion and dust production 12 p1638 N90-19410
Relationship of radiometric field measurements of wheat in the Assis-Safra region, 1988
[INPE-4949-RPE/598] 13 p1819 N90-20443
Agricultural yield estimation of sugarcane based on agrometeorological-spectral model
[INPE-5016-RPE/610] 14 p1996 N90-21441
Aerial photography as an aid for agricultural credit control
[INPE-5019-RPE/613] 14 p1999 N90-21455
Spectral response of wheat and its relationship with agronomic variables in the tropical region
[INPE-5018-RPE/612] 15 p2122 N90-22138
Field reports on radiometric campaigns of soybeans in the Federal district: Safra 88/89
[INPE-5021-RPE/615] 15 p2122 N90-22139
Proceedings of the Conference on Technology-Based Confidence Building: Energy and Environment
[CNSS-PAPERS-22] 15 p2125 N90-22152
Impact of meteorology on the agricultural sector: Compilation and analysis of projects
[INPE-4846-PRE/1475] 16 p2257 N90-22866
MARS (Monitoring Agro-ecological Resources with Remote sensing and Simulation) definition study: Results of the preparatory phase
[REPT-17] 19 p2706 N90-25395
Multisensor monitoring of deforestation in the Guinea Highlands of West Africa
[NASA-CR-186709] 19 p2706 N90-25396
Data Base Analyzer and Parameter Estimator (DBAPE) interactive computer program user's manual
[PB90-193053] 23 p3406 N90-29252

AGRISTARS PROJECT
Results of Agrisar-86 for the Flevopolder (Netherlands) test area
[BCRS-89-21] 11 p1527 N90-18789

AGROCLIMATOLOGY
From Penman to Makkink: A new method for the calculation of the climatological evaporation numbers
[KNMI-TR-111] 15 p2126 N90-22161

AGROMETEOROLOGY
LANDSAT-TM and agrometeorological data in the wheat crop yield estimation at the farm level
[INPE-4842-PRE/1471] 10 p1400 N90-18091
Wheat yield estimation at the farm level using LANDSAT TM and agrometeorological data
[INPE-5017-RPE/611] 14 p1996 N90-21439
Agricultural yield estimation of sugarcane based on agrometeorological-spectral model
[INPE-5016-RPE/610] 14 p1996 N90-21441
Impact of meteorology on the agricultural sector: Compilation and analysis of projects
[INPE-4846-PRE/1475] 16 p2257 N90-22866

AH-1G HELICOPTER
Investigation of difficult component effects on finite element model vibration prediction for the Bell AH-1G helicopter. Volume 1: Ground vibration test results
[NASA-CR-181916-VOL-1] 03 p0360 N90-12058
Investigation of difficult component effects on finite element model vibration prediction for the Bell AG-1G helicopter. Volume 2: Correlation results
[NASA-CR-181916-VOL-2] 05 p0654 N90-13814
Calculation of flight vibration levels of the AH-1G helicopter and correlation with existing flight vibration measurements
[NASA-CR-181923] 11 p1518 N90-18743
Calculation of flight vibration levels of the AH-1G helicopter and correlation with existing flight vibration measurements
[NASA-CR-182031] 19 p2702 N90-25375

AH-64 HELICOPTER
Preliminary airworthiness evaluation of the AH-64A equipped with the Air To Air Stinger (ATAS) missile system
[AD-A213030] 05 p0579 N90-13374
Aerodynamic performance of a 0.27-scale model of an AH-64 helicopter with baseline and alternate rotor blade sets
[NASA-TM-4201] 18 p2491 N90-24237
Plan, execute, and discuss vibration measurements and correlations to evaluate a NASTRAN finite element model of the AH-64 helicopter airframe
[NASA-CR-181973] 23 p3338 N90-28866

AILERONS
Nondestructive analysis of aileron fatigue and aging in a Mirage F1
[REPT-M6-594000] 05 p0580 N90-13378
Prediction of forces and moments for flight vehicle control effectors. Part 1: Validation of methods for predicting hypersonic vehicle controls forces and moments
[NASA-CR-186571] 15 p2047 N90-21734

AIR
NT COMPRESSED AIR
NT HIGH TEMPERATURE AIR
Surface-catalyzed air oxidation of hydrazines: Environmental chamber studies
02 p0203 N90-11159
Surface-catalyzed air oxidation reactions of hydrazines: Tubular reactor studies 02 p0204 N90-11167
Air breakdown photography in the picosecond domain
[DE89-016775] 03 p0322 N90-11830
An empirical formula for gas switch breakdown delay
[DE89-017233] 03 p0342 N90-11947
An air coupled transmission mode acoustic microscope for on-line non-destructive evaluation
[AD-A211416] 04 p0511 N90-12947
Test and evaluation of polymeric membranes for oxygen enrichment of air
[DE90-000555] 06 p0742 N90-14321
Reduction of erosion in elbows due to flow modifications, phase 2
[DE89-011702] 07 p0932 N90-15394
Two-dimensional calculation of sequential electron layer formation by crossed microwave beams in air at low pressure
[DE90-005254] 09 p1286 N90-17453
Two-dimensional, long-pulse computer calculation of microwave-induced electron layer formation in low-pressure air
[DE90-005994] 12 p1646 N90-19459
Sparse breakdown and statistical sneakthrough effects in low-altitude microwave propagation
[DE90-007252] 12 p1648 N90-19473
A technical and economic evaluation of oxygen-enriched combustion in diesel engines using water-emulsified fuels
[DE90-008095] 13 p1810 N90-20394
WINCOF-I code for prediction of fan compressor unit with water ingestion
[NASA-CR-185157] 15 p2045 N90-21724
Field evaluation of a passive sampling device for hydrazines in ambient air
[NASA-TM-103456] 18 p2578 N90-24686
The computer modeling of the combustion and extinction of methane-air premixed flames by thermally stable gases
[PB90-189432] 21 p2976 N90-26910
A review of reaction rates and thermodynamic and transport properties for an 11-species air model for chemical and thermal nonequilibrium calculations to 30000 K
[NASA-RP-1232] 21 p3002 N90-27064
Oxygen deficiency monitor system
[DE90-014866] 24 p3523 N90-29917

AIR BAG RESTRAINT DEVICES
Human factors: The human interface with aircraft interiors
[NIAR-90-18] 20 p2900 N90-26496

AIR BEARINGS
U GAS BEARINGS

AIR BLASTS
U AERIAL EXPLOSIONS

AIR BREATHING BOOSTERS
Conceptual work at Aerospatiale on air-breathing and non-air-breathing recoverable launchers
[REPT-892-422-104] 17 p2362 N90-23450
Ascent and descent optimizations of an air-breathing launch vehicle 22 p3130 N90-27761
Global optimization of air breathing launch vehicle trajectories 22 p3130 N90-27762

AIR BREATHING ENGINES
NT GAS TURBINE ENGINES
NT JET ENGINES
NT RAMJET ENGINES
NT SUPERSONIC COMBUSTION RAMJET ENGINES
NT TURBOFAN ENGINES
NT TURBOJET ENGINES
NT TURBOPROP ENGINES
NT TURBORAMJET ENGINES
Apollo lightcraft project
[NASA-CR-186055] 04 p0484 N90-12655
Aircraft propulsion: Leading the way in aviation
[LR-532] 05 p0583 N90-13395
A survey of missile aerodynamics
10 p1303 N90-17541
Appropriate aeroprediction accuracy in defining missile systems for aerodynamic flight 10 p1304 N90-17544
Use of semiempirical aerodynamic methods for preliminary design 10 p1304 N90-17546
A computational model for thickening boundary layers with mass addition for hypersonic engine inlet testing
[AD-A216246] 10 p1310 N90-17576
Effect of correlation on multi-engine rocket propulsion systems 11 p1471 N90-18467
AFOSR/ONR (Air Force Office of Scientific Research/Office of Naval Research) Contractors' Meeting on Combustion Rocket Propulsion Diagnostics of Reacting Flow
[AD-A216094] 11 p1476 N90-18491
Flight and driving optimization of air breathing aerodynamic space vehicle
[ETN-90-95379] 12 p1607 N90-19246
Proceedings of a contractors meeting on Combustion Rocket Propulsion Diagnostics of Reacting Flow
[AD-A216445] 12 p1617 N90-19297
Conceptual work at Aerospatiale on air-breathing and non-air-breathing recoverable launchers
[REPT-892-422-104] 17 p2362 N90-23450
Ramjet and ramrocket propulsion systems for missiles
21 p2973 N90-26897
Ascent and descent optimizations of an air-breathing launch vehicle 22 p3130 N90-27761

AIR CARGO
Fire hazards of aerosol cans in aircraft cargo compartments
[DOT/FAA/CT-89/32] 17 p2347 N90-23389

AIR CONDITIONING EQUIPMENT
Design and fabricate a metallic hydride heat pump with a cooling capacity of 9000 BTU/H
[AD-A213756] 07 p0931 N90-15388
Guidelines for evaluating energy analysis software
[AD-A214171] 07 p0976 N90-15640
An expert system for the design of heating, ventilating, and air-conditioning systems
[AD-A218287] 13 p1788 N90-20262

AIR CONDUCTIVITY
Transport processes through monomolecular films
[AD-A213609] 07 p0923 N90-15342
Conductive polymers of transition-metal complexes coordinated by a Diamino-Dichalcogen-Benzene compound
[AD-D014326] 12 p1629 N90-19360

AIR COOLING
Apparatus for cooling electronic components in aircraft
[AD-D014207] 05 p0579 N90-13373
The utilization of an infrared imaging system as a cooling slot blockage detector in the inspection of a transpiration cooled nozzle
[NASA-TM-102608] 12 p1663 N90-19555
Transpiration cooling in hypersonic flight
[NASA-CR-186435] 13 p1750 N90-20052
Acoustic convective system
[NASA-CASE-NPO-17278-1-CU]
14 p1959 N90-21215

AIR CURRENTS
NT JET STREAMS (METEOROLOGY)
NT MERIDIONAL FLOW
NT VERTICAL AIR CURRENTS
Characterization of thunderstorm induced Maxwell current densities in the middle atmosphere
12 p1634 N90-19391

A numerical study of wind forcing in the eastern boundary current system off Portugal
[AD-A219596] 17 p2430 N90-23847

AIR DATA SYSTEMS
Independent Orbiter Assessment (IOA): Assessment of the Orbiter Experiment (OEX) subsystem
[NASA-CR-185587] 02 p0171 N90-10962
Independent Orbiter Assessment (IOA): Analysis of the Orbiter Experiment (OEX) subsystem
[NASA-CR-185586] 02 p0171 N90-10963
Independent Orbiter Assessment (IOA): Assessment of the backup flight system FMEA/CIL
[NASA-CR-185566] 02 p0173 N90-10973
Preliminary results from a subsonic high angle-of-attack flush airdata sensing (HI-FADS) system: Design, calibration, and flight test evaluation
[NASA-TM-101713] 09 p1168 N90-16758
Wind-tunnel investigation of a flush airdata system at Mach numbers from 0.7 to 1.4
[NASA-TM-101697] 11 p1457 N90-18395
Experimental characterization of the effects of pneumatic tubing on unsteady pressure measurements
[NASA-TM-4171] 22 p3116 N90-27703
A real time evaluation of the use of a perspective format to promote situational awareness in users of air to air tactical displays 23 p3359 N90-28981
Design and evaluation of candidate pressure distribution and air data system tile penetration for the aeroassist flight experiment
[NASA-CR-4312] 24 p3471 N90-29615

AIR DEFENSE
NT ANTIMISSILE DEFENSE
Integrated G-suit/immersion suit
[AD-A212989] 06 p0821 N90-14774
Predicting Air Combat Maneuvering (ACM) performance 09 p1258 N90-17294
User's guide to OPUS (Optimal Preferential Utility and Strategies)
[AD-A214384] 10 p1424 N90-18217
Limitations of the conventional role of the B-1B in the European theater
[AD-A217285] 12 p1604 N90-19230
Comparison of oculometer and head-fixed reticle with voice or switch and touch panel for data entry on a generic tactical air combat display
[AD-A217231] 13 p1855 N90-20646
Visual behavior in the F-15 simulator for air-to-air combat
[AD-A218648] 16 p2262 N90-22893
A real time evaluation of the use of a perspective format to promote situational awareness in users of air to air tactical displays 23 p3359 N90-28981
Counterair situation awareness display for Army aviation 23 p3359 N90-28982

AIR DROP OPERATIONS
Modeling the effects of the use of GPS (Global Positioning System) derived altitude indication in the C-17A airdrop system
[AD-A215366] 09 p1166 N90-16748

AIR DUCTS
Study of active noise control in ducts
[DE89-772353] 10 p1425 N90-18224

AIR FILTERS
Aerosol separator for use in aircraft
[PB90-142217] 15 p2125 N90-22155

AIR FLOW
NT AIR CURRENTS
NT JET STREAMS (METEOROLOGY)
NT MERIDIONAL FLOW
NT VERTICAL AIR CURRENTS
Air velocity mapping of environmental test chambers
[AD-A212082] 03 p0310 N90-11764
Air flow over large scale topography
[AD-A211779] 04 p0519 N90-12998
Navier-Stokes solutions of 2-D transonic flow over unconventional airfoils 06 p0719 N90-14195
Numerical modeling of supersonic turbulent reacting free shear layers 06 p0719 N90-14197
Heat transfer to a stationary and moving sphere immersed in a fluidized bed 06 p0774 N90-14503
A wind tunnel study of a sting-mounted circulation control wing
[AD-A216248] 10 p1310 N90-17577
Experimental investigation to suppress flow-induced pressure oscillations in open cavities
[AD-A216285] 10 p1310 N90-17578
Passive venting technique for shallow cavities
[NASA-CASE-LAR-14031-1] 13 p1755 N90-20079
A comparison of two-and three-dimensional S809 airfoil properties for rough and smooth HAWT (Horizontal-Axis Wind Tunnel) rotor operation
[DE89-009512] 13 p1827 N90-20492
Study of possible solar heating effects on thermosonde probes: Error analysis
[AD-A218116] 13 p1903 N90-20917
The MANTA: An RPV design to investigate forces and moments on a lifting surface
[NASA-CR-186227] 14 p1915 N90-20971
Acoustic convective system
[NASA-CASE-NPO-17278-1-CU] 14 p1959 N90-21215
Fire propagation in concurrent flows
[PB90-151754] 15 p2066 N90-21834
Aerosol separator for use in aircraft
[PB90-142217] 15 p2125 N90-22155
An anomalous wind between valleys: Its characteristics and a proposed explanation
[DE90-008965] 15 p2133 N90-22189
Daytime wind valleys adjacent to the Great Salt Lake
[DE90-008991] 15 p2133 N90-22190
The ASCOT 1988 valley/tributary interaction study
[DE90-009043] 15 p2133 N90-22191
The effects of compressibility on a supersonic mixing layer
[AD-A219315] 16 p2197 N90-22543
Mechanical paint removal techniques for aircraft structures
[IAR-89-23] 19 p2682 N90-25254
Modeling of supersonic reacting flow fields 21 p2973 N90-26898
Numerical method for calculating indoor airflows using a turbulence model
[PB90-162009] 21 p3003 N90-27067
A numerical study of the role of meso beta and meso gamma scale vertical exchange processes in the evolution of upper tropospheric frontal systems
[AD-A222057] 21 p3031 N90-27230
Comparison of altitude test cell results 22 p3119 N90-27715
Comparison of ground-level test cells and ground-level to altitude test cells 22 p3119 N90-27716
General test plan 22 p3120 N90-27721
A nonhydrostatic numerical model in sigma-coordinates and simulations of mesoscale phenomena 23 p3350 N90-28932

AIR FREIGHT
U AIR CARGO

AIR INTAKES
NT ENGINE INLETS
NT HYPERSONIC INLETS
NT SUPERSONIC INLETS

AIR JETS
Rectangular subsonic jet flow field measurements
[NASA-CR-185962] 02 p0219 N90-11255
Rectangular subsonic jet flow field measurements
[NASA-CR-181925] 14 p2023 N90-21598
The entrainment rate for a row of turbulent jets
[NASA-CR-185278] 23 p3269 N90-28504
Particle dispersion in a turbulent shear flow
[AD-A224327] 24 p3467 N90-29590

AIR LAND INTERACTIONS
Global tropospheric chemistry: Chemical fluexes in the global atmosphere
[NASA-CR-186090] 03 p0369 N90-12109
Sounding and surface meteorological data from the Land/Sea Breeze Experiment (LASBEX)
[AD-A216269] 11 p1536 N90-18842
A PBL-radiation model for application to regional numerical weather prediction 12 p1635 N90-19394
Observations of atmospheric electricity, 1988
[GEOPHYSICAL-PUBL-10] 14 p2006 N90-21499
The applications of chemical thermodynamics and chemical kinetics to planetary atmospheres research 20 p2948 N90-26773
Grassland/atmosphere response to changing climate: Coupling regional and local scales
[DE90-015814] 24 p3487 N90-29710

AIR LAUNCHING
Low Earth Orbit Raider (LER) winged air launch vehicle concept
[NASA-CR-186057] 04 p0452 N90-12590

AIR LOCKS
Independent Orbiter Assessment (IOA): Assessment of the life support and airlock support systems, volume 1
[NASA-CR-185581-VOL-1] 02 p0174 N90-10977
Independent Orbiter Assessment (IOA): Assessment of the life support and airlock support systems, volume 2
[NASA-CR-185581-VOL-2] 02 p0174 N90-10978
Independent Orbiter Assessment (IOA): Analysis of the life support and airlock support subsystems
[NASA-CR-185539] 03 p0314 N90-11786
Columbus scientific airlock 18 p2541 N90-24503

AIR MASSES
Are ozone exceedance rates decreasing. Comment on extreme value analysis of environmental time-series: An application to trend detection in ground-level ozone
[AD-A211029] 02 p0239 N90-11357
Atmospheric aerosol size distributions and optical properties found in the marine boundary layer over the Atlantic Ocean
[AD-A210800] 02 p0252 N90-11431
The development of a spatial synoptic climatological index for environmental analysis 06 p0816 N90-14744
Structure and dynamics of the Arizona monsoon boundary
[AD-A217378] 13 p1844 N90-20586
Optimal control of an aircraft flying through a downburst 15 p2053 N90-21765
Calculation of IR propagation statistics in the eastern Atlantic for surveillance system performance assessment 15 p2085 N90-21938
Development and use of a passive technique for measuring nitrogen dioxide in the background atmosphere 16 p2331 N90-23285
Cloud optical parameters as derived from the multispectral cloud radiometer 22 p3215 N90-28239
Observations of anthropogenic cloud condensation nuclei 22 p3218 N90-28251
Instability bursts associated with Extratropical Cyclone Systems (ECSs) and a forecast index of 3 to 12 hour heavy precipitation
[NOAA-TM-NESDIS-30] 22 p3228 N90-28309
An investigation of forcing mechanisms during a surprise tornadic thunderstorm
[PB90-216805] 23 p3352 N90-28940

AIR NAVIGATION
NT ALL-WEATHER AIR NAVIGATION
NT AREA NAVIGATION
NT NAP-OF-THE-EARTH NAVIGATION
Federal Radionavigation Plan, 1988
[PB89-163075] 02 p0148 N90-10346
Design of a Kalman filter for transfer alignment 02 p0149 N90-10848
Control outside of independent surveillance coverage operational concept
[AD-A214163] 07 p0878 N90-15090
Navigation of autonomous air vehicles by passive imaging sensors 08 p1026 N90-15927
Navigation and guidance testing of the Lockheed/US Army Aquila remotely piloted vehicle 08 p1027 N90-15935
Advances in Techniques and Technologies for Air Vehicle Navigation and Guidance
[AGARD-CP-455] 09 p1163 N90-16731
Terrain-aided navigation and target acquisition on the AFTI/F-16 09 p1166 N90-16747
Interoperability issues in the use of satellite-based navigation systems for civil aviation purposes
[AD-A217279] 12 p1602 N90-19223
Joint University Program for Air Transportation Research, 1988-1989
[NASA-CP-3063] 14 p1905 N90-20921
Ridge regression processing 14 p1907 N90-20931
Application of optimal tracking methods to aircraft terrain following
[AD-A221099] 18 p2496 N90-24264
Cognitive requirements for aircraft navigation
[NASA-CR-186933] 21 p2955 N90-26804
FAA Loran early implementation project
[AD-A221866] 21 p2956 N90-26805
Analysis, Design and Synthesis Methods for Guidance and Control Systems
[AGARD-AG-314] 24 p3423 N90-29338
GPS integrity requirements for use by civil aviation 24 p3423 N90-29339
Combining LORAN and GPS: The best of both worlds 24 p3424 N90-29343
Techniques for autonomous GPS integrity monitoring 24 p3424 N90-29345
An analysis of GPS as the sole means navigation system in US Navy aircraft 24 p3425 N90-29350

AIR PIRACY
Aviation security: Corrective actions underway, but better inspection guidance still needed. Report to the Chairwoman, Government Activities and Transportation Subcommittee, Committee on Government Operations, House of Representatives
[GAO/RCED-88-160] 17 p2347 N90-23367

AIR POLLUTION
NT GLOBAL AIR POLLUTION
NT INDOOR AIR POLLUTION
International impacts of global climate change: Testimony to House Appropriations Subcommittee on Foreign Operations, Export Financing and Related Programs
[DE89-014004] 01 p0085 N90-10482
International Conference on Aerosols and Background Pollution Abstracts
[AD-A210970] 01 p0085 N90-10483
Geophysical monitoring for climatic change number 16
[PB89-159628] 01 p0087 N90-10494
Managing human exposure and health risks: An integrated approach and the role of uncertainty
[DE89-008611] 01 p0092 N90-10525
Hydrazine dosimetry 02 p0206 N90-11178

Potential effects of global climate change on the United States. Executive summary. Draft
[PB89-161046] 02 p0237 N90-11350
Potential effects of global climate change on the United States. Volume 1: Regional studies. Draft
[PB89-161053] 02 p0238 N90-11351
Potential effects of global climate change on the United States. Volume 2: National studies. Draft
[PB89-161061] 02 p0238 N90-11352
Improved pattern recognition techniques for real time operation
[AD-A211395] 03 p0324 N90-11840
Evaluation and sensitivity analyses results of the MESOPUFF 2 model with CAPTEX (Cross-Appalachian Tracer Experiment) measurements
[PB89-198253] 03 p0368 N90-12103
Methanol fueled vehicles and photochemical models: An evaluation of the state of knowledge
[PB89-214225] 03 p0419 N90-12410
Contribution of deforestation to atmospheric CO2 and reforestation as an option to control CO2
[DE89-017255] 04 p0516 N90-12979
Development of an inventory of materials potentially sensitive to ambient atmospheric acidity in the South Coast Air Basin
[PB89-224604] 04 p0516 N90-12982
Air quality simulation model performance for one-hour averages
[PB89-233506] 05 p0665 N90-13890
Observations of stratospheric HCl: 1975-1985
[AERONOMICA-ACTA-A-349-1989] 05 p0666 N90-13892
Profile measurements of sulfur dioxide, nitrogen oxides, and nitric acid deposition velocities in California's south coast air basin
[PB90-104001] 06 p0808 N90-14703
Proceedings of the US/FRG (Fed. Republic of Germany) research symposium: Effects of Atmospheric Pollutants on the Spruce-Fir Forests of the Eastern United States and the Fed. Republic of Germany
[PB90-107160] 06 p0808 N90-14704
International Conference on Global and Regional Atmospheric Environmental Chemistry and visit to Hangzhou, China, foreign trip report
[DE90-000099] 06 p0810 N90-14713
Strategy for monitoring the effects of land use change on atmospheric CO2 concentrations
[DE90-001635] 06 p0812 N90-14722
Nitrogen deposition to forest trees
[DE90-003285] 06 p0812 N90-14726
Extraterrestrial halogen and sulfur content of the stratosphere
[DE89-017623] 06 p0815 N90-14736
Characterization of chemicals on engine exhaust particles
[AD-A213566] 07 p0882 N90-15106
A methodology for evaluating heavy gas dispersion models
[AD-A214009] 07 p0887 N90-15131
Variability of cultivar responses to ozone
[PB89-225460] 07 p0956 N90-15528
Long-term worldwide environmental effects caused by acid rain from fossil fuels
[DE90-001534] 07 p0956 N90-15533
International aspects of restrictions of ozone-depleting substances
[DE90-001813] 07 p0957 N90-15534
Acid deposition
[DE90-003959] 07 p0958 N90-15544
Vertical distribution of pollutants in the presence of convective storms
[DE90-002590] 07 p0960 N90-15549
Environmental, health, and CFC substitution aspects of the ozone depletion issue
[DE90-004404] 08 p1099 N90-16383
Simulation of pollutant transport using a mesoscale grid circulation model
[GKSS-89/E/24] 08 p1099 N90-16385
Evaluation of the use of flat terrain models versus complex terrain screening models in estimating pollutant transport and deposition in complex terrain
[DE90-005271] 09 p1245 N90-17223
Chamber investigations of the fate of diesel emissions in the atmosphere, volume 1, task 3
[PB90-114422] 10 p1405 N90-18103
Chamber investigations of the fate of diesel emissions in the atmosphere. Volume 2: AMES assay and GCMS final data reports and gas phase projections
[PB90-114430] 10 p1405 N90-18104
Modeling the effects of air pollution on forest ecosystems: Considerations for applying a model to Southeast Asia
[DE90-004937] 10 p1406 N90-18110
Photointerpretation with instruments for evaluation of environmental impact: Mata Atlantica in Cubata
[INPE-4910-PRE/1511] 11 p1531 N90-18817
Tropospheric chemistry of natural hydrocarbons and energy-related pollutants: Biosphere/climate feedbacks
[DE90-005643] 11 p1532 N90-18820
Transport of atmospheric aerosols above the Sierra Nevada slopes
[PB90-120288] 12 p1685 N90-19675
Development of an atmospheric diffusion model in fog (1). Literature review of scavenging process by precipitation
[DE89-782318] 12 p1685 N90-19676
Chemical composition of precipitation and wet/dry deposition of sulfur compounds around the coastal area
[DE89-782324] 12 p1685 N90-19677
Proceedings of the 2nd United States/USSR Symposium on Air Pollution Effects on Vegetation Including Forest Ecosystems
[PB90-127119] 12 p1685 N90-19678
The RADM 2 gas-phase chemical mechanism
12 p1686 N90-19684
Simulation of the propagation of radiactive substances from the example of Chernobyl (USSR)
12 p1686 N90-19685
Implementation of the RADM/EURAD models on the great calculation system of the Juelich KFA
12 p1687 N90-19687
GeoNet 88: Calculation connection system concept for the EURAD project 12 p1687 N90-19688
Validation of the EURAD cloud modules
12 p1687 N90-19693
Estimation of the distribution of SO2 and NOX emission in Europe 12 p1688 N90-19699
Emission data for the EURAD project
12 p1688 N90-19700
The EURAD model in EUROTRAC
12 p1689 N90-19701
Predicting effects of global climate change on reservoir water quality and fish habitat
[DE90-003674] 12 p1689 N90-19704
Air pollution-caused changes in photosynthesis: Effects on plant growth and rhizosphere functions
[DE90-007184] 13 p1829 N90-20501
The Terrain-Responsive Atmospheric Code (TRAC) project plan: Development of a hazardous materials dispersion modeling capability with application to ambient air monitoring network design
[DE90-007293] 13 p1829 N90-20502
Transformation and deposition of airborne gaseous and particulate pollutants during transport over the Baltic Sea
[PUBL-AIR-QUALITY-5] 14 p2003 N90-21478
Effects of Air Pollution on Western Forests
[PB90-131111] 14 p2003 N90-21481
An evaluation of the relationship between the production and use of energy and atmospheric methane emissions
[DE90-007982] 14 p2004 N90-21487
Proceedings of the Conference on Technology-Based Confidence Building: Energy and Environment
[CNSS-PAPERS-22] 15 p2125 N90-22152
The laminar flow element: Its use as a flow standard
[PB90-129677] 15 p2126 N90-22157
The sources and chemistry of late winter Arctic tropospheric aerosols
[PB90-131988] 15 p2126 N90-22158
HCl monitor 16 p2209 N90-22599
Airliner cabin ozone: An updated review
[AD-A219264] 16 p2276 N90-22970
National emissions standards for hazardous air pollutants application for approval of construction SP-100 ground engineering system test site
[DE90-007985] 16 p2316 N90-23203
Effects of air temperature on atmospheric CO2-plant growth relationships
[DE90-010159] 17 p2420 N90-23793
Aerodynamic development perspective for traffic aeroplanes
[DGLR-89-141] 18 p2495 N90-24260
National Aeronautics and Space Administration (NASA)/American Society for Engineering Education (ASEE) Summer Faculty Fellowship Program-1989, volume 1
[NASA-CR-185601-VOL-1] 18 p2627 N90-24972
Remote sensing for better understanding of the system Earth 19 p2706 N90-25399
Global changes in tropospheric chemistry
19 p2708 N90-25411
Tools for mapping environmental monitoring data
[PB90-129685] 19 p2712 N90-25432
Southern California air quality study: Toxic air contaminants, task 1
[PB90-171570] 19 p2712 N90-25437
The effects of urban air pollution on solar radiation
[DE89-009455] 19 p2712 N90-25438
Catching our breath: Next steps for reducing urban ozone
[PB90-130451] 20 p2883 N90-26398
Measurements of tropospheric nitric acid over the Western United States and Northeastern Pacific Ocean
[NASA-TM-103470] 20 p2883 N90-26399
Results from global tropospheric sulphur simulations
20 p2885 N90-26413
Atmospheric dispersion of solid and liquid rocket propellants
[AD-A221293] 21 p3020 N90-27173
Evaluation of the role of ozone, acid deposition, and other airborne pollutants in the forests of eastern North America
[PB90-184896] 22 p3197 N90-28140
Aircraft measurements of pollution species near Bermuda and the east coast of the United States during CASE-WATOX
[PB90-159450] 22 p3197 N90-28141
Options for controlling the global warming impact from motor vehicles
[PB90-161688] 22 p3197 N90-28142
Lidar observations of stratospheric aerosols in 1988
[PB90-180670] 22 p3198 N90-28145
Quality assurance support for the National Atmospheric Deposition Program and national trends network monitoring activities: 1987-1990
[PB90-187162] 22 p3198 N90-28149
Source emission test of gas turbine engine test facility, Kelly AFB, TX
[AD-A223869] 23 p3282 N90-28571
The distribution of middle tropospheric carbon monoxide during early October 1984
[NASA-TM-103485] 23 p3346 N90-28906
National air pollutant emission estimates, 1940-1988
[PB90-199266] 23 p3346 N90-28908
National air quality and emissions trends report, 1988
[PB90-200114] 23 p3346 N90-28909
The global cycle of reactive nitrogen
[DE90-015041] 23 p3348 N90-28919
Acid deposition: No such thing as a free launch
[DE90-015085] 23 p3348 N90-28920
Tropospheric nitrogen: The influence of anthropogenic sources on distributions and deposition, executive summary
[DE90-015401] 23 p3348 N90-28922
Diffusion in the surface layer of the convective boundary layer
[AD-A224125] 23 p3349 N90-28924
Atmospheric methane data for the period 1983-1985 from the NOAA/GMCC global cooperative flask sampling network
[PB90-208588] 24 p3486 N90-29701
Success of EPA's stratospheric ozone engineering research
[PB90-246265] 24 p3487 N90-29706
Effects of increased CO2 on forest response
[DE90-015406] 24 p3487 N90-29708
SamTrack: A sample tracking system for environmental monitoring
[DE90-016026] 24 p3488 N90-29712

AIR PURIFICATION
Independent Orbiter Assessment (IOA): CIL issues resolution report, volume 2
[NASA-CR-185524-VOL-2] 02 p0170 N90-10955
Space Station Freedom environmental control and life support system phase 3 simplified integrated test detailed report
[NASA-TM-4204] 16 p2207 N90-22593

AIR QUALITY
Geophysical monitoring for climatic change number 16
[PB89-159628] 01 p0087 N90-10494
Interrelation of experimental exposure and ambient air quality data for comparison of ozone exposure indices and estimating agricultural losses
[PB89-195036] 02 p0238 N90-11353
Final Environmental Impact Statement for the Galileo Mission (Tier 2)
[NASA-TM-101825] 03 p0367 N90-12102
Review of the national ambient air quality standards for lead: Exposure analysis methodology and validation
[PB89-207914] 03 p0368 N90-12104
Sensitivity of a regional oxidant model to variations in climate parameters, volume 1 and 2
[PB89-224943] 04 p0516 N90-12981
Air quality simulation model performance for one-hour averages
[PB89-233506] 05 p0665 N90-13890
Variability of cultivar responses to ozone
[PB89-225460] 07 p0956 N90-15528
Environmental surveillance data
[DE90-001275] 07 p0956 N90-15532
Environmental, health, and safety concerns associated with nonpetroleum fuel use in US transportation
[DE90-004367] 08 p1099 N90-16362
Comparison of emissions of transit buses using methanol and diesel fuel
[DE90-005652] 10 p1391 N90-18044

Controlling Summer Heat Islands: Proceedings
[DE90-008075] 13 p1830 N90-20508
Final Safety Analysis Report for the Ulysses Mission. Volume 3 (Book 1): Nuclear risk analysis document
[DE90-008691] 14 p1939 N90-21101
Effects of Air Pollution on Western Forests
[PB90-131111] 14 p2003 N90-21481
Global distribution of organo-bromine gases
15 p2124 N90-22150
Prevention of significant deterioration application for approval to construct SP-100 Ground Engineering System Test Site
[DE90-007986] 15 p2166 N90-22381
HCl Vapor Characterization and Detection. JANNAF Safety and Environmental Protection Subcommittee Workshop
[AD-A216252] 16 p2208 N90-22596
Tools for mapping environmental monitoring data
[PB90-129685] 19 p2712 N90-25432
Southern California air quality study: Toxic air contaminants, task 1
[PB90-171570] 19 p2712 N90-25437
Pollutants: Production and methods of reduction
[CIT/SME/VKI/RS/6] 20 p2810 N90-25990
Investigation of the effects of acid deposition on materials
[PB90-158973] 22 p3197 N90-28143
Environmental Research Laboratories programs and plans. FY-1989 and FY-1990 plans
[PB90-169988] 22 p3197 N90-28144
Quality assurance support for the National Atmospheric Deposition Program and national trends network monitoring activities: 1987-1990
[PB90-187162] 22 p3198 N90-28149
Role of grid-based, reactive air quality modeling in policy analysis: Perspectives and implications, as drawn from a case study
[PB90-187204] 22 p3198 N90-28150
Source emission test of gas turbine engine test facility, Kelly AFB, TX
[AD-A223869] 23 p3282 N90-28571
National air quality and emissions trends report, 1988
[PB90-200114] 23 p3346 N90-28909
Diffusion in the surface layer of the convective boundary layer
[AD-A224125] 23 p3349 N90-28924
The Surface Air Sampling Program
[DE90-014873] 24 p3487 N90-29711

AIR SAMPLING
Interrelation of experimental exposure and ambient air quality data for comparison of ozone exposure indices and estimating agricultural losses
[PB89-195036] 02 p0238 N90-11353
Pilot investigation of indoor-outdoor and personal PM10 (thoracic) and associated ionic compounds and mutagenic activity
[PB89-222723] 05 p0673 N90-13920
Analysis of ambient polar volatile organic compounds using chemical ionization-ion trap detector
[PB90-106451] 07 p0956 N90-15529
HCl monitor, phase 2
[AD-A213572] 07 p0958 N90-15542
Aerosol separator for use in aircraft
[PB90-142217] 15 p2125 N90-22155
Development and use of a passive technique for measuring nitrogen dioxide in the background atmosphere 16 p2331 N90-23285
Feasibility study for a microwave-powered ozone sniffer aircraft
[NASA-CR-186660] 17 p2353 N90-23397
NASA/USRA high altitude reconnaissance aircraft
[NASA-CR-186685] 18 p2496 N90-24266
Field evaluation of a passive sampling device for hydrazines in ambient air
[NASA-TM-103456] 18 p2578 N90-24686
Airborne chemistry measurements
19 p2707 N90-25405
Terpene concentrations and emissions in a Scots pine forest 20 p2886 N90-26422
Laboratory and field evaluations of extrasensitive sulfur dioxide and nitrogen dioxide analyzers for acid deposition monitoring
[PB90-201062] 22 p3199 N90-28153
The affect of gravity on particle collection in inertial impactors
[DE90-013372] 23 p3393 N90-29173
The Surface Air Sampling Program
[DE90-014873] 24 p3487 N90-29711
SamTrack: A sample tracking system for environmental monitoring
[DE90-016026] 24 p3488 N90-29712

AIR SEA INTERACTIONS
U AIR WATER INTERACTIONS

AIR SICKNESS
U MOTION SICKNESS

AIR START
In flight relight tests on AM-X single engine fly-by-wire aircraft 02 p0152 N90-10869

AIR TO AIR MISSILES
NT SIDEWINDER MISSILES
Analysis and testing of a high performance air-air missile 01 p0014 N90-10069
Optimal and on-board near-optimal midcourse guidance 02 p0150 N90-10857
Preliminary airworthiness evaluation of the AH-64A equipped with the Air To Air Stinger (ATAS) missile system
[AD-A213030] 05 p0579 N90-13374
An autopilot design methodology for bank-to-turn missiles
[AD-A213379] 05 p0583 N90-13399
A real time evaluation of the use of a perspective format to promote situational awareness in users of air to air tactical displays 23 p3359 N90-28981

AIR TO AIR REFUELING
Visual servoing for autonomous aircraft refueling
[AD-A216042] 11 p1455 N90-18386

AIR TO AIR ROCKETS
U AIR TO AIR MISSILES

AIR TO SURFACE MISSILES
Navigation up-date using radar mapping: Assessment and optimisation simulation tool
08 p1026 N90-15928

AIR TRAFFIC
Safer skies with TCAS: Traffic Alert and Collision Avoidance System
[PB89-169221] 01 p0004 N90-10016
FAA air traffic activity: Fiscal year 1988
[AD-A211338] 04 p0449 N90-12570
National Airspace System airspace management operational concept
[DOT/FAA/DS-89/29] 05 p0577 N90-13361
Preliminary design of four aircraft to service the California Corridor in the year 2010: The California Condor, California Sky-Hopper, high capacity short range transport tilt rotor aircraft needed to simplify intercity transportation
[NASA-CR-186232] 06 p0724 N90-14226
Turbulence spectral widths view angle independence as observed by Doppler radar
[DOT/FAA/SA-89/2] 07 p0963 N90-15566
Dallas/Fort Worth simulation. Volume 2: Appendixes D, E, and F
[AD-A216613] 11 p1454 N90-18380
US civil airmen statistics: Calendar year 1989
[AD-A220438] 17 p2343 N90-23342
IFR aircraft handled forecast by air route traffic control center: Fiscal years 1990 to 2005
[AD-A220312] 18 p2496 N90-24263
An aircraft noise study in Norway
18 p2611 N90-24872
Public-sector aviation issues, 1987 to 1988 graduate research award papers
[PB90-191206] 22 p3110 N90-27667
Airport capacity enhancement plan 1989
[PB90-197997] 23 p3270 N90-28507
Communications Interface Driver (CID) software principles of operation
[DOT/FAA/CT-TN89/46] 24 p3526 N90-29937

AIR TRAFFIC CONTROL
NT AUTOMATED EN ROUTE ATC
NT RADAR APPROACH CONTROL
National airspace system approach and departure sequencing operational concept
[NAS-SR-1322] 01 p0004 N90-10017
Design of a final approach spacing tool for TRACON air traffic control
[NASA-TM-102229] 02 p0147 N90-10841
Ground and Obstacle Avoidance (GOA) concept of operations
[DOT/FAA/DS-89/08] 02 p0150 N90-10855
A simulation study of landing time allocation procedures for use in computer-assisted air traffic management systems
[AD-A212159] 03 p0303 N90-11722
On the generation of a variable structure airport surface traffic control system
[AD-A211306] 03 p0304 N90-11724
The 1987 survey of track keeping and altitudes on Heathrow and Gatwick standard instrument departure routes (DAY)
[CAA-PAPER-88010] 03 p0305 N90-11729
FAA air traffic activity: Fiscal year 1988
[AD-A211338] 04 p0449 N90-12570
Development and evaluation at ATCEU of executive and support operations, phase 4A/3D --- ATCEU (Air Traffic Control Evaluation Unit)
[CAA-PAPER-88017] 04 p0449 N90-12572
Operational trial of effect of raising minimum stack level in Heathrow stacks
[CAA-PAPER-89003] 04 p0449 N90-12573
Parallel approach separation and controller performance: A study of the impact of two separation standards
[DOT/FAA/CT-TN89/50] 04 p0449 N90-12574
Software fault tolerance
[RSRE-MEMO-4237] 04 p0450 N90-12575
Aircraft Reply and Interference Environment Simulator (ARIES) hardware principles of operation. Volume 2: Appendixes
[DOT/FAA/CT-TN88/4-2] 04 p0484 N90-12781
Aircraft Reply and Interference Environment Simulator (ARIES) hardware principles of operation, volume 1
[DOT/FAA/CT-TN88/4-1] 04 p0484 N90-12782
Assessment of voice coders for ATC/pilot voice communications via satellite digital communication channels
[CAA-PAPER-89004] 04 p0489 N90-12807
Fine resolution errors in secondary surveillance radar altitude reporting amongst aircraft transmitting the conspicuity codes 4321 and 4322
[RSRE-88004] 04 p0490 N90-12816
National Airspace System airspace management operational concept
[DOT/FAA/DS-89/29] 05 p0577 N90-13361
An update to the system safety study of TCAS 2
[DOT/FAA/SA-89/3] 05 p0577 N90-13363
Computer-based tools for assisting air traffic controllers with arrivals flow management
[RSRE-88001] 05 p0577 N90-13366
Flight deck automation: Promises and realities
[NASA-CP-10036] 05 p0580 N90-13384
National airspace system monitoring operational concept
[NAS-SR-1330] 06 p0722 N90-14214
Adaptive clutter rejection filters for airborne Doppler weather radar applied to the detection of low altitude windshear
[NASA-CR-186211] 06 p0766 N90-14453
Control outside of independent surveillance coverage operational concept
[AD-A214163] 07 p0878 N90-15090
Piloted simulation of a ground-based time-control concept for air traffic control
[NASA-TM-101085] 08 p1020 N90-15898
FAA air traffic control operations concepts. Volume 7: ATCT (Airport Traffic Control Towers) tower controllers
[AD-A210455] 09 p1163 N90-16730
National airspace system plan: Facilities, equipment, associated development and other capital needs
[AD-A215882] 11 p1453 N90-18373
Delivery performance of conventional aircraft by terminal-area, time-based air traffic control: A real-time simulation evaluation
[NASA-TP-2978] 11 p1454 N90-18378
Dallas/Fort Worth simulation. Volume 2: Appendixes D, E, and F
[AD-A216613] 11 p1454 N90-18380
Symposium on air traffic control training for tomorrow's technology
[PB90-127325] 12 p1601 N90-19216
Interoperability issues in the use of satellite-based navigation systems for civil aviation purposes
[AD-A217279] 12 p1602 N90-19223
Operational evaluation of initial data link air traffic control services, volume 1
[DOT/FAA/CT-90/1-VOL-1] 12 p1648 N90-19472
Joint University Program for Air Transportation Research, 1988-1989
[NASA-CP-3063] 14 p1905 N90-20921
Investigation of air transportation technology at the Massachusetts Institute of Technology, 1988-1989
14 p1905 N90-20922
Automatic speech recognition in air traffic control
14 p1905 N90-20923
Cockpit display of hazardous wind shear information
14 p1905 N90-20924
Investigation of air transportation technology at Princeton University, 1988-1989
14 p1907 N90-20935
Plan for the FAA air traffic operational evaluation of the Automated Surface Observing System (ASOS)
[DOT/FAA/CT-TN89/58] 14 p1914 N90-20968
Feasibility of using frequency offset on very high frequency air/ground voice channels
[DOT/FAA/CT-TN89/71] 14 p1964 N90-21248
National airspace system air-ground communications operational concept
[DOT/FAA/DS-90/2] 14 p1964 N90-21249
Meteorologist Weather Processor (MWP) integration test plan
[DOT/FAA/CT-TN89/62] 14 p2007 N90-21500
Windshear case study: Denver, Colorado, July 11, 1988
[DOT/FAA/DS-89/19] 14 p2008 N90-21509

A conflict analysis of 4D descent strategies in a metered, multiple-arrival route environment
[NASA-CR-182019] 15 p2055 N90-21772
FAA (Federal Aviation Administration) aviation forecasts, fiscal years 1990-2001
[AD-A219165] 16 p2195 N90-22530
Analysis of sequencing and scheduling methods for arrival traffic
[NASA-TM-102795] 17 p2348 N90-23373
Simulator evaluation of the final approach spacing tool
[NASA-TM-102807] 17 p2348 N90-23374
Preliminary evaluation of a small wearable display
[AD-A219867] 17 p2350 N90-23385
Effects of monitoring under high and low taskload on detection of flashing and colored radar targets
[AD-A220313] 17 p2439 N90-23895
IFR aircraft handled forecast by air route traffic control center: Fiscal years 1990 to 2005
[AD-A220312] 18 p2496 N90-24263
Automatic speech recognition in air-ground data link
18 p2640 N90-25037
National Airspace System (NAS) software life cycle management study
[AD-A221180] 19 p2657 N90-25122
The Federal Aviation Administration plan for research, engineering and development. Volume 2: Project descriptions
[AD-A221264] 19 p2800 N90-25931
Aviation safety: Serious problems continue to trouble the air traffic control work force. Report to congressional requesters
[GAO/RCED-89-112] 20 p2805 N90-25959
The disturbance processes on the data links of the mode-S air traffic control system
[ETN-90-99990] 20 p2806 N90-25965
Mobile satellite communications for civil aviation
[NLR-MP-88066-U] 20 p2855 N90-26238
A measurement of the effectiveness of the Airway Science Program to meet Federal Aviation Administration work force needs
[NIAR-90-5] 20 p2934 N90-26694
Dallas/Fort Worth simulation, volume 1
[DOT/FAA/CT-TN89/28-VOL-1] 21 p2955 N90-26802
Data link test and analysis system/ATCRBS transponder test system technical reference
[DOT/FAA/CT-TN90/7] 21 p2955 N90-26803
Atlanta tower simulation, volume 1
[DOT/FAA/CT-TN89/27-VOL-1] 21 p2961 N90-26835
Atlanta tower simulation. Volume 2: Appendixes
[DOT/FAA/CT-TN89/27-VOL-2] 21 p2961 N90-26836
Real-time adaptive aircraft scheduling
[NASA-CR-177558] 22 p3110 N90-27669
Flight service automation system, model 1 full capacity, NAS operational test and evaluation integration test plan
[DOT/FAA/CT-TN90/4] 22 p3111 N90-27672
Integrated Air Traffic Management
[DLR-MITT-89-23] 22 p3112 N90-27676
Air traffic management in Europe: Structure, tasks, potential 22 p3112 N90-27677
Airline requirements for a future air traffic management system 22 p3112 N90-27678
R and D aspects of the future operational concept of the BFS 22 p3112 N90-27679
Four-dimensional planner: A ground based planning system for time accurate approach guidance 22 p3113 N90-27683
Development of a COMPAS prototype for the ATC Centre at Frankfurt (Fed. Republic of Germany) 22 p3113 N90-27684
Safety net functions 22 p3113 N90-27685
Approach towards a future integrated airport surface traffic management 22 p3113 N90-27686
Experimental study towards a future airport ground movement simulator 22 p3113 N90-27687
Aspects of data link applications for ATC purposes 22 p3113 N90-27688
Application of a company data link at Lufthansa German Airlines 22 p3113 N90-27689
PHARE: Concept and programme 22 p3114 N90-27690
Integration of flight management and air traffic management systems
[RAE-TM-FM-41] 22 p3114 N90-27693
Dallas/Forth Worth simulation. Phase 2: Triple simultaneous parallel Instrument Landing System (ILS) approaches (turbojets)
[DOT/FAA/CT-90/2] 23 p3270 N90-28509
Communications Interface Driver (CID) test plan
[DOT/FAA/CT-TN89/35] 23 p3319 N90-28762
Analysis, Design and Synthesis Methods for Guidance and Control Systems
[AGARD-AG-314] 24 p3423 N90-29338
Study improvement training facilities ground control air traffic controllers. Part 1: Alternative solutions and their consequences
[FEL-89-A257-PT-1] 24 p3431 N90-29380
Study improvement training facilities ground control air traffic controllers. Part 2: Functional analysis approach control trainer
[FEL-89-A260-PT-2] 24 p3436 N90-29409

AIR TRAFFIC CONTROLLERS (PERSONNEL)

FAA air traffic control operations concepts. Volume 7: ATCT (Airport Traffic Control Towers) tower controllers
[AD-A210455] 09 p1163 N90-16730
Delivery performance of conventional aircraft by terminal-area, time-based air traffic control: A real-time simulation evaluation
[NASA-TP-2978] 11 p1454 N90-18378
Symposium on air traffic control training for tomorrow's technology
[PB90-127325] 12 p1601 N90-19216
Meteorologist Weather Processor (MWP) integration test plan
[DOT/FAA/CT-TN89/62] 14 p2007 N90-21500
Effects of monitoring under high and low taskload on detection of flashing and colored radar targets
[AD-A220313] 17 p2439 N90-23895
From where they look to what they think: Determining controller cognitive strategies from oculometer scanning data 18 p2641 N90-25041
Aviation safety: Conditions within the air traffic control work force. Fact sheet for congressional requesters
[GAO/RCED-89-113FS] 20 p2805 N90-25958
Aviation safety: Serious problems continue to trouble the air traffic control work force. Report to congressional requesters
[GAO/RCED-89-112] 20 p2805 N90-25959
A measurement of the effectiveness of the Airway Science Program to meet Federal Aviation Administration work force needs
[NIAR-90-5] 20 p2934 N90-26694
Atlanta tower simulation, volume 1
[DOT/FAA/CT-TN89/27-VOL-1] 21 p2961 N90-26835
Atlanta tower simulation. Volume 2: Appendixes
[DOT/FAA/CT-TN89/27-VOL-2] 21 p2961 N90-26836
Airline requirements for a future air traffic management system 22 p3112 N90-27678
R and D aspects of the future operational concept of the BFS 22 p3112 N90-27679
Four-dimensional planner: A ground based planning system for time accurate approach guidance 22 p3113 N90-27683
Approach towards a future integrated airport surface traffic management 22 p3113 N90-27686
Neurophysiological correlates of information processing abilities during divided attention situations in air traffic controllers 23 p3360 N90-28989
Study improvement training facilities ground control air traffic controllers. Part 2: Functional analysis approach control trainer
[FEL-89-A260-PT-2] 24 p3436 N90-29409
Ability and metacognitive determinants of skill acquisition and transfer
[AD-A224589] 24 p3499 N90-29776

AIR TRANSPORTATION

New energy conversion techniques in space, applicable to propulsion
[AIAA-79-1338] 01 p0028 N90-10145
Study of high-speed civil transports
[NASA-CR-4235] 05 p0578 N90-13370
Flight deck automation: Promises and realities
[NASA-CP-10036] 05 p0580 N90-13384
California air transportation study: A transportation system for the California Corridor of the year 2010
[NASA-CR-186219] 06 p0722 N90-14212
UK airmisses involving commercial air transport, September to December 1988
[ISSN-0951-6301] 08 p1019 N90-15897
Fire hardening of aircraft through upgrades of materials and designs 10 p1315 N90-17605
Joint University Program for Air Transportation Research, 1988-1989
[NASA-CP-3063] 14 p1905 N90-20921
Investigation of air transportation technology at the Massachusetts Institute of Technology, 1988-1989 14 p1905 N90-20922
Automatic speech recognition in air traffic control 14 p1905 N90-20923
Investigation of air transportation technology at Princeton University, 1988-1989 14 p1907 N90-20935
Aeronautics and space report of the President: 1987 activities 15 p2181 N90-22462
FAA (Federal Aviation Administration) aviation forecasts, fiscal years 1990-2001
[AD-A219165] 16 p2195 N90-22530
US civil airmen statistics: Calendar year 1989
[AD-A220438] 17 p2343 N90-23342
The cost of air service fragmentation
[TT-9010] 24 p3422 N90-29334

AIR WATER INTERACTIONS

Investigations of polar air stream cyclogenesis based on numerical simulations with a mesoscale model
[PB89-214563] 03 p0373 N90-12132
Equatorial oceanic response to forcing on time scales from days to months
[PB89-206775] 03 p0377 N90-12147
On the statistics of El Nino occurrences and the relationship of El Nino to volcanic and solar/geomagnetic activity
[NASA-TP-2948] 03 p0429 N90-12456
Current velocity and hydrographic observations in the southwestern North Atlantic Ocean: Subtropical Atlantic Climate Studies (STACS), 1988
[PB89-230825] 04 p0521 N90-13010
A forecasting system using the parabolic equation: Application to surface-to-air propagation in the presence of elevated layers 06 p0760 N90-14420
Physical models for aerosol in the marine mixed-layer 06 p0763 N90-14438
A low-order model of the equatorial ocean-atmosphere system 06 p0813 N90-14730
Further research on dynamics of marine atmospheres in tropical cyclones
[AD-A213882] 07 p0984 N90-15571
The chemistry and dynamics of marine stratocumulus 08 p1102 N90-16381
Sea surface temperature fields derived from aircraft and ship observations during FASINEX 1986
[AD-A215727] 09 p1250 N90-17250
Remote sensing: Environmental effects of surface films
[AD-A216190] 10 p1400 N90-18094
Drifting buoy data from Western Tropical Pacific for the period February 1, 1986 through February 28, 1989
[PB90-113978] 12 p1695 N90-19732
Theoretical modeling studies of the marine planetary
[AD-A217200] 13 p1841 N90-20567
Southern oscillation in the OSU coupled upper ocean/atmosphere GCM
[DE90-008415] 13 p1844 N90-20588
A modeling study of the cloud-topped marine boundary layer
[AD-A218103] 13 p1846 N90-20594
MECCA program documentation
[NOAA-TR-NESDIS-46] 14 p2003 N90-21477
The extension of rapid distortion theory to stratified shear flows 14 p2005 N90-21491
Predictability of weather and climate in a coupled ocean-atmosphere model: A dynamical systems approach
[NASA-CR-186499] 14 p2007 N90-21502
Numerical simulations of the cloud-capped marine boundary layer 14 p2008 N90-21506
Modeling the upper ocean and its interaction with the atmosphere
[DE90-008980] 14 p2008 N90-21511
The Mediterranean marine environment and its effects on aerosols and infrared transmission 15 p2079 N90-21909
The naval oceanic vertical aerosol model 15 p2082 N90-21921
Infrared propagation in the air-sea boundary layer 15 p2083 N90-21926
The relationship between the buoyancy of near-surface air and the potential temperature of the tropopause 15 p2128 N90-22165
Lagrangian model simulation of the turbulent transport of evaporating jet droplets 15 p2128 N90-22168
Southern oscillation simulation in coupled ocean/atmosphere global climate models 15 p2131 N90-22181
Impact of marine boundary layer parameterization on a numerical simulation of cyclogenesis during a cold air outbreak event 16 p2256 N90-22864
Predictability of weather and climate in a coupled ocean-atmosphere model: A dynamical systems approach 16 p2256 N90-22865
A study of the surface layers at an air-water interface
[AD-A219378] 16 p2260 N90-22882
A numerical study of the seasonal variability of the Somali current
[AD-A220708] 17 p2427 N90-23829
Modeling bottom stress in depth-averaged flows
[AD-A218605] 17 p2429 N90-23840
Kinematics under wind waves
[AD-A219541] 17 p2430 N90-23844
The effects of climatological and transient wind forcing on eddy generation in the California current system
[AD-A219858] 17 p2431 N90-23855

Measurements of tropospheric nitric acid over the Western United States and Northeastern Pacific Ocean
[NASA-TM-103470] 20 p2883 N90-26399
Mariners Weather Log, volume 33, number 2, Spring 1989
[PB90-146838] 20 p2889 N90-26443
Mariners Weather Log, volume 33, number 3, Summer 1989
[PB90-146846] 20 p2889 N90-26444
Mariners Weather Log, volume 33, number 4, Fall 1989
[PB90-146853] 20 p2890 N90-26445
Dependence of radar backscatter on the energetics of the air-sea interface
[AD-A221966] 21 p2996 N90-27028
Aircraft measurements of pollution species near Bermuda and the east coast of the United States during CASE-WATOX
[PB90-159450] 22 p3197 N90-28141
Comparative climatology of four marine stratocumulus regimes 22 p3213 N90-28225
An eight-month climatology of marine stratocumulus cloud fraction, albedo, and integrated liquid water 22 p3214 N90-28233
Mesoscale variability of free tropospheric humidity near San Nicolas Island during FIRE 22 p3214 N90-28234
The above-inversion moisture structure observed during FIRE 22 p3215 N90-28235
Diurnal variation in the turbulent structure of the cloudy marine boundary layer during FIRE 1987 22 p3217 N90-28248
Stratus: An interactive steady state mixed layer model for personal computers 22 p3219 N90-28255
Verification of the naval oceanic vertical aerosol model during FIRE 22 p3219 N90-28257
A cloudiness transition in a marine boundary layer 22 p3219 N90-28259
Vertical-velocity skewness in the marine stratus-topped boundary layer 22 p3220 N90-28262
The role of clouds in CO2-induced climate change
[DE90-014380] 23 p3346 N90-28911
Proceedings of the 14th Annual Climate Diagnostics Workshop
[PB90-198573] 23 p3351 N90-28938
Measuring the vertical directional spectra caused by sea surface sound
[AD-A223883] 23 p3354 N90-28957
Rates of vertical mixing, gas exchange, and new productions: Estimates from seasonal gas cycles in the upper ocean near Bermuda
[PB90-244781] 24 p3496 N90-29758

AIRBORNE EQUIPMENT
NT AIRBORNE/SPACEBORNE COMPUTERS
Meeting Review: Workshop on Airborne Instrumentation
[PB89-174775] 01 p0007 N90-10032
SOFIA (Stratospheric Observatory For Infrared Astronomy): A 3m class airborne telescope 05 p0659 N90-13846
Evaluation of the airborne visible-infrared imaging spectrometer for mapping subtle lithological variation
[NASA-CR-186213] 06 p0802 N90-14670
The development of an airborne synthetic aperture radar motion compensation system 09 p1165 N90-16745
Airborne electromagnetic sensing of sea ice thickness
[AD-A214460] 09 p1240 N90-17198
A CCIR aeronautical mobile satellite report 10 p1372 N90-17954
An improved airborne wind measurement technique for the NAE (National Aeronautical Establishment) Twin Otter
[AD-A217978] 13 p1842 N90-20575
Feasibility study for a microwave-powered ozone sniffer aircraft
[NASA-CR-186660] 17 p2353 N90-23397
A theoretical model for airborne radars
[AD-A220735] 17 p2390 N90-23615
Determination of tide heights from airborne bathymetric data
[AD-A220412] 17 p2430 N90-23848
NASA/USRA high altitude reconnaissance aircraft
[NASA-CR-186685] 18 p2496 N90-24266
Users guide for an Airborne Windshear Doppler Radar Simulation (AWDRS) program
[NASA-CR-182025] 19 p2657 N90-25121
Analysis and improved design considerations for airborne pulse Doppler radar signal processing in the detection of hazardous windshear
[NASA-CR-186792] 20 p2890 N90-26448
Aircraft measurements of the turbulence structure in cirrus clouds
[ISSN-0069-5882] 20 p2890 N90-26450
Aircraft measurements of pollution species near Bermuda and the east coast of the United States during CASE-WATOX
[PB90-159450] 22 p3197 N90-28141
Front range lidar, aircraft, and balloon experiment
[PB90-225301] 22 p3212 N90-28218
Airborne lidar/radiometric measurements of cirrus cloud parameters and their application to LOWTRAN radiance evaluations 22 p3227 N90-28298
The use of an airborne lidar for mapping cirrus clouds in FIRE, phase 2 22 p3228 N90-28304
Description of the MARC measuring system
[FEL-89-B170] 23 p3342 N90-28887
Characteristics of pushbroom scanning type radiometer utilizing linear sensors
[NAL-TR-1024] 24 p3472 N90-29625

AIRBORNE INTEGRATED RECONNAISSANCE SYSTEM
Further experiments in variable frame rate analysis for speech recognition
[RSRE-MEMO-4336] 22 p3165 N90-27951
Triphone clustering in the ARM system
[RSRE-MEMO-4357] 22 p3166 N90-27952
Improved front-end analysis in the ARM system: Linear transformations of SRUbank
[RSRE-MEMO-4358] 22 p3166 N90-27953
Experiments with grand variance in the ARM continuous speech recognition system
[RSRE-MEMO-4359] 22 p3166 N90-27954

AIRBORNE LASERS
China-built airborne synchronous laser ranger the new L-8 jet trainer aircraft
[AD-A213835] 07 p0936 N90-15422
An evaluation of an airborne laser profiling system for high precision terrain mapping
[AD-A217025] 11 p1525 N90-18780
Pre-study laser bathymetry
[BCRS-89-26] 15 p2134 N90-22198
Helicopter Airborne Laser Positioning System (HALPS)
[NASA-TM-102814] 17 p2354 N90-23399

AIRBORNE SURVEILLANCE RADAR
Application of superresolution methods for airborne radar 14 p1961 N90-21227
Airborne Doppler radar flight experiments for the detection of microbursts 14 p1963 N90-21243

AIRBORNE/SPACEBORNE COMPUTERS
Optimal and on-board near-optimal midcourse guidance 02 p0150 N90-10857
Realtime processing and display 02 p0155 N90-10886
Independent Orbiter Assessment (IOA): Analysis of the backup flight system
[NASA-CR-185567] 02 p0165 N90-10932
Software and hardware description of the helicopter motion equations for VAX computers
[AD-A213248] 05 p0579 N90-13375
Definition of avionics concepts for a heavy lift cargo vehicle, appendix A
[NASA-CR-183817] 05 p0580 N90-13380
True covariance simulation of the EUVE update filter 05 p0589 N90-13427
A knowledge-based system design/information tool for aircraft flight control systems
[NASA-TM-101704] 05 p0685 N90-13990
Space station Simulation Computer System (SCS) study for NASA/MSFC. Volume 1: Overview and summary
[NASA-CR-183840] 13 p1762 N90-20113
Animation graphic interface for the space shuttle onboard computer 13 p1859 N90-20667
Computer processing of multi-channel electromagnetic data from an airborne geophysical survey system
[PB90-138413] 14 p1965 N90-21253
A comparison of time-optimal interception trajectories for the F-8 and F-15
[NASA-CR-186300] 15 p2050 N90-21753
Preliminary development of an intelligent computer assistant for engine monitoring
[NASA-TM-101702] 15 p2157 N90-22322
A computer graphics system for visualizing spacecraft in orbit 16 p2272 N90-22952
Gamma Ray Observatory (GRO) dynamics simulator requirements and mathematical specifications, revision 1
[NASA-CR-183465] 17 p2362 N90-23447
Software maintenance on Airbus family
[REPT-892-111-101] 17 p2444 N90-23931
Columbus onboard FDIR concept 18 p2500 N90-24286
On-board expert system for manned rendezvous operation assistance 18 p2504 N90-24309
High performance processing system for embedded control applications in space 18 p2507 N90-24330
ACES: Space shuttle flight software analysis expert system 19 p2739 N90-25571
Space operations: NASA efforts to develop and deploy advanced spacecraft computers. Report to the Chairman, Subcommittee on Space Science and Applications, Committee on Science, Space, and Technology, House of Representatives
[GAO/IMTEC-89-17] 19 p2742 N90-25582
Aircraft condition monitoring system for future Airbus aircraft: New concept for programming and data recording 22 p3103 N90-27619
Start-up built-in test for the DISCUS fault tolerant, fly-by-wire computer system 22 p3104 N90-27625
Integration of flight management and air traffic management systems
[RAE-TM-FM-41] 22 p3114 N90-27693

AIRBUS
U EUROPEAN AIRBUS

AIRCRAFT ACCIDENT INVESTIGATION
Aircraft accident report: Aloha Airlines, Flight 243, Boeing 737-200, N73711, near Maui, Hawaii, April 28, 1988
[PB89-910404] 01 p0004 N90-10013
Post crash flight analysis: Visualizing flight recorder data
[AD-A212063] 03 p0302 N90-11715
Aircraft accident report: Delta Air Lines, Inc., Boeing 727-232, N473DA, Dallas-Fort Worth International Airport, Texas, August 31, 1988
[PB89-910406] 08 p1019 N90-15895
RAAF Orion aircraft A9-300 oxygen fire
[AD-A215496] 09 p1162 N90-16725
Aircraft accident report, United Airlines Flight 811, Boeing 747-122, N4713U, Honolulu, Hawaii, February 24, 1989
[PB90-910401] 15 p2050 N90-21748
UK airmisses involving commercial air transport: May - August 1989
[ISSN-0951-6301] 24 p3422 N90-29335

AIRCRAFT ACCIDENTS
NT BIRD-AIRCRAFT COLLISIONS
Aircraft accident report: Aloha Airlines, Flight 243, Boeing 737-200, N73711, near Maui, Hawaii, April 28, 1988
[PB89-910404] 01 p0004 N90-10013
Classification and reduction of pilot error
[NASA-CR-181867] 01 p0004 N90-10014
The human factors relating to escape and survival from helicopters ditching in water
[AGARD-AG-305(E)] 05 p0576 N90-13358
Flight in Adverse Environmental Conditions
[AGARD-CP-470] 07 p0869 N90-15041
The human element: The key to safe, civil operations in adverse weather 07 p0869 N90-15042
See and avoid/cockpit visibility
[AD-A214214] 07 p0877 N90-15084
International Aircraft Occupant Safety Conference and Workshop proceedings
[AD-A214452] 07 p0877 N90-15085
Aircraft accident report: Delta Air Lines, Inc., Boeing 727-232, N473DA, Dallas-Fort Worth International Airport, Texas, August 31, 1988
[PB89-910406] 08 p1019 N90-15895
RAAF Orion aircraft A9-300 oxygen fire
[AD-A215496] 09 p1162 N90-16725
Review of serious aircraft accidents in the Belgian Air Force: Causes and comparison with selection data 09 p1254 N90-17277
Accidents in fighter aircraft caused by human factors. Why do they occur 09 p1254 N90-17278
Psychological reactions of pilots involved in accidents in the Swedish Air Force 09 p1254 N90-17279
The descent from the Olimpus: The effect of accidents on aircrew survivors 09 p1255 N90-17280
Aircraft Fire Safety
[AGARD-CP-467] 10 p1311 N90-17581
Fire safety in civil aviation 10 p1312 N90-17586
Full scale study of a cabin fire in an A300 fuselage section 10 p1313 N90-17592
Aircraft fire safety in the Canadian Forces 10 p1315 N90-17604
The importance of pathophysiological parameters in fire modelling of aircraft accidents 10 p1317 N90-17618
A review of the analytical simulation of aircraft crash dynamics
[NASA-TM-102595] 13 p1753 N90-20068
Annual review of aircraft accident data: US general aviation calendar year 1987
[PB90-138066] 14 p1913 N90-20966
Aircraft accident report, United Airlines Flight 811, Boeing 747-122, N4713U, Honolulu, Hawaii, February 24, 1989
[PB90-910401] 15 p2050 N90-21748
Optimal control of an aircraft flying through a downburst 15 p2053 N90-21765
UK airmisses involving commercial air transport, January - April 1989
[ISSN-0951-6301] 16 p2197 N90-22544

Aircraft crash survival design guide. Volume 1: Design criteria and checklists
[AD-A218434] 16 p2198 N90-22545
Aircraft crash survival design guide. Volume 2: Aircraft design crash impact conditions and human tolerance
[AD-A218435] 16 p2198 N90-22546
Aircraft crash survival design guide. Volume 4: Aircraft seats, restraints, litters, and cockpit/cabin delethalization
[AD-A218437] 16 p2198 N90-22548
Aircraft crash survival design guide. Volume 5: Aircraft postcrash survival
[AD-A218438] 16 p2198 N90-22549
US civil airmen statistics: Calendar year 1989
[AD-A220436] 17 p2343 N90-23342
Economic values for evaluation of Federal Aviation Administration investment and regulatory programs
[AD-A219882] 17 p2343 N90-23343
Aeronautical decisionmaking for air ambulance program administrators
[DOT/FAA/DS-88/8] 17 p2347 N90-23368
Unique failure behavior of metal/composite aircraft structural components under crash type loads
[NASA-TM-102679] 18 p2572 N90-24660
Computational crash dynamics. Project 1.2: Computational crash dynamics analysis
[IAR-89-19] 20 p2804 N90-25956
Annual review of aircraft accident data: US general aviation, calender year 1987
[PB90-138066] 22 p3110 N90-27666
A review of research and development in crashworthiness of general aviation aircraft: Seats, restraints and floor structures
[AD-A221557] 22 p3115 N90-27698

AIRCRAFT APPROACH SPACING
National airspace system approach and departure sequencing operational concept
[NAS-SR-1322] 01 p0004 N90-10017
Design of a final approach spacing tool for TRACON air traffic control
[NASA-TM-102229] 02 p0147 N90-10841
UK airmisses involving commercial air transport, May-August 1988
[ISSN-0951-6301] 03 p0303 N90-11717
Parallel approach separation and controller performance: A study of the impact of two separation standards
[DOT/FAA/CT-TN89/50] 04 p0449 N90-12574
Piloted simulation of a ground-based time-control concept for air traffic control
[NASA-TM-101085] 08 p1020 N90-15898
Analysis of sequencing and scheduling methods for arrival traffic
[NASA-TM-102795] 17 p2348 N90-23373
Four-dimensional navigation and Flight Management Systems 22 p3112 N90-27681
Dallas/Forth Worth simulation. Phase 2: Triple simultaneous parallel Instrument Landing System (ILS) approaches (turbojets)
[DOT/FAA/CT-90/2] 23 p3270 N90-28509

AIRCRAFT BASES
U MILITARY AIR FACILITIES

AIRCRAFT BRAKES
Brake performance of the McDonnell Douglas DC-10-30/40 during high speed, high energy rejected takeoffs
[PB90-917004] 14 p1920 N90-21000

AIRCRAFT CABINS
U AIRCRAFT COMPARTMENTS

AIRCRAFT CARRIERS
Census of US civil aircraft
[PB90-120296] 14 p1905 N90-20920

AIRCRAFT COMMUNICATION
Fine resolution errors in secondary surveillance radar altitude reporting amongst aircraft transmitting the conspicuity codes 4321 and 4322
[RSRE-88004] 04 p0490 N90-12816
Data Link Processor (DLP) operational test and evaluation/integration test plan
[DOT/FAA/CT-TN89/32] 06 p0757 N90-14404
The application of queuing theory to the modelling of CP-140 aircraft communications
[AD-A213479] 07 p0918 N90-15310
Human factors issues in aircraft maintenance and inspection
[AD-A215724] 11 p1542 N90-18875
AIRNET: A real-time comunications network for aircraft
[NASA-CR-186140] 18 p2543 N90-24514
An aeronautical mobile satellite experiment
[NASA-CR-186971] 23 p3287 N90-28593

AIRCRAFT COMPARTMENTS
UHB demonstrator interior noise control flight tests and analysis
[NASA-CR-181697] 04 p0549 N90-13198
Objectives and results of cabin fire research in Germany 10 p1312 N90-17588
New aircraft cabin and cargo flammability standards for transport category aircraft 10 p1312 N90-17589
Fire prevention in transport airplane passenger cabins 10 p1313 N90-17590
Characteristics of transport, aircraft fires measured by full-scale tests 10 p1313 N90-17591
Aircraft internal fires 10 p1313 N90-17593
Fire science and aircraft safety 10 p1314 N90-17596
Forced and natural venting of aircraft cabin fires: A numerical simulation 10 p1314 N90-17597
Time development of convection flow patterns in aircraft cabins under post-crash fire exposure 10 p1314 N90-17598
Fire hardening of an aircraft passenger cabin 10 p1315 N90-17606
New materials for civil aircraft furnishing 10 p1316 N90-17609
Flammability testing of aircraft cabin materials 10 p1316 N90-17611
Method for the evaluation of toxicity of combustion products from aircraft cabin materials: Analysis and results 10 p1316 N90-17612
Smokehoods donned quickly. The impact of donning smokehoods on evacuation times 10 p1317 N90-17614
Preliminary fire extinguishing tests with handheld bottles: A comparison of extinguishing compounds
[DOT/FAA/CT-TN89/60] 10 p1368 N90-17930
Floor pull test of a transport airframe section
[DOT/FAA/CT-TN88/14] 13 p1754 N90-20072
Boeing 727-100 test project (high energy radiated field tests)
[DOT/FAA/CT-88/33] 14 p1964 N90-21247
The Shock and Vibration Digest, volume 21, no. 6 15 p2163 N90-22363
Noise transmission into propeller-driven airplanes 15 p2163 N90-22364
Airliner cabin ozone: An updated review
[AD-A219264] 16 p2276 N90-22970
Fire hazards of aerosol cans in aircraft cargo compartments
[DOT/FAA/CT-89/32] 17 p2347 N90-23369
Problems of internal acoustics in two and three dimensional cavities with deformable walls using the MSC/Nastran code
[DLC/STR-INT-TN-004] 18 p2612 N90-24876
Human factors: The human interface with aircraft interiors
[NIAR-90-18] 20 p2900 N90-26496
B-1B improved windshield development. Volume 2: Magna analysis: Baseline and parametric
[AD-A221501] 21 p2960 N90-26828
Toxicity of thermolysis products from the materials of airplane cockpits
[CEAT-PV-M6/5924/02] 22 p3156 N90-27895
Tests for aircraft interior materials in fire accident
[LR-622] 24 p3423 N90-29337

AIRCRAFT CONFIGURATIONS
A numerical method for solving transonic flow past aircraft in Cartesian coordinates
[NAL-TR-1008] 01 p0001 N90-10003
Computation of transonic flow about stores
[AD-A210402] 01 p0002 N90-10009
Supersonic flow computations over aerospace configurations using an Euler marching solver
[NASA-CR-4085] 01 p0003 N90-10012
Static aeroelastic analysis for generic configuration aircraft
[NASA-TM-89423] 01 p0009 N90-10042
Grid generation procedure using the integral equation method
[NAL-TR-1009] 01 p0111 N90-10630
Robust control design for flight control
[AD-A211957] 03 p0309 N90-11756
Installed tailplane lift-curve slope at subsonic speeds
[ESDU-89029] 07 p0876 N90-15081
Dynamic derivatives of missiles and fighter-type configurations at high angles of attack 10 p1306 N90-17554
Fuselage design for a specified Mach-sliced area distribution
[NASA-TP-2975] 11 p1455 N90-18385
Influence of forebody geometry on aerodynamic characteristics and a design guide for defining departure/spin resistant forebody configurations
[AD-A216714] 11 p1456 N90-18388
A user's manual for the method of moments Aircraft Modeling Code (AMC)
[NASA-CR-186371] 11 p1456 N90-18390
Subsonic flutter analysis using MSC/NASTRAN
[PB90-166786] 14 p1928 N90-21041
Prediction of forces and moments for flight vehicle control effectors. Part 1: Validation of methods for predicting hypersonic vehicle controls forces and moments
[NASA-CR-186571] 15 p2047 N90-21734
Grid patching approaches for complex three-dimensional configurations 15 p2094 N90-21985
Multiblock topology specification and grid generation for complete aircraft configurations 15 p2094 N90-21986
A discussion on issues relating to multiblock grid generation 15 p2095 N90-21991
Automatic grid generation in complex three-dimensional configurations using a frontal system 15 p2096 N90-21992
Unstructured finite element mesh generation and adaptive procedures for CFD 15 p2096 N90-21993
Dynamic ground-effect measurements on the F-15 STOL and Maneuver Technology Demonstrator (S/MTD) configuration
[NASA-TP-3000] 16 p2195 N90-22531
A modeling technique for STOVL ejector and volume dynamics
[NASA-TM-103167] 16 p2202 N90-22566
Supersonic flow computations for an ASTOVL aircraft configuration, phase 2, part 2
[NASA-CR-4284] 16 p2234 N90-22746
The influence of adjacent seating configurations on egress through a type 3 emergency exit
[AD-A218393] 17 p2348 N90-23371
Actuated forebody strakes
[NASA-CASE-LAR-13983-1] 17 p2352 N90-23390
Preliminary design of a supersonic Short Takeoff and Vertical Landing (STOVL) fighter aircraft
[NASA-CR-186670] 17 p2352 N90-23394
Composite reduced Navier Stokes procedures for flow problems with strong pressure interactions
[AD-A219621] 17 p2403 N90-23687
Activities report in aerospace and aerodynamics
[ETN-90-96774] 17 p2487 N90-24224
NASA/USRA high altitude reconnaissance aircraft
[NASA-CR-186685] 18 p2496 N90-24266
Helicopter controllability
[AD-A220078] 18 p2498 N90-24275
Feasibility study for a microwave-powered ozone sniffer aircraft, volume 2
[NASA-CR-186676] 20 p2806 N90-25967
ARLSUPER version 1.0, program users guide
[AD-A222693] 21 p2953 N90-26793
Aircraft lightning protection handbook
[AD-A222716] 22 p3110 N90-27668
Aircraft evacuations: The effect of passenger motivation and cabin configuration adjacent to the exit
[CAA-PAPER-89019] 24 p3423 N90-29336

AIRCRAFT CONSTRUCTION
U AIRCRAFT STRUCTURES

AIRCRAFT CONSTRUCTION MATERIALS
NT AIRFRAME MATERIALS
Conference on Aerospace Transparent Materials and Enclosures (15th) 16-20 January 1989. Volume 2: Sessions 6-9
[AD-A210201] 01 p0006 N90-10024
Composite Blade Structural Analyzer (COBSTRAN) theoretical/programmer's manual
[NASA-TM-101958] 01 p0033 N90-10181
Materials for engine applications above 3000 deg F: An overview
[NASA-TM-100169] 01 p0034 N90-10188
Castings Airworthiness
[AGARD-R-762] 01 p0042 N90-10231
Casting factors imposed by the French regulation for foundry castings used in military aircraft 01 p0042 N90-10233
The question of the casting factor 01 p0043 N90-10238
Choice and characterization of new materials for aerospace applications
[ETN-89-95219] 03 p0320 N90-11819
A new test procedure for a wing made with carbon fiber composites
[ETN-89-95220] 03 p0320 N90-11820
The evolution of light alloys in the aerospace industry
[ETN-89-95216] 03 p0329 N90-11872
Aluminium alloy development for aero engines
[PNR90548] 03 p0330 N90-11874
A vision of the future: The new engine technology
[PNR90566] 04 p0455 N90-12603
Material requirements for future aeroengines
[PNR90595] 04 p0456 N90-12610
Composite materials for future aeroengines
[PNR90584] 04 p0466 N90-12667
The future of non ferrous metals in aerospace engines
[PNR90572] 04 p0475 N90-12720

Fatigue behavior of specimens under compression load spectra
[ETN-89-95207] 04 p0512 N90-12954
An investigation on combined extension and bending of thin sheets with a central crack
[LR-561] 04 p0512 N90-12958
Some new techniques for aircraft fuselage skin tests
[LR-547] 05 p0580 N90-13379
Some aspects of test frequency influence on the fatigue behavior of ARALL
[LR-549] 05 p0620 N90-13616
Design and evaluation of a new biaxial testing method for sheet material (SUPERBAT)
[LR-548] 05 p0656 N90-13824
New Light Alloys
[AGARD-CP-444] 07 p0897 N90-15185
Properties of Al-Li alloys 07 p0898 N90-15191
Putting alloy 2091 to work 07 p0899 N90-15197
Bird impact tests on asymmetric sandwich structures made in Kevlar 49
[CEAT-NT-10/S/83-5] 09 p1162 N90-16727
Bird impact tests on curved structures of the type Sandwich-Kevlar-Nida for normal and angular shooting
[CEAT-NT-10/S/83-4] 09 p1162 N90-16728
New materials for civil aircraft furnishing
10 p1316 N90-17609
Heat release rate measurement for evaluating the flammability of aircraft materials
10 p1316 N90-17610
Flammability testing of aircraft cabin materials
10 p1316 N90-17611
Method for the evaluation of toxicity of combustion products from aircraft cabin materials: Analysis and results 10 p1316 N90-17612
Investigation of the failure modes in a metal matrix composite under thermal cycling
[AD-A216195] 10 p1349 N90-17825
Tensile mechanical properties in flat specimens of 7150-T7751
[INFORME-I-296/88] 10 p1356 N90-17860
Comparative analysis between the mechanical properties of conventional alloys and Al-Li
[INFORME-DT-317/89] 10 p1356 N90-17861
Simple shear tests of the FMI 23.5.06 adhesive cured at low pressure (12 PSI)
[INFORME-I-298/88] 10 p1357 N90-17871
Pressure air tightness tests of laminated panels for wing leading edge heat shields
[INFORME-I-377/89] 10 p1358 N90-17873
Bearing tests in Ti-6Al-4V plates made using superplastic forming
[INFORME-I-357/89] 10 p1396 N90-18068
The manufacturing procedures for composite materials, automation, and robotization
[ETN-90-96232] 11 p1482 N90-18528
Evaluation and choice algorithms of cost optimal prepreg-application processes: Production of strongly charged plane parts made of fiber reinforced plastics
[ETN-90-95895] 12 p1620 N90-19313
Compendium of abstracts and viewgraphs.
[AD-A217189] 13 p1767 N90-20140
Ultrasonic and radiographic evaluation of advanced aerospace materials: Ceramic composites
[NASA-TM-102540] 14 p1989 N90-21401
Boeing/NASA composite components flight service evaluation
[NASA-CR-181898] 16 p2210 N90-22609
Bird impact tests on Kevlar 29 and 49 sandwich structures under straight-on and glancing impact
[REPT-S3-4273-PARTIAL-6] 16 p2212 N90-22617
Bird impact tests on Kevlar plates. Sandwich Kevlar-nida submitted to straight-on and glancing impact
[REPT-S3-4273-PARTIAL-3] 16 p2212 N90-22619
Bird impact tests on structures made of Kevlar 49. Monolithic plates under straight-on impact
[REPT-S3-4273-PARTIAL-1] 16 p2213 N90-22620
The Trickett-Welch Solution to the Behrens-Fisher problem applied to one-sided tolerance limits for random effects model
[AD-A220416] 17 p2465 N90-24086
Investigation on sheet material of 8090 and 2091 aluminium-lithium alloy
[MBB-UT-122/89-PUB] 19 p2652 N90-25090
Damage tolerance demonstration for A310-300 CFPR components
[MBB-UT-012/89-PUB] 19 p2652 N90-25091
Nondestructive x ray methods for characterization of advanced aerospace materials
[DE90-011751] 19 p2699 N90-25356
Towards 2000: The composite engine
[PNR90646] 20 p2811 N90-26000
The impact and requirements of new materials on aeroengines
[PNR90671] 20 p2812 N90-26003
Metal matrix composites and powder processing for aero-engine applications
[PNR90617] 20 p2828 N90-26087
Materials and structures for 2000 and beyond: An attempted forecast by the DLR Materials and Structures Department
[ESA-TT-1154-REV] 20 p2843 N90-26173
Material selection and design: An expert system approach
[PNR90611] 20 p2908 N90-26544
AGARD highlights 90/1 20 p2951 N90-26788
Evaluation of energy absorption of new concepts of aircraft composite subfloor intersections
[NASA-TP-2951] 21 p2959 N90-26823
Design of helicopter components in metal matrix composites
[REPT-100-20-55] 21 p2972 N90-26894
Toxicity of thermolysis products from the materials of airplane cockpits
[CEAT-PV-M6/5924/02] 22 p3156 N90-27895
Toxicological aspects of fire onboard aircrafts: Role of the pressurization and ventilation in the cockpit
[ETN-90-97452] 22 p3233 N90-28335
Static and dynamic characterization of the ATR 72 rods made of Ti 10.2.3 titanium alloy
[REPT-49-238] 23 p3310 N90-28722
Tests for aircraft interior materials in fire accident
[LR-622] 24 p3423 N90-29337
Fatigue, static tensile strength and stress corrosion of aircraft materials and structures. Part 1: Text
[LR-630-PT-1-REV] 24 p3482 N90-29682
Fatigue, static tensile strength and stress corrosion of aircraft materials and structures. Part 2: Figures
[LR-630-PT-2] 24 p3482 N90-29683

AIRCRAFT CONTROL
NT HELICOPTER CONTROL
Classification and reduction of pilot error
[NASA-CR-181867] 01 p0004 N90-10014
Real-time support for high performance aircraft operation
[NASA-CR-185475] 01 p0015 N90-10075
The active flexible wing aeroservoelastic wind-tunnel test program 01 p0024 N90-10119
The active control of an unstable canard aircraft
02 p0156 N90-10894
Robust control design for flight control
[AD-A211957] 03 p0309 N90-11756
Evolution of flight commands in Aeritalia design
[ETN-89-95211] 03 p0309 N90-11759
Integration of a centralized multiplexed control unit into the cockpit of an aircraft
[F6150-DT410-1-88329] 04 p0458 N90-12622
Aircraft SAR simulation Sargen 1.0
[FEL-1989-44] 04 p0491 N90-12823
Aerodynamics of thrust vectoring
[NASA-CR-185074] 05 p0575 N90-13354
A knowledge-based system design/information tool for aircraft flight control systems
[NASA-TM-101704] 05 p0685 N90-13990
Laboratory test methodology for evaluating the effects of electromagnetic disturbances on fault-tolerant control systems
[NASA-TM-101665] 05 p0695 N90-14061
Design of a spanloader cargo aircraft
[NASA-CR-186046] 06 p0722 N90-14216
Turbulence effects of aircraft flight dynamics and control 07 p0871 N90-15055
Aircraft performance enhancement with active compressor stabilization
[AD-A213652] 07 p0879 N90-15097
Relative merits of reactive and forward-look detection for wind-shear encounters during landing approach for various microburst escape strategies
[NASA-TM-4158] 07 p0882 N90-15108
Experimental evaluation of impedance control for robotic aircraft refueling
[AD-A215532] 09 p1167 N90-16755
Results of aircraft open-loop tests of an experimental magnetic leader cable system for guidance during roll-out and turnoff
[NASA-TM-4135] 09 p1169 N90-16767
Design of integrated pitch axis for autopilot/autothrottle and integrated lateral axis for autopilot/yaw damper for NASA TSRV airplane using integral LQG methodology
[NASA-CR-4268] 09 p1169 N90-16768
The 59th Shock and Vibration Symposium, volume 1
[AD-A214578] 09 p1238 N90-17183
Stability characteristics of a combat aircraft with control surface failure
[AD-A216196] 10 p1323 N90-17646
Hypercube expert system shell-applying production parallelism
[AD-A215762] 10 p1418 N90-18173
Possible piloting techniques at hypersonic speeds
[ISL-CO-216/88] 11 p1456 N90-18392
Practical methods for robust multivariable control
[AD-A216937] 11 p1550 N90-18920
Unsteady aerodynamics of delta wings performing maneuvers to high angle of attack
12 p1598 N90-19196
Joint University Program for Air Transportation Research, 1988-1989
[NASA-CP-3063] 14 p1905 N90-20921
Neural networks for aircraft control
14 p1908 N90-20937
Perspectives on the use of rule-based control
14 p1908 N90-20940
Optimization and guidance of flight trajectories in the presence of windshear
[NASA-CR-186163] 15 p2049 N90-21747
The insertion of human dynamics models in the flight control loops of V/STOL research aircraft. Appendix 2: The optimal control model of a pilot in V/STOL aircraft control loops
[NASA-CR-186598] 15 p2055 N90-21776
An adaptive human response mechanism controlling the V/STOL aircraft. Appendix 3: The adaptive control model of a pilot in V/STOL aircraft control loops
[NASA-CR-186599] 15 p2056 N90-21777
Minimum flying qualities. Volume 1: Piloted simulation evaluation of multiple axis flying qualities
[AD-A218560] 16 p2200 N90-22560
Minimum flying qualities. Volume 2: Pilot modeling for flying qualities applications
[AD-A218561] 16 p2201 N90-22561
Minimum flying qualities. Volume 3: Program CC's implementation of the human optimal control model
[AD-A218562] 16 p2201 N90-22562
Application of numerical optimization techniques to control system design for nonlinear dynamic models of aircraft 16 p2287 N90-23032
Preliminary airworthiness evaluation of the RC-12K
[AD-A219545] 17 p2351 N90-23387
Actuated forebody strakes
[NASA-CASE-LAR-13983-1] 17 p2352 N90-23390
Aircrew neck injuries: A new, or an existing, misunderstood phenomenon 19 p2719 N90-25467
An investigation of the use of singular perturbation methods and modal control theory in the derivation of aircraft control schemes
[MATHS-REPT-A-106] 20 p2814 N90-26014
Aerodynamic/dynamic interaction
[AD-A222263] 21 p2954 N90-26798
Past, present and future: Aircraft integrated monitoring systems: An ever-developing technology
22 p3103 N90-27618
Observer or direct inversion 22 p3103 N90-27622
Performance assessment of MIL-STD-1553B on the avionic systems demonstrator rig of British Aerospace
22 p3104 N90-27624
Scope and conception of the pilot support system ASPIO
[LRT-WE-13-FB-88-1] 22 p3233 N90-28334
Aerodynamics of Combat Aircraft Controls and of Ground Effects
[AGARD-CP-465] 23 p3271 N90-28513
Combat aircraft control requirements
23 p3271 N90-28515
Control research in the NASA high-alpha technology program 23 p3272 N90-28516
Combat aircraft control requirements for agility
23 p3272 N90-28517
Effective optimal control of a fighter aircraft engine
23 p3277 N90-28548
A sensor stabilization/tracking system for unmanned air vehicles
[AD-A224008] 23 p3283 N90-28579
Proprioception in aircraft control
[IZF-1989-43] 23 p3377 N90-29082
An expert system to perform on-line controller restructuring for abrupt model changes
[NASA-TM-103609] 23 p3385 N90-29121
Evaluation for DLC-Flap Monitoring System of the VSRA
[NAL-TM-607] 24 p3433 N90-29391
Short period control using angular acceleration feedback: Compensation for first lag servo
[NAL-TM-600] 24 p3435 N90-29399

AIRCRAFT DESIGN
NT HELICOPTER DESIGN
Prediction of dynamic derivatives
01 p0012 N90-10055
Marginal release disturbances on advanced missiles
01 p0014 N90-10070
High temperature VSCF (Variable Speed Constant Frequency) generator system
[AD-A210823] 01 p0061 N90-10351
Turbulence management: Application aspects
01 p0066 N90-10378

Low-speed, high-lift aerodynamic characteristics of slender, hypersonic accelerator-type configurations
[NASA-TP-2945] 02 p0145 N90-10830
See and avoid/cockpit visibility
[DOT/FAA/CT-TN89/18] 02 p0148 N90-10843
ATTAS flight testing experiences 02 p0151 N90-10862
P-180 AVANTI: Project and flight test program comprehensive overview 02 p0151 N90-10863
The Experimental Aircraft Flight Test Programme 02 p0152 N90-10865
Flight test techniques adopted by Avions Marcel Dassault-Breguet Aviation 02 p0152 N90-10867
Flight testing and flight research: From the age of the tower jumper to the age of the astronaut 02 p0154 N90-10882
Integrated multidisciplinary design optimization of rotorcraft
[NASA-TM-101642] 02 p0155 N90-10889
Wind tunnel test of CAD USB-STOL semi-borne prototype
[NAL-TM-566] 03 p0299 N90-11696
Computer simulation of aircraft aerodynamics
[NASA-TM-102221] 03 p0300 N90-11699
Development of direct-inverse 3-D methods for applied transonic aerodynamic wing design and analysis
[NASA-CR-186036] 03 p0305 N90-11733
A design procedure for the handling qualities optimization of the X-29A aircraft
[NASA-TM-4142] 03 p0306 N90-11753
Evolution of flight commands in Aeritalia design
[ETN-89-95211] 03 p0309 N90-11759
Stall/spin/flight simulation
[DOT/FAA/CT-88/28] 03 p0310 N90-11765
The aerodynamic experimental center of Aeritalia: Combat aircraft group
[ETN-89-95213] 03 p0311 N90-11766
Choice and characterization of new materials for aerospace applications
[ETN-89-95219] 03 p0320 N90-11819
The evolution of light alloys in the aerospace industry
[ETN-89-95216] 03 p0329 N90-11872
General data processing support from project planning to workshop control
[MBB-UD-526/88-PUB] 03 p0388 N90-12208
On the occasion of the 100th birthday of Ernst Heinkel
[MBB/LW/3015/S/PUB/321] 03 p0436 N90-12494
LFC: A maturing concept
[DOUGLAS-PAPER-7878] 04 p0438 N90-12505
Lockheed laminar-flow control systems development and applications 04 p0438 N90-12506
Laminar flow: The Cessna perspective 04 p0439 N90-12507
Long-range LFC transport 04 p0439 N90-12508
Development flight tests of JetStar LFC leading-edge flight test experiment 04 p0439 N90-12509
The right wing of the LEFT airplane 04 p0439 N90-12510
Research in Natural Laminar Flow and Laminar-Flow Control, part 2
[NASA-CP-2487-PT-2] 04 p0440 N90-12519
Research in Natural Laminar Flow and Laminar-Flow Control, part 3
[NASA-CP-2487-PT-3] 04 p0443 N90-12539
The design of an airfoil for a high-altitude, long-endurance remotely piloted vehicle 04 p0445 N90-12545
The 757 NLF glove flight test results 04 p0445 N90-12546
Nacelle design 04 p0446 N90-12551
Project, implementation, and utilization of composite structures
[ETN-89-95209] 04 p0456 N90-12665
Study of high-speed civil transports
[NASA-CR-4235] 05 p0578 N90-13370
The S.D.G., P.S.D. and the nonlinear airplane
[NLR-MP-88018-U] 05 p0578 N90-13371
Efficient methods for integrated structural-aerodynamic wing optimum design 05 p0579 N90-13376
California air transportation study: A transportation system for the California Corridor of the year 2010
[NASA-CR-186219] 06 p0722 N90-14212
Design of a spanloader cargo aircraft
[NASA-CR-186046] 06 p0722 N90-14216
Preliminary design of four aircraft to service the California Corridor in the year 2010: The California Condor, California Sky-Hopper, high capacity short range transport tilt rotor aircraft needed to simplify intercity transportation
[NASA-CR-186232] 06 p0724 N90-14226
Canard versus aft-tail ride qualities performance and pilot command response 07 p0871 N90-15053
The interference of flightmechanical control laws with those of load alleviation and its influence on structural design 07 p0871 N90-15054
Turbulence effects of aircraft flight dynamics and control 07 p0871 N90-15055
Aircraft performance enhancement with active compressor stabilization
[AD-A213652] 07 p0879 N90-15097
Aluminum-lithium: Application of plate and sheet to fighter aircraft 07 p0900 N90-15202
Application of Lagrangian blending functions for grid generation around airplane geometries
[NASA-CR-186318] 08 p1018 N90-15891
Fuel Tank Technology
[AGARD-R-771] 08 p1021 N90-15904
The repair of aircraft integral fuel tanks in the RAF: A user's view of fuel tank technology 08 p1022 N90-15908
Integral fuel tank certification and test methods 08 p1023 N90-15916
Semi-empirical transition criteria for the design of laminar profiles 08 p1087 N90-16174
The use of prototypes in selected foreign fighter aircraft development programs: Rafale, EAP, Lavi, and Gripen
[AD-A214500] 09 p1159 N90-16707
NASA supercritical airfoils: A matrix of family-related airfoils
[NASA-TP-2969] 09 p1159 N90-16710
Analysis of indirect effects of lightning on a metallic A 300 wing: Test report
[REPT-E87/645800] 09 p1162 N90-16726
Terrain-aided navigation and target acquisition on the AFTI/F-16 09 p1166 N90-16747
Preliminary design of a family of three close air support aircraft
[NASA-CR-186070] 09 p1166 N90-16751
Further development and limited flight testing of the CycloCrane
[AD-A215519] 09 p1167 N90-16754
Preliminary results from a subsonic high angle-of-attack flush airdata sensing (HI-FADS) system: Design, calibration, and flight test evaluation
[NASA-TM-101713] 09 p1168 N90-16758
The integration of stores on modern tactical aircraft: Where we have been, and what we should do for the future 10 p1305 N90-17552
Objectives and results of cabin fire research in Germany 10 p1312 N90-17588
Characteristics of transport, aircraft fires measured by full-scale tests 10 p1313 N90-17591
Aircraft internal fires 10 p1313 N90-17593
Hot surface ignition studies of aviation fluids 10 p1314 N90-17600
US Navy aircraft fire protection technology 10 p1315 N90-17603
Fire hardening of an aircraft passenger cabin 10 p1315 N90-17606
Advanced materials for interior and equipment related to fire safety in aviation 10 p1316 N90-17608
The technology challenge of the advanced tactical fighter: A study of the technology transition process
[AD-A216109] 10 p1320 N90-17630
GTD/UTD: Brief history of successive development of theory and recent advances. Applications to antennas on ships and aircraft 10 p1370 N90-17939
Research on a two-dimensional inlet for a supersonic V/STOL propulsion system. Appendix A
[NASA-CR-174945] 11 p1451 N90-18364
Fuselage design for a specified Mach-sliced area distribution
[NASA-TP-2975] 11 p1455 N90-18385
Influence of forebody geometry on aerodynamic characteristics and a design guide for defining departure/spin resistant forebody configurations
[AD-A216714] 11 p1456 N90-18388
Analysis and design of symmetrical airfoils
[PD-CF-8943] 12 p1601 N90-19213
Flow simulation for aircraft
[NLR-MP-87082-U] 12 p1661 N90-19543
A note on an acoustic response during an engine nacelle flight experiment
[NASA-TM-102585] 12 p1710 N90-19821
Implications of Advanced Technologies for Air and Spacecraft Escape
[AGARD-CP-472] 13 p1751 N90-20054
Development of an ejection seat specification for a new fighter aircraft 13 p1751 N90-20057
Compression pylon
[NASA-CASE-LAR-13777-1] 13 p1755 N90-20078
The NASA digital VGH program. Exploration of methods and final results. Volume 1: Development of methods
[NASA-CR-181909-VOL-1] 13 p1756 N90-20081
The NASA digital VGH program. Exploration of methods and final results. Volume 3: B 727 data 1978-1980: 1765 hours
[NASA-CR-181909-VOL-3] 13 p1756 N90-20082
The NASA digital VGH program: Exploration of methods and final results. Volume 4: B 747 data 1978-1980, 1689 hours
[NASA-CR-181909-VOL-4] 13 p1756 N90-20083
The NASA digital VGH program: Exploration of methods and final results. Volume 5: DC 10 data 1981-1982, 129 hours
[NASA-CR-181909-VOL-5] 13 p1756 N90-20084
Aerofoil design techniques 14 p1916 N90-20978
A system for transonic wing design with geometric constraints based on an inverse method 14 p1917 N90-20983
Numerical optimization of wings in transonic flow 14 p1920 N90-20997
Aerodynamic design via control theory 14 p1920 N90-20998
Conceptual design optimization study
[NASA-CR-4298] 15 p2051 N90-21755
Applications of Mesh Generation to Complex 3-D Configurations
[AGARD-CP-464] 15 p2093 N90-21975
Design and testing of a multiblock grid-generation procedure for aircraft design and research 15 p2094 N90-21984
Multiblock topology specification and grid generation for complete aircraft configurations 15 p2094 N90-21986
Feature-associated mesh embedding for complex configurations 15 p2095 N90-21988
A3I visibility modeling project 15 p2140 N90-22230
Aircraft crash survival design guide. Volume 1: Design criteria and checklists
[AD-A218434] 16 p2198 N90-22545
Aircraft crash survival design guide. Volume 2: Aircraft design crash impact conditions and human tolerance
[AD-A218435] 16 p2198 N90-22546
Aircraft technology management and the related significance of the supercomputer 16 p2277 N90-22975
The use of supercomputers for the design and analysis of constructions 16 p2277 N90-22977
The automation management to support research and development 16 p2277 N90-22978
Design trends for Army/Air Force airplanes in the United States
[NASA-TM-4179] 16 p2342 N90-23338
Aircraft drawings index 17 p2343 N90-23340
Preliminary design of a supersonic Short Takeoff and Vertical Landing (STOVL) fighter aircraft
[NASA-CR-186670] 17 p2352 N90-23394
AVION: A detailed report on the preliminary design of a 79-passenger, high-efficiency, commercial transport aircraft
[NASA-CR-186663] 17 p2353 N90-23395
High speed civil transport
[NASA-CR-186661] 17 p2353 N90-23396
Feasibility study for a microwave-powered ozone sniffer aircraft
[NASA-CR-186660] 17 p2353 N90-23397
Nonflammable hydraulic power system for tactical aircraft. Volume 1: Aircraft system definition, design and analysis
[AD-A218493] 17 p2356 N90-23409
Conceptual design for aerospace vehicles 18 p2641 N90-25043
The FX/90: A proposal in response to a low Reynolds Number station keeping mission
[NASA-CR-186665] 19 p2659 N90-25131
Design of a low cost short takeoff-vertical landing export fighter/attack aircraft
[NASA-CR-186658] 19 p2659 N90-25132
From 1959-1989: 30 years of service experience with ramjets
[PNR90677] 19 p2660 N90-25139
Prediction methodologies for nonlinear aerodynamic characteristics of control surfaces
[NIAR-90-17] 20 p2801 N90-25937
Technical evaluation report on the Fluid Dynamics Panel Symposium on Computational Methods for Aerodynamic Design (Inverse) and Optimization
[AGARD-AR-267] 20 p2803 N90-25947
Formation of design envelope criterion in terms of deterministic spectral procedure
[RAE-TM-SS-9] 20 p2804 N90-25953
Feasibility study for a microwave-powered ozone sniffer aircraft, volume 2
[NASA-CR-186676] 20 p2806 N90-25967
Global Sentry: NASA/USRA high altitude reconnaissance aircraft design, volume 2
[NASA-CR-186820-VOL-2] 20 p2807 N90-25971
A contribution to the economic, optimal dimensioning, and shaping of aircraft structures using a design model
[ETN-90-96966] 20 p2808 N90-25976
Towards 2000: The composite engine
[PNR90646] 20 p2811 N90-26000

Prediction of rotating disc flow and heat transfer in gas turbine engines
[PNR90650] 20 p2812 N90-26001
A computer module used to calculate the horizontal control surface size of a conceptual aircraft design
[NASA-CR-186872] 20 p2903 N90-26515
Lessons learned from the T-46A durability and damage tolerance program 21 p2957 N90-26812
Photoelasticity: A cost effective design tool 21 p2958 N90-26819
The SKY SHARK: An RPV designed to investigate the pressure distribution on a lifting surface
[NASA-CR-186222] 21 p2959 N90-26824
Active control of aerothermoelastic effects for a conceptual hypersonic aircraft
[NASA-TM-102713] 22 p3122 N90-27725
Impact of Emerging NDE-NDI Methods on Aircraft Design, Manufacture, and Maintenance
[AGARD-CP-462] 22 p3184 N90-28068
Inspection reliability 22 p3184 N90-28072
Impact of NDE-NDI methods on aircraft design, manufacture, and maintenance, from the fundamental point of view 22 p3189 N90-28093
Hypersonic Arbitrary-Body Aerodynamics (HABA) for conceptual design
[DE90-014750] 23 p3268 N90-28495
Combat aircraft control requirements for agility 23 p3272 N90-28517
Effects of canard position on the aerodynamic characteristics of a close-coupled canard configuration at low speed 23 p3272 N90-28519
Innovative control concepts and component integration for a generic supercruise fighter 23 p3273 N90-28521
Control of vortex aerodynamics at high angles of attack 23 p3273 N90-28523
Inflight thrust vectoring: A further degree of freedom in the aerodynamic/flight mechanical design of modern fighter aircraft 23 p3274 N90-28528
Dynamic ground effects 23 p3275 N90-28531
Determination of the ground effect on the characteristics of the A320 aircraft 23 p3275 N90-28534
Life cycle cost in the conceptual design of subsonic commercial aircraft, volumes 1 and 2 23 p3275 N90-28535
System reliability optimization of aircraft wings 23 p3275 N90-28536
The aerodynamic design of the oblique flying wing supersonic transport
[NASA-CR-177552] 23 p3276 N90-28540
Energy efficient engine program technology benefit/cost study, volume 2
[NASA-CR-174766-VOL-2] 23 p3280 N90-28565
Situational Awareness in Aerospace Operations
[AGARD-CP-478] 23 p3357 N90-28972
A knowledge-based system design/information tool
[NASA-CR-4316] 23 p3389 N90-29143
Some topics in computational transonic aerodynamics: Revision
[NAL-TR-1018T] 24 p3422 N90-29332
Aircraft evacuations: The effect of passenger motivation and cabin configuration adjacent to the exit
[CAA-PAPER-89019] 24 p3423 N90-29336
Aircraft design for mission performance using nonlinear multiobjective optimization methods
[NASA-CR-4328] 24 p3432 N90-29384
WingDesign: Program for the structural design of a wing cross-section
[LR-627] 24 p3433 N90-29390
A human factors engineering approach to the development and dynamic evaluation of a prototype aircrew seat for military aircraft
[AD-A218283] 24 p3500 N90-29779

AIRCRAFT DETECTION
Identification Friend, Foe or Neutral Joint Test 02 p0154 N90-10881
Temporal attributes of the ambient seismo-acoustic environment: La Junta, Colorado
[AD-A219369] 16 p2249 N90-22825

AIRCRAFT ENERGY EFFICIENCY PROGRAM
U ACEE PROGRAM

AIRCRAFT ENGINES
NT HELICOPTER ENGINES
A supersonic through-flow fan engine airframe integration study
[NASA-CR-185140] 01 p0001 N90-10004
Full scale technology demonstration of a modern counterrotating unducted fan engine concept: Component test
[NASA-CR-180868] 01 p0010 N90-10047
Full scale technology demonstration of a modern counterrotating unducted fan engine concept. Design report
[NASA-CR-180867] 01 p0010 N90-10048
Full scale technology demonstration of a modern counterrotating unducted fan engine concept. Engine test
[NASA-CR-180869] 01 p0011 N90-10049
Combustor influence on fighter engine operability 01 p0035 N90-10193
Dynamic instability characteristics of aircraft turbine engine combustors 01 p0036 N90-10195
Advanced technologies impact on compressor design and development: A perspective
[NASA-TM-102341] 02 p0156 N90-10891
Future military powerplants --- fighter aircraft engines
[PNR90554] 03 p0308 N90-11749
Aluminium alloy development for aero engines
[PNR90548] 03 p0330 N90-11874
Flanged joints of aeroengines
[PNR90594] 04 p0455 N90-12609
Aviation Engine Test Facilities (AETF) fire protection study
[AD-A211483] 04 p0483 N90-12777
Effect of reduced aft diameter and increased blade number on high-speed counterrotation propeller performance
[NASA-TM-102077] 05 p0575 N90-13352
Study of the engine bird ingestion experience of the Boeing 737 aircraft
[DOT/FAA/CT-89/16] 05 p0576 N90-13360
AGARD Highlights 89/2 06 p0717 N90-14184
X.2 limited flight test plan
[AD-A214412] 07 p0880 N90-15099
An experimental investigation of thrust vectoring two-dimensional convergent-divergent nozzles installed in a twin-engine fighter model at high angles of attack
[NASA-TM-4155] 08 p1017 N90-15884
Using goal programming to determine the optimal engine mix for UH-1 helicopters
[AD-A214893] 09 p1168 N90-16762
Analysis of hydraulic fluids and lubricating oils for the formation of Trimethylolpropane Phosphate (TMP-P)
[AD-A215188] 09 p1198 N90-16939
AGARD/SMP Review: Damage Tolerance for Engine Structures. 2: Defects and Quantitative Materials Behaviour --- conference
[AGARD-R-769] 11 p1457 N90-18396
In-flight evaluations of turbine fuel extenders
[DOT/FAA/CT-89/33] 12 p1633 N90-19387
Structural tailoring of select fiber composite structures
[NASA-TM-102484] 14 p1946 N90-21137
Attachment of lead wires to thin film thermocouples mounted on high temperature materials using the parallel gap welding process
[NASA-TM-102442] 14 p1983 N90-21361
Aeropropulsion facilities configuration control: Procedures manual
[NASA-TM-102541] 14 p1989 N90-21399
Small business innovation research. Abstracts of completed 1987 phase 1 projects
[NASA-TM-101797] 14 p2036 N90-21681
Control of flow separation and mixing by aerodynamic excitation
[NASA-TM-103131] 15 p2047 N90-21733
Preliminary development of an intelligent computer assistant for engine monitoring
[NASA-TM-101702] 15 p2157 N90-22322
Preliminary airworthiness evaluation of the RC-12K
[AD-A219545] 17 p2351 N90-23387
Fatigue crack growth investigation of a Ti-6Al-4V forging under complex loading conditions: NATO/AGARD supplemental engine disk program
[AD-A220239] 17 p2377 N90-23538
Processing of advanced ceramics which have potential for use in gas turbine aero engines
[AD-A220988] 19 p2677 N90-25226
Stage 2 re-engining: The only way to achieve a real stage 3 aircraft
[PNR90636] 20 p2808 N90-25977
Towards 2000: The composite engine
[PNR90646] 20 p2811 N90-26000
Prediction of rotating disc flow and heat transfer in gas turbine engines
[PNR90650] 20 p2812 N90-26001
Prediction and measurement of rotor blade/stator vane dynamic characteristics of a modern aero-engine axial compressor
[PNR90667] 20 p2812 N90-26002
The impact and requirements of new materials on aeroengines
[PNR90671] 20 p2812 N90-26003
Aircraft exhaust emissions: An engine manufacturer's perspective
[PNR90675] 20 p2812 N90-26004
Handbook of uncertainty methodology for engine testing at Pyestock (England)
[RAE-TM-P-1179] 20 p2812 N90-26007
Metal matrix composites and powder processing for aero-engine applications
[PNR90617] 20 p2828 N90-26087
NDT in aerospace: The next decade (1990's)
[PNR90628] 20 p2874 N90-26348
Elevated temperature crack growth
[NASA-CR-182247] 20 p2875 N90-26355
Bringing aircraft noise testing down to Earth
[PNR90642] 20 p2924 N90-26637
Effective optimal control of a fighter aircraft engine 23 p3277 N90-28548
Energy efficient engine program technology benefit/cost study. Volume 1: Executive summary
[NASA-CR-174766-VOL-1] 23 p3280 N90-28564
Energy efficient engine program technology benefit/cost study, volume 2
[NASA-CR-174766-VOL-2] 23 p3280 N90-28565
Energy Efficient Engine: Control system preliminary definition report
[NASA-CR-179578] 23 p3281 N90-28569
High Temperature Surface Interactions
[AGARD-CP-461] 23 p3306 N90-28698
Fretting fatigue strength of Ti-6Al-4V at room and elevated temperatures and ways of improving it 23 p3308 N90-28709
Audibility and annoyance of en route noise of unducted fan engines
[AD-A223687] 24 p3543 N90-30035

AIRCRAFT EQUIPMENT
NT EJECTION SEATS
Electro-impulse de-icing testing analysis and design
[NASA-CR-4175] 01 p0007 N90-10031
Meeting Review: Workshop on Airborne Instrumentation
[PB89-174775] 01 p0007 N90-10032
Numerical simulation of aeroplane response to a lightning injection
[ETN-89-95271] 03 p0303 N90-11716
Acoustic recording systems for use in military aircraft
[RAE-TM-MM-11] 04 p0551 N90-13207
Conference Proceedings of the Human-Electronic Crew: Can They Work Together
[AD-A211871] 05 p0676 N90-13936
Results of aircraft open-loop tests of an experimental magnetic leader cable system for guidance during roll-out and turnoff
[NASA-TM-4135] 09 p1169 N90-16767
Failure analysis handbook
[AD-A219747] 17 p2413 N90-23752
Multichannel on-board load and fatigue monitoring 22 p3103 N90-27621
AIMS test and simulation equipment 22 p3104 N90-27623
Performance assessment of MIL-STD-1553B on the avionic systems demonstrator rig of British Aerospace 22 p3104 N90-27624
Integrated Air Traffic Management
[DLR-MITT-89-23] 22 p3112 N90-27678
A reliable, maintenance-free oxygen sensor for aircraft using an oxygen-sensitive coating on potentiometric electrodes
[AD-A222696] 23 p3277 N90-28545
Military aircrew seating: A human factors engineering approach
[AD-A218049] 23 p3362 N90-28999

AIRCRAFT FUEL SYSTEMS
Integral fuel tanks - design, production, aging, repair 08 p1021 N90-15906

AIRCRAFT FUELS
Aircraft fuel tank construction and testing experience 08 p1021 N90-15907
The repair of aircraft integral fuel tanks in the RAF: A user's view of fuel tank technology 08 p1022 N90-15908
Ignitability of jet-A fuel vapors in aircraft fuel tanks 10 p1313 N90-17594
The stability of fuel fires 10 p1315 N90-17601
Production of high density aviation fuels via novel zeolite catalyst routes
[AD-A216444] 11 p1494 N90-18801
Low-energy gamma ray attenuation characteristics of aviation fuels
[NASA-TP-2974] 11 p1543 N90-18882
Turbine fuel alternatives (near term)
[AD-A219405] 16 p2225 N90-22695
Micro separometer and ball-on-cylinder lubricity evaluator tests or corrosion inhibitor/lubricity improver additives
[AD-A221339] 19 p2678 N90-25228
Advanced fuel properties, phase 1
[AD-A219788] 19 p2679 N90-25236
Study of high-speed civil transports. Summary
[NASA-CR-4236] 20 p2806 N90-25966
Development of a mathematical model for the thermal decomposition of aviation fuels
[AD-A221673] 21 p2990 N90-26994

AIRCRAFT GUIDANCE
Guidance simulation and test support for differential GPS flight experiment
[NASA-CR-177471] 01 p0005 N90-10021
Trajectory optimization and guidance for an aerospace plane
[NASA-CR-185884] 05 p0578 N90-13369
Relative merits of reactive and forward-look detection for wind-shear encounters during landing approach for various microburst escape strategies
[NASA-TM-4158] 07 p0882 N90-15108
Guidance analysis of the aeroglide plane change maneuver as a turning point problem
[NASA-TM-101639] 07 p0883 N90-15110
Integrated flight guidance system using differential-GPS for landing approach guidance 09 p1163 N90-16735
Results of aircraft open-loop tests of an experimental magnetic leader cable system for guidance during roll-out and turnoff
[NASA-TM-4135] 09 p1169 N90-16767
A head up display format for application to V/STOL aircraft approach and landing
[NASA-TM-102216] 10 p1320 N90-17632
The Fourteenth Biennial Guidance Test Symposium, volume 1
[AD-A216925] 11 p1455 N90-18383
Automation of the readout, transcription and evaluation of digital flight data at DLR 22 p3106 N90-27645
On-board planning and control of 4D-trajectories in the TMA 22 p3112 N90-27680
Four-dimensional navigation and Flight Management Systems 22 p3112 N90-27681
Four-dimensional planner: A ground based planning system for time accurate approach guidance 22 p3113 N90-27683
Description of the primary flight display and flight guidance system logic in the NASA B-737 transport systems research vehicle
[NASA-TM-102710] 23 p3277 N90-28546

AIRCRAFT HANGARS
U HANGARS

AIRCRAFT HAZARDS
Remote sensing techniques of the Wave Propagation Laboratory for the measurement of supercooled liquid water: Applications to aircraft icing
[PB89-208102] 02 p0148 N90-10842
Meeting review: The Second NCAR (National Center for Atmospheric Research) Research Aircraft Fleet Workshop
[PB89-200901] 03 p0369 N90-12113
The human factors relating to escape and survival from helicopters ditching in water
[AGARD-AG-305(E)] 05 p0576 N90-13358
Flight in adverse environmental conditions
[AGARD-AR-277] 06 p0723 N90-14218
Wind shear models for aircraft hazard investigation 07 p0869 N90-15044
NASA's program on icing research and technology 07 p0873 N90-15062
Principal characteristics of lightning on aircraft 07 p0874 N90-15067
International Aircraft Occupant Safety Conference and Workshop proceedings
[AD-A214452] 07 p0877 N90-15085
The collection of non-conus aircraft icing data along with an identification of the geographical areas of potential severe icing and a study of a method of remote determining atmospheric icing data
[AD-A215055] 09 p1162 N90-16724
RAAF Orion aircraft A9-300 oxygen fire
[AD-A215496] 09 p1162 N90-16725
Investigation of air transportation technology at the Massachusetts Institute of Technology, 1988-1989 14 p1905 N90-20922
Cockpit display of hazardous wind shear information 14 p1905 N90-20924
Modeling of surface roughness effects on glaze ice accretion 14 p1905 N90-20925
Ultrasonic techniques for aircraft ice accretion measurement 14 p1906 N90-20926
Investigation of surface water behavior during glaze ice accretion 14 p1906 N90-20927
The influence of ice accretion physics on the forecasting of aircraft icing conditions 14 p1906 N90-20928
Cockpit display of hazardous weather information 14 p1906 N90-20929
Advanced instrumentation for aircraft icing research
[NASA-CR-185225] 14 p1921 N90-21006
Fire hazards of aerosol cans in aircraft cargo compartments
[DOT/FAA/CT-89/32] 17 p2347 N90-23389
A quantitative technique to estimate microburst wind shear hazard to aircraft 18 p2640 N90-25040
A NASA/university/industry consortium for research on aircraft ice protection
[IAR-89-18] 20 p2807 N90-25969

AIRCRAFT INDUSTRY
A review of Australian and New Zealand investigations on aeronautical fatigue during the period April 1987 to March 1989
[AD-A210373] 01 p0006 N90-10026
The use of prototypes in selected foreign fighter aircraft development programs: Rafale, EAP, Lavi, and Gripen
[AD-A214500] 09 p1159 N90-16707
FAA (Federal Aviation Administration) aviation forecasts, fiscal years 1990-2001
[AD-A219165] 16 p2195 N90-22530
Supercomputer and Technology
[NLR-PUB-8801] 16 p2277 N90-22974
Aircraft modifications cost analysis. Volume 1: Overview of the study
[AD-A220764] 19 p2649 N90-25074
The Federal Aviation Administration plan for research, engineering and development. Volume 1: Program plan
[AD-A221263] 19 p2800 N90-25930
Radiation-curable prepreg composites
[DE90-629740] 23 p3301 N90-28674

AIRCRAFT INSTRUMENTS
NT APPROACH INDICATORS
NT AUTOMATIC PILOTS
NT FLIGHT RECORDERS
Cockpit lighting compatibility with image intensification night imaging systems: issues and answers
[AD-A210503] 01 p0006 N90-10028
Optimal integral controller with sensor failure accommodation 01 p0024 N90-10123
Flight simulator evaluation of a head-down display
[NAL-TM-573] 02 p0157 N90-10898
Devices and procedures for the calibration of sensors and measurement: Systems of the flight test support system ATTAS
[DFVLR-MITT-89-06] 03 p0351 N90-12007
Principal characteristics of lightning on aircraft 07 p0874 N90-15067
Display interface concepts for automated fault diagnosis
[NASA-TM-101610] 07 p0881 N90-15102
A simulation evaluation of the engine monitoring and control system display
[NASA-TP-2960] 11 p1457 N90-18393
Three input concepts for flight crew interaction with information presented on a large-screen electronic cockpit display
[NASA-TM-4173] 11 p1457 N90-18394
Simulator comparison of thumball, thumb switch, and touch screen input concepts for interaction with a large screen cockpit display format
[NASA-TM-102587] 14 p1921 N90-21005
Continued development and analysis of a new extended Kalman filter for the Completely Integrated Reference Instrumentation System (CIRIS)
[AD-A220106] 17 p2354 N90-23400
Qualitative evaluation of a conformal velocity vector display for use at high angles-of-attack in fighter aircraft
[NASA-TM-102629] 20 p2809 N90-25981
Aircraft Integrated Monitoring Systems
[DLR-MITT-90-04] 22 p3103 N90-27617
Past, present and future: Aircraft integrated monitoring systems: An ever-developing technology 22 p3103 N90-27618
Harrier Information Management System (HIMS): The system and the approach 22 p3105 N90-27630
AIMS for helicopters 22 p3106 N90-27639
Airborne CO2 Doppler lidar for wind shear detection 22 p3106 N90-27640
The new US flight recorder regulations 22 p3106 N90-27642
The Canadian Aviation Safety Board's flight recorder facility 22 p3106 N90-27643
Australian experience in flight recorder readout and analysis 22 p3106 N90-27644
Automation of the readout, transcription and evaluation of digital flight data at DLR 22 p3106 N90-27645
Position finding and ground target direction finding by an aircraft with a gimballed video camera
[DLR-FB-89-62] 22 p3111 N90-27673
Scope and conception of the pilot support system ASPIO
[LRT-WE-13-FB-88-1] 22 p3233 N90-28334

AIRCRAFT INTERIORS
U AIRCRAFT COMPARTMENTS

AIRCRAFT LANDING
NT CRASH LANDING
NT DITCHING (LANDING)
A simulation study of landing time allocation procedures for use in computer-assisted air traffic management systems
[AD-A212159] 03 p0303 N90-11722
Ice runways near the South Pole
[AD-A211606] 03 p0335 N90-11908
Field-of-View variations and stripe-texturing effects on assault landing performance in the C-130 weapon system trainer
[AD-A212763] 04 p0459 N90-12634
Autonomous automatic landing through computer vision 09 p1163 N90-16734
Integrated flight guidance system using differential-GPS for landing approach guidance 09 p1163 N90-16735
A head up display format for application to V/STOL aircraft approach and landing
[NASA-TM-102216] 10 p1320 N90-17632
Airplane takeoff and landing performance monitoring system
[NASA-CASE-LAR-13734-1-CU] 13 p1758 N90-20096
Runaway rubber removal
[AD-A218349] 13 p1759 N90-20100
Optimization and guidance of flight trajectories in the presence of windshear
[NASA-CR-186163] 15 p2049 N90-21747
Dynamic ground-effect measurements on the F-15 STOL and Maneuver Technology Demonstrator (S/MTD, configuration
[NASA-TP-3000] 16 p2195 N90-22531
Preliminary airworthiness evaluation of the RC-12K
[AD-A219545] 17 p2351 N90-23387
Electro-optics engineering support for the integrated launch and recovery television surveillance system
[AD-A223450] 24 p3436 N90-29406

AIRCRAFT LIGHTS
The automatic detection of anti-collision lights
[RSRE-MEMO-4272] 08 p1019 N90-15896

AIRCRAFT MAINTENANCE
Aircraft accident report: Aloha Airlines, Flight 243, Boeing 737-200, N73711, near Maui, Hawaii, April 28, 1988
[PB89-910404] 01 p0004 N90-10013
An appraisal of a number of power assessment procedures being proposed for use in Chinook-Lycoming T55 engine
[AD-A210482] 01 p0009 N90-10041
The RB199: An in-service success
[PNR90544] 03 p0307 N90-11746
Repair of composites by means of wet-lay-up
[LR-551] 05 p0620 N90-13617
Integral fuel tanks - design, production, aging, repair 08 p1021 N90-15906
The repair of aircraft integral fuel tanks in the RAF: A user's view of fuel tank technology 08 p1022 N90-15908
Fuel resistant coatings for metal and composite fuel tanks 08 p1022 N90-15911
Spray sealing: A breakthrough in integral fuel tank sealing technology 08 p1022 N90-15912
Design philosophy and construction techniques for integral fuselage fuel tanks 08 p1023 N90-15913
Integral fuel tank certification and test methods 08 p1023 N90-15916
Cost effectiveness of composite materials on the F-15 and F-16 aircrafts
[AD-A216353] 10 p1320 N90-17631
Human factors issues in aircraft maintenance and inspection
[AD-A215724] 11 p1542 N90-18875
Environmental effects upon cross-servicing of aircraft in NATO
[AD-A218374] 17 p2343 N90-23341
A survey of human factors methodologies and models for improving the maintainability design of emerging Army aviation systems
[AD-A221159] 18 p2586 N90-24724
Damage tolerance demonstration for A310-300 CFRP components
[MBB-UT-012/89-PUB] 19 p2652 N90-25091
From 1959-1989: 30 years of service experience with ramjets
[PNR90677] 19 p2660 N90-25139
CREW CHIEF: A computer graphics simulation of an aircraft maintenance technician 19 p2729 N90-25515
Modeling strength data for CREW CHIEF 19 p2729 N90-25516
Success in tutoring electronic troubleshooting 19 p2739 N90-25568
Second Annual International Conference on Aging Aircraft
[AD-A222715] 20 p2805 N90-25961
Robotic-aided system for inspection of aging aircraft
[NIAR-90-9] 20 p2873 N90-26346
Computerized corrosion forecasting model for C-5 aircraft 21 p2957 N90-26815
Individual Helicopter Tracking Program (IHTP) for the MH-53J helicopter 21 p2958 N90-26818
Peak identification techniques 21 p2959 N90-26822

B-1B improved windshield development. Volume 2: Magna analysis: Baseline and parametric
[AD-A221501] 21 p2960 N90-26828
Impact of NDE-NDI methods on aircraft design, manufacture, and maintenance, from the fundamental point of view 22 p3189 N90-28093

AIRCRAFT MANEUVERS
Nonlinear maneuver autopilot for the F-15 aircraft
[NASA-CR-179442] 02 p0262 N90-11487
FPG2: A flight profile generator program
[AD-A212408] 04 p0453 N90-12595
Flow visualization of the effect of pitch rate on the vortex development on the scale model of a F-18 fighter aircraft
[AD-A214244] 07 p0876 N90-15080
Relative merits of reactive and forward-look detection for wind-shear encounters during landing approach for various microburst escape strategies
[NASA-TM-4158] 07 p0882 N90-15108
Preliminary results from a subsonic high angle-of-attack flush airdata sensing (HI-FADS) system: Design, calibration, and flight test evaluation
[NASA-TM-101713] 09 p1168 N90-16758
Estimation and control of nonlinear and hybrid systems with applications to air-to-air guidance
[AD-A214542] 09 p1170 N90-16770
Predicting Air Combat Maneuvering (ACM) performance 09 p1258 N90-17294
Unsteady aerodynamics of delta wings performing maneuvers to high angle of attack
12 p1598 N90-19196
A study of flows over highly-swept wings designed for maneuver at supersonic speeds
[AD-A216837] 12 p1599 N90-19202
A study of supermanuever aerodynamics
[AD-A218378] 17 p2344 N90-23349
Fighter agility metrics, research, and test
[NASA-CR-186118] 17 p2351 N90-23386
Tips on desert flying
[PB90-233222] 22 p3110 N90-27670
Aerodynamics of Combat Aircraft Controls and of Ground Effects
[AGARD-CP-465] 23 p3271 N90-28513
Combat aircraft control requirements
23 p3271 N90-28515
Observability of relative navigation using range-only measurements 24 p3427 N90-29360
Analysis of dynamic transient response and postflutter behavior of super-maneuvering airplane
[AD-A224126] 24 p3432 N90-29386
Fighter agility metrics
[NASA-CR-187289] 24 p3432 N90-29389

AIRCRAFT MODELS
Measurements of pressures on the tail and aft fuselage of an airplane model during rotary motions at spin attitudes
[NASA-TP-2939] 02 p0145 N90-10829
The spinning of aircraft: A discussion of spin prediction techniques including a chronological bibliography
[ARL-AERO-R-177] 02 p0155 N90-10888
Stability and control derivatives of the De Havilland DHC-2 BEAVER aircraft
[PB89-217525] 03 p0309 N90-11754
Sequential design of experiments with physically based models 23
[AD-A211918] 03 p0393 N90-12239
The precise calculation of the inviscid leading edge flow on a laminar airfoil using simple methods and verification by measurements on the TLF pilot model
08 p1068 N90-16180
Stability characteristics of a combat aircraft with control surface failure
[AD-A216196] 10 p1323 N90-17646
Automation of an RCS (Radar Cross Section) measurement system and its application to investigate the electromagnetic scattering from scale model aircraft canopies
[AD-A215741] 10 p1375 N90-17970
Aerofoil design techniques 14 p1916 N90-20978
Prediction methodologies for nonlinear aerodynamic characteristics of control surfaces
[NIAR-90-17] 20 p2801 N90-25937
Wind tunnel study of wake downwash behind A 6 percent scale model B1-B aircraft
[DE90-011783] 20 p2802 N90-25941
High resolution exponential modeling of fully polarized radar returns
[AD-A221432] 21 p2997 N90-27036
The effects of foreplanes on the static and dynamic characteristics of a combat aircraft model
23 p3273 N90-28520
Study of ground effects on flying scaled models
23 p3275 N90-28532

AIRCRAFT NOISE
NT BLADE SLAP NOISE
NT JET AIRCRAFT NOISE
NT PROPELLER NOISE
NT SONIC BOOMS
Measurement resolution of noise directivity patterns from acoustic flight tests
[NASA-TM-4134] 01 p0118 N90-10679
Propfan Test Assessment (PTA): Flight test report
[NASA-CR-182278] 03 p0306 N90-11738
The NASA experience in aeronautical R and D: Three case studies with analysis
[AD-A211486] 04 p0437 N90-12496
Near-field noise predictions of an aircraft in cruise
04 p0443 N90-12538
Acoustic design considerations: Review of rotor acoustic sources 04 p0451 N90-12585
UHB demonstrator interior noise control flight tests and analysis
[NASA-CR-181897] 04 p0549 N90-13198
Mobility power flow analysis of an L-shaped plate structure subjected to acoustic excitation
[NASA-CR-186130] 05 p0655 N90-13817
A two dimensional power spectral estimate for some nonstationary processes
[NASA-CR-186100] 06 p0833 N90-14843
Evaluation of analysis techniques for low frequency interior noise and vibration of commercial aircraft
[NASA-CR-181851] 06 p0837 N90-14866
Cumulative airport noise exposure metrics: An assessment of evidence for time-of-day weightings, revision
[AD-A214878] 09 p1170 N90-16773
Comparison between design and installed acoustic characteristics of NASA Lewis 9- by 15-foot low-speed wind tunnel acoustic treatment
[NASA-TP-2996] 12 p1606 N90-19242
Noise of a simulated installed model counterrotation propeller at angle-of-attack and takeoff/approach conditions
[NASA-TM-102440] 13 p1881 N90-20794
Lateral attenuation of military aircraft flight noise
[AD-A218041] 13 p1882 N90-20799
The Shock and Vibration Digest, volume 21, no. 6
15 p2163 N90-22363
Noise transmission into propeller-driven airplanes
15 p2163 N90-22364
Updating a dosage-effect relationship for the prevalence of annoyance due to general transportation noise
[AD-A219416] 17 p2421 N90-23794
Analyses of the predictability of noise-induced sleep disturbance
[AD-A220156] 17 p2435 N90-23876
Evaluation of speech recognizers for use in advanced combat helicopter crew station research and development
[NASA-CR-177547] 18 p2496 N90-24265
Fluid dynamic and acoustic experiments on turbomachine rotors subject to variable flow conditions
[AD-A220298] 18 p2552 N90-24565
FAA/NASA En Route Noise Symposium
[NASA-CP-3067] 18 p2608 N90-24853
Proposed definition of the term en route in en route aircraft noise 18 p2608 N90-24854
PTA en route noise measurements
18 p2608 N90-24855
En route noise: NASA propfan test aircraft (calculated source noise
[DOT-TSC-FA953-LR5] 18 p2609 N90-24857
En route noise of two turboprop aircraft
[DLR-MITT-89-18] 18 p2609 N90-24859
Sound propagation elements in evaluation of en route noise of advanced turbofan aircraft
18 p2609 N90-24861
Preliminary thoughts on an acoustic metric for the wilderness aircraft overflight study
18 p2609 N90-24862
US Forest Service and National Park Service Wilderness Aircraft Overflight Study: Sociological background and study plans 18 p2609 N90-24863
When propfans cruise, will LDN 65 fly
18 p2610 N90-24864
Agenda toward the development of a rational noise descriptor system relevant to human annoyance by en route aircraft noise 18 p2610 N90-24866
Additive evaluation criteria for aircraft noise
18 p2610 N90-24867
Social survey findings on en route noise annoyance issues 18 p2610 N90-24868
Predicting the audibility and annoyance of unducted fan engines 18 p2610 N90-24869
En route noise annoyance laboratory test: Preliminary results 18 p2611 N90-24870
Problems related to aircraft noise in Switzerland
18 p2611 N90-24871
An aircraft noise study in Norway
18 p2611 N90-24872
Problems of internal acoustics in two and three dimensional cavities with deformable walls using the MSC/Nastran code
[DLC/STR-INT-TN-004] 18 p2612 N90-24876
High speed turboprop aeroacoustic study (counterrotation). Volume 1: Model development
[NASA-CR-185241] 20 p2923 N90-26633
Bringing aircraft noise testing down to Earth
[PNR90642] 20 p2924 N90-26637
BASEOPS default profiles for civil aircraft
[AD-A223161] 21 p2959 N90-26825
Air Force procedure for predicting aircraft noise around airbases: Airbase operations program (BASEOPS) description
[AD-A223089] 21 p3072 N90-27466
Air Force procedure for predicting aircraft noise around airbases: Noise Exposure Model (NOISEMAP). User's manual
[AD-A223162] 21 p3072 N90-27467
Aviation acoustical noise measurement
[AD-A222014] 21 p3073 N90-27469
Public-sector aviation issues, 1987 to 1988 graduate research award papers
[PB90-191206] 22 p3110 N90-27667
Structure-borne noise estimates for the PTA aircraft
[NASA-CR-4315] 22 p3244 N90-28396
A process for analysis, evaluation, and development of aerial servicing noise reduction measures in civil aircraft
[ETN-90-97300] 22 p3244 N90-28398
Comparison of speech intelligibility in cockpit noise using SPH-4 flight helmet with and without active noise reduction
[NASA-CR-177564] 23 p3271 N90-28510
Audibility and annoyance of en route noise of unducted fan engines
[AD-A223687] 24 p3543 N90-30035
Assessment System for Aircraft Noise (ASAN): Development of alpha-test prototype system software
[AD-A223770] 24 p3543 N90-30036

AIRCRAFT NOISE PREDICTION
U NOISE PREDICTION (AIRCRAFT)

AIRCRAFT PARTS
Castings Airworthiness
[AGARD-R-762] 01 p0042 N90-10231
Casting factors imposed by the French regulation for foundry castings used in military aircraft
01 p0042 N90-10233
The question of the casting factor
01 p0043 N90-10238
Expert system diagnostics and parts life tracking as applied to the AV-8B aircraft for the USMC
22 p3104 N90-27629
Evaluation of composite components on the Bell 206L and Sikorsky S-76 helicopters
[NASA-TM-4195] 22 p3135 N90-27787
In-service inspection of composite components on aircraft at depot and field levels
22 p3186 N90-28078

AIRCRAFT PERFORMANCE
NT HELICOPTER PERFORMANCE
On the interactive computer program IPIS for aircraft parameter identification
[NAL-TR-1000] 01 p0103 N90-10586
Introduction to data items on flight path optimisation
[ESDU-89015] 06 p0723 N90-14221
Influence of windshear, downdraft and turbulence on flight safety 07 p0870 N90-15048
Classification of windshear severity
07 p0870 N90-15049
A pitch control law for compensation of the phugoid mode induced by windshears 07 p0870 N90-15051
Aircraft response and pilot behaviour during a wake vortex encounter perpendicular to the vortex axis
07 p0871 N90-15057
Ice induced aerodynamic performance degradation of rotorcraft: An overview 07 p0873 N90-15063
Aircraft performance enhancement with active compressor stabilization
[AD-A213652] 07 p0879 N90-15097
A UK perspective on the uniform engine test programme
[RAE-TM-P-1172] 08 p1025 N90-15922
Application of multifunction inertial reference systems to fighter aircraft 09 p1164 N90-16740
Longitudinal stability and control characteristics of the Quiet Short-Haul Research Aircraft (QSRA)
[NASA-TP-2965] 10 p1322 N90-17639
The effects of wind tunnel data uncertainty on aircraft point performance predictions
[AD-A216091] 11 p1456 N90-18387
Development of a preliminary high-angle-of-attack nose-down pitch control requirement for high-performance aircraft
[NASA-TM-101684] 12 p1600 N90-19206

Potential role of avionics in escape systems
13 p1752 N90-20060
The implementation and operation of a variable-response electronic throttle control system for a TF-104G aircraft
[NASA-TM-101696] 13 p1756 N90-20086
Airplane takeoff and landing performance monitoring system
[NASA-CASE-LAR-13734-1-CU]
13 p1758 N90-20096
Flight test investigation of certification issues pertaining to general-aviation-type aircraft with natural laminar flow
[NASA-CR-181967] 14 p1911 N90-20952
Flight path reconstruction using extended Kalman filtering techniques
[PD-FC-9001] 14 p1915 N90-20970
Supersonic through-flow fan engine and aircraft mission performance
[NASA-TM-102304] 14 p1927 N90-21038
The 1D-ISAR imaging of manoeuvering aircraft
14 p1963 N90-21241
Preliminary airworthiness evaluation of the RC-12K
[AD-A219545] 17 p2351 N90-23387
Initial flight test of half-scale unmanned air vehicle
[AD-A219584] 17 p2351 N90-23388
Overcoming the Bellman's curse of dimensionality in large optimization problems
[NASA-TM-102662] 17 p2352 N90-23391
Estimating short-period dynamics using an extended Kalman filter
[NASA-TM-101722] 17 p2352 N90-23392
Lateral-directional stability and control characteristics of the Quiet Short-Haul Research Aircraft (QSRA)
[NASA-TM-102250] 17 p2356 N90-23413
A quantitative technique to estimate microburst wind shear hazard to aircraft 18 p2640 N90-25040
Effects of simplifying assumptions on optimal trajectory estimation for a high-performance aircraft
[NASA-TM-101721] 19 p2661 N90-25142
Handbook of uncertainty methodology for engine testing at Pyestock (England)
[RAE-TM-P-1179] 20 p2812 N90-26007
Model tilt-rotor hover performance and surface pressure measurement
[AD-A222535] 21 p2959 N90-26827
Aircraft Integrated Monitoring Systems
[DLR-MITT-90-04] 22 p3103 N90-27617
Past, present and future: Aircraft integrated monitoring systems: An ever-developing technology
22 p3103 N90-27618
Comparative Engine Performance Measurements
[AGARD-LS-169] 22 p3118 N90-27711
Survivable penetration 24 p3428 N90-29363
Multi-disciplinary optimization of aeroservoelastic systems
[NASA-CR-185931] 24 p3432 N90-29385

AIRCRAFT PILOTS
NT TEST PILOTS
Scientific and technical report voice activated gun turrent control
[AD-A210350] 01 p0110 N90-10623
A comparison of two subject-controlled attitude measures during somatogravic illusion exposure
[AD-A212528] 04 p0525 N90-13031
Conference Proceedings of the Human-Electronic Crew: Can They Work Together
[AD-A211871] 05 p0676 N90-13936
Cockpit resource management: A selected annotated bibliography
[AD-A214272] 07 p0969 N90-15594
Peripheral nervous velocity of conduction in fighter pilots 09 p1256 N90-17287
Principle guidelines for the psychological screening of candidate pilots for the Belgian Air Force
09 p1257 N90-17292
Proximity compatibility and information display: The effects of space and color on the analysis of aircraft stall conditions
[AD-A214488] 09 p1260 N90-17309
Prescribing spectacles for aviators
[AD-A214830] 09 p1260 N90-17310
Pilot candidate selection
[AD-A217295] 12 p1696 N90-19742
The effect of windscreen bows and HUD pitch ladder format on pilot performance during simulated flight
[AD-A218139] 14 p2011 N90-21523
Field-of-view assessment of low-level flight and an airdrop in the C-130 Weapon System Trainer (WST)
[AD-A218504] 16 p2200 N90-22559
Relationship between flexibility of closure and success in pilot night vision sensor system training
[AD-A221439] 16 p2261 N90-22890
Peacetime replacement and crash damage factors for army aircraft
[AD-A218544] 17 p2348 N90-23372
Activities report of the National Aerospace Medical Center
[ETN-90-96936] 18 p2585 N90-24721
Radiological investigation of the vertebral column of candidates for military flying training the the Royal Norwegian Air Force 19 p2718 N90-25463
Data analysis in cervical trauma
19 p2718 N90-25464
Progressive cervical osteoarthritis in high performance aircraft pilots 19 p2718 N90-25465
Biochemical and physiological changes in glider pilots during multi-hour flights
[ESA-TT-1183] 19 p2722 N90-25484
The prediction of professional success of licenced pilots: The validity of flight experience in comparison with standardized psychological aptitude tests
[DLR-FB-89-53] 19 p2723 N90-25488
International application of the DLR test-system: First year of cooperation with IBERIA in pilot selection
[DLR-FB-90-05] 19 p2723 N90-25491
A trend analysis of women who hold Federal Aviation Administration certificates: Relationship to the representation of women in collegiate aviation faculty ranks
[IAR-90-3] 19 p2762 N90-25691
Biodynamic simulations of an aircraft pilot/passenger in various crash environments
[NIAR-90-6] 20 p2900 N90-26494
Cognitive requirements for aircraft navigation
[NASA-CR-186933] 21 p2955 N90-26804
Tips on desert flying
[PB90-233222] 22 p3110 N90-27670
Influence of gravito-inertial force on vestibular nystagmus in man
[IZF-1989-24] 22 p3231 N90-28325
Human factors and safety considerations of night vision systems flight
[USAARL-89-12] 22 p3233 N90-28332
Evaluation of existing aircraft operator data bases
[DOT/FAA/CT-90/18] 22 p3260 N90-28463

AIRCRAFT POWER SOURCES
U AIRCRAFT ENGINES

AIRCRAFT POWER SUPPLIES
The aerospace energy systems laboratory: Hardware and software implementation
[NASA-TM-101706] 01 p0107 N90-10610
Civil air transport: A fresh look at power-by-wire and fly-by-light
[NASA-TM-102574] 14 p1969 N90-21283
Preliminary design of a long-endurance Mars aircraft
[NASA-CR-185243] 15 p2052 N90-21763

AIRCRAFT PRODUCTION
Scenario 2000
[MBB-UD-500/89-PUB] 19 p2652 N90-25092

AIRCRAFT PRODUCTION COSTS
The manufacturing procedures for composite materials, automation, and robotization
[ETN-90-96232] 11 p1482 N90-18528
Aircraft modifications cost analysis. Volume 1: Overview of the study
[AD-A220764] 19 p2649 N90-25074

AIRCRAFT RELIABILITY
Aircraft accident report: Aloha Airlines, Flight 243, Boeing 737-200, N73711, near Maui, Hawaii, April 28, 1988
[PB89-910404] 01 p0004 N90-10013
Airworthiness and flight characteristics test of the UH-60A Black Hawk helicopter equipped with the XM-139 multiple mine dispensing system (VOLCANO)
[AD-A210271] 01 p0006 N90-10025
Castings Airworthiness
[AGARD-R-762] 01 p0042 N90-10231
Casting airworthiness joint European civil authorities view-point 01 p0042 N90-10234
Royal Aerospace Establishment: No place for a castings factor 01 p0042 N90-10235
Combined advanced foundry and quality control techniques to enhance reliability of castings for the aerospace industry 01 p0043 N90-10240
Preliminary airworthiness evaluation of the AH-64A equipped with the Air To Air Stinger (ATAS) missile system
[AD-A213030] 05 p0579 N90-13374
Preliminary airworthiness evaluation of the Woodward hydromechanical unit installed on T700-GE-700 engines in the UH-60A helicopter
[AD-A216751] 11 p1464 N90-18430
Activities report in civil aviation
[ETN-90-95471] 13 p1753 N90-20067
Airworthiness and flight characteristics evaluation of the McDonnell Douglas Helicopter Corporation (MDHC) 530FF helicopter
[AD-A218253] 13 p1755 N90-20076
The NASA digital VGH program. Exploration of methods and final results. Volume 1: Development of methods
[NASA-CR-181909-VOL-1] 13 p1756 N90-20081
The NASA digital VGH program. Exploration of methods and final results. Volume 3: B 727 data 1978-1980: 1765 hours
[NASA-CR-181909-VOL-3] 13 p1756 N90-20082
The NASA digital VGH program: Exploration of methods and final results. Volume 4: B 747 data 1978-1980, 1689 hours
[NASA-CR-181909-VOL-4] 13 p1756 N90-20083
The NASA digital VGH program: Exploration of methods and final results. Volume 5: DC 10 data 1981-1982, 129 hours
[NASA-CR-181909-VOL-5] 13 p1756 N90-20084
The role of structural analysis in airworthiness certification
[BR112064] 14 p1915 N90-20972
Preliminary airworthiness evaluation of the RC-12K
[AD-A219545] 17 p2351 N90-23387
From 1959-1989: 30 years of service experience with ramjets
[PNR90677] 19 p2660 N90-25139
Ground-simulation investigations of VTOL airworthiness criteria for terminal-area operations
[NASA-TM-102810] 19 p2660 N90-25141
Program plan: International aircraft operator data base
[IAR-90-1] 19 p2763 N90-25697
Second Annual International Conference on Aging Aircraft
[AD-A222715] 20 p2805 N90-25961
Estimation of defective rate of mechanic-hydraulic components
[ETN-90-97275] 21 p3011 N90-27120
Aircraft Integrated Monitoring Systems
[DLR-MITT-90-04] 22 p3103 N90-27617
Computer modeling and data processing methods: An essential part of jet engine condition monitoring and fault diagnosis 22 p3104 N90-27626
Impact of Emerging NDE-NDI Methods on Aircraft Design, Manufacture, and Maintenance
[AGARD-CP-462] 22 p3184 N90-28068
Inspection reliability 22 p3184 N90-28072
System reliability optimization of aircraft wings
23 p3275 N90-28536
Tests for aircraft interior materials in fire accident
[LR-622] 24 p3423 N90-29337
Application of multifunction inertial reference systems to fighter aircraft 24 p3423 N90-29341

AIRCRAFT SAFETY
Aircraft accident report: Aloha Airlines, Flight 243, Boeing 737-200, N73711, near Maui, Hawaii, April 28, 1988
[PB89-910404] 01 p0004 N90-10013
Safer skies with TCAS: Traffic Alert and Collision Avoidance System
[PB89-169221] 01 p0004 N90-10016
Electro-impulse de-icing testing analysis and design
[NASA-CR-4175] 01 p0007 N90-10031
Design of a final approach spacing tool for TRACON air traffic control
[NASA-TM-102229] 02 p0147 N90-10841
Test and evaluation: Reducing risks to military aircraft from bird collisions. Report to the Chairman, Legislation, and National Security Subcommittee, Committee on Goverment Operations, House of Representatives
[AD-A210670] 02 p0148 N90-10845
Aircraft cabin fire suppression by means of an interior water spray system
[CAA-PAPER-88014] 03 p0303 N90-11719
The 1987 survey of track keeping and altitudes on Heathrow and Gatwick standard instrument departure routes (DAY)
[CAA-PAPER-88010] 03 p0305 N90-11729
A comparison of two subject-controlled attitude measures during somatogravic illusion exposure
[AD-A212528] 04 p0525 N90-13031
The human factors relating to escape and survival from helicopters ditching in water
[AGARD-AG-305(E)] 05 p0576 N90-13358
Adverse weather operations during the Canadian Atlantic storms program 07 p0871 N90-15052
See and avoid/cockpit visibility
[AD-A214214] 07 p0877 N90-15084
International Aircraft Occupant Safety Conference and Workshop proceedings
[AD-A214452] 07 p0877 N90-15085
Application of experimental techniques to store release problems 10 p1304 N90-17545
Aircraft fires: A study of transport accidents from 1975 to the present 10 p1311 N90-17583
Aircraft fire safety: Learning from past accidents
10 p1312 N90-17584
Objectives and results of cabin fire research in Germany 10 p1312 N90-17588
New aircraft cabin and cargo flammability standards for transport category aircraft 10 p1312 N90-17589
Fire prevention in transport airplane passenger cabins
10 p1313 N90-17590

Characteristics of transport, aircraft fires measured by full-scale tests
10 p1313 N90-17591
Aircraft internal fires
10 p1313 N90-17593
Fire science and aircraft safety
10 p1314 N90-17596
The stability of fuel fires
10 p1315 N90-17601
US Navy aircraft fire protection technology
10 p1315 N90-17603
Aircraft fire safety in the Canadian Forces
10 p1315 N90-17604
New materials for civil aircraft furnishing
10 p1316 N90-17609
Modelling time to incapacitation and death from toxic and physical hazards in aircraft fires
10 p1318 N90-17619
Weather data dissemination to aircraft
14 p1907 N90-20934
Statistics on aircraft gas turbine engine rotor failures that occurred in US commercial aviation during 1986
[DOT/FAA/CT-89/30]
14 p1922 N90-21008
Aircraft accident report, United Airlines Flight 811, Boeing 747-122, N4713U, Honolulu, Hawaii, February 24, 1989
[PB90-910401]
15 p2050 N90-21748
Aviation security: Corrective actions underway, but better inspection guidance still needed. Report to the Chairwoman, Government Activities and Transportation Subcommittee, Committee on Government Operations, House of Representatives
[GAO/RCED-88-160]
17 p2347 N90-23367
Aeronautical decisionmaking for air ambulance program administrators
[DOT/FAA/DS-88/8]
17 p2347 N90-23368
Aviation safety: Conditions within the air traffic control work force. Fact sheet for congressional requesters
[GAO/RCED-89-113FS]
20 p2805 N90-25958
Aviation safety: Serious problems continue to trouble the air traffic control work force. Report to congressional requesters
[GAO/RCED-89-112]
20 p2805 N90-25959
Safety net functions
22 p3113 N90-27685
Scope and conception of the pilot support system ASPIO
[LRT-WE-13-FB-88-1]
22 p3233 N90-28334
Modeling and analysis of airport and aircraft operations
[PB90-222167]
23 p3271 N90-28511

AIRCRAFT SPECIFICATIONS

Aircraft/airport compatibility: Some strategic, tactical, and operational issues
[TT-8902]
05 p0585 N90-13409
Analysis of indirect effects of lightning on a metallic A 300 wing: Test report
[REPT-E87/645800]
09 p1162 N90-16726
Preliminary design of a family of three close air support aircraft
[NASA-CR-186070]
09 p1166 N90-16751

AIRCRAFT SPIN

Stall/spin aerodynamic data project
[DOT/FAA/CT-88/29]
06 p0723 N90-14222
AM-X high incidence trials, development and results
[ETN-90-97277]
20 p2814 N90-26016
A flight dynamic model of aircraft spinning
[AR-005-600]
23 p3283 N90-28576

AIRCRAFT STABILITY

NT HOVERING STABILITY
Structural stability augmentation system design using BODEDIRECT: A quick and accurate approach
01 p0023 N90-10116
The active control of an unstable canard aircraft
02 p0156 N90-10894
Stability and control derivatives of the De Havilland DHC-2 BEAVER aircraft
[PB89-217525]
03 p0309 N90-11754
Aerodynamics of thrust vectoring
[NASA-CR-185074]
05 p0575 N90-13354
On the application of modified stepwise regression for the estimation of aircraft stability and control parameters
[REPT-8905]
05 p0583 N90-13400
Design of a spanloader cargo aircraft
[NASA-CR-186046]
06 p0722 N90-14216
An aerodynamic tradeoff study of the scissor wing configuration
[NASA-CR-186576]
14 p1913 N90-20965
Helicopter controllability
[AD-A220078]
18 p2498 N90-24275
The role of C(sub n beta.dyn) in the aircraft stability at high angles of attack
[AD-A221586]
21 p2961 N90-26833
The DELTA MONSTER: An RPV designed to investigate the aerodynamics of a delta wing platform
[NASA-CR-186226]
24 p3431 N90-29381

AIRCRAFT STRUCTURES

NT AIRFRAMES
NT FUSELAGES
The application of TSIM software to act design and analysis on flexible aircraft
01 p0018 N90-10086
Modifying high-order aeroelastic math model of a jet transport using maximum likelihood estimation
01 p0021 N90-10106
Flexible aircraft dynamic modeling for dynamic analysis and control synthesis
01 p0022 N90-10112
Aircraft modal supression system: Existing design approach and its shortcomings
01 p0023 N90-10115
Structural stability augmentation system design using BODEDIRECT: A quick and accurate approach
01 p0023 N90-10116
Thin walled cast high-strength structural parts
01 p0043 N90-10242
Fatigue crack initiation mechanics of metal aircraft structures
[AD-A210567]
01 p0045 N90-10255
Transport composite fuselage technology: Impact dynamics and acoustic transmission
[NASA-CR-4035]
03 p0321 N90-11821
Investigation of difficult component effects on finite element model vibration prediction for the Bell AG-1G helicopter. Volume 2: Correlation results
[NASA-CR-181916-VOL-2]
05 p0654 N90-13814
The microstructure and properties of aluminum-lithium alloys
07 p0897 N90-15187
Fabrication of test-articles from Al-Li 2091 for Fokker 100
07 p0899 N90-15196
Current status of the application of conventional aluminium-lithium alloys and the potential for future developments
07 p0900 N90-15203
Integral fuel tanks - design, production, aging, repair
08 p1021 N90-15906
A dynamicist's view of fuel tank skin durability
08 p1023 N90-15915
Analysis of damaged components from DOE security helicopter N7EG
[DE90-004488]
09 p1162 N90-16729
Optimum element density studies for finite-element thermal analysis of hypersonic aircraft structures
[NASA-TM-4163]
09 p1219 N90-17074
Experimental investigation to suppress flow-induced pressure oscillations in open cavities
[AD-A216285]
10 p1310 N90-17578
Flammability testing of aircraft cabin materials
10 p1316 N90-17611
A CCIR aeronautical mobile satellite report
10 p1372 N90-17954
A study of the structural efficiency of fluted core graphite-epoxy panels
[NASA-TM-101681]
10 p1396 N90-18070
X-29A aircraft structural loads flight testing
[NASA-TM-101715]
12 p1603 N90-19225
A new method for measuring the transmissivity of aircraft transparencies
[AD-A216953]
12 p1714 N90-19842
Computer-aided structural optimisation of aircraft structures
[BR112837]
14 p1915 N90-20973
Robots for aircraft coatings removal: Parameters and requirements
[DE90-009429]
15 p2106 N90-22048
Multilevel decomposition approach to the preliminary sizing of a transport aircraft wing
[NASA-CR-4296]
16 p2200 N90-22557
NASA-UVA light aerospace alloy and structures technology program
[NASA-CR-182607]
16 p2217 N90-22651
Some 1-(diorganooxyphosphonyl)methyl-2,4- and -2,6-dinitro-benzenes
[NASA-CASE-ARC-11425-3]
17 p2367 N90-23475
Modeling growth of fatigue cracks which originate at rivet holes
18 p2645 N90-25060
Flexural fatigue life prediction of closed hat-section using materially nonlinear axial fatigue characteristics
18 p2645 N90-25062
Elevator tab assembly producibility study
[IAR-89-16]
19 p2659 N90-25133
The effect of aircraft size on cabin floor dynamic pulses
[DOT/FAA/CT-88/15]
19 p2659 N90-25136
Mechanical paint removal techniques for aircraft structures
[IAR-89-23]
19 p2682 N90-25254
Behavior of composite/metal aircraft structural elements and components under crash type loads: What are they telling us
[NASA-TM-102681]
19 p2701 N90-25368
Calculation of flight vibration levels of the AH-1G helicopter and correlation with existing flight vibration measurements
[NASA-CR-182031]
19 p2702 N90-25375
Computational crash dynamics. Project 1.2: Computational crash dynamics analysis
[IAR-89-19]
20 p2804 N90-25956
A contribution to the economic, optimal dimensioning, and shaping of aircraft structures using a design model
[ETN-90-96966]
20 p2808 N90-25976
Mechanical paint removal techniques for aircraft structures
[NIAR-90-12]
20 p2842 N90-26166
Materials and structures for 2000 and beyond: An attempted forecast by the DLR Materials and Structures Department
[ESA-TT-1154-REV]
20 p2843 N90-26173
Neural networks for detecting defects in aircraft structures
[IAR-90-4]
20 p2873 N90-26345
Proceedings of the 1987 Aircraft/Engine Structural Integrity Program (ASIP/ENSIP) Conference
[AD-A198037]
21 p2956 N90-26807
Lessons learned for composite aircraft structures qualification
21 p2956 N90-26808
An aluminum quality breakthrough for aircraft structural reliability
21 p2957 N90-26816
Application of damage tolerance
21 p2958 N90-26817
Photoelasticity: A cost effective design tool
21 p2958 N90-26819
Finite element models of USAF aircraft structures
21 p2958 N90-26820
Automated analysis of MXU-553 flight data
21 p2958 N90-26821
A review of crashworthiness of composite aircraft structures
[AD-A221555]
22 p3115 N90-27697
A Protection And Detection Surface (PADS) for damage tolerance
[NASA-TP-3011]
22 p3135 N90-27788
Reinforcing fibers and technology development for resin composites. Consequences for aircraft structures
[FOA-C-20777-2.5]
22 p3154 N90-27883
Characterization of the 7175 T7352. Dissection of a die casting standard spar
[CEAT-PV-M5/528900]
22 p3158 N90-27906
NDI-concept for composites in future military aircraft
22 p3184 N90-28070
An ultrasonic system for in-service non-destructive inspection of composite structures
22 p3185 N90-28076
A technique for rapid inspection of composite aircraft structure for impact damage
22 p3185 N90-28077
In-service inspection of composite components on aircraft at depot and field levels
22 p3186 N90-28078
Neutron radiography: Applications and systems
22 p3186 N90-28080
New aspects in aircraft inspection using eddy current methods
22 p3187 N90-28085
Inspection system for in-situ inspection of aircraft composite structures
22 p3188 N90-28091
Use of acoustic emission for continuous surveillance of aircraft structures
22 p3188 N90-28092
Aircraft battle damage repair of transparencies
[AD-A224168]
24 p3432 N90-29387
Evaluation of static and fatigue properties of thin sheets of 8090-T8 aluminum-lithium alloy and observation of its fracture surfaces
[NAL-TR-1039]
24 p3453 N90-29499
Fatigue, static tensile strength and stress corrosion of aircraft materials and structures. Part 1: Text
[LR-630-PT-1-REV]
24 p3482 N90-29682
Fatigue, static tensile strength and stress corrosion of aircraft materials and structures. Part 2: Figures
[LR-630-PT-2]
24 p3482 N90-29683

AIRCRAFT SURVIVABILITY

Aircraft live fire testing
02 p0154 N90-10879
In service life monitoring system using g-meter readings and mass configuration control
[ETN-89-95218]
03 p0356 N90-12035
Multichannel on-board load and fatigue monitoring
22 p3103 N90-27621
Advanced algorithms design and implementation in on-board microprocessor systems for engine life usage monitoring
22 p3104 N90-27628
Survivable penetration
24 p3428 N90-29363

AIRCRAFT TIRES

Evaluation of two transport aircraft and several ground test vehicle friction measurements obtained for various runway surface types and conditions. A summary of test results from joint FAA/NASA Runway Friction Program
[NASA-TP-2917]
08 p1021 N90-15902
Modeling and analysis of the space shuttle nose-gear tire with semianalytic finite elements
[NASA-TP-2977]
12 p1670 N90-19595
Runaway rubber removal
[AD-A218349]
13 p1759 N90-20100
Reliability and performance of friction measuring tires and friction equipment correlation
[AD-A223694]
24 p3436 N90-29408

AIRCRAFT WAKES
NT HELICOPTER WAKES
NT PROPELLER SLIPSTREAMS
NT SLIPSTREAMS
Development of a VSAERO (Vortex Separation Aerodynamics) model of the F/A-18
[AD-A212442] 04 p0448 N90-12566
Effect of pylon wake with and without pylon blowing on propeller thrust
[NASA-TM-4162] 06 p0718 N90-14190
Wind tunnel study of wake downwash behind A 6 percent scale model B1-B aircraft
[DE90-011783] 20 p2802 N90-25941
AIRCREWS
U FLIGHT CREWS
AIRDROPS
Modeling the effects of the use of GPS (Global Positioning System) derived altitude indication in the C-17A airdrop system
[AD-A215366] 09 p1166 N90-16748
Field-of-view assessment of low-level flight and an airdrop in the C-130 Weapon System Trainer (WST)
[AD-A218504] 16 p2200 N90-22559
Advanced recovery systems wind tunnel test report
[NASA-CR-177563] 22 p3108 N90-27653
AIRFIELDS
U AIRPORTS
AIRFOIL CHARACTERISTICS
U AIRFOILS
AIRFOIL OSCILLATIONS
NT WING OSCILLATIONS
Dynamic testing techniques and applications for an aeroelastic rotor test facility 05 p0584 N90-13406
Nonlinear phenomena in computational transonic aeroelasticity 07 p0874 N90-15070
An interactive boundary-layer method for unsteady airfoil flows. Part 1: Quasi-steady-state model
[AD-A221220] 18 p2493 N90-24250
Flow visualization of dynamic stall on an oscillating airfoil
[AD-A222202] 21 p2954 N90-26797
AIRFOIL PROFILES
NT WING PROFILES
Design of the low-speed NLF(1)-0414F and the high-speed HSNLF(1)-0213 airfoils with high-lift systems 04 p0444 N90-12540
Wind tunnel results of the high-speed NLF(1)-0213 airfoil 04 p0444 N90-12542
Design and test of a natural laminar flow/large Reynolds number airfoil with a high design cruise lift coefficient 04 p0444 N90-12543
Residual interference assessment in adaptive wall wind tunnels
[NASA-CR-181896] 04 p0458 N90-12625
Computation of unsteady transonic flow about airfoils in frequency domain using the full-potential equation 06 p0719 N90-14198
Detection of flow instabilities at airfoil profiles using piezoelectric arrays 08 p1067 N90-16175
Determination of dynamic surface forces using piezoelectric arrays 08 p1080 N90-16249
Use of the film-of-oil technique for profile measurements in the Transonic Wind tunnel Brunswick (TWB) 08 p1080 N90-16252
Definition, transformation-formulae and measurements of tipvane angles
[IW-R510] 08 p1097 N90-16351
CAST-10-2/DOA 2 Airfoil Studies Workshop Results
[NASA-CP-3052] 10 p1323 N90-17647
Investigation of CAST-10-2/DOA 2 airfoil in NAE high Reynolds number two-dimensional test facility 10 p1324 N90-17654
Experimental and theoretical aerodynamic characteristics of a high-lift semispan wing model
[NASA-TP-2990] 13 p1749 N90-20046
Optimum hypersonic airfoils with attached shocks 14 p1912 N90-20960
The MANTA: An RPV design to investigate forces and moments on a lifting surface
[NASA-CR-186227] 14 p1915 N90-20971
Inverse design of airfoil contours: Constraints, numerical method, and applications 14 p1917 N90-20980
An efficient airfoil design method using the Navier-Stokes equations 14 p1917 N90-20981
Numerical optimization of target pressure distributions for subsonic and transonic airfoil design 14 p1919 N90-20993
Adaptive grid embedding for the two-dimensional flux-split Euler equations
[NASA-CR-186533] 14 p2019 N90-21571
Graphs of the state of stress at rounded corners
[MEMT-1] 15 p2119 N90-22122
Aerodynamics of a full-scale, non rotating wind turbine blade under natural wind conditions
[RISOE-M-2768] 15 p2123 N90-22144
The SKY SHARK: An RPV designed to investigate the pressure distribution on a lifting surface
[NASA-CR-186222] 21 p2959 N90-26824
A two dimensional study of rotor/airfoil interaction in hover
[NASA-CR-183272] 22 p3114 N90-27694
WingDesign: Program for the structural design of a wing cross-section
[LR-627] 24 p3433 N90-29390
AIRFOIL SECTIONS
U AIRFOIL PROFILES
AIRFOIL THICKNESS
U AIRFOIL PROFILES
AIRFOILS
NT AERIAL RUDDERS
NT AILERONS
NT CIRCULATION CONTROL AIRFOILS
NT DELTA WINGS
NT ELEVATORS (CONTROL SURFACES)
NT ELEVONS
NT FIXED WINGS
NT FLAPS (CONTROL SURFACES)
NT FLEXIBLE WINGS
NT HORIZONTAL TAIL SURFACES
NT JET FLAPS
NT JOINED WINGS
NT LAMINAR FLOW AIRFOILS
NT LEADING EDGE FLAPS
NT LIFTING ROTORS
NT LOW ASPECT RATIO WINGS
NT OBLIQUE WINGS
NT PROPELLER BLADES
NT RECTANGULAR WINGS
NT RIGID ROTORS
NT RIGID WINGS
NT RING WINGS
NT ROTARY WINGS
NT SLENDER WINGS
NT SPOILERS
NT SUPERCRITICAL AIRFOILS
NT SUPERCRITICAL WINGS
NT SWEPT FORWARD WINGS
NT SWEPT WINGS
NT SWEPTBACK WINGS
NT TABS (CONTROL SURFACES)
NT THIN AIRFOILS
NT THIN WINGS
NT TILTING ROTORS
NT UPPER SURFACE BLOWN FLAPS
NT VARIABLE SWEEP WINGS
NT WINGS
Basic studies of the unsteady flow past high angle of attack airfoils
[AD-A210252] 01 p0002 N90-10008
Goertler instability on an airfoil: Comparison of marching solution with experimental observations 01 p0063 N90-10364
Simultaneous detection of separation and transition in surface shear layers 01 p0064 N90-10368
The structure of separated flow regions occurring near the leading edge of airfoils - including transition
[NASA-CR-185853] 03 p0299 N90-11695
Goertler instability on an airfoil 04 p0440 N90-12517
The design of an airfoil for a high-altitude, long-endurance remotely piloted vehicle 04 p0445 N90-12545
Studies of gas turbine heat transfer airfoil surfaces and end-wall cooling effects
[AD-A212451] 04 p0457 N90-12620
Analysis of experimental data for CAST 10-2/DOA 2 supercritical airfoil at low Reynolds numbers and application to high Reynolds number flow
[AD-A211654] 05 p0571 N90-13326
Convective heat transfer measurements from a NACA 0012 airfoil in flight and in the NASA Lewis Icing Research Tunnel
[NASA-TM-102448] 05 p0642 N90-13750
Navier-Stokes solutions of 2-D transonic flow over unconventional airfoils 06 p0719 N90-14195
A one equation turbulence model for transonic airfoils 06 p0719 N90-14199
Computational investigation of incompressible airfoil flows at high angles of attack
[AD-A205885] 06 p0720 N90-14201
Visualization of boundary layer transition zone movement on oscillating airfoils with shear-sensitive liquid-crystal coatings
[DE89-009570] 06 p0721 N90-14210
Stall/spin aerodynamic data project
[DOT/FAA/CT-88/29] 06 p0723 N90-14222
Effect of unshielded and shielded horn balances on hinge moment coefficients for controls at low speeds
[ESDU-89003-A] 06 p0726 N90-14238
Unsteady aerodynamics of oscillating and rapidly pitched airfoils 07 p0875 N90-15074
Experimental measurements of the laminar separation bubble on an Eppler 387 airfoil at low Reynolds numbers
[NASA-CR-186263] 07 p0929 N90-15380
Test techniques for cryogenic wind tunnels 08 p1030 N90-15952
Models for cryogenic wind tunnels 08 p1031 N90-15956
An interactive method for the flow calculation of airfoils with local separation regions 08 p1069 N90-16190
Convergence speeding up in the calculation of the viscous flow about an airfoil 08 p1070 N90-16194
Periodically unsteady effects on profiles, induced by separation 08 p1070 N90-16196
An improvement of convection fidelity in Euler calculations 09 p1159 N90-16709
Numerical solutions of the linearized Euler equations for unsteady vortical flows around lifting airfoils
[NASA-TM-102466] 10 p1307 N90-17562
Effect of riblets on flow separation from a cylinder and an airfoil in subsonic flow
[AD-A216197] 10 p1309 N90-17574
CAST-10-2/DOA 2 Airfoil Studies Workshop Results
[NASA-CP-3052] 10 p1323 N90-17647
Nonlinear transonic Wall-Interference Assessment/Correction (WIAC) procedures and application to cast-10 airfoil results from the NASA 0.3-m TCT 8- by 24-inch Slotted Wall Test Section (SWTS) 10 p1323 N90-17648
High Reynolds number tests of the CAST-10-2/DOA 2 transonic airfoil at ambient and cryogenic temper ature conditions 10 p1324 N90-17650
Some Navier-Stokes calculations for the CAST-10 airfoil 10 p1324 N90-17651
Main results of CAST-10 airfoil tested in T2 cryogenic wind tunnel 10 p1324 N90-17652
An experimental AWTS process and comparisons of ONERA T2 and 0.3-m TCT AWTS data for the ONERA CAST-10 aerofoil 10 p1324 N90-17653
Investigation of CAST-10-2/DOA 2 airfoil in NAE high Reynolds number two-dimensional test facility 10 p1324 N90-17654
Comparison of NAE porous wall and NASA adaptive wall test results using the NAE CAST-10 airfoil model 10 p1325 N90-17656
Comparison of two- and three-dimensional Navier-Stokes solutions with NASA experimental data for CAST-10 airfoil 10 p1325 N90-17658
Unsteady viscous calculation method for cascades with leading edge induced separation 11 p1459 N90-18408
Asymptotic analysis of transonic flow through oscillating cascades 11 p1462 N90-18421
Measurement of velocity profiles and Reynolds stresses on an oscillating airfoil 11 p1463 N90-18427
Calculation of excrescence drag magnification due to pressure gradient at high subsonic speeds
[ESDU-87004] 12 p1598 N90-19195
Heat transfer measurements from a NACA 0012 airfoil in flight and in the NASA Lewis icing research tunnel
[NASA-CR-4278] 12 p1599 N90-19203
Analysis and design of symmetrical airfoils
[PD-CF-8943] 12 p1601 N90-19213
Numerical simulations of supersonic flow through oscillating cascade sections
[NASA-TM-103100] 13 p1750 N90-20051
A comparison of two-and three-dimensional S809 airfoil properties for rough and smooth HAWT (Horizontal-Axis Wind Tunnel) rotor operation
[DE89-009512] 13 p1827 N90-20492
Ultrasonic techniques for aircraft ice accretion measurement 14 p1906 N90-20926
Comparison of C- and O-grid generation methods using a NACA 0012 airfoil
[AD-A216375] 14 p1910 N90-20948
Progress in inverse design and optimization in aerodynamics 14 p1916 N90-20977
An efficient airfoil design method using the Navier-Stokes equations 14 p1917 N90-20981
A fast collocation method for transonic airfoil design 14 p1917 N90-20984
A computational design method for shock free transonic cascades and airfoils 14 p1918 N90-20986
A tool for automatic design of airfoils in different operating conditions 14 p1919 N90-20994
The use of numerical optimization for helicopter airfoil and blade design 14 p1919 N90-20995
Aerodynamic design by optimization 14 p1920 N90-20996
Optimization of aerodynamic designs using computational fluid dynamics 14 p1920 N90-20999
The effects of compressor endwall flow on airfoil incidence and deviation 14 p1922 N90-21011
Research on cascade secondary and tip-leakage flows: Periodicity and surface flow visualization 14 p1925 N90-21026

Control of flow separation and mixing by aerodynamic excitation
[NASA-TM-103131] 15 p2047 N90-21735
A computer code for the prediction of aerodynamic characteristics of lifting airfoils at transonic speed
[DLC-EST-TN-030] 17 p2346 N90-23359
Prediction of aerodynamic performance of airfoils in low Reynolds number flows
[DLC-EST-TN-031] 17 p2346 N90-23360
Euler code predicted separation at the airfoil trailing edge
[FFA-TN-1989-30] 17 p2346 N90-23364
The computation of turbulent thin shear flows associated with flow around multielement aerofoils
18 p2491 N90-24240
Reduced order models for nonlinear aerodynamics
18 p2492 N90-24244
Aerodynamic pressure measurements on a rotating wind turbine blade
[DE90-000327] 18 p2494 N90-24256
An analytic study of nonsteady two-phase laminar boundary layer around an airfoil
18 p2643 N90-25051
DRAG-n-FLY: A proposal in response to a low Reynolds number station keeping mission
[NASA-CR-186666] 19 p2658 N90-25130
Computation of viscous aerodynamic characteristics of 2-D airfoils for helicopter applications
[NLR-MP-88052-U] 20 p2804 N90-25951
On central-difference and upwind schemes
[NASA-CR-182061] 20 p2917 N90-26595
Flow visualization of dynamic stall on an oscillating airfoil
[AD-A222202] 21 p2954 N90-26797
A heat transfer analysis for rough turbine airfoils
[AD-A221942] 21 p2960 N90-26831
A comparison of two central difference schemes for solving the Navier-Stokes equations
[NASA-TM-102815] 22 p3108 N90-27654
Development of a linearized unsteady aerodynamic analysis for cascade gust response predictions
[NASA-CR-4308] 22 p3108 N90-27655
Aerodynamics of a linear oscillating cascade
[NASA-TM-103250] 22 p3108 N90-27657
Two-dimensional wind tunnel test and comparison with calculations for a 15.2 percent thick airfoil section for wind turbines
[FFA-TN-1990-16] 23 p3269 N90-28501
The effect of rapid spoiler deployment on the transient forces on an aerofoil 23 p3274 N90-28527
Comparison of wind tunnel airfoil performance data with wind turbine blade data
[DE90-000343] 24 p3418 N90-29308
A boundary-layer transition model for the Navier-Stokes computation for a natural-laminar-flow airfoil
[NAL-TR-1038T] 24 p3421 N90-29328
The computation and analysis of acoustic waves in transonic airfoil-vortex interactions
24 p3542 N90-30031

AIRFRAME MATERIALS
New materials and structural concepts for space transportation systems 09 p1179 N90-16837
Aircraft crash survival design guide. Volume 5: Aircraft postcrash survival
[AD-A218438] 16 p2198 N90-22549
Experimental analysis of the buckling of composite plates under compression loads
[IMFL-89-28] 22 p3193 N90-28119
The stress and temperature dependence of creep in an Al-2.0 wt percent Li alloy
[AD-A223676] 24 p3449 N90-29480

AIRFRAMES
A supersonic through-flow fan engine airframe integration study
[NASA-CR-185140] 01 p0001 N90-10004
A review of Australian and New Zealand investigations on aeronautical fatigue during the period April 1987 to March 1989
[AD-A210373] 01 p0006 N90-10026
How to control unstable missile airframes: Methodology and limitations 01 p0013 N90-10060
Winged versus wingless airframes
01 p0015 N90-10073
Airframe structural dynamic considerations in rotor design optimization
[NASA-TM-101646] 03 p0360 N90-12057
Investigation of difficult component effects on finite element model vibration prediction for the Bell AH-1G helicopter. Volume 1: Ground vibration test results
[NASA-CR-181916-VOL-1] 03 p0360 N90-12058
Airframe design considerations: Overview --- rotor design optimization 04 p0451 N90-12586
Investigation of difficult component effects on finite element model vibration prediction for the Bell AG-1G helicopter. Volume 2: Correlation results
[NASA-CR-181916-VOL-2] 05 p0654 N90-13814
An experimental investigation of the interaction between a model rotor and airframe in forward flight
06 p0723 N90-14219
An analytical method for the prediction of unsteady rotor/airframe interactions in forward flight
06 p0724 N90-14223
Application of the joined wing to tiltrotor aircraft
[NASA-CR-177543] 07 p0879 N90-15093
The use of prototypes in selected foreign fighter aircraft development programs: Rafale, EAP, Lavi, and Gripen
[AD-A214500] 09 p1159 N90-16707
Hypersonic nozzle/afterbody performance at low Mach numbers
[AD-A216223] 10 p1309 N90-17575
Calculation of flight vibration levels of the AH-1G helicopter and correlation with existing flight vibration measurements
[NASA-CR-181923] 11 p1518 N90-18743
Fatigue crack initiation and small crack growth in several airframe alloys
[NASA-TM-102598] 11 p1518 N90-18746
Static strength and damage tolerance tests on the Fokker 100 airframe
[NLR-MP-88023-U] 12 p1604 N90-19228
Floor pull test of a transport airframe section
[DOT/FAA/CT-TN88/14] 13 p1754 N90-20072
Compendium of abstracts and viewgraphs.
[AD-A217189] 13 p1767 N90-20140
Plan, formulate, and discuss a NASTRAN finite element model of the UH-60A helicopter airframe
[NASA-CR-181975] 13 p1818 N90-20439
NASA airframe structural integrity program
[NASA-TM-102637] 14 p1993 N90-21422
Aircraft crash survival design guide. Volume 3: Aircraft structural crash resistance
[AD-A218436] 16 p2198 N90-22547
Flutter investigations on a Transavia PL12/T-400 aircraft
[AD-A219108] 16 p2203 N90-22570
Characterisation of fatigue of aluminium alloys by acoustic emission. Part 2: Discrimination between primary and other emissions
[AERE-R-13303-PT-2] 17 p2375 N90-23523
Ground shake test of the UH-60A helicopter airframe and comparison with NASTRAN finite element model predictions
[NASA-CR-181993] 19 p2661 N90-25143
Velocity measurements on a lifting rotor/airframe configuration in low speed forward flight
21 p2953 N90-26790
Aircraft lightning protection handbook
[AD-A222716] 22 p3110 N90-27668
Acoustic emission detection of crack presence and crack advance during flight 22 p3186 N90-28082
NASA Langley Research Center National Aero-Space Plane Mission simulation profile sets
[NASA-TM-102670] 23 p3276 N90-28541
Correlation of AH-1G airframe flight vibration data with a coupled rotor-fuselage analysis
[NASA-CR-181974] 23 p3338 N90-28865
Plan, execute, and discuss vibration measurements and correlations to evaluate a NASTRAN finite element model of the AH-64 helicopter airframe
[NASA-CR-181973] 23 p3338 N90-28866
Proceedings of damping '89. Volume 1: Pages AAB-1 through DCD-11
[AD-A223431] 24 p3479 N90-29664
Fractographic analysis of fatigue failures of airframe equipment parts: Examples of a rod end housing and a rod end cap
[NAL-TR-1047] 24 p3483 N90-29686

AIRGLOW
NT GEOCORONAL EMISSIONS
NT NIGHTGLOW
Ionospheric irregularities due to powerful HF radio transmissions 02 p0245 N90-11389
Investigation of atmospheric emissions in ultraviolet, vacuum ultraviolet, and extreme ultraviolet wavelength
[AD-A212169] 03 p0371 N90-12123
Comparison of the LOWTRAN 7 code and S3-4 satellite measurements of UV radiance
[AD-A211356] 03 p0372 N90-12124
Spatial characteristics of airglow and solar scatter radiance from the earth's atmosphere
[AD-A211358] 03 p0372 N90-12126
The effects of gravity waves on horizontal layers: Simulation and interpretation 05 p0660 N90-13852
Measurement of optical radiations in spacecraft environments
[AD-A213814] 07 p0950 N90-15497
Metal vaporisers: Bicentennial series of five historical monographs
[ISBN-0-642-13584-3] 08 p1052 N90-16081
Effects of gravity waves on the polar O2 and OH airglow 08 p1101 N90-16373
Study of the atmospheric emissions of OI wavelength 557.7 nm and O2 (0,0) wavelength 761.9 nm in the equatorial region utilizing measurement of photometer on-board a rocket
[INPE-4811-TDL/358] 11 p1533 N90-18827
Spacecraft optical contamination environment
[AD-A218088] 13 p1889 N90-20838
Optical instrumentation support for the airborne ionospheric observatory
[AD-A218207] 13 p1889 N90-20839
Low latitude F-region dynamical processes from atomic oxygen nightglow emissions
[INPE-4999-PRE/1561] 14 p2006 N90-21494

AIRLINE OPERATIONS
View on recent fuel costs in airlines
[NAL-TM-569] 02 p0289 N90-11653
National Airspace System flight planning operational concept
[DOT/FAA/DS-89/30] 05 p0577 N90-13362
Indianapolis Downtown Heliport: Operations analysis and marketing history
[REPT-90RR-13] 14 p1930 N90-21049
FAA (Federal Aviation Administration) aviation forecasts, fiscal years 1990-2001
[AD-A219165] 16 p2195 N90-22530
The effect of noise-abatement profiles on noise immissions and human annoyance underneath a subsequent climbpath 18 p2610 N90-24865
Stage 2 re-engining: The only way to achieve a real stage 3 aircraft
[PNR90636] 20 p2808 N90-25977
Application of a company data link at Lufthansa German Airlines 22 p3113 N90-27689
Evaluation of existing aircraft operator data bases
[DOT/FAA/CT-90/18] 22 p3260 N90-28463
Modeling and analysis of airport and aircraft operations
[PB90-222167] 23 p3271 N90-28511
Airline productivity relating on the fuel cost. (2): Fuel consumption values and fuel efficiency
[NAL-TM-604-2] 24 p3422 N90-29333

AIRLOCK MODULES
Independent Orbiter Assessment (IOA): Assessment of the life support and airlock support systems, volume 1
[NASA-CR-185581-VOL-1] 02 p0174 N90-10977
Independent Orbiter Assessment (IOA): Assessment of the life support and airlock support systems, volume 2
[NASA-CR-185581-VOL-2] 02 p0174 N90-10978
Columbus scientific airlock 18 p2541 N90-24503

AIRPORT BEACONS
NT DISCRETE ADDRESS BEACON SYSTEM

AIRPORT LIGHTS
NT RUNWAY LIGHTS

AIRPORT PLANNING
Development and evaluation at ATCEU of executive and support operations, phase 4A/3D --- ATCEU (Air Traffic Control Evaluation Unit)
[CAA-PAPER-88017] 04 p0449 N90-12572
Aircraft/airport compatibility: Some strategic, tactical, and operational issues
[TT-8902] 05 p0585 N90-13409
US civil airmen statistics: Calendar year 1989
[AD-A220438] 17 p2343 N90-23342
The Federal Aviation Administration plan for research, engineering and development. Volume 1: Program plan
[AD-A221263] 19 p2800 N90-25930
The potential for an extra runway at Heathrow: A preliminary feasibility study
[TT-9007] 24 p3435 N90-29403

AIRPORT SECURITY
Aviation security: Corrective actions underway, but better inspection guidance still needed. Report to the Chairwoman, Government Activities and Transportation Subcommittee, Committee on Government Operations, House of Representatives
[GAO/RCED-88-160] 17 p2347 N90-23357
Investigations of monopulse-assisted radio location systems for the safety of surface traffic
[ETN-90-97324] 21 p2956 N90-26806

AIRPORT SURFACE DETECTION EQUIPMENT
Investigations of monopulse-assisted radio location systems for the safety of surface traffic
[ETN-90-97324] 21 p2956 N90-26806
Approach towards a future integrated airport surface traffic management 22 p3113 N90-27686
Experimental study towards a future airport ground movement simulator 22 p3113 N90-27687

AIRPORT TOWERS
FAA air traffic activity: Fiscal year 1988
[AD-A211338] 04 p0449 N90-12570
FAA air traffic control operations concepts. Volume 7: ATCT (Airport Traffic Control Towers) tower controllers
[AD-A210455] 09 p1163 N90-16730
Atlanta tower simulation, volume 1
[DOT/FAA/CT-TN89/27-VOL-1] 21 p2961 N90-26835

Atlanta tower simulation. Volume 2: Appendixes
[DOT/FAA/CT-TN89/27-VOL-2] 21 p2961 N90-26836

AIRPORTS
NT HELIPORTS
ILS (Instrument Landing System) mathematical modeling study on the effects of proposed hangar construction west of runway 18R on localizer performance at Dallas-Fort Worth International Airport
[AD-A210631] 01 p0005 N90-10019
A simulation study of landing time allocation procedures for use in computer-assisted air traffic management systems
[AD-A212159] 03 p0303 N90-11722
Development and evaluation at ATCEU of executive and support operations, phase 4A/3D — ATCEU (Air Traffic Control Evaluation Unit)
[CAA-PAPER-88017] 04 p0449 N90-12572
California air transportation study: A transportation system for the California Corridor of the year 2010
[NASA-CR-186219] 06 p0722 N90-14212
National airspace system: Airport movement area control operational concept
[WP-89W00181] 07 p0878 N90-15086
Cumulative airport noise exposure metrics: An assessment of evidence for time-of-day weightings, revision
[AD-A214878] 09 p1170 N90-16773
Synthetic aperture radar imagery of airports and surrounding areas: Archived SAR data
[NASA-CR-4275] 11 p1453 N90-18371
Synthetic aperture radar imagery of airports and surrounding areas: Philadelphia Airport
[NASA-CR-4280] 11 p1453 N90-18372
Low-energy gamma ray attenuation characteristics of aviation fuels
[NASA-TP-2974] 11 p1543 N90-18882
Activities report in civil aviation
[ETN-90-95471] 13 p1753 N90-20067
Airfields on antarctic glacier ice
[AD-A217638] 13 p1759 N90-20097
Criteria for polymer concrete on airport pavements
[DOT/FAA/DS-89/18] 14 p1929 N90-21045
MLS mathematical model validation study using airborne MLS data from Midway Airport engineering flight tests, August 1988
[DOT/FAA/CT-TN90/2] 17 p2349 N90-23378
Synthetic aperture radar imagery of airports and surrounding areas: Denver Stapleton International Airport
[NASA-CR-4305] 18 p2495 N90-24257
Criteria for coal tar seal coats on airport pavements. Volume 2: Laboratory and field studies
[AD-A220167] 18 p2498 N90-24277
FAA/NASA En Route Noise Symposium
[NASA-CP-3067] 18 p2608 N90-24853
The effect of noise-abatement profiles on noise immissions and human annoyance underneath a subsequent climbpath 18 p2610 N90-24865
Predicting the audibility and annoyance of unducted fan engines 18 p2610 N90-24869
En route noise annoyance laboratory test: Preliminary results 18 p2611 N90-24870
An aircraft noise study in Norway 18 p2611 N90-24872
Replication of NASPAC Dallas/Fort Worth study
[DOT/FAA/CT-TN90/26] 19 p2657 N90-25123
Atlanta tower simulation, volume 1
[DOT/FAA/CT-TN89/27-VOL-1] 21 p2961 N90-26835
Atlanta tower simulation. Volume 2: Appendixes
[DOT/FAA/CT-TN89/27-VOL-2] 21 p2961 N90-26836
Air Force procedure for predicting aircraft noise around airbases: Airbase operations program (BASEOPS) description
[AD-A223069] 21 p3072 N90-27466
Public-sector aviation issues, 1987 to 1988 graduate research award papers
[PB90-191206] 22 p3110 N90-27667
Real-time adaptive aircraft scheduling
[NASA-CR-177558] 22 p3110 N90-27669
Approach towards a future integrated airport surface traffic management 22 p3113 N90-27686
Airport pavement drainage
[DOT/FAA/RD-90/24] 22 p3122 N90-27728
Airport capacity enhancement plan 1989
[PB90-197997] 23 p3270 N90-28507
Modeling and analysis of airport and aircraft operations
[PB90-222167] 23 p3271 N90-28511
Proceedings of a workshop on Future Airport Passenger Terminals
[PB90-213620] 23 p3284 N90-28580
Development of acceptance plans for airport pavement materials. Volume 1: Development
[DOT/FAA/RD-90/15] 23 p3284 N90-28581
Development of a thickness design procedure for stabilized layers under rigid airfield pavements
[DOT/FAA/RD-90/22] 23 p3284 N90-28582
The cost of air service fragmentation
[TT-9010] 24 p3422 N90-29334
The potential for an extra runway at Heathrow: A preliminary feasibility study
[TT-9007] 24 p3435 N90-29403

AIRS (RECONNAISSANCE SYS)
U AIRBORNE INTEGRATED RECONNAISSANCE SYSTEM

AIRSHIPS
Further development and limited flight testing of the CycloCrane
[AD-A215519] 09 p1167 N90-16754

AIRSPACE
National airspace system plan: Facilities, equipment, associated development and other capital needs
[AD-A215882] 11 p1453 N90-18373
An early overview of tiltrotor aircraft characteristics and pilot procedures in civil transport applications
[DOT/FAA/DS-89/37] 14 p1921 N90-21003
Effects of monitoring under high and low taskload on detection of flashing and colored radar targets
[AD-A220313] 17 p2439 N90-23895
Proposed definition of the term en route in en route aircraft noise 18 p2608 N90-24854
Airport capacity enhancement plan 1989
[PB90-197997] 23 p3270 N90-28507
An analysis of GPS as the sole means navigation system in US Navy aircraft 24 p3425 N90-29350

AIRSPEED
Evaluation of the improved OV-1D anti-icing system, phase 2
[AD-A213928] 07 p0877 N90-15083
Low air speed computation for helicopters: A new approach 09 p1165 N90-16744
Reducing C130E Hercules operating costs in the Royal Australian Air Force and the United States Air Force by increasing cruise speeds
[AD-A215747] 10 p1319 N90-17629
Optimal control of an aircraft flying through a downburst 15 p2053 N90-21765

AIRWORTHINESS
U AIRCRAFT RELIABILITY

AIRWORTHINESS REQUIREMENTS
U AIRCRAFT RELIABILITY

ALANINE
NT PHENYLALANINE
Boron analogues of amino acids and derivatives
[AD-A211311] 03 p0379 N90-12157

ALARMS
U WARNING SYSTEMS

ALASKA
HIPAS 1987-88: ULF research and campaign support
[AD-A211720] 03 p0339 N90-11933
Crustal structure studies utilizing earthquake sequences
[AD-A212916] 05 p0666 N90-13895
The interaction and variation of waves and turbulence from MST radar data
[AD-A212849] 05 p0670 N90-13906
Hypotheses testing of watershed/landscape dynamics in northern Alaska using digital analysis
[DE90-006721] 13 p1820 N90-20450
A cloud climatology for the North Pacific area centered at Shemya, Alaska
[AD-A217334] 13 p1844 N90-20585
The chemical and structural properties of sea ice in the southern Beaufort Sea
[AD-A219746] 17 p2418 N90-23776
Ecological study of peat landforms in Canada and Alaska
[NASA-CR-184923] 19 p2705 N90-25391
Geologic studies in Alaska by the US geological survey, 1988
[PB90-180993] 22 p3211 N90-28213

ALBEDO
NT EARTH ALBEDO
Senegalese land surface change analysis and biophysical parameter estimation using NOAA AVHRR spectral data
[NASA-CR-186120] 05 p0664 N90-13883
Atlas of albedo and absorbed solar radiation derived from Nimbus 6 earth radiation budget data set, July 1975 to May 1978
[NASA-RP-1230] 06 p0815 N90-14741
Quantitative studies of the Martian south polar region using spacecraft images 15 p2191 N90-22514
Physical parameterization of snow albedo for use in climate models
[PB90-167313] 19 p2712 N90-25433
An eight-month climatology of marine stratocumulus cloud fraction, albedo, and integrated liquid water 22 p3214 N90-28233
Spectral absorption of marine stratocumulus clouds derived from in situ cloud radiation measurements 22 p3215 N90-28238

ALBUMINS
Human serum albumin crystals and method of preparation
[NASA-CASE-MFS-28234-1] 13 p1850 N90-20616

ALCOHOLS
NT ETHYL ALCOHOL
NT GLYCOLS
NT ISOPROPYL ALCOHOL
NT METHYL ALCOHOL
NT PHENOLS
NT POLYVINYL ALCOHOL
An investigation of flame spread over shallow liquid pools in microgravity and nonair environments
[NASA-TM-102425] 05 p0630 N90-13880
Low frequency polarized and depolarized light scattering in H-bonded liquids: CH3(CH2)n-1OH (n=1,...5)
[PREPRINT-693] 05 p0700 N90-14100
Comparison of structural subunits of the core light-harvesting complexes of photosynthetic bacteria
[DE90-001412] 06 p0819 N90-14765
Orthobaric densities and molar volumes of liquids: Alcohols
[ESDU-89037] 07 p0897 N90-15184
Alcohol and blends as motor fuels
[DE90-003517] 08 p1053 N90-16085
Optimum catalytic process for alcohol fuels from syngas
[DE90-005290] 11 p1494 N90-18600
Optimum catalytic process for alcohol fuels from syngas
[DE90-007188] 11 p1495 N90-18604
Supersonic jet studies of benzyl alcohols: Minimum energy conformations and torsional motion
[AD-A221815] 21 p2980 N90-26934
Analysis of the T63-A-700 engine used in alcohol turbine fuel extender test
[DOT/FAA/CT-TN90/18] 23 p3278 N90-28549

ALDEHYDES
NT FORMALDEHYDE

ALERTNESS
Attention and vigilance in speech perception
[AD-A210493] 01 p0095 N90-10539
High peak power microwave pulses at 2.37 GHz: No effects on vigilance performance in monkeys
[AD-A219570] 17 p2433 N90-23863
Loss of alertness and consciousness from pilot position during long range flight 23 p3360 N90-28990

ALFVEN WAVES
U MAGNETOHYDRODYNAMIC WAVES

ALGAAS
U ALUMINUM GALLIUM ARSENIDES

ALGAE
Biochemical cycling and fluxes between the deep euphotic zone and other oceanic realms
[PB89-152458] 01 p0089 N90-10509
Free swimming organisms: Microgravity as an investigative tool 05 p0678 N90-13949
Utilization of non-conventional systems for conversion of biomass to food components
[NASA-CR-177545] 07 p0968 N90-15591
Design and operation of an outdoor microalgae test facility
[DE89-009493] 13 p1848 N90-20608
Carbon and hydrogen metabolism of green algae in light and dark
[DE90-008648] 13 p1849 N90-20612
Photosynthetic water splitting, phase 2
[PB90-132671] 15 p2066 N90-21833

ALGAL BLOOM
U ALGAE

ALGEBRA
NT ADJOINTS
NT AUTOMORPHISMS
NT BANACH SPACE
NT BINOMIALS
NT CANONICAL FORMS
NT CURRENT ALGEBRA
NT DETERMINANTS
NT DYADICS
NT EIGENVALUES
NT EIGENVECTORS
NT GROUP THEORY
NT HERMITIAN POLYNOMIAL
NT HESSIAN MATRICES
NT HILBERT SPACE
NT HOMOMORPHISMS
NT JORDAN FORM
NT LIE GROUPS
NT LINEAR EQUATIONS
NT LINEAR EVOLUTION EQUATIONS

NT LINEAR TRANSFORMATIONS
NT MATRICES (MATHEMATICS)
NT NONLINEAR EQUATIONS
NT NONLINEAR EVOLUTION EQUATIONS
NT POLYNOMIALS
NT QUADRATIC EQUATIONS
NT RICCATI EQUATION
NT SOBOLEV SPACE
NT SPINOR GROUPS
NT STATE VECTORS
NT STIFFNESS MATRIX
NT STOKES THEOREM (VECTOR CALCULUS)
NT STRESS TENSORS
NT SUBGROUPS
NT TENSORS
NT VECTOR SPACES
NT VECTORS (MATHEMATICS)
NT VORTICITY

Numerical methods for differential-algebraic equations: Current status and future directions
[DE89-015116] 01 p0111 N90-10632

Extended Weyl group for Kac-Moody algebras
[DE89-617525] 01 p0111 N90-10634

Applications of algebraic logic and universal algebra to computer science
[AD-A210556] 01 p0113 N90-10645

Module algebra (revised version)
[CWI-CS-R8844-REV] 02 p0260 N90-11474

Synchrony with empty process --- the algebra of synchronous processes
[CWI-CS-R8832] 02 p0261 N90-11481

On sufficient conditions for a function to be analytic
[DE89-618382] 02 p0264 N90-11503

General hulls in uniform algebras
[DE89-618383] 02 p0264 N90-11504

Analytic manifolds in uniform algebras
[DE89-618384] 02 p0264 N90-11505

Generalized BDF (Backward Differentiation Formula) methods applied to Hessenberg form DAEs
[DE89-017326] 02 p0267 N90-11522

An interpolation theorem in equational logic
[CWI-CS-R8838] 02 p0268 N90-11528

The realization of input-output maps using bialgebras
[NASA-CR-185362] 03 p0391 N90-12228

Some notes on perturbations of differential-algebraic equations
[PB89-218564] 03 p0393 N90-12243

Augmentations of grammatical categories in distributional-algebraic models of natural languages
[REPT-89-24] 03 p0396 N90-12262

Some techniques for anaphora resolution in algebraic linguistics
[REPT-89-28] 03 p0396 N90-12265

Two dimensional conformal supergravity and critical behavior
[DE89-611968] 03 p0420 N90-12414

Anaphoric trees and an extension of the model of anaphora resolution
[REPT-89-37] 04 p0540 N90-13130

An algebra for process creation
[CWI-CS-R8907] 04 p0543 N90-13155

Program transformation with abstract relation algebras
[AD-A213270] 05 p0688 N90-14011

Mathematical techniques for system realization and identification
[AD-A212088] 06 p0833 N90-14841

Classification of modular invariant partition functions for the twisted N=2 superconformal algebra, twisted SU(2) Kac-Moody algebra and D(sub 2K) parafermions
[DE90-600767] 06 p0835 N90-14853

Modular invariants for theta-functions with characteristics and the twisted N=2 superconformal and SU(2) Kac-Moody algebras
[DE89-635701] 07 p0982 N90-15671

Chern-Simons theories of symplectic super-diffeomorphisms
[DE89-635700] 07 p0987 N90-15703

The algebra of the NODEN analyser
[RSRE-89012] 08 p1111 N90-16432

Techniques for analyzing the dynamic response of structural systems using computer-derived Green's functions
[AD-A214523] 09 p1237 N90-17181

The bifurcation interpreter: A step towards the automatic analysis of dynamical systems
[AD-A214618] 09 p1265 N90-17336

Quantum sl(2) enveloping algebra and representations of braid group
[DE90-607044] 09 p1275 N90-17389

Design and implementation of the nested relational data model under the Exodus extensible database system
[AD-A215356] 09 p1296 N90-17515

Dynamic factorization in large-scale optimization
[AD-A214568] 10 p1416 N90-18161

New spacetime superalgebras and their Kac-Moody extension
[DE90-606949] 10 p1422 N90-18201

A simple algebraic grid adaptation scheme with applications to two- and three-dimensional flow problems
[NASA-TM-102446] 11 p1505 N90-18667

Parallel algorithms derivation
[AD-A216452] 11 p1545 N90-18894

Differential-geometric techniques for solving differential algebraic equations
[AD-A216503] 11 p1552 N90-18934

Schema-based theories of problem solving
[AD-A216717] 11 p1552 N90-18939

Uniqueness of closure of the constraint algebra for quantum gravity
[DE90-610476] 12 p1691 N90-19712

Superconformal algebra on meromorphic vector fields with three poles on super-Riemann sphere
[DE90-610423] 12 p1706 N90-19796

Banach C*-algebras not containing a subspace isomorphic to C(sub 0)
[DE90-610428] 12 p1706 N90-19798

Projective cohomology over a chain complex
[DE90-606958] 13 p1880 N90-20788

High accuracy solutions of incompressible Navier-Stokes equations
[NASA-TM-102539] 14 p2018 N90-21567

Weierstrass preparation and division theorems for the ring of germs of superanalytic functions
[DE90-612742] 14 p2020 N90-21576

Extension of the constraints algebra for the closed string with the fixed topology world sheet
[DE90-612745] 14 p2020 N90-21577

Extension of the Krichever-Novikov algebra in the closed string theory
[DE90-612746] 14 p2020 N90-21578

The N = 2 superconformal algebras on hyperelliptic surfaces and their Coulomb gas realization
[DE90-612790] 14 p2020 N90-21581

Fusion algebra and fusing matrices
[DE90-612798] 14 p2021 N90-21583

Differential-algebraic equations as stiff ordinary differential equations
[DE90-007922] 14 p2021 N90-21585

Comparison of the algebraic reconstruction technique with the maximum entropy reconstruction technique for a variety of detection tasks
[DE90-008933] 14 p2021 N90-21587

Finding the complete path and weight enumerators of convolutional codes 15 p2077 N90-21897

Algebraic block-structured grid generation based on a macro-block concept 15 p2093 N90-21978

Applications of algebraic grid generation 15 p2093 N90-21979

Incomparable elements in algebraic lattices with applications to formal language theory
[MEMO-INF-89-54] 15 p2148 N90-22269

Operator algebra from fusion rules: The infinite number of Ising theories
[NIKHEF-H/89-7] 15 p2165 N90-22374

Generalized killing equations and symmetries of spinning space
[NIKHEF-H/89-8] 15 p2165 N90-22375

Spatial operator algebra framework for multibody system dynamics 16 p2279 N90-22989

A survey on the structured singular value 16 p2281 N90-22998

Efficient computer algebra algorithms for polynomial matrices in control design 16 p2285 N90-23022

A computer program to implement the Chen method of dimensional analysis
[AD-A218557] 16 p2306 N90-23142

A computational method for general higher index nonlinear singular systems of differential equations
[AD-A219164] 16 p2307 N90-23147

Stability regimes in a rotating quadrupole focusing accelerator
[AD-A219513] 16 p2317 N90-23209

Automatic runtime consistency checking and debugging of formally specified programs
[AD-A218855] 17 p2442 N90-23916

A process specification formalism based on static COLD
[CWI-CS-R8930] 17 p2448 N90-23960

Numerical conformal mapping and applications
[AD-A219789] 17 p2457 N90-24019

Discrete mathematics for communication systems
[AD-A220430] 17 p2457 N90-24022

On models for propositional dynamic logic
[RUU-CS-89-3] 17 p2460 N90-24046

Optical computing strategies
[AD-A219433] 17 p2472 N90-24131

On the use of equational type logic for software engineering and protocol design
[MEMO-INF-89-52] 18 p2592 N90-24748

Design of a specification language by abstract syntax engineering
[CWI-CS-R8934] 18 p2599 N90-24789

G exchangeability and the construction of distribution-free statistics 18 p2605 N90-24837

Solution of exterior acoustic problems by the boundary element method 18 p2611 N90-24874

Data conversions in abstract data types
[RUU-CS-88-30] 18 p2634 N90-25006

Extensions of algebraic image operators: An approach to model-based vision 19 p2741 N90-25577

Interactive grid generation on small computers
[AD-A221234] 19 p2742 N90-25585

Automated angular momentum recoupling algebra
[DE90-011988] 19 p2750 N90-25626

Hopf-algebraic structure of combinatorial objects and differential operators
[NASA-CR-186360] 19 p2752 N90-25640

Application of symbolic computations to the constitutive modeling of structural materials
[NASA-TM-103225] 20 p2876 N90-26364

Principles of FP2: Term algebras for specification of parallel machines
[RR-789-I-IMAG-98-LIFIA] 20 p2913 N90-26571

Mathematical problem-solving transfer: The effects of cognitive load and attention a schema acquisition and rule automation 20 p2917 N90-26594

Unification and disunification: Theory and applications
[ETN-90-97247] 20 p2919 N90-26610

Applied mathematical modules for use in a linear algebra service course
[AD-A222814] 20 p2920 N90-26618

Linear algebra on a CRAY X-MP
[AD-A221780] 21 p3056 N90-27374

Toeplitz matrices: Algebra and algorithms
[AD-A223174] 21 p3064 N90-27416

On the theory and numerics of differential-algebraic equations
[AD-A222427] 21 p3065 N90-27422

Integrated structural/control design via multiobjective optimization
[AD-A223088] 21 p3071 N90-27459

Grid generation and processing for FINFLO flow solver
[PB90-189481] 22 p3169 N90-27975

Beltrami algebra and symmetry of Beltrami equation on Riemann surfaces
[DE90-627157] 23 p3388 N90-29135

The combinatorics computation for Casimir operators of the symplectic Lie algebra and the application for determining the center of the enveloping algebra of a semidirect product
[DE90-627161] 23 p3388 N90-29136

Superconformal algebra and central extension of meromorphic vector fields with multipoles on super-Riemann sphere
[DE90-627211] 23 p3390 N90-29153

The control point form of algebraic grid generation 24 p3470 N90-29609

Trees, bialgebras and intrinsic numerical algorithms
[NASA-CR-187031] 24 p3524 N90-29925

An algebraic hierarchical basis preconditioner
[DE90-015875] 24 p3538 N90-30008

ALGOL

A persistent heap for ALGOL 68
[RSRE-MEMO-4268] 08 p1110 N90-16427

Outline and realization of a polymorphic language extension for ELAN
[TR-89-23] 19 p2743 N90-25592

Investigation of x ray variability in highly active cool stars
[NASA-CR-183853] 24 p3560 N90-30143

ALGORITHMIC ORIENTED LANGUAGE

U ALGOL

ALGORITHMS

NT PARSING ALGORITHMS
NT SIMPLEX METHOD

Computation of transonic flow about stores
[AD-A210402] 01 p0002 N90-10009

A structured singular value approach to missile autopilot analysis 2 01 p0014 N90-10068

A performance comparison of integration algorithms in simulating flexible structures 01 p0021 N90-10101

Minimum-variance reduced-order estimation algorithms from Pontrygin's minimum principle 01 p0021 N90-10105

Use of the quasilinearization algorithm for the simulation of LSS slewing 01 p0022 N90-10110

Boost-phase discrimination research activities
[NASA-TM-101889] 01 p0032 N90-10176

Mechanical states in wound capacitors. Part 2: Optimization
[DE89-008116] 01 p0059 N90-10338

An algorithm to calculate the beam momentum distribution from flying wire profiles
[DE89-015587] 01 p0073 N90-10418

Stimulated rotational Raman scattering
[DE89-016427] 01 p0075 N90-10430
On learning from exercises
[AD-A210593] 01 p0101 N90-10574
An algorithm for the systematic disturbance of optimal rotational solutions
[NASA-TM-101089] 01 p0102 N90-10575
Performance evaluation of the Scheme86 and HP precision architectures
[AD-A209418] 01 p0102 N90-10578
A low-cost hypercube load-balance algorithm
[DE89-015739] 01 p0104 N90-10589
Tests of various finite difference algorithms applied to a simple water vapor transport problem on a staggered grid
[AD-A210229] 01 p0105 N90-10596
Cost metric algorithms for internetwork applications
[AD-A210324] 01 p0105 N90-10597
Primal barrier methods for linear programming
[AD-A210501] 01 p0105 N90-10600
Some results on learning
[AD-A210591] 01 p0110 N90-10624
Quotient-difference type generalizations of the power method and their analysis
[NASA-TM-102361] 01 p0112 N90-10635
An iterative method for systems of nonlinear hyperbolic equations
[NASA-CR-181919] 01 p0112 N90-10638
Tests of gating algorithms for tracking of multiple objects. Part 1: Theory, requirements and performance measures
[AD-A210519] 01 p0113 N90-10644
Research in mathematics and computer science: Calculation of the probability of undetected error for certain error detection codes, phase 1
[AD-A210302] 01 p0115 N90-10664
High accuracy coordinate determination using the global positioning system 02 p0150 N90-10858
Frequency domain design of robust controllers for space structures
[AD-A211172] 02 p0176 N90-10985
Modal analysis of space structures with the Ibrahim Time Domain method 02 p0181 N90-11026
An experimental SMI adaptive antenna array for weak interfering signals
[NASA-CR-185976] 02 p0212 N90-11211
Validation of NEC (Numerical Electromagnetics Code) for antennas near ground
[DE89-016502] 02 p0212 N90-11212
Rethinking synthesis of fine-motion strategies
[DE89-016671] 02 p0230 N90-11322
A technique to correlate fractography with NDE (Non-Destructive Evaluation) of small samples
[DE89-016904] 02 p0231 N90-11325
On algorithms for generating computationally simple piecewise linear classifiers
[NDRE/PUBL-89/1001] 02 p0258 N90-11459
An investigation of the usefulness of Earley's Algorithm in a general context-free recognizer
[DE89-016498] 02 p0258 N90-11463
Programs for numerical integration of piece-wise smooth functions
[DE89-620449] 02 p0258 N90-11464
Parameter estimation in functional and partial differential equations
[AD-A211040] 02 p0265 N90-11511
The upwind control volume scheme for unstructured triangular grids
[NASA-TM-101664] 03 p0301 N90-11703
On the generation of a variable structure airport surface traffic control system
[AD-A211306] 03 p0304 N90-11724
Vision-based navigation for autonomous ground vehicles
[AD-A211584] 03 p0304 N90-11725
Resistive block methods for electrostatic field solutions with internal elements
[DE89-017535] 03 p0337 N90-11920
Nearly optimal algorithms and bounds for multilayer channel routing
[AD-A211913] 03 p0343 N90-11955
Redundancies and don't cares in sequential logic synthesis
[AD-A211931] 03 p0343 N90-11956
A design methodology for self-tuning control of systems with inherent conflicts
[PB89-219505] 03 p0344 N90-11960
Viscous split algorithms for the time dependent incompressible Navier-Stokes equations
[AD-A211592] 03 p0348 N90-11985
Efficient finite element solution of Navier-Stokes equations and related topics
[AD-A211647] 03 p0348 N90-11986
Some new algorithms for boundary value problems in smooth particle hydrodynamics
[AD-A211728] 03 p0348 N90-11987
A multigrid algorithm for the incompressible Navier-Stokes equation
[GMD-374] 03 p0349 N90-11993
Error estimation and self-adaptive mesh refinement for boundary element method 03 p0356 N90-12037
Aerosol backscatter studies supporting LAWS 03 p0363 N90-12079
LAWS simulation: Sampling strategies and wind computation algorithms 03 p0364 N90-12081
Processing of DMSP magnetic data and its use in geomagnetic field modeling
[NASA-TM-100750] 03 p0370 N90-12115
The use of Lanczos's method to solve the large generalized symmetric definite eigenvalue problem
[NASA-CR-181914] 03 p0385 N90-12193
Tools to aid in the development high-performance algorithms
[DE89-012395] 03 p0386 N90-12194
An approximate max-flow min-cut theorem for uniform multicommodity flow problems with applications to approximation algorithms
[AD-A211908] 03 p0386 N90-12198
Parallel graph contraction
[AD-A211916] 03 p0386 N90-12199
Scheduling sporadic and aperiodic events in a hard real-time system
[AD-A211344] 03 p0387 N90-12205
Parallel architectures and parallel algorithms for integrated vision systems
[NASA-CR-185990] 03 p0389 N90-12215
Can perceptrons find Lyapunov functions: An algorithmic approach to systems stability
[RR-365] 03 p0391 N90-12224
Fast forward dynamics algorithm for robot arms using multiprocessing
[RR-367] 03 p0391 N90-12225
Numerical experience with a class of algorithms for nonlinear optimization using inexact function and gradient information
[NASA-CR-181927] 03 p0392 N90-12232
Dynamic embedding of trees in hypercubes with constant dilation and load
[AD-A211884] 03 p0392 N90-12236
Fast computation using faulty hypercubes
[AD-A211910] 03 p0393 N90-12238
Sequential design of experiments with physically based models 23
[AD-A211918] 03 p0393 N90-12239
On the communication complexity of solving a polynomial equation
[AD-A211945] 03 p0393 N90-12240
A matrix factorization and its application to large-scale linear programming
[AD-A211293] 03 p0394 N90-12244
Orthogonal least squares methods and their application to nonlinear system identification
[RR-343] 03 p0395 N90-12259
Temporal and spatial filtering remedies for dispersion in electromagnetic particle codes
[DE89-017534] 03 p0408 N90-12337
Problem of incomplete information in relational databases
[PB89-217533] 03 p0417 N90-12393
Numerical algorithms for steady and unsteady incompressible Navier-Stokes equations
[NASA-CR-186039] 04 p0437 N90-12499
Chordwise loading and camber for two-dimensional thin sections
[AD-A213318] 04 p0448 N90-12588
Automatic processing of images from the GRATE flight test tool
[DLR-FB-89-28] 04 p0454 N90-12599
Numerical analysis of notch test damage to laminated composite plates submitted to uniaxial traction
[CETIM-107310] 04 p0467 N90-12675
FLIC (FLame with Implicit Convection): A detailed, two-dimensional flame model
[AD-A212953] 04 p0473 N90-12710
Stable Kalman filters for processing clock measurement data 04 p0487 N90-12801
On a fast two-dimensional radar imaging process for rotating targets, and an analysis of its image quality
[ESA-TT-1142] 04 p0489 N90-12808
Automatic analysis and exploitation of the flow visualization images
[ETN-89-95712] 04 p0501 N90-12887
Self-tuning control of nonlinear Armax models --- Autoregressive Moving Average with eXogeneous (ARMAX) inputs
[RR-362] 04 p0508 N90-12930
Geodetic point positioning with GPS (Global Positioning System) carrier beat phase data from the CASA UNO experiment
[AD-A211955] 04 p0514 N90-12970
Cloud cover determination in polar regions from satellite imagery
[NASA-CR-186096] 04 p0520 N90-13003
A fast algorithm for the evaluation of heat potentials
[AD-A211316] 04 p0529 N90-13052
A fan-in algorithm for distributed sparse numerical factorization
[AD-A211569] 04 p0529 N90-13054
Algorithmic fault tolerance
[RSRE-MEMO-4214] 04 p0530 N90-13057
Solving 3D block bidiagonal linear systems on vector computers
[CWI-NM-R8819] 04 p0530 N90-13061
Multiplicative iterative algorithms for convex programming
[CWI-AM-R8808] 04 p0532 N90-13072
Towards a parallel algorithm for the many body problem
[CS-8813] 04 p0533 N90-13078
Subspace iteration algorithms in FORTRAN 77 and FORTRAN 8x
[AD-A212275] 04 p0533 N90-13083
Parallel and determinstic algorithms from MRF (Markov Random Fields): Surface reconstruction and integration
[AD-A212457] 04 p0533 N90-13084
Sequential quadratic programming algorithms for optimization
[AD-A212800] 04 p0534 N90-13088
Algorithm development for SDI weapons system allocation
[AD-A212973] 04 p0534 N90-13090
Formal calculations and parallelism. Solving linear systems
[ETN-89-95499] 04 p0536 N90-13098
Labeled trees and the efficient computation of derivations
[NASA-CR-185386] 04 p0538 N90-13113
Multigrid Monte Carlo in an external U(1) gauge field
[NIKHEF-ITFA-88-52] 04 p0538 N90-13114
A recursive algorithm for computing the frequency response of a class of nonlinear difference equation models
[RR-354] 04 p0539 N90-13123
Placing mirrors in grids
[CWI-CS-R8906] 04 p0543 N90-13154
Note on the convergence of simulated annealing algorithms
[MEMO-774] 04 p0544 N90-13162
The Painleve test for nonlinear ordinary and partial differential equations
[AD-A212894] 04 p0546 N90-13177
Monte Carlo (importance) sampling within a Benders' decomposition algorithm for stochastic linear programs
[AD-A212854] 04 p0548 N90-13189
Molecular dynamics of lipid bilayers
[AD-A211492] 04 p0552 N90-13214
Research in computer vision for autonomous systems
[AD-A212420] 04 p0555 N90-13235
Flux-corrected transport algorithms for two-dimensional compressible magnetohydrodynamics
[AD-A212757] 04 p0557 N90-13246
Automation of orbit determination functions for National Aeronautics and Space Administration (NASA)-supported satellite missions 05 p0590 N90-13434
Validation of the Hipparcos catalog 05 p0611 N90-13564
Linking Hipparcos to a quasi-inertial system 05 p0611 N90-13565
An algorithm for control volume analysis of cryogenic systems
[AD-A213394] 05 p0631 N90-13683
Test generation for highly sequential circuits
[AD-A211932] 05 p0634 N90-13698
Parameter estimation for the Gummel-Poon transistor model
[MA-53] 05 p0635 N90-13705
Inviscid 2D solutions on unstructured, adaptive grids 05 p0640 N90-13737
An improved algorithm for the modeling of vapor flow in heat pipes
[NASA-CR-185179] 05 p0642 N90-13748
Analysis of rotary engine combustion processes based on unsteady, three-dimensional computations
[NASA-TM-102469] 05 p0642 N90-13749
Probabilistic finite element analysis of dynamic structural response
[AD-A213249] 05 p0650 N90-13789
Time domain coupling of the boundary and finite element methods for elastodynamics
[AD-A213243] 05 p0654 N90-13811
Application of an optimal filter for inflatable sphere data processing 05 p0659 N90-13849
Parallelism in the discrete-event simulation algorithm
[AD-A213060] 05 p0682 N90-13970
Novel graph searching methods for image analysis
[AD-A213065] 05 p0682 N90-13971

A fault-tolerant software algorithm for a network of transputers
[AD-A213092] 05 p0682 N90-13972
Algorithm for atmospheric corrections of aircraft and satellite imagery
[NASA-TM-100751] 05 p0683 N90-13976
The cellular approach: A new method to speed up simulated annealing for macro placement
[MEMO-COSOR-88-29] 05 p0683 N90-13980
On the asymptotic convergence of the simulated annealing algorithm in the presence of a parameter dependent penalization
[MEMO-COSOR-89-16] 05 p0684 N90-13984
A multilevel parallel solver for block tridiagonal and banded linear systems
[AD-A213151] 05 p0688 N90-14008
FORTRAN subroutines for the evaluation of the confluent hypergeometric functions
[AD-A213308] 05 p0689 N90-14012
On the performance of on-line algorithms for partition problems
[MEMO-784] 05 p0689 N90-14015
Global optimization and simulated annealing
[MEMO-COSOR-88-21] 05 p0690 N90-14025
The weighted sum of two S-units being a square
[MEMO-792] 05 p0691 N90-14031
Measurement of arithmetic error and calculation perturbations
[IMAG-RR-767-M] 05 p0692 N90-14039
Data structures for the representation and manipulation of polyhedrons
[IMAG-RR-772-M] 05 p0692 N90-14042
Navier-Stokes solutions of 2-D transonic flow over unconventional airfoils 06 p0719 N90-14195
Advanced 3-D CFD algorithm for turbomachinery 06 p0725 N90-14233
The parabolic equation approach to predicting tropospheric propagation effects in operational environments 06 p0759 N90-14418
Pattern recognition techniques applied to the NASA-ACTS order-wire problem 06 p0764 N90-14446
Data compression techniques applied to high resolution high frame rate video technology
[NASA-CR-4263] 06 p0765 N90-14452
Numerical solution of the incompressible Navier-Stokes equations 06 p0774 N90-14501
An image compression algorithm for a high-resolution digital still camera
[NASA-CR-185079] 06 p0780 N90-14532
Numerical simulation of laser radiation propagation in non-uniform absorbing medium. Geometrical optics approximation
[DE89-632014] 06 p0787 N90-14585
Group implicit concurrent algorithms in nonlinear structural dynamics
[NASA-CR-185950] 06 p0796 N90-14638
A new uniformly valid asymptotic integration algorithm for elasto-plastic-creep and unified viscoplastic theories including continuum damage
[NASA-TM-102344] 06 p0799 N90-14655
Power spectral estimation algorithms
[NASA-CR-186189] 06 p0828 N90-14812
The phase gradient autofocus algorithm: An optimal estimator of the phase derivative
[DE90-000895] 06 p0828 N90-14814
Versatility of the CFR algorithm for limited angle reconstruction
[DE90-001421] 06 p0829 N90-14817
Program CICC flow and heat transfer in Cable-In-Conduit Conductors
[DE90-001519] 06 p0829 N90-14818
Algorithmic randomness, physical entropy, measurements, and the second law
[DE90-002413] 06 p0830 N90-14823
Interactive multidimensional data analysis and understanding
[DE90-001794] 06 p0830 N90-14824
Some numerical experiments concerning the equation of state algorithm for multi-material cells in HULL
[DE89-008240] 06 p0830 N90-14827
Architectures for reasoning in parallel
[NASA-CR-186237] 06 p0832 N90-14836
Parallel projected variable metric algorithms for unconstrained optimization
[NASA-CR-181930] 06 p0833 N90-14842
Numerical methodologies for solving partial differential equations
[DE90-001842] 06 p0834 N90-14849
Application of heuristic satellite plan synthesis algorithms to requirements of the WARC-88 allotment plan
[NASA-TM-102479] 06 p0835 N90-14856
Advanced detection, isolation, and accommodation of sensor failures in turbofan engines: Real-time microcomputer implementation
[NASA-TP-2925] 07 p0883 N90-15112
More efficient sensitivity testing
[DE90-002639] 07 p0916 N90-15298
Component presence-absence detection for automated visual inspection of hybrid microcircuits
[KCP-613-4050] 07 p0922 N90-15335
Array signal processing: New techniques for direction finding and spectrum estimation
[AD-A213883] 07 p0924 N90-15345
New transient algorithms for non-Newtonian flows
[AD-A213494] 07 p0930 N90-15385
Control of mechanical manipulators 07 p0938 N90-15432
Mesh refinement in finite element analysis by minimization of the stiffness matrix trace
[NASA-CR-185170] 07 p0938 N90-15434
A simple shell element formulation for large-scale elastoplastic analysis
[DE89-015452] 07 p0946 N90-15475
On the motion of compliantly-connected rigid bodies in contact. Part 1: The motion prediction problem
[AD-A214135] 07 p0948 N90-15489
On the motion of compliantly-connected rigid bodies in contact. Part 2: A system for analyzing designs for assembly
[AD-A214136] 07 p0948 N90-15490
Fatigue behavior of vertical axis wind turbine airfoils with two weld configurations
[DE90-002628] 07 p0955 N90-15525
An architectural model of visual motion understanding
[AD-A214327] 07 p0967 N90-15589
Designing machines for lattice physics and algorithm investigation
[DE90-003543] 07 p0969 N90-15596
A block QR factorization algorithm using restricted pivoting
[DE90-001921] 07 p0972 N90-15613
Sequential quadratic programming algorithms for optimization
[DE90-000022] 07 p0973 N90-15617
Optimizing and evaluating algorithms for replicated data concurrency control
[DE90-003080] 07 p0973 N90-15619
Software for a new modified Cholesky factorization
[AD-A213643] 07 p0975 N90-15630
On the correctness of orphan management algorithms
[AD-A213777] 07 p0975 N90-15632
Evaluation of a simple algorithm for estimating infrared signatures from multi-pixel to sub-pixel targets applied to AGA thermovision imagery
[AD-A214103] 07 p0976 N90-15639
A renormalization group approach to image processing: A new computational method for three-dimensional shapes in robot vision, and the computation complexity of the cooling algorithms
[AD-A214247] 07 p0977 N90-15643
Principles and algorithms for causal reasoning with uncertainty
[AD-A214248] 07 p0977 N90-15644
A paradigm for robust geometric algorithms
[AD-A214324] 07 p0978 N90-15647
MODTRAN: A moderate resolution model for LOWTRAN 7
[AD-A214337] 07 p0978 N90-15650
Neural network models for linear programming
[DE89-015974] 07 p0979 N90-15651
Estimating departure times from traffic counts using dynamic assignment
[DE89-016259] 07 p0979 N90-15653
Simulating the scheduling of parallel supercomputer applications
[DE90-003604] 07 p0979 N90-15655
Design and implementation of two concurrent multi-sensor integration algorithms for mobile robots
[DE90-003041] 07 p0981 N90-15663
Using mappings to prove timing properties
[AD-A213967] 07 p0981 N90-15666
Membership-set parameter estimation via optimal bounding ellipsoids
[AD-A213807] 07 p0984 N90-15685
Bounded polynomial randomized consensus
[AD-A213808] 07 p0984 N90-15686
Optimization of stochastic systems via simulation
[AD-A214011] 07 p0985 N90-15689
A structural factoring approach for analyzing probabilistic networks 07 p0986 N90-15697
Strong large deviation and local limit theorems
[AD-A213610] 07 p0986 N90-15698
Concurrence control for transactions with priorities
[NASA-CR-186241] 07 p0986 N90-15699
Systolic algorithms for imaging from space
[AD-A213870] 07 p0987 N90-15701
Personal computer study of finite-difference methods for the transonic small disturbance equation
[NASA-TM-102582] 08 p1019 N90-15892
Advances in techniques and technologies for air vehicle navigation and guidance
[AGARD-AR-276] 08 p1020 N90-15899
Navigation of autonomous air vehicles by passive imaging sensors 08 p1026 N90-15927
Experience with strain-gage balances for cryogenic wind tunnels 08 p1031 N90-15958
A numerical simulation of the flow in the diffuser of the NASA Lewis icing research tunnel
[NASA-TM-102480] 08 p1032 N90-15965
Digital system for monitoring and controlling remote processes
[DE90-003935] 08 p1054 N90-16094
MT's algorithm: A new algorithm to search for the optimum set of modulation indices for simultaneous range, command, and telemetry
[NASA-CR-186259] 08 p1057 N90-16110
Evaluation of a new charge algorithm for a lead-acid battery with gelled electrolyte using a 96V gel cell 4 as a test battery
[DE90-003420] 08 p1061 N90-16133
Parallel asynchronous systems and image processing algorithms 08 p1075 N90-16218
Element-by-element preconditioning techniques for large-scale, vectorized finite element analysis in nonlinear solid and structural mechanics 08 p1087 N90-16291
Ice floe identification in satellite images using mathematical morphology and clustering about principal curves
[AD-A213854] 08 p1090 N90-16311
Rainflow counting algorithm for the LIFE2 fatigue analysis code
[DE90-002834] 08 p1096 N90-16344
A space-time discretization procedure for wave propagation problems
[NASA-TM-102215] 08 p1105 N90-16399
Spanning trees of hypercubes with a maximum of sixteen peaks
[IMAG-RR-755-I] 08 p1107 N90-16406
Case tool evaluation system
[DE90-003698] 08 p1108 N90-16413
Algorithms for fault tolerant distributed systems
[AD-A214447] 08 p1109 N90-16416
An algorithm to compute the square root of 3x3 positive definite matrix
[DE89-635711] 08 p1109 N90-16417
The theory of hybrid stochastic algorithms
[DE90-003941] 08 p1109 N90-16421
Basic mathematical function libraries for scientific computation
[NASA-TM-102256] 08 p1110 N90-16423
The inside-outside algorithm: Further experiments on three and four letter word spelling and implementation on an array processor
[RSRE-MEMO-4256] 08 p1110 N90-16426
Beamforming pre-processors for high discrimination algorithms
[RSRE-MEMO-4304] 08 p1110 N90-16429
Optimization of monotonic inference algorithms in propositional and first order logic
[LAAS-89204] 08 p1111 N90-16436
Design and implementation of a multi-sensor fusion algorithm on a hypercube computer architecture
[DE90-003682] 08 p1112 N90-16438
Interpretation of CAD (Computer Aided Design) models through IGES (Initial Graphics Exchange Specification) interface
[PB90-121294] 08 p1112 N90-16441
Parallel algorithm for determining motion vectors in ice floe images by matching edge features 08 p1114 N90-16451
Optimal step sizes in semi-stochastic approximation procedures
[ETN-90-95888] 08 p1117 N90-16469
Solving time harmonic wave problems on vector processors
[DE90-003956] 08 p1119 N90-16480
Scaling study for SP-100 reactor technology
[NASA-TM-897140] 08 p1122 N90-16496
Abbreviated query interpretation in extended entity-relationship oriented databases
[DE90-003114] 08 p1137 N90-16587
Event-join optimization in temporal relational databases
[DE90-003117] 08 p1137 N90-16588
Estimation and control of nonlinear and hybrid systems with applications to air-to-air guidance
[AD-A214542] 09 p1170 N90-16770
Implementation of adaptive arrays in the block oriented systems simulator
[AD-A215545] 09 p1171 N90-16774

An autonomous orbit determination system for earth satellites
[AD-A215671] 09 p1172 N90-16779
Robustness of a moving-bank multiple model adaptive controller for a large space structure
[AD-A215670] 09 p1183 N90-16859
New approach to omega PPCs (Propagation Corrections)
[AD-A215610] 09 p1207 N90-17000
A distributed kernel for simulation of the VHSIC hardware description language
[AD-A215419] 09 p1213 N90-17032
Development of the Kalman filter application and a VHDL model for the AFIT (Air Force Institute of Technology) Floating Point Application Specific Processor (FPASP)
[AD-A215423] 09 p1213 N90-17033
An upwind-biased, point-implicit relaxation algorithm for viscous, compressible perfect-gas flows
[NASA-TP-2953] 09 p1214 N90-17042
Basic research in reliability for real systems
[AD-A214536] 09 p1234 N90-17158
Eigensolution of finite element problems in a completely connected parallel architecture
[NASA-TM-102450] 09 p1236 N90-17173
Efficient algorithms for dilated mappings of binary trees
[NASA-CR-181980] 09 p1262 N90-17317
Projection techniques for image restoration
09 p1263 N90-17322
Concurrency control for transactions with priorities
[NASA-CR-186268] 09 p1263 N90-17323
Vision-based navigation and parallel computing
[AD-A214481] 09 p1264 N90-17327
Piecewise linear-quadratic programming and its applications
[AD-A214489] 09 p1264 N90-17328
Network flow algorithms
[AD-A214689] 09 p1265 N90-17337
Matching extension in regular graphs
[AD-A214757] 09 p1268 N90-17339
Development of advanced WTA algorithms for parallel processing
[AD-A214874] 09 p1266 N90-17341
A note on Smale's global Newton method
[AD-A215139] 09 p1267 N90-17346
Two adaptive techniques let progressive refinement outperform the traditional radiosity algorithm
[AD-A215174] 09 p1267 N90-17347
The graphical representation of algorithmic processes, volume 1
[AD-A215359] 09 p1268 N90-17350
Computer-Aided Design for Built-In-Test (CADBIT). Volume 1: Technical issues
[AD-A215737] 09 p1268 N90-17353
Evaluation of the modal testing MODENT software with simulated data
[INPE-4885-NTE/291] 09 p1269 N90-17357
Parallel functional computation
[AD-A214627] 09 p1269 N90-17360
Large-scale optimization via distributed systems
[AD-A215136] 09 p1270 N90-17364
A genetic adaptive system for image understanding and learning research
[AD-A214810] 09 p1271 N90-17367
Symbol manipulation and applied mathematics
[AD-A214702] 09 p1273 N90-17378
Solving computer graphics problems through boolean combinations of polygons
[AD-A214788] 09 p1273 N90-17380
System identification and filtering of nonlinear controlled Markov processes by canonical variate analysis
[AD-A214873] 09 p1273 N90-17381
Localization of multiple broadband targets in spherical coordinates via adaptive beamforming and non-linear estimation
[AD-A215714] 09 p1274 N90-17387
A Doppler centroid estimation algorithm for SAR systems optimized for the quasi-homogeneous source
[NASA-CR-186229] 09 p1275 N90-17391
Studies in statistical signal processing
[AD-A214490] 09 p1275 N90-17393
An analysis of scatter decomposition
[NASA-CR-181978] 09 p1276 N90-17396
Adaptive multiple-band CFAR (Constant-False-Alarm-Rate) detection of an optical pattern with unknown spectral distribution
[AD-A214754] 09 p1281 N90-17429
Generating optimally evasive MaRV trajectories
[DE90-004496] 10 p1328 N90-17671
Report on the multicolor pyrometry session at the Second NASA Non-Contact Temperature-Measurement Workshop 10 p1367 N90-17926
Rain core structure statistics derived from radar and disdrometer measurements in the mid-Atlantic coast of the US 10 p1373 N90-17956
Evaluation of a delay-Doppler imaging algorithm based on the Wigner-Ville distribution
[AD-A215827] 10 p1377 N90-17980
Tracking a hypersonic aircraft from a space platform
[AD-A216399] 10 p1377 N90-17984
Shape from focus
[AD-A215959] 10 p1393 N90-18052
Adaptive vibration control of vibration isolation mounts, using an LMS-based control algorithm
[AD-A214386] 10 p1394 N90-18061
A study of near tip phenomena for cracks in a particulate composite 10 p1395 N90-18062
Finite element investigation of a composite cylindrical shell under transverse load with through thickness shear and snapping
[AD-A216377] 10 p1397 N90-18078
Finding minimum-cost flows by double scaling
[AD-A214498] 10 p1416 N90-18159
Hybrid (optical/electronic) computing and digital optical computing
[AD-A214502] 10 p1416 N90-18160
Faster scaling algorithms for general graph matching problems
[AD-A215112] 10 p1417 N90-18163
Research at New York University's Ultracomputer Research Laboratory
[DE90-005471] 10 p1417 N90-18167
A monotone surrogate algorithm for the 0-1 Multiknapsack problem
[INPE-4933-PRE/1423] 10 p1417 N90-18169
An exact algorithm for the p-median problem
[INPE-4914-PRE/1415] 10 p1418 N90-18172
Nonprocedural implementation of mathematical programming algorithms
[AD-A216039] 10 p1419 N90-18179
Numerical algorithms for parallel computers
[AD-A216812] 10 p1419 N90-18181
Theoretical and experimental analyses of parallel combinatorial algorithms
[AD-A216407] 10 p1420 N90-18186
The strength of weak learnability
[AD-A216389] 10 p1420 N90-18190
Factoring symmetric indefinite matrices on high-performance architectures
[NASA-CR-181982] 10 p1421 N90-18195
An algorithm for finding characteristic roots of quasi-triangular Markov chains
[AD-A215490] 10 p1421 N90-18196
A parallel iterative method for solving 3-dimensional elliptic partial differential equations
[DE90-005187] 10 p1422 N90-18199
Molecular dynamics simulation of sedimentation using the monotonic Lagrangian grid
[AD-A215099] 10 p1427 N90-18236
Model-reference adaptive control applied to loadfollowing of a space-nuclear power system
[DE89-014581] 10 p1429 N90-18245
A numerical solution of the time-dependent Boltzmann equation
[AD-A216397] 10 p1434 N90-18275
The design and analysis of algorithm and data structure for efficient solutions of minimum-cost network flow problems on MISD and MIMD 10 p1441 N90-18313
The design and analysis of new techniques for transaction management in database systems
10 p1441 N90-18314
Visual servoing for autonomous aircraft refueling
[AD-A216042] 11 p1455 N90-18386
Wind-tunnel investigation of a flush airdata system at Mach numbers from 0.7 to 1.4
[NASA-TM-101697] 11 p1457 N90-18395
Analysis of whisker-toughened ceramic components: A design engineer's viewpoint
[NASA-TM-102333] 11 p1478 N90-18504
Transient responses of coupled systems
[ONERA-RT-13/3596-RY-070-R]
11 p1509 N90-18687
A numerical solution to the Boltzmann equation for use in calculating pumping rates in a CO2 discharge laser
[AD-A216376] 11 p1514 N90-18718
Fast algorithms for calculating laser wavefront phase compensation given noisy measurements of phase gradient
[DE90-006357] 11 p1515 N90-18727
Resource Assessment Project: User needs survey results
[DE89-009502] 11 p1529 N90-18802
Spatial registration of TIROS-N weather satellite data
[AD-A216041] 11 p1536 N90-18841
Comparisons between the RTNEPH (Real-Time Nephanalysis) and AFGL cloud layer analysis algorithms
[AD-A216637] 11 p1538 N90-18844
A case study of the 24 August 1986 FLOWS microburst
[AD-A216939] 11 p1537 N90-18847
Teleoperator servoloop tuning using an expert system
[DE90-005674] 11 p1542 N90-18876
A scalable multiprocessor architecture using Cartesian network: Relative addressing
[AD-A216580] 11 p1542 N90-18878
An exact algorithm for the problem of p-medians
[INPE-4924-TDL/384] 11 p1544 N90-18885
DOA (Direction of Arrival) estimation by Eigendecomposition using single vector Lanczos' algorithm
[AD-A215802] 11 p1544 N90-18887
Determination of the underlying task scheduling algorithm for and Ada runtime system
[AD-A215880] 11 p1544 N90-18890
Distributed decomposition of block-angular linear programs on a hypercube computer
[AD-A216433] 11 p1545 N90-18893
Parallel algorithms derivation
[AD-A216452] 11 p1545 N90-18894
Optimum and heuristic algorithms for finite state machine decomposition and partitioning
[AD-A216778] 11 p1546 N90-18899
Derivation of efficient parallel programs: An example from genetic sequence analysis
[DE90-005654] 11 p1547 N90-18904
Parallelizing the SDI ACCESS algorithm for the Connection Machine-2
[DE90-006382] 11 p1548 N90-18909
Can the square law be validated
[DE90-007112] 11 p1553 N90-18945
On the depth of combinatorial optimization problems
[MEMO-803] 11 p1554 N90-18946
A streamwise upwind algorithm applied to vortical flow over a delta wing
[NASA-TM-102225] 12 p1599 N90-19201
Heli/SITAN: A terrain referenced navigation algorithm for helicopters
[DE90-005193] 12 p1602 N90-19217
Remote Attitude Measurement Sensor (RAMS)
12 p1611 N90-19271
Evaluation and choice algorithms of cost optimal prepreg-application processes: Production of strongly charged plane parts made of fiber reinforced plastics
[ETN-90-95895] 12 p1620 N90-19313
Hydrogen assay foil counting system
[DE90-007415] 12 p1624 N90-19332
Investigations into a new algorithm for calculating H infinity optimal controllers 12 p1637 N90-19406
A vectorized algorithm for 3D dynamics of a tethered satellite 12 p1640 N90-19423
Costas loop lock detection in the advanced receiver
12 p1643 N90-19441
Memory management in traceback Viterbi decoders
12 p1643 N90-19443
Some easily analyzable convolutional codes
12 p1644 N90-19444
Fast transform decoding of nonsystematic Reed-Solomon codes 12 p1644 N90-19447
Application of adaptive least-squares algorithm to multi-element array signal reconstruction
12 p1644 N90-19448
Signal processing
[DE90-006904] 12 p1647 N90-19464
Parallel distributed networks for image smoothing and segmentation in analog VSLI
[AD-A216780] 12 p1651 N90-19491
A high resolution automatic image measuring system
[WISS-ARB-VERMESSUNGSWESEN-154]
12 p1663 N90-19559
Selection of optimal textural features for maximum likelihood image classification
[DE90-006901] 12 p1678 N90-19638
Automated visibility and cloud cover measurements with a solid-state imaging system
[AD-A216906] 12 p1693 N90-19724
Random access transmission algorithms for data local area networks
[AD-A216443] 12 p1700 N90-19761
An optimized algorithm for solving the nodal diffusion method on shared memory multiprocessors
[DE90-002703] 12 p1700 N90-19762
Object detection and amplitude estimation based on maximum a posteriori reconstructions
[DE90-007511] 12 p1701 N90-19770
Theory and applications of belief functions
[AD-A217092] 12 p1702 N90-19774
Adaptive, asynchronous stochastic global optimization algorithms for sequential and parallel computation
[AD-A217093] 12 p1702 N90-19775
Parallel algorithms for boundary value problems
[NASA-TM-102498] 12 p1704 N90-19783
On the parallel efficiency of the Frederickson-McBryan multigrid
[NASA-CR-181999] 12 p1705 N90-19791

A tensor product B-spline method for numerical grid generation
[DE90-005979] 12 p1705 N90-19792
Hierarchical basis preconditioners for second order elliptic problems in three dimensions
[DE90-005980] 12 p1706 N90-19793
Convergence properties of iterative algorithms for solving the nodal diffusion equations
[DE89-016859] 12 p1707 N90-19804
Algorithms for calorimeter simulation with parameterized showers by example of H1 detectors
[MPI-PAE/EXP.EL-200] 12 p1711 N90-19828
Thermal infrared scene simulation
[DE90-006900] 12 p1714 N90-19845
Visibility problems in numerical models of terrain
[INPE-4921-TDL/382] 12 p1726 N90-19919
Viscous shock profiles and primitive formulations
[NASA-CR-182029] 13 p1750 N90-20049
Experimental validation of extended image reconstruction using bispectral speckle interferometry
[DE90-008545] 13 p1772 N90-20171
Numerical Arc Segmentation Algorithm for a Radio Conference-NASARC (version 4.0) technical manual
[NASA-TM-101453] 13 p1788 N90-20264
Tomographic processing of synthetic aperture radar signals for enhanced resolution
[AD-A217178] 13 p1789 N90-20265
Effects of additional interfering signals on adaptive array performance
[NASA-CR-186508] 13 p1790 N90-20271
Meteor observations using the 50 MHz MENTOR imaging Doppler interferometer
[AD-A217908] 13 p1790 N90-20276
High resolution radar target modeling using ARMA (Autoregressive Moving Average) models
[AD-A218212] 13 p1791 N90-20278
Statistical equipment modeling for VLSI manufacturing
[DE90-008527] 13 p1795 N90-20304
Parallel algorithms in the finite element approximation of flow problems
[AD-A217729] 13 p1802 N90-20341
Massively-parallel computational fluid dynamics
[AD-A217732] 13 p1802 N90-20342
Numerical modeling of airblast
[AD-A217993] 13 p1803 N90-20347
The design and implementation of a position measuring system for a remotely controlled video camera
[AD-A218077] 13 p1805 N90-20362
Control system design of the third flexible joint of PUMA 560 robot
[AD-A218075] 13 p1812 N90-20405
Comparison of two matrix data structures for advanced CSM testbed applications
[NASA-CR-181951] 13 p1815 N90-20421
Utilization of LANDSAT-5 and NOAA-9 satellite imagery in the identification of physical-chemical parameters of the water in the Guanabara Bay
[INPE-4761-TDL/349] 13 p1819 N90-20445
Synopsis of early field test results from the gravity gradiometer survey system 13 p1833 N90-20525
Methods for local gravity field approximation 13 p1834 N90-20532
The effects of structure and source complexity on waveforms: Crustal structure of Tibet and the recovery of complex seismic sources
[AD-A218202] 13 p1843 N90-20579
Downward shortwave surface irradiance from 17 sites for the FIRE/SRB Wisconsin experiment
[NASA-TM-102596] 13 p1844 N90-20583
A prototype expert system to forecast severe winds in the western Mediterranean Sea
[AD-A218017] 13 p1845 N90-20593
Three-dimensional medical image analysis using local dynamic algorithm selection on a multiple-instruction, multiple-data architecture
[AD-A218024] 13 p1852 N90-20630
NYU (New York University) ultracomputer
[AD-A217167] 13 p1863 N90-20688
(DURIP) Two-Processor Alliant FX/4 System
[AD-A217810] 13 p1864 N90-20692
Simplified linear-time Jordan sorting and polygon clipping
[AD-A215110] 13 p1864 N90-20693
An algorithm for efficient estimation of superimposed exponential signals
[AD-A217218] 13 p1865 N90-20698
Experiments in finding neural network weights
[DE90-007696] 13 p1865 N90-20702
ISLE (Image and Signal Processing LISP Environment) reference manual
[DE90-007858] 13 p1866 N90-20705
Parts of recognition
[AD-A217694] 13 p1868 N90-20714
Probabilistic analysis of algorithms for NP-complete problems
[AD-A217880] 13 p1868 N90-20716
Development of computer software for the analysis and design of modern control systems
[AD-A217924] 13 p1868 N90-20717
Free indexation: Combinatorial analysis and a compositional algorithm
[AD-A218219] 13 p1869 N90-20724
Optimization of series expressions. Part 1: User's manual for the series macro package
[AD-A218220] 13 p1869 N90-20725
Performance of concurrency control algorithms in distributed systems
[AD-A218280] 13 p1870 N90-20727
Almost-optimum parallel speed-ups of algorithms for bipartite matching and related problems
[AD-A215111] 13 p1871 N90-20728
Advanced parallel systems
[AD-A217175] 13 p1872 N90-20731
Parallel computer graphics algorithms for the connection machine
[AD-A217300] 13 p1872 N90-20733
Design of a simulation interface for a parellel computing environment
[DE90-008497] 13 p1873 N90-20737
A time stepping algorithm for parallel computers
[DE90-008163] 13 p1873 N90-20738
A model and implementation of multigrid for massively parallel computers
[DE90-008165] 13 p1873 N90-20739
Implementation of midcourse tracking and correlation on massively parallel computers
[DE90-008156] 13 p1873 N90-20740
Robotic mobility system: Road following algorithms
[AD-A218107] 13 p1874 N90-20748
Stereo feature matching in disparity space
[AD-A218170] 13 p1875 N90-20751
Maintaining bridge-connected and biconnected components on-line
[AD-A215107] 13 p1875 N90-20754
Exact algorithms for output encoding, state assignment and four-level Boolean minimization
[AD-A217121] 13 p1876 N90-20756
Algorithms for optimal processing of polarimetric radar data
[AD-A217330] 13 p1876 N90-20758
Three-dimensional route planning for a cruise missile for minimal detection by observer
[AD-A218336] 13 p1880 N90-20787
Lateral attenuation of military aircraft flight noise
[AD-A218041] 13 p1882 N90-20799
Theoretical studies of spin-forbidden processes within the Breit-Pauli approximation
[AD-A217778] 13 p1885 N90-20815
Comparison of C- and O-grid generation methods using a NACA 0012 airfoil
[AD-A216375] 14 p1910 N90-20948
An overlapped grid method for multigrid, finite volume/difference flow solvers: MaGGiE
[NASA-CR-182008] 14 p1911 N90-20953
A two-dimensional unsteady analysis for transonic and supersonic cascade flows 14 p1911 N90-20955
Flight path reconstruction using extended Kalman filtering techniques
[PD-FC-9001] 14 p1915 N90-20970
A homotopy approach to the solutions of minimum-fuel space-flight rendezvous problems 14 p1931 N90-21053
Numerical simulation model for hydrazine attitude control thrusters. Part 1: Model description
[INPE-4952-RPE/601] 14 p1942 N90-21115
Modeling the temperature dependence of the thermal conductivity of aluminum nitride
[DE90-009428] 14 p1949 N90-21154
Capabilities of bistatic synthetic aperture radar for covert battlefield surveillance 14 p1961 N90-21230
Concept and results of the DLR realtime SAR processor 14 p1963 N90-21244
Numerical Arc Segmentation Algorithm for a Radio Conference (NASARC), version 4.0: User's manual
[NASA-TM-101454] 14 p1964 N90-21250
The 4th Annual Review of Progress in Applied Computational Electromagnetics
[AD-A217912] 14 p1966 N90-21257
A correlation-spectral method for line detection on noisy data
[DE90-007925] 14 p1967 N90-21266
Electromechanical actuation for thrust vector control applications
[NASA-TM-102548] 14 p1968 N90-21272
Numerical simulation of vortex breakdown 14 p1970 N90-21288
A cost-effective strategy for nonoscillatory convection without clipping
[NASA-TM-102538] 14 p1971 N90-21291
Analysis and finite element approximation of some optimal control problems associated with the Navier-Stokes equations 14 p1972 N90-21299
Digital processing of TM/LANDSAT data in monitoring interior water
[INPE-4956-PRE/1533] 14 p1997 N90-21448
Editing wind profiler measurements
[PB90-130147] 14 p2007 N90-21503
Windshear case study: Denver, Colorado, July 11, 1988
[DOT/FAA/DS-89/19] 14 p2008 N90-21509
Strategies for concurrent processing of complex algorithms in data driven architectures
[NASA-CR-186515] 14 p2013 N90-21535
The parallel algorithm for solving the three-dimensional integral magnetostatic equations
[DE90-616529] 14 p2015 N90-21547
Parallel tridiagonalization of a general matrix using distributed-memory multiprocessors
[DE90-008902] 14 p2015 N90-21551
Performance bounds on parallel self-initiating discrete-event
[NASA-CR-182010] 14 p2016 N90-21556
NETRA: A parallel architecture for integrated vision systems 2: Algorithms and performance evaluation
[NASA-CR-186510] 14 p2017 N90-21557
Adaptive grid embedding for the two-dimensional flux-split Euler equations
[NASA-CR-186533] 14 p2019 N90-21571
Comparison of the algebraic reconstruction technique with the maximum entropy reconstruction technique for a variety of detection tasks
[DE90-008933] 14 p2021 N90-21587
Finite element algorithms for hyperbolic conservation laws with forcing terms
[INPE-5024-RPE/617] 14 p2022 N90-21595
Modeling high-temperature superconductors and metallic alloys on the Intel IPSC/860
[DE90-009402] 14 p2033 N90-21665
Extension of a streamwise upwind algorithm to a moving grid system
[NASA-TM-102800] 15 p2048 N90-21739
First-order weight corrections for real-time flight path management
[LR-580] 15 p2050 N90-21751
Accurate nonlinear control for satellites using reaction wheels
[INPE-4983-PRE/1546] 15 p2059 N90-21787
A trajectory generation and system characterization model for cislunar low-thrust spacecraft. Volume 2: Technical manual
[NASA-CR-185172] 15 p2061 N90-21807
Framework for a space shuttle main engine health monitoring system
[NASA-CR-185224]. 15 p2061 N90-21809
Finding the complete path and weight enumerators of convolutional codes 15 p2077 N90-21897
Adaptive frequency estimation by MUSIC (Multiple Signal Classification) method
[PB90-166794] 15 p2086 N90-21943
Convergence acceleration of upwind relaxation methods for the Navier-Stokes equations 15 p2092 N90-21973
Applications of Mesh Generation to Complex 3-D Configurations
[AGARD-CP-464] 15 p2093 N90-21975
Three-dimensional adaptive grids with limited skewness 15 p2095 N90-21987
Unstructured mesh generation by a generalized Delaunay algorithm 15 p2096 N90-21995
Nonlinear stability analysis and control of dynamical robotic systems 15 p2104 N90-22037
Trajectory generation for car-like robots
[DE90-008407] 15 p2106 N90-22047
The classification of defects from ultrasonic measurements
[AERE-R-13306] 15 p2108 N90-22056
Parallel asynchronous hardware implementation of image processing algorithms 15 p2138 N90-22219
Computation and parallel implementation for early vision 15 p2139 N90-22222
Algorithms and architectures for robot vision 15 p2141 N90-22236
Kalman filter based range estimation for autonomous navigation using imaging sensors 15 p2142 N90-22238
Intensity dependent spread processor and workstation 15 p2143 N90-22244
Optimal 3-dimensional methods for linear programming
[PB90-155391] 15 p2145 N90-22253
An algorithm and computer program for the calculation of envelope curves
[PB90-155409] 15 p2145 N90-22254
Symbolic pattern processing system for planar spatial structures
[DE90-001598] 15 p2146 N90-22256

Molecular dynamics simulations of short-range force systems on 1024-node hypercubes
[DE90-009833] 15 p2146 N90-22259
On decoding of multi-level MPSK modulation codes
[NASA-CR-186601] 15 p2146 N90-22261
Local mode smoothing analysis for various incomplete factorization iterative methods in three dimensions
[REPT-89-38] 15 p2147 N90-22263
An approach to rescheduling activities based on determination of priority and disruptivity
15 p2153 N90-22299
Space communications scheduler: A rule-based approach to adaptive deadline scheduling
15 p2153 N90-22300
Bounded-time fault-tolerant rule-based systems
15 p2157 N90-22318
Automating security monitoring and analysis for Space Station Freedom's electric power system
[NASA-TM-103148] 15 p2158 N90-22324
Branch point placement
[OUEL-1767/89] 15 p2158 N90-22329
Control of human arm movement via optimization
15 p2159 N90-22334
On the existence of a positive definite solution of the matrix equation X + A(sup tau)X(exp -1)A = I
[PB90-133976] 15 p2159 N90-22335
Orthogonal distance regression
[PB90-151747] 15 p2160 N90-22336
Spline function smoothing and differentiation of noisy data on a rectangular grid
[DE90-009319] 15 p2160 N90-22338
Dynamical approach study of spurious steady-state numerical solutions of nonlinear differential equations. Part 1: The ODE connection and its implications for algorithm development in computational fluid dynamics
[NASA-TM-102820] 15 p2160 N90-22339
Normal forms for weakly non-linear perturbed wave equations
[REPT-89-41] 15 p2161 N90-22343
Preference numbers and funnel dimension
[REPT-89-57] 15 p2161 N90-22346
Neural implementation of a method for solving systems of linear algebraic equations
[NPL-DITC-155/89] 15 p2162 N90-22356
Update on the OPAL opacity code
[DE90-009946] 15 p2184 N90-22480
Limiting performance based structural and control optimization for large vibrating structures
16 p2202 N90-22568
Automated star pattern recognition
16 p2211 N90-22612
Detection of bridging faults in DFCMOS combinational gates
[REPT-89-060] 16 p2231 N90-22726
Increased stuck-at fault coverage with reduced I(sub DDQ) test sets
[DE90-009509] 16 p2245 N90-22804
Guidelines, operational procedures, and quality control for the estimation of geodetic point positions from GPS data collected with the TI4100 receiver
[AD-A218460] 16 p2250 N90-22829
The analysis of polar clouds from AVHRR satellite data using pattern recognition techniques
[NASA-CR-183300] 16 p2257 N90-22868
Relationship between flexibility of closure and success in pilot night vision sensor system training
[AD-A221439] 16 p2261 N90-22890
Tracking in uncertain environments
[RAE-TM-AW-121] 16 p2261 N90-22891
Efficient specialization of relational concepts
[AD-A218889] 16 p2262 N90-22894
Spatial operator algebra framework for multibody system dynamics
16 p2279 N90-22989
An order (n) algorithm for the dynamics simulation of robotic systems
16 p2279 N90-22990
Recursive linearization of multibody dynamics equations of motion
16 p2280 N90-22993
An innovations approach to decoupling of multibody dynamics and control
16 p2280 N90-22994
Efficient dynamic simulation for multiple chain robotic mechanisms
16 p2280 N90-22995
Algorithms for computing the multivariable stability margin
16 p2281 N90-22999
Robustness analysis for real parametric uncertainty
16 p2281 N90-23000
A disturbance based control/structure design algorithm
16 p2282 N90-23003
Using deflation in the pole assignment problem with output feedback
16 p2282 N90-23004
Parallel processing of real-time dynamic systems simulation on OSCAR (Optimally SCheduled Advanced multiprocessoR)
16 p2282 N90-23006
A unifying framework for rigid multibody dynamics and serial and parallel computational issues
16 p2283 N90-23009
Parallel algorithms and architecture for computation of manipulator forward dynamics
16 p2283 N90-23010
Efficient computer algebra algorithms for polynomial matrices in control design
16 p2285 N90-23022
An algorithm for the solution of dynamic linear programs
16 p2286 N90-23026
An inverse kinematics algorithm for a highly redundant variable-geometry-truss manipulator
16 p2288 N90-23033
Characterization of robotics parallel algorithms and mapping onto a reconfigurable SIMD machine
16 p2289 N90-23039
A decoupled recursive approach for constrained flexible multibody system dynamics
16 p2289 N90-23042
Algorithmic considerations of integrated design for CSI on a hypercube architecture
16 p2289 N90-23043
A parallel structure transient response algorithm using independent substructure response computation
16 p2290 N90-23044
Parallel conjugate gradient algorithms for manipulator dynamic simulation
16 p2290 N90-23045
Implementation of generalized optimality criteria in a multidisciplinary environment
16 p2290 N90-23048
New multivariable capabilities of the INCA program
16 p2290 N90-23049
ASTEC: Controls analysis for personal computers
16 p2291 N90-23052
Control/structure interaction design methodology
16 p2291 N90-23053
OPTICON: Pro-Matlab software for large order controlled structure design
16 p2292 N90-23058
Distributed neural control of a hexapod walking vehicle
16 p2293 N90-23061
A new second-order integration algorithm for simulating mechanical dynamic systems
16 p2293 N90-23064
The use of real-time, hardware-in-the-loop simulation in the design and development of the new Hughes HS601 spacecraft attitude control system
16 p2293 N90-23065
A real time, FEM based optimal control algorithm and its implementation using parallel processing hardware (transistors) in a microprocessor environment
16 p2294 N90-23066
JPL control/structure interaction test bed real-time control computer architecture
16 p2294 N90-23070
Faster simulation plots
16 p2295 N90-23071
Component model reduction via the projection and assembly method
16 p2295 N90-23073
Issues in CSI analysis for large scale systems
16 p2296 N90-23076
The power and efficiency of advanced software and parallel processing
16 p2296 N90-23079
Numerical algorithms for computations of feedback laws arising in control of flexible systems
16 p2297 N90-23085
Robust modelling of sampled systems for time delay estimation
[REPT-89-047] 16 p2298 N90-23092
Program inversion: More than fun
[CS-8903] 16 p2299 N90-23095
About the order of Appel's algorithm
[CS-8910] 16 p2299 N90-23097
The visibility diagram: A data structure for visibility and motion planning problems. Part 1: Application to the visibility polygon query problem
[CS-8913-PT-1] 16 p2299 N90-23098
On the performance of parallel algorithms
[CS-8914] 16 p2299 N90-23099
Curvature-dependent parametrization of curves and surfaces
[CS-8915] 16 p2299 N90-23100
Concurrent computing: Numerical algorithms and some applications
[AD-A218570] 16 p2300 N90-23103
Kernel architecture manual
[AD-A219295] 16 p2301 N90-23115
Adaptive mesh experiments for hyperbolic partial differential equations
[AD-A219194] 16 p2307 N90-23148
Proceedings of the 9th International Conference on Computing Methods in Applied Science and Engineering
[AD-A219307] 16 p2307 N90-23149
Statistical inference from sampled data
[AD-A218731] 16 p2309 N90-23156
Looking at large data sets using binned data plots
[DE90-008206] 16 p2326 N90-23263
Towards a calculus of data refinement
[CS-8902] 16 p2326 N90-23264
Development of new methods for predicting the bistatic electromagnetic scattering from absorbing shapes
[AD-A219327] 17 p2388 N90-23600
Unfairness caused by quadratic backoff in a packet-radio network
[AD-A219635] 17 p2388 N90-23603
Neuromorphic optical signal processing and image understanding for automated target recognition
[AD-A219827] 17 p2437 N90-23884
Cumulative reports and publications through December 31, 1989
[NASA-CR-182041] 17 p2439 N90-23898
Area-time efficient adders
[MEMO-INF-89-61] 17 p2440 N90-23905
Proceeding of the Embedded AI Languages Workshop
[AD-A218531] 17 p2442 N90-23914
Gemini2: A second generation layout validation program
[AD-A220731] 17 p2444 N90-23926
The LORE-interpreter: Notes on the implementation
[REPT-89-60] 17 p2445 N90-23932
A survey of search directions in interior point methods for linear programming
[REPT-89-65] 17 p2445 N90-23934
A scanning algorithm for display of generalized cylinders
[REPT-89-77] 17 p2445 N90-23936
A tabular bottom up recognizer
[REPT-89-78] 17 p2445 N90-23937
Sequencing and scheduling: Algorithms and complexity
[CWI-BS-R8909] 17 p2446 N90-23942
Scheduling around a small common due date
[CWI-BS-R8914] 17 p2446 N90-23943
On linear time minor tests and depth first search
[RUU-CS-89-1] 17 p2446 N90-23944
Bit-optimal election in synchronous rings
[RUU-CS-89-2] 17 p2446 N90-23945
A vectorization algorithm for the solution of large, sparse triangular systems of equations
[AD-A219850] 17 p2446 N90-23947
A parallel algorithm for global routing
[NASA-CR-186152] 17 p2448 N90-23959
Finding minimum area k-gons
[RUU-CS-89-7] 17 p2449 N90-23967
Designing distributed algorithms by means of formal sequentially phased reasoning
[TR-89-8] 17 p2449 N90-23969
Distributed hierarchical routing
[RUU-CS-89-5] 17 p2452 N90-23986
Adaptive filtering and control
[AD-A219556] 17 p2454 N90-23998
Efficient motion planning for an L-shaped object
[RUU-CS-88-38] 17 p2463 N90-24073
Sparse approximations of inverse matrices
[ETN-90-96904] 17 p2464 N90-24074
Universal criteria for blind deconvolution
[AD-A220853] 17 p2465 N90-24087
Application of optimal tracking methods to aircraft terrain following
[AD-A221099] 18 p2496 N90-24264
Collision detection using linear programming
18 p2507 N90-24326
Signal processing on finite groups
[AD-A221129] 18 p2544 N90-24523
Vortex-induced boundary-layer separation
18 p2551 N90-24560
Turbulence modeling in the SHALE code
[DE90-010354] 18 p2553 N90-24574
Real time inverse kinematics with joint limits and spatial constraints
[AD-A220462] 18 p2586 N90-24723
On the performance of algorithms for large-scale bound constrained problems
[DE90-010084] 18 p2590 N90-24736
Experimental high speed/power ratio ASIC designs using residue numbers
[AD-A220302] 18 p2591 N90-24741
Exact coloring algorithm for weighted graphs applied to timetabling problems with lectures of different lengths
[MEMO-814] 18 p2592 N90-24747
Majority voting: Characterization and algorithms
[RUU-CS-88-32] 18 p2592 N90-24750
A simple output-sensitive algorithm for hidden surface removal
[RUU-CS-89-26] 18 p2592 N90-24751
Parallelizing the closure computation in automated deduction
[DE90-007792] 18 p2593 N90-24758
Input/output algorithm for M-dimensional rectangular domain decompositions on N-dimensional hypercube multicomputers
[DE90-010494] 18 p2594 N90-24762
Visual animation of parallel algorithms for matrix computations
[DE90-011076] 18 p2594 N90-24763
Embedded diagonally implicit Runge-Kutta algorithms on parallel computers
[CWI-NM-R8912] 18 p2595 N90-24765
The HK singular value decomposition of rank deficient matrix triplets
[DE90-010114] 18 p2598 N90-24784

Minimum loss scheduling
[MEMO-821] 18 p2600 N90-24796
Improved self-reduction algorithms for graphs with bounded tree width
[RUU-CS-88-29] 18 p2601 N90-24805
Ray shooting, implicit point location, and related queries in arrangements of segments
[RUU-CS-89-11] 18 p2601 N90-24807
Counting and reporting intersections in arrangements of line segments
[RUU-CS-89-12] 18 p2601 N90-24808
An input-size/output-size trade-off in the time-complexity of rectilinear hidden surface removal
[RUU-CS-89-24] 18 p2602 N90-24814
An improved technique for output-sensitive hidden surface removal
[RUU-CS-89-32] 18 p2602 N90-24817
Approximations of thermoelastic and viscoelastic control systems
[NASA-CR-182054] 18 p2604 N90-24834
Direct calculation of Newton steps without accumulating Jacobians
[DE90-009702] 18 p2607 N90-24847
En route noise: NASA propfan test aircraft (calculated source noise
[DOT-TSC-FA953-LR5] 18 p2609 N90-24857
A comparison of select image-compression algorithms for an electronic still camera 18 p2632 N90-24994
Optical rate sensor algorithms 18 p2632 N90-24997
Minimizing distortion and internal forces in truss structures by simulated annealing 18 p2644 N90-25055
Kharitonov's theorem: Generalizations and algorithms 18 p2646 N90-25064
Cloud field classification based on textural features 18 p2646 N90-25066
Evaluation of nonlinear motion-drive algorithms for flight simulators
[UTIAS-TN-272] 19 p2662 N90-25148
Conception and results of the DLR realtime azimuth processor for the E-SAR system
[ESA-TT-1184] 19 p2684 N90-25268
Performance of a self-aligning solar array tracking controller
[DE90-011184] 19 p2698 N90-25350
Cloud analysis with satellite data 19 p2707 N90-25401
Mobile transporter path planning 19 p2727 N90-25505
A comparison of two neural network schemes for navigation 19 p2733 N90-25536
Ocean feature recognition using genetic algorithms with fuzzy fitness functions (GA/F3) 19 p2740 N90-25576
Outline and realization of a polymorphic language extension for ELAN
[TR-89-23] 19 p2743 N90-25592
New multi-level codes over GF(q)
[NASA-CR-186862] 19 p2744 N90-25594
Depth buffer shadow algorithms
[DE90-012070] 19 p2744 N90-25595
Computer-aided design of advanced control algorithms for industrial robotics: An overview of ESPRIT project SACODY
[REPT-81-DT-89-47] 19 p2744 N90-25596
Random pseudo-polynomial algorithms in combinatorial programming
[REPT-89-067] 19 p2744 N90-25597
The Knuth-Bendix completion algorithm and its specification in Z
[RSRE-MEMO-4323] 19 p2745 N90-25601
Trajectory planning and control of a 6 DOF manipulator with Stewart platform-based mechanism
[NASA-CR-186813] 19 p2747 N90-25610
Non-linear systems identification using neural networks
[RR-370] 19 p2748 N90-25616
A parallel recursive prediction error algorithm for training layered neural networks
[RR-373] 19 p2748 N90-25617
A comparison of the backpropagation and recursive prediction error algorithms for training neural networks
[RR-379] 19 p2748 N90-25620
Modular arithmetic and randomization for exact matroid problems: Extended abstract
[REPT-89-064] 19 p2751 N90-25628
Non-linear systems identification using radial basis functions
[RR-378] 19 p2751 N90-25635
Synthesis and validation of feedback guidance laws for air-to-air interceptions
[LR-615] 19 p2752 N90-25639
Supersonic combustor modeling 20 p2810 N90-25992
Guidance and targeting for the strategic target system
[DE90-005239] 20 p2817 N90-26031
The origin of poorly conditioned susceptibility matrix within inverse CVM algorithm in the case of Pd(sub 3)V: A comparison to the case of Ni(sub 3)V
[DE90-012464] 20 p2833 N90-26110
Application of inertial instruments for DSN antenna pointing and tracking 20 p2853 N90-26224
Implementation of an algorithm for travelling-wave-based directional detection
[EUT-89-E-214] 20 p2855 N90-26239
Modeling, simulation, and analysis of optical remote sensing systems
[NASA-CR-186648] 20 p2878 N90-26376
A hybrid M-algorithm/sequential decoder for convolutional and trellis codes
[NASA-CR-186863] 20 p2906 N90-26528
Automated sensitivity analysis with the Gradient Enhanced Software System (GRESS)
[DE90-011291] 20 p2906 N90-26529
ANTIPASTO: An interactive mesh generator and preprocessor for two-dimensional analysis programs
[DE90-011755] 20 p2906 N90-26530
Parallel processors and nonlinear structural dynamics algorithms and software
[NASA-CR-186755] 20 p2907 N90-26536
An angular weighting approach for calculating gradients and divergences
[DE90-013164] 20 p2908 N90-26539
Efficient generalized conjugate gradient algorithms. Part 2: Implementation
[MATHS-REPT-A-118-PT-2] 20 p2908 N90-26543
A parallel algorithm for surface plane intersection
[IMAG-RR-794-M] 20 p2909 N90-26549
Study of a class of non convex optimization algorithms: Implementation and applications
[ETN-90-97241] 20 p2909 N90-26552
Adaptive and comparative studies of optimization algorithms: Implementations and applications
[ETN-90-97243] 20 p2910 N90-26553
Parallel programming with algorithmic skeletons
[DE90-010536] 20 p2911 N90-26562
MINAS: An algorithm for systematic state assignment of sequential machines: Computational aspects and results
[EUT-89-E-217] 20 p2912 N90-26566
From network to artwork: Automatic schematic diagram generation
[EUT-89-E-219] 20 p2912 N90-26567
Implementation of algorithms used in calculating the tensor product of matrices on a distributed memory machine
[IMAG-RR-786-I] 20 p2913 N90-26572
Parallel algorithm for distributed memory computers (applications to matricial algorithms)
[ETN-90-97252] 20 p2913 N90-26573
Multilayered neural networks: Learning algorithms, implementation on hypercube machines, applications
[ETN-90-97255] 20 p2913 N90-26574
On output deadbeat control of discrete-time multivariable systems
[MATHS-REPT-A-122] 20 p2915 N90-26583
Search of primitive polynomials over finite fields
[IMAG-RR-797-M] 20 p2918 N90-26607
Unification and disunification: Theory and applications
[ETN-90-97247] 20 p2919 N90-26610
Contribution to the study of differential equations and to the differences in the complex field
[ETN-90-97250] 20 p2919 N90-26612
Parallel/distributed direct method for solving linear systems
[NASA-TM-103229] 20 p2919 N90-26614
Causal distributed breakpoints
[AD-A222613] 20 p2921 N90-26622
Fluid Dynamics Panel Working Group 12 on Adaptive Wind Tunnel Walls: Technology and Applications
[AGARD-AR-269] 21 p2961 N90-26838
Streamlining algorithms for complete adaptation 21 p2962 N90-26841
Speech coding 21 p2992 N90-27009
Speech processing standards 21 p2993 N90-27013
Multistage estimation of received carrier signal parameters under very high dynamic conditions of the receiver
[NASA-CASE-NPO-17911-1-CU] 21 p2994 N90-27016
Nonlinear real-time signal processing
[AD-A222889] 21 p2994 N90-27020
A preliminary analysis of threshold signal detection in ambient and signal-dependent noise environments
[AD-A222089] 21 p2996 N90-27030
Specification for HF Lowest Usable Frequency (LUF) model
[AD-A222114] 21 p2996 N90-27031
Adaptive time series analysis using predictive inference and entropy
[AD-A222337] 21 p2997 N90-27033
High resolution exponential modeling of fully polarized radar returns
[AD-A221432] 21 p2997 N90-27036
Parallel numerical simulations of axisymmetric projectile flows using zonal-overlapped grids
[AD-A221711] 21 p3005 N90-27082
Basic data requirements for microwave radiometer systems 21 p3015 N90-27143
ERBE and CERES broadband scanning radiometers 21 p3016 N90-27149
Computer production of K-indices by a simple method based on linear elimination 21 p3024 N90-27194
Resource a ocation using constraint propagation 21 p3040 N90-27278
Genetic algorithm based fuzzy control of spacecraft autonomous rendezvous 21 p3041 N90-27281
Expert Sy tem Development Methodology (ESDM) 21 p3042 N90-27292
A diagnosis system using object-oriented fault tree models 21 p3046 N90-27313
An engineering approach to automatic programming 21 p3046 N90-27317
Some software implementation of the functions sine and cosine
[DE90-010398] 21 p3050 N90-27339
Modified fast frequency acquisition via adaptive least squares algorithm
[NASA-CASE-NPO-17845-1-CU] 21 p3050 N90-27341
Generalization in the presence of free variables: A mechanically-checked correctness proof for one algorithm
[AD-A222681] 21 p3051 N90-27346
Non-interactive zero knowledge
[AD-A222698] 21 p3052 N90-27347
An algorithm for automated surface modelling in unigraphics
[AD-A223219] 21 p3053 N90-27355
Some remarks on the generalised Bareiss and Levinson algorithms
[AD-A221957] 21 p3053 N90-27357
Recovery in distributed systems using optimistic message logging and checkpointing
[AD-A222104] 21 p3054 N90-27361
Maintenance of a minimum spanning forest in a dynamic planar graph
[AD-A221425] 21 p3054 N90-27362
Architectures for optical computing
[AD-A221435] 21 p3054 N90-27364
Algorithms to solve nonlinear time dependent problems of engineering and physics
[AD-A221463] 21 p3055 N90-27366
ROBFIT: A code for the analysis of histogram spectra with nonlinear regression and robust estimation
[AD-A221527] 21 p3055 N90-27369
EINMUF: An HF MUF, FOT, LUF prediction program
[AD-A221577] 21 p3055 N90-27371
A build-up interior method for linear programming: Affine scaling form
[AD-A221802] 21 p3056 N90-27375
Context propagation truth maintenance system
[RR-779-I] 21 p3057 N90-27380
The image of weighted combinatorial problems
[REPT-88-017] 21 p3057 N90-27382
A neural network for feature extraction
[AD-A223059] 21 p3058 N90-27387
Practical issues in the complexity of neural networks
[AD-A221420] 21 p3058 N90-27389
On parallel hashing and integer sorting
[AD-A221569] 21 p3058 N90-27390
Learning binary relations and total orders
[AD-A221643] 21 p3059 N90-27392
Parallel algorithms for computer vision
[AD-A221871] 21 p3059 N90-27394
Robotic space simulation integration of vision algorithms into an orbital operations simulation
[NASA-CR-185934] 21 p3059 N90-27395
Design of robust multivariable controllers
[AD-A222096] 21 p3060 N90-27397
Development, implementation, and validation of control algorithms for the dual-arm robotic manipulation of a single object
[AD-A222502] 21 p3060 N90-27402
On finding supernodes for sparse matrix computations
[DE90-013626] 21 p3063 N90-27410
Conjugate gradient methods for constrained least squares problems
[AD-A222706] 21 p3063 N90-27411
Toeplitz matrices: Algebra and algorithms
[AD-A223174] 21 p3064 N90-27416
Finding the maximum recoverable system state in optimistic rollback recovery methods
[AD-A222338] 21 p3064 N90-27419

Proving Boolean equivalence with Prolog
[AD-A221766] 21 p3065 N90-27427
Development and analysis of ARMA parameter estimation schemes in the presence of noise
[AD-A221794] 21 p3066 N90-27428
Generalized Voronoi diagrams: Initial results
[IMAG-RR-799-M] 21 p3066 N90-27429
Model-based Gaussian and non-Gaussian clustering
[AD-A222097] 21 p3066 N90-27430
Causal distributed breakpoints
[AD-A222103] 21 p3066 N90-27431
Advanced retrieval assistance for the DGIS gateway
[AD-A221592] 21 p3067 N90-27558
Advanced algorithms design and implementation in on-board microprocessor systems for engine life usage monitoring 22 p3104 N90-27628
Expert system diagnostics and parts life tracking as applied to the AV-8B aircraft for the USMC 22 p3104 N90-27629
Sideslip-induced static pressure errors in flight-test measurements
[NASA-TM-102846] 22 p3116 N90-27702
Multi-sensor analysis techniques for SSME safety monitoring
[NASA-CR-185260] 22 p3124 N90-27732
Optical communications system having a wide-core single-mode planar waveguide
[AD-D014485] 22 p3164 N90-27939
On unstructured grids and solvers 22 p3172 N90-27994
Towards a genuinely multi-dimensional upwind scheme 22 p3172 N90-27995
Remote sounding through semi-transparent cirrus cloud 22 p3226 N90-28296
Study of the ocean tides by the assimilation of marigraphic and altimetric satellite data in a hydrodynamic model
[ETN-90-97460] 22 p3231 N90-28320
Analysis and design of algorithm-based fault-tolerant systems
[NASA-CR-186884] 22 p3236 N90-28352
Local spatial frequency analysis for computer vision
[NASA-CR-186990] 22 p3237 N90-28356
Efficient algorithms for a class of partitioning problems
[NASA-CR-182073] 22 p3237 N90-28357
Algorithmic components in evaluating systems dependability
[REPT-88-044] 22 p3237 N90-28358
Algorithms and evaluation for regulation of linear, time-independent difference systems under position value limitation
[ETN-90-97308] 22 p3238 N90-28364
A Bayesian derivation of an iterative autofocus/super-resolution algorithm
[RSRE-MEMO-4337] 22 p3239 N90-28371
Interconnection networks and parallel processing
[FEL-1989-112] 22 p3240 N90-28376
Parallelisation of a dynamic programming algorithm suitable for feature detection
[RSRE-MEMO-4349] 22 p3241 N90-28377
Genetic algorithms: The state of the art and some research proposals
[REPT-89-058] 22 p3241 N90-28380
Polymatroids: Construction and random algorithms
[REPT-89-068] 22 p3242 N90-28388
Robust circle and sphere fitting by least squares
[NPL-DITC-153/89] 22 p3243 N90-28389
Theoretical thermodynamics: Equation of state and perturbation studies
[PB90-199332] 22 p3255 N90-28430
Studies in automatic speech recognition and its application in aerospace 23 p3318 N90-28759
Real-time aerodynamic heating and surface temperature calculations for hypersonic flight simulation
[NASA-TM-4222] 23 p3327 N90-28815
ROSES, a Robot Operating System Expert Scheduler: Methodological framework
[DE90-014782] 23 p3334 N90-28851
Tele-Autonomous control involving contact --- object localization
[NASA-CR-187004] 23 p3335 N90-28854
Selective learning algorithm for certain types of learning failure in multilayer perceptrons
[AD-A223982] 23 p3362 N90-28998
Methods and strategies of object localization 23 p3366 N90-29020
Robot Acting on Moving Bodies (RAMBO): Interaction with tumbling objects 23 p3366 N90-29022
Approximation algorithms for planning and control 23 p3370 N90-29042
Multiresolutional models of uncertainty generation and reduction 23 p3370 N90-29043
Efficient mapping algorithms for scheduling robot inverse dynamics computation on a multiprocessor system 23 p3375 N90-29071
Parallel algorithms for computation of the manipulator inertia matrix 23 p3376 N90-29072
Organising geometric computations for space telerobotics 23 p3376 N90-29074
Learning in stochastic neural networks for constraint satisfaction problems 23 p3377 N90-29078
LINTERP: A numerical algorithm for interpolating quadrilateral and hexahedral meshes
[DE90-014417] 23 p3379 N90-29090
The effect of multiprocessor radius on scaling
[DE90-014772] 23 p3380 N90-29095
Recursive least-squares learning algorithms for neural networks
[DE90-014926] 23 p3380 N90-29096
Block Lanczos algorithm
[AD-A224011] 23 p3383 N90-29111
Least-index resolution of degeneracy in linear complementarity problems with sufficient matrices
[DE90-014406] 23 p3390 N90-29145
Prediction, control, and decision-making aspects for chaotic systems
[DE90-014452] 23 p3402 N90-29224
Independent ground monitor coverage of Global Positioning System (GPS) satellites for use by civil aviation 24 p3428 N90-29364
Omega navigation signal characteristics 24 p3429 N90-29369
A land navigation demonstration vehicle with a color map display for tactical use 24 p3430 N90-29375
Optimal trajectories for hypervelocity flight 24 p3430 N90-29378
AutoPAVER: A software package for automated pavement evaluation
[AD-A224176] 24 p3458 N90-29531
Modeling and reconstruction algorithms for detection, location, and identification of subsurface anomalies
[AD-A224358] 24 p3459 N90-29539
High range resolution radar cross-section profiles: A preliminary analysis
[AD-A223448] 24 p3461 N90-29550
Performance analysis of subspace-based parameter estimation algorithms
[AD-A224523] 24 p3463 N90-29566
Macro cell placement with neural net algorithms
[REPT-90-020] 24 p3466 N90-29585
Unstructured mesh methods for CFD 24 p3470 N90-29611
A vector diagram approach to shaping inputs for vibration reduction
[AD-A223724] 24 p3480 N90-29671
Active vibration damping of flexible structures
[DLR-FB-90-03] 24 p3481 N90-29676
Studies of ionospheric dynamics utilizing data from DMSP
[AD-A223370] 24 p3492 N90-29733
Windshear estimation along the trajectory of an aircraft 24 p3494 N90-29745
Guidance algorithms for a free-flying space robot 24 p3503 N90-29798
Trinocular stereovision using figural continuity, dealing with curved objects 24 p3503 N90-29802
A fast 3-D object recognition algorithm for the vision system of a special-purpose dexterous manipulator 24 p3503 N90-29803
THREAD: A programming environment for interactive planning-level robotics applications 24 p3505 N90-29810
What kind of computation is intelligence. A framework for integrating different kinds of expertise 24 p3506 N90-29817
The flight telerobotic servicer: From functional architecture to computer architecture 24 p3507 N90-29823
Research and development activities at the Goddard Space Flight Center for the flight telerobotic servicer project 24 p3507 N90-29824
Test and validation for robot arm control dynamics simulation 24 p3507 N90-29826
Discrete-time adaptive control of robot manipulators 24 p3509 N90-29834
Optimal payload rate limit algorithm for zero-G manipulators 24 p3513 N90-29858
Efficient conjugate gradient algorithms for computation of the manipulator forward dynamics 24 p3514 N90-29864
Kinematics and control algorithm development and simulation for a redundant two-arm robotic manipulator system 24 p3516 N90-29877
Trees, bialgebras and intrinsic numerical algorithms
[NASA-CR-187031] 24 p3524 N90-29925
The development and evaluation of numerical algorithms for MIMD computers
[NASA-TM-101167] 24 p3526 N90-29939
Parallel architectures and algorithms for image understanding
[AD-A223479] 24 p3526 N90-29940
A comparison of hardware implementations for low-level vision algorithms
[AD-A223699] 24 p3527 N90-29945
Fast algorithms for parallel architectures
[AD-A223731] 24 p3528 N90-29947
Bispectral-based optimization algorithms for speckle imaging
[DE90-015610] 24 p3529 N90-29957
Developing tools for performance visualization of parallel algorithms
[DE90-015801] 24 p3530 N90-29960
Handbook of data compression algorithms
[ESA-TM-06] 24 p3531 N90-29969
Unstructured mesh relaxation
[DE90-015814] 24 p3534 N90-29989
The location of zeros using generalizations of Newton's method
[DE90-627168] 24 p3541 N90-30023
A canonical integration technique of arbitrary order
[DE90-628377] 24 p3541 N90-30025
Monte Carlo simulation of complex spectra for opacity calculations
[DE90-015198] 24 p3561 N90-30147

ALIGNMENT
NT SELF ALIGNMENT
Design of a Kalman filter for transfer alignment 02 p0149 N90-10848
Periodic permanent magnet structures
[AD-D014173] 03 p0398 N90-12280
Use of the NPL linac for x ray dosimetry --- linear accelerator (linac)
[NPL-RSA(EXT)-6] 03 p0404 N90-12314
Cold tests of quasi-optical gyrotron resonators
[AD-A212707] 04 p0498 N90-12868
Extended Kalman filter for attitude estimation of the earth radiation budget satellite 05 p0590 N90-13433
Segment alignment control system 05 p0595 N90-13457
Real-time sensing of optical alignment 05 p0599 N90-13479
Mechanical strain isolator mount
[NASA-CASE-LAR-13580-1] 08 p1084 N90-16272
B-Factory Final Focus System using superconducting quadrupoles
[DE90-004432] 08 p1131 N90-16552
Drag reduction by longitudinal riblets on the surface of a streamwise aligned body of revolution
[MPIS-MITT-92] 12 p1600 N90-19210
Development and testing of a universally implementable recording aligning system
[SER-C-349] 12 p1691 N90-19716
Tensile film clamps and mounting block for the rheovibron and autovibron viscoelastometer
[NASA-CASE-LAR-13696-1] 13 p1812 N90-20409
Error correction of the DEA (Digital Electronic Automation) coordinate measuring machines at LLNL
[DE90-008913] 14 p1983 N90-21365
Induction-type metal detector with increased scanning area capability
[NASA-CASE-KSC-11386-1] 15 p2101 N90-22023
Utilization of Moire patterns as an orbital docking aid to space shuttle/Space Station Freedom 18 p2629 N90-24980
Calibration technique for heat flux sensors used in fire experiments and standard fire tests
[DOT/FAA/CT-89/26] 19 p2694 N90-25329
Performance of a self-aligning solar array tracking controller
[DE90-011184] 19 p2698 N90-25350
Alignment positioning mechanism
[NASA-CASE-MSC-21502-1] 20 p2872 N90-26341
Quick connect coupling
[NASA-CASE-MSC-21539-1] 21 p3010 N90-27111
Near-field gain of pyramidal horns from 18 to 40 GHz
[PB90-155854] 22 p3164 N90-27941
Using the x ray region of the electromagnetic spectrum for alignment: Overview, geometric optics, and design considerations
[DE90-014798] 23 p3317 N90-28752
Kalman filter formulations for transfer alignment of strapdown inertial units 24 p3424 N90-29342
Guidance and control techniques for airborne transfer alignment and SAR motion compensation 24 p3429 N90-29372

ALIPHATIC COMPOUNDS
Pentafluorothio polynitroaliphatic explosives
[AD-D014221] 06 p0753 N90-14383

ALIPHATIC HYDROCARBONS
NT ACETYLENE
NT ALKANES
NT ALKENES
NT BUTADIENE
NT BUTANES
NT BUTENES
NT DIENES
NT ETHANE

NT ETHYLENE
NT METHANE
NT OCTANES
NT OXYACETYLENE
NT POLYBUTADIENE
NT PROPANE
NT PROPYLENE
NT VINYLIDENE
Thermal conductivity of gaseous aliphatic hydrocarbons. Part 1: Alkanes
[ESDU-89035-PT-1] 07 p0897 N90-15183

ALKALI HALIDES
NT CESIUM IODIDES
NT SODIUM CHLORIDES
NT SODIUM FLUORIDES
NT SODIUM IODIDES
Design and construction of systems for the single-crystals growth of ternary silver halides, alkali halides, and alkaline earth fluorides, and the dielectric investigation of silver halide
[ETN-89-94673] 02 p0286 N90-11632
On the choice of trial function in theoretical calculations of the thermal conductivity
[DE90-001733] 07 p0897 N90-15182
Atomic and molecular spectra from electron-excited alkali halides
[DE90-006160] 11 p1562 N90-19004

ALKALI METALS
NT CESIUM
NT CESIUM VAPOR
NT LIQUID LITHIUM
NT LIQUID SODIUM
NT LITHIUM
NT LITHIUM ISOTOPES
NT POTASSIUM
NT RUBIDIUM
NT SODIUM
Neutron scattering studies of premartensitic phenomena
[DE90-000025] 03 p0328 N90-11863
The onset of boiling of the liquid alkali metals
[DE90-002276] 08 p1044 N90-16036
Volatile divalent double metal alkoxides
[AD-D014355] 10 p1438 N90-18300
Positron-alkali atom scattering 11 p1556 N90-18958
Scattering of positrons and electrons by alkali atoms 11 p1556 N90-18959
Resonances in low-energy positron-alkali scattering 11 p1560 N90-18992
Interactions of molecules with surfaces
[DE90-007555] 13 p1883 N90-20806
Pre-concentration method for inductively coupled plasma-mass spectrometry
[PB90-181348] 19 p2673 N90-25202
A composition for the filling of gas-discharge tubes
[AD-A222818] 21 p2999 N90-27047
Photoelectron spectroscopy at limit surfaces of semiconductors with rare Earth and alkali metals
[ETN-90-97322] 22 p3249 N90-28427
Thermodynamics and structure of liquid alkali metals from the charged-hard-sphere reference fluid
[DE90-627792] 23 p3311 N90-28725

ALKALIES
NT LITHIUM HYDROXIDES
NT POTASSIUM HYDROXIDES
The effects of caustics in acoustic inverse scattering experiments
[AD-A218454] 16 p2313 N90-23185
Structure of metal overlayers by low energy alkali ion scattering: Cu/Ru(0001) and Sn/Pt(111)
[DE90-014453] 23 p3310 N90-28718

ALKALINE BATTERIES
Silver composite cathodes for alkaline secondary batteries
[AD-D014227] 06 p0767 N90-14462
Silver-nickel composite cathodes for alkaline secondary batteries
[AD-D014231] 06 p0767 N90-14464
Oxygen electrodes for rechargeable alkaline fuel cells-II 13 p1823 N90-20469
Non-noble electrocatalysts for alkaline fuel cells 13 p1824 N90-20470

ALKALINE EARTH COMPOUNDS
Chemiluminescent ion-molecule reactions of group-3 ions with halogens: New optical spectra and reaction dynamics
[MPIS-18/1988] 02 p0196 N90-11120

ALKALINE EARTH METALS
Excimer emission from alkali diatomic and alkaline-earth-noble-gas molecules
[AD-A214246] 07 p0896 N90-15179
Surface and interface studies by Auger electron spectroscopy
[ETN-90-96948] 18 p2522 N90-24398
Pre-concentration method for inductively coupled plasma-mass spectrometry
[PB90-181348] 19 p2673 N90-25202
Synthesis, structure, electric, and magnetic properties of CaNiN
[AD-A222273] 21 p2978 N90-26923

ALKALINE EARTH OXIDES
NT BARIUM OXIDES
NT BERYLLIUM OXIDES
NT CALCIUM OXIDES
NT MAGNESIUM OXIDES
Prospects for wavelength tunable lasers based on vacancy defects in alkaline-earth oxides
[DE90-001078] 06 p0789 N90-14592

ALKALINITY
Conductive polymers of transition-metal complexes coordinated by a Diamino-Dichalcogen-Benzene compound
[AD-D014326] 12 p1629 N90-19360

ALKALOIDS
NT ATROPINE
NT CAFFEINE

ALKANES
NT BUTANES
NT ETHANE
NT METHANE
NT OCTANES
NT PROPANE
A new method for the characterization of solutes and solvent phases using solvatochromic parameters
[AD-A211238] 02 p0196 N90-11116
Summary physical data tables: Alkanes
[ESDU-PD3] 07 p0893 N90-15162
Thermal conductivity of gaseous aliphatic hydrocarbons. Part 1: Alkanes
[ESDU-89035-PT-1] 07 p0897 N90-15183
Novel macrocyclic carriers for proton-coupled liquid membrane transport
[DE90-015529] 24 p3445 N90-29453

ALKENES
NT BUTENES
NT ETHYLENE
NT PROPYLENE
NT VINYLIDENE
Radical homopolymerization of a trisubstituted alkene: 1-cyclobutenecarboxylic acid and its polymer
[AD-A223188] 21 p2986 N90-26968

ALKYL COMPOUNDS
NT TRIMETHYL COMPOUNDS
The effect of degree of aromaticity and alkyl substitution of polyaromatic hydrocarbons on instrumental response factors
[DE89-000761] 02 p0196 N90-11117
Determination of the thermal stability of perfluoroalkylethers
[NASA-TM-102493] 10 p1358 N90-17875
X ray specular reflection studies of silicon coated by organic monolayers (alkylsiloxanes)
[AD-A217418] 13 p1779 N90-20213
Boron-containing organosilane polymers and ceramic materials thereof
[NASA-CASE-ARC-11649-2-SB] 14 p1952 N90-21177
Some 1-(diorganooxyphosphonyl)methyl-2,4- and -2,6-dinitro-benzenes
[NASA-CASE-ARC-11425-3] 17 p2367 N90-23475

ALKYLATION
Carboxyalkylated hemoglobin as a potential blood substitute
[AD-A213886] 07 p0966 N90-15582

ALKYNES
NT ACETYLENE
NT OXYACETYLENE

ALL SKY PHOTOGRAPHY
Theory of wide-angle photometry from standard stars
[NASA-CR-185964] 06 p0860 N90-14999
Fast classification of ROSAT sources on objective prism plates 19 p2788 N90-25871

ALL-WEATHER AIR NAVIGATION
Kalman Filter Integration of Modern Guidance and Navigation Systems
[AGARD-LS-166] 02 p0148 N90-10847
Development of the integrated all-weather navigation system for Tornado 02 p0149 N90-10849
Flight in Adverse Environmental Conditions
[AGARD-CP-470] 07 p0869 N90-15041
The human element: The key to safe, civil operations in adverse weather 07 p0869 N90-15042
The United States Air Force approach to all-weather testing 07 p0870 N90-15047
Adverse weather operations during the Canadian Atlantic storms program 07 p0871 N90-15052
Position computation without elevation information for computed centerline operations
[DOT/FAA/CT-TN89/42] 17 p2349 N90-23379
High mountain flying in ski country, USA
[PB90-180316] 22 p3107 N90-27651
The integration of multiple avionic sensors and technologies for future military helicopters 24 p3424 N90-29344

ALLENDE METEORITE
Identification of solar nebula condensates in interplanetary dust particles and unequilibrated ordinary chondrites 08 p1144 N90-16629
Nature and origin of interstellar diamond from the Allende CV3 meteorite 21 p3092 N90-27581

ALLOCATIONS
NT RESOURCE ALLOCATION
Finite methods for a nonlinear allocation problem
[AD-A209719] 01 p0111 N90-10629
A simulation study of landing time allocation procedures for use in computer-assisted air traffic management systems
[AD-A212159] 03 p0303 N90-11722
Name assignment techniques for relational schemas representing extended entity-relationship schemas
[DE90-003269] 07 p0974 N90-15623
Profiles-aeronautical/astronautical engineering: Human resources and funding
[PB90-103888] 09 p1203 N90-16969
Science requirements for passive microwave sensors on earth science geostationary platforms 12 p1608 N90-19251

ALLOYING
The effects of alloying and thermal factors on the solidification and mechanical properties of gray iron
[VTT-619] 05 p0625 N90-13651
A review of the effects of microalloying constituents on the formation and breakdown of protective oxide scales on high-temperature alloys at temperatures below 700 C
[DE90-001277] 07 p0902 N90-15216
Long term creep strength of silver alloyed copper
[DE90-602367] 08 p1045 N90-16039
Alloying of metals for corrosion resistance
[AD-D014313] 09 p1194 N90-16919
A fundamental understanding of the effect of alloying elements on the corrosion resistance of rapidly solidified Mg alloys
[AD-A216767] 11 p1486 N90-18553
A study of the influence of alloying additions on the passivity of aluminium
[AD-A219630] 17 p2376 N90-23532

ALLOYS
NT ALUMINUM ALLOYS
NT AUSTENITIC STAINLESS STEELS
NT BAINITIC STEEL
NT BERYLLIUM ALLOYS
NT BINARY ALLOYS
NT BISMUTH ALLOYS
NT BORON ALLOYS
NT BRASSES
NT CARBON STEELS
NT CAST ALLOYS
NT CHROMIUM ALLOYS
NT CHROMIUM STEELS
NT COBALT ALLOYS
NT COPPER ALLOYS
NT ERBIUM ALLOYS
NT FERRITIC STAINLESS STEELS
NT GALLIUM ALLOYS
NT GERMANIUM ALLOYS
NT HAFNIUM ALLOYS
NT HASTELLOY (TRADEMARK)
NT HEAT RESISTANT ALLOYS
NT HIGH STRENGTH ALLOYS
NT HIGH STRENGTH STEELS
NT INCONEL (TRADEMARK)
NT INDIUM ALLOYS
NT IRON ALLOYS
NT LANTHANUM ALLOYS
NT LEAD ALLOYS
NT LIGHT ALLOYS
NT LIQUID ALLOYS
NT LITHIUM ALLOYS
NT LOW CARBON STEELS
NT MAGNESIUM ALLOYS
NT MANGANESE ALLOYS
NT MANGANIN (TRADEMARK)
NT MARAGING STEELS
NT MARTENSITIC STAINLESS STEELS
NT MERCURY AMALGAMS
NT MOLYBDENUM ALLOYS
NT MONEL (TRADEMARK)
NT MONOTECTIC ALLOYS
NT NICKEL ALLOYS
NT NICKEL STEELS
NT NIOBIUM ALLOYS
NT NITINOL ALLOYS
NT PALLADIUM ALLOYS
NT QUATERNARY ALLOYS
NT RARE EARTH ALLOYS

NT REFRACTORY METAL ALLOYS
NT SHAPE MEMORY ALLOYS
NT SILICON ALLOYS
NT SOLDERS
NT STAINLESS STEELS
NT STEELS
NT TERNARY ALLOYS
NT TIN ALLOYS
NT TITANIUM ALLOYS
NT TUNGSTEN ALLOYS
NT UDIMET ALLOYS
NT URANIUM ALLOYS
NT VANADIUM ALLOYS
NT WASPALOY
NT WROUGHT ALLOYS
NT ZINC ALLOYS
NT ZIRCONIUM ALLOYS

Formation and modification of surface alloys by excimer laser melting and resolidification
[DE89-016968] 03 p0327 N90-11856

Electronic structure of transition metal alloys and intermetallics: Charge transfer and its implications for Moessbauer effect measurements
[DE89-017603] 03 p0327 N90-11860

Kinetic processes in advanced alloys
[AD-A212049] 03 p0329 N90-11867

Current research in advanced materials
[DE89-017466] 03 p0331 N90-11884

Superplasticity: An overview 06 p0743 N90-14326

Electrical properties of materials for high temperature strain gage applications
[NASA-CR-186192] 06 p0780 N90-14534

Thermal mechanical fatigue of coated blade materials
[AD-A214258] 07 p0882 N90-15107

Electron theory of long wavelength concentration fluctuations in liquid metal alloys
[DE89-636213] 07 p0904 N90-15225

Alloying of metals for corrosion resistance
[AD-D014313] 09 p1194 N90-16919

Application of high-rate cutting tools
[AD-A214644] 09 p1203 N90-16970

Construction of inelastic stress-strain curves from minimal materials data (computer program)
[ESDU-89052] 09 p1239 N90-17189

Computer simulation of electromigration in thin films
[AD-A216382] 10 p1357 N90-17867

Crystal growth and mechanical properties of semiconductor alloys
[AD-A216697] 11 p1570 N90-19035

Fracture toughness and tensile properties of alloy HT9 in thin sections under high neutron fluences
[DE90-008386] 15 p2069 N90-21851

Computational methods and plasticity
[LR-583] 15 p2119 N90-22120

High Intensity Electro-Magnetic and Ultrasonic Effects on Inorganic Materials Behavior and Processing Workshop
[AD-A218884] 16 p2215 N90-22640

Improved high temperature oxidation behavior of alloys by ion implantation
[AERE-R-13309] 16 p2217 N90-22650

The oxidation and corrosion of ODS alloys
[NASA-TM-102555] 19 p2675 N90-25211

Solidification processing of alloys using an applied electric field
[NASA-CASE-MFS-26083-1-CU] 21 p2981 N90-26940

Metallurgical processes in multi-component rare Earth-transition metal permanent magnet alloys
[AD-A222891] 21 p2982 N90-26942

Computational investigation of local material strength and toughness on crack growth
[AD-A223189] 21 p3012 N90-27127

Power beam technology at Los Alamos: A review of research and development activities
[DE90-009002] 22 p3182 N90-28057

Creep and creep rupture of strongly reinforced metallic composites
[NASA-CR-185286] 22 p3192 N90-28110

ALLUVIUM

Geochemical survey on faults overland with alluvial deposits, part 1. Application for the Neodani and the Atera faults survey
[DE89-782326] 12 p1690 N90-19707

ALMUCANTAR

U ELEVATION ANGLE

ALOUETTE SATELLITES

NT ALOUETTE 1 SATELLITE
NT ALOUETTE 2 SATELLITE

ALOUETTE 1 SATELLITE

Results from Alouette 1, Explorer 20, Alouette 2, and Explorer 31
[NASA-TM-101822] 24 p3483 N90-29690

ALOUETTE 2 SATELLITE

Results from Alouette 1, Explorer 20, Alouette 2, and Explorer 31
[NASA-TM-101822] 24 p3483 N90-29690

ALPHA PARTICLES

Theoretical plasma physics
[DE90-000009] 03 p0408 N90-12341

Stability of the Global Alfven Eigenmode in the presence of fusion alpha particles in an ignited tokamak plasma
[DE89-016618] 06 p0848 N90-14930

Destabilization of tokamak pressure-gradient driven instabilities by energetic alpha populations
[DE90-003716] 07 p0996 N90-15756

Quasilinear approach to the damping of LH waves in a reactor-grade plasma
[IPPCZ-292] 10 p1432 N90-18262

Thermonuclear instability of global-type shear Alfven modes
[DE90-007087] 11 p1568 N90-19026

Marginal test and analysis of DRAM with masked alpha radiation
[RB-4180] 12 p1699 N90-19754

Onboard detection of intrinsic Ly alpha radiation from a neutral particle beam
[DE90-010341] 18 p2511 N90-24346

Emission of quick neutrons and non-equilibrium phenomena by central shocks in the reaction 40 Ar + 40 Ca at 20 MeV/u
[ETN-90-97296] 24 p3544 N90-30043

Control of helium accumulation
[DE90-015658] 24 p3550 N90-30084

ALPHA RADIATION

U ALPHA PARTICLES

ALPHANUMERIC CHARACTERS

NT BINARY DIGITS
NT DIGITS

Source header list. Volume 1: A through K
[AD-A216000] 10 p1442 N90-18319

Source header list. Volume 2: L through Z
[AD-A216001] 10 p1442 N90-18320

ALPINE METEOROLOGY

Simulation of a weather situation with high ozone concentrations during ALPEX 12 p1686 N90-19686

ALS (LAUNCH SYSTEM)

U ADVANCED LAUNCH SYSTEM (STS)

ALTERATION

U REVISIONS

ALTERNATING CURRENT

Capacitive behavior in conducting polymers: The ac impedance and quartz crystal microbalance studies
[AD-A210754] 02 p0201 N90-11150

The theory of ac impedance of rough electrode-electrolyte interfaces
[DE89-017474] 02 p0217 N90-11243

Study of metal corrosion using ac impedance techniques in the STS launch environment 08 p1155 N90-16688

Ac loss measurements of two multifilamentary NbTi composite strands
[DE90-005388] 12 p1619 N90-19304

Critical current density and transition temperature measurements of Y-Ba-Cu-O rods
[AD-A216695] 12 p1719 N90-19875

A comparative study of electric power distribution systems for spacecraft
[NASA-CR-186531] 14 p1942 N90-21113

An ultrasonic-switching three phase current source inverter with insulated gate bipolar transistors
[EMV-89-11] 17 p2399 N90-23666

Evaluation of the state of charge of battery electrodes with ac impedance techniques
[AD-A219581] 17 p2420 N90-23789

Equivalent circuit models for ac impedance data analysis
[NASA-TM-100402] 19 p2686 N90-25277

Performance test plan for variable-speed ac superconducting motor
[DE90-016208] 24 p3465 N90-29579

ALTERNATING CURRENT GENERATORS

U AC GENERATORS

ALTERNATING DIRECTION IMPLICIT METHODS

Pressure correction splitting methods for the computation of oscillatory free convection in low Pr fluids
[CWI-NM-R8816] 02 p0222 N90-11271

Gas flows in rocket motors. Volume 2, appendix C: Time iterative solution of viscous supersonic flow
[AD-A213349] 05 p0615 N90-13592

Three-dimensional simulation of vortex breakdown
[NASA-TM-102664] 15 p2049 N90-21744

A fully implicit ADI method for quasi three-dimensional flows through straight blade rows
[ETN-90-96965] 20 p2863 N90-26283

ALTERNATIONS

Application of Chebyshev approximation to curve fitting
[MEMO-805] 11 p1554 N90-18947

ALTERNATIVES

US access to space: Launch vehicle choices for 1990 to 2010 16 p2205 N90-22579

ALTERNATORS (GENERATORS)

U AC GENERATORS

ALTIMETERS

NT LASER ALTIMETERS
NT RADIO ALTIMETERS

Geosat/ERM altimeter data analysis for the determination of global oceanic mesoscale variability 07 p0949 N90-15492

Modeling the effects of the use of GPS (Global Positioning System) derived altitude indication in the C-17A airdrop system
[AD-A215366] 09 p1166 N90-16748

User's guide: Programs for processing altimeter data over inland seas
[NASA-TM-100730] 13 p1841 N90-20572

Programmable generation of linear frequency modulated pulses 14 p1961 N90-21232

ALTIMETRY

NT SATELLITE ALTIMETRY

An update to the system safety study of TCAS 2
[DOT/FAA/SA-89/3] 05 p0577 N90-13363

Correction of ionospheric effects for the precise orbit determination of satellites 08 p0762 N90-14432

Study of the ocean tides by the assimilation of marigraphic and altimetric satellite data in a hydrodynamic model
[ETN-90-97460] 22 p3231 N90-28320

Impact of satellite altimetric data on the numerical simulation of the general oceanic currents: Sensitivity to orbit parameters
[ETN-90-97461] 22 p3231 N90-28321

ALTITUDE

NT FLIGHT ALTITUDE
NT HIGH ALTITUDE
NT LOW ALTITUDE
NT SEA LEVEL

Laser altimeter for use over the ocean
[AD-A211252] 02 p0224 N90-11286

Modeling the effects of the use of GPS (Global Positioning System) derived altitude indication in the C-17A airdrop system
[AD-A215366] 09 p1166 N90-16748

Cloud volume statistics for southern Sweden
[CM-77] 17 p2427 N90-23830

Space station contamination modeling
[NASA-CR-183871] 23 p3286 N90-28590

ALTITUDE CONTROL

Stability characteristics of a combat aircraft with control surface failure
[AD-A216196] 10 p1323 N90-17646

High altitude ozone research balloon
[NASA-CR-186653] 19 p2654 N90-25107

ALTITUDE SICKNESS

Effects of dexamethasone and high terrestrial altitude on cognitive performance and affect
[AD-A217897] 13 p1851 N90-20625

ALTITUDE SIMULATION

Contrasting landform perception with varied radar illumination geometries and at simulated resolutions of Venera and Magellan 03 p0423 N90-12430

Decompression sickness affecting the temporomandibular joint
[AD-A220959] 18 p2584 N90-24715

Experimental techniques in the field of low density aerodynamics
[AGARD-AG-318(FR)] 21 p2953 N90-26792

Evaluation of the performance capability of the aviator under hypoxic conditions operational experience 23 p3361 N90-28991

ALTITUDE TESTS

Altitude testing of the 2D V/STOL ADEN demonstrator on an F404 engine
[NASA-CR-174824] 10 p1321 N90-17638

Design of the UETP experiment 22 p3118 N90-27712

Comparison of altitude test cell results 22 p3119 N90-27715

Comparison of ground-level test cells and ground-level to altitude test cells 22 p3119 N90-27716

Experience in developing an improved altitude test capability 22 p3120 N90-27719

Very low height drop test. Conditioning and tandem dropping of two loads conditioned in two PC6 platforms assembled by rigid structures
[REPT-89/07] 22 p3193 N90-28116

Very low height drop test. Conditioning and tandem dropping of two loads conditioned in two PC6 platforms assembled by one PD9 platform and rigid structures
[REPT-89/04] 22 p3193 N90-28117

High altitude balloon flight test of the GRAD experiment
[AD-A224398] 24 p3432 N90-29388

ALU (COMPUTER COMPONENTS)
U ARITHMETIC AND LOGIC UNITS

ALUMINA
U ALUMINUM OXIDES

ALUMINATES
Growth and patterning of laser ablated superconducting YBa2Cu3O7 films on LaAlO3 substrates
[NASA-TM-102436] 15 p2173 N90-22421
Evaluation of room-temperature chloroaluminate molten salts as electrolytes for high energy density batteries
[AD-A223097] 20 p2860 N90-26267

ALUMINIDES
Exploratory study of niobium, titanium, zirconium and tantalum aluminides
[AD-A210658] 02 p0283 N90-11615
Weldability of ductile nickel aluminides
[DE89-017452] 03 p0327 N90-11859
Low temperature formation of titanium aluminide films using physical vapor deposition
[AD-A211877] 03 p0328 N90-11866
Thermal mechanical fatigue of coated blade materials
[AD-A214258] 07 p0882 N90-15107
Shock-induced reaction synthesis of aluminides and silicides
[DE90-003948] 08 p1049 N90-16066
An introduction to nickel aluminide alloy
[DE90-008565] 13 p1778 N90-20207
Improved toughness alloys based on titanium aluminides
[AD-A218149] 13 p1778 N90-20208
Titanium aluminides: Processing, properties and potential
[AERE-R-13198] 14 p1949 N90-21158
Surface characterization of hydrogen charged and uncharged alpha-2 and gamma titanium aluminide alloys using AES and REELS
[NASA-CR-186561] 14 p1951 N90-21171
Microstructure and mechanical properties of nickel aluminide powders consolidated by extrusion and hot isostatic pressing
[DE90-009777] 15 p2070 N90-21855
Oxide thermal stability on gamma titanium aluminide
[DE90-012054] 19 p2678 N90-25232
Crystal growth and deformation behavior of TiAl aluminides
[DE90-012972] 20 p2930 N90-26671
High temperature protective coatings: Recent trends
23 p3308 N90-28710
Powder processing of aluminides
[DE90-015314] 24 p3444 N90-29447

ALUMINIZING
U ALUMINUM COATINGS

ALUMINUM
NT ALUMINUM ISOTOPES
NT ALUMINUM 26
Application of superplastically formed and diffusion bonded aluminum to a laminar flow control leading edge
[NASA-CR-178316] 01 p0007 N90-10030
High-speed machining of aluminum
[DE89-014011] 01 p0077 N90-10441
Influence of grain refining on the casting, physical, mechanical, and electrochemical properties of technical aluminum
[ETN-89-94661] 02 p0199 N90-11135
Investigations into the infiltration kinetics, wettability, and interfacial bond strength of Al/SiC composites
[AD-A211924] 03 p0320 N90-11815
Deformation behavior of SiC/2014 Al metal-matrix composite
[AD-A212095] 03 p0320 N90-11816
Tribological properties of ceramic/Ti3Al-Nb sliding couples for use as candidate seal materials to 700 deg C
[NASA-TM-102401] 04 p0464 N90-12658
Biaxial flexing of a fiber-reinforced aluminum composite
[AD-A212742] 04 p0468 N90-12681
Rolling of ARALL laminates (an alternative method for post-stretching ARALL laminates)
[LR-560] 04 p0484 N90-12778
Impact tests on aluminum 2024 T3, aramid and glass reinforced aluminum laminates and thermoplastic composites
[LR-534] 05 p0619 N90-13613
A method of soldering aluminum
[AD-D014226] 06 p0792 N90-14611
Glancing angle x ray studies of oxide films
[DE89-017828] 06 p0852 N90-14953
Ultrasonic evaluation of porosity in aluminum cast materials
[AD-A213548] 07 p0905 N90-15232
Using small scale tests to estimate the failure diameter of a propellant
[DE90-001166] 07 p0913 N90-15281
Strengthening of aluminum by oxygen implantation: Experimental results and mechanical modeling
[DE90-005960] 09 p1195 N90-16924
Effect of reduced atmospheric pressure on the performance characteristics of pyrotechnic compositions containing aluminum
[AD-A214473] 09 p1200 N90-16953
Strain induced amorphization of aluminium by manganese implantation
[DE90-607259] 10 p1356 N90-17863
Process development and fabrication of space station type aluminum-clad graphite epoxy struts
[NASA-CR-181873] 11 p1468 N90-18454
The improved adhesion of organic polymers to silica and to aluminum metal with zirconium Schiff-base block copolymer coatings
[AD-A216669] 11 p1490 N90-18575
Nanolayer reactions in aluminum-metal interfaces
[DE90-004955] 12 p1626 N90-19342
Glancing angle XAFS (X ray Absorption Fine Structure) and x ray reflectivity studies of transition-metal/aluminum interfaces
[DE90-005575] 12 p1627 N90-19353
Creep behavior of alloys based on TiAl containing TiB2 and TiN particulates
[DE90-006489] 12 p1628 N90-19355
Origin and effect of pores in aluminum welded joints
[REPT-87M/43/05720/SCP/GRF] 12 p1675 N90-19620
Advanced high-temperature batteries
13 p1825 N90-20480
Stopping power for protons in Al for the whole range of velocities
[DE90-008558] 13 p1884 N90-20810
Formation of subsurface aluminum layers in beryllium by ion implantation and post-implant annealing
[DE90-007975] 14 p1951 N90-21172
The corrosion protection of 6061-T6 aluminum by a polyurethane-sealed anodized coat
[NASA-TM-100394] 14 p1955 N90-21191
Fatigue crack growth investigation of a Ti-6Al-4V forging under complex loading conditions: NATO/AGARD supplemental engine disk program
[AD-A220239] 17 p2377 N90-23538
An investigation of the chemistry of silane coupling agents for adhesive bonding of aluminum
[AD-A220797] 17 p2381 N90-23560
Subsurface hardening and flow of aluminum during the incubation period of solid particle erosion
[DE90-010141] 18 p2525 N90-24409
Effects of internal hydrogen on the vacancy loop formation probability in Al
[DE90-011114] 18 p2527 N90-24422
Applications of an acoustic-emission data-acquisition workstation: 2
[DE90-010941] 18 p2612 N90-24880
Heat sink effects on weld bead: VPPA process
[NASA-CR-186723] 19 p2697 N90-25349
Effect of casting procedures and diesel engine environment on the behavior of aluminum titanate
[AD-A223079] 20 p2835 N90-26126
The effect of impurity gasses on variable polarity plasma arc welded 2219 aluminum
[NASA-CR-183803] 21 p2980 N90-26935
The thermal radiative properties of metals at high temperature
[DE90-012468] 21 p2981 N90-26938
UNICOAT: Development of a primer/topcoat and flexible primer for aluminum
[AD-A221803] 21 p2989 N90-26986
Research on optogalvanic effects
[AD-A221512] 21 p3071 N90-27463
The effect of reinforcement stability on composition redistribution in cast aluminum metal matrix composites
[DE90-012469] 22 p3135 N90-27791
An examination of impact damage in glass-phenolic and aluminum honeycomb core composite panels
[NASA-TP-3042] 22 p3153 N90-27876
ARALL (ARamid ALuminum Laminate), a literature survey
[FOA-C-20782-2.5] 23 p3301 N90-28671
The stability of the martensitic phases in Cu-Zn-Al at an electron concentration of 1.534
[DE90-628628] 23 p3311 N90-28727

ALUMINUM ALLOYS
Microstructure morphology and quality of Al-Si castings 01 p0043 N90-10244
Emittance, catalysis, and dynamic oxidation of Ti-14Al-21Nb
[NASA-TP-2955] 01 p0044 N90-10248
Fatigue crack initiation mechanics of metal aircraft structures
[AD-A210567] 01 p0045 N90-10255
Fracture and three dimensional stress analyses of 7075 aluminum projectile components under spin and inertia load
[AD-A210986] 01 p0081 N90-10463
Theoretical and experimental investigation of thin-walled aluminum panels under cyclic shear load
02 p0177 N90-10996
Material properties of 2219-T851 aluminum alloy plasma welded compared to TIG welding
02 p0182 N90-11032
Effects of a heat cycle on material strength
[NAL-TM-562] 03 p0306 N90-11737
Elevated temperature aluminum-titanium alloy by powder metallurgy process
[AD-D014165] 03 p0326 N90-11852
A study of the hot workability of Al-8.5 wt pct Mg alloys for armor plate applications
[AD-A211680] 03 p0329 N90-11868
Effect of fretting on fatigue strength of aluminium alloys
[ESDU-89004] 03 p0329 N90-11870
Aluminium alloy development for aero engines
[PNR90548] 03 p0330 N90-11874
Axial compression buckling test on the H-2 launch vehicle satellite fairing structural element prototype (aluminum surface plate/aluminum honeycomb sandwiched curved surface plate)
[NAL-TM-563] 03 p0356 N90-12039
Superplastic forming and diffusion bonding of rapidly solidified, dispersion strengthened aluminum alloys for elevated temperature structural applications
[NASA-CR-181849] 04 p0474 N90-12718
An approach to low temperature high strain rate superplasticity in aluminum alloy 2090
[AD-A212271] 04 p0476 N90-12731
Corrosion and corrosion inhibition of metals/alloys in methylphosphonic difluoride and decontaminating solutions
[AD-A212404] 04 p0477 N90-12734
Quench sensitivity in Al-Cu-Li alloys
[AD-A213055] 05 p0624 N90-13639
The effect of composition and aging treatment on the microstructure and mechanical properties of aluminum-lithium-titanium alloys
[AD-A213144] 05 p0624 N90-13640
Implementation and analysis of adhesion in multimaterials of the type Al(Si)-ZrO2 and graphite, metal or ceramics
[ECL-89-004] 05 p0628 N90-13667
Threshold for fatigue crack propagation
[DLR-FB-89-33] 05 p0655 N90-13815
Advances and future directions in superplastic materials 06 p0744 N90-14328
The mechanical properties of superplastically formed titanium and aluminium alloys 06 p0744 N90-14331
The manufacture of superplastic alloys
06 p0745 N90-14333
Influence of hole surface finish, cyclic frequency and spectrum severity on the fatigue behavior of thick section aluminum alloy pin joints
[ARL-STRUC-R-430] 06 p0745 N90-14336
The strength-toughness combination of the aluminum-lithium alloys 2090 and 2091 at cryogenic temperatures
[DE90-001425] 06 p0746 N90-14338
The effect of hydrogen charging on the mechanical properties of aluminum alloy 2090
[DE90-000129] 06 p0746 N90-14341
Phases in lanthanum-nickel-aluminum intermetallic alloys
[DE90-000651] 06 p0746 N90-14343
A method of soldering aluminum
[AD-D014226] 06 p0792 N90-14611
Fatigue properties of SiC/Al composites
07 p0889 N90-15138
New Light Alloys
[AGARD-CP-444] 07 p0897 N90-15185
Al-Li alloy developed by Pechiney
07 p0897 N90-15186
The microstructure and properties of aluminum-lithium alloys 07 p0897 N90-15187
Mechanical properties and fracture toughness of 8090-T651 plate and 2091 and 8090 sheet
07 p0897 N90-15188
Fatigue properties of Al-Li alloys
07 p0898 N90-15189
Corrosion and stress corrosion of aluminium-lithium alloys 07 p0898 N90-15190
Properties of Al-Li alloys 07 p0898 N90-15191
Investigation on sheet material of 8090 and 2091 aluminium-lithium alloy 07 p0898 N90-15192
Aluminum lithium alloys for Navy aircraft
07 p0898 N90-15193
Fatigue, fracture mechanics and corrosion properties of some aluminium-lithium alloys 07 p0898 N90-15194

Fatigue and fracture behaviour of a PM Al-Li alloy
07 p0899 N90-15195
Fabrication of test-articles from Al-Li 2091 for Fokker 100
07 p0899 N90-15196
Putting alloy 2091 to work
07 p0899 N90-15197
Fabrication characteristics of 8090 alloy
07 p0899 N90-15198
Superplastic performance and properties of the Lital Alloys
07 p0899 N90-15199
Point of view of a civil aircraft manufacturer on Al-Li alloy
07 p0899 N90-15200
Uses and properties of Al-Li on the new EH101 helicopter
07 p0900 N90-15201
Aluminum-lithium: Application of plate and sheet to fighter aircraft
07 p0900 N90-15202
Current status of the application of conventional aluminium-lithium alloys and the potential for future developments
07 p0900 N90-15203
High performance powder metallurgy aluminum alloys: An overview
07 p0900 N90-15204
Microstructure/mechanical property relations in a mechanically alloyed aluminum
07 p0900 N90-15205
Report of the Advanced Neutron Source (ANS) Aluminum Cladding Corrosion Workshop
[DE90-001281]
07 p0903 N90-15217
Properties of aluminum-uranium alloys
[DE90-003889]
07 p0907 N90-15243
High temperature aluminum-base alloy
[AD-D014270]
08 p1043 N90-16028
Experimental evaluation of new alloy coatings
[AD-A214922]
09 p1194 N90-16916
Fatigue of aluminium alloy joints with various fastener systems. Low load transfer
[ESDU-89046]
09 p1239 N90-17193
Hardness-damage correlations in Ta implanted single crystal Ni3Al
[DE90-005270]
09 p1293 N90-17494
Development of an aluminium solar cell interconnector technology
10 p1341 N90-17771
Comparative analysis between the mechanical properties of conventional alloys and Al-Li
[INFORME-DT-317/89]
10 p1356 N90-17861
Effect of a single overload upon fatigue crack growth in an aluminum-lithium alloy
[AD-A216183]
10 p1356 N90-17865
Surface modification of steels and aluminum alloys to control corrosion and hydrogen embrittlement. Part 1: Chemical methods
[AD-A216272]
10 p1356 N90-17866
Phonon dispersion and Kohn anomalies in the alloy Cu(0.84)Al(0.16)
[DE90-005578]
10 p1428 N90-18239
A fundamental understanding of the effect of alloying elements on the corrosion resistance of rapidly solidified Mg alloys
[AD-A216767]
11 p1486 N90-18553
Processing and elevated temperature ductility of aluminum alloy 7475
[AD-A216840]
11 p1486 N90-18554
Significance of oxide skins on powder for the quality of PM Al materials
[ESA-TT-1178]
11 p1487 N90-18560
Cost and energy consumption estimates for the aluminum-air battery anode fuel cycle
[DE90-005810]
11 p1503 N90-18656
Optimizing superplastic response in navalite, a lithium containing aluminum-magnesium alloy
[AD-A216552]
12 p1626 N90-19346
Deformation and fracture of TiAl + W at elevated temperatures
[DE90-006490]
12 p1628 N90-19356
Liquid oxygen LOX compatibility evaluations of aluminum lithium (Al-Li) alloys: Investigation of the Alcoa 2090 and MMC weldalite 049 alloys
12 p1636 N90-19398
Evaluation of the response of aluminum alloys to single and multiple particle impacts
[DE90-003689]
12 p1676 N90-19626
Corrosion properties of Fe3Al in H2S-H2-H2O mixtures
[DE90-004936]
13 p1772 N90-20167
The effect of the SiC/Al interface on matrix microstructure in 2xxx-SiCp metal matrix
[AERE-R-13591]
13 p1775 N90-20184
Constitutive data acquisition and modelling in aluminium 2014 alloy
[AERE-R-13651]
13 p1775 N90-20186
The ageing effect of the matrix-reinforcement interface on the ageing response of an aluminium 6061 alloy reinforced with 20vol percent SiC particulates
[AERE-R-13361]
13 p1776 N90-20193
Evaluation of 2090-T8E48 aluminum-lithium plates
[AD-A217262]
13 p1776 N90-20196
Through-the-thickness fatigue crack closure behavior in an aluminum alloy
[NASA-TM-102590]
13 p1816 N90-20427
Crack stoppers and ARALL laminates
[PB90-166588]
14 p1947 N90-21142
Grain boundary precipitation in Ni3Al based alloys
[AERE-R-13382]
14 p1950 N90-21161
Lecture on ordered intermetallic alloys
[DE90-009011]
14 p1951 N90-21189
Fatigue crack growth from narrow-band Gaussian spectrum loading in 6063 aluminum alloy
[DE90-008957]
14 p1952 N90-21173
Determination of Li-Al alloy extent in tubular aluminum elements by small source neutron radiology
[DE90-009142]
14 p1952 N90-21174
Ductile alloy encapsulated ceramic armor development
[AD-A217632]
14 p1954 N90-21183
Fractographic analysis of the crack growth rate and the shear lip development of 2024-T3 specimens under simple variable-amplitude loading
[PB90-167032]
14 p1994 N90-21427
High-temperature deformation of mechanically-alloyed aluminum IN90211
16 p2216 N90-22645
Environment enhanced fatigue of advanced aluminum alloys and composites
16 p2218 N90-22652
Elevated temperature crack growth in advanced powder metallurgy aluminum alloys
16 p2218 N90-22653
Elevated temperature crack growth in aluminum alloys: Tensile deformation of 2618 and FVS0812 aluminum alloys
16 p2218 N90-22654
Deformation and fracture of thin sheet aluminum-lithium alloys: The effect of cryogenic temperatures
16 p2218 N90-22655
Measurements and mechanisms of localized aqueous corrosion in aluminum-lithium alloys
16 p2219 N90-22656
The effects of zinc addition on the environmental stability of Al-Li alloys
16 p2219 N90-22657
Deformation and fracture of aluminum-lithium alloys: The effect of dissolved hydrogen
16 p2219 N90-22658
The lithium concentration dependence of creep in binary aluminum-lithium alloys
[AD-A213706]
16 p2221 N90-22668
A comparison of CuAlNi and other high damping alloys for the purpose of naval ship silencing applications
[AD-A218801]
16 p2221 N90-22671
Structure-property relations in aluminum-lithium alloys
[AD-A219183]
16 p2222 N90-22672
Characterisation of fatigue of aluminium alloys by acoustic emission. Part 1: Identification of source mechanism
[AERE-R-13302-PT-1]
17 p2375 N90-23522
Characterisation of fatigue of aluminium alloys by acoustic emission. Part 2: Discrimination between primary and other emissions
[AERE-R-13303-PT-2]
17 p2375 N90-23523
A study of the influence of alloying additions on the passivity of aluminium
[AD-A219630]
17 p2376 N90-23532
The effects of slip character and crack closure on the growth of small fatigue cracks in titanium-aluminium alloys
[AD-A220714]
17 p2377 N90-23534
Fractographic observations on fatigue crack growth in 2024-T3 sheet material under flight-simulation loading
[LR-592]
17 p2415 N90-23760
J-integral and HRR field of a stably growing crack, an experimental analysis
[AD-A220418]
17 p2416 N90-23764
Metal matrix composites from dynamic consolidation of powder mixtures
[DE90-010951]
18 p2519 N90-24388
A study of the phase decomposition of Fe-Ni-Al-Mo alloys
[DE90-010143]
18 p2524 N90-24406
Grain growth and phase formation in ion irradiated/annealed thin Ni-Al alloys films
[DE90-010409]
18 p2525 N90-24407
Electronic structure and phase stability properties of Al-Li alloys
[DE90-010632]
18 p2525 N90-24410
Damping associated with incipient melting in aluminum-indium alloys
[AD-A220241]
18 p2525 N90-24412
Precipitation on dislocations in Al-Li-Cc-Mg-Zr
[AD-A221124]
18 p2526 N90-24415
Processing and properties of advanced aluminum alloys
[AD-A221292]
18 p2526 N90-24416
The effects of cooling rate XD (trademark) TiAl weld microstructure
[DE90-011975]
18 p2528 N90-24427
Phase stability in the Al(6-x)Cu(x)Zr2 system for 0 less than x less than 1.0
[DE90-010620]
18 p2620 N90-24925
Investigation on sheet material of 8090 and 2091 aluminium-lithium alloy
[MBB-UT-122/89-PUB]
19 p2652 N90-25090
The effect of trace amounts of antimony on the structure and properties of aluminum alloy A356.2
[DE90-010461]
19 p2674 N90-25207
Scratches and shot peening effects on the fatigue life of aluminum-lithium alloys
[NIAR-90-15]
19 p2674 N90-25208
Surface condition effect on the fatigue behavior of aluminum lithium alloys
[NIAR-90-13]
19 p2674 N90-25209
Deformation and fracture behavior of TiAl
[DE90-012212]
19 p2675 N90-25212
Weak-beam electron microscopy of dislocation splitting in TiAl: Relationship to plasticity
[ESA-TT-1159]
19 p2676 N90-25217
Mechanical paint removal techniques for aircraft structures
[IAR-89-23]
19 p2682 N90-25254
A study on ultrasonic detection and characterization of partially closed fatigue cracks
[DE90-011748]
19 p2702 N90-25371
Erosion mechanisms in composite materials and ripple formation mechanism in erosion
[IAR-89-4-PT-2]
20 p2826 N90-26079
The influence of microstructure on the tensile behavior of an aluminum metal matrix composite
[NASA-TM-102694]
20 p2827 N90-26082
Investigation of thermo-mechanical effects in silicon carbide Whisker/Al alloy composites
[AD-A222635]
20 p2828 N90-26089
A study of the fatigue behavior in scratched samples of Al-Li alloy (2090-T3)
[IAR-89-24]
20 p2832 N90-26107
Compendium of material test results on HY-130 and Ti-3Al2V metals in support of United States navy programs
[DE90-011754]
20 p2833 N90-26112
Damping capacity of aluminum 6061-indium alloys
[AD-A222802]
20 p2835 N90-26124
Fracture toughness and failure mechanisms in commercial 2091 Al-Li sheet at cryogenic temperatures
[AD-A222803]
20 p2835 N90-26125
Mechanical paint removal techniques for aircraft structures
[NIAR-90-12]
20 p2842 N90-26166
The blunt notch behaviour of metal laminates: ARALL and GLARE
[LR-617]
20 p2877 N90-26368
Investigation of crack-closure prediction models for fatigue in aluminium alloy sheet under flight-simulation loading
[LR-619]
20 p2877 N90-26369
Crystal growth and deformation behavior of TiAl aluminides
[DE90-012972]
20 p2930 N90-26671
An aluminum quality breakthrough for aircraft structural reliability
21 p2957 N90-26816
Corrosion protection of metal matrix composites
[AD-A222951]
21 p2971 N90-26888
Weldment mechanical properties of aluminum-copper-lithium alloy, 2090, at ambient and cryogenic temperatures
[DE90-014178]
21 p2981 N90-26941
Study of the behavior of Al metallic matrix + SiC composite materials under fatigue tests
[ETCA-89-R-077]
22 p3154 N90-27881
Corrosion of aluminum alloys by IRFNA
[AD-A223011]
22 p3157 N90-27897
Methodology of the fatigue under shocks. Experimental results: 7075 T6 and 35 NCD16
[ETCA-89-R-140]
22 p3157 N90-27901
Characterization of the pitting corrosion of aluminum-lithium alloys
[ETCA-89-R-176]
22 p3157 N90-27903
Characterization of the CP 214 T851. Dissection of a cast flat bar for a standard spar
[CEAT-PV-M4/462200]
22 p3158 N90-27905
Characterization of the 7175 T7352. Dissection of a die casting standard spar
[CEAT-PV-M5/528900]
22 p3158 N90-27906
Characterization of the 7175 T7352 101. Dissection of a die casting standard spar
[CEAT-PV-M5/5288]
22 p3158 N90-27907
Characterization of the 7010 T73651. Dissection of a sheet billet for a standard spar
[CEAT-PV-M5/521700]
22 p3158 N90-27908
High temperature oxidation of Al-Li alloys
23 p3307 N90-28705
Behavior of Al-Mg alloys in hot working and superplasticity
[DE90-015193]
23 p3310 N90-28723
Evaluation of ARALL-4: An aramid fiber reinforced aluminum
[AD-A223502]
24 p3443 N90-29443
Processability and high temperature behavior of emerging aerospace alloys
[AD-A224285]
24 p3448 N90-29475

The roles of strain and reheating interval in continuous recrystallization during the thermomechanical processing by warm rolling of an Al-Mg alloy
[AD-A223673] 24 p3449 N90-29479
The stress and temperature dependence of creep in an Al-2.0 wt percent Li alloy
[AD-A223676] 24 p3449 N90-29480
Oxidation of NiAl(110)
[DE90-015645] 24 p3451 N90-29487
Evaluation of static and fatigue properties of thin sheets of 8090-T8 aluminum-lithium alloy and observation of its fracture surfaces
[NAL-TR-1039] 24 p3453 N90-29499

ALUMINUM ARSENIDES
Field-effect spectroscopy of interface states
[AD-A212998] 05 p0703 N90-14112
Peeled film GaAs solar cells for space power
[NASA-TM-103125] 14 p1970 N90-21287

ALUMINUM BORON COMPOSITES
Limits to today's composites: Chances for tomorrow's developments
[MBB-Z-0287-89-PUB] 18 p2519 N90-24385

ALUMINUM CARBIDES
Investigation of commercial Al-Ti and Al-Ti-B master alloys and development of a new grain refining agent based on carbides for aluminum and aluminum alloys
[ETN-89-94663] 02 p0199 N90-11136
The application of cast SiC/Al to rotary engine components
[NASA-CR-179610] 05 p0581 N90-13385
Fabrication, phase transformation studies, and characterization of SiC-AlN-Al2OC ceramics
[DE90-006591] 12 p1631 N90-19371
Acoustic characterisation of an aluminium silicon carbide metal matrix composite
[AERE-R-13273] 14 p1943 N90-21121

ALUMINUM CHLORIDES
Heat capacities of 1-methyl-3-ethylimidazolium chloride-aluminum chloride molten salts
[AD-A212790] 04 p0472 N90-12707
Ionic equilibrium between octahedral and tetrahedral complexes in liquid aluminium-sodium fluoride mixtures
[DE90-613690] 14 p1948 N90-21150

ALUMINUM COATINGS
The substitution of IVD (Ion Vapor Deposition) aluminum for cadmium
[AD-A215633] 09 p1195 N90-16921
The improved adhesion of organic polymers to silica and to aluminum metal with zirconium Schiff-base block copolymer coatings
[AD-A216669] 11 p1490 N90-18575
Shaping radiation pattern of excimer laser by means of controllable intracavity mirror
16 p2310 N90-23166
High-temperature materials. Coating, welding, and service tests
[VTT-RR-645] 19 p2675 N90-25214

ALUMINUM COMPOUNDS
NT ALUMINATES
NT ALUMINIDES
NT ALUMINUM ARSENIDES
NT ALUMINUM CARBIDES
NT ALUMINUM CHLORIDES
NT ALUMINUM FLUORIDES
NT ALUMINUM NITRIDES
NT ALUMINUM OXIDES
NT BERYL
NT CRYOLITE
NT KAOLINITE
NT SAPPHIRE
Y-Si-Al-O-N glass fibers
[AD-A211170] 02 p0190 N90-11088
Heat treatment of pulsed Nd: YAG laser welds in a Ti-14.8 wt pct Al-21.3 wt pct Nb titanium aluminide
[DE90-003484] 07 p0905 N90-15228
Activation of methane by transition metal-substituted aluminophosphate molecular sieves
[DE90-005663] 12 p1624 N90-19331
High resolution transmission electron microscopy of aluminophosphates
[DE90-015632] 24 p3553 N90-30105

ALUMINUM FLUORIDES
Ionic equilibrium between octahedral and tetrahedral complexes in liquid aluminium-sodium fluoride mixtures
[DE90-613690] 14 p1948 N90-21150

ALUMINUM GALLIUM ARSENIDES
Experimental investigations of transport and optical properties of 3-5 quantum well structures grown via molecular beam epitaxy under optimal growth conditions
[AD-A210269] 01 p0132 N90-10758
High energy neutron irradiation effects in GaAs modulation-Doped Field Effect Transistors (MODFETS): Threshold voltage
[AD-A210502] 01 p0132 N90-10763
Electron transport in heterojunction superlattices
[AD-A212366] 04 p0560 N90-13265
GaAs gate dynamic memory technology
[AD-A212387] 04 p0560 N90-13266
The growth of epitaxial GaAs and GaAlAs on silicon substrates by OMVPE
[AD-A212873] 04 p0561 N90-13269
Method of making self-aligned GaAs/AlGaAs FET's
[AD-D014229] 06 p0849 N90-14935
Picosecond photoconductivity using a graded bandgap Al(x)Ga(1-x)As active detecting layer
[DE90-003452] 07 p1000 N90-15786
The growth of epitaxial GaAs and GaAlAs on silicon substrates by OMVPE
[AD-A214642] 09 p1288 N90-17469
Electronic properties of GaAs-(Al,Ga)As quasiperiodic
[AD-A214704] 09 p1289 N90-17472
Proceedings of the conference on Hot Carriers in Semiconductors
[AD-A215544] 09 p1291 N90-17482
Low temperature photoluminescence study of uranium implanted into III-V semiconductors and AlGaAs
[AD-A215710] 09 p1291 N90-17484
Selective excitation luminescence and photoluminescence investigations of ytterbium doped InP, GaAs and AlGaAs
[AD-A215713] 09 p1291 N90-17485
AlGaAs/GaAs solar cells with efficiencies greater than 22 percent
10 p1339 N90-17755
Luminescence of lanthanides and actinides implanted into binary III-V semiconductors and AlGaAs
[AD-A215759] 11 p1569 N90-19031
Low threshold current implanted-planar-buried-heterostructure, graded-index, separate-confinement-heterostructure GaAs-AlGaAs laser
[DE90-002579] 12 p1666 N90-19572
Investigation of the technological effects on the coupling behavior of parallel GaAlAs rib waveguide
[ETN-90-95323] 13 p1887 N90-20825
Differential measurements of the lateral photo effect in GaAs/AlGaAs heterostructures
[AERE-R-13557] 13 p1893 N90-20861
Apparatus for the efficient wavelength conversion of laser radiation
[AD-D014506] 20 p2866 N90-26305
Application of InAlAs/GaAs superlattice alloys to GaAs solar cells
[DE90-013070] 20 p2881 N90-26389
Investigation on the MBE growth and properties of AlGaInAs/InP and InGaAs-InAlAs superlattices
[DE90-012248] 21 p3080 N90-27515
Linear laser diode arrays for improvement in optical disk recording for space stations
[NASA-CR-4322] 22 p3180 N90-28047
High resistivity Al(x)Ga(1-x) As(y)Sb(1-y) epitaxial layers by sulfur compensation doping
[DE90-012228] 22 p3248 N90-28419
Manufacturing and characterization of liquid-phase epitaxy layers with atomic levels at the crystal surface and at the hetero limit surfaces in the system GaAs-AlGaAs
[ETN-90-97310] 24 p3554 N90-30113

ALUMINUM GRAPHITE COMPOSITES
Space structures concepts and materials
[NASA-CR-183727] 01 p0025 N90-10128
Damping characteristics of metal matrix composites
[AD-A213712] 07 p0891 N90-15151

ALUMINUM ISOTOPES
NT ALUMINUM 26
The Al-26(rho, gamma)Si-27 reaction: Stellar origins of galactic Al-26
15 p2188 N90-22498

ALUMINUM NITRIDES
Basic research on processing of ceramics for space structures
[AD-A205954] 02 p0199 N90-11139
Fabrication, phase transformation studies, and characterization of SiC-AlN-Al2OC ceramics
[DE90-006591] 12 p1631 N90-19371
Modeling the temperature dependence of the thermal conductivity of aluminum nitride
[DE90-009428] 14 p1949 N90-21154
Polymeric aluminasilazane precursors for aluminosilicon nitride
[AD-A222755] 20 p2841 N90-26158

ALUMINUM OXIDES
NT SAPPHIRE
Zirconia toughened SiC whisker reinforced alumina composites small business innovation research
[NASA-CR-179629] 01 p0052 N90-10294
A diffuse reflectance infrared Fourier transform spectroscopic study of adsorbed hydrazines
02 p0205 N90-11170
Kinetics and mechanisms of primary and steady state creep in B- and Al-containing alpha silicon carbide
[AD-A210739] 02 p0283 N90-11616
Processing and characterization of alumina platelet-reinforced mullite composites
[DE90-000057] 03 p0320 N90-11814
Significance of oxide skins on powder for the quality of PM Al material --- PM (press molded)
[DFVLR-FB-89-11] 03 p0329 N90-11873
Flexure strength of advanced ceramics: A round robin exercise
[AD-A212101] 03 p0332 N90-11889
Spall resistance of alumina
[AD-A213213] 04 p0477 N90-12735
The multivalent beta'-aluminas
[AD-A212103] 04 p0478 N90-12738
NBS/BAM (National Bureau of Standards/Bundesanstalt fuer Materialprufung) 1986 Symposium on Advanced Ceramics
[PB89-229074] 04 p0479 N90-12747
SEM (Scanning Electron Microscope) image analysis of grain growth in microwave-annealed alumina
[DE90-001606] 06 p0746 N90-14339
Ordered ceramic membranes
[DE89-017426] 06 p0750 N90-14364
Surface engineering by high energy beams
[DE90-001296] 07 p0908 N90-15250
Development of the RAIDS (Remote Atmospheric and Ionospheric Detector System) extreme ultraviolet wedge and strip detector
[AD-A213730] 07 p0949 N90-15495
Microstructures of Y123 films on SrTiO3, LaGaO3, and LaAlO3
[DE90-003367] 08 p1129 N90-16537
Extrusion of alumina-silicon carbide whisker composites
[DE90-004379] 09 p1186 N90-16869
Study of adherent oxide scales
[AD-A215189] 09 p1198 N90-16940
Adhesion of silver films to ion-bombarded alumina
[DE90-005642] 09 p1199 N90-16947
Significance of oxide skins on powder for the quality of PM Al materials
[ESA-TT-1178] 11 p1487 N90-18560
Sintering of a model nickel/alumina catalyst
[ETN-90-96270] 11 p1487 N90-18561
Microstructural variations in aluminum oxide coatings deposited using a dual beam ion system
[DE90-006040] 11 p1491 N90-18583
Comparison of tension, compression, and flexure creep for alumina and silicon nitride ceramics
[DE90-006154] 11 p1492 N90-18586
Ion implantation-induced amorphization of ceramic oxides
[DE90-006564] 11 p1571 N90-19041
Preparation and characterization of alumina films prepared by a novel spray pyrolysis method
[AD-A217570] 12 p1625 N90-19339
Experimentally determined wear behavior of an Al2O3-SiC composite from 25 to 1200 C
[NASA-TM-102549] 13 p1765 N90-20130
Synthesis of alumina-coated SiC whiskers for production of SiC whisker-reinforced alumina composite materials
[DE90-007778] 13 p1788 N90-20147
Techno-economic assessment of a carbothermic alumina reduction process
[DE90-007018] 13 p1772 N90-20170
Tensile fracture toughness of ceramic materials: Effects of dynamic loading and elevated temperatures
[DE90-008329] 13 p1781 N90-20223
Anisotropy of grain growth in alumina
[DE90-009045] 14 p2032 N90-21655
New corrosion resistant ceramic coatings by laser processing
[AERE-R-13166] 15 p2071 N90-21863
In-situ pulsed laser deposition of high-T(sub c) YBa(sub 2)Cu(sub 3)O(sub 7) superconducting thin films on (100) LaAlO3 substrates
[DE90-009861] 15 p2173 N90-22418
Optical spectroscopy of Ti(3+) doped YAlO3
[AD-A219043] 16 p2324 N90-23251
High temperature oxidation of Ni3Al composites
[DE90-010145] 18 p2517 N90-24373
Characterization of solid state bonding between Coors AD-999 alumina and niobium
[DE90-010653] 18 p2518 N90-24379
Electron microscopy of interfaces in silicon carbide whisker-reinforced alumina composites
[DE90-010439] 18 p2519 N90-24386
The influence of ion implantation on the near-surface mechanical properties of ceramics
[DE90-010139] 18 p2531 N90-24444
Properties of films prepared from low surface area/density alumina-silica
[DE90-011048] 18 p2531 N90-24446
Synthesis, characterization and evaluation of CO-oxidation catalysts for high repetition rate CO2 TEA lasers
18 p2557 N90-24593
Performance of alumina-supported Pt catalysts in an electron-beam-sustained CO2 laser amplifier
18 p2561 N90-24613

Effect of film adhesion on tribological properties of silver-coated alumina
[DE90-010090] 18 p2564 N90-24632
An investigation of a mathematical model of an optically pumped Ti(3+):Al2O3 laser system
18 p2646 N90-25063
Laboratory simulation of the effect of rocket thrust on a precessing space vehicle
[NASA-CR-186681] 19 p2669 N90-25182
Oxidation characteristics of Ti-14Al-21Nb ingot alloy
[NASA-TP-3012] 19 p2674 N90-25206
Mechanisms for solid particle erosion in ductile and brittle materials
[NIAR-90-11] 19 p2675 N90-25210
The application of HREELS to model catalysts: CO and C2H4 adsorption on Pt/Al2O3
[AD-A222744] 20 p2831 N90-26103
The effect of crystal orientation on damage accumulation in chromium-implanted Al2O3
[DE90-012294] 20 p2931 N90-26674
A study of the elastic properties of Al2O3 and Si3N4 matrix composites with SiC whisker reinforcement
[DE90-013674] 21 p2970 N90-26882
Advanced ceramic armor materials
[AD-A223227] 21 p2986 N90-26970
Study of the structure of ZrO2-Al2O3 plasma sprayed coatings
[ETCA-89-R-078] 22 p3161 N90-27924
Electronic conduction in molten cryolite saturated with alumina
[DE90-015090] 23 p3400 N90-29211
Non-destructive evaluation of infiltration-toughened ceramics
[DE90-629716] 24 p3453 N90-29501

ALUMINUM SILICATES
NT KAOLINITE

ALUMINUM 26
Gamma-ray observations and the distribution of interstellar aluminum-26
08 p1150 N90-16661

AM (MODULATION)
U AMPLITUDE MODULATION

AMALGAMS
U MERCURY AMALGAMS

AMAZON REGION (SOUTH AMERICA)
Connections between the circulation in altitude and convection over South America
[INPE-4923-TDL/383] 11 p1534 N90-18828
Availability of multitemporal LANDSAT data accompanying the variation of water surfaces in the program area of Careiro PDRI/AM
[INPE-4896-PRE/1496] 12 p1677 N90-19634
An observational study of squall lines in the Amazon
[INPE-4865-TDL/376] 12 p1693 N90-19723
Monitoring of agrocattle-raising projects through visual/digital analysis of LANDSAT-TM imagery south of Para state
[INPE-4982-PRE/1542] 14 p1996 N90-21442
Multitemporal analysis of LANDSAT/TM digital imagery in the detection of areas affected by caterpillar (sibine fusca) attack in the dende (elais guineensis) palm plantation
[INPE-4979-PRE/1544] 14 p1999 N90-21457
Radon concentration over the Brazilian Amazon Basin during the wet season (Belem-Manaus GTE-ABLE-2B flight of April 24, 1987)
[INPE-4892-PRE/1493] 14 p2004 N90-21486
Geographic information system: Coded data of agrocattle-raising projects in the Amazon
[INPE-4978-PRE/1543] 15 p2180 N90-22457
Characterization of biogenic aerosol particles from the Amazon Basin during dry and wet season
20 p2886 N90-26418
Activities report for the IBDF-INPE project SEQE, year 1987
[INPE-4534-RPE/565] 23 p3415 N90-29298

AMBIENCE
Wind speed dependence of acoustic ambient vertical directional spectra at high frequency
[AD-A214293] 07 p0989 N90-15712
Vertical directionality measurements of ambient noise in the NE Pacific
[AD-A220007] 17 p2432 N90-23856
A preliminary study of the masking of wind turbine noise by ambient sound
[FFA-TN-1990-01] 20 p2923 N90-26636
Methods for detecting low-frequency signals in the presence of strong winds
[AD-A223980] 23 p3320 N90-28769

AMBIENT TEMPERATURE
Measurement of respiratory air temperatures and calculation of respiratory heat loss when working at various ambient temperatures
[AD-A210378] 01 p0093 N90-10529
Advances in ambient temperature secondary lithium cells
13 p1825 N90-20481
Ambient-temperature creep failure of silver-aided diffusion bonds between steel
[DE90-010687] 18 p2527 N90-24420
Fatigue crack growth in ceramic materials at ambient and elevated temperatures
[DE90-008418] 18 p2531 N90-24443
Weldment mechanical properties of aluminum-copper-lithium alloy, 2090, at ambient and cryogenic temperatures
[DE90-014178] 21 p2981 N90-26941
A cost-effective realization of environmental temperature control
[DE90-011651] 24 p3458 N90-29532

AMBIGUITY
Alias-free Wigner distribution function and complex ambiguity function for discrete-time samples
[AD-A211050] 02 p0269 N90-11533
Phase ambiguity resolution for offset QPSK modulation systems
[NASA-CASE-NPO-17853-1-CU]
09 p1204 N90-16975
Ambiguity bootstrapping to determine GPS orbits and baselines
[AD-A218206] 14 p1931 N90-21052

AMBIT
U FIELD THEORY (PHYSICS)

AMERICIUM
Magnetic behavior of curium and americium-curium alloys
[DE89-017808] 07 p0902 N90-15213
Phase diagram and thermodynamic data for the Am-Pu system
[NPL-DMM(A)-5] 22 p3255 N90-28431

AMIDES
NT BISMALEIMIDE
NT CYANAMIDES
NT POLYIMIDES
NT UREAS
Chemical and photochemical reactivity in microemulsions and waterless microemulsions
[AD-A211776] 04 p0470 N90-12692
Composite materials with improved properties in compression: Synthesis and dimerization 2,3-dimethyl-5-silaspiro(4.4)nona-2,7-diene
[AD-A222552] 22 p3156 N90-27892

AMINES
NT ANILINE
NT CATECHOLAMINE
NT DIAMINES
NT DIMETHYLHYDRAZINES
NT EPINEPHRINE
NT FLUOROAMINES
NT TETRAFLUOROHYDRAZINE
Reactions of hydrogen chloride and boron trichloride with trimethylsilylamino groups
[AD-A209006] 01 p0038 N90-10209
Advanced biosensors for amino acid detection
[AD-A214029] 08 p1076 N90-16225

AMINO ACIDS
NT ALANINE
NT GLYCINE
NT PHENYLALANINE
NT TRYPTOPHAN
NT TYROSINE
Control of synthetic peptide tertiary structure
[AD-A210339] 01 p0049 N90-10281
Excitatory amino acids as transmitters in the brain
[AD-A210685] 01 p0093 N90-10532
Boron analogues of amino acids and derivatives
[AD-A211311] 03 p0379 N90-12157
Characterization of biopolymer surfaces using scanning microscopies
[AD-A216572] 11 p1490 N90-18572

AMINO RADICAL
Electrochemical surface finishing using amino-substrates on carbon fibers in organic media. Effects of the finishing on the mechanical properties of carbon-epoxy composites
[ONERA-RT-9/3549-M] 23 p3301 N90-28672

AMMETERS
Solid state voltammetry and sensors in solids and gases
[DE90-003234] 08 p1129 N90-16538
A fiber-optic current sensor for aerospace applications
[NASA-TM-103152] 16 p2239 N90-22773

AMMONIA
Low temperature spectroscope of hydrazine and ammonia complexes
02 p0205 N90-11169
Equation-of-state data of synthetic Uranus
[DE89-016509] 02 p0296 N90-11683
Intermittent Solar Ammonia Absorption Cycle (ISAAC) refrigeration for lesser developed countries
[DE90-006700] 11 p1496 N90-18610
A three-year study of the OH masers in Orion-KL and a study of the (3,2) transition of ammonia
15 p2183 N90-22471
Reactions of silane in active nitrogen
[AD-A220371] 17 p2373 N90-23511
Analysis of energy spectra of the ions in the coma of Halley's comet for the evaluation of the production ratio of methane and ammonia
[ETN-90-96489] 18 p2638 N90-25026
The 30-kW ammonia arcjet technology
[NASA-CR-186850] 19 p2670 N90-25190
Laboratory measurements and modeling of microwave absorption by ammonia in gas mixtures applicable to giant planet atmospheres
20 p2944 N90-26750

AMMONIUM COMPOUNDS
NT AMMONIUM NITRATES
NT AMMONIUM PERCHLORATES
An evaluation of metal salts of 3-nitro-1,2,4-triazol-5-one (NTO) as potential primary explosives
[MRL-TN-563] 14 p1956 N90-21202
Studies on the use of supercritical ammonia for ceramic nitride synthesis and fabrication
[NASA-TM-102570] 15 p2068 N90-21843

AMMONIUM NITRATES
Investigation of the phase stabilizing effect of potassium fluoride on ammonium nitrate
[AD-A213042] 06 p0753 N90-14381
Steady state model to determine lake resources at risk to acid deposition in the Sierra Nevada, California
[PB89-103995] 06 p0809 N90-14705
Properties and thermal decomposition of the double salts of uranyl nitrate-ammonium nitrate
[DE89-004909] 07 p0914 N90-15287
Analysis of liquid propellant exposed to elastomeric materials
[AD-A214465] 09 p1200 N90-16952
Crystal structure of Tetra-Ammonium Adamantyl Tetra-Nitrate (TAATN): High energy/density fuel candidate for liquid propellant
[AD-A215684] 09 p1201 N90-16955
Investigation of the phase stabilizing effect of 4 percent potassium fluoride on ammonium nitrate
[AD-A215313] 11 p1494 N90-18599

AMMONIUM PERCHLORATES
Using small scale tests to estimate the failure diameter of a propellant
[DE90-001166] 07 p0913 N90-15281
RSRM-9 (360L009): Ballistics mass properties
[NASA-CR-183944] 20 p2823 N90-26064

AMMONOLYSIS
Studies on the use of supercritical ammonia for ceramic nitride synthesis and fabrication
[NASA-TM-102570] 15 p2068 N90-21843

AMMUNITION
Remarks on certain aspects of solid explosive detonation via small projectile impact
[AD-A210648] 01 p0054 N90-10307
Fractographic analysis of long rod penetrator-armor ceramic interactions
[AD-A215172] 09 p1197 N90-16938
Taylor impact testing
[AD-A215018] 09 p1231 N90-17144
Measurement of gas leaks between a projectile and the walls of a tube in a ballistic compressor
[ISL-CO-250/88] 11 p1510 N90-18694
Jam resistant fluid power actuator for ballistic-damage tolerant redundant cylinder assemblies
[AD-D014360] 12 p1671 N90-19600
Evaluation of 2090-T8E48 aluminum-lithium plates
[AD-A217262] 13 p1776 N90-20196
Minutes of the 23rd Explosives Safety Seminar, volume 1
[AD-A218264] 14 p1958 N90-21213
Extraction of recovery of plasticizers from solid propellants and munitions
[AD-D014433] 15 p2072 N90-21868
Video camera system for locating bullet holes in targets at a ballistics tunnel
[NASA-TM-4197] 20 p2865 N90-26296
Very low height drop test. Conditioning and tandem dropping of two loads conditioned in two PC6 platforms assembled by one PD9 platform and rigid structures
[REPT-89/04] 22 p3193 N90-28117

AMORPHOUS MATERIALS
NT AMORPHOUS SILICON
Optical dispersion relations for diamondlike carbon films
[NASA-TM-102356] 01 p0129 N90-10738
Neutron scattering studies of amorphous Invar alloys
[DE89-016868] 02 p0197 N90-11126
Physical ageing and short term creep in amorphous and semicrystalline polymers
[NPL-DMA(A)-185] 04 p0479 N90-12745
Bulk acoustic waves resonators made of amorphous materials
[NOTE-TECHNIQUE-1989-4] 04 p0550 N90-13199
Computational studies of structural and transport properties of amorphous solids
[ETN-90-96027] 05 p0628 N90-13664

Dynamical structure of liquid and amorphous metals
[DE90-003805] 07 p0905 N90-15229
Metal film coatings on amorphous metallic alloys
[AD-D014308] 07 p0907 N90-15240
Epoxy-resin cable terminations
[AD-A213789] 07 p0942 N90-15454
Research on amorphous silicon-germanium alloys for tandem solar cells
[DE89-009436] 07 p0950 N90-15499
Proceedings of the Latin American Conference on the Applications of the Moessbauer Effect
[DE90-600819] 07 p1002 N90-15803
Researches on amorphous perovskite
[DE89-900733] 08 p1128 N90-16535
Effects of ion dose on the morphology and crystallization of amorphous germanium
[DE90-003564] 08 p1130 N90-16547
Experimental studies of gas trapping in amorphous ice and thermal modelling of comets: Implications for Rosetta 08 p1140 N90-16610
Studies of the structure and properties of amorphous a-Zr76Fe24Hx
[AD-A214646] 09 p1190 N90-16897
The 25-KVA amorphous metal-core transformer developmental test report
[AD-A215444] 09 p1213 N90-17035
Bulk acoustic wave resonators made of amorphous materials
[ONERA-NT-1989-4] 09 p1279 N90-17416
Strain induced amorphization of aluminium by manganese implantation
[DE90-607259] 10 p1356 N90-17863
Structural and fast ion transport properties of glassy and amorphous materials
[DE90-005587] 10 p1358 N90-17877
Statistical mechanical models for liquid and amorphous structure in covalently bonded systems
[DE90-607233] 10 p1428 N90-18240
Improved amorphous metal materials for magnetic pulse compression
[DE90-005723] 11 p1486 N90-18555
Ion implantation-induced amorphization of ceramic oxides
[DE90-006564] 11 p1571 N90-19041
International conference on Surface Modification of Metals by Ion Beams
[AD-A215872] 12 p1626 N90-19345
Optical studies of dynamical processes in disordered materials
[DE90-007080] 12 p1631 N90-19372
Evolution of ices and carbonaceous materials in the laboratory and in comets 12 p1739 N90-19998
Research on amorphous silicon-based thin film photovoltaic devices. Task B: Research on stable high efficiency large area, amorphous silicon-based submodules
[DE90-000320] 14 p2002 N90-21473
Low temperature properties of amorphous solids 15 p2171 N90-22405
Amorphization of metals by ion implantation and ion beam mixing
[DE90-620571] 16 p2221 N90-22667
Vibrational and optical properties of amorphous metals
[DE90-011427] 18 p2522 N90-24403
Process of three dimensional lithography in amorphous polymers
[AD-D014500] 19 p2676 N90-25221
Wear mechanisms of amorphous carbon and zirconia coatings on rigid disk magnetic recording media
[DE90-011053] 20 p2837 N90-26133
On diamond, graphitic and amorphous carbons in primitive extraterrestrial solar system materials 21 p3095 N90-27591
Processing Bi-Pb-Sr-Ca-Cu-O superconductors from amorphous state 22 p3150 N90-27860
Research on high-efficiency, multiple-gap, multi-junction amorphous silicon-based alloy thin-film solar cells
[DE90-000338] 23 p3344 N90-28896

AMORPHOUS SEMICONDUCTORS
NT AMORPHOUS SILICON
Ultrafast processes and spectroscopy with free electron lasers
[AD-A212889] 05 p0647 N90-13773
Structural instabilities, impurities, and defects in electronic materials
[AD-A215384] 09 p1290 N90-17481
International Summer School on Solid State Microbatteries
[AD-A213457] 10 p1434 N90-18277

AMORPHOUS SILICON
Structure of amorphous silicon alloy films
[DE89-009441] 01 p0128 N90-10734
Research on high-efficiency, single-junction, monolithic, thin-film amorphous silicon solar cells
[DE89-000846] 06 p0805 N90-14687
Instability of a-Si:H/Ag interface at 150 deg C
[DE89-009419] 07 p0950 N90-15498
Research on high-efficiency, single-junction, monolithic, thin-film amorphous silicon solar cells, phase 1
[DE89-009495] 07 p0951 N90-15502
Research on high-efficiency, single-junction, monolithic, thin-film amorphous silicon solar cells, phase 2
[DE89-009496] 07 p0951 N90-15503
Research on amorphous silicon based thin film photovoltaic devices. Phase 2: Research on stable high-efficiency, large area amorphous silicon based submodules
[DE89-009515] 09 p1243 N90-17209
Hydrogenated amorphous silicon films prepared by glow discharge of disilane
[DE90-000309] 11 p1491 N90-18581
Hydrogenated amorphous and microcrystalline silicon deposited from silane-hydrogen mixtures
[ETN-90-96267] 11 p1493 N90-18590
Chemical vapor deposition and photochemical vapor deposition of amorphous silicon photovoltaic devices
[DE89-009510] 11 p1529 N90-18803
Reactions of silane in active nitrogen
[AD-A220371] 17 p2373 N90-23511
Diagnostics of glow discharges used to produce hydrogenated amorphous silicon films
[DE90-000329] 18 p2522 N90-24402
Structural and electronic studies of a:SiGe:H alloys
[DE90-000313] 19 p2710 N90-25424
Optical properties and transport properties of hydrogenated amorphous silicon
[ETN-90-97215] 20 p2927 N90-26656
Research on the structural and electronic properties of defects in amorphous silicon
[DE90-000342] 23 p3312 N90-28730
Research on stable, large-area, amorphous silicon based submodules, phase 3
[DE90-000339] 23 p3399 N90-29204

AMOUNT
An introduction to Montague grammar
[REPT-89-46] 15 p2147 N90-22266

AMPERAGE
U ELECTRIC CURRENT

AMPHIBIA
NT FROGS
Experimental control of axis polarity in amphibian embryos 19 p2680 N90-25244
The first seven minutes of a Zenopus egg fertilised on a sounding rocket in space 19 p2680 N90-25245
Simulation of the inversion of amphibian eggs in a gravitational field using hollow glass spheres 19 p2681 N90-25251
Lens and limb regeneration in newt during and after 13-day long spaceflight 19 p2681 N90-25252

AMPLIFICATION
NT SOUND AMPLIFICATION
NT WAVE AMPLIFICATION
Master oscillator with power amplifiers: Performance of a two-element CW HF phased-laser array
[AD-A211141] 01 p0076 N90-10435
Minimized emittance growth with elliptical beam pipes in FEL (Free-Electron Laser)
[DE89-016982] 02 p0228 N90-11305
Base level management of radio frequency radiation protection program
[AD-A211787] 03 p0381 N90-12171
X-UV amplification in a plasma column of five centimeters. Five beams experiment 06 p0786 N90-14574
Proof-of-principle experiment for a hot electron pumped XUV amplifier
[DE90-000820] 06 p0787 N90-14586
Enhancement of microchannel plate gain by deposition of CsI on the channel walls
[DE90-003051] 07 p0922 N90-15334
Vorticity amplification in nonorthogonal stagnation flow 08 p1064 N90-16152
One-dimensional single-mode nonlinear FEL amplification code: User's manual
[DE90-719544] 09 p1227 N90-17121
Numeric model of a CO2 laser amplifier
[AD-A215818] 10 p1389 N90-18035
Research on free electron lasers
[AD-A215865] 11 p1514 N90-18715
Optical amplification in 45 deg - cut BaTiO3
[AD-A216043] 11 p1566 N90-19011
Development of an ultra-bright laser and an application to multi-photon ionization 14 p1984 N90-21372
LLE review
[DE90-008958] 14 p1985 N90-21378
Direct solar-pumped iodine laser amplifier
[NASA-CR-186442] 15 p2103 N90-22030
Telescope considered as a very high gain antenna
[ETN-90-96614] 17 p2473 N90-24138
Gain in waveguide laser at 10.6 micrometer
[FOA-C-30540-3.1] 18 p2563 N90-24624
The electrical characteristic and gain behavior as a function of the radial distance from the laser axis in a copper vapor laser
[DE90-615371] 18 p2564 N90-24630
Beam combining of excimer lasers by stimulated Raman scattering
[AD-A222973] 21 p3008 N90-27099

AMPLIFICATION FACTOR
U AMPLIFICATION

AMPLIFIER DESIGN
The 30-GHz monolithic receive module
[NASA-CR-180849] 18 p2545 N90-24528
The e-beam sustained CO2 laser amplifier 18 p2561 N90-24611

AMPLIFIERS
NT BROADBAND AMPLIFIERS
NT CARCINOTRONS
NT CYCLOTRON RESONANCE DEVICES
NT DISTRIBUTED AMPLIFIERS
NT FEEDBACK AMPLIFIERS
NT LIGHT AMPLIFIERS
NT LIMITER AMPLIFIERS
NT MICROWAVE AMPLIFIERS
NT OPERATIONAL AMPLIFIERS
NT PARAMETRIC AMPLIFIERS
NT PHOTOMULTIPLIER TUBES
NT POWER AMPLIFIERS
NT PREAMPLIFIERS
NT TRAVELING WAVE AMPLIFIERS
NT VOLTAGE AMPLIFIERS
A new semicustom integrated bipolar amplifier for silicon strip detectors
[DE89-015585] 02 p0215 N90-11229
Development of FIR arrays with integrating amplifiers 05 p0598 N90-13473
Electron beam sensitive devices for controllability
[IMAG-RR-761-I] 05 p0636 N90-13707
An experimental analysis of the waveguide modes in a high-gain free-electron laser amplifier 05 p0648 N90-13779
Optimization of the intermodulation performance of GaAs MESFET small-signal amplifiers
[AD-A215193] 09 p1212 N90-17026
Megawatt-klystron amplifiers in L-band
[DE90-004864] 10 p1379 N90-17992
Results of the PALADIN experiment
[DE90-006776] 12 p1667 N90-19578
Performance of zig-zag slab regenerative ring amplifier laser system
[DE90-006995] 13 p1806 N90-20371
Common source cascode amplifiers for integrating IR-FPA applications 14 p1977 N90-21324
Generation of ultrashort laser pulses from neodymium glass oscillator and regenerative amplifier 14 p1984 N90-21373
Relativistic klystron amplifiers driven by modulated intense relativistic electron beams
[AD-A221075] 18 p2607 N90-24849
DURIP: Instrumentation for laser switched power LINAC
[AD-A222629] 20 p2868 N90-26318
A solid-state multiple-pass amplifier for diode pumped coherent laser radar systems
[AD-A222537] 21 p3009 N90-27104
Solid state space harmonic amplifier
[AD-D014455] 22 p3166 N90-27955

AMPLITUDE DISTRIBUTION ANALYSIS
In-band amplitude dispersion on a microwave link 20 p2846 N90-26189

AMPLITUDE MODULATION
Experimental and theoretical study of CO2 staggered hollow-bore array lasers
[AD-A212921] 10 p1389 N90-18032
Auditory perception
[AD-A217012] 11 p1540 N90-18864
Active phase and amplitude modulator
[AD-D014318] 12 p1650 N90-19480
Multi-level trellis coded modulation and multi-stage decoding
[NASA-CR-186861] 19 p2743 N90-25593

AMPLITUDE PROBABILITY ANALYSIS
U AMPLITUDE DISTRIBUTION ANALYSIS

AMPLITUDES
NT PULSE AMPLITUDE
NT SCATTERING AMPLITUDE
Bordered surfaces, off-shell amplitudes, sewing, and string field theory
[DE90-000006] 03 p0414 N90-12378
A simulation of optical propagation through atmospheric turbulence using two-dimensional Fourier transform techniques
[AD-A216776] 11 p1566 N90-19013
Effects of amplitude distortions and IF equalization on satellite communication system bit-error rate performance
[NASA-TM-102415] 12 p1645 N90-19454

An algorithm for efficient estimation of superimposed exponential signals
[AD-A217218] 13 p1865 N90-20698
Application and extension of an analytical model of the confined acoustic beam generated by a transducer
[AD-A222994] 20 p2924 N90-26639
Introductory lectures on conformal field theory and strings
[DE90-627219] 24 p3556 N90-30120

AMPOULES
Method of preparing radially homogeneous mercury cadmium telluride crystals
[NASA-CASE-MFS-25786-2] 13 p1898 N90-20896

ANAEROBES
Effect of community structure on the kinetics of anaerobic degradation of aromatic compounds
[DE90-003666] 07 p0888 N90-15134
Anaerobic metabolism of aromatic compounds by phototrophic bacteria: Biochemical aspects
[DE90-009503] 14 p2009 N90-21516

ANALOG CIRCUITS
Current protections modelisation in a buck cell
10 p1335 N90-17723
Neurobeamformer 2: Further exploration of adaptive beamforming via neural networks
[AD-A215118] 10 p1426 N90-18226
Solid state research
[NASA-CR-186699] 17 p2476 N90-24160
Solid state research
[NASA-CR-186700] 17 p2477 N90-24161

ANALOG COMPUTERS
CAD work station for electronics designer
[DE90-616473] 14 p2015 N90-21546

ANALOG DATA
Acoustic studies of new materials: Quasicrystals, low-loss glasses and high Tc superconductors
[AD-A211281] 02 p0272 N90-11551
Resistive fuses: Analog hardware for detecting discontinuities in early vision
[AD-A211891] 05 p0634 N90-13696
An artificial intelligence approach to analog system diagnosis
[AD-A213135] 05 p0686 N90-13992
Analog electronic control differential transmitter
[AD-D014508] 19 p2685 N90-25272

ANALOG SIMULATION
Polarization coupling in the acousto-optic interaction of surface waves 15 p2164 N90-22365

ANALOG TO DIGITAL CONVERTERS
The 22 GHz Radioastron receiver: Development of prototype components during the year 1988
[PB89-212583] 07 p0920 N90-15323
Application of a buck-type MC2 regulated converter for a stepper motor control 10 p1335 N90-17722
Effective waveform recorder evaluation procedures
[DE90-005197] 10 p1387 N90-18027
A digitally controlled system for effecting and presenting a selected electrical resistance
[NASA-CASE-MFS-29149-1] 12 p1652 N90-19492
HCl monitor 16 p2209 N90-22599
Personal computer programs for the control of subnanosecond transient digitizers with applications for device damage testing
[AD-A221458] 21 p3054 N90-27365

ANALOGIES
A simple model for the stellar analogy of compact solar flares
[DE90-003215] 07 p1015 N90-15877
Systematicity as a selection constraint in analogical mapping
[AD-A216029] 11 p1541 N90-18869
Analogies between cometary, interplanetary, and interstellar matter 11 p1578 N90-19087
Frontal structure in a mesoscale model
15 p2132 N90-22187

ANALOGS
Continuum analogues of contragredient Lie algebras: Lie algebras with a Cartan operator and nonlinear dynamical systems
[DE89-635698] 07 p0985 N90-15691
Mathematical model for adaptive control system of ASEA robot at Kennedy Space Center
08 p1157 N90-16701
Laboratory studies of cometary ice analogues
12 p1739 N90-19997
Stable isotope studies of cometary analogue materials
12 p1740 N90-20001
Crustal strength of different model comet materials
12 p1740 N90-20003
CO2 depth profiles in cometary model substances of KOSI 12 p1742 N90-20014
Dynamics of crust formation and dust emission of comet nucleus analogues under isolation
12 p1743 N90-20020
Condensed phase kinetic deuterium isotope effects in high energy phenomena: Mechanistic investigations and relationships
[AD-A217161] 13 p1770 N90-20156
Introducing the VRT gas turbine combustor
[NASA-TM-103176] 17 p2386 N90-23591

ANALYSIS (MATHEMATICS)
NT ABEL FUNCTION
NT ANALYTIC FUNCTIONS
NT APPROXIMATION
NT ASYMPTOTES
NT ASYMPTOTIC SERIES
NT BANACH SPACE
NT BESSEL FUNCTIONS
NT BIHARMONIC EQUATIONS
NT BORN APPROXIMATION
NT BOUNDARY INTEGRAL METHOD
NT BURGER EQUATION
NT CALCULUS
NT CALCULUS OF VARIATIONS
NT CAMPBELL-HAUSDORFF SERIES
NT CHEBYSHEV APPROXIMATION
NT COMBINATIONS (MATHEMATICS)
NT COMBINATORIAL ANALYSIS
NT COMPLEX VARIABLES
NT COMPUTATIONAL CHEMISTRY
NT COMPUTATIONAL FLUID DYNAMICS
NT CONFORMAL MAPPING
NT CONJUGATE GRADIENT METHOD
NT CONJUGATES
NT CONTINUITY (MATHEMATICS)
NT CONVOLUTION INTEGRALS
NT COSINE SERIES
NT CURL (VECTORS)
NT DEPENDENT VARIABLES
NT DIFFERENCE EQUATIONS
NT DIFFERENTIAL CALCULUS
NT DIFFERENTIAL EQUATIONS
NT EDDINGTON APPROXIMATION
NT EINSTEIN EQUATIONS
NT ELLIPTIC DIFFERENTIAL EQUATIONS
NT ELLIPTIC FUNCTIONS
NT ERROR ANALYSIS
NT ESSENTIALLY NON-OSCILLATORY SCHEMES
NT EXISTENCE THEOREMS
NT EXPONENTIAL FUNCTIONS
NT EXTREMUM VALUES
NT FAST FOURIER TRANSFORMATIONS
NT FINITE DIFFERENCE THEORY
NT FINITE ELEMENT METHOD
NT FINITE VOLUME METHOD
NT FLUX VECTOR SPLITTING
NT FOKKER-PLANCK EQUATION
NT FOURIER ANALYSIS
NT FOURIER SERIES
NT FOURIER TRANSFORMATION
NT FREDHOLM EQUATIONS
NT FUNCTION SPACE
NT FUNCTIONAL ANALYSIS
NT FUNCTIONAL INTEGRATION
NT GAUSS EQUATION
NT GREEN'S FUNCTIONS
NT HALF PLANES
NT HALF SPACES
NT HANKEL FUNCTIONS
NT HARMONIC ANALYSIS
NT HARMONIC FUNCTIONS
NT HARTREE APPROXIMATION
NT HELMHOLTZ VORTICITY EQUATION
NT HILBERT SPACE
NT HILBERT TRANSFORMATION
NT HYPERBOLIC DIFFERENTIAL EQUATIONS
NT HYPERBOLIC FUNCTIONS
NT HYPERGEOMETRIC FUNCTIONS
NT HYPERPLANES
NT INTEGRAL CALCULUS
NT INTEGRAL EQUATIONS
NT INTEGRAL TRANSFORMATIONS
NT INTERPOLATION
NT ITERATION
NT ITERATIVE SOLUTION
NT J INTEGRAL
NT JACOBI INTEGRAL
NT JACOBI MATRIX METHOD
NT KERNEL FUNCTIONS
NT LAGUERRE FUNCTIONS
NT LAPLACE TRANSFORMATION
NT LEAST SQUARES METHOD
NT LEBESGUE THEOREM
NT LEGENDRE FUNCTIONS
NT LIAPUNOV FUNCTIONS
NT LIMITS (MATHEMATICS)
NT LINEAR EQUATIONS
NT LINEAR EVOLUTION EQUATIONS
NT LIOUVILLE EQUATIONS
NT LOGARITHMS
NT MAXIMA
NT MEAN SQUARE VALUES
NT MEASURE AND INTEGRATION
NT MEROMORPHIC FUNCTIONS
NT MINIMA
NT MONTE CARLO METHOD
NT MULTIGRID METHODS
NT NAKED SINGULARITIES
NT NEUMANN PROBLEM
NT NEWTON METHODS
NT NEWTON-RAPHSON METHOD
NT NOMOGRAPHS
NT NONHOLONOMIC EQUATIONS
NT NONLINEAR EQUATIONS
NT NONLINEAR EVOLUTION EQUATIONS
NT NUMERICAL ANALYSIS
NT NUMERICAL DIFFERENTIATION
NT NUMERICAL INTEGRATION
NT ORTHOGONAL FUNCTIONS
NT OSEEN APPROXIMATION
NT PADE APPROXIMATION
NT PARABOLIC DIFFERENTIAL EQUATIONS
NT PARTIAL DIFFERENTIAL EQUATIONS
NT PARTICLE IN CELL TECHNIQUE
NT PARTITIONS (MATHEMATICS)
NT PERIODIC FUNCTIONS
NT PERMUTATIONS
NT PHASE-SPACE INTEGRAL
NT POISSON EQUATION
NT POWER SERIES
NT PREDICTOR-CORRECTOR METHODS
NT QUADRATIC EQUATIONS
NT RAYLEIGH-RITZ METHOD
NT RELAXATION METHOD (MATHEMATICS)
NT RICCATI EQUATION
NT RUNGE-KUTTA METHOD
NT SERIES (MATHEMATICS)
NT SINE SERIES
NT SINGULAR INTEGRAL EQUATIONS
NT SINGULARITY (MATHEMATICS)
NT SOBOLEV SPACE
NT SPHERICAL HARMONICS
NT TANGENTS
NT TAYLOR SERIES
NT TRIGONOMETRIC FUNCTIONS
NT TRUNCATION ERRORS
NT TVD SCHEMES
NT VECTOR ANALYSIS
NT VLASOV EQUATIONS
NT VOLTERRA EQUATIONS
NT VORTICITY
NT VORTICITY EQUATIONS
NT WEIERSTRASS FUNCTIONS
NT WEIGHTING FUNCTIONS
NT WIENER HOPF EQUATIONS
NT ZONAL HARMONICS
Summaries of the FY 1989 Applied Mathematical Sciences Research program
[DE89-016694] 02 p0267 N90-11521
Backward analysis on higher order functions
[MEMO-INF-89-19] 02 p0268 N90-11526
A thermoelastic transversely isotropic thick walled cylinder/disk application: An analytical solution and study
[NASA-TM-102320] 04 p0511 N90-12950
Mathematical techniques for system realization and identification
[AD-A212088] 06 p0833 N90-14841
The kind of mathematics involved in applied superconductivity research
[DE90-003706] 07 p1002 N90-15798
Proceedings of a research workshop on Nonlinear Time Series Analysis and Applications
[AD-A216541] 10 p1423 N90-18214
Analytic solutions for the decay of turbulent swirling flow in a cylinder
[DE90-005744] 11 p1507 N90-18677
Rule matrices, degree vectors, and preimages for cellular automata
[DE90-007492] 12 p1707 N90-19805
Institute for Computational Mechanics in Propulsion (ICOMP) fourth annual review, 1989
[NASA-TM-102519] 13 p1878 N90-20769
On the existence of a positive definite solution of the matrix equation X + A(sup tau)X(exp -1)A = I
[PB90-133976] 15 p2159 N90-22335
Discrete variable structural optimization by the complex method
[LR-597] 15 p2161 N90-22341
An algebric approach to infinite data structures
[CS-8909] 16 p2327 N90-23265
Efficient representation of the hydrographic structure of the north atlantic ocean and aspects of the circulation from objective methods
[AD-A218606] 17 p2429 N90-23841

Cumulative reports and publications through December 31, 1989
[NASA-CR-182041] 17 p2439 N90-23898
The Clemson University, university research initiative program in discrete mathematics and computational analysis
[AD-A220103] 17 p2461 N90-24055
Dynamic jamming of networks
[AD-A223044] 20 p2856 N90-26247
Applied mathematical modules for use in a linear algebra service course
[AD-A222814] 20 p2920 N90-26618
A closed form solution to HZE propagation
[NASA-TM-103482] 20 p2924 N90-26640
Symmetry and global bifurcation in nonlinear solid mechanics
[AD-A221981] 21 p3013 N90-27129

ANALYSIS OF VARIANCE
Application of dimensional analysis to statistical process modeling
[AD-A211881] 03 p0335 N90-11905
A comparison of variance-controlled and non-controlled principal components
[AD-A220530] 18 p2598 N90-24782
Minimum variance control of nonlinear systems
[RR-369] 19 p2748 N90-25615
A new diagnostics approach for repeated measures designs
[AD-A223500] 24 p3540 N90-30020

ANALYTIC FUNCTIONS
On sufficient conditions for a function to be analytic
[DE89-618382] 02 p0264 N90-11503
General hulls in uniform algebras
[DE89-618383] 02 p0264 N90-11504
Some comments on the solvable Chiral Potts model
[PREPRINT-673] 05 p0696 N90-14070
Weierstrass preparation and division theorems for the ring of germs of superanalytic functions
[DE90-612742] 14 p2020 N90-21576
Hausdorff measure and boundary behavior of analytic functions
[ETN-90-96501] 18 p2605 N90-24835
Hybrid analysis: Coupling of the finite element method with analytical approaches
[MBB-UO-0048/89-PUB] 19 p2650 N90-25079
The Cousin problems for an overdetermined system of complex partial differential equations
[DE90-627170] 23 p3389 N90-29139
Some overdetermined systems of complex partial differential equations
[DE90-627162] 24 p3536 N90-29995

ANALYTIC GEOMETRY
NT CIRCUMFERENCES
NT CONICS
NT ELLIPSES
NT EPICYCLOIDS
NT PARABOLAS
NT PROLATE SPHEROIDS
NT TANGENTS
NT TORUSES
NT TRIGONOMETRY
Geometric considerations for a waypoint guidance method
[DE90-001803] 07 p0878 N90-15088
A scanning algorithm for display of generalized cylinders
[REPT-89-77] 17 p2445 N90-23936

ANALYTICAL CHEMISTRY
Analytical study of comet nucleus samples
08 p1140 N90-16608
Fundamental studies of surface processes and trace analysis using solid electrodes
[AD-A216538] 11 p1483 N90-18533

ANALYZERS
NT SIGNAL ANALYZERS
Real-time observations of aerosol composition changes
[DE89-012382] 01 p0073 N90-10422
COSTEP: A comprehensive suprathermal and energetic particle analyzer for SOHO 04 p0568 N90-13314
Two possible configurations for the top-hat electrostatic analyzer: A numerical study
[IFSI-88-18] 08 p1077 N90-16229
CIS-2 analyzer derivation of hardware parameters
[IFSI-89-13] 08 p1077 N90-16230
BEAR electrostatic analyzer: Flight results
[DE90-006511] 11 p1498 N90-18625
FOMA: A Fast Optical Multichannel Analyzer
[DE90-004093] 12 p1713 N90-19839
A linear filtering technique for removal of low-frequency noise
[DE90-006183] 13 p1794 N90-20296
Dynamic mechanical analysis of polymeric materials
18 p2513 N90-24353
Experimental determination of material damping using vibration analyzer 18 p2514 N90-24358
Personal Computer (PC) thermal analyzer
[AD-A221325] 18 p2548 N90-24546
Optical signal processing
[AD-A220332] 18 p2615 N90-24897
Dynamic jamming of networks
[AD-A223044] 20 p2856 N90-26247
GSHELL: Multichannel analyzer/multichannel scaler emulation software for IBM-PC-compatible computers
[DE90-015396] 24 p3529 N90-29956
Submicron particle analyzer
[AD-A223558] 24 p3545 N90-30050

ANATOMY
NT ADRENAL GLAND
NT ARM (ANATOMY)
NT ARTERIES
NT AUTONOMIC NERVOUS SYSTEM
NT BARORECEPTORS
NT BLADDER
NT BLOOD VESSELS
NT BONE MARROW
NT BONES
NT BRAIN
NT BRAIN STEM
NT CARDIOVASCULAR SYSTEM
NT CARTILAGE
NT CENTRAL NERVOUS SYSTEM
NT CEREBELLUM
NT CEREBRAL CORTEX
NT CEREBRUM
NT COLLAGENS
NT CONNECTIVE TISSUE
NT CONSTRICTORS
NT CORNEA
NT EAR
NT EFFERENT NERVOUS SYSTEMS
NT EYE (ANATOMY)
NT FEET (ANATOMY)
NT FEMUR
NT FINGERS
NT FOVEA
NT GANGLIA
NT GRAVIRECEPTORS
NT HAND (ANATOMY)
NT HEAD (ANATOMY)
NT HEART
NT HUMAN BODY
NT INTESTINES
NT JOINTS (ANATOMY)
NT LEG (ANATOMY)
NT LIVER
NT LUNGS
NT MUSCLES
NT MUSCULOSKELETAL SYSTEM
NT MYOCARDIUM
NT NECK (ANATOMY)
NT NERVES
NT NERVOUS SYSTEM
NT OTOLITH ORGANS
NT PERIPHERAL NERVOUS SYSTEM
NT PHOTORECEPTORS
NT PINEAL GLAND
NT PITUITARY GLAND
NT RETINA
NT SEMICIRCULAR CANALS
NT SKIN (ANATOMY)
NT SPINAL CORD
NT SPINE
NT SPLEEN
NT SYMPATHETIC NERVOUS SYSTEM
NT TESTES
NT THALAMUS
NT TIBIA
NT ULNA
NT VERTEBRAE
NT VESTIBULES
NT WRIST
Organization of a large-scale cortical network
[AD-A216829] 11 p1540 N90-18863

ANCHORS (FASTENERS)
Design and development activities on the candidate sample acquisition system for the Rosetta mission
12 p1738 N90-19993

ANDROMEDA GALAXY
Local normal galaxies 16 p2336 N90-23315

ANECHOIC CHAMBERS
Tower wake/blade interaction noise of a wind turbine
[NAL-TR-945] 02 p0236 N90-11344
Optical links for microwave application
[AD-A220574] 17 p2472 N90-24134
Tests of an ultra-light tunnel in the anechoic wind tunnel facility CEPRA 19
[ONERA-RF-20/7294-PH] 22 p3122 N90-27729
Acoustic qualification of an anechoic chamber
[RAE-TM-MAT/STR-1136] 22 p3245 N90-28400

ANELASTICITY
Dynamic and microphysical characteristics of cirrus clouds as revealed by aircraft, lidar, and other observations during FIRE 15 p2130 N90-22177
Rubberlike elasticity experiment
18 p2515 N90-24362

ANEMOMETERS
NT DRAG FORCE ANEMOMETERS
NT HOT-FILM ANEMOMETERS
NT HOT-WIRE ANEMOMETERS
NT LASER ANEMOMETERS
NT SONIC ANEMOMETERS
Miniature laser Doppler anemometer with a diode laser
[ISL-CO-224/88] 08 p1077 N90-16232

ANEMOMETRY
U VELOCITY MEASUREMENT

ANGLE OF ATTACK
NT ZERO ANGLE OF ATTACK
Basic studies of the unsteady flow past high angle of attack airfoils
[AD-A210252] 01 p0002 N90-10008
Analysis of flight data from a High-Incidence Research Model by system identification methods
[NASA-TP-2940] 01 p0015 N90-10074
A computational/experimental study of the flow around a body of revolution at angle of attack
[NASA-TM-88329] 02 p0219 N90-11254
Normal-force-curve and pitching-moment-curve slopes of forebody-cylinder combinations at zero angle of attack for Mach numbers up to 5
[ESDU-89008] 03 p0301 N90-11709
Flutter clearance of the F-18 high-angle-of-attack research vehicle with experimental wingtip instrumentation pods
[NASA-TM-4148] 03 p0305 N90-11732
Prediction of unsteady blade surface pressures on an advanced propeller at an angle of attack
[NASA-TM-102374] 04 p0447 N90-12560
Normal force, pitching moment, and side force of forebody-cylinder combinations for angles of attack up to 90 degrees and Mach numbers up to 5
[ESDU-89014] 06 p0718 N90-14192
Stability of a supersonic boundary layer on a sharp cone at a small angle of attack 06 p0775 N90-14510
Flow visualization of the effect of pitch rate on the vortex development on the scale model of a F-18 fighter aircraft
[AD-A214244] 07 p0876 N90-15080
Body effect on wing angle of attack and pitching moment at zero lift at low speeds
[ESDU-89042] 09 p1167 N90-16757
Preliminary results from a subsonic high angle-of-attack flush airdata sensing (HI-FADS) system: Design, calibration, and flight test evaluation
[NASA-TM-101713] 09 p1168 N90-16758
Dynamic derivatives of missiles and fighter-type configurations at high angles of attack
10 p1306 N90-17554
Unsteady Euler analysis of the flow field of a propfan at an angle of attack
[NASA-TM-102426] 10 p1426 N90-18229
Static and rotational aerodynamic data from 0 deg to 90 deg angle of attack for a series of basic and altered forebody shapes
[AD-A216582] 11 p1451 N90-18361
Influence of forebody geometry on aerodynamic characteristics and a design guide for defining departure/spin resistant forebody configurations
[AD-A216714] 11 p1456 N90-18388
Application of variable-gain output feedback for high-alpha control
[NASA-TM-102603] 11 p1484 N90-18434
Unsteady aerodynamics of delta wings performing maneuvers to high angle of attack
12 p1598 N90-19196
Development of a preliminary high-angle-of-attack nose-down pitch control requirement for high-performance aircraft
[NASA-TM-101684] 12 p1600 N90-19206
F-15B high angle-of-attack phenomena and spin prediction using bifurcation analysis
[AD-A217366] 13 p1754 N90-20073
Numerical simulation of hypersonic flow around a space plane. Part 2: Application to high angles of attack flow
[NAL-TR-1011T] 15 p2045 N90-21726
Flowfield measurements in the wake of a missile at high angle of attack
[AD-A219645] 17 p2345 N90-23351
An experimental investigation of support strut interference on a three-percent fighter model at high angles of attack
[AD-A219793] 17 p2345 N90-23353
Nonaxisymmetric body, supersonic, inviscid dynamic derivative prediction
[AD-A220839] 17 p2346 N90-23358

An experimental and theoretical investigation of the flow over plane delta wings with supersonic leading edges
[LR-586] 19 p2555 N90-25114
Qualitative evaluation of a conformal velocity vector display for use at high angles-of-attack in fighter aircraft
[NASA-TM-102629] 20 p2809 N90-25981
AM-X high incidence trials, development and results
[ETN-90-97277] 20 p2814 N90-26016
The role of C(sub n beta,dyn) in the aircraft stability at high angles of attack
[AD-A221586] 21 p2961 N90-26833
Control research in the NASA high-alpha technology program 23 p3272 N90-28516
Development of non-conventional control methods for high angle of attack flight using vortex manipulation 23 p3273 N90-28522
Control of vortex aerodynamics at high angles of attack 23 p3273 N90-28523
Aerodynamic parameters of High-Angle-of Attack Research Vehicle (HARV) estimated from flight data
[NASA-TM-102692] 23 p3283 N90-28578

ANGLES (GEOMETRY)
NT ANGLE OF ATTACK
NT BRAGG ANGLE
NT DIHEDRAL ANGLE
NT ELEVATION ANGLE
NT LEADING EDGE SWEEP
NT LOOK ANGLES (ELECTRONICS)
NT SWEEP ANGLE
NT ZERO ANGLE OF ATTACK
Some computational properties of rotation representations
[AD-A213888] 07 p0981 N90-15665
Angle of arrival detection through analysis of optical fiber intensity patterns
[AD-A215421] 09 p1218 N90-17065
Preliminary experimental measurement of isoplanatic angle
[AD-A215828] 10 p1407 N90-18115
Angle estimation in the presence of mainbeam interference
[AD-A216832] 11 p1498 N90-18621
Angle measurements using the laser gyro GG 1342
[DLR-FB-89-50] 18 p2555 N90-24579
Image of the angle by partially coherent lighting: Calculations and experiments
[ETN-90-96505] 18 p2616 N90-24900
Device and method for detecting and displaying crossover pattern in precision winding
[AD-D014539] 19 p2685 N90-25276
Laser radar angular tracking
[AD-A222741] 20 p2869 N90-26319
Small angle generating apparatus
[AD-D014467] 22 p3246 N90-28408

ANGULAR ACCELERATION
Dynamic interactions and globally optimal maneuver of distributed systems 09 p1236 N90-17172
Design and testing of a noninteracting control loop for the dynamically tuned dry gyro
[NAL-TR-1017] 13 p1803 N90-20350
Sliding control of pointing and tracking with operator spline estimation 16 p2281 N90-22997
Risk of cervical injury in real and simulated accidents 19 p2721 N90-25475
Special test and evaluation methods used for a nine-axis accelerometer
[PB90-209578] 23 p3329 N90-28822
Short period control using angular acceleration feedback: Compensation for first lag servo
[NAL-TM-600] 24 p3435 N90-29399

ANGULAR CORRELATION
Perturbed angular correlations in zirconia ceramics
[DE89-017272] 06 p0751 N90-14369
Angular correlation studies in noble gases 11 p1557 N90-18972
The effects on antenna-filtered scintillation parameters of non-zero antenna pointing angles
[AD-A223840] 24 p3462 N90-29554

ANGULAR DISTRIBUTION
A study of recoil protons in ultra-relativistic nucleus-nucleus collisions
[LUIP-8907] 06 p0838 N90-14873
Studies of elastic scattering and cross sections of the C-12 + Si-28 system
[DE89-635990] 08 p1120 N90-16486
Determination of solar flare accelerated ion angular distributions from SMM gamma ray and neutron measurements and determination of the He-3/H ratio in the solar photosphere from SMM gamma ray measurements
[NASA-CR-186038] 08 p1153 N90-16676
Fluctuations in cosmic background radiation
[INPE-4579-PRE/1313] 23 p3415 N90-29294

ANGULAR MOMENTUM
Electron-positron momentum distribution measurements of high-T superconductors and related systems
[DE90-002974] 07 p0999 N90-15780
Lower limit for the average angular momentum leading to fusion
[DE90-004027] 08 p1126 N90-16523
Accretion flows in high mass star formation
[DE90-007251] 12 p1744 N90-20027
US-Japan Workshop on Atomic Collisions in Solids: Abstracts of lectures
[DE90-008979] 14 p2025 N90-21611
Automated angular momentum recoupling algebra
[DE90-011988] 19 p2750 N90-25626

ANGULAR MOTION
U ANGULAR VELOCITY

ANGULAR RESOLUTION
Angle estimation in a multipath environment with an eight element linear array operating at 10.5 GHz
[FEL-1989-15] 04 p0491 N90-12826
Faster Phong shading via angular interpolation
[CWI-CS-R8909] 04 p0543 N90-13156
Design of a large angular aperture TeO2 acousto-optic tunable filter
[AD-A213999] 07 p0993 N90-15738
CIS-2 analyzer derivation of hardware parameters
[IFSI-89-13] 08 p1077 N90-16230
Enhanced resolution particle size distributions by multiple angle photon correlation spectroscopy 09 p1223 N90-17094
Perceived orientation, spatial layout and the geometry of pictures 16 p2269 N90-22933
Angle measurements using the laser gyro GG 1342
[DLR-FB-89-50] 18 p2555 N90-24579
The target pursuit of Giotto camera
[ETN-90-96496] 18 p2555 N90-24581

ANGULAR VELOCITY
Hybrid angular velocity reference system for the investigation of dynamic properties of strapdown gryos
[DFVLR-FB-89-25] 04 p0450 N90-12577
RTSIN1: A model of a strapdown INS on a two-axis rate table
[AD-A212406] 04 p0450 N90-12579
Extension to Eulers's theorem to n-dimensional spaces 05 p0589 N90-13431
Kinematic and kinetic analyses of drop landings 14 p2010 N90-21517
Sliding control of pointing and tracking with operator spline estimation 16 p2281 N90-22997
Nonaxisymmetric body, supersonic, inviscid dynamic derivative prediction
[AD-A220839] 17 p2346 N90-23358
Construction of a hybrid angular velocity reference system for investigation of the dynamic characteristics of strapdown gyros
[ESA-TT-1181] 19 p2694 N90-25332
Small angle generating apparatus
[AD-D014467] 22 p3246 N90-28408

ANHYDRIDES
NT PEROXIDES
Novel polyimide compositions based on 4,4': Isophthaloyldiphthalic anaydride (IDPA)
[NASA-CASE-LAR-14194-1] 07 p0890 N90-15148
Wet spinning of solid polyamic acid fibers
[NASA-CASE-LAR-14162-1] 07 p0910 N90-15259
LARC-IA: A flexible backbone polyimide
[NASA-TM-102586] 09 p1196 N90-16926
Copolyimide with a combination of flexibilizing groups
[NASA-CASE-LAR-13821-1] 09 p1199 N90-16950
Initiation precursors and initiators in laser-induced copolymerization of styrene and maleic anhydride in acetone
[NASA-TM-4166] 10 p1346 N90-17810
Modified maleic anhydride copolymers as e-beam resists
[AD-A218470] 16 p2223 N90-22679
Substituted 1,1,1-triaryl-2,2,2-trifluoroethanes and processes for their synthesis
[NASA-CASE-LEW-14345-2] 17 p2371 N90-23497
Molecular structure of interphases between DGEBA/BTDA adhesives and silver substances using surface-enhanced Raman scattering
[AD-A222750] 20 p2841 N90-26157
Aromatic polyimides containing a dimethylsilane-linked dianhydride
[NASA-CASE-LAR-14198-1] 21 p2984 N90-26956

ANILINE
Rechargeable lithium/polymer cathode batteries
[AD-A210978] 01 p0062 N90-10354
Transport studies of conducting polymers 02 p0200 N90-11140
Cell performance of ultra-thin polymer cathode system: Theoretical energy and power density projections
[AD-A210786] 02 p0202 N90-11151
Electroactive polyaniline film deposited from non-aqueous media. 2: Effect of acid concentration in solutions
[AD-A212084] 04 p0477 N90-12737
Quartz crystal microbalance analysis: Partial cation release during oxidation of conducting polymers
[AD-A221091] 18 p2530 N90-24439
Characterization of a solid-state microelectrochemical diode employing a poly(vinyl alcohol)/phosphoric acid solid-state electrolyte: Rectification at junctions between WO3 and polyaniline
[AD-A222025] 21 p3000 N90-27054
Potential dependence of the conductivity of highly oxidized polythiophenes, polypyrroles, and polyaniline: Finite windows of high conductivity
[AD-A222024] 22 p3159 N90-27912

ANIMALS
NT AMPHIBIA
NT BIRDS
NT COCKROACHES
NT DROSOPHILA
NT FISHES
NT FROGS
NT HUMAN BEINGS
NT INSECTS
NT MAMMALS
NT MANATEES
NT MICE
NT MONKEYS
NT PRIMATES
NT RATS
NT RODENTS
ELF (Extremely Low Frequency) communications system ecological monitoring program: Summary of 1988 progress
[AD-A216153] 10 p1377 N90-17981
Bioelectromagnetic effects of the Electromagnetic Pulse (EMP)
[AD-A221552] 21 p3033 N90-27243

ANIMATION
NT COMPUTER ANIMATION

ANIONS
Quartz crystal microbalance analysis. 1: Evidence of anion or cation insertion into electropolymerized conducting polymers
[AD-A212304] 04 p0480 N90-12755
The effects of trace anions on the voltammetry of single crystal gold surfaces
[AD-A211886] 04 p0558 N90-13254
Cell performance of ultra-thin polymer cathode systems. Part 1: Anion intercalating polymer cathode
[AD-A216037] 11 p1501 N90-18639
Threshold photodetachment spectroscopy of the I + HI transition state region
[AD-A218410] 16 p2260 N90-22883
Cation and anion tracer diffusion in YBa(sub 2)Cu(sub 3)O(sub 7-delta)
[DE90-009708] 18 p2620 N90-24927
Peak analysis in gas chromatography and the development of new stationary phases for anion chromatography
[DE90-014428] 23 p3304 N90-28687

ANISOTROPIC FLUIDS
The supersonic anisotropic collapse of Langmuir waves 06 p0783 N90-14550
Towards a two dimensional scheme of anisotropic Godunov type. On the calculation of the velocity of the nodes in the multidimensional Lagrangian codes
[ETN-90-97458] 22 p3175 N90-28017
Towards a two dimensional code of anisotropic Godunov type 22 p3175 N90-28018

ANISOTROPIC MEDIA
NT ANISOTROPIC FLUIDS
Direction-dependent stopping power and beam deflection in anisotropic solids
[DE90-001076] 06 p0840 N90-14883
Geometrical optics in inhomogeneous chiral media with application to polarization correction in inhomogeneous lens antennas
[PB90-110669] 08 p1122 N90-16497
Transport properties of anisotropic superconductors 15 p2170 N90-22404
Transient electromagnetic scattering on anisotropic media
[DE90-011802] 19 p2683 N90-25262

ANISOTROPIC PLATES
Nonlinear collapse simulation of anisotropic plates and corrugated panels 02 p0183 N90-11035
Measuring of the complete stiffness matrix for anisotropic laminated materials
[DLR-MITT-89-11] 05 p0618 N90-13606
Measuring of the complete stiffness matrix for anisotropic laminated materials
[DLR-MITT-89-12] 05 p0618 N90-13607

Modeling of composite beams and plates for static and dynamic analysis
[NASA-CR-186459] 20 p2874 N90-26354
Structural analysis and optimum design of geodesically stiffened composite panels
[NASA-CR-186944] 23 p3337 N90-28862

ANISOTROPIC SHELLS
Nonlinear collapse simulation of anisotropic plates and corrugated panels 02 p0183 N90-11035
Modeling and analysis of the space shuttle nose-gear tire with semianalytic finite elements
[NASA-TP-2977] 12 p1670 N90-19595
ANILISA: Computational module for Koiter's imperfection sensitivity theory
[LR-582] 15 p2119 N90-22119
Derivation of the governing equations of anisotropic conical shells
[LR-609] 19 p2704 N90-25387
Buckling of anisotropic cylindrical shells subjected to combined axial compression, normal pressure, bending and shear loading
[LR-611] 24 p3482 N90-29678

ANISOTROPY
NT ELASTIC ANISOTROPY
NT PLASTIC ANISOTROPY
International seminar on the inelastic behavior of solids: Models and utilization
[DE89-017420] 03 p0327 N90-11858
Anisotropy and microstructure of high-coercivity rare earth permanent magnets
[AD-A211905] 03 p0399 N90-12285
Development of texture analysis and its applications to titanium aero engine components
[PNR90561] 04 p0454 N90-12602
A cell-centered multigrid method for three-dimensional anisotropic-diffusion and interface problems
[REPT-89-35] 04 p0540 N90-13128
SWAN: A study of solar wind anisotropies 04 p0568 N90-13312
A four channel He-3 cooled balloon-borne bolometer radiometer 05 p0597 N90-13469
Anisotropy of electron distributions related to the anisotropy and polarization of the continuous emitted x rays 06 p0785 N90-14566
Anisotropy of oxygen tracer diffusion in YBa2Cu3O7-delta single crystals
[DE90-001931] 06 p0856 N90-14979
Multigrid methods for two- and three-dimensional Poisson-type equations on the sphere
[GMD-391] 08 p1117 N90-16468
Anisotropy and microstructure of high coercivity rare earth iron permanent magnets, list of papers published
[AD-A214160] 08 p1118 N90-16476
The modified Ginzburg-Landau theory for anisotropic high temperature superconductors
[DE89-635909] 08 p1128 N90-16532
Production of photons in anisotropic spacetimes
[DE90-600760] 08 p1135 N90-16576
Impingement characteristics of heated plane turbulent jets 09 p1215 N90-17047
Transient elastic waves on anisotropic half-spaces 10 p1396 N90-18074
Anisotropy and dimensionality in untwinned crystals of YBa2Cu3O(7-delta)
[DE90-004890] 10 p1436 N90-18287
Analysis of linear multigrid methods for elliptic differential equations with discontinuous and anisotropic coefficients
[ETN-90-96269] 11 p1553 N90-18944
Integrated optics anisotropic waveguides and devices
[AD-A217064] 12 p1715 N90-19849
The COBE cosmic 3 K anisotropy experiment: A gravity wave and cosmic string probe 12 p1732 N90-19959
Search for anisotropies in the underground cosmic ray muon flux 12 p1745 N90-20034
Shaping the insonifying pulse to optimise B-scans obtained in austenite
[AERE-R-13518] 13 p1775 N90-20187
Scattering sources: A spherical harmonics expansion
[DE90-008724] 13 p1867 N90-20711
Specific heat and critical fluctuations in anisotropic high-T(sub c) oxide superconductors
[DE90-613394] 14 p2031 N90-21651
Transport and relaxation properties in anisotropic superconductors 15 p2170 N90-22403
Effect on relaxation on nonlinear waves in crystals 16 p2310 N90-23165
Anisotropic inflation 16 p2331 N90-23286
Three-dimensional structure of plane mixing layers 17 p2344 N90-23347
Modelling and control of a balloon borne stabilized platform 17 p2355 N90-23408
Diffusion in lattices with anisotropic scatterers
[CWI-AM-R8921] 18 p2599 N90-24792
Investigations of ultrasonic wave interactions at imperfect boundaries separating anisotropic materials
[DE90-010061] 18 p2612 N90-24875
Large scale structure and microwave background anisotropies in cosmological models and stellar photometry techniques with the wide field/planetary camera of the Hubble space telescope 18 p2637 N90-25023
The yield and post-yield behavior of high-density polyethylene
[NASA-CR-186574] 19 p2676 N90-25219
Transient electromagnetic scattering on anisotropic media
[DE90-011802] 19 p2683 N90-25262
An approach for relating the results of quantitative nondestructive evaluation to intrinsic properties of high-performance materials
[NASA-CR-186484] 19 p2699 N90-25355
Earth radiation budget measurements from space 19 p2707 N90-25404
Reflection indicatrices of natural surfaces for AVHRR channels 1 and 2
[ESA-TT-1192] 19 p2709 N90-25417
Theory of circular dielectric waveguide with anisotropic sheet cover
[NASA-CR-186883] 20 p2855 N90-26235
High speed magneto-resistive random access memory
[NASA-CASE-NPO-17954-1-CU] 20 p2904 N90-26519
A comment on anisotropic spheres admitting one parameter group of conformal motions
[DE90-627195] 23 p3403 N90-29230
Evaluation of ARALL-4: An aramid fiber reinforced aluminum
[AD-A223502] 24 p3443 N90-29443
Ionospheric irregularities: Source, structure, plasma processes and effects on sensor systems
[AD-A223908] 24 p3490 N90-29723
Superconductivity and information exchange
[DE90-015767] 24 p3554 N90-30110

ANNEALING
NT LASER ANNEALING
Gaussmeter determination of 302 stainless steel material condition
[BDX-613-3941] 01 p0044 N90-10249
The effects of normal annealing cycles during IGFET fabrication on initial and radiation induced gate insulator defects
[AD-A210282] 01 p0049 N90-10278
Characterization of GaAs/Si/GaAs heterointerfaces
[DE89-016302] 01 p0131 N90-10752
Methods to decrease defect density in GaAs/Si heteroepitaxy
[DE89-016306] 01 p0131 N90-10753
Thin section casting program. Volume 4: Static cast product bending, straightening, and rolling
[DE89-009034] 02 p0210 N90-11202
Ion beam annealing of Ga-implanted Si
[DE89-016857] 02 p0282 N90-11610
On-orbit annealing of gallium arsenide solar cell arrays
[AD-A212087] 03 p0334 N90-11900
Effect of annealing conditions on the structural and superconducting properties of Y-Ba-Cu-O films
[AD-A211308] 03 p0413 N90-12371
Study of palladium and chromium silicides formation in liquid phase and in solid phase
[LAAS-89040] 04 p0470 N90-12695
Note on the convergence of simulated annealing algorithms
[MEMO-774] 04 p0544 N90-13162
Global optimization and simulated annealing
[MEMO-COSOR-88-21] 05 p0690 N90-14025
Unified model of charge build up and annealing of oxide charge and interface states in SiO2 due to stress
[HMI-B-465] 05 p0704 N90-14120
SEM (Scanning Electron Microscope) image analysis of grain growth in microwave-annealed alumina
[DE90-001606] 06 p0746 N90-14339
Research on mercury cadmium telluride
[AD-A213924] 07 p0906 N90-15237
Sintering studies on high field varistors
[DE90-002626] 07 p0926 N90-15359
Partial reduction of re-oxidation processing of Y-Ba-Cu-O sputtered thin films
[DE90-003655] 07 p0999 N90-15782
Processing and fabrication of YBa2Cu4O8 and YBa2Cu4O8/YBa2Cu3O(x) composites
[DE90-003559] 07 p1001 N90-15789
Defect control and denuded trap zones in the 3-5 semiconductors
[AD-A214099] 07 p1004 N90-15814
Irradiation creep and swelling of annealed type 304L stainless steel at approximately 390 C and high neutron fluence
[DE90-004521] 08 p1046 N90-16047
The influence of residual contamination on the structure and properties of metal/GaAs interfaces
[DE90-000549] 08 p1127 N90-16530
Ion beam annealing of Si co-implanted with Ga and As
[DE90-004297] 08 p1132 N90-16556
The growth of epitaxial GaAs and GaAlAs on silicon substrates by OMVPE
[AD-A214642] 09 p1288 N90-17469
Computer simulation of electromigration in thin films
[AD-A216382] 10 p1357 N90-17867
Materials processing of diamond: Etching, doping by ion implantation and contact formation
[AD-A216530] 10 p1438 N90-18301
Structure and reactivity of model thin film catalysts
[DE90-007365] 11 p1485 N90-18546
Effect of electron-excitation on radiation damage in ion-irradiated FCC metals
[DE90-719537] 12 p1626 N90-19344
Silicon carbide semiconductor device fabrication and characterization
[NASA-CR-186354] 12 p1719 N90-19873
Systematics in positron annihilation lifetime analysis of high (Tc) superconducting transitions
[DE90-008361] 13 p1896 N90-20884
Formation of subsurface aluminum layers in beryllium by ion implantation and post-implant annealing
[DE90-007975] 14 p1951 N90-21172
Proceedings of the Joint NOSC/NRL (Naval Ocean Systems Center/Naval Research Laboratory) InP Microwave/Millimeter Wave Technology Workshop
[AD-A218216] 14 p1966 N90-21259
Hydrogenation of stainless steels implanted with nitrogen
[DE90-617397] 16 p2221 N90-22666
Low temperature degradation of Y-TZP materials
[AD-A218841] 16 p2223 N90-22684
Lateral spreading of Au contacts on InP
[NASA-TM-103133] 16 p2252 N90-22843
Preliminary investigation into the effect of high temperature thermal anneals on the figure of merit of silicon germanium alloys
[AD-A218573] 17 p2375 N90-23527
The origin of multiple melting in polyurethane block copolymers
[AD-A220050] 17 p2381 N90-23563
Fundamental and applied aspects of defect engineering in G2As; EL2 and other nonstoichiometric defects
[AD-A218597] 17 p2475 N90-24152
Minimizing distortion and internal forces in truss structures by simulated annealing 18 p2644 N90-25055
Fabricating vanadium sheet to improve symmetry of drawn parts
[DE90-011253] 19 p2682 N90-25257
Parallelization of an annealing simulation applied to improving tetrahedric grids
[IMAG-RR-796-M] 20 p2913 N90-26570
Rapid thermal processing: A study of the silicon oxidation and of the implanted boron activation
[LAAS-90051] 20 p2932 N90-26681
Ellipsometric study of YBa2Cu3O(7-x) laser ablated and co-evaporated films
[NASA-TM-103223] 20 p2932 N90-26682
The effect of processing, deformation and annealing on the microstructure of Y1Ba2Cu3O7-(sub delta)
[DE90-011731] 21 p3079 N90-27510
Rapid annealing of iron implanted Hg(1-x)Cd(x)Te
[AD-A222777] 21 p3082 N90-27524
Microstructure and magnetization of doped Y-Ba-Ca-O materials prepared by melt quench and post annealing method 22 p3138 N90-27803
Preparation and characteristics of superconducting cuprate thin films: Nd(2-x)Ce(x)CuO4 and substituted Bi-system 22 p3140 N90-27813
Transient annealing characterization of irradiated MOSFETS
[AD-A223877] 23 p3401 N90-29220
Research on mercury cadmium telluride
[AD-A224250] 24 p3448 N90-29474
Ion-beam mixing of Fe/B layers for tribological applications
[DE90-010091] 24 p3456 N90-29518
Synthesis and property evaluation of Y-Ba2-Cu3-O(6+x) superconductors
[AD-A223494] 24 p3552 N90-30095

ANNIHILATION REACTIONS
NT POSITRON ANNIHILATION
Femtosecond dynamics of fluoro-aluminum phthalocyanine and linear alkane molecules
[AD-A210939] 01 p0133 N90-10766
Minimal total cross section for e(+)e(-) yields W(+)W(-)
[NIKHEF-H/88-12] 04 p0553 N90-13222
Model-independent analysis of the Z line shape in e+e- annihilation
[PREPRINT-679] 05 p0698 N90-14089

Unitarity limits on the mass and radius of dark matter particles
[NASA-CR-186079] 05 p0713 N90-14164
Gamma ray lines from dark matter annihilation
[DE90-000779] 06 p0864 N90-15021
Annihilation in Gases and Galaxies
[NASA-CP-3058] 11 p1555 N90-18957
Angular correlation studies in noble gases
11 p1557 N90-18972
Total cross sections for positrons scattered elastically from helium based on new measurements of total ionization cross sections 11 p1558 N90-18976
Multiple-ionization of xenon atoms by positron impact
11 p1558 N90-18978
Positron annihilation in gamma-ray bursts
11 p1559 N90-18983
Annihilation physics of exotic galactic dark matter particles 11 p1559 N90-18984
Optically excited states in positronium
11 p1559 N90-18985
Antiproton-matter interactions in antiproton applications 11 p1560 N90-18989
Positron-molecule bound states and positive ion production 11 p1561 N90-18994
Dislocation annihilation mechanism for the formation of dislocation free zone at a crack tip
[DE90-610552] 12 p1674 N90-19615
The effects of cold dark matter on Big Bang nucleosynthesis 12 p1698 N90-19749
Gamma ray cosmology: The extra galactic gamma spectrum and methods to detect the underlying source
16 p2337 N90-23321
Feasibility for EGRET detection of antimatter concentrations in the universe 16 p2338 N90-23323
Molecular dynamics of physical aging processes in polymer glasses (experiment and theory)
[AD-A222848] 21 p2984 N90-26959
Slow positron beam generator for lifetime studies
[NASA-CASE-LAR-14250-1-SB]
21 p3073 N90-27472
High temperature surface interactions: Overview
23 p3306 N90-28699

ANNOTATIONS
Medical subject headings: Annotated alphabetic list, 1990
[PB90-100009] 14 p2036 N90-21683

ANNUAL VARIATIONS
ELF (Extremely Low Frequency) Communications System Ecological Monitoring Program: Electromagnetic field measurements and engineering support, 1988
[AD-A210200] 01 p0056 N90-10321
A seasonal isotherm depth climatology for the eastern tropical Pacific
[PB89-193577] 01 p0090 N90-10512
Diagnostic study of atmosphere-terrain interaction leading to the formation of dust clouds and poor visibilities over near east desert areas
[AD-A211243] 02 p0239 N90-11358
Average diurnal and seasonal profiles of ionospheric storms 02 p0241 N90-11371
Solar radiation in Linkoeping (Sweden): Variations over half a year in irradiance and spectral composition in the interval 400-1000 nm
[FOA-C-30521-3.1] 02 p0250 N90-11417
Atlas of tropical sea surface temperature and surface winds
[PB89-223598] 04 p0521 N90-13009
An evaluation of trend detection techniques for use in water quality monitoring programs
[PB89-100058] 06 p0808 N90-14702
Climatology of Lawrence Livermore National Laboratory
[DE90-000905] 06 p0818 N90-14756
Distribution and seasonal variations of diffuse fraction
[DE90-601303] 09 p1246 N90-17228
Rain attenuation measurements: Variability and data quality assessment 10 p1373 N90-17955
US Navy regional climatic study of the Central East Asian coast and associated waters
[AD-A217448] 13 p1844 N90-20587
Use of microwave satellite data to study variations in rainfall over the Indian Ocean
[NASA-CR-186408] 14 p2007 N90-21501
Global and hemispheric annual temperature variations between 1861 and 1988
[DE90-007993] 16 p2257 N90-22869
Seasonal weather forecast verification
[DE90-009467] 17 p2425 N90-23818
A numerical study of the seasonal variability of the Somali current
[AD-A220708] 17 p2427 N90-23829
Trace metal sources for the atlantic inflow to the Mediterranean Sea
[AD-A218607] 17 p2429 N90-23842
In-band amplitude dispersion on a microwave link
20 p2846 N90-26189
Annual and interannual variations of Earth-emitted radiation based on a 10-year data set
[NASA-TM-103465] 20 p2887 N90-26432
An intercomparison of intraseasonal variability in general circulation models and observations
[NASA-TM-100764] 21 p3030 N90-27228
Relationship between solar activities and thunderstorm activities in the Beijing area and the northeast region of China 22 p3208 N90-28197
Seasonal and interannual changes in cirrus
22 p3222 N90-28272
Annual course of precipitation over much of the US: Observed versus GCM simulation
[PB90-221656] 23 p3352 N90-28942
An observational study of the circulation in the Southern Hemisphere stratosphere 24 p3488 N90-29715

ANNULAR FLOW
Decay of secondary flow and the associated loss variation downstream of an annual turbine stator cascade
[DE90-505520] 20 p2809 N90-25984

ANNULAR NOZZLES
Characterization of plasma flow through magnetic nozzles
[AD-A221044] 18 p2617 N90-24905

ANNULI
Green's functions for the elastic annulus and their application to various crack problems
15 p2120 N90-22129
On the natural frequencies of a short circular cylinder, including the effects of entrained mass
[LR-602] 19 p2704 N90-25383

ANODES
NT CELL ANODES
NT TUBE ANODES
Plasma-anode electron gun research
[AD-A211547] 03 p0312 N90-11773
Interfacial effects in monolithic solid oxide fuel cells
[DE90-001914] 06 p0806 N90-14690
Development of the RAIDS (Remote Atmospheric and Ionospheric Detector System) extreme ultraviolet wedge and strip detector
[AD-A213730] 07 p0949 N90-15495
Cost and energy consumption estimates for the aluminum-air battery anode fuel cycle
[DE90-005810] 11 p1503 N90-18656
Anode plasma formation as a possible mechanism for an electrical stress limit in cold cathode diodes
[DE90-007503] 12 p1655 N90-19516
Impedance studies of Ni/Cd and Ni/H2 cells using the cell case as a reference electrode
13 p1824 N90-20473
The development of a simulation program of the anode side for aluminum/air batteries
[PB90-165754] 14 p1970 N90-21286
Development of planar geometry solid oxide fuel cell technology, phase 2
[PB90-131293] 14 p2001 N90-21467
Anode materials for electrochemical waste destruction
18 p2514 N90-24354
Geometric effects in applied-field MPD thrusters
[NASA-TM-103259] 22 p3134 N90-27782

ANODIC COATINGS
Electrochemistry at very small electrodes
[AD-A213158] 05 p0621 N90-13823
Study of metal-insulator-semiconductor structures on indium phosphide, implemented by anodic oxidation
[ECL-88-10] 05 p0703 N90-14114
Corrosion control through a better understanding of the metallic substrate/organic coating interface
[AD-A220432] 17 p2377 N90-23533
Corrosion protection of metal matrix composites
[AD-A222951] 21 p2971 N90-26888
Research on mercury cadmium telluride
[AD-A224250] 24 p3448 N90-29474

ANODIZING
The corrosion protection of 6061-T6 aluminum by a polyurethane-sealed anodized coat
[NASA-TM-100394] 14 p1955 N90-21191

ANOMALIES
NT GRAVITY ANOMALIES
NT MAGNETIC ANOMALIES
Semi-monthly temperature and geopotential anomaly in the upper 500 meters along the Oahu-Farallon Islands great circle from November 15, 1967 through December 15, 1979
[AD-A210640] 01 p0091 N90-10518
Quantization of anomalous gauge theories on a lattice
[DE89-010247] 01 p0135 N90-10776
Device for inspection of materials by eddy current methods
[AD-D014205] 04 p0511 N90-12948
Research on mercury cadmium telluride
[AD-A213924] 07 p0906 N90-15237
Multiple flow regimes in the Northern Hemisphere winter 08 p1100 N90-16372
Phonon anomaly at T(sub c) in (Y/ER)Ba2Cu3O(7-delta)
[DE90-003562] 08 p1129 N90-16539
Spacecraft environmental anomalies handbook
[NASA-CR-186331] 09 p1182 N90-16852
Phonon dispersion and Kohn anomalies in the alloy Cu(0.84)Al(0.16)
[DE90-005578] 10 p1428 N90-18239
BRS current and related anomalies in two-dimensional gravity and string theories
[DE90-733095] 10 p1440 N90-18307
Process development and fabrication of space station type aluminum-clad graphite epoxy struts
[NASA-CR-181873] 11 p1468 N90-18454
Technique for evaluating the erosive properties of ablative internal insulation materials
11 p1471 N90-18466
A homotopy approach to the solutions of minimum-fuel space-flight rendezvous problems
14 p1931 N90-21053
MHD modes driven by anomalous electron viscosity and their role in fast sawtooth crashes
[DE90-009311] 14 p2029 N90-21639
Southern oscillation simulation in coupled ocean/atmosphere global climate models
15 p2131 N90-22181
Tropopause undulations and the development of extratropical cyclones 15 p2132 N90-22186
Low temperature properties of amorphous solids
15 p2171 N90-22405
The Al-26(rho, gamma)Si-27 reaction: Stellar origins of galactic Al-26 15 p2188 N90-22498
Tropical-extratropical interaction in a model atmosphere 17 p2422 N90-23800
An analytic/empirical model of the middle and low latitude ionosphere
[AD-A220004] 17 p2423 N90-23809
Communications and tracking expert systems study
[NASA-CR-185935] 21 p2992 N90-27004
The basis for facility comparison
22 p3118 N90-27713
Study of anomalies in transition vegetation in Alto Xingo-NT, through remote sensing techniques
[INPE-4601-TDL/334] 23 p3343 N90-28891
Causal simulation and sensor planning in predictive monitoring 23 p3369 N90-29037
Systematic approach to critical phenomena by the extended variational method and coherent-anomaly method
[DE90-627320] 23 p3392 N90-29185
Omega navigation signal characteristics
24 p3429 N90-29369
Modeling and reconstruction algorithms for detection, location, and identification of subsurface anomalies
[AD-A224358] 24 p3459 N90-29539

ANOXIA
Synergistic effects of nitrogen dioxide and carbon dioxide following acute inhalation exposures in rats
[PB89-214779] 03 p0377 N90-12150
The importance of pathophysiological parameters in fire modelling of aircraft accidents 10 p1317 N90-17618

ANTARCTIC ENVIRONMENT
U ICE ENVIRONMENTS

ANTARCTIC OCEAN
The sea ice margins: A summary of physical phenomena
[PB89-212328] 02 p0253 N90-11436

ANTARCTIC REGIONS
NT ROSS ICE SHELF
Improving snow roads and airstrips in Antarctica
[AD-A211588] 03 p0335 N90-11907
Ice runways near the South Pole
[AD-A211606] 03 p0335 N90-11908
Antarctic surface temperature and pressure data
[DE90-000971] 07 p0963 N90-15565
Environmental impact statement on the US Antarctic program
[DE90-004940] 09 p1245 N90-17221
Guide to the US collection of antarctic meteorites 1976-1988 (everything you wanted to know about the meteorite collection). Antarctic Meteorite Newsletter, Volume 13, Number 1
[NASA-TM-101939] 09 p1299 N90-17526
Psychophysiological correlates of human adaptation in antarctica
[AD-A216879] 10 p1412 N90-18142
An application of ocean wave-current refraction to the gulf stream using SEASAT SAR data
[AD-A216769] 11 p1537 N90-18851
Gravity field of the Western Weddell Sea: Comparison of airborne gravity and Geosat derived gravity
13 p1833 N90-20526
Satellite radar altimetry over ice. Volume 1: Processing and corrections of Seasat data over Greenland
[NASA-RP-1233-VOL-1] 13 p1840 N90-20562

Satellite radar altimetry over ice. Volume 4: Users' guide for Antarctica elevation data from Seasat
[NASA-RP-1233-VOL-4] 13 p1840 N90-20564
Opportunities for US-USSR cooperation in the investigation of Arctic stratospheric ozone
15 p2125 N90-22154
Site visit to US Antarctic Program (USAP) facilities and the Research Vessel Polar Duke
[DE90-009396] 15 p2126 N90-22159
JARE data reports, no. 140 (meteorology 21): Meteorological data at Asuka Camp, Antarctica in 1987
[ISSN-0075-3343] 15 p2132 N90-22188
SeaRISE: A Multidisciplinary Research Initiative to Predict Rapid Changes in Global Sea Level Caused by Collapse of Marine Ice Sheets
[NASA-CP-3075] 16 p2249 N90-22824
A study of auroral activity in the nightside polar cap
16 p2254 N90-22852
The analysis of polar clouds from AVHRR satellite data using pattern recognition techniques
[NASA-CR-183300] 16 p2257 N90-22868
On the effectiveness of the production of antarctic bottom water in the Weddell and Ross Seas
[AD-A218873] 16 p2259 N90-22880
Nimbus-7 TOMS Antarctic ozone atlas: August through November, 1989
[NASA-RP-1237] 17 p2428 N90-23837
Polar prospects: A minerals treaty for Antarctica
[OTA-O-428] 17 p2480 N90-24185
Spatial cross-correlation of Antarctic Sea ice and seabed topography
[NASA-CR-186815] 20 p2891 N90-26451
Proceedings of a Workshop on Antarctic Meteorite Stranding Surfaces
[NASA-CR-186575] 20 p2942 N90-26739
Proceedings of a workshop on Differences Between Antarctic and Non-Antarctic Meteorites
[NASA-CR-184918] 20 p2942 N90-26740
Wind tunnel simulation of Antarctic snowdrifting
[PB90-184565] 22 p3212 N90-28222
Ross Sea oceanographic data, 1983-1987: USCGC GLACIER, January-February 1983; USCGC POLAR SEA, January-February 1984; USCGC POLAR STAR, February 1984; USCGC POLAR SEA, February 1987
[PB90-243932] 23 p3354 N90-28955

ANTARCTICA
U ANTARCTIC REGIONS

ANTENNA ARRAYS
NT LINEAR ARRAYS
NT STEERABLE ANTENNAS
NT YAGI ANTENNAS
Submillimeter quantum electronics
[AD-A210439] 01 p0132 N90-10762
Antenna beamforming using optical processing
[NASA-CR-180844] 02 p0212 N90-11210
An experimental SMI adaptive antenna array for weak interfering signals
[NASA-CR-185976] 02 p0212 N90-11211
Proceedings of the 1988 Antenna Applications Symposium, volume 1
[AD-A211396] 03 p0338 N90-11928
Theory and simulation of the operation of a Doppler direction finder in a multipath environment
[FEL-1988-56] 03 p0340 N90-11939
The Owens Valley solar array
03 p0435 N90-12490
Application of the moment method to the design of slotted waveguide array antennas
04 p0484 N90-12780
Adaptive antenna arrays for satellite communication
[NASA-CR-185989] 04 p0485 N90-12784
Properties of density tapered arrays
[RSRE-MEMO-4210] 04 p0489 N90-12810
Statistical density and amplitude tapered arrays
[RSRE-MEMO-4211] 04 p0490 N90-12818
Performance analysis of large adaptive sidelobe canceller arrays with reused elements
[AD-A212888] 04 p0494 N90-12841
Vehicle antenna for the mobile satellite experiment
[NASA-CR-186109] 06 p0733 N90-14271
Proceedings of the Antenna Applications Symposium, volume 2
[AD-A213815] 07 p0919 N90-15313
High resolution imaging by phase retrieval and discrimination using speckle, volume 1
[AD-A214243] 07 p0919 N90-15317
Focal plane antenna array for millimeter waves
[AD-D014306] 07 p0920 N90-15322
Investigation of broadband microstrip antenna structures for application in monolithic millimeter wave arrays
[AD-A213856] 07 p0923 N90-15344
Scannable millimeter wave arrays, volume 1
[AD-A213895] 07 p0924 N90-15347
Scannable millimeter wave arrays, volume 2
[AD-A213896] 07 p0924 N90-15348
Large-aperture sparse array detector system for multiple emitter location
[AD-D014303] 07 p0925 N90-15355
Technology of fast-wave current drive antennas
[DE90-001972] 07 p0994 N90-15747
Stripline feed for a microstrip array of patch elements with teardrop shaped probes
[NASA-CASE-NPO-17548-1-CU]
08 p1056 N90-16104
Implementation of adaptive arrays in the block oriented systems simulator
[AD-A215545] 09 p1171 N90-16774
A study of loaded microstrip antennas and their applications to arrays
[AD-A214857] 09 p1205 N90-16985
Very broad band VHF/UHF omnidirectional antenna design study
[AD-A215358] 09 p1207 N90-16997
Planar array antenna design analysis, volume 1
[AD-A215537] 09 p1207 N90-16999
Power conditioning for active array SAR antennas
10 p1338 N90-17744
Lower bounds on multiple-source direction finding in the presence of direction-dependent antenna-array-calibration errors
[AD-A215825] 10 p1376 N90-17979
Reconfigurable antennas, monolithic microwave integrated circuits with feeding networks for microstrip antennas
[AD-A216916] 11 p1498 N90-18622
An investigation of the transfer of monopulse tracking between two coherent point sources
[AD-A217007] 12 p1646 N90-19457
Effects of additional interfering signals on adaptive array performance
[NASA-CR-186508] 13 p1790 N90-20271
Performance of a 300 Mbps 1:16 serial/parallel optoelectronic receiver module
[NASA-TM-103110] 13 p1795 N90-20302
Concepts for high resolution space based SAR/ISAR systems: Preliminary design considerations
14 p1960 N90-21224
Coplanar waveguide fed phased array antenna
[NASA-TM-102522] 14 p1968 N90-21273
Optical control of an 8-element Ka-band phased array using a high-speed optoelectronic interconnect
[NASA-TM-102550] 14 p1968 N90-21275
Large space systems antenna technology
15 p2060 N90-21798
A real-time signal combining system for Ka-band feed arrays using maximum-likelihood weight estimates
15 p2076 N90-21888
The effect of mechanical deformation on the radiation patterns of large space-based arrays
[AD-A219288] 16 p2230 N90-22719
Performance of adaptive nulling antennas in a jamming environment
[AD-A219305] 16 p2230 N90-22720
Model order determination methods for autoregressive radio direction finding techniques
[AD-A220707] 17 p2350 N90-23384
Beamforming devices and feed structures for a DBS flat-plate antenna
[BBC-RD-1989/12] 17 p2386 N90-23592
Low-sidelobe phased array antenna characteristics using the planar near-field Scanning technique: Theory and experiment
[AD-A220611] 17 p2390 N90-23613
Large aperture array measurements of the vertical ambient noise field
[AD-A220165] 17 p2432 N90-23859
High performance millimeter-wave microstrip circulators and isolators
[NASA-CR-186276] 19 p2685 N90-25270
Feasibility study of a synthesis procedure for array feeds to improve radiation performance of large distorted reflector antennas
[NASA-CR-186641] 20 p2851 N90-26213
Design of an optically controlled Ka-band GaAs MMIC phased-array antenna
[NASA-TM-103147] 20 p2857 N90-26250
Planar microstrip Yagi array antenna
[NASA-CASE-NPO-17873-1-CU]
21 p2994 N90-27015
Guidance and control techniques for airborne transfer alignment and SAR motion compensation
24 p3429 N90-29372

ANTENNA COMPONENTS
NT ANTENNA FEEDS
NT DIPLEXERS
Structural problems of accurate inflatable surfaces
02 p0184 N90-11044
Dielectric covered microstrip patch antennas
[AD-A211577] 03 p0344 N90-11963
Performance effects of tie-truss modifications for a 70-meter centerline beam waveguide antenna
04 p0486 N90-12791
Investigation of broadband microstrip antenna structures for application in monolithic millimeter wave arrays
[AD-A213856] 07 p0923 N90-15344
A Communications Antenna Pointing System (CAPS): A modular approach 18 p2537 N90-24474
Precision pointing and locking capabilities combined by a linear actuator 18 p2537 N90-24475
Some remarks on a hinge actuator for large spot antenna arm deployers 18 p2539 N90-24486
Hemispherical pointing mechanism
18 p2541 N90-24502
Optical signal processing
[AD-A220332] 18 p2615 N90-24897
Analysis and design of modifications for improved performance of the AFIT radar cross section measurement chamber
[AD-A223352] 24 p3460 N90-29545

ANTENNA COUPLERS
NT DIPLEXERS

ANTENNA DESIGN
Technology for large space systems: A bibliography with indexes (supplement 21)
[NASA-SP-7046(21)] 01 p0026 N90-10130
New electrodynamic and electrostatic models with applications to antenna theory, superconductor slots, and lasers 01 p0055 N90-10316
Maximization of directed electromagnetic radiation with an optimized antenna
[DE89-014045] 01 p0056 N90-10319
TWIRE: A test program for VLF airborne transmissions
[AD-A210516] 01 p0057 N90-10324
A high precision gravity compensation system for the deployment test of the ERS-1 SAR antenna
02 p0183 N90-11038
Structural problems of accurate inflatable surfaces
02 p0184 N90-11044
Test results on conceptual models of the large deployable antenna for mobile communications satellites
02 p0185 N90-11050
ESA-D: An integrated software for antenna design and analysis 02 p0185 N90-11052
A calibrated, omnidirectional, LF loop antenna for GWEN (Ground Wave Emergency Network)
[AD-A211264] 02 p0213 N90-11221
Recent advances to NEC (Numerical Electromagnetics Code): Applications and validation
[DE89-009231] 03 p0337 N90-11917
Dielectric covered microstrip patch antennas
[AD-A211577] 03 p0344 N90-11963
Application of the moment method to the design of slotted waveguide array antennas
04 p0484 N90-12780
Performance effects of tie-truss modifications for a 70-meter centerline beam waveguide antenna
04 p0486 N90-12791
DSN 70-meter antenna microwave optics design and performance improvements. Part 2: Comparison with measurements 04 p0487 N90-12800
Properties of density tapered arrays
[RSRE-MEMO-4210] 04 p0489 N90-12810
Spectrometer technology recommendations
05 p0597 N90-13468
Joint Services Electronics Program
[AD-A213015] 05 p0634 N90-13699
A study on the sensitivity and simultaneous adjustment of a hoop-column antenna surface
[NASA-TM-101538] 05 p0653 N90-13807
Vehicle antenna for the mobile satellite experiment
[NASA-CR-186109] 06 p0733 N90-14271
Frequency independent constant beamwidth directional lens antenna for very wideband and multi-channel electromagnetic communications
[AD-D014214] 06 p0765 N90-14449
Alternative techniques for some typical MIL-STD-461/462 types of measurements
[PB89-235139] 07 p0917 N90-15302
Scannable millimeter wave arrays, volume 1
[AD-A213895] 07 p0924 N90-15347
Scannable millimeter wave arrays, volume 2
[AD-A213896] 07 p0924 N90-15348
Technology of fast-wave current drive antennas
[DE90-001972] 07 p0994 N90-15747
Satellite broadcasting: Requirements for the receiving antenna
[BBC-RD-1989/5] 08 p1055 N90-16098
Very broad band VHF/UHF omnidirectional antenna design study
[AD-A215358] 09 p1207 N90-16997
Planar array antenna design analysis, volume 1
[AD-A215537] 09 p1207 N90-16999

Modern Antenna Design Using Computers and Measurement: Application to Antenna Problems of Military Interest
[AGARD-LS-165] 10 p1369 N90-17932
A selective survey of computational electromagnetics for antenna applications 10 p1369 N90-17933
Recent advances to NEC: Applications and validation 10 p1369 N90-17934
Some applications of model-based parameter estimation in computational electromagnetics 10 p1369 N90-17935
Measurement and computer simulation of antennas on ships and aircraft for results of operational reliability 10 p1369 N90-17936
HF wire antennas over real ground: Computer simulation and measurement 10 p1370 N90-17937
Antennas on land vehicles for improved communications 10 p1370 N90-17938
Antenna installation on aircraft: Theory and practice 10 p1371 N90-17941
Antenna design methods adapted to radio communication
[TELECOM-88-E-018] 10 p1375 N90-17971
Earth Science Geostationary Platform Technology
[NASA-CP-3040] 12 p1608 N90-19249
Large space antenna concepts for ESGP 12 p1608 N90-19253
Large-diameter geostationary millimeter wavelength antenna concept 12 p1609 N90-19254
Design of a low-frequency (5-20 GHz), 15-meter-diameter passive radiometer for geostationary earth science platforms 12 p1609 N90-19255
Structures for remotely deployable precision antennas 12 p1609 N90-19256
Unfurlable, continuous-surface reflector concept 12 p1609 N90-19257
Advances in large inflatable reflectors 12 p1609 N90-19258
Millimeter radiometer system technology 12 p1610 N90-19260
Synthetic Aperture Interferometric Radiometer (SAIR) 12 p1610 N90-19261
Rain radars for earth science geostationary platforms: Some possibilities 12 p1610 N90-19262
Large antenna measurement and compensation techniques 12 p1610 N90-19263
A comparison of reflector antenna designs for wide-angle scanning 12 p1610 N90-19264
Arrays for space applications 12 p1610 N90-19265
Conjugate field approaches for active array compensation 12 p1610 N90-19266
Reflector surface distortion analysis techniques (thermal distortion analysis of antennas in space) 12 p1611 N90-19267
Antennas for 20/30 GHz and beyond 12 p1611 N90-19269
The 32-GHz performance of the DSS-14 70-meter antenna: 1989 configuration 12 p1645 N90-19452
A spaceborne optical interferometer: The JPL CSI mission focus 14 p1933 N90-21063
Aperture taper determination for the half-scale accurate antenna reflector
[NASA-CR-185215] 14 p1969 N90-21282
Millimeter wavelength rectenna development 15 p2060 N90-21797
Inflatable antennas for microwave pwoer transmission 15 p2060 N90-21799
Dual-shaped offset reflector antenna designs from solutions of the geometrical optics first-order partial differential equations 15 p2076 N90-21887
Passive shape control of space antennas with determinate truss support structures 15 p2087 N90-21949
Beamforming devices and feed structures for a DBS flat-plate antenna
[BBC-RD-1989/12] 17 p2386 N90-23592
Parasitic coupling of the fringing fields of an Ion-Bernstein wave antenna
[DE90-009918] 17 p2387 N90-23596
Inmarsat omni-antenna deployment mechanism 18 p2542 N90-24508
Antennas for portable VHF-FM receivers
[BBC-RD-1990/1] 20 p2850 N90-26211
Design and performance analysis of the DSS-13 beam waveguide antenna 20 p2853 N90-26225
DSS 15, 45, and 65 34-meter high efficiency antenna radio frequency performance enhancement by tilt added to the subreflector during elevation angle changes 20 p2854 N90-26229
Planar microstrip Yagi array antenna
[NASA-CASE-NPO-17873-1-CU] 21 p2994 N90-27015
Thermal-distortion analysis of an antenna strongback for geostationary high-frequency microwave applications
[NASA-TP-3016] 22 p3125 N90-27738
Theory of planar near-field measurement
[FEL-89-B273] 22 p3244 N90-28395
ATDRS payload technology research and development
[NASA-TM-103256] 23 p3287 N90-28596

ANTENNA FEEDS
Ka-band MMIC beam steered transmitter array 04 p0488 N90-12803
Scannable millimeter wave arrays, volume 1
[AD-A213895] 07 p0924 N90-15347
Scannable millimeter wave arrays, volume 2
[AD-A213896] 07 p0924 N90-15348
Stripline feed for a microstrip array of patch elements with teardrop shaped probes
[NASA-CASE-NPO-17548-1-CU] 08 p1056 N90-16104
Reconfigurable antennas, monolithic microwave integrated circuits with feeding networks for microstrip antennas
[AD-A216916] 11 p1498 N90-18622
A comparison of reflector antenna designs for wide-angle scanning 12 p1610 N90-19264
Dual frequency launcher for circularly polarized antenna
[AD-D014361] 12 p1645 N90-19456
Ultralow noise performance of an 8.4-GHz maser-feedhorn system 15 p2076 N90-21889
An 8.4-GHz dual-maser front-end system for Parkes reimplementation 15 p2078 N90-21905
The 30-GHz monolithic receive module
[NASA-CR-180849] 18 p2545 N90-24528
Design and performance analysis of the DSS-13 beam waveguide antenna 20 p2853 N90-26225
ATDRS payload technology research and development
[NASA-TM-103256] 23 p3287 N90-28596

ANTENNA FIELDS
U ANTENNA RADIATION PATTERNS

ANTENNA RADIATION PATTERNS
NT SIDELOBES
The addition of Bendix MLS (Microwave Landing System) antenna patterns to MLS mathematical model
[AD-A210633] 01 p0005 N90-10020
Maximization of directed electromagnetic radiation with an optimized antenna
[DE89-014045] 01 p0056 N90-10319
Nonprincipal-plane scattering from flat plates: Second-order and corner diffraction and pattern control of horn antennas
[NASA-CR-185485] 02 p0211 N90-11205
Part B: Pattern control of horn antennas 02 p0211 N90-11207
Scalar Green function method for microstrip antenna analysis based on the exact image theory
[PB89-218838] 04 p0488 N90-12805
Properties of density tapered arrays
[RSRE-MEMO-4210] 04 p0489 N90-12810
Statistical density and amplitude tapered arrays
[RSRE-MEMO-4211] 04 p0490 N90-12818
Proceedings of the Antenna Applications Symposium, volume 2
[AD-A213815] 07 p0919 N90-15313
Modeling antennas and scatterers of arbitrary shape embedded in layered dielectric media
[AD-A214902] 09 p1211 N90-17023
Measurement and computer simulation of antennas on ships and aircraft for results of operational reliability 10 p1369 N90-17936
Antenna installation on aircraft: Theory and practice 10 p1371 N90-17941
Antenna design methods adapted to radio communication
[TELECOM-88-E-018] 10 p1375 N90-17971
ACIRF user's guide: Theory and examples
[AD-A216436] 11 p1496 N90-18613
Conjugate field approaches for active array compensation 12 p1610 N90-19266
Mesh surfaces for reflector applications 12 p1611 N90-19268
An investigation of the transfer of monopulse tracking between two coherent point sources
[AD-A217007] 12 p1648 N90-19457
An investigation of the extent of the fresnel region of aperture antennas with attention to superdirectivity
[AD-A217518] 13 p1794 N90-20294
Analysis of a high harmonic rectangular gyrotron using ribbon beams 15 p2061 N90-21801
The effect of mechanical deformation on the radiation patterns of large space-based arrays
[AD-A219288] 16 p2230 N90-22719
Spectral measurements of the cosmic microwave background 16 p2340 N90-23334
Critique of nondiffracting beams
[AD-A220722] 17 p2390 N90-23614
Feasibility study of a synthesis procedure for array feeds to improve radiation performance of large distorted reflector antennas
[NASA-CR-186641] 20 p2851 N90-26213
Scattering from coated structures and antenna pattern control using impedance surfaces, part A/B
[NASA-CR-186871] 20 p2854 N90-26233
Near-field gain of pyramidal horns from 18 to 40 GHz
[PB90-155854] 22 p3164 N90-27941
Annular slot antenna radiating into lossy material
[NPL-DITC-152/89] 22 p3165 N90-27945
The Helicopter Antenna Radiation Prediction Code (HARP)
[NASA-CR-186925] 22 p3165 N90-27946
Spatial array processing by the method CLEAN
[FEL-1989-144] 22 p3165 N90-27949

ANTENNAS
NT CASSEGRAIN ANTENNAS
NT DIPOLE ANTENNAS
NT DIRECTIONAL ANTENNAS
NT GRAVITATIONAL WAVE ANTENNAS
NT HOOP COLUMN ANTENNAS
NT HORN ANTENNAS
NT LENS ANTENNAS
NT LOOP ANTENNAS
NT MICROSTRIP ANTENNAS
NT MICROWAVE ANTENNAS
NT MONOPULSE ANTENNAS
NT MULTIBEAM ANTENNAS
NT OMNIDIRECTIONAL ANTENNAS
NT PARABOLIC ANTENNAS
NT RADAR ANTENNAS
NT RADIO ANTENNAS
NT RECTENNAS
NT REFLECTOR ANTENNAS
NT SATELLITE ANTENNAS
NT SLOT ANTENNAS
NT SPACECRAFT ANTENNAS
NT SPACETENNAS
NT STEERABLE ANTENNAS
NT WAVEGUIDE ANTENNAS
NT WHIP ANTENNAS
NT YAGI ANTENNAS
The addition of Bendix MLS (Microwave Landing System) antenna patterns to MLS mathematical model
[AD-A210633] 01 p0005 N90-10020
An experimental SMI adaptive antenna array for weak interfering signals
[NASA-CR-185976] 02 p0212 N90-11211
Validation of NEC (Numerical Electromagnetics Code) for antennas near ground
[DE89-016502] 02 p0212 N90-11212
Polarimetric SAR antenna characterization
[AD-A213438] 07 p0917 N90-15306
Proceedings of the Antenna Applications Symposium, volume 2
[AD-A213815] 07 p0919 N90-15313
Technology of fast-wave current drive antennas
[DE90-001972] 07 p0994 N90-15747
Theoretical analysis of microwave and millimeter wave integrated circuits based on magnetic films
[AD-A214772] 09 p1211 N90-17021
Disturbance torque rejection properties of the NASA/JPL 70-meter antenna axis servos 12 p1644 N90-19450
An investigation of the transfer of monopulse tracking between two coherent point sources
[AD-A217007] 12 p1648 N90-19457
Single antenna interferometry
[DE90-008120] 12 p1648 N90-19474
Lightning protection apparatus for RF equipment and the like
[AD-D014336] 12 p1650 N90-19483
Full wave computation of electromagnetic wave excitation, propagation, and absorption at the ion cyclotron frequency in fusion experiments
[DE90-009399] 14 p2030 N90-21642
Structural fatigue in the 34-meter HA-Dec antennas 15 p2078 N90-21902
Critique of nondiffracting beams
[AD-A220722] 17 p2390 N90-23614
Short range, close to ground, VHF/UHF propagation: A comparison of measured results with a simple ray-based model
[RSRE-MEMO-4335] 19 p2684 N90-25266
Structures for remotely deployable precision antennas
[NASA-CR-182065] 20 p2822 N90-26061
Antennas for portable VHF-FM receivers
[BBC-RD-1990/1] 20 p2850 N90-26211
Integrated radiometric profiler for atmospheric humidity and temperature measurements
[AD-A221931] 21 p3032 N90-27237
Activities of the Division of Microwave Technology
[FOA-C-30555-3.2] 24 p3459 N90-29537

The effects on antenna-filtered scintillation parameters of non-zero antenna pointing angles
[AD-A223840] 24 p3462 N90-29554

ANTHROPOLOGY
Pareto optimization design techniques for the AFIT (Air Force Institute of Technology)/AAMRL (Armstrong Aeronautical Medical Research Laboratory) anthropomorphic robotic manipulator
[AD-A216178] 10 p1414 N90-18150

ANTHROPOMETRY
Anthropometry of a fit test sample used in evaluating the current and improved MCU-2/P masks
[AD-A215173] 11 p1541 N90-18873
Software systems for modeling articulated figures 13 p1861 N90-20677
The predictability and efficiency of human walking: Metabolic, mechanical, and biophysical considerations 15 p2137 N90-22211
The application of kriging in the statistical analysis of anthropometric data, volume 1
[AD-A220613] 17 p2438 N90-23891
The application of kriging in the statistical analysis of anthropometric data, volume 2
[AD-A220614] 17 p2438 N90-23892
The application of kriging in the statistical analysis of anthropometric data, volume 3
[AD-A220615] 17 p2438 N90-23893
An investigation into techniques for landmark identification of 3D images of human subjects, phase 1
[AD-A218614] 18 p2583 N90-24713
The use of PLAID in the Space Station Freedom viewing analysis 19 p2729 N90-25517
Quantitative assessment of human motion using video motion analysis 19 p2730 N90-25518
The relationship of isometric grip strength, optimal dynamometer settings, and certain anthropometric factors
[AD-A222046] 21 p3037 N90-27264
Physiological reactions to heat stress; quantifying the effects of individual parameters
[IZF-1989-30] 22 p3232 N90-28326
Human factors model concerning the man-machine interface of mining crewstations 23 p3364 N90-29011

ANTIAIRCRAFT MISSILES
NT SIDEWINDER MISSILES
Investigation method for AA-proximity fuses
[FEL-89-A194] 24 p3459 N90-29535

ANTIBIOTICS
Study of rifampicin fixation on plasma proteins by derivative spectrophotometry
[CERMA-89-25] 11 p1540 N90-18866

ANTIBODIES
Experiment K-6-23. Effect of spaceflight on levels and function of immune cells 20 p2897 N90-26476
Pseudomonas diagnostic assay
[NASA-CASE-NPO-17653-1-CU] 21 p3032 N90-27239

ANTICYCLONES
Synoptic/planetary-scale interactions and blocking over the North Atlantic Ocean 03 p0360 N90-12061
A forecasting system using the parabolic equation: Application to surface-to-air propagation in the presence of elevated layers 06 p0760 N90-14420
The role of an upstream cyclone and corresponding synoptic/planetary-scale interactions during the development of a blocking anticyclone 08 p1150 N90-16659
Genesis of bow echoes: A rear-inflow induced meso-convective structure
[PB90-209776] 23 p3349 N90-28926

ANTIDIURETICS
Arginine vasopressin lowers pulmonary artery pressure in hypoxic rats by releasing artrial natriuretic peptide
[AD-A215986] 10 p1410 N90-18134

ANTIFERROMAGNETISM
Investigations of spontaneous nuclear order in copper by neutron diffraction
[ETN-90-96060] 05 p0698 N90-14090
Local pairing and antiferromagnetism in high-T sub c superconductors
[AD-A213004] 05 p0703 N90-14113
Macroscopic persistent currents in high temperature ceramic superconductors
[DE89-636232] 06 p0855 N90-14973
Further studies on possible coexistence of antiferromagnetism and superconductivity in 2D Heisenberg model
[DE90-601082] 07 p1000 N90-15783
Magnetic interactions in Sn-119 substituted for Cu in antiferromagnetic and superconducting lamellar cuprates
[DE90-003661] 08 p1132 N90-16560
Magnetic properties of surfaces and interfaces
[DE90-007348] 13 p1880 N90-20789
Preparation and properties of iron doped II-VI chalcogenides
[AD-A220802] 17 p2477 N90-24163
Synthesis, structure, and properties of a new ternary metal nitride, Ca3CrN3
[AD-A222274] 21 p2978 N90-26924
Spin bipolaron in the framework of emery model for high-T(sub c) copper oxide superconductors 22 p3149 N90-27856
Electron energy spectrum and magnetic interactions in high-T(sub c) superconductors 22 p3149 N90-27857
Studies of iron impurities in YxPr1-xBa2Cu3O7-delta 22 p3151 N90-27865
Surface and defect excitations in covalently bonded solids
[AD-A221995] 23 p3303 N90-28682
Effects of Al substitution by Fe in CeAl2
[DE90-627843] 23 p3311 N90-28726
Antiferromagnetism and enhanced heat in CeM2Sn (M = Ni, Ir, Cu, Rh, Pd, and Pt
[DE90-014924] 23 p3399 N90-29206
Susceptibility of the Potts model in an hierarchical lattice: Renormalisation group approach
[DE90-627324] 23 p3401 N90-29215

ANTIFOULING
Archaebacterial involvement in microbial metal corrosion: Metabolism of S and Fe
[AD-A219982] 17 p2377 N90-23537

ANTIFRICTION BEARINGS
NT BALL BEARINGS
NT ROLLER BEARINGS
Life of concentrated contacts in the mixed EHD and boundary film regimes
[AD-A216673] 11 p1517 N90-18738
Cryogenic anti-friction bearing with inner race
[NASA-CASE-MFS-28384-1] 21 p3010 N90-27112
Plastic superconductor bearings any size, any shape, 77 k and up 22 p3145 N90-27838

ANTIGENS
Experiment K-6-23. Effect of spaceflight on levels and function of immune cells 20 p2897 N90-26476

ANTIGRAVITY
The +Gz protection in the future: Review of scientific literature
[AD-A217887] 13 p1851 N90-20623

ANTIICING ADDITIVES
Flight and wind tunnel investigation of aerodynamic effects of aircraft ground deicing/antiicing fluids 07 p0873 N90-15064

ANTIMATTER
NT ANTINEUTRINOS
NT ANTINUCLEONS
NT ANTIPARTICLES
NT ANTIPROTONS
NT POSITRONS
Annihilation in Gases and Galaxies
[NASA-CP-3058] 11 p1555 N90-18957
Feasibility for EGRET detection of antimatter concentrations in the universe 16 p2338 N90-23323
Confinement of nonneutral plasma in unconventional geometries
[DE90-013048] 20 p2928 N90-26659
Measurement of gravitational acceleration of antimatter
[DE90-627464] 23 p3403 N90-29233

ANTIMISSILE DEFENSE
Tracking performance evaluation
[AD-A210499] 01 p0095 N90-10540
Algorithm development for SDI weapons system allocation
[AD-A212973] 04 p0534 N90-13090
High resolution imaging by phase retrieval and discrimination using speckle, volume 1
[AD-A214243] 07 p0919 N90-15317
Delta 181 sensor module command center
[AD-A214868] 09 p1182 N90-16855
Development of advanced WTA algorithms for parallel processing
[AD-A214874] 09 p1266 N90-17341
Defending against a space blockade: CADRE paper
[AD-A215681] 09 p1276 N90-17398
Multi-dimensional LADAR tracking and adaptive grasping for spaceborne assembly of SDI (Strategic Defense Initiative) platforms
[AD-A218236] 13 p1791 N90-20279
The thrust and parry of the SIOP (Single Integrated Operational Plan) and SDI
[AD-A217617] 13 p1880 N90-20784
Strategic defense initiative: Three reasons to stay the course
[AD-A222246] 21 p3070 N90-27456

ANTIMISSILE MISSILES
Brilliant pebbles
[DE90-010756] 18 p2606 N90-24845

ANTIMONIDES
NT GALLIUM ANTIMONIDES
NT INDIUM ANTIMONIDES

ANTIMONY
Trap gettering by isoelectronic doping of p-GaAs and n-GaAs grown by molecular beam epitaxy
[AD-A211162] 01 p0133 N90-10769
The effect of trace amounts of antimony on the structure and properties of aluminum alloy A356.2
[DE90-010461] 19 p2674 N90-25207

ANTIMONY COMPOUNDS
NT GALLIUM ANTIMONIDES
NT INDIUM ANTIMONIDES
The synthesis and structure of novel antimony thiametallacycles
[AD-A210888] 01 p0042 N90-10229
Ternary reactions among polymer substrate-organohalogen-antimony oxides under pyrolytic, oxidative and flaming conditions
[PB90-154766] 15 p2071 N90-21861
High resistivity Al(x)Ga(1-x) As(y)Sb(1-y) epitaxial layers by sulfur compensation doping
[DE90-012228] 22 p3248 N90-28419

ANTIMONY ISOTOPES
Tellurium-118/antimony-118 generator
[DE89-015225] 01 p0122 N90-10698

ANTINEUTRINOS
Experimental test of PCAC hypothesis in the reactions mu neutrino-proton giving muon(-)-proton-pion(+) and mu antineutrino-proton giving muon(+)-proton-pion(-) in the delta (1232) region --- partial conserved axial current
[MPE-PAE/EXP.EL.199] 03 p0403 N90-12309
First results from the MACRO (Monopole, Astrophysics, Cosmic Ray Observatory) detector at the Gran Sasso Laboratory
[DE90-003243] 07 p1011 N90-15858
Chopper for neutrinos and antineutrinos
[AD-A218402] 17 p2471 N90-24124
Exploding neutron stars near the minimum mass: The total energy release 19 p2774 N90-25769

ANTINUCLEONS
The creation of high energy densities with antimatter beams
[DE90-002383] 06 p0842 N90-14899

ANTIPARTICLES
NT ANTINEUTRINOS
NT ANTINUCLEONS
NT ANTIPROTONS
NT POSITRONS
Minimal total cross section for e(+)e(-) yields W(+)W(-)
[NIKHEF-H/88-12] 04 p0553 N90-13222
Possible measurement of the gravitational acceleration of molecules, atoms, nuclei, elementary particles, and antiparticles
[DE90-719559] 08 p1121 N90-16490
The effects of cold dark matter on Big Bang nucleosynthesis 12 p1698 N90-19749
US-Japan Workshop on Atomic Collisions in Solids: Abstracts of lectures
[DE90-008979] 14 p2025 N90-21611
Quark-antiquark pair production via gamma W fusion at high energy e(+)e(-) colliders
[PREPRINT-705] 16 p2316 N90-23205
Measurement of gravitational acceleration of antimatter
[DE90-627464] 23 p3403 N90-29233

ANTIPROTONS
Proceedings of the 10 May 1989 Antiproton Technology Workshop: Addendum
[AD-A212804] 04 p0554 N90-13227
Physics with ultra-low energy antiprotons
[DE90-002397] 06 p0840 N90-14888
The creation of high energy densities with antimatter beams
[DE90-002383] 06 p0842 N90-14899
LEAP: A balloon-borne search for low-energy cosmic ray antiprotons 07 p1015 N90-15878
Antihydrogen formation in collisions of positronium with antiprotons 11 p1560 N90-18988
Anitproton-matter interactions in antiproton applications 11 p1560 N90-18989
The inverse-square law and quantum gravity 12 p1731 N90-19949
A measurement of the gravitational acceleration of the antiproton
[DE90-008903] 14 p2025 N90-21612
A search for low energy cosmic ray antiprotons 24 p3564 N90-30161

ANTIREFLECTION COATINGS
High-efficiency CuInSe2 and CuInGaSe2 based cells and materials research
[DE89-009449] 01 p0083 N90-10471
Diamondlike carbon coatings for optical systems
[AD-A211255] 02 p0276 N90-11573

Vanadium dioxide protective devices
[AD-A212018] 03 p0332 N90-11887
Development of a unique laboratory standard indium gallium arsenide detector for the 500 to 1700 micron spectral region, phase 2
[NASA-CR-180482] 16 p2238 N90-22767
Development of an all silicon integrated optical modulator for high speed data communications and sensor applications
[AD-A220270] 18 p2547 N90-24535
Damage measurements on optical materials for use in high-peak-power lasers
[DE90-013489] 20 p2868 N90-26314
Laser damage database at 1064 nm
[DE90-013490] 20 p2868 N90-26315

ANTISEPTICS
Electrochemical control of iodine disinfectant for space transportation system and space station potable water 18 p2629 N90-24981
Ozone for trace organic contaminant removal
[PB90-221680] 23 p3347 N90-28916

ANTISHIP MISSILES
Suboptimal period design for a maneuvering missile to evade tracking filters 12 p1650 N90-19479

ANTISKID DEVICES
Guidance document for selecting antiskid materials applied to ice- and snow-covered roadways
[PB90-183658] 21 p2983 N90-26950

ANTISUBMARINE WARFARE
VLA missile development and high angle of attack behavior 10 p1305 N90-17553
Proceedings of a Workshop on the Geoelectric and Geomagnetic Environment of Continental Margins
[AD-A223743] 24 p3493 N90-29739

ANTISUBMARINE WARFARE AIRCRAFT
NT P-3 AIRCRAFT

ANTITANK MISSILES
Missile Aerodynamics: NEAR Conference on Missile Aerodynamics
[ISBN-0-9620629-1-X] 10 p1303 N90-17540
The use of lateral jet control at Aerospatiale 10 p1305 N90-17551

ANXIETY
Fear-potentiated startle as a model system for analyzing learning and memory
[AD-A212131] 04 p0525 N90-13029
Passenger behaviour in aircraft emergencies involving smoke and fire 10 p1317 N90-17613
Psychophysiological correlates of human adaptation in antarctica
[AD-A216679] 10 p1412 N90-18142

APATITES
U CALCIUM PHOSPHATES
U MINERALS

APERTURES
NT SYNTHETIC APERTURES
Properties of density tapered arrays
[RSRE-MEMO-4210] 04 p0489 N90-12810
Design of a large angular aperture TeO2 acousto-optic tunable filter
[AD-A213999] 07 p0993 N90-15738
Coded-aperture imaging in nuclear medicine 08 p1073 N90-16208
Diffraction limited dichroic combiner diode laser
[AD-D014291] 08 p1082 N90-16263
A finite element-boundary integral formulation for scattering by three-dimensional cavity-backed apertures
[NASA-CR-186332] 09 p1187 N90-16878
Radar transponder antenna pattern analysis for the space shuttle 12 p1638 N90-19414
Green's functions for a theoretical model of an aperture fed stacked-patch microstrip antenna
[AD-A216280] 12 p1645 N90-19455
An investigation of the extent of the fresnel region of aperture antennas with attention to superdirectivity
[AD-A217518] 13 p1794 N90-20294
Placement of multiple apertures for imaging telescopes
[DE90-006991] 13 p1888 N90-20833
Millimeter wave near-field study
[NASA-CR-182014] 14 p1932 N90-21058
An assessment of the potential of continuous-wave ranging for measuring the distance to a highly reflective, infinite sheet
[NASA-TM-101680] 14 p1969 N90-21279
Aperture taper determination for the half-scale accurate antenna reflector
[NASA-CR-185215] 14 p1969 N90-21282
Development of the CLAES instrument aperture door system 15 p2112 N90-22083
Agile multiple aperture imager receiver development
[AD-A218956] 16 p2318 N90-23215
Vertical directionality measurements of ambient noise in the NE Pacific
[AD-A220007] 17 p2432 N90-23856
Infrared observations of the solar system in support of Large Aperture Infrared Telescope (LARITS): Calibration. Appendices
[AD-A222245] 21 p3097 N90-27598
Analysis of a TM01 circular to TE10 rectangular waveguide mode converter
[AD-A224566] 24 p3464 N90-29568

APEXES
A graph theoretic characterization for the rank of the transfer matrix of a structured system
[CWI-OS-R8819] 05 p0695 N90-14064

APL (PROGRAMMING LANGUAGE)
Simulating simultaneous processes with APL
[MEMO-INF-89-47] 11 p1547 N90-18906

APNEA
U RESPIRATION

APOGEE BOOST MOTORS
The apogee boost motor 05 p0605 N90-13517

APOGEES
Hard start problem of the apogee engine for the ETS-6
[DE90-505525] 20 p2825 N90-26072

APOLLO FLIGHTS
NT APOLLO 15 FLIGHT

APOLLO SOYUZ TEST PROJECT
Systems interoperability approach Apollo/Soyuz test project 08 p1035 N90-15979

APOLLO 15 FLIGHT
The Apollo 15 coarse fines (4-10 mm)
[NASA-TM-101934] 06 p0865 N90-15027

APPEARANCE
Appearance analysis from CAD models
[IMAG-RR-756-I-IMAG-88-LIFIA] 08 p1111 N90-16434

APPENDAGES
NT ARM (ANATOMY)
NT FEET (ANATOMY)
NT FINGERS
NT HAND (ANATOMY)
NT LEG (ANATOMY)

APPLICATION
U UTILIZATION

APPLICATION SPECIFIC INTEGRATED CIRCUITS
A new semicustom integrated bipolar amplifier for silicon strip detectors
[DE89-015585] 02 p0215 N90-11229
ASIC (Application Specific Integrated Circuit) replacement for an SSI (Small Scale Integrated) component design: A case study
[DE89-013494] 02 p0215 N90-11232
GaAs ASIC design case study
[DE89-013934] 02 p0258 N90-11461
VLSI implementation of moment invariants for automated inspection
[DE90-005318] 12 p1652 N90-19493
Product assurance technology for procuring reliable, radiation-hard, custom LSI/VLSI electronics
[NASA-CR-185954] 13 p1791 N90-20281
Experimental high speed/power ratio ASIC designs using residue numbers
[AD-A220302] 18 p2591 N90-24741

APPLICATIONS OF MATHEMATICS
The fast Gauss transform
[AD-A211287] 02 p0266 N90-11517
Preference numbers and funnel dimension
[REPT-89-57] 15 p2161 N90-22346

APPLICATIONS PROGRAMS (COMPUTERS)
NT NASTRAN
Forecasting convection with the AFOS (Automation of Field Operations and Services) data analysis programs. (ADAP-version 2.0) (AFOS data analysis programs-version 2.0)
[PB89-145940] 01 p0086 N90-10492
String Search
[PB89-195986] 01 p0104 N90-10593
User's manual for PEPSIG NASA tip vortex version
[NASA-CR-182178] 02 p0146 N90-10835
A parallel numerical simulation for supersonic flows using zonal overlapped grids and local time steps for common and distributed memory multiprocessors
[DE89-015252] 02 p0147 N90-10839
Independent Orbiter Assessment (IOA): Analysis of the backup flight system
[NASA-CR-185567] 02 p0165 N90-10932
Modifications to the aerotherm charring material thermal response and ablation program (CMA) for carbon ablation analysis
[AD-A211069] 02 p0195 N90-11115
Applications of the hybrid automated reliability predictor: Revised edition
[NASA-TP-2760-REV] 02 p0257 N90-11454
Two VAX-PASCAL terminal interface modules for visualizing scanning and parsing
[MEMO-INF-89-17] 02 p0259 N90-11470
Offaxis radiance studies for infrared sensors
[AD-A210790] 02 p0275 N90-11570
NRL/VOA modifications to IONCAP as of 12 July 1988
[AD-A211546] 03 p0338 N90-11929
Description of a software library for the calculation of surface fluxes
[KNMI-TR-112] 03 p0375 N90-12141
A language for assembly instructions
[REPT-88-90] 03 p0388 N90-12209
Development of computer codes to model dynamics of the earth's magnetosphere
[AD-A211532] 04 p0517 N90-12987
Building a software package for solving large sparse nonlinear systems of equations
[AD-A211758] 04 p0529 N90-13055
A moving-grid interface for systems of one-dimensional time-dependent partial differential equations
[CWI-NM-R8904] 04 p0541 N90-13136
Gas flows in rocket motors. Volume 3, appendix D: Computer code listings
[AD-A213350] 05 p0616 N90-13593
MOBILE4 oxygenated fuels version user's guide
[PB89-230700] 05 p0629 N90-13674
Parameter estimation for the Gummel-Poon transistor model
[MA-53] 05 p0635 N90-13705
Software development for avionics SSME control and diagnostics
[NASA-CR-184894] 05 p0681 N90-13964
Algorithm for atmospheric corrections of aircraft and satellite imagery
[NASA-TM-100751] 05 p0683 N90-13976
Extended memory library for AFOS (Automation of Field Operations and Services) applications
[PB89-230858] 05 p0708 N90-14147
A composite numerical procedure for calculating the motion of vortex filaments 06 p0721 N90-14207
Guidance, steering, load relief and control of an asymmetric launch vehicle
[NASA-CR-185598] 06 p0730 N90-14257
The stability of Taylor-Couette flow with radial heating 06 p0774 N90-14502
The average ion model. Computation of the absorption and emission coefficients in hot plasmas 06 p0785 N90-14569
XRAD: A one dimensional Lagrangian code with radiative transport 06 p0785 N90-14570
Characteristics of an x ray source created by a laser plasma 06 p0786 N90-14575
JPL reuse program 06 p0825 N90-14795
Advanced Software Development Workstation Project 06 p0827 N90-14807
Some numerical experiments concerning the equation of state algorithm for multi-material cells in HULL
[DE89-008240] 06 p0830 N90-14827
Transverse (through-the-thickness) shear stiffnesses of fibre reinforced composite laminated plates (computer program)
[ESDU-89013] 07 p0891 N90-15152
Analysis of an elastohydrodynamic lubricated point contact: User's manual
[AD-A214257] 07 p0943 N90-15459
ZBTAB: Zenith-248 version of BLUGTAB
[AD-A214279] 08 p1108 N90-16415
Creating the next generation control system software
[DE90-003391] 08 p1109 N90-16419
Reusable navigation module 09 p1165 N90-16742
Construction of inelastic stress-strain curves from minimal materials data (computer program)
[ESDU-89052] 09 p1239 N90-17189
Evaluation of the modal testing MODENT software with simulated data
[INPE-4885-NTE/291] 09 p1269 N90-17357
WPK: Solar array dimensioning tool 10 p1348 N90-17808
GTD/UTD: Brief history of successive development of theory and recent advances. Applications to antennas on ships and aircraft 10 p1370 N90-17939
PRPSIM: A FORTRAN code to calculate properties of radio wave propagation in a structured ionized medium. Volume 2: Theory and models
[AD-A216299] 10 p1377 N90-17983
Software verification plan for GCS --- guidance and control software
[NASA-TM-101668] 10 p1394 N90-18057
Fifty year canon of lunar eclipses: 1986-2035
[NASA-RP-1216] 10 p1446 N90-18342
Satellite radar altimetry over ice. Volume 2: Users' guide for Greenland elevation data from Seasat
[NASA-RP-1233-VOL-2] 13 p1840 N90-20563
TAE Plus: Transportable Applications Environment Plus tools for building graphic-oriented applications 13 p1856 N90-20652
The Real Time Interactive Display Environment (RTIDE), a display building tool developed by Space Shuttle flight controllers 13 p1857 N90-20654

Applications of graphics to support a testbed for autonomous space vehicle operations
13 p1858 N90-20661
Automated analysis of measured turbulent boundary flow
[PB90-147844] 15 p2092 N90-21970
Design and testing of a multiblock grid-generation procedure for aircraft design and research
15 p2094 N90-21984
The computational structural mechanics testbed data library description
[NASA-TM-100645-REV-1] 15 p2121 N90-22135
Graphically-oriented nonlinear analysis of statically loaded plane frames on microcomputers
[PB90-165945] 15 p2144 N90-22248
Extension of a three-dimensional viscous wing flow analysis user's manual: VISTA 3-D code
[NASA-CR-182024] 16 p2197 N90-22538
Quantitative characterization of spatial distribution of particles in materials: Application to materials processing
16 p2219 N90-22660
An order (n) algorithm for the dynamics simulation of robotic systems 16 p2279 N90-22990
Space station dynamics, attitude control and momentum management 16 p2287 N90-23029
OPTICON: Pro-Matlab software for large order controlled structure design 16 p2292 N90-23058
Combining high performance simulation, data acquisition, and graphics display computers
16 p2293 N90-23062
The use of real-time, hardware-in-the-loop simulation in the design and development of the new Hughes HS601 spacecraft attitude control system
16 p2293 N90-23065
Control design and simulation of systems modeled using ADAMS 16 p2296 N90-23081
The Durra application debugger/monitor
[AD-A219290] 16 p2301 N90-23111
Basic graphics routine technical manual
[AD-A219409] 16 p2302 N90-23117
Predicting tidal displacements of the surface of the Earth, volume 1
[ETN-90-96690] 17 p2431 N90-23850
Predicting tidal displacements of the surface of the Earth, volume 2
[ETN-90-96691] 17 p2431 N90-23851
Knowledge-based control of an adaptive interface
18 p2630 N90-24987
A few modeling and rendering techniques for computer graphics and their implementation on ultra hardware
18 p2640 N90-25038
An approach to a real-time distribution system
19 p2733 N90-25535
ACES: Space shuttle flight software analysis expert system 19 p2739 N90-25571
Tools for distributed application management
[NASA-CR-186711] 19 p2742 N90-25586
Exploiting replication in distributed systems
[NASA-CR-186410] 19 p2746 N90-25603
CEBAF control system
[CEBAF-PR-89-013] 19 p2757 N90-25666
Tools for distributed application management
[NASA-CR-186646] 19 p2762 N90-25692
Computer aided handling qualities evaluation in frequency domain
[NAL-TM-SE-8902] 20 p2905 N90-26523
Digital signal processing software packages for IBM-PC and IBM-PC with DSP-16
[AD-A221679] 21 p3056 N90-27372
Guide to available mathematical software
[PB90-216508] 22 p3236 N90-28351
Software development tools
[PB90-250051] 23 p3381 N90-29103
Semiconductor measurement technology. EPROP: An interactive FORTRAN program for computing selected electronic properties of Gallium Arsenide and Silicon
[PB90-222738] 23 p3399 N90-29203
Variational formulation and finite element implementation of Pagano's theory of laminated plates
24 p3442 N90-29437
Development of a software package for automatic data acquisition, analysis, and controls in an axial flow compressor test rig
[PD-PR-8910] 24 p3524 N90-29926
An interactive optimization based, computer graphics software package. Phase 2: Users manual
[AD-A223654] 24 p3529 N90-29954
ESTEC software catalogue
[ESA-SP-1133] 24 p3531 N90-29968

APPLICATIONS TECHNOLOGY SATELLITES
U ATS

APPROACH
NT INSTRUMENT APPROACH
Simulations for computer centerline approach
[DOT/FAA/CT-TN89/41] 03 p0304 N90-11726
A head up display format for application to V/STOL aircraft approach and landing
[NASA-TM-102216] 10 p1320 N90-17632
Rosetta/CNSR, ESA's planetary cornerstone mission
12 p1738 N90-19990
Heliport visual approach surface high temperature and high altitude tests
[DOT/FAA/CT-TN89/34] 22 p3112 N90-27675
Vibration responses of two house structures during the Edwards Air Force Base phase of the national sonic boom program
[NASA-CR-182089] 23 p3393 N90-29169

APPROACH AND LANDING TESTS (STS)
Prediction of longitudinal pilot induced oscillations using the optimal control model
[AD-A220593] 17 p2356 N90-23412

APPROACH CONTROL
NT RADAR APPROACH CONTROL
National airspace system approach and departure sequencing operational concept
[NAS-SR-1322] 01 p0004 N90-10017
Operational trial of effect of raising minimum stack level in Heathrow stacks
[CAA-PAPER-89003] 04 p0449 N90-12573
Parallel approach separation and controller performance: A study of the impact of two separation standards
[DOT/FAA/CT-TN89/50] 04 p0449 N90-12574
Analysis of sequencing and scheduling methods for arrival traffic
[NASA-TM-102795] 17 p2348 N90-23373
Replication of NASPAC Dallas/Fort Worth study
[DOT/FAA/CT-TN90/26] 19 p2657 N90-25123
Four-dimensional planner: A ground based planning system for time accurate approach guidance
22 p3113 N90-27683
Approach towards a future integrated airport surface traffic management 22 p3113 N90-27686
Independent ground monitor coverage of Global Positioning System (GPS) satellites for use by civil aviation 24 p3428 N90-29364

APPROACH INDICATORS
Helicopter Visual Segment Approach Lighting System (HALS)
[ACD-330] 02 p0150 N90-10856
Tracking performance of the AN/GPN-22 precision approach radar
[FEL-1988-34] 12 p1647 N90-19467

APPROPRIATIONS
Federal funds for research and development: Fiscal years 1986, 1987, and 1988. Volume 36: Detailed statistical tables
[PB89-223523] 03 p0419 N90-12407
Federal funds for research and development. Fiscal years 1987, 1988, and 1989. Volume 37: Detailed statistical tables
[PB89-223531] 03 p0419 N90-12408
Departments of Veterans Affairs and Housing and Urban Development, and Independent Agencies Appropriations Bill, 1990
[H-REPT-101-150] 04 p0563 N90-13281
National Aeronautics and Space Administration
04 p0563 N90-13282
Fiscal year 1990 authorization request and budget estimates for the National Aeronautics and Space Administration
[GPO-96-945] 04 p0563 N90-13283
Departments of Veterans Affairs and Housing and Urban Development, and Independent Agencies Appropriation Bill, 1990
[S-REPT-101-128] 04 p0563 N90-13284
The 1990 National Aeronautics and Space Administration Authorization
[GPO-98-466] 04 p0563 N90-13285
Department of Veterans Affairs and Housing and Urban Development, and Independent Agencies Appropriations Act, 1990
[HR-2916-PP] 04 p0564 N90-13286
National Aeronautics and Space Administration
04 p0564 N90-13287
National Aeronautics and Space Administration Authorization Act, fiscal year 1990
[S-REPT-101-157] 04 p0564 N90-13288
National Aeronautics and Space Administration Authorization Act, fiscal year 1990
[S-REPT-101-157] 04 p0564 N90-13289
National Aeronautics and Space Administration Multiyear Authorization Act of 1989
05 p0709 N90-14148
National Aeronautics and Space Administration authorization
[S-HRG-101-348] 05 p0709 N90-14149
Space funding: NASA and DOD activities for fiscal years 1981 through 1989. Fact sheet for the Chairman and the Ranking Minority Member, Subcommittee on Science, Technology, and Space, Committee on Commerce, Science, and Transportation, US Senate
[GAO/NSIAD-89-102FS] 17 p2481 N90-24187
The 1991 NASA authorization: National Aeronautics and Space Administration fiscal year 1991 authorization request and budget estimates
[GPO-27-291] 17 p2481 N90-24188
Departments of Veterans Affairs and Housing and Urban Development, and Independent Agencies Appropriations for Fiscal Year 1990, part 2
[S-HRG-101-345-PT-2] 18 p2636 N90-25017
National Aeronautics and Space Administration, 2 May 1989 18 p2636 N90-25018
National Aeronautics and Space Administration, 3 May 1989 18 p2636 N90-25019
Departments of Veterans Affairs and Housing and Urban Development, and independent agencies appropriations for 1991. Part 4: National Aeronautics and Space Administration
[GPO-30-861] 21 p3088 N90-27561
NSF Tokyo reports. The 1989 survey of research and development in Japan
[PB90-199340] 22 p3265 N90-28487
Our changing planet: The FY 1991 US global change research program. A report by the committee on Earth Sciences to accompany the FY 1991 budget
[PB90-202623] 23 p3348 N90-28907
Federal support to universities, colleges, and selected nonprofit institutions: Fiscal year 1988 (detailed statistical tables)
[PB90-226887] 23 p3404 N90-29236
NASA authorization, 1991, volume 2
[GPO-32-196] 24 p3559 N90-30138

APPROXIMATION
NT BORN APPROXIMATION
NT CHEBYSHEV APPROXIMATION
NT EDDINGTON APPROXIMATION
NT ESSENTIALLY NON-OSCILLATORY SCHEMES
NT FINITE DIFFERENCE THEORY
NT FINITE ELEMENT METHOD
NT HARTREE APPROXIMATION
NT LEAST SQUARES METHOD
NT MEAN SQUARE VALUES
NT MULTIGRID METHODS
NT NEWTON METHODS
NT NEWTON-RAPHSON METHOD
NT NUMERICAL DIFFERENTIATION
NT OSEEN APPROXIMATION
NT PADE APPROXIMATION
NT PARTICLE IN CELL TECHNIQUE
NT PREDICTOR-CORRECTOR METHODS
NT RAYLEIGH-RITZ METHOD
NT RELAXATION METHOD (MATHEMATICS)
NT TVD SCHEMES
On lower confidence for PCS in truncated location parameter models
[AD-A210274] 01 p0115 N90-10661
The temporal development of collision cascades in the binary collision approximation
[DE89-015860] 01 p0122 N90-10699
An interactive program for constrained spline approximation of numerical data
[DE89-016674] 02 p0267 N90-11520
An approximate max-flow min-cut theorem for uniform multicommodity flow problems with applications to approximation algorithms
[AD-A211908] 03 p0386 N90-12198
Convergence results for pseudospectral approximations of hyperbolic systems by a penalty type boundary treatment
[NASA-CR-181929] 03 p0391 N90-12230
Rational expansion for nonlinear input-output maps
[RR-348] 03 p0394 N90-12248
Non-stationary computer model of the asymptotic region of an electric arc gas heater
[IPPCZ-288] 03 p0407 N90-12330
A linearized surface condition in low speed hydrodynamics
[REPT-89-04] 04 p0501 N90-12885
Multiplicative iterative algorithms for convex programming
[CWI-AM-R8808] 04 p0532 N90-13072
Stable summability and approximation theory
[AD-A211379] 04 p0539 N90-13118
A generalization of Moak's q-Laguerre polynomials
[REPT-89-21] 04 p0540 N90-13126
An Eigenvalue Analysis of finite-difference approximations for hyperbolic IBVPs
[NASA-TM-102241] 04 p0541 N90-13137
Explicit formulas for Hankel norm approximations of infinite-dimensional systems
[TW-289] 04 p0545 N90-13167

Berry-Esseen rates and bootstrap results for generalized L-statistics
[CWI-MS-R8808] 04 p0546 N90-13179
Random truncation models and Markov processes
[CWI-MS-R8817] 04 p0547 N90-13181
On new methods for computing with multivariate B-splines
[MEMO-783] 04 p0547 N90-13183
The physical optics approximation in the near-field region
[FEL-1989-100] 04 p0555 N90-13234
Time evolution of the electron swarm energy distribution function
[AD-A212967] 04 p0557 N90-13247
Small scale structure on cosmic strings
[NASA-CR-186075] 04 p0565 N90-13298
The weighted sum of two S-units being a square
[MEMO-792] 05 p0691 N90-14031
Practice of bivariate quadratic simplicial splines
[MEMO-800] 05 p0691 N90-14034
Computational aspects of pseudospectral Laguerre approximations
[NASA-CR-181934] 05 p0691 N90-14038
The fluid mechanics of filters
06 p0773 N90-14499
Approximate methods for dynamic plastic deformation of structures
[DE90-002214] 06 p0800 N90-14660
Quasi interpolants and approximation power of multivariate splines
[AD-A213535] 07 p0983 N90-15678
An improved toeplitz approximation method
[AD-A213994] 07 p0984 N90-15688
Optimization of stochastic systems via simulation
[AD-A214011] 07 p0985 N90-15689
A structural factoring approach for analyzing probabilistic networks 07 p0986 N90-15697
Triangle based TVD schemes for hyperbolic conservation laws
[NASA-CR-181984] 08 p1106 N90-16401
Optimal step sizes in semi-stochastic approximation procedures
[ETN-90-95888] 08 p1117 N90-16469
Approximation method for nonlinear integral equations of Hammerstein type
[DE90-600727] 09 p1272 N90-17372
Robustness of controllers designed using Galerkin type approximations
[NASA-CR-181986] 10 p1395 N90-18063
An approximate model for the performance and acoustic predictions of counterrotating propeller configurations
[NASA-CR-180667] 10 p1426 N90-18228
Approximations to joint distributions of definite quadratic forms
[AD-A216434] 11 p1551 N90-18930
Strong moderate deviation theorems
[MEMO-804] 11 p1555 N90-18954
Deterministic differential game solution: The approximate strategy method
[ESA-TT-1158] 11 p1555 N90-18956
Iterative procedures for space shuttle main engine performance models 12 p1639 N90-19416
Networks and the best approximation property
[AD-A216712] 12 p1703 N90-19778
The 0-1 multiknapsack problem: Heuristic and reduction methods
[INPE-4894-PRE/1495] 12 p1704 N90-19782
On the approximative normal values of multivalued operators in topological vector space
[DE90-610430] 12 p1707 N90-19800
Theory system reliability demonstration and burn-in design
[AD-A217775] 13 p1814 N90-20416
Methods for local gravity field approximation
13 p1834 N90-20532
High order filtering methods for approximating hyperbolic systems of conservation laws
[NASA-CR-182016] 13 p1856 N90-20650
Computing mean responses in nonlinear models
[AD-A217642] 13 p1865 N90-20700
Performance of concurrency control algorithms in distributed systems
[AD-A218260] 13 p1870 N90-20727
Observer based compensators for nonlinear systems
[AD-A217426] 13 p1876 N90-20760
An approximation theory for the identification of linear thermoelastic systems
[NASA-CR-182015] 13 p1877 N90-20764
Spectral line shape code for multielectron emitters
[DE90-008526] 13 p1891 N90-20853
An approximate viscous shock layer method for calculating the hypersonic flow over blunt-nosed bodies
14 p1910 N90-20947
On the dynamics of polymer mixtures in solution using the RPA
[DE90-613689] 14 p1948 N90-21149
Ordering mechanism in substitutional Ni-Cr alloys: Theory and experiment
[DE90-006268] 14 p1949 N90-21156
Modified tight-binding approximation and electron-phonon spectral function for transition metals
[DE90-614022] 14 p1950 N90-21166
Generalized random phase approximation for multicomponent polymer systems
[DE90-613691] 14 p1955 N90-21194
New ferrite-filled waveguiding structures analysed by the averaging method
[PB90-165671] 14 p1967 N90-21269
A review of approximate methods for determining the vibrational modes of membranes
15 p2109 N90-22063
Stability radius of polynomials occurring in the numerical solution of initial value problems
[TW-89-04] 15 p2162 N90-22350
The approximation of a composite Bezier cubic curve by a composite Bezier quadratic curve
[NPL-DITC-147/89] 15 p2162 N90-22354
Differential equation based method for accurate approximations in optimization
[NASA-TM-102639] 16 p2200 N90-22558
Approximation in LQG control of a thermoelastic rod
16 p2297 N90-23084
On approximation of nonlinear boundary integral equations for the combined method
[DE90-009784] 16 p2305 N90-23130
High order essentially non-oscillatory schemes for Hamilton-Jacobi equations
[NASA-CR-181995] 16 p2305 N90-23137
Analytic semigroups: Applications to inverse problems for flexible structures
[NASA-CR-182047] 16 p2306 N90-23138
An examination of the full-wave method for rough surface scattering
[AD-A218664] 16 p2308 N90-23155
On the parallel solution of parabolic equations
[NASA-CR-180363] 17 p2455 N90-24009
An averaging result for random differential equations
[AD-A220364] 17 p2457 N90-24021
Convergence of one-leg multistep methods for stiff nonlinear initial value problems
[CWI-NM-R8911] 17 p2459 N90-24040
Approximate interval estimation methods for the reliability of systems using component data with exponential and Weibull distributions
[AD-A219857] 17 p2460 N90-24048
Sparse approximations of inverse matrices
[ETN-90-96904] 17 p2464 N90-24074
Bounding separable recourse functions with limited distribution information
[AD-A219504] 17 p2465 N90-24084
Sojourn times in queueing networks
[CWI-BS-R8916] 17 p2467 N90-24102
On computational aspects of simplicial splines
[MEMO-818] 18 p2600 N90-24795
Second order asymptotics in level crossing problems for differences of renewal processes
[MEMO-824] 18 p2600 N90-24798
On the independence of B-splines on unordered knot sets
[MEMO-827] 18 p2600 N90-24800
A general method for approximating improper integrals
[AD-A221153] 18 p2604 N90-24830
More about general saddlepoint approximations
[AD-A221217] 18 p2604 N90-24832
The CFL condition for spectral approximations to hyperbolic initial-boundary value problems
[NASA-CR-182053] 18 p2604 N90-24833
Axions and SN 1987A: Axion trapping
[NASA-CR-186604] 18 p2612 N90-24881
Image of the angle by partially coherent lighting: Calculations and experiments
[ETN-90-96505] 18 p2616 N90-24900
An experimental and theoretical investigation of the flow over plane delta wings with supersonic leading edges
[LR-588] 19 p2655 N90-25114
Computational fluid dynamics for missiles
[RAE-TM-AERO-2171] 20 p2863 N90-26288
H-infinity control: An exploratory study
[EUT-88-E-211] 20 p2915 N90-26584
Comment on high resolution simulations of cosmic strings. 1: Network evoloution
[NASA-CR-186606] 20 p2941 N90-26734
An approximate method for calculating three-dimensional inviscid hypersonic flow fields
[NASA-TP-3018] 21 p3002 N90-27066
Investigations on improved iterative methods for solving sparse systems of linear equations
[AD-A221980] 21 p3064 N90-27417
Implicit solution of three-dimensional internal turbulent flows
[NASA-TM-103099] 22 p3170 N90-27982
Difference methods for hyperbolic problems with emphasis on space-centered approximations
22 p3172 N90-27998
An analysis of flow models: From Navier-Stokes to potential flow equations 22 p3173 N90-28002
Unsteady aerodynamics of controls
23 p3273 N90-28525
Finite element analysis of coupled thermoelasticity
[PB90-201211] 23 p3337 N90-28860
Planning 3-D collision-free paths using spheres
23 p3367 N90-29024
Approximation algorithms for planning and control
23 p3370 N90-29042
Recurrence relations and weight functions for approximation by orthonormal polynomials
[DE90-627156] 23 p3388 N90-29134
An enhanced integrated aerodynamic load/dynamic optimization procedure for helicopter rotor blades
[NASA-CR-4326] 24 p3432 N90-29383
Approximate equations for heat conduction in multi-layered cylindrical shells
[NAL-TR-1049] 24 p3471 N90-29614
Systems reliability and inference: Summary of accomplishments 1988-1990
[AD-A224433] 24 p3477 N90-29653
Estimation and representation of multidimensional mappings
[DLR-MITT-90-06] 24 p3531 N90-29967
Machine learning
[AD-A223732] 24 p3534 N90-29988
Saddlepoint approximations in conditional inference
[AD-A223280] 24 p3537 N90-30000
A comparative first principles study of phase stability in Ni-Ti and Ni-Al alloys around equiatomic composition
[DE90-016477] 24 p3554 N90-30111

APPROXIMATION METHODS
U APPROXIMATION

APSIDES
NT APOGEES

APTITUDE
Measuring learning ability by dynamic testing
[AD-A215273] 09 p1259 N90-17304
Appropriateness measurement for computerized adaptive tests
[AD-A216121] 11 p1541 N90-18870
The incremental validity of spatial and perceptual-psychomotor tests relative to the armed services vocational aptitude battery
[AD-A220903] 18 p2585 N90-24719
TOM: Test of multiple task performance, user manual
[DLR-FB-89-60] 19 p2723 N90-25490
International application of the DLR test-system: First year of cooperation with IBERIA in pilot selection
[DLR-FB-90-05] 19 p2723 N90-25491
Cross-validation of experimental USAF pilot training performance models
[AD-A222253] 21 p3035 N90-27257
Air Force Officer Qualifying Test (AFOQT): Development of quick score composites for forms P1 and P2
[AD-A223868] 23 p3362 N90-28997

AQUATIC PLANTS
NT PHYTOPLANKTON
Utilization of water hyacinths to upgrade heavily loaded wastewater treatment plant effluents
15 p2073 N90-21873

AQUEOUS SOLUTIONS
Dimensional analysis of continuous high-capacity electrodispersion of aqueous based liquids in an organic continuous phase
[DE90-003714] 07 p0888 N90-15136
Mechanistic modeling of corrosion fatigue crack growth of steels in aqueous solutions 18 p2524 N90-24404
Passivation of high temperature superconductors
[NASA-CASE-NPO-17949-1-CU]
20 p2932 N90-26684
Aqueous solution properties of ampholytic ionomers
[AD-A222152] 22 p3156 N90-27890

AQUIFERS
Image processing of LANDSAT MSS data for buried valley detection in northern Indiana
06 p0802 N90-14668

ARC DISCHARGES
Plasma centrifuge with vacuum arc discharge applied to the separation of stable isotopes
[INPE-4925-TDL/385] 12 p1716 N90-19854
Dissociation phenomena in electron-beam sustained carbon dioxide lasers 18 p2560 N90-24610

ARC HEATING
Hermes plasma wind tunnel. Preliminary study, phase A1: Text
[DVG-HER-TN-002-PT-1] 04 p0459 N90-12631
Aerodynamic simulation conditions in arc heated wind tunnels 09 p1180 N90-16843

Determination of the velocity, density, maximum flux, and enthalpy profiles for a very high temperature arc jet nozzle flow
[AD-A218390] 17 p2402 N90-23682
The arc-hot wind tunnel 18 p2489 N90-24230
Studies of surface heat transfer in an arc-heated wind tunnel
[NAL-TR-1048] 24 p3437 N90-29410

ARC JET ENGINES
The effect of electrode configuration on arcjet performance
[NASA-TM-102346] 02 p0189 N90-11081
Arcjet thruster research and technology. Phase 1: Executive summary
[NASA-CR-182106] 06 p0734 N90-14278
Electric propulsion options for 10 kW class earth-space missions 11 p1472 N90-18474
Test facility and preliminary performance of a 100 kW class MPD thruster 11 p1472 N90-18476
Arcjet cathode phenomena 11 p1473 N90-18477
Arcjet nozzle design impacts 11 p1473 N90-18478
Mission options for an electric propulsion demonstration flight test 11 p1473 N90-18479
Arcjet load characteristics
[NASA-TM-103190] 19 p2669 N90-25181
The 30-kW ammonia arcjet technology
[NASA-CR-186850] 19 p2670 N90-25190
Preliminary plume characteristics of an arcjet thruster
[NASA-TM-103241] 20 p2825 N90-26071
Advanced propulsion for LEO and GEO platforms
[NASA-TM-103228] 22 p3134 N90-27785
Low power arcjet performance
[NASA-TM-103280] 23 p3298 N90-28657
High power arcjet
[NASA-CR-183086] 23 p3298 N90-28658

ARC MELTING
Metal transfer in gas metal arc welding
[AD-A213390] 05 p0624 N90-13642

ARC SPRAYING
Improved process for HIP canning of composites
[NASA-CASE-LEW-14990-1-CU] 07 p0890 N90-15147
Arc-sprayed coatings for electromagnetic pulse protection: Assessment of physical and electrical properties
[AD-A213825] 07 p0912 N90-15275

ARC WELDING
NT GAS TUNGSTEN ARC WELDING
NT PLASMA ARC WELDING
Metal transfer in gas metal arc welding
[AD-A213390] 05 p0624 N90-13642
Arc current control of a robotic welding system: Modeling and control system design
[AD-A213150] 05 p0650 N90-13788
The feasibility of welding of irradiated materials
[DE90-002200] 06 p0795 N90-14631
The effect of nitrogen and titanium on the toughness of high strength saw weld deposits
[AD-A213400] 07 p0905 N90-15230
Submerged arc welding consumables for HSLA (High Strength Low Alloy)-100 steel
[AD-A213433] 07 p0941 N90-15452
A new model for hydrogen absorption in welds
[AD-A216951] 12 p1626 N90-19347
Trailer shield assembly for a welding torch
[NASA-CASE-MFS-29260-1] 12 p1672 N90-19602
The mathematical modeling of arc welding operation
[DE90-013700] 22 p3183 N90-28064
Materials studies for magnetic fusion energy applications at low temperatures, volume 12
[PB90-157553] 22 p3248 N90-28417
Investigation of weld bead cooling rate during startup of gas metal arc welding
[AD-A223567] 24 p3449 N90-29478
The dc arc weld starter
[DE90-014679] 24 p3475 N90-29641
Adaptive control of an arc welding process
[AD-A223626] 24 p3476 N90-29645

ARCHAEBACTERIA
Molecular biology and physiology of methanogenic archaebacteria
[AD-A210399] 01 p0091 N90-10522
A new class of lubricants derived from archaebacterial lipids
[AD-D014429] 14 p1954 N90-21185
Archaebacterial involvement in microbial metal corrosion: Metabolism of S and Fe
[AD-A219982] 17 p2377 N90-23537

ARCHAEOLOGY
A case for archaeological reconnaissance of the Cabo Catoche-Porvenir region of the northeastern Yucatan Peninsula
[NASA-TM-102248] 16 p2249 N90-22827

ARCHES
A study of incremental-iterative strategies for nonlinear analyses
[PB89-226005] 06 p0798 N90-14646

ARCHITECTURE
The astronomy of Andean myth: The history of a cosmology 02 p0291 N90-11660
Designing and designing knowledge in engineering and architecture
[PB89-219521] 03 p0415 N90-12383

ARCHITECTURE (COMPUTERS)
The organization of permutation architectures with bussed interconnections
[AD-A210832] 01 p0061 N90-10352
The role of sensor directed, model based control in robotics
[DE89-014133] 01 p0077 N90-10442
Performance evaluation of the Scheme86 and HP precision architectures
[AD-A209418] 01 p0102 N90-10578
A multiprocessor architecture using modular arithmetic for very high precision computation
[AD-A208154] 01 p0102 N90-10579
Effective resource utilization for multiprocessor join execution
[DE89-016303] 01 p0105 N90-10595
Cost metric algorithms for internetwork applications
[AD-A210324] 01 p0105 N90-10597
Using computer design and simulation to improve manufacturing productivity
[AD-A210338] 01 p0105 N90-10598
Applications of parallel supercomputers: Scientific results and computer science lessons
[DE89-016385] 01 p0107 N90-10611
Shared memory versus message passing architectures: An application based study
[AD-A210312] 01 p0108 N90-10615
Exploring the benefits of multiple hardware contexts in a multiprocessor architecture: Preliminary results
[AD-A210349] 01 p0108 N90-10616
The rewrite rule machine project
[AD-A210528] 01 p0109 N90-10617
Northeast Artificial Intelligence Consortium annual report for 1987. Volume 5: Building an intelligent assistant: The acquisition, integration and maintenance of complex distributed tasks
[AD-A210330] 01 p0109 N90-10621
The architecture of NEWTON: A general-purpose dynamics simulator
[NASA-CR-185489] 01 p0118 N90-10678
A comparison of real-time optical correlators for pattern recognition
[DE89-016416] 01 p0123 N90-10705
Development of Information Quality Engineering (IQE) methodology for information resource management
[AD-A210615] 01 p0137 N90-10791
Realtime processing and display 02 p0155 N90-10886
Hanford Meteorological Station computer codes. Volume 10: The ARCHIVE computer code
[DE89-016175] 02 p0252 N90-11429
Performance reports for EIM (Engineering Information Management) computer systems: A managerial perspective
[DE89-015194] 02 p0256 N90-11449
New computing systems and their impact on structural analysis and design
[NASA-CR-185831] 02 p0257 N90-11457
An investigation of the usefulness of Earley's Algorithm in a general context-free recognizer
[DE89-016498] 02 p0258 N90-11463
Computing the two dimensional fast Fourier transform on a general purpose mesh connected multiprocessor
[DE89-016515] 02 p0266 N90-11518
An interactive program for constrained spline approximation of numerical data
[DE89-016674] 02 p0267 N90-11520
Summaries of the FY 1989 Applied Mathematical Sciences Research program
[DE89-016694] 02 p0267 N90-11521
Adaptive gigabit fiber optics local area network
[AD-A210794] 02 p0275 N90-11571
LEXER: A tool for lexical analysis of program input
[DE89-016924] 02 p0288 N90-11649
Spacelab system analysis Marshall Avionics System Testbed (MAST)
[NASA-CR-183804] 03 p0317 N90-11802
A distributed pipelined architecture of the recursive Lagrangian equations of motion for robot manipulators with VLSI implementation — VLSI (very large scale integration)
[RR-353] 03 p0344 N90-11966
Optical arithmetic logic using the modified signed-digit redundant number representation
[AD-D014176] 03 p0384 N90-12186
On the design and implementation of a secure computer system
[RSRE-MEMO-4188] 03 p0385 N90-12189
Software package for 3-dimensional graphic display unit
[NAL-TM-559] 03 p0385 N90-12191
ISI's (Information Sciences Institute) SDI architecture simulator: An experiment in adding new software to the system
[AD-A211314] 03 p0387 N90-12204
Parallel architectures and parallel algorithms for integrated vision systems
[NASA-CR-185990] 03 p0389 N90-12215
Distributed VLSI architecture for fast Jacobian and inverse Jacobian formulations
[RR-346] 03 p0390 N90-12218
Robot inverse dynamics computation via VLSI distributed architectures
[RR-350] 03 p0390 N90-12223
Ground-state coding in partially connected neural networks
[NASA-TM-102239] 03 p0391 N90-12227
Distributed knowledge-based systems
[AD-A211984] 03 p0418 N90-12401
Development of an integrated mobile robot system at CMU (Carnegie-Mellon University)
[AD-A212555] 04 p0510 N90-12944
A hybrid architecture for feature labelling of oceanographic satellite images
[AD-A212236] 04 p0515 N90-12975
ISI's (Information Sciences Institute) SDI architecture simulator: Initial prototype user interface
[AD-A211325] 04 p0529 N90-13053
A Z specification of the MaCHO interface editor
[RSRE-MEMO-4247] 04 p0531 N90-13067
Area-universal networks
[AD-A211883] 04 p0535 N90-13092
LAIOS: A multiprocessor network for artificial intelligence applications
[ETN-89-95498] 04 p0537 N90-13109
A compilation strategy for numerical programs based on partial evaluation
[AD-A212759] 04 p0546 N90-13175
Definition of avionics concepts for a heavy lift cargo vehicle, appendix A
[NASA-CR-183817] 05 p0580 N90-13380
Overview of the Tycho data analysis 05 p0610 N90-13558
Computational and psychophysical study of human vision using neural networks
[AD-A213290] 05 p0674 N90-13924
Dynamic workload modeling of high speed token rings in a metropolitan area network
[MEMO-INF-89-21] 05 p0694 N90-14059
Architecture and language for a layered relational database 05 p0707 N90-14146
The Tactical Environmental Support System (TESS(3)) 06 p0757 N90-14409
The characteristics of the HF radio channel and its influence on modern HF data communication system design 06 p0765 N90-14448
A radar simulation program for a 1024-processor hypercube
[DE89-014494] 06 p0766 N90-14455
CTH: A three-dimensional shock wave physics code
[DE89-016529] 06 p0779 N90-14528
Parallel eigenanalysis of finite element models in a completely connected architecture
[NASA-CR-185166] 06 p0799 N90-14652
High performance parallel architectures
[DE90-001055] 06 p0823 N90-14782
High volume data storage architecture analysis
[NASA-CR-186239] 06 p0823 N90-14784
Selecting and effectively using a computer aided software engineering tool
[DE89-017876] 06 p0828 N90-14815
The High-Speed Channel (HSC) and ultra-speed networks
[DE89-015283] 06 p0829 N90-14819
The design of a computer system for image simulation and image processing of high resolution electron micrographs
[DE90-000179] 06 p0829 N90-14820
Using object-oriented development to support prototyping
[DE90-000547] 06 p0829 N90-14821
Interactive multidimensional data analysis and understanding
[DE90-001794] 06 p0830 N90-14824
A tutorial on software reliability engineering
[DE89-012368] 06 p0830 N90-14828
Multiple crossbar network: Integrated supercomputing framework
[DE89-012614] 06 p0831 N90-14831

The Delta-t transport protocol: Features and experience useful for high performance networks
[DE89-016542] 06 p0831 N90-14832
Generalization in backpropagation networks: An empirical study using image data
[DE89-012658] 06 p0832 N90-14835
Architectures for reasoning in parallel
[NASA-CR-186237] 06 p0832 N90-14836
NETRA: A parallel architecture for integrated vision systems. 1: Architecture and organization
[NASA-CR-185955] 06 p0832 N90-14839
Autonomous land navigation in a structured environment
[DE90-001625] 07 p0878 N90-15087
NOISE: A nonlinear optimization induction free-electron laser systems engineering code
[DE90-004438] 07 p0936 N90-15420
Sensor integration using concurrent computing on-board the ORNL mobile robot
[DE89-008740] 07 p0939 N90-15436
A semiautomated computer-interactive dynamic impact testing system
[DE90-002721] 07 p0946 N90-15479
An architectural model of visual motion understanding
[AD-A214327] 07 p0967 N90-15589
Designing machines for lattice physics and algorithm investigation
[DE90-003543] 07 p0969 N90-15596
ARGOS (A Research GMMP Operating System): Overvie w and interfaces
[AD-A213871] 07 p0970 N90-15599
The implementation of a coherent memory abstraction on a NUMA (Non-Uniform Memory Access) multiprocessor: Experiences with PLATINUM (Platform for Investigating Non-Uniform Memory)
[AD-A213909] 07 p0970 N90-15600
Memory management for large-scale NUMA (Non-Uniform Memory Access) multiprocessors
[AD-A213910] 07 p0970 N90-15601
An overview of PLATINUM: A Platform for Investiga ting Non-Uniform Memory (preliminary version)
[AD-A213911] 07 p0970 N90-15602
Evolution of an operating system for large-scale shared-memory multiprocessors
[AD-A213912] 07 p0970 N90-15603
Reconfigurable N-dimensional computer memory
[AD-D014309] 07 p0971 N90-15607
High level language memory management on parallel architectures
[DE89-015018] 07 p0971 N90-15609
An efficient UNICOS run-time system for functional programs on a CRAY X-MP
[DE89-016603] 07 p0972 N90-15610
Elicitation of natural language representations of uncertainty using computer technology
[DE90-001416] 07 p0972 N90-15611
Transport modeling and advanced computer techniques
[DE90-001481] 07 p0972 N90-15612
Name assignment techniques for relational schemas representing extended entity-relationship schemas
[DE90-003269] 07 p0974 N90-15623
Programs for control of an analog-signal switching network
[DE90-003645] 07 p0974 N90-15626
Optical neural nets for scene analysis
[AD-A213986] 07 p0976 N90-15637
MASC: Multiprocessor architecture for symbolic processing
[AD-A213504] 07 p0979 N90-15656
One-class generalization in second-order backpropagation networks for image classification
[DE89-015845] 07 p0980 N90-15661
Systolic algorithms for imaging from space
[AD-A213870] 07 p0987 N90-15701
Upgrade plans to handle 30 to 40 Mbytes of data for D3-D
[DE90-003291] 07 p0995 N90-15750
Procurement of an optical disk information storage and retrieval system
[DE90-001372] 07 p1010 N90-15849
Data file management in the D3-D data acquisition and analysis computer systems
[DE90-003289] 07 p1010 N90-15850
Issues and approaches for electronic document approval and transmittal using digital signatures and text authentication: Prototype documentation
[DE90-003382] 08 p1055 N90-16119
The Suprenum architecture and its application to computational fluid dynamics
[GMD-389] 08 p1065 N90-16161
Parallel asynchronous systems and image processing algorithms 08 p1075 N90-16218
Expert system control of a six-legged walking telerobot
[DE90-004661] 08 p1086 N90-16285
Dynamic architecture computer
[AD-A214262] 08 p1106 N90-16402
The SMITE approach to security
[RSRE-89014] 08 p1106 N90-16404
Spanning trees of hypercubes with a maximum of sixteen peaks
[IMAG-RR-755-I] 08 p1107 N90-16406
FRAC-IN-THE-BOX utilization
[DE90-003648] 08 p1108 N90-16412
Algorithms for fault tolerant distributed systems
[AD-A214447] 08 p1109 N90-16416
Creating the next generation control system software
[DE90-003391] 08 p1109 N90-16419
A 3-D measurement system using object-oriented FORTH
[DE90-003393] 08 p1109 N90-16420
Design and implementation of a multi-sensor fusion algorithm on a hypercube computer architecture
[DE90-003682] 08 p1112 N90-16438
Overview and extensions of a system for routing directed graphs on SIMD architectures 08 p1113 N90-16444
BLITZEN: A highly integrated massively parallel machine 08 p1115 N90-16453
On the efficient exploitation of speculation under data flow paradigms of control
[AD-A214112] 08 p1115 N90-16455
Abbreviated query interpretation in extended entity-relationship oriented databases
[DE90-003114] 08 p1137 N90-16587
Recent developments in TERPROM 09 p1163 N90-16732
Parallel processing implementation of a flight controller 09 p1165 N90-16743
Eigensolution of finite element problems in a completely connected parallel architecture
[NASA-TM-102450] 09 p1236 N90-17173
The use of computer programs to determine environmental compliance, predict performance, and assess impacts
[DE90-005230] 09 p1245 N90-17222
Supporting shared data structures on distributed memory architectures
[NASA-CR-181981] 09 p1262 N90-17318
Communication-efficient arbitration models for low-resolution data flow computing
[AD-A214768] 09 p1262 N90-17319
MPlus Database system
[DE90-004146] 09 p1263 N90-17325
The EPSILON-2 hybrid dataflow architecture
[DE90-003152] 09 p1263 N90-17326
Parallel functional computation
[AD-A214827] 09 p1269 N90-17360
Parallel logic programming and parallel systems software and hardware
[AD-A214635] 09 p1270 N90-17361
Merlin: A superglue for multicomputer systems
[NASA-CR-186330] 09 p1271 N90-17366
Hybrid optical/digital architecture for distortion invariant pattern recognition
[AD-A215628] 09 p1282 N90-17435
Database creation and/or reorganization over multiple database backends
[AD-A214939] 09 p1296 N90-17513
Design and implementation of the nested relational data model under the Exodus extensible database system
[AD-A215356] 09 p1296 N90-17515
Low elevation angle KU-band satellite measurements at Austin, Texas 10 p1373 N90-17959
Development of an integrated mobile robot system at Carnegie Mellon University: June 1988
[AD-A215955] 10 p1392 N90-18049
A flexible basis for software configuration management
[RSRE-MEMO-4127] 10 p1415 N90-18153
Cache for multi-threaded processors on a split-transaction bus
[AD-A216404] 10 p1415 N90-18156
Research at New York University's Ultracomputer Research Laboratory
[DE90-005471] 10 p1417 N90-18167
Logical architecture
[INPE-4792-RPE/585] 10 p1418 N90-18171
Numerical algorithms for parallel computers
[AD-A216812] 10 p1419 N90-18181
Writing parallel, discrete-event simulations in ModSim: Insight and experience
[DE90-001833] 10 p1419 N90-18183
Factoring symmetric indefinite matrices on high-performance architectures
[NASA-CR-181982] 10 p1421 N90-18195
Structured analysis tool interface to the strategic defense initiative architecture dataflow modeling technique
[AD-A216281] 10 p1424 N90-18218
Optical shared memory
[AD-A215090] 10 p1430 N90-18249
The design and analysis of new techniques for transaction management in database systems
10 p1441 N90-18314
Binary correlators for optical computing and pattern recognition 10 p1441 N90-18318
A microcode compiler that runs on the IBM AT and supports cascadable microcomputers, part 1
[AD-A215888] 11 p1542 N90-18877
A scalable multiprocessor architecture using Cartesian network: Relative addressing
[AD-A216580] 11 p1542 N90-18878
Performance characterization of the Convex C-240 computer system
[DE90-006425] 11 p1543 N90-18879
Cedar project: Original goals and progress to date
[DE90-006761] 11 p1543 N90-18880
L: A language for solution of incremental systems in a parallel processing environment
[INPE-4818-TDL/362] 11 p1543 N90-18884
Derivation of efficient parallel programs: An example from genetic sequence analysis
[DE90-005654] 11 p1547 N90-18904
Parallelizing the SDI ACCESS algorithm for the Connection Machine-2
[DE90-006382] 11 p1548 N90-18909
Summer institute in parallel computing
[DE90-005532] 11 p1548 N90-18910
Using special-purpose computing to examine chaotic behavior in nonlinear mappings
[AD-A216800] 11 p1549 N90-18916
Architecture for a human-robot symbiotic system
[DE90-005870] 11 p1550 N90-18921
Using the K-25 C/TD common file system: A guide to CFSI
[DE90-005815] 11 p1593 N90-19179
Flight crew aiding for recovery from subsystem failures
[NASA-CR-181905] 12 p1696 N90-19741
An approach to elemental task learning
[DE90-006614] 12 p1697 N90-19745
Design and architecture of fourth and fifth generation software engineering environments
[ETN-90-95365] 12 p1698 N90-19752
A virtual zero-time, monolithic systolic sorting array
[DE90-001000] 12 p1698 N90-19753
Flosolver Mk1B: An eight processor parallel machine
[PD-CF-8941] 12 p1699 N90-19755
Random access transmission algorithms for data local area networks
[AD-A216443] 12 p1700 N90-19761
Image manipulation in the SIGGRAPH Interactive Proceedings
[DE90-007542] 12 p1702 N90-19771
Space station Simulation Computer System (SCS) study for NASA/MSFC. Volume 3: Refined conceptual design report
[NASA-CR-183842] 13 p1762 N90-20115
Space station Simulation Computer System (SCS) study for NASA/MSFC. Volume 4: Conceptual design report
[NASA-CR-183843] 13 p1762 N90-20116
Joint services electronics program
[AD-A217961] 13 p1797 N90-20311
Integrated circuits for avionics
[AD-A217964] 13 p1797 N90-20312
Massively-parallel computational fluid dynamics
[AD-A217732] 13 p1802 N90-20342
Robot navigation research using the HERMIES mobile robot
[DE90-001952] 13 p1810 N90-20396
Robust performance of multiple tasks by a mobile robot
[DE90-001953] 13 p1811 N90-20397
Swing-free movement of simply suspended objects employing parameter estimation
[DE90-002238] 13 p1811 N90-20398
Transaction processing in a quality control laboratory
[DE90-004655] 13 p1813 N90-20414
Approximate evaluation of reliability and related quantities via perturbation techniques
[AD-A218340] 13 p1814 N90-20417
Three-dimensional medical image analysis using local dynamic algorithm selection on a multiple-instruction, multiple-data architecture
[AD-A218024] 13 p1852 N90-20630
Adaptive associative-processing optical computing architectures
[AD-D014317] 13 p1863 N90-20685
A unified approach to the synthesis of fully testable sequential machines
[AD-A217120] 13 p1863 N90-20687
NYU (New York University) ultracomputer
[AD-A217187] 13 p1863 N90-20688
Computer Science and Technology Board
[DE90-008292] 13 p1864 N90-20690
A real-time parallel pipelined data-flow image-processing system
[DE90-008324] 13 p1864 N90-20691

(DURIP) Two-Processor Alliant FX/4 System
[AD-A217810] 13 p1864 N90-20692
The contour model architecture and assembly language
[AD-A217114] 13 p1865 N90-20697
Using formal methods to develop a paradigm for software design
[DE90-005633] 13 p1866 N90-20703
ISLE (Image and Signal Processing LISP Environment) reference manual
[DE90-007858] 13 p1866 N90-20705
RIPE: An object-oriented Robot Independent Programming Environment
[DE90-008501] 13 p1866 N90-20707
Joint Japanese-American Workshop on Future Trends in Logic Programming
[DE90-008343] 13 p1867 N90-20709
A paradoxical result in unconditionally secure authentication codes, and an explanation
[DE90-008529] 13 p1867 N90-20710
Technical specifications requirements: Automated reasoning applications
[DE90-008799] 13 p1867 N90-20712
Advanced parallel systems
[AD-A217175] 13 p1872 N90-20731
Robust planning and control using neural networks
[AD-A217216] 13 p1872 N90-20732
Parallel computer graphics algorithms for the connection machine
[AD-A217300] 13 p1872 N90-20733
Asynchronous design for parallel processing architectures
[AD-A217421] 13 p1872 N90-20734
The Livermore distributed storage system: Implementation and experiences
[DE90-007257] 13 p1872 N90-20735
Implementation of a control system test environment in UNIX
[DE90-007485] 13 p1872 N90-20736
A parallel architecture for real-time simulation
[AD-A218321] 13 p1873 N90-20741
Irredundant sequential machines via optimal logic synthesis
[AD-A217119] 13 p1873 N90-20742
Hybrid intelligent perception system: Intelligent perception through combining artificial neural networks and an expert system
[DE90-007483] 13 p1874 N90-20746
Computation and graphics in mathematical research
[DE90-008429] 13 p1877 N90-20766
Towards SDS (Strategic Defense System) testing and evaluation: A collection of relevant topics
[AD-A217610] 13 p1880 N90-20783
Controlled multibody dynamics simulation for large space structures 14 p1934 N90-21068
Computational architecture for integrated controls and structures design 14 p1935 N90-21076
Application of optimization in design and motion control of robot manipulators 14 p1988 N90-21393
A knowledge-based information based for crop area estimation
[INPE-4990-PRE/1555] 14 p1996 N90-21444
Fault tolerant hypercube computer system architecture
[NASA-CASE-NPO-16859-1-CU] 14 p2012 N90-21527
Software Management Environment (SME) concepts and architecture
[NASA-TM-103306] 14 p2014 N90-21543
Software Engineering Laboratory (SEL) database organization and user's guide
[NASA-TM-103304] 14 p2015 N90-21545
Toward a new CIM (Computer Integrated Manufacturing) architecture for Sandia Laboratories
[DE90-008677] 14 p2015 N90-21548
Architecture independent environment for developing engineering software on MIMD computers
[NASA-CR-186562] 14 p2016 N90-21553
Performance bounds on parallel self-initiating discrete-event
[NASA-CR-182010] 14 p2016 N90-21556
NETRA: A parallel architecture for integrated vision systems 2: Algorithms and performance evaluation
[NASA-CR-186510] 14 p2017 N90-21557
Activities and operations of the Advanced Computing Research Facility
[DE90-007957] 14 p2017 N90-21559
STORM: A statistical object representation model
[DE90-009048] 14 p2036 N90-21686
Parallel asynchronous hardware implementation of image processing algorithms 15 p2138 N90-22219
Sparse distributed memory overview 15 p2141 N90-22235
Algorithms and architectures for robot vision 15 p2141 N90-22236
VCS: A networked Version Control System
[DE90-009805] 15 p2145 N90-22250
Understanding the computing system domain of advanced computing with microcomputers
[DE90-009825] 15 p2145 N90-22251
Scalable coherent interface
[DE90-008011] 15 p2149 N90-22277
The art of fault-tolerant system reliability modeling
[NASA-TM-102623] 15 p2152 N90-22292
The 1990 Goddard Conference on Space Applications of Artificial Intelligence
[NASA-CP-3068] 15 p2152 N90-22294
Resource Allocation Planning Helper (RALPH): Lessons learned 15 p2152 N90-22296
The role of artificial intelligence techniques in scheduling systems 15 p2152 N90-22297
SURE (Science User Resource Expert): A science planning and scheduling assistant for a resource based environment 15 p2153 N90-22302
Managing temporal relations 15 p2154 N90-22304
Autonomous power expert system 15 p2154 N90-22306
Spacecraft command verification: The AI solution 15 p2154 N90-22307
Adaptive pattern recognition by mini-max neural networks as a part of an intelligent processor 15 p2156 N90-22317
Guide to RMS-literature
[REPT-89-52] 15 p2158 N90-22326
An intelligent interface for the design of optimal control systems
[INPE-4917-PRE/1516] 15 p2159 N90-22332
Facilitating knowledge sharing in organizations: Semiautonomous agents that learn to gather, classify, and distribute environmental scanning knowledge 15 p2176 N90-22435
Update on the OPAL opacity code
[DE90-009946] 15 p2184 N90-22480
A candidate architecture for monitoring and control in chemical transfer propulsion systems
[NASA-TM-103161] 16 p2208 N90-22595
H2, fixed architecture, control design for large scale systems
[NASA-CR-180471] 16 p2226 N90-22698
Executive summary for the network assessment model
[AD-A218762] 16 p2229 N90-22718
Plan execution control and architecture for mobile robots
[LAAS-89-371] 16 p2243 N90-22793
A preliminary analysis of the SOAR architecture as a basis for general intelligence
[AD-A218913] 16 p2262 N90-22896
Towards the knowledge level in SOAR: The role of the architecture in the use of knowledge
[NASA-CR-186615] 16 p2262 N90-22897
Rules and maps in connectionist symbol processing
[AD-A219028] 16 p2264 N90-22903
Connectionism and compositional semantics
[AD-A219029] 16 p2264 N90-22904
Cognitive architectures and rational analysis: Comment
[AD-A219199] 16 p2264 N90-22907
Toward a SOAR theory of taking instructions for immediate reasoning tasks
[AD-A219201] 16 p2265 N90-22909
An instructable Connectionist/Control architecture: Using rule-based instructions to accomplish connectionist learning in a human time scale
[AD-A219274] 16 p2266 N90-22914
Non-LIFO (Last-In-First-Out) execution of cognitive procedures
[AD-A219277] 16 p2266 N90-22916
Encoding sequential structure in simple recurrent networks
[AD-A218928] 16 p2278 N90-22984
Parallel algorithms and architecture for computation of manipulator forward dynamics 16 p2283 N90-23010
Characterization of robotics parallel algorithms and mapping onto a reconfigurable SIMD machine 16 p2289 N90-23039
Algorithmic considerations of integrated design for CSI on a hypercube architecture 16 p2289 N90-23043
JPL control/structure interaction test bed real-time control computer architecture 16 p2294 N90-23070
Proceedings of the NATO Advanced Workshop on Supercomputing
[AD-A218508] 16 p2299 N90-23102
Fault tolerant multiprocessing and development of tools
[AD-A219216] 16 p2301 N90-23110
Kernal architecture manual
[AD-A219295] 16 p2301 N90-23115
Interconnection networks for highly parallel supercomputing architectures
[REPT-89-053] 16 p2302 N90-23118
Message handling in the post-2000 era: Executive summary
[AD-A219983] 17 p2393 N90-23628
Ultra high-speed compound semiconductors and real time signal processing
[AD-A220721] 17 p2396 N90-23651
VLSI architectures and CAD
[AD-A220736] 17 p2397 N90-23652
An expert system for the study of high duty bonded joints in aerospace structures
[REPT-892-430-110] 17 p2414 N90-23753
FASTER: The Fault Tolerant Architecture Simulation Tool for Evaluating Reliability, introduction and applications
[AD-A219941] 17 p2414 N90-23755
TUMULT-64: A real-time multi-processor system
[MEMO-INF-89-58] 17 p2440 N90-23904
The standard map machine
[AD-A219943] 17 p2441 N90-23908
Novel numerical algorithms for sensing, discrimination, and control
[AD-A220805] 17 p2444 N90-23929
Design of finite element systems for parallel computers 17 p2450 N90-23975
ISDN in the local environment: The CISLAN project
[MEMO-INF-89-70] 17 p2452 N90-23985
Northeast Artificial Intelligence Consortium. Volume 4. Distributed AI for communications network management
[AD-A218717] 17 p2453 N90-23994
A decision support system for control and automation of dynamical processes
[AD-A219501] 17 p2454 N90-23995
Northeast Artificial Intelligence Consortium annual report, 1988. Volume 12: Computer architectures for very large knowledge bases
[AD-A219599] 17 p2454 N90-23999
Neural networks applied to signal processing
[AD-A219605] 17 p2454 N90-24000
The Hermes robot arm teleoperation and control concept 18 p2503 N90-24301
The bi-arm servicer: A multimission concept and a technological model for space robotics 18 p2504 N90-24307
NASREM: A functional architecture for control of the flight telerobotic servicer 18 p2506 N90-24325
A low-cost PC-based telemetry data-reduction system
[DE90-000330] 18 p2509 N90-24339
AIRNET: A real-time comunications network for aircraft
[NASA-CR-186140] 18 p2543 N90-24514
SEU characterization and design dependence of the SA3300 microprocessor
[DE90-007678] 18 p2589 N90-24728
Recent experiences and future expectations in data storage technology
[DE90-011488] 18 p2589 N90-24729
CERC (Center for Energy Research Computation) report: Results of the CERC Project with recommendations for ANL (Argonne National Laboratory) institutional strategies in advanced scientific computing
[DE90-008238] 18 p2594 N90-24759
Input/output algorithm for M-dimensional rectangular domain decompositions on N-dimensional hypercube multicomputers
[DE90-010494] 18 p2594 N90-24762
Visual animation of parallel algorithms for matrix computations
[DE90-011076] 18 p2594 N90-24763
Determination of algorithm parallelism in NP complete problems for distributed architectures
[AD-A220192] 18 p2598 N90-24786
Enhancing a relational database: Stepwise, bottom-up design
[DE90-010834] 18 p2635 N90-25012
Conceptual design for aerospace vehicles 18 p2641 N90-25043
Privacy-enhanced electronic mail
[PCS-TR90-150-REV-1] 19 p2683 N90-25261
A task control architecture for autonomous robots 19 p2735 N90-25546
Behavioral networks as a model for intelligent agents 19 p2738 N90-25561
The application of NASREM to remote robot control 19 p2738 N90-25563
Multiprocessor architecture: Synthesis and evaluation
[NASA-CR-186618] 19 p2741 N90-25579
The basis system
[DE90-012077] 19 p2743 N90-25591
Modeling and synthesis of multicomputer interconnection networks
[NASA-CR-186619] 19 p2746 N90-25604
On the design of a concurrent image analysis system
[DE90-011388] 19 p2746 N90-25605

Neuromorphic learning of continuous-valued mappings from noise-corrupted data. Application to real-time adaptive control
[NASA-TM-4176] 19 p2747 N90-25607
Applying formal models and proofs to the verification of distributed systems
[IAR-89-7] 19 p2750 N90-25625
Center for Space Microelectronics Technology 1988-1989 technical report
[NASA-CR-186849] 19 p2753 N90-25642
Thermionic gun control system for the CEBAF injector
[CEBAF-PR-89-028] 19 p2755 N90-25654
Tools for distributed application management
[NASA-CR-186646] 19 p2762 N90-25692
Technical evaluation report on the Guidance and Control Panel 49th Symposium on Fault Tolerant Design Concepts for Highly Integrated Flight Critical Guidance and Control Systems
[AGARD-AR-281] 20 p2813 N90-26012
OASIS, LLNL version: Software maintenance manual
[DE90-013522] 20 p2868 N90-26313
Guidance and control system for an autonomous underwater vehicle
[AD-A222709] 20 p2873 N90-26343
Computer architecture evaluation for structural dynamics computations: Project summary
[NASA-CR-186137] 20 p2903 N90-26512
Applications for the scalable coherent interface
[DE90-011795] 20 p2903 N90-26514
ANTIPASTO: An interactive mesh generator and preprocessor for two-dimensional analysis programs
[DE90-011755] 20 p2906 N90-26530
SUPES version 2.1: A Software Utilities Package for the Engineering Sciences
[DE90-011763] 20 p2906 N90-26531
Level-2 system: Programmers-users manual
[DE90-013324] 20 p2908 N90-26540
Single-pass memory system evaluation for multiprogramming workloads
[NASA-CR-186553] 20 p2910 N90-26558
Language support for parallel computation
[AD-A223072] 20 p2911 N90-26560
Parallel programming with algorithmic skeletons
[DE90-010536] 20 p2911 N90-26562
Pacific missile test center information resources management organization (code 0300): The ORACLE client-server and distributed processing architecture
[DE90-013271] 20 p2912 N90-26565
Design of a universal protocol subsystem architecture: Specification of functions and services
[EUT-89-E-230] 20 p2912 N90-26569
Massively parallel architecture: Integrated cell network for image reconstruction
[ETN-90-97257] 20 p2913 N90-26575
Superconcurrent processing: A dynamic approach to heterogeneous parallelism
[AD-A222798] 20 p2914 N90-26576
Application of artificial intelligence to the architectural synthesis of VLSI integrated circuits
[ETN-90-97253] 20 p2916 N90-26589
High speed all optical networks
[NASA-CR-185311] 20 p2926 N90-26649
A methodology for benchmarking distributed database management systems
[DE90-007801] 20 p2935 N90-26702
Particle simulation of hypersonic flow
[AD-A222704] 21 p2954 N90-26794
Computational methods for problems in aerodynamics using parallel and vector architecture
[AD-A221979] 21 p2954 N90-26795
Local design methodologies for a hierarchic control architecture
[AD-A222006] 21 p2966 N90-26862
Optical wavefront computer for stabilizing large space structures
[AD-A221707] 21 p2967 N90-26866
Communications network analysis tool
[AD-A222061] 21 p2998 N90-27029
Parallel numerical simulations of axisymmetric projectile flows using zonal-overlapped grids
[AD-A221711] 21 p3005 N90-27082
Development of an integrated mobile robot system at Carnegie-Mellon University
[AD-A222494] 21 p3011 N90-27119
Symbolic architectures for cognition
[AD-A222909] 21 p3035 N90-27254
Special purpose parallel computer architecture for real-time control and simulation in robotic applications
[NASA-CASE-NPO-17629-1-CU] 21 p3038 N90-27268
A computer for low contest-switch time
[AD-A222883] 21 p3038 N90-27269
An architecture for intelligent task interruption 21 p3041 N90-27284
A knowledge-based approach to configuration layout, justification, and documentation 21 p3041 N90-27286
KIPSE1: A Knowledge-based Interactive Problem Solving Environment for data estimation and pattern classification 21 p3041 N90-27287
An architecture for rule based system explanation 21 p3042 N90-27288
A study on diagnosability of space station ECLSS 21 p3043 N90-27294
Graphical explanation in an expert system for Space Station Freedom rack integration 21 p3044 N90-27299
A knowledge base architecture for distributed knowledge agents 21 p3044 N90-27302
Creature co-op: Achieving robust remote operations with a community of low-cost robots 21 p3044 N90-27303
Capturing design knowledge 21 p3045 N90-27305
A tool for modeling concurrent real-time computation 21 p3047 N90-27321
Sisal on a message passing architecture
[DE90-008786] 21 p3051 N90-27342
Knowledge based quality assurance tools
[AD-A223064] 21 p3053 N90-27353
Architectures for optical computing
[AD-A221435] 21 p3054 N90-27364
Knowledge representation in PARKA
[AD-A221471] 21 p3055 N90-27367
A programming environment for parallel vision algorithms
[AD-A221486] 21 p3055 N90-27368
Analog hardware for learning neural networks
[NASA-CASE-NPO-17664-1-CU] 21 p3057 N90-27384
CSRD parallel service machine enhancement
[AD-A221951] 21 p3058 N90-27388
Multiprocessor realization of neural networks
[AD-A222146] 21 p3060 N90-27400
The development of the time-delayed neural network architecture
[AD-A221540] 21 p3061 N90-27403
The post-2000 MILSATCOM architecture 21 p3070 N90-27452
Aircraft condition monitoring system for future Airbus aircraft: New concept for programming and data recording 22 p3103 N90-27619
Multichannel on-board load and fatigue monitoring 22 p3103 N90-27621
Reconfigurable integrated system architecture for future monitoring systems 22 p3106 N90-27638
Video-rate visual servoing for robots
[AD-A218711] 22 p3181 N90-28052
Improving software reusability by program specialization: A case study
[REPT-90-011] 22 p3240 N90-28374
Fault-tolerance in massively parallel silicon architectures: The case of neural nets
[REPT-90-012] 22 p3240 N90-28375
Interconnection networks and parallel processing
[FEL-1989-112] 22 p3240 N90-28376
Proceedings of the Conference on Artificial Intelligence in the Department of Energy Complex
[DE90-011634] 22 p3241 N90-28378
Compact 4-D optical neural network architecture
[AD-A222160] 22 p3241 N90-28379
Using embedded microcontrollers in radar test equipment
[DE90-014997] 23 p3319 N90-28763
Target detection in Gaussian noise using artificial neural systems
[AD-A223983] 23 p3320 N90-28770
DOE/NIST Workshop on Common Architectures for Robotic Systems
[PB90-216839] 23 p3332 N90-28840
A system architecture for a planetary rover 23 p3365 N90-29015
The NASA/OAST telerobot testbed architecture 23 p3365 N90-29016
Three-dimensional motor schema based navigation 23 p3367 N90-29026
A hybrid architecture for the implementation of the Athena neural net model 23 p3368 N90-29032
A design philosophy for multi-layer neural networks with applications to robot control 23 p3368 N90-29033
State-based scheduling: An architecture for telescope observation scheduling 23 p3369 N90-29038
The JPL telerobot operator control station. Part 1: Hardware 23 p3371 N90-29049
Implementation and design of a teleoperation system based on a VMEBUS/68020 pipelined architecture 23 p3372 N90-29053
Integrating planning, execution, and learning 23 p3377 N90-29079
A personal computer-based, multitasking data acquisition system
[NASA-TM-4232] 23 p3382 N90-29107
A hardware/software environment to support R/D in intelligent machines and mobile robotic systems
[DE90-014458] 23 p3385 N90-29119
Information management directions: The integration challenge
[PB90-219866] 23 p3405 N90-29245
Distributed control architecture for CNI preprocessors 24 p3426 N90-29356
JTIDS relative navigation: Principles, architecture, and inertial mixing 24 p3426 N90-29357
High speed bus technology development
[AD-A224488] 24 p3463 N90-29565
Basic properties and limits of integrated arrays of dissipative circuit and logic elements
[AD-A224533] 24 p3464 N90-29567
Concept for a reference model Architecture for Real-Time Intelligent Control Systems (ARTICS)
[PB90-220286] 24 p3475 N90-29638
Controlling multiple manipulators using RIPS 24 p3505 N90-29814
The flight telerobotic servicer: From functional architecture to computer architecture 24 p3507 N90-29823
System architectures for telerobotic research 24 p3515 N90-29872
Optical symbolic processor for expert system execution
[AD-A224284] 24 p3525 N90-29931
Parallel architectures and algorithms for image understanding
[AD-A223479] 24 p3526 N90-29940
Computer-aided engineering environment for controlled mechanical systems
[AD-A223551] 24 p3527 N90-29942
Fast algorithms for parallel architectures
[AD-A223731] 24 p3528 N90-29947
MUSE: A systolic array for adaptive nulling with 64 degrees of freedom, using Givens transformations and wafer scale integration
[AD-A223812] 24 p3529 N90-29953
GSHELL: Multichannel analyzer/multichannel scaler emulation software for IBM-PC-compatible computers
[DE90-015396] 24 p3529 N90-29956
A manual for microcomputer image analysis
[DE90-015629] 24 p3529 N90-29958
Asynchronous design for parallel processing architectures
[AD-A223754] 24 p3533 N90-29981
Approach to telerobot computing architecture
[NASA-CR-186993] 24 p3534 N90-29984
Optical signal computing
[AD-A223624] 24 p3545 N90-30051
A survey of object-oriented database technology
[AD-A224490] 24 p3558 N90-30130
Small multipurpose stored data acquisition system
[DE90-010823] 24 p3558 N90-30134
Integration of information systems components
[DE90-011761] 24 p3559 N90-30136

ARCTIC ENVIRONMENTS
U ICE ENVIRONMENTS

ARCTIC OCEAN
The sea ice margins: A summary of physical phenomena
[PB89-212328] 02 p0253 N90-11436

ARCTIC REGIONS
Meteorological atlas of the Northern Hemisphere lower stratosphere for January and February 1989 during the Airborne Arctic Stratospheric Expedition
[NASA-TM-4145] 05 p0671 N90-13908
A rough transform technique for extracting lead features from sea ice imagery
[AD-A212758] 06 p0801 N90-14666
Decomposition in Arctic terrestrial environments
[DE90-001198] 06 p0809 N90-14706
A compact acoustic recorder
[AD-A213581] 07 p0933 N90-15403
Measurement of fluctuations in the tilt of Arctic ice at the CEAREX Oceanography Camp: Experiment review, data catalog, and preliminary results
[AD-A215059] 09 p1249 N90-17249
Opportunities for US-USSR cooperation in the investigation of Arctic stratospheric ozone 15 p2125 N90-22154
The sources and chemistry of late winter Arctic tropospheric aerosols
[PB90-131988] 15 p2126 N90-22158
On the antarctic ozone depletion during solar cycle 21
[NOTA-INTERNA-943] 16 p2253 N90-22849
The analysis of polar clouds from AVHRR satellite data using pattern recognition techniques
[NASA-CR-183300] 16 p2257 N90-22868

Comparison of Goretex laminated and Dermoflex coated fabrics
[AD-A219383] 17 p2368 N90-23481
Environmental measurements and analysis: Arctic acoustics experiments in the marginal ice zone
[AD-A220509] 18 p2582 N90-24708
Arctic cold weather medicine and accidental hypothermia
[AD-A223090] 20 p2899 N90-26487
Geologic studies in Alaska by the US geological survey, 1988
[PB90-180993] 22 p3211 N90-28213
An integrated system for land navigation
24 p3430 N90-29377
Wind tunnel, field, and numerical investigations of plume downwash and dispersion at an arctic industrial site
24 p3489 N90-29721

AREA
On the areas of various bodies in the Euclidean space: The case of irregular convex polygons
[DE89-618377] 02 p0264 N90-11500
Area-universal networks
[AD-A211883] 04 p0535 N90-13092

AREA NAVIGATION
Simulations for computer centerline approach
[DOT/FAA/CT-TN89/41] 03 p0304 N90-11726
A conflict analysis of 4D descent strategies in a metered, multiple-arrival route environment
[NASA-CR-182019] 15 p2055 N90-21772
An evaluation of the accuracy of a microwave landing system area navigation system at Miami/Tamiami Florida Airport
[DOT/FAA/CT-TN89/40] 17 p2349 N90-23377

ARGON
Spin-orbit relaxation rates of Bi(6p(3)) 2D(3/2) following photolysis of Bi(CH3)3 at lambda = 193 nm
[AD-A211792] 03 p0402 N90-12303
Survey of the response of standard limited streamer tubes over the complete range of three-component gas mixtures of isobutane, CO(sub 2), argon
[DE89-016692] 04 p0499 N90-12875
Hot spots Ar and Ne gas puff z-pinch
[IPPCZ-289] 05 p0701 N90-14103
The effect of electric field on attachment of electrons to solutes in liquid argon
[DE90-003969] 11 p1482 N90-18529
Numerical Green's functions in optical potential calculations for positron scattering from argon and neon
11 p1557 N90-18971
Effects of basis set contraction in relativistic calculations on neon, argon, and germanium
[AD-A223357] 24 p3446 N90-29460
Rates of vertical mixing, gas exchange, and new productions: Estimates from seasonal gas cycles in the upper ocean near Bermuda
[PB90-244781] 24 p3496 N90-29758

ARGON LASERS
Treatment of laser-induced retinal injuries
[AD-A210284] 01 p0092 N90-10526
Theoretical and experimental investigation of coupled Ar-ion lasers
[AD-A214908] 09 p1227 N90-17122
A study of the interaction of light with surfaces of sub-micron dimensions
[DE90-006646] 11 p1571 N90-19046
Picosecond Laser Facility
[AD-A217784] 13 p1808 N90-20384

ARGON PLASMA
An experimental study of microwave transmission through a decaying plasma
[AD-A210586] 01 p0127 N90-10726
Box experiments. Nonlinear effects at plasma resonance 06 p0783 N90-14555
Plasma modification of poly (p-phenylenebenzobisthiazole)
[AD-A215761] 10 p1433 N90-18272

ARGOS SYSTEM
Location systems: ARGOS, SARSAT
17 p2359 N90-23430
Comparison of location systems
17 p2360 N90-23437

ARGUMENTS (MATHEMATICS)
U INDEPENDENT VARIABLES

ARIANE LAUNCH VEHICLE
Dynamic substructuring for modular analysis and testing 02 p0180 N90-11015
Induced shock loads during the separation of the Ariane 5 VEB structure 02 p0184 N90-11045
Flight-mechanical environment on Ariane launch vehicle payloads 02 p0184 N90-11048
Ariane 5 structural design and development
02 p0186 N90-11057
Progress in Space Transportation
[ESA-SP-293] 09 p1173 N90-16782
Keynote address 09 p1173 N90-16783
ESA's space transportation programme
09 p1173 N90-16786
The Ariane-5 Programme 09 p1176 N90-16808
Ariane-5 upper stage EPS 09 p1176 N90-16809
Vulcain engine development status
09 p1176 N90-16810
Ariane-5 solid boosters stage development
09 p1176 N90-16811
Static test deflector for Ariane-5 SRM: Technical design and economical choice 09 p1176 N90-16812
The DLR technology programme on space transportation 09 p1180 N90-16841
Efficient calculation of Ariane ascent trajectories with recursive quadratic programming
09 p1180 N90-16844
A power system for ARTEP 10 p1331 N90-17694
The initial imperfection databank at the Delft University of Technology, part 3
[LR-568] 15 p2057 N90-21783
Seal requirements in rocket propulsion
[ETN-90-96611] 16 p2205 N90-22580
Conceptual work at Aerospatiale on air-breathing and non-air-breathing recoverable launchers
[REPT-892-422-104] 17 p2362 N90-23450
PLATO: A European plateform orbiter concept
[MBB-UO-0061/89-PUB] 19 p2652 N90-25095
Ascent and descent trajectory optimization of Ariane 5/Hermes 22 p3126 N90-27743
Hermes emergency reentry trajectories consequences on the Ariane 5 trajectories 22 p3127 N90-27747

ARIES SOUNDING ROCKET
Rocket and satellite observations of the local interstellar medium 02 p0292 N90-11668

ARIP (IMPACT PREDICTION)
U COMPUTERIZED SIMULATION
U IMPACT PREDICTION

ARITHMETIC
NT FIXED POINT ARITHMETIC
NT FLOATING POINT ARITHMETIC
A multiprocessor architecture using modular arithmetic for very high precision computation
[AD-A208154] 01 p0102 N90-10579
Non-separate arithmetic codes
[RSRE-MEMO-4215] 04 p0530 N90-13058
Measurement of arithmetic error and calculation perturbations
[IMAG-RR-767-M] 05 p0692 N90-14039
Ultra high performance, highly reliable, numeric intensive processors and systems
[AD-A214100] 07 p0980 N90-15659
Research equipment
[AD-A216515] 11 p1552 N90-18937
Euler's theorem for polynomials
[AD-A218148] 13 p1878 N90-20774
VLSI binary updown counter
[NASA-CASE-NPO-17205-1-CU]
14 p2011 N90-21525
Arithmetic classification of perfect models of stratified programs (extended version)
[CWI-CS-R8928] 17 p2462 N90-24063
A study of effects of instructional modes in a sequence of computer-assisted instruction lessons, with an introduction to computer-aided diagnosis of arithmetic errors 18 p2589 N90-24730
Rosser orderings and free variables
[ITLI-ML-89-03] 18 p2603 N90-24822
Sigma-completeness and bounded arithmetic
[ITLI-ML-89-05] 18 p2603 N90-24823

ARITHMETIC AND LOGIC UNITS
Measurement of arithmetic error and calculation perturbations
[IMAG-RR-767-M] 05 p0692 N90-14039
A genetic adaptive system for image understanding and learning research
[AD-A214810] 09 p1271 N90-17367

ARIZONA
Disturbances in the Arizona Monsoon
03 p0362 N90-12071
Winter cloud seeding potential on the Mogollon Rim
[PB89-190540] 07 p0962 N90-15562
Tropical squall lines of the Arizona monsoon
16 p2257 N90-22867
Anderson Mesa, Arizona as a site for an optical interferometric array 16 p2330 N90-23281

ARM (ANATOMY)
Criteria for a recommended standard: Occupational exposure to hand-arm vibration
[PB90-168048] 22 p3233 N90-28331

ARMATURES
Laser controlled semiconductor armature for electromagnetic launchers
[AD-D014435] 14 p1931 N90-21055
Feasibility of intercalated graphite railgun armatures
[NASA-TM-102546] 14 p1953 N90-21181

ARMED FORCES
NT ARMED FORCES (FOREIGN)
NT ARMED FORCES (UNITED STATES)
NT NAVY

ARMED FORCES (FOREIGN)
Physical performance and carbohydrate consumption in CF commandos during a 5-day field trial
[AD-A217204] 13 p1850 N90-20619

ARMED FORCES (UNITED STATES)
Human performance in continuous/sustained operations and the demands of extended work/rest schedules: An annotated bibliography, volume 2
[AD-A210504] 01 p0093 N90-10530
Twenty-five years of service, 1962-1987: Proceedings of the Air Force Studies Board Symposium on Air Force Research and Development, November 16, 1987
[PB89-198915] 03 p0415 N90-12384
Proceedings of the Army Symposium on Solid Mechanics, 1989: Mechanics of Engineered Materials and Applications
[AD-A211954] 04 p0511 N90-12951
Physical performance and carbohydrate consumption in CF commandos during a 5-day field trial
[AD-A217204] 13 p1850 N90-20619
Proceedings of the 28th Annual US Army Operations Research Symposium (AORS), volume 1
[AD-A219349] 18 p2606 N90-24842
Artificial intelligence within AFSC
19 p2727 N90-25504
United States Naval Academy summary of Research, Academic Departments, 1989-1990
[AD-A221219] 19 p2800 N90-25929
Space test range
[AD-A223259] 21 p2964 N90-26850
Research proposal
[AD-A221453] 21 p3085 N90-27545
United States Air Force research initiation program for 1988, volume 1
[AD-A223123] 21 p3101 N90-27613
United States Air Force research initiation program for 1988, volume 2
[AD-A223124] 21 p3102 N90-27614
United States Air Force research initiation program for 1988, volume 3
[AD-A223125] 21 p3102 N90-27615
United States Air Force research initiation program for 1988, volume 4
[AD-A223126] 21 p3102 N90-27616
Air Force Officer Qualifying Test (AFOQT): Development of quick score composites for forms P1 and P2
[AD-A223868] 23 p3362 N90-28997
Minimal sleep to maintain performance: Search for sleep quantum in sustained operations
[AD-A223815] 24 p3498 N90-29770
Software development: A product life-cycle perspective
[AD-A223783] 24 p3528 N90-29952

ARMOR
Alternative test methodology for ballistic performance ranking of armor ceramics
[AD-A210587] 01 p0051 N90-10290
Studies in penetration mechanics
[AD-A210713] 01 p0079 N90-10448
A study of the hot workability of Al-8.5 wt pct Mg alloys for armor plate applications
[AD-A211680] 03 p0329 N90-11868
Stand-off shields for hypervelocity particles
[DE89-016182] 07 p0939 N90-15437
Comparison of multidimensional calculations of long-rod impacts on oblique plates
[DE89-015275] 07 p0939 N90-15440
Fractographic analysis of long rod penetrator-armor ceramic interactions
[AD-A215172] 09 p1197 N90-16938
Taylor impact testing
[AD-A215018] 09 p1231 N90-17144
Evaluation of 2090-T8E48 aluminum-lithium plates
[AD-A217262] 13 p1776 N90-20196
Ductile alloy encapsulated ceramic armor development
[AD-A217632] 14 p1954 N90-21183
Large-scale simulations of monolithic and segmented projectiles impacting spaced armor
[AD-A219374] 16 p2244 N90-22800
Numerical simulation of semi-infinite target penetration by continuous and segmented rods
[AD-A219437] 17 p2412 N90-23743
X ray diffraction analysis of control and test fibers
[MTL-TR-89-58] 19 p2678 N90-25233
Motion sickness, visual displays, and armored vehicle design
[AD-A222678] 20 p2902 N90-26506
Advanced ceramic armor materials
[AD-A223227] 21 p2986 N90-26970

ARMS (ROBOTICS)
U ROBOT ARMS

AROMATIC COMPOUNDS
The effect of degree of aromaticity and alkyl substitution of polyaromatic hydrocarbons on instrumental response factors
[DE89-000781] 02 p0196 N90-11117
High temperature chemistry of aromatic hydrocarbons
[DE90-003664] 07 p0888 N90-15133
Effect of community structure on the kinetics of anaerobic degradation of aromatic compounds
[DE90-003666] 07 p0888 N90-15134

AROUSAL
Causes of aircrew error in the Royal Air Force
09 p1254 N90-17276

ARPA COMPUTER NETWORK
The internet worm
[NASA-CR-181576] 17 p2441 N90-23910

ARRAYS
NT ANTENNA ARRAYS
NT LINEAR ARRAYS
NT PHASED ARRAYS
NT SOLAR ARRAYS
NT SOLAR BLANKETS
NT STEERABLE ANTENNAS
NT SYSTOLIC ARRAYS
NT YAGI ANTENNAS
Laser diode array and transmission optics
01 p0030 N90-10163
A lunar far-side very low frequency array
[NASA-CP-3039] 01 p0139 N90-10805
On-orbit annealing of gallium arsenide solar cell arrays
[AD-A212087] 03 p0334 N90-11900
A SAW Slanted Array Correlator (SAC) with separate amplitude compensation channel
[AD-D014174] 03 p0336 N90-11914
Infrared detector array
[AD-D014170] 03 p0350 N90-11997
Sequential searching in multidimensional monotone arrays
[AD-A211938] 03 p0384 N90-12188
Development of FIR arrays with integrating amplifiers
05 p0598 N90-13473
Design of incoherent imaging arrays
[DE90-000861] 06 p0844 N90-14909
Detection of flow instabilities at airfoil profiles using piezoelectric arrays 08 p1067 N90-16175
Optical flow measuring method using diode lasers, phase coupled arrays, and high frequency pulsed diode lasers
08 p1067 N90-16176
A low-threshold EAS (Extensive-Air-Shower) array for gamma-ray astronomy at Los Alamos
[DE89-016780] 08 p1139 N90-16600
Status of the expansion of the CYGNUS array at Los Alamos
[DE89-016781] 08 p1139 N90-16601
Aerodynamic study on forced vibrations on stator rows of axial compressors 11 p1460 N90-18412
Performance of the IMP array processing algorithm: First results
[RSRE-MEMO-4291] 15 p2148 N90-22274
Anderson Mesa, Arizona as a site for an optical interferometric array 16 p2330 N90-23281
Artificial dielectrics
[AD-A219671] 17 p2389 N90-23605
Object orientated simulation on transputer arrays using time warp
[AD-A219795] 17 p2389 N90-23607
Vertical directionality measurements of ambient noise in the NE Pacific
[AD-A220007] 17 p2432 N90-23856
Observations of seafloor ambient noise with an ocean bottom seismometer array
[AD-A220159] 17 p2432 N90-23858
Gallium arsenide pilot line for high performance components
[AD-A220948] 18 p2547 N90-24540
Natural convection form an array of rectangular protrusions in an enclosure filled with dielectric fluid: Effects of boundary conditions, fluid Prandtl number, and selective powering
[AD-A219819] 18 p2552 N90-24563
A novel multireceiver communications system configuration based on optimal estimation theory
[NASA-CR-186847] 20 p2851 N90-26216
Non-contacting printed circuit waveguide elements
[AD-D014489] 22 p3166 N90-27957
Improved compact optical RF spectrum analyzer
[AD-D014481] 22 p3177 N90-28026
Serial interferometric fiber-optic sensor array
[AD-D014466] 22 p3246 N90-28407
Phoenix data analysis and numerical simulation
[AD-A224226] 23 p3320 N90-28772
Large aperture acoustic arrays in support of reverberation studies
[AD-A224002] 23 p3393 N90-29168
Dynamical properties of two-dimensional Josephson junction arrays
[AD-A223965] 23 p3402 N90-29221
Basic properties and limits of integrated arrays of dissipative circuit and logic elements
[AD-A224533] 24 p3464 N90-29567
Symmetrical layered thin film edge field-emitter-array and method for its production
[AD-D014594] 24 p3464 N90-29569

ARRIVALS
Computer-based tools for assisting air traffic controllers with arrivals flow management
[RSRE-88001] 05 p0577 N90-13366
Queues with negative arrivals
[AD-A213860] 07 p0984 N90-15687

ARSENIC
Effect of adsorbed arsenic on the decomposition rate of nickel hydride
[AD-A213245] 05 p0621 N90-13624
Improved SiAs BIBIB (Back-Illuminated Blocked-Impurity-Band) hybrid arrays
14 p1981 N90-21349
Ion/molecule reactions of arsenic and phosphorus cluster ions: Ionization potentials and novel reaction pathways
[AD-A222019] 21 p2977 N90-26918

ARSENIC COMPOUNDS
NT ALUMINUM ARSENIDES
NT ALUMINUM GALLIUM ARSENIDES
NT ARSENIDES
NT GALLIUM ARSENIDES
NT INDIUM ARSENIDES

ARSENIDES
NT ALUMINUM ARSENIDES
NT ALUMINUM GALLIUM ARSENIDES
NT GALLIUM ARSENIDES
NT INDIUM ARSENIDES
Energy relaxation of light holes in InAs(.15)Sb(.85)/InSb multiple quantum wells
[DE89-016035] 03 p0409 N90-12349

ARTERIES
Generation of free radicals during cold injury and rewarming
[AD-A213088] 05 p0672 N90-13915
Apparatus for imaging deep arterial and coronary lesions
[NASA-CASE-NPO-17439-1-CU]
08 p1104 N90-16391
Factor analytic reduction of the carotid-cardiac baroreflex parameters 08 p1155 N90-16693
Arginine vasopressin lowers pulmonary artery pressure in hypoxic rats by releasing artrial natriuretic peptide
[AD-A215986] 10 p1410 N90-18134

ARTHRITIS
Progressive cervical osteoarthritis in high performance aircraft pilots 19 p2718 N90-25465

ARTHROPODS
NT COCKROACHES
NT DROSOPHILA
NT INSECTS

ARTICULATION (SPEECH)
The effects of noise on speech and warning signals
[AD-A212520] 04 p0551 N90-13210

ARTIFICIAL CARDIAC PACEMAKER
The use of lithium batteries in biomedical devices
[AD-A210789] 01 p0061 N90-10350

ARTIFICIAL CLOUDS
NT CHEMICAL CLOUDS

ARTIFICIAL HEART VALVES
Durable heat diaphragm from ordered polymer films
[AD-A220794] 17 p2381 N90-23559

ARTIFICIAL INTELLIGENCE
NT EXPERT SYSTEMS
Identification of stability and control parameters of a brilliant ammunition 01 p0014 N90-10065
Real-time support for high performance aircraft operation
[NASA-CR-185475] 01 p0015 N90-10075
Knowledge-based machine vision systems for space station automation
[NASA-CR-185710] 01 p0025 N90-10124
Analysis and construction of contact and tactile sensors
[DE89-013992] 01 p0072 N90-10416
Autonomous mobile robot research using the HERMIES-3 robot
[DE89-015916] 01 p0078 N90-10443
Advancing automation and robotics technology for the space station Freedom and for the US economy
[NASA-TM-101561] 01 p0102 N90-10577
Northeast Artificial Intelligence Consortium annual report for 1987. Volume 5: Building an intelligent assistant: The acquisition, integration and maintenance of complex distributed tasks
[AD-A210330] 01 p0109 N90-10621
Northeast Artificial Intelligence Consortium annual report for 1987. Volume 7, part A: Time oriented problem solving
[AD-A210331] 01 p0110 N90-10622
Some results on learning
[AD-A210591] 01 p0110 N90-10624
The applicability and limitations of expert system shells
[AD-A210801] 01 p0110 N90-10625
The development of an expert system for the creative design of mechanisms
[AD-A211115] 01 p0110 N90-10628
Flight testing a newly-designed stand-off weapon dispenser 02 p0154 N90-10880
Systems analysis considerations in artificial intelligence/expert systems technology applications
[DE89-016847] 02 p0262 N90-11490
A survey of research methods to study design
[AD-A211213] 02 p0262 N90-11491
Electron transfer reactions
[AD-A210711] 02 p0271 N90-11545
Three dimensional object recognition employing combined visual and tactile sensing
[PB89-219489] 03 p0382 N90-12176
Navigation of robotic systems
[DE89-017507] 03 p0390 N90-12219
Taxonomic syntax for first order inference
[AD-A211618] 03 p0390 N90-12221
DOD Gateway Information System (DGIS) common command language: A retrospective on the introduction of prolog as the development tool
[AD-A211941] 03 p0418 N90-12400
Telerobotic control for teams of semi-autonomous agents, phase 1
[AD-A211648] 04 p0526 N90-13037
A knowledge-based approach to automated flow-field zoning for computational fluid dynamics
[NASA-TM-101072] 04 p0528 N90-13048
Truth maintenance systems and their implementation in PROLOG
[MEMO-INF-89-13] 04 p0531 N90-13064
Expert system for test program set fault candidate selection
[AD-A213338] 04 p0535 N90-13091
An on-line distributed minimum-time trajectory generator for intelligent robot manipulators
[RR-358] 04 p0536 N90-13102
Artificial intelligence for communication prospects
[FEL-1989-1] 04 p0537 N90-13107
Radar and sensor array design planning for a naval missile testing center. Artificial intelligence applications
[ETCA-88-R-099] 04 p0537 N90-13108
LAIOS: A multiprocessor network for artificial intelligence applications
[ETN-89-95498] 04 p0537 N90-13109
A theory of networks for approximation and learning
[AD-A212359] 04 p0538 N90-13110
NTRFACE for MAGIC
[AD-A212858] 04 p0538 N90-13112
Research in computer vision for autonomous systems
[AD-A212420] 04 p0555 N90-13235
User needs, benefits, and integration of robotic systems in a space station laboratory
[NASA-CR-185150] 05 p0651 N90-13794
Conference Proceedings of the Human-Electronic Crew: Can They Work Together
[AD-A211871] 05 p0676 N90-13936
A knowledge-based system design/information tool for aircraft flight control systems
[NASA-TM-101704] 05 p0685 N90-13990
An artificial intelligence approach to analog system diagnosis
[AD-A213135] 05 p0686 N90-13992
The problem of automation: Inappropriate feedback and interaction, not overautomation
[NASA-CR-186126] 05 p0686 N90-13994
A knowledge-based flight status monitor for real-time application in digital avionics systems
[NASA-TM-101710] 05 p0686 N90-13995
Decision-aid design factors in connection with HF communication and emitter location disciplines
06 p0758 N90-14413
A modern trans-ionospheric propagation sensing system 06 p0761 N90-14430
Automation and robotics in construction: Japanese research and development
[AD-A214170] 07 p0942 N90-15456
An architectural model of visual motion understanding
[AD-A214327] 07 p0967 N90-15589
Understanding developments in computer technology: A pragmatic and synthetic interpretation
07 p0971 N90-15608
Optical neural nets for scene analysis
[AD-A213986] 07 p0976 N90-15637
Tools for simulation-based training
[AD-A214307] 07 p0978 N90-15646

MASC: Multiprocessor architecture for symbolic processing
[AD-A213504] 07 p0979 N90-15656
Some computational properties of rotation representations
[AD-A213888] 07 p0981 N90-15665
Gaze controls with interactions and delays
[AD-A214286] 07 p0981 N90-15667
Automated observation scheduling for the VLT
[NASA-CR-186282] 07 p1012 N90-15861
Artificial intelligence approaches to astronomical observation scheduling
[NASA-CR-186277] 07 p1012 N90-15862
Automated telescope scheduling
[NASA-CR-186279] 07 p1012 N90-15863
An intelligence-driven RPV mission planner
08 p1027 N90-15932
NASA/ASEE Summer Faculty Fellowship Program
[NASA-CR-166837] 08 p1154 N90-16686
The DAB model of drawing processes
08 p1155 N90-16691
Target classification using SAR (Synthetic Aperture Radar) polarimetric data
[AD-A215672] 09 p1208 N90-17002
Applications of a fingertip sensor for the Salisbury robot hand
[DE90-005002] 09 p1231 N90-17142
Payload invariant control via neural networks: Development and experimental evaluation
[AD-A215740] 09 p1260 N90-17306
Job planning and execution monitoring for a human-robot symbiotic system
[DE90-004464] 09 p1261 N90-17315
Research and development in natural language understanding as part of the Strategic Computing Program
[AD-A214586] 09 p1264 N90-17330
Parallel logic programming and parallel systems software and hardware
[AD-A214635] 09 p1270 N90-17361
A genetic adaptive system for image understanding and learning research
[AD-A214810] 09 p1271 N90-17367
Representing knowledge intelligently: Production rules, frames, and transitional networks
[AD-A215098] 09 p1271 N90-17368
A model for comparing game theory and artificial intelligence decision making processes
[AD-A215418] 09 p1271 N90-17369
Use of hypermedia as a user interface for an artificial intelligence-based problem solver
[AD-A215551] 09 p1271 N90-17370
Hybrid optical/digital architecture for distortion invariant pattern recognition
[AD-A215628] 09 p1282 N90-17435
An Autonomous Platform Simulator (APS)
[AD-A215768] 10 p1392 N90-18048
Development of an integrated mobile robot system at Carnegie Mellon University: June 1988
[AD-A215955] 10 p1392 N90-18049
Advancing automation and robotics technology for the Space Station Freedom and for the US economy
[NASA-TM-101691] 10 p1414 N90-18151
An intelligent tool for the design of presentations: A system identification study
[AD-A215770] 10 p1418 N90-18174
High-Level Vision and Planning Workshop Proceedings
[AD-A215982] 10 p1420 N90-18188
Event-train restoration via backpropagation neural networks
[AD-A216308] 10 p1420 N90-18189
SHARP: A multi-mission artificial intelligence system for spacecraft telemetry monitoring and diagnosis
[NASA-CR-186285] 11 p1467 N90-18444
An approach centered in production rules for a partition of environment and planning in a visual navigation system (SNV)
[INPE-4813-TDL/360] 11 p1517 N90-18737
A self-organizing multiple-view representation of three-dimensional objects
[AD-A216711] 11 p1541 N90-18871
KAM: Automatic planning and interpretation of numerical experiments using geometrical methods
[AD-A216805] 11 p1546 N90-18900
A colony architecture for an artificial creature
[AD-A216802] 11 p1549 N90-18918
Architecture for a human-robot symbiotic system
[DE90-005670] 11 p1550 N90-18921
Teaching a new methodology for designing relational data bases: An experiment testing the effectiveness of an intelligent tutoring system on cognitive skill acquisition (volumes 1 and 2)
11 p1574 N90-19063
Artificial intelligence issues related to automated computing operations
12 p1637 N90-19404
Flight crew aiding for recovery from subsystem failures
[NASA-CR-181905] 12 p1696 N90-19741
An approach to elemental task learning
[DE90-006614] 12 p1697 N90-19745
High-level connectionist models
[AD-A216581] 12 p1698 N90-19751
Parallel neural net path-planner on hypercube and transputer
[DE90-006324] 12 p1703 N90-19777
Hybrid neural network and rule-based pattern recognition system capable of self-modification
[DE90-007482] 12 p1703 N90-19779
Concept formation and generalization based on experimentation by an autonomous mobile robot
[DE90-001731] 13 p1810 N90-20395
Parameter-scheduled trajectory planning for suppression of coupled horizontal and vertical vibrations in a flexible rod
[DE90-002313] 13 p1817 N90-20435
Free indexation: Combinatorial analysis and a compositional algorithm
[AD-A218219] 13 p1869 N90-20724
Artificial Intelligence (AI) Center of Excellence at the University of Pennsylvania
[AD-A217393] 13 p1874 N90-20743
A locally constrained parallel activation model for diagnostic reasoning
[AD-A217808] 13 p1874 N90-20747
CEREBRAL WEEVIL: A machine learning model for hemispheric categorization of complex visual patterns
[AD-A219143] 13 p1874 N90-20749
An investigation of the locality of memory accesses during symbolic program execution
[AD-A218168] 13 p1875 N90-20750
Stereo feature matching in disparity space
[AD-A218170] 13 p1875 N90-20751
Location recognition using stereo vision
[AD-A218218] 13 p1875 N90-20752
Three-dimensional route planning for a cruise missile for minimal detection by observer
[AD-A218336] 13 p1880 N90-20787
Time and truth in plans 14 p1906 N90-20930
Perspectives on the use of rule-based control
14 p1908 N90-20940
Vision Science and Technology at NASA: Results of a Workshop
[NASA-TM-102214-REV-1] 15 p2138 N90-22216
Sparse distributed memory overview
15 p2141 N90-22235
The 1990 Goddard Conference on Space Applications of Artificial Intelligence
[NASA-CP-3068] 15 p2152 N90-22294
The application of connectionism to query planning/scheduling in intelligent user interfaces
15 p2152 N90-22295
Resource Allocation Planning Helper (RALPH): Lessons learned
15 p2152 N90-22296
The role of artificial intelligence techniques in scheduling systems
15 p2152 N90-22297
PLAN-IT-2: The next generation planning and scheduling tool
15 p2153 N90-22298
Space communications scheduler: A rule-based approach to adaptive deadline scheduling
15 p2153 N90-22300
Constraint-based evaluation of sequential procedures
15 p2153 N90-22301
Managing temporal relations 15 p2154 N90-22304
Spacecraft command verification: The AI solution
15 p2154 N90-22307
Analyzing spacecraft configurations through specialization and default reasoning
15 p2155 N90-22308
Simulation-based reasoning about the physical propagation of fault effects 15 p2155 N90-22309
The JPL/KSC telerobotic inspection demonstration
15 p2155 N90-22312
System control of an autonomous planetary mobile spacecraft 15 p2155 N90-22313
Automated procedure execution for space vehicle autonomous control 15 p2156 N90-22314
Knowledge structure representation and automated updates in intelligent information management systems
15 p2156 N90-22316
Bounded-time fault-tolerant rule-based systems
15 p2157 N90-22318
A knowledge-based system with learning for computer communication network design
15 p2157 N90-22319
Guide to RMS-literature
[REPT-89-52] 15 p2158 N90-22326
Facilitating knowledge sharing in organizations: Semiautonomous agents that learn to gather, classify, and distribute environmental scanning knowledge
15 p2176 N90-22435
The Department of Defense critical technologies plan for the Committees on Armed Services United States Congress
[AD-A219300] 16 p2227 N90-22702
Efficient specialization of relational concepts
[AD-A218889] 16 p2262 N90-22894
Intelligent signal processing techniques for multi-sensor surveillance systems
[AD-A218890] 16 p2262 N90-22895
A preliminary analysis of the SOAR architecture as a basis for general intelligence
[AD-A218913] 16 p2262 N90-22896
Towards the knowledge level in SOAR: The role of the architecture in the use of knowledge
[NASA-CR-186515] 16 p2262 N90-22897
Stochastic interactive activation and the effect of context on perception
[AD-A218929] 16 p2262 N90-22898
Discovering problem solving strategies: What humans do and machines don't (yet)
[AD-A219008] 16 p2263 N90-22902
Learning events in the acquisition of three skills
[AD-A219038] 16 p2264 N90-22905
A connectionist implementation of cognitive phonology
[AD-A219095] 16 p2264 N90-22906
Cognitive architectures and rational analysis: Comment
[AD-A219199] 16 p2264 N90-22907
Toward a SOAR theory of taking instructions for immediate reasoning tasks
[AD-A219201] 16 p2265 N90-22909
Learning artificial grammars with competitive chunking
[AD-A219270] 16 p2265 N90-22911
A task-analytic approach to the automated design of information graphics
[AD-A219271] 16 p2265 N90-22912
Laboratory replication of scientific discovery processes
[AD-A219273] 16 p2266 N90-22913
An instructable Connectionist/Control architecture: Using rule-based instructions to accomplish connectionist learning in a human time scale
[AD-A219274] 16 p2266 N90-22914
Hatching a theory of incubation effects
[AD-A219275] 16 p2266 N90-22915
Automatic compiler construction
[AD-A218777] 16 p2278 N90-22983
Natural language processing: A tutorial
[AD-A219096] 16 p2300 N90-23108
Application of artificial intelligence in electronic circuit diagnosis 16 p2303 N90-23122
Adaptive Resonance Theory 1
[AD-A219044] 16 p2304 N90-23126
Scientific discovery as problem solving
[AD-A218887] 16 p2307 N90-23145
Learning environment for neural networks and transient acoustics
[AD-A219000] 16 p2314 N90-23186
Explanation generation in expert systems (a literature review and implementation)
[AD-A218741] 16 p2327 N90-23268
A study of supermanuever aerodynamics
[AD-A218378] 17 p2344 N90-23349
A neural network based speech recognition system
[AD-A219794] 17 p2389 N90-23606
Neuromorphic optical signal processing and image understanding for automated target recognition
[AD-A219827] 17 p2437 N90-23884
Advancing automation and robotics technology for the Space Station Freedom and for the US economy
[NASA-TM-102668] 17 p2439 N90-23899
Memory-based expert systems
[AD-A219875] 17 p2440 N90-23907
Proceeding of the Embedded AI Languages Workshop
[AD-A218531] 17 p2442 N90-23914
Improving upon standard pattern classification algorithms by implementing them as multi-layer perceptrons
[AD-A220048] 17 p2447 N90-23954
Formal methods in knowledge representation
[TR-89-11] 17 p2450 N90-23972
Northeast Artificial Intelligence Consortium. Volume 3: The Versatile Maintenance Expert System research project
[AD-A218716] 17 p2453 N90-23993
Northeast Artificial Intelligence Consortium. Volume 4. Distributed AI for communications network management
[AD-A218717] 17 p2453 N90-23994
Northeast Artificial Intelligence Consortium annual report, 1988. Volume 12: Computer architectures for very large knowledge bases
[AD-A219599] 17 p2454 N90-23999
Neural networks applied to signal processing
[AD-A219605] 17 p2454 N90-24000
A viewpoint on the contribution of expert systems of logistics
[REPT-892-320-101] 17 p2454 N90-24002

Intelligent, real-time problem solving
[AD-A219929] 17 p2455 N90-24006
Bayesian learning
[NASA-CR-181528] 17 p2465 N90-24082
Research in knowledge delivery
[AD-A219920] 17 p2480 N90-24180
Laser range camera modeling
[DE90-008220] 18 p2562 N90-24616
Real time automatic programming
[AD-A220162] 18 p2591 N90-24740
Parallelizing the closure computation in automated deduction
[DE90-007792] 18 p2593 N90-24758
A neural network for feature extraction
[AD-A220363] 18 p2597 N90-24775
Intelligent tutoring systems: An exploratory study of ITS and their implementation in Prolog
[RUU-CS-88-37] 18 p2597 N90-24779
Adaptive control of visually guided grasping in neural networks
[AD-A221387] 18 p2597 N90-24780
Brilliant pebbles
[DE90-010756] 18 p2606 N90-24845
National Aeronautics and Space Administration (NASA)/American Society for Engineering Education (ASEE) Summer Faculty Fellowship Program-1989, volume 1
[NASA-CR-185601-VOL-1] 18 p2627 N90-24972
National Aeronautics and Space Administration (NASA)/American Society for Engineering Education (ASEE) Summer Faculty Fellowship Program-1989, volume 2
[NASA-CR-185601-VOL-2] 18 p2630 N90-24985
A comparison of two neural network schemes for navigation 18 p2631 N90-24991
Acquiring generalizations to organize human databases
[AD-A219835] 18 p2634 N90-25004
Mars Rover imaging systems and directional filtering 18 p2648 N90-25071
MARS, an AI-based Mission Activities and Resource Scheduler
[MBB-0060/89-PUB] 19 p2650 N90-25083
Active perception and exploratory robotics
[MS-CIS-89-65] 19 p2726 N90-25501
Artificial intelligence within AFSC 19 p2727 N90-25504
Automation in the Space Station module power management and distribution Breadboard 19 p2728 N90-25509
Smart built-in test 19 p2728 N90-25512
Autonomous power expert fault diagnostic system for Space Station Freedom electrical power system testbed 19 p2730 N90-25521
Artificial intelligence for multi-mission planetary operations 19 p2732 N90-25532
A comparison of two neural network schemes for navigation 19 p2733 N90-25536
Sunspot prediction using neural networks 19 p2737 N90-25560
Behavioral networks as a model for intelligent agents 19 p2738 N90-25561
A research program in computer technology
[AD-A221184] 19 p2746 N90-25606
Operations mission planner
[NASA-CR-186846] 19 p2747 N90-25611
Adaptive robot control using artificial neural networks: An application in the theory of cognition
[RR-374] 19 p2748 N90-25618
Intelligent Real-Time Problem Solving
[AD-A220357] 19 p2750 N90-25621
Twilight zones and cornerstones: A gnat robot double feature
[AD-A220026] 20 p2870 N90-26326
Guidance and control system for an autonomous underwater vehicle
[AD-A222709] 20 p2873 N90-26343
Automatic line network extraction from aerial imagery of urban areas through knowledge based image analysis
[AD-A222675] 20 p2880 N90-26385
Grasping with mechanical intelligence
[NASA-CR-186864] 20 p2900 N90-26498
ATN design tool
[AD-A223030] 20 p2911 N90-26559
Multilayered neural networks: Learning algorithms, implementation on hypercube machines, applications
[ETN-90-97255] 20 p2913 N90-26574
A sum rule satisfied by optimized feed-forward layered networks
[RSRE-MEMO-4341] 20 p2914 N90-26579
On networks, optimized feature extraction, and the Bayes decision
[RSRE-MEMO-4342] 20 p2914 N90-26580
Application of artificial intelligence to the architectural synthesis of VLSI integrated circuits
[ETN-90-97253] 20 p2916 N90-26589
Rhetorical structure theory and text analysis
[AD-A222655] 20 p2941 N90-26733
Digital intelligent magnetic recording system DIMARS as the automated workstation at magnetic observatory 21 p3022 N90-27186
Evaluation of correlations between meteorological measurements and observations of lightning activity using artificial neural systems
[AD-A222659] 21 p3030 N90-27229
Symbolic architectures for cognition
[AD-A222909] 21 p3035 N90-27254
Knowledge and distributed computation
[AD-A223100] 21 p3039 N90-27270
Fifth Conference on Artificial Intelligence for Space Applications
[NASA-CP-3073] 21 p3040 N90-27275
Agent independent task planning 21 p3040 N90-27276
Spike: Artificial intelligence scheduling for Hubble space telescope 21 p3040 N90-27277
Resource allocation using constraint propagation 21 p3040 N90-27278
DEVS-based intelligent control of space adapted fluid mixing 21 p3040 N90-27279
Dynamic test input generation for multiple-fault isolation 21 p3040 N90-27280
The application of intelligent process control to space based systems 21 p3041 N90-27282
Knowledge representation for commonality 21 p3041 N90-27285
An automated tool for the design and assessment of space systems 21 p3042 N90-27289
Establishing a communications-intensive network to resolve artificial intelligence issues within NASA's Space Station Freedom research centers community 21 p3042 N90-27291
Attitude Determination and Control System (ADCS) and Maintenance and Diagnostic System (MDS): A maintenance and diagnostic system for Space Station Freedom 21 p3043 N90-27295
Space Station Freedom ECLSS: A step toward autonomous regenerative life support systems 21 p3043 N90-27297
Simulation-based intelligent robotic agent for Space Station Freedom 21 p3043 N90-27298
A development framework for artificial intelligence based distributed operations support systems 21 p3044 N90-27301
Design knowledge capture for a corporate memory facility 21 p3045 N90-27304
Capturing design knowledge 21 p3045 N90-27305
Case-based reasoning in design: An apologia 21 p3045 N90-27308
Artificial Intelligence Software Engineering (AISE) model 21 p3045 N90-27309
A diagnosis system using object-oriented fault tree models 21 p3046 N90-27313
Object oriented fault diagnosis system for space shuttle main engine redlines 21 p3046 N90-27315
Construction of dynamic stochastic simulation models using knowledge-based techniques 21 p3047 N90-27322
Intelligent tutoring systems for space applications 21 p3048 N90-27324
Documentation and knowledge acquisition 21 p3048 N90-27325
Using decision-tree classifier systems to extract knowledge from databases 21 p3048 N90-27328
Artificial intelligence techniques for modeling database user behavior 21 p3049 N90-27330
The sixth generation robot in space 21 p3049 N90-27332
Compiling knowledge-based systems from KEE to Ada 21 p3049 N90-27334
SDI satellite autonomy using AI and Ada 21 p3050 N90-27336
Soviet image pattern recognition research
[DE90-010912] 21 p3059 N90-27396
Collective computation of neural network
[AD-A221848] 21 p3061 N90-27405
NDI-concept for composites in future military aircraft 22 p3184 N90-28070
Use of acoustic emission for continuous surveillance of aircraft structures 22 p3188 N90-28092
Encoding techniques for complex information structures in connectionist systems
[NASA-CR-186942] 22 p3238 N90-28362
Fault-tolerance in massively parallel silicon architectures: The case of neural nets
[REPT-90-012] 22 p3240 N90-28375
Proceedings of the Conference on Artificial Intelligence in the Department of Energy Complex
[DE90-011634] 22 p3241 N90-28378
Genetic algorithms: The state of the art and some research proposals
[REPT-89-058] 22 p3241 N90-28380
Control of intelligent robots in space 23 p3365 N90-29013
Automation and robotics technology for intelligent mining systems 23 p3366 N90-29018
A design philosophy for multi-layer neural networks with applications to robot control 23 p3368 N90-29033
Coordinating the activities of a planner and an execution agent 23 p3369 N90-29035
Plan recognition for space telerobotics 23 p3369 N90-29038
Approximation algorithms for planning and control 23 p3370 N90-29042
Proceedings of the NASA Conference on Space Telerobotics, volume 2
[NASA-CR-186857] 23 p3370 N90-29044
HERMIES-3: A step toward autonomous mobility, manipulation, and perception 23 p3374 N90-29065
Rice-obot 1: An intelligent autonomous mobile robot 23 p3375 N90-29068
Organising geometric computations for space telerobotics 23 p3376 N90-29074
Integrating planning and reactive control 23 p3377 N90-29077
Learning in stochastic neural networks for constraint satisfaction problems 23 p3377 N90-29078
Integrating planning, execution, and learning 23 p3377 N90-29079
Who's who in scientific visualization at LLNL
[DE90-014720] 23 p3379 N90-29091
Designing intelligent computer aided instruction systems with integrated knowledge representation schemes
[AD-A224178] 23 p3383 N90-29113
Overcoming rule-based rigidity and connectionist limitations through massively-parallel case-based reasoning
[NASA-CR-186963] 23 p3384 N90-29117
A hardware/software environment to support R/D in intelligent machines and mobile robotic systems
[DE90-014458] 23 p3385 N90-29119
Model authoring system for fail safe analysis
[NASA-CR-4317] 23 p3389 N90-29142
A knowledge-based system design/information tool
[NASA-CR-4316] 23 p3389 N90-29143
Concept for a reference model Architecture for Real-Time Intelligent Control Systems (ARTICS)
[PB90-220286] 24 p3475 N90-29638
Robots, systems, and flexible automation
[DE90-015802] 24 p3476 N90-29649
Neural nets and eddy-current testing
[DE90-016044] 24 p3478 N90-29656
Guidance algorithms for a free-flying space robot 24 p3503 N90-29798
Reflections on the relationship between artificial intelligence and operations research 24 p3506 N90-29816
What kind of computation is intelligence. A framework for integrating different kinds of expertise 24 p3506 N90-29817
A design strategy for autonomous systems 24 p3506 N90-29818
Learning in tele-autonomous systems using Soar 24 p3506 N90-29819
Information management in an integrated space telerobot 24 p3511 N90-29846
Global models: Robot sensing, control, and sensory-motor skills 24 p3511 N90-29849
A layered abduction model of perception: Integrating bottom-up and top-down processing in a multi-sense agent 24 p3512 N90-29851
Determining robot actions for tasks requiring sensor interaction 24 p3514 N90-29868
The laboratory telerobotic manipulator program 24 p3515 N90-29869
Requirements for implementing real-time control functional modules on a hierarchical parallel pipelined system 24 p3518 N90-29891
Strategies for tutoring multiple bugs
[AD-A223921] 24 p3524 N90-29927
Tutorial on using LISP object-oriented programming for blackboards: Solving the radar tracking problem
[AD-A224272] 24 p3525 N90-29930
Knowledge base refinement as improving an incorrect and incomplete domain theory
[AD-A224441] 24 p3526 N90-29935
Machine recognition as representation and search
[AD-A223700] 24 p3528 N90-29946
Direct estimation of structure and motion from multiple frames
[AD-A223903] 24 p3534 N90-29985
Machine learning
[AD-A223732] 24 p3534 N90-29988
Optical signal computing
[AD-A223624] 24 p3545 N90-30051

ARTIFICIAL SATELLITES
NT ACTS
NT AERONAUTICAL SATELLITES
NT ALOUETTE 1 SATELLITE
NT ALOUETTE 2 SATELLITE
NT ASTRONOMICAL SATELLITES
NT ATS
NT BEACON EXPLORER A
NT BEACON SATELLITES
NT COLUMBUS SPACE STATION
NT COMMUNICATION SATELLITES
NT COMMUNICATIONS TECHNOLOGY SATELLITE
NT COSMIC BACKGROUND EXPLORER SATELLITE
NT COSMOS SATELLITES
NT DIRECT BROADCAST SATELLITES
NT DMSP SATELLITES
NT ENVIRONMENTAL RESEARCH SATELLITES
NT ERS-1 (ESA SATELLITE)
NT ESA SATELLITES
NT EUROPEAN COMMUNICATIONS SATELLITE
NT EXOSAT SATELLITE
NT EXPLORER SATELLITES
NT EXPLORER 20 SATELLITE
NT EXPLORER 31 SATELLITE
NT EXTREME ULTRAVIOLET EXPLORER SATELLITE
NT FRENCH SATELLITES
NT GAMMA RAY OBSERVATORY
NT GEODETIC SATELLITES
NT GEOPOTENTIAL RESEARCH MISSION
NT GEOS 1 SATELLITE
NT GEOS 2 SATELLITE
NT GEOSAT SATELLITES
NT GOES SATELLITES
NT GOES 4
NT HEAO
NT HEAO 1
NT HEAO 2
NT HIPPARCOS SATELLITE
NT HUBBLE SPACE TELESCOPE
NT INFRARED ASTRONOMY SATELLITE
NT INFRARED SPACE OBSERVATORY (ISO)
NT INTELSAT SATELLITES
NT INTERNATIONAL SUN EARTH EXPLORER 3
NT IRIS SATELLITES
NT ITOS SATELLITES
NT IUE
NT LAGEOS (SATELLITE)
NT LANDSAT SATELLITES
NT LANDSAT 5
NT LARGE DEPLOYABLE REFLECTOR
NT LONG DURATION EXPOSURE FACILITY
NT MAN TENDED FREE FLYERS
NT MARECS MARITIME SATELLITES
NT METEOROLOGICAL SATELLITES
NT METEOSAT SATELLITE
NT MIR SPACE STATION
NT MOLNIYA SATELLITES
NT MSAT
NT NAVIGATION SATELLITES
NT NAVIGATION TECHNOLOGY SATELLITES
NT NAVSTAR SATELLITES
NT NIMBUS 7 SATELLITE
NT NOAA SATELLITES
NT ORBITING LUNAR STATIONS
NT POGO
NT ROSAT MISSION
NT SAGE SATELLITE
NT SAN MARCO SATELLITES
NT SARSAT
NT SCATHA SATELLITE
NT SCIENTIFIC SATELLITES
NT SEASAT SATELLITES
NT SKYLAB 1
NT SOLAR POWER SATELLITES
NT SOVIET SATELLITES
NT SPACE INFRARED TELESCOPE FACILITY
NT SPACE STATION POLAR PLATFORMS
NT SPACE STATIONS
NT SPARTAN SATELLITES
NT SPOT (FRENCH SATELLITE)
NT SYNCHRONOUS SATELLITES
NT SYNCOM SATELLITES
NT TETHERED SATELLITES
NT TIROS N SERIES SATELLITES
NT TIROS SATELLITES
NT TRANSIT SATELLITES
NT X RAY ASTROPHYSICS FACILITY

On analytic modeling of lunar perturbations of artificial satellites of the earth
[AD-A210440] 01 p0016 N90-10078

Gyrotron development for space power beaming
01 p0028 N90-10148

Effects of rain attenuation on satellite EHF (Extremely High Frequency) communications in the US
[AD-A210517] 01 p0057 N90-10325

On-orbit annealing of gallium arsenide solar cell arrays
[AD-A212087] 03 p0334 N90-11900

Auroral and sub-auroral interaction at the F region ionosphere
[AD-A213284] 05 p0666 N90-13896

An assessment of potential markets for small satellites
[NASA-TM-101943] 09 p1181 N90-16848

The extension of technology and the control of production costs in advanced satellite systems
[AD-A215104] 09 p1183 N90-16857

Development and use of data analysis procedures for the CRRES (Combined Release and Radiation Effects Satellite) payloads AFGL-701-2/Dosimeter and AFGL-701-4/Fluxmeter and application of the data analysis results to improve the static and dynamic models of the Earth's radiation belts
[AD-A215953] 10 p1447 N90-18348

Orbit determination of artificial Earth satellites through estmation techniques combined with state smoothing techniques
[INPE-4959-TDL/388] 11 p1465 N90-18440

Evaluation of influences of errors involved in orbit propagation of artificial satellites
[INPE-4962-TDL/391] 11 p1466 N90-18441

Present and future risk of satellite and manned platforms collisions with other space objects and particles on earth orbits
[R-8841] 12 p1615 N90-19287

Present and future risk of collision of satellites and manned platforms with other space objects and particles in terrestrial orbit
[R-8840] 12 p1615 N90-19288

Low-cost small satellites for astrophysical missions
[DE90-007625] 12 p1616 N90-19293

A satellite simulation program
[AD-A218079] 13 p1764 N90-20124

Distributed earth model/orbiter simulation
13 p1860 N90-20671

Design of a digital model following controller of reaction wheel torques
[INPE-4753-PRE/1425] 14 p1938 N90-21093

Space environment simulation of the SCD-01 satellite through heating plates
[INPE-4988-PRE/1550] 14 p1940 N90-21105

Lessons learned in the transition to Ada from FORTRAN at NASA/Goddard
[NASA-TM-103311] 14 p2014 N90-21538

Analysis, selection, and implementation of procedures which approve optimal artificial satellite maneuvers
[INPE-5003-TDL/397] 15 p2058 N90-21786

Semianalytic satellite theory
[AD-A220744] 17 p2361 N90-23444

New generation power subsystems for satellites
[AD-A219540] 17 p2365 N90-23464

Analysis of phase retrieval in active imaging
[AD-A221080] 18 p2563 N90-24626

Theoretical principles of the FHP-GA trajectory calculation program
[FB-10-89] 19 p2663 N90-25156

An Earth orbiting satellite service and repair facility
[NASA-CR-186669] 19 p2665 N90-25166

StarPlan: A model-based diagnostic system for spacecraft 19 p2728 N90-25511

Satellite material contaminant optical properties
19 p2732 N90-25529

Engineering and the advancement of human welfare. Ten outstanding achievements 1964-1989
[ISBN-0-309-04185-6] 23 p3415 N90-29297

ARTILLERY
NT PRECISION GUIDED PROJECTILES

Active primary lithium thionyl chloride battery for artillery applications
[DE90-009511] 15 p2089 N90-21955

ARTS
NT ABILITIES
NT COMPUTER ANIMATION
NT GRAPHIC ARTS

ARYABHATA
U INDIAN SPACECRAFT

ARYL COMPOUNDS
U AROMATIC COMPOUNDS

ASBESTOS
Tribomaterial factors in space mechanism brake performance 15 p2114 N90-22096

ASCENT
NT CLIMBING FLIGHT

Optimal trajectories for the aeroassisted flight experiment. Part 4: Data, tables, and graphs
[NASA-CR-186164] 15 p2056 N90-21780

Random vibration analysis of space flight hardware using NASTRAN 18 p2570 N90-24645

Heliport visual approach surface high temperature and high altitude tests
[DOT/FAA/CT-TN89/34] 22 p3112 N90-27675

Flight control issues of the next generation space transportation launch vehicles 22 p3126 N90-27742

Optimal trajectories for Saenger-type vehicles
22 p3129 N90-27760

ASCENT PROPULSION SYSTEMS
Optimum ascent performance of winged two-stage vehicles 09 p1177 N90-16816

ETO (Earth-To-Orbit): A trajectory program for aerospace vehicles
[AD-A218157] 13 p1760 N90-20103

ASCENT TRAJECTORIES
GOES-I/M ascent maneuvers from transfer orbit to station 05 p0587 N90-13421

Efficient calculation of Ariane ascent trajectories with recursive quadratic programming
09 p1180 N90-16844

Ascent and descent trajectory optimization of Ariane 5/Hermes 22 p3126 N90-27743

Optimal trajectories for Saenger-type vehicles
22 p3129 N90-27760

ASDE
U AIRPORT SURFACE DETECTION EQUIPMENT

ASHES
NT FLY ASH

ASIA
Diagnostic study of atmosphere-terrain interaction leading to the formation of dust clouds and poor visibilities over near east desert areas
[AD-A211243] 02 p0239 N90-11358

Responding to the threat of global warming: Options for the Pacific and Asia
[DE90-003553] 07 p0957 N90-15539

Dust clouds Kosa from the east Asian dust storms in 1982-1988 as observed by the GMS satellite
21 p3028 N90-27214

Responding to the threat of global warming: Options for the Pacific and Asia
[DE90-014756] 23 p3347 N90-28918

ASIC
U APPLICATION SPECIFIC INTEGRATED CIRCUITS

ASPARTATES
Polypeptide inhibitors of mineral scaling and corrosion
[AD-A210507] 01 p0041 N90-10225

ASPECT RATIO
NT HIGH ASPECT RATIO
NT LOW ASPECT RATIO

Definition, transformation-formulae and measurements of tipvane angles
[IW-R510] 08 p1097 N90-16351

An iterative solution to aeroelastic effects in potential flow
[AD-A216291] 10 p1310 N90-17580

Magnetic surfaces in tokamaks
[DE90-628905] 24 p3549 N90-30076

ASPHALT
Evaluation of a neoprene latex modified SAMI (Stress Absorbing Membrane Interlayer)
[PB89-226435] 05 p0628 N90-13865

Design temperatures for flexible airfield pavement design
[AD-A214141] 07 p0884 N90-15115

Evaluation of two transport aircraft and several ground test vehicle friction measurements obtained for various runway surface types and conditions. A summary of test results from joint FAA/NASA Runway Friction Program
[NASA-TP-2917] 08 p1021 N90-15902

Criteria for coal tar seal coats on airport pavements. Volume 2: Laboratory and field studies
[AD-A220167] 18 p2498 N90-24277

ASPHERICITY
Surface topography measurements over the 1 meter to 10 micrometer spatial period bandwidth
[DE90-003642] 08 p1122 N90-16501

ASPIRATION
U VACUUM

ASRM (STS)
U ADVANCED SOLID ROCKET MOTOR (STS)

ASROC ENGINE
VLA missile development and high angle of attack behavior 10 p1305 N90-17553

ASSAULTING
U ATTACKING (ASSAULTING)

ASSAYING
ROBOCAL (Robotic Calorimetry): An automated NDA (Nondestructive Assay) calorimetry and gamma isotopic system
[DE90-003217] 07 p0894 N90-15168

Chamber investigations of the fate of diesel emissions in the atmosphere. Volume 2: AMES assay and GCMS final data reports and gas phase projections
[PB90-114430] 10 p1405 N90-18104

Pseudomonas diagnostic assay
[NASA-CASE-NPO-17653-1-CU]
21 p3032 N90-27239

ASSEMBLER ROUTINES
The function of the Interactive Model Assembly Program (IMAP) for a flight simulator
[NAL-TR-1034] 24 p3437 N90-29412
Assembler for a parallel computer
[NAL-TM-586] 24 p3532 N90-29974

ASSEMBLIES
NT TAIL ASSEMBLIES
Fatigue testing of welded steel assemblies with or without finishing treatments
[CETIM-107900] 04 p0513 N90-12961
Assembly, integration, and verification 05 p0605 N90-13519

ASSEMBLING
NT ORBITAL ASSEMBLY
Computer-aided design of flexible assembly systems
[PB89-216253] 03 p0354 N90-12025
Electrochemical cell for obtaining oxygen from carbon dioxide atmospheres
[NASA-CR-186225] 09 p1189 N90-16886
Development of an aluminium solar cell interconnector technology 10 p1341 N90-17771
Assembly technology of GaAs solar cell 10 p1341 N90-17772
RALPH: An automatic Robot Assembly Language Programmer: An overview
[PB90-120973] 11 p1548 N90-18912
Component count and preliminary assembly considerations for large space truss structures
[NASA-TM-102604] 13 p1763 N90-20121
Flexible automatic discrete parts assembly
[AD-A217401] 13 p1787 N90-20256
Component model reduction via the projection and assembly method 16 p2295 N90-23073
Strut-node joint conjugates for the assembly of semi-permanent or reusable truss structures 18 p2640 N90-25039
Assembly via disassembly: A case in machine perceptual development
[NASA-CR-186867] 20 p2900 N90-26497
How do robots take two parts apart 23 p3374 N90-29061

ASSEMBLY
Assembly of objects with not fully predefined shapes 24 p3513 N90-29859
Precedence relationship representations of mechanical assembly sequences 24 p3514 N90-29866
Using multiple sensors for printed circuit board insertion 24 p3514 N90-29867

ASSEMBLY LANGUAGE
Yaw rate control of an air bearing vehicle 12 p1639 N90-19420
The contour model architecture and assembly language
[AD-A217114] 13 p1865 N90-20697

ASSESSMENTS
NT DAMAGE ASSESSMENT
NT TECHNOLOGY ASSESSMENT
Independent Orbiter Assessment (IOA): Analysis of the Orbiter Experiment (OEX) subsystem
[NASA-CR-185586] 02 p0171 N90-10983
A critical assessment of thermodynamic and phase diagram data for the Ga-In system
[NPL-DMA(A)-174] 03 p0415 N90-12382
Assessment of voice coders for ATC/pilot voice communications via satellite digital communication channels
[CAA-PAPER-89004] 04 p0489 N90-12807
Error allocation and accuracy assessment 05 p0603 N90-13501
Safety evaluation report for Galileo, volume 2
[DE90-003087] 07 p0886 N90-15123
An assessment and comparison of fuel cells for transportation applications
[DE90-001807] 07 p0952 N90-15508
Risk assessment and its application to flight safety analysis
[DE90-004985] 09 p1161 N90-16722
Probability of failure and risk assessment of propulsion structural components 11 p1471 N90-18470
Global positioning system overview/status 21 p3069 N90-27446
Emerging technologies in electronics and their measurement needs, second edition
[PB90-188087] 23 p3320 N90-28773
The nuclear battery
[DE90-630400] 24 p3462 N90-29559
Techniques for developing a system safety risk assessment model
[AD-A223477] 24 p3477 N90-29654

ASSIGNMENT
U ALLOCATIONS

ASSIMILATION
Regulation of nitrogen uptake and assimilation: Effects of nitrogen source, root-zone pH, and aerial CO2 concentration on growth and productivity of soybeans
[NASA-CR-177546] 10 p1413 N90-18147
The effect of wave data assimilation on the numerical simulation of wave energy advection
[KNMI-TR-121] 24 p3496 N90-29760

ASSOCIATIONS
U ORGANIZATIONS

ASSOCIATIVE PROCESSING (COMPUTERS)
Optical computing based on the Hopfield model for neural networks
[AD-A211824] 03 p0389 N90-12216
On modeling resources in multiprocessor systems
[MEMO-INF-88-33] 04 p0535 N90-13095
An implementation-oriented specification of the TUMULT communication primitives
[MEMO-INF-88-34] 04 p0536 N90-13096
Adaptive associative-processing optical computing architectures
[AD-D014317] 13 p1863 N90-20685
Quadratic Hadamard Memories 1
[AD-A217224] 14 p2013 N90-21534
Neural networks
[AD-A222110] 21 p3060 N90-27398

ASTEROID BELTS
NT ASTEROIDS
Dust bands in the asteroid belt
[NASA-CR-186301] 07 p1014 N90-15873
Pioneers 10 and 11 deep space missions
[NASA-TM-102269] 10 p1448 N90-18355

ASTEROID MISSIONS
NT COMET RENDEZVOUS ASTEROID FLYBY MISSION

ASTEROIDS
The treatment of minor planets and planetary satellites 05 p0611 N90-13563
The volatile composition of comets
[NASA-CR-186281] 07 p1014 N90-15871
Dust bands in the asteroid belt
[NASA-CR-186301] 07 p1014 N90-15873
Comments on comet shapes and aggregation processes 08 p1142 N90-16622
The comet rendezvous asteroid flyby mission 08 p1145 N90-16639
Detecting extended solar system structures with COBE (Cosmic Background Explorer)
[AD-A216380] 10 p1447 N90-18349
Zodiacal dust bands: Their relation to asteroid families
[AD-A216025] 11 p1590 N90-19170
Optical constraints of kerogen from 0.15 to 40 microns: Comparison with meteoritic organics 20 p2948 N90-26776
Cosmic bombardment 2: Intercepting the bomblets cost-efficiently
[DE90-010401] 21 p3098 N90-27601

ASTP
U APOLLO SOYUZ TEST PROJECT

ASTRO MISSIONS (STS)
Seeing in a new light: Astro-1 teacher's guide with activities
[NASA-EP-274] 13 p1899 N90-20900

ASTRO VEHICLE
Microgravity conditions of a space vehicle 13 p1785 N90-20247

ASTROBIOLOGY
U EXOBIOLOGY

ASTRODYNAMICS
On mean elements for satellite orbits perturbed by the zonal harmonics of the geopotential
[AD-A212322] 04 p0461 N90-12642
The hyperbolic Kepler's equation, and the elliptic equation revisited
[RAE-TM-SPACE-369] 09 p1274 N90-17388
On universal elements, and conversion procedures to and from position and velocity
[RAE-TM-SPACE-370] 09 p1277 N90-17406
Satellite motion in axi-symmetric gravitational field. Part 2: Perturbations due to an arbitrary J(sub l)
[RAE-TR-89022] 16 p2206 N90-22586

ASTROMETRY
Astrometric telescope facility. Preliminary systems definition study. Volume 3: Cost estimate
[NASA-TM-89429-VOL-3] 01 p0140 N90-10808
A statistical study of radio-source structure effects on astrometric very long baseline interferometry observations 04 p0485 N90-12788
The Hipparcos Mission. Prelaunch status. Volume 2: The input catalog
[ESA-SP-1111-VOL-2] 05 p0606 N90-13529
Stellar content of the input catalog 05 p0607 N90-13535
Ground-based astrometric measurements 05 p0607 N90-13536
The compilation of astrometric data 05 p0607 N90-13537
Double stars 05 p0608 N90-13540
Minor planets and other solar system objects 05 p0608 N90-13545
Overview of the data acquisition and reductions 05 p0609 N90-13549
Astrometric parameter determination in FAST 05 p0610 N90-13556
The sphere solution and astrometric parameter determination in NDAC 05 p0610 N90-13557
Overview of the Tycho data analysis 05 p0610 N90-13558
Tycho astrometry 05 p0610 N90-13559
Double star reductions in NDAC 05 p0610 N90-13561
The treatment of minor planets and planetary satellites 05 p0611 N90-13563
Linking Hipparcos to a quasi-inertial system 05 p0611 N90-13565
Solar variability observed through changes in solar figure and mean diameter
[DE90-006600] 11 p1535 N90-18834
Photon statistical limitations for daytime optical tracking 12 p1643 N90-19442
Optical interferometers for tests of relativistic gravity in space 12 p1734 N90-19967
A higher density VLBI catalog for navigating Magellan and Galileo 15 p2078 N90-21904
Activities report of the Institute of Astronomical Calculations
[ETN-90-96461] 17 p2481 N90-24189
Nonlinear multi-mode coupling of the solar gravity modes in a rotationally split multiplet 21 p3100 N90-27608

ASTRONAUT LOCOMOTION
EVA space suit. General concepts of design and arrangement 08 p1034 N90-15976
The European EVA spacesuit mechanisms 18 p2538 N90-24481

ASTRONAUT MANEUVERING EQUIPMENT
NT MANNED MANEUVERING UNITS

ASTRONAUT PERFORMANCE
Pre- and postflight postural control of the D1 Spacelab mission astronauts examined with a tilting room
[IZF-1988-25] 04 p0527 N90-13039
On the wings of a dream: The Space Shuttle
[NASA-EP-269] 05 p0593 N90-13448
Issues in development, evaluation, and use of the NASA Preflight Adaptation Trainer (PAT)
[NASA-CR-185608] 15 p2137 N90-22212

ASTRONAUT TRAINING
On the wings of a dream: The Space Shuttle
[NASA-EP-269] 05 p0593 N90-13448
Activities report in German aerospace
[ISSN-0070-3966] 11 p1595 N90-19189
Working on the moon: The Apollo experience
[DE90-003662] 12 p1697 N90-19744
Issues in development, evaluation, and use of the NASA Preflight Adaptation Trainer (PAT)
[NASA-CR-185608] 15 p2137 N90-22212

ASTRONAUTICS
A foundation for the design of an astronautics specification system based on dynamic motivation analysis
[ILR-MITT-220] 08 p1033 N90-15969
Profiles-aeronautical/astronautical engineering: Human resources and funding
[PB90-103888] 09 p1203 N90-16969
FY 1989 scientific and technical reports, articles, papers, and presentations
[NASA-TM-100384] 12 p1725 N90-19916

ASTRONAUTS
NT ORBITAL WORKERS
Exercise countermeasures for bed rest deconditioning
[NASA-TM-101045] 05 p0674 N90-13926
TALON and CRADLE: Systems for the rescue of tumbling spacecraft and astronauts, a preliminary design 08 p1161 N90-16847
Reliability of equivalent sphere model in blood-forming organ dose estimation
[NASA-TM-4178] 12 p1746 N90-20036
Animation graphic interface for the space shuttle onboard computer 13 p1859 N90-20667
SES cupola interactive display design environment 13 p1862 N90-20679
Issues in visual support to real-time space system simulation solved in the Systems Engineering Simulator 13 p1862 N90-20680
Space adaptation syndrome induced by a long duration +3Gx centrifuge run
[AD-A218248] 14 p2010 N90-21518
Evolution of EVA capabilities for space station construction and maintenance: Soviet and American experience 18 p2502 N90-24295
The use of underwater dynamometry to evaluate two space suits 18 p2632 N90-24995

Improved model for solar cosmic ray exposure in manned Earth orbital flights
[NASA-TP-2987] 18 p2639 N90-25031
A direct-interface, fusible heat sink for astronaut cooling
[NASA-TM-102835] 19 p2689 N90-25292
A noncontacting motion monitoring system for an astronaut translation aid
[NASA-TM-102640] 19 p2693 N90-25325
An expert system to advise astronauts during experiments: The protocol manager module
19 p2730 N90-25522
Design of a Lunar farside observatory
[NASA-CR-186671] 19 p2765 N90-25709
Project Exodus
[NASA-CR-186836] 20 p2816 N90-26026
Rings of Earth detected by orbital debris radar
20 p2854 N90-26232
Human work in space: The astronaut's legal status. Introduction 20 p2938 N90-26719
The astronauts' legal status: The International Space Station 20 p2938 N90-26721

ASTRONOMICAL CATALOGS
New statistical approaches to galaxy clustering
02 p0294 N90-11674
From scientific proposals to the Inca data base
05 p0606 N90-13530
Stellar content of the input catalog
05 p0607 N90-13535
The catalogs produced by the Inca consortium
05 p0608 N90-13546
Validation of the Hipparcos catalog
05 p0611 N90-13564
Accuracy and characteristics of the Hipparcos catalog
05 p0611 N90-13566
The Tycho input catalog 05 p0612 N90-13575
Fifty year canon of lunar eclipses: 1986-2035
[NASA-RP-1216] 10 p1446 N90-18342
A comparison of void distributions in Abell cluster catalogue with numerical simulations
[DE90-610640] 11 p1590 N90-19173
Mathematics and physics studies: Multi-project support
[AD-A218208] 13 p1869 N90-20723
Fifth fundamental catalogue (FK5). Part 1: The basic fundamental stars
[REPT-32(1988)-PT-1] 16 p2330 N90-23282
Quantifying the FIR interaction enhancement in paired galaxies
[DE90-627485] 23 p3412 N90-29281

ASTRONOMICAL COORDINATES
Linking Hipparcos to a quasi-inertial system
05 p0611 N90-13565

ASTRONOMICAL MAPS
Analysis of the star mapper data
05 p0609 N90-13551
Data processing in the FAST consortium
05 p0611 N90-13567
Data processing in the NDAC consortium
05 p0611 N90-13568

ASTRONOMICAL MODELS
NT STELLAR MODELS
Theory and modeling group 03 p0430 N90-12462
Orion B: Anatomy of a star-forming region
05 p0710 N90-14155
Archival research on absorption lines in violently star-forming galaxies
[NASA-CR-185960] 05 p0712 N90-14163
Big Bang nucleosynthesis and the Quark-Hadron transition
[NASA-CR-186169] 05 p0713 N90-14168
String correlations and galaxies formation
[ROM1F-89-677] 05 p0713 N90-14170
Des Cloizeaux's law for strings and galaxies formation. Part 2: Non Abelian configurations
[ROM1F-89-682-PT-2] 05 p0714 N90-14173
Near-infrared polarimetry and spectroscopy of comets
07 p1011 N90-15857
Laboratory simulations of the solar wind-comet interactions 07 p1015 N90-15875
Neutrino oscillations: An essay in honor of Felix Boehm
[DE90-003223] 08 p1121 N90-16491
Study of primitive universe in the Bianchi 9 model
[DE89-635903] 08 p1134 N90-16572
Pulsations of delta Scuti stars
[DE90-003213] 08 p1139 N90-16598
The microwave background in steady-state cosmology
11 p1587 N90-19150
The Moon has set
[REPT-89-07] 12 p1728 N90-19933
Cosmic string in compactified gauge theory
[DE90-741463] 12 p1738 N90-19988
Physics and Mechanics of Cometary Materials
[ESA-SP-302] 12 p1738 N90-19989
Physical models of cometary nuclei: A review
12 p1738 N90-19991
Studies of the evolution of the x ray emission of clusters of galaxies
[NASA-CR-186471] 13 p1903 N90-20918
The large scale structure of the universe in pancake models of galaxy formation 14 p2040 N90-21701
Horizon problem in cosmological models with non zero
[DE90-613367] 14 p2042 N90-21708
Numerical investigations of nonlinear behavior in the Einstein equations 15 p2175 N90-22427
Origin of pulsed emission from the young supernova remnant SN 1987A
[CAL-377] 15 p2182 N90-22469
A three-year study of the OH masers in Orion-KL and a study of the (3,2) transition of ammonia
15 p2183 N90-22471
The emission lines in the ultra-violet spectrum of Beta Lyrae 15 p2183 N90-22474
The modeling of IRAS detections of classical novae and related objects 15 p2185 N90-22482
Herbig-Haro objects and stellar jets
15 p2186 N90-22487
The distribution of molecular clouds in spiral galaxies
15 p2186 N90-22489
The Sagittarius B2 molecular cloud: An extreme case of a galactic center giant molecular cloud
15 p2187 N90-22493
Kinematic models of cometary comae
15 p2188 N90-22495
The mass of the Coma cluster
15 p2188 N90-22496
A galaxy formation cookbook: Recipes and utensils
15 p2190 N90-22508
Skewering the universe with QSO lines of sight: Lyman alpha clouds as probes of large scale structure
16 p2329 N90-23278
Anisotropic inflation 16 p2331 N90-23286
The dynamical evolution of dense clusters of compact stars 16 p2331 N90-23287
The effect of a stellar wind on an expanding H II region 16 p2333 N90-23292
A model of the diffuse galactic gamma ray emission
16 p2334 N90-23297
Gamma rays from giant molecular clouds
16 p2334 N90-23298
Gamma radiation from radio pulsars
16 p2334 N90-23302
Gravitational collapse, Friedman models and cosmological constant: Does the universe oscillate
[DE90-620792] 16 p2338 N90-23324
Periodic signatures for the detection of cosmic axions
[NASA-CR-186608] 17 p2470 N90-24122
Probing the Big Bang with LEP
[NASA-CR-181060] 17 p2485 N90-24212
Large scale structure and microwave background anisotropies in cosmological models and stellar photometry techniques with the wide field/planetary camera of the Hubble space telescope
18 p2637 N90-25023
Synthetic spectra of accretion disks in DQ Her binaries
[NASA-CR-186837] 18 p2638 N90-25029
Small helium-cooled infrared telescope experiment for Spacelab-2 (IRT)
[NASA-CR-183983] 19 p2765 N90-25708
Astrophysical importance of the slim accretion disks
19 p2782 N90-25827
Theories of the X ray background
19 p2784 N90-25842
AGNs and the spectrum of the X ray background
19 p2787 N90-25858
QSO optical counts and constraints on the X ray background 19 p2789 N90-25877
Thermal comptonization in accretion disks
19 p2791 N90-25890
Spherical accretion with thermal pair production as models of AGN 19 p2793 N90-25897
X ray constraints on the beaming hypothesis for BL Lacertae objects 19 p2793 N90-25900
The iron abundance gradient in the intracluster medium of Perseus: A galactic wind model. Application to other clusters 19 p2793 N90-25901
A magnetic flare model for X ray variability in AGN
19 p2794 N90-25907
Neutral column density and soft excesses in active galactic nuclei 19 p2794 N90-25908
Origin of density fluctuations in extended inflation
[NASA-CR-182852] 19 p2795 N90-25915
Extended inflation from higher dimensional theories
[NASA-CR-180549] 19 p2796 N90-25916
Nonstandard big bang models
[DE90-625593] 20 p2941 N90-26736
Photon sputtering of H2O ices: A preliminary report
20 p2949 N90-26783
Optical imaging of IRAS galaxies: The evolution of infrared-bright galaxies 22 p3261 N90-28465
Gamma ray evidence for cosmic ray sources
23 p3414 N90-29292

ASTRONOMICAL OBSERVATORIES
NT ASTRONOMICAL SATELLITES
NT GAMMA RAY OBSERVATORY
NT HEAO
NT HEAO 1
NT HEAO 2
NT HUBBLE SPACE TELESCOPE
NT INFRARED ASTRONOMY SATELLITE
NT INFRARED SPACE OBSERVATORY (ISO)
NT IUE
NT LARGE DEPLOYABLE REFLECTOR
NT ROSAT MISSION
NT SPACE INFRARED TELESCOPE FACILITY
NT SPARTAN SATELLITES
NT X RAY ASTROPHYSICS FACILITY
Analysis of nearly simultaneous X-ray and optical observations of active galactic nuclei
01 p0139 N90-10806
System and performance analysis of a low density actively controlled mirror for astronomic observation
02 p0178 N90-11002
Long-lived space observatories for astronomy and astrophysics
[NASA-CR-185373] 06 p0731 N90-14261
Properties of evolved star circumstellar grains
06 p0861 N90-15003
The South African Astronomical Observatory
[NASA-CR-186258] 07 p1011 N90-15856
Science exploration opportunities for manned missions to the Moon, Mars, Phobos, and an asteroid
[NASA-CR-186295] 09 p1171 N90-16776
The James Clerk Maxwell telescope
11 p1589 N90-19166
Optical interferometer in space
12 p1731 N90-19953
Anderson Mesa, Arizona as a site for an optical interferometric array 16 p2330 N90-23281
Research and facilities handbook 1989
[ISSN-0267-6281] 19 p2784 N90-25840

ASTRONOMICAL PHOTOGRAPHY
Advances in photographic X-ray imaging for solar astronomy 01 p0139 N90-10803
Information reconstruction from speckle interferograms
[ETN-90-95918] 12 p1729 N90-19939
Diffraction-limited imaging on the 200-inch telescope
15 p2183 N90-22475
Galactical ultra wide angle Schmidt system
18 p2536 N90-24468
Super-diffraction limited measurements through the turbulent atmosphere by speckle interferometry
[AD-A221227] 18 p2581 N90-24699

ASTRONOMICAL PHOTOMETRY
NT STELLAR SPECTROPHOTOMETRY
Analysis of nearly simultaneous X-ray and optical observations of active galactic nuclei
01 p0139 N90-10806
Reexamination of data from the asteroid/meteoroid detector
[NASA-CR-185997] 05 p0714 N90-14175
Infrared properties of five spiral galaxies
11 p1587 N90-19154

ASTRONOMICAL SATELLITES
NT GAMMA RAY OBSERVATORY
NT HEAO
NT HEAO 1
NT HEAO 2
NT HUBBLE SPACE TELESCOPE
NT INFRARED ASTRONOMY SATELLITE
NT INFRARED SPACE OBSERVATORY (ISO)
NT IUE
NT LARGE DEPLOYABLE REFLECTOR
NT SPACE INFRARED TELESCOPE FACILITY
NT SPARTAN SATELLITES
NT X RAY ASTROPHYSICS FACILITY
Signposts to the future 19 p2788 N90-25867

ASTRONOMICAL SPECTROSCOPY
Integrating detectors and their application to infrared astronomy 02 p0290 N90-11659
The low-ion QSO absorption-line systems
05 p0712 N90-14162
Near-infrared polarimetry and spectroscopy of comets
07 p1011 N90-15857
IR spectroscopy of planets and satellites; Venus, Mars, giant planets, and Titan 11 p1578 N90-19085
Infrared spectroscopy of dust
11 p1579 N90-19094
Infrared heterodyne spectroscopy of polyatomic molecules in circumstellar envelopes
12 p1736 N90-19980
O-star parameters from line profiles of wind-blanketed model atmospheres 12 p1736 N90-19982

Stressed detector arrays for airborne astronomy
14 p1978 N90-21332
The 3S0114+65 and its peculiar companion
19 p2777 N90-25792
The formation and structure of circumstellar and interstellar dust 21 p3091 N90-27576

ASTRONOMICAL TELESCOPES
U TELESCOPES

ASTRONOMY
NT GAMMA RAY ASTRONOMY
NT INFRARED ASTRONOMY
NT RADAR ASTRONOMY
NT RADIO ASTRONOMY
NT SPACEBORNE ASTRONOMY
NT ULTRAVIOLET ASTRONOMY
NT X RAY ASTRONOMY
Institute of Geophysics and Planetary Physics, 1988
[DE89-014363] 01 p0137 N90-10794
National register of research projects, 1986/87. Part 2B: Natural sciences: Physical, engineering and related sciences (new projects)
[DE89-015033] 01 p0143 N90-10826
Meeting of intercosmos space physics group
02 p0158 N90-10902
The astronomy of Andean myth: The history of a cosmology 02 p0291 N90-11660
National Science Foundation
04 p0569 N90-13320
European Rocket and Balloon Programs and Related Research
[ESA-SP-291] 05 p0656 N90-13826
The German space science program
05 p0662 N90-13873
The Explorer program for astronomy and astrophysics
05 p0712 N90-14159
Analysis of coordinated observations of a giant stellar flare
[NASA-CR-185961] 05 p0715 N90-14176
Artificial intelligence approaches to astronomical observation scheduling
[NASA-CR-186277] 07 p1012 N90-15862
Reports of planetary astronomy, 1986
[NASA-TM-100776] 08 p1138 N90-16596
Proceedings of Colloquium 110 of the International Astronomical Union on Library and Information Services in Astronomy
[AD-A215612] 09 p1296 N90-17523
Preliminary experimental measurement of isoplanatic angle
[AD-A215828] 10 p1407 N90-18115
Software for image treatment of the FORCE system operating at the IFSI --- Ist. di Fisica dello Spazio Interplanetario (IFSI)
[IFSI-88-15] 10 p1417 N90-18164
Speckle interferometry for high resolution pictures of astronomical objects
[ETN-90-95827] 12 p1729 N90-19936
MAX 1991. The active sun: A plan for pursuing the study of the active sun at the time of the next maximum in solar activity, January 1985
[NASA-CR-186125] 12 p1745 N90-20030
Experimental validation of extended image reconstruction using bispectral speckle interferometry
[DE90-008545] 13 p1772 N90-20171
Bibliography of spatial interferometry in optical astronomy
[NASA-TM-100754] 13 p1901 N90-20911
Design and performance analysis of adaptive optical telescopes using laser guide stars
[AD-A218025] 13 p1902 N90-20913
Common source cascode amplifiers for integrating IR-FPA applications 14 p1977 N90-21324
Experience with the UKIRT InSb array camera
14 p1977 N90-21327
Initial astronomical results with a new 5-14 micron Si:Ga 58x62 DRO array camera 14 p1978 N90-21334
Laboratory and telescope use of the NICMOS2 128 x 128 HgCdTe array 14 p1979 N90-21338
HgCdTe 256x256 NWIR FPA
14 p1981 N90-21348
Tests of the Rockwell Si:As Back-Illuminated Blocked-Impurity Band (BIBIB) detectors
14 p1981 N90-21350
Motion detection in astronomical and ice floe images
15 p2140 N90-22231
NSSDC data listing
[NASA-TM-102980] 15 p2180 N90-22456
The optical night sky at low surface brightness: High latitude dust and faint field galaxies
15 p2185 N90-22481
Activities report of the Institute of Astronomical Calculations
[ETN-90-96461] 17 p2481 N90-24189
Activities report of the Institute for Astronomy and Astrophysics
[MITT-10] 18 p2636 N90-25020
Activities report of the Netherlands Space Research Organization
[ETN-90-96927] 18 p2636 N90-25021
Reports of planetary astronomy, 1990
[NASA-TM-4205] 20 p2940 N90-26730
Astronomy at ultra-high energies: Results from the CYGNUS experiment
[DE90-011979] 20 p2940 N90-26732
Astronomical observations of solid phase carbon
21 p3089 N90-27566
Spatial interferometry in optical astronomy
[NASA-RP-1245] 22 p3262 N90-28470
Theoretical specifications of the trajectory estimation for a space navigation system with the function of guidance and control
[NAL-TR-1032] 24 p3439 N90-29420
Bispectral-based optimization algorithms for speckle imaging
[DE90-015610] 24 p3529 N90-29957
Detector to study low-flex hard x ray/gamma ray sources
[UT-HE-90/08] 24 p3564 N90-30164
Some personal reminiscences. The ESRO-ESA space science story: Twenty-five years of European cooperation
[ESA-BR-66] 24 p3565 N90-30168

ASTROPHYSICS
NT COMPUTATIONAL ASTROPHYSICS
NT NUCLEAR ASTROPHYSICS
NT SOLAR PHYSICS
NT STELLAR PHYSICS
On the utility and ubiquity of atomic collision physics
[DE89-015356] 01 p0119 N90-10686
Institute of Geophysics and Planetary Physics, 1988
[DE89-014363] 01 p0137 N90-10794
Astrophysical and cosmological constraints to neutrino properties
[NASA-CR-185031] 01 p0140 N90-10809
Atomic effects of beta decay in astrophysics and in elementary particle physics 01 p0141 N90-10811
Meeting of intercosmos space physics group
02 p0158 N90-10902
A liquid xenon imaging telescope for 1-30 MeV gamma-ray astrophysics
[NASA-CR-185999] 02 p0291 N90-11662
Studying shocks in model astrophysical flows
[DE89-618786] 02 p0295 N90-11677
Detailed photonuclear cross-section calculations and astrophysical applications
[DE89-017531] 03 p0421 N90-12419
Research in cosmic and gamma ray astrophysics
[NASA-CR-185451] 04 p0569 N90-13316
Stellar content of the input catalog
05 p0607 N90-13535
European Rocket and Balloon Programs and Related Research
[ESA-SP-291] 05 p0656 N90-13826
The Swedish sounding rocket and balloon program
05 p0657 N90-13830
An implementation plan for priorities in solar-system space physics
[NASA-CR-185375] 05 p0710 N90-14154
The Explorer program for astronomy and astrophysics
05 p0712 N90-14159
The ultimate structure of matter: The US High Energy Physics Program from the 1950s through the 1980s
[DE90-001784] 06 p0840 N90-14887
An international discussion on research in solar and space physics 06 p0859 N90-14998
Astophysical opacities at LLNL
[DE90-003599] 07 p1014 N90-15872
Space operations: Listing of NASA scientific missions, 1980-2000. Fact sheet for the Chairman, Subcommittee on Space Science and Applications, Committee on Science, Space, and Technology, House of Representatives
[AD-A213493] 07 p1016 N90-15881
Variational problems in astrophysics
09 p1298 N90-17524
Particle theory and cosmology
[DE90-005338] 10 p1446 N90-18346
Gamma ray astronomy and black hole astrophysics
[NASA-CR-186496] 11 p1590 N90-19169
Particle physics and cosmology
[DE90-006547] 11 p1590 N90-19171
Current and future uses of accelerators in particle astrophysics
[DE90-006667] 11 p1595 N90-19186
Low-cost small satellites for astrophysical missions
[DE90-007625] 12 p1616 N90-19293
Measurement of cross sections: New needs and possibilities
[DE90-007248] 12 p1711 N90-19829
Experimental and theoretical high energy physics
[DE90-005974] 12 p1712 N90-19834
Astronomy and astrophysics
[REPT-33/89] 12 p1729 N90-19938
Pulsar timing and gravitational waves
12 p1732 N90-19955
LAGEOS 3 and the gravitomagnetic field
12 p1733 N90-19961
Very high energy gamma ray astrophysics
[DE90-006645] 12 p1737 N90-19983
Nuclear interactions of high energy heavy ions and applications in astrophysics
[DE90-006691] 12 p1737 N90-19984
The Advanced Composition Explorer
[DE90-006522] 12 p1737 N90-19987
Mercuric iodide room temperature gamma-ray detectors
[NASA-TM-103318] 13 p1804 N90-20357
Problems in radiative transfer in astrophysics: An escape probability treatment of line overlap and a model of the masers around VX Sgr 14 p2041 N90-21705
NSSDC data listing
[NASA-TM-102989] 15 p2180 N90-22456
Physics of systems containing neutron stars
[NASA-CR-186002] 15 p2182 N90-22467
A high galactic latitude survey of far ultraviolet excess objects 15 p2183 N90-22473
The Al-26(rho, gamma)Si-27 reaction: Stellar origins of galactic Al-26 15 p2188 N90-22498
An astrophysics data program investigation of cluster evolution
[NASA-CR-181296] 15 p2191 N90-22510
Molecular evolution in astrophysical environments
16 p2332 N90-23291
The illusive Geminga: What is it
16 p2335 N90-23307
Institute of Astronomy 17 p2481 N90-24190
Research and technology 1989
[NASA-TM-100369] 17 p2486 N90-24219
Activities report of the Institute for Astronomy and Astrophysics
[MITT-10] 18 p2636 N90-25020
Small helium-cooled infrared telescope experiment for Spacelab-2 (IRT)
[NASA-CR-183983] 19 p2765 N90-25708
The 23rd ESLAB Symposium on Two Topics in X Ray Astronomy. Volume 1: X Ray Binaries
[ESA-SP-296-VOL-1] 19 p2765 N90-25711
Astrophysical importance of the slim accretion disks
19 p2782 N90-25827
Laboratory studies of photodissociation processes relevant to the formation of cometary radicals
20 p2947 N90-26772
Proton irradiation of simple gas mixtures: Influence of irradiation parameters 20 p2949 N90-26782
Coulomb-dissociation of 156 MeV 6Li-projectiles
[KFK-4691] 21 p3075 N90-27482
Carbon in primitive meteorites
21 p3089 N90-27563
Astronomical observations of solid phase carbon
21 p3089 N90-27566
Down-to-earth studies of carbon clusters
21 p3091 N90-27573
FT-IR spectroscopic studies of polycyclic aromatic hydrocarbons 21 p3095 N90-27592
Data catalog series for space science and applications flight missions. Volume 5A: Descriptions of astronomy, astrophysics, and solar physics spacecraft and investigations. Volume 5B: Descriptions of data sets from astronomy, astrophysics, and solar physics spacecraft and investigations
[NASA-TM-101908] 24 p3437 N90-29413
Activities report of the Space Science Department
[ESA-SP-1126] 24 p3560 N90-30142
Some personal reminiscences. The ESRO-ESA space science story: Twenty-five years of European cooperation
[ESA-BR-66] 24 p3565 N90-30168

ASYMMETRY
A symplectic coherent beam-beam model
[DE89-015386] 01 p0122 N90-10701
Observations of azimuthal asymmetry for certain FRC operating regimes
[DE89-015300] 01 p0126 N90-10721
Radiationless transitions and excited-state absorption of low-field chromium complexes in solids
[AD-A210653] 02 p0194 N90-11105
Ionospheric total electron content, and far ultraviolet, near infrared oxygen emission 02 p0249 N90-11410
Building a software package for solving large sparse nonlinear systems of equations
[AD-A211758] 04 p0529 N90-13055
Exploring asymmetric heavy-ion reactions at the KX-ray method: The Ne20 + Tb159 reaction at 15 MeV/unit
[KVI-777] 04 p0552 N90-13216
Study of forces and moments on wing-bodies at high incidence, volumes 1 and 2 05 p0575 N90-13350

The linear study of zonally asymmetric barotropic flows 05 p0668 N90-13902
Rotation of the photospheric magnetic fields: A north-south asymmetry
[NASA-CR-186159] 05 p0715 N90-14177
Products of the hypochlorite oxidation of hydrazine fuels
[AD-A213557] 07 p0915 N90-15291
Study on edge plasma physics and particle control in the Heliotron E device
[DE90-719524] 09 p1284 N90-17443
Lateral asymmetry in pattern recognition: Understanding the effects of familiarity, distinction, and perspective change
[AD-A217739] 13 p1854 N90-20641
Analytical study of the origin and behavior of asymmetric vortices
[NASA-TM-102796] 15 p2049 N90-21746
Experimental investigation of the effect of cavitation on the rotordynamic forces on a whirling centrifugal pump impeller 15 p2105 N90-22039
A free electron laser master oscillator power amplifier experiment 16 p2239 N90-22776
Innovative design of composite structures: Axisymmetric deformations of unsymmetrically laminated cylinders loaded in axial compression
[NASA-CR-186635] 19 p2700 N90-25364
Trajectory optimization for an asymmetric launch vehicle
[NASA-CR-185630] 20 p2817 N90-26033
Baryogenesis in extended inflation. 2: Baryogenesis via primordial black holes
[NASA-CR-182843] 20 p2941 N90-26735
On the dynamic and thermodynamic structures of marine stratocumulus 22 p3216 N90-28244
Physically-based general circulation model parameterization of clouds and their radiative interaction 22 p3228 N90-28308
Development of non-conventional control methods for high angle of attack flight using vortex manipulation 23 p3273 N90-28522
Effects of flowfield turbulence on asymmetric vortices over a slender body
[AD-A224139] 23 p3328 N90-28819

ASYMPTOTES

Asymptotic bias of autoregressive estimators
[IMAG-RR-745-M] 03 p0395 N90-12255
On the maximum period of a permutation of N elements
[MEMO-771] 04 p0544 N90-13159
Robust adaptive control: Stability and asymptotic performance
[AD-A219259] 16 p2304 N90-23127

ASYMPTOTIC GIANT BRANCH STARS

Properties of evolved star circumstellar grains 06 p0861 N90-15003
Nonradial instability strips for post-AGB stars
[DE90-014922] 23 p3411 N90-29278

ASYMPTOTIC METHODS

Asymptotic robustness in regression and autoregression based on Lindeberg conditions
[AD-A210725] 01 p0114 N90-10654
Hopf bifurcation in the driven cavity
[NASA-TM-102334] 03 p0345 N90-11969
A study of the asymptotic behavior of linear difference equations with polynomial coefficients
[IMAG-RR-743-M] 03 p0395 N90-12254
Asymptotic analyses of the structures and characteristics of flames 04 p0468 N90-12683
Berry-Esseen rates and bootstrap results for generalized L-statistics
[CWI-MS-R8808] 04 p0546 N90-13179
Variational and asymptotic methods in open and closed waveguide analysis
[REPT-34] 04 p0554 N90-13229
A new uniformly valid asymptotic integration algorithm for elasto-plastic-creep and unified viscoplastic theories including continuum damage
[NASA-TM-102344] 06 p0799 N90-14655
High-frequency asymptotic methods for analyzing the EM scattering by open-ended waveguide cavities
[NASA-CR-186244] 08 p1056 N90-16103
Asymptotically fast triangularization of matrices over rings
[DE90-003161] 08 p1117 N90-16471
On some problems in reliability theory 09 p1233 N90-17155
Nonparametric estimation of reliability and related functions
[AD-A215138] 09 p1234 N90-17160
Conditions at the downstream boundary for simulations of viscous incompressible flow
[NASA-TM-102510] 10 p1422 N90-18198
Asymptotic analysis of transonic flow through oscillating cascades 11 p1462 N90-18421
Transient responses of coupled systems
[ONERA-RT-13/3596-RY-070-R] 11 p1509 N90-18687
Asymptotic boundary conditions for dissipative waves: General theory
[NASA-TM-102497] 11 p1551 N90-18927
An unsteady time asymptotic flow in the square driven cavity
[NASA-TM-103141] 15 p2099 N90-22016
On the theory of Heiser and Sherclift experiment. Part 1: MHD flow in an open channel in strong uniform magnetic field
[OUEL-1804/89-PT-1] 15 p2170 N90-22400
On the theory of Heiser and Sherclift experiment. Part 2: MHD flow between two cylinders in strong radical magnetic field
[OUEL-1805/89-PT-2] 15 p2170 N90-22401
The analysis and simulation of compressible turbulence
[NASA-CR-181997] 16 p2197 N90-22539
Nonlinear internal gravity wave critical layers 17 p2422 N90-23801
Concerning the interaction of non-stationary cross-flow vortices in a three-dimensional boundary layer
[NASA-CR-182037] 18 p2492 N90-24245
Second order asymptotics in level crossing problems for differences of renewal processes
[MEMO-824] 18 p2600 N90-24798
On the statistical analysis of growth
[ETN-90-96923] 18 p2606 N90-24841
A critical evaluation of two-equation models for near wall turbulence
[NASA-CR-182068] 20 p2860 N90-26270
Variance reduction for quantile estimates in simulations via nonlinear controls
[AD-A222653] 20 p2916 N90-26590
Asymptotic optimality of the fast randomized versions of GCV and C(sub L) in ridge regression and regularization
[IMAG-RR-793-M] 20 p2918 N90-26606
A study of the asymptotic properties of least square estimators for multiple phase regression problems
[ETN-90-97244] 20 p2921 N90-26620
Asymptotic behavior of solutions of diffusion-like partial differential equations invariant to a family of affine groups
[DE90-014792] 23 p3388 N90-29130
Asymptotics of Laplace-Dirichlet integrals
[DE90-627165] 23 p3388 N90-29137

ASYMPTOTIC PROPERTIES

Likelihood cross-validation bandwidth selection for nonparametric kernel density estimators
[REPT-89-10] 03 p0398 N90-12279
Stable and unstable subspaces of a critical functional differential equation
[PB89-220651] 04 p0538 N90-13115
On a rate of convergence of the multiknapsack value function
[CWI-MS-R8812] 04 p0542 N90-13144
Asymptotic expansions for two-stage rank tests
[MEMO-773] 04 p0544 N90-13161
Interpretation and manipulation of Edgeworth expansions
[MEMO-775] 04 p0544 N90-13163
On the asymptotic convergence of the simulated annealing algorithm in the presence of a parameter dependent penalization
[MEMO-COSOR-89-16] 05 p0684 N90-13984
Estimation of convolution tail behavior
[MEMO-COSOR-89-04] 05 p0693 N90-14051
The synergism of analytic and numerical techniques in general relativity: Calculation of radiative spacetimes 15 p2174 N90-22425
On rates of convergence and asymptotic normality in the multiknapsack problem
[CWI-BS-R8912] 17 p2460 N90-24045
Asymptotic analysis of wind-induced vibrations
[ETN-90-96903] 18 p2572 N90-24658
Asymptotic expansions of an integral containing a phase function with three saddle points
[CWI-AM-R8922] 18 p2599 N90-24793
Asymptotic law of the orthogonal empirical functions and applications, part 2
[IMAG-RR-792-M-PT-2] 20 p2918 N90-26605
A study of the asymptotic properties of least square estimators for multiple phase regression problems
[ETN-90-97244] 20 p2921 N90-26620
Asymptotic code vector density in topographic vector quantisers
[RSRE-MEMO-4392] 24 p3539 N90-30012

ASYMPTOTIC SERIES

Global existence and asymptotic stability for a nonlinear integrodifferential equation modeling heat flow
[AD-A210647] 01 p0071 N90-10408
A unified approach to estimating tail behavior
[AD-A210961] 01 p0117 N90-10672
Small sample theory for steady state confidence intervals
[AD-A212097] 03 p0393 N90-12242
Smoothed limit theorems for equilibrium processes
[AD-A212321] 04 p0547 N90-13186
Asymptotic analysis of performance of membrane modules for gas separations
[DE90-000699] 06 p0742 N90-14316
Strong large deviation and local limit theorems
[AD-A213610] 07 p0986 N90-15698
Asymptotic behaviour of solutions of a degenerate quasilinear hyperbolic equation
[DE89-635713] 09 p1276 N90-17400
Using the method of matched asymptotic expansions, analytically investigate the three-dimensional, atmosphere entry problem
[AD-A216287] 11 p1468 N90-18451
Effect on relaxation on nonlinear waves in crystals 16 p2310 N90-23165
M-estimators in linear models with long range dependent errors
[AD-A219921] 17 p2461 N90-24053
Vortex-induced boundary-layer separation 18 p2551 N90-24560
Contribution to the study of differential equations and to the differences in the complex field
[ETN-90-97250] 20 p2919 N90-26612
Asymptotic analysis of dissipative waves with applications to their numerical simulation
[NASA-TM-103231] 20 p2920 N90-26615
Asymptotic modal analysis and statistical energy analysis
[NASA-CR-186732] 20 p2923 N90-26634
Application and extension of an analytical model of the confined acoustic beam generated by a transducer
[AD-A222994] 20 p2924 N90-26639
Consistency and convergence for numerical radiation conditions
[NASA-TM-103262] 23 p3387 N90-29124
Tail and quantile estimation for strongly mixing stationary sequences
[AD-A223472] 24 p3540 N90-30019
Propagation of chaos and the McKean-Vlasov equation in duals of nuclear spaces
[AD-A224431] 24 p3543 N90-30039

ASYNCHRONOUS MOTORS

Coordinate transformation for an asynchronous, machine, and time discretization of a state observer
[EMV-88-30] 17 p2397 N90-23657
Design, simulation, and testing of a field-oriented ac servo-drive using a TMS 32010 signal processor
[EMV-88-42] 17 p2397 N90-23658
Design and use of brushless dc motor without detent torque 18 p2539 N90-24491
Identification method for estimation of electrical parameters of induction motors
[ETN-90-97306] 22 p3168 N90-27969

ATAXIA

The relationship between subjective and objective measures of simulator-induced ataxia
[AD-A213095] 05 p0673 N90-13922
Simulator induced sickness in the CP-140 (Aurora) flight deck simulator
[AD-A213096] 05 p0673 N90-13923
Simulator sickness in the AH-1S (Cobra) flight simulator
[AD-A214562] 09 p1250 N90-17254

ATHLETES

What should athletes know about low body temperature (hypothermia)
[AD-A218316] 13 p1854 N90-20637

ATHODYDS

U RAMJET ENGINES

ATLANTIC OCEAN

Mariners Weather Log, volume 32, number 3, Summer 1988
[PB88-248075] 01 p0086 N90-10491
US Navy regional climatic study of the United States Atlantic Coast and associated waters
[AD-A210198] 01 p0088 N90-10503
Evaluation of the North Atlantic seasonal nitrogen model, version 2
[DE89-016157] 01 p0090 N90-10515
Atmospheric aerosol size distributions and optical properties found in the marine boundary layer over the Atlantic Ocean
[AD-A210800] 02 p0252 N90-11431
Synoptic/planetary-scale interactions and blocking over the North Atlantic Ocean 03 p0360 N90-12061
Dynamics of the equatorial undercurrent and its termination
[PB89-198147] 03 p0377 N90-12146
Investigation of North Atlantic fog and development of a marine fog forecast system
[AD-A211750] 04 p0519 N90-12999

Current velocity and hydrographic observations in the southwestern North Atlantic Ocean: Subtropical Atlantic Climate Studies (STACS), 1988
[PB89-230825] 04 p0521 N90-13010
Analysis of propagation in an inhomogeneous atmosphere in the horizontal and vertical direction using the parabolic equation method 06 p0760 N90-14421
Intertropical Convergence Zone (ITCZ) and its relationship with the precipitation of the north-northeast Brazilian region
[INPE-4887-TDL/378] 11 p1535 N90-18839
Dynamics of an ERICA (Experiment on Rapidly Intensifying Cyclones over the Atlantic) cyclone
[AD-A216775] 11 p1536 N90-18846
Analysis of GALE (Genesis of Atlantic Lows Experiment) data
[AD-A217182] 13 p1844 N90-20584
Forecast of Atlantic seasonal hurricane activity for 1990 15 p2134 N90-22194
An investigation of meteorological effects on currents in the shelf and continental slope seas northwest of the United Kingdom. 2: Relationships between currents at different locations and with other variables
[PB90-151911] 15 p2134 N90-22195
US Navy regional climatic study of southern African waters
[AD-A218792] 16 p2258 N90-22874
The trace metal geochemistry of suspended oceanic particulate matter
[AD-A218604] 17 p2429 N90-23839
Efficient representation of the hydrographic structure of the north atlantic ocean and aspects of the circulation from objective methods
[AD-A218606] 17 p2429 N90-23841
Trace metal sources for the atlantic inflow to the Mediterranean Sea
[AD-A218607] 17 p2429 N90-23842

ATLANTIS (ORBITER)
Shuttle Atlantis to deploy Galileo probe toward Jupiter
[NASA-TM-101888] 02 p0175 N90-10982

ATMOSPHERIC ABSORPTION
U ATMOSPHERIC ATTENUATION

ATMOSPHERIC ATTENUATION
Atmospheric transmissivity update - 1988
[AD-A209130] 01 p0085 N90-10484
Tropospheric influences on satellite-Earth paths and their determination by means of radar measurements
[ESA-TT-1143] 04 p0460 N90-12639
Ultraviolet absorption cross-sections of bromoform in the temperature range 295-240 K
[AERONOMICA-ACTA-A-348-1989] 05 p0622 N90-13630
MODTRAN: A moderate resolution model for LOWTRAN 7
[AD-A214337] 07 p0978 N90-15650
X-band atmospheric attenuation for an Earth terminal measurement system
[PB90-100736] 08 p1056 N90-16101
Helsinki University of Technology Radio Laboratory
[PB90-110677] 08 p1056 N90-16102
The physical foundations of radiometry and their applications in the mm-waveband
[REPT-12-88] 08 p1058 N90-16114
Atmospheric transmittance determination from a two-angle measurement of radiance change
[AD-A213847] 08 p1101 N90-16375
Rain attenuation measurements: Variability and data quality assessment 10 p1373 N90-17955
Observations of attenuation at 20.6, 31.65 and 90.0 GHz: Preliminary results from Wallops Island, VA 10 p1373 N90-17957
Radiometric observations at 20.6, 31.65, and 90.0 GHz: Continuing studies 10 p1373 N90-17958
Low elevation angle KU-band satellite measurements at Austin, Texas 10 p1373 N90-17959
Atmospheric transmission calculations for optical frequencies 10 p1373 N90-17960
Recent achievements of OPEX 10 p1373 N90-17961
The ITALSAT experiment 10 p1374 N90-17962
ACTS propagation concerns, issues, and plans 10 p1374 N90-17963
US Activity with the OLYMPUS satellite 10 p1374 N90-17964
LOWTRAN 7: Status, review, and impact for short-to-long-wavelength infrared applications 15 p2081 N90-21917
Millimetre-wave propagation in the evaporation duct 15 p2084 N90-21929
Applications of remote sensing to studies of oceanic upper mixed layer dynamics 15 p2122 N90-22137
En route noise: NASA propfan test aircraft (calculated source noise
[DOT-TSC-FA953-LR5] 18 p2609 N90-24857
The effects of urban air pollution on solar radiation
[DE89-009455] 19 p2712 N90-25438
An outline for the RTNEPH infrared atmospheric water vapor attenuation study
[AD-A221753] 21 p3027 N90-27209
Study of a variable step network and comparison between the radii method and the parabolic equations, applied to the acoustic propagation in the atmosphere
[ONERA-RF-12/3641-PY] 22 p3245 N90-28401

ATMOSPHERIC BOUNDARY LAYER
Airborne profiles taken near San Nicolas Island, California, during Operation FIRE (First ISCCP (International Satellite Cloud Climatology Project) regional experiment) (1987): Aerosol size distributions, air and surface temperatures, cloud top temperatures, and relative humidities
[AD-A211664] 03 p0374 N90-12136
Description of a software library for the calculation of surface fluxes
[KNMI-TR-112] 03 p0375 N90-12141
Central Sudan surface wind data and climate characteristic
[KNMI-WR-88-01] 04 p0520 N90-13000
The shape of the probability density function of short-term concentration fluctuations of plumes in the atmospheric boundary layer
[AD-A212632] 04 p0548 N90-13188
Dynamics of baroclinic instability in rapid cyclogenesis 07 p0962 N90-15563
The response of the atmospheric convective boundary layer to surface inhomogeneities 08 p1100 N90-16389
Glancing shock-boundary layer interactions 10 p1309 N90-17571
Some aspects of atmospheric turbulence in forests
[INPE-4951-RPE/600] 11 p1532 N90-18818
Sounding and surface meteorological data from the Land/Sea Breeze Experiment (LASBEX)
[AD-A216269] 11 p1536 N90-18842
Wind tunnel design of heat island turbulent boundary layer
[IHW-ET/50] 12 p1660 N90-19542
Transport of atmospheric aerosols above the Sierra Nevada slopes
[PB90-120288] 12 p1685 N90-19675
Modelization of dry deposition in the Chemical Transport Model (CTM) of EURAD 12 p1688 N90-19698
A modeling study of the cloud-topped marine boundary layer
[AD-A218103] 13 p1846 N90-20594
The influence of lateral boundary conditions, fixed surface forcings, and synoptic situations upon predictability estimates using limited area numerical models 14 p2005 N90-21492
Sensitivity studies in a two-dimensional atmospheric transport model
[DAR-TP-18] 14 p2006 N90-21496
Numerical simulations of the cloud-capped marine boundary layer 14 p2008 N90-21506
Infrared propagation in the air-sea boundary layer 15 p2083 N90-21926
Effect of atmospheric turbulence on electro-optical systems 15 p2086 N90-21940
A linear analysis of monsoon base states associated with banded convection 15 p2130 N90-22179
Impact of marine boundary layer parameterization on a numerical simulation of cyclogenesis during a cold air outbreak event 16 p2256 N90-22864
A day in the life of a warm front
[AD-A220373] 17 p2426 N90-23826
The GIT model: An atmospheric boundary layer model along a trajectory
[FOA-E-40039-3.2] 18 p2579 N90-24693
Measurements of tropospheric nitric acid over the Western United States and Northeastern Pacific Ocean
[NASA-TM-103470] 20 p2883 N90-26399
An intercomparison of intraseasonal variability in general circulation models and observations
[NASA-TM-100764] 21 p3030 N90-27228
Vandenberg Boundary Layer Survey (VBLS): Results
[AD-A222517] 21 p3031 N90-27234
An eight-month climatology of marine stratocumulus cloud fraction, albedo, and integrated liquid water 22 p3214 N90-28233
Mesoscale variability of free tropospheric humidity near San Nicolas Island during FIRE 22 p3214 N90-28234
Diurnal variation in the turbulent structure of the cloudy marine boundary layer during FIRE 1987 22 p3217 N90-28248
Stratus: An interactive steady state mixed layer model for personal computers 22 p3219 N90-28255
A cloudiness transition in a marine boundary layer 22 p3219 N90-28259
Vertical-velocity skewness in the marine stratus-topped boundary layer 22 p3220 N90-28262
Turbulent statistics in the vicinity of an SST front: A north wind case, FASINEX February 16, 1986 22 p3221 N90-28266
Wind tunnel, field, and numerical investigations of plume downwash and dispersion at an arctic industrial site 24 p3489 N90-29721

ATMOSPHERIC CHEMISTRY
Paper 1. Impact of volcanic aerosols on stratospheric chemistry. Paper 2. O2 (1 sigma g +) and O2 (1 delta g) in the H + O2 reaction system. Paper 3. Barotropic instability of zonal jets on Mars, Earth and Venus 01 p0084 N90-10477
Study of the NO3 radical decomposition reaction and the N2O5 in equilibrium with NO3 + NO2 equilibrium constant
[PB89-208961] 01 p0085 N90-10480
Study of high frequency water vapor absorption parameters
[AD-A210676] 02 p0194 N90-11108
The Third Conference on the Environmental Chemistry of Hydrazine Fuels
[AD-A197632] 02 p0203 N90-11157
Atmospheric chemistry of the fuel hydrazines 02 p0203 N90-11158
An atmospheric pressure flow reactor: Gas phase kinetics and mechanism in tropospheric conditions without wall effects 02 p0203 N90-11160
The behavior of hydrazine vapor in an environmental chamber under simulated atmospheric conditions 02 p0203 N90-11161
Potential effects of global climate change on the United States. Executive summary. Draft
[PB89-161046] 02 p0237 N90-11350
NCAR (National Center for Atmospheric Research) master mechanism of the gas phase chemistry, version 2.0
[PB89-208979] 02 p0249 N90-11413
National Climate Program five-year plan, 1989-1993
[PB89-207369] 02 p0252 N90-11426
National Center For Atmospheric Research annual report, fiscal year 1988
[PB89-208987] 02 p0252 N90-11428
Atmospheric aerosol size distributions and optical properties found in the marine boundary layer over the Atlantic Ocean
[AD-A210800] 02 p0252 N90-11431
Ion bombardment of Io and Mercury 02 p0296 N90-11682
Global tropospheric chemistry: Chemical fluexes in the global atmosphere
[NASA-CR-186090] 03 p0369 N90-12109
LABCEDE fluorescence investigations
[AD-A210678] 03 p0370 N90-12114
Fundamental molecular data to support CARS diagnostics of temperature, pressure, and species concentration
[AD-A212411] 04 p0472 N90-12704
Infrared spectrometry of aerosols
[AD-A213303] 04 p0473 N90-12713
Retrieval of atomic oxygen and temperature in the thermosphere. Part 1: Feasibility of an experiment based on the spectrally resolved 147 micrometer limb emission
[AD-A211987] 04 p0517 N90-12985
Fundamentals of middle atmospheric dynamics
[AD-A211747] 04 p0518 N90-12988
Role of chemical effects in daytime high latitude trough formation
[AD-A211772] 04 p0518 N90-12989
Zonal average cloud characteristics for global atmospheric chemistry modeling
[CM-76] 04 p0518 N90-12992
Infrared water vapor continuum absorption: New atmospheric electrical measurements and theory
[AD-A212594] 04 p0519 N90-12994
Mesoscale acid deposition modeling studies
[NASA-CR-4262] 04 p0554 N90-13228
Proceedings: US/FRG (Federal Republic of Germany) Workshop on Photochemical Ozone Problem and Its Control: US Experiences and the Situation in Europe
[PB89-233514] 05 p0666 N90-13891
CANOES 2: Dynamics of atmospheric infrared thermochemical excitation, volume 1
[AD-A213341] 05 p0667 N90-13897
CANOES 2: Dynamics of atmospheric infrared thermochemical excitation, volume 2
[AD-A213342] 05 p0667 N90-13898
CANOES 2: Dynamics of atmospheric infrared thermochemical excitation, volume 3
[AD-A213343] 05 p0667 N90-13899
Global stratospheric change: Requirements for a Very-High-Altitude Aircraft for Atmospheric Research
[NASA-CP-10041] 06 p0723 N90-14220
On the mitigation of non-CO2 greenhouse gases
[DE89-016659] 06 p0809 N90-14710

International Conference on Global and Regional Atmospheric Environmental Chemistry and visit to Hangzhou, China, foreign trip report
[DE90-000099] 06 p0810 N90-14713
Nitrogen deposition to forest trees
[DE90-003285] 06 p0812 N90-14726
Characterization of cloud chemistry and frequency of canopy exposure to clouds in the Sierra Nevada
[PB89-104035] 06 p0817 N90-14753
Long-term worldwide environmental effects caused by acid rain from fossil fuels
[DE90-001534] 07 p0956 N90-15533
HCl monitor, phase 2
[AD-A213572] 07 p0958 N90-15542
Oxygen and other atmospheric gases
[AD-A214296] 07 p0961 N90-15557
NO2 photodissociation dynamics
[AD-A214422] 07 p0962 N90-15560
Anomalous absorption by atmospheric water vapor and stabilized water fogs in the infrared and CM-wave regions
[AD-A214202] 07 p0964 N90-15572
MODTRAN: A moderate resolution model for LOWTRAN 7
[AD-A214337] 07 p0978 N90-15650
ECC (Electrochemical Concentration Cell) ozonesonde observations at Mirny, Antarctica, during 1986
[PB90-113960] 08 p1098 N90-16357
Upper atmosphere research
[ISBN-0-642-13582-7] 08 p1100 N90-16368
The chemistry and dynamics of marine stratocumulus
08 p1102 N90-16381
Reactions of atmospheric species with clean and H, C, and O implanted species
[AD-A214602] 09 p1244 N90-17218
Plume flowfield analysis of the shuttle primary Reaction Control System (RCS) rocket engine
[NASA-CR-186315] 10 p1329 N90-17676
Report from upper atmospheric science
10 p1444 N90-18332
Tropospheric chemistry of natural hydrocarbons and energy-related pollutants: Biosphere/climate feedbacks
[DE90-005643] 11 p1532 N90-18820
The EURAD Model: Structure and First Results
[REPT-61] 12 p1686 N90-19680
Atmospheric chemiluminescence: COCHISE and FACELIF experiments
[AD-A218121] 13 p1843 N90-20578
The receiving system of a dual dye lidar to study molecular and aerosol densities at the base of the stratosphere
[AD-A218286] 13 p1843 N90-20581
Meteorological influences on mountain cloudwater chemistry in the eastern United States
[PB90-132432] 14 p2007 N90-21504
The sources and chemistry of late winter Arctic tropospheric aerosols
[PB90-131988] 15 p2126 N90-22158
Cloud chemistry and occurrence in the western United States: A synopsis of current information
[PB90-134248] 15 p2131 N90-22182
The diurnal ozone cycle in a coniferous forest: The importance of meteorology and chemistry
[CM-75] 17 p2421 N90-23795
A study of gravity wave variability, saturation, and turbulence generation in the mesosphere and lower thermosphere
[AD-A220018] 17 p2424 N90-23810
Effects of solar ultraviolet radiation on biogeochemical dynamics in aquatic environments
[AD-A221119] 18 p2578 N90-24687
Global changes in tropospheric chemistry
19 p2708 N90-25411
The effects of urban air pollution on solar radiation
[DE89-009455] 19 p2712 N90-25438
Diversiform processes of ozone in the atmosphere: Introduction study
[AERONOMICA-ACTA-A-352-1990]
19 p2713 N90-25439
Digital filtering of plume emission spectra
[NASA-TM-103135] 20 p2824 N90-26070
Nordic Symposium on Atmospheric Chemistry
[CM-78] 20 p2883 N90-26403
Further development and application of an atmospheric chemistry trajectory model 20 p2884 N90-26408
Natural and anthropogenic components in bulk precipitation at Blidoe (archipelago of Stockholm, Sweden) 20 p2884 N90-26409
Some results from the precipitation chemistry measurement programme in Sweden
20 p2884 N90-26410
Ice core studies and the past atmospheric environment of polar regions 20 p2885 N90-26411
The Renland ice core (Greenland): A source for climatic studies over 100,000 years 20 p2885 N90-26412
Results from global tropospheric sulphur simulations
20 p2885 N90-26413
The aqueous atmospheric chemistry of mercury
20 p2886 N90-26420
Terpene concentrations and emissions in a Scots pine forest 20 p2886 N90-26422
The diurnal ozone cycle in a coniferous forest: The importance of meteorology and chemistry
20 p2886 N90-26423
Stratospheric chemistry 20 p2886 N90-26424
Photodissociation of NO2: Influence of photolysis wavelength and temperature dependence on product formation 20 p2887 N90-26426
The collection and analysis of atmospheric peroxides
20 p2887 N90-26428
Destruction of peroxy radical by Cu ion catalysed reactions on atmospheric particles
20 p2887 N90-26429
Heterogeneous transformation of peroxyacetylnitrate
20 p2887 N90-26430
Formation and deactivation of vibrationally excited atmospheric molecules
[AD-A222660] 20 p2889 N90-26442
Submillimeter and millimeter observations of solar system objects
[NASA-CR-186636] 20 p2940 N90-26731
Absolute vacuum ultraviolet photoabsorption cross section studies of atomic and molecular species: Techniques and observational data
20 p2944 N90-26754
Novel laser gain and time-resolved FTIR studies of photochemistry 20 p2945 N90-26756
Kinetics and thermochemistry of polyatomic free radicals: New results and new understandings
20 p2946 N90-26764
A laboratory investigation of the production and properties of molecular and radical species pertinent to planetary atmospheres 20 p2946 N90-26766
The applications of chemical thermodynamics and chemical kinetics to planetary atmospheres research
20 p2948 N90-26773
Spectroscopy of ions and their clusters
[AD-A223109] 21 p2977 N90-26917
Tropospheric sounders 21 p3016 N90-27150
All-optical photochromic spatial light modulators based on photoinduced electron transfer in rigid matrices
[NASA-CASE-NPO-17612-1-CU]
21 p3076 N90-27487
Plasma cloaking: Air chemistry, broadband absorption, and plasma generation
[AD-A222044] 21 p3078 N90-27503
Atmospheric Sciences Research in the US EPA climate program
[PB90-221870] 22 p3212 N90-28219
Quenching of N(2D) by O(3P)
[AD-A221690] 23 p3303 N90-28683
Acid deposition: No such thing as a free launch
[DE90-015085] 23 p3348 N90-28920
Tropospheric nitrogen: The influence of anthropogenic sources on distributions and deposition
[DE90-015408] 24 p3487 N90-29709
A study of water vapor, electrical parameters, and radio propagation
[AD-A223582] 24 p3492 N90-29736
Optical emissions from bombarding atmospheric gases with heavy ions
[AD-A223544] 24 p3543 N90-30040
Interstellar magnetic fields: An observational perspective 24 p3560 N90-30144

ATMOSPHERIC CIRCULATION
NT ZONAL FLOW (METEOROLOGY)
Atmospheric environment for space shuttle (STS-29) launch
[NASA-TM-100376] 02 p0175 N90-10980
Atmospheric environment for space shuttle (STS-30) launch
[NASA-TM-100381] 02 p0175 N90-10981
Global ionospheric dynamics
02 p0240 N90-11366
Global ionospheric dynamics: A review
02 p0241 N90-11367
A fully analytic, low and middle latitude ionospheric model 02 p0241 N90-11368
Seasonal and geomagnetic response of the thermosphere and ionosphere 02 p0243 N90-11380
Stratiform clouds and their interaction with atmospheric motions 03 p0360 N90-12060
Studies of baroclinic instability in the presence of surface topography and stratospheric ozone
03 p0361 N90-12068
Use of satellite data and modeling to asses the influence of stratospheric processes on the troposphere
03 p0363 N90-12075
Laboratory and theoretical models of planetary-scale instabilities and waves 03 p0363 N90-12076
Development of high resolution simulations of the atmospheric environment using the MASS model
[NASA-CR-186040] 03 p0374 N90-12133
A new generation of atmospheric tracers: The biological connection
[AD-A212285] 04 p0517 N90-12983
Air flow over large scale topography
[AD-A211779] 04 p0519 N90-12998
Airdata calibration of a high-performance aircraft for measuring atmospheric wind profiles
[NASA-TM-101714] 06 p0725 N90-14228
An observational study of intramonthly quasi-periodicities in the Northern Hemisphere, extratropical geopotential height field
06 p0813 N90-14729
Beryllium dispersion near explosive firing tables: A comparison of computed and observed results
[DE90-002635] 07 p0960 N90-15550
Simulation of pollutant transport using a mesoscale grid circulation model
[GKSS-89/E/24] 08 p1099 N90-16365
The effect of orographic forcing on the mean flow of the stratosphere 08 p1099 N90-16367
The response of the atmospheric convective boundary layer to surface inhomogeneities
08 p1100 N90-16369
Multiple flow regimes in the Northern Hemisphere winter 08 p1100 N90-16372
USSR Climate Handbook Number 27. Part 1: Solar radiation, radiation balance and sunshine
[AD-A215647] 09 p1248 N90-17242
A 3-D dynamical/chemical GCM for simulating the anthropogenical effects on ozone
[DE90-004836] 10 p1406 N90-18108
Preliminary experimental measurement of isoplanatic angle
[AD-A215828] 10 p1407 N90-18115
An analysis of diurnal wind variability in the Santa Barbara Channel from SODAR measurements
[AD-A215769] 10 p1408 N90-18121
Perspectives on aerosol deposition to natural surfaces
[DE90-003398] 11 p1532 N90-18819
Connections between the circulation in altitude and convection over South America
[INPE-4923-TDL/383] 11 p1534 N90-18828
Summer Study Program in Geophysical Fluid Dynamics: The Influence of Convection on Large-Scale Circulations, 1988
[AD-A216024] 11 p1535 N90-18840
Dynamics of an ERICA (Experiment on Rapidly Intensifying Cyclones over the Atlantic) cyclone
[AD-A216775] 11 p1536 N90-18846
NAPAP (National Acid Precipitation Assessment Program) emissions inventory: Overview of allocation factors, 1985
[PB90-126012] 12 p1685 N90-19679
An observational study of squall lines in the Amazon
[INPE-4865-TDL/376] 12 p1693 N90-19723
Wind conditions near the ground in Federal Republic of Germany
[ISBN-3-88148-248-2] 12 p1694 N90-19727
Structure and dynamics of the Arizona monsoon boundary
[AD-A217378] 13 p1844 N90-20586
Atmospheric wind measurements using a 50 MHz imaging Doppler Interferometer radar
[AD-A218277] 13 p1847 N90-20601
Microwave brightness temperature and its relation to atmospheric general circulation features
[AD-A218312] 13 p1847 N90-20603
Mark 3 interferometer
[AD-A217188] 13 p1902 N90-20912
The influence of lateral boundary conditions, fixed surface forcings, and synoptic situations upon predictability estimates using limited area numerical models
14 p2005 N90-21492
Sensitivity studies in a two-dimensional atmospheric transport model
[DAR-TP-18] 14 p2006 N90-21496
Meteorological influences on mountain cloudwater chemistry in the eastern United States
[PB90-132432] 14 p2007 N90-21504
An investigation of turbulence structure in a low Reynolds number incompressible turbulent boundary layer
15 p2091 N90-21966
An anomalous wind between valleys: Its characteristics and a proposed explanation
[DE90-008965] 15 p2133 N90-22189
The multifractal nature of turbulence
16 p2235 N90-22752
Gravity wave and turbulence studies using a high-resolution ST radar
[AD-A218877] 16 p2255 N90-22860

Proceedings of Workshop on Atmospheric Density and Aerodynamic Drag Models for Air Force Operations, volume 1
[AD-A220381] 17 p2345 N90-23355
Proceedings of Workshop on Atmospheric Density and Aerodynamic Drag Models for Air Force Operations, volume 2
[AD-A220382] 17 p2345 N90-23356
Meteor radar studies of the mesopause region and nonlinear atmospheric waves 17 p2421 N90-23799
Atmospheric turbulence measurements in support of adaptive optics technology
[AD-A220445] 17 p2423 N90-23805
A numerical study of the seasonal variability of the Somali current
[AD-A220708] 17 p2427 N90-23829
Barotropic vortex adjustment to asymmetric forcing with application to tropical cyclone motion
[AD-A219883] 17 p2427 N90-23831
The role of eddy fluxes of momentum in hurricane formation
[AD-A219417] 18 p2581 N90-24700
Characterization of the surfaces of platinum/tin oxide based catalysts by Fourier transform spectroscopy (FTIR) 18 p2643 N90-25054
Studies in the parameterization of cloudiness in climate models and the analysis of radiation fields in general circulation models
[NASA-CR-186378] 19 p2715 N90-25448
Measurements of CH4, N2O, CO, H2O and O3 in the middle atmosphere by the ATMOS experiment on Spacelab 3
[NASA-TM-103476] 20 p2883 N90-26400
The long-term variation of lead-210 in relation to particle-bound sulphur in surface air in Finland 20 p2884 N90-26407
Further development and application of an atmospheric chemistry trajectory model 20 p2884 N90-26408
Measurement of diurnal variation in the Earth radiation budget
[MITT-69] 21 p3027 N90-27212
Meteorological Satellite Center Technical Note, no. 17, 1988
[ISSN-0388-9653] 21 p3028 N90-27213
Distribution and movement of smokes from forest fires that occurred along the boundary of the People's Republic of China and the USSR on April-May 1987 21 p3028 N90-27216
Behavior of dust clouds from Australian dust storms in 1982-1983 as observed by the GMS 21 p3029 N90-27221
Dust clouds from African dust storms in 1986-1987 as observed by Meteosat 21 p3029 N90-27222
Downwelled longwave surface irradiance data from five sites for the FIRE/SRB Wisconsin Experiment from October 12 through November 2, 1986
[NASA-TM-102597] 21 p3030 N90-27225
MECA Workshop on Dust on Mars 3
[NASA-CR-185065] 21 p3100 N90-27604
Lower thermosphere (80-100 km) dynamics response to solar and geomagnetic activity: Overview 22 p3207 N90-28194
Inhomogeneities of stratocumulus liquid water 22 p3213 N90-28228
Cloud optical parameters as derived from the multispectral cloud radiometer 22 p3215 N90-28239
Physically-based general circulation model parameterization of clouds and their radiative interaction 22 p3228 N90-28308
The global cycle of reactive nitrogen
[DE90-015041] 23 p3348 N90-28919
An observational study of the circulation in the Southern Hemisphere stratosphere 24 p3488 N90-29715
Zonal winds between 25 and 120 km retrieved from solar occultation spectra 24 p3489 N90-29718
A study of water vapor, electrical parameters, and radio propagation
[AD-A223582] 24 p3492 N90-29736
Absolute wind measurements in the lower thermosphere of Venus using infrared heterodyne spectroscopy 24 p3561 N90-30146

ATMOSPHERIC COMPOSITION

NT ATMOSPHERIC MOISTURE
NT IONOSPHERIC COMPOSITION

Meeting Review: Workshop on Airborne Instrumentation
[PB89-174775] 01 p0007 N90-10032
Kiruna geophysical data: Data Summary 88/7-9, July - September 1988
[PB89-210249] 01 p0086 N90-10487
Geophysical monitoring for climatic change number 16
[PB89-159628] 01 p0087 N90-10494
Human health studies of carbon monoxide (CO) under conditions of military weapons systems crewman exposures. Protocol 1: Formation of COHb
[AD-A210344] 01 p0092 N90-10528
Laboratory measurements of microwave and millimeter-wave properties of planetary atmospheric constituents
[NASA-CR-185914] 01 p0141 N90-10815
Atmospheric chemistry of the fuel hydrazines 02 p0203 N90-11158
Stratospheric ozone depletion
[PB89-207476] 02 p0238 N90-11354
Report of the 1988 2-D Intercomparison Workshop, chapter 3 02 p0248 N90-11407
Micrometeorological investigation of surface exchange of trace gases: A case study
[PB89-208375] 02 p0249 N90-11412
NCAR (National Center for Atmospheric Research) master mechanism of the gas phase chemistry, version 2.0
[PB89-208979] 02 p0249 N90-11413
Lidar observations of the stratospheric aerosol: Boulder, Colorado, 1985 to 1987
[PB89-203871] 02 p0251 N90-11425
A dynamical study of Jupiter's Great Red Spot 02 p0295 N90-11681
Ion bombardment of Io and Mercury 02 p0296 N90-11682
Progress of research on water vapor lidar
[NASA-CR-185970] 03 p0352 N90-12011
Studies of baroclinic instability in the presence of surface topography and stratospheric ozone 03 p0361 N90-12068
Aerosol in the Pacific troposphere 03 p0363 N90-12078
Ozone depletion, greenhouse gases, and climate change
[NASA-CR-185323] 03 p0367 N90-12101
A statistical intercomparison of temperature and precipitation predicted by four general circulation models with historical data
[DE89-017785] 03 p0369 N90-12108
Contribution of deforestation to atmospheric CO2 and reforestation as an option to control CO2
[DE89-017255] 04 p0516 N90-12979
Proceedings: US/FRG (Federal Republic of Germany) Workshop on Photochemical Ozone Problem and Its Control: US Experiences and the Situation in Europe
[PB89-233514] 05 p0666 N90-13891
A high-resolution atlas of the infrared spectrum of the Sun and the Earth atmosphere from space: A compilation of ATMOS spectra of the region from 650 to 4800 cm (2.3 to 16 micron). Volume 1: The Sun
[NASA-RP-1224-VOL-1] 05 p0666 N90-13893
The retrieval of the concentrations of nitric oxide and nitrogen dioxide from satellite solar occultation measurements at sunset and sunrise 06 p0814 N90-14733
The development of a spatial synoptic climatological index for environmental analysis 06 p0816 N90-14744
Evaluation of climatic models: Comparison of simulated and observed patterns for past climates
[DE90-001228] 06 p0817 N90-14755
Factors that may influence responses of the US transportation sector to policies for reducing greenhouse gas emissions
[DE90-000704] 07 p0958 N90-15543
Oxygen and other atmospheric gases
[AD-A214296] 07 p0961 N90-15557
The middle Martian atmosphere 07 p1014 N90-15874
ECC (Electrochemical Concentration Cell) ozonesonde observations at South Pole, Antarctica, during 1988
[PB90-110172] 08 p1098 N90-16355
Scientific linkages in global change
[PB90-112608] 08 p1098 N90-16356
ECC (Electrochemical Concentration Cell) ozonesonde observations at Mirny, Antarctica, during 1988
[PB90-113960] 08 p1098 N90-16357
Operational ozone monitoring with the Global Ozone Monitoring Radiometer (GOMR)
[PB90-114034] 08 p1098 N90-16359
Potential impact of stratospheric ozone depletion on marine ecosystems
[PB90-112616] 08 p1098 N90-16360
Upper atmosphere research
[ISBN-0-642-13582-7] 08 p1100 N90-16368
Time and spatially dependent estimates of pollutant trace gas emissions and their effect on tropospheric ozone 09 p1243 N90-17212
Prospect of new energy. Global warming (1988)
[DE90-702486] 09 p1244 N90-17217
Reactions of atmospheric species with clean and H, C, and O implanted species
[AD-A214602] 09 p1244 N90-17218
Methodology used for gas analysis and control of trace chemical contaminants at a hyperbaric facility. 1: Gas sampling
[AD-A216155] 10 p1325 N90-17659
A 3-D dynamical/chemical GCM for simulating the anthropogenical effects on ozone
[DE90-004836] 10 p1406 N90-18108
The role of clouds in the photochemistry of the background troposphere 12 p1688 N90-19694
Emission data for the EURAD project 12 p1688 N90-19700
Ultraviolet observations of the atmosphere of Io and the plasma torus 12 p1728 N90-19929
Draft global warming study
[DE90-008446] 13 p1830 N90-20507
Preliminary report on the demonstration of the VAS CO2 cloud parameters (cover, height, and amount) in support of ASOS
[NOAA-TM-NESDIS-29] 14 p2006 N90-21498
New spectral features of stratospheric trace gases 15 p2079 N90-21910
Global distribution of organo-bromine gases 15 p2124 N90-22150
Opportunities for US-USSR cooperation in the investigation of Arctic stratospheric ozone 15 p2125 N90-22154
The sources and chemistry of late winter Arctic tropospheric aerosols
[PB90-131988] 15 p2126 N90-22156
On the antarctic ozone depletion during solar cycle 21
[NOTA-INTERNA-943] 16 p2253 N90-22849
Airliner cabin ozone: An updated review
[AD-A219264] 16 p2276 N90-22970
Spectral measurements of the cosmic microwave background 16 p2340 N90-23334
Molecular studies of dense cores 17 p2484 N90-24207
Effects of solar ultraviolet radiation on biogeochemical dynamics in aquatic environments
[AD-A221119] 18 p2578 N90-24687
Space station contamination study: Assessment of contaminant spectral brightness
[NASA-CR-186173] 19 p2666 N90-25169
Remote sensing for better understanding of the system Earth 19 p2706 N90-25399
Airborne chemistry measurements 19 p2707 N90-25405
Global changes in tropospheric chemistry 19 p2708 N90-25411
Southern California air quality study: Toxic air contaminants, task 1
[PB90-171570] 19 p2712 N90-25437
Diversiform processes of ozone in the atmosphere: Introduction study
[AERONOMICA-ACTA-A-352-1990] 19 p2713 N90-25439
Research programs: Meteorological prediction. Oceanic processes. Climate and global change monitoring. Satellite instrumentation and calibration 19 p2714 N90-25447
Reports of workshops on Probe Measurements of Particles and Radiation in the Atmosphere of Titan
[NASA-TM-102218] 19 p2797 N90-25919
Measurements of CH4, N2O, CO, H2O and O3 in the middle atmosphere by the ATMOS experiment on Spacelab 3
[NASA-TM-103476] 20 p2883 N90-26400
The global consequences of increasing tropospheric ozone concentrations
[NASA-TM-103477] 20 p2883 N90-26401
Nordic Symposium on Atmospheric Chemistry
[CM-78] 20 p2883 N90-26403
Further development and application of an atmospheric chemistry trajectory model 20 p2884 N90-26408
The Renland ice core (Greenland): A source for climatic studies over 100,000 years 20 p2885 N90-26412
The diurnal ozone cycle in a coniferous forest: The importance of meteorology and chemistry 20 p2886 N90-26423
Formation kinetics of N2O in the atmosphere 20 p2886 N90-26425
Laboratory measurements of microwave and millimeter-wave properties of planetary constituents 20 p2943 N90-26745
Laboratory studies, analysis, and interpretation of the spectra of hydrocarbons present in planetary atmospheres including cyanoacetylene, acetylene, propane, and ethane 20 p2943 N90-26748
Infrared spectra of van de Waals complexes of importance in planetary atmospheres 20 p2943 N90-26749
Conceptual design study for Infrared Limb Experiment (IRLE)
[NASA-CR-186950] 21 p2968 N90-26869
Tropospheric sounders 21 p3016 N90-27150
Lidar observations of stratospheric aerosols in 1988
[PB90-180870] 22 p3198 N90-28145
Stratospheric effects of solar ultraviolet variations on the solar rotation time scale 22 p3204 N90-28176

The vertical ozone distribution during maximum and minimum solar activity 22 p3205 N90-28182
Diurnal and temporal variation of UV-flux and its dependence on stratospheric ozone 22 p3205 N90-28184
Numerical simulation of the middle atmosphere chemical composition and temperature under changing solar conditions 22 p3206 N90-28186
An influence of solar activity on latitudinal distribution of atmospheric ozone and temperature in 2-D radiative-photochemical model 22 p3206 N90-28187
A change of mesospheric ozone content under electron precipitation influence 22 p3207 N90-28191
Atmospheric Sciences Research in the US EPA climate program
[PB90-221870] 22 p3212 N90-28219
The distribution of middle tropospheric carbon monoxide during early October 1984
[NASA-TM-103485] 23 p3346 N90-28906
The role of clouds in CO2-induced climate change
[DE90-014380] 23 p3346 N90-28911
The global cycle of reactive nitrogen
[DE90-015041] 23 p3348 N90-28919
Tropospheric nitrogen: The influence of anthropogenic sources on distributions and deposition, executive summary
[DE90-015401] 23 p3348 N90-28922
Estimating the spatial variability of trace gas deposition velocities
[PB90-208570] 23 p3349 N90-28928
Present state of knowledge of the upper atmosphere 1990: An assessment report
[NASA-RP-1242] 23 p3350 N90-28929
Infrared spectroscopic measurements on planetary atmospheric gases 23 p3412 N90-29283
Atmospheric methane data for the period 1983-1985 from the NOAA/GMCC global cooperative flask sampling network
[PB90-208588] 24 p3486 N90-29701
Success of EPA's stratospheric ozone engineering research
[PB90-246265] 24 p3487 N90-29706
Effects of increased CO2 on forest response
[DE90-015406] 24 p3487 N90-29708
Grassland/atmosphere response to changing climate: Coupling regional and local scales
[DE90-015814] 24 p3487 N90-29710
The effects of a doubling of atmospheric CO2 on the stormtracks in the climate of a general circulation model
[KNMI-WR-90-01] 24 p3488 N90-29713
Meteorological conditions over the North Atlantic Ocean during GCE/CASE/WATOX
[PB90-252032] 24 p3494 N90-29747
Rates of vertical mixing, gas exchange, and new productions: Estimates from seasonal gas cycles in the upper ocean near Bermuda
[PB90-244781] 24 p3496 N90-29758
Oxygen deficiency monitor system
[DE90-014866] 24 p3523 N90-29917
Optical emissions from bombarding atmospheric gases with heavy ions
[AD-A223544] 24 p3543 N90-30040

ATMOSPHERIC CONDITIONS
U METEOROLOGY

ATMOSPHERIC CONDUCTIVITY
NT IONOSPHERIC CONDUCTIVITY

ATMOSPHERIC CORRECTION
Algorithm for atmospheric corrections of aircraft and satellite imagery
[NASA-TM-100751] 05 p0683 N90-13976
Atmospheric correction of satellite pictures in the framework of the project Friese Fronten
[BCRS-89-12] 17 p2419 N90-23786
Atmospheric correction of thematic mapping measurements about seabeds of the German Bay
[GKSS-89/E/47] 20 p2816 N90-26029
The skin temperature of mountain slopes and the determination of the sensible heat flux
[DLR-FB-90-07] 24 p3495 N90-29754

ATMOSPHERIC DENSITY
Neutral air turbulence in the middle and upper atmosphere observed during the MAC/EPSILON campaign 05 p0660 N90-13855
Integrated analytical evaluation and optimization of model parameters against preprocessed measurement data
[AD-A215518] 09 p1247 N90-17231
An investigation of long term orbits about the planet Mars using a dynamic atmosphere model
[AD-A216111] 10 p1447 N90-18351
MEGALIDAR proof-of-concept demonstration
[AD-A218787] 16 p2255 N90-22858
Proceedings of Workshop on Atmospheric Density and Aerodynamic Drag Models for Air Force Operations, volume 1
[AD-A220381] 17 p2345 N90-23355
Proceedings of Workshop on Atmospheric Density and Aerodynamic Drag Models for Air Force Operations, volume 2
[AD-A220382] 17 p2345 N90-23356
Atmospheric structure and variability
[AD-A223439] 24 p3492 N90-29734

ATMOSPHERIC DIFFUSION
The suitability of diffusion and wind-field techniques for an emergency-response dispersion model
[PB89-190219] 01 p0085 N90-10481
A new generation of atmospheric tracers: The biological connection
[AD-A212285] 04 p0517 N90-12983
Meteorological monitoring for environmental/dose assessment and emergency response modeling: How much is enough
[DE90-002726] 06 p0818 N90-14757
Development of an atmospheric diffusion model in fog (1). Literature review of scavenging process by precipitation
[DE89-782318] 12 p1685 N90-19676
Modelization of dry deposition in the Chemical Transport Model (CTM) of EURAD 12 p1688 N90-19698
PUFFY: A puff diffusion computer model
[FOA-C-40251-4.5] 17 p2421 N90-23796

ATMOSPHERIC EFFECTS
Development of a semiquantitative corrosion monitor
[AD-A208132] 01 p0072 N90-10414
Diagnostic study of atmosphere-terrain interaction leading to the formation of dust clouds and poor visibilities over near east desert areas
[AD-A211243] 02 p0239 N90-11358
Ionospheric irregularities and their effects on electromagnetic waves propagating through them 02 p0245 N90-11391
Small-scale irregularities and global plasma dynamics in the high-latitude ionosphere 02 p0246 N90-11394
Accurate measurements of the total angle of arrival of HF skywaves 02 p0248 N90-11402
Ionospheric limitations to the accuracy of SSL estimates of HF transmitter locations 02 p0248 N90-11403
NCAR (National Center for Atmospheric Research) master mechanism of the gas phase chemistry, version 2.0
[PB89-208979] 02 p0249 N90-11413
Turbulence effects for retroreflection
[FOA-C-30523-3.1] 02 p0276 N90-11575
Deducing the age of the dense Venus atmosphere 03 p0425 N90-12438
Atmospheric horizontal-inhomogeneity effects on the optical depths determined by the double-elevation-angle lidar technique
[AD-A212836] 04 p0493 N90-12839
Atmospheric drag model calibrations for spacecraft lifetime prediction 05 p0591 N90-13439
Lifetime predictions for the Solar Maximum Mission (SMM) and San Marco spacecraft 05 p0591 N90-13440
Hybrid PE-ray-mode formulation of high frequency propagation in a bilinear tropospheric surface duct 06 p0759 N90-14417
Design of a compensation filter for a quadratic phase communication channel 06 p0761 N90-14428
A modern trans-ionospheric propagation sensing system 06 p0761 N90-14430
Correction of ionospheric effects for the precise orbit determination of satellites 06 p0762 N90-14432
Remote sensing of the aerosol scattering coefficient with a multi-field-of view lidar 06 p0763 N90-14437
Physical models for aerosol in the marine mixed-layer 06 p0763 N90-14438
The effect of oblate spheroidal drops on rain attenuation at 94 GHz: Comparison between theory and experiment 06 p0763 N90-14440
TROPO: A technique for predicting propagation and modem performance of digital troposcatter systems 06 p0764 N90-14444
Pattern recognition techniques applied to the NASA-ACTS order-wire problem 06 p0764 N90-14446
Flight in Adverse Environmental Conditions
[AGARD-CP-470] 07 p0869 N90-15041
Adverse weather operations during the Canadian Atlantic storms program 07 p0871 N90-15052
A CCIR aeronautical mobile satellite report 10 p1372 N90-17954
Effect of marine atmosphere on performance of electrooptical systems
[AD-A215947] 10 p1430 N90-18252
LANDSAT-5 data in the study of wheat and bean crops
[INPE-4746-RPE/580] 13 p1819 N90-20444
Investigations into the properties, conditions, and effects of the ionosphere
[AD-A217807] 14 p2005 N90-21489
Atmospheric Propagation in the UV, Visible, IR, and mm-Wave Region and Related Systems Aspects
[AGARD-CP-454] 15 p2079 N90-21907
The Mediterranean marine environment and its effects on aerosols and infrared transmission 15 p2079 N90-21909
Minimizing the effects of the atmosphere in the observation of ultraviolet radiation 15 p2080 N90-21911
Report on STC/Technische Universiteit (TU) Delft Extremely High Frequency (EHF) radio relay study 15 p2081 N90-21915
Propagation environments, effects, and decision aids 15 p2081 N90-21918
Interpreting meteorological data reports for LOWTRAN Navy aerosol model extinction calculations 15 p2082 N90-21920
Modeling millimeter-wave propagation effects in the atmosphere 15 p2082 N90-21922
Lidar measurements of the optical propagation environment 15 p2084 N90-21930
Effect of atmospheric turbulence on electro-optical systems 15 p2086 N90-21940
Atmospheric modelling studies: A modelling comparison between IR and millimetric atmospheric propagation 15 p2086 N90-21941
Fast method for computing infrared transmission, computation examples 15 p2086 N90-21942
An experimental investigation of mixing in buoyant flows 15 p2090 N90-21963
Utilization of higher frequencies for satellite communications: Determination of atmospheric effects using experiments and models
[DLR-FB-89-46] 18 p2544 N90-24518
Ionic atmosphere effects on the energetics of thermal and optical electron-exchange reactions: Application to ferrocenium-ferrocene self exchange
[AD-A222605] 20 p2889 N90-26441
Investigation of the effects of acid deposition on materials
[PB90-158973] 22 p3197 N90-28143
Simulation of long range atmosphere effects in short range thermal infrared and CCD images
[IZF-1989-27] 22 p3247 N90-28413

ATMOSPHERIC ELECTRICITY
NT AURORAL ELECTROJETS
NT ELECTROJETS
NT EQUATORIAL ELECTROJET
NT IONOSPHERIC CURRENTS
The 1984 direct strike lightning data, part 1
[NASA-TM-87690-PT-1] 01 p0089 N90-10505
The 1984 direct strike lightning data, part 2
[NASA-TM-87690-PT-2] 01 p0089 N90-10506
The 1984 direct strike lightning data, part 3
[NASA-TM-87690-PT-3] 01 p0089 N90-10507
Infrared water vapor continuum absorption: New atmospheric electrical measurements and theory
[AD-A212594] 04 p0519 N90-12994
Airborne measurements of the electric field and the charge precipitation particles in convective clouds: Lower positive charge centres
[ESA-TT-1157] 11 p1535 N90-18836
Radar detection of lightning and electric fields
[AD-A217894] 13 p1842 N90-20574
Observations of atmospheric electricity, 1988
[GEOPHYSICAL-PUBL-10] 14 p2006 N90-21499
Local atmospheric electricity and its possible application in high energy cosmic ray air shower detection 16 p2340 N90-23335
Aircraft lightning protection handbook
[AD-A222716] 22 p3110 N90-27668
Solar activity influences on atmospheric electricity and on some structures in the middle atmosphere 22 p3207 N90-28196
A global model of thunderstorm electricity and the prediction of whistler duct formation 24 p3493 N90-29744

ATMOSPHERIC EMISSION
U AIRGLOW

ATMOSPHERIC ENTRY
NT HYPERSONIC REENTRY
NT REENTRY
NT SPACECRAFT REENTRY
NT UNCONTROLLED REENTRY (SPACECRAFT)
Project AENEAS: A feasibility study for crew emergency return vehicle
[PB89-217020] 03 p0317 N90-11799
Optimal trajectories for the Aeroassisted Flight Experiment. Part 1: Equations of motion in an Earth-fixed system
[NASA-CR-186134] 05 p0592 N90-13441
Optimal trajectories for the Aeroassisted Flight Experiment. Part 2: Equations of motion in an inertial system
[NASA-CR-186135] 05 p0592 N90-13442

Optimal trajectories for the aeroassisted flight experiment, 1988-89
[NASA-CR-186132] 05 p0592 N90-13443
Optimal trajectories for the aeroassisted flight experiment
[NASA-CR-186133] 06 p0729 N90-14250
Aerobraking characteristics for several potential manned Mars entry vehicles
[NASA-TM-101669] 06 p0733 N90-14272
Preliminary investigation of parameter sensitivities for atmospheric entry and aerobraking at Mars
[NASA-TM-101607] 10 p1327 N90-17667
Using the method of matched asymptotic expansions, analytically investigate the three-dimensional, atmosphere entry problem
[AD-A216287] 11 p1468 N90-18451
Use of random Martian atmosphere to evaluate potential entry guidance schemes
[NASA-TM-102606] 13 p1764 N90-20122
Optimal trajectories for the aeroassisted flight experiment. Part 3: Formulation, results, and analysis
[NASA-CR-186165] 14 p1930 N90-21051
Equilibrium radiative heating tables for Earth entry
[NASA-TM-102652] 17 p2401 N90-23675
Equilibrium radiative heating tables for aerobraking in the Martian atmosphere
[NASA-TM-102659] 19 p2688 N90-25290

ATMOSPHERIC ENTRY SIMULATION

Liquid infiltrated C/SiC: An alternative material for hot space structures 02 p0182 N90-11030
Optimal trajectories for the aeroassisted flight experiment. Part 3: Formulation, results, and analysis
[NASA-CR-186165] 14 p1930 N90-21051
The effect of interplanetary trajectory options on a manned Mars aerobrake configuration
[NASA-TP-3019] 20 p2818 N90-26036

ATMOSPHERIC GENERAL CIRCULATION MODELS

NASA/MSFC FY88 Global Scale Atmospheric Processes Research Program Review
[NASA-TM-100357] 03 p0360 N90-12059
Stratiform clouds and their interaction with atmospheric motions 03 p0360 N90-12060
Application of dynamical systems theory to global weather phenomena revealed by satellite imagery 03 p0361 N90-12063
Variational objective analysis for cyclone studies 03 p0361 N90-12064
Dynamics and energetics of the South Pacific Convergence Zone during FGGE SOP-1 and South Pacific Convergence Zone and global-scale 03 p0361 N90-12065
Low level remote sensing: Orographic winds 03 p0361 N90-12066
Global backscatter assessment 03 p0364 N90-12080
Measurements of aerosol properties needed to infer backscatter characteristics in support of the NASA Doppler Lidar program 03 p0364 N90-12082
Global environmental effects of impact-generated aerosols: Results from a general circulation model
[DE89-008033] 03 p0368 N90-12106
A statistical intercomparison of temperature and precipitation predicted by four general circulation models with historical data
[DE89-017785] 03 p0369 N90-12108
Analysis and modeling of summertime convective cloud and precipitation structure over the Southeastern United States
[NASA-CR-185436] 04 p0519 N90-12996
Climate system research studies of global and regional instrumental data
[DE90-001205] 06 p0809 N90-14707
Evaluation of climatic models: Comparison of simulated and observed patterns for past climates
[DE90-001228] 06 p0817 N90-14755
Research project on CO2-induced climate change
[DE90-003531] 07 p0957 N90-15538
Time and spatially dependent estimates of pollutant trace gas emissions and their effect on tropospheric ozone 09 p1243 N90-17212
Regional climate change predictions from the Goddard Institute for Space Studies high resolution GCM
[NASA-CR-186375] 12 p1693 N90-19725
USU center of excellence in theory and analysis of the geo-plasma environment
[AD-A217736] 13 p1759 N90-20101
Atmospheric Radiation Measurement Program Plan
[DE90-008108] 13 p1829 N90-20504
An intercomparison of general circulation model predictions of regional climate change
[DE90-008325] 13 p1845 N90-20589
On three-dimensional scaling and consistent truncation of global atmospheric models 15 p2127 N90-22164
Satellite versus GCM-simulated radiation balance: Comparisons and implications for climate modeling 15 p2131 N90-22180
Southern oscillation simulation in coupled ocean/atmosphere global climate models 15 p2131 N90-22181
Remote sensing for better understanding of the system Earth 19 p2706 N90-25399
Physical parameterization of snow albedo for use in climate models
[PB90-167313] 19 p2712 N90-25433
Studies in the parameterization of cloudiness in climate models and the analysis of radiation fields in general circulation models
[NASA-CR-186378] 19 p2715 N90-25448
A study of the effect of synoptic scale processes in GCM modelling
[NASA-CR-184804] 21 p3021 N90-27175
An intercomparison of intraseasonal variability in general circulation models and observations
[NASA-TM-100764] 21 p3030 N90-27228
July 16, 1987 revisited: Lessons for modelers 22 p3214 N90-28232
Reflectivities of uniform and broken stratiform clouds: An update 22 p3215 N90-28236
Observed cloud reflectivities and liquid water paths: An update 22 p3215 N90-28237
Comparison of 30 day integrations with and without interactive clouds 22 p3222 N90-28274
Moisture and heat budgets of a cirrus cloud from aircraft measurements during FIRE 22 p3223 N90-28279
A scheme for parameterizing cirrus cloud ice water content in general circulation models 22 p3226 N90-28292
Physically-based general circulation model parameterization of clouds and their radiative interaction 22 p3228 N90-28308
The role of clouds in CO2-induced climate change
[DE90-014380] 23 p3346 N90-28911
Annual course of precipitation over much of the US: Observed versus GCM simulation
[PB90-221656] 23 p3352 N90-28942
The effects of a doubling of atmospheric CO2 on the stormtracks in the climate of a general circulation model
[KNMI-WR-90-01] 24 p3488 N90-29713

ATMOSPHERIC HEAT BUDGET

Crau 1987: The KNMI contribution --- KNMI (Royal Netherlands Meteorological Institute)
[KNMI-TR-110] 03 p0375 N90-12140

ATMOSPHERIC HEATING

NT GLOBAL WARMING
NT STRATOSPHERIC WARMING
Ion heating events observed at the EISCAT radar 02 p0244 N90-11385
North-south tropical F2 layer asymmetry at west AFrican and Pacific longitudes 02 p0247 N90-11398
Global distribution of moisture, evaporation-precipitation, and diabatic heating rates 03 p0362 N90-12069
Atmospheric planetary waves induced by solar rotation 22 p3204 N90-28178
Inhomogeneities of stratocumulus liquid water 22 p3213 N90-28228
Low-frequency cloud-radiation interactions 22 p3225 N90-28289
Zonal winds between 25 and 120 km retrieved from solar occultation spectra 24 p3489 N90-29718

ATMOSPHERIC IMPURITIES

U AIR POLLUTION

ATMOSPHERIC IONIZATION

NT AURORAL IONIZATION

ATMOSPHERIC LASERS

Design and performance analysis of adaptive optical telescopes using laser guide stars
[AD-A218025] 13 p1902 N90-20913
Long pulse narrowband XeCl laser studies
[AD-A219774] 17 p2409 N90-23724

ATMOSPHERIC LOADING

U POLLUTION TRANSPORT

ATMOSPHERIC MODELS

NT ATMOSPHERIC GENERAL CIRCULATION MODELS
The suitability of diffusion and wind-field techniques for an emergency-response dispersion model
[PB89-190219] 01 p0085 N90-10481
Numerical simulations of a midlatitude squall line 01 p0087 N90-10497
Coordination of mesoscale meteorological research between ASL and European groups
[AD-A210902] 01 p0089 N90-10508
Potential effects of global climate change on the United States. Volume 1: Regional studies. Draft
[PB89-161053] 02 p0238 N90-11351
Ionospheric Structure and Variability on a Global Scale and Interactions with Atmosphere and Magnetosphere
[AGARD-CP-441] 02 p0239 N90-11361
Global ionospheric dynamics: A review 02 p0241 N90-11367
A fully analytic, low and middle latitude ionospheric model 02 p0241 N90-11368
Modelling ionospheric density structures 02 p0242 N90-11375
Seasonal and geomagnetic response of the thermosphere and ionosphere 02 p0243 N90-11380
Ionospheric irregularities and their effects on electromagnetic waves propagating through them 02 p0245 N90-11391
Auroral and sub-auroral F-layer irregularity studies in the Northern and Southern Hemisphere during the equinox transition study September 16-26, 1984 02 p0246 N90-11393
Multistation/multiparameter observations with a network of digital ionosondes 02 p0247 N90-11396
Coordinated multi-parameter measurements and predictions of the global-scale ionosphere 02 p0247 N90-11397
An ionospheric model for HF sky-wave backscatter radar 02 p0247 N90-11401
Ionospheric limitations to the accuracy of SSL estimates of HF transmitter locations 02 p0248 N90-11403
Two-Dimensional Intercomparison of Stratospheric Models
[NASA-CP-3042] 02 p0248 N90-11405
Report on the 2-D Model Intercomparison Workshop held January 11-16, 1987 in Fort Myers Beach, Florida, chapter 2 02 p0248 N90-11406
Report of the 1988 2-D Intercomparison Workshop, chapter 3 02 p0248 N90-11407
Model documentation, chapter 4 02 p0249 N90-11408
Introduction and data summary, chapter 5 02 p0249 N90-11409
Comparison of the LOWTRAN 7 code and S3-4 satellite measurements of UV radiance
[AD-A211356] 03 p0372 N90-12124
Spatial characteristics of airglow and solar scatter radiance from the earth's atmosphere
[AD-A211358] 03 p0372 N90-12126
TEC (Total Electron Content) models
[AD-A211553] 03 p0372 N90-12129
Investigations of polar air stream cyclogenesis based on numerical simulations with a mesoscale model
[PB89-214563] 03 p0373 N90-12132
Development of high resolution simulations of the atmospheric environment using the MASS model
[NASA-CR-186040] 03 p0374 N90-12133
Airborne profiles taken near San Nicolas Island, California, during Operation FIRE (First ISCCP (International Satellite Cloud Climatology Project) regional experiment) (1987): Aerosol size distributions, air and surface temperatures, cloud top temperatures, and relative humidities
[AD-A211664] 03 p0374 N90-12136
Deducing the age of the dense Venus atmosphere 03 p0425 N90-12438
Sensitivity of a regional oxidant model to variations in climate parameters, volume 1 and 2
[PB89-224943] 04 p0516 N90-12981
Development of computer codes to model dynamics of the earth's magnetosphere
[AD-A211532] 04 p0517 N90-12987
Air flow over large scale topography
[AD-A211779] 04 p0519 N90-12998
Cloud cover determination in polar regions from satellite imagery
[NASA-CR-186096] 04 p0520 N90-13003
Project WIND: Experiments with the UK Meteorological Office mesoscale model
[AD-A212291] 04 p0521 N90-13006
Mesoscale acid deposition modeling studies
[NASA-CR-4262] 04 p0554 N90-13228
Air quality simulation model performance for one-hour averages
[PB89-233506] 05 p0665 N90-13890
An evaluation of the Smith-Feddes model
[AD-A213237] 05 p0671 N90-13907
Three dimensional analysis of the structure of the atmosphere in polar environments by vertical satellite sounding. Interest for the meteorological forecasts at high latitudes
[ETN-90-95506] 05 p0671 N90-13911
Operational Decision Aids for Exploiting or Mitigating Electromagnetic Propagation Effects
[AGARD-CP-453] 06 p0757 N90-14405
Hybrid PE-ray-mode formulation of high frequency propagation in a bilinear tropospheric surface duct 06 p0759 N90-14417
The use of backscatter for modelling ionosphere and jamming in very short term forecasts 06 p0762 N90-14434
Physical models for aerosol in the marine mixed-layer 06 p0763 N90-14438

The effect of oblate spheroidal drops on rain attenuation at 94 GHz: Comparison between theory and experiment
06 p0763 N90-14440
A one-dimensional shipboard model for forecasting refractive effects in the planetary boundary layer
06 p0764 N90-14442
A low-order model of the equatorial ocean-atmosphere system
06 p0813 N90-14730
Laboratory evaluation and application of microwave absorption properties under simulated conditions for planetary atmospheres
[NASA-CR-185916] 06 p0865 N90-15025
Description of atmospheric turbulence
07 p0869 N90-15043
A methodology for evaluating heavy gas dispersion models
[AD-A214009] 07 p0887 N90-15131
Application of a mass-consistent wind model to chinook windstorms
[AD-A213622] 07 p0963 N90-15568
MODTRAN: A moderate resolution model for LOWTRAN 7
[AD-A214337] 07 p0978 N90-15650
A calculation of energetic proton spectra producedat substorm onset in the fields of the explosive reconnection model
07 p1013 N90-15866
The middle Martian atmosphere
07 p1014 N90-15874
Interconnectedness in nature and in science: The case of climate and climate modeling
[PB90-113986] 08 p1098 N90-16358
The effect of orographic forcing on the mean flow of the stratosphere
08 p1099 N90-16367
Lidar technique for adjusting aerosol model number densities to existing conditions
[AD-A213846] 08 p1101 N90-16374
Verification study of a three-dimensional local scale atmospheric model PHYSIC at seacoast region
[DE90-719560] 08 p1102 N90-16384
Enhanced satellite geodesy through the addition of a pseudorange observable
[AD-A214987] 09 p1241 N90-17200
Numerical modeling of the atmosphere with an isentropic vertical coordinate
09 p1246 N90-17226
Integrated analytical evaluation and optimization of model parameters against preprocessed measurement data
[AD-A215518] 09 p1247 N90-17231
A 3-D dynamical/chemical GCM for simulating the anthropogenical effects on ozone
[DE90-004836] 10 p1406 N90-18108
Super-micro computer weather prediction model
[AD-A216329] 10 p1409 N90-18124
Report from ionospheric science
10 p1444 N90-18333
An investigation of long term orbits about the planet Mars using a dynamic atmosphere model
[AD-A216111] 10 p1447 N90-18351
ACIRF user's guide: Theory and examples
[AD-A216436] 11 p1496 N90-18613
Perspectives on aerosol deposition to natural surfaces
[DE90-003398] 11 p1532 N90-18819
The mesoscale meteorological model MM4 and its modifications for EURAD
12 p1686 N90-19682
The Chemical Transfer Model (CTM) of EURAD: Development status
12 p1686 N90-19683
The RADM 2 gas-phase chemical mechanism
12 p1686 N90-19684
Simulation of the propagation of radiactive substances from the example of Chernobyl (USSR)
12 p1686 N90-19685
Simulation of a weather situation with high ozone concentrations during ALPEX
12 p1686 N90-19686
Implementation of the RADM/EURAD models on the great calculation system of the Juelich KFA
12 p1687 N90-19687
GeoNet 88: Calculation connection system concept for the EURAD project
12 p1687 N90-19688
Comparison of a 6-layer and a 15-layer version of the Chemical Transfer Model (CTM)
12 p1687 N90-19689
Control of the RADM chemistry mechanism of the gas phase
12 p1687 N90-19690
On the question of spray effects
12 p1687 N90-19691
Cloud parameterization in EURAD and its future development
12 p1687 N90-19692
Validation of the EURAD cloud modules
12 p1687 N90-19693
Initialization of EURAD. Part 1: Utilization of ECMWF analysis data
12 p1688 N90-19695
Initialization of EURAD, part 2
12 p1688 N90-19696
Boundary layer parameterization in CTM and MM4
12 p1688 N90-19697
Modelization of dry deposition in the Chemical Transport Model (CTM) of EURAD
12 p1688 N90-19698
Estimation of the distribution of SO2 and NOX emission in Europe
12 p1688 N90-19699
Emission data for the EURAD project
12 p1688 N90-19700
The EURAD model in EUROTRAC
12 p1689 N90-19701
Simulation of global Kr-85 and (14)CO2 distribution by means of a time-dependent, two dimensional model of the atmosphere
[ETN-90-95376] 12 p1689 N90-19702
Synoptic-scale forcing of the low-level jet in developing baroclinic waves
12 p1692 N90-19717
Exploiting surface observations of cloudiness for globalscale nephanalyses
12 p1692 N90-19719
The atmospheric energy cycle of stationary and transient waves
[ISSN-0069-5882] 12 p1694 N90-19728
USU center of excellence in theory and analysis of the geo-plasma environment
[AD-A217736] 13 p1759 N90-20101
Use of environmental monitoring data in evaluation of atmospheric modeling results
[DE90-008607] 13 p1831 N90-20510
Analysis of GALE (Genesis of Atlantic Lows Experiment) data
[AD-A217182] 13 p1844 N90-20584
Adiabatic and diabatic initialization of the AFGL (Air Force Geophysics Laboratory) global spectral model using dynamic normal mode and nonlinear normal mode methods
[AD-A218120] 13 p1846 N90-20595
Sensitivity studies in a two-dimensional atmospheric transport model
[DAR-TP-18] 14 p2006 N90-21496
Predictability of weather and climate in a coupled ocean-atmosphere model: A dynamical systems approach
[NASA-CR-186499] 14 p2007 N90-21502
Windshear case study: Denver, Colorado, July 11, 1988
[DOT/FAA/DS-89/19] 14 p2008 N90-21509
Modeling the upper ocean and its interaction with the atmosphere
[DE90-008980] 14 p2008 N90-21511
Model atmospheres for novae during the early stages
[NASA-CR-180498] 14 p2038 N90-21694
Atmospheric Propagation in the UV, Visible, IR, and mm-Wave Region and Related Systems Aspects
[AGARD-CP-454] 15 p2079 N90-21907
A survey of the maritime-aerosol data collected at South Uist and the implications for the LOWTRAN maritime aerosol model
15 p2079 N90-21908
Models of aerosols, clouds, and precipitation for atmospheric propagation studies
15 p2081 N90-21919
Interpreting meteorological data reports for LOWTRAN Navy aerosol model extinction calculations
15 p2082 N90-21920
The naval oceanic vertical aerosol model
15 p2082 N90-21921
Modeling millimeter-wave propagation effects in the atmosphere
15 p2082 N90-21922
Inclusion of clouds and rain in atmospheric slant path calculations
15 p2083 N90-21925
A temperature-dependent regular infrared band model for absorption and dispersion
15 p2083 N90-21927
Millimetre-wave propagation in the evaporation duct
15 p2084 N90-21929
Technique for selecting an aerosol model useful for infrared atmospheric transmittance calculations
15 p2085 N90-21934
Atmospheric modelling studies: A modelling comparison between IR and millimetric atmospheric propagation
15 p2086 N90-21941
Modeling the lateral diffusion of fluorescent particles within a forest canopy
15 p2121 N90-22136
Opportunities for US-USSR cooperation in the investigation of Arctic stratospheric ozone
15 p2125 N90-22154
Formulation of non-reflecting boundary conditions in numerical models of the atmosphere
15 p2129 N90-22175
Characteristics of cumulus bandclouds off the east coast of Hawaii
15 p2130 N90-22178
A linear analysis of monsoon base states associated with banded convection
15 p2130 N90-22179
Hail growth in a highly-glaciated central high plains multi-cellular hailstorm
15 p2131 N90-22184
A high galactic latitude survey of far ultraviolet excess objects
15 p2183 N90-22473
Spectrum formation in active galactic nuclei and Type 2 supernovae
15 p2187 N90-22490
Modelling late-time atmospheres of supernovae
15 p2189 N90-22500
Auroral ultraviolet darkening on the outer planets
15 p2192 N90-22518
The HCl/aerosol problem
16 p2208 N90-22597
Evolution of atmospheric baroclinic waves
16 p2254 N90-22855
Predictability of weather and climate in a coupled ocean-atmosphere model: A dynamical systems approach
16 p2256 N90-22865
Proceedings of Workshop on Atmospheric Density and Aerodynamic Drag Models for Air Force Operations, volume 1
[AD-A220381] 17 p2345 N90-23355
Proceedings of Workshop on Atmospheric Density and Aerodynamic Drag Models for Air Force Operations, volume 2
[AD-A220382] 17 p2345 N90-23356
Engineer's Refractive Effects Prediction System (EREPS), revision 2.0
[AD-A220742] 17 p2391 N90-23616
Tropical-extratropical interaction in a model atmosphere
17 p2422 N90-23800
An analytic/empirical model of the middle and low latitude ionosphere
[AD-A220004] 17 p2423 N90-23809
Ionospheric equivalent slab thickness and its modeling applications
[AD-A220105] 17 p2424 N90-23811
A description of tropical cyclone recurvature in terms of isentropic potential vorticity
[AD-A218482] 17 p2425 N90-23821
Barotropic vortex adjustment to asymmetric forcing with application to tropical cyclone motion
[AD-A219883] 17 p2427 N90-23831
Atmospheric transport and dispersion model hierarchy, part 2
[AD-A220138] 17 p2427 N90-23833
Transmission of infrared radiation through the Australian atmosphere: Predictions using the LOWTRAN model
[AD-A220340] 17 p2428 N90-23835
Abundance differences among G and K giants
17 p2484 N90-24208
Implementation of reflectance models in operational AVHRR radiation budget processing
[NOAA-TR-NESDIS-49] 18 p2578 N90-24688
The GIT model: An atmospheric boundary layer model along a trajectory
[FOA-E-40039-3.2] 18 p2579 N90-24693
Models of the external source contribution to magnetospheric magnetic fields for CRRES data analysis
[AD-A221059] 18 p2580 N90-24697
Effects of simplifying assumptions on optimal trajectory estimation for a high-performance aircraft
[NASA-TM-101721] 19 p2661 N90-25142
Sea breeze: Induced mesoscale systems and severe weather
[NASA-CR-186367] 19 p2715 N90-25450
Verification and improvement of the EMEP model for long-range transport and deposition of pollutants
20 p2884 N90-26405
An Eulerian transport model for NO(sub x)-compounds
20 p2884 N90-26406
Some results from the precipitation chemistry measurement programme in Sweden
20 p2884 N90-26410
Results from global tropospheric sulphur simulations
20 p2885 N90-26413
The NASA/MSFC Global Reference Atmospheric Model, 1990 version (GRAM-90)
[NASA-CR-186717] 20 p2888 N90-26435
Infrared line parameters at low temperatures relevant to planetary atmospheres
20 p2944 N90-26753
Gaussian quadrature exponential sum modeling of near infrared methane laboratory spectra obtained at temperatures from 106 to 297 K
20 p2945 N90-26758
Measurements of the methane relaxation times for application to the infrared emission models of the upper atmospheres of outer planets and Titan
20 p2945 N90-26759
Chemical kinetics and modeling of planetary atmospheres
20 p2946 N90-26763
Liquid-vapor equilibrium of multicomponent cryogenic systems
20 p2948 N90-26774
A regional forecasting model
[AD-A221556] 21 p3031 N90-27235
The QBO and weak external forcing by solar activity: A three dimensional model study
22 p3203 N90-28171
Solar activity influence on cosmic ray penetration in the middle atmosphere
22 p3207 N90-28192
Intensive MHD-structures penetration in the middle atmosphere initiated in the ionospheric cusp under quiet geomagnetic conditions
22 p3207 N90-28193

A new calculation of the radiative cooling by carbon dioxide in the middle atmosphere and the lower thermosphere 22 p3210 N90-28211
Inhomogeneities of stratocumulus liquid water 22 p3213 N90-28228
Cloud optical parameters as derived from the multispectral cloud radiometer 22 p3215 N90-28239
Turbulence structure in clear and cloudy regions of the 7 July 1987 Electra mission 22 p3217 N90-28247
A unified view of convective transports by stratocumulus clouds, shallow cumulus clouds, and deep convection 22 p3219 N90-28254
Stratus: An interactive steady state mixed layer model for personal computers 22 p3219 N90-28255
Verification of the naval oceanic vertical aerosol model during FIRE 22 p3219 N90-28257
Analysis of marine stratocumulus clearing events during FIRE 22 p3220 N90-28260
Radiative diffusivity factors in cirrus and stratocumulus clouds: Application to two-stream models 22 p3226 N90-28293
Tropospheric nitrogen: The influence of anthropogenic sources on distributions and deposition, executive summary
[DE90-015401] 23 p3348 N90-28922
Genesis of bow echoes: A rear-inflow induced meso-convective structure
[PB90-209776] 23 p3349 N90-28926
Present state of knowledge of the upper atmosphere 1990: An assessment report
[NASA-RP-1242] 23 p3350 N90-28929
A nonhydrostatic numerical model in sigma-coordinates and simulations of mesoscale phenomena 23 p3350 N90-28932
Grassland/atmosphere response to changing climate: Coupling regional and local scales
[DE90-015814] 24 p3487 N90-29710
Geophysical turbulence research at NCAR
[AD-A223361] 24 p3492 N90-29732
Atmospheric structure and variability
[AD-A223439] 24 p3492 N90-29734
Numerical simulation of the lightning return stroke 24 p3493 N90-29743
A global model of thunderstorm electricity and the prediction of whistler duct formation 24 p3493 N90-29744
Tests of initialization procedures with the NRL limited area numerical weather prediction model
[AD-A223549] 24 p3495 N90-29750
Coordination of mesoscale meteorological research between ASL and European groups
[AD-A223811] 24 p3495 N90-29751
Absolute wind measurements in the lower thermosphere of Venus using infrared heterodyne spectroscopy 24 p3561 N90-30146
Carbon monoxide isotopes and clumping in giant molecular clouds 24 p3562 N90-30151

ATMOSPHERIC MOISTURE
Global atmospheric moisture variability 03 p0361 N90-12062
Variational objective analysis for cyclone studies 03 p0361 N90-12064
Low level remote sensing: Orographic winds 03 p0361 N90-12066
Global distribution of moisture, evaporation-precipitation, and diabatic heating rates 03 p0362 N90-12069
Tropical Pacific moisture variability 03 p0362 N90-12070
Survey of the CLUSE main experiment Grand-CLUSE, May 1 - June 15, 1988 --- Humidity Exchange Over the Sea (HEXOS) experiment
[FEL-1988-43] 04 p0518 N90-12991
Infrared water vapor continuum absorption: New atmospheric electrical measurements and theory
[AD-A212594] 04 p0519 N90-12994
Dynamics of baroclinic instability in rapid cyclogenesis 07 p0962 N90-15563
Anomalous absorption by atmospheric water vapor and stabilized water fogs in the infrared and CM-wave regions
[AD-A214202] 07 p0964 N90-15572
Observations of attenuation at 20.6, 31.65 and 90.0 GHz: Preliminary results from Wallops Island, VA 10 p1373 N90-17957
On the relationship between water vapor over the oceans and sea surface temperature
[NASA-CR-186199] 10 p1409 N90-18127
A linear analysis of monsoon base states associated with banded convection 15 p2130 N90-22179
The GIT model: An atmospheric boundary layer model along a trajectory
[FOA-E-40039-3.2] 18 p2579 N90-24693
An outline for the RTNEPH infrared atmospheric water vapor attenuation study
[AD-A221753] 21 p3027 N90-27209
Low-frequency cloud-radiation interactions 22 p3225 N90-28289
Rain-fade simulation and power augmentation for satellite communication systems
[NASA-TM-103134] 23 p3319 N90-28768
An analysis of the characteristics of atmospheric profiles obtained with the High resolution Interferometer Sounder (HIS) 24 p3488 N90-29716
A documentation of icing-relevant cloud physical parameters on vertical soundings of stratiform clouds
[DLR-MITT-90-07] 24 p3495 N90-29753

ATMOSPHERIC NOISE
U ATMOSPHERICS

ATMOSPHERIC OPTICS
Turbulence effects for retroreflection
[FOA-C-30523-3.1] 02 p0276 N90-11575
Atmospheric horizontal-inhomogeneity effects on the optical depths determined by the double-elevation-angle lidar technique
[AD-A212836] 04 p0493 N90-12839

ATMOSPHERIC PHYSICS
NT CLOUD PHYSICS
Study of high frequency water vapor absorption parameters
[AD-A210676] 02 p0194 N90-11108
Ionospheric Structure and Variability on a Global Scale and Interactions with Atmosphere and Magnetosphere
[AGARD-CP-441] 02 p0239 N90-11361
Atmospheric gravity waves in the auroral source region of TIDs, studied with the EISCAT CP2-data 02 p0244 N90-11387
Small-scale irregularities and global plasma dynamics in the high-latitude ionosphere 02 p0246 N90-11394
Meteorological rocket observations
[PB89-168769] 02 p0250 N90-11419
National Center For Atmospheric Research annual report, fiscal year 1988
[PB89-208987] 02 p0252 N90-11428
Interannual variability of temperature in the upper layer of the North Pacific eastern boundary region, 1971-1987
[PB89-190227] 02 p0253 N90-11434
Middle Atmosphere Program. Handbook for MAP, volume 28
[NASA-CR-184972] 03 p0370 N90-12117
Comparison of the LOWTRAN 7 code and S3-4 satellite measurements of UV radiance
[AD-A211356] 03 p0372 N90-12124
A new generation of atmospheric tracers: The biological connection
[AD-A212285] 04 p0517 N90-12983
Fundamentals of middle atmospheric dynamics
[AD-A211747] 04 p0518 N90-12988
Infrared water vapor continuum absorption: New atmospheric electrical measurements and theory
[AD-A212594] 04 p0519 N90-12994
Comments on the use of LOWTRAN in transmission calculations for sites with the ground elevated relative to sea level
[AD-A212724] 04 p0519 N90-12995
The shape of the probability density function of short-term concentration fluctuations of plumes in the atmospheric boundary layer
[AD-A212632] 04 p0548 N90-13188
An implementation plan for priorities in solar-system space physics
[NASA-CR-185375] 05 p0710 N90-14154
Description of SHARC: The Strategic High-Altitude Radiance Code
[AD-A213806] 07 p0961 N90-15555
Oxygen and other atmospheric gases
[AD-A214296] 07 p0961 N90-15557
Anomalous absorption by atmospheric water vapor and stabilized water fogs in the infrared and CM-wave regions
[AD-A214202] 07 p0964 N90-15572
MODTRAN: A moderate resolution model for LOWTRAN 7
[AD-A214337] 07 p0978 N90-15650
Upper atmosphere research
[ISBN-0-642-13582-7] 08 p1100 N90-16368
Rocket-triggered lightning strikes and forest fire ignition 08 p1155 N90-16690
Integrated analytical evaluation and optimization of model parameters against preprocessed measurement data
[AD-A215518] 09 p1247 N90-17231
Kiruna geophysical data
[PB90-123985] 09 p1247 N90-17232
Activities report in DLR research field communication engineering and reconnaissance
[ISSN-0173-0118] 11 p1525 N90-18781
Studies of cubic ice crystals
[AD-A216574] 11 p1534 N90-18832
Active probing of space plasmas
[AD-A216867] 12 p1716 N90-19855
Atmospheric chemiluminescence: COCHISE and FACELIF experiments
[AD-A218121] 13 p1843 N90-20578
JPRS report. Science and technology. USSR: Earth sciences
[JPRS-UES-88-004] 14 p1995 N90-21431
JPRS report. Science and technology. USSR: Earth sciences
[JPRS-UES-89-002] 14 p1995 N90-21432
JPRS report: Science and technology. USSR: Earth sciences
[JPRS-UES-90-005] 14 p1995 N90-21433
Hybrid modeling of plasmas and applications to fusion and space physics 15 p2168 N90-22387
Handbook of climate of the USSR. Humidity of air, atmospheric precipitations, snow cover
[AD-A220454] 17 p2427 N90-23828
Atmospheric transport and dispersion model hierarchy, part 2
[AD-A220138] 17 p2427 N90-23833
Activities report in meteorological research and associated fields
[ISSN-0349-0068] 18 p2582 N90-24707
Cloud reflectance characteristics in the presence of variable Dimethylsulfide (DMS) sources
[AD-A222808] 21 p3024 N90-27197
Vandenberg Boundary Layer Survey (VBLS): Results
[AD-A222517] 21 p3031 N90-27234
Resonant Rossby waves and solar activity 22 p3205 N90-28179
Comparison of satellite derived dynamical quantities in the stratosphere of the Southern Hemisphere 22 p3210 N90-28210
Atmospheric Sciences Research in the US EPA climate program
[PB90-221870] 22 p3212 N90-28219
Tests of initialization procedures with the NRL limited area numerical weather prediction model
[AD-A223549] 24 p3495 N90-29750

ATMOSPHERIC PRESSURE
Independent Orbiter Assessment (IOA): Analysis of the electrical power generation/power reactant storage and distribution subsystem
[NASA-CR-185556] 02 p0162 N90-10918
Independent Orbiter Assessment (IOA): Assessment of the atmospheric revitalization pressure control subsystem FMEA/CIL
[NASA-CR-185594] 02 p0170 N90-10957
An atmospheric pressure flow reactor: Gas phase kinetics and mechanism in tropospheric conditions without wall effects 02 p0203 N90-11160
Instability mechanisms in a barotropic atmosphere
[KNMI-WR-89-01] 04 p0520 N90-13001
Saltation thresholds and entrainment of fine particles at Earth and Martian pressures
[NASA-TM-102193] 06 p0860 N90-14997
Cosmic ray NM-64 neutron monitor data 16
[IFSI-88-21] 08 p1154 N90-16684
Effect of reduced atmospheric pressure on the performance characteristics of pyrotechnic compositions containing aluminum
[AD-A214473] 09 p1200 N90-16953
Full scale catalytic combustion of methane under atmospheric pressure
[DE89-772354] 10 p1351 N90-17835
High growth rate diamond synthesis in a large area atmospheric pressure inductively coupled plasma
[AD-A216090] 11 p1567 N90-19019
A method for correcting and reducing the pressure data recorded at the PAM 2 stations during GALE
[AD-A218165] 13 p1846 N90-20596
Zones of feasibility for retrieval of surface pressure from observations of absorption in the A band of oxygen
[DAR-TP-19] 14 p2006 N90-21495
JARE data reports, no. 140 (meteorology 21): Meteorological data at Asuka Camp, Antarctica in 1987
[ISSN-0075-3343] 15 p2132 N90-22188
Temporal attributes of the ambient seismo-acoustic environment: La Junta, Colorado
[AD-A219369] 16 p2249 N90-22825
Cosmic ray NM-64 neutron monitor data-17
[NOTA-INTERNA-945] 16 p2341 N90-23337
Improved meteorological measurements from buoys and ships (IMET): Preliminary report on barometric pressure sensors
[PB90-242116] 24 p3494 N90-29748

ATMOSPHERIC RADIATION
NT AIRGLOW
NT AURORAL ARCS
NT AURORAS
NT GEOCORONAL EMISSIONS
NT IONOSPHERIC NOISE
NT NIGHTGLOW
NT RED ARCS

NT SKY RADIATION
NT TROPOSPHERIC RADIATION
NT WHISTLERS
Quantifying the link between change in radiative balance and atmospheric temperature
[DE90-000819] 06 p0811 N90-14721
A low-order model of the equatorial ocean-atmosphere system 06 p0813 N90-14730
USSR Climate Handbook Number 27. Part 1: Solar radiation, radiation balance and sunshine
[AD-A215647] 09 p1248 N90-17242
On the question of spray effects 12 p1687 N90-19691
Atmospheric Radiation Measurement Program plan
[DE90-006349] 12 p1689 N90-19705
Cloud types and the tropical Earth radiation budget, revised
[NASA-CR-180475] 13 p1843 N90-20582
A radiological assessment of nuclear power and propulsion operations near Space Station Freedom
[NASA-CR-185185] 14 p1941 N90-21108
Modelling UV-visible radiation observed from space 15 p2085 N90-21937
Implementation of reflectance models in operational AVHRR radiation budget processing
[NOAA-TR-NESDIS-49] 18 p2578 N90-24688
Current status of SHARC, the strategic high altitude radiance code, and description of its new auroral module
[AD-A221068] 18 p2580 N90-24698
Reports from the German Meteorological Service. No. 178: Climatological research about the atmospheric counter radiation and comparison of calculation processes by means of measurements in the Upper Rhine Valley (Fed. Republic of Germany) during a year
[ISBN-3-88148-249-0] 18 p2582 N90-24704
Downwelled longwave surface irradiance data from five sites for the FIRE/SRB Wisconsin Experiment from October 12 through November 2, 1986
[NASA-TM-102597] 21 p3030 N90-27225
Structural analysis of stratocumulus convection 22 p3216 N90-28243
A case study of cumulus formation beneath a stratocumulus sheet: Its structure and effect on boundary layer budgets 22 p3219 N90-28256
A preliminary ARM (Atmospheric Radiation Measurements) guide for climatic evaluations
[DE90-015135] 23 p3351 N90-28937

ATMOSPHERIC REFRACTION
A technique for the generation of range-height-angle charts
[AD-A214534] 09 p1204 N90-16979
Speckle imaging through the atmosphere
[AD-A214652] 09 p1281 N90-17428
Reactive atmosphere processing of BaTiO3 and origins of its photorefractive effect
[AD-A215034] 09 p1289 N90-17475
Remote sensing of evaporation ducts for Naval warfare
[AD-A214849] 10 p1374 N90-17965
Navigation experiment NAVEX data storage and processing
[ESA-TT-1175] 11 p1467 N90-18445
Visibility problems in numerical models of terrain
[INPE-4921-TDL/382] 12 p1726 N90-19919
Information reconstruction from speckle interferograms
[ETN-90-95918] 12 p1729 N90-19939
Tropospheric monitoring technology for gravity wave experiments 12 p1734 N90-19971
Infrared propagation in the air-sea boundary layer 15 p2083 N90-21926
Engineer's Refractive Effects Prediction System (EREPS), revision 2.0
[AD-A220742] 17 p2391 N90-23616
Understanding tropscatter propagation
[AD-A220969] 18 p2544 N90-24520
Impact of cirrus on the surface radiative environment at the FIRE ETLA Palisades, NY site 22 p3221 N90-28270

ATMOSPHERIC SCATTERING
NT TROPOSPHERIC SCATTERING
Lidar observations of the stratospheric aerosol: Boulder, Colorado, 1985 to 1987
[PB89-203871] 02 p0251 N90-11425
Atmospheric aerosol size distributions and optical properties found in the marine boundary layer over the Atlantic Ocean
[AD-A210800] 02 p0252 N90-11431
Propagation of an elliptical laser beam through the turbulent atmosphere (vertical beams)
[PB89-208680] 03 p0352 N90-12010
A stochastic model for the calculation of multiple scattered lidar returns
[DLR-FB-89-36] 05 p0648 N90-13778
A methodology for evaluating heavy gas dispersion models
[AD-A214009] 07 p0887 N90-15131
Atmospheric transmission calculations for optical frequencies 10 p1373 N90-17960
Quantitative studies of the Martian south polar region using spacecraft images 15 p2191 N90-22514
A study of auroral activity in the nightside polar cap 16 p2254 N90-22852
Engineer's Refractive Effects Prediction System (EREPS), revision 2.0
[AD-A220742] 17 p2391 N90-23616

ATMOSPHERIC SHELLS
U ATMOSPHERIC STRATIFICATION

ATMOSPHERIC SOUNDING
A study of the impact of simulated 183 GHz water vapor retrievals on numerical weather prediction
[AD-A210431] 01 p0088 N90-10504
Laser sounding from space: Report of the ESA Technology Working Group on Space Laser Sounding and Ranging
[ESA-SP-1108] 03 p0354 N90-12024
LAWS simulation: Sampling strategies and wind computation algorithms 03 p0364 N90-12081
Middle Atmosphere Program. Handbook for MAP, volume 28
[NASA-CR-184972] 03 p0370 N90-12117
Observation of wind corners in the middle atmosphere over Andenes (69 N) during winter 1983/84, summer 1987 and summer 1988 05 p0657 N90-13836
The electrodynamics of the polar ionosphere with special emphasis on the dayside cleft region 05 p0658 N90-13838
Some remarks on the working principle of the rocketborne nose tip dc probes in the D-region of the ionosphere 05 p0658 N90-13839
New perspectives for the inversion of backscatter ionograms 06 p0761 N90-14427
The use of backscatter for modelling ionosphere and jamming in very short term forecasts 06 p0762 N90-14434
Remote sensing of atmospheric water vapour by pressure modulation radiometry 06 p0802 N90-14667
Identification and quantification of synoptic structure in simulated Tiros N radiance soundings 07 p0959 N90-15546
Identification and quantification of synoptic structure in simulated TIROS N radiance soundings
[AD-A213729] 07 p0960 N90-15553
A dynamic model for forecasting new cloud development
[AD-A213939] 08 p1102 N90-16383
Preliminary comparison of temperature soundings obtained from simultaneous radiometric, radio-acoustic, and rawinsonde measurements
[PB90-119835] 11 p1535 N90-18838
Preliminary report on the demonstration of the VAS CO2 cloud parameters (cover, height, and amount) in support of ASOS
[NOAA-TM-NESDIS-29] 14 p2006 N90-21498
Atmospheric sounding with UV lidar
[FOA-C-30542-3.1] 18 p2579 N90-24692
Reports of workshops on Probe Measurements of Particles and Radiation in the Atmosphere of Titan
[NASA-TM-102218] 19 p2797 N90-25919
Lidar instruments proposed for Eos 21 p3016 N90-27145
Structural analysis of stratocumulus convection 22 p3216 N90-28243
A stratocumulus thermodynamic analysis: July 5 case study 22 p3217 N90-28245
Modification of the background flow by roll vortices 22 p3219 N90-28258
Intercomparison of standard resolution and high resolution TOVS soundings with radiosonde, lidar, and surface temperature/humidity data 22 p3228 N90-28306
An analysis of the characteristics of atmospheric profiles obtained with the High resolution Interferometer Sounder (HIS) 24 p3488 N90-29716
A documentation of icing-relevant cloud physical parameters on vertical soundings of stratiform clouds
[DLR-MITT-90-07] 24 p3495 N90-29753

ATMOSPHERIC STRATIFICATION
Flux parameterization techniques in the atmospheric surface layer 07 p0959 N90-15548
The diurnal ozone cycle in a coniferous forest: The importance of meteorology and chemistry
[CM-75] 17 p2421 N90-23795
A day in the life of a warm front
[AD-A220373] 17 p2426 N90-23826

ATMOSPHERIC TEMPERATURE
A study of the impact of simulated 183 GHz water vapor retrievals on numerical weather prediction
[AD-A210431] 01 p0088 N90-10504
Measurement of respiratory air temperatures and calculation of respiratory heat loss when working at various ambient temperatures
[AD-A210378] 01 p0093 N90-10529
Ozone depletion, greenhouse gases, and climate change
[NASA-CR-185323] 03 p0367 N90-12101
A statistical intercomparison of temperature and precipitation predicted by four general circulation models with historical data
[DE89-017785] 03 p0369 N90-12108
Retrieval of atomic oxygen and temperature in the thermosphere. Part 2: Feasibility of an experiment based on limb emission in the OI lines
[AD-A211807] 03 p0371 N90-12121
Retrieval of atomic oxygen and temperature in the thermosphere. Part 1: Feasibility of an experiment based on the spectrally resolved 147 micrometer limb emission
[AD-A211987] 04 p0517 N90-12986
Evidence for accurate temperatures from the inflatable falling sphere 05 p0657 N90-13835
Near-mesopause temperatures at 69 N latitude in late summer 05 p0658 N90-13837
Quantifying the link between change in radiative balance and atmospheric temperature
[DE90-000819] 06 p0811 N90-14721
Vibration damping composition suitable for outer space temperature variations
[AD-D014288] 08 p1088 N90-16296
ECC (Electrochemical Concentration Cell) ozonesonde observations at South Pole, Antarctica, during 1988
[PB90-110172] 08 p1098 N90-16355
Climatic summaries and documentation for the primary meteorological Station, H. J. Andrews Experimental Forest, 1972 to 1984
[PB90-104373] 08 p1102 N90-16382
Simultaneous observations of the emissions OI (5577), O2A(0.1), NaD(5893) and OH(9.4) and the rotational temperatures TO2 and TOH in the upper atmosphere
[INPE-4851-TDL/366] 10 p1407 N90-18113
Preliminary comparison of temperature soundings obtained from simultaneous radiometric, radio-acoustic, and rawinsonde measurements
[PB90-119835] 11 p1535 N90-18838
Ionospheric heating with oblique waves. Volume 1: Electron density perturbations
[AD-A216260] 12 p1690 N90-19709
United States Historical Climatology Network (HCN) serial temperature and precipitation data
[DE90-008029] 13 p1830 N90-20506
A cloud climatology for the North Pacific area centered at Shemya, Alaska
[AD-A217334] 13 p1844 N90-20585
Millimetric, infrared, and optical propagation studies over a 500 m path 15 p2080 N90-21913
Tropopause undulations and the development of extratropical cyclones 15 p2132 N90-22186
SeaRISE: A Multidisciplinary Research Initiative to Predict Rapid Changes in Global Sea Level Caused by Collapse of Marine Ice Sheets
[NASA-CP-3075] 16 p2249 N90-22824
Accuracy and precision of GOES data collection platforms for temperature measurements
[AD-A218798] 16 p2250 N90-22832
Global and hemispheric annual temperature variations between 1861 and 1988
[DE90-007993] 16 p2257 N90-22869
Effect of low air velocities on thermal homeostasis and comfort during exercise at space station operational temperature and humidity 18 p2628 N90-24975
Design and implementation of sensor systems for control of a closed-loop life support system
[NASA-CR-186675] 19 p2725 N90-25497
Photodissociation of NO2: Influence of photolysis wavelength and temperature dependence on product formation 20 p2887 N90-26426
Integrated radiometric profiler for atmospheric humidity and temperature measurements
[AD-A221931] 21 p3032 N90-27237
Effects of corpuscular radiation on weather and climate 22 p3201 N90-28164
Seasonal variation of the 11 year solar cycle effect on the middle atmosphere: Role of the quasi biennial oscillation 22 p3202 N90-28167
Influence of solar activity on middle atmosphere associated with phases of equatorial quasi-biennial oscillation 22 p3202 N90-28168
Solar activity influence on climatic variations of stratosphere and mesosphere in mid-latitudes 22 p3202 N90-28169
The planetary waves dynamics and interannual course of meteorological parameters of the high latitude stratosphere and mesosphere of the Northern and Southern Hemispheres during the 20th and 21st solar cycles and different phases of QBO 22 p3203 N90-28170

Solar activity, the QBO, and tropospheric responses
22 p3203 N90-28172
A search for solar related changes in tropospheric weather
22 p3203 N90-28173
The mesospheric responses to short-term solar ultraviolet variability
22 p3204 N90-28174
Response of the middle atmosphere to solar UV and dynamical perturbations
22 p3204 N90-28175
Stratospheric effects of solar ultraviolet variations on the solar rotation time scale
22 p3204 N90-28176
An influence of solar activity on latitudinal distribution of atmospheric ozone and temperature in 2-D radiative-photochemical model
22 p3206 N90-28187
An eight-month climatology of marine stratocumulus cloud fraction, albedo, and integrated liquid water
22 p3214 N90-28233
Structural analysis of stratocumulus convection
22 p3216 N90-28243
The effects of clouds on CO2 forcing
22 p3222 N90-28271
Remote sounding through semi-transparent cirrus cloud
22 p3226 N90-28296
Improved meteorological measurements from buoys and ships (IMET): Preliminary comparison of solar radiation air temperature shields
[PB90-241928] 22 p3229 N90-28314
Daily temperature, solar radiation, wind speed, cloud cover, and precipitation data recorded at the meteorological station for calendar years 1957--1988
[DE90-014399] 23 p3352 N90-28941
An analysis of the characteristics of atmospheric profiles obtained with the High resolution Interferometer Sounder (HIS)
24 p3488 N90-29716

ATMOSPHERIC TIDES
Zonal winds between 25 and 120 km retrieved from solar occultation spectra
24 p3489 N90-29718

ATMOSPHERIC TURBULENCE
NT CLEAR AIR TURBULENCE
NT GUSTS
Turbulence effects for retroreflection
[FOA-C-30523-3.1] 02 p0276 N90-11575
Some implications of the isotropic momentarily frozen assumptions for the SPAN-MAT program
[NASA-CR-181937] 03 p0301 N90-11704
Propagation of an elliptical laser beam through the turbulent atmosphere (vertical beams)
[PB89-206680] 03 p0352 N90-12010
Turbulence effects on reflected optical patterns (atmosphere and structure)
[PB89-206094] 03 p0404 N90-12315
The S.D.G., P.S.D. and the nonlinear airplane
[NLR-MP-88018-U] 05 p0578 N90-13371
Probability density function of optical scintillations (scintillation distribution)
[PB89-103912] 06 p0843 N90-14906
Description of atmospheric turbulence
07 p0669 N90-15043
Statistics of a reflected laser beam in the turbulent atmosphere (path correlation)
[PB90-113994] 08 p1082 N90-16261
New atmospheric turbulence model for shuttle applications
[NASA-TM-4168] 08 p1103 N90-16389
Response of structures to atmospheric turbulence. Response to across-wind turbulence components
[ESDU-89049] 09 p1239 N90-17191
Some aspects of atmospheric turbulence in forests
[INPE-4951-RPE/600] 11 p1532 N90-18818
Temporal response of atmospheric turbulence compensation
[DE90-006354] 11 p1535 N90-18837
A simulation of optical propagation through atmospheric turbulence using two-dimensional Fourier transform techniques
[AD-A216776] 11 p1566 N90-19013
Application of wavefront analysis techniques to restoring of images degraded by atmospheric turbulence
[ONERA-PUBL-1989-1] 11 p1589 N90-19168
Correlation of atmospheric optical turbulence and meteorological measurements
[AD-A218019] 13 p1842 N90-20576
Millimetric, infrared, and optical propagation studies over a 500 m path
15 p2080 N90-21913
Modelling of optically and IR effective atmospheric turbulence
15 p2082 N90-21923
Effect of atmospheric turbulence on electro-optical systems
15 p2086 N90-21940
The multifractal nature of turbulence
16 p2235 N90-22752
Gravity wave and turbulence studies using a high-resolution ST radar
[AD-A218877] 16 p2255 N90-22860
A study of turbulence near thunderstorm tops
[NASA-CR-186620] 16 p2258 N90-22870
A scattering center based numerical simulation of small scale atmospheric turbulence
16 p2312 N90-23179
Atmospheric turbulence measurements in support of adaptive optics technology
[AD-A220445] 17 p2423 N90-23805
Super-diffraction limited measurements through the turbulent atmosphere by speckle interferometry
[AD-A221227] 18 p2581 N90-24699
Aircraft measurements of the turbulence structure in cirrus clouds
[ISSN-0069-5882] 20 p2890 N90-26450
Program to perform research on use of lidar for range resolved turbulence measurements
[AD-A222189] 21 p3026 N90-27204
Turbulent statistics in the vicinity of an SST front: A north wind case, FASINEX February 16, 1986
22 p3221 N90-28266
Sound propagation through atmospheric turbulence: A literature summary
[RPI-MATH-184] 23 p3350 N90-28930
Geophysical turbulence research at NCAR
[AD-A223361] 24 p3492 N90-29732

ATMOSPHERIC WINDOWS
Analysis of cirrus optical properties with data from NASA ER2 High-resolution Interferometer Sounder (HIS)
[NASA-CR-186365] 21 p3030 N90-27227

ATMOSPHERICS
NT HISS
NT WHISTLERS
Long wave atmospheric noise model, phase 1. Volume 1: Lightning occurrence rates and propagation theory
[AD-A212794] 04 p0493 N90-12836
Long wave atmospheric noise model, phase 1. Volume 2: Mode parameters
[AD-A212795] 04 p0493 N90-12837
A communications system with an adaptive multi-functional architecture
06 p0759 N90-14415
Temporal response of atmospheric turbulence compensation
[DE90-006354] 11 p1535 N90-18837
Wind lidar for BEST
[CNES-NT-125] 23 p3353 N90-28947
Some personal reminiscences. The ESRO-ESA space science story: Twenty-five years of European cooperation
[ESA-BR-66] 24 p3565 N90-30168

ATOM CONCENTRATION
Retrieval of atomic oxygen and temperature in the thermosphere. Part 1: Feasibility of an experiment based on the spectrally resolved 147 micrometer limb emission
[AD-A211987] 04 p0517 N90-12986
Diurnal variation of the sodium layer at polar latitudes in summer
05 p0662 N90-13869
Mechanistic model for catalytic recombination during aerobraking maneuvers
[NASA-CR-185611] 14 p1932 N90-21059

ATOMIC BATTERIES
U RADIOISOTOPE BATTERIES

ATOMIC BEAMS
Laser cooling of neutral atoms
[AD-A214440] 09 p1279 N90-17418
Measurement of the space potential of a high-temperature plasma by fast atomic beam scattering on an ion probe beam
[DE90-006118] 11 p1567 N90-19020
Atom interferometry progress
[AD-A220875] 18 p2613 N90-24882
Traps for neutral atoms
[AD-A220925] 18 p2613 N90-24885

ATOMIC CLOCKS
Determining the effects of microwave power and C-field setting on the frequency of a cesium atomic frequency standard
[AD-A216599] 11 p1501 N90-18642
Synchronization of the ground station atomic clocks using three weighted transportable cesium time standards in the Navex navigation experiment
[ESA-TT-1153] 11 p1512 N90-18711
A review of atomic clock technology, the performance capability of present spaceborne and terrestrial atomic clocks, and a look toward the future
12 p1735 N90-19972
Atomic velocity distributions out of hydrogen maser dissociators
[AD-A219500] 17 p2408 N90-23721
Navigation experiment NAVEX: Measurements and performance of the spaceborne clocks
[DLR-FB-89-43] 18 p2555 N90-24580

ATOMIC COLLISIONS
On the utility and ubiquity of atomic collision physics
[DE89-015356] 01 p0119 N90-10688
Dielectronic excitation and recombination in crystal channels
[DE89-016864] 02 p0284 N90-11625
The process e(-)p giving gamma e(-)p as a fast luminosity for the HERA collider
[NIKHEF-H/88-13] 04 p0553 N90-13223
CANOES 2: Dynamics of atmospheric infrared thermochemical excitation, volume 1
[AD-A213341] 05 p0667 N90-13897
CANOES 2: Dynamics of atmospheric infrared thermochemical excitation, volume 2
[AD-A213342] 05 p0667 N90-13898
Interaction of radiation with matter: Atomic collision processes occurring in the presence of radiation fields
[AD-A213112] 05 p0697 N90-14078
Multiple electron capture in close ion-atom collisions
[DE90-001541] 06 p0840 N90-14885
Scattering of positrons and electrons by alkali atoms
11 p1556 N90-18959
Positron collisions with alkali-metal atoms
11 p1556 N90-18962
Theoretical survey on positronium formation and ionisation in positron atom scattering
11 p1556 N90-18965
New parameter-free polarization potentials in low-energy positron collisions
11 p1557 N90-18968
Ionisation of atomic hydrogen by positron impact
11 p1558 N90-18977
US-Japan Workshop on Atomic Collisions in Solids: Abstracts of lectures
[DE90-008979] 14 p2025 N90-21611
Support for the 16th International Conference on the Physics of Electronic and Atomic Collisions
[AD-A218567] 16 p2315 N90-23200
Polarization effects in ionizing collisions with Ne*(3-P2)- and Ne**(3-D3)-atoms
[ETN-90-96891] 17 p2471 N90-24127
Few-body collisions in a weakly interacting Bose gas
[ETN-90-96893] 18 p2613 N90-24886
Experimental investigations of low-energy (4 to 40 eV) collisions of O(-)(P2) ions and O(P3) atoms with surfaces
19 p2732 N90-25530
Support for the Forty-Second Annual Gaseous Electronics Conference
[AD-A222881] 21 p3073 N90-27473
Correlated charge changing ion-atom collisions
[DE90-014662] 23 p3393 N90-29171

ATOMIC ENERGY
U NUCLEAR ENERGY

ATOMIC ENERGY LEVELS
Laser production of soft x rays by multiquantum processes and the excitation of atomic inner-shell states
[AD-A211372] 03 p0353 N90-12021
Spin-orbit relaxation rates of Bi(6p(3)) 2D(3/2) following photolysis of Bi(CH3)3 at lambda = 193 nm
[AD-A211792] 03 p0402 N90-12303
Dynamics of an M-level atom interacting with cavity fields: Properties of photon statistics
[AD-A211321] 04 p0552 N90-13213
Theoretical study of the Townes-Merritt effect in level crossing experiments
[AD-A214909] 09 p1191 N90-16900
Laser cooling of neutral atoms
[AD-A214440] 09 p1279 N90-17418
Squeezing of many-atom radiation in an optical cavity
[AD-A215736] 09 p1280 N90-17422
The Huechel model for small metal clusters. 4: Orbital properties and cohesive energies for model clusters of up to several hundred atoms
[AD-A216161] 10 p1354 N90-17852
Inelastic collisions of positrons with one-valence-electron targets
11 p1556 N90-18963
Positron-rubidium scattering
11 p1556 N90-18964
Theoretical survey on positronium formation and ionisation in positron atom scattering
11 p1556 N90-18965
The calculation of the contributions to low energy e+H2 scattering from sigma u+ and Pion u symmetries using the Kohn variational method
11 p1557 N90-18969
Combined effect of isotopic substitution, temperature, and magnetic field on the lifetimes of triplet biradicals
[AD-A219711] 17 p2372 N90-23509
Microscopic aspects of the initial stages of epitaxial growth. A scanning tunneling microscopy study
[AD-A224325] 24 p3551 N90-30094

ATOMIC EXCITATIONS
Observation of excited H(sup 0) atoms produced by relativistic H(sup (minus)) ions in carbon and formvar foils
[DE89-015301] 01 p0120 N90-10688
Dielectronic excitation and recombination in crystal channels
[DE89-016864] 02 p0284 N90-11625
Theoretical study of the Townes-Merritt effect in level crossing experiments
[AD-A214909] 09 p1191 N90-16900
Inelastic collisions of positrons with one-valence-electron targets
11 p1556 N90-18963
Positron excitation of neon
11 p1558 N90-18973
Optically excited states in positronium
11 p1559 N90-18985

Positronium ions and molecules
11 p1560 N90-18990
Structure and vibrational excitations of reconstructed semiconductor surfaces
[DE90-006589] 11 p1571 N90-19044
Laser enhanced chemical reactions
[DE90-008273] 13 p1807 N90-20377
Interaction of atomic hydrogen with pico- and femtosecond laser pulses
[AD-A218426] 16 p2241 N90-22785
Fifteenth International Conference on X Ray and Inner-Shell Processes
[DE90-013024] 23 p3393 N90-29170

ATOMIC EXPLOSIONS
U NUCLEAR EXPLOSIONS

ATOMIC INTERACTIONS
NT ATOMIC COLLISIONS

ATOMIC MASS
U ATOMIC WEIGHTS

ATOMIC MOBILITIES
Mobility of sulfur in thermally altered meteorites
06 p0862 N90-15010

ATOMIC PHYSICS
Atomic effects of beta decay in astrophysics and in elementary particle physics 01 p0141 N90-10811
Theoretical atomic physics for fusion
[DE89-017363] 02 p0274 N90-11563
Atomic and molecular surface and volume processes in the analysis of negative hydrogen discharges
[DE89-015705] 03 p0401 N90-12294
Gordon Conference on Atomic Physics
[AD-A211946] 03 p0402 N90-12304
General contraction of Gaussian basis sets. Part 2: Atomic natural orbitals and the calculation of atomic and molecular properties
[NASA-CR-186201] 08 p1119 N90-16482
Atomic processes in plasmas under ultra-intense laser irradiation
[DE90-003221] 08 p1126 N90-16521
Annihilation physics of exotic galactic dark matter particles 11 p1559 N90-18984
Theoretical investigations in elementary particle physics
[DE90-007178] 13 p1883 N90-20802
Center for Atomic, Molecular, and Optical Physics: Technical activities
[PB90-133158] 14 p2022 N90-21591
Helium transport in plasma edge regions
14 p2027 N90-21625
Atomic processes in high temperature plasmas
[DE90-008873] 14 p2028 N90-21632
Report of research activity at the Research Laboratory of Electronics 17 p2486 N90-24217
Research and technology 1989
[NASA-TM-100369] 17 p2486 N90-24219

ATOMIC RECOMBINATION
NT OXYGEN RECOMBINATION
An Introduction to Hypersonic Aerodynamics
[VKI-LS-1989-01] 05 p0573 N90-13334
On catalytic recombination rates in hypersonic stagnation heat transfer 05 p0573 N90-13338

ATOMIC SPECTRA
Theory of atomic spectral emission intensity
[IRF-PREPRINT-110] 02 p0287 N90-11641
Interaction of radiation with matter: Atomic collision processes occurring in the presence of radiation fields
[AD-A213112] 05 p0697 N90-14078
Determination of iron in chromium plating and polishing solutions by atomic absorption spectrometry
[AD-A214467] 09 p1189 N90-16892
Theoretical study of the Townes-Merritt effect in level crossing experiments
[AD-A214909] 09 p1191 N90-16900
Shock layer vacuum UV spectroscopy in an arc-jet wind tunnel
[NASA-TM-102258] 09 p1226 N90-17112
Atomic and molecular spectra from electron-excited alkali halides
[DE90-006160] 11 p1562 N90-19004
Study of new technique of solid combustible materials to determination of volatile elements by flame atomic absorption spectrophotometry
[DE90-612907] 14 p1947 N90-21147
Atom interferometry progress
[AD-A220875] 18 p2613 N90-24882
Wear metal analysis in engine oil by microwave digestion and atomic absorption spectroscopy
[AD-A223070] 21 p2985 N90-26964

ATOMIC STRUCTURE
Bonding in transition metal silyl dimers. Molecular orbital theory
[AD-A208269] 01 p0046 N90-10260
Superconductivity from valence fluctuations with finite U
[DE89-015302] 01 p0129 N90-10742
Shock-induced atomic-scale structure in metals
[DE89-016539] 02 p0197 N90-11124
Proceedings of the Polycrystalline Thin Film Program Meeting
[DE89-009457] 02 p0237 N90-11348
Structure and properties of simple molecular systems at very high density
[DE89-016974] 02 p0273 N90-11557
A fermi liquid electric structure and the nature of the carriers in high-T(sub c) cuprates: A photoemission study
[DE89-016774] 02 p0284 N90-11624
Electronic structure of transition metal alloys and intermetallics: Charge transfer and its implications for Moessbauer effect measurements
[DE89-017603] 03 p0327 N90-11860
Multiple martensitic transformations, incommensurate/commensurate phases, and charge-density-wave states in plutonium metal: Their consequences
[DE90-001235] 06 p0748 N90-14350
Atomic structure and spectral perturbations in hot dense plasmas 06 p0785 N90-14567
Structural peculiarities and molecular properties of charge complexes formed on positive ion injection into dense inert gas media
[DE89-633953] 06 p0839 N90-14877
Exchange coupling in metals as understood then and now
[DE90-001271] 07 p0902 N90-15214
Phase transition in polymer blends and structure of ionomers
[DE90-003525] 07 p0911 N90-15266
Band-to-band transitions in poly (phenyl methyl silane)
[DE90-003575] 07 p0990 N90-15720
Relativistic self-consistent field studies of atoms and molecules
[AD-A214101] 07 p0991 N90-15724
Theoretical studies on the electronic structure of high-temperature superconductors
[DE90-001301] 07 p0998 N90-15771
Variational quantum Monte Carlo calculation of electronic and structural properties of crystals
[DE90-003265] 07 p0999 N90-15781
Magnetic and electronic correlations in YBa2Cu3O(sub 6+x)
[DE89-017604] 07 p1000 N90-15785
Magnetic mechanisms of high temperature superconductivity
[DE90-003625] 07 p1001 N90-15796
X ray absorption studies of YBa2Cu3O(6+x), La(2-x)Sr(x)CuO4, and Nd(2-x)Ce(x)CuO4
[DE90-003640] 07 p1002 N90-15797
Atomic scale structure of twin boundary in Y-Ba-Cu-O superconductors
[DE90-003955] 07 p1006 N90-15823
Surface studies at the NSLS
[DE90-003173] 08 p1043 N90-16027
Elastic moduli of copper: Electronic structure contributions from pseudopotentials and full-potential linear muffin-tin orbital band structure calculations
[DE90-004423] 08 p1044 N90-16037
Theoretical studies of chemisorption and surface reactions on nickel and silicon
[DE90-004849] 08 p1047 N90-16050
Pairs of chalcogen impurities in silicon
[DE89-635767] 08 p1049 N90-16063
Tailorable infrared sensing device with strain layer superlattice structure
[NASA-CASE-NPO-16617-2-CU]
09 p1227 N90-17118
Density of electronic states in a biased resonant tunneling structure
[AD-A215735] 09 p1291 N90-17486
Normal state electronic structure and the superconducting energy gap in HTSC's as determined from photoemission spectroscopy
[DE90-004857] 09 p1292 N90-17489
Structural and fast ion transport properties of glassy and amorphous materials
[DE90-005587] 10 p1358 N90-17877
Chemical activation of molecules by metals: Experimental studies of electron distributions and bonding
[DE90-005371] 10 p1428 N90-18238
Phonon dispersion and Kohn anomalies in the alloy Cu(0.84)Al(0.16)
[DE90-005578] 10 p1428 N90-18239
The electronic structure of sigma 5 grain boundaries in Cu
[DE90-005999] 10 p1437 N90-18294
Structure and vibrational excitations of reconstructed semiconductor surfaces
[DE90-006589] 11 p1571 N90-19044
Exchange and correlation effects in the Visscher-Falicov model for metal intercalated graphite
[DE90-610553] 12 p1627 N90-19349
Supercomputer applications for materials science: Ordering effects of hydrogen in palladium
[DE90-004864] 12 p1718 N90-19870
Band electronic structures and crystal packing forces
[DE90-007669] 12 p1723 N90-19898
Electronic structure, alloy phase stability, and phase diagrams
[DE90-008306] 13 p1778 N90-20203
The basis spline method and associated techniques
[DE90-008403] 13 p1877 N90-20763
Theoretical studies of spin-forbidden processes within the Breit-Pauli approximation
[AD-A217778] 13 p1885 N90-20815
Spectral line shape code for multielectron emitters
[DE90-008526] 13 p1891 N90-20853
Theory of defect process: Basic issues in quantitative understanding
[AERE-R-13661] 13 p1892 N90-20860
The geometry of disorder: Report 1987 to 1990
[DE90-008250] 13 p1896 N90-20882
Ordering mechanism in substitutional Ni-Cr alloys: Theory and experiment
[DE90-006268] 14 p1949 N90-21156
New surface atomic structures for column 5 overlayers on the (110) surfaces of 3-5 compound semiconductors
[DE90-009003] 14 p2033 N90-21663
Investigation of atomistic simulation of structural and dynamic differences in glassy and liquid states of atactic poly(propylene)
[AD-A218896] 16 p2224 N90-22687
Electronic theory of solids, surfaces, interfaces, and clusters 16 p2320 N90-23230
Investigation of Schottky barriers
[AD-A218422] 16 p2323 N90-23247
Optical phonons and electronic properties in double heterostructures
[AD-A219436] 17 p2475 N90-24153
Electronic structure and phase stability properties of Al-Li alloys
[DE90-010632] 18 p2525 N90-24410
Atomic structure of Ag/Ni interfaces
[DE90-010053] 18 p2618 N90-24914
Atomic scale imaging of the structure and chemistry of semiconductor interfaces
[DE90-011321] 18 p2626 N90-24965
One-dimensional sigma-conjugated polysilylenes: Science and technology
[DE90-012902] 20 p2839 N90-26146
Soft x ray resist characterization: Studies with a laser plasma x ray source
[DE90-013493] 20 p2928 N90-26661
New electronic states of NH and ND observed by resonance enhanced multiphoton ionization spectroscopy 20 p2945 N90-26760
Laboratory studies of the interaction of ions with condensed gases: Planetary applications
20 p2949 N90-26778
Ni impurity effects on hydrogen surface chemistry and etching of Si(111)
[AD-A222083] 21 p2977 N90-26921
Electronic and structural properties of Si10 cluster
[AD-A222429] 21 p3074 N90-27478
Electronic and molecular structure of carbon grains
21 p3091 N90-27574
Electronic structure Fermi liquid theory of high T(sub c) superconductors: Comparison with experiments
22 p3142 N90-27821
Accurate quantum chemical calculations
[NASA-TM-101932] 23 p3303 N90-28680
Research on the structural and electronic properties of defects in amorphous silicon
[DE90-000342] 23 p3312 N90-28730
Effects of basis set contraction in relativistic calculations on neon, argon, and germanium
[AD-A223357] 24 p3446 N90-29460
Thermochemical data for silicon-containing species from ab initio electronic structure calculations
[DE90-011024] 24 p3446 N90-29463
Oxidation of NiAl(110)
[DE90-015645] 24 p3451 N90-29487
Atomistic studies of grain boundaries in alloys and compounds
[DE90-012401] 24 p3452 N90-29492
Recent progress in electronic structure calculations for defects in metals
[DE90-016323] 24 p3452 N90-29494
Scanning tunneling microscopy of semiconductor surfaces
[AD-A223339] 24 p3552 N90-30095
Soft x ray emission spectra from laser-irradiated high-Z targets
[AD-A223552] 24 p3552 N90-30099

First principles calculation of oxygen ordering in YBa2Cu3O(7-y)
[DE90-015205] 24 p3553 N90-30102
A comparative first principles study of phase stability in Ni-Ti and Ni-Al alloys around equiatomic composition
[DE90-016477] 24 p3554 N90-30111

ATOMIC THEORY
NT HEISENBERG THEORY
A review of atomic clock technology, the performance capability of present spaceborne and terrestrial atomic clocks, and a look toward the future
12 p1735 N90-19972

ATOMIC WEIGHTS
Measurement of the masses and lifetimes of the charmed mesons D neutral, D plus and D (sub s) plus
[MPI-PAE/EXP-EL-220] 22 p3245 N90-28405

ATOMIZATION
U ATOMIZING

ATOMIZERS
Calculation on film preparation and film motion of a swirl atomizer
[ESA-TT-1096] 03 p0348 N90-11990
Effect of vane twist on the performance of dome swirlers for gas turbine airblast atomizers
[NASA-TM-103195] 19 p2688 N90-25289

ATOMIZING
NT GAS ATOMIZATION
NT LIQUID ATOMIZATION
Structures and energies for small borane compounds: One and two boron compounds
[AD-A212264] 04 p0471 N90-12701
Extended basis set calculations of atomization energies: Comparison of isogyric and direct results
[AD-A212268] 04 p0471 N90-12702
Fundamental mechanism of atomization
[AD-A213859] 07 p0915 N90-15293
Simulation of thermal dynamics of a vaporizing coal-water droplet in a combustor
[DE90-005356] 12 p1621 N90-19317
Assessment of research needs for laser technologies applied to advanced spectroscopic methods
[DE90-007402] 12 p1669 N90-19588
The glow discharge as an atomization and ionization source
[DE90-007693] 13 p1771 N90-20163
A technical and economic evaluation of oxygen-enriched combustion in diesel engines using water-emulsified fuels
[DE90-008095] 13 p1810 N90-20394
Effect of vane twist on the performance of dome swirlers for gas turbine airblast atomizers
[NASA-TM-103195] 19 p2688 N90-25289
Ignition and combustion characteristics of metallized propellants
[NASA-CR-186870] 21 p2976 N90-26911

ATOMS
NT HELIUM ATOMS
NT HYDROGEN ATOMS
NT METASTABLE ATOMS
NT NEUTRAL ATOMS
NT NITROGEN ATOMS
NT OXYGEN ATOMS
The temporal development of collision cascades in the binary collision approximation
[DE89-015860] 01 p0122 N90-10699
Dynamics of nucleation at electrochemical interfaces via surface EXAFS and standing wave measurements
[AD-A210733] 02 p0195 N90-11109
Development of laser excited atomic fluorescence and ionization spectrometric methods
[DE90-001567] 06 p0742 N90-14320
Multiple electron capture in close ion-atom collisions
[DE90-001541] 06 p0840 N90-14885
Atomic matching across internal interfaces
[DE90-002266] 06 p0841 N90-14889
Observation of atomic relaxation near an interface through detection of emitted fluorescence
[AD-A214308] 07 p0991 N90-15725
Theoretical investigations of the structures and binding energies of Be(sub n) and Mg(sub n) (n = 3-5) clusters
[NASA-TM-101931] 08 p1120 N90-16483
Possible measurement of the gravitational acceleration of molecules, atoms, nuclei, elementary particles, and antiparticles
[DE90-719559] 08 p1121 N90-16490
The Hueckel model for small metal clusters. 4: Orbital properties and cohesive energies for model clusters of up to several hundred atoms
[AD-A216161] 10 p1354 N90-17852
Time-dependent density-functional theory
[AD-A220993] 18 p2604 N90-24829
Absolute vacuum ultraviolet photoabsorption cross section studies of atomic and molecular species: Techniques and observational data
20 p2944 N90-26754
Rate constant for reaction of atomic hydrogen with germane
20 p2947 N90-26768
Structure and dynamics of excited atoms
[AD-A221973] 21 p3074 N90-27474
Theoretical studies of time-of-flight and atom and molecular surface collision
[AD-A221705] 21 p3075 N90-27480

ATP
U ADENOSINE TRIPHOSPHATE

ATROPHY
Experiment K-6-07. Metabolic and morphologic properties of muscle fibers after spaceflight
20 p2893 N90-26461
Experiment K-6-08. Biochemical and histochemical observations of vastus medialis
20 p2893 N90-26462
Experiment K-6-09. Morphological and biochemical investigation of microgravity-induced nerve and muscle breakdown. Part 1: Investigation of nerve and muscle breakdown during spaceflight; Part 2: Biochemical analysis of EDL and PLT muscles
20 p2893 N90-26463
Experiment K-6-10. Effects of zero gravity on myofibril protein content and isomyosin distribution in rodent skeletal muscle
20 p2894 N90-26464
Experiment K-6-11. Actin mRNA and cytochrome c mRNA concentrations in the tricepts brachia muscle of rats
20 p2894 N90-26465
Experiment K-6-21. Effect of microgravity on 1) metabolic enzymes of type 1 and type 2 muscle fibers and on 2) metabolic enzymes, neutransmitter amino acids, and neurotransmitter associated enzymes in motor and somatosensory cerebral cortex. Part 1: Metabolic enzymes of individual muscle fibers; part 2: metabolic enzymes of hippocampus and spinal cord
20 p2896 N90-26474

ATROPINE
Effects of cholinergic drugs on exercise performance and simple reaction time of rhesus monkeys
[AD-A219455] 17 p2433 N90-23862

ATS
Thermal analysis of Acetylene Terminated Sulfone (ATS) resin
[AD-A220775] 17 p2381 N90-23558

ATTACK AIRCRAFT
NT AH-64 HELICOPTER
NT B-1 AIRCRAFT
NT B-52 AIRCRAFT
NT B-58 AIRCRAFT
NT B-70 AIRCRAFT
NT BOMBER AIRCRAFT
NT F-4 AIRCRAFT
NT F-8 AIRCRAFT
NT F-14 AIRCRAFT
NT F-15 AIRCRAFT
NT F-16 AIRCRAFT
NT F-17 AIRCRAFT
NT F-18 AIRCRAFT
NT F-86 AIRCRAFT
NT F-104 AIRCRAFT
NT F-111 AIRCRAFT
NT FIGHTER AIRCRAFT
Estimating the relationships between the state of the art of technology and production cost for the US aircraft
[AD-A212127] 04 p0437 N90-12495
Evaluation of a damaged F/A-18 horizontal stabilator
[AD-A212573] 04 p0453 N90-12597
Development of a least squares time response lower-order equivalent systems technique
[AD-A220527] 17 p2351 N90-23389
AM-X high incidence trials, development and results
[ETN-90-97277] 20 p2814 N90-26016
Expert system for pilot assistance: The challenge of an intensive prototyping
[ETN-90-97274] 22 p3111 N90-27674
Combat aircraft control requirements
23 p3271 N90-28515
Combat aircraft control requirements for agility
23 p3272 N90-28517
The effects of foreplanes on the static and dynamic characteristics of a combat aircraft model
23 p3273 N90-28520
The steady and time-dependent aerodynamic characteristics of a combat aircraft with a delta or swept canard
23 p3274 N90-28526
The potential for digital databases in flight planning and flight aiding for combat aircraft
24 p3429 N90-29371

ATTACKING (ASSAULTING)
Field-of-View variations and stripe-texturing effects on assault landing performance in the C-130 weapon system trainer
[AD-A212763] 04 p0459 N90-12634
Time-optimal aircraft pursuit-evasion with a weapon envelope constraint
[NASA-CR-186640] 19 p2658 N90-25126

ATTENTION
Daytime sleepiness, performance, mood, nocturnal sleep: The effect of benzodiazepine and caffeine on their relationship
[AD-A210915] 01 p0093 N90-10533
Attention and vigilance in speech perception
[AD-A210493] 01 p0095 N90-10539
Electrophysiological studies of visual attention and resource allocation
[AD-A212287] 04 p0525 N90-13030
Watchfulness and attention during weightlessness simulations: Use of computerized psychometric tests
[REPT-89-TOU-3-1045] 05 p0674 N90-13928
The role of attention in visual processing
[AD-A214158] 07 p0967 N90-15588
A model for visual attention
[AD-A214505] 09 p1258 N90-17297
Proximity compatibility and information display: The effects of space and color on the analysis of aircraft stall conditions
[AD-A214488] 09 p1260 N90-17309
Visual selective attention
[AD-A219204] 16 p2265 N90-22910
DURIP: Improved eye movement monitoring capabilities for studies in visual cognition
[AD-A220355] 18 p2586 N90-24722
The role of attention in information processing implications for the design of displays
[AD-A219252] 19 p2723 N90-25486
Mathematical problem-solving transfer: The effects of cognitive load and attention a schema acquisition and rule automation
20 p2917 N90-26594
Conference on The Perception of Structure Program and Abstracts
[AD-A222437] 22 p3232 N90-28328
Evaluation of the Situational Awareness Rating Technique (SART) as a tool for aircrew systems design
23 p3358 N90-28977
Attention gradients in situation awareness
23 p3358 N90-28978
The three-dimensional structure of visual attention and its implications for display design
23 p3359 N90-28980
Neurophysiological correlates of information processing abilities during divided attention situations in air traffic controllers
23 p3360 N90-28989
Attention, imagery, and memory: A neuromagnetic investigation
[AD-A224560] 24 p3499 N90-29775

ATTENUATION
NT ACOUSTIC ATTENUATION
NT ATMOSPHERIC ATTENUATION
NT MICROWAVE ATTENUATION
NT RADIO ATTENUATION
NT SHOCK WAVE ATTENUATION
NT SIDELOBE REDUCTION
NT WAVE ATTENUATION
Effects of rain attenuation on satellite EHF (Extremely High Frequency) communications in the US
[AD-A210517] 01 p0057 N90-10325
Investigations of ultrasonic wave interactions at imperfect boundaries separating anisotropic materials
[DE90-010661] 18 p2612 N90-24875
Software set-up for data processing of depolarization due to rain and ice crystals in the Olympus project
[EUT-89-E-218] 20 p2855 N90-26240
Interaction of electromagnetic signals with particulate clouds
[AD-A222804] 20 p2856 N90-26244

ATTENUATION COEFFICIENTS
Vapor pressures of acetylene at low temperatures
20 p2949 N90-26777

ATTENUATORS
NT RESISTORS
NT THERMISTORS
Means for protecting electroexplosive devices which are subject to a wide variety of radio frequency
[AD-D014219] 06 p0753 N90-14382
Operational effects on crashworthy seat attenuators
[AD-A221148] 18 p2495 N90-24259

ATTITUDE (INCLINATION)
NT PITCH (INCLINATION)
NT ROLL
NT SATELLITE ORIENTATION
NT YAW
A comparison of two subject-controlled attitude measures during somatogravic illusion exposure
[AD-A212528] 04 p0525 N90-13031
Simultaneous quaternion estimation (QUEST) and bias determination
05 p0587 N90-13417
COBE nonspinning attitude propagation
05 p0587 N90-13418
Extension to Eulers's theorem to n-dimensional spaces
05 p0589 N90-13431

Analytical derivation and verification of zero-gyro control for the IUE satellite
[NASA-TM-100748] 05 p0645 N90-13767
Thermal analysis of fixed and tilting pad journal bearings including cross-film viscosity variations and deformations
07 p0937 N90-15429
TALON and CRADLE: Systems for the rescue of tumbling spacecraft and astronauts, a preliminary design
09 p1181 N90-16847
Measurement of fluctuations in the tilt of Arctic ice at the CEAREX Oceanography Camp: Experiment review, data catalog, and preliminary results
[AD-A215059] 09 p1249 N90-17249
Remote Attitude Measurement Sensor (RAMS)
12 p1611 N90-19271
Determination of the implementation of the 3-axis attitude motion simulator digital position controller
12 p1638 N90-19409
Optimization of the effective GPS data rate
14 p1907 N90-20932
Accurate nonlinear control for satellites using reaction wheels
[INPE-4983-PRE/1546] 15 p2059 N90-21787
Towards a Sarkovski order for the embedding of disks maintaining their orientation
[REPT-89-43] 15 p2151 N90-22289
Minimum attainable RMS attitude error using co-located rate sensors 16 p2288 N90-23038
Three approximate methods for estimating the best subset of GPS satellites for satellite position calculations
[AD-A220380] 17 p2350 N90-23383
NASA Lewis icing research tunnel user manual
[NASA-TM-102319] 17 p2355 N90-23407
An electronic spirit level tilt sensor
[ETN-90-96697] 17 p2406 N90-23710
Optical rate sensor algorithms
18 p2632 N90-24997
Coupled rotor-body equations of motion hover flight
[NASA-CR-186710] 19 p2655 N90-25111
Molecular dynamics simulations of grain-boundary diffusion for varying tilt angle geometries
[DE90-012919] 20 p2930 N90-26669
Maintaining spatial orientation awareness
23 p3361 N90-28993
Cognition versus sensation: A paradigm for reorientation
[IZF-1989-20] 23 p3361 N90-28995

ATTITUDE CONTROL
NT DIRECTIONAL CONTROL
NT LATERAL CONTROL
NT LONGITUDINAL CONTROL
NT SATELLITE ATTITUDE CONTROL
NT THRUST VECTOR CONTROL
The Spartan 1 mission
[NASA-TM-101887] 01 p0015 N90-10077
Explicit modeling and computational load distribution for concurrent processing simulation of the space station
01 p0020 N90-10096
Modeling, simulation, and analyses of attitude control for the Crew/Equipment Retriever (CER) proposed for space station
[AD-A208140] 01 p0025 N90-10125
Independent Orbiter Assessment (IOA): Analysis of the ascent thrust vector control actuator subsystem
[NASA-CR-185579] 02 p0164 N90-10929
Independent Orbiter Assessment (IOA): Analysis of the reaction control system, volume 1
[NASA-CR-185532-VOL-1] 02 p0166 N90-10938
Low-speed wind-tunnel study of reaction control-jet effectiveness for hover and transition of a STOVL fighter concept
[NASA-TM-4147] 03 p0308 N90-11751
Aircraft SAR simulation Sargen 1.0
[FEL-1989-44] 04 p0491 N90-12823
Aerodynamics of thrust vectoring
[NASA-CR-185074] 05 p0575 N90-13354
The effects of seasonal and latitudinal earth infrared radiance variations on ERBS attitude control
05 p0586 N90-13414
Spacecraft attitude determination using the earth's magnetic field 05 p0589 N90-13429
Analysis of the flight dynamics of the Solar Maximum Mission (SMM) off-sun scientific pointing
05 p0590 N90-13432
Overview of the Hipparcos satellite
05 p0603 N90-13502
The attitude and orbit control system
05 p0605 N90-13516
High precision rocket attitude reconstruction using star sensor and magnetometer data
05 p0659 N90-13844
The SN 1987A attitude control system
05 p0659 N90-13845
Development of a three-axis trim program
[AD-A212883] 06 p0726 N90-14237
Techniques for extreme attitude suspension of a wind tunnel model in a magnetic suspension and balance system
[NASA-CR-181895] 06 p0728 N90-14245
Plume shape optimization of small attitude control thrusters with respect to impingement and thrust
[ISL-CO-220/88] 08 p1064 N90-16153
Cooperative control of two active spacecraft during proximity operations
[NASA-CR-185596] 09 p1172 N90-16778
TALON and CRADLE: Systems for the rescue of tumbling spacecraft and astronauts, a preliminary design
09 p1181 N90-16847
Mission report on the Orbiter Camera Payload System (OCPS) Large Format Camera (LFC) and Attitude Reference System (ARS)
[NASA-CR-186273] 09 p1240 N90-17197
Possible piloting techniques at hypersonic speeds
[ISL-CO-216/88] 11 p1456 N90-18392
Data collection and location platforms experimental network: Description of an orbit routine
[INPE-4798-NTE/287] 11 p1485 N90-18439
Attitude estimation procedure for spin stabilized satellites
[INPE-4866-TDL/377] 11 p1467 N90-18449
LACE flight dynamics experiment
14 p1937 N90-21086
Design of a digital model following controller of reaction wheel torques
[INPE-4753-PRE/1425] 14 p1938 N90-21093
Attitude control modes for the MECB remote sensing satellites
[INPE-4755-PRE/1427] 14 p1938 N90-21094
Numerical simulation model for hydrazine attitude control thrusters. Part 1: Model description
[INPE-4952-RPE/601] 14 p1942 N90-21115
Direct inversion of rigid-body rotational dynamics
[NASA-TM-102798] 15 p2055 N90-21773
Numerical simulation model of hydrazine attitude control thrusters
[INPE-4965-PRE/1534] 15 p2068 N90-21848
Automated star pattern recognition
16 p2211 N90-22612
Space station dynamics, attitude control and momentum management 16 p2287 N90-23029
The use of real-time, hardware-in-the-loop simulation in the design and development of the new Hughes HS601 spacecraft attitude control system
16 p2293 N90-23065
Modeling and control of flexible space stations (slew maneuvers) 16 p2297 N90-23086
Gamma Ray Observatory (GRO) dynamics simulator requirements and mathematical specifications, revision 1
[NASA-CR-183465] 17 p2362 N90-23447
The large wheel actuator LDR 100-0: Development status and test results 18 p2539 N90-24487
A study of concept options for the evolution of Space Station Freedom
[NASA-TM-102675] 19 p2663 N90-25154
Fluid-loop reaction system
[NASA-CASE-NPO-17204-1-CU]
20 p2864 N90-26292
Lunar lander conceptual design
[NASA-CR-186233] 21 p2965 N90-26856
Flow induced nutation instability in spinning solid propellant rockets
[AD-A222504] 21 p2969 N90-26877
Attitude Determination and Control System (ADCS) and Maintenance and Diagnostic System (MDS): A maintenance and diagnostic system for Space Station Freedom 21 p3043 N90-27295
Spacecraft attitude dynamics: Evolution and current challenges 22 p3128 N90-27754
A model of the perturbed spinning motion of the San Marco 5th spacecraft 22 p3129 N90-27755
The instrument pointing system: Precision attitude control in space 22 p3129 N90-27756
A new method for a tethered system aided space station assembly 22 p3130 N90-27765
Effects of low bond number liquid motions on spacecraft attitude 22 p3131 N90-27768
Short period control using angular acceleration feedback: Compensation for first lag servo
[NAL-TM-600] 24 p3435 N90-29399
A new momentum management controller for the space station
[NASA-CR-187265] 24 p3440 N90-29425
The control of space manipulators subject to spacecraft attitude control saturation limits
24 p3515 N90-29871

ATTITUDE GYROS
On-ground attitude determination
05 p0609 N90-13552

ATTITUDE STABILITY
NT DIRECTIONAL STABILITY
NT GYROSCOPIC STABILITY
NT LATERAL STABILITY
NT LONGITUDINAL STABILITY
Modeling, simulation, and analyses of attitude control for the Crew/Equipment Retriever (CER) proposed for space station
[AD-A208140] 01 p0025 N90-10125
Techniques for extreme attitude suspension of a wind tunnel model in a magnetic suspension and balance system
[NASA-CR-181895] 06 p0728 N90-14245
A three axis attitude control of a satellite
[NASDA-TR-22] 24 p3439 N90-29421

ATTRACTION
Replica scaling analysis of interfaces in random media
[PREPRINT-713] 16 p2312 N90-23174

ATTRITION (MATERIALS)
U COMMINUTION

AUDIO EQUIPMENT
NT EARPHONES
NT MICROPHONES
Navigation software for the MPL vertical line array
[AD-A220166] 17 p2432 N90-23860
Copyright and home copying: Technology challenges the law
[PB90-151309] 21 p3086 N90-27547

AUDIO FREQUENCIES
A prototype microprocessor based audiometer for use by the CF (Canadian Forces) medical services for periodic hearing tests
[AD-A212990] 05 p0673 N90-13921
Auditory pattern memory: Mechanisms of tonal sequence discrimination by human observers
[AD-A214494] 09 p1250 N90-17253
Perception of long-period complex sounds
[AD-A216743] 11 p1539 N90-18861
Vertical directionality measurements of ambient noise in the NE Pacific
[AD-A220007] 17 p2432 N90-23856
Perception of complex auditory patterns
[AD-A219626] 17 p2434 N90-23867

AUDIO SIGNALS
Perceived urgency of warning signals determined using a forced choice pair comparison technique
[RAE-TM-MM-12] 04 p0551 N90-13206
A waveform capture and storage unit and its use for investigating disturbances on digital transmission links
[BBC-RD-1989/17] 12 p1649 N90-19478
Direct Radio Broadcasting by Satellite (DRBS): A review of the technical factors and system approaches suitable for mobile and fixed reception
[BBC-RD-1989/4] 14 p1960 N90-21221

AUDIO VISUAL EQUIPMENT
U TRAINING DEVICES
U VISUAL AIDS

AUDIOMETRY
Speech reception in quiet and in noisy conditions by individuals with noise-induced hearing loss in relation to their audiogram
[IZF-1989-11] 05 p0633 N90-13692
Evaluation of speech intelligibility through a bone conduction stimulator
[AD-A212002] 05 p0673 N90-13919
A prototype microprocessor based audiometer for use by the CF (Canadian Forces) medical services for periodic hearing tests
[AD-A212990] 05 p0673 N90-13921

AUDITORY PERCEPTION
Attention and vigilance in speech perception
[AD-A210493] 01 p0095 N90-10539
Inferences from images
[AD-A210710] 02 p0258 N90-11465
Binaural masking: An analysis of models
[AD-A211578] 03 p0381 N90-12168
The effects of hearing protectors on speech communication and the perception of warning signals
[AD-A212521] 04 p0492 N90-12832
Removal of noise from noise-degraded speech signals
[AD-A212876] 04 p0493 N90-12840
Time-frequency factors in auditory perception
[AD-A211491] 04 p0523 N90-13016
Shape instabilities of plate-like structures. 1: Experimental observations in heavily cold worked in situ composites
[AD-A212251] 04 p0523 N90-13021
Seminars of Applied Physics, Materials Physics and Biomedical Engineering, 1989
[PB89-218572] 04 p0548 N90-13192
Speech reception in quiet and in noisy conditions by individuals with noise-induced hearing loss in relation to their audiogram
[IZF-1989-11] 05 p0633 N90-13692
Voice preprocessor for digital voice applications
[AD-A214726] 09 p1205 N90-16982

Auditory pattern memory: Mechanisms of tonal sequence discrimination by human observers
[AD-A214494] 09 p1250 N90-17253
Recognition of environmental sounds
[AD-A214942] 09 p1259 N90-17302
On categorizing sounds
[AD-A216417] 10 p1427 N90-18232
Perception of long-period complex sounds
[AD-A216743] 11 p1539 N90-18861
Auditory perception
[AD-A217012] 11 p1540 N90-18864
Auditory spectro-temporal pattern analysis
[AD-A218416] 16 p2313 N90-23184
Perception of complex auditory patterns
[AD-A219626] 17 p2434 N90-23867
Auditory perception of complex sounds
[AD-A219927] 17 p2435 N90-23872
Binaural masking: An analysis of models
[AD-A221668] 21 p3035 N90-27252
Complex auditory signals
[AD-A224127] 23 p3356 N90-28969
Auditory processing of complex sounds across frequency channels
[AD-A224147] 23 p3356 N90-28970
The simulation of localized sounds for improved situational awareness 23 p3359 N90-28984
Techniques and applications for binaural sound manipulation in human-machine interfaces
[NASA-TM-102279] 23 p3362 N90-28996

AUDITORY SIGNALS
Binaural masking: An analysis of models
[AD-A211578] 03 p0381 N90-12168
Time-frequency factors in auditory perception
[AD-A211491] 04 p0523 N90-13016
Auditory pattern memory: Mechanisms of tonal sequence discrimination by human observers
[AD-A214494] 09 p1250 N90-17253
Evaluation of two objective measures of effective auditory stimulus level
[AD-A214669] 09 p1250 N90-17255
Neurobeamformer 2: Further exploration of adaptive beamforming via neural networks
[AD-A215118] 10 p1426 N90-18226
Auditory perception
[AD-A217012] 11 p1540 N90-18864
Auditory spectro-temporal pattern analysis
[AD-A218416] 16 p2313 N90-23184
Perception of complex auditory patterns
[AD-A219626] 17 p2434 N90-23867
Listening to turbulence: An example of scientific audiolization
[DE90-010637] 19 p2753 N90-25646
Binaural masking: An analysis of models
[AD-A221668] 21 p3035 N90-27252
Complex auditory signals
[AD-A224127] 23 p3356 N90-28969
Auditory processing of complex sounds across frequency channels
[AD-A224147] 23 p3356 N90-28970
The effects of acoustic orientation cues on instrument flight performance in a flight simulator
23 p3359 N90-28985

AUDITORY STIMULI
Sound Localization by Human Observers symposium proceedings
[AD-A212877] 04 p0524 N90-13026
Evaluation of two objective measures of effective auditory stimulus level
[AD-A214669] 09 p1250 N90-17255
Acetylcholinesterase inhibition and information processing in the auditory cortex
[AD-A216092] 10 p1411 N90-18139
Auditory perception
[AD-A217012] 11 p1540 N90-18864
Brain stem evoked responses in altered G environments
[AD-A220097] 17 p2435 N90-23874
Binaural masking: An analysis of models
[AD-A221668] 21 p3035 N90-27252
Complex auditory signals
[AD-A224127] 23 p3356 N90-28969

AUGER EFFECT
Surface characterization of hydrogen charged and uncharged alpha-2 and gamma titanium aluminide alloys using AES and REELS
[NASA-CR-186561] 14 p1951 N90-21171

AUGER SPECTROSCOPY
Quantitative interpretation of auger lineshapes and electron/photon stimulated desorption
[AD-A211550] 03 p0324 N90-11842
Quantitative AES and XPS: Determination of the electron spectrometer transmission function and the detector sensitivity energy dependencies for the production of true electron emission spectra in AES and XPS
[NPL-DMA(A)-194] 05 p0623 N90-13834
Auger and x ray absorption studies of solid molecular oxygen
[DE90-003966] 07 p1006 N90-15825
An Auger electron spectroscopy study of surface-preparation contaminants
[NASA-TP-2972] 09 p1203 N90-16968
Spectroscopic evidence for carbon-carbon bonding in carbide layers on metals
[AD-A216726] 11 p1479 N90-18512
Extracting chemical information form Auger line shapes
[AD-A216729] 11 p1483 N90-18537
Positron annihilation induced Auger electron spectroscopy 11 p1561 N90-18996
Magnetron sputtered boron films and Ti/B multilayer structures
[DE90-009190] 14 p1948 N90-21153
Long term intensity stability of Auger electron spectrometers: Instructions for the interlaboratory comparison
[NPL-DMM(A)-1] 15 p2102 N90-22027
Surface physics instrumentation
[AD-A220460] 17 p2373 N90-23512
Surface and interface studies by Auger electron spectroscopy
[ETN-90-96948] 18 p2522 N90-24398
Ni impurity effects on hydrogen surface chemistry and etching of Si(111)
[AD-A222083] 21 p2977 N90-26921
Face-specific interaction of MoS4(2-) with oriented crystals of (0001) CdX(X = Se, S)
[AD-A222405] 21 p3084 N90-27537
Use of electron spectroscopies in the tribological evaluation of diamond films
[DE90-014421] 23 p3334 N90-28848

AUGMENTATION
NT STABILITY AUGMENTATION
NT THRUST AUGMENTATION
Enhancement of microchannel plate gain by deposition of CsI on the channel walls
[DE90-003051] 07 p0922 N90-15334
Muzzle shunt augmentation of conventional railguns
[DE90-007505] 12 p1607 N90-19248
Multibody modeling and verification
12 p1640 N90-19422
Data analysis techniques 21 p3017 N90-27151
Variable mixture ratio performance through nitrogen augmentation 23 p3295 N90-28639

AURORAL ACTIVITY
U AURORAS

AURORAL ARCS
NT RED ARCS
Low frequency electrostatic waves observed in the vicinity of an auroral arc 02 p0243 N90-11378
A high spatial resolution study of the thermospheric response to a discrete auroral arc
[NASA-TM-102904] 07 p0961 N90-15559
A study of auroral activity in the nightside polar cap
16 p2254 N90-22852
A study of the spatial scales of discrete polar auroral arcs
[NASA-CR-186806] 19 p2714 N90-25444
Ionospheric irregularities: Source, structure, plasma processes and effects on sensor systems
[AD-A223908] 24 p3490 N90-29723

AURORAL ECHOES
First results from HF (High-Frequency) oblique backscatter soundings to the northwest of College, Alaska using a modified ULCAR digisonde D-256
[AD-A214931] 09 p1206 N90-16987

AURORAL ELECTROJETS
The auroral energy deposition over the polar ionosphere during substorms
[AD-A210522] 01 p0088 N90-10490

AURORAL IONIZATION
X ray spectrophotometric remote sensing of diffuse auroral ionization
[SD-TR-89-09] 08 p1139 N90-16599
Kiruna geophysical data
[PB90-123985] 09 p1247 N90-17232

AURORAL IRRADIATION
Actions of magnetospheres on planetary atmospheres
[IRF-SR-203] 17 p2486 N90-24215
Electron populations above the nightside auroral oval during magnetic quiet times
[IRF-PREPRINT-116] 19 p2714 N90-25445
Preliminary results from the quadrupole probe on NEED-1
[FFI-89/7015] 19 p2714 N90-25446

AURORAL ZONES
A review on radio studies of auroral E-region ionospheric irregularities 02 p0245 N90-11390
Auroral and sub-auroral F-layer irregularity studies in the Northern and Southern Hemisphere during the equinox transition study September 16-26, 1984
02 p0246 N90-11393
An ionospheric model for HF sky-wave backscatter radar 02 p0247 N90-11401
Observations of electrostatic hydrogen cyclotron waves and electric field fluctuations near one Hz in auroral acceleration regions 05 p0658 N90-13842
The auroral current - voltage relationship
05 p0658 N90-13843
Preliminary results of the rocket and scatter experiments ROSE: Measurements with the newly designed spherical probe 05 p0659 N90-13850
ALIS: An Auroral Large Imaging System in northern Scandinavia 05 p0663 N90-13877
Auroral and sub-auroral interaction at the F region ionosphere
[AD-A213284] 05 p0666 N90-13896
Quantifying and reducing uncertainty in the assimilative mapping of ionospheric electrodynamics
[AD-A218057] 13 p1842 N90-20577
Spacecraft optical contamination environment
[AD-A218088] 13 p1889 N90-20838
Polar BEAR UV imaging of airglow and aurora-image processing and results
[AD-A219480] 17 p2422 N90-23802
Evaluation of space plasma data: Effects upon spacecraft materials and predictions of hazardous conditions; polar ARCS
[AD-A219509] 17 p2474 N90-24145

AURORAS
NT AURORAL ARCS
NT RED ARCS
Observations of ionosphere/magnetosphere interactions from the Dynamics Explorer satellites
02 p0242 N90-11376
Empirical models of convection electric fields and electrostatic potential at high latitude from EISCAT observations: Preliminary results
02 p0243 N90-11377
Polar F layer lacuna irregularities at Dumont d'Urville
02 p0243 N90-11379
Quiet time conductivities of the auroral ionosphere
02 p0244 N90-11383
Atmospheric gravity waves in the auroral source region of TIDs, studied with the EISCAT CP2-data
02 p0244 N90-11387
On the possibility of producing artificial ionization and polar aurora in the ionosphere by radio-waves emitted from the ground 02 p0245 N90-11388
North-south tropical F2 layer asymmetry at west AFrican and Pacific longitudes 02 p0247 N90-11398
LABCEDE fluorescence investigations
[AD-A210678] 03 p0370 N90-12114
Distribution of auroral precipitation at midnight during a magnetic storm
[PB89-213136] 03 p0370 N90-12118
UV ionospheric remote sensing with the polar BEAR satellite
[AD-A211359] 03 p0372 N90-12127
Vacuum ultraviolet backgrounds from space - ten years after
[AD-A211353] 03 p0435 N90-12493
Development of computer codes to model dynamics of the earth's magnetosphere
[AD-A211532] 04 p0517 N90-12987
Auroral particle acceleration by dc and low frequency electric fields 05 p0658 N90-13841
Stable auroral red arc occurrences detected by the Pacific Northwest Laboratory photometer network: A decade of observations, 1978 - 1988
[DE90-004994] 09 p1298 N90-17522
Active probing of space plasmas
[AD-A216867] 12 p1716 N90-19855
Amplified spontaneous emission measurements on the aurora large-aperture module
[DE90-004841] 13 p1806 N90-20369
Optical instrumentation support for the airborne ionospheric observatory
[AD-A218207] 13 p1889 N90-20839
Auroral ultraviolet darkening on the outer planets
15 p2192 N90-22518
A study of auroral activity in the nightside polar cap
16 p2254 N90-22852
Quantifying and reducing uncertainty in the assimilative mapping of ionospheric electrodynamics
16 p2254 N90-22854
Polar BEAR UV imaging of airglow and aurora-image processing and results
[AD-A219480] 17 p2422 N90-23802
Diagnosis of auroral dynamics using global auroral imaging with emphasis on large-scale evolutions
[NASA-CR-186623] 17 p2422 N90-23804
Viking data analysis
[AD-A222609] 20 p2823 N90-26062

AUSFORMING
Austempered ductile iron data base: A cooperative program between industry and the Trade Adjustment Assistance Program of the Department of Commerce
[PB90-115569] 12 p1626 N90-19343
AUSTENITE
Fatigue growth and closure of short cracks
[AD-A210824] 01 p0081 N90-10462
Use of overlapped reflection for determining the retained austenite by X-ray diffraction
[DE89-615450] 02 p0198 N90-11128
Contribution to the transcrystalline stress crack corrosion of austenite chromium-nickel steels
[ETN-89-94665] 02 p0199 N90-11137
Heat-resistant steels containing 8 pct Cr
[PB90-108796] 09 p1193 N90-16912
Austempered ductile iron data base: A cooperative program between industry and the Trade Adjustment Assistance Program of the Department of Commerce
[PB90-115569] 12 p1626 N90-19343
Studies on phosphorus segregation in austenite
[ISBN-952-90-1488-0] 18 p2526 N90-24417
The effect of manganese on the onset of the stage 2 reaction in an austempered ductile iron matrix
[DE90-011804] 20 p2834 N90-26119
Microstructural development in HSLA-100 steel weld metals
[AD-A222105] 21 p2982 N90-26944
Single-phase solidification during rapid resolidification of stainless steel alloys
[DE90-015190] 24 p3450 N90-29483
Tensile behavior and swelling of ternary austenitic alloys irradiated in different neutron spectra
[DE90-015295] 24 p3450 N90-29485
Isotopic tailoring and other techniques used to study helium effects in austenitic alloys
[DE90-016344] 24 p3452 N90-29495
AUSTENITIC STAINLESS STEELS
The effects of temperature on fatigue crack propagation in 310 austenitic stainless steel
[DE90-000136] 03 p0328 N90-11865
How the common practice of heating plates of austenitic stainless steel during cooling affects their mechanical properties
[CETIM-104500] 04 p0476 N90-12725
Contribution to the electrochemical study of corrosion in the low conductivity media: Application to the study of the behavior of austenitic stainless steels in concentrated solutions of acetic acid
[ISAL-89-0014] 05 p0625 N90-13648
The metallurgical determinants of toughness as cryogenic temperature
[DE90-002331] 06 p0748 N90-14351
Microstructure induced by laser shock in an austenitic steel 06 p0784 N90-14558
Measuring the thickness of austenitic weld deposits on carbon steel walls using a magnetic method
[DE89-635446] 06 p0794 N90-14628
An investigation of the sensitization behavior of Fe-Mn-Cr austenitic steels
[DE90-002719] 07 p0904 N90-15226
Fusion reactor materials
[DE90-000976] 07 p0994 N90-15744
An XPS and electrochemical study of the influence of molybdenum and nitrogen on the passivity of austenitic stainless steel
[AD-A214267] 08 p1044 N90-16034
Interplanar spacing for various phases in austenitic stainless steels
[DE90-602350] 08 p1045 N90-16038
Heat-resistant steels containing 8 pct Cr
[PB90-108796] 09 p1193 N90-16912
Helium permeability through austenitic stainless steel
[DE90-007046] 11 p1488 N90-18562
Evaluation of radiation-induced sensitization using electrochemical potentiokinetic reactivation technique for austenitic stainless steels
[DE90-002708] 12 p1627 N90-19352
Shaping the insonifying pulse to optimise B-scans obtained in austenite
[AERE-R-13518] 13 p1775 N90-20187
Stochastic approach to the initiation of pitting corrosion
[AERE-R-13348] 13 p1775 N90-20190
Development and evaluation of advanced austenitic alloys
[DE90-011315] 18 p2528 N90-24425
Fatigue crack propagation in austenitic stainless steels at cryogenic temperatures
[DE90-011597] 18 p2528 N90-24426
Cyclic stress strain behavior of an austenitic stainless steel Polarit 778 under variable amplitude loading
[VTT-RR-647] 19 p2675 N90-25215
Methodology of the fatigue under shocks. Experimental results: 7075 T6 and 35 NCD16
[ETCA-89-R-140] 22 p3157 N90-27901
Influence of a surface finishing on the fatigue behavior of a 32CDV13 steel
[ETCA-89-R-164] 22 p3157 N90-27902
Evaluation of advanced austenitic alloys relative to alloy design criteria for steam service. Part 1: Lean stainless steel
[DE90-014765] 23 p3310 N90-28720
The effect of helium on microstructural evolution in austenitic steels as determined by spectral tailoring experiments
[DE90-016360] 24 p3452 N90-29496
AUSTRALIA
The development of over-the-horizon radar in Australia
[ISBN-0-642-13561-4] 08 p1055 N90-16099
An examination of the fatigue meter records from the RAAF Orion P-3C fleet
[AD-A214000] 10 p1319 N90-17628
Geopotential models in the Australian region
13 p1832 N90-20519
A requirement for Australian research: Access to big science facilities, a report by the Australian National Committee for Crystallography
[DE90-614784] 14 p1930 N90-21048
Transmission of infrared radiation through the Australian atmosphere: Predictions using the LOWTRAN model
[AD-A220340] 17 p2428 N90-23835
Behavior of dust clouds from Australian dust storms in 1982-1983 as observed by the GMS
21 p3029 N90-27221
AUTOCLAVING
Autoclavable addition polyimides for 371 C composite applications
[NASA-TM-103233] 22 p3153 N90-27874
AUTOCOLLIMATORS
U COLLIMATORS
AUTOCORRELATION
A simple fiber optic autocorrelation tachometer
[ETN-90-96146] 08 p1077 N90-16228
Online submicron particle sizing by dynamic light scattering using autodilution 09 p1223 N90-17095
Effects of strong scattering on transionospheric propagation
[AD-A216708] 11 p1497 N90-18617
Spanwise measurements of vertical components of atmospheric turbulence
[NASA-TP-2963] 12 p1692 N90-19718
Picosecond Laser Facility
[AD-A217784] 13 p1808 N90-20384
Model order determination methods for autoregressive radio direction finding techniques
[AD-A220707] 17 p2350 N90-23384
Pattern classification of textura by moment and distance autocorrelation function
[INPE-4976-PRE/1541] 20 p2879 N90-26379
Reversed residuals in autoregressive time series analysis
[AD-A222711] 20 p2921 N90-26624
Dynamics of fluids in bulk and near a vertical wall: Studied by photoncorrelation spectroscopy
[PB90-200452] 22 p3169 N90-27976
Near-angle scattering and binary optics
[AD-A224140] 23 p3396 N90-29186
AUTOMATA THEORY
An introduction to input/output automata
[AD-A210831] 01 p0106 N90-10604
Cellular automata and massively parallel physics
[DE89-016506] 02 p0220 N90-11257
Time bounds for real-time process control in the presence of timing uncertainty
[AD-A213791] 07 p0975 N90-15633
Using mappings to prove timing properties
[AD-A213967] 07 p0981 N90-15666
Rule matrices, degree vectors, and preimages for cellular automata
[DE90-007492] 12 p1707 N90-19805
Encoding sequential structure in simple recurrent networks
[AD-A218928] 16 p2278 N90-22984
Collective properties of neural systems and their relation to other physical models
[AD-A219071] 16 p2315 N90-23201
The bit full-decomposition of sequential machines
[EUT-89-E-223] 20 p2904 N90-26516
The full-decomposition of sequential machines with the separate realization of the next-state and output functions
[EUT-89-E-222] 20 p2909 N90-26547
Place/transition nets with debit arcs
[NASA-CR-186932] 21 p3058 N90-27386
AUTOMATED EN ROUTE ATC
Route data representation for ATC simulation experiments
[RSRE-MEMO-4133] 04 p0450 N90-12576
The MODE S operational test and evaluation/integration test plan
[DOT/FAA/CT-TN89/51] 22 p3111 N90-27671
AUTOMATED PILOT ADVISORY SYSTEM
The influence of ice accretion physics on the forecasting of aircraft icing conditions 14 p1906 N90-20928
AUTOMATIC CONTROL
NT ACTIVE CONTROL
NT ADAPTIVE CONTROL
NT AUTOMATIC FLIGHT CONTROL
NT AUTOMATIC FREQUENCY CONTROL
NT AUTOMATIC GAIN CONTROL
NT DYNAMIC CONTROL
NT FEEDBACK CONTROL
NT FEEDFORWARD CONTROL
NT LINEAR QUADRATIC GAUSSIAN CONTROL
NT LINEAR QUADRATIC REGULATOR
NT MACHINE LEARNING
NT MODEL REFERENCE ADAPTIVE CONTROL
NT NUMERICAL CONTROL
NT OPTIMAL CONTROL
NT PROPORTIONAL CONTROL
NT SELF ADAPTIVE CONTROL SYSTEMS
NT SELF ALIGNMENT
NT SEQUENTIAL CONTROL
NT TIME OPTIMAL CONTROL
Active participation in highly automated systems: Turning the wrong stuff into the right stuff
[AD-A210218] 01 p0101 N90-10572
Advancing automation and robotics technology for the space station Freedom and for the US economy
[NASA-TM-101561] 01 p0102 N90-10577
Autonomous control system for Czochralski growth of LEC GaAs
[AD-A210190] 01 p0131 N90-10754
Automatic classification of spectra from the Infrared Astronomical Satellite (IRAS)
[NASA-RP-1217] 01 p0140 N90-10807
Kinematic design NC optical generator
03 p0404 N90-12316
Batch LCAP2-linear control analysis, version 2.0: User's manual
[AD-A211670] 04 p0461 N90-12643
Automated monitor and control for deep space network subsystems 04 p0486 N90-12794
Automatic communications channel interference monitoring
[RSRE-MEMO-4243] 04 p0491 N90-12820
Automated Steerable Nulling Antenna Processor (SNAP) model
[PB89-231740] 04 p0509 N90-12937
Apparatus for cooling electronic components in aircraft
[AD-D014207] 05 p0579 N90-13373
Flight deck automation: Promises and realities
[NASA-CP-10036] 05 p0580 N90-13384
The economic impact of automation technology
[AD-A213363] 05 p0630 N90-13682
Arc current control of a robotic welding system: Modeling and control system design
[AD-A213150] 05 p0650 N90-13788
Kinematics and control of manipulation robots
[WTHD-187] 05 p0652 N90-13803
Flight software development for the isothermal dendritic growth experiment
[NASA-TM-102412] 05 p0685 N90-13988
Automated glass fiber drawing
[DE90-000894] 06 p0751 N90-14367
CCD TV focal plane guider development and comparison to SIRTF applications
[NASA-CR-185977] 06 p0842 N90-14900
CIS-lunar space infrastructure lunar technologies: Executive summary
[NASA-CR-186220] 06 p0865 N90-15029
Automated convection soldering
[KCP-613-4005] 07 p0916 N90-15300
Computer controlled MHD power consolidation and pulse-generation system
[DE90-001224] 07 p0981 N90-15662
Special Course on Advances in Cryogenic Wind Tunnel Technology
[AGARD-R-774] 08 p1028 N90-15939
Automatic control of KKK: Requirements, sensors, actuators, and control performance results
08 p1029 N90-15944
Automatic control of cryogenic wind tunnels
08 p1031 N90-15957
Automated information systems plan
[AD-A214982] 09 p1296 N90-17514
Development of an integrated mobile robot system at Carnegie Mellon University: June 1988
[AD-A215955] 10 p1392 N90-18049
Aurora upgrade. Volume 5: Machine monitoring and control system
[AD-A215963] 10 p1393 N90-18053
High-Level Vision and Planning Workshop Proceedings
[AD-A215982] 10 p1420 N90-18188

KAM: Automatic planning and interpretation of numerical experiments using geometrical methods
[AD-A216805] 11 p1546 N90-18900
RALPH: An automatic Robot Assembly Language Programmer: An overview
[PB90-120973] 11 p1548 N90-18912
A high resolution automatic image measuring system
[WISS-ARB-VERMESSUNGSWESEN-154] 12 p1663 N90-19559
Development of a passive robot-controlled reaction arm 13 p1809 N90-20389
Thermal control system corrosion study
[NASA-TM-102220] 14 p1971 N90-21294
Development of cable drive systems for an automated assembly project 15 p2116 N90-22105
Paving: A new approach to automated quadrilateral mesh generation
[DE90-010244] 15 p2148 N90-22260
A CSP model for distributed control software design
[OUEL-1789/89] 15 p2148 N90-22273
The procedure safety system 15 p2155 N90-22311
Automated procedure execution for space vehicle autonomous control 15 p2156 N90-22314
Automated electric power management and control for Space Station Freedom
[NASA-TM-103151] 16 p2304 N90-23125
ISO attitude and orbit control subsystem
[REPT-892-440-104] 17 p2366 N90-23467
ESPRIT 820:QUIC. QUIC toolkit demonstrator applications
[REPT-892-440-105] 17 p2386 N90-23590
Northeast Artificial Intelligence Consortium. Volume 4. Distributed AI for communications network management
[AD-A218717] 17 p2453 N90-23994
Sensor system for automatic traffic recording in free area
[ETN-90-96493] 18 p2565 N90-24634
Third Annual Workshop on Space Operations Automation and Robotics (SOAR 1989)
[NASA-CP-3059] 19 p2727 N90-25503
Automation in the Space Station module power management and distribution Breadboard 19 p2728 N90-25509
Solar array automation limitations 19 p2729 N90-25513
The environmental control and life support system advanced automation project. Phase 1: Application evaluation 19 p2730 N90-25523
Process and information integration via hypermedia 19 p2733 N90-25534
Space environments and their effects on space automation and robotics 19 p2735 N90-25543
Automated control of hierarchical systems using value-driven methods 19 p2735 N90-25547
Computer-aided design of advanced control algorithms for industrial robotics: An overview of ESPRIT project SACODY
[REPT-81-DT-89-47] 19 p2744 N90-25596
Multi-microprocessor control of a precision pan and tilt head
[RSRE-MEMO-4252] 19 p2747 N90-25613
Use of the TACL system at CEBAF for control of the cryogenic test facility
[CEBAF-PR-89-024] 19 p2755 N90-25652
Thermionic gun control system for the CEBAF injector
[CEBAF-PR-89-028] 19 p2755 N90-25654
CEBAF control system
[CEBAF-PR-89-013] 19 p2757 N90-25666
Guidance and control system for an autonomous underwater vehicle
[AD-A222709] 20 p2873 N90-26343
Pilot interaction with automated airborne decision making systems
[NASA-CR-186730] 20 p2899 N90-26492
Verification-correction of a program for including uncertainties in the robot automatic programming
[ETN-90-97246] 20 p2915 N90-26588
The test for automatic neph-analysis chart 21 p3029 N90-27219
Fifth Conference on Artificial Intelligence for Space Applications
[NASA-CP-3073] 21 p3040 N90-27275
DEVS-based intelligent control of space adapted fluid mixing 21 p3040 N90-27279
The application of intelligent process control to space based systems 21 p3041 N90-27282
An automated tool for the design and assessment of space systems 21 p3042 N90-27289
Space station advanced automation 21 p3044 N90-27300
A development framework for artificial intelligence based distributed operations support systems 21 p3044 N90-27301
A sensor stabilization/tracking system for unmanned air vehicles
[AD-A224008] 23 p3283 N90-28579
Robotic and automatic welding development at the Marshall Space Flight Center 23 p3298 N90-28656
Experiences with the JPL telerobot testbed: Issues and insights 23 p3373 N90-29059
Automated information system life-cycle management manual
[PB90-219288] 23 p3405 N90-29244
Computer-aided engineering environment for controlled mechanical systems
[AD-A223551] 24 p3527 N90-29942

AUTOMATIC CONTROL VALVES
NT PRESSURE REGULATORS
Analysis of high speed pneumatic actuation systems under rotary directional on-off flow control 04 p0507 N90-12926

AUTOMATIC DATA PROCESSING
U DATA PROCESSING

AUTOMATIC FLIGHT CONTROL
Application of multifunction inertial reference systems to fighter aircraft 09 p1164 N90-16740
Checklist reading problems in airplanes equipped with speech recognition systems
[ILR-MITT-223(1989)] 09 p1261 N90-17314
Design of a helicopter automatic flight control system using adaptive control 14 p1928 N90-21040
First-order weight corrections for real-time flight path management
[LR-580] 15 p2050 N90-21751
Helicopter controllability
[AD-A220078] 18 p2498 N90-24275
Flight service automation system, model 1 full capacity, NAS operational test and evaluation integration test plan
[DOT/FAA/CT-TN90/4] 22 p3111 N90-27672
Flight test investigation of flight director and autopilot functions for helicopter decelerating instrument approaches
[DOT/FAA/CT-TN89/54] 22 p3121 N90-27724

AUTOMATIC FREQUENCY CONTROL
Tracking performance of a combined Costas/AFC-loop under noisy Rayleigh/Rician channel conditions with additive Gaussian noise jamming
[ETN-90-96964] 20 p2855 N90-26237

AUTOMATIC GAIN CONTROL
Studies of ECCM improvements for frequency-hopping CPFSK systems
[AD-A222995] 21 p2995 N90-27023

AUTOMATIC PATTERN RECOGNITION
U PATTERN RECOGNITION

AUTOMATIC PILOTS
How to control unstable missile airframes: Methodology and limitations 01 p0013 N90-10060
A structured singular value approach to missile autopilot analysis 2 01 p0014 N90-10068
Flexible missile autopilot design studies with PC-MATLAB/386 01 p0018 N90-10088
Nonlinear maneuver autopilot for the F-15 aircraft
[NASA-CR-179442] 02 p0262 N90-11487
Pilotless airplanes
[AD-A211719] 03 p0305 N90-11734
Independent Orbiter Assessment (IOA): FMEA/CIL assessment
[NASA-CR-185550] 03 p0314 N90-11783
An autopilot design methodology for bank-to-turn missiles
[AD-A213379] 05 p0583 N90-13399
Design of integrated pitch axis for autopilot/autothrottle and integrated lateral axis for autopilot/yaw damper for NASA TSRV airplane using integral LQG methodology
[NASA-CR-4268] 09 p1169 N90-16768
Cooperative control of two active spacecraft during proximity operations
[NASA-CR-185596] 09 p1172 N90-16778
The NASA digital VGH program: Exploration of methods and final results. Volume 2: L 1011 data 1976-1979: 1619 hours
[NASA-CR-181909-VOL-2] 13 p1756 N90-20080
Robustness evaluation of H2 and H(infinity) control theory as applied to a transport aircraft
[AD-A222795] 20 p2814 N90-26018
Flight test investigation of flight director and autopilot functions for helicopter decelerating instrument approaches
[DOT/FAA/CT-TN89/54] 22 p3121 N90-27724
Scope and conception of the pilot support system ASPIO
[LRT-WE-13-FB-88-1] 22 p3233 N90-28334

AUTOMATIC ROCKET IMPACT PREDICTORS
U COMPUTERIZED SIMULATION
U IMPACT PREDICTION

AUTOMATIC TEST EQUIPMENT
Expert system for test program set fault candidate selection
[AD-A213338] 04 p0535 N90-13091
An artificial intelligence approach to analog system diagnosis
[AD-A213135] 05 p0686 N90-13992
A computer-controlled automated test system for fatigue and fracture testing
[DE90-002931] 06 p0800 N90-14661
Use of hypermedia as a user interface for an artificial intelligence-based problem solver
[AD-A215551] 09 p1271 N90-17370
Improved solar cells testing fixtures 10 p1346 N90-17807
Smart built-in test 19 p2728 N90-25512

AUTOMATIC WEATHER STATIONS
A program to improve performance of AFGL (Air Force Geophysical Laboratory) automated present weather observing sensors
[AD-A207669] 01 p0087 N90-10495

AUTOMATION
Automation of an RCS (Radar Cross Section) measurement system and its application to investigate the electromagnetic scattering from scale model aircraft canopies
[AD-A215741] 10 p1375 N90-17970
Advancing automation and robotics technology for the Space Station Freedom and for the US economy
[NASA-TM-101691] 10 p1414 N90-18151

AUTOMOBILE ACCIDENTS
Field evaluation of a Nissan laser collision avoidance system
[PB90-105602] 06 p0722 N90-14215
Electronystagmographic findings following cervical injuries 19 p2718 N90-25466
Biofidelity of a dummy's neck during automobile collision testing 19 p2721 N90-25477

AUTOMOBILE ENGINES
Advanced Turbine Technology Applications Project (ATTAP)
[NASA-CR-185133] 01 p0008 N90-10036
Automotive Stirling engine development program
[NASA-CR-180839] 02 p0289 N90-11654

AUTOMOBILE FUELS
CRC (Coordinating Research Council) octane number requirement survey 1988
[AD-A214845] 09 p1200 N90-16954

AUTOMOBILES
NT ELECTRIC AUTOMOBILES
Advanced Turbine Technology Applications Program, (ATTAP): A plan for improving the prototype production of ceramic components for the gas turbine engine, 1988--1992
[DE89-015566] 02 p0230 N90-11320
Methodology for the calibration of and data acquisition with a six-degree-of-freedom acceleration measurement device
[PB89-233597] 06 p0779 N90-14531
Flow visualization using the laser light sheet method in vehicle aerodynamics and combustion chamber engineering 08 p1079 N90-16246
Results from the third year of operation of the Federal Methanol Fleet at Lawrence Berkeley Laboratory
[DE90-003306] 08 p1084 N90-16277
Preliminary collection 891 of lectures/papers in Symposium by Society of Automotive Engineers of Japan
[DE90-710449] 10 p1391 N90-18045
Future automotive materials: Evolution or revolution 18 p2516 N90-24370
CRC low- and intermediate-temperature driveability program using gasoline-alcohol blends
[AD-A221321] 18 p2533 N90-24453
Special test and evaluation methods used for a nine-axis accelerometer
[PB90-209578] 23 p3329 N90-28822
Automotive Stirling engine development program
[NASA-CR-180840] 23 p3408 N90-29260
Satellite navigation systems for land vehicles 24 p3430 N90-29376

AUTOMORPHISMS
The algebraic basis of mathematical morphology. Part 2: Openings and closings
[CWI-AM-R8904-PT-2] 04 p0543 N90-13150
On distance-transitive graphs and involutions
[CWI-PM-R8808] 05 p0691 N90-14037
The algebraic basis of mathematical morphology. Part 1: Dilations and erosions
[CWI-AM-R8807] 05 p0695 N90-14065

AUTONOMIC NERVOUS SYSTEM
NT SYMPATHETIC NERVOUS SYSTEM
Extrathalamic modulation of cortical function
[AD-A211044] 01 p0094 N90-10535
Neurocontrol systems and wing-fluid interactions underlying dragonfly flight 12 p1606 N90-19240
Effects of choinergic drugs on exercise performance and simple reaction time of rhesus monkeys
[AD-A219455] 17 p2433 N90-23862

AUTONOMOUS NAVIGATION
Vision-based navigation for autonomous ground vehicles
[AD-A211584] 03 p0304 N90-11725
Autonomous land navigation in a structured environment
[DE90-001625] 07 p0878 N90-15087
Research in knowledge-based vision techniques for the Autonomous Land Vehicle Program
[AD-A213440] 07 p0942 N90-15453
Planning systems for autonomous legged vehicles
[AD-A214242] 07 p0942 N90-15458
Expert system for Kalman filter supervision: Application to autonomous satellite navigation
09 p1164 N90-16739
An autonomous orbit determination system for earth satellites
[AD-A215671] 09 p1172 N90-16779
Vision-based navigation and parallel computing
[AD-A214481] 09 p1264 N90-17327
A computer simulation study of a sensor-based heuristic navigation for three-dimensional rough terrain with obstacles
[AD-A215115] 10 p1318 N90-17622
An Autonomous Platform Simulator (APS)
[AD-A215768] 10 p1392 N90-18048
Robotic mobility system: Road following algorithms
[AD-A218107] 13 p1874 N90-20748
Location recognition using stereo vision
[AD-A218218] 13 p1875 N90-20752
Autonomous integrated GPS/INS navigation experiment for OMV. Phase 1: Feasibility study
[NASA-CR-4267] 14 p1914 N90-20969
Kalman filter based range estimation for autonomous navigation using imaging sensors
15 p2142 N90-22238
ALVINN: An Autonomous Land Vehicle In a Neural Network
[AD-A218975] 16 p2243 N90-22797
Color image processing for navigation: Two road trackers
[AD-A222667] 20 p2916 N90-26591
Genetic algorithm based fuzzy control of spacecraft autonomous rendezvous 21 p3041 N90-27281
Building an environment model using depth information 23 p3374 N90-29064
HERMIES-3: A step toward autonomous mobility, manipulation, and perception 23 p3374 N90-29065
The potential for digital databases in flight planning and flight aiding for combat aircraft 24 p3429 N90-29371

AUTONOMOUS SPACECRAFT CLOCKS
Navigation experiment NAVEX: Measurements and performance of the spaceborne clocks
[DLR-FB-89-43] 18 p2555 N90-24580

AUTONOMY
Autonomous mobile robot research using the HERMIES-3 robot
[DE89-015916] 01 p0078 N90-10443
Vision-based navigation for autonomous ground vehicles
[AD-A211584] 03 p0304 N90-11725
Squirt: The prototypical mobile robot for autonomous graduate students
[AD-A212337] 04 p0510 N90-12941
Research in computer vision for autonomous systems
[AD-A212420] 04 p0555 N90-13235
Navigation of autonomous air vehicles by passive imaging sensors 08 p1026 N90-15927
Technology and evaluation of unmanned air vehicles
08 p1027 N90-15934
Autonomous automatic landing through computer vision 09 p1163 N90-16734
Intelligent landmarks recognition in satellites images
09 p1165 N90-16741
Autonomous orbit determination using GPS
[INPE-4815-TDL/361] 11 p1466 N90-18442
Publications of the NASA Controlled Ecological Life Support System (CELSS) Program, 1979-1989
[NASA-CR-4297] 15 p2051 N90-21754
Positive lubrication system 15 p2115 N90-22097
Autonomous power expert system
15 p2154 N90-22306
System control of an autonomous planetary mobile spacecraft 15 p2155 N90-22313
Automated star pattern recognition
16 p2211 N90-22612
Soil Transport Implement
[NASA-CR-184931] 17 p2385 N90-23582
Design of an autonomous teleoperated cargo transporting vehicle for lunar base operations
[NASA-CR-186686] 18 p2565 N90-24633
Autonomous power expert system
[NASA-CR-185263] 19 p2670 N90-25187
Autonomous space processor for orbital debris
[NASA-CR-186691] 20 p2820 N90-26044
Closed-loop autonomous docking system
[NASA-CASE-MFS-28421-1] 21 p2966 N90-26861
A hybrid approach to space power control
21 p3043 N90-27293
Space Station Freedom ECLSS: A step toward autonomous regenerative life support systems
21 p3043 N90-27297
SDI satellite autonomy using AI and Ada
21 p3050 N90-27336
Dynamic interaction of multiple autonomous mobile robots 23 p3333 N90-28844
Control of intelligent robots in space
23 p3365 N90-29013
Automation and robotics technology for intelligent mining systems 23 p3366 N90-29018
Real-time edge tracking using a tactile sensor
23 p3367 N90-29023
Three-dimensional motor schema based navigation
23 p3367 N90-29026
Periodic gaits for the CMU ambler
23 p3367 N90-29027
Exploiting map plans as resources for action
23 p3367 N90-29028
Building an environment model using depth information 23 p3374 N90-29064
Rice-obot 1: An intelligent autonomous mobile robot
23 p3375 N90-29068
Integrating planning, execution, and learning
23 p3377 N90-29079
Techniques for autonomous GPS integrity monitoring
24 p3424 N90-29345
Tele-autonomous systems: New methods for projecting and coordinating intelligent action at a distance
24 p3502 N90-29794
A design strategy for autonomous systems
24 p3506 N90-29818
The flight telerobotic servicer project: A technical overview 24 p3506 N90-29821
Sensor-based fine telemanipulation for space robotics
24 p3510 N90-29841
Teleoperation experiments with a Utah/MIT hand and a VPL DataGlove 24 p3517 N90-29883
Instruction dialogues: Teaching new skills to a robot
24 p3517 N90-29884
Multi-level manual and autonomous control superposition for intelligent telerobot
24 p3518 N90-29888
The JPL telerobotic Manipulator Control and Mechanization (MCM) subsystem
24 p3519 N90-29892
Computed torque control of a free-flying cooperating-arm robot 24 p3520 N90-29898
Next generation space robot
24 p3520 N90-29899

AUTOPILOTS
U AUTOMATIC PILOTS

AUTORADIOGRAPHY
Biomedical studies with the free electron laser
[AD-A208927] 01 p0091 N90-10519
Neutron autoradiography of hydrogen
[DE90-612930] 14 p1948 N90-21148

AUTOREGRESSIVE PROCESSES
Adaptive noise cancellation for a class of nonlinear 2R filter
[RR-351] 03 p0344 N90-11965
Asymptotic bias of autoregressive estimators
[IMAG-RR-745-M] 03 p0395 N90-12255
Self-tuning control of nonlinear Armax models --- Autoregressive Moving Average with eXogeneous (ARMAX) inputs
[RR-362] 04 p0508 N90-12930
Adaptive clutter rejection filters for airborne Doppler weather radar applied to the detection of low altitude windshear
[NASA-CR-186211] 06 p0766 N90-14453
Analysis of nonlinear systems using ARMA (Autoregressive Moving Average) models
[DE90-002395] 08 p1088 N90-16297
Item identities and their related observables
[AD-A219559] 17 p2468 N90-24104
Percussive sound analysis using an autoregressive model. Application of modified covariance
[TELECOM-PARIS-89-D-016] 18 p2612 N90-24879
Strong consistency of the least squares estimator for a non-ergodic threshold autoregressive model
[IMAG-RR-791-M] 20 p2918 N90-26604
Autoregressive-moving average models for texture classification
[INPE-4987-PRE/1549] 23 p3380 N90-29092
Tail and quantile estimation for strongly mixing stationary sequences
[AD-A223472] 24 p3540 N90-30019

AUXILIARY POWER SOURCES
NT NUCLEAR AUXILIARY POWER UNITS
NT SPACE POWER REACTORS
NT SPACE POWER UNIT REACTORS
Independent Orbiter Assessment (IOA): Analysis of the auxiliary power unit
[NASA-CR-185568] 02 p0165 N90-10931
Independent Orbiter Assessment (IOA): Weibull analysis report
[NASA-CR-185534] 02 p0168 N90-10948
Independent Orbiter Assessment (IOA): Assessment of the auxiliary power unit
[NASA-CR-185580] 02 p0174 N90-10976
Power generation and distribution
05 p0604 N90-13515
Advanced Turbine Technology Applications Project (ATTAP)
[NASA-CR-185240] 20 p2939 N90-26728
Thermal analyses of power subsystem components
[NASA-CR-186314] 24 p3474 N90-29637

AUXILIARY PROPULSION
Advanced APS impacts on vehicle payloads
11 p1472 N90-18472
Low power arcjet performance
[NASA-TM-103280] 23 p3298 N90-28657

AVAILABILITY
A simulation model for dynamic system availability analysis
[AD-A213499] 07 p0974 N90-15628
Complex availability problems solved with simulation
[DE89-012610] 08 p1116 N90-16459
Sensitivity of space system availability predictions to underlying component reliability estimates
[AD-A215535] 09 p1183 N90-16858
Basic research in reliability for real systems
[AD-A214536] 09 p1234 N90-17158

AVALANCHE DIODES
Thermal model for double-drift IMPATT diodes on diamond heat sinks
[AD-A211746] 03 p0415 N90-12380
Photon counting modules using RCA silicon avalanche photodiodes 09 p1222 N90-17089
Characterization and development report for the SA3124, a 15-volt zener diode
[DE90-005711] 10 p1379 N90-17993
Growth, characterization and device development in monocrystalline diamond films
[AD-A218211] 13 p1898 N90-20895
Diluted magnetic semiconductors
[AD-A220444] 17 p2476 N90-24159
Fundamental studies and device development in beta silicon carbide
[AD-A219253] 19 p2676 N90-25220
High voltage picosecond pulse generation using avalanche diodes
[DE90-015194] 24 p3465 N90-29577

AVALANCHES
NT ELECTRON AVALANCHE
Avalanche photoconductive switching
[DE90-002980] 07 p0922 N90-15337

AVERAGE
NT MEAN
Development of a mass averaging temperature probe
11 p1461 N90-18418
Computational issue in the analysis of adaptive control systems 16 p2281 N90-23001

AVHRR
U ADVANCED VERY HIGH RESOLUTION RADIOMETER

AVIATION
U AERONAUTICS

AVIATION METEOROLOGY
A scalar/vector potential solution for aerodynamic coefficients in wind shear 02 p0147 N90-10838
Description of atmospheric turbulence
07 p0869 N90-15043
Proceedings of the Professional Pilots Meteorology Training Standards Conference
[AD-A216618] 11 p1536 N90-18843

AVIATION PSYCHOLOGY
Model for measuring complex performance in an aviation environment
[DE90-002055] 07 p0967 N90-15585
Personality factors in flight operations. Volume 1: Leader characteristics and crew performance in a full-mission air transport simulation
[NASA-TM-102259] 17 p2348 N90-23370

AVIATORS
U AIRCRAFT PILOTS

AVIONICS
Kalman Filter Integration of Modern Guidance and Navigation Systems
[AGARD-LS-166] 02 p0148 N90-10847
Development of the integrated all-weather navigation system for Tornado 02 p0149 N90-10849
The development of mission-specific advanced inertially-based avionics system
02 p0149 N90-10851
Flight Test Techniques
[AGARD-CP-452] 02 p0151 N90-10860

Flight testing of the Tornado Terrain Following System
02 p0153 N90-10875
Air Combat Environment Test and Evaluation Facility (ACETEF)
02 p0154 N90-10883
Flight test instrumentation and data processing at British Aerospace, Warton, U.K.
02 p0155 N90-10887
Spacelab system analysis Marshall Avionics System Testbed (MAST)
[NASA-CR-183804] 03 p0317 N90-11802
Acquisition and recording an AMX A/C. Aeritalia experience and present trends
[ETN-89-95217] 04 p0454 N90-12598
Definition of avionics concepts for a heavy lift cargo vehicle, appendix A
[NASA-CR-183817] 05 p0580 N90-13380
A new view of weapon system reliability and maintainability
[AD-A213281] 05 p0580 N90-13382
A new view of weapon system reliability and maintainability: Executive summary
[AD-A213282] 05 p0580 N90-13383
A knowledge-based flight status monitor for real-time application in digital avionics systems
[NASA-TM-101710] 05 p0686 N90-13995
Definition of avionics concepts for a heavy lift cargo vehicle. Volume 1: Executive summary
[NASA-CR-183818] 06 p0725 N90-14229
Definition of avionics concepts for a heavy lift cargo vehicle, volume 2
[NASA-CR-183819] 06 p0725 N90-14230
Preliminary design document: Ground based testbed for avionics systems
[NASA-CR-183821] 06 p0725 N90-14231
Preliminary design of the Shuttle-C avionics recovery system
[NASA-CR-186230] 06 p0730 N90-14258
Aircraft testing in the electromagnetic environment
07 p0873 N90-15066
Advances in techniques and technologies for air vehicle navigation and guidance
[AGARD-AR-276] 08 p1020 N90-15899
Synthesis of control law, on a RPV, in order to minimize the number of sensors 08 p1025 N90-15925
Mirach 100 flight control system
08 p1025 N90-15926
The use of prototypes in selected foreign fighter aircraft development programs: Rafale, EAP, Lavi, and Gripen
[AD-A214500] 09 p1159 N90-16707
Analysis and test of a wide angle spectrometer
[AD-A215819] 10 p1388 N90-18030
Marshall Avionics Testbed System (MAST)
12 p1639 N90-19417
Potential role of avionics in escape systems
13 p1752 N90-20060
Controllable propulsion for escape systems control
13 p1753 N90-20064
Integrated circuits for avionics
[AD-A217964] 13 p1797 N90-20312
Joint University Program for Air Transportation Research, 1988-1989
[NASA-CP-3063] 14 p1905 N90-20921
Optimization of the effective GPS data rate
14 p1907 N90-20932
Advanced Launch System (ALS): Electrical actuation and power systems improve operability and cost picture
[NASA-TM-102547] 14 p1968 N90-21271
Correlation/validation of finite element code analyses for vibration assessment of avionic equipment
[AD-A220393] 17 p2353 N90-23398
Research and development: Technical and scientific publications 1989
[ISSN-0931-9751] 19 p2649 N90-25075
Space shuttle avionics system
[NASA-SP-504] 19 p2664 N90-25160
Success in tutoring electronic troubleshooting
19 p2739 N90-25568
Hardware and software reliability estimation using simulations
[NASA-CR-186637] 19 p2741 N90-25580
Space Transportation Avionics Technology Symposium. Volume 1: Executive summary
[NASA-CP-3081-VOL-1] 20 p2809 N90-25980
Biconic cargo return vehicle with an advanced recovery system. Volume 1: Conceptual design
[NASA-CR-186520] 20 p2821 N90-26052
Equipment feasibility study: Very high frequency communication equipment (136-137 megahertz)
[DOT/FAA/CT-TN89/72] 20 p2850 N90-26210
Hover position sensing system
21 p3069 N90-27448
Performance assessment of MIL-STD-1553B on the avionic systems demonstrator rig of British Aerospace
22 p3104 N90-27624
Position finding and ground target direction finding by an aircraft with a gimballed video camera
[DLR-FB-89-62] 22 p3111 N90-27673
PHARE: Concept and programme
22 p3114 N90-27690
Economical graphics display system for flight simulation avionics
[NASA-CR-186886] 22 p3116 N90-27701
Advanced transport operating system software upgrade: Flight management/flight controls software description
[NASA-CR-181936] 22 p3239 N90-28366
Validation of the F-18 high alpha research vehicle flight control and avionics systems modifications
[NASA-TM-101723] 23 p3276 N90-28542
Liquid Rocket Booster (LRB) for the Space Transportion System (STS) systems study. Appendix D: Trade study summary for the liquid rocket booster
[NASA-CR-183790-APP-D] 23 p3289 N90-28604
Studies in automatic speech recognition and its application in aerospace 23 p3318 N90-28759
The integration of multiple avionic sensors and technologies for future military helicopters
24 p3424 N90-29344
Distributed control architecture for CNI preprocessors
24 p3426 N90-29356
Integrated strapdown avionics for precision guided vehicles 24 p3427 N90-29361
Integrated navigation/flight control for future high performance aircraft 24 p3427 N90-29362
Survivable penetration 24 p3428 N90-29363
The potential for digital databases in flight planning and flight aiding for combat aircraft 24 p3429 N90-29371
High speed bus technology development
[AD-A224486] 24 p3463 N90-29565

AVOIDANCE
NT COLLISION AVOIDANCE

AWARDS
AGARD Highlights 89/2 06 p0717 N90-14184

AXAF
U X RAY ASTROPHYSICS FACILITY

AXES (COORDINATES)
U COORDINATES

AXES (REFERENCE LINES)
NT AXES OF ROTATION
NT EARTH AXIS

AXES OF ROTATION
NT EARTH AXIS
Some computational properties of rotation representations
[AD-A213888] 07 p0981 N90-15665
Motion translator
[AD-D014452] 22 p3181 N90-28053

AXIAL COMPRESSION LOADS
The initial imperfection data bank at the Delft University of Technology, part 2
[LR-559-PT-2] 05 p0656 N90-13825
Analysis and testing of axial compression in imperfect slender truss struts
[NASA-TM-4174] 08 p1087 N90-16292
Compressive strength of synthetic comet nucleus samples 12 p1741 N90-20006
Theoretical analysis and pressure distribution of thin-walled metal inverbuckle energy absorbing tubes
17 p2414 N90-23758
Recent developments in shell stability analysis
[LR-633] 24 p3483 N90-29685

AXIAL COMPRESSORS
U TURBOCOMPRESSORS

AXIAL FLOW
Laser anemometer measurements in a transonic axial-flow fan rotor
[NASA-TP-2879] 02 p0218 N90-11245
Stage effects on stalling and recovery of a high-speed 10-stage axial-flow compressor
04 p0454 N90-12600
An interactive grid generation procedure for axial and radial flow turbomachinery
[NASA-CR-185167] 05 p0682 N90-13968
Temporally and spatially resolved flow in a two-stage axial compressor. Part 2: Computational assessment
[NASA-TM-102273] 06 p0726 N90-14236
Axial flow in corners at supersonic and hypersonic speeds 10 p1308 N90-17570
Relating flow between counter-rotating propellers to aerodynamic interaction noise 14 p1909 N90-20944
The modeling of drop-containing turbulent eddies
[NASA-CR-186805] 18 p2553 N90-24570
Flow coupling between a rotor and a stator in turbomachinery
[AD-A223882] 23 p3282 N90-28572

AXIAL FLOW COMPRESSORS
U TURBOCOMPRESSORS

AXIAL FLOW PUMPS
NT TURBINE PUMPS
An investigation of end-wall vortex cavitation in a high Reynolds number axial-flow pump
[AD-A211426] 03 p0347 N90-11982

AXIAL FLOW TURBINES
Innovative turbine concepts for open-cycle OTEC (Ocean Thermal Energy Conversion)
[DE90-000315] 13 p1827 N90-20493
Calculation of the secondary flow in an axial turbine
14 p1924 N90-21022
Research on cascade secondary and tip-leakage flows: Periodicity and surface flow visualization
14 p1925 N90-21026
Computational prediction and measurement of the flow in axial turbine cascades and stages
14 p1925 N90-21028

AXIAL LOADS
NT AXIAL COMPRESSION LOADS
Design and evaluation of a new biaxial testing method for sheet material (SUPERBAT)
[LR-548] 05 p0656 N90-13824
Elastic stress concentration factors. Geometric discontinuities in rods and tubes of isotropic materials
[ESDU-89048] 09 p1239 N90-17192
Analysis of ductile fracture under biaxial loading using moire interferometry 10 p1394 N90-18060
Compressive strength of carbon/epoxy laminated under multiaxial stress
[DE90-005552] 11 p1478 N90-18505
Inelastic response of metal matrix composites under biaxial loading 16 p2220 N90-22661
The behaviour of mechanically fastened joints in composite structures 16 p2242 N90-22789
J-integral and HRR field of a stably growing crack, an experimental analysis
[AD-A220418] 17 p2416 N90-23764
The yield and post-yield behavior of high-density polyethylene
[NASA-CR-186574] 19 p2676 N90-25219
Flexion, extension and lateral bending responses of the cervical spine 19 p2719 N90-25468
Evaluation of fracture strength properties of silicon carbide ceramics under cyclic/static axial loading at ultra-high temperature
[DE90-503402] 20 p2839 N90-26147
Behavior of aramid/epoxy wounded tubes under uniaxial and biaxial loading
[ETCA-89-R-150] 23 p3339 N90-28873

AXIAL MODES
Response of differently axial-excited spinning liquid columns
[LRT-WE-9-FB-16(1989)] 21 p3006 N90-27091

AXIAL STRAIN
Elastic buckling of imperfect cylindrical shells containing granular solids
[PB90-110362] 09 p1236 N90-17174
Damage in a perforated graphite-epoxy composite plate under monotonic and cyclic biaxial loading
[ESA-TT-1117] 11 p1480 N90-18521
Finite element analysis of structural components using viscoplastic models with application to a cowl lip problem
[NASA-CR-185189] 17 p2416 N90-23769
Innovative design of composite structures: Axisymmetric deformations of unsymmetrically laminated cylinders loaded in axial compression
[NASA-CR-186635] 19 p2700 N90-25364
Microstructure: Property correlation — multiaxial fatigue damage evolution in waspaloy
[NASA-CR-180406] 23 p3340 N90-28880

AXIAL STRESS
Elastic buckling of imperfect cylindrical shells containing granular solids
[PB90-110362] 09 p1236 N90-17174
Analysis of biaxial stress fields in plates cracking at elevated temperatures
[AD-A216271] 10 p1397 N90-18077
Steady state temperatures and thermal stresses in a spherical or cylindrical laminated shell
[ESDU-89027] 12 p1674 N90-19612
Flutter of slender bodies under axial stress
[PB90-167024] 14 p1994 N90-21425
High temperature multiaxiale creep testing of Nimonic 115
[RAE-TM-P-1182] 20 p2835 N90-26122
Study of the mechanical behavior of composites under complex stress systems
[ETN-90-97455] 22 p3154 N90-27879

AXIOMS
On axiomatizations for propositional logics of programs
[RUU-CS-88-34] 17 p2449 N90-23966
Extending the lambda calculus with surjective pairing is conservative
[ITLI-ML-89-02] 18 p2603 N90-24821
The axiomatization of randomness
[ITLI-ML-89-06] 18 p2603 N90-24824

AXISYMMETRIC BODIES
Laminar boundary layer along inviscid surface streamlines over inclined axisymmetric bodies in incompressible flow
[AD-A210202] 01 p0070 N90-10401
Tire modeling by finite elements
06 p0792 N90-14614
Formation of a pair of turbulent layers in the region of a flow around an axisymmetric body with an incidence angle
[ISL-R-130/87] 09 p1219 N90-17070
POS2D: A graphic program for analysing axisymmetric and two-dimensional structures
[DE90-608884] 10 p1417 N90-18168
Numerical study of laminar and turbulent flows past two-dimensional and axisymmetric bodies
15 p2100 N90-22020
Dimensional analysis of structures using wrapping techniques
[REPT-892-430-119] 16 p2247 N90-22815
The finite analytic method and its applications. Volume 1: Laminar and turbulent flows past two-dimensional and axisymmetric bodies
[AD-A222787] 20 p2864 N90-26294
Annular slot antenna radiating into lossy material
[NPL-DITC-152/89] 22 p3165 N90-27945
Sting-support interference on afterbody drag at transonic speeds
[NAL-TM-EA-8902] 23 p3267 N90-28492
Prediction of subsonic vortex shedding from forebodies with chines
[NASA-CR-4323] 23 p3268 N90-28494
AXISYMMETRIC DEFORMATION
U AXIAL STRAIN
AXISYMMETRIC FLOW
NT ANNULAR FLOW
NT KARMAN-BODEWADT FLOW
Chemical reactions in turbulent mixing flows
[AD-A211240] 02 p0220 N90-11263
Three component laser Doppler measurements in an axisymmetric jet
[NASA-CR-181908] 03 p0300 N90-11702
Coherent structures in a round jet
05 p0640 N90-13733
Applications of a new exact solution of the Navier-Stokes equations to flow in pipes of varying width
06 p0774 N90-14504
Heat transfer in convective boundary layer and channel flows 06 p0774 N90-14505
A numerical model for the axisymmetric equilibrium shape of drops in uniform motion: Effects of external flow, electric field and surface charge
07 p0874 N90-15071
Viscous effects on the instability of an axisymmetric jet
[NASA-TM-102396] 09 p1161 N90-16719
Separation bubbles at high Reynolds number: Measurement and computation
[CUED/A-AERO/15] 12 p1657 N90-19525
Fluid dynamics analysis of a rotating axisymmetric part using FIDAP
[DE90-008733] 13 p1802 N90-20340
The radiation of sound from a propeller at angle of attack
[NASA-CR-4264] 14 p2023 N90-21602
Theory and numerical analysis of single and multi-element nozzle propellers
[LR-579] 15 p2048 N90-21741
Numerical study of the onset of instability in the flow past a sphere 17 p2400 N90-23672
Symmetry in the dynamics of a polarized fluid
[ETN-90-96896] 18 p2552 N90-24567
Prediction of two-dimensional time-dependent gasdynamic flows for hypersonic studies
[UTIAS-335] 20 p2801 N90-25935
FINFLO: A finite-volume based computer program for two-dimensional and axisymmetric compressible flow
[PB90-189473] 22 p3169 N90-27974
Design of an axisymmetric, contoured nozzle for the HEG
[DLR-FB-90-04] 23 p3327 N90-28812
Structure in the near field of the transverse jet
[AD-A224502] 24 p3467 N90-29591
AXISYMMETRY
U SYMMETRY
AXLES
U SHAFTS (MACHINE ELEMENTS)
AZIDES (INORGANIC)
Informal conference on the Chemistry of Energetic Azides, Isocyanates, and Related Species
[AD-A219825] 17 p2373 N90-23514
AZIDES (ORGANIC)
Informal conference on the Chemistry of Energetic Azides, Isocyanates, and Related Species
[AD-A219825] 17 p2373 N90-23514
AZIMUTH
ILS/MLS comparison tests at Miami/Tamiami, Florida Airport
[ACD-330] 01 p0005 N90-10018
Observations of azimuthal asymmetry for certain FRC operating regimes
[DE89-015300] 01 p0126 N90-10721
Passive trajectography by azimuth: Improvement of estimation quality 02 p0150 N90-10854
AZO COMPOUNDS
NT HMX
NT RDX
AZOLES
NT PYRROLES
NT TRYPTOPHAN
Second-generation ordered polymers
[AD-A216126] 12 p1630 N90-19365
Polyimidazoles via aromatic nucleophilic displacement
[NASA-CASE-LAR-14145-1] 21 p2983 N90-26954
AZULENE
Impedance analysis of ionic transport in polypyrrole-polyazulene copolymer and its charge-discharge characteristics
[AD-A210979] 01 p0052 N90-10299
Rechargeable lithium/polymer cathode batteries
[AD-A210978] 01 p0062 N90-10354

B

B STARS
A theoretical study of circumstellar dust around Ae/Be stars 14 p2040 N90-21700
Evolutionary effects in B stars
14 p2041 N90-21704
A high galactic latitude survey of far ultraviolet excess objects 15 p2183 N90-22473
Interactions of massive stars with the interstellar medium: Bow shocks and superbubbles
15 p2186 N90-22485
The Sagittarius B2 molecular cloud: An extreme case of a galactic center giant molecular cloud
15 p2187 N90-22493
Ultraviolet and infrared studies of Be stars
16 p2329 N90-23275
Kappa effect pulsational instability for hot extreme helium stars
[DE90-014920] 23 p3411 N90-29277
Pulsations of B star models by an opacity mechanism
[DE90-014923] 23 p3412 N90-29279
B-1 AIRCRAFT
Wind tunnel study of wake downwash behind A 6 percent scale model B1-B aircraft
[DE90-011783] 20 p2802 N90-25941
B-1B improved windshield development. Volume 2: Magna analysis: Baseline and parametric
[AD-A221501] 21 p2960 N90-26828
B-52 AIRCRAFT
Application of fracture mechanics and half-cycle method to the prediction of fatigue life of B-52 aircraft pylon components
[NASA-TM-88277] 05 p0655 N90-13820
B-58 AIRCRAFT
Sonic boom signature data from cruciform microphone array experiments during the 1966-1967 EAFB national sonic boom evaluation program
[NASA-CR-182027] 14 p2024 N90-21605
B-70 AIRCRAFT
Sonic boom signature data from cruciform microphone array experiments during the 1966-1967 EAFB national sonic boom evaluation program
[NASA-CR-182027] 14 p2024 N90-21605
BACKGROUND NOISE
Binaural masking: An analysis of models
[AD-A211578] 03 p0381 N90-12168
The effects of noise on speech and warning signals
[AD-A212520] 04 p0551 N90-13210
Radio noise measurements in the long-wave band at Thule, Greenland
[NASA-CR-182824] 09 p1206 N90-16991
Recognition of environmental sounds
[AD-A214942] 09 p1259 N90-17302
An ultra-small capacitance Josephson junction
[DE90-613396] 14 p2032 N90-21653
Excess noise, anomalous effects and reliability of high frequency devices (Schottky diodes, MESFET and HEMT)
[LAAS-89-394] 16 p2231 N90-22728
A preliminary analysis of threshold signal detection in ambient and signal-dependent noise environments
[AD-A222089] 21 p2996 N90-27030
Methods for detecting low-frequency signals in the presence of strong winds
[AD-A223980] 23 p3320 N90-28769
BACKGROUND RADIATION
Thermal radiation from terrain: Measurements and first results
[FOA-C-30525-3.1] 02 p0236 N90-11342
Gamma radiation background measurements from Spacelab 2
[NASA-CR-183782] 02 p0297 N90-11689
Spatial characteristics of airglow and solar scatter radiance from the earth's atmosphere
[AD-A211358] 03 p0372 N90-12126
Design and tests of simple, inexpensive optical beacon for use on small satellites
[AD-A213325] 04 p0555 N90-13238
A four channel He-3 cooled balloon-borne bolometer radiometer 05 p0597 N90-13489
Diffraction, chopping, and background subtraction for LDR 05 p0598 N90-13476
The grand unified photon spectrum: A coherent view of the diffuse extragalactic background radiation
[NASA-CR-186077] 05 p0715 N90-14180
The thermal behavior of natural backgrounds and its prediction by means of numerical models
06 p0762 N90-14436
The disk-halo connection and the nature of the interstellar medium
[NASA-CR-186266] 07 p1012 N90-15860
Gravitational lens effect on the cosmic background radiation due to nonlinear inhomogeneities
[DE90-701753] 07 p1013 N90-15868
Natural and man-made emissions at 1.0 to 5.6 MHz measured between 10 and 18 R sub E
[MPE-PREPRINT-146] 08 p1058 N90-16116
The excess flux in the cosmic submillimeter background radiation and the primordial deuterium abundance
[NASA-CR-186312] 08 p1154 N90-16683
Detecting extended solar system structures with COBE (Cosmic Background Explorer)
[AD-A216380] 10 p1447 N90-18349
Sources of gravitational waves
12 p1730 N90-19942
The pregalactic cosmic gravitational wave background
12 p1730 N90-19945
The space microwave interferometer and the search for cosmic background gravitational wave radiation
12 p1731 N90-19952
The COBE cosmic 3 K anisotropy experiment: A gravity wave and cosmic string probe 12 p1732 N90-19959
Examination of the background by High Energy X ray Experiment (HEXE) on the space station MIR
[ETN-90-95735] 12 p1746 N90-20041
COS-B gamma ray sources beyond the predicted diffuse emission 16 p2335 N90-23308
COMPTEL observations of active galactic nuclei
16 p2337 N90-23319
Dipole analysis on EGRET data of extragalactic gamma ray background radiation 16 p2337 N90-23322
Spectral measurements of the cosmic microwave background 16 p2340 N90-23334
Cosmic Background Explorer (COBE) press kit
[PB9-10172] 17 p2364 N90-23459
Large scale structure and microwave background anisotropies in cosmological models and stellar photometry techniques with the wide field/planetary camera of the Hubble space telescope
18 p2637 N90-25023
Low-frequency measurements of the CMB (Cosmic Microwave Background) spectrum
[DE90-011589] 18 p2639 N90-25033
The 23rd ESLAB Symposium on Two Topics in X Ray Astronomy. Volume 2: AGN and the X Ray Background
[ESA-SP-296-VOL-2] 19 p2784 N90-25841
Theories of the X ray background
19 p2784 N90-25842
Spatial fluctuations in the diffuse X ray background
19 p2785 N90-25845
Einstein IPC observations of the 1 to 3 keV X ray background 19 p2785 N90-25846
Contributions of discrete sources to the X ray background 19 p2785 N90-25847
Active star-forming galaxies in the X ray foreground
19 p2785 N90-25848
Is AGN spectral evolution needed for the CXB
19 p2786 N90-25856
AGNs and the spectrum of the X ray background
19 p2787 N90-25858
The Einstein All-Sky IPC slew survey
19 p2787 N90-25865
Properties of sources that may contribute the other half of the cosmic X ray background
19 p2788 N90-25866
Signposts to the future 19 p2788 N90-25867
QSO optical counts and constraints on the X ray background 19 p2789 N90-25877
Pure luminosity evolution and the AGN contribution to the X ray background 19 p2790 N90-25883

Constraints on the high energy properties of active galactic nuclei 19 p2792 N90-25894
Spatial and spectral features of soft diffuse X ray background seen by the Einstein observatory 19 p2792 N90-25895
Effect of X ray spectra of Seyfert galaxies on the cosmic X ray background 19 p2792 N90-25896
Comparing measurements of AGN X ray spectra with the shape of the diffuse X ray background spectrum 19 p2793 N90-25902
Proceedings of workshop on Dark Matter and the Structure of the Universe [DE90-791308] 21 p3098 N90-27602
Fluctuations in cosmic background radiation [INPE-4579-PRE/1313] 23 p3415 N90-29294
Microwave background distortions from domain walls [NASA-CR-187272] 24 p3462 N90-29556
Characteristic microwave background distortions from collapsing domain wall bubbles [NASA-CR-187270] 24 p3462 N90-29557

BACKINGS
U BACKUPS

BACKSCATTERING
Global ionospheric dynamics 02 p0240 N90-11366
An ionospheric model for HF sky-wave backscatter radar 02 p0247 N90-11401
Aerosol backscatter studies supporting LAWS 03 p0363 N90-12079
Global backscatter assessment 03 p0364 N90-12080
Measurements of aerosol properties needed to infer backscatter characteristics in support of the NASA Doppler Lidar program 03 p0364 N90-12082
Infrared backscattering 03 p0364 N90-12083
Doppler statistics of ocean velocity variability [AD-A211687] 03 p0377 N90-12148
Ion beam analysis of diffusion in polymer glasses [AD-A212339] 04 p0480 N90-12756
Investigation of the properties of radar backscatter from sea ice [AD-A212808] 04 p0493 N90-12838
Improvement and extension of a radar forest backscattering model [NASA-CR-186083] 04 p0515 N90-12973
Workshop on Recent Progress in Surface and Volume Scattering [AD-A212455] 04 p0555 N90-13236
Analysis of high temperature superconductors by means of PIXE and RBS methods [DE89-630241] 04 p0558 N90-13252
Preliminary results of the rocket and scatter experiments ROSE: Measurements with the newly designed spherical probe 05 p0659 N90-13850
New perspectives for the inversion of backscatter ionograms 06 p0761 N90-14427
The use of backscatter for modelling ionosphere and jamming in very short term forecasts 06 p0762 N90-14434
Simulated Brillouin backscattering in optical fibers: A ring resonator 06 p0783 N90-14556
N-port theory applied to backscatter polarimetry and depolarization in foliage penetration [AD-A213437] 07 p0917 N90-15305
Flashlight radar: A three-dimensional imaging radar [AD-A213439] 07 p0918 N90-15307
Backscattering effects in DIAL due to water vapor [SER-WISS-ABHANDL-89] 08 p1082 N90-16265
Investigation of the backscatter behavior of selected test areas in two geocoded SEASAT-SAR scenes in greater Bonn (Fed. Republic of Germany) 08 p1094 N90-16331
Lidar technique for adjusting aerosol model number densities to existing conditions [AD-A213846] 08 p1101 N90-16374
First results from HF (High-Frequency) oblique backscatter soundings to the northwest of College, Alaska using a modified ULCAR digisonde D-256 [AD-A214931] 09 p1206 N90-16987
Active and passive remote sensing of ice [AD-A214863] 09 p1241 N90-17199
Nimbus 7 solar backscatter ultraviolet (SBUV) ozone products user's guide [NASA-RP-1234] 09 p1246 N90-17227
Polarization radar processing technology [AD-A215242] 10 p1374 N90-17967
Millimeter wave radar clutter program [AD-A215772] 10 p1376 N90-17978
CW (Continuous Wave) stimulated Brillouin scattering of long-pulse chemical laser beams [AD-A216409] 10 p1390 N90-18039
UV spectral simulations using LOWTRAN 7 15 p2083 N90-21928
Lidar measurements of the optical propagation environment 15 p2084 N90-21930
Cirrus cloud optical properties measured with the University of Wisconsin high spectral resolution and volume imaging lidars 15 p2084 N90-21932
Millimeter-wave bistatic scattering by terrain 15 p2085 N90-21936
Millimeter - wave radar scattering from terrain: Data handbook [AD-A220770] 17 p2391 N90-23617
A laboratory investigation into microwave backscattering from sea ice [NASA-CR-186621] 18 p2542 N90-24510
Radar clutter via waveguide methods [AD-A220237] 18 p2542 N90-24512
A laboratory investigation into microwave backscattering from sea ice [NASA-CR-186357] 19 p2705 N90-25390
Bermuda ionosonde tests in support of OTH-B [NASA-TM-89359] 19 p2713 N90-25442
LEP and CEBAF polarimeters [CEBAF-PR-89-010] 19 p2757 N90-25667
The 27-28 October 1986 FIRE IFO cirrus case study: Cirrus parameter relationships derived from satellite and lidar data [NASA-TM-103469] 20 p2890 N90-26447
Development of eye-safe lidar for aerosol measurements [NASA-CR-186905] 20 p2901 N90-26503
Backscatter enhancement in scattering from rough surfaces [AD-A223110] 21 p2995 N90-27024
Dependence of radar backscatter on the energetics of the air-sea interface [AD-A221966] 21 p2996 N90-27028
Aureole lidar: Ground based measurement [AD-A223207] 21 p3008 N90-27101
Lidar instruments proposed for Eos 21 p3016 N90-27145
Remote sensing of the ocean surface with C- and Ku-band airborne scatterometers 22 p3195 N90-28129
Radar clutter via ray methods [AD-A223796] 24 p3462 N90-29553

BACKUPS
Independent Orbiter Assessment (IOA): Assessment of the backup flight system FMEA/CIL [NASA-CR-185566] 02 p0173 N90-10973
The real-time roll-back and recovery of transactions in database systems [AD-A214471] 09 p1295 N90-17506
Impact tolerant material [NASA-CASE-LAR-12887-3] 15 p2064 N90-21822

BACKWARD DIFFERENCING
Generalized BDF (Backward Differentiation Formula) methods applied to Hessenberg form DAEs [DE89-017328] 02 p0267 N90-11522
Backward analysis on higher order functions [MEMO-INF-89-19] 02 p0268 N90-11526
Using Broyden updates to approximate the Jacobian in a semi-implicit backward differentiation code [AD-A213239] 05 p0688 N90-14010

BACKWARD FACING STEPS
An algebraic turbulence model for flow separation caused by forward and backward facing steps [AD-A213800] 07 p0931 N90-15389
Theoretical investigation of the stabilization of a diffusion flame above a recirculation region [ESA-TT-1149] 11 p1484 N90-18543
Separation bubbles at high Reynolds number: Measurement and computation [CUED/A-AERO/15] 12 p1657 N90-19525

BACKWARD WAVE TUBES
Experimental demonstration of an electromagnetically pumped free-electron laser with cyclotron harmonic idlers [AD-A218830] 17 p2408 N90-23719

BACKWARD WAVES
Low noise, high voltage supply for carcinotron backward wave oscillators 10 p1338 N90-17742

BACTERIA
NT ARCHAEBACTERIA
NT ESCHERICHIA
NT PSEUDOMONAS
NT SALMONELLA
Genetic engineering of single-domain magnetic particles [AD-A210332] 01 p0091 N90-10521
A structural basis for electron transfer in bacterial photosynthesis [DE89-015702] 01 p0120 N90-10687
Genetic engineering of enhanced microbial nitrification [PB89-208334] 03 p0378 N90-12155
Comparison of structural subunits of the core light-harvesting complexes of photosynthetic bacteria [DE90-001412] 06 p0819 N90-14765
Breeding of hydrogen producing anaerobic bacteria. Cellulase secretion from transformed Escherichia coli JM109 [DE90-710739] 10 p1410 N90-18133
Anaerobic metabolism of aromatic compounds by phototrophic bacteria: Biochemical aspects [DE90-009503] 14 p2009 N90-21516

BACTERIOLOGY
Effect of community structure on the kinetics of anaerobic degradation of aromatic compounds [DE90-003666] 07 p0888 N90-15134

BAFFLES
The baffles 05 p0604 N90-13509
Design of DIII-D advanced divertor [DE90-003343] 07 p0995 N90-15752
Diffraction about acoustically soft panels [AD-A220850] 17 p2469 N90-24115
Interaction of acoustic waves generated by coupled plate [NASA-CR-186873] 21 p3072 N90-27464
A study of mixed convection in large baffled rectangular chambers with and without internal heat sources [AD-A223158] 22 p3169 N90-27977

BAGGAGE
Fire hazards of aerosol cans in aircraft cargo compartments [DOT/FAA/CT-89/32] 17 p2347 N90-23369

BAGS
NT AIR BAG RESTRAINT DEVICES
Research and development on enhanced degradable plastics [AD-A217180] 13 p1779 N90-20212
Lunar regolith bagging system [NASA-CR-186683] 19 p2677 N90-25223
Lunar regolith bagging system [NASA-CR-186652] 19 p2677 N90-25224

BAINITE
Microstructural development in HSLA-100 steel weld metals [AD-A222105] 21 p2982 N90-26944

BAINITIC STEEL
Improvement in pre-constraint fatigue resistance of modular ferretic and bainitic steel by shot peening treatments [CETIM-106370] 04 p0476 N90-12727
Deformation and fracture of low alloy steels at high temperature [DE90-001274] 07 p0902 N90-15215

BAKEOUT
U DEGASSING

BALANCE
Effect of control surface mass unbalance on the stability of a closed-loop active control system [NASA-TP-2952] 03 p0357 N90-12042
Choice of a differential method for the attitude restitution in dynamic unbalance [CNES-CT/DTI/MS/CM/290] 05 p0613 N90-13582
Balance laws and centro velocity in dissipative systems [MEMO-797] 05 p0639 N90-13726
The relationship between subjective and objective measures of simulator-induced ataxia [AD-A213095] 05 p0673 N90-13922
Cryogenic temperature effects on sting-balance deflections in the National Transonic Facility [NASA-TM-4157] 06 p0727 N90-14244
A procedure for force-balancing planar linkages using counterweights [ESDU-89028] 07 p0940 N90-15446
Improved energy and power balance at Nova targets [DE90-007260] 13 p1807 N90-20372

BALANCING
MM and T advanced balancing/machining [AD-A213103] 05 p0648 N90-13775
A comparison of techniques for balancing planar linkages [ESDU-89043] 09 p1232 N90-17150
An applicational process for dynamic balancing of turbomachinery shafting [NASA-TM-102537] 13 p1810 N90-20392
Aerodynamic control design: Experience and results at Aermacchi 23 p3272 N90-28518

BALL BEARINGS
Fully articulated four-point-bend loading fixture [NASA-CASE-LEW-14776-1] 07 p0940 N90-15445
Traction modeling of military lubricants [AD-A213866] 09 p1230 N90-17139
A parametric heat transfer study for cryogenic ball bearings in SSME HPOTP 12 p1635 N90-19397
Positive lubrication system 15 p2115 N90-22097
Test results and flight experience of ball bearing momentum and reaction wheels 15 p2115 N90-22099
AX-5 space suit bearing torque investigation 15 p2115 N90-22101

Fourth European Space Mechanisms and Tribology Symposium
[ESA-SP-299] 18 p2535 N90-24462
Tribological properties of PVD-applied MoS2 coatings used on space mechanisms 18 p2537 N90-24470
Study of ball bearings for space use 18 p2537 N90-24477
Mechanisms add foldability to ROSAT solar panels 18 p2538 N90-24483
Some remarks on a hinge actuator for large spot antenna arm deployers 18 p2539 N90-24486
The performance of PTFE, lead, and MoS2 as lubricant films for ball bearings operating in vacuum at 20 K 18 p2540 N90-24495
Evolution and use of combined mechanical and thermal codes for cryogenic turbopump bearings 23 p3291 N90-28618
Determination of the SSME high pressure oxidizer turbopump bearing temperature 23 p3291 N90-28619
Cryogenic, high speed, turbopump bearing cooling requirements 23 p3291 N90-28620
Pool boiling from rotating and stationary spheres in liquid nitrogen 23 p3292 N90-28621
Bearing optimization for SSME HPOTP application 23 p3292 N90-28622
Development of improved self lubricating cages for SSME HPOTP bearings 23 p3292 N90-28623
Cage stability analysis for SSME HPOTP bearings 23 p3292 N90-28625
Rocketdyne LOX bearing tester program 23 p3293 N90-28626
Lubrication characteristics of rolling bearings lubricated by self-lubricating composite retainers. Part 1: Selection of bearings for Earth sensors
[NAL-TR-1019] 24 p3477 N90-29651

BALLAST
Ballast system for maintaining constant pressure in a glove box
[NASA-CASE-NPO-17786-1-CU] 09 p1224 N90-17104

BALLAST (MASS)
Schleicher ASK-21 glider (TG-9) stall and spin
[AD-A213513] 07 p0879 N90-15096

BALLISTIC MISSILE DECOYS
Comparison of laser and neutral particle beam discrimination
[DE89-017786] 03 p0353 N90-12018

BALLISTIC MISSILES
NT INTERCONTINENTAL BALLISTIC MISSILES
Brazil, the United States, and the missile technology control regime
[AD-A220551] 17 p2362 N90-23449
Extrapolation of missile flight lines
[ETN-90-96494] 18 p2508 N90-24336
Brilliant pebbles
[DE90-010756] 18 p2606 N90-24845

BALLISTIC RANGES
Spark camera annotation and control system for the BRL (Ballistic Research Laboratory) Transonic Range Facility
[AD-A212266] 04 p0459 N90-12633

BALLISTIC TRAJECTORIES
The vibro-acoustic mapping of low gravity trajectories on a Learjet aircraft
[NASA-TM-103103] 15 p2045 N90-21723

BALLISTICS
NT HYDROBALLISTICS
NT INTERIOR BALLISTICS
NT TERMINAL BALLISTICS
Aircraft live fire testing 02 p0154 N90-10879
RSRM-3 (360L003) ballistics/mass properties report
[NASA-CR-183716] 04 p0463 N90-12651
Ballistics/mass properties
[NASA-CR-183723] 04 p0463 N90-12652
Ballistic properties of composite materials for personnel protection
[MRL-TR-89-6] 04 p0465 N90-12661
Evaluation of selected computer models for modeling pyrotechnic and propellant devices
[AD-A213003] 05 p0629 N90-13671
Enhanced tracking of ballistic targets using forward looking infrared measurements with active target illumination
[AD-A215422] 09 p1282 N90-17434
External flow computations for a finned 60mm ramjet in steady supersonic flight
[AD-A216998] 12 p1605 N90-19233
Computational fluid dynamics method for low Reynolds number flow in a precessing/spinning, liquid filled cylinder with rounded endcaps
[AD-A216997] 12 p1659 N90-19531
Ductile alloy encapsulated ceramic armor development
[AD-A217632] 14 p1954 N90-21183
RSRM-9 (360L009): Ballistics mass properties
[NASA-CR-183944] 20 p2823 N90-26064
Flight motor set 360L007 (STS-33R)
[NASA-CR-183979] 20 p2824 N90-26067
Video camera system for locating bullet holes in targets at a ballistics tunnel
[NASA-TM-4197] 20 p2865 N90-26296
Phase-sensitive optical detection of ballistic phonon pulses using frequency-modulation spectroscopy and persistent spectral holes
[AD-A221521] 21 p2979 N90-26930
Advanced ceramic armor materials
[AD-A223227] 21 p2986 N90-26970
A planar rocket motor model for visualization of violent reaction due to fragment impact
[AD-A224273] 24 p3441 N90-29431
Evaluation of ARALL-4: An aramid fiber reinforced aluminum
[AD-A223502] 24 p3443 N90-29443

BALLOON FLIGHT
European Rocket and Balloon Programs and Related Research
[ESA-SP-291] 05 p0656 N90-13826
Swiss scientific balloon and sounding rocket experiments 1987-1989 05 p0656 N90-13827
The French balloon program and related space research 05 p0656 N90-13828
The Norwegian balloon and sounding rocket program 1989-1992 05 p0656 N90-13829
The Swedish sounding rocket and balloon program 05 p0657 N90-13830
The German scientific balloon and sounding rocket program 05 p0657 N90-13831
Evidence for accurate temperatures from the inflatable falling sphere 05 p0657 N90-13835
JACEE long duration balloon flights
[DE90-006008] 12 p1746 N90-20039
Hard X ray observations of galactic sources 19 p2771 N90-25752

BALLOON SOUNDING
New calculations of photodissociation cross-sections in the O2 Schumann-Runge system 05 p0657 N90-13834
Investigations into the properties, conditions, and effects of the ionosphere
[AD-A217807] 14 p2005 N90-21489
Measurements of the high altitude infrared characteristics of the atmosphere
[AD-A224401] 24 p3491 N90-29728

BALLOON-BORNE INSTRUMENTS
Design of scientific payloads and components
[AD-A211819] 03 p0351 N90-12005
Solar flare gamma-ray and hard x ray imaging with the GRID-on-a-balloon 03 p0432 N90-12474
A four channel He-3 cooled balloon-borne bolometer radiometer 05 p0597 N90-13469
Three-meter balloon-borne telescope 05 p0601 N90-13490
Deep detection of hot star populations at balloon ultraviolet wavelengths 05 p0661 N90-13865
Kestrel 3 Program
[DE90-001796] 06 p0721 N90-14209
A large detector for cosmic ray abundance and energy measurements 06 p0867 N90-15037
LEAP: A balloon-borne search for low-energy cosmic ray antiprotons 07 p1015 N90-15878
Wide-beam balloon observations of the 157.7 microns (CII) line 11 p1581 N90-19108
GPS-aided gravimetry at 30 km altitude from a balloon-borne platform 13 p1834 N90-20530
A general-purpose balloon-borne pointing system for solar scientific instruments
[NASA-TP-3013] 14 p1959 N90-21219
Modelling and control of a balloon borne stabilized platform 17 p2355 N90-23408
Rotating-unbalanced-mass devices and methods for scanning balloon-borne-experiments, free-flying spacecraft, and space shuttle/space station attached experiments
[NASA-CASE-MFS-28425-1] 20 p2866 N90-26304
Supersaturation, droplet spectra, and turbulent mixing in clouds 22 p3217 N90-28249
High altitude balloon flight test of the GRAD experiment
[AD-A224398] 24 p3432 N90-29388

BALLOONING MODES
Theory of high-n toroidicity-induced shear Alfven eigenmode in tokamaks
[DE89-016726] 02 p0277 N90-11582
Destabilization of tokamak pressure-gradient driven instabilities by energetic alpha populations
[DE90-003716] 07 p0996 N90-15756
Results of the H-mode experiments with JT-60 outer and lower divertors
[DE90-733146] 10 p1432 N90-18265
Resonant MHD modes with toroidal coupling
[DE90-015185] 23 p3397 N90-29196

BALLOONS
NT HIGH ALTITUDE BALLOONS
NT TETHERED BALLOONS
Operational activity in France and a new method of balloon temperature piloting 05 p0660 N90-13857
Large heavy duty balloons in Europe 05 p0661 N90-13858
The DYANA campaign 1990 05 p0662 N90-13870
Long duration balloon flights in the middle stratosphere 05 p0663 N90-13874

BALMER SERIES
Flare model sensitivity of the Balmer spectrum 03 p0432 N90-12477
Detection of emission lines from the secondary star in IX Vel (=CPD-48 deg 1577)
[MPE-PREPRINT-172] 22 p3265 N90-28485
Formation of hydrogen line and continuum emission in young stellar objects 24 p3562 N90-30150

BALTIC SEA
Transformation and deposition of airborne gaseous and particulate pollutants during transport over the Baltic Sea
[PUBL-AIR-QUALITY-5] 14 p2003 N90-21478
Wave propagation over sea: Tropospheric effects on communication, radar, and ESM systems; proposal for a measuring programme
[FOA-C-30544-8.3] 18 p2543 N90-24517
Deposition to the Baltic Sea 20 p2884 N90-26404
Phytoplankton and its contribution to the atmospheric sulfur budget of northern Europe 20 p2885 N90-26417

BANACH SPACE
NT HILBERT SPACE
NT SOBOLEV SPACE
Hahn-Banach type theorems for dual semigroups
[CWI-AM-R8903] 04 p0543 N90-13149
Uniform stability for time-varying infinite-dimensional discrete linear systems
[DE89-635712] 08 p1116 N90-16460
Existence, uniqueness, and approximation of a solution for a K-positive definite operator equation
[DE90-600728] 09 p1272 N90-17373
Iterative methods for nonlinear set-valued operators of the monotone type with applications to operator equations
[DE90-606950] 10 p1422 N90-18202
Banach C*-algebras not containing a subspace isomorphic to C(sub 0)
[DE90-610428] 12 p1706 N90-19798
Projection-iteration methods for solving nonlinear operator equations
[DE90-610433] 12 p1707 N90-19801
Classical mechanics on superspace
[DE90-608907] 12 p1724 N90-19906
Periodic solutions for Hamiltonian systems in a nonconvex potential well
[DE90-612752] 14 p2020 N90-21580
Reflexivity, the dual Radon-Nykodym property, and continuity of adjoint semigroups
[CWI-AM-R8908] 17 p2460 N90-24042
Applications of cone theory to boundary value problems
[AD-A220939] 18 p2603 N90-24828
Geometric theory for infinite dimensional systems
[ETN-90-96922] 23 p3389 N90-29144
For the definition of two person zero sum games
[ETN-90-97294] 24 p3541 N90-30022

BAND STRUCTURE OF SOLIDS
A fermi liquid electric structure and the nature of the carriers in high-T(sub c) cuprates: A photoemission study
[DE89-016774] 02 p0284 N90-11624
Normal state electronic structure and the superconducting energy gap in HTSC's as determined from photoemission spectroscopy
[DE90-004857] 09 p1292 N90-17489
Full vector wave calculation of photonic band structures in face-centered cubic dielectric media
[AD-A222616] 20 p2933 N90-26686

BANDGAP
U ENERGY GAPS (SOLID STATE)

BANDPASS FILTERS
NT TRACKING FILTERS
High resolution, wide band Chirp-Z signal analyzer
[AD-D014240] 06 p0768 N90-14465
Narrow band and wide angle hemispherical interference optical filter
[AD-D014238] 06 p0843 N90-14904
Transmission and reflection studies of thin films in the vacuum ultraviolet 12 p1638 N90-19412
The effects of sinusoidal interference on the second-order carrier tracking loop preceded by a bandpass limiter in the Block 4 receiver 12 p1644 N90-19449

Coplanar waveguide discontinuities for P-I-N diode switches and filter applications
[NASA-TM-102534] 14 p1969 N90-21278
Classification regions in remote sensing imagery utilizing spatial characteristics
[INPE-4913-PRE/1514] 20 p2879 N90-26381
Utilizations of an acoustic surface wave-convolver for signal processing in the measurement and information techniques
[ETN-90-97319] 22 p3165 N90-27947
Improved front-end analysis in the ARM system: Linear transformations of SRUbank
[RSRE-MEMO-4358] 22 p3166 N90-27953
Non-contacting printed circuit waveguide elements
[AD-D014489] 22 p3166 N90-27957

BANDSTOP FILTERS
Coplanar waveguide discontinuities for P-I-N diode switches and filter applications
[NASA-TM-102534] 14 p1969 N90-21278
Improved front-end analysis in the ARM system: Linear transformations of SRUbank
[RSRE-MEMO-4358] 22 p3166 N90-27953

BANDWIDTH
NT BROADBAND
NT NARROWBAND
NT SPECTRAL LINE WIDTH
Multi-level bandwidth efficient block modulation codes
[NASA-CR-185484] 01 p0056 N90-10317
Likelihood cross-validation bandwidth selection for nonparametric kernel density estimators
[REPT-89-10] 03 p0398 N90-12279
Ultra high performance, highly reliable, numeric intensive processors and systems
[AD-A214100] 07 p0980 N90-15659
Research in optical interconnection techniques
[AD-A214028] 07 p0993 N90-15739
Effect of contralateral masking parameters on difference limen for intensity
[AD-A214169] 10 p1411 N90-18135
A unified model for the 3.28 micron and 3.4 micron spectral feature in the interstellar medium and in comets
11 p1579 N90-19092
A coal model for the carriers of the unidentified IR bands
11 p1581 N90-19110
The influence of gamma-radiation on the bandwidth of optical fibres and the reduction of the induced attenuation by bleaching and hardening the fibre
[FEL-1988-62] 12 p1714 N90-19846
Broadening the interface bandwidth in simulation based training
13 p1859 N90-20666
HDTV bandwidth reduction using motion compensation and DATV
[BBC-RD-1989/10] 14 p1965 N90-21254
Radar RFI at Goldstone DSS 12 and DSS 16
15 p2078 N90-21900
Long pulse narrowband XeCl laser studies
[AD-A219774] 17 p2409 N90-23724
Spectral properties of a 1.3-micrometers InGaAsP diode laser under modulation
[AD-A220066] 17 p2409 N90-23729
Understanding tropscatter propagation
[AD-A220969] 18 p2544 N90-24520

BANKING FLIGHT
U TURNING FLIGHT

BARDEEN APPROXIMATION
U BARRIER LAYERS
U ELECTRICAL PROPERTIES
U SURFACE PROPERTIES

BARDEEN-COOPER-SCHRIEFFER THEORY
U BCS THEORY

BARENTS SEA
The Regional Polar Ice Prediction System, Berents Sea (RPIPS-B): A technical description
[AD-A213159] 04 p0522 N90-13012

BARIUM
Atomic and molecular surface and volume processes in the analysis of negative hydrogen discharges
[DE89-015705] 03 p0401 N90-12294
Generation of H-, H2v(double prime), and H atoms by H2+ and H3+ ions incident upon barium surfaces
[DE90-005549] 09 p1280 N90-17423
Low temperature elastic and dielectric properties of incommensurate barium sodium niobate
[AD-A216969] 12 p1709 N90-19815
Synthesis of Y1Ba2Cu3O(sub x) superconducting powders by intermediate phase reaction
22 p3149 N90-27855
Crystal chemical and quantum chemical studies of Ba(Sr)-Nb oxide compounds 22 p3150 N90-27858
Superconductivity in the Sn-Ba-Sr-Y-Cu-O system
22 p3151 N90-27863
A YBCO RF-SQUID magnetometer and its applications 22 p3151 N90-27867
Dynamical information for Fe doped YBa2Cu3O7 superconducting oxides obtained from high temperature Moessbauer studies
[DE90-627871] 23 p3401 N90-29218

BARIUM COMPOUNDS
NT BARIUM FLUORIDES
NT BARIUM OXIDES
NT BARIUM TITANATES
Muon SR investigation of magnetism and superconductivity in (Y(1-x)Pr(x))Ba2Cu3O7
[DE90-000689] 06 p0852 N90-14956
A (mu)SR-investigation of the mixed state of the high-Tc superconductor HoBa2Cu3O7-delta
[DE90-620802] 16 p2322 N90-23241
High resolution transmission electron microscopy of partial states of oxygen order in YBa2Cu3O(z)
[DE90-015637] 24 p3554 N90-30108

BARIUM FLUORIDES
The use of BaF2 buffer layers for the sputter-deposition of TlCaBaCuO thin-film superconductors
[DE90-004859] 09 p1292 N90-17490
Spectroscopy of laser properties of Nd(3+)-doped CaF2, SrF2, and BaF2
[DE90-012086] 19 p2695 N90-25337
Microstructures and properties of superconducting Y-Er-BaCu-O thin films obtained from disordered Y-Er-BaF2-Cu films 22 p3147 N90-27848

BARIUM OXIDES
A study of the tribological and surface micromechanical properties of YBa2Cu3O7-x
[DE89-015680] 02 p0281 N90-11607
Resistivity measurements of superconducting materials
[PB89-225700] 04 p0496 N90-12856
High resolution-angle resolved photoemission studies of high temperature superconductors
[DE89-017691] 06 p0852 N90-14950
Effects of shock-induced defects on flux pinning in YBa2Cu3O(7-delta)
[DE90-000824] 06 p0853 N90-14959
Anisotropy of oxygen tracer diffusion in YBa2Cu3O7-delta single crystals
[DE90-001931] 06 p0856 N90-14979
Partial reduction of re-oxidation processing of Y-Ba-Cu-O sputtered thin films
[DE90-003655] 07 p0999 N90-15782
Magnetic and electronic correlations in YBa2Cu3O(sub 6+x)
[DE89-017604] 07 p1000 N90-15785
Magnetic flux pinning in YBa2Cu3O7 films
[DE90-003709] 07 p1002 N90-15799
Cu-O chains in YBa2Cu3O(7-delta) and the phonon mechanism of high-Tc superconductivity
[DE90-603502] 07 p1003 N90-15805
Atomic scale structure of twin boundary in Y-Ba-Cu-O superconductors
[DE90-003955] 07 p1006 N90-15823
Electrical transport dissipation effects in epitaxial Y1Ba2Cu3O(7-x) thin films
[DE90-004301] 09 p1287 N90-17461
High-temperature deformation of YBa2Cu3O(7-delta) with Ag additions
[DE90-004884] 09 p1292 N90-17491
Effects of O2 ion bombardment of Y-BaCu-oxide during thin film growth
[DE90-005315] 09 p1293 N90-17495
Long laser-pulse method of producing Y-Ba-Cu-O superconducting films
[DE90-005202] 10 p1436 N90-18289
Hyper- and hypobaric processing of Tl-Ba-Ca-Cu-O superconductors
[DE90-005637] 10 p1437 N90-18292
Laser surface interactions of high-(Tc) superconductors
[DE90-006894] 12 p1669 N90-19587
Superconductivity in Ba(1-x)BiO3
[DE90-003781] 12 p1718 N90-19869
Y1Ba2Cu3O(7-x) laser-ablation plume dynamics measurement by nanosecond response ion probe: Comparison with optical measurements
[DE90-007658] 13 p1807 N90-20375
High resolution transmission electron microscopy study of defect structures in mixed-phase YBaCuO
[DE90-007767] 13 p1894 N90-20873
Synthesis and properties of polycrystalline Tl2Ba2Ca2Cu2O(x) and Tl2Ba2Ca2Cu3O(x)
[DE90-007528] 13 p1897 N90-20887
Deformation processing of YBa2Cu3O(sub x)
[DE90-007795] 14 p2030 N90-21644
Growth and patterning of laser ablated superconducting YBa2Cu3O7 films on LaAlO3 substrates
[NASA-TM-102436] 15 p2173 N90-22421
Photoresponse of YBa2Cu3O(7-delta) granular and epitaxial superconducting thin films
[NASA-TM-103144] 16 p2231 N90-22732
Influence of high energy radiation on critical parameters of superconducting ceramics YBa2Cu3O7
[DE90-620562] 16 p2322 N90-23239
In-situ processing of epitaxial and textured high (Tc) superconducting HoBa2Cu3O(7-x) thin films by pulsed laser evaporation technique
[DE90-009828] 17 p2474 N90-24148
Magnetic and resistive measurements of the upper critical field in intwinned single crystals of YBa2Cu3O(7-delta)
[DE90-010083] 18 p2619 N90-24918
The defect structure of ion and neutron irradiated YBa2Cu3O(7-delta) single crystals
[DE90-010100] 18 p2619 N90-24920
Valence-defect chemical equilibria in nonstoichiometric YBa2Cu3O(7-delta)
[DE90-010152] 18 p2619 N90-24921
Computer-controlled ion beam sputter deposition of multicomponent oxides
[DE90-010544] 18 p2619 N90-24923
Thermal and phase analysis of YBa2Cu3O(7-x) powder compacts with organic acid additives
[DE90-010142] 18 p2620 N90-24930
Transverse- and zero-field muon SR investigation of magnetism and superconductivity in (Y(1-x)Pr(x)Ba2Cu3O7)
[DE90-010597] 18 p2624 N90-24953
Practical superconductor development for electrical power applications
[DE90-010262] 18 p2625 N90-24957
Superconducting thin films of YBaCu oxides prepared by MOCVD
[DE90-011109] 18 p2625 N90-24961
Effect of Cu(2+) magnetic moments on the superconductivity of YBa2Cu3O7: The origin of the linear term in the specific heat; the volume fraction of superconductivity
[DE90-011214] 18 p2626 N90-24963
Highly-textured thallium-barium-calcium-copper-oxide polycrystalline superconducting films on silver substrates
[DE90-011972] 18 p2627 N90-24970
Sequentially evaporated thin film YBa2Cu3O(7-x) superconducting microwave ring resonator
[NASA-TM-103180] 19 p2685 N90-25273
Microstructures of superconducting YBa2Cu3O(7-x) thin films
[DE90-011976] 19 p2761 N90-25688
Large, orientation-dependent enhancements of critical currents in Y1Ba2Cu3O(7-x) epitaxial thin films: Evidence for intrinsic flux pinning
[DE90-009424] 20 p2929 N90-26666
Ellipsometric study of YBa2Cu3O(7-x) laser ablated and co-evaporated films
[NASA-TM-103223] 20 p2932 N90-26682
The effect of processing, deformation and annealing on the microstructure of Y1Ba2Cu3O7-(sub delta)
[DE90-011731] 21 p3079 N90-27510
Preparation and magnetic measurements of single crystal Tl2Ba2CaCu2O8
[DE90-013657] 21 p3081 N90-27519
Flux creep in Bi2Sr2CaCu2O8(sub +x) single crystals
22 p3136 N90-27794
Elliptical flux vortices in polycrystalline YBa2Cu3O7
22 p3136 N90-27795
Microstructure and magnetization of doped Y-Ba-Ca-O materials prepared by melt quench and post annealing method 22 p3138 N90-27803
Effect of shock pressure on the structure and superconducting properties of Y-Ba-Cu-O in explosively fabricated bulk metal-matrix composites
22 p3138 N90-27804
Laser ablated high T(sub c) superconducting thin YBa2Cu3O(7-x) films on substrates suitable for microwave applications 22 p3139 N90-27808
The effect of temperature cycling typical of low earth orbit satellites on thin films of YBa2Cu3O(7-x)
22 p3140 N90-27812
The effects of space radiation on thin films of YBa2Cu3O(sub 7-x) 22 p3147 N90-27845
Superconductivity in 2-2-3 Y2Ba2Cu3O(sub 8+ delta)
22 p3147 N90-27847
Comparative study of flux pinning flux creep and critical currents between YBaCuO crystals with and without Y2BaCuO5 inclusions 22 p3152 N90-27869
Synthesis and structural chemistry of Au(III)-substituted Ba2YCu3O(7-delta)
[NASA-TM-103292] 23 p3305 N90-28696
Investigation of YBa2Cu3O(7-sigma) by NMR and construction of an ultra low temperature cryostat
24 p3550 N90-30088
Synthesis and property evaluation of Y-Ba2-Cu3-O(6+x) superconductors
[AD-A223494] 24 p3552 N90-30098
First principles calculation of oxygen ordering in YBa2Cu3O(7-y)
[DE90-015205] 24 p3553 N90-30102

BARIUM TITANATES
Influence of core-shell grains on the internal stress state and permittivity response of zirconia modified barium titanate
[AD-A211245] 02 p0202 N90-11153
Reactive atmosphere processing of BaTiO3 and origins of its photorefractive effect
[AD-A215034] 09 p1289 N90-17475
Optical amplification in 45 deg - cut BaTiO3
[AD-A216043] 11 p1566 N90-19011
Image amplification in photoreactive crystals and utilization in optical reaction systems
[ETN-90-97285] 24 p3546 N90-30059
BARKHAUSEN EFFECT
Barkhausen noise analysis and ferromagnetic materials
[AD-A217989] 13 p1881 N90-20792
BAROCLINIC INSTABILITY
Dynamics and energetics of the South Pacific Convergence Zone during FGGE SOP-1 and South Pacific Convergence Zone and global-scale 03 p0361 N90-12065
Studies of baroclinic instability in the presence of surface topography and stratospheric ozone 03 p0361 N90-12068
Laboratory and theoretical studies of baroclinic processes 03 p0363 N90-12077
Instability mechanisms in a barotropic atmosphere
[KNMI-WR-89-01] 04 p0520 N90-13001
Dynamics of baroclinic instability in rapid cyclogenesis 07 p0962 N90-15563
Laboratory studies of isolated eddies in a rotating fluid
[AD-A213903] 08 p1063 N90-16146
Numerical simulations of the rapid cyclogenesis over Canada and evolution of a cold front observed on 25-26 April 1979 (SESAME-AVE-3) 09 p1247 N90-17234
Cyclogeneses and extratropical cyclones in the south-southeast region of Brazil and its influence in time
[INPE-4812-TDL/359] 12 p1693 N90-19722
Evolution of finite amplitude baroclinic waves in the atmosphere and ocean
[INPE-4752-TDL/346] 12 p1695 N90-19733
The instability mechanism of synoptic-scale eddies 22 p3211 N90-28217
BAROCLINIC WAVES
Dynamics of baroclinic wave systems 03 p0362 N90-12072
Numerical modeling of the atmosphere with an isentropic vertical coordinate 09 p1246 N90-17226
Synoptic-scale forcing of the low-level jet in developing baroclinic waves 12 p1692 N90-19717
The atmospheric energy cycle of stationary and transient waves
[ISSN-0069-5882] 12 p1694 N90-19728
Evolution of finite amplitude baroclinic waves in the atmosphere and ocean
[INPE-4752-TDL/346] 12 p1695 N90-19733
The observed three-dimensional structure of baroclinic waves in the Northern Hemisphere winter as revealed in a linear regression analysis 15 p2128 N90-22167
Evolution of atmospheric baroclinic waves 16 p2254 N90-22855
Planetary-scale flow on a two-layer beta-plane channel model with topography 23 p3350 N90-28931
BAROCLINITY
The influence of a steady baroclinic deep ocean on the shelf
[PB89-198188] 01 p0089 N90-10511
Global atmospheric moisture variability 03 p0361 N90-12062
Cyclogeneses and extratropical cyclones in the south-southeast region of Brazil and its influence in time
[INPE-4812-TDL/359] 12 p1693 N90-19722
Evolution of finite amplitude baroclinic waves in the atmosphere and ocean
[INPE-4752-TDL/346] 12 p1695 N90-19733
Planetary-scale flow on a two-layer beta-plane channel model with topography 23 p3350 N90-28931
Vorticity balance study for a tropical region, during the Southern Hemisphere summer
[INPE-4634-TDL/336] 23 p3353 N90-28949
BAROMETERS
Cosmic ray NM-64 neutron monitor data-17
[NOTA-INTERNA-945] 16 p2341 N90-23337
Improved meteorological measurements from buoys and ships (IMET): Preliminary report on barometric pressure sensors
[PB90-242116] 24 p3494 N90-29748
BAROMETRIC PRESSURE
U ATMOSPHERIC PRESSURE
BARORECEPTORS
Factor analytic reduction of the carotid-cardiac baroreflex parameters 08 p1155 N90-16693
BAROTROPIC FLOW
Paper 1. Impact of volcanic aerosols on stratospheric chemistry. Paper 2. O2 (1 sigma g +) and O2 (1 delta g) in the H + O2 reaction system. Paper 3. Barotropic instability of zonal jets on Mars, Earth and Venus 01 p0084 N90-10477
Laboratory and theoretical studies of baroclinic processes 03 p0363 N90-12077
Instability mechanisms in a barotropic atmosphere
[KNMI-WR-89-01] 04 p0520 N90-13001
The linear study of zonally asymmetric barotropic flows 05 p0668 N90-13902
Planetary-scale flow on a two-layer beta-plane channel model with topography 23 p3350 N90-28931
BAROTROPISM
NT PLANETARY WAVES
Evolution of atmospheric baroclinic waves 16 p2254 N90-22855
Barotropic vortex adjustment to asymmetric forcing with application to tropical cyclone motion
[AD-A219883] 17 p2427 N90-23831
Barotropic mechanisms associated with tropical plume formation 24 p3489 N90-29719
BARRED GALAXIES
Nuclear activity, morphology, and far infrared properties of spiral galaxies
[ETN-90-95373] 12 p1744 N90-20024
BARRELS (CONTAINERS)
The influence of large, cold objects on engulfing fire environments
[DE90-003342] 15 p2073 N90-21875
BARRICADES
U BARRIERS
BARRIER LAYERS
Elastic impurity scattering in double-barrier resonant tunneling structures
[AD-A212850] 05 p0702 N90-14110
Fabrication of NBN based electronic devices with silicon barriers
[AD-D014230] 06 p0767 N90-14463
Multiband photoconductive detector based on layered semiconductor quantum wells
[AD-D014232] 06 p0849 N90-14936
High temperature, flexible, thermal barrier seal
[NASA-CASE-LEW-14672-1] 07 p0940 N90-15444
Influence of heat treating on the mechanical values and the stability of heat barrier coatings
[ETN-90-95902] 12 p1631 N90-19375
Field effect transistor structures based on strain induced polarization charges
[DE90-007247] 12 p1655 N90-19515
Effect of barrier layers in burn-through experiments with 351-nm laser illumination
[DE90-006806] 12 p1667 N90-19577
System for venting gas from a liquid storage tank
[NASA-CASE-MSC-21253-1] 13 p1787 N90-20254
Microwave field effect transistor
[NASA-CASE-GSC-12442-2] 13 p1792 N90-20282
Investigation of Schottky barriers
[AD-A218422] 16 p2323 N90-23247
Quantum-confined hole states in double-barrier resonant tunneling structures
[AD-A221342] 18 p2623 N90-24946
Production of superconductor/carbon bicomponent fibers 22 p3138 N90-27805
Thermal analysis of thermal barrier coatings in a high heat flux environment 23 p3297 N90-28652
Vacuum application of thermal barrier plasma coatings 23 p3298 N90-28653
BARRIERS
The rodent research animal holding facility as a barrier to environmental contamination
[NASA-TM-102237] 03 p0378 N90-12151
A general approach to dominance in the plane
[RUU-CS-88-35] 17 p2463 N90-24072
BARS
Deformation of Ti-6Al-4V bar and extrusion under superplastic forming conditions
[RAE-TM-MAT/STR-1110] 03 p0330 N90-11875
Multilayer theory for delamination analysis of a composite curved bar subjected to end forces and end moments
[NASA-TM-4139] 04 p0466 N90-12669
Open-mode delamination stress concentrations in horseshoe and elliptic composite curved bars subjected to end forces
[NASA-TM-4164] 08 p1039 N90-16004
Characterization of the CP 214 T851. Dissection of a cast flat bar for a standard spar
[CEAT-PV-M4/462200] 22 p3158 N90-27905
BARYON RESONANCE
Q-2 and A dependence of delta (1232) electroexcitation in nuclei
[DE90-003470] 08 p1121 N90-16492
BARYONS
NT HYPERONS
Cosmic strings and baryon decay catalysis
[NASA-CR-186074] 04 p0566 N90-13299
The effects of cold dark matter on Big Bang nucleosynthesis 12 p1698 N90-19749
Gamma ray cosmology: The extra galactic gamma spectrum and methods to detect the underlying source 16 p2337 N90-23321
Baryogenesis in extended inflation. Part 1: Baryogenesis via production and decay of supermassive bosons
[NASA-CR-180615] 17 p2470 N90-24120
Cosmological baryon and lepton number in the presence of electroweak fermion-number violation
[NASA-CR-186609] 17 p2470 N90-24123
Cosmic strings and baryon decay
[NASA-CR-182842] 19 p2754 N90-25651
Baryogenesis in extended inflation. 2: Baryogenesis via primordial black holes
[NASA-CR-182843] 20 p2941 N90-26735
Biased clustering in a universe with hot dark matter and cosmic string
[FERMILAB-PUB-90/23-A] 22 p3262 N90-28473
BASALT
Meteoritic basalts
[NASA-CR-185949] 06 p0861 N90-15004
Stored mafic/ultramafic crust and early Archean mantle depletion
[NASA-CR-186460] 12 p1691 N90-19715
Geology of Espinhaco Meridional, including the Quadrilatero Ferrifero: Integration through remote sensing data
[INPE-4904-PRE/1505] 14 p1998 N90-21450
Ilmenite exsolution schemes in Apollo-17 high-Ti basalts
[DE90-011992] 21 p2976 N90-26912
BASE FLOW
A numerical and analytical study of normal stresses and pressure differences in non-Newtonian creeping flows 16 p2234 N90-22749
Numerical study of the onset of instability in the flow past a sphere 17 p2400 N90-23672
Direct numerical simulation of turbulent couette flow
[AD-A224287] 24 p3467 N90-29589
BASES (CHEMICAL)
NT ALKALIES
NT ATROPINE
NT CAFFEINE
NT LITHIUM HYDROXIDES
NT POTASSIUM HYDROXIDES
NT PYRIDINES
BASIC (PROGRAMMING LANGUAGE)
Personal computer process data acquisition
[DE89-017877] 06 p0828 N90-14816
BASINS
U STRUCTURAL BASINS
BATCH PROCESSING
Identification of impulsive interference channels
[AD-A213154] 05 p0688 N90-14009
Adaptive control of helicopter vibrations via the impulse response method
[AD-A213728] 07 p0883 N90-15113
Polynomial transfer lot sizing techniques for batch processing on consecutive machines
[AD-A214198] 07 p0980 N90-15660
Comparison of batch means and independent replications techniques to applications of the Kalman filter for simulation output analysis
[AD-A220656] 17 p2444 N90-23925
STATLIB: NSWC library of statistical programs and subroutines
[AD-A221538] 21 p3055 N90-27370
BATHYMETERS
Pre-study laser bathymetry
[BCRS-89-26] 15 p2134 N90-22198
Determination of tide heights from airborne bathymetric data
[AD-A220412] 17 p2430 N90-23848
BATHYMETRY
U BATHYMETERS
BATHYTHERMOGRAPHS
Environmental measurements and analysis: Arctic acoustics experiments in the marginal ice zone
[AD-A220509] 18 p2582 N90-24708
Oceanographic data exchange, 1988
[PB90-232596] 23 p3353 N90-28952
BATTERIES
U ELECTRIC BATTERIES
BATTERY CHARGERS
Evaluation of a new charge algorithm for a lead-acid battery with gelled electrolyte using a 96V gel cell 4 as a test battery
[DE90-003420] 08 p1061 N90-16133
All-solid-state thin-film rechargeable lithium batteries using solid redox polymerization electrodes
[DE90-008665] 13 p1796 N90-20306

Evaluation of the state of charge of battery electrodes with ac impedance techniques
[AD-A219561] 17 p2420 N90-23789
Performance of battery charge controllers
[DE90-011413] 19 p2686 N90-25279
Survey of applicability of electric vehicles (EVs) in specific regions such as resorts
[DE90-503592] 20 p2871 N90-26336

BATTERY SEPARATORS
U SEPARATORS

BAYES THEOREM
Number of test samples needed to obtain a desired Bayesian confidence interval for a proportion
[AD-A208157] 01 p0115 N90-10658
Empirical Bayes selection for the highest probability of success in negative binomial distributions
[AD-A210273] 01 p0115 N90-10660
A brief bibliography of statistical classification procedures: Decision-theoretic approach
[AD-A210276] 01 p0115 N90-10663
On finding the largest normal mean and estimating the selected mean
[AD-A211628] 03 p0394 N90-12245
Empirical Bayes estimation of binomial parameter with symmetric priors
[AD-A211646] 03 p0394 N90-12246
On the asymptotic optimality of certain empirical Bayes simultaneous testing procedures
[AD-A211649] 03 p0397 N90-12270
Different notions of uncertainty in quasi-probabilistic models
[CWI-CS-R8847] 04 p0547 N90-13182
Illustration of Bayesian inference in normal data models using Gibbs sampling
[AD-A212630] 04 p0547 N90-13187
An iterative Bayes procedure for reliability assessment
[DE90-002106] 07 p0944 N90-15466
Recurrence and ergodicity for exponential family state-space models
[AD-A213466] 07 p0983 N90-15677
On some problems in reliability theory
09 p1233 N90-17155
Application of Bayesian reliability concepts to cruise missile electronic components
[AD-A216208] 10 p1394 N90-18059
A sample reuse method for accurate parametric empirical Bayes confidence intervals
[AD-A216196] 10 p1424 N90-18216
Tracking in uncertain environments
[RAE-TM-AW-121] 16 p2261 N90-22891
Parametric models for A(sub n): Splitting processes and mixtures
[AD-A218421] 16 p2306 N90-23140
A theory of Bayesian data analysis
[AD-A218420] 16 p2308 N90-23152
Bayesian nonparametric prediction and statistical inference
[AD-A218473] 16 p2308 N90-23154
Selecting multinomial populations
[AD-A219256] 16 p2309 N90-23159
The application of kriging in the statistical analysis of anthropometric data, volume 1
[AD-A220613] 17 p2438 N90-23891
Bayesian learning
[NASA-CR-181528] 17 p2465 N90-24082
Bayesian characterization and detection of rare binary signature events
[AD-A221116] 18 p2606 N90-24844
A Bayesian approach to reliability and confidence
18 p2628 N90-24974
Explanation of Bayesian conditioning for decision support systems 18 p2633 N90-25002
Nonparametric selection, ranking and testing
[AD-A219254] 19 p2752 N90-25636
A Bayesian proportional model for software reliability
[IMAG-RR-795-M] 20 p2874 N90-26353
On networks, optimized feature extraction, and the Bayes decision
[RSRE-MEMO-4342] 20 p2914 N90-26580
Model-based Gaussian and non-Gaussian clustering
[AD-A222097] 21 p3066 N90-27430
A Bayesian derivation of an iterative autofocus/super-resolution algorithm
[RSRE-MEMO-4337] 22 p3239 N90-28371
Preference relations, Chisini-de Finetti means and Bayesian inference in retrieval-system modelling
[ESA-STR-230] 22 p3260 N90-28461
Systems reliability and inference: Summary of accomplishments 1988-1990
[AD-A224433] 24 p3477 N90-29653
Classical and Bayes-P subset selection procedures for double exponential populations
[AD-A223830] 24 p3538 N90-30006

BAYESIAN STATISTICS
U BAYES THEOREM

BAYS (STRUCTURAL UNITS)
Independent Orbiter Assessment (IOA): Assessment of the mechanical actuation subsystem, volume 1
[NASA-CR-185527-VOL-1] 02 p0169 N90-10952
Independent Orbiter Assessment (IOA): Assessment of the mechanical actuation subsystem, volume 2
[NASA-CR-185527-VOL-2] 02 p0169 N90-10953
Control of an experiment to measure acoustic noise in the space shuttle
[NPS62-89-022] 06 p0838 N90-14869
Onorbit electron beam welding experiment definition
[NASA-CR-183847] 07 p0938 N90-15431
Experimental investigation to suppress flow-induced pressure oscillations in open cavities
[AD-A216285] 10 p1310 N90-17578
Vibration test procedures for orbiter sidewall-mounted payloads, phase 2
[AD-A220774] 20 p2818 N90-26038
Dynamic structural analysis using boundary element techniques
[AD-A222943] 21 p3012 N90-27126

BAYS (TOPOGRAPHIC FEATURES)
NT CHESAPEAKE BAY (US)
Coastal Research Center Woods Hole Oceanographic Institution
[PB89-198238] 01 p0089 N90-10510
Continental shelf processes affecting the oceanography of the South Atlantic Bight
[DE90-008439] 13 p1848 N90-20606

BCC LATTICES
U BODY CENTERED CUBIC LATTICES

BCH CODES
A versatile integrated block codes encoder-decoder
20 p2848 N90-26197
Cyclic error correcting block codes for reliability increasing of VLSI networks
[ETN-90-97304] 22 p3168 N90-27968

BCS THEORY
BCS (Bardeen-Cooper-Schrieffer) primer: A guide to computational methods in superconductivity theory
[AD-A216393] 12 p1719 N90-19874
Superconductivity in mixed boson-fermion systems
[DE90-627491] 23 p3401 N90-29216

BE A
U BEACON EXPLORER A

BEACON EXPLORER A
Satellite radar altimetry over ice. Volume 4: Users' guide for Antarctica elevation data from Seasat
[NASA-RP-1233-VOL-4] 13 p1840 N90-20564

BEACON SATELLITES
NT BEACON EXPLORER A
Design and tests of simple, inexpensive optical beacon for use on small satellites
[AD-A213325] 04 p0555 N90-13238

BEACONS
NT DISCRETE ADDRESS BEACON SYSTEM
NT RADAR BEACONS
NT RADIO DIRECTION FINDERS
Data Link Processor (DLP) project transition plan
[DOT/FAA/CT-TN89/68] 14 p1965 N90-21256
The DORIS system 17 p2359 N90-23431
SILEX Beacon equipment
[ETN-90-96613] 17 p2409 N90-23726

BEADS
Model filled polymers I. Synthesis of crosslinked monodisperse polystyrene beads
[AD-A213228] 05 p0627 N90-13660
Model filled polymers 3. Rheological behavior of polystyrene containing crosslinked polystyrene beads
[AD-A215867] 11 p1489 N90-18567
Heat sink effects on weld bead: VPPA process
12 p1639 N90-19418
Heat sink effects on weld bead: VPPA process
[NASA-CR-186723] 19 p2697 N90-25349
Investigation of weld bead cooling rate during startup of gas metal arc welding
[AD-A223567] 24 p3449 N90-29478

BEAM CURRENTS
Simulation of an axially symmetric ion-optical system
[DE89-620129] 02 p0273 N90-11560
Broad-beam multi-ampere metal ion source
[DE90-003106] 08 p1059 N90-16123
Power threshold for neutral beam current drive
[DE90-008348] 13 p1886 N90-20822
Proposal for FY86 Lawrence Livermore National Laboratory particle beam research
[DE90-007936] 14 p2026 N90-21617
A simple beam position monitor system for CEBAF
[CEBAF-PR-89-015] 19 p2757 N90-25664

BEAM INJECTION
Fermilab fixed target beams from the main injector
[DE89-014355] 01 p0122 N90-10697
Simulation of an axially symmetric ion-optical system
[DE89-620129] 02 p0273 N90-11560
Projections for a steady-state tokamak reactor based on ITER
[DE89-016678] 02 p0278 N90-11589
Beam-plasma discharge in penetrating plasma
[DE89-630481] 02 p0280 N90-11597
International workshop on Beam Injection Assessment of Defects in Semiconductors
[AD-A210842] 02 p0283 N90-11617
Simulation of radial expansion of an electron beam injected into a background plasma
[NASA-CR-186188] 07 p0994 N90-15743
Intense REB (Relativistic Electron Beam) transport in a weakly magnetized plasma
[DE90-002978] 07 p0994 N90-15749
Broad-beam multi-ampere metal ion source
[DE90-003106] 08 p1059 N90-16123
To construct a linac/storage ring FEL facility
[AD-A214620] 09 p1211 N90-17020
Alfven wave stability in D III-D
[DE90-005555] 10 p1437 N90-18291
Injection parameters and beam oscillations during extraction
[NIKHEF-K/AMPS/89-07] 11 p1499 N90-18632
Negative ion surface plasma source development for plasma trap injectors in Novosibirsk
[DE90-006082] 12 p1716 N90-19856
Power threshold for neutral beam current drive
[DE90-008348] 13 p1886 N90-20822
PIC code modeling of spacecraft charging potential during electron beam injection into a background of neutral gas and plasma, part 1
[NASA-CR-186602] 15 p2059 N90-21792
Measurements and simulation of controlled beamfront motion in the Laser Controlled Collective Accelerator
[DE90-009992] 16 p2240 N90-22780
Plasma instabilities associated with the injection of artificial ion beams into the ionosphere
16 p2254 N90-22851
The beta limit in the DIII-D tokamak
[DE90-011896] 19 p2759 N90-25677
Proceedings of the US-Japan Fusion Cooperation Program Exchange P148 Workshop on Advanced Current Drive Concepts
[IPPJ-REV-4] 21 p3078 N90-27498
Some novel sources of x ray beams: Channeling, transition and Cherenkov radiation
[DE90-014442] 23 p3395 N90-29181

BEAM INTERACTIONS
Tangent map analysis of the beam-beam interaction
[DE89-015857] 01 p0120 N90-10689
Novel physical effects in intersecting optical waveguides 02 p0274 N90-11565
Experimental and theoretical study of artificial plasma layers produced by two intersecting beams in a chamber
[NASA-CR-184598] 05 p0701 N90-14102
Single beam interactions for the study of x ray lasers
06 p0786 N90-14573
Aerosol heating and vaporization of high-flux laser beams
[DE90-003471] 07 p0937 N90-15428
Lecture notes on supersonic molecular beam sources
[MPIS-20/1988] 08 p1121 N90-16494
High intensity laser beam interactions with single droplets 15 p2083 N90-21924
Overview of advanced fuel fusion
[DE90-015660] 24 p3550 N90-30085

BEAM SPLITTERS
Fermilab fixed target beams from the main injector
[DE89-014355] 01 p0122 N90-10697
Narrow-bandwidth unstable laser resonator
[AD-D014362] 12 p1665 N90-19568
Literature file on fast kickers and SEPTA: Components for deflection and separation of particle beams
[LINO-162] 12 p1727 N90-19924
Design of CEBAF's RF separator and results of cold tests
[CEBAF-PR-89-021] 19 p2756 N90-25658
Adaptive polarization diversity detection scheme for coherent communications and interferometric fiber sensors
[AD-D014479] 22 p3163 N90-27938
Near-angle scattering and binary optics
[AD-A224140] 23 p3396 N90-29186

BEAM SWITCHING
Antenna beamforming using optical processing
[NASA-CR-180844] 02 p0212 N90-11210
Cryogenic Schottky-mixer receiver front-end for 40-50 GHz
[PB89-221667] 03 p0343 N90-11959
The 32-GHz performance of the DSS-14 70-meter antenna: 1989 configuration 12 p1645 N90-19452
Dynamics of plasma injection along magnetic field lines in the PBFA 2 (Particle Beam Fusion Accelerator 2) plasma opening switch
[DE90-006751] 12 p1717 N90-19862

BEAM WAVEGUIDES
Performance effects of tie-truss modifications for a 70-meter centerline beam waveguide antenna
04 p0486 N90-12791
Design and performance analysis of the DSS-13 beam waveguide antenna 20 p2853 N90-26225
BEAMED POWER
U POWER BEAMING
BEAMS (RADIATION)
NT ATOMIC BEAMS
NT ELECTRON BEAMS
NT GAMMA RAY BEAMS
NT ION BEAMS
NT LASER BEAMS
NT LIGHT BEAMS
NT MOLECULAR BEAMS
NT NEUTRAL BEAMS
NT NEUTRINO BEAMS
NT NEUTRON BEAMS
NT PARTICLE BEAMS
NT PHOTON BEAMS
NT PION BEAMS
NT PROTON BEAMS
NT RADAR BEAMS
NT RELATIVISTIC ELECTRON BEAMS
Gyrotron development for space power beaming
01 p0028 N90-10148
Laser-powered Martian rover
01 p0029 N90-10157
Applicability of the beamed power concept to lunar rovers, construction, mining, explorers and other mobile equipment 01 p0030 N90-10159
Laser diode array and transmission optics
01 p0030 N90-10163
Beamed laser power in support of near-earth missions
01 p0031 N90-10167
An algorithm to calculate the beam momentum distribution from flying wire profiles
[DE89-015587] 01 p0073 N90-10418
A symplectic coherent beam-beam model
[DE89-015386] 01 p0122 N90-10701
Electromagnetic pulse interaction at a dielectric interface
[AD-A211081] 02 p0213 N90-11220
A solution to nonlinearity problems
[DE89-016975] 02 p0270 N90-11544
International workshop on Beam Injection Assessment of Defects in Semiconductors
[AD-A210842] 02 p0283 N90-11617
Microwave instability near transition energy
[DE90-000107] 03 p0338 N90-11922
Propagation of an elliptical laser beam through the turbulent atmosphere (vertical beams)
[PB89-208680] 03 p0352 N90-12010
Turbulence effects on reflected optical patterns (atmosphere and structure)
[PB89-208094] 03 p0404 N90-12315
Canonical formalism for coupled beam optics
[DE90-003764] 07 p0992 N90-15734
Optical guiding by plasma waves in the plasma beat wave accelerator
[AD-A214288] 07 p0997 N90-15763
Large angle off-axis beam steering of a phased telescope array
[AD-D014269] 08 p1060 N90-16127
Two-dimensional, long-pulse simulation of microwave-induced electron layer evolution in low-pressure air
[DE90-005180] 09 p1208 N90-17004
Optimization of Gaussian beam widths in acoustic propagation
[AD-A215893] 10 p1427 N90-18231
Determining the effects of microwave power and C-field setting on the frequency of a cesium atomic frequency standard
[AD-A216599] 11 p1501 N90-18642
Optically tunable gratings for optical interconnects
[AD-A216978] 12 p1714 N90-19844
Nonlinear optics in thin films
[AD-A217336] 13 p1887 N90-20829
Energy beam treatment for improved adhesion of coatings to surfaces
[AD-D014449] 14 p1954 N90-21190
Beamforming devices and feed structures for a DBS flat-plate antenna
[BBC-RD-1989/12] 17 p2386 N90-23592
Critique of nondiffracting beams
[AD-A220722] 17 p2390 N90-23614
Diffraction effects in directed radiation beams
[AD-A220785] 17 p2391 N90-23619
The effects of wiggler errors on free electron laser performance
[AD-A220421] 17 p2409 N90-23725
Fast acting optical beam deflection system
[AD-A220186] 17 p2473 N90-24141
Monoenergetic positron beam studies of near-surface phenomena
[ETN-90-96947] 18 p2613 N90-24887
A simple beam position monitor system for CEBAF
[CEBAF-PR-89-015] 19 p2757 N90-25664
X ray constraints on the beaming hypothesis for BL Lacertae objects 19 p2793 N90-25900
Structures for remotely deployable precision antennas
[NASA-CR-182065] 20 p2822 N90-26061
Application and extension of an analytical model of the confined acoustic beam generated by a transducer
[AD-A222994] 20 p2924 N90-26639
Crossed-microwave-beam air ionization laboratory experiments
[DE90-012056] 21 p3024 N90-27195
Slow positron beam generator for lifetime studies
[NASA-CASE-LAR-14250-1-SB]
21 p3073 N90-27472
Analysis of vibrational power transmission through a beam system including a flexible section
[ISVR-TR-176] 23 p3340 N90-28875
Status of the advanced light source
[DE90-015636] 23 p3395 N90-29185
High average power CW FELS (Free Electron Laser) for application to plasma heating: Designs and experiments
[DE90-011085] 24 p3474 N90-29633
Special purpose spatial light modulators
[AD-A223794] 24 p3545 N90-30052
Beam and plasma physics research
[AD-A224452] 24 p3548 N90-30067
BEAMS (SUPPORTS)
NT BOX BEAMS
NT CANTILEVER BEAMS
NT CURVED BEAMS
NT I BEAMS
NT TIMOSHENKO BEAMS
Analysis of delamination growth
02 p0183 N90-11036
The dynamic stability of an axially loaded beam with lateral elastic support and damping
02 p0232 N90-11331
Active control of the forced and transient response of a finite beam 03 p0357 N90-12040
Computation of generalized modal loads in an acoustic field define by a distribution of correlated pressures
[NASA-CR-186041] 03 p0358 N90-12047
Identification of equivalent modulus of a composite beam from nonmodal vibratory tests
[ECL-89-001] 05 p0656 N90-13821
Measurement of reflection and impedance in a beam by the structural intensity technique
[DE90-728212] 08 p1088 N90-16299
Dynamic modeling of flexible bodies in multibody systems 09 p1229 N90-17134
A statistical study of the surface accuracy of a planar truss beam
[NASA-TM-4161] 09 p1235 N90-17171
Dynamic interactions and globally optimal maneuver of distributed systems 09 p1236 N90-17172
Damage mechanisms and indenter size effects in cross plied carbon-carbon composites
[AD-A216413] 10 p1351 N90-17832
Plastic bending tests of cold-formed rectangular hollow sections
[PB90-124611] 12 p1674 N90-19613
Modal analysis of nonprismatic beams: Uniform segment method
[AD-A216952] 12 p1674 N90-19614
Development of finished beam and shell elements from engineering models for structures under high inelastic deformations
[ETN-90-95377] 12 p1675 N90-19619
Active control of the forced and transient response of a finite beam
[NASA-CR-181957] 13 p1816 N90-20430
Towards a unified analysis methodology for composite rotor blades 15 p2046 N90-21730
The Shock and Vibration Digest, volume 21, no. 8
15 p2110 N90-22068
Recent progress in the dynamic plastic behavior of structures, part 5 15 p2110 N90-22069
Pultrusion process development for long space boom model
[NASA-TM-4017] 16 p2214 N90-22628
Theory of filtering and control with application to control of large space structures
[AD-A219936] 17 p2366 N90-23468
Composite integrity monitoring
[AD-A220813] 17 p2369 N90-23487
A sequentially deployable structure for space applications. Part 2: Engineering model manufacturing and testing 18 p2541 N90-24504
Obtaining an equivalent beam
18 p2570 N90-24646
Transitioning of power flow in beam models with bends 18 p2570 N90-24648
Advanced buckling analyses of beams with arbitrary cross sections
[ISBN-90-9002808-0] 18 p2572 N90-24659
Dynamic analysis of space-related linear and non-linear structures
[NASA-TM-103490] 19 p2667 N90-25174
Loads analysis and testing of flight configuration solid rocket motor outer boot ring segments
[NASA-TP-3028] 19 p2701 N90-25366
Damage states in laminated composite three-point bend specimens: An experimental-analytical correlation study
[NASA-TM-101800] 20 p2827 N90-26083
Modeling of composite beams and plates for static and dynamic analysis
[NASA-CR-186459] 20 p2874 N90-26354
Local design methodologies for a hierarchic control architecture
[AD-A222006] 21 p2966 N90-26862
Tip-position control of a flexible beam: Modeling approaches and experimental verification
[AD-A224249] 24 p3476 N90-29643
BEAMSHAPING
U COLLIMATION
BEARING (DIRECTION)
Optimal observer motion for bearings-only localization and tracking 04 p0449 N90-12569
The relationship between subjective and objective measures of simulator-induced ataxia
[AD-A213095] 05 p0673 N90-13922
Grouping for recognition
[AD-A216716] 11 p1549 N90-18915
Visualization of three dimensional data
19 p2736 N90-25553
Implementation of an algorithm for travelling-wave-based directional detection
[EUT-89-E-214] 20 p2855 N90-26239
Tracking a head-mounted display in a room-sized environment with head-mounted cameras
[AD-A222545] 21 p3037 N90-27266
BEARINGS
NT ANTIFRICTION BEARINGS
NT BALL BEARINGS
NT FOIL BEARINGS
NT GAS BEARINGS
NT JOURNAL BEARINGS
NT MAGNETIC BEARINGS
NT ROLLER BEARINGS
NT THRUST BEARINGS
Three-dimensional analysis of surface crack-Hertzian stress field interaction
[NASA-CR-4254] 02 p0232 N90-11332
The nature and control of skidding in lightly loaded intershaft bearings
[PNR90591] 04 p0508 N90-12933
Vibration transmission through rolling element bearings in geared rotor system, part 1
[NASA-CR-186093] 04 p0509 N90-12936
Flight motor set 360L001 (STS-26R). Volume 5: Nozzle component
[NASA-CR-183771] 05 p0615 N90-13588
Friction in bearings
[ESDU-89044] 09 p1232 N90-17149
Investigation of applications of diamond film
[AD-A216104] 10 p1368 N90-17931
Bearing and gear steels for aerospace applications
[NASA-TM-102529] 13 p1809 N90-20391
Bearing elastohydrodynamic lubrication: A complex calculation made simple
[NASA-TM-102575] 15 p2105 N90-22041
NASA/GSFC split-rail parallel gripper
18 p2507 N90-24328
Solutions to the frictional dynamics problem and the reciprocal variable feedback methodology for design and control of robot mechanisms 23 p3333 N90-28846
BEAT
U SYNCHRONISM
BEAUFORT SEA (NORTH AMERICA)
The chemical and structural properties of sea ice in the southern Beaufort Sea
[AD-A219746] 17 p2418 N90-23776
BED REST
Exercise countermeasures for bed rest deconditioning
[NASA-TM-101045] 05 p0674 N90-13926
Noninvasive estimation of fluid shifts between body compartments by measurement of bioelectric characteristics 18 p2628 N90-24976
Research in human performance related to space: A compilation of three projects/proposals
18 p2629 N90-24983
Joint US/USSR study: Comparison of effects of horizontal and head-down bed rest
[NASA-TP-3037] 23 p3355 N90-28965

BEDDING EQUIPMENT
Laboratory evaluation of two new high-performance polyester batting insulation materials
[AD-A222291] 21 p2987 N90-26976
BEDROCK
Volcanism on Venus: Large shields and major accumulations of small domes 03 p0426 N90-12445
Erosional development of bedrock spur and gully topography in the Valles Marineris, Mars
[NASA-CR-180655] 17 p2424 N90-23813
BEDS (GEOLOGY)
Fundamental studies on hydrology, hydraulics and geometry of river networks
[AD-A218662] 16 p2250 N90-22830
BEDS (PROCESS ENGINEERING)
Thermohydraulics of a heat dissipating debris bed 19 p2691 N90-25310
Advanced heat pump
[AD-D014560] 22 p3170 N90-27979
BEECH AIRCRAFT
U BEECHCRAFT AIRCRAFT
BEECHCRAFT AIRCRAFT
Elevator tab assembly producibility study
[IAR-89-16] 19 p2659 N90-25133
BEHAVIOR
NT DECONDITIONING
NT HUMAN BEHAVIOR
Summarizing qualitative behavior from measurements of nonlinear circuits, revision
[AD-A210919] 01 p0061 N90-10353
Biological investigations of adaptive networks: Neuronal control of conditioned responses
[AD-A211043] 01 p0094 N90-10534
Study of the behavioral and biological effects of high intensity 60 Hz electric fields
[DE89-015528] 02 p0254 N90-11438
Analysis of three approaches to qualitative simulation
[MEMO-INF-89-32] 05 p0691 N90-14035
A structured connectionist approach to direct inferences and figurative adjective-noun combinations
[AD-A214326] 07 p0978 N90-15649
Traction modeling of military lubricants
[AD-A213866] 09 p1230 N90-17139
Local moduli of continuity of some classes of Gaussian processes
[AD-A217692] 13 p1879 N90-20778
Biological effects of ELF (Extremely-Low-Frequency) electric and magnetic fields
[DE90-008634] 14 p2009 N90-21514
Effects of cholinergic drugs on exercise performance and simple reaction time of rhesus monkeys
[AD-A219455] 17 p2433 N90-23862
Role of interfaces and interphases in the evolution mechanics of material systems
[AD-A222702] 21 p2971 N90-26885
BELL AIRCRAFT
NT UH-1 HELICOPTER
NT XV-15 AIRCRAFT
BELLOWS
Pressurized bellows flat contact heat exchanger interface
[NASA-CASE-MSC-21271-1] 15 p2097 N90-21999
BELTS
Investigation of the effects of external supports on manual lifting
[PB90-103367] 09 p1260 N90-17307
BENCHES
U SEATS
BEND TESTS
Stress intensity factors and displacements for arc bend samples using collocation
[AD-A210404] 01 p0080 N90-10460
Liquid infiltrated C/SiC: An alternative material for hot space structures 02 p0182 N90-11030
Small-radius bending loss in single-mode fibers
[AD-A211822] 03 p0405 N90-12323
Crack propagation failure of carbon/resin composites
[ONERA-RT-45/7086-M] 04 p0467 N90-12677
Buckling of delaminations in ARALL laminates
[LR-535] 05 p0619 N90-13614
Strength and toughness of monolithic and composite silicon nitrides
[NASA-TM-102423] 06 p0751 N90-14368
Mechanical behavior of laminated composites at elevated temperatures 07 p0889 N90-15141
Experiences with three-point bending test specimens for determining the crack-arrest fracture toughness K(sub Ia) in low-alloy steel
[DE90-004120] 08 p1089 N90-16306
Measuring strain in carbon fibre composite laminates using the Raman optomechanical strain gauge 11 p1477 N90-18503
Compact reinforced composite basic principles
[CBL-41] 11 p1480 N90-18520
Influence of a surface finishing on the fatigue behavior of a 32CDV13 steel
[ETCA-89-R-164] 22 p3157 N90-27902
Characterization of the CP 214 T851. Dissection of a cast flat bar for a standard spar
[CEAT-PV-M4/462200] 22 p3158 N90-27905
Characterization of the 7175 T7352. Dissection of a die casting standard spar
[CEAT-PV-M5/528900] 22 p3158 N90-27906
Characterization of the 7175 T7352 101. Dissection of a die casting standard spar
[CEAT-PV-M5/5288] 22 p3158 N90-27907
Characterization of the 7010 T73651. Dissection of a sheet billet for a standard spar
[CEAT-PV-M5/521700] 22 p3158 N90-27908
Surface effect for test piece on flexural test of carbon fiber reinforced plastic laminates
[NAL-TM-601] 24 p3442 N90-29436
BENDING
NT ELASTIC BENDING
Aircraft modal supression system: Existing design approach and its shortcomings 01 p0023 N90-10115
Structural stability augmentation system design using BODEDIRECT: A quick and accurate approach 01 p0023 N90-10116
Thin section casting program. Volume 4: Static cast product bending, straightening, and rolling
[DE89-009034] 02 p0210 N90-11202
Small-radius bending loss in single-mode fibers
[AD-A211822] 03 p0405 N90-12323
Multilayer theory for delamination analysis of a composite curved bar subjected to end forces and end moments
[NASA-TM-4139] 04 p0466 N90-12669
Dynamic interactions and globally optimal maneuver of distributed systems 09 p1236 N90-17172
Plastic bending tests of cold-formed rectangular hollow sections
[PB90-124611] 12 p1674 N90-19613
The reliability of clinical measurements of forward bending obtained by the use of the modified fingertip-to-floor method
[AD-A217907] 13 p1852 N90-20627
A modification of a low-order Reissner-Mindlin plate bending element
[PB90-165630] 14 p1994 N90-21428
Natural modes of cracked beams and identification of cracks 15 p2111 N90-22075
Rotor loading on a three-bladed wind turbine 15 p2123 N90-22145
Improved crystal bending techniques applied to the LLNL dual-arm Johann mounting x ray spectrometer
[DE90-009528] 15 p2173 N90-22415
Localization of vibration in disordered nearly cyclic structures 16 p2246 N90-22812
Transitioning of power flow in beam models with bends 18 p2570 N90-24648
Development of a finite element based delamination analysis for laminates subject to extension, bending, and torsion 18 p2642 N90-25049
Loads analysis and testing of flight configuration solid rocket motor outer boot ring segments
[NASA-TP-3028] 19 p2701 N90-25366
Flexion, extension and lateral bending responses of the cervical spine 19 p2719 N90-25468
Buckling and postbuckling behavior of square compression-loaded graphite-epoxy plates with circular cutouts
[NASA-TP-3007] 20 p2826 N90-26077
Damage states in laminated composite three-point bend specimens: An experimental-analytical correlation study
[NASA-TM-101800] 20 p2827 N90-26083
High-temperature deformation of silicon
[DE90-013628] 22 p3160 N90-27919
Inelastic analysis of laminated composites 23 p3301 N90-28669
Ascertaining the fracture toughness of ceramic materials by means of bending testpieces of various notch types at ambient and high temperatures
[ESA-TT-992] 23 p3312 N90-28733
A nonlinear finite element formulation for the large displacement analysis of plates 23 p3338 N90-28867
Green's functions for dislocations in bonded strips and related crack problems
[NASA-CR-185291] 23 p3340 N90-28878
BENDING FATIGUE
Stress intensity factors and displacements for arc bend samples using collocation
[AD-A210404] 01 p0080 N90-10460
An investigation on combined extension and bending of thin sheets with a central crack
[LR-581] 04 p0512 N90-12958
Cyclic fatigue of hot-isostatic-pressed silicon nitride
[PB90-122649] 08 p1090 N90-16308
Flexural fatigue life prediction of closed hat-section using materially nonlinear axial fatigue characteristics 18 p2645 N90-25062
BENDING MOMENTS
The response of helicopter rotors to vibratory airload
[AD-A215678] 09 p1167 N90-16756
BENDING THEORY
Effects of aeroelastic tailoring on anisotropic composite material beam models of helicopter blades
[AD-A213478] 07 p0879 N90-15095
Inelastic analysis of laminated composites 23 p3301 N90-28669
BENDING VIBRATION
Dynamic interactions and globally optimal maneuver of distributed systems 09 p1236 N90-17172
On a generalized laminate theory with application to bending, vibration, and delamination buckling in composite laminates 24 p3478 N90-29659
BENDS (PHYSIOLOGY)
U DECOMPRESSION SICKNESS
BENZENE
Monte Carlo simulations of small solute/solvent clusters: Cluster properties and phase transitions
[AD-A209559] 01 p0119 N90-10684
Calculation of the refractive index change in dissociating shocked benzene
[DE89-017737] 03 p0322 N90-11833
Thermophysical properties of benzene. Part 1: The ideal gas and the saturated liquid and vapour
[ESDU-89002-PT-1] 04 p0470 N90-12693
Thermophysical properties of benzene. Part 2: Thermodynamic properties at elevated pressures
[ESDU-89003-PT-2] 04 p0470 N90-12694
Extracting chemical information form Auger line shapes
[AD-A216729] 11 p1483 N90-18537
The 1-((diorganooxyphosphonyl)-methyl)-2,4- and -2,6-diamido benzenes
[NASA-CASE-ARC-11425-4] 13 p1766 N90-20133
Detailed mechanism for oxidation of benzene
[NASA-TM-102443] 15 p2067 N90-21842
Some 1-(diorganooxyphosphonyl)methyl-2,4- and -2,6-dinitro-benzenes
[NASA-CASE-ARC-11425-3] 17 p2367 N90-23475
Supersonic jet studies of benzyl alcohols: Minimum energy conformations and torsional motion
[AD-A221815] 21 p2980 N90-26934
BERING SEA
The sea ice margins: A summary of physical phenomena
[PB89-212328] 02 p0253 N90-11436
Tuning of the OSCURS (Ocean Surface Current Simulations) numerical model to ocean surface measurements in the Gulf of Alaska
[PB89-103979] 06 p0818 N90-14759
Circulation and property distributions in the Central Bering Sea, Spring, 1988
[PB90-155847] 22 p3230 N90-28317
BERNOULLI EQUATION
U BERNOULLI THEOREM
BERNOULLI THEOREM
Separable coordinate systems for PDE
[AD-A223052] 21 p3063 N90-27415
BERYL
Potential of solar-simulator-pumped alexandrite lasers
[NASA-TM-102701] 22 p3180 N90-28046
BERYLLIUM
A rate-dependent constitutive model for Be
[DE89-017755] 03 p0327 N90-11861
Beryllium dispersion near explosive firing tables: A comparison of computed and observed results
[DE90-002635] 07 p0960 N90-15550
High-purity beryllium foils
[DE90-006408] 12 p1626 N90-19348
The optical properties of beryllium
[DE90-006372] 12 p1715 N90-19848
Formation of subsurface aluminum layers in beryllium by ion implantation and post-implant annealing
[DE90-007975] 14 p1951 N90-21172
Reply to coupled S- and D-wave states in the thorium-doped heavy-fermion superconducting UBe13 by H. Pleiner and H. R. Brand
[AD-A220843] 17 p2477 N90-24164
BERYLLIUM ALLOYS
Nickel berylides and their properties
[DE90-001736] 07 p0903 N90-15220
BERYLLIUM COMPOUNDS
NT BERYL
NT BERYLLIUM HYDRIDES
NT BERYLLIUM OXIDES
Development of a reliable fabrication technique to produce intermetallic compounds
[AD-A215004] 09 p1194 N90-16918
Fabrication of intermetallic compounds by solid state reaction of roll-bonded materials
[AD-A221960] 21 p2982 N90-26943

BERYLLIUM HYDRIDES
A new low density, high porosity lithium hydride-beryllium hydride foam
[DE90-015150] 23 p3313 N90-28739
BERYLLIUM OXIDES
The role of polarity on the stability of graphitic compounds
[DE90-006528] 13 p1780 N90-20218
Reliability study of TWT output RF window
[AD-A223688] 24 p3465 N90-29574
Innovative techniques for the production of low cost 2D laser diode arrays
[AD-A223575] 24 p3474 N90-29632
BESSEL FUNCTIONS
NT HANKEL FUNCTIONS
Some exact solutions of the three-identical-particle problem with S-wave inverse square potentials
[DE89-618402] 02 p0267 N90-11524
Multiwave diffraction analysis of transmission phase gratings
[RSRE-MEMO-4325] 15 p2087 N90-21948
On a third q-Bessel function
[REPT-89-48] 15 p2161 N90-22344
Incomplete integrals of cylindrical functions
[AD-A219512] 16 p2310 N90-23161
Application and extension of an analytical model of the confined acoustic beam generated by a transducer
[AD-A222994] 20 p2924 N90-26639
Theory of biaxial graded-index optical fiber
[NASA-CR-186882] 20 p2927 N90-26652
BETA INTERACTIONS
U WEAK INTERACTIONS (FIELD THEORY)
BETA PARTICLES
Atomic effects of beta decay in astrophysics and in elementary particle physics 01 p0141 N90-10811
An experimental high energy physics program
[DE89-014695] 03 p0403 N90-12311
Cosmic ray half life of (54)Mn
[DE90-000134] 07 p1016 N90-15880
BETATRONS
Synchrotron-betatron parametric instability in free-electron lasers
[AD-A213373] 05 p0648 N90-13777
Anharmonic betatron motion in free electron lasers
[DE90-001515] 07 p0934 N90-15407
A microwiggler Free-Electron Laser at the Brookhaven Accelerator Test Facility
[DE90-003643] 07 p0936 N90-15418
Effects and tolerances of injection jitter in the SLC and future linear colliders
[DE90-014805] 23 p3394 N90-29179
BIAS
NT RESPONSE BIAS
Inherent bias in nonlinear least squares analysis of first-order kinetic data
[AD-A210677] 01 p0114 N90-10651
Bias and oxide thickness dependence of trapped charge buildup in MOS devices
[AD-A210264] 01 p0131 N90-10757
Asymptotic bias of autoregressive estimators
[IMAG-RR-745-M] 03 p0395 N90-12255
Simultaneous quaternion estimation (QUEST) and bias determination 05 p0587 N90-13417
Determination of the gravity disturbance by processing the gravity gradiometer surveying system: Processing procedure and results
[AD-A219992] 17 p2423 N90-23808
An accurate numerical technique for determining flight test rate gyroscope biases prior to takeoff
[AD-A220987] 19 p2660 N90-25138
Visualization of three dimensional data 19 p2736 N90-25553
The basis for facility comparison 22 p3118 N90-27713
A double-sided silicon strip detector with capacitive read out and a new method of integrated bias coupling 22 p3178 N90-28037
Dynamical properties of two-dimensional Josephson junction arrays
[AD-A223965] 23 p3402 N90-29221
Head-mounted spatial instruments II: Synthetic reality or impossible dream 24 p3508 N90-29828
BIBLIOGRAPHIES
Technology for large space systems: A bibliography with indexes (supplement 21)
[NASA-SP-7046(21)] 01 p0026 N90-10130
Space station systems: A bibliography with indexes (supplement 8)
[NASA-SP-7056(08)] 01 p0026 N90-10131
Aerospace medicine and biology: A continuing bibliography with indexes (supplement 328)
[NASA-SP-7011(328)] 01 p0092 N90-10524
Human performance in continuous/sustained operations and the demands of extended work/rest schedules: An annotated bibliography, volume 2
[AD-A210504] 01 p0093 N90-10530
NASA scientific and technical publications: A catalog of special publications, reference publications, conference publications, and technical papers, 1988
[NASA-SP-7063(03)] 01 p0136 N90-10782
National register of research projects, 1986/87. Part 2B: Natural sciences: Physical, engineering and related sciences (new projects)
[DE89-015033] 01 p0143 N90-10826
Aeronautical engineering: A continuing bibliography with indexes (supplement 243)
[NASA-SP-7037(243)] 03 p0299 N90-11693
Aeronautical engineering: A continuing bibliography with indexes (supplement 244)
[NASA-SP-7037(244)] 03 p0299 N90-11694
NDE (Non-Destructive Evaluation) publications, 1985
[PB89-229025] 03 p0356 N90-12036
Earth resources: A continuing bibliography with indexes (issue 63)
[NASA-SP-7041(63)] 03 p0366 N90-12091
Aerospace medicine and biology: A continuing bibliography with indexes (supplement 329)
[NASA-SP-7011(329)] 03 p0382 N90-12173
Working with people to improve productivity and quality: A bibliography with indexes, 1984-1988
[NASA-SP-7078] 03 p0415 N90-12385
Center for Electronics and Electrical Engineering technical publication announcements covering Center programs, January-March 1989 with 1989 CEEE events calendar
[PB89-228308] 03 p0418 N90-12402
Aeronautical engineering: A continuing bibliography with indexes (supplement 245)
[NASA-SP-7037(245)] 04 p0437 N90-12497
A semiparametric model for citation counts
[CWI-MS-R8814] 04 p0542 N90-13145
Publications of the National Institute of Standards and Technology, 1988 catalog
[PB89-218382] 04 p0563 N90-13279
Space station systems: A bibliography with indexes (supplement 9)
[NASA-SP-7056(09)] 05 p0613 N90-13580
Aerospace medicine and biology: A continuing bibliography with indexes (supplement 330)
[NASA-SP-7011(330)] 05 p0674 N90-13925
Rocket studies of the lower ionosphere
[NASA-CR-186187] 06 p0814 N90-14735
USSR Space Life Sciences Digest. Index to issues 21-25
[NASA-CR-3922(30)] 06 p0819 N90-14763
Publications of the Jet Propulsion Laboratory, 1988
[NASA-CR-185956] 06 p0859 N90-14995
Aeronautical engineering: A continuing bibliography with indexes (supplement 246)
[NASA-SP-7037(246)] 07 p0874 N90-15068
Cockpit resource management: A selected annotated bibliography
[AD-A214272] 07 p0969 N90-15594
Bibliography of Lewis Research Center technical publications announced in 1988
[NASA-TM-102034] 07 p1009 N90-15846
NASA Patent Abstracts Bibliography: A continuing bibliography. Section 1: Abstracts (supplement 36)
[NASA-SP-7039(36)-SECT-1] 07 p1010 N90-15851
AGARD index of publications, 1986-1988
[AGARD-INDEX-86-88] 08 p1136 N90-16585
JSC document index
[NASA-TM-102923] 08 p1137 N90-16589
Catalogue of ESA publications in 1987
[ESA-SP-1087] 08 p1137 N90-16590
Publications of the Exobiology Program for 1988: A special bibliography
[NASA-TM-4169] 09 p1262 N90-17316
Noise and sonic boom impact technology. Effects of aircraft noise and sonic booms on structures: An assessment of the current state-of-knowledge
[AD-A213919] 09 p1278 N90-17409
Aeronautical engineering: A continuing bibliography with indexes (supplement 247)
[NASA-SP-7037(247)] 10 p1303 N90-17537
Aerospace medicine and biology: A continuing bibliography with indexes (supplement 333)
[NASA-SP-7011(333)] 10 p1411 N90-18136
Aerospace medicine and biology: A continuing bibliography with indexes (supplement 331)
[NASA-SP-7011(331)] 10 p1411 N90-18137
NASA Patent Abstracts Bibliography: A continuing bibliography. Section 2: Indexes (supplement 36)
[NASA-SP-7039(36)-SECT-2] 10 p1441 N90-18317
Aeronautical engineering: A continuing bibliography with indexes (supplement 249)
[NASA-SP-7037(249)] 12 p1597 N90-19190
FY 1989 scientific and technical reports, articles, papers, and presentations
[NASA-TM-100384] 12 p1725 N90-19916
The NASA, Marshall Space Flight Center drop tube user's manual
[NASA-TM-100392] 13 p1786 N90-20251
Bibliography of spatial interferometry in optical astronomy
[NASA-TM-100754] 13 p1901 N90-20911
A compendium of sources of fracture toughness and fatigue crack growth data for metallic alloys, part 4
[NASA-TM-102646] 14 p1950 N90-21164
Microgravity science and applications bibliography, 1989 revision
[NASA-TM-4192] 14 p1957 N90-21207
JPRS report: Science and technology. USSR: Electronics and electrical engineering
[JPRS-UEE-90-002] 14 p1970 N90-21284
Tenth International Free Electron Laser Conference
[DE90-614773] 14 p1985 N90-21376
JPRS report. Science and technology. USSR: Earth sciences
[JPRS-UES-88-004] 14 p1995 N90-21431
JPRS report. Science and technology. USSR: Earth sciences
[JPRS-UES-89-002] 14 p1995 N90-21432
JPRS report: Science and technology. USSR: Earth sciences
[JPRS-UES-90-005] 14 p1995 N90-21433
JPRS report: Science and technology. USSR: Life sciences
[JPRS-ULS-90-002] 14 p1995 N90-21434
Geobotanical remote sensing: A review
[INPE-5026-PRE/1565] 14 p1996 N90-21440
Annotated bibliography of software engineering laboratory literature
[NASA-TM-103313] 14 p2013 N90-21536
Collected software engineering papers, volume 7
[NASA-TM-103312] 14 p2014 N90-21537
Collected software engineering papers, volume 6
[NASA-TM-103309] 14 p2014 N90-21540
JPRS report: Science and technology. USSR: Physics and mathematics
[JPRS-UPM-90-002] 14 p2022 N90-21593
The Shock and Vibration Digest, volume 22, no. 2 14 p2022 N90-21596
Current experiments in elementary particle physics
[DE90-008062] 14 p2024 N90-21607
Small business innovation research. Abstracts of 1988 phase 1 awards
[NASA-TM-102991] 14 p2036 N90-21680
Small business innovation research. Abstracts of completed 1987 phase 1 projects
[NASA-TM-101797] 14 p2036 N90-21681
Aeronautical engineering: A continuing bibliography with indexes (supplement 250)
[NASA-SP-7037(250)] 15 p2045 N90-21722
Publications of the NASA Controlled Ecological Life Support System (CELSS) Program, 1979-1989
[NASA-CR-4297] 15 p2051 N90-21754
The Shock and Vibration Digest, volume 21, no. 2 15 p2109 N90-22059
The Shock and Vibration Digest, volume 21, no. 1 15 p2109 N90-22061
The Shock and Vibration Digest, volume 21, no. 7 15 p2110 N90-22066
The Shock and Vibration Digest, volume 21, no. 8 15 p2110 N90-22068
The Shock and Vibration Digest, volume 22, no. 1 15 p2111 N90-22073
Aerospace medicine and biology: A continuing bibliography with indexes (supplement 334)
[NASA-SP-7011(334)] 15 p2136 N90-22207
Aerospace medicine and biology: A continuing bibliography with indexes (supplement 335)
[NASA-SP-7011(335)] 15 p2136 N90-22208
A Chinese bibliography on quadratic systems of differential equations
[REPT-89-39] 15 p2161 N90-22342
The Shock and Vibration Digest, volume 21, no. 6 15 p2163 N90-22363
Electronic transfer of information applications in the Societe Aerospatiale 15 p2179 N90-22454
Development of high-activity para- to ortho-hydrogen conversion catalysts, volume 2
[AD-A218700] 16 p2215 N90-22638
Aeronautical engineering: A continuing bibliography with indexes (supplement 251)
[NASA-SP-7037(251)] 17 p2343 N90-23344
Aeronautical engineering: A continuing bibliography with indexes (supplement 252)
[NASA-SP-7037(252)] 17 p2343 N90-23345
Aerospace medicine and biology: A continuing bibliography with indexes (supplement 336)
[NASA-SP-7011(336)] 17 p2436 N90-23877
The biogeochemistry of metal cycling
[NASA-CR-4295] 17 p2439 N90-23897

A bibliography of the qualitative theory of quadratic systems of differential equations in the plane
[REPT-89-71] 17 p2458 N90-24029
Management: A bibliography for NASA managers
[NASA-SP-7500(24)] 17 p2479 N90-24174
Aeronautical engineering: A cumulative index to a continuing bibliography (supplement 248)
[NASA-SP-7037(248)] 19 p2649 N90-25072
Aeronautical engineering: A continuing bibliography with indexes (supplement 253)
[NASA-SP-7037(253)] 19 p2654 N90-25105
Space station systems: A bibliography with indexes (supplement 10)
[NASA-SP-7056(10)] 19 p2666 N90-25171
Managing the global environment
[AD-A218615] 19 p2712 N90-25434
Aerospace medicine and biology: A cumulative index to a continuing bibliography (supplement 332)
[NASA-SP-7011(332)] 19 p2722 N90-25480
Aerospace medicine and biology: A continuing bibliography with indexes (supplement 337)
[NASA-SP-7011(337)] 19 p2722 N90-25481
Aerospace medicine and biology: A continuing bibliography with indexes (supplement 338)
[NASA-SP-7011(338)] 19 p2722 N90-25482
NASA Patent Abstracts Bibliography: A continuing bibliography. Section 1: Abstracts (supplement 37)
[NASA-SP-7039(37)-SECT-1] 19 p2763 N90-25698
Supersonic wind tunnel nozzles: A selected, annotated bibliography to aid in the development of quiet wind tunnel technology
[NASA-CR-4294] 20 p2814 N90-26019
Technology for large space systems: A bibliography with indexes (supplement 22)
[NASA-SP-7046(22)] 20 p2822 N90-26056
Aircrew life support systems enhancement
[AD-A222626] 20 p2902 N90-26505
NASA Patent Abstracts Bibliography: A continuing bibliography. Section 2: Indexes (supplement 37)
[NASA-SP-7039(37)-SECT-2] 20 p2935 N90-26700
Information resources management, 1984-1989: A bibliography with indexes
[NASA-SP-7079] 21 p3086 N90-27548
Index of USACERL publications, October 1984-December 1989
[AD-A221644] 21 p3088 N90-27559
Aeronautical engineering: A continuing bibliography with indexes (supplement 254)
[NASA-SP-7037(254)] 22 p3107 N90-27647
Aeronautical engineering: A continuing bibliography with indexes (supplement 255)
[NASA-SP-7037(255)] 22 p3107 N90-27648
NIST (National Institute of Standards and Technology) serial holdings, 1990 edition
[PB90-183245] 22 p3163 N90-27936
Center for Electronics and Electrical Engineering technical progress bulletin covering center programs, July to September 1989, with 1990 CEEE events calendar
[PB90-188095] 22 p3167 N90-27959
NASA geodynamics program: Bibliography
[NASA-TM-4220] 22 p3194 N90-28123
Bibliography of oceanography, meteorology, and geology of Louisiana, Texas, Mississippi, Alabama, and Florida
[PB90-194663] 22 p3194 N90-28124
Aerospace medicine and biology: A continuing bibliography with indexes (supplement 339)
[NASA-SP-7011(339)] 22 p3232 N90-28327
Scientific and technical information management
22 p3257 N90-28444
NASA scientific and technical information for the 1990s 22 p3257 N90-28445
Appendix A: NASA information services
22 p3258 N90-28451
Spatial interferometry in optical astronomy
[NASA-RP-1245] 22 p3262 N90-28470
Technical bibliography of high performance polyethylene fibers
[SNPE-NT-106/89/GTR/RP/NP]
23 p3313 N90-28736
Aerospace medicine and biology: A continuing bibliography with indexes (supplement 340)
[NASA-SP-7011(340)] 23 p3355 N90-28963
Biomedical and environmental sciences program publications, 1989
[DE90-014785] 23 p3406 N90-29250
FAA Rotorcraft Research, Engineering, and Development Bibliography 1962-1989
[AD-A224256] 24 p3417 N90-29299

BICARBONATES
U CARBONATES

BICRYSTALS
High voltage/high resolution studies of metal and semiconductor interfaces
[DE90-009065] 14 p2032 N90-21656
Application of microdesigned interfaces to studies of ceramic processing
[DE90-011633] 21 p2983 N90-26951

BIDIRECTIONAL REFLECTANCE
Spectral responses of soybeans and their relationship with agronomical parameters
[INPE-4832-PRE/1462] 10 p1398 N90-18084
Measuring and modeling near-surface reflected and emitted radiation fluxes at the FIFE site
[NASA-CR-180953] 20 p2879 N90-26378
Analysis of ER-2 radiometer and lidar observations from the 1987 marine stratus experiment
22 p3216 N90-28241

BIFURCATION (MATHEMATICS)
U BRANCHING (MATHEMATICS)

BIG BANG COSMOLOGY
The origin of the universe from quantum chaos: An introduction to current ideas
[AD-A210441] 01 p0141 N90-10813
Nuclear physics and cosmology
[NASA-CR-186166] 05 p0713 N90-14167
Big Bang nucleosynthesis and the Quark-Hadron transition
[NASA-CR-186169] 05 p0713 N90-14168
Cosmology and the weak interaction
[NASA-CR-186170] 05 p0713 N90-14169
Nuclear reaction uncertainties in standard and non-standard cosmologies
[DE90-003594] 08 p1151 N90-16666
The effects of cold dark matter on Big Bang nucleosynthesis 12 p1698 N90-19749
Big-bang nucleosynthesis revisited
[NASA-CR-186256] 15 p2174 N90-22426
Cosmic Background Explorer (COBE) press kit
[P89-10172] 17 p2364 N90-23459
Probing the Big Bang with LEP
[NASA-CR-181060] 17 p2485 N90-24212
Extended inflation from higher dimensional theories
[NASA-CR-180549] 19 p2796 N90-25916
Nonstandard big bang models
[DE90-625593] 20 p2941 N90-26736

BIGHTS
U BAYS (TOPOGRAPHIC FEATURES)

BIHARMONIC EQUATIONS
An H(m)sub 0 interpolation result
[AD-A219888] 17 p2461 N90-24051

BILLETS
Method of making a long life high current density cathode from tungsten and iridium powders using a quarternary compound as the impregnant
[AD-D014425] 14 p1958 N90-21211
Characterization of the 7010 T73651. Dissection of a sheet billet for a standard spar
[CEAT-PV-M5/521700] 22 p3158 N90-27908

BINARY ALLOYS
Electrical properties of materials for high temperature strain gage applications
[NASA-CR-186192] 06 p0780 N90-14534
Electronic structure, alloy phase stability, and phase diagrams
[DE90-008306] 13 p1778 N90-20203
Dynamics of the solidification front
13 p1785 N90-20243
The lithium concentration dependence of creep in binary aluminum-lithium alloys
[AD-A218706] 16 p2221 N90-22668
Damping associated with incipient melting in aluminum-indium alloys
[AD-A220241] 18 p2525 N90-24412
Hydrogen in palladium alloys: Experiments, models and simulations
[PB90-200429] 22 p3156 N90-27896
A comparative first principles study of phase stability in Ni-Ti and Ni-Al alloys around equiatomic composition
[DE90-016477] 24 p3554 N90-30111

BINARY CODES
Binary Gray codes and index systems
[REPT-89-29] 04 p0530 N90-13060
On linear structure and phase rotation invariant properties of block 2(sup l)-PSK modulation codes
[NASA-CR-186308] 12 p1641 N90-19429
Exact algorithms for output encoding, state assignment and four-level Boolean minimization
[AD-A217121] 13 p1876 N90-20756
Converses for write-unidirectional memories
[EUT-89-E-220] 20 p2909 N90-26546

BINARY DATA
FORTRAN program for x ray photoelectron spectroscopy data reformatting
[NASA-TP-2957] 03 p0409 N90-12348
Efficient algorithms for dilated mappings of binary trees
[NASA-CR-181980] 09 p1262 N90-17317
Binary correlators for optical computing and pattern recognition 10 p1441 N90-18318
Binary space partitioning trees and their uses
13 p1857 N90-20657
VLSI binary updown counter
[NASA-CASE-NPO-17205-1-CU]
14 p2011 N90-21525
Polar coordinate laser writer for binary optics fabrication
[AD-A222827] 21 p3008 N90-27097
Learning binary relations and total orders
[AD-A221643] 21 p3059 N90-27392

BINARY DIGITS
Comparison of DPCM prediction strategies for high-quality digital television bit-rate reduction
[BBC-RD-1989/8] 01 p0056 N90-10318
Long period pseudo random number sequence generator
[NASA-CASE-NPO-17241-1-CU]
17 p2394 N90-23636
Formal verification of mathematical software, volume 2
[AD-A223633] 24 p3527 N90-29943
Unique binary search tree representations and equality-testing of sets and sequences
[AD-A223643] 24 p3537 N90-30002

BINARY MIXTURES
NT EUTECTICS
Solidification front/viscous phase transitions, forward-backward heat equations
[AD-A211068] 02 p0195 N90-11114
Vapor-liquid equilibrium of binary mixtures in the extended critical region. Part 1: Thermodynamic model
[PB89-218374] 04 p0469 N90-12687
Preparation of binary ice layers by condensation from gas phase
[JUEL-2248] 05 p0622 N90-13631
Asymptotic analysis of performance of membrane modules for gas separations
[DE90-000699] 06 p0742 N90-14316
Molecular theory of fluid phase equilibria
[PB90-131277] 15 p2066 N90-21832

BINARY STARS
NT CATACLYSMIC VARIABLES
NT DWARF NOVAE
NT ECLIPSING BINARY STARS
NT SYMBIOTIC STARS
NT X RAY BINARIES
MOXE: An X-ray all-sky monitor for Soviet Spectrum-X-Gamma Mission
[NASA-TM-101266] 02 p0223 N90-11280
An improved algorithm for the determination of the system paramters of a visual binary by least squares
02 p0290 N90-11658
Proximity effects on adjacent and multiple stars
05 p0607 N90-13533
Double stars 05 p0608 N90-13540
Double star reductions in NDAC
05 p0610 N90-13561
Double star reductions in FAST
05 p0611 N90-13562
Properties of evolved star circumstellar grains
08 p0861 N90-15003
EXOSAT measurements of the pulse period of Vela X-1
[MPE-PREPRINT-157] 08 p1152 N90-16673
The emission lines in the ultra-violet spectrum of Beta Lyrae 15 p2183 N90-22474
Diffraction-limited imaging on the 200-inch telescope
15 p2183 N90-22475
Rapid mass transfer in binary systems
16 p2332 N90-23289
What can gamma rays tell us about binary x ray sources and SNR's 16 p2336 N90-23310
Observations of Cygnus X-2 at x ray, UV, optical and radio frequencies
[MPE-PREPRINT-163] 17 p2481 N90-24191
Multifrequency observations of Cyg X-2: X ray observations with Ginga 17 p2482 N90-24192
Observations of Cygnus X-2 with IUE: Ultraviolet results from a multiwavelength campaign
17 p2482 N90-24193
Optical spectroscopy of V1341 Cyg, the optical counterpart of Cyg X-2 17 p2482 N90-24194
Radio observations of the x ray binary Cygnus X-2
17 p2482 N90-24195
EXOSAT observations of Cygnus X-1: Study of the soft x ray excess 17 p2483 N90-24199
The pulsed light curve of Vela X-1
17 p2483 N90-24202
Spectral variability of LMC X-4
17 p2483 N90-24204
The role of comptonisation in energy spectra of standard QPO-sources 17 p2484 N90-24205
Synthetic spectra of accretion disks in DQ Her binaries
[NASA-CR-186837] 18 p2638 N90-25029

Pulsations of the white dwarf component in V471 tauri-like binaries
[DE90-014921] 23 p3409 N90-29267
Investigation of x ray variability in highly active cool stars
[NASA-CR-183853] 24 p3560 N90-30143

BINARY SUMMATORS
U ADDING CIRCUITS

BINARY SYSTEMS (DIGITAL)
U DIGITAL SYSTEMS

BINARY SYSTEMS (MATERIALS)
NT BINARY ALLOYS
NT BINARY MIXTURES
NT EUTECTICS
The propagation of time harmonic Rayleigh-Lamb waves in a bimaterial plate
[AD-A216834] 11 p1519 N90-18749
Luminescence of lanthanides and actinides implanted into binary III-V semiconductors and AlGaAs
[AD-A215759] 11 p1569 N90-19031

BINAURAL HEARING
Binaural masking: An analysis of models
[AD-A211578] 03 p0381 N90-12168
Binaural masking: An analysis of models
[AD-A221668] 21 p3035 N90-27252
Techniques and applications for binaural sound manipulation in human-machine interfaces
[NASA-TM-102279] 23 p3362 N90-28996

BINDERS (ADHESIVES)
U ADHESIVES

BINDERS (MATERIALS)
NT PROPELLANT BINDERS
Effects of binder concentration on the properties of plastic-bonded explosives
[DE89-007744] 01 p0053 N90-10301
A preliminary assessment of 3-Nitro-1,2,4-Triazol-5-One (NTO) as an insensitive high explosive
[AD-A215063] 10 p1360 N90-17889
High gloss corrosion-resistant coatings
[AD-D014403] 14 p1954 N90-21184
Methods for improving the flowability of a percussion primer composition
[MRL-TR-89-32] 14 p1956 N90-21201
Calculation of thick wall fiber binders for rotor components of modern helicopters
[MBB-UD-554/84-PUB] 19 p2660 N90-25137
Understanding silica binders
[PNR90625] 20 p2840 N90-26150
The optimum polymer binder for pressable high performance explosives: A preliminary evaluation
[ETN-90-97612] 24 p3457 N90-29524

BINOCULAR VISION
Disparity gradients and depth scaling
[AD-A218612] 17 p2453 N90-23992

BINOMIALS
Empirical Bayes selection for the highest probability of success in negative binomial distributions
[AD-A210273] 01 p0115 N90-10660
Empirical Bayes estimation of binomial parameter with symmetric priors
[AD-A211646] 03 p0394 N90-12246
Priority arbitration with busses
[AD-A216392] 12 p1704 N90-19784
The multifractal nature of turbulence
16 p2235 N90-22752

BIOASSAY
Amperometric biosensors for glucose, lactate, and glycolate based on oxidases and redox-modified siloxane polymers
[DE90-002301] 06 p0781 N90-14541
Advanced biosensors for amino acid detection
[AD-A214029] 08 p1076 N90-16225
Short-term bioassays may be useful in evaluating fiber/whisker hazards
[DE90-003707] 08 p1104 N90-16393

BIOASTRONAUTICS
Aerospace medicine and biology: A continuing bibliography with indexes (supplement 328)
[NASA-SP-7011(328)] 01 p0092 N90-10524
Aerospace medicine and biology: A continuing bibliography with indexes (supplement 329)
[NASA-SP-7011(329)] 03 p0382 N90-12173
Biology in microgravity: A guide for experimenters
[ESA-TM-02] 04 p0482 N90-12769
Aerospace medicine and biology: A continuing bibliography with indexes (supplement 330)
[NASA-SP-7011(330)] 05 p0674 N90-13925
USSR Space Life Sciences Digest. Index to issues 21-25
[NASA-CR-3922(30)] 06 p0819 N90-14763
Aerospace medicine and biology: A continuing bibliography with indexes (supplement 333)
[NASA-SP-7011(333)] 10 p1411 N90-18136
Aerospace medicine and biology: A continuing bibliography with indexes (supplement 331)
[NASA-SP-7011(331)] 10 p1411 N90-18137
Small business innovation research. Abstracts of 1988 phase 1 awards
[NASA-TM-102991] 14 p2036 N90-21680
Small business innovation research. Abstracts of completed 1987 phase 1 projects
[NASA-TM-101797] 14 p2036 N90-21681
USSR Space Life Sciences Digest, issue 25
[NASA-CR-3922(29)] 15 p2135 N90-22203
Aerospace medicine and biology: A continuing bibliography with indexes (supplement 334)
[NASA-SP-7011(334)] 15 p2136 N90-22207
Aerospace medicine and biology: A continuing bibliography with indexes (supplement 335)
[NASA-SP-7011(335)] 15 p2136 N90-22208
Aerospace medicine and biology: A continuing bibliography with indexes (supplement 336)
[NASA-SP-7011(336)] 17 p2436 N90-23877
USSR space life sciences digest, issue 27
[NASA-CR-3922(32)] 19 p2717 N90-25457
Aerospace medicine and biology: A cumulative index to a continuing bibliography (supplement 332)
[NASA-SP-7011(332)] 19 p2722 N90-25480
Aerospace medicine and biology: A continuing bibliography with indexes (supplement 337)
[NASA-SP-7011(337)] 19 p2722 N90-25481
Aerospace medicine and biology: A continuing bibliography with indexes (supplement 338)
[NASA-SP-7011(338)] 19 p2722 N90-25482
Aerospace medicine and biology: A continuing bibliography with indexes (supplement 339)
[NASA-SP-7011(339)] 22 p3232 N90-28327
Aerospace medicine and biology: A continuing bibliography with indexes (supplement 340)
[NASA-SP-7011(340)] 23 p3355 N90-28963

BIOCHEMICAL FUEL CELLS
Lightweight solid polymer electrolyte fuel cell with stack power density of 3 kW/lb (7 kW/kg)
[AD-A223964] 23 p3345 N90-28905

BIOCHEMISTRY
NT BIOGEOCHEMISTRY
NT ENZYMOLOGY
Biochemical cycling and fluxes between the deep euphotic zone and other oceanic realms
[PB89-152458] 01 p0089 N90-10509
Electroporation: Theory of basic mechanisms
[AD-A210196] 01 p0091 N90-10520
Synaptic plasticity and memory formation
[AD-A211368] 03 p0379 N90-12158
Cellular and molecular mechanisms of high pressure inotropy in cardiac muscle
[AD-A211695] 03 p0381 N90-12170
Biological and biochemical methane reactions
[PB89-232615] 04 p0516 N90-12977
Fear-potentiated startle as a model system for analyzing learning and memory
[AD-A212131] 04 p0525 N90-13029
Response of lymphocytes to a mitogenic stimulus during spaceflight
05 p0677 N90-13942
Capillary electrophoresis ionization-mass spectrometry and tandem mass spectrometry
[DE90-002664] 07 p0892 N90-15158
Introduction to extremely-low-frequency electric and magnetic fields
[DE90-002662] 07 p0966 N90-15578
The physical-organic chemistry of surfaces, and its relevance to molecular recognition
[AD-A215987] 10 p1354 N90-17850
Assessment of research needs for laser technologies applied to advanced spectroscopic methods
[DE90-007402] 12 p1669 N90-19588
Assessment of biobased materials
[DE90-000300] 13 p1780 N90-20220
Final safety analysis report for the Ulysses Mission. Volume 3 (Book 2): Nuclear risk analysis document-appendices
[DE90-008692] 14 p1939 N90-21102
JPRS report: Science and technology. USSR: Life sciences
[JPRS-ULS-90-002] 14 p1995 N90-21434
Biological effects of ELF (Extremely-Low-Frequency) electric and magnetic fields
[DE90-008634] 14 p2009 N90-21514
Anaerobic metabolism of aromatic compounds by phototrophic bacteria: Biochemical aspects
[DE90-009503] 14 p2009 N90-21516
Studies of 60-Hz exposure effects on human function
[DE90-009473] 15 p2137 N90-22210
Neurotransmitter and peptide localization in human brain
[AD-A219964] 17 p2435 N90-23873
Biochemical and physiological changes in glider pilots during multi-hour flights
[ESA-TT-1183] 19 p2722 N90-25484
Experiment K-6-08. Biochemical and histochemical observations of vastus medialis
20 p2893 N90-26462
Experiment K-6-09. Morphological and biochemical investigation of microgravity-induced nerve and muscle breakdown. Part 1: Investigation of nerve and muscle breakdown during spaceflight; Part 2: Biochemical analysis of EDL and PLT muscles 20 p2893 N90-26463
Experiment K-6-13. Morphological and biochemical examination of heart tissue. Part 1: Effects of microgravity on the myocardial fine structure of rats flown on Cosmos 1887. Ultrastructure studies. Part 2: Cellular distribution of cyclic ampdependent protein kinase regulatory subunits in heart muscle of rats flown on Cosmos 1887
20 p2894 N90-26467
Experiment K-6-14. Hepatic function in rats after spaceflight 20 p2895 N90-26468
Photosynthesis in intact plants
[DE90-013699] 20 p2898 N90-26482
Computer simulation of chemical reactions in synthetic model compounds and genetically engineered active sites
[AD-A222611] 20 p2898 N90-26483
Magnetic resonance elucidation of molecule/macromolecule interaction stereochemistry
[AD-A221444] 21 p2979 N90-26928
A design tool utilizing stoichiometric structure for the analysis of biochemical reaction networks
[AD-A223873] 23 p3355 N90-28961
Joint US/USSR study: Comparison of effects of horizontal and head-down bed rest
[NASA-TP-3037] 23 p3355 N90-28965

BIOCONTROL SYSTEMS
A Scheiner-principle pocket optometer for self-evaluation and biofeedback accommodation training
[AD-A213171] 04 p0524 N90-13027

BIOCONVERSION
Modern biofuel cells for waste recycling in life support systems
[NASA-CR-185963] 05 p0638 N90-13718
Low-temperature conversion of high-moisture biomass: Continuous reactor system results
[DE90-000984] 06 p0805 N90-14683
The Third Pacific Basin Biofuels Workshop: Proceedings
[DE90-002523] 07 p0953 N90-15513
Biofuels program summary. Volume 2: Research summaries
[DE89-009484] 18 p2576 N90-24678

BIODEGRADABILITY
Assessment of biobased materials
[DE90-000300] 13 p1780 N90-20220

BIODEGRADATION
Synaptic plasticity and memory formation
[AD-A211368] 03 p0379 N90-12158
Effect of community structure on the kinetics of anaerobic degradation of aromatic compounds
[DE90-003666] 07 p0888 N90-15134
The Third Pacific Basin Biofuels Workshop: Proceedings
[DE90-002523] 07 p0953 N90-15513
Research and development on enhanced degradable plastics
[AD-A217180] 13 p1779 N90-20212
Enhanced bioreclamation of jet fuels: A full-scale test at Eglin AFB, Florida
[AD-A222348] 21 p2990 N90-26992

BIODYNAMICS
Biomedical influences on spinal cord function
[AD-A210311] 01 p0092 N90-10527
Human factors in the naval environment: A review of motion sickness and biodynamic problems
[AD-A214733] 09 p1251 N90-17258
Guidelines for safe human exposure to impact acceleration, update A
[AD-A215287] 09 p1253 N90-17268
Investigation of the effects of external supports on manual lifting
[PB90-103367] 09 p1260 N90-17307
Escape systems research at RAE
13 p1751 N90-20058
Proceedings of Biostructures as Composite Materials ARO Workshop
[AD-A220262] 18 p2518 N90-24381
Electronystagmographic findings following cervical injuries 19 p2718 N90-25466
A kinematic/dynamic model for prediction of neck injury during impact acceleration 19 p2719 N90-25469
Analysis of the biomechanic and ergonomic aspects of the cervical spine under load 19 p2719 N90-25470
Dynamical modifications to the head, load factors from additional weight 19 p2720 N90-25472
Risk of cervical injury in real and simulated accidents
19 p2721 N90-25475
Biofidelity of a dummy's neck during automobile collision testing 19 p2721 N90-25477
Omni-directional human head-neck response
[SAE-861893] 19 p2721 N90-25478

Quantitative assessment of human motion using video motion analysis 19 p2730 N90-25518
Experiment K-6-02. Biomedical, biochemical and morphological alterations of muscle and dense, fibrous connective tissues during 14 days of spaceflight 20 p2892 N00-26456
Biodynamic simulations of an aircraft pilot/passenger in various crash environments
[NIAR-90-6] 20 p2900 N90-26494
A human factors engineering approach to the development and dynamic evaluation of a prototype aircrew seat for military aircraft
[AD-A218283] 24 p3500 N90-29779

BIOELECTRIC POTENTIAL
Electrophysiological studies of visual attention and resource allocation
[AD-A212287] 04 p0525 N90-13030
Transduction of nanovolt signals: Limits of electric-field detection
[AD-A219214] 16 p2312 N90-23177

BIOELECTRICITY
Coronary arterial capacitance and subendocardial vascular patency throughout the cardiac cycle 11 p1538 N90-18855
Life sciences: Lawrence Berkeley Laboratory, 1988
[DE90-008061] 13 p1849 N90-20611
Multimedia system control
[AD-A219392] 16 p2276 N90-22971
Noninvasive estimation of fluid shifts between body compartments by measurement of bioelectric characteristics 18 p2628 N90-24976
Multi-user facility for high performance optical recording of brain activity (DURIP)
[AD-A223491] 24 p3498 N90-29768

BIOENGINEERING
NT ANTHROPOMETRY
NT BIOINSTRUMENTATION
NT ELECTROCARDIOGRAPHY
NT ELECTROENCEPHALOGRAPHY
NT ELECTROMYOGRAPHY
NT MAGNETOCARDIOGRAPHY
NRL (Naval Research Laboratory) Review
[AD-A212886] 05 p0716 N90-14182
The United States Air Force School of Aerospace Medicine: Special report
[AD-A217740] 13 p1851 N90-20622
Instrumentation and robotic image processing using top-down model control 15 p2142 N90-22239
Proceedings of Biostructures as Composite Materials ARO Workshop
[AD-A220262] 18 p2518 N90-24381
ECUT: Energy Conversion and Utilization Technologies program. Biocatalysis project
[NASA-CR-186866] 19 p2717 N90-25458

BIOFEEDBACK
NT SENSORY FEEDBACK
Computer generation of a tutorial dialogue
[AD-A211976] 03 p0360 N90-12162
A Scheiner-principle pocket optometer for self-evaluation and biofeedback accommodation training
[AD-A213171] 04 p0524 N90-13027

BIOGENESIS
U BIOLOGICAL EVOLUTION

BIOGEOCHEMISTRY
Global tropospheric chemistry: Chemical fluexes in the global atmosphere
[NASA-CR-186090] 03 p0369 N90-12109
The biogeochemistry of metal cycling
[NASA-CR-4295] 17 p2439 N90-23897
Effects of solar ultraviolet radiation on biogeochemical dynamics in aquatic environments
[AD-A221119] 18 p2578 N90-24687
Nordic Symposium on Atmospheric Chemistry
[CM-78] 20 p2883 N90-26403

BIOGRAPHY
Space flight (selected articles)
[AD-A212068] 03 p0311 N90-11769

BIOINSTRUMENTATION
Synthetic polypeptide composites for sensor applications
[AD-A210797] 01 p0052 N90-10296
The use of lithium batteries in biomedical devices
[AD-A210789] 01 p0061 N90-10350
A new generation of atmospheric tracers: The biological connection
[AD-A212285] 04 p0517 N90-12983
Amperometric biosensors for glucose, lactate, and glycolate based on oxidases and redox-modified siloxane polymers
[DE90-002301] 06 p0781 N90-14541
The development of coherent x ray lasers for x ray holography
[DE90-000784] 06 p0789 N90-14595
Advanced biosensors for amino acid detection
[AD-A214029] 08 p1076 N90-16225
Bioluminescence for detection of trace compounds
[AD-A219435] 17 p2372 N90-23503
Biosensors for the detection of heavy metal ions
[MBB-Z-0289-89-PUB] 17 p2433 N90-23864

BIOLOGICAL ACTIVITY
U ACTIVITY (BIOLOGY)

BIOLOGICAL ANALYSIS
U BIOASSAY

BIOLOGICAL CELLS
U CELLS (BIOLOGY)

BIOLOGICAL CLOCKS
U RHYTHM (BIOLOGY)

BIOLOGICAL EFFECTS
NT DESYNCHRONIZATION (BIOLOGY)
NT JET LAG
Organic explosives and related compounds. Environmental and health considerations
[AD-A210554] 01 p0054 N90-10306
Aerospace medicine and biology: A continuing bibliography with indexes (supplement 328)
[NASA-SP-7011(328)] 01 p0092 N90-10524
Biological investigations of adaptive networks: Neuronal control of conditioned responses
[AD-A211043] 01 p0094 N90-10534
Study of the behavioral and biological effects of high intensity 60 Hz electric fields
[DE89-015528] 02 p0254 N90-11438
Aerospace medicine and biology: A continuing bibliography with indexes (supplement 329)
[NASA-SP-7011(329)] 03 p0382 N90-12173
Biology in microgravity: A guide for experimenters
[ESA-TM-02] 04 p0482 N90-12769
Aerospace medicine and biology: A continuing bibliography with indexes (supplement 330)
[NASA-SP-7011(330)] 05 p0674 N90-13925
Biological effects of hyperthermia and potential risk associated with ultrasonic exposure
[PB89-100702] 06 p0820 N90-14768
Introduction to extremely-low-frequency electric and magnetic fields
[DE90-002662] 07 p0966 N90-15578
A collaborative effort to model plant response to acidic rain
[DE90-003002] 09 p1244 N90-17215
The 1988-1989 NASA space/gravitational biology accomplishments
[NASA-TM-4160] 09 p1250 N90-17251
Method for the evaluation of toxicity of combustion products from aircraft cabin materials: Analysis and results 10 p1316 N90-17612
L x ray spectrometry in vivo with a Si(Li)-NaI(Tl)
[DE90-005649] 10 p1387 N90-18028
Aerospace medicine and biology: A continuing bibliography with indexes (supplement 333)
[NASA-SP-7011(333)] 10 p1411 N90-18136
Aerospace medicine and biology: A continuing bibliography with indexes (supplement 331)
[NASA-SP-7011(331)] 10 p1411 N90-18137
Risk analysis: Fundamental concepts, regulatory toxicology, and relative comparisons from radiation biology
[DE90-002466] 11 p1536 N90-18856
Biological applications and effects of optical masers
[AD-A217910] 13 p1808 N90-20385
Biological effects of ELF (Extremely-Low-Frequency) electric and magnetic fields
[DE90-008634] 14 p2009 N90-21514
Proceedings of the 6th Regional Symposium on Biophysics
[DE90-619618] 15 p2136 N90-22206
Aerospace medicine and biology: A continuing bibliography with indexes (supplement 334)
[NASA-SP-7011(334)] 15 p2136 N90-22207
Aerospace medicine and biology: A continuing bibliography with indexes (supplement 335)
[NASA-SP-7011(335)] 15 p2136 N90-22208
Studies of 60-Hz exposure effects on human function
[DE90-009473] 15 p2137 N90-22210
A study of low level laser retinal damage
[AD-A218919] 16 p2261 N90-22887
Exposure of human cells to electromagnetic fields
[AD-A219377] 16 p2261 N90-22889
Lack of behavioral effects of high-peak-power microwave pulses from an axially extracted virtual cathode oscillator
[AD-A220779] 17 p2391 N90-23618
Aerospace medicine and biology: A continuing bibliography with indexes (supplement 336)
[NASA-SP-7011(336)] 17 p2436 N90-23877
Shutter mechanism for controlling the exposure of samples to solar radiation 18 p2540 N90-24498
Mechanism for deployment and retraction of biological samples 18 p2540 N90-24499
Microgravity as a tool in developmental biology
[ESA-SP-1123] 19 p2680 N90-25239
Microgravity and mammalian cells 19 p2680 N90-25240
Epidermal Growth Factor (EGF) induced signal transduction in A431 cells is sensitive to gravity 19 p2680 N90-25241
Experimental control of axis polarity in amphibian embryos 19 p2680 N90-25244
The role of gravity in bird development 19 p2681 N90-25246
Simulation of the inversion of amphibian eggs in a gravitational field using hollow glass spheres 19 p2681 N90-25251
Lens and limb regeneration in newt during and after 13-day long spaceflight 19 p2681 N90-25252
Aerospace medicine and biology: A cumulative index to a continuing bibliography (supplement 332)
[NASA-SP-7011(332)] 19 p2722 N90-25480
Aerospace medicine and biology: A continuing bibliography with indexes (supplement 337)
[NASA-SP-7011(337)] 19 p2722 N90-25481
Aerospace medicine and biology: A continuing bibliography with indexes (supplement 338)
[NASA-SP-7011(338)] 19 p2722 N90-25482
Natural and anthropogenic components in bulk precipitation at Blidoe (archipelago of Stockholm, Sweden) 20 p2884 N90-26409
Experiment K-6-16. Morphological examination of rat testes. The effect of Cosmos 1887 flight on spermatogonial population and testosterone level in rat testes 20 p2895 N90-26489
Neurobehavioral effects of carbon monoxide (CO) exposure in humans: Elevated carboxyhemoglobin (COHb) and cerebrovascular responses
[AD-A222840] 21 p3034 N90-27246
Aerospace medicine and biology: A continuing bibliography with indexes (supplement 339)
[NASA-SP-7011(339)] 22 p3232 N90-28327
Criteria for a recommended standard: Occupational exposure to hand-arm vibration
[PB90-168048] 22 p3233 N90-28331
Research for electric energy systems
[DE90-014221] 23 p3321 N90-28775
Aerospace medicine and biology: A continuing bibliography with indexes (supplement 340)
[NASA-SP-7011(340)] 23 p3355 N90-28963

BIOLOGICAL EVOLUTION
Press abstracts of the 21st Lunar and Planetary Science Conference
[NASA-CR-186874] 20 p2941 N90-26738

BIOLOGICAL MODELS
U BIONICS

BIOLOGICAL MODELS (MATHEMATICS)
Computation of the unsteady facilitated transport of oxygen in hemoglobin
[NASA-TM-102251] 08 p1106 N90-16400

BIOLOGICAL RHYTHM
U RHYTHM (BIOLOGY)

BIOLUMINESCENCE
Bioluminescence for detection of trace compounds
[AD-A213458] 09 p1189 N90-16889
Some problems in oceanic radiative transfer
[AD-A215935] 10 p1410 N90-18131
Bioluminescence for detection of trace compounds
[AD-A219435] 17 p2372 N90-23503

BIOMAGNETISM
Seminars of Applied Physics, Materials Physics and Biomedical Engineering, 1989
[PB89-218572] 04 p0548 N90-13192
Attention, imagery, and memory: A neuromagnetic investigation
[AD-A224560] 24 p3499 N90-29775

BIOMASS
Low-temperature conversion of high-moisture biomass: Continuous reactor system results
[DE90-000984] 06 p0805 N90-14683
Utilization of non-conventional systems for conversion of biomass to food components
[NASA-CR-177545] 07 p0968 N90-15591
Dynamics of carbon dioxide exchange of a wheat community grown in a semi-closed environment 08 p1155 N90-16689
Biomass fuels in the developing countries: An overview
[DE90-002616] 09 p1241 N90-17201
Spectral responses of soybeans and their relationship with agronomical parameters
[INPE-4832-PRE/1462] 10 p1398 N90-18084
Relationships between the aerial biomass from ground layers of cerrado and its spectral reflectance
[INPE-4848-PRE/1477] 11 p1521 N90-18760
Hawaii integrated biofuels research program, phase 1
[DE90-006885] 11 p1530 N90-18811
Carbon dioxide and water exchange rates by a wheat crop in NASA's biomass production chamber: Results from an 86-day study (January to April 1989)
[NASA-TM-102788] 19 p2716 N90-25453

System development and early biological tests in NASA's biomass production chamber
[NASA-TM-103494] 19 p2716 N90-25456
Proximate composition of seed and biomass from soybean plants grown at different carbon monoxide (CO2) concentrations
[NASA-TM-103496] 20 p2897 N90-26480
Activities report for the IBDF-INPE project SEQE, year 1987
[INPE-4534-RPE/565] 23 p3415 N90-29298

BIOMASS ENERGY PRODUCTION
Low-temperature conversion of high-moisture biomass: Continuous reactor system results
[DE90-000984] 06 p0805 N90-14683
The Third Pacific Basin Biofuels Workshop: Proceedings
[DE90-002523] 07 p0953 N90-15513
Hawaii integrated biofuels research program, phase 1
[DE90-006885] 11 p1530 N90-18811
Testing of an advanced thermochemical conversion reactor system
[DE90-007989] 15 p2123 N90-22141
Biofuels program summary. Volume 2: Research summaries
[DE89-009484] 18 p2576 N90-24678

BIOMECHANICS
U BIODYNAMICS

BIOMEDICAL DATA
Biomedical applications of synchrotron x ray microscopy
[DE90-004957] 11 p1540 N90-18867
Potential biomedical application of the Los Alamos infrared free-electron laser: DNA spectroscopy
[DE90-006505] 12 p1667 N90-19575
Software quality assurance and software safety in the biomed control system
[DE90-008072] 13 p1866 N90-20706
The SPECIALIST: Natural language processing system
[PB90-240029] 23 p3381 N90-29098

BIOMETRICS
NT ANTHROPOMETRY
NT ELECTROCARDIOGRAPHY
NT ELECTROENCEPHALOGRAPHY
NT ELECTROMYOGRAPHY
NT MAGNETOCARDIOGRAPHY

BIONICS
Collective properties of neural systems and their relation to other physical models
[AD-A219071] 16 p2315 N90-23201
Effects of protracted ionizing radiation dosage on humans and animals: A brief review of selected investigations
[AD-A222240] 21 p3033 N90-27241
Microscopic models for electromagnetic wave propagation in highly dispersive media
[AD-A224382] 24 p3460 N90-29540
Directing an animated scene with autonomous actors
[REPT-89-041] 24 p3531 N90-29972

BIOPHYSICS
NT HEALTH PHYSICS
NT PUBLIC HEALTH
DOE/CEC Workshop on Critical Evaluation of Radiobiological Data to Biophysical Modeling
[DE89-015214] 02 p0254 N90-11437
The sensory transduction pathways in bacterial chemotaxis 05 p0677 N90-13944
Gravitropism in plants: Hydraulics and wall growth properties of responding cells 05 p0678 N90-13950
Life sciences: Lawrence Berkeley Laboratory, 1988
[DE90-008061] 13 p1849 N90-20611
Modelling of molecular structures and properties in physical chemistry and biophysics
[AD-A214561] 14 p1947 N90-21145
JPRS report: Science and technology. USSR: Life sciences
[JPRS-ULS-90-002] 14 p1995 N90-21434
Proceedings of the 6th Regional Symposium on Biophysics
[DE90-619618] 15 p2136 N90-22206
The predictability and efficiency of human walking: Metabolic, mechanical, and biophysical considerations 15 p2137 N90-22211
Proceedings of Biostructures as Composite Materials ARO Workshop
[AD-A220262] 18 p2518 N90-24381

BIOPOLYMERS
NT ALBUMINS
NT ASPARTATES
NT CARBOXYHEMOGLOBIN
NT CATALASE
NT CHOLINESTERASE
NT CYTOCHROMES
NT DEOXYRIBONUCLEIC ACID
NT ENZYMES
NT GLOBULINS
NT HEMOGLOBIN
NT MELANIN
NT OXIDASE
NT PROTEINS
NT RIBONUCLEIC ACIDS
The biocorrosion of copper by biopolymers as examined in situ, in real time FT-IR/CIR/ATR in conjunction with pre and post XPS/AES
[DE90-002086] 06 p0747 N90-14348
Characterization of biopolymer surfaces using scanning microscopies
[AD-A216572] 11 p1490 N90-18572
The flow of non Newtonian fluids in porous media 19 p2691 N90-25307
Polymer research
[PB90-246638] 23 p3313 N90-28737

BIOPROCESSING
Molecular biology and physiology of methanogenic archaebacteria
[AD-A210399] 01 p0091 N90-10522
Research in biological separations and cell culture
[NASA-CR-172060] 15 p2135 N90-22202
ECUT: Energy Conversion and Utilization Technologies program. Biocatalysis project
[NASA-CR-186866] 19 p2717 N90-25458

BIOREACTORS
Model system studies with a phase separated membrane bioreactor 05 p0679 N90-13954
Design challenges for space bioreactors 05 p0679 N90-13955
Fermentation and oxygen transfer in microgravity 05 p0679 N90-13956
Low-temperature conversion of high-moisture biomass: Continuous reactor system results
[DE90-000984] 06 p0805 N90-14683
Bio-reactor chamber
[NASA-CASE-MSC-20929-1] 09 p1250 N90-17252
Three-dimensional coculture process
[NASA-CASE-MSC-21560-1] 11 p1538 N90-18852
Research in biological separations and cell culture
[NASA-CR-172060] 15 p2135 N90-22202
The effects of simulated hypogravity on murine bone marrow cells 18 p2631 N90-24989

BIOREGENERATION
U REGENERATION (PHYSIOLOGY)

BIOREGENERATIVE LIFE SUPPORT SYSTEMS
U CLOSED ECOLOGICAL SYSTEMS

BIORHYTHMS
U RHYTHM (BIOLOGY)

BIOSENSORS
U BIOINSTRUMENTATION

BIOSIMULATION
U BIONICS

BIOSPHERE
Managing marine protected areas: An action plan
[PB89-158778] 06 p0808 N90-14701
Climate-biosphere interactions scope of work
[PB90-106444] 06 p0814 N90-14734
Strategic implementation plan
[NASA-TM-102907] 17 p2433 N90-23861
CNES space programmes related to climate 19 p2706 N90-25400

BIOSYNTHESIS
Biomedical studies with the free electron laser
[AD-A208927] 01 p0091 N90-10519
Membrane fusion: The role of polyphosphatidylinositol
[AD-A211289] 03 p0379 N90-12156
Metabolism, seizures, and blood flow in brain following organophosphate exposure: Mechanisms of action and possible therapeutic agents
[AD-A217098] 12 p1696 N90-19740
Assessment of biobased materials
[DE90-000300] 13 p1780 N90-20220
Microgravity and mammalian cells 19 p2680 N90-25240
Gas exchange characteristics as indicators of the basic limiting factors in photosynthesis
[DE90-012399] 20 p2898 N90-26481
A design tool utilizing stoichiometric structure for the analysis of biochemical reaction networks
[AD-A223873] 23 p3355 N90-28961
Interaction of electromagnetic fields with chondrocytes in gel culture
[AD-A223397] 24 p3497 N90-29765

BIOTECHNOLOGY
Army Science Conference Proceedings (16th) held in Fort Monroe, Virginia on 25-27 October 1988: Addenda
[AD-A210235] 01 p0143 N90-10827
Model system studies with a phase separated membrane bioreactor 05 p0679 N90-13954
Bio-reactor chamber
[NASA-CASE-MSC-20929-1] 09 p1250 N90-17252
Breeding of hydrogen producing anaerobic bacteria. Cellulase secretion from transformed Escherichia coli JM109
[DE90-710739] 10 p1410 N90-18133
Artificial life: The coming evolution
[DE90-008860] 14 p2009 N90-21515
Archaebacterial involvement in microbial metal corrosion: Metabolism of S and Fe
[AD-A219982] 17 p2377 N90-23537
Proceedings of Biostructures as Composite Materials ARO Workshop
[AD-A220262] 18 p2518 N90-24381
Understanding our genetic inheritance. The US Human genome project: The first five years, FY 1991-1995
[DE90-008240] 18 p2584 N90-24718

BIPLANES
The Stealth biplane: A proposal in response to a low Reynolds Number station keeping mission
[NASA-CR-186680] 19 p2658 N90-25127

BIPOLAR TRANSISTORS
Parameter estimation for the Gummel-Poon transistor model
[MA-53] 05 p0635 N90-13705
Design of a power component with IGBT insulated grid. Static and dynamic study
[ECL-88-22] 05 p0636 N90-13710
Modeling and measurement methods for high speed bipolar transistors
[REPT-11] 05 p0636 N90-13714
Defect control and denuded trap zones in the 3-5 semiconductors
[AD-A214099] 07 p1004 N90-15814
A physical and numerical study of the turn-off behavior of bipolar power transistors
[LAAS-89185] 08 p1061 N90-16136
Pulse-width dependent radiation effects on electronic components
[AD-A219517] 17 p2395 N90-23643
A high frequency (20 kHz) power electronics reactive-current compensator with insulated gate bipolar transistors as semiconductor switches
[EMV-88-54] 17 p2399 N90-23665
An ultrasonic-switching three phase current source inverter with insulated gate bipolar transistors
[EMV-89-11] 17 p2399 N90-23666
EHF heterojunction bipolar transistors
[AD-A220984] 18 p2548 N90-24541
Neutron and gamma irradiation effects on power semiconductor switches
[NASA-TM-103200] 19 p2686 N90-25278
Higher order diffusion model for a bipolar transistor
[PB90-190901] 22 p3167 N90-27960
Wideband impedance transformer for UHF power transistor time domain waveform measurement system
[PB90-210642] 22 p3167 N90-27962

BIPOLARITY
A new semicustom integrated bipolar amplifier for silicon strip detectors
[DE89-015585] 02 p0215 N90-11229
Sealing L-alloys/FeS(x) cells for a bipolar battery
[DE90-004887] 09 p1214 N90-17040
Characterization testing of a 40 AHR bipolar nickel-hydrogen battery 13 p1822 N90-20463
Development of a sealed bipolar Li-alloy/FeS2 battery for electric vehicles
[DE90-013650] 21 p2999 N90-27045

BIPROPELLANTS
U LIQUID ROCKET PROPELLANTS

BIRD-AIRCRAFT COLLISIONS
Definition and reduction of the F-18 windshield birdstrike hazard
[AD-A210700] 01 p0004 N90-10015
Test and evaluation: Reducing risks to military aircraft from bird collisions. Report to the Chairman, Legislation, and National Security Subcommittee, Committee on Goverment Operations, House of Representatives
[AD-A210670] 02 p0148 N90-10845
Study of the engine bird ingestion experience of the Boeing 737 aircraft
[DOT/FAA/CT-89/16] 05 p0576 N90-13360
Full-scale birdstrike testing of in-service aged F-111 ADBIRT windshield transparencies
[AD-A218035] 13 p1754 N90-20069
Bird impact tests on Kevlar 29 and 49 sandwich structures under straight-on and glancing impact
[REPT-S3-4273-PARTIAL-6] 16 p2212 N90-22617
Bird impact tests on Kevlar plates. Sandwich Kevlar-nida submitted to straight-on and glancing impact
[REPT-S3-4273-PARTIAL-3] 16 p2212 N90-22619
Bird impact tests on structures made of Kevlar 49. Monolithic plates under straight-on impact
[REPT-S3-4273-PARTIAL-1] 16 p2213 N90-22620
Forward canopy feasibility and Thru-The-Canopy (TTC) ejection system study
[AD-A220360] 18 p2495 N90-24258
Study of the engine bird ingestion experience of the Boeing 737 aircraft (October 1986 to September 1988)
[DOT/FAA/CT-89/29] 19 p2656 N90-25119

User's manual ROBIN: A research and notification system for bird migration
[FEL-1989-103] 23 p3270 N90-28508

BIRDS

Study of the engine bird ingestion experience of the Boeing 737 aircraft
[DOT/FAA/CT-89/16] 05 p0576 N90-13360
Bird impact tests on asymmetric sandwich structures made in Kevlar 49
[CEAT-NT-10/S/83-5] 09 p1162 N90-16727
Bird impact tests on curved structures of the type Sandwich-Kevlar-Nida for normal and angular shooting
[CEAT-NT-10/S/83-4] 09 p1162 N90-16728
Study of bird ingestions into small inlet area, aircraft turbine engines (May 1987 to April 1988)
[DOT/FAA/CT-89/17] 11 p1453 N90-18375
Bird impact tests on a Kevlar 49 structure. Monolithic plates. Oblique-angled impact
[REPT-S3-4273] 11 p1454 N90-18376
Remote sensing for the classification and quantification of vegetation in Spring staging areas of Brent geese on the Frisian Islands (Netherlands)
[BCRS-89-27] 11 p1527 N90-18790
The role of gravity in bird development
19 p2681 N90-25246

BIREFRINGENCE

Utilization of photorefractive crystals in optical image processing
[ISBN-3-923560-06-0] 02 p0225 N90-11292
Spectral contents readout of birefringent sensor
[NASA-CR-179444] 06 p0843 N90-14905
An illustrated guide of optical characteristics of aircraft transparencies
[AD-A214565] 09 p1167 N90-16752
Micro-miniature roll rate sensor
[AD-A214778] 09 p1225 N90-17107
Integrated optics anisotropic waveguides and devices
[AD-A217064] 12 p1715 N90-19849
Models of intracavity frequency doubled lasers
[AD-A221182] 18 p2563 N90-24628
Polarization contrast vision
[AD-A221423] 21 p3076 N90-27492
Adaptive polarization diversity detection scheme for coherent communications and interferometric fiber sensors
[AD-D014479] 22 p3163 N90-27938

BISMALEIMIDE

Modified bismaleimides for carbon fibre composites
11 p1476 N90-18495
Utilization of thermometric methods for the testing of carbon reinforced plastics
[ETN-90-96076] 12 p1621 N90-19314
Development of a graphite/bismaleimide leading edge for the F-111 (EF-111A) horizontal stabilizer
21 p2956 N90-26809
A characterization of V-391/H46-8B, A toughened BMI prepreg system produced by US Polymeric
[AD-A221772] 21 p2989 N90-26985
Thermal analysis of bismaleimide matrix resins
[DE90-016283] 24 p3457 N90-29523

BISMUTH

Spin-orbit relaxation rates of Bi(6p(3)) 2D(3/2) following photolysis of Bi(CH3)3 at lambda = 193 nm
[AD-A211792] 03 p0402 N90-12303
The effect of composition and processing on high T(sub c) superconductors containing bismuth
[DE90-002203] 06 p0854 N90-14965
Aligned bismuth, strontium, calcium cuprate coatings on polycrystalline substrates
[AD-D014522] 19 p2678 N90-25229

BISMUTH ALLOYS

Phase equilibria and solution thermodynamics of bismuth-lead alloys
[PB90-138421] 14 p1950 N90-21163

BISMUTH COMPOUNDS

NT BISMUTH OXIDES
NT BISMUTH SULFIDES
Synthesis conductivity, and x ray photoelectron spectrum of Bi2Sr2Cu(sub 7+x). A new ternary bismuth-oxide system exhibiting metallic conductivity
[DE90-003010] 07 p0999 N90-15778
An explanation for the rise in T(sub c) in the Tl- and Bi-based high temperature superconductors
22 p3142 N90-27822
Stabilization of high T(sub c) phase in bismuth cuprate superconductor by lead doping
22 p3144 N90-27832
Evidence for a coherence gap in Ce3Bi4Pt3
[DE90-014925] 23 p3399 N90-29207

BISMUTH OXIDES

Bi-Sr-Ca-Cu-O superconducting ceramics
[DE89-636225] 06 p0855 N90-14972
Development of planar geometry solid oxide fuel cells
[PB90-100769] 08 p1095 N90-16341
High temperature neutron diffraction study of the formation reaction of bismuth superconductors
[DE90-004883] 08 p1134 N90-16568
Evolution of structure and electrical properties during crystallization of rapidly solidified Bi4Ti3O12
[DE90-005221] 09 p1292 N90-17492
High temperature superconductivity
[AD-A215491] 10 p1436 N90-18286
Superconductivity in Ba(1-x)BiO3
[DE90-003781] 12 p1718 N90-19869
Synthesis of Bi-Sr-Ca-Cu oxide superconductor by solution technique
[DE90-008707] 13 p1897 N90-20888
Practical superconductor development for electrical power applications
[DE90-010262] 18 p2625 N90-24957
In-situ growth of superconducting films of Bi-Sr-Ca-Cu-O using magnetron sputtering
[DE90-011161] 18 p2626 N90-24962
Phenomenological theory of the normal and superconductive states of Cu-O and Bi-O metals
22 p3142 N90-27819
Magnetic properties of the 110K superconducting phase in Pb-doped Bi-Sr-Ca-Cu-O thin films
22 p3151 N90-27868
Optical and microwave detection using Bi-Sr-Ca-Cu-O thin films
22 p3152 N90-27870

BISMUTH SULFIDES

Scanning laser photocurrent spectroscopy of electrochemically grown bismuth sulphide films
[AERE-M-3709] 16 p2217 N90-22649

BISTABLE AMPLIFIERS

U FLIP-FLOPS

BISTABLE CIRCUITS

NT FLIP-FLOPS
Optically tunable gratings for optical interconnects
[AD-A216978] 12 p1714 N90-19844

BISTATIC RADAR

U MULTISTATIC RADAR

BISTATIC REFLECTIVITY

Millimeter wave radar clutter program
[AD-A215772] 10 p1376 N90-17978
The measurement of surface reflectivity at millimetre wavelengths
[MRL-TN-559] 14 p1960 N90-21222
Development of new methods for predicting the bistatic electromagnetic scattering from absorbing shapes
[AD-A219327] 17 p2388 N90-23600

BIT ERROR RATE

A performance comparison between block interleaved and helically interleaved concatenated coding systems
04 p0486 N90-12792
Performance of the image statistics decoder in conjunction with the Goldstone-VLA array
04 p0487 N90-12796
Binary Gray codes and index systems
[REPT-89-29] 04 p0530 N90-13060
Error detection and correction for a multiple frequency quaternary phase shift keyed signal
[AD-A215706] 09 p1208 N90-17003
Effects of amplitude distortions and IF equalization on satellite communication system bit-error rate performance
[NASA-TM-102415] 12 p1645 N90-19454
Bit-error-rate testing of fiber optic data links for MMIC-based phased array antennas
[NASA-TM-102523] 14 p1966 N90-21261
How to construct an atomic variable
[CWI-CS-R8939] 18 p2596 N90-24772
A versatile integrated block codes encoder-decoder
20 p2848 N90-26197
Converses for write-unidirectional memories
[EUT-89-E-220] 20 p2909 N90-26546

BIT SYNCHRONIZATION

Frame synchronization methods based on channel symbol measurements 04 p0486 N90-12795
Coordination of processing elements in a multiprocessor computer
[WO-PATENT-88/04075] 06 p0831 N90-14830
Bit-optimal election in synchronous rings
[RUU-CS-89-2] 17 p2446 N90-23945
Propagation Effects and Circuit Performance of Modern Military Radio Systems with Particular Emphasis on Those Employing Bandspreading
[AGARD-CP-442] 20 p2844 N90-26178
New synchronisation techniques applicable to multi-tone transmission systems 20 p2848 N90-26199
Synchronization of frequency shift transmission and the effect of oversampling 20 p2848 N90-26200
New approaches for rapid synchronisation frequency hoppers 20 p2849 N90-26201

BITS

The distributed bit complexity of the ring: From the anonymous to the non-anonymous case
[RUU-CS-88-33] 17 p2452 N90-23988
How to construct an atomic variable
[CWI-CS-R8939] 18 p2596 N90-24772

BIVARIATE ANALYSIS

Operational measures of central tendency
[DE89-016959] 03 p0392 N90-12234
Practice of bivariate quadratic simplicial splines
[MEMO-800] 05 p0691 N90-14034
Multivariate clustering based on entropy
[PB89-233993] 10 p1439 N90-18303
Use of Coxian-type distributions in a general model of the maximum of bivariate random variables
[PB90-121229] 12 p1704 N90-19780
Forecasting the tornadic intensities of thunderstorms by multivariate techniques
[AD-A218284] 13 p1847 N90-20602
The perceptual interaction of graphical attributes in thirteen bivariate displays
[AD-A217980] 13 p1868 N90-20720
Unification of statistical methods for continuous and discrete data
[AD-A224307] 24 p3540 N90-30017

BL LACERTAE OBJECTS

Analysis of nearly simultaneous X-ray and optical observations of active galactic nuclei
01 p0139 N90-10806
The ratio to X-ray spectral shape and variability of blazars 02 p0297 N90-11688
Short time scale variability of the BL Lac object OJ 287 in the near-infrared
[IFSI-89-3] 08 p1140 N90-16603
Spectral plane quasars, spectral turn-over, and frequency atlas
[INPE-5011-TDL/399] 16 p2329 N90-23277
BL Lacs from the EMSS: Number-counts and implications for the luminosity function
19 p2785 N90-25849
Multifrequency observation of blazars
19 p2786 N90-25857
Variability in BL Lac objects: A schematic model
19 p2787 N90-25861
Rapid X ray variability in BL Lacertae objects
19 p2787 N90-25862
X ray spectra of OVV QSOs 19 p2787 N90-25863
Multiwavelength observations of BL Lacertae
19 p2791 N90-25886
X ray emission from relativistic jets in AGNs and statistical implications 19 p2792 N90-25893
X ray constraints on the beaming hypothesis for BL Lacertae objects 19 p2793 N90-25900

BLACK BODY RADIATION

Development of the blackbody probe type pyrometer, part 1. Experimental study on the fundamental characteristics
[DE89-782288] 12 p1663 N90-19553
Analysis of methods to determine emissivity for ground surface targets in the spectral band 8 to 14 microns
[INPE-4984-TDL/394] 13 p1820 N90-20447
A modified Moebius inverse formula and its applications in physics
[DE90-612740] 14 p2022 N90-21594
Model atmospheres for novae during the early stages
[NASA-CR-180498] 14 p2038 N90-21694
Einstein SSS+MPC observations of Seyfert type galaxies 19 p2795 N90-25913
Stratocumulus cloud height variations determined from surface and satellite observations
22 p3214 N90-28230

BLACK HOLES (ASTRONOMY)

Scalar fields versus black holes
[DE89-611967] 03 p0420 N90-12413
Twistons
[RSRE-MEMO-4234] 04 p0562 N90-13275
Perturbation methods for the calculation of gravitational waves from slightly non-spherical spacetimes with applications to stellar core collapse
06 p0863 N90-15015
Black-hole decay and topological stability in quantum gravity
[DE89-618785] 06 p0863 N90-15017
An atlas of aperiodic variability in HMXB
[MPE-PREPRINT-158] 08 p1140 N90-16605
On quantum effects near a black hole singularity
[DE90-600754] 08 p1151 N90-16668
Infrared spectroscopy of the central few parsecs of the galaxy 11 p1585 N90-19140
Gamma ray astronomy and black hole astrophysics
[NASA-CR-186496] 11 p1590 N90-19169
Nearly simultaneous optical, ultraviolet, and x ray observations of three PG quasars
[NASA-CR-186355] 12 p1728 N90-19932
Relativistic Gravitational Experiments in Space
[NASA-CP-3046] 12 p1730 N90-19940
Sources of gravitational waves
12 p1730 N90-19942
Detecting gravity waves from binary black holes
12 p1730 N90-19943

Gravitational radiation from rotating gravitational collapse 12 p1730 N90-19944
General relativistic x ray (UV) polarization rotations as a quantitative test for black holes 12 p1732 N90-19957
Space telescope searches for black holes in galactic nuclei 12 p1732 N90-19958
LAGEOS 3 and the gravitomagnetic field 12 p1733 N90-19961
Toward quantum corrections in black hole thermodynamics 14 p2040 N90-21702
Multipole moments in general relativity and dynamical perturbations of black-hole magnetospheres 15 p2190 N90-22509
The dynamical evolution of dense clusters of compact stars 16 p2331 N90-23287
Studies in gravitational lensing and numerical hydrodynamics 16 p2332 N90-23290
What can gamma rays tell us about binary x ray sources and SNR's 16 p2336 N90-23310
Spectral evolution of active galactic nuclei Penrose Compton scattering processes and gamma ray emission from Seyfert galaxies 16 p2337 N90-23317
Contributions of the X Ray Astronomy Group of the Max-Planck-Institut fuer Extraterrestrische Physik [MPE-PREPRINT-165] 17 p2482 N90-24196
Observations of black hole candidates with the Mir-Kvant HEXE 17 p2483 N90-24198
EXOSAT observations of Cygnus X-1: Study of the soft x ray excess 17 p2483 N90-24199
Black holes in X ray binaries: X ray properties of the galactic black hole candidates 19 p2765 N90-25712
QPOs from black-hole candidates 19 p2770 N90-25743
EXOSAT observations of Cygnus X-1: Study of the soft X ray excess 19 p2771 N90-25750
The soft X ray spectrum of Cygnus X-1 19 p2771 N90-25751
Observations of black hole candidates with the Mir-Kvant HEXE 19 p2774 N90-25774
The optical light curve of Cygnus X-1 19 p2778 N90-25801
Constraints on the SS433 system from the Ginga observations 19 p2784 N90-25838
X ray AGN variability with hour to month timescales 19 p2788 N90-25869
X ray emission from relativistic jets in AGNs and statistical implications 19 p2792 N90-25893
Baryogenesis in extended inflation. 2: Baryogenesis via primordial black holes [NASA-CR-182843] 20 p2941 N90-26735
Information loss down a black hole [DE90-627482] 24 p3562 N90-30154

BLACK SEA
Analysis of altimetry over inland seas [NASA-TM-100729] 13 p1840 N90-20566

BLADDER
Rapidly quantifying the relative distention of a human bladder [NASA-CASE-LAR-13901-1-NP] 14 p2010 N90-21519

BLADE SLAP
U BLADE-VORTEX INTERACTION

BLADE SLAP NOISE
Data of aero acoustic measurements on ultra-light aircraft propellers [ESA-TT-1147] 19 p2754 N90-25648

BLADE TIPS
User's manual for PEPSIG NASA tip vortex version [NASA-CR-182178] 02 p0146 N90-10835
Computation of the tip vortex flowfield for advanced aircraft propellers [NASA-CR-182179] 02 p0146 N90-10836
Acoustical effects of a large ridge on low-frequency sound propagation in stationary and moving atmospheres [NASA-CR-186001] 03 p0400 N90-12290
Advanced clearance control systems --- blade tips [PNR90553] 04 p0454 N90-12601
Dynamic tip clearance measurements in axial flow compressors [PNR90597] 04 p0456 N90-12612
Flows with tip leakage 05 p0641 N90-13740
Rotor induced-inflow-ratio measurements and CAMRAD calculations [NASA-TP-2946] 08 p1017 N90-15882
An experimental investigation of viscous aspects of propeller blade flow 09 p1159 N90-16711
Turbine blade data acquisition system user's guide [AD-A214986] 09 p1169 N90-16763
Z-grid signal conditioning system user's guide and technical reference [AD-A215122] 10 p1395 N90-18067
Losses in the tip-leakage flow of a planar cascade of turbine blades 14 p1925 N90-21027
Analysis of the rotor tip leakage flow with tip cooling air ejection 14 p1926 N90-21029
The validation and application of a rotor acoustic prediction computer program [NASA-TM-101794] 21 p3072 N90-27465
Noise from tip vortex and bubble cavitation [AD-A221962] 21 p3072 N90-27468
Blade tip rubbing stress prediction 23 p3290 N90-28615
Structural testing and analytical research of turbine components [AD-A223516] 24 p3434 N90-29396
Noncontact measurement of rotating blade vibrations [NAL-TR-1033] 24 p3483 N90-29687

BLADE-VORTEX INTERACTION
User's manual for PEPSIG NASA tip vortex version [NASA-CR-182178] 02 p0146 N90-10835
Computation of the tip vortex flowfield for advanced aircraft propellers [NASA-CR-182179] 02 p0146 N90-10836
An investigation of counterrotating tip vortex interaction [NASA-CR-185135] 02 p0271 N90-11549
Review and analysis of the DNW/Model 360 rotor acoustic data base [NASA-TM-102253] 03 p0299 N90-11692
Application of a copper vapour laser to investigation of shock and blade interaction in a shock tube [PNR90578] 04 p0506 N90-12918
Rotor induced-inflow-ratio measurements and CAMRAD calculations [NASA-TP-2946] 08 p1017 N90-15882
Prediction of rotor blade-vortex interaction noise from 2-D aerodynamic calculations and measurements [ISL-CO-243/88] 11 p1451 N90-18365
Study of the blade/vortice interaction on a one-blade rotor during forward flight (incompressible, non viscous fluid) [ISL-R-115/88] 11 p1456 N90-18391
Development of a mass averaging temperature probe 11 p1461 N90-18418
Methods for making unsteady aerodynamic pressure measurements in a rotating turbine stage 11 p1463 N90-18426
Airloads, wakes, and aeroelasticity [NASA-CR-177551] 15 p2048 N90-21738
Extension of a three-dimensional viscous wing flow analysis [NASA-CR-182023] 17 p2344 N90-23348
Aerodynamic loads and blade vortex interaction noise prediction [ISL-PU-310/89] 20 p2802 N90-25942
Noise from tip vortex and bubble cavitation [AD-A221962] 21 p3072 N90-27468
The acoustic results of a United Technologies scale model helicopter rotor tested at DNW [NASA-TM-101879] 21 p3073 N90-27471
Numerical simulations of blade-vortex interactions and lifting hovering rotor flows [AD-A224238] 24 p3417 N90-29302

BLADES
Calculation of the unsteady two-dimensional, inviscid, compressible flow around a strongly cambered oscillating single blade 11 p1460 N90-18409

BLASIUS FLOW
Absolute determination of the wall shear stress by means of an interferometer [DFVLR-FB-89-13] 03 p0349 N90-11991

BLAST LOADS
Minutes of the 23rd Explosives Safety Seminar, volume 1 [AD-A218264] 14 p1958 N90-21213
Minutes of the 23rd Eplosives Safety Seminar, volume 2 [AD-A218265] 14 p1959 N90-21214
Design concepts for hardened communications structures [AD-A221233] 19 p2683 N90-25260

BLASTOFF
U ROCKET LAUNCHING

BLATTIDAE
U COCKROACHES

BLAZARS
NT BL LACERTAE OBJECTS
An optical and infrared study of blazars 12 p1728 N90-19930

BLEED-OFF
U PRESSURE REDUCTION

BLENDS
U MIXTURES

BLINDNESS
NT FLASH BLINDNESS

BLINDS
Shutter mechanism for controlling the exposure of samples to solar radiation 18 p2540 N90-24498

BLOCK COPOLYMERS
The improved adhesion of organic polymers to silica and to aluminum metal with zirconium Schiff-base block copolymer coatings [AD-A216669] 11 p1490 N90-18575
CO2 diffusion and solubility in a Polystyrene/Polybutadiene block copolymer with highly oriented lamellar morphology [AD-A217165] 13 p1779 N90-20211
Synthesis and characterization of aromatic polyester and polysiloxane containing block copolymers: Multiphase transparent atomic oxygen resistant damping materials, liquid crystal films, and toughening components of sol/gel glasses [AD-A218871] 16 p2224 N90-22685
The origin of multiple melting in polyurethane block copolymers [AD-A220050] 17 p2381 N90-23583
Compression molded polyurethane block copolymers. 3: Evaluation of microphase compositions [AD-A220160] 17 p2382 N90-23584
Compression molded polyurethane block copolymers. 1: Thermal and thermomechanical properties [AD-A220068] 18 p2529 N90-24431
Imide/arylene ether copolymers [NASA-CASE-LAR-14159-1-CU] 21 p2983 N90-26953
Modification of polystyrene/polybutadiene block copolymer films by chemical reaction with bromine and effect on gas permeability [AD-A223612] 24 p3455 N90-29513

BLOCK DIAGRAMS
The algebra of the NODEN analyser [RSRE-89012] 08 p1111 N90-16432
Block Runge-Kutta methods on parallel computers [CWI-NM-R8906] 17 p2452 N90-23982
Block Runge-Kutta methods [CWI-NM-R8913] 17 p2452 N90-23983
Large sets of block designs [ETN-90-97212] 20 p2918 N90-26602

BLOCKING
Effect of central obscuration on the LDR point spread function 05 p0598 N90-13475
The effects of nonselective and selective beta blockade upon nonshivering thermogenesis during an acute cold exposure in cold acclimated men 06 p0820 N90-14767
The role of an upstream cyclone and corresponding synoptic/planetary-scale interactions during the development of a blocking anticyclone 08 p1150 N90-16659
The utilization of an infrared imaging system as a cooling slot blockage detector in the inspection of a transpiration cooled nozzle [NASA-TM-102608] 12 p1663 N90-19555
An adaptive blocking strategy for matrix factorizations [DE90-011108] 21 p3051 N90-27343

BLOOD
High-frequency ventilation in dogs with three gases of different densities [AD-A212862] 06 p0819 N90-14762
Carboxyalkylated hemoglobin as a potential blood substitute [AD-A213886] 07 p0966 N90-15582
Arginine vasopressin lowers pulmonary artery pressure in hypoxic rats by releasing artrial natriuretic peptide [AD-A215986] 10 p1410 N90-18134
Performance of a coincidence based blood activity monitor [DE90-006105] 11 p1540 N90-18865
Neurobehavioral effects of carbon monoxide (CO) exposure in humans: Elevated carboxyhemoglobin (COHb) and cerebrovascular responses [AD-A222840] 21 p3034 N90-27246

BLOOD CELLS
NT ERYTHROCYTES
NT LEUKOCYTES
NT LYMPHOCYTES

BLOOD CIRCULATION
NT BRAIN CIRCULATION
NT CORONARY CIRCULATION
NT PULMONARY CIRCULATION
Generation of free radicals during cold injury and rewarming [AD-A213088] 05 p0672 N90-13915
Monitoring chaos of cardiac rhythms [DE90-000692] 07 p0968 N90-15580
United States Air Force research initiation program for 1988, volume 4 [AD-A223126] 21 p3102 N90-27616

BLOOD FLOW
Coronary arterial capacitance and subendocardial vascular patency throughout the cardiac cycle 11 p1538 N90-18855

BLOOD PLASMA
Study of rifampicin fixation on plasma proteins by derivative spectrophotometry
[CERMA-89-25] 11 p1540 N90-18866
Hypobaric hypoxia (380 torr) decreases intracellular and total body water in goats
[AD-A218192] 13 p1849 N90-20615
The effects of graded exercise at sea level on plasma proenkephalin peptide F and catecholamine responses
[AD-A218195] 13 p1853 N90-20633

BLOOD PRESSURE
NT HYPERTENSION
NT HYPOTENSION
NT LOWER BODY NEGATIVE PRESSURE
Arginine vasopressin lowers pulmonary artery pressure in hypoxic rats by releasing artrial natriuretic peptide
[AD-A215986] 10 p1410 N90-18134
The role of blood volume in determining the cardiovascular adjustments to exercise
11 p1538 N90-18854
Elevated central venous pressure: A consequence of exercise training-induced hypervolemia
[NASA-TM-102965] 13 p1850 N90-20617
Hemodynamic and ADH responses to central blood volume shifts in cardiac-denervated humans
[NASA-TM-103471] 20 p2898 N90-26485
Cardiovascular deconditioning of cosmonauts: Role, importance and applications of the lower body negative pressure
[ETN-90-97507] 23 p3355 N90-28964

BLOOD VESSELS
NT ARTERIES
Arginine vasopressin lowers pulmonary artery pressure in hypoxic rats by releasing artrial natriuretic peptide
[AD-A215986] 10 p1410 N90-18134

BLOOD VOLUME
Control of thermoregulatory sweating during exercise in the heat
[AD-A206001] 01 p0092 N90-10523
The role of blood volume in determining the cardiovascular adjustments to exercise
11 p1538 N90-18854
Elevated central venous pressure: A consequence of exercise training-induced hypervolemia
[NASA-TM-102965] 13 p1850 N90-20617
A comparison of the mechanisms of cold- and microgravity-induced fluid loss
[AD-A218098] 13 p1852 N90-20631
Hemodynamic and ADH responses to central blood volume shifts in cardiac-denervated humans
[NASA-TM-103471] 20 p2898 N90-26485

BLOWERS
The hypersonic vacuum wind tunnels: Status, research, and necessary developments 18 p2490 N90-24231

BLOWING
Numerical experiments on transition control in wall-bounded shear flows 04 p0443 N90-12536
Effect of pylon wake with and without pylon blowing on propeller thrust
[NASA-TM-4162] 06 p0718 N90-14190
Controlled vortical flow on delta wings through unsteady leading edge blowing
[NASA-CR-186267] 09 p1160 N90-16712
Control of vortex aerodynamics at high angles of attack 23 p3273 N90-28523

BLOWOFF (COMBUSTION)
U FLAMEOUT

BLOWOUTS
Blow-out of rubber blocks due to internal heating
[AD-A215730] 09 p1198 N90-16943

BLUE STARS
Ultraviolet properties of hot stars in globular clusters
06 p0862 N90-15007
Evolutionary effects in B stars
14 p2041 N90-21704
The shock process and light element production in supernovae envelopes
[NASA-CR-182854] 22 p3262 N90-28471

BLUFF BODIES
Characterization of nonpremixed turbulent bluff-body burner flames
[PB89-229447] 04 p0469 N90-12689
Fluctuating wind forces measured on a bluff body extending from a cavity
[AD-A216414] 10 p1386 N90-18020
A method for the reduction of aerodynamic drag of road vehicles
[NASA-TM-102589] 22 p3108 N90-27656
An investigation of the steady and unsteady near wake and its effect on a laminar boundary layer
23 p3324 N90-28794

BLUNT BODIES
Blunt-nose inviscid airflows with coupled nonequilibrium processes 05 p0573 N90-13336
Optimum shape of a blunt forebody in hypersonic flow
[NASA-CR-181955] 05 p0575 N90-13351
Computation of nonequilibrium gas flow past blunt bodies
[PREPRINT-488] 05 p0644 N90-13757
Measured and predicted aerodynamic coefficients and shock shapes for Aeroassist Flight Experiment (AFE) configuration
[NASA-TP-2956] 06 p0717 N90-14185
Demonstration of the feasibility of laser induced fluorescence for arc jet flow diagnostics
[NASA-CR-185595] 08 p1040 N90-16013
Computation of compressible viscous flows
10 p1308 N90-17567
Fluctuating wind forces measured on a bluff body extending from a cavity
[AD-A216414] 10 p1386 N90-18020
Interaction of an oblique shock wave with supersonic flow over a blunt body 12 p1598 N90-19197
An approximate viscous shock layer method for calculating the hypersonic flow over blunt-nosed bodies
14 p1910 N90-20947
Parallel computation of supersonic flows using a three-dimensional, zonal, Navier-Stokes code
[AD-A218824] 17 p2344 N90-23350
Equilibrium radiative heating tables for Earth entry
[NASA-TM-102652] 17 p2401 N90-23675
Temperature determination of shock layer using spectroscopic techniques 18 p2628 N90-24973
Equilibrium radiative heating tables for aerobraking in the Martian atmosphere
[NASA-TM-102659] 19 p2688 N90-25290
Numerical analysis of three-dimensional particle-laden flow equations
[IAR-90-2] 20 p2860 N90-26268
Nonequilibrium radiation and chemistry models for aerocapture vehicle flowfields
[NASA-CR-186728] 22 p3169 N90-27973
A numerical calculation of hypersonic flow around blunt bodies using upwind difference scheme
[NAL-TR-1025] 24 p3422 N90-29331

BLUNT LEADING EDGES
Effects of nose bluntness and shock-shock interactions on blunt bodies in viscous hypersonic flows
[NASA-CR-186451] 14 p1910 N90-20950

BLUNT TRAILING EDGES
A study on upstream moving pressure waves induced by vortex separation
[ISL-CO-203/88] 12 p1597 N90-19192

BLURRING
Model-based quantification of image quality
08 p1072 N90-16206

BMC
U BONE MINERAL CONTENT

BOATS
Sweep width determination for HU-25B airborne radars: Life raft and recreational boat targets
[AD-A221362] 18 p2545 N90-24524

BODIES OF REVOLUTION
NT CELESTIAL SPHERE
NT CONICAL BODIES
NT CYLINDRICAL BODIES
NT ROTATING CYLINDERS
NT ROTATING SPHERES
NT SPHERES
NT TORUSES
A computational/experimental study of the flow around a body of revolution at angle of attack
[NASA-TM-88329] 02 p0219 N90-11254
Incompressible flow about ellipsoids of revolution
[REPT-88-02] 03 p0302 N90-11713
Flow in the neighborhood of an ellipsoid cylinder of revolution model
[ONERA-RT-22/7252-AN-000A]
04 p0502 N90-12895
Drag reduction by longitudinal riblets on the surface of a streamwise aligned body of revolution
[MPIS-MITT-92] 12 p1600 N90-19210
Effect of vortex generators on the aerodynamic wing characteristics and body of revolution
[AD-A222813] 20 p2804 N90-25955

BODY CENTERED CUBIC LATTICES
Energetics of BCC-FCC lattice deformation in iron
[AD-A213801] 07 p0905 N90-15233
Surface studies at the NSLS
[DE90-003173] 08 p1043 N90-16027

BODY FLUIDS
NT BLOOD
NT CEREBROSPINAL FLUID
NT SWEAT
NT URINE
USSR Space Life Sciences Digest, issue 22
[NASA-CR-3922(26)] 03 p0378 N90-12153
Hypobaric hypoxia (380 torr) decreases intracellular and total body water in goats
[AD-A218192] 13 p1849 N90-20615
A comparison of the mechanisms of cold- and microgravity-induced fluid loss
[AD-A218098] 13 p1852 N90-20631
National Aeronautics and Space Administration (NASA)/American Society for Engineering Education (ASEE) Summer Faculty Fellowship Program-1989, volume 1
[NASA-CR-185601-VOL-1] 18 p2627 N90-24972
Noninvasive estimation of fluid shifts between body compartments by measurement of bioelectric characteristics 18 p2628 N90-24976
Conservation of body calcium by increased dietary intake of potassium: A potential measure to reduce the osteoporosis process during prolonged exposure to microgravity 18 p2631 N90-24993

BODY KINEMATICS
Spatial dynamics of deformable multibody systems with variable kinematic structure
[AD-A214098] 07 p0942 N90-15455
Quantitative assessment of human motion using video motion analysis 19 p2730 N90-25518

BODY MEASUREMENT (BIOLOGY)
NT ANTHROPOMETRY

BODY TEMPERATURE
Measurement of respiratory air temperatures and calculation of respiratory heat loss when working at various ambient temperatures
[AD-A210378] 01 p0093 N90-10529
Human body regional convective heat transfer determination using subliming naphthalene disks
[AD-A212170] 03 p0380 N90-12165
Prediction of thermal stress casualties
[AD-A212356] 04 p0523 N90-13022
Radio frequency (13.56 MHz) energy enhances rewarming from mild hypothermia
[AD-A212703] 04 p0524 N90-13024
Psychological and physiological responses of blacks and caucasians to hand cooling
[AD-A215646] 09 p1253 N90-17272
Alterations in the metabolic and sympathetic response to cold exposure after cold air acclimation
[AD-A216817] 10 p1412 N90-18144
What should athletes know about low body temperature (hypothermia)
[AD-A218316] 13 p1854 N90-20637
Comparison of light duty gloves with natural and synthetic materials under wet and dry conditions
[AD-A218119] 13 p1856 N90-20649
Heat exhaustion in a rat model: Lithium as a biochemical probe
[AD-A219361] 16 p2260 N90-22884
Effect of low air velocities on thermal homeostasis and comfort during exercise at space station operational temperature and humidity 18 p2628 N90-24975
Effects of a time zone shift of 9 hours on the circadian rhythms in cockpit aircrew members on longhaul flights
[ESA-TT-1185] 19 p2722 N90-25485
Adjustment and validation of the mathematical prediction model for sweat rate, heart rate, and body temperature under outdoor conditions
[AD-A222599] 20 p2898 N90-26486
Physical characteristics of clothing materials with regard to heat transport
[IZF-1989-10] 22 p3233 N90-28336
Pharmacological resetting of the circadian sleep-wake cycle effects of triazolam on reentrainment of circadian rhythms in a diurnal primate
[AD-A224227] 24 p3497 N90-29764
Evaluation of physiological and psychological impairment of human performance in cold stressed subjects
[AD-A223635] 24 p3498 N90-29769

BODY TEMPERATURE (NON-BIOLOGICAL)
U TEMPERATURE

BODY TEMPERATURE REGULATION
U THERMOREGULATION

BODY-WING CONFIGURATIONS
Low-speed, high-lift aerodynamic characteristics of slender, hypersonic accelerator-type configurations
[NASA-TP-2945] 02 p0145 N90-10830
Three-component laser Doppler velocimeter measurements in a juncture flow
04 p0441 N90-12525
Pivotal mono wing cruise missile with wing deployment and fastener mechanism
[AD-D014191] 04 p0452 N90-12594
Study of forces and moments on wing-bodies at high incidence, volumes 1 and 2 05 p0575 N90-13350
An experimental study of the time-dependent behavior of the appendage-body junction vortex
[AD-A213465] 07 p0930 N90-15384
Body effect on wing angle of attack and pitching moment at zero lift at low speeds
[ESDU-89042] 09 p1167 N90-16757
Initial flight test of half-scale unmanned air vehicle
[AD-A219584] 17 p2351 N90-23388

Three-dimensional model testing in the transonic self-streamlining wind tunnel 23 p3284 N90-28583
Effects of flowfield turbulence on asymmetric vortices over a slender body
[AD-A224139] 23 p3328 N90-28819
Studies of surface heat transfer in an arc-heated wind tunnel
[NAL-TR-1048] 24 p3437 N90-29410

BOEING AIRCRAFT
NT B-52 AIRCRAFT
NT BOEING 727 AIRCRAFT
NT BOEING 737 AIRCRAFT
NT BOEING 747 AIRCRAFT
NT BOEING 757 AIRCRAFT
NT C-135 AIRCRAFT
NT CH-47 HELICOPTER
Boeing 727-100 test project (high energy radiated field tests)
[DOT/FAA/CT-88/33] 14 p1964 N90-21247

BOEING MILITARY AIRCRAFT
U MILITARY AIRCRAFT

BOEING 727 AIRCRAFT
The NASA digital VGH program. Exploration of methods and final results. Volume 3: B 727 data 1978-1980: 1765 hours
[NASA-CR-181909-VOL-3] 13 p1756 N90-20082

BOEING 737 AIRCRAFT
Aircraft accident report: Aloha Airlines, Flight 243, Boeing 737-200, N73711, near Maui, Hawaii, April 28, 1988
[PB89-910404] 01 p0004 N90-10013
Study of the engine bird ingestion experience of the Boeing 737 aircraft (October 1986 to September 1988)
[DOT/FAA/CT-89/29] 19 p2656 N90-25119

BOEING 747 AIRCRAFT
The NASA digital VGH program: Exploration of methods and final results. Volume 4: B 747 data 1978-1980, 1689 hours
[NASA-CR-181909-VOL-4] 13 p1756 N90-20083
SOFIA: Stratospheric Observatory for Infrared Astronomy 14 p1980 N90-21346
Aircraft accident report, United Airlines Flight 811, Boeing 747-122, N4713U, Honolulu, Hawaii, February 24, 1989
[PB90-910401] 15 p2050 N90-21748
An experimental study of fault propagation in a jet-engine controller
[NASA-CR-181335] 17 p2354 N90-23401

BOEING 757 AIRCRAFT
Flight survey of the 757 wing noise field and its effects on laminar boundary layer transition. Volume 3: Extended data analysis
[NASA-CR-178419] 10 p1427 N90-18233

BOGOLIUBOV THEORY
On the construction of the scattering matrix for locally-noncommutative interactions of relativistic fields
[DE89-630138] 02 p0287 N90-11640
Few-body collisions in a weakly interacting Bose gas
[ETN-90-96893] 18 p2613 N90-24886

BOGS
U MARSHLANDS

BOILERS
Independent Orbiter Assessment (IOA): Analysis of the hydraulics/water spray boiler subsystem
[NASA-CR-185541] 02 p0165 N90-10934
Independent Orbiter Assessment (IOA): Assessment of the hydraulics/water spray boiler subsystem
[NASA-CR-185537] 03 p0316 N90-11792
Test results from a full-scale sodium reflux pool-boiler solar receiver
[DE90-003577] 12 p1684 N90-19671

BOILING
NT FILM BOILING
Semi-empirical theory of heat-transfer when boiling
[DE89-635418] 06 p0857 N90-14984
Radial heat flux limits in potassium heat pipes: An experimental and analytical investigation
[DE90-002655] 07 p0932 N90-15396
The onset of boiling of the liquid alkali metals
[DE90-002276] 08 p1044 N90-16036
Effect of reduced atmospheric pressure on the performance characteristics of pyrotechnic compositions containing aluminum
[AD-A214473] 09 p1200 N90-16953
Boiling inside tubes: Pressure drop in straitht tubes with upward or horizontal flow
[ESDU-89039] 09 p1220 N90-17078
Process for making a noble metal on tin oxide catalyst
[NASA-CASE-LAR-13741-1-SB] 13 p1774 N90-20180
Design and test of a compact optics system for the pool boiling experiment
[NASA-TM-102530] 13 p1786 N90-20253
Boron-containing organosilane polymers and ceramic materials thereof
[NASA-CASE-ARC-11649-2-SB] 14 p1952 N90-21177
Flow boiling with enhancement devices for cold plate coolant channel design
[NASA-CR-186358] 15 p2089 N90-21961
Thermohydraulics of a heat dissipating debris bed 19 p2691 N90-25310
Boiling/evaporative heat transfer from spheres in packed-bed thermal energy storage units
[DE90-012023] 19 p2711 N90-25430

BOILING WATER REACTORS
NT PATHFINDER NUCLEAR REACTOR

BOLOGRAMS
U BOLOMETERS

BOLOMETERS
A four channel He-3 cooled balloon-borne bolometer radiometer 05 p0597 N90-13469
Systematic errors in power measurements made with a dual six-port ANA
[PB90-145160] 14 p1968 N90-21276
A 100 micro Kelvin bolometer system for SIRTF 14 p1976 N90-21317
A progress report on using bolometers cooled by adiabatic demagnetization refrigeration 14 p1976 N90-21318
Upcoming planetary missions and the applicability of high temperature superconductor bolometers 22 p3140 N90-27811
Thermal response of large area high temperature superconducting YBaCuO infrared bolometer 22 p3146 N90-27839
Optical and microwave detection using Bi-Sr-Ca-Cu-O thin films 22 p3152 N90-27870

BOLTED JOINTS
Flanged joints of aeroengines
[PNR90594] 04 p0455 N90-12609
Experimental determination of thermal conductance in bolted joint impact in satellites
[INPE-4989-PRE/1551] 15 p2059 N90-21788
Review of analysis methods for mechanically fastened joints in composites
[LR-599] 15 p2107 N90-22050
The behaviour of mechanically fastened joints in composite structures 16 p2242 N90-22789
Simplified design procedures for fiber composite structural components/joints
[NASA-TM-103113] 18 p2519 N90-24384
Igniter adapter-to-igniter chamber deflection test
[NASA-CR-184002] 22 p3133 N90-27780

BOLTS
Eddy current test for bolts
[AD-A214829] 09 p1234 N90-17159
High resistance bolts: Test trials for plated bolts
[CRIF-MT-178] 17 p2413 N90-23748
Guidelines for threaded fasteners
[ESA-PSS-03-208-ISSUE-1] 22 p3182 N90-28061
Advanced NDE techniques for quantitative characterization of aircraft 22 p3188 N90-28088

BOLTZMANN DISTRIBUTION
Physics of high energy photoconductive switches
[AD-A210341] 01 p0060 N90-10345
Brownian trail rectified
[DE90-003339] 07 p0988 N90-15706
The Eighteenth Conference on Stochastic Processes and their Applications
[AD-A212301] 08 p1040 N90-16010
The neoclassical transport of toroidal momentum in tokamaks
[DE90-006864] 11 p1568 N90-19023

BOLTZMANN TRANSPORT EQUATION
Energy dependent transport problem with generalized boundary conditions
[DE89-617843] 01 p0118 N90-10676
Time evolution of the electron swarm energy distribution function
[AD-A212967] 04 p0557 N90-13247
Solution of the Boltzmann equation using an energy group method
[AD-A213138] 05 p0699 N90-14096
Nonlinear heat transfer and wave motion
[AD-A214911] 09 p1217 N90-17058
A numerical solution of the time-dependent Boltzmann equation
[AD-A216397] 10 p1434 N90-18275
A numerical solution to the Boltzmann equation for use in calculating pumping rates in a CO2 discharge laser
[AD-A216376] 11 p1514 N90-18718
The n-p bremsstrahlung in heavy ion collision processes
[DE90-008542] 13 p1886 N90-20823
Ensemble Monte Carlo simulation of electron transport in AlGaAs/GaAs heterostructures
[ISBN-90-9003048-4] 18 p2622 N90-24940
Constitutive laws for discrete velocity models of gas (continued)
[ETN-90-97451] 22 p3175 N90-28016

BOLTZMANN-VLASOV EQUATION
Nonlinear plasma and beam physics in plasma wake-fields
[DE90-008812] 13 p1892 N90-20855
Relativistic stimulated Brillouin and Raman scattering in a laser-produced plasma
[DE90-613123] 14 p2028 N90-21627
On the relativistic Vlasov equation in guiding-center coordinates
[DE90-613241] 14 p2028 N90-21629
Low-frequency oscillations in vlasov plasmas: The quadratic polarization approximation
[DE90-611309] 18 p2617 N90-24910
Reduced distribution functions and nonequilibrium thermodynamics of single component fluids
[PB90-189119] 22 p3254 N90-28428

BOMBER AIRCRAFT
NT B-1 AIRCRAFT
NT B-52 AIRCRAFT
NT B-58 AIRCRAFT
NT B-70 AIRCRAFT
Encyclopedia of US Air Force aircraft and missile systems. Volume 2: Post-World War 2 bombers, 1945-1973
[AD-A209273] 01 p0001 N90-10001
Proposed activities to prepare for testing advanced/stealth weapons systems
[AD-A214453] 07 p0920 N90-15321
Limitations of the conventional role of the B-1B in the European theater
[AD-A217285] 12 p1604 N90-19230

BOMBS (ORDNANCE)
Flight testing a newly-designed stand-off weapon dispenser 02 p0154 N90-10880
Pivotal mono wing cruise missile with wing deployment and fastener mechanism
[AD-D014191] 04 p0452 N90-12594
Limitations of the conventional role of the B-1B in the European theater
[AD-A217285] 12 p1604 N90-19230

BOMBS (PRESSURE GAGES)
U PRESSURE GAGES

BOMBS (SAMPLERS)
U SAMPLERS

BOND GRAPHS
The interface chemistry of phenolic and epoxy adhesives with a model aluminium surface
[MBB-Z-0288-89-PUB] 18 p2531 N90-24441

BONDING
NT ADHESIVE BONDING
NT CERAMIC BONDING
NT METAL BONDING
NT METAL-METAL BONDING
NT REACTION BONDING
NT RESIN BONDING
A characterization of the side bonding, upset plug welding process
[DE89-015181] 02 p0229 N90-11315
Apparatus and method for monitoring pressure leaks from a sealed system
[AD-D014168] 03 p0349 N90-11995
Field-assisted bonding of single crystal quartz
[DE89-015407] 03 p0410 N90-12353
Superplasticity
[AGARD-LS-168] 06 p0743 N90-14325
An investigation of elastic guided waves for ceramic joint evaluation
[DE90-004400] 08 p1050 N90-16071
Adhesion of silver films to ion-bombarded alumina
[DE90-005642] 09 p1199 N90-16947
Scuffing modelling and experiments for heavily loaded elastohydrodynamic lubricatic.1 contacts 10 p1391 N90-18047
Enhanced bonding of fiber reinforcements to thermoset resins 11 p1476 N90-18496
Method for maintaining precise suction strip porosities
[NASA-CASE-LAR-13638-1] 12 p1641 N90-19427
Study and sizing of bonded joints in space structures
[REPT-892-430-124] 16 p2207 N90-22591
Qualification of the RSRM case membrane case-to-insulation bondline inspection using the Thiokol Corporation ultrasonic RSRM bondline inspection system
[NASA-CR-183940] 16 p2209 N90-22602
Qualification of the RSRM field joint CF case-to-insulation bondline inspection using the Thiokol Corporation ultrasonic RSRM bondline inspection system
[NASA-CR-183931] 16 p2242 N90-22788
Ultrahigh carbon steels and their laminates
[AD-A218780] 17 p2376 N90-23530

An expert system for the study of high duty bonded joints in aerospace structures
[REPT-892-430-110] 17 p2414 N90-23753
Characterization of solid state bonding between Coors AD-999 alumina and niobium
[DE90-010653] 18 p2518 N90-24379
Joining engineering ceramics
[DE90-010819] 18 p2531 N90-24445
Acousto-optic signature analysis for inspection of the orbiter thermal protection tile bonds
[DE90-013089] 20 p2819 N90-26043
Field experience in using laser acoustic sensing for inspection
[DE90-012954] 20 p2873 N90-26347
Microwave spectra of van der Waals complexes of importance in planetary atmospheres
20 p2944 N90-26752
New core design for use with precision composite reflectors
[NASA-CASE-NPO-17858-1-CU]
21 p2970 N90-26880
Fabrication of intermetallic compounds by solid state reaction of roll-bonded materials
[AD-A221960] 21 p2982 N90-26943
Electronic and molecular structure of carbon grains
21 p3091 N90-27574
Advanced NDE techniques for quantitative characterization of aircraft 22 p3188 N90-28088
Nylon and teflon scribe effect on NBR to Chemlok 233 and NBR to NBR bond interfaces
[NASA-CR-184004] 22 p3189 N90-28095
Accurate quantum chemical calculations
[NASA-TM-101932] 23 p3303 N90-28680

BONE DEMINERALIZATION
Conservation of body calcium by increased dietary intake of potassium: A potential measure to reduce the osteoporosis process during prolonged exposure to microgravity 18 p2631 N90-24993
An in-vitro technique to study bone metabolism in developing mouse long bone rudiments under microgravity and compression 19 p2681 N90-25248
Experiment K-6-04. Trace element balance in rats during spaceflight 20 p2892 N90-26458

BONE MARROW
The effects of simulated hypogravity on murine bone marrow cells 18 p2631 N90-24989
The interaction of polymeric materials with ceramic surfaces with special reference to the behaviour of bioceramics 20 p2836 N90-26127
Experiment K-6-23. Effect of spaceflight on levels and function of immune cells 20 p2897 N90-26476

BONE MINERAL CONTENT
Bone mineral measurement using dual energy x ray densitometry 05 p0680 N90-13958
Effects of microgravity on rat bone, cartilage and connective tissues 20 p2891 N90-26454
Experiment K-6-01. Distribution and biochemistry of mineral and matrix in the femurs of rats
20 p2892 N90-26455
Experiment K-6-04. Trace element balance in rats during spaceflight 20 p2892 N90-26458
Experiment K-6-05. The maturaton of bone and dentin matrices in rats flown on Cosmos 1887
20 p2893 N90-26459
Experiment K-6-27. Analysis of radiographs and biosamples from primate studies
20 p2897 N90-26478

BONES
NT FEMUR
NT SPINE
NT TIBIA
NT ULNA
NT VERTEBRAE
Evaluation of speech intelligibility through a bone conduction stimulator
[AD-A212002] 05 p0673 N90-13919
The interaction of polymeric materials with ceramic surfaces with special reference to the behaviour of bioceramics 20 p2836 N90-26127
Effects of microgravity on rat bone, cartilage and connective tissues 20 p2891 N90-26454
Experiment K-6-02. Biomedical, biochemical and morphological alterations of muscle and dense, fibrous connective tissues during 14 days of spaceflight
20 p2892 N90-26456
Experiment K-6-03. Gravity and skeletal growth, part 1. Part 2: Morphology and histochemistry of bone cells and vasculature of the tibia; Part 3: Nuclear volume analysis of osteoblast histogenesis in periodontal ligament cells; Part 4: Intervertebral disc swelling pressure associated with microgravity 20 p2892 N90-26457
Experiment K-6-04. Trace element balance in rats during spaceflight 20 p2892 N90-26458
Experiment K-6-05. The maturaton of bone and dentin matrices in rats flown on Cosmos 1887
20 p2893 N90-26459
Experiment K-6-06. Morphometric and EM analyses of tibial epiphyseal plates from Cosmos 1887 rats
20 p2893 N90-26460

BOOLEAN ALGEBRA
NT BOOLEAN FUNCTIONS
Modular specifications in process algebra with curious queues
[CWI-CS-R8821] 04 p0543 N90-13152
Solving computer graphics problems through boolean combinations of polygons
[AD-A214788] 09 p1273 N90-17380
Boolean approaches in digital diagnosis
[AD-A215660] 09 p1274 N90-17386
Boolean minimization and algebraic factorization procedures for fully testable sequential machines
[AD-A216779] 11 p1553 N90-18940
Error detection in data processing devices by means of residue codes
[ETN-90-95370] 12 p1701 N90-19787
Binary space partitioning trees and their uses
13 p1857 N90-20657
Exact algorithms for output encoding, state assignment and four-level Boolean minimization
[AD-A217121] 13 p1876 N90-20756
VLSI binary updown counter
[NASA-CASE-NPO-17205-1-CU]
14 p2011 N90-21525
Automatic runtime consistency checking and debugging of formally specified programs
[AD-A218855] 17 p2442 N90-23916
Constraint-oriented specification in a constructive formal description technique
[MEMO-INF-89-44] 17 p2463 N90-24070
The axiomatization of randomness
[ITLI-ML-89-06] 18 p2603 N90-24824
Computer assisted analysis and modelling of structured problems
[AD-A222991] 21 p3052 N90-27350
Proving Boolean equivalence with Prolog
[AD-A221766] 21 p3065 N90-27427
Search strategies for computer-stored information: A microcomputer tutorial 24 p3557 N90-30126

BOOLEAN FUNCTIONS
Boolean functions, invariance groups and parallel complexity
[CWI-CS-R8836] 02 p0260 N90-11472
Optimal layout via Boolean satisfiability
[AD-A216777] 12 p1705 N90-19787
Computing Boolean functions on anonymous networks
[CWI-CS-R8935] 18 p2602 N90-24818

BOOMS (EQUIPMENT)
Space telescope solar array: Nonlinear test and analysis effects 02 p0185 N90-11051
Vibration tests of the ACPB canister flight unit of the RETE experiment, integrated with the tests of the booms from R. Piaggio
[IFSI-89-11] 10 p1328 N90-17670
Design and development of a spacecraft stability boom 18 p2540 N90-24494

BOOST
U ACCELERATION (PHYSICS)

BOOSTER RECOVERY
A two-stage earth-to-orbit transport with translating oblique wings for booster recovery
[NASA-CASE-LAR-14156-1] 09 p1173 N90-16781

BOOSTER ROCKET ENGINES
NT ADVANCED SOLID ROCKET MOTOR (STS)
NT APOGEE BOOST MOTORS
NT SPACE SHUTTLE BOOSTERS
Liquid rocket booster study. Volume 2, book 1
[NASA-CR-183600] 01 p0026 N90-10133
Liquid rocket booster study. Volume 2, book 5, appendix 9: LRB alternate applications and evolutionary growth
[NASA-CR-183604] 01 p0026 N90-10134
Liquid rocket booster study. Volume 2, book 4, appendices 6-8: Reports of Rocketdyne, Pratt and Whitney, and TRW
[NASA-CR-183603] 01 p0027 N90-10135
Liquid rocket booster study. Volume 2, book 2, appendix 1: Trades studies
[NASA-CR-183601] 01 p0027 N90-10136
Liquid rocket booster study. Volume 1: Executive summary
[NASA-CR-183599] 01 p0027 N90-10137
Liquid rocket booster study. Volume 2, book 6, appendix 10: Vehicle systems effects
[NASA-CR-183605] 01 p0027 N90-10138
Liquid rocket booster study. Volume 2, book 3, appendices 2-5: PPIP, transition plan, AMOS plan, and environmental analysis
[NASA-CR-183602] 01 p0027 N90-10139
Review of the Aerospace Safety Advisory Panel report for NASA fiscal year 1990 authorization
[GPO-24-234] 06 p0722 N90-14213
Transportation systems for manned space missions
09 p1176 N90-16805
Ariane-5 solid boosters stage development
09 p1176 N90-16811
The liquid rocket booster and its potential for the STS
09 p1179 N90-16833
Are reusable boosters cost-effective
09 p1179 N90-16834
Space transportation booster engine configuration study. Addendum: Design definition document
[NASA-CR-183854] 09 p1184 N90-16862
Booster propulsion/vehicle impact study, 2
[NASA-CR-179313] 10 p1346 N90-17809
A preliminary assessment of 3-Nitro-1,2,4-Triazol-5-One (NTO) as an insensitive high explosive
[AD-A215063] 10 p1360 N90-17889
Hydrocarbon-fuel/combustion-chamber-liner materials compatibility
[NASA-CR-185203] 14 p1950 N90-21165
Draft environmental impact statement for the Galileo Mission (Tier 2)
[NASA-TM-102926] 15 p2124 N90-22148
Earth-to-orbit vehicle providing a reusable orbital stage
[NASA-CASE-LAR-13486-1] 16 p2206 N90-22584
On the simulation test for the relative motion of separated sub-boosters on M-3S2 with nearly half a model vehicle ST-735 and their motion analyses using inertial sensors output
[ISAS-635] 17 p2366 N90-23471
First Vulcain engine test results
[MBB-UK-0054/88-PUB] 19 p2652 N90-25093
PDWAP: A preliminary design and weights analysis program for aerospace vehicles
[AD-A222614] 20 p2808 N90-25979
Report of the Defense Science Board 1989 summer study on national space launch strategy
[AD-A222419] 21 p2963 N90-26848
Hybrid propulsion technology program
[NASA-CR-183952] 21 p2968 N90-26870
Liquid Rocket Booster (LRB) for the Space Transportation System (STS) systems study. Volume 1: Executive summary
[NASA-CR-183822] 23 p3288 N90-28599
Liquid Rocket Booster (LRB) for the Space Transportation System (STS) systems study, volume 2
[NASA-CR-183786] 23 p3288 N90-28600
Liquid Rocket Booster (LRB) for the Space Transportation System (STS) systems study. Appendix A: Stress analysis report for the pump-fed and pressure-fed liquid rocket booster
[NASA-CR-183787-APP-A] 23 p3288 N90-28601
Liquid Rocket Booster (LRB) for the Space Transportation System (STS) systems study. Appendix B: Liquid rocket booster acoustic and thermal environments
[NASA-CR-183788-APP-B] 23 p3288 N90-28602
Liquid Rocket Booster (LRB) for the Space Transportion System (STS) systems study. Appendix D: Trade study summary for the liquid rocket booster
[NASA-CR-183790-APP-D] 23 p3289 N90-28604
Liquid Rocket Booster (LRB) for the Space Transportation System (STS) systems study. Appendix E: Pressure-fed booster test bed for the liquid rocket booster study
[NASA-CR-183791-APP-E] 23 p3289 N90-28605
Liquid Rocket Booster (LRB) for the Space Transportation System (STS) systems study. Appendix F: Performance and trajectory for ALS/LRB launch vehicles
[NASA-CR-183792-APP-F] 23 p3289 N90-28606
Liquid Rocket Booster (LRB) for the Space Transportation System (STS) systems study. Appendix G: LRB for the STS system study level 2 requirements, revision 1
[NASA-CR-183793-APP-G] 23 p3289 N90-28607
Summary of booster propulsion/vehicle impact study results 23 p3294 N90-28635
High/variable mixture ratio oxygen/hydrogen engines
23 p3295 N90-28637
Use of Ni63 overvoltage gap switches in the flight termination systems on boosters launched from US Army Kwajalein Atoll (USAKA)
[AD-A223866] 23 p3299 N90-28661

BOOSTERS (EXPLOSIVES)
An evaluation of ethylene-vinyl acetate copolymers as desensitizers for RDX in insensitive booster compositions prepared by slurry coating technology
[MRL-TR-89-33] 12 p1633 N90-19385
Preparation, characterisation and cookoff behaviour of booster compositions prepared from RDX and acrylic or ethylene-vinyl acetate dispersions
[MRL-TR-89-44] 14 p1957 N90-21203
Determination of detonation parameters of booster explosives at small charge diameters
[MRL-TR-89-45] 14 p1957 N90-21204

BORANES
NT CARBORANE
Metal-assisted syntheses of boranes and carboranes
[AD-A210728] 01 p0041 N90-10227

Structures and energies for small borane compounds: One and two boron compounds
[AD-A212264] 04 p0471 N90-12701
Metallaboranes as precursors to metallic glasses
[AD-A216946] 11 p1490 N90-18577

BORATES
NT LITHIUM BORATES

BORAZON (TRADEMARK)
U BORON NITRIDES

BOREDOM
Functional decor in the International Space Station: Body orientation cues and picture perception
[NASA-TM-102242] 05 p0675 N90-13931

BOREHOLES
In-situ permeable flow sensor
[DE90-008806] 14 p1983 N90-21364

BORES
U CAVITIES

BORIC ACIDS
Tribological properties of boric acid and boric-acid-forming surfaces. Part 2: Formation and self-lubrication mechanisms of boric acid films on boron- and boric-oxide-containing surfaces
[DE90-005632] 13 p1811 N90-20400
Tribological properties of boric acid and boric acid forming surfaces. Part 1: Crystal chemistry and self-lubricating mechanism of boric acid
[DE90-005665] 13 p1811 N90-20401

BORIDES
NT TITANIUM BORIDES
Collective-mode spectroscopy of textures in superfluid (3)He-B
[PB89-221634] 03 p0413 N90-12370
Preparation and properties of icosahedral borides
[DE90-003574] 07 p0896 N90-15180

BORING MACHINES
New tool-holding concept
[DE90-000880] 06 p0794 N90-14624
Proof of principal for staircase auger chip removal theory
[NASA-CR-184934] 17 p2385 N90-23583

BORN APPROXIMATION
Clutter models for subsurface electromagnetic applications
[PB89-229678] 03 p0338 N90-11925
The effective (3)He-nucleon force in a microscopic DWBA approach to the (3)He,t charge exchange reaction --- Distorted Wave-Borne Approximation (DWBA)
[KVI-763] 05 p0697 N90-14077
Positron collisions with alkali-metal atoms
11 p1556 N90-18962
The calculation of the contributions to low energy e+H2 scattering from sigma u+ and Pion u symmetries using the Kohn variational method 11 p1557 N90-18969
A scattering center based numerical simulation of small scale atmospheric turbulence 16 p2312 N90-23179

BORN-MAYER EQUATION
U BORN APPROXIMATION

BORON
NT BORON ISOTOPES
Photoreflectance study of boron ion-implanted (100) cadmium telluride
[SD-TR-88-89] 01 p0053 N90-10300
Boron analogues of amino acids and derivatives
[AD-A211311] 03 p0379 N90-12157
Development of a titanium/boron blending process
[DE90-001450] 06 p0754 N90-14386
Characterization of B and N implanted fused silica
[DE90-004198] 08 p1050 N90-16069
Cluster based reaction probabilities for boron with oxygen, hydrogen, water, nitrogen, nitrous oxide, carbon dioxide, carbon monoxide, methane, tetrafluoromethane, and silane
[AD-A214554] 09 p1190 N90-16894
Magnetron sputtered boron films and Ti/B multilayer structures
[DE90-009190] 14 p1948 N90-21153
Grain boundary precipitation in Ni3Al based alloys
[AERE-R-13362] 14 p1950 N90-21161
Lecture on ordered intermetallic alloys
[DE90-009011] 14 p1951 N90-21169
Boron-containing organosilane polymers and ceramic materials thereof
[NASA-CASE-ARC-11649-2-SB] 14 p1952 N90-21177
Production and coating of pure boron powders
[AD-A220272] 18 p2533 N90-24452
Effect of boron on intergranular hot cracking in Ni-Cr-Fe superalloys containing niobium
[NASA-CR-184038] 20 p2834 N90-26115
Rapid thermal processing: A study of the silicon oxidation and of the implanted boron activation
[LAAS-90051] 20 p2932 N90-26681
Regression and combustion characteristics of boron containing fuels for solid fuel ramjets
22 p3161 N90-27928
Ion-beam mixing of Fe/B layers for tribological applications
[DE90-010091] 24 p3456 N90-29518

BORON ALLOYS
Formation of Titanium-boron surface alloys by excimer laser mixing
[DE90-013172] 20 p2834 N90-26118
Tensile behavior of borated stainless steels, phase 1
[DE90-014368] 23 p3309 N90-28717

BORON CARBIDES
Shock compression and release in high-strength ceramics
[DE89-013995] 01 p0047 N90-10265
Characterizations of shock-loaded aluminum-infiltrated boron carbide cermets
[DE89-016773] 02 p0201 N90-11146
Synthesis and properties of new preceramic materials
[DE90-002562] 06 p0752 N90-14373
Preparation and properties of icosahedral borides
[DE90-003574] 07 p0896 N90-15180
Structural stability of heat treated W/B4C multilayers
[DE90-005322] 09 p1188 N90-16884
Dynamic properties of porous B4C
[AD-A222850] 21 p2985 N90-26960

BORON CHLORIDES
Reactions of hydrogen chloride and boron trichloride with trimethylsilylamino groups
[AD-A209006] 01 p0038 N90-10209
On the vapour phase deposition mechanism of carbon-boron-nitrogen compounds between 800 and 1000 C
[REPT-892-430-101] 16 p2214 N90-22632

BORON COMPOUNDS
NT BORANES
NT BORIC ACIDS
NT BORIDES
NT BORON CARBIDES
NT BORON CHLORIDES
NT BORON FLUORIDES
NT BORON HYDRIDES
NT BORON NITRIDES
NT BORON PHOSPHIDES
NT CARBORANE
NT LITHIUM BORATES
NT TITANIUM BORIDES
Metallized fuel particle size study in a solid fuel ramjet
[AD-A220079] 18 p2533 N90-24451

BORON FIBERS
Study on failure modes of boron fiber reinforced aluminum composite materials by AE method, part 2
[DE90-505522] 20 p2828 N90-26086
Development of dual fiber reinforced glass matrix composites for structural space based applications
[AD-A223801] 24 p3444 N90-29446

BORON FLUORIDES
Pyrromethene-BF2 complexes as laser dyes
[AD-A223562] 24 p3473 N90-29631

BORON HYDRIDES
NT BORANES
NT CARBORANE
Kinetics of boron hydride interconversion reactions
[AD-A215386] 09 p1192 N90-16906

BORON ISOTOPES
BOREX: Solar neutrino experiment via weak neutral and charged currents in boron-11
[DE90-003790] 09 p1300 N90-17530
The shock process and light element production in supernovae envelopes
[NASA-CR-182854] 22 p3262 N90-28471

BORON NITRIDES
New polymer precursors to boron and silicon nitrides
[AD-A210287] 01 p0049 N90-10279
Static tensile and tensile creep testing of four boron nitride coated ceramic fibers at elevated temperatures
[NASA-CR-184999] 03 p0318 N90-11807
Fundamental tribological properties of ion-beam-deposited boron nitride films
[NASA-TM-102088] 03 p0331 N90-11881
Synthesis and properties of new preceramic materials
[DE90-002562] 06 p0752 N90-14373
The effect of fiber coatings on interfacial shear strength and the mechanical behavior of ceramic composites
[DE90-007574] 12 p1632 N90-19380
Vibrational spectroscopy of boron nitride at high temperatures and pressures
[DE90-008633] 13 p1772 N90-20172
The role of polarity on the stability of graphitic compounds
[DE90-006528] 13 p1780 N90-20218
Status and applications of diamond and diamond-like materials: An emerging technology
[NASA-CR-186935] 21 p2985 N90-26963
Self-lubricating-diamond like coatings deposition
[AD-A221756] 21 p2988 N90-26983

BORON PHOSPHIDES
Preparation and properties of icosahedral borides
[DE90-003574] 07 p0896 N90-15180

BORON REINFORCED MATERIALS
NT ALUMINUM BORON COMPOSITES
Kinetics and mechanisms of primary and steady state creep in B- and Al-containing alpha silicon carbide
[AD-A210739] 02 p0283 N90-11616

BORON TRIFLUORIDE
U BORON FLUORIDES

BOROSILICATE GLASS
Toughening mechanisms in ceramic composites
[PB89-235907] 05 p0626 N90-13656
Characterization of B and N implanted fused silica
[DE90-004198] 08 p1050 N90-16069
Diffusion and germ formation in glasses
13 p1786 N90-20250
Strengthening and toughening mechanisms in ceramic fiber-reinforced glass matrix composites
23 p3300 N90-28666

BOSE-CHAUDHURI-HOCQUENGHEM CODES
U BCH CODES

BOSE-EINSTEIN STATISTICS
U QUANTUM STATISTICS

BOSONS
NT ALPHA PARTICLES
NT ETA-MESONS
NT MESONS
NT MUONS
NT PHOTONS
NT PIONS
The interacting boson approximation
[KVI-774] 04 p0552 N90-13215
Ground states of a two-dimensional charged-boson system
[AD-A212363] 04 p0553 N90-13226
Narrow one-channel resonances and their manifestation in the pure elastic scattering of unpolarized particles
[DE89-632177] 06 p0839 N90-14876
Proceedings of the 23rd Annual Seminar on Theoretical Physics
[DE90-601827] 08 p1135 N90-16577
Distributed bosonic states and condensed matter fusion
[AD-A217605] 12 p1718 N90-19868
Extension of the constraints algebra for the closed string with the fixed topology world sheet
[DE90-612745] 14 p2020 N90-21577
Extension of the Krichever-Novikov algebra in the closed string theory
[DE90-612746] 14 p2020 N90-21578
String dynamics in curved space-time revisited
[DE90-612796] 14 p2035 N90-21674
Baryogenesis in extended inflation. Part 1: Baryogenesis via production and decay of supermassive bosons
[NASA-CR-180615] 17 p2470 N90-24120
Few-body collisions in a weakly interacting Bose gas
[ETN-90-96893] 18 p2613 N90-24886
Superconductivity in mixed boson-fermion systems
[DE90-627491] 23 p3401 N90-29216
Effective actions for bosonic topological defects
[NASA-CR-187271] 24 p3544 N90-30041

BOTANY
NT GEOBOTANY
Life science research in space
[ESA-SP-1105] 05 p0672 N90-13917
The effect of clinostat rotation on plant protoplasts
19 p2681 N90-25247

BOUNDARIES
NT FLUID BOUNDARIES
NT FREE BOUNDARIES
NT GAS-SOLID INTERFACES
NT GRAIN BOUNDARIES
NT LIQUID-LIQUID INTERFACES
NT LIQUID-SOLID INTERFACES
NT LIQUID-VAPOR INTERFACES
Parameter estimation in functional and partial differential equations
[AD-A211040] 02 p0265 N90-11511
Boundary effects on the MHD dynamo in laboratory plasmas
[DE89-015207] 02 p0276 N90-11576
On the Hellinger type distances for filtered experiments
[CWI-MS-R8818] 04 p0542 N90-13146
On the smooth fit boundary conditions in the optimal stopping problem for semimartingales
[CWI-MS-R8819] 04 p0542 N90-13147
On the maximum period of a permutation of N elements
[MEMO-771] 04 p0544 N90-13159
Hamiltonian properties of graphs with large neighborhood unions
[MEMO-779] 05 p0689 N90-14013

Linear groups and distance-transitive graphs
[CWI-PM-R8805] 05 p0691 N90-14036
Computer-aided boundary delineation of agricultural lands
[NASA-TM-102243] 08 p1091 N90-16313
Harmonic mappings into manifolds with boundary
[DE90-606961] 09 p1277 N90-17402
Investigation of boundary for the negative ion extraction in the sheet-plasma negative ion source
[DE90-719532] 09 p1286 N90-17458
Boundary estimation problems arising in thermal tomography
[NASA-CR-181964] 10 p1421 N90-18193
Kinetic relations and the propagation of phase boundaries in solids
[AD-A215881] 11 p1519 N90-18747
Causal boundary construction for space-times of the general relativity theory
[ETN-90-95357] 12 p1725 N90-19915
A structured approach to interactive multiple block grid generation 15 p2094 N90-21983
Excitation of hypersound at boundary between Type-2 superconductor and a concentrated paramagnetic compound 16 p2310 N90-23164
Kharitonov's theorem: Generalizations and algorithms 18 p2646 N90-25064
A critical evaluation of two-equation models for near wall turbulence
[NASA-CR-182068] 20 p2860 N90-26270
On domain decomposition methods for solving partial differential equations
[AD-A222975] 21 p3063 N90-27414
Study of the reflection of surface acoustic wave from a material discontinuity boundary using a perturbation method 24 p3542 N90-30032

BOUNDARY CONDITIONS
Energy dependent transport problem with generalized boundary conditions
[DE89-617843] 01 p0118 N90-10676
Analysis of three- and four-sided uniform waveguides with unusual cross-section/boundary conditions
[AD-A212653] 04 p0493 N90-12834
Stability conditions for steady shearing. Stability conditions for simple shear under mixed thermal boundary conditions 04 p0499 N90-12873
On the smooth fit boundary conditions in the optimal stopping problem for semimartingales
[CWI-MS-R8819] 04 p0542 N90-13147
A new technique for simulating composite material. Task 2: Analytical solutions with Generalized Impedance Boundary Conditions (GIBCs)
[NASA-CR-186249] 07 p0890 N90-15146
Finite element calculations for transonic flows taking into account several far field boundary conditions 08 p1069 N90-16188
Estimation of thermodynamic properties of alloys from phase diagram and other loose boundary conditions
[DE90-719511] 08 p1135 N90-16579
Asymptotic boundary conditions for dissipative waves: General theory
[NASA-TM-102497] 11 p1551 N90-18927
The effect of elastic boundary conditions on the dynamic response of rectangular plates
[NASA-CR-186059] 14 p1990 N90-21405
The influence of lateral boundary conditions, fixed surface forcings, and synoptic situations upon predictability estimates using limited area numerical models 14 p2005 N90-21492
Formulation of non-reflecting boundary conditions in numerical models of the atmosphere 15 p2129 N90-22175
Stable boundary conditions for Cartesian grid calculations
[NASA-CR-182048] 16 p2306 N90-23139
Boundary conditions for the Navier-Stoke's equations at an artificial boundary intersecting a solid boundary
[FFA-TN-1990-11] 19 p2691 N90-25313
Numerical method for calculating indoor airflows using a turbulence model
[PB90-162009] 21 p3003 N90-27067
A finite difference treatment of Stokes-type flows: Preliminary report
[NASA-CR-186480] 22 p3168 N90-27970
Finite-volume application of high order ENO schemes to multi-dimensional boundary-value problems
[NASA-CR-186917] 22 p3242 N90-28387
Parallelization of implicit finite difference schemes in computational fluid dynamics
[NASA-CR-182081] 22 p3243 N90-28392
Secondary instabilities in compressible boundary layers
[NASA-CR-182091] 23 p3269 N90-28502
Calculation of temperature distribution in various turbine blades using a boundary-fitted coordinate transformation method 23 p3278 N90-28550
Electromagnetic scattering from two-dimensional thick material junctions
[NASA-CR-186468] 23 p3319 N90-28767
On the use of Lagrangian variables in descriptions of unsteady boundary-layer separation
[NASA-CR-182071] 23 p3323 N90-28789
An asymptotically induced domain decomposition method for parabolic boundary layer problems
[DE90-014620] 23 p3326 N90-28804
Consistency and convergence for numerical radiation conditions
[NASA-TM-103262] 23 p3387 N90-29124
Solution of nonlinear eigenvalue problems via parallel shooting
[LR-587] 24 p3539 N90-30013

BOUNDARY DETECTION (IMAGERY)
U EDGE DETECTION

BOUNDARY ELEMENT METHOD
Numerical models for exterior and interior fluid-structure interaction problems 02 p0188 N90-11073
Three-dimensional analysis of surface crack-Hertzian stress field interaction
[NASA-CR-4254] 02 p0232 N90-11332
Error estimation and self-adaptive mesh refinement for boundary element method 03 p0356 N90-12037
A two-dimensional hybrid experimental-numerical technique for elastic-plastic stress analysis 04 p0511 N90-12949
Numerical analysis of scattering by interface flaws
[AD-A212996] 05 p0654 N90-13810
Time domain coupling of the boundary and finite element methods for elastodynamics
[AD-A213243] 05 p0654 N90-13811
Boundary element analysis of single and multidomain problems in acoustics 06 p0837 N90-14867
Development of an integrated BEM approach for hot fluid structure interaction
[NASA-CR-186214] 07 p0927 N90-15364
Solution of potential flow past an elastic body using the boundary element technique
[AD-A213843] 07 p0931 N90-15390
Electroplating simulation
[DE90-003683] 08 p1054 N90-16091
Validation of the boundary element method applied to complex fracture mechanics conditions
[AD-A216412] 10 p1398 N90-18080
On the exponential convergence of the h-p version for boundary element Galerkin methods on polygons
[AD-A215814] 10 p1423 N90-18210
The h-p version of the boundary element method with geometric mesh on polygonal domains
[AD-A215815] 10 p1423 N90-18211
A combined finite element-boundary element formulation for solution of two-dimensional problems via CGFFT
[NASA-CR-186464] 12 p1620 N90-19309
Scattering of waves by inclusions in a nonhomogeneous elastic half space solved by boundary element methods
[PB90-145699] 15 p2116 N90-22107
Solution of exterior acoustic problems by the boundary element method 18 p2611 N90-24874
Stress intensity factors for arbitrary two-dimensional crack problems involving crack face loadings
[FFA-TN-1990-10] 19 p2703 N90-25380
Weight functions and stress intensity factors for mode 1 cracks in arbitrary 2D geometries under general crack surface loading
[FFA-TN-1990-17] 19 p2703 N90-25381
Dynamic structural analysis using boundary element techniques
[AD-A222943] 21 p3012 N90-27126
Development of an integrated BEM for hot fluid-structure interaction 23 p3291 N90-28617

BOUNDARY INTEGRAL METHOD
A combined finite element and boundary integral formulation for solution via CGFFT of 2-dimensional scattering problems
[NASA-CR-184781] 01 p0055 N90-10313
A finite element-boundary integral formulation for scattering by three-dimensional cavity-backed apertures
[NASA-CR-186332] 09 p1187 N90-16878
Effects of nonuniform potential and current distributions in electrochemical systems
[DE90-007349] 12 p1623 N90-19325
Area Over Length (AOL): A program for the calculation of effective two-dimensional thermal conductance through an arbitrarily shaped region
[DE90-008005] 13 p1801 N90-20335
Elastodynamic scattering and transmission problems in three dimensions by the boundary integral equation method 15 p2111 N90-22077
On approximation of nonlinear boundary integral equations for the combined method
[DE90-009784] 16 p2305 N90-23130
On a method for computing eigenvalues and eigenfunctions of linear differential operators
[PREPRINT-706] 17 p2456 N90-24013
Structural zooming research and development of an interactive computer graphical interface for stress analysis of cracks 18 p2641 N90-25042
SuperCHIEF: A modified CHIEF (Combined Helmholz Integral Equation Formulation) method
[DE90-014744] 23 p3387 N90-29123
Solution of the Stokes system by boundary integral equations and fixed point iterative schemes
[DE90-627166] 23 p3389 N90-29138
A potential-vorticity decomposition for the boundary integral equation analysis of viscous flows 24 p3417 N90-29301

BOUNDARY LAYER COMBUSTION
Transport phenomena and interfacial kinetics in multiphase combustion systems
[AD-A212932] 05 p0621 N90-13620
Regression and combustion characteristics of boron containing fuels for solid fuel ramjets 22 p3161 N90-27928

BOUNDARY LAYER CONTROL
NT POROUS BOUNDARY LAYER CONTROL
Application of superplastically formed and diffusion bonded aluminum to a laminar flow control leading edge
[NASA-CR-178316] 01 p0007 N90-10030
Laminar flow control perforated wing panel development
[NASA-CR-178166] 01 p0034 N90-10187
Stability of a supersonic boundary layer along a swept leading edge 01 p0063 N90-10359
Control and modification of turbulence 01 p0066 N90-10377
Turbulence management: Application aspects 01 p0066 N90-10378
Dynamics and control of turbulent shear flows
[AD-A210396] 01 p0070 N90-10402
Active control of unsteady and separated flow structures
[AD-A212109] 03 p0301 N90-11707
Research in Natural Laminar Flow and Laminar-Flow Control, part 1
[NASA-CP-2487-PT-1] 04 p0438 N90-12503
Laminar flow: Challenge and potential 04 p0438 N90-12504
LFC: A maturing concept
[DOUGLAS-PAPER-7878] 04 p0438 N90-12505
Lockheed laminar-flow control systems development and applications 04 p0438 N90-12506
Laminar flow: The Cessna perspective 04 p0439 N90-12507
Long-range LFC transport 04 p0439 N90-12508
Development flight tests of JetStar LFC leading-edge flight test experiment 04 p0439 N90-12509
The right wing of the LEFT airplane 04 p0439 N90-12510
Performance of laminar-flow leading-edge test articles in cloud encounters 04 p0439 N90-12511
Simulated airline service experience with laminar-flow control leading-edge systems 04 p0439 N90-12512
Stability theory applications to laminar-flow control 04 p0439 N90-12513
Nonparallel stability of boundary layers 04 p0440 N90-12514
Goertler instability on an airfoil 04 p0440 N90-12517
Effect of roughness on the stability of boundary layers 04 p0440 N90-12518
Research in Natural Laminar Flow and Laminar-Flow Control, part 2
[NASA-CP-2487-PT-2] 04 p0440 N90-12519
Advanced measurement techniques, part 1 04 p0441 N90-12520
Experimental studies on Goertler vortices 04 p0442 N90-12529
An experimental evaluation of slots versus porous strips for laminar-flow applications 04 p0442 N90-12530
Boundary-layer stability analysis of Langley Research Center 8-foot LFC experimental data 04 p0442 N90-12532
Sensitivity of LFC techniques in the non-linear regime 04 p0442 N90-12533
Numerical solutions of the compressible 3-D boundary-layer equations for aerospace configurations with emphasis on LFC 04 p0443 N90-12534
Theoretical methods and design studies for NLF and HLFC swept wings at subsonic and supersonic speeds 04 p0443 N90-12535
Numerical experiments on transition control in wall-bounded shear flows 04 p0443 N90-12536
Application of sound and temperature to control boundary-layer transition 04 p0443 N90-12537
Research in Natural Laminar Flow and Laminar-Flow Control, part 3
[NASA-CP-2487-PT-3] 04 p0443 N90-12539

Design and test of an NLF wing glove for the variable-sweep transition flight experiment
04 p0444 N90-12544
F-14 VSTFE and results of the cleanup flight test program
04 p0445 N90-12547
Status report on a natural laminar-flow nacelle flight experiment
04 p0445 N90-12550
Nacelle design
04 p0446 N90-12551
Nacelle aerodynamic performance
04 p0446 N90-12552
Supersonic laminar-flow control
04 p0446 N90-12554
The effects of wall surface defects on boundary-layer transition in quiet and noisy supersonic flow
04 p0446 N90-12556
Supersonic boundary-layer transition on the LaRC F-106 and the DFRF F-15 aircraft. Part 1: Transition measurements and stability analysis
04 p0447 N90-12558
Simulated-airline-service flight tests of laminar-flow control with perforated-surface suction system
[NASA-TP-2966] 10 p1319 N90-17627
Experimental and theoretical aerodynamic characteristics of a high-lift semispan wing model
[NASA-TP-2990] 13 p1749 N90-20046
A study of supermanuever aerodynamics
[AD-A218378] 17 p2344 N90-23349
Effect of suction on controlling the secondary instability of boundary layers
[NASA-CR-4306] 18 p2552 N90-24566
Application of laminar flow control to supersonic transport configurations
[NASA-CR-181917] 20 p2803 N90-25944
Jet vortex generators for turbulent flow separation control
[NASA-CR-186959] 22 p3109 N90-27659
Control of submersible vortex flows
[NASA-TM-102693] 23 p3267 N90-28493
A numerical study of the response of the laminar unsteady separated flow about a circular cylinder to changes of boundary conditions
[DLR-FB-90-10] 24 p3471 N90-29613

BOUNDARY LAYER EQUATIONS
A three-dimensional linear stability approach to transition on wings at incidence
01 p0065 N90-10373
Numerical computation of the viscous flow field around a prolate spheroid
[DFVLR-FB-89-22] 03 p0349 N90-11992
Boundary-layer receptivity and laminar-flow airfoil design
04 p0440 N90-12516
Numerical solutions of the compressible 3-D boundary-layer equations for aerospace configurations with emphasis on LFC
04 p0443 N90-12534
Theoretical methods and design studies for NLF and HLFC swept wings at subsonic and supersonic speeds
04 p0443 N90-12535
Unsteady three-dimensional thin-layer Navier Stokes solutions on dynamic blocked grids
[AD-A212377] 04 p0503 N90-12899
An introduction to Hypersonic Aerodynamics
[VKI-LS-1989-01] 05 p0573 N90-13334
Theory of stagnation point heat transfer in dissociated air
05 p0573 N90-13337
Effects of flame stretch on the propagation, extinction, and stability of premixed flames
06 p0739 N90-14301
An efficient solver of the Eigenvalue problem of the linear stability equations for three dimensional, compressible boundary-layer flows
08 p1066 N90-16172
Numerical boundary layer calculations on the DFVLR ellipsoid of revolution
08 p1070 N90-16193
Grid-independent wall layer turbulence model for complex flow calculations
[DE90-003500] 08 p1071 N90-16200
Super-micro computer weather prediction model
[AD-A216329] 10 p1409 N90-18124
Multicellular natural convection in a narrow vertical slot
[AD-A216411] 11 p1505 N90-18668
Composite-grid techniques and adaptive mesh refinement in computational fluid dynamics
[AD-A217383] 13 p1800 N90-20328
Extension of a three-dimensional viscous wing flow analysis user's manual: VISTA 3-D code
[NASA-CR-182024] 16 p2197 N90-22538
Three-dimensional separated flow prediction on fusiform body using Euler and boundary layer methods
16 p2234 N90-22745
Examination of microburst development in Colorado thunderstorm for the 5 August 1982 case
[AD-A218478] 17 p2425 N90-23820
Flow studies in impeller passages
18 p2551 N90-24558
Boundary conditions for the Navier-Stoke's equations at an artificial boundary intersecting a solid boundary
[FFA-TN-1990-11] 19 p2691 N90-25313
The discretization of the three dimensional boundary layer equations
[ETN-90-97292] 22 p3171 N90-27987
An analysis of flow models: From Navier-Stokes to potential flow equations
22 p3173 N90-28002
Calculation of unsteady two dimensional viscous incompressible flows by spectral methods
[ETN-90-97449] 22 p3175 N90-28015
An investigation of the steady and unsteady near wake and its effect on a laminar boundary layer
23 p3324 N90-28794
Supersonic/hypersonic aerodynamics and heat transfer for projectile design using viscous-inviscid interaction
[AD-A224354] 24 p3418 N90-29303

BOUNDARY LAYER FLOW
NT BOUNDARY LAYER SEPARATION
NT REATTACHED FLOW
NT SECONDARY FLOW
NT SEPARATED FLOW
On the interaction of stationary crossflow vortices and Tollmien-Schlichting waves in the boundary layer on a rotating disc
[NASA-CR-181859] 01 p0002 N90-10007
The three-dimensional vortex sheet structure on delta wings
01 p0064 N90-10367
A composite velocity procedure for the three-dimensional reduced Navier-Stokes equations
01 p0069 N90-10396
Low-Reynolds-number modeling of complex flows with and without density variation
02 p0146 N90-10832
An experimental study of surface roughness effects on turbulent boundary layer flow and heat transfer
[AD-A212099] 03 p0347 N90-11980
Numerical computation of the viscous flow field around a prolate spheroid
[DFVLR-FB-89-22] 03 p0349 N90-11992
Evaluation and sensitivity analyses results of the MESOPUFF 2 model with CAPTEX (Cross-Appalachian Tracer Experiment) measurements
[PB89-198253] 03 p0368 N90-12103
Three-component laser Doppler velocimeter measurements in a juncture flow
04 p0441 N90-12525
Recent tests at Langley with a University of Tennessee Space Institute (UTSI) skin friction balance
04 p0441 N90-12527
Experimental and numerical analyses of laminar boundary-layer flow stability over an aircraft fuselage forebody
04 p0445 N90-12549
Reduction of turbulent drag: Boundary layer manipulators
[CERT-RSF-OA-74/2259-AYD]
04 p0501 N90-12889
Fundamental studies of turbulent wall pressure fluctuations with applications to advanced acoustic sensor systems
[AD-A213041] 04 p0552 N90-13212
Theory of stagnation point heat transfer in dissociated air
05 p0573 N90-13337
The 3D LDA techniques in vortex studies and boundary layer surveys
05 p0574 N90-13346
Multiple paths to subharmonic laminar breakdown in a boundary layer
[NASA-CR-181948] 05 p0638 N90-13722
Generalized similarity solutions for three dimensional, laminar, steady, compressible boundary layer flows on swept profile cylinders
[DLR-FB-89-34] 05 p0639 N90-13725
Computation of nonequilibrium gas flow past blunt bodies
[PREPRINT-488] 05 p0644 N90-13757
Heat transfer in convective boundary layer and channel flows
06 p0774 N90-14505
Spatial evolution of nonlinear acoustic mode instabilities on hypersonic boundary layers
[NASA-TM-102431] 06 p0777 N90-14517
Flow visualization in the cryogenic wind tunnel
08 p1030 N90-15953
Application of the singularity-separating method to computing problems of solid-propellant combustion in a closed vessel
[PREPRINT-489] 08 p1053 N90-16086
Method for the primary stability analysis of the three dimensional, compressible boundary layer flows
08 p1066 N90-16171
Wake interaction effects on the transition process on turbine blades
[AD-A214492] 09 p1168 N90-16759
Colliding natural convection boundary layer flow in a rectangular enclosure
[DE90-005397] 10 p1384 N90-18009
Incompressible flow friction factors in a simulated heat pipe
[AD-A216288] 10 p1386 N90-18018
The effect of adverse pressure gradient on turbulent burst structure in low-Reynolds number equilibrium boundary layers
[AD-A217308] 13 p1799 N90-20327
Experimental investigation of the mechanisms underlying vortex kinematics in unsteady separated flows
[AD-A217889] 13 p1802 N90-20346
Relating flow between counter-rotating propellers to aerodynamic interaction noise
14 p1909 N90-20944
Comparison of C- and O-grid generation methods using a NACA 0012 airfoil
[AD-A216375] 14 p1910 N90-20948
On the instability of Goertler vortices to nonlinear travelling waves
[NASA-CR-181994] 14 p1970 N90-21289
The effects of forcing on a single stream shear layer and its parent boundary layer
[NASA-CR-186529] 14 p1973 N90-21301
An investigation of turbulence structure in a low Reynolds number incompressible turbulent boundary layer
15 p2091 N90-21966
Automated analysis of measured turbulent boundary flow
[PB90-147844] 15 p2092 N90-21970
Experimental observations on transition to turbulence in confined coaxial jets and other boundary layer flows
[DE90-008939] 15 p2098 N90-22005
Thin-layer Navier-Stokes solutions of the asymmetric vortical flow on a tangent ogive body
[AD-A220810] 17 p2403 N90-23690
Fluid oscillations in an open, flexible container
[REPT-89-89] 17 p2404 N90-23696
Concerning the interaction of non-stationary cross-flow vortices in a three-dimensional boundary layer
[NASA-CR-182037] 18 p2492 N90-24245
Low-density flow effects for hypervelocity vehicles, phase 2
[AD-A221034] 18 p2493 N90-24249
An interactive boundary-layer method for unsteady airfoil flows. Part 1: Quasi-steady-state model
[AD-A221220] 18 p2493 N90-24250
On the instability of hypersonic flow past a flat plate
[NASA-CR-182051] 18 p2493 N90-24252
Experimental investigation of Tollmien-Schlichting instability and transition in similar boundary layer flow in an adverse pressure gradient (Hartree beta = -0.14)
[LR-604] 19 p2692 N90-25318
Analysis of near-surface flow physics in a two-stage, 10 km/s, electromagnetic launcher
[DE90-013292] 21 p2964 N90-26852
Vortex-induced boundary layer separation
[AD-A221564] 21 p3005 N90-27078
Experimental study of an unsteady boundary layer on an oscillating plane plate. Optimization and validation of calculation code for the analysis of the potential flow/boundary layer coupling in the neighborhood of a plane plate and an oscillating profile
[ETN-90-97436] 22 p3175 N90-28013
Effects of flowfield turbulence on asymmetric vortices over a slender body
[AD-A224139] 23 p3328 N90-28819
Numeric fluid mechanics
23 p3392 N90-29161

BOUNDARY LAYER NOISE
U AERODYNAMIC NOISE
U BOUNDARY LAYERS

BOUNDARY LAYER PLASMAS
Numerical study of the current sheet and PSBL in a magnetotail model
[NASA-CR-183289] 02 p0293 N90-11669
Practical aspects of a 2-D edge-plasma model
[DE90-002995] 06 p0848 N90-14932
Propulsion research on the hybrid plume rocket
[AD-A214420] 07 p0887 N90-15132
On the structure of the tail magnetic field
[IFSI-88-19] 08 p1101 N90-16378

BOUNDARY LAYER SEPARATION
Laminar boundary layer along inviscid surface streamlines over inclined axisymmetric bodies in incompressible flow
[AD-A210202] 01 p0070 N90-10401
Dynamics and control of turbulent shear flows
[AD-A210396] 01 p0070 N90-10402
Active control of unsteady and separated flow structures
[AD-A212109] 03 p0301 N90-11707
Control of turbulent mixing layers
[AD-A211413] 03 p0301 N90-11708
Simulation of glancing shock wave and boundary layer interaction
[NASA-TM-102233] 03 p0345 N90-11970
Some observations on transitory stall in conical diffusers
[NASA-TM-102387] 04 p0447 N90-12561

A computationally efficient modelling of laminar separation bubbles
[NASA-CR-185854] 04 p0499 N90-12872
Computation of Navier-Stokes equations for three-dimensional flow separation
[NASA-TM-102266] 05 p0575 N90-13353
Navier-Stokes solutions of 2-D transonic flow over unconventional airfoils 06 p0719 N90-14195
Navier-Stokes analysis of airfoils with leading edge ice accretions 06 p0719 N90-14196
Computational investigation of incompressible airfoil flows at high angles of attack
[AD-A205885] 06 p0720 N90-14201
Experimental measurements of the laminar separation bubble on an Eppler 387 airfoil at low Reynolds numbers
[NASA-CR-186263] 07 p0929 N90-15380
An algebraic turbulence model for flow separation caused by forward and backward facing steps
[AD-A213800] 07 p0931 N90-15389
Computation of broadband mixing noise from turbomachinery
[AD-A214448] 07 p0989 N90-15713
Flow separation in shock wave boundary layer interactions at hypersonic speeds
[NASA-CR-4274] 08 p1017 N90-15885
A numerical and experimental investigation of multiple shock wave/turbulent boundary layer interactions in a rectangular duct 08 p1062 N90-16141
Flows with Separation
[DGLR-PAPERS-88-05] 08 p1066 N90-16169
An interactive method for the flow calculation of airfoils with local separation regions 08 p1069 N90-16190
Calculation of the flap profile flows with separation based on coupled potential and boundary layer solutions 08 p1069 N90-16191
Inverse solutions for boundary layers with separation or close to separation under locally infinite swept wing conditions 08 p1070 N90-16192
Periodically unsteady effects on profiles, induced by separation 08 p1070 N90-16196
A survey of missile aerodynamics 10 p1303 N90-17541
Special Course on Three-Dimensional Supersonic/Hypersonic Flows Including Separation
[AGARD-R-764] 10 p1308 N90-17565
Glancing shock-boundary layer interactions 10 p1309 N90-17571
Effect of riblets on flow separation from a cylinder and an airfoil in subsonic flow
[AD-A216197] 10 p1309 N90-17574
Experimental investigation of the influence of rotor wakes on the development of the profile boundary layer and the performance of an annular compressor cascade 11 p1463 N90-18425
Measurement of velocity profiles and Reynolds stresses on an oscillating airfoil 11 p1463 N90-18427
Contribution to the study of three-dimensional separation in turbulent incompressible flow
[ESA-TT-1169] 11 p1510 N90-18697
Influence of friction and separation phenomena on the dynamic blade loading of transonic turbine cascades
[MITT-88-04] 12 p1605 N90-19235
Separation bubbles at high Reynolds number: Measurement and computation
[CUED/A-AERO/15] 12 p1657 N90-19525
Unsteady three-dimensional marginal separation, including breakdown
[NASA-TM-102525] 13 p1801 N90-20337
Control of flow separation and mixing by aerodynamic excitation
[NASA-TM-103131] 15 p2047 N90-21733
Numerical investigation of some control methods for 3-D turbulent interactions due to sharp fins 15 p2053 N90-21764
Low temperature properties of amorphous solids 15 p2171 N90-22405
A study of supermanuever aerodynamics
[AD-A218378] 17 p2344 N90-23349
Euler code predicted separation at the airfoil trailing edge
[FFA-TN-1989-30] 17 p2346 N90-23364
Fluid dynamic mechanisms and interactions within separated flows
[AD-A219628] 17 p2403 N90-23689
An interactive boundary-layer method for unsteady airfoil flows. Part 1: Quasi-steady-state model
[AD-A221220] 18 p2493 N90-24250
Flow studies in impeller passages 18 p2551 N90-24558
Vortex-induced boundary-layer separation 18 p2551 N90-24560
A computational efficient modelling of laminar separation bubbles
[NASA-CR-186729] 19 p2688 N90-25291
Report of the Fluid Dynamics Panel Working Group 10 on calculation of 3D separate turbulent flows in boundary layer limit
[AGARD-AR-255] 20 p2862 N90-26280
Vortex-induced boundary layer separation
[AD-A221564] 21 p3005 N90-27078
United States Air Force research initiation program for 1988, volume 3
[AD-A223125] 21 p3102 N90-27615
Jet vortex generators for turbulent flow separation control
[NASA-CR-186959] 22 p3109 N90-27659
Experimental study on the vortices generated by the body of a missile during flight. Part 1: Laminar boundary layer
[ONERA-RT-40/1147-AY-130A-PT-1] 22 p3110 N90-27665
Wind tunnel investigation of periodic vortex separation from rough surface circular cylinders by means of acoustic measurements
[ESA-TT-1092] 23 p3268 N90-28499
In-flight flow visualization with pressure measurements at low speeds on the NASA F-18 high alpha research vehicle
[NASA-TM-101726] 23 p3270 N90-28505
On the use of Lagrangian variables in descriptions of unsteady boundary-layer separation
[NASA-CR-182071] 23 p3323 N90-28789
Dynamic separation: Search for the cause of dynamic stall and search for its control
[AD-A223412] 24 p3418 N90-29305
Structure in the near field of the transverse jet
[AD-A224502] 24 p3467 N90-29591
A numerical study of the response of the laminar unsteady separated flow about a circular cylinder to changes of boundary conditions
[DLR-FB-90-10] 24 p3471 N90-29613

BOUNDARY LAYER STABILITY

Fluid Dynamics of Three-Dimensional Turbulent Shear Flows and Transition
[AGARD-CP-438] 01 p0062 N90-10356
Stability and transition of three-dimensional boundary layers 01 p0062 N90-10357
Stability of a supersonic boundary layer along a swept leading edge 01 p0063 N90-10359
Direct numerical study of leading-edge contamination 01 p0063 N90-10361
Experimental study of transition and leading edge contamination on swept wings 01 p0063 N90-10362
Three-dimensional boundary layer transition on a concave surface 01 p0064 N90-10365
Curvature effects on the stability of three-dimensional laminar boundary layers 01 p0064 N90-10366
The three-dimensional vortex sheet structure on delta wings 01 p0064 N90-10367
Simultaneous detection of separation and transition in surface shear layers 01 p0064 N90-10368
Experimental study of instability modes in a three-dimensional boundary layer 01 p0064 N90-10369
Primary and secondary stability analysis applied to the DFVLR-transition swept-plate experiment 01 p0065 N90-10371
Numerical investigation of transition in 3D boundary layers 01 p0065 N90-10372
A three-dimensional linear stability approach to transition on wings at incidence 01 p0065 N90-10373
Trailing-edge sweep and three-dimensional vortex interactions in jets and mixing layers 01 p0066 N90-10379
Numerical simulation of coherent structures in an incompressible mixing layer 01 p0067 N90-10383
Wall-layer eruptions in turbulent flows
[NASA-TM-102362] 02 p0219 N90-11250
Nonparallel stability of boundary layers 04 p0440 N90-12514
Interaction of Tollmien-Schlichting waves and Goertler vortices 04 p0440 N90-12515
Boundary-layer receptivity and laminar-flow airfoil design 04 p0440 N90-12516
Effect of roughness on the stability of boundary layers 04 p0440 N90-12518
Predicted and hot-film measured Tollmien-Schlichting wave characteristics 04 p0441 N90-12523
Experimental studies on Goertler vortices 04 p0442 N90-12529
An experimental evaluation of slots versus porous strips for laminar-flow applications 04 p0442 N90-12530
Results of LFC experiment on slotted swept supercritical airfoil in Langley's 8-foot transonic pressure tunnel 04 p0442 N90-12531
Boundary-layer stability analysis of Langley Research Center 8-foot LFC experimental data 04 p0442 N90-12532
Sensitivity of LFC techniques in the non-linear regime 04 p0442 N90-12533
Numerical solutions of the compressible 3-D boundary-layer equations for aerospace configurations with emphasis on LFC 04 p0443 N90-12534
Theoretical methods and design studies for NLF and HLFC swept wings at subsonic and supersonic speeds 04 p0443 N90-12535
Research in Natural Laminar Flow and Laminar-Flow Control, part 3
[NASA-CP-2487-PT-3] 04 p0443 N90-12539
Design of the low-speed NLF(1)-0414F and the high-speed HSNLF(1)-0213 airfoils with high-lift systems 04 p0444 N90-12540
Design and test of an NLF wing glove for the variable-sweep transition flight experiment 04 p0444 N90-12544
Variable-Sweep Transition Flight Experiment (VSTFE): Stability code development and clean-up glove data analysis 04 p0445 N90-12548
Experimental and numerical analyses of laminar boundary-layer flow stability over an aircraft fuselage forebody 04 p0445 N90-12549
Experimental and theoretical investigation of boundary-layer instability mechanisms on a swept leading edge at Mach 3.5 04 p0447 N90-12557
Supersonic boundary-layer transition on the LaRC F-106 and the DFRF F-15 aircraft. Part 1: Transition measurements and stability analysis 04 p0447 N90-12558
Stability of a supersonic boundary layer on a sharp cone at a small angle of attack 06 p0775 N90-14510
Spatial evolution of nonlinear acoustic mode instabilities on hypersonic boundary layers
[NASA-TM-102431] 06 p0777 N90-14517
Experiments on the laminar-turbulent transition on swept wings 08 p1066 N90-16170
Method for the primary stability analysis of the three dimensional, compressible boundary layer flows 08 p1066 N90-16171
An efficient solver of the Eigenvalue problem of the linear stability equations for three dimensional, compressible boundary-layer flows 08 p1066 N90-16172
Detection of flow instabilities at airfoil profiles using piezoelectric arrays 08 p1067 N90-16175
Direct measurement of laminar instability amplification factors in flight 08 p1067 N90-16178
Numerical simulation of supersonic free shear layers
[AD-A216289] 10 p1310 N90-17579
Investigation of the development of laminar boundary-layer instabilities along a cooled-wall hollow cylinder at Mach number 8
[AD-A217672] 13 p1800 N90-20331
On the instability of Goertler vortices to nonlinear travelling waves
[NASA-CR-181994] 14 p1970 N90-21289
Boundary layer turbulence pulsed by acoustic waves
[ETN-90-96621] 16 p2236 N90-22759
On the instability of hypersonic flow past a flat plate
[NASA-CR-182051] 18 p2493 N90-24252
Effect of suction on controlling the secondary instability of boundary layers
[NASA-CR-4306] 18 p2552 N90-24566
Effects of forebody geometry on subsonic boundary-layer stability
[NASA-CR-4314] 20 p2802 N90-25939
Application of laminar flow control to supersonic transport configurations
[NASA-CR-181917] 20 p2803 N90-25944
Inviscid dynamics of unstable shear layers
[AD-A222297] 21 p3004 N90-27077
Vandenberg Boundary Layer Survey (VBLS): Results
[AD-A222517] 21 p3031 N90-27234
Experimental study of an unsteady boundary layer on an oscillating plane plate. Optimization and validation of calculation code for the analysis of the potential flow/boundary layer coupling in the neighborhood of a plane plate and an oscillating profile
[ETN-90-97436] 22 p3175 N90-28013
Experimental investigations on the stability and transition of three-dimensional boundary layers
[ESA-TT-1026] 23 p3325 N90-28803

BOUNDARY LAYER TRANSITION

On the interaction of stationary crossflow vortices and Tollmien-Schlichting waves in the boundary layer on a rotating disc
[NASA-CR-181859] 01 p0002 N90-10007
The measurement of boundary layers on a compressor blade in cascade. Volume 1: Experimental technique, analysis and results
[NASA-CR-185118-VOL-1] 01 p0009 N90-10038
The measurement of boundary layers on a compressor blade in cascade. Volume 2: Data tables
[NASA-CR-185118-VOL-2] 01 p0009 N90-10039
Fluid Dynamics of Three-Dimensional Turbulent Shear Flows and Transition
[AGARD-CP-438] 01 p0062 N90-10356

Stability and transition of three-dimensional boundary layers 01 p0062 N90-10357
Experimental investigation of attachment-line transition in low-speed, high-lift wind-tunnel testing 01 p0062 N90-10358
Leading edge transition by contamination in hypersonic flow 01 p0063 N90-10360
Direct numerical study of leading-edge contamination 01 p0063 N90-10361
Experimental study of transition and leading edge contamination on swept wings 01 p0063 N90-10362
Numerical investigation of the effects of longitudinal vortices on the onset of transition in a flat plate boundary layer 01 p0063 N90-10363
Three-dimensional boundary layer transition on a concave surface 01 p0064 N90-10365
Simultaneous detection of separation and transition in surface shear layers 01 p0064 N90-10368
Experimental study of instability modes in a three-dimensional boundary layer 01 p0064 N90-10369
Primary and secondary stability analysis applied to the DFVLR-transition swept-plate experiment 01 p0065 N90-10371
Numerical investigation of transition in 3D boundary layers 01 p0065 N90-10372
A three-dimensional linear stability approach to transition on wings at incidence 01 p0065 N90-10373
Numerically determined transition in separated internal flow 01 p0065 N90-10374
Control and modification of turbulence 01 p0066 N90-10377
An experimental investigation of transition in oscillating pipe flow 02 p0218 N90-11249
The structure of separated flow regions occurring near the leading edge of airfoils - including transition [NASA-CR-185853] 03 p0299 N90-11695
Normal-force-curve and pitching-moment-curve slopes of forebody-cylinder combinations at zero angle of attack for Mach numbers up to 5 [ESDU-89008] 03 p0301 N90-11709
Research in Natural Laminar Flow and Laminar-Flow Control, part 1 [NASA-CP-2487-PT-1] 04 p0438 N90-12503
Performance of laminar-flow leading-edge test articles in cloud encounters 04 p0439 N90-12511
Stability theory applications to laminar-flow control 04 p0439 N90-12513
Boundary-layer receptivity and laminar-flow airfoil design 04 p0440 N90-12516
Research in Natural Laminar Flow and Laminar-Flow Control, part 2 [NASA-CP-2487-PT-2] 04 p0440 N90-12519
Advanced measurement techniques, part 1 04 p0441 N90-12520
Flow quality measurements in compressible subsonic flows 04 p0441 N90-12521
Hot-film system for transition detection in cryogenic wind tunnels 04 p0441 N90-12522
Remote detection of boundary-layer transition by an optical system 04 p0441 N90-12524
Theoretical methods and design studies for NLF and HLFC swept wings at subsonic and supersonic speeds 04 p0443 N90-12535
Numerical experiments on transition control in wall-bounded shear flows 04 p0443 N90-12536
Application of sound and temperature to control boundary-layer transition 04 p0443 N90-12537
Research in Natural Laminar Flow and Laminar-Flow Control, part 3 [NASA-CP-2487-PT-3] 04 p0443 N90-12539
Wind tunnel results of the low-speed NLF(1)-0414F airfoil 04 p0444 N90-12541
Design and test of an NLF wing glove for the variable-sweep transition flight experiment 04 p0444 N90-12544
The 757 NLF glove flight test results 04 p0445 N90-12546
F-14 VSTFE and results of the cleanup flight test program 04 p0445 N90-12547
Variable-Sweep Transition Flight Experiment (VSTFE): Stability code development and clean-up glove data analysis 04 p0445 N90-12548
Experimental and numerical analyses of laminar boundary-layer flow stability over an aircraft fuselage forebody 04 p0445 N90-12549
Status report on a natural laminar-flow nacelle flight experiment 04 p0445 N90-12550
Nacelle design 04 p0446 N90-12551
Nacelle aerodynamic performance 04 p0446 N90-12552
Supersonic laminar-flow control 04 p0446 N90-12554
Design and fabrication requirements for low noise supersonic/hypersonic wind tunnels 04 p0446 N90-12555
The effects of wall surface defects on boundary-layer transition in quiet and noisy supersonic flow 04 p0446 N90-12556
Supersonic boundary-layer transition on the LaRC F-106 and the DFRF F-15 aircraft. Part 1: Transition measurements and stability analysis 04 p0447 N90-12558
Supersonic boundary-layer transition on the LaRC F-106 and the DFRF F-15 aircraft. Part 2: Aerodynamic predictions 04 p0447 N90-12559
A computationally efficient modelling of laminar separation bubbles [NASA-CR-185854] 04 p0499 N90-12872
Transition in surface boundary layers [CERT-RSF-OA-43/5018-AYD] 04 p0502 N90-12897
Multiple paths to subharmonic laminar breakdown in a boundary layer [NASA-CR-181948] 05 p0638 N90-13722
Numerical simulation of transition in three-dimensional boundary layers [DLR-FB-89-12] 05 p0639 N90-13728
Visualization of boundary layer transition zone movement on oscillating airfoils with shear-sensitive liquid-crystal coatings [DE89-009570] 06 p0721 N90-14210
On strongly nonlinear vortex/wave interactions in boundary-layer transition [NASA-CR-181963] 07 p0876 N90-15078
Numerical investigation of transition control of a flat plate boundary layer 07 p0926 N90-15361
Flows with Separation [DGLR-PAPERS-88-05] 08 p1066 N90-16169
Numerical simulation of the nonlinear evolution of a perturbation in a three dimensional boundary layer 08 p1067 N90-16173
Semi-empirical transition criteria for the design of laminar profiles 08 p1067 N90-16174
Determination of the N-factor in the Brunswick (Federal Rep. of Germany) transonic wind tunnel using measurements of pressure distributions and transition points, and the Sally method 08 p1067 N90-16177
Development of transition criteria on the basis of e to the N power for three dimensional wing boundary layers 08 p1067 N90-16179
Wake interaction effects on the transition process on turbine blades [AD-A214492] 09 p1168 N90-16759
A review of high-speed, convective, heat-transfer computation methods 10 p1305 N90-17548
Goertler vortices in growing boundary layers: The leading edge receptivity problem, linear growth and the nonlinear breakdown stage [NASA-CR-181962] 10 p1306 N90-17555
Opportunities for improved understanding of supersonic and hypersonic flows 10 p1308 N90-17566
Some Navier-Stokes calculations for the CAST-10 airfoil 10 p1324 N90-17651
Main results of CAST-10 airfoil tested in T2 cryogenic wind tunnel 10 p1324 N90-17652
An experimental AWTS process and comparisons of ONERA T2 and 0.3-m TCT AWTS data for the ONERA CAST-10 aerofoil 10 p1324 N90-17653
Investigation of CAST-10-2/DOA 2 airfoil in NAE high Reynolds number two-dimensional test facility 10 p1324 N90-17654
Numerical studies on laminar-turbulent transition in boundary layers 10 p1383 N90-18001
Effects of controlled three-dimensional perturbations on boundary layer transition [AD-A215080] 10 p1384 N90-18011
Flight survey of the 757 wing noise field and its effects on laminar boundary layer transition. Volume 3: Extended data analysis [NASA-CR-178419] 10 p1427 N90-18233
Modelling unsteady transition and its effects on profile loss 11 p1462 N90-18423
Experimental investigation of the influence of rotor wakes on the development of the profile boundary layer and the performance of an annular compressor cascade 11 p1463 N90-18425
Flight test investigation of certification issues pertaining to general-aviation-type aircraft with natural laminar flow [NASA-CR-181967] 14 p1911 N90-20952
Current Japanese supercomputers for computational fluid dynamics applications 16 p2311 N90-23172
Concerning the interaction of non-stationary cross-flow vortices in a three-dimensional boundary layer [NASA-CR-182037] 18 p2492 N90-24245
Flow unsteadiness effects on boundary layers [NASA-CR-186067] 18 p2550 N90-24557
Coherent structures, chaos and the role of modern dynamics in turbulent shear flows [AD-A220884] 18 p2552 N90-24562
A brief review of some mechanisms causing boundary layer transition at high speeds [NASA-TM-102834] 20 p2803 N90-25945
An investigation into the numerical prediction of boundary layer transition using the K.Y. Chien turbulence model [NASA-CR-185252] 20 p2860 N90-26269
Effects of 2 Hz imposed bulk flow unsteadiness on laminar-turbulent transition in a straight channel [AD-A223028] 20 p2864 N90-26295
Three-dimensional structure of boundary layers in transition to turbulence [AD-A223242] 21 p3004 N90-27076
FIRE aircraft observations of horizontal and vertical transport in marine stratocumulus 22 p3220 N90-28261
Two-dimensional wind tunnel test and comparison with calculations for a 15.2 percent thick airfoil section for wind turbines [FFA-TN-1990-16] 23 p3269 N90-28501
Use of liquid crystals for qualitative and quantitative 2-D studies of transition and skin friction [RAE-TM-AERO-2159] 23 p3325 N90-28800
Experimental investigations on the stability and transition of three-dimensional boundary layers [ESA-TT-1026] 23 p3325 N90-28803
Numeric fluid mechanics 23 p3392 N90-29161
A boundary-layer transition model for the Navier-Stokes computation for a natural-laminar-flow airfoil [NAL-TR-1038T] 24 p3421 N90-29328
Transition of the boundary layer [DERAT-RSF-50/5018-37] 24 p3469 N90-29600

BOUNDARY LAYERS

NT ATMOSPHERIC BOUNDARY LAYER
NT COMPRESSIBLE BOUNDARY LAYER
NT HYPERSONIC BOUNDARY LAYER
NT INCOMPRESSIBLE BOUNDARY LAYER
NT LAMINAR BOUNDARY LAYER
NT PLANETARY BOUNDARY LAYER
NT SUPERSONIC BOUNDARY LAYERS
NT THERMAL BOUNDARY LAYER
NT THREE DIMENSIONAL BOUNDARY LAYER
NT TURBULENT BOUNDARY LAYER
NT TWO DIMENSIONAL BOUNDARY LAYER
Atmospheric aerosol size distributions and optical properties found in the marine boundary layer over the Atlantic Ocean [AD-A210800] 02 p0252 N90-11431
Computer simulations of electromagnetic ion instabilities in the plasma sheet boundary layer [DE89-016596] 02 p0278 N90-11588
Upwind discretization of the steady Navier-Stokes equations [CWI-NM-R8810] 04 p0502 N90-12891
General buckling tests with thin-walled shells [DLR-MITT-89-13] 05 p0655 N90-13816
On the nonexistence of a strong solution in the boundary problem for a sticky Brownian motion [CWI-BS-R8901] 05 p0689 N90-14018
A note concerning the onset of three dimensionality and time dependence in Goertler vortices [NASA-CR-181956] 06 p0718 N90-14193
Convective boundary layer and modeling of dispersion 06 p0813 N90-14731
Numerical investigation of transition control of a flat plate boundary layer 07 p0926 N90-15361
Flow separation in shock wave boundary layer interactions at hypersonic speeds [NASA-CR-4274] 08 p1017 N90-15885
An experimental investigation of viscous aspects of propeller blade flow 09 p1159 N90-16711
Predicted and measured boundary layer refraction for advanced turboprop propeller noise [NASA-TM-102365] 09 p1279 N90-17413
Shock-shock boundary layer interactions 10 p1308 N90-17569
Glancing shock-boundary layer interactions 10 p1309 N90-17571
Some Navier-Stokes calculations for the CAST-10 airfoil 10 p1324 N90-17651
Investigation of CAST-10-2/DOA 2 airfoil in NAE high Reynolds number two-dimensional test facility 10 p1324 N90-17654
Experience with some repeat tests on the 9 inch chord CAST-10-2/DOA 2 airfoil model in the Langley 0.3-m TCT adaptive wall test section 10 p1325 N90-17657
Liquid transverse jets in compressible crossflows 10 p1385 N90-18012
Aerodynamics of unsteady systems. Numerical study of potential flow/boundary layer coupling [ETN-90-96257] 11 p1452 N90-18367
Experimental investigations of the unsteady boundary layer on an oscillating flat plate. Optimization and validation of a code, for calculating the potential flow/boundary layer coupling of a flat plate and of an oscillating profile [ETN-90-96254] 11 p1508 N90-18682

Swept shock/boundary layer interaction experiments in support of CFD code validation
[NASA-CR-186397] 12 p1659 N90-19535
Three-dimensional structure of plane mixing layers
17 p2344 N90-23347
The 3-D composite velocity solutions for subsonic/transonic flow over forebodies and afterbodies
[AD-A220370] 17 p2345 N90-23354
Flow unsteadiness effects on boundary layers
[NASA-CR-186067] 18 p2550 N90-24557
Flow studies in impeller passages
18 p2551 N90-24558
On computational aspects of simplicial splines
[MEMO-818] 18 p2600 N90-24795
On the receptivity problem for Goertler vortices: Vortex motions induced by wall roughness
[NASA-CR-182036] 19 p2654 N90-25109
A computational efficient modelling of laminar separation bubbles
[NASA-CR-186729] 19 p2688 N90-25291
A brief review of some mechanisms causing boundary layer transition at high speeds
[NASA-TM-102834] 20 p2803 N90-25945
Experimental techniques in the field of low density aerodynamics
[AGARD-AG-318(FR)] 21 p2953 N90-26792
Installation and pretest analysis of DARPA suboff model in the DTRC anechoic wind tunnel
[AD-A221497] 21 p2955 N90-26801
Toward the optimization of a non-diffusing, two-dimensional S-shaped duct
[IAR-89-3] 21 p3003 N90-27068
The radiation budget of stratocumulus clouds measured by tethered balloon instrumentation: Variability of flux measurements 22 p3216 N90-28242
Turbulence structure in clear and cloudy regions of the 7 July 1987 Electra mission 22 p3217 N90-28247
A case study of cumulus formation beneath a stratocumulus sheet: Its structure and effect on boundary layer budgets 22 p3219 N90-28256
FIRE aircraft observations of horizontal and vertical transport in marine stratocumulus
22 p3220 N90-28261
Unsteady aerodynamics of controls
23 p3273 N90-28525
An asymptotically induced domain decomposition method for parabolic boundary layer problems
[DE90-014620] 23 p3326 N90-28804
Extrapolation procedures at outflow boundaries for the Navier-Stokes equations
[FFA-TN-1990-23] 23 p3327 N90-28811
Simulation and measurement of the heat exchange between the urban canopy and boundary layers
24 p3486 N90-29702
Meteorological conditions over the North Atlantic Ocean during GCE/CASE/WATOX
[PB90-252032] 24 p3494 N90-29747

BOUNDARY LUBRICATION
Cold press lubrication: Fine tuning of the CETIM Forgelub test
[CETIM-105160] 04 p0509 N90-12938
Liquid lubrication in space
[NASA-RP-1240] 22 p3183 N90-28063

BOUNDARY VALUE PROBLEMS
NT CAUCHY PROBLEM
NT DIRICHLET PROBLEM
NT NEUMANN PROBLEM
Use of the quasilinearization algorithm for the simulation of LSS slewing 01 p0022 N90-10110
Two counter-rotating vortices approaching a free surface in a viscous fluid
[AD-A210495] 01 p0070 N90-10404
Stability of discontinuous shearing motions of a non-Newtonian fluid
[AD-A210643] 01 p0071 N90-10406
Stability of discontinuous steady states in shearing motion of a non-Newtonian fluid
[AD-A210644] 01 p0071 N90-10407
Global existence and asymptotic stability for a nonlinear integrodifferential equation modeling heat flow
[AD-A210647] 01 p0071 N90-10408
Mechanics of the crack path formation
[NASA-CR-185143] 01 p0080 N90-10455
Numerical methods for differential-algebraic equations: Current status and future directions
[DE89-015116] 01 p0111 N90-10632
Efficient algorithm for calculation of radar cross section
[AD-A210785] 02 p0213 N90-11217
Analytical and numerical studies in flow development
[DE89-017380] 02 p0221 N90-11269
Parameter estimation in functional and partial differential equations
[AD-A211040] 02 p0265 N90-11511
On the numerical solution of two-point boundary value problems
[AD-A211244] 02 p0266 N90-11516
Potential for parallelism in explicit linear methods
[DE89-017329] 02 p0267 N90-11523
On the equivalence of BS-stability and B-consistency
[CWI-NM-R8815] 02 p0268 N90-11530
Nearly optimal algorithms and bounds for multilayer channel routing
[AD-A211913] 03 p0343 N90-11955
Some new algorithms for boundary value problems in smooth particle hydrodynamics
[AD-A211728] 03 p0348 N90-11987
On the computation of normal modes of a rotating, viscous, incompressible fluid with a capillary free boundary
[REPT-89-01] 03 p0348 N90-11989
Buckling of axially compressed imperfect orthotropic shells with elastic edge supports
[PB89-217038] 03 p0357 N90-12043
Convergence results for pseudospectral approximations of hyperbolic systems by a penalty type boundary treatment
[NASA-CR-181929] 03 p0391 N90-12230
Goertler instability on an airfoil
04 p0440 N90-12517
Analysis of three- and four-sided uniform waveguides with unusual cross-section/boundary conditions
[AD-A212653] 04 p0493 N90-12834
A 2d-1 lower bound 2-layer knock-knee channel routing
[AD-A211948] 04 p0495 N90-12847
Stability conditions for steady shearing. Stability conditions for simple shear under mixed thermal boundary conditions 04 p0499 N90-12873
A simulation study of the overdetermined geodetic boundary value problem using collocation
[AD-A211785] 04 p0518 N90-12990
Smoothed predictor-corrector methods for solving partial differential equations
[CWI-NM-R8808] 04 p0540 N90-13131
Iterated theta method for hyperbolic equations
[CWI-NM-R8809] 04 p0540 N90-13132
An algebraic characterization of B-convergent Runge-Kutta methods
[CWI-NM-R8901] 04 p0541 N90-13133
Increasing the real stability boundary of explicit methods
[CWI-NM-R8902] 04 p0541 N90-13134
An Eigenvalue Analysis of finite-difference approximations for hyperbolic IBVPs
[NASA-TM-102241] 04 p0541 N90-13137
A practical approach for minimum time control of the Spacecraft Control Laboratory Experiment (SCOLE), appendix A
[NASA-CR-186008] 05 p0602 N90-13495
Magneto-elastic interactions in conducting structures in transient magnetic fields 05 p0632 N90-13686
The initial-boundary value problem for the Davey-Stewartson 1 equation; how to generate and drive localized coherent structures in multidimensions
[PREPRINT-684] 05 p0643 N90-13756
Time domain coupling of the boundary and finite element methods for elastodynamics
[AD-A213243] 05 p0654 N90-13811
Parabolic equations for curves on surfaces. 2: Intersections, blow up and generalized solutions
[AD-A212890] 05 p0687 N90-14004
The weighted sum of two S-units being a square
[MEMO-792] 05 p0691 N90-14031
Solving a specific Thue-Mahler equation
[MEMO-793] 05 p0691 N90-14032
Practice of bivariate quadratic simplicial splines
[MEMO-800] 05 p0691 N90-14034
Computational aspects of pseudospectral Laguerre approximations
[NASA-CR-181934] 05 p0691 N90-14038
Energy exchange of interacting solitons in multidimensions
[PREPRINT-662] 05 p0696 N90-14071
Evaluation of the indirect effects of lightning on a system: Double transfer function method
[RAE-TRANS-2172] 06 p0721 N90-14211
Dynamics and control of flexible spacecraft during and after slewing maneuvers
[NASA-CR-186123] 06 p0733 N90-14270
Analysis of metal matrix composite structures using a microchemical constitutive theory
06 p0737 N90-14290
The stability of Taylor-Couette flow with radial heating
06 p0774 N90-14502
Proceedings of the Focused Research Program on Spectral Theory and Boundary Value Problems. Volume 4: Nonlinear Differential Equations
[DE90-000920] 06 p0822 N90-14780
A tensor product b-spline method for 3D multi-block elliptic grid generation
[DE89-017440] 06 p0836 N90-14859
Boundary element analysis of single and multidomain problems in acoustics 06 p0837 N90-14867
A direct-inverse method for transonic and separated flows about airfoils
[NASA-CR-4270] 07 p0875 N90-15072
Numerical simulation of the unsteady two-dimensional flow in a time-dependent doubly-connected domain
07 p0875 N90-15073
Guidance analysis of the aeroglide plane change maneuver as a turning point problem
[NASA-TM-101639] 07 p0883 N90-15110
New transient algorithms for non-Newtonian flows
[AD-A213494] 07 p0930 N90-15385
Research in mathematics and computer science at Argonne
[DE90-000975] 07 p0969 N90-15595
On functional integral representations in the lower Hubbard band based on generalized coherent states
[DE90-602936] 07 p1003 N90-15804
Finite element calculations for transonic flows taking into account several far field boundary conditions
08 p1069 N90-16188
On the reciprocity of state vectors in boundary value models
[AD-A214104] 08 p1115 N90-16458
Solving time harmonic wave problems on vector processors
[DE90-003956] 08 p1119 N90-16480
High-order mixture homogenization of fiber-reinforced composites
[AD-A215247] 09 p1187 N90-16876
Upper semicontinuous global attractors for viscous flow
[NASA-CR-181976] 09 p1217 N90-17056
On the superconvergence of the SBB method
[DE89-635709] 09 p1272 N90-17375
Validation of the boundary element method applied to complex fracture mechanics conditions
[AD-A216412] 10 p1398 N90-18080
Boundary estimation problems arising in thermal tomography
[NASA-CR-181964] 10 p1421 N90-18193
Conditions at the downstream boundary for simulations of viscous incompressible flow
[NASA-TM-102510] 10 p1422 N90-18198
On the exponential convergence of the h-p version for boundary element Galerkin methods on polygons
[AD-A215814] 10 p1423 N90-18210
The h-p version of the boundary element method with geometric mesh on polygonal domains
[AD-A215815] 10 p1423 N90-18211
Asymptotic boundary conditions for dissipative waves: General theory
[NASA-TM-102497] 11 p1551 N90-18927
Initialization of EURAD. Part 1: Utilization of ECMWF analysis data 12 p1688 N90-19695
Parallel algorithms for boundary value problems
[NASA-TM-102498] 12 p1704 N90-19783
On the parallel efficiency of the Frederickson-McBryan multigrid
[NASA-CR-181999] 12 p1705 N90-19791
Hierarchical basis preconditioners for second order elliptic problems in three dimensions
[DE90-005980] 12 p1706 N90-19793
A unified integrated model for sputter coating uniformity
[DE90-008322] 13 p1778 N90-20205
Amplitude-dependent neutral modes in compressible boundary layer flows
[NASA-TM-102524] 13 p1799 N90-20326
A simple multicomponent fluid theory with accurate physics
[DE90-006537] 13 p1801 N90-20334
Geopotential coefficient determination and the gravimetric boundary value problem: A new approach
13 p1833 N90-20521
The role of topography in geodetic gravity field modelling 13 p1835 N90-20534
Very accurate upward continuation to low heights in a test of non-Newtonian theory 13 p1837 N90-20548
Domain decomposition for a boundary-value problem with a shock layer
[DE90-007857] 13 p1877 N90-20762
Magnetostatic boundary-value problems in the incompleto-nonlinear formulation and methods of their solution
[DE90-615185] 13 p1877 N90-20767
Micro SAINT programs for numerical methods of integration and differential equations
[AD-A218097] 13 p1878 N90-20772
A system for transonic wing design with geometric constraints based on an inverse method
14 p1917 N90-20983

Subsonic and transonic blade design by means of analysis codes
14 p1917 N90-20985
A computational design method for shock free transonic cascades and airfoils
14 p1918 N90-20986
Compact scheme for systems of equations applied to fundamental problems of mechanics of continua
[NASA-CR-186494] 14 p1971 N90-21292
Theory and application of nonlinear normal mode initialization
[PB90-166000] 14 p2006 N90-21497
Compact finite volume methods for the diffusion equation
[NASA-CR-186477] 14 p2019 N90-21568
Finite element algorithms for hyperbolic conservation laws with forcing terms
[INPE-5024-RPE/617] 14 p2022 N90-21595
High energy phenomena during solar flares
[INPE-4961-TDL/390] 14 p2043 N90-21713
Experimental and analytical investigations of granular materials: Shear flow and convective heat transfer
15 p2091 N90-21968
The solution of scattering and radiation problems for complex configurations based on 3-D grid and patch models
15 p2096 N90-21997
Analysis of a finite two-dimensional solid with an inclined crack and a rigid inclusion
15 p2120 N90-22127
Formulation of non-reflecting boundary conditions in numerical models of the atmosphere
15 p2129 N90-22175
Tropopause undulations and the development of extratropical cyclones
15 p2132 N90-22186
Normal forms for weakly non-linear perturbed wave equations
[REPT-89-41] 15 p2161 N90-22343
The theta-methods in the numerical solution of delay differential equations
[TW-89-03] 15 p2161 N90-22349
Stability radius of polynomials occurring in the numerical solution of initial value problems
[TW-89-04] 15 p2162 N90-22350
Stability criteria in the numerical solution of initial value problems
[TW-89-05] 15 p2162 N90-22351
The minimum drag profile in laminar flow: A numerical way
16 p2196 N90-22535
Adaptive mesh experiments for hyperbolic partial differential equations
[AD-A219194] 16 p2307 N90-23148
A study of supermanuever aerodynamics
[AD-A218378] 17 p2344 N90-23349
Parasitic coupling of the fringing fields of an Ion-Bernstein wave antenna
[DE90-009918] 17 p2387 N90-23596
Nonlinear internal gravity wave critical layers
17 p2422 N90-23801
Hypersingular integrals and the two dimensional Helmholtz equation
[DE90-009821] 17 p2456 N90-24012
Efficient smoothing for boundary value models
[AD-A218484] 17 p2456 N90-24014
Local and global order reduction of some LOD schemes
[CWI-NM-R8914] 17 p2459 N90-24041
A feedback extension to the numerical solution of nonlinear boundary value problems
[AD-A219886] 17 p2461 N90-24050
An H(m)sub 0 interpolation result
[AD-A219888] 17 p2461 N90-24051
Computational aspects of adaptive dimensional reduction for nonlinear boundary value problems
[AD-A219889] 17 p2461 N90-24052
Contractivity of Runge-Kutta methods
[TW-89-12] 17 p2464 N90-24079
Diffraction about acoustically soft panels
[AD-A220850] 17 p2469 N90-24115
Asymptotic analysis of wind-induced vibrations
[ETN-90-96903] 18 p2572 N90-24658
Multi-grid and B(ox)-splines
[MEMO-828] 18 p2600 N90-24801
On the use of stability regions in the numerical analysis of stability value problems
[TW-89-07] 18 p2603 N90-24826
On a generalization of the resolvent condition in the Kreiss matrix theorem
[TW-89-08] 18 p2603 N90-24827
Applications of cone theory to boundary value problems
[AD-A220939] 18 p2603 N90-24828
The CFL condition for spectral approximations to hyperbolic initial-boundary value problems
[NASA-CR-182053] 18 p2604 N90-24833
Finite amplitude surface waves in cooled plasmas with smeared interface
[DE90-611308] 18 p2617 N90-24909
Structural zooming research and development of an interactive computer graphical interface for stress analysis of cracks
18 p2641 N90-25042
Extension-torsion coupling behavior of advanced composite tilt-rotor blades
18 p2644 N90-25057
The role of the topography in gravity gradiometer reductions and in the solution of the geodetic boundary value problem using analytical downward continuation
[AD-A223107] 21 p3025 N90-27201
Free boundary problems for flow with vorticity
[AD-A218415] 22 p3168 N90-27971
Constitutive laws for discrete velocity models of gas (continued)
[ETN-90-97451] 22 p3175 N90-28016
Emitter and base recombination parameters in solar cells: Measurement process and dependence on temperature and injection
[ETN-90-97305] 22 p3196 N90-28138
Power bounded prolongations and Picard-Lindeloef iteration
[PB90-190877] 22 p3242 N90-28384
Linear iterative solvers for implicit ODE methods
[NASA-CR-182074] 22 p3242 N90-28386
Finite-volume application of high order ENO schemes to multi-dimensional boundary-value problems
[NASA-CR-186917] 22 p3242 N90-28387
Solution of the Stokes system by boundary integral equations and fixed point iterative schemes
[DE90-627166] 23 p3389 N90-29138
The fundamentals of adaptive grid movement
24 p3470 N90-29610
Proceedings of damping '89. Volume 1: Pages AAB-1 through DCD-11
[AD-A223431] 24 p3479 N90-29664
An existence theorem for periodic solutions and applications to some third order nonlinear differential equations
[DE90-627152] 24 p3536 N90-29992
Solution of nonlinear eigenvalue problems via parallel shooting
[LR-587] 24 p3539 N90-30013

BOUSSINESQ APPROXIMATION
Numerical solution of three-dimensional unsteady flows: Application to instability problems
01 p0065 N90-10375
A multigrid method for the Navier-Stokes and Boussinesq equations
[REPT-89-17] 04 p0501 N90-12886
Numerical simulation of vortex breakdown
14 p1970 N90-21288
Stability of a solitary wave solution to a set of coupled Boussinesq-like equations
[DE90-008927] 14 p2021 N90-21586
Numerical solution of a bifurcation problem for the Boussinesq equations at low Prandtl numbers by a multigrid method
[REPT-89-67] 17 p2458 N90-24026
A line relaxation smoother for the multigrid solution of the Boussinesq equations
[REPT-89-68] 17 p2458 N90-24027
On traveling wave solutions of a set of coupled Boussinesq-like equations
[DE90-013182] 20 p2917 N90-26597
Numerical method for calculating indoor airflows using a turbulence model
[PB90-162009] 21 p3003 N90-27067

BOW SHOCK WAVES
U BOW WAVES
U SHOCK WAVES

BOW WAVES
Plasma waves in the earth's foreshock, bow shock, and magnetosheath
01 p0086 N90-10486
Computer simulation of plasma interactions near Titan
01 p0142 N90-10816
Shock layer vacuum UV spectroscopy in an arc-jet wind tunnel
[NASA-TM-102258] 09 p1226 N90-17112
Glancing shock-boundary layer interactions
10 p1309 N90-17571
Liquid transverse jets in compressible crossflows
10 p1385 N90-18012
Investigation of plasma density bulge in front of Venus bow shock
[NASA-CR-186937] 22 p3262 N90-28476
Genesis of bow echoes: A rear-inflow induced meso-convective structure
[PB90-209776] 23 p3349 N90-28926

BOX BEAMS
Solar Concentrator Advanced Development Program
[NASA-CR-185173] 16 p2250 N90-22834

BOXES (CONTAINERS)
The rodent research animal holding facility as a barrier to environmental contamination
[NASA-TM-102237] 03 p0378 N90-12151
Advanced gearbox technology
[NASA-CR-179625] 18 p2498 N90-24274

BRAGG ANGLE
Bragg crystal polarimeters
[NASA-CR-181331] 01 p0073 N90-10423
First-order Bragg SAR imagery of Kelvin wakes and moving internal wave fields
[AD-A213361] 05 p0633 N90-13691
New approach to the dynamical diffraction theory in the case of three-dimensional perfect crystal
[DE90-620563] 16 p2322 N90-23240
Probing interfacial structure and composition with x ray standing waves
[AD-A223071] 21 p2977 N90-26916
Identification of tetragonal and cubic structures of zirconia
[AD-A222373] 21 p3083 N90-27535
An x ray source for lithography
[AD-D014596] 24 p3473 N90-29630

BRAGG CELLS
Optical excisor modeling
[AD-A219338] 16 p2230 N90-22722

BRAIN
NT BRAIN STEM
NT CEREBELLUM
NT CEREBRAL CORTEX
NT CEREBRUM
NT PINEAL GLAND
NT THALAMUS
Biomedical influences on spinal cord function
[AD-A210311] 01 p0092 N90-10527
Excitatory amino acids as transmitters in the brain
[AD-A210685] 01 p0093 N90-10532
Computational and psychophysical study of human vision using neural networks
[AD-A213290] 05 p0674 N90-13924
Investigation of a magnetostrictive fiber optic interferometric sensor
[AD-A215666] 09 p1226 N90-17111
Activation: Positive and negative effects of the alarm system in the brain
09 p1257 N90-17290
Computing with neural maps: Application to perceptual and cognitive functions
[AD-A216689] 10 p1412 N90-18143
Development of gamma-emitting, receptor-binding radiotracers for imaging the brain and pancreas
[DE90-008314] 13 p1851 N90-20621
Brain activity during tactical decision-making. Part 3: Relationships between probe-evoked potentials, simulation performance, and on-job performance
[AD-A217207] 13 p1854 N90-20638
Sparse distributed memory overview
15 p2141 N90-22235
Pyramid image codes
15 p2143 N90-22243
DURIP-Instrumentation for recording and analyzing multiple input/output saccadic eye movement neurosensory control
[AD-A219905] 17 p2435 N90-23871
Neurotransmitter and peptide localization in human brain
[AD-A219964] 17 p2435 N90-23873
Analysis of neural systems involved in modulation of memory storage
[AD-A220230] 18 p2584 N90-24714
Experiment K-6-18. Study of muscarinic and gaba (benzodiazepine) receptors in the sensory-motor cortex, hippcampus and spinal code
20 p2895 N90-26471
The integrated area measure of visual endogenous ERPs: Relation to cognitive workload and hemisphere
[AD-A223191] 21 p3035 N90-27255
Time, space and form in vision
[AD-A213889] 23 p3357 N90-28971
Multi-user facility for high performance optical recording of brain activity (DURIP)
[AD-A223491] 24 p3498 N90-29768
Attention, imagery, and memory: A neuromagnetic investigation
[AD-A224560] 24 p3499 N90-29775

BRAIN CIRCULATION
Metabolism, seizures, and blood flow in brain following organophosphate exposure: Mechanisms of action and possible therapeutic agents
[AD-A217098] 12 p1696 N90-19740
Neurobehavioral effects of carbon monoxide (CO) exposure in humans: Elevated carboxyhemoglobin (COHb) and cerebrovascular responses
[AD-A222840] 21 p3034 N90-27246

BRAIN STEM
Brain stem evoked responses in altered G environments
[AD-A220097] 17 p2435 N90-23874

BRAKES (FOR ARRESTING MOTION)
NT AERODYNAMIC BRAKES
NT AIRCRAFT BRAKES
NT DRAG CHUTES
NT LEADING EDGE FLAPS

Independent Orbiter Assessment (IOA): Analysis of the rudder/speed brake subsystem
[NASA-CR-185560] 02 p0161 N90-10916
Independent Orbiter Assessment (IOA): Assessment of the rudder/speed brake subsystem FMEA/CIL
[NASA-CR-185558] 02 p0174 N90-10975
Investigation into the effect of fibre size on the tribological behaviour of semi-metallic brake material
09 p1185 N90-16864
Bidirectional drive and brake mechanism
[NASA-CASE-MSC-21540-1] 20 p2872 N90-26342

BRAKING
Independent Orbiter Assessment (IOA): Analysis of the nose wheel steering subsystem
[NASA-CR-185548] 02 p0163 N90-10921
Independent Orbiter Assessment (IOA): Analysis of the landing/deceleration subsystem
[NASA-CR-185569] 02 p0167 N90-10943
Preliminary subsystem designs for the Assured Crew Return Vehicle (ACRV), volume 1
[NASA-CR-186677-VOL-1] 20 p2818 N90-26039

BRANCHING (MATHEMATICS)
NT PERIOD DOUBLING
An introduction to fractals and chaos
[AD-A210257] 01 p0117 N90-10675
Numerical analysis of chaotic symbol sequences generated by parabolic and triangle maps of the interval
[MPIS-22/1987] 04 p0539 N90-13124
Self-decomposable distributions and branching processes
[MEMO-COSOR-89-06] 05 p0693 N90-14052
Introduction to bifurcation theory
[DE90-003319] 07 p0982 N90-15673
Nonlinear maps with competitive interactions: Fixed-points, bifurcations, and chaotic attractors
[DE90-001858] 07 p0986 N90-15695
The bifurcation interpreter: A step towards the automatic analysis of dynamical systems
[AD-A214618] 09 p1265 N90-17336
New aspects in bifurcation with symmetry
[AD-A216506] 11 p1552 N90-18935
F-15B high angle-of-attack phenomena and spin prediction using bifurcation analysis
[AD-A217366] 13 p1754 N90-20073
Branch point placement
[OUEL-1767/89] 15 p2158 N90-22329
Bicausal representations and multivariable generalized predictive control
[OUEL-1781/89] 15 p2159 N90-22331
Hopf bifurcation with nonsemisimple 1:1 resonance e
[MEMO-808] 15 p2161 N90-22347
Bifurcational aspects of parametric resonance
[W-8904] 16 p2231 N90-22730
Nonlinear bifurcation study of plane Poiseuille flow
[DLR-FB-89-42] 16 p2236 N90-22756
Continuation and multi-grid methods for bifurcation problems
[AD-A218904] 16 p2307 N90-23146
Numerical solution of a bifurcation problem for the Boussinesq equations at low Prandtl numbers by a multigrid method
[REPT-89-67] 17 p2458 N90-24026
Quadratic systems with three saddles and one antisaddle
[REPT-89-80] 17 p2458 N90-24033
Concatenable structures for decomposable problems
[RUU-CS-89-16] 18 p2601 N90-24810
Three-dimensional viscous flow structures from bifurcation of a degenerate singularity with three zero eigenvalues
[LR-572] 19 p2692 N90-25314
Flow structures around non-hyperbolic singularities on the wall with one vanishing eigenvalue: A discussion of the flow structures and the unfoldings
[LR-586] 19 p2692 N90-25315
Limit cycles and bifurcation in piecewise-linear and piecewise-analytic systems. 1: General theory
[RR-372] 19 p2751 N90-25634
Perturbation methods in the theory of waves and bifurcation phenomena 20 p2916 N90-26593
The image of weighted combinatorial problems
[REPT-88-017] 21 p3057 N90-27382

BRANCHING (PHYSICS)
The 2.7/4.3 micron CO2 branching ratio measurement
[AD-A215952] 11 p1534 N90-18830
Bifurcations in viscous flow fields. On the genesis and development of topologically complicated separated flow structures
[PB90-167156] 15 p2099 N90-22012

BRASSES
Pulsed laser-induced melting of intermediate Cu-Zn phases
[DE90-005404] 11 p1513 N90-18713

BRAYTON CYCLE
Performance potential of an advanced technology Mach 3 turbojet engine installed on a conceptual high-speed civil transport
[NASA-TM-4144] 01 p0008 N90-10034
Advanced energy system program
[PB89-235170] 05 p0665 N90-13887
Conceptual design study of a 5 kilowatt solar dynamic Brayton power system using a dome Fresnel lens solar concentrator
[NASA-CR-185134] 06 p0735 N90-14281
Design study of a modular gas-cooled, closed-brayton cycle reactor for marine use
[AD-A213453] 07 p0953 N90-15518
Low cost Brayton engine for gas-fired cogeneration system, phase 1
[PB90-127457] 12 p1681 N90-19655
Analysis of thermal energy storage material with change-of-phase volumetric effects
[NASA-TM-102457] 15 p2092 N90-21974
Megawatt solar power systems for lunar surface operations
[NASA-CR-186509] 20 p2881 N90-26391

BRAZIL
The use of photographs for identification and analysis of urban residential sectors, with planning views
[INPE-4788-PRE/1448] 10 p1399 N90-18087
LANDSAT-TM and agrometeorological data in the wheat crop yield estimation at the farm level
[INPE-4842-PRE/1471] 10 p1400 N90-18091
Aerial photographs to support the fiscalization process of agriculture loans in the Irece-BA region
[INPE-4839-PRE/1468] 10 p1400 N90-18092
TVI: A mathematical model for global estimation of Brazilian cerrado phytomass
[INPE-4836-PRE/1465] 11 p1521 N90-18759
Remote sensing applied to the monitoring of mineral extraction in the proximity of urban areas: Pros and cons
[INPE-4867-PRE/1478] 11 p1522 N90-18766
Radiometric study of wheat and bean crops in three types of latossolo
[INPE-4843-PRE/1472] 11 p1523 N90-18767
Multistage forest volume estimation using a sampling system with probability variables
[INPE-4897-PRE/1498] 11 p1523 N90-18769
Development of the agricultural information system. Characteristics and results of the Distrito Federal model
[INPE-4940-PRE/1430] 11 p1524 N90-18773
Perspective revision of systematic mapping through orbital imagery
[INPE-4817-PRE/1453] 11 p1524 N90-18775
Photointerpretation with instruments for evaluation of environmental impact: Mata Atlantica in Cubata
[INPE-4910-PRE/1511] 11 p1531 N90-18817
Geological structure of the State of Rio de Janeiro viewed through MSS LANDSAT imagery
[INPE-4826-PRE/1457] 11 p1533 N90-18825
Quantification of structural field data in the Rio Grande do Norte basin and neighborhood
[INPE-4821-RPE/591] 11 p1533 N90-18826
The patterns of fracture and the conditioning tectonics in the region of the Quadrilatero Ferrifero and part of the Migmatitic-Gnanulitic Complex in Minas Gerais (Brazil)
[INPE-4895-PRE/1496] 11 p1534 N90-18829
Intertropical Convergence Zone (ITCZ) and its relationship with the precipitation of the north-northeast Brazilian region
[INPE-4887-TDL/378] 11 p1535 N90-18839
Areas of aquatic macrophytes classified through vegetative indexes extracted from LANDSAT/TM imagery
[INPE-4880-PRE/1489] 12 p1677 N90-19633
Analysis of tectonic movements utilizing remote sensor products in the Southern Espinhaco (SE) region
[INPE-4830-PRE/1451] 12 p1690 N90-19708
Evaluation of TM/LANDSAT and HRV/SPOT data in the identification of reforested areas in the Mogi-Guacu (SP) region
[INPE-4874-PRE/1485] 13 p1819 N90-20442
Utilization of LANDSAT-5 and NOAA-9 satellite imagery in the identification of physical-chemical parameters of the water in the Guanabara Bay
[INPE-4761-TDL/349] 13 p1819 N90-20445
Synthesis and analysis of 25 years (1961-1986) of INPE/SRE activities related to the vegetation/forest area
[INPE-4969-RPE/604] 13 p1819 N90-20446
Underwater physiography of the continental shelf of Rio Grande do Norte visible through satellite imagery
[INPE-4964-TDL/392] 13 p1820 N90-20448
Evolution of remote sensing applied to vegetation and forest at INPE
[INPE-4970-PRE/1538] 14 p1998 N90-21452
Analysis of water quality parameters of the Piaui River (SE), Brazil, through field and TM/LANDSAT sensor data
[INPE-4918-PRE/1417] 14 p1998 N90-21453
Aerial photography as an aid for agricultural credit control
[INPE-5019-RPE/613] 14 p1999 N90-21455
Contribution for the study of the evolution of part of the Espinhaco supergroup and its foundation through fracture analysis
[INPE-4907-PRE/1508] 14 p1999 N90-21459
Wheat productivity estimate through field radiometry
[INPE-4994-PRE/1556] 14 p2000 N90-21460
Regional remote sensing laboratory
[INPE-4922-PRE/1519] 14 p2001 N90-21465
Radon concentration over the Brazilian Amazon Basin during the wet season (Belem-Manaus GTE-ABLE-2B flight of April 24, 1987)
[INPE-4892-PRE/1493] 14 p2004 N90-21486
Field reports on radiometric campaigns of soybeans in the Federal district: Safra 88/89
[INPE-5021-RPE/615] 15 p2122 N90-22139
Impact of meteorology on the agricultural sector: Compilation and analysis of projects
[INPE-4846-PRE/1475] 16 p2257 N90-22866
Brazil, the United States, and the missile technology control regime
[AD-A220551] 17 p2362 N90-23449
Digital geometric correction for MSS-LANDSAT imagery
[INPE-4627-PRE/1345] 23 p3342 N90-28886
Study of anomalies in transition vegetation in Alto Xingo-NT, through remote sensing techniques
[INPE-4601-TDL/334] 23 p3343 N90-28891
Computer vision and its potential applications in Brazil
[INPE-4666-NTE/283] 23 p3381 N90-29100
Activities report for the IBDF-INPE project SEQE, year 1987
[INPE-4534-RPE/565] 23 p3415 N90-29298

BRAZILIAN SPACE PROGRAM
Qualification of the 4th stage propulsor of the Brazilian launcher. SLV: A new sounding rocket
05 p0661 N90-13860
The Brazilian space program: Actual state of the art
05 p0661 N90-13861
The MECB data collecting satellite power supply subsystem 10 p1332 N90-17699
Experimental proposition aboard the second data collecting satellite-SCD 2 of the MECB
[INPE-4980-RPE/606] 13 p1765 N90-20128
Space environment simulation of the SCD-01 satellite through heating plates
[INPE-4988-PRE/1550] 14 p1940 N90-21105

BRAZING
NT ULTRASONIC SOLDERING
Effects of titanium on some surface properties of nitride ceramics
[AERE-R-13566] 14 p1953 N90-21178
Review of the state of the technology for joining ceramics for high-temperature structural applications
[DE90-009224] 14 p1956 N90-21199
Joining engineering ceramics
[DE90-010819] 18 p2531 N90-24445
Advanced technology in welding, materials processing and evaluation
[DE90-010799] 19 p2697 N90-25347

BREADBOARD MODELS
Development of a traveling wave tube for the project X-SAR. Construction and testing of a breadboard model
[ETN-90-95900] 05 p0636 N90-13713
Knowledge-based imaging-sensor fusion system
08 p1075 N90-16220
A complete EPC simulation 10 p1337 N90-17741
Electronically Variable Pressure Regulator (EVPR)
11 p1474 N90-18484
An experimental evaluation of two nonazeotropic refrigerant mixtures in a water-to-water breadboard heat pump
[DE90-009016] 14 p1973 N90-21305
A soft actuation system for segmented reflector articulation and isolation 15 p2113 N90-22084
A spring-actuated spin and eject device for interplanetary missions 18 p2540 N90-24493
A laboratory breadboard system for dual-arm teleoperation 19 p2740 N90-25573
Hubble space telescope six-battery test bed
[NASA-TM-103506] 22 p3124 N90-27731
Force-reflective teleoperated system with shared and compliant control capabilities 24 p3510 N90-29845
Flight telerobotic servicer control from the Orbiter
24 p3517 N90-29882

BREAKAWAY
U BOUNDARY LAYER SEPARATION

BREAKDOWN
Investigations on hot spots effects in reverse biased spatial solar cells 10 p1344 N90-17789

BREAKERS (ELECTRIC)
U CIRCUIT BREAKERS
BREAKING
Security calculations of rip reached construction elements by means of probabilistic breaking mechanics and a Markov process
[ETN-90-95890] 12 p1676 N90-19624
BREATHING
Frequency and ventilation: A survey of theoretical and experimental ventilation modelling
[LR-625] 24 p3498 N90-29772
BREATHING APPARATUS
NT UNDERWATER BREATHING APPARATUS
High-frequency ventilation in dogs with three gases of different densities
[AD-A212862] 06 p0819 N90-14762
Performance evaluation of the Puritan-Bennett crew-member portable protective breathing device as prescribed by portions of FAA action notice A-8150.2
[AD-A211113] 06 p0821 N90-14772
Comparison of protective breathing equipment performance at ground level and 8,000 feet altitude using parameters prescribed by portions of FAA action notice A-8150.2
[AD-A212852] 06 p0821 N90-14773
Development of improved fire safety standards adopted by the Federal Aviation Administration 10 p1312 N90-17585
The research program at the Civil Aeromedical Institute concerning protective breathing equipment for use by crew and passengers in an aviation smoke/fume environment 10 p1317 N90-17616
The effects of wearing passenger protective breathing equipment on evacuation times through type 3 and type 4 emergency aircraft exits in clear air and smoke. Phase 1: Evacuations in clear air. Phase 2: Evacuations in smoke
[AD-A216798] 11 p1453 N90-18374
Evaluation of the Scott aviation portable protective breathing device for contaminant leakage as prescribed by FAA Action Notice A-8150.2. Phase 1: Original tests of the portable protective breathing device. Phase 2: Tests of the redesigned portable protective breathing device
[AD-A216799] 12 p1601 N90-19214
BREEDER REACTORS
NT LIQUID METAL FAST BREEDER REACTORS
Experience with model based display for advanced diagnostics and control
[DE89-015693] 01 p0082 N90-10469
Microstructural evolution of martensitic steels during fast neutron irradiation
[DE89-016231] 07 p0902 N90-15212
Fusion reactor materials
[DE90-000976] 07 p0994 N90-15744
BREEDING (REPRODUCTION)
Breeding of hydrogen producing anaerobic bacteria. Cellulase secretion from transformed Escherichia coli JM109
[DE90-710739] 10 p1410 N90-18133
BREMSSTRAHLUNG
The auroral energy deposition over the polar ionosphere during substorms
[AD-A210522] 01 p0086 N90-10490
The behavior of beams of relativistic non-thermal electrons under the influence of collisions and synchrotron losses
[NASA-CR-185983] 03 p0401 N90-12298
Proof of the feasibility of coherent and incoherent schemes for pumping a gamma-ray laser
[AD-A212315] 04 p0506 N90-12921
Numerical simulation of the preheating by x rays in spherical plasmas 06 p0784 N90-14564
X ray spectrophotometric remote sensing of diffuse auroral ionization
[SD-TR-89-09] 08 p1139 N90-16599
The inverse triax x ray diode: An alternate reduced-endpoint-energy bremsstrahlung source
[DE90-006366] 13 p1792 N90-20285
The n-p bremsstrahlung in heavy ion collision processes
[DE90-008542] 13 p1886 N90-20823
VLA observations of the coronal plasma
[NASA-CR-186540] 14 p2042 N90-21711
Flare stars at radio wavelengths
[NASA-CR-186539] 14 p2044 N90-21719
Numerical simulations of x rays and gamma rays from solar flares 16 p2339 N90-23330
Proof of the feasibility of coherent and incoherent schemes for pumping a gamma-ray laser
[AD-A219972] 18 p2562 N90-24620
Axions and SN 1987A: Axion trapping
[NASA-CR-186604] 18 p2612 N90-24881
U. radio emission from quiescent filaments
[NASA-CR-186538] 19 p2797 N90-25922
BRIDGES (STRUCTURES)
Inventory of program packages related to the project SIMONA
[ETN-90-96397] 15 p2148 N90-22270
BRIDGMAN METHOD
Bridgman crystal growth
[NASA-CR-186204] 07 p0997 N90-15766
Temperature profiles in high gradient furnaces 10 p1362 N90-17896
Temperature and melt solid interface control during crystal growth
[NASA-CR-186731] 20 p2929 N90-26664
BRIGHTNESS
Functional decor in the International Space Station: Body orientation cues and picture perception
[NASA-TM-102242] 05 p0675 N90-13931
Reexamination of data from the asteroid/meteoroid detector
[NASA-CR-185997] 05 p0714 N90-14175
Ultrahigh-brightness lasers and their applications
[DE90-000877] 06 p0789 N90-14596
Human factors evaluation of electroluminescent display Number 1
[DE90-002231] 06 p0822 N90-14777
Electron beam and high-speed optical diagnostics for the Los Alamos HIBAF (High Brightness Accelerator FEL) Facility
[DE90-007828] 11 p1515 N90-18725
A new method for measuring the transmissivity of aircraft transparencies
[AD-A216953] 12 p1714 N90-19842
The association of supernovae with regions of recent star formation in late-type galaxies 15 p2188 N90-22497
The large and small scale density structure in the solar corona 16 p2338 N90-23327
Space station contamination study: Assessment of contaminant spectral brightness
[NASA-CR-186173] 19 p2666 N90-25169
Infrared mapping with a two-dimensional infrared array
[AD-A221938] 21 p3096 N90-27596
BRIGHTNESS DISTRIBUTION
Multiwavelength constraints on gamma-ray burst sources 18 p2639 N90-25032
XB 1905+00: A very compact low-mass X ray binary viewed at low inclination 19 p2773 N90-25765
Search for large scale extended diffuse X ray emission from the Coma-A1367 supercluster 19 p2794 N90-25906
New Voyager radio spectrograms of Uranus
[NASA-CR-180381] 23 p3412 N90-29284
BRIGHTNESS TEMPERATURE
Radiometric observations at 20.6, 31.65, and 90.0 GHz: Continuing studies 10 p1373 N90-17958
Microwave brightness temperature and its relation to atmospheric general circulation features
[AD-A218312] 13 p1847 N90-20603
VLA observations of the coronal plasma
[NASA-CR-186540] 14 p2042 N90-21711
Flare stars at radio wavelengths
[NASA-CR-186539] 14 p2044 N90-21719
A laboratory study of the effects of diet and bright light countermeasures to jet lag
[AD-A220148] 17 p2435 N90-23875
U. radio emission from quiescent filaments
[NASA-CR-186538] 19 p2797 N90-25922
Disk mass densities in edge-on spiral galaxies 21 p3097 N90-27600
Stratocumulus cloud height variations determined from surface and satellite observations 22 p3214 N90-28230
BRILLOUIN EFFECT
Simulated Brillouin backscattering in optical fibers: A ring resonator 06 p0783 N90-14556
SBS (Stimulated Brillouin Scattering) pulse distortion in multimode optical fibers: Preliminary results
[DE90-003023] 07 p0992 N90-15731
Magnetostatic wave device characterization by Brillouin light scattering
[AD-A213798] 09 p1281 N90-17426
CW (Continuous Wave) stimulated Brillouin scattering of long-pulse chemical laser beams
[AD-A216409] 10 p1390 N90-18039
Relativistic stimulated Brillouin and Raman scattering in a laser-produced plasma
[DE90-613123] 14 p2028 N90-21627
Transient effects in Brillouin gain spectroscopy in solids
[DE90-009476] 15 p2067 N90-21839
High resolution stimulated Raman-Brillouin spectroscopy in gases and solids
[DE90-009535] 15 p2067 N90-21840
NMR and optical studies of piezoelectric polymers
[DE90-012459] 20 p2837 N90-26137
BRILLOUIN ZONES
Magnetically insulated electron flows in pulsed power systems
[AD-A212746] 04 p0549 N90-13196
Optical phonon modes in a double heterostructure of polar crystals
[AD-A214208] 07 p1004 N90-15816
High-resolution Brillouin gain spectroscopy in solids
[DE90-009475] 14 p1949 N90-21155
The role of the topography in gravity gradiometer reductions and in the solution of the geodetic boundary value problem using analytical downward continuation
[AD-A223107] 21 p3025 N90-27201
BRINES
The chemical and structural properties of sea ice in the southern Beaufort Sea
[AD-A219746] 17 p2418 N90-23776
BRITTLE MATERIALS
The response of isotropic brittle materials to abrasive processes
[DE89-016637] 01 p0045 N90-10251
A theory of damage in brittle and cementitious materials, part 1
[AD-A212940] 05 p0627 N90-13658
Mechanics of interaction of a crack with microcracks 06 p0798 N90-14650
Spallation and dynamic fracture as an effect of laser induced shock waves in carbon based composite materials
[AD-A216540] 11 p1478 N90-18509
Combining acoustic emission locations and a microcrack damage model to study development of damage in brittle materials
[DE90-005195] 15 p2117 N90-22111
A continuum damage model for the quasi-static response of brittle materials
[DE90-007681] 15 p2117 N90-22112
Controlled crack growth specimen for brittle systems
[NASA-TM-103126] 17 p2378 N90-23543
Computational aspects of adaptive dimensional reduction for nonlinear boundary value problems
[AD-A219889] 17 p2461 N90-24052
Indentation fracture of brittle materials
[DE90-010709] 18 p2572 N90-24857
Mechanisms for solid particle erosion in ductile and brittle materials
[NIAR-90-11] 19 p2675 N90-25210
Nonlinear material response to very rapid energy deposition
[AD-A221932] 21 p2989 N90-26988
Green's functions for dislocations in bonded strips and related crack problems
[NASA-CR-185291] 23 p3340 N90-28878
High performance brittle matrices and brittle matrix composites, book 1
[AD-A223273] 24 p3443 N90-29440
High performance brittle matrices and brittle matrix composites, book 2
[AD-A223274] 24 p3443 N90-29441
BRITTLENESS
The response of isotropic brittle materials to abrasive processes
[DE89-016637] 01 p0045 N90-10251
Microstructural effects on spall fracture in 1008 steel
[DE89-016770] 02 p0198 N90-11131
Mechanics of interaction of a crack with microcracks 06 p0798 N90-14650
The mechanical behavior of a fiber-reinforced brittle matrix composite 07 p0889 N90-15139
Effect of heat treatment on the fracture toughness transition properties of an A508 class 3 steel
[AERE-R-13548] 13 p1774 N90-20182
Strength and microstructure of ceramics
[AD-A217752] 13 p1782 N90-20227
Combining acoustic emission locations and a microcrack damage model to study development of damage in brittle materials
[DE90-005195] 15 p2117 N90-22111
Mechanics of necking, crazing, and crack growth in polymers 17 p2378 N90-23540
Controlled crack growth specimen for brittle systems
[NASA-TM-103126] 17 p2378 N90-23543
Mechanisms for solid particle erosion in ductile and brittle materials
[NIAR-90-11] 19 p2675 N90-25210
Evaluation of fracture strength properties of silicon carbide ceramics under cyclic/static axial loading at ultra-high temperature
[DE90-503402] 20 p2839 N90-26147
Development of ceramic hybrid combustor: Design and combustion test results
[DE90-503442] 20 p2839 N90-26149
Theory of ceramic/zirconia composites: Toughening, strengthening, and synergism
[AD-A222931] 21 p2985 N90-26961

Micromechanics of size effect in failure due to distributed cracking
[AD-A223211] 21 p3013 N90-27128
Superconducting film on metallic wire
22 p3146 N90-27840
Is there anything of practical value hidden amongst the composite toughening theories. A Jim Mueller prospective
[DE90-014905] 23 p3301 N90-28673
High performance brittle matrices and brittle matrix composites, book 1
[AD-A223273] 24 p3443 N90-29440
Alloy design of ordered intermetallics
[DE90-016031] 24 p3451 N90-29490

BROADBAND
Coherent multilchannel techniques for integrated broadband communications subscriber lines
[AD-A209323] 01 p0055 N90-10312
Performance of a broadbanded ultrasonic transducer with coaxially mounted, nondirectional receiver
[DE89-015838] 01 p0060 N90-10343
Comparison of sine dwell and broadband methods for modal testing 02 p0181 N90-11025
Wideband connectivity and support for Cronus cluster at USAF Electronic Systems Division
[AD-A210749] 02 p0212 N90-11215
Performance of four rake modems over the non-disturbed wideband HF channel
[AD-A211589] 03 p0339 N90-11930
Television systems with enhanced image quality for new broadband channels
[ETN-89-94622] 03 p0340 N90-11936
Wideband phase-locked angular modulator
04 p0487 N90-12798
Computation of broadband mixing noise from turbomachinery
[AD-A214448] 07 p0989 N90-15713
Near-infrared polarimetry and spectroscopy of comets
07 p1011 N90-15857
Localization of multiple broadband targets in spherical coordinates via adaptive beamforming and non-linear estimation
[AD-A215714] 09 p1274 N90-17387
A current disruption mechanism in the neutral sheet for triggering substorm expansions
[NASA-CR-186260] 09 p1298 N90-17525
A new broadband pulsed high voltage monitor
[DE90-006264] 11 p1502 N90-18651
Field theoretical analysis and synthesis of broadband waveguide: Height, plane shunt circulators with multiple layer material insertions
[ETN-90-95360] 12 p1647 N90-19469
Joint services electronics program
[AD-A217961] 13 p1797 N90-20311
Computation of broad spectral band electro-optical system transmittance response characteristics to military smokes and obscurants using field test data from transmissometer system measurements
15 p2086 N90-21939
Regional studies with broadband data
[AD-A219215] 16 p2256 N90-22861
Basic research in electronics (JSEP)
[AD-A219931] 17 p2398 N90-23661
Studies in the parameterization of cloudiness in climate models and the analysis of radiation fields in general circulation models
[NASA-CR-186378] 19 p2715 N90-25448
Progress and remaining issues in the development of a wideband HF channel model and simulation
20 p2845 N90-26182
Broadband analysis of ground wave propagation at a50 to 400 MHz 20 p2846 N90-26185
Estimation of the impulse response of a broadband mobile radio channel in suburbia at 910 MHz
20 p2846 N90-26187
Wideband characterization of forest propagation channels 20 p2846 N90-26188
An experimental medium speed wideband modem
20 p2847 N90-26194
Transient signal distortion and coupling in multilayer multiconductor MIC microstrips
[AD-A222989] 21 p3000 N90-27050
ERBE and CERES broadband scanning radiometers
21 p3016 N90-27149
Accurate determination of the complex permittivity of biological tissue at 90 GHz, 70 GHz, and over a broad band around 35 GHz
[AD-A222062] 21 p3033 N90-27240
Multispectral variable magnification glancing incidence x ray telescope
[NASA-CASE-MFS-28013-4] 21 p3096 N90-27595
Lightweight, broadband, pulsed, frequency agile, self-screening jammer for airborne deployment
[AD-D014488] 22 p3163 N90-27937
Stand-alone terrestrial and satellite networks for nationwide interoperation of broadband networks
[PB90-172404] 22 p3164 N90-27942
Congestion-reduction and service-restoration strategies for telecommunication networks
[PB90-207838] 22 p3164 N90-27944
Wideband impedance transformer for UHF power transistor time domain waveform measurement system
[PB90-210642] 22 p3167 N90-27962
Broadband studies of seismic sources at regional and teleseismic distances using advanced time series analysis methods
[AD-A223113] 22 p3211 N90-28215
New approach to HF channel modeling and simulation. Part 2: Stochastic model
[PB90-200338] 23 p3317 N90-28755
Microwave active filters based on coupled negative resistance method
[AD-A223269] 24 p3464 N90-29570
Audibility and annoyance of en route noise of unducted fan engines
[AD-A223687] 24 p3543 N90-30035

BROADBAND AMPLIFIERS
Broadband versus narrowband driver/power amplifier: A spectral purity comparison
[DOT/FAA/CT-TN89/73] 10 p1379 N90-17995
Compton amplifier
[DIGEL-1985-5] 12 p1654 N90-19506
Beam combining of excimer lasers by stimulated Raman scattering
[AD-A222973] 21 p3008 N90-27099

BROADCASTING
The use of broadcast signals for passive sensing in automated HF communication systems
06 p0762 N90-14433
Research in optical interconnection techniques
[AD-A214028] 07 p0993 N90-15739
Use of an HF active monitoring array in the presence of high level interference
[BBC-RD-1989/7] 08 p1055 N90-16096
Satellite broadcasting: Requirements for the receiving antenna
[BBC-RD-1989/5] 08 p1055 N90-16098
The use of efficient broadcast protocols in asynchronous distributed systems
[NASA-CR-186272] 09 p1269 N90-17358
Antennas on land vehicles for improved communications 10 p1370 N90-17938
Accuracy of global positioning system broadcast orbits for relative surveys
[PB90-125428] 12 p1602 N90-19218
Direct Radio Broadcasting by Satellite (DRBS): A review of the technical factors and system approaches suitable for mobile and fixed reception
[BBC-RD-1989/4] 14 p1960 N90-21221
Prediction of VHF/UHF mobile reception in urban areas: Comparison with measurements in London
[BBC-RD-1989/11] 14 p1965 N90-21255
JPRS report: Science and technology. USSR: Electronics and electrical engineering
[JPRS-UEE-90-002] 14 p1970 N90-21284
Broadcast file distribution on packet satellite networks
15 p2079 N90-21906
Texstar: The all-Texas educational satellite system
[NASA-CR-186654] 20 p2820 N90-26045
Experimentation of a transmission system data processing by meteor bursts 20 p2850 N90-26207
Applications of ISES for the oceans
21 p3017 N90-27156
Global positioning system overview/status
21 p3069 N90-27446
A radio frequency user's guide to the space environment services center geophysical alert broadcasts
[PB90-240631] 23 p3351 N90-28935

BROKEN SYMMETRY
Symmetry breaking bifurcations and the growth of chaos in a rotating fluid
[AD-A210969] 01 p0072 N90-10411
A theoretical high energy physics program
[DE89-012685] 01 p0121 N90-10696
Symmetry breaking phenomena in liquid Helium-4
[DE89-618686] 04 p0469 N90-12685
Fractional charging and reentrance in granular superconductors 04 p0557 N90-13248
Symmetry breaking bifurcations of a current sheet
[DE90-601005] 08 p0837 N90-14864
Existence of Bose-Einstein condensation in one and two dimensions
[DE89-635910] 09 p1294 N90-17498
Goldstone excitation and symmetry breaking mechanism in superfluid He-4
[DE90-610676] 12 p1720 N90-19881
Chiral interface at the finite temperature transition point of QCD
[NASA-CR-186605] 17 p2470 N90-24121
High temperature x ray diffraction and Landau theory investigations of order-disorder transition in defect NaCl-type solids
[DE90-011807] 20 p2930 N90-26673
Symmetry breaking oxygen displacement in superconducting oxides
[DE90-013670] 21 p3081 N90-27520
Surface and defect excitations in covalently bonded solids
[AD-A221995] 23 p3303 N90-28682
Z(6) model: Criticality and break-collape method
[DE90-627323] 23 p3401 N90-29214
Introduction to gauge theories and unification
[DE90-014473] 23 p3402 N90-29225
On the infrared behaviour of some non-Minkowskian quantum fields 23 p3410 N90-29273

BROMIDES
Carbon-13 nuclear magnetic resonance of heterocyclic salts and its precursors
[DE89-635768] 08 p1041 N90-16016
Ternary reciprocal system of lithium and potassium fluorides and bromides
[DE90-004938] 10 p1352 N90-17840
Effects of cholinergic drugs on exercise performance and simple reaction time of rhesus monkeys
[AD-A219455] 17 p2433 N90-23862
Effects of pyridostigmine bromide on A-10 pilots during execution of a simulated mission: Physiology
[AD-A221222] 18 p2584 N90-24717

BROMINATION
Brominated graphitized carbon fibers
[NASA-CASE-LEW-14698-2] 07 p0910 N90-15262

BROMINE
Brominated graphitized carbon fibers
[NASA-CASE-LEW-14698-2] 07 p0910 N90-15262
Rapidity densities and their fluctuations in central 200 A GeV S32 interations with Au and Ag,Br nuclei
[LUIP-8905] 07 p0989 N90-15715
Transition state spectroscopy of hydrogen transfer reactions
[AD-A215041] 09 p1191 N90-16901
Feasibility of a super high energy density battery of the Li/BrF3 electrochemical system
[AD-A216575] 11 p1528 N90-18799
Global distribution of organo-bromine gases
15 p2124 N90-22150
Modification of polystyrene/polybutadiene block copolymer films by chemical reaction with bromine and effect on gas permeability
[AD-A223612] 24 p3455 N90-29513

BROMINE COMPOUNDS
NT BROMIDES
Ultraviolet absorption cross-sections of bromoform in the temperature range 295-240 K
[AERONOMICA-ACTA-A-348-1989]
05 p0622 N90-13630
Feasibility of a super high energy density battery of the Li/BrF3 electrochemical system
[AD-A216794] 11 p1502 N90-18644

BROWN DWARF STARS
Discovery of low mass objects in Taurus
14 p1978 N90-21329

BROWNIAN MOVEMENTS
Stochastic propagation of an array of parallel cracks: Exploratory work on matrix fatigue damage in composite laminates
[DE89-017837] 03 p0319 N90-11813
On the nonexistence of a strong solution in the boundary problem for a sticky Brownian motion
[CWI-BS-R8901] 05 p0689 N90-14018
Brownian trail rectified
[DE90-003339] 07 p0988 N90-15706
A diffusion on a fractal state space
[AD-A213555] 07 p0988 N90-15707
Laser light scattering review 09 p1221 N90-17086
A posterior stochastic equation for quantum Brownian motion
[PREPRINT-715] 16 p2315 N90-23194
Hitting lines with two-dimensional Brownian motion
[AD-A223595] 24 p3541 N90-30027

BRUCETON TEST
U STATISTICAL TESTS

BRUSHES
NT BRUSHES (ELECTRICAL CONTACTS)
Design of a device to remove lunar dust from space suits for the proposed lunar base
[NASA-CR-186679] 19 p2724 N90-25496
Friction, wear and electric characteristics of slip-ring brush materials for space applications. Part 1: Screening by pin-on-disk friction tests
[NAL-TR-1040] 24 p3478 N90-29657

BRUSHES (ELECTRICAL CONTACTS)
Design and use of brushless dc motor without detent torque 18 p2539 N90-24491

Theoretical and experimental examinations of brushless monophase direct current motors
[ETN-90-97301] 24 p3466 N90-29580

BUBBLE CHAMBERS
Experimental test of PCAC hypothesis in the reactions mu neutrino-proton giving muon(-)-proton-pion(+) and mu antineutrino-proton giving muon(+)-proton-pion(-) in the delta (1232) region --- partial conserved axial current
[MPE-PAE/EXP.EL.199] 03 p0403 N90-12309

BUBBLES
Theory of droplet. Part 1: Renormalized laws of droplet vaporization in non-dilute sprays
01 p0068 N90-10390
Analytic theory for the selection of Saffman-Taylor fingers in the presence of thin film effects
[NASA-CR-181910] 01 p0118 N90-10677
Global morphology of plasma bubbles in the low latitude ionosphere 02 p0241 N90-11369
A computationally efficient modelling of laminar separation bubbles
[NASA-CR-185854] 04 p0499 N90-12872
Measurements of bubble properties using a multi-frequency sound field
[AD-A212591] 04 p0551 N90-13211
Gas evolution and bubble formation on electrodes
[DLR-FB-89-35] 05 p0622 N90-13629
Experimental measurements of the laminar separation bubble on an Eppler 387 airfoil at low Reynolds numbers
[NASA-CR-186263] 07 p0929 N90-15380
Numerical simulation of a bubble shaped bursting vortex 08 p1069 N90-16187
Vortex cores and vortex breakdown
[AD-A215266] 09 p1218 N90-17062
Underwater acoustic scattering from spherical particulates and bubbles
[AD-A214827] 09 p1279 N90-17414
False vacuum decay in Jordan-Brans-Dicke cosmologies
[NASA-CR-186257] 09 p1293 N90-17497
Non-Contact Temperature Requirements (NCTM) for drop and bubble physics 10 p1366 N90-17918
Numerical simulation of acoustic scatter from subsurface bubble clouds
[AD-A217068] 12 p1710 N90-19822
Diffusion and germ formation in glasses
13 p1786 N90-20250
Modeling studies of electrolyte flow and bubble behavior in advanced Hall cells
[DE90-007013] 13 p1795 N90-20303
Numerical simulation of liquid circulation in a bubbly column
[DE90-005226] 15 p2097 N90-22002
Gravitational couplings of the inflation in extended inflation
[NASA-CR-186595] 15 p2190 N90-22504
Soft inflation
[NASA-CR-186593] 15 p2190 N90-22506
Pseudo-steady diffusional growth or collapse of bubbles rising in time dependent pressure fields
[AD-A218825] 16 p2237 N90-22764
Numerical and physical modelling of bubbly flow phenomena
[DE90-009837] 17 p2401 N90-23677
Baryogenesis in extended inflation. Part 1: Baryogenesis via production and decay of supermassive bosons
[NASA-CR-180615] 17 p2470 N90-24120
A computational efficient modelling of laminar separation bubbles
[NASA-CR-186729] 19 p2688 N90-25291
Bubble, Drop and Particle Unit (BDPU): A multi-user microgravity facility
[IAF-89-431] 20 p2842 N90-26164
Noise from tip vortex and bubble cavitation
[AD-A221962] 21 p3072 N90-27468
Thermogravimetry-mass spectrometry analysis of gas bubbles in molten glass
[DE90-014116] 23 p3303 N90-28684
A plasma diagnostic study of two wind-blown shell nebulae: NGC 7635 and NGC 2359
23 p3410 N90-29271
Characteristic microwave background distortions from collapsing domain wall bubbles
[NASA-CR-187270] 24 p3462 N90-29557
Relic gravitational waves and extended inflation
[NASA-CR-186469] 24 p3493 N90-29740

BUCKLING
NT ELASTIC BUCKLING
NT THERMAL BUCKLING
Design guide for predicting nonlinear random response (including snap-through) of buckled plates
[NASA-CR-181877] 01 p0118 N90-10681
Overview of actual buckling calculation methods for space vehicle structures 02 p0177 N90-10995
Axial compression buckling test on the H-2 launch vehicle satellite fairing structural element prototype (aluminum surface plate/aluminum honeycomb sandwiched curved surface plate)
[NAL-TM-563] 03 p0356 N90-12039
Buckling of axially compressed imperfect orthotropic shells with elastic edge supports
[PB89-217038] 03 p0357 N90-12043
The use of Lanczos's method to solve the large generalized symmetric definite eigenvalue problem
[NASA-CR-181914] 03 p0385 N90-12193
Multilevel optimization with system Optsys
[FFA-TN-1988-60] 04 p0512 N90-12953
Buckling of delaminations in ARALL laminates
[LR-535] 05 p0619 N90-13614
General buckling tests with thin-walled shells
[DLR-MITT-89-13] 05 p0655 N90-13816
Buckling load analysis for imperfect cylindrical shells, part 1
[LR-543-PT-1] 05 p0656 N90-13823
The initial imperfection data bank at the Delft University of Technology, part 2
[LR-559-PT-2] 05 p0656 N90-13825
Flexural and torsional-flexural buckling of thin-walled open section struts
[ESDU-89007] 06 p0797 N90-14643
A review of the theory and methods for determining dynamic pulse buckling of cylindrical shells
[AD-A214764] 09 p1238 N90-17185
The behavior of a composite material in compression
[AD-A216324] 10 p1350 N90-17829
PATRAN-STAGS translator (PATSTAGS)
[NASA-TM-100388] 12 p1674 N90-19616
Interlaminar shear stress effects on the postbuckling response of graphite-epoxy panels
[NASA-TM-102626] 12 p1676 N90-19630
Innovative design of composite structures: The use of curvilinear fiber format to improve buckling resistance of composite plates with central circular holes
[NASA-CR-186454] 13 p1766 N90-20135
Innovative design of composite structures: The use of curvilinear fiber format in composite structure design
[NASA-CR-186453] 13 p1766 N90-20136
Perturbation solutions in D* for buckling, vibration, and static loading of specially orthotropic plates
13 p1814 N90-20419
Postbuckling behavior of laminated specially orthotropic plates by affine transformation 13 p1814 N90-20420
Experiments on buckling and critical buckling. Behavior of carbon fiber reinforced plastic shells submitted to tensile stresses
[ETN-90-95382] 13 p1816 N90-20429
Compressive behavior of laminated composite structures 14 p1945 N90-21134
User manual for VICONOPT: An exact analysis and optimum design program covering the buckling and vibration of prismatic assemblies of flat in-plane loaded, anisotropic plates, with approximations for discrete supports, and transverse stiffeners
[NASA-CR-181966] 14 p1991 N90-21413
Review of formulae for the buckling of simply-supported, orthotropic plates under shear load, including transverse shear effects
[PB90-167073] 14 p1994 N90-21429
Recent progress in the dynamic plastic behavior of structures, part 5 15 p2110 N90-22069
ANILISA: Computational module for Koiter's imperfection sensitivity theory
[LR-582] 15 p2119 N90-22119
Structural behavior of composites with progressive fracture
[NASA-TM-102370] 17 p2368 N90-23477
Theoretical analysis and pressure distribution of thin-walled metal inverbuckle energy absorbing tubes
17 p2414 N90-23758
Advanced buckling analyses of beams with arbitrary cross sections
[ISBN-90-9002808-0] 18 p2572 N90-24659
Incorporation of a progressive failure analysis method in the CSM testbed software system
18 p2640 N90-25036
Experimental observations and finite element analysis of the initiation of fiber microbuckling in notched composite laminates
[NASA-CR-186207] 19 p2699 N90-25359
Postbuckling response of long thick plates loaded in compression including higher order transverse shearing effects
[NASA-TM-102663] 19 p2700 N90-25363
A photoelastic analysis of the strain field around impact damage in a graphite fibre reinforced panel subjected to compression loads
[FFA-TN-1989-48] 19 p2703 N90-25379
A suitable transverse shear stiffness definition for buckling of laminates and sandwich plates
[LR-603] 19 p2704 N90-25384
Some kinematic relations of thin elastic shells
[LR-612] 19 p2704 N90-25388
From Lie group transformation to the generalized Koiter initial postbuckling theory of perfect shells
[LR-613] 19 p2704 N90-25389
Buckling and postbuckling behavior of square compression-loaded graphite-epoxy plates with circular cutouts
[NASA-TP-3007] 20 p2826 N90-26077
A comparison of the post-buckling behavior of metallic and composite plates with centrally located cutouts
[NIAR-90-14] 20 p2875 N90-26356
The use of Lanczo's method to solve the large generalized symmetric Eigenvalue problem in parallel
[NASA-CR-182072] 20 p2907 N90-26533
Compressive strength of rigid-rod polymer fibers
[AD-A221886] 21 p2989 N90-26987
Modal interaction in postbuckled plates. Theory
[NASA-TP-2943] 21 p3012 N90-27121
Energetics and crystal chemistry of Ruddlesden-Popper type structures in high T(sub c) ceramic superconductors
22 p3141 N90-27814
Postbuckling response of long thick isotropic plates loaded in compression including higher order transverse shearing effects
[NASA-TM-4199] 22 p3190 N90-28100
Lateral buckling of short I-beams under cyclic loading
[PB90-213653] 22 p3191 N90-28104
Experimental analysis of the buckling of composite plates under compression loads
[IMFL-89-28] 22 p3193 N90-28119
Liquid Rocket Booster (LRB) for the Space Transportation System (STS) systems study. Appendix A: Stress analysis report for the pump-fed and pressure-fed liquid rocket booster
[NASA-CR-183787-APP-A] 23 p3288 N90-28601
Buckling and postbuckling behavior of compression-loaded isotropic plates with cutouts
[NASA-TP-3024] 23 p3337 N90-28859
Structural analysis and optimum design of geodesically stiffened composite panels
[NASA-CR-186944] 23 p3337 N90-28862
Parametric solution of nonlinear structure problems
[ONERA-RT-21/3542-RY-082-R] 23 p3340 N90-28874
On a generalized laminate theory with application to bending, vibration, and delamination buckling in composite laminates 24 p3478 N90-29659
Investigation of the dynamic buckling of liquid-filled tanks 24 p3478 N90-29660
Buckling of anisotropic cylindrical shells subjected to combined axial compression, normal pressure, bending and shear loading
[LR-611] 24 p3482 N90-29678
Recent developments in shell stability analysis
[LR-633] 24 p3483 N90-29685

BUDGETING
Energy storage and distribution program summary. Volume 2: Research summaries, fiscal year 1988
[DE89-000867] 01 p0083 N90-10470
Studies of the European transonic wind tunnel
[ONERA-RSF-12/0694-GY] 04 p0562 N90-13278
Developing integrated parametric planning models for budgeting and managing complex projects
[NASA-CR-186006] 06 p0857 N90-14986

BUDGETS
International conference management
08 p1136 N90-16583
The Ariane-5 Programme 09 p1176 N90-16808

BUFFER STORAGE
Making extensible database technology work
09 p1203 N90-16973
Analysis of a queueing model of the Orwell slotted ring
[MEMO-812] 18 p2606 N90-24843

BUFFERS (CHEMISTRY)
The use of BaF2 buffer layers for the sputter-deposition of TlCaBaCuO thin-film superconductors
[DE90-004859] 09 p1292 N90-17490

BUFFETING
Assessment of computational prediction of tail buffeting
[NASA-TM-101613] 08 p1018 N90-15886

BUILDING MATERIALS
U CONSTRUCTION MATERIALS

BUILDING STRUCTURES
U BUILDINGS

BUILDINGS
Wind/seismic comparisons for upgrading existing structures
[DE89-016055] 03 p0357 N90-12044
Use of remote sensing data for land and building statistics 08 p1094 N90-16335
Lateral buckling of short I-beams under cyclic loading
[PB90-213653] 22 p3191 N90-28104

Torsional effects in structures subjected to strong ground motion
[PB90-226960] 23 p3339 N90-28869
Transferring building energy technologies by linking government and private-sector programs
[DE90-000346] 23 p3408 N90-29258

BULK MODULUS
Bulk and shear moduli of epoxy encapsulants
[DE90-000899] 06 p0751 N90-14371
Elastic properties of silica xerogels
[AD-A216528] 12 p1630 N90-19366

BUNCHING
NT ELECTRON BUNCHING
Instability investigation for storage mode. Microwave instability (single-bunch instability)
[NIKHEF-K/AMPS/89/05] 11 p1499 N90-18628

BUNDLES
Two dimensional modifications of Gaussian laser light bundles
[AD-A215207] 10 p1389 N90-18033

BUOYANCY
Relation of wind field and buoyancy to rainfall inferred from radar
[PB89-208326] 02 p0251 N90-11424
Buoyancy effects on the vapor condensation rate on a horizontal liquid surface
[NASA-TM-102437] 05 p0629 N90-13675
Facilities for microgravity combustion research
[NASA-TM-102014] 05 p0630 N90-13679
Premixed flames in microgravity 09 p1201 N90-16959
Measurements of mean and fluctuating temperature in microgravity 09 p1201 N90-16961
Polymer solution phase separation: Microgravity simulation 09 p1224 N90-17101
Modelling directional solidification
[NASA-CR-186181] 09 p1292 N90-17487
Non-contact temperature measurements in support of microgravity combustion experiments 10 p1363 N90-17900
Siphon flows in isolated magnetic flux tubes. 3: The equilibrium path of the flux tube arch
[NASA-CR-186297] 12 p1709 N90-19813
Nonintrusive optical measurements of turbulence and mixing in a stably stratified fluid 13 p1799 N90-20322
An experimental investigation of mixing in buoyant flows 15 p2090 N90-21983
The relationship between the buoyancy of near-surface air and the potential temperature of the tropopause 15 p2128 N90-22165
Current drive in a supernova 15 p2187 N90-22491
The role of gravity on macrosegregation in alloys
[NASA-CR-186530] 19 p2679 N90-25238
Turbulence spectra of the FIRE stratocumulus-topped boundary layers 22 p3217 N90-28246
Laboratory experiments on stability and entrainment of oceanic stratocumulus. Part 2: Entrainment experiment 22 p3220 N90-28264
Effect of a crystal-melt interface on Taylor-Vortex flow with buoyancy
[PB90-244401] 24 p3551 N90-30089

BUOYS
Statistical models for the optimal estimation of oceanic fields
[AD-A211786] 03 p0377 N90-12149
Near real time VHF telemetry of near shore oceanographic data
[AD-A215756] 10 p1327 N90-17666
Comparison of circulation obtained through the trajectory of a drifting buoy tracked by satellite and hydrographic data in the Bransfield Strait
[INPE-4946-TDL/387] 11 p1537 N90-18850
Drifting buoy data from Western Tropical Pacific for the period February 1, 1986 through February 28, 1989
[PB90-113978] 12 p1695 N90-19732
In situ investigation of sea surface noise from a depth of one meter
[AD-A220158] 17 p2432 N90-23857
Circulation and property distributions in the Central Bering Sea, Spring, 1988
[PB90-155847] 22 p3230 N90-28317

BURAN SPACE SHUTTLE
Landing tests for Buran shuttle with jet engine-equipped mock-up 02 p0158 N90-10904

BUREAUS (ORGANIZATIONS)
Navigation programmes: Financial and institutional aspects 17 p2361 N90-23441
Second Meeting of the Space Agency Forum on the International Space Year (SAFISY)
[ESA-SP-1115] 19 p2800 N90-25932

BURGER EQUATION
A control problem for Burgers' equation with bounded input/output
[NASA-CR-182062] 19 p2747 N90-25608

BURN-IN
Theory system reliability demonstration and burn-in design
[AD-A217775] 13 p1814 N90-20416

BURNERS
Characterization of nonpremixed turbulent bluff-body burner flames
[PB89-229447] 04 p0469 N90-12689
Externally vaporizing system for turbine combustor
[AD-D014284] 08 p1024 N90-15918
Investigation of the processes controlling the flame generation of refractory materials
[DE90-007564] 12 p1624 N90-19333
Modification and improvement of software for modeling multidimensional reacting fuel flows
[AD-A217789] 13 p1783 N90-20235
Extended range tankless water heater
[DE90-014474] 23 p3316 N90-28750
Radiative heat transfer
[PB90-247602] 23 p3327 N90-28813

BURNING
U COMBUSTION

BURNING PROCESS
U COMBUSTION

BURNING RATE
Flammability, smoke, and dry arc tracking tests of aircraft electrical wire insulations
[DOT/FAA/CT-89/21] 03 p0302 N90-11714
Ignition characteristics of the nickel-based alloy UNS N07718 in pressurized oxygen
[NASA-CR-185932] 03 p0326 N90-11850
RSRM-3 (360L003) ballistics/mass properties report
[NASA-CR-183716] 04 p0463 N90-12651
Ballistics/mass properties
[NASA-CR-183723] 04 p0463 N90-12652
Calculation of Einstein A coefficients and oscillator strengths for the A(perturbed)(2)A(1)-X(perturbed)(2)B(1) transition of NH(2)
[AD-A213837] 07 p0896 N90-15176
Burning rates of two cast nitramine explosives using a hybrid closed bomb-strand burner
[DE90-002785] 07 p0914 N90-15286
Effect of reduced atmospheric pressure on the performance characteristics of pyrotechnic compositions containing aluminum
[AD-A214473] 09 p1200 N90-16953
Droplet vaporisation and combustion in microgravity 09 p1202 N90-16963
RSRM-9 (360L009): Ballistics mass properties
[NASA-CR-183944] 20 p2823 N90-26064
Composite propellants with high burning rates
[FOA-C-20781-2.1] 23 p3315 N90-28744
An experimental investigation of strand burning metallized solid propellants
[AD-A224074] 24 p3457 N90-29526

BURNOUT
Burnout thresholds and cross section of power MOS transistors with heavy ions
[AD-A218998] 16 p2232 N90-22736
Hermes emergency reentry trajectories consequences on the Ariane 5 trajectories 22 p3127 N90-27747

BURNS (INJURIES)
Treatment of laser-induced retinal injuries
[AD-A210284] 01 p0092 N90-10526

BURST TESTS
Burst pressure prediction of metallic/fibre reinforced rocket motor cases using an elasto-plastic instability analysis
[RARDE-1/89] 08 p1038 N90-15997

BURSTS
NT GAMMA RAY BURSTS
NT RADIO BURSTS
NT SOLAR RADIO BURSTS
NT TYPE 3 BURSTS
Search for proton decay and supernova neutrino bursts with a lunar base neutron detector
[DE90-607644] 10 p1448 N90-18358
QPO from the rapid burster 19 p2770 N90-25741
SONA: A measurement system for the determination of the end-of-flight burst behaviour of projectiles equipped with proximity fuses
[FEL-89-A293] 24 p3459 N90-29536

BUS CONDUCTORS
Power generation and distribution 05 p0604 N90-13515
The 120 VDC test bed for Columbus power system 10 p1329 N90-17679
Laboratory implementation of the Continuously Reconfiguring Multi-Microprocessor Flight Control System (CRMMFCS)
[AD-A217730] 13 p1758 N90-20094
Applications for the scalable coherent interface
[DE90-011795] 20 p2903 N90-26514

BUSHINGS
Overcenter collet space station truss fastener
[NASA-CASE-MSC-21504-1] 21 p2966 N90-26859

BUSINESS MANAGEMENT
U INDUSTRIAL MANAGEMENT

BUTADIENE
Thermophysical properties of buta-1,3-diene
[ESDU-89005] 05 p0620 N90-13619
Synthesis and chemistry of unsaturated metal nitrogen compounds
[AD-A216550] 12 p1622 N90-19321

BUTANES
Survey of the response of standard limited streamer tubes over the complete range of three-component gas mixtures of isobutane, CO(sub 2), argon
[DE89-016692] 04 p0499 N90-12875
A comparison of the autoignition chemistry of n-butane and isobutane in an internal combustion engine
[DE90-009474] 15 p2067 N90-21838
Combustion of n-butane and isobutane in an internal combustion engine: A comparison of experimental and modeling results
[DE90-005993] 18 p2522 N90-24400

BUTENES
A model for long-term creep and the effects of physical ageing in poly (butylene terephthalate)
[NPL-DMA(A)-182] 03 p0333 N90-11895

BUTT JOINTS
The effect of nitrogen and titanium on the toughness of high strength saw weld deposits
[AD-A213400] 07 p0905 N90-15230
Static and fatigue strength of an adhesive bonded CFRP butt-strap joint: The effects of stacking sequence and temperature
[NLR-TR-88036-U] 20 p2877 N90-26370

BUTTERFLY VALVES
NT DAMPERS (VALVES)
Comments on compressible flow through butterfly valves
[DE89-015730] 07 p0928 N90-15371
Hybrid butterfly valve
[NASA-CASE-SSC-00004] 07 p0940 N90-15443

BUTYLENE
U BUTENES

BUTYLENE OXIDES
U TETRAHYDROFURAN

C

C (PROGRAMMING LANGUAGE)
PCP (Parallel C Preprocessor): A parallel extension of C that is 99 percent fat free
[DE90-002813] 06 p0831 N90-14834
Yaw rate control of an air bearing vehicle 12 p1639 N90-19420
Distributed simulation, no special tools required 15 p2150 N90-22281
A personal computer-based, multitasking data acquisition system
[NASA-TM-4232] 23 p3382 N90-29107

C BAND
The effectiveness of adaptive PRF (Pulse Repetition Frequency) selection in minimizing range obscuration in the TDWR (Terminal Doppler Weather Radar) system
[AD-A211267] 02 p0213 N90-11222
The PHARUS project: Design of a polarimetric C-band SAR in the Netherlands 14 p1961 N90-21228
A motion compensation study for the PHARUS project 14 p1962 N90-21235
Remote sensing of the ocean surface with C- and Ku-band airborne scatterometers 22 p3195 N90-28129
Design and realization of a two stage C-band low noise amplifier
[FEL-89-B265] 23 p3322 N90-28783

C STARS
U CARBON STARS

C-M DIAGRAM
U COLOR-MAGNITUDE DIAGRAM

C-5 AIRCRAFT
Computerized corrosion forecasting model for C-5 aircraft 21 p2957 N90-26815

C-130 AIRCRAFT
Improving snow roads and airstrips in Antarctica
[AD-A211588] 03 p0335 N90-11907
Reducing C130E Hercules operating costs in the Royal Australian Air Force and the United States Air Force by increasing cruise speeds
[AD-A215747] 10 p1319 N90-17629
A human factors engineering approach to the development and dynamic evaluation of a prototype aircrew seat for military aircraft
[AD-A218283] 24 p3500 N90-29779

C-135 AIRCRAFT
Combustion Experiments During KC-135 Parabolic Flights
[ESA-SP-1113] 09 p1201 N90-16958

C-140 AIRCRAFT
The right wing of the LEFT airplane
04 p0439 N90-12510
Simulated airline service experience with laminar-flow control leading-edge systems 04 p0439 N90-12512
Simulated-airline-service flight tests of laminar-flow control with perforated-surface suction system
[NASA-TP-2966] 10 p1319 N90-17627
C-141 AIRCRAFT
Stressed detector arrays for airborne astronomy
14 p1978 N90-21332
CABIN ATMOSPHERES
NT SPACECRAFT CABIN ATMOSPHERES
Characteristics of transport, aircraft fires measured by full-scale tests 10 p1313 N90-17591
CABLES
The effects of radiation on the mechanical properties of polymers used as electrical cable insulation and jacketing materials
[AERE-R-13286] 13 p1779 N90-20209
Cable suspended windmill
[NASA-CASE-LAR-13434-1] 17 p2412 N90-23742
CABLES (ROPES)
Estimating the time to fatigue failure of mooring cables
[PB89-220677] 04 p0511 N90-12946
An experimental investigation of the flow field around yawed stranded cables
[AD-A215782] 12 p1658 N90-19529
Development of cable drive systems for an automated assembly project 15 p2116 N90-22105
Modeling towed cable system dynamics
[AD-A223610] 24 p3476 N90-29644
CAD (DESIGN)
U COMPUTER AIDED DESIGN
CADASTRAL MAPPING
Aerial photographs to support the fiscalization process of agriculture loans in the Irece-BA region
[INPE-4839-PRE/1468] 10 p1400 N90-18092
Aerial photography as an aid for agricultural credit control
[INPE-5019-RPE/613] 14 p1999 N90-21455
CADMIUM
Experimental measurements of shock-induced vaporization in cadmium and lead
[DE89-016877] 02 p0194 N90-11103
The substitution of IVD (Ion Vapor Deposition) aluminum for cadmium
[AD-A215833] 09 p1195 N90-16921
Elastic scattering of e- and e+ from Rb and Cd
11 p1556 N90-18960
Impedance studies of Ni/Cd and Ni/H2 cells using the cell case as a reference electrode
13 p1824 N90-20473
UV photo-enhanced MOCVD of cadmium and cadmium telluride
[RSRE-MEMO-4208] 15 p2174 N90-22422
Trace metal sources for the atlantic inflow to the Mediterranean Sea
[AD-A218607] 17 p2429 N90-23842
Research on high-specific-heat dielectrics
[AD-A221215] 18 p2623 N90-24944
Laser induced surface chemical epitaxy
[AD-A222082] 21 p2977 N90-26920
CADMIUM COMPOUNDS
NT CADMIUM SULFIDES
NT CADMIUM TELLURIDES
CADMIUM MERCURY TELLURIDES
U MERCURY CADMIUM TELLURIDES
CADMIUM NICKEL BATTERIES
U NICKEL CADMIUM BATTERIES
CADMIUM SULFIDES
Stabilization of high (Tc) superconductivity in cadmium sulfide
[DE90-008249] 13 p1896 N90-20881
Preparation and properties of iron doped II-VI chalcogenides
[AD-A220802] 17 p2477 N90-24163
Optical nonlinearity due to structure defects and bistability in the band discontinuity area of CdS
[ETN-90-97303] 24 p3554 N90-30112
CADMIUM TELLURIDES
Photoreflectance study of boron ion-implanted (100) cadmium telluride
[SD-TR-88-89] 01 p0053 N90-10300
Thin film cadmium telluride, zinc telluride, and mercury zinc telluride solar cells
[DE89-009499] 06 p0804 N90-14681
High-efficiency large-area CdTe modules
[DE89-009498] 06 p0806 N90-14689
CdTe buffered GaAs thin-slab IR waveguide modulators and T/R filter
[AD-A215999] 12 p1651 N90-19488
CuInSe2 and CdTe: Scale-up for manufacturing
[DE89-009503] 13 p1827 N90-20489
UV photo-enhanced MOCVD of cadmium and cadmium telluride
[RSRE-MEMO-4208] 15 p2174 N90-22422
Polycrystalline thin film cadmium telluride n-i-p solar cells
[DE90-000351] 21 p3019 N90-27167
CAFFEINE
Daytime sleepiness, performance, mood, nocturnal sleep: The effect of benzodiazepine and caffeine on their relationship
[AD-A210915] 01 p0093 N90-10533
The effect of caffeine on endurance time to exhaustion at high altitude
[AD-A212069] 03 p0380 N90-12163
Influence of theobromine on heat production and body temperatures in cold-exposed humans: A preliminary report
[AD-A217203] 13 p1850 N90-20618
A laboratory study of the effects of diet and bright light countermeasures to jet lag
[AD-A220148] 17 p2435 N90-23875
CAI
U COMPUTER ASSISTED INSTRUCTION
CALCIFICATION
Experiment K-6-19. Pineal physiology in microgravity: Relation to rat gonadal function
20 p2895 N90-26472
CALCITE
Nonlinear material response to very rapid energy deposition
[AD-A221932] 21 p2989 N90-26988
CALCIUM
NT CALCIUM ISOTOPES
Investigation of resonant ac-dc magnetic field effects
[AD-A211612] 03 p0379 N90-12159
Calcium displacement caused by electromagnetic fields
[AD-A212690] 04 p0524 N90-13023
Conservation of body calcium by increased dietary intake of potassium: A potential measure to reduce the osteoporosis process during prolonged exposure to microgravity 18 p2631 N90-24993
Energy storage for a lunar base by the reversible chemical reaction: CaO+H2O reversible reaction Ca(OH)2
[NASA-TM-103145] 19 p2709 N90-25419
Experiment K-6-01. Distribution and biochemistry of mineral and matrix in the femurs of rats
20 p2892 N90-26455
Experiment K-6-19. Pineal physiology in microgravity: Relation to rat gonadal function
20 p2895 N90-26472
Synthesis, structure, and properties of Ca2ZnN2
[AD-A222012] 21 p3083 N90-27533
High T(sub c) copper-oxide superconductors
[AD-D014483] 22 p3247 N90-28416
CALCIUM CARBONATES
NT CALCITE
Polypeptide inhibitors of mineral scaling and corrosion
[AD-A210507] 01 p0041 N90-10225
Chemistry-structure-property interrelationships for calcareous deposits as stand-alone coatings
[AD-A216031] 10 p1359 N90-17881
Calcium carbonate scale dissolution in water stabilized by carbon dioxide treatment
[AD-A218502] 16 p2214 N90-22633
CALCIUM CHLORIDES
Advanced calcium-thionyl chloride high-power battery
[AD-A211856] 04 p0495 N90-12846
Advanced calcium thionyl chloride high power battery
[AD-A216685] 13 p1825 N90-20482
CALCIUM COMPOUNDS
NT CALCITE
NT CALCIUM CARBONATES
NT CALCIUM CHLORIDES
NT CALCIUM FLUORIDES
NT CALCIUM OXIDES
NT CALCIUM PHOSPHATES
NT CALCIUM SULFIDES
NT PEROVSKITES
MHD seed recovery and regeneration
[DE89-002711] 01 p0125 N90-10715
Advanced calcium-thionyl chloride high-power battery
[AD-A211856] 04 p0495 N90-12846
Cycle-life improvement of Zn/NiOOH cells by the addition of Ca(OH)2 to the zinc electrode
[DE90-004040] 08 p1062 N90-16139
Aligned bismuth, strontium, calcium cuprate coatings on polycrystalline substrates
[AD-D014522] 19 p2678 N90-25229
CALCIUM FLUORIDES
A viscoplastic model with application to LiF-22 percent CaF2 hypereutectic salt
[NASA-TM-103181] 17 p2417 N90-23770
Spectroscopy of laser properties of Nd(3+)-doped CaF2, SrF2, and BaF2
[DE90-012086] 19 p2695 N90-25337
Self-lubricating surfaces by ion beam processing
[AD-A222489] 21 p3011 N90-27118
CALCIUM ISOTOPES
Large-angle elastic and inelastic scattering of Pi+ and Pi- from Si28 and Ca40
[AD-A218163] 13 p1885 N90-20818
CALCIUM METABOLISM
Experiment K-6-19. Pineal physiology in microgravity: Relation to rat gonadal function
20 p2895 N90-26472
CALCIUM OXIDES
Prospects for wavelength tunable lasers based on vacancy defects in alkaline-earth oxides
[DE90-001078] 06 p0789 N90-14592
Bi-Sr-Ca-Cu-O superconducting ceramics
[DE89-636225] 06 p0855 N90-14972
Hyper- and hypobaric processing of Tl-Ba-Ca-Cu-O superconductors
[DE90-005637] 10 p1437 N90-18292
High temperature interaction of SO2 with oxide sorbents
[DE90-000435] 11 p1485 N90-18545
Synthesis and properties of polycrystalline Tl2Ba2CaCu2O(x) and Tl2Ba2Ca2Cu3O(x)
[DE90-007528] 13 p1897 N90-20887
Synthesis of Bi-Sr-Ca-Cu oxide superconductor by solution technique
[DE90-008707] 13 p1897 N90-20888
Practical superconductor development for electrical power applications
[DE90-010262] 18 p2625 N90-24957
In-situ growth of superconducting films of Bi-Sr-Ca-Cu-O using magnetron sputtering
[DE90-011161] 18 p2626 N90-24962
Highly-textured thallium-barium-calcium-copper-oxide polycrystalline superconducting films on silver substrates
[DE90-011972] 18 p2627 N90-24970
Preparation and magnetic measurements of single crystal Tl2Ba2CaCu2O8
[DE90-013657] 21 p3081 N90-27519
Flux creep in Bi2Sr2CaCu2O8(sub +x) single crystals
22 p3136 N90-27794
Magnetic properties of the 110K superconducting phase in Pb-doped Bi-Sr-Ca-Cu-O thin films
22 p3151 N90-27868
Optical and microwave detection using Bi-Sr-Ca-Cu-O thin films 22 p3152 N90-27870
Ion-beam-assisted deposition of silver films on zirconia ceramics for improved tribological behavior
[DE90-009706] 24 p3456 N90-29516
CALCIUM PHOSPHATES
Polypeptide inhibitors of mineral scaling and corrosion
[AD-A210507] 01 p0041 N90-10225
CALCIUM SULFIDES
Preparation, properties, and development of calcium lanthanum sulfide as an 8- to 12-micrometer transmitting ceramic
[AD-A220200] 17 p2382 N90-23565
CALCIUM 45
U CALCIUM ISOTOPES
CALCULATION
U COMPUTATION
CALCULUS
NT ASYMPTOTIC SERIES
NT CAMPBELL-HAUSDORFF SERIES
NT CONTINUITY (MATHEMATICS)
NT COSINE SERIES
NT CURL (VECTORS)
NT DIFFERENTIAL CALCULUS
NT FOURIER SERIES
NT INTEGRAL CALCULUS
NT LIMITS (MATHEMATICS)
NT PADE APPROXIMATION
NT POWER SERIES
NT SERIES (MATHEMATICS)
NT SINE SERIES
NT TAYLOR SERIES
NT VECTOR ANALYSIS
NT VORTICITY
Taxonomic syntax for first order inference
[AD-A211618] 03 p0390 N90-12221
A fractional calculus model of aeroelasticity
[AD-A216244] 10 p1423 N90-18212
Simplicial lattices in classical and quantum gravity: Mathematical structure and application
10 p1439 N90-18304
Should a function continue
[AD-A216406] 11 p1551 N90-18929
Monostable electrovalve
[INPE-4928-RPE/595] 12 p1651 N90-19487
A decoupled recursive approach for constrained flexible multibody system dynamics 16 p2289 N90-23042

Extending the lambda calculus with surjective pairing is conservative
[ITLI-ML-89-02] 18 p2603 N90-24821
Application of symbolic computations to the constitutive modeling of structural materials
[NASA-TM-103225] 20 p2876 N90-26364
Formal semantics of SQL queries
[REPT-89-069] 24 p3531 N90-29973

CALCULUS OF VARIATIONS
New theoretical approaches for studying electron collisions with small molecules
[DE89-017543] 02 p0273 N90-11558
Monte Carlo studies of nuclei and quantum liquid drops
[DE89-016914] 03 p0402 N90-12300
Application of a self-adaptive grid method to complex flows
[NASA-TM-102223] 05 p0571 N90-13324
Periodic solutions of Hamiltonian systems of 3-body type
[AD-A212891] 05 p0687 N90-14005
Variational quantum Monte Carlo calculation of electronic and structural properties of crystals
[DE90-003265] 07 p0999 N90-15781
On mean value iterations with application to variational inequality problems
[DE90-005556] 10 p1422 N90-18200
A Lagrangian formalism for nonequilibrium ensembles
[DE90-612748] 14 p2020 N90-21579
Linking numbers and variational method
[DE90-612793] 14 p2020 N90-21582
A variational approach to heteroclinic orbits for a class of Hamiltonian systems
[AD-A219853] 17 p2460 N90-24047
A white noise theory of infinite dimensional calculus
[AD-A221253] 18 p2607 N90-24850
The open-ended coaxial line: A rigorous variational treatment
[RSRE-MEMO-4331] 19 p2683 N90-25265
Dirac's equation as a geodesic in Riemann space
[DE90-627194] 23 p3390 N90-29152
Systematic approach to critical phenomena by the extended variational method and coherent-anomaly method
[DE90-627320] 23 p3392 N90-29165
Ignition and burn control characteristics of thermonuclear plasmas
[DE90-015385] 23 p3398 N90-29197

CALENDARS
Calendar of selected aeronautical and space meetings
[AGARD-CAL-90/1] 11 p1574 N90-19060

CALIBRATING
NT WIND TUNNEL CALIBRATION
Introduction to total- and partial-pressure measurements in vacuum systems
[NASA-RP-1219] 01 p0072 N90-10412
A FORTRAN program for the calculation of the calibration coefficients of a six-component strain gauge balance
[AD-A210375] 01 p0105 N90-10599
Autonomous control system for Czochralski growth of LEC GaAs
[AD-A210190] 01 p0131 N90-10754
Automatic classification of spectra from the Infrared Astronomical Satellite (IRAS)
[NASA-RP-1217] 01 p0140 N90-10807
NIST (National Institute of Standards and Technology) measurement services: The calibration of thermocouples and thermocouple materials
[PB89-209340] 02 p0222 N90-11274
Using self-calibrating thermocouples in industry
[DE89-013539] 02 p0223 N90-11278
Design and calibration of an electrodynamic driver for the Space Thermoacoustic Refrigerator (STAR)
[AD-A212022] 03 p0335 N90-11906
Calibration and de-embedding of microwave measurements using any combination of one- or two-port standards
[PB89-212674] 03 p0337 N90-11916
Contribution of the precision determination of noise powers in the MHz and lower GHz frequency range
[PTB-E-33] 03 p0340 N90-11935
Droplet sizing instrumentation used for icing research: Operation, calibration, and accuracy
[NASA-CR-182293] 03 p0350 N90-11999
Scintillating fiber ribbon - tungsten calorimeter
[DE89-016705] 03 p0350 N90-12001
Devices and procedures for the calibration of sensors and measurement: Systems of the flight test support system ATTAS
[DFVLR-MITT-89-06] 03 p0351 N90-12007
DSN 70-meter antenna microwave optics design and performance improvements. Part 2: Comparison with measurements 04 p0487 N90-12800
NIST (National Institute of Standards and Technology) measurement services: The ac-dc difference calibrations
[PB89-222616] 04 p0494 N90-12845
Optimum data weighting and error calibration for estimation of gravitational parameters
[NASA-TM-100737] 04 p0517 N90-12985
Catalog of absolutely calibrated, range normalized, wideband, electric field waveforms from located lightning flashes in Florida: July 24 and August 14, 1985 data
[AD-A212708] 04 p0521 N90-13008
Dynamic testing techniques and applications for an aeroelastic rotor test facility 05 p0584 N90-13406
A gyroscope calibration analysis for the Gamma Ray Observatory (GRO) 05 p0589 N90-13428
Extended Kalman filter for attitude estimation of the earth radiation budget satellite 05 p0590 N90-13433
The modulating grid 05 p0603 N90-13505
On-ground photometric calibration 05 p0605 N90-13523
In-orbit payload calibration 05 p0606 N90-13526
New ground-based photometric measurements 05 p0607 N90-13538
Standard stars and photometric calibration 05 p0607 N90-13539
Variable stars 05 p0608 N90-13541
The first-look data analysis at Utrecht 05 p0612 N90-13571
Liquid water content and droplet size calibration of the NASA Lewis Icing Research Tunnel
[NASA-TM-102447] 05 p0651 N90-13797
GRADIO: An error analysis of the spaceborne gravity gradiometer
[ETN-90-96010] 05 p0667 N90-13901
Airdata calibration of a high-performance aircraft for measuring atmospheric wind profiles
[NASA-TM-101714] 06 p0725 N90-14228
Calibration approach to electron probe microanalysis: A study with PWA-1480, a nickel base superalloy
[NASA-TM-102393] 06 p0745 N90-14335
Calibration curves for some standard Gap Tests
[DE89-016599] 06 p0754 N90-14389
Methodology for the calibration of and data acquisition with a six-degree-of-freedom acceleration measurement device
[PB89-233597] 06 p0779 N90-14531
Single particle friction tests with cellulose acetate sphere samples
[DE89-017537] 06 p0793 N90-14622
Results of the 1989 NASA/JPL balloon flight solar cell calibration program
[NASA-CR-186114] 06 p0803 N90-14872
MTX (Microwave Tokamak Experiment)/ELF (Electron Laser Facility) 2 microwave power measurements and calibration for the 2-GW, 140-GHz, ELF 2 Free Electron Laser (FEL)
[DE90-000825] 06 p0846 N90-14922
Design and calibration of an in-stack, low-pressure impactor
[AD-A213531] 07 p0882 N90-15105
N-port theory applied to backscatter polarimetry and depolarization in foliage penetration
[AD-A213437] 07 p0917 N90-15305
Flashlight radar: A three-dimensional imaging radar
[AD-A213439] 07 p0918 N90-15307
Calibration of seven-hole pressure probes for use in fluid flows with large angularity
[NASA-TM-102200] 07 p0933 N90-15399
Portable digital pressure indicator for calibrating magnetic tape recorders
[NASA-TM-101650] 07 p0933 N90-15401
Image enhancement using the IRAS (infrared Astronomy Satellite) survey data
[AD-A213811] 07 p0950 N90-15496
Outlier detection in multivariate calibration
[DE90-001502] 07 p0982 N90-15672
Cryogenic balances for the US NTF 08 p1031 N90-15959
Modeling a self-calibrating thermocouple for use in a smart temperature measurement system
[DE90-003697] 08 p1081 N90-16259
Calibration of a pulsed potential crack monitor for use in fatigue crack growth studies
[RAE-TM-M/S-1126] 08 p1089 N90-16301
New approach to omega PPCs (Propagation Corrections)
[AD-A215610] 09 p1207 N90-17000
Changes in the volt, ohm, and temperature and long range impact of using the Josephson voltage standard
[DE90-004493] 09 p1214 N90-17039
The 15th Transducer Workshop --- for telemetry applications
[AD-A215515] 10 p1327 N90-17665
Radiation thermometry at NIST: An update of services and research activities 10 p1364 N90-17903
Temperature control and calibration issues in the growth, processing and characterization of electronic materials 10 p1365 N90-17914
Millimeter wave radar clutter program
[AD-A215772] 10 p1376 N90-17978
Lower bounds on multiple-source direction finding in the presence of direction-dependent antenna-array-calibration errors
[AD-A215825] 10 p1376 N90-17979
Development of an alternative concentration probe calibration method
[AD-A216245] 10 p1388 N90-18031
Feasibility demonstration of a 445N high-performance rocket engine 11 p1473 N90-18481
A new broadband pulsed high voltage monitor
[DE90-006264] 11 p1502 N90-18651
Measurement of spectral emissivity by Fourier transform infrared spectrometer
[DE89-782319] 11 p1510 N90-18698
Construction and calibration of a gas pressure meter with high temporal resolution
[INPE-4953-RPE/602] 11 p1511 N90-18700
Electron beam and high-speed optical diagnostics for the Los Alamos HIBAF (High Brightness Accelerator FEL) Facility
[DE90-007828] 11 p1515 N90-18725
Measurement system of spectral irradiance in the near infrared 11 p1588 N90-19160
Radial response of the burst and transient source experiment 12 p1637 N90-19408
Transmission and reflection studies of thin films in the vacuum ultraviolet 12 p1638 N90-19412
The 32-GHz performance of the DSS-14 70-meter antenna: 1989 configuration 12 p1645 N90-19452
Calibration of the sonic measuring and control cross section in the gas feed installation of the solid fuel combustion chamber
[LR-552] 12 p1661 N90-19548
Development of the blackbody probe type pyrometer, part 1. Experimental study on the fundamental characteristics
[DE89-782288] 12 p1663 N90-19553
ARGUS/LLNL IR camera calibration and characterization
[AD-A217076] 12 p1664 N90-19563
Recalibrating software reliability models
[NASA-CR-186407] 12 p1700 N90-19763
Cosmic ray composition and muon decoherence at the knee of the all-particle cosmic ray spectrum 12 p1745 N90-20035
Analysis of radiometer calibration effects with TOUCHSTONE
[NASA-CR-186476] 13 p1792 N90-20284
Statistical equipment modeling for VLSI manufacturing
[DE90-008527] 13 p1795 N90-20304
Design and calibration of a vacuum compatible scanning tunneling microscope
[NASA-TM-102514] 13 p1804 N90-20353
Gravity field determination and error assessment techniques 13 p1832 N90-20517
An improved error assessment for the GEM-T1 gravitational model 13 p1832 N90-20518
Geopotential models in the Australian region 13 p1832 N90-20519
First year's results and field experience with the latest JILA absolute gravimeter 13 p1834 N90-20529
Effective calibration of heat flux transducers for experimental use
[AD-A218262] 13 p1853 N90-20636
Modification, testing, and calibration of infrared search and target designator hardware received from NSWC
[AD-A217920] 13 p1889 N90-20837
Calibration of Hewlett-Packard network analyzers: A precision viewpoint
[NASA-CR-181989] 14 p1966 N90-21262
Systematic errors in power measurements made with a dual six-port ANA
[PB90-145160] 14 p1968 N90-21276
Software to characterize tuning fork resonators used in the Quartz Digital Accelerometer
[DE90-007913] 14 p1983 N90-21363
Error correction of the DEA (Digital Electronic Automation) coordinate measuring machines at LLNL
[DE90-008913] 14 p1983 N90-21365
Absolute multilayer characterization at high spatial resolution via real-time soft x ray imaging
[DE90-009181] 14 p1984 N90-21371
Mechanics of interface fracture 14 p1990 N90-21408
Possible use of satellite data for flood plain mapping
[INPE-4968-PRE/1537] 14 p2000 N90-21452
SR90, strontium shaped-charge critical ionization velocity experiment
[NASA-CR-186501] 14 p2024 N90-21606
Precise estimation of tropospheric path delays with GPS techniques 15 p2074 N90-21881

Lidar measurements of the optical propagation environment 15 p2084 N90-21930
Radar scatterometry and polarimetry at 220 GHz 15 p2085 N90-21935
Millimeter-wave bistatic scattering by terrain 15 p2085 N90-21936
Computation of broad spectral band electro-optical system transmittance response characteristics to military smokes and obscurants using field test data from transmissometer system measurements 15 p2086 N90-21939
Homogeneous dilute turbulent particle-laden water flows 15 p2090 N90-21965
The calibration and measuring procedure of a five-hole hemispherical head probe in compressible flow
[LR-585] 15 p2099 N90-22013
Development of the CLAES instrument aperture door system 15 p2112 N90-22083
Self-calibration of robot-sensor system 15 p2144 N90-22246
A refrigerated Dewar for the Josephson array voltage calibration system
[DE90-005237] 15 p2172 N90-22412
Qualification of the RSRM case membrane case-to-insulation bondline inspection using the Thiokol Corporation ultrasonic RSRM bondline inspection system
[NASA-CR-183940] 16 p2209 N90-22602
Phase Doppler droplet sizing: Scattering angle effects
[DE90-009571] 16 p2236 N90-22754
Qualification of the RSRM field joint CF case-to-insulation bondline inspection using the Thiokol Corporation ultrasonic RSRM bondline inspection system
[NASA-CR-183931] 16 p2242 N90-22788
Characterization and calibration of coordinate measuring machines
[DE90-009320] 16 p2242 N90-22791
Local atmospheric electricity and its possible application in high energy cosmic ray air shower detection 16 p2340 N90-23335
Field calibration of two types of microphones in hyperbaric air
[AD-A219477] 17 p2395 N90-23642
A process for the measurement of the unsteady three dimensional stream vectors in turbomachines
[MITT-89-01] 17 p2405 N90-23702
Self-calibrating apparatus to find dynamic compressibility of organic solids
[AD-A219780] 17 p2415 N90-23763
Data quality analysis at the National Transonic Facility
[NASA-CR-4303] 17 p2448 N90-23957
Formula scoring: Basic theory and applications
[AD-A218368] 17 p2465 N90-24083
Angle measurements using the laser gyro GG 1342
[DLR-FB-89-50] 18 p2555 N90-24579
Laser range camera modeling
[DE90-008220] 18 p2562 N90-24618
Proof of the feasibility of coherent and incoherent schemes for pumping a gamma-ray laser
[AD-A219972] 18 p2562 N90-24620
Evaluating Statistical Process Control (SPC) techniques and computing the uncertainty of force calibrations 18 p2631 N90-24992
Evaluation of various thrust calculation techniques on an F404 engine
[NASA-TP-3001] 19 p2659 N90-25134
An accurate numerical technique for determining flight test rate gyroscope biases prior to takeoff
[AD-A220987] 19 p2660 N90-25138
Calibration technique for heat flux sensors used in fire experiments and standard fire tests
[DOT/FAA/CT-89/26] 19 p2694 N90-25329
On the calibration of an autocollimator-comparator guide of a vertical target levelling rod differing from the ABBE's principle
[ISBN-951-754-887-7] 19 p2694 N90-25331
Space radiation studies
[NASA-CR-183991] 19 p2798 N90-25925
Electric field strength meters for the HF, VHF, and UHF bands
[BBC-RD-1990/3] 20 p2851 N90-26212
Video camera system for locating bullet holes in targets at a ballistics tunnel
[NASA-TM-4197] 20 p2865 N90-26296
Optical characterization of clouds of fine liquid-nitrogen particles
[NASA-TM-103208] 20 p2865 N90-26299
An automated calibration laboratory for flight research instrumentation: Requirements and a proposed design approach
[NASA-TM-101719] 20 p2912 N90-26564
Absolute measurements of gravity
[AD-A222731] 20 p2922 N90-26629
Method and apparatus for applying a mechanical force to surface
[NASA-CASE-LAR-14009-1] 21 p3011 N90-27115
Calibration of the visible and near-infrared channels of the LANDSAT-5 Thematic Mapper using high-altitude aircraft measurements
[NASA-TM-102185] 21 p3015 N90-27138
Comparisons of the recording instruments. Description of the difference-plots 21 p3022 N90-27181
Experiences with modern absolute instruments 21 p3022 N90-27183
Reproduction of GMS IR calibration table 21 p3028 N90-27215
Diagnostics for hydrogen atoms and molecules in H-atom sources and beams using VUV laser light
[AD-A222340] 21 p3074 N90-27476
Infrared observations of the solar system in support of Large Aperture Infrared Telescope (LARITS): Calibration
[AD-A222222] 21 p3097 N90-27597
Infrared observations of the solar system in support of Large Aperture Infrared Telescope (LARITS): Calibration. Appendices
[AD-A222245] 21 p3097 N90-27598
A study of the sensitivity of an imaging telescope (GRITS) for high energy gamma-ray astronomy
[NASA-CR-186921] 22 p3261 N90-28468
Three-dimensional model testing in the transonic self-streamlining wind tunnel 23 p3284 N90-28583
Accurate quantum chemical calculations
[NASA-TM-101932] 23 p3303 N90-28680
A microprocessor controlled strain gauge calibration module
[AR-005-579] 23 p3329 N90-28821
Rheometer strain and strain-rate errors
[DE90-013845] 23 p3329 N90-28824
A laser spectrometer and wavemeter for pulsed lasers
[NASA-CR-181731] 23 p3331 N90-28832
Operation and calibration of MRL permeameter for measurement of DC magnetic properties of materials under stress
[MRL-TN-574] 23 p3338 N90-28863
Calibration of the PARC program for propulsion-type flows
[AD-A224253] 24 p3434 N90-29395
Procedure for calibrating fly-by-wire control chains of the flying testbed ATTAS
[DLR-MITT-90-02] 24 p3435 N90-29401
A 94 GHz transmissometer
[AD-A223309] 24 p3471 N90-29618
Long-term flat-field behavior in LLNL streak cameras: Preliminary results
[DE90-015615] 24 p3472 N90-29621
Noncontact measurement of rotating blade vibrations
[NAL-TR-1033] 24 p3483 N90-29687
A review of manganin gauge technology for measurements in the gigapascal range
[MRL-TR-90-5] 24 p3541 N90-30026
Database development for the DMSP experiments
[AD-A224346] 24 p3557 N90-30129

CALIFORNIA
Airborne profiles taken near San Nicolas Island, California, during Operation FIRE (First ISCCP (International Satellite Cloud Climatology Project) regional experiment) (1987): Aerosol size distributions, air and surface temperatures, cloud top temperatures, and relative humidities
[AD-A211664] 03 p0374 N90-12136
Correlation of AVHRR imagery with sub-surface features in California current
[AD-A218184] 13 p1848 N90-20607
Evaporation duct effects at millimeter wavelengths 15 p2080 N90-21914
The naval oceanic vertical aerosol model 15 p2082 N90-21921
The effects of climatological and transient wind forcing on eddy generation in the California current system
[AD-A219858] 17 p2431 N90-23855
Development of remote sensing techniques for the investigation of neotectonic activity, eastern transverse ranges and vicinity, southern California 18 p2573 N90-24662

CALORIMETERS
Thermophysical properties of ceramics. Part 2: Development of specific-heat-measurement apparatus at high temperature
[DE89-760382] 01 p0047 N90-10268
New tools for the simulation and design of calorimeters
[DE89-016323] 02 p0223 N90-11281
The 3-D heat transfer computer calculations of th e performance of the IAEA's air-bath calorimeters
[DE89-016908] 02 p0224 N90-11283
Scintillating fiber ribbon - tungsten calorimeter
[DE89-016705] 03 p0350 N90-12001
High resolution X-ray spectroscopy using germanium microcalorimeters
[DE89-017784] 03 p0351 N90-12004
Calorimetric measurements on electrochemical cells with Pd-D cathodes
[DE90-002198] 06 p0805 N90-14685
ROBOCAL (Robotic Calorimetry): An automated NDA (Nondestructive Assay) calorimetry and gamma isotopic system
[DE90-003217] 07 p0894 N90-15168
The digital data acquisition chain and the cosmic ray trigger system for the SLD warm iron calorimeter
[DE90-000943] 07 p1015 N90-15879
Design of a microwave calorimeter for the microwave tokamak experiment
[DE90-004486] 10 p1387 N90-18026
Microcalometric studies of gun propellant KKR 8
[FOA-C-20770-2.1] 11 p1495 N90-18606
Algorithms for calorimeter simulation with parameterized showers by example of H1 detectors
[MPI-PAE/EXP.EL-200] 12 p1711 N90-19828
A new thermal sensor for x ray microcalorimetry
[DE90-008547] 13 p1805 N90-20360
Improved Thermo-Oxidative-Deposition screening tests for turbine lubricants
[AD-A217795] 14 p1954 N90-21188
High power, high sensitivity microwave calorimeter
[AD-D014427] 14 p1982 N90-21355
A low temperature calorimetric study of several high-T(sub c) superconductors 16 p2322 N90-23237
Calibration technique for heat flux sensors used in fire experiments and standard fire tests
[DOT/FAA/CT-89/26] 19 p2694 N90-25329
NPL absorbed dose graphite calorimeter correction for the effect of the gaps around the core
[NPL-RSA(EXT)-12] 22 p3178 N90-28032
Study of the induction time in isothermal decomposition of explosives
[DE90-014906] 23 p3315 N90-28745

CALORIMETRY
U HEAT MEASUREMENT

CALUTRONS
U CYCLOTRONS

CAM (MANUFACTURING)
U COMPUTER AIDED MANUFACTURING

CAMBER
NT WING CAMBER
The maximum lift coefficient of plain wings at subsonic speeds
[ESDU-89034] 07 p0876 N90-15082
Calculation of the unsteady two-dimensional, inviscid, compressible flow around a strongly cambered oscillating single blade 11 p1460 N90-18409
A study of flows over highly-swept wings designed for maneuver at supersonic speeds
[AD-A216837] 12 p1599 N90-19202

CAMERA TUBES
NT IMAGE DISSECTOR TUBES
NT VIDICONS

CAMERAS
NT DIFFRACTION LIMITED CAMERAS
NT FAINT OBJECT CAMERA
NT FRAMING CAMERAS
NT HIGH SPEED CAMERAS
NT SCHMIDT CAMERAS
NT STREAK CAMERAS
NT TELEVISION CAMERAS
Robust spatial calibration of a planar positron camera
[AD-A210773] 02 p0224 N90-11284
Aspects of the development of a 1-5 micron infrared camera for astronomy 02 p0290 N90-11656
A survey of camera error sources in machine vision systems
[DE89-014072] 03 p0405 N90-12318
An imaging vector magnetograph for the next solar maximum 03 p0435 N90-12489
A high-speed digital camera system for the observation of rapid H-alpha fluctuations in solar flares 03 p0435 N90-12491
An image compression algorithm for a high-resolution digital still camera
[NASA-CR-185079] 06 p0780 N90-14532
Tomographic imagery by multislot coding applied to x ray diagnostics of laser plasmas: Implementation of a direct electronic detection camera 06 p0787 N90-14579
Sensor integration using concurrent computing on-board the ORNL mobile robot
[DE89-008740] 07 p0939 N90-15436
Knowledge-based imaging-sensor fusion system 08 p1075 N90-16220
A knowledge-based machine vision system for space station automation 08 p1075 N90-16221
On the geometry of a general three-camera headmounted system
[AD-A214790] 09 p1225 N90-17108

Mission report on the Orbiter Camera Payload System (OCPS) Large Format Camera (LFC) and Attitude Reference System (ARS)
[NASA-CR-186273] 09 p1240 N90-17197
First test results with a CCD camera developed by INPE
[INPE-4873-PRE/1484] 10 p1388 N90-18029
Visual navigation: Constructing and utilizing simple maps of an indoor environment
[AD-A216761] 11 p1455 N90-18382
High speed imaging with a tapped solid state sensor
[DE90-006116] 11 p1511 N90-18702
Refurbishment and modification of the Metric Camera (RMK) for reflight on EOM-1 Spacelab mission
[ETN-90-96284] 11 p1512 N90-18710
The microchannel plate camera as a detector at high resolution spectrographs: Experiments for velocity distribution in planetary nebulae
[ETN-90-95733] 12 p1664 N90-19560
ARGUS/LLNL IR camera calibration and characterization
[AD-A217076] 12 p1664 N90-19563
Very high energy gamma ray astrophysics
[DE90-006645] 12 p1737 N90-19983
Simple reflection holography
[DE90-008309] 13 p1805 N90-20359
The design and implementation of a position measuring system for a remotely controlled video camera
[AD-A218077] 13 p1805 N90-20362
Ga:Ge array development 14 p1977 N90-21323
Study of advanced InSb arrays for SIRTF (Space Infrared Telescope Facility) 14 p1977 N90-21325
Experience with the UKIRT InSb array camera 14 p1977 N90-21327
Reduction and analysis techniques for infrared imaging data 14 p1977 N90-21328
High resolution imaging of the Venus night side using a Rockwell 128x128 HgCdTe array 14 p1978 N90-21330
Initial astronomical results with a new 5-14 micron Si:Ga 58x62 DRO array camera 14 p1978 N90-21334
Low noise HgCdTe 128 x 128 SWIR FPA for Hubble space telescope 14 p1979 N90-21337
Future directions for NICMOS arrays 14 p1979 N90-21339
Status of the isophot detector development 14 p1980 N90-21342
ISO camera array development status 14 p1980 N90-21344
Space environment robot vision system 15 p2143 N90-22245
Wearing of cryomechanisms at 4 K
[REPT-892-440-103] 17 p2473 N90-24139
The target pursuit of Giotto camera
[ETN-90-96496] 18 p2555 N90-24581
Periphery camera system
[AD-A221281] 18 p2555 N90-24583
Laser range camera modeling
[DE90-008220] 18 p2562 N90-24618
A comparison of select image-compression algorithms for an electronic still camera 18 p2632 N90-24994
Video photographic considerations for measuring the proximity of a probe aircraft with a smoke seeded trailing vortex
[NASA-TM-102691] 19 p2657 N90-25120
Technology development: Future use of NASA's large format camera is uncertain
[GAO/NSIAD-90-142] 20 p2865 N90-26298
Multiple target tracking in a wide-field-of-view camera system
[DE90-013488] 20 p2865 N90-26300
Color image processing for navigation: Two road trackers
[AD-A222667] 20 p2916 N90-26591
Development of Planar Laser-Induced Fluorescence (PLIF) techniques for supersonic flows 21 p2974 N90-26900
Tracking a head-mounted display in a room-sized environment with head-mounted cameras
[AD-A222545] 21 p3037 N90-27266
Infrared mapping with a two-dimensional infrared array
[AD-A221938] 21 p3096 N90-27596
Towards an understanding of camera fixation
[PB90-160342] 22 p3177 N90-28027

CAMPBELL-HAUSDORFF SERIES
Limit cycles and bifurcation in piecewise-linear and piecewise-analytic systems. 1: General theory
[RR-372] 19 p2751 N90-25634

CAMS
Phase control mechanism for wave energy conversion
[AD-D014354] 12 p1681 N90-19657
A robot end effector exchange mechanism for space applications 15 p2113 N90-22088
Core sample extractor
[NASA-CR-182864] 17 p2411 N90-23740

CANADA
Adverse weather operations during the Canadian Atlantic storms program 07 p0871 N90-15052
Aircraft fire safety: Learning from past accidents 10 p1312 N90-17584
Aircraft fire safety in the Canadian Forces 10 p1315 N90-17604
GEOID '88: A gravimetric geoid for Canada 13 p1837 N90-20543
A study of auroral activity in the nightside polar cap 16 p2254 N90-22852
Ecological study of peat landforms in Canada and Alaska
[NASA-CR-184923] 19 p2705 N90-25391
Command and control in the age of space-based surveillance 21 p3069 N90-27445
Authors guide to the publishing procedures at Defence Research Establishment Suffield
[AD-A223101] 21 p3087 N90-27554
The Canadian Aviation Safety Board's flight recorder facility 22 p3106 N90-27643
The nuclear battery
[DE90-630400] 24 p3462 N90-29559

CANADAIR AIRCRAFT
CF 18 480 Gallon External Fuel Tank Stores Clearance Program 02 p0153 N90-10877

CANADAIR CF-104 AIRCRAFT
U CANADAIR AIRCRAFT
U F-104 AIRCRAFT

CANADIAN SPACECRAFT
NT ALOUETTE 1 SATELLITE
NT ALOUETTE 2 SATELLITE

CANALS
The use of remote sensing for the localization of seepage near the Twenthe canal, Netherlands
[BCRS-89-30] 18 p2575 N90-24669

CANARD CONFIGURATIONS
The active control of an unstable canard aircraft 02 p0156 N90-10894
Validation of a computer code for analysis of subsonic aerodynamic performance of wings with flaps in combination with a canard or horizontal tail and an application to optimization
[NASA-TP-2961] 06 p0717 N90-14187
Canard versus aft-tail ride qualities performance and pilot command response 07 p0871 N90-15053
Some recent developments in materials and techniques for model fabrication 08 p1031 N90-15955
Wind tunnel investigations on the configuration of the international vortex flow experiment 08 p1068 N90-16181
X-29A aircraft structural loads flight testing
[NASA-TM-101715] 12 p1603 N90-19225
Constrained spanload optimization for minimum drag of multi-lifting-surface configurations 14 p1919 N90-20992
Feasibility study for a microwave-powered ozone sniffer aircraft
[NASA-CR-186660] 17 p2353 N90-23397
Project Dawdler: A proposal in response to a low Reynolds number station keeping mission
[NASA-CR-186668] 19 p2658 N90-25128
Effect of tail size reductions on longitudinal aerodynamic characteristics of a three surface F-15 model with nonaxisymmetric nozzles
[NASA-TP-3036] 20 p2802 N90-25938
An in-flight interaction of the X-29A canard and flight control system
[NASA-TM-101718] 20 p2807 N90-25973
A computer module used to calculate the horizontal control surface size of a conceptual aircraft design
[NASA-CR-186872] 20 p2903 N90-26515
Aerodynamic and propulsive control development of the STOL and maneuver technology demonstrator 23 p3271 N90-28514
Effects of canard position on the aerodynamic characteristics of a close-coupled canard configuration at low speed 23 p3272 N90-28519
The effects of foreplanes on the static and dynamic characteristics of a combat aircraft model 23 p3273 N90-28520
The steady and time-dependent aerodynamic characteristics of a combat aircraft with a delta or swept canard 23 p3274 N90-28526
An in-flight investigation of ground effect on a forward-swept wing airplane 23 p3275 N90-28533

CANCELLATION
Performance analysis of large adaptive sidelobe canceller arrays with reused elements
[AD-A212888] 04 p0494 N90-12841
Adaptive canceller limitations caused by I,Q mismatch errors
[AD-A214287] 07 p0919 N90-15318

CANCELLATION CIRCUITS
Neurobeamformer 2: Further exploration of adaptive beamforming via neural networks
[AD-A215118] 10 p1426 N90-18226
Improvement of clutter rejection by scanning motion compensation in ground-based monopulse radar
[ETN-90-96550] 16 p2228 N90-22711

CANCER
Proceedings of the 10 May 1989 Antiproton Technology Workshop: Addendum
[AD-A212804] 04 p0554 N90-13227
Elicitation of natural language representations of uncertainty using computer technology
[DE90-001416] 07 p0972 N90-15611
Short-term bioassays may be useful in evaluating fiber/whisker hazards
[DE90-003707] 08 p1104 N90-16393
Proceedings of a workshop on Carcinogenic Potential of Extremely Low Frequency Magnetic Fields
[DE90-614340] 14 p2010 N90-21520

CANISTERS
U CANS

CANNING
One step HIP canning of powder metallurgy composites
[NASA-CASE-LEW-14719-1] 17 p2370 N90-23493

CANNONS
U GUNS (ORDNANCE)

CANONICAL FORMS
Canonical formalism for coupled beam optics
[DE90-003764] 07 p0992 N90-15734
On functional integral representations in the lower Hubbard band based on generalized coherent states
[DE90-602936] 07 p1003 N90-15804
System identification and filtering of nonlinear controlled Markov processes by canonical variate analysis
[AD-A214873] 09 p1273 N90-17381
On the structure of Mandelbrot's percolation process and other random Cantor sets
[REPT-89-54] 15 p2163 N90-22362
Robust fixed order dynamic compensation for large space structure control 16 p2292 N90-23059
Almost input-output decoupling with stability
[MEMO-819] 18 p2597 N90-24778

CANOPIES
Automation of an RCS (Radar Cross Section) measurement system and its application to investigate the electromagnetic scattering from scale model aircraft canopies
[AD-A215741] 10 p1375 N90-17970
A new method for measuring the transmissivity of aircraft transparencies
[AD-A216953] 12 p1714 N90-19842
Water-tunnel study results of a TF/A-18 and F/A-18 canopy flow visualization
[NASA-TM-101705] 16 p2195 N90-22532
Nondestructive measurement of residual stresses in aircraft transparencies
[AD-A218680] 17 p2415 N90-23762
Forward canopy feasibility and Thru-The-Canopy (TTC) ejection system study
[AD-A220360] 18 p2495 N90-24258
Measurement techniques, evaluation criteria and injury probability assessment methodologies developed for Navy ejection and crashworthy seat evaluations 19 p2721 N90-25479

CANOPIES (VEGETATION)
Canopy stomatal conductance
[DE89-016860] 06 p0809 N90-14711
Characterization of cloud chemistry and frequency of canopy exposure to clouds in the Sierra Nevada
[PB89-104035] 06 p0817 N90-14753
Dynamics of carbon dioxide exchange of a wheat community grown in a semi-closed environment 08 p1155 N90-16689
Continuous gas exchange measurements using individual fascicle cuvettes: The tubule system
[DE90-004932] 10 p1405 N90-18105
Relationships between the aerial biomass from ground layers of cerrado and its spectral reflectance
[INPE-4848-PRE/1477] 11 p1521 N90-18760
Thermal remote sensing in the differentiation of soybean crops (glycine max (L.) merrill) submitted to water deficit
[INPE-4900-PRE/1501] 11 p1522 N90-18762
Relationships between spectral parameters and agronomics of wheat and beam crops
[INPE-4791-RPE/584] 11 p1523 N90-18768
Evaluation of TM/LANDSAT and HRV/SPOT data in reforested areas
[INPE-4575-RPE/567] 11 p1524 N90-18772
Spectral response of wheat and its relationship with agronomical prameters
[INPE-4950-RPE/599] 11 p1524 N90-18774
Some aspects of atmospheric turbulence in forests
[INPE-4951-RPE/600] 11 p1532 N90-18818

Evaluation of TM/LANDSAT and HRV/SPOT data in the identification of reforested areas in the Mogi-Guacu (SP) region
[INPE-4874-PRE/1485] 13 p1819 N90-20442
Relationship of radiometric field measurements of wheat in the Assis-Safra region, 1988
[INPE-4949-RPE/598] 13 p1819 N90-20443
Principles of the radiosity method for canopy reflectance modeling
[DE90-008943] 14 p2001 N90-21466
Millimeter-wave bistatic scattering by terrain 15 p2085 N90-21936
Modeling the lateral diffusion of fluorescent particles within a forest canopy 15 p2121 N90-22136
Spectral response of wheat and its relationship with agronomic variables in the tropical region
[INPE-5018-RPE/612] 15 p2122 N90-22138
Seasonal LAI in slash pine estimated with LANDSAT TM
[NASA-TM-102278] 19 p2706 N90-25397
Measuring and modeling near-surface reflected and emitted radiation fluxes at the FIFE site
[NASA-CR-180953] 20 p2879 N90-26378
Remote sensing of Earth terrain
[NASA-CR-186888] 20 p2880 N90-26382
Modeling and measurement of tree canopy reflectance
[MITT-66] 21 p3018 N90-27162
Comparison of overstory canopy cover estimates on forest survey plots
[PB90-159484] 22 p3194 N90-28126
A manual for analysis of hemispherical canopy photography
[DE90-014718] 23 p3342 N90-28885
Simulation and measurement of the heat exchange between the urban canopy and boundary layers 24 p3486 N90-29702

CANS
Improved process for HIP canning of composites
[NASA-CASE-LEW-14990-1-CU] 07 p0890 N90-15147
Long term creep strength of silver alloyed copper
[DE90-602367] 08 p1045 N90-16039
Acceleration tests of the ACPB canister flight unit from RETE experiment
[IFSI-89-2] 10 p1328 N90-17669
Vibration tests of the ACPB canister flight unit of the RETE experiment, integrated with the tests of the booms from R. Piaggio
[IFSI-89-11] 10 p1328 N90-17670
Fire hazards of aerosol cans in aircraft cargo compartments
[DOT/FAA/CT-89/32] 17 p2347 N90-23369
Two-dimensional model of a Space Station Freedom thermal energy storage canister
[NASA-TM-103124] 20 p2862 N90-26279

CANT
U SLOPES

CANTILEVER BEAMS
Analysis of the non-planar response of a cantilever, with the aid of computerized symbolic manipulation
[AD-A212421] 04 p0545 N90-13172
Attitude and shape control of optimally designed large space structures 05 p0613 N90-13579
The adhesive bonding of thermoplastic composites
[AD-A213358] 05 p0618 N90-13605
Load-shortening behavior of an initially curved eccentrically loaded column
[NASA-TM-101643] 08 p1088 N90-16293
Effects of T-tabs and large deflections in DCB specimen tests
[NASA-TM-101677] 09 p1186 N90-16868
Damping loss factor determination of glass and graphite fiber composites
[AD-A214535] 10 p1347 N90-17816
Damping loss factor determination of glass and graphite epoxy laminated composites using vertically oriented cantilever beams
[AD-A216529] 10 p1351 N90-17833
Baseline experiment for active control of structural vibrations
[AD-A216194] 10 p1397 N90-18076
United States Air Force Academy get-away-special flexible beam experiment 14 p1937 N90-21088
Natural modes of cracked beams and identification of cracks 15 p2111 N90-22075
Localization of vibration in disordered nearly cyclic structures 16 p2246 N90-22812
Lateral buckling of short I-beams under cyclic loading
[PB90-213653] 22 p3191 N90-28104
Minimum weight design of a leaf spring tapered in thickness and width for the Hubble Space Telescope-space support equipment
[NASA-TM-4233] 23 p3340 N90-28879

CANTILEVER MEMBERS
NT CANTILEVER BEAMS

CANTILEVER WINGS
U WINGS

CAPACITANCE
Analysis of loss mechanisms in polycrystalline thin-film solar cells
[DE89-009454] 03 p0366 N90-12093
Capacitive behavior in conducting polymers
[AD-A212448] 04 p0481 N90-12760
A capacitive technique for real-time monitoring polymer coating thickness on carbon filaments during prepregging process
[NASA-TM-101682] 06 p0780 N90-14533
Coronary arterial capacitance and subendocardial vascular patency throughout the cardiac cycle 11 p1538 N90-18855
Temperature compensated crystal oscillator (TCXO) with improved temperature compensation
[AD-D014334] 12 p1650 N90-19482
Lightning protection apparatus for RF equipment and the like
[AD-D014336] 12 p1650 N90-19483
Development and utilization of new diagnostics for dense-phase pneumatic transport
[DE90-006787] 12 p1659 N90-19536
Deep level transient spectroscopy in resistive layers
[DE90-008349] 13 p1772 N90-20169
Advanced double layer capacitors 13 p1822 N90-20464
Simulator comparison of thumball, thumb switch, and touch screen input concepts for interaction with a large screen cockpit display format
[NASA-TM-102587] 14 p1921 N90-21005
Calibration of Hewlett-Packard network analyzers: A precision viewpoint
[NASA-CR-181989] 14 p1966 N90-21262
An ultra-small capacitance Josephson junction
[DE90-613396] 14 p2032 N90-21653
A capacitance process for contact-free microfile measurement on metallic surfaces
[ETN-90-96503] 18 p2549 N90-24549
Measurement of deep levels at InGaAs(P)/InP heterojunctions
[AD-A222890] 21 p3082 N90-27526
L-SWITCH: A PC-program for computing transient voltages and currents during switching off three-phase inductances
[PB90-191412] 22 p3167 N90-27961
A double-sided silicon strip detector with capacitive read out and a new method of integrated bias coupling 22 p3178 N90-28037

CAPACITANCE-VOLTAGE CHARACTERISTICS
Electron beam induced damage in PECVD Si3N4 and SiO2 films on InP
[NASA-TM-102544] 13 p1810 N90-20393

CAPACITORS
Mechanical states in wound capacitors. Part 1: Prediction
[DE89-008110] 01 p0059 N90-10337
Mechanical states in wound capacitors. Part 2: Optimization
[DE89-008116] 01 p0059 N90-10338
Capacitive energy storage at cryogenic temperatures, phase 2
[AD-A210366] 01 p0061 N90-10347
Advanced double layer capacitor
[AD-A210510] 01 p0061 N90-10348
Properties of devices prepared with epitaxial layers on InP
[AD-A210304] 01 p0132 N90-10759
Capacitive behavior in conducting polymers: The ac impedance and quartz crystal microbalance studies
[AD-A210754] 02 p0201 N90-11150
Lifetime testing of commercially available 3.0 (mu)f, 100 kV pulsed-power capacitors
[DE89-017230] 02 p0217 N90-11242
Advanced double layer capacitor
[AD-A211977] 04 p0469 N90-12688
Capacitive behavior in conducting polymers
[AD-A212448] 04 p0481 N90-12760
GaAs gate dynamic memory technology
[AD-A212387] 04 p0560 N90-13266
High temperature capacitive strain gage
[NASA-CR-4266] 05 p0644 N90-13760
Temperature stable ceramic dielectric compositions
[AD-D014209] 06 p0749 N90-14358
Advanced double layer capacitor
[AD-A213406] 07 p0923 N90-15341
Analysis of the behaviour of a current-fed multi-stage voltage multiplier with capacitive output 10 p1338 N90-17745
Spacecraft thermal control design data, volume 3
[ESA-PSS-03-108-ISSUE-1-VOL-3] 11 p1469 N90-18457
Reliability studies of ceramic capacitors
[AD-A216763] 11 p1501 N90-18643
Alternate film dielectric materials
[DE90-007213] 12 p1632 N90-19378
Advanced double layer capacitor
[AD-A217110] 12 p1656 N90-19518
Advanced double layer capacitors 13 p1822 N90-20464
Advanced double layer capacitor
[AD-A219419] 16 p2233 N90-22741
Application of ultracapacitors in electric vehicle propulsion systems
[DE90-010884] 18 p2550 N90-24554
Role of surface passivation in the integrated processing of MOS structures
[AD-A222630] 20 p2859 N90-26264
A double-sided silicon strip detector with capacitive read out and a new method of integrated bias coupling 22 p3178 N90-28037
Application of a rechargeable, small caliber railgun power supply
[AD-A224207] 24 p3438 N90-29418

CAPE KENNEDY LAUNCH COMPLEX
Atmospheric environment for space shuttle (STS-29) launch
[NASA-TM-100376] 02 p0175 N90-10980
Atmospheric environment for space shuttle (STS-30) launch
[NASA-TM-100381] 02 p0175 N90-10981

CAPILLARIES
Combined capillary electrophoresis and electrospray ionization mass spectrometry
[DE90-001903] 06 p0743 N90-14322

CAPILLARY CIRCULATION
U CAPILLARY FLOW

CAPILLARY FLOW
Capillary effects in steady-state flow in heterogeneous cores
[DE89-000758] 01 p0070 N90-10399
Analysis of spurt phenomena for a non-Newtonian fluid
[AD-A210560] 01 p0071 N90-10405
Vibration isolation technology: Sensitivity of selected classes of space experiments to residual accelerations
[NASA-CR-185443] 04 p0482 N90-12768
Capillary flow properties of mesh wicks
[AD-A214769] 09 p1217 N90-17057
Experimental investigation of the thermocapillary migration of water droplets in butylbenzoate
[MPIS-14/1988] 13 p1770 N90-20155
Development and integration of the capillary pumped loop GAS and Hitchhiker flight experiments
[NASA-TM-100756] 15 p2059 N90-21790
Plane Stokes flow driven by capillarity on a free surface: Overview and status
[DE90-009186] 15 p2098 N90-22008
Plane Stokes flow driven by capillarity on a free surface: Overview and status
[DE90-009290] 15 p2098 N90-22009
Fingering in 2-D porous media: Experiments, network simulators and statistical models 19 p2691 N90-25308
Viscous fingering in porous media: A discussion of the small length scale cut-off 19 p2691 N90-25311

CAPILLARY TUBES
Fluorescence and elastic scattering from laser dye-filled capillaries
[AD-A217026] 11 p1484 N90-18540
Ceramic heat pipe wick
[NASA-CASE-GSC-13199-1] 17 p2378 N90-23541

CAPILLARY WAVES
NT BAROCLINIC WAVES
NT GRAVITY WAVES
NT RIPPLES
On the temperature of surfaces 10 p1366 N90-17917
Survey of instrumental methods for the determination of the high frequency wave spectrum
[IOS-267] 15 p2135 N90-22200

CAPS (EXPLOSIVES)
Minutes of the 23rd Explosives Safety Seminar, volume 1
[AD-A218264] 14 p1958 N90-21213

CAPSULES (SPACECRAFT)
U SPACE CAPSULES

CAPTIVE TESTS
NT STATIC TESTS
Pivotal mono wing cruise missile with wing deployment and fastener mechanism
[AD-D014191] 04 p0452 N90-12594

CAPTURE CROSS SECTIONS
U ABSORPTION CROSS SECTIONS

CARBAMATES (TRADENAME)
NT URETHANES
Novel carbamates, their production and their use as fuels additives
[EP-PATENT-0-298-636-A-1] 05 p0629 N90-13676

CARBENES
Highly reduced carbene complexes: Formation of an alkoxymalonate by coupling of carbon dioxide with the nucleophilic carbene in Cr(CO4)=C(OMe)Ph2(-)
[AD-A215132] 09 p1191 N90-16902
CARBIDES
NT ALUMINUM CARBIDES
NT BORON CARBIDES
NT NIOBIUM CARBIDES
NT SILICON CARBIDES
NT TITANIUM CARBIDES
NT TUNGSTEN CARBIDES
Creep strength of niobium alloys, Nb-1%Zr and PWC-11
[NASA-TM-102390] 03 p0326 N90-11854
The effects of Mo2C morphology and strain distribution on the fatigue properties of Fe-C-Mo dual-phase steels 07 p0901 N90-15210
Application of high-rate cutting tools
[AD-A214644] 09 p1203 N90-16970
Continuous preparation of a thin refractory carbide deposit on the surface of carbon fibers: Characterization of the C/SiC fiber 11 p1477 N90-18501
Spectroscopic evidence for carbon-carbon bonding in carbide layers on metals
[AD-A216726] 11 p1479 N90-18512
Wetting of metallic carbides by non-reactive liquid metals
[AERE-M-3759] 13 p1775 N90-20185
The role of polarity on the stability of graphitic compounds
[DE90-006528] 13 p1780 N90-20218
CARBOHYDRATE METABOLISM
Heatstroke pathophysiology: The energy depletion model
[AD-A212156] 03 p0380 N90-12164
CARBOHYDRATES
NT CELLULOSE
NT GLUCOSE
NT GLUCOSIDES
NT STARCHES
Physical performance and carbohydrate consumption in CF commandos during a 5-day field trial
[AD-A217204] 13 p1850 N90-20619
Work enhancement and thermal changes during intermittent work in cool water after carbohydrate loading
[AD-A222877] 21 p3034 N90-27247
CARBON
NT CARBON ISOTOPES
NT CARBON 12
NT CARBON 13
NT CARBON 14
Research on ultra low wear materials for energy conservation
[DE89-015096] 01 p0046 N90-10263
Observation of excited H(sup 0) atoms produced by relativistic H(sup (minus)) ions in carbon and formvar foils
[DE89-015301] 01 p0120 N90-10688
Optical dispersion relations for diamondlike carbon films
[NASA-TM-102356] 01 p0129 N90-10738
Modifications to the aerotherm charring material thermal response and ablation program (CMA) for carbon ablation analysis
[AD-A211069] 02 p0195 N90-11115
Carbon in detonations
[DE89-016037] 02 p0208 N90-11189
Diamondlike carbon coatings for optical systems
[AD-A211255] 02 p0276 N90-11573
Plasma-deposited amorphous hydrogenated carbon films and their tribological properties
[NASA-TM-102379] 03 p0331 N90-11880
An investigation of diamond film deposition in a premixed oxyacetylene flame
[AD-A212595] 04 p0561 N90-13268
The conversion of carbonaceous materials to clean carbon and co-product gaseous fuel
[DE90-001561] 06 p0754 N90-14387
Phase changes in carbon and nitrogen systems: Their effects on the detonation properties of high explosives
[DE90-000829] 06 p0755 N90-14392
Effect of carbon on ion beam mixing of Fe-Ti bilayers
[DE90-003650] 08 p1048 N90-16056
The carbon chemistry of meteorites: Relationships to comets 08 p1141 N90-16615
Neptune's Triton: A moon rich in dry ice and carbon
[NASA-CR-186298] 08 p1152 N90-16675
Migration of carbon in tempered martensitic steel during excimer laser melting
[DE90-004838] 09 p1195 N90-16922
Reactions of atmospheric species with clean and H, C, and O implanted species
[AD-A214602] 09 p1244 N90-17218
Effect of propellant flowrate and purity on carbon deposition in LO2/methane gas generators 11 p1471 N90-18468
Spectroscopic evidence for carbon-carbon bonding in carbide layers on metals
[AD-A216726] 11 p1479 N90-18512
Wide-beam balloon observations of the 157.7 microns (CII) line 11 p1581 N90-19108
Carbon black/polyethylene composites for PTC (Positive Temperature Coefficient) thermistor applications
[AD-A215988] 12 p1619 N90-19307
The effect of fiber coatings on interfacial shear strength and the mechanical behavior of ceramic composites
[DE90-007574] 12 p1632 N90-19380
Techno-economic assessment of a carbothermic alumina reduction process
[DE90-007018] 13 p1772 N90-20170
Carbon and hydrogen metabolism of green algae in light and dark
[DE90-008648] 13 p1849 N90-20612
Direct sublimation of NaCl salt from carbon matrixes
[DE90-007927] 14 p1946 N90-21139
Testing carbon fabric for oxidation mass loss 15 p2063 N90-21819
Mechanical properties of carbon-implanted niobium
[DE90-009864] 15 p2064 N90-21823
Recombination lines of C I and N II in the interstellar medium 15 p2182 N90-22466
Analysis of gamma squared Velorum photometry from the South Pole 15 p2183 N90-22472
Fuel-rich catalytic combustion: A fuel processor for high-speed propulsion
[NASA-TM-103177] 17 p2374 N90-23518
Power density effects in the physical and chemical properties of sputtered diamond-like carbon thin films
[DE90-011587] 18 p2532 N90-24450
The effect of carbon type and processing on high rate thionyl chloride cathode collectors
[AD-A219823] 18 p2546 N90-24532
Potential technology transfers of research on low-temperature carbon monoxide-oxygen recombination catalysts 18 p2562 N90-24616
Use of high-dimensional spectral data to evaluate organic matter, reflectance relationships in soils
[NASA-CR-186650] 18 p2574 N90-24665
Open hole and post-impact compression fatigue of stitched and unstitched carbon/epoxy composites
[NASA-TM-102676] 19 p2701 N90-25370
Wear mechanisms of amorphous carbon and zirconia coatings on rigid disk magnetic recording media
[DE90-011053] 20 p2837 N90-26133
Application of the results of carbon pellet modeling to the problem of plasma penetration
[DE90-012713] 20 p2928 N90-26658
Carbon in the Galaxy: Studies from Earth and Space
[NASA-CP-3061] 21 p3089 N90-27562
Carbon in primitive meteorites 21 p3089 N90-27563
Carbon in comet dust 21 p3089 N90-27564
Carbon-rich particles in Comet Halley 21 p3089 N90-27565
Astronomical observations of solid phase carbon 21 p3089 N90-27566
Carbon stardust: From soot to diamonds 21 p3090 N90-27568
Carbon chemistry of circumstellar envelopes 21 p3090 N90-27570
Carbon chemistry in dense molecular clouds: Theory and observational constraints 21 p3090 N90-27571
CI, CII, and CO as tracers of gas phase carbon 21 p3091 N90-27572
Down-to-earth studies of carbon clusters 21 p3091 N90-27573
Electronic and molecular structure of carbon grains 21 p3091 N90-27574
A unifying picture of gas-phase formation and growth of PAH (Polycyclic Aromatic Hydrocarbons), soot, diamond and graphite 21 p3091 N90-27575
The formation and structure of circumstellar and interstellar dust 21 p3091 N90-27576
Nature and origin of interstellar diamond from the Allende CV3 meteorite 21 p3092 N90-27581
An ionic mechanism of carbon formation in flames 21 p3093 N90-27582
On planetary nebulae as sources of carbon dust: Infrared emission from planetary nebulae of the galactic halo 21 p3093 N90-27583
Diamonds in detonation soot 21 p3094 N90-27585
Raman spectroscopic studies of carbon in extra-terrestrial materials 21 p3095 N90-27589
On diamond, graphitic and amorphous carbons in primitive extraterrestrial solar system materials 21 p3095 N90-27591
Carbon in the outer solar system 21 p3096 N90-27593
Nonequilibrium radiation and chemistry models for aerocapture vehicle flowfields
[NASA-CR-186728] 22 p3169 N90-27973
Mechanical properties testing of diamond and diamond-like films by ultra-low load indentation
[DE90-014456] 23 p3337 N90-28861
CARBON COMPOUNDS
NT ALUMINUM CARBIDES
NT BORON CARBIDES
NT CALCITE
NT CALCIUM CARBONATES
NT CARBIDES
NT CARBON DIOXIDE
NT CARBON DISULFIDE
NT CARBON MONOXIDE
NT CARBON TETRACHLORIDE
NT CARBONATES
NT CHLOROCARBONS
NT DOLOMITE (MINERAL)
NT FLUOROCARBONS
NT HALOCARBONS
NT LEXAN (TRADEMARK)
NT NIOBIUM CARBIDES
NT POLYCARBONATES
NT SILICON CARBIDES
NT SODIUM CARBONATES
NT TITANIUM CARBIDES
NT TUNGSTEN CARBIDES
On the vapour phase deposition mechanism of carbon-boron-nitrogen compounds between 800 and 1000 C
[REPT-892-430-101] 16 p2214 N90-22632
CARBON CYCLE
Biochemical cycling and fluxes between the deep euphotic zone and other oceanic realms
[PB89-152458] 01 p0089 N90-10509
A simple, mass balance model of carbon flow in a controlled ecological life support system
[NASA-TM-102151] 01 p0101 N90-10571
Prospect of new energy. Global warming (1988)
[DE90-702486] 09 p1244 N90-17217
Modeling the upper ocean and its interaction with the atmosphere
[DE90-008980] 14 p2008 N90-21511
CARBON DIOXIDE
Biochemical cycling and fluxes between the deep euphotic zone and other oceanic realms
[PB89-152458] 01 p0089 N90-10509
Potential effects of global climate change on the United States. Executive summary. Draft
[PB89-161046] 02 p0237 N90-11350
Policies to encourage private sector responses to potential climate change
[DE89-017244] 03 p0368 N90-12107
A statistical intercomparison of temperature and precipitation predicted by four general circulation models with historical data
[DE89-017785] 03 p0369 N90-12108
Synergistic effects of nitrogen dioxide and carbon dioxide following acute inhalation exposures in rats
[PB89-214779] 03 p0377 N90-12150
Spin-orbit relaxation rates of Bi(6p(3)) 2D(3/2) following photolysis of Bi(CH3)3 at lambda = 193 nm
[AD-A211792] 03 p0402 N90-12303
Mechanisms of CO2 reduction metal and metal modified semiconductor electrodes
[AD-A213169] 04 p0473 N90-12712
Survey of the response of standard limited streamer tubes over the complete range of three-component gas mixtures of isobutane, CO(sub 2), argon
[DE89-016692] 04 p0499 N90-12875
Contribution of deforestation to atmospheric CO2 and reforestation as an option to control CO2
[DE89-017255] 04 p0516 N90-12979
Effects of atmospheric mix and toxic fumes on military performance
[PB89-223630] 04 p0522 N90-13015
Global energy and the greenhouse issue
[DE90-001394] 06 p0809 N90-14709
Canopy stomatal conductance
[DE89-016860] 06 p0809 N90-14711
Strategy for monitoring the effects of land use change on atmospheric CO2 concentrations
[DE90-001635] 06 p0812 N90-14722
Rayleigh-Taylor instability in compressible fluids
[DE90-003027] 07 p0929 N90-15376
Research project on CO2-induced climate change
[DE90-003531] 07 p0957 N90-15538
Responding to the threat of global warming: Options for the Pacific and Asia
[DE90-003553] 07 p0957 N90-15539
Solid-state electrolyte catalysis for methane and oxygen synthesis
[PB90-100231] 08 p1040 N90-16011

Mechanisms of the electrochemistry of small organic molecules
[PB90-100785] 08 p1040 N90-16012
Method of making carbon dioxide and chlorine free fluoride-based glass
[AD-D014260] 08 p1048 N90-16060
Dynamics of carbon dioxide exchange of a wheat community grown in a semi-closed environment 08 p1155 N90-16689
Electrochemical cell for obtaining oxygen from carbon dioxide atmospheres
[NASA-CR-186225] 09 p1189 N90-16886
New electronic materials and CO2 reduction
[AD-A214679] 09 p1191 N90-16899
Prospect of new energy. Global warming (1988)
[DE90-702486] 09 p1244 N90-17217
A numerical study of shock wave refraction at a CO2/CH4 interface
[DE90-005997] 10 p1386 N90-18022
Continuous gas exchange measurements using individual fascicle cuvettes: The tubule system
[DE90-004932] 10 p1405 N90-18105
Energy technology R and D and the greenhouse effect
[DE90-001339] 10 p1406 N90-18107
Oxygen electrode in molten carbonate fuel cells
[DE90-005377] 11 p1528 N90-18796
Natural and anthropogenic climate change
[DE90-006488] 11 p1532 N90-18822
The 2.7/4.3 micron CO2 branching ratio measurement
[AD-A215952] 11 p1534 N90-18830
Studies of atmospheric molecules by multiphoton spectroscopy
[DE90-005829] 11 p1534 N90-18833
Spectroscopy and physico-chemistry of CO:H2O and CO2:H2O ices 11 p1581 N90-19111
A preliminary analysis of US CO2 emissions reduction potential from energy conservation and the substitution of natural gas for coal in the period to 2010
[DOE/NBB-0085] 12 p1684 N90-19673
Simulation of global Kr-85 and (14)CO2 distribution by means of a time-dependent, two dimensional model of the atmosphere
[ETN-90-95376] 12 p1689 N90-19702
CO2 diffusion and solubility in a Polystyrene/Polybutadiene block copolymer with highly oriented lamellar morphology
[AD-A217165] 13 p1779 N90-20211
Global Warming: A Northwest Perspective
[DE90-008140] 13 p1830 N90-20505
Source attribution for tropospheric ozone in the US
[DE90-007994] 14 p2004 N90-21484
Preliminary report on the demonstration of the VAS CO2 cloud parameters (cover, height, and amount) in support of ASOS
[NOAA-TM-NESDIS-29] 14 p2006 N90-21498
Calcium carbonate scale dissolution in water stabilized by carbon dioxide treatment
[AD-A218502] 16 p2214 N90-22633
Effects of air temperature on atmospheric CO2-plant growth relationships
[DE90-010159] 17 p2420 N90-23793
The effects of climate change on energy planning and operations in the Pacific Northwest. Volume 2: Technical background
[DE90-009465] 17 p2425 N90-23817
CO-oxidation catalysts: Low-temperature CO oxidation over Noble-Metal Reducible Oxide (NMRO) catalysts 18 p2556 N90-24588
Pt/SnO2-based CO-oxidation catalysts for long-life closed-cycle CO2 lasers 18 p2556 N90-24589
Alternative catalysts for low-temperature CO-oxidation 18 p2557 N90-24594
A computer program for the design of optimum catalytic monoliths for CO2 lasers 18 p2558 N90-24595
Mechanistic studies of the CO-oxidation reaction on catalysts for use in long-life CO2 lasers 18 p2558 N90-24596
The effect of H2O and pretreatment on the activity of a Pt/SnO2 catalyst 18 p2558 N90-24597
Rare-isotope and kinetic studies of Pt/SnO2 catalysts 18 p2558 N90-24598
Characterization study of polycrystalline tin oxide surfaces before and after reduction in CO 18 p2559 N90-24601
Anthropogenic sources of NO(x), SO()x, CO, and CH4: Geographical distribution
[AERONOMICA-ACTA-A-353-1990] 19 p2713 N90-25440
Carbon dioxide and water exchange rates by a wheat crop in NASA's biomass production chamber: Results from an 86-day study (January to April 1989)
[NASA-TM-102788] 19 p2716 N90-25453
Aircraft exhaust emissions: An engine manufacturer's perspective
[PNR90675] 20 p2812 N90-26004
Gas exchange characteristics as indicators of the basic limiting factors in photosynthesis
[DE90-012399] 20 p2898 N90-26481
Development of membrane process for carbon dioxide separation from diving atmosphere
[AD-A222606] 20 p2901 N90-26504
Recent high resolution laboratory determinations of line broadening and intensity parameters: PH3, CH3D, and CO2 20 p2944 N90-26751
A new calculation of the radiative cooling by carbon dioxide in the middle atmosphere and the lower thermosphere 22 p3210 N90-28211
Study of power generation systems for CO2 collection: LNG combined cycle
[DE90-507881] 23 p3345 N90-28901
Natural and anthropogenic climate change
[DE90-015528] 23 p3348 N90-28923
Statistically designed study of the variables and parameters of carbon dioxide equations of state
[DE90-016196] 24 p3447 N90-29467
Effects of increased CO2 on forest response
[DE90-015406] 24 p3487 N90-29708

CARBON DIOXIDE CONCENTRATION

Assessment of crop response to increases in atmospheric carbon dioxide concentrations: Summary of research progress report, July 1, 1988--June 30, 1989
[DE89-016251] 02 p0239 N90-11360
Quantifying the link between change in radiative balance and atmospheric temperature
[DE90-000819] 06 p0811 N90-14721
Carbon dioxide and climate: Summaries of research in FY 1989
[DE90-001791] 06 p0812 N90-14723
US energy use: New technologies and policies in response to global warming
[DE90-002170] 06 p0812 N90-14724
Greenhouse gases: Changing the global climate
[DE90-002788] 07 p0957 N90-15535
Factors that may influence responses of the US transportation sector to policies for reducing greenhouse gas emissions
[DE90-000704] 07 p0958 N90-15543
A qualitative architecture for understanding policy responses to global change
[DE90-003936] 08 p1099 N90-16364
Dynamics of carbon dioxide exchange of a wheat community grown in a semi-closed environment 08 p1155 N90-16689
Biomass fuels in the developing countries: An overview
[DE90-002616] 09 p1241 N90-17201
Evaluating CO, CO2 and H2O concentration by partial integration of absorption band spectra
[ISL-R-110/88] 09 p1244 N90-17219
Survey on energy conversion of CO2 gas. Approach to solution of CO2 gas problems
[DE90-742055] 10 p1352 N90-17843
Variations in volatiles in magma bodies based on studies of melt inclusions
[DE90-006272] 11 p1532 N90-18821
CO2 depth profiles in cometary model substances of KOSI 12 p1742 N90-20014
Draft global warming study
[DE90-008446] 13 p1830 N90-20507
Sensitivity studies in a two-dimensional atmospheric transport model
[DAR-TP-18] 14 p2006 N90-21496
Kinetic and extraction measurements on 12C18O2
[AD-A220417] 17 p2472 N90-24133
Monitoring of catalyst performance in CO2 lasers using frequency modulation spectroscopy with diode lasers 18 p2561 N90-24614
Carbon dioxide and water exchange rates by a wheat crop in NASA's biomass production chamber: Results from an 86-day study (January to April 1989)
[NASA-TM-102788] 19 p2716 N90-25453
Proximate composition of seed and biomass from soybean plants grown at different carbon monoxide (CO2) concentrations
[NASA-TM-103496] 20 p2897 N90-26480
Effects of corpuscular radiation on weather and climate 22 p3201 N90-28164
The effects of clouds on CO2 forcing 22 p3222 N90-28271
The role of clouds in CO2-induced climate change
[DE90-014380] 23 p3346 N90-28911
Effects of increased CO2 on forest response
[DE90-015406] 24 p3487 N90-29708
Grassland/atmosphere response to changing climate: Coupling regional and local scales
[DE90-015814] 24 p3487 N90-29710
The effects of a doubling of atmospheric CO2 on the stormtracks in the climate of a general circulation model
[KNMI-WR-90-01] 24 p3488 N90-29713

CARBON DIOXIDE LASERS

Laser propulsion to earth orbit. Has its time come? 01 p0028 N90-10143
Low ppb level detection of toxic compounds with a fully automated CO2 laser photoacoustic detector 02 p0206 N90-11181
Construction of a picosecond laser system for the investigation of semiconductors using nonlinear optical methods
[ETN-89-94664] 03 p0352 N90-12013
Automated glass fiber drawing
[DE90-000894] 06 p0751 N90-14367
Eurolaser CO2 laser
[ETN-90-95907] 06 p0787 N90-14582
A compact, high-powered far-infrared (FIR) laser
[DE89-016786] 06 p0789 N90-14597
Experimental and theoretical study of CO2 staggered hollow-bore array lasers
[AD-A212921] 10 p1389 N90-18032
Numeric model of a CO2 laser amplifier
[AD-A215818] 10 p1389 N90-18035
A numerical solution to the Boltzmann equation for use in calculating pumping rates in a CO2 discharge laser
[AD-A216378] 11 p1514 N90-18718
Cloud hole-boring with infrared lasers: Theory and experiment
[DE90-006519] 11 p1515 N90-18723
Effects produced by pulsed CO2 lasers
[ISL-R-112/88] 11 p1516 N90-18731
Research on sliding spark preionization in a TEA CO2 laser
[ISL-R-113/88] 11 p1516 N90-18732
Study of discharge mechanisms and the stability of transverse electric discharges in the gas mixtures
[ISL-R-114/88] 11 p1516 N90-18733
CdTe buffered GaAs thin-slab IR waveguide modulators and T/R filter
[AD-A215999] 12 p1651 N90-19488
CO2 laser plus optimization for harmonic generation
[AD-D014341] 12 p1665 N90-19565
Results of the PALADIN experiment
[DE90-006776] 12 p1667 N90-19578
Cloud hole-boring with long pulse CO2 lasers
[DE90-008946] 14 p1985 N90-21377
High power CO2 laser instability and its corrections 15 p2102 N90-22028
Contributions to the development of SLM TEA CO2 laser sources for high resolution molecular spectroscopy 16 p2240 N90-22778
Kinetic and extraction measurements on 12C18O2
[AD-A220417] 17 p2472 N90-24133
Low-Temperature CO-Oxidation Catalysts for Long-Life CO2 Lasers
[NASA-CP-3076] 18 p2556 N90-24586
Pulsed-discharge carbon dioxide lasers 18 p2556 N90-24587
Pt/SnO2-based CO-oxidation catalysts for long-life closed-cycle CO2 lasers 18 p2556 N90-24589
LaRC-developed catalysts for CO2 lasers 18 p2557 N90-24591
Phillips CO-oxidation catalyts for long-lived CO2 lasers: Activity and initial characterization studies 18 p2557 N90-24592
Synthesis, characterization and evaluation of CO-oxidation catalysts for high repetition rate CO2 TEA lasers 18 p2557 N90-24593
Alternative catalysts for low-temperature CO-oxidation 18 p2557 N90-24594
A computer program for the design of optimum catalytic monoliths for CO2 lasers 18 p2558 N90-24595
Mechanistic studies of the CO-oxidation reaction on catalysts for use in long-life CO2 lasers 18 p2558 N90-24596
The effect of H2O and pretreatment on the activity of a Pt/SnO2 catalyst 18 p2558 N90-24597
Rare-isotope and kinetic studies of Pt/SnO2 catalysts 18 p2558 N90-24598
Effect of pretreatment on a platinized tin oxide catalyst used for low-temperature CO-oxidation 18 p2558 N90-24599
Platinized tin oxide catalysts for CO2 lasers: Effects of pretreatment 18 p2559 N90-24600
Dissociation phenomena in electron-beam sustained carbon dioxide lasers 18 p2560 N90-24610
The e-beam sustained CO2 laser amplifier 18 p2561 N90-24611
A compact, rugged, high repetition rate CO2 laser incorporating catalyst 18 p2561 N90-24612
Performance of alumina-supported Pt catalysts in an electron-beam-sustained CO2 laser amplifier 18 p2561 N90-24613
Monitoring of catalyst performance in CO2 lasers using frequency modulation spectroscopy with diode lasers 18 p2561 N90-24614
Applications of low temperature CO-oxidation catalysts to breathable gases 18 p2561 N90-24615

Potential technology transfers of research on low-temperature carbon monoxide-oxygen recombination catalysts 18 p2562 N90-24616
Gain in waveguide laser at 10.6 micrometer [FOA-C-30540-3.1] 18 p2563 N90-24624
Characterization of the surfaces of platinum/tin oxide based catalysts by Fourier transform spectroscopy (FTIR) 18 p2643 N90-25054
Advanced solar-propelled cargo spacecraft for Mars missions [NASA-CR-186218] 19 p2665 N90-25164
Mode-medium instability and its correction with a Gaussian reflectivity mirror [NASA-TP-3023] 19 p2758 N90-25673
New discharge pumping method for CO2 lasers [AD-A220898] 20 p2866 N90-26307
The effects of pretreatment conditions on a Pt/SnO2 catalyst for the oxidation of CO in CO2 lasers [NASA-TM-103487] 20 p2867 N90-26309
A compact, high-powered Far-Infrared (FIR) laser [DE90-009996] 20 p2867 N90-26312
Airborne CO2 Doppler lidar for wind shear detection 22 p3106 N90-27640
Modeling of carbon monoxide oxidation kinetics over NASA carbon dioxide laser catalysts [NASA-CR-186356] 22 p3155 N90-27885
Four techniques to measure complex refractive indices of liquids and solids at carbon dioxide laser wavelengths in the infrared spectral region [AD-A222007] 22 p3180 N90-28043
Scattering of CO2-laser radiation by water droplets [FOA-C-20776-2.3] 22 p3181 N90-28049
Design of a CO2 laser power control system for a Spacelab microgravity experiment [NASA-TM-103112] 23 p3331 N90-28833

CARBON DIOXIDE REMOVAL

Dissociation and vibrational relaxation of XeF by various collision partners [AD-A210769] 02 p0227 N90-11300
Space Station Freedom environmental control and life support system phase 3 simplified integrated test detailed report [NASA-TM-4204] 16 p2207 N90-22593

CARBON DISULFIDE

Pressure induced resonance Raman effects in shocked carbon disulfide [AD-A210665] 02 p0194 N90-11107

CARBON FIBER REINFORCED PLASTICS

Influence of the fiber/matrix interface on damage development in CFRP 02 p0183 N90-11037
Delamination tests under compression-compression and tension-compression loading 02 p0186 N90-11062
A new test procedure for a wing made with carbon fiber composites [ETN-89-95220] 03 p0320 N90-11820
Aging of CFRP due to longterm storage in heated air [ESA-TT-1124] 03 p0333 N90-11893
Damage tolerance of CFRP sandwich panels [FFA-TN-1988-70] 04 p0465 N90-12664
Textural and structural organization of the heat treated polymers: Mechanical properties relationships [ETN-89-95711] 04 p0478 N90-12744
Low temperature optical testing of CFRP telescope panels 05 p0596 N90-13463
SiO overcoating and polishing of CFRP telescope panels 05 p0599 N90-13478
Fractography of composite delamination [NASA-CR-183291] 05 p0617 N90-13599
Simple shear tests of the FMI 23.5.06 adhesive cured at low pressure (12 PSI) [INFORME-I-296/88] 10 p1357 N90-17871
Study of defect distribution in manufacturing test E8 No. 2 (program A-330/340) [INFORME-I-366/89] 10 p1358 N90-17872
Enhanced bonding of fiber reinforcements to thermoset resins 11 p1476 N90-18496
Calculation of mechanical properties variations depending on matrix parameters in a composite, as a function of the test temperature [DT-311/88] 11 p1481 N90-18526
Impact of composites in the aerospace industry [ETN-90-96231] 11 p1481 N90-18527
The manufacturing procedures for composite materials, automation, and robotization [ETN-90-96232] 11 p1482 N90-18528
Practical calculation of the liveload of carbon fiber reinforced plastics by the finite element method [ETN-90-95867] 12 p1620 N90-19311
Evaluation and choice algorithms of cost optimal prepreg-application processes: Production of strongly charged plane parts made of fiber reinforced plastics [ETN-90-95895] 12 p1620 N90-19313
Utilization of thermometric methods for the testing of carbon reinforced plastics [ETN-90-96076] 12 p1621 N90-19314
Experiments on buckling and critical buckling. Behavior of carbon fiber reinforced plastic shells submitted to tensile stresses [ETN-90-95382] 13 p1816 N90-20429
Failure analysis of woven hybrid composite using a finite element method [OUEL-1791/89] 15 p2065 N90-21828
The behaviour of mechanically fastened joints in composite structures 16 p2242 N90-22789
Demonstration centers for fiber reinforced materials [REPT-45/89] 17 p2370 N90-23495
Limits to today's composites: Chances for tomorrow's developments [MBB-Z-0287-89-PUB] 18 p2519 N90-24385
Damage tolerance demonstration for A310-300 CFPR components [MBB-UT-012/89-PUB] 19 p2652 N90-25091
Fractography of composite delamination [NASA-CR-181965] 19 p2702 N90-25372
Static and fatigue strength of an adhesive bonded CFRP butt-strap joint: The effects of stacking sequence and temperature [NLR-TR-88036-U] 20 p2877 N90-26370
Polyarylacetylene resin composites [AD-A221507] 21 p2972 N90-26890
Study of an impact on organic matrix and long fibers composite plates (thermal aspect) [ETCA-89-R-155] 22 p3154 N90-27882
Ultrasonic inspection of advanced CFRP structures by computer-controlled, pulse-echo technique 22 p3185 N90-28075
Study of failure processes in fiber reinforced composites using acoustic emission techniques 22 p3188 N90-28090
Ultrasonic verification of five wave fronts in unidirectional graphite epoxy composite [NASA-CR-185288] 23 p3337 N90-28858
Surface effect for test piece on flexural test of carbon fiber reinforced plastic laminates [NAL-TM-601] 24 p3442 N90-29436
Non-destructive method for environmental breakdown of graphite fiber reinforced polymer composites [AD-A223729] 24 p3455 N90-29515

CARBON FIBERS

Interfacial adsorption and crystallization of polycarbonate in carbon fiber composites [AD-A211230] 02 p0191 N90-11090
Carbon fiber reinforced glass matrix composites for structural space based applications [AD-A211682] 03 p0320 N90-11818
Project, implementation, and utilization of composite structures [ETN-89-95209] 04 p0466 N90-12665
Surface treatments of carbon fibers in an organic environment. Finite element analysis of pull-out tests [ONERA-RT-7/3549-M] 04 p0471 N90-12698
Analysis of carbon fiber's x ray microscopic structure [AD-A212215] 04 p0480 N90-12752
Impact tests of three composite materials with carbon fiber cores [REPT-M6-582500] 05 p0619 N90-13610
Method for stabilization of pan-based carbon fibers [AD-D014228] 06 p0736 N90-14288
Carbon fiber reinforced metal matrix composites [AD-D014245] 06 p0737 N90-14289
A capacitive technique for real-time monitoring polymer coating thickness on carbon filaments during prepregging process [NASA-TM-101682] 06 p0780 N90-14533
Brominated graphitized carbon fibers [NASA-CASE-LEW-14698-2] 07 p0910 N90-15262
Instrumented impact and residual tensile strength testing of eight-ply carbon epoxy specimens [NASA-TP-2981] 08 p1040 N90-16007
Compression testing of carbon fibers [AD-A215296] 09 p1187 N90-16877
Physical chemical characterization of the surface of carbon fibers: Test report [REPT-49-740/F] 09 p1188 N90-16881
Adhesive for composite bonding [DE90-005683] 09 p1188 N90-16885
Damping loss factor determination of glass and graphite fiber composites [AD-A214535] 10 p1347 N90-17816
Modified bismaleimides for carbon fibre composites 11 p1476 N90-18495
Interlaminar fracture testing of carbon fibre/PEEK composites validity and applications 11 p1477 N90-18497
Continuous preparation of a thin refractory carbide deposit on the surface of carbon fibers: Characterization of the C/SiC fiber 11 p1477 N90-18501
Measuring strain in carbon fibre composite laminates using the Raman optomechanical strain gauge 11 p1477 N90-18503
Fluorinated graphite fibers as a new engineering material: Promises and challenges [NASA-TM-102511] 12 p1618 N90-19301
Oxygen concentrations on surfaces of carbon fibers [AD-A217724] 13 p1769 N90-20152
Proceedings of the Advisory Committee on Standardization of Carbon-Phenolic Test Methods and Specifications [NASA-CR-186478] 15 p2063 N90-21817
Development of low thermal conductivity pan-based carbon fibers for solid rocket motor nozzle applications 15 p2063 N90-21818
Effect of surface oxygen on adhesion of carbon fiber-reinforced composites [AD-A220777] 17 p2369 N90-23486
Low velocity instrumented impact testing of four new damage tolerant carbon/epoxy composite systems [NASA-TP-3029] 19 p2672 N90-25198
A study on carbon Fiber (long fiber) reinforced copper matrix composite [AD-A221584] 21 p2972 N90-26891
Characterization of PMDI/HOPG interfaces by SERS using a silver overlayer configuration [AD-A223104] 21 p2985 N90-26966
Production of superconductor/carbon bicomponent fibers 22 p3138 N90-27805
Reinforcing fibers and technology development for resin composites. Consequences for aircraft structures [FOA-C-20777-2.5] 22 p3154 N90-27883
Elementary characterization of the pre-impregnated carbon/epoxy NCHR 914/155/34 percent-T300F from Brochier after the technical note CEAT number 1/M/87 [CEAT-PV-M7/6211] 22 p3154 N90-27884
Electrochemical surface finishing using amino-substrates on carbon fibers in organic media. Effects of the finishing on the mechanical properties of carbon-epoxy composites [ONERA-RT-9/3549-M] 23 p3301 N90-28672
Development of dual fiber reinforced glass matrix composites for structural space based applications [AD-A223801] 24 p3444 N90-29446
Precursor structure-fiber property relationships in polyacrylonitrile-based carbon fibers [AD-A224246] 24 p3454 N90-29503
Non-destructive method for environmental breakdown of graphite fiber reinforced polymer composites [AD-A223729] 24 p3455 N90-29515

CARBON ISOTOPES

NT CARBON 12
NT CARBON 13
NT CARBON 14
Carbon isotope ratios and lithium abundances in open cluster giants 02 p0292 N90-11664
Stable isotope studies of cometary analogue materials 12 p1740 N90-20001
Kinetic and extraction measurements on 12C18O2 [AD-A220417] 17 p2472 N90-24133
Probing the possibility of a C-12/C-13 galactic abundance gradient 21 p3094 N90-27586

CARBON LASERS

Inspection of carbon/epoxy and aluminum honeycomb paraboloidal components by HNDT [AD-A216796] 11 p1479 N90-18514

CARBON MONOXIDE

Human health studies of carbon monoxide (CO) under conditions of military weapons systems crewman exposures. Protocol 1: Formation of COHb [AD-A210344] 01 p0092 N90-10528
Catalogic hydrogenation of carbon monoxide [DE89-017813] 03 p0323 N90-11834
Fundamental molecular data to support CARS diagnostics of temperature, pressure, and species concentration [AD-A212411] 04 p0472 N90-12704
Computer simulation studies of the catalytic oxidation of carbon monoxide on platinum metals [PB89-223739] 04 p0475 N90-12721
Effects of atmospheric mix and toxic fumes on military performance [PB89-223630] 04 p0522 N90-13015
MOBILE4 oxygenated fuels version user's guide [PB89-230700] 05 p0629 N90-13674
Strategy for monitoring the effects of land use change on atmospheric CO2 concentrations [DE90-001635] 06 p0812 N90-14722
Mechanisms of the electrochemistry of small organic molecules [PB90-100785] 08 p1040 N90-16012
Time and spatially dependent estimates of pollutant trace gas emissions and their effect on tropospheric ozone 09 p1243 N90-17212
Evaluating CO, CO2 and H2O concentration by partial integration of absorption band spectra [ISL-R-110/88] 09 p1244 N90-17219
Observations of CO on Mars in the infrared and millimetre range 11 p1578 N90-19090

Spectroscopy and physico-chemistry of CO:H2O and CO2:H2O ices 11 p1581 N90-19111
CO infrared bands in atmospheres of long-period variables 11 p1584 N90-19128
Carbon monoxide in supernova 1987A 11 p1585 N90-19135
The strengths of the 2.3 micron CO band in luminous interacting and merging galaxies 11 p1587 N90-19148
A search for the CO feature in active galactic nuclei 11 p1587 N90-19151
Structure of model gas flames in nitramines [AD-A217578] 13 p1770 N90-20159
A comparison of photospheric and circumstellar (HCN)/(CO)-ratios for bright carbon stars [PB90-151101] 15 p2184 N90-22477
The distribution of molecular clouds in spiral galaxies 15 p2186 N90-22489
High spatial resolution isotopic CO and CS observations of M17 SW: The clumpy structure of the molecular cloud core [MPE-PREPRINT-161] 16 p2330 N90-23283
Catalyst for carbon monoxide oxidation [NASA-CASE-LAR-14155-1-SB] 17 p2374 N90-23517
Effects of air temperature on atmospheric CO2-plant growth relationships [DE90-010159] 17 p2420 N90-23793
The oxidation of carbon monoxide using tin oxide based catalysts 18 p2557 N90-24590
Mechanistic studies of the CO-oxidation reaction on catalysts for use in long-life CO2 lasers 18 p2558 N90-24596
ISS and TPD study of the adsorption and interaction of CO and H2 on polycrystalline Pt 18 p2559 N90-24602
In situ analysis of CO during chemisorption and oxidation on graphite: Supported Pt by FTIR-microspectrometry 18 p2559 N90-24605
Calorimetry, activity, and micro-FTIR analysis of CO chemisorption, titration, and oxidation on supported Pt 18 p2560 N90-24606
Analysis of Pt/SnO(sub x) during catalysis of CO oxidation 18 p2560 N90-24607
Mars in situ propellants: Carbon monoxide and oxygen ignition experiments [NASA-TM-103202] 20 p2823 N90-26065
The application of HREELS to model catalysts: CO and C2H4 adsorption on Pt/Al2O3 [AD-A222744] 20 p2831 N90-26103
Proximate composition of seed and biomass from soybean plants grown at different carbon monoxide (CO2) concentrations [NASA-TM-103496] 20 p2897 N90-26480
Tropospheric sounders 21 p3016 N90-27150
Neurobehavioral effects of carbon monoxide (CO) exposure in humans: Elevated carboxyhemoglobin (COHb) and cerebrovascular responses [AD-A222840] 21 p3034 N90-27246
Modeling of carbon monoxide oxidation kinetics over NASA carbon dioxide laser catalysts [NASA-CR-186356] 22 p3155 N90-27885
The distribution of middle tropospheric carbon monoxide during early October 1984 [NASA-TM-103485] 23 p3346 N90-28906
Long-range plan for a research project on carbon monoxide production and prediction [PB90-209602] 23 p3346 N90-28910
Carbon monoxide isotopes and clumping in giant molecular clouds 24 p3562 N90-30151

CARBON MONOXIDE LASERS
Platinized tin oxide catalysts for CO2 lasers: Effects of pretreatment 18 p2559 N90-24600

CARBON STARS
Properties of evolved star circumstellar grains 06 p0861 N90-15003
IR spectrophotometry of bright carbon stars 11 p1584 N90-19131
The evolution and geometry of the outer parts of the small Magellanic cloud 14 p2040 N90-21697
A comparison of photospheric and circumstellar (HCN)/(CO)-ratios for bright carbon stars [PB90-151101] 15 p2184 N90-22477

CARBON STEELS
NT LOW CARBON STEELS
Corrosion rates of structural materials on the ocean floor [DE89-015211] 02 p0197 N90-11123
Microstructural effects on spall fracture in 1008 steel [DE89-016770] 02 p0198 N90-11131
Carbonitrition response of steel plates not destined for heat treatments [CETIM-106960] 04 p0476 N90-12728
Effects of dislocation substructure and prestrain on fracture behavior in aluminum and steel alloys 06 p0745 N90-14334
Measuring the thickness of austenitic weld deposits on carbon steel walls using a magnetic method [DE89-635446] 06 p0794 N90-14628
Surface modification of steels and aluminum alloys to control corrosion and hydrogen embrittlement. Part 1: Chemical methods [AD-A216272] 10 p1356 N90-17866
The mechanism, measurement, and influence of properties on the galling of metals [DE90-006533] 11 p1487 N90-18558
Bearing and gear steels for aerospace applications [NASA-TM-102529] 13 p1809 N90-20391
Ultrahigh carbon steels and their laminates [AD-A218780] 17 p2376 N90-23530
Microbially influenced corrosion of carbon steels [DE90-012231] 21 p2980 N90-26936

CARBON TETRACHLORIDE
Carbon doping of compound semiconductor epitaxial layers using carbon tetrachloride [AD-A215053] 09 p1290 N90-17477

CARBON 12
Studies of elastic scattering and cross sections of the C-12 + Si-28 system [DE89-635990] 08 p1120 N90-16486

CARBON 13
Carbon-13 nuclear magnetic resonance of heterocyclic salts and its precursors [DE89-635768] 08 p1041 N90-16016
Plasma centrifuge with vacuum arc discharge applied to the separation of stable isotopes [INPE-4925-TDL/385] 12 p1716 N90-19854

CARBON 14
Simulation of global Kr-85 and (14)CO2 distribution by means of a time-dependent, two dimensional model of the atmosphere [ETN-90-95376] 12 p1689 N90-19702

CARBON-CARBON COMPOSITES
Thermal stability of the carbon-carbon bond in ethylene adsorbed on Si(100): An isotopic mixing study [AD-A211591] 04 p0470 N90-12691
Review of polyarylacetylene matrices for thin-walled composites [AD-A214921] 09 p1186 N90-16872
Effects of heat treatment on microstructure and flexural properties of unidirectional carbon-carbon composites [AD-A214985] 09 p1186 N90-16873
Program to study the oxidation of carbon-carbon composites and coatings on these materials [AD-A214989] 09 p1187 N90-16874
Coefficients of thermal expansion for a carbon-carbon composite [DE90-004484] 09 p1188 N90-16883
Damage mechanisms and indenter size effects in cross plied carbon-carbon composites [AD-A216413] 10 p1351 N90-17832
Third European Conference on Composite Materials [EOARD-LR-89-050] 11 p1476 N90-18494
State of the art and future prospects for high temperature composites 11 p1477 N90-18498
Spallation and dynamic fracture as an effect of laser induced shock waves in carbon based composite materials [AD-A216540] 11 p1478 N90-18509
Reusable high-temperature heat pipes and heat pipe panels [NASA-CASE-LAR-13761-1] 13 p1799 N90-20323
Lightweight piston architecture [NASA-CASE-LAR-13926-1] 15 p2105 N90-22042
The position of carbon/carbon composites among high temperature composites [REPT-892-430-126] 16 p2213 N90-22626
Micro-mechanical modeling of crack growth resistance in a carbon/carbon composite [DE90-009407] 17 p2368 N90-23479
Limits to today's composites: Chances for tomorrow's developments [MBB-Z-0287-89-PUB] 18 p2519 N90-24385
Carbon-carbon composites: Emerging materials for hypersonic flight [NASA-TM-103472] 20 p2827 N90-26080
Braided composite fasteners and method for producing same [NASA-CASE-LAR-14062-1] 21 p3010 N90-27114
United States Air Force research initiation program for 1988, volume 3 [AD-A223125] 21 p3102 N90-27615
TRANSTRAIN: A program to compute strain transformations in composite materials [NASA-TM-103509] 22 p3153 N90-27877
NASA Langley Research Center National Aero-Space Plane Mission simulation profile sets [NASA-TM-102670] 23 p3276 N90-28541
The effects of atomic oxygen on the thermal emittance of high temperature radiator surfaces [NASA-TM-103224] 23 p3301 N90-28670

CARBONACEOUS CHONDRITES
NT ALLENDE METEORITE
NT MURCHISON METEORITE
Evolution of carbonaceous chondrite parent bodies: Insights into cometary nuclei 08 p1145 N90-16638
On diamond, graphitic and amorphous carbons in primitive extraterrestrial solar system materials 21 p3095 N90-27591
Carbon in the outer solar system 21 p3096 N90-27593

CARBONACEOUS MATERIALS
NT GRAPHITE
NT PEAT
NT PYROLYTIC GRAPHITE
Modifications to the aerotherm charring material thermal response and ablation program (CMA) for carbon ablation analysis [AD-A211069] 02 p0195 N90-11115
Diamondlike carbon coatings for optical systems [AD-A211255] 02 p0276 N90-11573
The conversion of carbonaceous materials to clean carbon and co-product gaseous fuel [DE90-001561] 06 p0754 N90-14387
Laboratory analyses of micron-sized solid grains: Experimental techniques and recent results 08 p1141 N90-16616
A coal model for the carriers of the unidentified IR bands 11 p1581 N90-19110
Spatially high-resolution flame diagnosis by means of spontaneous Raman spectroscopy [ETN-90-95870] 12 p1623 N90-19328
Evolution of ices and carbonaceous materials in the laboratory and in comets 12 p1739 N90-19998
Status and applications of diamond and diamond-like materials: An emerging technology [NASA-CR-186935] 21 p2985 N90-26963
The possible presence of interstellar PAHs in meteorites and interplanetary dust particles 21 p3092 N90-27579
Laboratory simulation of interstellar grain chemistry and the production of complex organic molecules 21 p3092 N90-27580

CARBONACEOUS METEORITES
NT ALLENDE METEORITE
NT CARBONACEOUS CHONDRITES
NT MURCHISON METEORITE
The carbon chemistry of meteorites: Relationships to comets 08 p1141 N90-16615
Carbon stardust: From soot to diamonds 21 p3090 N90-27568

CARBONACEOUS ROCKS
NT COAL

CARBONATES
NT CALCITE
NT CALCIUM CARBONATES
NT DOLOMITE (MINERAL)
NT LEXAN (TRADEMARK)
NT POLYCARBONATES
NT SODIUM CARBONATES
Molten carbonate fuel cell technology improvement [DE90-001934] 07 p0950 N90-15501
Oxygen electrode in molten carbonate fuel cells [DE90-002871] 07 p0952 N90-15510
Characterization of new cathode materials for molten carbonate fuel cells [DE90-003547] 07 p0953 N90-15516
Determination of optimum electrolyte composition for molten carbonate fuel cells [DE90-000410] 09 p1243 N90-17210
Oxygen electrode in molten carbonate fuel cells [DE90-005377] 11 p1528 N90-18796
The oxidation of carbon monoxide using tin oxide based catalysts 18 p2557 N90-24590
Geochemistry and origin of regional dolomites [DE90-012589] 21 p3024 N90-27196
Wind tunnel simulation of Antarctic snowdrifting [PB90-184585] 22 p3212 N90-28222

CARBONIZATION
Low energy ion generator [DE90-759905] 14 p1955 N90-21195
The effects of carbonization on the confinement properties of the DIII-D H-mode [DE90-013297] 20 p2928 N90-26660
Raman spectroscopic studies of carbon in extra-terrestrial materials 21 p3095 N90-27589

CARBONYL COMPOUNDS
Polyimides with carbonyl and ether connecting groups between the aromatic rings [NASA-CASE-LAR-14001-1] 07 p0910 N90-15260
Use of ab initio theory in studying various chemical systems [AD-A220913] 18 p2521 N90-24396
Selective metallization of carbonyl-containing polymer films [AD-D014526] 19 p2678 N90-25230

Chemical stabilization of laser dyes
[AD-A224219] 24 p3473 N90-29627

CARBORANE
Monomers, polymers and transition metal complexes based upon carboranes
[AD-A210226] 01 p0040 N90-10221
Metal-assisted syntheses of boranes and carboranes
[AD-A210728] 01 p0041 N90-10227
N-Hexyl Carborane (NHC) as combustion catalyst in composite propellants
[FOA-C-20755-2.1] 02 p0209 N90-11193

CARBOXYHEMOGLOBIN
Neurobehavioral effects of carbon monoxide (CO) exposure in humans: Elevated carboxyhemoglobin (COHb) and cerebrovascular responses
[AD-A222840] 21 p3034 N90-27246

CARBOXYLATES
Comparison of carboxylated and sulfonated model polyurethane ionomers
[AD-A210438] 01 p0050 N90-10284

CARBOXYLATION
Carboxyalkylated hemoglobin as a potential blood substitute
[AD-A213886] 07 p0966 N90-15582

CARBOXYLIC ACIDS
NT ACETIC ACID
NT ACRYLIC ACID
NT ALANINE
NT FORMIC ACID
NT NICOTINIC ACID
NT TRYPTOPHAN
Cubane derivatives for propellant applications
[AD-A210368] 01 p0054 N90-10305
Electroactive polyaniline film deposited from non-aqueous media. 2: Effect of acid concentration in solutions
[AD-A212084] 04 p0477 N90-12737
Radical homopolymerization of a trisubstituted alkene: 1-cyclobutenecarboxylic acid and its polymer
[AD-A223188] 21 p2986 N90-26968

CARBURIZING
Advances and directions of ion nitriding/carburizing
[NASA-TM-102398] 03 p0334 N90-11902
Internal and external nitriding and nitrocarburizing of iron and iron-based alloys
[ETN-90-96012] 05 p0625 N90-13646

CARCINOGENS
Elicitation of natural language representations of uncertainty using computer technology
[DE90-001416] 07 p0972 N90-15611
Bioluminescence for detection of trace compounds
[AD-A213458] 09 p1189 N90-16889
Risk analysis: Fundamental concepts, regulatory toxicology, and relative comparisons from radiation biology
[DE90-002466] 11 p1538 N90-18856
Proceedings of a workshop on Carcinogenic Potential of Extremely Low Frequency Magnetic Fields
[DE90-614340] 14 p2010 N90-21520
DNA damage and repair in human skin: Pathways and questions
[DE90-015126] 23 p3356 N90-28966

CARCINOMA
U CANCER

CARCINOTRONS
Low noise, high voltage supply for carcinotron backward wave oscillators 10 p1338 N90-17742

CARDIOGRAPHY
NT ELECTROCARDIOGRAPHY
NT MAGNETOCARDIOGRAPHY

CARDIOVASCULAR SYSTEM
NT ARTERIES
NT BLOOD VESSELS
NT HEART
NT MYOCARDIUM
USSR Space Life Sciences Digest, issue 22
[NASA-CR-3922(26)] 03 p0378 N90-12153
USSR Space Life Sciences Digest, issue 23
[NASA-CR-3922(27)] 03 p0378 N90-12154
Heatstroke pathophysiology: The energy depletion model
[AD-A212156] 03 p0380 N90-12164
Cardiovascular, renal, electrolyte, and hormonal changes in man during gravitational stress, weightlessness, and simulated weightlessness: Lower body positive pressure applied by the antigravity suit
[NASA-TM-102232] 04 p0522 N90-13013
The development of a model of the human responses to load carriage 06 p0821 N90-14775
Monitoring chaos of cardiac rhythms
[DE90-000692] 07 p0966 N90-15580
The role of blood volume in determining the cardiovascular adjustments to exercise 11 p1538 N90-18854
Elevated central venous pressure: A consequence of exercise training-induced hypervolemia
[NASA-TM-102965] 13 p1850 N90-20617
A comparison of the mechanisms of cold- and microgravity-induced fluid loss
[AD-A218098] 13 p1852 N90-20631
Effect of fluid countermeasures of varying osmolarity on cardiovascular responses to orthostatic stress 18 p2628 N90-24978
Hemodynamic and ADH responses to central blood volume shifts in cardiac-denervated humans
[NASA-TM-103471] 20 p2898 N90-26485
Cardiovascular deconditioning of cosmonauts: Role, importance and applications of the lower body negative pressure
[ETN-90-97507] 23 p3355 N90-28964
Prevalence of hypertension among active duty personnel
[AD-A223892] 23 p3356 N90-28968
Fluid and electrolyte homeostasis during spaceflight: Elucidation of mechanisms in a primate
[NASA-CR-177548] 23 p3378 N90-29085
Optimism and cardiovascular reactivity to psychological and cold pressor stress
[AD-A223818] 24 p3498 N90-29771
Physiological metrics of mental workload: A review of recent progress
[NASA-CR-187290] 24 p3499 N90-29777

CARGO
NT AIR CARGO
NT BAGGAGE
Control of an experiment to measure acoustic noise in the space shuttle
[NPS62-89-022] 06 p0838 N90-14869
A Mars/Phobos transportation system
[NASA-CR-186217] 09 p1230 N90-17135
New aircraft cabin and cargo flammability standards for transport category aircraft 10 p1312 N90-17589
Electric propulsion for manned Mars exploration 11 p1473 N90-18480
Design of an unmanned lunar cargo lander that reconfigures into a shelter for a habitation module or disassembles into parts useful to a permanent manned lunar base
[NASA-CR-186687] 17 p2363 N90-23454
Design of an autonomous teleoperated cargo transporting vehicle for lunar base operations
[NASA-CR-186686] 18 p2565 N90-24633
Design of a thermal and micrometeorite protection system for an unmanned lunar cargo lander
[NASA-CR-186682] 19 p2664 N90-25161
Design of a versatile, teleoperable, towable lifting machine with robotic capabilities for use in NASA's lunar base operations
[NASA-CR-186688] 19 p2697 N90-25345
Biconic cargo return vehicle with an advanced recovery system. Volume 1: Conceptual design
[NASA-CR-186520] 20 p2821 N90-26052

CARGO AIRCRAFT
NT C-5 AIRCRAFT
NT C-130 AIRCRAFT
NT C-135 AIRCRAFT
NT C-140 AIRCRAFT
NT C-141 AIRCRAFT
NT SPANLOADER AIRCRAFT
Design of a spanloader cargo aircraft
[NASA-CR-186046] 06 p0722 N90-14216

CARGO SPACECRAFT
Advanced solar-propelled cargo spacecraft for Mars missions
[NASA-CR-186218] 19 p2665 N90-25164
Project Exodus
[NASA-CR-186836] 20 p2816 N90-26026
Winged cargo return vehicle. Volume 1: Conceptual design
[NASA-CR-186823] 20 p2821 N90-26050

CARIBBEAN REGION
Summary of 1989 Atlantic tropical cyclone activity and seasonal forecast verification 06 p0815 N90-14743
Forecast of Atlantic seasonal hurricane activity for 1990 15 p2134 N90-22194

CARIBBEAN SEA
Puerto Rico Workshop on Land-Based Sources of Marine Pollution in the Wider Caribbean Region
[PB90-184094] 23 p3348 N90-28921
Measuring the vertical directional spectra caused by sea surface sound
[AD-A223883] 23 p3354 N90-28957

CARRIAGES
New test techniques to evaluate near field effects for supersonic store carriage and separation 01 p0013 N90-10062
The integration of stores on modern tactical aircraft: Where we have been, and what we should do for the future 10 p1305 N90-17552

CARRIER DENSITY (SOLID STATE)
Modeling and measurement methods for high speed bipolar transistors
[REPT-11] 05 p0636 N90-13714
Luminescence from electroformed metal-isolator-metal-structures
[ETN-90-97295] 22 p3249 N90-28425

CARRIER FREQUENCIES
Time-frequency factors in auditory perception
[AD-A211491] 04 p0523 N90-13016
Processing of undifferences GPS carrier beat phase measurements and adjustment computations
[TR-5-1988] 05 p0578 N90-13368
Applications of acousto-optical correlation devices in radar signal processing
[AD-A216624] 11 p1497 N90-18616
Numerical Arc Segmentation Algorithm for a Radio Conference-NASARC (version 4.0) technical manual
[NASA-TM-101453] 13 p1788 N90-20264
QPSK carrier-acquisition performance in the advanced receiver 2 15 p2076 N90-21892
Radar RFI at Goldstone DSS 12 and DSS 16 15 p2078 N90-21900

CARRIER INJECTION
Extended characterization of the damage by hot charge carriers in gate oxide by short channel MOS field effect transistors
[ETN-90-97313] 24 p3555 N90-30114

CARRIER LIFETIME
A simple model for the determination of L(sub 0), D and tau in a semiconductor and their temperature dependence
[DE90-610564] 12 p1720 N90-19879
Experimental evaluation of chemical cleaning processes for high-lifetime silicon processing
[DE90-009332] 16 p2226 N90-22699
An influence of fast neutron irradiation on the properties of p-i-n wide-based diodes
[DE90-611148] 18 p2550 N90-24556
Development of a point-contact solar cell using high-volume processing techniques
[DE90-010330] 18 p2577 N90-24683
Radiation effects in InAsSb strained-layer superlattice photodiodes induced by dose-rate and transient x ray environments
[DE90-015000] 23 p3400 N90-29208

CARRIER MOBILITY
NT ELECTRON MOBILITY
NT HOLE MOBILITY

CARRIER MODULATION
U MODULATION

CARRIER ROCKETS
U LAUNCH VEHICLES

CARRIER TRANSPORT (SOLID STATE)
Costas loop lock detection in the advanced receiver 12 p1643 N90-19441

CARRINGTON ROTATION
U SOLAR ROTATION

CARTESIAN COORDINATES
A numerical method for solving transonic flow past aircraft in Cartesian coordinates
[NAL-TR-1008] 01 p0001 N90-10003
A scalable multiprocessor architecture using Cartesian network: Relative addressing
[AD-A216580] 11 p1542 N90-18878
Direct formulation of a 4-node hybrid shell element with rotational degrees of freedom
[NASA-CR-4282] 14 p1991 N90-21411
Coordinate systems for plastic yield surfaces stress and strain space theories
[PB90-164765] 15 p2117 N90-22110
Stable boundary conditions for Cartesian grid calculations
[NASA-CR-182048] 16 p2306 N90-23139
Finding squares and rectangles in sets of points
[RUU-CS-89-10] 18 p2601 N90-24806
A 3D visualization system for molecular structures 18 p2641 N90-25044
Galerkin finite difference Laplacian operators on isolated unstructured triangular meshes by linear combinations
[NASA-TM-103209] 20 p2861 N90-26276
Space station definitions, design, and development. Task 5: Multiple arm telerobot coordination and control: Manipulator design methodology
[NASA-CR-182043] 20 p2914 N90-26577
Cartesian closed categories of domains
[ETN-90-97284] 20 p2919 N90-26613
Computer program for converting rectangular coordinates to latitude-longitude coordinates
[PB90-231796] 23 p3342 N90-28883
Cartesian control of redundant robots 23 p3363 N90-29004
Measurement of hand dynamics in a microsurgery environment: Preliminary data in the design of a bimanual telemicro-operation test bed 23 p3364 N90-29010

CARTILAGE
Interaction of electromagnetic fields with chondrocytes in gel culture
[AD-A223397] 24 p3497 N90-29765
CARTOGRAPHY
U MAPPING
CARTRIDGE ACTUATED DEVICES
U ACTUATORS
U EXPLOSIVE DEVICES
CARTRIDGES
Evaluation of selected computer models for modeling pyrotechnic and propellant devices
[AD-A213003] 05 p0629 N90-13671
CARTS
A noncontacting motion monitoring system for an astronaut translation aid
[NASA-TM-102640] 19 p2693 N90-25325
Hitching mechanism for lunar dump train
[NASA-CR-183034] 19 p2697 N90-25344
CASCADE FLOW
The measurement of boundary layers on a compressor blade in cascade. Volume 1: Experimental technique, analysis and results
[NASA-CR-185118-VOL-1] 01 p0009 N90-10038
The measurement of boundary layers on a compressor blade in cascade. Volume 2: Data tables
[NASA-CR-185118-VOL-2] 01 p0009 N90-10039
Turbulence scale effects on heat transfer in a linear turbine cascade
[AD-A216222] 10 p1321 N90-17637
Maxwellian cascade model
[DE90-004389] 10 p1427 N90-18235
Unsteady Aerodynamic Phenomena in Turbomachines
[AGARD-CP-468] 11 p1459 N90-18405
Numerical investigation of unsteady flow in oscillating turbine and compressor cascades
11 p1459 N90-18407
Unsteady viscous calculation method for cascades with leading edge induced separation
11 p1459 N90-18408
Aerodynamic superposition principle in vibrating turbine cascades 11 p1460 N90-18410
Gust response analysis for cascades operating in nonuniform mean flows 11 p1461 N90-18415
High-resolution Euler computations of unsteady transonic flows in cascades 11 p1462 N90-18420
Asymptotic analysis of transonic flow through oscillating cascades 11 p1462 N90-18421
Experiments on the unsteady flow in a supersonic compressor stage 11 p1462 N90-18422
Time-dependent measurements on vibrating annular turbine cascades under various steady state conditions
11 p1463 N90-18424
Experimental investigation of the influence of rotor wakes on the development of the profile boundary layer and the performance of an annular compressor cascade
11 p1463 N90-18425
Influence of friction and separation phenomena on the dynamic blade loading of transonic turbine cascades
[MITT-88-04] 12 p1605 N90-19235
Digital determination of the three dimensional flow in turbomachines with the S1-S2 current function process
[ITSM-MITT-30] 12 p1605 N90-19236
A two-dimensional unsteady analysis for transonic and supersonic cascade flows 14 p1911 N90-20955
A computational design method for shock free transonic cascades and airfoils 14 p1918 N90-20986
An inverse method for the design of turbomachine blades 14 p1918 N90-20988
Secondary flows and Reynolds stress distributions downstream of a turbine cascade at different expansion ratios 14 p1923 N90-21015
An investigation of secondary flows in nozzle guide vanes 14 p1923 N90-21016
Secondary flow in a turbine guide vane with low aspect ratio 14 p1924 N90-21018
Measurement of the flow field in the blade passage and side-wall region of a plane turbine cascade
14 p1924 N90-21019
Centrifugal impeller geometry and its influence on secondary flows 14 p1924 N90-21020
Calculation of the three dimensional turbulent flow in a linear turbine blade 14 p1924 N90-21021
Research on cascade secondary and tip-leakage flows: Periodicity and surface flow visualization
14 p1925 N90-21026
Losses in the tip-leakage flow of a planar cascade of turbine blades 14 p1925 N90-21027
Computational prediction and measurement of the flow in axial turbine cascades and stages
14 p1925 N90-21028
Detailed heat transfer measurements in nozzle guide vane passages in linear and annular cascades in the presence of secondary flows 14 p1926 N90-21030
The effect of secondary flow on the redistribution of the total temperature field downstream of a stationary turbine cascade 14 p1926 N90-21033
Decay of secondary flow and the associated loss variation downstream of an annual turbine stator cascade
[DE90-505520] 20 p2809 N90-25984
A fully implicit ADI method for quasi three-dimensional flows through straight blade rows
[ETN-90-96965] 20 p2863 N90-26283
Aerodynamics of a linear oscillating cascade
[NASA-TM-103250] 22 p3108 N90-27657
CASCADES (FLUID DYNAMICS)
U FLUID DYNAMICS
CASCODE MOSFET
U FIELD EFFECT TRANSISTORS
CASE HISTORIES
The NASA experience in aeronautical R and D: Three case studies with analysis
[AD-A211486] 04 p0437 N90-12496
CAE (Computer-Aided Engineering) tools' limitations case study: An SSI (Small Scale Integrated) design to an ASIC (Application Specific Integrated Circuit)
[DE90-002902] 08 p1109 N90-16418
CASES (CONTAINERS)
NT ROCKET ENGINE CASES
Feasibility of a super high energy density battery of the Li/BrF3 electrochemical system
[AD-A216794] 11 p1502 N90-18644
CASING
Lunar drill footplate and casing
[NASA-CR-183153] 17 p2411 N90-23738
CASKS
U BARRELS (CONTAINERS)
CASPIAN SEA
Analysis of altimetry over inland seas
[NASA-TM-100729] 13 p1840 N90-20566
CASSEGRAIN ANTENNAS
Telescope considered as a very high gain antenna
[ETN-90-96614] 17 p2473 N90-24138
Development of an optimized compact test range
[MBB-0053/88-PUB] 19 p2651 N90-25085
CASSEGRAIN OPTICS
An approach to optical structures control
05 p0595 N90-13456
A comparison of reflector antenna designs for wide-angle scanning 12 p1610 N90-19264
Dual-shaped offset reflector antenna designs from solutions of the geometrical optics first-order partial differential equations 15 p2076 N90-21887
Telescope considered as a very high gain antenna
[ETN-90-96614] 17 p2473 N90-24138
Advanced multilayer x ray optics
[DE90-008228] 18 p2616 N90-24902
DSS 15, 45, and 65 34-meter high efficiency antenna radio frequency performance enhancement by tilt added to the subreflector during elevation angle changes
20 p2854 N90-26229
CASSINI MISSION
Reports of workshops on Probe Measurements of Particles and Radiation in the Atmosphere of Titan
[NASA-TM-102218] 19 p2797 N90-25919
Investigation of the Saturn dust environment from the analysis of energetic charged particle measurements
[NASA-CR-186727] 20 p2950 N90-26784
Upcoming planetary missions and the applicability of high temperature superconductor bolometers
22 p3140 N90-27811
CAST ALLOYS
Influence of grain refining on the casting, physical, mechanical, and electrochemical properties of technical aluminum
[ETN-89-94661] 02 p0199 N90-11135
A study of the hot workability of Al-8.5 wt pct Mg alloys for armor plate applications
[AD-A211680] 03 p0329 N90-11868
Constitutive modeling for isotropic materials (HOST)
[NASA-CR-179522] 05 p0582 N90-13390
Constitutive modeling for isotropic materials (HOST)
[NASA-CR-174718] 05 p0582 N90-13391
Magnesium alloy technology for aerospace applications 07 p0901 N90-15209
Cast stainless steel aging: Mechanisms and predictions
[DE90-003772] 07 p0907 N90-15241
Identification of a cast iron alloy containing nonstrategic elements
[NASA-CR-185174] 11 p1487 N90-18559
Ageing effects in welded cast CF3 stainless steel
[AERE-R-13559] 13 p1775 N90-20188
Micromechanisms of fatigue crack growth and fracture toughness in metal matrix composites
[AD-A223863] 23 p3302 N90-28676
CASTING
NT SLIP CASTING
Thin section casting program. Volume 1: Executive summary and overview
[DE89-009030] 02 p0209 N90-11198
Thin section casting program. Volume 2: Horizontal TSC (Thin-Section Casting) approach
[DE89-009031] 02 p0210 N90-11199
Thin section casting program. Volume 2-A: Appendix to volume 2
[DE89-009032] 02 p0210 N90-11200
Thin section casting program. Volume 3: Vertical TSC (Thin-Section Casting) approach
[DE89-009033] 02 p0210 N90-11201
Thin section casting program. Volume 4: Static cast product bending, straightening, and rolling
[DE89-009034] 02 p0210 N90-11202
Thin section casting program. Volume 5: Westinghouse MHD Project
[DE89-009035] 02 p0210 N90-11203
The manufacture of superplastic alloys
06 p0745 N90-14333
Magnesium alloy technology for aerospace applications 07 p0901 N90-15209
Fabrication of superconductor coils
[DE90-003571] 07 p0922 N90-15338
High temperature aluminum-base alloy
[AD-D014270] 08 p1043 N90-16028
A cure process model for resin transfer molding of advanced composites
[NASA-CR-186247] 09 p1185 N90-16867
High density tape casting system
[NASA-CASE-NPO-16901-1-CU]
12 p1640 N90-19425
Dispersion reinforced materials
13 p1785 N90-20244
Spray deposition: A fundamental study of droplet impingement, spreading and consolidation
[AD-A217202] 13 p1787 N90-20255
Strengthening mechanisms of tungsten powder reinforced uranium
[DE90-009331] 14 p1947 N90-21144
Pressure rig for repetitive casting
[NASA-CASE-LAR-14050-1] 14 p1959 N90-21216
A casting and imaging technique for determining void geometry and relative permeability behavior of a single fracture specimen
[DE90-009192] 14 p1989 N90-21403
The effect of thermal damage on the mechanical properties of polymer regrinds 18 p2515 N90-24363
The effect of trace amounts of antimony on the structure and properties of aluminum alloy A356.2
[DE90-010461] 19 p2674 N90-25207
The role of gravity on macrosegregation in alloys
[NASA-CR-186530] 19 p2679 N90-25238
Effect of casting procedures and diesel engine environment on the behavior of aluminum titanate
[AD-A223079] 20 p2835 N90-26126
A tough performance simultaneous semi-interpenetrating polymer network
[NASA-CASE-LAR-14339-1] 21 p2984 N90-26955
Characterization of the CP 214 T851. Dissection of a cast flat bar for a standard spar
[CEAT-PV-M4/462200] 22 p3158 N90-27905
Characterization of the 7175 T7352. Dissection of a die casting standard spar
[CEAT-PV-M5/528900] 22 p3158 N90-27906
Characterization of the 7175 T7352 101. Dissection of a die casting standard spar
[CEAT-PV-M5/5288] 22 p3158 N90-27907
Characterization of the 7010 T73651. Dissection of a sheet billet for a standard spar
[CEAT-PV-M5/521700] 22 p3158 N90-27908
High temperature oxidation of Al-Li alloys
23 p3307 N90-28705
CASTING SOLVENTS
U PLASTICIZERS
CASTINGS
NT INGOTS
Castings Airworthiness
[AGARD-R-762] 01 p0042 N90-10231
US Air Force certification of castings
01 p0042 N90-10232
Casting factors imposed by the French regulation for foundry castings used in military aircraft
01 p0042 N90-10233
Casting airworthiness joint European civil authorities view-point 01 p0042 N90-10234
Royal Aerospace Establishment: No place for a castings factor 01 p0042 N90-10235
Castings, from theory to practical application
01 p0042 N90-10236
Evaluation of titanium castings for aerospace components 01 p0043 N90-10237
The question of the casting factor
01 p0043 N90-10238
Quality control of castings 01 p0043 N90-10239

Combined advanced foundry and quality control techniques to enhance reliability of castings for the aerospace industry 01 p0043 N90-10240
The creation of quality: New directions in the production of aeronautics castings 01 p0043 N90-10241
Thin walled cast high-strength structural parts 01 p0043 N90-10242
Advances in the technology of titanium castings 01 p0043 N90-10243
Microstructure morphology and quality of Al-Si castings 01 p0043 N90-10244
The improved corrosion resistance of ultra high purity magnesium alloy castings 01 p0044 N90-10245
Influence of grain refining on the casting, physical, mechanical, and electrochemical properties of technical aluminum
[ETN-89-94661] 02 p0199 N90-11135
A theory of damage in brittle and cementitious materials, part 1
[AD-A212940] 05 p0627 N90-13658
Defects in monoblock cast turbine wheels 11 p1458 N90-18400
A casting and imaging technique for determining void geometry and relative permeability behavior of a single fracture specimen
[DE90-009192] 14 p1989 N90-21403

CASTOR OIL
UV-curable polyurethane-methacrylate co-networks and interpenetrating networks
[AD-A210445] 01 p0050 N90-10285

CASUALTIES
Prediction of thermal stress casualties
[AD-A212356] 04 p0523 N90-13022
Can the square law be validated
[DE90-007112] 11 p1553 N90-18945
Field assessment of wet bulb globe temperature: Present and future
[AD-A218224] 13 p1853 N90-20635

CAT SCANNER
U COMPUTER AIDED TOMOGRAPHY

CATABOLISM
A program for the study of skeletal muscle catabolism following physical trauma
[AD-A216569] 11 p1539 N90-18859

CATACLYSMIC VARIABLES
Theoretical statistics of zero-age cataclysmic variables 01 p0141 N90-10810
Galactic x ray astronomy with EXOSAT 08 p1139 N90-16597
Accretion shock geometries in the magnetic variables
[NASA-CR-186290] 08 p1150 N90-16664
The inter-outburst behavior of cataclysmic variables
[NASA-CR-186374] 13 p1902 N90-20914
Globular cluster X ray binaries 19 p2768 N90-25729
Is KO Vel (E1013-477) an intermediate polar 19 p2773 N90-25766
Long period variations in high mass X ray binaries and their possible relationship with SU UMa stars 19 p2777 N90-25796
Radiative shock oscillations in AM Her cataclysmic binaries 19 p2783 N90-25834
Detection of emission lines from the secondary star in IX Vel (=CPD-48 deg 1577)
[MPE-PREPRINT-172] 22 p3265 N90-28485
X ray spectra of cataclysmic variables
[NASA-CR-187002] 23 p3412 N90-29280

CATALASE
Biological applications and effects of optical masers
[AD-A217910] 13 p1808 N90-20385

CATALOGS
Publications of the National Institute of Standards and Technology, 1988 catalog
[PB89-218382] 04 p0563 N90-13279
The Weapons Laboratory technical library: Automating with STILAS 15 p2178 N90-22447
Activities report of the Institute of Astronomical Calculations
[ETN-90-96461] 17 p2481 N90-24189

CATALOGS (PUBLICATIONS)
NT ASTRONOMICAL CATALOGS
Software methodology catalog, second edition, revision
[AD-A210548] 01 p0106 N90-10801
NASA scientific and technical publications: A catalog of special publications, reference publications, conference publications, and technical papers, 1988
[NASA-SP-7063(03)] 01 p0136 N90-10782
Criss-cross directory of NASA N numbers and DOD AD numbers. Volume 2, part 1: AD to N, 1979-1986. N to AD, 1962-1986
[NASA-TM-101814] 03 p0416 N90-12388
Criss-cross directory of NASA N numbers and DOD AD numbers. Volume 2, part 2: AD to N, 1979-1986. N to AD, 1962-1986
[NASA-TM-101815] 03 p0416 N90-12389
Catalogue of ESA publications in 1987
[ESA-SP-1087] 08 p1137 N90-16590
A higher density VLBI catalog for navigating Magellan and Galileo 15 p2078 N90-21904
Photometric monitoring of early type emission line stars 15 p2184 N90-22478
Extended optical emission in 3CR radio galaxies 15 p2193 N90-22523
Activities report of the Institute for Astronomy and Astrophysics
[MITT-10] 18 p2636 N90-25020
A systematic approach to training: A training needs assessment 18 p2645 N90-25059
Mars landing site catalog
[NASA-RP-1238] 21 p3100 N90-27607
Guide to available mathematical software
[PB90-216508] 22 p3236 N90-28351
Data catalog series for space science and applications flight missions. Volume 5A: Descriptions of astronomy, astrophysics, and solar physics spacecraft and investigations. Volume 5B: Descriptions of data sets from astronomy, astrophysics, and solar physics spacecraft and investigations
[NASA-TM-101908] 24 p3437 N90-29413
Data catalog series for space science and applications flight flight missions. Volume 2B: Descriptions of data sets from geostationary and high-altitude scientific spacecraft and investigations
[NASA-TM-101909] 24 p3437 N90-29414
Data catalog series for space science and applications flight missions. Volume 1A: Descriptions of planetary and heliocentric spacecraft and investigations, second edition
[NASA-TM-101910] 24 p3438 N90-29415
Data catalog series for space science and applications flight missions. Volume 6: Master index volume
[NASA-TM-101913] 24 p3438 N90-29416
Catalog of strong motion stations in Eastern North America
[PB90-251984] 24 p3490 N90-29722
Data catalog series for space science and applications flight missions. Volume 4B: Descriptions of data sets from meteorological and terrestrial applications spacecraft and investigations
[NASA-TM-101880] 24 p3556 N90-30123
Data catalog series for space science and applications flight missions. Volume 3B: Descriptions of data sets from low- and medium-altitude scientific spacecraft and investigations
[NASA-TM-89680] 24 p3560 N90-30140
Data catalog series for space science and applications flight missions. Volume 1B: Descriptions of data sets from planetary and heliocentric spacecraft and investigations
[NASA-TM-89695] 24 p3561 N90-30148

CATALYSIS
Heterogeneous catalysts in water
[AD-A210742] 01 p0041 N90-10228
Emittance, catalysis, and dynamic oxidation of Ti-14Al-21Nb
[NASA-TP-2955] 01 p0044 N90-10248
Control of synthetic peptide tertiary structure
[AD-A210339] 01 p0049 N90-10281
Inherent bias in nonlinear least squares analysis of first-order kinetic data
[AD-A210677] 01 p0114 N90-10651
Enhanced oxidation and solovolysis reactions in chemically inert microheterogeneous systems
[AD-A210748] 02 p0195 N90-11110
Surface-catalyzed air oxidation reactions of hydrazines: Tubular reactor studies 02 p0204 N90-11167
Natural gas to liquids
[DE89-000982] 03 p0322 N90-11828
Electron density modulation of catalytic metal centers by substituted aryl-isocyanide ligands
[AD-A212875] 04 p0473 N90-12708
Mechanisms of CO2 reduction metal and metal modified semiconductor electrodes
[AD-A213169] 04 p0473 N90-12712
Computer simulation studies of the catalytic oxidation of carbon monoxide on platinum metals
[PB89-223739] 04 p0475 N90-12721
Synthesis and high temperature chemistry of methylsilsesquioxane polymers produced by titanium catalyzed redistribution of methylhydridooligo- and polysiloxanes
[AD-A212000] 04 p0477 N90-12736
Transition metal catalyzed synthesis of organmetallic polymers
[AD-A212133] 04 p0478 N90-12740
Cosmic strings and baryon decay catalysis
[NASA-CR-186074] 04 p0566 N90-13299
On catalytic recombination rates in hypersonic stagnation heat transfer 05 p0573 N90-13338
Electronic materials high-T(sub c) superconductivity polymers and composites structural materials surface science and catalysts industry participation
[NASA-CR-186063] 07 p0890 N90-15145
Interfacial systems for photochemical energy conversion
[DE90-003181] 07 p0953 N90-15514
Solid-state electrolyte catalysis for methane and oxygen synthesis
[PB90-100231] 08 p1040 N90-16011
New electronic materials and CO2 reduction
[AD-A214679] 09 p1191 N90-16899
Improved performance in co-processing through fundamental and mechanistic studies in hydrogen transfer and catalysis
[DE90-004794] 10 p1352 N90-17839
Chemistry at clusters, microstructures and surfaces
[AD-A215842] 10 p1353 N90-17844
A review of the mechanism and kinetics of electrochemical hydrogen entry and degradation of metallic systems
[AD-A216671] 10 p1355 N90-17857
Ligand-centered electron-transfer redox processes for manganese, iron, and cobalt complexes in relation to selected catalytic systems
[AD-A217957] 13 p1773 N90-20177
Model catalytic oxidation studies using supported monometallic and heterobimetallic oxides
[DE90-009984] 16 p2220 N90-22664
The effect of catalysts on gas-phase hydrocarbon ignition
[AD-A218775] 17 p2371 N90-23499
Morphology changes due to oxidative treatment of glassy carbon electrodes and its applications
[AD-A219425] 17 p2371 N90-23501
An evaluation of imbedded thermocouples as a solid-propellant combustion diagnostic
[AD-A219947] 17 p2406 N90-23711
CO-oxidation catalysts: Low-temperature CO oxidation over Noble-Metal Reducible Oxide (NMRO) catalysts 18 p2556 N90-24588
Review of model sensor studies on Pd/SnO2(110) surfaces 18 p2559 N90-24604
Calorimetry, activity, and micro-FTIR analysis of CO chemisorption, titration, and oxidation on supported Pt 18 p2560 N90-24606
Analysis of Pt/SnO(sub x) during catalysis of CO oxidation 18 p2560 N90-24607
Potential technology transfers of research on low-temperature carbon monoxide-oxygen recombination catalysts 18 p2562 N90-24616
ECUT: Energy Conversion and Utilization Technologies program. Biocatalysis project
[NASA-CR-186866] 19 p2717 N90-25458
Electrochemical, in situ Raman spectroscopic, and conductivity studies of polypyrrole incorporating large size anions: Conducting nature of reduced form
[AD-A222739] 20 p2831 N90-26102
The application of HREELS to model catalysts: CO and C2H4 adsorption on Pt/Al2O3
[AD-A222744] 20 p2831 N90-26103
The catalytic synthesis of inorganic polymers for high temperature applications and as ceramic precursors
[AD-A222620] 20 p2840 N90-26156
Modeling of carbon monoxide oxidation kinetics over NASA carbon dioxide laser catalysts
[NASA-CR-186356] 22 p3155 N90-27885
Catalytic synthesis of polymethylsilsesquioxanes
[AD-A222643] 22 p3159 N90-27910
A study of catalysts and mechanisms in synthesis reactions
[DE90-015064] 23 p3304 N90-28691

CATALYSTS
NT ELECTROCATALYSTS
Structural and surface characterization of dispersed metal catalysts
[DE89-014530] 01 p0038 N90-10208
Heterogeneous catalysts in water
[AD-A210742] 01 p0041 N90-10228
Photochemically-driven biomimetic oxidation of alkanes and olefins
[DE89-011536] 02 p0193 N90-11097
Homogeneous catalysts in hypersonic combustion
[DE89-015258] 02 p0193 N90-11098
Surface-catalyzed air oxidation of hydrazines: Environmental chamber studies 02 p0203 N90-11159
Trace metal catalysis of hydrazine decomposition: The role of chromium 02 p0204 N90-11163
N-Hexyl Carborane (NHC) as combustion catalyst in composite propellants
[FOA-C-20755-2.1] 02 p0209 N90-11193
In-situ spectroscopic studies of transition metal macrocycles as catalysts for the electrochemical reduction of oxygen
[PB89-219273] 03 p0321 N90-11826

Conversion of methane to liquid hydrocarbons
[DE89-017547] 03 p0322 N90-11831
Catalogic hydrogenation of carbon monoxide
[DE89-017813] 03 p0323 N90-11834
Correlations between surface structure and catalytic activity/selectivity
[DE90-003755] 07 p0896 N90-15181
New polymers made with well-characterized organometallic catalysts
[AD-A213592] 07 p0912 N90-15272
Survey on synthesis technologies of methanol as an alternative fuel
[DE89-901303] 07 p0914 N90-15284
Analysis of catalytically enhanced solar absorption chemical reactors: 1 - numerical model description
[DE89-014742] 07 p0951 N90-15505
Structure and reactivity of model thin film catalysts
[DE90-007365] 11 p1485 N90-18546
Sintering of a model nickel/alumina catalyst
[ETN-90-96270] 11 p1487 N90-18561
Morphological consequences of catalytic hydrogenation of polymers in the bulk
[DE90-007276] 11 p1494 N90-18598
Optimum catalytic process for alcohol fuels from syngas
[DE90-005290] 11 p1494 N90-18600
Production of high density aviation fuels via novel zeolite catalyst routes
[AD-A216444] 11 p1494 N90-18601
Optimum catalytic process for alcohol fuels from syngas
[DE30-007188] 11 p1495 N90-18604
Synthesis and properties of a novel catalyst for the combustion of methane
[PB90-127499] 12 p1622 N90-19320
Enhancement of processes for solar photocatalytic detoxification of water
[DE90-003949] 12 p1623 N90-19330
Isotope exchange in oxide-containing catalyst
[NASA-CASE-LAR-13542-2-SB] 13 p1769 N90-20154
Hydrous metal oxide-supported catalysts. Part 1: Preparation chemistry and physical and chemical properties
[DE90-007607] 13 p1771 N90-20161
Developments in solar photocatalysis for destruction of organics in water
[DE90-007685] 13 p1771 N90-20162
Analytical electron microscopy of catalyst preparations
[DE90-008699] 13 p1773 N90-20173
Process for making a noble metal on tin oxide catalyst
[NASA-CASE-LAR-13741-1-SB] 13 p1774 N90-20180
The chemical basis for the origin of the genetic code and the process of protein synthesis
[NASA-CR-186590] 15 p2136 N90-22205
Development of high-activity para- to ortho-hydrogen conversion catalysts, volume 2
[AD-A218700] 16 p2215 N90-22638
Model catalytic oxidation studies using supported monometallic and heterobimetallic oxides
[DE90-009984] 16 p2220 N90-22664
Dehydrogenative polymerization of silanes to polysilanes: A monomeric copper(2) siloxide
[AD-A218550] 16 p2223 N90-22681
The effect of catalysts on gas-phase hydrocarbon ignition
[AD-A218775] 17 p2371 N90-23499
Catalyst for carbon monoxide oxidation
[NASA-CASE-LAR-14155-1-SB] 17 p2374 N90-23517
Electronic and ionic transport in processable conducting polymers
[AD-A221045] 18 p2530 N90-24436
Low-Temperature CO-Oxidation Catalysts for Long-Life CO2 Lasers
[NASA-CP-3076] 18 p2556 N90-24586
CO-oxidation catalysts: Low-temperature CO oxidation over Noble-Metal Reducible Oxide (NMRO) catalysts 18 p2556 N90-24588
Pt/SnO2-based CO-oxidation catalysts for long-life closed-cycle CO2 lasers 18 p2556 N90-24589
The oxidation of carbon monoxide using tin oxide based catalysts 18 p2557 N90-24590
LaRC-developed catalysts for CO2 lasers 18 p2557 N90-24591
Phillips CO-oxidation catalyts for long-lived CO2 lasers: Activity and initial characterization studies 18 p2557 N90-24592
Synthesis, characterization and evaluation of CO-oxidation catalysts for high repetition rate CO2 TEA lasers 18 p2557 N90-24593
Alternative catalysts for low-temperature CO-oxidation 18 p2557 N90-24594
A computer program for the design of optimum catalytic monoliths for CO2 lasers 18 p2558 N90-24595
Mechanistic studies of the CO-oxidation reaction on catalysts for use in long-life CO2 lasers 18 p2558 N90-24596
The effect of H2O and pretreatment on the activity of a Pt/SnO2 catalyst 18 p2558 N90-24597
Rare-isotope and kinetic studies of Pt/SnO2 catalysts 18 p2558 N90-24598
Effect of pretreatment on a platinized tin oxide catalyst used for low-temperature CO-oxidation 18 p2558 N90-24599
Platinized tin oxide catalysts for CO2 lasers: Effects of pretreatment 18 p2559 N90-24600
Calorimetry, activity, and micro-FTIR analysis of CO chemisorption, titration, and oxidation on supported Pt 18 p2560 N90-24606
Characterization of the surfaces of platinum/tin oxide based catalysts by Fourier Transform Infrared Spectroscopy (FTIR) 18 p2560 N90-24608
Chemisorption studies of Pt/SnO2 catalysts 18 p2560 N90-24609
Dissociation phenomena in electron-beam sustained carbon dioxide lasers 18 p2560 N90-24610
The e-beam sustained CO2 laser amplifier 18 p2561 N90-24611
A compact, rugged, high repetition rate CO2 laser incorporating catalyst 18 p2561 N90-24612
Performance of alumina-supported Pt catalysts in an electron-beam-sustained CO2 laser amplifier 18 p2561 N90-24613
Monitoring of catalyst performance in CO2 lasers using frequency modulation spectroscopy with diode lasers 18 p2561 N90-24614
Applications of low temperature CO-oxidation catalysts to breathable gases 18 p2561 N90-24615
Potential technology transfers of research on low-temperature carbon monoxide-oxygen recombination catalysts 18 p2562 N90-24616
A direct absorber reactor/receiver for solar thermal applications
[DE90-006280] 18 p2577 N90-24679
Characterization of the surfaces of platinum/tin oxide based catalysts by Fourier transform spectroscopy (FTIR) 18 p2643 N90-25054
The effects of pretreatment conditions on a Pt/SnO2 catalyst for the oxidation of CO in CO2 lasers
[NASA-TM-103487] 20 p2867 N90-26309
Destruction of peroxy radical by Cu ion catalysed reactions on atmospheric particles 20 p2887 N90-26429
Computer simulation of chemical reactions in synthetic model compounds and genetically engineered active sites
[AD-A222611] 20 p2898 N90-26483
Experimental and kinetic modeling of acid/base redox reactions over metal oxide catalysts
[DE90-013835] 22 p3156 N90-27893
Catalytic ignition of hydrogen/oxygen 23 p3293 N90-28627
A study of catalysts and mechanisms in synthesis reactions
[DE90-015064] 23 p3304 N90-28691
Composite propellants with high burning rates
[FOA-C-20781-2.1] 23 p3315 N90-28744

CATALYTIC ACTIVITY
Full scale catalytic combustion of methane under atmospheric pressure
[DE89-772354] 10 p1351 N90-17835
Hydrous metal oxide-supported catalysts. Part 2: Catalytic properties and applications
[DE90-008098] 12 p1625 N90-19336
Non-noble electrocatalysts for alkaline fuel cells 13 p1824 N90-20470
Mechanistic model for catalytic recombination during aerobraking maneuvers
[NASA-CR-185611] 14 p1932 N90-21059
Model catalytic oxidation studies using supported monometallic and heterobimetallic oxides
[DE90-009984] 16 p2220 N90-22664
Low-Temperature CO-Oxidation Catalysts for Long-Life CO2 Lasers
[NASA-CP-3076] 18 p2556 N90-24586
Alternative catalysts for low-temperature CO-oxidation 18 p2557 N90-24594
Mechanistic studies of the CO-oxidation reaction on catalysts for use in long-life CO2 lasers 18 p2558 N90-24596
Effect of pretreatment on a platinized tin oxide catalyst used for low-temperature CO-oxidation 18 p2558 N90-24599
Platinized tin oxide catalysts for CO2 lasers: Effects of pretreatment 18 p2559 N90-24600
Analysis of Pt/SnO(sub x) during catalysis of CO oxidation 18 p2560 N90-24607
Destruction of peroxy radical by Cu ion catalysed reactions on atmospheric particles 20 p2887 N90-26429
Modeling of carbon monoxide oxidation kinetics over NASA carbon dioxide laser catalysts
[NASA-CR-186356] 22 p3155 N90-27885

CATCHMENT AREAS
U WATERSHEDS

CATECHOLAMINE
NT EPINEPHRINE
The effects of high intensity cycle exercise on sympatho-adrenal-medullary response patterns
[AD-A217962] 13 p1852 N90-20628
The effects of graded exercise at sea level on plasma proenkephalin peptide F and catecholamine responses
[AD-A218195] 13 p1853 N90-20633

CATEGORIES
The fine-structure of categorial semantics
[ITLI-LP-89-01] 17 p2464 N90-24075

CATHODE GLOW
An analysis of the anomalous high-current cathode emission in pseudospark and back-of-the-cathode lighted thyratron switches
[AD-A215328] 10 p1378 N90-17988
Electron beam generation by electron bombardment induced cathode emission
[AD-A218203] 13 p1798 N90-20318

CATHODE RAY TUBES
Effects of miniature CRT (Cathode Ray Tube) location upon primary and secondary task performances
[AD-A210223] 01 p0101 N90-10573
Effect of extraneous color-coded targets on identification of targets on CRT displays
[AD-A219473] 17 p2436 N90-23879
The interaction of chromostereopsis and stereopsis in stereoscopic CRT (Cathode Ray Tubes) displays
[AD-A217906] 23 p3277 N90-28544
Computer simulation of micro-triode performance
[DE90-014191] 23 p3320 N90-28774

CATHODES
NT CELL CATHODES
NT HOLLOW CATHODES
NT PHOTOCATHODES
NT THERMIONIC CATHODES
NT TUBE CATHODES
Rechargeable lithium/polymer cathode batteries
[AD-A210978] 01 p0062 N90-10354
Plasma gun with coaxial powder feed and adjustable cathode
[NASA-CASE-LEW-14901-1] 01 p0126 N90-10718
New secondary batteries utilizing electronically conductive polymer cathodes
[NASA-CR-185885] 02 p0215 N90-11227
Gas evolution and bubble formation on electrodes
[DLR-FB-89-35] 05 p0622 N90-13629
Silver-nickel composite cathodes for alkaline secondary batteries
[AD-D014231] 06 p0767 N90-14464
Gigatron: A new technology for microwave power devices
[DE90-001066] 06 p0771 N90-14483
Calorimetric measurements on electrochemical cells with Pd-D cathodes
[DE90-002198] 06 p0805 N90-14685
Characterization of new cathode materials for molten carbonate fuel cells
[DE90-003547] 07 p0953 N90-15516
Organic cathode for a secondary battery
[NASA-CASE-NPO-17604-1-CU] 08 p1059 N90-16124
Copper chloride cathode for a secondary battery
[NASA-CASE-NPO-17640-1-CU] 09 p1210 N90-17011
Performance of superconductive oxides as cathodes for lithium rechargeable batteries
[AD-A216030] 10 p1401 N90-18098
Arcjet cathode phenomena 11 p1473 N90-18477
Dual cathode system for electron beam instruments
[NASA-CASE-NPO-16878-1-CU] 13 p1803 N90-20351
Advanced rechargeable sodium batteries with novel cathodes 13 p1822 N90-20459
Corrosion testing of candidates for the alkaline fuel cell cathode 13 p1824 N90-20471
Impedance studies of Ni/Cd and Ni/H2 cells using the cell case as a reference electrode 13 p1824 N90-20473
Method of making a long life high current density cathode from tungsten and iridium powders using a quarternary compound as the impregnant
[AD-D014425] 14 p1958 N90-21211
An attempt to measure cold-fusion effects
[DE90-613248] 14 p2031 N90-21649
Advanced electric propulsion research, 1989
[NASA-CR-185237] 15 p2062 N90-21810
Method of making a cathode from tungsten powder
[AD-D014434] 15 p2069 N90-21850
Hollow cathode operation at high discharge currents
[NASA-CR-185238] 15 p2088 N90-21953

MHD channel development, part 1
[DE90-009549] 15 p2169 N90-22394
Corrosion control through a better understanding of the metallic substrate/organic coating interface
[AD-A220432] 17 p2377 N90-23533
The effect of carbon type and processing on high rate thionyl chloride cathode collectors
[AD-A219823] 18 p2546 N90-24532
Metal chloride cathode for a battery
[NASA-CASE-NPO-17809-1-CU] 21 p2998 N90-27041
A high temperature molten salt thermal electrochemical cell
[AD-D014469] 22 p3195 N90-28131
Unipolar arcing on the cathode surface of a high voltage diode
[AD-A224122] 23 p3322 N90-28787

CATHODIC COATINGS
Diamondlike carbon coatings for optical systems
[AD-A211255] 02 p0276 N90-11573
Chemistry-structure-property interrelationships for calcareous deposits as stand-alone coatings
[AD-A216031] 10 p1359 N90-17881
Advances in ambient temperature secondary lithium cells 13 p1825 N90-20481

CATHODOLUMINESCENCE
International workshop on Beam Injection Assessment of Defects in Semiconductors
[AD-A210842] 02 p0283 N90-11617
Photoelectron pumped phosphors
[AD-A213202] 04 p0505 N90-12912
An electron-beam controlled semiconductor switch
[AD-A217181] 13 p1793 N90-20286

CATIONS
Solvent effects on intervalence electron-transfer energies for biferrocene cations: Comparisons with molecular models of solvent reorganization
[AD-A210263] 01 p0120 N90-10691
Quantum chemical investigations of the mechanism of cationic polymerization and theoretical prediction of crystal densities and decomposition pathways of energetic molecules
[AD-A210322] 02 p0200 N90-11143
X ray diffraction patterns of metal aurocyanides
[DE89-015188] 03 p0326 N90-11851
Quartz crystal microbalance analysis. 1: Evidence of anion or cation insertion into electropolymerized conducting polymers
[AD-A212304] 04 p0480 N90-12755
Cation disordering in the Tl-2122 superconductors
[DE90-003579] 07 p1001 N90-15795
Superconductivity and stoichiometry in Tl2Ca2Ba2Cu3O(x) single crystals
[DE90-003838] 07 p1002 N90-15801
DURIP theoretical/experimental investigations of highly energetic dication species
[AD-A217771] 13 p1808 N90-20383
Laser temperature-jump kinetic studies of fast reactions in nonaqueous solutions
[AD-A218819] 17 p2371 N90-23500
Evaluation of ion intercalation in conducting polymers
[AD-A219423] 17 p2379 N90-23549
Observation of a magic number in the ion distribution of ethene clusters
[AD-A219837] 18 p2521 N90-24393
Quartz crystal microbalance analysis: Partial cation release during oxidation of conducting polymers
[AD-A221091] 18 p2530 N90-24439
Cation and anion tracer diffusion in YBa(sub 2)Cu(sub 3)O(sub 7-delta)
[DE90-009708] 18 p2620 N90-24927
Passive mechanisms of surfaces produced by ion beam mixing and ion implantation
[AD-A222432] 21 p2982 N90-26945
Cell performance of ultra-thin polymer cathode cell systems. Part 2: Cation intercalating composite polymer cathode
[AD-A221919] 21 p3020 N90-27172
Synthesis of Y1Ba2Cu3O(sub x) superconducting powders by intermediate phase reaction 22 p3149 N90-27855

CAUCHY PROBLEM
The nonconvex multi-dimensional Riemann problem for Hamilton-Jacobi equations
[NASA-CR-181887] 03 p0384 N90-12182
Parameter identification for an abstract Cauchy problem by quasilinearization
[NASA-CR-181933] 03 p0385 N90-12192
Green's functions for the elastic annulus and their application to various crack problems 15 p2120 N90-22129
Analysis of nonlinear internal waves observed by LANDSAT-TM
[PREPRINT-704] 16 p2249 N90-22828
Boundary conditions for nonlinear hyperbolic systems of conservation laws
[REPT-892-422-101] 17 p2404 N90-23694
Hyperbolic conservation laws and numerical methods 22 p3172 N90-27990
Computational Fluid Dynamics, Volume 2
[VKI-LS-1990-03-VOL-2] 22 p3172 N90-27993
Towards a two dimensional scheme of anisotropic Godunov type. On the calculation of the velocity of the nodes in the multidimensional Lagrangian codes
[ETN-90-97458] 22 p3175 N90-28017
Towards a two dimensional code of anisotropic Godunov type 22 p3175 N90-28018

CAUSES
Review of serious aircraft accidents in the Belgian Air Force: Causes and comparison with selection data 09 p1254 N90-17277

CAUSTICS
U ALKALIES

CAVITATION
U CAVITATION FLOW

CAVITATION FLOW
An investigation of end-wall vortex cavitation in a high Reynolds number axial-flow pump
[AD-A211426] 03 p0347 N90-11982
Elasticity effects on cavitation in a squeeze film damper undergoing noncentered circular whirl
[NASA-TM-102392] 05 p0649 N90-13786
Cavitation and superplasticity 06 p0744 N90-14329
Cavitation-controlled ultrasonic agitator
[DE90-002773] 06 p0838 N90-14871
Study on the thermodynamical and mechanical conditions for the generation of high operating pressures with liquefied gases for low and very low flow rates
[ESA-TT-1148] 11 p1510 N90-18696
Experimental investigation of the effect of cavitation on the rotordynamic forces on a whirling centrifugal pump impeller 15 p2105 N90-22039
Microstructural dependence of the cavitation damage function in FCC materials
[DE90-012898] 20 p2833 N90-26113
A high-speed photography study of cavitation in a dynamically loaded journal bearing
[NASA-TM-103178] 20 p2872 N90-26338
Noise from tip vortex and bubble cavitation
[AD-A221962] 21 p3072 N90-27468
Three-dimensional cavity flow fields at subsonic and transonic speeds
[NASA-TM-4209] 22 p3107 N90-27650
Current research in cavitating fluid films
[NASA-TM-103184] 23 p3323 N90-28791

CAVITIES
Numerical calculations of the collapse of a cavity in the vicinity of a compliant wall
[AD-A210489] 01 p0070 N90-10403
Worked-in holes in three-dimensional reinforced composites 02 p0186 N90-11060
Periodic permanent magnet structures
[AD-D014173] 03 p0398 N90-12280
Dynamics of an M-level atom interacting with cavity fields: Properties of photon statistics
[AD-A211321] 04 p0552 N90-13213
High-frequency asymptotic methods for analyzing the EM scattering by open-ended waveguide cavities
[NASA-CR-186244] 08 p1056 N90-16103
A finite element-boundary integral formulation for scattering by three-dimensional cavity-backed apertures
[NASA-CR-186332] 09 p1187 N90-16878
Squeezing of many-atom radiation in an optical cavity
[AD-A215736] 09 p1280 N90-17422
Experimental investigation to suppress flow-induced pressure oscillations in open cavities
[AD-A216285] 10 p1310 N90-17578
Fluctuating wind forces measured on a bluff body extending from a cavity
[AD-A216414] 10 p1386 N90-18020
Fast optical switch and limiter using quantum size effect in metal grain composites
[AD-D014332] 12 p1619 N90-19305
Elastomeric electrical isolation membrane
[AD-D014365] 12 p1651 N90-19490
Analysis of unsteady heat transfer by natural convection in a two-dimensional square cavity using a high order finite-volume method 12 p1657 N90-19521
Passive venting technique for shallow cavities
[NASA-CASE-LAR-14031-1] 13 p1755 N90-20079
Pressure rig for repetitive casting
[NASA-CASE-LAR-14050-1] 14 p1959 N90-21216
Thermal radiation characteristics of nonisothermal cylindrical enclosures using a numerical ray tracing technique
[NASA-TM-102527] 14 p1972 N90-21296
Current management for improved railgun performance 15 p2057 N90-21781
An unsteady time asymptotic flow in the square driven cavity
[NASA-TM-103141] 15 p2099 N90-22016
Origin of pulsed emission from the young supernova remnant SN 1987A
[CAL-377] 15 p2182 N90-22469
Circumferential pressure probe
[NASA-CASE-LAR-13775-1] 17 p2406 N90-23706
Problems of internal acoustics in two and three dimensional cavities with deformable walls using the MSC/Nastran code
[DLC/STR-INT-TN-004] 18 p2612 N90-24876
High repetition rate kickers for linear colliders
[CEBAF-PR-89-020] 19 p2756 N90-25661
Velocity selection to enable direct measurement of strong single atom-optical cavity coupling
[AD-A223060] 21 p3071 N90-27460
Cavity aeroacoustics
[AD-A223853] 24 p3418 N90-29307
An investigation of hole-edge crack problem by a combined complex variable and least square method
[LR-626] 24 p3482 N90-29679

CAVITONS
Dynamics of cavitons in strong Langmuir turbulence
[DE90-008918] 14 p2029 N90-21633

CAVITY RESONATORS
Efficient nonlinear conversion of laser diode pumped miniature solid state laser sources
[AD-A210708] 01 p0075 N90-10433
Coupled multiline CW HF lasers: Experimental performance
[AD-A210844] 01 p0075 N90-10434
Use of depletion edge translation for high-speed modulation and switching of lightwaves
[AD-A211186] 01 p0124 N90-10713
Measurement of pressure fluctuations in a resonant chamber with laser-induced iodine fluorescence
[ESA-TT-1123] 03 p0406 N90-12326
Cold tests of quasi-optical gyrotron resonators
[AD-A212707] 04 p0498 N90-12868
Cavity eigenmodes for the NIST/NRL (National Institute of Standards and Technology/Naval Research Laboratory) free electron laser
[AD-A212706] 04 p0507 N90-12923
Hydrogen radical enhanced growth of solar cells
[DE89-009497] 06 p0806 N90-14694
RF superconductivity research and development at Los Alamos National Laboratory
[DE90-002440] 06 p0855 N90-14969
Review of quasi-optical gyrotron development
[AD-A213491] 07 p0933 N90-15402
A simple method using MAFIA to calculate external Q values of waveguide-loaded cavities
[DE90-741487] 12 p1647 N90-19465
Field theoretical analysis and synthesis of broadband waveguide: Height, plane shunt circulators with multiple layer material insertions
[ETN-90-95360] 12 p1647 N90-19469
Narrow-bandwidth unstable laser resonator
[AD-D014362] 12 p1665 N90-19568
High-temperature ceramic superconductors
[AD-A218347] 13 p1783 N90-20233
Development and applications of a coupled cavity sodium-chloride laser 15 p2102 N90-22029
RF properties of high temperature superconductors: Cavity methods
[DE90-011961] 18 p2627 N90-24969
Resonant coupling through a slot to a loaded cylindrical cavity: Experimental results
[AD-A223000] 20 p2922 N90-26631
Approximation, synthesis, and development of bi-mode cavities microwave filters presenting unsymmetrical quasi-elliptic responses
[CNES-NT-124] 23 p3318 N90-28781

CCD
U CHARGE COUPLED DEVICES

CCD STAR TRACKER
Evaluation test of CCD area sensor for star sensor
[NAL-TM-570] 02 p0274 N90-11566
The MPI/AIT X ray Imager (MAXI): High speed PN-CCD's for x ray detection
[MPE-PREPRINT-154] 08 p1077 N90-16234

CD-ROM
U OPTICAL DISKS
U READ-ONLY MEMORY DEVICES

CDC COMPUTERS
NT CDC CYBER 205 COMPUTER

CDC CYBER 205 COMPUTER
Checking the Goldbach conjecture on a vector computer
[CWI-NM-R8812] 02 p0260 N90-11475
Solving 3D block bidiagonal linear systems on vector computers
[CWI-NM-R8819] 04 p0530 N90-13061

CDMA
U CODE DIVISION MULTIPLE ACCESS

CEILINGS (METEOROLOGY)
Calibration of a visioceilometer, a hand held lidar system
[FEL-1988-73] 03 p0374 N90-12137
A closer look at the visioceilometer
[FEL-1989-80] 03 p0374 N90-12138
CEILOMETERS
U CLOUD HEIGHT INDICATORS
CELESTIAL BODIES
NT A STARS
NT ACHONDRITES
NT ACTIVE GALAXIES
NT ALLENDE METEORITE
NT ANDROMEDA GALAXY
NT ASTEROID BELTS
NT ASTEROIDS
NT ASYMPTOTIC GIANT BRANCH STARS
NT B STARS
NT BARRED GALAXIES
NT BINARY STARS
NT BL LACERTAE OBJECTS
NT BLACK HOLES (ASTRONOMY)
NT BLAZARS
NT BLUE STARS
NT BROWN DWARF STARS
NT CARBON STARS
NT CARBONACEOUS CHONDRITES
NT CARBONACEOUS METEORITES
NT CATACLYSMIC VARIABLES
NT CEPHEID VARIABLES
NT CHARON
NT CHONDRITES
NT COMET HEADS
NT COMET NUCLEI
NT COMET TAILS
NT COMETS
NT COOL STARS
NT CRAB NEBULA
NT DEIMOS
NT DISK GALAXIES
NT DOUBLE STARS
NT DWARF GALAXIES
NT DWARF NOVAE
NT DWARF STARS
NT EARLY STARS
NT EARTH (PLANET)
NT ECLIPSING BINARY STARS
NT ELLIPTICAL GALAXIES
NT EXTRAGALACTIC RADIO SOURCES
NT F STARS
NT FAINT OBJECTS
NT FLARE STARS
NT G STARS
NT GALACTIC CLUSTERS
NT GALAXIES
NT GAS GIANT PLANETS
NT GIACOBINI-ZINNER COMET
NT GIANT STARS
NT GLOBULAR CLUSTERS
NT H I REGIONS
NT H II REGIONS
NT HALLEY'S COMET
NT HERBIG-HARO OBJECTS
NT HERCULES NOVA
NT HORIZONTAL BRANCH STARS
NT HOT STARS
NT IAPETUS
NT INFRARED SOURCES (ASTRONOMY)
NT INFRARED STARS
NT INTERACTING GALAXIES
NT IO
NT IRAS-ARAKI-ALCOCK COMET
NT IRON METEORITES
NT IRREGULAR GALAXIES
NT JUPITER (PLANET)
NT JUPITER SATELLITES
NT K STARS
NT LATE STARS
NT M STARS
NT MAGELLANIC CLOUDS
NT MAGNETIC STARS
NT MAIN SEQUENCE STARS
NT MARS (PLANET)
NT MERCURY (PLANET)
NT METALLIC STARS
NT METEORITES
NT METEOROID SHOWERS
NT METEOROIDS
NT MICROMETEORITES
NT MICROMETEOROIDS
NT MILKY WAY GALAXY
NT MIRA VARIABLES
NT MOON
NT MURCHISON METEORITE
NT NATURAL SATELLITES
NT NEBULAE
NT NEPTUNE (PLANET)
NT NEUTRON STARS
NT NOVAE
NT O STARS
NT OPEN CLUSTERS
NT ORION NEBULA
NT PECULIAR GALAXIES
NT PHOBOS
NT PHOEBE
NT PLANETARY NEBULAE
NT PLANETARY RINGS
NT PLANETS
NT PLEIADES CLUSTER
NT PLUTO (PLANET)
NT PRE-MAIN SEQUENCE STARS
NT PROTOPLANETS
NT PROTOSTARS
NT PULSARS
NT QUASARS
NT RADIO GALAXIES
NT RADIO JETS (ASTRONOMY)
NT RADIO SOURCES (ASTRONOMY)
NT RADIO STARS
NT RED GIANT STARS
NT REFERENCE STARS
NT REFLECTION NEBULAE
NT RHEA (ASTRONOMY)
NT SATURN (PLANET)
NT SATURN RINGS
NT SATURN SATELLITES
NT SEYFERT GALAXIES
NT SOLAR SYSTEM
NT SPIRAL GALAXIES
NT STAR CLUSTERS
NT STARBURST GALAXIES
NT STARS
NT STELLAR SYSTEMS
NT SUBDWARF STARS
NT SUN
NT SUPERGIANT STARS
NT SUPERNOVA 1987A
NT SUPERNOVAE
NT SYMBIOTIC STARS
NT T TAURI STARS
NT TERRESTRIAL PLANETS
NT TITAN
NT TITANIA
NT TRIPLE STARS
NT TRITON
NT URANUS (PLANET)
NT VARIABLE STARS
NT VENUS (PLANET)
NT VIRGO GALACTIC CLUSTER
NT WHITE DWARF STARS
NT WOLF-RAYET STARS
NT X RAY BINARIES
NT X RAY STARS
NT ZODIACAL DUST
CELESTIAL MECHANICS
On mean elements for satellite orbits perturbed by the zonal harmonics of the geopotential
[AD-A212322] 04 p0461 N90-12642
The hyperbolic Kepler's equation, and the elliptic equation revisited
[RAE-TM-SPACE-369] 09 p1274 N90-17388
On universal elements, and conversion procedures to and from position and velocity
[RAE-TM-SPACE-370] 09 p1277 N90-17406
Orbital mechanics: A learning tool on the main frame
[AD-A218799] 16 p2204 N90-22576
Satellite motion in axi-symmetric gravitational field. Part 2: Perturbations due to an arbitrary J(sub l)
[RAE-TR-89022] 16 p2206 N90-22586
Trajectory optimization of a bimodal nuclear powered spacecraft to Mars
[AD-A222974] 21 p2969 N90-26876
Observation model and parameter partials for the JPL geodetic (GPS) modeling software 'GPSOMC'
[NASA-CR-186972] 22 p3132 N90-27774
CELESTIAL NAVIGATION
Study of modern instrumentation and methods for astronomic positioning in the field
[AD-A213217] 05 p0710 N90-14157
CELESTIAL OBSERVATION
U ASTRONOMY
CELESTIAL SPHERE
Mark 3 interferometer
[AD-A217188] 13 p1902 N90-20912
CELL ANODES
Improved anode catalysts for coal gas-fueled phosphoric acid fuel cells
[DE90-004016] 08 p1096 N90-16347
A simple demonstration of corrosion cells
18 p2514 N90-24355
Evaluation of room-temperature chloroaluminate molten salts as electrolytes for high energy density batteries
[AD-A223097] 20 p2860 N90-26267
Field emitter array integrated distributed amplifiers
[AD-D014493] 22 p3166 N90-27958
CELL CATHODES
Cell performance of ultra-thin polymer cathode system: Theoretical energy and power density projections
[AD-A210786] 02 p0202 N90-11151
Electrochemical preparation of silver oxide electrodes having high thermal stability
[AD-D014224] 06 p0767 N90-14460
Silver composite cathodes for alkaline secondary batteries
[AD-D014227] 06 p0767 N90-14462
Cell performance of ultra-thin polymer cathode systems. Part 1: Anion intercalating polymer cathode
[AD-A216037] 11 p1501 N90-18639
Corrosion testing of candidates for the alkaline fuel cell cathode 13 p1824 N90-20471
Advances in ambient temperature secondary lithium cells 13 p1825 N90-20481
Catalysts for ultrahigh current density oxygen cathodes for space fuel cell applications
[NASA-CR-180650] 16 p2251 N90-22835
New liquid cathode electrolytes in high rate cells
[AD-A219822] 18 p2546 N90-24531
Evaluation of room-temperature chloroaluminate molten salts as electrolytes for high energy density batteries
[AD-A223097] 20 p2860 N90-26267
Cell performance of ultra-thin polymer cathode cell systems. Part 2: Cation intercalating composite polymer cathode
[AD-A221919] 21 p3020 N90-27172
Field emitter array integrated distributed amplifiers
[AD-D014493] 22 p3166 N90-27958
CELL DIVISION
Microgravity and mammalian cells
19 p2680 N90-25240
Insulin and insulin-like growth factor-1 induce pronounced hypertrophy of skeletal myofibers in tissue culture
[NASA-CR-187026] 23 p3354 N90-28960
CELL MEMBRANES (BIOLOGY)
Gravitropism in plants: Hydraulics and wall growth properties of responding cells 05 p0678 N90-13950
CELLS
Epidermal Growth Factor (EGF) induced signal transduction in A431 cells is sensitive to gravity
19 p2680 N90-25241
CELLS (BIOLOGY)
NT EGGS
NT ERYTHROCYTES
NT GAMETOCYTES
NT LEUKOCYTES
NT LYMPHOCYTES
NT MACROPHAGES
NT NEURONS
NT PROTOPLASTS
NT SPERMATOZOA
Electroporation: Theory of basic mechanisms
[AD-A210196] 01 p0091 N90-10520
Genetic engineering of single-domain magnetic particles
[AD-A210332] 01 p0091 N90-10521
Heatstroke pathophysiology: The energy depletion model
[AD-A212156] 03 p0380 N90-12164
A statistical analysis of spatial point patterns, a case study
[CWI-MS-R8813] 04 p0547 N90-13180
Generation of free radicals during cold injury and rewarming
[AD-A213088] 05 p0672 N90-13915
Life science research in space
[ESA-SP-1105] 05 p0672 N90-13917
Cells in Space
[NASA-CP-10034] 05 p0676 N90-13939
Fundamental results from microgravity cell experiments with possible commericial applications
05 p0676 N90-13940
The pituitary growth hormone cell in space
05 p0676 N90-13941
Polarity establishment, morphogenesis, and cultured plant cells in space 05 p0677 N90-13943
Physical phenomena and the microgravity response
05 p0677 N90-13945
How to detect when cells in space perceive gravity
05 p0678 N90-13946
Do the design concepts used for the space flight hardware directly affect cell structure and/or cell function ground based simulations 05 p0679 N90-13953
Three-dimensional coculture process
[NASA-CASE-MSC-21560-1] 11 p1538 N90-18852
Study of hydrazine metabolism and toxicity
[AD-A217103] 12 p1695 N90-19736

Biological soft x ray contact microscopy: Imaging living CHO-SC1 cells and other biological materials
[DE90-007560] 13 p1849 N90-20610
Does DNA cytometry have a place in the clinical laboratory
[DE90-007652] 14 p2009 N90-21512
Research in biological separations and cell culture
[NASA-CR-172060] 15 p2135 N90-22202
Exposure of human cells to electromagnetic fields
[AD-A219377] 16 p2261 N90-22889
The effects of simulated hypogravity on murine bone marrow cells 18 p2631 N90-24989
Experiment K-6-06. Morphometric and EM analyses of tibial epiphyseal plates from Cosmos 1887 rats 20 p2893 N90-26460
Experiment K-6-17. Structural changes and cell turnover in the rats small intestine induced by spaceflight 20 p2895 N90-26470
Experiment K-6-22. Growth hormone regulation, synthesis and secretion in microgravity. Part 1: Somatotroph physiology. Part 2: Immunohistochemical analysis of hypothalamic hormones. Part 3: Plasma analysis 20 p2896 N90-26475
Experiment K-6-23. Effect of spaceflight on levels and function of immune cells 20 p2897 N90-26476
Mechanisms of microwave induced damage in biologic materials
[AD-A222454] 21 p3033 N90-27242
Interaction of electromagnetic fields with chondrocytes in gel culture
[AD-A223397] 24 p3497 N90-29765

CELLULAR MATERIALS (NON BIOLOGICAL)
U FOAMS

CELLULOSE
Single particle friction tests with cellulose acetate sphere samples
[DE89-017537] 06 p0793 N90-14622
Breeding of hydrogen producing anaerobic bacteria. Cellulase secretion from transformed Escherichia coli JM109
[DE90-710739] 10 p1410 N90-18133
Recycling waste-paper 18 p2514 N90-24359

CELLULOSE NITRATE
Experimental and theoretical research on the injection of ignition gases into a bed of inert powder
[ISL-CO-251/88] 11 p1485 N90-18547

CEMENTATION
Surface reactions of the TA6V titanium alloy under laser irradiation
[ETCA-90-R-012] 22 p3158 N90-27904

CEMENTS
A numerical laboratory for granular solids
[DE89-016367] 03 p0358 N90-12045
Fiber reinforced cementitious composites technology
[PB89-227813] 05 p0619 N90-13608
Criteria for polymer concrete on airport pavements
[DOT/FAA/DS-89/18] 14 p1929 N90-21045
Transport of gases through concrete
[AERE-G-4977] 16 p2234 N90-22747
Development and testing of rapid repair methods for war damaged runways
[AD-A223970] 23 p3285 N90-28586

CENSUS
Census of US civil aircraft
[PB90-120296] 14 p1905 N90-20920

CENTAURUS CONSTELLATION
Project Longshot: A mission to Alpha Centauri
[NASA-CR-186052] 17 p2357 N90-23417
Orbitally modulated VHE gamma rays from Cen X-3 19 p2780 N90-25812

CENTER OF MASS
Exclusive production of p, p-, pi, and pi- in photon photon collisions
[NIKHEF-H/89-9] 15 p2165 N90-22376

CENTIMETER WAVES
Validity domain of the scalar Kirchhoff and Rayleigh-Sommerfeld diffraction theories in the near field of small phase objects: Comparison between calculation models and microwave measure
[ETN-90-96963] 20 p2855 N90-26236

CENTRAL AMERICA
Forecasters handbook for Central America and adjacent waters
[AD-A216752] 11 p1536 N90-18845
Evolution of finite amplitude baroclinic waves in the atmosphere and ocean
[INPE-4752-TDL/346] 12 p1695 N90-19733

CENTRAL BULGE (GALAXIES)
U GALACTIC BULGE

CENTRAL NERVOUS SYSTEM
NT BRAIN
NT BRAIN STEM
NT CEREBELLUM
NT CEREBRAL CORTEX
NT CEREBRUM
NT PINEAL GLAND
NT SPINAL CORD
NT THALAMUS
Reciprocal relationships between the immune and central nervous system
[AD-A221259] 18 p2583 N90-24712

CENTRAL PROCESSING UNITS
NT ARITHMETIC AND LOGIC UNITS
The M/G/1 processor sharing queue as the almost sure limit of feedback queues
[REPT-89-32] 04 p0528 N90-13044
Solving 3D block bidiagonal linear systems on vector computers
[CWI-NM-R8819] 04 p0530 N90-13061
Area-universal networks
[AD-A211883] 04 p0535 N90-13092
Definition of avionics concepts for a heavy lift cargo vehicle, appendix A
[NASA-CR-183817] 05 p0580 N90-13380
The role of the host in a cooperating mainframe and workstation environment, volumes 1 and 2
[NASA-CR-185463-VOL-1/2] 05 p0602 N90-13496
Concurrent processing adaptation of aeroplastic analysis of propfans
[NASA-TM-102455] 06 p0799 N90-14656
Coordination of processing elements in a multiprocessor computer
[WO-PATENT-88/04075] 06 p0831 N90-14830
Architectures for reasoning in parallel
[NASA-CR-186237] 06 p0832 N90-14836
Ultra high performance, highly reliable, numeric intensive processors and systems
[AD-A214100] 07 p0980 N90-15659
CPU timing routines for a CONVEX C220 computer system
[NASA-CR-181950] 08 p1110 N90-16424
The inside-outside algorithm: Further experiments on three and four letter word spelling and implementation on an array processor
[RSRE-MEMO-4256] 08 p1110 N90-16426
Beamforming pre-processors for high discrimination algorithms
[RSRE-MEMO-4304] 08 p1110 N90-16429
Dynamically allocating sets of fine-grained processors to running computations 08 p1114 N90-16447
Scan line graphics generation on the massively parallel processor 08 p1114 N90-16450
Loran C monitor: Facilities Central Processing Unit (FCPU) port evaluation
[DOT/FAA/CT-TN89/57] 10 p1318 N90-17623
Transient finite element computations on the transputer system
[NASA-CR-185199] 10 p1396 N90-18071
A scheme for supporting distributed data structures on multicomputers
[NASA-CR-181987] 10 p1415 N90-18152
Cache for multi-threaded processors on a split-transaction bus
[AD-A216404] 10 p1415 N90-18156
The mesoscale meteorological model MM4 and its modifications for EURAD 12 p1686 N90-19682
Parallel algorithms for boundary value problems
[NASA-TM-102498] 12 p1704 N90-19783
Onboard shuttle on-line software requirements system: Prototype 13 p1858 N90-20658
Performance tradeoffs in multithreaded processors
[AD-A217123] 13 p1871 N90-20729
Software techniques for non-von Neumann architectures
[AD-A220390] 17 p2440 N90-23902
TUMULT-64: A real-time multi-processor system
[MEMO-INF-89-58] 17 p2440 N90-23904
The incorporation of a multigrid method into the orthogonal curvilinear coordinate version of the Rolls-Royce PACE computer program
[TT-8804] 19 p2751 N90-25627
Practical applications of remote sensing technology
[NASA-CR-186810] 20 p2879 N90-26377
JTIDS relative navigation: Principles, architecture, and inertial mixing 24 p3426 N90-29357

CENTRIFUGAL COMPRESSORS
Flow in a forward swept centrifugal fan, volumes 1 and 2 14 p1912 N90-20959
An investigation of the three-dimensional flow field in a centrifugal compressor 16 p2235 N90-22751

CENTRIFUGAL FORCE
Study of vortex arrays induced artificially and from centrifugal instabilities
[AD-A216499] 11 p1506 N90-18669
Vortex motion phase separator for zero gravity liquid transfer
[NASA-CASE-KSC-11387-1] 13 p1783 N90-20236
Mobility of the head and load effects: Experimental approach in a centrifuge 19 p2720 N90-25473
Structural analysis and optimization of a propfan blade using a finite element method
[DLR-FB-90-01] 20 p2812 N90-26006
Rotating-unbalanced-mass devices and methods for scanning balloon-borne-experiments, free-flying spacecraft, and space shuttle/space station attached experiments
[NASA-CASE-MFS-28425-1] 20 p2866 N90-26304
Rotating flow in radial turbomachinery
[AD-A222885] 21 p3004 N90-27073
Target acquisition under load factors: Advantages and disadvantages of a helmet mounted sight 23 p3359 N90-28983
Unexpected properties of the centrifugal force
[DE90-627197] 23 p3392 N90-29164

CENTRIFUGAL PUMPS
A three-dimensional potential flow analysis of dynamic fluid forces acting on a whirling centrifugal impeller bounded by a volute 05 p0637 N90-13717
Experimental investigation of the effect of cavitation on the rotordynamic forces on a whirling centrifugal pump impeller 15 p2105 N90-22039
Design and use of high speed synchronous motor running in aggressive liquids 18 p2538 N90-24478
Experimental investigation of the hydrodynamic forces on the shroud of a centrifugal pump impeller
[NASA-CR-186952] 21 p3009 N90-27108

CENTRIFUGES
NT HUMAN CENTRIFUGES
VIBRAFUGE: A combined environment testing facility-vibration testing on a centrifuge
[DE89-015120] 01 p0080 N90-10458
Cross-axis synchronous flow through coil planet centrifuge for large-scale preparative countercurrent chromatography
[PB89-200174] 04 p0468 N90-12682
VIBRAFUGE: Combined vibration and centrifuge testing
[DE90-001091] 07 p0884 N90-15114
Acceleration tests of the ACPB canister flight unit from RETE experiment
[IFSI-89-2] 10 p1328 N90-17669
Plasma centrifuge with vacuum arc discharge applied to the separation of stable isotopes
[INPE-4925-TDL/385] 12 p1716 N90-19854
Space adaptation syndrome induced by a long duration +3Gx centrifuge run
[AD-A218248] 14 p2010 N90-21518

CENTRIPETAL FORCE
On the complexity analysis of the coriolis and centripetal effects of a 6 DOF robot manipulator --- Degrees of Freedom (DOF)
[RR-344] 03 p0355 N90-12030

CENTROIDS
A laboratory verification sensor 05 p0599 N90-13477
QPO from the rapid burster 19 p2770 N90-25741

CEPHEID VARIABLES
Cepheid masses for models with enhanced opacities
[DE90-014919] 23 p3409 N90-29266

CEPSTRAL ANALYSIS
A cepstral analysis of EEG (Electroencephalographic) signals in motion sickness studies
[AD-A215663] 09 p1253 N90-17273
Cepstrum analysis and applications to computational fluid dynamic solutions 14 p1973 N90-21302

CERAMAL PROTECTIVE COATINGS
U CERMETS
U PROTECTIVE COATINGS

CERAMALS
U CERMETS

CERAMIC BONDING
The processing and mechanical properties of high temperature/high performance composites. Book 4, section 3: Flow and creep strength
[AD-A216144] 10 p1349 N90-17822
Numerical model of bond strength measurements
[DE90-006000] 10 p1396 N90-18073
Interfacial chemistry of MoS2 films on Si
[AD-A216527] 11 p1482 N90-18532
Ductile alloy encapsulated ceramic armor development
[AD-A217632] 14 p1954 N90-21183

CERAMIC COATINGS
Japanese structural ceramics research and development 01 p0048 N90-10272
Vanadium dioxide protective devices
[AD-A212018] 03 p0332 N90-11887
Thermomechanical contact phenomena and wear of sliding components
[AD-A211290] 03 p0355 N90-12028
Implementation and analysis of adhesion in multimaterials of the type Al(Si)-ZrO2 and graphite, metal or ceramics
[ECL-89-004] 05 p0628 N90-13667

Mechanical aspects of interfaces in high performance composites 10 p1347 N90-17812
Laboratory for the processing and evaluation of inorganic matrix composites
[AD-A216881] 11 p1480 N90-18516
Influence of heat treating on the mechanical values and the stability of heat barrier coatings
[ETN-90-95902] 12 p1631 N90-19375
New corrosion resistant ceramic coatings by laser processing
[AERE-R-13166] 15 p2071 N90-21863
Quality evaluation of coatings by automatic scratch testing
[AD-A219331] 17 p2379 N90-23548
A computational study of the effectiveness of coating materials for KE projectile fins subjected to the combined effects of inbore and aerodynamic heating
[AD-A222595] 20 p2840 N90-26155
Scandia-stabilized zirconia coating for composites
[AD-D014550] 22 p3160 N90-27917
Study of the structure of ZrO2-Al2O3 plasma sprayed coatings
[ETCA-89-R-078] 22 p3161 N90-27924
High temperature protective coatings: Recent trends 23 p3308 N90-28710
Thermal shock and oxidation resistance of ceramic coatings 23 p3308 N90-28711

CERAMIC FIBERS

Static tensile and tensile creep testing of four boron nitride coated ceramic fibers at elevated temperatures
[NASA-CR-184999] 03 p0318 N90-11807
Oxide ceramic fibers by the sol-gel methods
[AD-A211315] 04 p0478 N90-12742
Sputter deposition of diffusion barrier coatings on SiC monofilaments for use in Ti-based composites 11 p1477 N90-18502
Processing, fabrication, characterization and device demonstration of high temperature superconducting ceramics
[AD-A218330] 13 p1782 N90-20231
Fatigue crack growth in a unidirectional SCS-6/Ti-15-3 composite
[NASA-TM-103095] 16 p2217 N90-22646
High temperature fatigue behavior of a SiC/Ti-24Al-11Nb composite
[NASA-TM-103157] 16 p2248 N90-22822
The effect of interfacial characteristics on the mechanical performance of ceramic-ceramic composites
[AD-A223031] 20 p2829 N90-26090
High temperature ceramic superconductors
[AD-A221743] 21 p3084 N90-27540

CERAMIC MATRIX COMPOSITES

Ceramic components in machines, Cologne and Aachen, West Germany; Maastricht, The Netherlands and Brussels, Belgium
[DE89-015831] 01 p0047 N90-10264
Zirconia toughened SiC whisker reinforced alumina composites small business innovation research
[NASA-CR-179629] 01 p0052 N90-10294
Liquid infiltrated C/SiC: An alternative material for hot space structures 02 p0182 N90-11030
Inorganic composite materials in Japan: Status and trends
[PB89-230015] 03 p0319 N90-11810
Toughening of a particulate-reinforced/ceramic-matrix composite
[AD-A213180] 05 p0618 N90-13604
Oxidation effects on the mechanical properties of SiC fiber-reinforced reaction-bonded silicon nitride matrix composites
[NASA-TM-102360] 06 p0736 N90-14287
The mechanical behavior of a fiber-reinforced brittle matrix composite 07 p0889 N90-15139
Effects of filament-matrix interfaces on the mechanical properties of SiC-reinforced Si3N4: A review
[DE90-001863] 07 p0890 N90-15144
High-performance LO2-CH4 engine with ceramic matrix composite materials 09 p1180 N90-16840
Mechanical aspects of interfaces in high performance composites 10 p1347 N90-17812
State of the art and future prospects for high temperature composites 11 p1477 N90-18498
Silicon carbo-nitride ceramic matrix composites by polymer pyrolysis 11 p1477 N90-18499
Ceramic matrix composites, new high performance materials 11 p1477 N90-18500
Characterization of ceramic matrix composites fabricated by chemical vapor infiltration
[DE90-008409] 13 p1768 N90-20149
Fundamental aspects of and failure modes in high-temperature composites
[NASA-TM-102558] 13 p1769 N90-20151
Nicalon/siliconoxycarbide ceramic composites
[NASA-TM-102563] 14 p1945 N90-21133
Small business innovation research. Abstracts of completed 1987 phase 1 projects
[NASA-TM-101797] 14 p2036 N90-21681
The position of carbon/carbon composites among high temperature composites
[REPT-892-430-126] 16 p2213 N90-22626
A comprehensive study on microstructure mechanics relationships of ceramic matrix composites
[AD-A219318] 16 p2213 N90-22627
Nondestructive Testing (NDT); Ceramic Matrix Composite Materials (CMCM) --- Nondestructive testing (ndc); ceramic matrix composite materials (CMMC)
[REPT-892-430-123] 16 p2222 N90-22677
Microcracking and toughness of ceramic-fiber/ceramic-matrix composites under high temperature
[AD-A218516] 16 p2223 N90-22680
MTS high temperature testing system
[AD-A219613] 17 p2369 N90-23483
Thermomechanical properties of new composite materials SiC/glass-ceramic
[REPT-892-430-118] 17 p2370 N90-23491
Theory and experimental technique for nondestructive evaluation of ceramic composites
[NASA-TM-102561] 17 p2414 N90-23754
Fracture toughness and solid-particle erosion of ceramic-matrix whisker-reinforced composites
[DE90-009713] 18 p2517 N90-24376
Influence of interfacial shear strength on the mechanical properties of SiC fiber reinforced reaction-bonded silicon nitride matrix composites
[NASA-TM-102462] 18 p2518 N90-24382
Alumina reinforced tetragonal zirconia (TZP) composites
[DE90-011871] 19 p2672 N90-25194
The application of engineering ceramics in gas turbines
[PNR90676] 20 p2812 N90-26005
Extension of a noninteractive reliability model for ceramic matrix composites
[NASA-CR-185267] 20 p2838 N90-26142
A study of the elastic properties of Al2O3 and Si3N4 matrix composites with SiC whisker reinforcement
[DE90-013674] 21 p2970 N90-26882
Interfacial studies of Chemical Vapor Infiltrated (CVI) ceramic matrix composites
[AD-A221867] 21 p2972 N90-26893
Inorganic composite materials in Japan: Status and trends
[PB90-174392] 22 p3135 N90-27789
Ceramic matrix composites in simulated SSME environments 23 p3298 N90-28655
Strengthening and toughening mechanisms in ceramic fiber-reinforced glass matrix composites 23 p3300 N90-28666

CERAMICS

Advanced Turbine Technology Applications Project (ATTAP)
[NASA-CR-185133] 01 p0008 N90-10036
Materials for engine applications above 3000 deg F: An overview
[NASA-TM-100169] 01 p0034 N90-10188
Raman characterization of high temperature materials using an imaging detector
[DE89-016308] 01 p0040 N90-10219
New structural materials
[AD-A209425] 01 p0044 N90-10246
Friction and wear of oxide-ceramic sliding against IN-718 nickel base alloy at 25 to 800 C in atmospheric air
[NASA-TM-102291] 01 p0046 N90-10262
Ceramic components in machines, Cologne and Aachen, West Germany; Maastricht, The Netherlands and Brussels, Belgium
[DE89-015831] 01 p0047 N90-10264
Shock compression and release in high-strength ceramics
[DE89-013995] 01 p0047 N90-10265
Thermophysical properties of ceramics. Part 2: Development of specific-heat-measurement apparatus at high temperature
[DE89-760382] 01 p0047 N90-10268
Japanese structural ceramics research and development 01 p0048 N90-10272
Structure-mechanical property relationships in ion implanted ceramics
[DE89-010129] 01 p0048 N90-10274
Alternative test methodology for ballistic performance ranking of armor ceramics
[AD-A210587] 01 p0051 N90-10290
The measurement of infrared spectra of dense ceramics by specular reflectance spectroscopy
[AD-A210609] 01 p0051 N90-10291
Improved silicon carbide for advanced heat engines
[NASA-CR-180831] 01 p0051 N90-10293
Zirconia toughened SiC whisker reinforced alumina composites small business innovation research
[NASA-CR-179629] 01 p0052 N90-10294
Composite ceramic superconducting wires for electric motor applications
[AD-A210345] 01 p0060 N90-10346
Capacitive energy storage at cryogenic temperatures, phase 2
[AD-A210366] 01 p0061 N90-10347
Plasma gun with coaxial powder feed and adjustable cathode
[NASA-CASE-LEW-14901-1] 01 p0126 N90-10718
Ceramic processing of bulk high-T(sub c) superconductors
[DE89-015703] 01 p0128 N90-10736
Precision materials characterization in the near millimeter and submillimeter wavelength range
[AD-A210655] 02 p0194 N90-11106
Basic research on processing of ceramics for space structures
[AD-A205954] 02 p0199 N90-11139
Fifth International Workshop on Glasses and Ceramics from Gels
[DE89-016899] 02 p0201 N90-11147
Influence of core-shell grains on the internal stress state and permittivity response of zirconia modified barium titanate
[AD-A211245] 02 p0202 N90-11153
Intergranular and interphase boundaries in ceramics
[DE89-016969] 02 p0202 N90-11154
Design of ceramic fabric heat pipe with water working fluid
[DE89-016565] 02 p0221 N90-11265
Advanced Turbine Technology Applications Program, (ATTAP)
[DE89-016067] 02 p0230 N90-11318
Advanced Turbine Technology Applications Program, (ATTAP): A plan for improving the prototype production of ceramic components for the gas turbine engine, 1988--1992
[DE89-015566] 02 p0230 N90-11320
Superconducting ceramics in the Bi1.5SrCaCu2O sub x system by melt quenching technique
[NASA-CR-185139] 02 p0281 N90-11606
Kinetics and mechanisms of primary and steady state creep in B- and Al-containing alpha silicon carbide
[AD-A210739] 02 p0283 N90-11616
High-temperature ceramic superconductors
[AD-A211070] 02 p0283 N90-11618
Physics and materials science of high temperature superconductors
[AD-A211246] 02 p0283 N90-11619
Origins of high-temperature superconductivity in the new copper oxide based ceramic superconductors
[DE89-016543] 02 p0284 N90-11622
Carbon fiber reinforced glass matrix composites for structural space based applications
[AD-A211682] 03 p0320 N90-11818
Sliding seal materials for low heat rejection engines
[NASA-CR-182262] 03 p0331 N90-11882
Photolithography: A new tool for ceramic science
[DE90-000135] 03 p0331 N90-11885
Densification of particulate ceramic composites: The role of heterogeneities
[DE90-000177] 03 p0331 N90-11886
Structure/reactivity relationships of polysilazane preceramics
[AD-A212028] 03 p0332 N90-11888
Flexure strength of advanced ceramics: A round robin exercise
[AD-A212101] 03 p0332 N90-11889
New mechanism for toughening ceramic materials
[AD-A211651] 03 p0332 N90-11892
Effect of annealing conditions on the structural and superconducting properties of Y-Ba-Cu-O films
[AD-A211308] 03 p0413 N90-12371
Synthesis and microstructure of highly oriented PbTiO3 thin films prepared by a sol-gel method
[AD-A211735] 03 p0414 N90-12377
Tribological properties of ceramic/Ti3Al-Nb sliding couples for use as candidate seal materials to 700 deg C
[NASA-TM-102401] 04 p0464 N90-12658
Laser probe vaporization/oxidation testing of high temperature composites
[AD-A211410] 04 p0465 N90-12663
Spall resistance of alumina
[AD-A213213] 04 p0477 N90-12735
Synthesis and high temperature chemistry of methylsilsesquioxane polymers produced by titanium catalyzed redistribution of methylhydridooligo- and polysiloxanes
[AD-A212000] 04 p0477 N90-12736
Oxide ceramic fibers by the sol-gel methods
[AD-A211315] 04 p0478 N90-12742

Pyrolytic production of ceramic composites from silicates
[ETCA-89-R-012] 04 p0479 N90-12746

NBS/BAM (National Bureau of Standards/Bundesanstalt fuer Materialprufung) 1988 Symposium on Advanced Ceramics
[PB89-229074] 04 p0479 N90-12747

Ion beam analysis of diffusion in polymer glasses
[AD-A212339] 04 p0480 N90-12756

Effects of hot corrosion on the room temperature strength of structural ceramics
[AD-A212568] 04 p0481 N90-12762

The 4th US Army Workshop on Low Heat Rejection Engines
[AD-A212378] 04 p0510 N90-12942

The 4th US Army Workshop on Low Heat Rejection Engines
[AD-A212379] 04 p0510 N90-12943

An air coupled transmission mode acoustic microscope for on-line non-destructive evaluation
[AD-A211416] 04 p0511 N90-12947

Proceedings of the Army Symposium on Solid Mechanics, 1989: Mechanics of Engineered Materials and Applications
[AD-A211954] 04 p0511 N90-12951

Development of an advanced fan blade containment system
[DOT/FAA/CT-89/20] 05 p0581 N90-13386

Thermal barrier coatings for gas turbine and diesel engines
[NASA-TM-102408] 05 p0623 N90-13636

Activities report of the metallic manufacturing industry
[ISSN-0524-7705] 05 p0625 N90-13649

Synthesis of inorganic polymers as glass precursors and for other uses. Preceramic block or graft copolymers as potential precursors to nanocomposite materials
[AD-A211978] 05 p0626 N90-13655

Toughening mechanisms in ceramic composites
[PB89-235907] 05 p0626 N90-13656

Surfaces and interfaces of ceramic materials
[AD-A212417] 05 p0627 N90-13657

MM and T for VHSIC multichip packages
[AD-A213259] 05 p0635 N90-13703

Sol-gel processing science using a Sol-Gel Optics Research Facility (SGORF)
[AD-A213056] 05 p0699 N90-14095

Preparation of 110K (Bi, Pb)-Sr-Ca-Cu-O superconductor from glass precursor
[NASA-CR-185162] 05 p0702 N90-14108

Advanced Turbine Technology Applications Project (ATTAP)
[NASA-CR-185109] 05 p0709 N90-14153

NRL (Naval Research Laboratory) Review
[AD-A212886] 05 p0716 N90-14182

Carbon fiber reinforced metal matrix composites
[AD-D014245] 06 p0737 N90-14289

Advances and future directions in superplastic materials 06 p0744 N90-14328

Temperature stable ceramic dielectric compositions
[AD-D014209] 06 p0749 N90-14358

Structure-property relationships in surface-modified ceramics. NATO Advanced Science Institutes, series E: Applied Sciences, volume 170
[AD-A212939] 06 p0749 N90-14359

Mechanisms of wear in structural ceramic materials 06 p0749 N90-14360

Ordered ceramic membranes
[DE89-017426] 06 p0750 N90-14364

Perturbed angular correlations in zirconia ceramics
[DE89-017272] 06 p0751 N90-14369

Computer synthesis of ceramic preforms for molten-metal infiltration
[DE90-000826] 06 p0751 N90-14370

Synthesis and properties of new preceram'c materials
[DE90-002582] 06 p0752 N90-14373

The 7th International Conference on Ceramics
[DE90-002144] 06 p0752 N90-14374

Numerical and empirical verification of the stress state in a ceramic, button-head, tensile specimen
[DE90-001645] 06 p0752 N90-14375

Thermal/structural analyses of several hydrogen-cooled leading-edge concepts for hypersonic flight vehicles
[NASA-TM-102391] 06 p0775 N90-14511

Field testing of a ceramic heat exchanger for heat recovery application
[DE90-002082] 06 p0778 N90-14523

Mechanics of interaction of a crack with microcracks 06 p0796 N90-14650

Interfacial effects in monolithic solid oxide fuel cells
[DE90-001914] 06 p0806 N90-14690

Ion beam analysis and modification of thin-film, high-temperature superconductors
[DE90-000918] 06 p0850 N90-14941

Solid State Division
[DE90-000979] 06 p0851 N90-14945

Bi-Sr-Ca-Cu-O superconducting ceramics
[DE89-636225] 06 p0855 N90-14972

Macroscopic persistent currents in high temperature ceramic superconductors
[DE89-636232] 06 p0855 N90-14973

Critical and subcritical crack-growth behavior along toughened ceramic/metal interfaces 07 p0889 N90-15140

Electronic materials high-T(sub c) superconductivity polymers and composites structural materials surface science and catalysts industry participation
[NASA-CR-186063] 07 p0890 N90-15145

Laser mixing of titanium on silicon carbide
[DE90-003216] 07 p0891 N90-15150

Processing and properties of nanophase oxides
[DE90-003826] 07 p0895 N90-15171

Surface modification of metals by ion beams
[DE90-001285] 07 p0903 N90-15218

Solid-state phase equilibria in the ZnS-Ga2S3 system
[AD-A213944] 07 p0906 N90-15238

Potential applications of structural ceramic composites in gas turbines
[DE90-001273] 07 p0908 N90-15248

Ceramic powder characterization
[DE90-001282] 07 p0908 N90-15249

Surface engineering by high energy beams
[DE90-001296] 07 p0908 N90-15250

Ceramic technology for advanced heat engines project
[DE90-001852] 07 p0908 N90-15251

Solid lubrication of ceramic surfaces by IAD (Ion-Assisted Deposition)-silver coatings for heat engine applications
[DE90-002860] 07 p0909 N90-15253

Crack tip toughening by inclusions with pairs of shear transformations
[DE89-007845] 07 p0909 N90-15254

Predicting the performance of ceramic filters by the use of silt density index
[DE90-001316] 07 p0909 N90-15258

Ceramic processing using inorganic polymers
[DE90-003638] 07 p0911 N90-15268

Development of NMR (Nuclear Magnetic Resonance) imaging probes for advanced ceramics
[DE90-003812] 07 p0911 N90-15269

IEA/Annex 2 powder characterization cooperative program
[AD-A213540] 07 p0911 N90-15271

Composite ceramic superconducting wires for electric motor applications
[AD-A213742] 07 p0912 N90-15274

Hardening and toughening of ZnS-Ga2S3 ceramics by solid-state reactions
[AD-A213875] 07 p0912 N90-15276

Silver coated superconducting ceramic powder
[AD-D014300] 07 p0913 N90-15278

Toughening behavior and interfacial properties of fiber-reinforced ceramic composites
[DE89-015351] 07 p0913 N90-15279

Development of glass-ceramic lasers
[AD-A214146] 07 p0936 N90-15423

Fabrication of porous ceramic electrode structures
[DE90-003548] 07 p0953 N90-15517

Characterization of MOCVD (Metal Organic Chemical Vapor Deposition) grown epitaxial ceramic oxide thin films
[DE90-003561] 07 p1001 N90-15790

Proceedings of the Latin American Conference on the Applications of the Moessbauer Effect
[DE90-600819] 07 p1002 N90-15803

High-temperature ceramic superconductors
[AD-A214251] 07 p1005 N90-15818

Structure-property relationships in ion-beam surface-modified ceramics: Theory and applications
[AD-A212785] 08 p1047 N90-16054

Porous ceramic bodies
[AD-D014277] 08 p1049 N90-16061

Metals and Ceramics Division Materials Sciences Program
[DE90-004371] 08 p1050 N90-16070

An investigation of elastic guided waves for ceramic joint evaluation
[DE90-004400] 08 p1050 N90-16071

Thermodynamic analysis of chemical stability of ceramic materials in hydrogen-containing atmospheres at high temperatures
[NASA-CR-4271] 08 p1050 N90-16072

Assessment of strength limiting flaws in ceramic heat exchanger components
[DE90-004086] 08 p1051 N90-16077

Analytical study on the decreasing method of thermal stress for ceramic gas turbines
[DE90-734934] 08 p1051 N90-16078

Basic studies on separative glass
[DE90-702436] 09 p1196 N90-16928

Study of the effect of ceramics gas turbine development
[DE90-702638] 09 p1196 N90-16929

Symposium on Chemical Precursors to Ceramics
[AD-A214499] 09 p1196 N90-16932

Crystallization of nanocomposite glasses made by the SSG process
[AD-A214572] 09 p1197 N90-16933

The preparation and characterisation of oxynitride glasses and glass-ceramics
[AD-A214783] 09 p1197 N90-16935

Fractographic analysis of long rod penetrator-armor ceramic interactions
[AD-A215172] 09 p1197 N90-16938

Novel approach for high resolution TEM (Transmission Electron Microscopy) studies of ceramic-ceramic interfaces
[DE90-005272] 09 p1199 N90-16945

Zirconia based ceramics
[DE90-606358] 09 p1199 N90-16946

Erosion of ceramic composites by various erodents
[DE90-005650] 09 p1199 N90-16948

Application of high-rate cutting tools
[AD-A214644] 09 p1203 N90-16970

Assessment of strength limiting flaws in ceramic heat exchanger tubes, phase 2
[DE90-004081] 09 p1220 N90-17080

Agglomeration of ceramic powders 09 p1223 N90-17098

Superconducting Bi1.5Pb0.5Sr2Ca2Cu3O(x) ceramics by rapid melt quenching and glass crystallization
[NASA-CR-185184] 09 p1288 N90-17465

Investigation of failure modes in a ceramic composite under off-axis loading
[AD-A216133] 10 p1348 N90-17820

The processing and mechanical properties of high temperature/high performance composites. Book 5, section 4: Processing: Matrices and composites, part 1
[AD-A216145] 10 p1349 N90-17823

The processing and mechanical properties of high temperature/high performance composites. Book 6, section 4: Processing: Matrices and composites, part 2
[AD-A216146] 10 p1349 N90-17824

Effects of elevated temperatures and thermal cycling on ceramic composite materials
[AD-A216242] 10 p1350 N90-17828

Control of titanium diboride SHS reactions by inert dilutions and mechanical constraint
[AD-A214378] 10 p1357 N90-17870

A finite element analysis of porosity effects on materials
[AD-A216225] 10 p1359 N90-17884

Materials properties numerical database system established and operational at CINDAS/Purdue University 10 p1366 N90-17919

Measurement of radiation property of long infrared emitter and examination of infrared radiation heating process
[DE90-741971] 10 p1425 N90-18222

Develop techniques for ion implantation of PLZT for adaptive optics
[AD-A216005] 10 p1431 N90-18253

Structural, magnetic and electrical properties of La(sub 2-x) Ba(sub x) NiO4
[AD-A214347] 10 p1434 N90-18278

Analysis of whisker-toughened ceramic components: A design engineer's viewpoint
[NASA-TM-102333] 11 p1478 N90-18504

Composite for smoothing the surface of ceramic substrates
[DE90-004005] 11 p1488 N90-18565

Colloid and interface chemistry aspects of ceramics
[AD-A216715] 11 p1490 N90-18576

Comparison of tension, compression, and flexure creep for alumina and silicon nitride ceramics
[DE90-006154] 11 p1492 N90-18586

Microwave radiation absorption by Ho(Y)-Ba-Cu-O superconducting ceramics
[DE90-610665] 11 p1492 N90-18588

The design of advanced ceramic composites
[DE90-006613] 11 p1493 N90-18592

Microstructural characterization of silicon nitride ceramics processed by pressureless sintering, overpressure sintering, and sinter/HIP
[DE90-007126] 11 p1493 N90-18594

Cohesive ceramic fabrication
[DE90-007333] 11 p1494 N90-18597

Reliability studies of ceramic capacitors
[AD-A216763] 11 p1501 N90-18643

Low cost filter development and control of permeability in high temperature, high pressure ceramic filter elements
[DE90-000403] 11 p1507 N90-18676

Biaxial strength and stress rupture of hot-pressed silicon nitride
[AD-A216950] 11 p1519 N90-18750

Ion implantation-induced amorphization of ceramic oxides
[DE90-006564] 11 p1571 N90-19041

Processing of advanced ceramics using microwaves thermal treatments
[DE90-606349] 12 p1629 N90-19362

Development of ceramic combustor for low BTU gases. Design and basic combustion characteristics
[DE89-782287] 12 p1629 N90-19363

Fracture strength analysis of silicon nitride and silicon carbide ceramics from an international cooperative research program
[DE90-005319] 12 p1630 N90-19368

Advanced ceramics
[DE90-608004] 12 p1630 N90-19370

Optical studies of dynamical processes in disordered materials
[DE90-007080] 12 p1631 N90-19372

The effect of fiber coatings on interfacial shear strength and the mechanical behavior of ceramic composites
[DE90-007574] 12 p1632 N90-19380

Proposal of arc driving type fault current limiter
[DE89-782290] 12 p1650 N90-19485

FWP executive summaries: Basic energy sciences materials sciences programs
[DE90-006373] 12 p1722 N90-19893

Materials Science Programs, fiscal year 1989
[DE90-008169] 13 p1765 N90-20131

Summary report of the Summer Conference of the DARPA-Materials Research Council
[AD-A217380] 13 p1767 N90-20143

Summary of the DoD Metal Matrix Composites (MMC) Steering Committee Meeting, hosted by the Institute for Defense Analysis
[AD-A217611] 13 p1768 N90-20145

Interface science in deformation processing of ceramics
[DE90-008424] 13 p1780 N90-20219

Radiation disorder and aperiodicity in irradiated ceramics
[DE90-008253] 13 p1781 N90-20222

Tensile fracture toughness of ceramic materials: Effects of dynamic loading and elevated temperatures
[DE90-008329] 13 p1781 N90-20223

Mechanical behavior of whisker reinforced ceramics
[DE90-008758] 13 p1781 N90-20224

Ceramic oxide thin film formation utilizing biological processes
[DE90-008599] 13 p1781 N90-20225

Strength and microstructure of ceramics
[AD-A217752] 13 p1782 N90-20227

High-temperature ceramic superconductors
[AD-A218347] 13 p1783 N90-20233

Nondestructive testing of ceramics by acoustic microscopy
[AERE-R-13350] 13 p1813 N90-20411

Nine-year aging behavior of the ceramic flatpack resonator
[DE90-008044] 13 p1813 N90-20412

Technology assessment of superconductivity
[AD-A217697] 13 p1897 N90-20889

Performance of Y-TZP materials between 800 C and 1200 C
[AD-A217723] 13 p1897 N90-20890

Nicalon/siliconoxycarbide ceramic composites
[NASA-TM-102563] 14 p1945 N90-21133

Boron-containing organosilane polymers and ceramic materials thereof
[NASA-CASE-ARC-11649-2-SB] 14 p1952 N90-21177

Effects of titanium on some surface properties of nitride ceramics
[AERE-R-13566] 14 p1953 N90-21178

Ductile alloy encapsulated ceramic armor development
[AD-A217632] 14 p1954 N90-21183

Fracture toughness and crack growth of Zerodur
[NASA-TM-4185] 14 p1954 N90-21187

Energy beam treatment for improved adhesion of coatings to surfaces
[AD-D014449] 14 p1954 N90-21190

ZELED analysis of aperiodicity and bond lengths in ceramic powders
[DE90-612932] 14 p1955 N90-21193

Research advances in fine ceramics
[DE90-008983] 14 p1956 N90-21197

Review of the state of the technology for joining ceramics for high-temperature structural applications
[DE90-009224] 14 p1956 N90-21199

Pressure rig for repetitive casting
[NASA-CASE-LAR-14050-1] 14 p1959 N90-21216

Ultrasonic and radiographic evaluation of advanced aerospace materials: Ceramic composites
[NASA-TM-102540] 14 p1989 N90-21401

Research programs in aeronautical engineering, solid state physics, and materials science at Technion-Israel Institute of Technology, Haifa, Israel
[EOARD-LR-89-068] 14 p2044 N90-21720

Studies on the use of supercritical ammonia for ceramic nitride synthesis and fabrication
[NASA-TM-102570] 15 p2068 N90-21843

Polysiloxanes derived from the controlled hydrolysis of tetraethoxysilane as precursors to silica for use in ceramic processing
[NASA-TM-102489] 15 p2070 N90-21858

A stress-strength interference approach to fast and delayed fracture reliability analysis for ceramic components 15 p2070 N90-21859

Fracture mechanics of monolithic ceramic materials under small scale microcracking conditions 15 p2070 N90-21860

Institute for Materials Science and Engineering, nondestructive evaluation: Technical activities
[PB90-132739] 15 p2108 N90-22055

On the design and development of a miniature ceramic gimbal bearing 15 p2115 N90-22100

Institute for Materials Science and Engineering, Fracture and Deformation Division: Technical activities, 1989
[PB90-155359] 15 p2116 N90-22106

Dynamic response of a complex encapsulated electronic assembly subjected to a severe shock environment
[DE90-007689] 15 p2118 N90-22114

Machining of new materials at Aerospatiale
[REPT-892-430-104] 16 p2213 N90-22622

Microcracking and toughness of ceramic-fiber/ceramic-matrix composites under high temperature
[AD-A218516] 16 p2223 N90-22680

Low temperature degradation of Y-TZP materials
[AD-A218841] 16 p2223 N90-22684

Low cost processing routes leading to high-performance ceramic tiles
[AD-A219034] 16 p2224 N90-22688

Composite ceramic superconducting wires for electric motor applications
[AD-A219131] 16 p2224 N90-22689

High temperature ceramic-tubed reformer
[DE90-009617] 16 p2236 N90-22755

Recent advances in nondestructive evaluation made possible by novel uses of video systems
[NASA-TM-102491] 16 p2244 N90-22801

Crack detection in silicon nitride by acoustic microscopy
[AERE-R-13196] 16 p2245 N90-22803

The pressure loaded volumetric ceramic receiver
[DLR-MITT-89-17] 16 p2252 N90-22842

What is going on in the La2CuO4 superconductors 16 p2311 N90-23171

Influence of high energy radiation on critical parameters of superconducting ceramics YBa2Cu3O7
[DE90-620562] 16 p2322 N90-23239

Ultrafine microstructure composites prepared by chemical vapor deposition
[AD-A219650] 17 p2369 N90-23484

Recent implementations on ceramic composites and thermostructural materials
[REPT-892-430-106] 17 p2370 N90-23489

Ceramic heat pipe wick
[NASA-CASE-GSC-13199-1] 17 p2378 N90-23541

Controlled crack growth specimen for brittle systems
[NASA-TM-103126] 17 p2378 N90-23543

Fracture mechanism maps for advanced structural ceramics. Part 1: Methodology and hot-pressed silicon nitride results
[AD-A220428] 17 p2380 N90-23556

Preparation, properties, and development of calcium lanthanum sulfide as an 8- to 12-micrometer transmitting ceramic
[AD-A220200] 17 p2382 N90-23565

Lightweight ceramic insulation and method
[NASA-CASE-MSC-20782-1] 17 p2382 N90-23566

Experiments on liquid immersion natural convection cooling of leadless chip carriers mounted on ceramic substrate
[AD-A219893] 17 p2478 N90-24167

Activities report in technical-physical research
[ETN-90-96771] 17 p2487 N90-24223

Friction and wear of whisker-reinforced ceramic composite bodies
[DE90-011313] 18 p2519 N90-24389

Cyclic damage zones ahead of tensile fatigue cracks in ceramic materials
[DE90-008372] 18 p2531 N90-24442

Fatigue crack growth in ceramic materials at ambient and elevated temperatures
[DE90-008418] 18 p2531 N90-24443

The influence of ion implantation on the near-surface mechanical properties of ceramics
[DE90-010139] 18 p2531 N90-24444

Joining engineering ceramics
[DE90-010819] 18 p2531 N90-24445

Ceramic epitaxial films and multilayers prepared by MOCVD
[DE90-011090] 18 p2532 N90-24447

Ceramic technology for advanced heat engines project data base
[DE90-011491] 18 p2532 N90-24448

Fracture behavior of surface modified ceramics
[DE90-011552] 18 p2532 N90-24449

NDE (NonDestructive Evaluation) of ceramic heat exchangers
[DE90-010977] 18 p2554 N90-24575

Mechanistic studies of the CO-oxidation reaction on catalysts for use in long-life CO2 lasers 18 p2558 N90-24596

Synthesis of ceramic superconductors under low oxygen pressure
[DE90-010415] 18 p2621 N90-24933

Preparation of high Tc superconducting ceramic materials of the Y-Ba-Cu-oxide type
[FOA-C-30550-3.2] 18 p2622 N90-24939

Research on high-specific-heat dielectrics
[AD-A221215] 18 p2623 N90-24944

Improved processing of ceramic superconductors
[DE90-009721] 18 p2624 N90-24951

Processing of advanced ceramics which have potential for use in gas turbine aero engines
[AD-A220988] 19 p2677 N90-25226

Crack bridging processes in toughened ceramics
[DE90-011650] 19 p2678 N90-25231

Outlook for ceramics in heat engines, 1990 - 2010: A technical and economic assessment based on a worldwide Delphi survey
[DE90-011262] 19 p2679 N90-25234

Sol-gel processing for fiber optic applications
[DE90-012083] 19 p2758 N90-25675

Towards 2000: The composite engine
[PNR90646] 20 p2811 N90-26000

Vitreous joining of SiC fiber reinforced SiC composites
[DE90-012951] 20 p2827 N90-26081

The effect of interfacial characteristics on the mechanical performance of ceramic-ceramic composites
[AD-A223031] 20 p2829 N90-26090

The interaction of polymeric materials with ceramic surfaces with special reference to the behaviour of bioceramics 20 p2836 N90-26127

Determination of the stress distributions in a ceramic: Tensile specimen using numerical techniques
[NASA-TM-101914] 20 p2837 N90-26132

Tensile strength measurement techniques for structural ceramics
[DE90-012193] 20 p2837 N90-26136

Real-time monitoring of ceramic sintering with laser ultrasonics
[DE90-012960] 20 p2838 N90-26140

Laser ultrasonic measurements on ceramic materials with rough surfaces
[DE90-012961] 20 p2838 N90-26141

Extension of a noninteractive reliability model for ceramic matrix composites
[NASA-CR-185267] 20 p2838 N90-26142

Evaluation of fracture strength properties of silicon carbide ceramics under cyclic/static axial loading at ultra-high temperature
[DE90-503402] 20 p2839 N90-26147

Development of ceramic fiber type combustor: Improvement of combustor and combustion test results
[DE90-503441] 20 p2839 N90-26148

Development of ceramic hybrid combustor: Design and combustion test results
[DE90-503442] 20 p2839 N90-26149

The catalytic synthesis of inorganic polymers for high temperature applications and as ceramic precursors
[AD-A222620] 20 p2840 N90-26156

Design of ceramic components with the NASA/CARES computer program
[NASA-TM-102369] 20 p2875 N90-26359

Advanced Turbine Technology Applications Project (ATTAP)
[NASA-CR-185240] 20 p2939 N90-26728

The 1990 Gordon Research Conference on Composites
[AD-A222849] 21 p2971 N90-26886

Application of microdesigned interfaces to studies of ceramic processing
[DE90-011633] 21 p2983 N90-26951

An initial comparison between two 3-D x ray CT algorithms for characterizing
[DE90-013656] 21 p2984 N90-26957

Dynamic properties of porous B4C
[AD-A222850] 21 p2985 N90-26960

Theory of ceramic/zirconia composites: Toughening, strengthening, and synergism
[AD-A222931] 21 p2985 N90-26961

Advanced ceramic armor materials
[AD-A223227] 21 p2986 N90-26970
Micromechanics of interfaces in high temperature ceramics
[AD-A222027] 21 p2987 N90-26973
Structure-property behavior of new organic-inorganic polymeric hybrid materials based on sol gel chemistry
[AD-A222168] 21 p2987 N90-26974
A summary of measurements of permittivities and permeabilities of some microwave absorbing materials
[AD-A223221] 21 p2995 N90-27026
Composite ceramic superconducting wires for electric motor applications
[AD-A222085] 21 p3001 N90-27055
Fabrication of composite high temperature superconductor wires from Ag/YBa2Cu3O(sub x) powder produced by AgNO3 decomposition
[AD-A221936] 21 p3083 N90-27532
Identification of tetragonal and cubic structures of zirconia
[AD-A222373] 21 p3083 N90-27535
Scaling behaviour of relaxation dependencies in metaloxide superconductors 22 p3138 N90-27802
Effect of shock pressure on the structure and superconducting properties of Y-Ba-Cu-O in explosively fabricated bulk metal-matrix composites
22 p3138 N90-27804
Production of superconductor/carbon bicomponent fibers 22 p3138 N90-27805
High-T(sub c) squid application in medicine and geophysics 22 p3139 N90-27806
Energetics and crystal chemistry of Ruddlesden-Popper type structures in high T(sub c) ceramic superconductors
22 p3141 N90-27814
Kinetics and thermodynamics of ceramic/metal interface reactions related to high T(sub c) superconducting applications 22 p3141 N90-27815
An EPR methodology for measuring the London penetration depth for the ceramic superconductors
22 p3143 N90-27828
Plastic superconductor bearings any size, any shape, 77 k and up 22 p3145 N90-27838
Low frequency electrical noise across contacts between a normal conductor and superconducting bulk YBa2Cu3O7 22 p3146 N90-27841
Composite superconducting wires obtained by high-rate tinning in molten Bi-Pb-Sr-Ca-Cu-O system
22 p3148 N90-27850
Grain orientation studies in superconductors
22 p3148 N90-27852
XES studies of density of states of high temperature superconductors 22 p3150 N90-27859
Processing Bi-Pb-Sr-Ca-Cu-O superconductors from amorphous state 22 p3150 N90-27860
Development of polysilsesquioxane composites
[NASA-CR-180263] 22 p3152 N90-27872
Catalytic synthesis of polymethylsilsesquioxanes
[AD-A222643] 22 p3159 N90-27910
Surfaces and interfaces of ceramics and metals
[DE90-014381] 22 p3160 N90-27920
Study of a method for measuring the dimensions of cracks on the surface of ceramics by Rayleigh waves
[ETCA-89-R-024] 22 p3160 N90-27922
Characterization by ultrasonic tests of ceramics submitted to thermal shocks: Influence of several parameters on the crack dimensioning
[ETCA-89-R-060] 22 p3160 N90-27923
Sintering of ceramics by laser irradiation
[ETCA-89-R-134] 22 p3161 N90-27926
Some design considerations for small piezo-electrical ceramic transducers
[FEL-1989-68] 22 p3178 N90-28034
Ceramics Analysis and Reliability Evaluation of Structures (CARES). Users and programmers manual
[NASA-TP-2916] 22 p3190 N90-28099
Micromechanical model of crack growth in fiber reinforced ceramics
[NASA-CR-4321] 22 p3192 N90-28113
Energy efficient engine pin fin and ceramic composite segmented liner combustor sector rig test report
[NASA-CR-179534] 23 p3281 N90-28567
Friction microprobe studies of composite surfaces
[DE90-014224] 23 p3299 N90-28662
Microdamage to ceramic surfaces under sliding conditions 23 p3308 N90-28708
Mechanical testing activities related to high-performance structural ceramics
[DE90-014299] 23 p3313 N90-28734
Improved silicon carbide for advanced heat engines
[NASA-CR-182186] 23 p3313 N90-28735
Proceedings of US Army Research Office Workshop on US Army Applications for Diamond and Diamondlike Materials
[AD-A224193] 23 p3314 N90-28741
In-flight investigation of shuttle tile pressure orifice installations
[NASA-TM-4219] 23 p3328 N90-28820
High performance brittle matrices and brittle matrix composites, book 1
[AD-A223273] 24 p3443 N90-29440
Effect of environment upon mechanical behavior of structural ceramics for application in the DOE ceramic technology for advanced heat engines project
[DE90-014770] 24 p3453 N90-29500
Non-destructive evaluation of infiltration-toughened ceramics
[DE90-629716] 24 p3453 N90-29501
Surface chemistry and structural effects in the stress corrosion of glass and ceramic materials
[AD-A223305] 24 p3454 N90-29507
Ion-beam-assisted deposition of silver films on zirconia ceramics for improved tribological behavior
[DE90-009706] 24 p3456 N90-29516
Wear of advanced ceramics: An overview
[DE90-012166] 24 p3456 N90-29519
Processing of nanocrystalline ceramics
[DE90-015700] 24 p3456 N90-29520
Reliability study of TWT output RF window
[AD-A223688] 24 p3485 N90-29574

CEREBELLUM
Biological investigations of adaptive networks: Neuronal control of conditioned responses
[AD-A211043] 01 p0094 N90-10534

CEREBRAL CORTEX
Extrathalamic modulation of cortical function
[AD-A211044] 01 p0094 N90-10535
Adaptive information processing in auditory cortex
[AD-A211294] 03 p0380 N90-12166
Role of retinocortical processing in spatial vision
[AD-A210995] 05 p0672 N90-13918
Acetylcholinesterase inhibition and information processing in the auditory cortex
[AD-A216092] 10 p1411 N90-18139
Organization of a large-scale cortical network
[AD-A216829] 11 p1540 N90-18863
Psychological studies of visual cortical function
[AD-A217029] 11 p1541 N90-18872
The boundaries of hemispheric processing in visual pattern recognition
[AD-A217675] 13 p1854 N90-20640
CEREBRAL WEEVIL: A machine learning model for hemispheric categorization of complex visual patterns
[AD-A218143] 13 p1874 N90-20749
Laser retinal effects: Electrophysiological determination in visual cortical cells of monkeys and cats
[AD-A218937] 16 p2261 N90-22888
Attention, imagery, and memory: A neuromagnetic investigation
[AD-A224560] 24 p3499 N90-29775

CEREBROSPINAL FLUID
Rheoencephalography in simulated aviation environmental stress
[AD-A221150] 18 p2584 N90-24716

CEREBRUM
NT CEREBRAL CORTEX
Metabolism, seizures, and blood flow in brain following organophosphate exposure: Mechanisms of action and possible therapeutic agents
[AD-A217098] 12 p1696 N90-19740

CERENKOV COUNTERS
A large detector for cosmic ray abundance and energy measurements 06 p0867 N90-15037
The detection of VHE gamma rays using the atmospheric Cerenkov technique 19 p2773 N90-25761
Search for neutrino events in the Kamiokande-2 detector in correlation with the solar-flare activity in March 1989
[DE90-508085] 24 p3563 N90-30160

CERENKOV EFFECT
U CERENKOV RADIATION

CERENKOV RADIATION
A large detector for cosmic ray abundance and energy measurements 06 p0867 N90-15037
Radiation of electromagnetic waves by an accelerated charged particle in medium
[DE90-610458] 12 p1646 N90-19461
Very high energy gamma ray astrophysics
[DE90-006645] 12 p1737 N90-19983
A balloon measurement of the isotopic composition of galactic cosmic ray iron 14 p2043 N90-21717
A search for very high energy gamma rays from the Crab pulsar-nebula 14 p2043 N90-21718
Very high energy gamma rays from the Crab nebula and pulsar 15 p2194 N90-22527
TeV radiation from the Crab nebula and other matters
16 p2335 N90-23306
Some novel sources of x ray beams: Channeling, transition and Cherenkov radiation
[DE90-014442] 23 p3395 N90-29181

CERIUM
Synthesis, characterization and evaluation of CO-oxidation catalysts for high repetition rate CO2 TEA lasers 18 p2557 N90-24593
Novel superconducting phases of Tl-based compounds 22 p3150 N90-27862
Effects of Al substitution by Fe in CeAl2
[DE90-627843] 23 p3311 N90-28726

CERIUM COMPOUNDS
NT CERIUM OXIDES
Searching for heavy fermion materials in Ce intermetallic compounds
[DE90-011809] 20 p2834 N90-26116
Antiferromagnetism and enhanced heat in CeM2Sn (M = Ni, Ir, Cu, Rh, Pd, and Pt
[DE90-014924] 23 p3399 N90-29206
Evidence for a coherence gap in Ce3Bi4Pt3
[DE90-014925] 23 p3399 N90-29207

CERIUM OXIDES
Enhanced ceria solid electrolyte fuel cell development. Reduction of electronic conductivity permits use of a solid ceria electrolyte in high efficiency high power density fuel cells at temperatures compatible with metallic cell hardware
[AD-A217840] 13 p1828 N90-20498
Enhanced ceria solid electrolyte fuel cell development. Reduction of electronic conductivity permits use of a solid ceria electrolyte in high efficiency high power density fuel cells at temperatures compatible with metallic cell hardware
[AD-A219297] 16 p2253 N90-22846

CERMETS
Characterizations of shock-loaded aluminum-infiltrated boron carbide cermets
[DE89-016773] 02 p0201 N90-11146
Research programs in aeronautical engineering, solid state physics, and materials science at Technion-Israel Institute of Technology, Haifa, Israel
[EOARD-LR-89-068] 14 p2044 N90-21720

CERTIFICATION
US Air Force certification of castings
01 p0042 N90-10232
Royal Aerospace Establishment: No place for a castings factor 01 p0042 N90-10235
CF 18 480 Gallon External Fuel Tank Stores Clearance Program 02 p0153 N90-10877
Realtime processing and display
02 p0155 N90-10886
Directory of International and Regional Organizations Conducting Standards-Related Activities, May 1989
[PB89-221147] 04 p0483 N90-12776
Integral fuel tank certification and test methods
08 p1023 N90-15916
Software verification plan for GCS --- guidance and control software
[NASA-TM-101668] 10 p1394 N90-18057
Structures and materials technology for hypersonic aerospacecraft
[NASA-TM-102583] 11 p1519 N90-18752
Assessment of crew workload measurement methods, techniques and procedures. Volume 2: Guidelines for the use of workload assessment techniques in aircraft certification
[AD-A217067] 12 p1697 N90-19748
GCS plan for software aspects of certification
[NASA-CR-181972] 13 p1864 N90-20694
Sole means navigation and integrity through hybrid Loran-C and NAVSTAR GPS 14 p1907 N90-20933
Brake performance of the McDonnell Douglas DC-10-30/40 during high speed, high energy rejected takeoffs
[PB90-917004] 14 p1920 N90-21000
An experimental evaluation of software redundancy as a strategy for improving reliability
[NASA-TM-102613] 17 p2448 N90-23958
Probabilistic approach to the certification for fatigue durability of composite structures
[DE90-505521] 20 p2828 N90-26085
Electric field strength meters for the HF, VHF, and UHF bands
[BBC-RD-1990/3] 20 p2851 N90-26212
The role of NDI in the certification of turbine engine components
[PNR90629] 20 p2874 N90-26349
Integration of externally carried weapon systems with military helicopters
[AGARD-AR-247] 22 p3115 N90-27696
Space shuttle descent flight verification by simulation: A challenge in implementing flight control system robustness 22 p3127 N90-27748
The role of NDI in the certification of turbine engine components 22 p3184 N90-28069
Ultrasonic inspection of advanced CFRP structures by computer-controlled, pulse-echo technique
22 p3185 N90-28075

An analysis of GPS as the sole means navigation system in US Navy aircraft 24 p3425 N90-29350

CESIUM
Determining the effects of microwave power and C-field setting on the frequency of a cesium atomic frequency standard
[AD-A216599] 11 p1501 N90-18642
Tellurium embrittlement of type 316 steel
[AERE-R-13440] 13 p1776 N90-20192

CESIUM COMPOUNDS
NT CESIUM IODIDES

CESIUM HALIDES
NT CESIUM IODIDES

CESIUM IODIDES
Enhancement of microchannel plate gain by deposition of CsI on the channel walls
[DE90-003051] 07 p0922 N90-15334
The problem of dead layer in gamma ray burst spectra recorded with NaI or CsI crystals 19 p2776 N90-25787

CESIUM IONS
Surface production of ions
[AD-A216470] 11 p1562 N90-19003

CESIUM PLASMA
True asymptotic plasma-sheath matching with an asymptotically correct collisional presheath
[AD-A212857] 05 p0701 N90-14104

CESIUM VAPOR
Development of a wet vapor homogeneous liquid metal MHD power system
[DE90-001468] 08 p1124 N90-16508

CESSNA AIRCRAFT
Laminar flow: The Cessna perspective 04 p0439 N90-12507

CESSNA MILITARY AIRCRAFT
U MILITARY AIRCRAFT

CF-104 AIRCRAFT
U CANADAIR AIRCRAFT
U F-104 AIRCRAFT

CFD
U CHARGE FLOW DEVICES

CFRP
U CARBON FIBER REINFORCED PLASTICS

CH-53 HELICOPTER
U H-53 HELICOPTER

CH-47 HELICOPTER
A rule-based paradigm for intelligent adaptive flight control 12 p1605 N90-19238
Simulator sickness in the CH-47 (Chinook) flight simulator
[AD-A218214] 13 p1853 N90-20634

CHAIRS
U SEATS

CHALCOGENIDES
NT ALKALINE EARTH OXIDES
NT ALUMINUM OXIDES
NT ANHYDRIDES
NT BARIUM OXIDES
NT BERYLLIUM OXIDES
NT BISMUTH OXIDES
NT BISMUTH SULFIDES
NT CADMIUM SULFIDES
NT CADMIUM TELLURIDES
NT CALCIUM OXIDES
NT CALCIUM SULFIDES
NT CARBON DIOXIDE
NT CARBON DISULFIDE
NT CARBON MONOXIDE
NT CERIUM OXIDES
NT CHROMIUM OXIDES
NT COBALT OXIDES
NT COPPER OXIDES
NT COPPER SELENIDES
NT DIOXIDES
NT DISULFIDES
NT GALLIUM OXIDES
NT HAFNIUM OXIDES
NT HEAVY WATER
NT HYDROGEN PEROXIDE
NT HYDROGEN SULFIDE
NT ILMENITE
NT LANTHANUM OXIDES
NT LEAD OXIDES
NT LEAD TELLURIDES
NT LITHIUM OXIDES
NT MAGNESIUM OXIDES
NT MANGANESE OXIDES
NT MERCURY TELLURIDES
NT METAL OXIDES
NT MIXED OXIDES
NT MOLYBDENUM DISULFIDES
NT MOLYBDENUM OXIDES
NT MOLYBDENUM SULFIDES
NT NICKEL OXIDES
NT NIOBIUM OXIDES
NT NITRIC OXIDE
NT NITROGEN DIOXIDE
NT NITROGEN OXIDES
NT NITROGEN TETROXIDE
NT NITROUS OXIDES
NT OXIDES
NT PEROXIDES
NT PLATINUM OXIDES
NT PLUTONIUM OXIDES
NT POLYSULFIDES
NT POTASSIUM OXIDES
NT QUARTZ
NT RUTILE
NT SAPPHIRE
NT SILICON DIOXIDE
NT SILICON OXIDES
NT SILVER OXIDES
NT SULFIDES
NT SULFUR DIOXIDES
NT SULFUR OXIDES
NT TANTALUM OXIDES
NT TIN OXIDES
NT TIN TELLURIDES
NT TITANIUM OXIDES
NT TUNGSTEN OXIDES
NT URANIUM OXIDES
NT VANADIUM OXIDES
NT YTTRIUM OXIDES
NT ZINC OXIDES
NT ZINC SELENIDES
NT ZINC SULFIDES
NT ZINC TELLURIDES
NT ZIRCONIUM OXIDES
Pairs of chalcogen impurities in silicon
[DE89-635767] 08 p1049 N90-16063
The preparation and properties of iron doped II-VI chalcogenides
[AD-A217569] 12 p1724 N90-19903

CHALLENGER (ORBITER)
America's shuttle returns to space 09 p1174 N90-16792
GPHS-RTG response to Challenger type accident 19 p2685 N90-25163

CHANCE-VOUGHT MILITARY AIRCRAFT
U MILITARY AIRCRAFT

CHANGE DETECTION
Satellite image sequences for motion analysis and change detection 08 p1092 N90-16323
Analysis of camera movement based on a sequence of images
[TELECOM-PARIS-89-D-008] 18 p2616 N90-24901
Optical motion detector detecting visible and near infrared light
[AD-D014515] 19 p2758 N90-25671

CHANNEL CAPACITY
Fellowships in information and stochastic systems
[AD-A212385] 04 p0563 N90-13280
Information capacity of the matched Gaussian channel with jamming. 1: Finite-dimensional channel
[AD-A214782] 09 p1205 N90-16984
Coding capacity for a class of additive channels
[AD-A215054] 09 p1206 N90-16993
Information capacity of dimension-limited channels
[AD-A215238] 09 p1207 N90-16996
Information capacity of the stationary Gaussian channel
[AD-A215408] 09 p1207 N90-16998
Quantization effects in Viterbi decoding rate 1/n convolutional codes 12 p1644 N90-19445
SAR image coding 14 p1964 N90-21246
Feasibility of using frequency offset on very high frequency air/ground voice channels
[DOT/FAA/CT-TN89/71] 14 p1964 N90-21248
Traffic placement policies for a multi-band network 15 p2149 N90-22279
Throughput and delay characteristics for a slow-frequency hopped aircraft-to-aircraft packet radio network
[AD-A220525] 17 p2389 N90-23609
Continuous on-line link error rate detector
[AD-D014510] 20 p2850 N90-26209

CHANNEL FLOW
NT OPEN CHANNEL FLOW
Numerical simulation of turbulent plane channel flows 01 p0067 N90-10382
Near-planar TS waves and longitudinal vortices in channel flow: Nonlinear interaction and focusing
[NASA-CR-181928] 03 p0300 N90-11698
Numerical experiments on transition control in wall-bounded shear flows 04 p0443 N90-12536
Investigation of turbulent flow in highly curved ducts with application to turbomachinery components
[NASA-CR-186060] 04 p0500 N90-12882
Evaluation of the near-wall k-epsilon turbulence model by comparison with direct simulations of turbulent channel flow
[AD-A212674] 04 p0503 N90-12903
Superfluid phase slippage in (3)He-B flow through a narrow channel
[PB89-218986] 04 p0559 N90-13258
Heat transfer in convective boundary layer and channel flows 06 p0774 N90-14505
Unsteady hydromagnetic flow of a radiating gas in a vertical channel with axial temperature variation
[DE90-600934] 06 p0778 N90-14525
Gelled propellant flow: Boundary layer theory for power-law fluids in a converging planar channel
[DE90-000923] 07 p0927 N90-15365
Experimental determination of the fluid velocity by spectral analysis of temperature fluctuations
[DE89-636430] 07 p0928 N90-15372
TS - Dean interactions in curved channel flow
[NASA-CR-181983] 10 p1306 N90-17559
Magnetohydrodynamic liquid-metal flows in a rectangular channel with an axial magnetic field, a moving conducting wall, and free surfaces
[AD-A216276] 10 p1425 N90-18223
Study of vortex arrays induced artificially and from centrifugal instabilities
[AD-A216499] 11 p1506 N90-18669
Carrier wing profile in nonstationary current
[ETN-90-95368] 12 p1600 N90-19208
Experimental investigations on channelized coplanar waveguide
[NASA-TM-102494] 13 p1792 N90-20286
Flow visualization studies in a curved rectangular channel with 40 to 1 aspect ratio and a straight channel with bulk flow unsteadiness
[AD-A218020] 13 p1803 N90-20348
Flow boiling with enhancement devices for cold plate coolant channel design
[NASA-CR-186358] 15 p2089 N90-21961
Automated analysis of measured turbulent boundary flow
[PB90-147844] 15 p2092 N90-21970
Some observations on liquid flow through filters
[AERE-R-13300] 16 p2234 N90-22748
Parallel channel flow excursions
[DE90-009129] 16 p2235 N90-22753
Computational simulation of transition to turbulence through inverse modeling 18 p2647 N90-25067
Flow resistance and critical shear stress in steep channels 19 p2687 N90-25282
Measurement of terms and parameters in turbulent models
[NASA-CR-183993] 20 p2860 N90-26271
The effect of a three-dimensional source on the flow through a channel with square cross section
[LR-512] 20 p2863 N90-26289
Effects of 2 Hz imposed bulk flow unsteadiness on laminar-turbulent transition in a straight channel
[AD-A223028] 20 p2864 N90-26295
An improved k-epsilon model for near-wall turbulence and comparison with direct numerical simulation
[NASA-TM-103221] 22 p3171 N90-27983
Numerical study of turbulence in the presence of walls
[ONERA-RSF-15/3419-AY-114A] 22 p3176 N90-28024
Free shear layer and swirl flow heat transfer enhancement
[PB90-226123] 23 p3325 N90-28798
Reynolds stress and the physics of turbulent momentum transport
[AD-A224172] 24 p3467 N90-29588
Direct numerical simulation of turbulent couette flow
[AD-A224287] 24 p3467 N90-29589
Effects of 1 Hz imposed bulk flow unsteadiness on laminar/turbulent transition in a straight channel
[AD-A223396] 24 p3468 N90-29594
Counter-current flow limitation in thin rectangular channels
[DE90-015124] 24 p3469 N90-29599

CHANNEL NOISE
Multi-stage noise-reducing system
[AD-D014179] 03 p0341 N90-11942
Absolute continuity and mutual information for Gaussian mixtures
[AD-A215185] 09 p1274 N90-17383
Trends in VLF/LF (Very Low Frequency/Low Frequency) modem performance testing
[AD-A216576] 11 p1497 N90-18614
Tracking performance of a combined Costas/AFC-loop under noisy Rayleigh/Rician channel conditions with additive Gaussian noise jamming
[ETN-90-96964] 20 p2855 N90-26237
An assessment of the application of in situ ion-density data from DMSP to modeling of transionospheric scintillation
[AD-A224392] 24 p3490 N90-29725

CHANNELS (DATA TRANSMISSION)
A new approach to HF (High Frequency) channel modeling and simulation. Part 1: Deterministic model
[PB89-203962] 03 p0336 N90-11913

Introduction to the Mil-Std-1553B serial multiplex data bus
[RAE-TM-MM-9] 03 p0418 N90-12405
Automatic communications channel interference monitoring
[RSRE-MEMO-4243] 04 p0491 N90-12820
MT's algorithm: A new algorithm to search for the optimum set of modulation indices for simultaneous range, command, and telemetry
[NASA-CR-186259] 08 p1057 N90-16110
Performance of cellular frequency-hopped spread-spectrum radio networks
[AD-A214480] 09 p1204 N90-16978
Classification of acousto-optic correlation signatures of spread spectrum signals using artificial neural networks
[AD-A215045] 09 p1206 N90-16992
Channel simulator upgrade to use field propagation data 10 p1372 N90-17948
Efficient interconnection schemes for VLSI and parallel computation
[AD-A216405] 10 p1420 N90-18185
An adaptive ARQ (Automatic Repeat Request) strategy for packet switching data communication networks
[AD-A216597] 11 p1497 N90-18615
Rate compatible punctured codes, their use in military satellite communication systems
[AD-A216723] 11 p1497 N90-18619
A linear systems theory approach to the range-independent acoustic channel
[AD-A216551] 12 p1710 N90-19817
Error control techniques for satellite and space communications
[NASA-CR-186221] 13 p1788 N90-20263
Traffic placement policies for a multi-band network 15 p2149 N90-22279
Alternative parallel ring protocols 15 p2150 N90-22282
Simulation and analysis of a MFQPSK signal transmitted through an acoustic medium
[AD-A220345] 17 p2393 N90-23633
CESAR LOCAL BUS
[FFI-89/7011] 17 p2440 N90-23903
Normal-mode and phase-integral methods for determining phase and group velocities in simple underwater acoustic ducts
[AD-A221393] 18 p2612 N90-24877
A digital Meteor-Burst Communication (MBC) propagation path simulator 20 p2847 N90-26190
Channel selection and control procedures in an automatic HF system 20 p2847 N90-26193
The need for headers: An impossibility result for communication over unreliable channels
[AD-A222623] 21 p2994 N90-27018
Spread-spectrum communications in non-Gaussian channels
[AD-A222886] 21 p2994 N90-27019
Studies in automatic speech recognition and its application in aerospace 23 p3318 N90-28759

CHAOS
Symmetry breaking bifurcations and the growth of chaos in a rotating fluid
[AD-A210969] 01 p0072 N90-10411
An introduction to fractals and chaos
[AD-A210257] 01 p0117 N90-10675
Theoretical investigations of chaotic dynamics
[AD-A207724] 01 p0134 N90-10772
The origin of the universe from quantum chaos: An introduction to current ideas
[AD-A210441] 01 p0141 N90-10813
Chaotic behavior in nonlinear polarization dynamics
[DE89-013453] 06 p0788 N90-14589
Hamiltonian chaos in a nonlinear polarized optical beam
[DE90-002437] 07 p0934 N90-15408
Monitoring chaos of cardiac rhythms
[DE90-000692] 07 p0966 N90-15580
Chaos and turbulence
[AD-A215310] 09 p1294 N90-17499
Concepts and experiments on space-time chaos
[ETN-90-96255] 11 p1508 N90-18683
Using special-purpose computing to examine chaotic behavior in nonlinear mappings
[AD-A216800] 11 p1549 N90-18916
Chaotic transients, higher dimensional phenomena, and coupled ordinary differential equations
[DE90-006641] 12 p1706 N90-19794
Nonlinear system vibration: The appearance of chaos
[DE90-007546] 12 p1708 N90-19810
Computation at the edge of chaos: Phase transition and emergent computation
[DE90-007488] 12 p1708 N90-19811
The role of chaos in hemispheric process and attention
[AD-A217674] 13 p1854 N90-20639
Homogeneous chaos, p-forms, scaling and the feynman integral
[AD-A218339] 13 p1879 N90-20777
Integrability and chaos in nonlinearly coupled optical beams
[DE90-007540] 13 p1888 N90-20834
The intrinsic stochasticity of near-integrable Hamiltonian systems
[IPPCZ-282] 15 p2167 N90-22386
Computational chaos in massively parallel neural networks 16 p2283 N90-23012
Intermittency and multifractality in magnetic dynamos
[PREPRINT-702] 16 p2319 N90-23226
Fields, particles, groups: Bertel Laurents 60th Anniversary Symposium
[ETN-90-96596] 17 p2478 N90-24170
Coherent structures, chaos and the role of modern dynamics in turbulent shear flows
[AD-A220884] 18 p2552 N90-24562
An investigation of chaotic Kolmogorov flows
[NASA-CR-182079] 23 p3328 N90-28816
Prediction, control, and decision-making aspects for chaotic systems
[DE90-014452] 23 p3402 N90-29224
Quantum chaos and dissipation: Lyapunov exponents
[DE90-627180] 23 p3403 N90-29228
Propagation of chaos and the McKean-Vlasov equation in duals of nuclear spaces
[AD-A224431] 24 p3543 N90-30039

CHAOTIC CLOUD PATTERNS
U CLOUDS (METEOROLOGY)

CHAPMAN SHEAR LAYER
U SHEAR LAYERS

CHAPMAN-JOUGET FLAME
U CHEMICAL EQUILIBRIUM
U DETONATION
U FLAME PROPAGATION

CHARACTER RECOGNITION
Proceedings of the Conference on Application of Scanning Methodologies in Libraries
[PB89-233415] 06 p0858 N90-14990
Alvey MMI007. Object identification from 2D images: The RSRE contribution
[RSRE-MEMO-4277] 08 p1110 N90-16428
Performance of the IMP array processing algorithm: First results
[RSRE-MEMO-4291] 15 p2148 N90-22274

CHARACTERISTIC EQUATIONS
U EIGENVALUES
U EIGENVECTORS

CHARACTERISTIC FUNCTIONS
U EIGENVALUES
U EIGENVECTORS

CHARACTERISTIC METHOD
U METHOD OF CHARACTERISTICS

CHARACTERISTICS
Fabrication characteristics of 8090 alloy 07 p0899 N90-15198

CHARACTERIZATION
A new method for the characterization of solutes and solvent phases using solvatochromic parameters
[AD-A211238] 02 p0196 N90-11116
Choice and characterization of new materials for aerospace applications
[ETN-89-95219] 03 p0320 N90-11819
Characterization and cycle tests of lightweight nickel electrodes
[NASA-TM-102399] 04 p0470 N90-12696
Polymer characterization by electrohydrodynamic ionization mass spectrometry
[AD-A212130] 04 p0478 N90-12739
Characterization of surfaces cut with a laser beam and thermal model of the process
[ISAL-89-0008] 05 p0648 N90-13780
Nondestructive evaluation of flaw clusters and thin layer interfaces 06 p0795 N90-14633
The processes of scientific research: The strategy of experimentation 06 p0824 N90-14788
Microwave characterization of high-temperature superconductors
[DE90-002408] 06 p0854 N90-14968
Characterization of chemicals on engine exhaust particles
[AD-A213566] 07 p0882 N90-15106
Ceramic powder characterization
[DE90-001282] 07 p0908 N90-15249
Simultaneous thermal analysis techniques for characterization of energetic materials
[DE90-003028] 07 p0914 N90-15289
Polarimetric SAR antenna characterization
[AD-A213438] 07 p0917 N90-15306
Advanced double layer capacitor
[AD-A213406] 07 p0923 N90-15341
Comprehensive, nonintercepting electron-beam diagnostics using spontaneous emission
[DE90-003211] 07 p0935 N90-15414
Characteristics of electromagnetic wave forms with lightning in winter season
[DE89-901256] 07 p0963 N90-15567
Piezoelectric ceramic modeling and characterization at high levels of mechanical activity
[ISAL-89-0030] 08 p1051 N90-16074
Candidate sample acquisition systems for the Rosetta 08 p1145 N90-16635
Physical chemical characterization of the surface of carbon fibers: Test report
[REPT-49-740/F] 09 p1188 N90-16881
Universal nondestructive MM-wave integrated circuit test fixture
[NASA-CASE-LEW-14746-1] 09 p1209 N90-17009
Signal processing applied to photothermal techniques for materials characterization 10 p1364 N90-17902
Materials thermal and thermoradiative properties/characterization technology 10 p1367 N90-17925
Space station technology summary 11 p1474 N90-18482
Characterization and development report for the SA3274-1 and SA3274-2 transient voltage suppressors
[DE90-005712] 11 p1502 N90-18649
Performance parameter characterisation of various types of IR single element detectors 11 p1588 N90-19161
Characterization of thunderstorm induced Maxwell current densities in the middle atmosphere 12 p1634 N90-19391
Liquid oxygen LOX compatibility evaluations of aluminum lithium (Al-Li) alloys: Investigation of the Alcoa 2090 and MMC weldalite 049 alloys 12 p1636 N90-19398
Mechanics of aeolian processes: Soil erosion and dust production 12 p1638 N90-19410
Construction and characterization of a valve for rapid gas injection
[INPE-4789-RPE/583] 12 p1651 N90-19486
Synthesis and analysis of 25 years (1961-1986) of INPE/SRE activities related to the vegetation/forest area
[INPE-4969-RPE/604] 13 p1819 N90-20446
Growth, characterization and device development in monocrystalline diamond films
[AD-A218211] 13 p1898 N90-20895
Surface characterization of hydrogen charged and uncharged alpha-2 and gamma titanium aluminide alloys using AES and REELS
[NASA-CR-186561] 14 p1951 N90-21171
Evolution of remote sensing applied to vegetation and forest at INPE
[INPE-4970-PRE/1538] 14 p1998 N90-21452
Characterization of the plasma in magnetic multidipole discharges
[DE90-613219] 14 p2028 N90-21628
Development of ultrasonic nondestructive methods for defect and damage characterization in composite materials 15 p2063 N90-21816
Development of low thermal conductivity pan-based carbon fibers for solid rocket motor nozzle applications 15 p2063 N90-21818
Preparation and characterization of Cu2ZnGeS(4-y)Se(y)
[AD-A217469] 15 p2171 N90-22407
Impact damage in graphite/epoxy laminates: Damage characterization, acoustic emission, and finite element simulation, volumes 1 and 2 16 p2211 N90-22610
Time-varying filter modelling and time-frequency characterisation of nonstationary sound fields due to a moving source 16 p2312 N90-23178
Characterisation of fatigue of aluminium alloys by acoustic emission. Part 2: Discrimination between primary and other emissions
[AERE-R-13303-PT-2] 17 p2375 N90-23523
Characterization by means of electrochemical impedance measurement and optoelectrochemical analysis of electrolytic, insulating, and semiconducting solution structures. Development of a cartographic analysis method for optoelectrochemical impedance
[ECL-89-15] 17 p2474 N90-24144
Characterization of solid state bonding between Coors AD-999 alumina and niobium
[DE90-010653] 18 p2518 N90-24379
Morphological and structural characterization of the spinodal decomposition of Fe-Cr alloys
[DE90-010496] 18 p2526 N90-24418
Majority voting: Characterization and algorithms
[RUU-CS-88-32] 18 p2592 N90-24750
Characterization of a Ho:Tm:Cr:YAG laser with a Cr:GSAG laser as pumping source 18 p2642 N90-25047
Modeling and Applications of Transport Phenomena in Porous Media, volume 2
[VKI-LS-1990-01-VOL-2] 19 p2690 N90-25302
Characterization of porous media: Pore level 19 p2690 N90-25303

Characterization of porous media: Field level
19 p2690 N90-25304
Characterization of fluids in porous media
19 p2690 N90-25305
Characterization of inspection performance
[NLR-MP-88068-U] 20 p2874 N90-26350
The system matrix characterisation of input-output equivalence
[MATHS-REPT-A-112] 20 p2918 N90-26600
Elementary characterization of the pre-impregnated carbon/epoxy NCHR 914/155/34 percent-T300F from Brochier after the technical note CEAT number 1/M/87
[CEAT-PV-M7/6211] 22 p3154 N90-27884
Assessment and demonstration of the capabilities of NDI processes, equipment, and personnel
22 p3184 N90-28071
Radiation-curable prepreg composites
[DE90-629740] 23 p3301 N90-28674
High temperature superconducting thin film microwave circuits: Fabrication, characterization, and applications
[NASA-TM-103235] 23 p3322 N90-28786
Quality function deployment as a mechanism for process characterization and control
[DE90-014755] 23 p3337 N90-28857
Omega navigation signal characteristics
24 p3429 N90-29369
Nondestructive material characterization
[DE90-015176] 24 p3477 N90-29652

CHARACTERS
U SYMBOLS

CHARGE CARRIERS
NT FREE ELECTRONS
NT HOLES (ELECTRON DEFICIENCIES)
NT MINORITY CARRIERS
Studies of high power density, pico-second rise-time light activated semiconductor switch
[AD-A210549] 01 p0061 N90-10349
Particle emission and charging effects induced by fracture
[AD-A210215] 01 p0080 N90-10459
Trap gettering by isoelectronic doping of p-GaAs and n-GaAs grown by molecular beam epitaxy
[AD-A211162] 01 p0133 N90-10769
International workshop on Beam Injection Assessment of Defects in Semiconductors
[AD-A210842] 02 p0283 N90-11617
A fermi liquid electric structure and the nature of the carriers in high-T(sub c) cuprates: A photoemission study
[DE89-016774] 02 p0284 N90-11624
Graded bandgap solar cells
[AD-A211537] 03 p0367 N90-12097
Energy relaxation of light holes in InAs(.15)Sb(.85)/InSb multiple quantum wells
[DE89-016035] 03 p0409 N90-12349
Magnetic mechanisms of high temperature superconductivity
[DE90-003625] 07 p1001 N90-15796
Defect control and denuded trap zones in the 3-5 semiconductors
[AD-A214099] 07 p1004 N90-15814
Discretization of the steady state semiconductor device equations
[AD-A215807] 10 p1438 N90-18298
Proceedings of the 6th Conference on Hot Carriers in Semiconductors
[AD-A215978] 11 p1569 N90-19032
Electronic properties of high-temperature superconductors
[AD-A217953] 13 p1898 N90-20892
Joint services electronics program: Electronics research at the University of Texas at Austin
[AD-A220834] 17 p2397 N90-23655
Hot carrier in subpicosecond photoconductive experiments
[AD-A219874] 17 p2477 N90-24166
The color of polarization in cuprate superconductors
22 p3144 N90-27830
Study of hot carrier relaxation in quantum wells by subpicosecond Raman scattering
[DE90-015635] 24 p3554 N90-30107

CHARGE COUPLED DEVICES
The detection of soft X-rays with charged coupled detectors
01 p0138 N90-10798
Evaluation test of CCD area sensor for star sensor
[NAL-TM-570] 02 p0274 N90-11566
Fast and objective MRTD measurement
[FEL-1988-24] 03 p0351 N90-12006
An imaging vector magnetograph for the next solar maximum
03 p0435 N90-12489
Efficient detection of small moving objects
[AD-A213314] 05 p0632 N90-13690
CCD TV focal plane guider development and comparison to SIRTF applications
[NASA-CR-185977] 06 p0842 N90-14900
Hybrid optical/digital architecture for distortion invariant pattern recognition
[AD-A215628] 09 p1282 N90-17435
A space qualified thermal imaging system using a Pt Si detector array
10 p1367 N90-17921
First test results with a CCD camera developed by INPE
[INPE-4873-PRE/1484] 10 p1388 N90-18029
Investigations of x ray sensitive PN-CCD's
[MPE-213] 12 p1653 N90-19499
Structural experiments of planetary nebulae: Charge-coupled devices, image reduction under MIDAS, information representation, and development of an evolution classification for PN's
[ETN-90-95736] 12 p1744 N90-20026
Space environment robot vision system
15 p2143 N90-22245
Optical rate sensor algorithms
18 p2632 N90-24997
Optical techniques for determination of normal shock position in supersonic flows for aerospace applications
[NASA-TM-103201] 19 p2693 N90-25323
CAESAR: Performance and first evaluation of application possibilities
[BCRS-89-06] 19 p2705 N90-25393
Multiple target tracking in a wide-field-of-view camera system
[DE90-013488] 20 p2865 N90-26300
Development of Planar Laser-Induced Fluorescence (PLIF) techniques for supersonic flows
21 p2974 N90-26900
Design of GaAs charge coupled devices
[DE90-012124] 21 p3080 N90-27513
Noise performance of microchannel plate imaging systems
[DE90-015037] 23 p3322 N90-28785
Long-term flat-field behavior in LLNL streak cameras: Preliminary results
[DE90-015615] 24 p3472 N90-29621
Bispectral-based optimization algorithms for speckle imaging
[DE90-015610] 24 p3529 N90-29957

CHARGE DISTRIBUTION
Synchrotron-radiation experiments with recoil ions
[DE89-017579] 03 p0402 N90-12301
A numerical model for the axisymmetric equilibrium shape of drops in uniform motion: Effects of external flow, electric field and surface charge
07 p0874 N90-15071
On the observation of a transition from fusion to multifragmentation in high multiplicity O16 induced reactions
[LUIP-8812] 08 p1119 N90-16481
Near contact phenomena and transient effects in far infrared photoconductors
14 p1976 N90-21316

CHARGE EFFICIENCY
Terrestrial nickel/hydrogen battery development at Johnson Controls, Inc.
[DE89-015843] 06 p0769 N90-14471
Sodium/sulfur evaluation at SNL
[DE89-015846] 06 p0769 N90-14472
Membrane and durability studies for the zinc/bromine battery
[DE89-016181] 07 p0920 N90-15324
Research and development of lithium/polyaniline battery, part 2
[DE90-734985] 09 p1211 N90-17018
Thermal study of battery charge control by temperature derivative reduction
10 p1332 N90-17704
Low earth orbit nickel cadmium battery lifetime testing
10 p1334 N90-17716
Preliminary study of rechargeable lithium cells for space applications
10 p1334 N90-17717
Performance of superconductive oxides as cathodes for lithium rechargeable batteries
[AD-A216030] 10 p1401 N90-18098
Evaluation of the state of charge of battery electrodes with ac impedance techniques
[AD-A219561] 17 p2420 N90-23789
Storage battery operation technique of photovoltaic system to prevent the imbalance of state of charge
[DE90-503032] 20 p2858 N90-26255

CHARGE EXCHANGE
The effective (3)He-nucleon force in a microscopic DWBA approach to the (3)He,t charge exchange reaction --- Distorted Wave-Borne Approximation (DWBA)
[KVI-763] 05 p0697 N90-14077
An effective He-3 nucleon force for the He-3, t) charge exchange reaction
[KVI-813] 16 p2315 N90-23198
Studies of Io's atmosphere and plasma torus
16 p2338 N90-23326

CHARGE FLOW DEVICES
Rolls-Royce and ERCOFTAC
[PNR90600] 04 p0456 N90-12615
Feedback charge amplifier integrated on the detector wafer
[REPT-89-037] 04 p0496 N90-12852
Integrated silicon flow sensors
[ETN-90-96906] 17 p2407 N90-23715

CHARGE INJECTION DEVICES
ISO camera array development status
14 p1980 N90-21344

CHARGE SEPARATION
U POLARIZATION (CHARGE SEPARATION)

CHARGE TRANSFER
Electron transfer reactions
[AD-A210711] 02 p0271 N90-11545
Electronic structure of transition metal alloys and intermetallics: Charge transfer and its implications for Moessbauer effect measurements
[DE89-017603] 03 p0327 N90-11860
Resonant-tunneling oscillators and multipliers for submillimeter receivers
05 p0597 N90-13467
Charge transfer and bond lengths in YBa2Cu(sub 3-x)M(sub x)O(sub 6+y)
[DE90-002241] 06 p0854 N90-14966
New organic synthetic metals derived from BEDT-TTF, Ni(dsit)2 and BEDO-TTF
[DE90-003793] 07 p0907 N90-15242
Phonons and charge-transfer excitations in HTS superconductors
[DE89-016616] 07 p0997 N90-15768
Solid state voltammetry and sensors in solids and gases
[DE90-003234] 08 p1129 N90-16538
Electronic energies for Neon dimer dication radiative charge transfer
[AD-A215817] 10 p1429 N90-18244
Electrochemical investigations of electronically conductive polymers. Part 4: By controlling the supermolecular structure, charge transport rates can be enhanced
[AD-A216603] 11 p1490 N90-18573
Modelling of molecular structures and properties in physical chemistry and biophysics
[AD-A214561] 14 p1947 N90-21145
Towards a quantum pump of electric charges and currents
[AD-A221257] 18 p2607 N90-24851
Fast plasma mixing: A new excitation method for CW gas lasers
[AD-A220290] 18 p2617 N90-24904
Valence-defect chemical equilibria in nonstoichiometric YBa2Cu3O(7-delta)
[DE90-010152] 18 p2619 N90-24921
Ion/molecule reactions of arsenic and phosphorus cluster ions: Ionization potentials and novel reaction pathways
[AD-A222019] 21 p2977 N90-26918
Non-destructive characterization of polymer/metal interfaces using Surface-Enhanced Raman Scattering (SERS)
[AD-A223105] 21 p2986 N90-26967
Non-destructive characterization of polymer/metal interphases using surface-enhanced Raman scattering
[AD-A222490] 21 p2988 N90-26980
State-to-state ion-molecule reaction dynamics at thermal energies
[AD-A221589] 21 p3074 N90-27479
Charge transfer polarisation wave and carrier pairing in the high T(sub c) copper oxides
22 p3142 N90-27820
The mechanism of high-T(sub c) superconductivity due to bound hole mediators: Relationship to ferroelectricity
22 p3143 N90-27826
Correlated charge changing ion-atom collisions
[DE90-014662] 23 p3393 N90-29171

CHARGE TRANSFER DEVICES
NT CHARGE COUPLED DEVICES
NT CHARGE INJECTION DEVICES

CHARGED PARTICLES
NT ALPHA PARTICLES
NT ANTIPROTONS
NT ARGON PLASMA
NT BETA PARTICLES
NT BOUNDARY LAYER PLASMAS
NT CESIUM PLASMA
NT COLD PLASMAS
NT COLLISIONAL PLASMAS
NT COLLISIONLESS PLASMAS
NT CONDUCTION ELECTRONS
NT COSMIC PLASMA
NT CYLINDRICAL PLASMAS
NT DENSE PLASMAS
NT DEUTERONS
NT ELECTRON PLASMA
NT ELECTRON-POSITRON PLASMAS
NT ELECTRONS
NT ENERGETIC PARTICLES
NT FREE ELECTRONS

NT HEAVY NUCLEI
NT HELIUM PLASMA
NT HIGH ENERGY ELECTRONS
NT HIGH TEMPERATURE PLASMAS
NT HOT ELECTRONS
NT HYDROGEN PLASMA
NT IONIZED GASES
NT LASER PLASMAS
NT MAGNETIC CLOUDS
NT METALLIC PLASMAS
NT NITROGEN PLASMA
NT NONEQUILIBRIUM PLASMAS
NT NONUNIFORM PLASMAS
NT NUCLEI (NUCLEAR PHYSICS)
NT ODD-ODD NUCLEI
NT OXYGEN PLASMA
NT PHOTOELECTRONS
NT PI-ELECTRONS
NT PLASMA CLOUDS
NT PLASMA FOCUS
NT PLASMA JETS
NT PLASMA LAYERS
NT PLASMA SHEATHS
NT PLASMAS (PHYSICS)
NT POLARONS
NT POSITRONS
NT PROTONS
NT RADIATION BELTS
NT RADIO JETS (ASTRONOMY)
NT RECOIL PROTONS
NT RELATIVISTIC ELECTRON BEAMS
NT RELATIVISTIC PLASMAS
NT ROTATING PLASMAS
NT SEMICONDUCTOR PLASMAS
NT SOLAR PROTONS
NT SOLAR WIND
NT SPACE PLASMAS
NT SPHERICAL PLASMAS
NT STELLAR WINDS
NT STRONGLY COUPLED PLASMAS
NT THERMAL PLASMAS
NT TOROIDAL PLASMAS
NT TRITONS

Molecular dynamics study of the primitive model of 1-3 electrolyte studies
[AD-A211653] 03 p0325 N90-11846

Laser production of soft x rays by multiquantum processes and the excitation of atomic inner-shell states
[AD-A211372] 03 p0353 N90-12021

Confinement of multiply charged ions in an ECRH mirror plasma
[DE89-016052] 03 p0406 N90-12327

Twistons
[RSRE-MEMO-4234] 04 p0562 N90-13275

Near-surface sputtered particle transport for an oblique incidence magnetic field plasma
[DE90-004422] 07 p0996 N90-15758

Stochastic simulation of charged particle transport on the massively parallel processor
08 p1114 N90-16448

Possible measurement of the gravitational acceleration of molecules, atoms, nuclei, elementary particles, and antiparticles
[DE90-719559] 08 p1121 N90-16490

Experimental investigation of relationship between nonlinear field energy and emittance growth
[AD-A215813] 10 p1430 N90-18246

Report from space plasma science
10 p1445 N90-18336

Identification and solution of a charging problem in a high-altitude detector
[DE90-008637] 12 p1616 N90-19296

Radiation of electromagnetic waves by an accelerated charged particle in medium
[DE90-610458] 12 p1646 N90-19461

Fifth-order aberrations in magnetic quadrupole-octupole systems
[DE90-007489] 12 p1712 N90-19831

The 41st Annual Gaseous Electronics Conference
[AD-A214540] 12 p1715 N90-19851

Electrical resistivity of strongly coupled plasmas in intense fields
[DE90-002236] 12 p1717 N90-19861

Physical sputtering of metallic systems by charged-particle impact
[DE90-007803] 13 p1777 N90-20201

Charged-particle beam research program
[DE90-007937] 14 p2026 N90-21618

Some global problems in gauge theories (variations on a theme of Aharonov and Bohm)
[DE90-009034] 14 p2035 N90-21678

Beam propagation in direct nuclear pumped laser amplifiers
[DE90-009613] 15 p2104 N90-22035

Dynamics of motion charged particles in a field of two electromagnetic waves
[DE90-620690] 16 p2228 N90-22706

Solar flares and magnetospheric particles: Investigations based upon the ONR-602 and ONR-604 experiments
[AD-A218844] 16 p2340 N90-23332

First International Conference on Laboratory Research for Planetary Atmospheres
[NASA-CP-3077] 20 p2942 N90-26744

Investigation of the Saturn dust environment from the analysis of energetic charged particle measurements
[NASA-CR-186727] 20 p2950 N90-26784

Concept for a neutron spectrometer based on optical detection of (3)He(n, p)-3H reactions in a gas
[DE90-014776] 23 p3330 N90-28826

Old and new ideas in the theory of quantum measurement
[DE90-627181] 23 p3403 N90-29229

CHARGING

Terrestrial nickel/hydrogen battery development at Johnson Controls, Inc.
[DE89-015843] 06 p0769 N90-14471

CHARM (PARTICLE PHYSICS)

Measurement of the masses and lifetimes of the charmed mesons D neutral, D plus and D (sub s) plus
[MPI-PAE/EXP-EL-220] 22 p3245 N90-28405

CHARON

Neptune's Triton: A moon rich in dry ice and carbon
[NASA-CR-186298] 08 p1152 N90-16675

Carbon in the outer solar system
21 p3096 N90-27593

CHARPY IMPACT TEST

Mechanical property characterization of VascoMax T-300
[AD-A212950] 05 p0823 N90-13837

Cast stainless steel aging: Mechanisms and predictions
[DE90-003772] 07 p0907 N90-15241

A semiautomated computer-interactive dynamic impact testing system
[DE90-002721] 07 p0946 N90-15479

Response of unirradiated and neutron-irradiated vanadium alloys to Charpy-impact loading
[DE90-004878] 11 p1486 N90-18551

Evaluation of material homogeneity as a function of thickness of low-alloy ferritic steel
[DE90-008069] 13 p1777 N90-20202

Characterization of weldments using advanced experimental techniques
[DE90-009418] 16 p2242 N90-22792

Irradiation effects on impact behavior of 12Cr-1MoVW and 2 1/4Cr-1Mo steels
[DE90-011075] 18 p2527 N90-24421

Influence of thermal conditioning media on Charpy specimen test temperature
[DE90-012784] 20 p2875 N90-26360

Determination of the NDT temperature and Charpy V-notch impact properties of AAR TC128 grades B steel and A 8XX grade B steel
[PB90-207804] 23 p3309 N90-28716

Mechanical properties and fracture toughness of AAR-TC128 Grade B steel and a micro-alloyed, control-rolled steel, A 8XX grade B, from -80F to +73F
[PB90-207796] 24 p3448 N90-29471

CHARRING

Modifications to the aerotherm charring material thermal response and ablation program (CMA) for carbon ablation analysis
[AD-A211069] 02 p0195 N90-11115

CHARTS

NT BOND GRAPHS
NT FLOW CHARTS
NT GRAPHS (CHARTS)
NT METEOROLOGICAL CHARTS

NORDA's pattern analysis laboratory: Current contributions to naval mapping, charting, and geodesy
[AD-A212731] 06 p0801 N90-14665

A technique for the generation of range-height-angle charts
[AD-A214534] 09 p1204 N90-16979

Charting and Geodetic Services
[PB90-116674] 09 p1240 N90-17196

The test for automatic neph-analysis chart
21 p3029 N90-27219

An experiment to make a new design of the Satellite Cloud Information Chart with the combination of visible and infrared data observed by the GMS
21 p3029 N90-27223

CHASSIS

Articulated suspension system
[NASA-CASE-NPO-17354-1-CU]
09 p1233 N90-17153

CHEBYSHEV APPROXIMATION

Elimination of spurious eigenvalues in the Chebyshev tau spectral method
[PB89-209282] 03 p0345 N90-11967

Modified Chebyshev pseudospectral method with O(N exp -1) time step restriction
[NASA-CR-181958] 06 p0834 N90-14848

Spectral multi-domain approximation of the Navier-Stokes equations in curved complex geometries
[ONERA-NT-1987-2] 11 p1508 N90-18685

Application of Chebyshev approximation to curve fitting
[MEMO-805] 11 p1554 N90-18947

Conforming Chebyshev spectral collocation methods for the solution of laminar flow in a constricted channel
[NASA-CR-182011] 12 p1660 N90-19539

Spectral simulation of unsteady compressible flow past a circular cylinder
[NASA-CR-182030] 13 p1750 N90-20050

Cell averaging Chebyshev methods for hyperbolic problems
[NASA-CR-182028] 13 p1877 N90-20768

Performance of adaptive nulling antennas in a jamming environment
[AD-A219305] 16 p2230 N90-22720

Explicitly solvable complex Chebyshev approximation problems related to sine polynomials
[NASA-CR-181575] 17 p2455 N90-24007

Chebyshev polynomials are not always optimal
[NASA-CR-181465] 17 p2455 N90-24008

On the parallel solution of parabolic equations
[NASA-CR-180363] 17 p2455 N90-24009

On Bernstein type inequalities and a weighted Chebyshev approximation problem on ellipses
[NASA-CR-180368] 17 p2456 N90-24011

Convergence properties of the Runge-Kutta-Chebyshev method
[CWI-NM-R8907] 17 p2459 N90-24038

Using implicit ODE methods with iterative linear equation solvers in spectral methods
[FFI-89/7017] 19 p2751 N90-25633

On the linear and nonlinear stability of non-parallel flow
21 p3002 N90-27065

Solution of the Orr-Sommerfeld equation for three dimensional incompressible flow using Galerkin method and Chebichev polynomials: The COCIP code
[CERT-46/5618-34-DERAT] 22 p3176 N90-28021

Linear iterative solvers for implicit ODE methods
[NASA-CR-182074] 22 p3242 N90-28386

CHECKOUT

Dependency-directed localization of software bugs
[AD-A210837] 01 p0106 N90-10606

A distributed debugger for Amoeba
[CWI-CS-R8828] 02 p0257 N90-11453

Truth maintenance systems and their implementation in PROLOG
[MEMO-INF-89-13] 04 p0531 N90-13064

Qualification of improved joint heaters
[NASA-CR-183827] 05 p0616 N90-13594

The US National Transonic Facility, NTF
08 p1028 N90-15942

The Kryo-Kanal Koeln (KKK): Description of the tunnel conversion. Thermal insulation, instrumentation, operational experience, test results and operating costs
08 p1029 N90-15943

RADC reliability engineer's TOOLKIT
[AD-A215977] 10 p1394 N90-18058

Conceptual design of an integrated system for software systems design implementation and testing
[ETN-90-97318] 21 p3057 N90-27381

Debugging and analysis of large-scale parallel programs
[AD-A221678] 21 p3059 N90-27393

Strategies for tutoring multiple bugs
[AD-A223921] 24 p3524 N90-29927

CHECKOUT EQUIPMENT

U TEST EQUIPMENT

CHELATION

Colloid and interface chemistry aspects of ceramics
[AD-A216715] 11 p1490 N90-18576

CHEMICAL ANALYSIS

NT CHROMATOGRAPHY
NT GAS ANALYSIS
NT GAS CHROMATOGRAPHY
NT LIQUID CHROMATOGRAPHY
NT MICROANALYSIS
NT NEUTRON ACTIVATION ANALYSIS
NT OZONOMETRY
NT POTENTIOMETRIC ANALYSIS
NT QUALITATIVE ANALYSIS
NT QUANTITATIVE ANALYSIS
NT SPECTROSCOPIC ANALYSIS
NT VOLUMETRIC ANALYSIS

Analysis of surface modified colloidal silicas
[DE89-015849] 01 p0047 N90-10267

A simulator for a hydrocarbon ramrocket fuel gas generator: First phase development
[AR-005-621] 02 p0189 N90-11080

Reporting environmental data of known quality
[DE89-016214] 02 p0239 N90-11359

Structure/reactivity relationships of polysilazane preceramics
[AD-A212028] 03 p0332 N90-11888
An atom probe study of phase decomposition in three iron meteorites
[DE89-017581] 03 p0421 N90-12420
Heat pipe and thermal energy storage and corrosion studies (1988)
[AD-A212655] 04 p0472 N90-12706
Laboratory testing of Sonnenschein DF6V180 6 volt traction battery
[DE90-002080] 06 p0771 N90-14486
Capillary electrophoresis ionization-mass spectrometry and tandem mass spectrometry
[DE90-002664] 07 p0892 N90-15158
Development of a robotics system for automated chemical analysis of sediment, sludges, and soils
[DE90-003637] 07 p0895 N90-15170
The effect of nitrogen and titanium on the toughness of high strength saw weld deposits
[AD-A213400] 07 p0905 N90-15230
Electrochemical investigation of electronically conductive polymers
[AD-A214019] 07 p0912 N90-15277
Properties and thermal decomposition of the double salts of uranyl nitrate-ammonium nitrate
[DE89-004909] 07 p0914 N90-15287
Performance of an Inductively Coupled Plasma-Mass Spectrometer Analyzer system
[DE90-004002] 08 p1043 N90-16025
Selection of corrosion-resistant materials for use in molten nitrate salts
[DE90-004351] 08 p1046 N90-16048
Silicon-based coatings on niobium metal
[DE90-003651] 08 p1048 N90-16057
Thermodynamic analysis of chemical stability of ceramic materials in hydrogen-containing atmospheres at high temperatures
[NASA-CR-4271] 08 p1050 N90-16072
Microstructures of Y123 films on SrTiO3, LaGaO3, and LaAlO3
[DE90-003367] 08 p1129 N90-16537
Workshop on Analysis of Returned Comet Nucleus Samples
[NASA-CR-184821] 08 p1140 N90-16607
On the isotope analysis of cometary dust 08 p1141 N90-16611
Electron beam analysis of particulate cometary material 08 p1141 N90-16613
Thermal and chemical processing of the outermost layer of cometary nuclei 08 p1141 N90-16614
Analysis of organic compounds in returned comet nucleus samples 08 p1142 N90-16617
Prompt Gamma Activation Analysis (PGAA): Technique of choice for nondestructive bulk analysis of returned comet samples 08 p1144 N90-16633
Methods for the mineralogical and textural analysis of comet nucleus samples 08 p1147 N90-16648
Determination of iron in chromium plating and polishing solutions by atomic absorption spectrometry
[AD-A214467] 09 p1189 N90-16892
Sealing L-alloys/FeS(x) cells for a bipolar battery
[DE90-004887] 09 p1214 N90-17040
Chemical effect of fuel composition changes on emissions from a DI Diesel engine
[DE90-004466] 09 p1232 N90-17151
Determination of trivalent chromium ions in chromium plating solutions by ultraviolet-visible spectrophotometry
[AD-A215688] 10 p1351 N90-17837
Characterization of tetrahydrogen via state-selected excitation of H2
[AD-A216239] 10 p1355 N90-17855
Comparison of emissions of transit buses using methanol and diesel fuel
[DE90-005652] 10 p1391 N90-18044
Assessment of the theory and hypotheses of the acidification of watersheds
[DE90-005528] 10 p1406 N90-18111
Multivariate clustering based on entropy
[PB89-233993] 10 p1439 N90-18303
Extracting chemical information form Auger line shapes
[AD-A216729] 11 p1483 N90-18537
Liquid oxygen LOX compatibility evaluations of aluminum lithium (Al-Li) alloys: Investigation of the Alcoa 2090 and MMC weldalite 049 alloys 12 p1636 N90-19398
Corrosion properties of Fe3Al in H2S-H2-H2O mixtures
[DE90-004936] 13 p1772 N90-20167
Techno-economic assessment of a carbothermic alumina reduction process
[DE90-007018] 13 p1772 N90-20170
DURIP FTIR studies of solid state reaction dynamics
[AD-A217713] 13 p1773 N90-20174
The effect of the SiC/Al interface on matrix microstructure in 2xxx-SiCp metal matrix
[AERE-R-13591] 13 p1775 N90-20184
Evaluation of material homogeneity as a function of thickness of low-alloy ferritic steel
[DE90-008069] 13 p1777 N90-20202
Pyrotechnic device technology
[DE90-007683] 13 p1783 N90-20234
Tribological properties of boric acid and boric acid forming surfaces. Part 1: Crystal chemistry and self-lubricating mechanism of boric acid
[DE90-005665] 13 p1811 N90-20401
High temperature chemistry of oxide superconductors
[DE90-007821] 13 p1895 N90-20875
A solution level indicator system
[DE90-007939] 14 p1948 N90-21151
Analytical sciences
[DE90-007965] 14 p1948 N90-21152
An evaluation of metal salts of 3-nitro-1,2,4-triazol-5-one (NTO) as potential primary explosives
[MRL-TN-563] 14 p1956 N90-21202
Thermal control system corrosion study
[NASA-TM-102220] 14 p1971 N90-21294
Aging characteristics of Li/SO(sub 2) cells
[NASA-CR-180432] 15 p2088 N90-21954
Reactions of N2A3 sigma u + and candidates for short wavelengths lasers
[DE90-009514] 15 p2103 N90-22033
Testing of an advanced thermochemical conversion reactor system
[DE90-007989] 15 p2123 N90-22141
The role of automation and robotics in the Lunar-Based Chemical Analysis Laboratory
[DE90-009401] 15 p2192 N90-22516
The first example of an organogallium compound containing a Ga-Te bond: Synthesis, properties, and molecular structure of ((Me3CCH2)2GaTeph)2
[AD-A219258] 16 p2210 N90-22608
Continued investigations of new concepts for improved spectrochemical analysis
[AD-A219403] 16 p2216 N90-22644
High temperature ceramic-tubed reformer
[DE90-009617] 16 p2236 N90-22755
The chemical and structural properties of sea ice in the southern Beaufort Sea
[AD-A219746] 17 p2418 N90-23776
HPLC analysis of helicopter rotor blade materials
[AD-A221121] 18 p2497 N90-24270
Characterization study of polycrystalline tin oxide surfaces before and after reduction in CO 18 p2559 N90-24601
Workshop on High-Field NMR and Biological Applications
[DE90-010002] 18 p2614 N90-24889
Oxidation and sulfidation of Type 310S stainless steel at elevated temperatures
[DE90-010149] 20 p2832 N90-26109
Short-range structure of fluorine-modified phosphate glass
[DE90-013494] 20 p2839 N90-26145
Electromagnetic inverse scattering of buried objects
[ETN-90-97216] 20 p2856 N90-26242
Nordic Symposium on Atmospheric Chemistry
[CM-78] 20 p2883 N90-26403
Deposition to the Baltic Sea 20 p2884 N90-26404
Natural and anthropogenic components in bulk precipitation at Blidoe (archipelago of Stockholm, Sweden) 20 p2884 N90-26409
Measurements of monoterpenes in a coniferous forest 20 p2886 N90-26421
Terpene concentrations and emissions in a Scots pine forest 20 p2886 N90-26422
The collection and analysis of atmospheric peroxides 20 p2887 N90-26428
Experiment K-6-09. Morphological and biochemical investigation of microgravity-induced nerve and muscle breakdown. Part 1: Investigation of nerve and muscle breakdown during spaceflight; Part 2: Biochemical analysis of EDL and PLT muscles 20 p2893 N90-26463
Symmetry breaking oxygen displacement in superconducting oxides
[DE90-013670] 21 p3081 N90-27520
Nature and origin of interstellar diamond from the Allende CV3 meteorite 21 p3092 N90-27581
Analysis of acid precipitation samples collected by state agencies: January to December 1988
[PB90-191784] 22 p3198 N90-28151
Mass spectrometric analysis of hydrogen isotopes in metals and metal hydrides
[DE90-014118] 23 p3303 N90-28685
Fuels research, volume 1
[DE90-015393] 23 p3305 N90-28695
A design tool utilizing stoichiometric structure for the analysis of biochemical reaction networks
[AD-A223873] 23 p3355 N90-28961
Solid-state N15 NMR of N15-labeled nylon 6 and nylon 11
[AD-A223271] 24 p3446 N90-29459
Progress toward synthesis of polymeric polyradicals
[AD-A223414] 24 p3455 N90-29510
Ion-beam-assisted deposition of silver films on zirconia ceramics for improved tribological behavior
[DE90-009706] 24 p3456 N90-29516
Planar waveguide spectrometer
[DE90-016308] 24 p3546 N90-30057

CHEMICAL ATTACK
NT INTERGRANULAR CORROSION
A review of the mechanism and kinetics of electrochemical hydrogen entry and degradation of metallic systems
[AD-A216671] 10 p1355 N90-17857
Combination primer/topcoat coating
[AD-D014445] 14 p1954 N90-21189

CHEMICAL BONDS
NT COVALENT BONDS
NT HYDROGEN BONDS
International Conference on Organometallic Chemistry (13th) held in Torino, Europe on 4-9 September 1988: Abstracts
[AD-A210617] 01 p0033 N90-10178
Reaction of oxygen with allene
[DE89-015219] 01 p0039 N90-10216
Bonding in transition metal silyl dimers. Molecular orbital theory
[AD-A208269] 01 p0046 N90-10260
New polymer precursors to boron and silicon nitrides
[AD-A210287] 01 p0049 N90-10279
Quantum chemical investigations of the mechanism of cationic polymerization and theoretical prediction of crystal densities and decomposition pathways of energetic molecules
[AD-A210322] 02 p0200 N90-11143
Vibrational spectroscopic study of the kaolinite-hydrazine intercalation complex 02 p0204 N90-11166
Low temperature spectroscope of hydrazine and ammonia complexes 02 p0205 N90-11169
Synthesis and high temperature chemistry of methylsilsesquioxane polymers produced by titanium catalyzed redistribution of methylhydridooligo- and polysiloxanes
[AD-A212000] 04 p0477 N90-12736
Molecular dynamics of lipid bilayers
[AD-A211492] 04 p0552 N90-13214
Interstitial formation, non-equilibrium and macroscopic processes in mercury cadmium telluride
[AD-A212412] 04 p0561 N90-13267
Computational solution of chemistry problems
[NASA-CR-186000] 05 p0620 N90-13618
The production and spectroscopy of molecular ions isolated in solid neon
[AD-A213723] 07 p0895 N90-15174
Cu-O chains in YBa2Cu3O(7-delta) and the phonon mechanism of high-Tc superconductivity
[DE90-603502] 07 p1003 N90-15805
Hydrogen desorption from the monohydride phase on Si(100)
[AD-A215237] 09 p1191 N90-16903
LARC-IA: A flexible backbone polyimide
[NASA-TM-102586] 09 p1196 N90-16926
Numerical model of bond strength measurements
[DE90-006000] 10 p1396 N90-18073
Chemical activation of molecules by metals: Experimental studies of electron distributions and bonding
[DE90-005371] 10 p1428 N90-18238
Perfluorinated ligands in organometallic chemistry
[AD-A216415] 11 p1476 N90-18493
Spectroscopic evidence for carbon-carbon bonding in carbide layers on metals
[AD-A216726] 11 p1479 N90-18512
Interfacial chemistry of MoS2 films on Si
[AD-A216527] 11 p1482 N90-18532
Ultrafast chemical dynamics of reactions in beams
[AD-A216319] 11 p1514 N90-18717
Quantum-theoretical methods and studies relating to properties of materials
[AD-A217843] 13 p1765 N90-20132
The 1-((diorganooxyphosphonyl)-methyl)-2,4- and -2,6-diamido benzenes
[NASA-CASE-ARC-11425-4] 13 p1766 N90-20133
Molecular organization and electrical properties of mixed Langmuir-Blodgett multilayer thin films of polypyrrole
[DE90-007627] 13 p1894 N90-20870
Modelling of molecular structures and properties in physical chemistry and biophysics
[AD-A214561] 14 p1947 N90-21145
Boron-containing organosilane polymers and ceramic materials thereof
[NASA-CASE-ARC-11649-2-SB] 14 p1952 N90-21177

A new class of lubricants derived from archaebacterial lipids
[AD-D014429] 14 p1954 N90-21185
New surface atomic structures for column 5 overlayers on the (110) surfaces of 3-5 compound semiconductors
[DE90-009003] 14 p2033 N90-21663
A comparison of the autoignition chemistry of n-butane and isobutane in an internal combustion engine
[DE90-009474] 15 p2067 N90-21838
The first example of an organogallium compound containing a Ga-Te bond: Synthesis, properties, and molecular structure of ((Me3CCH2)2GaTeph)2
[AD-A219258] 16 p2210 N90-22608
Modes of attachment of pyridine to gold surfaces
[AD-A219519] 17 p2372 N90-23504
An investigation of the chemistry of silane coupling agents for adhesive bonding of aluminum
[AD-A220797] 17 p2381 N90-23560
Short-range structure of fluorine-modified phosphate glass
[DE90-013494] 20 p2839 N90-26145
One-dimensional sigma-conjugated polysilylenes: Science and technology
[DE90-012902] 20 p2839 N90-26146
Surface reactions in the space environment
[AD-A221767] 21 p2979 N90-26932
Energetics and crystal chemistry of Ruddlesden-Popper type structures in high T(sub c) ceramic superconductors 22 p3141 N90-27814
Thermochemical data for silicon-containing species from ab initio electronic structure calculations
[DE90-011024] 24 p3446 N90-29463
Transition metal activation and functionalization of carbon-hydrogen bonds
[DE90-015826] 24 p3451 N90-29489

CHEMICAL CLEANING
Cleaning of printed circuit assemblies with surface-mounted components
[DE89-013609] 03 p0341 N90-11945
An ellipsometric measurement of optical properties for InP surfaces
[AD-A217185] 13 p1887 N90-20827
Experimental evaluation of chemical cleaning processes for high-lifetime silicon processing
[DE90-009332] 16 p2226 N90-22699

CHEMICAL CLOUDS
The EURAD Model: Structure and First Results
[REPT-61] 12 p1686 N90-19680

CHEMICAL COMPOSITION
NT CARBON DIOXIDE CONCENTRATION
NT STELLAR COMPOSITION
New structural materials
[AD-A209425] 01 p0044 N90-10246
Properties of HY-100 for naval construction
[MRL-R-1149] 01 p0044 N90-10247
Characterization and evaluation of acid rain in East Central Florida from 1978 to 1987: Ten year summary report
[NASA-TM-102149] 01 p0084 N90-10478
Evaluation of rocket motor exhaust and liner combustion by-products
[AD-A210747] 02 p0189 N90-11083
Compositional analysis of steels by X-ray fluorescence spectrometry
[DE89-630803] 02 p0198 N90-11129
Interactions of hydrazines with colloidal constituents of soils 02 p0204 N90-11164
Coating galvanized steel
[AD-A211775] 03 p0329 N90-11869
Correlating microemulsion fuel composition, structure and combustion properties
[DE89-017779] 03 p0333 N90-11898
KIVA reactive hydrodynamics code applied to detonations in high vacuum
[DE89-016979] 03 p0346 N90-11974
Fundamentals of middle atmospheric dynamics
[AD-A211747] 04 p0518 N90-12988
Semiconductor measurement technology: Database for and statistical analysis of the interlaboratory determination of the conversion coefficient for the measurement of the interstitial oxygen content of silicon by infrared absorption
[PB89-221170] 04 p0558 N90-13253
Effects of composition and age hardening on precious metal electrical contacts
[DE88-008791] 06 p0769 N90-14476
BES welding science contractors summary report, 1988 to 1989
[DE90-001004] 06 p0793 N90-14619
The effect of composition and processing on high T(sub c) superconductors containing bismuth
[DE90-002203] 06 p0854 N90-14965
Novel polyimide compositions based on 4,4': Isophthaloyldiphthalic anaydride (IDPA)
[NASA-CASE-LAR-14194-1] 07 p0890 N90-15148
Orthobaric densities and molar volumes of liquids: Alcohols
[ESDU-89037] 07 p0897 N90-15184
Superplastic performance and properties of the Lital Alloys 07 p0899 N90-15199
Magnetic viscosity in Ni/Cu compositionally-modulated alloys
[DE90-002303] 07 p0904 N90-15223
The effect of dissolved chlorine on the pitting behavior of 304L stainless steel in a 0.5 N NaCl solution
[AD-A213803] 07 p0905 N90-15234
The effect of dissolved ozone on the corrosion behavior of Cu-30 Ni and 304L stainless steel in 0.5 N NaCl solutions
[AD-A213804] 07 p0906 N90-15235
Thermal stability of jet fuel
[DE90-002760] 07 p0914 N90-15288
The volatile composition of comets
[NASA-CR-186281] 07 p1014 N90-15871
Improved performance polysulfide based sealant 08 p1022 N90-15910
On-line chemical composition analyzer development
[DE90-004079] 08 p1043 N90-16026
Researches on amorphous perovskite
[DE89-900733] 08 p1128 N90-16535
The origin, composition and history of cometary ices from spectroscopic studies 08 p1140 N90-16609
Direct determination of the morphology, structure and composition of cometary and interstellar ice analogs in the laboratory 08 p1141 N90-16612
The carbon chemistry of meteorites: Relationships to comets 08 p1141 N90-16615
From interstellar dust to comets 08 p1142 N90-16620
Modifications of comet materials by the sublimation process: Results from simulation experiments 08 p1142 N90-16621
Morphology and compositional differentiation of the surface of comets 08 p1143 N90-16624
Identification of solar nebula condensates in interplanetary dust particles and unequilibrated ordinary chondrites 08 p1144 N90-16629
Composition of dust from Comet P/Halley: The mineral fraction 08 p1144 N90-16631
Computer simulation of dust grain evolution 08 p1144 N90-16632
Solar nebula condensates and the composition of comets 08 p1144 N90-16634
Candidate sample acquisition systems for the Rosetta 08 p1145 N90-16635
The comet rendezvous asteroid flyby mission 08 p1145 N90-16639
What if chondritic porous interplanetary dust particles are not the real McCoy 08 p1146 N90-16642
Neptune's Triton: A moon rich in dry ice and carbon
[NASA-CR-186298] 08 p1152 N90-16675
Review of polyarylacetylene matrices for thin-walled composites
[AD-A214921] 09 p1186 N90-16872
Acquisition of analytical instruments for combustion research
[AD-A214495] 09 p1190 N90-16893
Study of chemical systems in static and time resolved mode by x ray absorption spectroscopy
[AD-A215383] 09 p1191 N90-16904
Chemical profiling of silicon nitride structures
[AD-A215643] 09 p1192 N90-16907
Ion beam modification of metals: Mechanical properties and structure
[AD-A214701] 09 p1194 N90-16915
Chemical effect of fuel composition changes on emissions from a DI Diesel engine
[DE90-004466] 09 p1232 N90-17151
Identification of a cast iron alloy containing nonstrategic elements
[NASA-CR-185174] 11 p1487 N90-18559
High-purity beryllium foils
[DE90-006408] 12 p1626 N90-19348
Chemical composition of precipitation and wet/dry deposition of sulfur compounds around the coastal area
[DE89-782324] 12 p1685 N90-19677
Geochemical survey on faults overland with alluvial deposits, part 1. Application for the Neodani and the Atera faults survey
[DE89-782326] 12 p1690 N90-19707
Tunneling microscopy of submonolayer adsorbates on Si3
[AD-A216985] 12 p1719 N90-19876
The composition of cometary nuclei 12 p1743 N90-20022
Oxygen concentrations on surfaces of carbon fibers
[AD-A217724] 13 p1769 N90-20152
Design and processing of strong-tough microcomposite steels
[DE90-007764] 13 p1777 N90-20197
A systematic study of the effects of metal substitutions for Cu in YBa(sub 2) (Cu(sub 1-x) M(sub x)3 O(sub 7-rho), M=Fe, Co, Al, Ga, Cr, Ni, and Zn
[DE90-003957] 13 p1892 N90-20857
Grain boundary precipitation in Ni3Al based alloys
[AERE-R-13362] 14 p1950 N90-21161
Methods for improving the flowability of a percussion primer composition
[MRL-TR-89-32] 14 p1956 N90-21201
Evolutionary effects in B stars 14 p2041 N90-21704
A balloon measurement of the isotopic composition of galactic cosmic ray iron 14 p2043 N90-21717
Welding behavior and welding metallurgy of ductile intermetallic alloys
[DE90-008908] 15 p2069 N90-21852
Application of x ray absorption edge spectrometry to the non-destructive determination of element concentrations, coating thickness and areal densities
[AERE-R-13030] 16 p2245 N90-22802
The effects of point defects and composition on structural phase transition
[DE90-010109] 16 p2322 N90-23238
Rheological and mechanical characteristics of poly-p-phenylene terephthalamide/nylon molecular and particulate composites
[AD-A219562] 17 p2368 N90-23482
HPLC analysis of helicopter rotor blade materials
[AD-A221121] 18 p2497 N90-24270
The measurement of composition during the early stages of the spinodal decomposition of Fe-Cr alloys
[DE90-010471] 18 p2525 N90-24408
Development and evaluation of advanced austenitic alloys
[DE90-011315] 18 p2528 N90-24425
The composition and physical properties of the Earth's mantle and core 18 p2579 N90-24689
The effect of trace amounts of antimony on the structure and properties of aluminum alloy A356.2
[DE90-010461] 19 p2674 N90-25207
Airborne chemistry measurements 19 p2707 N90-25405
A low NOx strategy for combusting high nitrogen content fuels
[PB90-155664] 19 p2712 N90-25435
Chemical structure and kinetics at liquid/solid interfaces
[AD-A222766] 20 p2831 N90-26105
Verification and improvement of the EMEP model for long-range transport and deposition of pollutants 20 p2884 N90-26405
Optical constraints of kerogen from 0.15 to 40 microns: Comparison with meteoritic organics 20 p2948 N90-26776
Laboratory studies of the interaction of ions with condensed gases: Planetary applications 20 p2949 N90-26778
Polyimidazoles via aromatic nucleophilic displacement
[NASA-CASE-LAR-14145-1] 21 p2983 N90-26954
Carbon chemistry of circumstellar envelopes 21 p3090 N90-27570
A systematic study of superconductivity in BiPb(Sn)-Sb Sr-Ca-Cu-O systems 22 p3144 N90-27831
Incoherent imaging of materials structure and composition by Z-contrast stem
[DE90-012789] 22 p3155 N90-27888
Analysis of acid precipitation samples collected by state agencies: January to December 1988
[PB90-191784] 22 p3198 N90-28151
Numerical simulation of the middle atmosphere chemical composition and temperature under changing solar conditions 22 p3206 N90-28186
Generation rates and chemical compositions of waste streams in a typical crewed space habitat
[NASA-TM-102799] 22 p3233 N90-28333
Tripropellant combustion process 23 p3293 N90-28631
Reflection Mass Spectrometry (REMS) during 3/5 MBE
[DE90-014568] 23 p3304 N90-28690
Tensile behavior of borated stainless steels, phase 1
[DE90-014368] 23 p3309 N90-28717
Evaluation of advanced austenitic alloys relative to alloy design criteria for steam service. Part 1: Lean stainless steel
[DE90-014765] 23 p3310 N90-28720
Geothermal fluid genesis in the Great Basin
[DE90-014438] 23 p3342 N90-28884

CHEMICAL DEFENSE
Effects of pyridostigmine bromide on A-10 pilots during execution of a simulated mission: Physiology
[AD-A221222] 18 p2584 N90-24717

CHEMICAL EFFECTS
Role of chemical effects in daytime high latitude trough formation
[AD-A211772] 04 p0518 N90-12989

The sensory transduction pathways in bacterial chemotaxis 05 p0677 N90-13944
Studies of the adsorption/desorption behavior of explosive-like molecules
[DE90-001867] 07 p0913 N90-15283
Chemical effect of fuel composition changes on emissions from a DI Diesel engine
[DE90-004466] 09 p1232 N90-17151
Anaerobic metabolism of aromatic compounds by phototrophic bacteria: Biochemical aspects
[DE90-009503] 14 p2009 N90-21516
The chemical effects of the Martian environment on power system component materials: A theoretical approach
[NASA-TM-103203] 20 p2825 N90-26074
Strengthening and toughening mechanisms in ceramic fiber-reinforced glass matrix composites 23 p3300 N90-28666

CHEMICAL ELEMENTS
NT ALKALI METALS
NT ALKALINE EARTH METALS
NT ALUMINUM
NT ALUMINUM ISOTOPES
NT ALUMINUM 26
NT AMERICIUM
NT AMORPHOUS SILICON
NT ANTIMONY
NT ANTIMONY ISOTOPES
NT ARGON
NT ARSENIC
NT BARIUM
NT BERYLLIUM
NT BISMUTH
NT BORON
NT BORON ISOTOPES
NT BROMINE
NT CADMIUM
NT CALCIUM
NT CALCIUM ISOTOPES
NT CARBON
NT CARBON ISOTOPES
NT CARBON 12
NT CARBON 13
NT CARBON 14
NT CERIUM
NT CESIUM
NT CESIUM VAPOR
NT CHLORINE
NT CHROMIUM
NT CHROMIUM ISOTOPES
NT COBALT
NT COBALT ISOTOPES
NT COBALT 60
NT COPPER
NT COPPER ISOTOPES
NT CURIUM
NT DEUTERIUM
NT ERBIUM
NT ERBIUM ISOTOPES
NT EUROPIUM ISOTOPES
NT FLUORINE
NT GADOLINIUM ISOTOPES
NT GALLIUM
NT GALLIUM ISOTOPES
NT GERMANIUM
NT GOLD
NT GOLD ISOTOPES
NT HAFNIUM
NT HALOGENS
NT HELIUM
NT HELIUM ISOTOPES
NT HOLMIUM
NT HYDROGEN
NT HYDROGEN ISOTOPES
NT INDIUM
NT IODINE
NT IODINE ISOTOPES
NT IRIDIUM
NT IRON
NT IRON ISOTOPES
NT ISOTOPES
NT KRYPTON
NT KRYPTON ISOTOPES
NT KRYPTON 85
NT LANTHANUM
NT LANTHANUM ISOTOPES
NT LEAD (METAL)
NT LEAD ISOTOPES
NT LIGHT ELEMENTS
NT LIQUID HELIUM
NT LIQUID HELIUM 2
NT LIQUID HYDROGEN
NT LIQUID LITHIUM
NT LIQUID NITROGEN
NT LIQUID OXYGEN
NT LIQUID SODIUM
NT LITHIUM
NT LITHIUM ISOTOPES
NT MAGNESIUM
NT MAGNESIUM ISOTOPES
NT MANGANESE
NT MANGANESE ISOTOPES
NT MERCURY (METAL)
NT MERCURY ISOTOPES
NT METALLOIDS
NT MOLYBDENUM
NT NEODYMIUM
NT NEON
NT NICKEL
NT NICKEL ISOTOPES
NT NIOBIUM
NT NIOBIUM ISOTOPES
NT NITROGEN
NT NUCLIDES
NT OXYGEN
NT OXYGEN ISOTOPES
NT OXYGEN 18
NT PALLADIUM
NT PHOSPHORUS
NT PLATINUM
NT PLUTONIUM
NT POLONIUM ISOTOPES
NT POTASSIUM
NT PRASEODYMIUM
NT RADIOACTIVE ISOTOPES
NT RADON
NT RADON ISOTOPES
NT RARE EARTH ELEMENTS
NT RARE GASES
NT RHODIUM
NT RUBIDIUM
NT RUTHENIUM
NT SCANDIUM
NT SELENIUM
NT SILICON
NT SILICON ISOTOPES
NT SILVER
NT SODIUM
NT STRONTIUM
NT SULFUR
NT TANTALUM
NT TELLURIUM
NT TELLURIUM ISOTOPES
NT TERBIUM
NT THALLIUM
NT THULIUM
NT TIN
NT TIN ISOTOPES
NT TITANIUM
NT TRITIUM
NT TUNGSTEN
NT URANIUM
NT URANIUM ISOTOPES
NT VANADIUM
NT XENON
NT YTTERBIUM
NT YTTRIUM
NT ZINC
NT ZIRCONIUM
The Periodic Law at high pressures
[DE90-000837] 06 p0742 N90-14319

CHEMICAL ENERGY
Acoustic-vortex-chemical interactions in an idealized ramjet 01 p0037 N90-10206
On the spectrum of the staggered Dirac operator at finite chemical potential
[ITFA-88-53] 04 p0561 N90-13272
Kinetics of boron hydride interconversion reactions
[AD-A215386] 09 p1192 N90-16906
Regional studies with broadband data
[AD-A219215] 16 p2256 N90-22861

CHEMICAL ENGINEERING
Systems analysis considerations in artificial intelligence/expert systems technology applications
[DE89-016847] 02 p0262 N90-11490
Structure/reactivity relationships of polysilazane preceramics
[AD-A212028] 03 p0332 N90-11888
Application of dimensional analysis to statistical process modeling
[AD-A211881] 03 p0335 N90-11905
Synthesis and properties of new preceramic materials
[DE90-002562] 06 p0752 N90-14373
New electronic materials and CO2 reduction
[AD-A214679] 09 p1191 N90-16899
The 10th Gordon Research Conference on Plasma Chemistry
[AD-A215161] 09 p1285 N90-17449
Compact scheme for systems of equations applied to fundamental problems of mechanics of continua
[NASA-CR-186494] 14 p1971 N90-21292
ECUT: Energy Conversion and Utilization Technologies program. Biocatalysis project
[NASA-CR-186866] 19 p2717 N90-25458
Development of microencapsulation techniques
[AD-A223032] 20 p2841 N90-26159

CHEMICAL EQUILIBRIUM
NT ACID BASE EQUILIBRIUM
Rotational and vibrational nonequilibrium effects in rarefied, hypersonic flow
[NASA-CR-182559] 04 p0437 N90-12498
Aerodynamic and kinetic processes in flames
[AD-A217796] 13 p1773 N90-20176
Ionic equilibrium between octahedral and tetrahedral complexes in liquid aluminium-sodium fluoride mixtures
[DE90-613690] 14 p1948 N90-21150
Controlled production and characterization of metastable intermetallics
[DE90-009384] 14 p1952 N90-21176
Valence-defect chemical equilibria in nonstoichiometric YBa2Cu3O(7-delta)
[DE90-010152] 18 p2619 N90-24921
Phase compatibilities of YBa2Cu3O(9-delta) type structure in quintenary systems Y-Ba-Cu-O-X (impurity) 22 p3145 N90-27834

CHEMICAL EVOLUTION
Workshop on Analysis of Returned Comet Nucleus Samples
[NASA-CR-184821] 08 p1140 N90-16607
Computer simulation of dust grain evolution 08 p1144 N90-16632
Evolution of carbonaceous chondrite parent bodies: Insights into cometary nuclei 08 p1145 N90-16638
The comet rendezvous asteroid flyby mission 08 p1145 N90-16639
Physical processing of cometary nuclei 08 p1148 N90-16653
Molecular evolution in astrophysical environments 16 p2332 N90-23291
Molecular gas in S106: Morphology, kinematics, and chemistry of a star forming region 17 p2484 N90-24209
Proton irradiation of simple gas mixtures: Influence of irradiation parameters 20 p2949 N90-26782
Interstellar grain chemistry and organic molecules 21 p3090 N90-27569
Chemical evolution of dwarf irregular galaxies 22 p3263 N90-28478

CHEMICAL EXPLOSIONS
NT GAS EXPLOSIONS
Effects of binder concentration on the properties of plastic-bonded explosives
[DE89-007744] 01 p0053 N90-10301
Time-resolved mass spectrometry technique for studying fast transient CHNO explosive decomposition kinetics
[DE89-016540] 02 p0193 N90-11101
Shock initiation of LX-17 as a function of its initial temperature
[DE89-017730] 02 p0208 N90-11192
Sensitivity relationships in energetic materials
[DE89-016967] 03 p0333 N90-11897
VISAR wave profile measurements in supra-compressed HE
[DE89-017736] 03 p0346 N90-11976
Fast transit gas- and condensed-phase chemistry of energetic materials
[DE90-001656] 06 p0755 N90-14395
Regional studies with broadband data
[AD-A219215] 16 p2256 N90-22861
Ultrafast laser investigation of a solid-state explosion
[AD-A218530] 17 p2408 N90-23718

CHEMICAL EXTINGUISHERS
U FIRE EXTINGUISHERS

CHEMICAL FUELS
NT AIRCRAFT FUELS
NT AUTOMOBILE FUELS
NT CRUDE OIL
NT DIESEL FUELS
NT ENDOTHERMIC FUELS
NT GASOLINE
NT HIGH ENERGY FUELS
NT HYDROCARBON FUELS
NT HYDROGEN FUELS
NT JET ENGINE FUELS
NT JP-4 JET FUEL
NT JP-8 JET FUEL
NT KEROSENE
NT LIQUID FUELS
NT METAL FUELS
NT NATURAL GAS
NT SYNTHETIC FUELS
Electrochemical phase diagrams for aqueous redox systems
[AD-A217168] 13 p1770 N90-20157
The effect of catalysts on gas-phase hydrocarbon ignition
[AD-A218775] 17 p2371 N90-23499

CHEMICAL INDICATORS
Flow visualization of water flows using the crystal violet method 08 p1081 N90-16253
Unsteady heat transfer measurement using thermochromatic liquid crystals as temperature indicators 08 p1081 N90-16254
CHEMICAL KINETICS
U REACTION KINETICS
CHEMICAL LASERS
Multiline multimode CW chemical laser performance [AD-A210613] 01 p0075 N90-10432
Master oscillator with power amplifiers: Performance of a two-element CW HF phased-laser array [AD-A211141] 01 p0076 N90-10435
Generation of iodine monofluoride in a supersonic multipurpose flowtube facility [AD-A213082] 05 p0647 N90-13774
Combustion of hydrogen and hydrocarbons in fluorine [AD-A214621] 09 p1190 N90-16896
Experimental investigation of a chemical laser cavity flowfield [AD-A216398] 10 p1390 N90-18038
CW (Continuous Wave) stimulated Brillouin scattering of long-pulse chemical laser beams [AD-A216409] 10 p1390 N90-18039
Chemical and laser sciences division [DE90-013532] 21 p3101 N90-27611
CHEMICAL MACHINING
Process development and fabrication of space station type aluminum-clad graphite epoxy struts [NASA-CR-181873] 11 p1468 N90-18454
CHEMICAL MILLING
U CHEMICAL MACHINING
CHEMICAL PROPERTIES
NT ACIDITY
NT HEAT OF COMBUSTION
NT HEAT OF FORMATION
NT LATENT HEAT
NT SALINITY
NT THERMOCHEMICAL PROPERTIES
Investigation of the pyrometallurgical, physical and mechanical behavior of weld metal [AD-A211114] 01 p0046 N90-10258
Properties of F-34 (JP-8) fuel for 1988 [AD-A210188] 01 p0053 N90-10303
Electronic and ionic transport in polymers [AD-A210654] 02 p0201 N90-11148
The multivalent beta'-aluminas [AD-A212103] 04 p0478 N90-12738
Surfaces and interfaces of ceramic materials [AD-A212417] 05 p0627 N90-13657
Properties of aluminum-uranium alloys [DE90-003889] 07 p0907 N90-15243
Spray sealing: A breakthrough in integral fuel tank sealing technology 08 p1022 N90-15912
Mechanoelectric conversion by uniaxial constraint in piezoelectric generators: Optimization of electrical, mechanical, and physico-chemical parameters of materials [ISAL-89-0020] 08 p1078 N90-16235
Nuclear weapon radiation effects on a space based interceptor weapon platform [DE89-016258] 09 p1181 N90-16850
New electronic materials and CO2 reduction [AD-A214679] 09 p1191 N90-16899
Chemistry at clusters, microstructures and surfaces [AD-A215842] 10 p1353 N90-17844
Study of alteration covers of part of the Sao Paulo State through remote sensing data [INPE-4849-TDL/364] 10 p1399 N90-18086
Spectroscopy and physico-chemistry of CO:H2O and CO2:H2O ices 11 p1581 N90-19111
The preparation and properties of iron doped II-VI chalcogenides [AD-A217569] 12 p1724 N90-19903
Physics and Mechanics of Cometary Materials [ESA-SP-302] 12 p1738 N90-19989
Symposium on High Temperature and Materials Chemistry [DE90-008047] 13 p1768 N90-20148
Hydrous metal oxide-supported catalysts. Part 1: Preparation chemistry and physical and chemical properties [DE90-007607] 13 p1771 N90-20161
High temperature chemistry of oxide superconductors [DE90-007821] 13 p1895 N90-20875
Surface structure and chemistry of high surface area silica gels [DE90-007684] 15 p2071 N90-21865
Methods for evaluation of thermally induced reactions in liquid propellants [AD-A218750] 16 p2225 N90-22694
The effect of catalysts on gas-phase hydrocarbon ignition [AD-A218775] 17 p2371 N90-23499
The chemical and structural properties of sea ice in the southern Beaufort Sea [AD-A219746] 17 p2418 N90-23776
Power density effects in the physical and chemical properties of sputtered diamond-like carbon thin films [DE90-011587] 18 p2532 N90-24450
Surface defects and chemistry on the SnO2(110) surface 18 p2559 N90-24603
Wear transition surfaces for long-term wear effects [DE90-011314] 19 p2698 N90-25351
Laboratory tests to determine the chemical and physical characteristics of propellant-solvent-fuel oil mixtures [AD-A222270] 21 p2990 N90-26991
An ionic mechanism of carbon formation in flames 21 p3093 N90-27582
Electrochemical evaluation of new fluorosulfonic and fluorophosphonic acids as fuel cell electrolytes [DE90-016626] 24 p3485 N90-29699
CHEMICAL PROPULSION
NT HYBRID PROPULSION
Low-earth-orbit to low-lunar-orbit laser freighter 01 p0030 N90-10160
Laser propulsion option 01 p0030 N90-10161
Present and future US and Soviet chemical missiles and chemical rocket projectiles [AD-A212199] 04 p0461 N90-12644
A candidate architecture for monitoring and control in chemical transfer propulsion systems [NASA-TM-103161] 16 p2208 N90-22595
Low thrust rocket test facility [NASA-TM-103206] 19 p2663 N90-25158
Integrated controls and health monitoring for chemical transfer propulsion [NASA-TM-103185] 19 p2668 N90-25178
Project LOCOST: Laser or Chemical Hybrid Orbital Space Transport [NASA-CR-186822] 20 p2819 N90-26042
CHEMICAL REACTION CONTROL
State-resolved reaction dynamics [AD-A211613] 03 p0403 N90-12307
Control of titanium diboride SHS reactions by inert dilutions and mechanical constraint [AD-A214378] 10 p1357 N90-17870
CHEMICAL REACTIONS
NT ALKYLATION
NT AMMONOLYSIS
NT ATOMIC RECOMBINATION
NT BROMINATION
NT CARBONIZATION
NT CARBOXYLATION
NT COPOLYMERIZATION
NT CRACKING (CHEMICAL ENGINEERING)
NT DEHYDROGENATION
NT DEIONIZATION
NT DENITROGENATION
NT DEOXIDIZING
NT DESULFURIZING
NT DIELS-ALDER REACTIONS
NT ELECTROCHEMICAL OXIDATION
NT EXOTHERMIC REACTIONS
NT FERMENTATION
NT FLUORINATION
NT GLYCOLYSIS
NT HALOGENATION
NT HYDROCRACKING
NT HYDROGENATION
NT HYDROGENOLYSIS
NT HYDROLYSIS
NT ION RECOMBINATION
NT METAL-WATER REACTIONS
NT METHANATION
NT NITRATION
NT NITRIDING
NT NITROGENATION
NT OXIDATION
NT OXIDATION-REDUCTION REACTIONS
NT OXYGEN RECOMBINATION
NT OXYGENATION
NT PHOSPHORYLATION
NT PHOTOCHEMICAL REACTIONS
NT PHOTOCHROMISM
NT PHOTODECOMPOSITION
NT PHOTOLYSIS
NT PHOTOOXIDATION
NT PHOTOSYNTHESIS
NT PYROLYSIS
NT REDUCTION (CHEMISTRY)
NT SULFATION
NT SULFIDATION
NT THERMAL DECOMPOSITION
NT TITRATION
Reactions of hydrogen chloride and boron trichloride with trimethylsilylamino groups [AD-A209006] 01 p0038 N90-10209
Chemistry of nitromethane at very high pressure [DE89-008016] 01 p0039 N90-10215
Reaction of oxygen with allene [DE89-015219] 01 p0039 N90-10216
Direct numerical simulation of turbulent free shear flows [AD-A210161] 01 p0040 N90-10218
Monomers, polymers and transition metal complexes based upon carboranes [AD-A210226] 01 p0040 N90-10221
Metal-assisted syntheses of boranes and carboranes [AD-A210728] 01 p0041 N90-10227
Cubane derivatives for propellant applications [AD-A210368] 01 p0054 N90-10305
On the utility and ubiquity of atomic collision physics [DE89-015356] 01 p0119 N90-10686
Solvent dynamical effects in electron transfer: Predicted influences of electron coupling upon the rate-dielectric friction dependence [AD-A210193] 01 p0120 N90-10690
Critical reaction rates in hypersonic combustion chemistry [DE89-014278] 02 p0156 N90-10892
Finite element analysis of cure-induced residual stress in composite materials 02 p0190 N90-11084
Simplified rate-law integration for reactions which are first order in each of two reactants [NASA-CR-185408] 02 p0192 N90-11093
Thermochemical model for shock-induced chemical reactions in porous thermite: The heat detonation model [DE89-016528] 02 p0193 N90-11100
Pressure induced resonance Raman effects in shocked carbon disulfide [AD-A210665] 02 p0194 N90-11107
Reactive ion etching of SiC thin films by mixtures of fluorinated gases and oxygen [AD-A211046] 02 p0195 N90-11113
Atmospheric chemistry of the fuel hydrazines 02 p0203 N90-11158
Modeling of hydrazine surface interactions in environmental reaction chambers 02 p0203 N90-11162
Interactions of hydrazines with colloidal constituents of soils 02 p0204 N90-11164
In-situ study of the chemically driven flow fields in initiating homogeneous and heterogeneous nitromethane explosives [DE89-008415] 02 p0207 N90-11186
Chemical reactions in turbulent mixing flows [AD-A211240] 02 p0220 N90-11263
In-situ cure monitoring of composites by fiber-optic molecular sensors [AD-A211495] 03 p0320 N90-11817
Shock dissociation of molecular fluids: A possibility of first-order phase change [DE89-016647] 03 p0322 N90-11829
Phase behavior of pure and mixed systems at high pressure [DE89-017734] 03 p0322 N90-11832
Synthesis and chemistry of strained and conjugated fluorocarbons [AD-A211633] 03 p0324 N90-11844
State-resolved reaction dynamics [AD-A211613] 03 p0403 N90-12307
Chemical and photochemical reactivity in microemulsions and waterless microemulsions [AD-A211776] 04 p0470 N90-12692
Measurement and correlation of the solubility and diffusion coefficient for oxygen and chlorine in basic hydrogen peroxide [AD-A212348] 04 p0472 N90-12703
FLIC (FLame with Implicit Convection): A detailed, two-dimensional flame model [AD-A212953] 04 p0473 N90-12710
An investigation of the irradiation swelling mechanisms in refractory metals at high temperatures [AD-A211406] 04 p0474 N90-12719
Chemical treatment of epoxy resins to reduce moisture sensitivity and to improve the mechanical properties [AD-A212360] 04 p0481 N90-12758
Role of chemical effects in daytime high latitude trough formation [AD-A211772] 04 p0518 N90-12989
Growth and characterization of zinc sulfide films by conversion of zinc oxide films with H2S [AD-A213345] 04 p0561 N90-13271
Physical phenomena and the microgravity response 05 p0677 N90-13945
Shock-induced solid state reactions and phase transitions: X ray profile studies on shock-modified Fe3O4 and ZrO2 powders [DE90-000669] 06 p0741 N90-14315
Photoconversion of inorganics to methane [PB89-230643] 06 p0753 N90-14379
Non-equilibrium effects of slow diffusion controlled reactions on the properties of explosives [DE90-000822] 06 p0754 N90-14391

The dissociation energy of N2
[NASA-TM-101930] 07 p0891 N90-15153
The behavior of matter under nonequilibrium conditions: Fundamental aspects and applications
[DE90-002522] 07 p0892 N90-15157
Theoretical methods for the study of chemical dynamics
[DE90-003122] 07 p0893 N90-15160
Dynamics of electron transfer for a nonsuperexchange coherent mechanism, 1
[AD-A213450] 07 p0990 N90-15721
The continuous crystallization of sulfur formed by the liquid-phase reaction of hydrogen sulfide and sulfur dioxide
[DE90-003991] 08 p1041 N90-16018
Selectivity of the reactions of oxygenates on transition metal surfaces
[DE90-003911] 08 p1045 N90-16040
Shock-induced reaction synthesis of aluminides and silicides
[DE90-003948] 08 p1049 N90-16066
High temperature neutron diffraction study of the formation reaction of bismuth superconductors
[DE90-004883] 08 p1134 N90-16568
Non-equilibrium chemistry in the solar nebula and early solar system: Implications for the chemistry of comets 08 p1142 N90-16618
Combustion of hydrogen and hydrocarbons in fluorine
[AD-A214621] 09 p1190 N90-16896
Descriptive simulation: Combining symbolic and numerical methods in the analysis of chemical reaction mechanisms
[AD-A214678] 09 p1190 N90-16898
Transition state spectroscopy of hydrogen transfer reactions
[AD-A215041] 09 p1191 N90-16901
Full scale study of a cabin fire in an A300 fuselage section 10 p1313 N90-17592
Improved performance in co-processing through fundamental and mechanistic studies in hydrogen transfer and catalysis
[DE90-004794] 10 p1352 N90-17839
Chemical reactions in turbulent mixing flows
[AD-A216273] 10 p1355 N90-17856
Response of a chemically reacting layer to streamwise vorticity
[NASA-TM-102288] 10 p1383 N90-18005
Chemistry on interstellar grains and implications for infrared spectroscopy 11 p1579 N90-19097
Nanolayer reactions in aluminum-metal interfaces
[DE90-004955] 12 p1626 N90-19342
Determination of the mechanism of decomposition of energetic molecules
[AD-A217061] 12 p1633 N90-19388
Laboratory studies of free radical reactions in cloudwater
[DE90-003961] 12 p1694 N90-19730
Ion mixing and surface modification in metal-semiconductor systems
[DE90-007557] 12 p1723 N90-19897
Techno-economic assessment of a carbothermic alumina reduction process
[DE90-007018] 13 p1772 N90-20170
The extinction and structure of counterflow premixed flames
[AD-A218106] 13 p1773 N90-20178
Infrared and X ray photoelectron spectroscopy studies of the polyimide/metal interface
[AD-A218249] 13 p1773 N90-20179
An investigation of the mechanisms of solid state powder reaction in the combustion synthesis and sintering of high temperature materials
[DE90-007880] 13 p1777 N90-20198
Modification and improvement of software for modeling multidimensional reacting fuel flows
[AD-A217789] 13 p1783 N90-20235
TiCl4 as a source of TiO2 particles for laser anemometry measurements in hot gas
[NASA-TM-102581] 13 p1805 N90-20358
Laser enhanced chemical reactions
[DE90-008273] 13 p1807 N90-20377
Reactive and anisotropic elastic scattering of highly laser-vibration-excited diatomic molecules
[MPIS-19/1988] 13 p1883 N90-20804
Growth, characterization and device development in monocrystalline diamond films
[AD-A218211] 13 p1898 N90-20895
Computation of nonequilibrium chemically reacting flows in hypersonic flow field 14 p1911 N90-20954
Modelling of molecular structures and properties in physical chemistry and biophysics
[AD-A214561] 14 p1947 N90-21145
Compatibility of Au base thick films with solder alloys: Solid state growth of intermetallics
[DE90-009285] 14 p1952 N90-21175
Shock initiation sensitivity of damaged TP-H1207C composite propellant
[DE90-008509] 14 p1957 N90-21205
Transformation and deposition of airborne gaseous and particulate pollutants during transport over the Baltic Sea
[PUBL-AIR-QUALITY-5] 14 p2003 N90-21478
Thermogravimetric analysis of Nd(2-x)Ce(x)CuO(4-delta)
[DE90-009184] 14 p2032 N90-21658
Studies on reactive flows 15 p2066 N90-21831
Infrared absorption spectroscopy and chemical kinetics of free radicals
[DE90-009469] 15 p2067 N90-21837
An experimental investigation of mixing in buoyant flows 15 p2090 N90-21963
Experimental study of mixing and combustion processes in a solid-propellant ducted rocket motor 17 p2367 N90-23472
Ultrafine microstructure composites prepared by chemical vapor deposition
[AD-A219650] 17 p2369 N90-23484
Combined effect of isotopic substitution, temperature, and magnetic field on the lifetimes of triplet biradicals
[AD-A219711] 17 p2372 N90-23509
Reactions of silane in active nitrogen
[AD-A220371] 17 p2373 N90-23511
Fundamental and practical studies of metal contacts on mercury zinc telluride
[AD-A218730] 17 p2376 N90-23528
Report of research activity at the Research Laboratory of Electronics 17 p2486 N90-24217
Chemistry within molecular clusters
[AD-A219836] 18 p2520 N90-24392
Observation of a magic number in the ion distribution of ethene clusters
[AD-A219837] 18 p2521 N90-24393
Joining engineering ceramics
[DE90-010819] 18 p2531 N90-24445
The composition and physical properties of the Earth's mantle and core 18 p2579 N90-24689
Chemical and crystallographic phase behavior in the Ba(1-x)K(x)BiO3 system
[DE90-010072] 18 p2618 N90-24917
Supersonic combustor modeling 20 p2810 N90-25992
Critical evaluation of Jet-A spray combustion using propane chemical kinetics in gas turbine combustion simulated by KIVA-2
[NASA-TM-103173] 20 p2843 N90-26170
Computer simulation of chemical reactions in synthetic model compounds and genetically engineered active sites
[AD-A222611] 20 p2898 N90-26483
Stibathiolanes: Synthesis, solid state structure, and solution behavior
[AD-A223255] 20 p2933 N90-26688
PDF modeling of chemical nonequilibrium effects in turbulent nonpremixed jet flames 21 p2975 N90-26908
Polyimidazoles via aromatic nucleophilic displacement
[NASA-CASE-LAR-14145-1] 21 p2983 N90-26954
Environmental integrity of coating/metal interface
[AD-A222426] 21 p2987 N90-26978
Carbon-rich particles in Comet Halley 21 p3089 N90-27565
A unifying picture of gas-phase formation and growth of PAH (Polycyclic Aromatic Hydrocarbons), soot, diamond and graphite 21 p3091 N90-27575
Synthesis of Y1Ba2Cu3O(sub x) superconducting powders by intermediate phase reaction 22 p3149 N90-27855
Model of turbulent diffusion flames and nitric oxide generation
[PB90-155557] 22 p3155 N90-27886
Modeling of knock in spark-ignition engines
[DE90-010875] 22 p3182 N90-28058
High T(sub c) copper-oxide superconductors
[AD-D014483] 22 p3247 N90-28416
Assessment of battery technologies for electric vehicles. Volume 2, part 2: Appendices
[DE90-014610] 23 p3321 N90-28778
Chemical kinetic and aerodynamic structures of flames
[AD-A224281] 24 p3445 N90-29455
Electrochemistry of metal surfaces
[AD-A224551] 24 p3445 N90-29458
Synthesis and property evaluation of Y-Ba2-Cu3-O(6+x) superconductors
[AD-A223494] 24 p3552 N90-30098

CHEMICAL REACTORS

Analysis of catalytically enhanced solar absorption chemical reactors. 2: Predicted characteristics of a 100 kW chemical reactor
[DE89-014743] 07 p0954 N90-15521
Radiative transport models for solar thermal receiver/reactors
[DE90-000303] 12 p1683 N90-19665
Developments in solar photocatalysis for destruction of organics in water
[DE90-007685] 13 p1771 N90-20162
Testing of an advanced thermochemical conversion reactor system
[DE90-007989] 15 p2123 N90-22141
High temperature ceramic-tubed reformer
[DE90-009617] 16 p2236 N90-22755
A direct absorber reactor/receiver for solar thermal applications
[DE90-006280] 18 p2577 N90-24679
Energy storage for a lunar base by the reversible chemical reaction: CaO+H2O reversible reaction Ca(OH)2
[NASA-TM-103145] 19 p2709 N90-25419

CHEMICAL RELAXATION

U MOLECULAR RELAXATION

CHEMICAL SHIFT

U CHEMICAL EQUILIBRIUM

CHEMICAL TESTS

NT CHEMICAL ANALYSIS
NT CHROMATOGRAPHY
NT GAS ANALYSIS
NT GAS CHROMATOGRAPHY
NT LIQUID CHROMATOGRAPHY
NT MICROANALYSIS
NT NEUTRON ACTIVATION ANALYSIS
NT OZONOMETRY
NT POTENTIOMETRIC ANALYSIS
NT QUALITATIVE ANALYSIS
NT QUANTITATIVE ANALYSIS
NT SPECTROSCOPIC ANALYSIS
NT VOLUMETRIC ANALYSIS

CHEMICAL VAPOR DEPOSITION

U VAPOR DEPOSITION

CHEMICAL WARFARE

Recovery of particle size distribution of ultrafine aerosols from diffusional decay measurements
[AD-A213006] 05 p0621 N90-13621
Physiological evaluation of men wearing three different toxicological protective systems
[AD-A215527] 09 p1261 N90-17313
Plasma and ion fluorination for chemical hardening of synthetic rubbers
[AD-A216388] 10 p1360 N90-17885

CHEMILUMINESCENCE

Chemiluminescent ion-molecule reactions of group-3 ions with halogens: New optical spectra and reaction dynamics
[MPIS-18/1988] 02 p0196 N90-11120
Description of a chemiluminescence detector system specifically designed for monitoring airborne hydrazine and oxidizer propellant vapors 02 p0206 N90-11179
Singlet oxygen and iodine monofluoride collisional energy transfer mechanism
[AD-A215711] 09 p1280 N90-17421
Atmospheric chemiluminescence: COCHISE and FACELIF experiments
[AD-A218121] 13 p1843 N90-20578
Reactions of silane in active nitrogen
[AD-A220371] 17 p2373 N90-23511
Spectroscopy of propellant-related flames
[AD-A224068] 24 p3457 N90-29525

CHEMISORPTION

Self-assembled organic monolayer films
[AD-A212006] 03 p0323 N90-11838
Excitation lifetimes and excited-state forces in chemisorbed molecules
[DE90-002578] 07 p0894 N90-15165
Chemisorption under stress
[AD-A213785] 07 p0895 N90-15175
Theoretical studies of chemisorption and surface reactions on nickel and silicon
[DE90-004849] 08 p1047 N90-16050
Reactions of atmospheric species with clean and H, C, and O implanted species
[AD-A214602] 09 p1244 N90-17218
Laser studies of chemical dynamics at the gas-solid interface
[DE90-008698] 14 p1986 N90-21380
Reactions of laser-generated free radicals at semiconductor surfaces
[AD-A218552] 16 p2232 N90-22733
In situ analysis of CO during chemisorption and oxidation on graphite: Supported Pt by FTIR-microspectrometry 18 p2559 N90-24605
Calorimetry, activity, and micro-FTIR analysis of CO chemisorption, titration, and oxidation on supported Pt 18 p2560 N90-24606
Analysis of Pt/SnO(sub x) during catalysis of CO oxidation 18 p2560 N90-24607

Characterization of the surfaces of platinum/tin oxide based catalysts by Fourier Transform Infrared Spectroscopy (FTIR) 18 p2560 N90-24608
Chemisorption studies of Pt/SnO2 catalysts 18 p2560 N90-24609
Ni impurity effects on hydrogen surface chemistry and etching of Si(111)
[AD-A222083] 21 p2977 N90-26921
High resolution electron energy loss spectroscopy studies of chemisorbed species on metal surfaces
[AD-A222272] 21 p2978 N90-26922
On hydrogen chemisorption on metals: The electron correlation effects
[DE90-627318] 24 p3448 N90-29473
Scanning tunneling microscopy studies of chemisorbed layers on metal surfaces
[DE90-015623] 24 p3450 N90-29486
Oxidation of NiAl(110)
[DE90-015645] 24 p3451 N90-29487

CHEMONUCLEAR PROPULSION
U CHEMICAL PROPULSION
U NUCLEAR PROPULSION

CHEMOTHERAPY
The effects of nonselective and selective beta blockade upon nonshivering thermogenesis during an acute cold exposure in cold acclimated men 06 p0820 N90-14767

CHESAPEAKE BAY (US)
Chesapeake Bay surface salinities, 1951-88
[PB89-194583] 01 p0090 N90-10513
MECCA program documentation
[NOAA-TR-NESDIS-46] 14 p2003 N90-21477
Prediction of episodic acidification in Maryland coastal plain streams
[PB90-194978] 22 p3199 N90-28152
Perspectives on the Chesapeake Bay, 1990: Advances in estuarine sciences
[PB90-248600] 23 p3354 N90-28954

CHEWING
U MASTICATION

CHILD-LANGMUIR LAW
LEO high voltage solar array arcing response model, continuation 5
[NASA-CR-186505] 19 p2709 N90-25418

CHILDREN
A study of effects of instructional modes in a sequence of computer-assisted instruction lessons, with an introduction to computer-aided diagnosis of arithmetic errors 18 p2589 N90-24730

CHILLING
U COOLING

CHIMES
U AUDITORY SIGNALS

CHINA
A Chinese bibliography on quadratic systems of differential equations
[REPT-89-39] 15 p2161 N90-22342

CHINA (COMMUNIST) MAINLAND
U CHINA

CHINESE PEOPLES REPUBLIC
U CHINA

CHINESE SPACE PROGRAM
Comparison of the space program performance of countries with space programs
[ILR-MITT-222] 05 p0709 N90-14150

CHINESE SPACECRAFT
The main products and their distribution of FY-1 meteorological satellite
[AD-A221582] 21 p2967 N90-26865

CHINOOK HELICOPTER
U CH-47 HELICOPTER

CHIPS
BLITZEN: A highly integrated massively parallel machine 08 p1115 N90-16453
Design of a rotary stepped auger for a lunar environment
[NASA-CR-184919] 17 p2384 N90-23577
Proof of principal for staircase auger chip removal theory
[NASA-CR-184934] 17 p2385 N90-23583

CHIPS (ELECTRONICS)
Laterally stacked Schottky diodes for infrared sensor applications
[NASA-CASE-NPO-17426-1-CU] 01 p0058 N90-10329
The organization of permutation architectures with bussed interconnections
[AD-A210832] 01 p0061 N90-10352
Performance of the CAMEX64 silicon strip readout chip
[DE89-014015] 01 p0130 N90-10747
A new semicustom integrated bipolar amplifier for silicon strip detectors
[DE89-015585] 02 p0215 N90-11229
Optical clock distribution to VLSI chips
[AD-A212269] 04 p0560 N90-13264
Resistive fuses: Analog hardware for detecting discontinuities in early vision
[AD-A211891] 05 p0634 N90-13696
MM and T for VHSIC multichip packages
[AD-A213259] 05 p0635 N90-13703
Testing and data path redesign of a high speed, 16-point Winograd Fourier transform processor
[AD-A215661] 09 p1213 N90-17036
Finite element modeling and thermal simulations of transistor integrated circuits
[AD-A215928] 10 p1380 N90-17997
A gate array structure for the efficient project of digital circuits: The unit cell array
[ETN-90-95364] 12 p1653 N90-19502
A virtual zero-time, monolithic systolic sorting array
[DE90-001000] 12 p1698 N90-19753
Flosolver Mk1B: An eight processor parallel machine
[PD-CF-8941] 12 p1699 N90-19755
Product assurance technology for procuring reliable, radiation-hard, custom LSI/VLSI electronics
[NASA-CR-185954] 13 p1791 N90-20281
ISITE: Automatic circuit synthesis for double-metal CMOS VLSI (Very Large Scale Integrated) circuits
[AD-A217459] 13 p1793 N90-20292
Fault simulator evaluation
[AD-A217782] 13 p1798 N90-20308
The design of high-performance circuits for digital signal processing
[AD-A217786] 13 p1796 N90-20309
Integrated circuits for avionics
[AD-A217964] 13 p1797 N90-20312
An experimental study of fault propagation in a jet-engine controller
[NASA-CR-181335] 17 p2354 N90-23401
Microelectronic device reliability
[AD-A218774] 17 p2394 N90-23638
Test diagnostics of RF effects in integrated circuits
[AD-A219737] 17 p2396 N90-23648
UW VLSI chip tester
[AD-A220789] 17 p2397 N90-23653
Miniaturization of flight deflection measurement system
[NASA-CASE-LAR-13628-1] 17 p2406 N90-23707
WireLisp: Combining graphics and procedures in a circuit specification language
[AD-A220740] 17 p2444 N90-23927
Experiments on liquid immersion natural convection cooling of leadless chip carriers mounted on ceramic substrate
[AD-A219893] 17 p2478 N90-24167
Experimental high speed/power ratio ASIC designs using residue numbers
[AD-A220302] 18 p2591 N90-24741
Highest integration in microelectronics: Development of digital ASICs for PARS3-LR
[MBB-UA-1151/89-PUB] 19 p2653 N90-25099
Multiple target tracking in a wide-field-of-view camera system
[DE90-013488] 20 p2865 N90-26300
LASER: A Layout Sensitivity Explorer. Report and user's manual
[EUT-89-E-216] 20 p2908 N90-26545
Comparative evaluation of Allison T56 engine chip detectors
[AD-A221864] 21 p2960 N90-26832
VLSI architecture for a Reed-Solomon decoder
[NASA-CASE-NPO-17897-1-CU] 21 p2998 N90-27040
Finding minimum width for single-layer channel routing in linear time
[AD-A221876] 21 p3002 N90-27062
Microprocessor chip incorporating optical signal coupling receiver
[AD-D014547] 22 p3167 N90-27964
Solid state circuitry with optical data interfacing
[AD-D014548] 22 p3248 N90-28422
A single wafer bit-sliced convolver: An optimum statistical solution for the implementation of redundancy
[REPT-89-019] 24 p3466 N90-29584
A VHDL interface for Altera design files
[AD-A224476] 24 p3523 N90-29920
A comparison of hardware implementations for low-level vision algorithms
[AD-A223699] 24 p3527 N90-29945

CHIPS (MEMORY DEVICES)
VLSI single-chip (255,223) Reed-Solomon encoder with interleaver
[NASA-CASE-NPO-17280-1-CU] 14 p1933 N90-21061
Gallium arsenide pilot line for high performance components
[AD-A220948] 18 p2547 N90-24540
Failure of the ERBE scanner instrument aboard NOAA 10 spacecraft and results of failure analysis
[NASA-TM-102661] 19 p2694 N90-25328

CHIRAL DYNAMICS
Quantization of anomalous gauge theories on a lattice
[DE89-010247] 01 p0135 N90-10776
Eigensolutions for the reflection problem involving the interface of two chiral half spaces
[PB89-221592] 03 p0338 N90-11926
Index formulas for generalized Wiener-Hopf operators and Boson-Fermion correspondence in 2N dimensions
[CWI-PM-R8811] 04 p0542 N90-13141
Some comments on the solvable Chiral Potts model
[PREPRINT-673] 05 p0696 N90-14070
Generalized WKB approximation for stratified isotropic chiral structures
[PB90-165689] 14 p1967 N90-21270
Studies in quantum field theory
[DE90-008731] 14 p2035 N90-21677
Chiral interface at the finite temperature transition point of QCD
[NASA-CR-186605] 17 p2470 N90-24121
On the zeta-function regularization of chiral Jacobians for singular Dirac operators
[DE90-627176] 23 p3390 N90-29150
Criticality of the three-state chiral clock model: A renormalisation group study
[DE90-627321] 23 p3400 N90-29212

CHIRP
NT CHIRP SIGNALS
The adaptive line enhancer applied to chirp detection
[DE90-006772] 13 p1789 N90-20268

CHIRP SIGNALS
High resolution, wide band Chirp-Z signal analyzer
[AD-D014240] 06 p0768 N90-14465
An experimental medium speed wideband modem 20 p2847 N90-26194

CHLORIDES
NT ALUMINUM CHLORIDES
NT BORON CHLORIDES
NT CALCIUM CHLORIDES
NT CARBON TETRACHLORIDE
NT COPPER CHLORIDES
NT HYDROCHLORIC ACID
NT HYDROGEN CHLORIDES
NT IRON CHLORIDES
NT LITHIUM CHLORIDES
NT SODIUM CHLORIDES
NT TITANIUM CHLORIDES
Active primary lithium thionyl chloride battery for artillery applications
[DE90-009511] 15 p2089 N90-21955
Evaluation of room-temperature chloroaluminate molten salts as electrolytes for high energy density batteries
[AD-A223097] 20 p2860 N90-26267
Metal chloride cathode for a battery
[NASA-CASE-NPO-17809-1-CU] 21 p2998 N90-27041

CHLORINE
Measurement and correlation of the solubility and diffusion coefficient for oxygen and chlorine in basic hydrogen peroxide
[AD-A212348] 04 p0472 N90-12703
The effect of dissolved chlorine on the pitting behavior of 304L stainless steel in a 0.5 N NaCl solution
[AD-A213803] 07 p0905 N90-15234
Method of making carbon dioxide and chlorine free fluoride-based glass
[AD-D014260] 08 p1048 N90-16060
Fluorescence from photoexcitation of Cl2 at 50 to 105 nm
[NASA-CR-186206] 09 p1189 N90-16888
State to state kinetics of XeCl*
[AD-A215895] 10 p1353 N90-17847
Chlorine reactive-ion-beam etching of InSb and InAs0.15Sb0.85/InSb strained-layer-superlattices
[DE90-010848] 18 p2625 N90-24958

CHLORINE COMPOUNDS
NT ALUMINUM CHLORIDES
NT AMMONIUM PERCHLORATES
NT BORON CHLORIDES
NT CALCIUM CHLORIDES
NT CARBON TETRACHLORIDE
NT CHLORIDES
NT CHLORINE FLUORIDES
NT CHLOROCARBONS
NT COPPER CHLORIDES
NT HYDROCHLORIC ACID
NT IRON CHLORIDES
NT LITHIUM CHLORIDES
NT LITHIUM PERCHLORATES
NT PERCHLORATES
NT POTASSIUM PERCHLORATES
NT SODIUM CHLORIDES
NT TITANIUM CHLORIDES
The chemistry of the hypochlorite neutralization of hydrazine fuels 02 p0205 N90-11173

Products of the hypochlorite oxidation of hydrazine fuels
[AD-A213557] 07 p0915 N90-15291

CHLORINE FLUORIDES
Experimental studies on energy storage
[AD-A219032] 16 p2252 N90-22845
Nonflammable hydraulic power system for tactical aircraft. Volume 1: Aircraft system definition, design and analysis
[AD-A218493] 17 p2356 N90-23409

CHLOROCARBONS
Potential technologies for collection and destruction of CFCs (Chlorofluorocarbons), halons, and related compounds
[PB89-219968] 03 p0368 N90-12105
Evaluate and characterize mechanisms controlling transport, fate, and effects of army smokes in the aerosol wind tunnel: Transport, transformations, fate, and terrestrial ecological effects of hexachloroethane obscurant smokes
[DE90-002923] 07 p0957 N90-15536
Success of EPA's stratospheric ozone engineering research
[PB90-246265] 24 p3487 N90-29706

CHLOROPHYLLS
Comparison of structural subunits of the core light-harvesting complexes of photosynthetic bacteria
[DE90-001412] 06 p0819 N90-14765
Some problems in oceanic radiative transfer
[AD-A215935] 10 p1410 N90-18131
LANDSAT-5 data in the study of wheat and bean crops
[INPE-4746-RPE/580] 13 p1819 N90-20444
Utilization of LANDSAT-5 and NOAA-9 satellite imagery in the identification of physical-chemical parameters of the water in the Guanabara Bay
[INPE-4761-TDL/349] 13 p1819 N90-20445
Ocean colour: Methods, technologies, applications 19 p2707 N90-25406

CHLOROPLASTS
Carbon and hydrogen metabolism of green algae in light and dark
[DE90-008648] 13 p1849 N90-20612
Gas exchange characteristics as indicators of the basic limiting factors in photosynthesis
[DE90-012399] 20 p2898 N90-26481

CHLOROPRENE RESINS
Evaluation of a neoprene latex modified SAMI (Stress Absorbing Membrane Interlayer)
[PB89-226435] 05 p0628 N90-13665

CHOICE
U SELECTION

CHOKES (RESTRICTIONS)
Adjustable choke for fluids nozzle
[NASA-CASE-NPO-17625-1-CU] 21 p3003 N90-27070

CHOLESKY FACTORIZATION
The great circle reductions 05 p0609 N90-13553
Software for a new modified Cholesky factorization
[AD-A213643] 07 p0975 N90-15630

CHOLINE
Neurotransmitter and peptide localization in human brain
[AD-A219964] 17 p2435 N90-23873

CHOLINERGICS
Analysis of neural systems involved in modulation of memory storage
[AD-A220230] 18 p2584 N90-24714

CHOLINESTERASE
Acetylcholinesterase inhibition and information processing in the auditory cortex
[AD-A216092] 10 p1411 N90-18139

CHONDRITES
NT ALLENDE METEORITE
NT CARBONACEOUS CHONDRITES
NT MURCHISON METEORITE
Abstracts for the 52nd Annual Meeting of the Meteoritical Society
[NASA-CR-186160] 06 p0860 N90-14998
Mobility of sulfur in thermally altered meteorites 06 p0862 N90-15010
Identification of solar nebula condensates in interplanetary dust particles and unequilibrated ordinary chondrites 08 p1144 N90-16629
What if chondritic porous interplanetary dust particles are not the real McCoy 08 p1146 N90-16642
Refractory solids in chondrites and comets: How similar 08 p1148 N90-16654
Press abstracts of the 21st Lunar and Planetary Science Conference
[NASA-CR-186874] 20 p2941 N90-26738
Carbon in primitive meteorites 21 p3089 N90-27563
Nature and origin of interstellar diamond from the Allende CV3 meteorite 21 p3092 N90-27581

CHONDRULE
Abstracts for the 52nd Annual Meeting of the Meteoritical Society
[NASA-CR-186160] 06 p0860 N90-14998

CHROMATES
High temperature chemistry of complex vaporization/decomposition processes
[DE89-016559] 06 p0740 N90-14306

CHROMATOGRAPHY
NT GAS CHROMATOGRAPHY
NT LIQUID CHROMATOGRAPHY
Cross-axis synchronous flow through coil planet centrifuge for large-scale preparative countercurrent chromatography
[PB89-200174] 04 p0468 N90-12682
On-line chemical composition analyzer development
[DE90-004079] 08 p1043 N90-16026
Copolymers for drag reduction in marine propulsion: New molecular structures with enhanced effectiveness
[AD-A214444] 08 p1049 N90-16062
Ion chromatography in the manufacture of multilayer circuit boards
[DE90-005560] 11 p1503 N90-18652
Analytical sciences
[DE90-007965] 14 p1948 N90-21152
Retention index monitoring of volatile organic compounds using thermal desorption gas chromatography
[AD-A221117] 18 p2521 N90-24397
Computer analysis of chromatographic data 20 p2905 N90-26521
Elastomers and other organic composites
[AD-A222772] 21 p2984 N90-26958

CHROME
U CHROMIUM

CHROMITES
Synthesis of air-sinterable lanthanum chromite powders
[DE90-004681] 08 p1046 N90-16049
Research on high-specific-heat dielectrics
[AD-A221215] 18 p2623 N90-24944

CHROMIUM
NT CHROMIUM ISOTOPES
Radiationless transitions and excited-state absorption of low-field chromium complexes in solids
[AD-A210653] 02 p0194 N90-11105
Trace metal catalysis of hydrazine decomposition: The role of chromium 02 p0204 N90-11163
New laser materials
[DE89-017524] 03 p0353 N90-12017
Magnetotransport studies of epitaxial Cr thin films
[DE90-001930] 06 p0856 N90-14975
Development of glass-ceramic lasers
[AD-A214146] 07 p0936 N90-15423
Spectroscopic and laser properties of Cr:LiCaAlF6 and Cr:LiSrAlF6 crystals
[DE90-000783] 07 p0998 N90-15770
Determination of iron in chromium plating and polishing solutions by atomic absorption spectrometry
[AD-A214467] 09 p1189 N90-16892
Epitaxial growth of Cr(011) on LiF(001)
[DE90-005635] 09 p1293 N90-17496
Determination of trivalent chromium ions in chromium plating solutions by ultraviolet-visible spectrophotometry
[AD-A215688] 10 p1351 N90-17837
Infrared and X ray photoelectron spectroscopy studies of the polyimide/metal interface
[AD-A218249] 13 p1773 N90-20179
The stress corrosion performance of diffusion bonded nickel base alloys
[DE90-008130] 13 p1777 N90-20199
L shell XANES (X ray Absorption Near Edge Structure) for solid metals: Ti, V, Cr, Fe, Ni, Cu
[DE90-008043] 13 p1896 N90-20880
Ilmenite exsolution schemes in Apollo-17 high-Ti basalts
[DE90-011992] 21 p2976 N90-26912
Effects of low Chromium(3) concentration in electrodeposition of low contraction chromium
[AD-A223338] 24 p3449 N90-29477

CHROMIUM ALLOYS
NT CHROMIUM STEELS
Precipitation strengthened high strength, high conductivity Cu-Cr-Nb alloys produced by chill block melt spinning
[NASA-CR-185144] 03 p0326 N90-11853
Fracture toughness data base for HT9 and modified 9Cr-1Mo irradiated in several reactors up to approximately 100 dpa
[DE90-000111] 03 p0328 N90-11864
The effects of heat treatment after welding on the functional properties of assemblies of CrMo alloys. Heat treatment of a mixed assembly of A48 and 10CD9.10 alloys
[CETIM-104320] 04 p0475 N90-12724
Deformation and fracture of low alloy steels at high temperature
[DE90-001274] 07 p0902 N90-15215
An investigation of the sensitization behavior of Fe-Mn-Cr austenitic steels
[DE90-002719] 07 p0904 N90-15226
Microstructural explanation for irradiation embrittlement of V-15Cr-5Ti
[DE90-004112] 08 p1045 N90-16041
Production and processing of Cu-Cr-Nb alloys
[NASA-TM-102495] 08 p1047 N90-16053
Ordering mechanism in substitutional Ni-Cr alloys: Theory and experiment
[DE90-006268] 14 p1949 N90-21156
High-temperature oxidation and sulfidation of Fe-20Cr-16Ni-4Al-1Y2O3 oxide-dispersion-strengthened alloy
[DE90-007897] 14 p1951 N90-21168
On the stability of amorphous silica coatings for high temperature service
[AERE-R-13425] 14 p1953 N90-21179
Morphological and structural characterization of the spinodal decomposition of Fe-Cr alloys
[DE90-010496] 18 p2526 N90-24418
A resistance strain gage with repeatable and cancellable apparent strain for use to 800 C
[NASA-CR-185256] 20 p2823 N90-26063
Relationship between microstructure, spinodal-like decomposition and selective electropolishing of irradiated invar-type alloys
[DE90-015293] 24 p3450 N90-29484
Isotopic tailoring and other techniques used to study helium effects in austenitic alloys
[DE90-016344] 24 p3452 N90-29495
The effect of helium on microstructural evolution in austenitic steels as determined by spectral tailoring experiments
[DE90-016360] 24 p3452 N90-29496

CHROMIUM COMPOUNDS
NT CHROMATES
NT CHROMIUM OXIDES
Study of palladium and chromium silicides formation in liquid phase and in solid phase
[LAAS-89040] 04 p0470 N90-12695

CHROMIUM ISOTOPES
Enrichment services for chromium isotopes for the GALLEX (gallium experiment) international collaboration experiment on solar neutrino flux
[DE90-014300] 23 p3413 N90-29285

CHROMIUM OXIDES
Transport properties of thermally grown Cr2O3
[DE89-016703] 02 p0284 N90-11623
Study of adherent oxide scales
[AD-A215189] 09 p1198 N90-16940
New corrosion resistant ceramic coatings by laser processing
[AERE-R-13166] 15 p2071 N90-21863
The effect of catalysts on gas-phase hydrocarbon ignition
[AD-A218775] 17 p2371 N90-23499

CHROMIUM STEELS
Contribution to the transcrystalline stress crack corrosion of austenite chromium-nickel steels
[ETN-89-94665] 02 p0199 N90-11137
Microstructural evolution of martensitic steels during fast neutron irradiation
[DE89-016231] 07 p0902 N90-15212
Heat-resistant steels containing 8 pct Cr
[PB90-108796] 09 p1193 N90-16912
Oscillation and damping behavior of fine steel test tubes, with particular consideration to destruction free proofs from hydrogen fragilization
[ETN-90-95371] 12 p1627 N90-19351
Modification of surface mechanical properties of high-chromium tool steel by carbon-implanted codeposited Fe-Ti films
[DE90-007502] 12 p1628 N90-19358
A study of the relation between grain boundary type and sensitisation in a partially-sensitised AISI 304 stainless steel using electron back-scattering patterns
[AERE-R-13327] 16 p2321 N90-23234
Influence of sinter technical limits for the manufacturing of oscillation strained pieces made of sinter steel
[LBF-FB-184(1989)] 18 p2526 N90-24413
Irradiation effects on impact behavior of 12Cr-1MoVW and 2 1/4Cr-1Mo steels
[DE90-011075] 18 p2527 N90-24421

CHROMOSOMES
Effects of pulsed and CW (Continuous Wave) 2450 MHz radiation on transformation and chromosomes of human lymphocytes in vitro
[AD-A216500] 11 p1539 N90-18857

CHROMOSPHERE
Flare model sensitivity of the Balmer spectrum 03 p0432 N90-12477

Heating and acceleration of coronal and chromospheric ions during solar flares 03 p0433 N90-12479
Chromospheric-coronal coupling during solar flares: Current systems and particle acceleration 03 p0433 N90-12480
The winds of high luminosity late-type bright stars [NASA-CR-182961] 05 p0712 N90-14160

CHRONOBIOLOGY
U RHYTHM (BIOLOGY)

CHRONOLOGY
NT GEOCHRONOLOGY
Carbon isotope ratios and lithium abundances in open cluster giants 02 p0292 N90-11664
Impact cratering and the surface age of Venus: The Pre-Magellan controversy 03 p0426 N90-12446
Chronology of KSC and KSC related events for 1988 [NASA-TM-101915] 06 p0867 N90-15040
The age of the galactic disk [NASA-CR-186292] 07 p1013 N90-15869
New developments in stellar ages and modelling of Pop. I stars [SER-C-PREPUBL-FASC-41] 08 p1151 N90-16669
The Age of the Universe: Concordance [DE90-004971] 09 p1299 N90-17529

CHRONOTRONS
U PULSE RATE
U TIME LAG

CHUGGING
U COMBUSTION STABILITY

CID
U CHARGE INJECTION DEVICES

CINDER CONES
U CONES (VOLCANOES)

CINEFLUOROGRAPHY
U MOTION PICTURES
U RADIOGRAPHY

CINEMATOGRAPHY
Application of holography to behavior simulators [ISL-R-111/88] 09 p1226 N90-17115
Holocinematography for studies of turbulent multiphase flow [AD-A219130] 16 p2237 N90-22765
On the efficacy of cinema, or what the visual system did not evolve to do 16 p2269 N90-22934

CINERADIOGRAPHY
U MOTION PICTURES
U RADIOGRAPHY

CIRCADIAN RHYTHMS
Human performance in continuous/sustained operations and the demands of extended work/rest schedules: An annotated bibliography, volume 2 [AD-A210504] 01 p0093 N90-10530
Studies on predicting the resynchronization of the circadian system after transmedian flights [DFVLR-FB-89-10] 03 p0382 N90-12172
Effects of a time zone shift of nine hours on the circadian rhythms in cockpit aircrew members on longhaul flights [DLR-FB-89-31] 04 p0523 N90-13019
A review of circadian effects on selected human information processing tasks [AD-A214673] 09 p1251 N90-17256
Identifying the circadian cycle in human information processing data using periodicity analysis: A synopsis [AD-A214674] 09 p1251 N90-17257
Studies on predicting the resynchronization of the circadian system after transmeridian flights [ESA-TT-1177] 19 p2722 N90-25483
Effects of a time zone shift of 9 hours on the circadian rhythms in cockpit aircrew members on longhaul flights [ESA-TT-1185] 19 p2722 N90-25485
Melatonin, light and, circadian cycles [AD-A223196] 21 p3035 N90-27256
The 1989 Gordon Research Conference on Chronobiology [AD-A221972] 22 p3231 N90-28322
Pharmacological resetting of the circadian sleep-wake cycle effects of triazolam on reentrainment of circadian rhythms in a diurnal primate [AD-A224227] 24 p3497 N90-29764
Exogenous and endogenous control of activity behavior and the fitness of fish [DLR-FB-90-14] 24 p3497 N90-29766

CIRCLES (GEOMETRY)
NT GREAT CIRCLES
A study of failure characteristics in thermoplastic composite laminates due to an eccentric circular discontinuity [AD-A216226] 10 p1349 N90-17827
Cyclotomy and association schemes [REPT-89-73] 17 p2458 N90-24030

CIRCUIT BOARDS
Magellan/Galileo solder joint failure analysis and recommendations [NASA-CR-186294] 09 p1233 N90-17157
Computer-Aided Design for Built-In-Test (CADBIT). Volume 1: Technical issues [AD-A215737] 09 p1268 N90-17353
Computer-Aided Design for Built-In-Test (CADBIT). Volume 2: BIT Library [AD-A215738] 09 p1268 N90-17354
Computer-Aided Design for Built-In-Test (CADBIT). Volume 3: Software specification [AD-A215739] 09 p1268 N90-17355
Ion chromatography in the manufacture of multilayer circuit boards [DE90-005560] 11 p1503 N90-18652
Correlation/validation of finite element code analyses for vibration assessment of avionic equipment [AD-A220393] 17 p2353 N90-23398
Personal Computer (PC) thermal analyzer [AD-A221325] 18 p2548 N90-24546
Selective metallization of carbonyl-containing polymer films [AD-D014526] 19 p2678 N90-25230
Finding minimum width for single-layer channel routing in linear time [AD-A221876] 21 p3002 N90-27062
Microprocessor chip incorporating optical signal coupling receiver [AD-D014547] 22 p3167 N90-27964
Using multiple sensors for printed circuit board insertion 24 p3514 N90-29867

CIRCUIT BREAKERS
Development of an expert system supporting short-circuit tests for circuit breakers [DE89-760384] 01 p0059 N90-10334
Independent Orbiter Assessment (IOA): Analysis of the backup flight system [NASA-CR-185567] 02 p0165 N90-10932
Contribution to the study of a self-protected static switch and its command strategy [ECL-89-002] 05 p0636 N90-13711
L-SWITCH: A PC-program for computing transient voltages and currents during switching off three-phase inductances [PB90-191412] 22 p3167 N90-27961

CIRCUIT DIAGRAMS
Circuit level modeling of inductive elements [DE89-015122] 01 p0032 N90-10173
Focused ion beam implantation [AD-A210977] 01 p0133 N90-10767
Elements of a 200 watt pulsed excimer laser 02 p0226 N90-11295
Nearly optimal algorithms and bounds for multilayer channel routing [AD-A211913] 03 p0343 N90-11955
Built-in generation for CMOS circuits [IMAG-RR-736-I] 04 p0496 N90-12855
The application of artificial intelligence techniques to tracing the interconnections in an integrated circuit [TELECOM-PARIS-89-E002] 04 p0537 N90-13105
On the design of a computer-aided design system for digital circuits 05 p0633 N90-13695
Intrinsically safe 5-V, 4-A rechargeable power supply [PB90-103235] 09 p1209 N90-17006
A test method for measuring corona inception voltage for transducer autotransformers [AD-A216818] 11 p1502 N90-18646
Optimal layout via Boolean satisfiability [AD-A216777] 12 p1705 N90-19787
An alternate interconnect method for joining flexible circuits using conductive adhesives [DE90-008194] 16 p2222 N90-22674
LASER: A Layout Sensitivity Explorer. Report and user's manual [EUT-89-E-216] 20 p2908 N90-26545
VLSI design for reliability [AD-A224264] 24 p3463 N90-29562
Macro cell placement with neural net algorithms [REPT-90-020] 24 p3466 N90-29585

CIRCUIT PROTECTION
Performance of transient limiters under laboratory, simulated, and rocket-triggered lightning conditions [DE89-015773] 02 p0216 N90-11238
Steep front impulse tests on a solid-state relay [DE90-004243] 08 p1062 N90-16140
Analysis of the 60-Hz power system at KSC: The Orsino substation 08 p1155 N90-16692
Intrinsically safe 5-V, 4-A rechargeable power supply [PB90-103235] 09 p1209 N90-17006
Thermal switch disc for short circuit protection of batteries [NASA-CASE-MSC-21428-1] 09 p1209 N90-17008
Current protections modelisation in a buck cell 10 p1335 N90-17723
Dynamical model of series-resonant converter with peak capacitor voltage predictor and switching frequency control 10 p1336 N90-17730
A low cost anticharging connection system for solar generators and its application on ASPERA solar array 10 p1341 N90-17765
Power diode switching behavior [ETN-90-95363] 12 p1653 N90-19501
Definition of a design methodology and study of the driving and protection functions of a smart power switch [LAAS-89-330] 16 p2231 N90-22727
The dielectric behavior of sulfur hexafluoride submitted to rapid transitory overvoltages [ECL-89-16] 17 p2374 N90-23520
Controling, cabling and protection of GTO thyristors in pulse inverters [ETN-90-96500] 18 p2549 N90-24548
Simulation of the electrical and thermal behavior of gapless metal oxide surge arresters under AC-operation condition [ETN-90-97309] 20 p2859 N90-26262

CIRCUIT RELIABILITY
Development of an expert system supporting short-circuit tests for circuit breakers [DE89-760384] 01 p0059 N90-10334
VLSI integrated circuit tests [IMAG-RR-763-I] 08 p1061 N90-16135
Testing and data path redesign of a high speed, 16-point Winograd Fourier transform processor [AD-A215661] 09 p1213 N90-17036
Product assurance technology for procuring reliable, radiation-hard, custom LSI/VLSI electronics [NASA-CR-185954] 13 p1791 N90-20281
Smart microsensors for high temperature applications, phase 1 [AD-A224151] 23 p3330 N90-28828
Reliability analysis/assessment of advanced technologies [AD-A223647] 24 p3485 N90-29573

CIRCUITS
NT ADDING CIRCUITS
NT ANALOG CIRCUITS
NT APPLICATION SPECIFIC INTEGRATED CIRCUITS
NT BISTABLE CIRCUITS
NT CANCELLATION CIRCUITS
NT CIRCULATORS (PHASE SHIFT CIRCUITS)
NT COINCIDENCE CIRCUITS
NT COUNTING CIRCUITS
NT COUPLING CIRCUITS
NT DELAY CIRCUITS
NT DIGITAL ELECTRONICS
NT DIGITAL INTEGRATORS
NT DIPLEXERS
NT DISCRIMINATORS
NT ELECTRIC BRIDGES
NT EQUIVALENT CIRCUITS
NT FEEDBACK CIRCUITS
NT FLIP-FLOPS
NT GATES (CIRCUITS)
NT HYBRID CIRCUITS
NT INTEGRATED CIRCUITS
NT ITERATIVE NETWORKS
NT LARGE SCALE INTEGRATION
NT LIMITER CIRCUITS
NT LINEAR INTEGRATED CIRCUITS
NT LOGIC CIRCUITS
NT MATRICES (CIRCUITS)
NT MICROWAVE CIRCUITS
NT MIXING CIRCUITS
NT NEGATIVE RESISTANCE CIRCUITS
NT PHASE DETECTORS
NT PHASE SHIFT CIRCUITS
NT POWER SUPPLY CIRCUITS
NT PRINTED CIRCUITS
NT SCALERS
NT SWITCHING CIRCUITS
NT THRESHOLD GATES
NT TRANSISTOR CIRCUITS
NT TRANSMISSION CIRCUITS
NT TRIGGER CIRCUITS
NT VERY LARGE SCALE INTEGRATION
NT VHSIC (CIRCUITS)
NT WHEATSTONE BRIDGES
NT WIRE BRIDGE CIRCUITS
Statistical modeling of electrical components [BDX-613-3939] 01 p0059 N90-10336
Summarizing qualitative behavior from measurements of nonlinear circuits, revision [AD-A210919] 01 p0061 N90-10353
Independent Orbiter Assessment (IOA): Analysis of the backup flight system [NASA-CR-185567] 02 p0165 N90-10932
A digital model for level-clocked circuitry [AD-A211937] 03 p0343 N90-11957
Linear (passive) and non-linear guided and studies in glass [AD-A211693] 03 p0406 N90-12325
Simulation of circuits adapted to signal processing [TELECOM-PARIS-89-E001] 04 p0489 N90-12811

Test generation for highly sequential circuits
[AD-A211932] 05 p0634 N90-13698
Laser probing non-cylindrical Z-pinch in near-isolator region of a discharged chamber
[DE89-632018] 06 p0844 N90-14912
Tuned-circuit Johnson noise thermometry
[DE89-016221] 07 p0925 N90-15356
Analysis of the 60-Hz power system at KSC: The Orsino substation 08 p1155 N90-16692
Intrinsically safe 5-V, 4-A rechargeable power supply
[PB90-103235] 09 p1209 N90-17006
The design of low inductance electrical circuits for slapper detonator systems
[AD-A214981] 09 p1212 N90-17024
Interference rejection and detection performance of the smallest of circuit
[AD-A215153] 09 p1212 N90-17025
Cache for multi-threaded processors on a split-transaction bus
[AD-A216404] 10 p1415 N90-18156
Output performance of idealized microwave power amplifiers
[AD-A216797] 11 p1502 N90-18645
Radiation-hard high-efficiency InP space solar cell development
[AD-A216857] 11 p1528 N90-18800
Boolean minimization and algebraic factorization procedures for fully testable sequential machines
[AD-A216779] 11 p1553 N90-18940
Muzzle shunt augmentation of conventional railguns
[DE90-007505] 12 p1607 N90-19248
Modeling A circuit switched multiprocessor interconnect
[AD-A217122] 12 p1656 N90-19519
Measurement of proton induced radiation damage to CMOS transistors and pin diodes
[DE90-007836] 13 p1792 N90-20283
A real-time rejection circuit to automatically reject multiple interfering hopping signals while passing a lower level desired signal
[AD-D014424] 14 p1965 N90-21251
JPRS report: Science and technology. USSR: Electronics and electrical engineering
[JPRS-UEE-90-002] 14 p1970 N90-21284
Common source cascode amplifiers for integrating IR-FPA applications 14 p1977 N90-21324
Short wavelength HgCdTe staring focal plane for low background astronomy applications
14 p1979 N90-21336
An ultra-small capacitance Josephson junction
[DE90-613396] 14 p2032 N90-21653
New flexible circuit material evaluation
[DE90-008313] 15 p2071 N90-21866
Application of artificial intelligence in electronic circuit diagnosis 16 p2303 N90-23122
VLSI architectures and CAD
[AD-A220736] 17 p2397 N90-23652
Gemini2: A second generation layout validation program
[AD-A220731] 17 p2444 N90-23926
WireLisp: Combining graphics and procedures in a circuit specification language
[AD-A220740] 17 p2444 N90-23927
An approach to systematic phase-lock loop design
[ETN-90-96905] 19 p2686 N90-25280
Electronics design of the infrared/ultrasonic sensing for a robot gripper
[PB90-160383] 21 p3010 N90-27109
Integration of picosecond GaAs photoconductive devices with silicon circuits for optical clocking and interconnects
[DE90-012096] 21 p3080 N90-27512
Higher order diffusion model for a bipolar transistor
[PB90-190901] 22 p3167 N90-27960
Solid state circuitry with optical data interfacing
[AD-D014548] 22 p3248 N90-28422
Robust controller design by contraction of a pole region
[ESA-TT-1042] 23 p3384 N90-29118

CIRCULAR CONES
Semidiscrete Galerkin modelling of compressible viscous flow past a circular cone at incidence
[NASA-CR-186323] 11 p1505 N90-18664

CIRCULAR CYLINDERS
Leading edge transition by contamination in hypersonic flow 01 p0063 N90-10360
The near-wake flow structure of wake-cylinder interaction and surface loading of cylinder
02 p0218 N90-11248
SSME LOX post flow analysis/fluid structure interaction. Volume 1: Flow analysis
[NASA-CR-183677] 05 p0637 N90-13715
Finite element investigation of a composite cylindrical shell under transverse load with through thickness shear and snapping
[AD-A216377] 10 p1397 N90-18078
Scattering from an arbitrary cylinder in the presence of a planar media interface using the bymoment method
[DE90-006465] 11 p1499 N90-18626
Computation of hypersonic unsteady viscous flow over a cylinder 12 p1597 N90-19194
Dual frequency launcher for circularly polarized antenna
[AD-D014361] 12 p1645 N90-19456
An experimental study of the aeroelastic behaviour of two parallel interfering circular cylinders
12 p1673 N90-19609
Spectral simulation of unsteady compressible flow past a circular cylinder
[NASA-CR-182030] 13 p1750 N90-20050
Free wave propagation in orthogonally stiffened cylinders 15 p2119 N90-22124
Secondary frequencies in the wake of a circular cylinder with vortex shedding
[NASA-CR-181998] 16 p2197 N90-22540
Estimation of extra drag force on a circular cylinder due to the presence of solid particles in subsonic compressible flow
[AD-A218635] 16 p2197 N90-22542
Transverse vibrations of a composite cylindrical tube of circular cross section
[AD-A219227] 16 p2248 N90-22820
Stability regimes in a rotating quadrupole focusing accelerator
[AD-A219513] 16 p2317 N90-23209
Some ray tracing problems related to circles and ellipses
[AD-A219306] 16 p2318 N90-23217
Computations of a horseshoe vortex around an endwall-mounted cylinder 17 p2400 N90-23673
Innovative design of composite structures: Axisymmetric deformations of unsymmetrically laminated cylinders loaded in axial compression
[NASA-CR-186635] 19 p2700 N90-25364
Optical high-speed parallel backplane
[AD-D014504] 19 p2757 N90-25670
Aerodynamic forces acting on a finite rectangular slender body
[NAL-TR-1035] 24 p3421 N90-29329

CIRCULAR ORBITS
An analytic development of orbit determination for a distant, planetary orbiter 04 p0485 N90-12787
Investigation of the observability of a satellite cluster in a near circular orbit
[AD-A216224] 10 p1326 N90-17662
Lunar orbiting microwave beam power system
[NASA-TM-103211] 19 p2667 N90-25173

CIRCULAR PLATES
The dynamics of circular plates with patch damping: A numerical and experimental study
02 p0232 N90-11329

CIRCULAR POLARIZATION
Stripline feed for a microstrip array of patch elements with teardrop shaped probes
[NASA-CASE-NPO-17548-1-CU]
08 p1056 N90-16104
Dual frequency launcher for circularly polarized antenna
[AD-D014361] 12 p1645 N90-19456
Structure and dynamics of excited atoms
[AD-A221973] 21 p3074 N90-27474

CIRCULAR TUBES
Limit analysis of welded tee end connections for hollow tubes
[PB89-191647] 01 p0079 N90-10452
Mechanism for shear band formation in the high strain rate torsion test
[PB89-215370] 03 p0356 N90-12038
A study of heat and fluid flow phenomena on the gas side of circular-tube plate-fin heat exchangers
23 p3324 N90-28795

CIRCULAR WAVEGUIDES
Electromagnetic wave propagation through circular waveguides containing radially inhomogeneous lossy media
[AD-A213062] 05 p0632 N90-13688
Rectangular-to-circular waveguide transitions for high-power circular overmoded waveguides
[AD-A213925] 07 p0924 N90-15349
Theory of circular dielectric waveguide with anisotropic sheet cover
[NASA-CR-186883] 20 p2855 N90-26235
Analysis of a TM01 circular to TE10 rectangular waveguide mode converter
[AD-A224566] 24 p3464 N90-29568

CIRCULATION
NT ATMOSPHERIC CIRCULATION
NT BLOOD CIRCULATION
NT BRAIN CIRCULATION
NT CARBOXYHEMOGLOBIN
NT CONGESTION
NT CORONARY CIRCULATION
NT EL NINO
NT GULF STREAM
NT OCEAN CURRENTS
NT PULMONARY CIRCULATION
NT WATER CIRCULATION
NT WATER CURRENTS
NT ZONAL FLOW (METEOROLOGY)
Expandable radiator
[AD-D014258] 08 p1063 N90-16147
Turbulent heat and momentum transfer in recirculating and impinging flows 09 p1215 N90-17043
Parameterization of small-scale processes
[AD-A215507] 10 p1398 N90-18082
High performance millimeter-wave microstrip circulators and isolators
[NASA-CR-186276] 19 p2685 N90-25270

CIRCULATION CONTROL AIRFOILS
Aeroelastic characteristics of aircraft with circulation control wings 13 p1754 N90-20070

CIRCULATION DISTRIBUTION
A formatting style for typesetting and distributing draft international standards
[NPL-DITC-143/89] 04 p0530 N90-13059
Optimum spanwise camber for minimum induced drag
[BU-403] 11 p1452 N90-18369
The application of the finite element method to an aerodynamic problem specific to propeller design
[LR-614] 19 p2656 N90-25116
A study of water vapor, electrical parameters, and radio propagation
[AD-A223582] 24 p3492 N90-29736

CIRCULATORS (PHASE SHIFT CIRCUITS)
Field theoretical analysis and synthesis of broadband waveguide: Height, plane shunt circulators with multiple layer material insertions
[ETN-90-95360] 12 p1647 N90-19469

CIRCULATORY SYSTEM
NT ARTERIES
NT BLOOD VESSELS
NT CARDIOVASCULAR SYSTEM
NT HEART
NT MYOCARDIUM

CIRCUMFERENCES
Circularity measuring system: A shape gauge designed especially for use on large objects
15 p2116 N90-22104
Circumferential pressure probe
[NASA-CASE-LAR-13775-1] 17 p2406 N90-23706

CIRCUMSTELLAR MATTER
U STELLAR ENVELOPES

CIRROSTRATUS CLOUDS
ETO lidar studies of cirrostratus altocumulogenitus: Another role for supercooled liquid water in cirrus cloud formation 22 p3221 N90-28269

CIRRUS CLOUDS
Exploiting surface observations of cloudiness for globalscale nephanalyses 12 p1692 N90-19719
Downward shortwave surface irradiance from 17 sites for the FIRE/SRB Wisconsin experiment
[NASA-TM-102596] 13 p1844 N90-20583
Cirrus cloud optical properties measured with the University of Wisconsin high spectral resolution and volume imaging lidars 15 p2084 N90-21932
Dynamic and microphysical characteristics of cirrus clouds as revealed by aircraft, lidar, and other observations during FIRE 15 p2130 N90-22177
The 27-28 October 1986 FIRE IFO Cirrus case study: Comparison of radiative transfer theory with observations by satellite and aircraft
[NASA-TM-103468] 20 p2890 N90-26446
The 27-28 October 1986 FIRE IFO cirrus case study: Cirrus parameter relationships derived from satellite and lidar data
[NASA-TM-103469] 20 p2890 N90-26447
Aircraft measurements of the turbulence structure in cirrus clouds
[ISSN-0069-5882] 20 p2890 N90-26450
Application of automatic method to estimating high-level cloud motion wind in operational system and the characteristics of the resultant wind vectors
21 p3028 N90-27218
Analysis of cirrus optical properties with data from NASA ER2 High-resolution Interferometer Sounder (HIS)
[NASA-CR-186365] 21 p3030 N90-27227
Lidar cloud studies for FIRE and ECLIPS
[NASA-CR-186384] 22 p3211 N90-28214
FIRE Science Results 1989
[NASA-CP-3079] 22 p3213 N90-28224
A comparison of ISCCP and FIRE satellite cloud parameters 22 p3221 N90-28267
Comparison of satellite based cloud retrieval methods for cirrus and stratocumulus 22 p3221 N90-28268
Impact of cirrus on the surface radiative environment at the FIRE ETLA Palisades, NY site
22 p3221 N90-28270

Seasonal and interannual changes in cirrus
22 p3222 N90-28272
Spatial scales of cirrus cloud properties
22 p3222 N90-28275
Interpretation of cirrus cloud properties using coincident satellite and lidar data during the FIRE cirrus IFO
22 p3223 N90-28276
Properties of cirrus from multispectral AVHRR imagery data
22 p3223 N90-28277
Summary of results and conclusions based on analysis of volume imaging and high spectral resolution lidar data acquired during FIRE phase 1, part 1
22 p3223 N90-28278
Moisture and heat budgets of a cirrus cloud from aircraft measurements during FIRE
22 p3223 N90-28279
The 27-28 October 1986 FIRE cirrus case study: Meteorology and clouds
22 p3223 N90-28280
Satellite-derived cloud fields during the FIRE cirrus IFO case study
22 p3223 N90-28281
The October 27-28, 1986, FIRE cirrus case study: Cloud microstructure
22 p3224 N90-28283
Cirrus microphysics and radiative transfer: Cloud field study on October 28, 1986
22 p3224 N90-28284
The 27-28 October 1986 FIRE IFO cirrus case study: Comparison of satellite and aircraft derived particle size
22 p3224 N90-28285
Cirrus radiative characteristics and the radiative impact of small particles
22 p3224 N90-28286
Regional conditions during the 25 October 1986 FIRE cirrus/altocumulus case study
22 p3225 N90-28287
Cirrus clouds and climate feedback: Is the sky falling and should we go tell the king
22 p3225 N90-28288
Preliminary simulations of the large-scale environment during the FIRE cirrus IFO
22 p3225 N90-28290
Microphysical fundamentals governing cirrus cloud growth: Modeling studies
22 p3225 N90-28291
A scheme for parameterizing cirrus cloud ice water content in general circulation models
22 p3226 N90-28292
Radiative diffusivity factors in cirrus and stratocumulus clouds: Application to two-stream models
22 p3226 N90-28293
A comparative study of infrared radiance measurements by an ER-2 based radiometer and the LANDSAT 5 Thematic Mapper (TM-6)
22 p3226 N90-28294
Radiative properties of cirrus clouds inferred from broadband measurements during FIRE
22 p3226 N90-28295
Remote sounding through semi-transparent cirrus cloud
22 p3226 N90-28296
IR spectral characteristics of cirrus clouds
22 p3226 N90-28297
Airborne lidar/radiometric measurements of cirrus cloud parameters and their application to LOWTRAN radiance evaluations
22 p3227 N90-28298
The Colorado/Misscuri 1989 cirrus mini IFO
22 p3227 N90-28299
Summary of results and conclusions based on analysis of volume imaging and high spectral resolution lidar data acquired during FIRE phase 1, part 2
22 p3227 N90-28300
Cirrus parameterization from the FIRE ER-2 observations
22 p3227 N90-28302
The 1973-1974 lidar observations of cirrus clouds at Kwajalein
22 p3227 N90-28303
The use of an airborne lidar for mapping cirrus clouds in FIRE, phase 2
22 p3228 N90-28304
On the use of IR lidar and K(sub a)-band radar for observing cirrus clouds
22 p3228 N90-28305

CISLUNAR SPACE
A trajectory generation and system characterization model for cislunar low-thrust spacecraft. Volume 2: Technical manual
[NASA-CR-185172] 15 p2061 N90-21807

CITIES
The use of photographs for identification and analysis of urban residential sectors, with planning views
[INPE-4788-PRE/1448] 10 p1399 N90-18087
Controlling Summer Heat Islands: Proceedings
[DE90-008075] 13 p1830 N90-20508
Possible use of satellite data for flood plain mapping
[INPE-4968-PRE/1537] 14 p2000 N90-21462
Performance evaluation of morphological edge detectors
[INPE-4975-PRE/1540] 14 p2000 N90-21464
Development and use of a passive technique for measuring nitrogen dioxide in the background atmosphere
16 p2331 N90-23285
The effects of urban air pollution on solar radiation
[DE89-009455] 19 p2712 N90-25438
Automatic line network extraction from aerial imagery of urban areas through knowledge based image analysis
[AD-A222675] 20 p2880 N90-26385
Integration of multispectral SPOT imagery and panchromatic aerial photography for study in urban land use
[INPE-4967-PRE/1536] 22 p3194 N90-28125

CIVIL AVIATION
Casting airworthiness joint European civil authorities view-point
01 p0042 N90-10234
Flight testing in the Netherlands: An overview
02 p0155 N90-10884
Simulated airline service experience with laminar-flow control leading-edge systems
04 p0439 N90-12512
Fine resolution errors in secondary surveillance radar altitude reporting amongst aircraft transmitting the conspicuity codes 4321 and 4322
[RSRE-88004] 04 p0490 N90-12816
Study of high-speed civil transports
[NASA-CR-4235] 05 p0578 N90-13370
Cockpit resource management: A selected annotated bibliography
[AD-A214272] 07 p0969 N90-15594
Aircraft accident report: Delta Air Lines, Inc., Boeing 727-232, N473DA, Dallas-Fort Worth International Airport, Texas, August 31, 1988
[PB89-910406] 08 p1019 N90-15895
Investigation and characteristics of major fire-related accidents in civil air transports over the past ten years
10 p1311 N90-17582
Aircraft fire safety: Learning from past accidents
10 p1312 N90-17584
Fire safety in civil aviation
10 p1312 N90-17586
Fire hardening of an aircraft passenger cabin
10 p1315 N90-17606
New materials for civil aircraft furnishing
10 p1316 N90-17609
Human factors issues in aircraft maintenance and inspection
[AD-A215724] 11 p1542 N90-18875
Interoperability issues in the use of satellite-based navigation systems for civil aviation purposes
[AD-A217279] 12 p1602 N90-19223
Activities report in civil aviation
[ETN-90-95471] 13 p1753 N90-20067
Census of US civil aircraft
[PB90-120296] 14 p1905 N90-20920
Civil air transport: A fresh look at power-by-wire and fly-by-light
[NASA-TM-102574] 14 p1969 N90-21283
US civil airmen statistics: Calendar year 1989
[AD-A220438] 17 p2343 N90-23342
Aerodynamic development perspective for traffic aeroplanes
[DGLR-89-141] 18 p2495 N90-24260
The 30th Airlines International Electronics Meeting Proceedings
[ETN-90-96973] 18 p2495 N90-24261
The effect of noise-abatement profiles on noise immissions and human annoyance underneath a subsequent climbpath
18 p2610 N90-24865
Study of high-speed civil transports. Summary
[NASA-CR-4236] 20 p2806 N90-25966
Mobile satellite communications for civil aviation
[NLR-MP-88066-U] 20 p2855 N90-26238
BASEOPS default profiles for civil aircraft
[AD-A223161] 21 p2959 N90-26825
Federal Aviation Administration small business innovation research 5-year project summaries
[AD-A221590] 21 p3086 N90-27546
New features of JAL's ground station
22 p3105 N90-27633
Swissair studies on the compressibility of aircraft data
22 p3105 N90-27637
Application of a company data link at Lufthansa German Airlines
22 p3113 N90-27689
High-speed civil transport study: Special factors
[NASA-CR-181881] 23 p3276 N90-28537
GPS integrity requirements for use by civil aviation
24 p3423 N90-29339
Independent ground monitor coverage of Global Positioning System (GPS) satellites for use by civil aviation
24 p3428 N90-29364

CLADDING
Report of the Advanced Neutron Source (ANS) Aluminum Cladding Corrosion Workshop
[DE90-001281] 07 p0903 N90-15217
Tellurium embrittlement of type 316 steel
[AERE-R-13440] 13 p1776 N90-20192
Ductile alloy encapsulated ceramic armor development
[AD-A217632] 14 p1954 N90-21183

CLAMPS
Effect of fretting on fatigue strength of aluminium alloys
[ESDU-89004] 03 p0329 N90-11870
Improvement of rules relating to clamp calculations
[CETIM-110610] 04 p0509 N90-12939
Quick disconnect duct coupler
[AD-D014265] 08 p1084 N90-16274
Releasable clamping apparatus
[NASA-CASE-MFS-28192-1] 09 p1233 N90-17154
Tensile film clamps and mounting block for the rheovibron and autovibron viscoelastometer
[NASA-CASE-LAR-13696-1] 13 p1812 N90-20409
Clamping device for pressurized module radiator panel
18 p2539 N90-24488
Analysis and test interaction in the development of a hold down and release mechanism
18 p2539 N90-24489
The tetrahedral wedge attachment mechanism
18 p2539 N90-24490
Detachable interface mechanism
18 p2540 N90-24497
Power saw
[NASA-CASE-MSC-21469-1] 20 p2872 N90-26340
Overcenter collet space station truss fastener
[NASA-CASE-MSC-21504-1] 21 p2966 N90-26859
Rotationally actuated prosthetic helping hand
[NASA-CASE-MFS-28426-1] 21 p3036 N90-27261

CLARK Y AIRFOIL
U AIRFOIL PROFILES

CLASSICAL MECHANICS
NT ASTRODYNAMICS
NT CELESTIAL MECHANICS
NT KEPLER LAWS
NT ORBITAL MECHANICS
On some stochastic properties of the infinitely dimensional Hamiltonian systems of classical mechanics
[DE89-618403] 02 p0267 N90-11525
On a new integrable Hamiltonian system with nearest neighbors interaction
[PREPRINT-667] 05 p0692 N90-14043
Quantum sl(2) enveloping algebra and representations of braid group
[DE90-607044] 09 p1275 N90-17389
Construction of second constant of motion for two dimensional classical super systems
[DE90-607046] 10 p1423 N90-18208
Velocity measurement using interferometry
[ISL-CO-221/88] 11 p1512 N90-18709
Classical mechanics on superspace
[DE90-608907] 12 p1724 N90-19906
Skew-symmetric matrices in classical mechanics
[MEMO-COSOR-89-23] 17 p2459 N90-24036
Unexpected properties of the centrifugal force
[DE90-627197] 23 p3392 N90-29164

CLASSIFICATIONS
NT DICHOTOMIES
NT HIERARCHIES
NT INDEXES (DOCUMENTATION)
NT SUBJECTS
Classification and reduction of pilot error
[NASA-CR-181867] 01 p0004 N90-10014
Defense Technical Information Center cataloging guidelines
[AD-A211000] 01 p0137 N90-10792
Automatic classification of spectra from the Infrared Astronomical Satellite (IRAS)
[NASA-RP-1217] 01 p0140 N90-10807
Investigation on analyzing computer-aided forest disease classifications
[DFVLR-FB-89-16] 03 p0369 N90-12112
Program distribution for unclassified scientific and technical reports: Instructions and category scope notes, revision 75
[DE89-005395] 03 p0416 N90-12391
From scientific proposals to the Inca data base
05 p0606 N90-13530
Gas identification system using graded temperature sensor and neural net interpretation
[AD-A213359] 05 p0622 N90-13627
Classification of modular invariant partition functions for the twisted N=2 superconformal algebra, twisted SU(2) Kac-Moody algebra and D(sub 2K) parafermions
[DE90-600767] 06 p0835 N90-14853
The Apollo 15 coarse fines (4-10 mm)
[NASA-TM-101934] 06 p0865 N90-15027
Classification of windshear severity
07 p0870 N90-15049
Design and calibration of an in-stack, low-pressure impactor
[AD-A213531] 07 p0882 N90-15105
A logic for the pixel assignment step of imagery classification predicated on class structure
07 p0949 N90-15493
Context dependent anti-aliasing image reconstruction
08 p1073 N90-16209
TM land use classification of a region. Utilization for planning and statistics
08 p1095 N90-16339
The upper main sequence of OB associations. Part 2: The single-lined O stars: Spectral classification of northern stars and lines of C and N
[SER-C-PREPUBL-FASC-39] 08 p1139 N90-16602

Evaluation of digital classification results of summer cultivation in a test area in the Parana-Ano state harvest 1986-1987
[INPE-4828-PRE/1459] 10 p1399 N90-18085
Impact of uncertainty and diagnosticity on classification of multidimensional data with integral and separable displays of system status
[AD-A215966] 10 p1424 N90-18215
On categorizing sounds
[AD-A216417] 10 p1427 N90-18232
Multiparameter scatterometer for remote sensing (RADSER). Project Scatter: State-of-the-art and future applications
[INPE-4871-PRE/1482] 11 p1511 N90-18701
Evaluation of two methods for acquisition of training statistics for digital analysis of areas prepared for plowing
[INPE-4901-PRE/1502] 11 p1522 N90-18763
Monitoring of reforested areas through digital analysis of TM data
[INPE-4930-PRE/1420] 11 p1522 N90-18764
Multistage forest volume estimation using a sampling system with probability variables
[INPE-4897-PRE/1498] 11 p1523 N90-18769
Classification of high resolution imagery using texture attributes
[INPE-4888-TDL/379] 11 p1525 N90-18778
Improvement of classification results from satellite imagery to update and differentiate land use classes on topographic maps
[BCRS-89-17] 11 p1526 N90-18786
Remote sensing for the classification and quantification of vegetation in Spring staging areas of Brent geese on the Frisian Islands (Netherlands)
[BCRS-89-27] 11 p1527 N90-18790
Geological structure of the State of Rio de Janeiro viewed through MSS LANDSAT imagery
[INPE-4826-PRE/1457] 11 p1533 N90-18825
An integrated vision on methodologies and environments for modeling and simulation assisted by computer
[INPE-4861-TDL/372] 11 p1544 N90-18886
Areas of aquatic macrophytes classified through vegetative indexes extracted from LANDSAT/TM imagery
[INPE-4880-PRE/1489] 12 p1677 N90-19633
Acute oral toxicity of DIGL-RP solid propellant in ICR mice
[AD-A217711] 13 p1849 N90-20613
Acute oral toxicity of DIGL-RP solid propellant in Sprague-Dawley rats
[AD-A217712] 13 p1849 N90-20614
Theory of defect process: Basic issues in quantitative understanding
[AERE-R-13661] 13 p1892 N90-20860
Modeling and control of flexible space platforms with articulated payloads 14 p1935 N90-21073
Automatic classification of images
[AD-D014437] 14 p1966 N90-21260
Survey of land use through remote sensing
[INPE-5032-MD/042] 14 p1996 N90-21443
Digital processing of TM/LANDSAT data in monitoring interior water
[INPE-4956-PRE/1533] 14 p1997 N90-21448
Multitemporal analysis of LANDSAT/TM digital imagery in the detection of areas affected by caterpillar (sibine fusca) attack in the dende (elais guineensis) palm plantation
[INPE-4979-PRE/1544] 14 p1999 N90-21457
Evaluation of classification performance and proportion estimate of the sugar cane crop through PROCEDURE-INPE utilizing LANDSAT data
[INPE-4899-PRE/1500] 14 p1999 N90-21458
Recognition and analysis of aircraft targets by radar, using structural pattern representations derived from polarimetric signatures 15 p2074 N90-21879
The association of supernovae with regions of recent star formation in late-type galaxies
15 p2188 N90-22497
Operational digital land use map 1:50,000; investigation of a multiple automatic classification based on SPOT and LANDSAT Thematic Mapper satellite pictures
[BCRS-89-10] 17 p2419 N90-23784
Topological classification of structurally stable quadratic systems without limit cycles
[REPT-89-66] 17 p2457 N90-24025
Automated segmentation and extraction of area terrain features from radar imagery
[AD-A221096] 18 p2544 N90-24522
Multispectral classification of overlapping classes with applications to forest damage areas
[DLR-FB-89-55] 18 p2574 N90-24666
Cloud field classification based on textural features
18 p2646 N90-25066
Initial results on fault diagnosis of DSN antenna control assemblies using pattern recognition techniques
20 p2854 N90-26228
Pattern classification of textura by moment and distance autocorrelation function
[INPE-4976-PRE/1541] 20 p2879 N90-26379
Classification regions in remote sensing imagery utilizing spatial characteristics
[INPE-4913-PRE/1514] 20 p2879 N90-26381
A sum rule satisfied by optimized feed-forward layered networks
[RSRE-MEMO-4341] 20 p2914 N90-26579
On networks, optimized feature extraction, and the Bayes decision
[RSRE-MEMO-4342] 20 p2914 N90-26580
Hazard classification testing of liquid propellants
[AD-A222070] 21 p2990 N90-26990
Data analysis techniques 21 p3017 N90-27151
Applications of ISES for meteorology
21 p3018 N90-27160
Model-based Gaussian and non-Gaussian clustering
[AD-A222097] 21 p3066 N90-27430
Experimental fault characterization of a neural network
[NASA-CR-186885] 22 p3240 N90-28373
A conceptual weather-type classification procedure for the Philadelphia, Pennsylvania area
[PB90-231705] 23 p3352 N90-28944
A hybrid architecture for the implementation of the Athena neural net model 23 p3368 N90-29032
Autoregressive-moving average models for texture classification
[INPE-4987-PRE/1549] 23 p3380 N90-29092
Efficiency and effectiveness of deep structure-based subject indexing languages: PRECIS vs. DSIS
23 p3406 N90-29248
Human error classification and data collection
[DE90-631408] 24 p3522 N90-29915

CLASSIFIERS
A logic for the pixel assignment step of imagery classification predicated on class structure
07 p0949 N90-15493
Evaluation of two methods for acquisition of training statistics for digital analysis of areas prepared for plowing
[INPE-4901-PRE/1502] 11 p1522 N90-18763
Classification of high resolution imagery using texture attributes
[INPE-4888-TDL/379] 11 p1525 N90-18778
Improving upon standard pattern classification algorithms by implementing them as multi-layer perceptrons
[AD-A220046] 17 p2447 N90-23954
Cloud field classification based on textural features
18 p2646 N90-25066
Using decision-tree classifier systems to extract knowledge from databases 21 p3048 N90-27328
A failure diagnosis system based on a neural network classifier for the space shuttle main engine
[NASA-TM-103607] 23 p3299 N90-28659

CLASSIFYING
Sort computation 08 p1113 N90-16446
A virtual zero-time, monolithic systolic sorting array
[DE90-001000] 12 p1698 N90-19753
Derivation of sorting programs
21 p3047 N90-27319

CLAYS
NT KAOLINITE
Interactions of hydrazines with colloidal constituents of soils 02 p0204 N90-11164

CLEAN FUELS
NT FUEL OILS
The conversion of carbonaceous materials to clean carbon and co-product gaseous fuel
[DE90-001561] 06 p0754 N90-14387

CLEAN ROOMS
Clean access platform for orbiter
15 p2116 N90-22103
An advanced telerobotic system for shuttle payload changeout room processing applications
24 p3502 N90-29795
Vacuum mechatronics 24 p3512 N90-29854

CLEANERS
NT AIR FILTERS

CLEANING
NT CHEMICAL CLEANING
NT HOUSEKEEPING (SPACECRAFT)
NT STERILIZATION
NT WASHING
Contamination removal using various solvents and methodologies
[NASA-CR-183747] 05 p0626 N90-13652
An Auger electron spectroscopy study of surface-preparation contaminants
[NASA-TP-2972] 09 p1203 N90-16968
The development of ultraviolet-ozone cleaning as a production process in the packaging of integrated circuits
[DE90-007960] 14 p1959 N90-21220
Clean access platform for orbiter
15 p2116 N90-22103
Design of a device to remove lunar dust from space suits for the proposed lunar base
[NASA-CR-186679] 19 p2724 N90-25496
Role of surface passivation in the integrated processing of MOS structures
[AD-A222630] 20 p2859 N90-26264
Electronics design of the infrared/ultrasonic sensing for a robot gripper
[PB90-160383] 21 p3010 N90-27109
Study and analysis of leaking underground storage tank remediation techniques incorporated in states in EPA Region 6
[PB90-214834] 23 p3333 N90-28847

CLEANLINESS
NT HOUSEKEEPING (SPACECRAFT)
Clean access platform for orbiter
15 p2116 N90-22103
Wearing of cryomechanisms at 4 K
[REPT-892-440-103] 17 p2473 N90-24139
Wearing of cryomechanisms at 4 K
18 p2537 N90-24476

CLEAR AIR TURBULENCE
Analysis of severe atmospheric disturbances from airline flight records 07 p0869 N90-15045
Effect of atmospheric turbulence on electro-optical systems 15 p2086 N90-21940

CLEARANCES
Marginal release disturbances on advanced missiles
01 p0014 N90-10070
CF 18 480 Gallon External Fuel Tank Stores Clearance Program 02 p0153 N90-10877
Heliport surface maneuvering test results
[ACD-330] 02 p0157 N90-10897
Flutter clearance of the F-18 high-angle-of-attack research vehicle with experimental wingtip instrumentation pods
[NASA-TM-4148] 03 p0305 N90-11732
An investigation of end-wall vortex cavitation in a high Reynolds number axial-flow pump
[AD-A211426] 03 p0347 N90-11982
Advanced clearance control systems — blade tips
[PNR90553] 04 p0454 N90-12601
Dynamic tip clearance measurements in axial flow compressors
[PNR90597] 04 p0456 N90-12612
Assessment of worm gearing for helicopter transmissions
[NASA-TM-102441] 08 p1025 N90-15923
Experimental investigation of the hydrodynamic forces on the shroud of a centrifugal pump impeller
[NASA-CR-186952] 21 p3009 N90-27108
NASA/GE Energy Efficient Engine low pressure turbine scaled test vehicle performance report
[NASA-CR-168290] 23 p3280 N90-28563

CLEARING
Cloud hole-boring with long pulse CO2 lasers
[DE90-008946] 14 p1985 N90-21377
Stratocumulus cloud height variations determined from surface and satellite observations
22 p3214 N90-28230
A cloudiness transition in a marine boundary layer
22 p3219 N90-28259
Analysis of marine stratocumulus clearing events during FIRE 22 p3220 N90-28260

CLEAVAGE
Ultrafast chemical dynamics of reactions in beams
[AD-A216319] 11 p1514 N90-18717
Effect of heat treatment on the fracture toughness transition properties of an A508 class 3 steel
[AERE-R-13548] 13 p1774 N90-20182
Hydrogen induced fracture characteristics of single crystal nickel-based superalloys
[NASA-CR-183992] 20 p2832 N90-26108
Mechanical properties and fracture toughness of AAR-TC128 Grade B steel and a micro-alloyed, control-rolled steel, A 8XX grade B, from -80F to +73F
[PB90-207796] 24 p3448 N90-29471

CLIMATE
Effects of rain attenuation on satellite EHF (Extremely High Frequency) communications in the US
[AD-A210517] 01 p0057 N90-10325
US Navy regional climatic study of the United States Atlantic Coast and associated waters
[AD-A210198] 01 p0088 N90-10503
Toward an understanding of global change: Initial priorities for US contributions to the International Geosphere-Biosphere Program
[NASA-CR-185873] 04 p0516 N90-12980

Central Sudan surface wind data and climate characteristic
[KNMI-WR-88-01] 04 p0520 N90-13000
Current velocity and hydrographic observations in the southwestern North Atlantic Ocean: Subtropical Atlantic Climate Studies (STACS), 1988
[PB89-230825] 04 p0521 N90-13010
An evaluation of the Smith-Feddes model
[AD-A213237] 05 p0671 N90-13907
Antarctic surface temperature and pressure data
[DE90-000971] 07 p0963 N90-15565
Surface Observation Climatic Summaries (SOCS) for Pease Air Force Base, New Hampshire
[AD-A215750] 10 p1408 N90-18117
Exploiting surface observations of cloudiness for globalscale nephanalyses 12 p1692 N90-19719
Large impact events and atmospheric evolution on the terrestrial planets 12 p1744 N90-20028
Global Warming: A Northwest Perspective
[DE90-008140] 13 p1830 N90-20505
Cloud types and the tropical Earth radiation budget, revised
[NASA-CR-180475] 13 p1843 N90-20582
Southern oscillation in the OSU coupled upper ocean/atmosphere GCM
[DE90-008415] 13 p1844 N90-20588
Modeling large-scale vegetation dynamics
[DE90-008883] 14 p2004 N90-21485
Predictability of weather and climate in a coupled ocean-atmosphere model: A dynamical systems approach
[NASA-CR-186499] 14 p2007 N90-21502
Optimization of power output from wind turbines
15 p2124 N90-22146
On three-dimensional scaling and consistent truncation of global atmospheric models 15 p2127 N90-22164
Satellite versus GCM-simulated radiation balance: Comparisons and implications for climate modeling
15 p2131 N90-22180
Southern oscillation simulation in coupled ocean/atmosphere global climate models
15 p2131 N90-22181
Predictability of weather and climate in a coupled ocean-atmosphere model: A dynamical systems approach 16 p2256 N90-22865
Global and hemispheric annual temperature variations between 1861 and 1988
[DE90-007993] 16 p2257 N90-22869
Climatic handbook of the USSR, issue 27. Kamchatskaya Oblast. Part 3: Wind
[AD-A218720] 16 p2258 N90-22872
US Navy regional climatic study of southern African waters
[AD-A218792] 16 p2258 N90-22874
US Navy regional climatic study of the Mozambique channel and adjacent waters
[AD-A218793] 16 p2258 N90-22875
Handbook of climate of the USSR. Humidity of air, atmospheric precipitations, snow cover
[AD-A220454] 17 p2427 N90-23828
Effects of solar ultraviolet radiation on biogeochemical dynamics in aquatic environments
[AD-A221119] 18 p2578 N90-24687
Physical parameterization of snow albedo for use in climate models
[PB90-167313] 19 p2712 N90-25433
Studies in the parameterization of cloudiness in climate models and the analysis of radiation fields in general circulation models
[NASA-CR-186378] 19 p2715 N90-25448
Annual and interannual variations of Earth-emitted radiation based on a 10-year data set
[NASA-TM-103465] 20 p2887 N90-26432
Environmental Research Laboratories programs and plans, FY-1989 and FY-1990 plans
[PB90-169988] 22 p3197 N90-28144
Policy options for stabilizing global climate. Volume 2: Chapters 7-9
[PB90-182312] 22 p3198 N90-28147
Climate change and America's forests
[PB90-205477] 22 p3199 N90-28155
Atmospheric Sciences Research in the US EPA climate program
[PB90-221870] 22 p3212 N90-28219
Inhomogeneities of stratocumulus liquid water
22 p3213 N90-28228
Climate of the Kennedy Space Center and vicinity
[NASA-TM-103498] 22 p3228 N90-28307
A preliminary ARM (Atmospheric Radiation Measurements) guide for climatic evaluations
[DE90-015135] 23 p3351 N90-28937
Proceedings of the 14th Annual Climate Diagnostics Workshop
[PB90-198573] 23 p3351 N90-28938
Annual course of precipitation over much of the US: Observed versus GCM simulation
[PB90-221656] 23 p3352 N90-28942
Program on development of basic understanding of severe weather phenomena
[PB90-226564] 23 p3352 N90-28943
Satellite image atlas of glaciers of the world: Irian Jaya, Indonesia, and New Zealand
[PB90-230095] 24 p3483 N90-29691

CLIMATE CHANGE
International impacts of global climate change: Testimony to House Appropriations Subcommittee on Foreign Operations, Export Financing and Related Programs
[DE89-014004] 01 p0085 N90-10482
Geophysical monitoring for climatic change number 16
[PB89-159628] 01 p0087 N90-10494
Coastal Research Center Woods Hole Oceanographic Institution
[PB89-198238] 01 p0089 N90-10510
Potential effects of global climate change on the United States. Executive summary. Draft
[PB89-161046] 02 p0237 N90-11350
Potential effects of global climate change on the United States. Volume 1: Regional studies. Draft
[PB89-161053] 02 p0238 N90-11351
Potential effects of global climate change on the United States. Volume 2: National studies. Draft
[PB89-161061] 02 p0238 N90-11352
Ozone depletion, greenhouse gases, and climate change
[NASA-CR-185323] 03 p0367 N90-12101
Global environmental effects of impact-generated aerosols: Results from a general circulation model
[DE89-008033] 03 p0368 N90-12106
Policies to encourage private sector responses to potential climate change
[DE89-017244] 03 p0368 N90-12107
Ozone depletion, greenhouse gases, and climate change
[PB89-216097] 03 p0369 N90-12110
Contribution of deforestation to atmospheric CO2 and reforestation as an option to control CO2
[DE89-017255] 04 p0516 N90-12979
Toward an understanding of global change: Initial priorities for US contributions to the International Geosphere-Biosphere Program
[NASA-CR-185873] 04 p0516 N90-12980
Sensitivity of a regional oxidant model to variations in climate parameters, volume 1 and 2
[PB89-224943] 04 p0516 N90-12981
South Pole surface radiation balance measurements, April 1986 to February 1988
[PB89-224018] 04 p0519 N90-12993
Climate predictability: A dynamical view
[AERONOMICA-ACTA-A-347-1989]
05 p0671 N90-13909
Climate system research studies of global and regional instrumental data
[DE90-001205] 06 p0809 N90-14707
Global energy and the greenhouse issue
[DE90-001394] 06 p0809 N90-14709
International Conference on Global and Regional Atmospheric Environmental Chemistry and visit to Hangzhou, China, foreign trip report
[DE90-000099] 06 p0810 N90-14713
Climate projections with regional resolution
[DE90-000858] 06 p0810 N90-14715
Quantifying the link between change in radiative balance and atmospheric temperature
[DE90-000819] 06 p0811 N90-14721
Carbon dioxide and climate: Summaries of research in FY 1989
[DE90-001791] 06 p0812 N90-14723
US energy use: New technologies and policies in response to global warming
[DE90-002170] 06 p0812 N90-14724
Climate-biosphere interactions scope of work
[PB90-106444] 06 p0814 N90-14734
Evaluation of climatic models: Comparison of simulated and observed patterns for past climates
[DE90-001228] 06 p0817 N90-14755
Greenhouse gases: Changing the global climate
[DE90-002788] 07 p0957 N90-15535
Research project on CO2-induced climate change
[DE90-003531] 07 p0957 N90-15538
Global climate change and NEPA (National Environmental Policy Act) analyses
[DE90-003704] 07 p0958 N90-15540
Global climate change: A fossil energy perspective
[DE90-003770] 07 p0958 N90-15541
Scientific linkages in global change
[PB90-112608] 08 p1098 N90-16356
Effects of global climate change on agroecosystems: Scope of work
[PB90-120023] 11 p1531 N90-18813
Perspectives on aerosol deposition to natural surfaces
[DE90-003398] 11 p1532 N90-18819
Natural and anthropogenic climate change
[DE90-006488] 11 p1532 N90-18822
Sensitivity of ecological landscapes and regions to global climatic change
[PB90-120072] 12 p1684 N90-19674
Predicting effects of global climate change on reservoir water quality and fish habitat
[DE90-003674] 12 p1689 N90-19704
Regional climate change predictions from the Goddard Institute for Space Studies high resolution GCM
[NASA-CR-186375] 12 p1693 N90-19725
Simulation of landscape disturbances and the effect of climatic change
[DE90-007565] 13 p1829 N90-20503
Processes of community development and responses of ecosystems to climate change
[DE90-008640] 13 p1831 N90-20512
An intercomparison of general circulation model predictions of regional climate change
[DE90-008325] 13 p1845 N90-20589
A fossil energy perspective on global climate change
[DE90-007894] 14 p2004 N90-21483
Modeling the upper ocean and its interaction with the atmosphere
[DE90-008980] 14 p2008 N90-21511
SeaRISE: A Multidisciplinary Research Initiative to Predict Rapid Changes in Global Sea Level Caused by Collapse of Marine Ice Sheets
[NASA-CP-3075] 16 p2249 N90-22824
The effects of climate change on energy planning and operations in the Pacific Northwest. Volume 1: Overview
[DE90-009464] 17 p2425 N90-23816
The effects of climate change on energy planning and operations in the Pacific Northwest. Volume 2: Technical background
[DE90-009465] 17 p2425 N90-23817
Remote sensing for better understanding of the system Earth 19 p2706 N90-25399
CNES space programmes related to climate
19 p2706 N90-25400
Earth radiation budget and climate
19 p2707 N90-25403
Solid Earth, gravity field and environment
19 p2708 N90-25412
Research programs: Meteorological prediction. Oceanic processes. Climate and global change monitoring. Satellite instrumentation and calibration
19 p2714 N90-25447
Options for controlling the global warming impact from motor vehicles
[PB90-161688] 22 p3197 N90-28142
Policy options for stabilizing global climate. Volume 1: Chapters 1-6
[PB90-182304] 22 p3198 N90-28146
Policy options for stabilizing global climate. Volume 2: Chapters 7-9
[PB90-182312] 22 p3198 N90-28147
Climate change and America's forests
[PB90-205477] 22 p3199 N90-28155
Global climate change: A proposed gas industry program on global climate issues
[PB90-219296] 22 p3199 N90-28156
Effects of corpuscular radiation on weather and climate 22 p3201 N90-28164
Solar activity influence on climatic variations of stratosphere and mesosphere in mid-latitudes
22 p3202 N90-28169
Atmospheric Sciences Research in the US EPA climate program
[PB90-221870] 22 p3212 N90-28219
Cirrus clouds and climate feedback: Is the sky falling and should we go tell the king 22 p3225 N90-28288
Physically-based general circulation model parameterization of clouds and their radiative interaction
22 p3228 N90-28308
Our changing planet: The FY 1991 US global change research program. A report by the committee on Earth Sciences to accompany the FY 1991 budget
[PB90-202623] 23 p3346 N90-28907
The role of clouds in CO2-induced climate change
[DE90-014380] 23 p3346 N90-28911
Chasing a specter: Risk management for global environmental change
[DE90-014455] 23 p3347 N90-28917
Responding to the threat of global warming: Options for the Pacific and Asia
[DE90-014756] 23 p3347 N90-28918
Natural and anthropogenic climate change
[DE90-015528] 23 p3348 N90-28923
Annual course of precipitation over much of the US: Observed versus GCM simulation
[PB90-221656] 23 p3352 N90-28942

Atmospheric methane data for the period 1983-1985 from the NOAA/GMCC global cooperative flask sampling network
[PB90-208588] 24 p3486 N90-29701
Global Climate Change: Seeking a Global Consensus
[S-HRG-101-842] 24 p3486 N90-29704
Effects of increased CO2 on forest response
[DE90-015406] 24 p3487 N90-29708
Grassland/atmosphere response to changing climate: Coupling regional and local scales
[DE90-015814] 24 p3487 N90-29710
The effects of a doubling of atmospheric CO2 on the stormtracks in the climate of a general circulation model
[KNMI-WR-90-01] 24 p3488 N90-29713

CLIMATOLOGY
NT AGROCLIMATOLOGY
NT MICROCLIMATOLOGY
NT PALEOCLIMATOLOGY
International impacts of global climate change: Testimony to House Appropriations Subcommittee on Foreign Operations, Export Financing and Related Programs
[DE89-014004] 01 p0085 N90-10482
US Navy regional climatic study of the United States Atlantic Coast and associated waters
[AD-A210198] 01 p0088 N90-10503
A seasonal isotherm depth climatology for the eastern tropical Pacific
[PB89-193577] 01 p0090 N90-10512
Potential effects of global climate change on the United States. Volume 1: Regional studies. Draft
[PB89-161053] 02 p0238 N90-11351
Potential effects of global climate change on the United States. Volume 2: National studies. Draft
[PB89-161061] 02 p0238 N90-11352
Spatial and temporal short range total cloud cover estimation by metric analysis of composite imagery
02 p0251 N90-11423
National Center For Atmospheric Research annual report, fiscal year 1988
[PB89-208987] 02 p0252 N90-11428
Airborne profiles taken near San Nicolas Island, California, during Operation FIRE (First ISCCP (International Satellite Cloud Climatology Project) regional experiment) (1987): Aerosol size distributions, air and surface temperatures, cloud top temperatures, and relative humidities
[AD-A211664] 03 p0374 N90-12136
Climatological data for the North Sea based on observations by voluntary observing ships over the period 1961-1980
[KNMI-WR-89-02] 04 p0520 N90-13002
Cloud cover determination in polar regions from satellite imagery
[NASA-CR-186096] 04 p0520 N90-13003
Current velocity and hydrographic observations in the southwestern North Atlantic Ocean: Subtropical Atlantic Climate Studies (STACS), 1988
[PB89-230825] 04 p0521 N90-13010
The interaction and variation of waves and turbulence from MST radar data
[AD-A212849] 05 p0670 N90-13906
Climate predictability: A dynamical view
[AERONOMICA-ACTA-A-347-1989] 05 p0671 N90-13909
A rough transform technique for extracting lead features from sea ice imagery
[AD-A212758] 06 p0801 N90-14666
Climate-biosphere interactions scope of work
[PB90-106444] 06 p0814 N90-14734
The identification of terrain-induced circulations using principal components
[DE90-001991] 06 p0815 N90-14739
The development of a spatial synoptic climatological index for environmental analysis
06 p0816 N90-14744
Inverted surface troughs accompanying Rocky Mountain lee-side cyclogenesis 06 p0816 N90-14746
Use of operational 0-6 and 3-9 h quantitative precipitation forecasts for predicting heavy rain events
[PB90-103946] 06 p0817 N90-14750
Climatology of Lawrence Livermore National Laboratory
[DE90-000905] 06 p0818 N90-14756
Measurements of horizontal visibility in the lowest 300 m over Northern Germany 07 p0872 N90-15059
Global climate change: A fossil energy perspective
[DE90-003770] 07 p0958 N90-15541
Interconnectedness in nature and in science: The case of climate and climate modeling
[PB90-113986] 08 p1098 N90-16358
The chemistry and dynamics of marine stratocumulus
08 p1102 N90-16381
Climatic summaries and documentation for the primary meteorological Station, H. J. Andrews Experimental Forest, 1972 to 1984
[PB90-104373] 08 p1102 N90-16382
USSR Climate Handbook Number 27. Part 1: Solar radiation, radiation balance and sunshine
[AD-A215647] 09 p1248 N90-17242
Surface Observation Climatic Summaries (SOCS) for Pease Air Force Base, New Hampshire
[AD-A215750] 10 p1408 N90-18117
Surface observation climatic summaries
[AD-A215786] 10 p1408 N90-18122
Effects of global climate change on agroecosystems: Scope of work
[PB90-120023] 11 p1531 N90-18813
Forecasters handbook for Central America and adjacent waters
[AD-A216752] 11 p1536 N90-18845
Predicting effects of global climate change on reservoir water quality and fish habitat
[DE90-003674] 12 p1689 N90-19704
Exploiting surface observations of cloudiness for globalscale nephanalyses 12 p1692 N90-19719
Colloquium on Synoptic Meteorology
[PB90-121112] 12 p1692 N90-19720
Cyclogeneses and extratropical cyclones in the south-southeast region of Brazil and its influence in time
[INPE-4812-TDL/359] 12 p1693 N90-19722
Regional climate change predictions from the Goddard Institute for Space Studies high resolution GCM
[NASA-CR-186375] 12 p1693 N90-19725
United States Historical Climatology Network (HCN) serial temperature and precipitation data
[DE90-008029] 13 p1830 N90-20506
A cloud climatology for the North Pacific area centered at Shemya, Alaska
[AD-A217334] 13 p1844 N90-20585
US Navy regional climatic study of the Central East Asian coast and associated waters
[AD-A217448] 13 p1844 N90-20587
A fossil energy perspective on global climate change
[DE90-007894] 14 p2004 N90-21483
Evaporation duct effects at millimeter wavelengths
15 p2080 N90-21914
From Penman to Makkink: A new method for the calculation of the climatological evaporation numbers
[KNMI-TR-111] 15 p2126 N90-22161
Dynamic and microphysical characteristics of cirrus clouds as revealed by aircraft, lidar, and other observations during FIRE 15 p2130 N90-22177
Southern oscillation simulation in coupled ocean/atmosphere global climate models
15 p2131 N90-22181
Impact of meteorology on the agricultural sector: Compilation and analysis of projects
[INPE-4846-PRE/1475] 16 p2257 N90-22866
Climatic handbook of the USSR, issue 27. Kamchatskaya Oblast. Part 3: Wind
[AD-A218720] 16 p2258 N90-22872
Monthly surface thermal forcing in the tropical Pacific from 1980 to 1983
[NASA-CR-183033] 16 p2259 N90-22877
US Navy hindcast spectral ocean wave model climatic atlas: Mediterranean Sea
[AD-A219755] 17 p2426 N90-23825
The effects of climatological and transient wind forcing on eddy generation in the California current system
[AD-A219858] 17 p2431 N90-23855
Reports from the German Meteorological Service. No. 178: Climatological research about the atmospheric counter radiation and comparison of calculation processes by means of measurements in the Upper Rhine Valley (Fed. Republic of Germany) during a year
[ISBN-3-88148-249-0] 18 p2582 N90-24704
Cloud field classification based on textural features
18 p2646 N90-25066
CNES space programmes related to climate
19 p2706 N90-25400
Cloud analysis with satellite data
19 p2707 N90-25401
Earth radiation budget and climate
19 p2707 N90-25403
The 27-28 October 1986 FIRE IFO Cirrus case study: Comparison of radiative transfer theory with observations by satellite and aircraft
[NASA-TM-103468] 20 p2890 N90-26446
Liquid-vapor equilibrium of multicomponent cryogenic systems 20 p2948 N90-26774
Downwelled longwave surface irradiance data from five sites for the FIRE/SRB Wisconsin Experiment from October 12 through November 2, 1986
[NASA-TM-102597] 21 p3030 N90-27225
Analysis of cirrus optical properties with data from NASA ER2 High-resolution Interferometer Sounder (HIS)
[NASA-CR-186365] 21 p3030 N90-27227
Policy options for stabilizing global climate. Volume 1: Chapters 1-6
[PB90-182304] 22 p3198 N90-28146
Policy options for stabilizing global climate. Volume 2: Chapters 7-9
[PB90-182312] 22 p3198 N90-28147
Climate change and America's forests
[PB90-205477] 22 p3199 N90-28155
Global climate change: A proposed gas industry program on global climate issues
[PB90-219296] 22 p3199 N90-28156
Lidar cloud studies for FIRE and ECLIPS
[NASA-CR-186384] 22 p3211 N90-28214
Atmospheric Sciences Research in the US EPA climate program
[PB90-221870] 22 p3212 N90-28219
World weather records, 1971-1980. Volume 1: North America
[PB90-182858] 22 p3212 N90-28221
FIRE Science Results 1989
[NASA-CP-3079] 22 p3213 N90-28224
Comparative climatology of four marine stratocumulus regimes 22 p3213 N90-28225
Intercomparisons of GOES-derived cloud parameters and surface observations over San Nicolas Island
22 p3214 N90-28229
Stratocumulus cloud height variations determined from surface and satellite observations
22 p3214 N90-28230
An eight-month climatology of marine stratocumulus cloud fraction, albedo, and integrated liquid water
22 p3214 N90-28233
Satellite-derived cloud and radiation fields over the marine stratocumulus IFO 22 p3216 N90-28240
Stratus: An interactive steady state mixed layer model for personal computers 22 p3219 N90-28255
A cloudiness transition in a marine boundary layer
22 p3219 N90-28259
Laboratory experiments on stability and entrainment of oceanic stratocumulus. Part 1: Instability experiment
22 p3220 N90-28263
A comparison of ISCCP and FIRE satellite cloud parameters 22 p3221 N90-28267
Moisture and heat budgets of a cirrus cloud from aircraft measurements during FIRE 22 p3223 N90-28279
Satellite-derived cloud fields during the FIRE cirrus IFO case study 22 p3223 N90-28281
Comparison of surface-derived and ISCCP cloud optical properties 22 p3224 N90-28282
Climate of the Kennedy Space Center and vicinity
[NASA-TM-103498] 22 p3228 N90-28307
Our changing planet: The FY 1991 US global change research program. A report by the committee on Earth Sciences to accompany the FY 1991 budget
[PB90-202623] 23 p3346 N90-28907
A preliminary ARM (Atmospheric Radiation Measurements) guide for climatic evaluations
[DE90-015135] 23 p3351 N90-28937
Proceedings of the 14th Annual Climate Diagnostics Workshop
[PB90-198573] 23 p3351 N90-28938
Wind lidar for BEST
[CNES-NT-125] 23 p3353 N90-28947
Atmospheric methane data for the period 1983-1985 from the NOAA/GMCC global cooperative flask sampling network
[PB90-208588] 24 p3486 N90-29701

CLIMBING FLIGHT
Airplane takeoff and landing performance monitoring system
[NASA-CASE-LAR-13734-1-CU] 13 p1758 N90-20096
Project Dawdler: A proposal in response to a low Reynolds number station keeping mission
[NASA-CR-186668] 19 p2658 N90-25128
The SKY SHARK: An RPV designed to investigate the pressure distribution on a lifting surface
[NASA-CR-186222] 21 p2959 N90-26824

CLINICAL MEDICINE
Daytime sleepiness, performance, mood, nocturnal sleep: The effect of benzodiazepine and caffeine on their relationship
[AD-A210915] 01 p0093 N90-10533
DOCTORD Database System user's guide, June 1989: dBase 3 PLUS Physician/(Part B Medicare): Personal computer reference system and user's guide
[PB90-100181] 07 p0986 N90-15579
Acute oral toxicity of DIGL-RP solid propellant in ICR mice
[AD-A217711] 13 p1849 N90-20613
Acute oral toxicity of DIGL-RP solid propellant in Sprague-Dawley rats
[AD-A217712] 13 p1849 N90-20614
Laser-produced plasmas in medicine
[DE90-007623] 13 p1891 N90-20849

JPRS report: Science and technology. USSR: Life sciences
[JPRS-ULS-90-002] 14 p1995 N90-21434
Interactive displays in medical art 16 p2271 N90-22940
Possibilities of Nd: YAG laser utilization in medicine
[MBB-UE-0002/88-PUB] 19 p2653 N90-25100

CLOCKS
NT ATOMIC CLOCKS
NT AUTONOMOUS SPACECRAFT CLOCKS
A digital model for level-clocked circuitry
[AD-A211937] 03 p0343 N90-11957
Stable Kalman filters for processing clock measurement data 04 p0487 N90-12801
Optical clock distribution to VLSI chips
[AD-A212269] 04 p0560 N90-13264
Periodic phase adjustment distributed clock synchronization in the hard realtime environment
[AD-A213842] 07 p0988 N90-15708
Rate compatible punctured codes, their use in military satellite communication systems
[AD-A216723] 11 p1497 N90-18619
Real-time simulation clock
[NASA-CASE-LAR-14056-1] 17 p2407 N90-23713
Stability of laser oscillator systems 18 p2641 N90-25045
Criticality of the three-state chiral clock model: A renormalisation group study
[DE90-627321] 23 p3400 N90-29212

CLOGGING
U PLUGGING

CLOSED BASINS
U STRUCTURAL BASINS

CLOSED CIRCUIT TELEVISION
Issues in visual support to real-time space system simulation solved in the Systems Engineering Simulator 13 p1862 N90-20680
Real-time graphics for the Space Station Freedom cupola, developed in the Systems Engineering Simulator 13 p1862 N90-20683
The Orbital Maneuvering Vehicle Training Facility visual system concept 13 p1863 N90-20684
The use of PLAID in the Space Station Freedom viewing analysis 19 p2729 N90-25517
PC-based closed-circuit television system
[DE90-013366] 21 p2994 N90-27017

CLOSED CYCLES
Nuclear closed-cycle gaseous heat engine concept
[DE89-016824] 03 p0404 N90-12313
Development of a low noise 10 K J-T refrigeration system
[AD-A213347] 04 p0484 N90-12779
LaRC-developed catalysts for CO2 lasers 18 p2557 N90-24591
Rare-isotope and kinetic studies of Pt/SnO2 catalysts 18 p2558 N90-24598
An approach to systematic phase-lock loop design
[ETN-90-96905] 19 p2686 N90-25280

CLOSED ECOLOGICAL SYSTEMS
Power from space for use on earth: An emerging global option 01 p0028 N90-10144
A simple, mass balance model of carbon flow in a controlled ecological life support system
[NASA-TM-102151] 01 p0101 N90-10571
Fermentation and oxygen transfer in microgravity 05 p0679 N90-13956
Engineering sciences design. Design and implementation of components for a bioregenerative system for growing higher order plants in space
[NASA-CR-186056] 06 p0819 N90-14761
Utilization of non-conventional systems for conversion of biomass to food components
[NASA-CR-177545] 07 p0968 N90-15591
Dynamics of carbon dioxide exchange of a wheat community grown in a semi-closed environment 08 p1155 N90-16689
Publications of the NASA Controlled Ecological Life Support System (CELSS) Program, 1979-1989
[NASA-CR-4297] 15 p2051 N90-21754
Space Station Freedom environmental control and life support system phase 3 simplified integrated test detailed report
[NASA-TM-4204] 16 p2207 N90-22593
Strategic implementation plan
[NASA-TM-102907] 17 p2433 N90-23861
Carbon dioxide and water exchange rates by a wheat crop in NASA's biomass production chamber: Results from an 86-day study (January to April 1989)
[NASA-TM-102788] 19 p2716 N90-25453
Utilization of the water soluable fraction of wheat straw as a plant nutrient source
[NASA-TM-103497] 19 p2716 N90-25455
System development and early biological tests in NASA's biomass production chamber
[NASA-TM-103494] 19 p2716 N90-25456
Implementation of sensor and control designs for bioregenerative systems
[NASA-CR-186655] 20 p2897 N90-26479
Design of sensors for control of closed loop life support systems
[NASA-CR-186656] 20 p2899 N90-26490
Genesis lunar outpost criteria and design
[NASA-CR-186831] 20 p2901 N90-26499
Automation of closed environments in space for human comfort and safety
[NASA-CR-186834] 20 p2901 N90-26500
Space Station Freedom pressurized element interior design process
[NASA-CR-181297] 23 p3287 N90-28597
Electrochemical incineration of wastes
[NASA-CR-187033] 23 p3317 N90-28753
Atmosphere and water quality monitoring on Space Station Freedom
[NASA-CR-186707] 23 p3378 N90-29084
A lunar space station
[NASA-CR-186223] 24 p3563 N90-30158

CLOSED FAULTS
U GEOLOGICAL FAULTS

CLOSED LOOP SYSTEMS
U FEEDBACK CONTROL

CLOSURE LAW
Turbulence modelling of three-dimensional shear flows 01 p0066 N90-10381
The generalized drift flux approach: Identification of the void-drift closure law 01 p0067 N90-10386
A point in betaZ/Z not contained in a maximal orbit closure
[REPT-89-26] 04 p0540 N90-13127
Development of a three-dimensional local scale atmospheric model with turbulence closure model
[DE90-710045] 07 p0960 N90-15551
Study of continuum higher order closure models evaluated by a statistical theory of shock structure 10 p1303 N90-17538
Uniqueness of closure of the constraint algebra for quantum gravity
[DE90-610476] 12 p1691 N90-19712
Theoretical modeling studies of the marine planetary
[AD-A217200] 13 p1841 N90-20567
Calculation of 3D turbulent jets in crossflow with a multigrid method and a second-moment closure model
[NASA-TM-103159] 20 p2862 N90-26282
Modeling of near-wall turbulence
[NASA-TM-103222] 22 p3174 N90-28009
Wind tunnel, field, and numerical investigations of plume downwash and dispersion at an arctic industrial site 24 p3489 N90-29721

CLOSURES
Fatigue crack growth rates as a function of delta K: Variability and material property 02 p0182 N90-11031
Application of two-point closures to subgrid scale modeling for homogeneous, 3D turbulence 05 p0640 N90-13732
Spectral study of a compressible isotropic turbulence
[ECL-88-16] 05 p0643 N90-13753
Solution of the Boltzmann equation using an energy group method
[AD-A213138] 05 p0699 N90-14096
Observational study of the macroscopic behavior of moist-convective processes 07 p0959 N90-15547
Automatic prestart or post shutoff engine lubricator
[AD-D014259] 08 p1084 N90-16273
Analytical methods for the development of Reynolds stress closures in turbulence
[NASA-CR-182017] 12 p1660 N90-19538

CLOTH
U FABRICS

CLOTHING
NT COTTON FIBERS
NT EXTRAVEHICULAR MOBILITY UNITS
NT FLIGHT CLOTHING
NT GARMENTS
NT GLOVES
NT GOGGLES
NT HELMETS
NT PRESSURE SUITS
NT PROTECTIVE CLOTHING
NT SHOES
NT SPACE SUITS
Thermoregulatory responses to intermittent exercise are influenced by knit structure of underwear
[AD-A209087] 01 p0095 N90-10541
New Fabric Development Program
[AD-A211549] 03 p0332 N90-11891
On the wings of a dream: The Space Shuttle
[NASA-EP-269] 05 p0593 N90-13446
Sensations of temperature and humidity during intermittent exercise and the influence of underwear knit structure
[AD-A215285] 09 p1252 N90-17266
The effect of moisture absorption in clothing on the human heat balance
[AD-A217899] 13 p1852 N90-20626
Comparison of Goretex laminated and Dermoflex coated fabrics
[AD-A219383] 17 p2368 N90-23481
Calculation of clothing insulation and vapour resistance
[IZF-1989-49] 22 p3234 N90-28338

CLOUD COVER
US Navy regional climatic study of the United States Atlantic Coast and associated waters
[AD-A210198] 01 p0088 N90-10503
Spatial and temporal short range total cloud cover estimation by metric analysis of composite imagery 02 p0251 N90-11423
Lightning data study in conjunction with geostationary satellite data
[NASA-CR-179286] 03 p0375 N90-12142
Cloud cover determination in polar regions from satellite imagery
[NASA-CR-186096] 04 p0520 N90-13003
Global distribution of total cloud cover and cloud type amounts over the ocean
[DE90-003187] 07 p0964 N90-15574
Comparisons between the RTNEPH (Real-Time Nephanalysis) and AFGL cloud layer analysis algorithms
[AD-A216637] 11 p1536 N90-18844
Exploiting surface observations of cloudiness for globalscale nephanalyses 12 p1692 N90-19719
Automated visibility and cloud cover measurements with a solid-state imaging system
[AD-A216906] 12 p1693 N90-19724
Cloud types and the tropical Earth radiation budget, revised
[NASA-CR-180475] 13 p1843 N90-20582
US Navy regional climatic study of the Central East Asian coast and associated waters
[AD-A217448] 13 p1844 N90-20587
Preliminary report on the demonstration of the VAS CO2 cloud parameters (cover, height, and amount) in support of ASOS
[NOAA-TM-NESDIS-29] 14 p2006 N90-21498
Satellite versus GCM-simulated radiation balance: Comparisons and implications for climate modeling 15 p2131 N90-22180
The analysis of polar clouds from AVHRR satellite data using pattern recognition techniques
[NASA-CR-183300] 16 p2257 N90-22868
Cloud volume statistics for southern Sweden
[CM-77] 17 p2427 N90-23830
Evaluation of Stochastic models for estimating the persistence probability of cloud-free lines-of-sight
[AD-A220283] 18 p2581 N90-24702
Reports from the German Meteorological Service. No. 178: Climatological research about the atmospheric counter radiation and comparison of calculation processes by means of measurements in the Upper Rhine Valley (Fed. Republic of Germany) during a year
[ISBN-3-88148-249-0] 18 p2582 N90-24704
Cloud analysis with satellite data 19 p2707 N90-25401
Cloud dynamics and cloud microphysics by radar measurements 19 p2707 N90-25402
Studies in the parameterization of cloudiness in climate models and the analysis of radiation fields in general circulation models
[NASA-CR-186378] 19 p2715 N90-25448
On airborne measurements of radiation from broken cloud fields
[MITT-67] 21 p3027 N90-27211
Comparative climatology of four marine stratocumulus regimes 22 p3213 N90-28225
On estimating scale invariance in stratocumulus cloud fields 22 p3213 N90-28227
Spectral absorption of marine stratocumulus clouds derived from in situ cloud radiation measurements 22 p3215 N90-28238
Satellite-derived cloud and radiation fields over the marine stratocumulus IFO 22 p3216 N90-28240
The radiation budget of stratocumulus clouds measured by tethered balloon instrumentation: Variability of flux measurements 22 p3216 N90-28242
A stratocumulus thermodynamic analysis: July 5 case study 22 p3217 N90-28245
Turbulence structure in clear and cloudy regions of the 7 July 1987 Electra mission 22 p3217 N90-28247
Optical properties of marine stratocumulus clouds modified by ship track effluents 22 p3218 N90-28253
A case study of cumulus formation beneath a stratocumulus sheet: Its structure and effect on boundary layer budgets 22 p3219 N90-28256
A cloudiness transition in a marine boundary layer 22 p3219 N90-28259

FIRE aircraft observations of horizontal and vertical transport in marine stratocumulus
22 p3220 N90-28261
Comparison of satellite based cloud retrieval methods for cirrus and stratocumulus 22 p3221 N90-28268
The effects of clouds on CO2 forcing
22 p3222 N90-28271
Seasonal and interannual changes in cirrus
22 p3222 N90-28272
Relationship between the longwave cloud radiative forcing at the surface and the top of the atmosphere
22 p3222 N90-28273
Comparison of 30 day integrations with and without interactive clouds 22 p3222 N90-28274
Spatial scales of cirrus cloud properties
22 p3222 N90-28275
Summary of results and conclusions based on analysis of volume imaging and high spectral resolution lidar data acquired during FIRE phase 1, part 1
22 p3223 N90-28278
The 27-28 October 1986 FIRE cirrus case study: Meteorology and clouds 22 p3223 N90-28280
Satellite-derived cloud fields during the FIRE cirrus IFO case study 22 p3223 N90-28281
Comparison of surface-derived and ISCCP cloud optical properties 22 p3224 N90-28282
The 27-28 October 1986 FIRE IFO cirrus case study: Comparison of satellite and aircraft derived particle size
22 p3224 N90-28285
Cirrus radiative characteristics and the radiative impact of small particles 22 p3224 N90-28286
Regional conditions during the 25 October 1986 FIRE cirrus/altocumulus case study 22 p3225 N90-28287
Preliminary simulations of the large-scale environment during the FIRE cirrus IFO 22 p3225 N90-28290
A scheme for parameterizing cirrus cloud ice water content in general circulation models
22 p3226 N90-28292
Radiative diffusivity factors in cirrus and stratocumulus clouds: Application to two-stream models
22 p3226 N90-28293
IR spectral characteristics of cirrus clouds
22 p3226 N90-28297
The Colorado/Missouri 1989 cirrus mini IFO
22 p3227 N90-28299
Summary of results and conclusions based on analysis of volume imaging and high spectral resolution lidar data acquired during FIRE phase 1, part 2
22 p3227 N90-28300
A system for recording physical properties of clouds
22 p3227 N90-28301
The 1973-1974 lidar observations of cirrus clouds at Kwajalein 22 p3227 N90-28303
The use of an airborne lidar for mapping cirrus clouds in FIRE, phase 2 22 p3228 N90-28304
On the use of IR lidar and K(sub a)-band radar for observing cirrus clouds 22 p3228 N90-28305
Physically-based general circulation model parameterization of clouds and their radiative interaction
22 p3228 N90-28308
A preliminary ARM (Atmospheric Radiation Measurements) guide for climatic evaluations
[DE90-015135] 23 p3351 N90-28937
Daily temperature, solar radiation, wind speed, cloud cover, and precipitation data recorded at the meteorological station for calendar years 1957--1988
[DE90-014399] 23 p3352 N90-28941
A conceptual weather-type classification procedure for the Philadelphia, Pennsylvania area
[PB90-231705] 23 p3352 N90-28944
Study of the relationships between radar structure and the electrical activity of clouds
[ETN-90-97488] 23 p3352 N90-28946
A documentation of icing-relevant cloud physical parameters on vertical soundings of stratiform clouds
[DLR-MITT-90-07] 24 p3495 N90-29753

CLOUD DISPERSAL

Cloud dynamics and cloud microphysics by radar measurements 19 p2707 N90-25402
Diffusion in the surface layer of the convective boundary layer
[AD-A224125] 23 p3349 N90-28924

CLOUD GLACIATION

A documentation of icing-relevant cloud physical parameters on vertical soundings of stratiform clouds
[DLR-MITT-90-07] 24 p3495 N90-29753

CLOUD HEIGHT INDICATORS

Calibration of a visioceilometer, a hand held lidar system
[FEL-1988-73] 03 p0374 N90-12137
Absolute wind measurements in the lower thermosphere of Venus using infrared heterodyne spectroscopy
[NASA-CR-4290] 21 p3100 N90-27605
Lidar cloud studies for FIRE and ECLIPS
[NASA-CR-186384] 22 p3211 N90-28214
Stratocumulus cloud height variations determined from surface and satellite observations
22 p3214 N90-28230
Analysis of ER-2 radiometer and lidar observations from the 1987 marine stratus experiment
22 p3216 N90-28241
Stratus: An interactive steady state mixed layer model for personal computers 22 p3219 N90-28255

CLOUD PHYSICS

Numerical simulations of a midlatitude squall line
01 p0087 N90-10497
Remote sensing techniques of the Wave Propagation Laboratory for the measurement of supercooled liquid water: Applications to aircraft icing
[PB89-208102] 02 p0148 N90-10842
An evaluation of the Smith-Feddes model
[AD-A213237] 05 p0671 N90-13907
Winter cloud seeding potential on the Mogollon Rim
[PB89-190540] 07 p0962 N90-15562
Airborne measurements of the electric field and the charge precipitation particles in convective clouds: Lower positive charge centres
[ESA-TT-1157] 11 p1535 N90-18836
Cirrus cloud optical properties measured with the University of Wisconsin high spectral resolution and volume imaging lidars 15 p2084 N90-21932
Cloud chemistry and occurrence in the western United States: A synopsis of current information
[PB90-134248] 15 p2131 N90-22182
Hail growth in a highly-glaciated central high plains multi-cellular hailstorm 15 p2131 N90-22184
Cloud dynamics and cloud microphysics by radar measurements 19 p2707 N90-25402
An outline for the RTNEPH infrared atmospheric water vapor attenuation study
[AD-A221753] 21 p3027 N90-27209
Lidar cloud studies for FIRE and ECLIPS
[NASA-CR-186384] 22 p3211 N90-28214
Large-scale variability in marine stratocumulus clouds defined from simultaneous aircraft and satellite measurements 22 p3213 N90-28226
Inhomogeneities of stratocumulus liquid water
22 p3213 N90-28228
Intercomparisons of GOES-derived cloud parameters and surface observations over San Nicolas Island
22 p3214 N90-28229
Reflectivities of uniform and broken stratiform clouds: An update 22 p3215 N90-28236
Cloud optical parameters as derived from the multispectral cloud radiometer 22 p3215 N90-28239
Analysis of ER-2 radiometer and lidar observations from the 1987 marine stratus experiment
22 p3216 N90-28241
The radiation budget of stratocumulus clouds measured by tethered balloon instrumentation: Variability of flux measurements 22 p3216 N90-28242
Supersaturation, droplet spectra, and turbulent mixing in clouds 22 p3217 N90-28249
The influence of continental sources of aerosols on the marine stratocumulus during FIRE IFO-1
22 p3218 N90-28250
Observations of anthropogenic cloud condensation nuclei 22 p3218 N90-28251
Direct and remote sensing observations of the effects of ships on clouds 22 p3218 N90-28252
A unified view of convective transports by stratocumulus clouds, shallow cumulus clouds, and deep convection
22 p3219 N90-28254
Verification of the naval oceanic vertical aerosol model during FIRE 22 p3219 N90-28257
Comparison of satellite based cloud retrieval methods for cirrus and stratocumulus 22 p3221 N90-28268
ETO lidar studies of cirrostratus altocumulogenitus: Another role for supercooled liquid water in cirrus cloud formation 22 p3221 N90-28269
Spatial scales of cirrus cloud properties
22 p3222 N90-28275
Interpretation of cirrus cloud properties using coincident satellite and lidar data during the FIRE cirrus IFO
22 p3223 N90-28276
The 27-28 October 1986 FIRE cirrus case study: Meteorology and clouds 22 p3223 N90-28280
Satellite-derived cloud fields during the FIRE cirrus IFO case study 22 p3223 N90-28281
Comparison of surface-derived and ISCCP cloud optical properties 22 p3224 N90-28282
The October 27-28, 1986, FIRE cirrus case study: Cloud microstructure 22 p3224 N90-28283
Cirrus microphysics and radiative transfer: Cloud field study on October 28, 1986 22 p3224 N90-28284
Cirrus radiative characteristics and the radiative impact of small particles 22 p3224 N90-28286
Cirrus clouds and climate feedback: Is the sky falling and should we go tell the king 22 p3225 N90-28288
Preliminary simulations of the large-scale environment during the FIRE cirrus IFO 22 p3225 N90-28290
Microphysical fundamentals governing cirrus cloud growth: Modeling studies 22 p3225 N90-28291
A comparative study of infrared radiance measurements by an ER-2 based radiometer and the LANDSAT 5 Thematic Mapper (TM-6) 22 p3226 N90-28294
Radiative properties of cirrus clouds inferred from broadband measurements during FIRE
22 p3226 N90-28295
IR spectral characteristics of cirrus clouds
22 p3226 N90-28297
Airborne lidar/radiometric measurements of cirrus cloud parameters and their application to LOWTRAN radiance evaluations 22 p3227 N90-28298
The Colorado/Missouri 1989 cirrus mini IFO
22 p3227 N90-28299
A system for recording physical properties of clouds
22 p3227 N90-28301
The 1973-1974 lidar observations of cirrus clouds at Kwajalein 22 p3227 N90-28303
The use of an airborne lidar for mapping cirrus clouds in FIRE, phase 2 22 p3228 N90-28304
On the use of IR lidar and K(sub a)-band radar for observing cirrus clouds 22 p3228 N90-28305
Intercomparison of standard resolution and high resolution TOVS soundings with radiosonde, lidar, and surface temperature/humidity data
22 p3228 N90-28306
The signals of an ice warning device in dependence on total water content and normalized icing degree
[ESA-TT-1207] 24 p3484 N90-29692

CLOUD SEEDING

Applied atmospheric resources research program in Thailand
[PB89-235402] 05 p0668 N90-13903
Winter cloud seeding potential on the Mogollon Rim
[PB89-190540] 07 p0962 N90-15562
Numerical modeling of atmospheric growth processes
[REPT-70] 12 p1693 N90-19726

CLOUDS

Turbulent stripping of interstellar clouds by interaction with supernova remnants
[DE90-003622] 08 p1152 N90-16674
Numerical simulation of acoustic scatter from subsurface bubble clouds
[AD-A217068] 12 p1710 N90-19822
Large impact events and atmospheric evolution on the terrestrial planets 12 p1744 N90-20028
Cloud hole-boring with long pulse CO2 lasers
[DE90-008946] 14 p1985 N90-21377
Unsteady group behavior of droplet clouds in swirling flows 16 p2233 N90-22743
Interaction of electromagnetic signals with particulate clouds
[AD-A222804] 20 p2856 N90-26244
Optical characterization of clouds of fine liquid-nitrogen particles
[NASA-TM-103208] 20 p2865 N90-26299
Dust clouds Kosa from the east Asian dust storms in 1982-1988 as observed by the GMS satellite
21 p3028 N90-27214
Behavior of dust clouds from Australian dust storms in 1982-1983 as observed by the GMS
21 p3029 N90-27221
Dust clouds from African dust storms in 1986-1987 as observed by Meteosat 21 p3029 N90-27222
Sources of cloud nuclei and development of remote sensing techniques for cloud parameters
[AD-A222464] 21 p3031 N90-27233

CLOUDS (METEOROLOGY)

NT CHEMICAL CLOUDS
NT CIRROSTRATUS CLOUDS
NT CIRRUS CLOUDS
NT CONVECTION CLOUDS
NT CUMULONIMBUS CLOUDS
NT CUMULUS CLOUDS
NT ICE CLOUDS
NT NIMBOSTRATUS CLOUDS
NT STRATOCUMULUS CLOUDS
NT STRATUS CLOUDS
Numerical simulations of a midlatitude squall line
01 p0087 N90-10497
Further guide for the retrieval of dropsize distributions in water clouds with a ground-based clear-air-sensing Doppler radar
[PB89-196000] 03 p0336 N90-11911
Lightning data study in conjunction with geostationary satellite data
[NASA-CR-179286] 03 p0375 N90-12142
Performance of laminar-flow leading-edge test articles in cloud encounters 04 p0439 N90-12511
Zonal average cloud characteristics for global atmospheric chemistry modeling
[CM-76] 04 p0518 N90-12992

Analysis and modeling of summertime convective cloud and precipitation structure over the Southeastern United States
[NASA-CR-185436] 04 p0519 N90-12996
Mesoscale acid deposition modeling studies
[NASA-CR-4262] 04 p0554 N90-13228
Characterization of cloud chemistry and frequency of canopy exposure to clouds in the Sierra Nevada
[PB89-104035] 06 p0817 N90-14753
Adverse weather operations during the Canadian Atlantic storms program 07 p0871 N90-15052
Global distribution of total cloud cover and cloud type amounts over the ocean
[DE90-003187] 07 p0964 N90-15574
Determination of optical porperties of clouds from NOAA-AVHRR data using Apollo
08 p1092 N90-16321
Recognition and distinction of clouds, snow, and ice using AVHRR data 08 p1092 N90-16322
Support of hydrological models calculations by satellite data 08 p1094 N90-16337
Cloud hole-boring with infrared lasers: Theory and experiment
[DE90-006519] 11 p1515 N90-18723
Validation of the EURAD cloud modules
12 p1687 N90-19693
The role of clouds in the photochemistry of the background troposphere 12 p1688 N90-19694
Exploiting surface observations of cloudiness for globalscale nephanalyses 12 p1692 N90-19719
Digital simulation of a Boenline
[ISSN-0069-5882] 12 p1694 N90-19729
Laboratory studies of free radical reactions in cloudwater
[DE90-003961] 12 p1694 N90-19730
Cloud types and the tropical Earth radiation budget, revised
[NASA-CR-180475] 13 p1843 N90-20582
A cloud climatology for the North Pacific area centered at Shemya, Alaska
[AD-A217334] 13 p1844 N90-20585
An aircraft investigation of a convective boundary layer over Lake Michigan
[AD-A218175] 13 p1846 N90-20598
Preliminary report on the demonstration of the VAS CO2 cloud parameters (cover, height, and amount) in support of ASOS
[NOAA-TM-NESDIS-29] 14 p2006 N90-21498
Meteorological influences on mountain cloudwater chemistry in the eastern United States
[PB90-132432] 14 p2007 N90-21504
Numerical simulations of the cloud-capped marine boundary layer 14 p2008 N90-21506
Models of aerosols, clouds, and precipitation for atmospheric propagation studies
15 p2081 N90-21919
Lidar measurement of concentration and turbulence in battlefield obscurants 15 p2084 N90-21931
Characterizing microwave propagation using the AFGL microwave attenuation/transmittance/brightness temperature code
[AD-A220248] 18 p2543 N90-24513
Advanced mesoscale weather forecasting to support tactical operations on the airland battlefield
[AD-A219421] 19 p2715 N90-25449
The aqueous atmospheric chemistry of mercury
20 p2886 N90-26420
Perspective transformation for wide-view sky scenes
[AD-A222694] 21 p3007 N90-27093
Cloud reflectance characteristics in the presence of variable Dimethylsulfide (DMS) sources
[AD-A222806] 21 p3024 N90-27197
Meteorological Satellite Center Technical Note, no. 17, 1988
[ISSN-0388-9653] 21 p3028 N90-27213
Investigation into position accuracy of typhoon center determined on GMS imagery 21 p3028 N90-27217
An experiment to make a new design of the Satellite Cloud Information Chart with the combination of visible and infrared data observed by the GMS
21 p3029 N90-27223
Downwelled longwave surface irradiance data from five sites for the FIRE/SRB Wisconsin Experiment from October 12 through November 2, 1986
[NASA-TM-102597] 21 p3030 N90-27225
Analysis of cirrus optical properties with data from NASA ER2 High-resolution Interferometer Sounder (HIS)
[NASA-CR-186365] 21 p3030 N90-27227
FIRE Science Results 1989
[NASA-CP-3079] 22 p3213 N90-28224
Intercomparisons of GOES-derived cloud parameters and surface observations over San Nicolas Island
22 p3214 N90-28229
High resolution infrared measurements
22 p3221 N90-28265
Comparison of surface-derived and ISCCP cloud optical properties 22 p3224 N90-28282
The role of clouds in CO2-induced climate change
[DE90-014380] 23 p3346 N90-28911
The global cycle of reactive nitrogen
[DE90-015041] 23 p3348 N90-28919
Genesis of bow echoes: A rear-inflow induced meso-convective structure
[PB90-209776] 23 p3349 N90-28926
A preliminary ARM (Atmospheric Radiation Measurements) guide for climatic evaluations
[DE90-015135] 23 p3351 N90-28937
The signals of an ice warning device in dependence on total water content and normalized icing degree
[ESA-TT-1207] 24 p3484 N90-29692
Observations of tornadoes and wall clouds with a portable FM-CW Doppler radar: 1989--1990 results
[DE90-013152] 24 p3495 N90-29752
A documentation of icing-relevant cloud physical parameters on vertical soundings of stratiform clouds
[DLR-MITT-90-07] 24 p3495 N90-29753

CLUMPS
Electronic and structural properties of Si10 cluster
[AD-A222429] 21 p3074 N90-27478
Down-to-earth studies of carbon clusters
21 p3091 N90-27573
Electronic and molecular structure of carbon grains
21 p3091 N90-27574
Carbon monoxide isotopes and clumping in giant molecular clouds 24 p3562 N90-30151

CLUSTER ANALYSIS
On algorithms for generating computationally simple piecewise linear classifiers
[NDRE/PUBL-89/1001] 02 p0258 N90-11459
A statistical analysis of spatial point patterns, a case study
[CWI-MS-R8813] 04 p0547 N90-13180
Fast algorithms for estimating mixture parameters
[AD-A213869] 07 p0976 N90-15636
Multivariate clustering based on entropy
[PB89-233993] 10 p1439 N90-18303
Clustering and uniqueness in mathematical models of percolation phenomena
[ETN-90-96400] 15 p2163 N90-22358
Multispectral classification of overlapping classes with applications to forest damage areas
[DLR-FB-89-55] 18 p2574 N90-24666
A hard X ray observation of the Coma Cluster
19 p2789 N90-25875
Predissimilarities, prefilters, and ultrametrics on an arbitrary set
[IMAG-RR-970-M] 20 p2918 N90-26603
Triphone clustering in the ARM system
[RSRE-MEMO-4357] 22 p3166 N90-27952

CLUSTERS
The Hueckel model for small metal clusters. 4: Orbital properties and cohesive energies for model clusters of up to several hundred atoms
[AD-A216161] 10 p1354 N90-17852

CLUTTER
Clutter models for subsurface electromagnetic applications
[PB89-229678] 03 p0338 N90-11925
ASR-9 weather channel test report
[AD-A211749] 03 p0339 N90-11934
Modeling of diffraction reflection and clutter loss in UHF radio wave propagation
[FEL-1988-28] 03 p0340 N90-11938
Estimated UV clutter levels at 10-100 meter sensor pixel resolution extrapolated from recent polar bear measurements
[AD-A211357] 03 p0372 N90-12125
Stochastic modelling of EM scattering from foliage
[AD-A213118] 05 p0632 N90-13689
Adaptive clutter rejection filters for airborne Doppler weather radar applied to the detection of low altitude windshear
[NASA-CR-186211] 06 p0766 N90-14453
The effects of clutter-rejection filtering on estimating weather spectrum parameters
[NASA-CR-186212] 06 p0817 N90-14754
Long term integration for radar detection of small targets in clutter 09 p1203 N90-16972
First results from HF (High-Frequency) oblique backscatter soundings to the northwest of College, Alaska using a modified ULCAR digisonde D-256
[AD-A214931] 09 p1206 N90-16987
Active and passive remote sensing of ice
[AD-A214863] 09 p1241 N90-17199
Adaptive multiple-band CFAR (Constant-False-Alarm-Rate) detection of an optical pattern with unknown spectral distribution
[AD-A214754] 09 p1281 N90-17429
Adaptive processor emulation development
[AD-A214392] 10 p1371 N90-17944
Polarization radar processing technology
[AD-A215242] 10 p1374 N90-17967
Millimeter wave radar clutter program
[AD-A215772] 10 p1376 N90-17978
Synthetic aperture radar imagery of airports and surrounding areas: Archived SAR data
[NASA-CR-4275] 11 p1453 N90-18371
Synthetic aperture radar imagery of airports and surrounding areas: Philadelphia Airport
[NASA-CR-4280] 11 p1453 N90-18372
Algorithms for optimal processing of polarimetric radar data
[AD-A217330] 13 p1876 N90-20758
Problems in ISAR processing with range resolution by stepped frequency bursts 14 p1962 N90-21238
Improvement of clutter rejection by scanning motion compensation in ground-based monopulse radar
[ETN-90-96550] 16 p2228 N90-22711
Specification for environmental measurements to assess radar sensors
[AD-A219127] 16 p2250 N90-22833
A theoretical model for airborne radars
[AD-A220735] 17 p2390 N90-23615
Temporal statistics of low-angle ground clutter
[AD-A220816] 17 p2391 N90-23621
Use of clutter residue editing maps during the Denver 1988 Terminal Doppler Weather Radar (TDWR) tests
[AD-A218696] 17 p2426 N90-23822
Synthetic aperture radar imagery of airports and surrounding areas: Denver Stapleton International Airport
[NASA-CR-4305] 18 p2495 N90-24257
Radar clutter via waveguide methods
[AD-A220237] 18 p2542 N90-24512
The variably trimmed mean CFAR detector for nonhomogeneous background
[AD-A222801] 20 p2856 N90-26243
Backscatter enhancement in scattering from rough surfaces
[AD-A223110] 21 p2995 N90-27024
Recognition of infrared images. Part 3: The effect of image processing with a size-contrast box filter on observation performance
[IZF-1989-39] 23 p3395 N90-29182
Radar clutter via ray methods
[AD-A223796] 24 p3462 N90-29553
A 94 GHz transmissometer
[AD-A223309] 24 p3471 N90-29618
Angle sample variance of azimuthally spread scattering processes, using a two-element array
[AD-A223572] 24 p3542 N90-30034

CMOS
Performance of the CAMEX64 silicon strip readout chip
[DE89-014015] 01 p0130 N90-10747
A single-phase clocked NOR/NOR CMOS programmable sequential array structure
[AD-A211297] 03 p0387 N90-12203
Built-in generation for CMOS circuits
[IMAG-RR-736-I] 04 p0496 N90-12855
European Solid State Device Research Conference (18th) ESSDERC 88 held in Montpellier, France on 13-16 September 1988
[AD-A210618] 04 p0558 N90-13250
Resistive fuses: Analog hardware for detecting discontinuities in early vision
[AD-A211891] 05 p0634 N90-13696
VHSIC/VHSIC-Like reliability prediction modeling
[AD-A214601] 09 p1288 N90-17468
Measurement of proton induced radiation damage to CMOS transistors and pin diodes
[DE90-007836] 13 p1792 N90-20283
Radiation-hardened wafer scale integration
[AD-A217332] 13 p1793 N90-20290
ISITE: Automatic circuit synthesis for double-metal CMOS VLSI (Very Large Scale Integrated) circuits
[AD-A217459] 13 p1793 N90-20292
Transient radiation hardened CMOS (Complementary Metal Oxide Semiconductor) operational amplifiers
[AD-A217972] 13 p1797 N90-20313
SiO(x) precipitation: Defect density correlation with the n+ substrate resistivity
[DE90-005593] 13 p1895 N90-20878
Common source cascode amplifiers for integrating IR-FPA applications 14 p1977 N90-21324
Low noise HgCdTe 128 x 128 SWIR FPA for Hubble space telescope 14 p1979 N90-21337
HgCdTe 256x256 NWIR FPA
14 p1981 N90-21348
Design for testability of stuck-open and stack-on CMOS combinatorial circuits
[REPT-89-044] 16 p2230 N90-22725
Detection of bridging faults in DFCMOS combinational gates
[REPT-89-060] 16 p2231 N90-22726

Definition of a design methodology and study of the driving and protection functions of a smart power switch
[LAAS-89-330] 16 p2231 N90-22727
CMOS IC I(sub DDQ) testing for the 1990s
[DE90-009508] 17 p2394 N90-23634
Test diagnostics of RF effects in integrated circuits
[AD-A219737] 17 p2396 N90-23648
CMOS analog four-quadrant multiplier
[AD-D014507] 19 p2685 N90-25271
Contribution to CMOS integrated circuit tests: Study of the stuck-on and stuck-open fault tests
[ETN-90-97256] 20 p2859 N90-26261
On the design and analysis of multiple-storage elements
[AD-A223095] 20 p2859 N90-26266
Double sided silicon strip detectors
[MPI-PAE/EXP-EL-217] 22 p3178 N90-28036
Readout of double sided silicon strip detectors with high intensity integrated electronics 22 p3179 N90-28038
VLSI design for reliability
[AD-A224264] 24 p3463 N90-29562
Parametric testing for the RSRE CMOS, silicon on sapphire process
[RSRE-MEMO-4369] 24 p3555 N90-30115

COAGULATION
Low velocity dust-dust collisions 12 p1741 N90-20011
Mechanical properties of fluffy agglomerates consisting of core-mantle-particles 12 p1743 N90-20019

COAL
Development of the electroacoustic dewatering (EAD) process for fine/ultrafine coal
[DE89-015883] 01 p0122 N90-10700
Chemistry of large molecules
[DE90-000813] 06 p0751 N90-14366
Analysis of acid rain and associated phenomena
[DE90-002555] 06 p0812 N90-14725
Development and evaluation of a process to produce hydrogen from coal
[DE90-003937] 08 p1052 N90-16084
Improved anode catalysts for coal gas-fueled phosphoric acid fuel cells
[DE90-004016] 08 p1096 N90-16347
A coal model for the carriers of the unidentified IR bands 11 p1581 N90-19110
Simulation of thermal dynamics of a vaporizing coal-water droplet in a combustor
[DE90-005356] 12 p1621 N90-19317
Analysis of competition among kinds of energy at the era of complexed energy. (Report on overseas study)
[DE89-910213] 12 p1680 N90-19650
Criteria for coal tar seal coats on airport pavements. Volume 2: Laboratory and field studies
[AD-A220167] 18 p2498 N90-24277
Heat engines
[DE90-000485] 20 p2882 N90-26393
Distributed communications and control network for robotic mining 24 p3520 N90-29901

COAL DERIVED GASES
Development of ceramic combustor for low BTU gases. Design and basic combustion characteristics
[DE89-782287] 12 p1629 N90-19363

COAL DERIVED LIQUIDS
Production of jet fuels from coal-derived liquids. Volume 11: Production of advanced endothermic fuel blends from Great Plains Gasification Plant naphtha by-product stream
[AD-A210251] 02 p0207 N90-11184
Production of jet fuels from coal derived liquids. Volume 10: Jet fuels production by-products, utility, and sulfur emissions control integration study
[AD-A213872] 09 p1200 N90-16951
Development and use of an advanced coal-fueled diesel engine cycle simulation with group effects
[DE90-000450] 12 p1672 N90-19607

COAL GASIFICATION
Development and evaluation of a process to produce hydrogen from coal
[DE90-003937] 08 p1052 N90-16084
Development of ceramic combustor for low BTU gases. Design and basic combustion characteristics
[DE89-782287] 12 p1629 N90-19363
Corrosion properties of Fe3Al in H2S-H2-H2O mixtures
[DE90-004936] 13 p1772 N90-20167
Production of jet fuels from coal-derived liquids. Volume 13: Evaluation of storage and thermal stability of jet fuels derived from coal liquids
[AD-A224576] 24 p3457 N90-29527

COAL LIQUEFACTION
Hydrous metal oxide-supported catalysts. Part 2: Catalytic properties and applications
[DE90-008098] 12 p1625 N90-19336

COALESCENCE
U COALESCING

COALESCING
Non-Contact Temperature Requirements (NCTM) for drop and bubble physics 10 p1366 N90-17918
Investigation of surface water behavior during glaze ice accretion 14 p1906 N90-20927
High energy phenomena during solar flares
[INPE-4961-TDL/390] 14 p2043 N90-21713

COANDA EFFECT
An experimental and theoretical study of the aeroacoustics of external-Coanda gas flares 06 p0773 N90-14495
Control of flow separation and mixing by aerodynamic excitation
[NASA-TM-103131] 15 p2047 N90-21733

COASTAL MARSHLANDS
U MARSHLANDS

COASTAL PLAINS
Prediction of episodic acidification in Maryland coastal plain streams
[PB90-194978] 22 p3199 N90-28152

COASTAL WATER
Sounding and surface meteorological data from the Land/Sea Breeze Experiment (LASBEX)
[AD-A216269] 11 p1536 N90-18842
US Navy regional climatic study of the Central East Asian coast and associated waters
[AD-A217448] 13 p1844 N90-20587
Continental shelf processes affecting the oceanography of the South Atlantic Bight
[DE90-008439] 13 p1848 N90-20606
Remote sensing applied to sea water quality researches in coastal regions: A review
[INPE-4935-PRE/1425] 14 p1995 N90-21438
Modelling bottom stress in depth-averaged flows
[AD-A218605] 17 p2429 N90-23840
Modeling studies of the LeeUwin current using a high-resolution primitive equation model
[AD-A219595] 17 p2430 N90-23846

COASTAL ZONE COLOR SCANNER
Ocean colour: Methods, technologies, applications 19 p2707 N90-25406
The instrument HOSS (Hydro Optical Sensor System)
[FOA-C-30554-3.1] 22 p3246 N90-28411

COASTS
US Navy regional climatic study of the United States Atlantic Coast and associated waters
[AD-A210198] 01 p0088 N90-10503
Coastal Research Center Woods Hole Oceanographic Institution
[PB89-198238] 01 p0089 N90-10510
Coastal subsea permafrost and bedrock observations using dc resistivity
[AD-A210784] 02 p0253 N90-11435
Airborne profiles taken near San Nicolas Island, California, during Operation FIRE (First ISCCP (International Satellite Cloud Climatology Project) regional experiment) (1987): Aerosol size distributions, air and surface temperatures, cloud top temperatures, and relative humidities
[AD-A211664] 03 p0374 N90-12136
Precipitation distributions associated with cyclones originating over the Gulf of Mexico and surrounding coastal regions
[AD-A213644] 07 p0963 N90-15569
Lightning observations on Japan Sea coast in winter
[DE90-702485] 08 p1103 N90-16387
A Geographic Information System (GIS) for the southern Louisiana deltaic environments
[AD-A214676] 09 p1296 N90-17511
Near real time VHF telemetry of near shore oceanographic data
[AD-A215756] 10 p1327 N90-17666
Aerial photographs to support the fiscalization process of agriculture loans in the Irece-BA region
[INPE-4839-PRE/1468] 10 p1400 N90-18092
Satellite imagery for water quality assessment in coastal regions
[INPE-4891-PRE/1492] 12 p1678 N90-19636
Cyclogeneses and extratropical cyclones in the south-southeast region of Brazil and its influence in time
[INPE-4812-TDL/359] 12 p1693 N90-19722
An observational study of squall lines in the Amazon
[INPE-4865-TDL/376] 12 p1693 N90-19723
Utilization of LANDSAT-5 and NOAA-9 satellite imagery in the identification of physical-chemical parameters of the water in the Guanabara Bay
[INPE-4761-TDL/349] 13 p1819 N90-20445
Analysis of GALE (Genesis of Atlantic Lows Experiment) data
[AD-A217182] 13 p1844 N90-20584
Coastal frontogenesis and associated severe weather on 13 March 1986 (GALE IOP 13)
[AD-A217708] 13 p1845 N90-20590
Correlation of AVHRR imagery with sub-surface features in California current
[AD-A218184] 13 p1848 N90-20607
MECCA program documentation
[NOAA-TR-NESDIS-46] 14 p2003 N90-21477
Evaporation duct effects at millimeter wavelengths 15 p2080 N90-21914
Characteristics of cumulus bandclouds off the east coast of Hawaii 15 p2130 N90-22178
US Navy regional climatic study of southern African waters
[AD-A218792] 16 p2258 N90-22874
US Navy regional climatic study of the Mozambique channel and adjacent waters
[AD-A218793] 16 p2258 N90-22875
A numerical study of basic coastal upwelling processes 16 p2259 N90-22878
Coastal field data collection program. Hurricane Gilbert storm surge data
[AD-A218752] 17 p2426 N90-23823
Trace metal sources for the atlantic inflow to the Mediterranean Sea
[AD-A218607] 17 p2429 N90-23842
A numerical study of wind forcing in the eastern boundary current system off Portugal
[AD-A219596] 17 p2430 N90-23847
The effects of climatological and transient wind forcing on eddy generation in the California current system
[AD-A219858] 17 p2431 N90-23855
Applications of ISES for coastal zone studies 21 p3018 N90-27157
Bibliography of oceanography, meteorology, and geology of Louisiana, Texas, Mississippi, Alabama, and Florida
[PB90-194663] 22 p3194 N90-28124
Aerial videotape survey of coastal Louisiana, 1986. Louisiana Barrier Island erosion and land loss study: 1986-1990
[PB90-194648] 22 p3195 N90-28128
A case study of cumulus formation beneath a stratocumulus sheet: Its structure and effect on boundary layer budgets 22 p3219 N90-28256

COATING
NT ANODIZING
NT ELECTROPLATING
NT ENCAPSULATING
NT METALLIZING
High-temperature ceramic superconductors
[AD-A214251] 07 p1005 N90-15818
Continuous preparation of a thin refractory carbide deposit on the surface of carbon fibers: Characterization of the C/SiC fiber 11 p1477 N90-18501
Sputter deposition of diffusion barrier coatings on SiC monofilaments for use in Ti-based composites 11 p1477 N90-18502
An evaluation of ethylene-vinyl acetate copolymers as desensitizers for RDX in insensitive booster compositions prepared by slurry coating technology
[MRL-TR-89-33] 12 p1633 N90-19385
Electromagnetic properties of material coated surfaces
[NASA-CR-186466] 12 p1647 N90-19466
Fluid dynamics analysis of a rotating axisymmetric part using FIDAP
[DE90-008733] 13 p1802 N90-20340
Novel pulsed plasma treatment and coating process: Multilayer structures for optical computing applications
[AD-A220737] 18 p2615 N90-24894
Computerized corrosion forecasting model for C-5 aircraft 21 p2957 N90-26815

COATINGS
NT ALUMINUM COATINGS
NT ANODIC COATINGS
NT ANTIREFLECTION COATINGS
NT CATHODIC COATINGS
NT CERAMIC COATINGS
NT ELECTROPLATING
NT ENCAPSULATING
NT GLASS COATINGS
NT GOLD COATINGS
NT INORGANIC COATINGS
NT MAGNETIC FILMS
NT METAL COATINGS
NT METALLIZING
NT PAINTS
NT PLASTIC COATINGS
NT PRIMERS (COATINGS)
NT PROTECTIVE COATINGS
NT REFRACTORY COATINGS
NT SPRAYED COATINGS
NT THERMAL CONTROL COATINGS
NT ZINC COATINGS
Coatings in electrical contacts
[DE89-787739] 02 p0216 N90-11234
Constitutive parameter measurements of lossy materials
[NASA-CR-183398] 02 p0281 N90-11603
Coatings for gas turbine compressors
[NLR-MP-88045-U] 03 p0308 N90-11750

Method of modifying the dielectric properties of an organic polymer film
[AD-D014171] 03 p0330 N90-11879
Ion-assisted deposition of high-temperature lubricious surfaces
[DE89-012397] 03 p0331 N90-11883
The 4th US Army Workshop on Low Heat Rejection Engines
[AD-A212379] 04 p0510 N90-12943
An investigation of diamond film deposition in a premixed oxyacetylene flame
[AD-A212595] 04 p0561 N90-13268
Evaluation of a neoprene latex modified SAMI (Stress Absorbing Membrane Interlayer)
[PB89-226435] 05 p0628 N90-13665
Low resistivity electrodeless streamer tubes
[PREPRINT-685-89] 05 p0636 N90-13712
Novel in situ spectroscopic ellipsometer for real time analysis of CVD diamond films
[AD-A213218] 05 p0644 N90-13762
Visualization of boundary layer transition zone movement on oscillating airfoils with shear-sensitive liquid-crystal coatings
[DE89-009570] 06 p0721 N90-14210
An electroformed nickel-sulfur alloy for a nose cone
[DE90-000866] 06 p0745 N90-14337
Dissipation measurement in high T(sub c) superconductors with electromagnetic probes
[DE90-002058] 06 p0854 N90-14963
Silicon-based coatings on niobium metal
[DE90-003651] 08 p1048 N90-16057
Program to study the oxidation of carbon-carbon composites and coatings on these materials
[AD-A214989] 00 p1187 N90-16874
High modulus coatings
[AD-A215448] 09 p1198 N90-16941
Novel approach for high resolution TEM (Transmission Electron Microscopy) studies of ceramic-ceramic interfaces
[DE90-005272] 09 p1199 N90-16945
Application of high-rate cutting tools
[AD-A214644] 09 p1203 N90-16970
NMR measurements of solvent self-diffusion coefficients in polymer solutions
[AD-A215276] 09 p1279 N90-17419
Principles and formulation of solar reflecting and low infrared emitting coatings for defence use
[MRL-TR-89-2] 10 p1358 N90-17874
Fuel-elastomer compatibility studies: Results of 80 C/14-day exposure experiments
[AD-A216015] 10 p1361 N90-17893
Acoustic radiation of cylindrical shells, with stiffening finishing and coated with masking materials
[ISAL-89-0035] 10 p1426 N90-18227
Calculations of braiding parameters
[AD-A216836] 11 p1479 N90-18515
Coating possibilities for magnetic switches
[DE90-006536] 11 p1504 N90-18659
Modification of surface mechanical properties of high-chromium tool steel by carbon-implanted codeposited Fe-Ti films
[DE90-007502] 12 p1628 N90-19358
Microstructural characterization of multiphase coatings produced by chemical vapor deposition
[DE90-007573] 12 p1632 N90-19379
The effect of fiber coatings on interfacial shear strength and the mechanical behavior of ceramic composites
[DE90-007574] 12 p1632 N90-19380
Electromagnetic properties of material coated surfaces
[NASA-CR-186466] 12 p1647 N90-19466
Synthesis of alumina-coated SiC whiskers for production of SiC whisker-reinforced alumina composite materials
[DE90-007778] 13 p1768 N90-20147
Process for making a noble metal on tin oxide catalyst
[NASA-CASE-LAR-13741-1-SB] 13 p1774 N90-20180
A unified integrated model for sputter coating uniformity
[DE90-008322] 13 p1778 N90-20205
Sol-gel derived polytitanosiloxane coatings
[DE90-004186] 13 p1779 N90-20210
Development and construction of external laser components for hardening and coating
[MT-15/87] 13 p1808 N90-20364
Tribological properties of boric acid and boric-acid-forming surfaces. Part 2: Formation and self-lubrication mechanisms of boric acid films on boron- and boric-oxide-containing surfaces
[DE90-005632] 13 p1811 N90-20400
Development and application of nonflammable, high-temperature beta fibers
[NASA-TM-102158] 13 p1855 N90-20645
Design and optimisation of thin foil x ray telescopes 14 p2038 N90-21690
Theoretical studies of silicon chemistry
[AD-A219232] 16 p2225 N90-22690
Application of x ray absorption edge spectrometry to the non-destructive determination of element concentrations, coating thickness and areal densities
[AERE-R-13030] 16 p2245 N90-22802
Microstructure of thin films
[AD-A219262] 16 p2324 N90-23255
Development of damped metal matrix composites for advanced structural applications
[AD-A219864] 18 p2518 N90-24380
Effects of microstructure and adhesion on performance of sputter-deposited MoS2 solid lubricant coatings
[AD-A220900] 18 p2530 N90-24434
Thick and compact MoS2 coatings 18 p2541 N90-24501
Tribology of MoS2: Effect of film thickness 18 p2541 N90-24505
Mechanistic studies of the CO-oxidation reaction on catalysts for use in long-life CO2 lasers 18 p2558 N90-24596
Effect of film adhesion on tribological properties of silver-coated alumina
[DE90-010090] 18 p2564 N90-24632
Development of elements of a high Tc superconducting cable
[AD-A221300] 18 p2623 N90-24945
Method of inserting predesigned disbond areas into composite laminates
[NASA-CASE-LAR-13225-1] 19 p2672 N90-25197
Aligned bismuth, strontium, calcium cuprate coatings on polycrystalline substrates
[AD-D014522] 19 p2678 N90-25229
Sol-gel coating on acoustic wave devices: Thin film characterization and chemical sensor development
[DE90-012224] 19 p2679 N90-25235
Design and fabrication of high damage threshold turning mirrors for the Nova laser
[DE90-012703] 19 p2696 N90-25341
Performance testing and qualification of Sandia's third baseline photovoltaic concentrator module
[DE90-012644] 19 p2711 N90-25431
A resistance strain gage with repeatable and cancellable apparent strain for use to 800 C
[NASA-CR-185256] 20 p2823 N90-26063
Mechanical properties of silica coatings
[DE90-012721] 20 p2837 N90-26138
Mechanical properties of coatings and interfaces
[DE90-012726] 20 p2838 N90-26139
Scattering from coated structures and antenna pattern control using impedance surfaces, part A/B
[NASA-CR-185871] 20 p2854 N90-26233
Self-lubricating-diamond like coatings deposition
[AD-A221756] 21 p2988 N90-26983
Self-lubricating surfaces by ion beam processing
[AD-A222489] 21 p3011 N90-27118
Engine testing of thermographic phosphors
[DE90-013269] 22 p3182 N90-28059
Research on high-efficiency, multiple-gap, multi-junction amorphous silicon-based alloy thin-film solar cells
[DE90-000338] 23 p3344 N90-28896
Extension of plasma source ion implantation to ion beam enhanced deposition
[AD-A224462] 24 p3454 N90-29506
Ion-beam-assisted deposition of silver films on zirconia ceramics for improved tribological behavior
[DE90-009706] 24 p3456 N90-29516
Adhesion of silver films to ion-bombarded zirconia
[DE90-010088] 24 p3456 N90-29517
Ion-beam mixing of Fe/B layers for tribological applications
[DE90-010091] 24 p3456 N90-29518

COAXIAL CABLES
Analysis of coaxial wire measurement of longitudinal coupling impedance
[DE89-015748] 02 p0215 N90-11230
Fiber optics: A brief introduction
[DE89-009337] 02 p0274 N90-11567
Theoretical and experimental investigation of axial power extraction from a magnetically insulated transmission line oscillator
[DE90-003486] 08 p1060 N90-16131
Thermal coefficient of delay for various coaxial and fiber-optic cables 12 p1643 N90-19439
Validation of shielding effectiveness of cables with pigtails
[AD-A220647] 17 p2396 N90-23650
The open-ended coaxial line: A rigorous variational treatment
[RSRE-MEMO-4331] 19 p2683 N90-25265

COAXIAL FLOW
Numerical modeling of supersonic turbulent reacting free shear layers 06 p0719 N90-14197
Experimental observations on transition to turbulence in confined coaxial jets and other boundary layer flows
[DE90-008939] 15 p2098 N90-22005

COAXIAL NOZZLES
Coaxial injection technology for hypergolic propellants 09 p1180 N90-16839
Design of an axisymmetric, contoured nozzle for the HEG
[DLR-FB-90-04] 23 p3327 N90-28812

COAXIAL PLASMA ACCELERATORS
Energy deposition in low power coaxial plasma thrusters 06 p0844 N90-14911

COAXIAL TRANSMISSION
U COAXIAL CABLES
U TRANSMISSION

COBALT
NT COBALT ISOTOPES
NT COBALT 60
Structural and surface characterization of dispersed metal catalysts
[DE89-014530] 01 p0038 N90-10208
Ligand-centered electron-transfer redox processes for manganese, iron, and cobalt complexes in relation to selected catalytic systems
[AD-A217957] 13 p1773 N90-20177

COBALT ALLOYS
Determination and description of the long term creep behavior of high temperature gas turbine materials
[ETN-89-94985] 03 p0329 N90-11871
Crystal and magnetic structure of Er(2)(Co(sub x)Fe(sub 1-x))(17) compounds
[DE90-004928] 10 p1436 N90-18288
Pulsed and modulated passage NMRON studies of cobalt-iron alloys 17 p2470 N90-24118

COBALT COMPOUNDS
NT COBALT OXIDES
Lithium cobalt oxide thin film and its electrochromism
[DE90-004570] 08 p1133 N90-16564
Fabrication of nanometer single crystal metallic CoSi2 structures on Si
[NASA-CASE-NPO-17736-1-CU] 09 p1286 N90-17455
A high temperature molten salt thermal electrochemical cell
[AD-D014469] 22 p3195 N90-28131

COBALT ISOTOPES
NT COBALT 60
Modelling late-time atmospheres of supernovae 15 p2189 N90-22500
Upper limits on Co-57 abundance in SN1987A according to the Kvant data 19 p2769 N90-25735
NPL absorbed dose graphite calorimeter correction for the effect of the gaps around the core
[NPL-RSA(EXT)-12] 22 p3178 N90-28032

COBALT OXIDES
Lithium cobalt oxide thin film and its electrochromism
[DE90-004570] 08 p1133 N90-16564

COBALT 60
The effects of space radiation on thin films of YBa2Cu3O(sub 7-x) 22 p3147 N90-27845

COBE
U COSMIC BACKGROUND EXPLORER SATELLITE

COCKPIT SIMULATORS
Flight simulation test facility: Function and specification of the simulator cockpit system
[NAL-TM-577] 02 p0157 N90-10899
Spatial tests for aviators
[IZF-1988-15] 04 p0527 N90-13041
Cockpit resource management: A selected annotated bibliography
[AD-A214272] 07 p0969 N90-15594
Effect of laser glare and aircraft windscreen on visual search performance under low ambient lighting
[AD-A219456] 17 p2437 N90-23888
Simulation of transport aeroplanes
[MBB-UT-007/89-PUB] 19 p2651 N90-25089
Human performance in cockpit-related systems
[NIAR-90-7] 20 p2900 N90-26495

COCKPITS
Cockpit lighting compatibility with image intensification night imaging systems: Issues and answers
[AD-A210503] 01 p0006 N90-10028
See and avoid/cockpit visibility
[DOT/FAA/CT-TN89/18] 02 p0148 N90-10843
Flight simulation test facility: Function and specification of the simulator cockpit system
[NAL-TM-577] 02 p0157 N90-10899
Integration of a centralized multiplexed control unit into the cockpit of an aircraft
[F6150-DT410-1-88329] 04 p0458 N90-12622
Flight deck automation: Promises and realities
[NASA-CP-10036] 05 p0580 N90-13384
Conference Proceedings of the Human-Electronic Crew: Can They Work Together
[AD-A211871] 05 p0676 N90-13936
Imaging probabilities, geometry and ergonomics in limited visibility helicopter operations 07 p0872 N90-15060

See and avoid/cockpit visibility
[AD-A214214] 07 p0877 N90-15084
Task-oriented display design: Concept and example
[NASA-TM-101685] 07 p0881 N90-15101
Display interface concepts for automated fault diagnosis
[NASA-TM-101610] 07 p0881 N90-15102
Keeping the pilot in the loop
[RAE-TM-FM-18] 08 p1105 N90-16396
Three input concepts for flight crew interaction with information presented on a large-screen electronic cockpit display
[NASA-TM-4173] 11 p1457 N90-18394
Human factors engineering testing of aircraft cockpit lighting systems
[AD-A216853] 12 p1697 N90-19743
A new method for measuring the transmissivity of aircraft transparencies
[AD-A216953] 12 p1714 N90-19842
Cockpit display of hazardous wind shear information
14 p1905 N90-20924
Simulator comparison of thumball, thumb switch, and touch screen input concepts for interaction with a large screen cockpit display format
[NASA-TM-102567] 14 p1921 N90-21005
The effect of windscreen bows and HUD pitch ladder format on pilot performance during simulated flight
[AD-A218139] 14 p2011 N90-21523
A3I visibility modeling project
15 p2140 N90-22230
Automatic speech recognition in air-ground data link
18 p2640 N90-25037
Choosing a pilot subjective workload scale to fit flight operational requirements
[IAR-89-21] 20 p2900 N90-26493
Human performance in cockpit-related systems
[NIAR-90-7] 20 p2900 N90-26495
Psychophysiological assessment of pilot workload in an applied setting
[AD-A222707] 20 p2902 N90-26507
Application of audio/speech recognition for military applications 21 p2993 N90-27014
Cockpit Ocular Recording System (CORS)
[NASA-CR-4281] 21 p3033 N90-27244
Toxicity of thermolysis products from the materials of airplane cockpits
[CEAT-PV-M6/5924/02] 22 p3156 N90-27895
Situational Awareness in Aerospace Operations
[AGARD-CP-478] 23 p3357 N90-28972
Towards a future cockpit: The prototyping and pilot integration of the Mission Management Aid (MMA)
23 p3358 N90-28979
The function of the Interactive Model Assembly Program (IMAP) for a flight simulator
[NAL-TR-1034] 24 p3437 N90-29412

COCKROACHES
Neural networks for real-time sensory data processing and sensorimotor control
[AD-A223096] 20 p2916 N90-26592

COD (CRACKS)
U CRACK OPENING DISPLACEMENT

CODE DIVISION MULTIPLE ACCESS
High-throughput, survivable protocols for CDMA packet-radio networks (SRNTN-74)
[AD-A220189] 17 p2393 N90-23631
Multiple-access techniques for communication over dispersive radio channels 20 p2848 N90-26196

CODERS
Advanced modulation technology development for earth station demodulator applications. Coded modulation system development
[NASA-CR-185149] 13 p1789 N90-20270
VLSI single-chip (255,223) Reed-Solomon encoder with interleaver
[NASA-CASE-NPO-17280-1-CU]
14 p1933 N90-21061
A VLSI decomposition of the deBruijn graph
15 p2077 N90-21895
A neural network based speech recognition system
[AD-A219794] 17 p2389 N90-23606

CODING
NT AMPLITUDE MODULATION
NT DECODING
NT DELTA MODULATION
NT DIFFERENTIAL PULSE CODE MODULATION
NT FREQUENCY MODULATION
NT FREQUENCY SHIFT KEYING
NT PHASE MODULATION
NT PHASE SHIFT KEYING
NT PULSE AMPLITUDE MODULATION
NT PULSE CODE MODULATION
NT PULSE DURATION MODULATION
NT PULSE MODULATION
NT PULSE POSITION MODULATION
NT REDUNDANCY ENCODING
NT SIGNAL ENCODING
Electrostatically suspended rotor for angular encoder
[NASA-CASE-MFS-28294-1] 01 p0054 N90-10310
Multi-level bandwidth efficient block modulation codes
[NASA-CR-185484] 01 p0056 N90-10317
Radon transform analysis of a probabilistic method for image generation
[AD-A207814] 01 p0123 N90-10702
Deep null antennas and their applications to tactical VHF radio communications
[AD-A210656] 02 p0212 N90-11214
Performance analysis of hybrid ARQ protocols in a slotted code division multiple-access network
[AD-A211078] 02 p0213 N90-11219
Optical arithmetic logic using the modified signed-digit redundant number representation
[AD-D014176] 03 p0384 N90-12186
Ground-state coding in partially connected neural networks
[NASA-TM-102239] 03 p0391 N90-12227
Wire grid modeling of the linear tapered slot antenna
[AD-A212977] 04 p0494 N90-12842
Subspace iteration algorithms in FORTRAN 77 and FORTRAN 8x
[AD-A212275] 04 p0533 N90-13083
Magnetically insulated electron flows in pulsed power systems
[AD-A212746] 04 p0549 N90-13196
Review and evaluation of a turbomachinery throughflow finite element code
[AD-A213058] 05 p0650 N90-13787
A prototype microprocessor based audiometer for use by the CF (Canadian Forces) medical services for periodic hearing tests
[AD-A212990] 05 p0673 N90-13921
Implementation issues in source coding
[NASA-CR-185327] 05 p0681 N90-13963
Compression of bitmapped graphic data
[AD-A213141] 05 p0683 N90-13974
Surface cooled, vacuum impregnated superconducting magnet systems: Design, construction, applications
[ETN-90-96014] 05 p0696 N90-14072
SAND DEVIL: A digital video link for telemetry applications
[DE90-001879] 06 p0730 N90-14259
Visual Information Processing for Television and Telerobotics
[NASA-CP-3053] 08 p1072 N90-16204
Coded-aperture imaging in nuclear medicine
08 p1073 N90-16208
Context dependent prediction and category encoding for DPCM image compression 08 p1073 N90-16210
Image gathering and coding for digital restoration: Information efficiency and visual quality
08 p1073 N90-16211
Data compression for the microgravity experiments
08 p1074 N90-16212
High compression image and image sequence coding
08 p1074 N90-16214
From primal sketches to the recovery of intensity and reflectance representations 08 p1074 N90-16216
Parallel asynchronous systems and image processing algorithms 08 p1075 N90-16218
Neural networks for data compression and invariant image recognition 08 p1075 N90-16219
A programmable image compression system
08 p1076 N90-16222
Hybrid LZW compression 08 p1076 N90-16223
Digital image coding and compression
[PB90-110958] 08 p1107 N90-16409
High-order mixture homogenization of fiber-reinforced composites
[AD-A215247] 09 p1187 N90-16876
Performance of cellular frequency-hopped spread-spectrum radio networks
[AD-A214480] 09 p1204 N90-16978
Coding capacity for a class of additive channels
[AD-A215054] 09 p1206 N90-16993
Compiling scientific code using partial evaluation
[AD-A215087] 09 p1270 N90-17363
Multiple symbol differential detection of uncoded and trellis coded MPSK
[NASA-CR-186288] 10 p1376 N90-17975
Source header list. Volume 1: A through K
[AD-A216000] 10 p1442 N90-18319
Source header list. Volume 2: L through Z
[AD-A216001] 10 p1442 N90-18320
Rate compatible punctured codes, their use in military satellite communication systems
[AD-A216723] 11 p1497 N90-18619
A microcode compiler that runs on the IBM AT and supports cascadable microcomputers, part 1
[AD-A215888] 11 p1542 N90-18877
DoD manual for standard data elements
[AD-A216441] 11 p1575 N90-19066
Dynamic reconfiguration and link fault tolerance in a transputer network
[AD-A215105] 12 p1642 N90-19433
Some easily analyzable convolutional codes
12 p1644 N90-19444
Quantization effects in Viterbi decoding rate 1/n convolutional codes 12 p1644 N90-19445
Big Viterbi Decoder (BVD) results for (7,1/2) convolutional code 12 p1644 N90-19446
Fast transform decoding of nonsystematic Reed-Solomon codes 12 p1644 N90-19447
Digital video: Studio signal processing
[BBC-RD-1989/14] 12 p1648 N90-19476
Error control techniques for satellite and space communications
[NASA-CR-186221] 13 p1788 N90-20263
Fractal-based image compression
[AD-A217302] 13 p1865 N90-20699
Exact algorithms for output encoding, state assignment and four-level Boolean minimization
[AD-A217121] 13 p1876 N90-20756
Spectral line shape code for multielectron emitters
[DE90-008526] 13 p1891 N90-20853
Direct Radio Broadcasting by Satellite (DRBS): A review of the technical factors and system approaches suitable for mobile and fixed reception
[BBC-RD-1989/4] 14 p1960 N90-21221
Lessons learned in the transition to Ada from FORTRAN at NASA/Goddard
[NASA-TM-103311] 14 p2014 N90-21538
An adaptive vector quantization scheme
15 p2077 N90-21898
Algebraic block-structured grid generation based on a macro-block concept 15 p2093 N90-21978
Networks for image acquisition, processing and display 15 p2138 N90-22218
Image gathering, coding, and processing: End-to-end optimization for efficient and robust acquisition of visual information 15 p2139 N90-22224
Ames vision group research overview
15 p2143 N90-22242
Pyramid image codes 15 p2143 N90-22243
FORTRAN coding guidelines
[DE90-009804] 15 p2146 N90-22258
Geographic information system: Coded data of agrocattle-raising projects in the Amazon
[INPE-4978-PRE/1543] 15 p2180 N90-22457
Encoding sequential structure in simple recurrent networks
[AD-A218928] 16 p2278 N90-22984
Parallel computation of supersonic flows using a three-dimensional, zonal, Navier-Stokes code
[AD-A218824] 17 p2344 N90-23350
Codice ETF-3D: Euler transonic flow user manual
[DLC/FLU-INT-TN-006] 17 p2346 N90-23362
Implementation of image action plus software for image analysis of solid propellant combustion holograms
[AD-A219644] 17 p2372 N90-23508
CESAR LOCAL BUS
[FFI-89/7011] 17 p2440 N90-23903
Encoding of the Burgess metal electrical resistivity model into SESAME format and its adaptation to the metal nickel
[DE90-010816] 18 p2526 N90-24419
HDTV: A chance to enhance television colorimetry
[BBC-RD-1990/2] 18 p2543 N90-24515
Acquiring generalizations to organize human databases
[AD-A219835] 18 p2634 N90-25004
Privacy-enhanced electronic mail
[PCS-TR90-150-REV-1] 19 p2683 N90-25261
Multi-level trellis coded modulation and multi-stage decoding
[NASA-CR-186861] 19 p2743 N90-25593
A versatile integrated block codes encoder-decoder
20 p2848 N90-26197
Direct-sequence spread spectrum system
[AD-A223021] 20 p2856 N90-26245
A hybrid M-algorithm/sequential decoder for convolutional and trellis codes
[NASA-CR-186863] 20 p2906 N90-26528
Converses for write-unidirectional memories
[EUT-89-E-220] 20 p2909 N90-26546
UEDIT: A full-scale, scrollable APL2 spreadsheet input/output editor
[AD-A222712] 20 p2910 N90-26557
Overview of requirements and networks for voice communications and speech processing
21 p2992 N90-27007
Speech coding 21 p2992 N90-27009
Quality evaluation of speech processing systems
21 p2993 N90-27012
Speech processing standards
21 p2993 N90-27013

Parallel numerical simulations of axisymmetric projectile flows using zonal-overlapped grids
[AD-A221711] 21 p3005 N90-27082
SDI satellite autonomy using AI and Ada
21 p3050 N90-27336
Efficient instruction sequencing with inline target insertion
[NASA-CR-185341] 21 p3052 N90-27348
ROBFIT: A code for the analysis of histogram spectra with nonlinear regression and robust estimation
[AD-A221527] 21 p3055 N90-27369
Tutorial on Reed-Solomon error correction coding
[NASA-TM-102162] 22 p3234 N90-28339
Hash functions: A tutorial and status report
[NPL-DITC-151/89] 22 p3238 N90-28361
Encoding techniques for complex information structures in connectionist systems
[NASA-CR-186942] 22 p3238 N90-28362
Book of abstracts of the 1st Benelux-Japan Workshop on Information and Communication Theory
[PB90-191446] 24 p3556 N90-30124

COEFFICIENT OF FRICTION
The limiting friction force
[ECL-89-005] 05 p0652 N90-13801
Finite element analysis of frictional contact problems
06 p0792 N90-14612
Friction in bearings
[ESDU-89044] 09 p1232 N90-17149
Studies of mechano-chemical interactions in the tribological behavior of materials
[NASA-TM-102545] 14 p1953 N90-21182
Internal rotor friction instability
[NASA-CR-183942] 14 p1988 N90-21395
Pressure and shear stress measurement uncertainty for DARPA SUBOFF experiment
[AD-A219109] 16 p2243 N90-22798
CVD diamond films for tribological applications
[AD-A220265] 17 p2413 N90-23750
On the application of similarity laws to a scaled railway bogie model
[DLR-FB-90-06] 23 p3335 N90-28853

COEFFICIENTS
NT AERODYNAMIC COEFFICIENTS
NT ATTENUATION COEFFICIENTS
NT COEFFICIENT OF FRICTION
NT COHERENCE COEFFICIENT
NT CORRELATION COEFFICIENTS
NT COUPLING COEFFICIENTS
NT DIFFUSION COEFFICIENT
NT DISCHARGE COEFFICIENT
NT HEAT TRANSFER COEFFICIENTS
NT INFLUENCE COEFFICIENT
NT NOZZLE THRUST COEFFICIENTS
NT RECOMBINATION COEFFICIENT
NT REGRESSION COEFFICIENTS
NT SCATTERING COEFFICIENTS
NT WIGNER COEFFICIENT
A FORTRAN program for the calculation of the calibration coefficients of a six-component strain gauge balance
[AD-A210375] 01 p0105 N90-10599
The realization of input-output maps using bialgebras
[NASA-CR-185362] 03 p0391 N90-12228
Generalizations of Laguerre polynomials
[REPT-89-25] 03 p0396 N90-12263
A simulation study of the overdetermined geodetic boundary value problem using collocation
[AD-A211785] 04 p0518 N90-12990
Operator product coefficients in non-diagonal conformal field theories
[NIKHEF-H/88-19] 04 p0553 N90-13224
Optimal processes described by a parabolic differential equation with control in the coefficients, part 4
[MEMO-785-PT-4] 05 p0689 N90-14016
Geopotential coefficient determination and the gravimetric boundary value problem: A new approach
13 p1833 N90-20521
Precise solution for a finite set of spherical coefficients from equiangular gridded data 13 p1833 N90-20522
Search of primitive polynomials over finite fields
[IMAG-RR-797-M] 20 p2918 N90-26607

COENZYMES
NT ADENOSINE TRIPHOSPHATE

COERCIVITY
Anisotropy and microstructure of high-coercivity rare earth permanent magnets
[AD-A211905] 03 p0399 N90-12285
Anisotropy and microstructure of high coercivity rare earth iron permanent magnets, list of papers published
[AD-A214160] 08 p1118 N90-16476

COGENERATION
Advanced energy system program
[PB89-235170] 05 p0665 N90-13887
Solid oxide fuel cell cogeneration system conceptual design, program 2
[PB90-114966] 12 p1681 N90-19653
Survey on the possibility of introducing new energy to regional development plans
[DE89-782627] 12 p1681 N90-19654
Low cost Brayton engine for gas-fired cogeneration system, phase 1
[PB90-127457] 12 p1681 N90-19655
Fuel cells: Their applications, technological status, market and opportunity
[DE90-796158] 23 p3344 N90-28895

COGNITION
Models of mental functioning
[AD-A210456] 01 p0094 N90-10538
Comprehension processes in mechanical reasoning
[AD-A210459] 02 p0255 N90-11442
Planning in writing: The cognition of a constructive process
[AD-A210434] 02 p0288 N90-11648
Adaptive information processing in auditory cortex
[AD-A211294] 03 p0380 N90-12166
Metacognition and retrieval from long-term memory at Mount Everest
[AD-A211629] 03 p0382 N90-12177
The effect of incentives on the reliability and validity of cognitive speed tests
[AD-A211346] 03 p0383 N90-12181
Optical computing based on the Hopfield model for neural networks
[AD-A211824] 03 p0389 N90-12216
Individual differences in associative learning and forgetting
[AD-A212765] 04 p0526 N90-13034
Spatial tests for aviators
[IZF-1988-15] 04 p0527 N90-13041
A guide to reasoning under uncertainty
[REPT-72/87/R486U] 05 p0675 N90-13932
Cognitive and Neural Sciences Division 1989 programs
[AD-A212634] 06 p0820 N90-14769
Workload induced spatio-temporal distortions and safety of flight
[DE89-016613] 06 p0820 N90-14771
Numerical facility: Convergence of cognitive and factor analytic models
[AD-A213627] 07 p0983 N90-15680
Causes of aircrew error in the Royal Air Force
09 p1254 N90-17276
Feedback effects in computer-based skill learning
[AD-A214560] 09 p1258 N90-17298
Measures of subjective variables in visual cognition
[AD-A215084] 09 p1259 N90-17303
Measuring learning ability by dynamic testing
[AD-A215273] 09 p1259 N90-17304
EDISON Project
[AD-A214724] 09 p1265 N90-17338
Computing with neural maps: Application to perceptual and cognitive functions
[AD-A216689] 10 p1412 N90-18143
Alterations in the metabolic and sympathetic response to cold exposure after cold air acclimation
[AD-A216817] 10 p1412 N90-18144
Teaching a new methodology for designing relational data bases: An experiment testing the effectiveness of an intelligent tutoring system on cognitive skill acquisition (volumes 1 and 2)
11 p1574 N90-19063
Effects of dexamethasone and high terrestrial altitude on cognitive performance and affect
[AD-A217897] 13 p1851 N90-20625
The role of chaos in hemispheric process and attention
[AD-A217674] 13 p1854 N90-20639
The boundaries of hemispheric processing in visual pattern recognition
[AD-A217675] 13 p1854 N90-20640
Lateral asymmetry in pattern recognition: Understanding the effects of familiarity, distinction, and perspective change
[AD-A217739] 13 p1854 N90-20641
Role of cognitive factors in the acquisition of cognitive skill
[AD-A218069] 13 p1854 N90-20642
Information gathering and decisionmaking under stress
[AD-A218233] 13 p1854 N90-20643
Aiding the decision maker: Perceptual and cognitive issues at the human-machine interface
[AD-A217862] 13 p1855 N90-20648
CEREBRAL WEEVIL: A machine learning model for hemispheric categorization of complex visual patterns
[AD-A218143] 13 p1874 N90-20749
Time and truth in plans 14 p1906 N90-20930
Visions of visualization aids: Design philosophy and experimental results 15 p2138 N90-22220
Vision science and technology for supervised intelligent space robots 15 p2139 N90-22221
Sparse distributed memory overview
15 p2141 N90-22235
Human cognitive and motor performance measures under typical cool white fluorescent illumination vs relatively high cool white illuminance/irradiance lighting
[AD-A218445] 16 p2262 N90-22892
Efficient specialization of relational concepts
[AD-A218889] 16 p2262 N90-22894
Cognitive efficiency considerations for good graphic design
[AD-A218976] 16 p2263 N90-22899
Discovering problem solving strategies: What humans do and machines don't (yet)
[AD-A219008] 16 p2263 N90-22902
Rules and maps in connectionist symbol processing
[AD-A219028] 16 p2264 N90-22903
Learning events in the acquisition of three skills
[AD-A219038] 16 p2264 N90-22905
A connectionist implementation of cognitive phonology
[AD-A219095] 16 p2264 N90-22906
Cognitive architectures and rational analysis: Comment
[AD-A219199] 16 p2264 N90-22907
Information processing approaches to cognitive development
[AD-A219200] 16 p2265 N90-22908
Toward a SOAR theory of taking instructions for immediate reasoning tasks
[AD-A219201] 16 p2265 N90-22909
A task-analytic approach to the automated design of information graphics
[AD-A219271] 16 p2265 N90-22912
Laboratory replication of scientific discovery processes
[AD-A219273] 16 p2266 N90-22913
An instructable Connectionist/Control architecture: Using rule-based instructions to accomplish connectionist learning in a human time scale
[AD-A219274] 16 p2266 N90-22914
Hatching a theory of incubation effects
[AD-A219275] 16 p2266 N90-22915
Non-LIFO (Last-In-First-Out) execution of cognitive procedures
[AD-A219277] 16 p2266 N90-22916
Motor and cognitive performance do not change during a ten-week submarine patrol
[AD-A218639] 16 p2276 N90-22969
Application of artificial intelligence in electronic circuit diagnosis 16 p2303 N90-23122
Hand shaping: A paradigm for cognitive/motoric interaction
[AD-A219908] 17 p2437 N90-23885
DURIP: Computational modeling of cognitive processes
[AD-A219934] 17 p2437 N90-23886
Designing distributed algorithms by means of formal sequentially phased reasoning
[TR-89-8] 17 p2449 N90-23969
Northeast Artificial Intelligence Consortium. Volume 3: The Versatile Maintenance Expert System research project
[AD-A218716] 17 p2453 N90-23993
DURIP: Improved eye movement monitoring capabilities for studies in visual cognition
[AD-A220355] 18 p2586 N90-24722
From where they look to what they think: Determining controller cognitive strategies from oculometer scanning data 18 p2641 N90-25041
Process and representation in graphical displays
19 p2740 N90-25574
Adaptive robot control using artificial neural networks: An application in the theory of cognition
[RR-374] 19 p2748 N90-25618
Mathematical problem-solving transfer: The effects of cognitive load and attention a schema acquisition and rule automation 20 p2917 N90-26594
Qualitative and quantitative reasoning about thermodynamics
[NASA-CR-186788] 20 p2933 N90-26689
Cognitive requirements for aircraft navigation
[NASA-CR-186933] 21 p2955 N90-26804
Symbolic architectures for cognition
[AD-A222909] 21 p3035 N90-27254
The integrated area measure of visual endogenous ERPs: Relation to cognitive workload and hemisphere
[AD-A223191] 21 p3035 N90-27255
Conference on The Perception of Structure Program and Abstracts
[AD-A222437] 22 p3232 N90-28328
Encoding techniques for complex information structures in connectionist systems
[NASA-CR-186942] 22 p3238 N90-28362
Cognition versus sensation: A paradigm for reorientation
[IZF-1989-20] 23 p3361 N90-28995
Evaluation of physiological and psychological impairment of human performance in cold stressed subjects
[AD-A223635] 24 p3498 N90-29769

Ability and metacognitive determinants of skill acquisition and transfer
[AD-A224569] 24 p3499 N90-29776

COGNITIVE PSYCHOLOGY
Formalisms for user interface specification and design
08 p1155 N90-16687
Symposium on air traffic control training for tomorrow's technology
[PB90-127325] 12 p1601 N90-19216
Workload induced spatio-temporal distortions and safety of flight: An investigation of cognitive intrusions in perceptual processes 23 p3360 N90-28986
Neurophysiological correlates of information processing abilities during divided attention situations in air traffic controllers 23 p3360 N90-28989
A design strategy for autonomous systems
24 p3506 N90-29818
A layered abduction model of perception: Integrating bottom-up and top-down processing in a multi-sense agent 24 p3512 N90-29851

COHERENCE
Optical coherence multiplexing for interprocessor communications
[DE89-016186] 02 p0275 N90-11568
Coherent structures in a round jet
05 p0640 N90-13733

COHERENCE COEFFICIENT
Cineholography: A relation between the coherence length of the laser and the object velocity
[ISL-CO-234/88] 11 p1515 N90-18724

COHERENT ANTI-STOKES RAMAN SPECTROSCOPY
U RAMAN SPECTROSCOPY

COHERENT ELECTROMAGNETIC RADIATION
NT COHERENT LIGHT
NT LASER BEAMS

COHERENT LIGHT
Propagation of an elliptical laser beam through the turbulent atmosphere (vertical beams)
[PB89-208680] 03 p0352 N90-12010
Excimer emission from alkali diatomic and alkaline-earth-noble-gas molecules
[AD-A214246] 07 p0896 N90-15179
Method for holographic correction of beams of coherent light
[AD-D014406] 14 p1981 N90-21353
Image of the angle by partially coherent lighting: Calculations and experiments
[ETN-90-96505] 18 p2616 N90-24900
Adaptive polarization diversity detection scheme for coherent communications and interferometric fiber sensors
[AD-D014479] 22 p3163 N90-27938
Energy transmission by means of coherent quasi-mono-chromatic light beams
23 p3392 N90-29163
Effects and control of the correlation properties of light sources
[AD-A224539] 24 p3545 N90-30049

COHERENT RADAR
Joint VHF coherent radar and oblique sounder observations for short term ionosphere forecasting
02 p0247 N90-11399
Parametric spectral estimation techniques for coherent millimeter-wave radar
[AD-A214355] 10 p1371 N90-17943
Coherent radar measurement of ocean currents from geostationary orbit 12 p1609 N90-19259
A solid-state multiple-pass amplifier for diode pumped coherent laser radar systems
[AD-A222537] 21 p3009 N90-27104
High range resolution radar cross-section profiles: A preliminary analysis
[AD-A223448] 24 p3461 N90-29550

COHERENT RADIATION
NT COHERENT LIGHT
NT LASER BEAMS
Shortwavelength coherent radiation: Generation and applications
[AD-A209847] 01 p0074 N90-10427
Proof of the feasibility of coherent and incoherent schemes for pumping a gamma-ray laser
[AD-A212882] 04 p0507 N90-12924
Laser probing non-cylindrical Z-pinch in near-isolator region of a discharged chamber
[DE89-632018] 06 p0844 N90-14912
Parametric spectral estimation techniques for coherent millimeter-wave radar
[AD-A214355] 10 p1371 N90-17943
Linear, nonlinear, and tunable guided wave modes for high-power (GaAl)As semiconductor lasers
15 p2104 N90-22036
Apparatus for the efficient wavelength conversion of laser radiation
[AD-D014506] 20 p2866 N90-26305

COHERENT SCATTERING
Effects of coherent scattering on infrared absorption in doped semiconductors
[AD-A210224] 01 p0131 N90-10756
On the explanation of anomalies in inelastic neutron scattering by high-T(sub c) superconductors
[DE90-620561] 17 p2475 N90-24149
Feasibility of the temperature measurements in hypersonic flow by multibeam coherent Raman anti-Stokes scattering
[ONERA-RF-56/7131-PY] 24 p3419 N90-29312
CARS spectroscopy and applications
24 p3420 N90-29321
Angle sample variance of azimuthally spread scattering processes, using a two-element array
[AD-A223572] 24 p3542 N90-30034

COHERENT SOURCES
U COHERENT RADIATION
U RADIATION SOURCES

COHERENT TRANSMISSION
U COHERENT RADIATION

COHESION
Determination of flow-regime boundaries for cohesive particles
[DE90-001405] 07 p0928 N90-15369
The Hueckel model for small metal clusters. 4: Orbital properties and cohesive energies for model clusters of up to several hundred atoms
[AD-A216161] 10 p1354 N90-17852
Some considerations on cohesive forces in sun-grazing comets 12 p1742 N90-20015
Determination of flow-regime boundaries for cohesive particles
[DE90-007425] 13 p1800 N90-20332

COHOMOLOGY
U HOMOLOGY

COILS
Electrical test of gyrotron coil
[INPE-4929-RPE/596] 09 p1214 N90-17041

COINCIDENCE CIRCUITS
Parallel memory addressing using coincident optical pulses
[AD-A216302] 11 p1501 N90-18641

COLD ACCLIMATIZATION
Alterations in the metabolic and sympathetic response to cold exposure after cold air acclimation
[AD-A216817] 10 p1412 N90-18144
Arctic cold weather medicine and accidental hypothermia
[AD-A223090] 20 p2899 N90-26487

COLD CATHODE TUBES
NT PHOTOMULTIPLIER TUBES
Plasma-anode electron gun research
[AD-A211547] 03 p0312 N90-11773
Research on optogalvanic effects
[AD-A221512] 21 p3071 N90-27463

COLD FLOW TESTS
Aerodynamic and heat transfer measurements on blading for a high rim-speed transonic turbine
[RAE-TM-P-1151] 08 p1024 N90-15920
Cold flow determination of the internal flow environment around the submerged TVC nozzle for the space shuttle SRM 11 p1470 N90-18465
Experimental study of mixing and combustion processes in a solid-propellant ducted rocket motor
17 p2367 N90-23472

COLD FORMING
U COLD WORKING

COLD FRONTS
Numerical simulations of the rapid cyclogenesis over Canada and evolution of a cold front observed on 25-26 April 1979 (SESAME-AVE-3) 09 p1247 N90-17234
Coastal frontogenesis and associated severe weather on 13 March 1986 (GALE IOP 13)
[AD-A217708] 13 p1845 N90-20590
A method for correcting and reducing the pressure data recorded at the PAM 2 stations during GALE
[AD-A218165] 13 p1846 N90-20596
Frontal structure in a mesoscale model
15 p2132 N90-22187
Derivation of wind fields from Doppler measurements of a single radar and application to a cold front with narrow rainband
[DLR-FB-89-61] 18 p2582 N90-24705

COLD GAS
Very high resolution radio observations of molecular cloud cores 06 p0863 N90-15013

COLD HARDENING
Precipitation strengthened high strength, high conductivity Cu-Cr-Nb alloys produced by chill block melt spinning
[NASA-CR-185144] 03 p0326 N90-11853

COLD NEUTRONS
The effects of cold dark matter on Big Bang nucleosynthesis 12 p1698 N90-19749

COLD PLASMAS
Strategic characteristics of Dynamics Explorer 1 retarding ion mass spectrometer and the consequences for core plasma measurements
[AD-A214013] 07 p0886 N90-15125
Studies of Io's atmosphere and plasma torus
16 p2338 N90-23326
Characterization of plasma flow through magnetic nozzles
[AD-A221044] 18 p2617 N90-24905
Finite amplitude surface waves in cooled plasmas with smeared interface
[DE90-611308] 18 p2617 N90-24909
Spectroscopy of ions and their clusters
[AD-A223109] 21 p2977 N90-26917
Plasma cloaking: Air chemistry, broadband absorption, and plasma generation
[AD-A222044] 21 p3078 N90-27503
Transport of nonneutral plasmas
[AD-A223457] 24 p3549 N90-30077

COLD PRESSING
Cold press lubrication: Fine tuning of the CETIM Forgelub test
[CETIM-105160] 04 p0509 N90-12938
Increased fragility of deep pressed thin plates
[CETIM-13-Y-313] 04 p0513 N90-12962
Crystallization behavior and properties of BaO-Al2O3-2SiO2 glass matrices
[NASA-CR-185209] 12 p1631 N90-19374
Millimeter wave surface resistance of RBa2Cu3O(7-delta) (R=Y,Eu,Dy,Sm,Er) superconductors
[NASA-TM-102571] 13 p1897 N90-20886
Realization of equipment for manufacturing titanium alloy electrodes for first step melting
[ONERA-RT-15/3578-M] 24 p3453 N90-29498

COLD ROLLING
Thin section casting program. Volume 1: Executive summary and overview
[DE89-009030] 02 p0209 N90-11198
Novel processing of HTS based conductors
[DE90-005956] 12 p1722 N90-19892
Crown and shape control in the rolling of thin, wide plates
[ETN-90-96946] 17 p2378 N90-23539

COLD SURFACES
Tunneling microscopy of superconductors and tunneling barriers
[AD-A212120] 04 p0559 N90-13257

COLD TOLERANCE
Pre-treatment with tyrosine reverses hypothermia induced behavioral depression
[AD-A215211] 09 p1252 N90-17265
Sensations of temperature and humidity during intermittent exercise and the influence of underwear knit structure
[AD-A215285] 09 p1252 N90-17266
Psychological and physiological responses of blacks and caucasians to hand cooling
[AD-A215646] 09 p1253 N90-17272
Evaluation of physiological and psychological impairment of human performance in cold stressed subjects
[AD-A223635] 24 p3498 N90-29769
Optimism and cardiovascular reactivity to psychological and cold pressor stress
[AD-A223818] 24 p3498 N90-29771
Coping strategies and mood during cold weather training
[AD-A223915] 24 p3498 N90-29773

COLD WALLS
U COLD SURFACES
U WALLS

COLD WATER
Use of self-induced hypnosis to modify thermal balance during cold water immersion
[AD-A216156] 10 p1412 N90-18140
Insulation, compressibility and absorbency of dry suit undergarments
[AD-A215944] 10 p1414 N90-18149
A range-dependent analysis of acoustic transmission across a cold filament in the California current
[AD-A220175] 18 p2583 N90-24709

COLD WEATHER
Definition of research needs to address airport pavement distress in cold regions
[DOT/FAA/DS-89/13] 02 p0157 N90-10896
Effects of serial wet-dry-wet cold exposure: Thermal balance, physical activity, and cognitive performance
[AD-A212704] 04 p0524 N90-13025
Some practical advice on cold weather clothing
[AD-A215936] 10 p1414 N90-18148
Feasibility of using lasers and infrared heaters as UNREP icing countermeasures
[AD-A219031] 19 p2695 N90-25333

Arctic cold weather medicine and accidental hypothermia
[AD-A223090] 20 p2899 N90-26487
Coping strategies and mood during cold weather training
[AD-A223915] 24 p3498 N90-29773

COLD WEATHER TESTS
Battery actuation of NITINOL at sub-zero temperatures
[AD-A211254] 02 p0216 N90-11237
Comparison of Goretex laminated and Dermoflex coated fabrics
[AD-A219383] 17 p2368 N90-23481

COLD WELDING
Microstructure/mechanical property relations in a mechanically alloyed aluminum
07 p0900 N90-15205

COLD WORKING
NT COLD ROLLING
NT EXPLOSIVE FORMING
A theoretical investigation of the column behavior of cold-formed square hollow sections
[PB89-225981] 06 p0797 N90-14645
A finite strip method for the elastic-plastic large displacement analysis of thin-walled and cold-formed steel sections
[PB89-226021] 06 p0798 N90-14647
Plastic bending tests of cold-formed rectangular hollow sections
[PB90-124611] 12 p1674 N90-19613
Ductile alloy encapsulated ceramic armor development
[AD-A217632] 14 p1954 N90-21183
A comparison of CuAlNi and other high damping alloys for the purpose of naval ship silencing applications
[AD-A218801] 16 p2221 N90-22671
Strengthening in heavily cold worked Cu-20 vol. percent Fe in situ composites
[DE90-011741] 22 p3135 N90-27790

COLLAGENS
Experiment K-6-01. Distribution and biochemistry of mineral and matrix in the femurs of rats
20 p2892 N90-26455

COLLAPSE
Numerical calculations of the collapse of a cavity in the vicinity of a compliant wall
[AD-A210489] 01 p0070 N90-10403
Nonlinear collapse simulation of anisotropic plates and corrugated panels 02 p0183 N90-11035
Investigation of collapse characteristics of cylindrical composite panels with large cutouts
[AD-A216378] 10 p1397 N90-18079
Pseudo-steady diffusional growth or collapse of bubbles rising in time dependent pressure fields
[AD-A218825] 16 p2237 N90-22764
Failure mechanism of urethane elastomer coated fabric collapsible fuel tanks
[AD-A221033] 18 p2530 N90-24435
Self-similar Langmuir collapse
[DE90-611310] 18 p2617 N90-24911
A historical supernova's lower limit to the galactic stellar-collapse rate
[FERMILAB-PUB-90/24-A] 22 p3262 N90-28472
Reliability analysis of maintained structural system vulnerable to fatigue and fracture
23 p3338 N90-28868
Characteristic microwave background distortions from collapsing domain wall bubbles
[NASA-CR-187270] 24 p3462 N90-29557

COLLECTION
Potential technologies for collection and destruction of CFCs (Chlorofluorocarbons), halons, and related compounds
[PB89-219968] 03 p0368 N90-12105
Beam collector and output window for a 35 GHz 100 kW gyrotron
[INPE-4958-RPE/603] 11 p1511 N90-18699
Semi-active orbital debris sweeper
[NASA-CASE-MSC-21534-1] 21 p2966 N90-26860
Robotic sampling system for an unmanned Mars mission 23 p3375 N90-29070

COLLECTORS
U ACCUMULATORS

COLLEGES
U UNIVERSITIES

COLLIMATION
An algorithm to calculate the beam momentum distribution from flying wire profiles
[DE89-015587] 01 p0073 N90-10418
Antenna beamforming using optical processing
[NASA-CR-180844] 02 p0212 N90-11210
Performance of the IMP array processing algorithm: First results
[RSRE-MEMO-4291] 15 p2148 N90-22274
Shaping radiation pattern of excimer laser by means of controllable intracavity mirror
16 p2310 N90-23166
Development of a hybrid adaptive beamformer
[AD-A219652] 17 p2471 N90-24128

COLLIMATORS
MEGALIDAR proof-of-concept demonstration
[AD-A218787] 16 p2255 N90-22858
Telescope considered as a very high gain antenna
[ETN-90-96614] 17 p2473 N90-24138
On the calibration of an autocollimator-comparator guide of a vertical target levelling rod differing from the ABBE's principle
[ISBN-951-754-887-7] 19 p2694 N90-25331
Small angle generating apparatus
[AD-D014467] 22 p3246 N90-28408

COLLISION AVOIDANCE
Safer skies with TCAS: Traffic Alert and Collision Avoidance System
[PB89-169221] 01 p0004 N90-10016
See and avoid/cockpit visibility
[DOT/FAA/CT-TN89/18] 02 p0148 N90-10843
Test and evaluation: Reducing risks to military aircraft from bird collisions. Report to the Chairman, Legislation, and National Security Subcommittee, Committee on Goverment Operations, House of Representatives
[AD-A210670] 02 p0148 N90-10845
Ground and Obstacle Avoidance (GOA) concept of operations
[DOT/FAA/DS-89/08] 02 p0150 N90-10855
UK airmisses involving commercial air transport, May-August 1988
[ISSN-0951-6301] 03 p0303 N90-11717
UK airmisses involving commercial air transport
[CAA-2/88] 03 p0303 N90-11718
An update to the system safety study of TCAS 2
[DOT/FAA/SA-89/3] 05 p0577 N90-13383
Field evaluation of a Nissan laser collision avoidance system
[PB90-105602] 06 p0722 N90-14215
Programmable near-infrared ranging system
[AD-D014237] 06 p0843 N90-14903
See and avoid/cockpit visibility
[AD-A214214] 07 p0877 N90-15084
The automatic detection of anti-collision lights
[RSRE-MEMO-4272] 08 p1019 N90-15896
UK airmisses involving commercial air transport, September to December 1988
[ISSN-0951-6301] 08 p1019 N90-15897
Development of an automatic ground collision avoidance system using a digital terrain database
[AD-A216247] 10 p1318 N90-17621
UK airmisses involving commercial air transport, January - April 1989
[ISSN-0951-6301] 16 p2197 N90-22544
Results of TCAS-2 simulations in reconstructed dangerous encounters (Jul. 1986 to Jun. 1989)
[ETN-90-96474] 17 p2349 N90-23375
Effects of monitoring under high and low taskload on detection of flashing and colored radar targets
[AD-A220313] 17 p2439 N90-23895
Numerical approach of collision avoidance and optimal control on robotic manipulators
19 p2736 N90-25552
A real-time robot arm collision detection system
[NASA-CR-185878] 20 p2915 N90-26582
The real-time learning mechanism of the Scientific Research Associates Advanced Robotic System (SRAARS) 21 p3046 N90-27312
High mountain flying in ski country, USA
[PB90-180316] 22 p3107 N90-27651
Safety net functions 22 p3113 N90-27685
Dynamic interaction of multiple autonomous mobile robots 23 p3333 N90-28844
A 17 degree of freedom anthropomorphic manipulator
23 p3362 N90-29001
Planning 3-D collision-free paths using spheres
23 p3367 N90-29024
UK airmisses involving commercial air transport: May - August 1989
[ISSN-0951-6301] 24 p3422 N90-29335
A collision avoidance system for a spaceplane manipulator arm 24 p3521 N90-29903
An Ada-based marine radar simulator for collision avoidance training
[ETN-90-97611] 24 p3531 N90-29970

COLLISION PARAMETERS
NT COLLISION RATES
Aspects of the physics of the standard model
[PREPRINT-670] 05 p0698 N90-14087
Model-independent analysis of the Z line shape in e+e- annihilation
[PREPRINT-679] 05 p0698 N90-14089
Polarization effects in ionizing collisions with Ne*(3-P2)- and Ne**(3-D3)-atoms
[ETN-90-96891] 17 p2471 N90-24127
Collision detection using linear programming
18 p2507 N90-24326
A real-time robot arm collision detection system
[NASA-CR-185878] 20 p2915 N90-26582

COLLISION RATES
Dissociation and vibrational relaxation of XeF by various collision partners
[AD-A210769] 02 p0227 N90-11300
A numerical solution to the Boltzmann equation for use in calculating pumping rates in a CO2 discharge laser
[AD-A216376] 11 p1514 N90-18718

COLLISION WARNING DEVICES
U COLLISION AVOIDANCE
U WARNING SYSTEMS

COLLISIONAL PLASMAS
NT STRONGLY COUPLED PLASMAS
Simultaneous multiple frequency interferometry: An application of homodyne phase measurement
[DE89-013975] 01 p0126 N90-10719
Research on heating, instabilities, turbulence and RF emission from electric field dominated plasmas
[AD-A212122] 04 p0557 N90-13243
Time evolution of the electron swarm energy distribution function
[AD-A212967] 04 p0557 N90-13247
True asymptotic plasma-sheath matching with an asymptotically correct collisional presheath
[AD-A212857] 05 p0701 N90-14104
The 41st Annual Gaseous Electronics Conference
[AD-A214540] 12 p1715 N90-19851
Observations of plasma structure freezing scale at equatorial latitudes
[AD-A222529] 21 p3026 N90-27207
Support for the Forty-Second Annual Gaseous Electronics Conference
[AD-A222881] 21 p3073 N90-27473
Plasma cloaking: Air chemistry, broadband absorption, and plasma generation
[AD-A222044] 21 p3078 N90-27503

COLLISIONLESS PLASMAS
Hybrid particle-fluid approach to low-frequency turbulence in magnetically confined plasmas
[DE89-015904] 02 p0277 N90-11579
Radiative shocks with electron thermal conduction
02 p0293 N90-11670
Ion collection by probing objects in flowing magnetized plasmas
[DE90-001711] 06 p0845 N90-14916
Single fluid simulations of plasma openings switch behavior
[DE90-002643] 07 p0921 N90-15330
Longitudinal traveling waves bifurcating from Vlasov plasma equilibria 12 p1715 N90-19850
Relativistic stimulated Brillouin and Raman scattering in a laser-produced plasma
[DE90-613123] 14 p2028 N90-21627
On the relativistic Vlasov equation in guiding-center coordinates
[DE90-613241] 14 p2028 N90-21629
A self-consistent theory of radial transport of field-aligned current by microturbulence
[DE90-007920] 14 p2028 N90-21631
Rigorous upper bounds for turbulent transport in bounded systems: Passive advection and reversed-field pinches 15 p2168 N90-22390
Low-frequency oscillations in vlasov plasmas: The quadratic polarization approximation
[DE90-611309] 18 p2617 N90-24910

COLLISIONS
NT ATOMIC COLLISIONS
NT BIRD-AIRCRAFT COLLISIONS
NT COULOMB COLLISIONS
NT INELASTIC COLLISIONS
NT IONIC COLLISIONS
NT METEORITE COLLISIONS
NT MIDAIR COLLISIONS
NT MOLECULAR COLLISIONS
NT PARTICLE COLLISIONS
The temporal development of collision cascades in the binary collision approximation
[DE89-015860] 01 p0122 N90-10699
The time evaluation of the number of space probes and debris at different orbit heights with a view to a future collision risk in space
[R-8718] 03 p0311 N90-11772
Global environmental effects of impact-generated aerosols: Results from a general circulation model
[DE89-008033] 03 p0368 N90-12106
Granular flow: Numerical simulation of dry granular flows and calculation of hydrodynamic interactions in suspensions
[DE89-017544] 06 p0777 N90-14518
Dust bands in the asteroid belt
[NASA-CR-186301] 07 p1014 N90-15873

Anomalous waves in shock wave - fluid interface collisions
[AD-A213584] 08 p1062 N90-16144
Colliding natural convection boundary layer flow in a rectangular enclosure
[DE90-005397] 10 p1384 N90-18009
Zodiacal dust bands: Their relation to asteroid families
[AD-A216025] 11 p1590 N90-19170
Hydrodynamical simulations of collisions between interstellar clouds
[DE90-006921] 11 p1590 N90-19172
Present and future risk of satellite and manned platforms collisions with other space objects and particles on earth orbits
[R-8841] 12 p1615 N90-19287
Present and future risk of collision of satellites and manned platforms with other space objects and particles in terrestrial orbit
[R-8840] 12 p1615 N90-19288
Satellites and debris in earth revolution orbits and first estimation of the collision probability
[R-8709] 12 p1615 N90-19289
Project for the European space organization in the area of space debris
[REPT-29/89] 12 p1615 N90-19290
Large impact events and atmospheric evolution on the terrestrial planets 12 p1744 N90-20028
The n-p bremsstrahlung in heavy ion collision processes
[DE90-008542] 13 p1886 N90-20823
Computer simulation of time-dependent spherically symmetric spacetimes containing radiating fluids: Formalism and code tests 15 p2185 N90-22483
Fast plasma mixing: A new excitation method for CW gas lasers
[AD-A220290] 18 p2617 N90-24904
A computer simulation model for studying cervical spine injury prevention 19 p2721 N90-25476
Baryogenesis in extended inflation. 2: Baryogenesis via primordial black holes
[NASA-CR-182843] 20 p2941 N90-26735
Atmospherically induced optical contamination from orbiting thrusters
[AD-A223112] 21 p3021 N90-27174
Structure and dynamics of excited atoms
[AD-A221973] 21 p3074 N90-27474
Survival of carbon grains in shocks 21 p3090 N90-27567
Nature and origin of interstellar diamond from the Allende CV3 meteorite 21 p3092 N90-27581
Impact fracture experiments simulating interstellar grain-grain collisions 21 p3093 N90-27584
Collision forces for compliant projectiles
[NASA-TM-4203] 22 p3192 N90-28111
Planning 3-D collision-free paths using spheres 23 p3367 N90-29024

COLLOCATION
A multidomain spectral collocation method for the Stokes problem
[NASA-CR-181876] 03 p0396 N90-12266
A simulation study of the overdetermined geodetic boundary value problem using collocation
[AD-A211785] 04 p0518 N90-12990
A panel process for the calculation of the flow around a wing with front angle damping
[ETN-90-95367] 12 p1600 N90-19207
Conforming Chebyshev spectral collocation methods for the solution of laminar flow in a constricted channel
[NASA-CR-182011] 12 p1660 N90-19539
Methods for local gravity field approximation 13 p1834 N90-20532
Local gravity disturbance estimation from multiple-high-single-low satellite-to-satellite tracking 13 p1839 N90-20555
Analysis of altimetry over inland seas
[NASA-TM-100729] 13 p1840 N90-20566
A fast collocation method for transonic airfoil design 14 p1917 N90-20984
Fourier analysis of finite element preconditioned collocation schemes
[NASA-CR-182040] 16 p2304 N90-23128
A parallel least squares collocation conjugate gradient approach for the advection diffusion equation
[DE90-015965] 24 p3530 N90-29961

COLLOIDS
NT AEROSOLS
NT FOG
Analysis of surface modified colloidal silicas
[DE89-015849] 01 p0047 N90-10267
Interactions of hydrazines with colloidal constituents of soils 02 p0204 N90-11164
Laser light scattering as a probe of fractal colloid aggregates 09 p1222 N90-17097
Colloid and interface chemistry aspects of ceramics
[AD-A216715] 11 p1490 N90-18576
An analytical study of tribochemical phases with colloidal additives. Contributions made by energy filtering electron microscopy
[ECL-89-009] 17 p2374 N90-23521

COLOR
NT WATER COLOR
Multicolor electrochromic displays exploratory development
[AD-A212004] 03 p0303 N90-11721
Transport systems research vehicle color display system operations manual
[NASA-TM-101577] 03 p0306 N90-11736
Functional decor in the International Space Station: Body orientation cues and picture perception
[NASA-TM-102242] 05 p0675 N90-13931
Near-infrared polarimetry and spectroscopy of comets 07 p1011 N90-15857
Plant features measurements for robotics 08 p1156 N90-16695
Proximity compatibility and information display: The effects of space and color on the analysis of aircraft stall conditions
[AD-A214488] 09 p1260 N90-17309
Principles and formulation of solar reflecting and low infrared emitting coatings for defence use
[MRL-TR-89-2] 10 p1358 N90-17874
A multicolor imaging pyrometer 10 p1364 N90-17905
Eutrophication assessment through remote sensing techniques
[INPE-4932-PRE/1422] 10 p1398 N90-18083
Relationships between the aerial biomass from ground layers of cerrado and its spectral reflectance
[INPE-4848-PRE/1477] 11 p1521 N90-18760
Evaluation of selection techniques for multispectral bands employed in the discrimination of carbonatic rocks
[INPE-4850-TDL/365] 11 p1522 N90-18765
Psychological studies of visual cortical function
[AD-A217029] 11 p1541 N90-18872
The computation of color
[AD-A216531] 11 p1548 N90-18914
A model of incomplete chromatic adaptation for calculating corresponding colors
[DE90-006905] 11 p1567 N90-19016
Comet Halley: An optical continuum study 12 p1736 N90-19981
LANDSAT-5 data in the study of wheat and bean crops
[INPE-4746-RPE/580] 13 p1819 N90-20444
The intensity dependent spread model and color constancy 15 p2140 N90-22228
Image segmentation with detection of highlights and inter-reflections using color
[AD-A218710] 16 p2317 N90-23213
Hybrid diffractive-refractive telescope
[AD-A219241] 16 p2318 N90-23216
Coloring a graph optimally with two colors
[MEMO-820] 17 p2449 N90-23961
Exact coloring algorithm for weighted graphs applied to timetabling problems with lectures of different lengths
[MEMO-814] 18 p2592 N90-24747
An analysis of the contact sintering process in III-V solar cells
[NASA-TM-103179] 19 p2709 N90-25420
Multicolor infrared photodetector
[AD-D014511] 20 p2865 N90-26297
The color of polarization in cuprate superconductors 22 p3144 N90-27830
Comparison of methods of space color transformations for enhancement of colored images
[INPE-4977-PRE/1542] 23 p3341 N90-28881
A land navigation demonstration vehicle with a color map display for tactical use 24 p3430 N90-29375
Satellite navigation systems for land vehicles 24 p3430 N90-29376
Digital color representation
[DE90-014580] 24 p3524 N90-29924

COLOR (PARTICLE PHYSICS)
U QUANTUM CHROMODYNAMICS

COLOR CENTERS
Prospects for wavelength tunable lasers based on vacancy defects in alkaline-earth oxides
[DE90-001078] 06 p0789 N90-14592
Phase-sensitive optical detection of ballistic phonon pulses using frequency-modulation spectroscopy and persistent spectral holes
[AD-A221521] 21 p2979 N90-26930

COLOR CODING
The photo-colorimetric space as a medium for the representation of spatial data 16 p2268 N90-22927
Effect of extraneous color-coded targets on identification of targets on CRT displays
[AD-A219473] 17 p2436 N90-23879
Comparison of methods of space color transformations for enhancement of colored images
[INPE-4977-PRE/1542] 23 p3341 N90-28881
Information processing and perceptual characteristics of display design: The role of emergent features and objects
[AD-A223683] 24 p3558 N90-30133

COLOR ENHANCEMENT
U COLOR CODING

COLOR PERCEPTION
U COLOR VISION

COLOR PHOTOGRAPHY
Aerial photographs to support the fiscalization process of agriculture loans in the Irece-BA region
[INPE-4839-PRE/1468] 10 p1400 N90-18092
Photointerpretation with instruments for evaluation of environmental impact: Mata Atlantica in Cubata
[INPE-4910-PRE/1511] 11 p1531 N90-18817
Aerial photography as an aid for agricultural credit control
[INPE-5019-RPE/613] 14 p1999 N90-21455
National mapping program. Fact sheet: Black and white photographs. NHAP (National High Altitude Photography Program)
[PB90-185042] 21 p3015 N90-27139
Integration of multispectral SPOT imagery and panchromatic aerial photography for study in urban land use
[INPE-4967-PRE/1536] 22 p3194 N90-28125

COLOR TELEVISION
HDTV: A chance to enhance television colorimetry
[BBC-RD-1990/2] 18 p2543 N90-24515

COLOR VISION
The 1988 year end report for road following at Carnegie-Mellon
[NASA-CR-185967] 01 p0078 N90-10446
Filling or outlining shapes with color: The effects on a visual search task
[AD-A211067] 02 p0255 N90-11444
Eye movements and spatial pattern vision
[AD-A211650] 03 p0381 N90-12169
The effects of luminance boundaries on color perception
[AD-A216741] 11 p1539 N90-18860
The computation of color
[AD-A216531] 11 p1548 N90-18914
A new method for measuring the transmissivity of aircraft transparencies
[AD-A216953] 12 p1714 N90-19842
Stanford/NASA-Ames Center of Excellence in model-based human performance 15 p2143 N90-22241
Ames vision group research overview 15 p2143 N90-22242
The photo-colorimetric space as a medium for the representation of spatial data 16 p2268 N90-22927
The effects of luminance boundaries on color perception
[AD-A221544] 21 p3034 N90-27251

COLOR-COLOR DIAGRAM
An atlas of aperiodic variability in HMXB
[MPE-PREPRINT-158] 08 p1140 N90-16605
Multifrequency observations of Cyg X-2: X ray observations with Ginga 17 p2482 N90-24192
Studies of the possible X ray triple 4U1915-05 19 p2768 N90-25727
The Z/atoll classification 19 p2769 N90-25740
IUE observations of Cyg X-2 and Sco X-1: Accretion disks and the z-shaped curve 19 p2783 N90-25832

COLOR-MAGNITUDE DIAGRAM
The evolution and geometry of the outer parts of the small Magellanic cloud 14 p2040 N90-21697
An observational study of disk-population globular clusters 24 p3560 N90-30145

COLORADO
The interaction and variation of waves and turbulence from MST radar data
[AD-A212849] 05 p0670 N90-13906
Processes of community development and responses of ecosystems to climate change
[DE90-008640] 13 p1831 N90-20512
Temporal attributes of the ambient seismo-acoustic environment: La Junta, Colorado
[AD-A219369] 16 p2249 N90-22825
Examination of microburst development in Colorado thunderstorm for the 5 August 1982 case
[AD-A218478] 17 p2425 N90-23820

COLORATION
U COLOR

COLORIMETRY
HDTV: A chance to enhance television colorimetry
[BBC-RD-1990/2] 18 p2543 N90-24515

COLUMBIA (ORBITER)
Syncom 4 deploy, LDEF retrieval highlight 10-day Columbia flight
[NASA-NEWS-RELEASE-89-180] 05 p0594 N90-13448

COLUMBIUM
U NIOBIUM

COLUMBUS SPACE STATION
Aeritalia Space Systems Group, Turin, Italy
[EOARD-LR-89-041] 02 p0159 N90-10908
Key structures mechanical issues of the European Space Station and platform program Columbus 02 p0188 N90-11072
Columbus: A user's introduction
[ESA-BR-62] 08 p1036 N90-15989
DNSS: German/Norwegian work team Space Subsea. Environmental control and life support subsystems (technical matters), phase 2
[ETN-90-95905] 08 p1105 N90-16398
Keynote address 09 p1173 N90-16783
The DLR technology programme on space transportation 09 p1180 N90-16841
The 120 VDC test bed for Columbus power system 10 p1329 N90-17679
Solar array designs for Columbus elements 10 p1340 N90-17764
Columbus onboard FDIR concept 18 p2500 N90-24286
Distributed mission planning technology for Columbus 18 p2501 N90-24288
HERA and EVA co-operation scenarios 18 p2502 N90-24299
Robot-based equipment manipulation and transportation for the Columbus free flying laboratory 18 p2503 N90-24300
The large wheel actuator LDR 100-0: Development status and test results 18 p2539 N90-24487
Clamping device for pressurized module radiator panel 18 p2539 N90-24488
Progress in the design of a microgravity facility for in-orbit experiments 18 p2540 N90-24496
Detachable interface mechanism 18 p2540 N90-24497
Columbus scientific airlock 18 p2541 N90-24503
Electrical connector for operation in space 18 p2541 N90-24507
Technical characteristics and functions of different types of space stations 20 p2937 N90-26712
The US/International Space Station: Legal aspects of space objects and jurisdiction and control 20 p2937 N90-26713
Damage responsibility and liability in space stations 20 p2937 N90-26714
The International Space Station: The legal framework 20 p2938 N90-26716
Crossborder movements: Goods, personnel and technologies 20 p2939 N90-26722
Space Station intellectual property rights and US patent law 20 p2939 N90-26723
Space law put to the test by the International Space Station 20 p2939 N90-26727
CUIS user's manual
[ESA-TM-03] 22 p3132 N90-27775
Applications of X windows in astronautics: Status and prospects
[MBB-UO-0082-90-PUB] 22 p3238 N90-28365

COLUMNS
A theoretical investigation of the column behavior of cold-formed square hollow sections
[PB89-225961] 06 p0797 N90-14645

COLUMNS (PROCESS ENGINEERING)
Optimal processes described by a parabolic differential equation with control in the coefficients, part 4
[MEMO-785-PT-4] 05 p0689 N90-14016
Construction of a UV cell for micro-liquid chromatography
[PML-1989-B] 22 p3156 N90-27894

COMBAT
Aircraft live fire testing 02 p0154 N90-10879
Air Combat Environment Test and Evaluation Facility (ACETEF) 02 p0154 N90-10883
Electronic warfare: Reliable equipment needed to test Air Force's electronic warfare systems
[AD-A212952] 05 p0632 N90-13687
Predicting Air Combat Maneuvering (ACM) performance 09 p1258 N90-17294
Comparison of oculometer and head-fixed reticle with voice or switch and touch panel for data entry on a generic tactical air combat display
[AD-A217231] 13 p1855 N90-20646
Evaluation of speech recognizers for use in advanced combat helicopter crew station research and development
[NASA-CR-177547] 18 p2496 N90-24265
Time-optimal aircraft pursuit-evasion with a weapon envelope constraint
[NASA-CR-186640] 19 p2658 N90-25126
Development of a meta-analytic technique to assess stress effects
[AD-A220468] 19 p2723 N90-25487
Synthesis and validation of feedback guidance laws for air-to-air interceptions
[LR-615] 19 p2752 N90-25639
Combat aircraft control requirements for agility 23 p3272 N90-28517
Multiband imaging systems
[AD-A223969] 23 p3343 N90-28893
Performance-based measures of merit for tactical situation awareness 23 p3358 N90-28976
Counterair situation awareness display for Army aviation 23 p3359 N90-28982
The potential for digital databases in flight planning and flight aiding for combat aircraft 24 p3429 N90-29371

COMBINATIONS (MATHEMATICS)
On the 2-extendability of planar graphs
[AD-A210289] 01 p0112 N90-10642
On the asymptotic convergence of the simulated annealing algorithm in the presence of a parameter dependent penalization
[MEMO-COSOR-89-16] 05 p0684 N90-13984
Strong moderate deviation theorems
[MEMO-804] 11 p1555 N90-18954
Applications of polyhedral combinatorics to multicommodity flows and compact surfaces
[CWI-BS-R8921] 17 p2482 N90-24060
The systematic construction of a one-combinator basis
[RUU-CS-89-14] 18 p2601 N90-24809

COMBINATORIAL ANALYSIS
NT COMBINATIONS (MATHEMATICS)
NT PARTITIONS (MATHEMATICS)
NT PERMUTATIONS
Stochastic control theory, nonlinear structural mechanics and applied combinatorics
[AD-A209042] 01 p0114 N90-10657
On the decoder error probability of linear codes 04 p0486 N90-12793
Constructing a calculus of programs
[CWI-CS-R8914] 05 p0683 N90-13979
On the performance of on-line algorithms for partition problems
[MEMO-784] 05 p0689 N90-14015
Theoretical and experimental analyses of parallel combinatorial algorithms
[AD-A216407] 10 p1420 N90-18186
On the depth of combinatorial optimization problems
[MEMO-803] 11 p1554 N90-18946
Free indexation: Combinatorial analysis and a compositional algorithm
[AD-A218219] 13 p1869 N90-20724
Exact coloring algorithm for weighted graphs applied to timetabling problems with lectures of different lengths
[MEMO-814] 18 p2592 N90-24747
A simple output-sensitive algorithm for hidden surface removal
[RUU-CS-89-26] 18 p2592 N90-24751
Finding squares and rectangles in sets of points
[RUU-CS-89-10] 18 p2601 N90-24806
The systematic construction of a one-combinator basis
[RUU-CS-89-14] 18 p2601 N90-24809
An improved technique for output-sensitive hidden surface removal
[RUU-CS-89-32] 18 p2602 N90-24817
A RUTCOR project in discrete applied mathematics
[AD-A221191] 18 p2604 N90-24831
Some convergence results for probabilistic Tabu search
[MEMO-822] 18 p2605 N90-24840
Minimizing distortion and internal forces in truss structures by simulated annealing 18 p2644 N90-25055
Random pseudo-polynomial algorithms in combinatorial programming
[REPT-89-067] 19 p2744 N90-25597
Modular arithmetic and randomization for exact matroid problems: Extended abstract
[REPT-89-064] 19 p2751 N90-25628
Hopf-algebraic structure of combinatorial objects and differential operators
[NASA-CR-186360] 19 p2752 N90-25640
Combinatorial problems using a hypercube and Hamming graphs
[ETN-90-97240] 20 p2919 N90-26609
The image of weighted combinatorial problems
[REPT-88-017] 21 p3057 N90-27382
Integrated structural/control design via multiobjective optimization
[AD-A223088] 21 p3071 N90-27459
The combinatorics computation for Casimir operators of the symplectic Lie algebra and the application for determining the center of the enveloping algebra of a semidirect product
[DE90-627161] 23 p3388 N90-29136

COMBINED CYCLE POWER GENERATION
Study of power generation systems for CO2 collection: LNG combined cycle
[DE90-507881] 23 p3345 N90-28901

COMBUSTIBILITY
U FLAMMABILITY

COMBUSTIBLE FLOW
Upward flame spread on vertical walls
[PB89-214787] 01 p0039 N90-10217
Numerical simulation of detonation transfer between gaseous explosive layers
[MRL-RR-1-89] 01 p0069 N90-10395
Chemical reactions in turbulent mixing flows
[AD-A211240] 02 p0220 N90-11263
A planar reacting shear layer system for the study of fluid dynamics-combustion interaction
[NASA-TM-102422] 05 p0582 N90-13393
Combustion characteristics of sprays
[AD-A213651] 07 p0895 N90-15173
Development of an integrated BEM approach for hot fluid structure interaction
[NASA-CR-186214] 07 p0927 N90-15364
Response of a chemically reacting layer to streamwise vorticity
[NASA-TM-102288] 10 p1383 N90-18005
AFOSR/ONR (Air Force Office of Scientific Research/Office of Naval Research) Contractors' Meeting on Combustion Rocket Propulsion Diagnostics of Reacting Flow
[AD-A216094] 11 p1476 N90-18491
An investigation of flow structure, mixing and chemical reaction in combusting turbulent flows
[AD-A216739] 11 p1483 N90-18538
Modification and improvement of software for modeling multidimensional reacting fuel flows
[AD-A217789] 13 p1783 N90-20235
Numerical investigation of turbulent flame sheets
[AD-A218553] 16 p2215 N90-22635
Numerical simulation of turbulent combustion using vortex methods
[AD-A219624] 17 p2372 N90-23507
Topology of three-dimensional, variable density flows
[NASA-CR-186622] 17 p2402 N90-23683
Subsonic combustor flow modeling: State of the art of CFD techniques for reacting and combusting flow 20 p2810 N90-25991
Development of Planar Laser-Induced Fluorescence (PLIF) techniques for supersonic flows 21 p2974 N90-26900
AFOSR/ONR Contractors' Meeting on Combustion Rocket Propulsion Diagnostics of Reacting Flow
[AD-A224411] 24 p3441 N90-29432

COMBUSTION
NT AFTERBURNING
NT BOUNDARY LAYER COMBUSTION
NT DEFLAGRATION
NT EROSIVE BURNING
NT FUEL COMBUSTION
NT HYDROCARBON COMBUSTION
NT HYPERSONIC COMBUSTION
NT METAL COMBUSTION
NT NUCLEAR FUEL BURNUP
NT PROPELLANT COMBUSTION
NT SOLID PROPELLANT COMBUSTION
NT SOLID PROPELLANT IGNITION
NT SPONTANEOUS COMBUSTION
NT SUPERSONIC COMBUSTION
Consequence of condensed-phase formation in transient burning of TiHx/KClO in a closed system
[DE89-013922] 02 p0208 N90-11188
Analytical studies of three-dimensional combustion processes
[AD-A211903] 03 p0323 N90-11837
Experimental and computational study of combustion limits in natural-gas fueled internal combustion engines
[PB89-235196] 05 p0629 N90-13673
Thermochemical calculations with inert compounds
[FOA-C-20759-2.1] 05 p0630 N90-13677
Acoustic-vortical-combustion interaction in a solid fuel ramjet simulator 06 p0726 N90-14234
Comprehensive mechanisms for combustion chemistry: An experimental and numerical study with emphasis on applied sensitivity analysis
[DE90-003904] 08 p1041 N90-16017
Droplet vaporisation and combustion in microgravity 09 p1202 N90-16963
Heterogeneous combustion processes under microgravity conditions 09 p1202 N90-16965
A comparison of European and American microgravity combustion experimental techniques 09 p1202 N90-16966

Full scale study of a cabin fire in an A300 fuselage section
10 p1313 N90-17592
Non-contact temperature measurements in support of microgravity combustion experiments
10 p1363 N90-17900
Combustion process science and technology
10 p1366 N90-17916
AFOSR/ONR (Air Force Office of Scientific Research/Office of Naval Research) Contractors' Meeting on Combustion Rocket Propulsion Diagnostics of Reacting Flow
[AD-A216094] 11 p1476 N90-18491
Proceedings of a contractors meeting on Combustion Rocket Propulsion Diagnostics of Reacting Flow
[AD-A216445] 12 p1617 N90-19297
Simulation of thermal dynamics of a vaporizing coal-water droplet in a combustor
[DE90-005356] 12 p1621 N90-19317
Synthesis and properties of a novel catalyst for the combustion of methane
[PB90-127499] 12 p1622 N90-19320
Effect of barrier layers in burn-through experiments with 351-nm laser illumination
[DE90-006806] 12 p1667 N90-19577
An investigation of the mechanisms of solid state powder reaction in the combustion synthesis and sintering of high temperature materials
[DE90-007880] 13 p1777 N90-20198
A numerical investigation of the compressible mixing layer
[AD-A217738] 13 p1802 N90-20343
A technical and economic evaluation of oxygen-enriched combustion in diesel engines using water-emulsified fuels
[DE90-008095] 13 p1810 N90-20394
Full-scale air transport category fuselage burnthrough tests
[DOT/FAA/CT-TN89/65] 14 p1913 N90-20967
Study of new technique of solid combustible materials to determination of volatile elements by flame atomic absorption spectrophotometry
[DE90-612907] 14 p1947 N90-21147
On the use of external burning to reduce aerospace vehicle transonic drag
[NASA-TM-103107] 15 p2052 N90-21762
Saturated fluorescence measurements of the hydroxyl radical in laminar high-pressure flames
[NASA-CR-185218] 15 p2101 N90-22022
Rapid mass transfer in binary systems
16 p2332 N90-23289
Periphery camera system
[AD-A221281] 18 p2555 N90-24583
DURIP: Spontaneous Raman system for the study of enhanced combustion and non-thermal plasmas
[AD-A221410] 18 p2564 N90-24629
Thermodynamic and fluid mechanic analysis of rapid pressurization in a dead-end tube
18 p2631 N90-24990
Combustion instrumentation 20 p2811 N90-25996
Flight motor set 360L007 (STS-33R)
[NASA-CR-183979] 20 p2824 N90-26067
Supersonic reacting internal flow fields
[NASA-TM-103480] 20 p2829 N90-26094
Carbon deposition model for oxygen-hydrocarbon combustion. Task 6: Data analysis and formulation of an empirical model
[NASA-CR-183986] 20 p2829 N90-26095
Critical evaluation of Jet-A spray combustion using propane chemical kinetics in gas turbine combustion simulated by KIVA-2
[NASA-TM-103173] 20 p2843 N90-26170
Modeling of supersonic reacting flow fields
21 p2973 N90-26898
Four-step kinetics for methane and implications for turbulent combustion 21 p2975 N90-26906
Ignition and combustion characteristics of metallized propellants
[NASA-CR-186870] 21 p2976 N90-26911
Structure and radiation properties of turbulent diffusion flames
[PB90-218777] 22 p3155 N90-27887
The reduction of smoke emissions from Allison T56 engines
[ARL-PROP-R-182] 23 p3277 N90-28547
Energy Efficient Engine combustor test hardware detailed design report
[NASA-CR-168301] 23 p3279 N90-28554
Shock dynamics in the sub-nanometer femtosecond domain
[DE90-014390] 23 p3304 N90-28689
Study of the radical OH in a high pressure flame by resonant DRASC
[ONERA-RF-57/7131-PY] 23 p3305 N90-28692
Ignition and combustion of liquid propellants
[AD-A224150] 23 p3316 N90-28746
Radiative heat transfer
[PB90-247602] 23 p3327 N90-28813
Development of advanced combustion technology for medium and high speed natural gas engines
[PB90-198565] 23 p3331 N90-28836
Activities report for the IBDF-INPE project SEQE, year 1987
[INPE-4534-RPE/565] 23 p3415 N90-29298
A comparison of scramjet engine performances of various cycles
[NAL-TR-1042] 24 p3434 N90-29397

COMBUSTION CHAMBERS
NT DUMP COMBUSTORS
Combustor influence on fighter engine operability
01 p0035 N90-10193
Dynamic instability characteristics of aircraft turbine engine combustors 01 p0036 N90-10195
Recent developments in Ramjet pressure oscillation technology 01 p0036 N90-10199
Numerical simulation of pressure oscillations in a ramjet combustor 01 p0037 N90-10202
Evaluation of rocket motor exhaust and liner combustion by-products
[AD-A210747] 02 p0189 N90-11083
Steam cooled rich-burn combustor liner
[NASA-CASE-LEW-13609-1] 03 p0321 N90-11824
Investigation of combustion instability in ramjet combustors 06 p0739 N90-14303
System design and performance prediction of a free-piston Stirling engine/magnetic coupling/compressor assembly in a gas residential heat pump
[DE89-016070] 06 p0807 N90-14696
Solid fuel combustion chamber, phase 10
[LR-536] 08 p1038 N90-16000
Solid fuel combustion chamber
[LR-555] 08 p1038 N90-16001
Conceptual design for the space station Freedom modular combustion facility
[NASA-TM-102037] 08 p1053 N90-16087
Flow visualization using the laser light sheet method in vehicle aerodynamics and combustion chamber engineering 08 p1079 N90-16246
MHD integrated topping cycle project
[DE90-004141] 08 p1126 N90-16525
High-pressure promoted combustion chamber
[NASA-CASE-MSC-21470-1] 09 p1170 N90-16771
Full scale catalytic combustion of methane under atmospheric pressure
[DE89-772354] 10 p1351 N90-17835
MATE (Materials for Advanced Turbine Engines) Program, Project 3. Volume 2: Design, fabrication and evaluation of an oxide dispersion strengthened sheet alloy combustor liner
[NASA-CR-180892] 10 p1357 N90-17868
Chamber investigations of the fate of diesel emissions in the atmosphere, volume 1, task 3
[PB90-114422] 10 p1405 N90-18103
Chamber investigations of the fate of diesel emissions in the atmosphere. Volume 2: AMES assay and GCMS final data reports and gas phase projections
[PB90-114430] 10 p1405 N90-18104
Combustion instability in solid propellant rockets
[AD-A216740] 11 p1476 N90-18492
Simulation of thermal dynamics of a vaporizing coal-water droplet in a combustor
[DE90-005356] 12 p1621 N90-19317
The use of the gas feed system and the vitiator for the solid fuel combustion chamber
[LR-528] 12 p1623 N90-19329
Development of ceramic combustor for low BTU gases. Design and basic combustion characteristics
[DE89-782287] 12 p1629 N90-19363
Calibration of the sonic measuring and control cross section in the gas feed installation of the solid fuel combustion chamber
[LR-552] 12 p1661 N90-19548
Design of a pyrometer for temperature measurements on the solid fuel combustion chamber
[LR-530] 12 p1664 N90-19561
Hydrocarbon-fuel/combustion-chamber-liner materials compatibility
[NASA-CR-185203] 14 p1950 N90-21165
The modelling of heat and mass transfer near solid boundaries and comparison with experimental results
[PB90-167040] 14 p1974 N90-21310
Microgravity acoustic mixing for particle cloud combustors
[NASA-CR-185159] 14 p2023 N90-21600
On the direct simulation of vortex shedding
[LR-513] 15 p2048 N90-21743
The pyrolysis of polymethylmethacrylate during combustion in a solid fuel combustion chamber
[LR-531] 15 p2068 N90-21845
Solid fuel combustion chamber
[LR-562] 15 p2068 N90-21846
Solid fuel combustion chamber
[LR-591] 15 p2068 N90-21847
Cooling of rocket thrust chambers with liquid oxygen
[NASA-TM-103146] 16 p2210 N90-22605
Introducing the VRT gas turbine combustor
[NASA-TM-103176] 17 p2386 N90-23591
Metallized fuel particle size study in a solid fuel ramjet
[AD-A220079] 18 p2533 N90-24451
Rocket combustion chamber life-enhancing design concepts
[NASA-CR-185257] 19 p2669 N90-25183
Effect of vane twist on the performance of dome swirlers for gas turbine airblast atomizers
[NASA-TM-103195] 19 p2688 N90-25289
Measurement of velocity and temperature profiles at the exit plane of a tubular gas turbine combustor
[DE90-505519] 20 p2809 N90-25983
Combustion in the gas turbine. Part 1: Combustor types and design
[CIT/SME/VKI/RS/1] 20 p2810 N90-25986
Combustion in the gas turbine. Part 2: Preliminary design and performance
[CIT/SME/VKI/RS/3] 20 p2810 N90-25987
Aircraft exhaust emissions: An engine manufacturer's perspective
[PNR90675] 20 p2812 N90-26004
Hard start problem of the apogee engine for the ETS-6
[DE90-505525] 20 p2825 N90-26072
Development of ceramic fiber type combustor: Improvement of combustor and combustion test results
[DE90-503441] 20 p2839 N90-26148
Development of ceramic hybrid combustor: Design and combustion test results
[DE90-503442] 20 p2839 N90-26149
A heat transfer analysis for rough turbine airfoils
[AD-A221942] 21 p2960 N90-26831
Ramjet and ramrocket propulsion systems for missiles
21 p2973 N90-26897
Modeling of supersonic reacting flow fields
21 p2973 N90-26898
Flame extinction in compressible flow
21 p2973 N90-26899
Development of Planar Laser-Induced Fluorescence (PLIF) techniques for supersonic flows
21 p2974 N90-26900
Concentration, temperature, and density in a hydrogen-air flame by excimer-induced Raman scattering 21 p2974 N90-26903
Modeling of knock in spark-ignition engines
[DE90-010875] 22 p3182 N90-28058
Reliability analysis of a structural ceramic combustion chamber
[NASA-TM-103264] 22 p3192 N90-28112
Energy Efficient Engine combustor test hardware detailed design report
[NASA-CR-168301] 23 p3279 N90-28554
Energy Efficient Engine (E3) combustion system component technology performance report
[NASA-CR-168274] 23 p3279 N90-28555
Energy efficient engine pin fin and ceramic composite segmented liner combustor sector rig test report
[NASA-CR-179534] 23 p3281 N90-28567
Development of comprehensive numerical schemes for predicting evaporating gas-droplets flow processes of a liquid-fueled combustor
[NASA-CR-187018] 23 p3305 N90-28693
Solid fuel combustion chamber
[LR-634] 24 p3441 N90-29433

COMBUSTION CHEMISTRY
Critical reaction rates in hypersonic combustion chemistry
[DE89-014278] 02 p0156 N90-10892
Transport phenomena and interfacial kinetics in multiphase combustion systems
[AD-A212932] 05 p0621 N90-13620
A theoretical model of double base propellant combustion
[ONERA-RTF-23/7128-EY] 05 p0629 N90-13672
Comprehensive mechanisms for combustion chemistry: An experimental and numerical study with emphasis on applied sensitivity analysis
[DE90-003904] 08 p1041 N90-16017
Fire science and aircraft safety
10 p1314 N90-17596
Time development of convection flow patterns in aircraft cabins under post-crash fire exposure
10 p1314 N90-17598
Fire hardening of an aircraft passenger cabin
10 p1315 N90-17606
Studies on reactive flows 15 p2066 N90-21831
Ternary reactions among polymer substrate-organohalogen-antimony oxides under pyrolytic, oxidative and flaming conditions
[PB90-154766] 15 p2071 N90-21861

Oxidation and ignition characteristics of hydrocarbon fuels
[AD-A218666] 16 p2215 N90-22637
Gas Turbine Combustion, volume 1
[VKI-LS-1990-02-VOL-1] 20 p2810 N90-25985
Turbulent combustion modeling for turbo-jet combustion chambers 20 p2811 N90-25993
Chemistry of combustion processes 20 p2811 N90-25994
Critical evaluation of Jet-A spray combustion using propane chemical kinetics in gas turbine combustion simulated by KIVA-2
[NASA-TM-103173] 20 p2843 N90-26170
Non-premixed turbulent CO/H2 flames at local extinction conditions 21 p2975 N90-26907
The computer modeling of the combustion and extinction of methane-air premixed flames by thermally stable gases
[PB90-189432] 21 p2976 N90-26910

COMBUSTION CONTROL
Evaporation and combustion of dense sprays with a bimodal droplet size distribution 02 p0192 N90-11094
Feedback control of combustion instabilities: A case study in active adaptive control of complex physical systems
[AD-A215385] 09 p1192 N90-16905
Control of titanium diboride SHS reactions by inert dilutions and mechanical constraint
[AD-A214378] 10 p1357 N90-17870

COMBUSTION EFFICIENCY
Cycle analysis of scramjet engines
[NAL-TR-1002] 01 p0008 N90-10035
Direct numerical simulation of turbulent free shear flows
[AD-A210161] 01 p0040 N90-10218
Homogeneous catalysts in hypersonic combustion
[DE89-015258] 02 p0193 N90-11098
Aircraft propulsion: Leading the way in aviation
[LR-532] 05 p0583 N90-13395
Steady flow combustion model for solid-fuel ramjet projectiles
[BRL-TR-2987] 07 p0893 N90-15163
Factors that may influence responses of the US transportation sector to policies for reducing greenhouse gas emissions
[DE90-000704] 07 p0958 N90-15543
Cluster based reaction probabilities for boron with oxygen, hydrogen, water, nitrogen, nitrous oxide, carbon dioxide, carbon monoxide, methane, tetrafluoromethane, and silane
[AD-A214554] 09 p1190 N90-16894
Full scale catalytic combustion of methane under atmospheric pressure
[DE89-772354] 10 p1351 N90-17835
US Army Methanol-Fueled Administrative Vehicle Demonstration Program
[AD-A216013] 10 p1393 N90-18054
Overview of the methodologies used to compile large scale emissions inventories
[DE90-008518] 13 p1830 N90-20509
Metallized fuel particle size study in a solid fuel ramjet
[AD-A220079] 18 p2533 N90-24451
Effect of vane twist on the performance of dome swirlers for gas turbine airblast atomizers
[NASA-TM-103195] 19 p2688 N90-25289
A low NOx strategy for combusting high nitrogen content fuels
[PB90-155664] 19 p2712 N90-25435
Gas Turbine Combustion, volume 1
[VKI-LS-1990-02-VOL-1] 20 p2810 N90-25985
Pollutants: Production and methods of reduction
[CIT/SME/VKI/RS/6] 20 p2810 N90-25990
Subsonic combustor flow modeling: State of the art of CFD techniques for reacting and combusting flow 20 p2810 N90-25991
Supersonic combustor modeling 20 p2810 N90-25992
Turbulent combustion modeling for turbo-jet combustion chambers 20 p2811 N90-25993
Subsonic combustor testing 20 p2811 N90-25997
Supersonic combustor testing 20 p2811 N90-25998
Heat engines
[DE90-000485] 20 p2882 N90-26393
Raman scattering measurements using UV excimer lasers 21 p2974 N90-26902
Calculation of the combustion distribution in a liquid-fuel ramjet 22 p3162 N90-27931
An investigation of solid-fuel, dual-mode combustion ramjets 22 p3162 N90-27933
Photo-sensitized ignition of hydrogen/oxygen mixtures for hypersonic flight vehicles 22 p3163 N90-27935
Energy Efficient Engine combustor test hardware detailed design report
[NASA-CR-168301] 23 p3279 N90-28554
Energy Efficient Engine (E3) combustion system component technology performance report
[NASA-CR-168274] 23 p3279 N90-28555
Energy efficient engine program technology benefit/cost study. Volume 1: Executive summary
[NASA-CR-174766-VOL-1] 23 p3280 N90-28564
Energy efficient engine program technology benefit/cost study, volume 2
[NASA-CR-174766-VOL-2] 23 p3280 N90-28565
Energy Efficient Engine: Combustor component performance program
[NASA-CR-179533] 23 p3281 N90-28568
Performance measurements and energy balance of an SPS V160 Stirling motor at the German Aerospace Research Establishment
[DLR-MITT-90-03] 23 p3345 N90-28903
Solid fuel combustion chamber
[LR-534] 24 p3441 N90-29433

COMBUSTION HEAT
U HEAT OF COMBUSTION

COMBUSTION INSTABILITY
U COMBUSTION STABILITY

COMBUSTION PHYSICS
Evaporation and combustion of dense sprays with a bimodal droplet size distribution 02 p0192 N90-11094
Droplet combustion experiment drop tower tests using models of the space flight apparatus
[NASA-TM-101472] 02 p0209 N90-11196
Facilities for microgravity combustion research
[NASA-TM-102014] 05 p0630 N90-13679
Solid fuel combustion chamber, phase 10
[LR-536] 08 p1038 N90-16000
MHD integrated topping cycle project
[DE90-004141] 08 p1126 N90-16525
Combustion Experiments During KC-135 Parabolic Flights
[ESA-SP-1113] 09 p1201 N90-16958
Polymer group microgravity combustion experiment 09 p1202 N90-16964
Chemical reactions in turbulent mixing flows
[AD-A216273] 10 p1355 N90-17856
Microgravity noncontact temperature requirements at NASA Lewis Research Center 10 p1362 N90-17897
Non-contact temperature measurements in support of microgravity combustion experiments 10 p1363 N90-17900
Effect of propellant flowrate and purity on carbon deposition in LO2/methane gas generators 11 p1471 N90-18468
Theoretical investigation of the stabilization of a diffusion flame above a recirculation region
[ESA-TT-1149] 11 p1484 N90-18543
On the dynamics of the combustion process of hydrogen-air and hydrogen-methane-air mixtures
[DLR-FB-89-39] 11 p1485 N90-18548
Spacelab qualified infrared imager for microgravity science experiments
[NASA-TM-102503] 13 p1804 N90-20352
Modeling of combustion processes in a solid fuel particle
[DE90-009140] 16 p2214 N90-22629
Experimental study of mixing and combustion processes in a solid-propellant ducted rocket motor 17 p2367 N90-23472
Contributions to the study of parietal flames due to turbulent diffusion
[ECL-89-22] 17 p2374 N90-23519
Structure of monopropellant spray flames at elevated pressures
[AD-A218676] 17 p2383 N90-23570
Thermodynamic and fluid mechanic analysis of rapid pressurization in a dead-end tube 18 p2631 N90-24990
Mars in situ propellants: Carbon monoxide and oxygen ignition experiments
[NASA-TM-103202] 20 p2823 N90-26065
New findings and instrumentation from the NASA Lewis microgravity facilities
[NASA-TM-103189] 20 p2842 N90-26163
Critical evaluation of Jet-A spray combustion using propane chemical kinetics in gas turbine combustion simulated by KIVA-2
[NASA-TM-103173] 20 p2843 N90-26170
Computational experience with a three-dimensional rotary engine combustion model
[NASA-TM-103104] 20 p2861 N90-26275
Summary of Discussions at the Eleventh Meeting of the Sandia Cooperative Group on the Aerothermochemistry of Turbulent Combustion
[DE89-001846] 21 p2973 N90-26896
PDF modeling of chemical nonequilibrium effects in turbulent nonpremixed jet flames 21 p2975 N90-26908
Scalar dissipation measurements in the developing region of a jet 21 p2976 N90-26909
Pyrolysis and combustion of solid fuels under both subsonic and supersonic conditions 22 p3161 N90-27929
Combustion characteristics of oxygen/hydrogen high pressure preburners for staged combustion cycle rocket engine
[NAL-TR-1044] 24 p3441 N90-29434

COMBUSTION PRODUCTS
A simulator for a hydrocarbon ramrocket fuel gas generator: First phase development
[AR-005-621] 02 p0189 N90-11080
Evaluation of rocket motor exhaust and liner combustion by-products
[AD-A210747] 02 p0189 N90-11083
Homogeneous catalysts in hypersonic combustion
[DE89-015258] 02 p0193 N90-11098
A remote sensor to monitor combustion products using a tunable acousto-optic filter 02 p0223 N90-11275
Transport phenomena and interfacial kinetics in multiphase combustion systems
[AD-A212932] 05 p0621 N90-13620
The mobile combustion diagnostic fixture and its application to the study of propellant combustion. Part 1: Investigation of the low pressure combustion of LOVA XM39 propellant
[AD-A213272] 05 p0621 N90-13626
A new simulation method for the efficient calculation of benchmarks for detonation products equations of state
[DE90-001837] 06 p0777 N90-14522
Environmental quality and the shift to alternative fuels: Progress and interim findings of a Department of Energy study of transition in vehicular power systems
[DE90-002178] 06 p0810 N90-14716
Analysis of acid rain and associated phenomena
[DE90-002555] 06 p0812 N90-14725
Characterization of chemicals on engine exhaust particles
[AD-A213566] 07 p0882 N90-15106
Spectral studies of solid propellant combustion. 2: Emission and absorption results for M-30 and HMX1 propellants
[AD-A213857] 07 p0915 N90-15292
Long-term worldwide environmental effects caused by acid rain from fossil fuels
[DE90-001534] 07 p0956 N90-15533
Global climate change: A fossil energy perspective
[DE90-003770] 07 p0958 N90-15541
HCl monitor, phase 2
[AD-A213572] 07 p0958 N90-15542
Workshop on the Effects of Combined Fire Products on Human Physiological and Psychological Performance
[AD-A215465] 09 p1253 N90-17270
Method for the evaluation of toxicity of combustion products from aircraft cabin materials: Analysis and results 10 p1316 N90-17612
Modelling time to incapacitation and death from toxic and physical hazards in aircraft fires 10 p1318 N90-17619
Chamber investigations of the fate of diesel emissions in the atmosphere, volume 1, task 3
[PB90-114422] 10 p1405 N90-18103
Chamber investigations of the fate of diesel emissions in the atmosphere. Volume 2: AMES assay and GCMS final data reports and gas phase projections
[PB90-114430] 10 p1405 N90-18104
A fossil energy perspective on global climate change
[DE90-007894] 14 p2004 N90-21483
Device for quickly sensing the amount of O2 in a combustion product gas
[NASA-CASE-LAR-13816-1] 15 p2102 N90-22025
Formation kinetics of N2O in the atmosphere 20 p2886 N90-26425
Atmospheric dispersion of solid and liquid rocket propellants
[AD-A221293] 21 p3020 N90-27173
The reduction of smoke emissions from Allison T56 engines
[ARL-PROP-R-182] 23 p3277 N90-28547
Spectroscopic study of combustion diagnostics on hydroxyl radicals
[NASA-CR-186998] 23 p3305 N90-28694
The distribution of middle tropospheric carbon monoxide during early October 1984
[NASA-TM-103485] 23 p3346 N90-28906

COMBUSTION STABILITY
NT FLAME STABILITY
Combustion Instabilities in Liquid-Fuelled Propulsion Systems
[AGARD-CP-450] 01 p0035 N90-10191
Combustion instabilities in liquid-fueled propulsion systems: An overview 01 p0035 N90-10192
Experimental study on the stability of small rocket engines with storable liquid propellants 01 p0036 N90-10196

Low frequency and high frequency combustion oscillation phenomena inside a rocket combustion chamber fed by liquid or gaseous propellants
01 p0036 N90-10197
Effects of low-frequency instabilities on the operation of Ramjet air inlets 01 p0036 N90-10198
Reheat buzz: An acoustically coupled combustion instability 01 p0036 N90-10200
Attenuation of reheat buzz by active control
01 p0036 N90-10201
Numerical simulation of unsteady combustion in a dump combustor 01 p0037 N90-10203
Very-low-frequency oscillations in liquid-fueled ramjets
01 p0037 N90-10204
Oscillations in non-axisymmetric dump combustors
01 p0037 N90-10205
Acoustic-vortex-chemical interactions in an idealized ramjet 01 p0037 N90-10206
Combustion-driven oscillation in large combustion systems for power generation 01 p0038 N90-10207
Upward flame spread on vertical walls
[PB89-214787] 01 p0039 N90-10217
LOX/hydrocarbon combustion instability investigation
[NASA-CR-182249] 05 p0615 N90-13589
A surface coupled flamelet approach to dynamic response in heterogeneous propellant combustion
06 p0739 N90-14302
Investigation of combustion instability in ramjet combustors 06 p0739 N90-14303
Feedback control of combustion instabilities: A case study in active adaptive control of complex physical systems
[AD-A215385] 09 p1192 N90-16905
Combustion instability in solid propellant rockets
[AD-A216740] 11 p1476 N90-18492
On the dynamics of the combustion process of hydrogen-air and hydrogen-methane-air mixtures
[DLR-FB-89-39] 11 p1485 N90-18548
Premixed turbulent flame propagation
[AD-A219834] 17 p2373 N90-23515
An evaluation of imbedded thermocouples as a solid-propellant combustion diagnostic
[AD-A219947] 17 p2406 N90-23711
Combustor design and analysis using the Rocket Combustor Interactive Design (ROCCID) methodology
[NASA-TM-103165] 18 p2513 N90-24349
A comparison of analytical results for 20 K LOX/hydrogen instabilities
[NASA-TM-103166] 19 p2670 N90-25186
Gas Turbine Combustion, volume 1
[VKI-LS-1990-02-VOL-1] 20 p2810 N90-25985
Combustion in the gas turbine. Part 3: Fuel injection, ignition and stability
[CIT/SME/VKI/RS/4] 20 p2810 N90-25988
Liquid fueled ramjet combustion instability: Acoustical and vortical interactions with burning sprays
[AD-A222752] 20 p2831 N90-26104
Calculation of the combustion distribution in a liquid-fuel ramjet 22 p3162 N90-27931
Numerical simulations of flowfields in a central-dump ramjet combustor. 3: Effects of chemistry
[AD-A224145] 23 p3282 N90-28573
Oxygen/methane combustion stability investigation
23 p3293 N90-28628
Combustion instability coupling with feed system acoustics 23 p3293 N90-28629
Tripropellant combustion process
23 p3293 N90-28631

COMBUSTION TEMPERATURE
Program for high speed computation of physical properties of propellants and combustion gas of an LH2/LOX rocket engine
[NAL-TM-564] 03 p0318 N90-11803
A theoretical model of double base propellant combustion
[ONERA-RTF-23/7128-EY] 05 p0629 N90-13672
Combustion of n-butane and isobutane in an internal combustion engine: A comparison of experimental and modeling results
[DE90-005993] 18 p2522 N90-24400
Swirl coaxial injector element characterization for booster engines 23 p3294 N90-28632

COMBUSTION WAVES
U FLAME PROPAGATION

COMBUSTORS
U COMBUSTION CHAMBERS

COMET HEADS
Analysis of energy spectra of the ions in the coma of Halley's comet for the evaluation of the production ratio of methane and ammonia
[ETN-90-96489] 18 p2638 N90-25026

COMET NUCLEI
Hypervelocity impact studies on the Giotto comet Halley mission 06 p0862 N90-15008
The volatile composition of comets
[NASA-CR-186281] 07 p1014 N90-15871
Workshop on Analysis of Returned Comet Nucleus Samples
[NASA-CR-184821] 08 p1140 N90-16607
Analytical study of comet nucleus samples
08 p1140 N90-16608
On the isotope analysis of cometary dust
08 p1141 N90-16611
Direct determination of the morphology, structure and composition of cometary and interstellar ice analogs in the laboratory 08 p1141 N90-16612
Electron beam analysis of particulate cometary material 08 p1141 N90-16613
Thermal and chemical processing of the outermost layer of cometary nuclei 08 p1141 N90-16614
Analysis of organic compounds in returned comet nucleus samples 08 p1142 N90-16617
Trace element abundance determinations by Synchrotron X Ray Fluorescence (SXRF) on returned comet nucleus mineral grains 08 p1142 N90-16619
From interstellar dust to comets
08 p1142 N90-16620
Comments on comet shapes and aggregation processes 08 p1142 N90-16622
Cosmogenic nuclides in cometary materials: Implications for rate of mass loss and exposure history
08 p1143 N90-16623
Morphology and compositional differentiation of the surface of comets 08 p1143 N90-16624
Role of dust to gas production rate ratio in cometary physics 08 p1143 N90-16625
Spectrophotometric observations of comet P/Giacobini-Zinner 08 p1144 N90-16630
Candidate sample acquisition systems for the Rosetta
08 p1145 N90-16635
Interstellar and cometary dust
08 p1145 N90-16636
The in-situ cometary particulate size distribution measured for one comet: P/Halley
08 p1145 N90-16637
Evolution of carbonaceous chondrite parent bodies: Insights into cometary nuclei 08 p1145 N90-16638
The comet rendezvous asteroid flyby mission
08 p1145 N90-16639
Measurements of long-lived cosmogenic nuclides in returned comet nucleus samples
08 p1146 N90-16640
What if chondritic porous interplanetary dust particles are not the real McCoy 08 p1146 N90-16642
Handling and analysis of ices in cryostats and glove boxes in view of cometary samples
08 p1146 N90-16643
Thermal histories of the samples of two KOSI comet nucleus simulation experiments
08 p1147 N90-16645
Analysis of particulates of comet nucleus samples: Possible use of olivine as indicator phase
08 p1147 N90-16646
Methods for the mineralogical and textural analysis of comet nucleus samples 08 p1147 N90-16648
Non-destructive trace element microanalysis of as-received cometary nucleus samples using synchrotron x ray fluorescence 08 p1147 N90-16649
Mechanical and SEM analysis of artificial comet nucleus samples 08 p1148 N90-16650
Electron Spin Resonance (ESR) studies of returned comet nucleus samples 08 p1148 N90-16651
Physical processing of cometary nuclei
08 p1148 N90-16653
Isotopic microanalysis of returned comet nucleus samples 08 p1149 N90-16655
Physics and Mechanics of Cometary Materials
[ESA-SP-302] 12 p1738 N90-19989
Rosetta/CNSR, ESA's planetary cornerstone mission
12 p1738 N90-19990
Physical models of cometary nuclei: A review
12 p1738 N90-19991
Petrographic working model of the Rosetta sampling and modelling subgroup for a comet nucleus
12 p1738 N90-19992
Design and development activities on the candidate sample acquisition system for the Rosetta mission
12 p1738 N90-19993
Comets: Dirty snowballs or icy dirtballs
12 p1739 N90-19994
A test of the interstellar dust model of comets
12 p1739 N90-19995
Physical processes in cometary ices inferred from laboratory studies 12 p1739 N90-19996
Laboratory studies of cometary ice analogues
12 p1739 N90-19997
Evolution of ices and carbonaceous materials in the laboratory and in comets 12 p1739 N90-19998
Thermal conductivities and diffusivities of porous ice samples at low pressures and temperatures and possible modes of heat transfer in near surface layers of comets
12 p1739 N90-19999
Physico-chemical properties of formaldehyde-ice-dust mixtures 12 p1740 N90-20000
Stable isotope studies of cometary analogue materials
12 p1740 N90-20001
Compressive strength of synthetic comet nucleus samples 12 p1741 N90-20006
Thermal perturbation of comet samples during their acquisition 12 p1741 N90-20008
Rosetta/CNSR altimeter and sounding radar
12 p1741 N90-20009
Hot OH and CN: Evidence for organic molecules close to the nucleus of comet Halley
12 p1742 N90-20012
Some considerations on cohesive forces in sun-grazing comets 12 p1742 N90-20015
Gas diffusion in a cometary crust
12 p1742 N90-20017
Porosity and ice-dust mixtures in cometary particles
12 p1743 N90-20018
Dynamics of crust formation and dust emission of comet nucleus analogues under isolation
12 p1743 N90-20020
Relevance of laboratory studies to comets
12 p1743 N90-20023
The thermo-mechanical behavior of cometary nuclei
14 p2041 N90-21703
Carbon in comet dust 21 p3089 N90-27564
Dust emission by Comet P/Halley 1982i
24 p3563 N90-30159

COMET RENDEZVOUS ASTEROID FLYBY MISSION
The comet rendezvous asteroid flyby mission
08 p1145 N90-16639
Relevance of laboratory studies to comets
12 p1743 N90-20023

COMET TAILS
Disturbance structures and its magnetic field features in plasma comet tail
[DE90-610636] 12 p1737 N90-19986
A mechanism for the formation of knots, kinks and discontinuous events in the plasma tail of comets
[DE90-613285] 14 p2041 N90-21707
The production and spatial distribution of neutral and ionized water vapor in Comet P/Halley
15 p2185 N90-22484
Nongravitational forces by Halley's comet
[ETN-90-96491] 18 p2638 N90-25027

COMETARY ATMOSPHERES
Near-infrared polarimetry and spectroscopy of comets
07 p1011 N90-15857
The volatile composition of comets
[NASA-CR-186281] 07 p1014 N90-15871
Role of dust to gas production rate ratio in cometary physics 08 p1143 N90-16625
Sulfur compounds in comets
08 p1143 N90-16627
The comet rendezvous asteroid flyby mission
08 p1145 N90-16639
What if chondritic porous interplanetary dust particles are not the real McCoy 08 p1146 N90-16642
Comet Halley: An optical continuum study
12 p1736 N90-19981
A test of the interstellar dust model of comets
12 p1739 N90-19995
Thermal conductivities and diffusivities of porous ice samples at low pressures and temperatures and possible modes of heat transfer in near surface layers of comets
12 p1739 N90-19999
Physico-chemical properties of formaldehyde-ice-dust mixtures 12 p1740 N90-20000
Gas diffusion in a cometary crust
12 p1742 N90-20017
Porosity and ice-dust mixtures in cometary particles
12 p1743 N90-20018
The composition of cometary nuclei
12 p1743 N90-20022
Kinematic models of cometary comae
15 p2188 N90-22495
Optical properties of cometary dust
[AD-A218790] 16 p2338 N90-23325
Laboratory studies of photodissociation processes relevant to the formation of cometary radicals
20 p2947 N90-26772
Carbon in comet dust 21 p3089 N90-27564
Carbon-rich particles in Comet Halley
21 p3089 N90-27565

COMETS
NT COMET HEADS
NT COMET NUCLEI
NT COMET TAILS
NT GIACOBINI-ZINNER COMET
NT HALLEY'S COMET
NT IRAS-ARAKI-ALCOCK COMET
Dust bands in the asteroid belt
[NASA-CR-186301] 07 p1014 N90-15873
Laboratory simulations of the solar wind-comet interactions 07 p1015 N90-15875

Workshop on Analysis of Returned Comet Nucleus Samples
[NASA-CR-184821] 08 p1140 N90-16607
The origin, composition and history of cometary ices from spectroscopic studies 08 p1140 N90-16609
Experimental studies of gas trapping in amorphous ice and thermal modelling of comets: Implications for Rosetta 08 p1140 N90-16610
On the isotope analysis of cometary dust 08 p1141 N90-16611
Electron beam analysis of particulate cometary material 08 p1141 N90-16613
The carbon chemistry of meteorites: Relationships to comets 08 p1141 N90-16615
Laboratory analyses of micron-sized solid grains: Experimental techniques and recent results 08 p1141 N90-16616
Non-equilibrium chemistry in the solar nebula and early solar system: Implications for the chemistry of comets 08 p1142 N90-16618
Modifications of comet materials by the sublimation process: Results from simulation experiments 08 p1142 N90-16621
Comments on comet shapes and aggregation processes 08 p1142 N90-16622
Cosmogenic nuclides in cometary materials: Implications for rate of mass loss and exposure history 08 p1143 N90-16623
Role of dust to gas production rate ratio in cometary physics 08 p1143 N90-16625
Radiation modification of cometary materials: Laboratory simulations 08 p1143 N90-16626
Spectrophotometric observations of comet P/Giacobini-Zinner 08 p1144 N90-16630
Prompt Gamma Activation Analysis (PGAA): Technique of choice for nondestructive bulk analysis of returned comet samples 08 p1144 N90-16633
Candidate sample acquisition systems for the Rosetta 08 p1145 N90-16635
Interstellar and cometary dust 08 p1145 N90-16636
Evolution of carbonaceous chondrite parent bodies: Insights into cometary nuclei 08 p1145 N90-16638
The comet rendezvous asteroid flyby mission 08 p1145 N90-16639
Measurements of long-lived cosmogenic nuclides in returned comet nucleus samples 08 p1146 N90-16640
Metamorphism of cosmic dust: Processing from circumstellar outflows to the cometary regolith 08 p1146 N90-16641
What if chondritic porous interplanetary dust particles are not the real McCoy 08 p1146 N90-16642
Trajectory-capture cell instrumentation for measurement of dust particle mass, velocity and trajectory, and particle capture 08 p1146 N90-16644
The nature of cometary materials 08 p1147 N90-16647
Methods for the mineralogical and textural analysis of comet nucleus samples 08 p1147 N90-16648
Mechanical and SEM analysis of artificial comet nucleus samples 08 p1148 N90-16650
Ion bombardment experiments suggesting an origin for organic particles in pre-cometary and cometary ices 08 p1148 N90-16652
Physical processing of cometary nuclei 08 p1148 N90-16653
The measurement of trace elements in interplanetary dust and cometary particles by ultra-high sensitivity INAA 08 p1149 N90-16656
Infrared cometary spectroscopy 11 p1578 N90-19086
Analogies between cometary, interplanetary, and interstellar matter 11 p1578 N90-19087
The unidentified IR bands in laboratory, in interstellar medium, and in comets 11 p1578 N90-19089
A unified model for the 3.28 micron and 3.4 micron spectral feature in the interstellar medium and in comets 11 p1579 N90-19092
Interpretation of the 10 micron and 20 micron absorption bands in comets, the interstellar medium, and in an external galaxy 11 p1579 N90-19093
Disturbance structures and its magnetic field features in plasma comet tail
[DE90-610636] 12 p1737 N90-19986
Physics and Mechanics of Cometary Materials
[ESA-SP-302] 12 p1738 N90-19989
A test of the interstellar dust model of comets 12 p1739 N90-19995
Laboratory studies of cometary ice analogues 12 p1739 N90-19997
Evolution of ices and carbonaceous materials in the laboratory and in comets 12 p1739 N90-19998
Thermal conductivities and diffusivities of porous ice samples at low pressures and temperatures and possible modes of heat transfer in near surface layers of comets 12 p1739 N90-19999
Crustal strength of different model comet materials 12 p1740 N90-20003
Fracture mechanical aspects of dust emission processes from a model comet surface 12 p1740 N90-20004
Simulation of radar and radiometer signals remote sensing cometary surface and subsurface structures 12 p1740 N90-20005
Rosetta/CNSR altimeter and sounding radar 12 p1741 N90-20009
Cometary bodies in the circumstellar disk around beta Pictoris 12 p1741 N90-20010
A method of estimating temperature profiles and chemical differentiation in the near surface layers of porous comet nuclei: First results for comet P/Churyumov-Gerasimenko 12 p1742 N90-20013
CO2 depth profiles in cometary model substances of KOSI 12 p1742 N90-20014
Some considerations on cohesive forces in sun-grazing comets 12 p1742 N90-20015
Possible targeting of particle emission by mechanical stress and penetration of sublimating ice-dust-surfaces 12 p1742 N90-20016
Gas diffusion in a cometary crust 12 p1742 N90-20017
Porosity and ice-dust mixtures in cometary particles 12 p1743 N90-20018
Dynamics of crust formation and dust emission of comet nucleus analogues under isolation 12 p1743 N90-20020
First impressions of the comet drilling problem 12 p1743 N90-20021
Large impact events and atmospheric evolution on the terrestrial planets 12 p1744 N90-20028
A mechanism for the formation of knots, kinks and discontinuous events in the plasma tail of comets
[DE90-613285] 14 p2041 N90-21707
Optical properties of cometary dust
[AD-A218790] 16 p2338 N90-23325
Dust environment modelling from encounters with comet P/Halley 17 p2485 N90-24210
Laboratory studies of photodissociation processes relevant to the formation of cometary radicals 20 p2947 N90-26772
Optical constraints of kerogen from 0.15 to 40 microns: Comparison with meteoritic organics 20 p2948 N90-26776
Study of the polyoxymethylene and its sputtered fragments: Implications for comets 20 p2949 N90-26781
Photon sputtering of H2O ices: A preliminary report 20 p2949 N90-26783
Carbon in the Galaxy: Studies from Earth and Space
[NASA-CP-3061] 21 p3089 N90-27562
Interstellar grain chemistry and organic molecules 21 p3090 N90-27569
The possible presence of interstellar PAHs in meteorites and interplanetary dust particles 21 p3092 N90-27579
Laboratory simulation of interstellar grain chemistry and the production of complex organic molecules 21 p3092 N90-27580
The Tempel 2 dust trail
[AD-A224395] 24 p3562 N90-30153
IUE-ULDA access guide no. 2: International Ultraviolet Explorer-Uniform Low Dispersion Archive: Comets
[ESA-SP-1134] 24 p3563 N90-30157
Dust emission by Comet P/Halley 1982i 24 p3563 N90-30159

COMFORT
Human factors: The human interface with aircraft interiors
[NIAR-90-18] 20 p2900 N90-26496
Teleoperator comfort and psychometric stability: Criteria for limiting master-controller forces of operation and feedback during telemanipulation 23 p3364 N90-29009

COMMAND AND CONTROL
Conceptual design of a synchronous Mars telecommunications satellite
[NASA-TP-2942] 01 p0141 N90-10814
Identification Friend, Foe or Neutral Joint Test 02 p0154 N90-10881
Requirements specification with Petri nets using the cube tool methodology
[AD-A212190] 04 p0492 N90-12829
Design and performance of an on-satellite laser diagnostic system for a free space optical heterodyne frequency-shift-keyed communication system
[AD-A211986] 04 p0505 N90-12915
Telerobotic control for teams of semi-autonomous agents, phase 1
[AD-A211648] 04 p0526 N90-13037
Algorithm development for SDI weapons system allocation
[AD-A212973] 04 p0534 N90-13090
Contribution to the study of a self-protected static switch and its command strategy
[ECL-89-002] 05 p0636 N90-13711
Applications of artificial intelligence to space station and automated software techniques: High level robot command language
[NASA-CR-182997] 05 p0686 N90-13991
Propagation-based decision aids in the U.S. Navy 06 p0757 N90-14410
Delta 181 sensor module command center
[AD-A214868] 09 p1182 N90-16855
A specification and analysis of the IEEE (Institute of Electrical and Electronic Engineers) token ring protocol
[AD-A214567] 09 p1269 N90-17359
Definition of a management information system to support performance risk assessment
[AD-A215464] 09 p1297 N90-17516
Performance analysis of Aloha networks with power capture and near/far effect
[AD-A218739] 16 p2229 N90-22717
JPL control/structure interaction test bed real-time control computer architecture 16 p2294 N90-23070
Throughput and delay characteristics for a slow-frequency hopped aircraft-to-aircraft packet radio network
[AD-A220525] 17 p2389 N90-23609
Software techniques for non-von Neumann architectures
[AD-A220390] 17 p2440 N90-23902
Northeast Artificial Intelligence Consortium annual report, 1988. Volume 12: Computer architectures for very large knowledge bases
[AD-A219599] 17 p2454 N90-23999
Automated control of hierarchical systems using value-driven methods 19 p2735 N90-25547
Functional description of a command and control language tutor 19 p2739 N90-25587
A research program in computer technology
[AD-A221184] 19 p2746 N90-25606
Automatic information processing and high performance skills: Application to training
[AD-A221709] 21 p3036 N90-27259
DEVS-based intelligent control of space adapted fluid mixing 21 p3040 N90-27279
Command and control in the age of space-based surveillance 21 p3069 N90-27445
Replay and transmission of AIMS-data to mainframe computer using remote transcribers 22 p3105 N90-27634
Distributed database concepts for command and control information systems
[FFI-90/7005] 22 p3260 N90-28462
Research in command and control for the Dutch Army Corps (1NL)
[IZF-1989-28] 23 p3318 N90-28760
Experiments in the dynamic and strategic control of cooperating manipulators 23 p3333 N90-28845

COMMAND LANGUAGES
NT QUERY LANGUAGES
DOD Gateway Information System (DGIS) common command language: A retrospective on the introduction of prolog as the development tool
[AD-A211941] 03 p0418 N90-12400
A user's manual for the method of moments Aircraft Modeling Code (AMC)
[NASA-CR-186371] 11 p1456 N90-18390
Adjustable impedance, force feedback and command language aids for telerobotics (parts 1-4 of an 8-part MIT progress report) 23 p3363 N90-29007

COMMAND SERVICE MODULES
Incorporation of a progressive failure analysis method in the CSM testbed software system 18 p2640 N90-25036

COMMAND-CONTROL
U COMMAND AND CONTROL

COMMERCE
Assessing the accuracy of vulnerability models by comparison with vulnerability experiments
[AD-A210871] 01 p0116 N90-10669
The economic impact of automation technology
[AD-A213363] 05 p0630 N90-13682
Small business innovation research: Program solicitation
[NASA-TM-101869] 05 p0705 N90-14126
Total quality management implementing plan: Office of small and disadvantaged business utilization
[AD-A212865] 05 p0705 N90-14129
Program manager's handbook
[AD-A214338] 07 p1009 N90-15844
An investigation into the effects which aerospace industry offset trade agreements have on United States Air Force mission performance
[AD-A215093] 09 p1294 N90-17502

COCOM (Coordinating Committee for Multilateral Exports), technology transfer and its impact on national security
[AD-A214569] 09 p1297 N90-17519
From invention to innovation: Commercialization of new technology by independent and small business inventors
[DE90-006944] 12 p1727 N90-19927
Quality at a glance
[AD-A217297] 14 p1989 N90-21400
Small business innovation research. Abstracts of 1988 phase 1 awards
[NASA-TM-102991] 14 p2036 N90-21680
Small business innovation research. Abstracts of completed 1987 phase 1 projects
[NASA-TM-101797] 14 p2036 N90-21681
Federal Aviation Administration small business innovation research 5-year project summaries
[AD-A221590] 21 p3086 N90-27546
Time-based competition for competitive advantage: An information technology perspective
[AD-A224474] 23 p3407 N90-29255
Software development: A product life-cycle perspective
[AD-A223783] 24 p3528 N90-29952

COMMERCIAL AIRCRAFT
NT A-300 AIRCRAFT
NT A-310 AIRCRAFT
NT A-320 AIRCRAFT
NT BOEING 727 AIRCRAFT
NT BOEING 737 AIRCRAFT
NT BOEING 747 AIRCRAFT
NT BOEING 757 AIRCRAFT
NT DC 10 AIRCRAFT
NT EUROPEAN AIRBUS
NT L-1011 AIRCRAFT
NT SUPERSONIC COMMERCIAL AIR TRANSPORT
UK airmisses involving commercial air transport
[CAA-2/88] 03 p0303 N90-11718
International Aircraft Occupant Safety Conference and Workshop proceedings
[AD-A214452] 07 p0877 N90-15085
UK airmisses involving commercial air transport, September to December 1988
[ISSN-0951-6301] 08 p1019 N90-15897
Human factors issues in aircraft maintenance and inspection
[AD-A215724] 11 p1542 N90-18875
Aircraft accident report, United Airlines Flight 811, Boeing 747-122, N4713U, Honolulu, Hawaii, February 24, 1989
[PB90-910401] 15 p2050 N90-21748
First-order weight corrections for real-time flight path management
[LR-580] 15 p2050 N90-21751
Aircraft drawings index 17 p2343 N90-23340
AVION: A detailed report on the preliminary design of a 79-passenger, high-efficiency, commercial transport aircraft
[NASA-CR-186663] 17 p2353 N90-23395
High speed civil transport
[NASA-CR-186661] 17 p2353 N90-23396
The 30th Airlines International Electronics Meeting Proceedings
[ETN-90-96973] 18 p2495 N90-24261
Study of high-speed civil transports. Summary
[NASA-CR-4236] 20 p2806 N90-25966
Knowledge-based system for flight information management
[NASA-TM-102685] 20 p2903 N90-26511
BASEOPS default profiles for civil aircraft
[AD-A223161] 21 p2959 N90-26825
World jet airplane inventory at year-end 1989
[PB90-207218] 23 p3267 N90-28489
Life cycle cost in the conceptual design of subsonic commercial aircraft, volumes 1 and 2
23 p3275 N90-28535
Airline productivity relating on the fuel cost. (2): Fuel consumption values and fuel efficiency
[NAL-TM-604-2] 24 p3422 N90-29333
UK airmisses involving commercial air transport: May - August 1989
[ISSN-0951-6301] 24 p3422 N90-29335

COMMERCIAL AVIATION
U CIVIL AVIATION
U COMMERCIAL AIRCRAFT

COMMERCIAL SPACECRAFT
US commercial launcher summary
09 p1174 N90-16793
Financial and commercial issues: A customer's perspective 09 p1174 N90-16794
Launch insurance: Its role in the future development of commerce in space 09 p1174 N90-16795
Legal aspects of commercial space transportation
09 p1175 N90-16796
Advanced onboard propulsion benefits and status
[NASA-TM-103174] 22 p3134 N90-27786

COMMINUTION
NT CRUSHING
Dust bands in the asteroid belt
[NASA-CR-186301] 07 p1014 N90-15873

COMMONALITY
Preliminary design of a family of three close air support aircraft
[NASA-CR-186070] 09 p1166 N90-16751
Knowledge representation for commonality
21 p3041 N90-27285
General test plan 22 p3120 N90-27721
Ring laser gyro marine inertial navigation systems
24 p3426 N90-29355

COMMUNICATING
NT AIRCRAFT COMMUNICATION
NT CONVERSATION
NT GROUND-AIR-GROUND COMMUNICATION
NT INFORMATION DISSEMINATION
NT MESSAGES
NT NASCOM NETWORK
NT SELECTIVE DISSEMINATION OF INFORMATION
NT VERBAL COMMUNICATION
Desk top publishing: What you need to know
15 p2178 N90-22449
Pictorial communication: Pictures and the synthetic universe 16 p2267 N90-22919

COMMUNICATION
NT OPTICAL COMMUNICATION
NT UNDERWATER COMMUNICATION
Technical communications in aeronautics: Results of an exploratory study. An analysis of managers' and nonmanagers' responses
[NASA-TM-101625] 02 p0288 N90-11647
Rotorcraft low altitude CNS benefit/cost analysis: Rotorcraft operations data
[DOT/FAA/DS-89/9] 03 p0419 N90-12406
Technical communications in aeronautics: Results of an exploratory study. An analysis of profit managers' and nonprofit managers' responses
[NASA-TM-101626] 07 p1009 N90-15848
Activities report of the Institute for Communication Technology
[ETN-90-95383] 12 p1747 N90-20043
NASA Information Sciences and Human Factors Program
[NASA-TM-4190] 15 p2194 N90-22529
Message handling in the post-2000 era: Executive summary
[AD-A219983] 17 p2393 N90-23628
Interdisciplinary research: Promoting collaboration between the life sciences and medicine and the physical sciences and engineering 17 p2478 N90-24171
Solid-state lasers for coherent communication and remote sensing
[NASA-CR-186634] 20 p2866 N90-26306
Communications Interface Driver (CID) test plan
[DOT/FAA/CT-TN89/35] 23 p3319 N90-28762

COMMUNICATION CABLES
NT BEAM WAVEGUIDES
NT CIRCULAR WAVEGUIDES
NT COAXIAL CABLES
NT OPTICAL FIBERS
NT OPTICAL WAVEGUIDES
NT PLASMAGUIDES
NT RECTANGULAR WAVEGUIDES
NT WAVEGUIDES
Coherent multilchannel techniques for integrated broadband communications subscriber lines
[AD-A209323] 01 p0055 N90-10312

COMMUNICATION EQUIPMENT
NT CLOSED CIRCUIT TELEVISION
NT DIPLEXERS
NT RADIO RECEIVERS
NT SATELLITE TELEVISION
NT SUPERHETERODYNE RECEIVERS
NT TRANSMITTER RECEIVERS
Independent Orbiter Assessment (IOA) CIL issues resolution report, volume 3
[NASA-CR-185524-VOL-3] 02 p0170 N90-10956
Independent Orbiter Assessment (IOA): Analysis of the communication and tracking subsystem
[NASA-CR-185582] 02 p0172 N90-10967
Independent Orbiter Assessment (IOA): Assessment of the communication and tracking subsystem, volume 1
[NASA-CR-185528-VOL-1] 03 p0315 N90-11789
Independent Orbiter Assessment (IOA): Assessment of the communication and tracking subsystem, volume 2
[NASA-CR-185528-VOL-2] 03 p0315 N90-11790
Independent Orbiter Assessment (IOA): Assessment of the communication and tracking subsystem, volume 3
[NASA-CR-185528-VOL-3] 03 p0315 N90-11791
Baseband development system implementation
[AD-A213464] 07 p0918 N90-15309
X-band atmospheric attenuation for an Earth terminal measurement system
[PB90-100736] 08 p1056 N90-16101
Helsinki University of Technology Radio Laboratory
[PB90-110677] 08 p1056 N90-16102
An approach to the development of software for computer-aided design of satellite communications receivers for operation in scintillating channels
[AD-A215299] 09 p1267 N90-17349
AIRNET: A real-time comunications network for aircraft
[NASA-CR-186140] 18 p2543 N90-24514
Development of an all silicon integrated optical modulator for high speed data communications and sensor applications
[AD-A220270] 18 p2547 N90-24535

COMMUNICATION NETWORKS
NT DEEP SPACE NETWORK
NT LOCAL AREA NETWORKS
NT NASCOM NETWORK
Network analyzer for nonstatic jamming
[AD-A210759] 02 p0212 N90-11216
A contribution to the synthesis of communication switching systems with decentralized control using modular components
[ETN-89-94660] 02 p0214 N90-11226
Influence of ionospheric variations on high-reliability HF systems utilizing large bases 02 p0248 N90-11404
Satellite-matrix-switched, time-division-multiple-access network simulator
[NASA-TP-2944] 03 p0336 N90-11915
DOD Gateway Information System (DGIS) common command language: A retrospective on the introduction of prolog as the development tool
[AD-A211941] 03 p0418 N90-12400
A literature study of wave propagation in the 1-60 GHz range. Application to transportable military communication systems
[FEL-1988-47] 04 p0491 N90-12825
Data handling and telecommunications
05 p0604 N90-13514
Data Link Processor (DLP) operational test and evaluation/integration test plan
[DOT/FAA/CT-TN89/32] 06 p0757 N90-14404
Configuration development for ROMENET
[AD-A213367] 06 p0765 N90-14450
Multiple crossbar network: A switched high-speed local network
[DE90-001839] 06 p0831 N90-14833
Network simulator definition
[AD-A213463] 07 p0918 N90-15308
Voice/data integration in mobile radio networks: Overview and future research directions
[AD-A214289] 07 p0919 N90-15319
The first year's work of race project 1036 WTDM broadband customer premises network
[BBC-RD-1989/6] 08 p1055 N90-16097
Performance of cellular frequency-hopped spread-spectrum radio networks
[AD-A214480] 09 p1204 N90-16978
Packet Radio Integrated System Module (PRISM): Design document
[AD-A214723] 09 p1205 N90-16981
An approach to the development of software for computer-aided design of satellite communications receivers for operation in scintillating channels
[AD-A215299] 09 p1267 N90-17349
An adaptive ARQ (Automatic Repeat Request) strategy for packet switching data communication networks
[AD-A216597] 11 p1497 N90-18615
Rate compatible punctured codes, their use in military satellite communication systems
[AD-A216723] 11 p1497 N90-18619
Low earth orbiting satellite for international information exchange system
[DE90-007186] 12 p1615 N90-19292
Packet radio networks under dynamic jamming
[AD-A217094] 12 p1648 N90-19475
Express cubes: Improving the performance of k-ary n-cube interconnection networks
[AD-A217117] 13 p1793 N90-20287
Fault tolerant hypercube computer system architecture
[NASA-CASE-NPO-16859-1-CU] 14 p2012 N90-21527
Alternative parallel ring protocols
15 p2150 N90-22282
Modelling high data rate communication network access protocol 15 p2150 N90-22285
Extensibility and limitations of FDDI
15 p2151 N90-22286
Fairness problems at the media access level for high-speed networks 15 p2151 N90-22287
A knowledge-based system with learning for computer communication network design
15 p2157 N90-22319
Document delivery via ISDN or satellite networks
15 p2178 N90-22446

Performance analysis of Aloha networks with power capture and near/far effect
[AD-A218739] 16 p2229 N90-22717
RF network selection in a rule-based system. NOSC project ZE68: Cost metric algorithms for internetwork applications
[AD-A219389] 16 p2301 N90-23116
NASA 60 GHz intersatellite communication link definition study. Addendum A: Mixed baseband and IF signals
[NASA-CR-186337] 17 p2387 N90-23593
NASA 60 GHz intersatellite communication link definition study. Baseline document
[NASA-CR-186339] 17 p2387 N90-23594
NASA 60 GHz intersatellite links definition study. Final Review
[NASA-CR-186338] 17 p2387 N90-23595
Single mode communication link
[AD-A219499] 17 p2388 N90-23601
Detecting black holes in packet-radio networks (SRNTN-56)
[AD-A219636] 17 p2389 N90-23604
Throughput and delay characteristics for a slow-frequency hopped aircraft-to-aircraft packet radio network
[AD-A220525] 17 p2389 N90-23609
Northeast Artificial Intelligence Consortium. Volume 4. Distributed AI for communications network management
[AD-A218717] 17 p2453 N90-23994
Some issues related to simulation of the tracking and communications computer network
18 p2630 N90-24988
CLEAR: Automating control centers with expert system technology
19 p2733 N90-25533
OMS FDIR: Initial prototyping
19 p2738 N90-25562
A new technique in the global reliability of cyclic communications network
[NASA-TM-103479] 20 p2851 N90-26214
A novel communication network simulator
[AD-A223045] 20 p2857 N90-26248
Overview of requirements and networks for voice communications and speech processing
21 p2992 N90-27007
Advanced Communication Processing Techniques
[AD-A223244] 21 p2996 N90-27027
Communications network analysis tool
[AD-A222061] 21 p2996 N90-27029
Stand-alone terrestrial and satellite networks for nationwide interoperation of broadband networks
[PB90-172404] 22 p3164 N90-27942
Communications and media services
22 p3258 N90-28449
Secure Data Network System (SDNS) network, transport, and message security protocols
[PB90-198946] 23 p3318 N90-28757
The NASA/OAST telerobot testbed architecture
23 p3365 N90-29016
Coordinating the activities of a planner and an execution agent
23 p3369 N90-29035
Design of a monitor and simulation terminal (master) for space station telerobotics and telescience
23 p3372 N90-29051
PLRS: A new spread spectrum position location reporting system
24 p3427 N90-29358
Enhancing PLRS with user-to-user data capability
24 p3427 N90-29359
Using minimal spanning trees to compare the reliability of network topologies
[NASA-TM-4208] 24 p3539 N90-30014

COMMUNICATION SATELLITES
NT ACTS
NT AERONAUTICAL SATELLITES
NT COMMUNICATIONS TECHNOLOGY SATELLITE
NT DIRECT BROADCAST SATELLITES
NT EUROPEAN COMMUNICATIONS SATELLITE
NT INTELSAT SATELLITES
NT MARECS MARITIME SATELLITES
NT MOLNIYA SATELLITES
NT MSAT
NT SYNCOM SATELLITES
Conceptual design of a synchronous Mars telecommunications satellite
[NASA-TP-2942] 01 p0141 N90-10814
Test results on conceptual models of the large deployable antenna for mobile communications satellites
02 p0185 N90-11050
Petite Amateur Navy Satellite (PANSAT)
[NASA-CR-186049] 03 p0317 N90-11800
Satellite-matrix-switched, time-division-multiple-access network simulator
[NASA-TP-2944] 03 p0336 N90-11915
SLCSAT (Submarine Laser Communication Satellite) communication system design study
[AD-A213403] 07 p0917 N90-15304
Financial and commercial issues: A customer's perspective
09 p1174 N90-16794
Launch insurance: Its role in the future development of commerce in space
09 p1174 N90-16795
Legal aspects of commercial space transportation
09 p1175 N90-16796
Investigation of liquid sloshing in spin-stabilized satellites
[AD-A214730] 09 p1182 N90-16853
The spacebus power conditioning application to the Eutelsat 2 spacecraft
10 p1330 N90-17689
Analysis of power bus topologies used in telecommunications satellites
10 p1331 N90-17691
Structural design of the Telecom 2 solar array
10 p1343 N90-17786
The ITALSAT solar array
10 p1343 N90-17787
The electrical design of solar arrays for communication satellites
10 p1344 N90-17792
In-orbit performance of CS-3a spacecraft GaAs solar array
10 p1346 N90-17804
Performance measurements for a laboratory-simulated 30/20 GHz communication satellite transponder
[NASA-TM-102424] 10 p1376 N90-17977
Investigation of a photovoltaic/battery hybrid system for powering the high arctic data communications system
[AD-A218353] 13 p1798 N90-20319
Land mobile communications from non geostationary orbits (review of Archimedes ESA study)
[REPT-892-440-106] 17 p2392 N90-23624
A Communications Antenna Pointing System (CAPS): A modular approach
18 p2537 N90-24474
Tactical Applications of Space Systems
[AGARD-CP-460] 21 p3067 N90-27438
Lightweight EHF communications satellites
21 p3070 N90-27453
Advanced onboard propulsion benefits and status
[NASA-TM-103174] 22 p3134 N90-27786
Congestion-reduction and service-restoration strategies for telecommunication networks
[PB90-207838] 22 p3164 N90-27944
Approximation, synthesis, and development of bi-mode cavities microwave filters presenting unsymmetrical quasi-elliptic responses
[CNES-NT-124] 23 p3318 N90-28761

COMMUNICATION SYSTEMS
U TELECOMMUNICATION

COMMUNICATION THEORY
NT WORDS (LANGUAGE)
Determinism yields (event structure isomorphism equals step sequence equivalence)
[CWI-CS-R8839] 02 p0263 N90-11492
Book of abstracts of the 1st Benelux-Japan Workshop on Information and Communication Theory
[PB90-191446] 24 p3556 N90-30124

COMMUNICATIONS TECHNOLOGY SATELLITE
Activities report in DLR research field communication engineering and reconnaissance
[ISSN-0173-0118] 11 p1525 N90-18781

COMMUNITIES
Processes of community development and responses of ecosystems to climate change
[DE90-008640] 13 p1831 N90-20512
Updating a dosage-effect relationship for the prevalence of annoyance due to general transportation noise
[AD-A219416] 17 p2421 N90-23794

COMMUTATION
Minimal prime ideals in semigroups without nilpotent elements
[DE90-606957] 10 p1423 N90-18207

COMMUTATORS
Development of an all solid state 6 kHz pulse generator for driving free electron laser amplifiers
[AD-A224105] 24 p3463 N90-29561

COMMUTER AIRCRAFT
Preliminary design of four aircraft to service the California Corridor in the year 2010: The California Condor, California Sky-Hopper, high capacity short range transport tilt rotor aircraft needed to simplify intercity transportation
[NASA-CR-186232] 06 p0724 N90-14226
Low-speed wind-tunnel investigation of the flight dynamic characteristics of an advanced turboprop business/commuter aircraft configuration
[NASA-TP-2982] 12 p1606 N90-19239

COMPACT DISK READ-ONLY MEMORY DEVICES
U OPTICAL DISKS
U READ-ONLY MEMORY DEVICES

COMPACTING
Improving snow roads and airstrips in Antarctica
[AD-A211588] 03 p0335 N90-11907
RTM user's guide
[NASA-CR-186091] 04 p0531 N90-13065
Superconducting and microstructural properties of shock-compacted high-T sub c oxide powders
[DE90-000823] 06 p0853 N90-14958
Effects of shock-induced defects on flux pinning in YBa2Cu3O(7-delta)
[DE90-000824] 06 p0853 N90-14959
Shock-induced defects and flux pinning in YBa2Cu3O sub 7-delta + Ag composites
[DE90-000827] 06 p0853 N90-14960
Micro-scale simulation of dynamic compaction of oxide and metal powder mixture
[DE90-002220] 06 p0856 N90-14978
Ceramic processing using inorganic polymers
[DE90-003638] 07 p0911 N90-15268
Method for refining microstructures on prealloyed titanium powder compacts
[AD-D014280] 08 p1043 N90-16030

COMPARATORS
Characteristics of CMOS analog integrated structures using MOSIS (Metal Oxide Semiconductor Implementation System)
[DE90-001630] 07 p0998 N90-15773
On the calibration of an autocollimator-comparator guide of a vertical target levelling rod differing from the ABBE's principle
[ISBN-951-754-887-7] 19 p2694 N90-25331
Optical motion detector detecting visible and near infrared light
[AD-D014515] 19 p2758 N90-25671

COMPARISON
A performance comparison of integration algorithms in simulating flexible structures
01 p0021 N90-10101
Low-earth-orbit to low-lunar-orbit laser freighter
01 p0030 N90-10160
Perceived urgency of warning signals determined using a forced choice pair comparison technique
[RAE-TM-MM-12] 04 p0551 N90-13206
A comparison of European and American microgravity combustion experimental techniques
09 p1202 N90-16966
Gemini2: A second generation layout validation program
[AD-A220731] 17 p2444 N90-23926
The systematic construction of a one-combinator basis
[RUU-CS-89-14] 18 p2601 N90-24809
International application of the DLR test-system: First year of cooperation with IBERIA in pilot selection
[DLR-FB-90-05] 19 p2723 N90-25491
Improved meteorological measurements from buoys and ships (IMET): Preliminary comparison of pyranometers
[PB90-241936] 22 p3229 N90-28315
Improved meteorological measurements from buoys and ships (IMET): Preliminary comparison of precipitation sensors
[PB90-241902] 22 p3229 N90-28316
Norms and perception of events
[AD-A224236] 24 p3499 N90-29774

COMPARTMENTS
NT AIR LOCKS
NT AIRCRAFT COMPARTMENTS
NT ANECHOIC CHAMBERS
NT HYPERBARIC CHAMBERS
NT PRESSURE CHAMBERS
NT PRESSURIZED CABINS
NT SPACECRAFT CABINS
NT TEST CHAMBERS
NT VACUUM CHAMBERS

COMPASSES
Apparatus for and a method of determining compass headings
[AD-D014436] 16 p2199 N90-22551

COMPATIBILITY
NT ELECTROMAGNETIC COMPATIBILITY
NT SYSTEMS COMPATIBILITY
Improved performance polysulfide based sealant
08 p1022 N90-15910
Compatibility conditions of structural mechanics for finite element analysis
[NASA-TM-102413] 09 p1237 N90-17180
The integration of stores on modern tactical aircraft: Where we have been, and what we should do for the future
10 p1305 N90-17552
Fuel-elastomer compatibility studies: Results of 80 C/14-day exposure experiments
[AD-A216015] 10 p1361 N90-17893
Liquid oxygen LOX compatibility evaluations of aluminum lithium (Al-Li) alloys: Investigation of the Alcoa 2090 and MMC weldalite 049 alloys
12 p1636 N90-19398
Elastomer compatibility studies
[BR106069] 17 p2378 N90-23542
Imide/arylene ether copolymers
[NASA-CASE-LAR-14159-1-CU]
21 p2983 N90-26953
Materials for high-density electronic packaging and interconnection
[NASA-CR-186934] 21 p3000 N90-27049
Ground-based weather radar compatibility with digital radio-relay microwave systems
[PB90-206236] 23 p3318 N90-28756

Compatibility of elastomeric seal compounds with MIL-H-6083 and MIL-H-46170 hydraulic fluid
[AD-A224248] 24 p3454 N90-29504

COMPENSATORS

Null offset voltage compensator for operational amplifier
[AD-D014189] 04 p0496 N90-12859
Towards a complete local solution of the nonlinear model matching problem
[MEMO-781] 04 p0545 N90-13166
Optimal stochastic modeling and control of flexible structures
[AD-A212347] 06 p0733 N90-14269
The development of an airborne synthetic aperture radar motion compensation system 09 p1165 N90-16745
Design and testing of a noninteracting control loop for the dynamically tuned dry gyro
[NAL-TR-1017] 13 p1803 N90-20350
Observer based compensators for nonlinear systems
[AD-A217426] 13 p1876 N90-20760
Robust fixed order dynamic compensation for large space structure control 16 p2292 N90-23059
Theory of filtering and control with application to control of large space structures
[AD-A219936] 17 p2366 N90-23468
A high frequency (20 kHz) power electronics reactive-current compensator with insulated gate bipolar transistors as semiconductor switches
[EMV-88-54] 17 p2399 N90-23665
Design and investigation of a dive plane sliding mode compensator for an autonomous underwater vehicle
[AD-A219552] 17 p2454 N90-23997
A capacitance process for contact-free microfile measurement on metallic surfaces
[ETN-90-96503] 18 p2549 N90-24549
Sample rate effects on disturbance rejection for digital control systems 24 p3435 N90-29400

COMPENSATORY TRACKING

Application of optimal tracking methods to aircraft terrain following
[AD-A221099] 18 p2496 N90-24264

COMPETITION

Manufacturing and the manufacturing engineer in the year 2000, revision
[DE89-017707] 03 p0335 N90-11904
Analysis of competition among the kinds of energy at the era of complexed energy: General review
[DE89-910215] 11 p1527 N90-18793
Analysis of competition among kinds of energy at the era of complexed energy. (Report on overseas study)
[DE89-910213] 12 p1680 N90-19650
Space shuttle: Follow-up evaluation of NASA's solid rocket motor procurement. Report to the Chairman, Committee on Government Operations, House of Representatives
[GAO/NSIAD-89-89] 20 p2824 N90-26066
Enhancing US competitiveness through Federal scientific and technical information: Issues and opportunities 22 p3258 N90-28450
Mode competition in the quasioptical gyrotron
[AD-A222181] 23 p3329 N90-28823
Time-based competition for competitive advantage: An information technology perspective
[AD-A224474] 23 p3407 N90-29255

COMPILATION (COMPUTERS)

U COMPILERS

COMPILER PROGRAMS

U COMPILERS

COMPILERS

A prototype silicon compiler in prolog
[AD-A210669] 02 p0257 N90-11452
A compilation strategy for numerical programs based on partial evaluation
[AD-A212759] 04 p0546 N90-13175
The inca data base 05 p0607 N90-13531
The compilation of astrometric data 05 p0607 N90-13537
The StarLite project
[AD-A214193] 07 p0977 N90-15642
A generic fine-grained parallel C 08 p1115 N90-16454
Parallel functional computation
[AD-A214627] 09 p1269 N90-17360
Compiling scientific code using partial evaluation
[AD-A215087] 09 p1270 N90-17363
A microcode compiler that runs on the IBM AT and supports cascadable microcomputers, part 2
[AD-A215889] 10 p1415 N90-18155
Research at New York University's Ultracomputer Research Laboratory
[DE90-005471] 10 p1417 N90-18167
A microcode compiler that runs on the IBM AT and supports cascadable microcomputers, part 1
[AD-A215888] 11 p1542 N90-18877
Determination of the underlying task scheduling algorithm for and Ada runtime system
[AD-A215880] 11 p1544 N90-18890
A theory of quantitative inference for artifact sets applied to a mechanical design compiler
[AD-A216535] 11 p1545 N90-18896
Automatic compiler construction
[AD-A218777] 16 p2278 N90-22983
Optimization of series expressions. Part 2: Over view of the theory and implementation
[AD-A219961] 17 p2447 N90-23952
Higher order attribute grammars
[RUU-CS-89-4] 18 p2590 N90-24735
Compiling knowledge-based systems from KEE to Ada 21 p3049 N90-27334
Efficient instruction sequencing with inline target insertion
[NASA-CR-185341] 21 p3052 N90-27348
An Ada evaluation report for the Verdix Corp. VADS version 5.5 release h compiler
[NPL-DITC-145/89] 22 p3235 N90-28342

COMPLEMENTARY METAL OXIDE SEMICONDUCTORS

U CMOS

COMPLEMENTS (MATHEMATICS)

A basic theorem of complementarity for the generalized variational-like inequality problem
[DE90-003102] 07 p0973 N90-15620
Generalized quasi-variational inequality and implicit complementarity problems
[AD-A215191] 13 p1875 N90-20755

COMPLETENESS

Completeness of resolution by transfinite induction
[CWI-CS-R8837] 02 p0260 N90-11473
Proving total correctness of recursive procedures
[CWI-CS-R8904] 04 p0532 N90-13075
On models for propositional dynamic logic
[RUU-CS-89-3] 17 p2460 N90-24046
On the independence of B-splines on unordered knot sets
[MEMO-827] 18 p2600 N90-24800
Sigma-completeness and bounded arithmetic
[ITLI-ML-89-05] 18 p2603 N90-24823

COMPLEX COMPOUNDS

NMR evidence for a planar arene intermediate in the electron-transfer induced eta 6 to eta 4 hapticity change of a rhodium arene complex
[AD-A210211] 01 p0033 N90-10177
International Conference on Organometallic Chemistry (13th) held in Torino, Europe on 4-9 September 1988: Abstracts
[AD-A210617] 01 p0033 N90-10178
Monomers, polymers and transition metal complexes based upon carboranes
[AD-A210226] 01 p0040 N90-10221
Theoretical investigation of gas-surface interactions
[NASA-CR-185492] 02 p0272 N90-11552
A high level Ab initio study of the anionic hydrogen-bonded complexes FH-CN-, FH-NC-, H2O-CN- and H2O-NC- 02 p0272 N90-11553
Luminescence in applied magnetic fields
[AD-A211551] 03 p0399 N90-12287
A graph-theoretical approach to block-copolymer complexes. Part 3: Loops and cycles
[MEMO-778-PT-3] 04 p0479 N90-12750
Synthesis and characterization of new low-dimensional metal complex conductors
[AD-A213189] 04 p0498 N90-12871
New electrically conducting solids based on nickel(II) - bis(1,3-dithiole-2-thione-4,5-diselenolate)
[DE90-003788] 08 p1042 N90-16020
Highly reduced carbene complexes: Formation of an alkoxymalonate by coupling of carbon dioxide with the nucleophilic carbene in Cr(CO4)=C(OMe)Ph2(-)
[AD-A215132] 09 p1191 N90-16902
Luminescence probe studies of ionomers. Part 3: Distribution of decay rate constants for tris bipyridyl Ruthenium(II) in Nafion membranes
[AD-A215885] 10 p1359 N90-17880
Perfluorinated ligands in organometallic chemistry
[AD-A216415] 11 p1476 N90-18493
Synthesis and chemistry of unsaturated metal nitrogen compounds
[AD-A216550] 12 p1622 N90-19321
Conductive polymers of transition-metal complexes coordinated by a Diamino-Dichalcogen-Benzene compound
[AD-D014326] 12 p1629 N90-19360
Ligand-centered electron-transfer redox processes for manganese, iron, and cobalt complexes in relation to selected catalytic systems
[AD-A217957] 13 p1773 N90-20177
Laser temperature-jump kinetic studies of fast reactions in nonaqueous solutions
[AD-A218819] 17 p2371 N90-23500
Transition metal activation and functionalization of carbon-hydrogen bonds
[DE90-015826] 24 p3451 N90-29489

COMPLEX SYSTEMS

Explicit formulas for Hankel norm approximations of infinite-dimensional systems
[TW-289] 04 p0545 N90-13167
Solution bias in complex systems modeling
[DE90-002001] 06 p0836 N90-14858
Basic research in reliability for real systems
[AD-A214536] 09 p1234 N90-17158
Decomposition for optimal synthesis in a parallel computing environment 10 p1419 N90-18184
Research in reliability, availability and maintainability for complex failure systems
[AD-A217744] 13 p1813 N90-20415
Theory of defect process: Basic issues in quantitative understanding
[AERE-R-13661] 13 p1892 N90-20860
Perspectives on the use of rule-based control 14 p1908 N90-20940
Insights into complex human performance
[DE90-006957] 15 p2137 N90-22214
Spatial operator algebra framework for multibody system dynamics 16 p2279 N90-22989
Adaptive tracking for complex systems using reduced-order models
[NASA-CR-183464] 19 p2747 N90-25609
Applications of different design methodologies in navigation systems and development at JPL 20 p2852 N90-26221
Closed-form solution of decomposable stochastic models
[NASA-TM-103466] 20 p2920 N90-26619
Improved computational strategy for predicting the response of complex systems
[AD-A221661] 21 p3014 N90-27135
Automated unit-level testing with heuristic rules 21 p3049 N90-27335
Spacecraft attitude dynamics: Evolution and current challenges 22 p3128 N90-27754
System architectures for telerobotic research 24 p3515 N90-29872

COMPLEX VARIABLES

NT ANALYTIC FUNCTIONS
NT BESSEL FUNCTIONS
NT CONFORMAL MAPPING
NT CONJUGATES
NT ELLIPTIC FUNCTIONS
NT EXPONENTIAL FUNCTIONS
NT HANKEL FUNCTIONS
NT HARMONIC FUNCTIONS
NT HYPERBOLIC FUNCTIONS
NT HYPERGEOMETRIC FUNCTIONS
NT LAGUERRE FUNCTIONS
NT LEGENDRE FUNCTIONS
NT LOGARITHMS
NT MEROMORPHIC FUNCTIONS
NT NAKED SINGULARITIES
NT NONHOLONOMIC EQUATIONS
NT ORTHOGONAL FUNCTIONS
NT SINGULARITY (MATHEMATICS)
NT SPHERICAL HARMONICS

Rational expansion for nonlinear input-output maps
[RR-348] 03 p0394 N90-12248
Discrete variable structural optimization by the complex method
[LR-597] 15 p2161 N90-22341
The stress intensity factor and stress concentration for a finite plate with a single crack emanating from a hole
[LR-607] 19 p2704 N90-25385
An investigation of hole-edge crack problem by a combined complex variable and least square method
[LR-626] 24 p3482 N90-29679

COMPLEXITY

NT TASK COMPLEXITY

On the expected complexity of the three-dimensional Voronoi diagram
[PB89-209332] 01 p0112 N90-10636
Boolean functions, invariance groups and parallel complexity
[CWI-CS-R8836] 02 p0260 N90-11472
On the complexity analysis of the coriolis and centripetal effects of a 6 DOF robot manipulator --- Degrees of Freedom (DOF)
[RR-344] 03 p0355 N90-12030
Kolmogorov complexity and its applications
[CWI-CS-R8901] 04 p0548 N90-13191
Auditory perception of complex sounds
[AD-A219927] 17 p2435 N90-23872
An O(square root of n) complexity reduction for the long-step path-following algorithm for linear programming
[REPT-89-85] 17 p2445 N90-23940

Sequencing and scheduling: Algorithms and complexity
[CWI-BS-R8909] 17 p2446 N90-23942
Arithmetic classification of perfect models of stratified programs (extended version)
[CWI-CS-R8928] 17 p2462 N90-24063
Majority voting: Characterization and algorithms
[RUU-CS-88-32] 18 p2592 N90-24750
A simple output-sensitive algorithm for hidden surface removal
[RUU-CS-89-26] 18 p2592 N90-24751
Minimum loss scheduling
[MEMO-821] 18 p2600 N90-24796
Heterogeneity description using fractal concepts
19 p2690 N90-25299
Using information to measure software complexity
[REPT-89-022] 22 p3238 N90-28359

COMPLIANCE (ELASTICITY)
U MODULUS OF ELASTICITY

COMPLICATION
U COMPLEXITY

COMPONENT RELIABILITY
Independent Orbiter Assessment (IOA) CIL issues resolution report, volume 3
[NASA-CR-185524-VOL-3] 02 p0170 N90-10956
Independent Orbiter Assessment (IOA): FMEA/CIL assessment
[NASA-CR-185589] 02 p0170 N90-10960
Independent Orbiter Assessment (IOA): Analysis of the communication and tracking subsystem
[NASA-CR-185582] 02 p0172 N90-10967
The role of component testing
[PNR90589] 04 p0455 N90-12608
Electrical testing 05 p0605 N90-13520
Mechanical and thermal testing
05 p0605 N90-13521
Sufficiency and necessity in reliability modeling
[NASA-CR-186119] 05 p0635 N90-13706
Advanced Turbine Technology Applications Project (ATTAP)
[NASA-CR-185109] 05 p0709 N90-14153
A study of variable geometry in advanced gas turbines
07 p0881 N90-15104
Sensitivity of space system availability predictions to underlying component reliability estimates
[AD-A215535] 09 p1183 N90-16858
Transient pressure test article test program
11 p1470 N90-18463
Effect of correlation on multi-engine rocket propulsion systems 11 p1471 N90-18467
Space Station Freedom electric power system availability study
[NASA-CR-185181] 13 p1763 N90-20120
Dual cathode system for electron beam instruments
[NASA-CASE-NPO-16678-1-CU]
13 p1803 N90-20351
A stress-strength interference approach to fast and delayed fracture reliability analysis for ceramic components 15 p2070 N90-21859
Reliability importance measures and their calculation
[DE90-620391] 15 p2108 N90-22057
Failure mechanisms of GaAs transistors: A literature survey
[AD-A221089] 18 p2548 N90-24543
Integrated controls and health monitoring for chemical transfer propulsion
[NASA-TM-103185] 19 p2668 N90-25178
Design of ceramic components with the NASA/CARES computer program
[NASA-TM-102369] 20 p2875 N90-26359
Closed-form solution of decomposable stochastic models
[NASA-TM-103466] 20 p2920 N90-26619
A general discussion of the retirement for cause inspection system 21 p2957 N90-26814
Estimation of defective rate of mechanic-hydraulic components
[ETN-90-97275] 21 p3011 N90-27120
An automated tool for the design and assessment of space systems 21 p3042 N90-27289
Data base for crack growth properties of materials
23 p3296 N90-28647
Ceramic matrix composites in simulated SSME environments 23 p3298 N90-28655
Recommended practices for measurement of gas path pressures and temperatures for performance assessment of aircraft turbine engines and components
[AGARD-AR-245] 24 p3433 N90-29393

COMPOSITE MATERIALS
NT ALUMINUM BORON COMPOSITES
NT ALUMINUM GRAPHITE COMPOSITES
NT BORON REINFORCED MATERIALS
NT CARBON FIBER REINFORCED PLASTICS
NT CARBON-CARBON COMPOSITES
NT CERAMIC MATRIX COMPOSITES
NT CERMETS
NT COMPOSITE PROPELLANTS
NT EPOXY MATRIX COMPOSITES
NT EUTECTIC COMPOSITES
NT FIBER COMPOSITES
NT GLASS FIBER REINFORCED PLASTICS
NT GLASSY CARBON
NT GRAPHITE-EPOXY COMPOSITES
NT LAMINATES
NT METAL MATRIX COMPOSITES
NT POLYMER MATRIX COMPOSITES
NT REINFORCED PLASTICS
NT RESIN MATRIX COMPOSITES
NT THREE DIMENSIONAL COMPOSITES
NT WHISKER COMPOSITES
Composite Blade Structural Analyzer (COBSTRAN) theoretical/programmer's manual
[NASA-TM-101958] 01 p0033 N90-10181
Failure behavior of PEEK and its short-fiber composite systems
[AD-A210729] 01 p0035 N90-10189
New structural materials
[AD-A209425] 01 p0044 N90-10246
Preparation and evaluation of composite membranes for zinc/bromine storage batteries
[DE89-009931] 01 p0059 N90-10339
Finite element analysis of cure-induced residual stress in composite materials 02 p0190 N90-11084
On the effective transport properties of composite materials 02 p0190 N90-11086
Effect of thermal and cyclic loads on silicon carbide yarn reinforced glass matrix composites
[DE89-016554] 02 p0191 N90-11091
Potential industrial applications for composite phase-change materials as thermal energy storage media
[DE89-015170] 02 p0237 N90-11346
Thermal conduction of SSC (Superconducting Super Collider) wire
[DE89-016710] 03 p0319 N90-11811
Processing and characterization of alumina platelet-reinforced mullite composites
[DE90-000057] 03 p0320 N90-11814
Investigations into the infiltration kinetics, wettability, and interfacial bond strength of Al/SiC composites
[AD-A211924] 03 p0320 N90-11815
In-situ cure monitoring of composites by fiber-optic molecular sensors
[AD-A211495] 03 p0320 N90-11817
Choice and characterization of new materials for aerospace applications
[ETN-89-95219] 03 p0320 N90-11819
Current research in advanced materials
[DE89-017466] 03 p0331 N90-11884
Densification of particulate ceramic composites: The role of heterogeneities
[DE90-000177] 03 p0331 N90-11886
Flexure strength of advanced ceramics: A round robin exercise
[AD-A212101] 03 p0332 N90-11889
Material requirements for future aeroengines
[PNR90595] 04 p0456 N90-12610
Optical fibre witnesses of fatigue damage in composite materials 04 p0465 N90-12660
Laser probe vaporization/oxidation testing of high temperature composites
[AD-A211410] 04 p0465 N90-12663
Multilayer theory for delamination analysis of a composite curved bar subjected to end forces and end moments
[NASA-TM-4139] 04 p0466 N90-12669
A study of the impact of a ball bearing on a long fiber composite plate with a carbon matrix, part 2
[ETCA-88-R-088-PT-2] 04 p0467 N90-12673
Modeling of the dielectric behavior of composite materials
[CERT-1/1398-MO] 04 p0467 N90-12674
Oxide ceramic fibers by the sol-gel methods
[AD-A211315] 04 p0478 N90-12742
Pyrolytic production of ceramic composites from silicates
[ETCA-89-R-012] 04 p0479 N90-12746
An air coupled transmission mode acoustic microscope for on-line non-destructive evaluation
[AD-A211416] 04 p0511 N90-12947
Proceedings of the Army Symposium on Solid Mechanics, 1989: Mechanics of Engineered Materials and Applications
[AD-A211954] 04 p0511 N90-12951
RTM user's guide
[NASA-CR-186091] 04 p0531 N90-13065
Nondestructive analysis of aileron fatigue and aging in a Mirage F1
[REPT-M6-594000] 05 p0580 N90-13378
The application of cast SiC/Al to rotary engine components
[NASA-CR-179610] 05 p0581 N90-13385
Advanced composite materials for precision segmented reflectors 05 p0596 N90-13481
The Materials Division: A case study
[NASA-TM-102380] 05 p0617 N90-13597
Failure processes in unidirectional composite materials
05 p0617 N90-13598
Fatigue behavior of silicon carbide Whisker/Aluminum composite
[AD-A213094] 05 p0618 N90-13603
The adhesive bonding of thermoplastic composites
[AD-A213358] 05 p0618 N90-13605
Repair of composites by means of wet-lay-up
[LR-551] 05 p0620 N90-13617
Wear-resistant coated object
[EP-PATENT-0-289-173-A1] 05 p0624 N90-13643
Toughening mechanisms in ceramic composites
[PB89-235907] 05 p0626 N90-13656
Model filled polymers I. Synthesis of crosslinked monodisperse polystyrene beads
[AD-A213228] 05 p0627 N90-13660
NRL (Naval Research Laboratory) Review
[AD-A212886] 05 p0716 N90-14182
AGARD Highlights 89/2 06 p0717 N90-14184
Application of neutron diffraction NDE to high-temperature superconducting composites
[DE90-002184] 06 p0738 N90-14295
Fiber-optic sensors for composite cure analysis and lifetime nondestructive evaluation
[DE90-001739] 06 p0738 N90-14296
High-temperature corrosion of heat exchanger materials
[DE90-001963] 06 p0748 N90-14352
Computer synthesis of ceramic preforms for molten-metal infiltration
[DE90-000826] 06 p0751 N90-14370
Reactive flow measurements and calculations for ZrH2-based composite explosives
[DE90-000831] 06 p0755 N90-14393
Silver-nickel composite cathodes for alkaline secondary batteries
[AD-D014231] 06 p0767 N90-14464
Effects of lightning on operations of aerospace vehicles 07 p0873 N90-15065
Empirical and analytical determination of the fracture resistance of a TiB2 particle/SiC matrix composite
[NASA-TM-101940] 07 p0890 N90-15143
Composite activities at Lawrence Livermore National Laboratory
[DE90-002979] 07 p0891 N90-15149
Potential applications of structural ceramic composites in gas turbines
[DE90-001273] 07 p0908 N90-15248
A future for LLNL (Lawrence Livermore National Laboratory) research in composite high explosives
[DE90-004442] 07 p0915 N90-15290
Advanced composite polar boss
[AD-D014287] 08 p1037 N90-15994
Assessing the flammability of composite materials
[PB90-112996] 08 p1039 N90-16002
Evaluation of potential cold x ray shield materials tested on Proto II
[DE90-004348] 08 p1039 N90-16003
The structure of silica-polysiloxane composites and its effects on their elastomeric properties
[DE89-014768] 08 p1039 N90-16005
Design of coupled or uncoupled multifilamentary SSC-type strands with almost zero retained magnetization at fields near 0.3 T
[DE90-005391] 08 p1047 N90-16052
The physical properties of microcellular composite foams
[DE90-003658] 08 p1048 N90-16058
Review of investigations on aeronautical fatigue in the Federal Republic of Germany
[LBF-S-182] 08 p1089 N90-16302
Material technology challenges in space transportation
09 p1179 N90-16836
A cure process model for resin transfer molding of advanced composites
[NASA-CR-186247] 09 p1185 N90-16867
Metal matrix composite: Strengthening mechanisms
[AD-A214843] 09 p1186 N90-16871
Utilization of focused acoustic beams to inspect composite materials
[ETN-90-96084] 09 p1188 N90-16880
Nondestructive control of composite materials by holographic interferometry
[ISL-CO-244/88] 09 p1188 N90-16882
Adhesive for composite bonding
[DE90-005683] 09 p1188 N90-16885
Erosion of ceramic composites by various erodents
[DE90-005650] 09 p1199 N90-16948
Analysis of some fracture mechanics test procedures for defence research applications
[MRL-TR-89-11] 09 p1236 N90-17175

Analysis of composite ring of compression test data
[DE90-004468] 09 p1239 N90-17194
Cost effectiveness of composite materials on the F-15 and F-16 aircrafts
[AD-A216353] 10 p1320 N90-17631
Internal failures in model elastomeric composites
[AD-A215923] 10 p1348 N90-17818
The processing and mechanical properties of high temperature/high performance composites. Book 1, section 1: Coatings and interfaces
[AD-A216141] 10 p1348 N90-17821
The processing and mechanical properties of high temperature/high performance composites. Book 5, section 4: Processing: Matrices and composites, part 1
[AD-A216145] 10 p1349 N90-17823
The processing and mechanical properties of high temperature/high performance composites. Book 6, section 4: Processing: Matrices and composites, part 2
[AD-A216146] 10 p1349 N90-17824
Materials properties numerical database system established and operational at CINDAS/Purdue University 10 p1366 N90-17919
Composites design handbook for space structure applications
[ESA-PSS-03-1101-ISSUE-1-REV-1] 11 p1469 N90-18459
Third European Conference on Composite Materials
[EOARD-LR-89-050] 11 p1476 N90-18494
The processing and mechanical properties of high temperature/high performance composites. Book 2, section 2: Strength and fracture resistance
[AD-A216142] 11 p1478 N90-18507
The processing and mechanical properties of high temperature/high performance composites. Book 3, section 2: Strength and fracture resistance, part
[AD-A216143] 11 p1478 N90-18508
Calculations of braiding parameters
[AD-A216836] 11 p1479 N90-18515
Compact reinforced composite basic principles
[CBL-41] 11 p1480 N90-18520
Structural study of thermo-hardenable matrices. Deformation processes of composite matrices as a function of their molecular structure
[ONERA-RT-10/3521-M] 11 p1481 N90-18522
Comparison between the damage modes of thermo-hardenable and thermo-plastic composite matrices
[ONERA-RT-47/7086-M] 11 p1481 N90-18523
Thermal analysis of polymer composites
[AD-A216947] 11 p1490 N90-18578
Electronic and ionic transport in polymers
[AD-A217028] 11 p1491 N90-18579
Three-dimensional structural analyses of reentry vehicles
[DE90-006278] 12 p1615 N90-19291
Ac loss measurements of two multifilamentary NbTi composite strands
[DE90-005388] 12 p1619 N90-19304
Fast optical switch and limiter using quantum size effect in metal grain composites
[AD-D014332] 12 p1619 N90-19305
Heterogeneous composite and method of making
[AD-D014337] 12 p1619 N90-19306
Carbon black/polyethylene composites for PTC (Positive Temperature Coefficient) thermistor applications
[AD-A215988] 12 p1619 N90-19307
The effect of fiber coatings on interfacial shear strength and the mechanical behavior of ceramic composites
[DE90-007574] 12 p1632 N90-19380
Viscoelastic adherend effects in adhesively bonded composite-to-composite joints 12 p1670 N90-19594
Symposium on High Temperature and Materials Chemistry
[DE90-008047] 13 p1768 N90-20148
Extended x ray absorption fine structure analysis applied to composite materials
[DE90-008575] 13 p1769 N90-20150
Determination of fundamental thermodynamic properties of constituent materials and performance screening of candidate systems
[AD-A218089] 13 p1769 N90-20153
Assessment of biobased materials
[DE90-000300] 13 p1780 N90-20220
Electronic and ionic transport in processable conducting polymers
[AD-A218093] 13 p1782 N90-20229
Spray deposition: A fundamental study of droplet impingement, spreading and consolidation
[AD-A217202] 13 p1787 N90-20255
Comparison of light duty gloves with natural and synthetic materials under wet and dry conditions
[AD-A218119] 13 p1856 N90-20649
Dielectric composite thin films
[AD-A217940] 13 p1881 N90-20791
Fracture of sandwiched composites 14 p1946 N90-21136
Resistance mechanics for laminated composite materials
[INPE-4919-RPE/594] 14 p1947 N90-21141
Combination primer/topcoat coating
[AD-D014445] 14 p1954 N90-21189
Toughened YBa2Cu3O(sub x)/ZrO2 composites
[DE90-007796] 14 p2031 N90-21645
Review of analysis methods for mechanically fastened joints in composites
[LR-599] 15 p2107 N90-22050
Institute for Materials Science and Engineering, Fracture and Deformation Division: Technical activities, 1989
[PB90-155359] 15 p2116 N90-22106
Damage analysis following slight deformations of composite materials
[RDS-1-007-64] 16 p2212 N90-22618
Polymerization of composites
[REPT-892-430-102] 16 p2213 N90-22621
Machining of new materials at Aerospatiale
[REPT-892-430-104] 16 p2213 N90-22622
Polymerization of composite materials: A technique developed by Aerospatiale
[REPT-892-430-107] 16 p2213 N90-22623
The surprising possibilities of wrapping
[REPT-892-430-108] 16 p2213 N90-22624
Low cost processing routes leading to high-performance ceramic tiles
[AD-A219034] 16 p2224 N90-22688
Composite ceramic superconducting wires for electric motor applications
[AD-A219131] 16 p2224 N90-22689
Micro-mechanical modeling of crack growth resistance in a carbon/carbon composite
[DE90-009407] 17 p2368 N90-23479
High temperature insulation barrier composite
[NASA-CASE-MFS-29241-1] 17 p2368 N90-23480
The microwave permeability of conducting spherical shells
[AD-A220746] 17 p2369 N90-23485
Instability-related delamination growth of embedded and edge delaminations
[NASA-TM-100655] 17 p2370 N90-23494
Undercooling and nucleation in rapid solidification rate metal powders using solid in solid emulsification
[AD-A218527] 17 p2375 N90-23526
Center for Analysis of Heterogeneous and Nonlinear Media
[AD-A219627] 17 p2403 N90-23688
US Army Research Office Workshop on Smart Materials, Structures and Mathematical Issues proceedings
[AD-A218528] 17 p2468 N90-24110
Advanced artificial dielectric materials for millimeter wavelength applications, part A
[AD-A220221] 17 p2469 N90-24112
Using template/hotwire cutting to demonstrate moldless composite fabrication 18 p2515 N90-24361
State of the art and future prospects for high temperature composites
[REPT-892-430-125] 18 p2517 N90-24375
Ta and Nb reinforced MoSi2
[DE90-010596] 18 p2517 N90-24377
Proceedings of Biostructures as Composite Materials ARO Workshop
[AD-A220262] 18 p2518 N90-24381
Use of neutron diffraction in determining strains in high-temperature superconducting composites
[DE90-010404] 18 p2621 N90-24931
Development of elements of a high Tc superconducting cable
[AD-A221300] 18 p2623 N90-24945
Decay rate and resonance fluorescence spectrum of a molecule near a composite material surface
[AD-A219692] 19 p2671 N90-25192
Introduction to compact reinforced composite
[CBL-REPRINT-5] 19 p2673 N90-25199
A numerical micromechanics analysis of the mechanical properties of a plain weave composite
[OUEL-1760/89] 19 p2673 N90-25201
Nondestructive x ray methods for characterization of advanced aerospace materials
[DE90-011751] 19 p2699 N90-25356
Computational crash dynamics. Project 1.2: Computational crash dynamics analysis
[IAR-89-19] 20 p2804 N90-25956
The impact and requirements of new materials on aeroengines
[PNR90671] 20 p2812 N90-26003
Erosion mechanisms in composite materials and ripple formation mechanism in erosion
[IAR-89-4-PT-2] 20 p2826 N90-26079
Composite materials with improved properties in compression: Synthesis of 3-methylene-1,1-Dichlorosilacyclobutane and 1,1-dichlorosilacyclopent-3-ene
[AD-A222615] 20 p2828 N90-26088
The effect of interfacial characteristics on the mechanical performance of ceramic-ceramic composites
[AD-A223031] 20 p2829 N90-26090
Development of ceramic fiber type combustor: Improvement of combustor and combustion test results
[DE90-503441] 20 p2839 N90-26148
New core design for use with precision composite reflectors
[NASA-CASE-NPO-17858-1-CU] 21 p2970 N90-26880
Study on failure modes of SiC fiber reinforced aluminum composite materials by AE method
[DE90-505518] 21 p2971 N90-26884
Role of interfaces and interphases in the evolution mechanics of material systems
[AD-A222702] 21 p2971 N90-26885
The 1990 Gordon Research Conference on Composites
[AD-A222849] 21 p2971 N90-26886
Applications of digital image processing in testing and evaluation of composite materials
[AD-A222939] 21 p2971 N90-26887
Composite materials with improved properties in compression. Appendix 1: Cyclopropanation of poly(1-methyl 1-phenyl 1-sila-cis-pent-3-ene). Synthesis and characterization of poly(1-methyl 3,4-methylene-1-phenyl 1-sila-cis-pent-3-ene)
[AD-A221494] 21 p2971 N90-26889
Composite materials with improved properties in compression: Copolymerization of 1,1-dimethyl-1-Silacyclopent-3-ene and 1,1-diphenyl-1-Silacyclopent-3-ene. Characterization of copolymer microstructures by H1, C13, and Si29 NMR spectroscopy
[AD-A221686] 21 p2972 N90-26892
Elastomers and other organic composites
[AD-A222772] 21 p2984 N90-26958
Micromechanics of interfaces in high temperature ceramics
[AD-A222027] 21 p2987 N90-26973
A characterization of V-391/H46-8B, A toughened BMI prepreg system produced by US Polymeric
[AD-A221772] 21 p2989 N90-26985
Evaluation of composite components on the Bell 206L and Sikorsky S-76 helicopters
[NASA-TM-4195] 22 p3135 N90-27787
Composite materials with improved properties in compression: Synthesis and dimerization 2,3-dimethyl-5-silaspiro(4.4)nona-2,7-diene
[AD-A222552] 22 p3156 N90-27892
In-service inspection of composite components on aircraft at depot and field levels 22 p3186 N90-28078
Radiation-curable prepreg composites
[DE90-629740] 23 p3301 N90-28674
Fabrication of spherical pressure vessels from composite materials
[INPE-4598-RPE/570] 23 p3302 N90-28675
Dissipation of mechanical work and temperature rise in AS4/PEEK thermoplastic composite
[NASA-CR-186893] 23 p3302 N90-28678
A constitutive model for AS4/PEEK thermoplastic composites under cyclic loading
[NASA-CR-180393] 23 p3302 N90-28679
Technical bibliography of high performance polyethylene fibers
[SNPE-NT-106/89/GTR/RP/NP] 23 p3313 N90-28736
Proceedings of US Army Research Office Workshop on US Army Applications for Diamond and Diamondlike Materials
[AD-A224193] 23 p3314 N90-28741
Green's functions for dislocations in bonded strips and related crack problems
[NASA-CR-185291] 23 p3340 N90-28878
Large hydrodynamic tunnel: Calculation of the acoustic transparency of the jet stream
[REPT-89/115] 23 p3393 N90-29167
Engineering and the advancement of human welfare. Ten outstanding achievements 1964-1989
[ISBN-0-309-04185-6] 23 p3415 N90-29297
The overall response of composite materials undergoing large elastic deformations
[AD-A224509] 24 p3442 N90-29439
High performance brittle matrices and brittle matrix composites, book 1
[AD-A223273] 24 p3443 N90-29440
High performance brittle matrices and brittle matrix composites, book 2
[AD-A223274] 24 p3443 N90-29441
Prediction and control of processing-induced residual stresses in composites. Part 2: AS4/PEEK composite
[AD-A223696] 24 p3443 N90-29445
Powder processing of aluminides
[DE90-015314] 24 p3444 N90-29447

The friction and wear of lubricated Si3N4/SiC(w) composites
[DE90-015790] 24 p3444 N90-29448
Wear of advanced ceramics: An overview
[DE90-012166] 24 p3456 N90-29519
Proceedings of Damping '89. Volume 3: Pages ICA-1 through KDC-15
[AD-A223433] 24 p3479 N90-29666

COMPOSITE PROPELLANTS
Nitramine composite solid propellant modeling
02 p0207 N90-11183
N-Hexyl Carborane (NHC) as combustion catalyst in composite propellants
[FOA-C-20755-2.1] 02 p0209 N90-11193
RSRM-3 (360L003) ballistics/mass properties report
[NASA-CR-183716] 04 p0463 N90-12651
Ballistics/mass properties
[NASA-CR-183723] 04 p0463 N90-12652
Spectral studies of solid propellant combustion. 2: Emission and absorption results for M-30 and HMX1 propellants
[AD-A213857] 07 p0915 N90-15292
A study of near tip phenomena for cracks in a particulate composite 10 p1395 N90-18062
Shock initiation sensitivity of damaged TP-H1207C composite propellant
[DE90-008509] 14 p1957 N90-21205
Workshop on ESD (Electrostatic Discharge) Ignition of Composite Solid Propellants
[AD-A218599] 17 p2382 N90-23569
RSRM-9 (360L009): Ballistics mass properties
[NASA-CR-183944] 20 p2823 N90-26064
Hard start problem of the apogee engine for the ETS-6
[DE90-505525] 20 p2825 N90-26072
Composite propellants with high burning rates
[FOA-C-20781-2.1] 23 p3315 N90-28744

COMPOSITE STRUCTURES
NT LAMINATES
PMR graphite engine duct development
[NASA-CR-182228] 01 p0008 N90-10037
Hygrothermal effects on the complex moduli of composite laminates 01 p0033 N90-10182
Development of pressure containment and damage tolerance technology for composite fuselage structures in large transport aircraft
[NASA-CR-3996] 01 p0034 N90-10186
Global/local stress analysis of composite structures
[NASA-TM-101640] 01 p0080 N90-10456
Equilibrium and stability in composite thin shell
02 p0178 N90-10998
Transverse shear stiffness of composite and sandwich finite elements 02 p0182 N90-11034
Study of the application of automation to composites manufacture
[AD-A211049] 02 p0190 N90-11087
Rational design of high-current cable-in-conduit superconductors
[DE89-016867] 02 p0284 N90-11626
An integrated methodology for optimizing structural composite damping
[NASA-TM-102343] 03 p0319 N90-11808
Transport composite fuselage technology: Impact dynamics and acoustic transmission
[NASA-CR-4035] 03 p0321 N90-11821
Natural frequencies of singly-curved laminated plates with simply-supported edges
[ESDU-89011] 03 p0359 N90-12052
Evaluation of a damaged F/A-18 horizontal stabilator
[AD-A212573] 04 p0453 N90-12597
Project, implementation, and utilization of composite structures
[ETN-89-95209] 04 p0466 N90-12665
A thermoelastic transversely isotropic thick walled cylinder/disk application: An analytical solution and study
[NASA-TM-102320] 04 p0511 N90-12950
Aeroelastic control of composite lifting surfaces: Integrated aeroelastic control optimization
05 p0583 N90-13396
Composite panel development at JPL
05 p0595 N90-13458
Status of Gr/glass composites technology at UTOS
05 p0596 N90-13459
Large Deployable Reflector (LDR) thermal characteristics 05 p0596 N90-13460
Lightweight composite reflector panels
05 p0596 N90-13462
Low temperature optical testing of CFRP telescope panels 05 p0596 N90-13463
Static and free-vibrational response of semi-circular graphite-epoxy frames with thin-walled open sections
[NASA-CR-186097] 05 p0617 N90-13600
Measurement of damping of graphite epoxy composite materials and structural joints
[NASA-CR-183802] 06 p0736 N90-14286
Analysis of metal matrix composite structures using a microchemical constitutive theory
06 p0737 N90-14290
Strength and toughness of monolithic and composite silicon nitrides
[NASA-TM-102423] 06 p0751 N90-14368
Improved process for HIP canning of composites
[NASA-CASE-LEW-14990-1-CU]
07 p0890 N90-15147
New Light Alloys
[AGARD-CP-444] 07 p0897 N90-15185
High performance powder metallurgy aluminum alloys: An overview 07 p0900 N90-15204
Proceedings of the 1988 Structural Integrity Program Conference
[AD-A213545] 07 p0947 N90-15486
Elastic-plastic analysis of a thick-walled composite tube subjected to internal pressure
[AD-A215258] 09 p1238 N90-17187
Fire resistance and breakdown of composite materials
10 p1316 N90-17607
Advanced materials for interior and equipment related to fire safety in aviation 10 p1316 N90-17608
New materials for civil aircraft furnishing
10 p1316 N90-17609
The behavior of a composite material in compression
[AD-A216324] 10 p1350 N90-17829
Eccentricity effects of square cutouts on the natural frequencies and mode shapes of curved rectangular composite panels
[AD-A216410] 10 p1350 N90-17831
Low cost tooling material and process for graphite and Kevlar composites
[NASA-CR-179427] 10 p1351 N90-17834
Investigation of collapse characteristics of cylindrical composite panels with large cutouts
[AD-A216378] 10 p1397 N90-18079
Threaded joint design for composites
[DE90-005553] 11 p1478 N90-18506
Preliminary evaluation of the strength of pin-joints in laminated composite materials
[DE90-006353] 11 p1481 N90-18524
The design of advanced ceramic composites
[DE90-006613] 11 p1493 N90-18592
Evaluation of repeated impact damage in composite structures 12 p1619 N90-19303
Carbon black/polyethylene composites for PTC (Positive Temperature Coefficient) thermistor applications
[AD-A215988] 12 p1619 N90-19307
Innovative design of composite structures: The use of curvilinear fiber format in structural design of composites
[NASA-CR-186406] 12 p1620 N90-19308
Demonstration of capabilities of high temperature composites analyzer code HITCAN
[NASA-TM-102560] 12 p1676 N90-19629
COCOMAT: A Computer Aided Engineering (CAE) system for composite structures design
[NLR-MP-87078-U] 12 p1699 N90-19756
A review of the analytical simulation of aircraft crash dynamics
[NASA-TM-102595] 13 p1753 N90-20068
Innovative design of composite structures: The use of curvilinear fiber format to improve buckling resistance of composite plates with central circular holes
[NASA-CR-186454] 13 p1766 N90-20135
Innovative design of composite structures: The use of curvilinear fiber format in composite structure design
[NASA-CR-186453] 13 p1766 N90-20136
Through-thickness strain response of thick composites in compression
[AD-A217233] 13 p1767 N90-20141
Nondestructive testing of ceramics by acoustic microscopy
[AERE-R-13350] 13 p1813 N90-20411
Computational simulation of damping in composite structures
[NASA-TM-102567] 13 p1817 N90-20432
Advanced double layer capacitors
13 p1822 N90-20464
Free indexation: Combinatorial analysis and a compositional algorithm
[AD-A218219] 13 p1869 N90-20724
Filament winding of composite cylinders
14 p1943 N90-21119
Fracture and longevity of composite structures
[AD-A217827] 14 p1944 N90-21127
Multi-objective shape and material optimization of composite structures including damping
[NASA-TM-102579] 14 p1945 N90-21132
Compressive behavior of laminated composite structures 14 p1945 N90-21134
Structural tailoring of select fiber composite structures
[NASA-TM-102484] 14 p1946 N90-21137
User manual for VICONOPT: An exact analysis and optimum design program covering the buckling and vibration of prismatic assemblies of flat in-plane loaded, anisotropic plates, with approximations for discrete supports, and transverse stiffeners
[NASA-CR-181966] 14 p1991 N90-21413
Research programs in aeronautical engineering, solid state physics, and materials science at Technion-Israel Institute of Technology, Haifa, Israel
[EOARD-LR-89-068] 14 p2044 N90-21720
Elastodynamic scattering and transmission problems in three dimensions by the boundary integral equation method 15 p2111 N90-22077
Boeing/NASA composite components flight service evaluation
[NASA-CR-181898] 16 p2210 N90-22609
Large deformation analysis of laminated composite structures by a continuum-based shell element with transverse deformation 16 p2211 N90-22613
A life prediction model for laminated composite structural components
[NASA-CR-186587] 16 p2212 N90-22614
The elastic-plastic behavior of composite materials
16 p2212 N90-22615
Pultrusion process development for long space boom model
[NASA-TM-4017] 16 p2214 N90-22628
Environment enhanced fatigue of advanced aluminum alloys and composites 16 p2218 N90-22652
Inelastic response of metal matrix composites under biaxial loading 16 p2220 N90-22661
The behaviour of mechanically fastened joints in composite structures 16 p2242 N90-22789
Explicit modeling of composite plates and beams in the dynamics of multibody systems
16 p2285 N90-23019
Impact response of orthotropic composite plates predicted by a one-parameter differential equation
[FFA-TN-1989-07] 17 p2369 N90-23488
Stress fields in composite materials by means of a nonclassical approach 18 p2517 N90-24372
Simplified design procedures for fiber composite structural components/joints
[NASA-TM-103113] 18 p2519 N90-24384
Friction and wear of whisker-reinforced ceramic composite bodies
[DE90-011313] 18 p2519 N90-24389
Unique failure behavior of metal/composite aircraft structural components under crash type loads
[NASA-TM-102679] 18 p2572 N90-24660
Non destructive testing of composite structures using embedded optical fibers: A mechanical interaction model
[ETN-90-97016] 18 p2573 N90-24661
Incorporation of a progressive failure analysis method in the CSM testbed software system
18 p2640 N90-25036
Extension-torsion coupling behavior of advanced composite tilt-rotor blades 18 p2644 N90-25057
Seamless metal-clad fiber-reinforced organic matrix composite structures and process for their manufacture
[NASA-CASE-LAR-13562-1] 19 p2672 N90-25196
Method of inserting predesigned disbond areas into composite laminates
[NASA-CASE-LAR-13225-1] 19 p2672 N90-25197
Intelligent composites containing measuring fibre optic networks for continuous self diagnosis
[ETN-90-97018] 19 p2673 N90-25200
Behavior of composite/metal aircraft structural elements and components under crash type loads: What are they telling us
[NASA-TM-102681] 19 p2701 N90-25368
A photoelastic analysis of the strain field around impact damage in a graphite fibre reinforced panel subjected to compression loads
[FFA-TN-1989-48] 19 p2703 N90-25379
Damage states in laminated composite three-point bend specimens: An experimental-analytical correlation study
[NASA-TM-101800] 20 p2827 N90-26083
Probabilistic approach to the certification for fatigue durability of composite structures
[DE90-505521] 20 p2828 N90-26085
Modeling of composite beams and plates for static and dynamic analysis
[NASA-CR-186459] 20 p2874 N90-26354
Scaling effects in the static and dynamic response of graphite-epoxy beam-columns
[NASA-TM-102697] 20 p2876 N90-26363
Proceedings of the 1987 Aircraft/Engine Structural Integrity Program (ASIP/ENSIP) Conference
[AD-A198037] 21 p2956 N90-26807
Lessons learned for composite aircraft structures qualification 21 p2956 N90-26808
The response and failure mechanisms of circular metal and composite plates subjected to underwater shock loading
[AD-A222200] 21 p3013 N90-27131

A review of crashworthiness of composite aircraft structures
[AD-A221555] 22 p3115 N90-27697
A Protection And Detection Surface (PADS) for damage tolerance
[NASA-TP-3011] 22 p3135 N90-27788
Investigation of the techniques for the analysis of composite structures: Analysis and representation of the static and dynamic behavior of glued metal insert assemblies
[IMFL-89-44] 22 p3153 N90-27878
NDI-concept for composites in future military aircraft 22 p3184 N90-28070
An ultrasonic system for in-service non-destructive inspection of composite structures 22 p3185 N90-28076
A technique for rapid inspection of composite aircraft structure for impact damage 22 p3185 N90-28077
Development of an automated ultrasonic inspection system for composite structure on in-service aircraft 22 p3186 N90-28079
The application of infrared thermography to the nondestructive testing of composite materials 22 p3187 N90-28084
Inspection system for in-situ inspection of aircraft composite structures 22 p3188 N90-28091
Creep and creep rupture of strongly reinforced metallic composites
[NASA-CR-185286] 22 p3192 N90-28110
Energy efficient engine pin fin and ceramic composite segmented liner combustor sector rig test report
[NASA-CR-179534] 23 p3281 N90-28567
Mechanical behavior of thick, curved, laminated composites 23 p3299 N90-28664
Structural analysis and optimum design of geodesically stiffened composite panels
[NASA-CR-186944] 23 p3337 N90-28862
A low cost shadow moire device for the nondestructive evaluation of impact damage in composite laminates
[AD-A223451] 24 p3443 N90-29442
On a generalized laminate theory with application to bending, vibration, and delamination buckling in composite laminates 24 p3478 N90-29659
Proceedings of damping '89. Volume 1: Pages AAB-1 through DCD-11
[AD-A223431] 24 p3479 N90-29664
Proceedings of damping '89. Volume 2: Pages FAA-1 through IBD-15
[AD-A223432] 24 p3479 N90-29665
Practical superconductor development for electrical power applications
[DE90-014836] 24 p3554 N90-30109

COMPOSITE WRAPPING
The surprising possibilities of wrapping
[REPT-892-430-108] 16 p2213 N90-22624
Production of a variety of shapes using wrapping and draping techniques
[REPT-892-430-122] 16 p2213 N90-22625
Dimensional analysis of structures using wrapping techniques
[REPT-892-430-119] 16 p2247 N90-22815

COMPOSITES
U COMPOSITE MATERIALS

COMPOSITION (PROPERTY)
NT ATMOSPHERIC COMPOSITION
NT ATMOSPHERIC MOISTURE
NT ATOM CONCENTRATION
NT CARBON DIOXIDE CONCENTRATION
NT CHEMICAL COMPOSITION
NT CONCENTRATION (COMPOSITION)
NT GAS COMPOSITION
NT IONOSPHERIC COMPOSITION
NT LOW CONCENTRATIONS
NT LUNAR COMPOSITION
NT METEORITIC COMPOSITION
NT METEOROID CONCENTRATION
NT MOISTURE CONTENT
NT PLANETARY COMPOSITION
NT PLASMA COMPOSITION
NT STELLAR COMPOSITION
Modeling of the dielectric behavior of composite materials
[CERT-1/1398-MO] 04 p0467 N90-12674
Resonance enhanced Raman studies of as-grown and laser-processed HgCdTe
[AD-A213855] 08 p1129 N90-16540

COMPOUNDING
Development of a titanium/boron blending process
[DE90-001450] 06 p0754 N90-14386

COMPRESSED AIR
Investigation and study on compressed air storage power generation system, part 2
[DE90-702648] 08 p1097 N90-16354

COMPRESSED GAS
NT HIGH PRESSURE OXYGEN
Electron production, electron attachment, and charge recombination process in high pressure gas discharges
[AD-A216301] 10 p1434 N90-18274
Martensitic transformation induced by stress pulses
[DE90-009534] 15 p2069 N90-21854

COMPRESSIBILITY
Compressibility of heavy nuclei at high temperatures
[KVI-792] 04 p0552 N90-13217
Spectral study of a compressible isotropic turbulence
[ECL-88-16] 05 p0643 N90-13753
Compression testing of carbon fibers
[AD-A215296] 09 p1187 N90-16877
New mixing-length model for numerical solution of turbulent supersonic flows 09 p1216 N90-17048
Elastic buckling of imperfect cylindrical shells containing granular solids
[PB90-110362] 09 p1236 N90-17174
Turbulence models for compressive flows 10 p1308 N90-17568
Insulation, compressibility and absorbency of dry suit undergarments
[AD-A215944] 10 p1414 N90-18149
Compression pylon
[NASA-CASE-LAR-13777-1] 13 p1755 N90-20078
Summary report of the Summer Conference of the DARPA-Materials Research Council
[AD-A217380] 13 p1767 N90-20143
Numerical simulation of vortex breakdown 14 p1970 N90-21288
An internal/external pressure, tension/compression multiaxial fatigue system
[DE90-009510] 14 p1994 N90-21430
Failure mechanisms under complex loading of glass-reinforced polyester composites and their matrices: The effect of superposed hydrostatic pressures up to 300 MPa on axial tensile and compressive strengths, and in-plane shear properties of unidirtionally reinforced glass-polyester composites and the relevant polyesters 15 p2110 N90-22072
Internal fractures in model elastomeric composites 15 p2121 N90-22133
Extra compressibility terms for Favre-averaged two-equation models of inhomogeneous turbulent flows
[NASA-CR-177556] 17 p2405 N90-23701
A comparison of the post-buckling behavior of metallic and composite plates with centrally located cutouts
[NIAR-90-14] 20 p2875 N90-26356
Isothermal compressibility of SPC/E water
[AD-A222723] 20 p2925 N90-26643
Study of the compressibility effects on the turbulence of supersonic drags
[ETN-90-97448] 22 p3109 N90-27661
Composite materials with improved properties in compression: Synthesis and dimerization 2,3-dimethyl-5-silaspiro(4.4)nona-2,7-diene
[AD-A222552] 22 p3156 N90-27692
Postbuckling response of long thick isotropic plates loaded in compression including higher order transverse shearing effects
[NASA-TM-4199] 22 p3190 N90-28100
Thermophysical properties of Helium-4 from 0.8 to 1500 K with pressures to 2000 MPa
[NASA-CR-186992] 23 p3303 N90-28681
An investigation of the inviscid spatial instability of compressible mixing layers
[AD-A223776] 24 p3468 N90-29596

COMPRESSIBILITY EFFECTS
Application of a Reynolds stress turbulence model to the compressible shear layer
[NASA-CR-182002] 12 p1660 N90-19537

COMPRESSIBLE BOUNDARY LAYER
Numerical solutions of the compressible 3-D boundary-layer equations for aerospace configurations with emphasis on LFC 04 p0443 N90-12534
Generalized similarity solutions for three dimensional, laminar, steady, compressible boundary layer flows on swept profile cylinders
[DLR-FB-89-34] 05 p0639 N90-13725
A computational model for thickening boundary layers with mass addition for hypersonic engine inlet testing
[AD-A216246] 10 p1310 N90-17576
Development of a defect stream function, law of the wall/wake method for compressible turbulent boundary layers
[NASA-CR-4286] 11 p1507 N90-18675
Amplitude-dependent neutral modes in compressible boundary layer flows
[NASA-TM-102524] 13 p1799 N90-20326
Surface-cooling effects on compressible boundary-layer instability
[NASA-CR-182003] 14 p1971 N90-21290
Development of a defect stream function, law of the wall/wake method for compressible turbulent boundary layers 15 p2100 N90-22019
Secondary instabilities in compressible boundary layers
[NASA-CR-182091] 23 p3269 N90-28502

COMPRESSIBLE FLOW
NT TRANSONIC FLOW
Three-dimensional unsteady transonic viscous-inviscid interaction 01 p0001 N90-10005
Numerical simulation of the compressible Orszag-Tang vortex
[AD-A210465] 01 p0127 N90-10725
Experimental research on swept shock Wave/Boundary layer interactions
[AD-A211744] 03 p0348 N90-11988
Flow quality measurements in compressible subsonic flows 04 p0441 N90-12521
Flux-corrected transport algorithms for two-dimensional compressible magnetohydrodynamics
[AD-A212757] 04 p0557 N90-13246
Inviscid 3D solution methods 05 p0640 N90-13736
Embedded function methods for compressible high speed turbulent flow
[NASA-CR-186131] 06 p0773 N90-14498
Irreversible processes from reversible mechanics
[DE90-001057] 07 p0927 N90-15368
Comments on compressible flow through butterfly valves
[DE89-015730] 07 p0928 N90-15371
Adaptive local grid refinement for the compressible 3-D Euler equations
[FFA-TN-1989-40] 08 p1064 N90-16155
Method for the primary stability analysis of the three dimensional, compressible boundary layer flows 08 p1066 N90-16171
An efficient solver of the Eigenvalue problem of the linear stability equations for three dimensional, compressible boundary-layer flows 08 p1066 N90-16172
Digital image interpretation for optical flow measurement methods: System description and preliminary application examples 08 p1079 N90-16244
Physical models for supersonic turbulent boundary layer structure
[AD-A215284] 09 p1160 N90-16716
An upwind-biased, point-implicit relaxation algorithm for viscous, compressible perfect-gas flows
[NASA-TP-2953] 09 p1214 N90-17042
New mixing-length model for numerical solution of turbulent supersonic flows 09 p1216 N90-17048
Pressure losses in flow through a sudden contraction of duct area
[ESDU-89040] 09 p1220 N90-17077
Skin friction measurements by laser interferometry in supersonic flows 10 p1306 N90-17557
Turbulence models for compressive flows 10 p1308 N90-17568
Liquid transverse jets in compressible crossflows 10 p1385 N90-18012
Numerical simulation of compressible vortices
[AD-A216221] 10 p1385 N90-18017
A numerical study of shock wave refraction at a CO2/CH4 interface
[DE90-005997] 10 p1386 N90-18022
Direct numerical simulation of aerodynamic noise
[AD-A214122] 10 p1426 N90-18225
Calculation of the unsteady two-dimensional, inviscid, compressible flow around a strongly cambered oscillating single blade 11 p1460 N90-18409
Semidiscrete Galerkin modelling of compressible viscous flow past a circular cone at incidence
[NASA-CR-186323] 11 p1505 N90-18664
Effect of a random wind field on thermal blooming instabilities
[DE90-007241] 11 p1532 N90-18823
Spectral simulation of unsteady compressible flow past a circular cylinder
[NASA-CR-182030] 13 p1750 N90-20050
Analysis of flow-, thermal-, and structural-interaction of hypersonic structures subjected to severe aerodynamic heating
[AD-A217882] 13 p1750 N90-20053
A numerical investigation of the compressible mixing layer
[AD-A217738] 13 p1802 N90-20343
Comparison of C- and O-grid generation methods using a NACA 0012 airfoil
[AD-A216375] 14 p1910 N90-20948
Numerical method for designing 3D turbomachinery blade rows 14 p1918 N90-20990
PROTEUS two-dimensional Navier-Stokes computer code, version 1.0. Volume 1: Analysis description
[NASA-TM-102551] 14 p1973 N90-21303
PROTEUS two-dimensional Navier-Stokes computer code, version 1.0. Volume 2: User's guide
[NASA-TM-102552] 14 p1973 N90-21306

Numerical investigation of separated transonic turbulent flows with a multiple-time-scale turbulence model
[NASA-TM-102499] 15 p2090 N90-21962
Partial acoustic filtering applied to the equations of compressible flow
[DE90-000673] 15 p2097 N90-22001
The calibration and measuring procedure of a five-hole hemispherical head probe in compressible flow
[LR-585] 15 p2099 N90-22013
The analysis and simulation of compressible turbulence
[NASA-CR-181997] 16 p2197 N90-22539
Estimation of extra drag force on a circular cylinder due to the presence of solid particles in subsonic compressible flow
[AD-A218635] 16 p2197 N90-22542
The effects of compressibility on a supersonic mixing layer
[AD-A219315] 16 p2197 N90-22543
Investigation of advanced counterrotation blade configuration concepts for high speed turboprop systems, task 1: Ducted propfan analysis
[NASA-CR-185217] 16 p2202 N90-22567
Nonstrictly hyperbolic conservation laws
[AD-A218525] 16 p2237 N90-22762
Computation of low Mach number compressible flow
17 p2344 N90-23346
Topology of three-dimensional, variable density flows
[NASA-CR-186522] 17 p2402 N90-23683
Computational modeling of three-dimensional compressible leading edge vortices
[AD-A221022] 18 p2553 N90-24569
Turbulence modeling in the SHALE code
[DE90-010354] 18 p2553 N90-24574
Thermodynamic and fluid mechanic analysis of rapid pressurization in a dead-end tube
18 p2631 N90-24990
Finite element formulations for compressible flows
18 p2632 N90-24996
Practical developments in holographic interferometry
[PNR90669] 20 p2866 N90-26302
Substitution principle theory for compressible flows
21 p2953 N90-26791
Summary of Discussions at the Eleventh Meeting of the Sandia Cooperative Group on the Aerothermochemistry of Turbulent Combustion
[DE89-001846] 21 p2973 N90-26896
Flame extinction in compressible flow
21 p2973 N90-26899
Direct numerical simulation of compressible free shear flows
21 p2974 N90-26901
Three-dimensional structure of boundary layers in transition to turbulence
[AD-A223242] 21 p3004 N90-27076
Parallel numerical simulations of axisymmetric projectile flows using zonal-overlapped grids
[AD-A221711] 21 p3005 N90-27082
Near-wall modelling of compressible turbulent flows
[NASA-CR-186961] 22 p3109 N90-27658
FINFLO: A finite-volume based computer program for two-dimensional and axisymmetric compressible flow
[PB90-189473] 22 p3169 N90-27974
Implicit solution of three-dimensional internal turbulent flows
[NASA-TM-103099] 22 p3170 N90-27982
The streamline diffusion finite element method for compressible and incompressible fluid flow
22 p3172 N90-27991
Computation of compressible, vortical flows
22 p3172 N90-27996
Development of turbulence models for the analysis of compressible or incompressible unsteady flow
[ETN-90-97486] 23 p3326 N90-28810
Numerical simulation supersonic free shear layers
[AD-A223771] 24 p3418 N90-29306
Thermal transfers in unsteady compressible inviscid flow
[ETN-90-97557] 24 p3419 N90-29311
An investigation of the inviscid spatial instability of compressible mixing layers
[AD-A223776] 24 p3468 N90-29596
Transition of the boundary layer
[DERAT-RSF-50/5018-37] 24 p3469 N90-29600

COMPRESSIBLE FLUIDS
Rayleigh-Taylor instability in compressible fluids
[DE90-003027] 07 p0929 N90-15376
Decay estimates for the compressible Navier-Stokes equations in the half-space
[PREPRINT-46] 08 p1065 N90-16163
Self-calibrating apparatus to find dynamic compressibility of organic solids
[AD-A219780] 17 p2415 N90-23763
Finite element formulations for coupled fluid/structure eigenvalue analysis
[AD-A220793] 17 p2416 N90-23766

COMPRESSING
NT PLASMA COMPRESSION
NT SPEECH BASEBAND COMPRESSION
The HEL (Hugoniot Elastic Limit) and rate-dependent yield behavior
[DE89-016981] 02 p0199 N90-11134
Magnetic flux compression
[DE89-016991] 02 p0271 N90-11546
Axial compression buckling test on the H-2 launch vehicle satellite fairing structural element prototype (aluminum surface plate/aluminum honeycomb sandwiched curved surface plate)
[NAL-TM-563] 03 p0356 N90-12039
Temperature effects in shock consolidation of metal powders
[DE89-016782] 04 p0474 N90-12716
Electric-gun studies of conductors in high magnetic fields and experiments in dynamic flux compression
[DE90-000815] 06 p0768 N90-14470
Comparison of protective breathing equipment performance at ground level and 8,000 feet altitude using parameters prescribed by portions of FAA action notice A-8150.2
[AD-A212852] 06 p0821 N90-14773
Compression phenomena in hard-saturated microwave amplifiers
[AD-A214546] 09 p1204 N90-16980
Comparison of tension, compression, and flexure creep for alumina and silicon nitride ceramics
[DE90-006154] 11 p1492 N90-18586
Shock compression of solids: A tutorial
[DE90-009185] 14 p2032 N90-21659
Fluid dynamic mechanisms and interactions within separated flows
[AD-A219628] 17 p2403 N90-23689
Compression molded polyurethane block copolymers. 1: Thermal and thermomechanical properties
[AD-A220068] 18 p2529 N90-24431
Thermodynamic and fluid mechanic analysis of rapid pressurization in a dead-end tube
18 p2631 N90-24990
A comparison of select image-compression algorithms for an electronic still camera 18 p2632 N90-24994
Innovative design of composite structures: Axisymmetric deformations of unsymmetrically laminated cylinders loaded in axial compression
[NASA-CR-186635] 19 p2700 N90-25364

COMPRESSION LOADS
NT AXIAL COMPRESSION LOADS
NT IMPACT LOADS
Dynamically compressed metals: Theory
[AD-A210741] 01 p0045 N90-10257
Short fibre and particulate reinforced metal matrix composites 07 p0901 N90-15207
Thermoelastic response of an epoxy
[AD-A215639] 09 p1198 N90-16942
Blow-out of rubber blocks due to internal heating
[AD-A215730] 09 p1198 N90-16943
Elastic buckling of imperfect cylindrical shells containing granular solids
[PB90-110362] 09 p1236 N90-17174
Piezoelectric polymer PVDF shock gauge: State of the research art
[ISL-CO-207/89] 11 p1512 N90-18705
Optimization of laminated composite plates
[AD-A217621] 13 p1768 N90-20146
Fracture and longevity of composite structures
[AD-A217827] 14 p1944 N90-21127
UNIVIMP: A universal instrument for the survey of initial imperfections of thin-walled shells
[PB90-167065] 14 p1984 N90-21369
Axisymmetric and cylindrically orthotropic analysis of filament winding 16 p2246 N90-22811
A computer simulation model for studying cervical spine injury prevention 19 p2721 N90-25476
Buckling and postbuckling behavior of square compression-loaded graphite-epoxy plates with circular cutouts
[NASA-TP-3007] 20 p2826 N90-26077
Experimental analysis of the buckling of composite plates under compression loads
[IMFL-89-28] 22 p3193 N90-28119

COMPRESSION RATIO
Development of advanced combustion technology for medium and high speed natural gas engines
[PB90-198565] 23 p3331 N90-28836

COMPRESSION TESTERS
U COMPRESSION TESTS

COMPRESSION TESTS
Delamination tests under static compression loading
02 p0186 N90-11061
Delamination tests under compression-compression and tension-compression loading 02 p0186 N90-11062
Nonlinear theories concerning laminated composites under compression with delamination
[ONERA-RT-19/3542-RY-081-R] 04 p0467 N90-12672
Orthotropic elasto-plastic behavior of AS4/APC-2 thermoplastic composite in compression
[NASA-CR-186080] 04 p0513 N90-12959
Mathematical simulation of dynamic compression tests using the Hopkinson bar method
[ISL-R-128/87] 04 p0513 N90-12960
Compression testing of carbon fibers
[AD-A215296] 09 p1187 N90-16877
Analysis of composite ring of compression test data
[DE90-004468] 09 p1239 N90-17194
Compression testing of thick-section composite materials
[AD-A217234] 13 p1767 N90-20142
Investigation of metal processing technology
[AD-A218835] 17 p2376 N90-23531
Self-calibrating apparatus to find dynamic compressibility of organic solids
[AD-A219780] 17 p2415 N90-23763

COMPRESSIVE STRENGTH
Characterizations of shock-loaded aluminum-infiltrated boron carbide cermets
[DE89-016773] 02 p0201 N90-11146
Orthotropic elasto-plastic behavior of AS4/APC-2 thermoplastic composite in compression
[NASA-CR-186080] 04 p0513 N90-12959
High modulus coatings
[AD-A215448] 09 p1198 N90-16941
Compressive strength of carbon/epoxy laminated under multiaxial stress
[DE90-005552] 11 p1478 N90-18505
Compressive strength of synthetic comet nucleus samples 12 p1741 N90-20006
Through-thickness strain response of thick composites in compression
[AD-A217233] 13 p1767 N90-20141
Compression testing of thick-section composite materials
[AD-A217234] 13 p1767 N90-20142
Compressive behavior of laminated composite structures 14 p1945 N90-21134
Experimental observations and finite element analysis of the initiation of fiber microbuckling in notched composite laminates
[NASA-CR-186207] 19 p2699 N90-25359
The interaction of polymeric materials with ceramic surfaces with special reference to the behaviour of bioceramics 20 p2836 N90-26127
Resistivity, adhesive strength, and residual stress measurements of thin film metallizations on single crystal quartz
[DE90-011902] 20 p2837 N90-26135
Compressive strength of rigid-rod polymer fibers
[AD-A221886] 21 p2989 N90-26987

COMPRESSOR BLADES
The measurement of boundary layers on a compressor blade in cascade. Volume 1: Experimental technique, analysis and results
[NASA-CR-185118-VOL-1] 01 p0009 N90-10038
The measurement of boundary layers on a compressor blade in cascade. Volume 2: Data tables
[NASA-CR-185118-VOL-2] 01 p0009 N90-10039
Dynamic analysis of rotors under interference rubs
02 p0229 N90-11312
Blading design for multi-storage HP compressor
[PNR90602] 04 p0456 N90-12616
Performance of a highly-loaded HP compressor
[RAE-TM-P-1149] 08 p1024 N90-15919
A method for the prediction of supersonic compressor blade performance
[CUED/A-TURBO/TR-126] 10 p1321 N90-17634
Inverse computation of transonic internal flows with application for multi-point-design of supercritical compressor blades 14 p1918 N90-20987
Forcing function effects on rotor row unsteady aerodynamic response in a multistage compressor
16 p2196 N90-22536
Application of neural networks to the F/A-18 engine condition monitoring system
[AD-A219820] 18 p2497 N90-24271
Structural testing and analytical research of turbine components
[AD-A223516] 24 p3434 N90-29396
Experimental study on the dynamic behavior of a revolving blade grill
[REPT-NT-89-CC-18] 24 p3470 N90-29604

COMPRESSOR EFFICIENCY
Dynamic tip clearance measurements in axial flow compressors
[PNR90597] 04 p0456 N90-12612
The development of a T53-L11 engine computer model
[AD-A214533] 09 p1188 N90-16780

Small displacement, long life on-orbit compressor design and fabrication 11 p1475 N90-18489
Energy Efficient Engine acoustic supporting technology report
[NASA-CR-174834] 23 p3279 N90-28557

COMPRESSOR ROTORS
Advanced technologies impact on compressor design and development: A perspective
[NASA-TM-102341] 02 p0156 N90-10891
Dynamic analysis of rotors under interference rubs 02 p0229 N90-11312
An experimental, analytical, and computational investigation of turbomachinery rotor flow fields 07 p0926 N90-15360
Flow in a forward swept centrifugal fan, volumes 1 and 2 14 p1912 N90-20959
Prediction and measurement of rotor blade/stator vane dynamic characteristics of a modern aero-engine axial compressor
[PNR90667] 20 p2812 N90-26002

COMPRESSORS
NT CENTRIFUGAL COMPRESSORS
NT SUPERCHARGERS
NT SUPERSONIC COMPRESSORS
NT TURBOCOMPRESSORS
Stage effects on stalling and recovery of a high-speed 10-stage axial-flow compressor 04 p0454 N90-12600
Space station gas compressor technology study program, phase 1
[NASA-CR-183758] 05 p0601 N90-13491
Externally vaporizing system for turbine combustor
[AD-D014284] 08 p1024 N90-15918
Numerical investigation of unsteady flow in oscillating turbine and compressor cascades 11 p1459 N90-18407
Experiments on the unsteady flow in a supersonic compressor stage 11 p1462 N90-18422
Experimental investigation of the influence of rotor wakes on the development of the profile boundary layer and the performance of an annular compressor cascade 11 p1463 N90-18425
Compressor performance tests in the compressor research facility 11 p1463 N90-18428
Small displacement, long life on-orbit compressor design and fabrication 11 p1475 N90-18489
Analyses of power consumption for two sliding vane type compressors
[AD-A218366] 13 p1812 N90-20406
Secondary flows and radial mixing predictions in axial compressors 14 p1922 N90-21010
WINCOF-I code for prediction of fan compressor unit with water ingestion
[NASA-CR-185157] 15 p2045 N90-21724
Unsteady flow phenomena in turbomachines
[AD-A218370] 17 p2402 N90-23680
Off-design loss measurements in a compressor cascade
[AD-A220094] 18 p2552 N90-24564
Performance evaluation of LE-7 high pressure pumps
[DE90-505523] 20 p2817 N90-26034
The effects of a compressor rebuild on gas turbine engine performance: Final results 23 p3306 N90-28701

COMPTON EFFECT
Proof of the feasibility of coherent and incoherent schemes for pumping a gamma-ray laser
[AD-A212315] 04 p0506 N90-12921
Background studies in gas ionizing x ray detectors 12 p1636 N90-19399
Compton amplifier
[DIGEL-1985-5] 12 p1654 N90-19506
QCD Compton scattering at HERA energy
[NIKHEF-H/89-3] 15 p2165 N90-22372
Spectral evolution of active galactic nuclei Penrose Compton scattering processes and gamma ray emission from Seyfert galaxies 16 p2337 N90-23317
OSSE observations of active galactic nuclei 16 p2337 N90-23320
LEP and CEBAF polarimeters
[CEBAF-PR-89-010] 19 p2757 N90-25667
Is the hard tail of X rays from GX339-4 a Compton scattering component 19 p2779 N90-25806
Self-consistent Comptonised models for the spectra of low mass X ray binaries 19 p2780 N90-25817
The role of comptonisation in energy spectra of standard QPO-sources 19 p2781 N90-25820
Ion-heated thermal comptonization models and X ray spectral correlations in active galactic nuclei 19 p2790 N90-25880
Thermal comptonization in accretion disks 19 p2791 N90-25890
X ray emission from relativistic jets in AGNs and statistical implications 19 p2792 N90-25893
X ray spectral index variability in NGC 4151 19 p2795 N90-25911
Ground level atmospheric gamma ray flux measurements in the 1 to 6 MeV range 22 p3264 N90-28483

COMPUTATION
NT COMPUTATIONAL GEOMETRY
NT ORBIT CALCULATION
Proceedings of the Workshop on Computational Aspects in the Control of Flexible Systems, part 1
[NASA-TM-101578-PT-1] 01 p0017 N90-10080
Proceedings of the Workshop on Computational Aspects in the Control of Flexible Systems, part 2
[NASA-TM-101578-PT-2] 01 p0021 N90-10103
On learning from exercises
[AD-A210593] 01 p0101 N90-10574
Regulation of nonlinear and generalized linear systems
[AD-A207725] 01 p0109 N90-10619
Computational aspects of sensitivity calculations in linear transient structural analysis 02 p0231 N90-11327
Calculated solar radiation incident upon slopes of different orientated surfaces in Finland
[FMI-MP-8] 03 p0370 N90-12116
The J-Machine: A fine grain concurrent computer
[AD-A211909] 03 p0384 N90-12187
Scheduling sporadic and aperiodic events in a hard real-time system
[AD-A211344] 03 p0387 N90-12205
Fast computation using faulty hypercubes
[AD-A211910] 03 p0393 N90-12238
Analysis of carbon fiber's x ray microscopic structure
[AD-A212215] 04 p0480 N90-12752
Direction-of-arrival calculations at VLF/LF (Very Low Frequency/Low Frequency)
[AD-A212620] 04 p0493 N90-12833
Comments on the use of LOWTRAN in transmission calculations for sites with the ground elevated relative to sea level
[AD-A212724] 04 p0519 N90-12995
Labeled trees and the efficient computation of derivations
[NASA-CR-185386] 04 p0538 N90-13113
Multivariable divided difference and B-splines
[MEMO-772] 04 p0544 N90-13160
On new methods for computing with multivariate B-splines
[MEMO-783] 04 p0547 N90-13183
Direct computation of 3D shape invariants and the focus of expansion
[AD-A212386] 04 p0549 N90-13195
Ground states of a two-dimensional charged-boson system
[AD-A212363] 04 p0553 N90-13226
Thermochemical calculations with inert compounds
[FOA-C-20759-2.1] 05 p0630 N90-13677
Computation of nonequilibrium gas flow past blunt bodies
[PREPRINT-488] 05 p0644 N90-13757
Comparison of analytical methods for calculation of wind loads
[NASA-TM-102782] 05 p0654 N90-13813
On the recurrence relation for multivariate B-splines with respect to dimension
[MEMO-786] 05 p0689 N90-14017
The weighted sum of two S-units being a square
[MEMO-792] 05 p0691 N90-14031
Solving a specific Thue-Mahler equation
[MEMO-793] 05 p0691 N90-14032
Measurement of arithmetic error and calculation perturbations
[IMAG-RR-767-M] 05 p0692 N90-14039
Towards ab initio calculation of electron energies in semiconductors
[ETN-90-96016] 05 p0704 N90-14121
Example of procedure in calculation of control hinge moments
[ESDU-89010] 06 p0727 N90-14240
Enhanced resolution concepts in large scale scientific computing
[AD-A214095] 07 p0932 N90-15393
Portable digital pressure indicator for calibrating magnetic tape recorders
[NASA-TM-101650] 07 p0933 N90-15401
Multi-dimensional modeling of convective heat transfer with application to I.C. engines
[DE90-003245] 07 p0941 N90-15451
Calculation of source and structure parameters at regional and teleseismic distances
[AD-A214297] 07 p0961 N90-15558
Specification for evaporation duct height calculations
[AD-A213841] 07 p0964 N90-15570
A paradigm for robust geometric algorithms
[AD-A214324] 07 p0978 N90-15647
Hierarchical process composition: Dynamic maintenance of structure in a distributed environment
[AD-A214325] 07 p0978 N90-15648
MASC: Multiprocessor architecture for symbolic processing
[AD-A213504] 07 p0979 N90-15656
An algorithm to compute the square root of 3x3 positive definite matrix
[DE89-635711] 08 p1109 N90-16417
Complexity of human language comprehension
[AD-A214591] 09 p1258 N90-17299
EDISON Project
[AD-A214724] 09 p1265 N90-17338
Two adaptive techniques let progressive refinement outperform the traditional radiosity algorithm
[AD-A215174] 09 p1267 N90-17347
Parallel functional computation
[AD-A214627] 09 p1269 N90-17360
On calculating analytic centers
[AD-A215635] 09 p1274 N90-17385
A review of high-speed, convective, heat-transfer computation methods 10 p1305 N90-17548
A computational model for thickening boundary layers with mass addition for hypersonic engine inlet testing
[AD-A216246] 10 p1310 N90-17576
Hypercube expert system shell-applying production parallelism
[AD-A215762] 10 p1418 N90-18173
A hundred impossibility proofs for distributed computing
[AD-A216391] 10 p1419 N90-18180
Measuring Day-Night Noise Levels (DNL) using the metrosonics db-310 sound level analyzer (Dosimeter)
[AD-A215757] 10 p1427 N90-18230
Calculations of braiding parameters
[AD-A216836] 11 p1479 N90-18515
Computation and control with neural nets
[DE90-006460] 11 p1548 N90-18911
Research equipment
[AD-A216515] 11 p1552 N90-18937
Speculative computation in multilisp
[AD-A216579] 11 p1575 N90-19067
Visual processing in texture segregation
[AD-A216539] 12 p1696 N90-19737
Adaptive, asynchronous stochastic global optimization algorithms for sequential and parallel computation
[AD-A217093] 12 p1702 N90-19775
Computation at the edge of chaos: Phase transition and emergent computation
[DE90-007488] 12 p1708 N90-19811
BCS (Bardeen-Cooper-Schrieffer) primer: A guide to computational methods in superconductivity theory
[AD-A216393] 12 p1719 N90-19874
A matrix-free locally-implicit scheme for Navier-Stokes equations
[AD-A218298] 13 p1803 N90-20349
Long range geoid control through the European GPS traverse: Final results 13 p1837 N90-20545
Research in programming languages and software engineering
[AD-A217765] 13 p1868 N90-20715
Optimization of series expressions. Part 1: User's manual for the series macro package
[AD-A218220] 13 p1869 N90-20725
Fast method for computing infrared transmission, computation examples 15 p2086 N90-21942
Bearing elastohydrodynamic lubrication: A complex calculation made simple
[NASA-TM-102575] 15 p2105 N90-22041
The Shock and Vibration Digest, volume 21, no. 2 15 p2109 N90-22059
Computation and parallel implementation for early vision 15 p2139 N90-22222
The preprocessed doacross loop
[NASA-CR-182056] 16 p2276 N90-22972
A nearly-linear computational-cost scheme for the forward dynamics of an N-body pendulum 16 p2280 N90-22996
Computational issue in the analysis of adaptive control systems 16 p2281 N90-23001
Parallel and vector computation for stochastic optimal control applications 16 p2282 N90-23007
A unifying framework for rigid multibody dynamics and serial and parallel computational issues 16 p2283 N90-23009
Parallel algorithms and architecture for computation of manipulator forward dynamics 16 p2283 N90-23010
Computational dynamics for robotics systems using a non-strict computational approach 16 p2283 N90-23011
Locality in parallel computation
[AD-A218733] 16 p2302 N90-23120
A computational method for general higher index nonlinear singular systems of differential equations
[AD-A219164] 16 p2307 N90-23147
Hypersonic aerodynamics of spacecraft
[DLC-EST-TD-032] 17 p2346 N90-23361
The standard map machine
[AD-A219943] 17 p2441 N90-23908

Calculation of Lie algebra cohomology by computer
[MEMO-833] 17 p2449 N90-23962
Inverting the flow of computation
[TR-89-10] 17 p2450 N90-23971
On the parallel solution of parabolic equations
[NASA-CR-180363] 17 p2455 N90-24009
Optical computing strategies
[AD-A219433] 17 p2472 N90-24131
On computational aspects of simplicial splines
[MEMO-818] 18 p2600 N90-24795
Computing Boolean functions on anonymous networks
[CWI-CS-R8935] 18 p2602 N90-24818
Distributed computing on transitive networks: The torus
[RUU-CS-88-31] 18 p2634 N90-25007
Effects of simplifying assumptions on optimal trajectory estimation for a high-performance aircraft
[NASA-TM-101721] 19 p2661 N90-25142
Computational crash dynamics. Project 1.2: Computational crash dynamics analysis
[IAR-89-19] 20 p2804 N90-25956
Superconcurrent processing: A dynamic approach to heterogeneous parallelism
[AD-A222798] 20 p2914 N90-26576
Causal distributed breakpoints
[AD-A222613] 20 p2921 N90-26622
Molecular interactions and properties with many-body methods
[AD-A222631] 20 p2924 N90-26642
Full vector wave calculation of photonic band structures in face-centered cubic dielectric media
[AD-A222616] 20 p2933 N90-26686
Information sciences experiment system
21 p3015 N90-27142
A LOWTRAN7 sensitivity study in the 8-12 and 3-5 micron bands: Includes comparison with LOWTRAN6 results
[AD-A222094] 21 p3031 N90-27231
Curvature estimation in orientation selection
[AD-A221481] 21 p3034 N90-27249
On finding supernodes for sparse matrix computations
[DE90-013626] 21 p3063 N90-27410
Consequences of monotonicity for Markov transition functions
[AD-A222852] 21 p3063 N90-27412
The Helicopter Antenna Radiation Prediction Code (HARP)
[NASA-CR-186925] 22 p3165 N90-27946
Techniques and potential capabilities of multi-resolutional information (knowledge) processing
23 p3374 N90-29062
Parallel algorithms for computation of the manipulator inertia matrix
23 p3376 N90-29072
Block Lanczos algorithm
[AD-A224011] 23 p3383 N90-29111
Thermal transfers in unsteady compressible inviscid flow
[ETN-90-97557] 24 p3419 N90-29311
Estimation of liquid heat capacities. 1: Review and evaluation of Misserard method
[AD-A224161] 24 p3445 N90-29454
Accurate calculations of neutron kerma and damage from ENDF/B-VI evaluations for silicon, chromium, iron and nickel, and comparison with ENDF/B-V results
[DE90-016020] 24 p3481 N90-29674
Recent developments in shell stability analysis
[LR-633] 24 p3483 N90-29685
MUSE: A systolic array for adaptive nulling with 64 degrees of freedom, using Givens transformations and wafer scale integration
[AD-A223812] 24 p3529 N90-29953
A canonical integration technique of arbitrary order
[DE90-628377] 24 p3541 N90-30025
On a calculation of the ground-state energy in quantum mechanics
[DE90-627182] 24 p3555 N90-30119

COMPUTATIONAL ASTROPHYSICS

The physics of double layers and their role in astrophysics
[TRITA-EPP-89-03] 03 p0421 N90-12421
Turbulization of shear flows in astrophysics
19 p2773 N90-25763

COMPUTATIONAL CHEMISTRY

Quantum-theoretical methods and studies relating to properties of materials
[AD-A217643] 13 p1765 N90-20132
On upwind formulations and non equilibrium chemistry
[DLC/FLU-INT-TN-014] 17 p2403 N90-23691
Computed structures of polyimides model compounds
[NASA-TM-101674] 19 p2672 N90-25195

COMPUTATIONAL FLUID DYNAMICS

Three-dimensional unsteady transonic viscous-inviscid interaction
01 p0001 N90-10005
An integrated CFD/experimental analysis of aerodynamic forces and moments
[NASA-TM-102195] 01 p0002 N90-10006
The measurement of boundary layers on a compressor blade in cascade. Volume 1: Experimental technique, analysis and results
[NASA-CR-185118-VOL-1] 01 p0009 N90-10038
The measurement of boundary layers on a compressor blade in cascade. Volume 2: Data tables
[NASA-CR-185118-VOL-2] 01 p0009 N90-10039
Stability and Control of Tactical Missile Systems
[AGARD-CP-451] 01 p0011 N90-10050
The present status and the future of missile aerodynamics
01 p0012 N90-10051
Prediction of tactical missile dynamics
01 p0012 N90-10056
Fluid Dynamics of Three-Dimensional Turbulent Shear Flows and Transition
[AGARD-CP-438] 01 p0062 N90-10356
Stability and transition of three-dimensional boundary layers
01 p0062 N90-10357
Direct numerical study of leading-edge contamination
01 p0063 N90-10361
Numerical investigation of the effects of longitudinal vortices on the onset of transition in a flat plate boundary layer
01 p0063 N90-10363
Primary and secondary stability analysis applied to the DFVLR-transition swept-plate experiment
01 p0065 N90-10371
Numerical investigation of transition in 3D boundary layers
01 p0065 N90-10372
Numerically determined transition in separated internal flow
01 p0065 N90-10374
Control and modification of turbulence
01 p0066 N90-10377
Turbulence modelling of three-dimensional shear flows
01 p0066 N90-10381
Numerical simulation of turbulent plane channel flows
01 p0067 N90-10382
Numerical simulation of coherent structures in an incompressible mixing layer
01 p0067 N90-10383
A composite velocity procedure for the three-dimensional reduced Navier-Stokes equations
01 p0069 N90-10396
A high-order Lagrangian-decoupling method for the incompressible Navier-Stokes equations
[NASA-CR-181903] 01 p0111 N90-10631
Linear instability of supersonic plane wakes
[NASA-CR-181911] 02 p0146 N90-10833
An experimental investigation of the aerodynamic characteristics of slanted base ogive cylinders using magnetic suspension technology
[NASA-CR-181708] 02 p0146 N90-10834
Computation of the tip vortex flowfield for advanced aircraft propellers
[NASA-CR-182179] 02 p0146 N90-10836
A parallel numerical simulation for supersonic flows using zonal overlapped grids and local time steps for common and distributed memory multiprocessors
[DE89-015252] 02 p0147 N90-10839
International conference on numerical grid generation in computational fluid dynamics
[AD-A211082] 02 p0220 N90-11262
Chemical reactions in turbulent mixing flows
[AD-A211240] 02 p0220 N90-11263
Pressure correction splitting methods for the computation of oscillatory free convection in low Pr fluids
[CWI-NM-R8816] 02 p0222 N90-11271
A conforming spectral collocation strategy for Stokes flow through a channel contraction
[NASA-CR-181912] 02 p0263 N90-11495
Computer simulation of aircraft aerodynamics
[NASA-TM-102221] 03 p0300 N90-11699
Analytical studies of three-dimensional combustion processes
[AD-A211903] 03 p0323 N90-11837
Hopf bifurcation in the driven cavity
[NASA-TM-102334] 03 p0345 N90-11969
Simulation of glancing shock wave and boundary layer interaction
[NASA-TM-102233] 03 p0345 N90-11970
Numerical analysis, scientific computing and fundamental studies of fluid mechanics
[DE89-017554] 03 p0346 N90-11975
Near-wall, three-dimensional turbulence measurements: A challenge for laser velocimetry
[NASA-TM-102252] 03 p0346 N90-11978
Computational methods for complex flowfields
[AD-A211485] 03 p0347 N90-11983
A simplified self-adaptive grid method, SAGE
[NASA-TM-102198] 03 p0388 N90-12211
Rotational and vibrational nonequilibrium effects in rarefied, hypersonic flow
[NASA-CR-182559] 04 p0437 N90-12498
Numerical algorithms for steady and unsteady incompressible Navier-Stokes equations
[NASA-CR-186039] 04 p0437 N90-12499
Research in Natural Laminar Flow and Laminar-Flow Control, part 2
[NASA-CP-2487-PT-2] 04 p0440 N90-12519
Sensitivity of LFC techniques in the non-linear regime
04 p0442 N90-12533
Numerical solutions of the compressible 3-D boundary-layer equations for aerospace configurations with emphasis on LFC
04 p0443 N90-12534
Numerical experiments on transition control in wall-bounded shear flows
04 p0443 N90-12536
CFD methods for drag prediction and analysis currently in use in UK
[RAE-TM-AERO-2146] 04 p0448 N90-12563
Aerodynamic test and analysis of a slender generic missile configuration
[AD-A212522] 04 p0448 N90-12567
Numerical study of three-dimensional spatial instability of a supersonic flat plate boundary layer
[NASA-CR-181931] 04 p0499 N90-12874
A multigrid method for the Navier-Stokes and Boussinesq equations
[REPT-89-17] 04 p0501 N90-12886
An implicit Navier-Stokes solver optimised for a vector-parallel computer
[VKI-TN-169] 04 p0501 N90-12890
A knowledge-based approach to automated flow-field zoning for computational fluid dynamics
[NASA-TM-101072] 04 p0528 N90-13048
Analysis of experimental data for CAST 10-2/DOA 2 supercritical airfoil at low Reynolds numbers and application to high Reynolds number flow
[AD-A211654] 05 p0571 N90-13326
Correlation of Puma airloads: Lifting-line and wake calculation
[NASA-TM-102212] 05 p0572 N90-13327
Computation of viscous incompressible flows
[NASA-TM-101090] 05 p0572 N90-13329
Block-structured solution of three-dimensional transonic flows using parallel processing
[AD-A212851] 05 p0572 N90-13330
Study of the integration of wind tunnel and computational methods for aerodynamic configurations
[NASA-TM-102196] 05 p0572 N90-13332
A CFD study of tilt rotor flowfields
[NASA-CR-186116] 05 p0575 N90-13349
Computation of Navier-Stokes equations for three-dimensional flow separation
[NASA-TM-102266] 05 p0575 N90-13353
Recent progress in research pertaining to estimates of gas-side heat transfer in an aircraft gas turbine
[NASA-TM-102460] 05 p0582 N90-13394
SSME LOX post flow analysis/fluid structure interaction. Volume 2: Fluid structure interaction
[NASA-CR-183678] 05 p0637 N90-13716
A three-dimensional potential flow analysis of dynamic fluid forces acting on a whirling centrifugal impeller bounded by a volute
05 p0637 N90-13717
Multigrid and defect correction for the steady Navier-Stokes equations: Applications to aerodynamics
[ETN-90-96011] 05 p0639 N90-13727
Numerical simulation of transition in three-dimensional boundary layers
[DLR-FB-89-12] 05 p0639 N90-13728
Turbulent Shear Flows
[VKI-LS-1989-03] 05 p0640 N90-13730
Numerical Methods for Flows in Turbomachinery, volume 1
[VKI-LS-1989-06-VOL-1] 05 p0640 N90-13735
Inviscid 3D solution methods
05 p0640 N90-13736
Inviscid 2D solutions on unstructured, adaptive grids
05 p0640 N90-13737
Flows with tip leakage
05 p0641 N90-13740
Navier-Stokes simulation of the crossflow instability in swept-wing flows
[NASA-CR-186122] 05 p0641 N90-13744
Numerical investigations in three-dimensional internal flows
[NASA-CR-186068] 06 p0718 N90-14189
Efficient real gas Navier-Stokes computations of high speed flows using an LU scheme
[NASA-TM-102429] 06 p0720 N90-14203
An analysis of the viscous flow through a compact radial turbine by the average passage approach
[NASA-TM-102471] 06 p0720 N90-14206
Advanced 3-D CFD algorithm for turbomachinery
06 p0725 N90-14233
Temporally and spatially resolved flow in a two-stage axial compressor. Part 2: Computational assessment
[NASA-TM-102273] 06 p0726 N90-14236
A dynamic multiblock approach to solving the unsteady Euler equations about complex configurations
06 p0773 N90-14497
An entropy based approach to nonlinear stability
06 p0773 N90-14500

Applications of a new exact solution of the Navier-Stokes equations to flow in pipes of varying width
06 p0774 N90-14504
A numerical technique for analysis of resistojet nozzle flow
06 p0775 N90-14506
An experimental investigation of shear layer mixing in supersonic flows
06 p0775 N90-14508
Comparative study of the vorticity field in turbulent flows: Theory, experiments, and computations
[DE90-001399] 06 p0776 N90-14516
Unsteady aerodynamics of oscillating and rapidly pitched airfoils
07 p0875 N90-15074
Finite difference techniques and rotor blade aeroelastic partial differential equations with quasisteady aerodynamics
07 p0875 N90-15075
Hypersonic nozzle design
[NASA-CR-186261] 07 p0876 N90-15077
Spatially-resolved, nonintrusive measurements in a nonreacting scramjet combustor using laser-induced iodine fluorescence
07 p0881 N90-15103
Explicit and implicit calculations of turbulent cavity flows with and without yaw angle
[NASA-CR-186293] 07 p0929 N90-15381
Research in mathematics and computer science at Argonne
[DE90-000975] 07 p0969 N90-15595
Assessment of computational prediction of tail buffeting
[NASA-TM-101613] 08 p1018 N90-15886
Weapon aerodynamics overview
[RAE-TM-AERO-2150] 08 p1018 N90-15888
A numerical simulation of the flow in the diffuser of the NASA Lewis icing research tunnel
[NASA-TM-102480] 08 p1032 N90-15965
The Suprenum architecture and its application to computational fluid dynamics
[GMD-389] 08 p1065 N90-16161
Decay estimates for the compressible Navier-Stokes equations in the half-space
[PREPRINT-46] 08 p1065 N90-16163
Calculation of the flow field of a multiblade helicopter rotor using a Euler method including the wake
08 p1069 N90-16189
Calculation of the flap profile flows with separation based on coupled potential and boundary layer solutions
08 p1069 N90-16191
A finite volume calculation method for three dimensional, complex flows
08 p1070 N90-16195
A space-time discretization procedure for wave propagation problems
[NASA-TM-102215] 08 p1105 N90-16399
A new finite element formulation for CFD:8. The Galerkin/least-squares method for advective-diffusive equations
[DE89-636437] 08 p1116 N90-16462
Investigation of liquid sloshing in spin-stabilized satellites
[AD-A214730] 09 p1182 N90-16853
Computational fluid dynamics
[NASA-TM-102922] 09 p1216 N90-17052
Appendage flow computations using the INS3D computer code
[AD-A215689] 09 p1218 N90-17066
Theoretical and experimental approach of wave phenomena in free jets
[ISL-CO-247/88] 09 p1219 N90-17069
Formation of a pair of turbulent layers in the region of a flow around an axisymmetric body with an incidence angle
[ISL-R-130/87] 09 p1219 N90-17070
Formation of turbulent layers in the separated region around a body with polygonal cross section at large incidence and rolling
[ISL-R-101/88] 09 p1219 N90-17071
Study for the dissipative structures geometry in three dimensional developed turbulence
[ETN-90-96102] 09 p1219 N90-17072
NASA aerodynamics program
[NASA-TM-4175] 09 p1247 N90-17235
An entropy-based approach to nonlinear stability
[NASA-TM-101086] 09 p1272 N90-17376
Sampling scattered data onto rectangular grids for volume visualization
[AD-A215533] 09 p1274 N90-17384
Missile Aerodynamics: NEAR Conference on Missile Aerodynamics
[ISBN-0-9620629-1-X] 10 p1303 N90-17540
The role of computational fluid dynamics in missile aerodynamics
10 p1304 N90-17547
Prediction methods for store separation
10 p1305 N90-17549
Numerical solutions of the linearized Euler equations for unsteady vortical flows around lifting airfoils
[NASA-TM-102466] 10 p1307 N90-17562
Analysis and numerical solution of flow over airfoil with control flap
10 p1307 N90-17564
Special Course on Three-Dimensional Supersonic/Hypersonic Flows Including Separation
[AGARD-R-764] 10 p1308 N90-17565
Opportunities for improved understanding of supersonic and hypersonic flows
10 p1308 N90-17566
Computation of compressible viscous flows
10 p1308 N90-17567
Turbulence models for compressive flows
10 p1308 N90-17568
Shock-shock boundary layer interactions
10 p1308 N90-17569
Axial flow in corners at supersonic and hypersonic speeds
10 p1308 N90-17570
Reacting flows
10 p1309 N90-17573
Viscous three-dimensional analyses for nozzles for hypersonic propulsion
[NASA-CR-185197] 10 p1321 N90-17635
Application of Jameson's type nonlinear artificial dissipation to the two-dimensional Navier-Stokes computation
[NAL-TR-1015T] 10 p1384 N90-18006
Conditions at the downstream boundary for simulations of viscous incompressible flow
[NASA-TM-102510] 10 p1422 N90-18198
Acoustic radiation of cylindrical shells, with stiffening finishing and coated with masking materials
[ISAL-89-0035] 10 p1426 N90-18227
Prediction of rotor blade-vortex interaction noise from 2-D aerodynamic calculations and measurements
[ISL-CO-243/88] 11 p1451 N90-18365
Aerodynamics of unsteady systems. Numerical study of potential flow/boundary layer coupling
[ETN-90-96257] 11 p1452 N90-18367
Study of the blade/vortice interaction on a one-blade rotor during forward flight (incompressible, non viscous fluid)
[ISL-R-115/88] 11 p1456 N90-18391
Unsteady Aerodynamic Phenomena in Turbomachines
[AGARD-CP-468] 11 p1459 N90-18405
Calculation of the unsteady two-dimensional, inviscid, compressible flow around a strongly cambered oscillating single blade
11 p1460 N90-18409
Aerodynamic superposition principle in vibrating turbine cascades
11 p1460 N90-18410
Unsteady blade loads due to wake influence
11 p1460 N90-18413
Unsteady aerodynamic phenomena in a simulated wake and shock wave passing experiment
11 p1461 N90-18414
Gust response analysis for cascades operating in nonuniform mean flows
11 p1461 N90-18415
Numerical prediction of axial turbine stage aerodynamics
11 p1461 N90-18416
Numerical simulation of three-dimensional unsteady flows in turbomachines
11 p1461 N90-18417
Blade row interaction effects on compressor measurements
11 p1462 N90-18419
High-resolution Euler computations of unsteady transonic flows in cascades
11 p1462 N90-18420
Modelling unsteady transition and its effects on profile loss
11 p1462 N90-18423
Methods for making unsteady aerodynamic pressure measurements in a rotating turbine stage
11 p1463 N90-18426
Measurement of velocity profiles and Reynolds stresses on an oscillating airfoil
11 p1463 N90-18427
Stall and recovery in multistage axial flow compressors
11 p1464 N90-18429
Cold flow determination of the internal flow environment around the submerged TVC nozzle for the space shuttle SRM
11 p1470 N90-18465
Experimental flow models for SSME flowfield characterization
11 p1471 N90-18469
Improved computational fluid dynamics for continuum hypersonic flow
[AD-A216981] 11 p1506 N90-18674
Direct simulation Monte Carlo of shock reflexion on a wedge with boundary layer
[ISL-CO-245/88] 11 p1508 N90-18681
Spectral multi-domain approximation of the Navier-Stokes equations in curved complex geometries
[ONERA-NT-1987-2] 11 p1508 N90-18685
Numerical simulation of the incompressible inhomogeneous turbulence in a plane channel flow
[ONERA-NT-1988-5] 11 p1508 N90-18686
Interaction between oblique-angled incident shock wave and turbulent boundary layer on a heated wall. Experimental results
[ONERA-RT-84/7078-AY] 11 p1509 N90-18688
Numerical simulation of the vortex breakdown
[ONERA-RSF-4/4368-AY-004A] 11 p1509 N90-18689
On the evaluation of aerodynamic influence coefficients
[NLR-MP-87019-U] 12 p1597 N90-19191
Computation of hypersonic unsteady viscous flow over a cylinder
12 p1597 N90-19194
A streamwise upwind algorithm applied to vortical flow over a delta wing
[NASA-TM-102225] 12 p1599 N90-19201
External flow computations for a finned 60mm ramjet in steady supersonic flight
[AD-A216998] 12 p1605 N90-19233
Experimental and theoretical investigations of flowfields and heat transfer in modern gas turbines
[AD-A217663] 12 p1605 N90-19237
Numerical study of diffusion jet flames
12 p1621 N90-19316
Potential theory of radiation
12 p1635 N90-19395
The influence of a wall function on turbine blade heat transfer prediction
12 p1640 N90-19421
Numerical and experimental analysis of a thin liquid film on a rotating disk related to development of a spacecraft absorption cooling system
[NASA-CR-183457] 12 p1657 N90-19523
Computational fluid dynamics method for low Reynolds number flow in a precessing/spinning, liquid filled cylinder with rounded endcaps
[AD-A216997] 12 p1659 N90-19531
Swept shock/boundary layer interaction experiments in support of CFD code validation
[NASA-CR-186397] 12 p1659 N90-19535
Flow simulation for aircraft
[NLR-MP-87082-U] 12 p1661 N90-19543
Viscous shock profiles and primitive formulations
[NASA-CR-182029] 13 p1750 N90-20049
Numerical simulations of supersonic flow through oscillating cascade sections
[NASA-TM-103100] 13 p1750 N90-20051
Comparison of 3-D viscous flow computations of Mach 5 inlet with experimental data
[NASA-TM-102518] 13 p1757 N90-20090
Composite-grid techniques and adaptive mesh refinement in computational fluid dynamics
[AD-A217383] 13 p1800 N90-20328
Interior fluid dynamics of liquid-filled projectiles
[AD-A217630] 13 p1800 N90-20330
Numerical simulation methods of incompressible flows and an application to the space shuttle main engine
[NASA-TM-100038] 13 p1800 N90-20333
Mass transfer from a sphere in an oscillating flow with zero mean velocity
[NASA-TM-102566] 13 p1801 N90-20338
Fluid dynamics analysis of a rotating axisymmetric part using FIDAP
[DE90-008733] 13 p1802 N90-20340
Massively-parallel computational fluid dynamics
[AD-A217732] 13 p1802 N90-20342
Evaluation of an adaptive unstructured remeshing technique for integrated fluid-thermal-structural analysis
[NASA-TM-102611] 13 p1815 N90-20426
Tools for 3D scientific visualization in computational aerodynamics
13 p1858 N90-20660
GRID2D/3D: A computer program for generating grid systems in complex-shaped two- and three-dimensional spatial domains. Part 2: User's manual and program listing
[NASA-TM-102454] 13 p1867 N90-20708
On total variation diminishing schemes for transonic turbulent flow computation
14 p1909 N90-20945
Comparison of C- and O-grid generation methods using a NACA 0012 airfoil
[AD-A216375] 14 p1910 N90-20948
Convergence acceleration of hypersonic flow calculations: A nonlinear relaxation factor
14 p1911 N90-20957
Computational Methods for Aerodynamic Design (Inverse) and Optimization
[AGARD-CP-463] 14 p1916 N90-20976
An efficient airfoil design method using the Navier-Stokes equations
14 p1917 N90-20981
A computational design method for shock free transonic cascades and airfoils
14 p1918 N90-20986
Inverse computation of transonic internal flows with application for multi-point-design of supercritical compressor blades
14 p1918 N90-20987
An inverse method for the design of turbomachine blades
14 p1918 N90-20988
Optimization of aerodynamic designs using computational fluid dynamics
14 p1920 N90-20999
Secondary Flows in Turbomachines
[AGARD-CP-469] 14 p1922 N90-21009
Secondary flows and radial mixing predictions in axial compressors
14 p1922 N90-21010
A study on secondary flow and spanwise mixing in axial flow compressors
14 p1923 N90-21012
Parabolized calculations of turbulent three dimensional flows in a turbine duct
14 p1923 N90-21013
Experimental and numerical study on basic phenomena of secondary flows in turbines
14 p1923 N90-21014

An investigation of secondary flows in nozzle guide vanes 14 p1923 N90-21016
Secondary flow predictions for a transonic nozzle guide vane 14 p1924 N90-21017
Secondary flow in a turbine guide vane with low aspect ratio 14 p1924 N90-21018
Centrifugal impeller geometry and its influence on secondary flows 14 p1924 N90-21020
Calculation of the three dimensional turbulent flow in a linear turbine blade 14 p1924 N90-21021
Calculation of the secondary flow in an axial turbine 14 p1924 N90-21022
Secondary flow calculations for axial and radial compressors 14 p1925 N90-21024
Computational prediction and measurement of the flow in axial turbine cascades and stages 14 p1925 N90-21026
Analysis of the rotor tip leakage flow with tip cooling air ejection 14 p1926 N90-21029
Theoretical study of the flow in a rotating channel. Experimental study through flow visualization in a curved channel 14 p1926 N90-21032
A cost-effective strategy for nonoscillatory convection without clipping
[NASA-TM-102538] 14 p1971 N90-21291
Cepstrum analysis and applications to computational fluid dynamic solutions 14 p1973 N90-21302
PROTEUS two-dimensional Navier-Stokes computer code, version 1.0. Volume 1: Analysis description
[NASA-TM-102551] 14 p1973 N90-21303
PROTEUS two-dimensional Navier-Stokes computer code, version 1.0. Volume 2: User's guide
[NASA-TM-102552] 14 p1973 N90-21306
PROTEUS two-dimensional Navier-Stokes computer code, version 1.0. Volume 3: Programmer's reference
[NASA-TM-102553] 14 p1974 N90-21307
Numerical simulation of hypersonic flow around a space plane. Part 2: Application to high angles of attack flow
[NAL-TR-1011T] 15 p2045 N90-21726
Swept wing ice accretion modeling
[NASA-TM-103114] 15 p2046 N90-21727
Extension of a streamwise upwind algorithm to a moving grid system
[NASA-TM-102800] 15 p2048 N90-21739
Three-dimensional simulation of vortex breakdown
[NASA-TM-102664] 15 p2049 N90-21744
A multiblock/multizone code (PAB 3D-v2) for the three-dimensional Navier-Stokes equations: Preliminary applications
[NASA-CR-182032] 15 p2049 N90-21745
Analytical study of the origin and behavior of asymmetric vortices
[NASA-TM-102796] 15 p2049 N90-21746
An upwind-differencing scheme for the incompressible Navier-Stokes equations
[NASA-TM-101051] 15 p2051 N90-21757
A dual potential formulation of the Navier-Stokes equations 15 p2092 N90-21972
Convergence acceleration of upwind relaxation methods for the Navier-Stokes equations 15 p2092 N90-21973
Applications of Mesh Generation to Complex 3-D Configurations
[AGARD-CP-464] 15 p2093 N90-21975
Recent developments in grid generation 15 p2093 N90-21976
Applications of algebraic grid generation 15 p2093 N90-21979
Geometry and grids of complex configurations for aerodynamic calculation 15 p2093 N90-21980
Mesh generation for flow computation in turbomachine 15 p2094 N90-21981
Unsteady Euler solutions on dynamic blocked grids for complex configurations 15 p2094 N90-21982
A structured approach to interactive multiple block grid generation 15 p2094 N90-21983
Design and testing of a multiblock grid-generation procedure for aircraft design and research 15 p2094 N90-21984
Grid patching approaches for complex three-dimensional configurations 15 p2094 N90-21985
Multiblock topology specification and grid generation for complete aircraft configurations 15 p2094 N90-21986
Three-dimensional adaptive grids with limited skewness 15 p2095 N90-21987
Feature-associated mesh embedding for complex configurations 15 p2095 N90-21988
On the way to an integrated mesh generation system for industrial applications 15 p2095 N90-21989
Generation, optimization, and adaptation of multidomain meshes around complex configurations 15 p2095 N90-21990
A discussion on issues relating to multiblock grid generation 15 p2095 N90-21991
Automatic grid generation in complex three-dimensional configurations using a frontal system 15 p2096 N90-21992
Unstructured finite element mesh generation and adaptive procedures for CFD 15 p2096 N90-21993
Generation and adaptation of 3-D unstructured grids for transient problems 15 p2096 N90-21994
Unstructured mesh generation by a generalized Delaunay algorithm 15 p2096 N90-21995
Application of the TRANAIR rectangular grid approach to the aerodynamic analysis of complex configurations 15 p2096 N90-21996
The solution of scattering and radiation problems for complex configurations based on 3-D grid and patch models 15 p2096 N90-21997
High order P-G finite elements for convection-dominated problems
[DE90-614743] 15 p2097 N90-21998
Development of a computational fluid dynamics and chemistry model for the fouling of jet fuels
[DE90-005664] 15 p2098 N90-22003
Computational modeling and validation for hypersonic inlets
[NASA-TM-103111] 15 p2099 N90-22011
European research on viscous flow (EuroVisc)
[NLR-TP-89077-U] 15 p2099 N90-22014
Numerical study of laminar and turbulent flows past two-dimensional and axisymmetric bodies 15 p2100 N90-22020
GRID2D/3D: A computer program for generating grid systems in complex-shaped two- and three-dimensional spatial domains. Part 1: Theory and method
[NASA-TM-102453] 15 p2147 N90-22262
Dynamical approach study of spurious steady-state numerical solutions of nonlinear differential equations. Part 1: The ODE connection and its implications for algorithm development in computational fluid dynamics
[NASA-TM-102820] 15 p2160 N90-22339
The minimum drag profile in laminar flow: A numerical way 16 p2196 N90-22535
Extension of a three-dimensional viscous wing flow analysis user's manual: VISTA 3-D code
[NASA-CR-182024] 16 p2197 N90-22538
The analysis and simulation of compressible turbulence
[NASA-CR-181997] 16 p2197 N90-22539
Secondary frequencies in the wake of a circular cylinder with vortex shedding
[NASA-CR-181998] 16 p2197 N90-22540
A modeling technique for STOVL ejector and volume dynamics
[NASA-TM-103167] 16 p2202 N90-22566
Investigation of advanced counterrotation blade configuration concepts for high speed turboprop systems, task 1: Ducted propfan analysis
[NASA-CR-185217] 16 p2202 N90-22567
Three-dimensional separated flow prediction on fusiform body using Euler and boundary layer methods 16 p2234 N90-22745
Supersonic flow computations for an ASTOVL aircraft configuration, phase 2, part 2
[NASA-CR-4284] 16 p2234 N90-22746
Numerical flow simulation and supercomputers: More than a digital wind tunnel 16 p2277 N90-22976
PLOT3D user's manual
[NASA-TM-101067] 16 p2298 N90-23090
Stable boundary conditions for Cartesian grid calculations
[NASA-CR-182048] 16 p2306 N90-23139
Proceedings of the 9th International Conference on Computing Methods in Applied Science and Engineering
[AD-A219307] 16 p2307 N90-23149
ONR Far East Scientific Information Bulletin, Volume 13, No. 4
[ONRFE-SCI-INFO-BULL-13(4)88] 16 p2311 N90-23168
Current Japanese supercomputers for computational fluid dynamics applications 16 p2311 N90-23172
Computation of low Mach number compressible flow 17 p2344 N90-23346
Extension of a three-dimensional viscous wing flow analysis
[NASA-CR-182023] 17 p2344 N90-23348
Parallel computation of supersonic flows using a three-dimensional, zonal, Navier-Stokes code
[AD-A216824] 17 p2344 N90-23350
Multiprocessing on supercomputers for computational aerodynamics
[NASA-TM-102806] 17 p2347 N90-23366
Computational analysis of the flowfield of a two-dimensional ejector nozzle
[NASA-CR-185255] 17 p2355 N90-23406
Advanced instrumentation for local measurement of gas-solid suspension flows
[DE90-008498] 17 p2400 N90-23671
Nonlinear interactions in mixing layers and compressible heated round jets
[NASA-CR-186303] 17 p2400 N90-23674
Algebraic turbulence modeling for unstructured and adaptive meshes
[NASA-CR-182035] 17 p2401 N90-23676
The stability of two-dimensional wakes and shear-layers at high Mach numbers
[NASA-CR-182050] 17 p2401 N90-23678
Unsteady flow phenomena in turbomachines
[AD-A218370] 17 p2402 N90-23680
Computational fluid dynamics
[AD-A219557] 17 p2403 N90-23686
Center for Analysis of Heterogeneous and Nonlinear Media
[AD-A219627] 17 p2403 N90-23688
Solution of the steady state incompressible Navier-Stokes equations at high Reynolds numbers
[VKI-TN-170] 17 p2404 N90-23692
Large eddy simulation of a fully turbulent plane channel flow
[VKI-TN-171] 17 p2404 N90-23693
Second moment models of turbulence: Complex or stratified flow
[ECL-90-02] 17 p2405 N90-23703
Modeling turbulent flow with mixed thermal convection transfer
[ECL-89-19] 17 p2405 N90-23704
Cumulative reports and publications through December 31, 1989
[NASA-CR-182041] 17 p2439 N90-23898
Numerical solution of a bifurcation problem for the Boussinesq equations at low Prandtl numbers by a multigrid method
[REPT-89-67] 17 p2458 N90-24026
Mission of LARVE 18 p2489 N90-24229
The computation of turbulent thin shear flows associated with flow around multielement aerofoils 18 p2491 N90-24240
Code ETF-3D. Euler transonic flow: Theoretical manual
[DLC/FLU-INT-TN-005] 18 p2493 N90-24247
Code ETF-3D. Euler transonic flow: Validation manual
[DLC/FLU-INT-TN-007] 18 p2493 N90-24248
Experimental and analytical study of close-coupled ventral nozzles for ASTOVL aircraft
[NASA-TM-103170] 18 p2498 N90-24273
Vortex-induced boundary-layer separation 18 p2551 N90-24560
Symmetry in the dynamics of a polarized fluid
[ETN-90-96896] 18 p2552 N90-24567
Computational modeling of three-dimensional compressible leading edge vortices
[AD-A221022] 18 p2553 N90-24569
Flipper user's manual
[AD-A220788] 18 p2590 N90-24734
LOX manifold tee analysis
[NASA-CR-183994] 19 p2670 N90-25188
Boundary conditions for the Navier-Stoke's equations at an artificial boundary intersecting a solid boundary
[FFA-TN-1990-11] 19 p2691 N90-25313
The incorporation of a multigrid method into the orthogonal curvilinear coordinate version of the Rolls-Royce PACE computer program
[TT-8804] 19 p2751 N90-25627
Technical evaluation report on the Fluid Dynamics Panel Symposium on Computational Methods for Aerodynamic Design (Inverse) and Optimization
[AGARD-AR-267] 20 p2803 N90-25947
Computation of viscous aerodynamic characteristics of 2-D airfoils for helicopter applications
[NLR-MP-88052-U] 20 p2804 N90-25951
The role of computational fluids dynamics in missile aerodynamics
[NLR-MP-88072-U] 20 p2804 N90-25952
Turbine blade heat transfer coefficient evaluation by modified version of STAN5. Comparison with experimental data
[ETN-90-97283] 20 p2813 N90-26008
Liquid fueled ramjet combustion instability: Acoustical and vortical interactions with burning sprays
[AD-A222752] 20 p2831 N90-26104
A computational study of the effectiveness of coating materials for KE projectile fins subjected to the combined effects of inbore and aerodynamic heating
[AD-A222595] 20 p2840 N90-26155
Computational experience with a three-dimensional rotary engine combustion model
[NASA-TM-103104] 20 p2861 N90-26275
Code enhancements and validation of GASP
[NPS-PAPER-44] 20 p2861 N90-26277
Report of the Fluid Dynamics Panel Working Group 10 on calculation of 3D separate turbulent flows in boundary layer limit
[AGARD-AR-255] 20 p2862 N90-26280

A fully implicit ADI method for quasi three-dimensional flows through straight blade rows
[ETN-90-96965] 20 p2863 N90-26283
Development of a system for the numerical simulation of Euler flows, with results of preliminary 3-D propeller-slipstream/exhaust-jet calculations
[NLR-TR-88008-U] 20 p2863 N90-26285
Computational fluid dynamics for missiles
[RAE-TM-AERO-2171] 20 p2863 N90-26288
Informatics aspects of large flow calculations on the SX-2 supercomputer
[NLR-MP-88037-U] 20 p2864 N90-26290
Computational fluid dynamics 3-D analysis for advanced transonic turbine design
[ETN-90-97282] 20 p2864 N90-26291
Fluid Dynamics Panel Working Group 12 on Adaptive Wind Tunnel Walls: Technology and Applications
[AGARD-AR-269] 21 p2961 N90-26838
Streamlining algorithms for complete adaptation
21 p2962 N90-26841
Advanced optical diagnostics in hypersonic research
21 p2975 N90-26905
Turbulent reacting flows and supersonic combustion
[AD-A221793] 21 p2979 N90-26933
Development of a mathematical model for the thermal decomposition of aviation fuels
[AD-A221673] 21 p2990 N90-26994
Parallel numerical simulations of axisymmetric projectile flows using zonal-overlapped grids
[AD-A221711] 21 p3005 N90-27082
Theoretical and computational aspects of turbulence
[AD-A221795] 21 p3005 N90-27083
A comparison of two central difference schemes for solving the Navier-Stokes equations
[NASA-TM-102815] 22 p3108 N90-27654
Aerodynamics of a linear oscillating cascade
[NASA-TM-103250] 22 p3108 N90-27657
FINFLO: A finite-volume based computer program for two-dimensional and axisymmetric compressible flow
[PB90-189473] 22 p3169 N90-27974
Progress and challenges in modeling turbulent aerodynamic flows
[NASA-TM-102811] 22 p3170 N90-27981
Flowfield computation of entry vehicles
[NASA-CR-186946] 22 p3171 N90-27986
Computational Fluid Dynamics, volume 1
[VKI-LS-1990-03-VOL-1] 22 p3171 N90-27989
Numerical methods for shallow water flow
22 p3172 N90-27992
Computation of compressible, vortical flows
22 p3172 N90-27996
Difference methods for hyperbolic problems with emphasis on space-centered approximations
22 p3172 N90-27998
Efficient solution of the steady Euler equations with a centered implicit method 22 p3173 N90-27999
Computational Fluid Dynamics for Industrial Flows
[VKI-LS-1990-04] 22 p3173 N90-28001
An analysis of flow models: From Navier-Stokes to potential flow equations 22 p3173 N90-28002
Discretization methods for the incompressible Navier-Stokes equations 22 p3173 N90-28003
An introduction to turbulence models
22 p3173 N90-28004
POLYFLOW theoretical background
22 p3173 N90-28005
The PHOENICS flow-simulation system
22 p3174 N90-28006
A finite element method for turbulent incompressible flow 22 p3174 N90-28007
FLUENT and FLUENT/BFC CFD computer programs
22 p3174 N90-28008
Turbulent thermal convection in rotating cavities, volume 1
[ETN-90-97433] 22 p3174 N90-28011
Turbulent thermal convection in rotating cavities, volume 2
[ETN-90-97434] 22 p3174 N90-28012
Experimental study of an unsteady boundary layer on an oscillating plane plate. Optimization and validation of calculation code for the analysis of the potential flow/boundary layer coupling in the neighborhood of a plane plate and an oscillating profile
[ETN-90-97436] 22 p3175 N90-28013
Towards a two dimensional scheme of anisotropic Godunov type. On the calculation of the velocity of the nodes in the multidimensional Lagrangian codes
[ETN-90-97458] 22 p3175 N90-28017
Solution of Euler equations using finite element method and the kinetic decomposition of the flows: Study of the self-adaptation of the grid and of the calculation field
[CERT-1/334700-DERI-GAN] 22 p3176 N90-28020
Experimental study of the effects of rotation on the homogeneous turbulence. Comparison with the EDQNM model
[ONERA-RSF-11/1145-AY-166A]
22 p3176 N90-28025
Parallelization of implicit finite difference schemes in computational fluid dynamics
[NASA-CR-182081] 22 p3243 N90-28392
The effect of rapid spoiler deployment on the transient forces on an aerofoil 23 p3274 N90-28527
Study of the ground effects in the CEAT aerohydrodynamic tunnel: Using the results
23 p3274 N90-28530
The aerodynamic design of the oblique flying wing supersonic transport
[NASA-CR-177552] 23 p3276 N90-28540
Measurement of the steady surface pressure distribution on a single rotation large scale advanced prop-fan blade at Mach numbers from 0.03 to 0.78
[NASA-CR-182124] 23 p3278 N90-28552
Development of comprehensive numerical schemes for predicting evaporating gas-droplets flow processes of a liquid-fueled combustor
[NASA-CR-187018] 23 p3305 N90-28693
Spectroscopic study of combustion diagnostics on hydroxyl radicals
[NASA-CR-186998] 23 p3305 N90-28694
Numerical simulation of reactive turbulent flows
[ETN-90-97476] 23 p3326 N90-28807
Numerical resolution of Navier-Stokes equations using several turbulence models and applications on turbomachines
[ETN-90-97478] 23 p3326 N90-28808
Development of turbulence models for the analysis of compressible or incompressible unsteady flow
[ETN-90-97486] 23 p3326 N90-28810
Scientific Colloquium in Honor of Prof. Dr. Rer. Nat. Hermann L. Jordan
[ESA-TT-1101] 23 p3391 N90-29159
Numeric fluid mechanics 23 p3392 N90-29161
A potential-vorticity decomposition for the boundary integral equation analysis of viscous flows
24 p3417 N90-29301
Numerical simulation of hypersonic viscous flow for the design of H-2 orbiting plane (HOPE)
[NAL-TR-1028] 24 p3422 N90-29330
Some topics in computational transonic aerodynamics: Revision
[NAL-TR-1018T] 24 p3422 N90-29332
Secondary flow in presence of wall jets: Incorporation of compression effects in a quasi-elliptic Navier-Stokes calculation code
[ETN-90-97559] 24 p3469 N90-29602
Optimization of tetrahedrical meshes for finite element calculation methods in fluids mechanics
[ETN-90-97560] 24 p3469 N90-29603
Numerical Grid Generation
[VKI-LS-1990-06] 24 p3470 N90-29606
Grid generation 24 p3470 N90-29607
Unstructured mesh methods for CFD
24 p3470 N90-29611

COMPUTATIONAL GEOMETRY

On the expected complexity of the three-dimensional Voronoi diagram
[PB89-209332] 01 p0112 N90-10636
Unstructured finite element mesh generation and adaptive procedures for CFD 15 p2096 N90-21993
Numerical Grid Generation
[VKI-LS-1990-06] 24 p3470 N90-29606
Unstructured mesh methods for CFD
24 p3470 N90-29611

COMPUTATIONAL GRIDS

Iterative performance and an adaptive procedure for viscous flow problems 01 p0069 N90-10397
Tests of various finite difference algorithms applied to a simple water vapor transport problem on a staggered grid
[AD-A210229] 01 p0105 N90-10596
A parallel numerical simulation for supersonic flows using zonal overlapped grids and local time steps for common and distributed memory multiprocessors
[DE89-015252] 02 p0147 N90-10839
Computation of transient three-dimensional interstage flowfields using the arbitrary Lagrangian-Eulerian method
02 p0219 N90-11253
The upwind control volume scheme for unstructured triangular grids
[NASA-TM-101664] 03 p0301 N90-11703
Error estimation and self-adaptive mesh refinement for boundary element method 03 p0356 N90-12037
A simplified self-adaptive grid method, SAGE
[NASA-TM-102198] 03 p0388 N90-12211
A multigrid method combined with defect correction for free convection problems at high Rayleigh numbers
[REPT-89-27] 03 p0396 N90-12264
An electromagnetic finite element particle code on an unstructured grid
[DE89-017532] 03 p0407 N90-12336
Solution of the thin-layer Navier-Stokes equations for laminar transonic flow
[PB89-221600] 04 p0500 N90-12879
A multigrid method for the Navier-Stokes and Boussinesq equations
[REPT-89-17] 04 p0501 N90-12886
Multigrid Monte Carlo in an external U(1) gauge field
[NIKHEF-ITFA-88-52] 04 p0538 N90-13114
Multigrid solution method for the Euler equations
[PB89-219463] 04 p0539 N90-13116
Local mode smoothing analysis of various incomplete factorization iterative methods in two dimensions
[REPT-89-36] 04 p0540 N90-13129
Multigrid calculations of 3-D turbulent viscous flows
[NASA-CR-185154] 05 p0571 N90-13323
Application of a self-adaptive grid method to complex flows
[NASA-TM-102223] 05 p0571 N90-13324
Great circle interactions: Attitude smoothing and grid-step inconsistencies 05 p0609 N90-13554
The first-look data analysis at Utrecht
05 p0612 N90-13571
Gas flows in rocket motors, volume 1
[AD-A213348] 05 p0615 N90-13591
Effect of spatial resolution on apparent sensitivity to initial conditions of a decaying flow as it becomes turbulent
[NASA-TM-102377] 05 p0638 N90-13719
Multigrid and defect correction for the steady Navier-Stokes equations: Applications to aerodynamics
[ETN-90-96011] 05 p0639 N90-13727
Calculation of flow fields by the solution of the Euler equations using an extended finite volume discretization scheme
[DLR-FB-89-38] 05 p0639 N90-13729
Application of two-point closures to subgrid scale modeling for homogeneous, 3D turbulence
05 p0640 N90-13732
Application of multi-grid methods for solving the Navier-Stokes equations
[NASA-TM-102359] 05 p0687 N90-14002
A numerical technique for analysis of resistojet nozzle flow 06 p0775 N90-14506
CTH: A three-dimensional shock wave physics code
[DE89-016529] 06 p0779 N90-14528
Modified Chebyshev pseudospectral method with O(N exp -1) time step restriction
[NASA-CR-181958] 06 p0834 N90-14848
Mesh refinement in finite element analysis by minimization of the stiffness matrix trace
[NASA-CR-185170] 07 p0938 N90-15434
Personal computer study of finite-difference methods for the transonic small disturbance equation
[NASA-TM-102582] 08 p1019 N90-15892
Euler and Navier-Stokes computations for two-dimensional geometries using unstructured meshes
[NASA-CR-181977] 08 p1019 N90-15893
Adaptive local grid refinement for the compressible 3-D Euler equations
[FFA-TN-1989-40] 08 p1064 N90-16155
Grid-independent wall layer turbulence model for complex flow calculations
[DE90-003500] 08 p1071 N90-16200
FRAC-IN-THE-BOX utilization
[DE90-003648] 08 p1108 N90-16412
Parallel algorithms for interactive manipulation of digital terrain models 08 p1113 N90-16445
Multigrid methods for two- and three-dimensional Poisson-type equations on the sphere
[GMD-391] 08 p1117 N90-16458
Computational fluid dynamics
[NASA-TM-102922] 09 p1216 N90-17052
A solution method for the time-dependent Navier-Stokes equations for laminar, incompressible flow
[FFA-146] 09 p1219 N90-17075
On the superconvergence of the SBB method
[DE89-835709] 09 p1272 N90-17375
Symbol manipulation and applied mathematics
[AD-A214702] 09 p1273 N90-17378
Use of beta-splines for digital elevation modeling
[INPE-4941-PRE/1431] 10 p1400 N90-18093
Domain decomposition with local mesh refinement
[AD-A215806] 10 p1418 N90-18175
Molecular dynamics simulation of sedimentation using the monotonic Lagrangian grid
[AD-A215099] 10 p1427 N90-18236
A simple algebraic grid adaptation scheme with applications to two- and three-dimensional flow problems
[NASA-TM-102446] 11 p1505 N90-18667
Analysis of linear multigrid methods for elliptic differential equations with discontinuous and anisotropic coefficients
[ETN-90-96269] 11 p1553 N90-18944

Comparison of a 6-layer and a 15-layer version of the Chemical Transfer Model (CTM)
12 p1687 N90-19689
The p- and h-p versions of the finite element method: An overview
[AD-A216902] 12 p1705 N90-19789
On the parallel efficiency of the Frederickson-McBryan multigrid
[NASA-CR-181999] 12 p1705 N90-19791
A tensor product B-spline method for numerical grid generation
[DE90-005979] 12 p1705 N90-19792
Finite element mesh generation starting from general geometric models
[REPT-88-93] 12 p1707 N90-19803
Composite-grid techniques and adaptive mesh refinement in computational fluid dynamics
[AD-A217383] 13 p1800 N90-20328
Precise solution for a finite set of spherical coefficients from equiangular gridded data 13 p1833 N90-20522
Satellite radar altimetry over ice. Volume 4: Users' guide for Antarctica elevation data from Seasat
[NASA-RP-1233-VOL-4] 13 p1840 N90-20564
GRID2D/3D: A computer program for generating grid systems in complex-shaped two- and three-dimensional spatial domains. Part 2: User's manual and program listing
[NASA-TM-102454] 13 p1867 N90-20708
Automated finite element modeling and simulation
13 p1875 N90-20753
Comparison of C- and O-grid generation methods using a NACA 0012 airfoil
[AD-A216375] 14 p1910 N90-20948
An overlapped grid method for multigrid, finite volume/difference flow solvers: MaGGiE
[NASA-CR-182008] 14 p1911 N90-20953
Convergence acceleration of hypersonic flow calculations: A nonlinear relaxation factor
14 p1911 N90-20957
A fast collocation method for transonic airfoil design
14 p1917 N90-20984
A computational design method for shock free transonic cascades and airfoils 14 p1918 N90-20986
Secondary flow predictions for a transonic nozzle guide vane 14 p1924 N90-21017
Resistivity of pristine and intercalated graphite fiber epoxy composites
[NASA-TM-102576] 14 p1955 N90-21192
A quasi-Lagrangian moving grid technique for investigating compressible flows
14 p1972 N90-21298
A time-accurate adaptive grid method and the numerical simulation of a shock-vortex interaction
[NASA-TP-2998] 14 p2011 N90-21524
Compact finite volume methods for the diffusion equation
[NASA-CR-186477] 14 p2019 N90-21568
Adaptive grid embedding for the two-dimensional flux-split Euler equations
[NASA-CR-186533] 14 p2019 N90-21571
Extension of a streamwise upwind algorithm to a moving grid system
[NASA-TM-102800] 15 p2048 N90-21739
Three-dimensional simulation of vortex breakdown
[NASA-TM-102664] 15 p2049 N90-21744
A multiblock/multizone code (PAB 3D-v2) for the three-dimensional Navier-Stokes equations: Preliminary applications
[NASA-CR-182032] 15 p2049 N90-21745
Applications of Mesh Generation to Complex 3-D Configurations
[AGARD-CP-464] 15 p2093 N90-21975
Recent developments in grid generation
15 p2093 N90-21976
General structured grid generation systems
15 p2093 N90-21977
Geometry and grids of complex configurations for aerodynamic calculation 15 p2093 N90-21980
Mesh generation for flow computation in turbomachine
15 p2094 N90-21981
Unsteady Euler solutions on dynamic blocked grids for complex configurations 15 p2094 N90-21982
A structured approach to interactive multiple block grid generation 15 p2094 N90-21983
Design and testing of a multiblock grid-generation procedure for aircraft design and research
15 p2094 N90-21984
Grid patching approaches for complex three-dimensional configurations
15 p2094 N90-21985
Three-dimensional adaptive grids with limited skewness 15 p2095 N90-21987
Feature-associated mesh embedding for complex configurations 15 p2095 N90-21988
On the way to an integrated mesh generation system for industrial applications 15 p2095 N90-21989
Generation, optimization, and adaptation of multidomain meshes around complex configurations
15 p2095 N90-21990
A discussion on issues relating to multiblock grid generation 15 p2095 N90-21991
Automatic grid generation in complex three-dimensional configurations using a frontal system
15 p2096 N90-21992
Unstructured finite element mesh generation and adaptive procedures for CFD 15 p2096 N90-21993
Generation and adaptation of 3-D unstructured grids for transient problems 15 p2096 N90-21994
Unstructured mesh generation by a generalized Delaunay algorithm 15 p2096 N90-21995
Application of the TRANAIR rectangular grid approach to the aerodynamic analysis of complex configurations
15 p2096 N90-21996
The solution of scattering and radiation problems for complex configurations based on 3-D grid and patch models 15 p2096 N90-21997
Paving: A new approach to automated quadrilateral mesh generation
[DE90-010244] 15 p2146 N90-22260
GRID2D/3D: A computer program for generating grid systems in complex-shaped two- and three-dimensional spatial domains. Part 1: Theory and method
[NASA-TM-102453] 15 p2147 N90-22262
Local mode smoothing analysis for various incomplete factorization iterative methods in three dimensions
[REPT-89-38] 15 p2147 N90-22263
Spline function smoothing and differentiation of noisy data on a rectangular grid
[DE90-009319] 15 p2160 N90-22338
A study of woven fabric-reinforced composite materials using an invariant-based orthotropic plasticity formulation
16 p2211 N90-22611
Multigrid acceleration of transonic flow computations
[ENSM-8024] 16 p2237 N90-22760
Calculation of 3-dimensional synthetic seismograms on the connection machine
[AD-A218472] 16 p2255 N90-22857
A real time, FEM based optimal control algorithm and its implementation using parallel processing hardware (transistors) in a microprocessor environment
16 p2294 N90-23086
PLOT3D user's manual
[NASA-TM-101067] 16 p2298 N90-23090
Stable boundary conditions for Cartesian grid calculations
[NASA-CR-182048] 16 p2306 N90-23139
Continuation and multi-grid methods for bifurcation problems
[AD-A218904] 16 p2307 N90-23146
Adaptive mesh experiments for hyperbolic partial differential equations
[AD-A219194] 16 p2307 N90-23148
Proceedings of the 9th International Conference on Computing Methods in Applied Science and Engineering
[AD-A219307] 16 p2307 N90-23149
Current Japanese supercomputers for computational fluid dynamics applications 16 p2311 N90-23172
Studies of Io's atmosphere and plasma torus
16 p2338 N90-23326
Parallel computation of supersonic flows using a three-dimensional, zonal, Navier-Stokes code
[AD-A218824] 17 p2344 N90-23350
Algebraic turbulence modeling for unstructured and adaptive meshes
[NASA-CR-182035] 17 p2401 N90-23676
Composite reduced Navier Stokes procedures for flow problems with strong pressure interactions
[AD-A219621] 17 p2403 N90-23687
Numerical solution of a bifurcation problem for the Boussinesq equations at low Prandtl numbers by a multigrid method
[REPT-89-67] 17 p2458 N90-24026
A line relaxation smoother for the multigrid solution of the Boussinesq equations
[REPT-89-68] 17 p2458 N90-24027
A uniform representation scheme for freeform geometric modeling
[REPT-89-70] 17 p2458 N90-24028
Application of frequency interpolation to acoustic-structure interaction problems
[AD-A219330] 17 p2469 N90-24113
Multi-grid and B(ox)-splines
[MEMO-828] 18 p2600 N90-24801
Finding complete bipartite subgraphs in bipartite graphs
[RUU-CS-89-30] 18 p2602 N90-24815
The implementation of the graphics of program EAGLE: A numerical grid generation code on NASA Langley SNS computer system 18 p2642 N90-25050
The incorporation of a multigrid method into the orthogonal curvilinear coordinate version of the Rolls-Royce PACE computer program
[TT-8804] 19 p2751 N90-25627
An adaptive finite element method for shock developing partial differential equation
[FFI-89/7014] 19 p2751 N90-25632
Euler analysis comparison with LDV data for an advanced counter-rotation propfan at cruise
[NASA-TM-103249] 20 p2803 N90-25946
Galerkin finite difference Laplacian operators on isolated unstructured triangular meshes by linear combinations
[NASA-TM-103209] 20 p2861 N90-26276
Calculation of 3D turbulent jets in crossflow with a multigrid method and a second-moment closure model
[NASA-TM-103159] 20 p2862 N90-26282
Informatics aspects of large flow calculations on the SX-2 supercomputer
[NLR-MP-88037-U] 20 p2864 N90-26290
The finite analytic method and its applications. Volume 1: Laminar and turbulent flows past two-dimensional and axisymmetric bodies
[AD-A222787] 20 p2864 N90-26294
An angular weighting approach for calculating gradients and divergences
[DE90-013164] 20 p2908 N90-26539
Parallelization of an annealing simulation applied to improving tetrahedric grids
[IMAG-RR-796-M] 20 p2913 N90-26570
Generation and improvement of meshes for finite elements methods in two and three dimensions
[ETN-90-97249] 20 p2919 N90-26611
Numerical interactive grid generation for 3-D flow calculations
[NLR-MP-88055-U] 21 p3003 N90-27069
Inviscid dynamics of unstable shear layers
[AD-A222297] 21 p3004 N90-27077
Parallel performance of domain-decomposed preconditioned Krylov methods for PDEs with adaptive refinement
[AD-A222339] 21 p3064 N90-27420
Proceedings of Workshop on Reliability in Computational Mechanics
[AD-A221694] 21 p3065 N90-27426
On computations of the integrated space shuttle flowfield using overset grids
[NASA-CR-186927] 22 p3124 N90-27734
On unstructured grids and solvers
22 p3172 N90-27994
Towards a genuinely multi-dimensional upwind scheme 22 p3172 N90-27995
Efficient solution of the steady Euler equations with a centered implicit method 22 p3173 N90-27999
Towards a two dimensional scheme of anisotropic Godunov type. On the calculation of the velocity of the nodes in the multidimensional Lagrangian codes
[ETN-90-97458] 22 p3175 N90-28017
On the calculation of the velocity of the nodes in the multidimensional Lagrangian codes
22 p3175 N90-28019
Solution of Euler equations using finite element method and the kinetic decomposition of the flows: Study of the self-adaptation of the grid and of the calculation field
[CERT-1/334700-DERI-GAN] 22 p3176 N90-28020
Parallelization of implicit finite difference schemes in computational fluid dynamics
[NASA-CR-182081] 22 p3243 N90-28392
Calculation of temperature distribution in various turbine blades using a boundary-fitted coordinate transformation method 23 p3278 N90-28550
Multigrid for hypersonic inviscid flows
[NASA-CR-182082] 23 p3387 N90-29125
Deterministic transport on an arbitrarily-connected grid
[DE90-015148] 23 p3388 N90-29131
Numerical Grid Generation
[VKI-LS-1990-06] 24 p3470 N90-29606
Grid generation 24 p3470 N90-29607
The fundamentals of adaptive grid movement
24 p3470 N90-29610
Unstructured mesh methods for CFD
24 p3470 N90-29611
Elliptic grid generation 24 p3471 N90-29612
Unstructured mesh relaxation
[DE90-015614] 24 p3534 N90-29989

COMPUTER AIDED DESIGN

Remote control missile model test
01 p0013 N90-10063
Proceedings of the Workshop on Computational Aspects in the Control of Flexible Systems, part 1
[NASA-TM-101578-PT-1] 01 p0017 N90-10080
Computational controls for aerospace systems
01 p0017 N90-10082
Additional software developments wanted for modeling and control of flexible space systems
01 p0017 N90-10083

Flexible structure control experiments using a real-time workstation for computer-aided control engineering
01 p0017 N90-10084
CONSOLE: A CAD tandem for optimization-based design interacting with user-supplied simulators
01 p0017 N90-10085
Flexible missile autopilot design studies with PC-MATLAB/386 01 p0018 N90-10088
DYSCO: A software system for modeling general dynamic systems 01 p0018 N90-10089
Modeling and control system design and analysis tools for flexible structures 01 p0018 N90-10090
Proceedings of the Workshop on Computational Aspects in the Control of Flexible Systems, part 2
[NASA-TM-101578-PT-2] 01 p0021 N90-10103
Relating tolerances and kinematic behavior
[AD-A211125] 01 p0055 N90-10311
An expert system for optimal gear design
01 p0077 N90-10439
Atmospheric transmissivity update - 1988
[AD-A209130] 01 p0085 N90-10484
Evaluation of computer-aided software engineering tools for data base development
[DE89-014007] 01 p0104 N90-10591
Low-cost three-dimensional stereoscopic display technique for computer-aided design
[DE89-011635] 01 p0104 N90-10594
Aerospace system unified life cycle engineering producibility measurement issues
[AD-A210937] 01 p0106 N90-10607
The development of an expert system for the creative design of mechanisms
[AD-A211115] 01 p0110 N90-10628
Qualification by simulation: Dream or reality
02 p0177 N90-10990
Experimental identification of modal momentum coefficients and modal identity parameters of the FLECS structure 02 p0177 N90-10991
Overview of actual buckling calculation methods for space vehicle structures 02 p0177 N90-10995
ASIC (Application Specific Integrated Circuit) replacement for an SSI (Small Scale Integrated) component design: A case study
[DE89-013494] 02 p0215 N90-11232
New tools for the simulation and design of calorimeters
[DE89-016323] 02 p0223 N90-11281
Considerations for a design and operations knowledge support system for Space Station Freedom
[NASA-TM-102156] 02 p0258 N90-11451
Engineering specification and system design for CAD/CAM of custom shoes. Phase 5: UMC involvement (January 1, 1989 - June 30, 1989)
[NASA-CR-185838] 02 p0257 N90-11456
Using PATRAN: From eyeballs to submarines and more
[DE89-016989] 02 p0259 N90-11469
A survey of research methods to study design
[AD-A211213] 02 p0262 N90-11491
Wind tunnel test of CAD USB-STOL semi-borne prototype
[NAL-TM-566] 03 p0299 N90-11696
Development of direct-inverse 3-D methods for applied transonic aerodynamic wing design and analysis
[NASA-CR-186036] 03 p0305 N90-11733
Advanced technology in military gas turbine design and manufacture
[PNR90545] 03 p0307 N90-11747
Coupling rule-based and object-oriented programming for the classification of machined features
[DE89-017705] 03 p0334 N90-11903
Recent advances to NEC (Numerical Electromagnetics Code): Applications and validation
[DE89-009231] 03 p0337 N90-11917
Computer-aided design of flexible assembly systems
[PB89-216253] 03 p0354 N90-12025
Requirements for multidisciplinary design of aerospace vehicles on high performance computers
[NASA-CR-181915] 03 p0384 N90-12183
Reasoning about change and exceptions in automated process planning
[DE89-017706] 03 p0386 N90-12195
Low-cost three-dimensional stereoscopic display technique for computer-aided design
[DE89-017732] 03 p0386 N90-12196
Design mechanism for interactive graphics mechanism design
[PB89-219513] 03 p0387 N90-12202
Structure based formal methods for software engineering
[AD-A211660] 03 p0388 N90-12207
General data processing support from project planning to workshop control
[MBB-UD-526/88-PUB] 03 p0388 N90-12208
Designing and designing knowledge in engineering and architecture
[PB89-219521] 03 p0415 N90-12383
ANDECS-PERLUDE 2.0: A databased, interactive system of control software user's guide
[DFVLR-MITT-89-07] 03 p0418 N90-12404
The design of an airfoil for a high-altitude, long-endurance remotely piloted vehicle
04 p0445 N90-12545
Supersonic boundary-layer transition on the LaRC F-106 and the DFRF F-15 aircraft. Part 2: Aerodynamic predictions 04 p0447 N90-12559
On the precision and reliability of GPS networks computed using the double difference observable
[ETN-89-95719] 04 p0449 N90-12571
Case study on rapid software prototyping and automated software generation: An inertial navigation system
[AD-A212272] 04 p0450 N90-12578
A vision of the future: The new engine technology
[PNR90566] 04 p0455 N90-12603
A computer integrated approach to dimensional inspection
[PNR90596] 04 p0456 N90-12611
Rolls-Royce and ERCOFTAC
[PNR90600] 04 p0456 N90-12615
Application of the moment method to the design of slotted waveguide array antennas
04 p0484 N90-12780
A theoretical method for the mechanical calculation of heat exchangers with sliding heads, phase 1 study
[CETIM-110240-PHASE-1] 04 p0502 N90-12896
Computer oriented methods of multibody dynamics for application in vehicle technology
[DFVLR-FB-89-17] 04 p0533 N90-13080
NAUTILE: A physical design environment based on an object-oriented data manager
[IMAG-RR-737-I] 04 p0535 N90-13094
The application of artificial intelligence techniques to tracing the interconnections in an integrated circuit
[TELECOM-PARIS-89-E002] 04 p0537 N90-13105
Efficient methods for integrated structural-aerodynamic wing optimum design 05 p0579 N90-13376
Composite panel development at JPL
05 p0595 N90-13458
On the design of a computer-aided design system for digital circuits 05 p0633 N90-13695
Parameter estimation for the Gummel-Poon transistor model
[MA-53] 05 p0635 N90-13705
Methodology for automating software systems. Task 1 of the foundations for automating software systems
[NASA-CR-180499] 05 p0681 N90-13965
The cellular approach: A new method to speed up simulated annealing for macro placement
[MEMO-COSOR-88-29] 05 p0683 N90-13980
Chemistry of large molecules
[DE90-000813] 06 p0751 N90-14366
Communication Overview Program (COP)
06 p0762 N90-14435
Integrating and enhancing tools for ASIC (Application-Specific Integrated Circuits) design using MOSIS (Metal Oxide Semiconductor Implementation Service) fabrication
[DE90-001601] 06 p0769 N90-14475
Reuse research plans at Langley Research Center
06 p0825 N90-14797
Selecting and effectively using a computer aided software engineering tool
[DE89-017876] 06 p0828 N90-14815
Aircraft performance enhancement with active compressor stabilization
[AD-A213652] 07 p0879 N90-15097
Computer aided design of monolithic microwave and millimeter wave integrated circuits and subsystems
[AD-A213656] 07 p0923 N90-15343
An executive system for modeling with rational b-splines
[AD-A213460] 07 p0974 N90-15627
A paradigm for robust geometric algorithms
[AD-A214324] 07 p0978 N90-15647
Case tool evaluation system
[DE90-003698] 08 p1108 N90-16413
CAE (Computer-Aided Engineering) tools' limitations case study: An SSI (Small Scale Integrated) design to an ASIC (Application Specific Integrated Circuit)
[DE90-002902] 08 p1109 N90-16418
Appearance analysis from CAD models
[IMAG-RR-756-I-IMAG-88-LIFIA]
08 p1111 N90-16434
Low-cost volumetric modeling
[CRIF-MC-85] 08 p1111 N90-16435
Computer aided design based optical system modeling
[DE90-003453] 08 p1112 N90-16440
Interpretation of CAD (Computer Aided Design) models through IGES (Initial Graphics Exchange Specification) interface
[PB90-121294] 08 p1112 N90-16441
NASA/ASEE Summer Faculty Fellowship Program
[NASA-CR-166837] 08 p1154 N90-16686
Investigation of IGES for CAD/CAE data transfer
08 p1157 N90-16702
Classification and simulation of single and multi-degree-of-freedom motions
[AD-A214925] 09 p1231 N90-17143
SAtool II: An IDEF0 syntax data manipulator and graphics editor
[AD-A215289] 09 p1263 N90-17321
EDISON Project
[AD-A214724] 09 p1265 N90-17338
An approach to the development of software for computer-aided design of satellite communications receivers for operation in scintillating channels
[AD-A215299] 09 p1267 N90-17349
Computer-Aided Design for Built-In-Test (CADBIT). Volume 1: Technical issues
[AD-A215737] 09 p1268 N90-17353
Computer-Aided Design for Built-In-Test (CADBIT). Volume 2: BIT Library
[AD-A215738] 09 p1268 N90-17354
Computer-Aided Design for Built-In-Test (CADBIT). Volume 3: Software specification
[AD-A215739] 09 p1268 N90-17355
Interim Design Database (IDDB) CADAM drawing retrieval program user's manual for the IBM 3081
[DE90-004491] 09 p1269 N90-17356
Use of semiempirical aerodynamic methods for preliminary design 10 p1304 N90-17546
The Columbus power system simulation programme
10 p1330 N90-17686
New power system modelling approaches on the basis of equivalent state variables 10 p1330 N90-17687
Simulation of regenerative fuel cell systems including thermal control 10 p1333 N90-17711
The electrical design of solar arrays for communication satellites 10 p1344 N90-17792
WPK: Solar array dimensioning tool
10 p1346 N90-17808
Modern Antenna Design Using Computers and Measurement: Application to Antenna Problems of Military Interest
[AGARD-LS-165] 10 p1369 N90-17932
Recent advances to NEC: Applications and validation
10 p1369 N90-17934
Rapid prototyping of tools
[AD-A215956] 10 p1392 N90-18050
DANCIR (device and circuit simulator): A three dimensional steady-state semiconductor device simulator
[DE90-006370] 11 p1504 N90-18658
A theory of quantitative inference for artifact sets applied to a mechanical design compiler
[AD-A216535] 11 p1545 N90-18896
RALPH: An automatic Robot Assembly Language Programmer: An overview
[PB90-120973] 11 p1548 N90-18912
Kinematic control of robotic manipulators with multiple interchangeable wrists 12 p1670 N90-19592
COCOMAT: A Computer Aided Engineering (CAE) system for composite structures design
[NLR-MP-87078-U] 12 p1699 N90-19756
User-friendly software for the design of digital line-of-sight radio links
[PB90-118472] 12 p1700 N90-19760
An expert system for the design of heating, ventilating, and air-conditioning systems
[AD-A218287] 13 p1788 N90-20262
The design of high-performance circuits for digital signal processing
[AD-A217786] 13 p1796 N90-20309
TAE Plus: Transportable Applications Environment Plus tools for building graphic-oriented applications
13 p1856 N90-20652
RenderMan design principles
13 p1857 N90-20653
Recent advances in 3D finite difference mesh generation using the BRL-CAD package
[DE90-007854] 13 p1866 N90-20704
A review of the suitability of available Computer Aided Software Engineering (CASE) tools for the small software development environment
[AD-A218276] 13 p1870 N90-20726
The role of structural analysis in airworthiness certification
[BR112084] 14 p1915 N90-20972
Computer-aided structural optimisation of aircraft structures
[BR112837] 14 p1915 N90-20973
Computer-aided design of flywheel transmission systems 14 p1988 N90-21392

CAD work station for electronics designer
[DE90-616473] 14 p2015 N90-21546
The CAD/CAM product data standards: IGES/PDES (Initial Graphics Exchange Specification/Product Data Exchange Standards, the present and the future
[DE90-008803] 14 p2015 N90-21549
Curvature continuity of cubic Bezier curves in the solid modeling aerospace research tools design software
[NASA-CR-186583] 14 p2016 N90-21554
Conceptual design optimization study
[NASA-CR-4298] 15 p2051 N90-21755
Geometry and grids of complex configurations for aerodynamic calculation 15 p2093 N90-21980
A3I visibility modeling project
15 p2140 N90-22230
Graphically-oriented nonlinear analysis of statically loaded plane frames on microcomputers
[PB90-165945] 15 p2144 N90-22248
Engineering specification and system design for CAD/CAM of custom shoes: UMC project effort
[NASA-CR-186547] 15 p2145 N90-22255
Aircraft technology management and the related significance of the supercomputer
16 p2277 N90-22975
Numerical flow simulation and supercomputers: More than a digital wind tunnel 16 p2277 N90-22976
The use of supercomputers for the design and analysis of constructions 16 p2277 N90-22977
The development of a system for the numerical simulation of Euler flows 16 p2277 N90-22980
Strategy of supercomputer development
16 p2278 N90-22981
New multivariable capabilities of the INCA program
16 p2290 N90-23049
Multidisciplinary Expert-aided Analysis and Design (MEAD) 16 p2291 N90-23050
Overview of computational control research at UT Austin 16 p2291 N90-23051
Control/structure interaction design methodology
16 p2291 N90-23053
Curvature-dependent parametrization of curves and surfaces
[CS-8915] 16 p2299 N90-23100
Comparative evaluations of four specification methods for real-time systems
[AD-A219187] 16 p2300 N90-23109
Qualitative models for space system engineering
[NASA-CR-180682] 17 p2385 N90-23585
Circuit recognition of VLSI layouts
[AD-A219806] 17 p2396 N90-23649
VLSI architectures and CAD
[AD-A220736] 17 p2397 N90-23652
Evaluation methodology for software engineering
[AD-A218474] 17 p2441 N90-23913
Guide for the use of intergraph randmicas structural software for Computer-Aided Design and Drafting(CADD)
[AD-A220624] 17 p2443 N90-23924
Gemini2: A second generation layout validation program
[AD-A220731] 17 p2444 N90-23926
WireLisp: Combining graphics and procedures in a circuit specification language
[AD-A220740] 17 p2444 N90-23927
Numerical optimization, system theoretic and software tools for the integrated design of flexible structures and their control systems
[AD-A219877] 17 p2447 N90-23949
A comparison of a relational and nested-relational IDEF0 data model
[AD-A220147] 17 p2448 N90-23956
A hierarchical approach to large space structure control
[DE90-010681] 18 p2511 N90-24347
Combustor design and analysis using the Rocket Combustor Interactive Design (ROCCID) methodology
[NASA-TM-103165] 18 p2513 N90-24349
Personal Computer (PC) thermal analyzer
[AD-A221325] 18 p2548 N90-24546
A computer program for the design of optimum catalytic monoliths for CO2 lasers 18 p2558 N90-24595
Computer-Aided Structural Engineering (CASE) project. User's guide: A Three-Dimensional Stability Analysis/Design Program (3DSAD). Report 2: General loads module
[AD-A220331] 18 p2591 N90-24742
The Army/Air Force RAMCAD (Reliability And Maintainability Computer-Aided Design) program
[AD-A220923] 18 p2593 N90-24753
Strut-node joint conjugates for the assembly of semi-permanent or reusable truss structures
18 p2640 N90-25039
Conceptual design for aerospace vehicles
18 p2641 N90-25043
A Cax success story
[MBB-FW-52/S/PUB-382] 19 p2649 N90-25076
Development and application of an optimization procedure for space and aircraft structures
[MBB-FW-522/S/PUB-383] 19 p2650 N90-25078
PLATO: A European plateform orbiter concept
[MBB-UO-0061/89-PUB] 19 p2652 N90-25095
Integral-equation methods in steady and unsteady subsonic, transonic and supersonic aerodynamics for interdisciplinary design
[NASA-TM-102677] 19 p2655 N90-25110
CREW CHIEF: A computer graphics simulation of an aircraft maintenance technician
19 p2729 N90-25515
Modeling strength data for CREW CHIEF
19 p2729 N90-25516
The use of PLAID in the Space Station Freedom viewing analysis 19 p2729 N90-25517
Knowledge representation to support reasoning based on multiple models 19 p2731 N90-25525
Computer-aided design of advanced control algorithms for industrial robotics: An overview of ESPRIT project SACODY
[REPT-81-DT-89-47] 19 p2744 N90-25596
Feasibility study for a microwave-powered ozone sniffer aircraft, volume 2
[NASA-CR-186676] 20 p2806 N90-25967
Supersonic combustor modeling
20 p2810 N90-25992
Extension of a noninteractive reliability model for ceramic matrix composites
[NASA-CR-185267] 20 p2838 N90-26142
Modeling and optimization of a regenerative fuel cell system using the ASPEN process simulator
[NASA-TM-103210] 20 p2882 N90-26396
A computer module used to calculate the horizontal control surface size of a conceptual aircraft design
[NASA-CR-186872] 20 p2903 N90-26515
CAD/CAM reinforces the competitive edge of European mouldmakers
[CRIF-MC-88] 20 p2908 N90-26542
Material selection and design: An expert system approach
[PNR90611] 20 p2908 N90-26544
Contribution to the definition and application of NAUTILE (A new environment for the conception and assembling of integrated circuits)
[ETN-90-97251] 20 p2910 N90-26554
ATN design tool
[AD-A223030] 20 p2911 N90-26559
Application of artificial intelligence to the architectural synthesis of VLSI integrated circuits
[ETN-90-97253] 20 p2916 N90-26589
Development of a method to design helicopter rotors
[REPT-100-30-03] 21 p2960 N90-26830
Numerical interactive grid generation for 3-D flow calculations
[NLR-MP-88055-U] 21 p3003 N90-27069
An automated tool for the design and assessment of space systems 21 p3042 N90-27289
Expert System Development Methodology (ESDM)
21 p3042 N90-27292
Capturing design knowledge 21 p3045 N90-27305
An application of design knowledge captured from multiple sources 21 p3045 N90-27306
The integration of automated knowledge acquisition with computer-aided software engineering for space shuttle expert systems 21 p3045 N90-27307
Case-based reasoning in design: An apologia
21 p3045 N90-27308
Automated extraction of knowledge for model-based diagnostics 21 p3047 N90-27318
Inductive knowledge acquisition experience with commercial tools for space shuttle main engine testing
21 p3048 N90-27326
VIP: A knowledge-based design aid for the engineering of space systems 21 p3048 N90-27327
Producing process plans out of CAD files through AI techniques
[ETN-90-97273] 21 p3050 N90-27338
An algorithm for automated surface modelling in unigraphics
[AD-A223219] 21 p3053 N90-27355
Modification of a cam facility
[AD-A221828] 21 p3056 N90-27376
OMNI development of an engineering product data management system
[DE90-002407] 21 p3086 N90-27550
Interim status and recommendations for the Engineering Information System (EIS) program
[AD-A222060] 21 p3087 N90-27555
United States Air Force research initiation program for 1988, volume 4
[AD-A223126] 21 p3102 N90-27616
Spent-beam refocusing analysis and multistage depressed collector design for a 75-W, 59- to 64-GHz coupled-cavity traveling-wave tube
[NASA-TP-3039] 22 p3167 N90-27965
Computer-aided design of high-contact-ratio gears for minimum dynamic load and stress
[NASA-TM-103275] 22 p3183 N90-28065
A concept for integrating computer-aided drafting and design with cost engineering and specification preparation
[AD-A223150] 22 p3237 N90-28354
Hypersonic Arbitrary-Body Aerodynamics (HABA) for conceptual design
[DE90-014750] 23 p3268 N90-28495
Flow coupling between a rotor and a stator in turbomachinery
[AD-A223882] 23 p3282 N90-28572
Summary of booster propulsion/vehicle impact study results 23 p3294 N90-28635
Design and realization of a two stage C-band low noise amplifier
[FEL-89-B265] 23 p3322 N90-28783
Automated simulation as part of a design workstation
[NASA-TM-102852] 23 p3378 N90-29083
Engineering and the advancement of human welfare. Ten outstanding achievements 1964-1989
[ISBN-0-309-04185-6] 23 p3415 N90-29297
WingDesign: Program for the structural design of a wing cross-section
[LR-627] 24 p3433 N90-29390
Assessment and improvement of aeroengine disc structural integrity 24 p3433 N90-29392
CAD models for inductive strips in homogeneous finline: The methodology
[AD-A224446] 24 p3463 N90-29564
Computer-Aided Structural Engineering (CASE) project: Investigation and design of U-frame structures using program CUFRBC. Volume A: Program criteria and documentation
[AD-A224387] 24 p3525 N90-29934
Computer-aided engineering environment for controlled mechanical systems
[AD-A223551] 24 p3527 N90-29942
MacRootLocus: A CAD design tool for feedback control systems
[AD-A223772] 24 p3528 N90-29951
An interactive optimization based, computer graphics software package. Phase 2: Users manual
[AD-A223854] 24 p3529 N90-29954

COMPUTER AIDED ENGINEERING
U COMPUTER AIDED DESIGN

COMPUTER AIDED MANUFACTURING
Relating tolerances and kinematic behavior
[AD-A211125] 01 p0055 N90-10311
Engineering specification and system design for CAD/CAM of custom shoes. Phase 5: UMC involvement (January 1, 1989 - June 30, 1989)
[NASA-CR-185838] 02 p0257 N90-11456
Using computer design and simulation to improve manufacturing productivity, report period 1, 2 and 3
[AD-A210255] 02 p0258 N90-11462
Advanced technology in military gas turbine design and manufacture
[PNR90545] 03 p0307 N90-11747
General data processing support from project planning to workshop control
[MBB-UD-526/88-PUB] 03 p0388 N90-12208
Fabrication of modulated vanes for a split-coaxial RFQ
[DE88-757235] 03 p0403 N90-12310
A vision of the future: The new engine technology
[PNR90566] 04 p0455 N90-12603
What is the balance sheet for investment in automated manufacturing
[CETIM-105490] 04 p0532 N90-13071
Computer-aided fabrication system implementation
[AD-A213005] 05 p0682 N90-13969
The problem of automation: Inappropriate feedback and interaction, not overautomation
[NASA-CR-186126] 05 p0686 N90-13994
Computer synthesis of ceramic preforms for molten-metal infiltration
[DE90-000826] 06 p0751 N90-14370
Computer-aided fabrication of integrated circuits
[AD-A215439] 09 p1268 N90-17352
Interim Design Database (IDDB) CADAM drawing retrieval program user's manual for the IBM 3081
[DE90-004491] 09 p1269 N90-17356
Rapid prototyping of tools
[AD-A215956] 10 p1392 N90-18050
The Executive Workshop on Cost/Performance Measurement. Volume 1: Executive summary
[AD-A216745] 11 p1546 N90-18898
COCOMAT: A Computer Aided Engineering (CAE) system for composite structures design
[NLR-MP-87078-U] 12 p1699 N90-19756
Flexible automatic discrete parts assembly
[AD-A217401] 13 p1787 N90-20256
Toward a new CIM (Computer Integrated Manufacturing) architecture for Sandia Laboratories
[DE90-008677] 14 p2015 N90-21548

The CAD/CAM product data standards: IGES/PDES (Initial Graphics Exchange Specification/Product Data Exchange Standards, the present and the future
[DE90-008803] 14 p2015 N90-21549
Development, implementation and test of a computer program for the production of axisymmetric pattern moulds on a numerically controlled milling machine
[LR-593] 15 p2074 N90-21877
Computerized inspection of gear tooth surfaces
[NASA-TM-102395] 15 p2107 N90-22054
Engineering specification and system design for CAD/CAM of custom shoes: UMC project effort
[NASA-CR-186547] 15 p2145 N90-22255
Evaluation of joints bonded with elastoplastic adhesives
[REPT-892-430-120] 16 p2247 N90-22816
An abstract data model for the IDEF sub 0 graphical analysis language
[AD-A219855] 17 p2446 N90-23948
A comparison of a relational and nested-relational IDEF0 data model
[AD-A220147] 17 p2448 N90-23956
Integrating expert systems with solid modeling through interprocess communications and the applications interface specification
[DE90-012996] 20 p2907 N90-26537
CAD/CAM reinforces the competitive edge of European mouldmakers
[CRIF-MC-88] 20 p2908 N90-26542
Contribution to the definition and application of NAUTILE (A new environment for the conception and assembling of integrated circuits)
[ETN-90-97251] 20 p2910 N90-26554
From network to artwork: Automatic schematic diagram generation
[EUT-89-E-219] 20 p2912 N90-26567
An algorithm for automated surface modelling in unigraphics
[AD-A223219] 21 p3053 N90-27355
Modification of a cam facility
[AD-A221828] 21 p3056 N90-27376
OMNI development of an engineering product data management system
[DE90-002407] 21 p3086 N90-27550
Computerization of Welding Data: Proceedings of the conference and workshop
[PB90-219551] 23 p3332 N90-28841
An improved method for choosing sampling points for the inspection of complex surfaces in a computer-aided manufacturing environment 23 p3380 N90-29093
Engineering and the advancement of human welfare. Ten outstanding achievements 1964-1989
[ISBN-0-309-04185-6] 23 p3415 N90-29297

COMPUTER AIDED MAPPING

Characterizing termination of logic problems with level mappings
[CWI-CS-R8912] 04 p0532 N90-13077
The Hipparcos Mission. Prelaunch status. Volume 3: The data reductions
[ESA-SP-1111-VOL-3] 05 p0609 N90-13548
The use of LANDSAT-TM data for the management of pine forestations in central Chile
[DLR-FB-89-44] 05 p0664 N90-13881
Thematic coupling between digital images and geographic information systems
[ETN-90-95723] 12 p1679 N90-19646
Guided boundary detection in a digital image using dynamic programming
[ETN-90-96688] 17 p2419 N90-23782
Operational digital land use map 1:50,000; investigation of a multiple automatic classification based on SPOT and LANDSAT Thematic Mapper satellite pictures
[BCRS-89-10] 17 p2419 N90-23784

COMPUTER AIDED TOMOGRAPHY

Computational and visible light experiments for x ray laser holography
[DE90-006774] 11 p1512 N90-18707
Object detection and amplitude estimation based on maximum a posteriori reconstructions
[DE90-007511] 12 p1701 N90-19770
Computed tomography of electronics
[AD-A217976] 13 p1797 N90-20314
High explosives (PBX9502) characterization using computerized tomography
[DE90-008170] 14 p1990 N90-21404
Large scale metrology by computer assisted photogrammetry
[REPT-892-430-116] 16 p2239 N90-22772
On-line x ray inspection of materials and structural components using discrete element x ray detectors for digital radiographic and computed tomographic evaluation
[AD-A218911] 16 p2245 N90-22806
Computer tomography of thermal batteries and other closed systems
[AD-A218379] 17 p2419 N90-23787
NDE (NonDestructive Evaluation) of ceramic heat exchangers
[DE90-010977] 18 p2554 N90-24575
A plan for scientific visualization at ANL
[DE90-013565] 21 p3051 N90-27344
Development and application of Computed Tomography (CT) for inspection of aerospace components 22 p3187 N90-28083
Geophysical diffraction tomography: A complementary remote sensing technique for hazardous waste site characterization
[DE90-013025] 23 p3341 N90-28882
Engineering and the advancement of human welfare. Ten outstanding achievements 1964-1989
[ISBN-0-309-04185-6] 23 p3415 N90-29297

COMPUTER ANIMATION

Graphics Technology in Space Applications (GTSA 1989)
[NASA-CP-3045] 13 p1856 N90-20651
Using an instrumented manikin for Space Station Freedom analysis 13 p1861 N90-20675
Software systems for modeling articulated figures 13 p1861 N90-20677
Human task animation from performance models and natural language input 13 p1861 N90-20678
Autonomous space processor for orbital debris
[NASA-CR-186691] 20 p2820 N90-26044
Computer animation in mathematics, science, and art
[DE90-013051] 20 p2908 N90-26538
From network to artwork: Automatic schematic diagram generation
[EUT-89-E-219] 20 p2912 N90-26567
Generation of animation sequences of three dimensional models
[NASA-CASE-MSC-21379-1-SB] 21 p3050 N90-27340
Animated computer-generated video-tape instruction using DIGLIB (Device Independent Graphics Library)
[DE90-015360] 23 p3382 N90-29105
Directing an animated scene with autonomous actors
[REPT-89-041] 24 p3531 N90-29972

COMPUTER ARCHITECTURE

U ARCHITECTURE (COMPUTERS)

COMPUTER ASSISTED INSTRUCTION

Northeast Artificial Intelligence Consortium annual report for 1987. Volume 5: Building an intelligent assistant: The acquisition, integration and maintenance of complex distributed tasks
[AD-A210330] 01 p0109 N90-10621
Research, development, training and education using the Ada programming language
[AD-A210760] 02 p0259 N90-11466
Effects of the advanced map interpretation and terrain analysis course on contour-level navigation performance
[AD-A212163] 03 p0304 N90-11723
Computer generation of a tutorial dialogue
[AD-A211976] 03 p0380 N90-12162
Computer-based tutors for explaining and managing the process of diagnostic reasoning
[AD-A211738] 03 p0390 N90-12222
Workshop on synoptic meteorology instruction
[PB90-109950] 06 p0817 N90-14751
Development of the AH-64 display symbology training module
[AD-A213456] 07 p0968 N90-15592
Tools for simulation-based training
[AD-A214307] 07 p0978 N90-15646
Feedback effects in computer-based skill learning
[AD-A214560] 09 p1258 N90-17298
A comparison of microcomputer training methods and sources
[AD-A216349] 10 p1413 N90-18146
Teaching a new methodology for designing relational data bases: An experiment testing the effectiveness of an intelligent tutoring system on cognitive skill acquisition (volumes 1 and 2) 11 p1574 N90-19063
Guide for the use of intergraph randmicas structural software for Computer-Aided Design and Drafting(CADD)
[AD-A220624] 17 p2443 N90-23924
National Educators' Workshop: Update 1989 Standard Experiments in Engineering Materials Science and Technology
[NASA-CP-3074] 18 p2513 N90-24350
Demo of three ways to use a computer to assist in lab 18 p2515 N90-24364
Manual and computer-aided materials selection for industrial production: An exercise in decision making 18 p2516 N90-24368
A NASTRAN trainer for dynamics 18 p2569 N90-24638
A study of effects of instructional modes in a sequence of computer-assisted instruction lessons, with an introduction to computer-aided diagnosis of arithmetic errors 18 p2589 N90-24730
Intelligent tutoring systems: An exploratory study of ITS and their implementation in Prolog
[RUU-CS-88-37] 18 p2597 N90-24779
The development of expertise on an intelligent tutoring system 18 p2630 N90-24984
An intelligent simulation training system 19 p2739 N90-25566
Functional description of a command and control language tutor 19 p2739 N90-25567
Success in tutoring electronic troubleshooting 19 p2739 N90-25568
Human factors research in aircrew performance and training
[AD-A221657] 21 p3037 N90-27267
A structure for maturing intelligent tutoring system student models 21 p3047 N90-27320
Intelligent tutoring systems for space applications 21 p3048 N90-27324
Aspects of data link applications for ATC purposes 22 p3113 N90-27688
Selective learning algorithm for certain types of learning failure in multilayer perceptrons
[AD-A223982] 23 p3362 N90-28998
Strategies of computer-based instructional design: A review of guidelines and empirical research
[AD-A224038] 23 p3383 N90-29112
Designing intelligent computer aided instruction systems with integrated knowledge representation schemes
[AD-A224178] 23 p3383 N90-29113
QTA (QUESTIONNAIRE-TASK-ANALYSIS): An electronic tool for job/task analysis
[DE90-008944] 24 p3499 N90-29778
Strategies for tutoring multiple bugs
[AD-A223921] 24 p3524 N90-29927

COMPUTER CODES

U COMPUTER PROGRAMS

COMPUTER COMPATIBLE TAPES

Introduction of digital image processing by remote sensors applied to geology
[INPE-5023-RPE/616] 14 p1999 N90-21456
Digital geometric correction for MSS-LANDSAT imagery
[INPE-4627-PRE/1345] 23 p3342 N90-28886

COMPUTER DESIGN

Evaluating local indirect addressing in SIMD proc essors
[NASA-CR-181845] 01 p0103 N90-10581
Using computer design and simulation to improve manufacturing productivity
[AD-A210338] 01 p0105 N90-10598
The rewrite rule machine project
[AD-A210528] 01 p0109 N90-10617
Area-universal networks
[AD-A211883] 04 p0535 N90-13092
High volume data storage architecture analysis
[NASA-CR-186239] 06 p0823 N90-14784
Locality in parallel computation
[AD-A218733] 16 p2302 N90-23120
Educational and research activities of the Dig ital Systems Laboratory at Helsinki University of Technology
[PB90-190893] 22 p3265 N90-28486

COMPUTER GRAPHICS

NT COMPUTER ANIMATION
BLOT: A mesh and curve plot program for the output of a finite element analysis
[DE89-013994] 01 p0104 N90-10590
Using PATRAN: From eyeballs to submarines and more
[DE89-016989] 02 p0259 N90-11469
Summaries of the FY 1989 Applied Mathematical Sciences Research program
[DE89-016694] 02 p0267 N90-11521
Vision-based navigation for autonomous ground vehicles
[AD-A211584] 03 p0304 N90-11725
Color printing for computer graphics. Or: How to get it off your screen and onto paper, in color
[PB89-208110] 03 p0384 N90-12184
Basic program for raster scan display unit
[NAL-TM-560] 03 p0384 N90-12185
Software package for 3-dimensional graphic display unit
[NAL-TM-559] 03 p0385 N90-12191
Low-cost three-dimensional stereoscopic display technique for computer-aided design
[DE89-017732] 03 p0386 N90-12196
Design mechanism for interactive graphics mechanism design
[PB89-219513] 03 p0387 N90-12202
Designing and designing knowledge in engineering and architecture
[PB89-219521] 03 p0415 N90-12383
Visualization of high-resolution digital terrain
[AD-A212149] 04 p0515 N90-12971
Research in computer vision for autonomous systems
[AD-A212420] 04 p0555 N90-13235

Resistive fuses: Analog hardware for detecting discontinuities in early vision
[AD-A211891] 05 p0634 N90-13696
Interface between MEDUSA and GIFTS for shell structures
[LR-553] 05 p0684 N90-13985
Engineer's Refractive Effects Prediction System (EREPS) 06 p0758 N90-14411
GRAFIN: GRAFIX interactive manual
[PB89-232136] 06 p0827 N90-14809
A graphically oriented specification language for automatic code generation. GRASP/Ada: A Graphical Representation of Algorithms, Structure, and Processes for Ada, phase 1
[NASA-CR-183212] 06 p0828 N90-14813
The High-Speed Channel (HSC) and ultra-speed networks
[DE89-015283] 06 p0829 N90-14819
Vision in dynamic environments
[AD-A213434] 07 p0967 N90-15587
An architectural model of visual motion understanding
[AD-A214327] 07 p0967 N90-15589
LLNL's plan for a prototype circuit switch, a potential gigabit LAN of the future
[DE90-003614] 07 p0969 N90-15597
Scry: A distributed image handling system, version 1.1
[DE90-003105] 07 p0973 N90-15621
Name assignment techniques for relational schemas representing extended entity-relationship schemas
[DE90-003269] 07 p0974 N90-15623
An executive system for modeling with rational b-splines
[AD-A213460] 07 p0974 N90-15627
A renormalization group approach to image processing: A new computational method for three-dimensional shapes in robot vision, and the computation complexity of the cooling algorithms
[AD-A214247] 07 p0977 N90-15643
Some computational properties of rotation representations
[AD-A213888] 07 p0981 N90-15665
Dynamic architecture computer
[AD-A214262] 08 p1106 N90-16402
EZVIDEO, FORTRAN graphics routines for the IBM AT
[DE90-004409] 08 p1109 N90-16422
Computer aided design based optical system modeling
[DE90-003453] 08 p1112 N90-16440
Interpretation of CAD (Computer Aided Design) models through IGES (Initial Graphics Exchange Specification) interface
[PB90-121294] 08 p1112 N90-16441
Parallel algorithms for interactive manipulation of digital terrain models 08 p1113 N90-16445
Scan line graphics generation on the massively parallel processor 08 p1114 N90-16450
NASA/ASEE Summer Faculty Fellowship Program
[NASA-CR-166837] 08 p1154 N90-16686
The DAB model of drawing processes
08 p1155 N90-16691
Investigation of IGES for CAD/CAE data transfer
08 p1157 N90-16702
Non-Fourier computer generated holography for 3-D display
[AD-A215369] 09 p1225 N90-17109
SAtool II: An IDEF0 syntax data manipulator and graphics editor
[AD-A215289] 09 p1263 N90-17321
Vision-based navigation and parallel computing
[AD-A214481] 09 p1264 N90-17327
Computer perception of three-dimensional objects
[AD-A215058] 09 p1267 N90-17345
The graphical representation of algorithmic processes, volume 1
[AD-A215359] 09 p1268 N90-17350
Interim Design Database (IDDB) CADAM drawing retrieval program user's manual for the IBM 3081
[DE90-004491] 09 p1269 N90-17356
Solving computer graphics problems through boolean combinations of polygons
[AD-A214788] 09 p1273 N90-17380
Sampling scattered data onto rectangular grids for volume visualization
[AD-A215533] 09 p1274 N90-17384
Use of semiempirical aerodynamic methods for preliminary design 10 p1304 N90-17546
An Autonomous Platform Simulator (APS)
[AD-A215768] 10 p1392 N90-18048
Raster Metafile and Raster Metafile Translator
[NASA-TM-102588] 10 p1417 N90-18166
POS2D: A graphic program for analysing axisymmetric and two-dimensional structures
[DE90-608864] 10 p1417 N90-18168
Decomposition for optimal synthesis in a parallel computing environment 10 p1419 N90-18184
Optimal planning method of underground distribution system, part 2. Application to various types of system configurations
[DE89-782323] 11 p1500 N90-18636
A self-organizing multiple-view representation of three-dimensional objects
[AD-A216711] 11 p1541 N90-18871
An interactive system applied to the linear quadratic problem
[INPE-4945-TDL/386] 11 p1548 N90-18913
Image manipulation in the SIGGRAPH Interactive Proceedings
[DE90-007542] 12 p1702 N90-19771
Harmonic generation mechanisms in short-wavelength free-electron lasers
[DE90-007622] 13 p1807 N90-20374
A split-and-merge method for creating polygonal homogeneous-vegetation regions from digitized terrain data
[AD-A218080] 13 p1821 N90-20453
Graphics Technology in Space Applications (GTSA 1989)
[NASA-CP-3045] 13 p1856 N90-20651
TAE Plus: Transportable Applications Environment Plus tools for building graphic-oriented applications
13 p1856 N90-20652
RenderMan design principles
13 p1857 N90-20653
Knowledge representation in space flight operations
13 p1857 N90-20655
The Real Time Display Builder (RTDB)
13 p1857 N90-20656
Applications of graphics to support a testbed for autonomous space vehicle operations
13 p1858 N90-20661
Efficient utilization of graphics technology for space animation 13 p1859 N90-20663
Engineering visualization utilizing advanced animation
13 p1859 N90-20664
Animation graphic interface for the space shuttle onboard computer 13 p1859 N90-20667
Operational computer graphics in the flight dynamics environment 13 p1859 N90-20668
The use of graphics in the design of the human-telerobot interface 13 p1860 N90-20670
Distributed earth model/orbiter simulation
13 p1860 N90-20671
Space Station Freedom integrated fault model
13 p1860 N90-20673
Using an instrumented manikin for Space Station Freedom analysis 13 p1861 N90-20675
The development of the Canadian Mobile Servicing System Kinematic Simulation Facility
13 p1861 N90-20676
History of visual systems in the Systems Engineering Simulator 13 p1862 N90-20681
Computer image generation: Reconfigurability as a strategy in high fidelity space applications
13 p1862 N90-20682
Real-time graphics for the Space Station Freedom cupola, developed in the Systems Engineering Simulator
13 p1862 N90-20683
MEASURE: An integrated data-analysis and model identification facility
[NASA-CR-186452] 13 p1863 N90-20686
The HS6000/20 development system
[LINO-1989-6] 13 p1865 N90-20696
Implementation of a hypertext help system for GLAD (Graphics LAnguage for Database)
[AD-A217936] 13 p1868 N90-20718
The perceptual interaction of graphical attributes in thirteen bivariate displays
[AD-A217980] 13 p1868 N90-20720
Parallel computer graphics algorithms for the connection machine
[AD-A217300] 13 p1872 N90-20733
Implementation of a control system test environment in UNIX
[DE90-007485] 13 p1872 N90-20736
Computation and graphics in mathematical research
[DE90-008429] 13 p1877 N90-20766
Modeling the temperature dependence of the thermal conductivity of aluminum nitride
[DE90-009428] 14 p1949 N90-21154
High explosives (PBX9502) characterization using computerized tomography
[DE90-008170] 14 p1990 N90-21404
The CAD/CAM product data standards: IGES/PDES (Initial Graphics Exchange Specification/Product Data Exchange Standards, the present and the future
[DE90-008803] 14 p2015 N90-21549
Simulated image maps for use in experimental high-resolution electron microscopy
[DE90-009178] 14 p2032 N90-21657
The psychology of computer displays in the modern mission control center
[NASA-TM-100451] 15 p2137 N90-22213
A3I visibility modeling project
15 p2140 N90-22230
Graphics mini manual
[NASA-TM-87622-REV] 15 p2144 N90-22247
Graphically-oriented nonlinear analysis of statically loaded plane frames on microcomputers
[PB90-165945] 15 p2144 N90-22248
Preliminary development of an intelligent computer assistant for engine monitoring
[NASA-TM-101702] 15 p2157 N90-22322
Spatial Displays and Spatial Instruments
[NASA-CP-10032] 16 p2267 N90-22918
Pictorial communication: Pictures and the synthetic universe 16 p2267 N90-22919
The photo-colorimetric space as a medium for the representation of spatial data 16 p2268 N90-22927
Spatial issues in user interface design from a graphic design perspective 16 p2270 N90-22939
Interactive displays in medical art
16 p2271 N90-22940
The interactive digital video interface
16 p2271 N90-22941
A computer graphics system for visualizing spacecraft in orbit 16 p2272 N90-22952
Interactive orbital proximity operations planning system 16 p2273 N90-22953
Experiences in teleoperation of land vehicles
16 p2273 N90-22954
Development of a stereo 3-D pictorial primary flight display 16 p2273 N90-22955
Synthetic perspective optical flow: Influence on pilot control tasks 16 p2273 N90-22956
Optical, gravitational, and kinesthetic determinants of judged eye level 16 p2274 N90-22959
The making of the mechanical universe
16 p2274 N90-22961
Synesthetic art through 3-D projection: The requirements of a computer-based supermedium
16 p2274 N90-22962
Wide-angle display developments by computer graphics 16 p2275 N90-22963
Volumetric visualization of 3D data
16 p2275 N90-22964
Determination of depth-viewing volumes for stereo three-dimensional graphic displays
[NASA-TP-2999] 16 p2275 N90-22965
Graphics equipment for data analysis
[AD-A218983] 16 p2278 N90-22985
Combining high performance simulation, data acquisition, and graphics display computers
16 p2293 N90-23062
Man-in-the-control-loop simulation of manipulators
16 p2293 N90-23063
PLOT3D user's manual
[NASA-TM-101067] 16 p2298 N90-23090
Basic graphics routine technical manual
[AD-A219409] 16 p2302 N90-23117
Sensor performance analysis
[NASA-RP-1241] 17 p2418 N90-23780
The Zenith Z-248 as a scientific workstation
[AD-A219991] 17 p2441 N90-23909
Shape discrimination research using an IBM PC
[AD-A219993] 17 p2447 N90-23953
Coloring a graph optimally with two colors
[MEMO-820] 17 p2449 N90-23961
Computational geometry and its application to computer graphics
[RUU-CS-89-8] 17 p2449 N90-23968
Computational tools for multi-linked flexible structures
[NASA-CR-186139] 17 p2462 N90-24058
Morphological and structural characterization of the spinodal decomposition of Fe-Cr alloys
[DE90-010496] 18 p2526 N90-24418
A generic interface between COSMIC/NASTRAN and PATRAN (R) 18 p2569 N90-24640
Interconnection of the graphics language for database system to the multi-lingual, multi-model, multi-backend database system over an Ethernet network
[AD-A220081] 18 p2591 N90-24739
Computer-Aided Structural Engineering (CASE) project. User's guide: A Three-Dimensional Stability Analysis/Design Program (3DSAD). Report 2: General loads module
[AD-A220331] 18 p2591 N90-24742
On the projective invariant representation of conics in computer graphics
[CWI-CS-R8938] 18 p2593 N90-24752
Development of a postprocessing and 3D graphical imaging facility
[AD-A221212] 18 p2593 N90-24755
Graph structure model
[DE90-008945] 18 p2594 N90-24760

HUGOFIT and HUGOPLOT: Computer codes for plane shock wave analysis with materials that have non-simple Hugoniots
[DE90-010284] 18 p2594 N90-24761
Visual animation of parallel algorithms for matrix computations
[DE90-011076] 18 p2594 N90-24763
Parallel algorithmic methods for volumetric rendering
[DE90-011326] 18 p2594 N90-24764
A few modeling and rendering techniques for computer graphics and their implementation on ultra hardware
18 p2640 N90-25038
Strut-node joint conjugates for the assembly of semi-permanent or reusable truss structures
18 p2640 N90-25039
Structural zooming research and development of an interactive computer graphical interface for stress analysis of cracks 18 p2641 N90-25042
Conceptual design for aerospace vehicles
18 p2641 N90-25043
The implementation of the graphics of program EAGLE: A numerical grid generation code on NASA Langley SNS computer system 18 p2642 N90-25050
A Cax success story
[MBB-FW-52/S/PUB-382] 19 p2649 N90-25076
Tools for mapping environmental monitoring data
[PB90-129685] 19 p2712 N90-25432
CREW CHIEF: A computer graphics simulation of an aircraft maintenance technician
19 p2729 N90-25515
A laboratory breadboard system for dual-arm teleoperation 19 p2740 N90-25573
Interactive grid generation on small computers
[AD-A221234] 19 p2742 N90-25585
CEBAF control system
[CEBAF-PR-89-013] 19 p2757 N90-25666
Feasibility study for a microwave-powered ozone sniffer aircraft, volume 2
[NASA-CR-186676] 20 p2806 N90-25967
Computer simulation of gear tooth manufacturing processes
[NASA-CR-185200] 20 p2843 N90-26171
OASIS, LLNL version: Software maintenance manual
[DE90-013522] 20 p2868 N90-26313
Graphics applications utilizing parallel processing
[NASA-CR-186719] 20 p2907 N90-26534
Computer animation in mathematics, science, and art
[DE90-013051] 20 p2908 N90-26538
The rationale and specification of the ELLA graphics systems
[RSRE-89017] 20 p2909 N90-26548
UEDIT: A full-scale, scrollable APL2 spreadsheet input/output editor
[AD-A222712] 20 p2910 N90-26557
ATN design tool
[AD-A223030] 20 p2911 N90-26559
An architecture for rule based system explanation
21 p3042 N90-27288
A study on diagnosability of space station ECLSS
21 p3043 N90-27294
Graphical explanation in an expert system for Space Station Freedom rack integration
21 p3044 N90-27299
Generation of animation sequences of three dimensional models
[NASA-CASE-MSC-21379-1-SB]
21 p3050 N90-27340
A plan for scientific visualization at ANL
[DE90-013565] 21 p3051 N90-27344
Expert system in software engineering using Structured Analysis and Design Technique (SADT)
[AD-A223022] 21 p3052 N90-27351
Post script code for grey-scaled displays
[AD-A223099] 21 p3053 N90-27354
An algorithm for automated surface modelling in unigraphics
[AD-A223219] 21 p3053 N90-27355
A programming environment for parallel vision algorithms
[AD-A221486] 21 p3055 N90-27368
Economical graphics display system for flight simulation avionics
[NASA-CR-186886] 22 p3116 N90-27701
The Helicopter Antenna Radiation Prediction Code (HARP)
[NASA-CR-186925] 22 p3165 N90-27946
Local spatial frequency analysis for computer vision
[NASA-CR-186990] 22 p3237 N90-28356
Time, space and form in vision
[AD-A213889] 23 p3357 N90-28971
Design of a monitor and simulation terminal (master) for space station telerobotics and telescience
23 p3372 N90-29051
Who's who in scientific visualization at LLNL
[DE90-014720] 23 p3379 N90-29091
A computer graphics package
[ARE-TM(UDT)-89111] 23 p3380 N90-29094
Graph structure model
[DE90-014930] 23 p3381 N90-29097
Fast interactive image generation of line and surface oriented objects in raster systems
[ETN-90-97290] 23 p3381 N90-29102
Animated computer-generated video-tape instruction using DIGLIB (Device Independent Graphics Library)
[DE90-015360] 23 p3382 N90-29105
The 2-D and 3-D characterizations of GPS navigation service 24 p3425 N90-29348
Satellite navigation systems for land vehicles
24 p3430 N90-29376
The function of the Interactive Model Assembly Program (IMAP) for a flight simulator
[NAL-TR-1034] 24 p3437 N90-29412
Telepresence system development for application to the control of remote robotic systems
24 p3503 N90-29799
Graphic overlays in high-precision teleoperation: Current and future work at JPL 24 p3508 N90-29827
Head-mounted spatial instruments II: Synthetic reality or impossible dream 24 p3508 N90-29828
Use of graphics in decision aids for telerobotic control: (Parts 5-8 of an 8-part MIT progress report)
24 p3508 N90-29829
Realtime multi-plot graphics system
[NASA-CR-4304] 24 p3523 N90-29919
Digital color representation
[DE90-014580] 24 p3524 N90-29924
Machine recognition as representation and search
[AD-A223700] 24 p3528 N90-29946
An interactive optimization based, computer graphics software package. Phase 2: Users manual
[AD-A223854] 24 p3529 N90-29954
Ray traced scalar fields with shaded polygonal output
[DE90-011023] 24 p3529 N90-29955
A manual for microcomputer image analysis
[DE90-015629] 24 p3529 N90-29958
Computing environments, interactive graphics and nonparametric methods for data analysis
[DE90-016127] 24 p3530 N90-29962
Computing environments, interactive graphics and nonparametric methods for data analysis
[DE90-016128] 24 p3530 N90-29964
Information processing and perceptual characteristics of display design: The role of emergent features and objects
[AD-A223683] 24 p3558 N90-30133

COMPUTER INFORMATION SECURITY

DDN Trusted Guard Gateway: Trusted Guard Gateway (TGG) technology assessment, phase 2
[AD-A210248] 01 p0108 N90-10614
On the design and implementation of a secure computer system
[RSRE-MEMO-4188] 03 p0385 N90-12189
A security model and its implementation
[RSRE-MEMO-4222] 03 p0385 N90-12190
Operating experience with the Sandia terminal switching network and fiber optic loop
[DE89-007422] 03 p0404 N90-12317
A Z specification of the MaCHO interface editor
[RSRE-MEMO-4247] 04 p0531 N90-13067
How robust are distributed systems
[NASA-CR-186242] 06 p0832 N90-14837
On the privacy problems involved in allowing access to computers via the public telephone system
[RSRE-88006] 07 p0917 N90-15303
Issues and approaches for electronic document approval and transmittal using digital signatures and text authentication: Prototype documentation
[DE90-003382] 08 p1058 N90-16119
The SMITE approach to security
[RSRE-89014] 08 p1106 N90-16404
Tool support for the production of high integrity software
[RSRE-89005] 08 p1111 N90-16433
Using the K-25 C/TD common file system: A guide to CFSI
[DE90-005815] 11 p1593 N90-19179
Software verification and validation: Its role in computer assurance and its relationship with software project management standards
[PB90-111691] 14 p2012 N90-21530
The internet worm
[NASA-CR-181576] 17 p2441 N90-23910
Graph structure model
[DE90-008945] 18 p2594 N90-24760
Privacy-enhanced electronic mail
[PCS-TR90-150-REV-1] 19 p2683 N90-25261
Computer access security code system
[NASA-CASE-NPO-17525-1-CU]
19 p2742 N90-25583
Theft of information in the take-grant protection model
[NASA-CR-186638] 19 p2763 N90-25702
Basic mechanisms for computer security
[RSRE-89024] 22 p3235 N90-28347
Hash functions: A tutorial and status report
[NPL-DITC-151/89] 22 p3238 N90-28361
Report of the Invitational Workshop on Data Integrity
[PB90-148123] 22 p3240 N90-28372
Secure Data Network System (SDNS) network, transport, and message security protocols
[PB90-198946] 23 p3318 N90-28757
A comparison of password techniques for multilevel authentication mechanisms
[AD-A224245] 23 p3379 N90-29089
A survey of object-oriented database technology
[AD-A224490] 24 p3558 N90-30130

COMPUTER METHODS

U COMPUTER PROGRAMS

COMPUTER NETWORKS

NT ARPA COMPUTER NETWORK
NT LOCAL AREA NETWORKS
Ada (trademark) projects at NASA. Runtime environment issues and recommendations
[NASA-CR-183435] 01 p0103 N90-10583
Cost metric algorithms for internetwork applications
[AD-A210324] 01 p0105 N90-10597
An introduction to input/output automata
[AD-A210831] 01 p0106 N90-10604
Network of dedicated processors for finding lowest-cost map path
[NASA-CASE-NPO-17716-1-CU]
01 p0107 N90-10608
Tools for application development in heterogeneous distributed environments
[AD-A210238] 01 p0108 N90-10613
DDN Trusted Guard Gateway: Trusted Guard Gateway (TGG) technology assessment, phase 2
[AD-A210248] 01 p0108 N90-10614
Transaction throughput in distributed systems: A modeling study using dynamic queueing networks
[MEMO-INF-89-25] 02 p0261 N90-11479
Fixed point iteration on point-symmetric interference graphs
[MEMO-INF-89-23] 02 p0269 N90-11535
Toward a national research network
[PB89-198709] 02 p0287 N90-11644
The conditional-event approach to distributed simulation
[NASA-CR-185890] 03 p0387 N90-12200
On the communication complexity of solving a polynomial equation
[AD-A211945] 03 p0393 N90-12240
Operating experience with the Sandia terminal switching network and fiber optic loop
[DE89-007422] 03 p0404 N90-12317
Interoperability of heterogeneous information systems: The COST 11(ter) Project
[PB89-217541] 03 p0417 N90-12394
Access to Max '91 information via computer networks
03 p0430 N90-12486
Telescience Testbed Pilot Program
[NASA-CR-184997] 04 p0528 N90-13047
A formatting style for typesetting and distributing draft international standards
[NPL-DITC-143/89] 04 p0530 N90-13059
Area-universal networks
[AD-A211883] 04 p0535 N90-13092
Work-preserving emulations of fixed-connection networks
[AD-A211915] 04 p0535 N90-13093
Extended performability modeling using dynamic queing networks
[MEMO-INF-89-15] 04 p0536 N90-13099
Activities report of the Kernfysisch Versneller Instituut
[ETN-89-95752] 04 p0553 N90-13219
Computational and psychophysical study of human vision using neural networks
[AD-A213290] 05 p0674 N90-13924
The structural memory: A network model for human perception of serial objects
[CWI-CS-R8829] 05 p0675 N90-13930
Compression of bitmapped graphic data
[AD-A213141] 05 p0683 N90-13974
Empirical analysis and refinement of expert system knowledge bases
[AD-A213240] 05 p0707 N90-14143
Configuration development for ROMENET
[AD-A213367] 06 p0765 N90-14450
NORDA's pattern analysis laboratory: Current contributions to naval mapping, charting, and geodesy
[AD-A212731] 06 p0801 N90-14665
Integrated computer-based tools to facilitate environmental monitoring, assessment, and restoration
[DE90-002732] 06 p0811 N90-14717
AdaNET services 06 p0827 N90-14806
The High-Speed Channel (HSC) and ultra-speed networks
[DE89-015283] 06 p0829 N90-14819

Multiple crossbar network: Integrated supercomputing framework
[DE89-012614] 06 p0831 N90-14831
The Delta-t transport protocol: Features and experience useful for high performance networks
[DE89-016542] 06 p0831 N90-14832
Generalization in backpropagation networks: An empirical study using image data
[DE89-012658] 06 p0832 N90-14835
How robust are distributed systems
[NASA-CR-186242] 06 p0832 N90-14837
On the privacy problems involved in allowing access to computers via the public telephone system
[RSRE-88006] 07 p0917 N90-15303
Temporal, processor, and spatial locality in multiprocessor memory references
[AD-A213790] 07 p0969 N90-15598
Scry: A distributed image handling system, version 1.1
[DE90-003105] 07 p0973 N90-15621
Programs for control of an analog-signal switching network
[DE90-003645] 07 p0974 N90-15626
On the correctness of orphan management algorithms
[AD-A213777] 07 p0975 N90-15632
Neural network models for linear programming
[DE89-015974] 07 p0979 N90-15651
A neural network for bounded linear programming
[DE89-015975] 07 p0979 N90-15652
A multichannel processing approach to real time network detection, phase association, and threshold monitoring
[AD-A213940] 07 p0980 N90-15657
Adaptive backoff synchronization techniques
[AD-A213966] 07 p0980 N90-15658
One-class generalization in second-order backpropagation networks for image classification
[DE89-015845] 07 p0980 N90-15661
Upgrade plans to handle 30 to 40 Mbytes of data for D3-D
[DE90-003291] 07 p0995 N90-15750
Data file management in the D3-D data acquisition and analysis computer systems
[DE90-003289] 07 p1010 N90-15850
PVM (Parallel Virtual Machine): A framework for parallel distributed computing
[DE90-004390] 08 p1106 N90-16403
Overview and extensions of a system for routing directed graphs on SIMD architectures 08 p1113 N90-16444
Communication-efficient arbitration models for low-resolution data flow computing
[AD-A214768] 09 p1262 N90-17319
MPlus Database system
[DE90-004146] 09 p1263 N90-17325
Network flow algorithms
[AD-A214689] 09 p1265 N90-17337
The graphical representation of algorithmic processes, volume 1
[AD-A215359] 09 p1268 N90-17350
A specification and analysis of the IEEE (Institute of Electrical and Electronic Engineers) token ring protocol
[AD-A214567] 09 p1269 N90-17359
Large-scale optimization via distributed systems
[AD-A215136] 09 p1270 N90-17364
Merlin: A superglue for multicomputer systems
[NASA-CR-186330] 09 p1271 N90-17366
Internet protocol handbook. Volume 4: The Domain Name System (DNS) handbook
[AD-A214698] 09 p1296 N90-17512
Fine tuning your search output: Word processors, desktop publishing, electronic mail, databases, and beyond
[DE90-005192] 09 p1297 N90-17517
Finding minimum-cost flows by double scaling
[AD-A214498] 10 p1416 N90-18159
Research at New York University's Ultracomputer Research Laboratory
[DE90-005471] 10 p1417 N90-18167
Efficient interconnection schemes for VLSI and parallel computation
[AD-A216405] 10 p1420 N90-18185
Report of the First Annual Airborne Weapons Training Technology Review
[DE90-007189] 12 p1697 N90-19747
Networks and the best approximation property
[AD-A216712] 12 p1703 N90-19778
Transaction processing in a quality control laboratory
[DE90-004655] 13 p1813 N90-20414
Supercomputer environments
[AD-A217682] 13 p1863 N90-20689
Robust planning and control using neural networks
[AD-A217216] 13 p1872 N90-20732
The Livermore distributed storage system: Implementation and experiences
[DE90-007257] 13 p1872 N90-20735
Design of a simulation interface for a parellel computing environment
[DE90-008497] 13 p1873 N90-20737
Micro SAINT programs for numerical methods of integration and differential equations
[AD-A218097] 13 p1878 N90-20772
CALS (Computer-aided Acquisition and Logistic Support) Test Network information exchange user's manual, revision 1
[DE90-008119] 13 p1900 N90-20904
High performance computing and networking for science
[PB90-131228] 14 p2011 N90-21526
Toward a new CIM (Computer Integrated Manufacturing) architecture for Sandia Laboratories
[DE90-008677] 14 p2015 N90-21548
VCS: A networked Version Control System
[DE90-009805] 15 p2145 N90-22250
Extremely high data-rate, reliable network systems research
[NASA-CR-186359] 15 p2149 N90-22278
CSMA/RN: A universal protocol for gigabit networks 15 p2150 N90-22280
Performance of gigabit FDDI 15 p2150 N90-22283
Distributed simulation of network protocols 15 p2150 N90-22284
Extensibility and limitations of FDDI 15 p2151 N90-22286
A carrier sensed multiple access protocol for high data base rate ring networks 15 p2151 N90-22288
SURE (Science User Resource Expert): A science planning and scheduling assistant for a resource based environment 15 p2153 N90-22302
A knowledge-based system with learning for computer communication network design 15 p2157 N90-22319
Executive summary for the network assessment model
[AD-A218762] 16 p2229 N90-22718
Rules and maps in connectionist symbol processing
[AD-A219028] 16 p2264 N90-22903
Cognitive architectures and rational analysis: Comment
[AD-A219199] 16 p2264 N90-22907
Proceedings of the 3rd Annual Conference on Aerospace Computational Control, volume 2
[NASA-CR-186447] 16 p2289 N90-23040
Reusing software components by specialization
[REPT-89-062] 16 p2298 N90-23094
Fault tolerant multiprocessing and development of tools
[AD-A219216] 16 p2301 N90-23110
The Durra application debugger/monitor
[AD-A219290] 16 p2301 N90-23111
Locality in parallel computation
[AD-A218733] 16 p2302 N90-23120
A distributed program composition system
[NASA-CR-181568] 17 p2441 N90-23911
Improving upon standard pattern classification algorithms by implementing them as multi-layer perceptrons
[AD-A220046] 17 p2447 N90-23954
Distributed user services for supercomputers
[NASA-CR-180370] 17 p2450 N90-23976
A network flow model for load balancing in circuit-switched multicomputers
[NASA-CR-182049] 17 p2451 N90-23977
Failure analysis and modeling of a multicomputer system
[NASA-CR-186697] 17 p2451 N90-23980
Distributed hierarchical routing
[RUU-CS-89-5] 17 p2452 N90-23986
The distributed bit complexity of the ring: From the anonymous to the non-anonymous case
[RUU-CS-88-33] 17 p2452 N90-23988
Northeast Artificial Intelligence Consortium. Volume 3: The Versatile Maintenance Expert System research project
[AD-A218716] 17 p2453 N90-23993
Interconnection of the graphics language for database system to the multi-lingual, multi-model, multi-backend database system over an Ethernet network
[AD-A220081] 18 p2591 N90-24739
Development of a postprocessing and 3D graphical imaging facility
[AD-A221212] 18 p2593 N90-24755
Graph structure model
[DE90-008945] 18 p2594 N90-24760
Sensitivity analysis of transputer workfarm topologies
[AD-A219821] 18 p2595 N90-24766
National Aeronautics and Space Administration (NASA)/American Society for Engineering Education (ASEE) Summer Faculty Fellowship Program-1989, volume 2
[NASA-CR-185601-VOL-2] 18 p2630 N90-24985
Some issues related to simulation of the tracking and communications computer network 18 p2630 N90-24988
Enhancing a relational database: Stepwise, bottom-up design
[DE90-010834] 18 p2635 N90-25012
Exploiting replication in distributed systems
[NASA-CR-186410] 19 p2746 N90-25603
Modeling and synthesis of multicomputer interconnection networks
[NASA-CR-186619] 19 p2746 N90-25604
Reliable broadcast protocols
[NASA-CR-186411] 19 p2762 N90-25696
Computer architecture evaluation for structural dynamics computations: Project summary
[NASA-CR-186137] 20 p2903 N90-26512
Applications for the scalable coherent interface
[DE90-011795] 20 p2903 N90-26514
Integrating expert systems with solid modeling through interprocess communications and the applications interface specification
[DE90-012996] 20 p2907 N90-26537
Language support for parallel computation
[AD-A223072] 20 p2911 N90-26560
Pacific missile test center information resources management organization (code 0300): The ORACLE client-server and distributed processing architecture
[DE90-013271] 20 p2912 N90-26565
High speed all optical networks
[NASA-CR-185311] 20 p2926 N90-26649
Analysis of random drop for gateway congestion control
[NASA-CR-186736] 20 p2935 N90-26698
INTERMAGNET 21 p3023 N90-27190
KIPSE1: A Knowledge-based Interactive Problem Solving Environment for data estimation and pattern classification 21 p3041 N90-27287
Establishing a communications-intensive network to resolve artificial intelligence issues within NASA's Space Station Freedom research centers community 21 p3042 N90-27291
A study on diagnosability of space station ECLSS 21 p3043 N90-27294
Knowledge-based systems and NASA's software support environment 21 p3043 N90-27296
Design knowledge capture for a corporate memory facility 21 p3045 N90-27304
Advanced retrieval assistance for the DGIS gateway
[AD-A221592] 21 p3087 N90-27558
Cyclic error correcting block codes for reliability increasing of VLSI networks
[ETN-90-97304] 22 p3168 N90-27968
Efficient algorithms for a class of partitioning problems
[NASA-CR-182073] 22 p3237 N90-28357
Proceedings of the Conference on Artificial Intelligence in the Department of Energy Complex
[DE90-011634] 22 p3241 N90-28378
A model parametric real-time logic
[REPT-90-010] 22 p3241 N90-28381
The new space and Earth science information systems at NASA's archive 22 p3257 N90-28443
An environment to support problem solving
[ISBN-90-9003151-0] 22 p3259 N90-28458
Evaluating recursive queries in distributed databases
[REPT-90-015] 22 p3260 N90-28460
Secure Data Network System (SDNS) network, transport, and message security protocols
[PB90-198946] 23 p3318 N90-28757
The effect of multiprocessor radius on scaling
[DE90-014772] 23 p3380 N90-29095
Graph structure model
[DE90-014930] 23 p3381 N90-29097
High energy physics at Tufts University
[DE90-014664] 23 p3394 N90-29174
International aircraft operator data base master requirements and implementation plan
[DOT/FAA/CT-90/17] 23 p3405 N90-29247
Distributed communications and control network for robotic mining 24 p3520 N90-29901
Graphic interface for attribute-based data language queries from a personal computer to the multi-lingual, multi-model, multi-backend database system over an Ethernet network
[AD-A223738] 24 p3528 N90-29948
Computing environments, interactive graphics and nonparametric methods for data analysis
[DE90-016127] 24 p3530 N90-29962
Supporting large scale applications on networks of workstations
[NASA-CR-186346] 24 p3532 N90-29975
Low cost management of replicated data in fault-tolerant distributed systems
[NASA-CR-186370] 24 p3532 N90-29976
Reliable communication in the presence of failures
[NASA-CR-183046] 24 p3533 N90-29977
Fault tolerant design for multistage routing networks
[AD-A224267] 24 p3533 N90-29978

Accessing network databases via SQL transactions in a multi-model database system
[AD-A223946] 24 p3557 N90-30128

COMPUTER PROGRAM INTEGRITY
Proving total correctness of recursive procedures
[CWI-CS-R8904] 04 p0532 N90-13075
An empirical comparison of software fault tolerance and fault elimination
[NASA-CR-186313] 08 p1108 N90-16414
Tool support for the production of high integrity software
[RSRE-89005] 08 p1111 N90-16433
Stochastic models in reliability
[AD-A215479] 09 p1234 N90-17163
Adapting software development policies to modern technology
[AD-A213391] 10 p1416 N90-18157
A formal mechanism for determining redundancy and irrelevance in Hypertext views
[TR-89-9] 17 p2450 N90-23970
Generalization in the presence of free variables: A mechanically-checked correctness proof for one algorithm
[AD-A222681] 21 p3051 N90-27346
The identification of software failure regions
[AD-A223058] 21 p3052 N90-27352
Basic mechanisms for computer security
[RSRE-89024] 22 p3235 N90-28347
Software design for high integrity systems
[ETN-90-97517] 24 p3530 N90-29966
Analysis and synthesis of robust data structures
[AD-A224568] 24 p3558 N90-30131

COMPUTER PROGRAMMING
NT ASSEMBLER ROUTINES
NT LANGUAGE PROGRAMMING
NT LOGIC PROGRAMMING
NT MICROPROGRAMMING
NT MULTIPROGRAMMING
NT PARALLEL PROGRAMMING
NT SYMBOLIC PROGRAMMING
Automated model formulation for time-varying flexible structures 01 p0022 N90-10107
Evaluation of computer-aided software engineering tools for data base development
[DE89-014007] 01 p0104 N90-10591
Structure flow diagram generator
[PB89-195978] 01 p0104 N90-10592
String Search
[PB89-195986] 01 p0104 N90-10593
Using computer design and simulation to improve manufacturing productivity
[AD-A210338] 01 p0105 N90-10598
Software methodology catalog, second edition, revision
[AD-A210548] 01 p0106 N90-10601
The impact of recovery on concurrency control
[AD-A210828] 01 p0106 N90-10603
Type reconstruction with first-class polymorphic values
[AD-A210833] 01 p0106 N90-10605
Tools for application development in heterogeneous distributed environments
[AD-A210238] 01 p0108 N90-10613
The applicability and limitations of expert system shells
[AD-A210801] 01 p0110 N90-10625
Applications of algebraic logic and universal algebra to computer science
[AD-A210556] 01 p0113 N90-10645
Toward a theory of representation design
[AD-A210885] 01 p0116 N90-10670
Rethinking synthesis of fine-motion strategies
[DE89-016671] 02 p0230 N90-11322
An investigation of the usefulness of Earley's Algorithm in a general context-free recognizer
[DE89-016498] 02 p0258 N90-11463
Checking the Goldbach conjecture on a vector computer
[CWI-NM-R8812] 02 p0260 N90-11475
A generalization of A. N. Habermann's theorem for semaphores
[REPT-88-98] 02 p0261 N90-11484
LEXER: A tool for lexical analysis of program input
[DE89-016924] 02 p0288 N90-11649
The Knowledge Representation Project
[AD-A211288] 02 p0288 N90-11650
Coupling rule-based and object-oriented programming for the classification of machined features
[DE89-017705] 03 p0334 N90-11903
Software package for 3-dimensional graphic display unit
[NAL-TM-559] 03 p0385 N90-12191
Experience with CST: Programming and implementation
[AD-A211882] 03 p0386 N90-12197
A single-phase clocked NOR/NOR CMOS programmable sequential array structure
[AD-A211297] 03 p0387 N90-12203
ISI's (Information Sciences Institute) SDI architecture simulator: An experiment in adding new software to the system
[AD-A211314] 03 p0387 N90-12204
Adoption of software engineering innovations in organizations
[AD-A211573] 03 p0387 N90-12206
Structure based formal methods for software engineering
[AD-A211660] 03 p0388 N90-12207
A language for assembly instructions
[REPT-88-90] 03 p0388 N90-12209
Computer-based tutors for explaining and managing the process of diagnostic reasoning
[AD-A211738] 03 p0390 N90-12222
Case study on rapid software prototyping and automated software generation: An inertial navigation system
[AD-A212272] 04 p0450 N90-12578
An expert system for VM performance analysis
[REPT-89-30] 04 p0528 N90-13045
ISI's (Information Sciences Institute) SDI architecture simulator: Initial prototype user interface
[AD-A211325] 04 p0529 N90-13053
Building a software package for solving large sparse nonlinear systems of equations
[AD-A211758] 04 p0529 N90-13055
Mathematical equivalence in a primitive Ella
[RSRE-MEMO-4225] 04 p0531 N90-13066
A table-driven approach to fast context-free parsing
[AD-A212210] 04 p0533 N90-13082
Software Engineering Exercise (SEE) guidelines
[AD-A212510] 04 p0534 N90-13085
Toward a formal model of the design and evolution of software
[AD-A212533] 04 p0534 N90-13087
NTRFACE for MAGIC
[AD-A212858] 04 p0538 N90-13112
A modified Newton method for unconstrained minimization
[AD-A212752] 04 p0546 N90-13174
Computer-based tools for assisting air traffic controllers with arrivals flow management
[RSRE-88001] 05 p0577 N90-13366
Apparatus for cooling electronic components in aircraft
[AD-D014207] 05 p0579 N90-13373
SIMOGEN: An object-oriented language for simulation
[AD-A213129] 05 p0682 N90-13973
Multi-level specification and verification of real-time software
[AD-A213227] 05 p0683 N90-13975
Ada programming guidelines for deterministic storage management
[NASA-CR-181308] 05 p0684 N90-13982
Extended memory library for AFOS (Automation of Field Operations and Services) applications
[PB89-230858] 05 p0708 N90-14147
Force user's manual: A portable, parallel FORTRAN
[NASA-CR-4265] 06 p0823 N90-14785
QUEST/Ada: Query utility environment for software testing of Ada
[NASA-CR-186121] 06 p0823 N90-14787
Impact of domain analysis on reuse methods 06 p0824 N90-14792
Classic-Ada(TM) 06 p0824 N90-14793
Prototype software reuse environment at Goddard Space Flight Center 06 p0825 N90-14794
Johnson Space Center software reuse activity 06 p0825 N90-14796
Reuse research plans at Langley Research Center 06 p0825 N90-14797
Reuse at the Software Productivity Consortium 06 p0825 N90-14798
SSFP approach to software reuse 06 p0826 N90-14799
Level 2 software reuse study 06 p0826 N90-14800
Support for life-cycle product reuse in NASA's SSE 06 p0826 N90-14802
Application of reusable software components at the SEI 06 p0826 N90-14804
Technology transfer in software engineering 06 p0827 N90-14805
AdaNET services 06 p0827 N90-14806
Advanced Software Development Workstation Project 06 p0827 N90-14807
A graphically oriented specification language for automatic code generation. GRASP/Ada: A Graphical Representation of Algorithms, Structure, and Processes for Ada, phase 1
[NASA-CR-183212] 06 p0828 N90-14813
Selecting and effectively using a computer aided software engineering tool
[DE89-017876] 06 p0828 N90-14815
Programmable near-infrared ranging system
[AD-D014237] 06 p0843 N90-14903
Fatigue behavior of vertical axis wind turbine airfoils with two weld configurations
[DE90-002628] 07 p0955 N90-15525
Paralation views: Abstractions for efficient scientific computing on the connection machine
[AD-A213935] 07 p0971 N90-15604
Utilization of a PC for finite element modeling
[AD-A214173] 07 p0971 N90-15605
Scry: A distributed image handling system, version 1.1
[DE90-003105] 07 p0973 N90-15621
An executive system for modeling with rational b-splines
[AD-A213460] 07 p0974 N90-15627
The StarLite project
[AD-A214193] 07 p0977 N90-15642
A structured connectionist approach to direct inferences and figurative adjective-noun combinations
[AD-A214326] 07 p0978 N90-15649
Investigation of the applicability of a functional programming model to fault-tolerant parallel processing for knowledge-based systems
[NASA-CR-181938] 07 p0979 N90-15654
Diesel starting system monitor: Prototype development
[DE90-004425] 08 p1084 N90-16276
Bus programmable slave module
[NASA-CASE-MSC-21387-1] 08 p1108 N90-16411
An empirical comparison of software fault tolerance and fault elimination
[NASA-CR-186313] 08 p1108 N90-16414
ZBTAB: Zenith-248 version of BLUGTAB
[AD-A214279] 08 p1108 N90-16415
EZVIDEO, FORTRAN graphics routines for the IBM AT
[DE90-004409] 08 p1109 N90-16422
The new programming
[RSRE-MEMO-4249] 08 p1110 N90-16425
A persistent heap for ALGOL 68
[RSRE-MEMO-4268] 08 p1110 N90-16427
Alvey MMI007. Object identification from 2D images: The RSRE contribution
[RSRE-MEMO-4277] 08 p1110 N90-16428
Tool support for the production of high integrity software
[RSRE-89005] 08 p1111 N90-16433
Computer aided design based optical system modeling
[DE90-003453] 08 p1112 N90-16440
Off-line robot programming and graphical verification of path planning 08 p1156 N90-16699
Spark source mass spectrometry software documentation and verification
[DE90-004463] 09 p1192 N90-16909
Analog hardware for delta-backpropagation neural networks
[NASA-CASE-NPO-17564-1-CU] 09 p1204 N90-16974
Study for the dissipative structures geometry in three dimensional developed turbulence
[ETN-90-96102] 09 p1219 N90-17072
Implementing fault-tolerant sensors
[NASA-CR-186269] 09 p1225 N90-17105
Supporting shared data structures on distributed memory architectures
[NASA-CR-181981] 09 p1262 N90-17318
SAtool II: An IDEF0 syntax data manipulator and graphics editor
[AD-A215289] 09 p1263 N90-17321
Access to multiple underlying systems in Janus
[AD-A214585] 09 p1264 N90-17329
The graphical representation of algorithmic processes, volume 1
[AD-A215359] 09 p1268 N90-17350
The use of efficient broadcast protocols in asynchronous distributed systems
[NASA-CR-186272] 09 p1269 N90-17358
Help design software project
[AD-A214883] 09 p1270 N90-17362
Compiling scientific code using partial evaluation
[AD-A215067] 09 p1270 N90-17363
Loran C monitor: Facilities Central Processing Unit (FCPU) port evaluation
[DOT/FAA/CT-TN89/57] 10 p1318 N90-17623
Software verification plan for GCS --- guidance and control software
[NASA-TM-101668] 10 p1394 N90-18057
A flexible basis for software configuration management
[RSRE-MEMO-4127] 10 p1415 N90-18153
Adapting software development policies to modern technology
[AD-A213391] 10 p1416 N90-18157

Proceedings of the 4th Annual Ada Software Engineering Education and Training Symposium
[AD-A214663] 10 p1417 N90-18162
Software for image treatment of the FORCE system operating at the IFSI — Ist. di Fisica dello Spazio Interplanetario (IFSI)
[IFSI-88-15] 10 p1417 N90-18164
A system for execution of JSD requirements
[INPE-4915-TDL/381] 10 p1417 N90-18170
Logical architecture
[INPE-4792-RPE/585] 10 p1418 N90-18171
KAPSE Interface Team (KIT) public report, volume 7
[AD-A215838] 10 p1418 N90-18176
KAPSE Interface Team (KIT) public report, volume 8, part 1
[AD-A215839] 10 p1418 N90-18177
KAPSE Interface Team (KIT) public report, volume 8, part 2
[AD-A215840] 10 p1419 N90-18178
Structured analysis tool interface to the strategic defense initiative architecture dataflow modeling technique
[AD-A216281] 10 p1424 N90-18218
On the kinematic behavior of robots while executing general robot level commands
[PB90-120965] 11 p1517 N90-18735
Guidelines for the use of the SAME
[AD-A215846] 11 p1544 N90-18886
Technology assessment of software engineering
[AD-A216943] 11 p1546 N90-18902
RALPH: An automatic Robot Assembly Language Programmer: An overview
[PB90-120973] 11 p1548 N90-18912
Derivation of an efficient rule system pattern matcher
[AD-A216801] 11 p1549 N90-18917
ROCOPT: A user friendly interactive code to optimize rocket structural components 12 p1639 N90-19415
Implementation of the RADM/EURAD models on the great calculation system of the Juelich KFA
12 p1687 N90-19687
Software development: A paradigm for the future
[NASA-CR-186456] 12 p1701 N90-19766
Deceit: A flexible distributed file system
[NASA-CR-186412] 12 p1726 N90-19923
A data acquisition parallel bus for wind tunnels at ARL (Aeronautical Research Laboratory)
[AD-A218052] 13 p1759 N90-20098
Flexible automatic discrete parts assembly
[AD-A217401] 13 p1787 N90-20256
Numerical Arc Segmentation Algorithm for a Radio Conference-NASARC (version 4.0) technical manual
[NASA-TM-101453] 13 p1788 N90-20264
TAE Plus: Transportable Applications Environment Plus tools for building graphic-oriented applications
13 p1856 N90-20652
Onboard shuttle on-line software requirements system: Prototype 13 p1858 N90-20658
GCS plan for software aspects of certification
[NASA-CR-181972] 13 p1864 N90-20694
The contour model architecture and assembly language
[AD-A217114] 13 p1865 N90-20697
RIPE: An object-oriented Robot Independent Programming Environment
[DE90-006501] 13 p1866 N90-20707
Research in programming languages and software engineering
[AD-A217765] 13 p1868 N90-20715
VHSIC Hardware Description Language (VHDL) benchmark suite
[AD-A217947] 13 p1868 N90-20719
Optimization of series expressions. Part 1: User's manual for the series macro package
[AD-A218220] 13 p1869 N90-20725
A review of the suitability of available Computer Aided Software Engineering (CASE) tools for the small software development environment
[AD-A218276] 13 p1870 N90-20726
Towards SDS (Strategic Defense System) testing and evaluation: A collection of relevant topics
[AD-A217610] 13 p1880 N90-20783
Human centrifuge controller
[NAL-TM-SE-8901] 14 p1929 N90-21043
Numerical Arc Segmentation Algorithm for a Radio Conference (NASARC), version 4.0: User's manual
[NASA-TM-101454] 14 p1964 N90-21250
Software to characterize tuning fork resonators used in the Quartz Digital Accelerometer
[DE90-007913] 14 p1983 N90-21363
Maintenance = reuse-oriented software development
[NASA-CR-186455] 14 p2012 N90-21531
Integrating automated support for a software management cycle into the TAME system
[NASA-CR-186457] 14 p2013 N90-21532
Annotated bibliography of software engineering laboratory literature
[NASA-TM-103313] 14 p2013 N90-21536
Collected software engineering papers, volume 7
[NASA-TM-103312] 14 p2014 N90-21537
Evolution of Ada technology in the flight dynamics area: Implementation/testing phase analysis
[NASA-TM-103310] 14 p2014 N90-21539
Collected software engineering papers, volume 6
[NASA-TM-103309] 14 p2014 N90-21540
System testing of a production Ada (trademark) project: The GRODY study
[NASA-TM-103308] 14 p2014 N90-21541
Evolution of Ada technology in the flight dynamics area: Design phase analysis
[NASA-TM-103307] 14 p2014 N90-21542
Software Management Environment (SME) concepts and architecture
[NASA-TM-103306] 14 p2014 N90-21543
Implementation of a production Ada project: The GRODY study
[NASA-TM-103305] 14 p2015 N90-21544
Software Engineering Laboratory (SEL) database organization and user's guide
[NASA-TM-103304] 14 p2015 N90-21545
Exploiting virtual synchrony in distributed systems
[NASA-CR-182855] 14 p2016 N90-21555
Numerical code AEOLUS-E1 for analysing free-boundary resistive MHD mode
[DE90-759903] 14 p2028 N90-21630
Program CICC: Flow and heat transfer in Cable In Conduit Conductors, user's manual
[DE90-007924] 14 p2033 N90-21661
Improving a data-acquisition software system with abstract data type components
15 p2078 N90-21901
Resource Allocation Planning Helper (RALPH): Lessons learned 15 p2152 N90-22296
Knowledge-based and integrated monitoring and diagnosis in autonomous power systems
15 p2155 N90-22310
Evaluation of a proposed expert system development methodology: Two case studies
15 p2157 N90-22320
Object-oriented databases: How are they different and what difference does it make
[REPT-89-55] 15 p2180 N90-22459
Using object-oriented analysis techniques to support system testing
[DE90-009540] 16 p2226 N90-22700
Designing good experiments to test bad hypotheses
[AD-A218977] 16 p2263 N90-22900
Synesthetic art through 3-D projection: The requirements of a computer-based supermedium
16 p2274 N90-22962
A tool for aiding in the reuse of software
[INPE-4981-PRE/1545] 16 p2298 N90-23091
Reusing software components by specialization
[REPT-89-062] 16 p2298 N90-23094
Proceedings of the NATO Advanced Workshop on Supercomputing
[AD-A218508] 16 p2299 N90-23102
Concurrent computing: Numerical algorithms and some applications
[AD-A218570] 16 p2300 N90-23103
An algebric approach to infinite data structures
[CS-8909] 16 p2327 N90-23265
Explanation generation in expert systems (a literature review and implementation)
[AD-A218741] 16 p2327 N90-23268
Modelling and control of a balloon borne stabilized platform 17 p2355 N90-23408
Knowledge based system for Hermes orbital operations ground support
[REPT-892-440-102] 17 p2361 N90-23443
Software techniques for non-von Neumann architectures
[AD-A220390] 17 p2440 N90-23902
A distributed program composition system
[NASA-CR-181568] 17 p2441 N90-23911
Evaluation methodology for software engineering
[AD-A218474] 17 p2441 N90-23913
Distributed object oriented programming
[AD-A219689] 17 p2442 N90-23918
Comparison of selection procedures and validation of criterion used in selection of significant control variates of a simulation model
[AD-A220459] 17 p2443 N90-23921
OOPS it's happening, part 1
[AD-A220498] 17 p2443 N90-23922
Deductive computer programming, revision
[AD-A219848] 17 p2446 N90-23946
Optimization of series expressions. Part 2: Over view of the theory and implementation
[AD-A219961] 17 p2447 N90-23952
Code ETF-3D. Euler transonic flow: Theoretical manual
[DLC/FLU-INT-TN-005] 18 p2493 N90-24247
Code ETF-3D. Euler transonic flow: Validation manual
[DLC/FLU-INT-TN-007] 18 p2493 N90-24248
PCI: A PATRAN-NASTRAN model translator
18 p2569 N90-24639
Higher order attribute grammars
[RUU-CS-89-4] 18 p2590 N90-24735
Real time automatic programming
[AD-A220162] 18 p2591 N90-24740
Sequentiality in orthogonal term rewriting systems
[CWI-CS-R8932] 18 p2592 N90-24744
Development of a microcomputer based software system for use in crewmember ejection analysis
[AD-A220398] 19 p2656 N90-25117
National Airspace System (NAS) software life cycle management study
[AD-A221180] 19 p2657 N90-25122
An object-oriented solution example: A flight simulator electrical system
[AD-A219190] 19 p2661 N90-25145
GCS support/development system configuration document
[NASA-CR-182046] 19 p2743 N90-25589
QATT: A natural language interface for QPE
[UIUCDCS-R-89-1535] 19 p2743 N90-25590
Operations mission planner
[NASA-CR-186846] 19 p2747 N90-25611
Center for Space Microelectronics Technology 1988-1989 technical report
[NASA-CR-186849] 19 p2753 N90-25642
Applications of different design methodologies in navigation systems and development at JPL
20 p2852 N90-26221
Software set-up for data processing of depolarization due to rain and ice crystals in the Olympus project
[EUT-89-E-218] 20 p2855 N90-26240
ISIS and META projects
[NASA-CR-186645] 20 p2905 N90-26524
An expert system based software sizing tool, phase 2
[NASA-CR-188706] 20 p2905 N90-26525
Software requirements: Guidance and control software development specification
[NASA-CR-182058] 20 p2906 N90-26527
ANTIPASTO: An interactive mesh generator and preprocessor for two-dimensional analysis programs
[DE90-011755] 20 p2906 N90-26530
SUPES version 2.1: A Software Utilities Package for the Engineering Sciences
[DE90-011763] 20 p2906 N90-26531
Object oriented programming
[DE90-011797] 20 p2907 N90-26532
Innovative design systems: Where are we, and where do we go from here
[AD-A222586] 20 p2910 N90-26556
From network to artwork: Automatic schematic diagram generation
[EUT-89-E-219] 20 p2912 N90-26567
Design of a universal protocol subsystem architecture: Specification of functions and services
[EUT-89-E-230] 20 p2912 N90-26569
Verification-correction of a program for including uncertainties in the robot automatic programming
[ETN-90-97246] 20 p2915 N90-26588
Installation and pretest analysis of DARPA suboff model in the DTRC anechoic wind tunnel
[AD-A221497] 21 p2955 N90-26801
Development of a method to design helicopter rotors
[REPT-100-30-03] 21 p2960 N90-26830
Design of helicopter components in metal matrix composites
[REPT-100-20-55] 21 p2972 N90-26894
Magnetic resonance elucidation of molecule/macromolecule interaction stereochemistry
[AD-A221444] 21 p2979 N90-26928
The need for headers: An impossibility result for communication over unreliable channels
[AD-A222823] 21 p2994 N90-27018
Resource allocation using constraint propagation
21 p3040 N90-27278
Knowledge representation for commonality
21 p3041 N90-27285
A study on diagnosability of space station ECLSS
21 p3043 N90-27294
Knowledge-based systems and NASA's software support environment 21 p3043 N90-27296
The integration of automated knowledge acquisition with computer-aided software engineering for space shuttle expert systems 21 p3045 N90-27307
Artificial Intelligence Software Engineering (AISE) model 21 p3045 N90-27309
An application generator for rapid prototyping of Ada real-time control software 21 p3046 N90-27316
Automated extraction of knowledge for model-based diagnostics 21 p3047 N90-27318
Automated unit-level testing with heuristic rules
21 p3049 N90-27335

Ada as an implementation language for knowledge based systems 21 p3050 N90-27337
Expert system in software engineering using Structured Analysis and Design Technique (SADT)
[AD-A223022] 21 p3052 N90-27351
The identification of software failure regions
[AD-A223058] 21 p3052 N90-27352
An algorithm for automated surface modelling in unigraphics
[AD-A223219] 21 p3053 N90-27355
ROBFIT: A code for the analysis of histogram spectra with nonlinear regression and robust estimation
[AD-A221527] 21 p3055 N90-27369
Guide for the management of expert systems development
[AD-A221847] 21 p3056 N90-27378
Critical problems in very large scale computer systems
[AD-A221603] 21 p3058 N90-27391
Causal distributed breakpoints
[AD-A222103] 21 p3066 N90-27431
Systems engineering management guide
[AD-A223168] 21 p3085 N90-27544
Aircraft condition monitoring system for future Airbus aircraft: New concept for programming and data recording 22 p3103 N90-27619
Observation model and parameter partials for the JPL geodetic (GPS) modeling software 'GPSOMC'
[NASA-CR-186972] 22 p3132 N90-27774
Tolerating failures of continuous-valued sensors
[NASA-CR-187028] 22 p3178 N90-28035
Concurrent Image Processing Executive (CIPE). Volume 2: Programmer's guide
[NASA-CR-186854] 22 p3236 N90-28349
Efficient algorithms for a class of partitioning problems
[NASA-CR-182073] 22 p3237 N90-28357
Using information to measure software complexity
[REPT-89-022] 22 p3238 N90-28359
Study of an environment using formal reasoning. DILOG: State of the art and prototype
[CERT-1/334300-DERI] 22 p3239 N90-28368
Updates and consistency in the LOGRES language
[REPT-90-017] 22 p3239 N90-28369
LANZ: Software solving the large sparse symmetric generalized eigenproblem
[NASA-CR-182086] 23 p3340 N90-28876
A design tool utilizing stoichiometric structure for the analysis of biochemical reaction networks
[AD-A223873] 23 p3355 N90-28961
Control of intelligent robots in space
23 p3365 N90-29013
The KALI multi-arm robot programming and control environment 23 p3373 N90-29060
Integrating planning and reactive control
23 p3377 N90-29077
Preparing software conversion studies
[PB90-235623] 23 p3381 N90-29099
Software development tools
[PB90-250051] 23 p3381 N90-29103
Technical writing for software engineers
[AD-A223872] 23 p3382 N90-29109
Strategies of computer-based instructional design: A review of guidelines and empirical research
[AD-A224038] 23 p3383 N90-29112
Second order tensor finite element
[NASA-CR-184008] 23 p3386 N90-29122
THREAD: A programming environment for interactive planning-level robotics applications
24 p3505 N90-29810
A VHDL interface for Altera design files
[AD-A224476] 24 p3523 N90-29920
Programming your way out of the past: ISIS and the META Project
[NASA-CR-186275] 24 p3524 N90-29922
Development of a software package for automatic data acquisition, analysis, and controls in an axial flow compressor test rig
[PD-PR-8910] 24 p3524 N90-29926
Strategies for tutoring multiple bugs
[AD-A223921] 24 p3524 N90-29927
Tutorial on using LISP object-oriented programming for blackboards: Solving the radar tracking problem
[AD-A224272] 24 p3525 N90-29930
Effects of parameter uncertainties on software development effort estimates
[AD-A223304] 24 p3526 N90-29938
Durra: A task-level description language user's manual
[AD-A223761] 24 p3528 N90-29950
Software development: A product life-cycle perspective
[AD-A223783] 24 p3528 N90-29952
GSHELL: Multichannel analyzer/multichannel scaler emulation software for IBM-PC-compatible computers
[DE90-015396] 24 p3529 N90-29956
Automated CADAM data transfer: User's manual
[DE90-014871] 24 p3530 N90-29963
Software design for high integrity systems
[ETN-90-97517] 24 p3530 N90-29966
Supporting large scale applications on networks of workstations
[NASA-CR-186346] 24 p3532 N90-29975
Assessment System for Aircraft Noise (ASAN): Development of alpha-test prototype system software
[AD-A223770] 24 p3543 N90-30036

COMPUTER PROGRAMS
NT APPLICATIONS PROGRAMS (COMPUTERS)
NT ASSEMBLER ROUTINES
NT COMPILERS
NT COMPUTER SYSTEMS PROGRAMS
NT DISK OPERATING SYSTEM (DOS)
NT EDITING ROUTINES (COMPUTERS)
NT INPUT/OUTPUT ROUTINES
NT NASTRAN
NT OBJECT PROGRAMS
NT OPERATING SYSTEMS (COMPUTERS)
NT SOURCE PROGRAMS
NT SUBROUTINE LIBRARIES (COMPUTERS)
NT SUBROUTINES
NT UNIX (OPERATING SYSTEM)
Initial flight qualification and operational maintenance of X-29A flight software
[NASA-TM-101703] 01 p0005 N90-10023
Stability and Control of Tactical Missile Systems
[AGARD-CP-451] 01 p0011 N90-10050
Missile Datcom: Enhancements for design applications
01 p0012 N90-10054
Prediction of dynamic derivatives
01 p0012 N90-10055
Prediction of tactical missile dynamics
01 p0012 N90-10056
Remote control missile model test
01 p0013 N90-10063
Analysis and testing of a high performance air-air missile 01 p0014 N90-10069
Marginal release disturbances on advanced missiles
01 p0014 N90-10070
The application of TSIM software to act design and analysis on flexible aircraft 01 p0018 N90-10086
DYSCO: A software system for modeling general dynamic systems 01 p0018 N90-10089
Control law synthesis and optimization software for large order aeroservoelastic systems
01 p0022 N90-10111
TWIRE: A test program for VLF airborne transmissions
[AD-A210516] 01 p0057 N90-10324
Summarizing qualitative behavior from measurements of nonlinear circuits, revision
[AD-A210919] 01 p0061 N90-10353
Numerical simulation of detonation transfer between gaseous explosive layers
[MRL-RR-1-89] 01 p0069 N90-10395
Two stage gear tooth dynamics program
[NASA-CR-185110] 01 p0077 N90-10437
The MHOST finite element program: 3-D inelastic analysis methods for hot section components. Volume 2: User's manual
[NASA-CR-182235-VOL-2] 01 p0079 N90-10450
The MHOST finite element program: 3-D inelastic analysis methods for hot section components. Volume 3: Systems' manual
[NASA-CR-182236] 01 p0079 N90-10451
A common distributed language approach to software integration
[NASA-CR-185499] 01 p0103 N90-10584
On the interactive computer program IPIS for aircraft parameter identification
[NAL-TR-1000] 01 p0103 N90-10586
Waveform generator signal processing software
[PB89-192660] 01 p0103 N90-10587
BLOT: A mesh and curve plot program for the output of a finite element analysis
[DE89-013994] 01 p0104 N90-10590
A FORTRAN program for the calculation of the calibration coefficients of a six-component strain gauge balance
[AD-A210375] 01 p0105 N90-10599
Software methodology catalog, second edition, revision
[AD-A210548] 01 p0106 N90-10601
Dependency-directed localization of software bugs
[AD-A210837] 01 p0106 N90-10606
Tools for application development in heterogeneous distributed environments
[AD-A210238] 01 p0108 N90-10613
Northeast Artificial Intelligence Consortium annual report for 1987. Volume 7, part A: Time oriented problem solving
[AD-A210331] 01 p0110 N90-10622
Robot vehicle video image compression, phase 1
[AD-A210974] 01 p0110 N90-10626
The architecture of NEWTON: A general-purpose dynamics simulator
[NASA-CR-185489] 01 p0118 N90-10678
Autonomous control system for Czochralski growth of LEC GaAs
[AD-A210190] 01 p0131 N90-10754
Focused ion beam implantation
[AD-A210977] 01 p0133 N90-10767
A preliminary sensitivity analysis of the Generalized Escape System Simulation (GESS) computer program
[DE89-016891] 02 p0148 N90-10844
High accuracy coordinate determination using the global positioning system 02 p0150 N90-10858
GRATE: A new flight test tool for flying qualities evaluation 02 p0152 N90-10868
Results and practical experience using parameter identification techniques on the AM-X program at Aermacchi 02 p0153 N90-10873
Flight testing of the Tornado Terrain Following System
02 p0153 N90-10875
Independent Orbiter Assessment (IOA): Analysis of the guidance, navigation, and control subsystem
[NASA-CR-185555] 02 p0162 N90-10920
Independent Orbiter Assessment (IOA): Analysis of the remote manipulator system
[NASA-CR-185585] 02 p0164 N90-10926
Frequency domain design of robust controllers for space structures
[AD-A211172] 02 p0176 N90-10985
GEMMES: A new tool for dynamic modeling
02 p0179 N90-11005
Integration of analytical and test software for optimal structural design under dynamic loads
02 p0179 N90-11007
Experiences using a major FEM package interactively for spacecraft applications 02 p0179 N90-11008
Calculation of sound transmission through a cylindrical shell using ASKA acoustics 02 p0179 N90-11009
Numerical analysis of nonlinear viscoelastic structures: Application to elastomers and rubber-like materials
02 p0180 N90-11013
Automated stress analysis of Shuttle orbiter thermal protection system 02 p0184 N90-11043
JOE: Jordan Optimized Eigensolver. A step toward a numerical Jordan form analyzer for control and interactive thermo-structural-dynamic applications
02 p0184 N90-11047
ESA-D: An integrated software for antenna design and analysis 02 p0185 N90-11052
Thermal and structural analysis of Hermes
02 p0186 N90-11058
Exploitation of data management facilities for finite element analysis in aerospace structural engineering applications 02 p0188 N90-11078
Consequence of condensed-phase formation in transient burning of TiHx/KClO in a closed system
[DE89-013922] 02 p0208 N90-11188
Validation of NEC (Numerical Electromagnetics Code) for antennas near ground
[DE89-016502] 02 p0212 N90-11212
A general-purpose computer program for the Volterra-series analysis of nonlinear microwave circuits
[AD-A210768] 02 p0216 N90-11236
The 3D-POLY: A robot vision system for recognizing objects in occluded environments
02 p0229 N90-11313
Simulation of the polar cap F region ionization using an experimental convection electric field
02 p0241 N90-11370
Empirical models of convection electric fields and electrostatic potential at high latitude from EISCAT observations: Preliminary results
02 p0243 N90-11377
Calculation of the temperature and velocity vector of the neutral gas using EISCAT CP3-data
02 p0244 N90-11384
Ion heating events observed at the EISCAT radar
02 p0244 N90-11385
Coordinated multi-parameter measurements and predictions of the global-scale ionosphere
02 p0247 N90-11397
Hanford Meteorological Station computer codes. Volume 10: The ARCHIVE computer code
[DE89-016175] 02 p0252 N90-11429
ANIMA: Image analyzer applied to remote sensing
[INPE-4766-PRE/1435] 02 p0256 N90-11447
Software configuration management: An overview
[PB89-193833] 02 p0258 N90-11458
Experiments in fault tolerant software reliability
[NASA-CR-185927] 02 p0258 N90-11460
Programs for numerical integration of piece-wise smooth functions
[DE89-620449] 02 p0258 N90-11464
Research, development, training and education using the Ada programming language
[AD-A210760] 02 p0259 N90-11466

Computer programs for measuring variations in speech
[AD-A211126] 02 p0259 N90-11467
Evaluating the performance of software cache coherence
[AD-A211164] 02 p0259 N90-11468
LINPACK routines based on the level 2 BLAS
[CWI-NM-R8811] 02 p0261 N90-11483
An interactive program for constrained spline approximation of numerical data
[DE89-016674] 02 p0267 N90-11520
Simulation of an axially symmetric ion-optical system
[DE89-620129] 02 p0273 N90-11560
LEXER: A tool for lexical analysis of program input
[DE89-016924] 02 p0288 N90-11649
Experimental database retrieval system DARTS (Handling Manual)
[DE89-906473] 02 p0289 N90-11652
Some implications of the isotropic momentarily frozen assumptions for the SPAN-MAT program
[NASA-CR-181937] 03 p0301 N90-11704
Development of direct-inverse 3-D methods for applied transonic aerodynamic wing design and analysis
[NASA-CR-186036] 03 p0305 N90-11733
Program for high speed computation of physical properties of propellants and combustion gas of an LH2/LOX rocket engine
[NAL-TM-564] 03 p0318 N90-11803
Recent advances to NEC (Numerical Electromagnetics Code): Applications and validation
[DE89-009231] 03 p0337 N90-11917
KIVA reactive hydrodynamics code applied to detonations in high vacuum
[DE89-016979] 03 p0346 N90-11974
Generation and tooth contact analysis of spiral bevel gears with predesigned parabolic functions of transmission errors
[NASA-CR-4259] 03 p0355 N90-12033
Natural frequencies of singly-curved laminated plates with simply-supported edges
[ESDU-89011] 03 p0359 N90-12052
WISPER: A standardized fatigue load sequence for HAWT-blades
[NLR-MP-88029-U] 03 p0359 N90-12055
Aerosol backscatter studies supporting LAWS 03 p0363 N90-12079
Development of high resolution simulations of the atmospheric environment using the MASS model
[NASA-CR-186040] 03 p0374 N90-12133
Structure based formal methods for software engineering
[AD-A211660] 03 p0388 N90-12207
A simplified self-adaptive grid method, SAGE
[NASA-TM-102198] 03 p0388 N90-12211
Navigation of robotic systems
[DE89-017507] 03 p0390 N90-12219
Four vector-matrix primitives
[AD-A211889] 03 p0392 N90-12237
Numerical solution of acoustic-structure interaction problems
[AD-A211505] 03 p0400 N90-12293
Non-stationary computer model of the asymptotic region of an electric arc gas heater
[IPPCZ-288] 03 p0407 N90-12330
FORTRAN program for x ray photoelectron spectroscopy data reformatting
[NASA-TP-2957] 03 p0409 N90-12348
GALAX: A two-dimensional N-body code for disk galaxy dynamics
[PB89-217780] 03 p0420 N90-12415
Additions and corrections to SUPER: A program for calculating steady and oscillatory supersonic flow over a thin wing, tail plane and fin
[AD-A211771] 04 p0438 N90-12501
Development of a VSAERO (Vortex Separation Aerodynamics) model of the F/A-18
[AD-A212442] 04 p0448 N90-12566
FPG2: A flight profile generator program
[AD-A212408] 04 p0453 N90-12595
Rolls-Royce and ERCOFTAC
[PNR90600] 04 p0456 N90-12615
Numerical analysis of notch test damage to laminated composite plates submitted to uniaxial traction
[CETIM-107310] 04 p0467 N90-12675
IBM PC analysis of polarization resistance data
[AD-A212294] 04 p0477 N90-12732
Specification of Viper1 in Z
[RSRE-MEMO-4195] 04 p0490 N90-12817
Specification of Viper2 in Z
[RSRE-MEMO-4217] 04 p0490 N90-12819
Aircraft SAR simulation Sargen 1.0
[FEL-1989-44] 04 p0491 N90-12823
Specification for radar free-space detection range and free-space intercept range calculations
[AD-A213158] 04 p0494 N90-12843
Automated Steerable Nulling Antenna Processor (SNAP) model
[PB89-231740] 04 p0509 N90-12937
Improvement of rules relating to clamp calculations
[CETIM-110610] 04 p0509 N90-12939
Visualization of high-resolution digital terrain
[AD-A212149] 04 p0515 N90-12971
A hybrid architecture for feature labelling of oceanographic satellite images
[AD-A212236] 04 p0515 N90-12975
Cloud cover determination in polar regions from satellite imagery
[NASA-CR-186096] 04 p0520 N90-13003
The effect of concurrent strength and endurance training on electromechanical delay, maximum voluntary contraction, and rate of force development
[AD-A213316] 04 p0525 N90-13028
Spacecraft Orbit Design and Analysis (SODA), version 1.0 user's guide
[NASA-CR-181932] 04 p0529 N90-13050
Characterizing termination of logic problems with level mappings
[CWI-CS-R8912] 04 p0532 N90-13077
Interactive computer program for the generation of enthalpy-entropy and temperature-entropy charts of nitrogen and hydrogen
[DLR-FB-89-27] 04 p0533 N90-13081
Subspace iteration algorithms in FORTRAN 77 and FORTRAN 8x
[AD-A212275] 04 p0533 N90-13083
Software Engineering Exercise (SEE) guidelines
[AD-A212510] 04 p0534 N90-13085
NAUTILE: A physical design environment based on an object-oriented data manager
[IMAG-RR-737-I] 04 p0535 N90-13094
On modeling resources in multiprocessor systems
[MEMO-INF-88-33] 04 p0535 N90-13095
Numerical evaluation of the far field wave pattern of the radiation Green's function
[AD-A212839] 04 p0546 N90-13176
The Painleve test for nonlinear ordinary and partial differential equations
[AD-A212894] 04 p0546 N90-13177
Research on heating, instabilities, turbulence and RF emission from electric field dominated plasmas
[AD-A212122] 04 p0557 N90-13243
Semiconductor measurement technology: A software program for aiding the analysis of ellipsometric measurements, simple models
[PB89-235923] 04 p0560 N90-13261
Application of a self-adaptive grid method to complex flows
[NASA-TM-102223] 05 p0571 N90-13324
Geodetic network adjustment using GPS triple difference observations and a priori stochastic information
[TR-1-1987] 05 p0577 N90-13367
Trajectory optimization and guidance for an aerospace plane
[NASA-CR-185884] 05 p0578 N90-13369
Software and hardware description of the helicopter motion equations for VAX computers
[AD-A213248] 05 p0579 N90-13375
Application of a two-dimensional unsteady viscous analysis code to a supersonic throughflow fan stage
[NASA-TM-4141] 05 p0581 N90-13387
Simulation of spacecraft attitude dynamics using TREETOPS and model-specific computer Codes 05 p0587 N90-13419
GOES-I/M ascent maneuvers from transfer orbit to station 05 p0587 N90-13421
Shuttle relative navigation of a tethered satellite mission with current on board software 05 p0588 N90-13423
Automation of orbit determination functions for National Aeronautics and Space Administration (NASA)-supported satellite missions 05 p0590 N90-13434
Control of optical systems 05 p0600 N90-13484
Validation of the Hipparcos catalog 05 p0611 N90-13564
The Tycho input catalog 05 p0612 N90-13575
Modelling of satellite control thruster plumes 05 p0613 N90-13578
The economic impact of automation technology
[AD-A213363] 05 p0630 N90-13682
An improved algorithm for the modeling of vapor flow in heat pipes
[NASA-CR-185179] 05 p0642 N90-13748
Analysis of rotary engine combustion processes based on unsteady, three-dimensional computations
[NASA-TM-102469] 05 p0642 N90-13749
A prototype microprocessor based audiometer for use by the CF (Canadian Forces) medical services for periodic hearing tests
[AD-A212990] 05 p0673 N90-13921
Project ORION microcomputer management system
[AD-A212945] 05 p0680 N90-13959
The development of a program analysis environment for Ada
[NASA-CR-185860] 05 p0681 N90-13962
A fault-tolerant software algorithm for a network of transputers
[AD-A213092] 05 p0682 N90-13972
Constructing a calculus of programs
[CWI-CS-R8914] 05 p0683 N90-13979
Validation of a computer code for analysis of subsonic aerodynamic performance of wings with flaps in combination with a canard or horizontal tail and an application to optimization
[NASA-TP-2961] 06 p0717 N90-14187
Program VSAERO theory document: A computer program for calculating nonlinear aerodynamic characteristics of arbitrary configurations
[NASA-CR-4023] 06 p0720 N90-14200
An analysis of the viscous flow through a compact radial turbine by the average passage approach
[NASA-TM-102471] 06 p0720 N90-14206
RAMSCRAM: A flexible ramjet/scramjet engine simulation program
[NASA-TM-102451] 06 p0726 N90-14235
Development of a three-axis trim program
[AD-A212883] 06 p0726 N90-14237
Fluid flow analysis of the SSME high pressure fuel and oxidizer turbine coolant systems
[NASA-CR-183736] 06 p0734 N90-14277
Thermophysical properties of isopropyl alcohol. Part 2: Thermodynamic properties at elevated pressures
[ESDU-89020-PT-2] 06 p0739 N90-14300
Data Link Processor (DLP) operational test and evaluation/integration test plan
[DOT/FAA/CT-TN89/32] 06 p0757 N90-14404
Long wave propagation assessment 06 p0758 N90-14414
TROPO: A technique for predicting propagation and modem performance of digital troposcatter systems 06 p0764 N90-14444
The FTZ HF propagation model for use on small computers and its accuracy 06 p0765 N90-14447
A software-based controller for generation of synchronized pulses for use with rotating machinery
[DE89-016672] 06 p0770 N90-14477
Surface flow and heating distributions on a cylinder in near wake of Aeroassist Flight Experiment (AFE) configuration at incidence in Mach 10 Air
[NASA-TP-2954] 06 p0772 N90-14493
An experimental investigation of shear layer mixing in supersonic flows 06 p0775 N90-14508
Granular flow: Numerical simulation of dry granular flows and calculation of hydrodynamic interactions in suspensions
[DE89-017544] 06 p0777 N90-14518
CTH: A three-dimensional shock wave physics code
[DE89-016529] 06 p0779 N90-14528
Numerical simulations of free-electron laser oscillators
[DE89-003488] 06 p0788 N90-14588
INEX (Integrated Numerical Experiment) simulations of the Los Alamos HIBAF (High-Brightness Accelerator Free-Electron Laser) free-electron laser MOPA (Master Oscillator Power Amplifier) experiment
[DE90-002387] 06 p0790 N90-14601
Verification of the NIKE3D structural analysis code by comparison against the analytic solution for a spherical cavity under a far-field uniaxial stress
[DE90-000929] 06 p0799 N90-14653
Critical time step estimation for three-dimensional explicit impact analysis
[DE90-002187] 06 p0801 N90-14662
Computer simulation of wind/diesel system operation
[DE89-009445] 06 p0805 N90-14688
User's guide to PMESH: A grid-generation program for single-rotation and counterrotation advanced turboprops
[NASA-CR-185156] 06 p0823 N90-14783
The processes of scientific research: The strategy of experimentation 06 p0824 N90-14788
Software Reuse Issues
[NASA-CP-3057] 06 p0824 N90-14789
Automated reuseable components system study results 06 p0824 N90-14790
Knowledge-based reusable software synthesis system 06 p0824 N90-14791
Impact of domain analysis on reuse methods 06 p0824 N90-14792
JPL reuse program 06 p0825 N90-14795
Initial Ada components evaluation 06 p0826 N90-14803
Application of reusable software components at the SEI 06 p0826 N90-14804
AdaNET services 06 p0827 N90-14806
Personal computer process data acquisition
[DE89-017877] 06 p0828 N90-14818
Program CICC flow and heat transfer in Cable-In-Conduit Conductors
[DE90-001519] 06 p0829 N90-14819

Using object-oriented development to support prototyping
[DE90-000547] 06 p0829 N90-14821
Parallel mathematical software
[DE90-002694] 06 p0829 N90-14822
Interactive multidimensional data analysis and understanding
[DE90-001794] 06 p0830 N90-14824
A tutorial on software reliability engineering
[DE89-012368] 06 p0830 N90-14828
The Aerospace Energy Systems Laboratory: A BITBUS networking application
[NASA-TM-4149] 06 p0831 N90-14829
Boundary element analysis of single and multidomain problems in acoustics 06 p0837 N90-14867
REFLECT: A computer program for the x ray reflectivity of bent perfect crystals
[DE90-001266] 06 p0851 N90-14946
Micro-scale simulation of dynamic compaction of oxide and metal powder mixture
[DE90-002220] 06 p0856 N90-14978
The instability and fragmentation of the envelope of supernova 1987A 06 p0862 N90-15011
Systems for airborne wind and turbulence measurement 07 p0869 N90-15046
Nonlinear phenomena in computational transonic aeroelasticity 07 p0874 N90-15070
A study of variable geometry in advanced gas turbines 07 p0881 N90-15104
Design and calibration of an in-stack, low-pressure impactor
[AD-A213531] 07 p0882 N90-15105
Design limitations on ultra-high velocity projectile launchers
[DE89-012933] 07 p0885 N90-15118
Research on mercury cadmium telluride
[AD-A213924] 07 p0906 N90-15237
Automated convection soldering
[KCP-613-4005] 07 p0916 N90-15300
Rectangular-to-circular waveguide transitions for high-power circular overmoded waveguides
[AD-A213925] 07 p0924 N90-15349
Solution of potential flow past an elastic body using the boundary element technique
[AD-A213843] 07 p0931 N90-15390
Geotechnical instrumentation
[PB89-198675] 07 p0933 N90-15398
Implementing fault-tolerant sensors
[NASA-CR-186251] 07 p0933 N90-15400
Waveguide effects in superradiant free-electron lasers
[DE90-003605] 07 p0935 N90-15417
NOISE: A nonlinear optimization induction free-electron laser systems engineering code
[DE90-004438] 07 p0936 N90-15420
MESA 3-D calculations of armor penetration by projectiles with combined obliquity and yaw
[DE89-015265] 07 p0939 N90-15438
Comparison of multidimensional calculations of long-rod impacts on oblique plates
[DE89-015275] 07 p0939 N90-15440
Fragmentation statistics from Eulerian hydrocode calculations
[DE90-002906] 07 p0941 N90-15449
Planning minimum-energy paths in an off-road environment with anisotropic traversal costs and motion constraints
[AD-A214181] 07 p0942 N90-15457
A semiautomated computer-interactive dynamic impact testing system
[DE90-002721] 07 p0946 N90-15479
Pipeline vibrations. Fluid transients in non-rigid, unbranched planar piping systems
[ESDU-89030] 07 p0948 N90-15491
Inclusion of nonlinear aerodynamics in the FLAP code
[DE89-009507] 07 p0954 N90-15519
Description of SHARC: The Strategic High-Altitude Radiance Code
[AD-A213806] 07 p0961 N90-15555
Development of the AH-64 display symbology training module
[AD-A213456] 07 p0968 N90-15592
MANPRINT methods monograph: Aiding the development of manned system performance criteria
[AD-A213543] 07 p0968 N90-15593
Designing machines for lattice physics and algorithm investigation
[DE90-003543] 07 p0969 N90-15596
High level language memory management on parallel architectures
[DE89-015018] 07 p0971 N90-15609
CryoTran user's manual, version 1.0
[NASA-TM-102468] 07 p0973 N90-15622
Developmental versions of FORTRAN/77 routines for the design and analysis of mixture experiments
[DE90-003513] 07 p0974 N90-15624
Programs for control of an analog-signal switching network
[DE90-003645] 07 p0974 N90-15626
A simulation model for dynamic system availability analysis
[AD-A213499] 07 p0974 N90-15628
Software for a new modified Cholesky factorization
[AD-A213643] 07 p0975 N90-15630
Optical neural nets for scene analysis
[AD-A213986] 07 p0976 N90-15637
Principles and algorithms for causal reasoning with uncertainty
[AD-A214248] 07 p0977 N90-15644
MODTRAN: A moderate resolution model for LOWTRAN 7
[AD-A214337] 07 p0978 N90-15650
Use of the linear variate method of Monte Carlo for estimating uncertainty in thermal-hydraulic codes
[DE89-017871] 07 p0985 N90-15694
The calculation of overground sound propagation in the presence of wind and temperature gradients
[ESDU-89036] 07 p0989 N90-15714
Theoretical studies on the electronic structure of high-temperature superconductors
[DE90-001301] 07 p0998 N90-15771
Automated observation scheduling for the VLT
[NASA-CR-186282] 07 p1012 N90-15861
Automated telescope scheduling
[NASA-CR-186279] 07 p1012 N90-15863
Astophysical opacities at LLNL
[DE90-003599] 07 p1014 N90-15872
Rotor induced-inflow-ratio measurements and CAMRAD calculations
[NASA-TP-2946] 08 p1017 N90-15882
Improved tangent-cone method for the Aerodynamic Preliminary Analysis System (APAS) version of the hypersonic arbitrary-body program
[NASA-TM-4165] 08 p1018 N90-15890
The application of Z to the specification of air traffic control systems. 1: An initial specification of the radar processing activity
[RSRE-MEMO-4280] 08 p1020 N90-15900
Automated search techniques applied to optical payloads in unmanned air vehicles 08 p1026 N90-15931
Distribution of hardware and software elements in unmanned air vehicle systems 08 p1027 N90-15933
A numerical simulation of the flow in the diffuser of the NASA Lewis icing research tunnel
[NASA-TM-102480] 08 p1032 N90-15965
Dynamics analyses of space power systems using the salt code
[DE90-002274] 08 p1038 N90-15995
MT's algorithm: A new algorithm to search for the optimum set of modulation indices for simultaneous range, command, and telemetry
[NASA-CR-186259] 08 p1057 N90-16110
Stand Alone Pressure Measurement Device (SAPMD) for the space shuttle Orbiter, part 2
[NASA-CR-172119-PT-2] 08 p1072 N90-16203
Stochastic model of the NASA/MSFC ground facility for large space structures with uncertain parameters: The maximum entropy approach, part 2
[NASA-CR-186009] 08 p1107 N90-16407
FRAC-IN-THE-BOX utilization
[DE90-003648] 08 p1108 N90-16412
Case tool evaluation system
[DE90-003698] 08 p1108 N90-16413
An empirical comparison of software fault tolerance and fault elimination
[NASA-CR-186313] 08 p1108 N90-16414
CPU timing routines for a CONVEX C220 computer system
[NASA-CR-181950] 08 p1110 N90-16424
Software dependability growth characterization, modeling and evaluation
[LAAS-89320] 08 p1112 N90-16437
Design and implementation of a multi-sensor fusion algorithm on a hypercube computer architecture
[DE90-003682] 08 p1112 N90-16438
Results of error correction techniques applied on two high accuracy coordinate measuring machines
[DE90-003341] 08 p1112 N90-16439
On the efficient exploitation of speculation under data flow paradigms of control
[AD-A214112] 08 p1115 N90-16455
An implicit time-integration procedure for a set of internal variable constitutive equations for isotropic elasto-viscoplasticity
[PB90-121302] 08 p1117 N90-16470
Modeling energy output of inertial storage devices for the DIII-D tokamak
[DE90-004096] 08 p1126 N90-16524
User's manual for MGMHD: A multigrid three-dimensional computer code for the analysis of magnetohydrodynamic generators and diffusers
[DE90-004453] 08 p1127 N90-16526
Estimation of thermodynamic properties of alloys from phase diagram and other loose boundary conditions
[DE90-719511] 08 p1135 N90-16579
A computer program to calculate the population numbers of multi-level species
[IFSI-89-15] 08 p1151 N90-16671
The DAB model of drawing processes 08 p1155 N90-16691
Off-line robot programming and graphical verification of path planning 08 p1156 N90-16699
Activities report of the National Electrotechnic Institute Galileo Ferraris
[ETN-90-96178] 08 p1157 N90-16705
Recent developments in TERPROM 09 p1163 N90-16732
Reusable navigation module 09 p1165 N90-16742
The development of an airborne synthetic aperture radar motion compensation system 09 p1165 N90-16745
Guidance and control considerations for a maneuvering aerial target system 09 p1165 N90-16746
SINS1: A model of a strapdown inertial navigation system
[AD-A215495] 09 p1166 N90-16749
Application of model based reasoning to diagnosis of faults in inertial navigation equipment
[AD-A215561] 09 p1166 N90-16750
Turbine blade data acquisition system software reference
[AD-A215134] 09 p1169 N90-16764
Debris/ice/TPS assessment and photographic analysis for Shuttle Mission STS-33R
[NASA-TM-102785] 09 p1180 N90-16846
Descriptive simulation: Combining symbolic and numerical methods in the analysis of chemical reaction mechanisms
[AD-A214678] 09 p1190 N90-16898
Spark source mass spectrometry software documentation and verification
[DE90-004463] 09 p1192 N90-16909
Application of high-rate cutting tools
[AD-A214644] 09 p1203 N90-16970
Planar array antenna design analysis, volume 1
[AD-A215537] 09 p1207 N90-16999
Target classification using SAR (Synthetic Aperture Radar) polarimetric data
[AD-A215672] 09 p1208 N90-17002
Error detection and correction for a multiple frequency quaternary phase shift keyed signal
[AD-A215706] 09 p1208 N90-17003
Two-dimensional, long-pulse simulation of microwave-induced electron layer evolution in low-pressure air
[DE90-005180] 09 p1208 N90-17004
Development of the Kalman filter application and a VHDL model for the AFIT (Air Force Institute of Technology) Floating Point Application Specific Processor (FPASP)
[AD-A215423] 09 p1213 N90-17033
A circuit extraction system and graphical display for VLSI (Very Large Scale Integrated) design
[AD-A215868] 09 p1214 N90-17038
Appendage flow computations using the INS3D computer code
[AD-A215689] 09 p1218 N90-17066
Implementing fault-tolerant sensors
[NASA-CR-186269] 09 p1225 N90-17105
Laser wave estimation
[AD-A213867] 09 p1227 N90-17119
Three-dimensional simulation of free-electron laser harmonics with FRED
[DE90-005253] 09 p1229 N90-17130
Validation of an exponentially decreasing failure rate software reliability model
[AD-A215546] 09 p1235 N90-17165
Techniques for analyzing the dynamic response of structural systems using computer-derived Green's functions
[AD-A214523] 09 p1237 N90-17181
The use of computer programs to determine environmental compliance, predict performance, and assess impacts
[DE90-005230] 09 p1245 N90-17222
AOIPS 3 user's guide. Volume 2: Program descriptions
[NASA-TM-100725] 09 p1247 N90-17236
Subjective Workload Assessment Technique (SWAT): A user's guide
[AD-A215405] 09 p1261 N90-17312
MPlus Database system
[DE90-004146] 09 p1263 N90-17325
The EPSILON-2 hybrid dataflow architecture
[DE90-003152] 09 p1263 N90-17326
Vision-based navigation and parallel computing
[AD-A214481] 09 p1264 N90-17327

The bifurcation interpreter: A step towards the automatic analysis of dynamical systems
[AD-A214618] 09 p1265 N90-17336

A guide to IRUS-2 application development
[AD-A214758] 09 p1266 N90-17340

A theory for graph-based language specification, analysis, and mapping with application to the development of parallel software
[AD-A214910] 09 p1266 N90-17342

A knowledge based approach to program debugging
[AD-A214941] 09 p1266 N90-17344

An approach to the development of software for computer-aided design of satellite communications receivers for operation in scintillating channels
[AD-A215299] 09 p1267 N90-17349

Fractal-based image compression
[AD-A215400] 09 p1268 N90-17351

Computer-Aided Design for Built-In-Test (CADBIT). Volume 1: Technical issues
[AD-A215737] 09 p1268 N90-17353

Computer-Aided Design for Built-In-Test (CADBIT). Volume 3: Software specification
[AD-A215739] 09 p1268 N90-17355

Evaluation of the modal testing MODENT software with simulated data
[INPE-4885-NTE/291] 09 p1269 N90-17357

Parallel functional computation
[AD-A214627] 09 p1269 N90-17360

Representing knowledge intelligently: Production rules, frames, and transitional networks
[AD-A215098] 09 p1271 N90-17368

Use of hypermedia as a user interface for an artificial intelligence-based problem solver
[AD-A215551] 09 p1271 N90-17370

Boolean approaches in digital diagnosis
[AD-A215660] 09 p1274 N90-17386

Noise and sonic boom impact technology. Initial development of an Assessment System for Aircraft Noise (ASAN). Volume 1: Executive summary
[AD-A214164] 09 p1278 N90-17410

Noise and sonic boom impact technology. Initial development of an Assessment System for Aircraft Noise (ASAN). Volume 3: Technical description
[AD-A214455] 09 p1278 N90-17412

Full surface interferometric testing of grazing incidence mirrors
[AD-A213590] 09 p1281 N90-17425

An investigation of application development process controls in an end-user setting: A field study
09 p1295 N90-17504

The Cronus distributed DBMS (Database Management System) project
[AD-A214478] 09 p1295 N90-17508

Automated information systems plan
[AD-A214982] 09 p1296 N90-17514

A survey of missile aerodynamics
10 p1303 N90-17541

Ignitability of jet-A fuel vapors in aircraft fuel tanks
10 p1313 N90-17594

Forced and natural venting of aircraft cabin fires: A numerical simulation 10 p1314 N90-17597

Time development of convection flow patterns in aircraft cabins under post-crash fire exposure
10 p1314 N90-17598

Analysis of the National Transonic Facility mishap
[NASA-TM-101686] 10 p1318 N90-17620

Viscous three-dimensional analyses for nozzles for hypersonic propulsion
[NASA-CR-185197] 10 p1321 N90-17635

The application of a computer data acquisition system for a new high temperature tribometer
[NASA-TM-102508] 10 p1347 N90-17811

The evaporation of sessile droplets. Part 1: Theoretical factors for a two-component system
[AD-A215946] 10 p1353 N90-17848

FLUSH: A tool for the design of slush hydrogen flow systems
[NASA-TM-102467] 10 p1361 N90-17890

Recent advances to NEC: Applications and validation
10 p1369 N90-17934

Measurement and computer simulation of antennas on ships and aircraft for results of operational reliability
10 p1369 N90-17936

GTD/UTD: Brief history of successive development of theory and recent advances. Applications to antennas on ships and aircraft 10 p1370 N90-17939

Compact ranges in antenna and RCS measurements
10 p1371 N90-17940

Low elevation angle KU-band satellite measurements at Austin, Texas 10 p1373 N90-17959

Recent achievements of OPEX
10 p1373 N90-17961

Multiple symbol differential detection of uncoded and trellis coded MPSK
[NASA-CR-186268] 10 p1376 N90-17975

Development of a small signal theory for the harmonic gyroklystron
[AD-A216274] 10 p1380 N90-17999

The effect of the virtual mass force term on the stability of transient two-phase flow analysis
[DE90-733142] 10 p1384 N90-18010

Development of an integrated mobile robot system at Carnegie Mellon University: June 1988
[AD-A215955] 10 p1392 N90-18049

CHIMERA 2: A real-time UNIX-compatible multiprocessor operating system for sensor-based control applications
[AD-A215958] 10 p1392 N90-18051

RADC reliability engineer's TOOLKIT
[AD-A215977] 10 p1394 N90-18058

Dynamics of column stability with partial end restraints
[NASA-TM-101651] 10 p1396 N90-18069

Validation of the boundary element method applied to complex fracture mechanics conditions
[AD-A216412] 10 p1398 N90-18080

A microcode compiler that runs on the IBM AT and supports cascadable microcomputers, part 2
[AD-A215889] 10 p1415 N90-18155

Preparing software conversion studies
10 p1416 N90-18158

Proceedings of the 4th Annual Ada Software Engineering Education and Training Symposium
[AD-A214663] 10 p1417 N90-18162

The procedures for easy running of the HULL computer code under VMS
[MRL-GD-0023] 10 p1417 N90-18165

Hypercube expert system shell-applying production parallelism
[AD-A215762] 10 p1418 N90-18173

KAPSE Interface Team (KIT) public report, volume 7
[AD-A215838] 10 p1418 N90-18176

KAPSE Interface Team (KIT) public report, volume 8, part 1
[AD-A215839] 10 p1418 N90-18177

Nonprocedural implementation of mathematical programming algorithms
[AD-A216039] 10 p1419 N90-18179

Expert systems development methodology
[AD-A216892] 10 p1421 N90-18191

Measuring Day-Night Noise Levels (DNL) using the metrosonics db-310 sound level analyzer (Dosimeter)
[AD-A215757] 10 p1427 N90-18230

Development of free-piston Stirling engine performance and optimization codes based on Martini simulation technique
[NASA-CR-182210] 10 p1443 N90-18326

A study of the evolution of solar active regions for improving solar flare forecasts
[AD-A216325] 10 p1448 N90-18356

A user's manual for the method of moments Aircraft Modeling Code (AMC)
[NASA-CR-186371] 11 p1456 N90-18390

Unsteady Aerodynamic Phenomena in Turbomachines
[AGARD-CP-468] 11 p1459 N90-18405

Numerical prediction of axial turbine stage aerodynamics 11 p1461 N90-18416

Blade row interaction effects on compressor measurements 11 p1462 N90-18419

Data collection and location platforms experimental network: Description of an orbit routine
[INPE-4798-NTE/287] 11 p1465 N90-18439

Theory and verification of the fiber composite damage model implemented in DYNA3D
[AD-A216600] 11 p1479 N90-18511

Development of a progressive failure model for strength of laminated composite structure
[AD-A216966] 11 p1480 N90-18517

Numerical simulations of coherent structures in a jet flame with a noncircular cross section
[AD-A216710] 11 p1483 N90-18535

Automation and extension of LDV (Laser-Doppler Velocimetry) measurements of off-design flow in a subsonic cascade wind tunnel
[AD-A216627] 11 p1506 N90-18670

Computer viruses and related threats: A management guide
[PB90-111683] 11 p1543 N90-18881

Guidelines for the use of the SAME
[AD-A215846] 11 p1544 N90-18888

Deceit: A flexible distributed file system
[NASA-CR-186402] 11 p1544 N90-18891

Approaches to the planning of coherent text
[AD-A216463] 11 p1545 N90-18895

Knowledge-based extensible natural language interface technology program
[AD-A216664] 11 p1545 N90-18897

KAM: Automatic planning and interpretation of numerical experiments using geometrical methods
[AD-A216805] 11 p1546 N90-18900

A perspective of software reuse
[AD-A216911] 11 p1546 N90-18901

Technology assessment of software engineering
[AD-A216943] 11 p1546 N90-18902

User manual for NEXT 1.2: NLR engineering X-pert system toolkit
[NLR-TR-87178-U] 11 p1547 N90-18905

Computational structure of GPSG (Generalized Phrase Structure Grammar) models: Revised generalized phrase structure grammar
[AD-A216803] 11 p1553 N90-18941

Configuration management and control for ESA space systems
[ESA-PSS-01-11-ISSUE-1] 11 p1574 N90-19061

Heat transfer measurements from a NACA 0012 airfoil in flight and in the NASA Lewis icing research tunnel
[NASA-CR-4278] 12 p1599 N90-19203

Conjugate field approaches for active array compensation 12 p1610 N90-19266

Reflector surface distortion analysis techniques (thermal distortion analysis of antennas in space)
12 p1611 N90-19267

Mesh surfaces for reflector applications
12 p1611 N90-19268

The measurement, modeling, and prediction of traction for rocket propellant 1
[NASA-CR-185186] 12 p1633 N90-19386

Augmenting and updating NASA spacelink electronic information system 12 p1634 N90-19392

Potential theory of radiation 12 p1635 N90-19395

Artificial intelligence issues related to automated computing operations 12 p1637 N90-19404

Evaluation of the heat transfer module (FAHT) of Failure Analysis Nonlinear Thermal And Structural Integrated Code (FANTASTIC) 12 p1637 N90-19407

ROCOPT: A user friendly interactive code to optimize rocket structural components 12 p1639 N90-19415

Marshall Avionics Testbed System (MAST)
12 p1639 N90-19417

Yaw rate control of an air bearing vehicle
12 p1639 N90-19420

The influence of a wall function on turbine blade heat transfer prediction 12 p1640 N90-19421

Multibody modeling and verification
12 p1640 N90-19422

Determination of Earth orientation using the Global Positioning System 12 p1642 N90-19435

Memory management in traceback Viterbi decoders
12 p1643 N90-19443

Quantization effects in Viterbi decoding rate 1/n convolutional codes 12 p1644 N90-19445

Big Viterbi Decoder (BVD) results for (7,1/2) convolutional code 12 p1644 N90-19446

Fast transform decoding of nonsystematic Reed-Solomon codes 12 p1644 N90-19447

A simple method using MAFIA to calculate external Q values of waveguide-loaded cavities
[DE90-741487] 12 p1647 N90-19465

Tracking performance of the AN/GPN-22 precision approach radar
[FEL-1988-34] 12 p1647 N90-19467

PATRAN-STAGS translator (PATSTAGS)
[NASA-TM-100388] 12 p1674 N90-19616

Demonstration of capabilities of high temperature composites analyzer code HITCAN
[NASA-TM-102560] 12 p1676 N90-19629

Development of software routines for remote sensing digital image processing
[ETN-90-95452] 12 p1679 N90-19640

User-friendly software for the design of digital line-of-sight radio links
[PB90-118472] 12 p1700 N90-19760

Recalibrating software reliability models
[NASA-CR-186407] 12 p1700 N90-19763

A nonparametric software reliability growth model
[NASA-CR-186438] 12 p1700 N90-19764

Software development: A paradigm for the future
[NASA-CR-186456] 12 p1701 N90-19766

Generic distributed systems model
[AD-A217078] 12 p1702 N90-19773

Local area network with fault-checking, priorities, and redundant backup
[NASA-CASE-NPO-16949-1-CU] 12 p1703 N90-19776

The 0-1 multiknapsack problem: Heuristic and reduction methods
[INPE-4894-PRE/1495] 12 p1704 N90-19782

Executive information systems for providing next generation strategic information: An evaluation of EIS (Executive Information System) software and recommended applicability within the FAA computing environment
[AD-A216672] 12 p1726 N90-19920

Conception of an automatic measurement installation for spatial resolution detectors
[ETN-90-95732] 12 p1729 N90-19935

Nuclear interactions of high energy heavy ions and applications in astrophysics
[DE90-006691] 12 p1737 N90-19984
Experimental and theoretical aerodynamic characteristics of a high-lift semispan wing model
[NASA-TP-2990] 13 p1749 N90-20046
The application of active controls technology to a generic hypersonic aircraft configuration
[NASA-TM-101689] 13 p1754 N90-20071
Comparison of 3-D viscous flow computations of Mach 5 inlet with experimental data
[NASA-TM-102518] 13 p1757 N90-20090
Laboratory implementation of the Continuously Reconfiguring Multi-Microprocessor Flight Control System (CRMMFCS)
[AD-A217730] 13 p1758 N90-20094
A data acquisition parallel bus for wind tunnels at ARL (Aeronautical Research Laboratory)
[AD-A218052] 13 p1759 N90-20098
ETO (Earth-To-Orbit): A trajectory program for aerospace vehicles
[AD-A218157] 13 p1760 N90-20103
Component count and preliminary assembly considerations for large space truss structures
[NASA-TM-102604] 13 p1763 N90-20121
Composite laminate tailoring with probabilistic constraints and loads
[NASA-TM-102515] 13 p1766 N90-20138
Electrochemical phase diagrams for aqueous redox systems
[AD-A217168] 13 p1770 N90-20157
Modification and improvement of software for modeling multidimensional reacting fuel flows
[AD-A217789] 13 p1783 N90-20235
Analysis of radiometer calibration effects with TOUCHSTONE
[NASA-CR-186476] 13 p1792 N90-20284
Recent improvements to the electromagnetic surface patch code
[AD-A217479] 13 p1794 N90-20293
Area Over Length (AOL): A program for the calculation of effective two-dimensional thermal conductance through an arbitrarily shaped region
[DE90-008005] 13 p1801 N90-20335
Numerical modeling of airblast
[AD-A217993] 13 p1803 N90-20347
Space mechanism of low velocity for an array of solar panels: Analysis and design of an experimental model; dimensions of bearings
[INPE-4859-TDL/370] 13 p1809 N90-20390
Robust performance of multiple tasks by a mobile robot
[DE90-001953] 13 p1811 N90-20397
Comparison of two matrix data structures for advanced CSM testbed applications
[NASA-CR-181951] 13 p1815 N90-20421
Computer simulation of the mathematical modeling involved in constitutive equation development: Via symbolic computations
[NASA-TM-102532] 13 p1816 N90-20428
COMGEN: A computer program for generating finite element models of composite materials at the micro level
[NASA-TM-102556] 13 p1818 N90-20438
Stress field near crack tip: An experimental evaluation of the three dimensional variation
[AD-A217878] 13 p1818 N90-20441
Small and great circle routines
[AD-A217652] 13 p1820 N90-20449
A split-and-merge method for creating polygonal homogeneous-vegetation regions from digitized terrain data
[AD-A218080] 13 p1821 N90-20453
Phase 1 supplemental development of a kinematic Stirling/Rankine commercial gas-fired heat pump system
[PB90-129974] 13 p1825 N90-20483
The Terrain-Responsive Atmospheric Code (TRAC) project plan: Development of a hazardous materials dispersion modeling capability with application to ambient air monitoring network design
[DE90-007293] 13 p1829 N90-20502
GEOID '88: A gravimetric geoid for Canada
13 p1837 N90-20543
User's guide: Programs for processing altimeter data over inland seas
[NASA-TM-100730] 13 p1841 N90-20572
A prototype expert system to forecast severe winds in the western Mediterranean Sea
[AD-A218017] 13 p1845 N90-20593
RenderMan design principles
13 p1857 N90-20653
Onboard shuttle on-line software requirements system: Prototype 13 p1858 N90-20658
Engineering visualization utilizing advanced animation
13 p1859 N90-20664
GCS plan for software aspects of certification
[NASA-CR-181972] 13 p1864 N90-20694
Recent advances in 3D finite difference mesh generation using the BRL-CAD package
[DE90-007854] 13 p1866 N90-20704
ISLE (Image and Signal Processing LISP Environment) reference manual
[DE90-007858] 13 p1866 N90-20705
Software quality assurance and software safety in the biomed control system
[DE90-008072] 13 p1866 N90-20706
GRID2D/3D: A computer program for generating grid systems in complex-shaped two- and three-dimensional spatial domains. Part 2: User's manual and program listing
[NASA-TM-102454] 13 p1867 N90-20708
Scattering sources: A spherical harmonics expansion
[DE90-008724] 13 p1867 N90-20711
VAPEPS user's reference manual, version 5.0
[NASA-CR-180781] 13 p1868 N90-20713
Research in programming languages and software engineering
[AD-A217765] 13 p1868 N90-20715
Development of computer software for the analysis and design of modern control systems
[AD-A217924] 13 p1868 N90-20717
Mathematics and physics studies: Multi-project support
[AD-A218208] 13 p1869 N90-20723
Implementation of midcourse tracking and correlation on massively parallel computers
[DE90-008166] 13 p1873 N90-20740
Computation and graphics in mathematical research
[DE90-008429] 13 p1877 N90-20766
Towards SDS (Strategic Defense System) testing and evaluation: A collection of relevant topics
[AD-A217610] 13 p1880 N90-20783
Air Force Boom Event Analyzer Recorder (BEAR): Sysstem description
[AD-A218048] 13 p1882 N90-20800
Optical instrumentation support for the airborne ionospheric observatory
[AD-A218207] 13 p1889 N90-20839
Theory of defect process: Basic issues in quantitative understanding
[AERE-R-13661] 13 p1892 N90-20860
An overlapped grid method for multigrid, finite volume/difference flow solvers: MaGGiE
[NASA-CR-182008] 14 p1911 N90-20953
Convergence acceleration of hypersonic flow calculations: A nonlinear relaxation factor
14 p1911 N90-20957
Aerofoil design techniques 14 p1916 N90-20978
Constrained spanload optimization for minimum drag of multi-lifting-surface configurations
14 p1919 N90-20992
Aerodynamic design by optimization
14 p1920 N90-20996
Numerical optimization of wings in transonic flow
14 p1920 N90-20997
Experimental and numerical study on basic phenomena of secondary flows in turbines 14 p1923 N90-21014
Secondary flow in a turbine guide vane with low aspect ratio 14 p1924 N90-21018
Generation and decay of secondary flows and their impact on aerodynamic performance of modern turbomachinery components 14 p1925 N90-21023
Computational prediction and measurement of the flow in axial turbine cascades and stages
14 p1925 N90-21028
Supersonic nozzle design of arbitrary cross-section
14 p1927 N90-21035
Controlled multibody dynamics simulation for large space structures 14 p1934 N90-21068
Detection of potential space station control/structure interaction with CO-ST-IN 14 p1935 N90-21074
Filament winding of composite cylinders
14 p1943 N90-21119
A computational model of the perforation of multi-layer metallic laminates
[MRL-RR-9-89] 14 p1944 N90-21128
Structural tailoring of select fiber composite structures
[NASA-TM-102484] 14 p1946 N90-21137
Computer processing of multi-channel electromagnetic data from an airborne geophysical survey system
[PB90-138413] 14 p1965 N90-21253
The 4th Annual Review of Progress in Applied Computational Electromagnetics
[AD-A217912] 14 p1966 N90-21257
The 5th Annual Review of Progress in Applied Computational Electromagnetics
[AD-A217994] 14 p1966 N90-21258
Thermal radiation characteristics of nonisothermal cylindrical enclosures using a numerical ray tracing technique
[NASA-TM-102527] 14 p1972 N90-21296
Computer codes for the evaluation of thermodynamic properties, transport properties, and equilibrium constants of an 11-species air model
[NASA-TM-102602] 14 p1972 N90-21297
PROTEUS two-dimensional Navier-Stokes computer code, version 1.0. Volume 1: Analysis description
[NASA-TM-102551] 14 p1973 N90-21303
PROTEUS two-dimensional Navier-Stokes computer code, version 1.0. Volume 2: User's guide
[NASA-TM-102552] 14 p1973 N90-21306
PROTEUS two-dimensional Navier-Stokes computer code, version 1.0. Volume 3: Programmer's reference
[NASA-TM-102553] 14 p1974 N90-21307
The modelling of heat and mass transfer near solid boundaries and comparison with experimental results
[PB90-167040] 14 p1974 N90-21310
Phase-only holographic filters and their applications
[PB90-166802] 14 p1984 N90-21368
Improved analytical capabilities for foil air bearings, phase 1
[AD-A218071] 14 p1987 N90-21389
Aeropropulsion facilities configuration control: Procedures manual
[NASA-TM-102541] 14 p1989 N90-21399
The computational structural mechanics testbed generic structural-element processor manual
[NASA-CR-181728] 14 p1991 N90-21410
Stress analysis and minimum weight design of honeycomb sandwich plates 14 p1992 N90-21418
An internal/external pressure, tension/compression multiaxial fatigue system
[DE90-009510] 14 p1994 N90-21430
MECCA program documentation
[NOAA-TR-NESDIS-46] 14 p2003 N90-21477
An outline for the analysis of wave induced bottom pressure fluctuations
[MRL-TN-558] 14 p2008 N90-21510
Software verification and validation: Its role in computer assurance and its relationship with software project management standards
[PB90-111691] 14 p2012 N90-21530
Integrating automated support for a software management cycle into the TAME system
[NASA-CR-186457] 14 p2013 N90-21532
Collected software engineering papers, volume 7
[NASA-TM-103312] 14 p2014 N90-21537
Lessons learned in the transition to Ada from FORTRAN at NASA/Goddard
[NASA-TM-103311] 14 p2014 N90-21538
Evolution of Ada technology in the flight dynamics area: Implementation/testing phase analysis
[NASA-TM-103310] 14 p2014 N90-21539
Collected software engineering papers, volume 6
[NASA-TM-103309] 14 p2014 N90-21540
Software Management Environment (SME) concepts and architecture
[NASA-TM-103306] 14 p2014 N90-21543
Implementation of a production Ada project: The GRODY study
[NASA-TM-103305] 14 p2015 N90-21544
CAD work station for electronics designer
[DE90-616473] 14 p2015 N90-21546
The CAD/CAM product data standards: IGES/PDES (Initial Graphics Exchange Specification/Product Data Exchange Standards, the present and the future
[DE90-008803] 14 p2015 N90-21549
SIGNIF: A C function to compute significant digits
[DE90-009242] 14 p2015 N90-21550
Hypercluster parallel processing library user's manual
[NASA-CR-185231] 14 p2016 N90-21552
Curvature continuity of cubic Bezier curves in the solid modeling aerospace research tools design software
[NASA-CR-186583] 14 p2016 N90-21554
OTTER (Organized Techniques for Theorem-proving and Effective Research) 2.0 users guide
[DE90-007978] 14 p2018 N90-21563
Modeling high-temperature superconductors and metallic alloys on the Intel IPSC/860
[DE90-009402] 14 p2033 N90-21665
STORM: A statistical object representation model
[DE90-009048] 14 p2036 N90-21686
WINCOF-I code for prediction of fan compressor unit with water ingestion
[NASA-CR-185157] 15 p2045 N90-21724
Prediction of forces and moments for flight vehicle control effectors. Part 2: An analysis of delta wing aerodynamic control effectiveness in ground effect
[NASA-CR-186572] 15 p2047 N90-21735
A computer program for the prediction of nozzle-propeller performance
[LR-578] 15 p2048 N90-21740
A multiblock/multizone code (PAB 3D-v2) for the three-dimensional Navier-Stokes equations: Preliminary applications
[NASA-CR-182032] 15 p2049 N90-21745

Computational simulation of structural fracture in fiber composites
[NASA-TM-102505] 15 p2064 N90-21821
METCAN verification status
[NASA-TM-103119] 15 p2064 N90-21824
Probabilistic analysis of bladed turbine disks and the effect of mistuning
[NASA-TM-102564] 15 p2072 N90-21871
Development, implementation and test of a computer program for the production of axisymmetric pattern moulds on a numerically controlled milling machine
[LR-593] 15 p2074 N90-21877
Finding the complete path and weight enumerators of convolutional codes 15 p2077 N90-21897
A survey of the maritime-aerosol data collected at South Uist and the implications for the LOWTRAN maritime aerosol model 15 p2079 N90-21908
The Mediterranean marine environment and its effects on aerosols and infrared transmission
15 p2079 N90-21909
LOWTRAN 7: Status, review, and impact for short-to-long-wavelength infrared applications
15 p2081 N90-21917
Propagation environments, effects, and decision aids
15 p2081 N90-21918
Models of aerosols, clouds, and precipitation for atmospheric propagation studies
15 p2081 N90-21919
Interpreting meteorological data reports for LOWTRAN Navy aerosol model extinction calculations
15 p2082 N90-21920
Modeling millimeter-wave propagation effects in the atmosphere 15 p2082 N90-21922
UV spectral simulations using LOWTRAN 7
15 p2083 N90-21928
Technique for selecting an aerosol model useful for infrared atmospheric transmittance calculations
15 p2085 N90-21934
Calculation of IR propagation statistics in the eastern Atlantic for surveillance system performance assessment 15 p2085 N90-21938
Atmospheric modelling studies: A modelling comparison between IR and millimetric atmospheric propagation
15 p2086 N90-21941
Theory of a periodic cylindrical waveguide with a nonuniform metal-dielectric filling
[DE90-620099] 15 p2087 N90-21945
General structured grid generation systems
15 p2093 N90-21977
Algebraic block-structured grid generation based on a macro-block concept 15 p2093 N90-21978
Mesh generation for flow computation in turbomachine
15 p2094 N90-21981
Numerical simulation of liquid circulation in a bubbly column
[DE90-005226] 15 p2097 N90-22002
Reliability importance measures and their calculation
[DE90-620391] 15 p2108 N90-22057
Elastic stability and nonlinear behavior of imperfect shells with initial stresses 15 p2110 N90-22070
Nonlinear fracture mechanics using semicircular specimens and tension-softening behavior
15 p2116 N90-22108
ANILISA: Computational module for Koiter's imperfection sensitivity theory
[LR-582] 15 p2119 N90-22119
A free surface Bryan-Cox-Semtner model
[IOS-270] 15 p2135 N90-22201
Graphics mini manual
[NASA-TM-87622-REV] 15 p2144 N90-22247
An algorithm and computer program for the calculation of envelope curves
[PB90-155409] 15 p2145 N90-22254
Paving: A new approach to automated quadrilateral mesh generation
[DE90-010244] 15 p2146 N90-22260
GRID2D/3D: A computer program for generating grid systems in complex-shaped two- and three-dimensional spatial domains. Part 1: Theory and method
[NASA-TM-102453] 15 p2147 N90-22262
Software quality assurance: Towards a measurable quality improvement
[REPT-89-42] 15 p2147 N90-22264
New algorithms for one-loop integrals
[NIKHEF-H/89-17] 15 p2148 N90-22268
Inventory of program packages related to the project SIMONA
[ETN-90-96397] 15 p2148 N90-22270
Traffic placement policies for a multi-band network
15 p2149 N90-22279
Distributed simulation, no special tools required
15 p2150 N90-22281
The WAVE model for advanced knowledge processing
[OUEL-1803/89] 15 p2151 N90-22291
The art of fault-tolerant system reliability modeling
[NASA-TM-102623] 15 p2152 N90-22292
PLAN-IT-2: The next generation planning and scheduling tool 15 p2153 N90-22298
Space communications scheduler: A rule-based approach to adaptive deadline scheduling
15 p2153 N90-22300
Simulation-based reasoning about the physical propagation of fault effects 15 p2155 N90-22309
Automated procedure execution for space vehicle autonomous control 15 p2156 N90-22314
Bounded-time fault-tolerant rule-based systems
15 p2157 N90-22318
The Weapons Laboratory technical library: Automating with STILAS 15 p2178 N90-22447
Update on the OPAL opacity code
[DE90-009946] 15 p2184 N90-22480
The modeling of IRAS detections of classical novae and related objects 15 p2185 N90-22482
Debris/ice/TPS assessment and photographic analysis for Shuttle Mission STS-36
[NASA-TM-102789] 16 p2205 N90-22583
A study of woven fabric-reinforced composite materials using an invariant-based orthotropic plasticity formulation
16 p2211 N90-22611
Large deformation analysis of laminated composite structures by a continuum-based shell element with transverse deformation 16 p2211 N90-22613
Modeling of combustion processes in a solid fuel particle
[DE90-009140] 16 p2214 N90-22629
Calcium carbonate scale dissolution in water stabilized by carbon dioxide treatment
[AD-A218502] 16 p2214 N90-22633
A theoretical and experimental investigation of an absorption refrigeration system for application with solar energy units 16 p2226 N90-22697
Side moment exerted by a spinning, coning, highly viscous liquid payload
[AD-A218746] 16 p2237 N90-22763
Cognitive efficiency considerations for good graphic design
[AD-A218976] 16 p2263 N90-22899
The development of a system for the numerical simulation of Euler flows 16 p2277 N90-22980
Parallel processing of real-time dynamic systems simulation on OSCAR (Optimally SCheduled Advanced multiprocessoR) 16 p2282 N90-23006
Modern CACSD using the Robust-Control Toolbox
16 p2286 N90-23024
Simulation studies using multibody dynamics code DART 16 p2288 N90-23036
On trajectory generation for flexible space crane: Inverse dynamics analysis by LATDYN 16 p2288 N90-23037
Enhanced modeling features within TREETOPS
16 p2290 N90-23047
Implementation of generalized optimality criteria in a multidisciplinary environment 16 p2290 N90-23048
New multivariable capabilities of the INCA program
16 p2290 N90-23049
Multidisciplinary Expert-aided Analysis and Design (MEAD) 16 p2291 N90-23050
ASTEC: Controls analysis for personal computers
16 p2291 N90-23052
Multibody dynamics model building using graphical interfaces 16 p2297 N90-23082
PLOT3D user's manual
[NASA-TM-101067] 16 p2298 N90-23090
About the order of Appel's algorithm
[CS-8910] 16 p2299 N90-23097
Vectors and matrices: Two turbo pascal units for fast program development
[AD-A218917] 16 p2300 N90-23105
Natural language processing: A tutorial
[AD-A219096] 16 p2300 N90-23108
Comparative evaluations of four specification methods for real-time systems
[AD-A219187] 16 p2300 N90-23109
Version description and installation guide Kernel version 3.0
[AD-A219292] 16 p2301 N90-23113
Kernel architecture manual
[AD-A219295] 16 p2301 N90-23115
A computer program to implement the Chen method of dimensional analysis
[AD-A218557] 16 p2306 N90-23142
Current Japanese supercomputers for computational fluid dynamics applications 16 p2311 N90-23172
Optimal helicopter trajectory planning for terrain following flight
[NASA-CR-186470] 17 p2349 N90-23376
Continued development and analysis of a new extended Kalman filter for the Completely Integrated Reference Instrumentation System (CIRIS)
[AD-A220106] 17 p2354 N90-23400
Computational analysis of the flowfield of a two-dimensional ejector nozzle
[NASA-CR-185255] 17 p2355 N90-23406
A test matrix sequencer for research test facility automation
[NASA-TM-103108] 17 p2357 N90-23416
Autonomous low earth orbit navigation
[REPT-892-440-101] 17 p2364 N90-23458
Geometric programming prediction of design trends for OMV protective structures
[NASA-TM-4206] 17 p2365 N90-23462
Modeling and control of flexible vehicles in space
[AD-A219822] 17 p2365 N90-23465
ISO attitude and orbit control subsystem
[REPT-892-440-104] 17 p2366 N90-23467
Implementation of image action plus software for image analysis of solid propellant combustion holograms
[AD-A219644] 17 p2372 N90-23508
Health management system for rocket engines
[NASA-CR-185223] 17 p2383 N90-23574
UW VLSI chip tester
[AD-A220789] 17 p2397 N90-23653
Computations of a horseshoe vortex around an endwall-mounted cylinder 17 p2400 N90-23673
Equilibrium radiative heating tables for Earth entry
[NASA-TM-102652] 17 p2401 N90-23675
An expert system for the study of high duty bonded joints in aerospace structures
[REPT-892-430-110] 17 p2414 N90-23753
STARS: An integrated general-purpose finite element structural, aeroelastic, and aeroservoelastic analysis computer program
[NASA-TM-101709] 17 p2416 N90-23768
PUFFY: A puff diffusion computer model
[FOA-C-40251-4.5] 17 p2421 N90-23796
Two dimensional Fourier analysis of the earth gravitational field using the program package TIM
[ETN-90-96696] 17 p2424 N90-23815
A Kalman filter with smoothing for hurricane tracking and prediction
[AD-A220413] 17 p2426 N90-23827
Atmospheric transport and dispersion model hierarchy, part 2
[AD-A220138] 17 p2427 N90-23833
Navigation software for the MPL vertical line array
[AD-A220166] 17 p2432 N90-23860
The application of kriging in the statistical analysis of anthropometric data, volume 3
[AD-A220615] 17 p2438 N90-23893
The internet worm
[NASA-CR-181576] 17 p2441 N90-23910
Evaluation methodology for software engineering
[AD-A218474] 17 p2441 N90-23913
Conceptual modeling via logic programming
[AD-A219785] 17 p2442 N90-23919
Generation of expert systems by partial evaluation
[AD-A220427] 17 p2443 N90-23920
Explanation and the theory of expert problem solving
[AD-A220861] 17 p2444 N90-23930
Conceptual dependency graphs and DJ
[REPT-89-62] 17 p2445 N90-23933
The Delfi3-interpreter: Notes on the implementation
[REPT-89-72] 17 p2445 N90-23935
Optimization of series expressions. Part 2: Over view of the theory and implementation
[AD-A219961] 17 p2447 N90-23952
Shape discrimination research using an IBM PC
[AD-A219993] 17 p2447 N90-23953
A comparison of a relational and nested-relational IDEF0 data model
[AD-A220147] 17 p2448 N90-23956
An experimental evaluation of software redundancy as a strategy for improving reliability
[NASA-TM-102613] 17 p2448 N90-23958
Calculation of Lie algebra cohomology by computer
[MEMO-833] 17 p2449 N90-23962
Specification modules in LOTOS
[MEMO-INF-89-48] 17 p2449 N90-23965
The semantics of TRIDL
[TR-89-17] 17 p2450 N90-23973
Parallel execution of LISP programs
[AD-A219623] 17 p2451 N90-23978
The design of a local area network configuration management system for the Naval Postgraduate School Administrative Sciences Department
[AD-A219643] 17 p2451 N90-23979
Northeast Artificial Intelligence Consortium. Volume 4. Distributed AI for communications network management
[AD-A218717] 17 p2453 N90-23994
A decision support system for control and automation of dynamical processes
[AD-A219501] 17 p2454 N90-23995
Northeast Artificial Intelligence Consortium annual report, 1988. Volume 12: Computer architectures for very large knowledge bases
[AD-A219599] 17 p2454 N90-23999
A modified fast Fourier transform
[AD-A220567] 17 p2457 N90-24023

A note on the Gaussian integration formula
[AD-A220053] 17 p2461 N90-24054
Fast casual multicast
[NASA-CR-186643] 17 p2462 N90-24059
Sample size for correlation estimates
[AD-A219810] 17 p2465 N90-24085
IAPSA 2 small-scale system specification
[NASA-CR-182006] 17 p2467 N90-24103
Columbus onboard FDIR concept
18 p2500 N90-24286
Distributed mission planning technology for Columbus
18 p2501 N90-24288
Combustor design and analysis using the Rocket Combustor Interactive Design (ROCCID) methodology
[NASA-TM-103165] 18 p2513 N90-24349
Encoding of the Burgess metal electrical resistivity model into SESAME format and its adaptation to the metal nickel
[DE90-010816] 18 p2526 N90-24419
Flow studies in impeller passages
18 p2551 N90-24558
Off-design loss measurements in a compressor cascade
[AD-A220094] 18 p2552 N90-24564
A computer program for the design of optimum catalytic monoliths for CO2 lasers 18 p2558 N90-24595
Advanced buckling analyses of beams with arbitrary cross sections
[ISBN-90-9002808-0] 18 p2572 N90-24659
Current status of SHARC, the strategic high altitude radiance code, and description of its new auroral module
[AD-A221068] 18 p2580 N90-24698
ISIS and META projects
[NASA-CR-186624] 18 p2590 N90-24733
Flipper user's manual
[AD-A220788] 18 p2590 N90-24734
Some comments on techniques for resisting computer viruses
[AD-A221097] 18 p2593 N90-24754
CERC (Center for Energy Research Computation) report: Results of the CERC Project with recommendations for ANL (Argonne National Laboratory) institutional strategies in advanced scientific computing
[DE90-008238] 18 p2594 N90-24759
Graph structure model
[DE90-008945] 18 p2594 N90-24760
HUGOFIT and HUGOPLOT: Computer codes for plane shock wave analysis with materials that have non-simple Hugoniots
[DE90-010284] 18 p2594 N90-24761
Solution of exterior acoustic problems by the boundary element method 18 p2611 N90-24874
TFE verification program
[DE90-008227] 18 p2614 N90-24891
Managing parallelism and resources in scientific dataflow programs
[AD-A221398] 18 p2635 N90-25010
A few modeling and rendering techniques for computer graphics and their implementation on ultra hardware
18 p2640 N90-25038
A 3D visualization system for molecular structures
18 p2641 N90-25044
The implementation of the graphics of program EAGLE: A numerical grid generation code on NASA Langley SNS computer system 18 p2642 N90-25050
AFE dynamic effects in inhomogeneous plasmas
18 p2643 N90-25053
Extension-torsion coupling behavior of advanced composite tilt-rotor blades 18 p2644 N90-25057
Flexural fatigue life prediction of closed hat-section using materially nonlinear axial fatigue characteristics
18 p2645 N90-25062
Computational simulation of transition to turbulence through inverse modeling 18 p264[illegible] N90-25067
MARS, an AI-based Mission Activities and Resource Scheduler
[MBB-0060/89-PUB] 19 p26[illegible] N90-25083
Solution of the optimal control problem using the software package STOMP
[MBB-FE-126/S/PUB-370] 19 p2651 N90-25087
Coupled rotor-body equations of motion hover flight
[NASA-CR-186710] 19 p2655 N90-25111
The application of the finite element method to an aerodynamic problem specific to propeller design
[LR-614] 19 p2656 N90-25116
Users guide for an Airborne Windshear Doppler Radar Simulation (AWDRS) program
[NASA-CR-182025] 19 p2657 N90-25121
Replication of NASPAC Dallas/Fort Worth study
[DOT/FAA/CT-TN90/26] 19 p2657 N90-25123
Thermal and orbital analysis of Earth monitoring Sun-synchronous space experiments
[NASA-TM-101630] 19 p2666 N90-25168
A comparison of analytical results for 20 K LOX/hydrogen instabilities
[NASA-TM-103166] 19 p2670 N90-25186
Advanced fuel properties, phase 1
[AD-A219788] 19 p2679 N90-25236
Infrared fiber-optical temperature sensor
[AD-D014519] 19 p2693 N90-25321
A simulation code for turbocompound diesel engines
[IAR-89-26] 19 p2697 N90-25348
Comparison of two computer codes for crack growth analysis: NASCRAC Versus NASA/FLAGRO
[NASA-TM-100383] 19 p2700 N90-25360
Loads analysis and testing of flight configuration solid rocket motor outer boot ring segments
[NASA-TP-3028] 19 p2701 N90-25366
Physical parameterization of snow albedo for use in climate models
[PB90-167313] 19 p2712 N90-25433
Advanced mesoscale weather forecasting to support tactical operations on the airland battlefield
[AD-A219421] 19 p2715 N90-25449
The application of NASREM to remote robot control
19 p2738 N90-25563
Hardware and software reliability estimation using simulations
[NASA-CR-186637] 19 p2741 N90-25580
Multi-version software reliability through fault-avoidance and fault-tolerance
[NASA-CR-186502] 19 p2742 N90-25584
Interactive grid generation on small computers
[AD-A221234] 19 p2742 N90-25585
GSC configuration management plan
[NASA-CR-182044] 19 p2743 N90-25587
Software quality assurance plan for GCS
[NASA-CR-182045] 19 p2743 N90-25588
GCS support/development system configuration document
[NASA-CR-182046] 19 p2743 N90-25589
MEXP: A programming tool for the CESAR programmable systolic array multiprocessor
[FFI-89/7020] 19 p2744 N90-25598
Automated angular momentum recoupling algebra
[DE90-011988] 19 p2750 N90-25626
The incorporation of a multigrid method into the orthogonal curvilinear coordinate version of the Rolls-Royce PACE computer program
[TT-8804] 19 p2751 N90-25627
Reliability model generator specification
[NASA-CR-182005] 19 p2752 N90-25638
One dimensional heavy ion beam transport: Energy independent model
[NASA-CR-186722] 19 p2754 N90-25650
On using a superconducting linac to drive a short wavelength FEL
[CEBAF-PR-89-019] 19 p2756 N90-25660
Technical guide on documentation requirements for open market contract acquisitions of information resources
[NASA-TM-102650] 19 p2762 N90-25695
NASA Marshall Space Flight Center solar observatory report, January to December 1989
[NASA-TM-100404] 19 p2797 N90-25923
Turbine blade heat transfer coefficient evaluation by modified version of STAN5. Comparison with experimental data
[ETN-90-97283] 20 p2813 N90-26008
Prediction of the ullage gas thermal stratification in a NASP vehicle propellant tank experimental simulation using FLOW-3D
[NASA-TM-103217] 20 p2841 N90-26160
Integrated support structure
[NASA-CR-186835] 20 p2841 N90-26162
Critical evaluation of Jet-A spray combustion using propane chemical kinetics in gas turbine combustion simulated by KIVA-2
[NASA-TM-103173] 20 p2843 N90-26170
L-SWITCH: A PC program for computing transient voltages and currents during switching off three-phase inductances
[EUT-89-E-221] 20 p2858 N90-26257
A possibility to incorporate saturation in the simple, global model of a synchronous machine with rectifier
[EUT-89-E-225] 20 p2858 N90-26258
Code enhancements and validation of GASP
[NPS-PAPER-44] 20 p2861 N90-26277
Informatics aspects of large flow calculations on the SX-2 supercomputer
[NLR-MP-88037-U] 20 p2864 N90-26290
Design of ceramic components with the NASA/CARES computer program
[NASA-TM-102369] 20 p2875 N90-26359
Qualification of concentrating mirror systems with the HERMES measurement system and the HELIOS simulation program
[DLR-FB-89-51] 20 p2882 N90-26394
A computer module used to calculate the horizontal control surface size of a conceptual aircraft design
[NASA-CR-186872] 20 p2903 N90-26515
An expert system based software sizing tool, phase 2
[NASA-CR-186706] 20 p2905 N90-26525
Software requirements: Guidance and control software development specification
[NASA-CR-182058] 20 p2906 N90-26527
A hybrid M-algorithm/sequential decoder for convolutional and trellis codes
[NASA-CR-186863] 20 p2906 N90-26528
Automated sensitivity analysis with the Gradient Enhanced Software System (GRESS)
[DE90-011291] 20 p2906 N90-26529
Level-2 system: Programmers-users manual
[DE90-013324] 20 p2908 N90-26540
Documentation of program Tankplot
[FFI-89/7019] 20 p2908 N90-26541
CAD/CAM reinforces the competitive edge of European mouldmakers
[CRIF-MC-88] 20 p2908 N90-26542
LASER: A Layout Sensitivity Explorer. Report and user's manual
[EUT-89-E-216] 20 p2908 N90-26545
Pacific missile test center information resources management organization (code 0300): The ORACLE client-server and distributed processing architecture
[DE90-013271] 20 p2912 N90-26565
MINAS: An algorithm for systematic state assignment of sequential machines: Computational aspects and results
[EUT-89-E-217] 20 p2912 N90-26566
From network to artwork: Automatic schematic diagram generation
[EUT-89-E-219] 20 p2912 N90-26567
Contribution to the study of differential equations and to the differences in the complex field
[ETN-90-97250] 20 p2919 N90-26612
Cartesian closed categories of domains
[ETN-90-97284] 20 p2919 N90-26613
Efficient implementation of minimal polynomial and reduced rank extrapolation methods
[NASA-TM-103240] 20 p2920 N90-26616
Sensitivity analysis with a simple charging code
[RAE-TM-SPACE-374] 20 p2929 N90-26662
ARLSUPER version 1.0, program users guide
[AD-A222693] 21 p2953 N90-26793
Computational methods for problems in aerodynamics using parallel and vector architecture
[AD-A221979] 21 p2954 N90-26795
Installation and pretest analysis of DARPA suboff model in the DTRC anechoic wind tunnel
[AD-A221497] 21 p2955 N90-26801
Proceedings of the 1987 Aircraft/Engine Structural Integrity Program (ASIP/ENSIP) Conference
[AD-A198037] 21 p2956 N90-26807
Application of damage tolerance
21 p2958 N90-26817
Automated analysis of MXU-553 flight data
21 p2958 N90-26821
BASEOPS default profiles for civil aircraft
[AD-A223161] 21 p2959 N90-26825
B-1B improved windshield development. Volume 2: Magna analysis: Baseline and parametric
[AD-A221501] 21 p2960 N90-26828
Communications and tracking expert systems study
[NASA-CR-185935] 21 p2992 N90-27004
RADC/EEV diagnostic rhyme test system improvements
[AD-A223187] 21 p2995 N90-27025
Parallel numerical simulations of axisymmetric projectile flows using zonal-overlapped grids
[AD-A221711] 21 p3005 N90-27082
Development of an integrated mobile robot system at Carnegie-Mellon University
[AD-A222494] 21 p3011 N90-27119
Atmospheric dispersion of solid and liquid rocket propellants
[AD-A221293] 21 p3020 N90-27173
Evaluation of magnetospheric internal magnetic field models and existing software
[AD-A221816] 21 p3027 N90-27210
Downwelled longwave surface irradiance data from five sites for the FIRE/SRB Wisconsin Experiment from October 12 through November 2, 1986
[NASA-TM-102597] 21 p3030 N90-27225
A LOWTRAN7 sensitivity study in the 8-12 and 3-5 micron bands: Includes comparison with LOWTRAN6 results
[AD-A222094] 21 p3031 N90-27231
ECOS: The ESA Costing Software
[ESA-BR-56] 21 p3039 N90-27274
A hybrid approach to space power control
21 p3043 N90-27293
Design knowledge capture for a corporate memory facility 21 p3045 N90-27304
An application of design knowledge captured from multiple sources 21 p3045 N90-27306

Some software implementation of the functions sine and cosine
[DE90-010398] 21 p3050 N90-27339
A user's manual for MCPRAM (Monte Carlo PReprocessor for AMEER) and for the fuze options in AMEER (Aero Mechanical Equation Evaluation Routines)
[DE90-013598] 21 p3051 N90-27345
An algorithm for automated surface modelling in unigraphics
[AD-A223219] 21 p3053 N90-27355
Zadok user guide
[AD-A222071] 21 p3054 N90-27360
Data and analysis center for software
[AD-A221434] 21 p3054 N90-27363
Personal computer programs for the control of subnanosecond transient digitizers with applications for device damage testing
[AD-A221458] 21 p3054 N90-27365
Modification of a cam facility
[AD-A221828] 21 p3056 N90-27376
Guide for the management of expert systems development
[AD-A221847] 21 p3056 N90-27378
The image of weighted combinatorial problems
[REPT-88-017] 21 p3057 N90-27382
Critical problems in very large scale computer systems
[AD-A221603] 21 p3058 N90-27391
Parallel algorithms for computer vision
[AD-A221871] 21 p3059 N90-27394
The operational feature exchange language
[AD-A222497] 21 p3060 N90-27401
Development, implementation, and validation of control algorithms for the dual-arm robotic manipulation of a single object
[AD-A222502] 21 p3060 N90-27402
Proceedings of Workshop on Reliability in Computational Mechanics
[AD-A221694] 21 p3065 N90-27426
The validation and application of a rotor acoustic prediction computer program
[NASA-TM-101794] 21 p3072 N90-27485
Interim status and recommendations for the Engineering Information System (EIS) program
[AD-A222060] 21 p3087 N90-27555
Experimental study on the vortices generated by the body of a missile during flight. Part 1: Laminar boundary layer
[ONERA-RT-40/1147-AY-130A-PT-1] 22 p3110 N90-27665
A review of crashworthiness of composite aircraft structures
[AD-A221555] 22 p3115 N90-27697
Measurement uncertainty in gas turbine performance determination 22 p3119 N90-27717
Computer code for predicting coolant flow and heat transfer in turbomachinery
[NASA-TP-2985] 22 p3120 N90-27722
Testing DoD space systems: The challenge 22 p3132 N90-27771
Observation model and parameter partials for the JPL geodetic (GPS) modeling software 'GPSOMC'
[NASA-CR-186972] 22 p3132 N90-27774
TRANSTRAIN: A program to compute strain transformations in composite materials
[NASA-TM-103509] 22 p3153 N90-27877
Calculation of the combustion distribution in a liquid-fuel ramjet 22 p3162 N90-27931
Annular slot antenna radiating into lossy material
[NPL-DITC-152/89] 22 p3165 N90-27945
The Helicopter Antenna Radiation Prediction Code (HARP)
[NASA-CR-188925] 22 p3165 N90-27946
Spatial array processing by the method CLEAN
[FEL-1989-144] 22 p3165 N90-27949
FINFLO: A finite-volume based computer program for two-dimensional and axisymmetric compressible flow
[PB90-189473] 22 p3169 N90-27974
Grid generation and processing for FINFLO flow solver
[PB90-189481] 22 p3169 N90-27975
Flowfield computation of entry vehicles
[NASA-CR-186946] 22 p3171 N90-27986
Experimental study of an unsteady boundary layer on an oscillating plane plate. Optimization and validation of calculation code for the analysis of the potential flow/boundary layer coupling in the neighborhood of a plane plate and an oscillating profile
[ETN-90-97436] 22 p3175 N90-28013
Modification of the SHABERTH bearing code to incorporate RP-1 and a discussion of the traction model
[NASA-TP-3017] 22 p3183 N90-28066
In-service inspection of composite components on aircraft at depot and field levels 22 p3186 N90-28078
Ceramics Analysis and Reliability Evaluation of Structures (CARES). Users and programmers manual
[NASA-TP-2916] 22 p3190 N90-28099
Graphically-oriented linear analysis of plane frames subjected to complex loadings on microcomputers
[PB90-173279] 22 p3190 N90-28102
Storage allocation in Ada
[NPL-DITC-156/90] 22 p3235 N90-28343
START: A module for image processing to IMAGE-BASE
[FOA-C-30551-8.3] 22 p3238 N90-28363
Applications of X windows in astronautics: Status and prospects
[MBB-UO-0082-90-PUB] 22 p3238 N90-28365
Improving software reusability by program specialization: A case study
[REPT-90-011] 22 p3240 N90-28374
Target acquisition probability as a function of distance, calculated with PHIND
[IZF-1989-46] 22 p3244 N90-28394
Applications of ripple analysis in hydro-acoustics
[ETN-90-97015] 22 p3244 N90-28397
A computerized data-base system for land-use and land-cover data collected at ground-water sampling sites in the pilot national water-quality assessment program
[PB90-181868] 22 p3258 N90-28453
Nonequilibrium radiation and chemistry models for aerocapture vehicle flowfields
[NASA-CR-186379] 23 p3267 N90-28490
Prediction of subsonic vortex shedding from forebodies with chines
[NASA-CR-4323] 23 p3268 N90-28494
Evolution and use of combined mechanical and thermal codes for cryogenic turbopump bearings 23 p3291 N90-28618
Bearing optimization for SSME HPOTP application 23 p3292 N90-28622
Computer code for the prediction of nozzle admittance 23 p3293 N90-28630
High variable mixture ratio oxygen/hydrogen engine 23 p3295 N90-28640
NASCRAC (trademark): A fracture mechanics analysis code 23 p3296 N90-28645
Comparison of two computer codes for crack growth analysis: NASCRAC versus NASA/FLAGRO 23 p3297 N90-28648
Bandwidth and signal-to-noise ratio enhancement of the NPS transient electromagnetic scattering laboratory
[AD-A224144] 23 p3320 N90-28771
Simulation of INPE's printed circuit laboratory production line
[INPE-4556-TDL/331] 23 p3322 N90-28784
DOE/NIST Workshop on Common Architectures for Robotic Systems
[PB90-216839] 23 p3332 N90-28840
LANZ: Software solving the large sparse symmetric generalized eigenproblem
[NASA-CR-182086] 23 p3340 N90-28876
Computer program for converting rectangular coordinates to latitude-longitude coordinates
[PB90-231796] 23 p3342 N90-28883
A design tool utilizing stoichiometric structure for the analysis of biochemical reaction networks
[AD-A223873] 23 p3355 N90-28961
Control of intelligent robots in space 23 p3365 N90-29013
Modularity in robotic systems 23 p3365 N90-29014
Planning 3-D collision-free paths using spheres 23 p3367 N90-29024
State-based scheduling: An architecture for telescope observation scheduling 23 p3369 N90-29038
Focus of attention in an activity-based scheduler 23 p3369 N90-29039
Planning robot actions under position and shape uncertainty 23 p3376 N90-29073
A computer graphics package
[ARE-TM(UDT)-89111] 23 p3380 N90-29094
Preparing software conversion studies
[PB90-235623] 23 p3381 N90-29099
A stucture dependent software development on a relational basis: An integral approach
[ETN-90-97289] 23 p3381 N90-29101
Inference engine for expert systems
[INPE-4565-PRE/1306] 23 p3382 N90-29104
Product integration rules at Clenshaw-Curtis and related points: A robust implementation
[DE90-627158] 23 p3382 N90-29106
A hardware/software environment to support R/D in intelligent machines and mobile robotic systems
[DE90-014458] 23 p3385 N90-29119
ELEFUNT test results under AST FORTRAN V1.8.0 on the sequent symmetry
[DE90-014932] 23 p3387 N90-29127
Model authoring system for fail safe analysis
[NASA-CR-4317] 23 p3389 N90-29142
Computerized simulation of phenomena in plasma via particles
[INPE-4595-RPE/569] 23 p3397 N90-29194
Data Base Analyzer and Parameter Estimator (DBAPE) interactive computer program user's manual
[PB90-193053] 23 p3406 N90-29252
NASA Marshall Space Flight Center Solar Observatory report, January - June 1990
[NASA-TM-103512] 23 p3409 N90-29268
Comparison of dose estimates using the buildup-factor method and a Baryon transport code (BRYNTRN) with Monte Carlo results
[NASA-TP-3021] 23 p3414 N90-29290
Supersonic/hypersonic aerodynamics and heat transfer for projectile design using viscous-inviscid interaction
[AD-A224354] 24 p3418 N90-29303
A package for 3-D unstructured grid generation, finite-element flow solution and flow field visualization
[NASA-CR-182090] 24 p3419 N90-29309
Integration of GPS and strapdown inertial subsystems into a single unit 24 p3423 N90-29340
Applications of differential GPS 24 p3425 N90-29349
Inertial navigation system simulator program: Top-level design
[AD-A223762] 24 p3431 N90-29379
WingDesign: Program for the structural design of a wing cross-section
[LR-627] 24 p3433 N90-29390
Generalized Advanced Propeller Analysis System (GAPAS). Volume 2: Computer program user manual
[NASA-CR-185277] 24 p3434 N90-29394
Structural testing and analytical research of turbine components
[AD-A223516] 24 p3434 N90-29396
The function of the Interactive Model Assembly Program (IMAP) for a flight simulator
[NAL-TR-1034] 24 p3437 N90-29412
Satellite Constellation Orbit Evaluation (SCORE) program
[AD-A223531] 24 p3438 N90-29417
AutoPAVER: A software package for automated pavement evaluation
[AD-A224176] 24 p3458 N90-29531
Sounder update and field strength software modifications for Special Operations Radio Frequency Management System (SORFMS). Volume 1: Program descriptions and testing
[AD-A224510] 24 p3460 N90-29543
The f2 dominance of the energy-momentum tensor
[DE90-508027] 24 p3460 N90-29544
High range resolution radar cross-section profiles: A preliminary analysis
[AD-A223448] 24 p3461 N90-29550
Specification for a standard electromagnetic propagation model
[AD-A223556] 24 p3461 N90-29551
CAD models for inductive strips in homogeneous finline: The methodology
[AD-A224446] 24 p3463 N90-29564
Utilization of a measurement process by the examination of universal motors
[ETN-90-97307] 24 p3466 N90-29581
Buckling of anisotropic cylindrical shells subjected to combined axial compression, normal pressure, bending and shear loading
[LR-611] 24 p3482 N90-29678
Effects of energy, momentum and particle transport in the near-earth solar terrestrial system
[AD-A224393] 24 p3490 N90-29726
Studies of ionospheric dynamics utilizing data from DMSP
[AD-A223370] 24 p3492 N90-29733
Frequency and ventilation: A survey of theoretical and experimental ventilation modelling
[LR-625] 24 p3498 N90-29772
Autonomous sensor-based dual-arm satellite grappling 24 p3504 N90-29809
THREAD: A programming environment for interactive planning-level robotics applications 24 p3505 N90-29810
Requirements for implementing real-time control functional modules on a hierarchical parallel pipelined system 24 p3518 N90-29891
A collision avoidance system for a spaceplane manipulator arm 24 p3521 N90-29903
Realtime multi-plot graphics system
[NASA-CR-4304] 24 p3523 N90-29919
Issues in expanding the software base management system supporting the Computer Aided Prototyping System (CAPS)
[AD-A224344] 24 p3525 N90-29933
The effect of software reusability on information theory based software metrics
[AD-A224472] 24 p3526 N90-29936

Formal verification of mathematical software, volume 2
[AD-A223633] 24 p3527 N90-29943
MacRootLocus: A CAD design tool for feedback control systems
[AD-A223772] 24 p3528 N90-29951
Software development: A product life-cycle perspective
[AD-A223783] 24 p3528 N90-29952
Developing tools for performance visualization of parallel algorithms
[DE90-015801] 24 p3530 N90-29960
Directing an animated scene with autonomous actors
[REPT-89-041] 24 p3531 N90-29972
An analysis of the distinction between deep and shallow expert systems
[AD-A224443] 24 p3534 N90-29987
Unstructured mesh relaxation
[DE90-015614] 24 p3534 N90-29989
Investigation of the application in the simulation program 'PSpice' of the Jiles-Atherton model for nonlinear magnetic materials in order to predict the degaussing of magnets
[LINO-1990-1] 24 p3541 N90-30029
Establishment of a capability to measure optical transition radiation
[AD-A224094] 24 p3545 N90-30047
Beam and plasma physics research
[AD-A224452] 24 p3548 N90-30067
Compact toroid research
[DE90-016123] 24 p3550 N90-30087
Theory of electronic states and formations energies of defect complexes, interstitial defects, and crystal growth in semiconductors
[AD-A224069] 24 p3551 N90-30093
Analysis and synthesis of robust data structures
[AD-A224568] 24 p3558 N90-30131

COMPUTER SECURITY
U COMPUTER INFORMATION SECURITY

COMPUTER SIMULATION
U COMPUTERIZED SIMULATION

COMPUTER STORAGE DEVICES
NT ACCUMULATORS (COMPUTERS)
NT BUFFER STORAGE
NT COMPUTER COMPATIBLE TAPES
NT MAGNETIC CORES
NT MAGNETIC DISKS
NT MAGNETIC TAPES
NT OPTICAL DISKS
NT RANDOM ACCESS MEMORY
NT READ-ONLY MEMORY DEVICES
NT REGISTERS (COMPUTERS)

Shared memory versus message passing architectures: An application based study
[AD-A210312] 01 p0108 N90-10615
Exploring the benefits of multiple hardware contexts in a multiprocessor architecture: Preliminary results
[AD-A210349] 01 p0108 N90-10616
Evaluating the performance of software cache coherence
[AD-A211164] 02 p0259 N90-11468
Sequential searching in multidimensional monotone arrays
[AD-A211938] 03 p0384 N90-12188
Optical computing based on the Hopfield model for neural networks
[AD-A211824] 03 p0389 N90-12216
Thin film magnetic memory elements
[AD-D014178] 03 p0398 N90-12281
An image compression algorithm for a high-resolution digital still camera
[NASA-CR-185079] 06 p0780 N90-14532
New devices using ferroelectric thin films
[DE90-000789] 07 p0921 N90-15328
Temporal, processor, and spatial locality in multiprocessor memory references
[AD-A213790] 07 p0969 N90-15598
Adaptive backoff synchronization techniques
[AD-A213966] 07 p0980 N90-15658
Bounded polynomial randomized consensus
[AD-A213808] 07 p0984 N90-15686
On the geometry of a general three-camera headmounted system
[AD-A214790] 09 p1225 N90-17108
Communication-efficient arbitration models for low-resolution data flow computing
[AD-A214768] 09 p1262 N90-17319
Carbon doping of compound semiconductor epitaxial layers using carbon tetrachloride
[AD-A215053] 09 p1290 N90-17477
CHIMERA 2: A real-time UNIX-compatible multiprocessor operating system for sensor-based control applications
[AD-A215958] 10 p1392 N90-18051
Cache for multi-threaded processors on a split-transaction bus
[AD-A216404] 10 p1415 N90-18156
Modeling A circuit switched multiprocessor interconnect
[AD-A217122] 12 p1656 N90-19519
Role of cognitive factors in the acquisition of cognitive skill
[AD-A218069] 13 p1854 N90-20642
(DURIP) Two-Processor Alliant FX/4 System
[AD-A217810] 13 p1864 N90-20692
The HS6000/20 development system
[LINO-1989-6] 13 p1865 N90-20696
A Locality-based multiprocessor cache interference model
[AD-A217126] 13 p1871 N90-20730
The Livermore distributed storage system: Implementation and experiences
[DE90-007257] 13 p1872 N90-20735
An investigation of the locality of memory accesses during symbolic program execution
[AD-A218168] 13 p1875 N90-20750
CAMAC memory module: MEMO-32
[DE90-759846] 14 p2012 N90-21528
Quadratic Hadamard Memories 1
[AD-A217224] 14 p2013 N90-21534
Two-dimensional shape recognition using sparse distributed memory 15 p2140 N90-22227
Sparse distributed memory overview
15 p2141 N90-22235
Understanding the computing system domain of advanced computing with microcomputers
[DE90-009825] 15 p2145 N90-22251
Object orientated simulation on transputer arrays using time warp
[AD-A219795] 17 p2389 N90-23607
Memory-based expert systems
[AD-A219875] 17 p2440 N90-23907
A modified fast Fourier transform
[AD-A220567] 17 p2457 N90-24023
Implementation of an I-structure memory controller
[AD-A221397] 18 p2588 N90-24726
Recent experiences and future expectations in data storage technology
[DE90-011488] 18 p2589 N90-24729
Storing line segments in partition trees
[RUU-CS-89-17] 18 p2601 N90-24811
A survey of concurrent readers and writers
[CWI-CS-R8936] 19 p2741 N90-25581
High speed magneto-resistive random access memory
[NASA-CASE-NPO-17954-1-CU] 20 p2904 N90-26519
Atomic snapshots of shared memory
[AD-A222765] 20 p2904 N90-26520
Single-pass memory system evaluation for multiprogramming workloads
[NASA-CR-186553] 20 p2910 N90-26558
Two-dimensional signal processing and storage, and theory and applications of electromagnetic measurements
[AD-A222984] 21 p2995 N90-27022
Modification of a cam facility
[AD-A221828] 21 p3056 N90-27376
Parallel performance of domain-decomposed preconditioned Krylov methods for PDEs with adaptive refinement
[AD-A222339] 21 p3064 N90-27420
Bloch-line memory element and RAM memory
[AD-D014488] 22 p3234 N90-28340
Storage allocation in Ada
[NPL-DITC-156/90] 22 p3235 N90-28343
Reliability analysis/assessment of advanced technologies
[AD-A223647] 24 p3485 N90-29573
Attention, imagery, and memory: A neuromagnetic investigation
[AD-A224560] 24 p3499 N90-29775
A high-speed KDL-RAM file system for parallel computers
[AD-A223299] 24 p3533 N90-29979

COMPUTER SYSTEMS DESIGN
Performance evaluation of the Scheme86 and HP precision architectures
[AD-A209418] 01 p0102 N90-10578
The development of an expert system for the creative design of mechanisms
[AD-A211115] 01 p0110 N90-10628
Independent Orbiter Assessment (IOA): Assessment of the data processing system FMEA/CIL
[NASA-CR-185546] 02 p0162 N90-10917
Evaluating the performance of software cache coherence
[AD-A211164] 02 p0259 N90-11468
A verification exercise relating to specification styles in LOTOS
[MEMO-INF-89-18] 02 p0259 N90-11471
Basic program for raster scan display unit
[NAL-TM-560] 03 p0384 N90-12185
On the design and implementation of a secure computer system
[RSRE-MEMO-4188] 03 p0385 N90-12189
Adoption of software engineering innovations in organizations
[AD-A211573] 03 p0387 N90-12206
Detailed description of the knowledge-based system for physical database design, volume 2
[PB89-229033] 03 p0417 N90-12395
State of the art of human/machine dialog tool prototypes
[TELECOM-PARIS-89-H001] 04 p0527 N90-13038
NAUTILE: A physical design environment based on an object-oriented data manager
[IMAG-RR-737-I] 04 p0535 N90-13094
A compilation strategy for numerical programs based on partial evaluation
[AD-A212759] 04 p0546 N90-13175
A knowledge-based system design/information tool for aircraft flight control systems
[NASA-TM-101704] 05 p0685 N90-13990
Reuse research plans at Langley Research Center
06 p0825 N90-14797
Continuation of research in software for space operations support
[NASA-CR-186092] 06 p0827 N90-14808
The design of a computer system for image simulation and image processing of high resolution electron micrographs
[DE90-000179] 06 p0829 N90-14820
Understanding developments in computer technology: A pragmatic and synthetic interpretation
07 p0971 N90-15608
Elicitation of natural language representations of uncertainty using computer technology
[DE90-001416] 07 p0972 N90-15611
The Suprenum architecture and its application to computational fluid dynamics
[GMD-389] 08 p1085 N90-16161
Dynamic architecture computer
[AD-A214262] 08 p1106 N90-16402
UNIX internals. Part 1: Intertask communication in UNIX. Part 2: UNIX file system
[CNES-NT-122-PT-1/2] 08 p1107 N90-16405
Creating the next generation control system software
[DE90-003391] 08 p1109 N90-16419
A circuit extraction system and graphical display for VLSI (Very Large Scale Integrated) design
[AD-A215668] 09 p1214 N90-17038
Access to multiple underlying systems in Janus
[AD-A214585] 09 p1264 N90-17329
Database creation and/or reorganization over multiple database backends
[AD-A214939] 09 p1296 N90-17513
Optical shared memory
[AD-A215090] 10 p1430 N90-18249
Local area network with fault-checking, priorities, and redundant backup
[NASA-CASE-NPO-16949-1-CU] 12 p1703 N90-19776
Development of computer software for the analysis and design of modern control systems
[AD-A217924] 13 p1868 N90-20717
System testing of a production Ada (trademark) project: The GRODY study
[NASA-TM-103308] 14 p2014 N90-21541
Evolution of Ada technology in the flight dynamics area: Design phase analysis
[NASA-TM-103307] 14 p2014 N90-21542
Resource Allocation Planning Helper (RALPH): Lessons learned 15 p2152 N90-22296
The role of artificial intelligence techniques in scheduling systems 15 p2152 N90-22297
Evaluation of a proposed expert system development methodology: Two case studies
15 p2157 N90-22320
Applications to the aerospace and defense R and D community: The DOD computer-aided acquisition and logistics support (CALS) initiative
15 p2179 N90-22453
Six-degree-of-freedom missile simulation using the ADI AD 100 digital computer and ADSIM simulation language
16 p2294 N90-23068
Concurrent computing: Numerical algorithms and some applications
[AD-A216570] 16 p2300 N90-23103
The Durra application debugger/monitor
[AD-A219290] 16 p2301 N90-23111
Interconnection networks for highly parallel supercomputing architectures
[REPT-89-053] 16 p2302 N90-23118
Control of randomly sampled robotic systems
[AD-A218948] 16 p2309 N90-23157
A model of a path expression based operating system shell
[MEMO-INF-89-71] 17 p2440 N90-23906

Tool support for VDM
[REPT-89-81] 17 p2445 N90-23938
Some elementary questions on software quality control
[REPT-89-83] 17 p2445 N90-23939
Concurrent Clean
[TR-89-18] 17 p2450 N90-23974
The wakeup problem
[AD-A220534] 17 p2451 N90-23981
Space operations: NASA efforts to develop and deploy advanced spacecraft computers. Report to the Chairman, Subcommittee on Space Science and Applications, Committee on Science, Space, and Technology, House of Representatives
[GAO/IMTEC-89-17] 19 p2742 N90-25582
A research program in computer technology
[AD-A221184] 19 p2746 N90-25606
Prototyping an in-house business intelligence database
[PNR90665] 20 p2937 N90-26709
Disconnected actions: An asynchronous extension to a nested atomic action system
[AD-A221937] 21 p3053 N90-27356
CSRD parallel service machine enhancement
[AD-A221951] 21 p3058 N90-27388
Optics and symbolic computing
[AD-A221443] 21 p3077 N90-27493
The EFA integrated monitoring and recording system: Requirements and concept for implementation
22 p3103 N90-27620
AIMS test and simulation equipment
22 p3104 N90-27623
Knowledge based diagnosis of jet engines under consideration of model based methods
22 p3105 N90-27631
On line diagnostics of rotating machinery using expert system technology 22 p3105 N90-27632
New features of JAL's ground station
22 p3105 N90-27633
Flight data replay and analysis system
22 p3105 N90-27635
Daily flight operation monitoring in JAL
22 p3105 N90-27636
Documenting the decision structure in software development
[NASA-CR-186865] 23 p3382 N90-29108
Realtime multi-plot graphics system
[NASA-CR-4304] 24 p3523 N90-29919
Reliable communication in the presence of failures
[NASA-CR-183046] 24 p3533 N90-29977
Asynchronous design for parallel processing architectures
[AD-A223754] 24 p3533 N90-29981
Accessing network databases via SQL transactions in a multi-model database system
[AD-A223946] 24 p3557 N90-30128

COMPUTER SYSTEMS PERFORMANCE

Generic system components of the Thiokol ultrasonic RSRM case-to-insulation bondline inspection system
[NASA-CR-183738] 01 p0031 N90-10171
Performance evaluation of the Scheme86 and HP precision architectures
[AD-A209418] 01 p0102 N90-10578
Evaluation of computer-aided software engineering tools for data base development
[DE89-014007] 01 p0104 N90-10591
Computer availability impact on the archiving of scientific and technical reports
[AD-A210283] 01 p0136 N90-10787
Independent Orbiter Assessment (IOA): Assessment of the data processing system FMEA/CIL
[NASA-CR-185546] 02 p0162 N90-10917
The 3-D heat transfer computer calculations of th e performance of the IAEA's air-bath calorimeters
[DE89-016908] 02 p0224 N90-11283
Evaluating the performance of software cache coherence
[AD-A211164] 02 p0259 N90-11468
LINPACK routines based on the level 2 BLAS
[CWI-NM-R8811] 02 p0261 N90-11483
Software package for 3-dimensional graphic display unit
[NAL-TM-559] 03 p0385 N90-12191
Processing rate sensitivities of a heterogeneous multiprocessor
[PB89-229017] 03 p0387 N90-12201
A unified framework for simulating Markovian models of highly dependable systems
[AD-A212164] 03 p0396 N90-12267
Detailed description of the knowledge-based system for physical database design, volume 2
[PB89-229033] 03 p0417 N90-12395
The computer age and traditional approximate, analytical methods 04 p0483 N90-12772
Specification of Viper2 in Z
[RSRE-MEMO-4217] 04 p0490 N90-12819
An expert system for VM performance analysis
[REPT-89-30] 04 p0528 N90-13045
Performance evaluations of a parallel and expandable database computer: The multi-backend database computer
[AD-A212761] 04 p0528 N90-13046
Software Engineering Exercise (SEE) guidelines
[AD-A212510] 04 p0534 N90-13085
Extended performability modeling using dynamic queing networks
[MEMO-INF-89-15] 04 p0536 N90-13099
A compilation strategy for numerical programs based on partial evaluation
[AD-A212759] 04 p0546 N90-13175
Efficient methods for integrated structural-aerodynamic wing optimum design 05 p0579 N90-13376
The role of the host in a cooperating mainframe and workstation environment, volumes 1 and 2
[NASA-CR-185463-VOL-1/2] 05 p0602 N90-13496
Efficient on-line simulations of tree machines and multidimensional turing machines by random access machines
[AD-A213152] 05 p0680 N90-13960
Parallelism in the discrete-event simulation algorithm
[AD-A213060] 05 p0682 N90-13970
Monotonicity of performance measures in a processor sharing queue
[CWI-BS-R8902] 05 p0689 N90-14019
MIPs and BIPs are megaflops: Limits of unidimensional assessments
[DE89-015707] 06 p0820 N90-14770
High performance parallel architectures
[DE90-001055] 06 p0823 N90-14782
Coordination of processing elements in a multiprocessor computer
[WO-PATENT-88/04075] 06 p0831 N90-14830
Multiple crossbar network: Integrated supercomputing framework
[DE89-012614] 06 p0831 N90-14831
Integrated approach fault tolerance-current state and future requirements
[AD-A214402] 07 p0944 N90-15465
LLNL's plan for a prototype circuit switch, a potential gigabit LAN of the future
[DE90-003614] 07 p0969 N90-15597
Temporal, processor, and spatial locality in multiprocessor memory references
[AD-A213790] 07 p0969 N90-15598
ARGOS (A Research GMMP Operating System): Overvie w and interfaces
[AD-A213871] 07 p0970 N90-15599
Simulating the scheduling of parallel supercomputer applications
[DE90-003604] 07 p0979 N90-15655
One-class generalization in second-order backpropagation networks for image classification
[DE89-015845] 07 p0980 N90-15661
Alternative representations for database responses
07 p1009 N90-15847
Dynamic architecture computer
[AD-A214262] 08 p1106 N90-16402
UNIX internals. Part 1: Intertask communication in UNIX. Part 2: UNIX file system
[CNES-NT-122-PT-1/2] 08 p1107 N90-16405
A 3-D measurement system using object-oriented FORTH
[DE90-003393] 08 p1109 N90-16420
The NODEN hardware description language
[RSRE-89011] 08 p1111 N90-16431
The algebra of the NODEN analyser
[RSRE-89012] 08 p1111 N90-16432
Low-cost volumetric modeling
[CRIF-MC-85] 08 p1111 N90-16435
Computer aided design based optical system modeling
[DE90-003453] 08 p1112 N90-16440
Solving time harmonic wave problems on vector processors
[DE90-003956] 08 p1119 N90-16480
New optimization techniques in database access and maintenance 08 p1137 N90-16586
Event-join optimization in temporal relational databases
[DE90-003117] 08 p1137 N90-16588
Performance characterization of the Convex C-240 computer system
[DE90-006425] 11 p1543 N90-18879
Computer viruses and related threats: A management guide
[PB90-111683] 11 p1543 N90-18881
A survey of performability modelling tools
[MEMO-INF-89-50] 11 p1547 N90-18907
Parallelizing the SDI ACCESS algorithm for the Connection Machine-2
[DE90-006382] 11 p1548 N90-18909
Using dynamic queueing networks as a tool for specifying performability models
[MEMO-INF-89-51] 11 p1554 N90-18949
Using Rexx to coordinate relational commands
[DE90-007589] 12 p1702 N90-19772
Express cubes: Improving the performance of k-ary n-cube interconnection networks
[AD-A217117] 13 p1793 N90-20287
Almost-optimum parallel speed-ups of algorithms for bipartite matching and related problems
[AD-A215111] 13 p1871 N90-20728
An investigation of the locality of memory accesses during symbolic program execution
[AD-A218168] 13 p1875 N90-20750
Selective automatic fire extinguisher for computers (SAFECOMP): Developmental test and evaluation/initial operational test and evaluation
[AD-A217790] 14 p1958 N90-21212
Strategies for concurrent processing of complex algorithms in data driven architectures
[NASA-CR-186515] 14 p2013 N90-21535
System testing of a production Ada (trademark) project: The GRODY study
[NASA-TM-103308] 14 p2014 N90-21541
Extremely high data-rate, reliable network systems research
[NASA-CR-186359] 15 p2149 N90-22278
Performance of gigabit FDDI
15 p2150 N90-22283
Distributed simulation of network protocols
15 p2150 N90-22284
A carrier sensed multiple access protocol for high data base rate ring networks 15 p2151 N90-22288
NASA ground terminal communication equipment automated fault isolation expert systems
15 p2154 N90-22305
Simulation-based reasoning about the physical propagation of fault effects 15 p2155 N90-22309
Evaluation of a proposed expert system development methodology: Two case studies
15 p2157 N90-22320
Inertial navigation system simulator: Behavioral specification, revision
[AD-A219294] 16 p2199 N90-22554
The preprocessed doacross loop
[NASA-CR-182056] 16 p2276 N90-22972
Communication overhead on the Intel iPSC-860 hypercube
[NASA-CR-182055] 16 p2278 N90-22982
Implementation of generalized optimality criteria in a multidisciplinary environment 16 p2290 N90-23048
Comparative evaluations of four specification methods for real-time systems
[AD-A219187] 16 p2300 N90-23109
BTOS database evaluation
[AD-A219304] 16 p2328 N90-23271
Software techniques for non-von Neumann architectures
[AD-A220390] 17 p2440 N90-23902
Hartstone: Synthetic benchmark requirements for hard real-time applications
[AD-A219326] 17 p2442 N90-23917
Testing of elementary functions in Ada
[CWI-NM-R8909] 17 p2446 N90-23941
Improving upon standard pattern classification algorithms by implementing them as multi-layer perceptrons
[AD-A220046] 17 p2447 N90-23954
A formal approach to conformance testing
[MEMO-INF-89-45] 17 p2449 N90-23964
Parallel execution of LISP programs
[AD-A219623] 17 p2451 N90-23978
On a class of N-dimensional associated random walks and the hitting point identity
[CWI-BS-R8911] 17 p2466 N90-24090
IAPSA 2 small-scale system specification
[NASA-CR-182006] 17 p2467 N90-24103
Development of cost-effective standards for Earth observation spacecraft 18 p2501 N90-24292
High performance processing system for embedded control applications in space 18 p2507 N90-24330
ISIS and META projects
[NASA-CR-186624] 18 p2590 N90-24733
On the performance of algorithms for large-scale bound constrained problems
[DE90-010084] 18 p2590 N90-24736
Sensitivity analysis of transputer workfarm topologies
[AD-A219821] 18 p2595 N90-24766
Experiences with the Amoeba distributed operating system
[CWI-CS-R8929] 18 p2596 N90-24770
Amoeba: High performance distributed computing
[CWI-CS-R8937] 18 p2596 N90-24771
SUPES version 2.1: A Software Utilities Package for the Engineering Sciences
[DE90-011763] 20 p2906 N90-26531

Closed-form solution of decomposable stochastic models
[NASA-TM-103466] 20 p2920 N90-26619
A computer for low contest-switch time
[AD-A222883] 21 p3038 N90-27269
Disconnected actions: An asynchronous extension to a nested atomic action system
[AD-A221937] 21 p3053 N90-27356
Zadok user guide
[AD-A222071] 21 p3054 N90-27360
Architectures for optical computing
[AD-A221435] 21 p3054 N90-27364
On parallel hashing and integer sorting
[AD-A221569] 21 p3058 N90-27390
Optics and symbolic computing
[AD-A221443] 21 p3077 N90-27493
An Ada evaluation report for the Verdix Corp. VADS version 5.5 release h compiler
[NPL-DITC-145/89] 22 p3235 N90-28342
Performance of the Intel iPSC/860 hypercube
[DE90-014697] 22 p3235 N90-28346
DSIM: A distributed simulator
[NASA-CR-186880] 22 p3237 N90-28353
Algorithmic components in evaluating systems dependability
[REPT-88-044] 22 p3237 N90-28358
Applications of X windows in astronautics: Status and prospects
[MBB-UO-0082-90-PUB] 22 p3238 N90-28365
Updates and consistency in the LOGRES language
[REPT-90-017] 22 p3239 N90-28369
The effect of multiprocessor radius on scaling
[DE90-014772] 23 p3380 N90-29095
Concepts of concurrent programming
[AD-A223897] 23 p3382 N90-29110
ELEFUNT test results under AST FORTRAN V1.8.0 on the sequent symmetry
[DE90-014932] 23 p3387 N90-29127
Assembler for a parallel computer
[NAL-TM-586] 24 p3532 N90-29974
Supporting large scale applications on networks of workstations
[NASA-CR-186346] 24 p3532 N90-29975
Reliable communication in the presence of failures
[NASA-CR-183046] 24 p3533 N90-29977
An analysis of the distinction between deep and shallow expert systems
[AD-A224443] 24 p3534 N90-29987
Analysis and synthesis of robust data structures
[AD-A224568] 24 p3558 N90-30131

COMPUTER SYSTEMS PROGRAMS
NT ASSEMBLER ROUTINES
NT DISK OPERATING SYSTEM (DOS)
NT INPUT/OUTPUT ROUTINES
NT OPERATING SYSTEMS (COMPUTERS)
NT SUBROUTINE LIBRARIES (COMPUTERS)
NT UNIX (OPERATING SYSTEM)
Flight Test Techniques
[AGARD-CP-452] 02 p0151 N90-10860
Software configuration management: An overview
[PB89-193833] 02 p0258 N90-11458
Software package for 3-dimensional graphic display unit
[NAL-TM-559] 03 p0385 N90-12191
ANDECS-PERLUDE 2.0: A databased, interactive system of control software user's guide
[DFVLR-MITT-89-07] 03 p0418 N90-12404
Truth maintenance systems and their implementation in PROLOG
[MEMO-INF-89-13] 04 p0531 N90-13064
On-board software 05 p0605 N90-13518
Great circle reductions: Implementation and simulations 05 p0611 N90-13569
Implementation and simulations of the sphere solution in FAST 05 p0612 N90-13570
Data simulations in the fast consortium 05 p0612 N90-13573
Data simulations in the NDAC consortium 05 p0612 N90-13574
On the design of a computer-aided design system for digital circuits 05 p0633 N90-13695
JPL reuse program 06 p0825 N90-14795
Control of an experiment to measure acoustic noise in the space shuttle
[NPS62-89-022] 06 p0838 N90-14869
Autonomous land navigation in a structured environment
[DE90-001625] 07 p0878 N90-15087
The NODEN hardware description language
[RSRE-89011] 08 p1111 N90-16431
Parallel logic programming and parallel systems software and hardware
[AD-A214635] 09 p1270 N90-17361
Aurora upgrade. Volume 5: Machine monitoring and control system
[AD-A215963] 10 p1393 N90-18053
A flexible basis for software configuration management
[RSRE-MEMO-4127] 10 p1415 N90-18153
Development of software routines for remote sensing digital image processing
[ETN-90-95452] 12 p1679 N90-19640
Architecture independent environment for developing engineering software on MIMD computers
[NASA-CR-186562] 14 p2016 N90-21553
Software quality assurance: Towards a measurable quality improvement
[REPT-89-42] 15 p2147 N90-22264
An introduction to selected structured methods
[RSRE-MEMO-4294] 15 p2148 N90-22275
Reusing software components by specialization
[REPT-89-062] 16 p2298 N90-23094
Program inversion: More than fun
[CS-8903] 16 p2299 N90-23095
Software techniques for non-von Neumann architectures
[AD-A220390] 17 p2440 N90-23902
TUMULT-64: A real-time multi-processor system
[MEMO-INF-89-58] 17 p2440 N90-23904
A model of a path expression based operating system shell
[MEMO-INF-89-71] 17 p2440 N90-23905
A formal approach to conformance testing
[MEMO-INF-89-45] 17 p2449 N90-23964
On axiomatizations for propositional logics of programs
[RUU-CS-88-34] 17 p2449 N90-23966
Minimum loss scheduling
[MEMO-821] 18 p2600 N90-24796
ICASE semiannual report, April 1 - September 30, 1989
[NASA-CR-181988] 19 p2727 N90-25502
Tools for distributed application management
[NASA-CR-186646] 19 p2762 N90-25692
Knowledge-based systems and NASA's software support environment 21 p3043 N90-27296
Start-up built-in test for the DISCUS fault tolerant, fly-by-wire computer system 22 p3104 N90-27625
Reconfigurable integrated system architecture for future monitoring systems 22 p3106 N90-27638
Development of a COMPAS prototype for the ATC Centre at Frankfurt (Fed. Republic of Germany) 22 p3113 N90-27684
Computational Fluid Dynamics for Industrial Flows
[VKI-LS-1990-04] 22 p3173 N90-28001
POLYFLOW theoretical background 22 p3173 N90-28005
The PHOENICS flow-simulation system 22 p3174 N90-28006
A finite element method for turbulent incompressible flow 22 p3174 N90-28007
FLUENT and FLUENT/BFC CFD computer programs 22 p3174 N90-28008
Development of acceptance plans for airport pavement materials. Volume 1: Development
[DOT/FAA/RD-90/15] 23 p3284 N90-28581
A stucture dependent software development on a relational basis: An integral approach
[ETN-90-97289] 23 p3381 N90-29101
System software for Soviet computers 24 p3523 N90-29921
Communications Interface Driver (CID) software principles of operation
[DOT/FAA/CT-TN89/46] 24 p3526 N90-29937

COMPUTER SYSTEMS SIMULATION
Using computer design and simulation to improve manufacturing productivity
[AD-A210338] 01 p0105 N90-10598
Human Operator Simulator (HOS) 4 user's guide
[AD-A212007] 03 p0310 N90-11763
The comparison of the airbase simulation models airbase and sustained
[FEL-1988-66] 04 p0459 N90-12629
Simulation of synthetic aperture radar 2: Simulating SAR (Synthetic Aperture Radar) using the advanced visual technology system
[AD-A213659] 09 p1204 N90-16976
A distributed kernel for simulation of the VHSIC hardware description language
[AD-A215419] 09 p1213 N90-17032
A satellite simulation program
[AD-A218079] 13 p1764 N90-20124
Assembler for a parallel computer
[NAL-TM-586] 24 p3532 N90-29974

COMPUTER TECHNIQUES
NT COMPUTER AIDED DESIGN
NT COMPUTER AIDED MANUFACTURING
NT COMPUTER AIDED MAPPING
NT COMPUTER AIDED TOMOGRAPHY
NT COMPUTER ANIMATION
NT COMPUTER ASSISTED INSTRUCTION
Relating tolerances and kinematic behavior
[AD-A211125] 01 p0055 N90-10311
General decomposition of sequential machines: Relationships to state assignment
[AD-A208189] 01 p0102 N90-10580
The aerospace energy systems laboratory: Hardware and software implementation
[NASA-TM-101706] 01 p0107 N90-10610
Topographic map reading
[AD-A211269] 02 p0236 N90-11340
Applications of the hybrid automated reliability predictor: Revised edition
[NASA-TP-2760-REV] 02 p0257 N90-11454
Using computer design and simulation to improve manufacturing productivity, report period 1, 2 and 3
[AD-A210255] 02 p0258 N90-11462
Research, development, training and education using the Ada programming language
[AD-A210760] 02 p0259 N90-11466
Preference propagation in temporal/capacity constraint graphs
[AD-A210668] 02 p0264 N90-11506
Effects of the advanced map interpretation and terrain analysis course on contour-level navigation performance
[AD-A212163] 03 p0304 N90-11723
Computer generation of a tutorial dialogue
[AD-A211976] 03 p0380 N90-12162
Design mechanism for interactive graphics mechanism design
[PB89-219513] 03 p0387 N90-12202
Novel techniques for data decomposition and load balancing for parallel processing of vision systems: Implementation and evaluation using a motion estimation system
[NASA-CR-185991] 03 p0389 N90-12214
Some techniques for anaphora resolution in algebraic linguistics
[REPT-89-28] 03 p0396 N90-12265
Computer problems in goodness-of-fit
[AD-A211411] 03 p0397 N90-12268
Calculation of the odd and even integral components of the wave resistance Green's function
[AD-A212384] 04 p0503 N90-12900
Abstract grammars based on transductions
[MEMO-INF-89-7-REV] 04 p0531 N90-13063
Trace theory --- concurrent processing
[MEMO-INF-89-16] 04 p0536 N90-13100
NTRFACE for MAGIC
[AD-A212858] 04 p0538 N90-13112
Recent progress in research pertaining to estimates of gas-side heat transfer in an aircraft gas turbine
[NASA-TM-102460] 05 p0582 N90-13394
Space telescope pointing control 05 p0595 N90-13454
An algorithm for control volume analysis of cryogenic systems
[AD-A213394] 05 p0631 N90-13683
A prototype microprocessor based audiometer for use by the CF (Canadian Forces) medical services for periodic hearing tests
[AD-A212990] 05 p0673 N90-13921
Methodology for automating software systems. Task 1 of the foundations for automating software systems
[NASA-CR-180499] 05 p0681 N90-13965
Computer-aided fabrication system implementation
[AD-A213005] 05 p0682 N90-13969
A fault-tolerant software algorithm for a network of transputers
[AD-A213092] 05 p0682 N90-13972
The DOD Gateway Information System: Operational prototype and transition period 1987-1988
[AD-A213044] 05 p0707 N90-14141
ERIS: Engineering Resource Information System
[AD-A213357] 05 p0707 N90-14144
Vision in dynamic environments
[AD-A213434] 07 p0967 N90-15587
XNUSIM: Graphical interface for a multiprocessor simulator
[AD-A214178] 07 p0971 N90-15606
Name assignment techniques for relational schemas representing extended entity-relationship schemas
[DE90-003269] 07 p0974 N90-15623
Studies of quantitative methods for imaging from scattered fields
[AD-A214047] 07 p0976 N90-15638
Guidelines for evaluating energy analysis software
[AD-A214171] 07 p0976 N90-15640
Polynomial transfer lot sizing techniques for batch processing on consecutive machines
[AD-A214198] 07 p0980 N90-15660
Periodic phase adjustment distributed clock synchronization in the hard realtime environment
[AD-A213842] 07 p0988 N90-15708
Computer-aided boundary delineation of agricultural lands
[NASA-TM-102243] 08 p1091 N90-16313

The development of two-dimensional object identification techniques
[NASA-CR-186203] 08 p1107 N90-16408
An empirical comparison of software fault tolerance and fault elimination
[NASA-CR-186313] 08 p1108 N90-16414
CAE (Computer-Aided Engineering) tools' limitations case study: An SSI (Small Scale Integrated) design to an ASIC (Application Specific Integrated Circuit)
[DE90-002902] 08 p1109 N90-16418
New optimization techniques in database access and maintenance 08 p1137 N90-16586
A technique for the generation of range-height-angle charts
[AD-A214534] 09 p1204 N90-16979
Development of the Kalman filter application and a VHDL model for the AFIT (Air Force Institute of Technology) Floating Point Application Specific Processor (FPASP)
[AD-A215423] 09 p1213 N90-17033
Survey of ERIM approaches applicable to semi-automatic target detection and cueing for multispectral and multisensor exploitation
[AD-A214241] 09 p1258 N90-17296
Feedback effects in computer-based skill learning
[AD-A214560] 09 p1258 N90-17298
SAtool II: An IDEF0 syntax data manipulator and graphics editor
[AD-A215289] 09 p1263 N90-17321
Industrial Modernization Incentives Program: Computer-aided log book
[AD-A214614] 09 p1265 N90-17335
RADC fault tolerant system reliability evaluation facility
[AD-A215298] 09 p1267 N90-17348
Computer-aided fabrication of integrated circuits
[AD-A215439] 09 p1268 N90-17352
Noise and sonic boom impact technology. Initial development of an Assessment System for Aircraft Noise (ASAN). Volume 2: System design strategy
[AD-A214454] 09 p1278 N90-17411
Noise and sonic boom impact technology. Initial development of an Assessment System for Aircraft Noise (ASAN). Volume 3: Technical description
[AD-A214455] 09 p1278 N90-17412
Hybrid optical/digital architecture for distortion invariant pattern recognition
[AD-A215626] 09 p1282 N90-17435
HF wire antennas over real ground: Computer simulation and measurement 10 p1370 N90-17937
Antennas on land vehicles for improved communications 10 p1370 N90-17938
Development of an integrated mobile robot system at Carnegie Mellon University: June 1988
[AD-A215955] 10 p1392 N90-18049
Nonprocedural implementation of mathematical programming algorithms
[AD-A216039] 10 p1419 N90-18179
Structured analysis tool interface to the strategic defense initiative architecture dataflow modeling technique
[AD-A216281] 10 p1424 N90-18218
An analysis of the impacts of computer-based information systems on research and development organizations
[AD-A216283] 10 p1442 N90-18324
Life of concentrated contacts in the mixed EHD and boundary film regimes
[AD-A216673] 11 p1517 N90-18738
Spatial registration of TIROS-N weather satellite data
[AD-A216041] 11 p1536 N90-18841
Appropriateness measurement for computerized adaptive tests
[AD-A216121] 11 p1541 N90-18870
Computerized analysis of hydrogen plasma in a compact H(sup -) cusp source
[DE90-006881] 11 p1569 N90-19029
Multibody modeling and verification
12 p1640 N90-19422
CRISP (Computer Retrieval of Information on Scientific Projects) thesauras, fiscal year 1990
[PB90-138652] 12 p1726 N90-19922
A matrix-free locally-implicit scheme for Navier-Stokes equations
[AD-A216298] 13 p1803 N90-20349
Picosecond nonlinear studies of complex materials using the free electron laser
[AD-A216215] 13 p1809 N90-20387
Approximate evaluation of reliability and related quantities via perturbation techniques
[AD-A216340] 13 p1814 N90-20417
A split-and-merge method for creating polygonal homogeneous-vegetation regions from digitized terrain data
[AD-A216060] 13 p1821 N90-20453
Three-dimensional medical image analysis using local dynamic algorithm selection on a multiple-instruction, multiple-data architecture
[AD-A216024] 13 p1852 N90-20630
Role of cognitive factors in the acquisition of cognitive skill
[AD-A216069] 13 p1854 N90-20642
Multi-tasking computer control of video related equipment 13 p1859 N90-20665
Computer image generation: Reconfigurability as a strategy in high fidelity space applications
13 p1862 N90-20682
A locally constrained parallel activation model for diagnostic reasoning
[AD-A217808] 13 p1874 N90-20747
Institute for Computational Mechanics in Propulsion (ICOMP) fourth annual review, 1989
[NASA-TM-102519] 13 p1878 N90-20769
CALS (Computer-aided Acquisition and Logistic Support) Test Network information exchange user's manual, revision 1
[DE90-008119] 13 p1900 N90-20904
Development of microcomputer-based mental acuity tests for repeated-measures studies
[NASA-CR-185607] 14 p2010 N90-21521
Multigrid on massively parallel computers
[DE90-008999] 14 p2017 N90-21560
The ultimate CASE tool
[DE90-009351] 14 p2037 N90-21687
A study of caching in capability computers
[RSRE-89015] 15 p2149 N90-22276
The role of artificial intelligence techniques in scheduling systems 15 p2152 N90-22297
Polarization coupling in the acousto-optic interaction of surface waves 15 p2164 N90-22365
Electronic Transfer of Information and its Impact on Aerospace and Defence Research and Development
[AGARD-CP-466] 15 p2177 N90-22440
Electronic publishing with Standard Generalized Markup Language (SGML) 15 p2179 N90-22450
Applications to the aerospace and defense R and D community: The DOD computer-aided acquisition and logistics support (CALS) initiative
15 p2179 N90-22453
Electronic transfer of information applications in the Societe Aerospatiale 15 p2179 N90-22454
NASA Information Sciences and Human Factors Program
[NASA-TM-4190] 15 p2194 N90-22529
Synesthetic art through 3-D projection: The requirements of a computer-based supermedium
16 p2274 N90-22962
The automation management to support research and development 16 p2277 N90-22978
Aspects of efficient and reliable multibody system simulation 16 p2279 N90-22991
Using deflation in the pole assignment problem with output feedback 16 p2282 N90-23004
Some ray tracing problems related to circles and ellipses
[AD-A219306] 16 p2318 N90-23217
Laser temperature-jump kinetic studies of fast reactions in nonaqueous solutions
[AD-A218819] 17 p2371 N90-23500
Computer-aided mathematical analysis of probability of intercept for ground-based communication intercept system
[AD-A219856] 17 p2392 N90-23627
FASTER: The Fault Tolerant Architecture Simulation Tool for Evaluating Reliability, introduction and applications
[AD-A219941] 17 p2414 N90-23755
Cumulative reports and publications through December 31, 1989
[NASA-CR-182041] 17 p2439 N90-23898
Generation of expert systems by partial evaluation
[AD-A220427] 17 p2443 N90-23920
OOPS it's happening, part 1
[AD-A220498] 17 p2443 N90-23922
Advanced development environments, continuation
[AD-A220510] 17 p2443 N90-23923
Novel numerical algorithms for sensing, discrimination, and control
[AD-A220805] 17 p2444 N90-23929
A formal approach to conformance testing
[MEMO-INF-89-45] 17 p2449 N90-23964
The wakeup problem
[AD-A220534] 17 p2451 N90-23981
Constraint-oriented specification in a constructive formal description technique
[MEMO-INF-89-44] 17 p2463 N90-24070
On the notion of currying
[MEMO-INF-89-57] 18 p2592 N90-24749
Results of the REALAN project: Replacing the Ethernet access mechanism by the real-time access mechanism of Twentenet
[MEMO-INF-89-55] 18 p2596 N90-24768
Amoeba: High performance distributed computing
[CWI-CS-R8937] 18 p2596 N90-24771
The development of expertise on an intelligent tutoring system 18 p2630 N90-24984
Some issues related to simulation of the tracking and communications computer network
18 p2630 N90-24988
Applying formal models and proofs to the verification of distributed systems
[IAR-89-7] 19 p2750 N90-25625
The incorporation of a multigrid method into the orthogonal curvilinear coordinate version of the Rolls-Royce PACE computer program
[TT-8804] 19 p2751 N90-25627
Research conducted at the Institute for Computer Applications in Science and Engineering in applied mathematics, numerical analysis, and computer science
[NASA-CR-182057] 20 p2903 N90-26510
Computer analysis of chromatographic data
20 p2905 N90-26521
Computer aided handling qualities evaluation in frequency domain
[NAL-TM-SE-8902] 20 p2905 N90-26523
Exact results for the structured liquid-solid interface
[AD-A222762] 20 p2922 N90-26630
Local design methodologies for a hierarchic control architecture
[AD-A222006] 21 p2966 N90-26862
Object oriented fault diagnosis system for space shuttle main engine redlines 21 p3046 N90-27315
Computer assisted analysis and modelling of structured problems
[AD-A222991] 21 p3052 N90-27350
An algorithm for automated surface modelling in unigraphics
[AD-A223219] 21 p3053 N90-27355
Recovery in distributed systems using optimistic message logging and checkpointing
[AD-A222104] 21 p3054 N90-27361
Critical problems in very large scale computer systems
[AD-A221603] 21 p3058 N90-27391
Multiprocessor realization of neural networks
[AD-A222146] 21 p3060 N90-27400
Transparent optimistic rollback recovery
[AD-A222102] 21 p3070 N90-27455
Computer modeling and data processing methods: An essential part of jet engine condition monitoring and fault diagnosis 22 p3104 N90-27626
Basic mechanisms for computer security
[RSRE-89024] 22 p3235 N90-28347
Computer support for conducting supportability trade-offs in a team setting
[AD-A222002] 22 p3237 N90-28355
Numerical analysis
[AD-A221982] 22 p3242 N90-28385
Computerization of Welding Data: Proceedings of the conference and workshop
[PB90-219551] 23 p3332 N90-28841
Computer aided mechanogenesis of skeletal muscle organs from single cells in vitro
[NASA-CR-187025] 23 p3354 N90-28959
Portable Dextrous Force Feedback Master for robot telemanipulation (PDMFF) 23 p3373 N90-29058
A personal computer-based, multitasking data acquisition system
[NASA-TM-4232] 23 p3382 N90-29107
A knowledge-based system design/information tool
[NASA-CR-4316] 23 p3389 N90-29143
Issues in expanding the software base management system supporting the Computer Aided Prototyping System (CAPS)
[AD-A224344] 24 p3525 N90-29933
Tool for studying the effects of range restriction in correlation coefficiant estimation
[AD-A224035] 24 p3537 N90-29996

COMPUTER VIRUSES

Computer viruses and related threats: A management guide
[PB90-111683] 11 p1543 N90-18881
Some comments on techniques for resisting computer viruses
[AD-A221097] 18 p2593 N90-24754

COMPUTER VISION

Knowledge-based machine vision systems for space station automation
[NASA-CR-185710] 01 p0025 N90-10124
Adaptive machine vision
[AD-A208130] 01 p0076 N90-10436
The 1988 year end report for road following at Carnegie-Mellon
[NASA-CR-185967] 01 p0078 N90-10446
The 3D-POLY: A robot vision system for recognizing objects in occluded environments
02 p0229 N90-11313
Three dimensional object recognition employing combined visual and tactile sensing
[PB89-219489] 03 p0382 N90-12176

Parallel implementation and evaluation of motion estimation system algorithms on a distributed memory multiprocessor using knowledge based mappings
[NASA-CR-185984] 03 p0389 N90-12213
Novel techniques for data decomposition and load balancing for parallel processing of vision systems: Implementation and evaluation using a motion estimation system
[NASA-CR-185991] 03 p0389 N90-12214
Parallel architectures and parallel algorithms for integrated vision systems
[NASA-CR-185990] 03 p0389 N90-12215
A survey of camera error sources in machine vision systems
[DE89-014072] 03 p0405 N90-12318
Development of an integrated mobile robot system at CMU (Carnegie-Mellon University)
[AD-A212555] 04 p0510 N90-12944
Parallel and deterministic algorithms from MRF (Markov Random Fields): Surface reconstruction and integration
[AD-A212457] 04 p0533 N90-13084
Research in computer vision for autonomous systems
[AD-A212420] 04 p0555 N90-13235
Resistive fuses: Analog hardware for detecting discontinuities in early vision
[AD-A211891] 05 p0634 N90-13696
Image segmentation for the stereoscopic vision of a mobile robot
[ONERA-RT-1/3692-SY] 05 p0652 N90-13800
An editor for 3D-models for image analysis
[FOA-C-30534-3.4] 05 p0684 N90-13986
Robotic vision system
[AD-D014246] 06 p0832 N90-14838
NETRA: A parallel architecture for integrated vision systems. 1: Architecture and organization
[NASA-CR-185955] 06 p0832 N90-14839
Component presence-absence detection for automated visual inspection of hybrid microcircuits
[KCP-613-4050] 07 p0922 N90-15335
Research in knowledge-based vision techniques for the Autonomous Land Vehicle Program
[AD-A213440] 07 p0942 N90-15453
Vision in dynamic environments
[AD-A213434] 07 p0967 N90-15587
A renormalization group approach to image processing: A new computational method for three-dimensional shapes in robot vision, and the computation complexity of the cooling algorithms
[AD-A214247] 07 p0977 N90-15643
Gaze controls with interactions and delays
[AD-A214286] 07 p0981 N90-15667
Visual Information Processing for Television and Telerobotics
[NASA-CP-3053] 08 p1072 N90-16204
Parallel asynchronous systems and image processing algorithms 08 p1075 N90-16218
A knowledge-based machine vision system for space station automation 08 p1075 N90-16221
Plant features measurements for robotics 08 p1156 N90-16695
Autonomous automatic landing through computer vision 09 p1163 N90-16734
Vision-based navigation and parallel computing
[AD-A214481] 09 p1264 N90-17327
Computer perception of three-dimensional objects
[AD-A215058] 09 p1267 N90-17345
A genetic adaptive system for image understanding and learning research
[AD-A214810] 09 p1271 N90-17367
A vision system for robotic inspection and manipulation
[DE90-005412] 09 p1283 N90-17440
Development of an integrated mobile robot system at Carnegie Mellon University: June 1988
[AD-A215955] 10 p1392 N90-18049
High-Level Vision and Planning Workshop Proceedings
[AD-A215982] 10 p1420 N90-18188
Visual navigation: Constructing and utilizing simple maps of an indoor environment
[AD-A216761] 11 p1455 N90-18382
An approach centered in production rules for a partition of environment and planning in a visual navigation system (SNV)
[INPE-4813-TDL/360] 11 p1517 N90-18737
The computation of color
[AD-A216531] 11 p1548 N90-18914
Flexible automatic discrete parts assembly
[AD-A217401] 13 p1787 N90-20256
A system for analysis and interpretation of lineaments in remote sensing images
[INPE-4893-PRE/1494] 13 p1840 N90-20565
Texture segmentation using localized spatial filtering
[AD-A218064] 13 p1869 N90-20722
Robotic mobility system: Road following algorithms
[AD-A218107] 13 p1874 N90-20748
NETRA: A parallel architecture for integrated vision systems 2: Algorithms and performance evaluation
[NASA-CR-186510] 14 p2017 N90-21557
Vision Science and Technology at NASA: Results of a Workshop
[NASA-TM-102214-REV-1] 15 p2138 N90-22216
Parallel asynchronous hardware implementation of image processing algorithms 15 p2138 N90-22219
Vision science and technology for supervised intelligent space robots 15 p2139 N90-22221
Computation and parallel implementation for early vision 15 p2139 N90-22222
Intensity dependent spread theory 15 p2139 N90-22223
Image gathering, coding, and processing: End-to-end optimization for efficient and robust acquisition of visual information 15 p2139 N90-22224
Hybrid vision activities at NASA Johnson Space Center 15 p2139 N90-22225
Two-dimensional shape recognition using sparse distributed memory 15 p2140 N90-22227
The intensity dependent spread model and color constancy 15 p2140 N90-22228
Algorithms and architectures for robot vision 15 p2141 N90-22236
Computer vision techniques for rotorcraft low altitude flight 15 p2142 N90-22237
Computer vision research at Marshall Space Flight Center 15 p2142 N90-22240
Ames vision group research overview 15 p2143 N90-22242
Space environment robot vision system 15 p2143 N90-22245
Object detection using structural matching
[INPE-4954-PRE/1532] 15 p2159 N90-22333
ALVINN: An Autonomous Land Vehicle In a Neural Nettwork
[AD-A218975] 16 p2243 N90-22797
Optical calculation of correlation filters for a robotic vision system 18 p2630 N90-24986
Mars Rover imaging systems and directional filtering 18 p2648 N90-25071
Telepresence and Space Station Freedom workstation operations 19 p2731 N90-25527
A helmet mounted display to adapt the telerobotic environment to human vision 19 p2737 N90-25555
A topological image matcher
[OUEL-1798/89] 19 p2744 N90-25600
Feasibility study for a microwave-powered ozone sniffer aircraft, volume 2
[NASA-CR-186676] 20 p2806 N90-25967
Development of an integrated mobile robot system at Carnegie-Mellon University
[AD-A222494] 21 p3011 N90-27119
A vision-based telerobotic control station 21 p3046 N90-27311
A programming environment for parallel vision algorithms
[AD-A221486] 21 p3055 N90-27368
ARMTRAK: A domain for the unified study of natural language, planning, and active vision
[AD-A221701] 21 p3056 N90-27373
Parallel algorithms for computer vision
[AD-A221871] 21 p3059 N90-27394
Robotic space simulation integration of vision algorithms into an orbital operations simulation
[NASA-CR-185934] 21 p3059 N90-27395
Collective computation of neural network
[AD-A221848] 21 p3061 N90-27405
Dynamic monocular machine vision and applications of dynamic monocular machine vision
[LRT-WE-13-FB-88-3] 21 p3061 N90-27406
Towards an understanding of camera fixation
[PB90-160342] 22 p3177 N90-28027
Local spatial frequency analysis for computer vision
[NASA-CR-186990] 22 p3237 N90-28356
How do robots take two parts apart 23 p3374 N90-29061
Techniques and potential capabilities of multi-resolutional information (knowledge) processing 23 p3374 N90-29062
Who's who in scientific visualization at LLNL
[DE90-014720] 23 p3379 N90-29091
Computer vision and its potential applications in Brazil
[INPE-4666-NTE/283] 23 p3381 N90-29100
Neural nets and eddy-current testing
[DE90-016044] 24 p3478 N90-29656
The 3D model control of image processing 24 p3503 N90-29800
Weighted feature selection criteria for visual servoing of a telerobot 24 p3503 N90-29801
Trinocular stereovision using figural continuity, dealing with curved objects 24 p3503 N90-29802
A fast 3-D object recognition algorithm for the vision system of a special-purpose dexterous manipulator 24 p3503 N90-29803
Use of 3D vision for fine robot motion 24 p3503 N90-29804
Telerobotic workstation design aid 24 p3504 N90-29805
Space robotic system for proximity operations 24 p3504 N90-29806
Modeling and sensory feedback control for space manipulators 24 p3504 N90-29807
Control strategies for a telerobot 24 p3504 N90-29808
Autonomous sensor-based dual-arm satellite grappling 24 p3504 N90-29809
The 3-D vision system integrated dexterous hand 24 p3511 N90-29850
Assembly of objects with not fully predefined shapes 24 p3513 N90-29859
A comparison of hardware implementations for low-level vision algorithms
[AD-A223699] 24 p3527 N90-29945
Graphic interface for attribute-based data language queries from a personal computer to the multi-lingual, multi-model, multi-backend database system over an Ethernet network
[AD-A223738] 24 p3528 N90-29948

COMPUTERIZED CONTROL
U NUMERICAL CONTROL

COMPUTERIZED DESIGN
U COMPUTER AIDED DESIGN

COMPUTERIZED SIMULATION
NT ANALOG SIMULATION
NT DIGITAL SIMULATION
Validation of missile simulation 01 p0014 N90-10066
Additional software developments wanted for modeling and control of flexible space systems 01 p0017 N90-10083
Flexible structure control experiments using a real-time workstation for computer-aided control engineering 01 p0017 N90-10084
The application of TSIM software to act design and analysis on flexible aircraft 01 p0018 N90-10086
A comparison of software for the modeling and control of flexible systems 01 p0019 N90-10092
Efficiency and capabilities of multi-body simulations 01 p0019 N90-10095
Explicit modeling and computational load distribution for concurrent processing simulation of the space station 01 p0020 N90-10096
Simulation of flexible structures with impact: Experimental validation 01 p0020 N90-10097
Simulation and control problems in elastic robots 01 p0020 N90-10098
Linearized flexibility models in multibody dynamics and control 01 p0020 N90-10099
Simulation of shuttle flight control system structural interaction with RMS deployed payloads 01 p0020 N90-10100
A performance comparison of integration algorithms in simulating flexible structures 01 p0021 N90-10101
Use of the quasilinearization algorithm for the simulation of LSS slewing 01 p0022 N90-10110
Modeling, simulation, and analyses of attitude control for the Crew/Equipment Retriever (CER) proposed for space station
[AD-A208140] 01 p0025 N90-10125
Boost-phase discrimination research activities
[NASA-TM-101889] 01 p0032 N90-10176
Numerical simulation of pressure oscillations in a ramjet combustor 01 p0037 N90-10202
Numerical simulation of unsteady combustion in a dump combustor 01 p0037 N90-10203
Computer simulations of polymer dynamics in the solid state
[DE89-010337] 01 p0048 N90-10275
Statistical modeling of electrical components
[BDX-613-3939] 01 p0059 N90-10336
Numerical simulation of coherent structures in an incompressible mixing layer 01 p0067 N90-10383
Analysis of a model and sequential numerical method for thermal reservoir simulation
[DE89-015117] 01 p0067 N90-10384
Numerical simulation of detonation transfer between gaseous explosive layers
[MRL-RR-1-89] 01 p0069 N90-10395
The role of sensor directed, model based control in robotics
[DE89-014133] 01 p0077 N90-10442
A comparison of wind turbulence simulation models for stochastic loads analysis for horizontal-axis wind turbines
[DE89-009442] 01 p0083 N90-10473
Tracking performance evaluation
[AD-A210499] 01 p0095 N90-10540
On the interactive computer program IPIS for aircraft parameter identification
[NAL-TR-1000] 01 p0103 N90-10586

A low-cost hypercube load-balance algorithm
[DE89-015739] 01 p0104 N90-10589
An introduction to input/output automata
[AD-A210831] 01 p0106 N90-10604
Computational and statistical issues in discrete-event simulation
[AD-A210743] 01 p0116 N90-10668
Assessing the accuracy of vulnerability models by comparison with vulnerability experiments
[AD-A210871] 01 p0116 N90-10669
Generation of 3/2 omega sub o radiation in inhomogeneous plasmas under the irradiation of intense electromagnetic waves
[DE89-015723] 01 p0126 N90-10722
Computer simulation of plasma interactions near Titan
01 p0142 N90-10816
A parallel numerical simulation for supersonic flows using zonal overlapped grids and local time steps for common and distributed memory multiprocessors
[DE89-015252] 02 p0147 N90-10839
A preliminary sensitivity analysis of the Generalized Escape System Simulation (GESS) computer program
[DE89-016891] 02 p0148 N90-10844
Design of a Kalman filter for transfer alignment
02 p0149 N90-10848
Qualification by simulation: Dream or reality
02 p0177 N90-10990
Experimental identification of modal momentum coefficients and modal identity parameters of the FLECS structure 02 p0177 N90-10991
GEMMES: A new tool for dynamic modeling
02 p0179 N90-11005
Calculation of sound transmission through a cylindrical shell using ASKA acoustics 02 p0179 N90-11009
Numerical treatment of the thermo-structural-dynamic problems: The interpolation techniques
02 p0180 N90-11016
Fluid-structure interaction effects in tank structures due to sloshing and hydrodynamic ram: Coupled Lagangian-Eulerian simulations
02 p0181 N90-11022
Modeling of liquid sloshing effects in multibody systems 02 p0181 N90-11023
Nonlinear collapse simulation of anisotropic plates and corrugated panels 02 p0183 N90-11035
Automated stress analysis of Shuttle orbiter thermal protection system 02 p0184 N90-11043
Numerical simulation of micrometeroids and debris hypervelocity impacts on Columbus pressurized modules
02 p0188 N90-11075
ANTHEM simulation of plasma opening switches
[DE89-016617] 02 p0217 N90-11239
Cellular automata and massively parallel physics
[DE89-016506] 02 p0220 N90-11257
Numerical simulation of turbulent flow downstream a sudden axisymmetric expansion
[FOA-C-20758-2.1] 02 p0222 N90-11272
New tools for the simulation and design of calorimeters
[DE89-016323] 02 p0223 N90-11281
A compact X-ray free electron laser
[DE89-017236] 02 p0226 N90-11297
Simulation of the polar cap F region ionization using an experimental convection electric field
02 p0241 N90-11370
Short wavelength striations on expanding plasma clouds
[DE89-016585] 02 p0250 N90-11416
Task analysis of the UH-60 mission and decision rules for developing a UH-60 workload prediction model. Volume 1: Summary report
[AD-A210763] 02 p0255 N90-11446
On algorithms for generating computationally simple piecewise linear classifiers
[NDRE/PUBL-89/1001] 02 p0258 N90-11459
Using computer design and simulation to improve manufacturing productivity, report period 1, 2 and 3
[AD-A210255] 02 p0258 N90-11462
Using PATRAN: From eyeballs to submarines and more
[DE89-016989] 02 p0259 N90-11469
DMC (Distinct Motion Code): A rigid body motion code for determining the interaction of multiple spherical particles
[DE89-016929] 02 p0270 N90-11543
Structure and properties of simple molecular systems at very high density
[DE89-016974] 02 p0273 N90-11557
Simulation of an axially symmetric ion-optical system
[DE89-620129] 02 p0273 N90-11560
Particle simulation in curvilinear coordinate systems
[DE89-016727] 02 p0277 N90-11583
Computer simulations of electromagnetic ion instabilities in the plasma sheet boundary layer
[DE89-016596] 02 p0278 N90-11588
Computer simulation of aircraft aerodynamics
[NASA-TM-102221] 03 p0300 N90-11699
Post crash flight analysis: Visualizing flight recorder data
[AD-A212063] 03 p0302 N90-11715
Numerical simulation of aeroplane response to a lightning injection
[ETN-89-95271] 03 p0303 N90-11716
A simulation study of landing time allocation procedures for use in computer-assisted air traffic management systems
[AD-A212159] 03 p0303 N90-11722
Simulations for computer centerline approach
[DOT/FAA/CT-TN89/41] 03 p0304 N90-11726
STOVL propulsion system volume dynamics approximations
[NASA-TM-102397] 03 p0306 N90-11740
Human Operator Simulator (HOS) 4 user's guide
[AD-A212007] 03 p0310 N90-11763
Program for high speed computation of physical properties of propellants and combustion gas of an LH2/LOX rocket engine
[NAL-TM-564] 03 p0318 N90-11803
Analysis of opposed jet hydrogen-air counter flow diffusion flame
[NASA-CR-182366] 03 p0321 N90-11825
Computer simulations of radiation damage in amorphous solids
[PB89-212682] 03 p0322 N90-11827
Microwave instability near transition energy
[DE90-000107] 03 p0338 N90-11922
Theory and simulation of the operation of a Doppler direction finder in a multipath environment
[FEL-1988-56] 03 p0340 N90-11939
Development of high frequency spice models for ferrite core inductors and transformers
[DE89-015121] 03 p0341 N90-11946
Simulation of glancing shock wave and boundary layer interaction
[NASA-TM-102233] 03 p0345 N90-11970
The dynamic performance of robot manipulators under different operating conditions
[RR-345] 03 p0355 N90-12031
Generation and tooth contact analysis of spiral bevel gears with predesigned parabolic functions of transmission errors
[NASA-CR-4259] 03 p0355 N90-12033
Disturbances in the Arizona Monsoon
03 p0362 N90-12071
Laboratory and theoretical models of planetary-scale instabilities and waves 03 p0363 N90-12076
User's guide for a personal computer model of turbulence at a wind turbine rotor
[DE89-017753] 03 p0366 N90-12095
Development of high resolution simulations of the atmospheric environment using the MASS model
[NASA-CR-186040] 03 p0374 N90-12133
Low-cost three-dimensional stereoscopic display technique for computer-aided design
[DE89-017732] 03 p0386 N90-12196
The conditional-event approach to distributed simulation
[NASA-CR-185890] 03 p0387 N90-12200
ISI's (Information Sciences Institute) SDI architecture simulator: An experiment in adding new software to the system
[AD-A211314] 03 p0387 N90-12204
Fast forward dynamics algorithm for robot arms using multiprocessing
[RR-367] 03 p0391 N90-12225
A unified framework for simulating Markovian models of highly dependable systems
[AD-A212164] 03 p0396 N90-12267
DART: A simulation code for charged particle beams, revision 1
[DE89-016697] 03 p0404 N90-12312
Computer controlled MHD power consolidation and pulse-generation system
[DE89-015600] 03 p0407 N90-12333
Wave particle interactions
[DE89-017527] 03 p0407 N90-12335
Temporal and spatial filtering remedies for dispersion in electromagnetic particle codes
[DE89-017534] 03 p0408 N90-12337
Computer simulations of two-dimensional quasiperiodic crystal and random tiling models
[DE89-016909] 03 p0410 N90-12355
GALAX: A two-dimensional N-body code for disk galaxy dynamics
[PB89-217780] 03 p0420 N90-12415
Development and evaluation at ATCEU of executive and support operations, phase 4A/3D --- ATCEU (Air Traffic Control Evaluation Unit)
[CAA-PAPER-88017] 04 p0449 N90-12572
Route data representation for ATC simulation experiments
[RSRE-MEMO-4133] 04 p0450 N90-12576
RTSIN1: A model of a strapdown INS on a two-axis rate table
[AD-A212406] 04 p0450 N90-12579
Real-time simulation of an F110/STOVL turbofan engine
[NASA-TM-102409] 04 p0457 N90-12618
Analysis and simulation of dynamics of spacecraft power systems 04 p0483 N90-12653
A study of the impact of a ball bearing on a long fiber composite plate with a carbon matrix, part 2
[ETCA-88-R-088-PT-2] 04 p0467 N90-12673
Properties of Lennard-Jones mixtures at various temperatures and energy ratios with a size ratio of two
[PB89-235204] 04 p0471 N90-12697
FLIC (FLame with Implicit Convection): A detailed, two-dimensional flame model
[AD-A212953] 04 p0473 N90-12710
Computer simulation studies of the catalytic oxidation of carbon monoxide on platinum metals
[PB89-223739] 04 p0475 N90-12721
Synthesis and crystallization behavior of fluoride glasses
[AD-A212142] 04 p0478 N90-12741
Ultrastructure processing and characterization of polymers
[AD-A211460] 04 p0478 N90-12743
Simulation of circuits adapted to signal processing
[TELECOM-PARIS-89-E001] 04 p0489 N90-12811
Aircraft SAR simulation Sargen 1.0
[FEL-1989-44] 04 p0491 N90-12823
Description and results of a multihop NACS simulation
[FEL-1988-46] 04 p0491 N90-12824
A 2-MeV microwave thermionic gun
[DE89-015640] 04 p0494 N90-12844
Improved 2D numerical simulation model for strongly coupled heat and fluid flow in a thermal storage
[PB89-218879] 04 p0500 N90-12878
Analysis of high speed pneumatic actuation systems under rotary directional on-off flow control
04 p0507 N90-12926
Mathematical simulation of dynamic compression tests using the Hopkinson bar method
[ISL-R-128/87] 04 p0513 N90-12960
Telerobotic control for teams of semi-autonomous agents, phase 1
[AD-A211648] 04 p0526 N90-13037
ISI's (Information Sciences Institute) SDI architecture simulator: Initial prototype user interface
[AD-A211325] 04 p0529 N90-13053
RTM user's guide
[NASA-CR-186091] 04 p0531 N90-13065
Computer oriented methods of multibody dynamics for application in vehicle technology
[DFVLR-FB-89-17] 04 p0533 N90-13080
Formal calculations and parallelism. Solving linear systems
[ETN-89-95499] 04 p0536 N90-13098
Real-time robot motion: The VLSI implementation via transputers
[RR-364] 04 p0537 N90-13104
LAIOS: A multiprocessor network for artificial intelligence applications
[ETN-89-95498] 04 p0537 N90-13109
Analysis of the non-planar response of a cantilever, with the aid of computerized symbolic manipulation
[AD-A212421] 04 p0545 N90-13172
The process e(-)p giving gamma e(-)p as a fast luminosity for the HERA collider
[NIKHEF-H/88-13] 04 p0553 N90-13223
Particle transport simulation for spaceborne, NaI gamma-ray spectrometers
[AD-A205150] 04 p0564 N90-13292
Evolution of domain walls in the early universe
[NASA-CR-186076] 04 p0565 N90-13297
The S.D.G., P.S.D. and the nonlinear airplane
[NLR-MP-88018-U] 05 p0578 N90-13371
STOVL aircraft simulation for integrated flight and propulsion control research
[NASA-TM-102419] 05 p0581 N90-13389
Mathematical model identification for flight simulation, based on flight and taxi tests
[LR-550] 05 p0585 N90-13410
Explicit modeling and concurrent processing in the simulation of multibody dynamic systems
05 p0599 N90-13481
Control of optical systems 05 p0600 N90-13484
PACOSS program 05 p0601 N90-13487
Mission simulations 05 p0607 N90-13532
The Hipparcos Mission. Prelaunch status. Volume 3: The data reductions
[ESA-SP-1111-VOL-3] 05 p0609 N90-13548
General and numerical approach to the sphere solution in FAST 05 p0610 N90-13555

Photometry: Main mission and Tycho
05 p0610 N90-13560
Great circle reductions: Implementation and simulations 05 p0611 N90-13569
Implementation and simulations of the sphere solution in FAST 05 p0612 N90-13570
Modeling of the Hipparcos optical system
05 p0612 N90-13572
Data simulations in the fast consortium
05 p0612 N90-13573
Data simulations in the NDAC consortium
05 p0612 N90-13574
Experiments towards a global sphere solution
05 p0612 N90-13576
Evaluation of selected computer models for modeling pyrotechnic and propellant devices
[AD-A213003] 05 p0629 N90-13671
Sufficiency and necessity in reliability modeling
[NASA-CR-186119] 05 p0635 N90-13706
A review of quasi-coherent structures in a numerically simulated turbulent boundary layer
[NASA-TM-102191] 05 p0638 N90-13723
Navier-Stokes simulation of the crossflow instability in swept-wing flows
[NASA-CR-186122] 05 p0641 N90-13744
Large eddy simulation of homogeneous turbulence undergoing shear and thermal gradients. Application to one point closing models
[ECL-88-23] 05 p0643 N90-13754
A stochastic model for the calculation of multiple scattered lidar returns
[DLR-FB-89-36] 05 p0648 N90-13778
The effects of gravity waves on horizontal layers: Simulation and interpretation 05 p0660 N90-13852
Methodology for automating software systems. Task 1 of the foundations for automating software systems
[NASA-CR-180499] 05 p0681 N90-13965
The APROS software for process simulation and model development
[VTT-618] 05 p0684 N90-13987
Modeling of power electronic systems with EMTP
[NASA-TM-102375] 05 p0695 N90-14060
Analytical and computer-aided models of InP-based MISFETs and heterojunction devices
[AD-A211861] 05 p0702 N90-14106
Unsteady aerodynamic simulation of multiple bodies in relative motion: A prototype method
[NASA-TM-102181] 06 p0717 N90-14188
An investigation of the bursting of trailing vortices using numerical simulation 06 p0718 N90-14191
RAMSCRAM: A flexible ramjet/scramjet engine simulation program
[NASA-TM-102451] 06 p0726 N90-14235
Temporally and spatially resolved flow in a two-stage axial compressor. Part 2: Computational assessment
[NASA-TM-102273] 06 p0726 N90-14236
Solving the blow-by problem in a two-stage gun
[DE90-000842] 06 p0728 N90-14246
Fluid flow analysis of the SSME high pressure fuel and oxidizer turbine coolant systems
[NASA-CR-183736] 06 p0734 N90-14277
Effects of dislocation substructure and prestrain on fracture behavior in aluminum and steel alloys
06 p0745 N90-14334
Characterization of nanophase materials by x ray diffraction and computer simulation
[DE90-002270] 06 p0752 N90-14378
Weather satellite and computer modeling approaches to assessing propagation over marine environments
06 p0764 N90-14443
A radar simulation program for a 1024-processor hypercube
[DE89-014494] 06 p0766 N90-14455
Testing and performance of a high-gain flux-compression generator
[DE90-002808] 06 p0772 N90-14492
Multigrid solutions of elliptic fluid flow problems
06 p0775 N90-14507
Perturbations in high-velocity gas flow
[DE90-000539] 06 p0777 N90-14520
A new simulation method for the efficient calculation of benchmarks for detonation products equations of state
[DE90-001837] 06 p0777 N90-14522
Pipe and bend erosion by pneumatic transport of solids at high temperature
[DE89-015741] 06 p0778 N90-14524
CTH: A three-dimensional shock wave physics code
[DE89-016529] 06 p0779 N90-14528
Numerical simulation of the preheating by x rays in spherical plasmas 06 p0784 N90-14564
Theoretical studies of solar lasers and converters
[NASA-CR-186194] 06 p0787 N90-14583
Numerical simulation of laser radiation propagation in non-uniform absorbing medium. Geometrical optics approximation
[DE89-632014] 06 p0787 N90-14585
Numerical simulations of free-electron laser oscillators
[DE89-003488] 06 p0788 N90-14588
INEX (Integrated Numerical Experiment) simulations of the Los Alamos HIBAF (High-Brightness Accelerator Free-Electron Laser) free-electron laser MOPA (Master Oscillator Power Amplifier) experiment
[DE90-002387] 06 p0790 N90-14601
Hypervelocity impact calculations using CTH: Case studies
[DE90-002891] 06 p0795 N90-14632
Computer simulation of wind/diesel system operation
[DE89-009445] 06 p0805 N90-14688
The effects of clutter-rejection filtering on estimating weather spectrum parameters
[NASA-CR-186212] 06 p0817 N90-14754
Evaluation of climatic models: Comparison of simulated and observed patterns for past climates
[DE90-001228] 06 p0817 N90-14755
Some edge-enhancing operators and their applications to image enhancement and edge detection
06 p0828 N90-14810
The design of a computer system for image simulation and image processing of high resolution electron micrographs
[DE90-000179] 06 p0829 N90-14820
Solution bias in complex systems modeling
[DE90-002001] 06 p0836 N90-14858
Symmetry breaking bifurcations of a current sheet
[DE90-601005] 06 p0837 N90-14864
Computation of electromagnetic effects in a tokamak due to a plasma disruption
[DE90-001764] 06 p0848 N90-14931
Particle simulations in magnetospheric plasmas
[NASA-CR-186238] 06 p0848 N90-14934
Micro-scale simulation of dynamic compaction of oxide and metal powder mixture
[DE90-002220] 06 p0856 N90-14978
Dynamical simulation of dislocation microstructure
[DE90-003192] 06 p0857 N90-14982
A model of the thermal and electrical properties of cosmic dust particles 06 p0863 N90-15014
Numerical simulation of the unsteady two-dimensional flow in a time-dependent doubly-connected domain
07 p0875 N90-15073
A study of variable geometry in advanced gas turbines
07 p0881 N90-15104
The behavior of matter under nonequilibrium conditions: Fundamental aspects and applications
[DE90-002522] 07 p0892 N90-15157
Interaction of hydrogen in palladium as prescribed by the embedded atom method
[DE90-003893] 07 p0907 N90-15244
More efficient sensitivity testing
[DE90-002639] 07 p0916 N90-15298
High resolution imaging by phase retrieval and discrimination using speckle, volume 1
[AD-A214243] 07 p0919 N90-15317
Single fluid simulations of plasma openings switch behavior
[DE90-002643] 07 p0921 N90-15330
Explicit and implicit calculations of turbulent cavity flows with and without yaw angle
[NASA-CR-186293] 07 p0929 N90-15381
Waveguide effects in superradiant free-electron lasers
[DE90-003605] 07 p0935 N90-15417
Numerical analysis and simulation of frictional particle systems 07 p0937 N90-15430
Hydrodynamics code calculations of debris clouds produced by ball-plate impacts
[DE89-015270] 07 p0939 N90-15439
Comparison of multidimensional calculations of long-rod impacts on oblique plates
[DE89-015275] 07 p0939 N90-15440
Fragmentation statistics from Eulerian hydrocode calculations
[DE90-002906] 07 p0941 N90-15449
Planning systems for autonomous legged vehicles
[AD-A214242] 07 p0942 N90-15458
Beryllium dispersion near explosive firing tables: A comparison of computed and observed results
[DE90-002635] 07 p0960 N90-15550
Antarctic surface temperature and pressure data
[DE90-000971] 07 p0963 N90-15565
Further research on dynamics of marine atmospheres in tropical cyclones
[AD-A213882] 07 p0964 N90-15571
The components of scientific visualization
[DE90-001992] 07 p0972 N90-15614
Knowledge representations for the automatic generation of numerical simulators for PDEs
[DE89-008036] 07 p0972 N90-15615
CryoTran user's manual, version 1.0
[NASA-TM-102468] 07 p0973 N90-15622
A simulation model for dynamic system availability analysis
[AD-A213499] 07 p0974 N90-15628
The StarLite project
[AD-A214193] 07 p0977 N90-15642
Tools for simulation-based training
[AD-A214307] 07 p0978 N90-15648
Simulating the scheduling of parallel supercomputer applications
[DE90-003604] 07 p0979 N90-15655
Optimization of stochastic systems via simulation
[AD-A214011] 07 p0985 N90-15689
Simulation of radial expansion of an electron beam injected into a background plasma
[NASA-CR-186188] 07 p0994 N90-15743
Computer simulation of laser plasma interaction
[DE90-002828] 07 p0994 N90-15748
Theoretical and computational studies of magnetic insulation and other plasma-opening-switch phenomena
[DE90-004421] 07 p0996 N90-15757
Progress in LTE and non-LTE transport calculations
[DE90-003394] 07 p0997 N90-15764
A signal realization data base generated by the multiple phase-screen method
[AD-A214004] 07 p1010 N90-15852
A simple model for the stellar analogy of compact solar flares
[DE90-003215] 07 p1015 N90-15877
Piloted simulation of a ground-based time-control concept for air traffic control
[NASA-TM-101085] 08 p1020 N90-15898
Navigation of autonomous air vehicles by passive imaging sensors 08 p1026 N90-15927
Navigation up-date using radar mapping: Assessment and optimisation simulation tool
08 p1026 N90-15928
Automatic control of KKK: Requirements, sensors, actuators, and control performance results
08 p1029 N90-15944
Probabilistic simulation of uncertainties in composite uniaxial strengths
[NASA-TM-102483] 08 p1040 N90-16008
Multidimensional numerical simulation of large caliber ignition processes
[ISL-CO-233/88] 08 p1042 N90-16021
Fundamental studies of beta phase decomposition modes in titanium alloys
[AD-A214424] 08 p1044 N90-16035
Electroplating simulation
[DE90-003683] 08 p1054 N90-16091
Sizing and selection of batteries for stand-alone photovoltaic systems
[DE90-002990] 08 p1060 N90-16129
Grid-independent wall layer turbulence model for complex flow calculations
[DE90-003500] 08 p1071 N90-16200
On-line estimation of mechanical nonlinearities in compliant two-link robot manipulators
08 p1085 N90-16280
Design of a spheromak compressor driven by high explosives
[DE90-003652] 08 p1086 N90-16283
Element-by-element preconditioning techniques for large-scale, vectorized finite element analysis in nonlinear solid and structural mechanics 08 p1087 N90-16291
Rainflow counting algorithm for the LIFE2 fatigue analysis code
[DE90-002834] 08 p1096 N90-16344
Simulation of pollutant transport using a mesoscale grid circulation model
[GKSS-89/E/24] 08 p1099 N90-16365
A dynamic model for forecasting new cloud development
[AD-A213939] 08 p1102 N90-16383
New atmospheric turbulence model for shuttle applications
[NASA-TM-4168] 08 p1103 N90-16389
Mechanisms of microwave induced damage in biologic materials
[AD-A213480] 08 p1104 N90-16390
Discrete event simulation tool for analysis of qualitative models of continuous processing systems
[NASA-CASE-MSC-21465-1] 08 p1107 N90-16410
FRAC-IN-THE-BOX utilization
[DE90-003648] 08 p1108 N90-16412
Use of computer simulations to analyze limitations of kinetic models for recrystallization
[DE90-003618] 08 p1130 N90-16548
The concept of axial-symmetry constraint and its significance in recrystallization
[DE90-003620] 08 p1131 N90-16549
On the interaction of a pulsar with the ambient medium utilizing x ray images of the Crab nebula
[MPE-215] 08 p1140 N90-16604

Computer simulation of dust grain evolution
08 p1144 N90-16632
Off-line robot programming and graphical verification of path planning 08 p1156 N90-16699
Advances in navigation support systems based on operational pilot's heuristics 09 p1164 N90-16737
SINS1: A model of a strapdown inertial navigation system
[AD-A215495] 09 p1166 N90-16749
The development of a T53-L11 engine computer model
[AD-A214533] 09 p1168 N90-16760
Implementation of adaptive arrays in the block oriented systems simulator
[AD-A215545] 09 p1171 N90-16774
Nuclear weapon radiation effects on a space based interceptor weapon platform
[DE89-016258] 09 p1181 N90-16850
Descriptive simulation: Combining symbolic and numerical methods in the analysis of chemical reaction mechanisms
[AD-A214678] 09 p1190 N90-16898
A study of loaded microstrip antennas and their applications to arrays
[AD-A214857] 09 p1205 N90-16985
Two-dimensional, long-pulse simulation of microwave-induced electron layer evolution in low-pressure air
[DE90-005180] 09 p1208 N90-17004
Rotary absorption heat pump sensitivity analysis
[DE90-002877] 09 p1216 N90-17053
Study for the dissipative structures geometry in three dimensional developed turbulence
[ETN-90-96102] 09 p1219 N90-17072
Improved performance of the Boeing/LANL FEL (Free-Electron Laser) experiment: Extraction efficiency and cavity length detuning effects
[DE90-004872] 09 p1228 N90-17129
Three-dimensional simulation of free-electron laser harmonics with FRED
[DE90-005253] 09 p1229 N90-17130
Traction modeling of military lubricants
[AD-A213866] 09 p1230 N90-17139
Integrated analytical evaluation and optimization of model parameters against preprocessed measurement data
[AD-A215518] 09 p1247 N90-1/231
NASA aerodynamics program
[NASA-TM-4175] 09 p1247 N90-17235
Observing systems simulation experiments: Their role in meteorology
[AD-A215705] 09 p1248 N90-17243
The perceptual buildup of three-dimensional structure from motion
[AD-A214640] 09 p1259 N90-17300
Checklist reading problems in airplanes equipped with speech recognition systems
[ILR-MITT-223(1989)] 09 p1261 N90-17314
A knowledge based approach to program debugging
[AD-A214941] 09 p1266 N90-17344
A model for comparing game theory and artificial intelligence decision making processes
[AD-A215418] 09 p1271 N90-17369
Localization of multiple broadband targets in spherical coordinates via adaptive beamforming and non-linear estimation
[AD-A215714] 09 p1274 N90-17387
Adaptive multiple-band CFAR (Constant-False-Alarm-Rate) detection of an optical pattern with unknown spectral distribution
[AD-A214754] 09 p1281 N90-17429
Infrared target detection: Signal and noise sensitivity analysis
[AD-A215707] 09 p1282 N90-17436
An investigation of application development process controls in an end-user setting: A field study
09 p1295 N90-17504
A current disruption mechanism in the neutral sheet for triggering substorm expansions
[NASA-CR-186260] 09 p1298 N90-17525
Reacting flows 10 p1309 N90-17573
A computer simulation study of a sensor-based heuristic navigation for three-dimensional rough terrain with obstacles
[AD-A215115] 10 p1318 N90-17622
Direct multivariable adaptive controller with application to wing flutter 10 p1322 N90-17642
Design of JT-60U ICRF launcher
[DE90-733145] 10 p1326 N90-17663
Generating optimally evasive MaRV trajectories
[DE90-004496] 10 p1328 N90-17671
Plume flowfield analysis of the shuttle primary Reaction Control System (RCS) rocket engine
[NASA-CR-186315] 10 p1329 N90-17676
The Columbus power system simulation programme
10 p1330 N90-17688
Electrical battery model for LEO application based on absolute instantaneous state of charge
10 p1332 N90-17702
A complete EPC simulation 10 p1337 N90-17741
Computer simulation of electromigration in thin films
[AD-A216382] 10 p1357 N90-17867
Modern Antenna Design Using Computers and Measurement: Application to Antenna Problems of Military Interest
[AGARD-LS-165] 10 p1369 N90-17932
A selective survey of computational electromagnetics for antenna applications 10 p1369 N90-17933
Some applications of model-based parameter estimation in computational electromagnetics
10 p1369 N90-17935
Measurement and computer simulation of antennas on ships and aircraft for results of operational reliability
10 p1369 N90-17936
HF wire antennas over real ground: Computer simulation and measurement 10 p1370 N90-17937
Compact ranges in antenna and RCS measurements
10 p1371 N90-17940
Adaptive processor emulation development
[AD-A214392] 10 p1371 N90-17944
Modeling the response of a monopulse radar to impulsive jamming signals using the Block Oriented System Simulator (BOSS)
[AD-A215560] 10 p1375 N90-17969
On multiple edge diffraction and multiple reflections of microwaves over terrain
[AD-A216418] 10 p1377 N90-17985
A model for evaporation of freely falling droplets
[PUBL-AIR-QUALITY-6] 10 p1384 N90-18007
Numerical simulation of unstably stratified sheared flows
[DE90-005396] 10 p1384 N90-18008
Numerical simulation of compressible vortices
[AD-A216221] 10 p1385 N90-18017
Incompressible flow friction factors in a simulated heat pipe
[AD-A216288] 10 p1386 N90-18018
An Autonomous Platform Simulator (APS)
[AD-A215788] 10 p1392 N90-18048
A 3-D dynamical/chemical GCM for simulating the anthropogenical effects on ozone
[DE90-004836] 10 p1406 N90-18108
Super-micro computer weather prediction model
[AD-A216329] 10 p1409 N90-18124
Writing parallel, discrete-event simulations in ModSim: Insight and experience
[DE90-001833] 10 p1419 N90-18183
Conditions at the downstream boundary for simulations of viscous incompressible flow
[NASA-TM-102510] 10 p1422 N90-18198
Structured analysis tool interface to the strategic defense initiative architecture dataflow modeling technique
[AD-A216281] 10 p1424 N90-18218
Numerical simulation of non-inductive current drive for tokamak plasmas with time-varying electron temperatures
[DE90-733144] 10 p1432 N90-18264
Simulation and quantification of high-resolution Z-contrast imaging of semiconductor interfaces
[DE90-006159] 10 p1438 N90-18297
Binary correlators for optical computing and pattern recognition 10 p1441 N90-18318
Development of free-piston Stirling engine performance and optimization codes based on Martini simulation technique
[NASA-CR-182210] 10 p1443 N90-18326
Research and development of a helium-4 based solar neutrino detector
[DE90-005416] 10 p1447 N90-18353
Delivery performance of conventional aircraft by terminal-area, time-based air traffic control: A real-time simulation evaluation
[NASA-TP-2978] 11 p1454 N90-18378
Numerical simulation of three-dimensional unsteady flows in turbomachines 11 p1461 N90-18417
Autonomous orbit determination using GPS
[INPE-4815-TDL/361] 11 p1466 N90-18442
Cold flow determination of the internal flow environment around the submerged TVC nozzle for the space shuttle SRM 11 p1470 N90-18465
Numerical simulations of coherent structures in a jet flame with a noncircular cross section
[AD-A216710] 11 p1483 N90-18535
The joint effect of surface microtopography and near-surface structure on microcontact conditions
[DE90-006494] 11 p1493 N90-18591
Rate compatible punctured codes, their use in military satellite communication systems
[AD-A216723] 11 p1497 N90-18619
Reliability assessment using finite element techniques
[AD-A216907] 11 p1502 N90-18647
Performance of a 500 watt Nd:GGG zigzag slab oscillator
[DE90-006263] 11 p1503 N90-18657
DANCIR (device and circuit simulator): A three dimensional steady-state semiconductor device simulator
[DE90-006370] 11 p1504 N90-18658
Strong source heat transfer simulations based on a GalerKin/gradient least squares method
[DE90-608613] 11 p1507 N90-18678
Computational and visible light experiments for x ray laser holography
[DE90-006774] 11 p1512 N90-18707
INEX (Integrated Numerical Experiment) simulations of the Boeing FEL system
[DE90-004848] 11 p1513 N90-18712
Fast algorithms for calculating laser wavefront phase compensation given noisy measurements of phase gradient
[DE90-006357] 11 p1515 N90-18727
Earth model selection for computer simulations
[AD-A216843] 11 p1525 N90-18779
Particle simulations in magnetospheric plasmas
[AD-A216256] 11 p1534 N90-18831
Organization of a large-scale cortical network
[AD-A216829] 11 p1540 N90-18863
A scalable multiprocessor architecture using Cartesian network: Relative addressing
[AD-A216580] 11 p1542 N90-18878
L: A language for solution of incremental systems in a parallel processing environment
[INPE-4816-TDL/362] 11 p1543 N90-18884
An integrated vision on methodologies and environments for modeling and simulation assisted by computer
[INPE-4861-TDL/372] 11 p1544 N90-18886
Comparison of two Navy environmental database models: Generalized Digital Environmental Model and Podeszwa sound speed profile model
[AD-A215848] 11 p1544 N90-18889
An interactive system applied to the linear quadratic problem
[INPE-4945-TDL/386] 11 p1548 N90-18913
The lower hybrid drift instability and the evolution of plasma gradients
[DE90-006521] 11 p1568 N90-19021
The interaction of polycrystalline copper films with dilute aqueous solutions of cupric chloride
[AD-A216465] 11 p1569 N90-19033
Hydrodynamical simulations of collisions between interstellar clouds
[DE90-006921] 11 p1590 N90-19172
Aeroservoelasticity
[NASA-TM-102620] 12 p1603 N90-19227
Antennas for 20/30 GHz and beyond
12 p1611 N90-19269
Evaluation and choice algorithms of cost optimal prepreg-application processes: Production of strongly charged plane parts made of fiber reinforced plastics
[ETN-90-95895] 12 p1620 N90-19313
Numerical study of diffusion jet flames
12 p1621 N90-19316
Analytical optical scattering in clouds
12 p1638 N90-19413
Costas loop lock detection in the advanced receiver
12 p1643 N90-19441
Two-dimensional, long-pulse computer calculation of microwave-induced electron layer formation in low-pressure air
[DE90-005994] 12 p1646 N90-19459
Numerical simulation of cross field amplifiers
[DE90-006459] 12 p1652 N90-19496
Laser-matter interaction at intensities of 10(sup 12) W/cm(sup 2) and below
[DE90-007536] 12 p1669 N90-19590
Advanced control schemes and kinematic analysis for a kinematically redundant 7 DOF manipulator
[NASA-CR-186175] 12 p1671 N90-19599
Development and use of an advanced coal-fueled diesel engine cycle simulation with group effects
[DE90-000450] 12 p1672 N90-19607
Comparison of a 6-layer and a 15-layer version of the Chemical Transfer Model (CTM)
12 p1687 N90-19689
Flight crew aiding for recovery from subsystem failures
[NASA-CR-181905] 12 p1696 N90-19741
Theory and applications of belief functions
[AD-A217092] 12 p1702 N90-19774
Parallel neural net path-planner on hypercube and transputer
[DE90-008324] 12 p1703 N90-19777
Electron energy distributions and vibrational population distributions
[DE90-005550] 12 p1711 N90-19825

Molecular theory and computer simulation studies of natural and synthetic gas mixtures
[PB90-130329] 12 p1711 N90-19826
Thermal infrared scene simulation
[DE90-006900] 12 p1714 N90-19845
Supercomputer applications for materials science: Ordering effects of hydrogen in palladium
[DE90-004664] 12 p1718 N90-19870
Computer simulation of recrystallization in the presence of second phase particles
[DE90-007531] 12 p1723 N90-19896
Time-dependent two-dimensional radiation hydrodynamics of accreting matter onto highly magnetized neutron stars
[DE90-006927] 12 p1737 N90-19985
Spectral simulation of unsteady compressible flow past a circular cylinder
[NASA-CR-182030] 13 p1750 N90-20050
Escape systems research at RAE
13 p1751 N90-20058
Design and performance of a multi-stage cylindrical reconnection launcher
[DE90-007820] 13 p1761 N90-20108
Space station Simulation Computer System (SCS) study for NASA/MSFC. Volume 1: Overview and summary
[NASA-CR-183840] 13 p1762 N90-20113
Space station Simulation Computer System (SCS) study for NASA/MSFC. Volume 2: Concept document
[NASA-CR-183841] 13 p1762 N90-20114
Space station Simulation Computer System (SCS) study for NASA/MSFC. Volume 3: Refined conceptual design report
[NASA-CR-183842] 13 p1762 N90-20115
Space station Simulation Computer System (SCS) study for NASA/MSFC. Volume 4: Conceptual design report
[NASA-CR-183843] 13 p1762 N90-20116
Space station Simulation Computer System (SCS) study for NASA/MSFC. Volume 5: Study analysis report
[NASA-CR-183844] 13 p1763 N90-20117
Space station Simulation Computer System (SCS) study for NASA/MSFC. Volume 6: Study issues report
[NASA-CR-183845] 13 p1763 N90-20118
Shaping the insonifying pulse to optimise B-scans obtained in austenite
[AERE-R-13518] 13 p1775 N90-20187
Physical sputtering of metallic systems by charged-particle impact
[DE90-007803] 13 p1777 N90-20201
A unified integrated model for sputter coating uniformity
[DE90-008322] 13 p1778 N90-20205
The thermal response of generic objects in JP-4 pool fires
[DE90-008503] 13 p1788 N90-20259
Advanced modulation technology development for earth station demodulator applications. Coded modulation system development
[NASA-CR-185149] 13 p1789 N90-20270
Simulation of radar scattering from rough surfaces
[AD-A217841] 13 p1790 N90-20275
Analysis of radiometer calibration effects with TOUCHSTONE
[NASA-CR-186476] 13 p1792 N90-20284
The inverse triax x ray diode: An alternate reduced-endpoint-energy bremsstrahlung source
[DE90-006366] 13 p1792 N90-20285
Relativistic klystron afterburner simulation techniques
[DE90-008539] 13 p1796 N90-20305
Fluid dynamics analysis of a rotating axisymmetric part using FIDAP
[DE90-008733] 13 p1802 N90-20340
Amplified spontaneous emission measurements on the aurora large-aperture module
[DE90-004841] 13 p1806 N90-20369
Harmonic generation mechanisms in short-wavelength free-electron lasers
[DE90-007622] 13 p1807 N90-20374
Measurement of the stimulated thermal Rayleigh scattering instability
[DE90-007849] 13 p1807 N90-20376
Laser line transport with refraction
[DE90-008683] 13 p1808 N90-20382
Dynamic damping control: Implementation issues and simulation results
[DE90-007687] 13 p1812 N90-20403
Computer simulation of the mathematical modeling involved in constitutive equation development: Via symbolic computations
[NASA-TM-102532] 13 p1816 N90-20428
Finite element models to predict the structural response of 120-mm sabot/rods during launch
[DE90-007497] 13 p1817 N90-20436
Computer simulations and experiments to study the fracture of rods by flying plates
[DE90-008308] 13 p1817 N90-20437
Controlling Summer Heat Islands: Proceedings
[DE90-008075] 13 p1830 N90-20508
Use of environmental monitoring data in evaluation of atmospheric modeling results
[DE90-008607] 13 p1831 N90-20510
Studies of an orbital gradiometer mission
13 p1839 N90-20558
Analysis of GALE (Genesis of Atlantic Lows Experiment) data
[AD-A217182] 13 p1844 N90-20584
Southern oscillation in the OSU coupled upper ocean/atmosphere GCM
[DE90-008415] 13 p1844 N90-20588
Tools for 3D scientific visualization in computational aerodynamics 13 p1858 N90-20660
Engineering visualization utilizing advanced animation
13 p1859 N90-20664
Broadening the interface bandwidth in simulation based training 13 p1859 N90-20666
Distributed earth model/orbiter simulation
13 p1860 N90-20671
Prototype part task trainer: A remote manipulator system simulator 13 p1860 N90-20672
Graphical programming and the use of simulation for space-based manipulators 13 p1861 N90-20674
Using an instrumented manikin for Space Station Freedom analysis 13 p1861 N90-20675
The development of the Canadian Mobile Servicing System Kinematic Simulation Facility
13 p1861 N90-20676
Software systems for modeling articulated figures
13 p1861 N90-20677
Human task animation from performance models and natural language input 13 p1861 N90-20678
Computational complexity of random access models
[AD-A217685] 13 p1865 N90-20701
Performance of concurrency control algorithms in distributed systems
[AD-A218280] 13 p1870 N90-20727
Implementation of a control system test environment in UNIX
[DE90-007485] 13 p1872 N90-20736
Design of a simulation interface for a parellel computing environment
[DE90-008497] 13 p1873 N90-20737
A parallel architecture for real-time simulation
[AD-A218321] 13 p1873 N90-20741
Dynamics of electronically excited species in gaseous and condensed phase
[AD-A217696] 13 p1884 N90-20812
A new technique for guiding of electron beams
[DE90-008660] 13 p1886 N90-20824
Spontaneous magnetic reconnection in a turbulent plasma 13 p1889 N90-20840
New methods in plasma simulation
[DE90-007507] 13 p1890 N90-20847
M51's spiral structure
[DE90-007624] 13 p1903 N90-20916
Study of possible solar heating effects on thermosonde probes: Error analysis
AD-A218116] 13 p1903 N90-20917
Autonomous integrated GPS/INS navigation experiment for OMV. Phase 1: Feasibility study
[NASA-CR-4267] 14 p1914 N90-20969
Calculation of the three dimensional turbulent flow in a linear turbine blade 14 p1924 N90-21021
The numerical simulation of multistage turbomachinery flows 14 p1925 N90-21025
Controlled multibody dynamics simulation for large space structures 14 p1934 N90-21068
Detection of potential space station control/structure interaction with CO-ST-IN 14 p1935 N90-21074
Computational architecture for integrated controls and structures design 14 p1935 N90-21076
LACE flight dynamics experiment
14 p1937 N90-21086
Filament winding of composite cylinders
14 p1943 N90-21119
Fiber pushout test: A three-dimensional finite element computational simulation
[NASA-TM-102565] 14 p1945 N90-21131
Minutes of the 23rd Explosives Safety Seminar, volume 2
[AD-A218265] 14 p1959 N90-21214
Radar observations of a formation of two fighters: A case study for ISAR imaging 14 p1963 N90-21240
Airborne Doppler radar flight experiments for the detection of microbursts 14 p1963 N90-21243
The development of a simulation program of the anode side for aluminum/air batteries
[PB90-165754] 14 p1970 N90-21286
Phase-only holographic filters and their applications
[PB90-166802] 14 p1984 N90-21368
Computer-aided design of flywheel transmission systems 14 p1988 N90-21392
Problems associated with residual and mismatch stresses in thin film structures 14 p1990 N90-21407
An internal/external pressure, tension/compression multiaxial fatigue system
[DE90-009510] 14 p1994 N90-21430
A time-accurate adaptive grid method and the numerical simulation of a shock-vortex interaction
[NASA-TP-2998] 14 p2011 N90-21524
SR90, strontium shaped-charge critical ionization velocity experiment
[NASA-CR-186501] 14 p2024 N90-21606
Helium transport in plasma edge regions
14 p2027 N90-21625
Design and optimisation of thin foil x ray telescopes
14 p2038 N90-21690
Swept wing ice accretion modeling
[NASA-TM-103114] 15 p2046 N90-21727
Three-dimensional simulation of vortex breakdown
[NASA-TM-102664] 15 p2049 N90-21744
A comparison of time-optimal interception trajectories for the F-8 and F-15
[NASA-CR-186300] 15 p2050 N90-21753
Quiet mode for nonlinear rotor models
[NASA-TM-102236] 15 p2051 N90-21758
Optimal control of an aircraft flying through a downburst 15 p2053 N90-21765
Computational simulation of structural fracture in fiber composites
[NASA-TM-102505] 15 p2064 N90-21821
Progression of damage and fracture in composites under dynamic loading
[NASA-TM-103118] 15 p2065 N90-21825
QPSK carrier-acquisition performance in the advanced receiver 2 15 p2076 N90-21892
UV spectral simulations using LOWTRAN 7
15 p2083 N90-21928
Computer simulation of ionospheric radio frequency heating
[DE90-009478] 15 p2087 N90-21944
Experimental and analytical investigations of granular materials: Shear flow and convective heat transfer
15 p2091 N90-21968
A dual potential formulation of the Navier-Stokes equations 15 p2092 N90-21972
Design and testing of a multiblock grid-generation procedure for aircraft design and research
15 p2094 N90-21984
Generation and adaptation of 3-D unstructured grids for transient problems 15 p2096 N90-21994
Practical nonlinear simulation of rotating machinery dynamics with application to turbine blade rubbing
15 p2104 N90-22038
Lagrangian model simulation of the turbulent transport of evaporating jet droplets 15 p2128 N90-22168
Southern oscillation simulation in coupled ocean/atmosphere global climate models
15 p2131 N90-22181
Frontal structure in a mesoscale model
15 p2132 N90-22187
Molecular dynamics simulations of short-range force systems on 1024-node hypercubes
[DE90-009833] 15 p2146 N90-22259
Inventory of program packages related to the project SIMONA
[ETN-90-96397] 15 p2148 N90-22270
Extremely high data-rate, reliable network systems research
[NASA-CR-186359] 15 p2149 N90-22278
Traffic placement policies for a multi-band network
15 p2149 N90-22279
Distributed simulation, no special tools required
15 p2150 N90-22281
Alternative parallel ring protocols
15 p2150 N90-22282
Distributed simulation of network protocols
15 p2150 N90-22284
Modelling high data rate communication network access protocol 15 p2150 N90-22285
Adaptive control of a flexible manipulator with unknown changing loads 15 p2152 N90-22293
Simulation-based reasoning about the physical propagation of fault effects 15 p2155 N90-22309
An expert system for simulating electric loads aboard Space Station Freedom
[NASA-TM-103150] 15 p2158 N90-22325
Engagement analysis study
[DE90-009529] 15 p2163 N90-22359
Hybrid modeling of plasmas and applications to fusion and space physics 15 p2168 N90-22387
Three-dimensional simulations of simple electron drift wave turbulence in tokamak geometry
[DE90-009581] 15 p2169 N90-22398
Computer simulation of time-dependent spherically symmetric spacetimes containing radiating fluids: Formalism and code tests 15 p2185 N90-22483

A galaxy formation cookbook: Recipes and utensils
15 p2190 N90-22508
Minimum flying qualities. Volume 3: Program CC's implementation of the human optimal control model
[AD-A218562] 16 p2201 N90-22562
Semianalytic study of high-eccentricity orbit stability and evolution 16 p2204 N90-22574
Investigation of atomistic simulation of structural and dynamic differences in glassy and liquid states of atactic poly(propylene)
[AD-A218896] 16 p2224 N90-22687
Using object-oriented analysis techniques to support system testing
[DE90-009540] 16 p2226 N90-22700
HF propagation through actively modified ionospheres
[DE90-008931] 16 p2227 N90-22705
A free electron laser master oscillator power amplifier experiment 16 p2239 N90-22776
Influence of linear profile modification and loading conditions on the dynamic tooth load and stress of high contact ratio gears
[NASA-TM-103136] 16 p2243 N90-22796
Large-scale simulations of monolithic and segmented projectiles impacting spaced armor
[AD-A219374] 16 p2244 N90-22800
Probabilistic structural analysis of aerospace components using NESSUS
[NASA-TM-102324] 16 p2248 N90-22823
Stochastic interactive activation and the effect of context on perception
[AD-A218929] 16 p2262 N90-22898
Learning artificial grammars with competitive chunking
[AD-A219270] 16 p2265 N90-22911
Displays for telemanipulation
16 p2272 N90-22948
A computer graphics system for visualizing spacecraft in orbit 16 p2272 N90-22952
Volumetric visualization of 3D data
16 p2275 N90-22964
Supercomputer and Technology
[NLR-PUB-8801] 16 p2277 N90-22974
Numerical flow simulation and supercomputers: More than a digital wind tunnel 16 p2277 N90-22976
An assessment of multibody simulation tools for articulated spacecraft 16 p2279 N90-22988
An order (n) algorithm for the dynamics simulation of robotic systems 16 p2279 N90-22990
Aspects of efficient and reliable multibody system simulation 16 p2279 N90-22991
Efficient dynamic simulation for multiple chain robotic mechanisms 16 p2280 N90-22995
A robot arm simulation with a shared memory multiprocessor machine 16 p2283 N90-23008
Parallel algorithms and architecture for computation of manipulator forward dynamics 16 p2283 N90-23010
Computational chaos in massively parallel neural networks 16 p2283 N90-23012
Multi-flexible-body dynamics capturing motion-induced stiffness 16 p2284 N90-23013
Nonlinear strain-displacement relations and flexible multibody dynamics 16 p2284 N90-23014
Development of efficient computer program for dynamic simulation of telerobotic manipulation
16 p2284 N90-23017
Explicit modeling of composite plates and beams in the dynamics of multibody systems
16 p2285 N90-23019
Experimental verification of dynamic simulation
16 p2285 N90-23020
Space station dynamics, attitude control and momentum management 16 p2287 N90-23029
Application of numerical optimization techniques to control system design for nonlinear dynamic models of aircraft 16 p2287 N90-23032
Simulation studies using multibody dynamics code DART 16 p2288 N90-23036
Proceedings of the 3rd Annual Conference on Aerospace Computational Control, volume 2
[NASA-CR-186447] 16 p2289 N90-23040
Concurrent processing simulation of the space station
16 p2289 N90-23041
Methodology for analysis and simulation of large multidisciplinary problems 16 p2290 N90-23046
Enhanced modeling features within TREETOPS
16 p2290 N90-23047
ASTEC: Controls analysis for personal computers
16 p2291 N90-23052
Combining high performance simulation, data acquisition, and graphics display computers
16 p2293 N90-23062
Man-in-the-control-loop simulation of manipulators
16 p2293 N90-23063
A new second-order integration algorithm for simulating mechanical dynamic systems 16 p2293 N90-23064
The use of real-time, hardware-in-the-loop simulation in the design and development of the new Hughes HS601 spacecraft attitude control system
16 p2293 N90-23065
Six-degree-of-freedom missile simulation using the ADI AD 100 digital computer and ADSIM simulation language
16 p2294 N90-23068
Real-time closed-loop simulation and upset evaluation of control systems in harsh electromagnetic environments 16 p2294 N90-23069
Faster simulation plots 16 p2295 N90-23071
Component model reduction via the projection and assembly method 16 p2295 N90-23073
Modal identities for multibody elastic spacecraft: An aid to selecting modes for simulation
16 p2296 N90-23075
Structural modeling for control design (articulated multibody component representation)
16 p2296 N90-23077
The power and efficiency of advanced software and parallel processing 16 p2296 N90-23079
Dynamic analysis of flexible mechanical systems using LATDYN 16 p2296 N90-23080
Control design and simulation of systems modeled using ADAMS 16 p2296 N90-23081
Multibody dynamics model building using graphical interfaces 16 p2297 N90-23082
A verification library for multibody simulation software
16 p2298 N90-23089
The (DURIP) computer simulations of plasmas, nonlinear systems, and control theory
[AD-A219070] 16 p2300 N90-23107
Experimental adaptive control of a hydraulic robot
16 p2303 N90-23121
Index and consistency analysis for DAE (Differential Algebraic Equation) systems for Stefan-Maxwell diffusion-reaction problems
[DE90-008188] 16 p2304 N90-23129
Scientific discovery as problem solving
[AD-A218867] 16 p2307 N90-23145
On randomness of random number generators
[MEMO-COSOR-89-20] 16 p2308 N90-23151
A scattering center based numerical simulation of small scale atmospheric turbulence 16 p2312 N90-23179
Theoretical and computer simulation study of the density fluctuations in liquid water
[PREPRINT-697] 16 p2314 N90-23191
VLA and VLBI angular broadening measurements: The distribution of interstellar scattering at low Galactic latitudes 16 p2330 N90-23279
Studies of Io's atmosphere and plasma torus
16 p2338 N90-23326
Simulator evaluation of the final approach spacing tool
[NASA-TM-102807] 17 p2348 N90-23374
Gamma Ray Observatory (GRO) dynamics simulator requirements and mathematical specifications, revision 1
[NASA-CR-183465] 17 p2362 N90-23447
Using simulation to determine a strategy for positively tracking a cruise missile by CMMCA
[AD-A220526] 17 p2362 N90-23448
Simulation and interdisciplinary design methodology for control-structure interaction systems
17 p2385 N90-23584
Nonlinear dynamics and control of flexible structures
[AD-A218372] 17 p2386 N90-23588
Nonlinear dynamics and control of flexible structures
[AD-A218476] 17 p2386 N90-23589
Introducing the VRT gas turbine combustor
[NASA-TM-103176] 17 p2386 N90-23591
Simulation and analysis of a MFQPSK signal transmitted through an acoustic medium
[AD-A220345] 17 p2393 N90-23633
VLSI architectures and CAD
[AD-A220736] 17 p2397 N90-23652
Study and simulation of the behavior of a high frequency transformer
[ECL-89-008] 17 p2399 N90-23667
Three-dimensional convection in cylindrical geometry
17 p2399 N90-23668
Large eddy simulation of a fully turbulent plane channel flow
[VKI-TN-171] 17 p2404 N90-23693
Real-time simulation clock
[NASA-CASE-LAR-14056-1] 17 p2407 N90-23713
Multiwavelength pyrometry to correct for reflected radiation
[NASA-TM-102578] 17 p2407 N90-23714
Numerical simulation of semi-infinite target penetration by continuous and segmented rods
[AD-A219437] 17 p2412 N90-23743
FASTER: The Fault Tolerant Architecture Simulation Tool for Evaluating Reliability, introduction and applications
[AD-A219941] 17 p2414 N90-23755
A day in the life of a warm front
[AD-A220373] 17 p2426 N90-23826
A Kalman filter with smoothing for hurricane tracking and prediction
[AD-A220413] 17 p2426 N90-23827
Analysis of the accuracy of a proposed target motion analysis procedure
[AD-A219481] 17 p2436 N90-23880
The cost of conservative synchronization in parallel discrete event simulations
[NASA-CR-182034] 17 p2441 N90-23912
Distributed object oriented programming
[AD-A219689] 17 p2442 N90-23918
Comparison of selection procedures and validation of criterion used in selection of significant control variates of a simulation model
[AD-A220459] 17 p2443 N90-23921
Comparison of batch means and independent replications techniques to applications of the Kalman filter for simulation output analysis
[AD-A220656] 17 p2444 N90-23925
SPHC (Smooth Particle Hydrodynamics Code) manual
[AD-A220743] 17 p2444 N90-23928
Intelligent, real-time problem solving
[AD-A219929] 17 p2455 N90-24006
Dose analysis of the model 112A Pulserad pulsed x ray generator by its CYLTRAN
[AD-A220372] 17 p2471 N90-24125
Dust environment modelling from encounters with comet P/Halley 17 p2485 N90-24210
Low-density flow effects for hypervelocity vehicles, phase 2
[AD-A221034] 18 p2493 N90-24249
Servicing test facility: A hardware simulator for telerobotic in-orbit servicing 18 p2501 N90-24287
DDTF improvements for more accurate space docking simulation 18 p2504 N90-24311
Docking berthing systems: Functions and simulation
18 p2505 N90-24313
Robotic simulation support to systems development
18 p2505 N90-24315
Equivalent flexibility modeling: A novel approach towards recursive simulation of flexible spacecraft manipulator dynamics 18 p2505 N90-24316
Simulation and ground-based testing of ORU-handling with a bi-arm robot 18 p2505 N90-24317
ROSED: Robotic Servicing Demonstrator
18 p2505 N90-24318
The real-time Hermes robot arm simulator: HSF-P
18 p2506 N90-24319
Effects of X radiation on the LAMPSHADE orbital debris satellite shield, 2
[DE90-008214] 18 p2510 N90-24341
Experiments and other methods for developing expertise with design of experiments in a classroom setting
18 p2516 N90-24367
Metal matrix composites microfracture: Computational simulation
[NASA-TM-103153] 18 p2518 N90-24383
A particle-level numerical simulation of the dynamic consolidation of a metal matrix composite material
[DE90-010950] 18 p2519 N90-24387
Thermodynamic calculations for mixtures of environmentally safe refrigerants using the Lee-Kesler-Ploecker equation of state
[DE90-010493] 18 p2542 N90-24509
Prediction of high-voltage, broadband RF pulse generation from an air gas avalanche switch
[DE90-010183] 18 p2549 N90-24551
Computational modeling of three-dimensional compressible leading edge vortices
[AD-A221022] 18 p2553 N90-24569
A survey of human factors methodologies and models for improving the maintainability design of emerging Army aviation systems
[AD-A221159] 18 p2586 N90-24724
Construction of an Ethernet model with the PROMISE simulation tool
[NLR-MP-88047-U] 18 p2593 N90-24757
CERC (Center for Energy Research Computation) report: Results of the CERC Project with recommendations for ANL (Argonne National Laboratory) institutional strategies in advanced scientific computing
[DE90-008238] 18 p2594 N90-24759
Performance analysis of local area networks
[NASA-CR-186639] 18 p2595 N90-24767
Adaptive control of visually guided grasping in neural networks
[AD-A221387] 18 p2597 N90-24780
X ray optics
[AD-A221218] 18 p2616 N90-24898
Atomic structure of Ag/Ni interfaces
[DE90-010053] 18 p2618 N90-24914
Studies on ion scattering and sputtering processes in ion beam sputter-deposition of high Tc superconducting films: The optimization of deposition parameters
[DE90-010538] 18 p2621 N90-24936

Ensemble Monte Carlo simulation of electron transport in AlGaAs/GaAs heterostructures
[ISBN-90-9003048-4] 18 p2622 N90-24940
Optical calculation of correlation filters for a robotic vision system 18 p2630 N90-24986
Some issues related to simulation of the tracking and communications computer network 18 p2630 N90-24988
Thermodynamic and fluid mechanic analysis of rapid pressurization in a dead-end tube 18 p2631 N90-24990
A comparison of two neural network schemes for navigation 18 p2631 N90-24991
Finite element formulations for compressible flows 18 p2632 N90-24996
A quantitative technique to estimate microburst wind shear hazard to aircraft 18 p2640 N90-25040
Computational simulation of transition to turbulence through inverse modeling 18 p2647 N90-25067
Convex models of malfunction diagnosis in high performance aircraft
[AD-A218514] 19 p2649 N90-25073
Realtime simulation at MBB today and future aspects
[MBB-UA-1134/89-PUB] 19 p2653 N90-25098
Users guide for an Airborne Windshear Doppler Radar Simulation (AWDRS) program
[NASA-CR-182025] 19 p2657 N90-25121
Replication of NASPAC Dallas/Fort Worth study
[DOT/FAA/CT-TN90/26] 19 p2657 N90-25123
Lecture notes on flight simulation techniques
[LR-596] 19 p2662 N90-25153
Development of a computer model to predict platform station keeping requirements in the Gulf of Mexico using remote sensing data
[NASA-CR-186678] 19 p2663 N90-25155
Fingering in 2-D porous media: Experiments, network simulators and statistical models 19 p2691 N90-25308
A simulation code for turbocompound diesel engines
[IAR-89-26] 19 p2697 N90-25348
Snow cover mapping and snowmelt runoff simulations on microcomputers 19 p2707 N90-25408
Neck Injury in Advanced Military Aircraft Environments
[AGARD-CP-471] 19 p2717 N90-25459
Analysis of the biomechanic and ergonomic aspects of the cervical spine under load 19 p2719 N90-25470
Effects of head mounted devices on head-neck dynamic response to +G(sub z) accelerations 19 p2720 N90-25471
A computer simulation model for studying cervical spine injury prevention 19 p2721 N90-25476
TOM: Test of multiple task performance, user manual
[DLR-FB-89-60] 19 p2723 N90-25490
Differential psychological analysis of a computer-based audio-visual test of vigilance
[ESA-TT-1136] 19 p2724 N90-25494
CREW CHIEF: A computer graphics simulation of an aircraft maintenance technician 19 p2729 N90-25515
Modeling strength data for CREW CHIEF 19 p2729 N90-25516
A laboratory breadboard system for dual-arm teleoperation 19 p2740 N90-25573
Hardware and software reliability estimation using simulations
[NASA-CR-186637] 19 p2741 N90-25580
Depth buffer shadow algorithms
[DE90-012070] 19 p2744 N90-25595
Listening to turbulence: An example of scientific audiolization
[DE90-010637] 19 p2753 N90-25646
On using a superconducting linac to drive a short wavelength FEL
[CEBAF-PR-89-019] 19 p2756 N90-25660
Simulation of the boundary layer in accretion disks with the SPH method 19 p2779 N90-25807
New results of numerical simulations of X ray binaries evolution 19 p2782 N90-25828
Simulations of high-resolution X ray spectra of AGNs 19 p2791 N90-25885
Two-dimensional Euler and Navier-Stokes Time accurate simulations of fan rotor flows
[NASA-TM-102402] 20 p2803 N90-25948
Performance of a supercharged direct-injection stratified-charge rotary combustion engine
[NASA-TM-103105] 20 p2809 N90-25982
Model following control system design: Preliminary ATTAS in-flight simulation test results
[PD-FC-9003] 20 p2813 N90-26010
An investigation of the use of singular perturbation methods and modal control theory in the derivation or aircraft control schemes
[MATHS-REPT-A-106] 20 p2814 N90-26014
Guidance and targeting for the strategic target system
[DE90-005239] 20 p2817 N90-26031
Modelling of the processing of incompatible polymer blends
[ETN-90-97211] 20 p2840 N90-26152
Simulated dynamic response of a servovalve controlled hydraulic actuator
[NASA-TM-101644] 20 p2842 N90-26167
Computer simulation of gear tooth manufacturing processes
[NASA-CR-185200] 20 p2843 N90-26171
Initial results on fault diagnosis of DSN antenna control assemblies using pattern recognition techniques 20 p2854 N90-26228
Simulation of the electrical and thermal behavior of gapless metal oxide surge arresters under AC-operation condition
[ETN-90-97309] 20 p2859 N90-26262
Modeling, simulation, and analysis of optical remote sensing systems
[NASA-CR-186648] 20 p2878 N90-26376
Qualification of concentrating mirror systems with the HERMES measurement system and the HELIOS simulation program
[DLR-FB-89-51] 20 p2882 N90-26394
Modeling and optimization of a regenerative fuel cell system using the ASPEN process simulator
[NASA-TM-103210] 20 p2882 N90-26396
Computer simulation of chemical reactions in synthetic model compounds and genetically engineered active sites
[AD-A222611] 20 p2898 N90-26483
Object oriented programming
[DE90-011797] 20 p2907 N90-26532
Parallelization of an annealing simulation applied to improving tetrahedric grids
[IMAG-RR-796-M] 20 p2913 N90-26570
Position control of redundant manipulators using an adaptive error-based control scheme
[NASA-CR-186812] 20 p2914 N90-26578
Beam rider for an Articulated Robot Manipulator (ARM) accurate positioning of long flexible manipulators
[NASA-CR-185151] 20 p2914 N90-26581
Variance reduction for quantile estimates in simulations via nonlinear controls
[AD-A222653] 20 p2916 N90-26590
Isothermal compressibility of SPC/E water
[AD-A222723] 20 p2925 N90-26643
Computer modeling wave propagation with a variation of the Helmholtz-Kirchhoff relation
[AD-A222746] 20 p2927 N90-26657
Sensitivity analysis with a simple charging code
[RAE-TM-SPACE-374] 20 p2929 N90-26662
Molecular dynamics simulations of grain-boundary diffusion for varying tilt angle geometries
[DE90-012919] 20 p2930 N90-26669
Structure and dynamics of water at the Pt (111) interface: Molecular dynamics study
[AD-A222628] 20 p2933 N90-26687
Particle simulation of hypersonic flow
[AD-A222704] 21 p2954 N90-26794
Dallas/Fort Worth simulation, volume 1
[DOT/FAA/CT-TN89/28-VOL-1] 21 p2955 N90-26802
Cognitive requirements for aircraft navigation
[NASA-CR-186933] 21 p2955 N90-26804
Atlanta tower simulation, volume 1
[DOT/FAA/CT-TN89/27-VOL-1] 21 p2961 N90-26835
Atlanta tower simulation. Volume 2: Appendixes
[DOT/FAA/CT-TN89/27-VOL-2] 21 p2961 N90-26836
The computer modeling of the combustion and extinction of methane-air premixed flames by thermally stable gases
[PB90-189432] 21 p2976 N90-26910
Noise adaptation and correlated maneuver gating of an extended Kalman filter
[AD-A221713] 21 p3001 N90-27060
On modeling the effect of pore shapes on ductile fracture
[AD-A221774] 21 p3014 N90-27136
Evaluation of magnetospheric internal magnetic field models and existing software
[AD-A221816] 21 p3027 N90-27210
Special purpose parallel computer architecture for real-time control and simulation in robotic applications
[NASA-CASE-NPO-17629-1-CU] 21 p3038 N90-27268
Simulation-based intelligent robotic agent for Space Station Freedom 21 p3043 N90-27298
Construction of dynamic stochastic simulation models using knowledge-based techniques 21 p3047 N90-27322
The composite load spectra project 21 p3047 N90-27323
A plan for scientific visualization at ANL
[DE90-013565] 21 p3051 N90-27344
Computer assisted analysis and modelling of structured problems
[AD-A222991] 21 p3052 N90-27350
Robotic space simulation integration of vision algorithms into an orbital operations simulation
[NASA-CR-185934] 21 p3059 N90-27395
Identification techniques for nonlinear differential equations of motion
[AD-A220895] 21 p3062 N90-27407
Computation of efficient solutions of discretely distributed stochastic optimization problems
[ETN-90-97330] 21 p3067 N90-27436
Space-based wide area surveillance system studies 21 p3068 N90-27444
Stability regimes in a helical quadrupole focusing accelerator: Theory and simulation
[AD-A221755] 21 p3079 N90-27507
United States Air Force research initiation program for 1988, volume 1
[AD-A223123] 21 p3101 N90-27613
United States Air Force research initiation program for 1988, volume 3
[AD-A223125] 21 p3102 N90-27615
The EFA integrated monitoring and recording system: Requirements and concept for implementation 22 p3103 N90-27620
Observer or direct inversion 22 p3103 N90-27622
AIMS test and simulation equipment 22 p3104 N90-27623
Experimental study towards a future airport ground movement simulator 22 p3113 N90-27687
Economical graphics display system for flight simulation avionics
[NASA-CR-186886] 22 p3116 N90-27701
On computations of the integrated space shuttle flowfield using overset grids
[NASA-CR-186927] 22 p3124 N90-27734
Deployment of large flexible space structures 22 p3131 N90-27766
Flexible space-based robot modelling and real-time simulation 22 p3131 N90-27769
Autonomous propulsion system requirements for placement of an STS (Space Transportation System) external tank in low Earth orbit
[PB90-183302] 22 p3133 N90-27777
Hydrogen in palladium alloys: Experiments, models and simulations
[PB90-200429] 22 p3156 N90-27896
An improved k-epsilon model for near-wall turbulence and comparison with direct numerical simulation
[NASA-TM-103221] 22 p3171 N90-27983
Tolerating failures of continuous-valued sensors
[NASA-CR-187028] 22 p3178 N90-28035
Power beam technology at Los Alamos: A review of research and development activities
[DE90-009002] 22 p3182 N90-28057
DEPEND: A design environment for prediction and evaluation of system dependability
[NASA-CR-186890] 22 p3189 N90-28094
An evaluation of three models designed for siting wind turbines in areas of complex terrain
[DE90-013625] 22 p3196 N90-28137
Subjective-probability-based scenarios for uncertain input parameters: Stratospheric ozone depletion
[N-3140-EPA/JMO/RC] 22 p3199 N90-28157
Vertically averaged spectral model for tidal circulation in estuaries. Part 1: Model formulation
[PB90-181678] 22 p3230 N90-28319
Impact of satellite altimetric data on the numerical simulation of the general oceanic currents: Sensitivity to orbit parameters
[ETN-90-97461] 22 p3231 N90-28321
Influence of gravito-inertial force on vestibular nystagmus in man
[IZF-1989-24] 22 p3231 N90-28325
DSIM: A distributed simulator
[NASA-CR-186880] 22 p3237 N90-28353
Simulation of long range atmosphere effects in short range thermal infrared and CCD images
[IZF-1989-27] 22 p3247 N90-28413
Theoretical thermodynamics: Equation of state and perturbation studies
[PB90-199332] 22 p3255 N90-28430
Dynamic load-sharing using predicted process resource requirements
[NASA-CR-186891] 22 p3255 N90-28433
Dallas/Forth Worth simulation. Phase 2: Triple simultaneous parallel Instrument Landing System (ILS) approaches (turbojets)
[DOT/FAA/CT-90/2] 23 p3270 N90-28509
Shock dynamics in the sub-nanometer femtosecond domain
[DE90-014390] 23 p3304 N90-28689
Computer simulation of micro-triode performance
[DE90-014191] 23 p3320 N90-28774

Simulation of INPE's printed circuit laboratory production line
[INPE-4556-TDL/331] 23 p3322 N90-28784
Numerical simulation of reactive turbulent flows
[ETN-90-97476] 23 p3326 N90-28807
Three-dimensional simulations of the generation of one Angstrom radiation by a self-amplified spontaneous emission free-electron laser
[DE90-015032] 23 p3330 N90-28830
Dynamic interaction of multiple autonomous mobile robots 23 p3333 N90-28844
Tele-Autonomous control involving contact --- object localization
[NASA-CR-187004] 23 p3335 N90-28854
Reliability analysis of maintained structural system vulnerable to fatigue and fracture 23 p3338 N90-28868
Complex auditory signals
[AD-A224127] 23 p3356 N90-28969
Three-dimensional motor schema based navigation 23 p3367 N90-29026
Causal simulation and sensor planning in predictive monitoring 23 p3369 N90-29037
Efficient mapping algorithms for scheduling robot inverse dynamics computation on a multiprocessor system 23 p3375 N90-29071
Automated simulation as part of a design workstation
[NASA-TM-102852] 23 p3378 N90-29083
LINTERP: A numerical algorithm for interpolating quadrilateral and hexahedral meshes
[DE90-014417] 23 p3379 N90-29090
Who's who in scientific visualization at LLNL
[DE90-014720] 23 p3379 N90-29091
Block Lanczos algorithm
[AD-A224011] 23 p3383 N90-29111
Computerized simulation of phenomena in plasma via particles
[INPE-4595-RPE/569] 23 p3397 N90-29194
TSC (Tokamak Simulation Code) simulations of Alcator C-MOD discharges 3: Study of axisymmetric stability
[DE90-015386] 23 p3398 N90-29198
Control of nonlinear space-charge emittance growth
[DE90-014752] 23 p3410 N90-29270
The formation of globular clusters 23 p3410 N90-29272
Investigation of ATP blades, part 2. Validation of two-dimensional viscous flow simulation codes around thin airfoils
[NAL-TR-1046] 24 p3421 N90-29326
Enhancing PLRS with user-to-user data capability 24 p3427 N90-29359
Inertial navigation system simulator program: Top-level design
[AD-A223762] 24 p3431 N90-29379
The function of the Interactive Model Assembly Program (IMAP) for a flight simulator
[NAL-TR-1034] 24 p3437 N90-29412
Suspension systems for ground testing large space structures
[NASA-CR-4325] 24 p3439 N90-29424
User's manual for the Trajectory Simulation and Analysis Program (TSAP)
[DE90-014850] 24 p3440 N90-29426
Bistatic radar cross section of a perfectly conducting rhombus-shaped flat plate
[AD-A223418] 24 p3460 N90-29546
Control of a Cossor CSP1250 ionospheric simulator in an automated HF test bed
[AD-A223446] 24 p3461 N90-29549
Long pulse diode experiments
[DE90-016218] 24 p3465 N90-29578
Macro cell placement with neural net algorithms
[REPT-90-020] 24 p3466 N90-29585
An additive turbulent decomposition of the Navier-Stokes equations implemented on highly parallel computer systems
[AD-A223678] 24 p3468 N90-29595
The ACR-program for automatic finite element model generation for part through cracks
[DE90-631545] 24 p3479 N90-29662
Simulation and measurement of the heat exchange between the urban canopy and boundary layers 24 p3486 N90-29702
Wind tunnel, field, and numerical investigations of plume downwash and dispersion at an arctic industrial site 24 p3489 N90-29721
Atmospheric structure and variability
[AD-A223439] 24 p3492 N90-29734
Three-dimensional numerical study of thunderstorm downdrafts and associated outflow boundaries 24 p3494 N90-29746
Autonomous sensor-based dual-arm satellite grappling 24 p3504 N90-29809
Response to reflected-force feedback to fingers in teleoperations 24 p3509 N90-29837
Test and training simulator for ground-based teleoperated in-orbit servicing 24 p3510 N90-29843
Application of recursive manipulator dynamics to hybrid software/hardware simulation 24 p3516 N90-29876
Kinematics and control algorithm development and simulation for a redundant two-arm robotic manipulator system 24 p3516 N90-29877
Inverse dynamics of a 3 degree of freedom spatial flexible manipulator 24 p3516 N90-29878
Computer simulation and design of a three degree-of-freedom shoulder module 24 p3520 N90-29902
An interactive optimization based, computer graphics software package. Phase 2: Users manual
[AD-A223854] 24 p3529 N90-29954
Ray traced scalar fields with shaded polygonal output
[DE90-011023] 24 p3529 N90-29955
A reduced-order extended Kalman filter for moving images
[AD-A223742] 24 p3541 N90-30028
Three dimensional studies of helical equilibria and magnetic surface breaking due to the finite beta effect
[DE90-508078] 24 p3548 N90-30071
Monte Carlo simulation of complex spectra for opacity calculations
[DE90-015198] 24 p3561 N90-30147
Dust emission by Comet P/Halley 1982i 24 p3563 N90-30159

COMPUTERS
NT AIRBORNE/SPACEBORNE COMPUTERS
NT ANALOG COMPUTERS
NT CDC CYBER 205 COMPUTER
NT CRAY COMPUTERS
NT DIGITAL COMPUTERS
NT EMBEDDED COMPUTER SYSTEMS
NT HEWLETT-PACKARD COMPUTERS
NT HYBRID COMPUTERS
NT HYPERCUBE MULTIPROCESSORS
NT IBM COMPUTERS
NT MASSIVELY PARALLEL PROCESSORS
NT MICROCOMPUTERS
NT MIMD (COMPUTERS)
NT MINICOMPUTERS
NT OPTICAL COMPUTERS
NT PARALLEL COMPUTERS
NT PERSONAL COMPUTERS
NT SEQUENTIAL COMPUTERS
NT SIMD (COMPUTERS)
NT SUPERCOMPUTERS
NT TRANSPUTERS
NT VAX COMPUTERS
NT VAX-11 SERIES COMPUTERS
Computer availability impact on the archiving of scientific and technical reports
[AD-A210283] 01 p0136 N90-10787
The J-Machine: A fine grain concurrent computer
[AD-A211909] 03 p0384 N90-12187
Automation and robotics in construction: Japanese research and development
[AD-A214170] 07 p0942 N90-15456
Understanding developments in computer technology: A pragmatic and synthetic interpretation 07 p0971 N90-15608
Bus programmable slave module
[NASA-CASE-MSC-21387-1] 08 p1108 N90-16411
Executive summary for designing online help systems: Report of year 1 activity
[AD-A214811] 09 p1262 N90-17320
Technology assessment of computer languages
[AD-A216940] 10 p1419 N90-18182
Decomposition for optimal synthesis in a parallel computing environment 10 p1419 N90-18184
Technology assessment of software engineering
[AD-A216943] 11 p1548 N90-18902
Integrated IMA (Information Mission Areas) IC (Information Center) guide
[AD-A216944] 11 p1547 N90-18903
Research equipment
[AD-A216515] 11 p1552 N90-18937
Space station Simulation Computer System (SCS) study for NASA/MSFC. Volume 4: Conceptual design report
[NASA-CR-183843] 13 p1762 N90-20116
Space station Simulation Computer System (SCS) study for NASA/MSFC. Volume 6: Study issues report
[NASA-CR-183845] 13 p1763 N90-20118
Selective automatic fire extinguisher for computers (SAFECOMP): Developmental test and evaluation/initial operational test and evaluation
[AD-A217790] 14 p1958 N90-21212
Graphics mini manual
[NASA-TM-87622-REV] 15 p2144 N90-22247
Computer conferencing: Minds meeting anywhere anytime 15 p2179 N90-22452
DURIP-Instrumentation for recording and analyzing multiple input/output saccadic eye movement neurosensory control
[AD-A219905] 17 p2435 N90-23871
Cumulative reports and publications through December 31, 1989
[NASA-CR-182041] 17 p2439 N90-23898
Software techniques for non-von Neumann architectures
[AD-A220390] 17 p2440 N90-23902
A note on the Gaussian integration formula
[AD-A220053] 17 p2461 N90-24054
Advanced technology in welding, materials processing and evaluation
[DE90-010799] 19 p2697 N90-25347
A research program in computer technology
[AD-A221184] 19 p2748 N90-25606
The CEBAF instrumentation and control system
[CEBAF-PR-89-037] 19 p2755 N90-25657
Self-checking on-line testable static RAM
[NASA-CASE-NPO-17939-1-CU] 20 p2904 N90-26518
ISIS and META projects
[NASA-CR-186645] 20 p2905 N90-26524
Closed-form solution of decomposable stochastic models
[NASA-TM-103466] 20 p2920 N90-26619
Optical wavefront computer for stabilizing large space structures
[AD-A221707] 21 p2967 N90-26866
Disconnected actions: An asynchronous extension to a nested atomic action system
[AD-A221937] 21 p3053 N90-27356
Guide to available mathematical software
[PB90-216508] 22 p3236 N90-28351
Purchase of computer equipment: Justification and cost appraisal
[RSRE-89023] 22 p3256 N90-28438
A Boltzmann machine for the organization of intelligent machines 23 p3370 N90-29040
Guide to charging for the CCF
[RSRE-89022] 23 p3404 N90-29238
The development and evaluation of numerical algorithms for MIMD computers
[NASA-TM-101167] 24 p3526 N90-29939

CONCATENATED CODES
A performance comparison between block interleaved and helically interleaved concatenated coding systems 04 p0486 N90-12792
Error control techniques for satellite and space communications
[NASA-CR-182751] 05 p0631 N90-13685

CONCAVITY
Three-dimensional boundary layer transition on a concave surface 01 p0064 N90-10365

CONCENTRATION (COMPOSITION)
NT ATMOSPHERIC MOISTURE
NT ATOM CONCENTRATION
NT CARBON DIOXIDE CONCENTRATION
NT LOW CONCENTRATIONS
NT METEOROID CONCENTRATION
NT MOISTURE CONTENT
Electrical field dependence of protein conformation and channel function in lipid membranes of different compositions
[AD-A210236] 01 p0040 N90-10222
Effects of binder concentration on the properties of plastic-bonded explosives
[DE89-007744] 01 p0053 N90-10301
Electroactive polyaniline film deposited from non-aqueous media. 2: Effect of acid concentration in solutions
[AD-A212084] 04 p0477 N90-12737
Profile measurements of sulfur dioxide, nitrogen oxides, and nitric acid deposition velocities in California's south coast air basin
[PB90-104001] 06 p0808 N90-14703
The effect of dissolved chlorine on the pitting behavior of 304L stainless steel in a 0.5 N NaCl solution
[AD-A213803] 07 p0905 N90-15234
Influence of wall strain rate, polymer concentration, and channel height upon drag reduction and turbulent structure
[AD-A215378] 09 p1218 N90-17064
Low NO(x) potential of gas turbine engines
[NASA-TM-102452] 10 p1321 N90-17636
Development of an alternative concentration probe calibration method
[AD-A216245] 10 p1388 N90-18031
Investigation of multiple scattering in aqueous suspensions of non-absorbing polystrene microspheres using spectrophotometry
[BCRS-89-09] 11 p1485 N90-18549
Variations in volatiles in magma bodies based on studies of melt inclusions
[DE90-006272] 11 p1532 N90-18821

KOH concentration effect on the cycle life of nickel-hydrogen cells. Part 4: Results of failure analyses
13 p1824 N90-20475
Estimation of the concentration-distance profile within the electrochemical diffusion layer by Raman microprobe spectroscopy
[AD-A219521] 17 p2372 N90-23506
Study of the radical OH in a high pressure flame by resonant DRASC
[ONERA-RF-57/7131-PY] 23 p3305 N90-28692

CONCENTRATORS
Structural concepts for very large (400-meter-diameter) solar concentrators 01 p0029 N90-10153
United States photovoltaic concentrator technology process and new program initiative
[DE89-013812] 01 p0083 N90-10475
Recent progress in photovoltaic concentrator module technology
[DE90-009007] 14 p2002 N90-21475
High-efficiency silicon solar cells for a 22-sun line-focus module
[DE90-010242] 16 p2251 N90-22840
Photovoltaic concentrator technology development
[DE90-011479] 18 p2577 N90-24684
The photovoltaic concentrator initiative
[DE90-011228] 19 p2710 N90-25425
Performance testing and qualification of Sandia's third baseline photovoltaic concentrator module
[DE90-012644] 19 p2711 N90-25431
Silicon concentrator solar cell development
[DE90-011782] 20 p2880 N90-26386
Some studies related to a new Hexagonal Compound Parabolic Concentrator (HCPC) as a secondary in tandem with a solar tower
[DLR-FB-90-12] 24 p3485 N90-29700

CONCENTRIC CYLINDERS
Effect of a crystal-melt interface on Taylor-vortex flow
[NASA-CR-186512] 15 p2171 N90-22408
Rheology and microstructure of concentrated suspensions
[DE90-009976] 18 p2520 N90-24391
Stabilization of Taylor-Couette flow due to time-periodic outer cylinder oscillation
[PB90-219130] 23 p3323 N90-28790

CONCORDE AIRCRAFT
The next generation supersonic transport engine: Critical issues
[PNR90576] 04 p0455 N90-12605

CONCRETE STRUCTURES
Transport of gases through concrete
[AERE-G-4977] 16 p2234 N90-22747
Introduction to compact reinforced composite
[CBL-REPRINT-5] 19 p2673 N90-25199

CONCRETES
Fiber reinforced cementitious composites technology
[PB89-227813] 05 p0619 N90-13608
Evaluation of two transport aircraft and several ground test vehicle friction measurements obtained for various runway surface types and conditions. A summary of test results from joint FAA/NASA Runway Friction Program
[NASA-TP-2917] 08 p1021 N90-15902
High-strength concrete development through 25 years
[CBL-REPRINT-17] 11 p1492 N90-18589
Development of finished beam and shell elements from engineering models for structures under high inelastic deformations
[ETN-90-95377] 12 p1675 N90-19619
Criteria for polymer concrete on airport pavements
[DOT/FAA/DS-89/18] 14 p1929 N90-21045
Perforation of a reinforced concrete wall by a rigid missile
[AD-A210025] 14 p1986 N90-21381
Transport of gases through concrete
[AERE-G-4977] 16 p2234 N90-22747
Introduction to compact reinforced composite
[CBL-REPRINT-5] 19 p2673 N90-25199
Fracture mechanics in integrated design of new, ultra-strong materials and structures
[CBL-REPRINT-21] 19 p2703 N90-25378
Investigation of the effects of acid deposition on materials
[PB90-158973] 22 p3197 N90-28143
Development and testing of rapid repair methods for war damaged runways
[AD-A223970] 23 p3285 N90-28586
Computer-Aided Structural Engineering (CASE) project: Investigation and design of U-frame structures using program CUFRBC. Volume A: Program criteria and documentation
[AD-A224387] 24 p3525 N90-29934

CONCURRENT PROCESSING
The impact of recovery on concurrency control
[AD-A210828] 01 p0106 N90-10603
Tools for application development in heterogeneous distributed environments
[AD-A210238] 01 p0108 N90-10613
The rewrite rule machine project
[AD-A210528] 01 p0109 N90-10617
Northeast Artificial Intelligence Consortium annual report for 1987. Volume 7, part A: Time oriented problem solving
[AD-A210331] 01 p0110 N90-10622
MSP: Modeling of concurrent processes. Version 1.00 General introduction and directions for use
[REPT-88-88] 02 p0260 N90-11477
Synchrony with empty process --- the algebra of synchronous processes
[CWI-CS-R8832] 02 p0261 N90-11481
A generalization of A. N. Habermann's theorem for semaphores
[REPT-88-98] 02 p0261 N90-11484
Determinism yields (event structure isomorphism equals step sequence equivalence)
[CWI-CS-R8839] 02 p0263 N90-11492
The J-Machine: A fine grain concurrent computer
[AD-A211909] 03 p0384 N90-12187
Experience with CST: Programming and implementation
[AD-A211882] 03 p0386 N90-12197
Parallel processing on transputer arrays for the recognition of objects in infrared images
[RSRE-MEMO-4197] 03 p0389 N90-12217
A simple definition for parallel composition of prime event structures
[CWI-CS-R8903] 04 p0532 N90-13074
Trace theory --- concurrent processing
[MEMO-INF-89-16] 04 p0536 N90-13100
Modular specifications in process algebra with curious queues
[CWI-CS-R8821] 04 p0543 N90-13152
An algebra for process creation
[CWI-CS-R8907] 04 p0543 N90-13155
The Tactical Environmental Support System (TESS(3))
06 p0757 N90-14409
Group implicit concurrent algorithms in nonlinear structural dynamics
[NASA-CR-185950] 06 p0796 N90-14638
Concurrent processing adaptation of aeroplastic analysis of propfans
[NASA-TM-102455] 06 p0799 N90-14656
Strand: A practical parallel programming language
[DE90-002861] 06 p0830 N90-14825
Concurrence control for transactions with priorities
[NASA-CR-186241] 07 p0986 N90-15699
Concurrency control for transactions with priorities
[NASA-CR-186268] 09 p1263 N90-17323
Real-time concurrency control and transaction scheduling
[AD-A218162] 13 p1901 N90-20909
Strategies for concurrent processing of complex algorithms in data driven architectures
[NASA-CR-186515] 14 p2013 N90-21535
Concurrent processing simulation of the space station
16 p2289 N90-23041
Concurrent computing: Numerical algorithms and some applications
[AD-A218570] 16 p2300 N90-23103
The Durra application debugger/monitor
[AD-A219290] 16 p2301 N90-23111
A process specification formalism based on static COLD
[CWI-CS-R8930] 17 p2448 N90-23960
Priority inversion and its prevention
[AD-A218613] 17 p2467 N90-24101
Construction of an Ethernet model with the PROMISE simulation tool
[NLR-MP-88047-U] 18 p2593 N90-24757
How to construct an atomic variable
[CWI-CS-R8939] 18 p2596 N90-24772
A survey of concurrent readers and writers
[CWI-CS-R8936] 19 p2741 N90-25581
On the design of a concurrent image analysis system
[DE90-011388] 19 p2746 N90-25605
The proposal of a high-level stochastic Petri net
[REPT-90-005] 19 p2752 N90-25637
Parallel processors and nonlinear structural dynamics algorithms and software
[NASA-CR-186755] 20 p2907 N90-26536
Knowledge and inhibition in asynchronous distributed systems
[TR-90-1139] 20 p2935 N90-26703
A tool for modeling concurrent real-time computation
21 p3047 N90-27321
Performance of the Intel iPSC/860 hypercube
[DE90-014697] 22 p3235 N90-28346
Concurrent Image Processing Executive (CIPE). Volume 1: Design overview
[NASA-CR-186853] 22 p3236 N90-28348
Concurrent Image Processing Executive (CIPE). Volume 2: Programmer's guide
[NASA-CR-186854] 22 p3236 N90-28349
Concurrent Image Processing Executive (CIPE). Volume 3: User's guide
[NASA-CR-186848] 22 p3236 N90-28350
Concepts of concurrent programming
[AD-A223897] 23 p3382 N90-29110
Inertial navigation system simulator program: Top-level design
[AD-A223762] 24 p3431 N90-29379
Programming your way out of the past: ISIS and the META Project
[NASA-CR-186275] 24 p3524 N90-29922
Language and system support for concurrent programming
[AD-A223760] 24 p3528 N90-29949
Reliable communication in the presence of failures
[NASA-CR-183046] 24 p3533 N90-29977
Fact system: A standardizing modelization processing for concurrent systems
[ETN-90-97286] 24 p3533 N90-29982

CONDENSATES
Reflux condensation in vertical tubes
[ESDU-89038] 07 p0932 N90-15397
Identification of solar nebula condensates in interplanetary dust particles and unequilibrated ordinary chondrites 08 p1144 N90-16629
Solar nebula condensates and the composition of comets 08 p1144 N90-16634
Existence of Bose-Einstein condensation in one and two dimensions
[DE89-635910] 09 p1294 N90-17498
Bose condensate in superfluid (sup 4)He and momentum distributions by deep inelastic scattering
[DE90-007541] 12 p1712 N90-19832
Physical processes in cometary ices inferred from laboratory studies 12 p1739 N90-19996
Laboratory measurements of microwave and millimeter-wave properties of planetary constituents
20 p2943 N90-26745
Optical constants of solid methane
20 p2948 N90-26775

CONDENSATION
Heat transfer in condensation of lithium vapors
[DE90-002081] 07 p0929 N90-15375

CONDENSATION NUCLEI
Study of phase transformations liquid-solid-solid of ultrafine particles
[ISAL-89-0019] 08 p1042 N90-16022
Disturbance structures and its magnetic field features in plasma comet tail
[DE90-610636] 12 p1737 N90-19986
Results from global tropospheric sulphur simulations
20 p2885 N90-26413
Characterization of biogenic aerosol particles from the Amazon Basin during dry and wet season
20 p2886 N90-26418
Observations of anthropogenic cloud condensation nuclei 22 p3218 N90-28251
Direct and remote sensing observations of the effects of ships on clouds 22 p3218 N90-28252

CONDENSATION TRAILS
U CONTRAILS

CONDENSED MATTER PHYSICS
Highlights of papers presented at the workshop on Cold Fusion Phenomena
[DE89-016956] 03 p0407 N90-12334
Interaction of low-energy electrons and positrons with condensed matter: Stopping powers and inelastic mean free paths from optical data
[DE90-001001] 06 p0840 N90-14882
Existence of Bose-Einstein condensation in one and two dimensions
[DE89-635910] 09 p1294 N90-17498
Modern theory of magnetism
[DE90-007374] 11 p1561 N90-18998
Distributed bosonic states and condensed matter fusion
[AD-A217605] 12 p1718 N90-19868
Linear and nonlinear electrical response of condensed matter: Ionic, dielectric, and mixed-conduction materials
[AD-A218771] 16 p2215 N90-22639
Electronic theory of solids, surfaces, interfaces, and clusters 16 p2320 N90-23230
Proceedings of a research workshop on Computational Condensed Matter Physics. Total Energy Methods and Physics of III-V Semiconductors
[AD-A219568] 17 p2476 N90-24156

CONDENSER RADIATORS
U CONDENSERS (LIQUEFIERS)
U HEAT RADIATORS

CONDENSERS (LIQUEFIERS)
Reflux condensation in vertical tubes
[ESDU-89038] 07 p0932 N90-15397
Experimental investigation of condensation of steam in the presence of noncondensable gases for open-cycle surface condensers
[DE90-003552] 08 p1097 N90-16353

CONDENSING
Consequence of condensed-phase formation in transient burning of TiHx/KClO in a closed system
[DE89-013922] 02 p0208 N90-11188
Preparation of binary ice layers by condensation from gas phase
[JUEL-2248] 05 p0622 N90-13631
Buoyancy effects on the vapor condensation rate on a horizontal liquid surface
[NASA-TM-102437] 05 p0629 N90-13675
Vapor condensation on liquid surface due to laminar jet-induced mixing: The effects of system parameters
[NASA-TM-102433] 05 p0643 N90-13751
Processing and properties of nanophase oxides
[DE90-003826] 07 p0895 N90-15171
Recent advances in magnetic heat pump technology
[DE89-013289] 07 p0928 N90-15370
Experimental investigation of condensation of steam in the presence of noncondensable gases for open-cycle surface condensers
[DE90-003552] 08 p1097 N90-16353
On condensation driven by electrostatic interactions in macroionic solutions
[DE89-636072] 08 p1120 N90-16487
Existence of Bose-Einstein condensation in one and two dimensions
[DE89-635910] 09 p1294 N90-17498
Condensation fluid dynamics and heat transfer on rotating spherical surfaces in a microgravitational field
[DE90-005540] 11 p1495 N90-18607
Down-to-earth studies of carbon clusters
21 p3091 N90-27573

CONDITIONED RESPONSES
U CONDITIONING (LEARNING)

CONDITIONING (LEARNING)
Biological investigations of adaptive networks: Neuronal control of conditioned responses
[AD-A211043] 01 p0094 N90-10534
Integration of neurobiological and computational analyses of the neural network essentials for conditioned taste aversions
[AD-A210228] 01 p0094 N90-10537
Individual differences in associative learning and forgetting
[AD-A212765] 04 p0526 N90-13034
Excitatory and inhibitory backward conditioning in the rat 15 p2135 N90-22204

CONDITIONS
NT ADIABATIC CONDITIONS
NT BOUNDARY CONDITIONS
NT FLIGHT CONDITIONS
NT KUTTA-JOUKOWSKI CONDITION
NT NONEQUILIBRIUM CONDITIONS
NT RUNWAY CONDITIONS
On conditions for the development of stable discrete-time sliding mode control systems
[MATHS-REPT-A-124] 19 p2747 N90-25812

CONDUCTING FLUIDS
Command operated liquid metal opening switch
[AD-D014262] 08 p1060 N90-16126

CONDUCTING MEDIA
U CONDUCTORS

CONDUCTING POLYMERS
Optical modulators based on polymers
[EP-PATENT-0-294-061-A1] 05 p0700 N90-14099
Novel high-rate, all solid-state, sodium and lithium/organosulfur batteries
[DE90-001014] 07 p0920 N90-15325
Application of polymer electrolytes to lithium batteries
[AD-A216038] 10 p1401 N90-18099
Electrochemical investigations of electronically conductive polymers. Part 4: By controlling the supermolecular structure, charge transport rates can be enhanced
[AD-A216603] 11 p1490 N90-18573
Electronic and ionic transport in processable conducting polymers
[AD-A218093] 13 p1782 N90-20229
Quartz crystal microbalance studies: Solvent effects in conducting polymer films
[AD-A219426] 17 p2372 N90-23502
Evaluation of ion intercalation in conducting polymers
[AD-A219423] 17 p2379 N90-23549
Theoretical studies of electrons and electron transfer processes in fluids
[DE90-008414] 17 p2470 N90-24117
Electronic and ionic transport in processable conducting polymers
[AD-A221045] 18 p2530 N90-24436
Quartz crystal microbalance analysis: Partial cation release during oxidation of conducting polymers
[AD-A221091] 18 p2530 N90-24439
A lightweight solid polymer electrolyte fuel cell with stack power density of 3 kW/lb (7kW/kg)
[AD-A223068] 21 p3020 N90-27169
Cell performance of ultra-thin polymer cathode cell systems. Part 2: Cation intercalating composite polymer cathode
[AD-A221919] 21 p3020 N90-27172
Approaches to orthogonally fused conducting polymers for molecular electronics
[AD-A222546] 22 p3159 N90-27915
Polymer research
[PB90-246638] 23 p3313 N90-28737

CONDUCTION BANDS
High energy neutron irradiation effects in GaAs modulation-Doped Field Effect Transistors (MODFETS): Threshold voltage
[AD-A210502] 01 p0132 N90-10763
Strain and density dependent valence-band masses in InGaAs/GaAs and GaAs/GaAsP strained-layer structures
[DE89-016882] 02 p0285 N90-11627
Theory of the electronic and optical properties of semiconductor heterostructures
[AD-A214132] 08 p1130 N90-16544
Quantum-confined hole states in double-barrier resonant tunneling structures
[AD-A221342] 18 p2623 N90-24946

CONDUCTION ELECTRONS
Radiative shocks with electron thermal conduction
02 p0293 N90-11670
Alternating gradient photodetector
[NASA-CASE-NPO-17235-1-CU]
14 p1982 N90-21358
Quantum-confined hole states in double-barrier resonant tunneling structures
[AD-A221342] 18 p2623 N90-24946
Field emitter array integrated distributed amplifiers
[AD-D014493] 22 p3166 N90-27958

CONDUCTIVE HEAT TRANSFER
Interlaboratory comparison of two types of line-source thermal-conductivity apparatus measuring five insulating materials
[PB89-218325] 02 p0200 N90-11142
Cooling flows in clusters of galaxies
06 p0862 N90-15009
Spacecraft thermal control design data, volume 1
[ESA-PSS-03-108-ISSUE-1-VOL-1]
11 p1468 N90-18455
Numerical modelling of shocks in gases and metals
[MRL-RR-8-89] 12 p1658 N90-19528
Evolution of midplate hotspot swells: Numerical solutions
[NASA-CR-186462] 12 p1691 N90-19713
An approximation theory for the identification of linear thermoelastic systems
[NASA-CR-182015] 13 p1877 N90-20764
Inverse problems of heat conduction
15 p2091 N90-21969
High-temperature deformation of mechanically-alloyed aluminum IN90211 16 p2216 N90-22645
Thermal phenomena in high-Tc thin film superconductors 16 p2321 N90-23233
Thermal conductivity of metals
18 p2514 N90-24356
New discharge pumping method for CO2 lasers
[AD-A220898] 20 p2866 N90-26307
Radiative heat transfer
[PB90-247602] 23 p3327 N90-28813
Frequency response of a thermocouple wire: Effects of axial conduction
[NASA-CR-180454] 23 p3330 N90-28827
Approximate equations for heat conduction in multi-layered cylindrical shells
[NAL-TR-1049] 24 p3471 N90-29614

CONDUCTIVITY
Numerical and analytical study of nonlinear bifurcations associated with the morphological stability of two-dimensional single crystals
[PB90-209594] 23 p3398 N90-29200

CONDUCTORS
NT BUS CONDUCTORS
NT CONDUCTING POLYMERS
NT ELECTRIC CONDUCTORS
NT ELECTRIC WIRE
NT ELECTROLYTES
NT HIGH TEMPERATURE SUPERCONDUCTORS
NT ION EXCHANGE MEMBRANE ELECTROLYTES
NT MOLTEN SALT ELECTROLYTES
NT NONAQUEOUS ELECTROLYTES
NT PHOTOCONDUCTORS
NT SOLID ELECTROLYTES
NT SUPERCONDUCTORS
NT THERMAL CONDUCTORS
Magneto-elastic interactions in conducting structures in transient magnetic fields 05 p0632 N90-13686
Further studies of transverse stress effects in cable-in-conduit conductors
[DE90-001517] 06 p0771 N90-14484
A new technique for imaging the logic state of passivated conductors: Biased resistive contrast imaging
[DE90-000666] 10 p1380 N90-18000
Solid-state proton conductors
[DE90-007595] 11 p1531 N90-18812
Measurements of the interaction of high-voltage biassed conductors with the ionosphere
[AD-A218285] 13 p1843 N90-20580
Program CICC: Flow and heat transfer in Cable In Conduit Conductors, user's manual
[DE90-007924] 14 p2033 N90-21661
Current management for improved railgun performance 15 p2057 N90-21781
Solar array arcing in plasmas
19 p2737 N90-25558
Analysis of microstrip lines with alternative implementation of conductors and superconductors
[NASA-TM-103182] 22 p3167 N90-27966

CONES
NT ABLATIVE NOSE CONES
NT CIRCULAR CONES
NT CONICAL BODIES
NT NOSE CONES
The inviscid stability of supersonic flow past a sharp cone
[NASA-CR-181996] 11 p1451 N90-18363

CONES (VOLCANOES)
Geology of coronae and domal structures on Venus and models of their origin 15 p2191 N90-22513

CONFERENCES
Conference on Aerospace Transparent Materials and Enclosures (15th) 16-20 January 1989. Volume 2: Sessions 6-9
[AD-A210201] 01 p0006 N90-10024
Stability and Control of Tactical Missile Systems
[AGARD-CP-451] 01 p0011 N90-10050
Proceedings of the Workshop on Computational Aspects in the Control of Flexible Systems, part 1
[NASA-TM-101578-PT-1] 01 p0017 N90-10080
Proceedings of the Workshop on Computational Aspects in the Control of Flexible Systems, part 2
[NASA-TM-101578-PT-2] 01 p0021 N90-10103
Second Beamed Space-Power Workshop
[NASA-CP-3037] 01 p0027 N90-10140
International Conference on Organometallic Chemistry (13th) held in Torino, Europe on 4-9 September 1988: Abstracts
[AD-A210617] 01 p0033 N90-10178
Combustion Instabilities in Liquid-Fuelled Propulsion Systems
[AGARD-CP-450] 01 p0035 N90-10191
Castings Airworthiness
[AGARD-R-762] 01 p0042 N90-10231
Fluid Dynamics of Three-Dimensional Turbulent Shear Flows and Transition
[AGARD-CP-438] 01 p0062 N90-10356
International Conference on Aerosols and Background Pollution Abstracts
[AD-A210970] 01 p0085 N90-10483
Coordination of mesoscale meteorological research between ASL and European groups
[AD-A210902] 01 p0089 N90-10508
Proceedings of the 2nd International Conference on Vector and Parallel Computing
[AD-A209401] 01 p0103 N90-10585
Deep traps and sidegating in GaAs devices
[AD-A210740] 01 p0133 N90-10765
A lunar far-side very low frequency array
[NASA-CP-3039] 01 p0139 N90-10805
Army Science Conference Proceedings (16th) held in Fort Monroe, Virginia on 25-27 October 1988: Addenda
[AD-A210235] 01 p0143 N90-10827
Kalman Filter Integration of Modern Guidance and Navigation Systems
[AGARD-LS-166] 02 p0148 N90-10847
Flight Test Techniques
[AGARD-CP-452] 02 p0151 N90-10860
Meeting of intercosmos space physics group
02 p0158 N90-10902
Spacecraft Structures and Mechanical Testing
[ESA-SP-289] 02 p0176 N90-10986
Fifth International Workshop on Glasses and Ceramics from Gels
[DE89-016899] 02 p0201 N90-11147
The Third Conference on the Environmental Chemistry of Hydrazine Fuels
[AD-A197632] 02 p0203 N90-11157
International conference on numerical grid generation in computational fluid dynamics
[AD-A211082] 02 p0220 N90-11262
Proceedings of the Polycrystalline Thin Film Program Meeting
[DE89-009457] 02 p0237 N90-11348
Ionospheric Structure and Variability on a Global Scale and Interactions with Atmosphere and Magnetosphere
[AGARD-CP-441] 02 p0239 N90-11361

Two-Dimensional Intercomparison of Stratospheric Models
[NASA-CP-3042] 02 p0248 N90-11405
DOE/CEC Workshop on Critical Evaluation of Radiobiological Data to Biophysical Modeling
[DE89-015214] 02 p0254 N90-11437
Report of the Specialists' Workshop on Phase Transition Studies on Hydrogen-Bonded Crystals by Neutron and X-ray Diffractometries
[DE89-906638] 02 p0285 N90-11631
Globalization of Technology: International Perspectives. Proceedings of the 6th Convocation of the Council of Academies of Engineering and Technological Sciences
[PB89-198840] 02 p0288 N90-11645
Proceedings of the 1988 Antenna Applications Symposium, volume 1
[AD-A211396] 03 p0338 N90-11928
Proceedings of the Workshop on Compound Semiconductor Devices and Integrated Circuits (13th) held in Cabourg, France on 10-12 May 1989
[AD-A211848] 03 p0343 N90-11954
Solid-State Sensor and Actuator
[AD-A211427] 03 p0344 N90-11961
Indexes for the proceedings of the symposia (international) on detonation, 1951 through 1985
[DE89-015178] 03 p0345 N90-11972
Global tropospheric chemistry: Chemical fluexes in the global atmosphere
[NASA-CR-186090] 03 p0369 N90-12109
Ozone depletion, greenhouse gases, and climate change
[PB89-216097] 03 p0369 N90-12110
Meeting review: The Second NCAR (National Center for Atmospheric Research) Research Aircraft Fleet Workshop
[PB89-200901] 03 p0369 N90-12113
Middle Atmosphere Program. Handbook for MAP, volume 28
[NASA-CR-184972] 03 p0370 N90-12117
Heatstroke pathophysiology: The energy depletion model
[AD-A212156] 03 p0380 N90-12164
Gordon Conference on Atomic Physics
[AD-A211946] 03 p0402 N90-12304
A Conference on Three-Dimensional Representation held in University of Minnesota on 24-26 May 1989
[AD-A211630] 03 p0406 N90-12324
Max '91 Workshop 2: Developments in Observations and Theory for Solar Cycle 22
[NASA-TM-101893] 03 p0429 N90-12459
Research in Natural Laminar Flow and Laminar-Flow Control, part 1
[NASA-CP-2487-PT-1] 04 p0438 N90-12503
Research in Natural Laminar Flow and Laminar-Flow Control, part 2
[NASA-CP-2487-PT-2] 04 p0440 N90-12519
Research in Natural Laminar Flow and Laminar-Flow Control, part 3
[NASA-CP-2487-PT-3] 04 p0443 N90-12539
Guidance and Control Panel Symposium on Guidance and Control of Unmanned Air Vehicles
[AGARD-AR-260] 04 p0458 N90-12623
Proceedings of the DOD Workshop on the Manufacturing/Producibility of Organic Matrix Composites
[AD-A212577] 04 p0468 N90-12680
NBS/BAM (National Bureau of Standards/Bundesanstalt fuer Materialprufung) 1986 Symposium on Advanced Ceramics
[PB89-229074] 04 p0479 N90-12747
Laser Induced Damage in Optical Materials: 1987
[PB89-221162] 04 p0505 N90-12913
The 4th US Army Workshop on Low Heat Rejection Engines
[AD-A212379] 04 p0510 N90-12943
Proceedings of the Army Symposium on Solid Mechanics, 1989: Mechanics of Engineered Materials and Applications
[AD-A211954] 04 p0511 N90-12951
Exertional heatstroke: An international perspective. An introduction: The role of exercise in the etiology of exertional heatstroke
[AD-A212242] 04 p0523 N90-13020
Sound Localization by Human Observers symposium proceedings
[AD-A212877] 04 p0524 N90-13026
International Conference on Operator Theory: Advances and applications
[AD-A212341] 04 p0545 N90-13170
International Conference on Fixed Point Theory and Applications
[AD-A212369] 04 p0545 N90-13171
Seminars of Applied Physics, Materials Physics and Biomedical Engineering, 1989
[PB89-218572] 04 p0548 N90-13192
Proceedings of the 10 May 1989 Antiproton Technology Workshop: Addendum
[AD-A212804] 04 p0554 N90-13227
Workshop on Recent Progress in Surface and Volume Scattering
[AD-A212455] 04 p0555 N90-13236
European Solid State Device Research Conference (18th) ESSDERC 88 held in Montpellier, France on 13-16 September 1988
[AD-A210618] 04 p0558 N90-13250
Flight deck automation: Promises and realities
[NASA-CP-10036] 05 p0580 N90-13384
Flight Mechanics/Estimation Theory Symposium, 1989
[NASA-CP-3050] 05 p0586 N90-13413
Introduction to the report of the Asilomar 3 LDR workshop 05 p0594 N90-13450
Space Station Engineering Design Issues
[NASA-CR-185978] 05 p0601 N90-13492
The Fourth Oxford International Conference on the Mechanical Properties of Materials at High Rates of Strain
[AD-A212293] 05 p0653 N90-13809
European Rocket and Balloon Programs and Related Research
[ESA-SP-291] 05 p0656 N90-13826
Proceedings: US/FRG (Federal Republic of Germany) Workshop on Photochemical Ozone Problem and Its Control: US Experiences and the Situation in Europe
[PB89-233514] 05 p0666 N90-13891
ULF/VLF (0.001 to 50 Hz) Seismo-Acoustic Noise in the Ocean
[AD-A212942] 05 p0671 N90-13913
Cells in Space
[NASA-CP-10034] 05 p0676 N90-13939
Flight in adverse environmental conditions
[AGARD-AR-277] 06 p0723 N90-14218
Superplasticity
[AGARD-LS-168] 06 p0743 N90-14325
The 7th International Conference on Ceramics
[DE90-002144] 06 p0752 N90-14374
Operational Decision Aids for Exploiting or Mitigating Electromagnetic Propagation Effects
[AGARD-CP-453] 06 p0757 N90-14405
Proceedings of the First Annual Fuel Cells Contractors Review Meeting
[DE89-011699] 06 p0803 N90-14675
International Conference on Global and Regional Atmospheric Environmental Chemistry and visit to Hangzhou, China, foreign trip report
[DE90-000099] 06 p0810 N90-14713
Workshop on synoptic meteorology instruction
[PB90-109950] 06 p0817 N90-14751
Mid-Oceanic Ridge: A Dynamic Global System
[PB89-198691] 06 p0818 N90-14758
Proceedings of the Focused Research Program on Spectral Theory and Boundary Value Problems. Volume 4: Nonlinear Differential Equations
[DE90-000920] 06 p0822 N90-14780
Software Reuse Issues
[NASA-CP-3057] 06 p0824 N90-14789
Proceedings of the Conference on High-Spin Nuclear Structure and Novel Nuclear Shapes
[DE88-013968] 06 p0839 N90-14875
NIKHEF-K contributions to the 1989 Particle Accelerator Conference
[NIKHEF/AMPS/89/03] 06 p0841 N90-14891
Proceedings of the Conference on Application of Scanning Methodologies in Libraries
[PB89-233415] 06 p0858 N90-14990
Nomenclature for physical mapping of complex genomes
[DE89-015173] 06 p0859 N90-14994
Abstracts for the 52nd Annual Meeting of the Meteoritical Society
[NASA-CR-186160] 06 p0860 N90-14998
Flight in Adverse Environmental Conditions
[AGARD-CP-470] 07 p0869 N90-15041
International Aircraft Occupant Safety Conference and Workshop proceedings
[AD-A214452] 07 p0877 N90-15085
New Light Alloys
[AGARD-CP-444] 07 p0897 N90-15185
Proceedings of the Antenna Applications Symposium, volume 2
[AD-A213815] 07 p0919 N90-15313
Proceedings of the 1988 Structural Integrity Program Conference
[AD-A213545] 07 p0947 N90-15486
Acid rain research
[DE90-003283] 07 p0957 N90-15537
Responding to the threat of global warming: Options for the Pacific and Asia
[DE90-003553] 07 p0957 N90-15539
Ada 9X project report. Revision request report
[AD-A213503] 07 p0975 N90-15629
The 17th AINSE Plasma Physics Conference: Conference handbook
[DE90-600936] 07 p0996 N90-15759
Proceedings of the Latin American Conference on the Applications of the Moessbauer Effect
[DE90-600819] 07 p1002 N90-15803
The age of the galactic disk
[NASA-CR-186292] 07 p1013 N90-15869
Advances in techniques and technologies for air vehicle navigation and guidance
[AGARD-AR-276] 08 p1020 N90-15899
Fuel Tank Technology
[AGARD-R-771] 08 p1021 N90-15904
Guidance and Control of Unmanned Air Vehicles
[AGARD-CP-436] 08 p1025 N90-15924
Special Course on Advances in Cryogenic Wind Tunnel Technology
[AGARD-R-774] 08 p1028 N90-15939
Crew Safety and Rescue in Space: An International Approach
[ESA-SP-300] 08 p1034 N90-15974
The Eighteenth Conference on Stochastic Processes and their Applications
[AD-A212301] 08 p1040 N90-16010
Structure-property relationships in ion-beam surface-modified ceramics: Theory and applications
[AD-A212785] 08 p1047 N90-16054
Ninth Battery and Electrochemical Contractors' Conference: Extended abstracts
[DE89-016837] 08 p1059 N90-16120
Visual Information Processing for Television and Telerobotics
[NASA-CP-3053] 08 p1072 N90-16204
Proceedings of the 5th User Seminar of the German Remote Sensing Data Center of the DFVLR
[DFVLR-MITT-89-04] 08 p1092 N90-16318
Proceedings of the Conference on Technology-Based Confidence Building: Energy and Environment
[DE90-003363] 08 p1099 N90-16366
The 2nd Symposium on the Frontiers of Massively Parallel Computations
[NASA-TM-101918] 08 p1113 N90-16442
Proceedings of the specialists' meeting on physics and engineering of fission and spallation
[DE90-719706] 08 p1125 N90-16519
International conference management
08 p1136 N90-16583
Proceedings of the 79th SEGJ Conference
[DE89-760006] 08 p1157 N90-16704
Advances in Techniques and Technologies for Air Vehicle Navigation and Guidance
[AGARD-CP-455] 09 p1163 N90-16731
Progress in Space Transportation
[ESA-SP-293] 09 p1173 N90-16782
Symposium on Chemical Precursors to Ceramics
[AD-A214499] 09 p1196 N90-16932
Assessment of ground-coupled heat pumps
[DE90-003977] 09 p1220 N90-17079
Proceedings of the 17th Conference on Toxicology
[AD-A215076] 09 p1252 N90-17263
Workshop on the Effects of Combined Fire Products on Human Physiological and Psychological Performance
[AD-A215465] 09 p1253 N90-17270
The 10th Gordon Research Conference on Plasma Chemistry
[AD-A215161] 09 p1285 N90-17449
Workshop on Hydrogen Effects in InP and Related Compounds
[AD-A215197] 09 p1290 N90-17479
Proceedings of the conference on Hot Carriers in Semiconductors
[AD-A215544] 09 p1291 N90-17482
Proceedings of Colloquium 110 of the International Astronomical Union on Library and Information Services in Astronomy
[AD-A215612] 09 p1298 N90-17523
Missile Aerodynamics: NEAR Conference on Missile Aerodynamics
[ISBN-0-9620629-1-X] 10 p1303 N90-17540
Aircraft Fire Safety
[AGARD-CP-467] 10 p1311 N90-17581
CAST-10-2/DOA 2 Airfoil Studies Workshop Results
[NASA-CP-3052] 10 p1323 N90-17647
The 15th Transducer Workshop --- for telemetry applications
[AD-A215515] 10 p1327 N90-17665
European Space Power, volume 1
[ESA-SP-294-VOL-1] 10 p1329 N90-17678
European Space Power, volume 2
[ESA-SP-294-VOL-2] 10 p1338 N90-17748
Proceedings of a workshop on Higher-Order Spectral Analysis
[AD-A215849] 10 p1353 N90-17845
Proceedings of the Second Noncontact Temperature Measurement Workshop
[NASA-CR-181289] 10 p1362 N90-17894

Proceedings of the Thirteenth NASA Propagation Experimenters Meeting (NAPEX 13)
[NASA-CR-186062] 10 p1371 N90-17945
Preliminary collection 891 of lectures/papers in Symposium by Society of Automotive Engineers of Japan
[DE90-710449] 10 p1391 N90-18045
Parameterization of small-scale processes
[AD-A215507] 10 p1398 N90-18082
Proceedings of the 4th Annual Ada Software Engineering Education and Training Symposium
[AD-A214663] 10 p1417 N90-18162
High-Level Vision and Planning Workshop Proceedings
[AD-A215982] 10 p1420 N90-18188
Solar-Terrestrial Science Strategy Workshop
[NASA-CP-3048] 10 p1444 N90-18329
Background of the workshop
10 p1444 N90-18330
AGARD/SMP Review: Damage Tolerance for Engine Structures. 2: Defects and Quantitative Materials Behaviour — conference
[AGARD-R-769] 11 p1457 N90-18396
Unsteady Aerodynamic Phenomena in Turbomachines
[AGARD-CP-468] 11 p1459 N90-18405
The 1989 JANNAF Propulsion Meeting, volume 1
[CPIA-PUBL-515-VOL-1] 11 p1470 N90-18462
Third European Conference on Composite Materials
[EOARD-LR-89-050] 11 p1476 N90-18494
Proceedings of the 38th International Wire and Cable Symposium
[AD-A216023] 11 p1501 N90-18638
Investigation report of the investigation commission for interchange of heat pump technology in Europe
[DE89-782293] 11 p1505 N90-18666
The Executive Workshop on Cost/Performance Measurement. Volume 1: Executive summary
[AD-A216745] 11 p1546 N90-18898
Calendar of selected aeronautical and space meetings
[AGARD-CAL-90/1] 11 p1574 N90-19060
Infrared Spectroscopy in Astronomy
[ESA-SP-290] 11 p1578 N90-19084
Symposium on air traffic control training for tomorrow's technology
[PB90-127325] 12 p1601 N90-19216
Earth Science Geostationary Platform Technology
[NASA-CP-3040] 12 p1608 N90-19249
Proceedings of a contractors meeting on Combustion Rocket Propulsion Diagnostics of Reacting Flow
[AD-A216445] 12 p1617 N90-19297
International conference on Surface Modification of Metals by Ion Beams
[AD-A215872] 12 p1626 N90-19345
Proceedings of the 2nd United States/USSR Symposium on Air Pollution Effects on Vegetation Including Forest Ecosystems
[PB90-127119] 12 p1685 N90-19678
The EURAD Model: Structure and First Results
[REPT-61] 12 p1686 N90-19680
Colloquium on Synoptic Meteorology
[PB90-121112] 12 p1692 N90-19720
The 41st Annual Gaseous Electronics Conference
[AD-A214540] 12 p1715 N90-19851
National Technical Information Service 1989 Users Conference proceedings
[PB90-142563] 12 p1726 N90-19921
Physics and Mechanics of Cometary Materials
[ESA-SP-302] 12 p1738 N90-19989
Implications of Advanced Technologies for Air and Spacecraft Escape
[AGARD-CP-472] 13 p1751 N90-20054
Summary report of the Summer Conference of the DARPA-Materials Research Council
[AD-A217380] 13 p1767 N90-20143
Symposium on High Temperature and Materials Chemistry
[DE90-008047] 13 p1768 N90-20148
Center of Gravity: Metallic Solidification
[DFVLR-IB-333-89/3] 13 p1784 N90-20238
Conference digest: Thirteenth International Conference on Infrared and Millimeter Waves, volume 1039
[AD-A217343] 13 p1793 N90-20291
Space Electrochemical Research and Technology (SERT), 1989
[NASA-CP-3056] 13 p1821 N90-20454
Assessment of crew workload measurement methods, techniques and procedures. Volume 1: Process, methods and results
[AD-A217699] 13 p1855 N90-20647
Graphics Technology in Space Applications (GTSA 1989)
[NASA-CP-3045] 13 p1856 N90-20651
Towards SDS (Strategic Defense System) testing and evaluation: A collection of relevant topics
[AD-A217610] 13 p1880 N90-20783
Optical Bistability, 1988
[AD-A217681] 13 p1888 N90-20832
Workshop on the Physics and Chemistry of Mercury Cadmium Telluride and Related II-VI compounds
[AD-A217496] 13 p1894 N90-20867
Joint University Program for Air Transportation Research, 1988-1989
[NASA-CP-3063] 14 p1905 N90-20921
Computational Methods for Aerodynamic Design (Inverse) and Optimization
[AGARD-CP-463] 14 p1916 N90-20976
Secondary Flows in Turbomachines
[AGARD-CP-469] 14 p1922 N90-21009
Proceedings of the 13th International Congress on Instrumentation in Aerospace Simulation Facilities
[EOARD-LR-89-069] 14 p1929 N90-21046
NASA/DOD Controls-Structures Interaction Technology 1989
[NASA-CP-3041] 14 p1933 N90-21062
Modelling of molecular structures and properties in physical chemistry and biophysics
[AD-A214561] 14 p1947 N90-21145
Minutes of the 23rd Explosives Safety Seminar, volume 1
[AD-A218264] 14 p1958 N90-21213
Minutes of the 23rd Eplosives Safety Seminar, volume 2
[AD-A218265] 14 p1959 N90-21214
The 4th Annual Review of Progress in Applied Computational Electromagnetics
[AD-A217912] 14 p1966 N90-21257
The 5th Annual Review of Progress in Applied Computational Electromagnetics
[AD-A217994] 14 p1966 N90-21258
Proceedings of the Joint NOSC/NRL (Naval Ocean Systems Center/Naval Research Laboratory) InP Microwave/Millimeter Wave Technology Workshop
[AD-A218216] 14 p1966 N90-21259
Proceedings of the Third Infrared Detector Technology Workshop
[NASA-TM-102209] 14 p1975 N90-21313
Tenth International Free Electron Laser Conference
[DE90-614773] 14 p1985 N90-21376
Proceedings of the 4th European Conference, volume 2
[AD-A216521] 14 p1986 N90-21382
US-Japan Workshop on Atomic Collisions in Solids: Abstracts of lectures
[DE90-008979] 14 p2025 N90-21611
Recent advances in the studies of the nova outburst
[DE90-008936] 14 p2038 N90-21691
Free-Space Power Transmission
[NASA-CP-10016] 15 p2060 N90-21795
Proceedings of the Advisory Committee on Standardization of Carbon-Phenolic Test Methods and Specifications
[NASA-CR-186478] 15 p2063 N90-21817
Applications of Mesh Generation to Complex 3-D Configurations
[AGARD-CP-464] 15 p2093 N90-21975
Recent developments in grid generation
15 p2093 N90-21976
The 24th Aerospace Mechanisms Symposium
[NASA-CP-3062] 15 p2112 N90-22079
Proceedings of the Conference on Technology-Based Confidence Building: Energy and Environment
[CNSS-PAPERS-22] 15 p2125 N90-22152
Topical Conference on the Origin of the Earth
[NASA-CR-185061] 15 p2128 N90-22166
Proceedings of the 6th Regional Symposium on Biophysics
[DE90-619618] 15 p2136 N90-22206
Vision Science and Technology at NASA: Results of a Workshop
[NASA-TM-102214-REV-1] 15 p2138 N90-22216
The 1990 Goddard Conference on Space Applications of Artificial Intelligence
[NASA-CP-3068] 15 p2152 N90-22294
Impurity control in toroidal devices
[DE90-618585] 15 p2170 N90-22399
Space Station Workshop: Commercial Missions and User Requirements
[NASA-TM-102912] 15 p2175 N90-22428
Computer conferencing: Minds meeting anywhere anytime 15 p2179 N90-22452
High Intensity Electro-Magnetic and Ultrasonic Effects on Inorganic Materials Behavior and Processing Workshop
[AD-A218884] 16 p2215 N90-22640
Spatial Displays and Spatial Instruments
[NASA-CP-10032] 16 p2267 N90-22918
Proceedings of the 3rd Annual Conference on Aerospace Computational Control, volume 1
[NASA-CR-186445] 16 p2279 N90-22987
Proceedings of the 3rd Annual Conference on Aerospace Computational Control, volume 2
[NASA-CR-186447] 16 p2289 N90-23040
Proceedings of the NATO Advanced Workshop on Supercomputing
[AD-A218508] 16 p2299 N90-23102
Proceedings of the 9th International Conference on Computing Methods in Applied Science and Engineering
[AD-A219307] 16 p2307 N90-23149
Transactions of the Seventh Army Conference on Applied Mathematics and Computing
[AD-A219220] 16 p2309 N90-23160
ONR Far East Scientific Information Bulletin, Volume 13, No. 4
[ONRFE-SCI-INFO-BULL-13(4)88]
16 p2311 N90-23168
Support for the 16th International Conference on the Physics of Electronic and Atomic Collisions
[AD-A218567] 16 p2315 N90-23200
The Energetic Gamma-Ray Experiment Telescope (EGRET) Science Symposium
[NASA-CP-3071] 16 p2333 N90-23294
Proceedings of Workshop on Atmospheric Density and Aerodynamic Drag Models for Air Force Operations, volume 1
[AD-A220381] 17 p2345 N90-23355
Proceedings of Workshop on Atmospheric Density and Aerodynamic Drag Models for Air Force Operations, volume 2
[AD-A220382] 17 p2345 N90-23356
Peacetime replacement and crash damage factors for army aircraft
[AD-A218544] 17 p2348 N90-23372
Location and Navigation Satellite Systems
[ISBN-2-85-428-242-6] 17 p2358 N90-23420
The 18th Informal Conference on Photochemistry
[AD-A219779] 17 p2373 N90-23510
Informal conference on the Chemistry of Energetic Azides, Isocyanates, and Related Species
[AD-A219825] 17 p2373 N90-23514
Workshop on ESD (Electrostatic Discharge) Ignition of Composite Solid Propellants
[AD-A218599] 17 p2382 N90-23569
Proceedings of the 12th Symposium on Signal and Image Processing English-Language Abstracts
[AD-A218806] 17 p2388 N90-23598
DURIP: Computational modeling of cognitive processes
[AD-A219934] 17 p2437 N90-23886
Proceeding of the Embedded AI Languages Workshop
[AD-A218531] 17 p2442 N90-23914
US Army Research Office Workshop on Smart Materials, Structures and Mathematical Issues proceedings
[AD-A218528] 17 p2468 N90-24110
Proceedings of a research workshop on Computational Condensed Matter Physics. Total Energy Methods and Physics of III-V Semiconductors
[AD-A219568] 17 p2476 N90-24156
The 30th Airlines International Electronics Meeting Proceedings
[ETN-90-96973] 18 p2495 N90-24261
Second European In-Orbit Operations Technology Symposium
[ESA-SP-297] 18 p2499 N90-24280
National Educators' Workshop: Update 1989 Standard Experiments in Engineering Materials Science and Technology
[NASA-CP-3074] 18 p2513 N90-24350
Proceedings of Biostructures as Composite Materials ARO Workshop
[AD-A220262] 18 p2518 N90-24381
Fourth European Space Mechanisms and Tribology Symposium
[ESA-SP-299] 18 p2535 N90-24462
Low-Temperature CO-Oxidation Catalysts for Long-Life CO2 Lasers
[NASA-CP-3076] 18 p2556 N90-24586
Eighteenth NASTRAN (R) Users' Colloquium
[NASA-CP-3069] 18 p2568 N90-24637
Effects of solar ultraviolet radiation on biogeochemical dynamics in aquatic environments
[AD-A221119] 18 p2578 N90-24687
Activities report in meteorological research and associated fields
[ISSN-0349-0068] 18 p2582 N90-24707
Symposium on Applied Probability
[AD-A218760] 18 p2605 N90-24838
Proceedings of the 28th Annual US Army Operations Research Symposium (AORS), volume 1
[AD-A219349] 18 p2606 N90-24842
FAA/NASA En Route Noise Symposium
[NASA-CP-3067] 18 p2608 N90-24853
Workshop on High-Field NMR and Biological Applications
[DE90-010002] 18 p2614 N90-24889

Proceedings of symposium on Production and Target Interaction of Particle Beam
[IPPJ-900] 18 p2616 N90-24903
Conference on the Science and Technology of Thin-Film Superconductors
[DE90-000326] 18 p2620 N90-24926
Geoscience and a Lunar Base: A Comprehensive Plan for Lunar Exploration
[NASA-CP-3070] 18 p2638 N90-25030
Modeling and Applications of Transport Phenomena in Porous Media, volume 1
[VKI-LS-1990-01-VOL-1] 19 p2689 N90-25296
Modeling and Applications of Transport Phenomena in Porous Media, volume 2
[VKI-LS-1990-01-VOL-2] 19 p2690 N90-25302
Conference on Instrumental Activation Analysis: IAA 89
[DE90-615661] 19 p2694 N90-25327
Remote Sensing and the Earth's Environment
[ESA-SP-301] 19 p2706 N90-25398
Neck Injury in Advanced Military Aircraft Environments
[AGARD-CP-471] 19 p2717 N90-25459
Third Annual Workshop on Space Operations Automation and Robotics (SOAR 1989)
[NASA-CP-3059] 19 p2727 N90-25503
The 23rd ESLAB Symposium on Two Topics in X Ray Astronomy. Volume 1: X Ray Binaries
[ESA-SP-296-VOL-1] 19 p2765 N90-25711
Reports of workshops on Probe Measurements of Particles and Radiation in the Atmosphere of Titan
[NASA-TM-102218] 19 p2797 N90-25919
Eleventh European Cosmic Ray Symposium
[DE90-611419] 19 p2798 N90-25926
Eleventh European Cosmic Ray Symposium
[DE90-611424] 19 p2798 N90-25927
Second Meeting of the Space Agency Forum on the International Space Year (SAFISY)
[ESA-SP-1115] 19 p2800 N90-25932
Second Annual International Conference on Aging Aircraft
[AD-A222715] 20 p2805 N90-25961
Proceedings of the Second Symposium on GPS Applications in space, volume 1
[AD-A219978] 20 p2806 N90-25962
Proceedings of the Second Symposium on GPS Applications in Space, volume 2
[AD-A219979] 20 p2806 N90-25963
Space Transportation Avionics Technology Symposium. Volume 1: Executive summary
[NASA-CP-3081-VOL-1] 20 p2809 N90-25980
Technical evaluation report on the Guidance and Control Panel 49th Symposium on Fault Tolerant Design Concepts for Highly Integrated Flight Critical Guidance and Control Systems
[AGARD-AR-281] 20 p2813 N90-26012
Proceedings of the LDEF Materials Data Analysis Workshop
[NASA-CP-10046] 20 p2826 N90-26075
The 5th International symposium on palaeolimnology
[AD-A219244] 20 p2887 N90-26431
Proceedings of a workshop on Lunar Volcanic Glasses: Scientific and Resource Potential
[NASA-CR-186631] 20 p2888 N90-26437
Motion sickness, visual displays, and armored vehicle design
[AD-A222678] 20 p2902 N90-26506
Press abstracts of the 21st Lunar and Planetary Science Conference
[NASA-CR-186874] 20 p2941 N90-26738
Proceedings of a Workshop on Antarctic Meteorite Stranding Surfaces
[NASA-CR-186575] 20 p2942 N90-26739
Proceedings of a workshop on Differences Between Antarctic and Non-Antarctic Meteorites
[NASA-CR-184918] 20 p2942 N90-26740
First International Conference on Laboratory Research for Planetary Atmospheres
[NASA-CP-3077] 20 p2942 N90-26744
Rotorcraft aeromechanical stability-methodology assessment. Phase 2: Workshop
[NASA-TM-102272] 21 p2955 N90-26800
Proceedings of the 1987 Aircraft/Engine Structural Integrity Program (ASIP/ENSIP) Conference
[AD-A198037] 21 p2956 N90-26807
Application of damage tolerance
21 p2958 N90-26817
Advanced propulsion concepts
[NASA-CR-185920] 21 p2969 N90-26872
The 1990 Gordon Research Conference on Composites
[AD-A222849] 21 p2971 N90-26886
Summary of Discussions at the Eleventh Meeting of the Sandia Cooperative Group on the Aerothermochemistry of Turbulent Combustion
[DE89-001846] 21 p2973 N90-26896
Advanced Communication Processing Techniques
[AD-A223244] 21 p2996 N90-27027
Earth Sciences Requirements for the Information Sciences Experiment System
[NASA-CP-3072] 21 p3015 N90-27140
Abstracts of 1989 Japan Solar Energy Society and Japan Wind Energy Association Joint Conference
[DE90-503616] 21 p3019 N90-27168
MEVTV Workshop on Early Tectonic and Volcanic Evolution of Mars
[NASA-CR-186098] 21 p3021 N90-27176
Proceedings of the International Workshop on Geomagnetic Observatory Data Acquisition and Processing
[GEOPHYSICAL-PUBL-15] 21 p3021 N90-27177
Proceedings of the 21st Joint Meeting of the US-Japan Cooperative Program in Natural Resources Panel Wind and Seismic Effects
[PB90-186826] 21 p3030 N90-27226
Fifth Conference on Artificial Intelligence for Space Applications
[NASA-CP-3073] 21 p3040 N90-27275
The Second Asilomar Workshop on Progress in Mathematical Programming
[AD-A221986] 21 p3053 N90-27358
Proceedings of Workshop on Reliability in Computational Mechanics
[AD-A221694] 21 p3065 N90-27426
Support for the Forty-Second Annual Gaseous Electronics Conference
[AD-A222881] 21 p3073 N90-27473
Proceedings of the US-Japan Fusion Cooperation Program Exchange P148 Workshop on Advanced Current Drive Concepts
[IPPJ-REV-4] 21 p3078 N90-27498
The 2nd International Conference on Low-Energy Dislocation Structures
[AD-A222887] 21 p3082 N90-27525
The 1990 Gordon Research Conference on Crystal Growth
[AD-A223218] 21 p3083 N90-27531
Carbon in the Galaxy: Studies from Earth and Space
[NASA-CP-3061] 21 p3089 N90-27562
Proceedings of workshop on Dark Matter and the Structure of the Universe
[DE90-791308] 21 p3098 N90-27602
MEVTV Workshop on Tectonic Features on Mars
[NASA-CR-186143] 21 p3100 N90-27609
Integrated Air Traffic Management
[DLR-MITT-89-23] 22 p3112 N90-27676
AGARD/SMP Review Damage Tolerance for Engine Structures. 3: Component Behaviour and Life Management
[AGARD-R-770] 22 p3117 N90-27704
Space Vehicle Flight Mechanics
[AGARD-CP-489] 22 p3126 N90-27741
AMSAHTS 1990: Advances in Materials Science and Applications of High Temperature Superconductors
[NASA-CP-10043] 22 p3136 N90-27792
The 26th JANNAF Combustion Meeting, volume 1
[CPIA-PUBL-529-VOL-1] 22 p3161 N90-27927
Laser induced damage in optical materials: 1988
[PB90-185570] 22 p3179 N90-28041
Impact of Emerging NDE-NDI Methods on Aircraft Design, Manufacture, and Maintenance
[AGARD-CP-462] 22 p3184 N90-28068
Workshop minutes on Remote Sensing of Hydrocarbons and Toxic Pollutants
[PB90-186370] 22 p3194 N90-28127
Middle Atmosphere Program. Handbook for MAP, volume 29. Part 1: Extended Abstracts, International Symposium on Solar Activity Forcing of the Middle Atmosphere. Part 2: MASH Workshop
[NASA-CR-186005] 22 p3201 N90-28161
Comparison of satellite derived dynamical quantities in the stratosphere of the Southern Hemisphere
22 p3210 N90-28210
FIRE Science Results 1989
[NASA-CP-3079] 22 p3213 N90-28224
Conference on The Perception of Structure Program and Abstracts
[AD-A222437] 22 p3232 N90-28328
Report of the Invitational Workshop on Data Integrity
[PB90-148123] 22 p3240 N90-28372
Proceedings of the Conference on Artificial Intelligence in the Department of Energy Complex
[DE90-011634] 22 p3241 N90-28378
Aerodynamics of Combat Aircraft Controls and of Ground Effects
[AGARD-CP-465] 23 p3271 N90-28513
Proceedings of a workshop on Future Airport Passenger Terminals
[PB90-213620] 23 p3284 N90-28580
Advanced Earth-to-Orbit Propulsion Technology 1988, volume 1
[NASA-CP-3012-VOL-1] 23 p3290 N90-28611
High Temperature Surface Interactions
[AGARD-CP-461] 23 p3306 N90-28698
Proceedings of US Army Research Office Workshop on US Army Applications for Diamond and Diamondlike Materials
[AD-A224193] 23 p3314 N90-28741
Computerization of Welding Data: Proceedings of the conference and workshop
[PB90-219551] 23 p3332 N90-28841
Puerto Rico Workshop on Land-Based Sources of Marine Pollution in the Wider Caribbean Region
[PB90-184094] 23 p3348 N90-28921
Drilling the oceanic lower crust and mantle: A global strategy for exploring the deep oceanic crust and mantle in the 1990's
[PB90-240953] 23 p3351 N90-28936
Proceedings of the 14th Annual Climate Diagnostics Workshop
[PB90-198573] 23 p3351 N90-28938
Situational Awareness in Aerospace Operations
[AGARD-CP-478] 23 p3357 N90-28972
Proceedings of the NASA Conference on Space Telerobotics, volume 1
[NASA-CR-186856] 23 p3362 N90-29000
Proceedings of the NASA Conference on Space Telerobotics, volume 2
[NASA-CR-186857] 23 p3370 N90-29044
Workshop on Neural Networks
[DE90-014794] 23 p3385 N90-29120
Fifteenth International Conference on X Ray and Inner-Shell Processes
[DE90-013024] 23 p3393 N90-29170
Information management directions: The integration challenge
[PB90-219866] 23 p3405 N90-29245
Crossroads of Information Technology Standards
[PB90-239732] 23 p3406 N90-29251
The Second ARO Workshop on Rotorcraft Interactional Aerodynamics
[AD-A223310] 24 p3418 N90-29304
Analysis, Design and Synthesis Methods for Guidance and Control Systems
[AGARD-AG-314] 24 p3423 N90-29338
AFOSR/ONR Contractors' Meeting on Combustion Rocket Propulsion Diagnostics of Reacting Flow
[AD-A224411] 24 p3441 N90-29432
Proceedings of the 45th Ohio State University Symposium on Molecular Spectroscopy
[AD-A224349] 24 p3445 N90-29457
IEEE Conference on Neural Information Processing Systems, Natural and Synthetic
[AD-A223611] 24 p3461 N90-29552
Proceedings of the 14th Annual Electronics Manufacturing Seminar
[AD-A224276] 24 p3463 N90-29563
Report on the International Workshop on Progress Towards Molecular Scale Electronics
[AD-A223758] 24 p3465 N90-29575
Proceedings of damping '89. Volume 1: Pages AAB-1 through DCD-11
[AD-A223431] 24 p3479 N90-29664
Proceedings of damping '89. Volume 2: Pages FAA-1 through IBD-15
[AD-A223432] 24 p3479 N90-29665
Proceedings of Damping '89. Volume 3: Pages ICA-1 through KDC-15
[AD-A223433] 24 p3479 N90-29666
Proceedings of the High Energy Density Materials Contractors Conference
[AD-A223793] 24 p3484 N90-29695
Proceedings of the 17th Annual Gravity Gradiometer Conference
[AD-A223568] 24 p3492 N90-29735
Proceedings of a Workshop on the Geoelectric and Geomagnetic Environment of Continental Margins
[AD-A223743] 24 p3493 N90-29739
Proceedings of the NASA Conference on Space Telerobotics, volume 3
[NASA-CR-186858] 24 p3500 N90-29780
Proceedings of the NASA Conference on Space Telerobotics, volume 4
[NASA-CR-186859] 24 p3508 N90-29830
Proceedings of the NASA Conference on Space Telerobotics, volume 5
[NASA-CR-186860] 24 p3516 N90-29874
Working implementation agreements for open systems interconnection protocols
[PB90-197948] 24 p3557 N90-30127

CONFIDENCE LIMITS
Number of test samples needed to obtain a desired Bayesian confidence interval for a proportion
[AD-A208157] 01 p0115 N90-10658
The computation and use of the asymptotic covariance matrix for measurement error models
[PB89-215321] 01 p0115 N90-10659

On lower confidence for PCS in truncated location parameter models
[AD-A210274] 01 p0115 N90-10661
Small sample theory for steady state confidence intervals
[AD-A212097] 03 p0393 N90-12242
Application of Bayesian reliability concepts to cruise missile electronic components
[AD-A216208] 10 p1394 N90-18059
Uncertainty analysis of the accident effect area of a BLEVE
[REPT-89-49] 15 p2126 N90-22160
Approximate interval estimation methods for the reliability of systems using component data with exponential and Weibull distributions
[AD-A219857] 17 p2460 N90-24048

CONFIGURATION INTERACTION
Computational modeling of pi-conjugated polyradicals
[AD-A210573] 01 p0113 N90-10648
A diagnostic for determining the quality of single-reference electron correlation methods
[NASA-TM-101929] 06 p0838 N90-14874
The dissociation energy of N2
[NASA-TM-101930] 07 p0891 N90-15153
General contraction of Gaussian basis sets. Part 2: Atomic natural orbitals and the calculation of atomic and molecular properties
[NASA-CR-186201] 08 p1119 N90-16482
Accurate quantum chemical calculations
[NASA-TM-101932] 23 p3303 N90-28680

CONFIGURATION MANAGEMENT
Independent Orbiter Assessment (IOA): FMEA/CIL assessment
[NASA-CR-185589] 02 p0170 N90-10960
A figure control sensor for the Large Deployable Reflector (LDR) 05 p0594 N90-13451
Expert systems for adaptive control of large space structures 05 p0595 N90-13452
Wavefront error sensing for LDR 05 p0595 N90-13455
Segment alignment control system 05 p0595 N90-13457
Distribution of hardware and software elements in unmanned air vehicle systems 08 p1027 N90-15933
Industrial Modernization Incentives Program: Computer-aided log book
[AD-A214614] 09 p1265 N90-17335
A flexible basis for software configuration management
[RSRE-MEMO-4127] 10 p1415 N90-18153
Configuration management and control for ESA space systems
[ESA-PSS-01-11-ISSUE-1] 11 p1574 N90-19061
Aeropropulsion facilities configuration control: Procedures manual
[NASA-TM-102541] 14 p1989 N90-21399
A soft actuation system for segmented reflector articulation and isolation 15 p2113 N90-22084
Analyzing spacecraft configurations through specialization and default reasoning 15 p2155 N90-22308
GSC configuration management plan
[NASA-CR-182044] 19 p2743 N90-25587
Method and apparatus for configuration control of redundant robots
[NASA-CASE-NPO-17801-1-CU] 21 p3010 N90-27110
A knowledge-based approach to configuration layout, justification, and documentation 21 p3041 N90-27286
A new approach to global control of redundant manipulators 23 p3363 N90-29002
Performance monitoring, fault detection, fault localization design guidance
[AD-A223619] 24 p3478 N90-29655

CONFINEMENT
Thermal initiation of confined primary explosives with a proton beam
[AD-A212954] 04 p0482 N90-12767
Structure properties of confined systems. Hard spheres between ideal walls
[DE90-600818] 07 p0929 N90-15378
Thermomechanically-induced convective motion and natural convection in confined gaseous helium subjected to boundary heating 15 p2089 N90-21960
Laser Doppler anemometry measurements of a confined turbulent water jet with a uniform background flow 15 p2092 N90-21971
Experimental observations on transition to turbulence in confined coaxial jets and other boundary layer flows
[DE90-008939] 15 p2098 N90-22005
Advances in spheromak understanding and parameters
[DE90-012052] 19 p2759 N90-25678
An experimental investigation of a single and multiphase confined coaxial jet 23 p3324 N90-28796

CONFIRMATION
U PROVING

CONFLUENCE
U CONVERGENCE

CONFORMAL MAPPING
Local structure of a 2-codimensional conformally flat submanifold in an Euclidean space R(sup n+2)
[DE89-618379] 02 p0264 N90-11501
On sufficient conditions for a function to be analytic
[DE89-618382] 02 p0264 N90-11503
Singularity theory and N = 2 superconformal field theories
[DE89-016582] 02 p0269 N90-11538
Bordered surfaces, off-shell amplitudes, sewing, and string field theory
[DE90-000006] 03 p0414 N90-12378
Operator product coefficients in non-diagonal conformal field theories
[NIKHEF-H/88-19] 04 p0553 N90-13224
The off-shell closed strings as the topological open membranes: Dynamical transmutation of world sheet dimension
[DE89-635721] 08 p1134 N90-16571
Analysis and numerical solution of flow over airfoil with control flap 10 p1307 N90-17564
Cubic interaction in conformal theory of integer higher-spin fields in four dimensional space-time
[DE90-607095] 10 p1425 N90-18220
Solution of a class of conformal quantum field theory models in D-dimensional space
[DE90-607094] 10 p1439 N90-18306
Small and great circle routines
[AD-A217652] 13 p1820 N90-20449
The N = 2 superconformal algebras on hyperelliptic surfaces and their Coulomb gas realization
[DE90-612790] 14 p2020 N90-21581
Fusion algebra and fusing matrices
[DE90-612798] 14 p2021 N90-21583
Conserved conformal currents in curved space-time
[DE90-612766] 14 p2034 N90-21672
Generation, optimization, and adaptation of multidomain meshes around complex configurations 15 p2095 N90-21990
Numerical conformal mapping and applications
[AD-A219789] 17 p2457 N90-24019
Free boundary problems for flow with vorticity
[AD-A218415] 22 p3168 N90-27971
Prediction of subsonic vortex shedding from forebodies with chines
[NASA-CR-4323] 23 p3268 N90-28494
Beltrami algebra and symmetry of Beltrami equation on Riemann surfaces
[DE90-627157] 23 p3388 N90-29135
Trajectories of renormalization group flows on the phase diagram of N=2 superconformal field theories
[DE90-627212] 23 p3391 N90-29154
Topology of singularities and phase diagram of N=2 superconformal field theories
[DE90-627213] 23 p3391 N90-29155
A canonical integration technique of arbitrary order
[DE90-628377] 24 p3541 N90-30025

CONFORMAL TRANSFORMATIONS
U CONFORMAL MAPPING

CONGESTION
Adaptive backoff synchronization techniques
[AD-A213966] 07 p0980 N90-15658
Rate-based congestion control in networks with smart links, revision
[NASA-CR-186698] 17 p2452 N90-23987
Analysis of random drop for gateway congestion control
[NASA-CR-186736] 20 p2935 N90-26698

CONGRESSES
U CONFERENCES

CONGRESSIONAL REPORTS
Safer skies with TCAS: Traffic Alert and Collision Avoidance System
[PB89-169221] 01 p0004 N90-10016
Advancing automation and robotics technology for the space station Freedom and for the US economy
[NASA-TM-101561] 01 p0102 N90-10577
Departments of Veterans Affairs and Housing and Urban Development, and Independent Agencies Appropriations Bill, 1990
[H-REPT-101-150] 04 p0563 N90-13281
National Aeronautics and Space Administration 04 p0563 N90-13282
Fiscal year 1990 authorization request and budget estimates for the National Aeronautics and Space Administration
[GPO-96-945] 04 p0563 N90-13283
Departments of Veterans Affairs and Housing and Urban Development, and Independent Agencies Appropriation Bill, 1990
[S-REPT-101-128] 04 p0563 N90-13284
The 1990 National Aeronautics and Space Administration Authorization
[GPO-98-466] 04 p0563 N90-13285
Department of Veterans Affairs and Housing and Urban Development, and Independent Agencies Appropriations Act, 1990
[HR-2916-PP] 04 p0564 N90-13286
National Aeronautics and Space Administration 04 p0564 N90-13287
National Aeronautics and Space Administration Authorization Act, fiscal year 1990
[S-REPT-101-157] 04 p0564 N90-13288
National Aeronautics and Space Administration Authorization Act, fiscal year 1990
[S-REPT-101-157] 04 p0564 N90-13289
NASA technology applications
[GPO-99-412] 04 p0564 N90-13290
National Aeronautics and Space Administration Multiyear Authorization Act of 1989 05 p0709 N90-14148
National Aeronautics and Space Administration authorization
[S-HRG-101-348] 05 p0709 N90-14149
Consumer Ozone Protection Act of 1989
[S-HRG-101-377] 06 p0809 N90-14708
Space operations: Listing of NASA scientific missions, 1980-2000. Fact sheet for the Chairman, Subcommittee on Space Science and Applications, Committee on Science, Space, and Technology, House of Representatives
[AD-A213493] 07 p1016 N90-15881
Round trip to orbit. Human spaceflight alternatives: Special report
[OTA-ISC-419] 08 p1033 N90-15966
Advancing automation and robotics technology for the Space Station Freedom and for the US economy: Submitted to the United States Congress
[NASA-TM-101647] 12 p1613 N90-19279
Managing Federal information resources
[PB90-100173] 15 p2175 N90-22429
Space Shuttle, NASA's major changes to flight hardware: Fact sheet for the Chairman, Committee on Science, Space, and Technology, House of Representatives
[GAO/NSIAD-88-173FS] 15 p2181 N90-22461
Nuclear power in space
[GPO-23-835] 16 p2316 N90-23202
Aviation security: Corrective actions underway, but better inspection guidance still needed. Report to the Chairwoman, Government Activities and Transportation Subcommittee, Committee on Government Operations, House of Representatives
[GAO/RCED-88-160] 17 p2347 N90-23367
Space funding: NASA and DOD activities for fiscal years 1981 through 1989. Fact sheet for the Chairman and the Ranking Minority Member, Subcommittee on Science, Technology, and Space, Committee on Commerce, Science, and Transportation, US Senate
[GAO/NSIAD-89-102FS] 17 p2481 N90-24187
The 1991 NASA authorization: National Aeronautics and Space Administration fiscal year 1991 authorization request and budget estimates
[GPO-27-291] 17 p2481 N90-24188
Space shuttle: The future of the Vandenberg launch site needs to be determined
[GAO/NSIAD-88-158] 18 p2509 N90-24337
Satellite data archiving: US and foreign activities and plans for environmental information
[GAO/RCED-88-201] 18 p2633 N90-25001
Military space operations: Shuttle and satellite computer systems do not meet performance objectives
[GAO/IMTEC-88-7] 18 p2635 N90-25014
Space exploration: NASA's deep space missions are experiencing long delays
[GAO/NSIAD-88-128BR] 18 p2635 N90-25015
Space shuttle: Changes to the solid rocket motor contract
[GAO/NSIAD-88-203] 18 p2636 N90-25016
Departments of Veterans Affairs and Housing and Urban Development, and Independent Agencies Appropriations for Fiscal Year 1990, part 2
[S-HRG-101-345-PT-2] 18 p2636 N90-25017
National Aeronautics and Space Administration, 2 May 1989 18 p2636 N90-25018
National Aeronautics and Space Administration, 3 May 1989 18 p2636 N90-25019
Space operations: NASA efforts to develop and deploy advanced spacecraft computers. Report to the Chairman, Subcommittee on Space Science and Applications, Committee on Science, Space, and Technology, House of Representatives
[GAO/IMTEC-89-17] 19 p2742 N90-25582
Technology transfer: US and foreign participation in R and D at Federal laboratories
[GAO/RCED-88-203BR] 19 p2764 N90-25706

Technology transfer: Implementation status of the Federal Technology Transfer Act of 1986. Report to Congressional requesters
[GAO/RCED-89-154] 19 p2764 N90-25707
Aviation safety: Conditions within the air traffic control work force. Fact sheet for congressional requesters
[GAO/RCED-89-113FS] 20 p2805 N90-25958
Aviation safety: Serious problems continue to trouble the air traffic control work force. Report to congressional requesters
[GAO/RCED-89-112] 20 p2805 N90-25959
Space exploration: Cost, schedule, and performance of NASA's Mars Observer Mission. Fact sheet for the Chairman, Subcommittee on Science, Technology, and Space, Committee on Commerce, Science, and Transportation, US Senate
[GAO/NSIAD-88-137FS] 20 p2815 N90-26021
Space exploration: Cost, schedule, and performance of NASA's Magellan Mission to Venus. Fact sheet for the Chairman, Subcommittee on Science, Technology, and Space, Committee on Commerce, Science, and Transportation, US Senate
[GAO/NSIAD-88-130FS] 20 p2815 N90-26022
Space exploration: Cost, schedule, and performance of NASA's Ulysses Mission to the Sun. Fact sheet for the Chairman, Subcommittee on Science, Technology, and Space, Committee on Commerce, Science, and Transportation, US Senate
[GAO/NSIAD-88-129FS] 20 p2815 N90-26023
Space program: Space debris a potential threat to Space Station and shuttle
[GAO/IMTEC-90-18] 20 p2815 N90-26024
Space exploration: Cost, schedule, and performance of NASA's Galileo Mission to Jupiter. Fact sheet for the Chairman, Subcommittee on Science, Technology, and Space, Committee on Commerce, Science, and Transportation, US Senate
[GAO/NSIAD-88-138FS] 20 p2816 N90-26025
Space transportation: NASA has no firm need for increasingly costly orbital maneuvering vehicle
[GAO/NSIAD-90-192] 20 p2819 N90-26041
Space shuttle: Follow-up evaluation of NASA's solid rocket motor procurement. Report to the Chairman, Committee on Government Operations, House of Representatives
[GAO/NSIAD-89-89] 20 p2824 N90-26066
NASA project status reports: Congressional requirements can be met, but reliability must be ensured
[GAO/NSIAD-90-40] 20 p2843 N90-26189
Space operations: NASA's communications support for Earth orbiting spacecraft. Report to Chairman, Subcommittee on Space Science and Applications, Committee on Science, Space and Technology, House of Representatives
[GAO/IMTEC-89-41] 20 p2851 N90-26215
Technology development: Future use of NASA's large format camera is uncertain
[GAO/NSIAD-90-142] 20 p2865 N90-26298
Space operations: NASA is not properly safeguarding valuable data from past missions
[GAO/IMTEC-90-1] 20 p2936 N90-26704
Helping America compete: The role of Federal scientific and technical information
[OTA-CIT-454] 21 p3086 N90-27549
Departments of Veterans Affairs and Housing and Urban Development, and independent agencies appropriations for 1991. Part 4: National Aeronautics and Space Administration
[GPO-30-861] 21 p3088 N90-27561
Affordable spacecraft: Design and launch alternatives. Background paper 22 p3125 N90-27737
Space program safety: Funding for NASA's safety organizations should be centralized
[GAO/NSIAD-90-187] 22 p3255 N90-28434
Space projects: Improvements needed in selecting future projects for private financing
[GAO/NSIAD-90-147] 22 p3256 N90-28439
Present state of knowledge of the upper atmosphere 1990: An assessment report
[NASA-RP-1242] 23 p3350 N90-28929
Federal support to universities, colleges, and selected nonprofit institutions: Fiscal year 1988 (detailed statistical tables)
[PB90-226887] 23 p3404 N90-29236
Global Climate Change: Seeking a Global Consensus
[S-HRG-101-842] 24 p3486 N90-29704
Environmental quality, 1970 - 1990
[PB90-214610] 24 p3487 N90-29705
NASA authorization, 1991, volume 2
[GPO-32-196] 24 p3559 N90-30138

CONGRUENCES
The perception of geometrical structure from congruence 16 p2270 N90-22935
Supercongruences
[CWI-AM-R8918] 18 p2599 N90-24791

CONICAL BODIES
A coning motion apparatus for hydrodynamic model testing in a non-planar cross-flow
[AD-A213431] 07 p0930 N90-15383
External flow computations for a finned 60mm ramjet in steady supersonic flight
[AD-A216998] 12 p1605 N90-19233
Series reversion/inversion of Lambert's time function
[AD-A216243] 12 p1607 N90-19245
Discrete-vortex model for the symmetric-vortex flow on cones
[NASA-TP-2989] 14 p1909 N90-20946
Side moment exerted by a spinning, coning, highly viscous liquid payload
[AD-A218746] 16 p2237 N90-22763
Measurement and analysis of the electromagnetic scattering of a geodesic array of triangular trihedral corner reflectors
[AD-A220457] 17 p2389 N90-23608
Spectral methods for electromagnetic propagation and diffraction
[AD-A220291] 17 p2393 N90-23632
A monotone complementarity problem in Hilbert space
[AD-A220819] 17 p2468 N90-24105
Applications of cone theory to boundary value problems
[AD-A220939] 18 p2603 N90-24828

CONICAL FLARE
U CONES

CONICAL FLOW
Some observations on transitory stall in conical diffusers
[NASA-TM-102387] 04 p0447 N90-12561
The experimental investigation of flow in the core of a vortex structure
[BR114893] 24 p3468 N90-29597

CONICAL NOZZLES
Arcjet nozzle design impacts 11 p1473 N90-18478

CONICAL SHELLS
Ablative cooling of aerodynamically heated radomes
[AD-D014426] 14 p1971 N90-21293
The initial imperfection databank at the Delft University of Technology, part 3
[LR-568] 15 p2057 N90-21783
Derivation of the governing equations of anisotropic conical shells
[LR-609] 19 p2704 N90-25387

CONICS
NT ELLIPSES
NT PARABOLAS
Can ion acceleration by double-cyclotron absorption produce O(+) ion conics
[IRF-PREPRINT-114] 02 p0280 N90-11600
On the projective invariant representation of conics in computer graphics
[CWI-CS-R8938] 18 p2593 N90-24752

CONIFERS
Proceedings of the US/FRG (Fed. Republic of Germany) research symposium: Effects of Atmospheric Pollutants on the Spruce-Fir Forests of the Eastern United States and the Fed. Republic of Germany
[PB90-107160] 06 p0808 N90-14704
Monitoring of reforested areas through digital analysis of TM data
[INPE-4930-PRE/1420] 11 p1522 N90-18764
Evaluation of TM/LANDSAT and HRV/SPOT data in reforested areas
[INPE-4575-RPE/567] 11 p1524 N90-18772
Evaluation of TM/LANDSAT and HRV/SPOT data in the identification of reforested areas in the Mogi-Guacu (SP) region
[INPE-4874-PRE/1485] 13 p1819 N90-20442
Measurements of monoterpenes in a coniferous forest 20 p2886 N90-26421
Terpene concentrations and emissions in a Scots pine forest 20 p2886 N90-26422
The diurnal ozone cycle in a coniferous forest: The importance of meteorology and chemistry 20 p2886 N90-26423

CONJUGATE GRADIENT METHOD
Gradient projection techniques for large-scale optimization problems
[DE90-001986] 07 p0973 N90-15618
Piecewise linear-quadratic programming and its applications
[AD-A214489] 09 p1264 N90-17328
A combined finite element-boundary element formulation for solution of two-dimensional problems via CGFFT
[NASA-CR-186464] 12 p1620 N90-19309
Parallel conjugate gradient algorithms for manipulator dynamic simulation 16 p2290 N90-23045
Neural networks applied to signal processing
[AD-A219605] 17 p2454 N90-24000
A fast, preconditioned conjugate gradient Toeplitz solver
[NASA-CR-180367] 18 p2589 N90-24731
Trajectory optimization for an asymmetric launch vehicle
[NASA-CR-185630] 20 p2817 N90-26033
Efficient generalized conjugate gradient algorithms. Part 2: Implementation
[MATHS-REPT-A-118-PT-2] 20 p2908 N90-26543
Numerical analysis
[AD-A221982] 22 p3242 N90-28385
Efficient conjugate gradient algorithms for computation of the manipulator forward dynamics 24 p3514 N90-29864
A parallel least squares collocation conjugate gradient approach for the advection diffusion equation
[DE90-015965] 24 p3530 N90-29961
A new look at conjugate direction methods of optimization
[MATHS-REPT-A-125] 24 p3539 N90-30010

CONJUGATES
Conjugate profiles on mating gear teeth
[MEMO-COSOR-89-01] 05 p0651 N90-13795
Conjugate field approaches for active array compensation 12 p1610 N90-19266
A new look at conjugate direction methods of optimization
[MATHS-REPT-A-125] 24 p3539 N90-30010

CONJUGATION
NT PHASE CONJUGATION
Synthesis and chemistry of strained and conjugated fluorocarbons
[AD-A211633] 03 p0324 N90-11844

CONNECTIONS
U JOINTS (JUNCTIONS)

CONNECTIVE TISSUE
NT BONE MARROW
NT CARTILAGE
NT COLLAGENS
Effects of microgravity on rat bone, cartilage and connective tissues 20 p2891 N90-26454
Experiment K-6-02. Biomedical, biochemical and morphological alterations of muscle and dense, fibrous connective tissues during 14 days of spaceflight 20 p2892 N90-26456

CONNECTORS
NT ELECTRIC CONNECTORS
NT UMBILICAL CONNECTORS
NT UNIONS (CONNECTORS)
Varistor-particle lightning arrestor connector performance under simulated extreme lightning currents
[DE89-012663] 01 p0060 N90-10342
Connector selection program implementation notes, version 1.0
[DE90-004983] 08 p1085 N90-16279
Vortex motion phase separator for zero gravity liquid transfer
[NASA-CASE-KSC-11387-1] 13 p1783 N90-20236
Systematic errors in power measurements made with a dual six-port ANA
[PB90-145160] 14 p1968 N90-21276
The resupply interface mechanism RMS compatibility test 15 p2113 N90-22090
The connector space reduction mechanism 15 p2114 N90-22092
SKITTER/implement mechanical interface
[NASA-CR-184920] 17 p2384 N90-23578
Interconnecting devices conceived for in-orbit operations 18 p2506 N90-24323
Fluid connectors for operation in space 18 p2536 N90-24465
Multichip packaging technology with laser-patterned interconnects
[DE90-010743] 18 p2549 N90-24552
Quick-connect coupler for remote manipulation
[DE90-015352] 24 p3476 N90-29648

CONNECTORS (ELECTRIC)
U ELECTRIC CONNECTORS

CONOIDS
U CONICAL BODIES

CONSCIOUSNESS
Development of an ejection seat specification for a new fighter aircraft 13 p1751 N90-20057
Hatching a theory of incubation effects
[AD-A219275] 16 p2266 N90-22915
Target acquisition under load factors: Advantages and disadvantages of a helmet mounted sight 23 p3359 N90-28983
Loss of alertness and consciousness from pilot position during long range flight 23 p3360 N90-28990

CONSERVATION
NT ENERGY CONSERVATION
Conservation of body calcium by increased dietary intake of potassium: A potential measure to reduce the osteoporosis process during prolonged exposure to microgravity 18 p2631 N90-24993

CONSERVATION EQUATIONS
Gas flows in rocket motors, volume 1
[AD-A213348] 05 p0615 N90-13591
Prediction of length scales in a Mach reflection flowfield 15 p2089 N90-21959
Numerical modelling of shocks in gases and metals
[AD-A218586] 17 p2402 N90-23684
Flowfield computation of entry vehicles
[NASA-CR-186946] 22 p3171 N90-27986
FLUENT and FLUENT/BFC CFD computer programs
22 p3174 N90-28008
Analyses of spray and droplet ignition for pure and multicomponent fuels 23 p3304 N90-28688

CONSERVATION LAWS
Interpretation and modeling of the averaged equations for a fluid-solid flow 01 p0068 N90-10388
Balance laws and centro velocity in dissipative systems
[MEMO-797] 05 p0639 N90-13726
On the application of subcell resolution to conservation laws with stiff source terms
[NASA-TM-102384] 06 p0833 N90-14844
Local error estimates for discontinuous solutions of nonlinear hyperbolic equations
[NASA-CR-181960] 06 p0834 N90-14847
An entropy-based approach to nonlinear stability
[NASA-TM-101086] 09 p1272 N90-17376
A kinetic equation with kinetic entropy functions for scalar conservation laws
[NASA-CR-181985] 09 p1277 N90-17401
Computation of compressible viscous flows
10 p1308 N90-17567
Interaction of minor ions with fast and slow shocks
[NASA-CR-186372] 11 p1594 N90-19181
Viscous shock profiles and primitive formulations
[NASA-CR-182029] 13 p1750 N90-20049
High order filtering methods for approximating hyberbolic systems of conservation laws
[NASA-CR-182016] 13 p1858 N90-20650
Conserved integral characteristics of the gravitational field
[DE90-615205] 13 p1899 N90-20898
Finite element algorithms for hyperbolic conservation laws with forcing terms
[INPE-5024-RPE/617] 14 p2022 N90-21595
Numerical simulation model of hydrazine attitude control thrusters
[INPE-4965-PRE/1534] 15 p2068 N90-21848
Topics in vortex methods for the computation of three- and two-dimensional incompressible unsteady flows
15 p2091 N90-21967
A weak formulation for phase-change problems with bulk movement due to unequal densities
[DE90-009398] 15 p2163 N90-22361
Nonstrictly hyperbolic conservation laws
[AD-A218525] 16 p2237 N90-22762
Boundary conditions for nonlinear hyperbolic systems of conservation laws
[REPT-892-422-101] 17 p2404 N90-23694
Flowfield computation of entry vehicles
[NASA-CR-186946] 22 p3171 N90-27986
Computational Fluid Dynamics, volume 1
[VKI-LS-1990-03-VOL-1] 22 p3171 N90-27989
Hyperbolic conservation laws and numerical methods
22 p3172 N90-27990
Difference methods for hyperbolic problems with emphasis on space-centered approximations
22 p3172 N90-27998
Fluctuation splitting for multidimensional convection problems: An alternative to finite volume and finite element methods 22 p3173 N90-28000
Shock-layer bounds for a singularly perturbed equation
[NASA-CR-182080] 22 p3243 N90-28391
Numerical experiments on the accuracy of ENO and modified ENO schemes
[NASA-CR-182083] 23 p3387 N90-29128
Numerical methods for systems of conservation laws of mixed type using flux splitting
[NASA-CR-182084] 23 p3387 N90-29129

CONSISTENCY
On the equivalence of BS-stability and B-consistency
[CWI-NM-R8815] 02 p0268 N90-11530
Semantics and consistency of rule-based expert systems
[CWI-CS-R8824] 04 p0543 N90-13153
Log-based recovery in asynchronous distributed systems
[NASA-CR-186190] 11 p1550 N90-18924
Updates and consistency in the LOGRES language
[REPT-90-017] 22 p3239 N90-28369
Integrating mono-valued functions in deductive databases: A recursive extension of MILANT
[REPT-90-018] 22 p3239 N90-28370
Consistency and convergance for numerical radiation conditions
[NASA-TM-103262] 23 p3387 N90-29124

CONSOLES
NT REMOTE CONSOLES
The Real Time Interactive Display Environment (RTIDE), a display building tool developed by Space Shuttle flight controllers 13 p1857 N90-20654
Lunar deep drill apparatus
[NASA-CR-182756] 20 p2869 N90-26322

CONSOLIDATION
Temperature effects in shock consolidation of metal powders
[DE89-016782] 04 p0474 N90-12716
Computer controlled MHD power consolidation and pulse-generation system
[DE90-001224] 07 p0981 N90-15662
Spray deposition: A fundamental study of droplet-impingement, spreading and consolidation
[AD-A217202] 13 p1787 N90-20255
Prospects for integration of satellite communications, navigation and monitoring functions
17 p2360 N90-23439
A particle-level numerical simulation of the dynamic consolidation of a metal matrix composite material
[DE90-010950] 18 p2519 N90-24387
Metal matrix composites from dynamic consolidation of powder mixtures
[DE90-010951] 18 p2519 N90-24388
Dynamic consolidation of super hard materials
[AD-A224460] 24 p3454 N90-29505

CONSTANT SPEED PROPELLERS
U VARIABLE PITCH PROPELLERS

CONSTANTS
NT GRAVITATIONAL CONSTANT
NT GRUNEISEN CONSTANT
NT SOLAR CONSTANT
State to state kinetics of XeCl*
[AD-A215895] 10 p1353 N90-17847
Luminescence probe studies of ionomers. Part 3: Distribution of decay rate constants for tris bipyridyl Ruthenium(II) in Nafion membranes
[AD-A215885] 10 p1359 N90-17890
Construction of second constant of motion for two dimensional classical super systems
[DE90-607046] 10 p1423 N90-18208
Rate constant for reaction of atomic hydrogen with germane 20 p2947 N90-26768
Role of the methylene amidogen (H2CN) radical in the atmospheres of Titan and Jupiter
20 p2947 N90-26769
Optical constants of solid methane
20 p2948 N90-26775

CONSTELLATIONS
NT CENTAURUS CONSTELLATION
NT CYGNUS CONSTELLATION
NT LYRA CONSTELLATION
NT SAGITTARIUS CONSTELLATION
NT SCUTUM CONSTELLATION

CONSTITUTIONAL DIAGRAMS
U PHASE DIAGRAMS

CONSTITUTIVE EQUATIONS
Constitutive Relationships and Models in Continuum Theories of Multiphase Flows --- conferences
[NASA-CP-3047] 01 p0067 N90-10385
Interpretation and modeling of the averaged equations for a fluid-solid flow 01 p0068 N90-10388
An evaluation of the Chaboche and Bodner-Partom viscoplastic constitutive theories for strain rate sensitive materials 02 p0232 N90-11330
International seminar on the inelastic behavior of solids: Models and utilization
[DE89-017420] 03 p0327 N90-11858
A rate-dependent constitutive model for Be
[DE89-017755] 03 p0327 N90-11861
Constitutive modeling for isotropic materials (HOST)
[NASA-CR-179522] 05 p0582 N90-13390
Constitutive modeling for isotropic materials (HOST)
[NASA-CR-174718] 05 p0582 N90-13391
Analysis of metal matrix composite structures using a microchemical constitutive theory
06 p0737 N90-14290
Development of a rate independent plasticity theory for general cyclic loading 07 p0945 N90-15471
Ductile failure
[AD-A213864] 07 p0948 N90-15488
An implicit time-integration procedure for a set of internal variable constitutive equations for isotropic elasto-viscoplasticity
[PB90-121302] 08 p1117 N90-16470
A summary of the Bodner-Stouffer constitutive model
[AD-A214532] 09 p1237 N90-17182
Kinetic relations and the propagation of phase boundaries in solids
[AD-A215881] 11 p1519 N90-18747
An objective time-integration procedure for isotropic rate-independent and rate-dependent elastic-plastic constitutive equations
[PB90-121245] 11 p1550 N90-18925
Computer simulation of the mathematical modeling involved in constitutive equation development: Via symbolic computations
[NASA-TM-102532] 13 p1816 N90-20428
Rate dependent constitutive models for fiber reinforced polymer composites
[NASA-TM-102665] 17 p2370 N90-23492
An elastic/viscoplastic constitutive model for fiber-reinforced thermoplastic composites
18 p2516 N90-24371
Application of symbolic computations to the constitutive modeling of structural materials
[NASA-TM-103225] 20 p2876 N90-26364
Constitutive laws for discrete velocity models of gas (continued)
[ETN-90-97451] 22 p3175 N90-28016

CONSTRAINTS
NT METEOROLOGICAL PARAMETERS
Astrophysical and cosmological constraints to neutrino properties
[NASA-CR-185031] 01 p0140 N90-10809
Nonlinear adjustment with or without constraints, applicable to geodetic models
[AD-A210820] 02 p0265 N90-11509
Three level constraints on conformal field theories and string models
[DE89-016942] 02 p0286 N90-11634
Some notes on perturbations of differential-algebraic equations
[PB89-218564] 03 p0393 N90-12243
Stopping rules for a class of random methods for detecting necessary linear inequality constraints
[MEMO-777] 05 p0683 N90-13977
The regular indefinite linear quadratic problem with linear endpoint constraints
[MEMO-COSOR-88-15] 05 p0690 N90-14022
Stability and dynamics of constrained flexible multibody systems 06 p0791 N90-14609
Use of an HF active monitoring array in the presence of high level interference
[BBC-RD-1989/7] 08 p1055 N90-16096
Dynamics of column stability with partial end restraints
[NASA-TM-101651] 10 p1396 N90-18069
Uniqueness of closure of the constraint algebra for quantum gravity
[DE90-610476] 12 p1691 N90-19712
Trajectory optimization in the presence of constraints
[AD-A218271] 13 p1760 N90-20104
Constraint-based evaluation of sequential procedures
15 p2153 N90-22301
Nonaxisymmetric body, supersonic, inviscid dynamic derivative prediction
[AD-A220839] 17 p2346 N90-23358
Constraint-oriented specification in a constructive formal description technique
[MEMO-INF-89-44] 17 p2483 N90-24070
Fundamental limitations of qualitative simulation
[MEMO-INF-89-56] 18 p2600 N90-24802
Human factors: The human interface with aircraft interiors
[NIAR-90-18] 20 p2900 N90-26496
A comparison of alternative families of transformations for variables constrained to lie on the interval (0,1)
[MATHS-REPT-A-126] 24 p3539 N90-30011

CONSTRICTORS
Low power arcjet performance
[NASA-TM-103280] 23 p3298 N90-28657

CONSTRUCTION
Properties of HY-100 for naval construction
[MRL-R-1149] 01 p0044 N90-10247
S7 without any construction of Lie group
[DE89-618380] 02 p0269 N90-11539
M.I.N.G., Mars Investment for a New Generation: Robotic construction of a permanently manned Mars base
[NASA-CR-186224] 06 p0865 N90-15028
Geotechnical instrumentation
[PB89-198675] 07 p0933 N90-15398
Aircraft fuel tank construction and testing experience
08 p1021 N90-15907
The US National Transonic Facility, NTF
08 p1028 N90-15942
The Kryo-Kanal Koeln (KKK): Description of the tunnel conversion. Thermal insulation, instrumentation, operational experience, test results and operating costs
08 p1029 N90-15943
The European Transonic Windtunnel (ETW)
08 p1029 N90-15945
Materials and techniques for model construction
08 p1030 N90-15954
Some recent developments in materials and techniques for model fabrication 08 p1031 N90-15955
Models for cryogenic wind tunnels
08 p1031 N90-15956
A Mars/Phobos transportation system
[NASA-CR-186217] 09 p1230 N90-17135

Technology development, demonstration, and orbital support requirements for manned lunar and Mars missions
[NASA-TM-101666] 10 p1447 N90-18350
Optimal planning method of underground distribution system, part 2. Application to various types of system configurations
[DE89-782323] 11 p1500 N90-18636
Construction and calibration of a gas pressure meter with high temporal resolution
[INPE-4953-RPE/602] 11 p1511 N90-18700
Construction and characterization of a valve for rapid gas injection
[INPE-4789-RPE/583] 12 p1651 N90-19486
Simple reflection holography
[DE90-008309] 13 p1805 N90-20359
Nonlinear and distributed parameter models of the mini-mast truss 14 p1934 N90-21070
A robotically constructed production and supply base on Phobos
[NASA-CR-186234] 15 p2073 N90-21872
Development of a unique laboratory standard indium gallium arsenide detector for the 500 to 1700 micron spectral region, phase 2
[NASA-CR-180482] 16 p2238 N90-22767
Conceptual design and analysis of roads and road construction machinery for initial lunar base operations
[NASA-CR-186673] 18 p2535 N90-24459
The systematic construction of a one-combinator basis
[RUU-CS-89-14] 18 p2601 N90-24809
Strut-node joint conjugates for the assembly of semi-permanent or reusable truss structures
18 p2640 N90-25039
Lunar regolith bagging system
[NASA-CR-186683] 19 p2677 N90-25223
Design of a versatile, teleoperable, towable lifting machine with robotic capabilities for use in NASA's lunar base operations
[NASA-CR-186688] 19 p2697 N90-25345
Design and performance analysis of the DSS-13 beam waveguide antenna 20 p2853 N90-26225
Design of an autonomous Lunar construction utility vehicle
[NASA-CR-186832] 20 p2870 N90-26330
Index of USACERL publications, October 1984-December 1989
[AD-A221644] 21 p3088 N90-27559
Aircraft lightning protection handbook
[AD-A222716] 22 p3110 N90-27668
The challenge of assembling a space station in orbit
22 p3130 N90-27763
In-space construction and dynamics of large space structures 22 p3130 N90-27764
A new method for a tethered system aided space station assembly 22 p3130 N90-27765
Optical communications system having a wide-core single-mode planar waveguide
[AD-D014485] 22 p3164 N90-27939

CONSTRUCTION IN SPACE
U ORBITAL ASSEMBLY

CONSTRUCTION MATERIALS
Special Course on Advances in Cryogenic Wind Tunnel Technology
[AGARD-R-774] 08 p1028 N90-15939

CONSUMABLES (SPACECRAFT)
NT STORABLE PROPELLANTS

CONSUMABLES (SPACECREW SUPPLIES)
On the wings of a dream: The Space Shuttle
[NASA-EP-269] 05 p0593 N90-13446
Utilization of non-conventional systems for conversion of biomass to food components
[NASA-CR-177545] 07 p0968 N90-15591

CONSUMERS
Consumer electronics testing to fast-rise EMP (Electromagnetic Pulse) VEMPS (Vertical Electromagnetic Pulse Simulator) 2 development
[AD-A210505] 01 p0057 N90-10323
Copyright and home copying: Technology challenges the law
[PB90-151309] 21 p3086 N90-27547

CONSUMPTION
NT ENERGY CONSUMPTION
NT FUEL CONSUMPTION
NT OXYGEN CONSUMPTION
Physical performance and carbohydrate consumption in CF commandos during a 5-day field trial
[AD-A217204] 13 p1850 N90-20619
A laboratory study of the effects of diet and bright light countermeasures to jet lag
[AD-A220148] 17 p2435 N90-23875

CONTACT LOADS
NT ROLLING CONTACT LOADS
Analysis and construction of contact and tactile sensors
[DE89-013992] 01 p0072 N90-10416
Analysis of a finite two-dimensional solid with an inclined crack and a rigid inclusion 15 p2120 N90-22127
Influence of linear profile modification and loading conditions on the dynamic tooth load and stress of high contact ratio gears
[NASA-TM-103136] 16 p2243 N90-22796
Computer-aided design of high-contact-ratio gears for minimum dynamic load and stress
[NASA-TM-103275] 22 p3183 N90-28065
Surface effect for test piece on flexural test of carbon fiber reinforced plastic laminates
[NAL-TM-601] 24 p3442 N90-29436

CONTACT RESISTANCE
Development of a unique laboratory standard indium gallium arsenide detector for the 500 to 1700 micron spectral region, phase 2
[NASA-CR-180482] 16 p2238 N90-22767
An analysis of the contact sintering process in III-V solar cells
[NASA-TM-103179] 19 p2709 N90-25420
Friction, wear and electric characteristics of slip-ring brush materials for space applications. Part 1: Screening by pin-on-disk friction tests
[NAL-TR-1040] 24 p3478 N90-29657

CONTACTS (ELECTRIC)
U ELECTRIC CONTACTS

CONTAINERLESS MELTS
Nucleation kinetics in undercooled, glass-forming metallic melts
[DLR-FB-89-32] 05 p0624 N90-13644
Containerless Processing of Metals: Undercooling and Solidification
[DLR-MITT-89-15] 05 p0625 N90-13645
Non-contact temperature measurement requirements of ground-based research and flight programs at JPL
10 p1362 N90-17895
Comments on containerless bulk crystal growth and epitaxy in space and on their implications regarding non-contact temperature measurements
10 p1365 N90-17911
The NASA, Marshall Space Flight Center drop tube user's manual
[NASA-TM-100392] 13 p1786 N90-20251
Containerless low gravity processing of glass forming and immiscible alloys
[NASA-CR-186999] 23 p3316 N90-28747

CONTAINMENT
An apparatus for the electrodynamic containment of charged macroparticles 04 p0486 N90-12789
Development of an advanced fan blade containment system
[DOT/FAA/CT-89/20] 05 p0581 N90-13386
Selection of phase-change and containment materials for thermal energy storage
[NASA-CR-186228] 07 p0952 N90-15506

CONTAMINANTS
NT RADIOACTIVE CONTAMINANTS
NT TRACE CONTAMINANTS
Measurement of hydrazine contamination in soils
02 p0206 N90-11180
Photolysis of spacecraft contaminants
[AD-A211715] 03 p0317 N90-11801
The rodent research animal holding facility as a barrier to environmental contamination
[NASA-TM-102237] 03 p0378 N90-12151
Standard method for measurement of nonvolatile residue on surfaces
[AD-A213324] 04 p0474 N90-12714
Effects of atmospheric mix and toxic fumes on military performance
[PB89-223630] 04 p0522 N90-13015
Contamination removal using various solvents and methodologies
[NASA-CR-183747] 05 p0626 N90-13652
Analysis of acid rain and associated phenomena
[DE90-002555] 06 p0812 N90-14725
Characterization of cloud chemistry and frequency of canopy exposure to clouds in the Sierra Nevada
[PB89-104035] 06 p0817 N90-14753
Performance evaluation of the Puritan-Bennett crew-member portable protective breathing device as prescribed by portions of FAA action notice A-8150.2
[AD-A211113] 06 p0821 N90-14772
An Auger electron spectroscopy study of surface-preparation contaminants
[NASA-TP-2972] 09 p1203 N90-16968
Ballast system for maintaining constant pressure in a glove box
[NASA-CASE-NPO-17786-1-CU]
09 p1224 N90-17104
Environmental Projects. Volume 9: Construction of hazardous materials storage facilities
[NASA-CR-186296] 09 p1244 N90-17216
Evaluation of the use of flat terrain models versus complex terrain screening models in estimating pollutant transport and deposition in complex terrain
[DE90-005271] 09 p1245 N90-17223
Methodology used for gas analysis and control of trace chemical contaminants at a hyperbaric facility. 1: Gas sampling
[AD-A216155] 10 p1325 N90-17659
Comparison of emissions of transit buses using methanol and diesel fuel
[DE90-005652] 10 p1391 N90-18044
Application of high performance liquid chromatography/mass spectrometry to environmental analysis
[PB90-116963] 11 p1531 N90-18814
Tropospheric chemistry of natural hydrocarbons and energy-related pollutants: Biosphere/climate feedbacks
[DE90-005643] 11 p1532 N90-18820
Evaluation of the Scott aviation portable protective breathing device for contaminant leakage as prescribed by FAA Action Notice A-8150.2. Phase 1: Original tests of the portable protective breathing device. Phase 2: Tests of the redesigned portable protective breathing device
[AD-A216799] 12 p1601 N90-19214
Development of inspection techniques for quantitatively measuring surface contamination on SRM hardware
[NASA-CR-183902] 12 p1673 N90-19608
The Chemical Transfer Model (CTM) of EURAD: Development status 12 p1686 N90-19683
The pollution hazard assessment system: Documentation and users manual
[AD-A217108] 12 p1689 N90-19706
Overview of the methodologies used to compile large scale emissions inventories
[DE90-008518] 13 p1830 N90-20509
Transformation and deposition of airborne gaseous and particulate pollutants during transport over the Baltic Sea
[PUBL-AIR-QUALITY-5] 14 p2003 N90-21478
Gaithersburg Nike control and launch area preliminary assessment/site inspection, Gaithersburg, Maryland
[AD-A217791] 14 p2003 N90-21482
Dissociation phenomena in electron-beam sustained carbon dioxide lasers 18 p2560 N90-24610
Identifying atmospheric monitoring needs for Space Station Freedom 18 p2628 N90-24977
The effects of acid fog and dew on materials
[PB90-157496] 19 p2712 N90-25436
Southern California air quality study: Toxic air contaminants, task 1
[PB90-171570] 19 p2712 N90-25437
Spacecraft contamination programs within the Air Force Systems Command Laboratories
19 p2727 N90-25507
Satellite material contaminant optical properties
19 p2732 N90-25529
An overview of the joint FAA/NASA aircraft/ground runway friction program
[NASA-TM-103486] 20 p2805 N90-25957
Workshop minutes on Remote Sensing of Hydrocarbons and Toxic Pollutants
[PB90-186370] 22 p3194 N90-28127
Evaluation of the role of ozone, acid deposition, and other airborne pollutants in the forests of eastern North America
[PB90-184896] 22 p3197 N90-28140
Investigation of the effects of acid deposition on materials
[PB90-158973] 22 p3197 N90-28143
Laboratory and field evaluations of extrasensitive sulfur dioxide and nitrogen dioxide analyzers for acid deposition monitoring
[PB90-201062] 22 p3199 N90-28153
Space station contamination modeling
[NASA-CR-183871] 23 p3286 N90-28590
National air pollutant emission estimates, 1940-1988
[PB90-199266] 23 p3346 N90-28908
National air quality and emissions trends report, 1988
[PB90-200114] 23 p3346 N90-28909

CONTAMINATION
NT SPACECRAFT CONTAMINATION
Direct numerical study of leading-edge contamination
01 p0063 N90-10361
Effects of tacky mat contamination on bond degradation for Chemlok/liner and NBR/liner bonds
[NASA-CR-183742] 05 p0626 N90-13653
Use of a krypton isotope for rapid ion changeover at the Lawrence Berkeley Laboratory 88-inch cyclotron
[NASA-CR-186107] 05 p0698 N90-14084
Optical properties monitor: Experiment definition phase
[NASA-CR-183836] 05 p0699 N90-14092
Method of making carbon dioxide and chlorine free fluoride-based glass
[AD-D014260] 08 p1048 N90-16060

The influence of residual contamination on the structure and properties of metal/GaAs interfaces
[DE90-000549] 08 p1127 N90-16530
Methodology used for gas analysis and control of trace chemical contaminants at a hyperbaric facility. 1: Gas sampling
[AD-A216155] 10 p1325 N90-17659
Research project in microelectronic engineering and imaging science
[DE90-006907] 11 p1503 N90-18653
Development of inspection techniques for quantitatively measuring surface contamination on SRM hardware
[NASA-CR-183902] 12 p1673 N90-19608
The pollution hazard assessment system: Documentation and users manual
[AD-A217108] 12 p1689 N90-19706
Clean access platform for orbiter
15 p2116 N90-22103
Development and use of a passive technique for measuring nitrogen dioxide in the background atmosphere 16 p2331 N90-23285
Quantitative determination of 1, 2-ethanediol contamination in used diesel lubricating oils by gas chromatography/mass spectrometry
[AD-A218592] 17 p2371 N90-23498
Pre-concentration method for inductively coupled plasma-mass spectrometry
[PB90-181348] 19 p2673 N90-25202
Contamination of spacecraft by recontact of dumped liquids 19 p2728 N90-25508
Gaseous optical contamination of the spacecraft environment: A review 19 p2730 N90-25519
Role of surface passivation in the integrated processing of MOS structures
[AD-A222630] 20 p2859 N90-26264
Investigations of polarized light scattering from rough surfaces
[AD-A221943] 21 p3076 N90-27491
M-52 spray booth qualification test
[NASA-CR-184003] 22 p3122 N90-27727
Nylon and teflon scribe effect on NBR to Chemlok 233 and NBR to NBR bond interfaces
[NASA-CR-184004] 22 p3189 N90-28095
SamTrack: A sample tracking system for environmental monitoring
[DE90-016026] 24 p3488 N90-29712

CONTENT
NT BONE MINERAL CONTENT

CONTEXT
Context dependent anti-aliasing image reconstruction
08 p1073 N90-16209
Context dependent prediction and category encoding for DPCM image compression 08 p1073 N90-16210
Stochastic interactive activation and the effect of context on perception
[AD-A218929] 16 p2262 N90-22898
A computer for low contest-switch time
[AD-A222883] 21 p3038 N90-27269
Context propagation truth maintenance system
[RR-779-I] 21 p3057 N90-27380

CONTEXT FREE LANGUAGES
An investigation of the usefulness of Earley's Algorithm in a general context-free recognizer
[DE89-016498] 02 p0258 N90-11463

CONTINENTAL MARGINS
U CONTINENTAL SHELVES

CONTINENTAL SHELVES
The influence of a steady baroclinic deep ocean on the shelf
[PB89-198188] 01 p0089 N90-10511
Physiographic and geological setting of the Coastal Engineering Research Center's field research facility
[AD-A210772] 02 p0238 N90-11356
Remote sensing data acquisition, analysis and archival
[PB89-142566] 03 p0365 N90-12085
Underwater physiography of the continental shelf of Rio Grande do Norte visible through satellite imagery
[INPE-4964-TDL/392] 13 p1820 N90-20448
Continental shelf processes affecting the oceanography of the South Atlantic Bight
[DE90-008439] 13 p1848 N90-20606
An investigation of meteorological effects on currents in the shelf and continental slope seas northwest of the United Kingdom. 2: Relationships between currents at different locations and with other variables
[PB90-151911] 15 p2134 N90-22195
On the effectiveness of the production of antarctic bottom water in the Weddell and Ross Seas
[AD-A218873] 16 p2259 N90-22880
Trace metal sources for the atlantic inflow to the Mediterranean Sea
[AD-A218607] 17 p2429 N90-23842
Spatial cross-correlation of Antarctic Sea ice and seabed topography
[NASA-CR-186815] 20 p2891 N90-26451
Outer continental shelf environmental assessment program. Volume 66: Principal investigators
[PB90-194747] 22 p3199 N90-28154
Proceedings of a Workshop on the Geoelectric and Geomagnetic Environment of Continental Margins
[AD-A223743] 24 p3493 N90-29739

CONTINENTS
NT AFRICA
NT ASIA
NT AUSTRALIA
NT EUROPE
NT NORTH AMERICA
NT SOUTH AMERICA
The influence of continental sources of aerosols on the marine stratocumulus during FIRE IFO-1
22 p3218 N90-28250

CONTINUITY
Local moduli of continuity of some classes of Gaussian processes
[AD-A217692] 13 p1879 N90-20778

CONTINUITY (MATHEMATICS)
An algebra for process creation
[CWI-CS-R8907] 04 p0543 N90-13155
Continuity properties of one-parameter families of linear-quadratic problems without stability
[MEMO-COSOR-88-17] 05 p0690 N90-14024
Reflexivity, the dual Radon-Nykodym property, and continuity of adjoint semigroups
[CWI-AM-R8908] 17 p2460 N90-24042
The gamma process and the Poisson distribution
[MEMO-COSOR-89-24] 17 p2466 N90-24089
G2-continuity in homogeneous co-ordinates
[MATHS-REPT-A-110] 20 p2917 N90-26599
Rational cubics with G2-continuity
[MATHS-REPT-A-113] 20 p2918 N90-26601
Unification of statistical methods for continuous and discrete data
[AD-A224307] 24 p3540 N90-30017

CONTINUITY EQUATION
Discretization of the steady state semiconductor device equations
[AD-A215807] 10 p1438 N90-18298
The Chemical Transfer Model (CTM) of EURAD: Development status 12 p1686 N90-19683
Curvature continuity of cubic Bezier curves in the solid modeling aerospace research tools design software
[NASA-CR-186583] 14 p2016 N90-21554
Numerical modelling of shocks in gases and metals
[AD-A218586] 17 p2402 N90-23684
Three-dimensional viscous flow structures from bifurcation of a degenerate singularity with three zero eigenvalues
[LR-572] 19 p2692 N90-25314
Flow structures around non-hyperbolic singularities on the wall with one vanishing eigenvalue: A discussion of the flow structures and the unfoldings
[LR-586] 19 p2692 N90-25315
Analytical resolution of the Oseens differential equation of inclined turning cylinder with gliding
[ETN-90-97316] 22 p3171 N90-27988

CONTINUOUS FLOW ELECTROPHORESIS
U ELECTROPHORESIS

CONTINUOUS RADIATION
Design and operating characteristics of a CW relevant quasi-optical gyrotron with variable mirror separation
[AD-A210611] 01 p0074 N90-10425
Anisotropy of electron distributions related to the anisotropy and polarization of the continuous emitted x rays 08 p0785 N90-14566
Effects of pulsed and CW (Continuous Wave) 2450 MHz radiation on transformation and chromosomes of human lymphocytes in vitro
[AD-A216500] 11 p1539 N90-18857
Progress in the CW operation of a 140 GHz gyrotron
[DE90-007382] 12 p1663 N90-19558
An assessment of the potential of continuous-wave ranging for measuring the distance to a highly reflective, infinite sheet
[NASA-TM-101680] 14 p1969 N90-21279
Test diagnostics of RF effects in integrated circuits
[AD-A219737] 17 p2396 N90-23648
SILEX Beacon equipment
[ETN-90-96613] 17 p2409 N90-23726

CONTINUOUS SPECTRA
The origin of the continuum of AGN and the X ray background 19 p2795 N90-25912

CONTINUOUS WAVE LASERS
Multiline multimode CW chemical laser performance
[AD-A210613] 01 p0075 N90-10432
Coupled multiline CW HF lasers: Experimental performance
[AD-A210844] 01 p0075 N90-10434
Master oscillator with power amplifiers: Performance of a two-element CW HF phased-laser array
[AD-A211141] 01 p0076 N90-10435
Biomedical studies with the free electron laser
[AD-A208927] 01 p0091 N90-10519
Dissociation and vibrational relaxation of XeF by various collision partners
[AD-A210769] 02 p0227 N90-11300
Novel thin-film CuInSe2 fabrication
[DE89-009440] 02 p0281 N90-11604
Theoretical studies of solar lasers and converters
[NASA-CR-186194] 06 p0787 N90-14583
Eurolaser definition phase: A comparison of high power lasers available
[ETN-90-96061] 08 p1083 N90-16268
CW ultraviolet laser excited with an electron beam
[AD-A214928] 09 p1227 N90-17123
CW (Continuous Wave) stimulated Brillouin scattering of long-pulse chemical laser beams
[AD-A216409] 10 p1390 N90-18039
Applications of FM-CW laser radar to antenna contour mapping 12 p1611 N90-19270
Proceedings of Air Force Office of Scientific Research workshop on Laser Propulsion
[AD-A216563] 12 p1666 N90-19569
Measurement of the stimulated thermal Rayleigh scattering instability
[DE90-007849] 13 p1807 N90-20376
SILEX Beacon equipment
[ETN-90-96613] 17 p2409 N90-23726
Fast plasma mixing: A new excitation method for CW gas lasers
[AD-A220290] 18 p2617 N90-24904
A tunable, continuous wave, thulium-doped, solid state laser cross-reference to related application
[AD-D014558] 22 p3180 N90-28045
Tunable CW single-frequency source for injection seeding 2-micrometer lasers
[AD-A223979] 23 p3331 N90-28834

CONTINUOUS WAVES
U CONTINUOUS RADIATION

CONTINUUM FLOW
Study of continuum higher order closure models evaluated by a statistical theory of shock structure
10 p1303 N90-17538
Improved computational fluid dynamics for continuum hypersonic flow
[AD-A216981] 11 p1506 N90-18674
Continuum approach and contaminant transport in ground water flows 19 p2690 N90-25301

CONTINUUM MECHANICS
Mechanics of damping for fiber composite laminates including hygro-thermal effects
[NASA-TM-102329] 01 p0034 N90-10185
Constitutive Relationships and Models in Continuum Theories of Multiphase Flows --- conferences
[NASA-CP-3047] 01 p0067 N90-10385
A generalized thermomechanical constitutive model for metal matrix composites with plastic strain and damage
06 p0737 N90-14293
A new uniformly valid asymptotic integration algorithm for elasto-plastic-creep and unified viscoplastic theories including continuum damage
[NASA-TM-102344] 06 p0799 N90-14655
Damage evaluation from surface displacement data
07 p0944 N90-15469
Nonlinear continuum mechanics and applied analysis
[AD-A213629] 12 p1709 N90-19812
Compact scheme for systems of equations applied to fundamental problems of mechanics of continua
[NASA-CR-186494] 14 p1971 N90-21292
Finite element analysis of elastic contact problems with friction 15 p2105 N90-22040
A study of creep damage using microradiography and continuum damage mechanics 15 p2117 N90-22109

CONTINUUM MODELING
Study of continuum higher order closure models evaluated by a statistical theory of shock structure
10 p1303 N90-17538
Characterization of reaction kinetics in a porous electrode
[NASA-CR-186504] 12 p1625 N90-19340
A continuum damage model for the quasi-static response of brittle materials
[DE90-007681] 15 p2117 N90-22112

CONTINUUMS
A point in betaZ/Z not contained in a maximal orbit closure
[REPT-89-26] 04 p0540 N90-13127
Global optimization and simulated annealing
[MEMO-COSOR-88-21] 05 p0690 N90-14025
Continuum analogues of contragredient Lie algebras: Lie algebras with a Cartan operator and nonlinear dynamical systems
[DE89-635698] 07 p0985 N90-15691
A kinetic equation with kinetic entropy functions for scalar conservation laws
[NASA-CR-181985] 09 p1277 N90-17401

Radio continuum maps at 22 GHz of the H II regions RCW57 and W49
[INPE-4787-TDL/353] 10 p1446 N90-18343
Geometric continuum regularization of quantum field theory
[DE90-006099] 11 p1573 N90-19058
Comet Halley: An optical continuum study
12 p1736 N90-19981
The interstellar medium of a starburst galaxy; millimeter interferometric observations of M82
16 p2329 N90-23276
Formation of hydrogen line and continuum emission in young stellar objects 24 p3562 N90-30150

CONTOUR SENSORS
Order filters, median recursive filter: Analysis and evaluation of performance in image processing
[ISAL-89-0017] 08 p1123 N90-16505
Improved processes for ultrasonic object recognition in robotics
[ETN-90-95362] 12 p1672 N90-19604
Surface reconstruction based on critical contours in a multi-image context
[RR-784-I-IMAG-94-LIFIA] 20 p2880 N90-26383

CONTOURS
A two-dimensional adaptive-wall test section with ventilated walls in the Ames 2- by 2-foot transonic wind tunnel
[NASA-TM-102207] 05 p0585 N90-13407
Isolating contour information from arbitrary images
08 p1074 N90-16217
Dynamics of a class of vortex rings
[NASA-TM-102257] 12 p1657 N90-19524
The contour model architecture and assembly language
[AD-A217114] 13 p1865 N90-20697
Inverse design of airfoil contours: Constraints, numerical method, and applications 14 p1917 N90-20980
Topics in vortex methods for the computation of three- and two-dimensional incompressible unsteady flows
15 p2091 N90-21967
Methods of perturbation theory as a means for interactive design from bodies in a flow
[ETN-90-96502] 18 p2553 N90-24573
Generation of circumferential velocity contours associated with pulsed point suction on a rotating disk
18 p2646 N90-25065
Simple graphical descriptions of natural land profiles and the application of fractal and sub-fractal models to them
[RSRE-MEMO-4305] 22 p3195 N90-28130
Non-contact contour gage
[DE90-014672] 24 p3475 N90-29642

CONTRACT INCENTIVES
Small business innovation research: Program solicitation
[NASA-TM-101869] 05 p0705 N90-14126

CONTRACT MANAGEMENT
Studies of the European transonic wind tunnel
[ONERA-RSF-12/0694-GY] 04 p0562 N90-13278
Total quality management: Directorate of Contract Management master plan
[AD-A212867] 05 p0705 N90-14131
Congressional involvement and relations: A guide for Department of Defense acquisition managers
[AD-A214408] 07 p1011 N90-15855
The influence of contract type in program execution/V-22 Osprey: A case study
[AD-A220011] 17 p2484 N90-24206
Federal Aviation Administration small business innovation research 5-year project summaries
[AD-A221590] 21 p3086 N90-27546

CONTRACT NEGOTIATION
Space shuttle: Changes to the solid rocket motor contract
[GAO/NSIAD-88-203] 18 p2636 N90-25016

CONTRACTION
Parallel graph contraction
[AD-A211916] 03 p0386 N90-12199
The effect of concurrent strength and endurance training on electromechanical delay, maximum voluntary contraction, and rate of force development
[AD-A213316] 04 p0525 N90-13028
General contraction of Gaussian basis sets. Part 2: Atomic natural orbitals and the calculation of atomic and molecular properties
[NASA-CR-186201] 08 p1119 N90-16482
Robust controller design by contraction of a pole region
[ESA-TT-1042] 23 p3384 N90-29118
Effects of basis set contraction in relativistic calculations on neon, argon, and germanium
[AD-A223357] 24 p3446 N90-29460

CONTRACTORS
The extension of technology and the control of production costs in advanced satellite systems
[AD-A215104] 09 p1183 N90-16857
Definition of a management information system to support performance risk assessment
[AD-A215464] 09 p1297 N90-17516
The technology challenge of the advanced tactical fighter: A study of the technology transition process
[AD-A216109] 10 p1320 N90-17630
RADC reliability engineer's TOOLKIT
[AD-A215977] 10 p1394 N90-18058
The environmental liabilities of government contractors and agencies 17 p2481 N90-24186
Procedures for DOE-Navy exchange and approval of engineering information and material management required for production of W88-0/Mk5 RBA (reentry body assembly)
[DE90-014763] 23 p3287 N90-28595

CONTRACTS
NT INSURANCE (CONTRACTS)
Forecasting contracting workload
[AD-A211935] 03 p0416 N90-12387
The improvement of technology transfer from space to industry 11 p1577 N90-19079
The influence of contract type in program execution/V-22 Osprey: A case study
[AD-A220011] 17 p2484 N90-24206
Production activities in space: The problems of protection 20 p2939 N90-26725
Research proposal
[AD-A221453] 21 p3085 N90-27545
Federal Aviation Administration small business innovation research 5-year project summaries
[AD-A221590] 21 p3086 N90-27546
A dictionary of acquisition and contracting terms
[AD-A221681] 21 p3088 N90-27560
Independent research and independent exploratory development programs
[AD-A222690] 21 p3101 N90-27612

CONTRAILS
Effects on electromagnetic wave propagation and rocket vapor trails of intense turbulence generated by breaking internal gravity waves
[AD-A211755] 03 p0373 N90-12130

CONTRAROTATING PROPELLERS
User's guide to PMESH: A grid-generation program for single-rotation and counterrotation advanced turboprops
[NASA-CR-185156] 06 p0823 N90-14783
In-plane forces and moments on installed inclined propellers at low forward speeds
[ESDU-89047] 09 p1161 N90-16720
An approximate model for the performance and acoustic predictions of counterrotating propeller configurations
[NASA-CR-180667] 10 p1426 N90-18228
Relating flow between counter-rotating propellers to aerodynamic interaction noise 14 p1909 N90-20944
Investigation of advanced counterrotation blade configuration concepts for high speed turboprop systems, task 1: Ducted propfan analysis
[NASA-CR-185217] 16 p2202 N90-22567
Experimental performance and acoustic investigation of modern, counterrotating blade concepts
[NASA-CR-185158] 17 p2352 N90-23393

CONTRAST
NT IMAGE CONTRAST
The assessment of visibility from automatic contrast Measurements 07 p0872 N90-15061
Effect of contrast on the perception of direction of a moving pattern
[NASA-TM-102234] 07 p0965 N90-15577
Dazzling glare: Protection criteria versus visual performance
[AD-A219676] 17 p2438 N90-23889
A voltage contrast detector with double channel energy analyzer in a scanning electron microscope
[ISBN-90-6275-568-2] 19 p2694 N90-25330
Polarization contrast vision
[AD-A221423] 21 p3076 N90-27492

CONTROL
An algorithm for control volume analysis of cryogenic systems
[AD-A213394] 05 p0631 N90-13683

CONTROL BOARDS
The JPL telerobot operator control station: Operational experiences 19 p2738 N90-25565
Selective multimode/multiconfigurable data acquisition and reduction processor system
[AD-D014551] 22 p3234 N90-28341
Description of the primary flight display and flight guidance system logic in the NASA B-737 transport systems research vehicle
[NASA-TM-102710] 23 p3277 N90-28546
Flight telerobotic servicer control from the Orbiter
24 p3517 N90-29882

CONTROL CONFIGURED VEHICLES
Flight-testing of the self-repairing flight control system using the F-15 highly integrated digital electronic control flight research facility
[NASA-TM-101725] 19 p2661 N90-25144

CONTROL DEVICES
U CONTROL EQUIPMENT

CONTROL EQUIPMENT
NT CONTROL STICKS
NT CRYOSTATS
NT PRESSURE REGULATORS
NT SPEED REGULATORS
NT TELEOPERATORS
NT THERMOSTATS
Independent Orbiter Assessment (IOA): Assessment of instrumental subsystem FMEA/CIL
[NASA-CR-185572] 02 p0173 N90-10972
Integration of a centralized multiplexed control unit into the cockpit of an aircraft
[F6150-DT410-1-88329] 04 p0458 N90-12622
Design of a new control system for hovercrafts
[ETN-90-96230] 11 p1485 N90-18435
Multibody modeling and verification
12 p1640 N90-19422
Prediction of forces and moments for flight vehicle control effectors. Part 1: Validation of methods for predicting hypersonic vehicle controls forces and moments
[NASA-CR-186571] 15 p2047 N90-21734
Prediction of forces and moments for flight vehicle control effectors. Part 2: An analysis of delta wing aerodynamic control effectiveness in ground effect
[NASA-CR-186572] 15 p2047 N90-21735
Development of the methods and means of precise forming and geometry control of superconducting current-carrying element for the UNR pulsed dipoles
[DE90-620108] 15 p2173 N90-22419
Autonomous power expert fault diagnostic system for Space Station Freedom electrical power system testbed
19 p2730 N90-25521
Minimum variance control of nonlinear systems
[RR-369] 19 p2748 N90-25615
Making real-time reactive systems reliable
[NASA-CR-186642] 20 p2873 N90-26344
Semi-active orbital debris sweeper
[NASA-CASE-MSC-21534-1] 21 p2966 N90-26860
Personal computer programs for the control of subnanosecond transient digitizers with applications for device damage testing
[AD-A221458] 21 p3054 N90-27365
Analysis, Design and Synthesis Methods for Guidance and Control Systems
[AGARD-AG-314] 24 p3423 N90-29338
Distributed communications and control network for robotic mining 24 p3520 N90-29901

CONTROL MOMENT GYROSCOPES
Periodic-disturbance accommodating control of the space station for asymptotic momentum management
05 p0586 N90-13416
A new momentum management controller for the space station
[NASA-CR-187265] 24 p3440 N90-29425

CONTROL PANELS
U CONTROL BOARDS

CONTROL SIMULATION
An assessment of robustness of flight control systems based on variable structure techniques
02 p0157 N90-10895
Computer-based tools for assisting air traffic controllers with arrivals flow management
[RSRE-88001] 05 p0577 N90-13366
Simulation of spacecraft attitude dynamics using TREETOPS and model-specific computer Codes
05 p0587 N90-13419
Planning systems for autonomous legged vehicles
[AD-A214242] 07 p0942 N90-15458
Linear and non-linear control of high-order converters after reducing the order by appropriate techniques
10 p1336 N90-17733
Variable structure control system applied to multilevel power conditioning converters 10 p1336 N90-17734
Performance of concurrency control algorithms in distributed systems
[AD-A218280] 13 p1870 N90-20727
Robotic mobility system: Road following algorithms
[AD-A218107] 13 p1874 N90-20748
Minimum flying qualities. Volume 2: Pilot modeling for flying qualities applications
[AD-A218561] 16 p2201 N90-22561
Space station dynamics, attitude control and momentum management 16 p2287 N90-23029
Control design and simulation of systems modeled using ADAMS 16 p2296 N90-23081
Simulator evaluation of the final approach spacing tool
[NASA-TM-102807] 17 p2348 N90-23374
Comparison of selection procedures and validation of criterion used in selection of significant control variates of a simulation model
[AD-A220459] 17 p2443 N90-23921
Pilot decision-making training
[AD-A221349] 18 p2585 N90-24720

Digital radio link: Controlled simulator for frequency selective fading
[FOA-C-30527-3.5] 19 p2683 N90-25259
Robustness evaluation of H2 and H(infinity) control theory as applied to a transport aircraft
[AD-A222795] 20 p2814 N90-26018
Variance reduction for quantile estimates in simulations via nonlinear controls
[AD-A222653] 20 p2916 N90-26590
Test and validation for robot arm control dynamics simulation 24 p3507 N90-29826

CONTROL STABILITY
Wind tunnel results of the low-speed NLF(1)-0414F airfoil 04 p0444 N90-12541
On the application of modified stepwise regression for the estimation of aircraft stability and control parameters
[REPT-8905] 05 p0583 N90-13400
Robustness of a moving-bank multiple model adaptive controller for a large space structure
[AD-A215670] 09 p1183 N90-16859
Control and stability of a spinning symmetric satellite in an elliptical orbit
[AD-A216284] 10 p1328 N90-17672
A robust stability result for generalised predictive control
[OUEL-1773/89] 15 p2158 N90-22330
Robust adaptive control: Stability and asymptotic performance
[AD-A219259] 16 p2304 N90-23127
STARS: An integrated general-purpose finite element structural, aeroelastic, and aeroservoelastic analysis computer program
[NASA-TM-101709] 17 p2416 N90-23768
H-infinity control: An exploratory study
[EUT-88-E-211] 20 p2915 N90-26584
Robust controller design by contraction of a pole region
[ESA-TT-1042] 23 p3384 N90-29118
Stability analysis of multiple-robot control systems 24 p3505 N90-29811
On the stability of robotic systems with random communication rates 24 p3514 N90-29865

CONTROL STICKS
Simulator comparison of thumball, thumb switch, and touch screen input concepts for interaction with a large screen cockpit display format
[NASA-TM-102587] 14 p1921 N90-21005
Development of a multipurpose hand controller for JEMRMS 15 p2113 N90-22087
Teleoperation of a force controlled robot manipulator without force feedback to a human operator 18 p2503 N90-24305

CONTROL SURFACES
NT AERIAL RUDDERS
NT AILERONS
NT ELEVATORS (CONTROL SURFACES)
NT ELEVONS
NT FLAPS (CONTROL SURFACES)
NT GUIDE VANES
NT HORIZONTAL TAIL SURFACES
NT JET FLAPS
NT JET VANES
NT LEADING EDGE FLAPS
NT RUDDERS
NT SPOILERS
NT TABS (CONTROL SURFACES)
NT UPPER SURFACE BLOWN FLAPS
Aeroelastic tailoring procedure for controlling fin hinge moments 01 p0013 N90-10058
Aeroelastic analysis of missile control surfaces with structural non-linearity 01 p0015 N90-10071
The active flexible wing aeroservoelastic wind-tunnel test program 01 p0024 N90-10119
Effect of control surface mass unbalance on the stability of a closed-loop active control system
[NASA-TP-2952] 03 p0357 N90-12042
Stall/spin aerodynamic data project
[DOT/FAA/CT-88/29] 06 p0723 N90-14222
Example of procedure in calculation of control hinge moments
[ESDU-89010] 06 p0727 N90-14240
Numerical investigation of transition control of a flat plate boundary layer 07 p0926 N90-15361
Discrete proportional Plus Integral (PI) multivariable control laws for the Control Reconfigurable Combat Aircraft (CRCA)
[AD-A215664] 11 p1464 N90-18431
Prediction of forces and moments for flight vehicle control effectors. Part 1: Validation of methods for predicting hypersonic vehicle controls forces and moments
[NASA-CR-186571] 15 p2047 N90-21734
Research at NASA's NFAC wind tunnels
[NASA-TM-102827] 20 p2801 N90-25933
Prediction methodologies for nonlinear aerodynamic characteristics of control surfaces
[NIAR-90-17] 20 p2801 N90-25937
A computer module used to calculate the horizontal control surface size of a conceptual aircraft design
[NASA-CR-186872] 20 p2903 N90-26515
Aerodynamic/dynamic interaction
[AD-A222263] 21 p2954 N90-26798
Development of an automated ultrasonic inspection system for composite structure on in-service aircraft 22 p3186 N90-28079
Control of submersible vortex flows
[NASA-TM-102693] 23 p3267 N90-28493
Aerodynamic control design: Experience and results at Aermacchi 23 p3272 N90-28518
Development of non-conventional control methods for high angle of attack flight using vortex manipulation 23 p3273 N90-28522
Control of vortex aerodynamics at high angles of attack 23 p3273 N90-28523
Unsteady aerodynamics of controls 23 p3273 N90-28525

CONTROL SYSTEMS
U CONTROL

CONTROL SYSTEMS DESIGN
Identification of stability and control parameters of a brilliant ammunition 01 p0014 N90-10065
Investigations of thrust vector control for high-alpha pitchover 01 p0014 N90-10067
Real-time support for high performance aircraft operation
[NASA-CR-185475] 01 p0015 N90-10075
Proceedings of the Workshop on Computational Aspects in the Control of Flexible Systems, part 1
[NASA-TM-101578-PT-1] 01 p0017 N90-10080
NASA'S controls-structures interaction program 01 p0017 N90-10081
Computational controls for aerospace systems 01 p0017 N90-10082
Additional software developments wanted for modeling and control of flexible space systems 01 p0017 N90-10083
Flexible structure control experiments using a real-time workstation for computer-aided control engineering 01 p0017 N90-10084
CONSOLE: A CAD tandem for optimization-based design interacting with user-supplied simulators 01 p0017 N90-10085
Control/structure interaction methods for space station power systems 01 p0018 N90-10087
Flexible missile autopilot design studies with PC-MATLAB/386 01 p0018 N90-10088
Modeling and control system design and analysis tools for flexible structures 01 p0018 N90-10090
A comparison of software for the modeling and control of flexible systems 01 p0019 N90-10092
Proceedings of the Workshop on Computational Aspects in the Control of Flexible Systems, part 2
[NASA-TM-101578-PT-2] 01 p0021 N90-10103
Controlling flexible structures: A survey of methods 01 p0023 N90-10114
Structural stability augmentation system design using BODEDIRECT: A quick and accurate approach 01 p0023 N90-10116
Input-output oriented computation algorithms for the control of large flexible structures 01 p0023 N90-10118
Active vibration mitigation of distributed parameter, smart-type structures using Pseudo-Feedback Optimal Control (PFOC) 01 p0024 N90-10121
Bidirectional power converter control electronics
[NASA-CR-175070] 01 p0032 N90-10175
ATTAS flight testing experiences 02 p0151 N90-10862
The active control of an unstable canard aircraft 02 p0156 N90-10894
An assessment of robustness of flight control systems based on variable structure techniques 02 p0157 N90-10895
Independent Orbiter Assessment (IOA): Analysis of the ascent thrust vector control actuator subsystem
[NASA-CR-185579] 02 p0164 N90-10929
Independent Orbiter Assessment (IOA): Analysis of the electrical power distribution and control/electrical power generation subsystem
[NASA-CR-185538] 02 p0165 N90-10933
Independent Orbiter Assessment (IOA): Analysis of the reaction control system, volume 1
[NASA-CR-185532-VOL-1] 02 p0166 N90-10938
Independent Orbiter Assessment (IOA): Analysis of the reaction control system, volume 2
[NASA-CR-185532-VOL-2] 02 p0167 N90-10939
Independent Orbiter Assessment (IOA): Analysis of the reaction control system, volume 3
[NASA-CR-185532-VOL-3] 02 p0167 N90-10940
Independent Orbiter Assessment (IOA): Analysis of the electrical power distribution and control subsystem, volume 1
[NASA-CR-185529-VOL-1] 02 p0167 N90-10941
Independent Orbiter Assessment (IOA): Analysis of the electrical power distribution and control subsystem, volume 2
[NASA-CR-185529-VOL-2] 02 p0167 N90-10942
Independent Orbiter Assessment (IOA): CIL issues resolution report, volume 1
[NASA-CR-185524-VOL-1] 02 p0169 N90-10954
Independent Orbiter Assessment (IOA) CIL issues resolution report, volume 3
[NASA-CR-185524-VOL-3] 02 p0170 N90-10956
Independent Orbiter Assessment (IOA): Assessment of the atmospheric revitalization pressure control subsystem FMEA/CIL
[NASA-CR-185594] 02 p0170 N90-10957
Independent Orbiter Assessment (IOA): Assessment of the ascent thrust vector control actuator subsystem FMEA/CIL
[NASA-CR-185590] 02 p0170 N90-10959
Independent Orbiter Assessment (IOA): Assessment of the displays and controls subsystem
[NASA-CR-185588] 02 p0171 N90-10961
Independent Orbiter Assessment (IOA): Assessment of the EPD and C/remote manipulator system FMEA/CIL
[NASA-CR-185583] 02 p0172 N90-10965
Frequency domain design of robust controllers for space structures
[AD-A211172] 02 p0176 N90-10985
System and performance analysis of a low density actively controlled mirror for astronomic observation 02 p0178 N90-11002
The large European Acoustic Facility at ESTEC 02 p0187 N90-11067
A contribution to the synthesis of communication switching systems with decentralized control using modular components
[ETN-89-94660] 02 p0214 N90-11228
Modeling and simulation of spatial robotic manipulators with flexible links and joint drives for control strategies implementation and evaluation 02 p0228 N90-11311
Using computer design and simulation to improve manufacturing productivity, report period 1, 2 and 3
[AD-A210255] 02 p0258 N90-11452
Control and optimization for observations of systems governed by controlled partial differential equations
[AD-A211122] 02 p0266 N90-11513
Guaranteed cost control of flexible space structures 02 p0287 N90-11643
Applications of flight control system methods to an advanced combat rotorcraft
[NASA-TM-101054] 03 p0308 N90-11752
A design procedure for the handling qualities optimization of the X-29A aircraft
[NASA-TM-4142] 03 p0308 N90-11753
Robust control design for flight control
[AD-A211957] 03 p0309 N90-11756
Independent Orbiter Assessment (IOA): Assessment of the electrical power distribution and control subsystem, volume 1
[NASA-CR-185557-VOL-1] 03 p0313 N90-11779
Independent Orbiter Assessment (IOA): Assessment of the electrical power distribution and control subsystem, volume 2
[NASA-CR-185557-VOL-2] 03 p0313 N90-11780
Independent Orbiter Assessment (IOA): Assessment of the electrical power distribution and control subsystem, volume 3
[NASA-CR-185557-VOL-3] 03 p0313 N90-11781
Computer controlled MHD power consolidation and pulse-generation system
[DE89-015600] 03 p0407 N90-12333
Advanced clearance control systems --- blade tips
[PNR90553] 04 p0454 N90-12601
Spark camera annotation and control system for the BRL (Ballistic Research Laboratory) Transonic Range Facility
[AD-A212266] 04 p0459 N90-12633
Automated monitor and control for deep space network subsystems 04 p0486 N90-12794
Self-tuning control of nonlinear Armax models --- Autoregressive Moving Average with eXogeneous (ARMAX) inputs
[RR-362] 04 p0508 N90-12930
Visual perception processing in a hierarchical control system: Level 1
[PB89-221188] 04 p0536 N90-13101
Identification of robot dynamics: A parallel processing approach
[RR-361] 04 p0537 N90-13103
Discretization and model reduction for a class of nonlinear systems 05 p0583 N90-13397

An autopilot design methodology for bank-to-turn missiles
[AD-A213379] 05 p0583 N90-13399
Report of the Asilomar 3 LDR Workshop
[NASA-CR-184656] 05 p0594 N90-13449
A figure control sensor for the Large Deployable Reflector (LDR) 05 p0594 N90-13451
Space telescope pointing control 05 p0595 N90-13454
Wavefront error sensing for LDR 05 p0595 N90-13455
An approach to optical structures control 05 p0595 N90-13456
Segment alignment control system 05 p0595 N90-13457
LDR structural technology activities at JPL 05 p0601 N90-13488
A practical approach for minimum time control of the Spacecraft Control Laboratory Experiment (SCOLE), appendix A
[NASA-CR-186008] 05 p0602 N90-13495
Attitude and shape control of optimally designed large space structures 05 p0613 N90-13579
Adaptive strategies for controls of flexible arms
[NASA-CR-185868] 05 p0649 N90-13783
Arc current control of a robotic welding system: Modeling and control system design
[AD-A213150] 05 p0650 N90-13788
A knowledge-based system design/information tool for aircraft flight control systems
[NASA-TM-101704] 05 p0685 N90-13990
Laboratory test methodology for evaluating the effects of electromagnetic disturbances on fault-tolerant control systems
[NASA-TM-101665] 05 p0695 N90-14061
Control of an experiment to measure acoustic noise in the space shuttle
[NPS62-89-022] 06 p0838 N90-14889
Effect of modal truncation on derivatives of closed-loop damping ratios in structural control 07 p0882 N90-15109
Fly-by-light flight control system technology development plan
[NASA-CR-181953] 07 p0883 N90-15111
On the privacy problems involved in allowing access to computers via the public telephone system
[RSRE-88006] 07 p0917 N90-15303
Implementing fault-tolerant sensors
[NASA-CR-186251] 07 p0933 N90-15400
Control of mechanical manipulators 07 p0938 N90-15432
A semiautomated computer-interactive dynamic impact testing system
[DE90-002721] 07 p0946 N90-15479
Concurrence control for transactions with priorities
[NASA-CR-186241] 07 p0986 N90-15699
Crew emergency return vehicle autoland feasibility study
[NASA-CR-181940] 08 p1028 N90-15937
The US National Transonic Facility, NTF 08 p1028 N90-15942
Automatic control of KKK: Requirements, sensors, actuators, and control performance results 08 p1029 N90-15944
On-line chemical composition analyzer development
[DE90-004079] 08 p1043 N90-16026
D3-D cryogenic control system upgrade
[DE90-003290] 08 p1054 N90-16092
Digital system for monitoring and controlling remote processes
[DE90-003935] 08 p1054 N90-16094
Diesel starting system monitor: Prototype development
[DE90-004425] 08 p1084 N90-16276
Expert system control of a six-legged walking telerobot
[DE90-004861] 08 p1086 N90-16285
Stochastic model of the NASA/MSFC ground facility for large space structures with uncertain parameters: The maximum entropy approach, part 2
[NASA-CR-186009] 08 p1107 N90-16407
Guidance and control considerations for a maneuvering aerial target system 09 p1165 N90-16746
Applications of modern control theory synthesis to a super-augmented aircraft
[AD-A215431] 09 p1167 N90-16753
Design of integrated pitch axis for autopilot/autothrottle and integrated lateral axis for autopilot/yaw damper for NASA TSRV airplane using integral LQG methodology
[NASA-CR-4268] 09 p1169 N90-16768
Estimation and control of nonlinear and hybrid systems with applications to air-to-air guidance
[AD-A214542] 09 p1170 N90-16770
Overview of the Hermes in-orbit control system 09 p1178 N90-16824
Delta 181 sensor module command center
[AD-A214888] 09 p1182 N90-16855
Design of a robust controller for an unstable nonminimum phase guided missile
[AD-A216147] 10 p1323 N90-17645
Thermal study of battery charge control by temperature derivative reduction 10 p1332 N90-17704
Linear and non-linear control of high-order converters after reducing the order by appropriate techniques 10 p1336 N90-17733
Variable structure control system applied to multilevel power conditioning converters 10 p1336 N90-17734
High speed digital control of high frequency PWM converters 10 p1337 N90-17736
Comparison of control structures for a bidirectional high-frequency dc-dc converter 10 p1337 N90-17737
Simple pole/zero modelling of conductance controllers 10 p1337 N90-17739
Learning-based position control of a closed-kinematic chain robot end-effector
[NASA-CR-186283] 10 p1391 N90-18043
Aurora upgrade. Volume 5: Machine monitoring and control system
[AD-A215963] 10 p1393 N90-18053
Robustness of controllers designed using Galerkin type approximations
[NASA-CR-181986] 10 p1395 N90-18063
The implications of using integrated software support environment for design of guidance and control systems software
[AGARD-AR-229] 11 p1464 N90-18432
Application of variable-gain output feedback for high-alpha control
[NASA-TM-102603] 11 p1464 N90-18434
Spacecraft thermal control design data, volume 4
[ESA-PSS-03-108-ISSUE-1-VOL-4] 11 p1469 N90-18458
Application of artificial intelligence control to the vapor-liquid-solid silicon carbide whisker process
[DE90-007835] 11 p1480 N90-18519
Preliminary design of a pointer for movement of a solar simulator
[INPE-4864-TDL/375] 11 p1517 N90-18736
Computation and control with neural nets
[DE90-006460] 11 p1548 N90-18911
Practical methods for robust multivariable control
[AD-A216937] 11 p1550 N90-18920
Feasibility of Mealy design for processor controlpaths
[MEMO-INF-89-53] 11 p1550 N90-18923
Nonlinear model matching: A local solution and two worked examples
[MEMO-809] 11 p1554 N90-18948
Induction motor control
[NASA-TM-102533] 12 p1605 N90-19234
Self-tuning control techniques, implicit and explicit, with parameter estimation in Kalman filters, applied to artificial satellite attitude
[INPE-4857-TDL/368] 12 p1613 N90-19276
Application of attachment modes in the control of large space structures
[NASA-CR-185604] 12 p1613 N90-19280
Integrated control/structure optimization by multilevel decomposition
[NASA-TM-102619] 12 p1613 N90-19281
A computer control system for the alternating gradient magnetometer 12 p1636 N90-19402
Experiments in end-point control of a flexible robot with a mini-manipulator 12 p1671 N90-19596
Dynamics and control of robot manipulators with closed-kinematic chain mechanism 12 p1671 N90-19598
Laboratory implementation of the Continuously Reconfiguring Multi-Microprocessor Flight Control System (CRMMFCS)
[AD-A217730] 13 p1758 N90-20094
Discrete-time control of a spacecraft with retargetable flexible antennas 13 p1763 N90-20119
Docking mechanism for spacecraft
[NASA-CASE-MSC-21386-1] 13 p1764 N90-20126
Error control techniques for satellite and space communications
[NASA-CR-186221] 13 p1788 N90-20263
Design and testing of a noninteracting control loop for the dynamically tuned dry gyro
[NAL-TR-1017] 13 p1803 N90-20350
Design of a telerobotic controller with joint torque sensors
[DE90-008753] 13 p1812 N90-20404
Control system design of the third flexible joint of PUMA 560 robot
[AD-A216075] 13 p1812 N90-20405
The Rapid Geodetic Survey System (RGSS) 13 p1834 N90-20528
A learning regulator for the plane longitudinal movement
[ETN-90-95381] 13 p1864 N90-20695
Development of computer software for the analysis and design of modern control systems
[AD-A217924] 13 p1868 N90-20717
Observer based compensators for nonlinear systems
[AD-A217426] 13 p1876 N90-20760
Joint University Program for Air Transportation Research, 1988-1989
[NASA-CP-3063] 14 p1905 N90-20921
Rule-based mechanisms of learning for intelligent adaptive flight control 14 p1908 N90-20939
Perspectives on the use of rule-based control 14 p1908 N90-20940
Stochastic robustness of linear control systems 14 p1908 N90-20941
Design of a helicopter automatic flight control system using adaptive control 14 p1928 N90-21040
Human centrifuge controller
[NAL-TM-SE-8901] 14 p1929 N90-21043
NASA/DOD Controls-Structures Interaction Technology 1989
[NASA-CP-3041] 14 p1933 N90-21062
A spaceborne optical interferometer: The JPL CSI mission focus 14 p1933 N90-21063
Zenith Star: A structural control challenge 14 p1933 N90-21064
PACOSS program status and results 14 p1933 N90-21065
Controlled multibody dynamics simulation for large space structures 14 p1934 N90-21068
A distributed finite-element modeling and control approach for large flexible structures 14 p1934 N90-21071
Effective techniques for the identification and accommodation of disturbances 14 p1934 N90-21072
Modeling and control of flexible space platforms with articulated payloads 14 p1935 N90-21073
Detection of potential space station control/structure interaction with CO-ST-IN 14 p1935 N90-21074
Optimization of the structural and control system for LSS with reduced-order model 14 p1935 N90-21075
Computational architecture for integrated controls and structures design 14 p1935 N90-21076
Controller reduction for effective interdisciplinary design of active structures 14 p1935 N90-21077
Recent experience in simultaneous control-structure optimization 14 p1936 N90-21078
A survey of experiments and experimental facilities for active control of flexible structures 14 p1936 N90-21079
NASA CSI suspension methods overview 14 p1936 N90-21080
ASCIE: An integrated experiment to study CSI in large segmented optical systems 14 p1936 N90-21082
CSI sensing and control: Analytical and experimental results 14 p1936 N90-21083
Experimental evaluation of active-member control of precision structures 14 p1936 N90-21084
Controls, Astrophysics, and Structures Experiment in Space (CASES) 14 p1937 N90-21085
CSI technology validation on an LSS ground experiment facility 14 p1937 N90-21089
Initial operational capability of the ASTREX large space structures test bed 14 p1938 N90-21091
In-house experiments in large space structures at the Air Force Wright Aeronautical Laboratories Flight Dynamics Laboratory 14 p1938 N90-21092
Attitude control modes for the MECB remote sensing satellites
[INPE-4755-PRE/1427] 14 p1938 N90-21094
A general-purpose balloon-borne pointing system for solar scientific instruments
[NASA-TP-3013] 14 p1959 N90-21219
Microwave Landing System (MLS) remote monitoring subsystem/remote maintenance monitoring system
[DOT/FAA/PS-89/2] 15 p2050 N90-21749
Advances in optimal active control techniques for aerospace systems; application to aircraft active landing gear 15 p2054 N90-21769
A decentralized linear quadratic control design method for flexible structures 15 p2054 N90-21770
Balanced bridge feedback control system
[NASA-CASE-NPO-17430-1-CU] 15 p2088 N90-21951
A methodology for knowledge-based restructurable control to accommodate system failures 15 p2109 N90-22058
Relatchable launch restraint mechanism for deployable booms 15 p2114 N90-22091
VCS: A networked Version Control System
[DE90-009805] 15 p2145 N90-22250
The art of fault-tolerant system reliability modeling
[NASA-TM-102623] 15 p2152 N90-22292
Adaptive control of a flexible manipulator with unknown changing loads 15 p2152 N90-22293

System control of an autonomous planetary mobile spacecraft 15 p2155 N90-22313
An intelligent interface for the design of optimal control systems
[INPE-4917-PRE/1516] 15 p2159 N90-22332
A candidate architecture for monitoring and control in chemical transfer propulsion systems
[NASA-TM-103161] 16 p2208 N90-22595
H2, fixed architecture, control design for large scale systems
[NASA-CR-180471] 16 p2226 N90-22698
Using object-oriented analysis techniques to support system testing
[DE90-009540] 16 p2226 N90-22700
Elements of active vibration control for rotating machinery
[NASA-TM-102368] 16 p2227 N90-22703
Robust control of vibration in flexible structures 16 p2241 N90-22787
Plan execution control and architecture for mobile robots
[LAAS-89-371] 16 p2243 N90-22793
Proceedings of the 3rd Annual Conference on Aerospace Computational Control, volume 1
[NASA-CR-185446] 16 p2279 N90-22987
Experimental experience with flexible structures 16 p2281 N90-23002
A disturbance based control/structure design algorithm 16 p2282 N90-23003
Using deflation in the pole assignment problem with output feedback 16 p2282 N90-23004
Combined control-structure optimization 16 p2282 N90-23005
A robot arm simulation with a shared memory multiprocessor machine 16 p2283 N90-23008
Computational dynamics for robotics systems using a non-strict computational approach 16 p2283 N90-23011
Efficient computer algebra algorithms for polynomial matrices in control design 16 p2285 N90-23022
Integrated control-system design via generalized LQG (GLQG) theory 16 p2286 N90-23023
Modern CACSD using the Robust-Control Toolbox 16 p2286 N90-23024
H(2)- and H(infinity)-design tools for linear time-invariant systems 16 p2286 N90-23025
A methodology for formulating a minimal uncertainty model for robust control system design and analysis 16 p2287 N90-23028
Application of numerical optimization techniques to control system design for nonlinear dynamic models of aircraft 16 p2287 N90-23032
Control of a flexible planar truss using proof mass actuators 16 p2288 N90-23035
Minimum attainable RMS attitude error using co-located rate sensors 16 p2288 N90-23038
Proceedings of the 3rd Annual Conference on Aerospace Computational Control, volume 2
[NASA-CR-186447] 16 p2289 N90-23040
Algorithmic considerations of integrated design for CSI on a hypercube architecture 16 p2289 N90-23043
Enhanced modeling features within TREETOPS 16 p2290 N90-23047
New multivariable capabilities of the INCA program 16 p2290 N90-23049
Multidisciplinary Expert-aided Analysis and Design (MEAD) 16 p2291 N90-23050
Overview of computational control research at UT Austin 16 p2291 N90-23051
Substructural controller synthesis 16 p2292 N90-23055
OPTICON: Pro-Matlab software for large order controlled structure design 16 p2292 N90-23058
Robust fixed order dynamic compensation for large space structure control 16 p2292 N90-23059
Multivariable frequency weighted model order reduction for control synthesis
[AIAA-89-3558] 16 p2292 N90-23060
Distributed neural control of a hexapod walking vehicle 16 p2293 N90-23061
Combining high performance simulation, data acquisition, and graphics display computers 16 p2293 N90-23062
A real time, FEM based optimal control algorithm and its implementation using parallel processing hardware (transistors) in a microprocessor environment 16 p2294 N90-23066
Six-degree-of-freedom aircraft simulation with mixed-data structure using the applied dynamics simulation language, ADSIM 16 p2294 N90-23067
Six-degree-of-freedom missile simulation using the ADI AD 100 digital computer and ADSIM simulation language 16 p2294 N90-23068
JPL control/structure interaction test bed real-time control computer architecture 16 p2294 N90-23070
Multibody dynamics: Modeling component flexibility with fixed, free, loaded, constraint, and residual modes 16 p2295 N90-23072
Component model reduction via the projection and assembly method 16 p2295 N90-23073
Model reduction in the physical coordinate system 16 p2295 N90-23074
Modal identities for multibody elastic spacecraft: An aid to selecting modes for simulation 16 p2296 N90-23075
Issues in CSI analysis for large scale systems 16 p2296 N90-23076
Structural modeling for control design (articulated multibody component representation) 16 p2296 N90-23077
Significance of norms and completeness in variational based methods 16 p2296 N90-23078
Dynamic analysis of flexible mechanical systems using LATDYN 16 p2296 N90-23080
Control design and simulation of systems modeled using ADAMS 16 p2296 N90-23081
Multibody dynamics model building using graphical interfaces 16 p2297 N90-23082
Controlling flexible structures with second order actuator dynamics 16 p2297 N90-23083
Numerical algorithms for computations of feedback laws arising in control of flexible systems 16 p2297 N90-23085
Modeling and control of flexible space stations (slew maneuvers) 16 p2297 N90-23086
Mini-mast dynamic analysis using the truss-beam model 16 p2297 N90-23087
Controlling real-time systems with parallel processes
[CS-8918] 16 p2302 N90-23119
About linear systems robustness: Linear programming approach
[LAAS-89-384] 16 p2303 N90-23123
Control of randomly sampled robotic systems
[AD-A218948] 16 p2309 N90-23157
Modeling and control of flexible vehicles in space
[AD-A219622] 17 p2365 N90-23465
Simulation and interdisciplinary design methodology for control-structure interaction systems 17 p2385 N90-23584
Long period pseudo random number sequence generator
[NASA-CASE-NPO-17241-1-CU] 17 p2394 N90-23636
Numerical optimization, system theoretic and software tools for the integrated design of flexible structures and their control systems
[AD-A219877] 17 p2447 N90-23949
Real time adaptive control of an Autonomous Underwater Vehicle (AUV)
[AD-A219544] 17 p2454 N90-23996
Teleoperation of a force controlled robot manipulator without force feedback to a human operator 18 p2503 N90-24305
The bi-arm servicer: A multimission concept and a technological model for space robotics 18 p2504 N90-24307
NASREM: A functional architecture for control of the flight telerobotic servicer 18 p2506 N90-24325
High performance processing system for embedded control applications in space 18 p2507 N90-24330
Dynamic modeling and control of a flexible arm holding a non-rigid payload 18 p2507 N90-24331
Dynamics and control of free-flying inspection and maintenance vehicle with manipulators 18 p2508 N90-24332
Supervisory controlled telemanipulation and vision systems for inspection and maintenance operations 18 p2508 N90-24333
Control of large space structures
[AD-A221216] 18 p2511 N90-24345
A hierarchical approach to large space structure control
[DE90-010881] 18 p2511 N90-24347
Multi-application scanning mechanism 18 p2537 N90-24473
The problem of robust compensation for systems with unmodeled dynamics
[AD-A221246] 18 p2548 N90-24545
Approximations of thermoelastic and viscoelastic control systems
[NASA-CR-182054] 18 p2604 N90-24834
Modeling flexible aircraft for flight control design
[AD-A219123] 19 p2660 N90-25140
Dynamic analysis of space-related linear and non-linear structures
[NASA-TM-103490] 19 p2667 N90-25174
A linearly controlled direct-current power source for high-current inductive loads in a magnetic suspension wind tunnel
[NASA-TM-4198] 19 p2692 N90-25319
Control structure interaction instrumentation
[AD-A221375] 19 p2693 N90-25320
Out-reach in-space technology experiments program: Control of flexible robot manipulators in zero gravity, experiment definition phase
[NASA-CR-183849] 19 p2696 N90-25343
Robot vibration control using inertial damping forces
[NASA-CR-186808] 19 p2698 N90-25352
Robust controller designs for second-order dynamic system: A virtual passive approach
[NASA-TM-102666] 19 p2701 N90-25369
A task control architecture for autonomous robots 19 p2735 N90-25546
Automated control of hierarchical systems using value-driven methods 19 p2735 N90-25547
The JPL telerobot operator control station: Operational experiences 19 p2738 N90-25565
Adaptive tracking for complex systems using reduced-order models
[NASA-CR-183464] 19 p2747 N90-25609
Use of the TACL system at CEBAF for control of the cryogenic test facility
[CEBAF-PR-89-024] 19 p2755 N90-25652
RF control system development at CEBAF
[CEBAF-PR-89-026] 19 p2755 N90-25653
The CEBAF instrumentation and control system
[CEBAF-PR-89-037] 19 p2755 N90-25657
CEBAF control system
[CEBAF-PR-89-013] 19 p2757 N90-25666
Conceptual task modeling
[TR-89-14] 19 p2762 N90-25693
Synthesis of individual rotor blade control system for gust alleviation
[NASA-TM-101886] 20 p2807 N90-25972
Hot gas ingestion characteristics and flow visualization of a vectored thrust STOVL concept
[NASA-TM-103212] 20 p2813 N90-26009
Model following control system design: Preliminary ATTAS in-flight simulation test results
[PD-FC-9003] 20 p2813 N90-26010
H-infinity based integrated flight-propulsion control design for a STOVL aircraft in transition flight
[NASA-TM-103198] 20 p2813 N90-26011
An investigation of the use of singular perturbation methods and modal control theory in the derivation of aircraft control schemes
[MATHS-REPT-A-106] 20 p2814 N90-26014
Design and implementation of robust decentralized control laws for the ACES structure at Marshall Space Flight Center
[NASA-CR-4310] 20 p2820 N90-26046
Packet radio network concepts for the Norwegian field army 20 p2850 N90-26206
A model of the synchronous machine with rectifier, especially for control purposes
[EUT-89-E-215] 20 p2858 N90-26256
On controller choice for robust sliding mode performance
[MATHS-REPT-A-107] 20 p2872 N90-26337
Local design methodologies for a hierarchic control architecture
[AD-A222006] 21 p2966 N90-26862
Control of orbiting large space structural systems with discrete time observational data and random measurement noise
[AD-A222476] 21 p2967 N90-26863
Flow induced nutation instability in spinning solid propellant rockets
[AD-A222504] 21 p2969 N90-26877
DEVS-based intelligent control of space adapted fluid mixing 21 p3040 N90-27279
The application of intelligent process control to space based systems 21 p3041 N90-27282
An architecture for intelligent task interruption 21 p3041 N90-27284
A hybrid approach to space power control 21 p3043 N90-27293
Attitude Determination and Control System (ADCS) and Maintenance and Diagnostic System (MDS): A maintenance and diagnostic system for Space Station Freedom 21 p3043 N90-27295
Space Station Freedom ECLSS: A step toward autonomous regenerative life support systems 21 p3043 N90-27297
Simulation-based intelligent robotic agent for Space Station Freedom 21 p3043 N90-27298
A vision-based telerobotic control station 21 p3046 N90-27311
An application generator for rapid prototyping of Ada real-time control software 21 p3046 N90-27316
A tool for modeling concurrent real-time computation 21 p3047 N90-27321
SDI satellite autonomy using AI and Ada 21 p3050 N90-27336
Design of robust multivariable controllers
[AD-A222096] 21 p3060 N90-27397

Analysis and design methods for nonlinear control systems
[AD-A221621] 21 p3061 N90-27404
Nonlinear dynamics and control of SDI structural components
[AD-A222472] 21 p3071 N90-27458
Integrated structural/control design via multiobjective optimization
[AD-A223088] 21 p3071 N90-27459
Aircraft Integrated Monitoring Systems
[DLR-MITT-90-04] 22 p3103 N90-27617
Observer or direct inversion 22 p3103 N90-27622
AIMS test and simulation equipment
22 p3104 N90-27623
Performance assessment of MIL-STD-1553B on the avionic systems demonstrator rig of British Aerospace
22 p3104 N90-27624
New features of JAL's ground station
22 p3105 N90-27633
Experimental characterization of the effects of pneumatic tubing on unsteady pressure measurements
[NASA-TM-4171] 22 p3116 N90-27703
Hermes rendezvous with the space station
22 p3128 N90-27753
Flexible structure control and rigid body dynamics
22 p3129 N90-27757
Robust adaptive control: Handling the excitation problem 22 p3241 N90-28382
Aerodynamics of Combat Aircraft Controls and of Ground Effects
[AGARD-CP-465] 23 p3271 N90-28513
Aerodynamic and propulsive control development of the STOL and maneuver technology demonstrator
23 p3271 N90-28514
Combat aircraft control requirements
23 p3271 N90-28515
Aerodynamic control design: Experience and results at Aermacchi 23 p3272 N90-28518
Innovative control concepts and component integration for a generic supercruise fighter
23 p3273 N90-28521
Development of non-conventional control methods for high angle of attack flight using vortex manipulation
23 p3273 N90-28522
Unsteady aerodynamics of controls
23 p3273 N90-28525
Validation of the F-18 high alpha research vehicle flight control and avionics systems modifications
[NASA-TM-101723] 23 p3276 N90-28542
Propulsion system-flight control integration and optimization: Flight evaluation and technology transition
[NASA-TM-4207] 23 p3278 N90-28551
Energy Efficient Engine: Control system preliminary definition report
[NASA-CR-179578] 23 p3281 N90-28569
A conceptual framework for fighter flight control systems
[PD-CF-9009] 23 p3283 N90-28577
A microprocessor controlled strain gauge calibration module
[AR-005-579] 23 p3329 N90-28821
Design of a CO2 laser power control system for a Spacelab microgravity experiment
[NASA-TM-103112] 23 p3331 N90-28833
Cartesian control of redundant robots
23 p3363 N90-29004
The NASA/OAST telerobot testbed architecture
23 p3365 N90-29016
Exploiting map plans as resources for action
23 p3367 N90-29028
Computational neural learning formalisms for manipulator inverse kinematics
23 p3368 N90-29030
Multi-layer neural networks for robot control
23 p3368 N90-29031
Plan recognition for space telerobotics
23 p3369 N90-29036
Trajectory generation of space telerobots
23 p3372 N90-29055
Planning robot actions under position and shape uncertainty 23 p3376 N90-29073
Integrating planning and reactive control
23 p3377 N90-29077
An expert system to perform on-line controller restructuring for abrupt model changes
[NASA-TM-103609] 23 p3385 N90-29121
Analysis, Design and Synthesis Methods for Guidance and Control Systems
[AGARD-AG-314] 24 p3423 N90-29338
Integrated navigation/flight control for future high performance aircraft 24 p3427 N90-29362
Guidance and control techniques for airborne transfer alignment and SAR motion compensation
24 p3429 N90-29372
Multi-disciplinary optimization of aeroservoelastic systems
[NASA-CR-185931] 24 p3432 N90-29385
Sample rate effects on disturbance rejection for digital control systems 24 p3435 N90-29400
A three axis attitude control of a satellite
[NASDA-TR-22] 24 p3439 N90-29421
High frequency bundle protection
[DIGEL-1990-1] 24 p3466 N90-29582
Robust design of LQG controllers
24 p3475 N90-29639
Proceedings of the NASA Conference on Space Telerobotics, volume 3
[NASA-CR-186858] 24 p3500 N90-29780
Capture of free-flying payloads with flexible space manipulators 24 p3500 N90-29784
Technology and task parameters relating to the effectiveness of the bracing strategy
24 p3500 N90-29785
Manipulators with flexible links: A simple model and experiments 24 p3501 N90-29786
Experiments in identification and control of flexible-link manipulators 24 p3501 N90-29787
Impedance hand controllers for increasing efficiency in teleoperations 24 p3502 N90-29793
Stability analysis of multiple-robot control systems
24 p3505 N90-29811
Experiments in cooperative manipulation: A system perspective 24 p3505 N90-29812
On the manipulability of dual cooperative robots
24 p3505 N90-29813
Controlling multiple manipulators using RIPS
24 p3505 N90-29814
Time optimal movement of cooperating robots
24 p3505 N90-29815
Design of a structural and functional hierarchy for planning and control of telerobotic systems
24 p3506 N90-29820
The flight telerobotic servicer project: A technical overview 24 p3506 N90-29821
The flight telerobotic servicer Tinman concept: System design drivers and task analysis
24 p3506 N90-29822
The flight telerobotic servicer: From functional architecture to computer architecture
24 p3507 N90-29823
The Goddard Space Flight Center (GSFC) robotics technology testbed 24 p3507 N90-29825
Direct adaptive control of a PUMA 560 industrial robot
24 p3508 N90-29832
Model based manipulator control
24 p3509 N90-29833
Discrete-time adaptive control of robot manipulators
24 p3509 N90-29834
A discrete decentralized variable structure robotic controller 24 p3509 N90-29835
Construction and demonstration of a 9-string 6 DOF force reflecting joystick for telerobotics
24 p3509 N90-29836
Response to reflected-force feedback to fingers in teleoperations 24 p3509 N90-29837
The JAU-JPL anthropomorphic telerobot
24 p3509 N90-29838
A procedure concept for local reflex control of grasping 24 p3509 N90-29839
Performance limitations of bilateral force reflection imposed by operator dynamic characteristics
24 p3510 N90-29840
Sensor-based fine telemanipulation for space robotics
24 p3510 N90-29841
ROTEX-TRIIFEX: Proposal for a joint FRG-USA telerobotic flight experiment 24 p3510 N90-29842
Test and training simulator for ground-based teleoperated in-orbit servicing 24 p3510 N90-29843
Concept synthesis of an equipment manipulation and transportation system EMATS 24 p3510 N90-29844
Force-reflective teleoperated system with shared and compliant control capabilities 24 p3510 N90-29845
Information management in an integrated space telerobot 24 p3511 N90-29846
Redundancy in sensors, control and planning of a robotic system for space telerobotics 24 p3511 N90-29847
RCTS: A flexible environment for sensor integration and control of robot systems; the distributed processing approach 24 p3512 N90-29852
Real-time cartesian force feedback control of a teleoperated robot 24 p3513 N90-29857
Determining robot actions for tasks requiring sensor interaction 24 p3514 N90-29868
The laboratory telerobotic manipulator program
24 p3515 N90-29869
Robotic control of the seven-degree-of-freedom NASA laboratory telerobotic manipulator
24 p3515 N90-29870
System architectures for telerobotic research
24 p3515 N90-29872
The telerobot workstation testbed for the shuttle aft flight deck: A project plan for integrating human factors into system design 24 p3518 N90-29887
Multi-level manual and autonomous control superposition for intelligent telerobot
24 p3518 N90-29888
An alternative control structure for telerobotics
24 p3518 N90-29889
Requirements for implementing real-time control functional modules on a hierarchical parallel pipelined system 24 p3518 N90-29891
The JPL telerobotic Manipulator Control and Mechanization (MCM) subsystem
24 p3519 N90-29892
On discrete control of nonlinear systems with applications to robotics 24 p3519 N90-29893
Flight experiments in telerobotics-Orbiter middeck concept 24 p3519 N90-29895
Computed torque control of a free-flying cooperating-arm robot 24 p3520 N90-29898
Coordination in a hierarchical multi-actuator controller
24 p3520 N90-29900
A comparison of the Shuttle remote manipulator system and the Space Station Freedom mobile servicing center
24 p3522 N90-29910
Computer-aided engineering environment for controlled mechanical systems
[AD-A223551] 24 p3527 N90-29942
MacRootLocus: A CAD design tool for feedback control systems
[AD-A223772] 24 p3528 N90-29951
Directing an animated scene with autonomous actors
[REPT-89-041] 24 p3531 N90-29972

CONTROL THEORY

How to control unstable missile airframes: Methodology and limitations 01 p0013 N90-10060
Proceedings of the Workshop on Computational Aspects in the Control of Flexible Systems, part 1
[NASA-TM-101578-PT-1] 01 p0017 N90-10080
Simulation and control problems in elastic robots
01 p0020 N90-10098
Linearized flexibility models in multibody dynamics and control 01 p0020 N90-10099
Optical processing for distributed sensors in control of flexible spacecraft 01 p0021 N90-10102
Flexible robot control: Modeling and experiments
01 p0021 N90-10104
Modifying high-order aeroelastic math model of a jet transport using maximum likelihood estimation
01 p0021 N90-10106
Automated model formulation for time-varying flexible structures 01 p0022 N90-10107
Control law synthesis and optimization software for large order aeroservoelastic systems
01 p0022 N90-10111
Flexible aircraft dynamic modeling for dynamic analysis and control synthesis 01 p0022 N90-10112
Experimental validation of flexible robot arm modeling and control 01 p0023 N90-10113
Controlling flexible structures: A survey of methods
01 p0023 N90-10114
Aircraft modal supression system: Existing design approach and its shortcomings
01 p0023 N90-10115
Optimal q-Markov COVER for finite precision implementation 01 p0023 N90-10117
Stochastic control theory, nonlinear structural mechanics and applied combinatorics
[AD-A209042] 01 p0114 N90-10657
Frequency domain design of robust controllers for space structures
[AD-A211172] 02 p0176 N90-10985
Performance and robustness of adaptive controllers for linear stochastic systems 02 p0261 N90-11485
Nonlinear maneuver autopilot for the F-15 aircraft
[NASA-CR-179442] 02 p0262 N90-11487
Principal components in multivariate control charts
[DE89-016828] 02 p0262 N90-11489
Adaptive control law design for model uncertainty compensation
[AD-A211712] 03 p0309 N90-11758
Efficient finite element solution of Navier-Stokes equations and related topics
[AD-A211647] 03 p0348 N90-11986
An autopilot design methodology for bank-to-turn missiles
[AD-A213379] 05 p0583 N90-13399
The dynamics and control of large flexible space structures - 12, supplement 11
[NASA-CR-185966] 05 p0602 N90-13494
Attitude and shape control of optimally designed large space structures 05 p0613 N90-13579
A new approach to control single-link flexible arms. Part 3: Adaptive control of the tip position with payload changes
[AD-A213337] 05 p0650 N90-13792

On control of manipulators
[ISBN-90-9002789-0] 05 p0652 N90-13804
Compensatory tracking in disturbance tasks and target following tasks. The influence of cockpit motion on performance and control behavior
[LR-511] 05 p0675 N90-13933
The cellular approach: A new method to speed up simulated annealing for macro placement
[MEMO-COSOR-88-29] 05 p0683 N90-13980
Model reduction of weakly damped mechanical systems
[MEMO-798] 05 p0686 N90-13993
A priori results in linear quadratic optimal control theory
[MEMO-COSOR-89-02] 05 p0686 N90-13996
The quadratic matrix inequality in singular H infinity control with state feedback
[MEMO-COSOR-89-03] 05 p0686 N90-13997
The singular zero sum differential game with stability using H infinity control theory
[MEMO-COSOR-89-09] 05 p0687 N90-13999
The singular H infinity control problem with dynamic measurement feedback
[MEMO-COSOR-89-14] 05 p0687 N90-14000
The output-stabilizable subspace and linear optimal control
[MEMO-COSOR-89-15] 05 p0687 N90-14001
Survey of adaptive control theory and its applications
[DE89-901270] 06 p0833 N90-14840
A pitch control law for compensation of the phugoid mode induced by windshears 07 p0870 N90-15051
The interference of flightmechanical control laws with those of load alleviation and its influence on structural design 07 p0871 N90-15054
Adaptive control of helicopter vibrations via the impulse response method
[AD-A213728] 07 p0883 N90-15113
Control of mechanical manipulators 07 p0938 N90-15432
The application of optimal control theory for analysis of human jumping and pedaling 07 p0968 N90-15590
On the identification of local minimizers in inertia-controlling methods for quadratic programming
[DE89-017330] 07 p0973 N90-15616
Optimal periodic control and regulator theory based on the second variation 07 p0987 N90-15704
Guidance and Control of Unmanned Air Vehicles
[AGARD-CP-436] 08 p1025 N90-15924
Synthesis of control law, on a RPV, in order to minimize the number of sensors 08 p1025 N90-15925
Automatic control of cryogenic wind tunnels 08 p1031 N90-15957
Bilateral force reflection for teleoperators with masters and slaves with dissimilar and possibly redundant kinematics
[DE90-004392] 08 p1061 N90-16132
Parallel processing implementation of a flight controller 09 p1165 N90-16743
Applications of modern control theory synthesis to a super-augmented aircraft
[AD-A215431] 09 p1167 N90-16753
Investigation of liquid sloshing in spin-stabilized satellites
[AD-A214730] 09 p1182 N90-16853
The 1989 National Convention Record IEE Japan, part 8
[DE89-910081] 09 p1210 N90-17013
Design of a robust controller for an unstable nonminimum phase guided missile
[AD-A216147] 10 p1323 N90-17645
A fractional calculus model of aeroelasticity
[AD-A216244] 10 p1423 N90-18212
Application of variable-gain output feedback for high-alpha control
[NASA-TM-102603] 11 p1464 N90-18434
Practical methods for robust multivariable control
[AD-A216937] 11 p1550 N90-18920
System theory and mechanics
[MEMO-807] 11 p1550 N90-18922
Aeroservoelasticity
[NASA-TM-102620] 12 p1603 N90-19227
Output model-following control synthesis for an oblique-wing aircraft
[NASA-TM-100454] 12 p1606 N90-19241
A complete description of robot manipulator dynamics based on Lagrangian mechanics
[DE90-741467] 12 p1672 N90-19603
Drag-free satellite control 12 p1735 N90-19974
Digital-flutter-suppression-system investigations for the active flexible wing wind-tunnel model
[NASA-TM-102618] 13 p1758 N90-20093
Optimal, impulsive, time-fixed orbital rendezvous and interception with path constraints 13 p1760 N90-20102
Discrete-time control of a spacecraft with retargetable flexible antennas 13 p1763 N90-20119
Aiming control: Theory and applications to dynamic control of space structures
[AD-A217877] 13 p1764 N90-20123
Discrete-time control of a spacecraft with retargetable flexible antennas
[AD-A218345] 13 p1764 N90-20125
Development of computer software for the analysis and design of modern control systems
[AD-A217924] 13 p1868 N90-20717
Robust planning and control using neural networks
[AD-A217216] 13 p1872 N90-20732
Joint University Program for Air Transportation Research, 1988-1989
[NASA-CP-3063] 14 p1905 N90-20921
An expert system for wind shear avoidance 14 p1908 N90-20938
Experimental and theoretical investigation of optimal control methods with model reduction 14 p1928 N90-21039
Suboptimal and hybrid numerical solution schemes for orbit transfer manoeuvres
[INPE-4991-PRE/1556] 14 p1931 N90-21054
Modeling and control of flexible space platforms with articulated payloads 14 p1935 N90-21073
CSI sensing and control: Analytical and experimental results 14 p1936 N90-21083
Integrated modeling and analysis of a space-truss article
[NASA-TM-102615] 14 p1991 N90-21412
Optimal and near-optimal medium range air-to-air missile guidance against maneuvering targets 15 p2053 N90-21766
Advances in optimal active control techniques for aerospace systems; application to aircraft active landing gear 15 p2054 N90-21769
Nonlinear stability analysis and control of dynamical robotic systems 15 p2104 N90-22037
Perturbation techniques in the dynamics and control of flexible manipulators
[OUEL-1772/89] 15 p2107 N90-22053
On the existence of a positive definite solution of the matrix equation X + A(sup tau)X(exp -1)A = I
[PB90-133976] 15 p2159 N90-22335
Dynamics and control of tethered antennas/reflectors in orbit
[AD-A219316] 16 p2207 N90-22594
Plan execution control and architecture for mobile robots
[LAAS-89-371] 16 p2243 N90-22793
Recursive linearization of multibody dynamics equations of motion 16 p2280 N90-22993
Experimental experience with flexible structures 16 p2281 N90-23002
Frequency response modeling and control of flexible structures: Computational methods 16 p2285 N90-23021
Integrated control-system design via generalized LQG (GLQG) theory 16 p2286 N90-23023
Modern CACSD using the Robust-Control Toolbox 16 p2286 N90-23024
Control of a flexible planar truss using proof mass actuators 16 p2288 N90-23035
Extensions of output variance constrained controllers to hard constraints 16 p2292 N90-23056
Minimal complexity control law synthesis 16 p2292 N90-23057
Multivariable frequency weighted model order reduction for control synthesis
[AIAA-89-3558] 16 p2292 N90-23060
Numerical algorithms for computations of feedback laws arising in control of flexible systems 16 p2297 N90-23085
The (DURIP) computer simulations of plasmas, nonlinear systems, and control theory
[AD-A219070] 16 p2300 N90-23107
A priori results in linear-quadratic optimal control theory (extended version)
[MEMO-COSOR-89-17] 16 p2304 N90-23124
Optimal helicopter trajectory planning for terrain following flight
[NASA-CR-186470] 17 p2349 N90-23376
Prediction of longitudinal pilot induced oscillations using the optimal control model
[AD-A220593] 17 p2356 N90-23412
Theory of filtering and control with application to control of large space structures
[AD-A219936] 17 p2366 N90-23468
A theory of control for infinite dimensional systems with application to large scale space structures
[AD-A219937] 17 p2366 N90-23469
Simulation and interdisciplinary design methodology for control-structure interaction systems 17 p2365 N90-23584
Nonlinear dynamics and control of flexible structures
[AD-A218372] 17 p2386 N90-23588
Adaptive control methods for mechanical manipulators: A comparative study
[AD-A219965] 17 p2413 N90-23749
Adaptive control of a system with periodic dynamics: Application of an impulse response method to the helicopter vibration problem 17 p2453 N90-23990
Completion of the squares in the finite horizon H infinity control problem by measurement feedback
[MEMO-COSOR-89-27] 17 p2455 N90-24004
Numerical solution of large Lyapunov equations
[NASA-CR-180359] 17 p2456 N90-24010
Linear-quadratic problems and the Riccati equation
[MEMO-COSOR-89-26] 17 p2459 N90-24037
The Hermes robot arm teleoperation and control concept 18 p2503 N90-24301
On the theory of nonlinear control systems
[MEMO-813] 18 p2597 N90-24776
Almost input-output decoupling with stability
[MEMO-819] 18 p2597 N90-24778
Automated control of hierarchical systems using value-driven methods 19 p2735 N90-25547
Kinematically redundant arm formulations for coordinated multiple arm implementations 19 p2736 N90-25551
Neuromorphic learning of continuous-valued mappings from noise-corrupted data. Application to real-time adaptive control
[NASA-TM-4176] 19 p2747 N90-25607
On conditions for the development of stable discrete-time sliding mode control systems
[MATHS-REPT-A-124] 19 p2747 N90-25612
An investigation of the use of singular perturbation methods and modal control theory in the derivation or aircraft control schemes
[MATHS-REPT-A-106] 20 p2814 N90-26014
Low-speed wind tunnel investigation of the static stability and control characteristics of an advanced turboprop configuration with the propellers placed over the tail
[NASA-CR-186900] 20 p2814 N90-26017
Robustness evaluation of H2 and H(infinity) control theory as applied to a transport aircraft
[AD-A222795] 20 p2814 N90-26018
Design and implementation of robust decentralized control laws for the ACES structure at Marshall Space Flight Center
[NASA-CR-4310] 20 p2820 N90-26046
Manufacturing control: A basis for analysis
[PNR90639] 20 p2844 N90-26174
Inference and control mechanisms in NEXT 2.0
[NLR-MP-88062-U] 20 p2844 N90-26175
Control strategy for cooperating disparate manipulators
[NASA-CR-186809] 20 p2870 N90-26328
Guidance and control system for an autonomous underwater vehicle
[AD-A222709] 20 p2873 N90-26343
Assembly via disassembly: A case in machine perceptual development
[NASA-CR-186867] 20 p2900 N90-26497
Research conducted at the Institute for Computer Applications in Science and Engineering in applied mathematics, numerical analysis, and computer science
[NASA-CR-182057] 20 p2903 N90-26510
On the robust stability of MIMO linear feedback systems
[EUT-88-E-212] 20 p2915 N90-26585
Aiming control: Theory and applications to dynamic control of space structures
[AD-A221532] 21 p2967 N90-26864
Generalized interpolation theory for the design and analysis of robust feedback systems
[AD-A222130] 21 p3060 N90-27399
Analysis and design methods for nonlinear control systems
[AD-A221621] 21 p3061 N90-27404
Nonlinear dynamics and control of SDI structural components
[AD-A222472] 21 p3071 N90-27458
Development and testing of methodology for evaluating the performance of multi-input/multi-output digital control systems
[NASA-TM-102704] 22 p3115 N90-27699
Active control of aerothermoelastic effects for a conceptual hypersonic aircraft
[NASA-TM-102713] 22 p3122 N90-27725
Aerodynamic and propulsive control development of the STOL and maneuver technology demonstrator 23 p3271 N90-28514
Control research in the NASA high-alpha technology program 23 p3272 N90-28516
Innovative control concepts and component integration for a generic supercruise fighter 23 p3273 N90-28521

Real time guidance and propulsion control for single-stage-to-orbit airbreathing vehicles
23 p3285 N90-28587
An LQR controller design approach for a Large Gap Magnetic Suspension System (LGMSS)
[NASA-TM-101606] 23 p3316 N90-28751
Preliminary results on noncollocated torque control of space robot actuators 23 p3373 N90-29057
Control and estimation for aerospace applications with system time delays 24 p3428 N90-29367
Proceedings of damping '89. Volume 1: Pages AAB-1 through DCD-11
[AD-A223431] 24 p3479 N90-29664
Capture of free-flying payloads with flexible space manipulators 24 p3500 N90-29784
Control strategies for a telerobot
24 p3504 N90-29808
Stability analysis of multiple-robot control systems
24 p3505 N90-29811
Performance constraints and compensation for teleoperation with delay 24 p3517 N90-29881
Software design for high integrity systems
[ETN-90-97517] 24 p3530 N90-29966
Optimal control law phenomena in certain adaptive second-order observation systems
[AD-A224274] 24 p3534 N90-29986

CONTROL UNITS (COMPUTERS)
OOPS it's happening, part 1
[AD-A220498] 17 p2443 N90-23922
CESAR sequencer
[FFI-89/7021] 19 p2744 N90-25599
Computer-aided engineering environment for controlled mechanical systems
[AD-A223551] 24 p3527 N90-29942

CONTROL VALVES
Independent Orbiter Assessment (IOA): Analysis of the hydraulics/water spray boiler subsystem
[NASA-CR-185541] 02 p0165 N90-10934

CONTROLLABILITY
A design procedure for the handling qualities optimization of the X-29A aircraft
[NASA-TM-4142] 03 p0308 N90-11753
Preliminary airworthiness evaluation of the AH-64A equipped with the Air To Air Stinger (ATAS) missile system
[AD-A213030] 05 p0579 N90-13374
Electron beam sensitive devices for controllability
[IMAG-RR-761-I] 05 p0636 N90-13707
End point control of flexible manipulators
[AD-A217319] 14 p1986 N90-21383
Elements of active vibration control for rotating machinery
[NASA-TM-102368] 16 p2227 N90-22703
Prediction of longitudinal pilot induced oscillations using the optimal control model
[AD-A220593] 17 p2356 N90-23412
Numerical solution of large Lyapunov equations
[NASA-CR-180359] 17 p2456 N90-24010
Static wind-tunnel and radio-controlled flight test investigation of a remotely piloted vehicle having a delta wing planform
[NASA-TM-4200] 18 p2491 N90-24238
Helicopter controllability
[AD-A220078] 18 p2498 N90-24275
Orbiter utilization as an ACRV
[NASA-TM-102700] 20 p2817 N90-26032
Computer aided handling qualities evaluation in frequency domain
[NAL-TM-SE-8902] 20 p2905 N90-26523
Space shuttle descent flight verification by simulation: A challenge in implementing flight control system robustness 22 p3127 N90-27748
Combat aircraft control requirements
23 p3271 N90-28515
Combat aircraft control requirements for agility
23 p3272 N90-28517
Aerodynamic control design: Experience and results at Aermacchi 23 p3272 N90-28518
Innovative control concepts and component integration for a generic supercruise fighter
23 p3273 N90-28521
Noncontact measurement of rotating blade vibrations
[NAL-TR-1033] 24 p3483 N90-29687

CONTROLLED ATMOSPHERES
NT CABIN ATMOSPHERES
NT SPACECRAFT CABIN ATMOSPHERES
Effects of tacky mat contamination on bond degradation for Chemlok/liner and NBR/liner bonds
[NASA-CR-183742] 05 p0626 N90-13653
Regulation of nitrogen uptake and assimilation: Effects of nitrogen source, root-zone pH, and aerial CO2 concentration on growth and productivity of soybeans
[NASA-CR-177546] 10 p1413 N90-18147

CONTROLLED FUSION
Massachusetts Institute of Technology Plasma Fusion Center
[DE89-016050] 01 p0126 N90-10723
Compact torus configurations with high frequency driven currents
[ETN-89-94674] 02 p0290 N90-11598
Hybrid modeling of plasmas and applications to fusion and space physics 15 p2168 N90-22387

CONTROLLED STABILITY
U CONTROL

CONTROLLERS
NT POWER FACTOR CONTROLLERS
NT SERVOMECHANISMS
NT SERVOMOTORS
Explicit modeling and computational load distribution for concurrent processing simulation of the space station
01 p0020 N90-10096
Optical processing for distributed sensors in control of flexible spacecraft 01 p0021 N90-10102
Proceedings of the Workshop on Computational Aspects in the Control of Flexible Systems, part 2
[NASA-TM-101578-PT-2] 01 p0021 N90-10103
Flexible robot control: Modeling and experiments
01 p0021 N90-10104
Flexible aircraft dynamic modeling for dynamic analysis and control synthesis 01 p0022 N90-10112
Experimental validation of flexible robot arm modeling and control 01 p0023 N90-10113
Controlling flexible structures: A survey of methods
01 p0023 N90-10114
Optimal q-Markov COVER for finite precision implementation 01 p0023 N90-10117
Active vibration mitigation of distributed parameter, smart-type structures using Pseudo-Feedback Optimal Control (PFOC) 01 p0024 N90-10121
Optimal integral controller with sensor failure accommodation 01 p0024 N90-10123
An adaptive controller for enhancing operator performance during teleoperation
[NASA-CR-183445] 01 p0077 N90-10438
Adaptive robust control 01 p0109 N90-10820
Independent Orbiter Assessment (IOA): Analysis of the manned maneuvering unit
[NASA-CR-185565] 02 p0161 N90-10913
Independent Orbiter Assessment (IOA): Analysis of the electrical power generation/fuel cell powerplant subsystem
[NASA-CR-185561] 02 p0161 N90-10915
Independent Orbiter Assessment (IOA): Analysis of the electrical power generation/power reactant storage and distribution subsystem
[NASA-CR-185556] 02 p0162 N90-10918
Independent Orbiter Assessment (IOA): Analysis of the electrical power distribution and control/electrical power generation subsystem
[NASA-CR-185538] 02 p0165 N90-10933
Independent Orbiter Assessment (IOA): Analysis of the electrical power distribution and control/remote manipulator system subsystem
[NASA-CR-185526] 02 p0166 N90-10936
Independent Orbiter Assessment (IOA): Analysis of the reaction control system, volume 1
[NASA-CR-185532-VOL-1] 02 p0166 N90-10938
Independent Orbiter Assessment (IOA): Analysis of the reaction control system, volume 2
[NASA-CR-185532-VOL-2] 02 p0167 N90-10939
Independent Orbiter Assessment (IOA): Analysis of the reaction control system, volume 3
[NASA-CR-185532-VOL-3] 02 p0167 N90-10940
Independent Orbiter Assessment (IOA): Analysis of the electrical power distribution and control subsystem, volume 1
[NASA-CR-185529-VOL-1] 02 p0167 N90-10941
Independent Orbiter Assessment (IOA): Analysis of the electrical power distribution and control subsystem, volume 2
[NASA-CR-185529-VOL-2] 02 p0167 N90-10942
Independent Orbiter Assessment (IOA): Assessment of the backup flight system FMEA/CIL
[NASA-CR-185566] 02 p0173 N90-10973
Performance and robustness of adaptive controllers for linear stochastic systems 02 p0261 N90-11485
Independent Orbiter Assessment (IOA): Assessment of the reaction control system, volume 1
[NASA-CR-185543-VOL-1] 03 p0316 N90-11793
Independent Orbiter Assessment (IOA): Assessment of the reaction control system, volume 2
[NASA-CR-185543-VOL-2] 03 p0316 N90-11794
Independent Orbiter Assessment (IOA): Assessment of the reaction control system, volume 3
[NASA-CR-185543-VOL-3] 03 p0316 N90-11795
Independent Orbiter Assessment (IOA): Assessment of the reaction control system, volume 4
[NASA-CR-185543-VOL-4] 03 p0316 N90-11796
Independent Orbiter Assessment (IOA): Assessment of the reaction control system, volume 5
[NASA-CR-185543-VOL-5] 03 p0316 N90-11797
A design methodology for self-tuning control of systems with inherent conflicts
[PB89-219505] 03 p0344 N90-11960
Control of plasma position in the CASTOR tokamak
[IPPCZ-284] 03 p0407 N90-12332
Automated monitor and control for deep space network subsystems 04 p0486 N90-12794
Self-tuning control of nonlinear Armax models --- Autoregressive Moving Average with eXogeneous (ARMAX) inputs
[RR-362] 04 p0508 N90-12930
Control of optical systems 05 p0600 N90-13484
Research on the controllability of integrated circuits by means of electron beams
[ETN-90-95710] 05 p0636 N90-13708
Design and control of a two-degree-of-freedom lightweight flexible arm
[AD-A213335] 05 p0650 N90-13790
Optimal control of aero-assisted orbit transfer vehicles
06 p0727 N90-14241
A helicopter flight path controller design via a nonlinear transformation technique 06 p0727 N90-14242
Controller design for a robotic manipulator
06 p0792 N90-14615
Control of an experiment to measure acoustic noise in the space shuttle
[NPS62-89-022] 06 p0838 N90-14869
Effect of modal truncation on derivatives of closed-loop damping ratios in structural control
07 p0882 N90-15109
A versatile stepping motor controller for systems with many motors
[DE90-001556] 07 p0921 N90-15327
Tuned-circuit Johnson noise thermometry
[DE89-016221] 07 p0925 N90-15356
Architectural study of the design and operation of advanced force feedback manual controllers
[NASA-CR-185948] 07 p0981 N90-15664
Knowledge-based imaging-sensor fusion system
08 p1075 N90-16220
Expert system control of a six-legged walking telerobot
[DE90-004661] 08 p1086 N90-16285
Artificial intelligence in process control: Knowledge base for the shuttle ECS model 08 p1156 N90-16697
Mathematical model for adaptive control system of ASEA robot at Kennedy Space Center
08 p1157 N90-16701
Parallel processing implementation of a flight controller 09 p1165 N90-16743
Design of integrated pitch axis for autopilot/autothrottle and integrated lateral axis for autopilot/yaw damper for NASA TSRV airplane using integral LQG methodology
[NASA-CR-4268] 09 p1169 N90-16768
Overview of the Hermes in-orbit control system
09 p1178 N90-16824
Multiple model adaptive estimation techniques for adaptive model-based robot control
[AD-A215742] 09 p1231 N90-17146
Concurrency control for transactions with priorities
[NASA-CR-186268] 09 p1263 N90-17323
Active control of a flexible structure using a modal positive position feedback controller
[NASA-CR-186336] 09 p1272 N90-17371
The 120V 10A SSPC for the Columbus programme
10 p1330 N90-17683
Simple pole/zero modelling of conductance controllers 10 p1337 N90-17739
Dynamic response for thermal control and measurement and fast radiation thermometry
10 p1367 N90-17924
Robustness of controllers designed using Galerkin type approximations
[NASA-CR-181986] 10 p1395 N90-18063
Payload vibration isolation in a microgravity environment
[NASA-CR-186191] 11 p1518 N90-18744
A rule-based paradigm for intelligent adaptive flight control 12 p1605 N90-19238
Output model-following control synthesis for an oblique-wing aircraft
[NASA-TM-100454] 12 p1606 N90-19241
Investigations into a new algorithm for calculating H infinity optimal controllers 12 p1637 N90-19406
Determination of the implementation of the 3-axis attitude motion simulator digital position controller
12 p1638 N90-19409
Disturbance torque rejection properties of the NASA/JPL 70-meter antenna axis servos
12 p1644 N90-19450
Deceit: A flexible distributed file system
[NASA-CR-186412] 12 p1726 N90-19923

Potential role of avionics in escape systems
13 p1752 N90-20060
The implementation and operation of a variable-response electronic throttle control system for a TF-104G aircraft
[NASA-TM-101696] 13 p1756 N90-20086
Interaction of switch actuation on tracking with a four-axis flight control (cross-coupling)
[AD-A217981] 13 p1758 N90-20095
Space station Simulation Computer System (SCS) study for NASA/MSFC. Volume 4: Conceptual design report
[NASA-CR-183843] 13 p1762 N90-20116
Design and testing of a noninteracting control loop for the dynamically tuned dry gyro
[NAL-TR-1017] 13 p1803 N90-20350
Prototype part task trainer: A remote manipulator system simulator 13 p1860 N90-20672
Perspectives on the use of rule-based control
14 p1908 N90-20940
Experimental and theoretical investigation of optimal control methods with model reduction
14 p1928 N90-21039
Human centrifuge controller
[NAL-TM-SE-8901] 14 p1929 N90-21043
Effective techniques for the identification and accommodation of disturbances
14 p1934 N90-21072
Computational architecture for integrated controls and structures design 14 p1935 N90-21076
Controller reduction for effective interdisciplinary design of active structures 14 p1935 N90-21077
Design of a digital model following controller of reaction wheel torques
[INPE-4753-PRE/1425] 14 p1938 N90-21093
Electromechanical actuation for thrust vector control applications
[NASA-TM-102548] 14 p1968 N90-21272
Development of a dynamic modeling technique and its application to the analysis and control of a high-precision robotic manipulator 14 p1987 N90-21391
Active control of multi-dimensional random sound in ducts
[NASA-TM-102653] 14 p2024 N90-21603
A comparison of time-optimal interception trajectories for the F-8 and F-15
[NASA-CR-186300] 15 p2050 N90-21753
A decentralized linear quadratic control design method for flexible structures 15 p2054 N90-21770
Bi-directional thruster development and test report
[NASA-CR-182013] 15 p2058 N90-21785
An 8.4-GHz dual-maser front-end system for Parkes reimplementation 15 p2078 N90-21905
Nonlinear stability analysis and control of dynamical robotic systems 15 p2104 N90-22037
Development of a multipurpose hand controller for JEMRMS 15 p2113 N90-22087
A new six-degree-of-freedom force-reflecting hand controller for space telerobotics
15 p2113 N90-22089
Limiting performance based structural and control optimization for large vibrating structures
16 p2202 N90-22568
Field oriented control of induction motors
[NASA-TM-103154] 16 p2231 N90-22731
The interactive digital video interface
16 p2271 N90-22941
Multi-axis control of telemanipulators
16 p2271 N90-22943
Proceedings of the 3rd Annual Conference on Aerospace Computational Control, volume 1
[NASA-CR-186446] 16 p2279 N90-22967
A disturbance based control/structure design algorithm 16 p2282 N90-23003
A robot arm simulation with a shared memory multiprocessor machine 16 p2283 N90-23008
Enhanced modeling features within TREETOPS
16 p2290 N90-23047
Substructural controller synthesis
16 p2292 N90-23055
Extensions of output variance constrained controllers to hard constraints 16 p2292 N90-23056
Minimal complexity control law synthesis
16 p2292 N90-23057
Distributed neural control of a hexapod walking vehicle 16 p2293 N90-23061
Real-time closed-loop simulation and upset evaluation of control systems in harsh electromagnetic environments 16 p2294 N90-23069
An experimental study of fault propagation in a jet-engine controller
[NASA-CR-181335] 17 p2354 N90-23401
Statistical techniques for designing a decoupled controller to be robust to model and sensor noise
[AD-A220476] 17 p2412 N90-23745
An expert system to perform on-line controller tuning
[NASA-TM-103101] 17 p2453 N90-23991
Dynamic stabilization of large flexible space structures
[ETN-90-96926] 18 p2511 N90-24344
Implementation of an I-structure memory controller
[AD-A221397] 18 p2588 N90-24726
Performance of battery charge controllers
[DE90-011413] 19 p2686 N90-25279
Control structure interaction instrumentation
[AD-A221375] 19 p2693 N90-25320
Performance of a self-aligning solar array tracking controller
[DE90-011184] 19 p2698 N90-25350
Robust controller designs for second-order dynamic system: A virtual passive approach
[NASA-TM-102666] 19 p2701 N90-25369
Automation in the Space Station module power management and distribution Breadboard
19 p2728 N90-25509
The application of NASREM to remote robot control
19 p2738 N90-25563
A control problem for Burgers' equation with bounded input/output
[NASA-CR-182082] 19 p2747 N90-25808
The CEBAF instrumentation and control system
[CEBAF-PR-89-037] 19 p2755 N90-25657
H-infinity based integrated flight-propulsion control design for a STOVL aircraft in transition flight
[NASA-TM-103198] 20 p2813 N90-26011
Literature concerning control and display technology applicable to the Orbital Maneuvering Vehicle (OMV)
[NASA-CR-186790] 20 p2820 N90-26048
Intergration of system identification and robust controller designs for flexible structures in space
[NASA-TM-102695] 20 p2876 N90-26362
Position control of redundant manipulators using an adaptive error-based control scheme
[NASA-CR-186812] 20 p2914 N90-26578
A new scheme for identification and control
[EUT-88-E-213] 20 p2915 N90-26586
Temperature and melt solid interface control during crystal growth
[NASA-CR-186731] 20 p2929 N90-26664
Closed-loop autonomous docking system
[NASA-CASE-MFS-28421-1] 21 p2966 N90-26861
The real-time learning mechanism of the Scientific Research Associates Advanced Robotic System (SRAARS) 21 p3046 N90-27312
The sixth generation robot in space
21 p3049 N90-27332
SDI satellite autonomy using AI and Ada
21 p3050 N90-27336
Generation of animation sequences of three dimensional models
[NASA-CASE-MSC-21379-1-SB]
21 p3050 N90-27340
Development and testing of methodology for evaluating the performance of multi-input/multi-output digital control systems
[NASA-TM-102704] 22 p3115 N90-27699
Fiber-optic projected-fringe digital interferometry
[NASA-TM-103252] 22 p3178 N90-28033
Robust adaptive control: Handling the excitation problem 22 p3241 N90-28382
Real time guidance and propulsion control for single-stage-to-orbit airbreathing vehicles
23 p3285 N90-28587
Using embedded microcontrollers in radar test equipment
[DE90-014997] 23 p3319 N90-28763
Dynamic modeling and payload-adaptation control of a flexible one-link manipulator 23 p3333 N90-28843
Experiments in the dynamic and strategic control of cooperating manipulators 23 p3333 N90-28845
Cartesian control of redundant robots
23 p3363 N90-29004
Teleoperator comfort and psychometric stability: Criteria for limiting master-controller forces of operation and feedback during telemanipulation
23 p3364 N90-29009
A neural network for controlling the configuration of frame structure with elastic members
23 p3368 N90-29034
Multiple cooperating manipulators: The case of kinematically redundant arms 23 p3371 N90-29046
The JPL telerobot operator control station. Part 2: Software 23 p3371 N90-29050
Design of a monitor and simulation terminal (master) for space station telerobotics and telescience
23 p3372 N90-29051
Performance evaluation of a 6 axis high fidelity generalized force reflecting teleoperator
23 p3372 N90-29052
Implementation and design of a teleoperation system based on a VMEBUS/68020 pipelined architecture
23 p3372 N90-29053
Human machine interaction via the transfer of power and information signals 23 p3372 N90-29054
Trajectory generation of space telerobots
23 p3372 N90-29055
On the simulation of space based manipulators with contact 23 p3373 N90-29056
Planning robot actions under position and shape uncertainty 23 p3376 N90-29073
Robust controller design by contraction of a pole region
[ESA-TT-1042] 23 p3384 N90-29118
Sample rate effects on disturbance rejection for digital control systems 24 p3435 N90-29400
A digital controller for active aeroelastic controls
[NAL-TR-1014] 24 p3435 N90-29402
A new momentum management controller for the space station
[NASA-CR-187265] 24 p3440 N90-29425
Concept for a reference model Architecture for Real-Time Intelligent Control Systems (ARTICS)
[PB90-220286] 24 p3475 N90-29638
Robust design of LQG controllers
24 p3475 N90-29639
Adaptive control of an arc welding process
[AD-A223626] 24 p3476 N90-29645
Experiments in identification and control of flexible-link manipulators 24 p3501 N90-29787
Autonomous dexterous end-effectors for space robotics 24 p3501 N90-29788
Design and control of a multi-fingered robot hand provided with tactile feedback 24 p3501 N90-29789
Impedance hand controllers for increasing efficiency in teleoperations 24 p3502 N90-29793
Control strategies for a telerobot
24 p3504 N90-29808
Experiments in cooperative manipulation: A system perspective 24 p3505 N90-29812
Direct adaptive control of a PUMA 560 industrial robot
24 p3508 N90-29832
Discrete-time adaptive control of robot manipulators
24 p3509 N90-29834
A discrete decentralized variable structure robotic controller 24 p3509 N90-29835
Construction and demonstration of a 9-string 6 DOF force reflecting joystick for telerobotics
24 p3509 N90-29836
The JAU-JPL anthropomorphic telerobot
24 p3509 N90-29838
A procedure concept for local reflex control of grasping 24 p3509 N90-29839
Force-reflective teleoperated system with shared and compliant control capabilities 24 p3510 N90-29845
Real-time cartesian force feedback control of a teleoperated robot 24 p3513 N90-29857
An alternative control structure for telerobotics
24 p3518 N90-29889
Flight experiments in telerobotics-Orbiter middeck concept 24 p3519 N90-29895
Coordination in a hierarchical multi-actuator controller
24 p3520 N90-29900
An efficient temporal logic for robotic task planning
24 p3521 N90-29906
Approach to telerobot computing architecture
[NASA-CR-186993] 24 p3534 N90-29984

CONVAIR MILITARY AIRCRAFT
U MILITARY AIRCRAFT

CONVECTION
NT FORCED CONVECTION
NT FREE CONVECTION
NT MARANGONI CONVECTION
NT RAYLEIGH-BENARD CONVECTION
Forecasting convection with the AFOS (Automation of Field Operations and Services) data analysis programs. (ADAP-version 2.0) (AFOS data analysis programs-version 2.0)
[PB89-145940] 01 p0086 N90-10492
Simulation of the polar cap F region ionization using an experimental convection electric field
02 p0241 N90-11370
Viscous split algorithms for the time dependent incompressible Navier-Stokes equations
[AD-A211592] 03 p0348 N90-11985
Heat transfer in convective boundary layer and channel flows 06 p0774 N90-14505
Multigrid solutions of elliptic fluid flow problems
06 p0775 N90-14507
Convective boundary layer and modeling of dispersion
06 p0813 N90-14731
The dynamics of simulated convective storms in hurricane environments 06 p0816 N90-14747
Semi-empirical theory of heat-transfer when boiling
[DE89-635418] 06 p0857 N90-14984
Observational study of the macroscopic behavior of moist-convective processes 07 p0959 N90-15547
The response of the atmospheric convective boundary layer to surface inhomogeneities
08 p1100 N90-16369

An improvement of convection fidelity in Euler calculations 09 p1159 N90-16709
A numerical study of the formation of mesoscale convective complexes 09 p1245 N90-17225
Modelling directional solidification
[NASA-CR-186181] 09 p1292 N90-17487
Variational problems in astrophysics 09 p1298 N90-17524
Time development of convection flow patterns in aircraft cabins under post-crash fire exposure 10 p1314 N90-17598
Non-contact temperature measurements in support of microgravity combustion experiments 10 p1363 N90-17900
Development of an infrared imaging system for the surface tension driven convection experiment 10 p1367 N90-17922
NCTM workshop splinter session, IR thermal measurement instruments 10 p1367 N90-17923
Colliding natural convection boundary layer flow in a rectangular enclosure
[DE90-005397] 10 p1384 N90-18009
Nuclear driving of stellar oscillations and their coupling to convection 10 p1446 N90-18345
Connections between the circulation in altitude and convection over South America
[INPE-4923-TDL/383] 11 p1534 N90-18828
A PBL-radiation model for application to regional numerical weather prediction 12 p1635 N90-19394
Analysis of unsteady heat transfer by natural convection in a two-dimensional square cavity using a high order finite-volume method 12 p1657 N90-19521
Application of a Reynolds stress turbulence model to the compressible shear layer
[NASA-CR-182002] 12 p1660 N90-19537
An observational study of squall lines in the Amazon
[INPE-4865-TDL/376] 12 p1693 N90-19723
Spacelab qualified infrared imager for microgravity science experiments
[NASA-TM-102503] 13 p1804 N90-20352
An aircraft investigation of a convective boundary layer over Lake Michigan
[AD-A218175] 13 p1846 N90-20598
A case study of a quasi-stationary tropical convective line
[AD-A218325] 13 p1847 N90-20604
A cost-effective strategy for nonoscillatory convection without clipping
[NASA-TM-102538] 14 p1971 N90-21291
Finite element algorithms for hyperbolic conservation laws with forcing terms
[INPE-5024-RPE/617] 14 p2022 N90-21595
Thermal decay of an initially hot isothermal water body with application to thermal energy storage
[DE90-614742] 14 p2035 N90-21675
Analytical study of the origin and behavior of asymmetric vortices
[NASA-TM-102796] 15 p2049 N90-21746
Thermomechanically-induced convective motion and natural convection in confined gaseous helium subjected to boundary heating 15 p2089 N90-21960
The relationship between the buoyancy of near-surface air and the potential temperature of the tropopause 15 p2128 N90-22165
Current drive in a supernova 15 p2187 N90-22491
A new stochastic model of turbulent dispersion in the convective planetary boundary layer and the results of the Atterbury-87 field study 16 p2254 N90-22853
Quantifying and reducing uncertainty in the assimilative mapping of ionospheric electrodynamics 16 p2254 N90-22854
An interactive method for estimating hailstone size and convectively-driven wind gusts from forecast soundings
[AD-A218499] 16 p2258 N90-22871
High temperature insulation barrier composite
[NASA-CASE-MFS-29241-1] 17 p2368 N90-23480
The dynamic instability of adiabatic blastwaves
[NASA-CR-182498] 17 p2401 N90-23679
Sea breeze: Induced mesoscale systems and severe weather
[NASA-CR-186367] 19 p2715 N90-25450
On the viscosity in accretion disks 19 p2774 N90-25775
Estimation of convective rain volumes utilizing the are-time-integral technique
[NASA-CR-186814] 20 p2890 N90-26449
A lattice gas model for thermohydrodynamics
[DE90-011964] 20 p2933 N90-26690
Case study on Pre-Typhoon Active Convective Clouds (PTACC) 21 p3029 N90-27220
Investigations on improved iterative methods for solving sparse systems of linear equations
[AD-A221980] 21 p3064 N90-27417
Fluctuation splitting for multidimensional convection problems: An alternative to finite volume and finite element methods 22 p3173 N90-28000
Structural analysis of stratocumulus convection 22 p3216 N90-28243
A unified view of convective transports by stratocumulus clouds, shallow cumulus clouds, and deep convection 22 p3219 N90-28254
Oscillatory convection
[ESA-TT-890] 23 p3325 N90-28801
Diffusion in the surface layer of the convective boundary layer
[AD-A224125] 23 p3349 N90-28924
Genesis of bow echoes: A rear-inflow induced meso-convective structure
[PB90-209776] 23 p3349 N90-28926
Influence of convection on microstructure
[NASA-CR-186506] 24 p3448 N90-29470
Numerical simulations of the structure of supersonic shear layers
[AD-A224164] 24 p3467 N90-29587
An investigation of the inviscid spatial instability of compressible mixing layers
[AD-A223776] 24 p3468 N90-29596
Investigation of structure and transport processes in the high latitude ionospheric plasma using ground based and airborne digisondes
[AD-A224397] 24 p3491 N90-29727
Three-dimensional numerical study of thunderstorm downdrafts and associated outflow boundaries 24 p3494 N90-29746
Effect of a crystal-melt interface on Taylor-Vortex flow with buoyancy
[PB90-244401] 24 p3551 N90-30089

CONVECTION CLOUDS
NT CUMULONIMBUS CLOUDS
NT CUMULUS CLOUDS
Mesoscale analysis by numerical modelling coupled with satellite-based sounding 08 p1100 N90-16370
A dynamic model for forecasting new cloud development
[AD-A213939] 08 p1102 N90-16383
Cloud parameterization in EURAD and its future development 12 p1687 N90-19692
Theoretical modeling studies of the marine planetary
[AD-A217200] 13 p1841 N90-20567
Precipitation mechanisms in tropical and midlatitude convective clouds 14 p2008 N90-21507
Second National Winter Weather Workshop Conducted by the National Weather Service
[PB90-147414] 15 p2131 N90-22183
Gravity wave initiated convection
[NASA-CR-186868] 23 p3350 N90-28933

CONVECTION CURRENTS
Vertical distribution of pollutants in the presence of convective storms
[DE90-002590] 07 p0960 N90-15549
Polymer solution phase separation: Microgravity simulation 09 p1224 N90-17101
An optical white light speckle process in forward dispersion for measurement of the velocity field in free convective currents
[ETN-90-95913] 12 p1661 N90-19546
Next generation weather radar (NEXRAD) initial operational test and evaluation. Phase 2: (IOT and E(2))
[AD-A218770] 16 p2258 N90-22873

CONVECTIVE FLOW
NT RAYLEIGH-BENARD CONVECTION
Symmetry breaking bifurcations and the growth of chaos in a rotating fluid
[AD-A210969] 01 p0072 N90-10411
Convection of a pattern c' vorticity through a reacting shock wave
[NASA-CR-181921] 01 p0102 N90-10576
Studies of time-dependent polar cap convection patterns 02 p0251 N90-11421
A nonoscillatory, characteristically convected, finite volume scheme for multidimensional convection problems
[NASA-TM-102354] 02 p0263 N90-11497
Large eddy simulation of homogeneous turbulence undergoing shear and thermal gradients. Application to one point closing models
[ECL-88-23] 05 p0643 N90-13754
Feed back Petrov-Galerkin methods for convection dominated problems
[DE89-636436] 08 p1063 N90-16148
Simultaneous determination of temperature and velocity fields in a thermal convection flow with non-enclosed liquid crystal tracers 08 p1078 N90-16239
Electric field-induced flame convection in the absence of gravity 09 p1202 N90-16962
Multicellular natural convection in a narrow vertical slot
[AD-A216411] 11 p1505 N90-18668
Modeling convective Marangoni flows with void movement in the presence of solid-liquid phase change
[DE90-006474] 11 p1509 N90-18690
Summer Study Program in Geophysical Fluid Dynamics: The Influence of Convection on Large-Scale Circulations, 1988
[AD-A216024] 11 p1535 N90-18840
Acoustic convective system
[NASA-CASE-NPO-17278-1-CU] 14 p1959 N90-21215
A cost-effective strategy for nonoscillatory convection without clipping
[NASA-TM-102538] 14 p1971 N90-21291
High order P-G finite elements for convection-dominated problems
[DE90-614743] 15 p2097 N90-21998
A linear analysis of monsoon base states associated with banded convection 15 p2130 N90-22179
Three-dimensional convection in cylindrical geometry 17 p2399 N90-23668
Low Prandtl number convection in a rectangular cavity with longitudinal thermal gradient and transverse g-jitters
[REPT-892-430-109] 17 p2404 N90-23695
Influence of non-stationary field of magnetospheric convection on the D-region 22 p3210 N90-28209
Geophysical turbulence research at NCAR
[AD-A223361] 24 p3492 N90-29732

CONVECTIVE HEAT TRANSFER
Numerical solutions of turbulent flow with heat transfer over rough surfaces 02 p0218 N90-11246
Convective heat transfer in hypobaric environments
[AD-A212060] 03 p0347 N90-11979
Human body regional convective heat transfer determination using sublimating naphthalene disks
[AD-A212170] 03 p0380 N90-12165
Phase change material for spacecraft thermal management
[AD-A211404] 04 p0462 N90-12648
FLIC (FLame with Implicit Convection): A detailed, two-dimensional flame model
[AD-A212953] 04 p0473 N90-12710
Prediction of thermal stress casualties
[AD-A212356] 04 p0523 N90-13022
Convective heat transfer measurements from a NACA 0012 airfoil in flight and in the NASA Lewis Icing Research Tunnel
[NASA-TM-102448] 05 p0642 N90-13750
Automated convection soldering
[KCP-613-4005] 07 p0916 N90-15300
Multi-dimensional modeling of convective heat transfer with application to I.C. engines
[DE90-003245] 07 p0941 N90-15451
Analysis of catalytically enhanced solar absorption chemical reactors. 2: Predicted characteristics of a 100 kW chemical reactor
[DE89-014743] 07 p0954 N90-15521
A review of high-speed, convective, heat-transfer computation methods 10 p1305 N90-17548
Flammability testing of aircraft cabin materials 10 p1316 N90-17611
A model for evaporation of freely falling droplets
[PUBL-AIR-QUALITY-6] 10 p1384 N90-18007
A parametric heat transfer study for cryogenic ball bearings in SSME HPOTP 12 p1635 N90-19397
A method of estimating temperature profiles and chemical differentiation in the near surface layers of porous comet nuclei: First results for comet P/Churyumov-Gerasimenko 12 p1742 N90-20013
Heat transfer near the entrance to a film cooling hole in a gas turbine blade
[AD-A217396] 13 p1757 N90-20089
Acoustic convective system
[NASA-CASE-NPO-17278-1-CU] 14 p1959 N90-21215
ULTRA-SHARP nonoscillatory convection schemes for high-speed steady multidimensional flow
[NASA-TM-102568] 14 p2019 N90-21570
Experimental and analytical investigations of granular materials: Shear flow and convective heat transfer 15 p2091 N90-21968
Frontal structure in a mesoscale model 15 p2132 N90-22187
Effect of a crystal-melt interface on Taylor-vortex flow
[NASA-CR-186512] 15 p2171 N90-22408
Sulphur silicate interactions on the Jovian satellite Io 15 p2192 N90-22515
Natural convection liquid immersion cooling of high density columns of discrete heat sources in a vertical channel
[AD-A218388] 17 p2402 N90-23681
Modeling turbulent flow with mixed thermal convection transfer
[ECL-89-19] 17 p2405 N90-23704

Experiments on liquid immersion natural convection cooling of leadless chip carriers mounted on ceramic substrate
[AD-A219893] 17 p2478 N90-24167
Natural convection form an array of rectangular protrusions in an enclosure filled with dielectric fluid: Effects of boundary conditions, fluid Prandtl number, and selective powering
[AD-A219819] 18 p2552 N90-24563
A numerical investigation of thermal convection in highly viscous spherical shells with applications to mantle dynamics in the Earth and other terrestrial planets
18 p2579 N90-24691
Transients in turbulent convective heat transfer to a flow of supercritical helium
[ETN-90-97217] 20 p2863 N90-26286
A study of mixed convection in large baffled rectangular chambers with and without internal heat sources
[AD-A223158] 22 p3169 N90-27977
Turbulent thermal convection in rotating cavities, volume 1
[ETN-90-97433] 22 p3174 N90-28011
Turbulent thermal convection in rotating cavities, volume 2
[ETN-90-97434] 22 p3174 N90-28012
Calculation of temperature distribution in various turbine blades using a boundary-fitted coordinate transformation method 23 p3278 N90-28550
Free shear layer and swirl flow heat transfer enhancement
[PB90-228123] 23 p3325 N90-28798
Thermographic phosphor technique
24 p3421 N90-29324

CONVENTIONS
Polar prospects: A minerals treaty for Antarctica
[OTA-O-428] 17 p2480 N90-24185

CONVERGENCE
Primal barrier methods for linear programming
[AD-A210501] 01 p0105 N90-10600
Numerical methods for differential-algebraic equations: Current status and future directions
[DE89-015116] 01 p0111 N90-10632
Estimation on nonlinear damping in second order distributed parameter systems
[NASA-CR-181890] 02 p0263 N90-11494
Generalized BDF (Backward Differentiation Formula) methods applied to Hessenberg form DAEs
[DE89-017328] 02 p0267 N90-11522
Global atmospheric moisture variability
03 p0361 N90-12062
Dynamics and energetics of the South Pacific Convergence Zone during FGGE SOP-1 and South Pacific Convergence Zone and global-scale
03 p0361 N90-12065
Convergence results for pseudospectral approximations of hyperbolic systems by a penalty type boundary treatment
[NASA-CR-181929] 03 p0391 N90-12230
Some observations on the convergence behavior of GMRES
[REPT-89-09] 03 p0395 N90-12252
The convergence behavior of some iterative solution methods
[REPT-89-19] 03 p0396 N90-12260
A multigrid method combined with defect correction for free convection problems at high Rayleigh numbers
[REPT-89-27] 03 p0396 N90-12264
An algebraic characterization of B-convergent Runge-Kutta methods
[CWI-NM-R8901] 04 p0541 N90-13133
Tail triviality for sums of stationary random variables
[CWI-MS-R8810] 04 p0542 N90-13143
On a rate of convergence of the multiknapsack value function
[CWI-MS-R8812] 04 p0542 N90-13144
On the Hellinger type distances for filtered experiments
[CWI-MS-R8818] 04 p0542 N90-13146
Note on the convergence of simulated annealing algorithms
[MEMO-774] 04 p0544 N90-13162
Berry-Esseen rates and bootstrap results for generalized L-statistics
[CWI-MS-R8808] 04 p0546 N90-13179
Extended Kalman filter for attitude estimation of the earth radiation budget satellite 05 p0590 N90-13433
On the asymptotic convergence of the simulated annealing algorithm in the presence of a parameter dependent penalization
[MEMO-COSOR-89-16] 05 p0684 N90-13984
Convergence properties of indefinite linear quadratic problems with receding horizon
[MEMO-COSOR-88-25] 05 p0690 N90-14026
Parallel projected variable metric algorithms for unconstrained optimization
[NASA-CR-181930] 06 p0833 N90-14842
Effect of modal truncation on derivatives of closed-loop damping ratios in structural control
07 p0882 N90-15109
Sequential quadratic programming algorithms for optimization
[DE90-000022] 07 p0973 N90-15617
Mixed singular linear elliptic equations
[DE90-600722] 07 p0982 N90-15674
Convergence speeding up in the calculation of the viscous flow about an airfoil 08 p1070 N90-16194
On the superconvergence of the SBB method
[DE89-635709] 09 p1272 N90-17375
On the exponential convergence of the h-p version for boundary element Galerkin methods on polygons
[AD-A215814] 10 p1423 N90-18210
The h-p version of the boundary element method with geometric mesh on polygonal domains
[AD-A215815] 10 p1423 N90-18211
Intertropical Convergence Zone (ITCZ) and its relationship with the precipitation of the north-northeast Brazilian region
[INPE-4887-TDL/378] 11 p1535 N90-18839
Techniques for studying the effects of microgravity on model particle/cell systems 12 p1640 N90-19424
Banach C*-algebras not containing a subspace isomorphic to C(sub 0)
[DE90-610428] 12 p1706 N90-19798
Convergence properties of iterative algorithms for solving the nodal diffusion equations
[DE89-016859] 12 p1707 N90-19804
Dual cathode system for electron beam instruments
[NASA-CASE-NPO-16878-1-CU]
13 p1803 N90-20351
Techniques for accelerating iterative methods for the solution of mathematical problems
[AD-A218272] 13 p1878 N90-20775
Convergence acceleration of hypersonic flow calculations: A nonlinear relaxation factor
14 p1911 N90-20957
A modification of a low-order Reissner-Mindlin plate bending element
[PB90-165630] 14 p1994 N90-21428
Differential-algebraic equations as stiff ordinary differential equations
[DE90-007922] 14 p2021 N90-21585
Convergence acceleration of upwind relaxation methods for the Navier-Stokes equations
15 p2092 N90-21973
High order P-G finite elements for convection-dominated problems
[DE90-614743] 15 p2097 N90-21998
Multilevel decomposition approach to the preliminary sizing of a transport aircraft wing
[NASA-CR-4296] 16 p2200 N90-22557
Convergence of hyperspherical adiabatic expansion for helium-like systems
[DE90-620526] 16 p2214 N90-22631
Estimation of Hilbert space valued parameters by the method of sieves
[AD-A218565] 16 p2306 N90-23143
Computation of low Mach number compressible flow
17 p2344 N90-23346
Convergent strand array liquid pumping system
[NASA-CASE-NPO-17301-1-CU]
17 p2385 N90-23587
Convergence properties of the Runge-Kutta-Chebyshev method
[CWI-NM-R8907] 17 p2459 N90-24038
Convergence of one-leg multistep methods for stiff nonlinear initial value problems
[CWI-NM-R8911] 17 p2459 N90-24040
Local and global order reduction of some LOD schemes
[CWI-NM-R8914] 17 p2459 N90-24041
On rates of convergence and asymptotic normality in the multiknapsack problem
[CWI-BS-R8912] 17 p2460 N90-24045
Low-density flow effects for hypervelocity vehicles, phase 2
[AD-A221034] 18 p2493 N90-24249
Uniform limit theorems for synchronous processes with applications to queues
[AD-A220224] 18 p2599 N90-24788
Some convergence results for probabilistic Tabu search
[MEMO-822] 18 p2605 N90-24840
Efficient generalized conjugate gradient algorithms. Part 2: Implementation
[MATHS-REPT-A-118-PT-2] 20 p2908 N90-26543
A numerical study of the role of meso beta and meso gamma scale vertical exchange processes in the evolution of upper tropospheric frontal systems
[AD-A222057] 21 p3031 N90-27230
The Second Asilomar Workshop on Progress in Mathematical Programming
[AD-A221986] 21 p3053 N90-27358
A build-up interior method for linear programming: Affine scaling form
[AD-A221802] 21 p3056 N90-27375
Proceedings of Workshop on Reliability in Computational Mechanics
[AD-A221694] 21 p3065 N90-27426
Newton methods for large-scale linear equality-constrained minimization
[AD-A222310] 21 p3070 N90-27457
Tailoring explicit time-marching schemes to improve convergence characteristics 22 p3172 N90-27997
An asymptotically induced domain decomposition method for parabolic boundary layer problems
[DE90-014620] 23 p3326 N90-28804
An investigation of forcing mechanisms during a surprise tornadic thunderstorm
[PB90-216805] 23 p3352 N90-28940
Consistency and convergence for numerical radiation conditions
[NASA-TM-103262] 23 p3387 N90-29124
Numerical methods for systems of conservation laws of mixed type using flux splitting
[NASA-CR-182084] 23 p3387 N90-29129
An algebraic hierarchical basis preconditioner
[DE90-015875] 24 p3538 N90-30008

CONVERGENT-DIVERGENT NOZZLES
An experimental investigation of thrust vectoring two-dimensional convergent-divergent nozzles installed in a twin-engine fighter model at high angles of attack
[NASA-TM-4155] 08 p1017 N90-15884
Static investigation of a two-dimensional convergent-divergent exhaust nozzle with multiaxis thrust-vectoring capability
[NASA-TP-2973] 12 p1597 N90-19193
Computation of hypersonic unsteady viscous flow over a cylinder 12 p1597 N90-19194
Internal performance of two nozzles utilizing gimbal concepts for thrust vectoring
[NASA-TP-2991] 12 p1599 N90-19200
An optical study of the flow start-up process in four convergent-divergent nozzles
[AD-A222918] 21 p2963 N90-26846

CONVERSATION
A study of mental models through communication between users and advisors solving software manipulation problems 15 p2176 N90-22434

CONVERTAPLANES
U V/STOL AIRCRAFT

CONVEXITY
On the areas of various bodies in the Euclidean space: The case of irregular convex polygons
[DE89-618377] 02 p0264 N90-11500
Optimal matching of 3-D convex polyhedra
[TELECOM-PARIS-89C003] 03 p0395 N90-12258
Description and manipulation of convex polygons using polarity
[IMAG-RR-771-M] 05 p0692 N90-14041
A monotone complementarity problem in Hilbert space
[DE90-009755] 14 p2022 N90-21590
Design of cryogenic tanks for launch vehicles
16 p2220 N90-22662
Computational geometry and its application to computer graphics
[RUU-CS-89-8] 17 p2449 N90-23968
A study of non-uniqueness and instability for convex materials
[DE90-012060] 19 p2689 N90-25294

CONVOLUTION INTEGRALS
Inf-convolution splines
[IMAG-RR-749-M] 03 p0395 N90-12256
Estimation of convolution tail behavior
[MEMO-COSOR-89-04] 05 p0693 N90-14051
Utilizations of an acoustic surface wave-convolver for signal processing in the measurement and information techniques
[ETN-90-97319] 22 p3165 N90-27947
SAR processing methods
[FEL-1989-131] 22 p3165 N90-27948
Novel numerical analysis method for the study of convolution equations in appearance potential spectroscopy
[ETN-90-97288] 23 p3400 N90-29210

CONVOLUTIONS (MATHEMATICS)
U CONVOLUTION INTEGRALS

CONVULSIONS
Metabolism, seizures, and blood flow in brain following organophosphate exposure: Mechanisms of action and possible therapeutic agents
[AD-A217098] 12 p1696 N90-19740

COOL STARS
NT CARBON STARS
NT FLARE STARS
NT K STARS
NT M STARS
NT MIRA VARIABLES

Carbon chemistry of circumstellar envelopes
21 p3090 N90-27570
The formation and structure of circumstellar and interstellar dust
21 p3091 N90-27576
Investigation of x ray variability in highly active cool stars
[NASA-CR-183853] 24 p3560 N90-30143

COOLANT LOSS
U LOSS OF COOLANT

COOLANTS
NT ENGINE COOLANTS
A new inexpensive electrochemical meter for oxygen in sodium coolant
[DE89-630802] 02 p0194 N90-11104
Fluid flow analysis of the SSME high pressure fuel and oxidizer turbine coolant systems
[NASA-CR-183736] 06 p0734 N90-14277
The onset of boiling of the liquid alkali metals
[DE90-002276] 08 p1044 N90-16036
An experimental evaluation of two nonazeotropic refrigerant mixtures in a water-to-water breadboard heat pump
[DE90-009016] 14 p1973 N90-21305
Gas production and behavior in the coolant of the SP-100 space nuclear power system
[DE90-010674] 18 p2614 N90-24890

COOLERS
Feasibility of cool storage systems in refrigeration
[DE90-728179] 08 p1054 N90-16093

COOLING
NT ABSORPTION COOLING
NT AIR COOLING
NT CRYOGENIC COOLING
NT EVAPORATIVE COOLING
NT FILM COOLING
NT GAS COOLING
NT LIQUID COOLING
NT MAGNETIC COOLING
NT PLASMA COOLING
NT QUENCHING (COOLING)
NT RADIANT COOLING
NT REGENERATIVE COOLING
NT SOLAR COOLING
NT SPACE COOLING (BUILDINGS)
NT SUPERCOOLING
NT SURFACE COOLING
NT SWEAT COOLING
NT THERMOELECTRIC COOLING
Application of formal optimization techniques in thermal/structural design of a heat-pipe-cooled panel for a hypersonic vehicle
[NASA-TM-89131] 01 p0071 N90-10409
Steam cooled rich-burn combustor liner
[NASA-CASE-LEW-13609-1] 03 p0321 N90-11824
Estimation of time to maximum supercooling during dynamic frazil ice formation
[AD-A212204] 04 p0471 N90-12699
A closed-cycle refrigerator for cooling maser amplifiers below 4 Kelvin
04 p0487 N90-12797
Cryogenics for LDR
05 p0598 N90-13471
Effect of suction and cooling on the stability of subsonic and supersonic boundary layers
05 p0642 N90-13745
Generation of free radicals during cold injury and rewarming
[AD-A213088] 05 p0672 N90-13915
Design and demonstration of heat pipe cooling for NASP and evaluation of heating methods at high heating rates
[DE89-016995] 06 p0724 N90-14227
Thermal/structural analyses of several hydrogen-cooled leading-edge concepts for hypersonic flight vehicles
[NASA-TM-102391] 06 p0775 N90-14511
New heating and cooling technology: Regenerative heat pump according to the Vuilleumier principle
[DE90-002701] 06 p0807 N90-14699
Retractable gas cooled leads for ASTROMAG
[DE90-002679] 07 p0921 N90-15331
High power density spray cooling
[AD-A213575] 07 p0930 N90-15386
Design and fabricate a metallic hydride heat pump with a cooling capacity of 9000 BTU/H
[AD-A213756] 07 p0931 N90-15388
A renormalization group approach to image processing: A new computational method for three-dimensional shapes in robot vision, and the computation complexity of the cooling algorithms
[AD-A214247] 07 p0977 N90-15643
Productivity and cryogenic wind tunnels
08 p1032 N90-15961
Synthesis of tetrafluorohydrazine
[AD-D014281] 08 p1052 N90-16083
Design and testing of a superfluid liquid helium cooling loop
[NASA-CR-182776] 09 p1216 N90-17050
Pre-treatment with tyrosine reverses hypothermia induced behavioral depression
[AD-A215211] 09 p1252 N90-17265
Phase properties of the rapid cooled palladium-silicon alloy in the concentration range 40 to 58 at. percent Si
[DE90-719525] 09 p1284 N90-17444
Effects of heating/cooling on changes in sea surface temperature: Consequences for computation of surface advection from satellite images
[AD-A214125] 10 p1409 N90-18129
Flexible heat pipe cold plate
[AD-A216053] 11 p1464 N90-18433
Dryout stability and inception at low flowrates
[DE90-006955] 11 p1509 N90-18692
Spallation of oxide scales from 20 percent Cr/25 percent Ni/Nb stainless steel
[AERE-R-13464] 13 p1775 N90-20189
Core cooling studies at LLNL (Lawrence Livermore National Laboratory) and Sandia
[DE90-008303] 13 p1795 N90-20300
Phase 1 supplemental development of a kinematic Stirling/Rankine commercial gas-fired heat pump system
[PB90-129974] 13 p1825 N90-20483
Analysis of the rotor tip leakage flow with tip cooling air ejection
14 p1926 N90-21029
Detailed heat transfer measurements in nozzle guide vane passages in linear and annular cascades in the presence of secondary flows
14 p1926 N90-21030
Thermal decay of an initially hot isothermal water body with application to thermal energy storage
[DE90-614742] 14 p2035 N90-21675
Cooling of rocket thrust chambers with liquid oxygen
[NASA-TM-103146] 16 p2210 N90-22605
High temperature electric arc furnace and method
[NASA-CASE-MFS-28281-1] 17 p2357 N90-23415
Solidification of highly undercooled liquid droplets
[AD-A218776] 17 p2376 N90-23529
The effects of cooling rate XD (trademark) TiAl weld microstructure
[DE90-011975] 18 p2528 N90-24427
Axions and SN 1987A: Axion trapping
[NASA-CR-186604] 18 p2612 N90-24881
Nucleation kinetics in undercooled, class-forming metallic melts
[ESA-TT-1186] 19 p2676 N90-25218
The accelerated cooling in GTS plate mill
[ETN-90-97019] 19 p2682 N90-25256
The application of engineering ceramics in gas turbines
[PNR90676] 20 p2812 N90-26005
Time temperature relations during rubber forming continuous fiber reinforced thermoplastics
[LR-620] 20 p2840 N90-26151
Advanced heat pump
[AD-D014560] 22 p3170 N90-27979
A new calculation of the radiative cooling by carbon dioxide in the middle atmosphere and the lower thermosphere
22 p3210 N90-28211
Cryogenic, high speed, turbopump bearing cooling requirements
23 p3291 N90-28620
Transient cooling of a hot surface by droplets evaporation
[PB90-227968] 23 p3325 N90-28799
Prediction and control of processing-induced residual stresses in composites. Part 2: AS4/PEEK composite
[AD-A223696] 24 p3443 N90-29445
Investigation of weld bead cooling rate during startup of gas metal arc welding
[AD-A223567] 24 p3449 N90-29478
The influence of solidification rate on solute redistribution and second-phase formation in stainless steel alloys
[DE90-015189] 24 p3450 N90-29482

COOLING FLOWS (ASTROPHYSICS)
Cooling flows in clusters of galaxies
06 p0862 N90-15009

COOLING SYSTEMS
LDR cryogenics
05 p0598 N90-13472
Fluid flow analysis of the SSME high pressure fuel and oxidizer turbine coolant systems
[NASA-CR-183736] 06 p0734 N90-14277
Beam collector and output window for a 35 GHz 100 kW gyrotron
[INPE-4958-RPE/603] 11 p1511 N90-18699
An advanced cooled grating spectrometer for UKIRT-CGS4
11 p1589 N90-19165
Flow boiling with enhancement devices for cold plate coolant channel design
[NASA-CR-186358] 15 p2089 N90-21961
Gas production and behavior in the coolant of the SP-100 space nuclear power system
[DE90-010674] 18 p2614 N90-24890
A direct-interface, fusible heat sink for astronaut cooling
[NASA-TM-102835] 19 p2689 N90-25292
Combustor cooling aspects
[CIT/SME/VKI/RS/5] 20 p2810 N90-25989
High/variable mixture ratio oxygen/hydrogen engines
23 p3295 N90-28637
Analysis of scramjet engine characteristics
[NAL-TR-1041] 24 p3434 N90-29398
Thermal analyses of power subsystem components
[NASA-CR-186314] 24 p3474 N90-29637

COOPERATION
A comparison of software for the modeling and control of flexible systems
01 p0019 N90-10092
Interdisciplinary research: Promoting collaboration between the life sciences and medicine and the physical sciences and engineering
17 p2478 N90-24171

COORDINATE SYSTEMS
U COORDINATES

COORDINATE TRANSFORMATIONS
Self-calibration of robot-sensor system
15 p2144 N90-22246
Generalized killing equations and symmetries of spinning space
[NIKHEF-H/89-8] 15 p2165 N90-22375
Coordinate transformation for an asynchronous, machine, and time discretization of a state observer
[EMV-88-30] 17 p2397 N90-23657
Calculation of temperature distribution in various turbine blades using a boundary-fitted coordinate transformation method
23 p3278 N90-28550
Local interpolation functions for curve generation with the multi-surface transformation
24 p3470 N90-29608
The control point form of algebraic grid generation
24 p3470 N90-29609

COORDINATES
NT ASTRONOMICAL COORDINATES
NT CARTESIAN COORDINATES
NT COMPUTATIONAL GRIDS
NT GEODETIC COORDINATES
NT HYPERBOLIC COORDINATES
NT LAGRANGE COORDINATES
NT POLAR COORDINATES
NT SPHERICAL COORDINATES
Wave-mode coordinate analysis of L junction in LSS
[AD-A211116] 02 p0176 N90-10984
Conjugate profiles on mating gear teeth
[MEMO-COSOR-89-01] 05 p0651 N90-13795
A 3-D measurement system using object-oriented FORTH
[DE90-003393] 08 p1109 N90-16420
Results of error correction techniques applied on two high accuracy coordinate measuring machines
[DE90-003341] 08 p1112 N90-16439
Numerical modeling of the atmosphere with an isentropic vertical coordinate
09 p1246 N90-17226
Symbol manipulation and applied mathematics
[AD-A214702] 09 p1273 N90-17378
Control and stability of a spinning symmetric satellite in an elliptical orbit
[AD-A216284] 10 p1328 N90-17672
Spatial registration of TIROS-N weather satellite data
[AD-A216041] 11 p1536 N90-18841
Analysis and design of symmetrical airfoils
[PD-CF-8943] 12 p1601 N90-19213
Development of a standardized three axis sensor for inertial data achievement for future flight rule systems
[ETN-90-96075] 12 p1604 N90-19231
Estimation of modeled object pose from monocular images
[DE90-001678] 13 p1804 N90-20354
Error correction of the DEA (Digital Electronic Automation) coordinate measuring machines at LLNL
[DE90-008913] 14 p1983 N90-21365
Characterization and calibration of coordinate measuring machines
[DE90-009320] 16 p2242 N90-22791
Error cancellation in HPBL derivation of elastic hole-pressure error
[AD-A219854] 17 p2417 N90-23771
On a class of N-dimensional associated random walks and the hitting point identity
[CWI-BS-R8911] 17 p2466 N90-24090
G2-continuity in homogeneous co-ordinates
[MATHS-REPT-A-110] 20 p2917 N90-26599
Rational cubics with G2-continuity
[MATHS-REPT-A-113] 20 p2918 N90-26601
A nonhydrostatic numerical model in sigma-coordinates and simulations of mesoscale phenomena
23 p3350 N90-28932
Multiple cooperating manipulators: The case of kinematically redundant arms
23 p3371 N90-29048
The control point form of algebraic grid generation
24 p3470 N90-29609
Brorfelde Geomagnetic Observatory: Magnetic results, 1987
[ISBN-87-7478-297-5] 24 p3496 N90-29756

COORDINATION
The interface with the data reduction consortia
05 p0606 N90-13528

National airspace system monitoring operational concept
[NAS-SR-1330] 06 p0722 N90-14214
Motion coordination for mobile robots in unstructured environments
[PB90-199498] 23 p3332 N90-28837
Motion coordination for a mobile manipulator system
[PB90-203076] 23 p3332 N90-28839
Multiple cooperating manipulators: The case of kinematically redundant arms 23 p3371 N90-29046
Parallel algorithms for computation of the manipulator inertia matrix 23 p3376 N90-29072
Coordination in a hierarchical multi-actuator controller 24 p3520 N90-29900

COORDINATION POLYMERS
Transport studies of conducting polymers 02 p0200 N90-11140
Metal coordination polymers as potential high-energy lithographic resists
[AD-A216668] 11 p1490 N90-18574
The improved adhesion of organic polymers to silica and to aluminum metal with zirconium Schiff-base block copolymer coatings
[AD-A216669] 11 p1490 N90-18575

COPILOTS
U AIRCRAFT PILOTS

COPOLYMERIZATION
Suppression of side chain crystallization and transformation of monotropic mesophases into enantiotropic mesophases by copolymerization of the parent polymers' monomer pairs containing constitutional isomeric mesogenic side groups
[AD-A209066] 03 p0330 N90-11878
Curable polyether compositions
[AD-D014200] 04 p0468 N90-12679
Model filled polymers I. Synthesis of crosslinked monodisperse polystyrene beads
[AD-A213228] 05 p0627 N90-13660
The structure and properties of liquid crystal polymers 06 p0749 N90-14356
Initiation precursors and initiators in laser-induced copolymerization of styrene and maleic anhydride in acetone
[NASA-TM-4166] 10 p1346 N90-17810
Modified bismaleimides for carbon fibre composites 11 p1476 N90-18495
Control of phase structure in polymer blends
[AD-A217034] 11 p1491 N90-18580
Graft copolymers of rigid-rod poly(p-phenylenebenzobisimidazole)
[AD-A220369] 17 p2380 N90-23550
Composite materials with improved properties in compression: Copolymerization of 1,1-dimethyl-1-Silacyclopent-3-ene and 1,1-diphenyl-1-Silacyclopent-3-ene. Characterization of copolymer microstructures by H1, C13, and Si29 NMR spectroscopy
[AD-A221686] 21 p2972 N90-26892

COPOLYMERS
NT BLOCK COPOLYMERS
NT VINYL COPOLYMERS
NT VITON RUBBER (TRADEMARK)
Comparison of carboxylated and sulfonated model polyurethane ionomers
[AD-A210438] 01 p0050 N90-10284
Synthesis and physical properties of poly(perfluoroalkylether) urethanes
[AD-A210500] 01 p0050 N90-10287
Polyheterocycle Langmuir-Blodgett films
[AD-A210625] 01 p0051 N90-10292
Hierarchical structure in polymeric solids and its influence on properties
[AD-A210918] 01 p0052 N90-10297
Impedance analysis of ionic transport in polypyrrole-polyazulene copolymer and its charge-discharge characteristics
[AD-A210979] 01 p0052 N90-10299
Composites reinforced with thermotropic liquid crystal copolyester fibers
[AD-A211226] 02 p0191 N90-11089
Behaviour of VF(sub 2)/VF(sub 3) piezoelectric copolymers under shock loading
[DE89-016538] 02 p0201 N90-11145
Electronic and ionic transport in polymers
[AD-A210654] 02 p0201 N90-11148
Suppression of side chain crystallization and transformation of monotropic mesophases into enantiotropic mesophases by copolymerization of the parent polymers' monomer pairs containing constitutional isomeric mesogenic side groups
[AD-A209066] 03 p0330 N90-11878
Curable polyether compositions
[AD-D014200] 04 p0468 N90-12679
Ultrastructure processing and characterization of polymers
[AD-A211460] 04 p0478 N90-12743
A graph-theoretical approach to block-copolymer complexes. Part 3: Loops and cycles
[MEMO-778-PT-3] 04 p0479 N90-12750
Synthesis of energetic single phase and multi-phase polymers
[AD-A212539] 04 p0481 N90-12761
A center for advanced electrical and structural polymers
[AD-A212853] 04 p0482 N90-12764
Studies of Aflas fluoroelastomers
[AD-A213046] 05 p0621 N90-13622
Synthesis of inorganic polymers as glass precursors and for other uses. Preceramic block or graft copolymers as potential precursors to nanocomposite materials
[AD-A211978] 05 p0626 N90-13655
Process for producing a shaped, extruded product from a crosslinkable polymeric composition
[GB-PATENT-2-201-677-A] 05 p0627 N90-13662
Crosslinkable polymer
[GB-PATENT-2-205-846-A] 05 p0628 N90-13663
Electronic and ionic transport in polymers
[AD-A213410] 07 p0911 N90-15270
New polymers made with well-characterized organometallic catalysts
[AD-A213592] 07 p0912 N90-15272
Copolymers for drag reduction in marine propulsion: New molecular structures with enhanced effectiveness
[AD-A214444] 08 p1049 N90-16062
Diblock copolymers at surfaces
[DE90-005406] 08 p1051 N90-16079
Copolyimide with a combination of flexibilizing groups
[NASA-CASE-LAR-13821-1] 09 p1199 N90-16950
Composite for smoothing the surface of ceramic substrates
[DE90-004005] 11 p1488 N90-18565
Control of phase structure in polymer blends
[AD-A217034] 11 p1491 N90-18580
Synthesis of poly(dimethylsiloxane) - nylon 6 diblock copolymers
[AD-A216850] 12 p1630 N90-19367
An evaluation of ethylene-vinyl acetate copolymers as desensitizers for RDX in insensitive booster compositions prepared by slurry coating technology
[MRL-TR-89-33] 12 p1633 N90-19385
CO2 diffusion and solubility in a Polystyrene/Polybutadiene block copolymer with highly oriented lamellar morphology
[AD-A217165] 13 p1779 N90-20211
Copolymer-like structures of nematic nitroimine dimers
[AD-A217574] 13 p1780 N90-20215
Synthesis of new polyphosphazene elastomers
[AD-A217585] 13 p1780 N90-20216
Assessment of biobased materials
[DE90-000300] 13 p1780 N90-20220
Electronic and ionic transport in processable conducting polymers
[AD-A218093] 13 p1782 N90-20229
Nicalon/siliconoxycarbide ceramic composites
[NASA-TM-102563] 14 p1945 N90-21133
On the dynamics of polymer mixtures in solution using the RPA
[DE90-613689] 14 p1948 N90-21149
Generalized random phase approximation for multicomponent polymer systems
[DE90-613691] 14 p1955 N90-21194
Stability studies of a pH-sensitive polymer matrix: Applications to fiber optic pH sensors
[DE90-009579] 15 p2072 N90-21867
Modified maleic anhydride copolymers as e-beam resists
[AD-A218470] 16 p2223 N90-22679
Graft copolymers of rigid-rod poly(p-phenylenebenzobisimidazole)
[AD-A220369] 17 p2380 N90-23555
NMR studies of polymeric solid electrolytes
[AD-A219833] 17 p2381 N90-23562
Density profile of terminally adsorbed polymers
[AD-A220897] 18 p2529 N90-24433
NMR and optical studies of piezoelectric polymers
[DE90-012459] 20 p2837 N90-26137
The catalytic synthesis of inorganic polymers for high temperature applications and as ceramic precursors
[AD-A222620] 20 p2840 N90-26156
Composite materials with improved properties in compression: Copolymerization of 1,1-dimethyl-1-Silacyclopent-3-ene and 1,1-diphenyl-1-Silacyclopent-3-ene. Characterization of copolymer microstructures by H1, C13, and Si29 NMR spectroscopy
[AD-A221686] 21 p2972 N90-26892
Fluorescent probe investigation of a water-soluble polyphosphazene
[AD-A222317] 21 p2978 N90-26925
Silicon containing electroconductive polymers and structures made therefrom
[NASA-CASE-NPO-17826-1-CU] 21 p2983 N90-26952
Imide/arylene ether copolymers
[NASA-CASE-LAR-14159-1-CU] 21 p2983 N90-26953
Solubility characteristics of a methacrylate copolymer
[AD-A222938] 21 p2985 N90-26962
Synthesis of energetic single phase and multi-phase polymers
[AD-A222491] 21 p2988 N90-26981
Catalytic synthesis of polymethylsilsesquioxanes
[AD-A222643] 22 p3159 N90-27910
Novel side-chain liquid cyrstalline polymers
[AD-A221998] 22 p3159 N90-27911
Toughening of SAN copolymers by an SAN emulsion grafted rubber
[AD-A224213] 24 p3453 N90-29502

COPPER
NT COPPER ISOTOPES
Solvent effects on the kinetics of electroreduction of Cu(I) at mercury
[AD-A209423] 01 p0038 N90-10211
Shock-induced atomic-scale structure in metals
[DE89-016539] 02 p0197 N90-11124
Temperature dependent effects during Ag deposition on Cu(110)
[DE89-016987] 03 p0327 N90-11857
Investigations of spontaneous nuclear order in copper by neutron diffraction
[ETN-90-96060] 05 p0698 N90-14090
The biocorrosion of copper by biopolymers as examined in situ, in real time FT-IR/CIR/ATR in conjunction with pre and post XPS/AES
[DE90-002086] 06 p0747 N90-14348
Critical and subcritical crack-growth behavior along toughened ceramic/metal interfaces 07 p0889 N90-15140
Secondary electron emission characteristics of molybdenum-masked, ion-textured OFHC copper
[NASA-TP-2967] 07 p0902 N90-15211
Surface studies at the NSLS
[DE90-003173] 08 p1043 N90-16027
Elastic moduli of copper: Electronic structure contributions from pseudopotentials and full-potential linear muffin-tin orbital band structure calculations
[DE90-004423] 08 p1044 N90-16037
Long term creep strength of silver alloyed copper
[DE90-602367] 08 p1045 N90-16039
High-efficiency copper ternary thin film solar cells
[DE89-009470] 09 p1242 N90-17207
Plating nickel-63 on copper coupons
[DE90-005023] 10 p1356 N90-17862
The electronic structure of sigma 5 grain boundaries in Cu
[DE90-005999] 10 p1437 N90-18294
The mechanism, measurement, and influence of properties on the galling of metals
[DE90-006533] 11 p1487 N90-18558
Study of the dynamical behavior of copper in a shock wave
[ISL-R-123/88] 11 p1507 N90-18679
Nanolayer reactions in aluminum-metal interfaces
[DE90-004955] 12 p1626 N90-19342
Defect structures in copper and gold irradiated with fast neutrons, 14 MeV neutrons and 600 to 800 MeV protons
[DE90-007529] 12 p1629 N90-19359
Infrared and X ray photoelectron spectroscopy studies of the polyimide/metal interface
[AD-A218249] 13 p1773 N90-20179
CuInSe2 and CdTe: Scale-up for manufacturing
[DE89-009503] 13 p1827 N90-20489
A systematic study of the effects of metal substitutions for Cu in YBa(sub 2) (Cu(sub 1-x) M(sub x)3 O(sub 7-rho), M=Fe, Co, Al, Ga, Cr, Ni, and Zn
[DE90-003957] 13 p1892 N90-20857
Copper and oxygen NMR studies on the magnetic properties of YBa2Cu3O(7-y)
[DE90-007889] 13 p1893 N90-20863
L shell XANES (X ray Absorption Near Edge Structure) for solid metals: Ti, V, Cr, Fe, Ni, Cu
[DE90-008043] 13 p1895 N90-20880
Hydrocarbon-fuel/combustion-chamber-liner materials compatibility
[NASA-CR-185203] 14 p1950 N90-21165
Preparation and characterization of Cu2ZnGeS(4-y)Se(y)
[AD-A217469] 15 p2171 N90-22407
Trace metal sources for the atlantic inflow to the Mediterranean Sea
[AD-A218607] 17 p2429 N90-23842
Cascade collapse in copper and nickel
[DE90-011115] 18 p2527 N90-24423

The electrical characteristic and gain behavior as a function of the radial distance from the laser axis in a copper vapor laser
[DE90-615371] 18 p2564 N90-24630
Microstructure and stability of TiB2 and Cu multilayers
[DE90-011955] 18 p2627 N90-24968
Destruction of peroxy radical by Cu ion catalysed reactions on atmospheric particles
20 p2887 N90-26429
A study on carbon Fiber (long fiber) reinforced copper matrix composite
[AD-A221584] 21 p2972 N90-26891
The epitaxial growth of copper on the (111) surface of silicon
[DE90-013817] 21 p3082 N90-27523
Microstructures and properties of superconducting Y-Er-BaCu-O thin films obtained from disordered Y-Er-BaF2-Cu films 22 p3147 N90-27848
Superconductivity in the Sn-Ba-Sr-Y-Cu-O system
22 p3151 N90-27863
A YBCO RF-SQUID magnetometer and its applications 22 p3151 N90-27867
Structure of metal overlayers by low energy alkali ion scattering: Cu/Ru(0001) and Sn/Pt(111)
[DE90-014453] 23 p3310 N90-28718
The stability of the martensitic phases in Cu-Zn-Al at an electron concentration of 1.534
[DE90-628628] 23 p3311 N90-28727
Studies of central interactions of Si ions at 14.5 x A GeV/c in Au and Cu
[DE90-015095] 23 p3397 N90-29195
Reliability study of TWT output RF window
[AD-A223688] 24 p3465 N90-29574
The MTL Torsional Split-Hopkinson bar
[AD-A223278] 24 p3479 N90-29663

COPPER ALLOYS
NT BRASSES
NT MANGANIN (TRADEMARK)
Precipitation strengthened high strength, high conductivity Cu-Cr-Nb alloys produced by chill block melt spinning
[NASA-CR-185144] 03 p0326 N90-11853
Determination of the gaseous hydrogen ductile-brittle transition in copper-nickel alloys
[NASA-TM-86494] 04 p0474 N90-12715
Quench sensitivity in Al-Cu-Li alloys
[AD-A213055] 05 p0624 N90-13639
Magnetic viscosity in Ni/Cu compositionally-modulated alloys
[DE90-002303] 07 p0904 N90-15223
The effect of dissolved ozone on the corrosion behavior of Cu-30 Ni and 304L stainless steel in 0.5 N NaCl solutions
[AD-A213804] 07 p0906 N90-15235
Fusion reactor materials
[DE90-000976] 07 p0994 N90-15744
Production and processing of Cu-Cr-Nb alloys
[NASA-TM-102495] 08 p1047 N90-16053
Method of forming low cost, formable High T(subc) superconducting wire
[NASA-CASE-LEW-14676-2] 09 p1286 N90-17454
Phonon dispersion and Kohn anomalies in the alloy Cu(0.84)Al(0.16)
[DE90-005578] 10 p1428 N90-18239
Processing and elevated temperature ductility of aluminum alloy 7475
[AD-A216840] 11 p1486 N90-18554
High temperature fatigue behavior of tungsten copper composites
[NASA-TM-102404] 14 p1946 N90-21138
A comparison of CuAlNi and other high damping alloys for the purpose of naval ship silencing applications
[AD-A218801] 16 p2221 N90-22671
The mechanical properties of Cu/TiB2 multilayer structures
[DE90-010608] 18 p2517 N90-24378
Precipitation on dislocations in Al-Li-Cc-Mg-Zr
[AD-A221124] 18 p2526 N90-24415
Phase stability in the Al(6-x)Cu(x)Zr2 system for 0 less than x less than 1.0
[DE90-010620] 18 p2620 N90-24925
Weldment mechanical properties of aluminum-copper-lithium alloy, 2090, at ambient and cryogenic temperatures
[DE90-014178] 21 p2981 N90-26941
Advanced processing and properties of high performance alloys
[AD-A221776] 21 p2983 N90-26948
Strengthening in heavily cold worked Cu-20 vol. percent Fe in situ composites
[DE90-011741] 22 p3135 N90-27790
Density changes of generation 1.5 and 2.0 copper alloys irradiated at 411 to 414 C and 529 C in FFTF-MOTA
[DE90-015291] 23 p3311 N90-28724

COPPER CHLORIDES
Copper chloride cathode for a secondary battery
[NASA-CASE-NPO-17640-1-CU]
09 p1210 N90-17011
The interaction of polycrystalline copper films with dilute aqueous solutions of cupric chloride
[AD-A216465] 11 p1569 N90-19033

COPPER COMPOUNDS
NT COPPER CHLORIDES
NT COPPER OXIDES
NT COPPER SELENIDES
Aligned bismuth, strontium, calcium cuprate coatings on polycrystalline substrates
[AD-D014522] 19 p2678 N90-25229
The superconducting state of the high-transition temperature superconductors: Experimental basis
22 p3136 N90-27793
Synthesis of Y1Ba2Cu3O(sub x) superconducting powders by intermediate phase reaction
22 p3149 N90-27855
Antiferromagnetism and enhanced heat in CeM2Sn (M = Ni, Ir, Cu, Rh, Pd, and Pt
[DE90-014924] 23 p3399 N90-29206

COPPER ISOTOPES
Magnetic correlations in La(2-x)Sr(x)CuO4 from NQR relaxation and specific heat 22 p3143 N90-27827

COPPER OXIDES
Study of deposition of YBa2Cu3O7-x on cubic zirconia
[NASA-TM-102350] 01 p0128 N90-10737
Adaptation of the theory of superconductivity to the behavior of oxides
[DE89-016518] 02 p0282 N90-11608
Defect structures preceding amorphization by ion irradiations in YBa2Cu3O(7-delta)
[DE89-016905] 02 p0282 N90-11612
Origins of high-temperature superconductivity in the new copper oxide based ceramic superconductors
[DE89-016543] 02 p0284 N90-11622
A fermi liquid electric structure and the nature of the carriers in high-T(sub c) cuprates: A photoemission study
[DE89-016774] 02 p0284 N90-11624
High-temperature superconducting current leads for cryogenic apparatus
[DE89-017680] 03 p0411 N90-12361
Effects of grain boundary chemistry on critical current density in oxide superconductors
[DE89-017780] 03 p0412 N90-12365
Effect of annealing conditions on the structural and superconducting properties of Y-Ba-Cu-O films
[AD-A211308] 03 p0413 N90-12371
High temperature superconducting compounds
[AD-A211511] 03 p0413 N90-12374
Resistivity measurements of superconducting materials
[PB89-225700] 04 p0496 N90-12856
Composite vs constituent particle aspects of hole motion in the CuO2 plane
[DE89-618864] 04 p0558 N90-13251
Local pairing and antiferromagnetism in high-T sub c superconductors
[AD-A213004] 05 p0703 N90-14113
Static and dynamic magnetization properties of Y1Ba2Cu3O(sub z) thin films
[DE89-017584] 06 p0850 N90-14940
Muon SR investigation of magnetism and superconductivity in (Y(1-x)Pr(x))Ba2Cu3O7
[DE90-000689] 06 p0852 N90-14956
Bi-Sr-Ca-Cu-O superconducting ceramics
[DE89-636225] 06 p0855 N90-14972
On the free carrier-negative U center interacting model for the high-T(sub c) oxide superconductor
[DE89-635908] 07 p0998 N90-15775
Synthesis conductivity, and x ray photoelectron spectrum of Bi2Sr2Cu(sub 7+x). A new ternary bismuth-oxide system exhibiting metallic conductivity
[DE90-003010] 07 p0999 N90-15778
Linear electron-hole-electron pair model of high-temperature superconductivity in La(2-x)M(x)CuO4 and YBa2Cu3O(7-y): Part 2. Dependence of the superconducting transition temperatures on pressure and on hole concentration
[DE90-003012] 07 p0999 N90-15779
Partial reduction of re-oxidation processing of Y-Ba-Cu-O sputtered thin films
[DE90-003655] 07 p0999 N90-15782
Magnetic and electronic correlations in YBa2Cu3O(sub 6+x)
[DE89-017604] 07 p1000 N90-15785
Processing YBa2Cu3O(x) wires in O3/O2
[DE90-003570] 07 p1001 N90-15794
Magnetic flux pinning in YBa2Cu3O7 films
[DE90-003709] 07 p1002 N90-15799
Superconductivity and stoichiometry in Tl2Ca2Ba2Cu3O(x) single crystals
[DE90-003838] 07 p1002 N90-15801
Ion-irradiation effects in Tl2Ca2Ba2Cu3O10 superconductors
[DE90-003840] 07 p1002 N90-15802
Cu-O chains in YBa2Cu3O(7-delta) and the phonon mechanism of high-Tc superconductivity
[DE90-603502] 07 p1003 N90-15805
Atomic scale structure of twin boundary in Y-Ba-Cu-O superconductors
[DE90-003955] 07 p1006 N90-15823
Rotational magnetic processes in YB2Cu3O7
[DE90-000541] 08 p1128 N90-16533
The effects of oxygen and strontium vacancies on the superconductivity of single crystals of Bi2Sr(2-x)CuO(6-y)
[DE90-004242] 08 p1133 N90-16561
Physical properties of Bi2Sr2CuO6, the semiconducting phase, structurally distinct from the n = 1 Bi-cuprate superconductor
[DE90-004299] 08 p1133 N90-16563
A new approach for the utilization of electron paramagnetic resonance and an investigation of copper oxide superconductors
[AD-A213833] 09 p1277 N90-17404
Diffusion and processing of YBa2Cu3O(x)
[DE90-003569] 09 p1286 N90-17457
Oxidation and reduction of Bi2Sr1.85CuO(6-y) crystals
[DE90-004246] 09 p1287 N90-17460
High-temperature deformation of YBa2Cu3O(7-delta) with Ag additions
[DE90-004884] 09 p1292 N90-17491
Effects of O2 ion bombardment of Y-BaCu-oxide during thin film growth
[DE90-005315] 09 p1293 N90-17495
Anisotropy and dimensionality in untwinned crystals of YBa2Cu3O(7-delta)
[DE90-004890] 10 p1436 N90-18287
Long laser-pulse method of producing Y-Ba-Cu-O superconducting films
[DE90-005202] 10 p1436 N90-18289
What influences order parameters across the superconducting phase boundary
[DE90-610663] 11 p1572 N90-19047
Band electronic structures and crystal packing forces
[DE90-007689] 12 p1723 N90-19898
Preparation and properties of the system Cu(x)Pd(1-x)O (0 less than or equal to x less than or equal to 0.175)
[AD-A217567] 12 p1723 N90-19901
Y1Ba2Cu3O(7-x) laser-ablation plume dynamics measurement by nanosecond response ion probe: Comparison with optical measurements
[DE90-007658] 13 p1807 N90-20375
High resolution transmission electron microscopy study of defect structures in mixed-phase YBaCuO
[DE90-007767] 13 p1894 N90-20873
Synthesis and properties of polycrystalline Tl2Ba2CaCu2O(x) and Tl2Ba2Ca2Cu3O(x)
[DE90-007528] 13 p1897 N90-20887
Synthesis of Bi-Sr-Ca-Cu oxide superconductor by solution technique
[DE90-008707] 13 p1897 N90-20888
Deformation processing of YBa2Cu3O(sub x)
[DE90-007795] 14 p2030 N90-21644
Growth and patterning of laser ablated superconducting YBa2Cu3O7 films on LaAlO3 substrates
[NASA-TM-102436] 15 p2173 N90-22421
Photoresponse of YBa2Cu3O(7-delta) granular and epitaxial superconducting thin films
[NASA-TM-103144] 16 p2231 N90-22732
What is going on in the La2CuO4 superconductors
16 p2311 N90-23171
Influence of high energy radiation on critical parameters of superconducting ceramics YBa2Cu3O7
[DE90-620562] 16 p2322 N90-23239
In-situ processing of epitaxial and textured high (Tc) superconducting HoBa2Cu3O(7-x) thin films by pulsed laser evaporation technique
[DE90-009828] 17 p2474 N90-24148
Stability projections for high temperature superconductors
[AD-A218945] 18 p2618 N90-24913
Magnetic and resistive measurements of the upper critical field in intwinned single crystals of YBa2Cu3O(7-delta)
[DE90-010083] 18 p2619 N90-24918
The defect structure of ion and neutron irradiated YBa2Cu3O(7-delta) single crystals
[DE90-010100] 18 p2619 N90-24920
Valence-defect chemical equilibria in nonstoichiometric YBa2Cu3O(7-delta)
[DE90-010152] 18 p2619 N90-24921
Thermal and phase analysis of YBa2Cu3O(7-x) powder compacts with organic acid additives
[DE90-010142] 18 p2620 N90-24930
Transverse- and zero-field muon SR investigation of magnetism and superconductivity in (Y(1-x)Pr(x)Ba2Cu3O7)
[DE90-010597] 18 p2624 N90-24953

Superconducting thin films of YBaCu oxides prepared by MOCVD
[DE90-011109] 18 p2625 N90-24961
In-situ growth of superconducting films of Bi-Sr-Ca-Cu-O using magnetron sputtering
[DE90-011151] 18 p2626 N90-24962
Effect of Cu(2+) magnetic moments on the superconductivity of YBa2Cu3O7: The origin of the linear term in the specific heat; the volume fraction of superconductivity
[DE90-011214] 18 p2626 N90-24963
Highly-textured thallium-barium-calcium-copper-oxide polycrystalline superconducting films on silver substrates
[DE90-011972] 18 p2627 N90-24970
Sequentially evaporated thin film YBa2Cu3O(7-x) superconducting microwave ring resonator
[NASA-TM-103180] 19 p2685 N90-25273
Microstructures of superconducting YBa2Cu3O(7-x) thin films
[DE90-011976] 19 p2761 N90-25686
Large, orientation-dependent enhancements of critical currents in Y1Ba2Cu3O(7-x) epitaxial thin films: Evidence for intrinsic flux pinning
[DE90-009424] 20 p2929 N90-26666
NDE (Nondestructive evaluation) of critical currents in high T(sub c) superconductors
[DE90-012953] 20 p2930 N90-26670
Ellipsometric study of YBa2Cu3O(7-x) laser ablated and co-evaporated films
[NASA-TM-103223] 20 p2932 N90-26682
The effect of processing, deformation and annealing on the microstructure of Y1Ba2Cu3O7-(sub delta)
[DE90-011731] 21 p3079 N90-27510
Preparation and magnetic measurements of single crystal Tl2Ba2CaCu2O8
[DE90-013657] 21 p3081 N90-27519
Flux creep in Bi2Sr2CaCu2O8(sub +x) single crystals 22 p3135 N90-27794
Elliptical flux vortices in polycrystalline YBa2Cu3O7 22 p3136 N90-27795
Microstructure and magnetization of doped Y-Ba-Ca-O materials prepared by melt quench and post annealing method 22 p3138 N90-27803
Effect of shock pressure on the structure and superconducting properties of Y-Ba-Cu-O in explosively fabricated bulk metal-matrix composites 22 p3138 N90-27804
Oxide superconductors under magnetic field 22 p3139 N90-27807
Laser ablated high T(sub c) superconducting thin YBa2Cu3O(7-x) films on substrates suitable for microwave applications 22 p3139 N90-27808
The effect of temperature cycling typical of low earth orbit satellites on thin films of YBa2Cu3O(7-x) 22 p3140 N90-27812
Thermal and electric properties of Nd(1.85)Ce(0.15)CuO(4-y) and Pr(1.85)Ce(0.15)CuO(4-y) 22 p3141 N90-27816
Effect of oxygen stoichiometry on T(sub c) of Bi-based superconductors 22 p3142 N90-27818
Phenomenological theory of the normal and superconductive states of Cu-O and Bi-O metals 22 p3142 N90-27819
Charge transfer polarisation wave and carrier pairing in the high T(sub c) copper oxides 22 p3142 N90-27820
Electronic structure Fermi liquid theory of high T(sub c) superconductors: Comparison with experiments 22 p3142 N90-27821
Study of local structure and magnetism in high-T(sub c) copper oxide superconductors 22 p3143 N90-27824
The mechanism of high-T(sub c) superconductivity due to bound hole mediators: Relationship to ferroelectricity 22 p3143 N90-27826
Magnetic correlations in La(2-x)Sr(x)CuO4 from NQR relaxation and specific heat 22 p3143 N90-27827
Magnetism and superconductivity of some Tl-Cu oxides 22 p3143 N90-27829
The color of polarization in cuprate superconductors 22 p3144 N90-27830
A systematic study of superconductivity in BiPb(Sn)-Sb Sr-Ca-Cu-O systems 22 p3144 N90-27831
Stabilization of high T(sub c) phase in bismuth cuprate superconductor by lead doping 22 p3144 N90-27832
Structure and superconducting properties of ((Ln(1-x)Ln*(x) 1/2 (Ba(1-y)Sr(y) 1/3 Ce 1/6) 8Cu6O(z) 22 p3144 N90-27833
Plastic superconductor bearings any size, any shape, 77 k and up 22 p3145 N90-27838
Thermal response of large area high temperature superconducting YBaCuO infrared bolometer 22 p3146 N90-27839
Electronic state and superconductivity of YBa2Cu3-xO7-y (M=Al,Zn and Sn) systems 22 p3146 N90-27842
Effects of grain size and grain boundary on critical current density of high T(sub c) superconducting oxides 22 p3146 N90-27843
Microwave conductivity of laser ablated YBaCuO superconducting films and its relation to microstrip transmission line 22 p3147 N90-27844
The effects of space radiation on thin films of YBa2Cu3O(sub 7-x) 22 p3147 N90-27845
Superconductivity in 2-2-3 Y2Ba2Cu3O(sub 8+ delta) 22 p3147 N90-27847
Spin bipolaron in the framework of emery model for high-T(sub c) copper oxide superconductors 22 p3149 N90-27856
Comparative study of flux pinning flux creep and critical currents between YBaCuO crystals with and without Y2BaCuO5 inclusions 22 p3152 N90-27869
Incoherent imaging of materials structure and composition by Z-contrast stem
[DE90-012789] 22 p3155 N90-27888
High T(sub c) copper-oxide superconductors
[AD-D014483] 22 p3247 N90-28416
Synthesis and structural chemistry of Au(III)-substituted Ba2YCu3O(7-delta)
[NASA-TM-103292] 23 p3305 N90-28896
Electron microscopy of transition-metal doped BiCaSrCuO
[DE90-014184] 23 p3398 N90-29202
Investigation of YBa2Cu3O(7-sigma) by NMR and construction of an ultra low temperature cryostat 24 p3550 N90-30088
Synthesis and property evaluation of Y-Ba2-Cu3-O(6+x) superconductors
[AD-A223494] 24 p3552 N90-30098

COPPER SELENIDES
Investigations of CuInSe2 thin films and contacts
[DE90-000301] 12 p1721 N90-19886

COPYRIGHTS
Copyright and home copying: Technology challenges the law
[PB90-151309] 21 p3086 N90-27547
Legal ramifications of intellectual property 22 p3258 N90-28448

CORDITE
U DOUBLE BASE PROPELLANTS

CORE FLOW
Energy Efficient Engine core design and performance report
[NASA-CR-168069] 23 p3279 N90-28559

CORE SAMPLING
Analytical study of comet nucleus samples 08 p1140 N90-16608
The nature of cometary materials 08 p1147 N90-16647
Rosetta/CNSR, ESA's planetary cornerstone mission 12 p1738 N90-19990
Design and development activities on the candidate sample acquisition system for the Rosetta mission 12 p1738 N90-19993
Introduction to drilling technology 12 p1740 N90-20002
Compressive strength of synthetic comet nucleus samples 12 p1741 N90-20006
Rosetta/CNSR altimeter and sounding radar 12 p1741 N90-20009
First impressions of the comet drilling problem 12 p1743 N90-20021
Relevance of laboratory studies to comets 12 p1743 N90-20023
Core sample extractor
[NASA-CR-182864] 17 p2411 N90-23740
Lunar polar coring lander
[NASA-CR-186684] 19 p2796 N90-25917
Micro coring apparatus
[NASA-CR-183072] 20 p2869 N90-26321
Lunar deep drill apparatus
[NASA-CR-182756] 20 p2869 N90-26322
Ice core studies and the past atmospheric environment of polar regions 20 p2885 N90-26411
The Renland ice core (Greenland): A source for climatic studies over 100,000 years 20 p2885 N90-26412
Robotic sampling system for an unmanned Mars mission 23 p3375 N90-29070

CORES
NT EARTH CORE
NT HONEYCOMB CORES
NT MAGNETIC CORES
NT PLANETARY CORES
NT REACTOR CORES
Capillary effects in steady-state flow in heterogeneous cores
[DE89-000758] 01 p0070 N90-10399
Very high resolution radio observations of molecular cloud cores 06 p0863 N90-15013
Gas turbine regenerators: A method for selecting the optimum plate-finned surface pair for minimum core volume
[AD-A213430] 07 p0930 N90-15382
Vortex cores and vortex breakdown
[AD-A215266] 09 p1218 N90-17062
Understanding electronegative effects in core-level electron spectroscopies; application to the high temperature superconductors
[AD-A216728] 11 p1570 N90-19037
Counterrotating cores in elliptical galaxies 16 p2332 N90-23288
The chemical and structural properties of sea ice in the southern Beaufort Sea
[AD-A219746] 17 p2418 N90-23776
Molecular studies of dense cores 17 p2484 N90-24207
Micro coring apparatus
[NASA-CR-183072] 20 p2869 N90-26321
Lunar deep drill apparatus
[NASA-CR-182756] 20 p2869 N90-26322
New core design for use with precision composite reflectors
[NASA-CASE-NPO-17858-1-CU] 21 p2970 N90-26880

CORIOLIS EFFECT
On the complexity analysis of the coriolis and centripetal effects of a 6 DOF robot manipulator --- Degrees of Freedom (DOF)
[RR-344] 03 p0355 N90-12030
Dynamic interactions and globally optimal maneuver of distributed systems 09 p1236 N90-17172
The application of fiber optic technology to flowmeters
[AD-A214389] 10 p1430 N90-18247
Finite element analysis of a quartz rotation sensor
[DE90-006959] 12 p1664 N90-19562
A numerical study of the role of meso beta and meso gamma scale vertical exchange processes in the evolution of upper tropospheric frontal systems
[AD-A222057] 21 p3031 N90-27230

CORK (MATERIALS)
Thiokol/Wasatch installation evaluation of the redesigned field joint protection system (concepts 1 and 3)
[NASA-CR-183860] 13 p1765 N90-20127
Evaluation of EA-934NA with 2.5 percent Cab-O-Sil
[NASA-CR-184005] 22 p3158 N90-27909

CORNEA
Structural alterations in the cornea from exposure to infrared radiation
[AD-A215340] 09 p1253 N90-17269

CORNER FLOW
Observation of wind corners in the middle atmosphere over Andenes (69 N) during winter 1983/84, summer 1987 and summer 1988 05 p0657 N90-13836
Graphs of the state of stress at rounded corners
[MEMT-1] 15 p2119 N90-22122

CORNERS
Axial flow in corners at supersonic and hypersonic speeds 10 p1308 N90-17570

CORONA DISCHARGES
U ELECTRIC CORONA

CORONAGRAPHS
Optical detection of space debris using a large achromatic coronagraph
[AD-A211362] 04 p0462 N90-12647
The SOHO mission. Scientific and technical aspects of the instruments
[ESA-SP-1104] 04 p0566 N90-13302
UVCS: An Ultraviolet Coronagraph Spectrometer for SOHO 04 p0568 N90-13310
LASCO: A wide-field white light and spectrometric coronagraph for SOHO 04 p0588 N90-13311

CORONAL HOLES
The observation of possible reconnection events in the boundary changes of solar coronal holes 01 p0138 N90-10801
Correspondence between solar fine-scale structures in the corona, transition region, and lower atmosphere from collaborative observations 01 p0139 N90-10804
Shear-induced inflation of coronal magnetic fields
[NASA-CR-186103] 05 p0715 N90-14178
Interaction of minor ions with fast and slow shocks
[NASA-CR-186372] 11 p1594 N90-19181
The large and small scale density structure in the solar corona 16 p2338 N90-23327

CORONAL LOOPS
Solar X-ray Astronomy Sounding Rocket Program
[NASA-CR-183447] 01 p0138 N90-10796
As observational and theoretical investigation of stellar flares 06 p0862 N90-15012
VLA observations of the coronal plasma
[NASA-CR-186540] 14 p2042 N90-21711
Cyclotron maser and plasma wave growth in magnetic loops
[NASA-CR-179862] 15 p2170 N90-22402

Vlasov-Maxwell equilibria of solar coronal loops
[DE90-015025] 23 p3414 N90-29289
CORONARY CIRCULATION
Coronary arterial capacitance and subendocardial vascular patency throughout the cardiac cycle
11 p1538 N90-18855
CORONAS
NT CORONAL HOLES
NT CORONAL LOOPS
NT ELECTRIC CORONA
NT SOLAR CORONA
NT STELLAR CORONAS
Venus and the Archean Earth: Thermal considerations
03 p0427 N90-12448
The disk-halo connection and the nature of the interstellar medium
[NASA-CR-186286] 07 p1012 N90-15860
Geology of coronae and domal structures on Venus and models of their origin 15 p2191 N90-22513
Slow shocks in coronal mass ejections
[NASA-CR-186578] 15 p2193 N90-22522
The large and small scale density structure in the solar corona 16 p2338 N90-23327
Infrared coronal line novae 16 p2339 N90-23328
A review of self generated B-field in ICF corona
[DE90-627479] 24 p3547 N90-30063
CORPUSCULAR RADIATION
NT BETA PARTICLES
NT ELECTRON BEAMS
NT ELECTRON PRECIPITATION
NT ELECTRON RADIATION
NT ENERGETIC PARTICLES
NT RADIATION BELTS
NT RELATIVISTIC ELECTRON BEAMS
NT SOLAR CORPUSCULAR RADIATION
NT SOLAR COSMIC RAYS
NT SOLAR NEUTRONS
NT SOLAR PROTONS
CORRECTION
NT ATMOSPHERIC CORRECTION
NT OPTICAL CORRECTION PROCEDURE
Pressure correction splitting methods for the computation of oscillatory free convection in low Pr fluids
[CWI-NM-R8816] 02 p0222 N90-11271
Application of matrix correction methods on a plate and a truss structure
[NLR-MP-88042-U] 03 p0359 N90-12056
A multigrid method combined with defect correction for free convection problems at high Rayleigh numbers
[REPT-89-27] 03 p0396 N90-12264
Pressure correction calculation procedures for 3D viscous flow 05 p0641 N90-13738
New approach to omega PPCs (Propagation Corrections)
[AD-A215610] 09 p1207 N90-17000
Residual interference and wind tunnel wall adaption
10 p1324 N90-17655
First-order weight corrections for real-time flight path management
[LR-580] 15 p2050 N90-21751
Computerized inspection of gear tooth surfaces
[NASA-TM-102395] 15 p2107 N90-22054
Feasibility study of a synthesis procedure for array feeds to improve radiation performance of large distorted reflector antennas
[NASA-CR-186641] 20 p2851 N90-26213
Alignment positioning mechanism
[NASA-CASE-MSC-21502-1] 20 p2872 N90-26341
An outline for the RTNEPH infrared atmospheric water vapor attenuation study
[AD-A221753] 21 p3027 N90-27209
Adaptive optics correction in real-time for dynamic wavefront errors
[AD-A221588] 21 p3077 N90-27495
Tool for studying the effects of range restriction in correlation coefficient estimation
[AD-A224035] 24 p3537 N90-29996
CORRELATION
NT ANGULAR CORRELATION
NT AUTOCORRELATION
NT CORRELATION COEFFICIENTS
NT CORRELATION DETECTION
NT CROSS CORRELATION
NT DATA CORRELATION
NT SPECTRAL CORRELATION
NT STATISTICAL CORRELATION
Differences in writers initial task representations
[AD-A210433] 01 p0136 N90-10788
Lightning data study in conjunction with geostationary satellite data
[NASA-CR-179286] 03 p0375 N90-12142
On the effects of an uncertainty on evolution law in dynamical systems
[PREPRINT-689] 05 p0693 N90-14047
Perturbed angular correlations in zirconia ceramics
[DE89-017272] 06 p0751 N90-14369
A diagnostic for determining the quality of single-reference electron correlation methods
[NASA-TM-101929] 06 p0838 N90-14874
Correlations between surface structure and catalytic activity/selectivity
[DE90-003755] 07 p0896 N90-15181
Relativistic self-consistent field studies of atoms and molecules
[AD-A214101] 07 p0991 N90-15724
Classification of acousto-optic correlation signatures of spread spectrum signals using artificial neural networks
[AD-A215045] 09 p1206 N90-16992
On the temperature of surfaces
10 p1366 N90-17917
Modeling the pressure-strain correlation of turbulence: An invariant dynamical systems approach
[NASA-CR-181979] 10 p1383 N90-18003
The correlation between radio and far-infrared emission for disk galaxies 11 p1588 N90-19158
Correlation-induced changes of spectra
[AD-A217087] 12 p1669 N90-19591
Implementation of midcourse tracking and correlation on massively parallel computers
[DE90-008166] 13 p1873 N90-20740
Motion detection in astronomical and ice floe images
15 p2140 N90-22231
Sample size for correlation estimates
[AD-A219810] 17 p2465 N90-24085
Case study on Pre-Typhoon Active Convective Clouds (PTACC) 21 p3029 N90-27220
Evaluation of correlations between meteorological measurements and observations of lightning activity using artificial neural systems
[AD-A222659] 21 p3030 N90-27229
Reliability and performance of friction measuring tires and friction equipment correlation
[AD-A223694] 24 p3436 N90-29408
Tool for studying the effects of range restriction in correlation coefficient estimation
[AD-A224035] 24 p3537 N90-29996
Sensitivity of the error in multivariate statistical interpolation to parameter values
[AD-A224076] 24 p3540 N90-30015
Effects and control of the correlation properties of light sources
[AD-A224539] 24 p3545 N90-30049
New real space correlated-basis-functions approach for the electron correlations of the semiconductor inversion layer
[DE90-627315] 24 p3551 N90-30090
CORRELATION COEFFICIENTS
Correlative analyses for geomagnetic indices, cosmic-ray intensities and sunspot numbers recorded since 1937
[IFSI-89-4] 08 p1151 N90-16670
Review and statistical analysis of the ultrasonic velocity method for estimating the porosity fraction in polycrystalline materials
[NASA-TM-102501-REV] 14 p1989 N90-21402
Spectral response of wheat and its relationship with agronomic variables in the tropical region
[INPE-5018-RPE/612] 15 p2122 N90-22138
Field reports on radiometric campaigns of soybeans in the Federal district: Safra 88/89
[INPE-5021-RPE/615] 15 p2122 N90-22139
Tool for studying the effects of range restriction in correlation coefficient estimation
[AD-A224035] 24 p3537 N90-29996
CORRELATION DETECTION
Characteristics of the IAEA correlation monitor material for surveillance programmes
[VTT-RR-639] 19 p2682 N90-25258
Binary pseudo random phase correlation in radar systems: A new approach
[RSRE-MEMO-4223] 19 p2683 N90-25263
CORRELATION FUNCTIONS
U CORRELATION
CORRELATORS
NT IMAGE CORRELATORS
A comparison of real-time optical correlators for pattern recognition
[DE89-016416] 01 p0123 N90-10705
A SAW Slanted Array Correlator (SAC) with separate amplitude compensation channel
[AD-D014174] 03 p0336 N90-11914
Advanced instrumentation for QELS experiments
09 p1223 N90-17093
Hybrid optical/digital architecture for distortion invariant pattern recognition
[AD-A215628] 09 p1282 N90-17435
Binary correlators for optical computing and pattern recognition 10 p1441 N90-18318
Visual processing of object velocity and acceleration
[AD-A216509] 11 p1539 N90-18858
Optical calculation of correlation filters for a robotic vision system 18 p2630 N90-24986
CORRIDORS
En route noise annoyance laboratory test: Preliminary results 18 p2611 N90-24870
CORROSION
NT ELECTROCHEMICAL CORROSION
NT HOT CORROSION
NT INTERGRANULAR CORROSION
NT SCALE (CORROSION)
NT STRESS CORROSION
NT STRESS CORROSION CRACKING
Polypeptide inhibitors of mineral scaling and corrosion
[AD-A210507] 01 p0041 N90-10225
Development of a semiquantitative corrosion monitor
[AD-A208132] 01 p0072 N90-10414
Corrosion rates of structural materials on the ocean floor
[DE89-015211] 02 p0197 N90-11123
Thermomechanical contact phenomena and wear of sliding components
[AD-A211290] 03 p0355 N90-12028
Long endurance underwater power system
[AD-A211386] 03 p0366 N90-12096
Heat pipe and thermal energy storage and corrosion studies (1988)
[AD-A212655] 04 p0472 N90-12706
Development of an inventory of materials potentially sensitive to ambient atmospheric acidity in the South Coast Air Basin
[PB89-224604] 04 p0516 N90-12982
NDI (Nondestructive Inspection) oriented corrosion control for Army aircraft. Phase 1: Inspection methods
[AD-A213368] 05 p0576 N90-13359
Contribution to the electrochemical study of corrosion in the low conductivity media: Application to the study of the behavior of austenitic stainless steels in concentrated solutions of acetic acid
[ISAL-89-0014] 05 p0625 N90-13648
Laser Raman spectroscopy in studies of corrosion and electrocatalysis
[DE90-001414] 06 p0741 N90-14311
The biocorrosion of copper by biopolymers as examined in situ, in real time FT-IR/CIR/ATR in conjunction with pre and post XPS/AES
[DE90-002086] 06 p0747 N90-14348
High-temperature corrosion of heat exchanger materials
[DE90-001963] 06 p0748 N90-14352
Sodium/sulfur post-test analysis at ANL
[DE90-001911] 06 p0771 N90-14488
Report of the Advanced Neutron Source (ANS) Aluminum Cladding Corrosion Workshop
[DE90-001281] 07 p0903 N90-15217
Niobium 1 percent zirconium/potassium and titanium/potassium life-test heat pipe design and testing
[DE90-002430] 07 p0954 N90-15522
Study of metal corrosion using ac impedance techniques in the STS launch environment
08 p1155 N90-16688
A fundamental understanding of the effect of alloying elements on the corrosion resistance of rapidly solidified Mg alloys
[AD-A216767] 11 p1486 N90-18553
Corrosion fatigue of iron-chromium-nickel alloys: Fracture mechanics and chemistry
[DE90-006318] 11 p1487 N90-18556
Fastener design manual
[NASA-RP-1228] 11 p1517 N90-18740
Corrosion properties of Fe3Al in H2S-H2-H2O mixtures
[DE90-004936] 13 p1772 N90-20167
Stochastic approach to the initiation of pitting corrosion
[AERE-R-13348] 13 p1775 N90-20190
Corrosion testing of candidates for the alkaline fuel cell cathode 13 p1824 N90-20471
A corrosion fatigue/stress corrosion testing facility at Materials Research Laboratory
[MRL-TN-568] 14 p1929 N90-21044
Current fluctuations associated with localised corrosion: Mechanistic studies of the early stages of pitting and stress corrosion cracking of stainless steel
[AERE-R-13531] 14 p1950 N90-21159
Corrosion behavior of mild steel ih high pH aqueous media
[PB90-131152] 14 p1950 N90-21162
High-temperature oxidation and sulfidation of Fe-20Cr-16Ni-4Al-1Y2O3 oxide-dispersion-strengthened alloy
[DE90-007897] 14 p1951 N90-21168
The corrosion protection of 6061-T6 aluminum by a polyurethane-sealed anodized coat
[NASA-TM-100394] 14 p1955 N90-21191

A study of the influence of alloying additions on the passivity of aluminium
[AD-A219630] 17 p2376 N90-23532
Corrosion control through a better understanding of the metallic substrate/organic coating interface
[AD-A220432] 17 p2377 N90-23533
Archaebacterial involvement in microbial metal corrosion: Metabolism of S and Fe
[AD-A219982] 17 p2377 N90-23537
A simple demonstration of corrosion cells
18 p2514 N90-24355
Mechanistic modeling of corrosion fatigue crack growth of steels in aqueous solutions 18 p2524 N90-24404
Corrosion fatigue crack propagation in metals
[NASA-CR-4301] 18 p2524 N90-24405
The feasibility of detecting corrosion in electric fuzes using the thermal transient technique
[AD-A221385] 18 p2549 N90-24547
The oxidation and corrosion of ODS alloys
[NASA-TM-102555] 19 p2675 N90-25211
The effects of acid fog and dew on materials
[PB90-157496] 19 p2712 N90-25436
Flight set 360L001 (STS-26) igniter, post flight
[NASA-CR-183957] 20 p2870 N90-26325
Computerized corrosion forecasting model for C-5 aircraft 21 p2957 N90-26815
Microbially influenced corrosion of carbon steels
[DE90-012231] 21 p2980 N90-26936
Corrosion-inhibiting coating composition
[AD-D014546] 22 p3159 N90-27916
High-temperature, corrosion-preventive coating
[AD-D014557] 22 p3160 N90-27918
Investigation of the effects of acid deposition on materials
[PB90-158973] 22 p3197 N90-28143
Effect of protective coatings on mechanical properties of superalloys 23 p3308 N90-28707
Investigation of the effects of microalloy constituents, surface treatment and oxidation conditions on the development and breakdown of protective oxide scales
[DE90-015710] 24 p3451 N90-29488

CORROSION PREVENTION
Polypeptide inhibitors of mineral scaling and corrosion
[AD-A210507] 01 p0041 N90-10225
Corrosion and corrosion inhibition of metals/alloys in methylphosphonic difluoride and decontaminating solutions
[AD-A212404] 04 p0477 N90-12734
Polyelectrolyte-diffused zinc phosphate conversion coatings and polyacid coupling primers for corrosion protection of steel and aluminum, and alkali-catalyzed hydrolysis of polyimide-based materials
[AD-A212240] 04 p0480 N90-12754
NDI (Nondestructive Inspection) oriented corrosion control for Army aircraft. Phase 1: Inspection methods
[AD-A213368] 05 p0576 N90-13359
Glancing angle x ray studies of oxide films
[DE89-017828] 06 p0852 N90-14953
Development of a high temperature storage unit for integration with solar dynamic systems
10 p1335 N90-17720
Surface modification of steels and aluminum alloys to control corrosion and hydrogen embrittlement. Part 1: Chemical methods
[AD-A216272] 10 p1356 N90-17866
Chemistry-structure-property interrelationships for calcareous deposits as stand-alone coatings
[AD-A216031] 10 p1359 N90-17881
Development of fuel wear tests using the Cameron-Plint high-frequency reciprocating machine
[AD-A216003] 10 p1361 N90-17892
Investigation of applications of diamond film
[AD-A216104] 10 p1368 N90-17931
Mitigation of stress corrosion cracking of AISI 304 stainless steel in oxygenated water at 289 C by organic species at low concentration
[DE90-005631] 12 p1628 N90-19354
High gloss corrosion-resistant coatings
[AD-D014403] 14 p1954 N90-21184
Combination primer/topcoat coating
[AD-D014445] 14 p1954 N90-21189
The corrosion protection of 6061-T6 aluminum by a polyurethane-sealed anodized coat
[NASA-TM-100394] 14 p1955 N90-21191
New corrosion resistant ceramic coatings by laser processing
[AERE-R-13166] 15 p2071 N90-21863
Nonflammable hydraulic power system for tactical aircraft. Volume 1: Aircraft system definition, design and analysis
[AD-A218493] 17 p2356 N90-23409
Corrosion control through a better understanding of the metallic substrate/organic coating interface
[AD-A220432] 17 p2377 N90-23533
High resistance bolts: Test trials for plated bolts
[CRIF-MT-178] 17 p2413 N90-23748
Micro separometer and ball-on-cylinder lubricity evaluator tests or corrosion inhibitor/lubricity improver additives
[AD-A221339] 19 p2678 N90-25228
Corrosion protection of metal matrix composites
[AD-A222951] 21 p2971 N90-26888
UNICOAT: Development of a primer/topcoat and flexible primer for aluminum
[AD-A221803] 21 p2989 N90-26986
Corrosion-inhibiting coating composition
[AD-D014546] 22 p3159 N90-27916
High-temperature, corrosion-preventive coating
[AD-D014557] 22 p3160 N90-27918

CORROSION RESISTANCE
NT OXIDATION RESISTANCE
The improved corrosion resistance of ultra high purity magnesium alloy castings 01 p0044 N90-10245
Corrosion rates of structural materials on the ocean floor
[DE89-015211] 02 p0197 N90-11123
How the common practice of heating plates of austenitic stainless steel during cooling affects their mechanical properties
[CETIM-104500] 04 p0476 N90-12725
Corrosion and corrosion inhibition of metals/alloys in methylphosphonic difluoride and decontaminating solutions
[AD-A212404] 04 p0477 N90-12734
Aluminum lithium alloys for Navy aircraft
07 p0898 N90-15193
Fatigue, fracture mechanics and corrosion properties of some aluminium-lithium alloys 07 p0898 N90-15194
The effect of dissolved ozone on the corrosion behavior of Cu-30 Ni and 304L stainless steel in 0.5 N NaCl solutions
[AD-A213804] 07 p0906 N90-15235
Stainless steel passivity
[AD-A214108] 08 p1044 N90-16033
Selection of corrosion-resistant materials for use in molten nitrate salts
[DE90-004351] 08 p1046 N90-16048
MHD integrated topping cycle project
[DE90-004141] 08 p1126 N90-16525
Study of metal corrosion using ac impedance techniques in the STS launch environment
08 p1155 N90-16688
The effects of hydrogen embrittlement of titanium
08 p1156 N90-16698
Alloying of metals for corrosion resistance
[AD-D014313] 09 p1194 N90-16919
Compound for metallic surface treatment
[DE90-004121] 09 p1196 N90-16927
A fundamental understanding of the effect of alloying elements on the corrosion resistance of rapidly solidified Mg alloys
[AD-A216767] 11 p1486 N90-18553
The mechanism, measurement, and influence of properties on the galling of metals
[DE90-006533] 11 p1487 N90-18558
An attempt of improving high-temperature fatigue properties of Ni-Cr-W superalloys in HTGR helium
[DE90-741482] 12 p1627 N90-19350
Heat-resistant and anticorrosive paint
[DE90-006077] 12 p1630 N90-19369
Corrosion properties of Fe3Al in H2S-H2-H2O mixtures
[DE90-004936] 13 p1772 N90-20167
The stress corrosion performance of diffusion bonded nickel base alloys
[DE90-008130] 13 p1777 N90-20199
Sol-gel derived polytitanosiloxane coatings
[DE90-004186] 13 p1779 N90-20210
High-temperature oxidation and sulfidation of Fe-20Cr-16Ni-4Al-1Y2O3 oxide-dispersion-strengthened alloy
[DE90-007897] 14 p1951 N90-21168
High gloss corrosion-resistant coatings
[AD-D014403] 14 p1954 N90-21184
New corrosion resistant ceramic coatings by laser processing
[AERE-R-13166] 15 p2071 N90-21863
Improved high temperature oxidation behavior of alloys by ion implantation
[AERE-R-13309] 16 p2217 N90-22650
A study of the relation between grain boundary type and sensitisation in a partially-sensitised AISI 304 stainless steel using electron back-scattering patterns
[AERE-R-13327] 16 p2321 N90-23234
Modeling and experimental studies of oxide covered metal surfaces
[DE90-009961] 17 p2375 N90-23525
A study of the influence of alloying additions on the passivity of aluminium
[AD-A219630] 17 p2376 N90-23532
Archaebacterial involvement in microbial metal corrosion: Metabolism of S and Fe
[AD-A219982] 17 p2377 N90-23537
Evaluation of abrasion-resistant metallized coatings for civil works applications
[AD-A221078] 18 p2530 N90-24438
Fracture-tough, corrosion-resistant bearing steels
[NASA-CR-186796] 19 p2675 N90-25213
Passive mechanisms of surfaces produced by ion beam mixing and ion implantation
[AD-A222432] 21 p2982 N90-26945
Characterization of the pitting corrosion of aluminum-lithium alloys
[ETCA-89-R-176] 22 p3157 N90-27903
New aspects in aircraft inspection using eddy current methods 22 p3187 N90-28085
High Temperature Surface Interactions
[AGARD-CP-461] 23 p3306 N90-28698
Developments in test procedures for hot-salt corrosion of superalloys 23 p3306 N90-28700
Molten salt induced high temperature degradation of thermal barrier coatings 23 p3307 N90-28704
Overview on hot gas tests and molten salt corrosion experiments at the DLR 23 p3309 N90-28714
Evaluation of advanced austenitic alloys relative to alloy design criteria for steam service. Part 1: Lean stainless steel
[DE90-014765] 23 p3310 N90-28720
Proceedings of US Army Research Office Workshop on US Army Applications for Diamond and Diamondlike Materials
[AD-A224193] 23 p3314 N90-28741
Adhesion of silver films to ion-bombarded zirconia
[DE90-010088] 24 p3456 N90-29517

CORROSION TESTS
Development of a semiquantitative corrosion monitor
[AD-A208132] 01 p0072 N90-10414
Coatings for gas turbine compressors
[NLR-MP-88045-U] 03 p0308 N90-11750
NDI (Nondestructive Inspection) oriented corrosion control for Army aircraft. Phase 1: Inspection methods
[AD-A213368] 05 p0576 N90-13359
Contribution to the electrochemical study of corrosion in the low conductivity media: Application to the study of the behavior of austenitic stainless steels in concentrated solutions of acetic acid
[ISAL-89-0014] 05 p0625 N90-13648
Corrosion testing of candidates for the alkaline fuel cell cathode 13 p1824 N90-20471
A corrosion fatigue/stress corrosion testing facility at Materials Research Laboratory
[MRL-TN-568] 14 p1929 N90-21044

CORRUGATED PLATES
Nonlinear collapse simulation of anisotropic plates and corrugated panels 02 p0183 N90-11035

CORRUGATED SHELLS
Nonlinear collapse simulation of anisotropic plates and corrugated panels 02 p0183 N90-11035

CORTICOSTEROIDS
Effects of dexamethasone and high terrestrial altitude on cognitive performance and affect
[AD-A217897] 13 p1851 N90-20625

CORUNDUM
U ALUMINUM OXIDES

COSINE SERIES
Significance of norms and completeness in variational based methods 16 p2296 N90-23078

COSMIC BACKGROUND EXPLORER SATELLITE
COBE nonspinning attitude propagation
05 p0587 N90-13418
Detecting extended solar system structures with COBE (Cosmic Background Explorer)
[AD-A216380] 10 p1447 N90-18349
The COBE cosmic 3 K anisotropy experiment: A gravity wave and cosmic string probe 12 p1732 N90-19959
Overview of battery usage in NASA/GSFC LEO and GEOspacecrafts 13 p1821 N90-20455
Cosmic Background Explorer (COBE) press kit
[P89-10172] 17 p2364 N90-23459
CLEAR: Automating control centers with expert system technology 19 p2733 N90-25533

COSMIC DUST
NT INTERPLANETARY DUST
NT ZODIACAL DUST
Small grains in reflection nebulae: A study of diffuse interstellar bands, elemental depletions and infrared flux
02 p0293 N90-11672
A model of the thermal and electrical properties of cosmic dust particles 06 p0863 N90-15014
The volatile composition of comets
[NASA-CR-186281] 07 p1014 N90-15871
Dust bands in the asteroid belt
[NASA-CR-186301] 07 p1014 N90-15873
The carbon chemistry of meteorites: Relationships to comets 08 p1141 N90-16615

Trace element abundance determinations by Synchrotron X Ray Fluorescence (SXRF) on returned comet nucleus mineral grains 08 p1142 N90-16619
From interstellar dust to comets 08 p1142 N90-16620
Role of dust to gas production rate ratio in cometary physics 08 p1143 N90-16625
Computer simulation of dust grain evolution 08 p1144 N90-16632
Interstellar and cometary dust 08 p1145 N90-16636
Metamorphism of cosmic dust: Processing from circumstellar outflows to the cometary regolith 08 p1146 N90-16641
Detecting extended solar system structures with COBE (Cosmic Background Explorer) [AD-A216380] 10 p1447 N90-18349
Chemistry on interstellar grains and implications for infrared spectroscopy 11 p1579 N90-19097
Infrared spectroscopy of novae and related objects 11 p1583 N90-19123
Zodiacal dust bands: Their relation to asteroid families [AD-A216025] 11 p1590 N90-19170
Cosmic Dust Collection Facility: Scientific objectives and programmatic relations [NASA-TM-102160] 14 p1939 N90-21098
The optical night sky at low surface brightness: High latitude dust and faint field galaxies 15 p2185 N90-22481
The Sagittarius B2 molecular cloud: An extreme case of a galactic center giant molecular cloud 15 p2187 N90-22493
Electric dipole antennae used as micrometeoroid detectors [AERONOMICA-ACTA-A-351-1989] 17 p2392 N90-23623
Activities report of the Institute for Astronomy and Astrophysics [MITT-10] 18 p2636 N90-25020
Interstellar grain chemistry and organic molecules 21 p3090 N90-27569
The formation and structure of circumstellar and interstellar dust 21 p3091 N90-27576
Research opportunities on the Space Station 21 p3092 N90-27578
Impact fracture experiments simulating interstellar grain-grain collisions 21 p3093 N90-27584
The Tempel 2 dust trail [AD-A224395] 24 p3562 N90-30153

COSMIC GAMMA RAY BURSTS
U GAMMA RAY BURSTS

COSMIC GASES
NT INTERSTELLAR GAS
Implications of the IRAS data for galactic gamma-ray astronomy and EGRET [NASA-TM-103452] 22 p3261 N90-28466

COSMIC NOISE
Post-flare effects in the lower ionosphere of middle latitudes 22 p3209 N90-28205

COSMIC PLASMA
Ion bombardment of Io and Mercury 02 p0296 N90-11682
Correlative analyses for geomagnetic indices, cosmic-ray intensities and sunspot numbers recorded since 1937 [IFSI-89-4] 08 p1151 N90-16670

COSMIC RADIATION
U COSMIC RAYS

COSMIC RADIO WAVES
U EXTRATERRESTRIAL RADIO WAVES

COSMIC RAY SHOWERS
The determination of the muon content of EAS from Cygnus X-3 05 p0715 N90-14179
A low-threshold EAS (Extensive-Air-Shower) array for gamma-ray astronomy at Los Alamos [DE89-016780] 08 p1139 N90-16600
Status of the expansion of the CYGNUS array at Los Alamos [DE89-016781] 08 p1139 N90-16601
Relative muon content of UHE showers associated with Hercules X-1 [DE90-000609] 08 p1151 N90-16665
Research in theoretical physics [DE90-005558] 11 p1562 N90-19001
Search for anisotropies in the underground cosmic ray muon flux 12 p1745 N90-20034
Cosmic ray composition and muon decoherence at the knee of the all-particle cosmic ray spectrum 12 p1745 N90-20035
Very high energy gamma rays from the Crab nebula and pulsar 15 p2194 N90-22527

COSMIC RAYS
NT COSMIC RAY SHOWERS
NT GALACTIC COSMIC RAYS
NT GAMMA RAY BURSTS
NT SECONDARY COSMIC RAYS
NT SOLAR COSMIC RAYS
Cosmic strings and ultra-high energy cosmic rays [NASA-CR-185924] 03 p0435 N90-12492
Research in cosmic and gamma ray astrophysics [NASA-CR-185451] 04 p0569 N90-13316
The cosmic radiation effects and activation monitor [RAE-TM-SPACE-364] 04 p0569 N90-13318
Solar-geophysical data number 538, June 1989. Part 1: (Prompt reports). Data for May, April 1989, and late data [PB89-223838] 06 p0866 N90-15031
First results from the MACRO (Monopole, Astrophysics, Cosmic Ray Observatory) detector at the Gran Sasso Laboratory [DE90-003243] 07 p1011 N90-15858
Gravitational lens effect on the cosmic background radiation due to nonlinear inhomogeneities [DE90-701753] 07 p1013 N90-15868
The digital data acquisition chain and the cosmic ray trigger system for the SLD warm iron calorimeter [DE90-000943] 07 p1015 N90-15879
Stochastic simulation of charged particle transport on the massively parallel processor 08 p1114 N90-16448
Correlative analyses for geomagnetic indices, cosmic-ray intensities and sunspot numbers recorded since 1937 [IFSI-89-4] 08 p1151 N90-16670
A database of fragmentation cross section measurements applicable to cosmic ray propagation calculations [NASA-CR-186328] 08 p1153 N90-16681
The excess flux in the cosmic submillimeter background radiation and the primordial deuterium abundance [NASA-CR-186312] 08 p1154 N90-16683
Cosmic ray NM-64 neutron monitor data 16 [IFSI-88-21] 08 p1154 N90-16684
Activities report of the Institute of Interplanetary Stellar Physics [IFSI-89-8] 09 p1298 N90-17520
Report on scientific activity and funds management for 1988 [IFSI-89-9] 09 p1298 N90-17521
Elementary particle physics: Experimental [DE90-005973] 10 p1429 N90-18242
Activities report of the Institute of Interplanetary Stellar Physics [IFSI-88-22] 10 p1445 N90-18339
Scientific activity programs for 1988-1990 [IFSI-88-23] 10 p1445 N90-18340
Scientific activity program for 1989 [IFSI-89-10] 10 p1445 N90-18341
Development and use of data analysis procedures for the CRRES (Combined Release and Radiation Effects Satellite) payloads AFGL-701-2/Dosimeter and AFGL-701-4/Fluxmeter and application of the data analysis results to improve the static and dynamic models of the Earth's radiation belts [AD-A215953] 10 p1447 N90-18348
Studies of (mu)(prime)s underground with the Soudan 2 Tracker [DE90-005656] 10 p1449 N90-18360
The track-etch detector for the MACRO experiment at the Gran Sasso Laboratory [DE90-003235] 11 p1594 N90-19182
Current and future uses of accelerators in particle astrophysics [DE90-006667] 11 p1595 N90-19186
Measurement of cross sections: New needs and possibilities [DE90-007248] 12 p1711 N90-19829
The pregalactic cosmic gravitational wave background 12 p1730 N90-19945
The space microwave interferometer and the search for cosmic background gravitational wave radiation 12 p1731 N90-19952
Cosmic ray events in Soudan 2 [DE90-005657] 12 p1746 N90-20037
JACEE long duration balloon flights [DE90-006008] 12 p1746 N90-20039
Fragmentation of relativistic heavy nuclei with application to cosmic ray propagation 14 p2043 N90-21716
Gamma rays, cosmic rays, and local molecular clouds 15 p2193 N90-22524
Ultrahigh-energy particle flux from cosmic strings [NASA-CR-186592] 15 p2194 N90-22525
Very high energy gamma rays from the Crab nebula and pulsar 15 p2194 N90-22527
A model of the diffuse galactic gamma ray emission 16 p2334 N90-23297
Gamma rays from giant molecular clouds 16 p2334 N90-23298
More data on (possible) gamma ray (point) sources 16 p2335 N90-23309
What is learned from high energy bursts and flares 16 p2336 N90-23314
Local normal galaxies 16 p2336 N90-23315
Local atmospheric electricity and its possible application in high energy cosmic ray air shower detection 16 p2340 N90-23335
The ground-level cosmic-ray event of September 29, 1989 as recorded by the Rome detectors [NOTA-INTERNA-944] 16 p2340 N90-23336
Cosmic ray NM-64 neutron monitor data-17 [NOTA-INTERNA-945] 16 p2341 N90-23337
Low-frequency measurements of the CMB (Cosmic Microwave Background) spectrum [DE90-011589] 18 p2639 N90-25033
Is AGN spectral evolution needed for the CXB 19 p2786 N90-25856
Properties of sources that may contribute the other half of the cosmic X ray background 19 p2788 N90-25866
Eleventh European Cosmic Ray Symposium [DE90-611419] 19 p2798 N90-25926
Eleventh European Cosmic Ray Symposium [DE90-611424] 19 p2798 N90-25927
Solar activity influence on cosmic ray penetration in the middle atmosphere 22 p3207 N90-28192
Implications of the IRAS data for galactic gamma-ray astronomy and EGRET [NASA-TM-103452] 22 p3261 N90-28466
Measurements of the single event upset environment in the upper atmosphere [RAE-TM-SPACE-373] 23 p3351 N90-28934
Gamma ray evidence for cosmic ray sources 23 p3414 N90-29292
Fluctuations in cosmic background radiation [INPE-4579-PRE/1313] 23 p3415 N90-29294
Heavy Nucleus Collector (HNC) project for the NASA Long Duration Exposure Facility (LDEF) [NASA-CR-182094] 24 p3544 N90-30045
A search for low energy cosmic ray antiprotons 24 p3564 N90-30161
Re-analysis of data on the space radiation environment above southeast Asia [AD-A224155] 24 p3564 N90-30162
An advanced single event upset tester [AD-A223613] 24 p3564 N90-30163
Re-analysis of data on the space radiation environment above south-east Asia [RAE-TR-89048] 24 p3565 N90-30166

COSMIC X RAYS
The BATSE experiment on the Gamma Ray Observatory: Solar flare hard x ray and gamma-ray capabilities 03 p0431 N90-12469
Solar flare gamma-ray and hard x ray imaging with the GRID-on-a-balloon 03 p0432 N90-12474
Underground muons from the direction of Cygnus X-3 [DE90-005646] 12 p1746 N90-20038
EXOSAT observations of Seyfert type galaxies 13 p1901 N90-20910
Recent advances in the studies of the nova outburst [DE90-008936] 14 p2038 N90-21691

COSMOCHEMISTRY
Cosmogenic nuclides in cometary materials: Implications for rate of mass loss and exposure history 08 p1143 N90-16623
Metamorphism of cosmic dust: Processing from circumstellar outflows to the cometary regolith 08 p1146 N90-16641
Physical processing of cometary nuclei 08 p1148 N90-16653

COSMOGONY
U COSMOLOGY

COSMOLOGY
NT BIG BANG COSMOLOGY
Research program in theoretical high energy physics [DE89-013963] 01 p0121 N90-10695
Astrophysical and cosmological constraints to neutrino properties [NASA-CR-185031] 01 p0140 N90-10809
The origin of the universe from quantum chaos: An introduction to current ideas [AD-A210441] 01 p0141 N90-10813
The astronomy of Andean myth: The history of a cosmology 02 p0291 N90-11660
Gauge invariant cosmological perturbations with cold dark matter [DE89-790940] 02 p0295 N90-11679
Particle physics and cosmology using stellar evolution theory [DE89-017529] 03 p0421 N90-12418
Evolution of domain walls in the early universe [NASA-CR-186076] 04 p0565 N90-13297

Small scale structure on cosmic strings
[NASA-CR-186075] 04 p0565 N90-13298
Cosmic strings and baryon decay catalysis
[NASA-CR-186074] 04 p0566 N90-13299
Observational physics of mirror world
[NASA-CR-185923] 05 p0697 N90-14076
On thick domain walls in general relativity
[NASA-CR-185926] 05 p0704 N90-14124
Des Cloizeaux's law for strings and galaxies formation. Part 1: Abelian configurations
[ROM1F-89-681-PT-1] 05 p0714 N90-14172
Des Cloizeaux's law for strings and galaxies formation. Part 2: Non Abelian configurations
[ROM1F-89-682-PT-2] 05 p0714 N90-14173
The ultimate structure of matter: The US High Energy Physics Program from the 1950s through the 1980s
[DE90-001784] 06 p0840 N90-14887
Supersymmetric dark matter above the W mass
[NASA-CR-186168] 06 p0863 N90-15016
Is the number of photons conserved in an expanding universe
[DE89-618836] 06 p0864 N90-15018
Classical approach to higher-derivative gravity
[DE89-631649] 06 p0864 N90-15019
Small scale structure on cosmic strings
[DE90-003126] 07 p1013 N90-15867
Gravitational lens effect on the cosmic background radiation due to nonlinear inhomogeneities
[DE90-701753] 07 p1013 N90-15868
Study of primitive universe in the Bianchi 9 model
[DE89-635903] 08 p1134 N90-16572
Universe as a topological defect in a higher-dimensional Einstein-Yang-Mills theory
[DE90-719507] 08 p1135 N90-16578
Cosmogenic nuclides in cometary materials: Implications for rate of mass loss and exposure history
08 p1143 N90-16623
Measurements of long-lived cosmogenic nuclides in returned comet nucleus samples
08 p1146 N90-16640
Quantum fields in cosmological space-times: A soluble example
[DE89-618837] 08 p1150 N90-16662
Dissipative effects in Friedmann universes
[DE89-618838] 08 p1150 N90-16663
Determination of solar flare accelerated ion angular distributions from SMM gamma ray and neutron measurements and determination of the He-3/H ratio in the solar photosphere from SMM gamma ray measurements
[NASA-CR-186038] 08 p1153 N90-16676
False vacuum decay in Jordan-Brans-Dicke cosmologies
[NASA-CR-186257] 09 p1293 N90-17497
Cosmological observations in an inhomogeneous universe
[DE90-733096] 09 p1299 N90-17528
The Age of the Universe: Concordance
[DE90-004971] 09 p1299 N90-17529
Particle theory and cosmology
[DE90-005338] 10 p1446 N90-18346
Theoretical and experimental high energy physics
[DE90-006168] 11 p1565 N90-19006
The microwave background in steady-state cosmology
11 p1587 N90-19150
Particle physics and cosmology
[DE90-006547] 11 p1590 N90-19171
Quantum cosmological origin of large scale structures of the universe
[DE90-610647] 11 p1591 N90-19176
Elementary particles and cosmology
[DE90-610648] 11 p1591 N90-19177
Propagation of electromagnetic waves in multidimensional homogeneous cosmologies
[DE90-610474] 12 p1647 N90-19462
The ultimate structure of matter: The high energy physics program from the 1950s through the 1980s
[DE90-005682] 12 p1713 N90-19836
Dimensional transition of the universe
[DE90-741461] 12 p1724 N90-19910
Cosmic string in compactified gauge theory
[DE90-741463] 12 p1738 N90-19988
Activities report in nuclear physics
[ETN-90-95322] 13 p1883 N90-20803
The Inevitable Universe: Parker-Rhodes' peculiar mixture of ontology and physics
[DE90-006453] 13 p1902 N90-20915
Studies in quantum field theory
[DE90-008731] 14 p2035 N90-21677
The large scale structure of the universe in pancake models of galaxy formation 14 p2040 N90-21701
Horizon problem in cosmological models with non zero
[DE90-613367] 14 p2042 N90-21708
Numerical investigations of nonlinear behavior in the Einstein equations 15 p2175 N90-22427
Stability of compactification during inflation
[NASA-CR-186597] 15 p2189 N90-22502
Gravitational effects of global textures
[NASA-CR-186596] 15 p2189 N90-22503
Gravitational couplings of the inflation in extended inflation
[NASA-CR-186595] 15 p2190 N90-22504
Topological defects in extended inflation
[NASA-CR-186594] 15 p2190 N90-22505
Soft inflation
[NASA-CR-186593] 15 p2190 N90-22506
Ultrahigh-energy particle flux from cosmic strings
[NASA-CR-186592] 15 p2194 N90-22525
Spectral plane quasars, spectral turn-over, and frequency atlas
[INPE-5011-TDL/399] 16 p2329 N90-23277
Skewering the universe with QSO lines of sight: Lyman alpha clouds as probes of large scale structure
16 p2329 N90-23278
A general low-harmonic cosmic string and its self-intersection and fragmentation
16 p2331 N90-23284
Anisotropic inflation 16 p2331 N90-23286
Reconstructing primordial density fluctuations
16 p2333 N90-23293
Complementary information from mm-wave-, infrared-, and gamma ray astronomy 16 p2334 N90-23299
Gamma ray cosmology: The extra galactic gamma spectrum and methods to detect the underlying source
16 p2337 N90-23321
Dipole analysis on EGRET data of extragalactic gamma ray background radiation 16 p2337 N90-23322
Feasibility for EGRET detection of antimatter concentrations in the universe 16 p2338 N90-23323
Gravitational collapse, Friedman models and cosmological constant: Does the universe oscillate
[DE90-620792] 16 p2338 N90-23324
Cosmological baryon and lepton number in the presence of electroweak fermion-number violation
[NASA-CR-186609] 17 p2470 N90-24123
Institute of Astronomy 17 p2481 N90-24190
Evolution of light domain walls interacting with dark matter, part 1
[NASA-CR-181123] 17 p2485 N90-24211
Thermal relics: Do we know their abundances
[NASA-CR-183334] 17 p2485 N90-24213
Classical theory of radiating strings
[NASA-CR-186607] 17 p2485 N90-24214
Large scale structure and microwave background anisotropies in cosmological models and stellar photometry techniques with the wide field/planetary camera of the Hubble space telescope
18 p2637 N90-25023
Cosmic strings and baryon decay
[NASA-CR-182842] 19 p2754 N90-25651
Identifying decohering paths in closed quantum systems
[NASA-CR-182853] 19 p2761 N90-25690
Research and facilities handbook 1989
[ISSN-0267-6281] 19 p2784 N90-25840
Origin of density fluctuations in extended inflation
[NASA-CR-182852] 19 p2795 N90-25915
A research program in theoretical high energy physics
[DE90-013322] 20 p2926 N90-26648
Comment on high resolution simulations of cosmic strings. 1: Network evoloution
[NASA-CR-186606] 20 p2941 N90-26734
A research program in physics of the early universe
[DE90-013319] 20 p2942 N90-26742
Proceedings of workshop on Dark Matter and the Structure of the Universe
[DE90-791308] 21 p3098 N90-27602
Biased clustering in a universe with hot dark matter and cosmic string
[FERMILAB-PUB-90/23-A] 22 p3262 N90-28473
Quasar pairs and quasar's peculiar velocity
[FERMILAB-PUB-90/25-A] 22 p3262 N90-28474
Viscous causal cosmologies
[DE90-627487] 23 p3412 N90-29282
Relic gravitational waves and extended inflation
[NASA-CR-186469] 24 p3493 N90-29740
A new vector-tensor theory and higher-dimensional cosmology
[DE90-507990] 24 p3555 N90-30117

COSMONAUTS

Evolution of EVA capabilities for space station construction and maintenance: Soviet and American experience 18 p2502 N90-24295
Cardiovascular deconditioning of cosmonauts: Role, importance and applications of the lower body negative pressure
[ETN-90-97507] 23 p3355 N90-28964

COSMOS SATELLITES

Orbit determination and analysis for Cosmos 236 at 15th-order resonance
[RAE-TR-88058] 04 p0461 N90-12641
Re-entry hazards and cosmos 1900
[FOA-C-30535-9.4] 05 p0613 N90-13583
The US Experiments Flown on the Soviet Biosatellite Cosmos 1887
[NASA-TM-102254] 20 p2891 N90-26452

COST ANALYSIS

Statistical modeling of electrical components
[BDX-613-3939] 01 p0059 N90-10336
Cost metric algorithms for internetwork applications
[AD-A210324] 01 p0105 N90-10597
Planning an Integrated On-line Library System (IOLS)
[AD-A209406] 01 p0136 N90-10783
Lessons learned from the integration of flight systems
02 p0153 N90-10874
Guaranteed cost control of flexible space structures
02 p0287 N90-11643
Adoption of software engineering innovations in organizations
[AD-A211573] 03 p0387 N90-12206
Rotorcraft low altitude CNS benefit/cost analysis: Rotorcraft operations data
[DOT/FAA/DS-89/9] 03 p0419 N90-12406
What is the balance sheet for investment in automated manufacturing
[CETIM-105490] 04 p0532 N90-13071
The Explorer program for astronomy and astrophysics
05 p0712 N90-14159
Assessment of costs and benefits of flexible and alternative fuel use in the US transportation sector. Technical report three: Methanol production and transportation costs
[DE90-002625] 06 p0755 N90-14396
A review of gas-cooled reactor concepts for SDI (Strategic Defense Initiative)
[DE89-016962] 06 p0842 N90-14898
A nickel/hydrogen battery for PV systems
[DE90-001537] 07 p0926 N90-15358
Planning minimum-energy paths in an off-road environment with anisotropic traversal costs and motion constraints
[AD-A214181] 07 p0942 N90-15457
Analysis of the financial factors governing the profitability of lunar helium-3 07 p1008 N90-15838
A qualitative architecture for understanding policy responses to global change
[DE90-003936] 08 p1099 N90-16364
HOTOL: A future launcher for Europe
09 p1175 N90-16800
Cost optimisation of reusable aerospaceplane transportation systems 09 p1175 N90-16803
The extension of technology and the control of production costs in advanced satellite systems
[AD-A215104] 09 p1183 N90-16857
Improper use of economic analysis in materiel cost comparison studies
[AD-A214888] 09 p1297 N90-17518
Reducing C130E Hercules operating costs in the Royal Australian Air Force and the United States Air Force by increasing cruise speeds
[AD-A215747] 10 p1319 N90-17629
Cost effectiveness of composite materials on the F-15 and F-16 aircrafts
[AD-A216353] 10 p1320 N90-17631
Challenges for future space power systems
10 p1331 N90-17695
The 25 kWe spaceborne solar dynamic generator
10 p1331 N90-17696
CNES-CEA comparative evaluation study of various candidate 20 kWe space power systems
10 p1331 N90-17697
The GSR3: A new approach for solar array deployments 10 p1340 N90-17762
Finding minimum-cost flows by double scaling
[AD-A214498] 10 p1416 N90-18159
The Executive Workshop on Cost/Performance Measurement. Volume 1: Executive summary
[AD-A216745] 11 p1545 N90-18898
Survivability and effectiveness of near-term strategic defense
[DE90-005805] 11 p1555 N90-18955
Selection and design of a stretched-membrane heliostat for today's markets
[DE90-007997] 13 p1828 N90-20495
Criteria for polymer concrete on airport pavements
[DOT/FAA/DS-89/18] 14 p1929 N90-21045
Mars in this century: The Olympia Project
[DE90-008356] 14 p2042 N90-21709
RF network selection in a rule-based system. NOSC project ZE68: Cost metric algorithms for internetwork applications
[AD-A219389] 16 p2301 N90-23116
Use of optical storage devices as shared resources in local area networks
[AD-A219198] 16 p2327 N90-23269

Peacetime replacement and crash damage factors for army aircraft
[AD-A218544] 17 p2348 N90-23372
Preliminary design of a supersonic Short Takeoff and Vertical Landing (STOVL) fighter aircraft
[NASA-CR-186670] 17 p2352 N90-23394
Back to the stars 17 p2359 N90-23429
Implementation of location programmes 17 p2360 N90-23440
Joint tactical anti-jam communications: A systems approach
[AD-A219592] 17 p2388 N90-23602
Lunar shelter
[ILR-MITT-233(1989)] 17 p2439 N90-23896
An interactive life cycle cost forecasting tool
[AD-A220472] 17 p2480 N90-24184
System analysis and project of a laser-moved spaceship
[ILR-MITT-232(1989)] 18 p2513 N90-24348
Limits to today's composites: Chances for tomorrow's developments
[MBB-Z-0287-89-PUB] 18 p2519 N90-24385
Brilliant pebbles
[DE90-010756] 18 p2606 N90-24845
Operations and support cost modeling using Markov chains 18 p2648 N90-25070
Aircraft modifications cost analysis. Volume 1: Overview of the study
[AD-A220764] 19 p2649 N90-25074
Estimating the cost of major ongoing cost plus hardware development programs
[NASA-TM-100401] 19 p2764 N90-25705
Long-range planning cost model for support of future space missions by the deep space network 20 p2854 N90-26231
Strategic defense initiative: Three reasons to stay the course
[AD-A222246] 21 p3070 N90-27456
Design optimization of short focal length photovoltaic modules
[PB90-182221] 22 p3195 N90-28133
The production potential of wind power in Finland
[DE90-796157] 22 p3196 N90-28136
Purchase of computer equipment: Justification and cost appraisal
[RSRE-89023] 22 p3256 N90-28438
Guide to charging for the CCF
[RSRE-89022] 23 p3404 N90-29238
Airline productivity relating on the fuel cost. (2): Fuel consumption values and fuel efficiency
[NAL-TM-604-2] 24 p3422 N90-29333
Effects of parameter uncertainties on software development effort estimates
[AD-A223304] 24 p3526 N90-29938

COST EFFECTIVENESS

Environmental testing: An approach to more cost efficiency 02 p0176 N90-10988
Study of the application of automation to composites manufacture
[AD-A211049] 02 p0190 N90-11087
Designing for reliable and low maintenance cost aero engines
[PNR90570] 04 p0455 N90-12604
Guidance and Control Panel Symposium on Guidance and Control of Unmanned Air Vehicles
[AGARD-AR-260] 04 p0458 N90-12623
Aviation Engine Test Facilities (AETF) fire protection study
[AD-A211483] 04 p0483 N90-12777
Repair of composites by means of wet-lay-up
[LR-551] 05 p0620 N90-13617
Decision-aid design factors in connection with HF communication and emitter location disciplines 06 p0758 N90-14413
Fly-by-light flight control system technology development plan
[NASA-CR-181953] 07 p0883 N90-15111
A strategy for concurrent product and process design of aerospace components
[DE90-002926] 07 p0916 N90-15299
The European Transonic Windtunnel (ETW) 08 p1029 N90-15945
Guidance and control considerations for a maneuvering aerial target system 09 p1165 N90-16746
Are reusable boosters cost-effective 09 p1179 N90-16834
Cost effectiveness of composite materials on the F-15 and F-16 aircrafts
[AD-A216353] 10 p1320 N90-17631
A concept of a pilot production plant for directly glassed silicon 10 p1341 N90-17770
Assessment of solar cell quality criteria 10 p1342 N90-17776
US Army Methanol-Fueled Administrative Vehicle Demonstration Program
[AD-A216013] 10 p1393 N90-18054
Orbital fluid resupply assessment 11 p1475 N90-18487
A perspective of software reuse
[AD-A216911] 11 p1546 N90-18901
A cost-effective strategy for nonoscillatory convection without clipping
[NASA-TM-102538] 14 p1971 N90-21291
Optimization of power output from wind turbines 15 p2124 N90-22146
Evaluation of optical storage technology for decision support databases 15 p2176 N90-22436
The RACE (research and development in advanced technologies for Europe) program: A 1989 update
[AD-A218509] 16 p2228 N90-22713
Economic values for evaluation of Federal Aviation Administration investment and regulatory programs
[AD-A219882] 17 p2343 N90-23343
Development of cost-effective standards for Earth observation spacecraft 18 p2501 N90-24292
Quantitative assessment of human motion using video motion analysis 19 p2730 N90-25518
A parallel Newton-Euler formulation for fast dynamic simulation of robot manipulators
[RR-368] 19 p2748 N90-25614
The aerobraking space transfer vehicle
[NASA-CR-186819] 20 p2821 N90-26053
Individual Helicopter Tracking Program (IHTP) for the MH-53J helicopter 21 p2958 N90-26818
Photoelasticity: A cost effective design tool 21 p2958 N90-26819
Finite element models of USAF aircraft structures 21 p2958 N90-26820
Cost effective technology
[PNR90654] 21 p2991 N90-27002
Space projects: Improvements needed in selecting future projects for private financing
[GAO/NSIAD-90-147] 22 p3256 N90-28439
Life cycle cost in the conceptual design of subsonic commercial aircraft, volumes 1 and 2 23 p3275 N90-28535
Energy efficient engine program technology benefit/cost study. Volume 1: Executive summary
[NASA-CR-174766-VOL-1] 23 p3280 N90-28564
Energy Efficient Engine: High-pressure compressor test hardware detailed design report
[NASA-CR-180850] 23 p3281 N90-28570
Ring laser gyro principles and techniques 24 p3426 N90-29352
Ring laser gyro marine inertial navigation systems 24 p3426 N90-29355

COST ESTIMATES

Projections for a steady-state tokamak reactor based on ITER
[DE89-016678] 02 p0278 N90-11589
Estimating the relationships between the state of the art of technology and production cost for the US aircraft
[AD-A212127] 04 p0437 N90-12495
Definition of avionics concepts for a heavy lift cargo vehicle. Volume 1: Executive summary
[NASA-CR-183818] 06 p0725 N90-14229
Definition of avionics concepts for a heavy lift cargo vehicle, volume 2
[NASA-CR-183819] 06 p0725 N90-14230
Developing integrated parametric planning models for budgeting and managing complex projects
[NASA-CR-186006] 06 p0857 N90-14986
A guide for estimating potential energy savings from increased solar reflectance of a low-sloped roof
[DE90-003720] 07 p0955 N90-15526
Improper use of economic analysis in materiel cost comparison studies
[AD-A214888] 09 p1297 N90-17518
Preparing software conversion studies 10 p1416 N90-18158
Cost and energy consumption estimates for the aluminum-air battery anode fuel cycle
[DE90-005810] 11 p1503 N90-18656
An interactive life cycle cost forecasting tool
[AD-A220472] 17 p2480 N90-24184
Space funding: NASA and DOD activities for fiscal years 1981 through 1989. Fact sheet for the Chairman and the Ranking Minority Member, Subcommittee on Science, Technology, and Space, Committee on Commerce, Science, and Transportation, US Senate
[GAO/NSIAD-89-102FS] 17 p2481 N90-24187
Weight and cost forecasting for advanced manned space vehicles 18 p2632 N90-24998
Military space operations: Shuttle and satellite computer systems do not meet performance objectives
[GAO/IMTEC-88-7] 18 p2635 N90-25014
Space shuttle: Changes to the solid rocket motor contract
[GAO/NSIAD-88-203] 18 p2636 N90-25016
Aircraft modifications cost analysis. Volume 1: Overview of the study
[AD-A220764] 19 p2649 N90-25074
The Penguin: A low Reynolds number powered glider for station keeping missions
[NASA-CR-186667] 19 p2658 N90-25129
Estimating the cost of major ongoing cost plus hardware development programs
[NASA-TM-100401] 19 p2764 N90-25705
Mars in this decade: The great exploration
[DE90-011232] 19 p2797 N90-25920
Space exploration: Cost, schedule, and performance of NASA's Mars Observer Mission. Fact sheet for the Chairman, Subcommittee on Science, Technology, and Space, Committee on Commerce, Science, and Transportation, US Senate
[GAO/NSIAD-88-137FS] 20 p2815 N90-26021
Space exploration: Cost, schedule, and performance of NASA's Magellan Mission to Venus. Fact sheet for the Chairman, Subcommittee on Science, Technology, and Space, Committee on Commerce, Science, and Transportation, US Senate
[GAO/NSIAD-88-130FS] 20 p2815 N90-26022
Space exploration: Cost, schedule, and performance of NASA's Galileo Mission to Jupiter. Fact sheet for the Chairman, Subcommittee on Science, Technology, and Space, Committee on Commerce, Science, and Transportation, US Senate
[GAO/NSIAD-88-138FS] 20 p2816 N90-26025
Space transportation: NASA has no firm need for increasingly costly orbital maneuvering vehicle
[GAO/NSIAD-90-192] 20 p2819 N90-26041
Long-range planning cost model for support of future space missions by the deep space network 20 p2854 N90-26231
ECOS: The ESA Costing Software
[ESA-BR-56] 21 p3039 N90-27274
Knowledge representation for commonality 21 p3041 N90-27285
Departments of Veterans Affairs and Housing and Urban Development, and independent agencies appropriations for 1991. Part 4: National Aeronautics and Space Administration
[GPO-30-861] 21 p3088 N90-27561
A concept for integrating computer-aided drafting and design with cost engineering and specification preparation
[AD-A223150] 22 p3237 N90-28354
Extensions to the learning curve: An analysis of factors influence unit cost of weapon systems
[AD-A224119] 23 p3407 N90-29256
Effects of parameter uncertainties on software development effort estimates
[AD-A223304] 24 p3526 N90-29938

COST REDUCTION

US Navy principal site testing concept and the F-18 02 p0151 N90-10861
Environmental testing: An approach to more cost efficiency 02 p0176 N90-10988
Qualification by simulation: Dream or reality 02 p0177 N90-10990
Evaluation of copper slag blast media for railcar maintenance
[NASA-CR-183744] 05 p0630 N90-13681
Aluminum-lithium: Application of plate and sheet to fighter aircraft 07 p0900 N90-15202
IEA/Annex 2 powder characterization cooperative program
[AD-A213540] 07 p0911 N90-15271
Cost optimisation of reusable aerospaceplane transportation systems 09 p1175 N90-16803
Reducing C130E Hercules operating costs in the Royal Australian Air Force and the United States Air Force by increasing cruise speeds
[AD-A215747] 10 p1319 N90-17629
Lightweight, low cost, thin silicon cell arrays 10 p1345 N90-17800
Phase 1 supplemental development of a kinematic Stirling/Rankine commercial gas-fired heat pump system
[PB90-129974] 13 p1825 N90-20483
The Italian approach to small satellites for low cost access to space developments
[ETN-90-96552] 16 p2206 N90-22587
Rocket combustion chamber life-enhancing design concepts
[NASA-CR-185257] 19 p2669 N90-25183
Minimization of the cost of information transfer in HF spread spectrum transmission 20 p2848 N90-26198
Affordable spacecraft: Design and launch alternatives. Background paper 22 p3125 N90-27737
Energy efficient engine program technology benefit/cost study, volume 2
[NASA-CR-174766-VOL-2] 23 p3280 N90-28565
How can research and development leadtime be reduced
[AD-A224063] 23 p3404 N90-29240
The cost of air service fragmentation
[TT-9010] 24 p3422 N90-29334

COSTS
NT AIRCRAFT PRODUCTION COSTS
NT FREIGHT COSTS
NT LIFE CYCLE COSTS
NT LOW COST
NT OPERATING COSTS
Energy storage and distribution program summary. Volume 2: Research summaries, fiscal year 1988
[DE89-000867] 01 p0083 N90-10470
Structure based formal methods for software engineering
[AD-A211660] 03 p0388 N90-12207
Convergence properties of indefinite linear quadratic problems with receding horizon
[MEMO-COSOR-88-25] 05 p0690 N90-14026
Elastomeric impulse energy storage and transfer system
[AD-D014223] 06 p0730 N90-14255
Using goal programming to determine the optimal engine mix for UH-1 helicopters
[AD-A214893] 09 p1168 N90-16762
Technology maturity assessment methodology SDIO systems SETA
[AD-A214571] 09 p1294 N90-17501
Improper use of economic analysis in materiel cost comparison studies
[AD-A214888] 09 p1297 N90-17518
A perspective of software reuse
[AD-A216911] 11 p1546 N90-18901
An all electronic transportation system from LEO to GEO and beyond 15 p2060 N90-21796
Space Shuttle, NASA's major changes to flight hardware: Fact sheet for the Chairman, Committee on Science, Space, and Technology, House of Representatives
[GAO/NSIAD-88-173FS] 15 p2181 N90-22461
Economic values for evaluation of Federal Aviation Administration investment and regulatory programs
[AD-A219882] 17 p2343 N90-23343
The cost of conservative synchronization in parallel discrete event simulations
[NASA-CR-182034] 17 p2441 N90-23912
Weight and cost forecasting for advanced manned space vehicles 18 p2632 N90-24998
Space exploration: NASA's deep space missions are experiencing long delays
[GAO/NSIAD-88-128BR] 18 p2635 N90-25015
Space exploration: Cost, schedule, and performance of NASA's Magellan Mission to Venus. Fact sheet for the Chairman, Subcommittee on Science, Technology, and Space, Committee on Commerce, Science, and Transportation, US Senate
[GAO/NSIAD-88-130FS] 20 p2815 N90-26022
Space exploration: Cost, schedule, and performance of NASA's Ulysses Mission to the Sun. Fact sheet for the Chairman, Subcommittee on Science, Technology, and Space, Committee on Commerce, Science, and Transportation, US Senate
[GAO/NSIAD-88-129FS] 20 p2815 N90-26023
Preliminary designs for 25 kWe advanced Stirling conversion systems for dish electric applications
[NASA-TM-103188] 20 p2940 N90-26729
Individual Helicopter Tracking Program (IHTP) for the MH-53J helicopter 21 p2958 N90-26818
High productivity testing 21 p2962 N90-26843
Extensions to the learning curve: An analysis of factors influence unit cost of weapon systems
[AD-A224119] 23 p3407 N90-29256

COTTON
Variability of cultivar responses to ozone
[PB89-225460] 07 p0956 N90-15528

COTTON FIBERS
New Fabric Development Program
[AD-A211549] 03 p0332 N90-11891

COUETTE FLOW
Analytical and numerical studies in flow development
[DE89-017380] 02 p0221 N90-11269
The thermal stability between rotating cylinders in a radially symmetrical gravitational field
[DE89-618548] 02 p0287 N90-11638
Numerical analysis, scientific computing and fundamental studies of fluid mechanics
[DE89-017554] 03 p0346 N90-11975
The stability of Taylor-Couette flow with radial heating 06 p0774 N90-14502
Comments on ER (Electrorheological) fluid rheology
[DE90-002892] 07 p0894 N90-15168
The evolution of linearized perturbations of parallel flows
[DE90-005978] 09 p1221 N90-17082
Numerical simulation of unstably stratified sheared flows
[DE90-005396] 10 p1384 N90-18008
Experimental feasibility of investigating acoustic waves in Couette flow with entropy and pressure gradients
[NASA-TM-102621] 13 p1882 N90-20795
Effect of a crystal-melt interface on Taylor-vortex flow
[NASA-CR-185512] 15 p2171 N90-22408
A numerical and analytical study of normal stresses and pressure differences in non-Newtonian creeping flows 16 p2234 N90-22749
Analysis of near-surface flow physics in a two-stage, 10 km/s, electromagnetic launcher
[DE90-013292] 21 p2964 N90-26852
Stabilization of Taylor-Couette flow due to time-periodic outer cylinder oscillation
[PB90-219130] 23 p3323 N90-28790
Direct numerical simulation of turbulent couette flow
[AD-A224287] 24 p3467 N90-29589

COULOMB COLLISIONS
True asymptotic plasma-sheath matching with an asymptotically correct collisional presheath
[AD-A212857] 05 p0701 N90-14104
Controller design for a robotic manipulator 06 p0792 N90-14615
Current drive in a supernova 15 p2187 N90-22491
The sensitivity of EGRET to gamma ray polarization 16 p2335 N90-23305
Coulomb-dissociation of 156 MeV 6Li-projectiles
[KFK-4691] 21 p3075 N90-27482

COULOMB POTENTIAL
Auxiliary-field transformations for repulsive potentials: A physical approach
[DE89-016677] 02 p0214 N90-11223
On the role of Coulomb forces in atomic radiative emission
[IRF-PREPRINT-106] 03 p0403 N90-12308
Lower limit for the average angular momentum leading to fusion
[DE90-004027] 08 p1126 N90-16523
Kosterlitz-Thouless phase transition in two-dimensional hierarchical Coulomb gases
[DE89-618399] 09 p1189 N90-16890
Exchange and correlation effects in the Visscher-Falicov model for metal intercalated graphite
[DE90-610553] 12 p1627 N90-19349
Elastic and viscoelastic analysis of two multiply layered cylinders rolling over each other with Coulomb friction
[REPT-89-50] 15 p2107 N90-22051
New calculations and measurements of the Coulomb cross-section for the production of direct electron pairs by high energy nuclei
[NASA-TM-101280] 15 p2165 N90-22371
Localization effects in radiationally disordered high-temperature superconductors: Theoretical interpretation 22 p3148 N90-27853

COULOMETERS
Quartz crystal microbalance studies: Solvent effects in conducting polymer films
[AD-A219426] 17 p2372 N90-23502

COUNTER ROTATION
Full scale technology demonstration of a modern counterrotating unducted fan engine concept: Component test
[NASA-CR-180868] 01 p0010 N90-10047
Full scale technology demonstration of a modern counterrotating unducted fan engine concept. Design report
[NASA-CR-180867] 01 p0010 N90-10048
Full scale technology demonstration of a modern counterrotating unducted fan engine concept. Engine test
[NASA-CR-180869] 01 p0011 N90-10049
Two counter-rotating vortices approaching a free surface in a viscous fluid
[AD-A210495] 01 p0070 N90-10404
Acoustic test and analysis of a counterrotating prop-fan model
[NASA-CR-179590] 01 p0119 N90-10683
An investigation of counterrotating tip vortex interaction
[NASA-CR-185135] 02 p0271 N90-11549
Effect of reduced aft diameter and increased blade number on high-speed counterrotation propeller performance
[NASA-TM-102077] 05 p0575 N90-13352
Noise of a simulated installed model counterrotation propeller at angle-of-attack and takeoff/approach conditions
[NASA-TM-102440] 13 p1881 N90-20794
Studies on reactive flows 15 p2066 N90-21831
Unsteady Euler solutions on dynamic blocked grids for complex configurations 15 p2094 N90-21982
Counterrotating cores in elliptical galaxies 16 p2332 N90-23288
Advanced gearbox technology
[NASA-CR-179625] 18 p2498 N90-24274
Euler analysis comparison with LDV data for an advanced counter-rotation propfan at cruise
[NASA-TM-103249] 20 p2803 N90-25946
High speed turboprop aeroacoustic study (counterrotation). Volume 1: Model development
[NASA-CR-185241] 20 p2923 N90-26833
Response of a liquid column to counter-directional excitation under zero-gravity
[LRT-WE-9-FB-6(1989)] 21 p2991 N90-26998
Response of a liquid column to unequal counter-directional excitation under zero-gravity
[LRT-WE-9-FB-7(1989)] 21 p2991 N90-26999

COUNTER-ROTATING WHEELS
Theory of gearing
[NASA-RP-1212] 12 p1670 N90-19593
The large wheel actuator LDR 100-0: Development status and test results 18 p2539 N90-24487

COUNTERBALANCES
A procedure for force-balancing planar linkages using counterweights
[ESDU-89028] 07 p0940 N90-15448
Design and development of a spacecraft stability boom 18 p2540 N90-24494

COUNTERFLOW
Analysis of opposed jet hydrogen-air counter flow diffusion flame
[NASA-CR-182366] 03 p0321 N90-11825
Superflow induced phase transition in the axial vortex-free texture of rotating superfluid He-3-B
[PB90-110388] 08 p1127 N90-16531
The extinction and structure of counterflow premixed flames
[AD-A218106] 13 p1773 N90-20178
Experiments on the breakdown of heat transfer in liquid helium 2
[MPIS-13/1989] 16 p2326 N90-23259
A parametric study of counterflow heat exchanger transients
[IAR-89-10] 19 p2689 N90-25293
Counter-current flow limitation in thin rectangular channels
[DE90-015124] 24 p3469 N90-29599

COUNTERMEASURES
NT BALLISTIC MISSILE DECOYS
NT ELECTRONIC COUNTERMEASURES
NT JAMMING
NT OPTICAL COUNTERMEASURES
Countermeasures to microgravity 05 p0680 N90-13957
Use of lower body negative pressure as a countermeasure to negative Gz acceleration
[AD-A213927] 07 p0967 N90-15583
Atmospheric Propagation in the UV, Visible, IR, and mm-Wave Region and Related Systems Aspects
[AGARD-CP-454] 15 p2079 N90-21907
Computation of broad spectral band electro-optical system transmittance response characteristics to military smokes and obscurants using field test data from transmissometer system measurements 15 p2086 N90-21939
Effect of fluid countermeasures of varying osmolarity on cardiovascular responses to orthostatic stress 18 p2628 N90-24978
Counterair situation awareness display for Army aviation 23 p3359 N90-28982

COUNTERS
NT CERENKOV COUNTERS
NT NEUTRON COUNTERS
NT NEUTRON SPECTROMETERS
NT PARTICLE TELESCOPES
NT PROPORTIONAL COUNTERS
NT QUANTUM COUNTERS
NT RADIATION COUNTERS
NT SCINTILLATION COUNTERS
Instability of the behavior of high resistivity silicon detectors due to the presence of oxide charges
[REPT-89-038] 04 p0559 N90-13260
A counter gating circuit for acoustic emission monitoring of structures cracking under repetitive alternating loads
[ARL-MAT-TM-398] 05 p0653 N90-13808
Apparatus for using a time interval counter to measure frequency stability
[NASA-CASE-NPO-17325-1-CU] 09 p1208 N90-17005
VLSI binary updown counter
[NASA-CASE-NPO-17205-1-CU] 14 p2011 N90-21525
Local atmospheric electricity and its possible application in high energy cosmic ray air shower detection 16 p2340 N90-23335
Front range lidar, aircraft, and balloon experiment
[PB90-225301] 22 p3212 N90-28218

COUNTING
Estimating methods for counting process intensities: Non-parametric methods
[IMAG-RR-774-M] 06 p0834 N90-14846
The solid state photomultiplier: Status of photon counting beyond the near-infrared 14 p1976 N90-21319

Transformational part-count in layered octahedral-tetrahedral truss configurations
[NASA-TM-102635] 23 p3287 N90-28598
COUNTING CIRCUITS
NT SCALERS
Technology development and circuit design for a parallel laser programmable floating point application specific processor
[AD-A215870] 11 p1500 N90-18637
COUPLED MODES
A well conditioned formulation for the analysis of multi-layered frequency selective surfaces using a cascaded matrix approach, revised
[RSRE-MEMO-4289-REV] 04 p0496 N90-12858
An air coupled transmission mode acoustic microscope for on-line non-destructive evaluation
[AD-A211416] 04 p0511 N90-12947
Report from upper atmospheric science
10 p1444 N90-18332
Positioning control of highest accuracy for very dynamic coupled system
[ETN-90-95893] 12 p1701 N90-19769
Coupled magnetoplasmon-phonon modes at the surface of a semi-infinite semiconductor superlattice
[DE90-612904] 14 p2031 N90-21647
Nonlinear multi-mode coupling of the solar gravity modes in a rotationally split multiplet 21 p3100 N90-27608
Approximation, synthesis, and development of bi-mode cavities microwave filters presenting unsymmetrical quasi-elliptic responses
[CNES-NT-124] 23 p3318 N90-28761
COUPLERS
NT COUPLING CIRCUITS
NT DIPLEXERS
Quick disconnect duct coupler
[AD-D014265] 08 p1084 N90-16274
Discontinuous-taper directional coupler
[AD-D014324] 12 p1650 N90-19481
Optically tunable gratings for optical interconnects
[AD-A216978] 12 p1714 N90-19844
Direct writing of microstructures for solid-state electronics
[AD-A220996] 18 p2535 N90-24460
Quick-connect coupler for remote manipulation
[DE90-015352] 24 p3476 N90-29648
COUPLING
NT ACOUSTIC COUPLING
NT ELECTROMAGNETIC COUPLING
NT GYROSCOPIC COUPLING
NT MAGNETOSPHERE-IONOSPHERE COUPLING
NT MICROWAVE COUPLING
NT OPTICAL COUPLING
NT SPIN-SPIN COUPLING
NT THERMODYNAMIC COUPLING
Effect of particle velocity fluctuations on the inertia coupling in two-phase flow 01 p0068 N90-10391
Design and operating characteristics of a CW relevant quasi-optical gyrotron with variable mirror separation
[AD-A210611] 01 p0074 N90-10425
Stormtime coupling of the neutral and ionized upper atmosphere at middle latitudes
02 p0243 N90-11381
Ionosphere-thermosphere coupling at high latitudes: Aspect angle dependence of non-thermal plasmas
02 p0244 N90-11382
Chromospheric-coronal coupling during solar flares: Current systems and particle acceleration
03 p0433 N90-12480
Canonical formalism for coupled beam optics
[DE90-003764] 07 p0992 N90-15734
Highly reduced carbene complexes: Formation of an alkoxymalonate by coupling of carbon dioxide with the nucleophilic carbene in Cr(CO4)=C(OMe)Ph2(-)
[AD-A215132] 09 p1191 N90-16902
Innovations in the design and matching of magnetic components and semiconductors up performance and reliability of power converters 10 p1336 N90-17731
Optically tunable gratings for optical interconnects
[AD-A216978] 12 p1714 N90-19844
Relatchable launch restraint mechanism for deployable booms 15 p2114 N90-22091
Parasitic coupling of the fringing fields of an Ion-Bernstein wave antenna
[DE90-009918] 17 p2387 N90-23596
Temperature and coupling behavior of resonators and transducers of lithium tetraborate driven by lateral and thickness fields
[AD-A219548] 17 p2395 N90-23644
Statistical techniques for designing a decoupled controller to be robust to model and sensor noise
[AD-A220476] 17 p2412 N90-23745
Resonant coupling through a slot to a loaded cylindrical cavity: Experimental results
[AD-A223000] 20 p2922 N90-26631
The effect of nonlinearities on flexible structures
[AD-A222705] 21 p3012 N90-27124
Engineering test results for the Moog Single Line Disconnect
[NASA-TM-100755] 22 p3132 N90-27776
Microprocessor chip incorporating optical signal coupling receiver
[AD-D014547] 22 p3167 N90-27964
A double-sided silicon strip detector with capacitive read out and a new method of integrated bias coupling
22 p3178 N90-28037
The effects of structural flap-lag and pitch-lag coupling on soft inplane hingeless rotor stability in hover
[NASA-TP-3002] 23 p3269 N90-28503
Flow coupling between a rotor and a stator in turbomachinery
[AD-A223882] 23 p3282 N90-28572
COUPLING CIRCUITS
Magnetic coupled current sensing techniques for spacecraft power systems 10 p1335 N90-17725
Coupled strip line circuit
[AD-D014487] 22 p3166 N90-27956
Microwave active filters based on coupled negative resistance method
[AD-A223269] 24 p3464 N90-29570
COUPLING COEFFICIENTS
Solvent dynamical effects in electron transfer: Predicted influences of electron coupling upon the rate-dielectric friction dependence
[AD-A210193] 01 p0120 N90-10690
Transfer functions for nonlinear systems via Fourier-Borel transforms
[NASA-TM-100034] 02 p0145 N90-10828
Auxiliary-field transformations for repulsive potentials: A physical approach
[DE89-016677] 02 p0214 N90-11223
Dissociation and vibrational relaxation of XeF by various collision partners
[AD-A210769] 02 p0227 N90-11300
Resonances in low-energy positron-alkali scattering
11 p1560 N90-18992
Discontinuous-taper directional coupler
[AD-D014324] 12 p1650 N90-19481
Hybrid analysis: Coupling of the finite element method with analytical approaches
[MBB-UO-0048/89-PUB] 19 p2650 N90-25079
Temporal response of coupled one-dimensional dynamic systems
[AD-A222375] 21 p3073 N90-27470
COUPLINGS
Interchangeable end effector tools utilized on the protoflight manipulator arm
[NASA-CR-179374] 01 p0078 N90-10447
Dynamic characteristics concerned in the design of a free-piston Stirling engine/magnetic coupling/compressor system
[DE89-015981] 02 p0230 N90-11317
Docking system for spacecraft
[NASA-CASE-MSC-21327-1] 03 p0317 N90-11798
Docking mechanism for spacecraft
[NASA-CASE-MSC-21386-1] 13 p1764 N90-20126
Modeling and control of flexible space platforms with articulated payloads 14 p1935 N90-21073
The connector space reduction mechanism
15 p2114 N90-22092
Quick connect coupling
[NASA-CASE-MSC-21539-1] 21 p3010 N90-27111
Quick-connect coupler for remote manipulation
[DE90-015352] 24 p3476 N90-29648
COURSES
U PATHS
COVALENCE
Electronic theory of solids, surfaces, interfaces, and clusters 16 p2320 N90-23230
COVALENT BONDS
Statistical mechanical models for liquid and amorphous structure in covalently bonded systems
[DE90-607233] 10 p1428 N90-18240
Interfacial chemistry of MoS2 films on Si
[AD-A216527] 11 p1482 N90-18532
Extracting chemical information form Auger line shapes
[AD-A216729] 11 p1483 N90-18537
Theory of electronic states and formations energies of defect complexes, interstitial defects, and crystal growth in semiconductors
[AD-A224069] 24 p3551 N90-30093
COVARIANCE
Optimal q-Markov COVER for finite precision implementation 01 p0023 N90-10117
General covariance and strings
[DE89-016505] 02 p0286 N90-11633
A simulation study of the overdetermined geodetic boundary value problem using collocation
[AD-A211785] 04 p0518 N90-12990
True covariance simulation of the EUVE update filter
05 p0589 N90-13427
Bilinear modeling and nonlinear estimation
05 p0589 N90-13430
Error modeling of bias-type parameters for TOPEX orbit determination 07 p0884 N90-15117
An improved toeplitz approximation method
[AD-A213994] 07 p0984 N90-15688
A covariant multiple scattering series for elastic projectile-target scattering
[NASA-TM-101942] 09 p1279 N90-17417
Adaptive state estimation and sampling rate analysis for invariant linear dynamic systems in time
[INPE-4960-TDL/389] 11 p1554 N90-18951
Kreim factorization of covariance operators of 2-parameter random fields and application to the likelihood ratio
[MEMO-802] 11 p1555 N90-18953
Comparison of artificial matrices and covariance functions
[ETN-90-95722] 12 p1679 N90-19645
Derivation of kinematic fields using wind profiler data from the 1985 pre-storm experiment
[AD-A217952] 13 p1845 N90-20592
Spectral analytic methods for the estimation of number of signals and directions of arrival
[AD-A217219] 13 p1876 N90-20757
Extensions of output variance constrained controllers to hard constraints 16 p2292 N90-23056
Percussive sound analysis using an autoregressive model. Application of modified covariance
[TELECOM-PARIS-89-D-016] 18 p2612 N90-24879
Model-based Gaussian and non-Gaussian clustering
[AD-A222097] 21 p3066 N90-27430
Turbulent statistics in the vicinity of an SST front: A north wind case, FASINEX February 16, 1986
22 p3221 N90-28266
An error estimate for Tremolieres method for the discretization of parabolic variational inequalities
[DE90-627169] 24 p3541 N90-30024
COVERINGS
Hatch cover
[NASA-CASE-MSC-21356-1] 12 p1613 N90-19278
COVES
U BAYS (TOPOGRAPHIC FEATURES)
COWELL METHOD
U NUMERICAL INTEGRATION
COWLINGS
Finite element analysis of structural components using viscoplastic models with application to a cowl lip problem
[NASA-CR-185189] 17 p2416 N90-23769
CRAB NEBULA
On the interaction of a pulsar with the ambient medium utilizing x ray images of the Crab nebula
[MPE-215] 08 p1140 N90-16604
Infrared spectroscopy and imaging of supernova remnants 11 p1580 N90-19104
IRAS LRS spectra of extended objects: The Crab nebula 11 p1581 N90-19107
High energy x ray observations on the Crab nebula and the double star source GX 1+4
[ETN-90-95829] 12 p1729 N90-19937
Very high energy gamma rays from the Crab nebula and pulsar 15 p2194 N90-22527
Gamma radiation from radio pulsars
16 p2334 N90-23302
Gamma radiation from the Crab and Vela pulsars
16 p2334 N90-23303
TeV radiation from the Crab nebula and other matters
16 p2335 N90-23306
Spectral determinations for discrete sources with EGRET 16 p2336 N90-23312
CRACK ARREST
Experimental and numerical investigations of the crack arrest behavior of steels and cast iron materials
[MPA-TWB-88-03] 05 p0623 N90-13635
Experiences with three-point bending test specimens for determining the crack-arrest fracture toughness K(sub Ia) in low-alloy steel
[DE90-004120] 08 p1089 N90-16306
Analysis of some fracture mechanics test procedures for defence research applications
[MRL-TR-89-11] 09 p1236 N90-17175
Crack stoppers and ARALL laminates
[PB90-166588] 14 p1947 N90-21142
Fatigue crack growth in a unidirectional SCS-6/Ti-15-3 composite
[NASA-TM-103095] 16 p2217 N90-22646
CRACK CLOSURE
Fatigue growth and closure of short cracks
[AD-A210824] 01 p0081 N90-10462
A re-evaluation of fatigue threshold test procedures and the simulation and prediction of fatigue crack growth under conditions of low crack closure
02 p0231 N90-11328
Threshold for fatigue crack propagation
[DLR-FB-89-33] 05 p0655 N90-13815

Through-the-thickness fatigue crack closure behavior in an aluminum alloy
[NASA-TM-102590] 13 p1816 N90-20427
Three-dimensional fatigue crack closure behavior of metals 15 p2070 N90-21857
The effects of slip character and crack closure on the growth of small fatigue cracks in titanium-aluminium alloys
[AD-A220714] 17 p2377 N90-23534
A numerical study of plasticity induced closure in short cracks by the finite element method
[AD-A220471] 18 p2571 N90-24654
A study on ultrasonic detection and characterization of partially closed fatigue cracks
[DE90-011748] 19 p2702 N90-25371
Small crack growth and its influence in near alpha-titanium alloys
[RAE-TM-P-1171] 20 p2835 N90-26121
Elevated temperature crack growth
[NASA-CR-182247] 20 p2875 N90-26355
Investigation of crack-closure prediction models for fatigue in aluminium alloy sheet under flight-simulation loading
[LR-619] 20 p2877 N90-26369
Comparison of crack closure result obtained by 3D elastic-plastic FEM and modified Dugdale model
[FFA-TN-1990-18] 24 p3481 N90-29675
Effects of blocks of overloads and underloads on fatigue crack growth in 2024-T351 sheet specimens: Fractographic analysis and crack closure predictions
[LR-629] 24 p3482 N90-29681

CRACK FORMATION
U CRACK INITIATION

CRACK GEOMETRY
Potential difference applied to the measurement of small fatigue crack growth at notches in Ti-6Al-4V
[FFA-TN-1989-09] 04 p0512 N90-12952
Unilateral contact analysis of a crack with friction. Applications
[ETN-89-95511] 04 p0512 N90-12956
Hydrogen, thermal ageing and the role of carbides in fatigue of a high strength steel
[AERE-R-13590] 13 p1774 N90-20183
A numerical study of plasticity induced closure in short cracks by the finite element method
[AD-A220471] 18 p2571 N90-24654
Modeling growth of fatigue cracks which originate at rivet holes 18 p2645 N90-25060
The stress intensity factor and stress concentration for a finite plate with a single crack emanating from a hole
[LR-607] 19 p2704 N90-25385
A finite width plate with a single crack at the edge of a central hole. The K-value of the crack and sigma peak at the other side of the hole
[LR-608] 19 p2704 N90-25386
A framework to correlate a/W ratio effects on elastic-plastic fracture toughness (J (sub c))
[AD-A222822] 21 p3012 N90-27125
Study of a method for measuring the dimensions of cracks on the surface of ceramics by Rayleigh waves
[ETCA-89-R-024] 22 p3160 N90-27922
Characterization by ultrasonic tests of ceramics submitted to thermal shocks: Influence of several parameters on the crack dimensioning
[ETCA-89-R-060] 22 p3160 N90-27923

CRACK INITIATION
Fatigue crack initiation mechanics of metal aircraft structures
[AD-A210567] 01 p0045 N90-10255
Porosity and crack initiation during low cycle fatigue
[AD-A210989] 01 p0081 N90-10464
Review of the ESA fracture control policy
02 p0182 N90-11029
Influence of the fiber/matrix interface on damage development in CFRP 02 p0183 N90-11037
Elastic indentation fractures
[ETCA-88-R-116] 04 p0512 N90-12955
Unilateral contact analysis of a crack with friction. Applications
[ETN-89-95511] 04 p0512 N90-12956
Thermal fatigue durability for advanced propulsion materials
[NASA-TM-102348] 06 p0797 N90-14641
On the domain of dominance of the asymptotic elastodynamic crack-tip fields 07 p0944 N90-15468
Micromechanics of an extrusion in high-cycle fatigue with creep
[AD-A213509] 07 p0947 N90-15485
Numerical simulation of creep crack growth experiments
[IWM-W-4/88] 08 p1089 N90-16303
Observations of fatigue crack initiation and damage growth in notched titanium matrix composites
[NASA-TM-101688] 10 p1347 N90-17815
Analysis of ductile fracture under biaxial loading using moire interferometry 10 p1394 N90-18060
Fatigue crack initiation and small crack growth in several airframe alloys
[NASA-TM-102598] 11 p1518 N90-18746
Combined effect of matrix cracking and stress-free edge on delamination
[NASA-TM-102591] 14 p1944 N90-21126
Micromechanics analysis of space simulated thermal deformations and stresses in continuous fiber reinforced composites
[NASA-TM-102633] 14 p1946 N90-21140
A comprehensive study on microstructure mechanics relationships of ceramic matrix composites
[AD-A219318] 16 p2213 N90-22627
The initiation of intergranular stress corrosion-cracking on sensitized stainless steel in dilute thiosulphate solutions
[AERE-R-13317] 16 p2217 N90-22648
Deformation and fracture of thin sheet aluminum-lithium alloys: The effect of cryogenic temperatures
16 p2218 N90-22655
Fracture toughness and fatigue crack initiation tests of welded precipitation-hardening stainless steel
[AD-A218745] 16 p2221 N90-22669
Ply cracking in composite laminates
17 p2368 N90-23478
Brittle torsional fatigue crack initiation in an otherwise ductile environment
[AD-A220858] 17 p2416 N90-23767
Damage states in laminated composite three-point bend specimens: An experimental-analytical correlation study
[NASA-TM-101800] 20 p2827 N90-26083
Microstructural design for fatigue crack growth resistance in Ni-base alloy
[PNR90632] 20 p2834 N90-26120
Small crack growth and its influence in near alpha-titanium alloys
[RAE-TM-P-1171] 20 p2835 N90-26121
Study of the behavior of Al metallic matrix + SiC composite materials under fatigue tests
[ETCA-89-R-077] 22 p3154 N90-27881
New aspects in aircraft inspection using eddy current methods 22 p3187 N90-28085
Fatigue crack monitoring from initiation to through cracking in welded thick steel sections
[ARE-TM(UHS)-90203] 22 p3194 N90-28122
An investigation of crack-tip stress field criteria for predicting cleavage-crack initiation
[DE90-015597] 24 p3480 N90-29672
Fractographic analysis of fatigue crack growth under two-blocks loading on 2024-T351 sheet specimens
[LR-628] 24 p3482 N90-29680
Effects of blocks of overloads and underloads on fatigue crack growth in 2024-T351 sheet specimens: Fractographic analysis and crack closure predictions
[LR-629] 24 p3482 N90-29681

CRACK OPENING DISPLACEMENT
An interferometric strain-displacement measurement system
[NASA-TM-101638] 01 p0080 N90-10454
Stress intensity factors and displacements for arc bend samples using collocation
[AD-A210404] 01 p0080 N90-10460
The effect of a rigid elliptical inclusion on a straight crack
[AD-A212263] 04 p0513 N90-12965
Crack problems for elastic-plastic materials under antiplane shear loadings 06 p0799 N90-14651
Fracture of sandwiched composites
14 p1946 N90-21136
Elevated temperature crack growth in aluminum alloys: Tensile deformation of 2618 and FVS0812 aluminum alloys 16 p2218 N90-22654
Ply cracking in composite laminates
17 p2368 N90-23478
Mechanics of necking, crazing, and crack growth in polymers 17 p2378 N90-23540

CRACK PROPAGATION
Raman characterization of high temperature materials using an imaging detector
[DE89-016308] 01 p0040 N90-10219
Mechanics of the crack path formation
[NASA-CR-185143] 01 p0080 N90-10455
Particle emission and charging effects induced by fracture
[AD-A210215] 01 p0080 N90-10459
Fatigue growth and closure of short cracks
[AD-A210824] 01 p0081 N90-10462
Review of the ESA fracture control policy
02 p0182 N90-11029
Fatigue crack growth rates as a function of delta K: Variability and material property
02 p0182 N90-11031
A re-evaluation of fatigue threshold test procedures and the simulation and prediction of fatigue crack growth under conditions of low crack closure
02 p0231 N90-11328
Effects of a heat cycle on material strength
[NAL-TM-562] 03 p0306 N90-11737
Stochastic propagation of an array of parallel cracks: Exploratory work on matrix fatigue damage in composite laminates
[DE89-017837] 03 p0319 N90-11813
Processing and characterization of alumina platelet-reinforced mullite composites
[DE90-000057] 03 p0320 N90-11814
The effects of temperature on fatigue crack propagation in 310 austenitic stainless steel
[DE90-000136] 03 p0328 N90-11865
Fractographic and microstructural analysis of fatigue crack growth in a Ti-6Al-4V fan disc forging
[NLR-MP-88028-U] 03 p0330 N90-11877
A numerical laboratory for granular solids
[DE89-016367] 03 p0358 N90-12045
An application of the J-integral to an incremental analysis of blunting crack behavior
[DE89-016844] 03 p0358 N90-12046
A study of progressive cracking damage to carbon-epoxy composites and methods of crack reduction
[REPT-RE-49-324/F] 04 p0467 N90-12676
Crack propagation failure of carbon/resin composites
[ONERA-RT-45/7086-M] 04 p0467 N90-12677
Mechanical behavior of carbon/resin composites under delamination and cracking of transverse layers
[ONERA-RT-46/7086-M] 04 p0467 N90-12678
Biaxial flexing of a fiber-reinforced aluminum composite
[AD-A212742] 04 p0468 N90-12681
Potential difference applied to the measurement of small fatigue crack growth at notches in Ti-6Al-4V
[FFA-TN-1989-09] 04 p0512 N90-12952
Elastic indentation fractures
[ETCA-88-R-116] 04 p0512 N90-12955
Unilateral contact analysis of a crack with friction. Applications
[ETN-89-95511] 04 p0512 N90-12956
An investigation on combined extension and bending of thin sheets with a central crack
[LR-561] 04 p0512 N90-12958
Fatigue behavior of silicon carbide Whisker/Aluminum composite
[AD-A213094] 05 p0618 N90-13803
The adhesive bonding of thermoplastic composites
[AD-A213358] 05 p0618 N90-13805
Some aspects of test frequency influence on the fatigue behavior of ARALL
[LR-549] 05 p0620 N90-13616
Threshold for fatigue crack propagation
[DLR-FB-89-33] 05 p0655 N90-13815
Application of fracture mechanics and half-cycle method to the prediction of fatigue life of B-52 aircraft pylon components
[NASA-TM-88277] 05 p0655 N90-13820
An evaluation of a fatigue crack growth prediction model for variable-amplitude loading (PREFFAS)
[LR-537] 05 p0656 N90-13822
Effects of dislocation substructure and prestrain on fracture behavior in aluminum and steel alloys
06 p0745 N90-14334
The 4.2 K fracture toughness of 304 stainless steel in a magnetic field
[DE90-002083] 06 p0747 N90-14347
Failure probability estimate of Type 304 stainless steel piping
[DE90-000659] 06 p0796 N90-14635
A nonlinear high temperature fracture mechanics basis for strainrange partitioning
[NASA-TM-4133] 06 p0797 N90-14642
Fracture mechanics of porous materials
[DE90-000023] 06 p0800 N90-14657
Engineering approaches to the application of fracture toughness data in the nuclear industry
[DE90-001596] 06 p0800 N90-14659
Thermal mechanical fatigue of coated blade materials
[AD-A214258] 07 p0882 N90-15107
Critical and subcritical crack-growth behavior along toughened ceramic/metal interfaces
07 p0889 N90-15140
Fatigue properties of Al-Li alloys
07 p0898 N90-15189
Fatigue and fracture behaviour of a PM Al-Li alloy
07 p0899 N90-15195
Helium-induced weld cracking in irradiated 304 stainless steel
[DE90-001312] 07 p0903 N90-15219
Guide to the selection of surface treatments for the improvement of fatigue strength of steels
[ESDU-89031] 07 p0907 N90-15245
Crack tip toughening by inclusions with pairs of shear transformations
[DE89-007845] 07 p0909 N90-15254
Fractal dimension of the fractured surface of materials
[DE89-635764] 07 p0946 N90-15477

Experience with J testing of 304/308 stainless steel weldment
[DE90-002046] 07 p0946 N90-15478
Ductile failure
[AD-A213864] 07 p0948 N90-15488
Calibration of a pulsed potential crack monitor for use in fatigue crack growth studies
[RAE-TM-M/S-1126] 08 p1089 N90-16301
Numerical simulation of creep crack growth experiments
[IWM-W-4/88] 08 p1089 N90-16303
A quantitative analysis of slip phenomena along a dry contact surface between two bodies in comparison to interfacial crack propagation
[ISAL-89-0032] 08 p1089 N90-16304
BAM: German Federal Institute for Materials Research and Testing, Berlin
[DE90-004293] 08 p1090 N90-16307
Effects of moisture on composite materials
09 p1185 N90-16866
Fatigue crack propagation rates for titanium alloy sheet
[ESDU-89051] 09 p1201 N90-16956
Heavy-section steel technology program fracture issues
[DE90-005264] 09 p1240 N90-17195
Observations of fatigue crack initiation and damage growth in notched titanium matrix composites
[NASA-TM-101688] 10 p1347 N90-17815
Investigation of failure modes in a ceramic composite under off-axis loading
[AD-A216133] 10 p1348 N90-17820
Effect of a single overload upon fatigue crack growth in an aluminum-lithium alloy
[AD-A216183] 10 p1356 N90-17865
Effect of oxygen on the tear strength of elastomers
[AD-A215845] 10 p1359 N90-17879
The damage tolerance of disc materials: Metallurgical factors; relationship with processing parameters
11 p1458 N90-18398
Crack propagation from artificial defects in typical engine disk materials; interpretation of experimental results by means of 3D J integral
11 p1458 N90-18401
Corrosion fatigue of iron-chromium-nickel alloys: Fracture mechanics and chemistry
[DE90-006318] 11 p1487 N90-18556
Softening mechanisms and microstructural instabilities during high temperature, low cycle fatigue of Ni, Ni3Al, and their metal matrix composites
[DE90-006487] 11 p1487 N90-18557
Fatigue crack initiation and small crack growth in several airframe alloys
[NASA-TM-102598] 11 p1518 N90-18746
Biaxial strength and stress rupture of hot-pressed silicon nitride
[AD-A216950] 11 p1519 N90-18750
Hydrogen, thermal ageing and the role of carbides in fatigue of a high strength steel
[AERE-R-13599] 13 p1774 N90-20183
Fatigue crack growth in martensitic 2 1/4Cr-1Mo steel at elevated temperatures
[AERE-R-13524] 13 p1776 N90-20191
Strength and microstructure of ceramics
[AD-A217752] 13 p1782 N90-20227
Limitations and applications of fracture assessment with R6
[AERE-R-13012] 13 p1815 N90-20425
Through-the-thickness fatigue crack closure behavior in an aluminum alloy
[NASA-TM-102590] 13 p1816 N90-20427
A corrosion fatigue/stress corrosion testing facility at Materials Research Laboratory
[MRL-TN-568] 14 p1929 N90-21044
Three-dimensional elastic-plastic analysis of shallow cracks in single-edge-crack-tension specimens
[NASA-TM-102636] 14 p1945 N90-21130
Crack stoppers and ARALL laminates
[PB90-166588] 14 p1947 N90-21142
A compendium of sources of fracture toughness and fatigue crack growth data for metallic alloys, part 4
[NASA-TM-102646] 14 p1950 N90-21164
Fatigue crack growth from narrow-band Gaussian spectrum loading in 6063 aluminum alloy
[DE90-008957] 14 p1952 N90-21173
Fracture toughness and crack growth of Zerodur
[NASA-TM-4185] 14 p1954 N90-21187
Development of a fracture analysis technique for use with a general-purpose finite element program
14 p1992 N90-21416
NASA airframe structural integrity program
[NASA-TM-102637] 14 p1993 N90-21422
An evaluation of the pressure proof test concept for thin sheet 2024-T3
[NASA-TM-101675] 14 p1994 N90-21424
Fractographic analysis of the crack growth rate and the shear lip development of 2024-T3 specimens under simple variable-amplitude loading
[PB90-167032] 14 p1994 N90-21427
Energy release rate analysis of interfacial cracks in composites
15 p2065 N90-21829
Contact mechanics for three-dimensional geometries
15 p2111 N90-22076
Combining acoustic emission locations and a microcrack damage model to study development of damage in brittle materials
[DE90-005195] 15 p2117 N90-22111
A continuum damage model for the quasi-static response of brittle materials
[DE90-007681] 15 p2117 N90-22112
Inclusion of unstable ductile tearing and extrapolated crack-arrest toughness data in PWR vessel integrity assessment
[DE90-009427] 15 p2118 N90-22116
Fatigue crack growth in unidirectional metal matrix composite
[NASA-TM-103102] 15 p2118 N90-22117
Fatigue crack growth predictions for variable-amplitude and spectrum loading
[LR-526] 15 p2118 N90-22118
Green's functions for the elastic annulus and their application to various crack problems
15 p2120 N90-22129
Fatigue crack growth in a unidirectional SCS-6/Ti-15-3 composite
[NASA-TM-103095] 16 p2217 N90-22646
The initiation of intergranular stress corrosion-cracking on sensitized stainless steel in dilute thiosulphate solutions
[AERE-R-13317] 16 p2217 N90-22648
Environment enhanced fatigue of advanced aluminum alloys and composites
16 p2218 N90-22652
Elevated temperature crack growth in advanced powder metallurgy aluminum alloys
16 p2218 N90-22653
Elevated temperature crack growth in aluminum alloys: Tensile deformation of 2618 and FVS0812 aluminum alloys
16 p2218 N90-22654
Deformation and fracture of thin sheet aluminum-lithium alloys: The effect of cryogenic temperatures
16 p2218 N90-22655
Structure-property relations in aluminum-lithium alloys
[AD-A219183] 16 p2222 N90-22672
Fracture mechanics assessment of a cracked 16-inch inner diameter 1945 vintage-jacketed pressure vessel
[AD-A219135] 16 p2248 N90-22819
Micro-mechanical modeling of crack growth resistance in a carbon/carbon composite
[DE90-009407] 17 p2368 N90-23479
Characterisation of fatigue of aluminium alloys by acoustic emission. Part 2: Discrimination between primary and other emissions
[AERE-R-13303-PT-2] 17 p2375 N90-23523
The effects of slip character and crack closure on the growth of small fatigue cracks in titanium-aluminium alloys
[AD-A220714] 17 p2377 N90-23534
Fatigue crack growth investigation of a Ti-6Al-4V forging under complex loading conditions: NATO/AGARD supplemental engine disk program
[AD-A220239] 17 p2377 N90-23538
Mechanics of necking, crazing, and crack growth in polymers
17 p2378 N90-23540
Controlled crack growth specimen for brittle systems
[NASA-TM-103126] 17 p2378 N90-23543
Fracture mechanism maps for advanced structural ceramics. Part 1: Methodology and hot-pressed silicon nitride results
[AD-A220428] 17 p2380 N90-23556
Fatigue testing apparatus
[NASA-CASE-LEW-14124-1] 17 p2407 N90-23712
Fractographic observations on fatigue crack growth in 2024-T3 sheet material under flight-simulation loading
[LR-592] 17 p2415 N90-23760
Wide range stress intensity factor and crack-mouth-opening displacement expressions suitable for short crack fracture testing with arc bend-chord support samples
[AD-A218395] 17 p2415 N90-23761
J-integral and HRR field of a stably growing crack, an experimental analysis
[AD-A220418] 17 p2416 N90-23764
Mechanistic modeling of corrosion fatigue crack growth of steels in aqueous solutions
18 p2524 N90-24404
Corrosion fatigue crack propagation in metals
[NASA-CR-4301] 18 p2524 N90-24405
Processing and properties of advanced aluminum alloys
[AD-A221292] 18 p2526 N90-24416
Fatigue crack propagation in austenitic stainless steels at cryogenic temperatures
[DE90-011597] 18 p2528 N90-24426
Cyclic damage zones ahead of tensile fatigue cracks in ceramic materials
[DE90-008372] 18 p2531 N90-24442
Fatigue crack growth in ceramic materials at ambient and elevated temperatures
[DE90-008418] 18 p2531 N90-24443
Indentation fracture of brittle materials
[DE90-010709] 18 p2572 N90-24657
Modeling growth of fatigue cracks which originate at rivet holes
18 p2645 N90-25060
Comparison of two computer codes for crack growth analysis: NASCRAC Versus NASA/FLAGRO
[NASA-TM-100383] 19 p2700 N90-25360
A study on ultrasonic detection and characterization of partially closed fatigue cracks
[DE90-011748] 19 p2702 N90-25371
Weight functions and stress intensity factors for mode 1 cracks in arbitrary 2D geometries under general crack surface loading
[FFA-TN-1990-17] 19 p2703 N90-25381
Microstructural design for fatigue crack growth resistance in Ni-base alloy
[PNR90632] 20 p2834 N90-26120
Small crack growth and its influence in near alpha-titanium alloys
[RAE-TM-P-1171] 20 p2835 N90-26121
Elevated temperature crack growth
[NASA-CR-182247] 20 p2875 N90-26355
Fatigue life assessment using a short crack growth model
[PNR90663] 20 p2877 N90-26367
Computerized corrosion forecasting model for C-5 aircraft
21 p2957 N90-26815
Application of damage tolerance
21 p2958 N90-26817
Theory of ceramic/zirconia composites: Toughening, strengthening, and synergism
[AD-A222931] 21 p2985 N90-26961
Micromechanics of interfaces in high temperature ceramics
[AD-A222027] 21 p2987 N90-26973
Engineering fracture mechanics
[AD-A222699] 21 p3012 N90-27123
A framework to correlate a/W ratio effects on elastic-plastic fracture toughness (J (sub c))
[AD-A222822] 21 p3012 N90-27125
Computational investigation of local material strength and toughness on crack growth
[AD-A223189] 21 p3012 N90-27127
Fracture mechanics analysis for short cracks
[AD-A222170] 21 p3013 N90-27130
Strength under various modes of deformation
[AD-A222412] 21 p3013 N90-27132
Improved transverse crack detection in composites
[NASA-TM-103261] 22 p3153 N90-27875
Acoustic emission detection of crack presence and crack advance during flight
22 p3186 N90-28082
New aspects in aircraft inspection using eddy current methods
22 p3187 N90-28085
Acoustic emission from a growing crack
22 p3188 N90-28089
Micromechanical model of crack growth in fiber reinforced ceramics
[NASA-CR-4321] 22 p3192 N90-28113
Damage tolerance of woven graphite-epoxy buffer strip panels
[NASA-TM-102702] 22 p3192 N90-28114
A comparison of single-cycle versus multiple-cycle proof testing strategies
[NASA-CR-4318] 22 p3193 N90-28115
Fatigue crack monitoring from initiation to through cracking in welded thick steel sections
[ARE-TM(UHS)-90203] 22 p3194 N90-28122
Damage tolerance of the fighter aircraft 37 Viggen. Part 1: Analytical assessment
[FFA-TN-1990-12-PT-1] 23 p3276 N90-28538
Damage tolerance of the fighter aircraft 37 Viggen. Part 2: Experimental verification
[FFA-TN-1990-13-PT-2] 23 p3276 N90-28539
NASCRAC (trademark): A fracture mechanics analysis code
23 p3296 N90-28645
A comparison of single-cycle versus multi-cycle proof testing strategies
23 p3296 N90-28648
Data base for crack growth properties of materials
23 p3296 N90-28647
Comparison of two computer codes for crack growth analysis: NASCRAC versus NASA/FLAGRO
23 p3297 N90-28648
Micromechanisms of fatigue crack growth and fracture toughness in metal matrix composites
[AD-A223863] 23 p3302 N90-28676
Crack layer analysis of fatigue fracture of a beta titanium alloy
23 p3338 N90-28864
Green's functions for dislocations in bonded strips and related crack problems
[NASA-CR-185291] 23 p3340 N90-28878

Assessment and improvement of aeroengine disc structural integrity 24 p3433 N90-29392
Powder processing of aluminides
[DE90-015314] 24 p3444 N90-29447
Evaluation of static and fatigue properties of thin sheets of 8090-T8 aluminum-lithium alloy and observation of its fracture surfaces
[NAL-TR-1039] 24 p3453 N90-29499
Effect of environment upon mechanical behavior of structural ceramics for application in the DOE ceramic technology for advanced heat engines project
[DE90-014770] 24 p3453 N90-29500
Surface chemistry and structural effects in the stress corrosion of glass and ceramic materials
[AD-A223305] 24 p3454 N90-29507
An investigation of crack-tip stress field criteria for predicting cleavage-crack initiation
[DE90-015597] 24 p3480 N90-29672
Fractographic observations on fatigue crack growth under miniTWIST flight-simulation loading (2024-T3 material)
[LR-631] 24 p3483 N90-29684

CRACK TIPS
An application of the J-integral to an incremental analysis of blunting crack behavior
[DE89-016844] 03 p0358 N90-12046
An experimental and analytical program to develop crack tip fracture criteria
[AD-A211565] 03 p0359 N90-12051
Modeling the temperature rise at the tip of a fast crack
[AD-A212418] 04 p0514 N90-12966
Mechanics of interaction of a crack with microcracks 06 p0798 N90-14650
Crack problems for elastic-plastic materials under antiplane shear loadings 06 p0799 N90-14651
Crack tip toughening by inclusions with pairs of shear transformations
[DE89-007845] 07 p0909 N90-15254
On the domain of dominance of the asymptotic elastodynamic crack-tip fields 07 p0944 N90-15468
A study of near tip phenomena for cracks in a particulate composite 10 p1395 N90-18062
Dislocation annihilation mechanism for the formation of dislocation free zone at a crack tip
[DE90-610552] 12 p1674 N90-19615
Stress field near crack tip: An experimental evaluation of the three dimensional variation
[AD-A217878] 13 p1818 N90-20441
Mechanics of interface fracture 14 p1990 N90-21408
Energy release rate analysis of interfacial cracks in composites 15 p2065 N90-21829
Natural modes of cracked beams and identification of cracks 15 p2111 N90-22075
Analysis of a finite two-dimensional solid with an inclined crack and a rigid inclusion 15 p2120 N90-22127
An investigation into the foundations of elastic-plastic fracture mechanics 15 p2120 N90-22130
Measurements and mechanisms of localized aqueous corrosion in aluminum-lithium alloys 16 p2219 N90-22656
J-integral and HRR field of a stably growing crack, an experimental analysis
[AD-A220418] 17 p2416 N90-23764
Mechanistic modeling of corrosion fatigue crack growth of steels in aqueous solutions 18 p2524 N90-24404
Corrosion fatigue crack propagation in metals
[NASA-CR-4301] 18 p2524 N90-24405
Crack bridging processes in toughened ceramics
[DE90-011650] 19 p2678 N90-25231
A study on ultrasonic detection and characterization of partially closed fatigue cracks
[DE90-011748] 19 p2702 N90-25371
Fracture mechanics analysis for short cracks
[AD-A222170] 21 p3013 N90-27130
Characterization by ultrasonic tests of ceramics submitted to thermal shocks: influence of several parameters on the crack dimensioning
[ETCA-89-R-060] 22 p3160 N90-27923
Studies on crack mechanics
[AD-A223634] 24 p3480 N90-29670
An investigation of hole-edge crack problem by a combined complex variable and least square method
[LR-626] 24 p3482 N90-29679

CRACKING (CHEMICAL ENGINEERING)
NT HYDROCRACKING
NT PYROLYSIS
Experimental and kinetic modeling of acid/base redox reactions over metal oxide catalysts
[DE90-013835] 22 p3156 N90-27893

CRACKING (FRACTURING)
NT STRESS CORROSION CRACKING
Porosity and crack initiation during low cycle fatigue
[AD-A210989] 01 p0081 N90-10464
Nonlinear theories concerning laminated composites under compression with delamination
[ONERA-RT-19/3542-RY-081-R] 04 p0467 N90-12672
A study of progressive cracking damage to carbon-epoxy composites and methods of crack reduction
[REPT-RE-49-324/F] 04 p0467 N90-12676
Elastic indentation fractures
[ETCA-88-R-116] 04 p0512 N90-12955
Stress intensity factors for cracking metal structures under rapid thermal loading. Volume 2: Theoretical background
[AD-A213297] 05 p0654 N90-13812
A computer-controlled automated test system for fatigue and fracture testing
[DE90-002931] 06 p0800 N90-14661
Thermal mechanical fatigue of coated blade materials
[AD-A214258] 07 p0882 N90-15107
Microstructure/mechanical property relations in a mechanically alloyed aluminum 07 p0900 N90-15205
Mechanical aspects of interfaces in high performance composites 10 p1347 N90-17812
Investigation of failure modes in a ceramic composite under off-axis loading
[AD-A216133] 10 p1348 N90-17820
Impact damage tolerance of composite cylindrical panels
[AD-A216401] 10 p1350 N90-17830
Defects in monoblock cast turbine wheels 11 p1458 N90-18400
Compact reinforced composite basic principles
[CBL-41] 11 p1480 N90-18520
Limitations and applications of fracture assessment with R6
[AERE-R-13012] 13 p1815 N90-20425
Cooling of rocket thrust chambers with liquid oxygen
[NASA-TM-103146] 16 p2210 N90-22605
Low temperature degradation of Y-TZP materials
[AD-A218841] 16 p2223 N90-22684
The effects of slip character and crack closure on the growth of small fatigue cracks in titanium-aluminium alloys
[AD-A220714] 17 p2377 N90-23534
ESA fracture control requirements
[ESA-PSS-01-401-ISSUE-1] 19 p2703 N90-25376
Effect of boron on intergranular hot cracking in Ni-Cr-Fe superalloys containing niobium
[NASA-CR-184038] 20 p2834 N90-26115

CRACKS
NT CRACK TIPS
NT MICROCRACKS
NT SHORT CRACKS
NT SURFACE CRACKS
Mechanics of the crack path formation
[NASA-CR-185143] 01 p0080 N90-10455
Effect of thermal and cyclic loads on silicon carbide yarn reinforced glass matrix composites
[DE89-016554] 02 p0191 N90-11091
Stochastic propagation of an array of parallel cracks: Exploratory work on matrix fatigue damage in composite laminates
[DE89-017837] 03 p0319 N90-11813
Weldability of ductile nickel aluminides
[DE89-017452] 03 p0327 N90-11859
A numerical laboratory for granular solids
[DE89-016367] 03 p0358 N90-12045
The effect of a rigid elliptical inclusion on a straight crack
[AD-A212263] 04 p0513 N90-12965
Stress intensity factors for cracking metal structures under rapid thermal loading. Volume 2: Theoretical background
[AD-A213297] 05 p0654 N90-13812
The feasibility of welding of irradiated materials
[DE90-002200] 06 p0795 N90-14631
Crack problems for elastic-plastic materials under antiplane shear loadings 06 p0799 N90-14651
Design temperatures for flexible airfield pavement design
[AD-A214141] 07 p0884 N90-15115
Electroplating simulation
[DE90-003683] 08 p1054 N90-16091
Fracto-fusion. Mechanism of cold fusion
[DE90-719573] 08 p1125 N90-16518
Inspection development for T-37 wing spar cap lug
[AD-A214826] 09 p1159 N90-16708
Effects of moisture on composite materials 09 p1185 N90-16866
Eddy current test for bolts
[AD-A214829] 09 p1234 N90-17159
Investigation of failure modes in a ceramic composite under off-axis loading
[AD-A216133] 10 p1348 N90-17820
Effects of elevated temperatures and thermal cycling on ceramic composite materials
[AD-A216242] 10 p1350 N90-17828
Damage mechanisms and indenter size effects in cross plied carbon-carbon composites
[AD-A216413] 10 p1351 N90-17832
Effect of a single overload upon fatigue crack growth in an aluminum-lithium alloy
[AD-A216183] 10 p1356 N90-17865
Analysis of biaxial stress fields in plates cracking at elevated temperatures
[AD-A216271] 10 p1397 N90-18077
Validation of the boundary element method applied to complex fracture mechanics conditions
[AD-A216412] 10 p1398 N90-18080
Arcjet cathode phenomena 11 p1473 N90-18477
Technology evaluation for space station atmospheric leakage
[DE90-007844] 12 p1616 N90-19294
Fatigue crack growth in martensitic 2 1/4Cr-1Mo steel at elevated temperatures
[AERE-R-13524] 13 p1776 N90-20191
Strength and microstructure of ceramics
[AD-A217752] 13 p1782 N90-20227
The diffraction of ultrasound by cracks: Comparison of experiment with theory
[AERE-R-13334] 13 p1813 N90-20410
The stress-driven redistribution of point defects in the vicinity of crack-like singularities
[AERE-R-12898] 13 p1815 N90-20424
Three-dimensional elastic-plastic analysis of shallow cracks in single-edge-crack-tension specimens
[NASA-TM-102636] 14 p1945 N90-21130
Fourier series methods for plates and shells with cracks and inclusions 14 p1990 N90-21406
An evaluation of the pressure proof test concept for thin sheet 2024-T3
[NASA-TM-101675] 14 p1994 N90-21424
Fractographic analysis of the crack growth rate and the shear lip development of 2024-T3 specimens under simple variable-amplitude loading
[PB90-167032] 14 p1994 N90-21427
Structural fatigue in the 34-meter HA-Dec antennas 15 p2078 N90-21902
The classification of defects from ultrasonic measurements
[AERE-R-13306] 15 p2108 N90-22056
Natural modes of cracked beams and identification of cracks 15 p2111 N90-22075
Contact mechanics for three-dimensional geometries 15 p2111 N90-22076
Combining acoustic emission locations and a microcrack damage model to study development of damage in brittle materials
[DE90-005195] 15 p2117 N90-22111
Dynamic response of a complex encapsulated electronic assembly subjected to a severe shock environment
[DE90-007689] 15 p2118 N90-22114
Inclusion of unstable ductile tearing and extrapolated crack-arrest toughness data in PWR vessel integrity assessment
[DE90-009427] 15 p2118 N90-22116
The stress field due to an edge dislocation and some fracture problems for a three-phase composite cylinder model 15 p2120 N90-22126
Analysis of a finite two-dimensional solid with an inclined crack and a rigid inclusion 15 p2120 N90-22127
Green's functions for the elastic annulus and their application to various crack problems 15 p2120 N90-22129
An investigation into the foundations of elastic-plastic fracture mechanics 15 p2120 N90-22130
Ultrasonic detection of critical damage in carbon-epoxy composite materials
[ONERA-RT-5/7256-RY-081-R] 16 p2212 N90-22616
Scattering of a plane electromagnetic wave from a semicircular crack in a perfectly conducting ground plane
[AD-A219310] 16 p2230 N90-22721
Crack detection in silicon nitride by acoustic microscopy
[AERE-R-13196] 16 p2245 N90-22803
Wide range stress intensity factor and crack-mouth-opening displacement expressions suitable for short crack fracture testing with arc bend-chord support samples
[AD-A218395] 17 p2415 N90-23761
Hypersingular integrals and the two dimensional Helmholtz equation
[DE90-009821] 17 p2456 N90-24012
Stress fields in composite materials by means of a nonclassical approach 18 p2517 N90-24372

Influence of interfacial shear strength on the mechanical properties of SiC fiber reinforced reaction-bonded silicon nitride matrix composites
[NASA-TM-102462] 18 p2518 N90-24382
Use of neutron diffraction in determining strains in high-temperature superconducting composites
[DE90-010404] 18 p2621 N90-24931
Structural zooming research and development of an interactive computer graphical interface for stress analysis of cracks 18 p2641 N90-25042
Inspection of welds with eddy current
[TTR-RR-644] 19 p2699 N90-25358
Comparison of two computer codes for crack growth analysis: NASCRAC Versus NASA/FLAGRO
[NASA-TM-100383] 19 p2700 N90-25360
Stress intensity factors for arbitrary two-dimensional crack problems involving crack face loadings
[FFA-TN-1990-10] 19 p2703 N90-25380
Development of creep-fatigue damage detection method of rotor steel by ultrasonic wave measurement
[DE90-503792] 20 p2877 N90-26365
Dynamic properties of porous B4C
[AD-A222850] 21 p2985 N90-26960
Engineering fracture mechanics
[AD-A222699] 21 p3012 N90-27123
Computational investigation of local material strength and toughness on crack growth
[AD-A223189] 21 p3012 N90-27127
Micromechanics of size effect in failure due to distributed cracking
[AD-A223211] 21 p3013 N90-27128
Load-point compliance for the arc bend-arc support fracture toughness specimen
[AD-A221618] 21 p3014 N90-27134
Progress in the detection of cracks under installed fasteners using eddy currents 22 p3186 N90-28081
Acoustic emission detection of crack presence and crack advance during flight 22 p3186 N90-28082
Acoustic emission from a growing crack
22 p3188 N90-28089
Theory of stress transfer in a cross-ply laminate containing a parallel array of transverse cracks
[NPL-DMA(A)-189] 22 p3192 N90-28109
Crack layer analysis of fatigue fracture of a beta titanium alloy 23 p3338 N90-28864
A welding metallurgy study of Hastelloy Alloys B-2 and W
[DE90-011910] 24 p3449 N90-29481
The ACR-program for automatic finite element model generation for part through cracks
[DE90-631545] 24 p3479 N90-29662
Fatigue, static tensile strength and stress corrosion of aircraft materials and structures. Part 1: Text
[LR-630-PT-1-REV] 24 p3482 N90-29682
Fatigue, static tensile strength and stress corrosion of aircraft materials and structures. Part 2: Figures
[LR-630-PT-2] 24 p3482 N90-29683

CRAF MISSION
U COMET RENDEZVOUS ASTEROID FLYBY MISSION

CRAFT
U VEHICLES

CRANES
Robot crane technology program
[PB90-111667] 11 p1516 N90-18734
On trajectory generation for flexible space crane: Inverse dynamics analysis by LATDYN 16 p2288 N90-23037
Lunar crane hook
[NASA-CR-184921] 17 p2384 N90-23579
Obtaining an equivalent beam
18 p2570 N90-24646
Design of a versatile, teleoperable, towable lifting machine with robotic capabilities for use in NASA's lunar base operations
[NASA-CR-186688] 19 p2697 N90-25345
Man-machine interface for the control of a lunar transport machine
[NASA-CR-184935] 19 p2724 N90-25495

CRANKED WINGS
U SWEPT WINGS

CRASH LANDING
NT DITCHING (LANDING)
Post crash flight analysis: Visualizing flight recorder data
[AD-A212063] 03 p0302 N90-11715
Aircraft crash survival design guide. Volume 2: Aircraft design crash impact conditions and human tolerance
[AD-A218435] 16 p2198 N90-22546

CRASHES
NT CRASH LANDING
NT DITCHING (LANDING)
Waveform generator signal processing software
[PB89-192660] 01 p0103 N90-10587
The impact of recovery on concurrency control
[AD-A210828] 01 p0106 N90-10603
Methodology for the calibration of and data acquisition with a six-degree-of-freedom acceleration measurement device
[PB89-233597] 06 p0779 N90-14531
International Aircraft Occupant Safety Conference and Workshop proceedings
[AD-A214452] 07 p0877 N90-15085
Aircraft accident report: Delta Air Lines, Inc., Boeing 727-232, N473DA, Dallas-Fort Worth International Airport, Texas, August 31, 1988
[PB89-910406] 08 p1019 N90-15895
Analysis of the National Transonic Facility mishap
[NASA-TM-101686] 10 p1318 N90-17620
A review of the analytical simulation of aircraft crash dynamics
[NASA-TM-102595] 13 p1753 N90-20068
Peacetime replacement and crash damage factors for army aircraft
[AD-A218544] 17 p2348 N90-23372
The effect of aircraft size on cabin floor dynamic pulses
[DOT/FAA/CT-88/15] 19 p2659 N90-25136
Behavior of composite/metal aircraft structural elements and components under crash type loads: What are they telling us
[NASA-TM-102681] 19 p2701 N90-25368
Measurement techniques, evaluation criteria and injury probability assessment methodologies developed for Navy ejection and crashworthy seat evaluations
19 p2721 N90-25479
Computational crash dynamics. Project 1.2: Computational crash dynamics analysis
[IAR-89-19] 20 p2804 N90-25956
Biodynamic simulations of an aircraft pilot/passenger in various crash environments
[NIAR-90-6] 20 p2900 N90-26494
Special test and evaluation methods used for a nine-axis accelerometer
[PB90-209578] 23 p3329 N90-28822

CRASHWORTHINESS
International Aircraft Occupant Safety Conference and Workshop proceedings
[AD-A214452] 07 p0877 N90-15085
Aircraft fires: A study of transport accidents from 1975 to the present 10 p1311 N90-17583
Floor pull test of a transport airframe section
[DOT/FAA/CT-TN88/14] 13 p1754 N90-20072
Aircraft crash survival design guide. Volume 1: Design criteria and checklists
[AD-A218434] 16 p2198 N90-22545
Aircraft crash survival design guide. Volume 2: Aircraft design crash impact conditions and human tolerance
[AD-A218435] 16 p2198 N90-22546
Aircraft crash survival design guide. Volume 3: Aircraft structural crash resistance
[AD-A218436] 16 p2198 N90-22547
Aircraft crash survival design guide. Volume 4: Aircraft seats, restraints, litters, and cockpit/cabin delethalization
[AD-A218437] 16 p2198 N90-22548
Aircraft crash survival design guide. Volume 5: Aircraft postcrash survival
[AD-A218438] 16 p2198 N90-22549
Operational effects on crashworthy seat attenuators
[AD-A221148] 18 p2495 N90-24259
Computational crash dynamics. Project 1.2: Computational crash dynamics analysis
[IAR-89-19] 20 p2804 N90-25956
Human factors: The human interface with aircraft interiors
[NIAR-90-18] 20 p2900 N90-26496
Evaluation of energy absorption of new concepts of aircraft composite subfloor intersections
[NASA-TP-2951] 21 p2959 N90-26823
A review of crashworthiness of composite aircraft structures
[AD-A221555] 22 p3115 N90-27697
A review of research and development in crashworthiness of general aviation aircraft: Seats, restraints and floor structures
[AD-A221557] 22 p3115 N90-27698

CRATERING
NT PROJECTILE CRATERING
State-of-the-art of measuring ground shock and cratering phenomena 09 p1235 N90-17170
Astronaut's guide to terrestrial impact craters
[NASA-TM-102902] 17 p2421 N90-23798

CRATERS
NT LUNAR CRATERS
NT METEORITE CRATERS
NT PLANETARY CRATERS
Astronaut's guide to terrestrial impact craters
[NASA-TM-102902] 17 p2421 N90-23798

CRAY COMPUTERS
New computing systems and their impact on structural analysis and design
[NASA-CR-185831] 02 p0257 N90-11457
Multiple crossbar network: Integrated supercomputing framework
[DE89-012614] 06 p0831 N90-14831
An efficient UNICOS run-time system for functional programs on a CRAY X-MP
[DE89-016603] 07 p0972 N90-15610
Modeling high-temperature superconductors and metallic alloys on the Intel IPSC/860
[DE90-009402] 14 p2033 N90-21665
The incorporation of a multigrid method into the orthogonal curvilinear coordinate version of the Rolls-Royce PACE computer program
[TT-8804] 19 p2751 N90-25627
Particle simulation of hypersonic flow
[AD-A222704] 21 p2954 N90-26794
Linear algebra on a CRAY X-MP
[AD-A221780] 21 p3056 N90-27374

CRAZING
U SURFACE CRACKS

CREATION
U CREATIVITY

CREATIVITY
An algebra for process creation
[CWI-CS-R8907] 04 p0543 N90-13155
EDISON Project
[AD-A214724] 09 p1265 N90-17338
On the creation of gravitational wave by photon in external electromagnetic field
[DE90-613366] 14 p1967 N90-21265
Assuring both quality and creativity in basic research
[DE90-011489] 22 p3256 N90-28435

CREEP ANALYSIS
Physical ageing and short term creep in amorphous and semicrystalline polymers
[NPL-DMA(A)-185] 04 p0479 N90-12745
Numerical simulation of creep crack growth experiments
[IWM-W-4/88] 08 p1089 N90-16303
Characterization of the creep compliances J22 and J66 of orthotropic composites with PEEK and epoxy matrices using the nonlinear viscoelastic response of the neat resins
[MBB-Z-0258/89-PUB] 19 p2650 N90-25082

CREEP PROPERTIES
NT SHEAR CREEP
NT STEADY STATE CREEP
NT TENSILE CREEP
Determination and description of the long term creep behavior of high temperature gas turbine materials
[ETN-89-94985] 03 p0329 N90-11871
The effect of flux creep on the magnetization field in the SSC diopole magnets
[DE90-000124] 03 p0399 N90-12284
Application of neutron diffraction NDE to high-temperature superconducting composites
[DE90-002184] 06 p0738 N90-14295
BES welding science contractors summary report, 1988 to 1989
[DE90-001004] 06 p0793 N90-14619
A nonlinear high temperature fracture mechanics basis for strainrange partitioning
[NASA-TM-4133] 06 p0797 N90-14642
Micromechanics of an extrusion in high-cycle fatigue with creep
[AD-A213509] 07 p0947 N90-15485
Effects of non-linearity in the variation of pinning potential with current-density on magnetic flux creep in high and low T(sub c) superconductors
[DE90-003952] 07 p1005 N90-15822
Non Newtonian gravity creeping flow
[DE90-600816] 07 p1006 N90-15828
Method of marking titanium alloy articles having distinct microstructural regions corresponding to high creep and fatigue resistance
[AD-D014283] 08 p1043 N90-16031
Irradiation creep and swelling of annealed type 304L stainless steel at approximately 390 C and high neutron fluence
[DE90-004521] 08 p1046 N90-16047
Modeling dislocation evolution in irradiated alloys
[DE90-004921] 08 p1047 N90-16051
Theoretical study on creep damage detection by ultra-sonic wave measurement
[DE90-702472] 08 p1087 N90-16290
A summary of the Bodner-Stouffer constitutive model
[AD-A214532] 09 p1237 N90-17182
Steady-state and transient Zener parameters in viscoplasticity: Drag strength versus yield strength
[NASA-TM-102487] 10 p1395 N90-18064
The 59th Shock and Vibration Symposium, volume 3
[AD-A214580] 10 p1395 N90-18066
Comparison of tension, compression, and flexure creep for alumina and silicon nitride ceramics
[DE90-006154] 11 p1492 N90-18586

The creep behavior of an aramide fiber reinforced wound tow-strap
[LR-546] 12 p1620 N90-19312
Radiation-induced density changes and creep in surface layers of glass
[DE90-008112] 12 p1633 N90-19383
Evaluation of thermal cycling creep-fatigue damage for a molten salt receiver
[DE90-002907] 12 p1684 N90-19670
Titanium aluminides: Processing, properties and potential
[AERE-R-13198] 14 p1949 N90-21158
A study of creep damage using microradiography and continuum damage mechanics 15 p2117 N90-22109
The lithium concentration dependence of creep in binary aluminum-lithium alloys
[AD-A218706] 16 p2221 N90-22668
A numerical and analytical study of normal stresses and pressure differences in non-Newtonian creeping flows 16 p2234 N90-22749
Characterization of weldments using advanced experimental techniques
[DE90-009418] 16 p2242 N90-22792
Experimental study of mixing and combustion processes in a solid-propellant ducted rocket motor 17 p2367 N90-23472
An orthotropic theory of viscoplasticity based on overstress for thermomechanical deformation and its application to laminated metal matrix composites 17 p2415 N90-23759
A viscoplastic model with application to LiF-22 percent CaF2 hypereutectic salt
[NASA-TM-103181] 17 p2417 N90-23770
Error cancellation in HPBL derivation of elastic hole-pressure error
[AD-A219854] 17 p2417 N90-23771
Stress versus temperature dependent activation energies in creep
[NASA-TM-103192] 17 p2417 N90-23773
A creep model for metallic composites based on matrix testing: Application to Kanthal composites
[NASA-TM-103172] 19 p2672 N90-25193
Development of a design methodology for high temperature cyclic applications of materials which experience cyclic softening
[DE90-006722] 19 p2674 N90-25205
Study on application of ultrasonic wave measurement to creep-fatigue damage detection
[DE89-782317] 19 p2700 N90-25361
High-temperature creep under a nonuniform temperature distribution
[ATR-88(3728-02)-1] 19 p2702 N90-25373
Microstructural dependence of the cavitation damage function in FCC materials
[DE90-012898] 20 p2833 N90-26113
Development of creep-fatigue damage detection method of rotor steel by ultrasonic wave measurement
[DE90-503792] 20 p2877 N90-26365
Diffusion-accommodated grain boundary sliding in a polycrystal
[DE90-012727] 20 p2930 N90-26668
Critical current density, flux creep, and microstructure in a Bi-Sr-Ca-Cu-O system
[DE90-010457] 20 p2931 N90-26676
Flux motion effects in Tl-Ca-Ba-Cu-O thin films
[DE90-012176] 21 p3080 N90-27514
Characterization of superconducting materials with muon spin rotation
[DE90-013755] 21 p3081 N90-27522
Flux creep in Bi2Sr2CaCu2O8(sub +x) single crystals 22 p3136 N90-27794
Nonlogarithmic magnetization relaxation at the initial time intervals and magnetic field dependence of the flux creep rate in Bi2Sr2Ca(sub I)Cu2Ox single crystals 22 p3137 N90-27801
Comparative study of flux pinning flux creep and critical currents between YBaCuO crystals with and without Y2BaCuO5 inclusions 22 p3152 N90-27869
Creep and creep rupture of strongly reinforced metallic composites
[NASA-CR-185286] 22 p3192 N90-28110
NASCRAC (trademark): A fracture mechanics analysis code 23 p3296 N90-28645
Inelastic analysis of laminated composites 23 p3301 N90-28669
The overall response of composite materials undergoing large elastic deformations
[AD-A224509] 24 p3442 N90-29439
The stress and temperature dependence of creep in an Al-2.0 wt percent Li alloy
[AD-A223676] 24 p3449 N90-29480
Multiaxial fatigue criterion for 2-1/4 Cr-1 Mo steel for use in high-temperature structural design
[DE90-016039] 24 p3452 N90-29491

CREEP RESISTANCE
U CREEP STRENGTH

CREEP RUPTURE STRENGTH
The influence of carbide precipitation on the creep rupture behavior of high temperature alloys
[JUEL-2211] 08 p1046 N90-16044
Identification of a cast iron alloy containing nonstrategic elements
[NASA-CR-185174] 11 p1487 N90-18559
Biaxial strength and stress rupture of hot-pressed silicon nitride
[AD-A216950] 11 p1519 N90-18750
Mechanical properties of pure nickel alloys after long term exposures to LiOH and vacuum at 775 K
[NASA-TM-102403] 13 p1774 N90-20181
Fracture mechanism maps for advanced structural ceramics. Part 1: Methodology and hot-pressed silicon nitride results
[AD-A220428] 17 p2380 N90-23556
Ambient-temperature creep failure of silver-aided diffusion bonds between steel
[DE90-010687] 18 p2527 N90-24420

CREEP STRENGTH
Development of metastable processing paths for high temperature alloys
[AD-A210550] 01 p0045 N90-10254
Creep strength of niobium alloys, Nb-1%Zr and PWC-11
[NASA-TM-102390] 03 p0326 N90-11854
Dispersion strengthening of high temperature niobium alloys
[AD-A213829] 07 p0906 N90-15236
Long term creep strength of silver alloyed copper
[DE90-602367] 08 p1045 N90-16039
The processing and mechanical properties of high temperature/high performance composites. Book 4, section 3: Flow and creep strength
[AD-A216144] 10 p1349 N90-17822
The processing and mechanical properties of high temperature/high performance composites. Book 2, section 2: Strength and fracture resistance
[AD-A216142] 11 p1478 N90-18507
A creep model for metallic composites based on matrix testing: Application to Kanthal composites
[NASA-TM-103172] 19 p2672 N90-25193
Application of high performance metals in gas turbine engines
[PNR90640] 20 p2811 N90-25999
Development of metastable processing paths for high temperature alloys
[AD-A223144] 22 p3157 N90-27898
Evaluation of advanced austenitic alloys relative to alloy design criteria for steam service. Part 1: Lean stainless steel
[DE90-014765] 23 p3310 N90-28720
High performance brittle matrices and brittle matrix composites, book 2
[AD-A223274] 24 p3443 N90-29441

CREEP TESTS
Creep and fracture behavior of heat resistant steels in characteristic cases of variable fatigue loading
[ETN-89-94671] 03 p0326 N90-11855
A model for long-term creep and the effects of physical ageing in poly (butylene terephthalate)
[NPL-DMA(A)-182] 03 p0333 N90-11895
The influence of carbide precipitation on the creep rupture behavior of high temperature alloys
[JUEL-2211] 08 p1046 N90-16044
Theoretical study on creep damage detection by ultra-sonic wave measurement
[DE90-702472] 08 p1087 N90-16290
Mechanical testing of selected engineering plastics
[DE90-008186] 16 p2222 N90-22673
A creep model for metallic composites based on matrix testing: Application to Kanthal composites
[NASA-TM-103172] 19 p2672 N90-25193
The effect of local thinning on the remaining life of superheater tubes
[VTT-RR-631] 19 p2703 N90-25377
High temperature multiaxiale creep testing of Nimonic 115
[RAE-TM-P-1182] 20 p2835 N90-26122

CRESTATRONS
U TRAVELING WAVE TUBES

CREVASSES
NT GLACIERS

CREVICES
U CRACKS

CREW PROCEDURES (INFLIGHT)
Payload crew utilization for spacelab missions
[NASA-TP-2976] 06 p0730 N90-14256
Causes of aircrew error in the Royal Air Force 09 p1254 N90-17276
Reactions to emergency situations in actual and simulated flight 09 p1255 N90-17283
Simulation-based reasoning about the physical propagation of fault effects 15 p2155 N90-22309

CREW SIZE
Lunar base 2 (the second thousand days of a base on the Moon)
[ILR-MITT-230(1989)] 16 p2275 N90-22968

CREW STATIONS
U CREW WORKSTATIONS

CREW WORKSTATIONS
The first 1000 days of a future lunar base
[ILR-MITT-224] 08 p1033 N90-15970
The determination of offgassing products from materials and assembled articles to be used in a manned space vehicle crew compartment
[ESA-PSS-01-729-ISSUE-1] 11 p1469 N90-18461
Evaluation of speech recognizers for use in advanced combat helicopter crew station research and development
[NASA-CR-177547] 18 p2496 N90-24265
Space Station Freedom pressurized element interior design process
[NASA-CR-181297] 23 p3287 N90-28597
Human factors model concerning the man-machine interface of mining crewstations 23 p3364 N90-29011

CREWS
NT FLIGHT CREWS
NT SPACECREWS
Evaluation of rocket motor exhaust and liner combustion by-products
[AD-A210747] 02 p0189 N90-11083
Air Force flight feeding. Volume 1: Evaluation of current system and alternative concepts
[AD-A212789] 04 p0527 N90-13043
Conference Proceedings of the Human-Electronic Crew: Can They Work Together
[AD-A211871] 05 p0676 N90-13936
Environmental quality and occupational health Special Emphasis Area Plan (SEAP)
[AD-A214738] 09 p1251 N90-17259
Assessment of crew workload measurement methods, techniques and procedures. Volume 1: Process, methods and results
[AD-A217699] 13 p1855 N90-20647
A comparative analysis of work-hour forecasting techniques at the crew level
[AD-A220706] 17 p2438 N90-23894
Operational effects on crashworthy seat attenuators
[AD-A221148] 18 p2495 N90-24259

CRIME
The astronauts' legal status: The International Space Station 20 p2938 N90-26721

CRIMPING
U FOLDING

CRITERIA
NT STRUCTURAL DESIGN CRITERIA
MANPRINT methods monograph: Aiding the development of manned system performance criteria
[AD-A213543] 07 p0968 N90-15593
Case tool evaluation system
[DE90-003698] 08 p1108 N90-16413
VULCAIN: An expert system dedicated to fire risk analysis within complex industrial environments 10 p1314 N90-17599
Optimization of sensors and actuators positioning aimed at obtaining reduced models for the synthesis of optimal control regulators of flexible structures
[INPE-4760-TDL/348] 11 p1468 N90-18450
Contribution to the study of stability robustness of nonlinear multivariable regulators
[INPE-4801-TDL/356] 11 p1554 N90-18950
First impressions of the comet drilling problem 12 p1743 N90-20021
Amplitude-dependent neutral modes in compressible boundary layer flows
[NASA-TM-102524] 13 p1799 N90-20326
Green's functions for the elastic annulus and their application to various crack problems 15 p2120 N90-22129
Measurements and mechanisms of localized aqueous corrosion in aluminum-lithium alloys 16 p2219 N90-22656
Additive evaluation criteria for aircraft noise 18 p2610 N90-24867
Statistical treatment of slow strain rate data for assessment of hydrogen embrittlement in low alloy high strength steel
[ARL-MAT-R-122] 20 p2832 N90-26106
Cloud top entrainment instability and cloud top distributions 22 p3214 N90-28231
A constitutive model for AS4/PEEK thermoplastic composites under cyclic loading
[NASA-CR-180393] 23 p3302 N90-28679
Periodic gaits for the CMU ambler 23 p3367 N90-29027
Search strategies for computer-stored information: A microcomputer tutorial 24 p3557 N90-30126

CRITICAL EXPERIMENTS
Analysis and evaluation of ZPPR (Zero Power Physics Reactor) critical experiments for a 100 kilowatt-electric space reactor
[DE90-005634] 12 p1713 N90-19835
CRITICAL FLOW
Experimental and analytical investigation of adiabatic critical water air two phase flow in small diameter tubes
[TB-88/1] 12 p1660 N90-19540
Nonlinear internal gravity wave critical layers
17 p2422 N90-23801
CRITICAL LOADING
Elastic-plastic instability of plane frames
14 p1992 N90-21415
Failure mechanisms under complex loading of glass-reinforced polyester composites and their matrices: The effect of superposed hydrostatic pressures up to 300 MPa on axial tensile and compressive strengths, and in-plane shear properties of unidirtionally reinforced glass-polyester composites and the relevant polyesters
15 p2110 N90-22072
Buckling of anisotropic cylindrical shells subjected to combined axial compression, normal pressure, bending and shear loading
[LR-611] 24 p3482 N90-29678
CRITICAL MACH NUMBER
U CRITICAL VELOCITY
U MACH NUMBER
CRITICAL MASS
Neon novae, recurrent novae, and type I supernovae
[DE90-003188] 12 p1728 N90-19931
Rapid mass transfer in binary systems
16 p2332 N90-23289
CRITICAL PATH METHOD
Project ORION microcomputer management system
[AD-A212945] 05 p0680 N90-13959
CRITICAL POINT
Critical magnetic fields (H(sub c2), H(sub c1)) and kappa in YBa2(Cu0.98M0.02)3O(7+delta), M=Ni, Al, and Cu
[DE89-016412] 01 p0130 N90-10745
Thermophysical properties of supercritical fluids and fluid mixtures
[DE89-016568] 02 p0193 N90-11102
Vapour pressures and critical points of liquids. Halogenated hydrocarbons
[ESDU-89006] 03 p0325 N90-11848
Thermophysical properties of isopropyl alcohol. Part 2: Thermodynamic properties at elevated pressures
[ESDU-89020-PT-2] 06 p0739 N90-14300
Orthobaric densities and molar volumes of liquids: Alcohols
[ESDU-89037] 07 p0897 N90-15184
Critical fluid light scattering 09 p1222 N90-17087
Vapor-liquid equilibria for complex mixtures with special emphasis on the critical region
[PB90-130345] 12 p1622 N90-19324
Critical point wetting drop tower experiment
[NASA-CR-186513] 14 p1957 N90-21208
CRITICAL PRESSURE
Vapor-liquid equilibrium of binary mixtures in the extended critical region. Part 1: Thermodynamic model
[PB89-218374] 04 p0469 N90-12687
Thermal conductivity of gaseous aliphatic hydrocarbons. Part 1: Alkanes
[ESDU-89035-PT-1] 07 p0897 N90-15183
Summary of a study to determine low-velocity impact damage and residual tension strength for a thick graphite/epoxy motor case
[NASA-TM-102678] 19 p2702 N90-25374
CRITICAL REYNOLDS NUMBER
U CRITICAL VELOCITY
U REYNOLDS NUMBER
CRITICAL SPEED
U CRITICAL VELOCITY
CRITICAL STRESS
U CRITICAL LOADING
CRITICAL TEMPERATURE
The effect of twins on critical currents of high Tc superconductors
[AD-A210988] 01 p0133 N90-10768
Physics and materials science of high temperature superconductors
[AD-A211246] 02 p0283 N90-11619
Vapor-liquid equilibrium of binary mixtures in the extended critical region. Part 1: Thermodynamic model
[PB89-218374] 04 p0469 N90-12687
Summary physical data tables: Alkanes
[ESDU-PD3] 07 p0893 N90-15162
Thermal conductivity of gaseous aliphatic hydrocarbons. Part 1: Alkanes
[ESDU-89035-PT-1] 07 p0897 N90-15183
Critical fluid light scattering 09 p1222 N90-17087
Critical field enhancement due to field penetration in fine-filament superconductors
[DE90-005389] 10 p1435 N90-18282
Superconducting and normal compounds: Some high field/high pressure effects 16 p2320 N90-23229
The onset of superconductivity in two-dimensional disordered systems 16 p2321 N90-23232
Influence of high energy radiation on critical parameters of superconducting ceramics YBa2Cu3O7
[DE90-620562] 16 p2322 N90-23239
CRITICAL VELOCITY
SR90, strontium shaped-charge critical ionization velocity experiment
[NASA-CR-186501] 14 p2024 N90-21606
CROP GROWTH
A collaborative effort to model plant response to acidic rain
[DE90-003002] 09 p1244 N90-17215
Spectral responses of soybeans and their relationship with agronomical parameters
[INPE-4832-PRE/1462] 10 p1398 N90-18084
Regulation of nitrogen uptake and assimilation: Effects of nitrogen source, root-zone pH, and aerial CO2 concentration on growth and productivity of soybeans
[NASA-CR-177546] 10 p1413 N90-18147
Relationships between spectral parameters and agronomics of wheat and beam crops
[INPE-4791-RPE/584] 11 p1523 N90-18768
Spectral response of wheat and its relationship with agronomical prameters
[INPE-4950-RPE/599] 11 p1524 N90-18774
Results of Agrisar-86 for the Flevopolder (Netherlands) test area
[BCRS-89-21] 11 p1527 N90-18789
Continuous hydroponic wheat production using a recirculating system
[NASA-TM-102784] 11 p1538 N90-18853
Relationship of radiometric field measurements of wheat in the Assis-Safra region, 1988
[INPE-4949-RPE/598] 13 p1819 N90-20443
Agricultural yield estimation of sugarcane based on agrometeorological-spectral model
[INPE-5016-RPE/610] 14 p1996 N90-21441
A knowledge-based information based for crop area estimation
[INPE-4990-PRE/1555] 14 p1996 N90-21444
Wheat productivity estimate through field radiometry
[INPE-4994-PRE/1556] 14 p2000 N90-21460
Carbon dioxide and water exchange rates by a wheat crop in NASA's biomass production chamber: Results from an 86-day study (January to April 1989)
[NASA-TM-102788] 19 p2716 N90-25453
System development and early biological tests in NASA's biomass production chamber
[NASA-TM-103494] 19 p2716 N90-25456
A computerized data-base system for land-use and land-cover data collected at ground-water sampling sites in the pilot national water-quality assessment program
[PB90-181868] 22 p3258 N90-28453
CROP IDENTIFICATION
Multiparameter scatterometer for remote sensing (RADSER). Project Scatter: State-of-the-art and future applications
[INPE-4871-PRE/1482] 11 p1511 N90-18701
Results of Agrisar-86 for the Flevopolder (Netherlands) test area
[BCRS-89-21] 11 p1527 N90-18789
Segmentation of Side-Looking Airborne Radar (SLAR) images using a priori knowledge
[BCRS-89-03] 12 p1679 N90-19644
CROP INVENTORIES
Quantitative evaluation of object-changes in multitemporal AGRISAR imagery
[FIM-195] 08 p1091 N90-16314
Use of remote sensing in operational inventory and monitoring agricultural and forestry tasks
08 p1094 N90-16336
Operational satellite environmental monitoring for food security by FAO: The ARTEMIS system
19 p2708 N90-25413
CROP INVENTORIES BY REMOTE SENSING
U AGRISTARS PROJECT
CROPLANDS
U FARMLANDS
CROPS
Impact of meteorology on the agricultural sector: Compilation and analysis of projects
[INPE-4846-PRE/1475] 16 p2257 N90-22866
CROSS CORRELATION
Spanwise measurements of vertical components of atmospheric turbulence
[NASA-TP-2963] 12 p1692 N90-19718
General forms and properties of zero cross-correlation radar waveforms
[AD-A217779] 13 p1790 N90-20273
Long term multi-frequency study of 3C 273
19 p2790 N90-25879
Spatial cross-correlation of Antarctic Sea ice and seabed topography
[NASA-CR-186815] 20 p2891 N90-26451
Application of automatic method to estimating high-level cloud motion wind in operational system and the characteristics of the resultant wind vectors
21 p3028 N90-27218
Progress in high temperature speckle-shift strain measurement system
[NASA-TM-103255] 22 p3177 N90-28031
CROSS FAULTS
U GEOLOGICAL FAULTS
CROSS FLOW
On the interaction of stationary crossflow vortices and Tollmien-Schlichting waves in the boundary layer on a rotating disc
[NASA-CR-181859] 01 p0002 N90-10007
Doubly-fluted tubes and enhanced tubes in confined crossflow
[PB89-217921] 03 p0345 N90-11971
Design and test of an NLF wing glove for the variable-sweep transition flight experiment
04 p0444 N90-12544
The 757 NLF glove flight test results
04 p0445 N90-12546
Cross-axis synchronous flow through coil planet centrifuge for large-scale preparative countercurrent chromatography
[PB89-200174] 04 p0468 N90-12682
Numerical evaluation of a solution representing a jet in cross-flow
[RAE-TM-AERO-2137] 04 p0502 N90-12893
Unsteady forces induced on finite-span cylinders in a cross-flow 05 p0642 N90-13746
A coning motion apparatus for hydrodynamic model testing in a non-planar cross-flow
[AD-A213431] 07 p0930 N90-15383
Response of structures to atmospheric turbulence. Response to across-wind turbulence components
[ESDU-89049] 09 p1239 N90-17191
Low cost filter development and control of permeability in high temperature, high pressure ceramic filter elements
[DE90-000403] 11 p1507 N90-18676
A streamwise upwind algorithm applied to vortical flow over a delta wing
[NASA-TM-102225] 12 p1599 N90-19201
Application of a three-dimensional Navier-Stokes model for a subsonic jet in a crossflow
13 p1749 N90-20045
The interaction between a plane shock wave and a cylindrical afterbody 15 p2046 N90-21728
Concerning the interaction of non-stationary cross-flow vortices in a three-dimensional boundary layer
[NASA-CR-182037] 18 p2492 N90-24245
Nonlinear development of Goertler and crossflow vortices and Goertler/Tollmien-Schlichting wave interaction
[AD-A221107] 18 p2553 N90-24571
Generation of circumferential velocity contours associated with pulsed point suction on a rotating disk
18 p2646 N90-25065
Calculation of 3D turbulent jets in crossflow with a multigrid method and a second-moment closure model
[NASA-TM-103159] 20 p2862 N90-26282
Wind tunnel investigation of periodic vortex separation from rough surface circular cylinders by means of acoustic measurements
[ESA-TT-1092] 23 p3268 N90-28499
Experimental investigations on the stability and transition of three-dimensional boundary layers
[ESA-TT-1026] 23 p3325 N90-28803
Structure in the near field of the transverse jet
[AD-A224502] 24 p3467 N90-29591
CROSS POLARIZATION
Eigensolutions for the reflection problem involving the interface of two chiral half spaces
[PB89-221592] 03 p0338 N90-11926
The Australian experiment with ETS-V
10 p1372 N90-17949
Polarization correction of Luneburg lens with chiral medium
[PB90-189127] 24 p3544 N90-30046
CROSS SECTIONS
Aircraft drawings index 17 p2343 N90-23340
The effect of a three-dimensional source on the flow through a channel with square cross section
[LR-512] 20 p2863 N90-26289
CROSSINGS
Higher order crossings from a parametric family of linear filters
[AD-A213427] 07 p0983 N90-15676
Theoretical study of the Townes-Merritt effect in level crossing experiments
[AD-A214909] 09 p1191 N90-16900

CROSSLINKING
Positron annihilation studies of interpenetrating polymer networks
[AD-A212162] 03 p0332 N90-11890
Model filled polymers I. Synthesis of crosslinked monodisperse polystyrene beads
[AD-A213228] 05 p0627 N90-13660
Process for producing a shaped, extruded product from a crosslinkable polymeric composition
[GB-PATENT-2-201-677-A] 05 p0627 N90-13662
Crosslinkable polymer
[GB-PATENT-2-205-846-A] 05 p0628 N90-13663
Crosslinked, flexible, low-molecular-weight polyacrylamide gels for mobility control
[DE90-000202] 07 p0913 N90-15280
Fundamental studies of time-dependent response and fracture of cross-linked polymers
[AD-A216694] 10 p1360 N90-17886
Thermal crystallization of polytetrahydrofuran networks
[AD-A215336] 10 p1436 N90-18285
Modified bismaleimides for carbon fibre composites
11 p1476 N90-18495
Interfacial chemistry of MoS2 films on Si
[AD-A216527] 11 p1482 N90-18532
Model filled polymers 3. Rheological behavior of polystyrene containing crosslinked polystyrene beads
[AD-A215867] 11 p1489 N90-18567
Carbon black/polyethylene composites for PTC (Positive Temperature Coefficient) thermistor applications
[AD-A215988] 12 p1619 N90-19307
Rigid rod molecules as liquid crystal thermosets
[AD-A217573] 13 p1770 N90-20158
Process for crosslinking methylene-containing aromatic polymers with ionizing radiation
[NASA-CASE-LAR-13448-1] 14 p1956 N90-21198
Conceptual definition of a high voltage power supply test facility
[NASA-CR-185216] 19 p2666 N90-25172
A tough high performance composite matrix
[NASA-CASE-LAR-14338-1] 21 p2970 N90-26881
A tough performance simultaneous semi-interpenetrating polymer network
[NASA-CASE-LAR-14339-1] 21 p2984 N90-26955
Structural and optical properties of DMP-128 holograms during environmental testing
[AD-A221691] 21 p3007 N90-27094

CROSSTALK
Single mode communication link
[AD-A219499] 17 p2388 N90-23601

CRUDE OIL
Devices and methods for in-situ combustion ignition
[DE89-000766] 06 p0740 N90-14309
The laminar to slug flow transition in Hele-Shaw flow
[DE90-000636] 06 p0777 N90-14521
Statistically designed study of the variables and parameters of carbon dioxide equations of state
[DE90-016196] 24 p3447 N90-29467

CRUISE MISSILES
Pivotal mono wing cruise missile with wing deployment and fastener mechanism
[AD-D014191] 04 p0452 N90-12594
Missile Aerodynamics: NEAR Conference on Missile Aerodynamics
[ISBN-0-9620629-1-X] 10 p1303 N90-17540
Use of semiempirical aerodynamic methods for preliminary design 10 p1304 N90-17546
High performance missiles of the future
10 p1305 N90-17550
Application of Bayesian reliability concepts to cruise missile electronic components
[AD-A216208] 10 p1394 N90-18059
Using simulation to determine a strategy for positively tracking a cruise missile by CMMCA
[AD-A220526] 17 p2362 N90-23448

CRUISING FLIGHT
Reducing C130E Hercules operating costs in the Royal Australian Air Force and the United States Air Force by increasing cruise speeds
[AD-A215747] 10 p1319 N90-17629
An approach to on-board optimization of cruise at constant altitude
[LR-581] 15 p2050 N90-21752

CRUSADER AIRCRAFT
U F-8 AIRCRAFT

CRUSHING
The effect of aircraft size on cabin floor dynamic pulses
[DOT/FAA/CT-88/15] 19 p2659 N90-25136

CRUSTAL DYNAMICS
U EARTH CRUST
U GEODYNAMICS

CRUSTAL FRACTURES
Supplementing geodetic data with prior information for crustal deformation in the Imperial Valley, California
[TR-6-1988] 05 p0668 N90-13904
Fracture mechanical aspects of dust emission processes from a model comet surface 12 p1740 N90-20004
In-situ fracture stiffness determination
[DE90-009202] 15 p2129 N90-22173

CRUSTS
NT EARTH CRUST
NT PLANETARY CRUSTS
Radiation modification of cometary materials: Laboratory simulations 08 p1143 N90-16626
Physical models of cometary nuclei: A review
12 p1738 N90-19991
Crustal strength of different model comet materials
12 p1740 N90-20003

CRYOGENIC COOLING
Design and calibration of an electrodynamic driver for the Space Thermoacoustic Refrigerator (STAR)
[AD-A212022] 03 p0335 N90-11906
Reduced voltage and restart testing of the 1-watt integral cryogenic cooler (HD-1033B/C/D)
[AD-A215133] 09 p1203 N90-16971
Reliability testing of the Hughes temperature controlled 1/4 watt split cycle cryogenic cooler (HD-1045 (V)/UA)
[AD-A216696] 12 p1641 N90-19426
Mechano-caloric cooling device
[NASA-CR-186316] 12 p1662 N90-19552
Multicomponent gas sorption Joule-Thomson refrigerator
[NASA-CASE-NPO-17569-1-CU]
20 p2844 N90-26176
High temperature superconductivity applications for electronic warfare and microwave systems
[AD-A222972] 21 p3082 N90-27528
Spacecraft thermal control design data, volume 5. Section R: Cryogenic cooling. Section S: Existing satellites
[ESA-PSS-03-108-ISSUE-1-VOL-5]
22 p3132 N90-27772

CRYOGENIC EQUIPMENT
Cryogenic Schottky-mixer receiver front-end for 40-50 GHz
[PB89-221667] 03 p0343 N90-11959
High-temperature superconducting current leads for cryogenic apparatus
[DE89-017680] 03 p0411 N90-12361
A closed-cycle refrigerator for cooling maser amplifiers below 4 Kelvin 04 p0487 N90-12797
Cryostatless high temperature supercurrent bearings for rocket engine turbopumps
[NASA-CR-183807] 04 p0509 N90-12935
Cryogenic systems for the large deployable reflector
05 p0597 N90-13470
Cryogenics for LDR 05 p0598 N90-13471
LDR cryogenics 05 p0598 N90-13472
Efficiency measurement of high pressure cryogenic rocket pumps
[NAL-TR-1022] 10 p1391 N90-18042
A refrigerated Dewar for the Josephson array voltage calibration system
[DE90-005237] 15 p2172 N90-22412
Initial experimentation on the nonvented fill of a 0.14m3 (5 ft. 3) dewar with nitrogen and hydrogen
[NASA-TM-103155] 20 p2862 N90-26278
Spacecraft thermal control design data, volume 5. Section R: Cryogenic cooling. Section S: Existing satellites
[ESA-PSS-03-108-ISSUE-1-VOL-5]
22 p3132 N90-27772

CRYOGENIC FLUID STORAGE
Evaluation of supercritical cryogen storage and transfer systems for future NASA missions
[NASA-TM-102394] 02 p0160 N90-10912
Independent Orbiter Assessment (IOA): Analysis of the electrical power distribution and control/electrical power generation subsystem
[NASA-CR-185538] 02 p0165 N90-10933
Evolutionary space station fluids management strategies
[NASA-CR-185137] 02 p0175 N90-10983
Liquid Transfer Cryogenic Test Facility: Initial hydrogen and nitrogen no-vent fill data
[NASA-TM-102572] 14 p1972 N90-21295
Spacecraft attitude impacts on COLD-SAT non-vacuum jacketed LH2 supply tank thermal performance
[NASA-TM-103158] 16 p2207 N90-22592
Design of cryogenic tanks for launch vehicles
16 p2220 N90-22662
Acquisition and correlation of cryogenic nitrogen mass flow data through a multiple orifice Joule-Thomson device
[NASA-TM-103121] 16 p2237 N90-22761
Numerical investigation of the thermal stratification in cryogenic tanks subjected to wall heat flux
[NASA-TM-103194] 22 p3171 N90-27984

CRYOGENIC FLUIDS
NT FERMI LIQUIDS
NT LIQUID HELIUM
NT LIQUID HELIUM 2
NT LIQUID HYDROGEN
NT LIQUID NITROGEN
NT LIQUID OXYGEN
Evolutionary space station fluids management strategies
[NASA-CR-185137] 02 p0175 N90-10983
Gas-phase flowrate effect on disintegrating cryogenic liquid-jets
[NASA-TM-102357] 02 p0223 N90-11277
Tank pressure control experiment on the space shuttle
[NASA-TM-102313] 05 p0615 N90-13590
CryoTran user's manual, version 1.0
[NASA-TM-102468] 07 p0973 N90-15622
On the selection of materials for cryogenic seals and the testing of their performance
08 p1156 N90-16696
Zero-gravity vortex vent and PVT gaging system
11 p1475 N90-18486
Scattered-light scanner measurements of cryogenic liquid-jet breakup
[NASA-TM-102432] 15 p2101 N90-22021
Pratt and Whitney cryogenic turbopump bearing experience 23 p3292 N90-28624

CRYOGENIC ROCKET PROPELLANTS
Evaluation of supercritical cryogen storage and transfer systems for future NASA missions
[NASA-TM-102394] 02 p0160 N90-10912
Evolutionary space station fluids management strategies
[NASA-CR-185137] 02 p0175 N90-10983
Thermal protection systems for reentry and hypersonic flight
[DLR-MITT-89-14] 05 p0613 N90-13577
The Ariane-5 Programme 09 p1176 N90-16808
Vulcain engine development status
09 p1176 N90-16810
Propellant trends in advanced rocket propulsion
09 p1179 N90-16838
Advanced APS impacts on vehicle payloads
11 p1472 N90-18472
RF modal quantity gaging 11 p1474 N90-18483
Technical accomplishments of the NASA Lewis Research Center, 1989
[NASA-TM-102296] 17 p2486 N90-24220
First Vulcain engine test results
[MBB-UK-0054/88-PUB] 19 p2652 N90-25093

CRYOGENIC TEMPERATURE
Capacitive energy storage at cryogenic temperatures, phase 2
[AD-A210366] 01 p0061 N90-10347
Cryogenic free jets
[ESA-TT-1128] 03 p0311 N90-11767
The strength-toughness combination of the aluminum-lithium alloys 2090 and 2091 at cryogenic temperatures
[DE90-001425] 06 p0746 N90-14338
The metallurgical determinants of toughness as cryogenic temperature
[DE90-002331] 06 p0748 N90-14351
Proton responses on MOS (Metal-Oxide-Semiconductor) electronics operating at cryogenic temperatures
[AD-A217622] 13 p1894 N90-20868
Deformation and fracture of thin sheet aluminum-lithium alloys: The effect of cryogenic temperatures
16 p2218 N90-22655
Computer controlled cryogenic temperature controller
[AD-A218785] 16 p2227 N90-22701
Experimental evaluation of a tuned electromagnetic damper for vibration control of cryogenic turbopump rotors
[NASA-TP-3005] 17 p2354 N90-23403
Fatigue crack propagation in austenitic stainless steels at cryogenic temperatures
[DE90-011597] 18 p2528 N90-24426
Fracture toughness and failure mechanisms in commercial 2091 Al-Li sheet at cryogenic temperatures
[AD-A222803] 20 p2835 N90-26125
Weldment mechanical properties of aluminum-copper-lithium alloy, 2090, at ambient and cryogenic temperatures
[DE90-014178] 21 p2981 N90-26941

CRYOGENIC WIND TUNNELS
Hot-film system for transition detection in cryogenic wind tunnels 04 p0441 N90-12522
Residual interference assessment in adaptive wall wind tunnels
[NASA-CR-181896] 04 p0458 N90-12625
Special Course on Advances in Cryogenic Wind Tunnel Technology
[AGARD-R-774] 09 p1028 N90-15939

Introduction to cryogenic wind tunnels
08 p1028 N90-15940
The NASA Langley 0.3-meter transonic cryogenic tunnel 08 p1028 N90-15941
The Kryo-Kanal Koeln (KKK): Description of the tunnel conversion. Thermal insulation, instrumentation, operational experience, test results and operating costs
08 p1029 N90-15943
Automatic control of KKK: Requirements, sensors, actuators, and control performance results
08 p1029 N90-15944
The cryogenic induction tunnel T2 at Toulouse
08 p1029 N90-15946
The cryogenic Ludwieg tube tunnel at Goettingen
08 p1029 N90-15947
Other cryogenic wind tunnel projects
08 p1029 N90-15948
Instrumentation for cryogenic wind tunnels
08 p1030 N90-15950
Fundamental considerations in testing in cryogenic wind tunnels 08 p1030 N90-15951
Test techniques for cryogenic wind tunnels
08 p1030 N90-15952
Flow visualization in the cryogenic wind tunnel
08 p1030 N90-15953
Materials and techniques for model construction
08 p1030 N90-15954
Some recent developments in materials and techniques for model fabrication 08 p1031 N90-15955
Models for cryogenic wind tunnels
08 p1031 N90-15956
Automatic control of cryogenic wind tunnels
08 p1031 N90-15957
Experience with strain-gage balances for cryogenic wind tunnels 08 p1031 N90-15958
Safety and cryogenic wind tunnels
08 p1032 N90-15960
Productivity and cryogenic wind tunnels
08 p1032 N90-15961
Energy management and recovery
08 p1032 N90-15962
An experimental AWTS process and comparisons of ONERA T2 and 0.3-m TCT AWTS data for the ONERA CAST-10 aerofoil 10 p1324 N90-17653
Method of forming a multiple layer dielectric and a hot film sensor therewith
[NASA-CASE-LAR-13678-1] 17 p2478 N90-24168

CRYOGENICS
Telescope structure for cryogenic application
02 p0180 N90-11019
Aspects of the development of a 1-5 micron infrared camera for astronomy 02 p0290 N90-11656
An algorithm for control volume analysis of cryogenic systems
[AD-A213394] 05 p0631 N90-13683
Cryogenic temperature effects on sting-balance deflections in the National Transonic Facility
[NASA-TM-4157] 06 p0727 N90-14244
Cryogenic mechanical properties of low density superplastic Al-Mg-Sc alloys
[DE90-002120] 07 p0904 N90-15222
Retractable gas cooled leads for ASTROMAG
[DE90-002679] 07 p0921 N90-15331
Analysis of ambient polar volatile organic compounds using chemical ionization-ion trap detector
[PB90-106451] 07 p0956 N90-15529
The NASA Langley 0.3-meter transonic cryogenic tunnel 08 p1028 N90-15941
The US National Transonic Facility, NTF
08 p1028 N90-15942
Cryogenic engineering and materials
08 p1030 N90-15949
Cryogenic balances for the US NTF
08 p1031 N90-15959
D3-D cryogenic control system upgrade
[DE90-003290] 08 p1054 N90-16092
Analysis of particulates of comet nucleus samples: Possible use of olivine as indicator phase
08 p1147 N90-16646
On the selection of materials for cryogenic seals and the testing of their performance
08 p1156 N90-16696
Debris/ice/TPS assessment and photographic analysis for Shuttle Mission STS-33R
[NASA-TM-102785] 09 p1180 N90-16846
Design and testing of a superfluid liquid helium cooling loop
[NASA-CR-182776] 09 p1216 N90-17050
Lightweight transformer demonstration
[DE90-001470] 10 p1379 N90-17991
Materials and selection criteria analysis for the compact ignition tokamak toroidal field coil turn-to-turn insulation system: Photographic summary oflaboratory testing
[DE90-008020] 13 p1891 N90-20850
Advanced Launch System (ALS): Electrical actuation and power systems improve operability and cost picture
[NASA-TM-102547] 14 p1968 N90-21271
Liquid Transfer Cryogenic Test Facility: Initial hydrogen and nitrogen no-vent fill data
[NASA-TM-102572] 14 p1972 N90-21295
Experience with the UKIRT InSb array camera
14 p1977 N90-21327
Status of the isophot detector development
14 p1980 N90-21342
Program CICC: Flow and heat transfer in Cable In Conduit Conductors, user's manual
[DE90-007924] 14 p2033 N90-21661
Nonoptimal entropy generation by heat transfer in cryogenic domain
[DE90-007544] 14 p2034 N90-21667
Ultralow noise performance of an 8.4-GHz maser-feedhorn system 15 p2076 N90-21889
Institute for Materials Science and Engineering, Fracture and Deformation Division: Technical activities, 1989
[PB90-155359] 15 p2116 N90-22106
A refrigerated Dewar for the Josephson array voltage calibration system
[DE90-005237] 15 p2172 N90-22412
Study to identify future cryogen payload elements/users for space shuttle launch during period 1990 to 2000
[NASA-CR-186311] 17 p2363 N90-23452
Wearing of cryomechanisms at 4 K
[REPT-892-440-103] 17 p2473 N90-24139
Interconnecting devices conceived for in-orbit operations 18 p2506 N90-24323
Rome air development center cryo test facility
[AD-A220067] 19 p2662 N90-25147
Use of the TACL system at CEBAF for control of the cryogenic test facility
[CEBAF-PR-89-024] 19 p2755 N90-25652
Use of high-temperature superconductors in superconducting magnetic energy power sources
[DE90-011119] 19 p2761 N90-25686
Debris/ice/TPS assessment and photographic analysis for shuttle mission STS-31R
[NASA-TM-102790] 20 p2819 N90-26040
Liquid-vapor equilibrium of multicomponent cryogenic systems 20 p2948 N90-26774
Cryogenic anti-friction bearing with inner race
[NASA-CASE-MFS-28384-1] 21 p3010 N90-27112
Debrix/ice/TPS assessment and photographic analysis of Shuttle Mission STS-32R
[NASA-TM-102787] 22 p3124 N90-27733
Cryogenic, high speed, turbopump bearing cooling requirements 23 p3291 N90-28620
Proceedings of Damping '89. Volume 3: Pages ICA-1 through KDC-15
[AD-A223433] 24 p3479 N90-29666
Proceedings of the High Energy Density Materials Contractors Conference
[AD-A223793] 24 p3484 N90-29695

CRYOLITE
Electronic conduction in molten cryolite saturated with alumina
[DE90-015090] 23 p3400 N90-29211

CRYOPUMPING
Mechano-caloric cooling device
[NASA-CR-186316] 12 p1662 N90-19552
BASG thermomechanical pump helium 2 transfer tests
[NASA-CR-177541] 14 p1939 N90-21097

CRYOSORPTION
U SORPTION

CRYOSTATS
High-temperature superconducting current leads for cryogenic apparatus
[DE89-017680] 03 p0411 N90-12361
Construction of the rotating cryostat ROTA2, its use for zero sound experiments in (3)He-B, and calculations of ion mobility in (3)He-A and (3)He-P
[ISBN-952-90091-3-5] 05 p0645 N90-13765
Thermal design of a 10-kW helium refrigerator
[DE90-701785] 06 p0756 N90-14403
Handling and analysis of ices in cryostats and glove boxes in view of cometary samples
08 p1146 N90-16643
Research and development of a helium-4 based solar neutrino detector
[DE90-005416] 10 p1447 N90-18353
Nonoptimal entropy generation by heat transfer in cryogenic domain
[DE90-007544] 14 p2034 N90-21667
A technique to measure the thermal diffusivity of high T(sub c) superconductors 22 p3147 N90-27846
Investigation of YBa2Cu3O(7-sigma) by NMR and construction of an ultra low temperature cryostat
24 p3550 N90-30088

CRYOTRAPPING
Experimental studies of gas trapping in amorphous ice and thermal modelling of comets: Implications for Rosetta 08 p1140 N90-16610
Traps for neutral atoms
[AD-A221331] 19 p2754 N90-25649

CRYPTOGRAPHY
A paradoxical result in unconditionally secure authentication codes, and an explanation
[DE90-008529] 13 p1867 N90-20710
Knowledge and distributed computation
[AD-A223100] 21 p3039 N90-27270
Hash functions: A tutorial and status report
[NPL-DITC-151/89] 22 p3238 N90-28361
Secure Data Network System (SDNS) network, transport, and message security protocols
[PB90-198946] 23 p3318 N90-28757

CRYSTAL DEFECTS
NT CRYSTAL DISLOCATIONS
NT EDGE DISLOCATIONS
NT POINT DEFECTS
NT VACANCIES (CRYSTAL DEFECTS)
The effects of normal annealing cycles during IGFET fabrication on initial and radiation induced gate insulator defects
[AD-A210282] 01 p0049 N90-10278
Defect structures preceding amorphization by ion irradiations in YBa2Cu3O(7-delta)
[DE89-016905] 02 p0282 N90-11612
Passage of ultrarelativistic electrons through real crystals
[DE89-618624] 02 p0282 N90-11613
Computer simulations of radiation damage in amorphous solids
[PB89-212682] 03 p0322 N90-11827
Mechanism of electrochemical activation of carbon electrodes: Role of graphite lattice defects
[AD-A211644] 03 p0325 N90-11845
Characterization of the Structure and Chemistry of Defects in Materials: Proceedings, volume 138
[DE89-014796] 03 p0410 N90-12352
Interaction of hydrogen isotopes with metals: Deuterium trapped at lattice defects in palladium
[DE90-000811] 06 p0747 N90-14344
Pairs of chalcogen impurities in silicon
[DE89-635767] 08 p1049 N90-16063
Slow positron defect profiling of silicon epilayers
[DE90-003958] 08 p1087 N90-16288
Fracto-fusion. Mechanism of cold fusion
[DE90-719573] 08 p1125 N90-16518
La(sub 2)MO(sub 4 + delta) (M = Cu, Ni, Co): Phase separation and superconductivity resulting from excess oxygen defects
[DE90-001988] 08 p1128 N90-16534
The 1MeV-electron irradiation induced defects in epitaxially grown 3C-SiC
[DE90-719574] 08 p1131 N90-16554
Diffusion and defect characterization studies of mercury cadmium telluride
[AD-A214655] 09 p1289 N90-17470
Structural instabilities, impurities, and defects in electronic materials
[AD-A215384] 09 p1290 N90-17481
Search for far infrared radiation from optically pumped defect modes
[AD-A216976] 12 p1714 N90-19843
Digital capacity transient spectroscopy of deep structure defects in III-V-Semiconductor structures
[ETN-90-96057] 12 p1722 N90-19890
NMR (Nuclear Magnetic Resonance) imaging development for the study of solids
[AD-A217073] 12 p1723 N90-19899
Research of the interaction between hydrogen and deuterium with atomic eigen defects and dislocations in nickel and iron
[ETN-90-95380] 13 p1776 N90-20195
Magnetic properties of surfaces and interfaces
[DE90-007348] 13 p1880 N90-20789
Workshop on the Physics and Chemistry of Mercury Cadmium Telluride and Related II-VI compounds
[AD-A217496] 13 p1894 N90-20867
SiO(x) precipitation: Defect density correlation with the n+ substrate resistivity
[DE90-005593] 13 p1895 N90-20878
Identification of defects in SOI (Silicon-On-Insulator) wafers
[DE90-006020] 13 p1895 N90-20879
Progress in the material development of LiCaAlF(6):Cr(3+) laser crystals
[DE90-009542] 14 p2034 N90-21666
The lithium concentration dependence of creep in binary aluminum-lithium alloys
[AD-A218706] 16 p2221 N90-22668
Fundamental and applied aspects of defect engineering in G2As; EL2 and other nonstoichiometric defects
[AD-A218597] 17 p2475 N90-24152
Cascade collapse in copper and nickel
[DE90-011115] 18 p2527 N90-24423

The defect structure of ion and neutron irradiated YBa2Cu3O(7-delta) single crystals
[DE90-010100] 18 p2619 N90-24920
HREM defects in GaAs/Ga(1-x)In(x)As strained layer superlattices
[DE90-010610] 18 p2620 N90-24924
Protons and lattice defects in perovskite-related oxides
[DE90-010957] 18 p2624 N90-24955
Twin boundaries, interfaces and modulated structures in martensites
[DE90-012899] 20 p2833 N90-26111
Crystal growth and deformation behavior of TiAl aluminides
[DE90-012972] 20 p2930 N90-26671
High temperature x ray diffraction and Landau theory investigations of order-disorder transition in defect NaCl-type solids
[DE90-011807] 20 p2930 N90-26673
Critical current density, flux creep, and microstructure in a Bi-Sr-Ca-Cu-O system
[DE90-010457] 20 p2931 N90-26676
Application of microdesigned interfaces to studies of ceramic processing
[DE90-011633] 21 p2983 N90-26951
Problems of enclosed crystal interfaces
[DE90-011594] 21 p3079 N90-27509
Hyperthermal atomic oxygen generator
[NASA-CR-186573] 22 p3155 N90-27689
Recent progress in electronic structure calculations for defects in metals
[DE90-016323] 24 p3452 N90-29494
Theory of electronic states and formations energies of defect complexes, interstitial defects, and crystal growth in semiconductors
[AD-A224069] 24 p3551 N90-30093
Optical nonlinearity due to structure defects and bistability in the band discontinuity area of CdS
[ETN-90-97303] 24 p3554 N90-30112

CRYSTAL DISLOCATIONS
NT EDGE DISLOCATIONS
Field-effect spectroscopy of interface states
[AD-A212998] 05 p0703 N90-14112
Quasicrystals and grain boundaries
[DE90-002213] 06 p0857 N90-14981
Modeling dislocation evolution in irradiated alloys
[DE90-004921] 08 p1047 N90-16051
Dislocation behaviour in Ge(x)Si(1-x) epilayers on (001) Si
[DE90-007063] 11 p1572 N90-19051
Modified dislocation structures in Ge(x)Si(1-x) double epilayers on (001) Si
[DE90-007078] 11 p1572 N90-19052
Microstructural simulations of dynamic recrystallization
[DE90-007504] 12 p1722 N90-19695
Research of the interaction between hydrogen and deuterium with atomic eigen defects and dislocations in nickel and iron
[ETN-90-95380] 13 p1776 N90-20195
An investigation of the dislocation structure of the Ni/Ag phase boundary
[DE90-008426] 13 p1895 N90-20876
Deformation and microstructure of rutile
[DE90-614113] 14 p2032 N90-21654
Precipitation on dislocations in Al-Li-Cc-Mg-Zr
[AD-A221124] 18 p2526 N90-24415
Effects of internal hydrogen on the vacancy loop formation probability in Al
[DE90-011114] 18 p2527 N90-24422
Cascade collapse in copper and nickel
[DE90-011115] 18 p2527 N90-24423
Electromigration in metallic microstructures
[AD-A221208] 18 p2622 N90-24942
Weak-beam electron microscopy of dislocation splitting in TiAl: Relationship to plasticity
[ESA-TT-1159] 19 p2676 N90-25217
Molecular beam epitaxial growth, characterization, and devices of modulated semiconductor structures
[AD-A221545] 21 p3084 N90-27538

CRYSTAL GROWTH
NT CZOCHRALSKI METHOD
NT DIRECTIONAL SOLIDIFICATION (CRYSTALS)
NT EPITAXY
NT LIQUID PHASE EPITAXY
NT MOLECULAR BEAM EPITAXY
NT PROTEIN CRYSTAL GROWTH
NT VAPOR PHASE EPITAXY
Quartz crystal microbalance studies of electrochemical growth of conducting polymers
[AD-A210788] 01 p0052 N90-10295
Morphological aspects of the friction of hot-filament-grown diamond thin films
[DE89-015986] 01 p0130 N90-10750
Autonomous control system for Czochralski growth of LEC GaAs
[AD-A210190] 01 p0131 N90-10754
Effects of gravity on equilibrium crystal shapes
02 p0281 N90-11602
Design and construction of systems for the single-crystals growth of ternary silver halides, alkali halides, and alkaline earth fluorides, and the dielectric investigation of silver halide
[ETN-89-94673] 02 p0286 N90-11632
Growth and characterization of materials for tunable lasers in the near infrared spectral region
[NASA-CR-185832] 03 p0352 N90-12009
New laser materials
[DE89-017524] 03 p0353 N90-12017
Process for single crystal growth of high T(sub c) superconductors
[AD-D014167] 03 p0409 N90-12346
Characterization of the Structure and Chemistry of Defects in Materials: Proceedings, volume 138
[DE89-014796] 03 p0410 N90-12352
Estimation of time to maximum supercooling during dynamic frazil ice formation
[AD-A212204] 04 p0471 N90-12699
Method for growing patterned thin films of superconductors
[AD-D014195] 04 p0560 N90-13262
Flight software development for the isothermal dendritic growth experiment
[NASA-TM-102412] 05 p0685 N90-13988
SEM (Scanning Electron Microscope) image analysis of grain growth in microwave-annealed alumina
[DE90-001606] 06 p0746 N90-14339
Primary arm spacing in directionally solidified Pb-10 wt percent Sn alloys
[NASA-CR-185190] 06 p0756 N90-14396
Electronic materials high-T(sub c) superconductivity polymers and composites structural materials surface science and catalysts industry participation
[NASA-CR-186063] 07 p0890 N90-15145
Processing and properties of nanophase oxides
[DE90-003826] 07 p0895 N90-15171
Research on mercury cadmium telluride
[AD-A213924] 07 p0906 N90-15237
Development of high performance beta-SiC field-effect transistors
[AD-A213885] 07 p0924 N90-15346
Research on amorphous silicon-germanium alloys for tandem solar cells
[DE89-009436] 07 p0950 N90-15499
Bridgman crystal growth
[NASA-CR-186204] 07 p0997 N90-15766
Irradition-induced grain growth: Role of dislocations
[DE90-003565] 07 p1001 N90-15792
Phase equilibrium and crystal growth studies on AgGaSe2 and related nonlinear optical materials
[AD-A213650] 07 p1003 N90-15809
Use of computer simulations to analyze limitations of kinetic models for recrystallization
[DE90-003618] 08 p1130 N90-16548
The concept of axial-symmetry constraint and its significance in recrystallization
[DE90-003620] 08 p1131 N90-16549
Eurolaser. High power excimer laser: Optical crystals
[ETN-90-95901] 08 p1132 N90-16558
Plasma assisted chemical vapor deposition of diamond films
[AD-A214641] 09 p1197 N90-16934
Reactive atmosphere processing of BaTiO3 and origins of its photorefractive effect
[AD-A215034] 09 p1289 N90-17475
Effects of O2 ion bombardment of Y-BaCu-oxide during thin film growth
[DE90-005315] 09 p1293 N90-17495
Temperature profiles in high gradient furnaces
10 p1362 N90-17896
Use of anomolous thermal imaging effects for multi-mode systems control during crystal growth
10 p1365 N90-17910
Experiments on large single crystals of the superconducting oxides YBa2Cu3O7, La sub 2-xBa sub xCuO4, and Bi-Ca-Sr-O
[AD-A215283] 10 p1435 N90-18284
Application of artificial intelligence control to the vapor-liquid-solid silicon carbide whisker process
[DE90-007835] 11 p1480 N90-18519
Studies of cubic ice crystals
[AD-A216574] 11 p1534 N90-18832
Crystal growth and mechanical properties of semiconductor alloys
[AD-A216697] 11 p1570 N90-19035
Solid State Photovoltaic Research Branch
[DE89-009463] 12 p1682 N90-19660
Opto-Em and devices investigation
[AD-A215033] 12 p1709 N90-19814
Computer simulation of recrystallization in the presence of second phase particles
[DE90-007531] 12 p1723 N90-19896
Human serum albumin crystals and method of preparation
[NASA-CASE-MFS-28234-1] 13 p1850 N90-20616
Apparatus for mixing solutions in low gravity environments
[NASA-CASE-MFS-26047-1] 14 p1958 N90-21209
Contract crystal growth and fabrication services
[AD-A218327] 14 p2031 N90-21646
Anisotropy of grain growth in alumina
[DE90-009045] 14 p2032 N90-21655
Linear, nonlinear, and tunable guided wave modes for high-power (GaAl)As semiconductor lasers
15 p2104 N90-22036
UV photo-enhanced MOCVD of cadmium and cadmium telluride
[RSRE-MEMO-4208] 15 p2174 N90-22422
The effect of elevated gravity on the crystallization of the MFI zeolites, ZSM-5, and silicalite
16 p2320 N90-23231
Hanging drop crystal growth apparatus and method
[NASA-CASE-MFS-28206-1-SB]
16 p2322 N90-23242
Advanced gas phase reactor for growth of Ge sub x Si sub 1-x
[AD-A219012] 16 p2323 N90-23250
High temperature electric arc furnace and method
[NASA-CASE-MFS-28281-1] 17 p2357 N90-23415
Solidification of dilute alloys under fluctuating residual gravity
[REPT-892-430-112] 17 p2377 N90-23535
Fundamental and applied aspects of defect engineering in G2As; EL2 and other nonstoichiometric defects
[AD-A218597] 17 p2475 N90-24152
Crystal growth apparatus
[NASA-CASE-MFS-28182-1] 17 p2478 N90-24169
Grain growth and phase formation in ion irradiated/annealed thin Ni-Al alloys films
[DE90-010409] 18 p2525 N90-24407
Contract crystal growth and fabrication services
[AD-A221357] 18 p2623 N90-24947
Hydrogen induced fracture characteristics of single crystal nickel-based superalloys
[NASA-CR-183992] 20 p2832 N90-26108
Dendritic web silicon photovoltaic cell research
[DE90-011788] 20 p2880 N90-26387
Temperature and melt solid interface control during crystal growth
[NASA-CR-186731] 20 p2929 N90-26664
Crystal growth and deformation behavior of TiAl aluminides
[DE90-012972] 20 p2930 N90-26671
MBE growth technology for high quality strained III-V layers
[NASA-CASE-NPO-17723-1-CU]
20 p2932 N90-26685
Intracavity frequency doubling of a Nd:YAG laser with an organic nonlinear optical crystal
[AD-A222392] 21 p3008 N90-27102
Growth of III-V films by control of MBE growth front stoichiometry
[NASA-CASE-NPO-17724-1-CU]
21 p3081 N90-27517
Preparation and magnetic measurements of single crystal Tl2Ba2CaCu2O8
[DE90-013657] 21 p3081 N90-27519
The 2nd International Conference on Low-Energy Dislocation Structures
[AD-A222887] 21 p3082 N90-27525
The 1990 Gordon Research Conference on Crystal Growth
[AD-A223218] 21 p3083 N90-27531
Design of organic nonlinear optical materials
[AD-A222400] 21 p3084 N90-27536
Diamonds in detonation soot
21 p3094 N90-27585
Grain orientation studies in superconductors
22 p3148 N90-27852
Microphysical fundamentals governing cirrus cloud growth: Modeling studies 22 p3225 N90-28291
Optoelectronics Research Center
[AD-A221926] 22 p3246 N90-28410
High resistivity Al(x)Ga(1-x) As(y)Sb(1-y) epitaxial layers by sulfur compensation doping
[DE90-012228] 22 p3248 N90-28419
Kinetic pathway in Stranski-Krastanov growth of Ge on Si(001)
[AD-A224324] 24 p3445 N90-29456
Influence of convection on microstructure
[NASA-CR-186506] 24 p3448 N90-29470
Research on mercury cadmium telluride
[AD-A224250] 24 p3448 N90-29474
Dynamic consolidation of super hard materials
[AD-A224460] 24 p3454 N90-29505
Mechanism of habit change for atmospheric ice crystal growth 24 p3489 N90-29717

Theory of electronic states and formations energies of defect complexes, interstitial defects, and crystal growth in semiconductors
[AD-A224069] 24 p3551 N90-30093
High throughput MBE materials for MODFET's
[AD-A223452] 24 p3552 N90-30097
Integrated technology in MCT/GaAs and MCT/Si for medium and long wavelength infrared
[AD-A223557] 24 p3552 N90-30100
Manufacturing and characterization of liquid-phase epitaxy layers with atomic levels at the crystal surface and at the hetero limit surfaces in the system GaAs-AlGaAs
[ETN-90-97310] 24 p3554 N90-30113

CRYSTAL LATTICES
NT BODY CENTERED CUBIC LATTICES
NT CUBIC LATTICES
NT FACE CENTERED CUBIC LATTICES
NT SUPERLATTICES
The structure determination of molecular adsorbates with large unit cells or lattice-gas disorder on metal surfaces
[AD-A210926] 01 p0042 N90-10230
Shock-induced atomic-scale structure in metals
[DE89-016539] 02 p0197 N90-11124
Ion beam annealing of Ga-implanted Si
[DE89-016857] 02 p0282 N90-11610
Deformation and defects in Laves-phase intermetallic compounds
[DE89-017798] 03 p0328 N90-11862
Energy concentration induced by phase transitions in hydrogenated metals
[PREPRINT-672] 05 p0625 N90-13650
Interaction of hydrogen isotopes with metals: Deuterium trapped at lattice defects in palladium
[DE90-000811] 06 p0747 N90-14344
Solid oxide fuel cells electrodes based on In(sub 2)O(sub 3)-PrO(sub 1.83)-ZrO(sub 2)
[DE90-002666] 06 p0806 N90-14691
Atomic matching across internal interfaces
[DE90-002266] 06 p0841 N90-14889
Ion beam processing of advanced electronic materials
[DE89-017342] 06 p0851 N90-14944
X ray studies of strain, interface, and impurity in semiconductors
[DE90-001525] 06 p0851 N90-14947
Practical limitations of ALCHEMI measurements on ordered intermetallic alloys
[DE90-000700] 06 p0853 N90-14957
Theory of the energetics and nonclassical nucleation for martensitic transformations from partially soft lattice modes
[DE90-002182] 06 p0854 N90-14964
Quasicrystals and grain boundaries
[DE90-002213] 06 p0857 N90-14981
A diffusion on a fractal state space
[AD-A213555] 07 p0988 N90-15707
Molecular-dynamics study of the amorphization of CuTi
[DE90-003563] 07 p1001 N90-15791
Cation disordering in the Tl-2122 superconductors
[DE90-003579] 07 p1001 N90-15795
High resolution electron microscopy of grain boundaries in nanophase palladium
[DE90-003823] 07 p1002 N90-15800
Epitaxial iron films
[AD-A213551] 07 p1003 N90-15807
Host materials for transition-metal ions
[AD-A213605] 07 p1003 N90-15808
Atomic scale structure of twin boundary in Y-Ba-Cu-O superconductors
[DE90-003955] 07 p1006 N90-15823
Elastic moduli of copper: Electronic structure contributions from pseudopotentials and full-potential linear muffin-tin orbital band structure calculations
[DE90-004423] 08 p1044 N90-16037
Interplanar spacing for various phases in austenitic stainless steels
[DE90-602350] 08 p1045 N90-16038
Contribution to the study of order effects in the Ising model framework: Ground states and phase diagrams
[ESA-TT-1118] 08 p1132 N90-16557
Kosterlitz-Thouless phase transition in two-dimensional hierarchical Coulomb gases
[DE89-618399] 09 p1189 N90-16890
Mechanics of iron, its stability and phase transformation
[DE89-636210] 09 p1193 N90-16913
Hardness-damage correlations in Ta implanted single crystal Ni3Al
[DE90-005270] 09 p1293 N90-17494
The Hueckel model for small metal clusters. 4: Orbital properties and cohesive energies for model clusters of up to several hundred atoms
[AD-A216161] 10 p1354 N90-17852
Environmental embrittlement: A major cause for low ductility of ordered intermetallics
[DE90-006161] 10 p1356 N90-17864
Flux lattice melting in the high Tc superconductors
10 p1366 N90-17915
Phonon dispersion and Kohn anomalies in the alloy Cu(0.84)Al(0.16)
[DE90-005578] 10 p1428 N90-18239
Simulation and quantification of high-resolution Z-contrast imaging of semiconductor interfaces
[DE90-006159] 10 p1438 N90-18297
Ion implantation-induced amorphization of ceramic oxides
[DE90-006564] 11 p1571 N90-19041
Dopant site location in dual-implanted GaP using (111) planar channeling
[DE90-006565] 11 p1571 N90-19042
Toda lattice with transverse degree of freedom
[DE90-002414] 11 p1572 N90-19049
The renormalization group and lattice QCD
[DE90-004860] 12 p1724 N90-19905
Research of the interaction between hydrogen and deuterium with atomic eigen defects and dislocations in nickel and iron
[ETN-90-95380] 13 p1776 N90-20195
A systematic study of the effects of metal substitutions for Cu in YBa(sub 2) (Cu(sub 1-x) M(sub x)3 O(sub 7-rho), M=Fe, Co, Al, Ga, Cr, Ni, and Zn
[DE90-003957] 13 p1892 N90-20857
On the substitution of Sr ions at Y sites in YB(suba2)Cu3O(sub7-d)
[DE90-613395] 14 p2031 N90-21652
Improved crystal bending techniques applied to the LLNL dual-arm Johann mounting x ray spectrometer
[DE90-009528] 15 p2173 N90-22415
Single-crystal diffraction analysis of 2-(trimethylsilylethynyl) 4-nitro-N,N-dimethylaniline
[AD-A218955] 16 p2216 N90-22642
Displacement flow and deuteron drag in a metal: A path towards cold fusion
[PREPRINT-703] 16 p2320 N90-23227
New approach to the dynamical diffraction theory in the case of three-dimensional perfect crystal
[DE90-620563] 16 p2322 N90-23240
Lattice field theory
[PREPRINT-719] 16 p2323 N90-23245
Electronic structure and lubrication properties of MoS2: A qualitative molecular orbital approach
[AD-A220566] 17 p2380 N90-23557
Valence-defect chemical equilibria in nonstoichiometric YBa2Cu3O(7-delta)
[DE90-010152] 18 p2619 N90-24921
Phase stability in the Al(6-x)Cu(x)Zr2 system for 0 less than x less than 1.0
[DE90-010620] 18 p2620 N90-24925
Thermal and phase analysis of YBa2Cu3O(7-x) powder compacts with organic acid additives
[DE90-010142] 18 p2620 N90-24930
Atomic scale imaging of the structure and chemistry of semiconductor interfaces
[DE90-011321] 18 p2626 N90-24965
Adlayer physics
[AD-A221064] 19 p2673 N90-25203
The origin of poorly conditioned susceptibility matrix within inverse CVM algorithm in the case of Pd(sub 3)V: A comparison to the case of Ni(sub 3)V
[DE90-012464] 20 p2833 N90-26110
MBE growth technology for high quality strained III-V layers
[NASA-CASE-NPO-17723-1-CU]
20 p2932 N90-26685
Problems of enclosed crystal interfaces
[DE90-011594] 21 p3079 N90-27509
Growth of III-V films by control of MBE growth front stoichiometry
[NASA-CASE-NPO-17724-1-CU]
21 p3081 N90-27517
Molecular beam epitaxial growth, characterization, and devices of modulated semiconductor structures
[AD-A221545] 21 p3084 N90-27538
Shock dynamics in the sub-nanometer femtosecond domain
[DE90-014390] 23 p3304 N90-28689
The stability of the martensitic phases in Cu-Zn-Al at an electron concentration of 1.534
[DE90-628628] 23 p3311 N90-28727
The first order phase transition for six-state Potts model on two dimensional random triangle lattice
[DE90-627210] 23 p3389 N90-29140
Criticality of the three-state chiral clock model: A renormalisation group study
[DE90-627321] 23 p3400 N90-29212
A generalised Hubbard Hamiltonian: Influence of temperature and fractality
[DE90-627322] 23 p3400 N90-29213
Z(6) model: Criticality and break-collape method
[DE90-627323] 23 p3401 N90-29214
Susceptibility of the Potts model in an hierarchical lattice: Renormalisation group approach
[DE90-627324] 23 p3401 N90-29215
Mechanism of habit change for atmospheric ice crystal growth 24 p3489 N90-29717

CRYSTAL OPTICS
Trapezoidal crystal in the six beam implosion
06 p0786 N90-14577
REFLECT: A computer program for the x ray reflectivity of bent perfect crystals
[DE90-001266] 08 p0851 N90-14946
Apparatus for the efficient wavelength conversion of laser radiation
[AD-D014506] 20 p2866 N90-26305
Image amplification in photoreactive crystals and utilization in optical reaction systems
[ETN-90-97285] 24 p3546 N90-30059

CRYSTAL OSCILLATORS
Temperature compensated crystal oscillator (TCXO) with improved temperature compensation
[AD-D014334] 12 p1650 N90-19482
Image amplification in photoreactive crystals and utilization in optical reaction systems
[ETN-90-97285] 24 p3546 N90-30059

CRYSTAL STRUCTURE
Structural and surface characterization of dispersed metal catalysts
[DE89-014530] 01 p0038 N90-10208
Raman spectroscopic study of the rare earth sesquisulfides
[AD-A210610] 01 p0041 N90-10226
The measurement of infrared spectra of dense ceramics by specular reflectance spectroscopy
[AD-A210609] 01 p0051 N90-10291
Face-specific interaction of MoS4(2-1) with oriented crystals of (0001) CdX (X = Se, S)
[AD-A209519] 01 p0128 N90-10732
Ordered structures and metastable alloys grown by OMVPE
[DE89-016370] 01 p0129 N90-10744
Atomic imaging and interfacial analysis
[DE89-015339] 01 p0130 N90-10748
Structural aspects of the phase separation in La2CuO4.032
[DE89-016183] 01 p0130 N90-10751
The effect of twins on critical currents of high Tc superconductors
[AD-A210988] 01 p0133 N90-10768
X-ray and gamma-ray spectroscopy of solids under pressure
[DE89-017271] 02 p0196 N90-11118
Intergranular and interphase boundaries in ceramics
[DE89-016969] 02 p0202 N90-11154
Effects of gravity on equilibrium crystal shapes
02 p0281 N90-11602
Defect structures preceding amorphization by ion irradiations in YBa2Cu3O(7-delta)
[DE89-016905] 02 p0282 N90-11612
Exploratory study of niobium, titanium, zirconium and tantalum aluminides
[AD-A210658] 02 p0283 N90-11615
High pressure 129I Moessbauer studies of GeI4 molecular crystals
[DE89-015269] 02 p0283 N90-11620
Chevron layer structures in Surface Stabilized Ferroelectric Liquid Crystal (SSFLC) cells filled witth a material which exhibits the chiral nematic to smectic C* phase transition
[DE89-016985] 02 p0285 N90-11628
Report of the Specialists' Workshop on Phase Transition Studies on Hydrogen-Bonded Crystals by Neutron and X-ray Diffractometries
[DE89-906638] 02 p0285 N90-11631
Deformation and defects in Laves-phase intermetallic compounds
[DE89-017798] 03 p0328 N90-11862
New laser materials
[DE89-017524] 03 p0353 N90-12017
Computer simulations of two-dimensional quasiperiodic crystal and random tiling models
[DE89-016909] 03 p0410 N90-12355
Effect of annealing conditions on the structural and superconducting properties of Y-Ba-Cu-O films
[AD-A211308] 03 p0413 N90-12371
Synthesis and microstructure of highly oriented PbTiO3 thin films prepared by a sol-gel method
[AD-A211735] 03 p0414 N90-12377
Development of texture analysis and its applications to titanium aero engine components
[PNR90561] 04 p0454 N90-12602
Electrically conducting organic materials: Design, synthesis and characterization
[AD-A212214] 04 p0471 N90-12700

Structural studies of sputter-deposited MoS2 solid lubricant films
[AD-A212407] 04 p0481 N90-12759
Studies of structure and switching dynamics in ferroelectric crystal and liquid crystal thin films
[AD-A212650] 05 p0702 N90-14109
The Periodic Law at high pressures
[DE90-000837] 06 p0742 N90-14319
Perturbed angular correlations in zirconia ceramics
[DE89-017272] 06 p0751 N90-14369
Prospects for wavelength tunable lasers based on vacancy defects in alkaline-earth oxides
[DE90-001078] 06 p0789 N90-14592
REFLECT: A computer program for the x ray reflectivity of bent perfect crystals
[DE90-001266] 06 p0851 N90-14946
X ray studies of strain, interface, and impurity in semiconductors
[DE90-001525] 06 p0851 N90-14947
High-temperature/high-pressure x ray diffraction: Recent developments
[DE89-015255] 06 p0851 N90-14949
Oxygen stoichiometry, structural transitions, and thermodynamic behavior of the YBa2Cu3O(x) system
[DE89-017894] 06 p0852 N90-14951
Superconductivity from finite-U valence fluctuations
[DE90-000603] 06 p0852 N90-14954
Powder neutron diffraction study of the structural phase diagram of the Ba(sub 1-x)K(sub x)BiO3 system
[DE90-002264] 06 p0854 N90-14967
Anisotropy of oxygen tracer diffusion in YBa2Cu3O7-delta single crystals
[DE90-001931] 06 p0856 N90-14979
Quasicrystals and grain boundaries
[DE90-002213] 06 p0857 N90-14981
Preparation and properties of icosahedral borides
[DE90-003574] 07 p0896 N90-15180
Interaction of hydrogen in palladium as prescribed by the embedded atom method
[DE90-003893] 07 p0907 N90-15244
Instability of a-Si:H/Ag interface at 150 deg C
[DE89-009419] 07 p0950 N90-15498
Deformation twinning in ordered intermetallic compounds
[DE89-014779] 07 p0997 N90-15767
Theoretical studies on the electronic structure of high-temperature superconductors
[DE90-001301] 07 p0998 N90-15771
The possible occurrence of multi-phase behavior in the high T(sub c) superconductor YBa2Cu3O(sub x)
[DE90-002999] 07 p0999 N90-15777
Variational quantum Monte Carlo calculation of electronic and structural properties of crystals
[DE90-003265] 07 p0999 N90-15781
Orientation of rf-sputter-deposited MoS2 films
[ATR-89(4752)-1] 07 p1000 N90-15784
Preparation, structure and properties of VO(sub x) and TiO2 thin films by MOCVD
[DE90-003566] 07 p1001 N90-15793
Cation disordering in the Tl-2122 superconductors
[DE90-003579] 07 p1001 N90-15795
Proceedings of the Latin American Conference on the Applications of the Moessbauer Effect
[DE90-600819] 07 p1002 N90-15803
Optical phonon modes in a double heterostructure of polar crystals
[AD-A214208] 07 p1004 N90-15816
Properties of high Tc superconducting oxides
[DE90-003792] 07 p1005 N90-15821
ZrO2 sintered compact and method for its production
[DE90-004125] 08 p1039 N90-16006
Fundamental studies of beta phase decomposition modes in titanium alloys
[AD-A214424] 08 p1044 N90-16035
Conformation, orientation and interaction in molecular monolayers: A surface second harmonic and sum frequency generation study
[DE90-003108] 08 p1128 N90-16536
Phonon anomaly at T(sub c) in (Y/ER)Ba2Cu3O(7-delta)
[DE90-003562] 08 p1129 N90-16539
Group 2 cubic fluorides as dielectrics for III-V compound semiconductors
[AD-A214096] 08 p1129 N90-16542
Scanning tunneling microscope studies of surface defects
[AD-A214121] 08 p1130 N90-16543
Fundamental issues in heteroepitaxy (condensed from the DOE panel report)
[DE90-003980] 08 p1132 N90-16555
Physical properties of Bi2Sr2CuO6, the semiconducting phase, structurally distinct from the n = 1 Bi-cuprate superconductor
[DE90-004299] 08 p1133 N90-16563
Electron beam induced oxygen in YBa2Cu3O(7-x) superconductors
[DE90-004839] 08 p1133 N90-16565
Development of a reliable fabrication technique to produce intermetallic compounds
[AD-A215004] 09 p1194 N90-18918
Crystal structure of Tetra-Ammonium Adamantyl Tetra-Nitrate (TAATN): High energy/density fuel candidate for liquid propellant
[AD-A215684] 09 p1201 N90-16955
Growth of epitaxical SiC layers onto on- and off-axis 6H-SiC substrates by ion beam deposition
[DE90-004236] 09 p1287 N90-17459
Flexibility of the zeolite RHO framework: In situ x ray and neutron powder structural characterization of divalent cation-exchanged zeolite RHO
[AD-A214573] 09 p1288 N90-17467
Point defects and interfaces in insulating solids
[AD-A214668] 09 p1289 N90-17471
Electronic properties of GaAs-(Al,Ga)As quasiperiodic
[AD-A214704] 09 p1289 N90-17472
Structural instabilities, impurities, and defects in electronic materials
[AD-A215384] 09 p1290 N90-17481
Use of anomolous thermal imaging effects for multi-mode systems control during crystal growth
10 p1365 N90-17910
Statistical mechanical models for liquid and amorphous structure in covalently bonded systems
[DE90-607233] 10 p1428 N90-18240
Anisotropy and dimensionality in untwinned crystals of YBa2Cu3O(7-delta)
[DE90-004890] 10 p1436 N90-18287
Crystal and magnetic structure of Er(2)(Co(sub x)Fe(sub 1-x))(17) compounds
[DE90-004928] 10 p1436 N90-18288
Chemistry of the doping mechanism in Ba(1-x)K(x)BiO3 and La2CuO(sub 4 + delta) oxide superconductors
[DE90-005640] 10 p1437 N90-18293
Structure and vibrational excitations of reconstructed semiconductor surfaces
[DE90-006589] 11 p1571 N90-19044
Modified dislocation structures in Ge(x)Si(1-x) double epilayers on (001) Si
[DE90-007078] 11 p1572 N90-19052
Fundamental studies of new magnetic heterostructures: Their growth, crystallographic structure, magnetic, and electronic properties
[DE90-007381] 11 p1572 N90-19053
Creep behavior of alloys based on TiAl containing TiB2 and TiN particulates
[DE90-006489] 12 p1628 N90-19355
Diffraction studies of the structure of glasses and liquids
[DE90-007662] 12 p1632 N90-19381
Laser surface interactions of high-(Tc) superconductors
[DE90-006894] 12 p1669 N90-19587
Supercomputer applications for materials science: Ordering effects of hydrogen in palladium
[DE90-004664] 12 p1718 N90-19870
Neutron scattering measurements of the magnetic excitations of high-temperature superconducting materials
[DE90-006567] 12 p1721 N90-19885
The effects of gradients on boundary stability
[DE90-007428] 12 p1722 N90-19894
Band electronic structures and crystal packing forces
[DE90-007669] 12 p1723 N90-19898
Vibrational spectroscopy of boron nitride at high temperatures and pressures
[DE90-008633] 13 p1772 N90-20172
Reactive sputtering of molybdenum
[DE90-008307] 13 p1778 N90-20204
An introduction to nickel aluminide alloy
[DE90-008565] 13 p1778 N90-20207
The role of polarity on the stability of graphitic compounds
[DE90-006528] 13 p1780 N90-20218
Ultrastructure processing of ordered polymers
[AD-A218331] 13 p1783 N90-20232
Ionic disorder in crystals at high temperatures with emphasis on fluorites
[AERE-R-13544] 13 p1893 N90-20862
An investigation of the dislocation structure of the Ni/Ag phase boundary
[DE90-008428] 13 p1895 N90-20876
Theoretical and experimental study of solid phase miscibility gaps in III/V quaternary alloys
[DE90-008430] 13 p1895 N90-20877
The geometry of disorder: Report 1987 to 1990
[DE90-008250] 13 p1896 N90-20882
Performance of Y-TZP materials between 800 C and 1200 C
[AD-A217723] 13 p1897 N90-20890
ZELED analysis of aperiodicity and bond lengths in ceramic powders
[DE90-612932] 14 p1955 N90-21193
Heat engine based on shape memory alloys
[AD-D014400] 14 p1986 N90-21385
Contract crystal growth and fabrication services
[AD-A218327] 14 p2031 N90-21646
Shock compression of solids: A tutorial
[DE90-009185] 14 p2032 N90-21659
In-situ pulsed laser deposition of high-T(sub c) YBa(sub 2)Cu(sub 3)O(sub 7) superconducting thin films on (100) LaAlO3 substrates
[DE90-009861] 15 p2173 N90-22418
The lithium concentration dependence of creep in binary aluminum-lithium alloys
[AD-A218706] 16 p2221 N90-22668
Ultrahigh carbon steels and their laminates
[AD-A218780] 17 p2376 N90-23530
In-situ processing of epitaxial and textured high (Tc) superconducting HoBa2Cu3O(7-x) thin films by pulsed laser evaporation technique
[DE90-009828] 17 p2474 N90-24148
A first principles examination of phase stability in FCC-based ordered Ni-V alloys
[DE90-010635] 18 p2525 N90-24411
Ceramic epitaxial films and multilayers prepared by MOCVD
[DE90-011090] 18 p2532 N90-24447
Chemical and crystallographic phase behavior in the Ba(1-x)K(x)BiO3 system
[DE90-010072] 18 p2618 N90-24917
Valence-defect chemical equilibria in nonstoichiometric YBa2Cu3O(7-delta)
[DE90-010152] 18 p2619 N90-24921
Real space method of powder diffraction for non-periodic and nearly periodic materials
[DE90-010537] 18 p2621 N90-24935
Protons and lattice defects in perovskite-related oxides
[DE90-010957] 18 p2624 N90-24955
Formation of cubic LI2 phases from Al3Ti and Al3Zr by transition metal substitutions for Al
[DE90-012288] 20 p2834 N90-26117
Exact results for the structured liquid-solid interface
[AD-A222762] 20 p2922 N90-26630
Large, orientation-dependent enhancements of critical currents in Y1Ba2Cu3O(7-x) epitaxial thin films: Evidence for intrinsic flux pinning
[DE90-009424] 20 p2929 N90-26666
Molecular dynamics simulations of grain-boundary diffusion for varying tilt angle geometries
[DE90-012919] 20 p2930 N90-26669
Optical constants of solid methane
20 p2948 N90-26775
Synthesis, structure, and properties of a new ternary metal nitride, Ca3CrN3
[AD-A222274] 21 p2978 N90-26924
Microstructural development in HSLA-100 steel weld metals
[AD-A222105] 21 p2982 N90-26944
Theory of ceramic/zirconia composites: Toughening, strengthening, and synergism
[AD-A222931] 21 p2985 N90-26961
Self-lubricating-diamond like coatings deposition
[AD-A221756] 21 p2988 N90-26983
Problems of enclosed crystal interfaces
[DE90-011594] 21 p3079 N90-27509
The effect of processing, deformation and annealing on the microstructure of Y1Ba2Cu3O7-(sub delta)
[DE90-011731] 21 p3079 N90-27510
Symmetry breaking oxygen displacement in superconducting oxides
[DE90-013670] 21 p3081 N90-27520
The epitaxial growth of copper on the (111) surface of silicon
[DE90-013817] 21 p3082 N90-27523
Synthesis, structure, and properties of Ca2ZnN2
[AD-A222012] 21 p3083 N90-27533
Identification of tetragonal and cubic structures of zirconia
[AD-A222373] 21 p3083 N90-27535
Face-specific interaction of MoS4(2-) with oriented crystals of (0001) CdX(X = Se, S)
[AD-A222405] 21 p3084 N90-27537
On diamond, graphitic and amorphous carbons in primitive extraterrestrial solar system materials
21 p3095 N90-27591
Pinning, flow and plastic deformation of flux vortices in high T(sub c) superconductors 22 p3136 N90-27796
Energetics and crystal chemistry of Ruddlesden-Popper type structures in high T(sub c) ceramic superconductors
22 p3141 N90-27814
Magnetism and superconductivity of some Tl-Cu oxides 22 p3143 N90-27829

Structure and superconducting properties of (((Ln(1-x)Ln*(x) 1/2 (Ba(1-y)Sr(y) 1/3 Ce 1/6) 8Cu6O(z)
22 p3144 N90-27833
Electronic state and superconductivity of YBa2Cu3-xO7-y (M = Al,Zn and Sn) systems
22 p3146 N90-27842
The relation between ferroelasticity and superconductivity 22 p3150 N90-27861
Measurement of H(sub c1) in a single crystal of YBa2Cu3O7 with low pinning 22 p3151 N90-27864
Studies of iron impurities in YxPr1-xBa2Cu3O7-delta
22 p3151 N90-27865
Twisted crystals: Propagation, genesis, and relationships with optical activity and molecular symmetry (excerpts)
[DE90-014259] 23 p3399 N90-29205
Antiferromagnetism and enhanced heat in CeM2Sn (M = Ni, Ir, Cu, Rh, Pd, and Pt
[DE90-014924] 23 p3399 N90-29206
X ray scattering studies of non-equilibrium ordering processes
[DE90-015066] 23 p3400 N90-29209
Kinetic pathway in Stranski-Krastanov growth of Ge on Si(001)
[AD-A224324] 24 p3445 N90-29456
Microscopic aspects of the initial stages of epitaxial growth. A scanning tunneling microscopy study
[AD-A224325] 24 p3551 N90-30094
Scanning tunneling microscopy of semiconductor surfaces
[AD-A223339] 24 p3552 N90-30095
First principles calculation of oxygen ordering in YBa2Cu3O(7-y)
[DE90-015205] 24 p3553 N90-30102
Transmission electron microscopy study of ICB Al on Ge and Si(001) substrates
[DE90-015299] 24 p3553 N90-30103
High resolution transmission electron microscopy of aluminophosphates
[DE90-015632] 24 p3553 N90-30105
High resolution transmission electron microscopy of partial states of oxygen order in YBa2Cu3O(z)
[DE90-015637] 24 p3554 N90-30108
A comparative first principles study of phase stability in Ni-Ti and Ni-Al alloys around equiatomic composition
[DE90-016477] 24 p3554 N90-30111

CRYSTAL SURFACES

Dynamics of nucleation at electrochemical interfaces via surface EXAFS and standing wave measurements
[AD-A210733] 02 p0195 N90-11109
The effects of trace anions on the voltammetry of single crystal gold surfaces
[AD-A211886] 04 p0558 N90-13254
Non-linear optical studies of adsorbates: Spectroscopy and dynamics
[DE90-001543] 06 p0741 N90-14312
Surface studies at the NSLS
[DE90-003173] 08 p1043 N90-16027
An evaluation of ethylene-vinyl acetate copolymers as desensitizers for RDX in insensitive booster compositions prepared by slurry coating technology
[MRL-TR-89-33] 12 p1633 N90-19385
Interactions of molecules with surfaces
[DE90-007555] 13 p1883 N90-20806
Picosecond laser pulse interactions with metallic and semiconducting surfaces
[AD-A219680] 17 p2408 N90-23723
Review of model sensor studies on Pd/SnO2(110) surfaces 18 p2559 N90-24604
The catalytic reactivity of thin film crystal surfaces
[DE90-010579] 18 p2622 N90-24937
Structure and dynamics of water at the Pt(111) interface: Molecular dynamics study
[AD-A222628] 20 p2933 N90-26687
Surfaces and interfaces of ceramics and metals
[DE90-014381] 22 p3160 N90-27920
High resolution technique and instrument for measuring lattice parameters in single crystals
[AD-D014549] 22 p3177 N90-28029
Manufacturing and characterization of liquid-phase epitaxy layers with atomic levels at the crystal surface and at the hetero limit surfaces in the system GaAs-AlGaAs
[ETN-90-97310] 24 p3554 N90-30113

CRYSTALLINITY

Study of microcrystalline, silicon-carbon p-layers prepared by photo-CVD and glow discharge
[DE89-009438] 06 p0850 N90-14939
An investigation of mechanical behavior of crystalline solids
[DE90-003530] 07 p1000 N90-15787
Modelling directional solidification
[NASA-CR-186181] 09 p1292 N90-17487
LaRC TPI 1500 series polymers
[NASA-CR-181899] 14 p1945 N90-21129
The influence of ion implantation on the near-surface mechanical properties of ceramics
[DE90-010139] 18 p2531 N90-24444
The composition and physical properties of the Earth's mantle and core 18 p2579 N90-24689
Crystalline photovoltaic cell research, status, and future direction
[DE90-011478] 19 p2710 N90-25427
Liquid crystalline polymers
[NASA-CR-186949] 21 p2986 N90-26971
Raman spectroscopic studies of carbon in extra-terrestrial materials 21 p3095 N90-27589
Effect of a crystal-melt interface on Taylor-Vortex flow with buoyancy
[PB90-244401] 24 p3551 N90-30089

CRYSTALLIZATION

NT DIRECTIONAL SOLIDIFICATION (CRYSTALS)
NT MELT SPINNING
NT RECRYSTALLIZATION

Computer simulations of polymer dynamics in the solid state
[DE89-010337] 01 p0048 N90-10275
Interfacial adsorption and crystallization of polycarbonate in carbon fiber composites
[AD-A211230] 02 p0191 N90-11090
Low temperature formation of titanium aluminide films using physical vapor deposition
[AD-A211877] 03 p0328 N90-11866
Suppression of side chain crystallization and transformation of monotropic mesophases into enantiotropic mesophases by copolymerization of the parent polymers' monomer pairs containing constitutional isomeric mesogenic side groups
[AD-A209066] 03 p0330 N90-11878
Synthesis and crystallization behavior of fluoride glasses
[AD-A212142] 04 p0478 N90-12741
A new model for the structure of silica glass
[AD-A212972] 05 p0627 N90-13659
Novel polyimide compositions based on 4,4': Isophthaloyldiphthalic anaydride (IDPA)
[NASA-CASE-LAR-14194-1] 07 p0890 N90-15148
The continuous crystallization of sulfur formed by the liquid-phase reaction of hydrogen sulfide and sulfur dioxide
[DE90-003991] 08 p1041 N90-16018
Effects of ion dose on the morphology and crystallization of amorphous germanium
[DE90-003564] 08 p1130 N90-16547
Ion beam annealing of Si co-implanted with Ga and As
[DE90-004297] 08 p1132 N90-16556
Crystallization of nanocomposite glasses made by the SSG process
[AD-A214572] 09 p1197 N90-16933
The preparation and characterisation of oxynitride glasses and glass-ceramics
[AD-A214783] 09 p1197 N90-16935
Protein crystal growth in microgravity
09 p1224 N90-17102
Superconducting Bi1.5Pb0.5Sr2Ca2Cu3O(x) ceramics by rapid melt quenching and glass crystallization
[NASA-CR-185184] 09 p1288 N90-17465
Evolution of structure and electrical properties during crystallization of rapidly solidified Bi4Ti3O12
[DE90-005221] 09 p1292 N90-17492
Thermal crystallization of polytetrahydrofuran networks
[AD-A215336] 10 p1436 N90-18285
Crystallization behavior and properties of BaO-Al2O3-2SiO2 glass matrices
[NASA-CR-185209] 12 p1631 N90-19374
Principles of metallic solidification
13 p1784 N90-20241
Dielectric composite thin films
[AD-A217940] 13 p1881 N90-20791
LaRC TPI 1500 series polymers
[NASA-CR-181899] 14 p1945 N90-21129
ZELED analysis of aperiodicity and bond lengths in ceramic powders
[DE90-612932] 14 p1955 N90-21193
Apparatus for mixing solutions in low gravity environments
[NASA-CASE-MFS-26047-1] 14 p1958 N90-21209
Interfacial studies in fiber-reinforced thermoplastic-matrix composites
15 p2062 N90-21814
The effect of elevated gravity on the crystallization of the MFI zeolites, ZSM-5, and silicalite
16 p2320 N90-23231
Solidification of highly undercooled liquid droplets
[AD-A218776] 17 p2376 N90-23529
Picosecond laser pulse interactions with metallic and semiconducting surfaces
[AD-A219680] 17 p2408 N90-23723
Protein crystal growth in low gravity
[NASA-CR-186243] 20 p2929 N90-26663
Mathematical simulation of heat exchanges and thermoelastic constraints in Czochralski crystal growth
[ETN-90-97242] 20 p2931 N90-26680
Transcrystalline morphology in carbon fibre composites with thermoplastic matrix and its influence on the mechanical properties
[FOA-C-20783-2.1] 22 p3248 N90-28423
Twisted crystals: Propagation, genesis, and relationships with optical activity and molecular symmetry (excerpts)
[DE90-014259] 23 p3399 N90-29205

CRYSTALLOGRAPHY

Mott transition: Low-energy excitations and superconductivity
[DE89-617778] 01 p0129 N90-10741
The growth of gallium nitride films via the innovative technique of atomic layer epitaxy
[AD-A210380] 01 p0132 N90-10760
Single crystal diffraction
[DE90-000024] 03 p0412 N90-12366
Spectral properties of one dimensional quasi-crystals
[PREPRINT-659] 06 p0850 N90-14938
Diffusion and defect characterization studies of mercury cadmium telluride
[AD-A214655] 09 p1289 N90-17470
Fundamental studies of new magnetic heterostructures: Their growth, crystallographic structure, magnetic, and electronic properties
[DE90-007381] 11 p1572 N90-19053
Crystallographic and magnetic properties of (C6 D11 ND3)CuBr3 and (Zn(1-x)Mn(x))3As2: A neutron scattering study
[ECN-219] 11 p1573 N90-19055
Techno-economic assessment of a carbothermic alumina reduction process
[DE90-007018] 13 p1772 N90-20170
Crystallography, spectroscopic analysis, and lasing properties of Nd3+:Y3Sc2Al3O12
[AD-A217792] 13 p1897 N90-20891
A requirement for Australian research: Access to big science facilities, a report by the Australian National Committee for Crystallography
[DE90-614784] 14 p1930 N90-21048
Retabulation of space group extinctions for electron diffraction
[DE90-612933] 14 p2031 N90-21648
Chemical and crystallographic phase behavior in the Ba(1-x)K(x)BiO3 system
[DE90-010072] 18 p2618 N90-24917
Use of neutron diffraction in determining strains in high-temperature superconducting composites
[DE90-010404] 18 p2621 N90-24931
Adlayer physics
[AD-A221064] 19 p2673 N90-25203
The effect of crystal orientation on damage accumulation in chromium-implanted Al2O3
[DE90-012294] 20 p2931 N90-26674
Macromolecular calculations for the XTAL-system of crystallographic programs
[AD-A222345] 22 p3248 N90-28421
Polycrystalline diamond Junction Field Effect Transistors (JFETS)
[AD-A223784] 24 p3465 N90-29576

CRYSTALS

NT BICRYSTALS
NT CRYSTAL OSCILLATORS
NT DENDRITIC CRYSTALS
NT DOPED CRYSTALS
NT IONIC CRYSTALS
NT LIQUID CRYSTALS
NT METAL CRYSTALS
NT MICROCRYSTALS
NT MIXED CRYSTALS
NT POLYCRYSTALS
NT QUARTZ CRYSTALS
NT SINGLE CRYSTALS
NT WHISKERS (CRYSTALS)

Bragg crystal polarimeters
[NASA-CR-181331] 01 p0073 N90-10423
Face-specific interaction of MoS4(2-1) with oriented crystals of (0001) CdX (X = Se, S)
[AD-A209519] 01 p0128 N90-10732
Crystal orientation effects in PETN explosive with 4 GPa shocks
[DE89-016996] 02 p0208 N90-11190
Utilization of photorefractive crystals in optical image processing
[ISBN-3-923560-06-0] 02 p0225 N90-11292
Acoustic studies of new materials: Quasicrystals, low-loss glasses and high Tc superconductors
[AD-A211281] 02 p0272 N90-11551
High pressure 129I Moessbauer studies of GeI4 molecular crystals
[DE89-015269] 02 p0283 N90-11620
Dielectronic excitation and recombination in crystal channels
[DE89-016864] 02 p0284 N90-11625

Energy transfer and non-linear optical properties at near ultraviolet wavelengths: Rare earth 4f(yields)5d transitions in crystals and glasses
[DE90-000065] 03 p0405 N90-12321
Computer simulations of two-dimensional quasiperiodic crystal and random tiling models
[DE89-016909] 03 p0410 N90-12355
Anomalous ion-channeling behavior across the superconducting transition in high-T(sub c) materials
[DE89-017677] 03 p0411 N90-12360
A prototype microprocessor based audiometer for use by the CF (Canadian Forces) medical services for periodic hearing tests
[AD-A212990] 05 p0673 N90-13921
Atomic matching across internal interfaces
[DE90-002266] 06 p0841 N90-14889
Dynamical structure of liquid and amorphous metals
[DE90-003805] 07 p0905 N90-15229
Energetics of BCC-FCC lattice deformation in iron
[AD-A213801] 07 p0905 N90-15233
Laser-induced surface ablation and optical damage of ZnS crystals caused by single- and multiple-pulse laser-irradiation
[DE90-003807] 07 p0936 N90-15419
Spectroscopic and laser properties of Cr:LiCaAlF6 and Cr:LiSrAlF6 crystals
[DE90-000783] 07 p0998 N90-15770
Thermal expansion of LATGS crystals
[DE89-636239] 08 p1130 N90-16546
Spectroscopic techniques for the analysis of CdTe substrates used for the growth of HgCdTe
[AD-A214545] 09 p1288 N90-17466
Thermal crystallization of polytetrahydrofuran networks
[AD-A215336] 10 p1436 N90-18285
Performance of a 500 watt Nd:GGG zigzag slab oscillator
[DE90-006263] 11 p1503 N90-18657
Studies of cubic ice crystals
[AD-A216574] 11 p1534 N90-18832
Crystal growth and mechanical properties of semiconductor alloys
[AD-A216697] 11 p1570 N90-19035
Synthesis and properties of a novel catalyst for the combustion of methane
[PB90-127499] 12 p1622 N90-19320
A new thermal sensor for x ray microcalorimetry
[DE90-008547] 13 p1805 N90-20360
Tribological properties of boric acid and boric acid forming surfaces. Part 1: Crystal chemistry and self-lubricating mechanism of boric acid
[DE90-005665] 13 p1811 N90-20401
Interactions of molecules with surfaces
[DE90-007555] 13 p1883 N90-20806
Crystal preparation at LBL, 1976 to 1986
[DE90-007754] 13 p1894 N90-20871
CCST (Center for Compound Semiconductor Technology) research briefs
[DE90-007782] 13 p1895 N90-20874
High temperature chemistry of oxide superconductors
[DE90-007821] 13 p1895 N90-20875
Method of preparing radially homogeneous mercury cadmium telluride crystals
[NASA-CASE-MFS-25786-2] 13 p1898 N90-20896
Modeling the temperature dependence of the thermal conductivity of aluminum nitride
[DE90-009428] 14 p1949 N90-21154
Contract crystal growth and fabrication services
[AD-A218327] 14 p2031 N90-21646
Simulated image maps for use in experimental high-resolution electron microscopy
[DE90-009176] 14 p2032 N90-21657
Transient effects in Brillouin gain spectroscopy in solids
[DE90-009476] 15 p2067 N90-21839
High resolution stimulated Raman-Brillouin spectroscopy in gases and solids
[DE90-009535] 15 p2067 N90-21840
Brillouin gain spectroscopy in glasses and crystals
[DE90-009536] 15 p2067 N90-21841
Photovoltaic Program Branch
[DE90-000318] 15 p2123 N90-22142
Effect of a crystal-melt interface on Taylor-vortex flow
[NASA-CR-186512] 15 p2171 N90-22408
Improved crystal bending techniques applied to the LLNL dual-arm Johann mounting x ray spectrometer
[DE90-009528] 15 p2173 N90-22415
JPRS report: Science and technology. USSR: Physics and mathematics
[JPRS-UPM-89-001] 16 p2310 N90-23162
Effect on relaxation on nonlinear waves in crystals
16 p2310 N90-23165
The effect of elevated gravity on the crystallization of the MFI zeolites, ZSM-5, and silicalite
16 p2320 N90-23231
Reflection oscillators employing series resonant crystals'
[NASA-CASE-GSC-13173-1] 17 p2394 N90-23635
Piezoelectric and pyroelectric effects of a crystalline polymer 18 p2515 N90-24360
Indentation fracture of brittle materials
[DE90-010709] 18 p2572 N90-24857
The defect structure of ion and neutron irradiated YBa2Cu3O(7-delta) single crystals
[DE90-010100] 18 p2619 N90-24920
Protein crystal growth in low gravity
[NASA-CR-186243] 20 p2929 N90-26863
A number-theoretic approach to subgroups of dihedral groups
[AD-A222857] 21 p3063 N90-27413
Face-specific interaction of MoS4(2-) with oriented crystals of (0001) CdX(X = Se, S)
[AD-A222405] 21 p3084 N90-27537
Grain orientation studies in superconductors
22 p3148 N90-27852
Crystal chemical and quantum chemical studies of Ba(Sr)-Nb oxide compounds 22 p3150 N90-27858
XES studies of density of states of high temperature superconductors 22 p3150 N90-27859
The relation between ferroelasticity and superconductivity 22 p3150 N90-27861
Comparative study of flux pinning flux creep and critical currents between YBaCuO crystals with and without Y2BaCuO5 inclusions 22 p3152 N90-27869
High-temperature deformation of silicon
[DE90-013628] 22 p3160 N90-27919
Twisted crystals: Propagation, genesis, and relationships with optical activity and molecular symmetry (excerpts)
[DE90-014259] 23 p3399 N90-29205
Effect of a crystal-melt interface on Taylor-Vortex flow with buoyancy
[PB90-244401] 24 p3551 N90-30089

CSM
U COMMAND SERVICE MODULES

CUBANE
Cubane derivatives for propellant applications
[AD-A210368] 01 p0054 N90-10305

CUBIC LATTICES
NT BODY CENTERED CUBIC LATTICES
NT FACE CENTERED CUBIC LATTICES
Temperature dependence of positron diffusion in cubic metals
[PB89-222020] 04 p0475 N90-12722
The Hueckel model for small metal clusters. 4: Orbital properties and cohesive energies for model clusters of up to several hundred atoms
[AD-A216161] 10 p1354 N90-17852
Molecular dynamics simulations of grain-boundary diffusion for varying tilt angle geometries
[DE90-012919] 20 p2930 N90-26669

CUES
Functional decor in the International Space Station: Body orientation cues and picture perception
[NASA-TM-102242] 05 p0675 N90-13931
Workload induced spatio-temporal distortions and safety of flight
[DE89-016613] 06 p0820 N90-14771
Imaging probabilities, geometry and ergonomics in limited visibility helicopter operations
07 p0872 N90-15060
Stereopsis cueing effects on hover-in-turbulence performance in a simulated rotorcraft
[NASA-TP-2980] 14 p1921 N90-21004
Fighter agility metrics, research, and test
[NASA-CR-186118] 17 p2351 N90-23386
Evaluation of nonlinear motion-drive algorithms for flight simulators
[UTIAS-TN-272] 19 p2662 N90-25148
The need for platform motion in modern piloted flight training simulators
[AD-A221720] 21 p2963 N90-26847

CUESTAS
U RIDGES

CULTIVATION
NT PLOWING
Statistical information system for cultivation of the soil. Use of remote sensing in official statistics
08 p1095 N90-16338
Evaluation of digital classification results of summer cultivation in a test area in the Parana-Ano state harvest 1986-1987
[INPE-4828-PRE/1459] 10 p1399 N90-18085
Multisensor monitoring of deforestation in the Guinea Highlands of West Africa
[NASA-CR-186709] 19 p2706 N90-25396

CULTURE TECHNIQUES
Genetic engineering of single-domain magnetic particles
[AD-A210332] 01 p0091 N90-10521
Response of lymphocytes to a mitogenic stimulus during spaceflight 05 p0677 N90-13942
Polarity establishment, morphogenesis, and cultured plant cells in space 05 p0677 N90-13943
Bio-reactor chamber
[NASA-CASE-MSC-20929-1] 09 p1250 N90-17252
Three-dimensional coculture process
[NASA-CASE-MSC-21560-1] 11 p1538 N90-18852
Research in biological separations and cell culture
[NASA-CR-172060] 15 p2135 N90-22202
Insulin and insulin-like growth factor-1 induce pronounced hypertrophy of skeletal myofibers in tissue culture
[NASA-CR-187026] 23 p3354 N90-28960
Definition of a near real time microbiological monitor for space vehicles
[NASA-CR-185599] 24 p3441 N90-29430
Interaction of electromagnetic fields with chondrocytes in gel culture
[AD-A223397] 24 p3497 N90-29765

CUMULATIVE DAMAGE
Porosity and crack initiation during low cycle fatigue
[AD-A210989] 01 p0081 N90-10464
Evaluation of a damaged F/A-18 horizontal stabilator
[AD-A212573] 04 p0453 N90-12597
Failure processes in unidirectional composite materials
05 p0617 N90-13598
Study of fatigue degradation mechanisms in unidirectional composite materials. Application to cumulative damage
[ECL-88-12] 05 p0619 N90-13611
Fatigue life estimates for helicopter loading spectra
[NASA-CR-181941] 08 p1088 N90-16294
Monoenergetic positron beam studies of near-surface phenomena
[ETN-90-96947] 18 p2613 N90-24887

CUMULONIMBUS CLOUDS
Cloud phase discrimination by near-infrared remote sensing 08 p1090 N90-16310
Case study on Pre-Typhoon Active Convective Clouds (PTACC) 21 p3029 N90-27220

CUMULUS CLOUDS
A numerical study of the formation of mesoscale convective complexes 09 p1245 N90-17225
Summer Study Program in Geophysical Fluid Dynamics: The Influence of Convection on Large-Scale Circulations, 1988
[AD-A216024] 11 p1535 N90-18840
Characteristics of cumulus bandclouds off the east coast of Hawaii 15 p2130 N90-22178
A unified view of convective transports by stratocumulus clouds, shallow cumulus clouds, and deep convection
22 p3219 N90-28254
A cloudiness transition in a marine boundary layer
22 p3219 N90-28259
Regional conditions during the 25 October 1986 FIRE cirrus/altocumulus case study 22 p3225 N90-28287

CURING
UV-curable polyurethane-methacrylate co-networks and interpenetrating networks
[AD-A210445] 01 p0050 N90-10285
In-situ cure monitoring of composites by fiber-optic molecular sensors
[AD-A211495] 03 p0320 N90-11817
Curable polyether compositions
[AD-D014200] 04 p0468 N90-12679
Structure and properties of polymer interphases
[AD-A212796] 04 p0481 N90-12763
Fiber-optic sensors for composite cure analysis and lifetime nondestructive evaluation
[DE90-001739] 06 p0738 N90-14296
Mechanistic modeling of epoxy resins
[DE89-015119] 07 p0908 N90-15247
A cure process model for resin transfer molding of advanced composites
[NASA-CR-186247] 09 p1185 N90-16867
Simple shear tests of the FMI 23.5.06 adhesive cured at low pressure (12 PSI)
[INFORME-I-298/88] 10 p1357 N90-17871
The viscoelasticity of curing thermosets
[DE90-006535] 13 p1781 N90-20221
Composite curing: A new process
[REPT-892-430-114] 17 p2370 N90-23490
Nonintrusive method and apparatus for monitoring the cure of polymeric materials
[NASA-CASE-LAR-13465-1] 17 p2378 N90-23544
Characterization of a thermally imidized soluble polyimide film
[NASA-TM-103484] 20 p2836 N90-26131
Evolution of structure and viscoelasticity in diethanolamine-cured epoxy
[DE90-011256] 20 p2837 N90-26134
New core design for use with precision composite reflectors
[NASA-CASE-NPO-17858-1-CU]
21 p2970 N90-26880
Radiation-curable prepreg composites
[DE90-629740] 23 p3301 N90-28674

CURIUM
Magnetic behavior of curium and americium-curium alloys
[DE89-017808] 07 p0902 N90-15213
The use of curium as a rare Earth substitute in high T(sub c)-related compounds
[DE90-009724] 18 p2620 N90-24928
CURL (VECTORS)
NT VORTICITY
Direct discretization of planar div-curl problems
[NASA-CR-181935] 02 p0263 N90-11498
Application of a generalized Leibniz rule for calculating electromagnetic fields within continuous source regions
[AD-A212470] 04 p0492 N90-12831
CURRENT ALGEBRA
SL(2,R) current algebra in two-dimensional conformal quantum gravity
[DE90-600755] 07 p0983 N90-15675
Quantum gravity in two dimensions and the SL(2,R) current algebra
[DE90-627215] 23 p3391 N90-29156
CURRENT AMPLIFIERS
NT PHOTOMULTIPLIER TUBES
CURRENT CONVERTERS (AC TO DC)
NIST (National Institute of Standards and Technology) measurement services: The ac-dc difference calibrations
[PB89-222616] 04 p0494 N90-12845
Voltage source ac-to-dc converters for high-power transmitters 15 p2075 N90-21886
Linear averaged and sampled data models for large signal control of high power factor ac-dc converters
[AD-A221976] 21 p3020 N90-27170
CURRENT DENSITY
Studies of high power density, pico-second rise-time light activated semiconductor switch
[AD-A210549] 01 p0061 N90-10349
Pinning of curved flux lines on the boundary between two phases of high temperature superconductors
[DE89-618865] 02 p0283 N90-11614
Resistive block methods for electrostatic field solutions with internal elements
[DE89-017535] 03 p0337 N90-11920
Superconducting switch program
[AD-A211580] 03 p0344 N90-11964
Effects of grain boundary chemistry on critical current density in oxide superconductors
[DE89-017780] 03 p0412 N90-12365
Heat and mass transfer design issues in PEM fuel cell hardware
[DE89-016779] 06 p0804 N90-14677
Polarization of Li/SOCl2 cells
[DE90-000883] 06 p0804 N90-14680
Calorimetric measurements on electrochemical cells with Pd-D cathodes
[DE90-002198] 06 p0805 N90-14685
Static and dynamic magnetization properties of Y1Ba2Cu3O(sub z) thin films
[DE89-017584] 06 p0850 N90-14940
Flux pinning and microstructure in YBa2Cu3O7
[DE90-001562] 06 p0851 N90-14948
A simple figure of merit for high temperature superconducting switches
[DE90-000610] 06 p0852 N90-14955
Processing YBa2Cu3O(x) wires in O3/O2
[DE90-003570] 07 p1001 N90-15794
Effects of non-linearity in the variation of pinning potential with current-density on magnetic flux creep in high and low T(sub c) superconductors
[DE90-003952] 07 p1005 N90-15822
Magnetic penetration depth and intragrain critical current density in gain-aligned Tl2Ca2Ba2Cu3O10 superconductor
[DE90-004245] 08 p1133 N90-16562
A lightweight solid polymer electrolyte fuel cell with stack power density of 3kW/lb (7 kW/kg)
[AD-A216253] 10 p1401 N90-18100
Research on free electron lasers
[AD-A215865] 11 p1514 N90-18715
Absorption experiments on electron-beam pumped rare gases
[DE90-006504] 11 p1515 N90-18722
Ac loss measurements of two multifilamentary NbTi composite strands
[DE90-005388] 12 p1619 N90-19304
Effects of nonuniform potential and current distributions in electrochemical systems
[DE90-007349] 12 p1623 N90-19325
Characterization of thunderstorm induced Maxwell current densities in the middle atmosphere
12 p1634 N90-19391
An electrical model for plasma armature voltage
[DE90-007530] 12 p1718 N90-19866
Critical current density and transition temperature measurements of Y-Ba-Cu-O rods
[AD-A216695] 12 p1719 N90-19875
Electron beam generation by electron bombardment induced cathode emission
[AD-A218203] 13 p1798 N90-20318
The application of Dow Chemical's perfluorinated membranes in proton-exchange membrane fuel cells
13 p1823 N90-20466
Power threshold for neutral beam current drive
[DE90-008348] 13 p1886 N90-20822
Method of making a long life high current density cathode from tungsten and iridium powders using a quarternary compound as the impregnant
[AD-D014425] 14 p1958 N90-21211
Observations of atmospheric electricity, 1988
[GEOPHYSICAL-PUBL-10] 14 p2006 N90-21499
Hollow cathode operation at high discharge currents
[NASA-CR-185238] 15 p2088 N90-21953
MHD channel development, part 1
[DE90-009549] 15 p2169 N90-22394
Catalysts for ultrahigh current density oxygen cathodes for space fuel cell applications
[NASA-CR-180650] 16 p2251 N90-22835
Current distribution in cylindrical porous electrodes
[DE90-009707] 18 p2546 N90-24530
Superconducting permanent magnets
[AD-A218944] 18 p2618 N90-24912
RF surface resistance measurements in the Pb-Bi-Sr-Ca-Cu-O system
[DE90-010412] 18 p2621 N90-24932
The effect of magnetic field on the critical current density of bulk superconducting wires
[DE90-010458] 18 p2621 N90-24934
Critical current density, flux creep, and microstructure in a Bi-Sr-Ca-Cu-O system
[DE90-010457] 20 p2931 N90-26676
Background effects in ESDIAD measurements on Si(111)-(7x7)
[AD-A222242] 21 p3001 N90-27056
Stabilization of high T(sub c) phase in bismuth cuprate superconductor by lead doping
22 p3144 N90-27832
Progress of research of high-T(sub c) superconductors
22 p3145 N90-27835
Low frequency electrical noise across contacts between a normal conductor and superconducting bulk YBa2Cu3O7 22 p3146 N90-27841
Effects of grain size and grain boundary on critical current density of high T(sub c) superconducting oxides
22 p3146 N90-27843
Microwave conductivity of laser ablated YBaCuO superconducting films and its relation to microstrip transmission line 22 p3147 N90-27844
Effects of friction and end losses on MHD thruster efficiency
[DE90-013673] 23 p3289 N90-28608
Measurement of localized corrosion using current density mapping
[DE90-015086] 23 p3310 N90-28721
Unipolar arcing on the cathode surface of a high voltage diode
[AD-A224122] 23 p3322 N90-28787
VLSI design for reliability
[AD-A224264] 24 p3463 N90-29562
CURRENT DISTRIBUTION
The physics of double layers and their role in astrophysics
[TRITA-EPP-89-03] 03 p0421 N90-12421
Characteristic impedance of microstrip lines
[NASA-TM-101581] 05 p0633 N90-13694
Some remarks on the working principle of the rocketborne nose tip dc probes in the D-region of the ionosphere 05 p0658 N90-13839
Effects of nonuniform potential and current distributions in electrochemical systems
[DE90-007349] 12 p1623 N90-19325
Current distribution in cylindrical porous electrodes
[DE90-009707] 18 p2546 N90-24530
Transversal, longitudinal, and three dimensional eddy currents in cylindrical guides with elliptic diameters
[ETN-90-97302] 22 p3188 N90-27967
Further studies of 60 Hz exposure effects on human function
[DE90-014377] 23 p3355 N90-28962
CURRENT REGULATORS
Research on the controllability of integrated circuits by means of electron beams
[ETN-90-95710] 05 p0636 N90-13708
Arc current control of a robotic welding system: Modeling and control system design
[AD-A213150] 05 p0650 N90-13788
Current protections modelisation in a buck cell
10 p1335 N90-17723
Magnetic coupled current sensing techniques for spacecraft power systems 10 p1335 N90-17725
State variable modelling for the audiosusceptibility evaluations of current controlled zero ripple structures
10 p1337 N90-17735
CURRENT SHEETS
Numerical study of the current sheet and PSBL in a magnetotail model
[NASA-CR-183289] 02 p0293 N90-11669
Symmetry breaking bifurcations of a current sheet
[DE90-601005] 06 p0837 N90-14864
A current disruption mechanism in the neutral sheet for triggering substorm expansions
[NASA-CR-186260] 09 p1298 N90-17525
Slow shocks in coronal mass ejections
[NASA-CR-186578] 15 p2193 N90-22522
The large and small scale density structure in the solar corona 16 p2338 N90-23327
CURRENT STABILIZERS
U CURRENT REGULATORS
CURRENTS (OCEANOGRAPHY)
U WATER CURRENTS
CURTISS-WRIGHT MILITARY AIRCRAFT
U MILITARY AIRCRAFT
CURVATURE
Curvature effects on the stability of three-dimensional laminar boundary layers 01 p0064 N90-10366
Compact surface in three-dimensional ellipsoid with prescribed mean curvature (I)
[DE89-618381] 02 p0264 N90-11502
Natural frequencies of singly-curved laminated plates with simply-supported edges
[ESDU-89011] 03 p0359 N90-12052
Some aspects of curvature in general relativity
05 p0704 N90-14122
The structure of supersonic turbulent boundary layers subjected to concave surface curvature
08 p1017 N90-15883
Load-shortening behavior of an initially curved eccentrically loaded column
[NASA-TM-101643] 08 p1088 N90-16293
Eccentricity effects of square cutouts on the natural frequencies and mode shapes of curved rectangular composite panels
[AD-A216410] 10 p1350 N90-17831
Theory of gearing
[NASA-RP-1212] 12 p1670 N90-19593
Curvature continuity of cubic Bezier curves in the solid modeling aerospace research tools design software
[NASA-CR-186583] 14 p2016 N90-21554
On the equation: Delta u+c=Ke(sup u)
[DE90-612741] 14 p2020 N90-21575
The curvature of conjugate profiles in points of contract
[MEMO-COSOR-89-18] 16 p2243 N90-22795
Near field curvature at parallel phase objects: Model examination with microwaves
[ETN-90-96499] 18 p2545 N90-24525
Data analysis in cervical trauma
19 p2718 N90-25464
Origin of density fluctuations in extended inflation
[NASA-CR-182852] 19 p2795 N90-25915
Curvature estimation in orientation selection
[AD-A221481] 21 p3034 N90-27249
Algorithms to solve nonlinear time dependent problems of engineering and physics
[AD-A221463] 21 p3055 N90-27366
The effects of grid-generated turbulence on flat and concave turbulent boundary layers
23 p3324 N90-28797
Free shear layer and swirl flow heat transfer enhancement
[PB90-228123] 23 p3325 N90-28798
Twisted crystals: Propagation, genesis, and relationships with optical activity and molecular symmetry (excerpts)
[DE90-014259] 23 p3399 N90-29205
Trinocular stereovision using figural continuity, dealing with curved objects 24 p3503 N90-29802
CURVE FITTING
An interactive program for constrained spline approximation of numerical data
[DE89-016674] 02 p0267 N90-11520
Computer problems in goodness-of-fit
[AD-A211411] 03 p0397 N90-12268
Evaluation of the modal testing MODENT software with simulated data
[INPE-4885-NTE/291] 09 p1269 N90-17357
Application of Chebyshev approximation to curve fitting
[MEMO-805] 11 p1554 N90-18947
Identification of XV-15 aeroelastic modes using frequency-domain methods
[NASA-TM-101021] 15 p2051 N90-21756
An algorithm and computer program for the calculation of envelope curves
[PB90-155409] 15 p2145 N90-22254
The approximation of a composite Bezier cubic curve by a composite Bezier quadratic curve
[NPL-DITC-147/89] 15 p2162 N90-22354

Laser temperature-jump kinetic studies of fast reactions in nonaqueous solutions
[AD-A218819] 17 p2371 N90-23500
Robust circle and sphere fitting by least squares
[NPL-DITC-153/89] 22 p3243 N90-28389

CURVED BEAMS
Numerical solutions of the nonlinear theory of curved beams 15 p2110 N90-22071

CURVED PANELS
Eccentricity effects of square cutouts on the natural frequencies and mode shapes of curved rectangular composite panels
[AD-A216410] 10 p1350 N90-17831

CURVED SURFACES
U CONTOURS
U SHAPES
U SURFACES

CURVES
Stochastic action of dynamical systems on curved manifolds. The isokinetic developing map on trajectories
[PREPRINT-666] 08 p1117 N90-16466
Theory of gearing
[NASA-RP-1212] 12 p1670 N90-19593

CURVES (GEOMETRY)
NT EPICYCLOIDS
Parabolic equations for curves on surfaces. 2: Intersections, blow up and generalized solutions
[AD-A212890] 05 p0687 N90-14004
On distance-transitive graphs and involutions
[CWI-PM-R8808] 05 p0691 N90-14037
Ice floe identification in satellite images using mathematical morphology and clustering about principal curves
[AD-A213854] 08 p1090 N90-16311
Curvature-dependent parametrization of curves and surfaces
[CS-8915] 16 p2299 N90-23100
Infinite separatrix cycles in the critical case, divergence and uniqueness of limit cycles of a quadratic differential system
[REPT-89-87] 17 p2458 N90-24034
On the projective invariant representation of conics in computer graphics
[CWI-CS-R8938] 18 p2593 N90-24752
Calculation of the algebraic curves parameterization: Hamburger-Noether expansions
[IMAG-RR-798-M] 20 p2919 N90-26608
Local interpolation functions for curve generation with the multi-surface transformation
24 p3470 N90-29608

CURVILINEAR COORDINATES
U SPHERICAL COORDINATES

CUSTOM INTEGRATED CIRCUITS
U APPLICATION SPECIFIC INTEGRATED CIRCUITS

CUT-OUTS
U OPENINGS

CUTANEOUS PERCEPTION
U TOUCH

CUTTERS
NT DRILL BITS
NT DRILLS
NT SAWS
High-speed machining of aluminum
[DE89-014011] 01 p0077 N90-10441
New tool-holding concept
[DE90-000880] 06 p0794 N90-14624
Application of high-rate cutting tools
[AD-A214644] 09 p1203 N90-16970
Using template/hotwire cutting to demonstrate moldless composite fabrication 18 p2515 N90-24361

CUTTING
NT LASER CUTTING
NT METAL CUTTING
NT MILLING (MACHINING)
NT SHEARING
NT SPARK MACHINING
Basic investigations of cutting machinability of inorganic glasses using single-point tools
[W-15/87] 02 p0210 N90-11204
Autonomous space processor for orbital debris
[NASA-CR-186043] 03 p0311 N90-11770
Electrode/workpiece combinations
[DE90-003919] 08 p1054 N90-16095
Application of high-rate cutting tools
[AD-A214644] 09 p1203 N90-16970
Fabrication of ultra thin GaAs and Ge substrates for high efficiency solar cells 10 p1339 N90-17753
Machining of new materials at Aerospatiale
[REPT-892-430-104] 16 p2213 N90-22622
Lunar stone saw
[NASA-CR-182438] 17 p2412 N90-23741
Using template/hotwire cutting to demonstrate moldless composite fabrication 18 p2515 N90-24361
Power saw
[NASA-CASE-MSC-21469-1] 20 p2872 N90-26340
New core design for use with precision composite reflectors
[NASA-CASE-NPO-17858-1-CU] 21 p2970 N90-26880

CVD (DEPOSITION)
U VAPOR DEPOSITION

CYANAMIDES
Non-destructive characterization of epoxy/dicyandiamide interphases using surface-enhanced Raman scattering
[AD-A215894] 10 p1353 N90-17846

CYANATES
Multiple internal reflection Fourier transform infrared spectroscopy studies of thiocyanate adsorption on silver and gold
[AD-A210245] 01 p0041 N90-10223

CYANIDES
NT ACETONITRILE
X ray diffraction patterns of metal aurocyanides
[DE89-015188] 03 p0326 N90-11851
A comparison of photospheric and circumstellar (HCN)/(CO)-ratios for bright carbon stars
[PB90-151101] 15 p2184 N90-22477

CYANO COMPOUNDS
NT CYANAMIDES
NT CYANOACETYLENE
NT ISOCYANATES
Electron density modulation of catalytic metal centers by substituted aryl-isocyanide ligands
[AD-A212875] 04 p0473 N90-12708
The heat of formation of CN radicals and radiative lifetimes of the A 1 Sigma - state of C2N2
20 p2946 N90-26765

CYANOACETYLENE
Laboratory studies, analysis, and interpretation of the spectra of hydrocarbons present in planetary atmospheres including cyanoacetylene, acetylene, propane, and ethane 20 p2943 N90-26748

CYBERNETICS
Conceptual dependency theory and robot programming
[REPT-89-20] 04 p0537 N90-13106
Computing with neural maps: Application to perceptual and cognitive functions
[AD-A216689] 10 p1412 N90-18143
An expert system for the design of heating, ventilating, and air-conditioning systems
[AD-A218287] 13 p1788 N90-20262
Guide to RMS-literature
[REPT-89-52] 15 p2158 N90-22326
Multimedia system control
[AD-A219392] 16 p2276 N90-22971
The human factors of workstation telepresence
19 p2732 N90-25528
Compact 4-D optical neural network architecture
[AD-A222160] 22 p3241 N90-28379

CYCLES
NT ACTIVITY CYCLES (BIOLOGY)
NT BRAYTON CYCLE
NT CARBON CYCLE
NT HYDROLOGICAL CYCLE
NT RANKINE CYCLE
NT SOLAR CYCLES
NT STIRLING CYCLE
NT STRESS CYCLES
NT SUNSPOT CYCLE
NT THERMODYNAMIC CYCLES
NT WORK-REST CYCLE
Long dominating cycles and paths in graphs with large neighborhood unions
[MEMO-769] 04 p0544 N90-13157
Hamiltonian properties of graphs with large neighborhood unions
[MEMO-779] 05 p0689 N90-14013
Changes in impedance of Ni electrodes upon standing and cycling
[NASA-TM-102438] 10 p1401 N90-18097
Periodic ARMA models: Optimal prediction and minimum-phase condition
[REPT-89-006] 16 p2305 N90-23131
The biogeochemistry of metal cycling
[NASA-CR-4295] 17 p2439 N90-23897
Cyclotomy and association schemes
[REPT-89-73] 17 p2458 N90-24030
EXOSAT medium energy observations of binary X ray pulsar 4U1538-52 19 p2783 N90-25837

CYCLIC ACCELERATORS
NT BETATRONS
NT STORAGE RINGS (PARTICLE ACCELERATORS)
NT SYNCHROTRONS
Beam diagnostics in circular machines: Review of new developments
[DE90-014986] 23 p3394 N90-29176

CYCLIC COMPOUNDS
NT ADENOSINE TRIPHOSPHATE
NT ATROPINE
NT AZOLES
NT AZULENE
NT BENZENE
NT CAFFEINE
NT CYCLIC HYDROCARBONS
NT CYCLOBUTANE
NT CYCLOHEXANE
NT ETHYLENE OXIDE
NT HETEROCYCLIC COMPOUNDS
NT HMX
NT NAPHTHALENE
NT NICOTINIC ACID
NT PHTHALOCYANIN
NT PYRIDINES
NT PYRROLES
NT RDX
NT TETRAHYDROFURAN
NT TRYPTOPHAN
The synthesis and structure of novel antimony thiametallacycles
[AD-A210888] 01 p0042 N90-10229

CYCLIC HYDROCARBONS
NT BENZENE
NT CYCLOBUTANE
NT CYCLOHEXANE
NT NAPHTHALENE
NMR evidence for a planar arene intermediate in the electron-transfer induced eta 6 to eta 4 hapticity change of a rhodium arene complex
[AD-A210211] 01 p0033 N90-10177
An implication of the IR identification of PAHs: The heating of the diffuse is gas 11 p1582 N90-19113
A survey of PAH emission in HII regions, planetary and proto-planetary nebulae 11 p1584 N90-19129
Electronic and molecular structure of carbon grains
21 p3091 N90-27574
A unifying picture of gas-phase formation and growth of PAH (Polycyclic Aromatic Hydrocarbons), soot, diamond and graphite 21 p3091 N90-27575
FT-IR spectroscopic studies of polycyclic aromatic hydrocarbons 21 p3095 N90-27592
Novel macrocyclic carriers for proton-coupled liquid membrane transport
[DE90-015529] 24 p3445 N90-29453

CYCLIC LOADS
Theoretical and experimental investigation of thin-walled aluminum panels under cyclic shear load
02 p0177 N90-10996
Effect of thermal and cyclic loads on silicon carbide yarn reinforced glass matrix composites
[DE89-016554] 02 p0191 N90-11091
Development of a rate independent plasticity theory for general cyclic loading 07 p0945 N90-15471
Cyclic fatigue of hot-isostatic-pressed silicon nitride
[PB90-122649] 08 p1090 N90-16308
Thermoelastic response of an epoxy
[AD-A215639] 09 p1198 N90-16942
Cyclic deformation of Sn-60 to Pb-40 solder joints during thermomechanical fatigue
[DE90-004197] 09 p1237 N90-17178
Effect of a single overload upon fatigue crack growth in an aluminum-lithium alloy
[AD-A216183] 10 p1356 N90-17865
Characterization of failure processes in tungsten copper composites under fatigue loading conditions
[NASA-TM-102371] 14 p1943 N90-21123
Cycle life machine for AX-5 space suit
15 p2112 N90-22080
Probabilistic finite elements: Applications to fracture and fatigue 15 p2121 N90-22134
Rotor loading on a three-bladed wind turbine
15 p2123 N90-22145
Rubberlike elasticity experiment
18 p2515 N90-24362
Mechanistic modeling of corrosion fatigue crack growth of steels in aqueous solutions 18 p2524 N90-24404
Computational methods and plasticity
[PB90-167917] 18 p2571 N90-24652
A numerical study of plasticity induced closure in short cracks by the finite element method
[AD-A220471] 18 p2571 N90-24654
Cyclic stress strain behavior of an austenitic stainless steel Polarit 778 under variable amplitude loading
[VTT-RR-647] 19 p2675 N90-25215
Calculation of service life of turbomachine components 22 p3117 N90-27706
The role of inflight engine condition monitoring on life cycle management of CF-18/F404 engine components
22 p3118 N90-27708
Methodology of the fatigue under shocks. Experimental results: 7075 T6 and 35 NCD16
[ETCA-89-R-140] 22 p3157 N90-27901

Lateral buckling of short I-beams under cyclic loading
[PB90-213653] 22 p3191 N90-28104
A constitutive model for AS4/PEEK thermoplastic composites under cyclic loading
[NASA-CR-180393] 23 p3302 N90-28679

CYCLING
U CYCLES

CYCLOBUTANE
Composite materials with improved properties in compression: Synthesis of 3-methylene-1,1-Dichlorosilacyclobutane and 1,1-dichlorosilacyclopent-3-ene
[AD-A222615] 20 p2828 N90-26088

CYCLOGENESIS
Thermodynamic and dynamic processes in the updraft region of GALE (Genesis of Atlantic Lows Experiment) IOP (Intensive Observation Period) 9
[AD-A208139] 01 p0087 N90-10496
Investigations of polar air stream cyclogenesis based on numerical simulations with a mesoscale model
[PB89-214563] 03 p0373 N90-12132
Inverted surface troughs accompanying Rocky Mountain lee-side cyclogenesis 06 p0816 N90-14746
Dynamics of baroclinic instability in rapid cyclogenesis 07 p0962 N90-15563
Potential vorticity in extratropical cyclones 07 p0962 N90-15564
Numerical simulations of the rapid cyclogenesis over Canada and evolution of a cold front observed on 25-26 April 1979 (SESAME-AVE-3) 09 p1247 N90-17234
Simulation of a weather situation with high ozone concentrations during ALPEX 12 p1686 N90-19686
Colloquium on Synoptic Meteorology
[PB90-121112] 12 p1692 N90-19720
Semigeostrophic flow over orography in a stratified rotating atmosphere 15 p2127 N90-22163
Second National Winter Weather Workshop Conducted by the National Weather Service
[PB90-147414] 15 p2131 N90-22183
Impact of marine boundary layer parameterization on a numerical simulation of cyclogenesis during a cold air outbreak event 16 p2256 N90-22864
A case study of explosive cyclogenesis in the eastern Pacific Ocean 14 to 17 December 1987
[AD-A219543] 17 p2426 N90-23824
A day in the life of a warm front
[AD-A220373] 17 p2426 N90-23826
Boundary layer parameterization for use in a limited area forecast model 21 p3029 N90-27224

CYCLOHEXANE
Extracting chemical information form Auger line shapes
[AD-A216729] 11 p1483 N90-18537

CYCLONES
NT HURRICANES
NT TYPHOONS
Variational objective analysis for cyclone studies 03 p0361 N90-12064
Air flow over large scale topography
[AD-A211779] 04 p0519 N90-12998
Inverted surface troughs accompanying Rocky Mountain lee-side cyclogenesis 06 p0816 N90-14746
Potential vorticity in extratropical cyclones 07 p0962 N90-15564
Precipitation distributions associated with cyclones originating over the Gulf of Mexico and surrounding coastal regions
[AD-A213644] 07 p0963 N90-15569
Further research on dynamics of marine atmospheres in tropical cyclones
[AD-A213882] 07 p0964 N90-15571
The role of an upstream cyclone and corresponding synoptic/planetary-scale interactions during the development of a blocking anticyclone 08 p1150 N90-16659
Numerical simulations of the rapid cyclogenesis over Canada and evolution of a cold front observed on 25-26 April 1979 (SESAME-AVE-3) 09 p1247 N90-17234
ONR tropical cyclone motion research initiative: Data assimilation considerations for field experiment analyses
[AD-A215726] 09 p1248 N90-17244
Dynamics of an ERICA (Experiment on Rapidly Intensifying Cyclones over the Atlantic) cyclone
[AD-A216775] 11 p1536 N90-18846
Cyclogeneses and extratropical cyclones in the south-southeast region of Brazil and its influence in time
[INPE-4812-TDL/359] 12 p1693 N90-19722
Analysis of GALE (Genesis of Atlantic Lows Experiment) data
[AD-A217182] 13 p1844 N90-20584
Applications of microwave radiometric measurements to infer tropical cyclone intensity and strength
[AD-A218273] 13 p1847 N90-20600
The invertibility principle for a simple hurricane model
[AD-A218344] 13 p1848 N90-20605
Tropopause undulations and the development of extratropical cyclones 15 p2132 N90-22186
Application of the lagged-averaged technique to tropical cyclone track predictions
[AD-A218389] 17 p2425 N90-23819
A description of tropical cyclone recurvature in terms of isentropic potential vorticity
[AD-A218482] 17 p2425 N90-23821
A day in the life of a warm front
[AD-A220373] 17 p2426 N90-23826
Barotropic vortex adjustment to asymmetric forcing with application to tropical cyclone motion
[AD-A219883] 17 p2427 N90-23831
Tropical cyclones, 1989: Central north Pacific
[PB90-182536] 17 p2428 N90-23836
Initiation and propagation of thunderstorm mesocyclones 17 p2428 N90-23838
Mariners Weather Log, volume 33, number 2, Spring 1989
[PB90-146838] 20 p2889 N90-26443
Wind field derivatives of extratropical cyclones observed by Doppler radar
[AD-A222188] 21 p3031 N90-27232
Instability bursts associated with Extratropical Cyclone Systems (ECSs) and a forecast index of 3 to 12 hour heavy precipitation
[NOAA-TM-NESDIS-30] 22 p3228 N90-28309

CYCLONES (EQUIPMENT)
U CENTRIFUGES

CYCLOTETRAMETHYLENE TETRANITRAMINE
U HMX

CYCLOTRIMETHYLENE TRINITRAMINE
U RDX

CYCLOTRON FREQUENCY
Observations of electrostatic hydrogen cyclotron waves and electric field fluctuations near one Hz in auroral acceleration regions 05 p0658 N90-13842
Full wave computation of electromagnetic wave excitation, propagation, and absorption at the ion cyclotron frequency in fusion experiments
[DE90-009399] 14 p2030 N90-21642

CYCLOTRON RADIATION
NT ION CYCLOTRON RADIATION
Electron cyclotron emission and absorption experiment on the CASTOR tokamak
[IPPCZ-285] 03 p0407 N90-12331
Operation of a step tunable megawatt gyrotron 15 p2061 N90-21802
Cyclotron maser and plasma wave growth in magnetic loops
[NASA-CR-179862] 15 p2170 N90-22402
Experimental demonstration of an electromagnetically pumped free-electron laser with cyclotron harmonic idlers
[AD-A218830] 17 p2408 N90-23719
A survey of equatorial magnetospheric wave activity between 5 and 8 R(sub E)
[AD-A220137] 17 p2424 N90-23812
Cyclotron absorption in gamma ray bursts seen with Ginga 19 p2769 N90-25736
Linearly extended cyclotron emission regions in AM Herculis systems 19 p2775 N90-25778
Hard X ray pulses from Vela X-1 19 p2777 N90-25791
Combined electron cyclotron ray tracing and transport code studies in the compact ignition tokamak
[DE90-014097] 23 p3396 N90-29189

CYCLOTRON RESONANCE
Producing of an ECR plasma using 2450MHz Whistler wave and the investigating of its parameters
[DE89-618689] 02 p0278 N90-11586
Investigation of resonant ac-dc magnetic field effects
[AD-A211612] 03 p0379 N90-12159
Propulsion research on the hybrid plume rocket
[AD-A214420] 07 p0887 N90-15132
The 17th AINSE Plasma Physics Conference: Conference handbook
[DE90-600936] 07 p0996 N90-15759
Density clamping phenomena in electron cyclotron resonance heated plasmas on Heliotron E
[DE90-719523] 09 p1284 N90-17442
Quasilinear approach to the damping of LH waves in a reactor-grade plasma
[IPPCZ-292] 10 p1432 N90-18262
Activities report of the Institute for Plasma Research
[ETN-90-96467] 16 p2319 N90-23225

CYCLOTRON RESONANCE DEVICES
Gyrotron development for space power beaming 01 p0028 N90-10148
History and status of beamed power technology and applications at 2.45 Gigahertz 01 p0029 N90-10150
Design and operating characteristics of a CW relevant quasi-optical gyrotron with variable mirror separation
[AD-A210611] 01 p0074 N90-10425
Cold tests of quasi-optical gyrotron resonators
[AD-A212707] 04 p0498 N90-12868
Scaling of an 85 GHz gyrotron to operate at 94 GHz
[AD-A212756] 04 p0504 N90-12909
Use of a krypton isotope for rapid ion changeover at the Lawrence Berkeley Laboratory 88-inch cyclotron
[NASA-CR-186107] 05 p0698 N90-14084
Review of quasi-optical gyrotron development
[AD-A213491] 07 p0933 N90-15402
Mechanical design of the inside launch system for electron cyclotron heating in D3-D
[DE90-003292] 07 p0995 N90-15751
Electrical test of gyrotron coil
[INPE-4929-RPE/596] 09 p1214 N90-17041
Development of a small signal theory for the harmonic gyroklystron
[AD-A216274] 10 p1380 N90-17999
Beam collector and output window for a 35 GHz 100 kW gyrotron
[INPE-4958-RPE/603] 11 p1511 N90-18699
Design considerations in achieving 1 MW CW operation with a whispering-gallery-mode gyrotron
[DE90-007283] 12 p1663 N90-19557
Progress in the CW operation of a 140 GHz gyrotron
[DE90-007382] 12 p1663 N90-19558
Low frequency gyrotron amplifier investigation, phase 2
[AD-A217096] 14 p1981 N90-21352
Free-Space Power Transmission
[NASA-CP-10016] 15 p2060 N90-21795
Analysis of a high harmonic rectangular gyrotron using ribbon beams 15 p2061 N90-21801
Operation of a step tunable megawatt gyrotron 15 p2061 N90-21802
The 10-100 kW submillimeter gyrotron 15 p2061 N90-21803
High power millimeter wave source development program 15 p2061 N90-21805
Measurement of plasma-neutralized super-vacuum currents in a gyrotron configuration
[AD-A218505] 16 p2316 N90-23207
Mode competition in the quasioptical gyrotron
[AD-A222181] 23 p3329 N90-28823

CYCLOTRONS
National Science Foundation 04 p0569 N90-13320
Coulomb-dissociation of 156 MeV 6Li-projectiles
[KFK-4691] 21 p3075 N90-27482

CYGNUS CONSTELLATION
The determination of the muon content of EAS from Cygnus X-3 05 p0715 N90-14179
Relative muon content of UHE showers associated with Hercules X-1
[DE90-000609] 08 p1151 N90-16665
Thermal pair cloud models of MeV gamma ray emissions from Cygnus X-1 and the Galactic Center
[DE90-001168] 09 p1301 N90-17536
Infrared spectroscopy and imaging of supernova remnants 11 p1580 N90-19104
Search for anisotropies in the underground cosmic ray muon flux 12 p1745 N90-20034
Underground muons from the direction of Cygnus X-3
[DE90-005646] 12 p1746 N90-20038
The 1989 outburst of V404 Cygni: A very unusual x ray nova
[DE90-008935] 14 p2038 N90-21693
Gamma rays from pulsar wind shock acceleration 16 p2336 N90-23311
Infrared coronal line novae 16 p2339 N90-23328
Observations of Cygnus X-2 at x ray, UV, optical and radio frequencies
[MPE-PREPRINT-163] 17 p2481 N90-24191
Radiation-driven evolution of low-mass x ray binaries 18 p2637 N90-25022
EXOSAT observations of Cygnus X-1: Study of the soft X ray excess 19 p2771 N90-25750
The soft X ray spectrum of Cygnus X-1 19 p2771 N90-25751
Noise variability in Cyg X-1 and Her X-1 19 p2771 N90-25753
The behaviour of SS433 and Cygnus X-3 at low frequency 19 p2772 N90-25756
Evidence of a 12 ms pulsar in Cygnus X-3 19 p2772 N90-25759
The optical light curve of Cygnus X-1 19 p2778 N90-25801
The interstellar D1 line at high resolution
[NASA-CR-184915] 20 p2941 N90-26737

CYLINDRICAL AFTERBODIES
U AFTERBODIES
U CYLINDRICAL BODIES

CYLINDRICAL BODIES
NT ROTATING CYLINDERS
An experimental investigation of the aerodynamic characteristics of slanted base ogive cylinders using magnetic suspension technology
[NASA-CR-181708] 02 p0146 N90-10834

Internal voltages and currents in well-shielded cylindrical objects due to simulated direct-strike lightning
[DE89-012664] 02 p0215 N90-11231
A computational/experimental study of the flow around a body of revolution at angle of attack
[NASA-TM-88329] 02 p0219 N90-11254
Normal-force-curve and pitching-moment-curve slopes of forebody-cylinder combinations at zero angle of attack for Mach numbers up to 5
[ESDU-89008] 03 p0301 N90-11709
Small particle scattering and absorption
[AD-A213168] 04 p0473 N90-12711
Stress waves through projectile joints and interfaces
[AD-A212201] 04 p0513 N90-12963
Method and apparatus to enhance the sensitivity of cylindrical magnetostrictive transducer to magnetic fields
[AD-D014218] 06 p0767 N90-14459
Surface flow and heating distributions on a cylinder in near wake of Aeroassist Flight Experiment (AFE) configuration at incidence in Mach 10 Air
[NASA-TP-2954] 06 p0772 N90-14493
Flow separation in shock wave boundary layer interactions at hypersonic speeds
[NASA-CR-4274] 08 p1017 N90-15885
Computation of fluid flow and heat transfer in rotating disc-systems 09 p1215 N90-17044
Effect of riblets on flow separation from a cylinder and an airfoil in subsonic flow
[AD-A216197] 10 p1309 N90-17574
Impact damage tolerance of composite cylindrical panels
[AD-A216401] 10 p1350 N90-17830
Oblique impact of two cylinders in a uniform flow
[AD-A215933] 10 p1385 N90-18015
Investigation of collapse characteristics of cylindrical composite panels with large cutouts
[AD-A216378] 10 p1397 N90-18079
Acoustic radiation of cylindrical shells, with stiffening finishing and coated with masking materials
[ISAL-89-0035] 10 p1426 N90-18227
Computational fluid dynamics method for low Reynolds number flow in a precessing/spinning, liquid filled cylinder with rounded endcaps
[AD-A216997] 12 p1659 N90-19531
Jam resistant fluid power actuator for ballistic-damage tolerant redundant cylinder assemblies
[AD-D014360] 12 p1671 N90-19600
Diagnostics and firing control for the cylindrical reconnection launcher
[DE90-007677] 13 p1761 N90-20107
Filament winding of composite cylinders
14 p1943 N90-21119
The interaction between a plane shock wave and a cylindrical afterbody 15 p2046 N90-21728
Theory of a periodic cylindrical waveguide with a nonuniform metal-dielectric filling
[DE90-620099] 15 p2087 N90-21945
On the theory of Heiser and Shercliff experiment. Part 2: MHD flow between two cylinders in strong radical magnetic field
[OUEL-1805/89-PT-2] 15 p2170 N90-22401
Three-dimensional separated flow prediction on fusiform body using Euler and boundary layer methods
16 p2234 N90-22745
Side moment exerted by a spinning, coning, highly viscous liquid payload
[AD-A216746] 16 p2237 N90-22763
Nonaxisymmetric body, supersonic, inviscid dynamic derivative prediction
[AD-A220639] 17 p2346 N90-23358
Controlled crack growth specimen for brittle systems
[NASA-TM-103126] 17 p2378 N90-23543
Three-dimensional convection in cylindrical geometry
17 p2399 N90-23668
Thin-layer Navier-Stokes solutions of the asymmetric vortical flow on a tangent ogive body
[AD-A220810] 17 p2403 N90-23690
Subsonic sting interference on the aerodynamic characteristics of a family of slanted-base ogive-cylinders
[NASA-CR-4299] 18 p2492 N90-24242
Low velocity impact analysis with NASTRAN
18 p2570 N90-24647
Device and method for detecting and displaying crossover pattern in precision winding
[AD-D014539] 19 p2685 N90-25276
On the natural frequencies of a short circular cylinder, including the effects of entrained mass
[LR-602] 19 p2704 N90-25383
Hydroelastic problems in space flight vehicles
[LRT-WE-9-FB-11(1989)] 21 p2967 N90-26868
Fabrication of microwave guides using high Tc superconductors
[AD-A221560] 21 p3001 N90-27059
Heat and momentum transfer to test samples in the high velocity plasma furnace
[AD-A222182] 21 p3079 N90-27505
Analytical resolution of the Oseens differential equation of inclined turning cylinder with gliding
[ETN-90-97316] 22 p3171 N90-27988
On Einsteinian 4-submanifolds in E(sup 6)
[DE90-627149] 23 p3402 N90-29226
Effect of a crystal-melt interface on Taylor-Vortex flow with buoyancy
[PB90-244401] 24 p3551 N90-30089

CYLINDRICAL PLASMAS
Rigorous upper bounds for turbulent transport in bounded systems: Passive advection and reversed-field pinches 15 p2168 N90-22390
Resonant MHD modes with toroidal coupling
[DE90-010077] 16 p2319 N90-23222

CYLINDRICAL SHELLS
Overview of actual buckling calculation methods for space vehicle structures 02 p0177 N90-10995
Calculation of sound transmission through a cylindrical shell using ASKA acoustics 02 p0179 N90-11009
A thermoelastic transversely isotropic thick walled cylinder/disk application: An analytical solution and study
[NASA-TM-102320] 04 p0511 N90-12950
Unsteady forces induced on finite-span cylinders in a cross-flow 05 p0642 N90-13746
The initial imperfection data bank at the Delft University of Technology, part 2
[LR-559-PT-2] 05 p0656 N90-13825
Colinear fluctuating wall shear stress and fluctuating pressure transducer
[AD-D014296] 08 p1076 N90-16226
Elastic buckling of imperfect cylindrical shells containing granular solids
[PB90-110362] 09 p1236 N90-17174
A review of the theory and methods for determining dynamic pulse buckling of cylindrical shells
[AD-A214764] 09 p1238 N90-17185
Steady state temperatures and thermal stresses in a spherical or cylindrical laminated shell
[ESDU-89027] 12 p1674 N90-19612
Modal interactions in shell dynamics
13 p1814 N90-20418
Transient response of a cylindrical shell of finite length to transverse impact
[OUEL-1780/89] 15 p2119 N90-22123
Transverse vibrations of a composite cylindrical tube of circular cross section
[AD-A219227] 16 p2248 N90-22820
Eigenvalue computations with the QUAD4 consistent-mass matrix 18 p2569 N90-24642
Generation of an axisymmetric cylindrical shell element using a shooting method
[ACTA-POLYTEC-SCAND-CI-93] 19 p2700 N90-25362
Engineering fracture mechanics
[AD-A222699] 21 p3012 N90-27123
Approximate equations for heat conduction in multi-layered cylindrical shells
[NAL-TR-1049] 24 p3471 N90-29614
Application of the complex variable solution to some problems in linear elastic materials with voids
24 p3478 N90-29658
Buckling of anisotropic cylindrical shells subjected to combined axial compression, normal pressure, bending and shear loading
[LR-611] 24 p3482 N90-29678

CYLINDRICAL TANKS
Linear liquid oscillations in cylindrical containers under zero-gravity
[LRT-WE-9-FB-5(1989)] 08 p1066 N90-16168
Surface dilation and fluid-dynamical behaviour of Newtonian liquids in an overflowing cylinder. 1: Pure liquids
[LR-601] 19 p2692 N90-25317
Numerical investigation of the thermal stratification in cryogenic tanks subjected to wall heat flux
[NASA-TM-103194] 22 p3171 N90-27984
Investigation of the dynamic buckling of liquid-filled tanks 24 p3478 N90-29660

CYLINDROIDS
U CYLINDRICAL BODIES

CYTOCHROMES
Experiment K-6-11. Actin mRNA and cytochrome c mRNA concentrations in the tricepts brachia muscle of rats 20 p2894 N90-26465

CYTOGENESIS
NT CELL DIVISION
NT DIFFERENTIATION (BIOLOGY)
NT MITOSIS
Computer aided mechanogenesis of skeletal muscle organs from single cells in vitro
[NASA-CR-187025] 23 p3354 N90-28959

CYTOLOGY
Cellular and molecular mechanisms of high pressure inotropy in cardiac muscle
[AD-A211695] 03 p0381 N90-12170
Fundamental results from microgravity cell experiments with possible commericial applications
05 p0676 N90-13940
Physical phenomena and the microgravity response
05 p0677 N90-13945
Does DNA cytometry have a place in the clinical laboratory
[DE90-007652] 14 p2009 N90-21512
The effect of clinostat rotation on plant protoplasts
19 p2681 N90-25247

CYTOMETRY
Does DNA cytometry have a place in the clinical laboratory
[DE90-007652] 14 p2009 N90-21512
The effects of simulated hypogravity on murine bone marrow cells 18 p2631 N90-24989

CYTOPHOTOMETRY
U CYTOMETRY

CYTOPLASM
Carbon and hydrogen metabolism of green algae in light and dark
[DE90-008648] 13 p1849 N90-20612

CZOCHRALSKI METHOD
Autonomous control system for Czochralski growth of LEC GaAs
[AD-A210190] 01 p0131 N90-10754
Optical spectroscopy of Ti(3+) doped YAlO3
[AD-A219043] 16 p2324 N90-23251
Three-dimensional convection in cylindrical geometry
17 p2399 N90-23668
Development of a large scale Nd:YAG growth process
[DE90-010746] 18 p2624 N90-24954
Mathematical simulation of heat exchanges and thermoelastic constraints in Czochralski crystal growth
[ETN-90-97242] 20 p2931 N90-26680

D

D LAYER
U D REGION

D REGION
HIPAS 1987-88: ULF research and campaign support
[AD-A211720] 03 p0339 N90-11933
Some remarks on the working principle of the rocketborne nose tip dc probes in the D-region of the ionosphere 05 p0658 N90-13839
Variation of D-region nitric-oxide density with solar activity and season at the dip equator
22 p3205 N90-28183
General overview of the solar activity effects on the lower ionosphere 22 p3208 N90-28198
Electron density profiles in the background of LF absorption during Forbush-decrease and PSE
22 p3208 N90-28199
The influence of IMF on the lower ionosphere plasma in high and middle latitudes 22 p3208 N90-28200
Solar cosmic ray effects in the lower ionosphere
22 p3208 N90-28201
On the relation between the electron content of the ionospheric D-region, variations of the riometer absorption, and the H-component of the geomagnetic field
22 p3210 N90-28208
Influence of non-stationary field of magnetospheric convection on the D-region 22 p3210 N90-28209
A study of water vapor, electrical parameters, and radio propagation
[AD-A223582] 24 p3492 N90-29736
A feasibility study for D-region equatorial ionosphere research using VLF radiowaves
[AD-A223685] 24 p3492 N90-29738

DAEMO (DATA ANALYSIS)
U DATA PROCESSING
U DATA REDUCTION
U DATA TRANSMISSION

DAMAGE
NT CUMULATIVE DAMAGE
NT FIRE DAMAGE
NT FLOOD DAMAGE
NT FROST DAMAGE
NT IMPACT DAMAGE
NT LASER DAMAGE
NT METEORITIC DAMAGE
NT PROTON DAMAGE
NT RADIATION DAMAGE
NT STORM DAMAGE
US Air Force certification of castings
01 p0042 N90-10232
Numerical analysis of a class of problems in the mathematical theory of plasticity and damage
[AD-A210731] 01 p0114 N90-10655

Influence of the fiber/matrix interface on damage development in CFRP 02 p0183 N90-11037
Numerical simulation of micrometeroids and debris hypervelocity impacts on Columbus pressurized modules 02 p0188 N90-11075
A theory of damage in brittle and cementitious materials, part 1
[AD-A212940] 05 p0627 N90-13658
Cavitation and superplasticity 06 p0744 N90-14329
Mechanisms of wear in structural ceramic materials 06 p0749 N90-14360
Review of surface flashover theory
[DE90-000806] 06 p0768 N90-14469
Hypervelocity impact calculations using CTH: Case studies
[DE90-002891] 06 p0795 N90-14632
A new uniformly valid asymptotic integration algorithm for elasto-plastic-creep and unified viscoplastic theories including continuum damage
[NASA-TM-102344] 06 p0799 N90-14655
Design temperatures for flexible airfield pavement design
[AD-A214141] 07 p0884 N90-15115
Point of view of a civil aircraft manufacturer on Al-Li alloy 07 p0899 N90-15200
Damage evaluation from surface displacement data 07 p0944 N90-15469
Fatigue loading history reconstruction based on the rain-flow technique
[NASA-CR-181942] 07 p0947 N90-15482
Theoretical study on creep damage detection by ultra-sonic wave measurement
[DE90-702472] 08 p1087 N90-16290
Effects of moisture on composite materials 09 p1185 N90-16866
Analysis of the National Transonic Facility mishap
[NASA-TM-101686] 10 p1318 N90-17620
Stability characteristics of a combat aircraft with control surface failure
[AD-A216196] 10 p1323 N90-17646
Observations of fatigue crack initiation and damage growth in notched titanium matrix composites
[NASA-TM-101688] 10 p1347 N90-17815
Damage mechanisms and indenter size effects in cross plied carbon-carbon composites
[AD-A216413] 10 p1351 N90-17832
AGARD/SMP Review: Damage Tolerance for Engine Structures. 2: Defects and Quantitative Materials Behaviour --- conference
[AGARD-R-769] 11 p1457 N90-18396
The damage tolerance of disc materials: Metallurgical factors; relationship with processing parameters 11 p1458 N90-18398
Future technology requirements (related to defects and quantitative material behavior to aid in implementation of damage tolerance for design of engine structures) 11 p1459 N90-18403
The need for a common approach within AGARD --- engine component defects 11 p1459 N90-18404
The processing and mechanical properties of high temperature/high performance composites. Book 2, section 2: Strength and fracture resistance
[AD-A216142] 11 p1478 N90-18507
The processing and mechanical properties of high temperature/high performance composites. Book 3, section 2: Strength and fracture resistance, part
[AD-A216143] 11 p1478 N90-18508
Theory and verification of the fiber composite damage model implemented in DYNA3D
[AD-A216600] 11 p1479 N90-18511
Jam resistant fluid power actuator for ballistic-damage tolerant redundant cylinder assemblies
[AD-D014360] 12 p1671 N90-19600
Simulation fidelity in lightning penetration studies
[DE90-006367] 12 p1694 N90-19731
Ion mixing and surface modification in metal-semiconductor systems
[DE90-007557] 12 p1723 N90-19897
The NASA, Marshall Space Flight Center drop tube user's manual
[NASA-TM-100392] 13 p1786 N90-20251
Nondestructive testing of ceramics by acoustic microscopy
[AERE-R-13350] 13 p1813 N90-20411
Damage characteristics of time domain histories
[DE90-008787] 13 p1842 N90-20573
Use of unbalanced laminates as a screening method for microcracking
[NASA-TM-102517] 14 p1944 N90-21124
Two-dimensional damage models of fiber-reinforced composites 14 p1946 N90-21135
Advances in optimal active control techniques for aerospace systems; application to aircraft active landing gear 15 p2054 N90-21769
Current management for improved railgun performance 15 p2057 N90-21781
Progression of damage and fracture in composites under dynamic loading
[NASA-TM-103118] 15 p2065 N90-21825
An assessment of the hardness of miniature vacuum tubes to high-voltage transients
[DE90-009541] 15 p2089 N90-21956
Natural modes of cracked beams and identification of cracks 15 p2111 N90-22075
A continuum damage model for the quasi-static response of brittle materials
[DE90-007681] 15 p2117 N90-22112
Impact damage in graphite/epoxy laminates: Damage characterization, acoustic emission, and finite element simulation, volumes 1 and 2 16 p2211 N90-22610
Peacetime replacement and crash damage factors for army aircraft
[AD-A218544] 17 p2348 N90-23372
An experimental study of fault propagation in a jet-engine controller
[NASA-CR-181335] 17 p2354 N90-23401
Effects of X radiation on the LAMPSHADE orbital debris satellite shield, 2
[DE90-008214] 18 p2510 N90-24341
The effect of thermal damage on the mechanical properties of polymer regrinds 18 p2515 N90-24363
Cyclic damage zones ahead of tensile fatigue cracks in ceramic materials
[DE90-008372] 18 p2531 N90-24442
Multispectral classification of overlapping classes with applications to forest damage areas
[DLR-FB-89-55] 18 p2574 N90-24666
Damage tolerance demonstration for A310-300 CFPR components
[MBB-UT-012/89-PUB] 19 p2652 N90-25091
Study of the engine bird ingestion experience of the Boeing 737 aircraft (October 1986 to September 1988)
[DOT/FAA/CT-89/29] 19 p2656 N90-25119
GPHS-RTG response to Challenger type accident 19 p2665 N90-25163
Design and fabrication of high damage threshold turning mirrors for the Nova laser
[DE90-012703] 19 p2696 N90-25341
Study on application of ultrasonic wave measurement to creep-fatigue damage detection
[DE89-782317] 19 p2700 N90-25361
Open hole and post-impact compression fatigue of stitched and unstitched carbon/epoxy composites
[NASA-TM-102676] 19 p2701 N90-25370
Fractography of composite delamination
[NASA-CR-181965] 19 p2702 N90-25372
The effects of acid fog and dew on materials
[PB90-157496] 19 p2712 N90-25436
Radiological investigation of the vertebral column of candidates for military flying training the the Royal Norwegian Air Force 19 p2718 N90-25463
Flexion, extension and lateral bending responses of the cervical spine 19 p2719 N90-25468
Space environments and their effects on space automation and robotics 19 p2735 N90-25543
Vibration test procedures for orbiter sidewall-mounted payloads, phase 1
[AD-A220773] 20 p2818 N90-26037
Vibration test procedures for orbiter sidewall-mounted payloads, phase 2
[AD-A220774] 20 p2818 N90-26038
Damage states in laminated composite three-point bend specimens: An experimental-analytical correlation study
[NASA-TM-101800] 20 p2827 N90-26083
Microstructural dependence of the cavitation damage function in FCC materials
[DE90-012898] 20 p2833 N90-26113
Mechanical paint removal techniques for aircraft structures
[NIAR-90-12] 20 p2842 N90-26166
Flight set 360L001 (STS-26) igniter, post flight
[NASA-CR-183957] 20 p2870 N90-26325
Development of creep-fatigue damage detection method of rotor steel by ultrasonic wave measurement
[DE90-503792] 20 p2877 N90-26365
Lessons learned for composite aircraft structures qualification 21 p2956 N90-26808
An expert system advisor for damage repair of composite wing skins (repairman) 21 p2956 N90-26810
Lessons learned from the T-45A durability and damage tolerance program 21 p2957 N90-26812
Computerized corrosion forecasting model for C-5 aircraft 21 p2957 N90-26815
Application of damage tolerance 21 p2958 N90-26817
Individual Helicopter Tracking Program (IHTP) for the MH-53J helicopter 21 p2958 N90-26818
Peak identification techniques 21 p2959 N90-26822
Semi-active orbital debris sweeper
[NASA-CASE-MSC-21534-1] 21 p2966 N90-26860
The effect of nonlinearities on flexible structures
[AD-A222705] 21 p3012 N90-27124
Personal computer programs for the control of subnanosecond transient digitizers with applications for device damage testing
[AD-A221458] 21 p3054 N90-27365
Rapid annealing of iron implanted Hg(1-x)Cd(x)Te
[AD-A222777] 21 p3082 N90-27524
Annual review of aircraft accident data: US general aviation, calender year 1987
[PB90-138066] 22 p3110 N90-27666
Scandia-stabilized zirconia coating for composites
[AD-D014550] 22 p3160 N90-27917
Creep and creep rupture of strongly reinforced metallic composites
[NASA-CR-185286] 22 p3192 N90-28110
Investigation of the effects of acid deposition on materials
[PB90-158973] 22 p3197 N90-28143
Damage tolerance of the fighter aircraft 37 Viggen. Part 1: Analytical assessment
[FFA-TN-1990-12-PT-1] 23 p3276 N90-28538
Damage tolerance of the fighter aircraft 37 Viggen. Part 2: Experimental verification
[FFA-TN-1990-13-PT-2] 23 p3276 N90-28539
Development and testing of rapid repair methods for war damaged runways
[AD-A223970] 23 p3285 N90-28586
Oxidation, sulfidation, and hot corrosion: Mechanisms and interrelationships 23 p3307 N90-28702
Evaluation of high temperature protective coatings for gas turbine engines under simulated service conditions 23 p3309 N90-28712
Damage resistant optical coatings prepared using high temperature, plasma chemical-vapor-deposition
[DE90-015042] 23 p3313 N90-28738
Minimum weight design of a leaf spring tapered in thickness and width for the Hubble Space Telescope-space support equipment
[NASA-TM-4233] 23 p3340 N90-28879
DNA damage and repair in human skin: Pathways and questions
[DE90-015126] 23 p3356 N90-28966
Aircraft battle damage repair of transparencies
[AD-A224168] 24 p3432 N90-29387
Non-destructive method for environmental breakdown of graphite fiber reinforced polymer composites
[AD-A223729] 24 p3455 N90-29515

DAMAGE ASSESSMENT

Hierarchical damage tolerant controllers for smart structures
[AD-A209422] 01 p0005 N90-10022
Debris/ice/TPS assessment and photographic analysis for Shuttle Mission STS-28R
[NASA-TM-102152] 01 p0016 N90-10079
Development of pressure containment and damage tolerance technology for composite fuselage structures in large transport aircraft
[NASA-CR-3996] 01 p0034 N90-10186
Aircraft live fire testing 02 p0154 N90-10879
The use of damage characterization for life prediction methodologies 02 p0185 N90-11053
Delamination tests under compression-compression and tension-compression loading 02 p0186 N90-11062
Intrinsic damage and strength criteria for advanced composite laminates in space applications 02 p0187 N90-11071
Computer simulations of radiation damage in amorphous solids
[PB89-212682] 03 p0322 N90-11827
Lightning and surge protection of photovoltaic installations: Two case histories, Vulcano and Kythnos
[PB89-229058] 03 p0374 N90-12135
Optical fibre witnesses of fatigue damage in composite materials 04 p0465 N90-12660
Damage tolerance of CFRP sandwich panels
[FFA-TN-1988-70] 04 p0465 N90-12664
Study of the engine bird ingestion experience of the Boeing 737 aircraft
[DOT/FAA/CT-89/16] 05 p0576 N90-13360
Debris/ice/TPS assessment and photographic analysis for Shuttle Mission STS-34
[NASA-TM-102153] 05 p0594 N90-13447
Impact tests of three composite materials with carbon fiber cores
[REPT-M8-582500] 05 p0619 N90-13610
Study of fatigue degradation mechanisms in unidirectional composite materials. Application to cumulative damage
[ECL-88-12] 05 p0619 N90-13611
Contribution to the fatigue behavior study of composite materials reinforced with unidirectional glass fibers
[ECL-88-20] 05 p0619 N90-13612

Mean stress and the exhaustion of fatigue-damage resistance
[NASA-TM-101311] 05 p0655 N90-13819
Risk-based fire safety experiment definition for manned spacecraft
[NASA-CR-183835] 06 p0731 N90-14262
Damage evaluation from surface displacement data 07 p0944 N90-15469
Analysis of damaged components from DOE security helicopter N7EG
[DE90-004488] 09 p1162 N90-16729
Noise and sonic boom impact technology. Sonic boom damage to conventional structures
[AD-A213594] 09 p1237 N90-17178
Noise and sonic boom impact technology. Effects of aircraft noise and sonic booms on structures: An assessment of the current state-of-knowledge
[AD-A213919] 09 p1278 N90-17409
Review of synergistic environmental interactions: Guidelines for new testing approaches on future solar arrays 10 p1345 N90-17803
Micrometeoroid impacts on silver bus bar targets at elevated voltages 10 p1346 N90-17805
Impact damage tolerance of composite cylindrical panels
[AD-A216401] 10 p1350 N90-17830
AGARD/SMP Review: Damage Tolerance for Engine Structures. 2: Defects and Quantitative Materials Behaviour — conference
[AGARD-R-769] 11 p1457 N90-18396
Damage assessment in composites by acousto-ultrasonic technique
[AD-A216590] 11 p1479 N90-18510
Damage in a perforated graphite-epoxy composite plate under monotonic and cyclic biaxial loading
[ESA-TT-1117] 11 p1480 N90-18521
The effects of radiation on the mechanical properties of polymers used as electrical cable insulation and jacketing materials
[AERE-R-13286] 13 p1779 N90-20209
Relevance of impacter shape to nonvisible damage and residual tensile strength of a thick graphite/epoxy laminate
[NASA-TM-102599] 14 p1943 N90-21122
Cross-sectional examination of the damage zone in impacted specimens of carbon/epoxy and carbon/PEEK composites
[NASA-TM-100391] 14 p1944 N90-21125
The controlled-damage concept in design of laminated composites 15 p2065 N90-21830
A study of creep damage using microradiography and continuum damage mechanics 15 p2117 N90-22109
Damage analysis following slight deformations of composite materials
[RDS-1-007-64] 16 p2212 N90-22618
Center for surface radiation damage studies
[AD-A218452] 16 p2222 N90-22678
Low velocity instrumented impact testing of four new damage tolerant carbon/epoxy composite systems
[NASA-TP-3029] 19 p2672 N90-25198
Characterization of impact damage in composites 21 p2957 N90-26811
Damage tolerance analysis for manned hypervelocity vehicles. Volume 2: Software user's manual
[AD-A222136] 21 p2959 N90-26826
Aircraft lightning protection handbook
[AD-A222716] 22 p3110 N90-27668
AGARD/SMP Review Damage Tolerance for Engine Structures. 3: Component Behaviour and Life Management
[AGARD-R-770] 22 p3117 N90-27704
AGARD damage tolerance concepts for engine structures Workshop 3, Component Behaviour and Life Management 22 p3117 N90-27705
Calculation of service life of turbomachine components 22 p3117 N90-27706
Component behaviour and life management: The need for common AGARD approaches and actions 22 p3118 N90-27710
Ultrasonic inspection of advanced CFRP structures by computer-controlled, pulse-echo technique 22 p3185 N90-28075
Study of failure processes in fiber reinforced composites using acoustic emission techniques 22 p3186 N90-28090
Inspection system for in-situ inspection of aircraft composite structures 22 p3188 N90-28091
Damage tolerance analysis for manned hypervelocity vehicles. Volume 1: Final technical report
[AD-A221970] 22 p3191 N90-28106
The fatigue damage behavior of a single crystal superalloy 23 p3296 N90-28644
Microdamage to ceramic surfaces under sliding conditions 23 p3308 N90-28708
Activities report for the IBDF-INPE project SEQE, year 1987
[INPE-4534-RPE/565] 23 p3415 N90-29298
A planar rocket motor model for visualization of violent reaction due to fragment impact
[AD-A224273] 24 p3441 N90-29431

DAMAGE THRESHOLD
U YIELD POINT

DAMPERS (VALVES)
Elasticity effects on cavitation in a squeeze film damper undergoing noncentered circular whirl
[NASA-TM-102392] 05 p0649 N90-13786

DAMPING
NT ELASTIC DAMPING
NT VIBRATION DAMPING
NT VISCOELASTIC DAMPING
NT VISCOUS DAMPING
Prediction of dynamic derivatives 01 p0012 N90-10055
On modelling nonlinear damping in distributed parameter systems 01 p0022 N90-10109
Aircraft modal supression system: Existing design approach and its shortcomings 01 p0023 N90-10115
Mechanics of damping for fiber composite laminates including hygro-thermal effects
[NASA-TM-102329] 01 p0034 N90-10185
Numerical simulation of unsteady combustion in a dump combustor 01 p0037 N90-10203
The effect of twins on critical currents of high Tc superconductors
[AD-A210988] 01 p0133 N90-10768
Use of Lanczos vectors in structural dynamics 02 p0179 N90-11011
Numerical analysis of nonlinear viscoelastic structures: Application to elastomers and rubber-like materials 02 p0180 N90-11013
The dynamic stability of an axially loaded beam with lateral elastic support and damping 02 p0232 N90-11331
Estimation on nonlinear damping in second order distributed parameter systems
[NASA-CR-181890] 02 p0263 N90-11494
An integrated methodology for optimizing structural composite damping
[NASA-TM-102343] 03 p0319 N90-11808
Non linear vibrations in a drive train when coupled to constant torque and constant power loads
[PNR90593] 04 p0508 N90-12934
Effect of modal truncation on derivatives of closed-loop damping ratios in structural control 07 p0882 N90-15109
Damping characteristics of metal matrix composites
[AD-A213712] 07 p0891 N90-15151
Underwater acoustic scattering from spherical particulates and bubbles
[AD-A214827] 09 p1279 N90-17414
Damping loss factor determination of glass and graphite fiber composites
[AD-A214535] 10 p1347 N90-17816
Quasilinear approach to the damping of LH waves in a reactor-grade plasma
[IPPCZ-292] 10 p1432 N90-18262
Robot crane technology program
[PB90-111667] 11 p1516 N90-18734
Control and stabilization of linear and nonlinear distributed systems
[AD-A216446] 11 p1547 N90-18908
Oscillation and damping behavior of fine steel test tubes, with particular consideration to destruction free proofs from hydrogen fragilization
[ETN-90-95371] 12 p1627 N90-19351
An experimental study of the aeroelastic behaviour of two parallel interfering circular cylinders 12 p1673 N90-19609
Dynamic damping control: Implementation issues and simulation results
[DE90-007687] 13 p1812 N90-20403
United States Air Force Academy get-away-special flexible beam experiment 14 p1937 N90-21088
Robust control of flexible structures 15 p2058 N90-21784
The Shock and Vibration Digest, volume 21, no. 1 15 p2109 N90-22061
Elastic stability and nonlinear behavior of imperfect shells with initial stresses 15 p2110 N90-22070
An investigation of the generation and radiation of aerodynamic noise in real piping systems 15 p2164 N90-22368
A comparison of CuAlNi and other high damping alloys for the purpose of naval ship silencing applications
[AD-A218801] 16 p2221 N90-22671
Sliding control of pointing and tracking with operator spline estimation 16 p2281 N90-22997
Theory of filtering and control with application to control of large space structures
[AD-A219936] 17 p2366 N90-23468
Statistical techniques for designing a decoupled controller to be robust to model and sensor noise
[AD-A220476] 17 p2412 N90-23745
Damping associated with incipient melting in aluminum-indium alloys
[AD-A220241] 18 p2525 N90-24412
Requirements for longitudinal HOM damping in superconducting recirculating linacs
[CEBAF-PR-89-018] 19 p2756 N90-25662
Damping capacity of aluminum 6061-indium alloys
[AD-A222802] 20 p2835 N90-26124
A critical evaluation of two-equation models for near wall turbulence
[NASA-CR-182068] 20 p2860 N90-26270
Increasing the margin of stability of arbitrarily finite modes of flexible large space structures with damping
[AD-A221742] 21 p2967 N90-26867
Approximate natural damped frequencies of a finite viscous floating-zone under zero-gravity condition
[LRT-WE-9-FB-8(1988)] 21 p2990 N90-26995
Oscillatory response of a liquid column to counter rotational excitation
[LRT-WE-9-FB-12(1989)] 21 p3006 N90-27088
Response of a liquid bridge with rotationally excited bottom
[LRT-WE-9-FB-13(1989)] 21 p3006 N90-27089
Effects and tolerances of injection jitter in the SLC and future linear colliders
[DE90-014805] 23 p3394 N90-29179

DAMPING FACTOR
U DAMPING

DAMPING IN PITCH
U DAMPING
U PITCH (INCLINATION)

DAMPING IN ROLL
U DAMPING
U ROLL

DAMPING IN YAW
U DAMPING
U YAW

DAMPNESS
U MOISTURE CONTENT

DAMS
Technical and administrative feasibility of microlight remote sensing applications for river boards
[BCRS-89-01] 12 p1679 N90-19643

DANGER
U HAZARDS

DARK ADAPTATION
Three stages and two systems of visual processing
[AD-A212670] 04 p0525 N90-13032
The assessment of visibility from automatic contrast Measurements 07 p0872 N90-15061
A scheiner-principle vernier optometer
[AD-D014304] 07 p0934 N90-15405
The kinetics of dark adaptation in hypoxic subjects
[AD-A218641] 16 p2260 N90-22885
The measurement of dark adaptation level in the presence of glare
[PB90-155987] 22 p3231 N90-28323

DARK MATTER
Rocket and satellite observations of the local interstellar medium 02 p0292 N90-11668
Gauge invariant cosmological perturbations with cold dark matter
[DE89-790940] 02 p0295 N90-11679
An experiment to search for galactic axions 05 p0710 N90-14158
Unitarity limits on the mass and radius of dark matter particles
[NASA-CR-186079] 05 p0713 N90-14164
Cosmology and the weak interaction
[NASA-CR-186170] 05 p0713 N90-14169
Supersymmetric dark matter above the W mass
[NASA-CR-186188] 06 p0863 N90-15016
Gamma ray lines from dark matter annihilation
[DE90-000779] 06 p0864 N90-15021
Dark matter and the solar neutrino problem: Can particle physics provide a single solution
[DE90-001827] 06 p0864 N90-15024
Annihilation physics of exotic galactic dark matter particles 11 p1559 N90-18984
Particle physics and cosmology
[DE90-006547] 11 p1590 N90-19171
The effects of cold dark matter on Big Bang nucleosynthesis 12 p1698 N90-19749
Studies of the evolution of the x ray emission of clusters of galaxies
[NASA-CR-186471] 13 p1903 N90-20918
The mass of the Coma cluster 15 p2188 N90-22496

Skewering the universe with QSO lines of sight: Lyman alpha clouds as probes of large scale structure
16 p2329 N90-23278
The dynamical evolution of dense clusters of compact stars
16 p2331 N90-23287
Reconstructing primordial density fluctuations
16 p2333 N90-23293
Periodic signatures for the detection of cosmic axions
[NASA-CR-186608] 17 p2470 N90-24122
Evolution of light domain walls interacting with dark matter, part 1
[NASA-CR-181123] 17 p2485 N90-24211
Probing the Big Bang with LEP
[NASA-CR-181060] 17 p2485 N90-24212
An X ray pulsar in the dark cloud Lynds 1457
19 p2767 N90-25723
Proceedings of workshop on Dark Matter and the Structure of the Universe
[DE90-791308] 21 p3098 N90-27602
Biased clustering in a universe with hot dark matter and cosmic string
[FERMILAB-PUB-90/23-A] 22 p3262 N90-28473

DARKENING

Auroral ultraviolet darkening on the outer planets
15 p2192 N90-22518

DARKNESS

A Scheiner-principle pocket optometer for self-evaluation and biofeedback accommodation training
[AD-A213171] 04 p0524 N90-13027

DART TURBOPROP ENGINES

U TURBOPROP ENGINES

DATA ACQUISITION

Development of an automated probe for thermal conductivity measurements
[PB89-209324] 01 p0073 N90-10419
Kiruna geophysical data: Data Summary 88/7-9, July - September 1988
[PB89-210249] 01 p0086 N90-10487
Extreme hurricanes in the nineteenth century
[PB89-201305] 01 p0087 N90-10498
Meteorological support: Descriptions of application programs for accessing and displaying data
[PB89-194625] 01 p0088 N90-10500
Research highlights of the NMC (National Meteorological Center) Development Division: 1987-1988
[PB89-206478] 01 p0088 N90-10501
Waveform generator signal processing software
[PB89-192660] 01 p0103 N90-10587
Independent Orbiter Assessment (IOA): Analysis of the DPS subsystem
[NASA-CR-185549] 02 p0163 N90-10924
Robust spatial calibration of a planar positron camera
[AD-A210773] 02 p0224 N90-11284
Reporting environmental data of known quality
[DE89-016214] 02 p0239 N90-11359
Meteorological rocket observations
[PB89-168769] 02 p0250 N90-11419
Contemporary China's meteorological enterprises (selected portions)
[AD-A210697] 03 p0373 N90-12131
Noise data of four small propeller-driven airplanes
[PB89-216980] 03 p0400 N90-12291
Characterizations of electrical properties of highT(sub c) superconducting materials
[NASA-TM-100380] 03 p0409 N90-12345
CALS (Computer-aided Acquisition and Logistic Support) Test Network information exchange: User's manual
[DE89-016700] 03 p0418 N90-12399
Preliminary experience with high response pressure measurements in a multistage, high speed compressor
[RAE-TM-P-1141] 04 p0457 N90-12619
A data acquisition and processing system for six component solid rocket motor testing
[AD-A212200] 04 p0464 N90-12657
The Telecommunications and Data Acquisition Report
[NASA-CR-185093] 04 p0485 N90-12786
Mode S data link trials, 10-11 January 1989
[RSRE-MEMO-4267] 04 p0490 N90-12815
Climatological data for the North Sea based on observations by voluntary observing ships over the period 1961-1980
[KNMI-WR-89-02] 04 p0520 N90-13002
A real-time wind model using digital data from aircraft
[RSRE-MEMO-4309] 04 p0521 N90-13005
Air Force flight feeding. Volume 1: Evaluation of current system and alternative concepts
[AD-A212789] 04 p0527 N90-13043
Berne solar observations
[REPT-55] 04 p0566 N90-13301
Measurement Techniques in Aerodynamics
[VKI-LS-1989-05] 05 p0573 N90-13339
Data acquisition in aerodynamic research
05 p0574 N90-13340
Pressure measurement techniques in use at the Royal Aerospace Establishment
05 p0574 N90-13347
Control of optical systems
05 p0600 N90-13484
Successive iterations of the input catalog
05 p0607 N90-13534
The SIMBAD data base
05 p0608 N90-13547
Overview of the data acquisition and reductions
05 p0609 N90-13549
Analysis of the image dissector tube data
05 p0609 N90-13550
Analysis of the star mapper data
05 p0609 N90-13551
High precision rocket attitude reconstruction using star sensor and magnetometer data
05 p0659 N90-13844
Normal points: Compression of satellite laser ranging data
[ETN-90-96008] 05 p0707 N90-14145
Methodology for the calibration of and data acquisition with a six-degree-of-freedom acceleration measurement device
[PB89-233597] 06 p0779 N90-14531
Derivation of synthetic mission profiles from electric vehicle field data
[DE89-011125] 06 p0793 N90-14620
Beyond the IDMY (International Daylighting Measurements Year): A network instrument for low-cost data acquisition
[DE90-002722] 06 p0815 N90-14740
Application of reusable software components at the SEI
06 p0826 N90-14804
Personal computer process data acquisition
[DE89-017877] 06 p0828 N90-14816
Publications of the Jet Propulsion Laboratory, 1988
[NASA-CR-185956] 06 p0859 N90-14995
Instrumentation for a facility for the test, analysis and active control of spacecraft truss structures
[AD-A213655] 07 p0886 N90-15124
MF/HF multistatic mid-ocean radar experiments in support of SWOTHR (Surface-Wave Over-The-Horizon Radar)
[AD-A213830] 07 p0919 N90-15314
NTES (Nuclear Test and Experimental Sciences) program laser facility for physics experiments Building 391 High Bay Option
[DE90-001795] 07 p0935 N90-15411
Upgrade plans to handle 30 to 40 Mbytes of data for D3-D
[DE90-003291] 07 p0995 N90-15750
Data file management in the D3-D data acquisition and analysis computer systems
[DE90-003289] 07 p1010 N90-15850
The digital data acquisition chain and the cosmic ray trigger system for the SLD warm iron calorimeter
[DE90-000943] 07 p1015 N90-15879
D3-D cryogenic control system upgrade
[DE90-003290] 08 p1054 N90-16092
Stand Alone Pressure Measurement Device (SAPMD) for the space shuttle Orbiter, part 1
[NASA-CR-172119-PT-1] 08 p1072 N90-16202
Stand Alone Pressure Measurement Device (SAPMD) for the space shuttle Orbiter, part 2
[NASA-CR-172119-PT-2] 08 p1072 N90-16203
Turbine blade data acquisition system user's guide
[AD-A214986] 09 p1169 N90-16763
Turbine blade data acquisition system software reference
[AD-A215134] 09 p1169 N90-16764
Turbine blade data acquisition system technical reference
[AD-A215135] 09 p1169 N90-16765
ONR tropical cyclone motion research initiative: Data assimilation considerations for field experiment analyses
[AD-A215726] 09 p1248 N90-17244
Measurement of the impulse response of the human visual system using correlation techniques
[AD-A215667] 09 p1254 N90-17274
Validity of empirical studies of information system effectiveness
[AD-A214474] 09 p1295 N90-17507
The application of a computer data acquisition system for a new high temperature tribometer
[NASA-TM-102508] 10 p1347 N90-17811
Proposition for an airborne remote sensing system
[INPE-4872-PRE/1483] 10 p1399 N90-18090
Data collection and location platforms experimental network: Description of an orbit routine
[INPE-4798-NTE/287] 11 p1465 N90-18439
Electronically Variable Pressure Regulator (EVPR)
11 p1474 N90-18484
Experimental investigations of the unsteady boundary layer on an oscillating flat plate. Optimization and validation of a code, for calculating the potential flow/boundary layer coupling of a flat plate and of an oscillating profile
[ETN-90-96254] 11 p1508 N90-18682
TVI: A mathematical model for global estimation of Brazilian cerrado phytomass
[INPE-4836-PRE/1465] 11 p1521 N90-18759
Paper on geography in environmental management: Research and new techniques
[INPE-4840-PRE/1469] 11 p1531 N90-18816
The Telecommunications and Data Acquisition Report
[NASA-CR-185033] 12 p1642 N90-19434
Data reduction of GOES (Geostationary Operational Environmental Satellite) information from DCP (Data Collection Platform) networks
[AD-A215844] 12 p1678 N90-19637
FOMA: A Fast Optical Multichannel Analyzer
[DE90-004093] 12 p1713 N90-19839
Physical models of cometary nuclei: A review
12 p1738 N90-19991
The USAF Advanced Dynamic Anthropomorphic Manikin (ADAM)
13 p1752 N90-20062
A data acquisition parallel bus for wind tunnels at ARL (Aeronautical Research Laboratory)
[AD-A218052] 13 p1759 N90-20098
Diagnostics and firing control for the cylindrical reconnection launcher
[DE90-007677] 13 p1761 N90-20107
PC-based PCM telemetry data reduction system software
[DE90-000317] 13 p1761 N90-20111
Experimental proposition aboard the second data collecting satellite-SCD 2 of the MECB
[INPE-4980-RPE/606] 13 p1765 N90-20128
Constitutive data acquisition and modelling in aluminium 2014 alloy
[AERE-R-13651] 13 p1775 N90-20186
The NASA, Marshall Space Flight Center drop tube user's manual
[NASA-TM-100392] 13 p1786 N90-20251
Spectral solar radiation data base documentation, volume 1
[DE89-009447] 13 p1841 N90-20571
Correlation of AVHRR imagery with sub-surface features in California current
[AD-A218184] 13 p1848 N90-20607
Diagnostic development and support of MHD (Magnetohydrodynamics) test facilities
[DE90-004969] 13 p1890 N90-20845
CALS (Computer-aided Acquisition and Logistic Support) Test Network information exchange user's manual, revision 1
[DE90-008119] 13 p1900 N90-20904
The MANTA: An RPV design to investigate forces and moments on a lifting surface
[NASA-CR-186227] 14 p1915 N90-20971
Performance evaluation of MSS/LANDSAT data in the estimation of fluvial channel width
[INPE-4906-PRE/1507] 14 p2000 N90-21463
CAMAC memory module: MEMO-32
[DE90-759846] 14 p2012 N90-21528
Enhanced Low Level Wind Shear (LLWAS) 6-sensor improvement user's manual for data processing of field data
[DOT/FAA/CT-TN90/8] 15 p2052 N90-21759
The Telecommunications and Data Acquisition Report
[NASA-CR-186479] 15 p2074 N90-21880
Improving a data-acquisition software system with abstract data type components
15 p2078 N90-21901
Small strain gage applications 2
[DE90-008312] 15 p2102 N90-22026
The AGRISCATT-87 campaign: Processing of the Dutscat data
[BCRS-89-20] 15 p2122 N90-22140
Site visit to US Antarctic Program (USAP) facilities and the Research Vessel Polar Duke
[DE90-009396] 15 p2126 N90-22159
Regional wind energy assessment
[DE90-009380] 15 p2133 N90-22192
Networks for image acquisition, processing and display
15 p2138 N90-22218
How to get it: A guide to defense-related information resources
[AD-A201600] 15 p2176 N90-22433
The ground-level cosmic-ray event of September 29, 1989 as recorded by the Rome detectors
[NOTA-INTERNA-944] 16 p2340 N90-23336
Cosmic ray NM-64 neutron monitor data-17
[NOTA-INTERNA-945] 16 p2341 N90-23337
Navigation software for the MPL vertical line array
[AD-A220166] 17 p2432 N90-23860
Data quality analysis at the National Transonic Facility
[NASA-CR-4303] 17 p2448 N90-23957
A low-cost PC-based telemetry data-reduction system
[DE90-000330] 18 p2509 N90-24339
Ceramic technology for advanced heat engines project data base
[DE90-011491] 18 p2532 N90-24448
Off-design loss measurements in a compressor cascade
[AD-A220094] 18 p2552 N90-24564

US Forest Service and National Park Service Wilderness Aircraft Overflight Study: Sociological background and study plans 18 p2609 N90-24863
Applications of an acoustic-emission data-acquisition workstation: 2
[DE90-010941] 18 p2612 N90-24880
Satellite data archiving: US and foreign activities and plans for environmental information
[GAO/RCED-88-201] 18 p2633 N90-25001
SERI solar radiation resource assessment project
[DE90-000307] 19 p2711 N90-25428
The development of the July 1989 1 deg x 1 deg and 30' x 30' terrestrial mean free-air anomaly data bases
[NASA-CR-186475] 19 p2713 N90-25441
Active perception and exploratory robotics
[MS-CIS-89-65] 19 p2726 N90-25501
Modeling strength data for CREW CHIEF 19 p2729 N90-25516
A human factors review of data entry devices
[DE90-012009] 19 p2763 N90-25703
The Telecommunications and Data Acquisition Report
[NASA-CR-186852] 20 p2852 N90-26217
The browse file of NASA/JPL quick-look radar images from the Loch Linnhe 1989 experiment
[NASA-CR-186855] 20 p2935 N90-26701
ARLSUPER version 1.0, program users guide
[AD-A222693] 21 p2953 N90-26793
Applications of ISES for the atmospheric sciences 21 p3017 N90-27155
Applications of ISES for coastal zone studies 21 p3018 N90-27157
Application of Meteorological Satellite (METSAT) data to support United States forces in the North Atlantic Treaty Organization (NATO) 21 p3068 N90-27440
On line diagnostics of rotating machinery using expert system technology 22 p3105 N90-27632
The Langley 14- by 22-foot subsonic tunnel: Description, flow characteristics, and guide for users
[NASA-TP-3006] 22 p3107 N90-27649
Measurement uncertainty in gas turbine performance determination 22 p3119 N90-27717
General test plan 22 p3120 N90-27721
Acoustic emission detection of crack presence and crack advance during flight 22 p3186 N90-28082
Size, duration, and rate of growth of nocturnal lightning events appearing on space shuttle video tapes
[NASA-CR-4313] 22 p3229 N90-28310
Improved meteorological measurements from buoys and ships (IMET): Preliminary conventions from buoys and standards data and file formats
[PB90-241910] 22 p3229 N90-28312
Selective multimode/multiconfigurable data acquisition and reduction processor system
[AD-D014551] 22 p3234 N90-28341
Building a user interface using SQL*Forms and an intermediate table
[DE90-012729] 22 p3259 N90-28455
Providing dynamic sorting and searching capabilities using SQL*Forms
[DE90-012735] 22 p3259 N90-28456
Analysis of heliport environmental data, Intracoastal City
[DOT/FAA/CT-TN89/43] 23 p3284 N90-28584
On-line object feature extraction for multispectral scene representation
[NASA-CR-187006] 23 p3342 N90-28888
A method of classification for multisource data in remote sensing based on interval-valued probabilities
[NASA-CR-187007] 23 p3343 N90-28889
How do robots take two parts apart 23 p3374 N90-29061
A personal computer-based, multitasking data acquisition system
[NASA-TM-4232] 23 p3382 N90-29107
The DELTA MONSTER: An RPV designed to investigate the aerodynamics of a delta wing platform
[NASA-CR-186226] 24 p3431 N90-29381
Human error classification and data collection
[DE90-631408] 24 p3522 N90-29915
Development of a software package for automatic data acquisition, analysis, and controls in an axial flow compressor test rig
[PD-PR-8910] 24 p3524 N90-29926
Diagnostic development and support of MHD test facilities
[DE90-015403] 24 p3550 N90-30083
Small multipurpose stored data acquisition system
[DE90-010823] 24 p3558 N90-30134

DATA ADAPTIVE EVALUATOR/MONITOR

U DATA PROCESSING
U DATA REDUCTION
U DATA TRANSMISSION

DATA ANALYSIS

U DATA PROCESSING
U DATA REDUCTION

DATA BASE MANAGEMENT SYSTEMS

Evaluation of computer-aided software engineering tools for data base development
[DE89-014007] 01 p0104 N90-10591
Effective resource utilization for multiprocessor join execution
[DE89-016303] 01 p0105 N90-10595
Performance reports for EIM (Engineering Information Management) computer systems: A managerial perspective
[DE89-015194] 02 p0256 N90-11449
Software configuration management: An overview
[PB89-193833] 02 p0258 N90-11458
The Knowledge Representation Project
[AD-A211288] 02 p0288 N90-11650
Experimental database retrieval system DARTS (Handling Manual)
[DE89-906473] 02 p0289 N90-11652
Program distribution for unclassified scientific and technical reports: Instructions and category scope notes, revision 75
[DE89-005395] 03 p0416 N90-12391
Role of conceptual models in the design and use of information systems
[PB89-217376] 03 p0416 N90-12392
Problem of incomplete information in relational databases
[PB89-217533] 03 p0417 N90-12393
Interoperability of heterogeneous information systems: The COST 11(ter) Project
[PB89-217541] 03 p0417 N90-12394
A real-time locking protocol
[AD-A211514] 03 p0418 N90-12403
Performance evaluations of a parallel and expandable database computer: The multi-backend database computer
[AD-A212761] 04 p0528 N90-13048
The integration of structured and formal methods
[RSRE-MEMO-4293] 04 p0531 N90-13068
The Inca data base 05 p0607 N90-13531
Retrieving and integrating IC fabrication data from dissimilar databases
[AD-A211890] 05 p0707 N90-14140
Integrated computer-based tools to facilitate environmental monitoring, assessment, and restoration
[DE90-002732] 06 p0811 N90-14717
An expert system for quality assurance (a.k.a.) QA Express
[DE90-003887] 07 p0944 N90-15467
Name assignment techniques for relational schemas representing extended entity-relationship schemas
[DE90-003269] 07 p0974 N90-15623
Programs for control of an analog-signal switching network
[DE90-003645] 07 p0974 N90-15626
Procurement of an optical disk information storage and retrieval system
[DE90-001372] 07 p1010 N90-15849
Young Investigator's Award and distributed self-adaptive databases
[AD-A214194] 07 p1010 N90-15854
RETE experiment activity at the TSS-1 POCC
[IFSI-89-12] 06 p1036 N90-15988
Connector selection program implementation notes, version 1.0
[DE90-004983] 08 p1085 N90-16279
Introduction to the framework and tasks of the DFD --- German Remote Sensing Data Center (DFD) 08 p1092 N90-16319
Computer aided design based optical system modeling
[DE90-003453] 08 p1112 N90-16440
Abbreviated query interpretation in extended entity-relationship oriented databases
[DE90-003114] 08 p1137 N90-16587
Event-join optimization in temporal relational databases
[DE90-003117] 08 p1137 N90-16588
Database design using NIAM (Nijssen Information Analysis Method) modeling
[DE89-014631] 08 p1138 N90-16592
A database of fragmentation cross section measurements applicable to cosmic ray propagation calculations
[NASA-CR-186328] 08 p1153 N90-16681
Making extensible database technology work 09 p1203 N90-16973
Computer-Aided Design for Built-In-Test (CADBIT). Volume 1: Technical issues
[AD-A215737] 09 p1268 N90-17353
Computer-Aided Design for Built-In-Test (CADBIT). Volume 2: BIT Library
[AD-A215738] 09 p1268 N90-17354
Computer-Aided Design for Built-In-Test (CADBIT). Volume 3: Software specification
[AD-A215739] 09 p1268 N90-17355
Interim Design Database (IDDB) CADAM drawing retrieval program user's manual for the IBM 3081
[DE90-004491] 09 p1269 N90-17356
The real-time roll-back and recovery of transactions in database systems
[AD-A214471] 09 p1295 N90-17506
The Cronus distributed DBMS (Database Management System) project
[AD-A214478] 09 p1295 N90-17508
Database creation and/or reorganization over multiple database backends
[AD-A214939] 09 p1296 N90-17513
Design and implementation of the nested relational data model under the Exodus extensible database system
[AD-A215356] 09 p1296 N90-17515
Fine tuning your search output: Word processors, desktop publishing, electronic mail, databases, and beyond
[DE90-005192] 09 p1297 N90-17517
The design and analysis of new techniques for transaction management in database systems 10 p1441 N90-18314
Source header list. Volume 1: A through K
[AD-A216000] 10 p1442 N90-18319
Source header list. Volume 2: L through Z
[AD-A216001] 10 p1442 N90-18320
Guidelines for the use of the SAME
[AD-A215846] 11 p1544 N90-18888
A human factors experimental comparison of two database query languages 11 p1574 N90-19064
DoD manual for standard data elements
[AD-A216441] 11 p1575 N90-19066
Data reduction of GOES (Geostationary Operational Environmental Satellite) information from DCP (Data Collection Platform) networks
[AD-A215844] 12 p1678 N90-19637
Using Rexx to coordinate relational commands
[DE90-007569] 12 p1702 N90-19772
Searching for existing nuclear data
[DE90-007535] 12 p1727 N90-19925
Spectral solar radiation data base documentation
[DE89-009448] 12 p1745 N90-20033
Hypotheses testing of watershed/landscape dynamics in northern Alaska using digital analysis
[DE90-006721] 13 p1820 N90-20450
The Terrain-Responsive Atmospheric Code (TRAC) project plan: Development of a hazardous materials dispersion modeling capability with application to ambient air monitoring network design
[DE90-007293] 13 p1829 N90-20502
Design considerations for a space database 13 p1858 N90-20659
Software quality assurance and software safety in the biomed control system
[DE90-008072] 13 p1866 N90-20706
Mathematics and physics studies: Multi-project support
[AD-A218208] 13 p1869 N90-20723
A model research archive: Archive and research implications for original records and support documents
[DE90-008248] 13 p1900 N90-20906
Designing an experimenters database using the Nijssen Information Analysis Methodology (NIAM)
[DE90-008548] 13 p1900 N90-20907
The Chemkin Thermodynamic Data Base
[DE90-007953] 14 p2035 N90-21676
The ultimate CASE tool
[DE90-009351] 14 p2037 N90-21687
Object-oriented databases: How are they different and what differnece does it make
[REPT-89-55] 15 p2180 N90-22459
Knowledge management: An abstraction of knowledge base and database management systems
[NASA-CR-4273] 16 p2278 N90-22986
A verification library for multibody simulation software 16 p2298 N90-23089
Object-oriented query languages: The notion and the issues
[REPT-89-054] 16 p2298 N90-23093
Assessment System for Aircraft Noise (ASAN) citation database. Volume 2: Database update manual
[AD-A219176] 16 p2314 N90-23189
Assessment System for Aircraft Noise (ASAN) citation database. Volume 3: New citation review procedures
[AD-A219177] 16 p2314 N90-23190
BTOS database evaluation
[AD-A219304] 16 p2328 N90-23271
A comparison of a relational and nested-relational IDEF0 data model
[AD-A220147] 17 p2448 N90-23956
The design of a local area network configuration management system for the Naval Postgraduate School Administrative Sciences Department
[AD-A219643] 17 p2451 N90-23979

Development of a consolidated environmental data base
[DE90-009419] 17 p2479 N90-24177
Interconnection of the graphics language for database system to the multi-lingual, multi-model, multi-backend database system over an Ethernet network
[AD-A220081] 18 p2591 N90-24739
Knowledge-based control of an adaptive interface
18 p2630 N90-24987
Using integrity constraints to control search in knowledge base systems
[AD-A221291] 18 p2634 N90-25009
Enhancing a relational database: Stepwise, bottom-up design
[DE90-010834] 18 p2635 N90-25012
TRENDS: The aeronautical post-test database management system
[NASA-TM-101025] 19 p2662 N90-25149
The EISI (Elemental and Interplanar Spacing Index) index: A search/match tool for electron diffraction phase analysis
[DE90-010832] 20 p2830 N90-26097
Compendium of material test results on HY-130 and Ti-3Al2V metals in support of United States navy programs
[DE90-011754] 20 p2833 N90-26112
Damage measurements on optical materials for use in high-peak-power lasers
[DE90-013489] 20 p2868 N90-26314
Laser damage database at 1064 nm
[DE90-013490] 20 p2868 N90-26315
Pacific missile test center information resources management organization (code 0300): The ORACLE client-server and distributed processing architecture
[DE90-013271] 20 p2912 N90-26565
International standards for text preparation and interchange
[DE90-011868] 20 p2935 N90-26699
A methodology for benchmarking distributed database management systems
[DE90-007801] 20 p2935 N90-26702
Construction of geological and geotechnical information database
[DE90-503417] 20 p2936 N90-26708
Prototyping an in-house business intelligence database
[PNR90665] 20 p2937 N90-26709
The composite load spectra project
21 p3047 N90-27323
Inductive knowledge acquisition experience with commercial tools for space shuttle main engine testing
21 p3048 N90-27326
Artificial intelligence techniques for modeling database user behavior 21 p3049 N90-27330
Representing processes in the extended entity-relationship model
[DE90-013350] 21 p3086 N90-27551
Status report on image information systems and image data base technology
[AD-A221488] 21 p3087 N90-27556
Swissair studies on the compressibility of aircraft data
22 p3105 N90-27637
Selective multimode/multiconfigurable data acquisition and reduction processor system
[AD-D014551] 22 p3234 N90-28341
Building a user interface using SQL*Forms and an intermediate table
[DE90-012729] 22 p3259 N90-28455
Providing dynamic sorting and searching capabilities using SQL*Forms
[DE90-012735] 22 p3259 N90-28456
Relational databases with NIAM models bid so long to top-down designs
[DE90-013496] 22 p3259 N90-28457
Object database management systems: Concepts and features
[PB90-216813] 23 p3405 N90-29243
System software for Soviet computers
24 p3523 N90-29921
Issues in expanding the software base management system supporting the Computer Aided Prototyping System (CAPS)
[AD-A224344] 24 p3525 N90-29933
Graphic interface for attribute-based data language queries from a personal computer to the multi-lingual, multi-model, multi-backend database system over an Ethernet network
[AD-A223738] 24 p3528 N90-29948
Computing environments, interactive graphics and nonparametric methods for data analysis
[DE90-016128] 24 p3530 N90-29964
ESTEC software catalogue
[ESA-SP-1133] 24 p3531 N90-29968
Formal semantics of SQL queries
[REPT-89-069] 24 p3531 N90-29973
A high-speed KDL-RAM file system for parallel computers
[AD-A223299] 24 p3533 N90-29979
Accessing network databases via SQL transactions in a multi-model database system
[AD-A223946] 24 p3557 N90-30128
A survey of object-oriented database technology
[AD-A224490] 24 p3558 N90-30130
Integration of information systems components
[DE90-011761] 24 p3559 N90-30136
FEDIX: An on-line information service for universities and other research organizations: User's guide
[DE90-014835] 24 p3559 N90-30137

DATA BASES

Evaluation of computer-aided software engineering tools for data base development
[DE89-014007] 01 p0104 N90-10591
An introduction to input/output automata
[AD-A210831] 01 p0106 N90-10604
Communications Data Base (CDB), phase 3 (with software documentation)
[AD-A210540] 01 p0137 N90-10789
Precision materials characterization in the near millimeter and submillimeter wavelength range
[AD-A210655] 02 p0194 N90-11106
Robust spatial calibration of a planar positron camera
[AD-A210773] 02 p0224 N90-11284
Multistation/multiparameter observations with a network of digital ionosondes 02 p0247 N90-11396
Two-Dimensional Intercomparison of Stratospheric Models
[NASA-CP-3042] 02 p0248 N90-11405
Introduction and data summary, chapter 5
02 p0249 N90-11409
Two enhancements of the logarithmic least-squares method for analyzing subjective comparisons
[AD-A211192] 02 p0266 N90-11514
Experimental database retrieval system DARTS (Handling Manual)
[DE89-906473] 02 p0289 N90-11652
Review and analysis of the DNW/Model 360 rotor acoustic data base
[NASA-TM-102253] 03 p0299 N90-11692
Remote sensing data acquisition, analysis and archival
[PB89-142566] 03 p0365 N90-12085
Global data bases on distribution, characteristics and methane emission of natural wetlands: Documentation of archived data tape
[NASA-TM-4153] 03 p0365 N90-12090
Airborne profiles taken near San Nicolas Island, California, during Operation FIRE (First ISCCP (International Satellite Cloud Climatology Project) regional experiment) (1987): Aerosol size distributions, air and surface temperatures, cloud top temperatures, and relative humidities
[AD-A211664] 03 p0374 N90-12136
Statistical models for the optimal estimation of oceanic fields
[AD-A211786] 03 p0377 N90-12149
Interoperability of heterogeneous information systems: The COST 11(ter) Project
[PB89-217541] 03 p0417 N90-12394
Detailed description of the knowledge-based system for physical database design, volume 2
[PB89-229033] 03 p0417 N90-12395
Development and use of a tribology research-in-progress database
[PB89-228274] 03 p0417 N90-12396
FEDIX: An on-line information service for universities and other research organizations: User's guide, version 2.0, release 1
[DE89-016695] 03 p0417 N90-12398
ANDECS-PERLUDE 2.0: A databased, interactive system of control software user's guide
[DFVLR-MITT-89-07] 03 p0418 N90-12404
The role of component testing
[PNR90589] 04 p0455 N90-12608
Central Sudan surface wind data and climate characteristic
[KNMI-WR-88-01] 04 p0520 N90-13000
Mesoscale acid deposition modeling studies
[NASA-CR-4262] 04 p0554 N90-13228
The Hipparcos Mission. Prelaunch status. Volume 2: The input catalog
[ESA-SP-1111-VOL-2] 05 p0606 N90-13529
From scientific proposals to the Inca data base
05 p0606 N90-13530
The Inca data base 05 p0607 N90-13531
Stellar content of the input catalog
05 p0607 N90-13535
Variable stars 05 p0608 N90-13541
The catalogs produced by the Inca consortium
05 p0608 N90-13546
The SIMBAD data base 05 p0608 N90-13547
The Hipparcos Mission. Prelaunch status. Volume 3: The data reductions
[ESA-SP-1111-VOL-3] 05 p0609 N90-13548
Overview of the Tycho data analysis
05 p0610 N90-13558
Tycho astrometry 05 p0610 N90-13559
Photometry: Main mission and Tycho
05 p0610 N90-13560
Validation of the Hipparcos catalog
05 p0611 N90-13564
Implementation and simulations of the sphere solution in FAST 05 p0612 N90-13570
The Tycho input catalog 05 p0612 N90-13575
The initial imperfection data bank at the Delft University of Technology, part 2
[LR-559-PT-2] 05 p0656 N90-13825
Database interfaces on NASA's heterogeneous distributed database system
[NASA-CR-185420] 05 p0706 N90-14133
Retrieving and integrating IC fabrication data from dissimilar databases
[AD-A211890] 05 p0707 N90-14140
The DOD Gateway Information System: Operational prototype and transition period 1987-1988
[AD-A213044] 05 p0707 N90-14141
Architecture and language for a layered relational database 05 p0707 N90-14146
Stall/spin aerodynamic data project
[DOT/FAA/CT-88/29] 06 p0723 N90-14222
SRB thermal environments
[NASA-CR-183801] 06 p0734 N90-14276
The importance of environmental data
06 p0757 N90-14406
The FTZ HF propagation model for use on small computers and its accuracy 06 p0765 N90-14447
Advanced Software Development Workstation Project
06 p0827 N90-14807
The development of an Ada programming support environment database: SEAD (Software Engineering and Ada Database), user's manual
[NASA-CR-181219] 06 p0828 N90-14811
The design and implementation of an intelligent interface for information retrieval 06 p0858 N90-14991
Current launch vehicle reliability practice and data base assessment. Volume 1: Executive summary and report body
[AD-A213600] 07 p0885 N90-15121
Identification and quantification of synoptic structure in simulated TIROS N radiance soundings
[AD-A213729] 07 p0960 N90-15553
DOCTORD Database System user's guide, June 1989: dBase 3 PLUS Physician/(Part B Medicare): Personal computer reference system and user's guide
[PB90-100181] 07 p0966 N90-15579
Ultra high performance, highly reliable, numeric intensive processors and systems
[AD-A214100] 07 p0980 N90-15659
Periodic phase adjustment distributed clock synchronization in the hard realtime environment
[AD-A213842] 07 p0988 N90-15708
A signal realization data base generated by the multiple phase-screen method
[AD-A214004] 07 p1010 N90-15852
Young Investigator's Award and distributed self-adaptive databases
[AD-A214194] 07 p1010 N90-15854
Connector selection program implementation notes, version 1.0
[DE90-004983] 08 p1085 N90-16279
A persistent heap for ALGOL 68
[RSRE-MEMO-4268] 08 p1110 N90-16427
New optimization techniques in database access and maintenance 08 p1137 N90-16586
Event-join optimization in temporal relational databases
[DE90-003117] 08 p1137 N90-16588
Experiences with knowledge-base and large database integration
[DE90-000686] 08 p1137 N90-16591
Database design using NIAM (Nijssen Information Analysis Method) modeling
[DE89-014631] 08 p1138 N90-16592
A database of fragmentation cross section measurements applicable to cosmic ray propagation calculations
[NASA-CR-186328] 08 p1153 N90-16681
The DAB model of drawing processes
08 p1155 N90-16691
Investigation of IGES for CAD/CAE data transfer
08 p1157 N90-16702
The collection of non-conus aircraft icing data along with an identification of the geographical areas of potential severe icing and a study of a method of remote determining atmospheric icing data
[AD-A215055] 09 p1162 N90-16724

A methodology for the concept definition of advanced space transportation systems 09 p1176 N90-16813
Verification of aerothermodynamic codes by means of a winged experimental re-entry vehicle 09 p1180 N90-16842
Descriptive simulation: Combining symbolic and numerical methods in the analysis of chemical reaction mechanisms [AD-A214678] 09 p1190 N90-16898
Making extensible database technology work 09 p1203 N90-16973
Case studies in data analysis [AD-A215342] 09 p1248 N90-17241
Executive summary for designing online help systems: Report of year 1 activity [AD-A214811] 09 p1262 N90-17320
MPlus Database system [DE90-004146] 09 p1263 N90-17325
Noise and sonic boom impact technology. Effects of aircraft noise and sonic booms on structures: An assessment of the current state-of-knowledge [AD-A213919] 09 p1278 N90-17409
The real-time roll-back and recovery of transactions in database systems [AD-A214471] 09 p1295 N90-17506
GRASS/GIS (Geographic Resources Analysis Support System/Geographic Information System) implementation guide [AD-A214623] 09 p1296 N90-17510
Database creation and/or reorganization over multiple database backends [AD-A214939] 09 p1296 N90-17513
Fine tuning your search output: Word processors, desktop publishing, electronic mail, databases, and beyond [DE90-005192] 09 p1297 N90-17517
Proceedings of Colloquium 110 of the International Astronomical Union on Library and Information Services in Astronomy [AD-A215612] 09 p1298 N90-17523
Historical review of missile aerodynamic developments 10 p1304 N90-17542
Development of an automatic ground collision avoidance system using a digital terrain database [AD-A216247] 10 p1318 N90-17621
Materials properties numerical database system established and operational at CINDAS/Purdue University 10 p1366 N90-17919
Materials thermal and thermoradiative properties/characterization technology 10 p1367 N90-17925
Connected digit recognition in a multilingual environment [AD-A196150] 10 p1371 N90-17942
NASA Propagation Information Center 10 p1371 N90-17946
The Australian experiment with ETS-V 10 p1372 N90-17949
Rain attenuation measurements: Variability and data quality assessment 10 p1373 N90-17955
ELF (Extremely Low Frequency) communications system ecological monitoring program: Summary of 1988 progress [AD-A216153] 10 p1377 N90-17981
Processing of DMSP magnetic data: Handbook of programs, tapes, and datasets [NASA-TM-100757] 10 p1407 N90-18114
Structured analysis tool interface to the strategic defense initiative architecture dataflow modeling technique [AD-A216281] 10 p1424 N90-18218
Future technology requirements (related to defects and quantitative material behavior to aid in implementation of damage tolerance for design of engine structures) 11 p1459 N90-18403
A battery data base for electric vehicle applications [DE90-007085] 11 p1503 N90-18655
SPOT for landscape: Development of a method for the use of SPOT pictures for the updating of the data base scale of the landscape [BCRS-89-18] 11 p1526 N90-18787
Comparison of two Navy environmental database models: Generalized Digital Environmental Model and Podeszwa sound speed profile model [AD-A215848] 11 p1544 N90-18889
Teaching a new methodology for designing relational data bases: An experiment testing the effectiveness of an intelligent tutoring system on cognitive skill acquisition (volumes 1 and 2) 11 p1574 N90-19063
Defense Technical Information Center Executive Information System: Documentation and user's manual [AD-A216235] 11 p1575 N90-19065
DTE and space technology transfer 11 p1576 N90-19071
Austempered ductile iron data base: A cooperative program between industry and the Trade Adjustment Assistance Program of the Department of Commerce [PB90-115569] 12 p1626 N90-19343
High throughput data communication system [AD-D014342] 12 p1642 N90-19432
Development of an Ada programming support environment database SEAD (Software Engineering and Ada Database) administration manual [NASA-CR-186064] 12 p1699 N90-19757
An equational language for specifying, querying, and updating database domains [PB90-124694] 12 p1726 N90-19918
Executive information systems for providing next generation strategic information: An evaluation of EIS (Executive Information System) software and recommended applicability within the FAA computing environment [AD-A216672] 12 p1726 N90-19920
CRISP (Computer Retrieval of Information on Scientific Projects) thesauras, fiscal year 1990 [PB90-138652] 12 p1726 N90-19922
Spectral solar radiation data base documentation [DE89-009448] 12 p1745 N90-20033
Satellite radar altimetry over ice. Volume 1: Processing and corrections of Seasat data over Greenland [NASA-RP-1233-VOL-1] 13 p1840 N90-20562
Satellite radar altimetry over ice. Volume 2: Users' guide for Greenland elevation data from Seasat [NASA-RP-1233-VOL-2] 13 p1840 N90-20563
Satellite radar altimetry over ice. Volume 4: Users' guide for Antarctica elevation data from Seasat [NASA-RP-1233-VOL-4] 13 p1840 N90-20564
Spectral solar radiation data base documentation, volume 1 [DE89-009447] 13 p1841 N90-20571
Acute oral toxicity of DIGL-RP solid propellant in Sprague-Dawley rats [AD-A217712] 13 p1849 N90-20614
Design considerations for a space database 13 p1858 N90-20659
Implementation of a hypertext help system for GLAD (Graphics LAnguage for Database) [AD-A217936] 13 p1868 N90-20718
Maintaining bridge-connected and biconnected components on-line [AD-A215107] 13 p1875 N90-20754
Implementation of a hypercube database system [DE90-008440] 13 p1900 N90-20905
Designing an experimenters database using the Nijssen Information Analysis Methodology (NIAM) [DE90-008548] 13 p1900 N90-20907
Real-time concurrency control and transaction scheduling [AD-A218162] 13 p1901 N90-20909
The influence of ice accretion physics on the forecasting of aircraft icing conditions 14 p1906 N90-20928
Software Engineering Laboratory (SEL) database organization and user's guide [NASA-TM-103304] 14 p2015 N90-21545
The Chemkin Thermodynamic Data Base [DE90-007953] 14 p2035 N90-21676
A formal approach to user models in data retrieval [PB90-124728] 14 p2036 N90-21682
The initial imperfection databank at the Delft University of Technology, part 3 [LR-568] 15 p2057 N90-21783
Calculation of IR propagation statistics in the eastern Atlantic for surveillance system performance assessment 15 p2085 N90-21938
The computational structural mechanics testbed data library description [NASA-TM-100645-REV-1] 15 p2121 N90-22135
Computer vision techniques for rotorcraft low altitude flight 15 p2142 N90-22237
Evaluation of optical storage technology for decision support databases 15 p2176 N90-22436
The Weapons Laboratory technical library: Automating with STILAS 15 p2178 N90-22447
Electronic mail systems 15 p2179 N90-22451
Applications to the aerospace and defense R and D community: The DOD computer-aided acquisition and logistics support (CALS) initiative 15 p2179 N90-22453
Electronic transfer of information applications in the Societe Aerospatiale 15 p2179 N90-22454
NSSDC data listing [NASA-TM-102989] 15 p2180 N90-22456
Object-oriented databases: How are they different and what difference does it make [REPT-89-55] 15 p2180 N90-22459
SGTE data for pure elements [NPL-DMA(A)-195] 15 p2181 N90-22460
Update on the OPAL opacity code [DE90-009946] 15 p2184 N90-22480
The modeling of IRAS detections of classical novae and related objects 15 p2185 N90-22482
Executive summary for the network assessment model [AD-A218762] 16 p2229 N90-22718
Assessment System for Aircraft Noise (ASAN) citation database. Volume 1: User's manual [AD-A219175] 16 p2314 N90-23188
Assessment System for Aircraft Noise (ASAN) citation database. Volume 3: New citation review procedures [AD-A219177] 16 p2314 N90-23190
Looking at large data sets using binned data plots [DE90-008206] 16 p2326 N90-23263
Data exchange strategy. Part 1: Review of digital data exchange technology [AD-A218506] 16 p2327 N90-23267
BTOS database evaluation [AD-A219304] 16 p2328 N90-23271
Ionospheric equivalent slab thickness and its modeling applications [AD-A220105] 17 p2424 N90-23811
A comparison of lightning network data with surface weather observations [AD-A220003] 17 p2427 N90-23832
Extreme quantile estimation in binary response models [AD-A220150] 17 p2466 N90-24093
Development of a consolidated environmental data base [DE90-009419] 17 p2479 N90-24177
Ceramic technology for advanced heat engines project data base [DE90-011491] 18 p2532 N90-24448
The INEL battery data base [DE90-010914] 18 p2550 N90-24555
Flow unsteadiness effects on boundary layers [NASA-CR-186067] 18 p2550 N90-24557
A correlation study of wind speed as measured by the special sensor microwave/imager and the GEOSAT altimeter [AD-A219841] 18 p2581 N90-24701
Implementation of an I-structure memory controller [AD-A221397] 18 p2588 N90-24726
Interconnection of the graphics language for database system to the multi-lingual, multi-model, multi-backend database system over an Ethernet network [AD-A220081] 18 p2591 N90-24739
Knowledge-based control of an adaptive interface 18 p2630 N90-24987
Line simplification and digital cartographic databases [DE90-010194] 18 p2634 N90-25003
Acquiring generalizations to organize human databases [AD-A219835] 18 p2634 N90-25004
A user-friendly, menu-driven, language-free laser characteristics curves graphing program for desk-top IBM PC compatible computers 18 p2644 N90-25056
A Cax success story [MBB-FW-52/S/PUB-382] 19 p2649 N90-25076
TRENDS: The aeronautical post-test database management system [NASA-TM-101025] 19 p2662 N90-25149
Operational satellite environmental monitoring for food security by FAO: The ARTEMIS system 19 p2708 N90-25413
The development of the July 1989 1 deg x 1 deg and 30' x 30' terrestrial mean free-air anomaly data bases [NASA-CR-186475] 19 p2713 N90-25441
Tools for distributed application management [NASA-CR-186711] 19 p2742 N90-25586
CEBAF control system [CEBAF-PR-89-013] 19 p2757 N90-25666
Tools for distributed application management [NASA-CR-186646] 19 p2762 N90-25692
Program plan: International aircraft operator data base [IAR-90-1] 19 p2763 N90-25697
A framework for query optimization in temporal databases [DE90-011339] 19 p2763 N90-25700
Proceedings of the LDEF Materials Data Analysis Workshop [NASA-CP-10046] 20 p2826 N90-26075
Compendium of material test results on HY-130 and Ti-3Al2V metals in support of United States navy programs [DE90-011754] 20 p2833 N90-26112
Reusable rocket engine turbopump health monitoring system, part 3 [NASA-CR-182294] 20 p2869 N90-26320
Application of symbolic computations to the constitutive modeling of structural materials [NASA-TM-103225] 20 p2876 N90-26364
An automated calibration laboratory for flight research instrumentation: Requirements and a proposed design approach [NASA-TM-101719] 20 p2912 N90-26564

Creating a VAPEPS database: A VAPEPS tutorial
[NASA-CR-186629] 20 p2936 N90-26705
Energy data base: Subject categories and scope
[DE90-009212] 20 p2936 N90-26706
Construction of geological and geotechnical information database
[DE90-503417] 20 p2936 N90-26708
Chemical kinetics and modeling of planetary atmospheres 20 p2946 N90-26763
BASEOPS default profiles for civil aircraft
[AD-A223161] 21 p2959 N90-26825
Solubility characteristics of a methacrylate copolymer
[AD-A222938] 21 p2985 N90-26962
Development of a mathematical model for the thermal decomposition of aviation fuels
[AD-A221673] 21 p2990 N90-26994
Evaluation of magnetospheric internal magnetic field models and existing software
[AD-A221816] 21 p3027 N90-27210
The composite load spectra project 21 p3047 N90-27323
Using decision-tree classifier systems to extract knowledge from databases 21 p3048 N90-27328
DEB: A Diagnostic Experience Browser using similarity networks 21 p3048 N90-27329
Artificial intelligence techniques for modeling database user behavior 21 p3049 N90-27330
Maintenance of a minimum spanning forest in a dynamic planar graph
[AD-A221425] 21 p3054 N90-27362
Data and analysis center for software
[AD-A221434] 21 p3054 N90-27363
Status report on image information systems and image data base technology
[AD-A221488] 21 p3087 N90-27556
Infrared observations of the solar system in support of Large Aperture Infrared Telescope (LARITS): Calibration
[AD-A222222] 21 p3097 N90-27597
Bibliography of oceanography, meteorology, and geology of Louisiana, Texas, Mississippi, Alabama, and Florida
[PB90-194663] 22 p3194 N90-28124
Analysis of acid precipitation samples collected by state agencies: January to December 1988
[PB90-191784] 22 p3198 N90-28151
Updates and consistency in the LOGRES language
[REPT-90-017] 22 p3239 N90-28369
Integrating mono-valued functions in deductive databases: A recursive extension of MILANT
[REPT-90-018] 22 p3239 N90-28370
Government Information Quarterly. Volume 7, no. 2: National Aeronautics and Space Administration Scientific and Technical Information Programs. Special issue
[ISSN-0740-624X] 22 p3257 N90-28440
The new space and Earth science information systems at NASA's archive 22 p3257 N90-28443
Scientific and technical information management 22 p3257 N90-28444
NASA scientific and technical information for the 1990s 22 p3257 N90-28445
Appendix A: NASA information services 22 p3258 N90-28451
A computerized data-base system for land-use and land-cover data collected at ground-water sampling sites in the pilot national water-quality assessment program
[PB90-181868] 22 p3258 N90-28453
Providing dynamic sorting and searching capabilities using SQL*Forms
[DE90-012735] 22 p3259 N90-28456
Relational databases with NIAM models bid so long to top-down designs
[DE90-013496] 22 p3259 N90-28457
Distributed transitive closure computations: The disconnection set approach
[REPT-90-014] 22 p3259 N90-28459
Evaluating recursive queries in distributed databases
[REPT-90-015] 22 p3260 N90-28460
Evaluation of existing aircraft operator data bases
[DOT/FAA/CT-90/18] 22 p3260 N90-28463
A flight dynamic model of aircraft spinning
[AR-005-600] 23 p3283 N90-28576
Data base for crack growth properties of materials 23 p3296 N90-28647
High energy-density liquid rocket fuel performance
[NASA-CR-185279] 23 p3315 N90-28742
Measuring the vertical directional spectra caused by sea surface sound
[AD-A223883] 23 p3354 N90-28957
A design tool utilizing stoichiometric structure for the analysis of biochemical reaction networks
[AD-A223873] 23 p3355 N90-28961
Object database management systems: Concepts and features
[PB90-216813] 23 p3405 N90-29243
International aircraft operator data base master requirements and implementation plan
[DOT/FAA/CT-90/17] 23 p3405 N90-29247
Data Base Analyzer and Parameter Estimator (DBAPE) interactive computer program user's manual
[PB90-193053] 23 p3406 N90-29252
The 2-D and 3-D characterizations of GPS navigation service 24 p3425 N90-29348
The potential for digital databases in flight planning and flight aiding for combat aircraft 24 p3429 N90-29371
Data catalog series for space science and applications flight missions. Volume 5A: Descriptions of astronomy, astrophysics, and solar physics spacecraft and investigations. Volume 5B: Descriptions of data sets from astronomy, astrophysics, and solar physics spacecraft and investigations
[NASA-TM-101908] 24 p3437 N90-29413
Data catalog series for space science and applications flight flight missions. Volume 2B: Descriptions of data sets from geostationary and high-altitude scientific spacecraft and investigations
[NASA-TM-101909] 24 p3437 N90-29414
Data catalog series for space science and applications flight missions. Volume 1A: Descriptions of planetary and heliocentric spacecraft and investigations, second edition
[NASA-TM-101910] 24 p3438 N90-29415
Data catalog series for space science and applications flight missions. Volume 6: Master index volume
[NASA-TM-101913] 24 p3438 N90-29416
Results from Alouette 1, Explorer 20, Alouette 2, and Explorer 31
[NASA-TM-101822] 24 p3483 N90-29690
The worldwide ionospheric data base
[NASA-TM-101823] 24 p3488 N90-29714
Graphic interface for attribute-based data language queries from a personal computer to the multi-lingual, multi-model, multi-backend database system over an Ethernet network
[AD-A223738] 24 p3528 N90-29948
An interactive optimization based, computer graphics software package. Phase 2: Users manual
[AD-A223854] 24 p3529 N90-29954
Computing environments, interactive graphics and nonparametric methods for data analysis
[DE90-016128] 24 p3530 N90-29964
Data catalog series for space science and applications flight missions. Volume 4B: Descriptions of data sets from meteorological and terrestrial applications spacecraft and investigations
[NASA-TM-101880] 24 p3556 N90-30123
Textual regularities applicable to full text searching: The case of family history literature 24 p3557 N90-30125
Accessing network databases via SQL transactions in a multi-model database system
[AD-A223946] 24 p3557 N90-30128
Integration of information systems components
[DE90-011761] 24 p3559 N90-30136
FEDIX: An on-line information service for universities and other research organizations: User's guide
[DE90-014835] 24 p3559 N90-30137
Data catalog series for space science and applications flight missions. Volume 3B: Descriptions of data sets from low- and medium-altitude scientific spacecraft and investigations
[NASA-TM-89680] 24 p3560 N90-30140
Data catalog series for space science and applications flight missions. Volume 1B: Descriptions of data sets from planetary and heliocentric spacecraft and investigations
[NASA-TM-89695] 24 p3561 N90-30148
Interplanetary medium data book, supplement 4, 1985-1988
[NASA-TM-101867] 24 p3561 N90-30149
A guide to the National Space Science Data Center
[NASA-TM-89637] 24 p3565 N90-30167

DATA BUSSES
U CHANNELS (DATA TRANSMISSION)

DATA COLLECTION PLATFORMS
Data reduction of GOES (Geostationary Operational Environmental Satellite) information from DCP (Data Collection Platform) networks
[AD-A215844] 12 p1678 N90-19637
The MANTA: An RPV design to investigate forces and moments on a lifting surface
[NASA-CR-186227] 14 p1915 N90-20971
Monitoring vegetation of Brazil: Potentialities of multi-sensors approach
[INPE-4993-PRE/1555] 14 p1998 N90-21451
Accuracy and precision of GOES data collection platforms for temperature measurements
[AD-A218798] 16 p2250 N90-22832

DATA COMPACTION
U DATA COMPRESSION

DATA COMPRESSION
Robot vehicle video image compression, phase 1
[AD-A210974] 01 p0110 N90-10626
Radon transform analysis of a probabilistic method for image generation
[AD-A207814] 01 p0123 N90-10702
Gridded environmental data compaction: An investigation
[AD-A210580] 02 p0252 N90-11430
Overview of the data acquisition and reductions 05 p0609 N90-13549
Compression of bitmapped graphic data
[AD-A213141] 05 p0683 N90-13974
Normal points: Compression of satellite laser ranging data
[ETN-90-96008] 05 p0707 N90-14145
Data compression techniques applied to high resolution high frame rate video technology
[NASA-CR-4263] 06 p0765 N90-14452
An image compression algorithm for a high-resolution digital still camera
[NASA-CR-185079] 06 p0780 N90-14532
Context dependent prediction and category encoding for DPCM image compression 08 p1073 N90-16210
Data compression for the microgravity experiments 08 p1074 N90-16212
From primal sketches to the recovery of intensity and reflectance representations 08 p1074 N90-16216
Neural networks for data compression and invariant image recognition 08 p1075 N90-16219
A programmable image compression system 08 p1076 N90-16222
Hybrid LZW compression 08 p1076 N90-16223
Digital image coding and compression
[PB90-110958] 08 p1107 N90-16409
Image segmentation by iterative parallel region growing with application to data compression and image analysis 08 p1114 N90-16452
Fractal-based image compression
[AD-A215400] 09 p1268 N90-17351
Event-train restoration via backpropagation neural networks
[AD-A216308] 10 p1420 N90-18189
Attitude estimation procedure for spin stabilized satellites
[INPE-4866-TDL/377] 11 p1467 N90-18449
Evaluation and analysis of the orbital maneuvering vehicle video system 12 p1638 N90-19411
Fractal-based image compression
[AD-A217302] 13 p1865 N90-20699
Weather data dissemination to aircraft 14 p1907 N90-20934
Concept and results of the DLR realtime SAR processor 14 p1963 N90-21244
The performance of wavelets for data compression in selected military applications
[AD-A219230] 18 p2614 N90-24892
The performance of wavelets for data compression in selected military applications. Volume 2: Supplementary tables and graphs
[AD-A219231] 18 p2615 N90-24893
Automated analysis of MXU-553 flight data 21 p2958 N90-26821
Swissair studies on the compressibility of aircraft data 22 p3105 N90-27637
Digital color representation
[DE90-014580] 24 p3524 N90-29924
Handbook of data compression algorithms
[ESA-TM-06] 24 p3531 N90-29969
Image compression
[AD-A224242] 24 p3537 N90-29998
Book of abstracts of the 1st Benelux-Japan Workshop on Information and Communication Theory
[PB90-191446] 24 p3556 N90-30124

DATA CONVERSION ROUTINES
NT SUBROUTINES
Automated information systems plan
[AD-A214982] 09 p1296 N90-17514
Preparing software conversion studies 10 p1416 N90-18158
Data conversions in abstract data types
[RUU-CS-88-30] 18 p2634 N90-25006
Logic level data conversion system
[AD-D014545] 22 p3167 N90-27963
Solid state circuitry with optical data interfacing
[AD-D014548] 22 p3248 N90-28422

DATA CONVERTERS
NT ANALOG TO DIGITAL CONVERTERS
NT DIGITAL TO ANALOG CONVERTERS
Data conversions in abstract data types
[RUU-CS-88-30] 18 p2634 N90-25006

DATA CORRELATION
Applications of acousto-optical correlation devices in radar signal processing
[AD-A216624] 11 p1497 N90-18616

Characterization of fluid flow by digital correlation of scattered light
[NASA-CR-186403] 13 p1799 N90-20324
Time series, statistics, and information
[AD-A224317] 24 p3540 N90-30018

DATA FLOW ANALYSIS
Structure flow diagram generator
[PB89-195978] 01 p0104 N90-10592
Stochastic flows in networks
[AD-A211209] 02 p0266 N90-11515
An approximate max-flow min-cut theorem for uniform multicommodity flow problems with applications to approximation algorithms
[AD-A211908] 03 p0386 N90-12198
The integration of structured and formal methods
[RSRE-MEMO-4293] 04 p0531 N90-13068
The application of artificial intelligence techniques to tracing the interconnections in an integrated circuit
[TELECOM-PARIS-89-E002] 04 p0537 N90-13105
Normal points: Compression of satellite laser ranging data
[ETN-90-96008] 05 p0707 N90-14145
The development of a low cost data logging system for flight trials based on an IBM compatible PC
[RAE-TM-FM-16] 08 p1023 N90-15917
The EPSILON-2 hybrid dataflow architecture
[DE90-003152] 09 p1263 N90-17326
Network flow algorithms
[AD-A214689] 09 p1265 N90-17337
Finding minimum-cost flows by double scaling
[AD-A214498] 10 p1416 N90-18159
Architecture independent environment for developing engineering software on MIMD computers
[NASA-CR-186562] 14 p2016 N90-21553
Structured NC
[RUU-CS-89-6] 17 p2452 N90-23989
An asymmetric shortest queue problem
[MEMO-COSOR-89-22] 17 p2459 N90-24035
The semantics of data flow diagrams
[TR-89-16] 17 p2480 N90-24181
Construction of an Ethernet model with the PROMISE simulation tool
[NLR-MP-88047-U] 18 p2593 N90-24757
Maintaining multiple representations of dynamic data structures
[RUU-CS-88-27] 18 p2634 N90-25005
Basic data requirements for microwave radiometer systems 21 p3015 N90-27143
SAGE 3: A visible wavelength limb sounder 21 p3016 N90-27147
Past, present and future: Aircraft integrated monitoring systems: An ever-developing technology 22 p3103 N90-27618
Communications Interface Driver (CID) software principles of operation
[DOT/FAA/CT-TN89/46] 24 p3526 N90-29937

DATA HANDLING SYSTEMS
U DATA SYSTEMS

DATA INTEGRATION
Voice/data integration in mobile radio networks: Overview and future research directions
[AD-A214289] 07 p0919 N90-15319
Experiences with knowledge-base and large database integration
[DE90-000686] 08 p1137 N90-16591
Process and information integration via hypermedia 19 p2733 N90-25534
The value of real experience
[PNR90619] 20 p2934 N90-26696

DATA LINKS
Toward a national research network
[PB89-198709] 02 p0287 N90-11644
Independent Orbiter Assessment (IOA): Assessment of the communication and tracking subsystem, volume 1
[NASA-CR-185528-VOL-1] 03 p0315 N90-11789
Independent Orbiter Assessment (IOA): Assessment of the communication and tracking subsystem, volume 2
[NASA-CR-185528-VOL-2] 03 p0315 N90-11790
Independent Orbiter Assessment (IOA): Assessment of the communication and tracking subsystem, volume 3
[NASA-CR-185528-VOL-3] 03 p0315 N90-11791
Mode S data link trials, 10-11 January 1989
[RSRE-MEMO-4267] 04 p0490 N90-12815
The role of the ground segment 05 p0606 N90-13527
The link to extragalactic objects 05 p0608 N90-13544
Linking Hipparcos to a quasi-inertial system 05 p0611 N90-13565
Data Link Processor (DLP) operational test and evaluation/integration test plan
[DOT/FAA/CT-TN89/32] 06 p0757 N90-14404
Satellite systems integrated with the terrestrial cellular network for mobile communications
[ESA-STR-228] 08 p1057 N90-16113
Development of a parallel link model for meteor burst communication
[AD-A215629] 09 p1208 N90-17001
Communication-efficient arbitration models for low-resolution data flow computing
[AD-A214768] 09 p1262 N90-17319
Field measurements in MSAT-X 10 p1371 N90-17947
Channel simulator upgrade to use field propagation data 10 p1372 N90-17948
Atmospheric transmission calculations for optical frequencies 10 p1373 N90-17960
Advanced tracking systems design and analysis
[NASA-CR-183459] 10 p1376 N90-17976
Dynamic reconfiguration and link fault tolerance in a transputer network
[AD-A215105] 12 p1642 N90-19433
Operational evaluation of initial data link air traffic control services, volume 1
[DOT/FAA/CT-90/1-VOL-1] 12 p1648 N90-19472
User-friendly software for the design of digital line-of-sight radio links
[PB90-118472] 12 p1700 N90-19760
High stability radio links 12 p1734 N90-19970
OMV mission simulator 13 p1860 N90-20669
Weather data dissemination to aircraft 14 p1907 N90-20934
Data Link Processor (DLP) project transition plan
[DOT/FAA/CT-TN89/68] 14 p1965 N90-21256
Bit-error-rate testing of fiber optic data links for MMIC-based phased array antennas
[NASA-TM-102523] 14 p1966 N90-21261
Microwave Landing System (MLS) remote monitoring subsystem/remote maintenance monitoring system
[DOT/FAA/PS-89/2] 15 p2050 N90-21749
Microwave Landing System (MLS) multiple system design interoperability interface control report
[DOT/FAA/SA-89/2] 15 p2050 N90-21750
The GEOSTAR location and messaging system 17 p2360 N90-23435
LOCSTAR: A satellite radiodetermination system for Europe 17 p2360 N90-23436
NASA 60 GHz intersatellite communication link definition study. Addendum A: Mixed baseband and IF signals
[NASA-CR-186337] 17 p2387 N90-23593
NASA 60 GHz intersatellite communication link definition study. Baseline document
[NASA-CR-186339] 17 p2387 N90-23594
NASA 60 GHz intersatellite links definition study. Final Review
[NASA-CR-186338] 17 p2387 N90-23595
Joint tactical anti-jam communications: A systems approach
[AD-A219592] 17 p2388 N90-23602
Rate-based congestion control in networks with smart links, revision
[NASA-CR-186698] 17 p2452 N90-23987
Performance analysis of local area networks
[NASA-CR-186639] 18 p2595 N90-24767
Automatic speech recognition in air-ground data link 18 p2640 N90-25037
CLEAR: Automating control centers with expert system technology 19 p2733 N90-25533
The disturbance processes on the data links of the mode-S air traffic control system
[ETN-90-96960] 20 p2806 N90-25965
Experimental analysis of the HF linkage 20 p2845 N90-26181
Experimental study of a digital mobile radio spread spectrum in an urban site 20 p2849 N90-26205
Continuous on-line link error rate detector
[AD-D014510] 20 p2850 N90-26209
Space operations: NASA's communications support for Earth orbiting spacecraft. Report to Chairman, Subcommittee on Space Science and Applications, Committee on Science, Space and Technology, House of Representatives
[GAO/IMTEC-89-41] 20 p2851 N90-26215
Data link test and analysis system/ATCRBS transponder test system technical reference
[DOT/FAA/CT-TN90/7] 21 p2955 N90-26803
The need for headers: An impossibility result for communication over unreliable channels
[AD-A222823] 21 p2994 N90-27018
Aspects of data link applications for ATC purposes 22 p3113 N90-27688
Application of a company data link at Lufthansa German Airlines 22 p3113 N90-27689
Stand-alone terrestrial and satellite networks for nationwide interoperation of broadband networks
[PB90-172404] 22 p3164 N90-27942
An aeronautical mobile satellite experiment
[NASA-CR-186971] 23 p3287 N90-28593
A FAA Technical Center project transition plan: Mode S
[DOT/FAA/CT-TN90/17] 23 p3319 N90-28765

DATA MANAGEMENT
Exploitation of data management facilities for finite element analysis in aerospace structural engineering applications 02 p0188 N90-11078
Toward a national research network
[PB89-198709] 02 p0287 N90-11644
The integration of structured and formal methods
[RSRE-MEMO-4293] 04 p0531 N90-13068
NAUTILE: A physical design environment based on an object-oriented data manager
[IMAG-RR-737-I] 04 p0535 N90-13094
Illustration of Bayesian inference in normal data models using Gibbs sampling
[AD-A212630] 04 p0547 N90-13187
The catalogs produced by the Inca consortium 05 p0608 N90-13546
Double star reductions in FAST 05 p0611 N90-13562
Data processing in the FAST consortium 05 p0611 N90-13567
Data processing in the NDAC consortium 05 p0611 N90-13568
Implementation and simulations of the sphere solution in FAST 05 p0612 N90-13570
The first-look data analysis at Utrecht 05 p0612 N90-13571
Data simulations in the fast consortium 05 p0612 N90-13573
Data simulations in the NDAC consortium 05 p0612 N90-13574
Transferring data objects: A focused Ada investigation
[NASA-CR-186065] 06 p0823 N90-14786
SSFP approach to software reuse 06 p0826 N90-14799
Data file management in the D3-D data acquisition and analysis computer systems
[DE90-003289] 07 p1010 N90-15850
Hybrid LZW compression 08 p1076 N90-16223
Experiences with knowledge-base and large database integration
[DE90-000686] 08 p1137 N90-16591
A Geographic Information System (GIS) for the southern Louisiana deltaic environments
[AD-A214676] 09 p1296 N90-17511
An adaptive ARQ (Automatic Repeat Request) strategy for packet switching data communication networks
[AD-A216597] 11 p1497 N90-18615
PC-based PCM telemetry data reduction system software
[DE90-000317] 13 p1761 N90-20111
Three-dimensional medical image analysis using local dynamic algorithm selection on a multiple-instruction, multiple-data architecture
[AD-A218024] 13 p1852 N90-20630
Architecture independent environment for developing engineering software on MIMD computers
[NASA-CR-186562] 14 p2016 N90-21553
A study of caching in capability computers
[RSRE-89015] 15 p2149 N90-22276
The application of connectionism to query planning/scheduling in intelligent user interfaces 15 p2152 N90-22295
Using expert systems to implement a semantic data model of a large mass storage system 15 p2156 N90-22315
Program inversion: More than fun
[CS-8903] 16 p2299 N90-23095
An abstract data model for the IDEF sub 0 graphical analysis language
[AD-A219855] 17 p2446 N90-23948
Knowledge-based control of an adaptive interface 18 p2630 N90-24987
Managing parallelism and resources in scientific dataflow programs
[AD-A221398] 18 p2635 N90-25010
Future developments of remote sensing systems: Data management and processing 19 p2709 N90-25416
Space operations: NASA is not properly safeguarding valuable data from past missions
[GAO/IMTEC-90-1] 20 p2936 N90-26704
VISTA (Vertical Integration of Science, Technology, and Applications) user interface software study
[DE90-010003] 20 p2936 N90-26707
Producing process plans out of CAD files through AI techniques
[ETN-90-97273] 21 p3050 N90-27338
OMNI development of an engineering product data management system
[DE90-002407] 21 p3086 N90-27550
Interim status and recommendations for the Engineering Information System (EIS) program
[AD-A222060] 21 p3087 N90-27555
Harrier Information Management System (HIMS): The system and the approach 22 p3105 N90-27630

Concurrent Image Processing Executive (CIPE). Volume 1: Design overview
[NASA-CR-186853] 22 p3236 N90-28348
Information management directions: The integration challenge
[PB90-219866] 23 p3405 N90-29245
Low cost management of replicated data in fault-tolerant distributed systems
[NASA-CR-186370] 24 p3532 N90-29976
External information sources and aerospace R/D: The use and importance of technical reports by US Aerospace engineers and scientists
[NASA-TM-101232] 24 p3558 N90-30132

DATA PROCESSING
NT ASSOCIATIVE PROCESSING (COMPUTERS)
NT BATCH PROCESSING
NT CEPSTRAL ANALYSIS
NT CONCURRENT PROCESSING
NT DATA CORRELATION
NT DATA REDUCTION
NT DATA RETRIEVAL
NT DATA SMOOTHING
NT DATA STORAGE
NT DATA TRANSFER (COMPUTERS)
NT DISTRIBUTED PROCESSING
NT MULTIPROCESSING (COMPUTERS)
NT ONBOARD DATA PROCESSING
NT OPTICAL DATA PROCESSING
NT PARALLEL PROCESSING (COMPUTERS)
NT PIPELINING (COMPUTERS)
NT SCENE ANALYSIS
NT SIGNAL ANALYSIS
NT SIGNAL PROCESSING
NT VECTOR PROCESSING (COMPUTERS)
NT VOICE DATA PROCESSING
Guidance simulation and test support for differential GPS flight experiment
[NASA-CR-177471] 01 p0005 N90-10021
Satellite Data Processing System (SDPS) users manual V1.0
[NASA-CR-183054] 01 p0082 N90-10468
Meteorological support: Descriptions of application programs for accessing and displaying data
[PB89-194625] 01 p0088 N90-10500
Data processing in lightning warning systems
[DE89-012495] 01 p0088 N90-10502
Advances in regression: Use of models in spectroscopic data analysis
[AD-A210541] 01 p0116 N90-10665
Motivating the notion of generic design within information processing theory: The design problem space
[AD-A210266] 01 p0136 N90-10786
Defense Technical Information Center cataloging guidelines
[AD-A211000] 01 p0137 N90-10792
Flight Test Techniques
[AGARD-CP-452] 02 p0151 N90-10860
The Experimental Aircraft Flight Test Programme 02 p0152 N90-10865
Flight test techniques adopted by Avions Marcel Dassault-Breguet Aviation 02 p0152 N90-10867
Flight test instrumentation and data processing at British Aerospace, Warton, U.K. 02 p0155 N90-10887
New data handling system (MDH) for mechanical tests at ESTEC 02 p0187 N90-11066
The large European Acoustic Facility at ESTEC 02 p0187 N90-11067
Hanford Meteorological Station computer codes. Volume 10: The ARCHIVE computer code
[DE89-016175] 02 p0252 N90-11429
Gridded environmental data compaction: An investigation
[AD-A210580] 02 p0252 N90-11430
Quantitative methods for waves in space plasmas
[PB89-210256] 02 p0280 N90-11599
Inferring data base requirements from examples in forms 02 p0288 N90-11646
The Knowledge Representation Project
[AD-A211288] 02 p0288 N90-11650
Navigation experiment NAVEX: Data storage and processing
[DFVLR-MITT-89-09] 03 p0304 N90-11727
NASA/MSFC FY88 Global Scale Atmospheric Processes Research Program Review
[NASA-TM-100357] 03 p0360 N90-12059
Global distribution of moisture, evaporation-precipitation, and diabatic heating rates 03 p0362 N90-12069
Laboratory and theoretical models of planetary-scale instabilities and waves 03 p0363 N90-12076
UV ionospheric remote sensing with the polar BEAR satellite
[AD-A211359] 03 p0372 N90-12127
World Weather Watch: Implementation
[WMO-714] 03 p0375 N90-12139
Crau 1987: The KNMI contribution --- KNMI (Royal Netherlands Meteorological Institute)
[KNMI-TR-110] 03 p0375 N90-12140
General data processing support from project planning to workshop control
[MBB-UD-526/88-PUB] 03 p0388 N90-12208
Operating experience with the Sandia terminal switching network and fiber optic loop
[DE89-007422] 03 p0404 N90-12317
Single crystal diffraction
[DE90-000024] 03 p0412 N90-12366
Problem of incomplete information in relational databases
[PB89-217533] 03 p0417 N90-12393
Stable Kalman filters for processing clock measurement data 04 p0487 N90-12801
Conception and results of the DLR realtime azimuth processor for the E-SAR system
[DLR-FB-89-30] 04 p0492 N90-12827
Automatic analysis and exploitation of the flow visualization images
[ETN-89-95712] 04 p0501 N90-12887
A Z specification of the MaCHO interface editor
[RSRE-MEMO-4247] 04 p0531 N90-13067
User manual of the force structure model scenario editor SCENE
[FEL-1988-101] 04 p0531 N90-13069
Process expressions and Hoare's logic
[CWI-CS-R8905] 04 p0532 N90-13076
Data acquisition in aerodynamic research 05 p0574 N90-13340
Optimum data weighting and error calibration for estimation of gravitational parameters 05 p0591 N90-13437
The in-orbit initialization phase 05 p0606 N90-13525
Proximity effects on adjacent and multiple stars 05 p0607 N90-13533
Successive iterations of the input catalog 05 p0607 N90-13534
The compilation of astrometric data 05 p0607 N90-13537
The choice of stars in the Magellanic clouds 05 p0608 N90-13543
On-ground attitude determination 05 p0609 N90-13552
Data processing in the FAST consortium 05 p0611 N90-13567
Data processing in the NDAC consortium 05 p0611 N90-13568
Data simulations in the fast consortium 05 p0612 N90-13573
Data simulations in the NDAC consortium 05 p0612 N90-13574
Application of an optimal filter for inflatable sphere data processing 05 p0659 N90-13849
Micro-based fact collection tool user's manual
[NASA-CR-180414] 05 p0684 N90-13981
Ada programming guidelines for deterministic storage management
[NASA-CR-181308] 05 p0684 N90-13982
Coordination of processing elements in a multiprocessor computer
[WO-PATENT-88/04075] 06 p0831 N90-14830
The AMY Experiment
[DE90-001153] 06 p0839 N90-14880
A dynamic systems engineering methodology research study. Phase 2: Evaluating methodologies, tools, and techniques for applicability to NASA's systems projects
[NASA-CR-181319] 06 p0857 N90-14985
Flashlight radar: A three-dimensional imaging radar
[AD-A213439] 07 p0918 N90-15307
A multichannel processing approach to real time network detection, phase association, and threshold monitoring
[AD-A213940] 07 p0980 N90-15657
Ultra high performance, highly reliable, numeric intensive processors and systems
[AD-A214100] 07 p0980 N90-15659
Upgrade plans to handle 30 to 40 Mbytes of data for D3-D
[DE90-003291] 07 p0995 N90-15750
The development of a low cost data logging system for flight trials based on an IBM compatible PC
[RAE-TM-FM-16] 08 p1023 N90-15917
The new programming
[RSRE-MEMO-4249] 08 p1110 N90-16425
Pattern matching in ML: A case study in refinement
[RSRE-89004] 08 p1111 N90-16430
Sort computation 08 p1113 N90-16446
On the efficient exploitation of speculation under data flow paradigms of control
[AD-A214112] 08 p1115 N90-16455
New optimization techniques in database access and maintenance 08 p1137 N90-16586
FY 1989 update to the Information Resources Management review plan
[DE90-004185] 08 p1138 N90-16593
USAF/GL meteor scatter data analysis program: A user's guide
[AD-A214988] 09 p1206 N90-16989
AOIPS 3 user's guide. Volume 2: Program descriptions
[NASA-TM-100725] 09 p1247 N90-17236
Case studies in data analysis
[AD-A215342] 09 p1248 N90-17241
ONR tropical cyclone motion research initiative: Data assimilation considerations for field experiment analyses
[AD-A215726] 09 p1248 N90-17244
A review of circadian effects on selected human information processing tasks
[AD-A214673] 09 p1251 N90-17256
Identifying the circadian cycle in human information processing data using periodicity analysis: A synopsis
[AD-A214674] 09 p1251 N90-17257
Communication-efficient arbitration models for low-resolution data flow computing
[AD-A214768] 09 p1262 N90-17319
EDISON Project
[AD-A214724] 09 p1265 N90-17338
Finite word length considerations in high resolution spectral estimation
[AD-A214684] 09 p1273 N90-17377
Modern Antenna Design Using Computers and Measurement: Application to Antenna Problems of Military Interest
[AGARD-LS-165] 10 p1369 N90-17932
Tracking a hypersonic aircraft from a space platform
[AD-A216399] 10 p1377 N90-17984
International course in remote sensing ONU/INPE, Brazil
[INPE-4802-NTE/288] 10 p1399 N90-18089
Proposition for an airborne remote sensing system
[INPE-4872-PRE/1483] 10 p1399 N90-18090
Processing of DMSP magnetic data: Handbook of programs, tapes, and datasets
[NASA-TM-100757] 10 p1407 N90-18114
Study on advanced information processing system
[NASA-CR-186342] 10 p1415 N90-18154
Preparing software conversion studies 10 p1416 N90-18158
A general method of using prior information in a simultaneous equation system
[NOAA-TR-NESDIS-47] 10 p1423 N90-18209
Impact of uncertainty and diagnosticity on classification of multidimensional data with integral and separable displays of system status
[AD-A215966] 10 p1424 N90-18215
Time and frequency-domain identification and verification of BO-105 dynamic models
[AD-A216828] 11 p1456 N90-18389
Navigation experiment NAVEX data storage and processing
[ESA-TT-1175] 11 p1467 N90-18445
Fast algorithms for calculating laser wavefront phase compensation given noisy measurements of phase gradient
[DE90-006357] 11 p1515 N90-18727
A global approach for the identification of structural connection properties
[NASA-TM-102502] 11 p1518 N90-18745
Resource Assessment Project: User needs survey results
[DE89-009502] 11 p1529 N90-18802
Feasibility of Mealy design for processor controlpaths
[MEMO-INF-89-53] 11 p1550 N90-18923
DoD manual for standard data elements
[AD-A216441] 11 p1575 N90-19066
Measurement system of spectral irradiance in the near infrared 11 p1588 N90-19160
GeoNet 88: Calculation connection system concept for the EURAD project 12 p1687 N90-19688
Error detection in data processing devices by means of residue codes
[ETN-90-95370] 12 p1701 N90-19767
Electron energy distributions and vibrational population distributions
[DE90-005550] 12 p1711 N90-19825
A guide to performing and documenting safety analyses
[DE90-008687] 13 p1788 N90-20260
Laser line transport with refraction
[DE90-008683] 13 p1808 N90-20382
Transaction processing in a quality control laboratory
[DE90-004655] 13 p1813 N90-20414
Controlling Summer Heat Islands: Proceedings
[DE90-008075] 13 p1830 N90-20508
Overview of the methodologies used to compile large scale emissions inventories
[DE90-008518] 13 p1830 N90-20509
Performance of FFT methods in local gravity field modelling 13 p1835 N90-20537

High resolution analysis of satellite gradiometry
13 p1840 N90-20561
Satellite radar altimetry over ice. Volume 2: Users' guide for Greenland elevation data from Seasat
[NASA-RP-1233-VOL-2] 13 p1840 N90-20563
User's guide: Programs for processing altimeter data over inland seas
[NASA-TM-100730] 13 p1841 N90-20572
Comparison of oculometer and head-fixed reticle with voice or switch and touch panel for data entry on a generic tactical air combat display
[AD-A217231] 13 p1855 N90-20646
Animation graphic interface for the space shuttle onboard computer 13 p1859 N90-20667
MEASURE: An integrated data-analysis and model identification facility
[NASA-CR-186452] 13 p1863 N90-20686
A paradoxical result in unconditionally secure authentication codes, and an explanation
[DE90-008529] 13 p1867 N90-20710
Mathematics and physics studies: Multi-project support
[AD-A218208] 13 p1869 N90-20723
Implementation of a control system test environment in UNIX
[DE90-007485] 13 p1872 N90-20736
Principles of the radiosity method for canopy reflectance modeling
[DE90-008943] 14 p2001 N90-21466
Meteorologist Weather Processor (MWP) integration test plan
[DOT/FAA/CT-TN89/62] 14 p2007 N90-21500
The CAD/CAM product data standards: IGES/PDES (Initial Graphics Exchange Specification/Product Data Exchange Standards, the present and the future
[DE90-008803] 14 p2015 N90-21549
Small business innovation research. Abstracts of 1988 phase 1 awards
[NASA-TM-102991] 14 p2036 N90-21680
Enhanced Low Level Wind Shear (LLWAS) 6-sensor improvement user's manual for data processing of field data
[DOT/FAA/CT-TN90/8] 15 p2052 N90-21759
The AGRISCATT-87 campaign: Processing of the Dutscat data
[BCRS-89-20] 15 p2122 N90-22140
The WAVE model for advanced knowledge processing
[OUEL-1803/89] 15 p2151 N90-22291
Spline function smoothing and differentiation of noisy data on a rectangular grid
[DE90-009319] 15 p2160 N90-22338
The approximation of a composite Bezier cubic curve by a composite Bezier quadratic curve
[NPL-DITC-147/89] 15 p2162 N90-22354
The use of local polynomial approximations in a knot-placement strategy for least squares spline fitting
[NPL-DITC-148/89] 15 p2162 N90-22355
The automation plan of the General Directorate 1 (search) of the European Patent Office
15 p2178 N90-22448
The role of orbit errors in processing of satellite altimeter data
[ETN-90-96699] 16 p2204 N90-22575
Tracking in uncertain environments
[RAE-TM-AW-121] 16 p2261 N90-22891
Towards a calculus of data refinement
[CS-8902] 16 p2326 N90-23264
Application of novel data processing techniques to the analysis of Ion Mobility Spectrometry (IMS) data
[AD-A219976] 17 p2374 N90-23516
Real-time simulation clock
[NASA-CASE-LAR-14056-1] 17 p2407 N90-23713
The VIERS-1 project. The Delft wind/wave experiment: Experiment and first results, part 1
[BCRS-89-24-PT-1] 17 p2418 N90-23779
Determination of the gravity disturbance by processing the gravity gradiometer surveying system: Processing procedure and results
[AD-A219992] 17 p2423 N90-23808
A model of a path expression based operating system shell
[MEMO-INF-89-71] 17 p2440 N90-23906
The Zenith Z-248 as a scientific workstation
[AD-A219991] 17 p2441 N90-23909
Automatic runtime consistency checking and debugging of formally specified programs
[AD-A218855] 17 p2442 N90-23916
Symbolic reasoning in model-based diagnosis: Efficient and effective information processing
[MEMO-INF-89-03] 17 p2452 N90-23984
Fields, particles, groups: Bertel Laurents 60th Anniversary Symposium
[ETN-90-96596] 17 p2478 N90-24170
Development of an all silicon integrated optical modulator for high speed data communications and sensor applications
[AD-A220270] 18 p2547 N90-24535
Spectral feature design in high dimensional multispectral data
[NASA-CR-186647] 18 p2574 N90-24664
Summary results of an assessment of research projects in the national photovoltaics program
[DE90-008222] 18 p2577 N90-24680
Models of the external source contribution to magnetospheric magnetic fields for CRRES data analysis
[AD-A221059] 18 p2580 N90-24897
How to construct an atomic variable
[CWI-CS-R8939] 18 p2596 N90-24772
Maintaining multiple representations of dynamic data structures
[RUU-CS-88-27] 18 p2634 N90-25005
Distributed computing on transitive networks: The torus
[RUU-CS-88-31] 18 p2634 N90-25007
Conference on Instrumental Activation Analysis: IAA 89
[DE90-615661] 19 p2694 N90-25327
An atlas of ECMWF analyses (1980-1987). Part 2: Second moment quantities
[NASA-TM-100762-PT-2] 19 p2715 N90-25451
The role of attention in information processing implications for the design of displays
[AD-A219252] 19 p2723 N90-25486
Active perception and exploratory robotics
[MS-CIS-89-65] 19 p2726 N90-25501
Multiprocessor architecture: Synthesis and evaluation
[NASA-CR-186618] 19 p2741 N90-25579
On the design of a concurrent image analysis system
[DE90-011388] 19 p2746 N90-25605
Neuromorphic learning of continuous-valued mappings from noise-corrupted data. Application to real-time adaptive control
[NASA-TM-4176] 19 p2747 N90-25607
Technical guide on documentation requirements for open market contract acquisitions of information resources
[NASA-TM-102650] 19 p2762 N90-25695
Object-oriented design: Deriving conceptual solutions to large-scale information processing problems
[DE90-011189] 19 p2763 N90-25699
A framework for query optimization in temporal databases
[DE90-011339] 19 p2763 N90-25700
M15:AC211/X2127+119: Optical curve, improved ephemeris, and phasing of EXOSAT X ray data
19 p2771 N90-25749
Observations of black hole candidates with the Mir-Kvant HEXE 19 p2774 N90-25774
Einstein SSS and MPC observations of Aql X-1 and 4U1820-30 19 p2777 N90-25790
The soft X ray excess in Einstein quasar spectra
19 p2794 N90-25910
Einstein SSS+MPC observations of Seyfert type galaxies 19 p2795 N90-25913
Software set-up for data processing of depolarization due to rain and ice crystals in the Olympus project
[EUT-89-E-218] 20 p2855 N90-26240
Documentation of program Tankplot
[FFI-89/7019] 20 p2908 N90-26541
UEDIT: A full-scale, scrollable APL2 spreadsheet input/output editor
[AD-A222712] 20 p2910 N90-26557
Neural networks for real-time sensory data processing and sensorimotor control
[AD-A223096] 20 p2916 N90-26592
Automated analysis of MXU-553 flight data
21 p2958 N90-26821
Radars in space 21 p3015 N90-27144
Description of SAFIRE for ISES
21 p3016 N90-27148
Applications of ISES for the atmospheric sciences
21 p3017 N90-27155
Applications of ISES for coastal zone studies
21 p3018 N90-27157
Applications of ISES for vegetation and land use
21 p3018 N90-27158
An experiment to make a new design of the Satellite Cloud Information Chart with the combination of visible and infrared data observed by the GMS
21 p3029 N90-27223
Automatic information processing and high performance skills: Application to training
[AD-A221709] 21 p3036 N90-27259
Automatic information processing and high performance skills: Acquisition, transfer, and retention
[AD-A221744] 21 p3036 N90-27260
An engineering approach to automatic programming
21 p3046 N90-27317
The composite load spectra project
21 p3047 N90-27323
Disconnected actions: An asynchronous extension to a nested atomic action system
[AD-A221937] 21 p3053 N90-27356
Representing processes in the extended entity-relationship model
[DE90-013350] 21 p3086 N90-27551
Further research on heading in text
[AD-A221511] 21 p3087 N90-27557
Computer modeling and data processing methods: An essential part of jet engine condition monitoring and fault diagnosis 22 p3104 N90-27626
On line diagnostics of rotating machinery using expert system technology 22 p3105 N90-27632
The MODE S operational test and evaluation/integration test plan
[DOT/FAA/CT-TN89/51] 22 p3111 N90-27671
Air traffic management in Europe: Structure, tasks, potential 22 p3112 N90-27677
Application of a company data link at Lufthansa German Airlines 22 p3113 N90-27689
Design of the UETP experiment
22 p3118 N90-27712
Measurement uncertainty in gas turbine performance determination 22 p3119 N90-27717
Experience in developing an improved design of experiment (lessons learned) 22 p3120 N90-27718
General test plan 22 p3120 N90-27721
Spatial array processing by the method CLEAN
[FEL-1989-144] 22 p3165 N90-27949
Using information to measure software complexity
[REPT-89-022] 22 p3238 N90-28359
Distributed transitive closure computations: The disconnection set approach
[REPT-90-014] 22 p3259 N90-28459
Phoenix data analysis and numerical simulation
[AD-A224226] 23 p3320 N90-28772
Techniques and potential capabilities of multi-resolutional information (knowledge) processing
23 p3374 N90-29062
The SPECIALIST: Natural language processing system
[PB90-240029] 23 p3381 N90-29098
Preparing software conversion studies
[PB90-235623] 23 p3381 N90-29099
INPE geographic data base
[INPE-4636-PRE/1348] 23 p3407 N90-29253
AutoPAVER: A software package for automated pavement evaluation
[AD-A224176] 24 p3458 N90-29531
Noncontact measurement of rotating blade vibrations
[NAL-TR-1033] 24 p3483 N90-29687
The effect of wave data assimilation on the numerical simulation of wave energy advection
[KNMI-TR-121] 24 p3496 N90-29760
An advanced telerobotic system for shuttle payload changeout room processing applications
24 p3502 N90-29795
Short encodings of evolving structures
[AD-A223641] 24 p3527 N90-29944
Computing environments, interactive graphics and nonparametric methods for data analysis
[DE90-016128] 24 p3530 N90-29964
Handbook of data compression algorithms
[ESA-TM-06] 24 p3531 N90-29969
Information processing and perceptual characteristics of display design: The role of emergent features and objects
[AD-A223683] 24 p3558 N90-30133
IUE-ULDA access guide no. 2. International Ultraviolet Explorer-Uniform Low Dispersion Archive: Comets
[ESA-SP-1134] 24 p3563 N90-30157
A search for low energy cosmic ray antiprotons
24 p3564 N90-30161

DATA PROCESSING EQUIPMENT

NT AIRBORNE/SPACEBORNE COMPUTERS
NT ANALOG COMPUTERS
NT CDC CYBER 205 COMPUTER
NT COMPUTERS
NT CRAY COMPUTERS
NT DATA PROCESSING TERMINALS
NT DIGITAL COMPUTERS
NT EMBEDDED COMPUTER SYSTEMS
NT HEWLETT-PACKARD COMPUTERS
NT HYBRID COMPUTERS
NT HYPERCUBE MULTIPROCESSORS
NT IBM COMPUTERS
NT MASSIVELY PARALLEL PROCESSORS
NT MICROCOMPUTERS
NT MICROPROCESSORS
NT MIMD (COMPUTERS)
NT MINICOMPUTERS
NT OPTICAL COMPUTERS
NT PARALLEL COMPUTERS
NT PERSONAL COMPUTERS
NT PRINTERS (DATA PROCESSING)

NT REMOTE CONSOLES
NT SEQUENTIAL COMPUTERS
NT SIMD (COMPUTERS)
NT SUPERCOMPUTERS
NT TRANSPUTERS
NT VAX COMPUTERS
NT VAX-11 SERIES COMPUTERS
Independent Orbiter Assessment (IOA): Assessment of the data processing system FMEA/CIL
[NASA-CR-185546] 02 p0162 N90-10917
Independent Orbiter Assessment (IOA): Analysis of the DPS subsystem
[NASA-CR-185549] 02 p0163 N90-10924
Independent Orbiter Assessment (IOA): CIL issues resolution report, volume 1
[NASA-CR-185524-VOL-1] 02 p0169 N90-10954
A methodology for the design of continuous-dataflow synchronous systems
[PB89-184360] 02 p0274 N90-11564
SN 1987: A telemetry decoding system
05 p0663 N90-13875
Data Link Processor (DLP) operational test and evaluation/integration test plan
[DOT/FAA/CT-TN89/32] 06 p0757 N90-14404
Instrumentation for a facility for the test, analysis and active control of spacecraft truss structures
[AD-A213655] 07 p0886 N90-15124
Understanding developments in computer technology: A pragmatic and synthetic interpretation
07 p0971 N90-15608
Polynomial transfer lot sizing techniques for batch processing on consecutive machines
[AD-A214198] 07 p0980 N90-15660
Preparing software conversion studies
10 p1416 N90-18158
Throughput and delay characteristics for a slow-frequency hopped aircraft-to-aircraft packet radio network
[AD-A220525] 17 p2369 N90-23609
A human factors review of data entry devices
[DE90-012009] 19 p2763 N90-25703
Earth Sciences Requirements for the Information Sciences Experiment System
[NASA-CP-3072] 21 p3015 N90-27140

DATA PROCESSING TERMINALS
Software package for 3-dimensional graphic display unit
[NAL-TM-559] 03 p0385 N90-12191
Theoretical and material studies of thin-film electroluminescent devices
[NASA-CR-186104] 06 p0768 N90-14468
The development of an Ada programming support environment database: SEAD (Software Engineering and Ada Database), user's manual
[NASA-CR-181219] 06 p0828 N90-14811
Criteria for device selection: A comparison between a mouse and a touchscreen as an input device for interactive video
[NPL-DITC-158/90] 22 p3235 N90-28344

DATA PROCESSORS
U DATA PROCESSING EQUIPMENT

DATA READOUT SYSTEMS
U DATA SYSTEMS
U DISPLAY DEVICES

DATA RECORDERS
The NASA digital VGH program: Exploration of methods and final results. Volume 2: L 1011 data 1978-1979: 1619 hours
[NASA-CR-181909-VOL-2] 13 p1756 N90-20080
The NASA digital VGH program. Exploration of methods and final results. Volume 1: Development of methods
[NASA-CR-181909-VOL-1] 13 p1756 N90-20081
The NASA digital VGH program. Exploration of methods and final results. Volume 3: B 727 data 1978-1980: 1765 hours
[NASA-CR-181909-VOL-3] 13 p1756 N90-20082
The NASA digital VGH program: Exploration of methods and final results. Volume 4: B 747 data 1978-1980, 1689 hours
[NASA-CR-181909-VOL-4] 13 p1756 N90-20083
The NASA digital VGH program: Exploration of methods and final results. Volume 5: DC 10 data 1981-1982, 129 hours
[NASA-CR-181909-VOL-5] 13 p1756 N90-20084
Evaluation of EDR-3 vibration, shock, temperature, and humidity recording unit
[NASA-CR-184006] 22 p3177 N90-28028

DATA RECORDING
A closer look at the visioceilometer
[FEL-1989-80] 03 p0374 N90-12138
Acoustic recording systems for use in military aircraft
[RAE-TM-MM-11] 04 p0551 N90-13207
Aircraft condition monitoring system for future Airbus aircraft: New concept for programming and data recording
22 p3103 N90-27619
The EFA integrated monitoring and recording system: Requirements and concept for implementation
22 p3103 N90-27620

DATA REDUCTION
NT DATA SMOOTHING
System identification for large space structures
01 p0025 N90-10126
The Experimental Aircraft Flight Test Programme
02 p0152 N90-10865
The Knowledge Representation Project
[AD-A211288] 02 p0288 N90-11650
The interface with the data reduction consortia
05 p0606 N90-13528
The Hipparcos Mission. Prelaunch status. Volume 2: The input catalog
[ESA-SP-1111-VOL-2] 05 p0606 N90-13529
New ground-based photometric measurements
05 p0607 N90-13538
Double stars 05 p0608 N90-13540
The Hipparcos Mission. Prelaunch status. Volume 3: The data reductions
[ESA-SP-1111-VOL-3] 05 p0609 N90-13548
Overview of the data acquisition and reductions
05 p0609 N90-13549
The great circle reductions 05 p0609 N90-13553
Great circle interactions: Attitude smoothing and grid-step inconsistencies 05 p0609 N90-13554
General and numerical approach to the sphere solution in FAST 05 p0610 N90-13555
Astrometric parameter determination in FAST
05 p0610 N90-13556
The sphere solution and astrometric parameter determination in NDAC 05 p0610 N90-13557
Overview of the Tycho data analysis
05 p0610 N90-13558
Tycho astrometry 05 p0610 N90-13559
Photometry: Main mission and Tycho
05 p0610 N90-13560
Double star reductions in NDAC
05 p0610 N90-13561
Double star reductions in FAST
05 p0611 N90-13562
The treatment of minor planets and planetary satellites 05 p0611 N90-13563
Linking Hipparcos to a quasi-inertial system
05 p0611 N90-13565
Data processing in the FAST consortium
05 p0611 N90-13567
Data processing in the NDAC consortium
05 p0611 N90-13568
Great circle reductions: Implementation and simulations 05 p0611 N90-13569
The first-look data analysis at Utrecht
05 p0612 N90-13571
The Tycho input catalog 05 p0612 N90-13575
Micro-based fact collection tool user's manual
[NASA-CR-180414] 05 p0684 N90-13981
Ada programming guidelines for deterministic storage management
[NASA-CR-181308] 05 p0684 N90-13982
MERLIN and VLBI observations of the radio galaxy Virgo A 06 p0860 N90-15001
RETE experiment activity at the TSS-1 POCC
[IFSI-89-12] 08 p1036 N90-15988
ONR tropical cyclone motion research initiative: Data assimilation considerations for field experiment analyses
[AD-A215726] 09 p1248 N90-17244
Sea surface temperature fields derived from aircraft and ship observations during FASINEX 1986
[AD-A215727] 09 p1250 N90-17250
PC-based PCM (Pulse Code Modulation) telemetry data reduction system hardware
[DE90-000316] 12 p1612 N90-19273
Data reduction of GOES (Geostationary Operational Environmental Satellite) information from DCP (Data Collection Platform) networks
[AD-A215844] 12 p1678 N90-19637
PC-based PCM telemetry data reduction system software
[DE90-000317] 13 p1761 N90-20111
The reduction correction in North America
13 p1836 N90-20540
A VLSI design for a systolic Viterbi decoder
15 p2077 N90-21899
Godhavn (Greenland) Geophysical Observatory: Magnetic results, 1984
[ISBN-87-7478-289-4] 17 p2423 N90-23807
Linear-quadratic problems and the Riccati equation
[MEMO-COSOR-89-26] 17 p2459 N90-24037
A low-cost PC-based telemetry data-reduction system
[DE90-000330] 18 p2509 N90-24339
Maintaining multiple representations of dynamic data structures
[RUU-CS-88-27] 18 p2634 N90-25005
Prediction methodologies for nonlinear aerodynamic characteristics of control surfaces
[NIAR-90-17] 20 p2801 N90-25937
Automated analysis of MXU-553 flight data
21 p2958 N90-26821
Description of SAFIRE for ISES
21 p3016 N90-27148
Selective multimode/multiconfigurable data acquisition and reduction processor system
[AD-D014551] 22 p3234 N90-28341

DATA RETRIEVAL
The impact of recovery on concurrency control
[AD-A210828] 01 p0106 N90-10603
The Inca data base 05 p0607 N90-13531
Mission simulations 05 p0607 N90-13532
The SIMBAD data base 05 p0608 N90-13547
High volume data storage architecture analysis
[NASA-CR-186239] 06 p0823 N90-14784
Document preservation by electronic imaging. Volume 1: Synopsis
[PB89-226526] 06 p0858 N90-14987
Document preservation by electronic imaging. Volume 2: System and experiment description
[PB89-226534] 06 p0858 N90-14988
Document preservation by electronic imaging. Volume 3: Appendices
[PB89-226542] 06 p0858 N90-14989
EXOSAT measurements of the pulse period of Vela X-1
[MPE-PREPRINT-157] 08 p1152 N90-16673
A formal approach to user models in data retrieval
[PB90-124728] 14 p2036 N90-21682
Building a user interface using SQL*Forms and an intermediate table
[DE90-012729] 22 p3259 N90-28455
Providing dynamic sorting and searching capabilities using SQL*Forms
[DE90-012735] 22 p3259 N90-28456

DATA SAMPLING
Number of test samples needed to obtain a desired Bayesian confidence interval for a proportion
[AD-A208157] 01 p0115 N90-10658
Boundary kernel estimation of the two sample comparison density function
[AD-A210757] 02 p0268 N90-11532
Fast sampling and stability of nonlinear sampled data systems. Part 2: Sampling rate estimations
[RR-341] 03 p0397 N90-12271
Fast sampling and stability of nonlinear sampled-data systems. Part 1: Existence theorems
[RR-340-PT-1] 03 p0398 N90-12276
Slow sampling and stability of nonlinear sampled-data systems
[RR-342] 03 p0398 N90-12277
Calculating the time domain average of gear vibration data sampled at less than the Nyquist frequency
[OUEL-1768/89] 15 p2107 N90-22052
Statistical inference from sampled data
[AD-A218731] 16 p2309 N90-23156
Control of randomly sampled robotic systems
[AD-A218948] 16 p2309 N90-23157
Reconstructing primordial density fluctuations
16 p2333 N90-23293
On airborne measurements of radiation from broken cloud fields
[MITT-67] 21 p3027 N90-27211
Impact of satellite altimetric data on the numerical simulation of the general oceanic currents: Sensitivity to orbit parameters
[ETN-90-97451] 22 p3231 N90-28321
Sample rate effects on disturbance rejection for digital control systems 24 p3435 N90-29400

DATA SIMULATION
Route data representation for ATC simulation experiments
[RSRE-MEMO-4133] 04 p0450 N90-12576
Aircraft SAR simulation Sargen 1.0
[FEL-1989-44] 04 p0491 N90-12823
The APROS software for process simulation and model development
[VTT-618] 05 p0684 N90-13987
Pattern recognition techniques applied to the NASA-ACTS order-wire problem
06 p0764 N90-14446
Simulating simultaneous processes with APL
[MEMO-INF-89-47] 11 p1547 N90-18906
A new stochastic model of turbulent dispersion in the convective planetary boundary layer and the results of the Atterbury-87 field study 16 p2254 N90-22853
Robust modelling of sampled systems for time delay estimation
[REPT-89-047] 16 p2298 N90-23092

DATA SMOOTHING
Minimum-variance reduced-order estimation algorithms from Pontrygin's minimum principle
01 p0021 N90-10105

Splines and equations of nonlinear parameters
[IMAG-RR-750-M] 03 p0395 N90-12257
A cell-centered multigrid method for three-dimensional anisotropic-diffusion and interface problems
[REPT-89-35] 04 p0540 N90-13128
Local mode smoothing analysis of various incomplete factorization iterative methods in two dimensions
[REPT-89-36] 04 p0540 N90-13129
Smoothed predictor-corrector methods for solving partial differential equations
[CWI-NM-R8808] 04 p0540 N90-13131
Iterated theta method for hyperbolic equations
[CWI-NM-R8809] 04 p0540 N90-13132
Great circle interactions: Attitude smoothing and grid-step inconsistencies 05 p0609 N90-13554
Identification and quantification of synoptic structure in simulated Tiros N radiance soundings
07 p0959 N90-15546
Adaptive state estimation and sampling rate analysis for invariant linear dynamic systems in time
[INPE-4960-TDL/389] 11 p1554 N90-18951
Local mode smoothing analysis for various incomplete factorization iterative methods in three dimensions
[REPT-89-38] 15 p2147 N90-22263
A Kalman filter with smoothing for hurricane tracking and prediction
[AD-A220413] 17 p2426 N90-23827
A line relaxation smoother for the multigrid solution of the Boussinesq equations
[REPT-89-68] 17 p2458 N90-24027
The test for automatic neph-analysis chart
21 p3029 N90-27219
The existence of smooth densities for the prediction filtering and smoothing problems
[AD-A222108] 21 p3066 N90-27432

DATA STORAGE
The MHOST finite element program: 3-D inelastic analysis methods for hot section components. Volume 3: Systems' manual
[NASA-CR-182236] 01 p0079 N90-10451
Computer availability impact on the archiving of scientific and technical reports
[AD-A210283] 01 p0136 N90-10787
A methodology for the design of continuous-dataflow synchronous systems
[PB89-184360] 02 p0274 N90-11564
Navigation experiment NAVEX: Data storage and processing
[DFVLR-MITT-89-09] 03 p0304 N90-11727
The interface with the data reduction consortia
05 p0606 N90-13526
The SIMBAD data base 05 p0608 N90-13547
High volume data storage architecture analysis
[NASA-CR-186239] 06 p0823 N90-14784
Document preservation by electronic imaging. Volume 1: Synopsis
[PB89-226526] 06 p0858 N90-14987
Document preservation by electronic imaging. Volume 2: System and experiment description
[PB89-226534] 06 p0858 N90-14988
Document preservation by electronic imaging. Volume 3: Appendices
[PB89-226542] 06 p0858 N90-14989
Procurement of an optical disk information storage and retrieval system
[DE90-001372] 07 p1010 N90-15849
IUE-ULDA access guide number 1: International Ultraviolet Explorer-Uniform Low Dispersion Archive. Dwarf novae and nova-like stars
[ESA-SP-1114] 08 p1152 N90-16672
Noise and sonic boom impact technology. Initial development of an Assessment System for Aircraft Noise (ASAN). Volume 3: Technical description
[AD-A214455] 09 p1278 N90-17412
Deceit: A flexible distributed file system
[NASA-CR-186402] 11 p1544 N90-18891
A waveform capture and storage unit and its use for investigating disturbances on digital transmission links
[BBC-RD-1989/17] 12 p1649 N90-19478
Comparison of two matrix data structures for advanced CSM testbed applications
[NASA-CR-181951] 13 p1815 N90-20421
A Locality-based multiprocessor cache interference model
[AD-A217126] 13 p1871 N90-20730
A model research archive: Archive and research implications for original records and support documents
[DE90-008246] 13 p1900 N90-20906
Rapidly quantifying the relative distention of a human bladder
[NASA-CASE-LAR-13901-1-NP]
14 p2010 N90-21519
Using expert systems to implement a semantic data model of a large mass storage system
15 p2156 N90-22315
Assessment System for Aircraft Noise (ASAN) citation database. Volume 2: Database update manual
[AD-A219176] 16 p2314 N90-23189
Looking at large data sets using binned data plots
[DE90-008206] 16 p2326 N90-23263
The Zenith Z-248 as a scientific workstation
[AD-A219991] 17 p2441 N90-23909
Recent experiences and future expectations in data storage technology
[DE90-011488] 18 p2589 N90-24729
A comparison of select image-compression algorithms for an electronic still camera 18 p2632 N90-24994
Satellite data archiving: US and foreign activities and plans for environmental information
[GAO/RCED-88-201] 18 p2633 N90-25001
On rectilinear link distance
[RUU-CS-89-13] 18 p2634 N90-25008
Using integrity constraints to control search in knowledge base systems
[AD-A221291] 18 p2634 N90-25009
OMS FDIR: Initial prototyping
19 p2738 N90-25562
On the design and analysis of multiple-storage elements
[AD-A223095] 20 p2859 N90-26266
Space operations: NASA is not properly safeguarding valuable data from past missions
[GAO/IMTEC-90-1] 20 p2936 N90-26704
Producing process plans out of CAD files through AI techniques
[ETN-90-97273] 21 p3050 N90-27338
Analog hardware for learning neural networks
[NASA-CASE-NPO-17664-1-CU]
21 p3057 N90-27384
Finding the maximum recoverable system state in optimistic rollback recovery methods
[AD-A222338] 21 p3064 N90-27419
Bloch-line memory element and RAM memory
[AD-D014488] 22 p3234 N90-28340
Storage allocation in Ada
[NPL-DITC-156/90] 22 p3235 N90-28343
Theoretical investigations of Pi-conjugated polyradicals as models for organic magnetic materials
[AD-A223411] 24 p3446 N90-29461
A high-speed KDL-RAM file system for parallel computers
[AD-A223299] 24 p3533 N90-29979

DATA STRUCTURES
Route data representation for ATC simulation experiments
[RSRE-MEMO-4133] 04 p0450 N90-12576
Spatial data structures for robotic vehicle route planning
[AD-A212806] 04 p0538 N90-13111
Data structures for the representation and manipulation of polyhedrons
[IMAG-RR-772-M] 05 p0692 N90-14042
Transferring data objects: A focused Ada investigation
[NASA-CR-186065] 06 p0823 N90-14786
Supporting shared data structures on distributed memory architectures
[NASA-CR-181981] 09 p1262 N90-17318
Loran C monitor: Facilities Central Processing Unit (FCPU) port evaluation
[DOT/FAA/CT-TN89/57] 10 p1318 N90-17623
A scheme for supporting distributed data structures on multicomputers
[NASA-CR-181987] 10 p1415 N90-18152
The design and analysis of algorithm and data structure for efficient solutions of minimum-cost network flow problems on MISD and MIMD 10 p1441 N90-18313
Comparison of two matrix data structures for advanced CSM testbed applications
[NASA-CR-181951] 13 p1815 N90-20421
Binary space partitioning trees and their uses
13 p1857 N90-20657
Knowledge structure representation and automated updates in intelligent information management systems
15 p2156 N90-22316
Document delivery via ISDN or satellite networks
15 p2178 N90-22446
Parallel and vector computation for stochastic optimal control applications 16 p2282 N90-23007
Factoring homomorphisms
[CS-8908] 16 p2299 N90-23096
The visibility diagram: A data structure for visibility and motion planning problems. Part 1: Application to the visibility polygon query problem
[CS-8913-PT-1] 16 p2299 N90-23098
An algebric approach to infinite data structures
[CS-8909] 16 p2327 N90-23265
Linear-quadratic problems and the Riccati equation
[MEMO-COSOR-89-26] 17 p2459 N90-24037
Distributed mission planning technology for Columbus
18 p2501 N90-24288
Conca enable structures for decomposable problems
[RUU-CS-89-16] 18 p2601 N90-24810
Trade-offs in non-reversing diameter
[RUU-CS-89-22] 18 p2602 N90-24813
Maintaining multiple representations of dynamic data structures
[RUU-CS-88-27] 18 p2634 N90-25005
On rectilinear link distance
[RUU-CS-89-13] 18 p2634 N90-25008
Atomic snapshots of shared memory
[AD-A222765] 20 p2904 N90-26520
A structure for maturing intelligent tutoring system student models 21 p3047 N90-27320
Maintenance of a minimum spanning forest in a dynamic planar graph
[AD-A221425] 21 p3054 N90-27362
Encoding techniques for complex information structures in connectionist systems
[NASA-CR-186942] 22 p3238 N90-28362
Treatment of systematic errors 2: Fusion of ultrasound and visual sensor data
[DE90-014780] 23 p3334 N90-28850
Analysis and synthesis of robust data structures
[AD-A224568] 24 p3558 N90-30131

DATA SYSTEMS
NT AIR DATA SYSTEMS
The large European Acoustic Facility at ESTEC
02 p0187 N90-11067
A methodology for the design of continuous-dataflow synchronous systems
[PB89-184360] 02 p0274 N90-11564
Fast sampling and stability of nonlinear sampled-data systems. Part 1: Existence theorems
[RR-340-PT-1] 03 p0398 N90-12276
Slow sampling and stability of nonlinear sampled-data systems
[RR-342] 03 p0398 N90-12277
Building a user-friendly data dictionary system in ORACLE
[DE89-014878] 03 p0417 N90-12397
The Hipparcos Mission. Prelaunch status. Volume 1: The Hipparcos satellite
[ESA-SP-1111-VOL-1] 05 p0603 N90-13499
Data handling and telecommunications
05 p0604 N90-13514
On-board software 05 p0605 N90-13518
The SIMBAD data base 05 p0608 N90-13547
Micro-based fact collection tool user's manual
[NASA-CR-180414] 05 p0684 N90-13981
Ada programming guidelines for deterministic storage management
[NASA-CR-181308] 05 p0684 N90-13982
Prototype software reuse environment at Goddard Space Flight Center 06 p0825 N90-14794
MT's algorithm: A new algorithm to search for the optimum set of modulation indices for simultaneous range, command, and telemetry
[NASA-CR-186259] 08 p1057 N90-16110
IUE-ULDA access guide number 1: International Ultraviolet Explorer-Uniform Low Dispersion Archive. Dwarf novae and nova-like stars
[ESA-SP-1114] 08 p1152 N90-16672
Cosmic ray NM-64 neutron monitor data 16
[IFSI-88-21] 08 p1154 N90-16684
Investigation of IGES for CAD/CAE data transfer
08 p1157 N90-16702
The use of efficient broadcast protocols in asynchronous distributed systems
[NASA-CR-186272] 09 p1269 N90-17358
Impact of uncertainty and diagnosticity on classification of multidimensional data with integral and separable displays of system status
[AD-A215966] 10 p1424 N90-18215
Comparison of oculometer and head-fixed reticle with voice or switch and touch panel for data entry on a generic tactical air combat display
[AD-A217231] 13 p1855 N90-20646
The Real Time Interactive Display Environment (RTIDE), a display building tool developed by Space Shuttle flight controllers 13 p1857 N90-20654
The Real Time Display Builder (RTDB)
13 p1857 N90-20656
Cockpit display of hazardous wind shear information
14 p1905 N90-20924
Weather data dissemination to aircraft
14 p1907 N90-20934
On board cross support scenarios
[INPE-5005-PRE/1562] 14 p1967 N90-21268
Analysis and modelling of spatial data proposal of a system for CBERS
[INPE-4911-PRE/1512] 14 p1997 N90-21445
NSSDC data listing
[NASA-TM-102989] 15 p2180 N90-22456
NASA Information Sciences and Human Factors Program
[NASA-TM-4190] 15 p2194 N90-22529

A test matrix sequencer for research test facility automation
[NASA-TM-103108] 17 p2357 N90-23416
Performance analysis of CCSDS path service
[NASA-CR-180699] 17 p2364 N90-23457
Research and technology 1989
[NASA-TM-100369] 17 p2486 N90-24219
Satellite data archiving: US and foreign activities and plans for environmental information
[GAO/RCED-88-201] 18 p2633 N90-25001
Data conversions in abstract data types
[RUU-CS-88-30] 18 p2634 N90-25006
Military space operations: Shuttle and satellite computer systems do not meet performance objectives
[GAO/IMTEC-88-7] 18 p2635 N90-25014
Artificial intelligence for multi-mission planetary operations 19 p2732 N90-25532
An approach to a real-time distribution system 19 p2733 N90-25535
A global common-user system for the provision of HF propagation data 20 p2845 N90-26180
Application of audio/speech recognition for military applications 21 p2993 N90-27014
Lidar instruments proposed for Eos 21 p3016 N90-27145
Onboard processor technology review 21 p3017 N90-27152
Evaluation of EDR-3 vibration, shock, temperature, and humidity recording unit
[NASA-CR-184006] 22 p3177 N90-28028
A guide to the National Space Science Data Center
[NASA-TM-89637] 24 p3565 N90-30167

DATA TRANSFER (COMPUTERS)
Transferring data objects: A focused Ada investigation
[NASA-CR-186065] 06 p0823 N90-14786
Multiple crossbar network: A switched high-speed local network
[DE90-001839] 06 p0831 N90-14833
Access to multiple underlying systems in Janus
[AD-A214585] 09 p1264 N90-17329
Loran C monitor: Facilities Central Processing Unit (FCPU) port evaluation
[DOT/FAA/CT-TN89/57] 10 p1318 N90-17623
Packet telemetry standard
[ESA-PSS-04-106-ISSUE-1] 11 p1467 N90-18447
Simulating simultaneous processes with APL
[MEMO-INF-89-47] 11 p1547 N90-18906
A scheme for supporting automatic data migration on multicomputers
[NASA-CR-182038] 16 p2276 N90-22973
Godhavn (Greenland) Geophysical Observatory: Magnetic results, 1984
[ISBN-87-7478-289-4] 17 p2423 N90-23807
CESAR LOCAL BUS
[FFI-89/7011] 17 p2440 N90-23903
JTIDS relative navigation: Principles, architecture, and inertial mixing 24 p3426 N90-29357

DATA TRANSMISSION
NT CODE DIVISION MULTIPLE ACCESS
NT MULTIPLE ACCESS
NT PACKET TRANSMISSION
A prototype silicon compiler in prolog
[AD-A210669] 02 p0257 N90-11452
A methodology for the design of continuous-dataflow synchronous systems
[PB89-184360] 02 p0274 N90-11564
Optical data transmission systems in radiation environment
[DE90-000174] 03 p0405 N90-12322
Spacelab system analysis: The modified free access protocol: An access protocol for communication systems with periodic and Poisson traffic
[NASA-CR-183805] 05 p0602 N90-13497
Data handling and telecommunications 05 p0604 N90-13514
The role of the ground segment 05 p0606 N90-13527
The interface with the data reduction consortia 05 p0606 N90-13528
The use of digital signal processing in satellite communication 05 p0631 N90-13684
Mitigating Doppler shift effect in HF multitone data modem 06 p0764 N90-14441
The characteristics of the HF radio channel and its influence on modern HF data communication system design 06 p0765 N90-14448
Research in optical interconnection techniques
[AD-A214028] 07 p0993 N90-15739
Implementation of adaptive arrays in the block oriented systems simulator
[AD-A215545] 09 p1171 N90-16774
Development of a parallel link model for meteor burst communication
[AD-A215629] 09 p1208 N90-17001
An adaptive ARQ (Automatic Repeat Request) strategy for packet switching data communication networks
[AD-A216597] 11 p1497 N90-18615
Performance of the all-digital data-transition tracking loop in the advanced receiver 12 p1643 N90-19440
Operational evaluation of initial data link air traffic control services, volume 1
[DOT/FAA/CT-90/1-VOL-1] 12 p1648 N90-19472
Investigation of a photovoltaic/battery hybrid system for powering the high arctic data communications system
[AD-A218353] 13 p1798 N90-20319
A real-time parallel pipelined data-flow image-processing system
[DE90-008324] 13 p1864 N90-20691
Optimization of the effective GPS data rate 14 p1907 N90-20932
VLSI single-chip (255,223) Reed-Solomon encoder with interleaver
[NASA-CASE-NPO-17280-1-CU] 14 p1933 N90-21061
SAR image coding 14 p1964 N90-21246
An introduction to high frequency radioteletype systems
[PB90-145533] 14 p1965 N90-21252
A correlation-spectral method for line detection on noisy data
[DE90-007925] 14 p1967 N90-21266
Subsystem TM Precision: Progress and perspective
[INPE-5006-PRE/1563] 14 p2000 N90-21461
CAMAC memory module: MEMO-32
[DE90-759846] 14 p2012 N90-21526
Microwave Landing System (MLS) remote monitoring subsystem/remote maintenance monitoring system
[DOT/FAA/PS-89/2] 15 p2050 N90-21749
Scalable coherent interface
[DE90-008011] 15 p2149 N90-22277
Extremely high data-rate, reliable network systems research
[NASA-CR-186359] 15 p2149 N90-22278
Performance of gigabit FDDI 15 p2150 N90-22283
Modelling high data rate communication network access protocol 15 p2150 N90-22285
Extensibility and limitations of FDDI 15 p2151 N90-22286
A carrier sensed multiple access protocol for high data base rate ring networks 15 p2151 N90-22288
Technologies for electronic transfer of information: The present state and trends in Europe 15 p2177 N90-22441
Technology for electronic transfer of information: The present and future in North America 15 p2177 N90-22442
Megatendances 15 p2178 N90-22445
Document delivery via ISDN or satellite networks 15 p2178 N90-22446
Evaluation of a prototype 6 tone modem
[RAE-TM-FM-28] 16 p2228 N90-22708
Performance analysis of Aloha networks with power capture and near/far effect
[AD-A218739] 16 p2229 N90-22717
Applicability of Asynchronous Transfer Mode (ATM) techniques to satellite communications systems
[MBB-UK-0059-89-PUB] 17 p2392 N90-23625
ISDN in the local environment: The CISLAN project
[MEMO-INF-89-70] 17 p2452 N90-23985
Rate-based congestion control in networks with smart links, revision
[NASA-CR-186698] 17 p2452 N90-23987
Automatic speech recognition in air-ground data link 18 p2640 N90-25037
A few modeling and rendering techniques for computer graphics and their implementation on ultra hardware 18 p2640 N90-25038
The disturbance processes on the data links of the mode-S air traffic control system
[ETN-90-96960] 20 p2806 N90-25965
Experimental analysis of the HF linkage 20 p2845 N90-26181
Channel selection and control procedures in an automatic HF system 20 p2847 N90-26193
Experimentation of a transmission system data processing by meteor bursts 20 p2850 N90-26207
System factors to be considered in assessing propagation effects on modern digital satellite communications systems 20 p2850 N90-26208
Microspacecraft and Earth observation: Electrical field (ELF) measurement project
[NASA-CR-186821] 20 p2888 N90-26436
Applications for the scalable coherent interface
[DE90-011795] 20 p2903 N90-26514
Design of a universal protocol subsystem architecture: Specification of functions and services
[EUT-89-E-230] 20 p2912 N90-26569
A methodology for benchmarking distributed database management systems
[DE90-007801] 20 p2935 N90-26702
Meteor burst communications systems
[AD-A221675] 21 p2997 N90-27037
Brief state-of-the-art review on optical communications for the NASA ISES workshop 21 p3017 N90-27153
Applications of ISES for geology 21 p3017 N90-27154
New features of JAL's ground station 22 p3105 N90-27633
Replay and transmission of AIMS-data to mainframe computer using remote transcribers 22 p3105 N90-27634
Adaptive polarization diversity detection scheme for coherent communications and interferometric fiber sensors
[AD-D014479] 22 p3163 N90-27938
Secure Data Network System (SDNS) network, transport, and message security protocols
[PB90-198946] 23 p3318 N90-28757
Automated CADAM data transfer: User's manual
[DE90-014871] 24 p3530 N90-29963

DATING
U CHRONOLOGY
U TIME MEASUREMENT

DAYTIME
Role of chemical effects in daytime high latitude trough formation
[AD-A211772] 04 p0518 N90-12989
Beyond the IDMY (International Daylighting Measurements Year): A network instrument for low-cost data acquisition
[DE90-002722] 06 p0815 N90-14740
Cumulative airport noise exposure metrics: An assessment of evidence for time-of-day weightings, revision
[AD-A214878] 09 p1170 N90-16773
Study of the atmospheric emissions of OI wavelength 557.7 nm and O2 (0,0) wavelength 761.9 nm in the equatorial region utilizing measurement of photometer on-board a rocket
[INPE-4811-TDL/358] 11 p1533 N90-18827
Photon statistical limitations for daytime optical tracking 12 p1643 N90-19442
Daytime wind valleys adjacent to the Great Salt Lake
[DE90-008991] 15 p2133 N90-22190
Comparison of 30 day integrations with and without interactive clouds 22 p3222 N90-28274

DBS (SATELLITES)
U DIRECT BROADCAST SATELLITES

DC (CURRENT)
U DIRECT CURRENT

DC 10 AIRCRAFT
The NASA digital VGH program: Exploration of methods and final results. Volume 5: DC 10 data 1981-1982, 129 hours
[NASA-CR-181909-VOL-5] 13 p1756 N90-20084
Brake performance of the McDonnell Douglas DC-10-30/40 during high speed, high energy rejected takeoffs
[PB90-917004] 14 p1920 N90-21000

DE HAVILLAND AIRCRAFT
NT DHC 2 AIRCRAFT

DE LAVAL NOZZLES
U CONVERGENT-DIVERGENT NOZZLES

DEACCLIMATIZATION
U ACCLIMATIZATION

DEACTIVATION
Space shuttle: The future of the Vandenberg launch site needs to be determined
[GAO/NSIAD-88-158] 18 p2509 N90-24337

DEAD RECKONING
Carin and GPS: The combination of dead reckoning, map matching and satellite navigation in a hybrid automobile navigation system
[ETN-90-95451] 12 p1602 N90-19220
Observability of relative navigation using range-only measurements 24 p3427 N90-29360

DEADWEIGHT
U STATIC LOADS

DEATH
The investigation of particulate matter in the lungs of smoke inhalation death victims 10 p1317 N90-17617
The importance of pathophysiological parameters in fire modelling of aircraft accidents 10 p1317 N90-17618
Modelling time to incapacitation and death from toxic and physical hazards in aircraft fires 10 p1318 N90-17619

DEBRIS
NT SPACE DEBRIS
Debris/ice/TPS assessment and photographic analysis for Shuttle Mission STS-28R
[NASA-TM-102152] 01 p0016 N90-10079

Debris/ice/TPS assessment and photographic analysis for Shuttle Mission STS-34
[NASA-TM-102153] 05 p0594 N90-13447
Hydrodynamics code calculations of debris clouds produced by ball-plate impacts
[DE89-015270] 07 p0939 N90-15439
Dust bands in the asteroid belt
[NASA-CR-186301] 07 p1014 N90-15873
Studies of density distributions in one-dimensional shock-induced debris clouds
[DE90-004089] 08 p1085 N90-16282
Zodiacal dust bands: Their relation to asteroid families
[AD-A216025] 11 p1590 N90-19170
In-line wear monitor
[AD-A217799] 13 p1757 N90-20091
Debris/ice/TPS assessment and photographic analysis for Shuttle Mission STS-36
[NASA-TM-102789] 16 p2205 N90-22583
Wear of gold-plated contacts: Microscopic aspects, role of oxygen 18 p2538 N90-24479
Debris/ice/TPS assessment and photographic analysis for shuttle mission STS-31R
[NASA-TM-102790] 20 p2819 N90-26040
Hypervelocity impact shield
[NASA-CASE-MSC-21420-1] 21 p2966 N90-26858
Debrix/ice/TPS assessment and photographic analysis of Shuttle Mission STS-32R
[NASA-TM-102787] 22 p3124 N90-27733

DEBUGGING
U CHECKOUT

DEBYE TEMPERATURE
U SPECIFIC HEAT

DECAMETRIC WAVES
Jupiter's drifting decametric bursts with the changing time scale
[DE90-618870] 15 p2192 N90-22517

DECARBURIZATION
The influence of carbide precipitation on the creep rupture behavior of high temperature alloys
[JUEL-2211] 08 p1046 N90-16044

DECAY
NT NEUTRON EMISSION
NT PLASMA DECAY
NT RADIOACTIVE DECAY
NT SPACECRAFT GLOW
NT WEAK ENERGY INTERACTIONS
NT WEAK INTERACTIONS (FIELD THEORY)
Atomic effects of beta decay in astrophysics and in elementary particle physics 01 p0141 N90-10811
The behavior of hydrazine vapor in an environmental chamber under simulated atmospheric conditions 02 p0203 N90-11161
The decay of viscoelastic fluid jets
[ETN-89-94667] 02 p0221 N90-11270
Cosmic strings and baryon decay catalysis
[NASA-CR-186074] 04 p0566 N90-13299
Biomodal spontaneous fission
[DE90-001516] 06 p0840 N90-14886
Thermal and statistical properties of nuclei and nuclear systems
[DE90-000183] 07 p0990 N90-15717
Combined effect of isotopic substitution, temperature, and magnetic field on the lifetimes of triplet biradicals
[AD-A219711] 17 p2372 N90-23509
The decay of neutron star magnetic fields 19 p2769 N90-25737

DECAY RATES
Dissociation and vibrational relaxation of XeF by various collision partners
[AD-A210789] 02 p0227 N90-11300
Luminescence probe studies of ionomers. Part 3: Distribution of decay rate constants for tris bipyridyl Ruthenium(II) in Nafion membranes
[AD-A215885] 10 p1359 N90-17880
Decay rate and other properties of the positronium negative ion 11 p1560 N90-18987
Pulsed and modulated passage NMRON studies of cobalt-iron alloys 17 p2470 N90-24118
Decay rate and resonance fluorescence spectrum of a molecule near a composite material surface
[AD-A219692] 19 p2671 N90-25192
Scaling behaviour of relaxation dependencies in metaloxide superconductors 22 p3138 N90-27802

DECELERATION
Independent Orbiter Assessment (IOA): Assessment of the landing/deceleration (LDG/DEC) subsystem FMEA/CIL
[NASA-CR-185570] 02 p0172 N90-10966
An open-loop transient thermodynamic model of the Cougar turbojet
[AD-A211774] 03 p0307 N90-11745
Flight test investigation of flight director and autopilot functions for helicopter decelerating instrument approaches
[DOT/FAA/CT-TN89/54] 22 p3121 N90-27724
Reentry trajectory optimization and control 22 p3127 N90-27746

DECELERATORS
U BRAKES (FOR ARRESTING MOTION)

DECISION ELEMENTS
U LOGICAL ELEMENTS

DECISION MAKING
Cost metric algorithms for internetwork applications
[AD-A210324] 01 p0105 N90-10597
A decision support approach to the file allocation problem in a distributed computing system 01 p0107 N90-10609
Learning to make decisions: When incentives help and hinder
[AD-A210185] 01 p0135 N90-10779
A theory of collective induction
[AD-A210553] 01 p0135 N90-10780
Effects of stress on judgment and decision making in dynamic tasks
[AD-A210605] 01 p0135 N90-10781
Comprehension processes in mechanical reasoning
[AD-A210459] 02 p0255 N90-11442
Electronic publishing: Guide to selection
[PB89-214753] 02 p0256 N90-11448
Preference propagation in temporal/capacity constraint graphs
[AD-A210668] 02 p0264 N90-11506
On the generation of a variable structure airport surface traffic control system
[AD-A211306] 03 p0304 N90-11724
On the asymptotic optimality of certain empirical Bayes simultaneous testing procedures
[AD-A211649] 03 p0397 N90-12270
Three stages and two systems of visual processing
[AD-A212670] 04 p0525 N90-13032
Operational Decision Aids for Exploiting or Mitigating Electromagnetic Propagation Effects
[AGARD-CP-453] 06 p0757 N90-14405
Propagation assessment and tactical decision aids 06 p0757 N90-14407
Human factors aspects of decision support systems 06 p0757 N90-14408
Propagation-based decision aids in the U.S. Navy 06 p0757 N90-14410
Engineer's Refractive Effects Prediction System (EREPS) 06 p0758 N90-14411
PROPHET and future signal warfare decision aids 06 p0758 N90-14412
Decision-aid design factors in connection with HF communication and emitter location disciplines 06 p0758 N90-14413
The parabolic equation approach to predicting tropospheric propagation effects in operational environments 06 p0759 N90-14418
Communication Overview Program (COP) 06 p0762 N90-14435
TROPO: A technique for predicting propagation and modem performance of digital troposcatter systems 06 p0764 N90-14444
Planning systems for autonomous legged vehicles
[AD-A214242] 07 p0942 N90-15458
International aspects of restrictions of ozone-depleting substances
[DE90-001813] 07 p0957 N90-15534
Model for measuring complex performance in an aviation environment
[DE90-002055] 07 p0967 N90-15585
Where to from here. Future applications of mental models of complex performance
[DE90-002091] 07 p0967 N90-15586
A qualitative architecture for understanding policy responses to global change
[DE90-003936] 08 p1099 N90-16364
Using goal programming to determine the optimal engine mix for UH-1 helicopters
[AD-A214893] 09 p1168 N90-16762
Expertise, stress, and pilot judgment 09 p1255 N90-17284
Job planning and execution monitoring for a human-robot symbiotic system
[DE90-004464] 09 p1261 N90-17315
Piecewise linear-quadratic programming and its applications
[AD-A214489] 09 p1264 N90-17328
A model for comparing game theory and artificial intelligence decision making processes
[AD-A215418] 09 p1271 N90-17369
Decision-analytic approach to rule-based expert system development using GPS (Global Positioning System) as the model
[AD-A216179] 10 p1319 N90-17626
Application of Bayesian reliability concepts to cruise missile electronic components
[AD-A216208] 10 p1394 N90-18059
Expert systems development methodology
[AD-A216892] 10 p1421 N90-18191
A colony architecture for an artificial creature
[AD-A216802] 11 p1549 N90-18918
Optimum selection procedures in multi-stage screening, reliability, and time
[AD-A216811] 11 p1553 N90-18942
Artificial intelligence issues related to automated computing operations 12 p1637 N90-19404
Distributed detection by a large team of sensors in tandem
[AD-A216607] 12 p1708 N90-19807
Executive information systems for providing next generation strategic information: An evaluation of EIS (Executive Information System) software and recommended applicability within the FAA computing environment
[AD-A216672] 12 p1726 N90-19920
On optimal distributed decision architectures in a hypothesis testing environment
[AD-A217824] 13 p1790 N90-20274
Controlling Summer Heat Islands: Proceedings
[DE90-008075] 13 p1830 N90-20508
Brain activity during tactical decision-making. Part 3: Relationships between probe-evoked potentials, simulation performance, and on-job performance
[AD-A217207] 13 p1854 N90-20638
Information gathering and decisionmaking under stress
[AD-A218233] 13 p1854 N90-20643
Aiding the decision maker: Perceptual and cognitive issues at the human-machine interface
[AD-A217862] 13 p1855 N90-20648
Design decision making with multiple interacting criteria and varying relative weights
[AD-A218027] 13 p1869 N90-20721
Insights into complex human performance
[DE90-006957] 15 p2137 N90-22214
The RACE (research and development in advanced technologies for Europe) program: A 1989 update
[AD-A218509] 16 p2228 N90-22713
RF network selection in a rule-based system. NOSC project ZE68: Cost metric algorithms for internetwork applications
[AD-A219389] 16 p2301 N90-23116
Economic values for evaluation of Federal Aviation Administration investment and regulatory programs
[AD-A219882] 17 p2343 N90-23343
Aeronautical decisionmaking for air ambulance program administrators
[DOT/FAA/DS-88/8] 17 p2347 N90-23368
The effects of climate change on energy planning and operations in the Pacific Northwest. Volume 1: Overview
[DE90-009464] 17 p2425 N90-23816
The effects of climate change on energy planning and operations in the Pacific Northwest. Volume 2: Technical background
[DE90-009465] 17 p2425 N90-23817
Perception of complex auditory patterns
[AD-A219626] 17 p2434 N90-23867
Northeast Artificial Intelligence Consortium. Volume 3: The Versatile Maintenance Expert System research project
[AD-A218716] 17 p2453 N90-23993
A decision support system for control and automation of dynamical processes
[AD-A219501] 17 p2454 N90-23995
A solution for the variance-penalized Markov decision problem based on parametric linear programming
[TW-90-02] 17 p2467 N90-24100
Multiple beam optical processing
[AD-A219048] 17 p2471 N90-24129
National Educators' Workshop: Update 1989 Standard Experiments in Engineering Materials Science and Technology
[NASA-CP-3074] 18 p2513 N90-24350
Manual and computer-aided materials selection for industrial production: An exercise in decision making 18 p2516 N90-24368
Pilot decision-making training
[AD-A221349] 18 p2585 N90-24720
A RUTCOR project in discrete applied mathematics
[AD-A221191] 18 p2604 N90-24831
Solving problems by interrogating sets of knowledge systems: Toward a theory of multiple knowledge systems 18 p2629 N90-24979
Keeping the dream alive: Managing the Space Station Program, 1982 to 1986
[NASA-CR-4272] 18 p2633 N90-25000
Explanation of Bayesian conditioning for decision support systems 18 p2633 N90-25002
Materials and processes for spacecraft: The ESTEC approach
[ESA-STM-244] 19 p2667 N90-25176
Nonparametric selection, ranking and testing
[AD-A219254] 19 p2752 N90-25636

Object-oriented design: Deriving conceptual solutions to large-scale information processing problems
[DE90-011189] 19 p2763 N90-25699
NASA project status reports: Congressional requirements can be met, but reliability must be ensured
[GAO/NSIAD-90-40] 20 p2843 N90-26169
Survey of applicability of electric vehicles (EVs) in specific regions such as resorts
[DE90-503592] 20 p2871 N90-26336
Pilot interaction with automated airborne decision making systems
[NASA-CR-186730] 20 p2899 N90-26492
A study of the asymptotic properties of least square estimators for multiple phase regression problems
[ETN-90-97244] 20 p2921 N90-26620
Effect of organizational structure on performance of decision making teams
[AD-A223160] 20 p2934 N90-26697
The lessons of Varsovian's reconnaissance
[NASA-TM-103207] 20 p2951 N90-26789
Case-based reasoning in design: An apologia
21 p3045 N90-27308
Automated extraction of knowledge for model-based diagnostics 21 p3047 N90-27318
Documentation and knowledge acquisition
21 p3048 N90-27325
Application of Meteorological Satellite (METSAT) data to support United States forces in the North Atlantic Treaty Organization (NATO) 21 p3068 N90-27440
Effects of organizational structure on performance: Experimental results
[AD-A222871] 21 p3085 N90-27543
Replay and transmission of AIMS-data to mainframe computer using remote transcribers
22 p3105 N90-27634
Severe thunderstorm cases of July 1988 through June 1989
[PB90-226424] 22 p3229 N90-28311
An environment to support problem solving
[ISBN-90-9003151-0] 22 p3259 N90-28458
Research in command and control for the Dutch Army Corps (1NL)
[IZF-1989-28] 23 p3318 N90-28760
Chasing a specter: Risk management for global environmental change
[DE90-014455] 23 p3347 N90-28917
A methodology for the objective measurement of pilot situation awareness 23 p3357 N90-28974
Situational Awareness Rating Technique (SART): The development of a tool for aircrew systems design
23 p3357 N90-28975
Towards a future cockpit: The prototyping and pilot integration of the Mission Management Aid (MMA)
23 p3358 N90-28979
Cognition versus sensation: A paradigm for reorientation
[IZF-1989-20] 23 p3361 N90-28995
Exploiting map plans as resources for action
23 p3367 N90-29028
Perceptual telerobotics 23 p3374 N90-29063
Inference engine for expert systems
[INPE-4565-PRE/1306] 23 p3382 N90-29104
Documenting the decision structure in software development
[NASA-CR-186865] 23 p3382 N90-29108
Overcoming rule-based rigidity and connectionist limitations through massively-parallel case-based reasoning
[NASA-CR-186963] 23 p3384 N90-29117
Prediction, control, and decision-making aspects for chaotic systems
[DE90-014452] 23 p3402 N90-29224
The effects of management support on the successful implementation of group decision support systems
[AD-A224473] 23 p3404 N90-29241
QTA (QUESTIONNAIRE-TASK-ANALYSIS): An electronic tool for job/task analysis
[DE90-008944] 24 p3499 N90-29778
What kind of computation is intelligence. A framework for integrating different kinds of expertise
24 p3506 N90-29817
Use of graphics in decision aids for telerobotic control: (Parts 5-8 of an 8-part MIT progress report)
24 p3508 N90-29829
Coordination in a hierarchical multi-actuator controller
24 p3520 N90-29900
Temporal logics meet telerobotics
24 p3521 N90-29905
Reactive behavior, learning, and anticipation
24 p3521 N90-29908

DECISION THEORY
NT STATISTICAL DECISION THEORY
A brief bibliography of statistical classification procedures: Decision-theoretic approach
[AD-A210276] 01 p0115 N90-10663
Application of a hybrid generation/utility assessment heuristic to a class of scheduling problems
[NASA-TM-102367] 01 p0117 N90-10674
Task analysis of the UH-60 mission and decision rules for developing a UH-60 workload prediction model. Volume 1: Summary report
[AD-A210763] 02 p0255 N90-11446
On finding the largest normal mean and estimating the selected mean
[AD-A211628] 03 p0394 N90-12245
A new decision rule for model structure identification of a class of nonlinear dynamic systems
[RR-360] 04 p0539 N90-13122
Defending against a space blockade: CADRE paper
[AD-A215681] 09 p1276 N90-17398
Decision-analytic approach to rule-based expert system development using GPS (Global Positioning System) as the model
[AD-A216179] 10 p1319 N90-17626
Impact of uncertainty and diagnosticity on classification of multidimensional data with integral and separable displays of system status
[AD-A215966] 10 p1424 N90-18215
Distributed detection by a large team of sensors in tandem
[AD-A216607] 12 p1708 N90-19807
On optimal distributed decision architectures in a hypothesis testing environment
[AD-A217824] 13 p1790 N90-20274
Design decision making with multiple interacting criteria and varying relative weights
[AD-A218027] 13 p1869 N90-20721
Automatic classification of images
[AD-D014437] 14 p1966 N90-21260
Recognition and analysis of aircraft targets by radar, using structural pattern representations derived from polarimetric signatures 15 p2074 N90-21879
A decision-making aid for multi-layer radar absorbent coverings
[ESA-TT-1173] 19 p2684 N90-25267
Communications and tracking expert systems study
[NASA-CR-185935] 21 p2992 N90-27004
The composite load spectra project
21 p3047 N90-27323
Using decision-tree classifier systems to extract knowledge from databases 21 p3048 N90-27328
A hypothesis test of cumulative sums of multinomial parameters
[AD-A221466] 21 p3067 N90-27434
A design philosophy for multi-layer neural networks with applications to robot control 23 p3368 N90-29033
Problems in probability, statistics, and reliability
[AD-A224152] 24 p3540 N90-30016

DECISIONS
Establishing viable task domains for telerobot demonstrations 24 p3518 N90-29886

DECKS (FLOORS)
U FLOORS

DECLINATION
Galileo Earth approach navigation using connected-element interferometer phase-delay tracking
15 p2075 N90-21884

DECODERS
NT VITERBI DECODERS
On the decoder error probability of linear codes
04 p0486 N90-12793
Performance of the image statistics decoder in conjunction with the Goldstone-VLA array
04 p0487 N90-12796
Memory management in traceback Viterbi decoders
12 p1643 N90-19443
Quantization effects in Viterbi decoding rate 1/n convolutional codes 12 p1644 N90-19445
Big Viterbi Decoder (BVD) results for (7,1/2) convolutional code 12 p1644 N90-19446
Fast transform decoding of nonsystematic Reed-Solomon codes 12 p1644 N90-19447
A VLSI decomposition of the deBruijn graph
15 p2077 N90-21895
Validity of the two-level model for Viterbi decoder gap-cycle performance 15 p2077 N90-21896
Finding the complete path and weight enumerators of convolutional codes 15 p2077 N90-21897
A VLSI design for a systolic Viterbi decoder
15 p2077 N90-21899
Miniaturization of flight deflection measurement system
[NASA-CASE-LAR-13628-1] 17 p2406 N90-23707
HDTV: A chance to enhance television colorimetry
[BBC-RD-1990/2] 18 p2543 N90-24515
A hybrid M-algorithm/sequential decoder for convolutional and trellis codes
[NASA-CR-186863] 20 p2906 N90-26528
VLSI architecture for a Reed-Solomon decoder
[NASA-CASE-NPO-17897-1-CU]
21 p2998 N90-27040

DECODING
On the decoder error probability of linear codes
04 p0486 N90-12793
Frame synchronization methods based on channel symbol measurements 04 p0486 N90-12795
Error control techniques for satellite and space communications
[NASA-CR-182751] 05 p0631 N90-13685
SN 1987: A telemetry decoding system
05 p0663 N90-13875
Fractal-based image compression
[AD-A217302] 13 p1865 N90-20699
A VLSI decomposition of the deBruijn graph
15 p2077 N90-21895
An adaptive vector quantization scheme
15 p2077 N90-21898
A VLSI design for a systolic Viterbi decoder
15 p2077 N90-21899
On decoding of multi-level MPSK modulation codes
[NASA-CR-186601] 15 p2146 N90-22261
The LORE-interpreter: Notes on the implementation
[REPT-89-60] 17 p2445 N90-23932
The Delfi3-interpreter: Notes on the implementation
[REPT-89-72] 17 p2445 N90-23935
HDTV: A chance to enhance television colorimetry
[BBC-RD-1990/2] 18 p2543 N90-24515
Failure of the ERBE scanner instrument aboard NOAA 10 spacecraft and results of failure analysis
[NASA-TM-102661] 19 p2694 N90-25328
Multi-level trellis coded modulation and multi-stage decoding
[NASA-CR-186861] 19 p2743 N90-25593
A hybrid M-algorithm/sequential decoder for convolutional and trellis codes
[NASA-CR-186863] 20 p2906 N90-26528
The speech signal 21 p2992 N90-27008
Tutorial on Reed-Solomon error correction coding
[NASA-TM-102162] 22 p3234 N90-28339
Automated system for meteorological analysis
[INPE-4586-TDL/332] 23 p3352 N90-28945
Book of abstracts of the 1st Benelux-Japan Workshop on Information and Communication Theory
[PB90-191446] 24 p3556 N90-30124

DECOMPOSITION
NT AMMONOLYSIS
NT CRACKING (CHEMICAL ENGINEERING)
NT GLYCOLYSIS
NT HYDROCRACKING
NT HYDROGENOLYSIS
NT PHOTODECOMPOSITION
NT PHOTODISSOCIATION
NT PHOTOLYSIS
NT PROPELLANT DECOMPOSITION
NT PYROLYSIS
NT THERMAL DECOMPOSITION
Chemistry of nitromethane at very high pressure
[DE89-008016] 01 p0039 N90-10215
Development of metastable processing paths for high temperature alloys
[AD-A210550] 01 p0045 N90-10254
Study of the NO3 radical decomposition reaction and the N2O5 in equilibrium with NO3 + NO2 equilibrium constant
[PB89-208961] 01 p0085 N90-10480
Time-resolved mass spectrometry technique for studying fast transient CHNO explosive decomposition kinetics
[DE89-016540] 02 p0193 N90-11101
Enhanced oxidation and solovolysis reactions in chemically inert microheterogeneous systems
[AD-A210748] 02 p0195 N90-11110
Quantum chemical investigations of the mechanism of cationic polymerization and theoretical prediction of crystal densities and decomposition pathways of energetic molecules
[AD-A210322] 02 p0200 N90-11143
Trace metal catalysis of hydrazine decomposition: The role of chromium 02 p0204 N90-11163
A prototype silicon compiler in prolog
[AD-A210669] 02 p0257 N90-11452
A multidomain spectral collocation method for the Stokes problem
[NASA-CR-181876] 03 p0396 N90-12266
An atom probe study of phase decomposition in three iron meteorites
[DE89-017581] 03 p0421 N90-12420
Metallo-organic decomposition process for dielectric films
[AD-A211590] 04 p0495 N90-12849
Effect of adsorbed arsenic on the decomposition rate of nickel hydride
[AD-A213245] 05 p0621 N90-13624
High temperature chemistry of complex vaporization/decomposition processes
[DE89-016559] 06 p0740 N90-14306

Fast transit gas- and condensed-phase chemistry of energetic materials
[DE90-001656] 06 p0755 N90-14395
Iterative methods of domain decomposition with cross-points for the solution of discrete elliptic problems
[DE90-000719] 06 p0835 N90-14854
A novel heat resistant blend produced by compositional quenching: A thermoplastic polyimide impact modified with a fluoroelastomer
[AD-A213724] 07 p0912 N90-15273
Simultaneous thermal analysis techniques for characterization of energetic materials
[DE90-003028] 07 p0914 N90-15289
The parallel decomposition of linear programs
[DE90-003538] 07 p0974 N90-15625
Fundamental studies of beta phase decomposition modes in titanium alloys
[AD-A214424] 08 p1044 N90-16035
Reactions of atmospheric species with clean and H, C, and O implanted species
[AD-A214602] 09 p1244 N90-17218
An analysis of scatter decomposition
[NASA-CR-181978] 08 p1276 N90-17396
Breeding of hydrogen producing anaerobic bacteria. Cellulase secretion from transformed Escherichia coli JM109
[DE90-710739] 10 p1410 N90-18133
Decomposition for optimal synthesis in a parallel computing environment 10 p1419 N90-18184
Thermal analysis of polymer composites
[AD-A216947] 11 p1490 N90-18578
Distributed decomposition of block-angular linear programs on a hypercube computer
[AD-A216433] 11 p1545 N90-18893
Determination of the mechanism of decomposition of energetic molecules
[AD-A217061] 12 p1633 N90-19388
A comparison between the propagators method and the decomposition method for nonlinear equations
[DE90-005783] 12 p1704 N90-19781
Condensed phase kinetic deuterium isotope effects in high energy phenomena: Mechanistic investigations and relationships
[AD-A217161] 13 p1770 N90-20156
Developments in solar photocatalysis for destruction of organics in water
[DE90-007685] 13 p1771 N90-20162
Domain decomposition for a boundary-value problem with a shock layer
[DE90-007857] 13 p1877 N90-20762
Conceptual design optimization study
[NASA-CR-4298] 15 p2051 N90-21755
A discussion on issues relating to multiblock grid generation 15 p2095 N90-21991
Multilevel decomposition approach to the preliminary sizing of a transport aircraft wing
[NASA-CR-4296] 16 p2200 N90-22557
Overcoming the Bellman's curse of dimensionality in large optimization problems
[NASA-TM-102662] 17 p2352 N90-23391
Thermal analysis of Acetylene Terminated Sulfone (ATS) resin
[AD-A220775] 17 p2381 N90-23558
Spectral methods for electromagnetic propagation and diffraction
[AD-A220291] 17 p2393 N90-23632
Discrete mathematics for communication systems
[AD-A220430] 17 p2457 N90-24022
A study of the phase decomposition of Fe-Ni-Al-Mo alloys
[DE90-010143] 18 p2524 N90-24406
The measurement of composition during the early stages of the spinodal decomposition of Fe-Cr alloys
[DE90-010471] 18 p2525 N90-24408
Interaction of the large eddy structure in the inner-half of a turbulent boundary layer 18 p2551 N90-24561
Input/output algorithm for M-dimensional rectangular domain decompositions on N-dimensional hypercube multicomputers
[DE90-010494] 18 p2594 N90-24762
The HK singular value decomposition of rank deficient matrix triplets
[DE90-010114] 18 p2598 N90-24784
Improved self-reduction algorithms for graphs with bounded tree width
[RUU-CS-88-29] 18 p2601 N90-24805
Arcjet load characteristics
[NASA-TM-103190] 19 p2669 N90-25181
The bit full-decomposition of sequential machines
[EUT-89-E-223] 20 p2904 N90-26516
The full-decomposition of sequential machines with the separate realization of the next-state and output functions
[EUT-89-E-222] 20 p2909 N90-26547
Closed-form solution of decomposable stochastic models
[NASA-TM-103466] 20 p2920 N90-26619
Microstructural development in HSLA-100 steel weld metals
[AD-A222105] 21 p2982 N90-26944
Synthesis of Y1Ba2Cu3O(sub x) superconducting powders by intermediate phase reaction 22 p3149 N90-27855
Study of the induction time in isothermal decomposition of explosives
[DE90-014906] 23 p3315 N90-28745
A complete analytical solution for the inverse instantaneous kinematics of a spherical-revolute-spherical (7R) redundant manipulator 23 p3363 N90-29006
Relationship between microstructure, spinodal-like decomposition and selective electropolishing of irradiated invar-type alloys
[DE90-015293] 24 p3450 N90-29484
An additive turbulent decomposition of the Navier-Stokes equations implemented on highly parallel computer systems
[AD-A223678] 24 p3468 N90-29595

DECOMPRESSION
U PRESSURE REDUCTION

DECOMPRESSION SICKNESS
Potential for reduction of decompression sickness by prebreathing with 100 percent oxygen while exercising
[AD-A213449] 07 p0966 N90-15581
Statistically based decompression tables 5: Haldane-Vann models for air diving
[AD-A214934] 09 p1251 N90-17261
Decompression sickness affecting the temporomandibular joint
[AD-A220959] 18 p2584 N90-24715
Aircrew life support systems enhancement
[AD-A222626] 20 p2902 N90-26505
Decompression sickness presenting as a viral syndrome
[AD-A223880] 23 p3356 N90-28967

DECONDITIONING
Cardiovascular deconditioning of cosmonauts: Role, importance and applications of the lower body negative pressure
[ETN-90-97507] 23 p3355 N90-28964

DECONTAMINATION
Heterogeneous catalysts in water
[AD-A210742] 01 p0041 N90-10228
Evaluation of mid-to-long term basic research for environmental restoration
[DE89-015621] 02 p0238 N90-11355
Corrosion and corrosion inhibition of metals/alloys in methylphosphonic difluoride and decontaminating solutions
[AD-A212404] 04 p0477 N90-12734
Contamination removal using various solvents and methodologies
[NASA-CR-183747] 05 p0626 N90-13652

DECOUPLING
NT SPIN DECOUPLING
A high-order Lagrangian-decoupling method for the incompressible Navier-Stokes equations
[NASA-CR-181903] 01 p0111 N90-10631
Using the physical structure of a system for control: An illustration
[MEMO-782] 05 p0689 N90-14014
Relatchable launch restraint mechanism for deployable booms 15 p2114 N90-22091
An innovations approach to decoupling of multibody dynamics and control 16 p2280 N90-22994
Almost disturbance decoupling by measurement feedback: A frequency domain analysis
[CWI-BS-R8910] 17 p2455 N90-24005
Dynamic disturbance decoupling for nonlinear systems
[MEMO-835] 17 p2463 N90-24069
The tetrahedral wedge attachment mechanism 18 p2539 N90-24490
Geometric theory for infinite dimensional systems
[PB90-190216] 22 p3242 N90-28383
Geometric theory for infinite dimensional systems
[ETN-90-96922] 23 p3389 N90-29144

DECOYS
NT BALLISTIC MISSILE DECOYS
User's guide to OPUS (Optimal Preferential Utility and Strategies)
[AD-A214364] 10 p1424 N90-18217

DEDUCTION
Expert systems as deductive systems
[CWI-CS-R8825] 04 p0532 N90-13073
On the safe approximation of PROLOG programs
[CWI-CS-R8913] 05 p0683 N90-13978
Optimization of monotonic inference algorithms in propositional and first order logic
[LAAS-89204] 08 p1111 N90-16436
Deductive computer programming, revision
[AD-A219848] 17 p2446 N90-23946
Integrating mono-valued functions in deductive databases: A recursive extension of MILANT
[REPT-90-018] 22 p3239 N90-28370

DEEP SPACE
NT INTERPLANETARY SPACE
NT INTERSTELLAR SPACE
JPRS Report: Science and technology. USSR: Space. Soviet space program to the year 2000
[JPRS-USP-89-008] 06 p0728 N90-14248
Manned spacecraft
[AD-A214218] 07 p0887 N90-15129
Pioneers 10 and 11 deep space missions
[NASA-TM-102269] 10 p1448 N90-18355
High stability radio links 12 p1734 N90-19970
Preliminary results of the peak experiment. ALTAIR deep-space measurements
[AD-A218622] 16 p2229 N90-22714
Space exploration: NASA's deep space missions are experiencing long delays
[GAO/NSIAD-88-128BR] 18 p2635 N90-25015

DEEP SPACE NETWORK
The Telecommunications and Data Acquisition Report
[NASA-CR-185093] 04 p0485 N90-12786
Automated monitor and control for deep space network subsystems 04 p0486 N90-12794
Frame synchronization methods based on channel symbol measurements 04 p0486 N90-12795
DSN 70-meter antenna microwave optics design and performance improvements. Part 2: Comparison with measurements 04 p0487 N90-12800
Stable Kalman filters for processing clock measurement data 04 p0487 N90-12801
A simple model for DSS-14 outage times 04 p0488 N90-12802
The NASA SETI sky survey: Recent developments 04 p0488 N90-12804
JPL reuse program 06 p0825 N90-14795
Environmental Projects. Volume 9: Construction of hazardous materials storage facilities
[NASA-CR-186296] 09 p1244 N90-17216
The Telecommunications and Data Acquisition Report
[NASA-CR-185033] 12 p1642 N90-19434
Determination of Earth orientation using the Global Positioning System 12 p1642 N90-19435
Environmental projects, volume 11. Environmental assessment: Addition to operations building, Mars site
[NASA-CR-186449] 14 p2003 N90-21479
Environmental projects, volume 10. Environmental assessment: New 34-meter antenna at Apollo site
[NASA-CR-186448] 14 p2003 N90-21480
The Telecommunications and Data Acquisition Report
[NASA-CR-186479] 15 p2074 N90-21880
Precise estimation of tropospheric path delays with GPS techniques 15 p2074 N90-21881
The determination of maximum deep space station slew rates for a high Earth orbiter 15 p2075 N90-21882
Microwave analog fiber-optic link for use in the deep space network 15 p2075 N90-21883
Galileo Earth approach navigation using connected-element interferometer phase-delay tracking 15 p2075 N90-21884
Voltage source ac-to-dc converters for high-power transmitters 15 p2075 N90-21886
A real-time signal combining system for Ka-band feed arrays using maximum-likelihood weight estimates 15 p2076 N90-21888
Radiometric tests on wet and dry antenna reflector surface panels 15 p2076 N90-21890
A functional description of the advanced receiver 15 p2076 N90-21891
A VLSI decomposition of the deBruijn graph 15 p2077 N90-21895
Radar RFI at Goldstone DSS 12 and DSS 16 15 p2078 N90-21900
Structural fatigue in the 34-meter HA-Dec antennas 15 p2078 N90-21902
A higher density VLBI catalog for navigating Magellan and Galileo 15 p2078 N90-21904
An 8.4-GHz dual-maser front-end system for Parkes reimplementation 15 p2078 N90-21905
A novel multireceiver communications system configuration based on optimal estimation theory
[NASA-CR-186847] 20 p2851 N90-26216
The Telecommunications and Data Acquisition Report
[NASA-CR-186852] 20 p2852 N90-26217
Goldstone intracomplex connected element interferometry 20 p2852 N90-26218
Information content of a single pass of phase-delay data from a short baseline connected element interferometer 20 p2852 N90-26220
Applications of different design methodologies in navigation systems and development at JPL 20 p2852 N90-26221
Application of inertial instruments for DSN antenna pointing and tracking 20 p2853 N90-26224

Design and performance analysis of the DSS-13 beam waveguide antenna 20 p2853 N90-26225
Initial results on fault diagnosis of DSN antenna control assemblies using pattern recognition techniques 20 p2854 N90-26228
Long-range planning cost model for support of future space missions by the deep space network 20 p2854 N90-26231

DEFECTS
NT CRYSTAL DEFECTS
NT CRYSTAL DISLOCATIONS
NT EDGE DISLOCATIONS
NT INCLUSIONS
NT POINT DEFECTS
NT SURFACE DEFECTS
NT VACANCIES (CRYSTAL DEFECTS)
Two photon absorption characterization
[AD-A210508] 01 p0121 N90-10694
Methods to decrease defect density in GaAs/Si heteroepitaxy
[DE89-016306] 01 p0131 N90-10753
Deformation and defects in Laves-phase intermetallic compounds
[DE89-017798] 03 p0328 N90-11862
A robot which will investigate the condition of underground pipe
[PB89-230650] 04 p0508 N90-12928
Reflection by defective diffusion bonds
[AD-A212995] 05 p0623 N90-13638
Theoretical evaluation of defects in pressure vessels and pipings
[CRIF-MT-174] 05 p0651 N90-13798
The initial imperfection data bank at the Delft University of Technology, part 2
[LR-559-PT-2] 05 p0656 N90-13825
Effects of shock-induced defects on flux pinning in YBa2Cu3O(7-delta)
[DE90-000824] 06 p0853 N90-14959
Shock-induced defects and flux pinning in YBa2Cu3O sub 7-delta + Ag composites
[DE90-000827] 06 p0853 N90-14960
Fuel resistant coatings for metal and composite fuel tanks 08 p1022 N90-15911
Assessment of strength limiting flaws in ceramic heat exchanger components
[DE90-004086] 08 p1051 N90-16077
Analysis and testing of axial compression in imperfect slender truss struts
[NASA-TM-4174] 08 p1087 N90-16292
Heteroepitaxy of GaAs on Si: Methods to decrease the defect density in the epilayer
[DE90-004028] 08 p1131 N90-16551
Universe as a topological defect in a higher-dimensional Einstein-Yang-Mills theory
[DE90-719507] 08 p1135 N90-16578
An illustrated guide of optical characteristics of aircraft transparencies
[AD-A214565] 09 p1167 N90-16752
Assessment of strength limiting flaws in ceramic heat exchanger tubes, phase 2
[DE90-004081] 09 p1220 N90-17080
Study of defect distribution in manufacturing test E8 No. 2 (program A-330/340)
[INFORME-I-366/89] 10 p1358 N90-17872
Boundary estimation problems arising in thermal tomography
[NASA-CR-181964] 10 p1421 N90-18193
Defects: Their behaviour and related design assumptions 11 p1457 N90-18397
Review of component defects, their relationship to manufacturing process, and their effect on materials behaviour (for critical rotating parts) 11 p1458 N90-18399
Defects in monoblock cast turbine wheels 11 p1458 N90-18400
Crack propagation from artificial defects in typical engine disk materials; interpretation of experimental results by means of 3D J integral 11 p1458 N90-18401
Review of modelling methods to take account of material structure and defects 11 p1458 N90-18402
Future technology requirements (related to defects and quantitative material behavior to aid in implementation of damage tolerance for design of engine structures) 11 p1459 N90-18403
The need for a common approach within AGARD --- engine component defects 11 p1459 N90-18404
Arcjet cathode phenomena 11 p1473 N90-18477
Transport effects and spectroscopy of defects in microstructures
[AD-A216718] 11 p1570 N90-19036
Defect structures in copper and gold irradiated with fast neutrons, 14 MeV neutrons and 600 to 800 MeV protons
[DE90-007529] 12 p1629 N90-19359
Interaction between implanted ions and intrinsic defects in silica
[DE90-006589] 13 p1892 N90-20858
Theory of defect process: Basic issues in quantitative understanding
[AERE-R-13661] 13 p1892 N90-20860
UNIVIMP: A universal instrument for the survey of initial imperfections of thin-walled shells
[PB90-167065] 14 p1984 N90-21369
Compendium of fracture mechanics problems
[NASA-TM-100393] 14 p1992 N90-21414
The initial imperfection databank at the Delft University of Technology, part 3
[LR-568] 15 p2057 N90-21783
Development of ultrasonic nondestructive methods for defect and damage characterization in composite materials 15 p2063 N90-21816
The classification of defects from ultrasonic measurements
[AERE-R-13306] 15 p2108 N90-22056
Positron trapping in semiconductors
[PB90-165606] 15 p2172 N90-22410
Topological defects in extended inflation
[NASA-CR-186594] 15 p2190 N90-22505
Localization of vibration in disordered nearly cyclic structures 16 p2246 N90-22812
StarPlan: A model-based diagnostic system for spacecraft 19 p2728 N90-25511
Comparison of currents predicted by NASCAP/LEO model simulations with elementary Langmuir-type bare probe models for an insulated cable containing a single pinhole
[NASA-TM-102486] 20 p2821 N90-26054
Neural networks for detecting defects in aircraft structures
[IAR-90-4] 20 p2873 N90-26345
Advanced processing and properties of high performance alloys
[AD-A221776] 21 p2983 N90-26948
Estimation of defective rate of mechanic-hydraulic components
[ETN-90-97275] 21 p3011 N90-27120
Magnetic flux leakage versus ultrasonic correlation
[AD-A222112] 21 p3071 N90-27462
Defects associated with the incorporation of germanium in gallium arsenide
[AD-A222953] 21 p3082 N90-27527
Development and application of Computed Tomography (CT) for inspection of aerospace components 22 p3187 N90-28083
Inspection system for in-situ inspection of aircraft composite structures 22 p3188 N90-28091
Experimental fault characterization of a neural network
[NASA-CR-186885] 22 p3240 N90-28373
Research on the structural and electronic properties of defects in amorphous silicon
[DE90-000342] 23 p3312 N90-28730
An improved method for choosing sampling points for the inspection of complex surfaces in a computer-aided manufacturing environment 23 p3380 N90-29093
Recent progress in electronic structure calculations for defects in metals
[DE90-016323] 24 p3452 N90-29494
Utilization of a measurement process by the examination of universal motors
[ETN-90-97307] 24 p3466 N90-29581
Nondestructive material characterization
[DE90-015176] 24 p3477 N90-29652
Effective actions for bosonic topological defects
[NASA-CR-187271] 24 p3544 N90-30041
Light scattering from surface and sub-surface defects
[DE90-016311] 24 p3546 N90-30058

DEFENSE COMMUNICATIONS SYSTEM (DCS)
Artificial intelligence for communication prospects
[FEL-1989-1] 04 p0537 N90-13107
Tactical UK military satellite ground terminals: A research and development review
[RSRE-MEMO-4262] 08 p1033 N90-15972

DEFENSE INDUSTRY
NT WEAPONS INDUSTRY
Domestic technology transfer program regulation
[PB89-195374] 01 p0137 N90-10793
Adoption of software engineering innovations in organizations
[AD-A211573] 03 p0387 N90-12206
A guide to quality assurance indicators for the defense electronics industry
[AD-A215630] 09 p1235 N90-17166
Research and development: Technical and scientific publications 1989
[ISSN-0931-9751] 19 p2649 N90-25075
AGARD highlights 90/1 20 p2951 N90-26788

DEFENSE METEOROLOGICAL SATELLITE PROGRAM
U DMSP SATELLITES

DEFENSE PROGRAM
Forecasting contracting workload
[AD-A211935] 03 p0416 N90-12387
FY 1990/FY 1991 biennial budget descriptive summaries for the Strategic Defense Initiative Organization
[AD-A211985] 03 p0419 N90-12409
Recommended changes in US military space policies and programs: A paper submitted to the Commission on Integrated Long-Term Strategy
[PB89-219364] 04 p0480 N90-12636
Concerning advanced architectures for strategic defense
[DE90-001894] 06 p0836 N90-14857
DOD (Department of Defense) Freedom of Information Act Program (incorporating changes 1 and 2)
[PB90-104753] 06 p0859 N90-14993
Prospects for space arms control
[DE90-003392] 07 p0987 N90-15700
Congressional involvement and relations: A guide for Department of Defense acquisition managers
[AD-A214408] 07 p1011 N90-15855
United States Department of Energy stategic defense initiative: New and innovative concepts program
[DE90-005006] 09 p1276 N90-17399
Defense Small Business Innovation Research (SBIR) Program: Program solicitation 90.1, FY-1990
[AD-A215350] 09 p1294 N90-17503
The technology challenge of the advanced tactical fighter: A study of the technology transition process
[AD-A216109] 10 p1320 N90-17630
The use of technology transfer centers by department of defense industrial facilities
[AD-A216863] 10 p1443 N90-18328
The Executive Workshop on Cost/Performance Measurement. Volume 1: Executive summary
[AD-A216745] 11 p1546 N90-18898
A perspective of software reuse
[AD-A216911] 11 p1546 N90-18901
Survivability and effectiveness of near-term strategic defense
[DE90-005805] 11 p1555 N90-18955
Assessing the morality of using the space environment as a platform for weapons
[AD-A217348] 13 p1879 N90-20780
The essence of spacepower: Important influences on the evolution of national spacepower
[AD-A217498] 13 p1879 N90-20781
The thrust and parry of the SIOP (Single Integrated Operational Plan) and SDI
[AD-A217617] 13 p1880 N90-20784
The Weapons Laboratory technical library: Automating with STILAS 15 p2178 N90-22447
The Department of Defense critical technologies plan for the Committees on Armed Services United States Congress
[AD-A219300] 16 p2227 N90-22702
International treaties and active experiments in space
[AD-A219368] 16 p2328 N90-23272
Environmental effects upon cross-servicing of aircraft in NATO
[AD-A218374] 17 p2343 N90-23341
Aircraft modifications cost analysis. Volume 1: Overview of the study
[AD-A220764] 19 p2649 N90-25074
SDIO robotics in space applications 19 p2729 N90-25514
Department of Energy Strategic Defense Initiative programs: Potential programmatic and facility impacts due to a prospective defense and space treaty
[DE90-012717] 21 p3067 N90-27437
Space-based wide area surveillance system studies 21 p3068 N90-27444
Potential new tactical applications of the Global Positioning System (GPS) 21 p3069 N90-27449
The NATO thesaurus project
[NASA-CR-186931] 21 p3087 N90-27552
Impact of the whole national economy of defense spending and space in the US: A literature analysis
[ISSN-0342-0787] 22 p3260 N90-28464
The personal computer: An untapped source for the United States Army War College
[AD-A223976] 23 p3379 N90-29087
An analysis of GPS as the sole means navigation system in US Navy aircraft 24 p3425 N90-29350
Database development for the DMSP experiments
[AD-A224346] 24 p3557 N90-30129

DEFINITION
A simple definition for parallel composition of prime event structures
[CWI-CS-R8903] 04 p0532 N90-13074
Liquid Rocket Booster (LRB) for the Space Transportation System (STS) systems study. Appendix G: LRB for the STS system study level 2 requirements, revision 1
[NASA-CR-183793-APP-G] 23 p3289 N90-28607
A glossary of terms, definitions, acronyms, and abbreviations related to the National Airspace System
[DOT/FAA/CT-TN89/53] 23 p3406 N90-29249

DEFLAGRATION
On the dynamics of the combustion process of hydrogen-air and hydrogen-methane-air mixtures
[DLR-FB-89-39] 11 p1485 N90-18548
DEFLATING
U INFLATABLE STRUCTURES
U PRESSURE REDUCTION
DEFLECTION
Field evaluation of the multi-depth deflectometers
[PB89-207708] 03 p0349 N90-11994
Bilinear modeling and nonlinear estimation 05 p0589 N90-13430
Cryogenic temperature effects on sting-balance deflections in the National Transonic Facility
[NASA-TM-4157] 06 p0727 N90-14244
Finite element analysis of laminated composite plates 06 p0737 N90-14291
A theoretical investigation of the column behavior of cold-formed square hollow sections
[PB89-225981] 06 p0797 N90-14845
Direction-dependent stopping power and beam deflection in anisotropic solids
[DE90-001076] 06 p0840 N90-14883
Effects of T-tabs and large deflections in DCB specimen tests
[NASA-TM-101677] 09 p1186 N90-16868
Application of attachment modes in the control of large space structures
[NASA-CR-185604] 12 p1613 N90-19280
Internal fractures in model elastomeric composites 15 p2121 N90-22133
Nonlinear strain-displacement relations and flexible multibody dynamics 16 p2284 N90-23014
Miniaturization of flight deflection measurement system
[NASA-CASE-LAR-13628-1] 17 p2406 N90-23707
Out-reach in-space technology experiments program: Control of flexible robot manipulators in zero gravity, experiment definition phase
[NASA-CR-183849] 19 p2696 N90-25343
Relativistic light bending near neutron stars 19 p2779 N90-25810
Refractive error analysis in the interferometric measurement of 2-D density fields containing strong gradients
[LR-616] 20 p2927 N90-26655
Igniter adapter-to-igniter chamber deflection test
[NASA-CR-184002] 22 p3133 N90-27780
Structural testing and analytical research of turbine components
[AD-A223516] 24 p3434 N90-29396
DEFLECTORS
NT FLAME DEFLECTORS
Static test deflector for Ariane-5 SRM: Technical design and economical choice 09 p1176 N90-16812
Literature file on fast kickers and SEPTA: Components for deflection and separation of particle beams
[LINO-162] 12 p1727 N90-19924
DEFOCUSING
Gas optics applicable to free electron laser technology
[AD-A214285] 07 p0993 N90-15741
Image of the angle by partially coherent lighting: Calculations and experiments
[ETN-90-96505] 18 p2616 N90-24900
DEFORESTATION
Contribution of deforestation to atmospheric CO2 and reforestation as an option to control CO2
[DE89-017255] 04 p0516 N90-12979
Strategy for monitoring the effects of land use change on atmospheric CO2 concentrations
[DE90-001635] 06 p0812 N90-14722
Multisensor monitoring of deforestation in the Guinea Highlands of West Africa
[NASA-CR-186709] 19 p2706 N90-25396
Characterization of biogenic aerosol particles from the Amazon Basin during dry and wet season 20 p2886 N90-26418
DEFORMATION
NT AXIAL STRAIN
NT ELASTIC BENDING
NT ELASTIC BUCKLING
NT ELASTIC DEFORMATION
NT PLASTIC DEFORMATION
NT STATIC DEFORMATION
NT TENSILE DEFORMATION
NT WAVE FRONT DEFORMATION
Hygrothermal deformations of composite shells 02 p0185 N90-11055
Deformation induced microstructural and microchemical changes during thermomechanical treatment
[DE89-017266] 02 p0197 N90-11127
An improved beam model for the vibrations of rotor blades 02 p0232 N90-11333
Evaluation of integrals related to the Debye function
[DE89-016930] 02 p0264 N90-11499
Deformation and defects in Laves-phase intermetallic compounds
[DE89-017798] 03 p0328 N90-11862
Field evaluation of the multi-depth deflectometers
[PB89-207708] 03 p0349 N90-11994
Crustal deformation: Earth vs Venus 03 p0427 N90-12450
Anomalous strain rate dependence of the serrated flow in Ni-H and Ni-C-H alloys
[AD-A213244] 05 p0624 N90-13641
The use of a deformation model for sampling digitalized stereoscopic images
[IMAG-RR-753-I] 05 p0664 N90-13884
Cavitation and superplasticity 06 p0744 N90-14329
Further studies of transverse stress effects in cable-in-conduit conductors
[DE90-001517] 06 p0771 N90-14484
CTH: A three-dimensional shock wave physics code
[DE89-016529] 06 p0779 N90-14528
Stability and dynamics of constrained flexible multibody systems 06 p0791 N90-14609
Dynamical simulation of dislocation microstructure
[DE90-003192] 06 p0857 N90-14982
Design temperatures for flexible airfield pavement design
[AD-A214141] 07 p0884 N90-15115
Deformation and fracture of low alloy steels at high temperature
[DE90-001274] 07 p0902 N90-15215
Energetics of BCC-FCC lattice deformation in iron
[AD-A213801] 07 p0905 N90-15233
Geotechnical instrumentation
[PB89-198675] 07 p0933 N90-15398
Thermal analysis of fixed and tilting pad journal bearings including cross-film viscosity variations and deformations 07 p0937 N90-15429
Spatial dynamics of deformable multibody systems with variable kinematic structure
[AD-A214098] 07 p0942 N90-15455
Statistical model for particle-void deformation kinetics in granular materials during shock wave propagation
[DE89-017729] 07 p0946 N90-15476
Effects of high rate shear on the microstructure and deformation and fracture behavior of two high strength steels
[AD-A214107] 08 p1044 N90-16032
An implicit time-integration procedure for a set of internal variable constitutive equations for isotropic elasto-viscoplasticity
[PB90-121302] 08 p1117 N90-16470
Metal matrix composite: Strengthening mechanisms
[AD-A214843] 09 p1186 N90-16871
Stress analysis in pressure vessels by mixed finite element methods taking into account shear deformation
[DE90-606755] 09 p1233 N90-17152
Cyclic deformation of Sn-60 to Pb-40 solder joints during thermomechanical fatigue
[DE90-004197] 09 p1237 N90-17179
High-temperature deformation of YBa2Cu3O(7-delta) with Ag additions
[DE90-004884] 09 p1292 N90-17491
High-order mixture homogenization of periodic nonlinear composites 10 p1347 N90-17814
Studies on deformation and fracture of viscoelastic composite materials
[AD-A216095] 10 p1348 N90-17819
The behavior of a composite material in compression
[AD-A216324] 10 p1350 N90-17829
A higher-order plate theory with ideal finite element suitability
[AD-A216163] 10 p1397 N90-18075
Finite element investigation of a composite cylindrical shell under transverse load with through thickness shear and snapping
[AD-A216377] 10 p1397 N90-18078
Threaded joint design for composites
[DE90-005553] 11 p1478 N90-18506
Comparison of tension, compression, and flexure creep for alumina and silicon nitride ceramics
[DE90-006154] 11 p1492 N90-18586
Irradiation-induced amorphization and elastic shear instability in intermetallic compounds
[DE90-004845] 12 p1625 N90-19341
Analysis of tectonic movements utilizing remote sensor products in the Southern Espinhaco (SE) region
[INPE-4830-PRE/1451] 12 p1690 N90-19708
P-T condition to deformation from fluid inclusions in mylonites
[NASA-CR-186377] 12 p1690 N90-19710
Interface science in deformation processing of ceramics
[DE90-008424] 13 p1780 N90-20219
Design and performance analysis of adaptive optical telescopes using laser guide stars
[AD-A218025] 13 p1902 N90-20913
A computational model of the perforation of multi-layer metallic laminates
[MRL-RR-9-89] 14 p1944 N90-21128
Micromechanics analysis of space simulated thermal deformations and stresses in continuous fiber reinforced composites
[NASA-TM-102633] 14 p1946 N90-21140
Modeling elastomer displacements for tactile sensing applications
[DE90-007959] 14 p1984 N90-21370
Heat engine based on shape memory alloys
[AD-D014400] 14 p1986 N90-21385
Improved analytical capabilities for foil air bearings, phase 1
[AD-A218071] 14 p1987 N90-21389
Thermomechanical deformation testing and modeling in the presence of metallurgical instabilities
[NASA-CR-185188] 14 p1993 N90-21420
Review of formulae for the buckling of simply-supported, orthotropic plates under shear load, including transverse shear effects
[PB90-167073] 14 p1994 N90-21429
Results of the Gondwana Project: An example of intercontinental geologic correlation utilizing LANDSAT imagery
[INPE-4870-PRE/1481] 14 p1995 N90-21437
Contribution for the study of the evolution of part of the Espinhaco supergroup and its foundation through fracture analysis
[INPE-4907-PRE/1508] 14 p1999 N90-21459
Deformation processing of YBa2Cu3O(sub x)
[DE90-007795] 14 p2030 N90-21644
Residual stresses in laminated thermoplastic matrix composites 15 p2063 N90-21815
The effect of hydrogen and microstructure on the deformation and fracture behavior of a single crystal nickel-base superalloy
[NASA-CR-185219] 15 p2068 N90-21849
Nonlinear spline operator interpolation and sliding control of deformable maneuvering bodies 15 p2074 N90-21878
Combining acoustic emission locations and a microcrack damage model to study development of damage in brittle materials
[DE90-005195] 15 p2117 N90-22111
Coupled behavior of rock joints
[DE90-009222] 15 p2129 N90-22174
Large deformation analysis of laminated composite structures by a continuum-based shell element with transverse deformation 16 p2211 N90-22613
Damage analysis following slight deformations of composite materials
[RDS-1-007-64] 16 p2212 N90-22618
High-temperature deformation of mechanically-alloyed aluminum IN90211 16 p2216 N90-22645
Deformation and fracture of thin sheet aluminum-lithium alloys: The effect of cryogenic temperatures 16 p2218 N90-22655
Deformation and fracture of aluminum-lithium alloys: The effect of dissolved hydrogen 16 p2219 N90-22658
The effect of mechanical deformation on the radiation patterns of large space-based arrays
[AD-A219288] 16 p2230 N90-22719
A multipulsed dynamic diffraction moire interferometer
[DE90-009765] 16 p2230 N90-22723
Large scale metrology by computer assisted photogrammetry
[REPT-892-430-116] 16 p2239 N90-22772
Sliding control of pointing and tracking with operator spline estimation 16 p2281 N90-22997
Nonlinear strain-displacement relations and flexible multibody dynamics 16 p2284 N90-23014
Nonlinear finite element formulation for the large displacement analysis in multibody system dynamics 16 p2284 N90-23015
The coupling effects of kinematics and flexibility on the Lagrangian dynamic formulation of open chain deformable links 16 p2284 N90-23018
Explicit modeling of composite plates and beams in the dynamics of multibody systems 16 p2285 N90-23019
Modal identities for multibody elastic spacecraft: An aid to selecting modes for simulation 16 p2296 N90-23075
An orthotropic theory of viscoplasticity based on overstress for thermomechanical deformation and its application to laminated metal matrix composites 17 p2415 N90-23759
A day in the life of a warm front
[AD-A220373] 17 p2426 N90-23826
Subsurface hardening and flow of aluminum during the incubation period of solid particle erosion
[DE90-010141] 18 p2525 N90-24409
Deformation-induced structural developments of ultra-high molecular weight polyethylene
[ETN-90-96899] 18 p2529 N90-24432

Fatigue crack growth in ceramic materials at ambient and elevated temperatures
[DE90-008418] 18 p2531 N90-24443
Obtaining an equivalent beam
18 p2570 N90-24646
Low velocity impact analysis with NASTRAN
18 p2570 N90-24647
Cation and anion tracer diffusion in YBa(sub 2)Cu(sub 3)O(sub 7-delta)
[DE90-009708] 18 p2620 N90-24927
Deformation and fracture behavior of TiAl
[DE90-012212] 19 p2675 N90-25212
Innovative design of composite structures: Axisymmetric deformations of unsymmetrically laminated cylinders loaded in axial compression
[NASA-CR-186635] 19 p2700 N90-25364
Flexion, extension and lateral bending responses of the cervical spine 19 p2719 N90-25468
Structural analysis and optimization of a propfan blade using a finite element method
[DLR-FB-90-01] 20 p2812 N90-26006
Crystal growth and deformation behavior of TiAl aluminides
[DE90-012972] 20 p2930 N90-26671
Determination of the heat dissipated from a specimen undergoing cyclic plasticity by a hybrid numerical/experimental method
[AD-A221575] 21 p2982 N90-26946
The sensitivity of several explosives to ignition in the launch environment
[AD-A221581] 21 p2990 N90-26993
The 2nd International Conference on Low-Energy Dislocation Structures
[AD-A222887] 21 p3082 N90-27525
High-temperature deformation of silicon
[DE90-013628] 22 p3160 N90-27919
Postbuckling response of long thick isotropic plates loaded in compression including higher order transverse shearing effects
[NASA-TM-4199] 22 p3190 N90-28100
Behavior of Al-Mg alloys in hot working and superplasticity
[DE90-015193] 23 p3310 N90-28723
High-temperature deformation and microstructural analysis for Si3N4-Sc2O3
[NASA-TM-103239] 23 p3314 N90-28740
A nonlinear finite element formulation for the large displacement analysis of plates
23 p3338 N90-28867
Twisted crystals: Propagation, genesis, and relationships with optical activity and molecular symmetry (excerpts)
[DE90-014259] 23 p3399 N90-29205
Nonlinear static and dynamic modeling of composite rotor blades including warping effects
24 p3431 N90-29382
Rheology of filler rubber: Silica-silicone
[AD-A223600] 24 p3455 N90-29511

DEGASSING

Trap gettering by isoelectronic doping of p-GaAs and n-GaAs grown by molecular beam epitaxy
[AD-A211162] 01 p0133 N90-10769
Significance of oxide skins on powder for the quality of PM Al material --- PM (press molded)
[DFVLR-FB-89-11] 03 p0329 N90-11873
Intrinsic properties of high voltage wires that may cause sporadic discharges in space vacuum
10 p1338 N90-17743
Significance of oxide skins on powder for the quality of PM Al materials
[ESA-TT-1178] 11 p1487 N90-18560

DEGENERATION

Experiment K-6-09. Morphological and biochemical investigation of microgravity-induced nerve and muscle breakdown. Part 1: Investigation of nerve and muscle breakdown during spaceflight; Part 2: Biochemical analysis of EDL and PLT muscles 20 p2893 N90-26463

DEGENERATIVE FEEDBACK

U NEGATIVE FEEDBACK

DEGRADATION

NT BIODEGRADATION
NT THERMAL DEGRADATION
Grain boundary chemistry in irradiated stainless steel and its influence on environmental degradation
[DE89-016827] 02 p0197 N90-11125
Effects of hot corrosion on the room temperature strength of structural ceramics
[AD-A212568] 04 p0481 N90-12762
Shape instabilities of plate-like structures. 1: Experimental observations in heavily cold worked in situ composites
[AD-A212251] 04 p0523 N90-13021
Tunneling microscopy of superconductors and tunneling barriers
[AD-A212120] 04 p0559 N90-13257
Further studies of transverse stress effects in cable-in-conduit conductors
[DE90-001517] 06 p0771 N90-14484
Sodium/sulfur post-test analysis at ANL
[DE90-001911] 06 p0771 N90-14488
Ice induced aerodynamic performance degradation of rotorcraft: An overview 07 p0873 N90-15063
A review of the effects of microalloying constituents on the formation and breakdown of protective oxide scales on high-temperature alloys at temperatures below 700 C
[DE90-001277] 07 p0902 N90-15216
Dual task performance with LPC (Linear Predictive Coding) degraded speech in a sentence verification task
[AD-A214298] 07 p0920 N90-15320
Fracture toughness of ferritic alloys at very high neutron exposures
[DE90-004519] 08 p1046 N90-16046
Application of ac impedance method for diagnosis of lithium secondary battery degradation. Preliminary study with AA size Li/MoS2 cells
[DE90-702474] 08 p1061 N90-16137
Model-based quantification of image quality
08 p1072 N90-16206
Effects of moisture on composite materials
09 p1185 N90-16866
Fuel-elastomer compatibility studies: Results of 80 C/14-day exposure experiments
[AD-A216015] 10 p1361 N90-17893
Feasibility demonstration of a 445N high-performance rocket engine 11 p1473 N90-18481
Development of a progressive failure model for strength of laminated composite structure
[AD-A216966] 11 p1480 N90-18517
Reliability studies of ceramic capacitors
[AD-A216763] 11 p1501 N90-18643
Photointerpretation with instruments for evaluation of environmental impact: Mata Atlantica in Cubata
[INPE-4910-PRE/1511] 11 p1531 N90-18817
Research and development on enhanced degradable plastics
[AD-A217180] 13 p1779 N90-20212
Advanced modulation technology development for earth station demodulator applications. Coded modulation system development
[NASA-CR-185149] 13 p1789 N90-20270
The application of electrochemical impedance spectroscopy for characterizing the degradation of Ni(OH)2/NiOOH electrodes 13 p1824 N90-20474
Evaluation of the mangrove areas of the Rio Piaui (SE) through remote sensing
[INPE-4909-PRE/1510] 14 p1998 N90-21454
Failure and degradation modes in selected solar materials: A review
[DE90-009075] 14 p2002 N90-21476
The effect of thermal damage on the mechanical properties of polymer regrinds 18 p2515 N90-24363
Investigation of lubrication characteristics of MoS2 films in space environment 18 p2537 N90-24472
Wear of gold-plated contacts: Microscopic aspects, role of oxygen 18 p2538 N90-24479
Scientific guidelines for preservation of samples collected from Mars
[NASA-TM-4184] 19 p2796 N90-25918
Aeolian removal of dust from radiator surfaces on Mars
[NASA-TM-103205] 20 p2824 N90-26068
The chemical effects of the Martian environment on power system component materials: A theoretical approach
[NASA-TM-103203] 20 p2825 N90-26074
Quantitative confirmation of diffusion-limited oxidation theories
[DE90-012997] 20 p2838 N90-26143
Reusable rocket engine turbopump health monitoring system, part 3
[NASA-CR-182294] 20 p2869 N90-26320
Space operations: NASA is not properly safeguarding valuable data from past missions
[GAO/IMTEC-90-1] 20 p2936 N90-26704
Computerized corrosion forecasting model for C-5 aircraft 21 p2957 N90-26815
B-1B improved windshield development. Volume 2: Magna analysis: Baseline and parametric
[AD-A221501] 21 p2960 N90-26828
Surface reactions in the space environment
[AD-A221767] 21 p2979 N90-26932
Laboratory evaluation of two new high-performance polyester batting insulation materials
[AD-A222291] 21 p2987 N90-26976
The effects of space radiation on thin films of YBa2Cu3O(sub 7-x) 22 p3147 N90-27845
A technique for rapid inspection of composite aircraft structure for impact damage 22 p3185 N90-28077
Molten salt induced high temperature degradation of thermal barrier coatings 23 p3307 N90-28704
Effect of protective coatings on mechanical properties of superalloys 23 p3308 N90-28707
Study of meteorological processes important in the degradation of materials through surface temperature
[PB90-222720] 23 p3336 N90-28856

DEGREES OF FREEDOM

Shape control of high degree-of-freedom variable geometry trusses 01 p0024 N90-10122
Optimized resolved rate control of seven-degree-of-freedom Laboratory Telerobotic Manipulator (LTM) with application to three-dimensional graphics simulation
[NASA-TP-2938] 01 p0109 N90-10618
Dynamic analysis of rotors under interference rubs
02 p0229 N90-11312
Design and control of a two-degree-of-freedom lightweight flexible arm
[AD-A213335] 05 p0650 N90-13790
Classification and simulation of single and multi-degree-of-freedom motions
[AD-A214925] 09 p1231 N90-17143
BRS current and related anomalies in two-dimensional gravity and string theories
[DE90-733095] 10 p1440 N90-18307
KAM: Automatic planning and interpretation of numerical experiments using geometrical methods
[AD-A216805] 11 p1546 N90-18900
Approximations to joint distributions of definite quadratic forms
[AD-A216434] 11 p1551 N90-18930
Toda lattice with transverse degree of freedom
[DE90-002414] 11 p1572 N90-19049
Direct formulation of a 4-node hybrid shell element with rotational degrees of freedom
[NASA-CR-4282] 14 p1991 N90-21411
Dynamics of an oscillator with three-degrees-of-freedom in a uniform windfield
[REPT-89-56] 15 p2119 N90-22121
Dynamic substructuring by the boundary flexibility vector method of component mode synthesis
[NASA-CR-182445] 16 p2247 N90-22813
Experimental verification of dynamic simulation
16 p2285 N90-23020
Real time inverse kinematics with joint limits and spatial constraints
[AD-A220462] 18 p2586 N90-24723
Short time-dynamometer system for shock wave channels
[MBB-UT-115/89-PUB] 19 p2651 N90-25084
Coupled rotor-body equations of motion hover flight
[NASA-CR-186710] 19 p2655 N90-25111
Reaction-compensation technology for microgravity laboratory robots
[NASA-TM-103271] 22 p3183 N90-28062
Inflight thrust vectoring: A further degree of freedom in the aerodynamic/flight mechanical design of modern fighter aircraft 23 p3274 N90-28528
A 17 degree of freedom anthropomorphic manipulator
23 p3362 N90-29001
Kinematic functions for the 7 DOF robotics research arm 23 p3363 N90-29003
A complete analytical solution for the inverse instantaneous kinematics of a spherical-revolute-spherical (7R) redundant manipulator 23 p3363 N90-29006
Characterization and control of self-motions in redundant manipulators 23 p3370 N90-29045
Reflexive obstacle avoidance for kinematically-redundant manipulators
23 p3371 N90-29047
Suspension systems for ground testing large space structures
[NASA-CR-4325] 24 p3439 N90-29424
The Goddard Space Flight Center (GSFC) robotics technology testbed 24 p3507 N90-29825

DEHYDRATION

Heat exhaustion
[AD-A212128] 04 p0522 N90-13014
Hydration effects on human physiology and exercise-heat performance
[AD-A217969] 13 p1852 N90-20629
Effect of fluid countermeasures of varying osmolarity on cardiovascular responses to orthostatic stress
18 p2628 N90-24978
The effects of pretreatment conditions on a Pt/SnO2 catalyst for the oxidation of CO in CO2 lasers
[NASA-TM-103487] 20 p2867 N90-26309

DEHYDROGENATION

Dehydrogenative polymerization of silanes to polysilanes: A monomeric copper(2) siloxide
[AD-A218550] 16 p2223 N90-22681

DEICERS

Evaluation of the improved OV-ID anti-icing system, phase 2
[AD-A213928] 07 p0877 N90-15083

Feasibility of using lasers and infrared heaters as UNREP icing countermeasures
[AD-A219031] 19 p2695 N90-25333
A NASA/university/industry consortium for research on aircraft ice protection
[IAR-89-18] 20 p2807 N90-25969
DEICING
Electro-impulse de-icing testing analysis and design
[NASA-CR-4175] 01 p0007 N90-10031
NASA's program on icing research and technology 07 p0873 N90-15062
Flight and wind tunnel investigation of aerodynamic effects of aircraft ground deicing/antiicing fluids 07 p0873 N90-15064
Modeling of surface roughness effects on glaze ice accretion 14 p1905 N90-20925
DEICING SYSTEMS
U DEICERS
DEIMOS
Stable orbits about the Martian moons
[AD-A216400] 10 p1447 N90-18352
DEIONIZATION
Process for making a noble metal on tin oxide catalyst
[NASA-CASE-LAR-13741-1-SB] 13 p1774 N90-20180
Plasma cloaking: Air chemistry, broadband absorption, and plasma generation
[AD-A222044] 21 p3078 N90-27503
DEKATRONS
U COUNTERS
DELAMINATING
Analysis of delamination growth 02 p0183 N90-11038
Delamination tests under static compression loading 02 p0186 N90-11061
Delamination tests under compression-compression and tension-compression loading 02 p0186 N90-11062
The 2.5D- and 3D-fabrics for delamination resistant composite laminates and sandwich structures 02 p0186 N90-11063
Multilayer theory for delamination analysis of a composite curved bar subjected to end forces and end moments
[NASA-TM-4139] 04 p0466 N90-12669
Nonlinear theories concerning laminated composites under compression with delamination
[ONERA-RT-19/3542-RY-061-R] 04 p0467 N90-12672
Fractography of composite delamination
[NASA-CR-183291] 05 p0617 N90-13599
Buckling of delaminations in ARALL laminates
[LR-535] 05 p0619 N90-13614
An analysis of drilling of composite materials 07 p0889 N90-15142
Open-mode delamination stress concentrations in horseshoe and elliptic composite curved bars subjected to end forces
[NASA-TM-4164] 08 p1039 N90-16004
Two new techniques for predicting delamination growth in laminated plates 09 p1185 N90-16865
Fatigue delamination onset prediction in tapered composite laminates
[NASA-TM-101673] 09 p1236 N90-17177
Studies on deformation and fracture of viscoelastic composite materials
[AD-A216095] 10 p1348 N90-17819
Investigation of the failure modes in a metal matrix composite under thermal cycling
[AD-A216195] 10 p1349 N90-17825
Cross-sectional examination of the damage zone in impacted specimens of carbon/epoxy and carbon/PEEK composites
[NASA-TM-100391] 14 p1944 N90-21125
Combined effect of matrix cracking and stress-free edge on delamination
[NASA-TM-102591] 14 p1944 N90-21126
Fracture and longevity of composite structures
[AD-A217827] 14 p1944 N90-21127
Compressive behavior of laminated composite structures 14 p1945 N90-21134
Delamination failure in a unidirectional curved composite laminate
[NASA-CR-182018] 14 p1993 N90-21421
Development of planar geometry solid oxide fuel cell technology, phase 2
[PB90-131293] 14 p2001 N90-21467
Energy release rate analysis of interfacial cracks in composites 15 p2065 N90-21829
The controlled-damage concept in design of laminated composites 15 p2065 N90-21830
Three-dimensional finite element formulations for thick and thin laminated plates 15 p2121 N90-22132
Elevated temperature crack growth in advanced powder metallurgy aluminum alloys 16 p2218 N90-22653
Instability-related delamination growth of embedded and edge delaminations
[NASA-TM-100655] 17 p2370 N90-23494
Development of a finite element based delamination analysis for laminates subject to extension, bending, and torsion 18 p2642 N90-25049
Tension fatigue of glass/epoxy and graphite/epoxy tapered laminates
[NASA-TM-102628] 19 p2671 N90-25191
Fractography of composite delamination
[NASA-CR-181965] 19 p2702 N90-25372
Strain energy release rate analysis of delamination in a tapered laminate subjected to tension load
[NASA-TM-102592] 20 p2826 N90-26076
Characterization of impact damage in composites 21 p2957 N90-26811
Green's functions for dislocations in bonded strips and related crack problems
[NASA-CR-185291] 23 p3340 N90-28878
On a generalized laminate theory with application to bending, vibration, and delamination buckling in composite laminates 24 p3478 N90-29659
DELAY
Navigation experiment NAVEX: The equipment delay times in the Spacelab mission D1
[DFVLR-MITT-89-10] 03 p0304 N90-11728
Gaze controls with interactions and delays
[AD-A214286] 07 p0981 N90-15667
Navigation experiment NAVEX: The self-test delay times in the D1 Spacelab mission
[ESA-TT-1176] 11 p1467 N90-18446
A stress-strength interference approach to fast and delayed fracture reliability analysis for ceramic components 15 p2070 N90-21859
Minimum loss scheduling
[MEMO-821] 18 p2600 N90-24796
Replication of NASPAC Dallas/Fort Worth study
[DOT/FAA/CT-TN90/26] 19 p2657 N90-25123
Device and method for detecting and displaying crossover pattern in precision winding
[AD-D014539] 19 p2685 N90-25276
Space exploration: Cost, schedule, and performance of NASA's Galileo Mission to Jupiter. Fact sheet for the Chairman, Subcommittee on Science, Technology, and Space, Committee on Commerce, Science, and Transportation, US Senate
[GAO/NSIAD-88-138FS] 20 p2816 N90-26025
Active lag angle device
[AD-D014538] 20 p2857 N90-26249
Investigation of weld bead cooling rate during startup of gas metal arc welding
[AD-A223567] 24 p3449 N90-29478
DELAY CIRCUITS
Delay test generation for synchronous sequential circuits
[AD-A211917] 05 p0634 N90-13697
Long period pseudo random number sequence generator
[NASA-CASE-NPO-17241-1-CU] 17 p2394 N90-23636
Magnetostatic wave transducers, resonators and dispersion control
[AD-A223437] 24 p3464 N90-29571
DELAY LINES
Satellite range delay simulator for a matrix-switched time division multiple-access network simulator
[NASA-TM-102407] 04 p0489 N90-12813
Design of a compensation filter for a quadratic phase communication channel 06 p0761 N90-14428
Fiber optic transversal filter/variable delay line
[AD-D014328] 10 p1430 N90-18248
Beamforming devices and feed structures for a DBS flat-plate antenna
[BBC-RD-1989/12] 17 p2386 N90-23592
Magnetostatic wave transducers, resonators and dispersion control
[AD-A223437] 24 p3464 N90-29571
DELINEATION
Computer-aided boundary delineation of agricultural lands
[NASA-TM-102243] 08 p1091 N90-16313
DELIVERY
NT PAYLOAD DELIVERY (STS)
NT WEAPONS DELIVERY
Document delivery via ISDN or satellite networks 15 p2178 N90-22446
DELPHI METHOD (FORECASTING)
The future of aircraft paint removal methods
[AD-A214946] 09 p1197 N90-16936
Outlook for ceramics in heat engines, 1990 - 2010: A technical and economic assessment based on a worldwide Delphi survey
[DE90-011262] 19 p2679 N90-25234
DELTA MODULATION
An experimental study of voice communication over a bandlimited channel using variable bit width delta modulation
[AD-A223445] 24 p3481 N90-29548
DELTA WINGS
An integrated CFD/experimental analysis of aerodynamic forces and moments
[NASA-TM-102195] 01 p0002 N90-10006
The three-dimensional vortex sheet structure on delta wings 01 p0064 N90-10367
Unsteady aerodynamics with applications to flight mechanics
[AD-A211944] 03 p0301 N90-11706
Experimental transonic flutter characteristics of two 72 deg-sweep delta-wing models
[NASA-TM-101659] 06 p0720 N90-14205
Flows with Separation
[DGLR-PAPERS-88-05] 08 p1066 N90-16169
Flow field visualization study on a 65 deg delta wing at M = 0.85 08 p1068 N90-16182
Research on three different Euler's schemes applied to a delta wing with vortical flows 08 p1068 N90-16184
Force and moment measurements on delta wings in unsteady flow 08 p1068 N90-16185
Numerical simulation of the laminar and turbulent three dimensional flow on a delta wing with sharp leading edge 08 p1069 N90-16186
Controlled vortical flow on delta wings through unsteady leading edge blowing
[NASA-CR-186267] 09 p1160 N90-16712
A two-stage earth-to-orbit transport with translating oblique wings for booster recovery
[NASA-CASE-LAR-14156-1] 09 p1173 N90-16781
An experimental study of the effect of streamwise vortices on unsteady turbulent boundary-layer separation 09 p1215 N90-17045
Surface pressure distributions on a delta wing undergoing large amplitude pitching oscillations
[NASA-CR-186326] 10 p1306 N90-17558
Numerical simulation of compressible vortices
[AD-A216221] 10 p1385 N90-18017
Unsteady aerodynamics of delta wings performing maneuvers to high angle of attack 12 p1598 N90-19196
Leading edge vortex dynamics on a pitching delta wing
[NASA-CR-186327] 12 p1598 N90-19198
A streamwise upwind algorithm applied to vortical flow over a delta wing
[NASA-TM-102225] 12 p1599 N90-19201
Conical Euler solution for a highly-swept delta wing undergoing wing-rock motion
[NASA-TM-102609] 12 p1600 N90-19211
A video-based experimental investigation of wing rock
[AD-A218244] 13 p1755 N90-20075
Experimental and numerical investigation of the vortex flow over a sharp edged delta wing; with and without sideslip
[PB90-167131] 14 p1913 N90-20964
Prediction of forces and moments for flight vehicle control effectors. Part 2: An analysis of delta wing aerodynamic control effectiveness in ground effect
[NASA-CR-186572] 15 p2047 N90-21735
A video-based experimental investigation of wing rock 15 p2054 N90-21771
An experimental and theoretical investigation of the flow over plane delta wings with supersonic leading edges
[LR-588] 19 p2655 N90-25114
Investigation of the vortex flow over a sharp-edged delta wing in the transonic speed regime
[LR-594] 19 p2656 N90-25115
Experimental study on vortex and shock wave development on a 65 deg delta wing
[NLR-MP-88033-U] 20 p2804 N90-25950
Experiments with unsteady, free surface, three-dimensional vortices in a thermally stable, stratified fluid
[AD-A222088] 21 p2954 N90-26796
Experimental investigations on the stability and vorticity of the vortex breakdown phenomenon above delta wings, measured by the ultrasonic laser method
[ESA-TT-1079] 23 p3268 N90-28498
Control of vortex aerodynamics at high angles of attack 23 p3273 N90-28523
The steady and time-dependent aerodynamic characteristics of a combat aircraft with a delta or swept canard 23 p3274 N90-28526
The aerodynamic design of the oblique flying wing supersonic transport
[NASA-CR-177552] 23 p3276 N90-28540
The DELTA MONSTER: An RPV designed to investigate the aerodynamics of a delta wing platform
[NASA-CR-185226] 24 p3431 N90-29381

DEMAGNETIZATION
A survey of the current state-of-the-art in high-energy-product permanent magnets
[AD-A211761] 04 p0549 N90-13193
Measurement of H(sub c1) in a single crystal of YBa2Cu3O7 with low pinning 22 p3151 N90-27864
Investigation of the application in the simulation program 'PSpice' of the Jiles-Atherton model for nonlinear magnetic materials in order to predict the degaussing of magnets
[LINO-1990-1] 24 p3541 N90-30029
DEMAND (ECONOMICS)
How far can the world get on energy efficiency alone
[DE90-001349] 06 p0805 N90-14686
DEMINERALIZING
NT BONE DEMINERALIZATION
DEMODULATION
Phase ambiguity resolution for offset QPSK modulation systems
[NASA-CASE-NPO-17853-1-CU] 09 p1204 N90-16975
Complex demodulation for bearing fault detection
[AD-A218367] 13 p1812 N90-20407
A functional description of the advanced receiver 15 p2076 N90-21891
Frequency domain techniques for analyzing picosecond optical pulses
[AD-A218856] 16 p2318 N90-23214
New approaches for rapid synchronisation frequency hoppers 20 p2849 N90-26201
QPSK loop lock detection in the advanced receiver 20 p2854 N90-26230
Spread-spectrum communications in non-Gaussian channels
[AD-A222686] 21 p2994 N90-27019
DEMODULATORS
NT MODEMS
NT PHASE LOCK DEMODULATORS
Robust spatial calibration of a planar positron camera
[AD-A210773] 02 p0224 N90-11284
OPFET (Optical Field-Effect Transistor) demodulator-downconverter for detecting microwave modulated optical signals
[AD-D014294] 08 p1060 N90-16128
Advanced modulation technology development for earth station demodulator applications. Coded modulation system development
[NASA-CR-185149] 13 p1789 N90-20270
An experimental study of voice communication over a bandlimited channel using variable bit width delta modulation
[AD-A223445] 24 p3461 N90-29548
DEMOGRAPHY
US Coast guard radionavigation system user survey
[AD-A218480] 17 p2349 N90-23380
The effects of climate change on energy planning and operations in the Pacific Northwest. Volume 2: Technical background
[DE90-009465] 17 p2425 N90-23817
In situ investigation of sea surface noise from a depth of one meter
[AD-A220158] 17 p2432 N90-23857
Formula scoring: Basic theory and applications
[AD-A218368] 17 p2465 N90-24083
A trend analysis of women who hold Federal Aviation Administration certificates: Relationship to the representation of women in collegiate aviation faculty ranks
[IAR-90-3] 19 p2762 N90-25691
Diagnostics for hydrogen atoms and molecules in H-atom sources and beams using VUV laser light
[AD-A222340] 21 p3074 N90-27476
The Tempel 2 dust trail
[AD-A224395] 24 p3562 N90-30153
DEMONSTRATION
U PROVING
DEMULTIPLEXING
The first year's work of race project 1036 WTDM broadband customer premises network
[BBC-RD-1989/6] 08 p1055 N90-16097
DENDRITIC CRYSTALS
Flight software development for the isothermal dendritic growth experiment
[NASA-TM-102412] 05 p0685 N90-13988
Primary arm spacing in directionally solidified Pb-10 wt percent Sn alloys
[NASA-CR-185190] 06 p0756 N90-14398
Dendritic web silicon photovoltaic cell research
[DE90-011786] 20 p2880 N90-26387
DENITROGENATION
Properties and thermal decomposition of the double salts of uranyl nitrate-ammonium nitrate
[DE89-004909] 07 p0914 N90-15287
DENSE PLASMAS
NT PLASMA FOCUS
NT STRONGLY COUPLED PLASMAS
The dense Z-pinch as a plasma radiation source. 1: Quasi-static Bennett model
[AD-A210600] 01 p0127 N90-10727
A fully electromagnetic hybrid model for high density plasma simulations
[DE89-016771] 02 p0279 N90-11593
Atomic structure and spectral perturbations in hot dense plasmas 06 p0785 N90-14567
Transversal inhomogeneity and radiative transfer in plasmas obtained by laser impact 06 p0785 N90-14568
Equation of state and opacity of dense plasmas
[DE90-002223] 06 p0847 N90-14926
Large scale calculations of the structure and dynamics of dense matter
[DE90-003654] 07 p0991 N90-15726
Equation of state of partially-ionized dense plasmas
[DE90-005246] 09 p1286 N90-17452
Producing dense plasmas with x rays
[DE90-009539] 15 p2169 N90-22393
DENSIFICATION
Preparation, purification and densification of zinc sulfide powder from organometallics
[AD-A210943] 01 p0052 N90-10298
Densification of particulate ceramic composites: The role of heterogeneities
[DE90-000177] 03 p0331 N90-11886
Densification studies of refractory materials using Hot Isostatic Pressing (HIP) and tantalum containment
[DE90-013481] 20 p2833 N90-26114
DENSITOMETERS
NT MICRODENSITOMETERS
Application of x ray absorption edge spectrometry to the non-destructive determination of element concentrations, coating thickness and areal densities
[AERE-R-13030] 16 p2245 N90-22802
DENSITY (MASS/VOLUME)
NT ATMOSPHERIC DENSITY
NT GAS DENSITY
NT SPACE DENSITY
Density of states in a resonant tunneling structure
[AD-A209508] 01 p0128 N90-10731
Orthobaric densities and molar volumes of liquids. Aromatic hydrocarbons
[ESDU-89019] 06 p0738 N90-14299
Density of intercalated graphite fibers
[NASA-TM-102411] 06 p0750 N90-14362
Simultaneous multipoint measurements of density gradients and temperature in a flame
[DE90-001719] 07 p0892 N90-15155
Orthobaric densities and molar volumes of liquids: Alcohols
[ESDU-89037] 07 p0897 N90-15184
Theory of microemulsions in a gravitational field 09 p1224 N90-17099
A small, inexpensive apparatus for the determination of the density of powdered materials
[AD-A215393] 09 p1225 N90-17110
Nonintrusive optical measurements of turbulence and mixing in a stably stratified fluid 13 p1799 N90-20322
A weak formulation for phase-change problems with bulk movement due to unequal densities
[DE90-009398] 15 p2163 N90-22361
Theoretical and computer simulation study of the density fluctuations in liquid water
[PREPRINT-697] 16 p2314 N90-23191
Analysis of turbulent density fluctuations by means of spontaneous Raman diffusion
[ISL-R-103/89] 20 p2863 N90-26287
Experiment K-6-12. Morphometric studies of atrial or granules and hepatocytes. Part 1: Morphometric study of the liver; Part 2: The atrial granular accumulations 20 p2894 N90-26466
Numerical investigation of the incompressible plane shear layer between two gases with different densities
[ETN-90-97315] 21 p3006 N90-27084
Density changes of generation 1.5 and 2.0 copper alloys irradiated at 411 to 414 C and 529 C in FFTF-MOTA
[DE90-015291] 23 p3311 N90-28724
DENSITY (NUMBER/VOLUME)
NT CARRIER DENSITY (SOLID STATE)
NT ELECTRON DENSITY (CONCENTRATION)
NT ELECTRON DENSITY PROFILES
NT ELECTRON DISTRIBUTION
NT ION DENSITY (CONCENTRATION)
NT IONOSPHERIC ELECTRON DENSITY
NT IONOSPHERIC ION DENSITY
NT MAGNETOSPHERIC ELECTRON DENSITY
NT METEOROID CONCENTRATION
NT PACKING DENSITY
NT PARTICLE DENSITY (CONCENTRATION)
NT PLASMA DENSITY
NT SPACE DENSITY
Nonpotential scattering for the density matrix and quantum gravity
[PREPRINT-688] 05 p0697 N90-14080
Large scale calculations of the structure and dynamics of dense matter
[DE90-003654] 07 p0991 N90-15726
DENSITY (RATE/AREA)
U FLUX DENSITY
DENSITY DISTRIBUTION
An evaluation of the Smith-Feddes model
[AD-A213237] 05 p0671 N90-13907
Rapidity densities and their fluctuations in central 200 A GeV S32 interations with Au and Ag,Br nuclei
[LUIP-8905] 07 p0989 N90-15715
Laboratory studies of isolated eddies in a rotating fluid
[AD-A213903] 08 p1063 N90-16146
Studies of density distributions in one-dimensional shock-induced debris clouds
[DE90-004089] 08 p1085 N90-16282
The lower hybrid drift instability and the evolution of plasma gradients
[DE90-006521] 11 p1568 N90-19021
Inclusion of clouds and rain in atmospheric slant path calculations 15 p2083 N90-21925
A study of creep damage using microradiography and continuum damage mechanics 15 p2117 N90-22109
Ability distributions pattern probabilities and quasidensities
[AD-A218471] 16 p2308 N90-23153
Reconstructing primordial density fluctuations 16 p2333 N90-23293
The large and small scale density structure in the solar corona 16 p2338 N90-23327
Data analysis of a two-lidar experiment
[AD-A220289] 17 p2428 N90-23834
Formula scoring: Basic theory and applications
[AD-A218368] 17 p2465 N90-24083
Applications of non-parametric density estimation
[AD-A220206] 17 p2466 N90-24094
A nonlocal free energy density functional approximation for the electrical double layer
[AD-A220664] 18 p2607 N90-24848
Origin of density fluctuations in extended inflation
[NASA-CR-182852] 19 p2795 N90-25915
An analysis of the Palomar-Green subdwarfs and white dwarfs 23 p3409 N90-29263
Non-destructive evaluation of infiltration-toughened ceramics
[DE90-629716] 24 p3453 N90-29501
DENSITY MEASUREMENT
NT X RAY DENSITY MEASUREMENT
The middle and high latitude ionosphere at approximately 550 km altitude 02 p0242 N90-11374
Modelling ionospheric density structures 02 p0242 N90-11375
Orthobaric densities and molar volumes of liquids. Introduction to data items issued after July 1989
[ESDU-89018] 06 p0738 N90-14298
Orthobaric densities and molar volumes of liquids. Aromatic hydrocarbons
[ESDU-89019] 06 p0738 N90-14299
Shock thickness measurements with laser beams
[MPIS-7/1989] 08 p1083 N90-16267
Upper atmosphere research
[ISBN-0-642-13582-7] 08 p1100 N90-16368
RF modal quantity gaging 11 p1474 N90-18483
Critical current density and transition temperature measurements of Y-Ba-Cu-O rods
[AD-A216695] 12 p1719 N90-19875
Application of x ray absorption edge spectrometry to the non-destructive determination of element concentrations, coating thickness and areal densities
[AERE-R-13030] 16 p2245 N90-22802
MEGALIDAR proof-of-concept demonstration
[AD-A218787] 16 p2255 N90-22858
Measurement Techniques for Hypersonic Flows
[VKI-LS-1990-05] 24 p3419 N90-29314
CARS spectroscopy and applications 24 p3420 N90-29321
Determination of density using simultaneous interferometry methods
[IMFL-90/04] 24 p3547 N90-30061
DEOXIDIZING
Isotope exchange in oxide-containing catalyst
[NASA-CASE-LAR-13542-2-SB] 13 p1769 N90-20154
DEOXYRIBONUCLEIC ACID
Biomedical studies with the free electron laser
[AD-A208927] 01 p0091 N90-10519
Nomenclature for physical mapping of complex genomes
[DE89-015173] 06 p0859 N90-14994
Mechanisms of microwave induced damage in biologic materials
[AD-A213480] 08 p1104 N90-16390

Potential biomedical application of the Los Alamos infrared free-electron laser: DNA spectroscopy
[DE90-006505] 12 p1667 N90-19575
Does DNA cytometry have a place in the clinical laboratory
[DE90-007652] 14 p2009 N90-21512
In vitro photoreactivation of transforming DNA of bacillus subtilis spores after irradiation with UV light
[DLR-FB-89-45] 18 p2583 N90-24710
Understanding our genetic inheritance. The US Human genome project: The first five years, FY 1991-1995
[DE90-008240] 18 p2584 N90-24718
Imaging and spectroscopy of small molecules by scanning tunneling microscopy
[AD-A222572] 20 p2924 N90-26641
DNA damage and repair in human skin: Pathways and questions
[DE90-015126] 23 p3356 N90-28966

DEPENDENCE
NT SPATIAL DEPENDENCIES
NT TEMPERATURE DEPENDENCE
NT TIME DEPENDENCE

DEPENDENT VARIABLES
A comparison of alternative families of transformations for variables constrained to lie on the interval (0,1)
[MATHS-REPT-A-126] 24 p3539 N90-30011

DEPERSONALIZATION
Passenger behaviour in aircraft emergencies involving smoke and fire 10 p1317 N90-17613

DEPLETION
NT OZONE DEPLETION
Ozone depletion, greenhouse gases, and climate change
[PB89-216097] 03 p0369 N90-12110
Frequency doubled operation of a ground state depleted laser using the Nd(3+)(4)F(sub 3/2)-(4)I(sub 9/2) transition in Y2SiO5
[DE90-012089] 19 p2695 N90-25338
Depletion mode pumping of solid state lasers
[DE90-012090] 19 p2696 N90-25339

DEPLOYMENT
Simulation of shuttle flight control system structural interaction with RMS deployed payloads 01 p0020 N90-10100
The third generation rigid solar array GSR3 02 p0180 N90-11017
A high precision gravity compensation system for the deployment test of the ERS-1 SAR antenna 02 p0183 N90-11038
Deployment simulation for 3rd generation solar array GSR3 02 p0188 N90-11074
Modeling and control of the rapid deployment of towed airborne devices 07 p0879 N90-15092
Structural and operational aspects of the concentrating SARA-Louver solar generator 10 p1340 N90-17760
SFU solar array 10 p1340 N90-17761
The GSR3: A new approach for solar array deployments 10 p1340 N90-17762
Deployment simulation for the third generation solar arrays GSR3 10 p1340 N90-17763
Solar array designs for Columbus elements 10 p1340 N90-17764
Structures for remotely deployable precision antennas 12 p1609 N90-19256
Advances in large inflatable reflectors 12 p1609 N90-19258
Kalman estimation for SEDS measurements 12 p1634 N90-19393
An inverse kinematics algorithm for a highly redundant variable-geometry-truss manipulator 16 p2288 N90-23033
In situ investigation of sea surface noise from a depth of one meter
[AD-A220158] 17 p2432 N90-23857
A cable-rigidized 3D pantograph 18 p2538 N90-24484
ADELE: Deployment hinge using wraparound strips 18 p2538 N90-24485
Some remarks on a hinge actuator for large spot antenna arm deployers 18 p2539 N90-24486
Mechanism for deployment and retraction of biological samples 18 p2540 N90-24499
A sequentially deployable structure for space applications. Part 2: Engineering model manufacturing and testing 18 p2541 N90-24504
Inmarsat omni-antenna deployment mechanism 18 p2542 N90-24508
The development of expertise on an intelligent tutoring system 18 p2630 N90-24984
Yaw fin deployment apparatus for ejection seat
[AD-D014512] 19 p2656 N90-25118
SEDS experiment design definition
[NASA-CR-183909] 19 p2665 N90-25165
Structures for remotely deployable precision antennas
[NASA-CR-182065] 20 p2822 N90-26061
Potential new tactical applications of the Global Positioning System (GPS) 21 p3069 N90-27449
Optimization of the deployment of a pair of satellites in inclined eccentric geosynchronous orbits 22 p3128 N90-27751
Dynamics and dynamics experiments in TSS-1 22 p3129 N90-27758
Deployment of large flexible space structures 22 p3131 N90-27766
Lightweight, broadband, pulsed, frequency agile, self-screening jammer for airborne deployment
[AD-D014468] 22 p3163 N90-27937
The effect of rapid spoiler deployment on the transient forces on an aerofoil 23 p3274 N90-28527
Shuttle remote manipulator system mission preparation and operations 24 p3521 N90-29909

DEPOLARIZATION
N-port theory applied to backscatter polarimetry and depolarization in foliage penetration
[AD-A213437] 07 p0917 N90-15305
Software set-up for data processing of depolarization due to rain and ice crystals in the Olympus project
[EUT-89-E-218] 20 p2855 N90-26240
Asymmetric depolarization in powerful extragalactic radio sources 22 p3264 N90-28484

DEPOLARIZERS
U DEPOLARIZATION

DEPOSITION
NT ANODIZING
NT ELECTRODEPOSITION
NT ELECTROPLATING
NT VACUUM DEPOSITION
NT VAPOR DEPOSITION
Alternative fabrication techniques for high-efficiency CuInSe2 and CuInSe2-alloy films and cells
[DE89-009451] 01 p0083 N90-10474
The auroral energy deposition over the polar ionosphere during substorms
[AD-A210522] 01 p0086 N90-10490
CuInSe2 solar cell research by sputter deposition
[DE89-009450] 02 p0236 N90-11345
The Si(1-x)Nx Rugate
[AD-A211236] 02 p0275 N90-11572
Diamondlike carbon coatings for optical systems
[AD-A211255] 02 p0276 N90-11573
Photolysis of spacecraft contaminants
[AD-A211715] 03 p0317 N90-11801
Temperature dependent effects during Ag deposition on Cu(110)
[DE89-016987] 03 p0327 N90-11857
Plasma-deposited amorphous hydrogenated carbon films and their tribological properties
[NASA-TM-102379] 03 p0331 N90-11880
Fundamental tribological properties of ion-beam-deposited boron nitride films
[NASA-TM-102088] 03 p0331 N90-11881
Ion-assisted deposition of high-temperature lubricious surfaces
[DE89-012397] 03 p0331 N90-11883
Ion beam deposition of epitaxial germanium and gallium arsenide layers
[DE89-017439] 03 p0411 N90-12357
High temperature superconducting compounds
[AD-A211511] 03 p0413 N90-12374
Metallo-organic decomposition process for dielectric films
[AD-A211590] 04 p0495 N90-12849
Mesoscale acid deposition modeling studies
[NASA-CR-4262] 04 p0554 N90-13228
Effect of adsorbed arsenic on the decomposition rate of nickel hydride
[AD-A213245] 05 p0621 N90-13624
Elaboration and characterization of MISFET transistors on InP
[ECL-88-19] 05 p0636 N90-13709
Preparation and properties of high deposition a-Si:H films and solar cells using disilane
[DE89-009467] 06 p0804 N90-14679
Profile measurements of sulfur dioxide, nitrogen oxides, and nitric acid deposition velocities in California's south coast air basin
[PB90-104001] 06 p0808 N90-14703
Steady state model to determine lake resources at risk to acid deposition in the Sierra Nevada, California
[PB89-103995] 06 p0809 N90-14705
Application of surface analysis methods to studies of atmospheric deposition in forests
[DE90-000562] 06 p0810 N90-14714
Enhancement of microchannel plate gain by deposition of CsI on the channel walls
[DE90-003051] 07 p0922 N90-15334
Acid deposition
[DE90-003959] 07 p0958 N90-15544
Partial reduction of re-oxidation processing of Y-Ba-Cu-O sputtered thin films
[DE90-003655] 07 p0999 N90-15782
Orientation of rf-sputter-deposited MoS2 films
[ATR-89(4752)-1] 07 p1000 N90-15784
The fabrication of YBa2Cu3O7 thin films by thermal coevaporation in oxygen
[DE90-003960] 07 p1006 N90-15824
The influence of residual contamination on the structure and properties of metal/GaAs interfaces
[DE90-000549] 08 p1127 N90-16530
Alloying of metals for corrosion resistance
[AD-D014313] 09 p1194 N90-16919
Adhesion of silver films to ion-bombarded alumina
[DE90-005642] 09 p1199 N90-16947
Dispelling the North American acid rain clouds: Developing a framework for political consensus through the identification of elite viewpoints, volumes 1 and 2 09 p1243 N90-17213
Evaluation of the use of flat terrain models versus complex terrain screening models in estimating pollutant transport and deposition in complex terrain
[DE90-005271] 09 p1245 N90-17223
Growth of epitaxical SiC layers onto on- and off-axis 6H-SiC substrates by ion beam deposition
[DE90-004236] 09 p1287 N90-17459
The use of BaF2 buffer layers for the sputter-deposition of TlCaBaCuO thin-film superconductors
[DE90-004859] 09 p1292 N90-17490
Epitaxial growth of Cr(011) on LiF(001)
[DE90-005635] 09 p1293 N90-17496
Effect of propellant flowrate and purity on carbon deposition in LO2/methane gas generators 11 p1471 N90-18468
Sputter deposition of diffusion barrier coatings on SiC monofilaments for use in Ti-based composites 11 p1477 N90-18502
Surface intermediates in thin film deposition on silicon
[AD-A216662] 11 p1483 N90-18534
Structure and reactivity of model thin film catalysts
[DE90-007385] 11 p1485 N90-18546
Perspectives on aerosol deposition to natural surfaces
[DE90-003398] 11 p1532 N90-18819
Pulsed laser deposition of high T(sub c) superconducting thin films
[AD-A216507] 11 p1569 N90-19034
The effect of fiber coatings on interfacial shear strength and the mechanical behavior of ceramic composites
[DE90-007574] 12 p1632 N90-19380
NAPAP (National Acid Precipitation Assessment Program) emissions inventory: Overview of allocation factors, 1985
[PB90-126012] 12 p1685 N90-19679
Analysis of tectonic movements utilizing remote sensor products in the Southern Espinhaco (SE) region
[INPE-4830-PRE/1451] 12 p1690 N90-19708
Characterization of ceramic matrix composites fabricated by chemical vapor infiltration
[DE90-008409] 13 p1768 N90-20149
Spray deposition: A fundamental study of droplet impingement, spreading and consolidation
[AD-A217202] 13 p1787 N90-20255
Tribological properties of boric acid and boric-acid-forming surfaces. Part 2: Formation and self-lubrication mechanisms of boric acid films on boron- and boric-oxide-containing surfaces
[DE90-005632] 13 p1811 N90-20400
Dielectric composite thin films
[AD-A217940] 13 p1881 N90-20791
Influence of the deposition conditions on radiofrequency magnetron sputtered MoS2 films
[NASA-TP-2994] 14 p1958 N90-21210
Improvement of small-area, amorphous-silicon thin-film photovoltaics on polymer substrate
[DE90-000314] 14 p2002 N90-21472
Transformation and deposition of airborne gaseous and particulate pollutants during transport over the Baltic Sea
[PUBL-AIR-QUALITY-5] 14 p2003 N90-21478
Effects of Air Pollution on Western Forests
[PB90-131111] 14 p2003 N90-21481
Development of a computational fluid dynamics and chemistry model for the fouling of jet fuels
[DE90-005664] 15 p2098 N90-22003
A study of mesoscale acid deposition in the lower Ohio River Valley 16 p2253 N90-22848
Fundamental and practical studies of metal contacts on mercury zinc telluride
[AD-A218730] 17 p2376 N90-23528
The diurnal ozone cycle in a coniferous forest: The importance of meteorology and chemistry
[CM-75] 17 p2421 N90-23795
Novel pulsed plasma treatment and coating process: Multilayer structures for optical computing applications
[AD-A220737] 18 p2615 N90-24894
Computer-controlled ion beam sputter deposition of multicomponent oxides
[DE90-010544] 18 p2619 N90-24923

Studies on ion scattering and sputtering processes in ion beam sputter-deposition of high Tc superconducting films: The optimization of deposition parameters
[DE90-010538] 18 p2621 N90-24936
SiC film deposited by pulsed excimer laser ablation
[DE90-010634] 18 p2622 N90-24938
Preparation and properties of superconducting thin films by excimer laser ablation
[DE90-011929] 18 p2626 N90-24967
Processing polymeric powders
18 p2647 N90-25069
Fundamental studies and device development in beta silicon carbide
[AD-A219253] 19 p2676 N90-25220
Carbon deposition model for oxygen-hydrocarbon combustion. Task 6: Data analysis and formulation of an empirical model
[NASA-CR-183986] 20 p2829 N90-26095
Measurements of tropospheric nitric acid over the Western United States and Northeastern Pacific Ocean
[NASA-TM-103470] 20 p2883 N90-26399
Laser induced surface chemical epitaxy
[AD-A222082] 21 p2977 N90-26920
Microbially influenced corrosion of carbon steels
[DE90-012231] 21 p2980 N90-26936
Self-lubricating-diamond like coatings deposition
[AD-A221756] 21 p2988 N90-26983
Preparation and characterization of thin films based on sol-gel technique and development of spectroscopic probe for film formation and characterization
[AD-A221762] 21 p2988 N90-26984
Nonlinear material response to very rapid energy deposition
[AD-A221932] 21 p2989 N90-26988
Development of a mathematical model for the thermal decomposition of aviation fuels
[AD-A221673] 21 p2990 N90-26994
In-situ integrated processing and characterization of thin films of high temperature superconductors, dielectrics and semiconductors by MOCVD 22 p3148 N90-27851
Quality assurance support for the National Atmospheric Deposition Program and national trends network monitoring activities: 1987-1990
[PB90-187162] 22 p3198 N90-28149
Acid deposition in Maryland: Summary of results through 1989
[PB90-229782] 22 p3200 N90-28160
Acid deposition: No such thing as a free launch
[DE90-015085] 23 p3348 N90-28920
Tropospheric nitrogen: The influence of anthropogenic sources on distributions and deposition, executive summary
[DE90-015401] 23 p3348 N90-28922
Estimating the spatial variability of trace gas deposition velocities
[PB90-208570] 23 p3349 N90-28928
Extension of plasma source ion implantation to ion beam enhanced deposition
[AD-A224462] 24 p3454 N90-29506
Ion-beam-assisted deposition of silver films on zirconia ceramics for improved tribological behavior
[DE90-009706] 24 p3456 N90-29516
Adhesion of silver films to ion-bombarded zirconia
[DE90-010088] 24 p3456 N90-29517
Ion-beam mixing of Fe/B layers for tribological applications
[DE90-010091] 24 p3456 N90-29518
Tropospheric nitrogen: The influence of anthropogenic sources on distributions and deposition
[DE90-015408] 24 p3487 N90-29709
Transmission electron microscopy study of ICB Al on Ge and Si(001) substrates
[DE90-015299] 24 p3553 N90-30103

DEPOSITS
Measuring the thickness of austenitic weld deposits on carbon steel walls using a magnetic method
[DE89-635446] 06 p0794 N90-14628
Chemistry-structure-property interrelationships for calcareous deposits as stand-alone coatings
[AD-A216031] 10 p1359 N90-17881
Geochemical survey on faults overland with alluvial deposits, part 1. Application for the Neodani and the Atera faults survey
[DE89-782326] 12 p1690 N90-19707
Geology, distribution of hot springs and hydrothermal alteration zones of major geothermal areas in Japan
[DE90-753026] 13 p1820 N90-20451
Development of a mathematical model for the thermal decomposition of aviation fuels
[AD-A221673] 21 p2990 N90-26994

DEPRESSIONS (TOPOGRAPHY)
U STRUCTURAL BASINS

DEPRESSURIZATION
U PRESSURE REDUCTION

DEPRIVATION
NT SLEEP DEPRIVATION
NT WATER DEPRIVATION

DEPTH
Determination of Q as a function of depth and tectonic province
[AD-A213805] 07 p0960 N90-15554
On the depth of combinatorial optimization problems
[MEMO-803] 11 p1554 N90-18948
A solution level indicator system
[DE90-007939] 14 p1948 N90-21151
Spatial constraints of stereopsis in video displays
16 p2267 N90-22920
Paradoxical monocular stereopsis and perspective vergence 16 p2267 N90-22922
The perception of three-dimensionality across continuous surfaces 16 p2268 N90-22924
How to reinforce perception of depth in single two-dimensional pictures 16 p2270 N90-22937
Determination of depth-viewing volumes for stereo three-dimensional graphic displays
[NASA-TP-2999] 16 p2275 N90-22965
Disparity gradients and depth scaling
[AD-A218612] 17 p2453 N90-23992
Design and investigation of a dive plane sliding mode compensator for an autonomous underwater vehicle
[AD-A219552] 17 p2454 N90-23997
An injective far-field pattern operator and inverse scattering problem in a finite depth ocean
[PB90-159294] 22 p3230 N90-28318
Building an environment model using depth information 23 p3374 N90-29064

DEPTH MEASUREMENT
Adjustable depth gage
[NASA-CASE-LEW-14880-1] 01 p0072 N90-10415
Use of ground penetrating radar to define recharge areas in the Central Sand Plain
[PB89-224885] 04 p0490 N90-12814
CO2 depth profiles in cometary model substances of KOSI 12 p1742 N90-20014
Real-time stereo-microradiography
[AD-A218433] 16 p2245 N90-22805
Determination of tide heights from airborne bathymetric data
[AD-A220412] 17 p2430 N90-23848

DEPTH PERCEPTION
U SPACE PERCEPTION

DERIVATION
Incompressible flow about ellipsoids of revolution
[REPT-88-02] 03 p0302 N90-11713
Tensor methods for unconstrained optimization using second derivatives
[AD-A213642] 07 p0983 N90-15681
Vector fields, linear spaces and tensors in physics. Part 3: Tensor analysis and its applications
[INPE-5000-MD/41] 11 p1561 N90-18997
On a non classical oblique derivative problem for parabolic singular integro-differential operators
[DE90-612739] 14 p2020 N90-21574
Adaptive node movement in finite-difference solutions of partial differential equations with applications to gasdynamics, part 1
[UTIAS-333-PT-1] 19 p2750 N90-25622

DERIVATION CALCULUS
U DIFFERENTIAL CALCULUS

DESALINIZATION
Planning for hybrid-cycle OTEC experiments using the HMTSTA test facility at the Natural Energy Laboratory of Hawaii
[DE89-013278] 02 p0237 N90-11349
Conceptual design analysis for hybrid-cycle OTEC plants for co-production of electric power and desalinated water
[DE90-003551] 08 p1097 N90-16350

DESCENT
NT PARACHUTE DESCENT
Piloted simulation of a ground-based time-control concept for air traffic control
[NASA-TM-101085] 08 p1020 N90-15898
Optimal control of an aircraft flying through a downburst 15 p2053 N90-21765
A conflict analysis of 4D descent strategies in a metered, multiple-arrival route environment
[NASA-CR-182019] 15 p2055 N90-21772
Preliminary Subsystem Designs for the Assured Crew Return Vehicle (ACRV), volumes 1-3
[NASA-CR-186662] 17 p2363 N90-23455
Reentry trajectory optimization and control
22 p3127 N90-27746
Space shuttle descent flight verification by simulation: A challenge in implementing flight control system robustness 22 p3127 N90-27748
Dynamic ground effects 23 p3275 N90-28531

DESCENT TRAJECTORIES
NT REENTRY TRAJECTORIES
Ascent and descent trajectory optimization of Ariane 5/Hermes 22 p3126 N90-27743

DESCRIPTIONS
Simulating simultaneous processes with APL
[MEMO-INF-89-47] 11 p1547 N90-18906

DESCRIPTIVE GEOMETRY
Rotary-Jet thrust augmentor with jet-flapped blades
18 p2492 N90-24243
On the projective invariant representation of conics in computer graphics
[CWI-CS-R8938] 18 p2593 N90-24752

DESERTS
NT MOJAVE DESERT (CA)
NT SAHARA DESERT (AFRICA)
Diagnostic study of atmosphere-terrain interaction leading to the formation of dust clouds and poor visibilities over near east desert areas
[AD-A211243] 02 p0239 N90-11358
Tips on desert flying
[PB90-233222] 22 p3110 N90-27670

DESICCANTS
Moisture control in sealed electronic packages
[DE90-008136] 13 p1771 N90-20166

DESICCATION
U DRYING

DESIGN ANALYSIS
Large scale prop-fan structural design study. Volume 1: Initial concepts
[NASA-CR-174992] 01 p0010 N90-10043
Large scale prop-fan structural design study. Volume 2: Preliminary design of SR-7
[NASA-CR-174993] 01 p0010 N90-10044
Full scale technology demonstration of a modern counterrotating unducted fan engine concept. Design report
[NASA-CR-180867] 01 p0010 N90-10048
Computational controls for aerospace systems
01 p0017 N90-10082
Castings, from theory to practical application
01 p0042 N90-10236
Relating tolerances and kinematic behavior
[AD-A211125] 01 p0055 N90-10311
Design and operating characteristics of a CW relevant quasi-optical gyrotron with variable mirror separation
[AD-A210611] 01 p0074 N90-10425
A design assessment for metallic pressure vessels circumferentially reinforced with a pre-tensioned high-specific-strength anisotropic composite overwind
[AD-A209108] 01 p0079 N90-10453
Stochastic control theory, nonlinear structural mechanics and applied combinatorics
[AD-A209042] 01 p0114 N90-10657
Integrated multidisciplinary design optimization of rotorcraft
[NASA-TM-101642] 02 p0155 N90-10889
An assessment of robustness of flight control systems based on variable structure techniques
02 p0157 N90-10895
Spacecraft Structures and Mechanical Testing
[ESA-SP-289] 02 p0176 N90-10986
Qualification by simulation: Dream or reality
02 p0177 N90-10990
Overview of actual buckling calculation methods for space vehicle structures 02 p0177 N90-10995
Viscoelastic tuned dampers for control of structural dynamics 02 p0178 N90-10999
Integration of analytical and test software for optimal structural design under dynamic loads
02 p0179 N90-11007
Advances in design and testing of spacecraft structures 02 p0180 N90-11018
ESA-D: An integrated software for antenna design and analysis 02 p0185 N90-11052
Two years experience with the ESTEC multishaker system 02 p0187 N90-11065
Deployment simulation for 3rd generation solar array GSR3 02 p0188 N90-11074
ASIC (Application Specific Integrated Circuit) replacement for an SSI (Small Scale Integrated) component design: A case study
[DE89-013494] 02 p0215 N90-11232
Laser dynamics: The system dynamics and network theory of optoelectronic integrated circuit design
02 p0226 N90-11296
GaAs ASIC design case study
[DE89-013934] 02 p0258 N90-11461
A survey of research methods to study design
[AD-A211213] 02 p0262 N90-11491
Performance and quality of a wing type parachute: Parametric analysis
[REPT-88-19] 03 p0302 N90-11710
Development of direct-inverse 3-D methods for applied transonic aerodynamic wing design and analysis
[NASA-CR-186036] 03 p0305 N90-11733
Design of a solar sail mission to Mars
[NASA-CR-186045] 03 p0311 N90-11771

An integrated methodology for optimizing structural composite damping
[NASA-TM-102343] 03 p0319 N90-11808
Current research in advanced materials
[DE89-017466] 03 p0331 N90-11884
Kinematic design NC optical generator 03 p0404 N90-12316
An introduction to effectiveness: NTU relationships
[ESDU-89016] 03 p0415 N90-12381
On the precision and reliability of GPS networks computed using the double difference observable
[ETN-89-95719] 04 p0449 N90-12571
Low Earth Orbit Raider (LER) winged air launch vehicle iconcept
[NASA-CR-186057] 04 p0452 N90-12590
Rolls-Royce and ERCOFTAC
[PNR90600] 04 p0456 N90-12615
Blading design for multi-storage HP compressor
[PNR90602] 04 p0456 N90-12616
Analysis and simulation of dynamics of spacecraft power systems 04 p0463 N90-12653
Mathematical models for the linear induction motor
[RR-WB-88-17] 04 p0496 N90-12853
The design, construction, performance and calibration of pulse generators to fulfil the requirements of specifications defence standard 59-41, FS(F) 510 and FS(S) 457
[RAE-TM-FS(F)-550] 04 p0496 N90-12857
A review of focal reducer interferometer systems
[RSRE-MEMO-3486] 04 p0554 N90-13231
Overview of the Hipparcos satellite 05 p0603 N90-13502
The payload structure 05 p0604 N90-13510
Spacecraft thermal control 05 p0604 N90-13513
Development of a shuttle plume radiation heating indicator
[NASA-CR-183679] 05 p0614 N90-13584
Flight motor set 360L001 (STS-26R). Volume 5: Nozzle component
[NASA-CR-183771] 05 p0615 N90-13588
Design of a power component with IGBT insulated grid. Static and dynamic study
[ECL-88-22] 05 p0636 N90-13710
Design and control of a two-degree-of-freedom lightweight flexible arm
[AD-A213335] 05 p0650 N90-13790
On control of manipulators
[ISBN-90-9002789-0] 05 p0652 N90-13804
A double focusing mass-spectrometer for simultaneous ion measurements in the stratosphere 05 p0659 N90-13848
Bone mineral measurement using dual energy x ray densitometry 05 p0680 N90-13958
The problem of automation: Inappropriate feedback and interaction, not overautomation
[NASA-CR-186126] 05 p0686 N90-13994
Fundamental quantum 1/f noise in ultrasmall semiconductor devices and their optimal design principles
[AD-A211947] 05 p0702 N90-14107
The space station tethered elevator system
[NASA-CR-186051] 06 p0732 N90-14265
Partial gravity habitat study: With application to lunar base design
[NASA-CR-186048] 06 p0732 N90-14267
The United States Air Force approach to all-weather testing 07 p0870 N90-15047
Task-oriented display design: Concept and example
[NASA-TM-101685] 07 p0881 N90-15101
Shuttle-C utilization for assembly of the rephased Freedom configuration
[NASA-TM-101658] 07 p0885 N90-15120
Modifications of the Penn State Boundary Layer Research Facility for boundary layer/structure interaction experimental research
[AD-A213874] 07 p0931 N90-15391
On the analysis and optimization of a platform manipulator 07 p0938 N90-15433
On the motion of compliantly-connected rigid bodies in contact. Part 1: The motion prediction problem
[AD-A214135] 07 p0948 N90-15489
On the motion of compliantly-connected rigid bodies in contact. Part 2: A system for analyzing designs for assembly
[AD-A214136] 07 p0948 N90-15490
High-efficiency silicon concentrator solar cells for use with prismatic covers
[DE90-002644] 07 p0952 N90-15509
Architectural study of the design and operation of advanced force feedback manual controllers
[NASA-CR-185948] 07 p0981 N90-15664
Performance of a highly-loaded HP compressor
[RAE-TM-P-1149] 08 p1024 N90-15919
EVA space suit. General concepts of design and arrangement 08 p1034 N90-15976
The visible channel of OMEGA-VIMS
[IFSI-89-14] 08 p1077 N90-16231
Low risk low power heat pipe/thermoelectric space power supply
[DE89-014817] 08 p1095 N90-16342
Conceptual design analysis for hybrid-cycle OTEC plants for co-production of electric power and desalinated water
[DE90-003551] 08 p1097 N90-16350
ATF-2 studies
[DE90-004380] 08 p1124 N90-16510
Properties and design of multifilamentary NbTi composite superconductors
[DE90-004904] 08 p1134 N90-16569
Space shuttle solid rocket booster redesign and testing 09 p1175 N90-16804
A methodology for the concept definition of advanced space transportation systems 09 p1176 N90-16813
Performance integration of a reusable launch vehicle with hybrid airbreathing rocket propulsion 09 p1177 N90-16820
The Hermes system: Its design objectives and solutions 09 p1177 N90-16821
Hermes propulsion system 09 p1178 N90-16823
Environmental constraints for polar platform design
[RAE-TR-89014] 09 p1181 N90-16849
Planar array antenna design analysis, volume 1
[AD-A215537] 09 p1207 N90-16999
High-efficiency Schottky-Varactor frequency multipliers at millimeter waves
[PB90-110701] 09 p1209 N90-17007
Space station wardroom habitability and equipment study
[NASA-CR-4246] 09 p1260 N90-17308
A design procedure for a slotted waveguide with probe-fed slots radiating into plasma
[DE90-004168] 09 p1284 N90-17446
Conceptual design of high Tc superconducting power cable and its economic evaluation
[DE90-734940] 09 p1287 N90-17462
Use of semiempirical aerodynamic methods for preliminary design 10 p1304 N90-17546
Numerical solutions of the linearized Euler equations for unsteady vortical flows around lifting airfoils
[NASA-TM-102466] 10 p1307 N90-17562
The Hermes power system 10 p1330 N90-17682
Autonomous electrical power supply subsystem for the Vesta mission 10 p1331 N90-17692
Design considerations and lessons learned on the European retrievable carrier 10 p1332 N90-17698
Space Station Freedom energy storage system design and development 10 p1332 N90-17701
Contribution to the study of design methods for numerical filters with finite pulse response and applications to image processing
[TELECOM-89-E-007] 10 p1376 N90-17974
Research on a two-dimensional inlet for a supersonic V/STOL propulsion system. Appendix A
[NASA-CR-174945] 11 p1451 N90-18364
Defects: Their behaviour and related design assumptions 11 p1457 N90-18397
The design of advanced ceramic composites
[DE90-006613] 11 p1493 N90-18592
Fastener design manual
[NASA-RP-1228] 11 p1517 N90-18740
Development of an experimental space station model for structural dynamics research
[NASA-TM-102601] 11 p1519 N90-18751
An interactive system applied to the linear quadratic problem
[INPE-4945-TDL/386] 11 p1548 N90-18913
Hamiltonian analysis and simulation of free electron lasers
[INPE-4785-TDL/351] 11 p1567 N90-19018
The ISO short wavelength spectrometer 11 p1589 N90-19162
The Infrared Space Observatory 11 p1589 N90-19163
Spectrophotometry of dust with Isophot 11 p1589 N90-19164
An advanced cooled grating spectrometer for UKIRT-CGS4 11 p1589 N90-19165
Solid oxide fuel cell cogeneration system conceptual design, program 2
[PB90-114968] 12 p1681 N90-19653
Aerodynamic analysis of a US Navy and Marine Corps unmanned air vehicle
[AD-A218282] 13 p1755 N90-20077
The NASA digital VGH program: Exploration of methods and final results. Volume 4: B 747 data 1978-1980, 1689 hours
[NASA-CR-181909-VOL-4] 13 p1756 N90-20083
Space station Simulation Computer System (SCS) study for NASA/MSFC. Volume 3: Refined conceptual design report
[NASA-CR-183842] 13 p1762 N90-20115
Space station Simulation Computer System (SCS) study for NASA/MSFC. Volume 4: Conceptual design report
[NASA-CR-183843] 13 p1762 N90-20116
Composite laminate tailoring with probabilistic constraints and loads
[NASA-TM-102515] 13 p1766 N90-20138
Design and test of a compact optics system for the pool boiling experiment
[NASA-TM-102530] 13 p1786 N90-20253
An applicational process for dynamic balancing of turbomachinery shafting
[NASA-TM-102537] 13 p1810 N90-20392
Plan, formulate, and discuss a NASTRAN finite element model of the UH-60A helicopter airframe
[NASA-CR-181975] 13 p1818 N90-20439
Multi-mission Ni-H2 battery cells for the 1990's 13 p1825 N90-20477
RenderMan design principles 13 p1857 N90-20653
Design decision making with multiple interacting criteria and varying relative weights
[AD-A218027] 13 p1869 N90-20721
Design of a natural laminar flow airfoil for an unmanned aircraft
[PD-CF-9004] 14 p1916 N90-20975
Aerodynamic design techniques at DLR Institute for Design Aerodynamics 14 p1916 N90-20979
Inverse design of airfoil contours: Constraints, numerical method, and applications 14 p1917 N90-20980
An efficient airfoil design method using the Navier-Stokes equations 14 p1917 N90-20981
A system for transonic wing design with geometric constraints based on an inverse method 14 p1917 N90-20983
A fast collocation method for transonic airfoil design 14 p1917 N90-20984
Subsonic and transonic blade design by means of analysis codes 14 p1917 N90-20985
A computational design method for shock free transonic cascades and airfoils 14 p1918 N90-20986
Inverse computation of transonic internal flows with application for multi-point-design of supercritical compressor blades 14 p1918 N90-20987
An inverse method for the design of turbomachine blades 14 p1918 N90-20988
Application of an inverse method to the design of a radial inflow turbine 14 p1918 N90-20989
Aerodynamic optimization by simultaneously updating flow variables and design parameters 14 p1918 N90-20991
Numerical optimization of target pressure distributions for subsonic and transonic airfoil design 14 p1919 N90-20993
A tool for automatic design of airfoils in different operating conditions 14 p1919 N90-20994
The use of numerical optimization for helicopter airfoil and blade design 14 p1919 N90-20995
Aerodynamic design by optimization 14 p1920 N90-20996
Numerical optimization of wings in transonic flow 14 p1920 N90-20997
Aerodynamic design via control theory 14 p1920 N90-20998
Optimization of aerodynamic designs using computational fluid dynamics 14 p1920 N90-20999
Recent experience in simultaneous control-structure optimization 14 p1936 N90-21078
Global nonlinear optimization of spacecraft protective structures design
[NASA-TM-100387] 14 p1938 N90-21095
Design and status of the detector block for the ISO-SWS 14 p1980 N90-21341
Conceptual design optimization study
[NASA-CR-4298] 15 p2051 N90-21755
Operation of a step tunable megawatt gyrotron 15 p2061 N90-21802
The 10-100 kW submillimeter gyrotron 15 p2061 N90-21803
Principles of Very Large Scale Integrated (VLSI) system planning 15 p2088 N90-21950
Thermomechanically-induced convective motion and natural convection in confined gaseous helium subjected to boundary heating 15 p2089 N90-21960
Application of the TRANAIR rectangular grid approach to the aerodynamic analysis of complex configurations 15 p2096 N90-21996
Review of analysis methods for mechanically fastened joints in composites
[LR-599] 15 p2107 N90-22050
Clean access platform for orbiter 15 p2116 N90-22103
Human motion perception: Higher-order organization 15 p2140 N90-22226
An investigation of narrow-bandgap semiconductors: Devices, circuits, and systems 15 p2171 N90-22406

Aircraft crash survival design guide. Volume 1: Design criteria and checklists
[AD-A218434] 16 p2198 N90-22545
Multilevel decomposition approach to the preliminary sizing of a transport aircraft wing
[NASA-CR-4296] 16 p2200 N90-22557
Differential equation based method for accurate approximations in optimization
[NASA-TM-102639] 16 p2200 N90-22558
Limiting performance based structural and control optimization for large vibrating structures
16 p2202 N90-22568
Design for testability of stuck-open and stack-on CMOS combinatorial circuits
[REPT-89-044] 16 p2230 N90-22725
Design of high-performance negative-feedback oscillators
[ETN-90-96698] 16 p2231 N90-22729
Supersonic flow computations for an ASTOVL aircraft configuration, phase 2, part 2
[NASA-CR-4284] 16 p2234 N90-22746
Lunar base 2 (the second thousand days of a base on the Moon)
[ILR-MITT-230(1989)] 16 p2275 N90-22968
Integrated control-system design via generalized LQG (GLQG) theory 16 p2286 N90-23023
H(2)- and H(infinity)-design tools for linear time-invariant systems 16 p2286 N90-23025
Application of numerical optimization techniques to control system design for nonlinear dynamic models of aircraft 16 p2287 N90-23032
Algorithmic considerations of integrated design for CSI on a hypercube architecture 16 p2289 N90-23043
Methodology for analysis and simulation of large multidisciplinary problems 16 p2290 N90-23046
Nonflammable hydraulic power system for tactical aircraft. Volume 1: Aircraft system definition, design and analysis
[AD-A218493] 17 p2356 N90-23409
Geometric programming prediction of design trends for OMV protective structures
[NASA-TM-4206] 17 p2365 N90-23462
Lunar crane hook
[NASA-CR-184921] 17 p2384 N90-23579
Data quality analysis at the National Transonic Facility
[NASA-CR-4303] 17 p2448 N90-23957
Designing distributed algorithms by means of formal sequentially phased reasoning
[TR-89-8] 17 p2449 N90-23969
A formal mechanism for determining redundancy and irrelevance in Hypertext views
[TR-89-9] 17 p2450 N90-23970
Combustor design and analysis using the Rocket Combustor Interactive Design (ROCCID) methodology
[NASA-TM-103165] 18 p2513 N90-24349
Experiments and other methods for developing expertise with design of experiments in a classroom setting
18 p2516 N90-24367
Simplified design procedures for fiber composite structural components/joints
[NASA-TM-103113] 18 p2519 N90-24384
Conceptual design and analysis of roads and road construction machinery for initial lunar base operations
[NASA-CR-186673] 18 p2535 N90-24459
Multi-application scanning mechanism
18 p2537 N90-24473
Design and use of high speed synchronous motor running in aggressive liquids 18 p2538 N90-24478
The European EVA spacesuit mechanisms
18 p2538 N90-24481
EVA power tool prototype 18 p2538 N90-24482
Columbus scientific airlock 18 p2541 N90-24503
A compact, rugged, high repetition rate CO2 laser incorporating catalyst 18 p2561 N90-24612
Photovoltaic concentrator technology development
[DE90-011479] 18 p2577 N90-24684
A survey of human factors methodologies and models for improving the maintainability design of emerging Army aviation systems
[AD-A221159] 18 p2586 N90-24724
Traps for neutral atoms
[AD-A220925] 18 p2613 N90-24885
An investigation of a mathematical model of an optically pumped Ti(3+):Al2O3 laser system
18 p2646 N90-25063
An approach for design and analysis of composite rotor blades
[AD-A219257] 19 p2657 N90-25125
Ground shake test of the UH-60A helicopter airframe and comparison with NASTRAN finite element model predictions
[NASA-CR-181993] 19 p2661 N90-25143
SEDS experiment design definition
[NASA-CR-183909] 19 p2665 N90-25165
A design optimization process for Space Station Freedom
[NASA-CR-186851] 19 p2667 N90-25175
A computational efficient modelling of laminar separation bubbles
[NASA-CR-186729] 19 p2688 N90-25291
Feasibility study for the advanced one-dimensional high temperature optical strain measurement system, phase 3
[NASA-CR-185254] 19 p2693 N90-25324
Depletion mode pumping of solid state lasers
[DE90-012090] 19 p2696 N90-25339
Calculation of flight vibration levels of the AH-1G helicopter and correlation with existing flight vibration measurements
[NASA-CR-182031] 19 p2702 N90-25375
Fracture mechanics in integrated design of new, ultra-strong materials and structures
[CBL-REPRINT-21] 19 p2703 N90-25378
Research on design and fabrication of high-efficiency solar cells
[DE90-012010] 19 p2711 N90-25429
Solar array automation limitations
19 p2729 N90-25513
Modeling and synthesis of multicomputer interconnection networks
[NASA-CR-186619] 19 p2746 N90-25604
Design of a Lunar farside observatory
[NASA-CR-186671] 19 p2765 N90-25709
The detection of VHE gamma rays using the atmospheric Cerenkov technique 19 p2773 N90-25761
Prediction methodologies for nonlinear aerodynamic characteristics of control surfaces
[NIAR-90-17] 20 p2801 N90-25937
PDWAP: A preliminary design and weights analysis program for aerospace vehicles
[AD-A222614] 20 p2808 N90-25979
Structural analysis and optimization of a propfan blade using a finite element method
[DLR-FB-90-01] 20 p2812 N90-26006
Background, current status, and prognosis of the ongoing slush hydrogen technology development program for the NASP
[NASA-TM-103220] 20 p2822 N90-26055
Computational fluid dynamics 3-D analysis for advanced transonic turbine design
[ETN-90-97282] 20 p2864 N90-26291
Design of an autonomous Lunar construction utility vehicle
[NASA-CR-186832] 20 p2870 N90-26330
The structural dynamics analysis of the main injector LOX inlet tee and its redesign
[NASA-CR-186764] 20 p2875 N90-26358
Parametric design studies of toroidal magnetic energy storage units
[DE90-013086] 20 p2881 N90-26390
Design of sensors for control of closed loop life support systems
[NASA-CR-186656] 20 p2899 N90-26490
A computer module used to calculate the horizontal control surface size of a conceptual aircraft design
[NASA-CR-186872] 20 p2903 N90-26515
Conception of a reconfigurable microprocessor
[ETN-90-97248] 20 p2904 N90-26517
Space station definitions, design, and development. Task 5: Multiple arm telerobot coordination and control: Manipulator design methodology
[NASA-CR-182043] 20 p2914 N90-26577
Surface acoustic wave filters in ZnO-SiO2-Si layered structures: Design, technology, and monolithic integration with electronic circuitry
[ETN-90-97218] 20 p2924 N90-26638
Lessons learned from the T-46A durability and damage tolerance program 21 p2957 N90-26812
Finite element models of USAF aircraft structures
21 p2958 N90-26820
Toward the optimization of a non-diffusing, two-dimensional S-shaped duct
[IAR-89-3] 21 p3003 N90-27068
Electronics design of the infrared/ultrasonic sensing for a robot gripper
[PB90-160383] 21 p3010 N90-27109
Case-based reasoning in design: An apologia
21 p3045 N90-27308
Generalized interpolation theory for the design and analysis of robust feedback systems
[AD-A222130] 21 p3060 N90-27399
Integrated structural/control design via multiobjective optimization
[AD-A223088] 21 p3071 N90-27459
Design of GaAs charge coupled devices
[DE90-012124] 21 p3080 N90-27513
Device for the dilution of hot exhaust jets
[ETN-90-97435] 22 p3120 N90-27723
Global optimization of air breathing launch vehicle trajectories 22 p3130 N90-27762
Hydrocarbon-fueled scramjet combustor component development tests 22 p3162 N90-27934
Spent-beam refocusing analysis and multistage depressed collector design for a 75-W, 59- to 64-GHz coupled-cavity traveling-wave tube
[NASA-TP-3039] 22 p3167 N90-27965
Design optimization of short focal length photovoltaic modules
[PB90-182221] 22 p3195 N90-28133
Energy Efficient Engine integrated core/low spool test hardware design report
[NASA-CR-168137] 23 p3281 N90-28566
Energy Efficient Engine: High-pressure compressor test hardware detailed design report
[NASA-CR-180850] 23 p3281 N90-28570
Development of a thickness design procedure for stabilized layers under rigid airfield pavements
[DOT/FAA/RD-90/22] 23 p3284 N90-28582
Liquid Rocket Booster (LRB) for the Space Transportation System (STS) systems study. Appendix G: LRB for the STS system study level 2 requirements, revision 1
[NASA-CR-183793-APP-G] 23 p3289 N90-28607
Design optimization of gas generator hybrid propulsion boosters
[NASA-CR-181096] 23 p3299 N90-28660
Extended range tankless water heater
[DE90-014474] 23 p3316 N90-28750
Using embedded microcontrollers in radar test equipment
[DE90-014997] 23 p3319 N90-28763
Minimum weight design of a leaf spring tapered in thickness and width for the Hubble Space Telescope-space support equipment
[NASA-TM-4233] 23 p3340 N90-28879
Military aircrew seating: A human factors engineering approach
[AD-A218049] 23 p3362 N90-28999
Strategies of computer-based instructional design: A review of guidelines and empirical research
[AD-A224038] 23 p3383 N90-29112
A knowledge-based system design/information tool
[NASA-CR-4316] 23 p3389 N90-29143
An enhanced integrated aerodynamic load/dynamic optimization procedure for helicopter rotor blades
[NASA-CR-4326] 24 p3432 N90-29383
Aircraft design for mission performance using nonlinear multiobjective optimization methods
[NASA-CR-4328] 24 p3432 N90-29384
Assessment and improvement of aeroengine disc structural integrity 24 p3433 N90-29392
Robust design of LQG controllers
24 p3475 N90-29639
Performance monitoring, fault detection, fault localization design guidance
[AD-A223619] 24 p3478 N90-29655
The flight telerobotic servicer Tinman concept: System design drivers and task analysis
24 p3506 N90-29822
Discrete-time adaptive control of robot manipulators
24 p3509 N90-29834
Construction and demonstration of a 9-string 6 DOF force reflecting joystick for telerobotics
24 p3509 N90-29836
RCTS: A flexible environment for sensor integration and control of robot systems; the distributed processing approach 24 p3512 N90-29852
System architectures for telerobotic research
24 p3515 N90-29872
Computer simulation and design of a three degree-of-freedom shoulder module
24 p3520 N90-29902
A comparison of the Shuttle remote manipulator system and the Space Station Freedom mobile servicing center
24 p3522 N90-29910
Computer-Aided Structural Engineering (CASE) project: Investigation and design of U-frame structures using program CUFRBC. Volume A: Program criteria and documentation
[AD-A224387] 24 p3525 N90-29934

DESIGN OF EXPERIMENTS

U EXPERIMENT DESIGN

DESIGN TO COST

General introduction to location and navigation capabilities 17 p2358 N90-23421

DESORPTION

Modeling of hydrazine surface interactions in environmental reaction chambers
02 p0203 N90-11162
Photolysis of spacecraft contaminants
[AD-A211715] 03 p0317 N90-11801
Quantitative interpretation of auger lineshapes and electron/photon stimulated desorption
[AD-A211550] 03 p0324 N90-11842

Studies of the adsorption/desorption behavior of explosive-like molecules
[DE90-001867] 07 p0913 N90-15283
Hydrogen desorption from the monohydride phase on Si(100)
[AD-A215237] 09 p1191 N90-16903
Lower limits on the absolute dissociative electron attachment cross section from O2 condensed on rare-gas films
[AD-A216727] 11 p1483 N90-18536
Absolute cross-sections for dissociative electron attachment in O2 condensed on Kr films
[AD-A216730] 11 p1570 N90-19038
Electron stimulated O(-) desorption from O2 condensed on a rare-gas film: Evidence for an indirect Bounce trajectory
[AD-A216725] 12 p1622 N90-19322
Experiments on oxygen desorption from surface warm seawater under Open-Cycle Ocean Thermal Energy Conversion (OC-OTEC) conditions
[DE90-000308] 12 p1683 N90-19666
Production and analysis by mass spectrometry of beams of polyglycol ions 15 p2066 N90-21835
Studies of chemistry and diffusion on silicon and gallium arsenide surfaces using laser-induced thermal desorption
[AD-A220946] 18 p2547 N90-24539
Characterization study of polycrystalline tin oxide surfaces before and after reduction in CO 18 p2559 N90-24601
ISS and TPD study of the adsorption and interaction of CO and H2 on polycrystalline Pt 18 p2559 N90-24602
The catalytic reactivity of thin film crystal surfaces
[DE90-010579] 18 p2622 N90-24937
Mass spectrometry of poly(methyl methacrylate)s of low molecular weight 20 p2829 N90-26091
Multicomponent gas sorption Joule-Thomson refrigerator
[NASA-CASE-NPO-17569-1-CU] 20 p2844 N90-26176
Ni impurity effects on hydrogen surface chemistry and etching of Si(111)
[AD-A222083] 21 p2977 N90-26921
PH3 surface chemistry on Si(111)-(7x7): A study by Auger spectroscopy and electron stimulated desorption methods
[AD-A221508] 21 p2979 N90-26929
Background effects in ESDIAD measurements on Si(111)-(7x7)
[AD-A222242] 21 p3001 N90-27056

DESTABILIZATION
Destabilization of tokamak pressure-gradient driven instabilities by energetic alpha populations
[DE90-003716] 07 p0996 N90-15756
Instabilities and subharmonic resonances of subsonic heated round jets, volume 2
[NASA-CR-186058] 15 p2100 N90-22017
Destabilization of supersonic free shear layers by parametric excitation using Mach waves generated by a wavy wall
[AD-A219655] 17 p2345 N90-23352

DESTRUCTION
Potential technologies for collection and destruction of CFCs (Chlorofluorocarbons), halons, and related compounds
[PB89-219968] 03 p0368 N90-12105
Developments in solar photocatalysis for destruction of organics in water
[DE90-007685] 13 p1771 N90-20162
Anode materials for electrochemical waste destruction 18 p2514 N90-24354

DESTRUCTIVE TESTS
NT BURST TESTS
Floor pull test of a transport airframe section
[DOT/FAA/CT-TN88/14] 13 p1754 N90-20072
Impact damage in graphite/epoxy laminates: Damage characterization, acoustic emission, and finite element simulation, volumes 1 and 2 16 p2211 N90-22610
Nondestructive evaluation of adhesively-bonded joints 22 p3185 N90-28074

DESULFURIZING
Improved performance in co-processing through fundamental and mechanistic studies in hydrogen transfer and catalysis
[DE90-004794] 10 p1352 N90-17839
Regenerative Cu La zeolite supported desulfurizing sorbents
[NASA-CASE-NPO-17480-1-CU] 20 p2830 N90-26098

DESYNCHRONIZATION (BIOLOGY)
Effects of a time zone shift of nine hours on the circadian rhythms in cockpit aircrew members on longhaul flights
[DLR-FB-89-31] 04 p0523 N90-13019
Studies on predicting the resynchronization of the circadian system after transmeridian flights
[ESA-TT-1177] 19 p2722 N90-25483

DESYNCHRONIZED SLEEP
U RAPID EYE MOVEMENT STATE

DETECTION
NT AIRCRAFT DETECTION
NT CHANGE DETECTION
NT CORRELATION DETECTION
NT EDGE DETECTION
NT MISSILE DETECTION
NT RADAR DETECTION
NT REMOTE SENSING
NT SIGNAL DETECTION
NT TARGET RECOGNITION
NT ULTRASONIC FLAW DETECTION
Data processing in lightning warning systems
[DE89-012495] 01 p0088 N90-10502
Improved pattern recognition techniques for real time operation
[AD-A211395] 03 p0324 N90-11840
Microwave signal detection using modulation of polymeric optical waveguides
[DE89-017545] 03 p0337 N90-11921
Statistical models for the optimal estimation of oceanic fields
[AD-A211786] 03 p0377 N90-12149
The detectors 05 p0604 N90-13507
Stabilizability and detectability of discrete-time time-varying systems
[MEMO-COSOR-88-16] 05 p0690 N90-14023
Detection of a chirping electromagnetic signal
[DE90-002105] 06 p0766 N90-14457
Noncontacting laser ultrasonic generation and detection at the surface of molten metal
[DE90-002020] 06 p0791 N90-14605
Process monitoring using optical ultrasonic wave detection
[DE90-002021] 06 p0838 N90-14870
Interferometric surface distortion detector
[AD-D014211] 06 p0842 N90-14901
Relative merits of reactive and forward-look detection for wind-shear encounters during landing approach for various microburst escape strategies
[NASA-TM-4158] 07 p0882 N90-15108
Laser detection and discrimination system
[AD-D014301] 07 p0937 N90-15426
RAIDS: An orbiting observatory for ionospheric remote sensing from space
[AD-A213717] 07 p0949 N90-15494
Observation of atomic relaxation near an interface through detection of emitted fluorescence
[AD-A214308] 07 p0991 N90-15725
Study of silicon nitride pH response to the fabrication of microelectronic sensors
[LAAS-89229] 08 p1042 N90-16023
An empirical comparison of software fault tolerance and fault elimination
[NASA-CR-186313] 08 p1108 N90-16414
Inspection development for T-37 wing spar cap lug
[AD-A214826] 09 p1159 N90-16708
A method for the early detection of instabilities in rotordynamics
[NASA-CR-186307] 09 p1170 N90-16769
Interference rejection and detection performance of the smallest of circuit
[AD-A215153] 09 p1212 N90-17025
Angle of arrival detection through analysis of optical fiber intensity patterns
[AD-A215421] 09 p1218 N90-17065
Formulation and verification of a technique for compensation of pneumatic attenuation errors in airborne pressure sensing devices 09 p1221 N90-17084
Micro-miniature roll rate sensor
[AD-A214778] 09 p1225 N90-17107
Tailorable infrared sensing device with strain layer superlattice structure
[NASA-CASE-NPO-16617-2-CU] 09 p1227 N90-17118
Airborne electromagnetic sensing of sea ice thickness
[AD-A214460] 09 p1240 N90-17198
A statistical model of the infrared signature of a wind roughened sea
[AD-A214531] 09 p1249 N90-17245
Survey of ERIM approaches applicable to semi-automatic target detection and cueing for multispectral and multisensor exploitation
[AD-A214241] 09 p1258 N90-17296
Adaptive multiple-band CFAR (Constant-False-Alarm-Rate) detection of an optical pattern with unknown spectral distribution
[AD-A214754] 09 p1281 N90-17429
Aggregate filter
[AD-A215029] 09 p1282 N90-17432
Stable auroral red arc occurrences detected by the Pacific Northwest Laboratory photometer network: A decade of observations, 1978 - 1988
[DE90-004994] 09 p1298 N90-17522
The GALLEX Project
[DE90-005573] 09 p1300 N90-17534
Signal processing applied to photothermal techniques for materials characterization 10 p1364 N90-17902
Polarization radar processing technology
[AD-A215242] 10 p1374 N90-17967
Analysis and test of a wide angle spectrometer
[AD-A215819] 10 p1388 N90-18030
Detecting extended solar system structures with COBE (Cosmic Background Explorer)
[AD-A216380] 10 p1447 N90-18349
Particle detection via rotons in helium-4 superfluid
[DE90-005417] 10 p1448 N90-18354
The signals of an ice warning device in dependence on total water content and normalized icing degree
[DLR-FB-89-52] 11 p1454 N90-18377
Fluorescence and elastic scattering from laser dye-filled capillaries
[AD-A217026] 11 p1484 N90-18540
Visual target detection and recognition
[DE90-006903] 11 p1567 N90-19015
The adaptive line enhancer applied to chirp detection
[DE90-006772] 13 p1789 N90-20268
A linear filtering technique for removal of low-frequency noise
[DE90-006183] 13 p1794 N90-20296
Algorithms for optimal processing of polarimetric radar data
[AD-A217330] 13 p1876 N90-20758
Determination of Li-Al alloy extent in tubular aluminum elements by small source neutron radiology
[DE90-009142] 14 p1952 N90-21174
A correlation-spectral method for line detection on noisy data
[DE90-007925] 14 p1967 N90-21266
Modeling elastomer displacements for tactile sensing applications
[DE90-007959] 14 p1984 N90-21370
The effect of windscreen bows and HUD pitch ladder format on pilot performance during simulated flight
[AD-A218139] 14 p2011 N90-21523
Device for quickly sensing the amount of O2 in a combustion product gas
[NASA-CASE-LAR-13816-1] 15 p2102 N90-22025
Motion detection in astronomical and ice floe images 15 p2140 N90-22231
Bioluminescence for detection of trace compounds
[AD-A219435] 17 p2372 N90-23503
Electric dipole antennae used as micrometeoroid detectors
[AERONOMICA-ACTA-A-351-1989] 17 p2392 N90-23623
A comparison of lightning network data with surface weather observations
[AD-A220003] 17 p2427 N90-23832
Biosensors for the detection of heavy metal ions
[MBB-Z-0289-89-PUB] 17 p2433 N90-23864
Perception of complex auditory patterns
[AD-A219626] 17 p2434 N90-23867
Retention index monitoring of volatile organic compounds using thermal desorption gas chromatography
[AD-A221117] 18 p2521 N90-24397
The feasibility of detecting corrosion in electric fuzes using the thermal transient technique
[AD-A221385] 18 p2549 N90-24547
Use of the Xybion ISG-camera in the RETRA-1000 TV-Holography unit
[AD-A219842] 18 p2554 N90-24577
Field evaluation of a passive sampling device for hydrazines in ambient air
[NASA-TM-103456] 18 p2578 N90-24686
Bayesian characterization and detection of rare binary signature events
[AD-A221116] 18 p2606 N90-24844
The effect of random variations of radiosonde data on the predicted FLIR performance calculated by the program UFLR
[AD-A220034] 18 p2615 N90-24896
Use of neutron diffraction in determining strains in high-temperature superconducting composites
[DE90-010404] 18 p2621 N90-24931
Rocket engine failure detection using system identification techiques
[NASA-CR-185259] 19 p2664 N90-25159
Device and method for detecting and displaying crossover pattern in precision winding
[AD-D014539] 19 p2685 N90-25276
A noncontacting motion monitoring system for an astronaut translation aid
[NASA-TM-102640] 19 p2693 N90-25325

On the relation between various levels of target acquisition
[IZF-1989-38] 19 p2724 N90-25492
PHIND, an analytical model to predict target acquisition distance with image intensifiers
[IZF-1989-45] 19 p2724 N90-25493
Design and implementation of sensor systems for control of a closed-loop life support system
[NASA-CR-186675] 19 p2725 N90-25497
StarPlan: A model-based diagnostic system for spacecraft 19 p2728 N90-25511
Smart built-in test 19 p2728 N90-25512
Autonomous power expert fault diagnostic system for Space Station Freedom electrical power system testbed 19 p2730 N90-25521
Artificial intelligence for multi-mission planetary operations 19 p2732 N90-25532
Detection of 2.93 ms pulsations in Sco X-1 19 p2774 N90-25772
The variably trimmed mean CFAR detector for nonhomogeneous background
[AD-A222801] 20 p2856 N90-26243
Laser radar angular tracking
[AD-A222741] 20 p2869 N90-26319
Neural networks for detecting defects in aircraft structures
[IAR-90-4] 20 p2873 N90-26345
Field experience in using laser acoustic sensing for inspection
[DE90-012954] 20 p2873 N90-26347
A study of positrons from Soviet nuclear powered satellites as tracers for magnetospheric research
[DE90-013157] 20 p2888 N90-26438
Analysis and improved design considerations for airborne pulse Doppler radar signal processing in the detection of hazardous windshear
[NASA-CR-186792] 20 p2890 N90-26448
A real-time robot arm collision detection system
[NASA-CR-185878] 20 p2915 N90-26582
Resonant coupling through a slot to a loaded cylindrical cavity: Experimental results
[AD-A223000] 20 p2922 N90-26631
An initial comparison between two 3-D x ray CT algorithms for characterizing
[DE90-013656] 21 p2984 N90-26957
Pseudomonas diagnostic assay
[NASA-CASE-NPO-17653-1-CU] 21 p3032 N90-27239
Detecting perceptual groupings in textures by continuity considerations 21 p3045 N90-27310
A model for a space shuttle safing and failure-detection expert 21 p3046 N90-27314
Optical and microwave detection using Bi-Sr-Ca-Cu-O thin films 22 p3152 N90-27870
Image fusion through multi-resolution contrast decomposition
[IZF-1989-19] 22 p3247 N90-28412
Target detection in Gaussian noise using artificial neural systems
[AD-A223983] 23 p3320 N90-28770
Building an environment model using depth information 23 p3374 N90-29064
Airborne target detection, acquisition, and tracking devices
[AD-A223852] 24 p3462 N90-29555
Leak detection aid
[DE90-014678] 24 p3471 N90-29616
The Surface Air Sampling Program
[DE90-014873] 24 p3487 N90-29711
Light scattering from surface and sub-surface defects
[DE90-016311] 24 p3546 N90-30058
New developments in low-energy cosmic gamma-ray detection
[UT-HE-90/07] 24 p3564 N90-30165

DETECTORS
Raman characterization of high temperature materials using an imaging detector
[DE89-016308] 01 p0040 N90-10219
A new semicustom integrated bipolar amplifier for silicon strip detectors
[DE89-015585] 02 p0215 N90-11229
Control of plasma position in the CASTOR tokamak
[IPPCZ-284] 03 p0407 N90-12332
Center for X Ray Optics, 1988
[DE90-003300] 07 p0992 N90-15732
A voltage contrast detector with double channel energy analyzer in a scanning electron microscope
[ISBN-90-6275-568-2] 19 p2694 N90-25330
Definition of a near real time microbiological monitor for space vehicles
[NASA-CR-185599] 24 p3441 N90-29430
Detectors and signal processing for the speed measuring system 4-01
[FEL-1989-64] 24 p3472 N90-29623

DETERIORATION
Auroral and sub-auroral interaction at the F region ionosphere
[AD-A213284] 05 p0666 N90-13896
Damage evaluation from surface displacement data 07 p0944 N90-15469
The effect of thermal damage on the mechanical properties of polymer regrinds 18 p2515 N90-24363
Progressive cervical osteoarthritis in high performance aircraft pilots 19 p2718 N90-25465
Space operations: NASA is not properly safeguarding valuable data from past missions
[GAO/IMTEC-90-1] 20 p2936 N90-26704
Applications of digital image processing in testing and evaluation of composite materials
[AD-A222939] 21 p2971 N90-26887
Guidelines for pressure vessel safety assessment
[PB90-219619] 23 p3316 N90-28749

DETERMINANTS
Deterministic differential game solution: The approximate strategy method
[ESA-TT-1158] 11 p1555 N90-18956

DETERMINATION
U MEASUREMENT

DETONABLE GAS MIXTURES
Phase changes in carbon and nitrogen systems: Their effects on the detonation properties of high explosives
[DE90-000829] 06 p0755 N90-14392

DETONATION
Free-expansion experiments and modeling in detonation: Chemistry and hydrodynamics on a laboratory scale
[DE89-007748] 01 p0053 N90-10302
Remarks on certain aspects of solid explosive detonation via small projectile impact
[AD-A210648] 01 p0054 N90-10307
Shock behavior of explosives about the C-J (Chapman-Juget) point
[DE89-007642] 01 p0070 N90-10400
Laser initiation of secondary explosives
[DE89-010229] 01 p0075 N90-10431
Thermochemical model for shock-induced chemical reactions in porous thermite: The heat detonation model
[DE89-016528] 02 p0193 N90-11100
A shock initiation model for fine-grained hexanitrostilbene
[DE89-007641] 02 p0207 N90-11185
In-situ study of the chemically driven flow fields in initiating homogeneous and heterogeneous nitromethane explosives
[DE89-008415] 02 p0207 N90-11186
Estimation of the C-J pressure of explosives
[DE89-013811] 02 p0208 N90-11187
Carbon in detonations
[DE89-016037] 02 p0208 N90-11189
Crystal orientation effects in PETN explosive with 4 GPa shocks
[DE89-016996] 02 p0208 N90-11190
Shock initiation of LX-17 as a function of its initial temperature
[DE89-017730] 02 p0208 N90-11192
Acceleration of metal plates
[DE89-016816] 02 p0209 N90-11197
Sharp shock model for propagating detonation waves
[DE89-016772] 02 p0221 N90-11266
Shock induced dissociation of polyethylene
[DE89-016983] 02 p0221 N90-11267
Response of standardized PVDF piezoelectric polymer gauges to direct shock pressures between 8 and 32 GPa
[DE89-016811] 02 p0224 N90-11282
Laser-driven miniature flyer plates for shock initiation of secondary explosives
[DE89-016587] 02 p0225 N90-11288
Effects of shock-modification on superconductivity in Tl2Ca2Ba2Cu3Oy and Bi2CaSr2Cu2Ox
[DE89-017231] 02 p0285 N90-11629
A critical assessment of models available for the shock initiation of heterogeneous explosives
[MRL-TR-89-17] 03 p0333 N90-11896
Sensitivity relationships in energetic materials
[DE89-016967] 03 p0333 N90-11897
Indexes for the proceedings of the symposia (international) on detonation, 1951 through 1985
[DE89-015178] 03 p0345 N90-11972
KIVA reactive hydrodynamics code applied to detonations in high vacuum
[DE89-016979] 03 p0346 N90-11974
VISAR wave profile measurements in supra-compressed HE
[DE89-017736] 03 p0346 N90-11976
Lagrangian analysis of MIV (Magnetic Impulse-Velocity) gauge experiments on PBX 9502 using the mass-displacement moment function
[DE89-016612] 03 p0350 N90-12000
Shock pressure determination in detonator wires
[DE89-017756] 03 p0350 N90-12002
Thermal initiation of confined primary explosives with a proton beam
[AD-A212954] 04 p0482 N90-12767
Flame acceleration studies in the MINIFLAME facility
[DE90-000041] 06 p0740 N90-14310
Detonation product equation of state for Baratol
[DE90-001050] 06 p0753 N90-14384
Calibration curves for some standard Gap Tests
[DE89-016599] 06 p0754 N90-14389
Non-equilibrium effects of slow diffusion controlled reactions on the properties of explosives
[DE90-000822] 06 p0754 N90-14391
Phase changes in carbon and nitrogen systems: Their effects on the detonation properties of high explosives
[DE90-000829] 06 p0755 N90-14392
Reactive flow measurements and calculations for ZrH2-based composite explosives
[DE90-000831] 06 p0755 N90-14393
Reaction zone structure in supracompressed detonating explosives
[DE90-000832] 06 p0755 N90-14394
A new simulation method for the efficient calculation of benchmarks for detonation products equations of state
[DE90-001837] 06 p0777 N90-14522
Using small scale tests to estimate the failure diameter of a propellant
[DE90-001166] 07 p0913 N90-15281
On the dynamics of the combustion process of hydrogen-air and hydrogen-methane-air mixtures
[DLR-FB-89-39] 11 p1485 N90-18548
A program of fundamental research on explosives at Los Alamos
[DE90-006509] 11 p1495 N90-18602
Determination of detonation parameters of booster explosives at small charge diameters
[MRL-TR-89-45] 14 p1957 N90-21204
Discrete modeling of beds of propellant exposed to strong stimulus
[DE90-008932] 14 p1957 N90-21206
Diamonds in detonation soot 21 p3094 N90-27585
Shock dynamics in the sub-nanometer femtosecond domain
[DE90-014390] 23 p3304 N90-28689
Analysis of pyrotechnic devices by laser-illuminated high speed photography
[DE90-015741] 24 p3458 N90-29530

DETONATION WAVES
Laser propulsion to earth orbit. Has its time come? 01 p0028 N90-10143
Numerical simulation of detonation transfer between gaseous explosive layers
[MRL-RR-1-89] 01 p0069 N90-10395
Convection of a pattern of vorticity through a reacting shock wave
[NASA-CR-181921] 01 p0102 N90-10576
Sharp shock model for propagating detonation waves
[DE89-016772] 02 p0221 N90-11266
Wave combustors for trans-atmospheric vehicles
[NASA-TM-102238] 03 p0307 N90-11742
Indexes for the proceedings of the symposia (international) on detonation, 1951 through 1985
[DE89-015178] 03 p0345 N90-11972
Propagation of detonation waves from an impact region
[DE90-001184] 06 p0776 N90-14515
Laser-supported detonation waves and pulsed laser propulsion
[DE90-002753] 07 p0935 N90-15412
Numerical study of unsteady flows in large air-driven blast simulators with single and multiple drivers
[UTIAS-334] 17 p2405 N90-23699

DETONATORS
RF and dc desensitized electroexplosive device
[AD-D014206] 04 p0497 N90-12862
Detonation product equation of state for Baratol
[DE90-001050] 06 p0753 N90-14384
Electrothermal response testing more than a quality assurance tool
[DE90-001449] 06 p0780 N90-14536
The design of low inductance electrical circuits for slapper detonator systems
[AD-A214981] 09 p1212 N90-17024
Excess transit time as a function of burst current in an exploding bridgewire detonator
[DE90-007168] 11 p1512 N90-18708
Ignition testing of low-energy laser diode ignited components
[DE90-009968] 16 p2214 N90-22630

DEUTERIUM
A laser-driven source of polarized hydrogen and deuterium
[DE89-015130] 01 p0075 N90-10429

Structure of amorphous silicon alloy films
[DE89-009441] 01 p0128 N90-10734
Solid fiber Z-pinches: Cold-start computations
[DE89-016768] 02 p0279 N90-11592
Spin-orbit relaxation rates of Bi(6p(3)) 2D(3/2) following photolysis of Bi(CH3)3 at lambda = 193 nm
[AD-A211792] 03 p0402 N90-12303
Interaction of hydrogen isotopes with metals: Deuterium trapped at lattice defects in palladium
[DE90-000811] 06 p0747 N90-14344
Cold fusion: Alchemist's dream
[DE90-000865] 06 p0847 N90-14925
In-situ ion beam measurements of deuterium loading in thin foil electrochemical cells
[DE90-003162] 07 p0952 N90-15511
Tritium and neutron measurements of a solid state cell
[DE90-003657] 07 p1005 N90-15820
Initial deuterium confinement studies in DIII-D tokamak: DIII-D milestone report number 58
[DE90-003942] 08 p1124 N90-16509
Theoretical study of cold nuclear fusion using barrier penetration approach
[DE90-601096] 08 p1124 N90-16513
Some theoretical aspects of cold fusion: A report
[DE90-601098] 08 p1125 N90-16514
The excess flux in the cosmic submillimeter background radiation and the primordial deuterium abundance
[NASA-CR-186312] 08 p1154 N90-16683
Results of an attempt to measure increased rates of the reaction D-2 + D-2 yields He-3 + n in a nonelectrochemical cold fusion experiment
[NASA-TM-102430] 09 p1280 N90-17424
Measurements of the D/H ratio in planetary atmospheres by ground based infrared spectroscopy
11 p1578 N90-19088
Research of the interaction between hydrogen and deuterium with atomic eigen defects and dislocations in nickel and iron
[ETN-90-95380] 13 p1776 N90-20195
Investigation of the effect of mechanical stress on cold fusion
[AD-A220123] 17 p2474 N90-24147
The beta limit in the DIII-D tokamak
[DE90-011896] 19 p2759 N90-25677
Mass spectrometric analysis of hydrogen isotopes in metals and metal hydrides
[DE90-014118] 23 p3303 N90-28685

DEUTERIUM COMPOUNDS
NT HEAVY WATER
Isotope driven critical scattering and phase separation from mixtures of deuterated and protonated polymers
[DE90-003976] 08 p1051 N90-16076
Overview of advanced fuel fusion
[DE90-015660] 24 p3550 N90-30085

DEUTERIUM OXIDES
U HEAVY WATER

DEUTERON IRRADIATION
Displacement flow and deuteron drag in a metal: A path towards cold fusion
[PREPRINT-703] 16 p2320 N90-23227

DEUTERONS
Ignition and burn criteria for D3He tokamak and spherical torus reactors
[DE89-015059] 01 p0125 N90-10716
Cold fusion: Alchemist's dream
[DE90-000865] 06 p0847 N90-14925
Alfven wave stability in D III-D
[DE90-005555] 10 p1437 N90-18291
Distributed bosonic states and condensed matter fusion
[AD-A217605] 12 p1718 N90-19868
Polarization observables in deuteron photo- and electro-disintegration
[CEBAF-PR-89-022] 19 p2756 N90-25659
Relativistic effects in low energy nucleon-nucleon scattering
[CEBAF-PR-89-025] 21 p3075 N90-27483

DEVELOPING NATIONS
Wider horizons: Potential contributions by space systems to socio-economic advancement in developing countries
[ESA-SP-1106] 04 p0562 N90-13276
Utilization of remote sensing in geoscientific development and projects 08 p1094 N90-16334

DEVELOPMENT
Information system life-cycle and documentation standards, volume 1
[NASA-TM-101856] 05 p0706 N90-14135
Product specification documentation standard and Data Item Descriptions (DID). Volume of the information system life-cycle and documentation standards, volume 3
[NASA-TM-101858] 05 p0706 N90-14137
Assurance specification documentation standard and Data Item Descriptions (DID). Volume of the information system life-cycle and documentation standards, volume 4
[NASA-TM-101859] 05 p0706 N90-14138

DEVIATION
Strong moderate deviation theorems for m-dependent random variables
[AD-A212618] 04 p0548 N90-13173
Large deviation estimates in the stochastic quantization of phi sub 2 exp 4
[PREPRINT-686] 05 p0693 N90-14050
The effects of compressor endwall flow on airfoil incidence and deviation 14 p1922 N90-21011

DEVITRIFICATION
U CRYSTALLIZATION

DEW
The effects of acid fog and dew on materials
[PB90-157496] 19 p2712 N90-25436

DEW POINT
JARE data reports, no. 140 (meteorology 21): Meteorological data at Asuka Camp, Antarctica in 1987
[ISSN-0075-3343] 15 p2132 N90-22188
Daily temperature, solar radiation, wind speed, cloud cover, and precipitation data recorded at the meteorological station for calendar years 1957--1988
[DE90-014399] 23 p3352 N90-28941

DEWAR SYSTEMS
U CRYOGENIC EQUIPMENT

DEWATERING
Development of the electroacoustic dewatering (EAD) process for fine/ultrafine coal
[DE89-015883] 01 p0122 N90-10700

DEWETTING
U DRYING

DHC BEAVER AIRCRAFT
U DHC 2 AIRCRAFT

DHC 2 AIRCRAFT
Stability and control derivatives of the De Havilland DHC-2 BEAVER aircraft
[PB89-217525] 03 p0309 N90-11754

DIAGNOSIS
Experience with model based display for advanced diagnostics and control
[DE89-015693] 01 p0082 N90-10469
Demonstration of the feasibility of laser induced fluorescence for arc jet flow diagnostics
[NASA-CR-185595] 08 p1040 N90-16013
Method and apparatus for characterizing reflected ultrasonic pulses
[NASA-CASE-LAR-13966-1] 09 p1278 N90-17408
VULCAIN: An expert system dedicated to fire risk analysis within complex industrial environments
10 p1314 N90-17599
Gear noise, vibration, and diagnostic studies at NASA Lewis Research Center
[NASA-TM-102435] 10 p1390 N90-18041
Development and utilization of new diagnostics for dense-phase pneumatic transport
[DE90-006787] 12 p1659 N90-19536
Common-mode rejector for pulse power diagnostics
[AD-A218090] 13 p1798 N90-20316
A locally constrained parallel activation model for diagnostic reasoning
[AD-A217808] 13 p1874 N90-20747
Application of artificial intelligence in electronic circuit diagnosis 16 p2303 N90-23122
A study of effects of instructional modes in a sequence of computer-assisted instruction lessons, with an introduction to computer-aided diagnosis of arithmetic errors 18 p2589 N90-24730
Convex models of malfunction diagnosis in high performance aircraft
[AD-A218514] 19 p2649 N90-25073
Smart built-in test 19 p2728 N90-25512
Autonomous power expert fault diagnostic system for Space Station Freedom electrical power system testbed
19 p2730 N90-25521
CLEAR: Automating control centers with expert system technology 19 p2733 N90-25533
Photovoltaic array space power plus diagnostics experiment 19 p2737 N90-25559
Robustness, diagnostics, computing, and graphics in statistics
[AD-A222688] 21 p3052 N90-27349
Beam diagnostics in circular machines: Review of new developments
[DE90-014986] 23 p3394 N90-29176
Diagnostic development and support of MHD test facilities
[DE90-015403] 24 p3550 N90-30083

DIAGRAMS
NT BLOCK DIAGRAMS
NT CIRCUIT DIAGRAMS
NT COLOR-COLOR DIAGRAM
NT COLOR-MAGNITUDE DIAGRAM
NT FEYNMAN DIAGRAMS
NT HERTZSPRUNG-RUSSELL DIAGRAM
NT NYQUIST DIAGRAM
NT PHASE DIAGRAMS
NT STRESS-STRAIN DIAGRAMS
On the expected complexity of the three-dimensional Voronoi diagram
[PB89-209332] 01 p0112 N90-10636

DIAMAGNETISM
Measuring the shielding effectiveness of superconductive composites
[DE89-015164] 01 p0033 N90-10180
Dissipation measurement in high T(sub c) superconductors with electromagnetic probes
[DE90-002058] 06 p0854 N90-14963
Optical paramagnetic/diamagnetic gas sensor
[AD-D014368] 12 p1663 N90-19554
Preparation and characteristics of superconducting cuprate thin films: Nd(2-x)Ce(x)CuO4 and substituted Bi-system 22 p3140 N90-27813
Magnetism and superconductivity of some Tl-Cu oxides 22 p3143 N90-27829
Phase compatibilities of YBa2Cu3O(9-delta) type structure in quintenary systems Y-Ba-Cu-O-X (impurity)
22 p3145 N90-27834
Plastic superconductor bearings any size, any shape, 77 k and up 22 p3145 N90-27838
Superconductivity in 2-2-3 Y2Ba2Cu3O(sub 8+ delta)
22 p3147 N90-27847

DIAMETERS
Effect of reduced aft diameter and increased blade number on high-speed counterrotation propeller performance
[NASA-TM-102077] 05 p0575 N90-13352
Precision segmented reflector, figure verification sensor 12 p1611 N90-19272
Determination of detonation parameters of booster explosives at small charge diameters
[MRL-TR-89-45] 14 p1957 N90-21204
Trade-offs in non-reversing diameter
[RUU-CS-89-22] 18 p2602 N90-24813
Accuracy analysis of the space shuttle solid rocket motor profile measuring device
[NASA-TM-101131] 21 p2968 N90-26871
Real-time concentration monitoring of large aerodynamic diameter fiber aerosols using the geometric optic inversion technique
[AD-A224167] 24 p3545 N90-30048

DIAMINES
Wet spinning of solid polyamic acid fibers
[NASA-CASE-LAR-14162-1] 07 p0910 N90-15259
Polyimides with carbonyl and ether connecting groups between the aromatic rings
[NASA-CASE-LAR-14001-1] 07 p0910 N90-15260
LARC-IA: A flexible backbone polyimide
[NASA-TM-102586] 09 p1196 N90-16926
Copolyimide with a combination of flexibilizing groups
[NASA-CASE-LAR-13821-1] 09 p1199 N90-16950
Acetylene terminated aspartimides and resins therefrom
[NASA-CASE-LAR-14188-1] 17 p2379 N90-23545

DIAMOND WINGS
U LOW ASPECT RATIO WINGS
U SWEPT WINGS

DIAMONDS
NT METEORITIC DIAMONDS
Characterization of diamond films by thermogravimetric analysis and infrared spectroscopy
[AD-A210564] 01 p0050 N90-10288
Morphological aspects of the friction of hot-filament-grown diamond thin films
[DE89-015986] 01 p0130 N90-10750
Diamondlike carbon coatings for optical systems
[AD-A211255] 02 p0276 N90-11573
Thermal model for double-drift IMPATT diodes on diamond heat sinks
[AD-A211746] 03 p0415 N90-12380
An investigation of diamond film deposition in a premixed oxyacetylene flame
[AD-A212595] 04 p0561 N90-13268
Novel in situ spectroscopic ellipsometer for real time analysis of CVD diamond films
[AD-A213218] 05 p0644 N90-13762
Characterization and in situ testing of diamond films
[DE90-003155] 07 p0911 N90-15265
Development of a diamond insulator for thermionic applications
[DE90-002849] 08 p1048 N90-16055
Plasma assisted chemical vapor deposition of diamond films
[AD-A214641] 09 p1197 N90-16934
Investigation of applications of diamond film
[AD-A216104] 10 p1388 N90-17931
Materials processing of diamond: Etching, doping by ion implantation and contact formation
[AD-A216530] 10 p1438 N90-18301

High growth rate diamond synthesis in a large area atmospheric pressure inductively coupled plasma
[AD-A216090] 11 p1567 N90-19019
Fluorinated diamond thin films for tribological applications
[AD-A217452] 13 p1779 N90-20214
Growth, characterization and device development in monocrystalline diamond films
[AD-A218211] 13 p1898 N90-20895
Studies of mechano-chemical interactions in the tribological behavior of materials
[NASA-TM-102545] 14 p1953 N90-21182
Diamond: A high power optical material
[DE90-008941] 14 p1955 N90-21196
Institute for Materials Science and Engineering, nondestructive evaluation: Technical activities
[PB90-132739] 15 p2108 N90-22055
CVD diamond films for tribological applications
[AD-A220265] 17 p2413 N90-23750
Power density effects in the physical and chemical properties of sputtered diamond-like carbon thin films
[DE90-011587] 18 p2532 N90-24450
Status and applications of diamond and diamond-like materials: An emerging technology
[NASA-CR-186935] 21 p2985 N90-26963
Ion beam processing of diamond
[AD-A221475] 21 p3001 N90-27058
Polycrystalline diamond Junction Field Effect Transistors (JFETS)
[AD-A222238] 21 p3083 N90-27534
Carbon stardust: From soot to diamonds
21 p3090 N90-27568
A unifying picture of gas-phase formation and growth of PAH (Polycyclic Aromatic Hydrocarbons), soot, diamond and graphite 21 p3091 N90-27575
Nature and origin of interstellar diamond from the Allende CV3 meteorite 21 p3092 N90-27581
On diamond, graphitic and amorphous carbons in primitive extraterrestrial solar system materials
21 p3095 N90-27591
Proceedings of US Army Research Office Workshop on US Army Applications for Diamond and Diamondlike Materials
[AD-A224193] 23 p3314 N90-28741
Use of electron spectroscopies in the tribological evaluation of diamond films
[DE90-014421] 23 p3334 N90-28848
Mechanical properties testing of diamond and diamond-like films by ultra-low load indentation
[DE90-014456] 23 p3337 N90-28861
Mechanical property measurement of polycrystalline diamond films
[AD-A224037] 23 p3402 N90-29222
Dynamic consolidation of super hard materials
[AD-A224460] 24 p3454 N90-29505
Polycrystalline diamond Junction Field Effect Transistors (JFETS)
[AD-A223784] 24 p3465 N90-29576

DIATOMIC MOLECULES
Particle kinetic simulation of high altitude hypervelocity flight
[NASA-CR-186003] 02 p0147 N90-10840
Extended basis set calculations of atomization energies: Comparison of isogyric and direct results
[AD-A212268] 04 p0471 N90-12702
Excimer emission from alkali diatomic and alkaline-earth-noble-gas molecules
[AD-A214246] 07 p0896 N90-15179
Characterization of tetrahydrogen via state-selected excitation of H2
[AD-A216239] 10 p1355 N90-17855
DURIP FTIR studies of solid state reaction dynamics
[AD-A217713] 13 p1773 N90-20174
Reactive and anisotropic elastic scattering of highly laser-vibration-excited diatomic molecules
[MPIS-19/1988] 13 p1883 N90-20804
Electronically metastable molecules of high symmetry
[AD-A217768] 13 p1885 N90-20814
Molecular theory of fluid phase equilibria
[PB90-131277] 15 p2066 N90-21832
Rotational and translational effects in collisions of electronically excited diatomic hydrides
[NASA-CR-186770] 20 p2829 N90-26093

DIATOMS (UNICELLULAR PLANTS)
U ALGAE

DICHOTOMIES
Dichotomies for certain product measures and stable processes
[AD-A222568] 20 p2921 N90-26621

DICHROISM
Diffraction limited dichroic combiner diode laser
[AD-D014291] 08 p1082 N90-16263

DICHROMATES
U CHROMATES

DICTIONARIES
Building a user-friendly data dictionary system in ORACLE
[DE89-014878] 03 p0417 N90-12397
Structured analysis tool interface to the strategic defense initiative architecture dataflow modeling technique
[AD-A216281] 10 p1424 N90-18218
Quick guide of the essential concepts used in optical digital data disk technology 17 p2479 N90-24175
Space Station Freedom: List of acronyms
17 p2479 N90-24176
IRDS prototyping with applications to the representation of EA/RA models
[NASA-CR-186066] 21 p3039 N90-27273
A dictionary of acquisition and contracting terms
[AD-A221681] 21 p3088 N90-27560
A glossary of terms, definitions, acronyms, and abbreviations related to the National Airspace System
[DOT/FAA/CT-TN89/53] 23 p3406 N90-29249

DIELECTRIC CONSTANT
U PERMITTIVITY

DIELECTRIC MATERIALS
U DIELECTRICS

DIELECTRIC PERMEABILITY
The microwave permeability of conducting spherical shells
[AD-A220746] 17 p2369 N90-23485
Advanced artificial dielectric materials for millimeter wavelength applications, part A
[AD-A220221] 17 p2469 N90-24112

DIELECTRIC POLARIZATION
Electromagnetic pulse interaction at a dielectric interface
[AD-A211081] 02 p0213 N90-11220
Time-resolved swarm studies in gases with emphasis on electron detachment and ion conversion
[ISBN-90-9003013-1] 18 p2613 N90-24883

DIELECTRIC PROPERTIES
NT PERMITTIVITY
Dynamically compressed metals: Theory
[AD-A210741] 01 p0045 N90-10257
The high-frequency dielectric properties of glass fibre reinforced plastic and honeycomb layers
[AD-A210581] 01 p0051 N90-10289
The measurement of infrared spectra of dense ceramics by specular reflectance spectroscopy
[AD-A210609] 01 p0051 N90-10291
Analysis of the performance of gallium arsenide photoavalanche switches
[DE89-015774] 01 p0129 N90-10739
Mott transition: Low-energy excitations and superconductivity
[DE89-617778] 01 p0129 N90-10741
Precision materials characterization in the near millimeter and submillimeter wavelength range
[AD-A210655] 02 p0194 N90-11106
Design and construction of systems for the single-crystals growth of ternary silver halides, alkali halides, and alkaline earth fluorides, and the dielectric investigation of silver halide
[ETN-89-94673] 02 p0286 N90-11632
Method of modifying the dielectric properties of an organic polymer film
[AD-D014171] 03 p0330 N90-11879
Time-domain analytic and numeric analysis of vertical dipoles in front of dielectric planar interface
[PB89-221642] 03 p0338 N90-11927
Characteristic impedance of microstrip lines
[NASA-TM-101581] 05 p0633 N90-13894
Mechanoelectric conversion by uniaxial constraint in piezoelectric generators: Optimization of electrical, mechanical, and physico-chemical parameters of materials
[ISAL-89-0020] 08 p1078 N90-16235
Group 2 cubic fluorides as dielectrics for III-V compound semiconductors
[AD-A214096] 08 p1129 N90-16542
Evolution of structure and electrical properties during crystallization of rapidly solidified Bi4Ti3O12
[DE90-005221] 09 p1292 N90-17492
Electronic and ionic transport in polymers
[AD-A217028] 11 p1491 N90-18579
Reliability studies of ceramic capacitors
[AD-A216763] 11 p1501 N90-18643
Discontinuous-taper directional coupler
[AD-D014324] 12 p1650 N90-19481
Low temperature elastic and dielectric properties of incommensurate barium sodium niobate
[AD-A216969] 12 p1709 N90-19815
Wetting of metallic carbides by non-reactive liquid metals
[AERE-M-3759] 13 p1775 N90-20185
Molecular organization and electrical properties of mixed Langmuir-Blodgett multilayer thin films of polypyrrole
[DE90-007627] 13 p1894 N90-20870
The dielectric behavior of sulfur hexafluoride submitted to rapid transitory overvoltages
[ECL-89-16] 17 p2374 N90-23520
Advanced artificial dielectric materials for millimeter wavelength applications, part A
[AD-A220221] 17 p2469 N90-24112
Electrical transport through tunnel barriers and thin dielectric layers and physical properties of the high Tc oxide superconductors
[AD-A219880] 17 p2477 N90-24165
Flight model discharge system
[AD-A220261] 18 p2510 N90-24342
The study of VF2/VF3 piezoelectric copolymeteres submitted to shocks
[ISL-CO-210/9] 20 p2931 N90-26679
Ellipsometric study of YBa2Cu3O(7-x) laser ablated and co-evaporated films
[NASA-TM-103223] 20 p2932 N90-26682
Dielectric function of InGaAs in the visible
[NASA-TM-103246] 20 p2932 N90-26683
Electric properties of highly oriented rigid chain, polymeric liquid crystals
[ETN-90-97287] 22 p3248 N90-28424
Semiconductor measurement technology: A software program for aiding the analysis of ellipsometric measurements, simple spectroscopic models
[PB90-216847] 23 p3398 N90-29201

DIELECTRICS
NT LOSSLESS MATERIALS
The high-frequency dielectric properties of glass fibre reinforced plastic and honeycomb layers
[AD-A210581] 01 p0051 N90-10289
Mott transition: Low-energy excitations and superconductivity
[DE89-617778] 01 p0129 N90-10741
Properties of devices prepared with epitaxial layers on InP
[AD-A210304] 01 p0132 N90-10759
Influence of core-shell grains on the internal stress state and permittivity response of zirconia modified barium titanate
[AD-A211245] 02 p0202 N90-11153
Electromagnetic pulse interaction at a dielectric interface
[AD-A211081] 02 p0213 N90-11220
Spectral-domain analysis of finite frequency selective surfaces
[AD-A211669] 03 p0339 N90-11932
Dielectric covered microstrip patch antennas
[AD-A211577] 03 p0344 N90-11963
Analysis of the efficiency of a dielectric solar energy collector
[PB89-212716] 03 p0366 N90-12092
Metallo-organic decomposition process for dielectric films
[AD-A211590] 04 p0495 N90-12849
Dielectric spectroscopy of semiconductors
[AD-A211989] 04 p0559 N90-13255
Growth and characterization of zinc sulfide films by conversion of zinc oxide films with H2S
[AD-A213345] 04 p0561 N90-13271
Joint Services Electronics Program
[AD-A213015] 05 p0634 N90-13699
Reorganization free energy for electron transfers at liquid-liquid and dielectric semiconductor-liquid interfaces
[AD-A212985] 05 p0703 N90-14111
Temperature stable ceramic dielectric compositions
[AD-D014209] 06 p0749 N90-14358
Laser-material interactions
[AD-A214421] 07 p0937 N90-15425
Modeling antennas and scatterers of arbitrary shape embedded in layered dielectric media
[AD-A214902] 09 p1211 N90-17023
Materials properties numerical database system established and operational at CINDAS/Purdue University 10 p1366 N90-17919
Electron-beam induced damage in thin insulating films on compound semiconductors
[NASA-CR-185177] 10 p1378 N90-17987
Investigation of low temperature multilevel dielectrics for application for radiation tolerant, submicron-scaled IC technology
[AD-A216114] 10 p1433 N90-18273
Reliability studies of ceramic capacitors
[AD-A216763] 11 p1501 N90-18643
Coating possibilities for magnetic switches
[DE90-006536] 11 p1504 N90-18659
Fast optical switch and limiter using quantum size effect in metal grain composites
[AD-D014332] 12 p1619 N90-19305
Heterogeneous composite and method of making
[AD-D014337] 12 p1619 N90-19306
Alternate film dielectric materials
[DE90-007213] 12 p1632 N90-19378
Thermal coefficient of delay for various coaxial and fiber-optic cables 12 p1643 N90-19439

Electromagnetic properties of material coated surfaces
[NASA-CR-186466] 12 p1647 N90-19466
Elastomeric electrical isolation membrane
[AD-D014365] 12 p1651 N90-19490
Microwave field effect transistor
[NASA-CASE-GSC-12442-2] 13 p1792 N90-20282
Dielectric composite thin films
[AD-A217940] 13 p1881 N90-20791
Refractive index profiles of thermally grown and chemically vapor deposited films on silicon
[AD-A217187] 13 p1893 N90-20865
Proceedings of the Joint NOSC/NRL (Naval Ocean Systems Center/Naval Research Laboratory) InP Microwave/Millimeter Wave Technology Workshop
[AD-A218216] 14 p1966 N90-21259
An assessment of the potential of continuous-wave ranging for measuring the distance to a highly reflective, infinite sheet
[NASA-TM-101680] 14 p1969 N90-21279
Theory of a periodic cylindrical waveguide with a nonuniform metal-dielectric filling
[DE90-620099] 15 p2087 N90-21945
Contributions to the development of SLM TEA CO2 laser sources for high resolution molecular spectroscopy 16 p2240 N90-22778
Development of new methods for predicting the bistatic electromagnetic scattering from absorbing shapes
[AD-A219327] 17 p2388 N90-23600
Artificial dielectrics
[AD-A219671] 17 p2389 N90-23605
Advanced artificial dielectric materials for millimeter wavelength applications, part A
[AD-A220221] 17 p2469 N90-24112
Electrical transport through tunnel barriers and thin dielectric layers and physical properties of the high Tc oxide superconductors
[AD-A219860] 17 p2477 N90-24165
Experiments on liquid immersion natural convection cooling of leadless chip carriers mounted on ceramic substrate
[AD-A219893] 17 p2478 N90-24167
Method of forming a multiple layer dielectric and a hot film sensor therewith
[NASA-CASE-LAR-13678-1] 17 p2478 N90-24168
Dielectric determination of the glass transition temperature (T sub g) 18 p2513 N90-24352
Natural convection form an array of rectangular protrusions in an enclosure filled with dielectric fluid: Effects of boundary conditions, fluid Prandtl number, and selective powering
[AD-A219819] 18 p2552 N90-24563
Research on high-specific-heat dielectrics
[AD-A221215] 18 p2623 N90-24944
Protons and lattice defects in perovskite-related oxides
[DE90-010957] 18 p2624 N90-24955
Transient electromagnetic scattering on anisotropic media
[DE90-011802] 19 p2683 N90-25262
Chemical structure and kinetics at liquid/solid interfaces
[AD-A222766] 20 p2831 N90-26105
Theory of circular dielectric waveguide with anisotropic sheet cover
[NASA-CR-186883] 20 p2855 N90-26235
Aromatic polyimides containing a dimethylsilane-linked dianhydride
[NASA-CASE-LAR-14198-1] 21 p2984 N90-26956
Nonlinear material response to very rapid energy deposition
[AD-A221932] 21 p2989 N90-26988
Subthreshold technique for fixed and interface trapped charge separation in irradiated MOSFETs
[AD-A221861] 21 p3001 N90-27061
Polarization contrast vision
[AD-A221423] 21 p3076 N90-27492
In-situ integrated processing and characterization of thin films of high temperature superconductors, dielectrics and semiconductors by MOCVD 22 p3148 N90-27851
Coupled strip line circuit
[AD-D014487] 22 p3166 N90-27956
Field emitter array integrated distributed amplifiers
[AD-D014493] 22 p3166 N90-27958
Spectroscopic ellipsometry in vacuum ultraviolet spectral area
[ETN-90-97317] 22 p3249 N90-28426
Damage resistant optical coatings prepared using high temperature, plasma chemical-vapor-deposition
[DE90-015042] 23 p3313 N90-28738
Research for electric energy systems
[DE90-014221] 23 p3321 N90-28775
Investigations into the use of dielectric coatings in magnetic switches
[DE90-014331] 23 p3321 N90-28776
Chiral Maxwell-Garnett mixing formula
[PB90-189143] 23 p3391 N90-29158

DIELS-ALDER REACTIONS
Curable polyether compositions
[AD-D014200] 04 p0468 N90-12679
Bis(4-(3,4-dimethylenepyrrolidyl)-phenyl) methane
[NASA-CASE-LAR-13965-1-CU] 14 p1942 N90-21118

DIENCEPHALON
NT PINEAL GLAND
NT THALAMUS

DIENES
NT BUTADIENE
NT POLYBUTADIENE
Curable polyether compositions
[AD-D014200] 04 p0468 N90-12679
Quantitative confirmation of diffusion-limited oxidation theories
[DE90-012997] 20 p2838 N90-26143

DIES
Characterization of the 7175 T7352. Dissection of a die casting standard spar
[CEAT-PV-M5/528900] 22 p3158 N90-27906
Characterization of the 7175 T7352 101. Dissection of a die casting standard spar
[CEAT-PV-M5/5288] 22 p3158 N90-27907

DIESEL ENGINES
Sliding seal materials for low heat rejection engines
[NASA-CR-182262] 03 p0331 N90-11882
Two-dimensional analysis of two-phase reacting flow in a firing direct-injection diesel engine
[NASA-TM-102069] 05 p0582 N90-13392
Computer simulation of wind/diesel system operation
[DE89-009445] 06 p0805 N90-14688
Design and fabricate a metallic hydride heat pump with a cooling capacity of 9000 BTU/H
[AD-A213756] 07 p0931 N90-15388
Diesel starting system monitor: Prototype development
[DE90-004425] 08 p1084 N90-16276
Chemical effect of fuel composition changes on emissions from a DI Diesel engine
[DE90-004466] 09 p1232 N90-17151
Development of fuel wear tests using the Cameron-Plint high-frequency reciprocating machine
[AD-A216003] 10 p1361 N90-17892
Preliminary collection 891 of lectures/papers in Symposium by Society of Automotive Engineers of Japan
[DE90-710449] 10 p1391 N90-18045
Development and use of an advanced coal-fueled diesel engine cycle simulation with group effects
[DE90-000450] 12 p1672 N90-19607
A technical and economic evaluation of oxygen-enriched combustion in diesel engines using water-emulsified fuels
[DE90-008095] 13 p1810 N90-20394
Contributions to the study of parietal flames due to turbulent diffusion
[ECL-89-22] 17 p2374 N90-23519
Assessment of fundamental materials needs for Thick Thermal Barrier Coatings (TTBC's) for truck diesel engines
[NASA-TM-103130] 17 p2377 N90-23536
Diesel engine condition monitoring: Laser-based diagnostic techniques 17 p2410 N90-23733
Development of a spark assisted direct injection multifuel diesel engine especially for alcohol fuels
[ACTA-POLYTEC-SCAND-ME-94] 17 p2412 N90-23747
A simulation code for turbocompound diesel engines
[IAR-89-26] 19 p2697 N90-25348
Effect of casting procedures and diesel engine environment on the behavior of aluminum titanate
[AD-A223079] 20 p2835 N90-26126
Heat engines
[DE90-000485] 20 p2882 N90-26393
Influence of diesel engine exposure on the rupture strength of silicon nitride and partially stabilized zirconia
[DE90-014759] 23 p3334 N90-28849

DIESEL FUELS
Mutagenic responses of some petroleum-base obscurants in the Ames test
[AD-A214201] 07 p0915 N90-15295
Development of fuel wear tests using the Cameron-Plint high-frequency reciprocating machine
[AD-A216003] 10 p1361 N90-17892
Comparison of emissions of transit buses using methanol and diesel fuel
[DE90-005652] 10 p1391 N90-18044
Chamber investigations of the fate of diesel emissions in the atmosphere, volume 1, task 3
[PB90-114422] 10 p1405 N90-18103
Chamber investigations of the fate of diesel emissions in the atmosphere. Volume 2: AMES assay and GCMS final data reports and gas phase projections
[PB90-114430] 10 p1405 N90-18104
A technical and economic evaluation of oxygen-enriched combustion in diesel engines using water-emulsified fuels
[DE90-008095] 13 p1810 N90-20394
Quantitative determination of 1, 2-ethanediol contamination in used diesel lubricating oils by gas chromatography/mass spectrometry
[AD-A218592] 17 p2371 N90-23498
Development of a spark assisted direct injection multifuel diesel engine especially for alcohol fuels
[ACTA-POLYTEC-SCAND-ME-94] 17 p2412 N90-23747
Regenerative Cu La zeolite supported desulfurizing sorbents
[NASA-CASE-NPO-17480-1-CU] 20 p2830 N90-26098
Heat engines
[DE90-000485] 20 p2882 N90-26393
Investigation of particulate formation during diesel spray combustion
[DE90-012682] 24 p3446 N90-29464

DIETS
A laboratory study of the effects of diet and bright light countermeasures to jet lag
[AD-A220148] 17 p2435 N90-23875
Conservation of body calcium by increased dietary intake of potassium: A potential measure to reduce the osteoporosis process during prolonged exposure to microgravity 18 p2631 N90-24993

DIFFERENCE EQUATIONS
Some observations on the convergence behavior of GMRES
[REPT-89-09] 03 p0395 N90-12252
A study of the asymptotic behavior of linear difference equations with polynomial coefficients
[IMAG-RR-743-M] 03 p0395 N90-12254
A long time tail for random walk in random scenery
[REPT-89-08] 03 p0398 N90-12278
Numerical solution of the incompressible Navier-Stokes equations 06 p0774 N90-14501
On the stability of a certain difference scheme
[PB90-165614] 14 p2021 N90-21588
On spurious steady-state solutions of explicit Runge-Kutta schemes
[NASA-TM-102819] 15 p2160 N90-22340
Computational fluid dynamics
[AD-A219557] 17 p2403 N90-23686
A comparison of the K-pulse and E-pulse techniques for aspect independent radar target identification
[AD-A220172] 18 p2542 N90-24511
Second order asymptotics in level crossing problems for differences of renewal processes
[MEMO-824] 18 p2600 N90-24798
Minimum variance control of nonlinear systems
[RR-369] 19 p2748 N90-25615
Difference methods for hyperbolic problems with emphasis on space-centered approximations 22 p3172 N90-27998
Numerical methods for systems of conservation laws of mixed type using flux splitting
[NASA-CR-182084] 23 p3387 N90-29129
A numerical calculation of hypersonic flow around blunt bodies using upwind difference scheme
[NAL-TR-1025] 24 p3422 N90-29331

DIFFERENCES
Multivariable divided difference and B-splines
[MEMO-772] 04 p0544 N90-13160

DIFFERENTIAL ALGEBRA
U DIFFERENTIAL CALCULUS
U MATRICES (MATHEMATICS)

DIFFERENTIAL CALCULUS
Computation and graphics in mathematical research
[DE90-008429] 13 p1877 N90-20766

DIFFERENTIAL EQUATIONS
NT BIHARMONIC EQUATIONS
NT BURGER EQUATION
NT COSINE SERIES
NT ELLIPTIC DIFFERENTIAL EQUATIONS
NT FOKKER-PLANCK EQUATION
NT GAUSS EQUATION
NT HELMHOLTZ VORTICITY EQUATION
NT HYPERBOLIC DIFFERENTIAL EQUATIONS
NT LIOUVILLE EQUATIONS
NT PARABOLIC DIFFERENTIAL EQUATIONS
NT PARTIAL DIFFERENTIAL EQUATIONS
NT POISSON EQUATION
NT RICCATI EQUATION
NT VLASOV EQUATIONS
NT VORTICITY EQUATIONS
Improved propagation models for discrete random media
[AD-A211085] 01 p0057 N90-10327
Numerical methods for differential-algebraic equations: Current status and future directions
[DE89-015116] 01 p0111 N90-10632

On the coefficients of differentiated expansions of ultraspherical polynomials
[NASA-CR-181913] 01 p0112 N90-10637
Periodic solutions of spatially periodic Hamiltonian systems
[AD-A210645] 01 p0113 N90-10649
Stochastic quantization
[AD-A210942] 01 p0117 N90-10671
Asynchronous integration of ordinary differential equations on multiprocessors
[DE89-014169] 02 p0263 N90-11493
Parameter estimation in functional and partial differential equations
[AD-A211040] 02 p0265 N90-11511
On the numerical solution of two-point boundary value problems
[AD-A211244] 02 p0266 N90-11516
Generalized BDF (Backward Differentiation Formula) methods applied to Hessenberg form DAEs
[DE89-017328] 02 p0267 N90-11522
Some exact solutions of the three-identical-particle problem with S-wave inverse square potentials
[DE89-618402] 02 p0267 N90-11524
The realization of input-output maps using bialgebras
[NASA-CR-185362] 03 p0391 N90-12228
Some notes on perturbations of differential-algebraic equations
[PB89-218564] 03 p0393 N90-12243
Mapping nonlinear integro-differential equations into the frequency domain
[RR-366] 03 p0394 N90-12249
A simple proof of a differential equation for generalizations of Laguerre polynomials
[REPT-89-15] 03 p0395 N90-12253
Vortex dynamics
[AD-A212119] 04 p0499 N90-12877
Stable and unstable subspaces of a critical functional differential equation
[PB89-220651] 04 p0538 N90-13115
A recursive algorithm for computing the frequency response of a class of nonlinear difference equation models
[RR-354] 04 p0539 N90-13123
Increasing the real stability boundary of explicit methods
[CWI-NM-R8902] 04 p0541 N90-13134
Transformations and representations of nonlinear systems
[MEMO-776] 04 p0544 N90-13164
Operator product coefficients in non-diagonal conformal field theories
[NIKHEF-H/88-19] 04 p0553 N90-13224
Using Broyden updates to approximate the Jacobian in a semi-implicit backward differentiation code
[AD-A213239] 05 p0688 N90-14010
Analysis of three approaches to qualitative simulation
[MEMO-INF-89-32] 05 p0691 N90-14035
The stability of Taylor-Couette flow with radial heating 06 p0774 N90-14502
Proceedings of the Focused Research Program on Spectral Theory and Boundary Value Problems. Volume 4: Nonlinear Differential Equations
[DE90-000920] 06 p0822 N90-14780
Block predictor (low order) corrector methods to solve ordinary differential equations on parallel computers
[IMAG-RR-757-M] 06 p0834 N90-14845
A comparison result and elliptic equations involving subcritical exponents
[DE90-001772] 06 p0834 N90-14850
Introduction to bifurcation theory
[DE90-003319] 07 p0982 N90-15673
Flow of harmonic applications of a compact variety on a bordered variety
[DE89-635699] 07 p0985 N90-15692
Nonlinear maps with competitive interactions: Fixed-points, bifurcations, and chaotic attractors
[DE90-001858] 07 p0986 N90-15695
Nonlocality and stochastic quantization of field theory
[DE89-633913] 07 p1007 N90-15833
Integrable classical systems in higher dimensions
[DE90-600737] 08 p1118 N90-16473
Numerical solutions of the linearized Euler equations for unsteady vortical flows around lifting airfoils
[NASA-TM-102466] 10 p1307 N90-17562
A selective survey of computational electromagnetics for antenna applications 10 p1369 N90-17933
Discretization of the steady state semiconductor device equations
[AD-A215807] 10 p1438 N90-18298
Direct and inverse scattering problem associated with the elliptic Sinh-Gordon equation
[AD-A216455] 11 p1551 N90-18931
Differential-geometric techniques for solving differential algebraic equations
[AD-A216503] 11 p1552 N90-18934
Waveform methods for ordinary differential equations
[DE90-006593] 11 p1553 N90-18943
Deterministic differential game solution: The approximate strategy method
[ESA-TT-1158] 11 p1555 N90-18956
A vectorized algorithm for 3D dynamics of a tethered satellite 12 p1640 N90-19423
Chaotic transients, higher dimensional phenomena, and coupled ordinary differential equations
[DE90-006641] 12 p1706 N90-19794
Differential operators associated with Gegenbauer polynomials. 3: The regular case
[DE90-610422] 12 p1706 N90-19795
Longitudinal traveling waves bifurcating from Vlasov plasma equilibria 12 p1715 N90-19850
A general existence and uniqueness theorem for implicit differential-algebraic equations
[AD-A217965] 13 p1878 N90-20770
Micro SAINT programs for numerical methods of integration and differential equations
[AD-A218097] 13 p1878 N90-20772
Numerical simulation model for hydrazine attitude control thrusters. Part 1: Model description
[INPE-4952-RPE/601] 14 p1942 N90-21115
PROTEUS two-dimensional Navier-Stokes computer code, version 1.0. Volume 3: Programmer's reference
[NASA-TM-102553] 14 p1974 N90-21307
Compact finite volume methods for the diffusion equation
[NASA-CR-186477] 14 p2019 N90-21568
Adaptive grid embedding for the two-dimensional flux-split Euler equations
[NASA-CR-186533] 14 p2019 N90-21571
On a non classical oblique derivative problem for parabolic singular integro-differential operators
[DE90-612739] 14 p2020 N90-21574
Differential-algebraic equations as stiff ordinary differential equations
[DE90-007922] 14 p2021 N90-21585
Electromagnetic inverse profiling of stratified media
[ETN-90-96402] 15 p2087 N90-21947
Instabilities and subharmonic resonances of subsonic heated round jets, volume 2
[NASA-CR-186058] 15 p2100 N90-22017
Dynamical approach study of spurious steady-state numerical solutions of nonlinear differential equations. Part 1: The ODE connection and its implications for algorithm development in computational fluid dynamics
[NASA-TM-102820] 15 p2160 N90-22339
On spurious steady-state solutions of explicit Runge-Kutta schemes
[NASA-TM-102819] 15 p2160 N90-22340
A Chinese bibliography on quadratic systems of differential equations
[REPT-89-39] 15 p2161 N90-22342
Normal forms for weakly non-linear perturbed wave equations
[REPT-89-41] 15 p2161 N90-22343
On a third q-Bessel function
[REPT-89-48] 15 p2161 N90-22344
Efficient estimation in the Clayton-Cuzick model for survival data
[TW-88-06] 15 p2161 N90-22348
The theta-methods in the numerical solution of delay differential equations
[TW-89-03] 15 p2161 N90-22349
Stability criteria in the numerical solution of initial value problems
[TW-89-05] 15 p2162 N90-22351
Stability analysis of numerical methods for delay differential equations
[TW-89-09] 15 p2162 N90-22353
Application of a dynamic stall model to rotor trim and aeroelastic response 16 p2200 N90-22556
Differential equation based method for accurate approximations in optimization
[NASA-TM-102639] 16 p2200 N90-22558
Aspects of efficient and reliable multibody system simulation 16 p2279 N90-22991
Systematic generation of multibody equations of motion suitable for recursive and parallel manipulation 16 p2280 N90-22992
A nearly-linear computational-cost scheme for the forward dynamics of an N-body pendulum 16 p2280 N90-22996
A new second-order integration algorithm for simulating mechanical dynamic systems 16 p2293 N90-23064
Index and consistency analysis for DAE (Differential Algebraic Equation) systems for Stefan-Maxwell diffusion-reaction problems
[DE90-008188] 16 p2304 N90-23129
Estimation of Hilbert space valued parameters by the method of sieves
[AD-A218565] 16 p2306 N90-23143
Parameter estimation in linear filtering
[AD-A218566] 16 p2307 N90-23144
A computational method for general higher index nonlinear singular systems of differential equations
[AD-A219164] 16 p2307 N90-23147
Computation of low Mach number compressible flow 17 p2344 N90-23346
Impact response of orthotropic composite plates predicted by a one-parameter differential equation
[FFA-TN-1989-07] 17 p2369 N90-23488
Block Runge-Kutta methods on parallel computers
[CWI-NM-R8906] 17 p2452 N90-23982
Block Runge-Kutta methods
[CWI-NM-R8913] 17 p2452 N90-23983
On a method for computing eigenvalues and eigenfunctions of linear differential operators
[PREPRINT-706] 17 p2456 N90-24013
An averaging result for random differential equations
[AD-A220364] 17 p2457 N90-24021
A bibliography of the qualitative theory of quadratic systems of differential equations in the plane
[REPT-89-71] 17 p2458 N90-24029
Quadratic systems with three saddles and one antisaddle
[REPT-89-80] 17 p2458 N90-24033
Infinite separatrix cycles in the critical case, divergence and uniqueness of limit cycles of a quadratic differential system
[REPT-89-87] 17 p2458 N90-24034
Local and global order reduction of some LOD schemes
[CWI-NM-R8914] 17 p2459 N90-24041
Polynomial asymptotic estimates of Gegenbauer, Laguerre, and Jacobi polynomials
[CWI-AM-R8911] 17 p2460 N90-24043
Contractivity of Runge-Kutta methods
[TW-89-12] 17 p2464 N90-24079
Models of intracavity frequency doubled lasers
[AD-A221182] 18 p2563 N90-24628
Asymptotic analysis of wind-induced vibrations
[ETN-90-96903] 18 p2572 N90-24658
Embedded diagonally implicit Runge-Kutta algorithms on parallel computers
[CWI-NM-R8912] 18 p2595 N90-24765
Potential performance of methods for parallelism across time in ODEs
[DE90-010992] 18 p2596 N90-24774
Sustained resonance in very slowly varying oscillatory Hamiltonian systems
[DE90-010422] 18 p2598 N90-24783
Ground states of semi-linear diffusion equations
[DE90-010419] 18 p2598 N90-24785
Fundamental limitations of qualitative simulation
[MEMO-INF-89-56] 18 p2600 N90-24802
Formal groups and differential equations
[ETN-90-96924] 18 p2603 N90-24825
On the use of stability regions in the numerical analysis of stability value problems
[TW-89-07] 18 p2603 N90-24826
On a generalization of the resolvent condition in the Kreiss matrix theorem
[TW-89-08] 18 p2603 N90-24827
Solution of the optimal control problem using the software package STOMP
[MBB-FE-126/S/PUB-370] 19 p2651 N90-25087
Time-optimal aircraft pursuit-evasion with a weapon envelope constraint
[NASA-CR-186640] 19 p2658 N90-25126
Hopf-algebraic structure of combinatorial objects and differential operators
[NASA-CR-186380] 19 p2752 N90-25640
Code enhancements and validation of GASP
[NPS-PAPER-44] 20 p2861 N90-26277
Contribution to the study of differential equations and to the differences in the complex field
[ETN-90-97250] 20 p2919 N90-26612
Theory of biaxial graded-index optical fiber
[NASA-CR-186882] 20 p2927 N90-26652
Substitution principle theory for compressible flows 21 p2953 N90-26791
Symmetry and global bifurcation in nonlinear solid mechanics
[AD-A221981] 21 p3013 N90-27129
Identification techniques for nonlinear differential equations of motion
[AD-A220895] 21 p3062 N90-27407
The stability of differential systems with delay
[RR-377] 21 p3062 N90-27408
Conjugate gradient methods for constrained least squares problems
[AD-A222706] 21 p3063 N90-27411
On the theory and numerics of differential-algebraic equations
[AD-A222427] 21 p3065 N90-27422
Transition to complicated behavior in infinite dimensional dynamical systems
[AD-A221502] 21 p3077 N90-27494

FINFLO: A finite-volume based computer program for two-dimensional and axisymmetric compressible flow
[PB90-189473] 22 p3169 N90-27974
The discretization of the three dimensional boundary layer equations
[ETN-90-97292] 22 p3171 N90-27987
Linear iterative solvers for implicit ODE methods
[NASA-CR-182074] 22 p3242 N90-28386
A nonlinear finite element formulation for the large displacement analysis of plates
23 p3338 N90-28867
Beltrami algebra and symmetry of Beltrami equation on Riemann surfaces
[DE90-627157] 23 p3388 N90-29135
Theory of biaxial graded-index optical fiber
[NASA-CR-186977] 23 p3395 N90-29180
Applications of differential GPS
24 p3425 N90-29349
Trees, bialgebras and intrinsic numerical algorithms
[NASA-CR-187031] 24 p3524 N90-29925
An instability theorem for a certain sixth order differential equation
[DE90-627150] 24 p3536 N90-29990
Uniform dissipative solutions for some fourth order nonlinear differential equations
[DE90-627151] 24 p3536 N90-29991
An existence theorem for periodic solutions and applications to some third order nonlinear differential equations
[DE90-627152] 24 p3536 N90-29992
Oscillatory and nonoscillatory behaviour of solutions of an equation alternately of retarded and advanced type
[DE90-627159] 24 p3536 N90-29993
Periodic solutions of certain fifth order differential equations
[DE90-627160] 24 p3536 N90-29994
Structure of magnetic field in tokamaks
[DE90-628904] 24 p3549 N90-30075

DIFFERENTIAL GEOMETRY
NT LIE GROUPS
NT RIEMANN MANIFOLD
NT SPINOR GROUPS
NT TENSOR ANALYSIS
Compact surface in three-dimensional ellipsoid with prescribed mean curvature (I)
[DE89-618381] 02 p0264 N90-11502
On geometry of inhomogeneous Heisenberg ferromagnet: Nonintegrable case
[MEMO-789] 05 p0691 N90-14030
The Eighteenth Conference on Stochastic Processes and their Applications
[AD-A212301] 08 p1040 N90-16010
Differential-geometric techniques for solving differential algebraic equations
[AD-A216503] 11 p1552 N90-18934
A scanning algorithm for display of generalized cylinders
[REPT-89-77] 17 p2445 N90-23936

DIFFERENTIAL INTERFEROMETRY
Remote detection of boundary-layer transition by an optical system 04 p0441 N90-12524
Quantative interferometry 08 p1078 N90-16237
Interferometry 24 p3419 N90-29315

DIFFERENTIAL OPERATORS
U DIFFERENTIAL EQUATIONS
U OPERATORS (MATHEMATICS)

DIFFERENTIAL PRESSURE
Measurements of coefficients of discharge for concentric flange-tapped square-edged orifice meters in water over the Reynolds number range 600 to 2,700,000
[PB89-235147] 04 p0502 N90-12892
Liquid Transfer Cryogenic Test Facility: Initial hydrogen and nitrogen no-vent fill data
[NASA-TM-102572] 14 p1972 N90-21295

DIFFERENTIAL PULSE CODE MODULATION
Context dependent prediction and category encoding for DPCM image compression 08 p1073 N90-16210

DIFFERENTIAL THERMAL ANALYSIS
U THERMAL ANALYSIS

DIFFERENTIATION
Modified Chebyshev pseudospectral method with O(N exp -1) time step restriction
[NASA-CR-181958] 06 p0834 N90-14848

DIFFERENTIATION (BIOLOGY)
Polarity establishment, morphogenesis, and cultured plant cells in space 05 p0677 N90-13943
Gravity and animal embryos 05 p0678 N90-13951
Three-dimensional coculture process
[NASA-CASE-MSC-21560-1] 11 p1538 N90-18852
Microgravity as a tool in developmental biology
[ESA-SP-1123] 19 p2680 N90-25239
Early mammalian development and possible involvement of gravity 19 p2680 N90-25242
Experimental control of axis polarity in amphibian embryos 19 p2680 N90-25244
Computer aided mechanogenesis of skeletal muscle organs from single cells in vitro
[NASA-CR-187025] 23 p3354 N90-28959
Insulin and insulin-like growth factor-1 induce pronounced hypertrophy of skeletal myofibers in tissue culture
[NASA-CR-187026] 23 p3354 N90-28960

DIFFERENTIATORS
Optical rate sensor algorithms
18 p2632 N90-24997

DIFFRACTION
NT ELECTRON DIFFRACTION
NT FRESNEL DIFFRACTION
NT NEUTRON DIFFRACTION
NT PULSE DIFFRACTION
NT WAVE DIFFRACTION
NT X RAY DIFFRACTION
Nonprincipal-plane scattering from flat plates: Second-order and corner diffraction and pattern control of horn antennas
[NASA-CR-185485] 02 p0211 N90-11205
Part A: Nonprincipal-plane scattering from flat plates: Second-order and corner diffractions
02 p0211 N90-11206
Diffraction, chopping, and background subtraction for LDR 05 p0598 N90-13476
Binary optics technology: The theory and design of multi-level diffractive optical elements
[AD-A213404] 07 p0992 N90-15735
Diffraction limited dichroic combiner diode laser
[AD-D014291] 08 p1082 N90-16263
On multiple edge diffraction and multiple reflections of microwaves over terrain
[AD-A216418] 10 p1377 N90-17985
Laser diffraction particle sizing: Instrument probe volume relocation and elongation
[NASA-TM-102512] 10 p1387 N90-18025
The diffraction of ultrasound by cracks: Comparison of experiment with theory
[AERE-R-13334] 13 p1813 N90-20410
Engineer's Refractive Effects Prediction System (EREPS), revision 2.0
[AD-A220742] 17 p2391 N90-23616
Diffraction effects in directed radiation beams
[AD-A220785] 17 p2391 N90-23619
Spectral methods for electromagnetic propagation and diffraction
[AD-A220291] 17 p2393 N90-23632
Real space method of powder diffraction for non-periodic and nearly periodic materials
[DE90-010537] 18 p2621 N90-24935
Scattering from coated structures and antenna pattern control using impedance surfaces, part A/B
[NASA-CR-186871] 20 p2854 N90-26233
Probing interfacial structure and composition with x ray standing waves
[AD-A223071] 21 p2977 N90-26916
High resolution technique and instrument for measuring lattice parameters in single crystals
[AD-D014549] 22 p3177 N90-28029
Geophysical diffraction tomography: A complementary remote sensing technique for hazardous waste site characterization
[DE90-013025] 23 p3341 N90-28882
Near-angle scattering and binary optics
[AD-A224140] 23 p3396 N90-29186

DIFFRACTION GRATINGS
U GRATINGS (SPECTRA)

DIFFRACTION LIMITED CAMERAS
Introduction to the report of the Asilomar 3 LDR workshop 05 p0594 N90-13450
Diffraction-limited imaging on the 200-inch telescope
15 p2183 N90-22475
Super-diffraction limited measurements through the turbulent atmosphere by speckle interferometry
[AD-A221227] 18 p2581 N90-24699

DIFFRACTION PATTERNS
Part A: Nonprincipal-plane scattering from flat plates: Second-order and corner diffractions
02 p0211 N90-11206
X ray diffraction patterns of metal aurocyanides
[DE89-015188] 03 p0326 N90-11851
A sampled-grating model of moire patterns from digital imaging
[AD-A213364] 06 p0843 N90-14902
Non-Fourier computer generated holography for 3-D display
[AD-A215369] 09 p1225 N90-17109
X ray microimaging by diffractive techniques
[DE90-008444] 13 p1804 N90-20356
Method for holographic correction of beams of coherent light
[AD-D014406] 14 p1981 N90-21353
Diffraction of light by ultrasonic pulses
15 p2164 N90-22366
A multipulsed dynamic diffraction moire interferometer
[DE90-009765] 16 p2230 N90-22723
A compact portable diffraction moire interferometer
[DE90-009780] 16 p2238 N90-22768
Diffraction patterns and vortex rollup
[AD-A219876] 17 p2461 N90-24049
A numerical simulation of the quasi-heterodyne technique for double-pulsed holographic vibration measurements
[PNR90622] 20 p2865 N90-26301
Analysis of strain relaxation in Au/Ni multilayers by x ray diffraction
[IAR-89-25] 20 p2875 N90-26357
Computer modeling wave propagation with a variation of the Helmholtz-Kirchhoff relation
[AD-A222746] 20 p2927 N90-26657

DIFFRACTION PROPAGATION
Low level range coverage performance prediction for VHF radar 06 p0763 N90-14439
Modelling UHF propagation for frequency assignment in radio relay networks 06 p0764 N90-14445

DIFFRACTION RADIATION
Custom diffraction gratings
[AD-A211002] 01 p0124 N90-10712
Multiwave diffraction analysis of transmission phase gratings
[RSRE-MEMO-4325] 15 p2087 N90-21948
Diffraction effects in directed radiation beams
[AD-A220785] 17 p2391 N90-23619

DIFFRACTION TELESCOPES
U SPECTROSCOPIC TELESCOPES

DIFFUSE RADIATION
Spatially high-resolution flame diagnosis by means of spontaneous Raman spectroscopy
[ETN-90-95870] 12 p1623 N90-19328
The diffuse galactic gamma ray emission
16 p2333 N90-23296
A model of the diffuse galactic gamma ray emission
16 p2334 N90-23297
COS-B gamma ray sources beyond the predicted diffuse emission 16 p2335 N90-23308
Feasibility for EGRET detection of antimatter concentrations in the universe 16 p2338 N90-23323
Cosmic Background Explorer (COBE) press kit
[PB9-10172] 17 p2364 N90-23459
Stenopic radiography: A non-destructive test without contact 22 p3187 N90-28086

DIFFUSERS
User's manual for MGMHD: A multigrid three-dimensional computer code for the analysis of magnetohydrodynamic generators and diffusers
[DE90-004453] 08 p1127 N90-16526

DIFFUSION
NT ATMOSPHERIC DIFFUSION
NT ELECTRON DIFFUSION
NT GASEOUS DIFFUSION
NT IONIC DIFFUSION
NT MAGNETIC DIFFUSION
NT MOLECULAR DIFFUSION
NT PARTICLE DIFFUSION
NT PLASMA DIFFUSION
NT SELF DIFFUSION (SOLID STATE)
NT SELF PROPAGATION
NT SPECIES DIFFUSION
NT SURFACE DIFFUSION
NT THERMAL DIFFUSION
NT TURBULENT DIFFUSION
Lithium compensation of GaAs
[DE89-616080] 01 p0129 N90-10740
Wavefront propagation for reaction-diffusion systems of PDE
[AD-A210862] 02 p0265 N90-11510
Kinetics of diffusion-controlled reactions
[AD-A212161] 03 p0399 N90-12286
Some observations on transitory stall in conical diffusers
[NASA-TM-102387] 04 p0447 N90-12561
Ion beam analysis of diffusion in polymer glasses
[AD-A212339] 04 p0480 N90-12756
Gravimetric measurements of materials outgassing applied to graphite-epoxy laminates
[NASA-TM-100753] 05 p0619 N90-13609
Physical phenomena and the microgravity response
05 p0677 N90-13945
Predictive aging of elastomers in air: The importance of understanding diffusion-limited oxidation effects
[DE90-001385] 06 p0751 N90-14372
Non-equilibrium effects of slow diffusion controlled reactions on the properties of explosives
[DE90-000822] 06 p0754 N90-14391
Anisotropy of oxygen tracer diffusion in YBa2Cu3O7-delta single crystals
[DE90-001931] 06 p0856 N90-14979
Interaction of hydrogen in palladium as prescribed by the embedded atom method
[DE90-003893] 07 p0907 N90-15244

Time-dependent free convection in low Prandtl number fluids
[DE90-003053] 07 p0929 N90-15377
Thin films under chemical stress
[DE90-003754] 07 p0947 N90-15484
Defect control and denuded trap zones in the 3-5 semiconductors
[AD-A214099] 07 p1004 N90-15814
And still, a new beginning: The Galerkin least-squares gradient method
[DE89-636435] 08 p1116 N90-16461
Solid state voltammetry and sensors in solids and gases
[DE90-003234] 08 p1129 N90-16538
Effects of moisture on composite materials
09 p1185 N90-16866
Evaluation of a diffusion/trapping model for hydrogen ingress in high strength alloys
[AD-A215528] 09 p1194 N90-16920
Distribution and seasonal variations of diffuse fraction
[DE90-601303] 09 p1246 N90-17228
Diffusion and processing of YBa2Cu3O(x)
[DE90-003589] 09 p1286 N90-17457
Diffusion and defect characterization studies of mercury cadmium telluride
[AD-A214655] 09 p1289 N90-17470
Self similar solutions of the second kind of nonlinear diffusion-type equations
[DE90-606953] 10 p1422 N90-18204
An overview of radiation-induced interface traps in MOS (Metal-Oxide Semiconductor) structures
[AD-A216101] 10 p1438 N90-18299
A new model for hydrogen absorption in welds
[AD-A216951] 12 p1626 N90-19347
Frequency response of electrochemical cells
12 p1639 N90-19419
Convergence properties of iterative algorithms for solving the nodal diffusion equations
[DE89-016859] 12 p1707 N90-19804
CO2 diffusion and solubility in a Polystyrene/Polybutadiene block copolymer with highly oriented lamellar morphology
[AD-A217165] 13 p1779 N90-20211
Diffusion and germ formation in glasses
13 p1786 N90-20250
Hydrodynamic interactions and transport coefficients in a suspension of spherical particles
[DE90-008301] 13 p1801 N90-20336
Generalized random phase approximation for multicomponent polymer systems
[DE90-613691] 14 p1955 N90-21194
Mixing of viscous fluids: Behavior of microstructures and chaos
[DE90-008871] 14 p1973 N90-21304
Compact finite volume methods for the diffusion equation
[NASA-CR-186477] 14 p2019 N90-21568
An experimental investigation of mixing in buoyant flows
15 p2090 N90-21963
On dual Lagrangian hyperbolic models for one dimensional two phase flow problems
[DE90-007012] 15 p2098 N90-22004
Modeling the lateral diffusion of fluorescent particles within a forest canopy 15 p2121 N90-22136
Pseudo-steady diffusional growth or collapse of bubbles rising in time dependent pressure fields
[AD-A218825] 16 p2237 N90-22764
Index and consistency analysis for DAE (Differential Algebraic Equation) systems for Stefan-Maxwell diffusion-reaction problems
[DE90-008188] 16 p2304 N90-23129
Contributions to the study of parietal flames due to turbulent diffusion
[ECL-89-22] 17 p2374 N90-23519
Diffusion in the thermal degradation of NC base propellants
[AD-A219831] 17 p2383 N90-23572
Bilateral prediction
[AD-A219564] 17 p2456 N90-24016
Nonlocal free energy density functional approximations for the electrical double layer; comparison with Monte Carlo results for 2:1 salt
[AD-A220911] 18 p2521 N90-24395
Ground states of semi-linear diffusion equations
[DE90-010419] 18 p2598 N90-24785
Cation and anion tracer diffusion in YBa(sub 2)Cu(sub 3)O(sub 7-delta)
[DE90-009708] 18 p2620 N90-24927
Sunlight diffusing tent for lunar worksite
[NASA-CR-186651] 19 p2677 N90-25225
The effects of different diffusion sources on silicon solar cell recombination properties
[DE90-011235] 19 p2710 N90-25426
Quantitative confirmation of diffusion-limited oxidation theories
[DE90-012997] 20 p2838 N90-26143
Determination of the heat dissipated from a specimen undergoing cyclic plasticity by a hybrid numerical/experimental method
[AD-A221575] 21 p2982 N90-26946
Investigations on improved iterative methods for solving sparse systems of linear equations
[AD-A221980] 21 p3064 N90-27417
Characterization of superconducting materials with muon spin rotation
[DE90-013755] 21 p3081 N90-27522
Higher order diffusion model for a bipolar transistor
[PB90-190901] 22 p3167 N90-27960
The streamline diffusion finite element method for compressible and incompressible fluid flow
22 p3172 N90-27991
Asymptotic behavior of solutions of diffusion-like partial differential equations invariant to a family of affine groups
[DE90-014792] 23 p3388 N90-29130
A parallel least squares collocation conjugate gradient approach for the advection diffusion equation
[DE90-015965] 24 p3530 N90-29961
Hitting lines with two-dimensional Brownian motion
[AD-A223595] 24 p3541 N90-30027
Stochastic properties of the plasma wave heating map
[DE90-508077] 24 p3548 N90-30070

DIFFUSION BONDING
U DIFFUSION WELDING

DIFFUSION COEFFICIENT
Measurement and correlation of the solubility and diffusion coefficient for oxygen and chlorine in basic hydrogen peroxide
[AD-A212348] 04 p0472 N90-12703
Temperature dependence of positron diffusion in cubic metals
[PB89-222020] 04 p0475 N90-12722
Kinetics of the graphite/oxygen reaction in the in-pore diffusion controlled regime. Part 3: Influence of boundary layer diffusion in kinetic experiments at temperatures 970K to 1170K
[JUEL-2284-PT-3] 08 p1042 N90-16024
NMR measurements of solvent self-diffusion coefficients in polymer solutions
[AD-A215276] 09 p1279 N90-17419
Direct measurements of the physical diffusion of redox active species: Microelectrochemical experiments and their simulation
[AD-A215680] 09 p1280 N90-17420
The temperature variation of hydrogen diffusion coefficients in metal alloys
[NASA-TM-100397] 15 p2067 N90-21836
Diffusion in lattices with anisotropic scatterers
[CWI-AM-R8921] 18 p2599 N90-24792
A lightweight solid polymer electrolyte fuel cell with stack power density of 3 kW/lb (7kW/kg)
[AD-A223068] 21 p3020 N90-27169
Frequency and ventilation: A survey of theoretical and experimental ventilation modelling
[LR-625] 24 p3498 N90-29772

DIFFUSION EFFECT
U DIFFUSION

DIFFUSION ELECTRODES
Effect of electrical double layer on transport limited currents at microelectrodes
[AD-A211586] 03 p0324 N90-11843
In-situ ion beam measurements of deuterium loading in thin foil electrochemical cells
[DE90-003162] 07 p0952 N90-15511
Direct measurements of the physical diffusion of redox active species: Microelectrochemical experiments and their simulation
[AD-A215680] 09 p1280 N90-17420
Fundamental studies of surface processes and trace analysis using solid electrodes
[AD-A216538] 11 p1483 N90-18533
Electrocatalysis for oxygen electrodes in fuel cells and water electrolyzers for space applications
13 p1823 N90-20468
Estimation of the concentration-distance profile within the electrochemical diffusion layer by Raman microprobe spectroscopy
[AD-A219521] 17 p2372 N90-23506
Use of microelectrode arrays to directly measure diffusion of ions in solid electrolytes: Physical diffusion of Ag(+) in a solid polymer electrolyte
[AD-A222026] 22 p3159 N90-27913
Cyclic voltammetry at a rotating disk, electroreduction of nitrate in acidic nickel solutions, and frequency-response analysis of porous electrodes
[DE90-015317] 24 p3447 N90-29466

DIFFUSION FLAMES
Analysis of opposed jet hydrogen-air counter flow diffusion flame
[NASA-CR-182366] 03 p0321 N90-11825
Asymptotic analyses of the structures and characteristics of flames 04 p0468 N90-12683
Investigation of fuel additive effects on sooting flames
[AD-A212925] 04 p0473 N90-12709
FLIC (FLame with Implicit Convection): A detailed, two-dimensional flame model
[AD-A212953] 04 p0473 N90-12710
Flow field observation of a hot He-CO2 jet in microgravity 09 p1201 N90-16960
Liquid transverse jets in compressible crossflows
10 p1385 N90-18012
Wick-type liquid-metal combustion
[AD-A216019] 11 p1482 N90-18530
Theoretical investigation of the stabilization of a diffusion flame above a recirculation region
[ESA-TT-1149] 11 p1484 N90-18543
Numerical study of diffusion jet flames
12 p1621 N90-19316
Investigation of the processes controlling the flame generation of refractory materials
[DE90-007564] 12 p1624 N90-19333
Structure of model gas flames in nitramines
[AD-A217578] 13 p1770 N90-20159
Aerodynamic and kinetic processes in flames
[AD-A217796] 13 p1773 N90-20178
Studies on reactive flows 15 p2066 N90-21831
Topology of three-dimensional, variable density flows
[NASA-CR-186622] 17 p2402 N90-23683
Flame extinction in compressible flow
21 p2973 N90-26899
Raman scattering measurements using UV excimer lasers 21 p2974 N90-26902
Four-step kinetics for methane and implications for turbulent combustion 21 p2975 N90-26906
Non-premixed turbulent CO/H2 flames at local extinction conditions 21 p2975 N90-26907
A theoretical study of flow structure and radiation for multiphase turbulent diffusion flames
[AD-A222934] 21 p2976 N90-26913
Model of turbulent diffusion flames and nitric oxide generation
[PB90-155557] 22 p3155 N90-27886
Structure and radiation properties of turbulent diffusion flames
[PB90-218777] 22 p3155 N90-27887
The 26th JANNAF Combustion Meeting, volume 1
[CPIA-PUBL-529-VOL-1] 22 p3161 N90-27927
Chemical kinetic and aerodynamic structures of flames
[AD-A224281] 24 p3445 N90-29455

DIFFUSION LENGTH
A simple model for the determination of L(sub 0), D and tau in a semiconductor and their temperature dependence
[DE90-610564] 12 p1720 N90-19879
Alternating gradient photodetector
[NASA-CASE-NPO-17235-1-CU]
14 p1982 N90-21358
Estimation of minority carrier diffusion lengths in InP/GaAs solar cells
[NASA-TM-103213] 20 p2824 N90-26069
Emitter and base recombination parameters in solar cells: Measurement process and dependence on temperature and injection
[ETN-90-97305] 22 p3196 N90-28138

DIFFUSION THEORY
Time evolution of the electron swarm energy distribution function
[AD-A212967] 04 p0557 N90-13247
Electrochemistry using nanometer-sized electrodes
[AD-A223890] 23 p3305 N90-28697

DIFFUSION WAVES
Photoinduced and holographically reinforced light diffusion in electrooptic crystals
[ETN-90-97321] 24 p3547 N90-30060

DIFFUSION WELDING
Application of superplastically formed and diffusion bonded aluminum to a laminar flow control leading edge
[NASA-CR-178316] 01 p0007 N90-10030
Superplastic forming and diffusion bonding of rapidly solidified, dispersion strengthened aluminum alloys for elevated temperature structural applications
[NASA-CR-181849] 04 p0474 N90-12718
Reflection by defective diffusion bonds
[AD-A212995] 05 p0623 N90-13638
Diffusion bonding of metals 06 p0744 N90-14330
Designing for superplastic alloys
06 p0744 N90-14332
Fatigue and impact strength of diffusion bonded titanium alloy joints
[RAE-TM-MAT/STR-1123] 08 p1045 N90-16043
Time-dependent failure of silver-interlayer diffusion bonds between non-deforming base-metals
[DE90-006925] 12 p1628 N90-19357
Time-dependent failure of silver interlayer welds
[DE90-008015] 13 p1818 N90-20440

Ambient-temperature creep failure of silver-aided diffusion bonds between steel
[DE90-010687] 18 p2527 N90-24420
The investigation and production of titanium-tantalum junctions diffusion bonded at high temperature (855 C to 920 C): The influence of temperature, time pressure and roughness on the mechanical properties, and the optimisation of the bonded conditions
[BR114894] 24 p3476 N90-29646

DIFFUSIVITY
Transport properties of thermally grown Cr2O3
[DE89-016703] 02 p0284 N90-11623
Hyperthermal atomic oxygen generator
[NASA-CR-186573] 22 p3155 N90-27889
Radiative diffusivity factors in cirrus and stratocumulus clouds: Application to two-stream models 22 p3226 N90-28293
Rates of vertical mixing, gas exchange, and new productions: Estimates from seasonal gas cycles in the upper ocean near Bermuda
[PB90-244781] 24 p3496 N90-29758

DIFLUORIDES
NT CALCIUM FLUORIDES
Corrosion and corrosion inhibition of metals/alloys in methylphosphonic difluoride and decontaminating solutions
[AD-A212404] 04 p0477 N90-12734

DIFLUORO COMPOUNDS
NT POLYTETRAFLUOROETHYLENE
NT TEFLON (TRADEMARK)
Research in energetic compounds
[AD-A214106] 10 p1360 N90-17887

DIGESTING
Wear metal analysis in engine oil by microwave digestion and atomic absorption spectroscopy
[AD-A223070] 21 p2985 N90-26964

DIGESTIVE SYSTEM
NT INTESTINES

DIGITAL CIRCUITS
U DIGITAL ELECTRONICS
U LOGIC CIRCUITS

DIGITAL COMMAND SYSTEMS
Robotic vehicle message format
[AD-A210996] 01 p0110 N90-10627
High speed digital control of high frequency PWM converters 10 p1337 N90-17736
Digital beam position regulation of the superconducting accelerator at Darmstadt
[ETN-90-97293] 22 p3246 N90-28406

DIGITAL COMMUNICATION
U PULSE COMMUNICATION

DIGITAL COMPUTERS
NT CDC CYBER 205 COMPUTER
NT HEWLETT-PACKARD COMPUTERS
NT MASSIVELY PARALLEL PROCESSORS
NT MICROCOMPUTERS
NT MIMD (COMPUTERS)
NT MINICOMPUTERS
NT PARALLEL COMPUTERS
NT PERSONAL COMPUTERS
NT SEQUENTIAL COMPUTERS
NT SIMD (COMPUTERS)
NT VAX COMPUTERS
NT VAX-11 SERIES COMPUTERS
Processing rate sensitivities of a heterogeneous multiprocessor
[PB89-229017] 03 p0387 N90-12201
The Shock and Vibration Digest, volume 21, no. 10 04 p0483 N90-12771
The computer age and traditional approximate, analytical methods 04 p0483 N90-12772
Laboratory test methodology for evaluating the effects of electromagnetic disturbances on fault-tolerant control systems
[NASA-TM-101665] 05 p0695 N90-14061
Data compression techniques applied to high resolution high frame rate video technology
[NASA-CR-4263] 06 p0765 N90-14452
Synthesis of control law, on a RPV, in order to minimize the number of sensors 08 p1025 N90-15925
Critical problems in very large scale computer systems
[AD-A215190] 09 p1270 N90-17365
High throughput data communication system
[AD-D014342] 12 p1642 N90-19432
High speed modem
[AD-D014319] 12 p1698 N90-19750
Data Link Processor (DLP) project transition plan
[DOT/FAA/CT-TN89/68] 14 p1965 N90-21256
Activities and operations of the Advanced Computing Research Facility
[DE90-007957] 14 p2017 N90-21559
Parallel asynchronous hardware implementation of image processing algorithms 15 p2138 N90-22219
Conceptual design for aerospace vehicles 18 p2641 N90-25043
Optical storage technology
[AD-A224028] 23 p3407 N90-29254
Control and estimation for aerospace applications with system time delays 24 p3428 N90-29367

DIGITAL DATA
Applications of artificial intelligence to digital photogrammetry 02 p0262 N90-11486
Inferring data base requirements from examples in forms 02 p0288 N90-11646
A real-time wind model using digital data from aircraft
[RSRE-MEMO-4309] 04 p0521 N90-13005
An image compression algorithm for a high-resolution digital still camera
[NASA-CR-185079] 06 p0780 N90-14532
The digital data acquisition chain and the cosmic ray trigger system for the SLD warm iron calorimeter
[DE90-000943] 07 p1015 N90-15879
Multidimensional numerical simulation of large caliber ignition processes
[ISL-CO-233/88] 08 p1042 N90-16021
Direct Monte Carlo calculations on expansion wave structure near a wall
[ISL-CO-249/88] 08 p1064 N90-16154
Context dependent anti-aliasing image reconstruction 08 p1073 N90-16209
Digital image coding and compression
[PB90-110958] 08 p1107 N90-16409
Fractal-based image compression
[AD-A215400] 09 p1268 N90-17351
Simulation of synthetic aperture radar 3: Evaluation of prototype digital feature analysis data
[AD-A216750] 11 p1498 N90-18620
Monitoring of reforested areas through digital analysis of TM data
[INPE-4930-PRE/1420] 11 p1522 N90-18764
A waveform capture and storage unit and its use for investigating disturbances on digital transmission links
[BBC-RD-1989/17] 12 p1649 N90-19478
Thematic coupling between digital images and geographic information systems
[ETN-90-95723] 12 p1679 N90-19646
A split-and-merge method for creating polygonal homogeneous-vegetation regions from digitized terrain data
[AD-A218080] 13 p1821 N90-20453
Data Link Processor (DLP) project transition plan
[DOT/FAA/CT-TN89/68] 14 p1965 N90-21256
Bit-error-rate testing of fiber optic data links for MMIC-based phased array antennas
[NASA-TM-102523] 14 p1966 N90-21261
Digital processing of TM/LANDSAT data in monitoring interior water
[INPE-4956-PRE/1533] 14 p1997 N90-21448
Introduction of digital image processing by remote sensors applied to geology
[INPE-5023-RPE/616] 14 p1999 N90-21456
Multitemporal analysis of LANDSAT/TM digital imagery in the detection of areas affected by caterpillar (sibine fusca) attack in the dende (elais guineensis) palm plantation
[INPE-4979-PRE/1544] 14 p1999 N90-21457
Guided boundary detection in a digital image using dynamic programming
[ETN-90-96688] 17 p2419 N90-23782
Quick guide of the essential concepts used in optical digital data disk technology 17 p2479 N90-24175
Fast classification of ROSAT sources on objective prism plates 19 p2788 N90-25871
About the derivation of geomagnetic indices from digital data 21 p3023 N90-27191
A FAA Technical Center project transition plan: Mode S
[DOT/FAA/CT-TN90/17] 23 p3319 N90-28765
Survivable penetration 24 p3428 N90-29363
Digital color representation
[DE90-014580] 24 p3524 N90-29924

DIGITAL ELECTRONICS
NT LOGIC CIRCUITS
NT THRESHOLD GATES
Free-world microelectronic manufacturing equipment
[FASAC-TAR-4070] 02 p0215 N90-11228
Inferring data base requirements from examples in forms 02 p0288 N90-11646
On the design of a computer-aided design system for digital circuits 05 p0633 N90-13695
Advanced detection, isolation, and accommodation of sensor failures in turbofan engines: Real-time microcomputer implementation
[NASA-TP-2925] 07 p0883 N90-15112
High speed digital control of high frequency PWM converters 10 p1337 N90-17736
A gate array structure for the efficient project of digital circuits: The unit cell array
[ETN-90-95364] 12 p1653 N90-19502
An investigation of narrow-bandgap semiconductors: Devices, circuits, and systems 15 p2171 N90-22406
An approach to systematic phase-lock loop design
[ETN-90-96905] 19 p2686 N90-25280
Improvements in fluxgate magnetometers at Danish Meteorological Institute's Magnetic Observatories 21 p3023 N90-27187
About the derivation of geomagnetic indices from digital data 21 p3023 N90-27191
Energy Efficient Engine: Control system preliminary definition report
[NASA-CR-179578] 23 p3281 N90-28569

DIGITAL FILTERS
NT FIR FILTERS
Optimal q-Markov COVER for finite precision implementation 01 p0023 N90-10117
Improved pattern recognition techniques for real time operation
[AD-A211395] 03 p0324 N90-11840
Compensation for peak shifts and variable background responses in fluorescence spectroscopy
[DE90-001102] 07 p0892 N90-15154
Contribution to the study of design methods for numerical filters with finite pulse response and applications to image processing
[TELECOM-89-E-007] 10 p1376 N90-17974
Optimization of digital filters for a short-scan interferometer
[AD-A217997] 13 p1798 N90-20315
Low order FIR and IIR filters in dynamic vision
[OUEL-1785/89] 15 p2167 N90-22384
Digital filtering of plume emission spectra
[NASA-TM-103135] 20 p2824 N90-26070
Alternative solutions for Hilbert filtering in a pulse compression radar
[FEL-89-C226] 22 p3165 N90-27950
Identification method for estimation of electrical parameters of induction motors
[ETN-90-97306] 22 p3168 N90-27969
Improvement of the detail reconnaissance in radiographic irradiation images by digital image restoration
[ETN-90-97311] 22 p3189 N90-28096

DIGITAL INTEGRATORS
Digital integrator
[DIGEL-1989-2] 12 p1654 N90-19508

DIGITAL NAVIGATION
Development of an automatic ground collision avoidance system using a digital terrain database
[AD-A216247] 10 p1318 N90-17621
JTIDS relative navigation: Principles, architecture, and inertial mixing 24 p3426 N90-29357

DIGITAL RADAR SYSTEMS
Simulation of synthetic aperture radar 1: Feature density and accuracy requirements
[AD-A211019] 02 p0213 N90-11218
Data Link Processor (DLP) operational test and evaluation/integration test plan
[DOT/FAA/CT-TN89/32] 06 p0757 N90-14404
Automatic thresholding multichannel digital radar early warning system
[AD-D014323] 12 p1642 N90-19431

DIGITAL SIMULATION
Analysis and testing of a high performance air-air missile 01 p0014 N90-10069
Numerical simulation of leading-edge vortex rollup and bursting 02 p0145 N90-10831
A digital model for level-clocked circuitry
[AD-A211937] 03 p0343 N90-11957
Experimental investigation of a planar shock wave over a double wedge
[AD-A211366] 03 p0347 N90-11981
A robust digital model following controller for helicopters
[ESA-TT-1041] 04 p0457 N90-12621
Performance of the split-symbol moments SNR estimator in the presence of inter-symbol interference 04 p0487 N90-12799
Analytical control of special numerical calculations of pressure propagation in a fluid
[GRS-70] 04 p0501 N90-12884
Visualization of high-resolution digital terrain
[AD-A212149] 04 p0515 N90-12971
Parallelism in the discrete-event simulation algorithm
[AD-A213060] 05 p0682 N90-13970
Aircraft response and pilot behaviour during a wake vortex encounter perpendicular to the vortex axis 07 p0871 N90-15057
Flows with Separation
[DGLR-PAPERS-88-05] 08 p1066 N90-16169
Numerical simulation of the nonlinear evolution of a perturbation in a three dimensional boundary layer 08 p1067 N90-16173
Numerical simulation of the laminar and turbulent three dimensional flow on a delta wing with sharp leading edge 08 p1069 N90-16186
Numerical simulation of a bubble shaped bursting vortex 08 p1069 N90-16187

Numerical simulation of laminar hypersonic flows about an ellipsoid 08 p1071 N90-16198
Power system modeling for a six legged walking vehicle 09 p1221 N90-17083
Variable structure control system applied to multilevel power conditioning converters 10 p1336 N90-17734
Response of a chemically reacting layer to streamwise vorticity
[NASA-TM-102288] 10 p1383 N90-18005
Direct numerical simulation of aerodynamic noise
[AD-A214122] 10 p1426 N90-18225
Computational aerodynamics of ordered vortex flows
[ETN-90-96272] 11 p1452 N90-18368
Orbit determination of artificial Earth satellites through estmation techniques combined with state smoothing techniques
[INPE-4959-TDL/388] 11 p1465 N90-18440
Simulation of synthetic aperture radar 3: Evaluation of prototype digital feature analysis data
[AD-A216750] 11 p1498 N90-18620
Comparison of two Navy environmental database models: Generalized Digital Environmental Model and Podeszwa sound speed profile model
[AD-A215848] 11 p1544 N90-18889
Flow simulation for aircraft
[NLR-MP-87082-U] 12 p1661 N90-19543
Feasibility of using Extreme Ultraviolet Explorer (EUVE) reaction wheels to satisfy Space Infrared Telescope Facility (SIRTF) maneuver requirements
[NASA-TM-100389] 12 p1663 N90-19556
Noise behavior of semiconductor lasers by optic feedback
[ETN-90-95728] 12 p1668 N90-19583
Digital treatment of elastic-plastic structures by means of quadratic optimization processes from the finite element method
[ETN-90-95823] 12 p1675 N90-19621
Initialization of EURAD. Part 1: Utilization of ECMWF analysis data 12 p1688 N90-19695
Numerical modeling of atmospheric growth processes
[REPT-70] 12 p1693 N90-19726
Digital simulation of a Boenline
[ISSN-0069-5882] 12 p1694 N90-19729
Digital production of perspective images
[SER-C-347] 12 p1701 N90-19768
Positioning control of highest accuracy for very dynamic coupled system
[ETN-90-95893] 12 p1701 N90-19769
Numerical simulation of acoustic scatter from subsurface bubble clouds
[AD-A217068] 12 p1710 N90-19822
A numerical investigation of the compressible mixing layer
[AD-A217738] 13 p1802 N90-20343
Comparison of C- and O-grid generation methods using a NACA 0012 airfoil
[AD-A216375] 14 p1910 N90-20948
Generation of triangular form models in a microcomputer environment
[INPE-4974-PRE/1539] 14 p1997 N90-21447
UD filtering and smoothing applied to orbit determination
[INPE-4966-PRE/1535] 15 p2189 N90-22501
Numerical flow simulation and supercomputers: More than a digital wind tunnel 16 p2277 N90-22976
The automation management to support research and development 16 p2277 N90-22978
The development of a system for the numerical simulation of Euler flows 16 p2277 N90-22980
Numerical simulation of turbulent combustion using vortex methods
[AD-A219624] 17 p2372 N90-23507
The use of additional Global Positioning System (GPS) observations in large scale photogrammetry
[ETN-90-96693] 17 p2418 N90-23778
Numerical investigation of the incompressible plane shear layer between two gases with different densities
[ETN-90-97315] 21 p3006 N90-27084
START: A module for image processing to IMAGE-BASE
[FOA-C-30551-8.3] 22 p3238 N90-28363
Numerical simulations of the structure of supersonic shear layers
[AD-A224164] 24 p3467 N90-29587
Numerical simulation of the lightning return stroke 24 p3493 N90-29743
Investigation of the application in the simulation program 'PSpice' of the Jiles-Atherton model for nonlinear magnetic materials in order to predict the degaussing of magnets
[LINO-1990-1] 24 p3541 N90-30029

DIGITAL SYSTEMS
NT DIGITAL NAVIGATION
NT DIGITAL RADAR SYSTEMS
Subpicosecond optical digital computation using conjugate parametric generators
[AD-A207908] 01 p0058 N90-10330
Radon transform analysis of a probabilistic method for image generation
[AD-A207814] 01 p0123 N90-10702
Autonomous control system for Czochralski growth of LEC GaAs
[AD-A210190] 01 p0131 N90-10754
Flight test results of a complex precise digital flight control system 02 p0152 N90-10870
Analysis of forest fire smoke using satellite imagery
[AD-A210657] 02 p0236 N90-11339
Applications of flight control system methods to an advanced combat rotorcraft
[NASA-TM-101054] 03 p0308 N90-11752
On-orbit annealing of gallium arsenide solar cell arrays
[AD-A212087] 03 p0334 N90-11900
Video imaging systems: A survey
[DE89-016920] 03 p0337 N90-11919
A digital model for level-clocked circuitry
[AD-A211937] 03 p0343 N90-11957
Advanced actuation systems development, volume 1
[AD-A213334] 04 p0458 N90-12624
Height and gradient from shading
[AD-A212338] 04 p0504 N90-12908
Advanced actuation systems development, volume 2
[AD-A213378] 05 p0583 N90-13398
A knowledge-based flight status monitor for real-time application in digital avionics systems
[NASA-TM-101710] 05 p0686 N90-13995
SAND DEVIL: A digital video link for telemetry applications
[DE90-001879] 06 p0730 N90-14259
A sampled-grating model of moire patterns from digital imaging
[AD-A213364] 06 p0843 N90-14902
Document preservation by electronic imaging. Volume 1: Synopsis
[PB89-226526] 06 p0858 N90-14987
Document preservation by electronic imaging. Volume 2: System and experiment description
[PB89-226534] 06 p0858 N90-14988
Document preservation by electronic imaging. Volume 3: Appendices
[PB89-226542] 06 p0858 N90-14989
Research in optical interconnection techniques
[AD-A214028] 07 p0993 N90-15739
Microwave screening on digital radio communication links due to multicircuit power transmission lines
[DE90-734950] 08 p1058 N90-16118
Linear digital imaging system fidelity analysis 08 p1072 N90-16205
Digital image interpretation for optical flow measurement methods: System description and preliminary application examples 08 p1079 N90-16244
Testing and data path redesign of a high speed, 16-point Winograd Fourier transform processor
[AD-A215661] 09 p1213 N90-17036
Boolean approaches in digital diagnosis
[AD-A215660] 09 p1274 N90-17386
Hybrid optical/digital architecture for distortion invariant pattern recognition
[AD-A215628] 09 p1282 N90-17435
Development of the triplex digital flight control system of the STOL research aircraft ASKA
[NAL-TR-1013] 10 p1322 N90-17640
The Advanced Digital-Optical Control System (ADOCS) user demonstration program
[AD-A215984] 10 p1323 N90-17644
High throughput data communication system
[AD-D014342] 12 p1642 N90-19432
Performance of the all-digital data-transition tracking loop in the advanced receiver 12 p1643 N90-19440
Costas loop lock detection in the advanced receiver 12 p1643 N90-19441
High speed modem
[AD-D014319] 12 p1698 N90-19750
User-friendly software for the design of digital line-of-sight radio links
[PB90-118472] 12 p1700 N90-19760
Priority arbitration with busses
[AD-A216392] 12 p1704 N90-19784
Digital-flutter-suppression-system investigations for the active flexible wing wind-tunnel model
[NASA-TM-102618] 13 p1758 N90-20093
LANDSAT-5 data in the study of wheat and bean crops
[INPE-4746-RPE/580] 13 p1819 N90-20444
A split-and-merge method for creating polygonal homogeneous-vegetation regions from digitized terrain data
[AD-A218080] 13 p1821 N90-20453
Fractal-based image compression
[AD-A217302] 13 p1865 N90-20699
Mathematics and physics studies: Multi-project support
[AD-A218208] 13 p1869 N90-20723
Implementation of a control system test environment in UNIX
[DE90-007485] 13 p1872 N90-20736
Error correction of the DEA (Digital Electronic Automation) coordinate measuring machines at LLNL
[DE90-008913] 14 p1983 N90-21365
A real-time signal combining system for Ka-band feed arrays using maximum-likelihood weight estimates 15 p2076 N90-21888
Geographic information system: Coded data of agrocattle-raising projects in the Amazon
[INPE-4978-PRE/1543] 15 p2180 N90-22457
On-line x ray inspection of materials and structural components using discrete element x ray detectors for digital radiographic and computed tomographic evaluation
[AD-A218911] 16 p2245 N90-22806
Data exchange strategy. Part 1: Review of digital data exchange technology
[AD-A218506] 16 p2327 N90-23267
Proceedings of the 12th Symposium on Signal and Image Processing English-Language Abstracts
[AD-A218806] 17 p2388 N90-23598
Single mode communication link
[AD-A219499] 17 p2388 N90-23601
Serrodyning by means of a digital phase shifter
[AD-A219593] 17 p2396 N90-23646
Digital terrain elevation data compact disk-read only memory prototype evaluation
[AD-A218545] 17 p2442 N90-23915
Multiple beam optical processing
[AD-A219048] 17 p2471 N90-24129
Optical computing strategies
[AD-A219433] 17 p2472 N90-24131
An assessment of the CD-FLIR as an ARGUS sensor
[AD-A220841] 17 p2473 N90-24137
Feasibility study for the advanced one-dimensional high temperature optical strain measurement system, phase 3
[NASA-CR-185254] 19 p2693 N90-25324
Applications of PC-based digital imaging for storing microscopy images on optical disks
[DE90-011355] 19 p2763 N90-25701
Radio channel measurement and modelling for future mobile radio systems 20 p2845 N90-26184
System factors to be considered in assessing propagation effects on modern digital satellite communications systems 20 p2850 N90-26208
Applications of digital image processing in testing and evaluation of composite materials
[AD-A222939] 21 p2971 N90-26887
Current methods of digital speech processing 21 p2993 N90-27010
RADC/EEV diagnostic rhyme test system improvements
[AD-A223187] 21 p2995 N90-27025
Improvements of automatic magnetic observatories in Italy 21 p3022 N90-27185
Digital intelligent magnetic recording system DIMARS as the automated workstation at magnetic observatory 21 p3022 N90-27186
Digital signal processing software packages for IBM-PC and IBM-PC with DSP-16
[AD-A221679] 21 p3056 N90-27372
Neural network with dynamically adaptable neurons
[NASA-CASE-NPO-17803-1-CU] 21 p3057 N90-27385
Status report on image information systems and image data base technology
[AD-A221488] 21 p3087 N90-27556
Development and testing of methodology for evaluating the performance of multi-input/multi-output digital control systems
[NASA-TM-102704] 22 p3115 N90-27699
Educational and research activities of the Dig ital Systems Laboratory at Helsinki University of Technology
[PB90-190893] 22 p3265 N90-28486
A conceptual framework for fighter flight control systems
[PD-CF-9009] 23 p3283 N90-28577
ATDRS payload technology research and development
[NASA-TM-103256] 23 p3287 N90-28596
Use of a three-axis monolithic ring laser gyro and digital signal processor in an inertial sensor element 24 p3426 N90-29354
Sample rate effects on disturbance rejection for digital control systems 24 p3435 N90-29400
A digital controller for active aeroelastic controls
[NAL-TR-1014] 24 p3435 N90-29402
An experimental study of voice communication over a bandlimited channel using variable bit width delta modulation
[AD-A223445] 24 p3461 N90-29548
Fault tolerant design for multistage routing networks
[AD-A224267] 24 p3533 N90-29978

DIGITAL TECHNIQUES
Engine controls for the 1990's
[PNR90546] 03 p0308 N90-11748
The use of digital signal processing in satellite communication 05 p0631 N90-13684
Data compression techniques applied to high resolution high frame rate video technology
[NASA-CR-4263] 06 p0765 N90-14452
Proceedings of the 5th User Seminar of the German Remote Sensing Data Center of the DFVLR
[DFVLR-MITT-89-04] 08 p1092 N90-16318
Attempt to draw conclusions concerning the geological subsoil from the vegetation using digital image processing of TM data 08 p1093 N90-16329
Focal research effort points of the Institute of Applied Geodesy in the field of digital image processing 08 p1094 N90-16333
Digital image coding and compression
[PB90-110958] 08 p1107 N90-16409
Phase ambiguity resolution for offset QPSK modulation systems
[NASA-CASE-NPO-17853-1-CU] 09 p1204 N90-16975
Digital to position converter
[DIGEL-1984-4] 12 p1654 N90-19509
Development of software routines for remote sensing digital image processing
[ETN-90-95452] 12 p1679 N90-19640
User-friendly software for the design of digital line-of-sight radio links
[PB90-118472] 12 p1700 N90-19760
Characterization of fluid flow by digital correlation of scattered light
[NASA-CR-186403] 13 p1799 N90-20324
Onboard shuttle on-line software requirements system: Prototype 13 p1858 N90-20658
Coordinate transformation for an asynchronous, machine, and time discretization of a state observer
[EMV-88-30] 17 p2397 N90-23657
Multispectral classification of overlapping classes with applications to forest damage areas
[DLR-FB-89-55] 18 p2574 N90-24666

DIGITAL TELEVISION
Comparison of DPCM prediction strategies for high-quality digital television bit-rate reduction
[BBC-RD-1989/8] 01 p0056 N90-10318
Digital video: Studio signal processing
[BBC-RD-1989/14] 12 p1648 N90-19476
A digital HDTV recorder using a cluster of four D1 DVTRs
[BBC-RD-1989/13] 12 p1649 N90-19477

DIGITAL TO ANALOG CONVERTERS
Application of a buck-type MC2 regulated converter for a stepper motor control 10 p1335 N90-17722

DIGITAL TRANSDUCERS
Data acquisition in aerodynamic research 05 p0574 N90-13340
Digital system for monitoring and controlling remote processes
[DE90-003935] 08 p1054 N90-16094

DIGITIZERS
U ANALOG TO DIGITAL CONVERTERS

DIGITS
NT BINARY DIGITS
SIGNIF: A C function to compute significant digits
[DE90-009242] 14 p2015 N90-21550

DIHEDRAL ANGLE
A number-theoretic approach to subgroups of dihedral groups
[AD-A222857] 21 p3063 N90-27413

DIHEDRAL EFFECT
U LATERAL STABILITY

DILATATION
U STRETCHING

DILATOMETERS
U EXTENSOMETERS

DILUTION
NT GEOMETRIC DILUTION OF PRECISION
Quality control programs for isotope dilution mass spectrometry
[DE90-004259] 09 p1189 N90-16891
Online submicron particle sizing by dynamic light scattering using autodilution 09 p1223 N90-17095
Control of titanium diboride SHS reactions by inert dilutions and mechanical constraint
[AD-A214378] 10 p1357 N90-17870
Molecular theory of fluid phase equilibria
[PB90-131277] 15 p2066 N90-21832
A modified Ubbelohde viscometer with improved dilution characteristics
[NIAR-90-16] 19 p2693 N90-25326

DIMENSIONAL ANALYSIS
Realization theoretic solution of two analytic matrix equations with applications to stabilization of infinite-dimensional systems
[AD-A211118] 02 p0265 N90-11512
Application of dimensional analysis to statistical process modeling
[AD-A211881] 03 p0335 N90-11905
MIPs and BIPs are megaflops: Limits of unidimensional assessments
[DE89-015707] 06 p0820 N90-14770
Dimensional analysis of continuous high-capacity electrodispersion of aqueous based liquids in an organic continuous phase
[DE90-003714] 07 p0888 N90-15136
A renormalization group approach to image processing: A new computational method for three-dimensional shapes in robot vision, and the computation complexity of the cooling algorithms
[AD-A214247] 07 p0977 N90-15643
WPK: Solar array dimensioning tool 10 p1346 N90-17808
Fiber pushout test: A three-dimensional finite element computational simulation
[NASA-TM-102565] 14 p1945 N90-21131
Dimensional analysis of structures using wrapping techniques
[REPT-892-430-119] 16 p2247 N90-22815
A computer program to implement the Chen method of dimensional analysis
[AD-A218557] 16 p2306 N90-23142
Study and simulation of the behavior of a high frequency transformer
[ECL-89-008] 17 p2399 N90-23667
Development and application of an optimization procedure for space and aircraft structures
[MBB-FW-522/S/PUB-383] 19 p2650 N90-25078
A contribution to the economic, optimal dimensioning, and shaping of aircraft structures using a design model
[ETN-90-96966] 20 p2808 N90-25976
Scaling effects in the static and dynamic response of graphite-epoxy beam-columns
[NASA-TM-102697] 20 p2876 N90-26363
Two-phase heat transport systems for spacecraft scaling with respect to gravity
[NLR-TP-89127-U] 21 p2965 N90-26857

DIMENSIONAL MEASUREMENT
Algorithmic randomness, physical entropy, measurements, and the second law
[DE90-002413] 06 p0830 N90-14823
Application of x ray absorption edge spectrometry to the non-destructive determination of element concentrations, coating thickness and areal densities
[AERE-R-13030] 16 p2245 N90-22802
Dimensional analysis of structures using wrapping techniques
[REPT-892-430-119] 16 p2247 N90-22815
Full surface interferometric testing of grazing incidence mirrors
[AD-A219394] 16 p2318 N90-23218

DIMENSIONAL STABILITY
NT SHELL STABILITY
NT STRUCTURAL STABILITY
Production of a variety of shapes using wrapping and draping techniques
[REPT-892-430-122] 16 p2213 N90-22625
Modified maleic anhydride copolymers as e-beam resists
[AD-A218470] 16 p2223 N90-22679
Solar Concentrator Advanced Development Program
[NASA-CR-185173] 16 p2250 N90-22834
High-temperature creep under a nonuniform temperature distribution
[ATR-88(3728-02)-1] 19 p2702 N90-25373

DIMENSIONLESS NUMBERS
NT HIGH REYNOLDS NUMBER
NT LOW REYNOLDS NUMBER
NT MACH NUMBER
NT PRANDTL NUMBER
NT RAYLEIGH NUMBER
NT REYNOLDS NUMBER
NT SCHMIDT NUMBER
NT SIMILARITY NUMBERS
NT STROUHAL NUMBER
A space-time discretization procedure for wave propagation problems
[NASA-TM-102215] 08 p1105 N90-16399

DIMENSIONS
NT DEPTH
NT DIAMETERS
NT DIFFUSION LENGTH
NT FILM THICKNESS
NT FRACTALS
NT HEIGHT
NT LENGTH
NT RADII
NT SCALE HEIGHT
NT TARGET THICKNESS
NT WIDTH
Dimensional reduction at high temperature revisited
[KVI-791] 04 p0549 N90-13194
On the recurrence relation for multivariate B-splines with respect to dimension
[MEMO-786] 05 p0689 N90-14017
A self-organizing multiple-view representation of three-dimensional objects
[AD-A216711] 11 p1541 N90-18871
Preference numbers and funnel dimension
[REPT-89-57] 15 p2161 N90-22346
Stability of compactification during inflation
[NASA-CR-186597] 15 p2189 N90-22502
Adding a dimension: Time as a factor in the generalizability of predictive relationships
[AD-A219679] 17 p2438 N90-23890

DIMERIZATION
Strongly coupled one-dimensional system and the polymer
[AD-A216330] 11 p1489 N90-18571
Composite materials with improved properties in compression: Synthesis and dimerization 2,3-dimethyl-5-silaspiro(4.4)nona-2,7-diene
[AD-A222552] 22 p3156 N90-27892

DIMERS
Bonding in transition metal silyl dimers. Molecular orbital theory
[AD-A208269] 01 p0046 N90-10260
Electrically conducting organic materials: Design, synthesis and characterization
[AD-A212214] 04 p0471 N90-12700
Structures and energies for small borane compounds: One and two boron compounds
[AD-A212264] 04 p0471 N90-12701
New electrically conducting solids based on nickel(II) - bis(1,3-dithiole-2-thione-4,5-diselenolate)
[DE90-003788] 08 p1042 N90-16020
Electronic energies for Neon dimer dication radiative charge transfer
[AD-A215817] 10 p1429 N90-18244
Chemical and electrochemical studies in ionic liquids
[AD-A217742] 13 p1773 N90-20175
Copolymer-like structures of nematic nitroimine dimers
[AD-A217574] 13 p1780 N90-20215
Composite materials with improved properties in compression: Synthesis and dimerization 2,3-dimethyl-5-silaspiro(4.4)nona-2,7-diene
[AD-A222552] 22 p3156 N90-27892

DIMETHYLHYDRAZINES
Ozonation of hydrazines and their associated impurities 02 p0205 N90-11174
Field evaluation of a passive sampling device for hydrazines in ambient air
[NASA-TM-103456] 18 p2578 N90-24686

DIODES
NT AVALANCHE DIODES
NT GUNN DIODES
NT JUNCTION DIODES
NT LIGHT EMITTING DIODES
NT PHOTODIODES
NT PLASMA DIODES
NT SCHOTTKY DIODES
NT SEMICONDUCTOR DIODES
NT THERMIONIC DIODES
NT VARACTOR DIODES
Laser diode array and transmission optics 01 p0030 N90-10163
Micro-cavity integrable vacuum diodes and triodes
[DE89-016649] 01 p0060 N90-10344
Studies of high power density, pico-second rise-time light activated semiconductor switch
[AD-A210549] 01 p0061 N90-10349
Efficient nonlinear conversion of laser diode pumped miniature solid state laser sources
[AD-A210708] 01 p0075 N90-10433
Quantum 1/F noise in solid state devices in particular Hg1-(sub x)Cd(sub x)Te N(+)-P diodes
[AD-A209365] 01 p0128 N90-10730
Calculations of soft x ray emission of REB-heated plasma
[IPPCZ-287] 03 p0407 N90-12329
Null offset voltage compensator for operational amplifier
[AD-D014189] 04 p0496 N90-12859
Monolithic laser diode structure for microwave generation
[AD-D014210] 06 p0782 N90-14543
Miniature laser Doppler anemometer with a diode laser
[ISL-CO-224/88] 08 p1077 N90-16232
Diode pumped monolithic Nd:YLF 1.053 micron mini-laser and its application to injection seeding
[DE90-005323] 10 p1390 N90-18040
Power diode switching behavior
[ETN-90-95363] 12 p1653 N90-19501
Experimental results of aging and thermal effects in high-power laser diodes
[DE90-005955] 12 p1686 N90-19573

Measurement of proton induced radiation damage to CMOS transistors and pin diodes
[DE90-007836] 13 p1792 N90-20283
The inverse triax x ray diode: An alternate reduced-endpoint-energy bremsstrahlung source
[DE90-006366] 13 p1792 N90-20285
A progress report on the Livermore Miniature Vacuum Tube Project
[DE90-008302] 13 p1794 N90-20299
Coplanar waveguide discontinuities for P-I-N diode switches and filter applications
[NASA-TM-102534] 14 p1969 N90-21278
The potential for high performance HgCdTe arrays at 4 microns 14 p1976 N90-21320
InSb DRO array characteristics 14 p1977 N90-21326
Laboratory and telescope use of the NICMOS2 128 x 128 HgCdTe array 14 p1979 N90-21338
Spectral properties of a 1.3-micrometers InGaAsP diode laser under modulation
[AD-A220066] 17 p2409 N90-23729
An influence of fast neutron irradiation on the properties of p-i-n wide-based diodes
[DE90-611148] 18 p2550 N90-24556
High-order mode dependencies in gain-guided twin-stripe laser diode arrays
[AD-A220868] 18 p2562 N90-24617
A viologen/ruthenium oxide-based microelectrochemical diode with pH-dependent current-voltage characteristics
[AD-A221961] 21 p3000 N90-27052
Ion divergence and the stability of magnetically insulated diodes
[DE90-014565] 23 p3321 N90-28777
PBFA 2 applied B ion diode beam characteristics at high voltages
[DE90-014419] 23 p3396 N90-29190
Long pulse diode experiments
[DE90-016218] 24 p3465 N90-29578

DIOPHANTINE EQUATION
The weighted sum of two S-units being a square
[MEMO-792] 05 p0691 N90-14031
Solving a specific Thue-Mahler equation
[MEMO-793] 05 p0691 N90-14032
Efficient computer algebra algorithms for polynomial matrices in control design 16 p2285 N90-23022

DIOXIDES
NT CARBON DIOXIDE
NT HYDROGEN PEROXIDE
NT QUARTZ
NT SILICON DIOXIDE
NT SULFUR DIOXIDES
Selective electrocatalysis of anodic oxygen-transfer reactions at chemically modified, thin-film lead dioxide electrodes
[DE90-011747] 20 p2857 N90-26252

DIPLEXERS
Millimeter-wave multiplexers
[AD-D014518] 19 p2685 N90-25274

DIPOLE ANTENNAS
Millimeter-wave/infrared rectenna development at Georgia Tech 01 p0028 N90-10147
Very broad band VHF/UHF omnidirectional antenna design study
[AD-A215358] 09 p1207 N90-16997
Dual frequency launcher for circularly polarized antenna
[AD-D014361] 12 p1645 N90-19456
Electric dipole antennae used as micrometeoroid detectors
[AERONOMICA-ACTA-A-351-1989] 17 p2392 N90-23623

DIPOLE MOMENTS
NT MAGNETIC MOMENTS
Time-domain analytic and numeric analysis of vertical dipoles in front of dielectric planar interface
[PB89-221642] 03 p0338 N90-11927
A search for the electric dipole of the electron
[DE90-001572] 08 p1120 N90-16484
Dipole analysis on EGRET data of extragalactic gamma ray background radiation 16 p2337 N90-23322

DIPOLES
Development of the methods and means of precise forming and geometry control of superconducting current-carrying element for the UNR pulsed dipoles
[DE90-620108] 15 p2173 N90-22419

DIRAC EQUATION
Reduction of the Dirac equation to the Dirac-Kaehler equation
[DE89-630111] 02 p0270 N90-11541
On the spectrum of the staggered Dirac operator at finite chemical potential
[ITFA-88-53] 04 p0561 N90-13272
Theory of singular Lagrangians
[DE90-600735] 08 p1115 N90-16456
Proceedings of the 23rd Annual Seminar on Theoretical Physics
[DE90-601827] 08 p1135 N90-16577
The basis spline method and associated techniques
[DE90-008403] 13 p1877 N90-20783
Local supersymmetry in non-relativistic systems
[DE90-612751] 14 p2034 N90-21670
Theory of a charged spinning particle in a gravitational and electromagnetic field
[NIKHEF-H/89-4] 15 p2165 N90-22373
On the zeta-function regularization of chiral Jacobians for singular Dirac operators
[DE90-627176] 23 p3390 N90-29150
Dirac's equation as a geodesic in Riemann space
[DE90-627194] 23 p3390 N90-29152
On Dirac's conjecture for Hamiltonian systems with first and second class constraints
[DE90-627206] 24 p3555 N90-30116

DIRECT BROADCAST SATELLITES
Beamforming devices and feed structures for a DBS flat-plate antenna
[BBC-RD-1989/12] 17 p2386 N90-23592

DIRECT CURRENT
A new semicustom integrated bipolar amplifier for silicon strip detectors
[DE89-015585] 02 p0215 N90-11229
Design of a high power density, permanent magnet, axial gap dc motor
[DE90-005449] 12 p1655 N90-19514
A comparative study of electric power distribution systems for spacecraft
[NASA-CR-186531] 14 p1942 N90-21113
A linearly controlled direct-current power source for high-current inductive loads in a magnetic suspension wind tunnel
[NASA-TM-4198] 19 p2692 N90-25319
Experiments on initial behaviour of corona generated with electrical pulses superimposed on DC bias
[EUT-89-E-226] 20 p2858 N90-26259
Liquid Rocket Booster (LRB) for the Space Transportation System (STS) systems study. Appendix C: Battery report for the liquid rocket booster TVC actuators
[NASA-CR-183789-APP-C] 23 p3288 N90-28603
Theoretical and experimental examinations of brushless monophase direct current motors
[ETN-90-97301] 24 p3466 N90-29580

DIRECT LIFT CONTROLS
Evaluation for DLC-Flap Monitoring System of the VSRA
[NAL-TM-607] 24 p3433 N90-29391

DIRECT POWER GENERATORS
NT ALKALINE BATTERIES
NT BIOCHEMICAL FUEL CELLS
NT FUEL CELLS
NT HYDROGEN OXYGEN FUEL CELLS
NT MAGNETOHYDRODYNAMIC GENERATORS
NT METAL AIR BATTERIES
NT NICKEL ZINC BATTERIES
NT PHOSPHORIC ACID FUEL CELLS
NT PHOTOVOLTAIC CELLS
NT PRIMARY BATTERIES
NT RADIOISOTOPE BATTERIES
NT REGENERATIVE FUEL CELLS
NT SODIUM SULFUR BATTERIES
NT SOLAR BLANKETS
NT SOLAR CELLS
NT SOLAR SEA POWER PLANTS
NT THERMAL BATTERIES
NT THERMIONIC CONVERTERS
NT THERMOELECTRIC GENERATORS
Electrical performance characteristics of high power converters for space power applications
[NASA-CR-185947] 06 p0734 N90-14279

DIRECTION
Direction-of-arrival calculations at VLF/LF (Very Low Frequency/Low Frequency)
[AD-A212620] 04 p0493 N90-12833
Effect of contrast on the perception of direction of a moving pattern
[NASA-TM-102234] 07 p0965 N90-15577
The effects of training on errors of perceived direction in perspective displays
[NASA-TM-102792] 22 p3232 N90-28329

DIRECTION FINDERS (RADIO)
U RADIO DIRECTION FINDERS

DIRECTION FINDING
Array signal processing: New techniques for direction finding and spectrum estimation
[AD-A213883] 07 p0924 N90-15345
Large-aperture sparse array detector system for multiple emitter location
[AD-D014303] 07 p0925 N90-15355
Lower bounds on multiple-source direction finding in the presence of direction-dependent antenna-array-calibration errors
[AD-A215825] 10 p1376 N90-17979
Evaluation of VHF intercept and direction finding systems
[AD-A219805] 17 p2350 N90-23382
Model order determination methods for autoregressive radio direction finding techniques
[AD-A220707] 17 p2350 N90-23384
Frequency assignments for HFDF receivers in a search and rescue network
[AD-A220529] 17 p2390 N90-23610
Estimation of noise field directionality: Comparison with Fourier series method
[AD-A220366] 17 p2469 N90-24114
Man-made noise in a military environment 20 p2847 N90-26191
Implementation of an algorithm for travelling-wave-based directional detection
[EUT-89-E-214] 20 p2855 N90-26239

DIRECTIONAL ANTENNAS
NT DIPOLE ANTENNAS
NT HORN ANTENNAS
NT LENS ANTENNAS
NT LOOP ANTENNAS
NT PARABOLIC ANTENNAS
NT RADAR ANTENNAS
NT REFLECTOR ANTENNAS
NT SLOT ANTENNAS
NT STEERABLE ANTENNAS
NT YAGI ANTENNAS
Maximization of directed electromagnetic radiation with an optimized antenna
[DE89-014045] 01 p0056 N90-10319
Theory and simulation of the operation of a Doppler direction finder in a multipath environment
[FEL-1988-56] 03 p0340 N90-11939
Frequency independent constant beamwidth directional lens antenna for very wideband and multi-channel electromagnetic communications
[AD-D014214] 06 p0765 N90-14449
An investigation of the extent of the fresnel region of aperture antennas with attention to superdirectivity
[AD-A217518] 13 p1794 N90-20294
Design concepts for hardened communications structures
[AD-A221233] 19 p2683 N90-25260

DIRECTIONAL CONTROL
NT THRUST VECTOR CONTROL
Independent Orbiter Assessment (IOA): Analysis of the rudder/speed brake subsystem
[NASA-CR-185560] 02 p0161 N90-10916
Independent Orbiter Assessment (IOA): Analysis of the guidance, navigation, and control subsystem
[NASA-CR-185555] 02 p0162 N90-10920
Independent Orbiter Assessment (IOA): Analysis of the ascent thrust vector control actuator subsystem
[NASA-CR-185579] 02 p0164 N90-10929
Design of a new control system for hovercrafts
[ETN-90-96230] 11 p1455 N90-18435
Development of a passive robot-controlled reaction arm 13 p1809 N90-20389

DIRECTIONAL SOLIDIFICATION (CRYSTALS)
Primary arm spacing in directionally solidified Pb-10 wt percent Sn alloys
[NASA-CR-185190] 06 p0756 N90-14398
Directional solidification of superalloys
[NASA-CASE-MFS-28314-1] 07 p0904 N90-15227
Modelling directional solidification
[NASA-CR-186181] 09 p1292 N90-17487
Composite ceramic superconducting wires for electric motor applications
[AD-A222085] 21 p3001 N90-27055

DIRECTIONAL STABILITY
NT GYROSCOPIC STABILITY
Yaw rate control of an air bearing vehicle 12 p1639 N90-19420
The effects of foreplanes on the static and dynamic characteristics of a combat aircraft model 23 p3273 N90-28520

DIRECTIVITY
Measurement resolution of noise directivity patterns from acoustic flight tests
[NASA-TM-4134] 01 p0118 N90-10679
An investigation of the extent of the fresnel region of aperture antennas with attention to superdirectivity
[AD-A217518] 13 p1794 N90-20294

DIRECTORIES
Criss-cross directory of NASA N numbers and DOD AD numbers. Volume 2, part 1: AD to N, 1979-1986. N to AD, 1962-1986
[NASA-TM-101814] 03 p0416 N90-12388

Criss-cross directory of NASA N numbers and DOD AD numbers. Volume 2, part 2: AD to N, 1979-1986. N to AD, 1962-1986
[NASA-TM-101815] 03 p0416 N90-12389
Directory of International and Regional Organizations Conducting Standards-Related Activities, May 1989
[PB89-221147] 04 p0483 N90-12776
The DOD Gateway Information System: Operational prototype and transition period 1987-1988
[AD-A213044] 05 p0707 N90-14141
Accessing Japanese technical information: A group of essays extracted from the NTIS (National Technical Information Service) Directory of Japanese Technical Resources in the United States for 1987 and 1988
[PB90-100165] 06 p0858 N90-14992
Who's who in scientific visualization at LLNL
[DE90-014720] 23 p3379 N90-29091
The worldwide ionospheric data base
[NASA-TM-101823] 24 p3488 N90-29714

DIRICHLET PROBLEM
On some problems in reliability theory 09 p1233 N90-17155
A parallel iterative method for solving 3-dimensional elliptic partial differential equations
[DE90-005187] 10 p1422 N90-18199
Inverse design of airfoil contours: Constraints, numerical method, and applications 14 p1917 N90-20980
Analysis and finite element approximation of some optimal control problems associated with the Navier-Stokes equations 14 p1972 N90-21299
An examination of the full-wave method for rough surface scattering
[AD-A218664] 16 p2308 N90-23155
Asymptotics of Laplace-Dirichlet integrals
[DE90-627165] 23 p3388 N90-29137

DIRIGIBLES
U AIRSHIPS

DISASTERS
A decision support system for control and automation of dynamical processes
[AD-A219501] 17 p2454 N90-23995

DISCHARGE COEFFICIENT
Effect of pipe roughness on orifice flow measurement
[PB89-231484] 04 p0500 N90-12880
Measurements of coefficients of discharge for concentric flange-tapped square-edged orifice meters in water over the Reynolds number range 600 to 2,700,000
[PB89-235147] 04 p0502 N90-12892

DISCHARGE TUBES
U GAS DISCHARGE TUBES

DISCONNECT DEVICES
Pressure sensitive release device
[AD-D014220] 06 p0792 N90-14610
Quick disconnect duct coupler
[AD-D014265] 08 p1084 N90-16274
Shape memory alloys for robot grippers and mechanical hands 18 p2536 N90-24466
Analysis and test interaction in the development of a hold down and release mechanism 18 p2539 N90-24489
The tetrahedral wedge attachment mechanism 18 p2539 N90-24490
A spring-actuated spin and eject device for interplanetary missions 18 p2540 N90-24493
Detachable interface mechanism 18 p2540 N90-24497
Underwater connect and disconnect plug and receptacle
[AD-D014175] 21 p2998 N90-27039
Engineering test results for the Moog Single Line Disconnect
[NASA-TM-100755] 22 p3132 N90-27776

DISCONNECTORS
U DISCONNECT DEVICES

DISCONTINUITY
NT SHOCK DISCONTINUITY
Local error estimates for discontinuous solutions of nonlinear hyperbolic equations
[NASA-CR-181960] 06 p0834 N90-14847
Evolution of overlapping spreading centers: A Sea Mark 2 investigation
[AD-A214278] 07 p0965 N90-15576
A study of a new time-domain method of lines and its application for the characterization of microstrip line and its discontinuities
[AD-A215441] 09 p1213 N90-17034
A study of failure characteristics in thermoplastic composite laminates due to an eccentric circular discontinuity
[AD-A216226] 10 p1349 N90-17827
Validation of the boundary element method applied to complex fracture mechanics conditions
[AD-A216412] 10 p1398 N90-18080
Algebraic block-structured grid generation based on a macro-block concept 15 p2093 N90-21978
The dynamic instability of adiabatic blastwaves
[NASA-CR-182498] 17 p2401 N90-23679
Numerical modelling of shocks in gases and metals
[AD-A218586] 17 p2402 N90-23684
Detecting perceptual groupings in textures by continuity considerations 21 p3045 N90-27310
Numerical solutions to steady-state problems with discontinuities
[AD-A222205] 21 p3064 N90-27418
Study of the reflection of surface acoustic wave from a material discontinuity boundary using a perturbation method 24 p3542 N90-30032

DISCRETE ADDRESS BEACON SYSTEM
Aircraft Reply and Interference Environment Simulator (ARIES) hardware principles of operation. Volume 2: Appendixes
[DOT/FAA/CT-TN88/4-2] 04 p0484 N90-12781
Aircraft Reply and Interference Environment Simulator (ARIES) hardware principles of operation, volume 1
[DOT/FAA/CT-TN88/4-1] 04 p0484 N90-12782

DISCRETE FUNCTIONS
Discrete-time conversion for simulating finite-horizon Markov processes
[AD-A210683] 01 p0116 N90-10666
Computational and statistical issues in discrete-event simulation
[AD-A210743] 01 p0116 N90-10668
Multi-sample functional statistical data analysis
[AD-A210992] 01 p0117 N90-10673
The discrete-time single-server queueing model
[MEMO-780] 04 p0544 N90-13165
Discretization and model reduction for a class of nonlinear systems 05 p0583 N90-13397
A transient response method for linear coupled substructures
[NASA-TP-2926] 05 p0592 N90-13444
A unified algebraic approach to integral and discrete evolution equations
[PREPRINT-668] 05 p0692 N90-14044
Numerical methodologies for solving partial differential equations
[DE90-001842] 06 p0834 N90-14849
Estimation in a discrete tail rate family of recapture sampling models
[NASA-CR-180452] 10 p1421 N90-18197
An analysis of the finite-differenced, even-parity discrete-ordinates equations in slab geometry
[DE90-006479] 15 p2160 N90-22337
Discrete variable structural optimization by the complex method
[LR-597] 15 p2161 N90-22341
The discrete time H infinity control problem: The full-information case
[MEMO-COSOR-89-25] 17 p2455 N90-24003
A modified fast Fourier transform
[AD-A220567] 17 p2457 N90-24023
On output deadbeat control of discrete-time multivariable systems
[MATHS-REPT-A-122] 20 p2915 N90-26583
The discretization of the three dimensional boundary layer equations
[ETN-90-97292] 22 p3171 N90-27987
Discretization methods for the incompressible Navier-Stokes equations 22 p3173 N90-28003
Numerical analysis
[AD-A221982] 22 p3242 N90-28385
The structure of random discrete spacetime
[NASA-CR-182841] 22 p3255 N90-28429
A digital controller for active aeroelastic controls
[NAL-TR-1014] 24 p3435 N90-29402
Computer-Aided Structural Engineering (CASE) project: Investigation and design of U-frame structures using program CUFRBC. Volume A: Program criteria and documentation
[AD-A224387] 24 p3525 N90-29934
Unification of statistical methods for continuous and discrete data
[AD-A224307] 24 p3540 N90-30017

DISCRIMINANT ANALYSIS (STATISTICS)
A brief bibliography of statistical classification procedures: Decision-theoretic approach
[AD-A210276] 01 p0115 N90-10663
Selecting multinomial populations
[AD-A219256] 18 p2309 N90-23159

DISCRIMINANT FUNCTIONS
U DISCRIMINANT ANALYSIS (STATISTICS)

DISCRIMINATION
NT SENSORY DISCRIMINATION
NT TACTILE DISCRIMINATION
NT VISUAL DISCRIMINATION
Gas identification system using graded temperature sensor and neural net interpretation
[AD-A213359] 05 p0622 N90-13627
Recognition and distinction of clouds, snow, and ice using AVHRR data 08 p1092 N90-16322
Aggregate filter
[AD-A215029] 09 p1282 N90-17432
Visual processing of object velocity and acceleration
[AD-A216509] 11 p1539 N90-18858
Perception of long-period complex sounds
[AD-A216743] 11 p1539 N90-18861
Auditory perception
[AD-A217012] 11 p1540 N90-18864

DISCRIMINATORS
Spatiotemporal characteristics of visual localization, phase 2
[AD-A212934] 05 p0674 N90-13929
Beamforming pre-processors for high discrimination algorithms
[RSRE-MEMO-4304] 08 p1110 N90-16429

DISEASED VEGETATION
U PLANT DISEASES

DISEASES
NT ARTHRITIS
NT ATAXIA
NT BONE DEMINERALIZATION
NT CANCER
NT HEART DISEASES
NT OCCUPATIONAL DISEASES
NT OSTEOPOROSIS
NT PARALYSIS
NT RADIATION SICKNESS
NT RESPIRATORY DISEASES
NT TUMORS
Evaluation of rocket motor exhaust and liner combustion by-products
[AD-A210747] 02 p0189 N90-11083
Investigation on analyzing computer-aided forest disease classifications
[DFVLR-FB-89-16] 03 p0369 N90-12112
Preliminary study of pharmacological control of space disease
[ETN-90-95015] 05 p0674 N90-13927
Progressive cervical osteoarthritis in high performance aircraft pilots 19 p2718 N90-25465

DISHES
U PARABOLIC REFLECTORS

DISILICIDES
Improvement study of iron disilicide thermoelectric materials
[AD-A218946] 16 p2252 N90-22844

DISINFECTANTS
U ANTISEPTICS

DISINTEGRATION
Polarization observables in deuteron photo- and electro-disintegration
[CEBAF-PR-89-022] 19 p2756 N90-25659

DISK GALAXIES
GALAX: A two-dimensional N-body code for disk galaxy dynamics
[PB89-217780] 03 p0420 N90-12415
The disk-halo connection and the nature of the interstellar medium
[NASA-CR-186286] 07 p1012 N90-15860
The correlation between radio and far-infrared emission for disk galaxies 11 p1588 N90-19158
Cometary bodies in the circumstellar disk around beta Pictoris 12 p1741 N90-20010
The distribution of molecular clouds in spiral galaxies 15 p2186 N90-22489

DISK OPERATING SYSTEM (DOS)
PC-based PCM (Pulse Code Modulation) telemetry data reduction system hardware
[DE90-000316] 12 p1612 N90-19273
An approximation for the response time of an open CP-disk system
[MEMO-COSOR-89-19] 16 p2327 N90-23266
IRDS prototyping with applications to the representation of EA/RA models
[NASA-CR-186066] 21 p3039 N90-27273
Turbo pascal implementation of a distributed processing network of MS-DOS microcomputers connected in a master-slave configuration
[AD-A223925] 24 p3525 N90-29928

DISKS
Hybrid butterfly valve
[NASA-CASE-SSC-00004] 07 p0940 N90-15443
Application of advanced coating techniques to rocket engine components 23 p3298 N90-28654

DISKS (SHAPES)
NT ROTATING DISKS
A thermoelastic transversely isotropic thick walled cylinder/disk application: An analytical solution and study
[NASA-TM-102320] 04 p0511 N90-12950
Computation of fluid flow and heat transfer in rotating disc-systems 09 p1215 N90-17044
Towards a Sarkovski order for the embedding of disks maintaining their orientation
[REPT-89-43] 15 p2151 N90-22289

Evaluation of plane-of-light noninterference stress measurement systems for measuring bladed disk vibrations
[AD-A223487] 24 p3479 N90-29667

DISLOCATIONS (MATERIALS)
NT CRYSTAL DISLOCATIONS
NT EDGE DISLOCATIONS
A two-parameter representation of dynamic dislocation distributions
[AD-A212249] 04 p0560 N90-13263
Anomalous strain rate dependence of the serrated flow in Ni-H and Ni-C-H alloys
[AD-A213244] 05 p0624 N90-13641
Determination of the heat dissipated from a specimen undergoing cyclic plasticity by a hybrid numerical/experimental method
[AD-A221575] 21 p2982 N90-26946
The 2nd International Conference on Low-Energy Dislocation Structures
[AD-A222887] 21 p3082 N90-27525

DISORIENTATION
NT DESYNCHRONIZATION (BIOLOGY)
NT JET LAG
Spatial tests for aviators
[IZF-1988-15] 04 p0527 N90-13041
Passenger behaviour in aircraft emergencies involving smoke and fire 10 p1317 N90-17613
Spatial disorientation incidents in the RNLAF F16 and F5 aircraft and suggestions for prevention 23 p3357 N90-28973

DISPERSING
The suitability of diffusion and wind-field techniques for an emergency-response dispersion model
[PB89-190219] 01 p0085 N90-10481
Performance of four rake modems over the non-disturbed wideband HF channel
[AD-A211589] 03 p0339 N90-11930
Convective boundary layer and modeling of dispersion 06 p0813 N90-14731
A methodology for evaluating heavy gas dispersion models
[AD-A214009] 07 p0887 N90-15131
Dimensional analysis of continuous high-capacity electrodispersion of aqueous based liquids in an organic continuous phase
[DE90-003714] 07 p0888 N90-15136
Beryllium dispersion near explosive firing tables: A comparison of computed and observed results
[DE90-002635] 07 p0960 N90-15550
A study on deformation and break-up of dispersed particles in elongational flow
[ETN-90-96268] 11 p1508 N90-18684
A temperature-dependent regular infrared band model for absorption and dispersion 15 p2083 N90-21927
The ASCOT 1988 valley/tributary interaction study
[DE90-009043] 15 p2133 N90-22191
Microscopic models for electromagnetic wave propagation in highly dispersive media
[AD-A224382] 24 p3460 N90-29540
Particle dispersion in a turbulent shear flow
[AD-A224327] 24 p3467 N90-29590

DISPERSION
MATE (Materials for Advanced Turbine Engines) Program, Project 3. Volume 2: Design, fabrication and evaluation of an oxide dispersion strengthened sheet alloy combustor liner
[NASA-CR-180892] 10 p1357 N90-17868

DISPERSION PRECIPITATION HARDENING
U PRECIPITATION HARDENING

DISPERSIONS
NT AEROSOLS
NT COLLOIDS
NT EMULSIONS
NT FOG
NT LIQUID-GAS MIXTURES
NT NUCLEAR EMULSIONS
NT SMOKE
Superplastic forming and diffusion bonding of rapidly solidified, dispersion strengthened aluminum alloys for elevated temperature structural applications
[NASA-CR-181849] 04 p0474 N90-12718
Containerless low gravity processing of glass forming and immiscible alloys
[NASA-CR-186999] 23 p3316 N90-28747

DISPLACEMENT
NT CRACK OPENING DISPLACEMENT
Two stage gear tooth dynamics program
[NASA-CR-185110] 01 p0077 N90-10437
Planar sliding of a rigid body with dry friction: Limit surfaces and dynamics of motion 02 p0229 N90-11314
Computational aspects of sensitivity calculations in linear transient structural analysis 02 p0231 N90-11327
Calcium displacement caused by electromagnetic fields
[AD-A212690] 04 p0524 N90-13023
Finite element analysis of laminated composite plates 06 p0737 N90-14291
A finite strip method for the elastic-plastic large displacement analysis of thin-walled and cold-formed steel sections
[PB89-226021] 06 p0798 N90-14647
Damage evaluation from surface displacement data 07 p0944 N90-15469
Nonlinear strain-displacement relations for thin axisymmetric shells
[PB89-226013] 07 p0945 N90-15470
Pipeline vibrations. Fluid transients in non-rigid, unbranched planar piping systems
[ESDU-89030] 07 p0948 N90-15491
Self compensation of rigid displacements in holographic interferometry
[ISL-CO-219/88] 09 p1226 N90-17113
Transient elastic waves on anisotropic half-spaces 10 p1396 N90-18074
A higher-order plate theory with ideal finite element suitability
[AD-A216163] 10 p1397 N90-18075
Validation of the boundary element method applied to complex fracture mechanics conditions
[AD-A216412] 10 p1398 N90-18080
Integrated force method versus displacement method for finite element analysis
[NASA-TP-2937] 10 p1398 N90-18081
Small displacement, long life on-orbit compressor design and fabrication 11 p1475 N90-18489
Intertropical Convergence Zone (ITCZ) and its relationship with the precipitation of the north-northeast Brazilian region
[INPE-4887-TDL/378] 11 p1535 N90-18839
Modeling elastomer displacements for tactile sensing applications
[DE90-007959] 14 p1984 N90-21370
Age constraints for the present fault configuration in the Imperial Valley, California: Evidence for northwestward propagation of the Gulf of California rift system
[NASA-CR-186541] 14 p2006 N90-21493
Limiting performance based structural and control optimization for large vibrating structures 16 p2202 N90-22568
Computations of weight functions in fracture mechanics 16 p2246 N90-22809
Adapting to variable prismatic displacement 16 p2271 N90-22945
Nonlinear finite element formulation for the large displacement analysis in multibody system dynamics 16 p2284 N90-23015
Significance of norms and completeness in variational based methods 16 p2296 N90-23078
Predicting tidal displacements of the surface of the Earth, volume 1
[ETN-90-96690] 17 p2431 N90-23850
Predicting tidal displacements of the surface of the Earth, volume 2
[ETN-90-96691] 17 p2431 N90-23851
Review of probabilistic analysis of dynamic response of systems with random parameters
[NASA-CR-186171] 18 p2568 N90-24636
Accuracy improvements in finite element stress analysis 18 p2571 N90-24651
Discrete approach: Percolation theory 19 p2689 N90-25297
Instabilities: Miscible and immiscible flows 19 p2689 N90-25298
Polyimidazoles via aromatic nucleophilic displacement
[NASA-CASE-LAR-14145-1] 21 p2983 N90-26954
Symmetry breaking oxygen displacement in superconducting oxides
[DE90-013670] 21 p3081 N90-27520
Acoustic emission from a growing crack 22 p3188 N90-28089
Fatigue testing apparatus
[AD-D014544] 22 p3192 N90-28108
Mechanical behavior of thick, curved, laminated composites 23 p3299 N90-28664
A nonlinear finite element formulation for the large displacement analysis of plates 23 p3338 N90-28867
Parametric solution of nonlinear structure problems
[ONERA-RT-21/3542-RY-082-R] 23 p3340 N90-28874
Rotordynamic properties of high pressure seals: An experimental approach 24 p3475 N90-29640

DISPLACEMENT MEASUREMENT
Three-in-one gage
[NASA-CR-183714] 01 p0072 N90-10413
An interferometric strain-displacement measurement system
[NASA-TM-101638] 01 p0080 N90-10454
Dynamic analysis of the geodetic networks originating from the Navstar/Global Positioning System (GPS) satellites
[SER-C-346] 08 p1091 N90-16316
Preliminary experiences with a novel method for the determination of displacement vector fields and satellite image sequences 08 p1093 N90-16324
The 59th Shock and Vibration Symposium, volume 1
[AD-A214576] 09 p1238 N90-17183
Circularity measuring system: A shape gauge designed especially for use on large objects 15 p2116 N90-22104
Evaluation of plane-of-light noninterference stress measurement systems for measuring bladed disk vibrations
[AD-A223487] 24 p3479 N90-29667

DISPLAY DEVICES
NT APPROACH INDICATORS
NT FLOW DIRECTION INDICATORS
NT HEAD-UP DISPLAYS
NT HELMET MOUNTED DISPLAYS
NT POSITION INDICATORS
NT RADIO DIRECTION FINDERS
NT SPEED INDICATORS
NT TACHOMETERS
NT WIND VANES
Classification and reduction of pilot error
[NASA-CR-181867] 01 p0004 N90-10014
Satellite Data Processing System (SDPS) users manual V1.0
[NASA-CR-183054] 01 p0082 N90-10468
Experience with model based display for advanced diagnostics and control
[DE89-015693] 01 p0082 N90-10469
Low-cost three-dimensional stereoscopic display technique for computer-aided design
[DE89-011635] 01 p0104 N90-10594
Flight simulator evaluation of a head-down display
[NAL-TM-573] 02 p0157 N90-10898
Independent Orbiter Assessment (IOA): Analysis of the backup flight system
[NASA-CR-185567] 02 p0165 N90-10932
Independent Orbiter Assessment (IOA): Assessment of the displays and controls subsystem
[NASA-CR-185588] 02 p0171 N90-10961
HDTV displays: Subjective effects of scanning standards and domestic picture sizes
[BBC-RD-1989/9] 02 p0211 N90-11208
Techniques for optimizing human-machine information transfer related to real-time interactive display systems
[NASA-TM-100450] 02 p0254 N90-11441
Filling or outlining shapes with color: The effects on a visual search task
[AD-A211067] 02 p0255 N90-11444
Multicolor electrochromic displays exploratory development
[AD-A212004] 03 p0303 N90-11721
Transport systems research vehicle color display system operations manual
[NASA-TM-101577] 03 p0306 N90-11736
Independent Orbiter Assessment (IOA): Analysis of the displays and controls subsystem
[NASA-CR-185563] 03 p0312 N90-11774
Analysis of two-pass Modified Hough Transform (MHT) technique for the detection of wake like signals
[AD-A211982] 03 p0338 N90-11924
Color printing for computer graphics. Or: How to get it off your screen and onto paper, in color
[PB89-208110] 03 p0384 N90-12184
Basic program for raster scan display unit
[NAL-TM-560] 03 p0384 N90-12185
Software package for 3-dimensional graphic display unit
[NAL-TM-559] 03 p0385 N90-12191
Integration of a centralized multiplexed control unit into the cockpit of an aircraft
[F6150-DT410-1-88329] 04 p0458 N90-12622
Characterization of liquid crystal displays for optical signal processing applications
[AD-A212832] 04 p0505 N90-12910
State of the art of human/machine dialog tool prototypes
[TELECOM-PARIS-89-H001] 04 p0527 N90-13038
A Z specification of the MaCHO interface editor
[RSRE-MEMO-4247] 04 p0531 N90-13067
Image enhancement software for underwater recovery operations: User's manual
[AD-A212943] 05 p0699 N90-14094
Studies of structure and switching dynamics in ferroelectric crystal and liquid crystal thin films
[AD-A212650] 05 p0702 N90-14109
A candidate concept for display of forward-looking wind shear information
[NASA-TM-101585] 06 p0725 N90-14232
Engineer's Refractive Effects Prediction System (EREPS) 06 p0758 N90-14411

Theoretical and material studies of thin-film electroluminescent devices
[NASA-CR-186104] 06 p0788 N90-14468
Human factors evaluation of electroluminescent display Number 1
[DE90-002231] 06 p0822 N90-14777
Task-oriented display design: Concept and example
[NASA-TM-101685] 07 p0881 N90-15101
Display interface concepts for automated fault diagnosis
[NASA-TM-101610] 07 p0881 N90-15102
Voice Multiplex System (VMS)
[AD-A213902] 07 p0919 N90-15315
Development of the AH-64 display symbology training module
[AD-A213456] 07 p0968 N90-15592
Studies of quantitative methods for imaging from scattered fields
[AD-A214047] 07 p0976 N90-15638
An electronic pressure profile display system for aeronautic test facilities
[NASA-TM-102478] 08 p1032 N90-15964
Sequential rapid communication visual displays
[AD-D014282] 08 p1056 N90-16106
Image processing by Intensity-Dependent Spread (IDS) 08 p1074 N90-16215
Liquid level measurement system for analog and digital readout
[AD-D014297] 08 p1076 N90-16227
Keeping the pilot in the loop
[RAE-TM-FM-18] 08 p1105 N90-16396
Assessment of visual function in aerospace medicine
[BMVG-FBWM-89-5] 08 p1105 N90-16397
Application of multifunction inertial reference systems to fighter aircraft 09 p1164 N90-16740
A circuit extraction system and graphical display for VLSI (Very Large Scale Integrated) design
[AD-A215668] 09 p1214 N90-17038
Proximity compatibility and information display: The effects of space and color on the analysis of aircraft stall conditions
[AD-A214488] 09 p1260 N90-17309
Attenuating the luminous output of the AN/PVS-5A night vision goggles and its effects on visual acuity
[AD-A214895] 09 p1261 N90-17311
Executive summary for designing online help systems: Report of year 1 activity
[AD-A214811] 09 p1262 N90-17320
The moving platform simulator 2: A networked real-time visual simulator with distributed processing and line-of-sight displays
[AD-A214936] 09 p1266 N90-17343
Fine tuning your search output: Word processors, desktop publishing, electronic mail, databases, and beyond
[DE90-005192] 09 p1297 N90-17517
An update of commercial infrared sensing and imaging instruments 10 p1366 N90-17920
Sensitivity of the peripheral vision to simulated aircraft ascent and descent 10 p1413 N90-18145
Impact of uncertainty and diagnosticity on classification of multidimensional data with integral and separable displays of system status
[AD-A215966] 10 p1424 N90-18215
Optical anti-aliasing filters
[AD-A215826] 10 p1430 N90-18251
A simulation evaluation of the engine monitoring and control system display
[NASA-TP-2960] 11 p1457 N90-18393
Three input concepts for flight crew interaction with information presented on a large-screen electronic cockpit display
[NASA-TM-4173] 11 p1457 N90-18394
Visual processing in texture segregation
[AD-A216539] 12 p1696 N90-19737
Comparison of oculometer and head-fixed reticle with voice or switch and touch panel for data entry on a generic tactical air combat display
[AD-A217231] 13 p1855 N90-20646
Graphics Technology in Space Applications (GTSA 1989)
[NASA-CP-3045] 13 p1856 N90-20651
The Real Time Interactive Display Environment (RTIDE), a display building tool developed by Space Shuttle flight controllers 13 p1857 N90-20654
Knowledge representation in space flight operations 13 p1857 N90-20655
The Real Time Display Builder (RTDB) 13 p1857 N90-20656
Design considerations for a space database 13 p1858 N90-20659
Applications of graphics to support a testbed for autonomous space vehicle operations 13 p1858 N90-20661
Large screen display for the Mission Control Center 13 p1858 N90-20662
Engineering visualization utilizing advanced animation 13 p1859 N90-20664
Broadening the interface bandwidth in simulation based training 13 p1859 N90-20666
Animation graphic interface for the space shuttle onboard computer 13 p1859 N90-20667
OMV mission simulator 13 p1860 N90-20669
Graphical programming and the use of simulation for space-based manipulators 13 p1861 N90-20674
SES cupola interactive display design environment 13 p1862 N90-20679
History of visual systems in the Systems Engineering Simulator 13 p1862 N90-20681
Real-time graphics for the Space Station Freedom cupola, developed in the Systems Engineering Simulator 13 p1862 N90-20683
The HS6000/20 development system
[LINO-1989-6] 13 p1865 N90-20696
The perceptual interaction of graphical attributes in thirteen bivariate displays
[AD-A217980] 13 p1868 N90-20720
Investigation of air transportation technology at the Massachusetts Institute of Technology, 1988-1989 14 p1905 N90-20922
Cockpit display of hazardous wind shear information 14 p1905 N90-20924
Cockpit display of hazardous weather information 14 p1906 N90-20929
Stereopsis cueing effects on hover-in-turbulence performance in a simulated rotorcraft
[NASA-TP-2980] 14 p1921 N90-21004
Simulator comparison of thumball, thumb switch, and touch screen input concepts for interaction with a large screen cockpit display format
[NASA-TM-102587] 14 p1921 N90-21005
A note on overdispersed exponential families
[AD-A216277] 14 p2018 N90-21565
The psychology of computer displays in the modern mission control center
[NASA-TM-100451] 15 p2137 N90-22213
Visions of visualization aids: Design philosophy and experimental results 15 p2138 N90-22220
Human motion perception: Higher-order organization 15 p2140 N90-22226
Stanford/NASA-Ames Center of Excellence in model-based human performance 15 p2143 N90-22241
Model-based method for terrain-following display design
[AD-A219302] 16 p2201 N90-22563
Cognitive efficiency considerations for good graphic design
[AD-A218976] 16 p2263 N90-22899
A task-analytic approach to the automated design of information graphics
[AD-A219271] 16 p2265 N90-22912
Spatial Displays and Spatial Instruments
[NASA-CP-10032] 16 p2267 N90-22918
Spatial constraints of stereopsis in video displays 16 p2267 N90-22920
Perceiving environmental properties from motion information: Minimal conditions 16 p2268 N90-22925
The photo-colorimetric space as a medium for the representation of spatial data 16 p2268 N90-22927
Distortions in memory for visual displays 16 p2268 N90-22929
Separate visual representations for perception and for visually guided behavior 16 p2269 N90-22931
The effects of viewpoint on the virtual space of pictures 16 p2269 N90-22932
The perception of geometrical structure from congruence 16 p2270 N90-22935
Exocentric direction judgements in computer-generated displays and actual scenes 16 p2270 N90-22936
How to reinforce perception of depth in single two-dimensional pictures 16 p2270 N90-22937
The eyes prefer real images 16 p2270 N90-22938
Spatial issues in user interface design from a graphic design perspective 16 p2270 N90-22939
Interactive displays in medical art 16 p2271 N90-22940
The interactive digital video interface 16 p2271 N90-22941
Displays, instruments, and the multi-dimensional world of cartography 16 p2271 N90-22942
Visual enhancements in pick-and-place tasks: Human operators controlling a simulated cylindrical manipulator 16 p2271 N90-22946
Displays for telemanipulation 16 p2272 N90-22948
Perception-action relationships reconsidered in light of spatial display instruments 16 p2272 N90-22949
A commentary on perception-action relationships in spatial display instruments 16 p2272 N90-22950
Spatial displays as a means to increase pilot situational awareness 16 p2272 N90-22951
A computer graphics system for visualizing spacecraft in orbit 16 p2272 N90-22952
Experiences in teleoperation of land vehicles 16 p2273 N90-22954
Development of a stereo 3-D pictorial primary flight display 16 p2273 N90-22955
Synthetic perspective optical flow: Influence on pilot control tasks 16 p2273 N90-22956
Sensory conflict in motion sickness: An observer theory approach 16 p2273 N90-22957
Optical, gravitational, and kinesthetic determinants of judged eye level 16 p2274 N90-22959
Voluntary presetting of the vestibular ocular reflex permits gaze stabilization despite perturbation of fast head movements 16 p2274 N90-22960
Simulator evaluation of the final approach spacing tool
[NASA-TM-102807] 17 p2348 N90-23374
Preliminary evaluation of a small wearable display
[AD-A219867] 17 p2350 N90-23385
Effect of extraneous color-coded targets on identification of targets on CRT displays
[AD-A219473] 17 p2436 N90-23879
The Zenith Z-248 as a scientific workstation
[AD-A219991] 17 p2441 N90-23909
A PC-based imaging system for the Naval Postgraduate School Infrared Search and Target Designation (NPS-IRSTD) system
[AD-A220109] 17 p2448 N90-23955
The effect of random variations of radiosonde data on the predicted FLIR performance calculated by the program UFLR
[AD-A220034] 18 p2615 N90-24896
Automatic speech recognition in air-ground data link 18 p2640 N90-25037
A 3D visualization system for molecular structures 18 p2641 N90-25044
The role of attention in information processing implications for the design of displays
[AD-A219252] 19 p2723 N90-25486
Visualization of three dimensional data 19 p2736 N90-25553
Remote operation of an orbital maneuvering vehicle in simulated docking maneuvers 19 p2736 N90-25554
A helmet mounted display to adapt the telerobotic environment to human vision 19 p2737 N90-25555
Process and representation in graphical displays 19 p2740 N90-25574
Evaluation of off-road terrain with static stereo and monoscopic displays 19 p2740 N90-25575
A human factors review of data entry devices
[DE90-012009] 19 p2763 N90-25703
Qualitative evaluation of a conformal velocity vector display for use at high angles-of-attack in fighter aircraft
[NASA-TM-102629] 20 p2809 N90-25981
Literature concerning control and display technology applicable to the Orbital Maneuvering Vehicle (OMV)
[NASA-CR-186790] 20 p2820 N90-26048
Choosing a pilot subjective workload scale to fit flight operational requirements
[IAR-89-21] 20 p2900 N90-26493
Motion sickness, visual displays, and armored vehicle design
[AD-A222678] 20 p2902 N90-26506
Knowledge-based system for flight information management
[NASA-TM-102685] 20 p2903 N90-26511
Cognitive requirements for aircraft navigation
[NASA-CR-186933] 21 p2955 N90-26804
The preparation of ACEL thin films
[AD-A222919] 21 p2999 N90-27048
Perspective transformation for wide-view sky scenes
[AD-A222694] 21 p3007 N90-27093
Aureole lidar: Ground based measurement
[AD-A223207] 21 p3008 N90-27101
ATS displays: A reasoning visualization tool for expert systems 21 p3042 N90-27290
Robot dynamics in reduced gravity environment 21 p3049 N90-27333
Post script code for grey-scaled displays
[AD-A223099] 21 p3053 N90-27354
The Canadian Aviation Safety Board's flight recorder facility 22 p3106 N90-27643
Australian experience in flight recorder readout and analysis 22 p3106 N90-27644
Economical graphics display system for flight simulation avionics
[NASA-CR-186886] 22 p3116 N90-27701
The dynamics of orbital maneuvering: Design and evaluation of a visual display aid for human controllers 22 p3131 N90-27767
The effects of training on errors of perceived direction in perspective displays
[NASA-TM-102792] 22 p3232 N90-28329

Development of a methodology for icon evaluation
[NPL-DITC-159/90] 22 p3235 N90-28345
The interaction of chromostereopsis and stereopsis in stereoscopic CRT (Cathode Ray Tubes) displays
[AD-A217906] 23 p3277 N90-28544
Description of the primary flight display and flight guidance system logic in the NASA B-737 transport systems research vehicle
[NASA-TM-102710] 23 p3277 N90-28546
Situational Awareness in Aerospace Operations
[AGARD-CP-478] 23 p3357 N90-28972
The three-dimensional structure of visual attention and its implications for display design
23 p3359 N90-28980
A real time evaluation of the use of a perspective format to promote situational awareness in users of air to air tactical displays 23 p3359 N90-28981
Counterair situation awareness display for Army aviation 23 p3359 N90-28982
Experimental tests on the minimal visual acuity required for safe air crew and air control personnel performance
23 p3360 N90-28987
Design of a monitor and simulation terminal (master) for space station telerobotics and telescience
23 p3372 N90-29051
Strategies of computer-based instructional design: A review of guidelines and empirical research
[AD-A224038] 23 p3383 N90-29112
Head-mounted spatial instruments II: Synthetic reality or impossible dream 24 p3508 N90-29828
Flight telerobotic servicer control from the Orbiter
24 p3517 N90-29882
Computing environments, interactive graphics and nonparametric methods for data analysis
[DE90-016128] 24 p3530 N90-29964
Information processing and perceptual characteristics of display design: The role of emergent features and objects
[AD-A223683] 24 p3558 N90-30133

DISPLAY SYSTEMS
U DISPLAY DEVICES

DISPOSAL
NT WASTE DISPOSAL

DISRUPTING
The internet worm
[NASA-CR-181576] 17 p2441 N90-23910

DISSECTION
Flexion, extension and lateral bending responses of the cervical spine 19 p2719 N90-25468

DISSIPATION
NT ENERGY DISSIPATION
NT OHMIC DISSIPATION
Dynamics of baroclinic wave systems
03 p0362 N90-12072
The analysis and modeling of dilatational terms in compressible turbulence
[NASA-CR-181959] 06 p0776 N90-14513
Dissipation measurement in high T(sub c) superconductors with electromagnetic probes
[DE90-002058] 06 p0854 N90-14963
Dissipation mechanism of the large-amplitude collective motion. Dynamical evolution of a collective bundle of trajectories in the TDHF phase space for a simple soluble model
[DE90-719557] 08 p1118 N90-16477
Dissipative effects in Friedmann universes
[DE89-618838] 08 p1150 N90-16663
Electrical transport dissipation effects in epitaxial Y1Ba2Cu3O(7-x) thin films
[DE90-004301] 09 p1287 N90-17461
Application of Jameson's type nonlinear artificial dissipation to the two-dimensional Navier-Stokes computation
[NAL-TR-1015T] 10 p1384 N90-18006
Asymptotic boundary conditions for dissipative waves: General theory
[NASA-TM-102497] 11 p1551 N90-18927
Heterogeneous composite and method of making
[AD-D014337] 12 p1619 N90-19306
On dissipative states in narrow current-carrying superconducting filaments
[ETN-90-95915] 12 p1721 N90-19889
Analysis of velocity and temperature fluctuations in turbulent shear flows 16 p2233 N90-22744
Evolution of atmospheric baroclinic waves
16 p2254 N90-22855
Structure of linear-quadratic control
[ETN-90-96894] 18 p2602 N90-24819
Analysis and mitigation of numerical dissipation in inviscid and viscid computation of vortex-dominated flows
[NASA-CR-186887] 20 p2862 N90-26281
On central-difference and upwind schemes
[NASA-CR-182061] 20 p2917 N90-26595
Asymptotic analysis of dissipative waves with applications to their numerical simulation
[NASA-TM-103231] 20 p2920 N90-26615
Scalar dissipation measurements in the developing region of a jet 21 p2976 N90-26909
FIRE aircraft observations of horizontal and vertical transport in marine stratocumulus
22 p3220 N90-28261
Dissipation of mechanical work and temperature rise in AS4/PEEK thermoplastic composite
[NASA-CR-186893] 23 p3302 N90-28678
Dissipative quantum maps
[DE90-627179] 23 p3402 N90-29227
Quantum chaos and dissipation: Lyapunov exponents
[DE90-627180] 23 p3403 N90-29228
Basic properties and limits of integrated arrays of dissipative circuit and logic elements
[AD-A224533] 24 p3464 N90-29567

DISSIPATORS
U DISSIPATION

DISSOCIATION
NT BIODEGRADABILITY
NT GAS DISSOCIATION
NT PHOTODISSOCIATION
Shock induced dissociation of polyethylene
[DE89-016983] 02 p0221 N90-11267
Shock dissociation of molecular fluids: A possibility of first-order phase change
[DE89-016647] 03 p0322 N90-11829
Atomic and molecular surface and volume processes in the analysis of negative hydrogen discharges
[DE89-015705] 03 p0401 N90-12294
Ion formation by electron impact
[AD-A211367] 03 p0403 N90-12305
The dissociation energy of N2
[NASA-TM-101930] 07 p0891 N90-15153
Theory of the dissociation dynamics of small molecules on metal surfaces: Finite temperature studies
[DE90-005217] 09 p1195 N90-16923
Generation of H-, H2v(double prime), and H atoms by H2+ and H3+ ions incident upon barium surfaces
[DE90-005549] 09 p1280 N90-17423
Photoinduced electron transfer processes in homogeneous and microheterogeneous solutions
[DE90-006048] 10 p1352 N90-17842
Lower limits on the absolute dissociative electron attachment cross section from O2 condensed on rare-gas films
[AD-A216727] 11 p1483 N90-18536
Absolute cross-sections for dissociative electron attachment in O2 condensed on Kr films
[AD-A216730] 11 p1570 N90-19038
Electron stimulated O(-) desorption from O2 condensed on a rare-gas film: Evidence for an indirect Bounce trajectory
[AD-A216725] 12 p1622 N90-19322
Ion and electron interactions at thermal and suprathermal energies
[AD-A216905] 12 p1622 N90-19323
The 18th Informal Conference on Photochemistry
[AD-A219779] 17 p2373 N90-23510
Informal conference on the Chemistry of Energetic Azides, Isocyanates, and Related Species
[AD-A219825] 17 p2373 N90-23514
Atomic velocity distributions out of hydrogen maser dissociators
[AD-A219500] 17 p2408 N90-23721
Rare-isotope and kinetic studies of Pt/SnO2 catalysts
18 p2558 N90-24598
Dissociation phenomena in electron-beam sustained carbon dioxide lasers 18 p2560 N90-24610
Excimer laser fragmentation studies of selected oximes: Nascent OH internal energy distributions and the search of H2CN fluorescence
[AD-A222622] 20 p2868 N90-26317
Dissociative recombination of molecular ions with electrons 20 p2946 N90-26767
The adsorption and thermal decomposition of PH3 on Si(111)-(7x7)
[AD-A222417] 21 p2978 N90-26927
Hyperthermal atomic oxygen generator
[NASA-CR-186573] 22 p3155 N90-27889

DISSOLUTION
U DISSOLVING

DISSOLVED GASES
Deformation and fracture of aluminum-lithium alloys: The effect of dissolved hydrogen 18 p2219 N90-22658

DISSOLVING
The interaction of polycrystalline copper films with dilute aqueous solutions of cupric chloride
[AD-A216465] 11 p1569 N90-19033
Calcium carbonate scale dissolution in water stabilized by carbon dioxide treatment
[AD-A218502] 16 p2214 N90-22633
Laboratory tests to determine the chemical and physical characteristics of propellant-solvent-fuel oil mixtures
[AD-A222270] 21 p2990 N90-26991

DISSYMMETRY
U ASYMMETRY

DISTANCE
NT DIFFUSION LENGTH
NT MISS DISTANCE
NT RADAR RANGE
NT RANGE AND RANGE RATE TRACKING
Jacobi functions as limit cases of q-ultraspherical polynomials
[CWI-PM-R8807] 04 p0541 N90-13139
On the Hellinger type distances for filtered experiments
[CWI-MS-R8818] 04 p0542 N90-13146
A validation of the proposed NATO standard method to determine target acquisition distances with image intensifiers
[IZF-1988-8] 04 p0554 N90-13230
Linear groups and distance-transitive graphs
[CWI-PM-R8805] 05 p0691 N90-14036
On distance-transitive graphs and involutions
[CWI-PM-R8808] 05 p0691 N90-14037
Evaluation of selection techniques for multispectral bands employed in the discrimination of carbonatic rocks
[INPE-4850-TDL/365] 11 p1522 N90-18765
An assessment of the potential of continuous-wave ranging for measuring the distance to a highly reflective, infinite sheet
[NASA-TM-101680] 14 p1969 N90-21279
Orthogonal distance regression
[PB90-151747] 15 p2160 N90-22336
Stereoscopic distance perception
16 p2267 N90-22921
Establishing a GPS-baseline between Seattle, Washington and Monterey, California
[AD-A220069] 18 p2495 N90-24262
AFE dynamic effects in inhomogeneous plasmas
18 p2643 N90-25053
Taxiway sign effectiveness under reduced visibility conditions
[DOT/FAA/CT-TN90/20] 19 p2662 N90-25150
Target acquisition probability as a function of distance, calculated with PHIND
[IZF-1989-46] 22 p3244 N90-28394

DISTANCE MEASURING EQUIPMENT
NT ALTIMETERS
NT LASER ALTIMETERS
NT LASER RANGE FINDERS
NT RADIO ALTIMETERS
NT RANGE FINDERS
Adjustable depth gage
[NASA-CASE-LEW-14880-1] 01 p0072 N90-10415
Distance measurement using laser diodes
[ETN-90-96144] 08 p1082 N90-16264

DISTANCE PERCEPTION
U SPACE PERCEPTION

DISTILLATION
On-line chemical composition analyzer development
[DE90-004079] 08 p1043 N90-16026
Design and construction of a packed column simulator operating under atmospheric and reduced pressure
[ISAL-89-60] 16 p2236 N90-22757
Method and apparatus for assessing distillate fuel stability by oxygen overpressure
[AD-D014499] 19 p2679 N90-25237

DISTILLATION EQUIPMENT
Reflux condensation in vertical tubes
[ESDU-89038] 07 p0932 N90-15397

DISTORTION
NT FLOW DISTORTION
NT SIGNAL DISTORTION
NT SURFACE DISTORTION
Microwave instability near transition energy
[DE90-000107] 03 p0338 N90-11922
A Scheiner-principle pocket optometer for self-evaluation and biofeedback accommodation training
[AD-A213171] 04 p0524 N90-13027
Workload induced spatio-temporal distortions and safety of flight
[DE89-016613] 06 p0820 N90-14771
Reduction of residual stress and distortion in HY100 and HY130 high strength steels during welding
[AD-A213532] 07 p0905 N90-15231
SBS (Stimulated Brillouin Scattering) pulse distortion in multimode optical fibers: Preliminary results
[DE90-003023] 07 p0992 N90-15731
An illustrated guide of optical characteristics of aircraft transparencies
[AD-A214565] 09 p1167 N90-16752
Speckle imaging through the atmosphere
[AD-A214652] 09 p1281 N90-17428

Engine inlet distortion in a 9.2 percent scale vectored thrust STOVL model in ground effect
[NASA-TM-102358] 10 p1307 N90-17561
Element-specific modal formulations for large-displacement multibody dynamics
14 p1934 N90-21069
Wave receptance analysis of vibrating beams and stiffened plates 14 p1993 N90-21419
The extension of rapid distortion theory to stratified shear flows 14 p2005 N90-21491
Free-field propagation of high intensity noise
[NASA-CR-186577] 14 p2024 N90-21604
High intensity laser beam interactions with single droplets 15 p2083 N90-21924
Distortions in memory for visual displays
16 p2268 N90-22929
The effects of viewpoint on the virtual space of pictures 16 p2269 N90-22932
Hybrid diffractive-refractive telescope
[AD-A219241] 16 p2318 N90-23216
Nonlinear interactions in mixing layers and compressible heated round jets
[NASA-CR-186303] 17 p2400 N90-23674
Remote sensing of Earth terrain
[NASA-CR-186888] 20 p2880 N90-26382
Microwave background distortions from domain walls
[NASA-CR-187272] 24 p3462 N90-29556
Characteristic microwave background distortions from collapsing domain wall bubbles
[NASA-CR-187270] 24 p3462 N90-29557

DISTRIBUTED AMPLIFIERS

High efficiency octave bandwidth millimeter wave power amplifier
[AD-A218245] 14 p1969 N90-21280
Field emitter array integrated distributed amplifiers
[AD-D014493] 22 p3166 N90-27958

DISTRIBUTED FEEDBACK LASERS

Noise behavior of semiconductor lasers by optic feedback
[ETN-90-95728] 12 p1668 N90-19583

DISTRIBUTED PARAMETER SYSTEMS

On modelling nonlinear damping in distributed parameter systems 01 p0022 N90-10109
Active vibration mitigation of distributed parameter, smart-type structures using Pseudo-Feedback Optimal Control (PFOC) 01 p0024 N90-10121
Transaction throughput in distributed systems: A modeling study using dynamic queueing networks
[MEMO-INF-89-25] 02 p0261 N90-11479
Estimation on nonlinear damping in second order distributed parameter systems
[NASA-CR-181890] 02 p0263 N90-11494
Parameter estimation in functional and partial differential equations
[AD-A211040] 02 p0265 N90-11511
Software development for avionics SSME control and diagnostics
[NASA-CR-184894] 05 p0681 N90-13964
Energy decay and boundary control for distributed parameter systems with viscoelastic damping
[AD-A216468] 11 p1519 N90-18748
Log-based recovery in asynchronous distributed systems
[NASA-CR-186190] 11 p1550 N90-18924
A distributed finite-element modeling and control approach for large flexible structures
14 p1934 N90-21071
On the continuous dependence with respect to sampling of the linear quadratic regulator problem for distributed parameter systems
[NASA-CR-182012] 14 p2018 N90-21568
Proceedings of the 3rd Annual Conference on Aerospace Computational Control, volume 2
[NASA-CR-186447] 16 p2289 N90-23040
Distributed neural control of a hexapod walking vehicle 16 p2293 N90-23061
Experiences with the Amoeba distributed operating system
[CWI-CS-R8929] 18 p2596 N90-24770
Amoeba: High performance distributed computing
[CWI-CS-R8937] 18 p2596 N90-24771
Autonomous power expert system
[NASA-CR-185263] 19 p2670 N90-25187
ISIS and META projects
[NASA-CR-186645] 20 p2905 N90-26524
Autoplan: A self-processing network model for an extended blocks world planning environment
[NASA-CR-186733] 20 p2905 N90-26526
Space Station Freedom ECLSS: A step toward autonomous regenerative life support systems
21 p3043 N90-27297
Nonlinear dynamics and control of SDI structural components
[AD-A222472] 21 p3071 N90-27458
Dynamic load-sharing using predicted process resource requirements
[NASA-CR-186891] 22 p3255 N90-28433
Active control of flexible structures
23 p3282 N90-28575
Distributed control architecture for CNI preprocessors
24 p3426 N90-29356
A distributed control and monitor system used in laser fusion research
[DE90-011483] 24 p3549 N90-30078

DISTRIBUTED PROCESSING

A decision support approach to the file allocation problem in a distributed computing system
01 p0107 N90-10609
The aerospace energy systems laboratory: Hardware and software implementation
[NASA-TM-101706] 01 p0107 N90-10610
Parallel processing and learning in simple systems
[AD-A210225] 01 p0108 N90-10612
Tools for application development in heterogeneous distributed environments
[AD-A210238] 01 p0108 N90-10613
Northeast Artificial Intelligence Consortium annual report for 1987. Volume 5: Building an intelligent assistant: The acquisition, integration and maintenance of complex distributed tasks
[AD-A210330] 01 p0109 N90-10621
Northeast Artificial Intelligence Consortium annual report for 1987. Volume 7, part A: Time oriented problem solving
[AD-A210331] 01 p0110 N90-10622
Advanced manned space flight simulation and training: An investigation of simulation host computer system concepts
[NASA-CR-185998] 02 p0160 N90-10911
A distributed debugger for Amoeba
[CWI-CS-R8828] 02 p0257 N90-11453
A verification exercise relating to specification styles in LOTOS
[MEMO-INF-89-18] 02 p0259 N90-11471
An integrated distributed processing interface for supercomputers and workstations
[DE89-016769] 02 p0260 N90-11478
On the Amoeba protocol
[CWI-CS-R8827] 02 p0261 N90-11480
Fixed point iteration on point-symmetric interference graphs
[MEMO-INF-89-23] 02 p0269 N90-11535
Spacelab system analysis Marshall Avionics System Testbed (MAST)
[NASA-CR-183804] 03 p0317 N90-11802
Parallel implementation and evaluation of motion estimation system algorithms on a distributed memory multiprocessor using knowledge based mappings
[NASA-CR-185984] 03 p0389 N90-12213
Distributed VLSI architecture for fast Jacobian and inverse Jacobian formulations
[RR-346] 03 p0390 N90-12218
Fast forward dynamics algorithm for robot arms using multiprocessing
[RR-367] 03 p0391 N90-12225
A fan-in algorithm for distributed sparse numerical factorization
[AD-A211569] 04 p0529 N90-13054
Waiting times in polling systems with Markovian server routing
[CWI-BS-R8905] 05 p0685 N90-13989
Monotonicity of performance measures in a processor sharing queue
[CWI-BS-R8902] 05 p0689 N90-14019
Workloads and waiting times in single-server systems with multiple customer classes
[CWI-BS-R8906] 05 p0689 N90-14020
Simple appoximations for second moment characteristics of the sojurn time in the M/G/1 processor sharing queue
[CWI-BS-R8907] 05 p0694 N90-14055
Database interfaces on NASA's heterogeneous distributed database system
[NASA-CR-185420] 05 p0706 N90-14133
Retrieving and integrating IC fabrication data from dissimilar databases
[AD-A211890] 05 p0707 N90-14140
The role of order in distributed programs
[NASA-CR-186252] 06 p0830 N90-14826
The Aerospace Energy Systems Laboratory: A BITBUS networking application
[NASA-TM-4149] 06 p0831 N90-14829
How robust are distributed systems
[NASA-CR-186242] 06 p0832 N90-14837
Implementing fault-tolerant sensors
[NASA-CR-186251] 07 p0933 N90-15400
Optimizing and evaluating algorithms for replicated data concurrency control
[DE90-003080] 07 p0973 N90-15619
Scry: A distributed image handling system, version 1.1
[DE90-003105] 07 p0973 N90-15621
An overview of lynx
[AD-A213714] 07 p0975 N90-15631
On the correctness of orphan management algorithms
[AD-A213777] 07 p0975 N90-15632
Optimistic concurrency control for nested distributed transactions
[AD-A213828] 07 p0976 N90-15634
Hierarchical process composition: Dynamic maintenance of structure in a distributed environment
[AD-A214325] 07 p0978 N90-15648
Periodic phase adjustment distributed clock synchronization in the hard realtime environment
[AD-A213842] 07 p0988 N90-15708
Young Investigator's Award and distributed self-adaptive databases
[AD-A214194] 07 p1010 N90-15854
PVM (Parallel Virtual Machine): A framework for parallel distributed computing
[DE90-004390] 08 p1106 N90-16403
Algorithms for fault tolerant distributed systems
[AD-A214447] 08 p1109 N90-16416
A distributed kernel for simulation of the VHSIC hardware description language
[AD-A215419] 09 p1213 N90-17032
Supporting shared data structures on distributed memory architectures
[NASA-CR-181981] 09 p1262 N90-17318
Communication-efficient arbitration models for low-resolution data flow computing
[AD-A214768] 09 p1262 N90-17319
The moving platform simulator 2: A networked real-time visual simulator with distributed processing and line-of-sight displays
[AD-A214936] 09 p1266 N90-17343
The use of efficient broadcast protocols in asynchronous distributed systems
[NASA-CR-186272] 09 p1269 N90-17358
Large-scale optimization via distributed systems
[AD-A215136] 09 p1270 N90-17364
The Cronus distributed DBMS (Database Management System) project
[AD-A214478] 09 p1295 N90-17508
Methodology for developing realtime distributed systems
[AD-A214570] 09 p1296 N90-17509
The Saguaro distributed operating system
[AD-A215083] 10 p1374 N90-17966
An Autonomous Platform Simulator (APS)
[AD-A215768] 10 p1392 N90-18048
Development of an integrated mobile robot system at Carnegie Mellon University: June 1988
[AD-A215955] 10 p1392 N90-18049
A scheme for supporting distributed data structures on multicomputers
[NASA-CR-181987] 10 p1415 N90-18152
A hundred impossibility proofs for distributed computing
[AD-A216391] 10 p1419 N90-18180
The design and analysis of new techniques for transaction management in database systems
10 p1441 N90-18314
Deceit: A flexible distributed file system
[NASA-CR-186402] 11 p1544 N90-18991
High-level connectionist models
[AD-A216581] 12 p1698 N90-19751
Generic distributed systems model
[AD-A217078] 12 p1702 N90-19773
Deceit: A flexible distributed file system
[NASA-CR-186412] 12 p1726 N90-19923
RIPE: An object-oriented Robot Independent Programming Environment
[DE90-008501] 13 p1866 N90-20707
Performance of concurrency control algorithms in distributed systems
[AD-A218280] 13 p1870 N90-20727
The Livermore distributed storage system: Implementation and experiences
[DE90-007257] 13 p1872 N90-20735
Cooperating intelligent systems
[NASA-CR-184982] 14 p2012 N90-21529
Fast causal multicast
[NASA-CR-186495] 14 p2013 N90-21533
Parallel tridiagonalization of a general matrix using distributed-memory multiprocessors
[DE90-008902] 14 p2015 N90-21551
Exploiting virtual synchrony in distributed systems
[NASA-CR-182855] 14 p2016 N90-21555
Two-dimensional shape recognition using sparse distributed memory 15 p2140 N90-22227
A CSP model for distributed control software design
[OUEL-1789/89] 15 p2148 N90-22273
Distributed simulation, no special tools required
15 p2150 N90-22281

A scheme for supporting automatic data migration on multicomputers
[NASA-CR-182038] 16 p2276 N90-22973
Methodology for analysis and simulation of large multidisciplinary problems 16 p2290 N90-23046
Sentence comprehension: A parallel distributed processing approach
[AD-A218886] 16 p2300 N90-23104
DARK (Distributed Ada Real-Time Kernel) porting and extension guide Kernel version 3.0
[AD-A219291] 16 p2301 N90-23112
Locality in parallel computation
[AD-A218733] 16 p2302 N90-23120
Real-time simulation clock
[NASA-CASE-LAR-14056-1] 17 p2407 N90-23713
A distributed program composition system
[NASA-CR-181568] 17 p2441 N90-23911
Distributed object oriented programming
[AD-A219689] 17 p2442 N90-23918
Advanced development environments, continuation
[AD-A220510] 17 p2443 N90-23923
Designing distributed algorithms by means of formal sequentially phased reasoning
[TR-89-8] 17 p2449 N90-23969
Distributed user services for supercomputers
[NASA-CR-180370] 17 p2450 N90-23976
The wakeup problem
[AD-A220534] 17 p2451 N90-23981
Distributed hierarchical routing
[RUU-CS-89-5] 17 p2452 N90-23986
Fast casual multicast
[NASA-CR-186643] 17 p2462 N90-24059
Priority inversion and its prevention
[AD-A218613] 17 p2467 N90-24101
ISIS and META projects
[NASA-CR-186624] 18 p2590 N90-24733
Visual animation of parallel algorithms for matrix computations
[DE90-011076] 18 p2594 N90-24763
Determination of algorithm parallelism in NP complete problems for distributed architectures
[AD-A220192] 18 p2598 N90-24786
Execution time supports for adaptive scientific algorithms on distributed memory machines
[NASA-CR-182052] 19 p2741 N90-25578
Tools for distributed application management
[NASA-CR-186711] 19 p2742 N90-25586
Exploiting replication in distributed systems
[NASA-CR-186410] 19 p2746 N90-25603
Applying formal models and proofs to the verification of distributed systems
[IAR-89-7] 19 p2750 N90-25625
Tools for distributed application management
[NASA-CR-186646] 19 p2762 N90-25692
Reliable broadcast protocols
[NASA-CR-186411] 19 p2762 N90-25696
ISIS and META projects
[NASA-CR-186645] 20 p2905 N90-26524
Autoplan: A self-processing network model for an extended blocks world planning environment
[NASA-CR-186733] 20 p2905 N90-26526
Formal verification of distributed computing systems: Logic characterization of behaviour equivalence
[LAAS-89386] 20 p2910 N90-26555
An automated calibration laboratory for flight research instrumentation: Requirements and a proposed design approach
[NASA-TM-101719] 20 p2912 N90-26564
Pacific missile test center information resources management organization (code 0300): The ORACLE client-server and distributed processing architecture
[DE90-013271] 20 p2912 N90-26565
Parallel algorithm for distributed memory computers (applications to matricial algorithms)
[ETN-90-97252] 20 p2913 N90-26573
Superconcurrent processing: A dynamic approach to heterogeneous parallelism
[AD-A222798] 20 p2914 N90-26576
Parallel/distributed direct method for solving linear systems
[NASA-TM-103229] 20 p2919 N90-26614
Causal distributed breakpoints
[AD-A222613] 20 p2921 N90-26622
A methodology for benchmarking distributed database management systems
[DE90-007801] 20 p2935 N90-26702
Knowledge and inhibition in asynchronous distributed systems
[TR-90-1139] 20 p2935 N90-26703
Knowledge and distributed computation
[AD-A223100] 21 p3039 N90-27270
A development framework for artificial intelligence based distributed operations support systems 21 p3044 N90-27301
A knowledge base architecture for distributed knowledge agents 21 p3044 N90-27302
An engineering approach to automatic programming 21 p3046 N90-27317
Sisal on a message passing architecture
[DE90-008786] 21 p3051 N90-27342
A theoretical model of optimistic recovery in distributed systems
[AD-A222055] 21 p3054 N90-27359
Recovery in distributed systems using optimistic message logging and checkpointing
[AD-A222104] 21 p3054 N90-27361
Architectures for optical computing
[AD-A221435] 21 p3054 N90-27364
Neural networks
[AD-A222110] 21 p3060 N90-27398
Finding the maximum recoverable system state in optimistic rollback recovery methods
[AD-A222338] 21 p3064 N90-27419
Causal distributed breakpoints
[AD-A222103] 21 p3066 N90-27431
Transparent optimistic rollback recovery
[AD-A222102] 21 p3070 N90-27455
Performance assessment of MIL-STD-1553B on the avionic systems demonstrator rig of British Aerospace 22 p3104 N90-27624
Tolerating failures of continuous-valued sensors
[NASA-CR-187028] 22 p3178 N90-28035
Efficient algorithms for a class of partitioning problems
[NASA-CR-182073] 22 p3237 N90-28357
Distributed transitive closure computations: The disconnection set approach
[REPT-90-014] 22 p3259 N90-28459
Evaluating recursive queries in distributed databases
[REPT-90-015] 22 p3260 N90-28460
Distributed database concepts for command and control information systems
[FFI-90/7005] 22 p3260 N90-28462
Educational and research activities of the Dig ital Systems Laboratory at Helsinki University of Technology
[PB90-190893] 22 p3265 N90-28486
Three-dimensional motor schema based navigation 23 p3367 N90-29026
Parallelization of a software relating to aerodynamics on MIMD type computers
[ONERA-RT-31/3479-CY] 23 p3384 N90-29114
Piecewise linear models of processor utilization
[DE90-014774] 23 p3384 N90-29115
Information management directions: The integration challenge
[PB90-219866] 23 p3405 N90-29245
JTIDS relative navigation: Principles, architecture, and inertial mixing 24 p3426 N90-29357
RCTS: A flexible environment for sensor integration and control of robot systems; the distributed processing approach 24 p3512 N90-29852
Programming your way out of the past: ISIS and the META Project
[NASA-CR-186275] 24 p3524 N90-29922
AHTO project: Software technology for open distributed processing
[PB90-190943] 24 p3524 N90-29923
Turbo pascal implementation of a distributed processing network of MS-DOS microcomputers connected in a master-slave configuration
[AD-A223925] 24 p3525 N90-29928
Supporting large scale applications on networks of workstations
[NASA-CR-186346] 24 p3532 N90-29975
Low cost management of replicated data in fault-tolerant distributed systems
[NASA-CR-186370] 24 p3532 N90-29976
Reliable communication in the presence of failures
[NASA-CR-183046] 24 p3533 N90-29977
Knowledge-based expert system configurator
[DE90-011711] 24 p3558 N90-30135

DISTRIBUTION
Tail triviality for sums of stationary random variables
[CWI-MS-R8810] 04 p0542 N90-13143

DISTRIBUTION (PROPERTY)
NT ANGULAR DISTRIBUTION
NT ANTENNA RADIATION PATTERNS
NT BOLTZMANN DISTRIBUTION
NT BRIGHTNESS DISTRIBUTION
NT CHARGE DISTRIBUTION
NT CURRENT DISTRIBUTION
NT DIFFRACTION PATTERNS
NT ELECTRON DENSITY PROFILES
NT ELECTRON DISTRIBUTION
NT ENERGY DISTRIBUTION
NT FLOW DISTRIBUTION
NT FORCE DISTRIBUTION
NT FREQUENCY DISTRIBUTION
NT ION DISTRIBUTION
NT LOAD DISTRIBUTION (FORCES)
NT MASS DISTRIBUTION
NT MOMENT DISTRIBUTION
NT PRESSURE DISTRIBUTION
NT RADIATION DISTRIBUTION
NT SIDELOBES
NT SPATIAL DISTRIBUTION
NT SPECTRAL ENERGY DISTRIBUTION
NT STAR DISTRIBUTION
NT STRAIN DISTRIBUTION
NT STRESS CONCENTRATION
NT STRESS DISTRIBUTION
NT TEMPERATURE DISTRIBUTION
NT VELOCITY DISTRIBUTION
NT VERTICAL DISTRIBUTION
Distribution of auroral precipitation at midnight during a magnetic storm
[PB89-213136] 03 p0370 N90-12118
Electron-positron momentum distribution measurements of high-T(sub c) superconductors and related systems
[DE89-017538] 03 p0411 N90-12358
Associated distributions in the analysis of two-dimensional random walks
[CWI-BS-R8917] 17 p2466 N90-24095
Hitting lines with two-dimensional Brownian motion
[AD-A223595] 24 p3541 N90-30027

DISTRIBUTION FUNCTIONS
Multi-sample functional statistical data analysis
[AD-A210992] 01 p0117 N90-10673
Balance equations for ionospheric plasmas with different partial temperatures 02 p0240 N90-11364
Boundary kernel estimation of the two sample comparison density function
[AD-A210757] 02 p0268 N90-11532
Resonance effect on the oscillator distribution function
[DE89-630105] 02 p0271 N90-11548
Molecular dynamics study of the primitive model of 1-3 electrolyte studies
[AD-A211653] 03 p0325 N90-11846
Some 1(sub p) invariant probability measures
[REPT-88-91] 03 p0397 N90-12273
A simple model for DSS-14 outage times 04 p0488 N90-12802
Removing stripes in GOES (Geostationary Operational Environmental Satellites) images by matching empirical distribution functions
[PB89-213359] 04 p0514 N90-12968
Domain of attraction of an operator between supremum and sum
[REPT-89-05] 04 p0539 N90-13119
Estimation of convolution tail behavior
[MEMO-COSOR-89-04] 05 p0693 N90-14051
Self-decomposable distributions and branching processes
[MEMO-COSOR-89-06] 05 p0693 N90-14052
Note on Urbanik's class L(sub n) --- self-decomposability of functions
[MEMO-COSOR-89-07] 05 p0694 N90-14053
Reverse self-decomposability --- for characteristic functions
[MEMO-COSOR-89-08] 05 p0694 N90-14054
Is the number of photons conserved in an expanding universe
[DE89-618836] 06 p0864 N90-15018
An iterative Bayes procedure for reliability assessment
[DE90-002106] 07 p0944 N90-15466
Dissipation mechanism of the large-amplitude collective motion. Dynamical evolution of a collective bundle of trajectories in the TDHF phase space for a simple soluble model
[DE90-719557] 08 p1118 N90-16477
Nonparametric estimation of reliability and related functions
[AD-A215138] 09 p1234 N90-17160
A further note on generalized hyperexponential distributions
[AD-A214881] 09 p1275 N90-17394
Multi-dimensional discrete ordinates solutions to combined mode radiation heat transfer problems and their application to a free-falling particle, direct absorption solar receiver
[DE90-004987] 09 p1300 N90-17531
Use of Coxian-type distributions in a general model of the maximum of bivariate random variables
[PB90-121229] 12 p1704 N90-19780
Bose condensate in superfluid (sup 4)He and momentum distributions by deep inelastic scattering
[DE90-007541] 12 p1712 N90-19832
Analysis of distributions of Visual Meteorological Conditions (VMC) heliport data
[DOT/FAA/CT-TN89/67] 14 p2008 N90-21508
Molecular theory of fluid phase equilibria
[PB90-131277] 15 p2066 N90-21832
A stress-strength interference approach to fast and delayed fracture reliability analysis for ceramic components 15 p2070 N90-21859
Second order asymptotics in level crossing problems for differences of renewal processes
[MEMO-824] 18 p2600 N90-24798

Neuromorphic learning of continuous-valued mappings from noise-corrupted data. Application to real-time adaptive control
[NASA-TM-4176] 19 p2747 N90-25607
Some observations for the pigeon hole principle
[RUU-CS-88-39] 19 p2750 N90-25624
Nonparametric selection, ranking and testing
[AD-A219254] 19 p2752 N90-25636
A linear-eddy model of turbulent shear layer mixing
21 p2974 N90-26904
Reduced distribution functions and nonequilibrium thermodynamics of single component fluids
[PB90-189119] 22 p3254 N90-28428
Saddlepoint approximations in conditional inference
[AD-A223280] 24 p3537 N90-30000

DISTRIBUTION MOMENTS
NT MEAN
NT ORTHOGONALITY
NT STANDARD DEVIATION
Simple appoximations for second moment characteristics of the sojurn time in the M/G/1 processor sharing queue
[CWI-BS-R8907] 05 p0694 N90-14055
Statistical methodologies for non-Gaussian noisy environments
[AD-A222137] 21 p3066 N90-27433

DISTRIBUTORS
An experimental and analytical examination of stratified thermal storage 09 p1215 N90-17046

DISTURBANCE THEORY
U PERTURBATION THEORY

DISTURBANCES
Disturbance torque rejection properties of the NASA/JPL 70-meter antenna axis servos
12 p1644 N90-19450
Effective techniques for the identification and accommodation of disturbances
14 p1934 N90-21072

DISTURBING FUNCTIONS
An algorithm for the systematic disturbance of optimal rotational solutions
[NASA-TM-101089] 01 p0102 N90-10575
Improved estimation of the disturbance variance in a linear regression model
[AD-A210272] 01 p0112 N90-10641
Another approach to the local disturbance decoupling problem with stability for nonlinear systems
[MEMO-799] 05 p0691 N90-14033
Almost disturbance decoupling by measurement feedback: A frequency domain analysis
[CWI-BS-R8910] 17 p2455 N90-24005

DISULFIDES
NT CARBON DISULFIDE
Advanced high-temperature batteries
13 p1825 N90-20480

DITCHING (LANDING)
The human factors relating to escape and survival from helicopters ditching in water
[AGARD-AG-305(E)] 05 p0576 N90-13358

DITHERS
Ring laser gyro principles and techniques
24 p3426 N90-29352

DITHIOLS
U THIOLS

DIURESIS
A comparison of the mechanisms of cold- and microgravity-induced fluid loss
[AD-A218098] 13 p1852 N90-20631

DIURNAL RHYTHMS
U CIRCADIAN RHYTHMS

DIURNAL VARIATIONS
Average diurnal and seasonal profiles of ionospheric storms 02 p0241 N90-11371
Diurnal variation of the sodium layer at polar latitudes in summer 05 p0662 N90-13869
The retrieval of the concentrations of nitric oxide and nitrogen dioxide from satellite solar occultation measurements at sunset and sunrise
06 p0814 N90-14733
New approach to omega PPCs (Propagation Corrections)
[AD-A215610] 09 p1207 N90-17000
An analysis of diurnal wind variability in the Santa Barbara Channel from SODAR measurements
[AD-A215769] 10 p1408 N90-18121
Niacin ingested at night causes severe hypotension
[AD-A217896] 13 p1851 N90-20624
Comparison of quiet time geomagnetic daily variation (Sq) in H component at Eusebio and Cachoeira Paulista
[INPE-4985-PRE/1547] 14 p2043 N90-21714
The diurnal ozone cycle in a coniferous forest: The importance of meteorology and chemistry
[CM-75] 17 p2421 N90-23795
Earth radiation budget measurements from space
19 p2707 N90-25404
New observations of stratospheric N2O5
[NASA-TM-103478] 20 p2883 N90-26402
The collection and analysis of atmospheric peroxides
20 p2887 N90-26428
Measurement of diurnal variation in the Earth radiation budget
[MITT-59] 21 p3027 N90-27212
Reproduction of GMS IR calibration table
21 p3028 N90-27215
Gases of the middle atmosphere and short-term solar radiation variations 22 p3204 N90-28177
Diurnal and temporal variation of UV-flux and its dependence on stratospheric ozone
22 p3205 N90-28184
Diurnal variation in the turbulent structure of the cloudy marine boundary layer during FIRE 1987
22 p3217 N90-28248
Pharmacological resetting of the circadian sleep-wake cycle effects of triazolam on reentrainment of circadian rhythms in a diurnal primate
[AD-A224227] 24 p3497 N90-29764

DIVERGENCE
NT MAGNETIC CHARGE DENSITY
A multidomain spectral collocation method for the Stokes problem
[NASA-CR-181876] 03 p0396 N90-12266
Ion divergence and the stability of magnetically insulated diodes
[DE90-014565] 23 p3321 N90-28777
On the infrared behaviour of some non-Minkowskian quantum fields 23 p3410 N90-29273

DIVERGENT NOZZLES
Exhaust environment measurements of a turbofan engine equipped with an afterburner and 2D nozzle
[NASA-CR-4289] 15 p2052 N90-21760

DIVERTERS
Analysis of results from wind tunnel tests of inlets for an advanced turboprop nacelle installation
[NASA-CR-174937] 01 p0003 N90-10011
Results of the H-mode experiments with JT-60 outer and lower divertors
[DE90-733146] 10 p1432 N90-18265

DIVIDING (MATHEMATICS)
Multivariable divided difference and B-aplines
[MEMO-772] 04 p0544 N90-13160
Counterexamples to Robertson's conjecture
[MEMO-COSOR-88-32] 05 p0693 N90-14048
Supercongruences
[CWI-AM-R8918] 18 p2599 N90-24791

DIVING (UNDERWATER)
Effects of serial wet-dry-wet cold exposure: Thermal balance, physical activity, and cognitive performance
[AD-A212704] 04 p0524 N90-13025
High-frequency ventilation in dogs with three gases of different densities
[AD-A212862] 06 p0819 N90-14762
Statistically based decompression tables 5: Haldane-Vann models for air diving
[AD-A214934] 09 p1251 N90-17261
Methodology used for gas analysis and control of trace chemical contaminants at a hyperbaric facility. 1: Gas sampling
[AD-A216155] 10 p1325 N90-17659
Use of self-induced hypnosis to modify thermal balance during cold water immersion
[AD-A216156] 10 p1412 N90-18140
Insulation, compressibility and absorbency of dry suit undergarments
[AD-A215944] 10 p1414 N90-18149
Field management of accidental hypothermia during diving
[AD-A219560] 17 p2434 N90-23866
Real time adaptive control of an Autonomous Underwater Vehicle (AUV)
[AD-A219544] 17 p2454 N90-23996
Design and investigation of a dive plane sliding mode compensator for an autonomous underwater vehicle
[AD-A219552] 17 p2454 N90-23997
Arctic cold weather medicine and accidental hypothermia
[AD-A223090] 20 p2899 N90-26487
Development of membrane process for carbon dioxide separation from diving atmosphere
[AD-A222606] 20 p2901 N90-26504
Underwater connect and disconnect plug and receptacle
[AD-D014175] 21 p2998 N90-27039

DME-A SATELLITE
U EXPLORER 31 SATELLITE

DMSP SATELLITES
Processing of DMSP magnetic data: Handbook of programs, tapes, and datasets
[NASA-TM-100757] 10 p1407 N90-18114
Impact of a unified DMSP meteorological sensor retrieval methodology on global numerical weather prediction
[AD-A220306] 18 p2581 N90-24703
Tactical applications of Defense Meteorological Satellite Program (DMSP) environmental data
21 p3067 N90-27439
DMSP's interactive tactical terminal
21 p3068 N90-27441
Block 6: The future DMSP space systems
21 p3068 N90-27443
An assessment of the application of in situ ion-density data from DMSP to modeling of transionospheric scintillation
[AD-A222695] 24 p3491 N90-29730
Studies of ionospheric dynamics utilizing data from DMSP
[AD-A223370] 24 p3492 N90-29733

DNA
U DEOXYRIBONUCLEIC ACID

DOCKING
U SPACECRAFT DOCKING

DOCUMENT STORAGE
Computer availability impact on the archiving of scientific and technical reports
[AD-A210283] 01 p0136 N90-10787
The new space and Earth science information systems at NASA's archive 22 p3257 N90-28443

DOCUMENTATION
Documentation of the current fault detection, isolation and reconfiguration software of the AIPS fault-tolerant processor
[NASA-TM-89154] 01 p0106 N90-10602
Laser Raman spectroscopy: A literature review
[FOA-C-20753-2.3] 02 p0196 N90-11121
Electronic publishing: Guide to selection
[PB89-214753] 02 p0256 N90-11448
Criss-cross directory of NASA N numbers and DOD AD numbers. Volume 2, part 1: AD to N, 1979-1986. N to AD, 1962-1986
[NASA-TM-101814] 03 p0416 N90-12388
Criss-cross directory of NASA N numbers and DOD AD numbers. Volume 2, part 2: AD to N, 1979-1986. N to AD, 1962-1986
[NASA-TM-101815] 03 p0416 N90-12389
A semiparametric model for citation counts
[CWI-MS-R8814] 04 p0542 N90-13145
Executive overview and introduction to the SMAP information system life-cycle and documentation standards
[NASA-TM-101765] 05 p0706 N90-14134
Information system life-cycle and documentation standards, volume 1
[NASA-TM-101856] 05 p0706 N90-14135
Management plan documentation standard and Data Item Descriptions (DID). Volume of the information system life-cycle and documentation standards, volume 2
[NASA-TM-101857] 05 p0706 N90-14136
Product specification documentation standard and Data Item Descriptions (DID). Volume of the information system life-cycle and documentation standards, volume 3
[NASA-TM-101858] 05 p0706 N90-14137
Assurance specification documentation standard and Data Item Descriptions (DID). Volume of the information system life-cycle and documentation standards, volume 4
[NASA-TM-101859] 05 p0706 N90-14138
Management control and status reports documentation standard and Data Item Descriptions (DID). Volume of the information system life-cycle and documentation standards, volume 5
[NASA-TM-101860] 05 p0706 N90-14139
Technical guide on documentation requirements for open market contract acquisitions of information resources
[NASA-TM-102650] 19 p2762 N90-25695
Documentation of program Tankplot
[FFI-89/7019] 20 p2908 N90-26541

DOCUMENTS
NT ABSTRACTS
NT ASTRONOMICAL CATALOGS
NT BIBLIOGRAPHIES
NT CATALOGS (PUBLICATIONS)
NT ENGINEERING DRAWINGS
NT HANDBOOKS
NT MANUALS
NT PERIODICALS
NT POSTLAUNCH REPORTS
NT PRESIDENTIAL REPORTS
NT TEXTBOOKS
NT TEXTS
NT USER MANUALS (COMPUTER PROGRAMS)
NT VIDEO DISKS
Publications of the National Institute of Standards and Technology, 1988 catalog
[PB89-218382] 04 p0563 N90-13279
AFOSR technical report summaries
[AD-A213148] 05 p0707 N90-14142
Publications of the Jet Propulsion Laboratory, 1988
[NASA-CR-185958] 06 p0859 N90-14995

Photochromic papers or films for noncopyable documents
[DE90-004006] 10 p1441 N90-18316
Augmenting and updating NASA spacelink electronic information system 12 p1634 N90-19392
Topics in HPM (High-Power Microwave) generation, coupling, and interaction
[AD-A216882] 12 p1682 N90-19658
Document delivery via ISDN or satellite networks 15 p2178 N90-22446
The automation plan of the General Directorate 1 (search) of the European Patent Office 15 p2178 N90-22448
Desk top publishing: What you need to know 15 p2178 N90-22449
Atlas/data abstract for the United States and selected areas, fiscal year 1989
[AD-A219289] 16 p2327 N90-23270
The application of SAW devices in expanded frequency spectrum communications
[AD-A222958] 21 p2994 N90-27021
Authors guide to the publishing procedures at Defence Research Establishment Suffield
[AD-A223101] 21 p3087 N90-27554
National Archives preservation research priorities: Past and present
[PB90-206210] 23 p3405 N90-29242

DOLOMITE (MINERAL)
Geochemistry and origin of regional dolomites
[DE90-012589] 21 p3024 N90-27196

DOMAIN WALL
Evolution of domain walls in the early universe
[NASA-CR-186076] 04 p0565 N90-13297
On thick domain walls in general relativity
[NASA-CR-185926] 05 p0704 N90-14124
An exact solution for a thick domain wall in general relativity
[NASA-CR-185013] 07 p1006 N90-15826
The dynamics of domain walls and strings
[NASA-CR-186255] 07 p1007 N90-15832
Nonlinear dynamics of domain walls and vortices in two-dimensional systems
[DE90-004840] 10 p1425 N90-18221
Chiral interface at the finite temperature transition point of QCD
[NASA-CR-186605] 17 p2470 N90-24121
Evolution of light domain walls interacting with dark matter, part 1
[NASA-CR-181123] 17 p2485 N90-24211
Microwave background distortions from domain walls
[NASA-CR-187272] 24 p3462 N90-29556
Characteristic microwave background distortions from collapsing domain wall bubbles
[NASA-CR-187270] 24 p3462 N90-29557

DOMAINS
A multidomain spectral collocation method for the Stokes problem
[NASA-CR-181876] 03 p0396 N90-12266
Time-domain Green function corresponding to a time-harmonic point source in complex space
[PB89-218846] 04 p0539 N90-13117
Corrections to the thin wall approximation in general relativity
[NASA-CR-186078] 04 p0562 N90-13274
Structural zooming research and development of an interactive computer graphical interface for stress analysis of cracks 18 p2641 N90-25042
Cartesian closed categories of domains
[ETN-90-97284] 20 p2919 N90-26613

DOMES (GEOLOGY)
Characteristics, distribution and geologic/terrain associations of small dome-like hills on Venus 03 p0422 N90-12425
Volcanism on Venus: Large shields and major accumulations of small domes 03 p0426 N90-12445

DOMES (STRUCTURAL FORMS)
NT RADOMES

DOMINANCE
A general approach to dominance in the plane
[RUU-CS-88-35] 17 p2463 N90-24072
The f2 dominance of the energy-momentum tensor
[DE90-508027] 24 p3460 N90-29544

DONNELL EQUATIONS
ANILISA: Computational module for Koiter's imperfection sensitivity theory
[LR-582] 15 p2119 N90-22119

DONOR MATERIALS
Hydrogen-assisted thermal donor formation in silicon
[DE89-016809] 02 p0279 N90-11594

DOORS
Independent Orbiter Assessment (IOA): Analysis of the mechanical actuation subsystem
[NASA-CR-185525] 02 p0168 N90-10944
Independent Orbiter Assessment (IOA): Assessment of the mechanical actuation subsystem, volume 1
[NASA-CR-185527-VOL-1] 02 p0169 N90-10952
Independent Orbiter Assessment (IOA): Assessment of the mechanical actuation subsystem, volume 2
[NASA-CR-185527-VOL-2] 02 p0169 N90-10953
Aircraft accident report, United Airlines Flight 811, Boeing 747-122, N4713U, Honolulu, Hawaii, February 24, 1989
[PB90-910401] 15 p2050 N90-21748
Development of the CLAES instrument aperture door system 15 p2112 N90-22083
Driving and latching of the Starlab pointing mirror doors 15 p2114 N90-22093
Columbus scientific airlock 18 p2541 N90-24503
Aircraft evacuations: The effect of passenger motivation and cabin configuration adjacent to the exit
[CAA-PAPER-89019] 24 p3423 N90-29336

DOPED CRYSTALS
Effects of coherent scattering on infrared absorption in doped semiconductors
[AD-A210224] 01 p0131 N90-10756
Strong-inversion model of threshold voltage in modulation doped field effect transistors: The role of unintentional acceptors
[AD-A212750] 04 p0498 N90-12870
Electron scattering by native defects in uniformly and modulation doped semiconductor structures
[DE90-006084] 10 p1437 N90-18296
Dopant site location in dual-implanted GaP using (111) planar channeling
[DE90-006565] 11 p1571 N90-19042
Power diode switching behavior
[ETN-90-95363] 12 p1653 N90-19501
Digital capacity transient spectroscopy of deep structure defects in III-V-Semiconductor structures
[ETN-90-96057] 12 p1722 N90-19890
Chemically prepared PZT films doped with niobium
[DE90-006811] 13 p1892 N90-20859
Continued development and characterization of doped layers, contacts, and associated electronic devices in silicon carbide
[AD-A219211] 16 p2232 N90-22737
Continued development and characterization of doped layers, contacts and associated electronic devices in silicon carbide
[AD-A219234] 16 p2232 N90-22738
Optical spectroscopy of Ti(3+) doped YAlO3
[AD-A219043] 16 p2324 N90-23251
XPS studies of doped polypyrrole films
[AD-A219424] 17 p2379 N90-23550
Preparation and properties of iron doped II-VI chalcogenides
[AD-A220802] 17 p2477 N90-24163
Chemical and crystallographic phase behavior in the Ba(1-x)K(x)BiO3 system
[DE90-010072] 18 p2618 N90-24917
Development of a large scale Nd:YAG growth process
[DE90-010746] 18 p2624 N90-24954
Protons and lattice defects in perovskite-related oxides
[DE90-010957] 18 p2624 N90-24955
A room-temperature, laser diode-pumped, Q-switched, 2 micron, thulium-doped, solid state laser
[AD-D014527] 19 p2695 N90-25334
Spectroscopy of laser properties of Nd(3+)-doped CaF2, SrF2, and BaF2
[DE90-012086] 19 p2695 N90-25337
Nondestructive one- and two-dimensional doping profiling by inverse methods
[ETN-90-97264] 20 p2874 N90-26351
Characterization of superconducting materials with muon spin rotation
[DE90-013755] 21 p3081 N90-27522
Microstructure and magnetization of doped Y-Ba-Ca-O materials prepared by melt quench and post annealing method 22 p3138 N90-27803
Preparation and characteristics of superconducting cuprate thin films: Nd(2-x)Ce(x)CuO4 and substituted Bi-system 22 p3140 N90-27813
Dynamics of the iron spins in superconducting YBa2(Cu(1-x)Fe(x))O7 22 p3143 N90-27825
Electronic state and superconductivity of YBa2Cu3-xO7-y (M=Al,Zn and Sn) systems 22 p3146 N90-27842
Titanium-doped sapphire lasers with high energy pumping
[RSRE-MEMO-4290] 22 p3181 N90-28050
High-temperature deformation and microstructural analysis for Si3N4-Sc2O3
[NASA-TM-103239] 23 p3314 N90-28740
Electron microscopy of transition-metal doped BiCaSrCuO
[DE90-014184] 23 p3398 N90-29202
Parity violation and superconductivity in doped Mott insulators
[DE90-627493] 23 p3401 N90-29217
Dynamical information for Fe doped YBa2Cu3O7 superconducting oxides obtained from high temperature Moessbauer studies
[DE90-627871] 23 p3401 N90-29218
XANES and EXAFS study of Au-substituted YBa2Cu3O(7-delta)
[NASA-TM-103291] 23 p3401 N90-29219

DOPING (ADDITIVES)
U ADDITIVES

DOPPLER EFFECT
Multiline multimode CW chemical laser performance
[AD-A210613] 01 p0075 N90-10432
A laser Doppler anemometry investigation of single-phase and particle-laden jet flows
[AD-A210660] 02 p0220 N90-11261
Theory and simulation of the operation of a Doppler direction finder in a multipath environment
[FEL-1988-56] 03 p0340 N90-11939
Doppler statistics of ocean velocity variability
[AD-A211687] 03 p0377 N90-12143
Development of an anti-Stokes coherent Raman diffusion system for measuring hypersonic flow
[ONERA-RSF-1/7301-PY] 04 p0459 N90-12630
Photochemical observation of ion flows in membrane channels
[AD-A212449] 04 p0472 N90-12705
Multiparameter radar estimation of raindrop size distribution
[AD-A212410] 04 p0521 N90-13007
The interaction and variation of waves and turbulence from MST radar data
[AD-A212849] 05 p0670 N90-13906
Mitigating Doppler shift effect in HF multitone data modem 06 p0764 N90-14441
High resolution Doppler lidar
[NASA-CR-183288] 06 p0781 N90-14542
Rotating Doppler frequency shifter
[AD-D014279] 08 p1118 N90-16475
In situ measurement of neutral beam components using the Doppler-shifted H(sub alpha) emissions in Heliotron E
[DE90-719521] 08 p1125 N90-16516
Doppler imagery for the visualisation of velocity fields
[ISL-CO-232/88] 09 p1226 N90-17114
Adaptive processor emulation development
[AD-A214392] 10 p1371 N90-17944
Evaluation of a delay-Doppler imaging algorithm based on the Wigner-Ville distribution
[AD-A215827] 10 p1377 N90-17980
Efficient detection and signal parameter estimation with application to high dynamic GPS receiver
[NASA-CASE-NPO-17820-1-CU] 11 p1454 N90-18379
An error sensitivity model for Doppler positioning using transit satellites
[AD-A216724] 11 p1455 N90-18381
Doppler spectra from incoherent backscatter: Principles and examples for application for POLDIRAD
[DLR-FB-89-48] 11 p1499 N90-18630
Coherent radar measurement of ocean currents from geostationary orbit 12 p1609 N90-19259
Correlation-induced changes of spectra
[AD-A217087] 12 p1669 N90-19591
Modelling Doppler broadening in Raman propagation
[DE90-008042] 13 p1789 N90-20269
Meteor observations using the 50 MHz MENTOR imaging Doppler interferometer
[AD-A217908] 13 p1790 N90-20276
Digital Doppler extraction demonstration with the advanced receiver 15 p2076 N90-21893
Phase Doppler droplet sizing: Scattering angle effects
[DE90-009571] 16 p2236 N90-22754
Innovative techniques for high-resolution imaging and precision tracking
[AD-A221380] 18 p2616 N90-24899
Study of short-lived unstable nuclei by means of laser optical pumping
[AD-A222561] 21 p3009 N90-27105
Velocity selection to enable direct measurement of strong single atom-optical cavity coupling
[AD-A223060] 21 p3071 N90-27460
Laser spectroscopy of plasmas
[AD-A221978] 21 p3078 N90-27502
Velocity Interferometer System for Any Reflector (VISAR): Displacement mode data reduction
[DE90-015027] 23 p3395 N90-29184
Laser velocimetry 24 p3420 N90-29317
High power oblique incidence HF ionospheric modification
[AD-A224402] 24 p3491 N90-29729

DOPPLER NAVIGATION
Development of the integrated all-weather navigation system for Tornado 02 p0149 N90-10849
Using connected-element interferometer phase-delay data for Magellan navigation in Venus orbit 15 p2075 N90-21885

GPS navigational performance in space rendezvous operations 18 p2504 N90-24310
DOPPLER RADAR
NT MULTISTATIC RADAR
A study of the impact of simulated satellite lidar wind observations
[AD-A210430] 01 p0086 N90-10468
The effectiveness of adaptive PRF (Pulse Repetition Frequency) selection in minimizing range obscuration in the TDWR (Terminal Doppler Weather Radar) system
[AD-A211267] 02 p0213 N90-11222
Further guide for the retrieval of dropsize distributions in water clouds with a ground-based clear-air-sensing Doppler radar
[PB89-196000] 03 p0336 N90-11911
Low level remote sensing: The Doppler Radar wind profiler 03 p0361 N90-12067
Measurements of aerosol properties needed to infer backscatter characteristics in support of the NASA Doppler Lidar program 03 p0364 N90-12082
Subjective uses of wind profiler data in warm season analysis and forecasting: Wind profiler training manual number 3
[PB89-223333] 04 p0520 N90-13004
Adaptive clutter rejection filters for airborne Doppler weather radar applied to the detection of low altitude windshear
[NASA-CR-186211] 06 p0766 N90-14453
Turbulence spectral widths view angle independence as observed by Doppler radar
[DOT/FAA/SA-89/2] 07 p0963 N90-15566
Analysis of significant weather on meso-alpha scales using conventional and remotely sensed data: Exploratory studies
[AD-A214563] 09 p1248 N90-17238
Doppler spectra from incoherent backscatter: Principles and examples for application for POLDIRAD
[DLR-FB-89-48] 11 p1499 N90-18630
A case study of the 24 August 1986 FLOWS microburst
[AD-A216939] 11 p1537 N90-18847
Doppler lidar working group report
[ESA-SP-1112] 11 p1537 N90-18848
Advanced Doppler tracking experiments 12 p1731 N90-19951
Tropospheric monitoring technology for gravity wave experiments 12 p1734 N90-19971
Doppler radar with multiphase modulation of transmitted and reflected signal
[NASA-CASE-MSC-18808-1] 13 p1791 N90-20280
Atmospheric wind measurements using a 50 MHz imaging Doppler interferometer radar
[AD-A218277] 13 p1847 N90-20601
Advanced instrumentation for aircraft icing research
[NASA-CR-185225] 14 p1921 N90-21006
Airborne Doppler radar flight experiments for the detection of microbursts 14 p1963 N90-21243
Dynamic and microphysical characteristics of cirrus clouds as revealed by aircraft, lidar, and other observations during FIRE 15 p2130 N90-22177
Turbulence spectral widths view angle independence as observed by Doppler radar
[AD-A219169] 16 p2199 N90-22550
Next generation weather radar (NEXRAD) initial operational test and evaluation. Phase 2: (IOT and E(2))
[AD-A218770] 16 p2258 N90-22873
Atmospheric turbulence measurements in support of adaptive optics technology
[AD-A220445] 17 p2423 N90-23805
Use of clutter residue editing maps during the Denver 1988 Terminal Doppler Weather Radar (TDWR) tests
[AD-A218896] 17 p2426 N90-23822
Kinetic and extraction measurements on 12C18O2
[AD-A220417] 17 p2472 N90-24133
Derivation of wind fields from Doppler measurements of a single radar and application to a cold front with narrow rainband
[DLR-FB-89-61] 18 p2582 N90-24705
Binary pseudo random phase correlation in radar systems: A new approach
[RSRE-MEMO-4223] 19 p2683 N90-25283
Combining zero Doppler filter calculations with MTI filter calculations to increase computational speed
[AD-A222468] 21 p2997 N90-27034
Wind field derivatives of extratropical cyclones observed by Doppler radar
[AD-A222188] 21 p3031 N90-27232
Phoenix data analysis and numerical simulation
[AD-A224226] 23 p3320 N90-28772
Observations of tornadoes and wall clouds with a portable FM-CW Doppler radar: 1989--1990 results
[DE90-013152] 24 p3495 N90-29752
DOSAGE
NT RADIATION DOSAGE
Meteorological monitoring for environmental/dose assessment and emergency response modeling: How much is enough
[DE90-002726] 06 p0818 N90-14757
Study of hydrazine metabolism and toxicity
[AD-A217103] 12 p1695 N90-19736
Acute oral toxicity of JA-2 solid propellant in ICR mice
[AD-A217264] 13 p1848 N90-20609
Acute oral toxicity of DIGL-RP solid propellant in ICR mice
[AD-A217711] 13 p1849 N90-20613
Acute oral toxicity of DIGL-RP solid propellant in Sprague-Dawley rats
[AD-A217712] 13 p1849 N90-20614
Effects of cholinergic drugs on exercise performance and simple reaction time of rhesus monkeys
[AD-A219455] 17 p2433 N90-23862
Dose analysis of the model 112A Pulserad pulsed x ray generator by its CYLTRAN
[AD-A220372] 17 p2471 N90-24125
DOSE
U DOSAGE
DOSIMETERS
Hydrazine dosimetry 02 p0206 N90-11178
Use of the NPL linac for x ray dosimetry --- linear accelerator (linac)
[NPL-RSA(EXT)-6] 03 p0404 N90-12314
Assessment of research needs for laser technologies applied to advanced spectrographic methods
[DE90-001154] 06 p0788 N90-14587
Measuring Day-Night Noise Levels (DNL) using the metrosonics db-310 sound level analyzer (Dosimeter)
[AD-A215757] 10 p1427 N90-18230
Energy deposition measurements for E-beam pumped excimer lasers
[DE90-007545] 13 p1806 N90-20365
Determinations of photon spectra
[AD-A218003] 13 p1885 N90-20816
Field evaluation of a passive sampling device for hydrazines in ambient air
[NASA-TM-103456] 18 p2578 N90-24686
Space radiation studies
[NASA-CR-183991] 19 p2798 N90-25925
Experiment K-6-24, K-6-25, K-6-26. Radiation dosimetry and spectrometry 20 p2897 N90-26477
A tandem system of ionization chambers for effective energy determination of unknown X-radiation fields
[DE90-630463] 24 p3436 N90-29405
DOSIMETRY
U DOSIMETERS
DOUBLE BASE PROPELLANTS
NT DOUBLE BASE ROCKET PROPELLANTS
Temperature measurements through a solid-propellant combustion wave using imbedded fine wire thermocouples
[AD-A218642] 16 p2225 N90-22683
Renewed aging control of adhesion of inhibitor on the gas generator charges for RB 24
[FOA-C-20780-2.1] 20 p2840 N90-26153
DOUBLE BASE ROCKET PROPELLANTS
A theoretical model of double base propellant combustion
[ONERA-RTF-23/7128-EY] 05 p0629 N90-13672
Propellant trends in advanced rocket propulsion 09 p1179 N90-16838
DOUBLE STARS
NT BINARY STARS
NT CATACLYSMIC VARIABLES
NT DWARF NOVAE
NT ECLIPSING BINARY STARS
NT SYMBIOTIC STARS
NT X RAY BINARIES
Speckle interferometry for high resolution pictures of astronomical objects
[ETN-90-95827] 12 p1729 N90-19936
High energy x ray observations on the Crab nebula and the double star source GX 1+4
[ETN-90-95829] 12 p1729 N90-19937
DOUGHNUT SHAPE WHEELS
U TOROIDAL WHEELS
DOUGLAS AIRCRAFT
NT DC 10 AIRCRAFT
DOUGLAS MILITARY AIRCRAFT
U MILITARY AIRCRAFT
DOVAP
U DOPPLER EFFECT
DOWN-CONVERTERS
OPFET (Optical Field-Effect Transistor) demodulator-downconverter for detecting microwave modulated optical signals
[AD-D014294] 08 p1060 N90-16128
An 8.4-GHz dual-maser front-end system for Parkes reimplementation 15 p2078 N90-21905
DOWNLINKING
SLCSAT (Submarine Laser Communication Satellite) communication system design study
[AD-A213403] 07 p0917 N90-15304
Advanced modulation technology development for earth station demodulator applications. Coded modulation system development
[NASA-CR-185149] 13 p1789 N90-20270
VLSI single-chip (255,223) Reed-Solomon encoder with interleaver
[NASA-CASE-NPO-17280-1-CU] 14 p1933 N90-21061
Microspacecraft and Earth observation: Electrical field (ELF) measurement project
[NASA-CR-186821] 20 p2888 N90-26436
DOWNRANGE
Down-range imaging of radar targets
[AD-A221084] 18 p2544 N90-24521
DOWNTIME
A simple model for DSS-14 outage times 04 p0488 N90-12802
DOWNWASH
Analysis of heliport environmental data: Indianapolis downtown heliport, Wall Street heliport. Volume 2: Wall Street heliport data plots
[DOT/FAA/CT-TN87/54-VOL-2] 03 p0310 N90-11761
Analysis of heliport environmental data: Indianapolis downtown heliport, Wall Street heliport. Volume 3: Indianapolis downtown heliport data plots
[AD-A217412] 13 p1829 N90-20500
Wind tunnel study of wake downwash behind A 6 percent scale model B1-B aircraft
[DE90-011783] 20 p2802 N90-25941
Analysis of heliport environmental data, Intracoastal City
[DOT/FAA/CT-TN89/43] 23 p3284 N90-28584
Wind tunnel, field, and numerical investigations of plume downwash and dispersion at an arctic industrial site 24 p3489 N90-29721
Three-dimensional numerical study of thunderstorm downdrafts and associated outflow boundaries 24 p3494 N90-29746
DPCM (MODULATION)
U DIFFERENTIAL PULSE CODE MODULATION
DRAFTING (DRAWING)
Guide for the use of intergraph randmicas structural software for Computer-Aided Design and Drafting(CADD)
[AD-A220624] 17 p2443 N90-23924
A concept for integrating computer-aided drafting and design with cost engineering and specification preparation
[AD-A223150] 22 p3237 N90-28354
DRAG
NT AERODYNAMIC DRAG
NT FRICTION DRAG
NT INTERFERENCE DRAG
NT MINIMUM DRAG
NT PRESSURE DRAG
NT SATELLITE DRAG
NT SUPERSONIC DRAG
NT VISCOUS DRAG
NT WAVE DRAG
New test techniques to evaluate near field effects for supersonic store carriage and separation 01 p0013 N90-10062
Reduction of profile drag by modifying the structure next to the wake area
[IMFL-88/35] 05 p0576 N90-13356
Induced drag for non-planar wings
[LR-521] 05 p0576 N90-13357
Lifetime predictions for the Solar Maximum Mission (SMM) and San Marco spacecraft 05 p0591 N90-13440
Crew emergency return vehicle autoland feasibility study
[NASA-CR-181940] 08 p1028 N90-15937
Calculation of excrescence drag magnification due to pressure gradient at high subsonic speeds
[ESDU-87004] 12 p1598 N90-19195
Estimation of extra drag force on a circular cylinder due to the presence of solid particles in subsonic compressible flow
[AD-A218635] 16 p2197 N90-22542
Modelling bottom stress in depth-averaged flows
[AD-A218605] 17 p2429 N90-23840
An analytic study of nonsteady two-phase laminar boundary layer around an airfoil 18 p2643 N90-25051
A user's manual for MCPRAM (Monte Carlo PReprocessor for AMEER) and for the fuze options in AMEER (Aero Mechanical Equation Evaluation Routines)
[DE90-013598] 21 p3051 N90-27345

Autonomous propulsion system requirements for placement of an STS (Space Transportation System) external tank in low Earth orbit
[PB90-183302] 22 p3133 N90-27777
Study of the ground effects in the CEAT aerohydrodynamic tunnel: Using the results
23 p3274 N90-28530
Shear-resistant drag reduction polymers. Part 1: Molecular investigations of polymer drag reduction and the development of laboratory screening methods
[AD-A223353] 24 p3454 N90-29508

DRAG BALANCE
U AERODYNAMIC BALANCE
U LIFT DRAG RATIO

DRAG CHUTES
An experimental investigation of wall-interference effects for parachutes in closed wind tunnels
[DE90-001802] 07 p0875 N90-15076

DRAG DEVICES
NT AERODYNAMIC BRAKES
NT DRAG CHUTES
NT LEADING EDGE FLAPS
NT SPOILERS
Study of the structure of the vortices created by the drag of a natched edge by thermal tracing
[IMFL-89-26] 22 p3109 N90-27660

DRAG EFFECT
U DRAG

DRAG FORCE ANEMOMETERS
Skin friction measurements with hot elements
05 p0574 N90-13345

DRAG MEASUREMENT
Study of the flow around the prototype of A300: Results of the third test campaign at F2 and comparison with calculations
[CERT-33/5025-29-DERAT] 22 p3109 N90-27663

DRAG REDUCTION
Control and modification of turbulence
01 p0066 N90-10377
Turbulence management: Application aspects
01 p0066 N90-10378
An experimental investigation of helicopter rotor hub fairing drag characteristics
[NASA-TM-102182] 03 p0300 N90-11701
Application of sound and temperature to control boundary-layer transition 04 p0443 N90-12537
Design of the low-speed NLF(1)-0414F and the high-speed HSNLF(1)-0213 airfoils with high-lift systems
04 p0444 N90-12540
Experimental and numerical analyses of laminar boundary-layer flow stability over an aircraft fuselage forebody 04 p0445 N90-12549
Status report on a natural laminar-flow nacelle flight experiment 04 p0445 N90-12550
Nacelle design 04 p0446 N90-12551
Reduction of turbulent drag: Boundary layer manipulators
[CERT-RSF-OA-74/2259-AYD]
04 p0501 N90-12889
Copolymers for drag reduction in marine propulsion: New molecular structures with enhanced effectiveness
[AD-A214444] 08 p1049 N90-16062
A two-stage earth-to-orbit transport with translating oblique wings for booster recovery
[NASA-CASE-LAR-14156-1] 09 p1173 N90-16781
Influence of wall strain rate, polymer concentration, and channel height upon drag reduction and turbulent structure
[AD-A215378] 09 p1218 N90-17064
NASA aerodynamics program
[NASA-TM-4175] 09 p1247 N90-17235
Effect of riblets on flow separation from a cylinder and an airfoil in subsonic flow
[AD-A216197] 10 p1309 N90-17574
Optimum spanwise camber for minimum induced drag
[BU-403] 11 p1452 N90-18369
Drag reduction by longitudinal riblets on the surface of a streamwise aligned body of revolution
[MPIS-MITT-92] 12 p1600 N90-19210
Drag-free satellite control 12 p1735 N90-19974
Aerodynamic analysis of a US Navy and Marine Corps unmanned air vehicle
[AD-A218282] 13 p1755 N90-20077
Compression pylon
[NASA-CASE-LAR-13777-1] 13 p1755 N90-20078
Passive venting technique for shallow cavities
[NASA-CASE-LAR-14031-1] 13 p1755 N90-20079
Investigation into the mechanism of polymer thread drag reduction
[AD-A217492] 13 p1800 N90-20329
A fast collocation method for transonic airfoil design
14 p1917 N90-20984
Constrained spanload optimization for minimum drag of multi-lifting-surface configurations
14 p1919 N90-20992
On the use of external burning to reduce aerospace vehicle transonic drag
[NASA-TM-103107] 15 p2052 N90-21762
Fundamental hydrodynamics research
[AD-A219179] 16 p2238 N90-22766
A laser-induced fluorescence technique for measurement of slot-injected fluid concentration profiles in a plate turbulent boundary layer
[AD-A221388] 18 p2553 N90-24572
Aero-acoustic investigations of the magnetic train Transrapid 06
[MBB-UW-0009/89-PUB] 19 p2654 N90-25104
A method for the reduction of aerodynamic drag of road vehicles
[NASA-TM-102589] 22 p3108 N90-27656
Study of the structure of the vortices created by the drag of a natched edge by thermal tracing
[IMFL-89-26] 22 p3109 N90-27660
Shear-resistant drag reduction polymers. Part 1: Molecular investigations of polymer drag reduction and the development of laboratory screening methods
[AD-A223353] 24 p3454 N90-29508

DRAGULATORS
U BRAKES (FOR ARRESTING MOTION)
U DRAG DEVICES

DRAINAGE
Independent Orbiter Assessment (IOA): Assessment of the purge, vent and drain subsystem
[NASA-CR-185535] 02 p0168 N90-10949
Independent Orbiter Assessment (IOA): Analysis of the purge, vent and drain subsystem
[NASA-CR-185547] 02 p0172 N90-10969
Analytical and experimental study of runway runoff with wind effects
[PTI-8948] 04 p0458 N90-12627
Remote sensing and run-off modelling in the Lake Victoria Basin, Kenya
[BCRS-89-19] 11 p1526 N90-18788
Characterization of linear structures from remote sensing data; Espinhaco Meridional (MG) sierra
[INPE-4905-PRE/1506] 14 p1997 N90-21449
Geographic information system: Coded data of agrocattle-raising projects in the Amazon
[INPE-4978-PRE/1543] 15 p2180 N90-22457
Erosional development of bedrock spur and gully topography in the Valles Marineris, Mars
[NASA-CR-180655] 17 p2424 N90-23813
Snow cover mapping and snowmelt runoff simulations on microcomputers 19 p2707 N90-25408
Airport pavement drainage
[DOT/FAA/RD-90/24] 22 p3122 N90-27728

DRAINING
U DRAINAGE

DRAWING
Designing and designing knowledge in engineering and architecture
[PB89-219521] 03 p0415 N90-12383
Processing of thermotropic liquid crystalline polymers and their blends
[AD-A218804] 16 p2223 N90-22683

DRAWINGS
NT ENGINEERING DRAWINGS
Aircraft drawings index 17 p2343 N90-23340

DRIFT (INSTRUMENTATION)
Simultaneous quaternion estimation (QUEST) and bias determination 05 p0587 N90-13417
True covariance simulation of the EUVE update filter
05 p0589 N90-13427
Changes in the volt, ohm, and temperature and long range impact of using the Josephson voltage standard
[DE90-004493] 09 p1214 N90-17039
Improvements of automatic magnetic observatories in Italy 21 p3022 N90-27185
Improvements in fluxgate magnetometers at Danish Meteorological Institute's Magnetic Observatories
21 p3023 N90-27187

DRIFT RATE
The behaviour of the L3 muon chambers in a magnetic field
[ETN-90-96920] 18 p2613 N90-24884

DRILL BITS
Design and development activities on the candidate sample acquisition system for the Rosetta mission
12 p1738 N90-19993
Introduction to drilling technology
12 p1740 N90-20002
Design of a rotary stepped auger for a lunar environment
[NASA-CR-184919] 17 p2384 N90-23577
Proof of principal for staircase auger chip removal theory
[NASA-CR-184934] 17 p2385 N90-23583
Lunar drill and test apparatus
[NASA-CR-183052] 17 p2411 N90-23736
Lunar drill footplate and casing
[NASA-CR-183153] 17 p2411 N90-23738

DRILLING
Adjustable depth gage
[NASA-CASE-LEW-14880-1] 01 p0072 N90-10415
Coastal subsea permafrost and bedrock observations using dc resistivity
[AD-A210784] 02 p0253 N90-11435
An analysis of drilling of composite materials
07 p0889 N90-15142
The nature of cometary materials
08 p1147 N90-16647
Introduction to drilling technology
12 p1740 N90-20002
Hot dry rock geothermal energy: A renewable energy resource that is ready for development now
[DE90-007509] 13 p1826 N90-20485
Machining of new materials at Aerospatiale
[REPT-892-430-104] 16 p2213 N90-22622
Rod gripper, changer, and storage system
[NASA-CR-183154] 17 p2411 N90-23739
Core sample extractor
[NASA-CR-182864] 17 p2411 N90-23740
Vertically reciprocating auger
[NASA-CR-182822] 18 p2535 N90-24458
Lunar deep drill apparatus
[NASA-CR-182756] 20 p2869 N90-26322
Drilling the oceanic lower crust and mantle: A global strategy for exploring the deep oceanic crust and mantle in the 1990's
[PB90-240953] 23 p3351 N90-28936

DRILLS
Design and development activities on the candidate sample acquisition system for the Rosetta mission
12 p1738 N90-19993
Compressive strength of synthetic comet nucleus samples 12 p1741 N90-20006
Design of a rotary stepped auger for a lunar environment
[NASA-CR-184919] 17 p2384 N90-23577
Proof of principal for staircase auger chip removal theory
[NASA-CR-184934] 17 p2385 N90-23583
Lunar drill and test apparatus
[NASA-CR-183052] 17 p2411 N90-23736
Lunar drill footplate and casing
[NASA-CR-183153] 17 p2411 N90-23738
Vertically reciprocating auger
[NASA-CR-182822] 18 p2535 N90-24458

DRINKING
Effect of fluid countermeasures of varying osmolarity on cardiovascular responses to orthostatic stress
18 p2628 N90-24978

DROGUE PARACHUTES
U DRAG CHUTES

DROGUES
U TOWED BODIES

DRONE AIRCRAFT
NT TARGET DRONE AIRCRAFT

DRONE HELICOPTERS
U HELICOPTERS

DRONE VEHICLES
NT TARGET DRONE AIRCRAFT

DROP SIZE
Evaporation and combustion of dense sprays with a bimodal droplet size distribution
02 p0192 N90-11094
Further guide for the retrieval of dropsize distributions in water clouds with a ground-based clear-air-sensing Doppler radar
[PB89-196000] 03 p0336 N90-11911
Two dimensional orifice array, monodisperse drop source, phase 1
[AD-A211319] 04 p0500 N90-12881
Multiparameter radar estimation of raindrop size distribution
[AD-A212410] 04 p0521 N90-13007
Liquid water content and droplet size calibration of the NASA Lewis Icing Research Tunnel
[NASA-TM-102447] 05 p0651 N90-13797
Comparison of two droplet sizing systems in an icing wind tunnel
[NASA-TM-102456] 06 p0793 N90-14617
Comparison of drop size distributions from two droplet sizing systems
[NASA-TM-102520] 09 p1232 N90-17147
Rain core structure statistics derived from radar and disdrometer measurements in the mid-Atlantic coast of the US 10 p1373 N90-17956
On the question of spray effects
12 p1687 N90-19691
Precipitation mechanisms in tropical and midlatitude convective clouds 14 p2008 N90-21507
Scattered-light scanner measurements of cryogenic liquid-jet breakup
[NASA-TM-102432] 15 p2101 N90-22021
NASA Lewis icing research tunnel user manual
[NASA-TM-102319] 17 p2355 N90-23407

Comparison test of droplet sizing instruments used in icing research
[DOT/FAA/CT-TN90/13] 19 p2693 N90-25322
Optical characterization of clouds of fine liquid-nitrogen particles
[NASA-TM-103208] 20 p2865 N90-26299
Nature and origin of interstellar diamond from the Allende CV3 meteorite 21 p3092 N90-27581
Spectral absorption of marine stratocumulus clouds derived from in situ cloud radiation measurements 22 p3215 N90-28238

DROP TESTS
Very low height drop test. Conditioning and tandem dropping of two loads conditioned in two PC6 platforms assembled by rigid structures
[REPT-89/07] 22 p3193 N90-28116
Very low height drop test. Conditioning and tandem dropping of two loads conditioned in two PC6 platforms assembled by one PD9 platform and rigid structures
[REPT-89/04] 22 p3193 N90-28117
Very low height drop test. Conditioning and tandem dropping of two loads conditionned in two PC6 platforms assembled by rigid structures
[REPT-89/08] 22 p3193 N90-28118

DROP TOWERS
Droplet combustion experiment drop tower tests using models of the space flight apparatus
[NASA-TM-101472] 02 p0209 N90-11196
Non-contact temperature measurement requirements 10 p1363 N90-17898
IR optical fiber-based noncontact pyrometer for drop tube instrumentation 10 p1365 N90-17909
Non-contact temperature measurement of a falling drop 10 p1365 N90-17912
The NASA, Marshall Space Flight Center drop tube user's manual
[NASA-TM-100392] 13 p1786 N90-20251
Critical point wetting drop tower experiment
[NASA-CR-186513] 14 p1957 N90-21208
Nucleation kinetics in undercooled, class-forming metallic melts
[ESA-TT-1186] 19 p2676 N90-25218
Noncontact measurement of high temperature using optical fiber sensors
[NASA-CR-186975] 23 p3329 N90-28825

DROP TRANSFER
Bubble, Drop and Particle Unit (BDPU): A multi-user microgravity facility
[IAF-89-431] 20 p2842 N90-26164

DROP TUBES
U DROP TOWERS

DROP WEIGHT TESTS
U DROP TESTS

DROPS (LIQUIDS)
NT RAINDROPS
Theory of droplet. Part 1: Renormalized laws of droplet vaporization in non-dilute sprays 01 p0068 N90-10390
Conceptual design of liquid droplet radiator shuttle-attached experiment
[NASA-CR-185164] 03 p0318 N90-11805
Conceptual design of liquid droplet radiator shuttle-attached experiment technical requirements document
[NASA-CR-185165] 03 p0318 N90-11806
Further guide for the retrieval of dropsize distributions in water clouds with a ground-based clear-air-sensing Doppler radar
[PB89-196000] 03 p0336 N90-11911
Droplet sizing instrumentation used for icing research: Operation, calibration, and accuracy
[NASA-CR-182293] 03 p0350 N90-11999
Monte Carlo studies of nuclei and quantum liquid drops
[DE89-016914] 03 p0402 N90-12300
Continuing studies of liquid propellant drops in hot, high-pressure environments
[AD-A212265] 04 p0482 N90-12765
Two dimensional orifice array, monodisperse drop source, phase 1
[AD-A211319] 04 p0500 N90-12881
Survey of the CLUSE main experiment Grand-CLUSE, May 1 - June 15, 1988 --- Humidity Exchange Over the Sea (HEXOS) experiment
[FEL-1988-43] 04 p0518 N90-12991
Metal transfer in gas metal arc welding
[AD-A213390] 05 p0624 N90-13642
Facilities for microgravity combustion research
[NASA-TM-102014] 05 p0630 N90-13679
Thermocapillary migration of liquid droplets in a temperature gradient in a density matched system
[NASA-CR-185178] 06 p0776 N90-14512
Dense-spray properties: Structure and turbulence modulation
[AD-A213671] 07 p0931 N90-15387
Anomalous absorption by atmospheric water vapor and stabilized water fogs in the infrared and CM-wave regions
[AD-A214202] 07 p0964 N90-15572
Droplet vaporisation and combustion in microgravity 09 p1202 N90-16963
Comparison of drop size distributions from two droplet sizing systems
[NASA-TM-102520] 09 p1232 N90-17147
The evaporation of sessile droplets. Part 1: Theoretical factors for a two-component system
[AD-A215946] 10 p1353 N90-17848
Non-Contact Temperature Requirements (NCTM) for drop and bubble physics 10 p1366 N90-17918
A model for evaporation of freely falling droplets
[PUBL-AIR-QUALITY-6] 10 p1384 N90-18007
A study on deformation and break-up of dispersed particles in elongational flow
[ETN-90-96268] 11 p1508 N90-18884
Cloud hole-boring with infrared lasers: Theory and experiment
[DE90-006519] 11 p1515 N90-18723
Simulation of thermal dynamics of a vaporizing coal-water droplet in a combustor
[DE90-005356] 12 p1621 N90-19317
Effects of turbulence mixing, variable properties, and vaporization on spray droplet combustion
[NASA-CR-186463] 12 p1623 N90-19326
Experimental investigation of the thermocapillary migration of water droplets in butylbenzoate
[MPIS-14/1988] 13 p1770 N90-20155
Spray deposition: A fundamental study of droplet impingement, spreading and consolidation
[AD-A217202] 13 p1787 N90-20255
High intensity laser beam interactions with single droplets 15 p2083 N90-21924
Flow visualization in supersonic turbulent boundary layers 16 p2195 N90-22533
Sticking coefficient of HCl on aerosols 16 p2208 N90-22598
Nonlinear spectroscopy of multicomponent droplets and 2- and 3-dimensional measurements in flames
[AD-A218569] 16 p2215 N90-22636
Unsteady group behavior of droplet clouds in swirling flows 16 p2233 N90-22743
Phase Doppler droplet sizing: Scattering angle effects
[DE90-009571] 16 p2236 N90-22754
Hanging drop crystal growth apparatus and method
[NASA-CASE-MFS-28205-1-SB] 16 p2322 N90-23242
Crystal growth apparatus
[NASA-CASE-MFS-28182-1] 17 p2478 N90-24169
Fundamental studies on spray combustion and turbulent combustion
[AD-A219840] 18 p2521 N90-24394
The modeling of drop-containing turbulent eddies
[NASA-CR-186805] 18 p2553 N90-24570
Comparison test of droplet sizing instruments used in icing research
[DOT/FAA/CT-TN90/13] 19 p2693 N90-25322
Liquid fueled ramjet combustion instability: Acoustical and vortical interactions with burning sprays
[AD-A222752] 20 p2831 N90-26104
Bubble, Drop and Particle Unit (BDPU): A multi-user microgravity facility
[IAF-89-431] 20 p2842 N90-26164
The 27-28 October 1986 FIRE IFO Cirrus case study: Comparison of radiative transfer theory with observations by satellite and aircraft
[NASA-TM-103468] 20 p2890 N90-26446
Sources of cloud nuclei and development of remote sensing techniques for cloud parameters
[AD-A222464] 21 p3031 N90-27233
Scattering of CO2-laser radiation by water droplets
[FOA-C-20776-2.3] 22 p3181 N90-28049
Supersaturation, droplet spectra, and turbulent mixing in clouds 22 p3217 N90-28249
Observations of anthropogenic cloud condensation nuclei 22 p3218 N90-28251
Direct and remote sensing observations of the effects of ships on clouds 22 p3218 N90-28252
Optical properties of marine stratocumulus clouds modified by ship track effluents 22 p3218 N90-28253
Analyses of spray and droplet ignition for pure and multicomponent fuels 23 p3304 N90-28688
Ignition and combustion of liquid propellants
[AD-A224150] 23 p3316 N90-28746
Transient cooling of a hot surface by droplets evaporation
[PB90-227968] 23 p3325 N90-28799
Particle dispersion in a turbulent shear flow
[AD-A224327] 24 p3467 N90-29590

DROSOPHILA
Microgravity effects on insect development and aging 19 p2680 N90-25243

DROWSINESS
U SLEEP

DRUG THERAPY
U CHEMOTHERAPY

DRUGS
NT ADRENERGICS
NT ANTIBIOTICS
NT ANTIDIURETICS
NT ATROPINE
NT CAFFEINE
NT CHOLINERGICS
NT EPINEPHRINE
NT INSULIN
NT MOTION SICKNESS DRUGS
NT STIMULANTS
The effects of nonselective and selective beta blockade upon nonshivering thermogenesis during an acute cold exposure in cold acclimated men 06 p0820 N90-14767
Human serum albumin crystals and method of preparation
[NASA-CASE-MFS-28234-1] 13 p1850 N90-20616
Influence of theobromine on heat production and body temperatures in cold-exposed humans: A preliminary report
[AD-A217203] 13 p1850 N90-20618
Melatonin, light and, circadian cycles
[AD-A223196] 21 p3035 N90-27258

DRY CELLS
NT NICKEL ZINC BATTERIES

DRY FRICTION
Planar sliding of a rigid body with dry friction: Limit surfaces and dynamics of motion 02 p0229 N90-11314
Evaluation of newly formulated Dow Corning 321 dry film lubricant
[NASA-CR-183828] 05 p0627 N90-13661
Space mechanism of low velocity for an array of solar panels: Analysis and design of an experimental model; dimensions of bearings
[INPE-4859-TDL/370] 13 p1809 N90-20390

DRY HEAT
Pressurized bellows flat contact heat exchanger interface
[NASA-CASE-MSC-21271-1] 15 p2097 N90-21999

DRYING
NT DEHYDRATION
NT FREEZE DRYING
Freeze-dried processing of tungsten heavy alloys
[DE89-015171] 02 p0197 N90-11122
Structure and properties of polymer interphases
[AD-A212796] 04 p0481 N90-12763
Porous ceramic bodies
[AD-D014277] 08 p1049 N90-16061
Process for making a noble metal on tin oxide catalyst
[NASA-CASE-LAR-13741-1-SB] 13 p1774 N90-20180
Comparison of light duty gloves with natural and synthetic materials under wet and dry conditions
[AD-A218119] 13 p1856 N90-20649
Wheat productivity estimate through field radiometry
[INPE-4994-PRE/1556] 14 p2000 N90-21460
Spectral response of wheat and its relationship with agronomic variables in the tropical region
[INPE-5018-RPE/612] 15 p2122 N90-22138
Thermohydraulics of a heat dissipating debris bed 19 p2691 N90-25310

DSN (SPACE NETWORK)
U DEEP SPACE NETWORK

DTA (ANALYSIS)
U THERMAL ANALYSIS

DUAL FREQUENCY RADAR
U MULTISPECTRAL RADAR

DUAL MODE PROPULSION
U HYBRID PROPULSION

DUALITY PRINCIPLE
On the manipulability of dual cooperative robots 24 p3505 N90-29813

DUALITY THEOREM
Hahn-Banach type theorems for dual semigroups
[CWI-AM-R8903] 04 p0543 N90-13149
Description and manipulation of convex polygons using polarity
[IMAG-RR-771-M] 05 p0692 N90-14041
The algebraic basis of mathematical morphology. Part 1: Dilations and erosions
[CWI-AM-R8807] 05 p0695 N90-14065
Note on p-semisimple BCI-algebras
[DE90-606955] 10 p1423 N90-18206
Multi-Hilbertian spaces and their duals
[AD-A222344] 21 p3064 N90-27421

DUCT GEOMETRY
Toward the optimization of a non-diffusing, two-dimensional S-shaped duct
[IAR-89-3] 21 p3003 N90-27068

DUCTED FLOW
NT KNUDSEN FLOW
Investigation of turbulent flow in highly curved ducts with application to turbomachinery components
[NASA-CR-186060] 04 p0500 N90-12882
A numerical and experimental investigation of multiple shock wave/turbulent boundary layer interactions in a rectanular duct 08 p1062 N90-16141
Pressure losses in flow through a sudden contraction of duct area
[ESDU-89040] 09 p1220 N90-17077
Analysis of internal flow in a ventral nozzle for STOVL aircraft
[NASA-TM-103123] 17 p2355 N90-23404
DUCTED PROPELLERS
U SHROUDED PROPELLERS
DUCTED ROCKET ENGINES
A simulator for a hydrocarbon ramrocket fuel gas generator: First phase development
[AR-005-621] 02 p0189 N90-11080
Analytical studies of three-dimensional combustion processes
[AD-A211903] 03 p0323 N90-11837
Experimental study of mixing and combustion processes in a solid-propellant ducted rocket motor
17 p2367 N90-23472
DUCTILITY
Numerical analysis of a class of problems in the mathematical theory of plasticity and damage
[AD-A210731] 01 p0114 N90-10655
Weldability of ductile nickel aluminides
[DE89-017452] 03 p0327 N90-11859
A study of the hot workability of Al-8.5 wt pct Mg alloys for armor plate applications
[AD-A211680] 03 p0329 N90-11868
Ductile failure
[AD-A212975] 05 p0618 N90-13601
Superplastic sheet forming 06 p0743 N90-14327
Ductile failure
[AD-A213864] 07 p0948 N90-15488
The effects of hydrogen embrittlement of titanium
08 p1156 N90-16698
Environmental embrittlement: A major cause for low ductility of ordered intermetallics
[DE90-006161] 10 p1356 N90-17864
Analysis of ductile fracture under biaxial loading using moire interferometry 10 p1394 N90-18060
The processing and mechanical properties of high temperature/high performance composites. Book 2, section 2: Strength and fracture resistance
[AD-A216142] 11 p1478 N90-18507
Processing and elevated temperature ductility of aluminum alloy 7475
[AD-A216840] 11 p1486 N90-18554
High-strength concrete development through 25 years
[CBL-REPRINT-17] 11 p1492 N90-18589
Austempered ductile iron data base: A cooperative program between industry and the Trade Adjustment Assistance Program of the Department of Commerce
[PB90-115569] 12 p1626 N90-19343
Optimizing superplastic response in navalite, a lithium containing aluminum-magnesium alloy
[AD-A216552] 12 p1626 N90-19346
Evaluation of material homogeneity as a function of thickness of low-alloy ferritic steel
[DE90-008069] 13 p1777 N90-20202
An introduction to nickel aluminide alloy
[DE90-008565] 13 p1778 N90-20207
Welding behavior and welding metallurgy of ductile intermetallic alloys
[DE90-008908] 15 p2069 N90-21852
Inclusion of unstable ductile tearing and extrapolated crack-arrest toughness data in PWR vessel integrity assessment
[DE90-009427] 15 p2118 N90-22116
Ultrahigh carbon steels and their laminates
[AD-A218780] 17 p2376 N90-23530
J-integral and HRR field of a stably growing crack, an experimental analysis
[AD-A220418] 17 p2416 N90-23764
The effect of trace amounts of antimony on the structure and properties of aluminum alloy A356.2
[DE90-010461] 19 p2674 N90-25207
Mechanisms for solid particle erosion in ductile and brittle materials
[NIAR-90-11] 19 p2675 N90-25210
Formation of cubic LI2 phases from Al3Ti and Al3Zr by transition metal substitutions for Al
[DE90-012288] 20 p2834 N90-26117
The effect of manganese on the onset of the stage 2 reaction in an austempered ductile iron matrix
[DE90-011804] 20 p2834 N90-26119
Processing and characterization of high strength, high ductility Hadfield steel
[AD-A221769] 21 p2982 N90-26947
Theory of ceramic/zirconia composites: Toughening, strengthening, and synergism
[AD-A222931] 21 p2985 N90-26961
Computational investigation of local material strength and toughness on crack growth
[AD-A223189] 21 p3012 N90-27127
On modeling the effect of pore shapes on ductile fracture
[AD-A221774] 21 p3014 N90-27136
Is there anything of practical value hidden amongst the composite toughening theories. A Jim Mueller prospective
[DE90-014905] 23 p3301 N90-28673
Tensile behavior of borated stainless steels, phase 1
[DE90-014368] 23 p3309 N90-28717
The roles of strain and reheating interval in continuous recrystallization during the thermomechanical processing by warm rolling of an Al-Mg alloy
[AD-A223673] 24 p3449 N90-29479
Tensile behavior and swelling of ternary austenitic alloys irradiated in different neutron spectra
[DE90-015295] 24 p3450 N90-29485
Alloy design of ordered intermetallics
[DE90-016031] 24 p3451 N90-29490
DUCTS
NT ACOUSTIC DUCTS
NT AIR DUCTS
PMR graphite engine duct development
[NASA-CR-182228] 01 p0008 N90-10037
Reheat buzz: An acoustically coupled combustion instability 01 p0036 N90-10200
Oscillations in non-axisymmetric dump combustors
01 p0037 N90-10205
Turbulent reacting flows in solid-propellant ducted rocket combustors 02 p0189 N90-11079
A forecasting system using the parabolic equation: Application to surface-to-air propagation in the presence of elevated layers 06 p0760 N90-14420
Propagation modeling for some horizontally varying tropospheric ducts 06 p0760 N90-14422
Laser velocimeter and total pressure measurements in circular-to-rectangular transition ducts
[NASA-CR-182286] 06 p0772 N90-14494
Heat transfer in convective boundary layer and channel flows 06 p0774 N90-14505
Low-altitude millimeter-wave propagation in the evaporation duct
[AD-A214432] 08 p1057 N90-16108
Depressurization test on hot gas duct
[DE90-710058] 09 p1236 N90-17176
Vortex motion phase separator for zero gravity liquid transfer
[NASA-CASE-KSC-11387-1] 13 p1783 N90-20236
Numerical method for designing 3D turbomachinery blade rows 14 p1918 N90-20990
Inflatable fuel tank buffer
[AD-D014446] 14 p1921 N90-21002
Parabolized calculations of turbulent three dimensional flows in a turbine duct 14 p1923 N90-21013
Effects of secondary flow on heat transfer in rotating passages 14 p1926 N90-21031
Active control of multi-dimensional random sound in ducts
[NASA-TM-102653] 14 p2024 N90-21603
An analysis of propagation in a surface duct over a periodically rough Earth
[AD-A220565] 17 p2390 N90-23612
Experimental and analytical study of close-coupled ventral nozzles for ASTOVL aircraft
[NASA-TM-103170] 18 p2498 N90-24273
Experimental validation study of an analytical model of discrete frequency sound propagation in closed-test-section wind tunnels
[NASA-TM-102801] 19 p2754 N90-25647
Measurement of terms and parameters in turbulent models
[NASA-CR-183993] 20 p2860 N90-26271
Toward the optimization of a non-diffusing, two-dimensional S-shaped duct
[IAR-89-3] 21 p3003 N90-27068
Spectral structure and generation mechanism of ducted VLF whistler mode sideband waves
24 p3489 N90-29720
DUMMIES
The USAF Advanced Dynamic Anthropomorphic Manikin (ADAM) 13 p1752 N90-20062
Biofidelity of a dummy's neck during automobile collision testing 19 p2721 N90-25477
DUMMY LOADS
U IMPEDANCE
U OUTPUT
DUMP COMBUSTORS
Numerical simulation of unsteady combustion in a dump combustor 01 p0037 N90-10203
Very-low-frequency oscillations in liquid-fueled ramjets
01 p0037 N90-10204
Oscillations in non-axisymmetric dump combustors
01 p0037 N90-10205
Calculation of the combustion distribution in a liquid-fuel ramjet 22 p3162 N90-27931
DUMPING
Lunar material transport vehicle
[NASA-CR-185929] 18 p2534 N90-24458
DUNGEYS WIND SHEAR MECHANISM
U WIND SHEAR
DUPLEXERS
Channel simulator upgrade to use field propagation data 10 p1372 N90-17948
Design, implementation and test of an RS-232 compatible bi-directional, full duplex, fiber-optic interface with provision for hardware handshaking on a minimum of fiber-optic lines
[AD-A216604] 11 p1566 N90-19012
DUPLICATING
U REPRODUCTION (COPYING)
DURABILITY
Considerations about the acceptance inspection of HS fasteners intended for controlled tightening
[CRIF-MT-175] 05 p0653 N90-13806
A dynamicist's view of fuel tank skin durability
08 p1023 N90-15915
Structural characterization of Spacelab
[ETN-90-95214] 08 p1087 N90-16289
LARC-IA: A flexible backbone polyimide
[NASA-TM-102586] 09 p1196 N90-16926
Compound for metallic surface treatment
[DE90-004121] 09 p1196 N90-16927
Feasibility demonstration of a 445N high-performance rocket engine 11 p1473 N90-18481
The effect of leveling coatings on the atomic oxygen durability of solar concentrator surfaces
[NASA-TM-102557] 14 p1941 N90-21110
Computational simulation of structural fracture in fiber composites
[NASA-TM-102505] 15 p2064 N90-21821
Progression of damage and fracture in composites under dynamic loading
[NASA-TM-103118] 15 p2065 N90-21825
Introducing the VRT gas turbine combustor
[NASA-TM-103176] 17 p2386 N90-23591
High-temperature materials. Coating, welding, and service tests
[VTT-RR-645] 19 p2675 N90-25214
Probabilistic approach to the certification for fatigue durability of composite structures
[DE90-505521] 20 p2828 N90-26085
Advanced Turbine Technology Applications Project (ATTAP)
[NASA-CR-185240] 20 p2939 N90-26728
Lessons learned from the T-46A durability and damage tolerance program 21 p2957 N90-26812
The effects of atomic oxygen on the thermal emittance of high temperature radiator surfaces
[NASA-TM-103224] 23 p3301 N90-28670
DURATION
U TIME
DUST
NT COSMIC DUST
NT INTERPLANETARY DUST
NT LUNAR DUST
NT ZODIACAL DUST
Diagnostic study of atmosphere-terrain interaction leading to the formation of dust clouds and poor visibilities over near east desert areas
[AD-A211243] 02 p0239 N90-11358
A study of the infrared emission of galactic supernova remnants 06 p0861 N90-15006
Hypervelocity impact studies on the Giotto comet Halley mission 06 p0862 N90-15008
Ambient flow studies and particulate collection measurements: A laminar flow, reduced entrainment electrostatic precipitator
[DE90-001457] 08 p1063 N90-16149
Workshop on Analysis of Returned Comet Nucleus Samples
[NASA-CR-184821] 08 p1140 N90-16607
On the isotope analysis of cometary dust
08 p1141 N90-16611
Laboratory analyses of micron-sized solid grains: Experimental techniques and recent results
08 p1141 N90-16616
Organic chemistry of cometary dust as derived from PUMA 1 data 08 p1143 N90-16628
Composition of dust from Comet P/Halley: The mineral fraction 08 p1144 N90-16631
The in-situ cometary particulate size distribution measured for one comet: P/Halley
08 p1145 N90-16637
Trajectory-capture cell instrumentation for measurement of dust particle mass, velocity and trajectory, and particle capture 08 p1146 N90-16644

Mechanical and SEM analysis of artificial comet nucleus samples 08 p1148 N90-16650
Refractory solids in chondrites and comets: How similar 08 p1148 N90-16654
The dynamics of dust in planetary magnetospheres 08 p1149 N90-16658
Aeolian removal of dust from photovoltaic surfaces on Mars
[NASA-TM-102507] 12 p1617 N90-19299
Mechanics of aeolian processes: Soil erosion and dust production 12 p1638 N90-19410
Comet Halley: An optical continuum study 12 p1736 N90-19981
Petrographic working model of the Rosetta sampling and modelling subgroup for a comet nucleus 12 p1738 N90-19992
Comets: Dirty snowballs or icy dirtballs 12 p1739 N90-19994
A test of the interstellar dust model of comets 12 p1739 N90-19995
Physico-chemical properties of formaldehyde-ice-dust mixtures 12 p1740 N90-20000
Cometary bodies in the circumstellar disk around beta Pictoris 12 p1741 N90-20010
Low velocity dust-dust collisions 12 p1741 N90-20011
Possible targeting of particle emission by mechanical stress and penetration of sublimating ice-dust-surfaces 12 p1742 N90-20016
Gas diffusion in a cometary crust 12 p1742 N90-20017
The composition of cometary nuclei 12 p1743 N90-20022
Large impact events and atmospheric evolution on the terrestrial planets 12 p1744 N90-20028
A theoretical study of circumstellar dust around Ae/Be stars 14 p2040 N90-21700
Photometric monitoring of early type emission line stars 15 p2184 N90-22478
The evolution of the supernova remnant IC 443 15 p2186 N90-22486
Estimation of extra drag force on a circular cylinder due to the presence of solid particles in subsonic compressible flow
[AD-A218635] 16 p2197 N90-22542
Optical properties of cometary dust
[AD-A218790] 16 p2338 N90-23325
Dust environment modelling from encounters with comet P/Halley 17 p2485 N90-24210
Design of a device to remove lunar dust from space suits for the proposed lunar base
[NASA-CR-186679] 19 p2724 N90-25496
Aeolian removal of dust from radiator surfaces on Mars
[NASA-TM-103205] 20 p2824 N90-26068
Investigation of the Saturn dust environment from the analysis of energetic charged particle measurements
[NASA-CR-186727] 20 p2950 N90-26784
Behavior of dust clouds from Australian dust storms in 1982-1983 as observed by the GMS 21 p3029 N90-27221
Dust clouds from African dust storms in 1986-1987 as observed by Meteosat 21 p3029 N90-27222
On planetary nebulae as sources of carbon dust: Infrared emission from planetary nebulae of the galactic halo 21 p3093 N90-27583
MECA Workshop on Dust on Mars 3
[NASA-CR-185065] 21 p3100 N90-27604
Generation rates and chemical compositions of waste streams in a typical crewed space habitat
[NASA-TM-102799] 22 p3233 N90-28333
Near-infrared speckle observations of T Tauri stars and a multi-wavelength study of the prototype star T Tauri 23 p3409 N90-29264
Interstellar magnetic fields: An observational perspective 24 p3560 N90-30144
Dust emission by Comet P/Halley 1982i 24 p3563 N90-30159

DUST COLLECTORS
Trajectory-capture cell instrumentation for measurement of dust particle mass, velocity and trajectory, and particle capture 08 p1146 N90-16644
Research opportunities on the Space Station 21 p3092 N90-27578

DUST STORMS
Aeolian removal of dust from photovoltaic surfaces on Mars
[NASA-TM-102507] 12 p1617 N90-19299
Meteorological Satellite Center Technical Note, no. 17, 1988
[ISSN-0388-9653] 21 p3026 N90-27213
Dust clouds Kosa from the east Asian dust storms in 1982-1988 as observed by the GMS satellite 21 p3026 N90-27214
Behavior of dust clouds from Australian dust storms in 1982-1983 as observed by the GMS 21 p3029 N90-27221
Dust clouds from African dust storms in 1986-1987 as observed by Meteosat 21 p3029 N90-27222

DWARF GALAXIES
UV observations of NGC 205
[NASA-CR-185975] 02 p0291 N90-11661
On the mass to light ratios of dwarf spheroidal galaxies
[DE90-610645] 11 p1591 N90-19175
Photometric analyses of abundances in dwarf spheroidal galaxies and globular clusters 12 p1736 N90-19978
Chemical evolution of dwarf irregular galaxies 22 p3263 N90-28478

DWARF NOVAE
Recent progress in understanding the eruptions of classical novae
[NASA-CR-186280] 07 p1014 N90-15870
IUE-ULDA access guide number 1: International Ultraviolet Explorer-Uniform Low Dispersion Archive. Dwarf novae and nova-like stars
[ESA-SP-1114] 08 p1152 N90-16672
Infrared spectroscopy of novae and related objects 11 p1583 N90-19123
The inter-outburst behavior of cataclysmic variables
[NASA-CR-186374] 13 p1902 N90-20914
The modeling of IRAS detections of classical novae and related objects 15 p2185 N90-22482
Superhumps in accretion disks 19 p2768 N90-25728

DWARF STARS
NT DWARF NOVAE
NT FLARE STARS
Magnetic fields in late-type dwarfs: Preliminary results from a multiline approach
[SER-C-PREPUB-FASC-31] 12 p1728 N90-19928
Fast spectroscopic variations on rapidly-rotating, cool dwarfs. 3: Masses of circumstellar absorbing clouds on AB Doradus
[NASA-CR-186563] 15 p2184 N90-22479

DYADICS
Scalar Green function method for microstrip antenna analysis based on the exact image theory
[PB89-218838] 04 p0488 N90-12805
Characteristic impedance of microstrip lines
[NASA-TM-101581] 05 p0633 N90-13694

DYE LASERS
Nonlinear dynamics of broad-band lasers
[DE89-017442] 02 p0228 N90-11307
Construction of a picosecond laser system for the investigation of semiconductors using nonlinear optical methods
[ETN-89-94664] 03 p0352 N90-12013
Fluorescence and elastic scattering from laser dye-filled capillaries
[AD-A217026] 11 p1484 N90-18540
Absorption experiments on electron-beam pumped rare gases
[DE90-006504] 11 p1515 N90-18722
Investigation of a simulated tritium plasma using Coherent Anti-Stokes Raman Spectroscopy (CARS)
[DE90-005696] 12 p1622 N90-19319
Blue upconversion thulium laser
[DE90-006517] 12 p1668 N90-19584
DURIP theoretical/experimental investigations of highly energetic dication species
[AD-A217771] 13 p1808 N90-20383
Picosecond Laser Facility
[AD-A217784] 13 p1808 N90-20384
The receiving system of a dual dye lidar to study molecular and aerosol densities at the base of the stratosphere
[AD-A218286] 13 p1843 N90-20581
Dynamics and instabilities in homogeneously broadened lasers
[AD-A218427] 16 p2241 N90-22786
Theoretical studies of solar pumped lasers
[NASA-CR-186712] 20 p2867 N90-26308
Characterization of a high-intensity, subpicosecond XeCl laser system
[DE90-011970] 20 p2867 N90-26310
Intracavity Dye-Laser Absorption Spectroscopy (IDLAS) for application to planetary molecules 20 p2945 N90-26761
High pulse energy flashlamp pumpable laser dyes
[AD-A223075] 22 p3180 N90-28042
Titanium-doped sapphire lasers with high energy pumping
[RSRE-MEMO-4290] 22 p3181 N90-28050
Chemical stabilization of laser dyes
[AD-A224219] 24 p3473 N90-29627
Pyrromethene-BF2 complexes as laser dyes
[AD-A223562] 24 p3473 N90-29631
Study of a 1-Hz hypocycloidal pinch (HCP) pump for production of ultraviolet lasers
[AD-A224091] 24 p3547 N90-30064

DYES
Flow visualization techniques for flight research 02 p0153 N90-10878
Photochromic papers or films for noncopyable documents
[DE90-004006] 10 p1441 N90-18316
A simple model for amplified spontaneous emission in dyes
[DE90-007249] 11 p1516 N90-18730
Diffusion of penetrants in polymers
[AD-A223217] 21 p2986 N90-26969
Chemical stabilization of laser dyes
[AD-A224219] 24 p3473 N90-29627

DYNAMIC CHARACTERISTICS
NT AERODYNAMIC DRAG
NT AERODYNAMIC STABILITY
NT AIRCRAFT STABILITY
NT ATTITUDE STABILITY
NT BOUNDARY LAYER STABILITY
NT COMBUSTION STABILITY
NT CONTROL STABILITY
NT DIRECTIONAL STABILITY
NT DRAG
NT DYNAMIC PRESSURE
NT DYNAMIC STABILITY
NT FLAME STABILITY
NT FLOW CHARACTERISTICS
NT FLOW DISTRIBUTION
NT FLOW STABILITY
NT FLOW VELOCITY
NT FREQUENCY STABILITY
NT FRICTION DRAG
NT GYROSCOPIC STABILITY
NT HOVERING STABILITY
NT INTERFERENCE DRAG
NT LATERAL STABILITY
NT LIFT
NT LONGITUDINAL STABILITY
NT LOW SPEED STABILITY
NT MAGNETOHYDRODYNAMIC STABILITY
NT MINIMUM DRAG
NT MOTION STABILITY
NT PRESSURE DRAG
NT ROTARY STABILITY
NT SATELLITE DRAG
NT SOLAR WIND VELOCITY
NT SPACECRAFT STABILITY
NT SUPERSONIC DRAG
NT TRANSIENT RESPONSE
NT VISCOUS DRAG
NT WAVE DRAG
NT ZERO LIFT
Prediction of dynamic derivatives 01 p0012 N90-10055
Summarizing qualitative behavior from measurements of nonlinear circuits, revision
[AD-A210919] 01 p0061 N90-10353
Analysis of spurt phenomena for a non-Newtonian fluid
[AD-A210560] 01 p0071 N90-10405
Solvent dynamical effects in electron transfer: Predicted influences of electron coupling upon the rate-dielectric friction dependence
[AD-A210193] 01 p0120 N90-10690
A review of the Error of Matrix Method (EMM) for structural dynamic model comparison 02 p0177 N90-10993
Dynamic characteristics concerned in the design of a free-piston Stirling engine/magnetic coupling/compressor system
[DE89-015981] 02 p0230 N90-11317
Stochastic optimization by simulation: Some experiments with a simple steady-state queue
[AD-A210762] 02 p0265 N90-11508
Markov processes in Hilbert space and continuous spontaneous localization of systems of identical particles
[DE89-618396] 02 p0270 N90-11540
Molecular dynamics study of the primitive model of 1-3 electrolyte studies
[AD-A211653] 03 p0325 N90-11846
Analysis and simulation of dynamics of spacecraft power systems 04 p0463 N90-12653
Choice of a differential method for the attitude restitution in dynamic unbalance
[CNES-CT/DTI/MS/CM/290] 05 p0613 N90-13582
Design of a power component with IGBT insulated grid. Static and dynamic study
[ECL-88-22] 05 p0636 N90-13710
Identification of equivalent modulus of a composite beam from nonmodal vibratory tests
[ECL-89-001] 05 p0656 N90-13821
The DYANA campaign 1990 05 p0662 N90-13870

Non-linear vibrations, stability, and dynamics of structures and mechanisms
[AD-A212152] 06 p0796 N90-14639
Theoretical methods for the study of chemical dynamics
[DE90-003122] 07 p0893 N90-15160
Base reaction optimization of redundant manipulators for space applications
[NASA-CR-186274] 07 p0941 N90-15447
Spatial dynamics of deformable multibody systems with variable kinematic structure
[AD-A214098] 07 p0942 N90-15455
Further research on dynamics of marine atmospheres in tropical cyclones
[AD-A213882] 07 p0964 N90-15571
Vision in dynamic environments
[AD-A213434] 07 p0967 N90-15587
Hierarchical process composition: Dynamic maintenance of structure in a distributed environment
[AD-A214325] 07 p0978 N90-15648
The use of hypervelocity launchers to explore previously inaccessible states of matter
[DE90-004088] 08 p1034 N90-15973
Performance predictions for an intermediate-sized VAWT based on performance of the 34-m VAWT test bed
[DE90-002835] 08 p1096 N90-16345
Continuous spontaneous reduction model involving gravity
[DE90-600730] 08 p1135 N90-16573
Gasdynamic phenomena in nuclear-reactor-pumped lasers
[DE90-005428] 09 p1229 N90-17131
Dynamic modeling of flexible bodies in multibody systems 09 p1229 N90-17134
Chaos and turbulence
[AD-A215310] 09 p1294 N90-17499
A new vision to model the parallel resonant converter 10 p1336 N90-17727
Analysis of the behaviour of a current-fed multi-stage voltage multiplier with capacitive output 10 p1338 N90-17745
Dynamics of column stability with partial end restraints
[NASA-TM-101651] 10 p1396 N90-18069
Proceedings of a research workshop on Nonlinear Time Series Analysis and Applications
[AD-A216541] 10 p1423 N90-18214
Molecular dynamics simulation of sedimentation using the monotonic Lagrangian grid
[AD-A215099] 10 p1427 N90-18236
Model filled polymers 3. Rheological behavior of polystyrene containing crosslinked polystyrene beads
[AD-A215867] 11 p1489 N90-18567
Study of the dynamical behavior of copper in a shock wave
[ISL-R-123/88] 11 p1507 N90-18679
The dynamics of electrons in very intense lasers
[DE90-007246] 11 p1516 N90-18729
Kinetic relations and the propagation of phase boundaries in solids
[AD-A215881] 11 p1519 N90-18747
System theory and mechanics
[MEMO-807] 11 p1550 N90-18922
Leading edge vortex dynamics on a pitching delta wing
[NASA-CR-186327] 12 p1598 N90-19198
Compensating for pneumatic distortion in pressure sensing devices
[NASA-TM-101716] 12 p1603 N90-19224
Performance of an optimized rotor blade at off-design flight conditions
[NASA-CR-4288] 12 p1603 N90-19226
Low-speed wind-tunnel investigation of the flight dynamic characteristics of an advanced turboprop business/commuter aircraft configuration
[NASA-TP-2982] 12 p1606 N90-19239
DURIP FTIR studies of solid state reaction dynamics
[AD-A217713] 13 p1773 N90-20174
Y1Ba2Cu3O(7-x) laser-ablation plume dynamics measurement by nanosecond response ion probe: Comparison with optical measurements
[DE90-007658] 13 p1807 N90-20375
An applicational process for dynamic balancing of turbomachinery shafting
[NASA-TM-102537] 13 p1810 N90-20392
Plan, formulate, and discuss a NASTRAN finite element model of the UH-60A helicopter airframe
[NASA-CR-181975] 13 p1818 N90-20439
Coastal frontogenesis and associated severe weather on 13 March 1986 (GALE IOP 13)
[AD-A217708] 13 p1845 N90-20590
Correlation of AVHRR imagery with sub-surface features in California current
[AD-A218184] 13 p1848 N90-20607
Implementation of a control system test environment in UNIX
[DE90-007485] 13 p1872 N90-20736
Dynamics of electronically excited species in gaseous and condensed phase
[AD-A217696] 13 p1884 N90-20812
Development of a dynamic modeling technique and its application to the analysis and control of a high-precision robotic manipulator 14 p1987 N90-21391
Modeling large-scale vegetation dynamics
[DE90-008883] 14 p2004 N90-21485
Towards a unified analysis methodology for composite rotor blades 15 p2046 N90-21730
Severe shock and vibration environments for electronic components
[DE90-007686] 15 p2117 N90-22113
Dynamics of an oscillator with three-degrees-of-freedom in a uniform windfield
[REPT-89-56] 15 p2119 N90-22121
Dynamic and microphysical characteristics of cirrus clouds as revealed by aircraft, lidar, and other observations during FIRE 15 p2130 N90-22177
Characteristics of cumulus bandclouds off the east coast of Hawaii 15 p2130 N90-22178
A galaxy formation cookbook: Recipes and utensils 15 p2190 N90-22508
Femtosecond studies of electron photodetachment of simple ions in liquid water: Solvation and geminate recombination dynamics
[AD-A218520] 16 p2215 N90-22634
Application of numerical optimization techniques to control system design for nonlinear dynamic models of aircraft 16 p2287 N90-23032
Combined effect of isotopic substitution, temperature, and magnetic field on the lifetimes of triplet biradicals
[AD-A219711] 17 p2372 N90-23509
Informal conference on the Chemistry of Energetic Azides, Isocyanates, and Related Species
[AD-A219825] 17 p2373 N90-23514
High frequency, high temperature specific core loss and dynamic B-H hysteresis loop characteristics of soft magnetic alloys
[NASA-TM-103164] 17 p2398 N90-23663
Non-linear dynamic analysis of geared systems, part 2
[NASA-CR-180495] 17 p2410 N90-23732
Diagnosis of auroral dynamics using global auroral imaging with emphasis on large-scale evolutions
[NASA-CR-186623] 17 p2422 N90-23804
Bit-optimal election in synchronous rings
[RUU-CS-89-2] 17 p2446 N90-23945
Sharing memory robustly in message-passing systems
[AD-A219923] 17 p2447 N90-23950
Investigation of the effect of mechanical stress on cold fusion
[AD-A220123] 17 p2474 N90-24147
Investigations on docking and berthing dynamics 18 p2504 N90-24312
Docking berthing systems: Functions and simulation 18 p2505 N90-24313
Equivalent flexibility modeling: A novel approach towards recursive simulation of flexible spacecraft manipulator dynamics 18 p2505 N90-24316
Dynamics and control of free-flying inspection and maintenance vehicle with manipulators 18 p2508 N90-24332
Damping associated with incipient melting in aluminum-indium alloys
[AD-A220241] 18 p2525 N90-24412
Dynamics of bulk and surface-adsorbed polyacrylates
[AD-A221046] 18 p2530 N90-24437
IR transition moments and collisional dynamics of vibrationally excited OH radicals via time-resolved laser absorption spectroscopy
[AD-A221005] 18 p2580 N90-24696
The low-speed wind tunnel at DFVLR in Brunswick (status 1988)
[ESA-TT-1163] 19 p2662 N90-25152
Behavior of composite/metal aircraft structural elements and components under crash type loads: What are they telling us
[NASA-TM-102681] 19 p2701 N90-25368
Chemical structure and kinetics at liquid/solid interfaces
[AD-A222766] 20 p2831 N90-26105
Flow visualization of dynamic stall on an oscillating airfoil
[AD-A222202] 21 p2954 N90-26797
Molecular dynamics of physical aging processes in polymer glasses (experiment and theory)
[AD-A222848] 21 p2984 N90-26959
Dynamic properties of porous B4C
[AD-A222850] 21 p2985 N90-26960
Noise adaptation and correlated maneuver gating of an extended Kalman filter
[AD-A221713] 21 p3001 N90-27060
Maintenance of a minimum spanning forest in a dynamic planar graph
[AD-A221425] 21 p3054 N90-27362
A new method for a tethered system aided space station assembly 22 p3130 N90-27765
The dynamics of orbital maneuvering: Design and evaluation of a visual display aid for human controllers 22 p3131 N90-27767
Study of the origin of three dimensional structures in shear flows through external forcing
[AD-A221923] 22 p3170 N90-27980
Dynamics of multistage gear transmission with effects of gearbox vibrations
[NASA-TM-103109] 22 p3182 N90-28060
Analysis of ER-2 radiometer and lidar observations from the 1987 marine stratus experiment 22 p3216 N90-28241
The effects of foreplanes on the static and dynamic characteristics of a combat aircraft model 23 p3273 N90-28520
Crash-impact behavior of graphite/epoxy composite sine wave webs 23 p3300 N90-28667
Static and dynamic characterization of the ATR 72 rods made of Ti 10.2.3 titanium alloy
[REPT-49-238] 23 p3310 N90-28722
Mode competition in the quasioptical gyrotron
[AD-A222181] 23 p3329 N90-28823
Dynamic interaction of multiple autonomous mobile robots 23 p3333 N90-28844
Dynamical properties of two-dimensional Josephson junction arrays
[AD-A223965] 23 p3402 N90-29221
Chemical kinetic and aerodynamic structures of flames
[AD-A224281] 24 p3445 N90-29455
Thermal imaging assessment
[AD-A224400] 24 p3460 N90-29542
Reynolds stress and the physics of turbulent momentum transport
[AD-A224172] 24 p3467 N90-29588
Modeling towed cable system dynamics
[AD-A223610] 24 p3476 N90-29644
Studies of ionospheric dynamics utilizing data from DMSP
[AD-A223370] 24 p3492 N90-29733

DYNAMIC CONTROL

Analysis of flight data from a High-Incidence Research Model by system identification methods
[NASA-TP-2940] 01 p0015 N90-10074
Viscoelastic tuned dampers for control of structural dynamics 02 p0178 N90-10999
Adaptive control law design for model uncertainty compensation
[AD-A211712] 03 p0309 N90-11758
Robot inverse dynamics computation via VLSI distributed architectures
[RR-350] 03 p0390 N90-12223
Path expression based operating systems
[MEMO-INF-88-68] 04 p0536 N90-13097
Remarks on the control of discrete time nonlinear systems
[MEMO-770] 04 p0544 N90-13158
Using the physical structure of a system for control: An illustration
[MEMO-782] 05 p0689 N90-14014
Optimal stochastic modeling and control of flexible structures
[AD-A212347] 06 p0733 N90-14269
Gaze controls with interactions and delays
[AD-A214286] 07 p0981 N90-15667
Power system modeling for a six legged walking vehicle 09 p1221 N90-17083
CHIMERA 2: A real-time UNIX-compatible multiprocessor operating system for sensor-based control applications
[AD-A215958] 10 p1392 N90-18051
Optimization of sensors and actuators positioning aimed at obtaining reduced models for the synthesis of optimal control regulators of flexible structures
[INPE-4760-TDL/348] 11 p1468 N90-18450
Energy decay and boundary control for distributed parameter systems with viscoelastic damping
[AD-A216468] 11 p1519 N90-18748
Advanced topics in structural dynamics: The maneuver of flexible spacecraft, and on-off decentralized control of flexible structures 12 p1612 N90-19274
Kinematic control of robotic manipulators with multiple interchangeable wrists 12 p1670 N90-19592
Discrete-time control of a spacecraft with retargetable flexible antennas 13 p1763 N90-20119
Aiming control: Theory and applications to dynamic control of space structures
[AD-A217877] 13 p1764 N90-20123
Dynamic damping control: Implementation issues and simulation results
[DE90-007687] 13 p1812 N90-20403

Sensor and actuator selection for fault-tolerant control of flexible structures
[AD-A217384] 13 p1817 N90-20433
Robust planning and control using neural networks
[AD-A217216] 13 p1872 N90-20732
Controlled multibody dynamics simulation for large space structures 14 p1934 N90-21068
End point control of flexible manipulators
[AD-A217319] 14 p1986 N90-21383
Integrated modeling and analysis of a space-truss article
[NASA-TM-102615] 14 p1991 N90-21412
Robust control of flexible structures
15 p2058 N90-21784
Dynamics and control of tethered antennas/reflectors in orbit
[AD-A219316] 16 p2207 N90-22594
Robust control of vibration in flexible structures
16 p2241 N90-22787
An innovations approach to decoupling of multibody dynamics and control 16 p2280 N90-22994
Frequency response modeling and control of flexible structures: Computational methods
16 p2285 N90-23021
Controlling flexible structures with second order actuator dynamics 16 p2297 N90-23083
Nonlinear dynamics and control of flexible structures
[AD-A218372] 17 p2386 N90-23586
Nonlinear dynamics and control of flexible structures
[AD-A218476] 17 p2386 N90-23589
Timing optimization of multi-phase sequential logic
[AD-A220836] 17 p2397 N90-23656
Statistical techniques for designing a decoupled controller to be robust to model and sensor noise
[AD-A220476] 17 p2412 N90-23745
Adaptive control methods for mechanical manipulators: A comparative study
[AD-A219965] 17 p2413 N90-23749
Self-calibrating apparatus to find dynamic compressibility of organic solids
[AD-A219780] 17 p2415 N90-23763
Rate-based congestion control in networks with smart links, revision
[NASA-CR-186698] 17 p2452 N90-23987
A three fingered multijointed gripper as a working tool for experimental use 18 p2507 N90-24329
Models of intracavity frequency doubled lasers
[AD-A221182] 18 p2563 N90-24628
Dynamic optimisation of thermal energy systems
[ETN-90-96900] 18 p2576 N90-24676
Dynamic analysis of space-related linear and non-linear structures
[NASA-TM-103490] 19 p2667 N90-25174
An inverse dynamic method yielding flexible manipulator state trajectories
[NASA-CR-186807] 20 p2870 N90-26329
On controller choice for robust sliding mode performance
[MATHS-REPT-A-107] 20 p2872 N90-26337
Dallas/Fort Worth simulation, volume 1
[DOT/FAA/CT-TN89/28-VOL-1]
21 p2955 N90-26802
Aiming control: Theory and applications to dynamic control of space structures
[AD-A221532] 21 p2967 N90-26864
Robot dynamics in reduced gravity environment
21 p3049 N90-27333
Nonlinear dynamics and control of SDI structural components
[AD-A222472] 21 p3071 N90-27458
Flexible structure control and rigid body dynamics
22 p3129 N90-27757
Dynamic modeling and payload-adaptation control of a flexible one-link manipulator 23 p3333 N90-28843
Experiments in the dynamic and strategic control of cooperating manipulators 23 p3333 N90-28845
Dynamic separation: Search for the cause of dynamic stall and search for its control
[AD-A223412] 24 p3418 N90-29305
Tip-position control of a flexible beam: Modeling approaches and experimental verification
[AD-A224249] 24 p3476 N90-29643
Proceedings of Damping '89. Volume 3: Pages ICA-1 through KDC-15
[AD-A223433] 24 p3479 N90-29666
Modeling, design, and control of flexible manipulator arms: Status and trends 24 p3500 N90-29782
Experiments in cooperative manipulation: A system perspective 24 p3505 N90-29812
Construction and demonstration of a 9-string 6 DOF force reflecting joystick for telerobotics
24 p3509 N90-29836
Response to reflected-force feedback to fingers in teleoperations 24 p3509 N90-29837
The JAU-JPL anthropomorphic telerobot
24 p3509 N90-29838
Performance limitations of bilateral force reflection imposed by operator dynamic characteristics
24 p3510 N90-29840
The 3-D vision system integrated dexterous hand
24 p3511 N90-29850
Linear analysis of a force reflective teleoperator
24 p3513 N90-29856
Real-time cartesian force feedback control of a teleoperated robot 24 p3513 N90-29857
Optimal payload rate limit algorithm for zero-G manipulators 24 p3513 N90-29858
Recursive multibody dynamics and discrete-time optimal control 24 p3513 N90-29860
Kinematics and control algorithm development and simulation for a redundant two-arm robotic manipulator system 24 p3516 N90-29877
A control approach for robots with flexible links and rigid end-effectors 24 p3516 N90-29879
Preshaping command inputs to reduce telerobotic system oscillations 24 p3517 N90-29880
Teleoperation experiments with a Utah/MIT hand and a VPL DataGlove 24 p3517 N90-29883
An alternative control structure for telerobotics
24 p3518 N90-29889
On discrete control of nonlinear systems with applications to robotics 24 p3519 N90-29893
Experimental study on two-dimensional free-flying robot satellite model 24 p3519 N90-29896
Computed torque control of a free-flying cooperating-arm robot 24 p3520 N90-29898
Computer-aided engineering environment for controlled mechanical systems
[AD-A223551] 24 p3527 N90-29942

DYNAMIC LOADS
NT AERODYNAMIC LOADS
NT BLAST LOADS
NT CONTACT LOADS
NT CYCLIC LOADS
NT GUST LOADS
NT IMPACT LOADS
NT ROLLING CONTACT LOADS
NT SHOCK LOADS
NT THRUST LOADS
NT TRANSIENT LOADS
NT VIBRATORY LOADS
NT WING LOADING
Two stage gear tooth dynamics program
[NASA-CR-185110] 01 p0077 N90-10437
Integration of analytical and test software for optimal structural design under dynamic loads
02 p0179 N90-11007
The dynamic stability of an axially loaded beam with lateral elastic support and damping
02 p0232 N90-11331
Flight motor set 360L001 (STS-26R). (Reconstructed dynamic loads analysis)
[NASA-CR-183811] 04 p0484 N90-12656
SSME LOX post flow analysis/fluid structure interaction. Volume 1: Flow analysis
[NASA-CR-183677] 05 p0637 N90-13715
Elasticity effects on cavitation in a squeeze film damper undergoing noncentered circular whirl
[NASA-TM-102392] 05 p0649 N90-13786
Comparison of analytical methods for calculation of wind loads
[NASA-TM-102782] 05 p0654 N90-13813
Critical time step estimation for three-dimensional explicit impact analysis
[DE90-002187] 06 p0801 N90-14662
Survey of adaptive control theory and its applications
[DE89-901270] 06 p0833 N90-14840
Investigation of loads generated by temperature transients in pipes
[DE89-636433] 07 p0932 N90-15395
Location of interior impact source in randomly excited structures
[DE90-001092] 07 p0945 N90-15474
Prediction of stochastic blade loads for three-bladed, rigid-hub rotors
[DE89-009508] 07 p0954 N90-15520
High-order mixture homogenization of fiber-reinforced composites
[AD-A215247] 09 p1187 N90-16876
Boundary walls, fences and hoardings: Mean and peak wind loads and overturning moments
[ESDU-89050] 09 p1239 N90-17190
Response of structures to atmospheric turbulence. Response to across-wind turbulence components
[ESDU-89049] 09 p1239 N90-17191
Analysis of biaxial stress fields in plates cracking at elevated temperatures
[AD-A216271] 10 p1397 N90-18077
Vertical axis wind turbine turbulent response model. Part 2: Response of Sandia National laboratories' 34-meter VAWT with aeroelastic effects
[DE90-005721] 11 p1529 N90-18804
Influence of friction and separation phenomena on the dynamic blade loading of transonic turbine cascades
[MITT-88-04] 12 p1605 N90-19235
Tensile fracture toughness of ceramic materials: Effects of dynamic loading and elevated temperatures
[DE90-008329] 13 p1781 N90-20223
Fatigue crack growth from narrow-band Gaussian spectrum loading in 6063 aluminum alloy
[DE90-008957] 14 p1952 N90-21173
Fracture toughness and crack growth of Zerodur
[NASA-TM-4185] 14 p1954 N90-21187
A numerical model for the determination of periodic solutions of pipes subjected to non-conservative loads
[DE90-614756] 14 p1993 N90-21423
Progression of damage and fracture in composites under dynamic loading
[NASA-TM-103118] 15 p2065 N90-21825
Practical nonlinear simulation of rotating machinery dynamics with application to turbine blade rubbing
15 p2104 N90-22038
Influence of linear profile modification and loading conditions on the dynamic tooth load and stress of high contact ratio gears
[NASA-TM-103136] 16 p2243 N90-22796
Theoretical analysis and pressure distribution of thin-walled metal inverbuckle energy absorbing tubes
17 p2414 N90-23758
Analysis of shell-type structures subjected to time-dependent mechanical and thermal loading
[NASA-CR-185077] 18 p2571 N90-24653
Scaling effects in the static and dynamic response of graphite-epoxy beam-columns
[NASA-TM-102697] 20 p2876 N90-26363

DYNAMIC MODELS
GEMMES: A new tool for dynamic modeling
02 p0179 N90-11005
A direct two response approach for updating analytical dynamic models of structures with emphasis on uniqueness 02 p0182 N90-11028
Adaptive control law design for model uncertainty compensation
[AD-A211712] 03 p0309 N90-11758
Dynamic robot models using the Manutec r3 as an example
[ESA-TT-1132] 04 p0458 N90-12626
Analysis of high speed pneumatic actuation systems under rotary directional on-off flow control
04 p0507 N90-12926
Fundamentals of middle atmospheric dynamics
[AD-A211747] 04 p0518 N90-12988
Extended performability modeling using dynamic queing networks
[MEMO-INF-89-15] 04 p0536 N90-13099
Unified model of charge build up and annealing of oxide charge and interface states in SiO2 due to stress
[HMI-B-465] 05 p0704 N90-14120
AcSim: Aircraft simulation program with application to flight profile generation
[AD-A212466] 06 p0723 N90-14217
Wind shear models for aircraft hazard investigation
07 p0869 N90-15044
Adaptive control of helicopter vibrations via the impulse response method
[AD-A213728] 07 p0883 N90-15113
Ductile failure
[AD-A213864] 07 p0948 N90-15488
Theoretical models of earthquake phenomena and the physical significance of seismic moment tensor expansions
[AD-A213813] 07 p0961 N90-15556
Investigation of liquid sloshing in spin-stabilized satellites
[AD-A214730] 09 p1182 N90-16853
Formulation and verification of a technique for compensation of pneumatic attenuation errors in airborne pressure sensing devices 09 p1221 N90-17084
Traction modeling of military lubricants
[AD-A213866] 09 p1230 N90-17139
Fire science and aircraft safety
10 p1314 N90-17596
Dynamical model of series-resonant converter with peak capacitor voltage predictor and switching frequency control 10 p1336 N90-17730
Linear and non-linear control of high-order converters after reducing the order by appropriate techniques
10 p1336 N90-17733
State variable modelling for the audiosusceptibility evaluations of current controlled zero ripple structures
10 p1337 N90-17735
Analysis of the CUK converter in delta V mode by charge and flux balances 10 p1337 N90-17738
Modelling the buck-type converter transient response with pulsating load 10 p1337 N90-17740
Time and frequency-domain identification and verification of BO-105 dynamic models
[AD-A216828] 11 p1456 N90-18389

Autonomous orbit determination using GPS
[INPE-4815-TDL/361] 11 p1466 N90-18442
Attitude estimation procedure for spin stabilized satellites
[INPE-4866-TDL/377] 11 p1467 N90-18449
Cold flow determination of the internal flow environment around the submerged TVC nozzle for the space shuttle SRM 11 p1470 N90-18465
A global approach for the identification of structural connection properties
[NASA-TM-102502] 11 p1518 N90-18745
Dynamics of an ERICA (Experiment on Rapidly Intensifying Cyclones over the Atlantic) cyclone
[AD-A216775] 11 p1536 N90-18846
Feasibility of using Extreme Ultraviolet Explorer (EUVE) reaction wheels to satisfy Space Infrared Telescope Facility (SIRTF) maneuver requirements
[NASA-TM-100389] 12 p1663 N90-19556
Modelling of molecular structures and properties in physical chemistry and biophysics
[AD-A214561] 14 p1947 N90-21145
Development of a dynamic modeling technique and its application to the analysis and control of a high-precision robotic manipulator 14 p1987 N90-21391
Perturbation techniques in the dynamics and control of flexible manipulators
[OUEL-1772/89] 15 p2107 N90-22053
Pseudo-steady diffusional growth or collapse of bubbles rising in time dependent pressure fields
[AD-A218825] 16 p2237 N90-22764
Plan execution control and architecture for mobile robots
[LAAS-89-371] 16 p2243 N90-22793
Experimental verification of dynamic simulation 16 p2285 N90-23020
Approximate minimum-time trajectories for 2-link flexible manipulators 16 p2287 N90-23030
Application of numerical optimization techniques to control system design for nonlinear dynamic models of aircraft 16 p2287 N90-23032
Modeling and control of flexible space stations (slew maneuvers) 16 p2297 N90-23086
A homing missile guidance law based on new target maneuver models
[AD-A220392] 17 p2356 N90-23410
A passive homing missile guidance law based on new target maneuver models
[AD-A220419] 17 p2356 N90-23411
Nonlinear dynamics and control of flexible structures
[AD-A218372] 17 p2386 N90-23588
Nonlinear dynamics and control of flexible structures
[AD-A218476] 17 p2386 N90-23589
Non-linear dynamic analysis of geared systems, part 2
[NASA-CR-180495] 17 p2410 N90-23732
Effect of constitutive modeling on the dynamic development of shear bands in viscoplastic materials
[AD-A220443] 17 p2416 N90-23765
Application of the lagged-averaged technique to tropical cyclone track predictions
[AD-A218389] 17 p2425 N90-23819
Dynamic constraints networks
[AD-A219778] 17 p2457 N90-24018
Applications of dynamical systems theory to fractals: A study of cookie-cutter Cantor sets
[REPT-89-76] 17 p2458 N90-24032
Eigenvalues of dynamic max-min systems
[REPT-89-84] 17 p2465 N90-24088
Dynamic modeling and control of a flexible arm holding a non-rigid payload 18 p2507 N90-24331
Dynamic and photometric evolutionary models of tidal tails and ripples 18 p2637 N90-25024
Convex models of malfunction diagnosis in high performance aircraft
[AD-A218514] 19 p2649 N90-25073
Conceptual task modeling
[TR-89-14] 19 p2762 N90-25693
The conceptual task model: A specification technique between requirements engineering and program development
[TR-89-15] 19 p2762 N90-25694
Research at NASA's NFAC wind tunnels
[NASA-TM-102827] 20 p2801 N90-25933
Formation of design envelope criterion in terms of deterministic spectral procedure
[RAE-TM-SS-9] 20 p2804 N90-25953
A reduced-dynamic technique for precise orbit determination 20 p2852 N90-26219
A model of the synchronous machine with rectifier, especially for control purposes
[EUT-89-E-215] 20 p2858 N90-26256
Method and apparatus for configuration control of redundant robots
[NASA-CASE-NPO-17801-1-CU] 21 p3010 N90-27110
Construction of dynamic stochastic simulation models using knowledge-based techniques 21 p3047 N90-27322
United States Air Force research initiation program for 1988, volume 1
[AD-A223123] 21 p3101 N90-27613
A new method for a tethered system aided space station assembly 22 p3130 N90-27765
Investigation of the techniques for the analysis of composite structures: Analysis and representation of the static and dynamic behavior of glued metal insert assemblies
[IMFL-89-44] 22 p3153 N90-27878
A flight dynamic model of aircraft spinning
[AR-005-600] 23 p3283 N90-28576
On the application of similarity laws to a scaled railway bogie model
[DLR-FB-90-06] 23 p3335 N90-28853
Time, space and form in vision
[AD-A213889] 23 p3357 N90-28971
A new approach to global control of redundant manipulators 23 p3363 N90-29002
State estimation for systems moving through random fields 24 p3429 N90-29373
Nonlinear static and dynamic modeling of composite rotor blades including warping effects 24 p3431 N90-29382
Experimental study on the dynamic behavior of a revolving blade grill
[REPT-NT-89-CC-18] 24 p3470 N90-29604
Tip-position control of a flexible beam: Modeling approaches and experimental verification
[AD-A224249] 24 p3476 N90-29643
A vector diagram approach to shaping inputs for vibration reduction
[AD-A223724] 24 p3480 N90-29671
Manipulators with flexible links: A simple model and experiments 24 p3501 N90-29786
Direct adaptive control of a PUMA 560 industrial robot 24 p3508 N90-29832
Performance limitations of bilateral force reflection imposed by operator dynamic characteristics 24 p3510 N90-29840
Preshaping command inputs to reduce telerobotic system oscillations 24 p3517 N90-29880
Multi-level manual and autonomous control superposition for intelligent telerobot 24 p3518 N90-29888
Symmetry and island structure of the standard map
[DE90-508076] 24 p3548 N90-30069

DYNAMIC PRESSURE
Determination of dynamic surface forces using piezoelectric arrays 08 p1080 N90-16249
A comparison of scramjet engine performances of various cycles
[NAL-TR-1042] 24 p3434 N90-29397
Analysis of scramjet engine characteristics
[NAL-TR-1041] 24 p3434 N90-29398

DYNAMIC PROGRAMMING
A survey of performability modelling tools
[MEMO-INF-89-50] 11 p1547 N90-18907
Using dynamic queueing networks as a tool for specifying performability models
[MEMO-INF-89-51] 11 p1554 N90-18949
Contribution to the study of stability robustness of nonlinear multivariable regulators
[INPE-4801-TDL/356] 11 p1554 N90-18950
Orbital maneuvers optimization for station acquisition of geostationary satellites. Deterministic and stochastic approaches
[LAAS-89-359] 16 p2206 N90-22589
Parallel and vector computation for stochastic optimal control applications 16 p2282 N90-23007
An algorithm for the solution of dynamic linear programs 16 p2286 N90-23026
Overcoming the Bellman's curse of dimensionality in large optimization problems
[NASA-TM-102662] 17 p2352 N90-23391
Guided boundary detection in a digital image using dynamic programming
[ETN-90-96688] 17 p2419 N90-23782
On linear time minor tests and depth first search
[RUU-CS-89-1] 17 p2446 N90-23944
Finding minimum area k-gons
[RUU-CS-89-7] 17 p2449 N90-23967
Minimum loss scheduling
[MEMO-821] 18 p2600 N90-24796
Stochastic dynamic programming for reservoir optimal control: Dense discretization and inflow correlation assumption made possible by parallel computing
[REPT-89-056] 22 p3238 N90-28360
Parallelisation of a dynamic programming algorithm suitable for feature detection
[RSRE-MEMO-4349] 22 p3241 N90-28377
Robot Acting on Moving Bodies (RAMBO): Interaction with tumbling objects 23 p3366 N90-29022

DYNAMIC PROPERTIES
U DYNAMIC CHARACTERISTICS

DYNAMIC RESPONSE
NT TRANSIENT RESPONSE
Analysis of spurt phenomena for a non-Newtonian fluid
[AD-A210560] 01 p0071 N90-10405
Design guide for predicting nonlinear random response (including snap-through) of buckled plates
[NASA-CR-181877] 01 p0118 N90-10681
Frequency domain design of robust controllers for space structures
[AD-A211172] 02 p0176 N90-10985
Reduction of dynamic response of spacecraft structures and payloads 02 p0178 N90-11000
Rotor blade dynamic design 04 p0451 N90-12583
The Shock and Vibration Digest, volume 21, no. 10 04 p0483 N90-12771
A survey on nonproportional damping 04 p0483 N90-12773
Pyrotechnic shock structural response 04 p0483 N90-12774
A recursive algorithm for computing the frequency response of a class of nonlinear difference equation models
[RR-354] 04 p0539 N90-13123
Probabilistic finite element analysis of dynamic structural response
[AD-A213249] 05 p0650 N90-13789
Manipulation strategies for massive space payloads
[NASA-CR-186081] 06 p0728 N90-14247
A surface coupled flamelet approach to dynamic response in heterogeneous propellant combustion 06 p0739 N90-14302
Stability and dynamics of constrained flexible multibody systems 06 p0791 N90-14609
Structural dynamics division research and technology accomplishments for FY 1989 and plans for FY 1990
[NASA-TM-101683] 08 p1019 N90-15894
Interdisciplinary research in viscoelasticity and rheology
[AD-A213630] 08 p1063 N90-16145
Restoring force method and response estimation
[DE90-002394] 08 p1116 N90-16463
Taylor impact testing
[AD-A215018] 09 p1231 N90-17144
Wind-excited behavior of structures, 5 09 p1235 N90-17169
Techniques for analyzing the dynamic response of structural systems using computer-derived Green's functions
[AD-A214523] 09 p1237 N90-17181
Boundary walls, fences and hoardings: Mean and peak wind loads and overturning moments
[ESDU-89050] 09 p1239 N90-17190
Response of structures to atmospheric turbulence. Response to across-wind turbulence components
[ESDU-89049] 09 p1239 N90-17191
Dynamic response for thermal control and measurement and fast radiation thermometry 10 p1367 N90-17924
Hydride heat pumps for upgrading spacecraft waste heat 10 p1385 N90-18013
Baseline experiment for active control of structural vibrations
[AD-A216194] 10 p1397 N90-18076
Reliability assessment using finite element techniques
[AD-A216907] 11 p1502 N90-18647
System properties from frequency response functions, part 1
[ISVR-TR-166-PT-1] 11 p1520 N90-18754
Advanced topics in structural dynamics: The maneuver of flexible spacecraft, and on-off decentralized control of flexible structures 12 p1612 N90-19274
Application of attachment modes in the control of large space structures
[NASA-CR-185604] 12 p1613 N90-19280
Applications of frequency and wavenumber nonlinear digital signal processing to nonlinear hydrodynamics research
[AD-A216259] 12 p1658 N90-19530
Study of the optimization of reference parameters to the dynamic constraints of solar panels
[INPE-4793-TDL/355] 12 p1681 N90-19656
Modal interactions in shell dynamics 13 p1814 N90-20418
Experimental aeroelasticity history, status and future in brief
[NASA-TM-102651] 14 p1930 N90-21047
Nonlinear and distributed parameter models of the mini-mast truss 14 p1934 N90-21070
Controller reduction for effective interdisciplinary design of active structures 14 p1935 N90-21077
The effect of elastic boundary conditions on the dynamic response of rectangular plates
[NASA-CR-186059] 14 p1990 N90-21405

Development and application of a generalized dynamic wake theory for lifting rotors 15 p2046 N90-21731
Natural modes of cracked beams and identification of cracks 15 p2111 N90-22075
Dynamic response of a complex encapsulated electronic assembly subjected to a severe shock environment [DE90-007689] 15 p2118 N90-22114
Dynamic response of structures with uncertain parameters 15 p2119 N90-22125
Application of a dynamic stall model to rotor trim and aeroelastic response 16 p2200 N90-22556
Influence of linear profile modification and loading conditions on the dynamic tooth load and stress of high contact ratio gears [NASA-TM-103136] 16 p2243 N90-22796
Dynamic substructuring by the boundary flexibility vector method of component mode synthesis [NASA-CR-182445] 16 p2247 N90-22813
Flat plate vibration analysis experimental and numerical fillet study [AD-A218789] 16 p2247 N90-22818
Nonlinear strain-displacement relations and flexible multibody dynamics 16 p2284 N90-23014
Explicit modeling of composite plates and beams in the dynamics of multibody systems 16 p2285 N90-23019
Frequency response modeling and control of flexible structures: Computational methods 16 p2285 N90-23021
Control/structure interaction design methodology 16 p2291 N90-23053
Model reduction in the physical coordinate system 16 p2295 N90-23074
Structural modeling for control design (articulated multibody component representation) 16 p2296 N90-23077
The power and efficiency of advanced software and parallel processing 16 p2296 N90-23079
Controlling flexible structures with second order actuator dynamics 16 p2297 N90-23083
A verification library for multibody simulation software 16 p2298 N90-23089
Impact response of orthotropic composite plates predicted by a one-parameter differential equation [FFA-TN-1989-07] 17 p2369 N90-23488
Nonlinear dynamics and control of flexible structures [AD-A218476] 17 p2386 N90-23589
Fractional state feedback control of undamped and viscoelastically-damped structures [AD-A220477] 17 p2412 N90-23746
Finite element formulations for coupled fluid/structure eigenvalue analysis [AD-A220793] 17 p2416 N90-23766
Dynamic predicate logic: Towards a compositional, non-representational semantics of discourse [ITLI-LP-89-02] 17 p2464 N90-24076
Experimental determination of material damping using vibration analyzer 18 p2514 N90-24358
Review of probabilistic analysis of dynamic response of systems with random parameters [NASA-CR-186171] 18 p2568 N90-24636
Dynamic analysis of flexible multibody structures 18 p2642 N90-25048
Coupled rotor-body equations of motion hover flight [NASA-CR-186710] 19 p2655 N90-25111
The effect of aircraft size on cabin floor dynamic pulses [DOT/FAA/CT-88/15] 19 p2659 N90-25136
Construction of a hybrid angular velocity reference system for investigation of the dynamic characteristics of strapdown gyros [ESA-TT-1181] 19 p2694 N90-25332
A kinematic/dynamic model for prediction of neck injury during impact acceleration 19 p2719 N90-25469
Effects of head mounted devices on head-neck dynamic response to +G(sub z) accelerations 19 p2720 N90-25471
The interpretation of nonlinear frequency response functions [RR-375] 19 p2753 N90-25643
Computational crash dynamics. Project 1.2: Computational crash dynamics analysis [IAR-89-19] 20 p2804 N90-25956
An in-flight interaction of the X-29A canard and flight control system [NASA-TM-101718] 20 p2807 N90-25973
An investigation of the use of singular perturbation methods and modal control theory in the derivation or aircraft control schemes [MATHS-REPT-A-106] 20 p2814 N90-26014
Simulated dynamic response of a servovalve controlled hydraulic actuator [NASA-TM-101644] 20 p2842 N90-26167
The structural dynamics analysis of the main injector LOX inlet tee and its redesign [NASA-CR-186764] 20 p2875 N90-26358
Scaling effects in the static and dynamic response of graphite-epoxy beam-columns [NASA-TM-102697] 20 p2876 N90-26363
Structural dynamics branch research and accomplishments [NASA-TM-102488] 20 p2878 N90-26373
Biodynamic simulations of an aircraft pilot/passenger in various crash environments [NIAR-90-6] 20 p2900 N90-26494
Local design methodologies for a hierarchic control architecture [AD-A222006] 21 p2966 N90-26862
Response of a liquid column to counter-directional excitation under zero-gravity [LRT-WE-9-FB-6(1989)] 21 p2991 N90-26998
Response of a liquid column to unequal counter-directional excitation under zero-gravity [LRT-WE-9-FB-7(1989)] 21 p2991 N90-26999
Response of a viscous liquid column to pitching- and roll-excitation in zero-gravity environment [LRT-WE-9-FB-10(1989)] 21 p2991 N90-27000
Response of a spinning liquid column to axial excitation [LRT-WE-9-FB-10(1988)] 21 p3006 N90-27085
Response of a liquid column with respect to oscillatory rotational top- and bottom excitation [LRT-WE-9-FB-8(1989)] 21 p3006 N90-27086
Response of differently axial-excited spinning liquid columns [LRT-WE-9-FB-16(1989)] 21 p3006 N90-27091
The effect of nonlinearities on flexible structures [AD-A222705] 21 p3012 N90-27124
Stochastic structural dynamics for aerospace applications [AD-A221517] 21 p3013 N90-27133
Improved computational strategy for predicting the response of complex systems [AD-A221661] 21 p3014 N90-27135
Temporal response of coupled one-dimensional dynamic systems [AD-A222375] 21 p3073 N90-27470
Development of a linearized unsteady aerodynamic analysis for cascade gust response predictions [NASA-CR-4308] 22 p3108 N90-27655
The dynamic electric microfield in ionic and polar media [AD-A222534] 22 p3156 N90-27891
Impulse response operators for structural complexes [AD-A222374] 22 p3191 N90-28107
Lower thermosphere (80-100 km) dynamics response to solar and geomagnetic activity: Overview 22 p3207 N90-28194
Effective optimal control of a fighter aircraft engine 23 p3277 N90-28548
Blade tip rubbing stress prediction 23 p3290 N90-28615
Cartesian control of redundant robots 23 p3363 N90-29004
Kinematics, controls, and path planning results for a redundant manipulator 23 p3363 N90-29005
Analysis of dynamic transient response and postflutter behavior of super-maneuvering airplane [AD-A224126] 24 p3432 N90-29386
Computer-aided engineering environment for controlled mechanical systems [AD-A223551] 24 p3527 N90-29942

DYNAMIC STABILITY
NT AERODYNAMIC STABILITY
NT AIRCRAFT STABILITY
NT ATTITUDE STABILITY
NT BOUNDARY LAYER STABILITY
NT COMBUSTION STABILITY
NT CONTROL STABILITY
NT DIRECTIONAL STABILITY
NT FLAME STABILITY
NT FLOW STABILITY
NT FREQUENCY STABILITY
NT GYROSCOPIC STABILITY
NT HOVERING STABILITY
NT LATERAL STABILITY
NT LONGITUDINAL STABILITY
NT LOW SPEED STABILITY
NT MAGNETOHYDRODYNAMIC STABILITY
NT MOTION STABILITY
NT ROTARY STABILITY
NT SPACECRAFT STABILITY

Combustor influence on fighter engine operability 01 p0035 N90-10193
Dynamic instability characteristics of aircraft turbine engine combustors 01 p0036 N90-10195
The dynamic stability of an axially loaded beam with lateral elastic support and damping 02 p0232 N90-11331
Vortex dynamics [AD-A212119] 04 p0499 N90-12877
SSME LOX post flow analysis/fluid structure interaction. Volume 1: Flow analysis [NASA-CR-183677] 05 p0637 N90-13715
A comparison of techniques for balancing planar linkages [ESDU-89043] 09 p1232 N90-17150
Energy decay and boundary control for distributed parameter systems with viscoelastic damping [AD-A216468] 11 p1519 N90-18748
The effects of gradients on boundary stability [DE90-007428] 12 p1722 N90-19894
Aeroelastic and stability behaviour of the WTS 3 Maglarp wind turbine. Calculations and comparisons with tests [FFA-TN-1989-23] 17 p2420 N90-23792
Models of intracavity frequency doubled lasers [AD-A221182] 18 p2563 N90-24628
Rotorcraft aeromechanical stability-methodology assessment. Phase 2: Workshop [NASA-TM-102272] 21 p2955 N90-26800
Inviscid dynamics of unstable shear layers [AD-A222297] 21 p3004 N90-27077
Transition to complicated behavior in infinite dimensional dynamical systems [AD-A221502] 21 p3077 N90-27494
Investigation of the dynamic buckling of liquid-filled tanks 24 p3478 N90-29660
Model based manipulator control 24 p3509 N90-29833

DYNAMIC STRUCTURAL ANALYSIS
Proceedings of the Workshop on Computational Aspects in the Control of Flexible Systems, part 1 [NASA-TM-101578-PT-1] 01 p0017 N90-10080
A finite element approach for large motion dynamic analysis of multibody structures in space 01 p0019 N90-10093
Enhanced element-specific modal formulations for flexible multibody dynamics 01 p0019 N90-10094
A performance comparison of integration algorithms in simulating flexible structures 01 p0021 N90-10101
Proceedings of the Workshop on Computational Aspects in the Control of Flexible Systems, part 2 [NASA-TM-101578-PT-2] 01 p0021 N90-10103
Flexible aircraft dynamic modeling for dynamic analysis and control synthesis 01 p0022 N90-10112
Experimental validation of flexible robot arm modeling and control 01 p0023 N90-10113
Controlling flexible structures: A survey of methods 01 p0023 N90-10114
Updating of finite element model by means of normal mode parameters 02 p0177 N90-10992
Viscoelastic tuned dampers for control of structural dynamics 02 p0178 N90-10999
A super element for multibody dynamics 02 p0178 N90-11004
Employment of modal survey methodologies in dynamic analysis procedures 02 p0179 N90-11006
Integration of analytical and test software for optimal structural design under dynamic loads 02 p0179 N90-11007
Use of Lanczos vectors in structural dynamics 02 p0179 N90-11011
Numerical treatment of the thermo-structural-dynamic problems: The interpolation techniques 02 p0180 N90-11016
Comparison of sine dwell and broadband methods for modal testing 02 p0181 N90-11025
Induced shock loads during the separation of the Ariane 5 VEB structure 02 p0184 N90-11045
The dynamics of circular plates with patch damping: A numerical and experimental study 02 p0232 N90-11329
Effects of mistuning and matrix structure on the topology of frequency response curves [NASA-TM-102290] 03 p0357 N90-12041
Airframe structural dynamic considerations in rotor design optimization [NASA-TM-101646] 03 p0360 N90-12057
RAN (Royal Australian Navy) vibration analysis system operator's guide [AD-A212441] 04 p0453 N90-12596
Flight motor set 360L001 (STS-26R). (Reconstructed dynamic loads analysis) [NASA-CR-183811] 04 p0464 N90-12656
Julia-Fatou-Sullivan theory for real one-dimensional dynamics [REPT-88-100] 04 p0548 N90-13190
Pointing control for LDR 05 p0595 N90-13453
Space telescope pointing control 05 p0595 N90-13454
Segment alignment control system 05 p0595 N90-13457
Initial test results for the mini-mast 05 p0600 N90-13482
Flight motor set 360L001 (STS-26R). Volume 5: Nozzle component [NASA-CR-183771] 05 p0615 N90-13588

Joint Services Electronics Program
[AD-A213015] 05 p0634 N90-13699
Investigation of difficult component effects on finite element model vibration prediction for the Bell AG-1G helicopter. Volume 2: Correlation results
[NASA-CR-181916-VOL-2] 05 p0654 N90-13814
Manipulation strategies for massive space payloads
[NASA-CR-186081] 06 p0728 N90-14247
Measurement of damping of graphite epoxy composite materials and structural joints
[NASA-CR-183802] 06 p0736 N90-14286
Stability and dynamics of constrained flexible multibody systems 06 p0791 N90-14609
Group implicit concurrent algorithms in nonlinear structural dynamics
[NASA-CR-185950] 06 p0796 N90-14638
Non-linear vibrations, stability, and dynamics of structures and mechanisms
[AD-A212152] 06 p0796 N90-14639
Active control system for gust load alleviation and structural damping 07 p0871 N90-15056
Location of interior impact source in randomly excited structures
[DE90-001092] 07 p0945 N90-15474
Structural dynamics division research and technology accomplishments for FY 1989 and plans for FY 1990
[NASA-TM-101683] 08 p1019 N90-15894
Dynamic analysis of geared rotors by finite elements
[NASA-TM-102349] 08 p1086 N90-16286
Elastic buckling of imperfect cylindrical shells containing granular solids
[PB90-110362] 09 p1236 N90-17174
Techniques for analyzing the dynamic response of structural systems using computer-derived Green's functions
[AD-A214523] 09 p1237 N90-17181
The 59th Shock and Vibration Symposium, volume 4
[AD-A214581] 09 p1238 N90-17184
Boundary walls, fences and hoardings: Mean and peak wind loads and overturning moments
[ESDU-89050] 09 p1239 N90-17190
Response of structures to atmospheric turbulence. Response to across-wind turbulence components
[ESDU-89049] 09 p1239 N90-17191
Analysis of the National Transonic Facility mishap
[NASA-TM-101686] 10 p1318 N90-17620
Deployment simulation for the third generation solar arrays GSR3 10 p1340 N90-17763
The 59th Shock and Vibration Symposium, volume 3
[AD-A214580] 10 p1395 N90-18066
Z-grid signal conditioning system user's guide and technical reference
[AD-A215122] 10 p1395 N90-18067
A global approach for the identification of structural connection properties
[NASA-TM-102502] 11 p1518 N90-18745
Biaxial strength and stress rupture of hot-pressed silicon nitride
[AD-A216950] 11 p1519 N90-18750
Development of an experimental space station model for structural dynamics research
[NASA-TM-102601] 11 p1519 N90-18751
Remote Attitude Measurement Sensor (RAMS) 12 p1611 N90-19271
Advanced topics in structural dynamics: The maneuver of flexible spacecraft, and on-off decentralized control of flexible structures 12 p1612 N90-19274
Investigation of SSME alternate high pressure fuel turbopump lift-off seal fluid and structural dynamic interaction 12 p1636 N90-19400
An experimental study of the aeroelastic behaviour of two parallel interfering circular cylinders 12 p1673 N90-19609
Modal analysis of nonprismatic beams: Uniform segment method
[AD-A216952] 12 p1674 N90-19614
A review of the analytical simulation of aircraft crash dynamics
[NASA-TM-102595] 13 p1753 N90-20068
Computational simulation of damping in composite structures
[NASA-TM-102567] 13 p1817 N90-20432
Plan, formulate, and discuss a NASTRAN finite element model of the UH-60A helicopter airframe
[NASA-CR-181975] 13 p1818 N90-20439
Localization and delocalization in periodic one-dimensional dynamic systems
[AD-A217939] 13 p1882 N90-20797
Performance data from a wind-tunnel test of two main-rotor blade designs for a utility-class helicopter
[NASA-TM-4183] 14 p1916 N90-20974
Nonlinear and distributed parameter models of the mini-mast truss 14 p1934 N90-21070
Controller reduction for effective interdisciplinary design of active structures 14 p1935 N90-21077
Controls, Astrophysics, and Structures Experiment in Space (CASES) 14 p1937 N90-21085
Space truss zero gravity dynamics 14 p1937 N90-21087
Fourier series methods for plates and shells with cracks and inclusions 14 p1990 N90-21406
User manual for VICONOPT: An exact analysis and optimum design program covering the buckling and vibration of prismatic assemblies of flat in-plane loaded, anisotropic plates, with approximations for discrete supports, and transverse stiffeners
[NASA-CR-181966] 14 p1991 N90-21413
Wave receptance analysis of vibrating beams and stiffened plates 14 p1993 N90-21419
Elasto-plastic large deformation analysis of thin-walled structures
[PB90-164757] 14 p1994 N90-21426
Development and application of a generalized dynamic wake theory for lifting rotors 15 p2046 N90-21731
Airloads, wakes, and aeroelasticity
[NASA-CR-177551] 15 p2048 N90-21738
Progression of damage and fracture in composites under dynamic loading
[NASA-TM-103118] 15 p2065 N90-21825
A review of approximate methods for determining the vibrational modes of membranes 15 p2109 N90-22063
Optimum design of structures under shock and vibration environment 15 p2110 N90-22067
Natural modes of cracked beams and identification of cracks 15 p2111 N90-22075
Aircraft crash survival design guide. Volume 3: Aircraft structural crash resistance
[AD-A218436] 16 p2198 N90-22547
Robust control of vibration in flexible structures 16 p2241 N90-22787
Dynamic substructuring by the boundary flexibility vector method of component mode synthesis
[NASA-CR-182445] 16 p2247 N90-22813
Flat plate vibration analysis experimental and numerical fillet study
[AD-A218789] 16 p2247 N90-22818
Transverse vibrations of a composite cylindrical tube of circular cross section
[AD-A219227] 16 p2248 N90-22820
Nonlinear strain-displacement relations and flexible multibody dynamics 16 p2284 N90-23014
Explicit modeling of composite plates and beams in the dynamics of multibody systems 16 p2285 N90-23019
Frequency response modeling and control of flexible structures: Computational methods 16 p2285 N90-23021
Simulation studies using multibody dynamics code DART 16 p2288 N90-23036
On trajectory generation for flexible space crane: Inverse dynamics analysis by LATDYN 16 p2288 N90-23037
A parallel structure transient response algorithm using independent substructure response computation 16 p2290 N90-23044
Control/structure interaction design methodology 16 p2291 N90-23053
Model reduction in the physical coordinate system 16 p2295 N90-23074
The power and efficiency of advanced software and parallel processing 16 p2296 N90-23079
Controlling flexible structures with second order actuator dynamics 16 p2297 N90-23083
Mini-mast dynamic analysis using the truss-beam model 16 p2297 N90-23087
Analytic semigroups: Applications to inverse problems for flexible structures
[NASA-CR-182047] 16 p2306 N90-23138
Impact response of orthotropic composite plates predicted by a one-parameter differential equation
[FFA-TN-1989-07] 17 p2369 N90-23488
Aeroelastic and stability behaviour of the WTS 3 Maglarp wind turbine. Calculations and comparisons with tests
[FFA-TN-1989-23] 17 p2420 N90-23792
Reduced order models for nonlinear aerodynamics 18 p2492 N90-24244
Experimental determination of material damping using vibration analyzer 18 p2514 N90-24358
Random vibration analysis of space flight hardware using NASTRAN 18 p2570 N90-24645
Unique failure behavior of metal/composite aircraft structural components under crash type loads
[NASA-TM-102679] 18 p2572 N90-24660
Ground shake test of the UH-60A helicopter airframe and comparison with NASTRAN finite element model predictions
[NASA-CR-181993] 19 p2661 N90-25143
A study of concept options for the evolution of Space Station Freedom
[NASA-TM-102675] 19 p2663 N90-25154
Calculation of flight vibration levels of the AH-1G helicopter and correlation with existing flight vibration measurements
[NASA-CR-182031] 19 p2702 N90-25375
An in-flight interaction of the X-29A canard and flight control system
[NASA-TM-101718] 20 p2807 N90-25973
Modeling of composite beams and plates for static and dynamic analysis
[NASA-CR-186459] 20 p2874 N90-26354
The structural dynamics analysis of the main injector LOX inlet tee and its redesign
[NASA-CR-186764] 20 p2875 N90-26358
Structural dynamics branch research and accomplishments
[NASA-TM-102488] 20 p2878 N90-26373
Parallel processors and nonlinear structural dynamics algorithms and software
[NASA-CR-186755] 20 p2907 N90-26536
Power flow analysis of two coupled plates with arbitrary characteristics
[NASA-CR-182033] 20 p2923 N90-26632
Dynamic structural analysis using boundary element techniques
[AD-A222943] 21 p3012 N90-27126
Stochastic structural dynamics for aerospace applications
[AD-A221517] 21 p3013 N90-27133
Improved computational strategy for predicting the response of complex systems
[AD-A221661] 21 p3014 N90-27135
A transient response analysis of the space shuttle vehicle during liftoff
[NASA-TM-103505] 22 p3125 N90-27735
In-space construction and dynamics of large space structures 22 p3130 N90-27764
Impulse response operators for structural complexes
[AD-A222374] 22 p3191 N90-28107
A nonlinear finite element formulation for the large displacement analysis of plates 23 p3338 N90-28867
Reliability analysis of maintained structural system vulnerable to fatigue and fracture 23 p3338 N90-28868
Interface formation and percusory dynamics
[AD-A224128] 23 p3402 N90-29223
Nonlinear static and dynamic modeling of composite rotor blades including warping effects 24 p3431 N90-29382
Investigation of the dynamic buckling of liquid-filled tanks 24 p3478 N90-29660
Proceedings of Damping '89. Volume 3: Pages ICA-1 through KDC-15
[AD-A223433] 24 p3479 N90-29666
Evaluation of plane-of-light noninterference stress measurement systems for measuring bladed disk vibrations
[AD-A223487] 24 p3479 N90-29667

DYNAMIC TESTS

Full scale technology demonstration of a modern counterrotating unducted fan engine concept: Component test
[NASA-CR-180868] 01 p0010 N90-10047
Dynamic substructuring for modular analysis and testing 02 p0180 N90-11015
Comparison of phase resonance, mode separation, and driven-base modal identification methods applied to the FLECS test structure 02 p0181 N90-11027
Transient tests for spacecraft structures 02 p0183 N90-11040
Dynamic testing techniques and applications for an aeroelastic rotor test facility 05 p0584 N90-13406
Static and free-vibrational response of semi-circular graphite-epoxy frames with thin-walled open sections
[NASA-CR-186097] 05 p0617 N90-13600
VIBRAFUGE: Combined vibration and centrifuge testing
[DE90-001091] 07 p0884 N90-15114
Geotechnical instrumentation
[PB89-198675] 07 p0933 N90-15398
A semiautomated computer-interactive dynamic impact testing system
[DE90-002721] 07 p0946 N90-15479
Conceptual design of a moving belt radiator shuttle-attached experiments: Technical requirement Document
[NASA-CR-185168] 08 p1038 N90-15996
Load-shortening behavior of an initially curved eccentrically loaded column
[NASA-TM-101643] 08 p1088 N90-16293
Results of aircraft open-loop tests of an experimental magnetic leader cable system for guidance during roll-out and turnoff
[NASA-TM-4135] 09 p1169 N90-16767

Dynamic derivatives of missiles and fighter-type configurations at high angles of attack
10 p1306 N90-17554
The 59th Shock and Vibration Symposium, volume 2
[AD-A214579] 10 p1395 N90-18065
The use of underwater dynamometry to evaluate two space suits 18 p2632 N90-24995
Measurement techniques, evaluation criteria and injury probability assessment methodologies developed for Navy ejection and crashworthy seat evaluations
19 p2721 N90-25479
Dynamic test input generation for multiple-fault isolation 21 p3040 N90-27280
Experimental identification of helicopter engine dynamics from closed loop data
22 p3104 N90-27627
Military aircrew seating: A human factors engineering approach
[AD-A218049] 23 p3362 N90-28999
Nonlinear modeling of joint dominated structures
[NASA-CR-4324] 24 p3439 N90-29423

DYNAMICAL SYSTEMS
The application of TSIM software to act design and analysis on flexible aircraft 01 p0018 N90-10086
DYSCO: A software system for modeling general dynamic systems 01 p0018 N90-10089
Explicit modeling and computational load distribution for concurrent processing simulation of the space station
01 p0020 N90-10096
Proceedings of the Workshop on Computational Aspects in the Control of Flexible Systems, part 2
[NASA-TM-101578-PT-2] 01 p0021 N90-10103
Theoretical investigations of chaotic dynamics
[AD-A207724] 01 p0134 N90-10772
Application of dynamical systems theory to global weather phenomena revealed by satellite imagery
03 p0361 N90-12063
The realization of input-output maps using bialgebras
[NASA-CR-185362] 03 p0391 N90-12228
Nonlinear systems and Kolmogorov's representation theorem
[RR-363] 04 p0508 N90-12931
A new decision rule for model structure identification of a class of nonlinear dynamic systems
[RR-360] 04 p0539 N90-13122
Numerical analysis of chaotic symbol sequences generated by parabolic and triangle maps of the interval
[MPIS-22/1987] 04 p0539 N90-13124
Remarks on the control of discrete time nonlinear systems
[MEMO-770] 04 p0544 N90-13158
Explicit modeling and concurrent processing in the simulation of multibody dynamic systems
05 p0599 N90-13481
Quadratic dynamical systems describing shear flow of non-Newtonian fluids
[AD-A212692] 05 p0638 N90-13720
Balance laws and centro velocity in dissipative systems
[MEMO-797] 05 p0639 N90-13726
Climate predictability: A dynamical view
[AERONOMICA-ACTA-A-347-1989]
05 p0671 N90-13909
Using the physical structure of a system for control: An illustration
[MEMO-782] 05 p0689 N90-14014
On the effects of an uncertainty on evolution law in dynamical systems
[PREPRINT-689] 05 p0693 N90-14047
Chaotic behavior in nonlinear polarization dynamics
[DE89-013453] 06 p0788 N90-14589
A simulation model for dynamic system availability analysis
[AD-A213499] 07 p0974 N90-15628
Introduction to bifurcation theory
[DE90-003319] 07 p0982 N90-15673
Continuum analogues of contragredient Lie algebras: Lie algebras with a Cartan operator and nonlinear dynamical systems
[DE89-635698] 07 p0985 N90-15691
Integrable classical systems in higher dimensions
[DE90-600737] 08 p1118 N90-16473
On gauge fixing and quantization of constrained Hamiltonian systems
[DE90-600732] 08 p1135 N90-16574
The bifurcation interpreter: A step towards the automatic analysis of dynamical systems
[AD-A214618] 09 p1265 N90-17336
Modeling the pressure-strain correlation of turbulence: An invariant dynamical systems approach
[NASA-CR-181979] 10 p1383 N90-18003
Construction of second constant of motion for two dimensional classical super systems
[DE90-607046] 10 p1423 N90-18208
Waveform methods for ordinary differential equations
[DE90-006593] 11 p1553 N90-18943
The free energy principle, negative energy modes, and stability
[DE90-005368] 11 p1573 N90-19056
A PBL-radiation model for application to regional numerical weather prediction 12 p1635 N90-19394
Development of dynamic equivalent network structures with a universal identification and optimization process
[ETN-90-95822] 12 p1654 N90-19507
Localization and delocalization in periodic one-dimensional dynamic systems
[AD-A217939] 13 p1882 N90-20797
Periodic solutions for Hamiltonian systems in a nonconvex potential well
[DE90-612752] 14 p2020 N90-21580
Nonlinear stability analysis and control of dynamical robotic systems 15 p2104 N90-22037
The Shock and Vibration Digest, volume 22, no. 1
15 p2111 N90-22073
Stable response of damped mechanical systems, 4
15 p2111 N90-22074
Approximate optimal guidance schemes for atmospheric orbital maneuvering 16 p2206 N90-22585
Qualitative aspects of signal processing through dynamical neural networks
[PREPRINT-711] 16 p2228 N90-22709
Modelling and computer control of a mechanical system
[W-8908] 16 p2243 N90-22794
Predictability of weather and climate in a coupled ocean-atmosphere model: A dynamical systems approach 16 p2256 N90-22865
Proceedings of the 3rd Annual Conference on Aerospace Computational Control, volume 1
[NASA-CR-186446] 16 p2279 N90-22987
Parallel processing of real-time dynamic systems simulation on OSCAR (Optimally SCheduled Advanced multiprocessoR) 16 p2282 N90-23006
Parallel and vector computation for stochastic optimal control applications 16 p2282 N90-23007
Optimum control forces for multibody systems with intermittent motion 16 p2284 N90-23016
Model reduction in the physical coordinate system
16 p2295 N90-23074
Non-symmetric double well and Euclidean functional integral
[PREPRINT-709] 16 p2305 N90-23133
The LORE-interpreter: Notes on the implementation
[REPT-89-60] 17 p2445 N90-23932
On models for propositional dynamic logic
[RUU-CS-89-3] 17 p2460 N90-24046
On the relationship between energy density and net power (intensity) in coupled one-dimensional dynamic systems
[AD-A221071] 19 p2709 N90-25421
A contribution to the improvement of the accuracy in the parameter identification of nonlinear processes, by example of the aircraft motion
[ETN-90-96961] 20 p2808 N90-25974
A new scheme for identification and control
[EUT-88-E-213] 20 p2915 N90-26586
Temporal response of coupled one-dimensional dynamic systems
[AD-A222375] 21 p3073 N90-27470
Transition to complicated behavior in infinite dimensional dynamical systems
[AD-A221502] 21 p3077 N90-27494
Spacecraft attitude dynamics: Evolution and current challenges 22 p3128 N90-27754
Robust eigensystem assignment for second-order estimators
[NASA-TM-102696] 22 p3191 N90-28103
Impulse response operators for structural complexes
[AD-A222374] 22 p3191 N90-28107

DYNAMO THEORY
The electrodynamics of the polar ionosphere with special emphasis on the dayside cleft region
05 p0658 N90-13838
The disk-halo connection and the nature of the interstellar medium
[NASA-CR-186286] 07 p1012 N90-15860

DYNAMOMETERS
Short time-dynamometer system for shock wave channels
[MBB-UT-115/89-PUB] 19 p2651 N90-25084
The relationship of isometric grip strength, optimal dynamometer settings, and certain anthropometric factors
[AD-A222046] 21 p3037 N90-27264

DYNAMOS
U ROTATING GENERATORS

DYSPROSIUM COMPOUNDS
Resistivity measurements of superconducting materials
[PB89-225700] 04 p0496 N90-12856
Terbium-dysprosium magnetostrictive high power transducers
[AD-D014509] 19 p2753 N90-25641

E

E GLASS
NT S GLASS
Characterization and role of an elastomeric interphase within polyepoxy reinforced glass, both particulate and fibrous
[ISAL-89-0064] 16 p2222 N90-22676

E LAYERS
U E REGION

E REGION
NT SPORADIC E LAYER
Quiet time conductivities of the auroral ionosphere
02 p0244 N90-11383
A review on radio studies of auroral E-region ionospheric irregularities 02 p0245 N90-11390
An ionospheric model for HF sky-wave backscatter radar 02 p0247 N90-11401
Preliminary results of the rocket and scatter experiments ROSE: Measurements with the newly designed spherical probe 05 p0659 N90-13850

EAR
NT OTOLITH ORGANS
NT SEMICIRCULAR CANALS
NT VESTIBULES
Test procedures for the evaluation of helmet and headset mounted active noise reduction systems
[AD-A212991] 05 p0676 N90-13937
Auditory perception
[AD-A217012] 11 p1540 N90-18864
The effects of blast trauma (impulse noise) on hearing: A parametric study source 2
[AD-A221731] 21 p3035 N90-27253

EAR PROTECTORS
The effects of hearing protectors on speech communication and the perception of warning signals
[AD-A212521] 04 p0492 N90-12832
Shape instabilities of plate-like structures. 1: Experimental observations in heavily cold worked in situ composites
[AD-A212251] 04 p0523 N90-13021
Application of active noise reduction for hearing protection and speech intelligibility improvement
[IZF-1988-21] 04 p0527 N90-13042
Evaluation of two objective measures of effective auditory stimulus level
[AD-A214669] 09 p1250 N90-17255

EARLY STARS
NT A STARS
NT B STARS
NT BLUE STARS
NT HOT STARS
NT O STARS
NT WHITE DWARF STARS
NT WOLF-RAYET STARS
Infrared diagnostics of interstellar shocks
11 p1582 N90-19115
The environment of young stellar objects studied by high-resolution infrared spectroscopy
11 p1583 N90-19120
Photometric monitoring of early type emission line stars 15 p2184 N90-22478
Probing the possibility of a C-12/C-13 galactic abundance gradient 21 p3094 N90-27586

EARLY WARNING SYSTEMS
Automatic thresholding multichannel digital radar early warning system
[AD-D014323] 12 p1642 N90-19431
A theoretical model for airborne radars
[AD-A220735] 17 p2390 N90-23615

EARPHONES
Techniques and applications for binaural sound manipulation in human-machine interfaces
[NASA-TM-102279] 23 p3362 N90-28996

EARTH (PLANET)
Offaxis radiance studies for infrared sensors
[AD-A210790] 02 p0275 N90-11570
Distributed earth model/orbiter simulation
13 p1860 N90-20671
JPRS report. Science and technology. USSR: Earth sciences
[JPRS-UES-88-004] 14 p1995 N90-21431

EARTH ALBEDO
Atlas of albedo and absorbed solar radiation derived from Nimbus 7 Earth radiation budget data set, November 1978 to October 1985
[NASA-RP-1231] 09 p1247 N90-17233

EARTH ATMOSPHERE
NT D REGION
NT E REGION
NT EARTH IONOSPHERE

NT EXOSPHERE
NT F REGION
NT F 2 REGION
NT FREE ATMOSPHERE
NT LOWER ATMOSPHERE
NT LOWER IONOSPHERE
NT MESOPAUSE
NT MESOSPHERE
NT MIDDLE ATMOSPHERE
NT MIDLATITUDE ATMOSPHERE
NT OZONOSPHERE
NT SPORADIC E LAYER
NT STRATOPAUSE
NT STRATOSPHERE
NT THERMOSPHERE
NT TROPOPAUSE
NT TROPOSPHERE
NT UPPER ATMOSPHERE
NT UPPER IONOSPHERE

Potential effects of global climate change on the United States. Volume 1: Regional studies. Draft
[PB89-161053] 02 p0238 N90-11351

Potential effects of global climate change on the United States. Volume 2: National studies. Draft
[PB89-161061] 02 p0238 N90-11352

Spatial characteristics of airglow and solar scatter radiance from the earth's atmosphere
[AD-A211358] 03 p0372 N90-12126

Crau 1987: The KNMI contribution --- KNMI (Royal Netherlands Meteorological Institute)
[KNMI-TR-110] 03 p0375 N90-12140

Vacuum ultraviolet backgrounds from space - ten years after
[AD-A211353] 03 p0435 N90-12493

European Rocket and Balloon Programs and Related Research
[ESA-SP-291] 05 p0656 N90-13826

A self-consistent model of the most common nightglow emissions 05 p0660 N90-13853

A high-resolution atlas of the infrared spectrum of the Sun and the Earth atmosphere from space: A compilation of ATMOS spectra of the region from 650 to 4800 cm (2.3 to 16 micron). Volume 1: The Sun
[NASA-RP-1224-VOL-1] 05 p0666 N90-13893

Development of a three-dimensional local scale atmospheric model with turbulence closure model
[DE90-710045] 07 p0960 N90-15551

The Polar Ice Prediction System: A sea ice forecasting system
[AD-A214600] 09 p1249 N90-17246

Two-dimensional calculation of sequential electron layer formation by crossed microwave beams in air at low pressure
[DE90-005254] 09 p1286 N90-17453

Quick, reliable estimates of high-power microwave fluences: The SNEAKY-2 program
[DE90-006347] 11 p1498 N90-18624

Fast algorithms for calculating laser wavefront phase compensation given noisy measurements of phase gradient
[DE90-006357] 11 p1515 N90-18727

Large impact events and atmospheric evolution on the terrestrial planets 12 p1744 N90-20028

Spectral solar radiation data base documentation, volume 1
[DE89-009447] 13 p1841 N90-20571

Southern oscillation in the OSU coupled upper ocean/atmosphere GCM
[DE90-008415] 13 p1844 N90-20588

Modelling UV-visible radiation observed from space 15 p2085 N90-21937

Earth observation from the interstellar space
[REPT-44/89] 17 p2418 N90-23781

Meteor radar studies of the mesopause region and nonlinear atmospheric waves 17 p2421 N90-23799

The effects of climate change on energy planning and operations in the Pacific Northwest. Volume 2: Technical background
[DE90-009465] 17 p2425 N90-23817

Transmission of infrared radiation through the Australian atmosphere: Predictions using the LOWTRAN model
[AD-A220340] 17 p2428 N90-23835

Ice core studies and the past atmospheric environment of polar regions 20 p2885 N90-26411

Crossed-microwave-beam air ionization laboratory experiments
[DE90-012056] 21 p3024 N90-27195

EARTH AXIS

Application of inertial instruments for DSN antenna pointing and tracking 20 p2853 N90-26224

EARTH CORE

Investigations of Eurasian seismic sources and upper mantle structure
[AD-A211806] 03 p0371 N90-12120

Geophysical studies related to geodetic reference frames
[AD-A220249] 18 p2574 N90-24863

Use of geomagnetic data for studies on the Earth's deep interior 21 p3023 N90-27192

EARTH CRUST

A search for layering in the oceanic crust
[PB89-198220] 01 p0090 N90-10514

Surface wave ray tracing and Ms:yield determination in a laterally heterogeneous earth
[AD-A210241] 01 p0090 N90-10516

Institute of Geophysics and Planetary Physics, 1988
[DE89-014363] 01 p0137 N90-10794

Global environmental effects of impact-generated aerosols: Results from a general circulation model
[DE89-008033] 03 p0368 N90-12106

Strain accumulation and surface deformation along the San Andreas, California
[NASA-CR-185893] 05 p0666 N90-13894

Crustal structure studies utilizing earthquake sequences
[AD-A212916] 05 p0666 N90-13895

Workshop on the Archean Mantle
[NASA-CR-186156] 06 p0814 N90-14736

Dynamics of mid-ocean ridge systems 07 p0965 N90-15575

Evolution of overlapping spreading centers: A Sea Mark 2 investigation
[AD-A214278] 07 p0965 N90-15576

The interpretation of crustal dynamics data in terms of plate interactions and active tectonics of the Anatolian plate and surrounding regions in the Middle East
[NASA-CR-186200] 11 p1533 N90-18624

Stored mafic/ultramafic crust and early Archean mantle depletion
[NASA-CR-186460] 12 p1691 N90-19715

The effects of structure and source complexity on waveforms: Crustal structure of Tibet and the recovery of complex seismic sources
[AD-A218202] 13 p1843 N90-20579

Surface roughness and the physical properties of fractures
[DE90-006046] 15 p2128 N90-22169

Analysis of regional phases using three-component data
[AD-A219482] 17 p2422 N90-23803

Heat and fluid flow within the Earth's crust: In situ measurements and mathematical models 18 p2579 N90-24690

Some aspects of the structure and evolution of oceanic spreading centers 24 p3496 N90-29757

EARTH ENVIRONMENT

The French balloon program and related space research 05 p0656 N90-13828

EARTH FIGURE

U GEODESY

EARTH GRAVITATION

Optimum data weighting and error calibration for estimation of gravitational parameters
[NASA-TM-100737] 04 p0517 N90-12985

Modeling of the Earth's gravity field using the New Global Earth Model (NEWGEM) 13 p1833 N90-20523

A framework for modelling kinematic measurements in gravity field applications 13 p1833 N90-20524

Synopsis of early field test results from the gravity gradiometer survey system 13 p1833 N90-20525

Terrestrial gravity instrumentation in the 20th Century: A brief review 13 p1834 N90-20527

Critique of the vertical gradient of gravity 13 p1834 N90-20531

The inverse gravimetric problem in gravity modelling 13 p1835 N90-20535

GEOID '88: A gravimetric geoid for Canada 13 p1837 N90-20543

Very accurate upward continuation to low heights in a test of non-Newtonian theory 13 p1837 N90-20548

A model of the general ocean circulation determined from a joint solution for the Earth's gravity field 13 p1838 N90-20550

Refinement of Earth's gravity field with Topex GPS measurements 13 p1838 N90-20553

Gravity field information from Gravity Probe-B 13 p1839 N90-20554

Satellite-to-satellite tracking experiment for global gravity field mapping 13 p1839 N90-20556

ARISTOTELES: A European approach for an Earth gravity field recovery mission 13 p1839 N90-20559

Critical point wetting drop tower experiment
[NASA-CR-186513] 14 p1957 N90-21208

Determination of the general ocean circulation using satellite altimetry from a simultaneous solution for the Earth's gravity field 16 p2203 N90-22569

Two dimensional Fourier analysis of the earth gravitational field using the program package TIM
[ETN-90-96696] 17 p2424 N90-23815

EARTH IONOSPHERE

NT D REGION
NT E REGION
NT F REGION
NT F 2 REGION
NT LOWER IONOSPHERE
NT SPORADIC E LAYER
NT UPPER IONOSPHERE

The auroral energy deposition over the polar ionosphere during substorms
[AD-A210522] 01 p0086 N90-10490

Long-term solar-terrestrial observations
[DE89-016318] 01 p0143 N90-10825

Balance equations for ionospheric plasmas with different partial temperatures 02 p0240 N90-11364

Global ionospheric dynamics: A review 02 p0241 N90-11367

A fully analytic, low and middle latitude ionospheric model 02 p0241 N90-11368

VLF/LF radio wave studies of the structure and variability of the equatorial, mid-latitude and polar ionosphere below 100 km 02 p0242 N90-11373

Seasonal and geomagnetic response of the thermosphere and ionosphere 02 p0243 N90-11380

Ionosphere-thermosphere coupling at high latitudes: Aspect angle dependence of non-thermal plasmas 02 p0244 N90-11382

Calculation of the temperature and velocity vector of the neutral gas using EISCAT CP3-data 02 p0244 N90-11384

Ion heating events observed at the EISCAT radar 02 p0244 N90-11385

Small-scale irregularities and global plasma dynamics in the high-latitude ionosphere 02 p0246 N90-11394

Short wavelength striations on expanding plasma clouds
[DE89-016585] 02 p0250 N90-11416

UV ionospheric remote sensing with the polar BEAR satellite
[AD-A211359] 03 p0372 N90-12127

TEC (Total Electron Content) models
[AD-A211553] 03 p0372 N90-12129

The electrodynamics of the polar ionosphere with special emphasis on the dayside cleft region 05 p0658 N90-13838

Resonance cone diagnostics in the mid-latitude ionosphere 05 p0658 N90-13840

Background electrodynamics measured by EISCAT during the NEED campaign 05 p0660 N90-13851

Auroral and sub-auroral interaction at the F region ionosphere
[AD-A213284] 05 p0666 N90-13896

Long wave propagation assessment 06 p0758 N90-14414

Correction of ionospheric effects for the precise orbit determination of satellites 06 p0762 N90-14432

Rocket studies of the lower ionosphere
[NASA-CR-186187] 06 p0814 N90-14735

RAIDS: An orbiting observatory for ionospheric remote sensing from space
[AD-A213717] 07 p0949 N90-15494

Development of the RAIDS (Remote Atmospheric and Ionospheric Detector System) extreme ultraviolet wedge and strip detector
[AD-A213730] 07 p0949 N90-15495

Report from upper atmospheric science 10 p1444 N90-18332

Report from ionospheric science 10 p1444 N90-18333

Incoherent retrodiffusion of radiowaves in plasma with particle impulse
[ETN-90-95375] 12 p1718 N90-19864

USU center of excellence in theory and analysis of the geo-plasma environment
[AD-A217736] 13 p1759 N90-20101

Quantifying and reducing uncertainty in the assimilative mapping of ionospheric electrodynamics
[AD-A218057] 13 p1842 N90-20577

Measurements of the interaction of high-voltage biassed conductors with the ionosphere
[AD-A218285] 13 p1843 N90-20580

Optical instrumentation support for the airborne ionospheric observatory
[AD-A218207] 13 p1889 N90-20839

Ionospheric equivalent slab thickness and its modeling applications
[AD-A220105] 17 p2424 N90-23811

Ion neutral gas coupling in the polar atmosphere: Use of EISCAT for the calculation of thermospheric parameters
[ETN-90-96490] 18 p2580 N90-24694

Preliminary results from the quadrupole probe on NEED-1
[FFI-89/7015] 19 p2714 N90-25446

Viking data analysis
[AD-A222609] 20 p2823 N90-26062

The near-Earth orbital environment coupling to its energy sources
[AD-A222435] 21 p3026 N90-27206
Report from GPS MANPACK tests in Spitsbergen area (Norway)
[FFI-90/7007] 22 p3114 N90-27692
Intensive MHD-structures penetration in the middle atmosphere initiated in the ionospheric cusp under quiet geomagnetic conditions 22 p3207 N90-28193
The worldwide ionospheric data base
[NASA-TM-101823] 24 p3488 N90-29714
High power oblique incidence HF ionospheric modification
[AD-A224402] 24 p3491 N90-29729
Studies of ionospheric dynamics utilizing data from DMSP
[AD-A223370] 24 p3492 N90-29733
Atmospheric structure and variability
[AD-A223439] 24 p3492 N90-29734
A feasibility study for D-region equatorial ionosphere research using VLF radiowaves
[AD-A223685] 24 p3492 N90-29738

EARTH LIMB
Offaxis radiance studies for infrared sensors
[AD-A210790] 02 p0275 N90-11570
Retrieval of atomic oxygen and temperature in the thermosphere. Part 2: Feasibility of an experiment based on limb emission in the OI lines
[AD-A211807] 03 p0371 N90-12121
Retrieval of atomic oxygen and temperature in the thermosphere. Part 1: Feasibility of an experiment based on the spectrally resolved 147 micrometer limb emission
[AD-A211987] 04 p0517 N90-12986
Conceptual design study for Infrared Limb Experiment (IRLE)
[NASA-CR-186950] 21 p2968 N90-26869
SAGE 3: A visible wavelength limb sounder 21 p3016 N90-27147

EARTH MAGNETOSPHERE
NT GEOMAGNETIC TAIL
NT MAGNETOSHEATH
User's guide to the Space Environment Services Center geophysical alert broadcasts
[PB89-194617] 02 p0249 N90-11411
Substorm associated pulsations: A study of plasmaspheric cavity resonance, mid-latitude polarisation and geostationary orbit signatures 02 p0251 N90-11422
Development of computer codes to model dynamics of the earth's magnetosphere
[AD-A211532] 04 p0517 N90-12987
Relationship between the current and the width of the POGO electrojet during the solstices
[DE89-619725] 04 p0565 N90-13294
Spacecraft attitude determination using the earth's magnetic field 05 p0589 N90-13429
Particle simulations in magnetospheric plasmas
[NASA-CR-186238] 06 p0848 N90-14934
Strategic characteristics of Dynamics Explorer 1 retarding ion mass spectrometer and the consequences for core plasma measurements
[AD-A214013] 07 p0886 N90-15125
Terrestrial magnetosphere magnetic field models
[REPT-89/CT/DTI/MS/AS/154] 08 p1102 N90-16380
Stable auroral red arc occurrences detected by the Pacific Northwest Laboratory photometer network: A decade of observations, 1978 - 1988
[DE90-004994] 09 p1298 N90-17522
Report from magnetospheric science 10 p1444 N90-18334
Development and use of data analysis procedures for the CRRES (Combined Release and Radiation Effects Satellite) payloads AFGL-701-2/Dosimeter and AFGL-701-4/Fluxmeter and application of the data analysis results to improve the static and dynamic models of the Earth's radiation belts
[AD-A215953] 10 p1447 N90-18348
Active probing of space plasmas
[AD-A216867] 12 p1716 N90-19855
USU center of excellence in theory and analysis of the geo-plasma environment
[AD-A217736] 13 p1759 N90-20101
Quantifying and reducing uncertainty in the assimilative mapping of ionospheric electrodynamics
[AD-A216057] 13 p1842 N90-20577
Center of excellence in theoretical geoplasma research
[AD-A215035] 14 p2005 N90-21488
Substorms: Their expansion and recovery phases
[DE90-008970] 14 p2042 N90-21712
Equilibrium and stability analysis of magnetospheric plasmas 15 p2057 N90-21782
Solar flares and magnetospheric particles: Investigations based upon the ONR-602 and ONR-604 experiments
[AD-A218844] 16 p2340 N90-23332
Diagnosis of auroral dynamics using global auroral imaging with emphasis on large-scale evolutions
[NASA-CR-186623] 17 p2422 N90-23804
A survey of equatorial magnetospheric wave activity between 5 and 8 R(sub E)
[AD-A220137] 17 p2424 N90-23812
Models of the external source contribution to magnetospheric magnetic fields for CRRES data analysis
[AD-A221059] 18 p2580 N90-24697
Viking data analysis
[AD-A222609] 20 p2823 N90-26062
A study of positrons from Soviet nuclear powered satellites as tracers for magnetospheric research
[DE90-013157] 20 p2888 N90-26438
Analytical studies of magnetospheric pulsations
[AD-A222275] 21 p3026 N90-27205
The near-Earth orbital environment coupling to its energy sources
[AD-A222435] 21 p3026 N90-27206
Evaluation of magnetospheric internal magnetic field models and existing software
[AD-A221816] 21 p3027 N90-27210
Influence of non-stationary field of magnetospheric convection on the D-region 22 p3210 N90-28209
A study of magnetic field reconnection and plasma processes in the magnetosphere
[DE90-016117] 24 p3493 N90-29741

EARTH MAGNETOTAIL
U GEOMAGNETIC TAIL

EARTH MANTLE
A search for layering in the oceanic crust
[PB89-196220] 01 p0090 N90-10514
Investigations of Eurasian seismic sources and upper mantle structure
[AD-A211806] 03 p0371 N90-12120
Workshop on the Archean Mantle
[NASA-CR-186156] 06 p0814 N90-14736
Determination of Q as a function of depth and tectonic province
[AD-A213805] 07 p0960 N90-15554
Evolution of overlapping spreading centers: A Sea Mark 2 investigation
[AD-A214278] 07 p0965 N90-15576
The composition and physical properties of the Earth's mantle and core 18 p2579 N90-24689
Use of geomagnetic data for studies on the Earth's deep interior 21 p3023 N90-27192

EARTH MOVEMENTS
NT EARTHQUAKES
Supplementing geodetic data with prior information for crustal deformation in the Imperial Valley, California
[TR-6-1988] 05 p0668 N90-13904

EARTH OBSERVATIONS (FROM SPACE)
NT SATELLITE OBSERVATION
NT SPOT (FRENCH SATELLITE)
Laser sounding from space: Report of the ESA Technology Working Group on Space Laser Sounding and Ranging
[ESA-SP-1108] 03 p0354 N90-12024
Strategy for earth explorers in global earth sciences
[NASA-CR-185933] 03 p0364 N90-12084
The use of LANDSAT-TM data for the management of pine forestations in central Chile
[DLR-FB-89-44] 05 p0664 N90-13881
Necessity and benefit of the X-SAR Space Shuttle experiment
[ESA-TT-1164] 08 p1057 N90-16112
Introduction to the framework and tasks of the DFD --- German Remote Sensing Data Center (DFD) 08 p1092 N90-16319
SPOT after two years in operation: An appraisal of results and a review of selected applications 08 p1093 N90-16326
Focal research effort points of the Institute of Applied Geodesy in the field of digital image processing 08 p1094 N90-16333
Refurbishment and modification of the Metric Camera (RMK) for reflight on EOM-1 Spacelab mission
[ETN-90-96284] 11 p1512 N90-18710
Paper on geography in environmental management: Research and new techniques
[INPE-4840-PRE/1469] 11 p1531 N90-18816
Activities report in German aerospace
[ISSN-0070-3966] 11 p1595 N90-19189
ESRIN
[ESA-BR-58] 12 p1677 N90-19631
Visibility problems in numerical models of terrain
[INPE-4921-TDL/382] 12 p1726 N90-19919
Trade-offs in a space based surveillance radar 14 p1960 N90-21225
Spaceborne radar observations: A guide for Magellan radar-image analysis
[NASA-CR-184998] 16 p2249 N90-22826
The VIERS-1 project. The Delft wind/wave experiment: Experiment and first results, part 1
[BCRS-89-24-PT-1] 17 p2418 N90-23779
Earth observation from the interstellar space
[REPT-44/89] 17 p2418 N90-23781
Vision of the Remote Sensing Management Commission on the ESA long term Earth observation program
[BCRS-89-11] 17 p2419 N90-23785
Concepts for high resolution space based SAR/ISAR systems
[MBB-UK-0057/89-PUB] 19 p2652 N90-25096
CAESAR: Performance and first evaluation of application possibilities
[BCRS-89-06] 19 p2705 N90-25393
Remote Sensing and the Earth's Environment
[ESA-SP-301] 19 p2706 N90-25398
Remote sensing for better understanding of the system Earth 19 p2706 N90-25399
CNES space programmes related to climate 19 p2706 N90-25400
Cloud analysis with satellite data 19 p2707 N90-25401
Ocean colour: Methods, technologies, applications 19 p2707 N90-25406
Snow and land ice in the climate system: Research problems and possibilities of remote sensing 19 p2707 N90-25407
Geocoded spaceborne SAR products for geological applications 19 p2708 N90-25410
Second Meeting of the Space Agency Forum on the International Space Year (SAFISY)
[ESA-SP-1115] 19 p2800 N90-25932
Microspacecraft and Earth observation: Electrical field (ELF) measurement project
[NASA-CR-186821] 20 p2888 N90-26436
Applications of ISES for the atmospheric sciences 21 p3017 N90-27155
Size, duration, and rate of growth of nocturnal lightning events appearing on space shuttle video tapes
[NASA-CR-4313] 22 p3229 N90-28310
Mesoscale Lightning Experiment (MLE): A view of lightning as seen from space during the STS-26 mission
[NASA-TM-103513] 23 p3353 N90-28951

EARTH OBSERVING SYSTEM (EOS)
Strategy for earth explorers in global earth sciences
[NASA-CR-185933] 03 p0364 N90-12084
Science and applications on the space station: A strategic vision
[NASA-TM-101863] 05 p0601 N90-13493
SURE (Science User Resource Expert): A science planning and scheduling assistant for a resource based environment 15 p2153 N90-22302
Modelling and synergism: Optical and microwave remote sensing. Partial report 1: Preliminary study
[BCRS-89-23] 18 p2575 N90-24688
Ocean colour: Methods, technologies, applications 19 p2707 N90-25406
Modeling, simulation, and analysis of optical remote sensing systems
[NASA-CR-186648] 20 p2878 N90-26376
Earth Sciences Requirements for the Information Sciences Experiment System
[NASA-CP-3072] 21 p3015 N90-27140
Information sciences experiment system 21 p3015 N90-27142
Lidar instruments proposed for Eos 21 p3016 N90-27145
Eos visible imagers 21 p3016 N90-27146
Applications of ISES for meteorology 21 p3018 N90-27160
Applications of ISES for instrument science 21 p3018 N90-27161

EARTH ORBITAL ENVIRONMENTS
Orbital debris research at NASA Johnson Space Center, 1986-1988
[NASA-TM-102155] 01 p0138 N90-10795
Environmental constraints for polar platform design
[RAE-TR-89014] 09 p1181 N90-16849
Status of the cycling tests performed with SAFT NiH2 cells dedicated to space applications 10 p1334 N90-17715
Low earth orbit nickel cadmium battery lifetime testing 10 p1334 N90-17716
Design development, qualification, and flight production of an ATOX resistant flexible solar array for low earth orbit mission 10 p1344 N90-17796
The advanced photovoltaic solar array program 10 p1345 N90-17797
Review of synergistic environmental interactions: Guidelines for new testing approaches on future solar arrays 10 p1345 N90-17803
Radio interference in the near-earth environment
[NASA-CR-180479] 11 p1498 N90-18623
Simplified model for solar cosmic ray exposure in manned Earth orbital flights
[NASA-TM-4182] 14 p2043 N90-21715

International treaties and active experiments in space
[AD-A219368] 16 p2328 N90-23272
Solar flares and magnetospheric particles: Investigations based upon the ONR-602 and ONR-604 experiments
[AD-A218844] 16 p2340 N90-23332
Orbit recovery of a low Earth orbiter from GPS and ground tracking stations
[FFI-89/7012] 17 p2361 N90-23446
SILEX Beacon equipment
[ETN-90-96613] 17 p2409 N90-23726
Laboratory investigations: Low Earth orbit environment chemistry with spacecraft surfaces
19 p2732 N90-25531

EARTH ORBITING SPACE STATIONS
U SPACE STATIONS

EARTH ORBITS
NT GEOSYNCHRONOUS ORBITS
Laser propulsion to earth orbit. Has its time come?
01 p0028 N90-10143
Low-earth-orbit to low-lunar-orbit laser freighter
01 p0030 N90-10160
Earth orbit laser systems 01 p0030 N90-10162
The time evaluation of the number of space probes and debris at different orbit heights with a view to a future collision risk in space
[R-8718] 03 p0311 N90-11772
On mean elements for satellite orbits perturbed by the zonal harmonics of the geopotential
[AD-A212322] 04 p0461 N90-12642
Design considerations for space flight hardware
[NASA-TM-102300] 06 p0734 N90-14275
An autonomous orbit determination system for earth satellites
[AD-A215671] 09 p1172 N90-16779
A two-stage earth-to-orbit transport with translating oblique wings for booster recovery
[NASA-CASE-LAR-14156-1] 09 p1173 N90-16781
Radiation of plasma waves from large space structures in low earth orbit
[AD-A215062] 09 p1182 N90-16856
Defending against a space blockade: CADRE paper
[AD-A215681] 09 p1276 N90-17398
Technology development, demonstration, and orbital support requirements for manned lunar and Mars missions
[NASA-TM-101666] 10 p1447 N90-18350
Spatial registration of TIROS-N weather satellite data
[AD-A216041] 11 p1536 N90-18841
Series reversion/inversion of Lambert's time function
[AD-A216243] 12 p1607 N90-19245
Low earth orbiting satellite for international information exchange system
[DE90-007186] 12 p1615 N90-19292
ETO (Earth-To-Orbit): A trajectory program for aerospace vehicles
[AD-A218157] 13 p1760 N90-20103
A satellite simulation program
[AD-A218079] 13 p1764 N90-20124
Measurements of the interaction of high-voltage biassed conductors with the ionosphere
[AD-A218285] 13 p1843 N90-20580
Optimal trajectories for the aeroassisted flight experiment. Part 3: Formulation, results, and analysis
[NASA-CR-186165] 14 p1930 N90-21051
SIRTF in high earth orbit 14 p1980 N90-21345
Orbital mechanics: A learning tool on the main frame
[AD-A218799] 16 p2204 N90-22576
The influence of the gas surface interaction on spacecraft orbital motion 17 p2365 N90-23461
Laboratory investigations: Low Earth orbit environment chemistry with spacecraft surfaces
19 p2732 N90-25531
Discharge transient coupling in large space power systems 19 p2735 N90-25544
Space operations: NASA's communications support for Earth orbiting spacecraft. Report to Chairman, Subcommittee on Space Science and Applications, Committee on Science, Space and Technology, House of Representatives
[GAO/IMTEC-89-41] 20 p2851 N90-26215
Atmospherically induced optical contamination from orbiting thrusters
[AD-A223112] 21 p3021 N90-27174
Final design for a comprehensive orbital debris management program
[NASA-CR-186674] 22 p3126 N90-27739
Possible trajectory profiles to achieve the geostationary orbit without any drift phase 22 p3127 N90-27745
Spacecraft attitude dynamics: Evolution and current challenges 22 p3128 N90-27754
The effect of temperature cycling typical of low earth orbit satellites on thin films of YBa2Cu3O(7-x)
22 p3140 N90-27812

EARTH PLANETARY STRUCTURE
Earth model selection for computer simulations
[AD-A216843] 11 p1525 N90-18779
Topical Conference on the Origin of the Earth
[NASA-CR-185061] 15 p2128 N90-22186

EARTH RADIATION
U TERRESTRIAL RADIATION

EARTH RADIATION BUDGET
South Pole surface radiation balance measurements, April 1986 to February 1988
[PB89-224018] 04 p0519 N90-12993
Extended Kalman filter for attitude estimation of the earth radiation budget satellite 05 p0590 N90-13433
Atlas of albedo and absorbed solar radiation derived from Nimbus 6 earth radiation budget data set, July 1975 to May 1978
[NASA-RP-1230] 06 p0815 N90-14741
Evaluation of climatic models: Comparison of simulated and observed patterns for past climates
[DE90-001228] 06 p0817 N90-14755
Atlas of albedo and absorbed solar radiation derived from Nimbus 7 Earth radiation budget data set, November 1978 to October 1985
[NASA-RP-1231] 09 p1247 N90-17233
USSR Climate Handbook Number 27. Part 1: Solar radiation, radiation balance and sunshine
[AD-A215647] 09 p1248 N90-17242
Cloud types and the tropical Earth radiation budget, revised
[NASA-CR-180475] 13 p1843 N90-20582
Satellite versus GCM-simulated radiation balance: Comparisons and implications for climate modeling
15 p2131 N90-22180
Implementation of reflectance models in operational AVHRR radiation budget processing
[NOAA-TR-NESDIS-49] 18 p2578 N90-24888
Earth radiation budget and climate
19 p2707 N90-25403
Earth radiation budget measurements from space
19 p2707 N90-25404
Modeling and measurement of tree canopy reflectance
[MITT-66] 21 p3018 N90-27162
Measurement of diurnal variation in the Earth radiation budget
[MITT-69] 21 p3027 N90-27212
The effects of clouds on CO2 forcing
22 p3222 N90-28271
Physically-based general circulation model parameterization of clouds and their radiative interaction
22 p3228 N90-28308

EARTH RADIATION BUDGET EXPERIMENT
The effects of seasonal and latitudinal earth infrared radiance variations on ERBS attitude control
05 p0586 N90-13414
Failure of the ERBE scanner instrument aboard NOAA 10 spacecraft and results of failure analysis
[NASA-TM-102661] 19 p2694 N90-25328
Earth radiation budget measurements from space
19 p2707 N90-25404
Earth Radiation Budget Experiment (ERBE) validation
[NASA-TM-103481] 20 p2888 N90-26433
ERBE and CERES broadband scanning radiometers
21 p3016 N90-27149
Measurement of diurnal variation in the Earth radiation budget
[MITT-69] 21 p3027 N90-27212

EARTH RESOURCES
NT AQUIFERS
NT COAL
NT CRUDE OIL
NT FORESTS
NT FOSSIL FUELS
NT GEOTHERMAL RESOURCES
NT GEYSERS
NT GLACIERS
NT ICEBERGS
NT KEROGEN
NT LAND ICE
NT NATURAL GAS
NT PEAT
NT RAIN FORESTS
NT WATER RESOURCES
Potential effects of global climate change on the United States. Volume 1: Regional studies. Draft
[PB89-161053] 02 p0238 N90-11351
Potential effects of global climate change on the United States. Volume 2: National studies. Draft
[PB89-161061] 02 p0238 N90-11352
Earth resources: A continuing bibliography with indexes (issue 63)
[NASA-SP-7041(63)] 03 p0366 N90-12091
How far can the world get on energy efficiency alone
[DE90-001349] 06 p0805 N90-14686
International course in remote sensing ONU/INPE, Brazil
[INPE-4802-NTE/288] 10 p1399 N90-18089
Sensitivity of ecological landscapes and regions to global climatic change
[PB90-120072] 12 p1684 N90-19674
Monitoring vegetation of Brazil: Potentialities of multi-sensors approach
[INPE-4993-PRE/1555] 14 p1998 N90-21451
Mission to planet Earth 15 p2125 N90-22153
Natural resources information system for the state of Oklahoma
[DE90-009483] 15 p2180 N90-22458
Remote Sensing and the Earth's Environment
[ESA-SP-301] 19 p2706 N90-25398
Operational satellite environmental monitoring for food security by FAO: The ARTEMIS system
19 p2708 N90-25413
Integration of multispectral SPOT imagery and panchromatic aerial photography for study in urban land use
[INPE-4967-PRE/1536] 22 p3194 N90-28125

EARTH RESOURCES PROGRAM
NT SEASAT PROGRAM

EARTH RESOURCES SURVEY PROGRAM
NT SEASAT PROGRAM

EARTH RESOURCES TECHNOLOGY SATELLITES
U LANDSAT SATELLITES

EARTH ROTATION
RTSIN1: A model of a strapdown INS on a two-axis rate table
[AD-A212406] 04 p0450 N90-12579
Determination of Earth orientation using the Global Positioning System 12 p1642 N90-19435
Geophysical studies related to geodetic reference frames
[AD-A220249] 18 p2574 N90-24663

EARTH SHAPE
U GEODESY

EARTH SURFACE
Crustal deformation: Earth vs Venus
03 p0427 N90-12450
Senegalese land surface change analysis and biophysical parameter estimation using NOAA AVHRR spectral data
[NASA-CR-186120] 05 p0664 N90-13883
Orbital remote sensing in the decade of the nineties: New approaches and challenges in geology
[INPE-4838-PRE/1467] 11 p1521 N90-18758
Mechanics of aeolian processes: Soil erosion and dust production 12 p1638 N90-19410
An analysis of propagation in a surface duct over a periodically rough Earth
[AD-A220565] 17 p2390 N90-23612
Astronaut's guide to terrestrial impact craters
[NASA-TM-102902] 17 p2421 N90-23798
Ecological study of peat landforms in Canada and Alaska
[NASA-CR-184923] 19 p2705 N90-25391
Thermal imaging assessment
[AD-A224400] 24 p3460 N90-29542

EARTH TERMINAL MEASUREMENT SYSTEM
X-band atmospheric attenuation for an Earth terminal measurement system
[PB90-100736] 08 p1056 N90-16101

EARTH TERMINALS
Harrier Information Management System (HIMS): The system and the approach 22 p3105 N90-27630

EARTH TIDES
Earth tidal analysis based on gravimeter observations and the influence of ocean tides
[ETN-90-95721] 12 p1695 N90-19734
Predicting tidal displacements of the surface of the Earth, volume 1
[ETN-90-96690] 17 p2431 N90-23850
Predicting tidal displacements of the surface of the Earth, volume 2
[ETN-90-96691] 17 p2431 N90-23851
Geophysical studies related to geodetic reference frames
[AD-A220249] 18 p2574 N90-24663

EARTH-MOON SYSTEM
Determination of parameters of the Earth-Moon system: A contribution to model extension, evaluation, results
[SER-C-353] 22 p3263 N90-28479

EARTH-MOON TRAJECTORIES
Calculation of double-lunar swingby trajectories: I. Keplerian foundation 05 p0590 N90-13435

EARTHNET
ESA/Earthnet 08 p1093 N90-16325
Future developments of remote sensing systems: Data management and processing 19 p2709 N90-25416

EARTHQUAKE RESISTANT STRUCTURES
Wind/seismic comparisons for upgrading existing structures
[DE89-016055] 03 p0357 N90-12044

EARTHQUAKES
Hydrophone investigations of earthquakes and explosion generated high-frequency seismic phases
[AD-A212055] 03 p0371 N90-12122
Crustal structure studies utilizing earthquake sequences
[AD-A212916] 05 p0666 N90-13895
Comparison of shock severity measures
[DE90-000790] 06 p0799 N90-14654
Determination of Q as a function of depth and tectonic province
[AD-A213805] 07 p0960 N90-15554
Theoretical models of earthquake phenomena and the physical significance of seismic moment tensor expansions
[AD-A213813] 07 p0961 N90-15556
Proceedings of the 79th SEGJ Conference
[DE89-760006] 08 p1157 N90-16704
Self-similar growth of three-dimensional fault
[DE90-608162] 10 p1407 N90-18112
Damage characteristics of time domain histories
[DE90-008787] 13 p1842 N90-20573
The effects of structure and source complexity on waveforms: Crustal structure of Tibet and the recovery of complex seismic sources
[AD-A218202] 13 p1843 N90-20579
Scattering of waves by inclusions in a nonhomogeneous elastic half space solved by boundary element methods
[PB90-145699] 15 p2116 N90-22107
Propagation and attenuation of Lg waves in South America
[AD-A218853] 16 p2255 N90-22859
Proceedings of the 21st Joint Meeting of the US-Japan Cooperative Program in Natural Resources Panel Wind and Seismic Effects
[PB90-186826] 21 p3030 N90-27226
Lateral buckling of short I-beams under cyclic loading
[PB90-213653] 22 p3191 N90-28104
NASA geodynamics program: Bibliography
[NASA-TM-4220] 22 p3194 N90-28123
Torsional effects in structures subjected to strong ground motion
[PB90-226960] 23 p3339 N90-28869
Catalog of strong motion stations in Eastern North America
[PB90-251984] 24 p3490 N90-29722

EATING
Air Force flight feeding. Volume 1: Evaluation of current system and alternative concepts
[AD-A212789] 04 p0527 N90-13043

EBULLITION
U BOILING

ECCENTRIC ORBITS
Orbit acquisition and control strategy for small satellites in inclined eccentric orbits
[ETN-90-96551] 16 p2203 N90-22573
Optimization of the deployment of a pair of satellites in inclined eccentric geosynchronous orbits
22 p3128 N90-27751

ECCENTRICITY
Rotordynamic properties of high pressure seals: An experimental approach 24 p3475 N90-29640

ECHELON FAULTS
U GEOLOGICAL FAULTS

ECHO SOUNDING
Polar mesosphere summer echoes and associated atmospheric gravity waves 05 p0660 N90-13856

ECHOES
NT AURORAL ECHOES
NT CLUTTER
NT RADAR ECHOES
NT SIGNAL REFLECTION
Method for eliminating self-screening noise jamming in radar systems
[AD-D014271] 08 p1056 N90-16105
Pulsed and modulated passage NMRON studies of cobalt-iron alloys 17 p2470 N90-24118
Genesis of bow echoes: A rear-inflow induced meso-convective structure
[PB90-209776] 23 p3349 N90-28926

ECLIPSES
NT LUNAR ECLIPSES
A source of observational constraints on the structure of Wolf-Rayet winds
[DE90-001236] 06 p0864 N90-15023
Ginga observations of SS 433
19 p2776 N90-25789

ECLIPSING BINARY STARS
NT DWARF NOVAE
A source of observational constraints on the structure of Wolf-Rayet winds
[DE90-001236] 06 p0864 N90-15023
Constraints on the SS433 system from the Ginga observations 19 p2784 N90-25838
Detection of emission lines from the secondary star in IX Vel (=CPD-48 deg 1577)
[MPE-PREPRINT-172] 22 p3265 N90-28485

ECOLOGICAL SYSTEMS
U ECOSYSTEMS

ECOLOGY
ELF (Extremely Low Frequency) Communications System Ecological Monitoring Program: Electromagnetic field measurements and engineering support, 1988
[AD-A210200] 01 p0056 N90-10321
Acid rain research
[DE90-003283] 07 p0957 N90-15537
ELF (Extremely Low Frequency) communications system ecological monitoring program: Summary of 1988 progress
[AD-A216153] 10 p1377 N90-17981
Perspectives on aerosol deposition to natural surfaces
[DE90-003398] 11 p1532 N90-18819
Sensitivity of ecological landscapes and regions to global climatic change
[PB90-120072] 12 p1684 N90-19674
Hypotheses testing of watershed/landscape dynamics in northern Alaska using digital analysis
[DE90-006721] 13 p1820 N90-20450
MARS (Monitoring Agro-ecological Resources with Remote sensing and Simulation) definition study: Results of the preparatory phase
[REPT-17] 19 p2706 N90-25395
Outer continental shelf environmental assessment program. Volume 66: Principal investigators
[PB90-194747] 22 p3199 N90-28154

ECONOMETRICS
Computing mean responses in nonlinear models
[AD-A217642] 13 p1865 N90-20700

ECONOMIC ANALYSIS
Study of the application of automation to composites manufacture
[AD-A211049] 02 p0190 N90-11087
View on recent fuel costs in airlines
[NAL-TM-569] 02 p0289 N90-11653
What is the balance sheet for investment in automated manufacturing
[CETIM-105490] 04 p0532 N90-13071
International Conference on Fixed Point Theory and Applications
[AD-A212369] 04 p0545 N90-13171
The economic impact of automation technology
[AD-A213363] 05 p0630 N90-13682
California air transportation study: A transportation system for the California Corridor of the year 2010
[NASA-CR-186219] 06 p0722 N90-14212
The conversion of carbonaceous materials to clean carbon and co-product gaseous fuel
[DE90-001561] 06 p0754 N90-14387
Markets for high-speed intercity Maglev technology: A systems analysis approach
[DE89-017683] 06 p0794 N90-14623
Report of NASA Lunar Energy Enterprise Case Study Task Force
[NASA-TM-101652] 07 p1007 N90-15836
Report of the NASA lunar energy enterprise case study task force 07 p1008 N90-15837
Analysis of the financial factors governing the profitability of lunar helium-3 07 p1008 N90-15838
The Solar Power Satellite (SPS): Progress so far
07 p1008 N90-15840
Lunar power system summary of studies for the lunar enterprise task force NASA-office of exploration
07 p1008 N90-15841
Feasibility of cool storage systems in refrigeration
[DE90-728179] 08 p1054 N90-16093
Industrial heat pump assessment study
[DE90-004541] 08 p1071 N90-16201
FY 1989 update to the Information Resources Management review plan
[DE90-004185] 08 p1138 N90-16593
Are reusable boosters cost-effective
09 p1179 N90-16834
Assessment of ground-coupled heat pumps
[DE90-003977] 09 p1220 N90-17079
A new method for power generation and distribution in outer space
[DE90-005571] 09 p1243 N90-17211
Measuring the demand for environmental studies
[PB90-100207] 09 p1244 N90-17214
Conceptual design of high Tc superconducting power cable and its economic evaluation
[DE90-734940] 09 p1287 N90-17462
Improper use of economic analysis in materiel cost comparison studies
[AD-A214888] 09 p1297 N90-17518
Hydrogen energy coordinating committee: Summary of DOE hydrogen programs
[DE90-004480] 10 p1361 N90-17891
Modeling the effects of air pollution on forest ecosystems: Considerations for applying a model to Southeast Asia
[DE90-004937] 10 p1406 N90-18110
Analysis of inter-energy competition in the age of complex energies
[DE89-910216] 11 p1527 N90-18794
Energy markets in the 1990's and beyond: A comparison of energy intensity in the United States and Japan
[DE90-005535] 11 p1528 N90-18797
Programs in Renewable Energy
[DE89-009489] 11 p1530 N90-18809
Promotion of European Space Technology Transfer
[ESA-SP-1122] 11 p1575 N90-19068
Space technology transfers in Europe
11 p1576 N90-19070
French approach to space technology transfer
11 p1576 N90-19074
Solid oxide fuel cell cogeneration system conceptual design, program 2
[PB90-114968] 12 p1681 N90-19653
Techno-economic assessment of a carbothermic alumina reduction process
[DE90-007018] 13 p1772 N90-20170
Photovoltaic energy
[DE89-009473] 13 p1826 N90-20486
Wind Energy Program summary. Volume 1: Overview
[DE89-009479] 13 p1827 N90-20491
International science and technology policies: Testimony before the Subcommittee on International Scientific Cooperation, Committee on Science, Space, and Technology, United States House of Representatives
[DE90-009416] 15 p2181 N90-22463
Economic values for evaluation of Federal Aviation Administration investment and regulatory programs
[AD-A219882] 17 p2343 N90-23343
Space funding: NASA and DOD activities for fiscal years 1981 through 1989. Fact sheet for the Chairman and the Ranking Minority Member, Subcommittee on Science, Technology, and Space, Committee on Commerce, Science, and Transportation, US Senate
[GAO/NSIAD-89-102FS] 17 p2481 N90-24187
Solar thermal program summary. Volume 2: Research summaries
[DE89-009476] 18 p2576 N90-24874
Outlook for ceramics in heat engines, 1990 - 2010: A technical and economic assessment based on a worldwide Delphi survey
[DE90-011262] 19 p2679 N90-25234
The effects of different diffusion sources on silicon solar cell recombination properties
[DE90-011235] 19 p2710 N90-25426
A contribution to the economic, optimal dimensioning, and shaping of aircraft structures using a design model
[ETN-90-96966] 20 p2808 N90-25976
ASATs vs Brilliant Pebbles
[DE90-010348] 20 p2922 N90-26626
Airline productivity relating on the fuel cost. (2): Fuel consumption values and fuel efficiency
[NAL-TM-604-2] 24 p3422 N90-29333

ECONOMIC DEVELOPMENT
A quasi-economic role for lunar science
[DE90-000679] 07 p1015 N90-15876
Space Station Freedom Pre-Workshop Session
[NASA-TM-102913] 17 p2479 N90-24172
State science and technology indicators: An exploratory profile and analysis
[PB90-246711] 23 p3408 N90-29259

ECONOMIC FACTORS
New energy conversion techniques in space, applicable to propulsion
[AIAA-79-1338] 01 p0028 N90-10145
An interactive life cycle cost forecasting tool
[AD-A220472] 17 p2480 N90-24184
Space program safety: Funding for NASA's safety organizations should be centralized
[GAO/NSIAD-90-187] 22 p3255 N90-28434

ECONOMIC IMPACT
Manufacturing and the manufacturing engineer in the year 2000, revision
[DE89-017707] 03 p0335 N90-11904
The economic impact of automation technology
[AD-A213363] 05 p0630 N90-13682
Impact of the whole national economy of defense spending and space in the US: A literature analysis
[ISSN-0342-0787] 22 p3260 N90-28464

ECONOMICS
NT DEMAND (ECONOMICS)
The transfer and diffusion of new technologies: A review of the economics literature
[DE89-015671] 02 p0290 N90-11655
Remarks on the control of discrete time nonlinear systems
[MEMO-770] 04 p0544 N90-13158

An assessment of potential markets for small satellites
[NASA-TM-101943] 09 p1181 N90-16848
Remote sensing applied to the monitoring of mineral extraction in the proximity of urban areas: Pros and cons
[INPE-4867-PRE/1478] 11 p1522 N90-18766
Survey on the social and economic influences of wide-spreading heat-pump technology
[DE89-782294] 12 p1658 N90-19526
Synthesis and analysis of 25 years (1961-1986) of INPE/SRE activities related to the vegetation/forest area
[INPE-4969-RPE/604] 13 p1819 N90-20446
Evolution of remote sensing applied to vegetation and forest at INPE
[INPE-4970-PRE/1538] 14 p1998 N90-21452
Advanced manufacturing technology: A Department of Energy technology transfer initiative
[DE90-008601] 14 p2037 N90-21688
Preference numbers and funnel dimension
[REPT-89-57] 15 p2161 N90-22346
FAA (Federal Aviation Administration) aviation forecasts, fiscal years 1990-2001
[AD-A219165] 16 p2195 N90-22530
The effects of climate change on energy planning and operations in the Pacific Northwest. Volume 1: Overview
[DE90-009464] 17 p2425 N90-23816
The effects of climate change on energy planning and operations in the Pacific Northwest. Volume 2: Technical background
[DE90-009465] 17 p2425 N90-23817
National patterns of research and development resources: 1989
[NSF-89-308] 17 p2486 N90-24218
Photovoltaic concentrator technology development
[DE90-011479] 18 p2577 N90-24684
Managing the global environment
[AD-A218615] 19 p2712 N90-25434
Study of high-speed civil transports. Summary
[NASA-CR-4236] 20 p2806 N90-25966
Survey of applicability of electric vehicles (EVs) in specific regions such as resorts
[DE90-503592] 20 p2871 N90-26336
Copyright and home copying: Technology challenges the law
[PB90-151309] 21 p3086 N90-27547
Sandia's CONCEPT-90 photovoltaic concentrator module
[DE90-012243] 22 p3196 N90-28134
Proceedings of a workshop on Future Airport Passenger Terminals
[PB90-213620] 23 p3284 N90-28580

ECONOMY
Advancing automation and robotics technology for the Space Station Freedom and for the US economy: Submitted to the United States Congress
[NASA-TM-101647] 12 p1613 N90-19279
The cost of air service fragmentation
[TT-9010] 24 p3422 N90-29334

ECOSYSTEMS
ELF (Extremely Low Frequency) Communications System Ecological Monitoring Program: Electromagnetic field measurements and engineering support, 1988
[AD-A210200] 01 p0056 N90-10321
Biochemical cycling and fluxes between the deep euphotic zone and other oceanic realms
[PB89-152458] 01 p0089 N90-10509
Coastal Research Center Woods Hole Oceanographic Institution
[PB89-198238] 01 p0089 N90-10510
Adaptation and resistance of ecosystems to stress
[AD-A212999] 05 p0665 N90-13889
Utilization of non-conventional systems for conversion of biomass to food components
[NASA-CR-177545] 07 p0968 N90-15591
Potential impact of stratospheric ozone depletion on marine ecosystems
[PB90-112616] 08 p1098 N90-16360
Modeling the effects of air pollution on forest ecosystems: Considerations for applying a model to Southeast Asia
[DE90-004937] 10 p1406 N90-18110
Assessment of the theory and hypotheses of the acidification of watersheds
[DE90-005528] 10 p1406 N90-18111
Effects of global climate change on agroecosystems: Scope of work
[PB90-120023] 11 p1531 N90-18813
Atlantic outer continental shelf: Description of the Mid-Atlantic environment
[PB90-100033] 11 p1537 N90-18849
Sensitivity of ecological landscapes and regions to global climatic change
[PB90-120072] 12 p1684 N90-19674
Proceedings of the 2nd United States/USSR Symposium on Air Pollution Effects on Vegetation Including Forest Ecosystems
[PB90-127119] 12 p1685 N90-19678
Underwater physiography of the continental shelf of Rio Grande do Norte visible through satellite imagery
[INPE-4964-TDL/392] 13 p1820 N90-20448
Hypotheses testing of watershed/landscape dynamics in northern Alaska using digital analysis
[DE90-006721] 13 p1820 N90-20450
Processes of community development and responses of ecosystems to climate change
[DE90-008640] 13 p1831 N90-20512
Publications of the NASA Controlled Ecological Life Support System (CELSS) Program, 1979-1989
[NASA-CR-4297] 15 p2051 N90-21754
Site visit to US Antarctic Program (USAP) facilities and the Research Vessel Polar Duke
[DE90-009396] 15 p2126 N90-22159
Utilization of the water soluable fraction of wheat straw as a plant nutrient source
[NASA-TM-103497] 19 p2716 N90-25455
Evaluation of the role of ozone, acid deposition, and other airborne pollutants in the forests of eastern North America
[PB90-184896] 22 p3197 N90-28140
Perspectives on the Chesapeake Bay, 1990: Advances in estuarine sciences
[PB90-248600] 23 p3354 N90-28954
Biomedical and environmental sciences program publications, 1989
[DE90-014785] 23 p3406 N90-29250

ECS
U EUROPEAN COMMUNICATIONS SATELLITE

EDDIES
U VORTICES

EDDINGTON APPROXIMATION
Electron positron pair winds and the Eddington limit
19 p2791 N90-25888

EDDY CURRENTS
Questions from the Willmarth Workshop on New Directions in Research on Turbulent Wall-Layer Structures
[AD-A211282] 02 p0221 N90-11264
Sensors for nondestructive testing and evaluation of materials
[DE89-014763] 02 p0223 N90-11279
Parametric study of power absorption from electromagnetic waves by small ferrite spheres
[NASA-TP-2949] 03 p0399 N90-12282
Device for inspection of materials by eddy current methods
[AD-D014205] 04 p0511 N90-12948
Eddy-current inspection of shuttle heat exchanger tube welds
[NASA-CR-186302] 07 p0943 N90-15462
Inspection development for T-37 wing spar cap lug
[AD-A214826] 09 p1159 N90-16708
The 1989 National Convention Record IEE Japan, part 7
[DE89-910080] 09 p1210 N90-17012
Electrical test of gyrotron coil
[INPE-4929-RPE/596] 09 p1214 N90-17041
Eddy current test for bolts
[AD-A214829] 09 p1234 N90-17159
Superconductive microprobes for eddy current evaluation of materials
[AD-A217776] 13 p1805 N90-20361
Institute for Materials Science and Engineering, nondestructive evaluation: Technical activities
[PB90-132739] 15 p2108 N90-22055
The effects of climatological and transient wind forcing on eddy generation in the California current system
[AD-A219858] 17 p2431 N90-23855
The role of eddy fluxes of momentum in hurricane formation
[AD-A219417] 18 p2581 N90-24700
Eddy current inspection at the nuclear power plants
[VTT-RR-653] 19 p2699 N90-25357
Inspection of welds with eddy current
[TTR-RR-644] 19 p2699 N90-25358
Artificial intelligence in the materials processing laboratory 21 p3041 N90-27283
Transversal, longitudinal, and three dimensional eddy currents in cylindrical guides with elliptic diameters
[ETN-90-97302] 22 p3168 N90-27967
Inspection reliability 22 p3184 N90-28072
Progress in the detection of cracks under installed fasteners using eddy currents 22 p3186 N90-28081
New aspects in aircraft inspection using eddy current methods 22 p3187 N90-28085
Analysis of three-dimensional eddy current field. Application to calculation of magnetic screening effect of the damper system in a model superconducting generator
[DE90-507869] 23 p3321 N90-28779
Neural nets and eddy-current testing
[DE90-016044] 24 p3478 N90-29656

EDDY DIFFUSION
U TURBULENT DIFFUSION

EDDY VISCOSITY
Application of large eddy interaction model to a mixing layer
[NASA-CR-185123] 05 p0572 N90-13328
Navier-Stokes solutions of 2-D transonic flow over unconventional airfoils 06 p0719 N90-14195
Group-kinetic theory and modeling of atmospheric turbulence
[NASA-CR-183776] 06 p0813 N90-14728
PROTEUS two-dimensional Navier-Stokes computer code, version 1.0. Volume 2: User's guide
[NASA-TM-102552] 14 p1973 N90-21306
PROTEUS two-dimensional Navier-Stokes computer code, version 1.0. Volume 3: Programmer's reference
[NASA-TM-102553] 14 p1974 N90-21307
Development of a defect stream function, law of the wall/wake method for compressible turbulent boundary layers 15 p2100 N90-22019
Algebraic turbulence modeling for unstructured and adaptive meshes
[NASA-CR-182035] 17 p2401 N90-23676
The computation of turbulent thin shear flows associated with flow around multielement aerofoils
18 p2491 N90-24240
An improved k-epsilon model for near-wall turbulence and comparison with direct numerical simulation
[NASA-TM-103221] 22 p3171 N90-27983
Modeling of near-wall turbulence
[NASA-TM-103222] 22 p3174 N90-28009

EDEMA
Experiment K-6-09. Morphological and biochemical investigation of microgravity-induced nerve and muscle breakdown. Part 1: Investigation of nerve and muscle breakdown during spaceflight; Part 2: Biochemical analysis of EDL and PLT muscles 20 p2893 N90-26463

EDGE DETECTION
Some edge-enhancing operators and their applications to image enhancement and edge detection
06 p0826 N90-14810
Detection of edges using local geometry
08 p1074 N90-16213
Isolating contour information from arbitrary images
08 p1074 N90-16217
Alvey MMI007. Object identification from 2D images: The RSRE contribution
[RSRE-MEMO-4277] 08 p1110 N90-16428
Order filters, median recursive filter: Analysis and evaluation of performance in image processing
[ISAL-89-0017] 08 p1123 N90-16505
The effects of luminance boundaries on color perception
[AD-A216741] 11 p1539 N90-18860
Performance evaluation of morphological edge detectors
[INPE-4975-PRE/1540] 14 p2000 N90-21464
Computation and parallel implementation for early vision 15 p2139 N90-22222
Intensity dependent spread theory
15 p2139 N90-22223
Edge recognition using image-processing hardware
[OUEL-1777/89] 15 p2148 N90-22271
Implementing the Canny edge recognizer with datacube image-processing hardware
[OUEL-1786/89] 15 p2148 N90-22272
Extensions of algebraic image operators: An approach to model-based vision 19 p2741 N90-25577
A topological image matcher
[OUEL-1798/89] 19 p2744 N90-25600
Robot Acting on Moving Bodies (RAMBO): Interaction with tumbling objects 23 p3366 N90-29022
Real-time edge tracking using a tactile sensor
23 p3367 N90-29023
Learned navigation in unknown terrains: A retraction method 23 p3368 N90-29029
Trinocular stereovision using figural continuity, dealing with curved objects 24 p3503 N90-29802

EDGE DISLOCATIONS
Crack tip toughening by inclusions with pairs of shear transformations
[DE89-007845] 07 p0909 N90-15254
Dislocation annihilation mechanism for the formation of dislocation free zone at a crack tip
[DE90-610552] 12 p1674 N90-19615
The stress field due to an edge dislocation and some fracture problems for a three-phase composite cylinder model 15 p2120 N90-22126

EDGE LOADING
Combined effect of matrix cracking and stress-free edge on delamination
[NASA-TM-102591] 14 p1944 N90-21126

Weight functions and stress intensity factors for mode 1 cracks in arbitrary 2D geometries under general crack surface loading
[FFA-TN-1990-17] 19 p2703 N90-25381

EDGES
NT BLUNT LEADING EDGES
NT BLUNT TRAILING EDGES
NT LEADING EDGES
NT SHARP LEADING EDGES
NT TRAILING EDGES

Interlaminar stress concentration in fiber composites
[ETN-89-94670] 03 p0319 N90-11809

Research in knowledge-based vision techniques for the Autonomous Land Vehicle Program
[AD-A213440] 07 p0942 N90-15453

Detection of edges using local geometry
08 p1074 N90-16213

From primal sketches to the recovery of intensity and reflectance representations 08 p1074 N90-16216

Instability-related delamination growth of embedded and edge delaminations
[NASA-TM-100655] 17 p2370 N90-23494

Symmetrical layered thin film edge field-emitter-array and method for its production
[AD-D014594] 24 p3464 N90-29569

An investigation of hole-edge crack problem by a combined complex variable and least square method
[LR-626] 24 p3482 N90-29679

EDITING

An investigation of the usefulness of Earley's Algorithm in a general context-free recognizer
[DE89-016498] 02 p0258 N90-11463

An executive system for modeling with rational b-splines
[AD-A213460] 07 p0974 N90-15627

Multi-tasking computer control of video related equipment 13 p1859 N90-20665

Editing wind profiler measurements
[PB90-130147] 14 p2007 N90-21503

Generation of animation sequences of three dimensional models
[NASA-CASE-MSC-21379-1-SB] 21 p3050 N90-27340

EDITING ROUTINES (COMPUTERS)

A Z specification of the MaCHO interface editor
[RSRE-MEMO-4247] 04 p0531 N90-13067

User manual of the force structure model scenario editor SCENE
[FEL-1988-101] 04 p0531 N90-13069

An editor for 3D-models for image analysis
[FOA-C-30534-3.4] 05 p0684 N90-13986

Issues and approaches for electronic document approval and transmittal using digital signatures and text authentication: Prototype documentation
[DE90-003382] 08 p1058 N90-16119

SAtool II: An IDEF0 syntax data manipulator and graphics editor
[AD-A215289] 09 p1263 N90-17321

Editing wind profiler measurements
[PB90-130147] 14 p2007 N90-21503

FASTER: The Fault Tolerant Architecture Simulation Tool for Evaluating Reliability, introduction and applications
[AD-A219941] 17 p2414 N90-23755

Towards elegant design of highly interactive information systems using an object-oriented approach
[REPT-89-75] 17 p2480 N90-24179

UEDIT: A full-scale, scrollable APL2 spreadsheet input/output editor
[AD-A222712] 20 p2910 N90-26557

EDUCATION
NT ASTRONAUT TRAINING
NT EJECTION TRAINING
NT FLIGHT TRAINING
NT GUNNERY TRAINING
NT MAINTENANCE TRAINING
NT PILOT TRAINING
NT SPACE FLIGHT TRAINING

Higher education for science and technology: A background paper
[PB89-191290] 02 p0287 N90-11642

Planning in writing: The cognition of a constructive process
[AD-A210434] 02 p0288 N90-11648

National Science Foundation
04 p0569 N90-13320

Software engineering and Ada (Trademark) training: An implementation model for NASA
[NASA-CR-186071] 05 p0681 N90-13986

Elementary and middle school science improvement project
[NASA-CR-183768] 05 p0705 N90-14125

Workshop on synoptic meteorology instruction
[PB90-109950] 06 p0817 N90-14751

Human behavior
[PB90-780008] 07 p0967 N90-15584

Where to from here. Future applications of mental models of complex performance
[DE90-002091] 07 p0967 N90-15586

Cockpit resource management: A selected annotated bibliography
[AD-A214272] 07 p0969 N90-15594

Tools for simulation-based training
[AD-A214307] 07 p0978 N90-15646

Electrical safety in the high voltage laboratory
[DE90-003026] 08 p1060 N90-16130

Structural understanding in problem solving
[AD-A214776] 09 p1273 N90-17379

Flight crew training for fire fighting
10 p1317 N90-17615

Remote sensing in agriculture: Basic concepts, methodology and applications
[INPE-4806-MD/39] 10 p1399 N90-18088

International course in remote sensing ONU/INPE, Brazil
[INPE-4802-NTE/288] 10 p1399 N90-18089

Proceedings of the 4th Annual Ada Software Engineering Education and Training Symposium
[AD-A214663] 10 p1417 N90-18162

KAPSE Interface Team (KIT) public report, volume 8, part 2
[AD-A215840] 10 p1419 N90-18178

The employment of SITIM-150 as an instructional objective for training in remote sensing
[INPE-4833-PRE/1463] 10 p1440 N90-18310

Evaluation of two methods for acquisition of training statistics for digital analysis of areas prepared for plowing
[INPE-4901-PRE/1502] 11 p1522 N90-18763

Calendar of selected aeronautical and space meetings
[AGARD-CAL-90/1] 11 p1574 N90-19060

The United States Air Force School of Aerospace Medicine: Special report
[AD-A217740] 13 p1851 N90-20622

Broadening the interface bandwidth in simulation based training 13 p1859 N90-20666

Seeing in a new light: Astro-1 teacher's guide with activities
[NASA-EP-274] 13 p1899 N90-20900

ONR (Office of Naval Research) summer scholars for the 1989 PREFACE Program
[AD-A217746] 13 p1903 N90-20919

Programme of the International Training Course on Remote Sensing for African Specialists
[INPE-4878-NTE/290] 14 p1995 N90-21435

The ultimate CASE tool
[DE90-009351] 14 p2037 N90-21687

The International Space University
[NASA-TM-103163] 16 p2209 N90-22604

National Educators' Workshop: Update 1989 Standard Experiments in Engineering Materials Science and Technology
[NASA-CP-3074] 18 p2513 N90-24350

Thermal conductivity of metals
18 p2514 N90-24356

Rubberlike elasticity experiment
18 p2515 N90-24362

The magnetization process: Hysteresis
18 p2515 N90-24365

Tensile and shear strength of adhesives
18 p2515 N90-24366

Experiments and other methods for developing expertise with design of experiments in a classroom setting
18 p2516 N90-24367

Electronics principles inventory, Sheppard Technical Training Center
[AD-A219935] 18 p2547 N90-24534

A study of effects of instructional modes in a sequence of computer-assisted instruction lessons, with an introduction to computer-aided diagnosis of arithmetic errors 18 p2589 N90-24730

The development of expertise on an intelligent tutoring system 18 p2630 N90-24984

National Aeronautics and Space Administration (NASA)/American Society for Engineering Education (ASEE) Summer Faculty Fellowship Program-1989, volume 2
[NASA-CR-185601-VOL-2] 18 p2630 N90-24985

NASA/American Society for Engineering Education (ASEE) Summer Faculty Fellowship Program 1989
[NASA-CR-181894] 18 p2639 N90-25034

A systematic approach to training: A training needs assessment 18 p2645 N90-25059

A survey of cervical pain in pilots of a Belgian F-16 Air Defence Wing 19 p2718 N90-25462

An intelligent simulation training system
19 p2739 N90-25566

Functional description of a command and control language tutor 19 p2739 N90-25567

Success in tutoring electronic troubleshooting
19 p2739 N90-25568

Outline and realization of a polymorphic language extension for ELAN
[TR-89-23] 19 p2743 N90-25592

United States Naval Academy summary of Research, Academic Departments, 1989-1990
[AD-A221219] 19 p2800 N90-25929

Texstar: The all-Texas educational satellite system
[NASA-CR-186654] 20 p2820 N90-26045

Applied mathematical modules for use in a linear algebra service course
[AD-A222814] 20 p2920 N90-26618

A measurement of the effectiveness of the Airway Science Program to meet Federal Aviation Administration work force needs
[NIAR-90-5] 20 p2934 N90-26694

Payload training methodology study
[NASA-CR-183907] 21 p2964 N90-26849

NASA/USRA University advanced design program
[NASA-CR-186050] 21 p2965 N90-26855

Automatic information processing and high performance skills: Application to training
[AD-A221709] 21 p3036 N90-27259

Automatic information processing and high performance skills: Acquisition, transfer, and retention
[AD-A221744] 21 p3036 N90-27260

NASA's educational programs
22 p3258 N90-28447

NSF Tokyo reports. Twenty-one new areas added for support under Monbusho's priority research area grants
[PB90-199589] 22 p3265 N90-28488

Selective learning algorithm for certain types of learning failure in multilayer perceptrons
[AD-A223982] 23 p3362 N90-28998

The personal computer: An untapped source for the United States Army War College
[AD-A223976] 23 p3379 N90-29087

Animated computer-generated video-tape instruction using DIGLIB (Device Independent Graphics Library)
[DE90-015360] 23 p3382 N90-29105

Workshop on Low Level Flight Training
[AGARD-AR-288] 24 p3436 N90-29404

Strategies for tutoring multiple bugs
[AD-A223921] 24 p3524 N90-29927

Search strategies for computer-stored information: A microcomputer tutorial 24 p3557 N90-30126

EEG (ELECTROENCEPHALOGRAMS)
U ELECTROENCEPHALOGRAPHY

EFFECTIVE PERCEIVED NOISE LEVELS

Noise levels from a VSTOL aircraft measured at ground level and at 1.2 m above the ground
[NPL-RSA(EXT)-009] 11 p1562 N90-18999

EFFECTIVENESS
NT COST EFFECTIVENESS
NT SYSTEM EFFECTIVENESS

EFFERENT NERVOUS SYSTEMS

Age-related changes in human posture control: Motor coordination tests
[NASA-CR-185855] 03 p0383 N90-12178

EFFICIENCY
NT CHARGE EFFICIENCY
NT COMBUSTION EFFICIENCY
NT COMPRESSOR EFFICIENCY
NT ENERGY CONVERSION EFFICIENCY
NT NOZZLE EFFICIENCY
NT POWER EFFICIENCY
NT PROPELLER EFFICIENCY
NT PROPULSIVE EFFICIENCY
NT THERMODYNAMIC EFFICIENCY
NT TRANSMISSION EFFICIENCY

Efficiency and capabilities of multi-body simulations
01 p0019 N90-10095

On learning from exercises
[AD-A210593] 01 p0101 N90-10574

A method to model fuze-performance. Part 3: Diffraction of electromagnetic radiation by an edge
[FEL-1989-22-PT-3] 03 p0340 N90-11940

Scaling of an 85 GHz gyrotron to operate at 94 GHz
[AD-A212756] 04 p0504 N90-12909

Large heavy duty balloons in Europe
05 p0661 N90-13858

Identification of impulsive interference channels
[AD-A213154] 05 p0688 N90-14009

Selection of the energy-efficient enhancement geometry for single-phase turbulent flow inside tubes
[DE89-017690] 06 p0777 N90-14519

Assessment of the efficiency of nondestructive techniques in materials testing studies based on the information criterion
[DE89-635444] 06 p0796 N90-14634

How far can the world get on energy efficiency alone
[DE90-001349] 06 p0805 N90-14686

High-efficient solar cells for space application
10 p1342 N90-17777

On-orbit results of the LIPS 3/InP homojunction solar cell experiment 10 p1344 N90-17794

Lightweight, low cost, thin silicon cell arrays
10 p1345 N90-17800
Outline of high voltage solar array experiment using SFU platform
10 p1345 N90-17801
Efficiency measurement of high pressure cryogenic rocket pumps
[NAL-TR-1022] 10 p1391 N90-18042
Test method for fire extinguishing powder, Nordtest project 675-87
[PB90-166984] 15 p2073 N90-21874
Electron beam pumped XeF(C yields A) laser scaling
[AD-A220022] 17 p2409 N90-23728
Area-time efficient adders
[MEMO-INF-89-61] 17 p2440 N90-23905
Symbolic reasoning in model-based diagnosis: Efficient and effective information processing
[MEMO-INF-89-03] 17 p2452 N90-23984
The integration of GPS heights into the Australian height datum
19 p2705 N90-25392
Combining zero Doppler filter calculations with MTI filter calculations to increase computational speed
[AD-A222468] 21 p2997 N90-27034
Non-interactive zero knowledge
[AD-A222698] 21 p3052 N90-27347
Computation of efficient solutions of discretely distributed stochastic optimization problems
[ETN-90-97330] 21 p3067 N90-27436

EFFLUENTS
Utilization of water hyacinths to upgrade heavily loaded wastewater treatment plant effluents
15 p2073 N90-21873
Optical properties of marine stratocumulus clouds modified by ship track effluents
22 p3218 N90-28253

EGGS
The role of gravity in bird development
19 p2681 N90-25246

EGRESS
The influence of adjacent seating configurations on egress through a type 3 emergency exit
[AD-A218393] 17 p2348 N90-23371

EGYPT
LANDSAT Thematic Mapper for hydrogeological mapping in Egypt
[BCRS-89-28] 11 p1527 N90-18791

EIGENFUNCTIONS
U EIGENVECTORS

EIGENSTATES
U EIGENVECTORS

EIGENVALUES
Quotient-difference type generalizations of the power method and their analysis
[NASA-TM-102361] 01 p0112 N90-10635
JOE: Jordan Optimized Eigensolver. A step toward a numerical Jordan form analyzer for control and interactive thermo-structural-dynamic applications
02 p0184 N90-11047
Two enhancements of the logarithmic least-squares method for analyzing subjective comparisons
[AD-A211192] 02 p0266 N90-11514
Elimination of spurious eigenvalues in the Chebyshev tau spectral method
[PB89-209282] 03 p0345 N90-11967
On the computation of normal modes of a rotating, viscous, incompressible fluid with a capillary free boundary
[REPT-89-01] 03 p0348 N90-11989
The use of Lanczos's method to solve the large generalized symmetric definite eigenvalue problem
[NASA-CR-181914] 03 p0385 N90-12193
An Eigenvalue Analysis of finite-difference approximations for hyperbolic IBVPs
[NASA-TM-102241] 04 p0541 N90-13137
AcSim: Aircraft simulation program with application to flight profile generation
[AD-A212466] 06 p0723 N90-14217
Parallel eigenanalysis of finite element models in a completely connected architecture
[NASA-CR-185166] 06 p0799 N90-14652
An efficient solver of the Eigenvalue problem of the linear stability equations for three dimensional, compressible boundary-layer flows
08 p1066 N90-16172
An algorithm to compute the square root of 3x3 positive definite matrix
[DE89-635711] 08 p1109 N90-16417
A fractional calculus model of aeroelasticity
[AD-A216244] 10 p1423 N90-18212
A comparison of flutter calculations based on eigenvalue and energy method
11 p1459 N90-18406
Initialization of EURAD. Part 1: Utilization of ECMWF analysis data
12 p1688 N90-19695
Parallel tridiagonalization of a general matrix using distributed-memory multiprocessors
[DE90-008902] 14 p2015 N90-21551
Bicausal representations and multivariable generalized predictive control
[OUEL-1781/89] 15 p2159 N90-22331
Using deflation in the pole assignment problem with output feedback
16 p2282 N90-23004
Fourier analysis of finite element preconditioned collocation schemes
[NASA-CR-182040] 16 p2304 N90-23128
Continuation and multi-grid methods for bifurcation problems
[AD-A218904] 16 p2307 N90-23146
Finite element formulations for coupled fluid/structure eigenvalue analysis
[AD-A220793] 17 p2416 N90-23766
On a method for computing eigenvalues and eigenfunctions of linear differential operators
[PREPRINT-706] 17 p2456 N90-24013
Eigenvalues of dynamic max-min systems
[REPT-89-84] 17 p2465 N90-24088
Eigenvalue computations with the QUAD4 consistent-mass matrix
18 p2569 N90-24642
Obtaining eigensolutions for multiple frequency ranges in a single NASTRAN execution
18 p2570 N90-24644
Normal-mode and phase-integral methods for determining phase and group velocities in simple underwater acoustic ducts
[AD-A221393] 18 p2612 N90-24877
Flow structures around non-hyperbolic singularities on the wall with one vanishing eigenvalue: A discussion of the flow structures and the unfoldings
[LR-586] 19 p2692 N90-25315
The use of Lanczo's method to solve the large generalized symmetric Eigenvalue problem in parallel
[NASA-CR-182072] 20 p2907 N90-26533
Canonical eigenvalues. Part 1: General theory
[AD-A222812] 20 p2920 N90-26617
On the spatial eigenvalue approach to high Reynolds number flow in a rotating and nutating cylinder
[AD-A221710] 21 p3005 N90-27081
Robust eigensystem assignment for second-order estimators
[NASA-TM-102696] 22 p3191 N90-28103
LANZ: Software solving the large sparse symmetric generalized eigenproblem
[NASA-CR-182086] 23 p3340 N90-28876
Factorization of the characteristic equation for three layer ducts
[AD-A223867] 23 p3354 N90-28956
Block Lanczos algorithm
[AD-A224011] 23 p3383 N90-29111
SuperCHIEF: A modified CHIEF (Combined Helmholz Integral Equation Formulation) method
[DE90-014744] 23 p3387 N90-29123
A corollary to Kodaira-Spencer's theorem on continuity of eigenvalues
[DE90-627164] 23 p3390 N90-29148
On the zeta-function regularization of chiral Jacobians for singular Dirac operators
[DE90-627176] 23 p3390 N90-29150
Fast algorithms for parallel architectures
[AD-A223731] 24 p3528 N90-29947
Solution of nonlinear eigenvalue problems via parallel shooting
[LR-587] 24 p3539 N90-30013

EIGENVECTORS
JOE: Jordan Optimized Eigensolver. A step toward a numerical Jordan form analyzer for control and interactive thermo-structural-dynamic applications
02 p0184 N90-11047
AcSim: Aircraft simulation program with application to flight profile generation
[AD-A212466] 06 p0723 N90-14217
Parallel eigenanalysis of finite element models in a completely connected architecture
[NASA-CR-185166] 06 p0799 N90-14652
DOA (Direction of Arrival) estimation by Eigendecomposition using single vector Lanczos' algorithm
[AD-A215802] 11 p1544 N90-18887
Adaptive frequency estimation by MUSIC (Multiple Signal Classification) method
[PB90-166794] 15 p2086 N90-21943
Bicausal representations and multivariable generalized predictive control
[OUEL-1781/89] 15 p2159 N90-22331
On a method for computing eigenvalues and eigenfunctions of linear differential operators
[PREPRINT-706] 17 p2456 N90-24013
Obtaining eigensolutions for multiple frequency ranges in a single NASTRAN execution
18 p2570 N90-24644
On the spatial eigenvalue approach to high Reynolds number flow in a rotating and nutating cylinder
[AD-A221710] 21 p3005 N90-27081
Improving the accuracy of inverse iteration
[AD-A221848] 21 p3056 N90-27377
A comparison of two central difference schemes for solving the Navier-Stokes equations
[NASA-TM-102815] 22 p3108 N90-27654
Robust eigensystem assignment for second-order estimators
[NASA-TM-102696] 22 p3191 N90-28103
Factorization of the characteristic equation for three layer ducts
[AD-A223867] 23 p3354 N90-28956
Block Lanczos algorithm
[AD-A224011] 23 p3383 N90-29111
Active vibration damping of flexible structures
[DLR-FB-90-03] 24 p3481 N90-29676
Fast algorithms for parallel architectures
[AD-A223731] 24 p3528 N90-29947
Solution of nonlinear eigenvalue problems via parallel shooting
[LR-587] 24 p3539 N90-30013

EINSTEIN EQUATIONS
Are there causal vacuum solutions with the symmetries of the Goedel universe in higher-derivative gravity
[DE89-611966] 01 p0134 N90-10770
Gravitational nonminimally coupled electromagnetic fields: A possible solution to some idiosincrasies of Einstein-Maxwell theory
[DE89-618430] 02 p0286 N90-11635
General exact solution for homogeneous time-dependent self-gravitating perfect fluids
[DE89-618425] 06 p0776 N90-14514
An exact solution for a thick domain wall in general relativity
[NASA-CR-185013] 07 p1006 N90-15826
On Einsteinization of background curved space in the induced quantum gravity
[DE90-610477] 12 p1724 N90-19907
Dimensional transition of the universe
[DE90-741461] 12 p1724 N90-19910
Linearized analysis of (2+1)-dimensional Einstein-Maxwell theory
[DE90-741470] 12 p1725 N90-19913
Experimental constraints on metric and non-metric theories of gravity
12 p1730 N90-19946
Gravitational consequences of modern field theories
12 p1730 N90-19947
Applied general relativity
12 p1731 N90-19950
The monad construction and Hermetian-Einstein metrics
[DE90-612738] 14 p2019 N90-21573
String dynamics in curved space-time revisited
[DE90-612786] 14 p2035 N90-21674
The dynamics of scalar fields in the early universe
14 p2039 N90-21696
The synergism of analytic and numerical techniques in general relativity: Calculation of radiative spacetimes
15 p2174 N90-22425
Numerical investigations of nonlinear behavior in the Einstein equations
15 p2175 N90-22427
Background connection: A necessary object in general relativity
[DE90-620463] 16 p2325 N90-23258
A comment on anisotropic spheres admitting one parameter group of conformal motions
[DE90-627195] 23 p3403 N90-29230

EINSTEIN OBSERVATORY
U HEAO 2

EISCAT RADAR SYSTEM (EUROPE)
Enhanced electron density layers in the high-latitude lower ionosphere
05 p0657 N90-13832
Background electrodynamics measured by EISCAT during the NEED campaign
05 p0660 N90-13851
Polar mesosphere summer echoes and associated atmospheric gravity waves
05 p0660 N90-13856
Ion neutral gas coupling in the polar atmosphere: Use of EISCAT for the calculation of thermospheric parameters
[ETN-90-96490] 18 p2580 N90-24694

EJECTA
Stability and fragmentation of ejecta in hypervelocity impact
[DE90-004087] 08 p1085 N90-16278

EJECTION
NT STELLAR MASS EJECTION
Integrated G-suit/immersion suit
[AD-A212989] 06 p0821 N90-14774
Calculation of two-neutron multiplicity in photonuclear reactions
[NASA-TP-2968] 06 p0841 N90-14890
Herbig-Haro objects and stellar jets
15 p2186 N90-22487
A spring-actuated spin and eject device for interplanetary missions
18 p2540 N90-24493
Laboratory studies of the interaction of ions with condensed gases: Planetary applications
20 p2949 N90-26778

EJECTION INJURIES
Development of a microcomputer based software system for use in crewmember ejection analysis
[AD-A220398] 19 p2656 N90-25117
EJECTION SEATS
A preliminary sensitivity analysis of the Generalized Escape System Simulation (GESS) computer program
[DE89-016891] 02 p0148 N90-10844
On the selection of crewmember rescue means for manned space launch systems
08 p1035 N90-15978
Development of acceleration exposure limits for advanced escape systems 13 p1751 N90-20055
Parachute opening shocks during high speed ejections: Normalization 13 p1751 N90-20056
Development of an ejection seat specification for a new fighter aircraft 13 p1751 N90-20057
Escape systems research at RAE
13 p1751 N90-20058
Fighter escape system: The next step forward
13 p1752 N90-20059
Ejection seat training of jet pilots and weapon system officers at the German Air Force School of Aviation Medicine 13 p1752 N90-20061
The USAF Advanced Dynamic Anthropomorphic Manikin (ADAM) 13 p1752 N90-20062
Windblast protection for advanced ejection seats
13 p1752 N90-20063
Spacecraft escape 13 p1753 N90-20066
Yaw fin deployment apparatus for ejection seat
[AD-D014512] 19 p2656 N90-25118
Measurement techniques, evaluation criteria and injury probability assessment methodologies developed for Navy ejection and crashworthy seat evaluations
19 p2721 N90-25479
EJECTION TRAINING
Ejection seat training of jet pilots and weapon system officers at the German Air Force School of Aviation Medicine 13 p1752 N90-20061
EJECTORS
Investigation of advanced mixer-ejector exhaust system
[AD-A211943] 03 p0301 N90-11705
Computational analysis of the flowfield of a two-dimensional ejector nozzle
[NASA-CR-185255] 17 p2355 N90-23406
Rotary-Jet thrust augmentor with jet-flapped blades
18 p2492 N90-24243
EKMAN LAYER
A numerical study of basic coastal upwelling processes 16 p2259 N90-22878
The instability mechanism of synoptic-scale eddies
22 p3211 N90-28217
EL NINO
Interannual variability of temperature in the upper layer of the North Pacific eastern boundary region, 1971-1987
[PB89-190227] 02 p0253 N90-11434
On the statistics of El Nino occurrences and the relationship of El Nino to volcanic and solar/geomagnetic activity
[NASA-TP-2948] 03 p0429 N90-12456
Proceedings of the 14th Annual Climate Diagnostics Workshop
[PB90-198573] 23 p3351 N90-28938
ELASTIC ANISOTROPY
Numerical analysis of a class of problems in the mathematical theory of plasticity and damage
[AD-A210731] 01 p0114 N90-10655
Low temperature properties of glasses
02 p0200 N90-11141
Materials characterization using holographic mapping of transient lamb waves
[AD-A211414] 03 p0358 N90-12050
Seismic anisotropy and large-scale porosity in the ocean floor
[AD-A220453] 17 p2431 N90-23849
Improved transverse crack detection in composites
[NASA-TM-103261] 22 p3153 N90-27875
A hybrid-stress finite element for linear anisotropic elasticity 23 p3290 N90-28614
ELASTIC BENDING
Two dimensional laminated shell theory including parabolic transverse shear
[AD-A213817] 07 p0948 N90-15487
ELASTIC BODIES
Simulation and control problems in elastic robots
01 p0020 N90-10098
Solution of potential flow past an elastic body using the boundary element technique
[AD-A213843] 07 p0931 N90-15390
Explicit modeling of composite plates and beams in the dynamics of multibody systems
16 p2285 N90-23019
ELASTIC BUCKLING
Elastic buckling of imperfect cylindrical shells containing granular solids
[PB90-110362] 09 p1236 N90-17174
Influence of microslidings on the macroscopic behavior of composite textiles
[ETN-90-97459] 22 p3154 N90-27880
ELASTIC COLLISIONS
U ELASTIC SCATTERING
ELASTIC CONSTANTS
U ELASTIC PROPERTIES
ELASTIC CYLINDERS
Application of the complex variable solution to some problems in linear elastic materials with voids
24 p3478 N90-29658
ELASTIC DAMPING
NT VISCOELASTIC DAMPING
Research into traveling wave control in flexible structures
[AD-A224504] 24 p3479 N90-29661
ELASTIC DEFORMATION
NT ELASTIC BENDING
NT ELASTIC BUCKLING
Numerical analysis of a class of problems in the mathematical theory of plasticity and damage
[AD-A210731] 01 p0114 N90-10655
Deformation behavior of SiC/2014 Al metal-matrix composite
[AD-A212095] 03 p0320 N90-11816
An application of the J-integral to an incremental analysis of blunting crack behavior
[DE89-016844] 03 p0358 N90-12046
Mathematical simulation of dynamic compression tests using the Hopkinson bar method
[ISL-R-128/87] 04 p0513 N90-12960
Analysis of the non-planar response of a cantilever, with the aid of computerized symbolic manipulation
[AD-A212421] 04 p0545 N90-13172
Strain accumulation and surface deformation along the San Andreas, California
[NASA-CR-185893] 05 p0686 N90-13894
Field-effect spectroscopy of interface states
[AD-A212998] 05 p0703 N90-14112
Mechanical behavior of laminated composites at elevated temperatures 07 p0889 N90-15141
The elastic properties of woven polymeric fabric
[DE89-015391] 07 p0909 N90-15255
A simple shell element formulation for large-scale elastoplastic analysis
[DE89-015452] 07 p0946 N90-15475
Dynamic modeling of flexible bodies in multibody systems 09 p1229 N90-17134
Studies on deformation and fracture of viscoelastic composite materials
[AD-A216095] 10 p1348 N90-17819
A higher-order plate theory with ideal finite element suitability
[AD-A216163] 10 p1397 N90-18075
An objective time-integration procedure for isotropic rate-independent and rate-dependent elastic-plastic constitutive equations
[PB90-121245] 11 p1550 N90-18925
Three-dimensional Fe analysis of the surface distribution in notched compact samples of 20 MnMoNi 55
[W-1/89] 12 p1676 N90-19625
Static aeroelastic analysis of a three-dimensional generic wing
[NASA-TM-102231] 13 p1757 N90-20087
A review of gear housing dynamics and acoustics literature
[NASA-CR-185148] 14 p1987 N90-21387
Elasto-plastic large deformation analysis of thin-walled structures
[PB90-164757] 14 p1994 N90-21426
Deformation and microstructure of rutile
[DE90-614113] 14 p2032 N90-21654
Simulation of inelastic deformation in glassy polypropylene and polycarbonate
[AD-A218891] 16 p2224 N90-22686
Multibody dynamics: Modeling component flexibility with fixed, free, loaded, constraint, and residual modes
16 p2295 N90-23072
Transactions of the Seventh Army Conference on Applied Mathematics and Computing
[AD-A219220] 16 p2309 N90-23160
Dynamic analysis of flexible multibody structures
18 p2642 N90-25048
Nonlinear material response to very rapid energy deposition
[AD-A221932] 21 p2989 N90-26988
Strength under various modes of deformation
[AD-A222412] 21 p3013 N90-27132
Collision forces for compliant projectiles
[NASA-TM-4203] 22 p3192 N90-28111
Analysis of dynamic transient response and postflutter behavior of super-maneuvering airplane
[AD-A224126] 24 p3432 N90-29386
The overall response of composite materials undergoing large elastic deformations
[AD-A224509] 24 p3442 N90-29439
Studies on crack mechanics
[AD-A223634] 24 p3480 N90-29670
Comparison of crack closure result obtained by 3D elastic-plastic FEM and modified Dugdale model
[FFA-TN-1990-18] 24 p3481 N90-29675
ELASTIC MEDIA
Crack problems for elastic-plastic materials under antiplane shear loadings 06 p0799 N90-14651
Defects: Their behaviour and related design assumptions 11 p1457 N90-18397
Elastodynamic scattering and transmission problems in three dimensions by the boundary integral equation method 15 p2111 N90-22077
ELASTIC MODULUS
U MODULUS OF ELASTICITY
ELASTIC PLATES
A finite element formulation for inelastic plates and shells based on a mixed variational principle
02 p0233 N90-11334
Materials characterization using holographic mapping of transient lamb waves
[AD-A211414] 03 p0358 N90-12050
A higher-order plate theory with ideal finite element suitability
[AD-A216163] 10 p1397 N90-18075
The propagation of time harmonic Rayleigh-Lamb waves in a bimaterial plate
[AD-A216834] 11 p1519 N90-18749
Through-thickness strain response of thick composites in compression
[AD-A217233] 13 p1767 N90-20141
Application of the complex variable solution to some problems in linear elastic materials with voids
24 p3478 N90-29658
ELASTIC PROPERTIES
NT AEROELASTICITY
NT AEROTHERMOELASTICITY
NT ANELASTICITY
NT ELASTOPLASTICITY
NT HYDROELASTICITY
NT MAGNETOSTRICTION
NT MODULUS OF ELASTICITY
NT PHOTOELASTICITY
NT PROPORTIONAL LIMIT
NT THERMOELASTICITY
NT VISCOELASTICITY
Mechanical states in wound capacitors. Part 1: Prediction
[DE89-008110] 01 p0059 N90-10337
Fatigue growth and closure of short cracks
[AD-A210824] 01 p0081 N90-10462
Acoustic studies of new materials: Quasicrystals, low-loss glasses and high Tc superconductors
[AD-A211281] 02 p0272 N90-11551
International seminar on the inelastic behavior of solids: Models and utilization
[DE89-017420] 03 p0327 N90-11858
New mechanism for toughening ceramic materials
[AD-A211651] 03 p0332 N90-11892
Buckling of axially compressed imperfect orthotropic shells with elastic edge supports
[PB89-217038] 03 p0357 N90-12043
Autofrettage-stress distribution under load and retained stresses after depressurization
[AD-A212090] 03 p0358 N90-12048
Numerical solution of acoustic-structure interaction problems
[AD-A211505] 03 p0400 N90-12293
Free-field response from inclined body waves in viscoelastic random medium
[REPT-88-99] 04 p0499 N90-12878
Elastic indentation fractures
[ETCA-88-R-116] 04 p0512 N90-12955
Energy concentration induced by phase transitions in hydrogenated metals
[PREPRINT-672] 05 p0625 N90-13650
A theory of damage in brittle and cementitious materials, part 1
[AD-A212940] 05 p0627 N90-13658
Analysis of new phenomena in shear flow of non-Newtonian fluids
[AD-A212893] 05 p0638 N90-13721
Elastic softening in nanocrystalline silicon
[DE90-002268] 06 p0752 N90-14377
Wide-angle propagation in inhomogeneous fluids and elastic solids using perturbation methods
06 p0837 N90-14868
Nickel beryllides and their properties
[DE90-001736] 07 p0903 N90-15220

Interdisciplinary research in viscoelasticity and rheology
[AD-A213630] 08 p1063 N90-16145
The redetermination of the elastic, piezoelectric, and dielectric constants of quartz and their variation with temperature
[AD-A215025] 09 p1197 N90-16937
A summary of the Bodner-Stouffer constitutive model
[AD-A214532] 09 p1237 N90-17182
Elastic-plastic analysis of a thick-walled composite tube subjected to internal pressure
[AD-A215258] 09 p1238 N90-17187
Internal failures in model elastomeric composites
[AD-A215923] 10 p1348 N90-17818
Threaded joint design for composites
[DE90-005553] 11 p1478 N90-18506
An objective time-integration procedure for isotropic rate-independent and rate-dependent elastic-plastic constitutive equations
[PB90-121245] 11 p1550 N90-18925
Elastic solutions in a semi-infinite solid with an ellipsoidal inclusion
[AD-A217063] 12 p1625 N90-19338
Elastic properties of silica xerogels
[AD-A216528] 12 p1630 N90-19366
A transient plasticity study and low cycle fatigue analysis of the Space Station Freedom photovoltaic solar array blanket
[NASA-TM-102516] 12 p1674 N90-19617
Error analysis of some Galerkin least squares methods for the elasticity equations
[DE90-608611] 12 p1705 N90-19790
Low temperature elastic and dielectric properties of incommensurate barium sodium niobate
[AD-A216969] 12 p1709 N90-19815
Dynamics of electronically excited species in gaseous and condensed phase
[AD-A217696] 13 p1884 N90-20812
Three-dimensional elastic-plastic analysis of shallow cracks in single-edge-crack-tension specimens
[NASA-TM-102636] 14 p1945 N90-21130
Review and statistical analysis of the ultrasonic velocity method for estimating the porosity fraction in polycrystalline materials
[NASA-TM-102501-REV] 14 p1989 N90-21402
Mechanics of interface fracture 14 p1990 N90-21408
Delamination failure in a unidirectional curved composite laminate
[NASA-CR-182018] 14 p1993 N90-21421
Towards a unified analysis methodology for composite rotor blades 15 p2046 N90-21730
Approximate analysis for the formation of adiabatic shear bands
[AD-A218751] 16 p2221 N90-22670
Nonstrictly hyperbolic conservation laws
[AD-A218525] 16 p2237 N90-22762
Thermomechanical properties of new composite materials SiC/glass-ceramic
[REPT-892-430-118] 17 p2370 N90-23491
HYPUF upgrade
[AD-A218400] 17 p2379 N90-23547
Stress fields in composite materials by means of a nonclassical approach 18 p2517 N90-24372
Computational methods and plasticity
[PB90-167917] 18 p2571 N90-24652
A numerical micromechanics analysis of the mechanical properties of a plain weave composite
[OUEL-1760/89] 19 p2673 N90-25201
An approach for relating the results of quantitative nondestructive evaluation to intrinsic properties of high-performance materials
[NASA-CR-186484] 19 p2699 N90-25355
Investigation of the mechanical properties of superconducting coils
[DE90-012020] 19 p2761 N90-25689
A study of the elastic properties of Al2O3 and Si3N4 matrix composites with SiC whisker reinforcement
[DE90-013674] 21 p2970 N90-26882
The relation between ferroelasticity and superconductivity 22 p3150 N90-27861
A theoretical investigation into the inelastic behavior of metal-matrix composites
[AD-A223973] 23 p3302 N90-28677
Factorization of the characteristic equation for three layer ducts
[AD-A223867] 23 p3354 N90-28956
Surface effect for test piece on flexural test of carbon fiber reinforced plastic laminates
[NAL-TM-601] 24 p3442 N90-29436
Percolation and low density materials: Theory and applications
[AD-A224237] 24 p3442 N90-29438
Tip-position control of a flexible beam: Modeling approaches and experimental verification
[AD-A224249] 24 p3476 N90-29643

ELASTIC SCATTERING
New theoretical approaches for studying electron collisions with small molecules
[DE89-017543] 02 p0273 N90-11558
Elastic impurity scattering in double-barrier resonant tunneling structures
[AD-A212850] 05 p0702 N90-14110
Narrow one-channel resonances and their manifestation in the pure elastic scattering of unpolarized particles
[DE89-632177] 06 p0839 N90-14876
Studies of elastic scattering and cross sections of the C-12 + Si-28 system
[DE89-635990] 08 p1120 N90-16486
Q-2 and A dependence of delta (1232) electroexcitation in nuclei
[DE90-003470] 08 p1121 N90-16492
Maximum likelihood techniques in QELS 09 p1222 N90-17091
Advanced instrumentation for QELS experiments 09 p1223 N90-17093
A covariant multiple scattering series for elastic projectile-target scattering
[NASA-TM-101942] 09 p1279 N90-17417
Fluorescence and elastic scattering from laser dye-filled capillaries
[AD-A217026] 11 p1484 N90-18540
Positron-alkali atom scattering 11 p1556 N90-18958
Elastic scattering of e- and e+ from Rb and Cd 11 p1556 N90-18960
Positron-rubidium scattering 11 p1556 N90-18964
Positron scattering by atomic hydrogen using optical potentials and with positronium formation 11 p1557 N90-18966
Numerical Green's functions in optical potential calculations for positron scattering from argon and neon 11 p1557 N90-18971
Positron excitation of neon 11 p1558 N90-18973
Positron-inert gas differential elastic scattering 11 p1558 N90-18974
Differential elastic scattering cross sections for 54.9eV positrons incident on helium 11 p1558 N90-18975
Total cross sections for positrons scattered elastically from helium based on new measurements of total ionization cross sections 11 p1558 N90-18976
Background studies in gas ionizing x ray detectors 12 p1636 N90-19399
The electron momentum-transfer cross sections of tungsten, silicon, and silicon dioxide at energies from 0.1 to 10,000 eV
[DE90-009041] 12 p1712 N90-19833
Reactive and anisotropic elastic scattering of highly laser-vibration-excited diatomic molecules
[MPIS-19/1988] 13 p1883 N90-20804
Large-angle elastic and inelastic scattering of Pi+ and Pi- from Si28 and Ca40
[AD-A218163] 13 p1885 N90-20818
Helium transport in plasma edge regions 14 p2027 N90-21625
Contributions of individual structural modes to the scattered acoustic field
[AD-A219128] 16 p2314 N90-23187
Chopper for neutrinos and antineutrinos
[AD-A218402] 17 p2471 N90-24124
Electromigration in metallic microstructures
[AD-A221208] 18 p2622 N90-24942
Concept for a neutron spectrometer based on optical detection of (3)He(n, p)-3H reactions in a gas
[DE90-014776] 23 p3330 N90-28826

ELASTIC SHELLS
A finite element formulation for inelastic plates and shells based on a mixed variational principle 02 p0233 N90-11334
Development of finished beam and shell elements from engineering models for structures under high inelastic deformations
[ETN-90-95377] 12 p1675 N90-19619

ELASTIC STABILITY
U DAMPING

ELASTIC STRENGTH
U PROPORTIONAL LIMIT

ELASTIC WAVES
NT AERODYNAMIC NOISE
NT AIRCRAFT NOISE
NT BAROCLINIC WAVES
NT BLADE SLAP NOISE
NT CAPILLARY WAVES
NT DETONATION WAVES
NT ELECTROSTATIC WAVES
NT ENGINE NOISE
NT GRAVITY WAVES
NT ION ACOUSTIC WAVES
NT JET AIRCRAFT NOISE
NT LAMB WAVES
NT LOVE WAVES
NT MAGNETOACOUSTIC WAVES
NT MAGNETOHYDRODYNAMIC WAVES
NT NOISE (SOUND)
NT NORMAL SHOCK WAVES
NT OBLIQUE SHOCK WAVES
NT P WAVES
NT PHONONS
NT PLASMA WAVES
NT POLARIZED ELASTIC WAVES
NT PROPELLER NOISE
NT RAYLEIGH WAVES
NT RIEMANN WAVES
NT RIPPLES
NT S WAVES
NT SEISMIC WAVES
NT SH WAVES
NT SHOCK WAVES
NT SONIC BOOMS
NT SOUND WAVES
NT STRESS WAVES
NT THERMAL NOISE
NT TOLLMIEN-SCHLICHTING WAVES
NT ULTRASONIC RADIATION
Analytical control of special numerical calculations of pressure propagation in a fluid
[GRS-70] 04 p0501 N90-12884
Bulk acoustic waves resonators made of amorphous materials
[NOTE-TECHNIQUE-1989-4] 04 p0550 N90-13199
An investigation of elastic guided waves for ceramic joint evaluation
[DE90-004400] 08 p1050 N90-16071
Direct Monte Carlo calculations on expansion wave structure near a wall
[ISL-CO-249/88] 08 p1064 N90-16154
Transient elastic waves on anisotropic half-spaces 10 p1396 N90-18074
Piezoelectric polymer PVDF shock gauge: State of the research art
[ISL-CO-207/89] 11 p1512 N90-18705
A study on upstream moving pressure waves induced by vortex separation
[ISL-CO-203/88] 12 p1597 N90-19192
Partial acoustic filtering applied to the equations of compressible flow
[DE90-000673] 15 p2097 N90-22001
Institute for Materials Science and Engineering, nondestructive evaluation: Technical activities
[PB90-132739] 15 p2108 N90-22055
Free wave propagation in orthogonally stiffened cylinders 15 p2119 N90-22124
Calculation of 3-dimensional synthetic seismograms on the connection machine
[AD-A218472] 16 p2255 N90-22857
Seismic anisotropy and large-scale porosity in the ocean floor
[AD-A220453] 17 p2431 N90-23849
Real-time monitoring of ceramic sintering with laser ultrasonics
[DE90-012960] 20 p2838 N90-26140
Laser ultrasonic measurements on ceramic materials with rough surfaces
[DE90-012961] 20 p2838 N90-26141
Factorization of the characteristic equation for three layer ducts
[AD-A223867] 23 p3354 N90-28956

ELASTICITY
U ELASTIC PROPERTIES

ELASTICIZERS
U PLASTICIZERS

ELASTODYNAMICS
NT ELASTIC DAMPING
NT ELASTOHYDRODYNAMICS
NT VISCOELASTIC DAMPING
An analytical and experimental study of the elastodynamic response characteristics of planar linkage mechanism with bearing clearances 02 p0233 N90-11336
Time domain coupling of the boundary and finite element methods for elastodynamics
[AD-A213243] 05 p0654 N90-13811
Element-specific modal formulations for large-displacement multibody dynamics 14 p1934 N90-21069
The Gauss beam method for surface waves. Theory and utilization for a lateral heterogeneous spheric Earth
[ETN-90-96492] 18 p2580 N90-24695

ELASTOHYDRODYNAMICS
Analysis of an elastohydrodynamic lubricated point contact: User's manual
[AD-A214257] 07 p0943 N90-15459
Investigation of rough elastohydrodynamic contact
[ISAL-89-0029] 08 p1085 N90-16281
Bearing elastohydrodynamic lubrication: A complex calculation made simple
[NASA-TM-102575] 15 p2105 N90-22041

ELASTOMERS
NT CHLOROPRENE RESINS
NT VITON RUBBER (TRADEMARK)
NT VULCANIZED ELASTOMERS
Adhesion of encapsulating elastomer to polyolefin sleeve
[BDX-613-3985] 01 p0048 N90-10271
Development of elastomeric polypeptide biomaterials
[AD-A210295] 01 p0049 N90-10280
Numerical analysis of nonlinear viscoelastic structures: Application to elastomers and rubber-like materials
02 p0180 N90-11013
High temperature insulators
[AD-D014193] 04 p0479 N90-12751
Synthesis of energetic single phase and multi-phase polymers
[AD-A212539] 04 p0481 N90-12761
Studies of Aflas fluoroelastomers
[AD-A213046] 05 p0621 N90-13622
Elastomeric impulse energy storage and transfer system
[AD-D014223] 06 p0730 N90-14255
Predictive aging of elastomers in air: The importance of understanding diffusion-limited oxidation effects
[DE90-001385] 06 p0751 N90-14372
A novel heat resistant blend produced by compositional quenching: A thermoplastic polyimide impact modified with a fluoroelastomer
[AD-A213724] 07 p0912 N90-15273
Spray sealing: A breakthrough in integral fuel tank sealing technology 08 p1022 N90-15912
Development of an elastomeric additive to improve the impact resistance of unsaturated polyester networks
[ISAL-89-0006] 06 p1050 N90-16073
Analysis of liquid propellant exposed to elastomeric materials
[AD-A214465] 09 p1200 N90-16952
Fuel-elastomer compatibility studies: Results of 80 C/14-day exposure experiments
[AD-A216015] 10 p1361 N90-17893
Elastic recovery and polymer-polymer interactions
[AD-A217085] 12 p1633 N90-19384
Elastomeric electrical isolation membrane
[AD-D014365] 12 p1651 N90-19490
Synthesis of new polyphosphazene elastomers
[AD-A217585] 13 p1780 N90-20216
Modeling elastomer displacements for tactile sensing applications
[DE90-007959] 14 p1984 N90-21370
Internal fractures in modal elastomeric composites
15 p2121 N90-22133
Elastomer compatibility studies
[BR106069] 17 p2378 N90-23542
Compression molded polyurethane block copolymers. 3: Evaluation of microphase compositions
[AD-A220160] 17 p2382 N90-23564
Equilibrium swelling of elastomeric materials in solvent environments
[DE90-010164] 18 p2529 N90-24430
Failure mechanism of urethane elastomer coated fabric collapsible fuel tanks
[AD-A221033] 18 p2530 N90-24435
Elastomers and other organic composites
[AD-A222772] 21 p2984 N90-26958
Model studies of the effect of surface roughness and mechanical interlocking on adhesion
[AD-A222402] 21 p2987 N90-26977
Synthesis of energetic single phase and multi-phase polymers
[AD-A222491] 21 p2988 N90-26981
Strength under various modes of deformation
[AD-A222412] 21 p3013 N90-27132
Elastomeric mount for thrust bearing shoe
[AD-D014465] 22 p3181 N90-28054
Compatibility of elastomeric seal compounds with MIL-H-6083 and MIL-H-46170 hydraulic fluid
[AD-A224248] 24 p3454 N90-29504
Rheology of filler rubber: Silica-silicone
[AD-A223600] 24 p3455 N90-29511
Effect of particulate fillers on the rheology of polymer melts
[AD-A223601] 24 p3455 N90-29512

ELASTOMETERS
The optimum polymer binder for pressable high performance explosives: A preliminary evaluation
[ETN-90-97612] 24 p3457 N90-29524

ELASTOPLASTICITY
The MHOST finite element program: 3-D inelastic analysis methods for hot section components. Volume 2: User's manual
[NASA-CR-182235-VOL-2] 01 p0079 N90-10450
The MHOST finite element program: 3-D inelastic analysis methods for hot section components. Volume 3: Systems' manual
[NASA-CR-182236] 01 p0079 N90-10451
Design of glued joints, elastoplastic adhesives
[DRIC-T-8168] 03 p0333 N90-11894
A two-dimensional hybrid experimental-numerical technique for elastic-plastic stress analysis
04 p0511 N90-12949
Orthotropic elasto-plastic behavior of AS4/APC-2 thermoplastic composite in compression
[NASA-CR-186080] 04 p0513 N90-12959
Elasto-plastic analysis of unidirectional fiber-reinforced composites subjected to transverse normal loading using the finite element method 06 p0737 N90-14292
Shear strain localization phenomenon in viscoplastic materials 06 p0798 N90-14649
A new uniformly valid asymptotic integration algorithm for elasto-plastic-creep and unified viscoplastic theories including continuum damage
[NASA-TM-102344] 06 p0799 N90-14655
A simple shell element formulation for large-scale elastoplastic analysis
[DE89-015452] 07 p0946 N90-15475
Ductile failure
[AD-A213864] 07 p0948 N90-15488
Development of finished beam and shell elements from engineering models for structures under high inelastic deformations
[ETN-90-95377] 12 p1675 N90-19619
Digital treatment of elastic-plastic structures by means of quadratic optimization processes from the finite element method
[ETN-90-95823] 12 p1675 N90-19621
Development of finite beam and shell elements for structures under great inelastic deformations
[ETN-90-95869] 12 p1675 N90-19623
Elastic-plastic instability of plane frames
14 p1992 N90-21415
Elasto-plastic large deformation analysis of thin-walled structures
[PB90-164757] 14 p1994 N90-21426
Elastic stability and nonlinear behavior of imperfect shells with initial stresses 15 p2110 N90-22070
Elasto-plastic analysis for contact fatigue failure
15 p2112 N90-22078
Coordinate systems for plastic yield surfaces stress and strain space theories
[PB90-164765] 15 p2117 N90-22110
An investigation into the foundations of elastic-plastic fracture mechanics 15 p2120 N90-22130
Evaluation of joints bonded with elastoplastic adhesives
[REPT-892-430-120] 16 p2247 N90-22816
On the performance of algorithms for large-scale bound constrained problems
[DE90-010084] 18 p2590 N90-24736
A framework to correlate a/W ratio effects on elastic-plastic fracture toughness (J (sub c))
[AD-A222822] 21 p3012 N90-27125
A comparison of single-cycle versus multiple-cycle proof testing strategies
[NASA-CR-4318] 22 p3193 N90-28115

ELASTOSTATICS
Ultrastructure processing of ordered polymers
[AD-A218331] 13 p1783 N90-20232
Two-dimensional damage models of fiber-reinforced composites 14 p1946 N90-21135
Finite element analysis of elastic contact problems with friction 15 p2105 N90-22040
Green's functions for dislocations in bonded strips and related crack problems
[NASA-CR-185291] 23 p3340 N90-28878

ELECTRIC AIRCRAFT
U FLY BY WIRE CONTROL

ELECTRIC ARCS
NT MERCURY ARCS
Non-stationary computer model of the asymptotic region of an electric arc gas heater
[IPPCZ-288] 03 p0407 N90-12330
Proposal of arc driving type fault current limiter
[DE89-782290] 12 p1650 N90-19485
Unipolar arcing on the cathode surface of a high voltage diode
[AD-A224122] 23 p3322 N90-28787

ELECTRIC AUTOMOBILES
Advanced battery development
[DE90-006073] 11 p1529 N90-18806
Advanced high-temperature batteries
13 p1825 N90-20480
Laboratory testing of Energy Research Corporation ERC 160 NiCd 6 volt traction battery
[DE90-009629] 15 p2089 N90-21957
Laboratory testing of Saft SEH-5-200 6 volt traction battery
[DE90-009787] 15 p2089 N90-21958
Engineering evaluation testing of the Soleq dual battery van
[DE90-012685] 19 p2698 N90-25354

ELECTRIC BATTERIES
NT ALKALINE BATTERIES
NT LEAD ACID BATTERIES
NT LITHIUM SULFUR BATTERIES
NT METAL AIR BATTERIES
NT NICKEL CADMIUM BATTERIES
NT NICKEL HYDROGEN BATTERIES
NT NICKEL IRON BATTERIES
NT NICKEL ZINC BATTERIES
NT PRIMARY BATTERIES
NT REDOX CELLS
NT SILVER ZINC BATTERIES
NT SODIUM SULFUR BATTERIES
NT STORAGE BATTERIES
NT THERMAL BATTERIES
NT ZINC-BROMIDE BATTERIES
The use of lithium batteries in biomedical devices
[AD-A210789] 01 p0061 N90-10350
The aerospace energy systems laboratory: Hardware and software implementation
[NASA-TM-101706] 01 p0107 N90-10610
New secondary batteries utilizing electronically conductive polymer cathodes
[NASA-CR-185885] 02 p0215 N90-11227
Lithium polymer electrolyte battery, electrochemical behavior of cathode materials
[AD-A210755] 02 p0216 N90-11235
Battery actuation of NITINOL at sub-zero temperatures
[AD-A211254] 02 p0216 N90-11237
Assessment of thin film batteries based on polymer electrolytes. Part 1: Energy density
[AD-A212111] 03 p0343 N90-11958
Design and commissioning test results for the hypervelocity launcher research complex battery power supply
[AD-A211320] 04 p0495 N90-12848
Assessment of thin film batteries based on polymer electrolytes. Part 3: Specific energy versus specific power
[AD-A212141] 04 p0515 N90-12976
Modeling of sodium/metal chloride batteries
[DE89-017685] 06 p0770 N90-14478
Battery technology assessment and R and D plan
[DE90-002007] 06 p0772 N90-14489
A cost effective battery bank for I(sup 2)T testing and evaluation of electrical switchgear
[DE90-002350] 06 p0772 N90-14490
Characterization of electric vehicle velocity and power profiles using road test data
[DE90-002085] 06 p0795 N90-14630
Technology Base Research Project for electrochemical energy storage
[DE90-002604] 06 p0806 N90-14693
The Aerospace Energy Systems Laboratory: A BITBUS networking application
[NASA-TM-4149] 06 p0831 N90-14829
Status and results of ANL life evaluation of valve-regulated lead-acid load-leveling batteries
[DE90-001918] 07 p0921 N90-15329
Rechargable molten-electrolyte lithium batteries
[DE90-003774] 07 p0923 N90-15339
An assessment and comparison of fuel cells for transportation applications
[DE90-001807] 07 p0952 N90-15508
Ninth Battery and Electrochemical Contractors' Conference: Extended abstracts
[DE89-016837] 08 p1059 N90-16120
Assessment of battery technologies for electric vehicles, volume 1
[DE90-002049] 08 p1059 N90-16122
Organic cathode for a secondary battery
[NASA-CASE-NPO-17604-1-CU] 08 p1059 N90-16124
Sizing and selection of batteries for stand-alone photovoltaic systems
[DE90-002990] 08 p1060 N90-16129
An approach for testing fuel-cell/battery hybrid power sources for bus applications
[DE90-002090] 08 p1083 N90-16270
Electric and hybrid vehicles: Technical background report for the DOE flexible and alternative fuels study
[DE90-002218] 08 p1084 N90-16271
Fault tree analysis: A tool for battery safety and reliability studies
[DE90-002582] 08 p1086 N90-16287
Intrinsically safe 5-V, 4-A rechargeable power supply
[PB90-103235] 09 p1209 N90-17006
Thermal switch disc for short circuit protection of batteries
[NASA-CASE-MSC-21428-1] 09 p1209 N90-17008
Copper chloride cathode for a secondary battery
[NASA-CASE-NPO-17640-1-CU] 09 p1210 N90-17011

Evaluation of a prototype lithium molybdenum disulfide secondary battery for load conditioner: Characteristics and performance of 70Wh class BC cell
[DE90-702460] 09 p1210 N90-17016
Research and development of lithium/polyaniline battery, part 2
[DE90-734985] 09 p1211 N90-17018
Sealing L-alloys/FeS(x) cells for a bipolar battery
[DE90-004887] 09 p1214 N90-17040
Overview of photovoltaic and battery applications
[PB90-120536] 09 p1242 N90-17206
A power system for ARTEP 10 p1331 N90-17694
Mathematical modelling and expert system for battery management 10 p1332 N90-17703
Preliminary study of rechargeable lithium cells for space applications 10 p1334 N90-17717
Surveys concerning the effect to introduce electric vehicles. On the possibility of new technology and introducing measures
[DE90-742057] 10 p1391 N90-18046
Performance of superconductive oxides as cathodes for lithium rechargeable batteries
[AD-A216030] 10 p1401 N90-18098
Application of polymer electrolytes to lithium batteries
[AD-A216038] 10 p1401 N90-18099
Cell performance of ultra-thin polymer cathode systems. Part 1: Anion intercalating polymer cathode
[AD-A216037] 11 p1501 N90-18639
Lithium ambient-temperature battery reliability
[DE90-005758] 11 p1502 N90-18650
A battery data base for electric vehicle applications
[DE90-007085] 11 p1503 N90-18655
Feasibility of a super high energy density battery of the Li/BrF3 electrochemical system
[AD-A216575] 11 p1528 N90-18799
Advanced battery development
[DE90-006073] 11 p1529 N90-18806
Flight termination system battery guidelines
[AD-A217310] 13 p1758 N90-20092
All-solid-state thin-film rechargeable lithium batteries using solid redox polymerization electrodes
[DE90-008665] 13 p1796 N90-20306
Space Electrochemical Research and Technology (SERT), 1989
[NASA-CP-3056] 13 p1821 N90-20454
Overview of battery usage in NASA/GSFC LEO and GEOspacecrafts 13 p1821 N90-20455
The application of electrochemical impedance spectroscopy for characterizing the degradation of Ni(OH)2/NiOOH electrodes 13 p1824 N90-20474
Advanced high-temperature batteries 13 p1825 N90-20480
Advanced calcium thionyl chloride high power battery
[AD-A216685] 13 p1825 N90-20482
Energy storage and distribution
[DE89-009487] 13 p1826 N90-20488
Active primary lithium thionyl chloride battery for artillery applications
[DE90-009511] 15 p2089 N90-21955
New generation power subsystems for satellites
[AD-A219540] 17 p2365 N90-23464
Evaluation of the state of charge of battery electrodes with ac impedance techniques
[AD-A219561] 17 p2420 N90-23789
Current distribution in cylindrical porous electrodes
[DE90-009707] 18 p2546 N90-24530
New liquid cathode electrolytes in high rate cells
[AD-A219822] 18 p2548 N90-24531
Performance of battery charge controllers
[DE90-011413] 19 p2686 N90-25279
Engineering evaluation testing of the Soleq dual battery van
[DE90-012685] 19 p2698 N90-25354
Electrochemical, in situ Raman spectroscopic, and conductivity studies of polypyrrole incorporating large size anions: Conducting nature of reduced form
[AD-A222739] 20 p2831 N90-26102
The development and characterization of ion exchange membranes for selected electrochemical power sources
[DE90-009741] 20 p2857 N90-26251
Evaluation of room-temperature chloroaluminate molten salts as electrolytes for high energy density batteries
[AD-A223097] 20 p2860 N90-26267
Metal chloride cathode for a battery
[NASA-CASE-NPO-17809-1-CU] 21 p2998 N90-27041
Electric and hybrid vehicles program
[DE90-013560] 21 p2998 N90-27043
Electric vehicle battery R/D in the context of a propulsion system
[DE90-013667] 21 p2999 N90-27046
Assessment of battery technologies for electric vehicles. Volume 2, part 2: Appendices
[DE90-014610] 23 p3321 N90-28778
The nuclear battery
[DE90-630400] 24 p3462 N90-29559

ELECTRIC BRIDGES
NT WHEATSTONE BRIDGES
NT WIRE BRIDGE CIRCUITS
High power density dc/dc converter: Selection of converter topology
[NASA-CR-186129] 06 p0768 N90-14467
Very low energy ignition of pyrotechnics using a Semiconductor Bridge (SCB)
[DE90-002645] 08 p1052 N90-16082
Microconvective heating of granular explosives by a semiconductor bridge
[DE90-005710] 11 p1484 N90-18541
Evaluation of a thermistior power measurement system for use on the NPL antenna extrapolation range
[NPL-DES-89] 24 p3466 N90-29583

ELECTRIC CHARGE
NT ELECTRIC DIPOLES
NT ELECTROSTATIC CHARGE
NT SPACE CHARGE
Capacitive behavior in conducting polymers: The ac impedance and quartz crystal microbalance studies
[AD-A210754] 02 p0201 N90-11150
On the extremum electric charge problem of steady electromagnetic equilibria
[TRITA-EPP-89-04] 04 p0489 N90-12809
Instability of the behavior of high resistivity silicon detectors due to the presence of oxide charges
[REPT-89-038] 04 p0559 N90-13260
The dynamics of dust in planetary magnetospheres 08 p1149 N90-16658
Airborne measurements of the electric field and the charge precipitation particles in convective clouds: Lower positive charge centres
[ESA-TT-1157] 11 p1535 N90-18836
Towards a quantum pump of electric charges and currents
[AD-A221257] 18 p2607 N90-24851
Pulsed field sample neutralization
[DE90-015131] 24 p3445 N90-29452

ELECTRIC CIRCUITS
U CIRCUITS

ELECTRIC COILS
NT MAGNET COILS
NT MAGNETIC COILS
Mechanical states in wound capacitors. Part 1: Prediction
[DE89-008110] 01 p0059 N90-10337
The 1989 National Convention Record IEE Japan, part 7
[DE89-910080] 09 p1210 N90-17012
Investigation of the mechanical properties of superconducting coils
[DE90-012020] 19 p2761 N90-25689

ELECTRIC CONDUCTORS
NT CONDUCTING POLYMERS
Testing results of the MIT Probe
[DE89-016679] 02 p0278 N90-11590
Synthesis and characterization of new low-dimensional metal complex conductors
[AD-A213189] 04 p0498 N90-12871
Chemical-like behavior of electrons and holes in polymeric conductors
[AD-A214496] 09 p1196 N90-16931
Flexible heat pipe cold plate
[AD-A216053] 11 p1464 N90-18433
Electrochemical investigations of electronically conductive polymers. Part 4: By controlling the supermolecular structure, charge transport rates can be enhanced
[AD-A216603] 11 p1490 N90-18573
Thermoelectric conversion with ion conductors
[AD-A217822] 13 p1828 N90-20497
NMR studies of polymeric solid electrolytes
[AD-A219833] 17 p2381 N90-23562
Microwigglers for submillimeter wavelength free-electron lasers
[AD-A220185] 17 p2409 N90-23730
Optical high-speed parallel backplane
[AD-D014504] 19 p2757 N90-25670
A technique to measure the thermal diffusivity of high T(sub c) superconductors 22 p3147 N90-27846
Transversal, longitudinal, and three dimensional eddy currents in cylindrical guides with elliptic diameters
[ETN-90-97302] 22 p3168 N90-27967

ELECTRIC CONNECTORS
Nearly optimal algorithms and bounds for multilayer channel routing
[AD-A211913] 03 p0343 N90-11955
High-temperature superconducting current leads for cryogenic apparatus
[DE89-017680] 03 p0411 N90-12361
Silicon hybrid wafer scale integration interconnect evaluation
[AD-A215353] 09 p1212 N90-17031
Efficient interconnection schemes for VLSI and parallel computation
[AD-A216405] 10 p1420 N90-18185
Elastomeric electrical isolation membrane
[AD-D014365] 12 p1651 N90-19490
Modeling A circuit switched multiprocessor interconnect
[AD-A217122] 12 p1656 N90-19519
Random access transmission algorithms for data local area networks
[AD-A216443] 12 p1700 N90-19761
Electrical connector for operation in space 18 p2541 N90-24507
CMOS analog four-quadrant multiplier
[AD-D014507] 19 p2685 N90-25271
Electrical resistance measurements of connector-panel interfaces
[AD-A221431] 21 p3001 N90-27057
Solid state circuitry with optical data interfacing
[AD-D014548] 22 p3248 N90-28422

ELECTRIC CONTACTS
Coatings in electrical contacts
[DE89-787739] 02 p0216 N90-11234
Niobium and niobium nitride contacts on semiconducting material
[AD-D014177] 03 p0409 N90-12347
Electrolitic deposited ohmic contacts on III-V compound semiconductors: A review
[PB89-217400] 03 p0410 N90-12350
Effects of composition and age hardening on precious metal electrical contacts
[DE88-008791] 06 p0769 N90-14476
On the numerical solution of the dynamically loaded hydrodynamic lubrication of the point contact problem
[NASA-TM-102427] 09 p1220 N90-17076
Contact formation on (Hg,Cd) Te
[AD-A217088] 12 p1723 N90-19900
Continued development and characterization of doped layers, contacts, and associated electronic devices in silicon carbide
[AD-A219211] 16 p2232 N90-22737
Continued development and characterization of doped layers, contacts and associated electronic devices in silicon carbide
[AD-A219234] 16 p2232 N90-22738
Lateral spreading of Au contacts on InP
[NASA-TM-103133] 16 p2252 N90-22843
Wear of gold-plated contacts: Microscopic aspects, role of oxygen 18 p2538 N90-24479
EHF heterojunction bipolar transistors
[AD-A220984] 18 p2548 N90-24541
Failure mechanisms of GaAs transistors: A literature survey
[AD-A221089] 18 p2548 N90-24543
Au-Ge-Ni-Ti ohmic contacts on gallium arsenide
[DE90-011064] 18 p2625 N90-24960
Ion beam processing of diamond
[AD-A221475] 21 p3001 N90-27058
Low frequency electrical noise across contacts between a normal conductor and superconducting bulk YBa2Cu3O7 22 p3146 N90-27841
Application of a rechargeable, small caliber railgun power supply
[AD-A224207] 24 p3438 N90-29418

ELECTRIC CORONA
The adhesive bonding of thermoplastic composites
[AD-A213358] 05 p0618 N90-13605
A test method for measuring corona inception voltage for transducer autotransformers
[AD-A216818] 11 p1502 N90-18646
Experiments on initial behaviour of corona generated with electrical pulses superimposed on DC bias
[EUT-89-E-226] 20 p2858 N90-26259
Research for electric energy systems
[DE90-014221] 23 p3321 N90-28775

ELECTRIC CURRENT
NT ALTERNATING CURRENT
NT ARC DISCHARGES
NT AURORAL ELECTROJETS
NT BEAM CURRENTS
NT DIRECT CURRENT
NT EDDY CURRENTS
NT ELECTRIC ARCS
NT ELECTRIC CORONA
NT ELECTRIC DISCHARGES
NT ELECTRIC SPARKS
NT ELECTRODELESS DISCHARGES
NT ELECTROJETS
NT EQUATORIAL ELECTROJET
NT EXTERNAL SURFACE CURRENTS
NT FIELD ALIGNED CURRENTS
NT FLASHOVER
NT GAS DISCHARGES
NT GLOW DISCHARGES
NT HIGH CURRENT
NT IONOSPHERIC CURRENTS

NT LIGHTNING
NT LINE CURRENT
NT MERCURY ARCS
NT PENNING DISCHARGE
NT PLASMA CURRENTS
NT RADIO FREQUENCY DISCHARGE
NT SHORT CIRCUIT CURRENTS
NT THRESHOLD CURRENTS
Internal voltages and currents in well-shielded cylindrical objects due to simulated direct-strike lightning
[DE89-012664] 02 p0215 N90-11231
HIPAS 1987-88: ULF research and campaign support
[AD-A211720] 03 p0339 N90-11933
The characterization of Nb3Sn superconductors for use in magnets of 19 T and greater
[DE89-017758] 03 p0412 N90-12364
Evaluation of a diffusion/trapping model for hydrogen ingress in high strength alloys
[AD-A215526] 09 p1194 N90-16920
Preliminary evaluation of space station transmission line in a ring configuration
[NASA-TM-102461] 10 p1329 N90-17677
Measurements of the interaction of high-voltage biassed conductors with the ionosphere
[AD-A218285] 13 p1843 N90-20580
Power transmission device
[AD-D014430] 14 p1969 N90-21281
The RAP unit: A remote autoranging picoammeter
[DE90-007711] 14 p1982 N90-21357
Solar flares and dynamics of Langmuir waves in current-carrying plasmas
[IPPCZ-291] 14 p2042 N90-21710
Current management for improved railgun performance 15 p2057 N90-21781
Development of the methods and means of precise forming and geometry control of superconducting current-carrying element for the UNR pulsed dipoles
[DE90-620108] 15 p2173 N90-22419
A fiber-optic current sensor for aerospace applications
[NASA-TM-103152] 16 p2239 N90-22773
Towards a quantum pump of electric charges and currents
[AD-A221257] 18 p2607 N90-24851
Parametric design studies of toroidal magnetic energy storage units
[DE90-013086] 20 p2881 N90-26390
Research on optogalvanic effects
[AD-A221512] 21 p3071 N90-27463
Measurement of localized corrosion using current density mapping
[DE90-015086] 23 p3310 N90-28721
Magnetic surfaces in tokamaks
[DE90-628905] 24 p3549 N90-30078

ELECTRIC DIPOLES
Time-domain analytic and numeric analysis of vertical dipoles in front of dielectric planar interface
[PB89-221642] 03 p0338 N90-11927
A search for the electric dipole of the electron
[DE90-001572] 08 p1120 N90-16484
Quasi-static analysis of scattering from a chiral sphere
[PB90-189135] 22 p3164 N90-27943

ELECTRIC DISCHARGES
NT ARC DISCHARGES
NT ELECTRIC ARCS
NT ELECTRIC CORONA
NT ELECTRIC SPARKS
NT ELECTRODELESS DISCHARGES
NT FLASHOVER
NT GAS DISCHARGES
NT GLOW DISCHARGES
NT LIGHTNING
NT MERCURY ARCS
NT PENNING DISCHARGE
NT RADIO FREQUENCY DISCHARGE
Method and apparatus for determining time, direction and composition of impacting space particles
[NASA-CASE-LAR-13392-1-CU] 01 p0026 N90-10132
Capacitive behavior in conducting polymers: The ac impedance and quartz crystal microbalance studies
[AD-A210754] 02 p0201 N90-11150
A severe human ESD (Electrostatic Discharge) model for safety and high reliability system qualification testing
[DE89-016177] 02 p0216 N90-11233
Simulation of the EMP (Electromagnetic Pulse) from ESD (Electrostatic Discharge)
[DE89-014484] 03 p0337 N90-11918
An empirical formula for gas switch breakdown delay
[DE89-017233] 03 p0342 N90-11947
Electrical breakdown in vacuum
[DE90-001623] 06 p0771 N90-14485
Electrode/workpiece combinations
[DE90-003919] 08 p1054 N90-16095
Study on lightning parameters in the light of long gap discharge phenomena
[DE90-734987] 09 p1248 N90-17237
Intrinsic properties of high voltage wires that may cause sporadic discharges in space vacuum 10 p1338 N90-17743
A low cost anticharging connection system for solar generators and its application on ASPERA solar array 10 p1341 N90-17765
Study of discharge mechanisms and the stability of transverse electric discharges in the gas mixtures
[ISL-R-114/88] 11 p1516 N90-18733
A simplified theoretical model for the laser-induced optogalvanic effect
[DE90-613121] 14 p2028 N90-21626
Workshop on ESD (Electrostatic Discharge) Ignition of Composite Solid Propellants
[AD-A218599] 17 p2382 N90-23589
Transient pulse monitor
[AD-A220353] 18 p2508 N90-24335
Storage battery operation technique of photovoltaic system to prevent the imbalance of state of charge
[DE90-503032] 20 p2858 N90-26255
Development of a sealed bipolar Li-alloy/FeS2 battery for electric vehicles
[DE90-013650] 21 p2999 N90-27045
Research on optogalvanic effects
[AD-A221512] 21 p3071 N90-27463
Spacecraft charging effects
[RAE-TM-SPACE-375] 23 p3287 N90-28594

ELECTRIC ENERGY STORAGE
Technology Base Research Project for electrochemical energy storage
[DE90-002604] 06 p0806 N90-14693
Space Electrochemical Research and Technology (SERT), 1989
[NASA-CP-3056] 13 p1821 N90-20454
New generation power subsystems for satellites
[AD-A219540] 17 p2365 N90-23464

ELECTRIC EQUIPMENT TESTS
Development of an expert system supporting short-circuit tests for circuit breakers
[DE89-760384] 01 p0059 N90-10334
Testing results of the MIT Probe
[DE89-016679] 02 p0278 N90-11590
The 25-KVA amorphous metal-core transformer developmental test report
[AD-A215444] 09 p1213 N90-17035
Thermal study of battery charge control by temperature derivative reduction 10 p1332 N90-17704
The ground testing of nickel hydrogen batteries prior to launch 10 p1333 N90-17705
Nickel hydrogen cell design for space applications 10 p1334 N90-17714
Status of the cycling tests performed with SAFT NiH2 cells dedicated to space applications 10 p1334 N90-17715
Low earth orbit nickel cadmium battery lifetime testing 10 p1334 N90-17716
The RAP unit: A remote autoranging picoammeter
[DE90-007711] 14 p1982 N90-21357
Evaluation for DLC-Flap Monitoring System of the VSRA
[NAL-TM-607] 24 p3433 N90-29391

ELECTRIC FIELD STRENGTH
Continuing current in cloud-to-ground lightning
[DE90-741969] 10 p1408 N90-18119
Analytical theory of the Bunemann instability for electron runaway
[IPF-88-3] 16 p2319 N90-23224
Electric field strength meters for the HF, VHF, and UHF bands
[BBC-RD-1990/3] 20 p2851 N90-26212
Resonant coupling through a slot to a loaded cylindrical cavity: Experimental results
[AD-A223000] 20 p2922 N90-26831

ELECTRIC FIELDS
Electrical field dependence of protein conformation and channel function in lipid membranes of different compositions
[AD-A210236] 01 p0040 N90-10222
Studies of high power density, pico-second rise-time light activated semiconductor switch
[AD-A210549] 01 p0061 N90-10349
Grid generation procedure using the integral equation method
[NAL-TR-1009] 01 p0111 N90-10630
Development of the electroacoustic dewatering (EAD) process for fine/ultrafine coal
[DE89-015883] 01 p0122 N90-10700
Analysis of the performance of gallium arsenide photoavalanche switches
[DE89-015774] 01 p0129 N90-10739
Thermodynamic principles of the process of the effect of electromagnetic fields on a polymer melt
[AD-A210698] 02 p0201 N90-11149
Simulation of the polar cap F region ionization using an experimental convection electric field 02 p0241 N90-11370
Empirical models of convection electric fields and electrostatic potential at high latitude from EISCAT observations: Preliminary results 02 p0243 N90-11377
Substorm associated pulsations: A study of plasmaspheric cavity resonance, mid-latitude polarisation and geostationary orbit signatures 02 p0251 N90-11422
Biological effects of power frequency electric and magnetic fields: Background paper
[PB89-209985] 02 p0254 N90-11439
Chevron layer structures in Surface Stabilized Ferroelectric Liquid Crystal (SSFLC) cells filled with a material which exhibits the chiral nematic to smectic C* phase transition
[DE89-016985] 02 p0285 N90-11628
Clutter models for subsurface electromagnetic applications
[PB89-229678] 03 p0338 N90-11925
Stellarator transport theory
[DE89-016371] 03 p0406 N90-12328
Field-assisted bonding of single crystal quartz
[DE89-015407] 03 p0410 N90-12353
Scalar Green function method for microstrip antenna analysis based on the exact image theory
[PB89-218838] 04 p0488 N90-12805
Catalog of absolutely calibrated, range normalized, wideband, electric field waveforms from located lightning flashes in Florida: July 24 and August 14, 1985 data
[AD-A212708] 04 p0521 N90-13008
Auroral particle acceleration by dc and low frequency electric fields 05 p0658 N90-13841
Review of surface flashover theory
[DE90-000806] 06 p0768 N90-14489
A numerical model for the axisymmetric equilibrium shape of drops in uniform motion: Effects of external flow, electric field and surface charge 07 p0874 N90-15071
Dimensional analysis of continuous high-capacity electrodispersion of aqueous based liquids in an organic continuous phase
[DE90-003714] 07 p0888 N90-15136
Comments on ER (Electrorheological) fluid rheology
[DE90-002892] 07 p0894 N90-15166
Geometrical optics in inhomogeneous chiral media with application to polarization correction in inhomogeneous lens antennas
[PB90-110669] 08 p1122 N90-16497
Rocket-triggered lightning strikes and forest fire ignition 08 p1155 N90-16690
Electric field-induced flame convection in the absence of gravity 09 p1202 N90-16962
Energy conversion efficiency in high current Raman regime Free Electron Laser (FEL). 1: Single mode analysis
[DE90-719527] 09 p1227 N90-17120
Continuing current in cloud-to-ground lightning
[DE90-741969] 10 p1408 N90-18119
Multilayer optical elements for generation and analysis of circularly polarized x rays
[DE90-006103] 10 p1430 N90-18250
Thermal conductivity of quasi-one dimensional conductors
[DE90-004844] 10 p1435 N90-18281
The effect of electric field on attachment of electrons to solutes in liquid argon
[DE90-003969] 11 p1482 N90-18529
A study of the interaction of light with surfaces of sub-micron dimensions
[DE90-006646] 11 p1571 N90-19048
Causality of plasma permittivity with loss and restoring terms
[NASA-TM-101671] 12 p1645 N90-19453
Two-dimensional, long-pulse computer calculation of microwave-induced electron layer formation in low-pressure air
[DE90-005994] 12 p1646 N90-19459
Numerical simulation of cross field amplifiers
[DE90-006459] 12 p1652 N90-19496
Field effect transistor structures based on strain induced polarization charges
[DE90-007247] 12 p1655 N90-19515
Energy transfer and photochemistry in biomimetic solar conversion
[PB90-114582] 12 p1681 N90-19652
Ionospheric heating with oblique waves. Volume 1: Electron density perturbations
[AD-A216260] 12 p1690 N90-19709
Modelling Doppler broadening in Raman propagation
[DE90-008042] 13 p1789 N90-20269
Radar detection of lightning and electric fields
[AD-A217894] 13 p1842 N90-20574
Quantifying and reducing uncertainty in the assimilative mapping of ionospheric electrodynamics
[AD-A218057] 13 p1842 N90-20577

Generalized WKB approximation for stratified isotropic chiral structures
[PB90-165689] 14 p1967 N90-21270
Proceedings of a workshop on Carcinogenic Potential of Extremely Low Frequency Magnetic Fields
[DE90-614340] 14 p2010 N90-21520
Langmuir wave interaction with ion acoustic wave
[DE90-615407] 14 p2027 N90-21624
Linear and nonlinear electrical response of condensed matter: Ionic, dielectric, and mixed-conduction materials
[AD-A218771] 16 p2215 N90-22639
Transduction of nanovolt signals: Limits of electric-field detection
[AD-A219214] 16 p2312 N90-23177
A capacitance process for contact-free microfile measurement on metallic surfaces
[ETN-90-96503] 18 p2549 N90-24549
Dissociation phenomena in electron-beam sustained carbon dioxide lasers 18 p2560 N90-24610
A study of the spatial scales of discrete polar auroral arcs
[NASA-CR-186806] 19 p2714 N90-25444
Inhomogeneous electric field effects in a linear RF quadruple trap 20 p2853 N90-26222
Microspacecraft and Earth observation: Electrical field (ELF) measurement project
[NASA-CR-186821] 20 p2888 N90-26436
Confinement of nonneutral plasma in unconventional geometries
[DE90-013048] 20 p2928 N90-26659
Facilities for improving evaluations of electromagnetic susceptibilities of weapon systems and electronic equipment
[PB90-155862] 21 p2961 N90-26837
Field-induced surface chemistry of NO
[AD-A223007] 21 p2977 N90-26915
Solidification processing of alloys using an applied electric field
[NASA-CASE-MFS-26083-1-CU] 21 p2981 N90-26940
Non-destructive characterization of polymer/metal interfaces using Surface-Enhanced Raman Scattering (SERS)
[AD-A223105] 21 p2986 N90-26967
Non-destructive characterization of polymer/metal interphases using surface-enhanced Raman scattering
[AD-A222490] 21 p2988 N90-26980
Ionospheric heating with oblique waves. Volume 2: Applications to high-frequency radio propagation
[AD-A223111] 21 p3025 N90-27202
Electrodynamics of the high latitude ionosphere
[AD-A223229] 21 p3026 N90-27203
Applications of gauge theories to enhance numerical solutions of mixed potential integral equations
[AD-A221520] 21 p3065 N90-27424
Structure and dynamics of excited atoms
[AD-A221973] 21 p3074 N90-27474
The dynamic electric microfield in ionic and polar media
[AD-A222534] 22 p3156 N90-27891
Quasi-static analysis of scattering from a chiral sphere
[PB90-189135] 22 p3164 N90-27943
Lower thermosphere (80-100 km) dynamics response to solar and geomagnetic activity: Overview 22 p3207 N90-28194
Further studies of 60 Hz exposure effects on human function
[DE90-014377] 23 p3355 N90-28962
Satellite measurements of magnetospheric Poynting flux
[AD-A224391] 24 p3490 N90-29724
Investigation of structure and transport processes in the high latitude ionospheric plasma using ground based and airborne digisondes
[AD-A224397] 24 p3491 N90-29727
Studies of ionospheric dynamics utilizing data from DMSP
[AD-A223370] 24 p3492 N90-29733
A global model of thunderstorm electricity and the prediction of whistler duct formation 24 p3493 N90-29744
Anomalous decay of Langmuir turbulence. High power, high frequency radiation from beam-plasma interaactions
[AD-A224282] 24 p3547 N90-30065

ELECTRIC FILTERS
NT BANDSTOP FILTERS
NT DIGITAL FILTERS
NT FIR FILTERS
NT MICROWAVE FILTERS
NT RADIO FILTERS
NT TRACKING FILTERS
NT WAVEGUIDE FILTERS
High speed imaging with a tapped solid state sensor
[DE90-006116] 11 p1511 N90-18702
A linear filtering technique for removal of low-frequency noise
[DE90-006183] 13 p1794 N90-20296
Bilateral prediction
[AD-A219564] 17 p2456 N90-24016
Combining zero Doppler filter calculations with MTI filter calculations to increase computational speed
[AD-A222468] 21 p2997 N90-27034
Design of sharp cutoff filters with low quality factors
[AD-A223130] 21 p3000 N90-27051

ELECTRIC FUSES
Resistive fuses: Analog hardware for detecting discontinuities in early vision
[AD-A211891] 05 p0634 N90-13696
Analysis and evaluation of technical data on the photochromic and non-linear optical properties of materials. Appendix: Eye/sensor protection by an optical fuse mirror at a focal plane: Feasibility assessment
[AD-A214051] 07 p0896 N90-15177

ELECTRIC GENERATORS
NT AC GENERATORS
NT ALKALINE BATTERIES
NT BIOCHEMICAL FUEL CELLS
NT DIRECT POWER GENERATORS
NT DYNAMOMETERS
NT FUEL CELLS
NT HOMOPOLAR GENERATORS
NT HYDROGEN OXYGEN FUEL CELLS
NT MAGNETOHYDRODYNAMIC GENERATORS
NT METAL AIR BATTERIES
NT NICKEL ZINC BATTERIES
NT PHOSPHORIC ACID FUEL CELLS
NT PHOTOVOLTAIC CELLS
NT PRIMARY BATTERIES
NT RADIOISOTOPE BATTERIES
NT REGENERATIVE FUEL CELLS
NT ROTATING GENERATORS
NT SODIUM SULFUR BATTERIES
NT SOLAR BLANKETS
NT SOLAR CELLS
NT SOLAR DYNAMIC POWER SYSTEMS
NT SOLAR GENERATORS
NT SOLAR SEA POWER PLANTS
NT THERMAL BATTERIES
NT THERMIONIC CONVERTERS
NT THERMOELECTRIC GENERATORS
NT TURBOGENERATORS
Laser-powered lunar base 01 p0029 N90-10156
Independent Orbiter Assessment (IOA): Assessment of the Electrical Power Distribution and Control/Electrical Power Generation (EPD and C/EPG) FMEA/CIL
[NASA-CR-185542] 03 p0314 N90-11785
An assessment of technology for self-powered gas appliances: A GATC (Gas Appliance Technology Center)
[PB89-219265] 03 p0354 N90-12026
Control of the variable speed generator on the Sandia 34-metre vertical axis wind turbine
[DE90-000803] 06 p0803 N90-14674
Design of a high-gain flux-compression generator
[DE90-002795] 07 p0922 N90-15333
Design and fabricate a metallic hydride heat pump with a cooling capacity of 9000 BTU/H
[AD-A213756] 07 p0931 N90-15388
Mechanoelectric conversion by uniaxial constraint in piezoelectric generators: Optimization of electrical, mechanical, and physico-chemical parameters of materials
[ISAL-89-0020] 08 p1078 N90-16235
The design of low inductance electrical circuits for slapper detonator systems
[AD-A214981] 09 p1212 N90-17024
Overview of photovoltaic and battery applications
[PB90-120536] 09 p1242 N90-17206
Developmental condition and technical problems on electric insulation for super-conducting electric power machine
[DE90-741973] 10 p1379 N90-17994
Stirling engine technologies in Japan
[DE89-782296] 11 p1528 N90-18795
Assessment of High Temperature Superconducting (HTS) electric motors for rotorcraft propulsion
[NASA-CR-185222] 15 p2052 N90-21761
Generalized averaging method for power conversion circuits
[AD-A221977] 21 p3020 N90-27171
Analysis of three-dimensional eddy current field. Application to calculation of magnetic screening effect of the damper system in a model superconducting generator
[DE90-507869] 23 p3321 N90-28779
A 10kW class molten carbonate fuel cell test: The stack with electrolyte plate prepared with paper-making method
[DE90-507841] 23 p3344 N90-28900
Performance measurements and energy balance of an SPS V160 Stirling motor at the German Aerospace Research Establishment
[DLR-MITT-90-03] 23 p3345 N90-28903
Energy transmission by means of coherent quasi-mono-chromatic light beams 23 p3392 N90-29163

ELECTRIC HYBRID VEHICLES
National program plan for electric vehicle battery research and development: Technical plan
[DE90-002023] 08 p1083 N90-16269
Electric and hybrid vehicles: Technical background report for the DOE flexible and alternative fuels study
[DE90-002218] 08 p1084 N90-16271
Electric and hybrid vehicles program
[DE90-013560] 21 p2998 N90-27043

ELECTRIC IGNITION
Electrical ignition of HAN-based liquid propellants
[AD-A223272] 24 p3458 N90-29528

ELECTRIC IMPULSES
U ELECTRIC PULSES

ELECTRIC MOTOR VEHICLES
Safety considerations for sodium-sulfur batteries for electric vehicles
[DE89-017682] 03 p0342 N90-11949
DSEP (Dual Shaft Electric Propulsion) operation and maintenance manual for the NVH and TB-2 vehicles: Advanced Dual Shaft Electric Propulsion System technology development program
[DE89-017549] 03 p0420 N90-12411
Derivation of synthetic mission profiles from electric vehicle field data
[DE89-011125] 06 p0793 N90-14620
Characterization of electric vehicle velocity and power profiles using road test data
[DE90-002085] 06 p0795 N90-14630
Assessment of battery technologies for electric vehicles, volume 1
[DE90-002049] 08 p1059 N90-16122
National program plan for electric vehicle battery research and development: Technical plan
[DE90-002023] 08 p1083 N90-16269
Surveys concerning the effect to introduce electric vehicles. On the possibility of new technology and introducing measures
[DE90-742057] 10 p1391 N90-18046
A battery data base for electric vehicle applications
[DE90-007085] 11 p1503 N90-19655
Life-cycle cost comparisons of advanced storage batteries and fuel cells for utility, stand-alone, and electric vehicle applications
[DE90-008090] 13 p1794 N90-20298
Analytical and experimental study of high phase order induction motors
[NASA-CR-186580] 15 p2088 N90-21952
Application of ultracapacitors in electric vehicle propulsion systems
[DE90-010884] 18 p2550 N90-24554
Survey of applicability of electric vehicles (EVs) in specific regions such as resorts
[DE90-503592] 20 p2871 N90-26336
Development of a sealed bipolar Li-alloy/FeS2 battery for electric vehicles
[DE90-013650] 21 p2999 N90-27045
Electric vehicle battery R/D in the context of a propulsion system
[DE90-013667] 21 p2999 N90-27046
Assessment of battery technologies for electric vehicles. Volume 2, part 2: Appendices
[DE90-014610] 23 p3321 N90-28778

ELECTRIC MOTORS
NT ASYNCHRONOUS MOTORS
NT INDUCTION MOTORS
NT STEPPING MOTORS
NT SYNCHRONOUS MOTORS
NT TORQUE MOTORS
Composite ceramic superconducting wires for electric motor applications
[AD-A210345] 01 p0060 N90-10346
Composite ceramic superconducting wires for electric motor applications
[AD-A213742] 07 p0912 N90-15274
Adjustable speed drive study, June 1985 to September 1988. Part 2: Appendices
[DE90-002771] 07 p0922 N90-15332
A simple fiber optic autocorrelation tachometer
[ETN-90-96146] 08 p1077 N90-16228
Electric and hybrid vehicles: Technical background report for the DOE flexible and alternative fuels study
[DE90-002218] 08 p1084 N90-16271
Design of a high power density, permanent magnet, axial gap dc motor
[DE90-005449] 12 p1655 N90-19514
Assessment of High Temperature Superconducting (HTS) electric motors for rotorcraft propulsion
[NASA-CR-185222] 15 p2052 N90-21761

Composite ceramic superconducting wires for electric motor applications
[AD-A219131] 16 p2224 N90-22689
Composite ceramic superconducting wires for electric motor applications
[AD-A222085] 21 p3001 N90-27055
Performance test plan for variable-speed ac superconducting motor
[DE90-016208] 24 p3465 N90-29579
Theoretical and experimental examinations of brushless monophase direct current motors
[ETN-90-97301] 24 p3466 N90-29580

ELECTRIC NETWORKS
A 2d-1 lower bound 2-layer knock-knee channel routing
[AD-A211948] 04 p0495 N90-12847
Memory matrix
[WO-PATENT-88/04096] 05 p0680 N90-13961
Sneak circuit analysis for the common man
[AD-A215275] 09 p1212 N90-17029
Boolean approaches in digital diagnosis
[AD-A215660] 09 p1274 N90-17386
Development of dynamic equivalent network structures with a universal identification and optimization process
[ETN-90-95822] 12 p1654 N90-19507
Modeling A circuit switched multiprocessor interconnect
[AD-A217122] 12 p1656 N90-19519
Parallel methods for solving nonlinear block bordered systems of equations
[AD-A217062] 12 p1707 N90-19806

ELECTRIC POTENTIAL
NT BIOELECTRIC POTENTIAL
NT COULOMB POTENTIAL
NT LOW VOLTAGE
NT OPEN CIRCUIT VOLTAGE
NT PHOTOVOLTAGES
NT QUANTUM WELLS
NT THRESHOLD VOLTAGE
Deep traps and sidegating in GaAs devices
[AD-A210740] 01 p0133 N90-10765
Internal voltages and currents in well-shielded cylindrical objects due to simulated direct-strike lightning
[DE89-012664] 02 p0215 N90-11231
Empirical models of convection electric fields and electrostatic potential at high latitude from EISCAT observations: Preliminary results
02 p0243 N90-11377
Effect of electrical double layer on transport limited currents at microelectrodes
[AD-A211586] 03 p0324 N90-11843
Capacitive behavior in conducting polymers
[AD-A212448] 04 p0481 N90-12760
Strong-inversion model of threshold voltage in modulation doped field effect transistors: The role of unintentional acceptors
[AD-A212750] 04 p0498 N90-12870
An iterative method to solve the nonlinear Poisson's equation in the case of plasma tangential discontinuities
[AERONOMICA-ACTA-A-346-1989]
05 p0692 N90-14045
Single element magnetic suspension actuator
[NASA-CASE-LAR-13981-1] 07 p0940 N90-15442
Changes in impedance of Ni electrodes upon standing and cycling
[NASA-TM-102438] 10 p1401 N90-18097
A test method for measuring corona inception voltage for transducer autotransformers
[AD-A216818] 11 p1502 N90-18646
Simple analytic potentials for linear ion traps
12 p1642 N90-19436
Lightning surge characteristics of transmission towers. Lightning surge characteristics of 15-meter-high scale model tower
[DE89-782322] 12 p1692 N90-19721
An electrical model for plasma armature voltage
[DE90-007530] 12 p1718 N90-19866
Tunneling microscopy of submonolayer adsorbates on Si3
[AD-A216985] 12 p1719 N90-19876
Electronic precipitator control
[NASA-CASE-LAR-13273-2] 13 p1798 N90-20320
The application of Dow Chemical's perfluorinated membranes in proton-exchange membrane fuel cells
13 p1823 N90-20466
Hydrogen-oxygen proton-exchange membrane fuel cells and electrolyzers 13 p1823 N90-20467
Measurements of the interaction of high-voltage biassed conductors with the ionosphere
[AD-A218285] 13 p1843 N90-20580
Alternating gradient photodetector
[NASA-CASE-NPO-17235-1-CU]
14 p1982 N90-21358
An ultra-small capacitance Josephson junction
[DE90-613396] 14 p2032 N90-21653
Voltage source ac-to-dc converters for high-power transmitters 15 p2075 N90-21886
Induction-type metal detector with increased scanning area capability
[NASA-CASE-KSC-11386-1] 15 p2101 N90-22023
Device for quickly sensing the amount of O2 in a combustion product gas
[NASA-CASE-LAR-13816-1] 15 p2102 N90-22025
A refrigerated Dewar for the Josephson array voltage calibration system
[DE90-005237] 15 p2172 N90-22412
Nonintrusive method and apparatus for monitoring the cure of polymeric materials
[NASA-CASE-LAR-13485-1] 17 p2378 N90-23544
Electric dipole antennae used as micrometeoroid detectors
[AERONOMICA-ACTA-A-351-1989]
17 p2392 N90-23623
Gallium arsenide pilot line for high performance components
[AD-A220948] 18 p2547 N90-24540
Millimeter-wave gyroklystron amplifier experiment using a relativistic electron beam
[AD-A221209] 18 p2548 N90-24544
Research studies on extreme ultraviolet and soft x ray lasers
[AD-A220271] 18 p2562 N90-24621
Conceptual definition of a high voltage power supply test facility
[NASA-CR-185216] 19 p2666 N90-25172
CMOS analog four-quadrant multiplier
[AD-D014507] 19 p2685 N90-25271
A voltage contrast detector with double channel energy analyzer in a scanning electron microscope
[ISBN-90-6275-568-2] 19 p2694 N90-25330
Comparison of currents predicted by NASCAP/LEO model simulations with elementary Langmuir-type bare probe models for an insulated cable containing a single pinhole
[NASA-TM-102486] 20 p2821 N90-26054
A possibility to incorporate saturation in the simple, global model of a synchronous machine with rectifier
[EUT-89-E-225] 20 p2858 N90-26258
High speed magneto-resistive random access memory
[NASA-CASE-NPO-17954-1-CU]
20 p2904 N90-26519
Low frequency electrical noise across contacts between a normal conductor and superconducting bulk YBa2Cu3O7 22 p3146 N90-27841
Corrosion-inhibiting coating composition
[AD-D014548] 22 p3159 N90-27916
L-SWITCH: A PC-program for computing transient voltages and currents during switching off three-phase inductances
[PB90-191412] 22 p3167 N90-27961
Logic level data conversion system
[AD-D014545] 22 p3167 N90-27963
Millimeter-wave generation via plasma three-wave mixing
[AD-A222010] 22 p3247 N90-28415
Unipolar arcing on the cathode surface of a high voltage diode
[AD-A224122] 23 p3322 N90-28787
Pulsed field sample neutralization
[DE90-015131] 24 p3445 N90-29452

ELECTRIC POWER CONVERSION
U ELECTRIC GENERATORS

ELECTRIC POWER PLANTS
NT FUEL CELL POWER PLANTS
NT NUCLEAR POWER PLANTS
NT SOLAR THERMAL ELECTRIC POWER PLANTS
Impact of fundamental technical improvements
[PB89-218010] 01 p0083 N90-10472
Stretched-membrane heliostats for solar central-receiver power plants
[DE89-016034] 01 p0084 N90-10476
Conceptual design analysis for hybrid-cycle OTEC plants for co-production of electric power and desalinated water
[DE90-003551] 08 p1097 N90-16350
Investigation and study on compressed air storage power generation system, part 2
[DE90-702648] 08 p1097 N90-16354
The 1989 National Convention Record IEE Japan, part 8
[DE89-910081] 09 p1210 N90-17013
Vision for the introduction of the wind power generation system. Survey on the prospective market, part 2
[DE89-910386] 12 p1680 N90-19651
Advanced on-site power plant development technology program
[DE90-000443] 13 p1826 N90-20484
Innovative turbine concepts for open-cycle OTEC (Ocean Thermal Energy Conversion)
[DE90-000315] 13 p1827 N90-20493

ELECTRIC POWER SUPPLIES
NT AIRCRAFT POWER SUPPLIES
NT SOLAR DYNAMIC POWER SYSTEMS
NT SPACE STATION POWER SUPPLIES
NT SPACECRAFT POWER SUPPLIES
Impact of fundamental technical improvements
[PB89-218010] 01 p0083 N90-10472
Biological effects of power frequency electric and magnetic fields: Background paper
[PB89-209985] 02 p0254 N90-11439
Independent Orbiter Assessment (IOA): Assessment of the reaction control system, volume 3
[NASA-CR-185543-VOL-3] 03 p0316 N90-11795
The US space station and its electric power system
[NASA-TM-101974] 05 p0616 N90-13596
Intrinsically safe 5-V, 4-A rechargeable power supply
[PB90-103235] 09 p1209 N90-17006
Conceptual design of high Tc superconducting power cable and its economic evaluation
[DE90-734940] 09 p1287 N90-17462
Autonomous electrical power supply subsystem for the Vesta mission 10 p1331 N90-17692
Design of a power supply system based in two quasi-resonant converters 10 p1336 N90-17728
Low noise, high voltage supply for carcinotron backward wave oscillators 10 p1338 N90-17742
High power medium voltage electronic load
10 p1338 N90-17747
Low weight variable GRV power supply as part of the injector electronics to be developed for the electron accelerator MEA
[DIGEL-1989-6] 11 p1504 N90-18661
Development of dynamic equivalent network structures with a universal identification and optimization process
[ETN-90-95822] 12 p1654 N90-19507
Flight termination system battery guidelines
[AD-A217310] 13 p1758 N90-20092
Space Station Freedom electric power system availability study
[NASA-CR-185181] 13 p1763 N90-20120
Power conditioning techniques
[NASA-TM-102577] 13 p1795 N90-20301
Advanced Launch System (ALS): Electrical actuation and power systems improve operability and cost picture
[NASA-TM-102547] 14 p1968 N90-21271
Nuclear technology and the space exploration missions
[NASA-TM-103156] 16 p2253 N90-22847
New generation power subsystems for satellites
[AD-A219540] 17 p2365 N90-23464
A linearly controlled direct-current power source for high-current inductive loads in a magnetic suspension wind tunnel
[NASA-TM-4198] 19 p2692 N90-25319
The development and characterization of ion exchange membranes for selected electrochemical power sources
[DE90-009741] 20 p2857 N90-26251
Practical superconductor development for electrical power applications
[DE90-014836] 24 p3554 N90-30109

ELECTRIC POWER TRANSMISSION
Independent Orbiter Assessment (IOA): Analysis of the electrical power distribution and control/electrical power generation subsystem
[NASA-CR-185538] 02 p0165 N90-10933
Independent Orbiter Assessment (IOA): Analysis of the electrical power distribution and control/remote manipulator system subsystem
[NASA-CR-185526] 02 p0166 N90-10936
Independent Orbiter Assessment (IOA): Analysis of the reaction control system, volume 2
[NASA-CR-185532-VOL-2] 02 p0167 N90-10939
Independent Orbiter Assessment (IOA): Analysis of the reaction control system, volume 3
[NASA-CR-185532-VOL-3] 02 p0167 N90-10940
Independent Orbiter Assessment (IOA): Analysis of the electrical power distribution and control subsystem, volume 1
[NASA-CR-185529-VOL-1] 02 p0167 N90-10941
Independent Orbiter Assessment (IOA): Analysis of the electrical power distribution and control subsystem, volume 2
[NASA-CR-185529-VOL-2] 02 p0167 N90-10942
Electron beam welding: Model of high voltage bias transmission line and termination circuits
[DE89-016900] 02 p0230 N90-11323
Independent Orbiter Assessment (IOA): Assessment of the reaction control system, volume 1
[NASA-CR-185543-VOL-1] 03 p0316 N90-11793
Independent Orbiter Assessment (IOA): Assessment of the reaction control system, volume 2
[NASA-CR-185543-VOL-2] 03 p0316 N90-11794
Independent Orbiter Assessment (IOA): Assessment of the reaction control system, volume 4
[NASA-CR-185543-VOL-4] 03 p0316 N90-11796

Independent Orbiter Assessment (IOA): Assessment of the reaction control system, volume 5
[NASA-CR-185543-VOL-5] 03 p0316 N90-11797
A physical and numerical study of the turn-off behavior of bipolar power transistors
[LAAS-89185] 08 p1061 N90-16136
Analysis of the 60-Hz power system at KSC: The Orsino substation 08 p1155 N90-16692
Conceptual design of high Tc superconducting power cable and its economic evaluation
[DE90-734940] 09 p1287 N90-17462
The 120V 20A PWM switch for applications in high power distribution 10 p1335 N90-17724
Power conditioning for active array SAR antennas 10 p1338 N90-17744
High power medium voltage electronic load 10 p1338 N90-17747
Proposal of arc driving type fault current limiter
[DE89-782290] 12 p1650 N90-19485
Lightning surge characteristics of transmission towers. Lightning surge characteristics of 15-meter-high scale model tower
[DE89-782322] 12 p1692 N90-19721
A comparative study of electric power distribution systems for spacecraft
[NASA-CR-186531] 14 p1942 N90-21113
An expert system for simulating electric loads aboard Space Station Freedom
[NASA-TM-103150] 15 p2158 N90-22325
A high frequency (20 kHz) power electronics reactive-current compensator with insulated gate bipolar transistors as semiconductor switches
[EMV-88-54] 17 p2399 N90-23665

ELECTRIC PROPULSION
NT ELECTROMAGNETIC PROPULSION
NT ION PROPULSION
NT LASER PROPULSION
NT PLASMA PROPULSION
Assessment of thin film batteries based on polymer electrolytes. Part 3: Specific energy versus specific power
[AD-A212141] 04 p0515 N90-12976
Design of a thrust stand for high power electric propulsion devices
[NASA-TM-102372] 08 p1037 N90-15992
Power processing unit for 20mN-class ion engine system 10 p1336 N90-17732
The 1989 JANNAF Propulsion Meeting, volume 1
[CPIA-PUBL-515-VOL-1] 11 p1470 N90-18462
Electric propulsion options for 10 kW class earth-space missions 11 p1472 N90-18474
Mission options for an electric propulsion demonstration flight test 11 p1473 N90-18479
Electric propulsion for manned Mars exploration 11 p1473 N90-18480
Advanced electric propulsion research, 1989
[NASA-CR-185237] 15 p2062 N90-21810
Transport properties of plasmas in microwave electrothermal thrusters
[AD-A219408] 16 p2320 N90-23228
Advanced propulsion for LEO and GEO platforms
[NASA-TM-103228] 22 p3134 N90-27785
Advanced onboard propulsion benefits and status
[NASA-TM-103174] 22 p3134 N90-27786
Low power arcjet performance
[NASA-TM-103280] 23 p3298 N90-28657
Development of the electric vehicle analyzer
[AD-A224201] 23 p3323 N90-28788
Application of a rechargeable, small caliber railgun power supply
[AD-A224207] 24 p3438 N90-29418

ELECTRIC PULSES
Elements of a 200 watt pulsed excimer laser 02 p0226 N90-11295
Local atmospheric electricity and its possible application in high energy cosmic ray air shower detection 16 p2340 N90-23335
Transient pulse monitor
[AD-A220353] 18 p2508 N90-24335
Experiments on initial behaviour of corona generated with electrical pulses superimposed on DC bias
[EUT-89-E-226] 20 p2858 N90-26259
A 6.4 kV pulse generator with transformers
[DIGEL-1989-1] 21 p3002 N90-27063

ELECTRIC REACTORS
NT SATURABLE REACTORS

ELECTRIC RELAYS
Steep front impulse tests on a solid-state relay
[DE90-004243] 08 p1062 N90-16140

ELECTRIC ROCKET ENGINES
NT ARC JET ENGINES
NT ELECTROTHERMAL ENGINES
NT ION ENGINES
NT MERCURY ION ENGINES
NT PLASMA ENGINES
NT RESISTOJET ENGINES
Arcjet nozzle design impacts 11 p1473 N90-18478
The 30-kW ammonia arcjet technology
[NASA-CR-186850] 19 p2670 N90-25190
Geometric effects in applied-field MPD thrusters
[NASA-TM-103259] 22 p3134 N90-27782

ELECTRIC SPARKS
Air breakdown photography in the picosecond domain
[DE89-016775] 03 p0322 N90-11830
Research on sliding spark preionization in a TEA CO2 laser
[ISL-R-113/88] 11 p1516 N90-18732

ELECTRIC SWITCHES
NT THERMOSTATS
Physics of high energy photoconductive switches
[AD-A210341] 01 p0060 N90-10345
Studies of high power density, pico-second rise-time light activated semiconductor switch
[AD-A210549] 01 p0061 N90-10349
Contribution to the study of a self-protected static switch and its command strategy
[ECL-89-002] 05 p0636 N90-13711
PWM converter topologies 10 p1335 N90-17721
The 120V 20A PWM switch for applications in high power distribution 10 p1335 N90-17724
Techniques for high frequency power conversion 10 p1336 N90-17729
Prediction of high-voltage, broadband RF pulse generation from an air gas avalanche switch
[DE90-010183] 18 p2549 N90-24551

ELECTRIC WELDING
NT ARC WELDING
NT ELECTRON BEAM WELDING
NT GAS TUNGSTEN ARC WELDING
NT PLASMA ARC WELDING
A characterization of the side bonding, upset plug welding process
[DE89-015181] 02 p0229 N90-11315
Resistance welding large parts
[DE89-010462] 03 p0354 N90-12027

ELECTRIC WIRE
Flammability, smoke, and dry arc tracking tests of aircraft electrical wire insulations
[DOT/FAA/CT-89/21] 03 p0302 N90-11714
Intrinsic properties of high voltage wires that may cause sporadic discharges in space vacuum 10 p1338 N90-17743
Proceedings of the 38th International Wire and Cable Symposium
[AD-A216023] 11 p1501 N90-18638
The RAP unit: A remote autoranging picoammeter
[DE90-007711] 14 p1982 N90-21357
RF surface resistance measurements in the Pb-Bi-Sr-Ca-Cu-O system
[DE90-010412] 18 p2621 N90-24932
Development of elements of a high Tc superconducting cable
[AD-A221300] 18 p2623 N90-24945
Finding minimum width for single-layer channel routing in linear time
[AD-A221876] 21 p3002 N90-27062
Evaluations of new polyimide films for flexible circuit applications at EG and G Mound Applied Technologies
[DE90-014117] 23 p3312 N90-28731

ELECTRIC WIRING
U ELECTRIC WIRE
U WIRING

ELECTRICAL BREAKDOWN
U ELECTRICAL FAULTS

ELECTRICAL CONDUCTIVITY
U ELECTRICAL RESISTIVITY

ELECTRICAL ENGINEERING
Center for Electronics and Electrical Engineering technical publication announcements covering Center programs, January-March 1989 with 1989 CEEE events calendar
[PB89-226308] 03 p0418 N90-12402
The 120V 10A SSPC for the Columbus programme 10 p1330 N90-17683
JPRS report: Science and technology. USSR: Electronics and electrical engineering
[JPRS-UEE-90-002] 14 p1970 N90-21284
Basic research in electronics (JSEP)
[AD-A219931] 17 p2398 N90-23661
An object-oriented solution example: A flight simulator electrical system
[AD-A219190] 19 p2661 N90-25145
Center for Electronics and Electrical Engineering technical progress bulletin covering center programs, July to September 1989, with 1990 CEEE events calender
[PB90-188095] 22 p3167 N90-27959
Emerging technologies in electronics and their measurement needs, second edition
[PB90-188087] 23 p3320 N90-28773
Performance analysis of subspace-based parameter estimation algorithms
[AD-A224523] 24 p3463 N90-29566

ELECTRICAL FAULTS
NT SHORT CIRCUITS
Built-in generation for CMOS circuits
[IMAG-RR-736-I] 04 p0496 N90-12855
Electrical breakdown in vacuum
[DE90-001623] 06 p0771 N90-14485
Boolean approaches in digital diagnosis
[AD-A215660] 09 p1274 N90-17386
Improvement of impulse breakdown strength of an XLPE cable by modifing semiconducting layer
[DE90-734942] 09 p1287 N90-17463
VHSIC/VHSIC-Like reliability prediction modeling
[AD-A214601] 09 p1288 N90-17468
Investigations on hot spots effects in reverse biased spatial solar cells 10 p1344 N90-17789
Proposal of arc driving type fault current limiter
[DE89-782290] 12 p1650 N90-19485
Velocity matched optical transmitter
[AD-A217413] 13 p1887 N90-20830
Knowledge-based and integrated monitoring and diagnosis in autonomous power systems 15 p2155 N90-22310
An experimental study of fault propagation in a jet-engine controller
[NASA-CR-181335] 17 p2354 N90-23401
A gas-phase high voltage electrical isolator with controlled breakdown
[RAE-TR-78030] 19 p2669 N90-25180
Autonomous power expert fault diagnostic system for Space Station Freedom electrical power system testbed 19 p2730 N90-25521
Implementation of an algorithm for travelling-wave-based directional detection
[EUT-89-E-214] 20 p2855 N90-26239
LASER: A Layout Sensitivity Explorer. Report and user's manual
[EUT-89-E-216] 20 p2908 N90-26545
Evaluations of new polyimide films for flexible circuit applications at EG and G Mound Applied Technologies
[DE90-014117] 23 p3312 N90-28731

ELECTRICAL GROUNDING
Cable coupling lightning transient qualification
[NASA-CR-183826] 05 p0584 N90-13405

ELECTRICAL IMPEDANCE
NT CONTACT RESISTANCE
NT ELECTRICAL RESISTANCE
NT REACTANCE
NT TRANSCONDUCTANCE
Magnetically insulated electron flows in pulsed power systems
[AD-A212746] 04 p0549 N90-13196
First International Symposium on Electrochemical Impedance Spectroscopy. Extended abstracts
[AD-A214406] 07 p0925 N90-15354
Very broad band VHF/UHF omnidirectional antenna design study
[AD-A215358] 09 p1207 N90-16997
Simple pole/zero modelling of conductance controllers 10 p1337 N90-17739
Impedance characteristics of terawatt ion diodes
[DE90-006276] 12 p1652 N90-19494
A contribution to the theory of transient conductor simulations
[ETN-90-95891] 12 p1654 N90-19511
The 5th Annual Review of Progress in Applied Computational Electromagnetics
[AD-A217994] 14 p1966 N90-21258
The open-ended coaxial line: A rigorous variational treatment
[RSRE-MEMO-4331] 19 p2683 N90-25265
Characteristic impedances and loss data for a common stripline pickup geometry
[CEBAF-PR-89-038] 19 p2755 N90-25656
An experimental system for measuring the wavenumber-frequency response of Timoshenko beams
[AD-A222569] 20 p2878 N90-26374

ELECTRICAL INSULATION
Flammability, smoke, and dry arc tracking tests of aircraft electrical wire insulations
[DOT/FAA/CT-89/21] 03 p0302 N90-11714
Cable coupling lightning transient qualification
[NASA-CR-183826] 05 p0584 N90-13405
Stress analysis of the Princeton Plasma Physics Laboratory 1/2- x 1/2-inch shear/compression test fixture
[DE90-004401] 08 p1124 N90-16512
Improvement of impulse breakdown strength of an XLPE cable by modifing semiconducting layer
[DE90-734942] 09 p1287 N90-17463
Developmental condition and technical problems on electric insulation for super-conducting electric power machine
[DE90-741973] 10 p1379 N90-17994

Elastomeric electrical isolation membrane
[AD-D014365] 12 p1651 N90-19490
The effects of radiation on the mechanical properties of polymers used as electrical cable insulation and jacketing materials
[AERE-R-13286] 13 p1779 N90-20209
Materials and selection criteria analysis for the compact ignition tokamak toroidal field coil turn-to-turn insulation system: Photographic summary ofllaboratory testing
[DE90-008020] 13 p1891 N90-20850
Study and simulation of the behavior of a high frequency transformer
[ECL-89-008] 17 p2399 N90-23667
Current distribution in cylindrical porous electrodes
[DE90-009707] 18 p2546 N90-24530
Evaluations of new polyimide films for flexible circuit applications at EG and G Mound Applied Technologies
[DE90-014117] 23 p3312 N90-28731
Investigations into the use of dielectric coatings in magnetic switches
[DE90-014331] 23 p3321 N90-28776
Characterization of electron flow in positive-polarity linear-induction accelerators
[DE90-014998] 23 p3394 N90-29177

ELECTRICAL LEADS
U ELECTRIC CONDUCTORS

ELECTRICAL MEASUREMENT
Coastal subsea permafrost and bedrock observations using dc resistivity
[AD-A210784] 02 p0253 N90-11435
Infrared water vapor continuum absorption: New atmospheric electrical measurements and theory
[AD-A212594] 04 p0519 N90-12994
The effects of trace anions on the voltammetry of single crystal gold surfaces
[AD-A211886] 04 p0558 N90-13254
Electrochemistry at very small electrodes
[AD-A213156] 05 p0621 N90-13623
Inspection development for T-37 wing spar cap lug
[AD-A214826] 09 p1159 N90-16708
High voltage pickup plate
[LINO-1989-3] 12 p1654 N90-19510
The RAP unit: A remote autoranging picoammeter
[DE90-007711] 14 p1982 N90-21357
The initiation of intergranular stress corrosion-cracking on sensitized stainless steel in dilute thiosulphate solutions
[AERE-R-13317] 16 p2217 N90-22648
A fiber-optic current sensor for aerospace applications
[NASA-TM-103152] 16 p2239 N90-22773
OSSE observations of active galactic nuclei
16 p2337 N90-23320
Self-calibrating apparatus to find dynamic compressibility of organic solids
[AD-A219780] 17 p2415 N90-23763
Noninvasive estimation of fluid shifts between body compartments by measurement of bioelectric characteristics 18 p2628 N90-24976
Nondestructive one- and two-dimensional doping profiling by inverse methods
[ETN-90-97264] 20 p2874 N90-26351
Electrical resistance measurements of connector-panel interfaces
[AD-A221431] 21 p3001 N90-27057
Electrical characterization of a Mapham inverter using pulse testing techniques
[NASA-TM-103254] 22 p3134 N90-27784
Measurement of localized corrosion using current density mapping
[DE90-015086] 23 p3310 N90-28721
Effects of Al substitution by Fe in CeAl2
[DE90-627843] 23 p3311 N90-28726
Emerging technologies in electronics and their measurement needs, second edition
[PB90-188087] 23 p3320 N90-28773
Evaluation of a thermistor power measurement system for use on the NPL antenna extrapolation range
[NPL-DES-89] 24 p3466 N90-29583

ELECTRICAL PROPERTIES
NT CAPACITANCE
NT CAPACITANCE-VOLTAGE CHARACTERISTICS
NT CHARGE DISTRIBUTION
NT CONTACT RESISTANCE
NT DIELECTRIC PROPERTIES
NT ELECTRICAL IMPEDANCE
NT ELECTRICAL RESISTANCE
NT ELECTRICAL RESISTIVITY
NT ELECTRON MOBILITY
NT ELECTROSTRICTION
NT FERROELECTRICITY
NT HOLE MOBILITY
NT INDUCTANCE
NT IONOSPHERIC CONDUCTIVITY
NT KONDO EFFECT
NT MAGNETORESISTIVITY
NT PERMITTIVITY
NT PHOTOCONDUCTIVITY
NT PHOTOVOLTAIC EFFECT
NT PIEZOELECTRICITY
NT PLASMA CONDUCTIVITY
NT PYROELECTRICITY
NT REACTANCE
NT SUPERCONDUCTIVITY
NT TRANSCONDUCTANCE
Impact of fundamental technical improvements
[PB89-218010] 01 p0083 N90-10472
Electroporation: Theory of basic mechanisms
[AD-A210196] 01 p0091 N90-10520
Two photon absorption characterization
[AD-A210508] 01 p0121 N90-10694
Ceramic processing of bulk high-T(sub c) superconductors
[DE89-015703] 01 p0128 N90-10736
Properties of devices prepared with epitaxial layers on InP
[AD-A210304] 01 p0132 N90-10759
Advanced GaAs process modeling, volume 1
[AD-A210385] 01 p0132 N90-10761
Coastal subsea permafrost and bedrock observations using dc resistivity
[AD-A210784] 02 p0253 N90-11435
Characterizations of electrical properties of highT(sub c) superconducting materials
[NASA-TM-100380] 03 p0409 N90-12345
Ultrastructure processing and characterization of polymers
[AD-A211460] 04 p0478 N90-12743
A center for advanced electrical and structural polymers
[AD-A212853] 04 p0482 N90-12784
Structural and electrical properties of thin films and superlattices composed of II-VI semiconductors
04 p0558 N90-13249
Study of the electrical and optical properties of the vanadium and nickel impurities in GaAs
[ISAL-89-0028] 04 p0559 N90-13259
A literature survey of inherently conducting polymers
[FOA-C-20763-2.4] 05 p0628 N90-13668
Joint Services Electronics Program
[AD-A213015] 05 p0634 N90-13699
Practical superconductor development for electrical power applications
[DE90-001804] 06 p0771 N90-14487
Electrical properties of materials for high temperature strain gage applications
[NASA-CR-186192] 06 p0780 N90-14534
Microstructure and electrical properties of bulk high-T(sub c) superconductors
[DE90-001762] 06 p0855 N90-14974
Magnetic and electrical properties
[DE90-002183] 06 p0856 N90-14977
A model of the thermal and electrical properties of cosmic dust particles 06 p0863 N90-15014
Arc-sprayed coatings for electromagnetic pulse protection: Assessment of physical and electrical properties
[AD-A213825] 07 p0912 N90-15275
RF transistor thermal/electrical characterization
[DE90-001427] 07 p0920 N90-15326
Development of tunable excimer lasers
[AD-A213521] 07 p0936 N90-15421
Thermally stable metal/GaAs contacts
[DE90-002122] 07 p0998 N90-15774
Properties of high Tc superconducting oxides
[DE90-003792] 07 p1005 N90-15821
The 25-KVA amorphous metal-core transformer developmental test report
[AD-A215444] 09 p1213 N90-17035
Electrical test of gyrotron coil
[INPE-4929-RPE/596] 09 p1214 N90-17041
The use of BaF2 buffer layers for the sputter-deposition of TlCaBaCuO thin-film superconductors
[DE90-004859] 09 p1292 N90-17490
Evolution of structure and electrical properties during crystallization of rapidly solidified Bi4Ti3O12
[DE90-005221] 09 p1292 N90-17492
Assessment of solar cell quality criteria
10 p1342 N90-17776
CIC type thin diode for solar array
10 p1344 N90-17788
Characterization and development report for the SA3124, a 15-volt zener diode
[DE90-005711] 10 p1379 N90-17993
Research on high-efficiency, multi-gap, multi-junction amorphous silicon-based alloy thin-film solar cells
[DE89-009492] 10 p1402 N90-18101
Research relating to crystalline silicon-film on a foreign substrate
[DE90-005720] 11 p1491 N90-18582
Zirconia-based electrodes for solid oxide fuel cells
[DE90-000462] 12 p1655 N90-19513
Modeling studies of electrolyte flow and bubble behavior in advanced Hall cells
[DE90-007013] 13 p1795 N90-20303
A nonintrusive method for measuring the operating temperature of a solenoid-operated valve
[DE90-007576] 13 p1804 N90-20355
The electronic properties of high (Tc) superconductors probed by positron annihilation
[DE90-008354] 13 p1896 N90-20883
Alternative materials for solid oxide fuel cells
[DE90-008615] 14 p2001 N90-21468
New flexible circuit material evaluation
[DE90-008313] 15 p2071 N90-21866
Active primary lithium thionyl chloride battery for artillery applications
[DE90-009511] 15 p2089 N90-21955
Laboratory testing of Energy Research Corporation ERC 160 NiCd 6 volt traction battery
[DE90-009629] 15 p2089 N90-21957
Laboratory testing of Saft SEH-5-200 6 volt traction battery
[DE90-009787] 15 p2089 N90-21958
Fundamental and practical studies of metal contacts on mercury zinc telluride
[AD-A218730] 17 p2376 N90-23528
New liquid cathode electrolytes in high rate cells
[AD-A219822] 18 p2546 N90-24531
Multichip packaging technology with laser-patterned interconnects
[DE90-010743] 18 p2549 N90-24552
The electrical characteristic and gain behavior as a function of the radial distance from the laser axis in a copper vapor laser
[DE90-615371] 18 p2564 N90-24630
Performance of battery charge controllers
[DE90-011413] 19 p2686 N90-25279
Crystalline photovoltaic cell research, status, and future direction
[DE90-011478] 19 p2710 N90-25427
Synthesis, structure, electric, and magnetic properties of CaNiN
[AD-A222273] 21 p2978 N90-26923
Silicon containing electroconductive polymers and structures made therefrom
[NASA-CASE-NPO-17826-1-CU]
21 p2983 N90-26952
Transient signal distortion and coupling in multilayer multiconductor MIC microstrips
[AD-A222989] 21 p3000 N90-27050
Investigation on the MBE growth and properties of AlGaInAs/InP and InGaAs-InAlAs superlattices
[DE90-012248] 21 p3080 N90-27515
Aircraft lightning protection handbook
[AD-A222716] 22 p3110 N90-27668
Oxygen stabilization induced enhancement in J(sub c) and T(sub c) of superconducting oxides
22 p3137 N90-27800
Preparation and characteristics of superconducting cuprate thin films: Nd(2-x)Ce(x)CuO4 and substituted Bi-system 22 p3140 N90-27813
Thermal and electric properties of Nd(1.85)Ce(0.15)CuO(4-y) and Pr(1.85)Ce(0.15)CuO(4-y)
22 p3141 N90-27816
Phase compatibilities of YBa2Cu3O(9-delta) type structure in quintenary systems Y-Ba-Cu-O-X (impurity)
22 p3145 N90-27834
Study of the superconducting properties of the Bi-Ca-Sr-Cu-O system 22 p3151 N90-27866
Identification method for estimation of electrical parameters of induction motors
[ETN-90-97306] 22 p3168 N90-27969
Friction, wear and electric characteristics of slip-ring brush materials for space applications. Part 1: Screening by pin-on-disk friction tests
[NAL-TR-1040] 24 p3478 N90-29657
A study of water vapor, electrical parameters, and radio propagation
[AD-A223582] 24 p3492 N90-29736

ELECTRICAL RESISTANCE
NT CONTACT RESISTANCE
NT TRANSCONDUCTANCE
Coastal subsea permafrost and bedrock observations using dc resistivity
[AD-A210784] 02 p0253 N90-11435
Resistance welding large parts
[DE89-010462] 03 p0354 N90-12027
A solvable self-similar model of the sausage instability in a resistive Z-pinch
[AD-A213137] 05 p0688 N90-14006
Inductive store opening switch and tests for energy transfer to a load
[DE90-002818] 06 p0770 N90-14482
Structural, magnetic and electrical properties of La(sub 2-x) Ba(sub x) NiO4
[AD-A214347] 10 p1434 N90-18278

A digitally controlled system for effecting and presenting a selected electrical resistance
[NASA-CASE-MFS-29149-1] 12 p1652 N90-19492
Enhanced ceria solid electrolyte fuel cell development. Reduction of electronic conductivity permits use of a solid ceria electrolyte in high efficiency high power density fuel cells at temperatures compatible with metallic cell hardware
[AD-A217840] 13 p1828 N90-20498
Noninvasive estimation of fluid shifts between body compartments by measurement of bioelectric characteristics 18 p2628 N90-24976
Quantum ballistic and adiabatic electron transport, studied with quantum point contacts
[ETN-90-97262] 20 p2889 N90-26440
Electrical resistance measurements of connector-panel interfaces
[AD-A221431] 21 p3001 N90-27057

ELECTRICAL RESISTIVITY
NT IONOSPHERIC CONDUCTIVITY
NT KONDO EFFECT
NT MAGNETORESISTIVITY
NT PHOTOCONDUCTIVITY
NT PLASMA CONDUCTIVITY
NT SUPERCONDUCTIVITY
Transport studies of conducting polymers
02 p0200 N90-11140
New secondary batteries utilizing electronically conductive polymer cathodes
[NASA-CR-185885] 02 p0215 N90-11227
Studies of a strongly coupled plasma produced in a capillary discharge
[DE89-016611] 02 p0277 N90-11581
Transport properties of thermally grown Cr2O3
[DE89-016703] 02 p0284 N90-11623
Resistive block methods for electrostatic field solutions with internal elements
[DE89-017535] 03 p0337 N90-11920
RF performance of polycrystalline high-T(sub c) superconductors
[DE89-017671] 03 p0411 N90-12359
Electrically conducting organic materials: Design, synthesis and characterization
[AD-A212214] 04 p0471 N90-12700
Capacitive behavior in conducting polymers
[AD-A212448] 04 p0481 N90-12760
Resistivity measurements of superconducting materials
[PB89-225700] 04 p0496 N90-12856
Synthesis and characterization of new low-dimensional metal complex conductors
[AD-A213189] 04 p0498 N90-12871
Assessment of thin film batteries based on polymer electrolytes. Part 3: Specific energy versus specific power
[AD-A212141] 04 p0515 N90-12976
Microwave microstrip resonator measurements of Y1Ba2Cu3O(7-x) and Bi2Sr2Ca1Cu2O(8-y) thin films
[NASA-TM-102159] 05 p0635 N90-13704
Solid oxide fuel cells electrodes based on In(sub 2)O(sub 3)-PrO(sub 1.83)-ZrO(sub 2)
[DE90-002666] 06 p0806 N90-14691
Electrochemical investigation of electronically conductive polymers
[AD-A214019] 07 p0912 N90-15277
Introduction to extremely-low-frequency electric and magnetic fields
[DE90-002662] 07 p0966 N90-15578
The measurement of transport properties in strongly coupled plasmas
[DE90-003451] 07 p0996 N90-15755
Electrical characteristics measurements for the TSS-1 satellite painting
[IFSI-89-7] 08 p1036 N90-15987
New electrically conducting solids based on nickel(II) - bis(1,3-dithiole-2-thione-4,5-diselenolate)
[DE90-003788] 08 p1042 N90-16020
Command operated liquid metal opening switch
[AD-D014262] 08 p1060 N90-16126
Solid state electrical switch employing materials with reversible phase transistors
[NASA-CASE-NPO-17621-1-CU]
09 p1209 N90-17010
Electromagnetic scale models using emulsions
[AD-A214855] 09 p1211 N90-17022
Development and application of diagnostic instrumentation for measurements of electron density and conductivity
[DE90-004076] 09 p1228 N90-17127
Thermal conductivity of quasi-one dimensional conductors
[DE90-004844] 10 p1435 N90-18281
Effect of manganese additions on the physical and superconducting properties of Nb-46.5Ti
[DE90-005393] 10 p1436 N90-18290
Electrochemical investigations of electronically conductive polymers. Part 4: By controlling the supermolecular structure, charge transport rates can be enhanced
[AD-A216603] 11 p1490 N90-18573
Reliability studies of ceramic capacitors
[AD-A216763] 11 p1501 N90-18643
Fast optical switch and limiter using quantum size effect in metal grain composites
[AD-D014332] 12 p1619 N90-19305
Heterogeneous composite and method of making
[AD-D014337] 12 p1619 N90-19306
Electrical resistivity of strongly coupled plasmas in intense fields
[DE90-002236] 12 p1717 N90-19861
Deep level transient spectroscopy in resistive layers
[DE90-008349] 13 p1772 N90-20169
Electronic and ionic transport in processable conducting polymers
[AD-A218093] 13 p1782 N90-20229
High-temperature ceramic superconductors
[AD-A218347] 13 p1783 N90-20233
Differential measurements of the lateral photo effect in GaAs/AiGaAs heterostructures
[AERE-R-13557] 13 p1893 N90-20861
SiO(x) precipitation: Defect density correlation with the n+ substrate resistivity
[DE90-005593] 13 p1895 N90-20878
Resistivity of pristine and intercalated graphite fiber epoxy composites
[NASA-TM-102576] 14 p1955 N90-21192
Near contact phenomena and transient effects in far infrared photoconductors 14 p1976 N90-21316
Alternating gradient photodetector
[NASA-CASE-NPO-17235-1-CU]
14 p1982 N90-21358
Viscosity, density and conductivity of ImCl(HCl) sub 1.3
[AD-A218902] 16 p2216 N90-22641
Scattering of a plane electromagnetic wave from a semicircular crack in a perfectly conducting ground plane
[AD-A219310] 16 p2230 N90-22721
A low temperature calorimetric study of several high-T(sub c) superconductors 16 p2322 N90-23237
High temperature electric arc furnace and method
[NASA-CASE-MFS-28281-1] 17 p2357 N90-23415
Preliminary investigation into the effect of high temperature thermal anneals on the figure of merit of silicon germanium alloys
[AD-A218573] 17 p2375 N90-23527
Fundamental and applied aspects of defect engineering in G2As; EL2 and other nonstoichiometric defects
[AD-A218597] 17 p2475 N90-24152
Encoding of the Burgess metal electrical resistivity model into SESAME format and its adaptation to the metal nickel
[DE90-010816] 18 p2526 N90-24419
Electronic and ionic transport in processable conducting polymers
[AD-A221045] 18 p2530 N90-24436
Resistivity measurements of halide-salt/MgO separators for thermal cells
[DE90-009740] 18 p2550 N90-24553
An influence of fast neutron irradiation on the properties of p-i-n wide-based diodes
[DE90-611148] 18 p2550 N90-24556
The composition and physical properties of the Earth's mantle and core 18 p2579 N90-24689
Magnetic and resistive measurements of the upper critical field in intwinned single crystals of YBa2Cu3O(7-delta)
[DE90-010083] 18 p2619 N90-24918
Electromigration in metallic microstructures
[AD-A221208] 18 p2622 N90-24942
High-temperature superconductors for space power transmission lines
[NASA-TM-103459] 18 p2624 N90-24952
An analysis of the contact sintering process in III-V solar cells
[NASA-TM-103179] 19 p2709 N90-25420
Searching for heavy fermion materials in Ce intermetallic compounds
[DE90-011809] 20 p2834 N90-26116
Resistivity, adhesive strength, and residual stress measurements of thin film metallizations on single crystal quartz
[DE90-011902] 20 p2837 N90-26135
The development and characterization of ion exchange membranes for selected electrochemical power sources
[DE90-009741] 20 p2857 N90-26251
High speed magneto-resistive random access memory
[NASA-CASE-NPO-17954-1-CU]
20 p2904 N90-26519
Experiments on superconductor imaging surface magnetometry
[DE90-008925] 20 p2929 N90-26865
Silicon containing electroconductive polymers and structures made therefrom
[NASA-CASE-NPO-17826-1-CU]
21 p2983 N90-26952
Preparation and characteristics of superconducting cuprate thin films: Nd(2-x)Ce(x)CuO4 and substituted Bi-system 22 p3140 N90-27813
Potential dependence of the conductivity of highly oxidized polythiophenes, polypyrroles, and polyaniline: Finite windows of high conductivity
[AD-A222024] 22 p3159 N90-27912
Method of obtaining current-conducting polymer materials
[AD-A222129] 22 p3159 N90-27914
High resistivity Al(x)Ga(1-x) As(y)Sb(1-y) epitaxial layers by sulfur compensation doping
[DE90-012228] 22 p3248 N90-28419
Electric properties of highly oriented rigid chain, polymeric liquid crystals
[ETN-90-97287] 22 p3248 N90-28424
Electronic conduction in molten cryolite saturated with alumina
[DE90-015090] 23 p3400 N90-29211

ELECTRICITY
NT ALTERNATING CURRENT
NT ATMOSPHERIC ELECTRICITY
NT AURORAL ELECTROJETS
NT ELECTROJETS
NT EQUATORIAL ELECTROJET
NT HYDROELECTRICITY
NT IONOSPHERIC CURRENTS
NT STATIC ELECTRICITY
Conductive polymers of transition-metal complexes coordinated by a Diamino-Dichalcogen-Benzene compound
[AD-D014326] 12 p1629 N90-19360
Perspectives on solar energy and the environment
[DE90-007680] 13 p1828 N90-20494
Solar electricity and solar fuels
[DE90-796156] 22 p3196 N90-28135
Study of the relationships between radar structure and the electrical activity of clouds
[ETN-90-97488] 23 p3352 N90-28946

ELECTRO-OPTICAL EFFECT
Propagation environments, effects, and decision aids
15 p2081 N90-21918

ELECTRO-OPTICAL SWITCHING
U OPTICAL SWITCHING

ELECTRO-OPTICS
Stimulated rotational Raman scattering
[DE89-016427] 01 p0075 N90-10430
Second-order nonlinear optical devices in poled polymers
[DE89-015842] 01 p0123 N90-10703
Use of depletion edge translation for high-speed modulation and switching of lightwaves
[AD-A211186] 01 p0124 N90-10713
Polarization matrices of lithium tetraborate
[AD-A210774] 02 p0195 N90-11112
Sensitivity of optoelectronic receivers
[AD-A211823] 03 p0338 N90-11923
Proceedings of the Workshop on Compound Semiconductor Devices and Integrated Circuits (13th) held in Cabourg, France on 10-12 May 1989
[AD-A211848] 03 p0343 N90-11954
The multivalent beta'-aluminas
[AD-A212103] 04 p0478 N90-12738
Workshop on Recent Progress in Surface and Volume Scattering
[AD-A212455] 04 p0555 N90-13236
European Solid State Device Research Conference (18th) ESSDERC 88 held in Montpellier, France on 13-16 September 1988
[AD-A210618] 04 p0558 N90-13250
Optics and opto-electronics systems
[AD-A212340] 05 p0699 N90-14093
Integrated optoelectronic receivers
[AD-A213376] 05 p0700 N90-14098
Physical models for aerosol in the marine mixed-layer
06 p0763 N90-14438
Photovoltaic Measurements and Performance Branch
[DE89-009500] 06 p0807 N90-14695
Analysis and evaluation of technical data on the photochromic and non-linear optical properties of materials. Appendix: Eye/sensor protection by an optical fuse mirror at a focal plane: Feasibility assessment
[AD-A214051] 07 p0896 N90-15177
A new kind of heterodyne fiber-optic gyroscope
[AD-A213953] 07 p0933 N90-15404
Laser-material interactions
[AD-A214421] 07 p0937 N90-15425
Research in optical interconnection techniques
[AD-A214028] 07 p0993 N90-15739

Solid state research
[AD-A213405] 07 p1003 N90-15808
Research on materials and components for opto-electronic signal processing and computing
[AD-A213740] 07 p1003 N90-15811
Innovative optoelectronic materials and structures using OMVPE
[AD-A214192] 07 p1004 N90-15815
Electro-optic sensors for surveillance and target acquisition 08 p1026 N90-15929
Analysis and evaluation of technical data on the photochromic and non-linear optical properties of materials
[AD-A214050] 08 p1041 N90-16014
High speed signal extraction using electro-optic techniques
[AD-A214446] 08 p1122 N90-16500
Polarization matrices of quartz
[AD-A215198] 09 p1212 N90-17027
Proposition for an airborne remote sensing system
[INPE-4872-PRE/1483] 10 p1399 N90-18090
Optical anti-aliasing filters
[AD-A215826] 10 p1430 N90-18251
Effect of marine atmosphere on performance of electrooptical systems
[AD-A215947] 10 p1430 N90-18252
Analysis and evaluation of technical data on the photochromic and non-linear optical properties of materials
[AD-A216124] 10 p1431 N90-18254
Electron production, electron attachment, and charge recombination process in high pressure gas discharges
[AD-A216301] 10 p1434 N90-18274
Colloid and interface chemistry aspects of ceramics
[AD-A216715] 11 p1490 N90-18576
Optical amplification in 45 deg - cut BaTiO3
[AD-A216043] 11 p1566 N90-19011
The III-V semiconductor quantum well lasers and related optoelectronic devices on silicon
[AD-A216980] 12 p1666 N90-19570
Opto-Em and devices investigation
[AD-A215033] 12 p1709 N90-19814
Performance of a 300 Mbps 1:16 serial/parallel optoelectronic receiver module
[NASA-TM-103110] 13 p1795 N90-20302
Joint Services Electronics Program research in electronics
[AD-A217745] 13 p1796 N90-20307
Joint services electronics program
[AD-A217961] 13 p1797 N90-20311
Picosecond Laser Facility
[AD-A217784] 13 p1808 N90-20384
Bibliography of spatial interferometry in optical astronomy
[NASA-TM-100754] 13 p1901 N90-20911
Modelling of optically and IR effective atmospheric turbulence 15 p2082 N90-21923
Computation of broad spectral band electro-optical system transmittance response characteristics to military smokes and obscurants using field test data from transmissometer system measurements
15 p2086 N90-21939
Effect of atmospheric turbulence on electro-optical systems 15 p2086 N90-21940
Atmospheric modelling studies: A modelling comparison between IR and millimetric atmospheric propagation
15 p2086 N90-21941
Optical bistability in semiconducting material
15 p2174 N90-22424
Application of high-temperature superconducting thin-film devices to electro-optical and electronic warfare systems
[AD-A218805] 16 p2323 N90-23249
Negative electron affinity for infrared detection
[AD-A218816] 17 p2395 N90-23639
Sensor performance analysis
[NASA-RP-1241] 17 p2418 N90-23780
Advanced guided wave electro-optical switches
[AD-A219784] 17 p2472 N90-24132
Investigations of laterally coupled all optical switches and detectors on silica fibers
[AD-A220297] 17 p2473 N90-24142
Photorefractive damage mechanisms in electro-optic materials
[AD-A219786] 17 p2476 N90-24157
Solid state research
[NASA-CR-186699] 17 p2476 N90-24160
Solid state research
[NASA-CR-186700] 17 p2477 N90-24161
Workshop on III-V Integrated Optoelectronics
[AD-A218759] 18 p2546 N90-24529
Development of an all silicon integrated optical modulator for high speed data communications and sensor applications
[AD-A220270] 18 p2547 N90-24535
Optical high-speed parallel backplane
[AD-D014504] 19 p2757 N90-25670
Optical wavefront computer for stabilizing large space structures
[AD-A221707] 21 p2967 N90-26866
Defects associated with the incorporation of germanium in gallium arsenide
[AD-A222953] 21 p3082 N90-27527
Perspectives on high temperature superconducting electronics 22 p3139 N90-27810
Optoelectronics Research Center
[AD-A221926] 22 p3246 N90-28410
Laboratory for Laser Energetics review
[DE90-014666] 23 p3330 N90-28829
The III-V semiconductor quantum well lasers and related optoelectronic devices on silicon
[AD-A224120] 23 p3331 N90-28835
Electro-optics engineering support for the integrated launch and recovery television surveillance system
[AD-A223450] 24 p3436 N90-29406
Parallel architectures and algorithms for image understanding
[AD-A223479] 24 p3526 N90-29940
Special purpose spatial light modulators
[AD-A223794] 24 p3545 N90-30052
Comparison of electro-optic diagnostic systems
[DE90-015819] 24 p3546 N90-30056
Photoinduced and holographically reinforced light diffusion in electrooptic crystals
[ETN-90-97321] 24 p3547 N90-30060
Study of a 1-Hz hypocycloidal pinch (HCP) pump for production of ultraviolet lasers
[AD-A224091] 24 p3547 N90-30064

ELECTROACOUSTIC TRANSDUCERS
NT HYDROPHONES
NT MICROPHONES
Design and calibration of an electrodynamic driver for the Space Thermoacoustic Refrigerator (STAR)
[AD-A212022] 03 p0335 N90-11906
Pulsed EMAT (Electromagnetic Acoustic Transducer) acoustic measurements on a horizontal continuous caster for internal temperature determination
[DE90-002735] 07 p0988 N90-15709
A test method for measuring corona inception voltage for transducer autotransformers
[AD-A216818] 11 p1502 N90-18646
Foundations of millimeter-wave frequency acoustic microscopy 12 p1709 N90-19816
Millimeter-wave acoustic transducers
[AD-A221402] 18 p2612 N90-24878
Application and extension of an analytical model of the confined acoustic beam generated by a transducer
[AD-A222994] 20 p2924 N90-26639

ELECTROACOUSTICS
Design and calibration of an electrodynamic driver for the Space Thermoacoustic Refrigerator (STAR)
[AD-A212022] 03 p0335 N90-11906

ELECTROCARDIOGRAMS
U ELECTROCARDIOGRAPHY

ELECTROCARDIOGRAPHY
Electrocardiogram of military aircraft pilots measured during real flight missions: Study of the variability of the cardiac rhythm in correlation with working stress
[ETN-90-97453] 22 p3231 N90-28324

ELECTROCATALYSTS
Electronic and ionic transport in polymers
[AD-A210654] 02 p0201 N90-11148
Laser Raman spectroscopy in studies of corrosion and electrocatalysis
[DE90-001414] 06 p0741 N90-14311
Proceedings of the First Annual Fuel Cells Contractors Review Meeting
[DE89-011699] 06 p0803 N90-14675
Improved anode catalysts for coal gas-fueled phosphoric acid fuel cells
[DE90-004016] 08 p1096 N90-16347
Electronic and ionic transport in polymers
[AD-A217028] 11 p1491 N90-18579
Gas cooled fuel cell systems technology development program
[DE90-000448] 12 p1683 N90-19668
Space Electrochemical Research and Technology (SERT), 1989
[NASA-CP-3056] 13 p1821 N90-20454
Electrocatalysis for oxygen electrodes in fuel cells and water electrolyzers for space applications
13 p1823 N90-20468
Non-noble electrocatalysts for alkaline fuel cells
13 p1824 N90-20470
Catalysts for ultrahigh current density oxygen cathodes for space fuel cell applications
[NASA-CR-180650] 16 p2251 N90-22835
Selective electrocatalysis of anodic oxygen-transfer reactions at chemically modified, thin-film lead dioxide electrodes
[DE90-011747] 20 p2857 N90-26252

ELECTROCHEMICAL CELLS
NT ALKALINE BATTERIES
NT BIOCHEMICAL FUEL CELLS
NT ELECTRIC BATTERIES
NT FUEL CELLS
NT HYDROGEN OXYGEN FUEL CELLS
NT LEAD ACID BATTERIES
NT LITHIUM SULFUR BATTERIES
NT METAL AIR BATTERIES
NT NICKEL CADMIUM BATTERIES
NT NICKEL HYDROGEN BATTERIES
NT NICKEL IRON BATTERIES
NT NICKEL ZINC BATTERIES
NT PHOSPHORIC ACID FUEL CELLS
NT PRIMARY BATTERIES
NT REDOX CELLS
NT REGENERATIVE FUEL CELLS
NT SILVER ZINC BATTERIES
NT SODIUM SULFUR BATTERIES
NT STORAGE BATTERIES
NT THERMAL BATTERIES
NT ZINC-BROMIDE BATTERIES
Photoelectrochemical behavior of type n of GaAs in concentrated iodide media and realization of an experimental device
[ECL-88-18] 05 p0703 N90-14117
Electrochemical preparation of silver oxide electrodes having high thermal stability
[AD-D014224] 06 p0767 N90-14460
Calorimetric measurements on electrochemical cells with Pd-D cathodes
[DE90-002198] 06 p0805 N90-14685
Electrochemistry in near-critical and supercritical fluids. 8: Methyl viologen, decamethylferrocene, Os(bpy)3(sup 2+) and ferrocene in acetonitrile and the effect of pressure on diffusion coefficients under supercritical conditions
[AD-A213407] 07 p0895 N90-15172
Advanced double layer capacitor
[AD-A213406] 07 p0923 N90-15341
In-situ ion beam measurements of deuterium loading in thin foil electrochemical cells
[DE90-003162] 07 p0952 N90-15511
Tritium and neutron measurements of a solid state cell
[DE90-003657] 07 p1005 N90-15820
Solid-state electrolyte catalysis for methane and oxygen synthesis
[PB90-100231] 08 p1040 N90-16011
Application of ac impedance method for diagnosis of lithium secondary battery degradation. Preliminary study with AA size Li/MoS2 cells
[DE90-702474] 08 p1061 N90-16137
ECC (Electrochemical Concentration Cell) ozonesonde observations at South Pole, Antarctica, during 1988
[PB90-110172] 08 p1098 N90-16355
ECC (Electrochemical Concentration Cell) ozonesonde observations at Mirny, Antarctica, during 1988
[PB90-113960] 08 p1098 N90-16357
Electrochemical cell for obtaining oxygen from carbon dioxide atmospheres
[NASA-CR-186225] 09 p1189 N90-16886
A preliminary investigation of cold fusion by electrolysis of heavy water
[DE90-004383] 09 p1285 N90-17447
International Summer School on Solid State Microbatteries
[AD-A213457] 10 p1434 N90-18277
Effects of nonuniform potential and current distributions in electrochemical systems
[DE90-007349] 12 p1623 N90-19325
Frequency response of electrochemical cells
12 p1639 N90-19419
Advanced double layer capacitor
[AD-A217110] 12 p1656 N90-19518
The electrochemical generation of useful chemical species from lunar materials 13 p1822 N90-20461
KOH concentration effect on the cycle life of nickel-hydrogen cells. Part 4: Results of failure analyses
13 p1824 N90-20475
Advances in ambient temperature secondary lithium cells 13 p1825 N90-20481
Advanced double layer capacitor
[AD-A219419] 16 p2233 N90-22741
The effect of carbon type and processing on high rate thionyl chloride cathode collectors
[AD-A219823] 18 p2546 N90-24532
Construction of a UV cell for micro-liquid chromatography
[PML-1989-B] 22 p3156 N90-27894
Corrosion of aluminum alloys by IRFNA
[AD-A223011] 22 p3157 N90-27897
Metallurgical analysis of leaking tray packs
[AD-A223157] 22 p3157 N90-27899
A high temperature molten salt thermal electrochemical cell
[AD-D014469] 22 p3195 N90-28131

Monolithic solid oxide fuel cell technology development, phase 1A
[PB90-183237] 22 p3195 N90-28132

ELECTROCHEMICAL CORROSION
IBM PC analysis of polarization resistance data
[AD-A212294] 04 p0477 N90-12732
Corrosion and corrosion inhibition of metals/alloys in methylphosphonic difluoride and decontaminating solutions
[AD-A212404] 04 p0477 N90-12734
Advanced calcium-thionyl chloride high-power battery
[AD-A211856] 04 p0495 N90-12846
The effect of dissolved chlorine on the pitting behavior of 304L stainless steel in a 0.5 N NaCl solution
[AD-A213803] 07 p0905 N90-15234
The effect of dissolved ozone on the corrosion behavior of Cu-30 Ni and 304L stainless steel in 0.5 N NaCl solutions
[AD-A213804] 07 p0906 N90-15235
Surface modification of steels and aluminum alloys to control corrosion and hydrogen embrittlement. Part 1: Chemical methods
[AD-A216272] 10 p1356 N90-17866
Feasibility of a super high energy density battery of the Li/BrF3 electrochemical system
[AD-A216794] 11 p1502 N90-18644
Electrochemical phase diagrams for aqueous redox systems
[AD-A217168] 13 p1770 N90-20157
Thermal control system corrosion study
[NASA-TM-102220] 14 p1971 N90-21294
Evaluation of abrasion-resistant metallized coatings for civil works applications
[AD-A221078] 18 p2530 N90-24438
Corrosion protection of metal matrix composites
[AD-A222951] 21 p2971 N90-26888
Corrosion of aluminum alloys by IRFNA
[AD-A223011] 22 p3157 N90-27897
Metallurgical analysis of leaking tray packs
[AD-A223157] 22 p3157 N90-27899
Characterization of the pitting corrosion of aluminum-lithium alloys
[ETCA-89-R-176] 22 p3157 N90-27903
High temperature surface interactions: Overview
23 p3306 N90-28699

ELECTROCHEMICAL OXIDATION
Scanning tunneling microscopy etching of micrometer level features on p-type GaAs
[AD-A209216] 01 p0058 N90-10328
Mechanism of electrochemical activation of carbon electrodes: Role of graphite lattice defects
[AD-A211644] 03 p0325 N90-11845
New electrically conducting solids based on nickel(II) - bis(1,3-dithiole-2-thione-4,5-diselenolate)
[DE90-003788] 08 p1042 N90-16020
International conference on Surface Modification of Metals by Ion Beams
[AD-A215872] 12 p1626 N90-19345
Morphology changes due to oxidative treatment of glassy carbon electrodes and its applications
[AD-A219425] 17 p2371 N90-23501
Anode materials for electrochemical waste destruction
18 p2514 N90-24354
Electrochemical incineration of wastes
[NASA-CR-187033] 23 p3317 N90-28753

ELECTROCHEMISTRY
NT ELECTROLYSIS
NT PHOTOELECTROCHEMISTRY
Potential dependence of the elementary steps in the kinetics of electrode reactions involving amalgam formation
[AD-A209424] 01 p0038 N90-10212
Combining spontaneous molecular assembly with microfabrication to pattern surfaces: Selective binding of isonitriles to platinum microwires and characterization by electrochemistry and surface spectroscopy
[AD-A209528] 01 p0039 N90-10213
Electrochemistry in near-critical and supercritical fluids. Part 7: SO2
[AD-A208207] 01 p0039 N90-10214
Polyheterocycle Langmuir-Blodgett films
[AD-A210625] 01 p0051 N90-10292
Quartz crystal microbalance studies of electrochemical growth of conducting polymers
[AD-A210788] 01 p0052 N90-10295
Advanced double layer capacitor
[AD-A210510] 01 p0061 N90-10348
Electroporation: Theory of basic mechanisms
[AD-A210196] 01 p0091 N90-10520
Face-specific interaction of MoS4(2-1) with oriented crystals of (0001) CdX (X = Se, S)
[AD-A209519] 01 p0128 N90-10732
Dynamics of nucleation at electrochemical interfaces via surface EXAFS and standing wave measurements
[AD-A210733] 02 p0195 N90-11109
Polarization matrices of lithium tetraborate
[AD-A210774] 02 p0195 N90-11112
Electronic and ionic transport in polymers
[AD-A210654] 02 p0201 N90-11148
Electrolyte dependence of charge injection processes for electroactive polymer films
[AD-A210787] 02 p0202 N90-11152
Lithium polymer electrolyte battery, electrochemical behavior of cathode materials
[AD-A210755] 02 p0216 N90-11235
The theory of ac impedance of rough electrode-electrolyte interfaces
[DE89-017474] 02 p0217 N90-11243
In-situ spectroscopic studies of transition metal macrocycles as catalysts for the electrochemical reduction of oxygen
[PB89-219273] 03 p0321 N90-11826
Effect of electrical double layer on transport limited currents at microelectrodes
[AD-A211586] 03 p0324 N90-11843
Highlights of papers presented at the workshop on Cold Fusion Phenomena
[DE89-016956] 03 p0407 N90-12334
Effects of grain boundary chemistry on critical current density in oxide superconductors
[DE89-017780] 03 p0412 N90-12365
Advanced double layer capacitor
[AD-A211977] 04 p0469 N90-12688
Electrically conducting organic materials: Design, synthesis and characterization
[AD-A212214] 04 p0471 N90-12700
Mechanisms of CO2 reduction metal and metal modified semiconductor electrodes
[AD-A213169] 04 p0473 N90-12712
Electrochemistry at very small electrodes
[AD-A213156] 05 p0621 N90-13623
Electrochemical study of the etching of III to V semiconductors
[ETN-90-96015] 05 p0623 N90-13633
Refurbishment of one-person regenerative air revitalization system
[NASA-CR-183757] 05 p0675 N90-13934
An evaluation of electrochemical potentiokinetic reactivation techniques for in-service measurements on Type 304 stainless steel
[DE89-017859] 06 p0746 N90-14340
Proceedings of the First Annual Fuel Cells Contractors Review Meeting
[DE89-011699] 06 p0803 N90-14675
Polarization of Li/SOCl2 cells
[DE90-000883] 06 p0804 N90-14680
Electrode development in monolithic solid oxide fuel cells
[DE90-001910] 06 p0805 N90-14684
Interfacial effects in monolithic solid oxide fuel cells
[DE90-001914] 06 p0806 N90-14690
Electrochemistry in near-critical and supercritical fluids. 8: Methyl viologen, decamethylferrocene, Os(bpy)3(sup 2+) and ferrocene in acetonitrile and the effect of pressure on diffusion coefficients under supercritical conditions
[AD-A213407] 07 p0895 N90-15172
Electronic and ionic transport in polymers
[AD-A213410] 07 p0911 N90-15270
Electrochemical investigation of electronically conductive polymers
[AD-A214019] 07 p0912 N90-15277
First International Symposium on Electrochemical Impedance Spectroscopy. Extended abstracts
[AD-A214406] 07 p0925 N90-15354
Mechanisms of the electrochemistry of small organic molecules
[PB90-100785] 08 p1040 N90-16012
Electrochemical parameterization of metal complex redox potentials, using the ruthenium(III)/ruthenium(II) couple to generate a ligand electrochemical series
[AD-A214439] 08 p1041 N90-16015
An XPS and electrochemical study of the influence of molybdenum and nitrogen on the passivity of austenitic stainless steel
[AD-A214267] 08 p1044 N90-16034
Ninth Battery and Electrochemical Contractors' Conference: Extended abstracts
[DE89-016837] 08 p1059 N90-16120
Organic cathode for a secondary battery
[NASA-CASE-NPO-17604-1-CU]
08 p1059 N90-16124
Solid state microelectrochemical devices: Transistor and diode devices employing a solid polymer electrolyte
[AD-A214206] 09 p1211 N90-17019
Direct measurements of the physical diffusion of redox active species: Microelectrochemical experiments and their simulation
[AD-A215680] 09 p1280 N90-17420
A review of the mechanism and kinetics of electrochemical hydrogen entry and degradation of metallic systems
[AD-A216671] 10 p1355 N90-17857
Electronic and ionic transport in polymers
[AD-A217028] 11 p1491 N90-18579
Electrochemical investigations of novel solid redox polymerization electrodes
[DE90-006087] 11 p1492 N90-18584
Feasibility of a super high energy density battery of the Li/BrF3 electrochemical system
[AD-A216575] 11 p1528 N90-18799
Advanced battery development
[DE90-006073] 11 p1529 N90-18806
Evaluation of radiation-induced sensitization using electrochemical potentiokinetic reactivation technique for austenitic stainless steels
[DE90-002708] 12 p1627 N90-19352
Linear free energy relations for multielectron transfer kinetics: A brief look at the Bronsted/Tafel analogy
[AD-A215078] 12 p1710 N90-19823
Chemical and electrochemical studies in ionic liquids
[AD-A217742] 13 p1773 N90-20175
Electronic and ionic transport in processable conducting polymers
[AD-A218093] 13 p1782 N90-20229
An electrochemical and spectroscopic study of electrode processes
[AD-A217261] 13 p1793 N90-20289
Exploratory battery technology development and testing report for 1988
[DE90-007996] 13 p1794 N90-20297
Fluid dynamics analysis of a rotating axisymmetric part using FIDAP
[DE90-008733] 13 p1802 N90-20340
Space Electrochemical Research and Technology (SERT), 1989
[NASA-CP-3056] 13 p1821 N90-20454
Advanced double layer capacitors
13 p1822 N90-20464
Novel electrodes for advanced energy storage systems
[DE90-008667] 13 p1828 N90-20496
Identification of defects in SOI (Silicon-On-Insulator) wafers
[DE90-006020] 13 p1895 N90-20879
Analytical sciences
[DE90-007965] 14 p1948 N90-21152
Application of neural nets to system identification and bifurcation analysis of real world experimental data
[DE90-007539] 14 p2017 N90-21558
An attempt to measure cold-fusion effects
[DE90-613248] 14 p2031 N90-21649
Electrochemical impregnation and cycle life of lightweight nickel electrodes for nickel-hydrogen cells
[NASA-TM-103140] 15 p2068 N90-21844
Electrochemical synthesis of ultrathin film composite membranes
[AD-A219041] 16 p2216 N90-22643
The initiation of intergranular stress corrosion-cracking on sensitized stainless steel in dilute thiosulphate solutions
[AERE-R-13317] 16 p2217 N90-22648
Quartz crystal microbalance studies: Solvent effects in conducting polymer films
[AD-A219426] 17 p2372 N90-23502
Estimation of the concentration-distance profile within the electrochemical diffusion layer by Raman microprobe spectroscopy
[AD-A219521] 17 p2372 N90-23506
Corrosion control through a better understanding of the metallic substrate/organic coating interface
[AD-A220432] 17 p2377 N90-23533
Evaluation of ion intercalation in conducting polymers
[AD-A219423] 17 p2379 N90-23549
Selective removal of organics for water reclamation
[NASA-TM-101890] 17 p2421 N90-23797
National Educators' Workshop: Update 1989 Standard Experiments in Engineering Materials Science and Technology
[NASA-CP-3074] 18 p2513 N90-24350
Current distribution in cylindrical porous electrodes
[DE90-009707] 18 p2546 N90-24530
Direct conversion technology
[NASA-CR-186795] 18 p2576 N90-24675
Electrochemical control of iodine disinfectant for space transportation system and space station potable water
18 p2629 N90-24981
Electrochemical, in situ Raman spectroscopic, and conductivity studies of polypyrrole incorporating large size anions: Conducting nature of reduced form
[AD-A222739] 20 p2831 N90-26102
The development and characterization of ion exchange membranes for selected electrochemical power sources
[DE90-009741] 20 p2857 N90-26251

Structured electrode interfaces
[AD-A222763] 20 p2859 N90-26265
Environmental integrity of coating/metal interface
[AD-A222426] 21 p2987 N90-26978
Metal chloride cathode for a battery
[NASA-CASE-NPO-17809-1-CU] 21 p2998 N90-27041
Potential dependence of the conductivity of highly oxidized polythiophenes, polypyrroles, and polyaniline: Finite windows of high conductivity
[AD-A222024] 22 p3159 N90-27912
A high temperature molten salt thermal electrochemical cell
[AD-D014489] 22 p3195 N90-28131
Electrochemical surface finishing using amino-substrates on carbon fibers in organic media. Effects of the finishing on the mechanical properties of carbon-epoxy composites
[ONERA-RT-9/3549-M] 23 p3301 N90-28672
Electrochemistry using nanometer-sized electrodes
[AD-A223890] 23 p3305 N90-28697
Zinc-bromine battery development
[DE90-014751] 23 p3321 N90-28781
Electrochemistry of metal surfaces
[AD-A224551] 24 p3445 N90-29458
Cyclic voltammetry at a rotating disk, electroreduction of nitrate in acidic nickel solutions, and frequency-response analysis of porous electrodes
[DE90-015317] 24 p3447 N90-29466
Non-destructive method for environmental breakdown of graphite fiber reinforced polymer composites
[AD-A223729] 24 p3455 N90-29515
Electrochemical characteristics of acid electrolytes for fuel cells
[PB90-244385] 24 p3484 N90-29693
Advanced materials and electrochemical processes in high-temperature solid electrolytes
[DE90-015552] 24 p3553 N90-30104

ELECTROCHROMISM
Lithium cobalt oxide thin film and its electrochromism
[DE90-004570] 08 p1133 N90-16564
Reflectance modulation with electrochromic Li(sub x)WO(3) films
[DE90-004571] 10 p1435 N90-18279

ELECTROCONDUCTIVITY
U ELECTRICAL RESISTIVITY

ELECTRODE MATERIALS
Water removal studies on high power hydrogen-oxygen fuel cells with alkaline electrolytes 10 p1333 N90-17712
Space Electrochemical Research and Technology (SERT), 1989
[NASA-CP-3056] 13 p1821 N90-20454
Catalysts for ultrahigh current density oxygen cathodes for space fuel cell applications
[NASA-CR-180650] 16 p2251 N90-22835
Electrochemical incineration of wastes
[NASA-CR-187033] 23 p3317 N90-28753

ELECTRODELESS DISCHARGES
Low resistivity electrodeless streamer tubes
[PREPRINT-685-89] 05 p0636 N90-13712

ELECTRODEPOSITION
NT ELECTROPLATING
Proceedings of the Polycrystalline Thin Film Program Meeting
[DE89-009457] 02 p0237 N90-11348
Fe-Ni-Cr alloys for coatings and electroforms
[PB89-195846] 03 p0325 N90-11849
Electroactive polyaniline film deposited from non-aqueous media. 2: Effect of acid concentration in solutions
[AD-A212084] 04 p0477 N90-12737
Technology Base Research Project for electrochemical energy storage
[DE90-002604] 06 p0806 N90-14693
High-efficiency copper ternary thin film solar cells
[DE89-009470] 09 p1242 N90-17207
Suitability of electrodeposition processes for high temperature superconductors
[IAR-89-22] 19 p2760 N90-25685
A study on carbon Fiber (long fiber) reinforced copper matrix composite
[AD-A221584] 21 p2972 N90-26891
Electrodeposition of wear resistant coatings
[PB90-221839] 23 p3312 N90-28732
Electrochemistry of metal surfaces
[AD-A224551] 24 p3445 N90-29458
Effects of low Chromium(3) concentration in electrodeposition of low contraction chromium
[AD-A223338] 24 p3449 N90-29477

ELECTRODES
NT ANODES
NT CATHODES
NT CELL ANODES
NT CELL CATHODES
NT DIFFUSION ELECTRODES
NT HOLLOW CATHODES
NT PHOTOCATHODES
NT PLASMA ELECTRODES
NT SOLID ELECTRODES
NT THERMIONIC CATHODES
NT TUBE ANODES
NT TUBE CATHODES
Potential dependence of the elementary steps in the kinetics of electrode reactions involving amalgam formation
[AD-A209424] 01 p0038 N90-10212
Combining spontaneous molecular assembly with microfabrication to pattern surfaces: Selective binding of isonitriles to platinum microwires and characterization by electrochemistry and surface spectroscopy
[AD-A209528] 01 p0039 N90-10213
Microsensor and pattern recognition techniques in hydrazine detection 02 p0206 N90-11177
Lithium polymer electrolyte battery, electrochemical behavior of cathode materials
[AD-A210755] 02 p0216 N90-11235
The theory of ac impedance of rough electrode-electrolyte interfaces
[DE89-017474] 02 p0217 N90-11243
Multicolor electrochromic displays exploratory development
[AD-A212004] 03 p0303 N90-11721
Mechanism of electrochemical activation of carbon electrodes: Role of graphite lattice defects
[AD-A211644] 03 p0325 N90-11845
Characterization and cycle tests of lightweight nickel electrodes
[NASA-TM-102399] 04 p0470 N90-12696
Influence of the composition of the metal deposited on carbon manganese welds on the work properties of the melted area depending on the operating mode of the weld
[CETIM-104530] 04 p0476 N90-12726
The effects of trace anions on the voltammetry of single crystal gold surfaces
[AD-A211886] 04 p0558 N90-13254
Electrochemistry at very small electrodes
[AD-A213156] 05 p0621 N90-13623
Electrochemical preparation of silver oxide electrodes having high thermal stability
[AD-D014224] 06 p0767 N90-14460
Sodium/sulfur post-test analysis at ANL
[DE90-001911] 06 p0771 N90-14488
Interfacial effects in monolithic solid oxide fuel cells
[DE90-001914] 06 p0806 N90-14690
Technology Base Research Project for electrochemical energy storage
[DE90-002604] 06 p0806 N90-14693
Dimensional analysis of continuous high-capacity electrodispersion of aqueous based liquids in an organic continuous phase
[DE90-003714] 07 p0888 N90-15136
Electrochemical investigation of electronically conductive polymers
[AD-A214019] 07 p0912 N90-15277
Advanced double layer capacitor
[AD-A213406] 07 p0923 N90-15341
Oxygen electrode in molten carbonate fuel cells
[DE90-002871] 07 p0952 N90-15510
Interfacial systems for photochemical energy conversion
[DE90-003181] 07 p0953 N90-15514
Fabrication of porous ceramic electrode structures
[DE90-003548] 07 p0953 N90-15517
Design of DIII-D advanced divertor
[DE90-003343] 07 p0995 N90-15752
Solid-state electrolyte catalysis for methane and oxygen synthesis
[PB90-100231] 08 p1040 N90-16011
Electrode/workpiece combinations
[DE90-003919] 08 p1054 N90-16095
Command operated liquid metal opening switch
[AD-D014262] 08 p1060 N90-16126
Cycle-life improvement of Zn/NiOOH cells by the addition of Ca(OH)2 to the zinc electrode
[DE90-004040] 08 p1062 N90-16139
Solid state microelectrochemical devices: Transistor and diode devices employing a solid polymer electrolyte
[AD-A214206] 09 p1211 N90-17019
Generation of H-, H2v(double prime), and H atoms by H2+ and H3+ ions incident upon barium surfaces
[DE90-005549] 09 p1280 N90-17423
Edge geometry superconducting tunnel junctions utilizing an NbN/MgO/NbN thin film structure
[NASA-CASE-NPO-17812-1-CU] 09 p1286 N90-17456
Rigorous calculations of lumped electrical parameters for a microstrip interdigitated electrode structure
[AD-A215337] 10 p1378 N90-17989
Changes in impedance of Ni electrodes upon standing and cycling
[NASA-TM-102438] 10 p1401 N90-18097
Cohesive ceramic fabrication
[DE90-007333] 11 p1494 N90-18597
Oxygen electrode in molten carbonate fuel cells
[DE90-005377] 11 p1528 N90-18796
Solid-state proton conductors
[DE90-007592] 11 p1531 N90-18812
Studies of photochemically and electrochemically driven electron transport in zeolites
[DE90-007659] 12 p1624 N90-19335
Characterization of reaction kinetics in a porous electrode
[NASA-CR-186504] 12 p1625 N90-19340
Frequency response of electrochemical cells 12 p1639 N90-19419
Zirconia-based electrodes for solid oxide fuel cells
[DE90-000462] 12 p1655 N90-19513
Advanced double layer capacitor
[AD-A217110] 12 p1656 N90-19518
Enhancement of mass transfer to a rotating cylinder electrode by inert particles suspended in the electrolyte
[DE90-008054] 13 p1771 N90-20165
Techno-economic assessment of a carbothermic alumina reduction process
[DE90-007018] 13 p1772 N90-20170
Microwave field effect transistor
[NASA-CASE-GSC-12442-2] 13 p1792 N90-20282
An electrochemical and spectroscopic study of electrode processes
[AD-A217261] 13 p1793 N90-20289
The electrochemical generation of useful chemical species from lunar materials 13 p1822 N90-20461
Recent advances in solid polymer electrolyte fuel cell technology with low platinum loading electrodes 13 p1823 N90-20465
Oxygen electrodes for rechargeable alkaline fuel cells-II 13 p1823 N90-20469
Corrosion testing of candidates for the alkaline fuel cell cathode 13 p1824 N90-20471
Structural comparison of nickel electrodes and precursor phases 13 p1824 N90-20472
Impedance studies of Ni/Cd and Ni/H2 cells using the cell case as a reference electrode 13 p1824 N90-20473
The application of electrochemical impedance spectroscopy for characterizing the degradation of Ni(OH)2/NiOOH electrodes 13 p1824 N90-20474
KOH concentration effect on the cycle life of nickel-hydrogen cells. Part 4: Results of failure analyses 13 p1824 N90-20475
Advances in lightweight nickel electrode technology 13 p1825 N90-20476
Nickel-hydrogen capacity loss on storage 13 p1825 N90-20478
Advanced high-temperature batteries 13 p1825 N90-20480
Novel electrodes for advanced energy storage systems
[DE90-008867] 13 p1828 N90-20496
GaAs traveling-wave optical modulators using modulated coplanar electrodes with periodic cross-tie overlays
[AD-A217731] 13 p1888 N90-20835
O2 reduction at the IFC orbiter fuel cell O2 electrode
[NASA-TM-102580] 14 p2001 N90-21469
Effect of LEO cycling on 125 Ah advanced design IPV nickel-hydrogen battery cells
[NASA-TM-103128] 15 p2061 N90-21808
Electrochemical impregnation and cycle life of lightweight nickel electrodes for nickel-hydrogen cells
[NASA-TM-103140] 15 p2068 N90-21844
Stability studies of a pH-sensitive polymer matrix: Applications to fiber optic pH sensors
[DE90-009579] 15 p2072 N90-21867
MHD channel development, part 2
[DE90-009550] 15 p2169 N90-22395
MHD channel development, part 3
[DE90-009551] 15 p2169 N90-22396
Morphology changes due to oxidative treatment of glassy carbon electrodes and its applications
[AD-A219425] 17 p2371 N90-23501
Modes of attachment of pyridine to gold surfaces
[AD-A219519] 17 p2372 N90-23504
An examination of the relationship between SERS intensities and surface concentration for pyridine adsorbed at the gold/aqueous solution interface
[AD-A219520] 17 p2372 N90-23505
Evaluation of the state of charge of battery electrodes with ac impedance techniques
[AD-A219561] 17 p2420 N90-23789
Current distribution in cylindrical porous electrodes
[DE90-009707] 18 p2546 N90-24530
New liquid cathode electrolytes in high rate cells
[AD-A219822] 18 p2548 N90-24531

Direct conversion technology
[NASA-CR-186795] 18 p2576 N90-24675
Electrode carrying wire for GTAW welding
[NASA-CASE-MFS-29491-1] 20 p2842 N90-26168
Selective electrocatalysis of anodic oxygen-transfer reactions at chemically modified, thin-film lead dioxide electrodes
[DE90-011747] 20 p2857 N90-26252
Structured electrode interfaces
[AD-A222763] 20 p2859 N90-26265
A viologen/ruthenium oxide-based microelectrochemical diode with pH-dependent current-voltage characteristics
[AD-A221961] 21 p3000 N90-27052
Integrated optics interdigitated-electrode switches
[AD-A223245] 21 p3076 N90-27490
Infrared reflection-adsorption spectroscopy of the electrode/electrolyte solution interface: Optical considerations
[AD-A221935] 22 p3246 N90-28409
Electrochemistry using nanometer-sized electrodes
[AD-A223890] 23 p3305 N90-28697
A tandem system of ionization chambers for effective energy determination of unknown X-radiation fields
[DE90-630463] 24 p3436 N90-29405
Electrochemistry of metal surfaces
[AD-A224551] 24 p3445 N90-29458
Realization of equipment for manufacturing titanium alloy electrodes for first step melting
[ONERA-RT-15/3578-M] 24 p3453 N90-29498
Electrical ignition of HAN-based liquid propellants
[AD-A223272] 24 p3458 N90-29528
Advanced materials and electrochemical processes in high-temperature solid electrolytes
[DE90-015552] 24 p3553 N90-30104

ELECTRODISSOLUTION
Research in biological separations and cell culture
[NASA-CR-172060] 15 p2135 N90-22202

ELECTRODYNAMICS
NT ELECTROHYDRODYNAMICS
NT ELECTROMECHANICS
NT QUANTUM ELECTRODYNAMICS
New electrodynamic and electrostatic models with applications to antenna theory, superconductor slots, and lasers 01 p0055 N90-10316
Observations of ionosphere/magnetosphere interactions from the Dynamics Explorer satellites 02 p0242 N90-11376
Polar F layer lacuna irregularities at Dumont d'Urville 02 p0243 N90-11379
Biological effects of power frequency electric and magnetic fields: Background paper
[PB89-209985] 02 p0254 N90-11439
Magneto-elastic interactions in conducting structures in transient magnetic fields 05 p0632 N90-13686
The electrodynamics of the polar ionosphere with special emphasis on the dayside cleft region 05 p0658 N90-13838
Background electrodynamics measured by EISCAT during the NEED campaign 05 p0660 N90-13851
Solar cell electrodynamic characteristics test equipment 10 p1344 N90-17791
Quantifying and reducing uncertainty in the assimilative mapping of ionospheric electrodynamics
[AD-A218057] 13 p1842 N90-20577
Theory of a periodic cylindrical waveguide with a nonuniform metal-dielectric filling
[DE90-620099] 15 p2087 N90-21945
Quantifying and reducing uncertainty in the assimilative mapping of ionospheric electrodynamics 16 p2254 N90-22854
Dynamics and dynamics experiments in TSS-1 22 p3129 N90-27758

ELECTRODYNAMOMETERS
U DYNAMOMETERS

ELECTROENCEPHALOGRAM
U ELECTROENCEPHALOGRAPHY

ELECTROENCEPHALOGRAPHY
Extrathalamic modulation of cortical function
[AD-A211044] 01 p0094 N90-10535
Test-retest reliability of oxford Medilog 9000 sleep recording and SS-90-3 sleep stage scoring
[AD-A211165] 02 p0254 N90-11440
Use of superconducting plates and shells to deflect magnetic noise fields: Application to MEG
[DE89-012592] 06 p0803 N90-14676
An exploratory analysis of motion sickness data: A time series approach
[AD-A215534] 09 p1253 N90-17271
A cepstral analysis of EEG (Electroencephalographic) signals in motion sickness studies
[AD-A215663] 09 p1253 N90-17273
Measurement of the impulse response of the human visual system using correlation techniques
[AD-A215667] 09 p1254 N90-17274
Multimedia system control
[AD-A219392] 16 p2276 N90-22971
Physiological metrics of mental workload: A review of recent progress
[NASA-CR-187290] 24 p3499 N90-29777

ELECTROEROSION
U SPARK MACHINING

ELECTROEXPLOSIVE DEVICES
U INITIATORS (EXPLOSIVES)

ELECTROFORMING
An electroformed nickel-sulfur alloy for a nose cone
[DE90-000866] 06 p0745 N90-14337
Luminescence from electroformed metal-isolator-metal-structures
[ETN-90-97295] 22 p3249 N90-28425

ELECTROGENERATORS
U ELECTRIC GENERATORS

ELECTROHYDRAULIC CONTROL
U HYDRAULIC CONTROL

ELECTROHYDRODYNAMICS
Polymer characterization by electrohydrodynamic ionization mass spectrometry
[AD-A212130] 04 p0478 N90-12739

ELECTROJETS
NT AURORAL ELECTROJETS
NT EQUATORIAL ELECTROJET
A review on radio studies of auroral E-region ionospheric irregularities 02 p0245 N90-11390
Relationship between the current and the width of the POGO electrojet during the solstices
[DE89-619725] 04 p0565 N90-13294

ELECTROLUMINESCENCE
Growth and characterization of zinc sulfide films by conversion of zinc oxide films with H2S
[AD-A213345] 04 p0561 N90-13271
Theoretical and material studies of thin-film electroluminescent devices
[NASA-CR-186104] 06 p0768 N90-14468
Human factors evaluation of electroluminescent display Number 1
[DE90-002231] 06 p0822 N90-14777
Luminescence from electroformed metal-isolator-metal-structures
[ETN-90-97295] 22 p3249 N90-28425

ELECTROLUMINESCENT LAMPS
U ELECTROLUMINESCENCE
U LUMINAIRES

ELECTROLYSIS
Selective removal of organics for water reclamation
[NASA-CR-185959] 02 p0255 N90-11445
Gas evolution and bubble formation on electrodes
[DLR-FB-89-35] 05 p0622 N90-13629
Lithium cobalt oxide thin film and its electrochromism
[DE90-004570] 08 p1133 N90-16564
A preliminary investigation of cold fusion by electrolysis of heavy water
[DE90-004383] 09 p1285 N90-17447
Solid polymer electrolyte water electrolysis as a mean of energy storage for space applications 10 p1334 N90-17713
Integrated regenerative fuel cell experimental evaluation
[NASA-CR-185183] 11 p1530 N90-18808
IEA (International Energy Agency) implementing agreement for a program of research and development on the production of hydrogen from water. Task 9: Hydrogen production
[DE90-007354] 12 p1625 N90-19337
Electrocatalysis for oxygen electrodes in fuel cells and water electrolyzers for space applications 13 p1823 N90-20468
An attempt to measure cold-fusion effects
[DE90-613248] 14 p2031 N90-21649
Impact of low gravity on water electrolysis operation
[NASA-CR-185521] 15 p2072 N90-21870

ELECTROLYTE METABOLISM
Cardiovascular, renal, electrolyte, and hormonal changes in man during gravitational stress, weightlessness, and simulated weightlessness: Lower body positive pressure applied by the antigravity suit
[NASA-TM-102232] 04 p0522 N90-13013
Fluid and electrolyte homeostasis during spaceflight: Elucidation of mechanisms in a primate
[NASA-CR-177548] 23 p3378 N90-29085
Renal response to seven days of lower body positive pressure in the squirrel monkey
[NASA-CR-183355] 24 p3497 N90-29761

ELECTROLYTES
NT ION EXCHANGE MEMBRANE ELECTROLYTES
NT MOLTEN SALT ELECTROLYTES
NT NONAQUEOUS ELECTROLYTES
NT SOLID ELECTROLYTES
Lithium polymer electrolyte battery, electrochemical behavior of cathode materials
[AD-A210755] 02 p0216 N90-11235
The theory of ac impedance of rough electrode-electrolyte interfaces
[DE89-017474] 02 p0217 N90-11243
Effect of electrical double layer on transport limited currents at microelectrodes
[AD-A211586] 03 p0324 N90-11843
Molecular dynamics study of the primitive model of 1-3 electrolyte studies
[AD-A211653] 03 p0325 N90-11846
Assessment of thin film batteries based on polymer electrolytes. Part 1: Energy density
[AD-A212111] 03 p0343 N90-11958
Heat capacities of 1-methyl-3-ethylimidazolium chloride-aluminum chloride molten salts
[AD-A212790] 04 p0472 N90-12707
Assessment of thin film batteries based on polymer electrolytes. Part 3: Specific energy versus specific power
[AD-A212141] 04 p0515 N90-12976
Heat exhaustion
[AD-A212128] 04 p0522 N90-13014
Electrochemistry at very small electrodes
[AD-A213156] 05 p0621 N90-13623
Surfaces and interfaces of ceramic materials
[AD-A212417] 05 p0627 N90-13657
Electrochemical preparation of silver oxide electrodes having high thermal stability
[AD-D014224] 06 p0767 N90-14460
Sodium/sulfur post-test analysis at ANL
[DE90-001911] 06 p0771 N90-14488
Heat and mass transfer design issues in PEM fuel cell hardware
[DE89-016779] 06 p0804 N90-14677
Technology Base Research Project for electrochemical energy storage
[DE90-002604] 06 p0806 N90-14693
Rechargable molten-electrolyte lithium batteries
[DE90-003774] 07 p0923 N90-15339
Evaluation of a new charge algorithm for a lead-acid battery with gelled electrolyte using a 96V gel cell 4 as a test battery
[DE90-003420] 08 p1061 N90-16133
Study of metal corrosion using ac impedance techniques in the STS launch environment 08 p1155 N90-16688
Research and development of lithium/polyaniline battery, part 2
[DE90-734985] 09 p1211 N90-17018
Solid state microelectrochemical devices: Transistor and diode devices employing a solid polymer electrolyte
[AD-A214206] 09 p1211 N90-17019
Determination of optimum electrolyte composition for molten carbonate fuel cells
[DE90-000410] 09 p1243 N90-17210
Integrated regenerative fuel cell experimental evaluation
[NASA-CR-185183] 11 p1530 N90-18808
Enhancement of mass transfer to a rotating cylinder electrode by inert particles suspended in the electrolyte
[DE90-008054] 13 p1771 N90-20165
Exploratory battery technology development and testing report for 1988
[DE90-007996] 13 p1794 N90-20297
Monolithic solid oxide fuel cell development 13 p1822 N90-20460
Advanced double layer capacitors 13 p1822 N90-20464
KOH concentration effect on the cycle life of nickel-hydrogen cells. Part 4: Results of failure analyses 13 p1824 N90-20475
Nickel-hydrogen capacity loss on storage 13 p1825 N90-20478
Advanced high-temperature batteries 13 p1825 N90-20480
Advances in ambient temperature secondary lithium cells 13 p1825 N90-20481
Effect of KOH concentration on LEO cycle life of IPV nickel-hydrogen flight battery cells
[NASA-TM-103127] 14 p1942 N90-21116
Effect of LEO cycling on 125 Ah advanced design IPV nickel-hydrogen battery cells
[NASA-TM-103128] 15 p2061 N90-21808
Linear and nonlinear electrical response of condensed matter: Ionic, dielectric, and mixed-conduction materials
[AD-A218771] 16 p2215 N90-22639
Advanced double layer capacitor
[AD-A219419] 16 p2233 N90-22741
Quartz crystal microbalance studies: Solvent effects in conducting polymer films
[AD-A219426] 17 p2372 N90-23502
Evaluation of ion intercalation in conducting polymers
[AD-A219423] 17 p2379 N90-23549
Current distribution in cylindrical porous electrodes
[DE90-009707] 18 p2546 N90-24530
New liquid cathode electrolytes in high rate cells
[AD-A219822] 18 p2548 N90-24531

Resistivity measurements of halide-salt/MgO separators for thermal cells
[DE90-009740] 18 p2550 N90-24553
Conservation of body calcium by increased dietary intake of potassium: A potential measure to reduce the osteoporosis process during prolonged exposure to microgravity 18 p2631 N90-24993
Storage battery operation technique of photovoltaic system to prevent the imbalance of state of charge
[DE90-503032] 20 p2856 N90-26255
Ionic atmosphere effects on the energetics of thermal and optical electron-exchange reactions: Application to ferrocenium-ferrocene self exchange
[AD-A222605] 20 p2889 N90-26441
Potential dependence of the conductivity of highly oxidized polythiophenes, polypyrroles, and polyaniline: Finite windows of high conductivity
[AD-A222024] 22 p3159 N90-27912
Infrared reflection-adsorption spectroscopy of the electrode/electrolyte solution interface: Optical considerations
[AD-A221935] 22 p3246 N90-28409
Assessment of battery technologies for electric vehicles. Volume 2, part 2: Appendices
[DE90-014810] 23 p3321 N90-28778
A 10kW class molten carbonate fuel cell test: The stack with electrolyte plate prepared with paper-making method
[DE90-507841] 23 p3344 N90-28900
Electronic conduction in molten cryolite saturated with alumina
[DE90-015090] 23 p3400 N90-29211
Electrochemical evaluation of new fluorosulfonic and fluorophosphonic acids as fuel cell electrolytes
[DE90-016626] 24 p3485 N90-29699

ELECTROLYTIC CELLS
Impedance studies of the cell Pt/Ag+ conducting glass/Ag beta-alumina/Pt
[AD-A209820] 01 p0038 N90-10210
Cell performance of ultra-thin polymer cathode system: Theoretical energy and power density projections
[AD-A210786] 02 p0202 N90-11151
Multicolor electrochromic displays exploratory development
[AD-A212004] 03 p0303 N90-11721
A lightweight solid polymer electrolyte fuel cell with stack power density of 3 kW/lb (7 kW/kg)
[AD-A211542] 03 p0367 N90-12098
Capacitive behavior in conducting polymers
[AD-A212448] 04 p0481 N90-12760
Assessment of thin film batteries based on polymer electrolytes. Part 3: Specific energy versus specific power
[AD-A212141] 04 p0515 N90-12976
Patents on solid electrolyte fuel cells: Japan
[DE90-702639] 09 p1241 N90-17202
Patents on solid electrolyte fuel cells: US and Britain
[DE90-702640] 09 p1241 N90-17203
Patents on solid electrolyte fuel cells: West Germany, Netherlands and Sweden
[DE90-702641] 09 p1242 N90-17204
Determination of optimum electrolyte composition for molten carbonate fuel cells
[DE90-000410] 09 p1243 N90-17210
A lightweight solid polymer electrolyte fuel cell with stack power density of 3kW/lb (7 kW/kg)
[AD-A216253] 10 p1401 N90-18100
Modeling studies of electrolyte flow and bubble behavior in advanced Hall cells
[DE90-007013] 13 p1795 N90-20303
Recent advances in solid polymer electrolyte fuel cell technology with low platinum loading electrodes 13 p1823 N90-20465
Impedance studies of Ni/Cd and Ni/H2 cells using the cell case as a reference electrode 13 p1824 N90-20473
Enhanced ceria solid electrolyte fuel cell development. Reduction of electronic conductivity permits use of a solid ceria electrolyte in high efficiency high power density fuel cells at temperatures compatible with metallic cell hardware
[AD-A217840] 13 p1828 N90-20498
Enhanced ceria solid electrolyte fuel cell development. Reduction of electronic conductivity permits use of a solid ceria electrolyte in high efficiency high power density fuel cells at temperatures compatible with metallic cell hardware
[AD-A219297] 16 p2253 N90-22846
Very high frequency measurements of geometric factors in transmission line lead acid cells
[AD-A219463] 17 p2420 N90-23788
A simple demonstration of corrosion cells 18 p2514 N90-24355
New liquid cathode electrolytes in high rate cells
[AD-A219822] 18 p2546 N90-24531
Evaluation of room-temperature chloroaluminate molten salts as electrolytes for high energy density batteries
[AD-A223097] 20 p2860 N90-26267
A lightweight solid polymer electrolyte fuel cell with stack power density of 3 kW/lb (7kW/kg)
[AD-A223068] 21 p3020 N90-27169
Cell performance of ultra-thin polymer cathode cell systems. Part 2: Cation intercalating composite polymer cathode
[AD-A221919] 21 p3020 N90-27172
Lightweight solid polymer electrolyte fuel cell with stack power density of 3 kW/lb (7 kW/kg)
[AD-A223964] 23 p3345 N90-28905
Electrochemical characteristics of acid electrolytes for fuel cells
[PB90-244385] 24 p3484 N90-29693
Electrochemical evaluation of new fluorosulfonic and fluorophosphonic acids as fuel cell electrolytes
[DE90-016626] 24 p3485 N90-29699

ELECTROLYTIC POLISHING
U ELECTROPOLISHING

ELECTROMAGNETIC ABSORPTION
NT GAMMA RAY ABSORPTION
NT INFRARED ABSORPTION
NT MULTIPHOTON ABSORPTION
NT PHOTOABSORPTION
NT POLAR CAP ABSORPTION
NT ULTRAVIOLET ABSORPTION
NT X RAY ABSORPTION
Two photon absorption characterization
[AD-A210508] 01 p0121 N90-10694
Radiationless transitions and excited-state absorption of low-field chromium complexes in solids
[AD-A210653] 02 p0194 N90-11105
Generation of axial and lateral magnetic fields in laser produced plasmas
[DE90-607470] 10 p1432 N90-18260
The 16-O photodisintegration at low energies
[NOTA-INTERNA-941] 16 p2315 N90-23196
Combined effect of isotopic substitution, temperature, and magnetic field on the lifetimes of triplet biradicals
[AD-A219711] 17 p2372 N90-23509
Method and apparatus for determining optical absorption and emission characteristics of a crystal or non-crystalline fiber
[NASA-CASE-LAR-13963-1] 17 p2475 N90-24150
Time-dependent density-functional theory
[AD-A220993] 18 p2604 N90-24829
Advanced multilayer x ray optics
[DE90-008228] 18 p2616 N90-24902
Laboratory measurements and modeling of microwave absorption by ammonia in gas mixtures applicable to giant planet atmospheres 20 p2944 N90-26750
Optical signatures of molecular particles via mass-selected cluster spectroscopy 20 p2949 N90-26780
The thermal radiative properties of metals at high temperature
[DE90-012468] 21 p2981 N90-26938
Solar cosmic ray effects in the lower ionosphere 22 p3208 N90-28201
The 27-day versus 13.5-day variations in the solar Lyman-alpha radiation and the radio wave absorption in the lower ionosphere over Europe 22 p3209 N90-28203
On the relation between the electron content of the ionospheric D-region, variations of the riometer absorption, and the H-component of the geomagnetic field 22 p3210 N90-28208
Laser induced fluorescence imaging applications 24 p3420 N90-29322

ELECTROMAGNETIC ACCELERATION
Railgun performance with a two-stage light-gas gun injector
[DE90-009183] 14 p1932 N90-21057
Control of surface melting and ablation in electromagnetic launchers via the magnetic vapor shielding mechanism
[AD-A219035] 16 p2204 N90-22578
Advanced space transportation technologies 18 p2645 N90-25061
Analysis of near-surface flow physics in a two-stage, 10 km/s, electromagnetic launcher
[DE90-013292] 21 p2964 N90-26852

ELECTROMAGNETIC COMPATIBILITY
Handbook of radio wave propagation loss (100-20,000 MHz), part 2
[PB89-195473] 03 p0336 N90-11912
The design, construction, performance and calibration of pulse generators to fulfil the requirements of specifications defence standard 59-41, FS(F) 510 and FS(S) 457
[RAE-TM-FS(F)-550] 04 p0496 N90-12857
Electrical testing 05 p0605 N90-13520
Alternative techniques for some typical MIL-STD-461/462 types of measurements
[PB89-235139] 07 p0917 N90-15302
The 5th Annual Review of Progress in Applied Computational Electromagnetics
[AD-A217994] 14 p1966 N90-21258
Validation of shielding effectiveness of cables with pigtails
[AD-A220647] 17 p2396 N90-23650
Resonant coupling through a slot to a loaded cylindrical cavity: Experimental results
[AD-A223000] 20 p2922 N90-26631
Ground-based weather radar compatibility with digital radio-relay microwave systems
[PB90-206236] 23 p3318 N90-28756

ELECTROMAGNETIC CONTROL
U ELECTROMAGNETS
U REMOTE CONTROL

ELECTROMAGNETIC COUPLING
NT MICROWAVE COUPLING
NT OPTICAL COUPLING
JPS heater and sensor lightning qualification
[NASA-CR-183830] 06 p0779 N90-14530
Metal film coatings on amorphous metallic alloys
[AD-D014308] 07 p0907 N90-15240
Computation of coupling elements between waveguides and modes for large launching structures
[IPPCZ-290] 13 p1890 N90-20842
Boeing 727-100 test project (high energy radiated field tests)
[DOT/FAA/CT-88/33] 14 p1964 N90-21247
Use of geomagnetic data for studies on the Earth's deep interior 21 p3023 N90-27192
Millimeter-wave generation via plasma three-wave mixing
[AD-A222010] 22 p3247 N90-28415

ELECTROMAGNETIC DEDUCTION
U MAGNETIC INDUCTION

ELECTROMAGNETIC FIELDS
NT FAR FIELDS
NT NEAR FIELDS
NT SYSTEM GENERATED ELECTROMAGNETIC PULSES
Electro-impulse de-icing testing analysis and design
[NASA-CR-4175] 01 p0007 N90-10031
On canonical quantization of the electromagnetic field in terms of field strengths
[DE89-615389] 01 p0055 N90-10314
ELF (Extremely Low Frequency) Communications System Ecological Monitoring Program: Electromagnetic field measurements and engineering support, 1988
[AD-A210200] 01 p0056 N90-10321
Thermodynamic principles of the process of the effect of electromagnetic fields on a polymer melt
[AD-A210698] 02 p0201 N90-11149
Generation of higher-order squeezing of quantum electromagnetic fields by degenerate four-wave mixing and other processes
[DE89-618392] 02 p0212 N90-11213
Deep null antennas and their applications to tactical VHF radio communications
[AD-A210856] 02 p0212 N90-11214
Auxiliary-field transformations for repulsive potentials: A physical approach
[DE89-016677] 02 p0214 N90-11223
New tools for the simulation and design of calorimeters
[DE89-016323] 02 p0223 N90-11281
Study of the behavioral and biological effects of high intensity 60 Hz electric fields
[DE89-015528] 02 p0254 N90-11438
Biological effects of power frequency electric and magnetic fields: Background paper
[PB89-209985] 02 p0254 N90-11439
Computer simulations of electromagnetic ion instabilities in the plasma sheet boundary layer
[DE89-016596] 02 p0278 N90-11588
A fully electromagnetic hybrid model for high density plasma simulations
[DE89-016771] 02 p0279 N90-11593
Gravitational nonminimally coupled electromagnetic fields: A possible solution to some idiosincrasies of Einstein-Maxwell theory
[DE89-618430] 02 p0286 N90-11635
Numerical study of the current sheet and PSBL in a magnetotail model
[NASA-CR-183289] 02 p0293 N90-11669
Electromagnetic jets in pulsar magnetospheres and near magnetized accretion disks 02 p0294 N90-11675
Resistive block methods for electrostatic field solutions with internal elements
[DE89-017535] 03 p0337 N90-11920
An electromagnetic finite element particle code on an unstructured grid
[DE89-017532] 03 p0407 N90-12336

Temporal and spatial filtering remedies for dispersion in electromagnetic particle codes
[DE89-017534] 03 p0408 N90-12337
On the extremum electric charge problem of steady electromagnetic equilibria
[TRITA-EPP-89-04] 04 p0489 N90-12809
Application of a generalized Leibniz rule for calculating electromagnetic fields within continuous source regions
[AD-A212470] 04 p0492 N90-12831
Wire grid modeling of the linear tapered slot antenna
[AD-A212977] 04 p0494 N90-12842
Calcium displacement caused by electromagnetic fields
[AD-A212690] 04 p0524 N90-13023
Time-domain Green function corresponding to a time-harmonic point source in complex space
[PB89-218846] 04 p0539 N90-13117
Liquid and solid ion plasmas
[AD-A212415] 04 p0557 N90-13244
Research in cosmic and gamma ray astrophysics
[NASA-CR-185451] 04 p0569 N90-13316
Countermeasures to microgravity
05 p0680 N90-13957
Computation of electromagnetic effects in a tokamak due to a plasma disruption
[DE90-001764] 06 p0848 N90-14931
Design of a bounded wave EMP (Electromagnetic Pulse) simulator
[AD-A214137] 07 p0919 N90-15316
Introduction to extremely-low-frequency electric and magnetic fields
[DE90-002662] 07 p0966 N90-15578
On averaged force acting on a particle in HF electromagnetic field
[DE90-600984] 08 p1057 N90-16109
Characteristics of electromagnetic wave forms with lightning in winter season (2): Characteristics in frequency domain
[DE90-734989] 08 p1103 N90-16388
Modeling antennas and scatterers of arbitrary shape embedded in layered dielectric media
[AD-A214902] 09 p1211 N90-17023
ELF (Extremely Low Frequency) communications system ecological monitoring program: Summary of 1988 progress
[AD-A216153] 10 p1377 N90-17981
Scattering from an arbitrary cylinder in the presence of a planar media interface using the bymoment method
[DE90-006465] 11 p1499 N90-18626
The dynamics of electrons in very intense lasers
[DE90-007246] 11 p1516 N90-18729
Muzzle shunt augmentation of conventional railguns
[DE90-007505] 12 p1607 N90-19248
Radiation of electromagnetic waves by an accelerated charged particle in medium
[DE90-610458] 12 p1646 N90-19461
Finite element analysis of a quartz rotation sensor
[DE90-006959] 12 p1664 N90-19562
Integrability and chaos in nonlinearly coupled optical beams
[DE90-007540] 13 p1888 N90-20834
Boeing 727-100 test project (high energy radiated field tests)
[DOT/FAA/CT-88/33] 14 p1964 N90-21247
The 5th Annual Review of Progress in Applied Computational Electromagnetics
[AD-A217994] 14 p1966 N90-21258
A new rectangular waveguide to coplanar waveguide transition
[NASA-TM-102477] 14 p1966 N90-21263
On the creation of gravitational wave by photon in external electromagnetic field
[DE90-613366] 14 p1967 N90-21265
Proceedings of a workshop on Carcinogenic Potential of Extremely Low Frequency Magnetic Fields
[DE90-614340] 14 p2010 N90-21520
Polarization: Effects on second harmonic power in light scattering by free electrons
[DE90-612842] 14 p2025 N90-21608
Electromagnetic inverse profiling of stratified media
[ETN-90-96402] 15 p2087 N90-21947
Studies of 60-Hz exposure effects on human function
[DE90-009473] 15 p2137 N90-22210
Theory of a charged spinning particle in a gravitational and electromagnetic field
[NIKHEF-H/89-4] 15 p2165 N90-22373
Dynamics of motion charged particles in a field of two electromagnetic waves
[DE90-620690] 16 p2228 N90-22706
ELF (Extremely Low Frequency) communications system ecological monitoring program: Slime mold studies
[AD-A218623] 16 p2229 N90-22715
ELF (Extremely Low Frequency) communications systems ecological monitoring program: Wetland studies
[AD-A218632] 16 p2229 N90-22716
Exposure of human cells to electromagnetic fields
[AD-A219377] 16 p2261 N90-22889
Quantum mechanics in Riemannian space-time
[DE90-620448] 16 p2325 N90-23257
Electromagnetic machines which utilize microgeometry field structures
[AD-A219828] 17 p2398 N90-23660
Bioelectromagnetic effects of the Electromagnetic Pulse (EMP)
[AD-A221552] 21 p3033 N90-27243
Research for electric energy systems
[DE90-014221] 23 p3321 N90-28775
Analysis of a TM01 circular to TE10 rectangular waveguide mode converter
[AD-A224566] 24 p3464 N90-29568
An x ray source for lithography
[AD-D014596] 24 p3473 N90-29630
Interaction of electromagnetic fields with chondrocytes in gel culture
[AD-A223397] 24 p3497 N90-29765

ELECTROMAGNETIC INTERACTIONS
NT LASER PLASMA INTERACTIONS
NT PHOTOPRODUCTION
NT PLASMA-ELECTROMAGNETIC INTERACTION
Electromagnetic pulse interaction at a dielectric interface
[AD-A211081] 02 p0213 N90-11220
Laser production of soft x rays by multiquantum processes and the excitation of atomic inner-shell states
[AD-A211372] 03 p0353 N90-12021
On the role of Coulomb forces in atomic radiative emission
[IRF-PREPRINT-106] 03 p0403 N90-12308
Hollow-cathode experiments to support electrodynamic tether applications
[IFSI-89-5] 08 p1036 N90-15986
Millimeter wave radar clutter program
[AD-A215772] 10 p1376 N90-17978
The 4th Annual Review of Progress in Applied Computational Electromagnetics
[AD-A217912] 14 p1966 N90-21257
Once more about the sizes of fast-moving objects
[DE90-615204] 14 p2022 N90-21592
Computer simulation of ionospheric radio frequency heating
[DE90-009478] 15 p2087 N90-21944
Interaction of atomic hydrogen with pico- and femtosecond laser pulses
[AD-A218426] 16 p2241 N90-22785
Optical properties of cometary dust
[AD-A218790] 16 p2338 N90-23325
Interaction of electromagnetic signals with particulate clouds
[AD-A222804] 20 p2856 N90-26244
Laser surface interactions of high-T(sub c) superconductors 22 p3139 N90-27809
The f2 dominance of the energy-momentum tensor
[DE90-508027] 24 p3460 N90-29544

ELECTROMAGNETIC INTERFERENCE
NT ATMOSPHERICS
NT CHIRP
NT CHIRP SIGNALS
NT COSMIC NOISE
NT CROSSTALK
NT ELECTROMAGNETIC NOISE
NT HISS
NT IONOSPHERIC NOISE
NT JAMMING
NT RADIO FREQUENCY INTERFERENCE
NT SHOT NOISE
NT THERMAL NOISE
NT WHISTLERS
NT WHITE NOISE
Laboratory test methodology for evaluating the effects of electromagnetic disturbances on fault-tolerant control systems
[NASA-TM-101665] 05 p0695 N90-14061
The parabolic equation approach to predicting tropospheric propagation effects in operational environments 06 p0759 N90-14418
Aircraft testing in the electromagnetic environment
07 p0873 N90-15066
Interference rejection and detection performance of the smallest of circuit
[AD-A215153] 09 p1212 N90-17025
Trends in VLF/LF (Very Low Frequency/Low Frequency) modem performance testing
[AD-A216576] 11 p1497 N90-18614
Effects of additional interfering signals on adaptive array performance
[NASA-CR-186508] 13 p1790 N90-20271
Test diagnostics of RF effects in integrated circuits
[AD-A219737] 17 p2396 N90-23648
Validation of shielding effectiveness of cables with pigtails
[AD-A220647] 17 p2396 N90-23650
Interactions between the Space Station and the environment: A preliminary assessment of EMI
19 p2737 N90-25557
The disturbance processes on the data links of the mode-S air traffic control system
[ETN-90-96960] 20 p2806 N90-25965
Minimization of the cost of information transfer in HF spread spectrum transmission 20 p2848 N90-26198
Center for Electronics and Electrical Engineering technical progress bulletin covering center programs, July to September 1989, with 1990 CEEE events calender
[PB90-188095] 22 p3167 N90-27959

ELECTROMAGNETIC MEASUREMENT
NT ELECTROMAGNETIC NOISE MEASUREMENT
The 1984 direct strike lightning data, part 1
[NASA-TM-87690-PT-1] 01 p0089 N90-10505
The 1984 direct strike lightning data, part 2
[NASA-TM-87690-PT-2] 01 p0089 N90-10506
The 1984 direct strike lightning data, part 3
[NASA-TM-87690-PT-3] 01 p0089 N90-10507
RF transistor thermal/electrical characterization
[DE90-001427] 07 p0920 N90-15326
Pulsed EMAT (Electromagnetic Acoustic Transducer) acoustic measurements on a horizontal continuous caster for internal temperature determination
[DE90-002735] 07 p0988 N90-15709
The 1985 and 1986 direct strike lightning data, part 1
[NASA-TM-100533-PT-1] 10 p1409 N90-18125
The 1985 and 1986 direct strike lightning data, part 2
[NASA-TM-100533-PT-2] 10 p1409 N90-18126
NDE (Nondestructive evaluation) of critical currents in high T(sub c) superconductors
[DE90-012953] 20 p2930 N90-26670
Two-dimensional signal processing and storage and theory and applications of electromagnetic measurements
[AD-A224239] 24 p3459 N90-29538

ELECTROMAGNETIC NOISE
NT ATMOSPHERICS
NT COSMIC NOISE
NT HISS
NT IONOSPHERIC NOISE
NT SHOT NOISE
NT THERMAL NOISE
NT WHISTLERS
NT WHITE NOISE
Quantum 1/F noise in solid state devices in particular Hg1-(sub x)Cd(sub x)Te N(+)-P diodes
[AD-A209365] 01 p0128 N90-10730
Nonlinear dynamics of broad-band lasers
[DE89-017442] 02 p0228 N90-11307
Sensitivity of optoelectronic receivers
[AD-A211823] 03 p0338 N90-11923
SIS (Superconductor-Insulator-Superconductor) mixer research
[AD-A211607] 03 p0414 N90-12375
Performance analysis of large adaptive sidelobe canceller arrays with reused elements
[AD-A212888] 04 p0494 N90-12841
Sound Localization by Human Observers symposium proceedings
[AD-A212877] 04 p0524 N90-13026
Numerical evaluation of the far field wave pattern of the radiation Green's function
[AD-A212839] 04 p0546 N90-13176
Use of superconducting plates and shells to deflect magnetic noise fields: Application to MEG
[DE89-012592] 06 p0803 N90-14676
Adaptive canceller limitations caused by I,Q mismatch errors
[AD-A214287] 07 p0919 N90-15318
Method for eliminating self-screening noise jamming in radar systems
[AD-D014271] 08 p1056 N90-16105
Radio noise measurements in the long-wave band at Thule, Greenland
[NASA-CR-182824] 09 p1206 N90-16991
A current disruption mechanism in the neutral sheet for triggering substorm expansions
[NASA-CR-186260] 09 p1298 N90-17525
Lower bounds on multiple-source direction finding in the presence of direction-dependent antenna-array-calibration errors
[AD-A215825] 10 p1376 N90-17979
Analysis and test of a wide angle spectrometer
[AD-A215819] 10 p1388 N90-18030
High-resolution radar imaging
[AD-A220809] 17 p2391 N90-23620
Laser gyros and field diagnostics
[AD-A220832] 17 p2406 N90-23709
Studies of ECCM improvements for frequency-hopping CPFSK systems
[AD-A222995] 21 p2995 N90-27023
Noise adaptation and correlated maneuver gating of an extended Kalman filter
[AD-A221713] 21 p3001 N90-27060

Novel approaches to sensitivity enhancement of ring laser gyros
[AD-A224335] 24 p3471 N90-29617
ELECTROMAGNETIC NOISE MEASUREMENT
Contribution of the precision determination of noise powers in the MHz and lower GHz frequency range
[PTB-E-33] 03 p0340 N90-11935
ELECTROMAGNETIC PROPAGATION
U ELECTROMAGNETIC WAVE TRANSMISSION
ELECTROMAGNETIC PROPERTIES
NT ABSORPTIVITY
NT BIDIRECTIONAL REFLECTANCE
NT BIREFRINGENCE
NT BRIGHTNESS
NT BRIGHTNESS DISTRIBUTION
NT COLOR
NT DICHROISM
NT FARADAY EFFECT
NT INDUCTANCE
NT KERR MAGNETOOPTICAL EFFECT
NT LUMINOSITY
NT MAGNETORESISTIVITY
NT OPACITY
NT OPTICAL BISTABILITY
NT OPTICAL PROPERTIES
NT OPTICAL REFLECTION
NT PHOSPHORESCENCE
NT PHOTOCONDUCTIVITY
NT PHOTOELASTICITY
NT RADIANCE
NT REFLECTANCE
NT REFRACTIVITY
NT SKY BRIGHTNESS
NT SPECTRAL REFLECTANCE
NT STELLAR LUMINOSITY
NT TRANSMISSIVITY
NT TRANSMITTANCE
NT TRANSPARENCE
NT WATER COLOR
High-temperature ceramic superconductors
[AD-A211070] 02 p0283 N90-11618
Nucleon polarizabilities in the constituent quark model
[NOTA-INTERNA-936] 05 p0698 N90-14082
Electromagnetic scale models using emulsions
[AD-A214855] 09 p1211 N90-17022
Electromagnetic properties of material coated surfaces
[NASA-CR-186486] 12 p1647 N90-19466
The measurement of surface reflectivity at millimetre wavelengths
[MRL-TN-559] 14 p1960 N90-21222
The microwave permeability of conducting spherical shells
[AD-A220746] 17 p2369 N90-23485
Spectral methods for electromagnetic propagation and diffraction
[AD-A220291] 17 p2393 N90-23632
Joint services electronics program
[AD-A220815] 17 p2397 N90-23654
Optical signal processing
[AD-A220332] 18 p2615 N90-24897
ELECTROMAGNETIC PROPULSION
Proceedings of a contractors meeting on Combustion Rocket Propulsion Diagnostics of Reacting Flow
[AD-A216445] 12 p1617 N90-19297
Laser controlled semiconductor armature for electromagnetic launchers
[AD-D014435] 14 p1931 N90-21055
A superconducting quenchgun for delivering lunar derived oxygen to lunar orbit
[NASA-CR-185161] 15 p2061 N90-21806
Control of surface melting and ablation in electromagnetic launchers via the magnetic vapor shielding mechanism
[AD-A219035] 16 p2204 N90-22578
ELECTROMAGNETIC PULSES
NT SYSTEM GENERATED ELECTROMAGNETIC PULSES
Consumer electronics testing to fast-rise EMP (Electromagnetic Pulse) VEMPS (Vertical Electromagnetic Pulse Simulator) 2 development
[AD-A210505] 01 p0057 N90-10323
Electromagnetic pulse interaction at a dielectric interface
[AD-A211081] 02 p0213 N90-11220
Acceleration of thin foil targets using fiber-coupled optical pulses
[DE89-016526] 02 p0275 N90-11569
Simulation of the EMP (Electromagnetic Pulse) from ESD (Electrostatic Discharge)
[DE89-014484] 03 p0337 N90-11918
The design, construction, performance and calibration of pulse generators to fulfil the requirements of specifications defence standard 59-41, FS(F) 510 and FS(S) 457
[RAE-TM-FS(F)-550] 04 p0496 N90-12857
Modeling of power electronic systems with EMTP
[NASA-TM-102375] 05 p0695 N90-14060
Detection of a chirping electromagnetic signal
[DE90-002105] 06 p0766 N90-14457
Flight in Adverse Environmental Conditions
[AGARD-CP-470] 07 p0869 N90-15041
Arc-sprayed coatings for electromagnetic pulse protection: Assessment of physical and electrical properties
[AD-A213825] 07 p0912 N90-15275
Design of a bounded wave EMP (Electromagnetic Pulse) simulator
[AD-A214137] 07 p0919 N90-15316
Proposed activities to prepare for testing advanced/stealth weapons systems
[AD-A214453] 07 p0920 N90-15321
Technology of fast spark gaps
[AD-A214199] 07 p0925 N90-15353
Frequency shift induced in laser pulses by plasma density variations
[AD-A214195] 07 p0936 N90-15424
On the HEMP (High-Altitude Electromagnetic Pulse) response of protective relays
[DE90-003718] 08 p1061 N90-16138
Steep front impulse tests on a solid-state relay
[DE90-004243] 08 p1062 N90-16140
Characteristics of electromagnetic wave forms with lightning in winter season (2): Characteristics in frequency domain
[DE90-734989] 08 p1103 N90-16388
Nonlinear modulational stability and propagation of an electromagnetic pulse in a two-component, neutral plasma
[AD-A215131] 09 p1207 N90-16994
Two-dimensional, long-pulse simulation of microwave-induced electron layer evolution in low-pressure air
[DE90-005180] 09 p1208 N90-17004
Optical nutation in polymers irradiated by ultrashort laser pulses
[AD-A212927] 10 p1357 N90-17869
New type of optical bistability in polymers mediated by phonons
[AD-A216102] 10 p1359 N90-17882
Parallel memory addressing using coincident optical pulses
[AD-A216302] 11 p1501 N90-18641
Development and applications of a coupled cavity sodium-chloride laser 15 p2102 N90-22029
Origin of pulsed emission from the young supernova remnant SN 1987A
[CAL-377] 15 p2182 N90-22469
Interaction of atomic hydrogen with pico- and femtosecond laser pulses
[AD-A218426] 16 p2241 N90-22785
Real-time closed-loop simulation and upset evaluation of control systems in harsh electromagnetic environments 16 p2294 N90-23069
Frequency domain techniques for analyzing picosecond optical pulses
[AD-A218856] 16 p2318 N90-23214
Diffraction effects in directed radiation beams
[AD-A220785] 17 p2391 N90-23619
Pulse-width dependent radiation effects on electronic components
[AD-A219517] 17 p2395 N90-23643
High peak power microwave pulses at 2.37 GHz: No effects on vigilance performance in monkeys
[AD-A219570] 17 p2433 N90-23863
Hot carrier in subpicosecond photoconductive experiments
[AD-A219874] 17 p2477 N90-24166
Prediction of high-voltage, broadband RF pulse generation from an air gas avalanche switch
[DE90-010183] 18 p2549 N90-24551
Phase-sensitive optical detection of ballistic phonon pulses using frequency-modulation spectroscopy and persistent spectral holes
[AD-A221521] 21 p2979 N90-26930
Bioelectromagnetic effects of the Electromagnetic Pulse (EMP)
[AD-A221552] 21 p3033 N90-27243
Personal computer programs for the control of subnanosecond transient digitizers with applications for device damage testing
[AD-A221458] 21 p3054 N90-27365
Serial interferometric fiber-optic sensor array
[AD-D014466] 22 p3246 N90-28407
Microscopic models for electromagnetic wave propagation in highly dispersive media
[AD-A224382] 24 p3460 N90-29540
ELECTROMAGNETIC PUMPS
Experimental demonstration of an electromagnetically pumped free-electron laser with cyclotron harmonic idlers
[AD-A218830] 17 p2408 N90-23719
Heat exchanger with oscillating flow
[NASA-CASE-LAR-14033-1] 21 p3004 N90-27072
ELECTROMAGNETIC RADIATION
NT AIRGLOW
NT BLACK BODY RADIATION
NT BREMSSTRAHLUNG
NT CENTIMETER WAVES
NT CERENKOV RADIATION
NT COHERENT LIGHT
NT COSMIC X RAYS
NT CYCLOTRON RADIATION
NT DECAMETRIC WAVES
NT DIFFRACTION RADIATION
NT ELECTROMAGNETIC PULSES
NT ELECTROMAGNETIC SURFACE WAVES
NT EXTRATERRESTRIAL RADIO WAVES
NT EXTREME ULTRAVIOLET RADIATION
NT FAR INFRARED RADIATION
NT FAR ULTRAVIOLET RADIATION
NT GAMMA RAY BEAMS
NT GAMMA RAY BURSTS
NT GAMMA RAYS
NT GEOCORONAL EMISSIONS
NT HYDROXYL EMISSION
NT INFRARED RADIATION
NT ION CYCLOTRON RADIATION
NT LASER BEAMS
NT LIGHT (VISIBLE RADIATION)
NT LIGHT BEAMS
NT LONG WAVE RADIATION
NT LYMAN ALPHA RADIATION
NT MICROWAVE EMISSION
NT MICROWAVES
NT MILLIMETER WAVES
NT MONOCHROMATIC RADIATION
NT NEAR INFRARED RADIATION
NT NEAR ULTRAVIOLET RADIATION
NT NIGHTGLOW
NT NONEQUILIBRIUM RADIATION
NT NONTHERMAL RADIATION
NT PHOTON BEAMS
NT PLANETARY RADIATION
NT PLASMONS
NT POLARIZED ELECTROMAGNETIC RADIATION
NT POLARIZED LIGHT
NT RADIO BURSTS
NT RADIO EMISSION
NT RADIO WAVES
NT SHORT WAVE RADIATION
NT SKY RADIATION
NT SKY WAVES
NT SOLAR RADIO BURSTS
NT SOLAR RADIO EMISSION
NT SOLAR X-RAYS
NT SUBMILLIMETER WAVES
NT SUNLIGHT
NT SYNCHROTRON RADIATION
NT SYSTEM GENERATED ELECTROMAGNETIC PULSES
NT TERRESTRIAL RADIATION
NT THERMAL RADIATION
NT TROPOSPHERIC RADIATION
NT TYPE 3 BURSTS
NT ULTRAVIOLET RADIATION
NT WHISTLERS
NT X RAYS
NT ZODIACAL LIGHT
Maximization of directed electromagnetic radiation with an optimized antenna
[DE89-014045] 01 p0056 N90-10319
Efficient algorithm for calculation of radar cross section
[AD-A210785] 02 p0213 N90-11217
Ionospheric irregularities and their effects on electromagnetic waves propagating through them 02 p0245 N90-11391
A new approach to HF (High Frequency) channel modeling and simulation. Part 1: Deterministic model
[PB89-203962] 03 p0336 N90-11913
A method to model fuze-performance. Part 3: Diffraction of electromagnetic radiation by an edge
[FEL-1989-22-PT-3] 03 p0340 N90-11940
Parametric study of power absorption from electromagnetic waves by small ferrite spheres
[NASA-TP-2949] 03 p0399 N90-12282
Specification for radar free-space detection range and free-space intercept range calculations
[AD-A213158] 04 p0494 N90-12843
Catalog of absolutely calibrated, range normalized, wideband, electric field waveforms from located lightning flashes in Florida: July 24 and August 14, 1985 data
[AD-A212708] 04 p0521 N90-13008
Stochastic modelling of EM scattering from foliage
[AD-A213118] 05 p0632 N90-13689

Operational Decision Aids for Exploiting or Mitigating Electromagnetic Propagation Effects
[AGARD-CP-453] 06 p0757 N90-14405
Propagation prediction for the North Sea environment
06 p0760 N90-14423
The effect of oblate spheroidal drops on rain attenuation at 94 GHz: Comparison between theory and experiment
06 p0763 N90-14440
Characteristics of electromagnetic wave forms with lightning in winter season
[DE89-901256] 07 p0963 N90-15567
Design of JT-60U ICRF launcher
[DE90-733145] 10 p1326 N90-17663
Effects of pulsed and CW (Continuous Wave) 2450 MHz radiation on transformation and chromosomes of human lymphocytes in vitro
[AD-A216500] 11 p1539 N90-18857
Apparatus and method for minimizing polarization-induced signal fading in an interferometric fiber-optic sensor using input-polarization modulation
[AD-D014315] 12 p1642 N90-19430
Propagation of electromagnetic waves in multidimensional homogeneous cosmologies
[DE90-610474] 12 p1647 N90-19462
Is Galerkin's method really better
[DE90-008804] 14 p1967 N90-21267
Center of excellence in theoretical geoplasma research
[AD-A215035] 14 p2005 N90-21488
Proceedings of a workshop on Carcinogenic Potential of Extremely Low Frequency Magnetic Fields
[DE90-614340] 14 p2010 N90-21520
Induction-type metal detector with increased scanning area capability
[NASA-CASE-KSC-11386-1] 15 p2101 N90-22023
High Intensity Electro-Magnetic and Ultrasonic Effects on Inorganic Materials Behavior and Processing Workshop
[AD-A218884] 16 p2215 N90-22640
Artificial dielectrics
[AD-A219671] 17 p2389 N90-23605
Diffraction effects in directed radiation beams
[AD-A220785] 17 p2391 N90-23619
A model of electromagnetic leakage through joints at radio frequencies
[BAE-WES-RP-GEN-EMC-049-T2.2]
17 p2392 N90-23626
Basic research in electronics (JSEP)
[AD-A219931] 17 p2398 N90-23661
A survey of equatorial magnetospheric wave activity between 5 and 8 R(sub E)
[AD-A220137] 17 p2424 N90-23812
Transient electromagnetic scattering on anisotropic media
[DE90-011802] 19 p2683 N90-25262
A decision-making aid for multi-layer radar absorbent coverings
[ESA-TT-1173] 19 p2684 N90-25267
Transmission, reflection, and radiation at junction planes of different open waveguides
[ISBN-90-9002864-1] 20 p2855 N90-26241
Remote sensing of Earth terrain
[NASA-CR-186888] 20 p2880 N90-26382
Resonant coupling through a slot to a loaded cylindrical cavity: Experimental results
[AD-A223000] 20 p2922 N90-26631
Mechanisms of microwave induced damage in biologic materials
[AD-A222454] 21 p3033 N90-27242
Laser diagnostics of plasma thrusters
[AD-A221682] 21 p3079 N90-27506
Stability regimes in a helical quadrupole focusing accelerator: Theory and simulation
[AD-A221755] 21 p3079 N90-27507
Simple graphical descriptions of natural land profiles and the application of fractal and sub-fractal models to them
[RSRE-MEMO-4305] 22 p3195 N90-28130
Small angle generating apparatus
[AD-D014467] 22 p3246 N90-28408
Propagation of electromagnetic radiation in a random field of gravitational waves and space radio interferometry
[DE90-627196] 23 p3319 N90-28764

ELECTROMAGNETIC SCATTERING
NT HALOS
NT IONOSPHERIC F-SCATTER PROPAGATION
NT LIGHT SCATTERING
NT MICROWAVE SCATTERING
NT MIE SCATTERING
NT RAMAN SPECTRA
NT RAYLEIGH SCATTERING
NT THOMSON SCATTERING
NT X RAY SCATTERING
Plasma theory and simulation
[AD-A207952] 01 p0125 N90-10714
Small particle scattering and absorption
[AD-A213168] 04 p0473 N90-12711
The physical optics approximation in the near-field region
[FEL-1989-100] 04 p0555 N90-13234
Workshop on Recent Progress in Surface and Volume Scattering
[AD-A212455] 04 p0555 N90-13236
Stochastic modelling of EM scattering from foliage
[AD-A213118] 05 p0632 N90-13689
N-port theory applied to backscatter polarimetry and depolarization in foliage penetration
[AD-A213437] 07 p0917 N90-15305
Studies of quantitative methods for imaging from scattered fields
[AD-A214047] 07 p0976 N90-15638
High-frequency asymptotic methods for analyzing the EM scattering by open-ended waveguide cavities
[NASA-CR-186244] 08 p1056 N90-16103
Plasmon excitation in the scattering of electromagnetic waves from good conductors
[AD-A214026] 08 p1056 N90-16107
A finite element-boundary integral formulation for scattering by three-dimensional cavity-backed apertures
[NASA-CR-186332] 09 p1187 N90-16878
Oblique ionospheric heating and effects on radio propagation
[AD-A214756] 09 p1205 N90-16983
USAF/GL meteor scatter data analysis program: A user's guide
[AD-A214988] 09 p1206 N90-16989
A study of a new time-domain method of lines and its application for the characterization of microstrip line and its discontinuities
[AD-A215441] 09 p1213 N90-17034
Simulation of rough surface scattering in three-dimensions
[AD-A215171] 09 p1277 N90-17405
Automation of an RCS (Radar Cross Section) measurement system and its application to investigate the electromagnetic scattering from scale model aircraft canopies
[AD-A215741] 10 p1375 N90-17970
Millimeter wave radar clutter program
[AD-A215772] 10 p1376 N90-17978
ACIRF user's guide: Theory and examples
[AD-A216436] 11 p1496 N90-18613
Effects of strong scattering on transionospheric propagation
[AD-A216708] 11 p1497 N90-18617
Scattering from an arbitrary cylinder in the presence of a planar media interface using the bymoment method
[DE90-006465] 11 p1499 N90-18626
A combined finite element-boundary element formulation for solution of two-dimensional problems via CGFFT
[NASA-CR-186464] 12 p1620 N90-19309
The 4th Annual Review of Progress in Applied Computational Electromagnetics
[AD-A217912] 14 p1966 N90-21257
Scattering of a plane electromagnetic wave from a semicircular crack in a perfectly conducting ground plane
[AD-A219310] 16 p2230 N90-22721
Development of new methods for predicting the bistatic electromagnetic scattering from absorbing shapes
[AD-A219327] 17 p2388 N90-23600
Measurement and analysis of the electromagnetic scattering of a geodesic array of triangular trihedral corner reflectors
[AD-A220457] 17 p2389 N90-23608
Understanding tropscatter propagation
[AD-A220969] 18 p2544 N90-24520
Transient electromagnetic scattering on anisotropic media
[DE90-011802] 19 p2683 N90-25262
Electromagnetic inverse scattering of buried objects
[ETN-90-97216] 20 p2856 N90-26242
Separable coordinate systems for PDE
[AD-A223052] 21 p3063 N90-27415
Free boundary problems for flow with vorticity
[AD-A218415] 22 p3168 N90-27971
Electromagnetic scattering from two-dimensional thick material junctions
[NASA-CR-186468] 23 p3319 N90-28767
Bandwidth and signal-to-noise ratio enhancement of the NPS transient electromagnetic scattering laboratory
[AD-A224144] 23 p3320 N90-28771

ELECTROMAGNETIC SHIELDING
JPS heater and sensor lightning qualification
[NASA-CR-183830] 06 p0779 N90-14530
Arc-sprayed coatings for electromagnetic pulse protection: Assessment of physical and electrical properties
[AD-A213825] 07 p0912 N90-15275
Aircraft lightning protection handbook
[AD-A222716] 22 p3110 N90-27668

ELECTROMAGNETIC SPECTRA
NT BALMER SERIES
NT ELECTRONIC SPECTRA
NT FRAUNHOFER LINES
NT GAMMA RAY SPECTRA
NT H ALPHA LINE
NT H BETA LINE
NT H LINES
NT INFRARED SPECTRA
NT K LINES
NT LINE SPECTRA
NT LYMAN SPECTRA
NT MICROWAVE SPECTRA
NT RADIO SPECTRA
NT RAMAN SPECTRA
NT RYDBERG SERIES
NT SOLAR SPECTRA
NT STELLAR SPECTRA
NT UBV SPECTRA
NT ULTRAVIOLET SPECTRA
NT VIBRATIONAL SPECTRA
NT VISIBLE SPECTRUM
NT X RAY SPECTRA
Research investigation directed toward extending the useful range of the electromagnetic spectrum
[AD-A217460] 13 p1789 N90-20267
Seeing in a new light: Astro-1 teacher's guide with activities
[NASA-EP-274] 13 p1899 N90-20900
A laboratory comparison of field techniques for measurement of the liquid water fraction of snow
[AD-A219587] 17 p2417 N90-23774
Improved compact optical RF spectrum analyzer
[AD-D014481] 22 p3177 N90-28026
Using the x ray region of the electromagnetic spectrum for alignment: Overview, geometric optics, and design considerations
[DE90-014798] 23 p3317 N90-28752
Methods for multisource data analysis in remote sensing
[NASA-CR-187005] 23 p3343 N90-28890

ELECTROMAGNETIC SURFACE WAVES
Recent improvements to the electromagnetic surface patch code
[AD-A217479] 13 p1794 N90-20293

ELECTROMAGNETIC WAVE FILTERS
NT BANDPASS FILTERS
NT BANDSTOP FILTERS
NT DIGITAL FILTERS
NT ELECTRIC FILTERS
NT FIR FILTERS
NT INFRARED FILTERS
NT MATCHED FILTERS
NT MICROWAVE FILTERS
NT OPTICAL FILTERS
NT RADIO FILTERS
NT TRACKING FILTERS
NT WAVEGUIDE FILTERS
Internal transmission line filter element
[AD-D014353] 12 p1651 N90-19489
Magnetostatic wave transducers, resonators and dispersion control
[AD-A223437] 24 p3464 N90-29571

ELECTROMAGNETIC WAVE TRANSMISSION
NT HALOS
NT IONOSPHERIC F-SCATTER PROPAGATION
NT IONOSPHERIC PROPAGATION
NT LIGHT SCATTERING
NT LIGHT TRANSMISSION
NT MICROWAVE ATTENUATION
NT MICROWAVE TRANSMISSION
NT MULTIPATH TRANSMISSION
NT RADAR TRANSMISSION
NT RADIO TRANSMISSION
NT SCATTER PROPAGATION
NT SHORT WAVE RADIO TRANSMISSION
NT SPREAD SPECTRUM TRANSMISSION
NT TELEVISION TRANSMISSION
TWIRE: A test program for VLF airborne transmissions
[AD-A210516] 01 p0057 N90-10324
Improved propagation models for discrete random media
[AD-A211085] 01 p0057 N90-10327
Validation of NEC (Numerical Electromagnetics Code) for antennas near ground
[DE89-016502] 02 p0212 N90-11212
Effects on electromagnetic wave propagation and rocket vapor trails of intense turbulence generated by breaking internal gravity waves
[AD-A211755] 03 p0373 N90-12130
Long wave atmospheric noise model, phase 1. Volume 1: Lightning occurrence rates and propagation theory
[AD-A212794] 04 p0493 N90-12836

Long wave atmospheric noise model, phase 1. Volume 2: Mode parameters
[AD-A212795] 04 p0493 N90-12837
Electromagnetic wave propagation through circular waveguides containing radially inhomogeneous lossy media
[AD-A213062] 05 p0632 N90-13688
The parabolic equation approach to predicting tropospheric propagation effects in operational environments 06 p0759 N90-14418
Weather satellite and computer modeling approaches to assessing propagation over marine environments 06 p0764 N90-14443
Remote sensing of evaporation ducts for Naval warfare
[AD-A214849] 10 p1374 N90-17965
A simulation of optical propagation through atmospheric turbulence using two-dimensional Fourier transform techniques
[AD-A216776] 11 p1566 N90-19013
Propagation of electromagnetic waves in multidimensional homogeneous cosmologies
[DE90-610474] 12 p1647 N90-19462
Vector circuit theory for multilayered isotropic and chiral structures: Reflection and transmission
[PB90-122474] 12 p1652 N90-19495
Active probing of space plasmas
[AD-A216867] 12 p1716 N90-19855
Ultrarelativistic envelope solitons in electron-positron plasma of the pulsar magnetosphere
[DE90-613289] 14 p1967 N90-21264
Full wave computation of electromagnetic wave excitation, propagation, and absorption at the ion cyclotron frequency in fusion experiments
[DE90-009399] 14 p2030 N90-21642
Multiwave diffraction analysis of transmission phase gratings
[RSRE-MEMO-4325] 15 p2087 N90-21948
Superheterodyne three-wave detection of gravitation waves
[DE90-620465] 16 p2255 N90-22856
Engineer's Refractive Effects Prediction System (EREPS), revision 2.0
[AD-A220742] 17 p2391 N90-23616
Remote optical sensing
[AD-A220780] 17 p2473 N90-24136
Understanding tropscatter propagation
[AD-A220969] 18 p2544 N90-24520
Millimeter-wave acoustic transducers
[AD-A221402] 18 p2612 N90-24878
Transmission, reflection, and radiation at junction planes of different open waveguides
[ISBN-90-9002864-1] 20 p2855 N90-26241
Propagation of electromagnetic radiation in a random field of gravitational waves and space radio interferometry
[DE90-627196] 23 p3319 N90-28764
Microscopic models for electromagnetic wave propagation in highly dispersive media
[AD-A224382] 24 p3460 N90-29540
Specification for a standard electromagnetic propagation model
[AD-A223556] 24 p3461 N90-29551

ELECTROMAGNETIC WAVES
U ELECTROMAGNETIC RADIATION

ELECTROMAGNETICS
U ELECTROMAGNETISM

ELECTROMAGNETISM
NT MAGNETOSTATICS
Magnetically levitated micro-robotics 02 p0270 N90-11542
Recent advances to NEC (Numerical Electromagnetics Code): Applications and validation
[DE89-009231] 03 p0337 N90-11917
Joint Services Electronics Program
[AD-A212309] 04 p0497 N90-12864
Airborne electromagnetic sensing of sea ice thickness
[AD-A214460] 09 p1240 N90-17198
Spectral emissivities and optical constants of electromagnetically levitated liquid metals as functions of temperature and wavelength 10 p1364 N90-17907
A selective survey of computational electromagnetics for antenna applications 10 p1369 N90-17933
Recent advances to NEC: Applications and validation 10 p1369 N90-17934
Some applications of model-based parameter estimation in computational electromagnetics 10 p1369 N90-17935
Measurement and computer simulation of antennas on ships and aircraft for results of operational reliability 10 p1369 N90-17936
Plasma diagnostics generated in the Compact Torus of UNICAMP
[INPE-4862-RPE/593] 10 p1433 N90-18271
Earth Science Geostationary Platform Technology
[NASA-CP-3040] 12 p1608 N90-19249
Large space antenna concepts for ESGP 12 p1608 N90-19253
Potential theory of radiation 12 p1635 N90-19395
Radar transponder antenna pattern analysis for the space shuttle 12 p1638 N90-19414
Superconductive microprobes for eddy current evaluation of materials
[AD-A217776] 13 p1805 N90-20361
Computer processing of multi-channel electromagnetic data from an airborne geophysical survey system
[PB90-138413] 14 p1965 N90-21253
Biological effects of ELF (Extremely-Low-Frequency) electric and magnetic fields
[DE90-008634] 14 p2009 N90-21514
Experimental evaluation of a tuned electromagnetic damper for vibration control of cryogenic turbopump rotors
[NASA-TP-3005] 17 p2354 N90-23403
Electromagnetic machines which utilize microgeometry field structures
[AD-A219828] 17 p2398 N90-23660
A linearly controlled direct-current power source for high-current inductive loads in a magnetic suspension wind tunnel
[NASA-TM-4198] 19 p2692 N90-25319
Non-destructive characterization of polymer/metal interphases using surface-enhanced Raman scattering
[AD-A222490] 21 p2988 N90-26980
Application of a rechargeable, small caliber railgun power supply
[AD-A224207] 24 p3438 N90-29418

ELECTROMAGNETS
NT SUPERCONDUCTING MAGNETS
An electromagnetic finite element particle code on an unstructured grid
[DE89-017532] 03 p0407 N90-12336
Temporal and spatial filtering remedies for dispersion in electromagnetic particle codes
[DE89-017534] 03 p0408 N90-12337
Permanent magnet flux-biased magnetic actuator with flux feedback
[NASA-CASE-LAR-13785-1] 09 p1277 N90-17403

ELECTROMECHANICAL DEVICES
Design of scientific payloads and components
[AD-A211819] 03 p0351 N90-12005
The effect of concurrent strength and endurance training on electromechanical delay, maximum voluntary contraction, and rate of force development
[AD-A213316] 04 p0525 N90-13028
Induction motor control
[NASA-TM-102533] 12 p1605 N90-19234
The connector space reduction mechanism 15 p2114 N90-22092
Electromagnetic machines which utilize microgeometry field structures
[AD-A219828] 17 p2398 N90-23660
Computer tomography of thermal batteries and other closed systems
[AD-A218379] 17 p2419 N90-23787
A possibility to incorporate saturation in the simple, global model of a synchronous machine with rectifier
[EUT-89-E-225] 20 p2858 N90-26258

ELECTROMECHANICS
Coatings in electrical contacts
[DE89-787739] 02 p0216 N90-11234
Aerospace induction motor actuators driven from a 20-kHz power link
[NASA-TM-102482] 13 p1756 N90-20085

ELECTROMIGRATION
Computer simulation of electromigration in thin films
[AD-A216382] 10 p1357 N90-17867
Electromigration in metallic microstructures
[AD-A221208] 18 p2622 N90-24942
VLSI design for reliability
[AD-A224264] 24 p3463 N90-29562

ELECTROMOTIVE FORCES
NT PONDEROMOTIVE FORCES

ELECTROMYOGRAMS
U ELECTROMYOGRAPHY

ELECTROMYOGRAPHS
U ELECTROMYOGRAPHY

ELECTROMYOGRAPHY
Age-related changes in human posture control: Motor coordination tests
[NASA-CR-185855] 03 p0383 N90-12178
Method and apparatus for applying a mechanical force to surface
[NASA-CASE-LAR-14009-1] 21 p3011 N90-27115

ELECTRON ACCELERATION
Joule heating and runaway electron acceleration in a solar flare 03 p0432 N90-12478
Development of computer codes to model dynamics of the earth's magnetosphere
[AD-A211532] 04 p0517 N90-12987

ELECTRON ACCELERATORS
NT BETATRONS
Bunch length in internal target mode
[NIKHEF-AMPS/89/04] 04 p0496 N90-12854
Electron beam propagation through a magnetic wiggler with random field errors
[AD-A212705] 04 p0498 N90-12867
Characteristics of an electron-beam rocket pellet accelerator
[DE90-001595] 06 p0729 N90-14252
Modification of MEA modulator-klystron units enabling short pulse injection into a pulse-stretcher ring 06 p0841 N90-14894
Performance and modification of the MEA RF drive system 06 p0842 N90-14895
An Energy Spectrum Compressor system (ESC) for the Amsterdam pulse stretcher (AmPS) 06 p0842 N90-14896
Intense REB (Relativistic Electron Beam) transport in a weakly magnetized plasma
[DE90-002978] 07 p0994 N90-15749
Low weight variable GRV power supply as part of the injector electronics to be developed for the electron accelerator MEA
[DIGEL-1989-6] 11 p1504 N90-18661
Pulse-width dependent radiation effects on electronic components
[AD-A219517] 17 p2395 N90-23643
Proof of the feasibility of coherent and incoherent schemes for pumping a gamma-ray laser
[AD-A219972] 18 p2562 N90-24620
Status of the CEBAF injector
[CEBAF-PR-89-027] 19 p2755 N90-25655
Design of CEBAF's RF separator and results of cold tests
[CEBAF-PR-89-021] 19 p2756 N90-25658
Impedance and wakefields beyond cutoff
[CEBAF-PR-89-016] 19 p2756 N90-25663
CEBAF control system
[CEBAF-PR-89-013] 19 p2757 N90-25666
DURIP: Instrumentation for laser switched power LINAC
[AD-A222629] 20 p2868 N90-26318
Digital beam position regulation of the superconducting accelerator at Darmstadt
[ETN-90-97293] 22 p3246 N90-28406

ELECTRON AFFINITY
Threshold photodetachment spectroscopy of the I + HI transition state region
[AD-A218410] 16 p2260 N90-22883

ELECTRON ATTACHMENT
Electron attachment and molecular fragmentation in laser-excited plasmas
[AD-A212098] 03 p0409 N90-12343
Electron production, electron attachment, and charge recombination process in high pressure gas discharges
[AD-A216301] 10 p1434 N90-18274
Lower limits on the absolute dissociative electron attachment cross section from O2 condensed on rare-gas films
[AD-A216727] 11 p1483 N90-18536
Absolute cross-sections for dissociative electron attachment in O2 condensed on Kr films
[AD-A216730] 11 p1570 N90-19038
Ion and electron interactions at thermal and suprathermal energies
[AD-A216905] 12 p1622 N90-19323
Electron-impact ionization and electron attachment cross sections of radicals important in transient gaseous discharges
[AD-A217510] 13 p1806 N90-20366
An ionic mechanism of carbon formation in flames 21 p3093 N90-27582

ELECTRON AVALANCHE
Prediction of high-voltage, broadband RF pulse generation from an air gas avalanche switch
[DE90-010183] 18 p2549 N90-24551
Time-resolved swarm studies in gases with emphasis on electron detachment and ion conversion
[ISBN-90-9003013-1] 18 p2613 N90-24883

ELECTRON BEAM WELDING
Characterization of electron-beam weld processes in uranium by acoustic emission monitoring
[DE89-016044] 01 p0078 N90-10444
Electron beam welding: Model of high voltage bias transmission line and termination circuits
[DE89-016900] 02 p0230 N90-11323
Deformation of electron beam welded Ti-6Al-4V alloy sheet under superplastic conditions
[RAE-TM-MAT/STR-1109] 03 p0359 N90-12053
Onorbit electron beam welding experiment definition
[NASA-CR-183847] 07 p0938 N90-15431
Power beam technology at Los Alamos: A review of research and development activities
[DE90-009002] 22 p3182 N90-28057

ELECTRON BEAMS
NT RELATIVISTIC ELECTRON BEAMS

Characterization of electron-beam weld processes in uranium by acoustic emission monitoring
[DE89-016044] 01 p0078 N90-10444
Negative-working electron beam resist based on poly(methyl methacrylate)
[AD-A207834] 01 p0128 N90-10733
A compact X-ray free electron laser
[DE89-017236] 02 p0226 N90-11297
Free-electron laser theory
[DE89-620145] 02 p0226 N90-11298
Stability requirements of RF linac-driven free-electron lasers
[DE89-016609] 02 p0227 N90-11303
Minimized emittance growth with elliptical beam pipes in FEL (Free-Electron Laser)
[DE89-016982] 02 p0228 N90-11305
Launched electrons in plasma opening switches
[DE89-016886] 02 p0279 N90-11596
Beam-plasma discharge in penetrating plasma
[DE89-630481] 02 p0280 N90-11597
International workshop on Beam Injection Assessment of Defects in Semiconductors
[AD-A210842] 02 p0283 N90-11617
A beam induced upset during the flight of the ECHO-7 rocket
[NASA-CR-186089] 03 p0309 N90-11755
Development and evaluation of an instrument for rapid electroreflectance of semiconductor materials
[AD-A211690] 03 p0414 N90-12376
Current limiting mechanisms in electron and ion beams experiments
[AD-A212295] 04 p0460 N90-12637
Bunch length in internal target mode
[NIKHEF-AMPS/89/04] 04 p0496 N90-12854
B factory via conversion of 1 TeV electron beams into 1 TeV photon beams
[DE89-017692] 04 p0505 N90-12914
Electron beam sensitive devices for controllability
[IMAG-RR-761-I] 05 p0636 N90-13707
Research on the controllability of integrated circuits by means of electron beams
[ETN-90-95710] 05 p0636 N90-13708
Evolution of the EPR procedure for polycrystalline Si ribbon drawing for photovoltaic cell manufacturing
[ISAL-89-0027] 05 p0665 N90-13888
Influence of RF-parameters on beam lifetime
[NIKHEF-K/AMPS/89-06] 05 p0699 N90-14091
Characteristics of an electron-beam rocket pellet accelerator
[DE90-001595] 06 p0729 N90-14252
Recent developments of gigatron technology
[DE90-001067] 06 p0769 N90-14474
Gigatron: A new technology for microwave power devices
[DE90-001066] 06 p0771 N90-14483
Electrical breakdown in vacuum
[DE90-001623] 06 p0771 N90-14485
Self-field-induced chaotic electron motion in free electron lasers
[DE90-001710] 06 p0790 N90-14598
Compact RF-linac free-electron lasers
[DE90-002386] 06 p0790 N90-14600
Analytical treatment of electron trajectory straightener issues in free-electron lasers
[DE90-002405] 06 p0790 N90-14603
An Energy Spectrum Compressor system (ESC) for the Amsterdam pulse stretcher (AmPS)
06 p0842 N90-14896
Microwave Transport Systems for the MTX (Microwave Tokamak Experiment)
[DE90-000821] 06 p0846 N90-14921
RF superconductivity research and development at Los Alamos National Laboratory
[DE90-002440] 06 p0855 N90-14969
Surface engineering by high energy beams
[DE90-001296] 07 p0908 N90-15250
Theory for high gain, high power free electron lasers
[DE90-003024] 07 p0934 N90-15409
Comprehensive, nonintercepting electron-beam diagnostics using spontaneous emission
[DE90-003211] 07 p0935 N90-15414
Initial optical transition radiation measurements of the electron beam for the Boeing free-electron laser experiment
[DE90-003396] 07 p0935 N90-15416
Waveguide effects in superradiant free-electron lasers
[DE90-003605] 07 p0935 N90-15417
A microwiggler Free-Electron Laser at the Brookhaven Accelerator Test Facility
[DE90-003643] 07 p0936 N90-15418
Simulation of radial expansion of an electron beam injected into a background plasma
[NASA-CR-186188] 07 p0994 N90-15743
Recent progress in relativistic klystron research
[DE90-000942] 08 p1059 N90-16121
Remote use of an Electron Beam Tester (EBT)
[IMAG-RR-760-I] 08 p1077 N90-16233
Proposal for a study of laser acceleration of electrons using micrograting structures at ATF
[DE90-003699] 08 p1082 N90-16262
Electron beam induced oxygen in YBa2Cu3O(7-x) superconductors
[DE90-004839] 08 p1133 N90-16565
To construct a linac/storage ring FEL facility
[AD-A214620] 09 p1211 N90-17020
Energy conversion efficiency in high current Raman regime Free Electron Laser (FEL). 1: Single mode analysis
[DE90-719527] 09 p1227 N90-17120
CW ultraviolet laser excited with an electron beam
[AD-A214928] 09 p1227 N90-17123
Electron-beam phase-only spatial light modulator for matched filtering
[AD-A215026] 09 p1282 N90-17431
Possibility of low-frequency electron wave in a beam-plasma system
[DE90-601021] 09 p1284 N90-17441
Stability of hollow beams in longitudinal phase space
[DE90-004284] 10 p1427 N90-18234
Electron production, electron attachment, and charge recombination process in high pressure gas discharges
[AD-A216301] 10 p1434 N90-18274
Research project in microelectronic engineering and imaging science
[DE90-006907] 11 p1503 N90-18653
Toroid monitor
[DIGEL-1989-8] 11 p1504 N90-18663
Absorption experiments on electron-beam pumped rare gases
[DE90-006504] 11 p1515 N90-18722
Electron beam and high-speed optical diagnostics for the Los Alamos HIBAF (High Brightness Accelerator FEL) Facility
[DE90-007828] 11 p1515 N90-18725
Positronium reflection and positronium beams
11 p1559 N90-18980
A continuous plasma final focus
[DE90-006096] 11 p1568 N90-19024
Anode plasma formation as a possible mechanism for an electrical stress limit in cold cathode diodes
[DE90-007503] 12 p1655 N90-19516
Time resolved gain/loss studies under low and high power loading for the XeF C-A transition
[DE90-007506] 12 p1655 N90-19517
On 140 GHz microwave FEL experiments using ELF-2
[DE90-006764] 12 p1667 N90-19576
First direct observation of FEL (Free-Electron Laser) from lambda=20 to 45 microns
[DE90-007508] 12 p1669 N90-19589
The EGS4 Code System: Solution of gamma-ray and electron transport problems
[DE90-008100] 12 p1713 N90-19838
An electron-beam controlled semiconductor switch
[AD-A217181] 13 p1793 N90-20288
Relativistic klystron afterburner simulation techniques
[DE90-008539] 13 p1796 N90-20305
Electron beam generation by electron bombardment induced cathode emission
[AD-A218203] 13 p1798 N90-20318
Dual cathode system for electron beam instruments
[NASA-CASE-NPO-16878-1-CU]
13 p1803 N90-20351
Energy deposition measurements for E-beam pumped excimer lasers
[DE90-007545] 13 p1806 N90-20365
Strategies for high efficiency operation of the E-beam excited atomic xenon laser using high-power and high-energy loading
[DE90-005196] 13 p1806 N90-20370
Electron beam induced damage in PECVD Si3N4 and SiO2 films on InP
[NASA-TM-102544] 13 p1810 N90-20393
Production rates for electron beams and swarms in nitrogen
[AD-A218145] 13 p1885 N90-20817
A new technique for guiding of electron beams
[DE90-008660] 13 p1886 N90-20824
Nonlinear plasma and beam physics in plasma wake-fields
[DE90-008812] 13 p1892 N90-20855
On storage rings for short wavelength FELs
[DE90-009059] 14 p1985 N90-21379
Proposal for FY86 Lawrence Livermore National Laboratory particle beam research
[DE90-007936] 14 p2026 N90-21617
PIC code modeling of spacecraft charging potential during electron beam injection into a background of neutral gas and plasma, part 1
[NASA-CR-186602] 15 p2059 N90-21792
Jupiter's drifting decametric bursts with the changing time scale
[DE90-618870] 15 p2192 N90-22517
Modified maleic anhydride copolymers as e-beam resists
[AD-A218470] 16 p2223 N90-22679
Forced scattering of electromagnetic waves on electron beam in periodically inhomogeneous plasma
[DE90-620705] 16 p2228 N90-22707
Measurements and simulation of controlled beamfront motion in the Laser Controlled Collective Accelerator
[DE90-009992] 16 p2240 N90-22780
Intense electron beam propagation across a magnetic field
[DE90-009993] 16 p2316 N90-23204
Foil focusing of electron beams
[AD-A219511] 16 p2317 N90-23208
Stability regimes in a rotating quadrupole focusing accelerator
[AD-A219513] 16 p2317 N90-23209
Composite curing: A new process
[REPT-892-430-114] 17 p2370 N90-23490
Long pulse narrowband XeCl laser studies
[AD-A219774] 17 p2409 N90-23724
The effects of wiggler errors on free electron laser performance
[AD-A220421] 17 p2409 N90-23725
Dose analysis of the model 112A Pulserad pulsed x ray generator by its CYLTRAN
[AD-A220372] 17 p2471 N90-24125
Molecular beam epitaxial growth of heterostructures to study quantum interference phenomena
[AD-A219442] 17 p2475 N90-24154
Dissociation phenomena in electron-beam sustained carbon dioxide lasers 18 p2560 N90-24610
The e-beam sustained CO2 laser amplifier
18 p2561 N90-24611
Performance of alumina-supported Pt catalysts in an electron-beam-sustained CO2 laser amplifier
18 p2561 N90-24613
RF control system development at CEBAF
[CEBAF-PR-89-026] 19 p2755 N90-25653
Status of the CEBAF injector
[CEBAF-PR-89-027] 19 p2755 N90-25655
Impedance and wakefields beyond cutoff
[CEBAF-PR-89-016] 19 p2756 N90-25663
Microstructures of superconducting YBa2Cu3O(7-x) thin films
[DE90-011976] 19 p2761 N90-25688
Solid rocket propellant initiation via particle beam heating
[AD-A221900] 21 p2969 N90-26878
Advanced optical diagnostics in hypersonic research
21 p2975 N90-26905
Background effects in ESDIAD measurements on Si(111)-(7x7)
[AD-A222242] 21 p3001 N90-27056
Free electron laser injection oscillator
[AD-D014180] 21 p3007 N90-27095
Self-lubricating surfaces by ion beam processing
[AD-A222489] 21 p3011 N90-27118
Stability regimes in a helical quadrupole focusing accelerator: Theory and simulation
[AD-A221755] 21 p3079 N90-27507
Digital beam position regulation of the superconducting accelerator at Darmstadt
[ETN-90-97293] 22 p3246 N90-28406
Radiation-curable prepreg composites
[DE90-629740] 23 p3301 N90-28674
Computer simulation of micro-triode performance
[DE90-014191] 23 p3320 N90-28774
UV-induced degradation of the Si-SiO2 interface: Applications to the point contact solar cell
[DE90-013843] 23 p3344 N90-28898
Characterization of electron flow in positive-polarity linear-induction accelerators
[DE90-014998] 23 p3394 N90-29177
Some novel sources of x ray beams: Channeling, transition and Cherenkov radiation
[DE90-014442] 23 p3395 N90-29181
Electron acoustic and magnetoacoustic modes in a magnetized beam plasma system
[DE90-627473] 23 p3398 N90-29199
Electron-beam fluorescence measurements in hypersonic flows 24 p3420 N90-29318
Electron beam for velocity determination
24 p3420 N90-29319
Microstructure of alpha-Al base matrix/SiC particulate composites
[DE90-014894] 24 p3444 N90-29449
Electrochemistry of metal surfaces
[AD-A224551] 24 p3445 N90-29458
Adhesion of silver films to ion-bombarded zirconia
[DE90-010088] 24 p3456 N90-29517
Long pulse diode experiments
[DE90-016218] 24 p3465 N90-29578

Establishment of a capability to measure optical transition radiation
[AD-A224094] 24 p3545 N90-30047
Anomalous decay of Langmuir turbulence. High power, high frequency radiation from beam-plasma interactions
[AD-A224282] 24 p3547 N90-30065

ELECTRON BOMBARDMENT
Secondary electron emission characteristics of molybdenum-masked, ion-textured OFHC copper
[NASA-TP-2967] 07 p0902 N90-15211
Electron beam generation by electron bombardment induced cathode emission
[AD-A218203] 13 p1798 N90-20318

ELECTRON BUNCHING
Bunch length in internal target mode
[NIKHEF-AMPS/89/04] 04 p0496 N90-12854
High repetition rate kickers for linear colliders
[CEBAF-PR-89-020] 19 p2756 N90-25661
Analytic study of the high-frequency impedance
[CEBAF-PR-89-014] 19 p2757 N90-25665

ELECTRON CAPTURE
Electron attachment and molecular fragmentation in laser-excited plasmas
[AD-A212098] 03 p0409 N90-12343
Multiple electron capture in close ion-atom collisions
[DE90-001541] 06 p0840 N90-14885
Defect control and denuded trap zones in the 3-5 semiconductors
[AD-A214099] 07 p1004 N90-15814
The electron momentum-transfer cross sections of tungsten, silicon, and silicon dioxide at energies from 0.1 to 10,000 eV
[DE90-009041] 12 p1712 N90-19833
Absolute pressure dependence of the second ionization level of EL2 in GaAs
[DE90-007761] 13 p1894 N90-20872
Atomic processes in high temperature plasmas
[DE90-008873] 14 p2028 N90-21632

ELECTRON COLLISIONS
U ELECTRON SCATTERING

ELECTRON COMPOUNDS
U INTERMETALLICS

ELECTRON CYCLOTRON HEATING
Microwave Tokamak Experiment (MTX) first year of operation and future plans
[DE90-000817] 06 p0846 N90-14920
Microwave Tokamak Experiment: An overview of the construction and checkout phase
[DE90-000834] 06 p0847 N90-14924
Review of quasi-optical gyrotron development
[AD-A213491] 07 p0933 N90-15402
Mechanical design of the inside launch system for electron cyclotron heating in D3-D
[DE90-003292] 07 p0995 N90-15751
Second harmonic electron cyclotron heating in low and over density plasmas in Heliotron DR
[DE90-719519] 08 p1125 N90-16515
Spectroscopic diagnostics of high temperature plasmas
[DE90-003912] 08 p1126 N90-16522
Microwave free-electron laser applications for electron cyclotron heating of plasmas
[DE90-005203] 10 p1431 N90-18257
Design considerations in achieving 1 MW CW operation with a whispering-gallery-mode gyrotron
[DE90-007283] 12 p1663 N90-19557
Applied plasma physics
[DE90-007932] 14 p2029 N90-21635
Activities report of the Institute for Plasma Research
[ETN-90-96467] 16 p2319 N90-23225
Microwave generation for magnetic fusion energy applications
[DE90-011042] 18 p2617 N90-24906
High average power CW FELS (Free Electron Laser) for application to plasma heating: Designs and experiments
[DE90-011085] 24 p3474 N90-29833

ELECTRON DENSITY (CONCENTRATION)
NT CARRIER DENSITY (SOLID STATE)
NT ELECTRON DENSITY PROFILES
NT IONOSPHERIC ELECTRON DENSITY
NT MAGNETOSPHERIC ELECTRON DENSITY
A diagnostic for determining the quality of single-reference electron correlation methods
02 p0272 N90-11554
TEC (Total Electron Content) models
[AD-A211553] 03 p0372 N90-12129
Stellarator transport theory
[DE89-016371] 03 p0406 N90-12328
Electron density modulation of catalytic metal centers by substituted aryl-isocyanide ligands
[AD-A212875] 04 p0473 N90-12708
Resonance cone diagnostics in the mid-latitude ionosphere 05 p0658 N90-13840
Background electrodynamics measured by EISCAT during the NEED campaign 05 p0660 N90-13851
Numerical simulation of laser radiation propagation in non-uniform absorbing medium. Geometrical optics approximation
[DE89-632014] 06 p0787 N90-14585
Electron theory of long wavelength concentration fluctuations in liquid metal alloys
[DE89-636213] 07 p0904 N90-15225
Microfluctuations of plasma density in a theta-pinch and spatial coherency of a probing laser beam
[DE90-603347] 07 p0996 N90-15760
Atomic processes in plasmas under ultra-intense laser irradiation
[DE90-003221] 08 p1126 N90-16521
Two-dimensional, long-pulse simulation of microwave-induced electron layer evolution in low-pressure air
[DE90-005180] 09 p1208 N90-17004
Development and application of diagnostic instrumentation for measurements of electron density and conductivity
[DE90-004076] 09 p1228 N90-17127
Two-dimensional calculation of sequential electron layer formation by crossed microwave beams in air at low pressure
[DE90-005254] 09 p1286 N90-17453
X ray spectra produced by NaF implosions
[AD-A215803] 10 p1429 N90-18243
Alfven wave stability in D III-D
[DE90-005555] 10 p1437 N90-18291
Effects of strong scattering on transionospheric propagation
[AD-A216708] 11 p1497 N90-18617
Quick, reliable estimates of high-power microwave fluences: The SNEAKY-2 program
[DE90-006347] 11 p1498 N90-18624
Theory for high gain, high power free electron lasers
[DE90-005548] 11 p1514 N90-18714
The rapid inward diffusion of cold ions in tokamaks and their effect on ion transport
[DE90-006863] 11 p1568 N90-19022
Computerized analysis of hydrogen plasma in a compact H(sup -) cusp source
[DE90-006881] 11 p1569 N90-19029
Two-dimensional, long-pulse computer calculation of microwave-induced electron layer formation in low-pressure air
[DE90-005994] 12 p1646 N90-19459
Ionospheric heating with oblique waves. Volume 1: Electron density perturbations
[AD-A216260] 12 p1690 N90-19709
Wetting of metallic carbides by non-reactive liquid metals
[AERE-M-3759] 13 p1775 N90-20185
Difference in electron thermal diffusivity and profile between interior and exterior of TFTR L-mode plasmas
[DE90-007479] 13 p1890 N90-20846
Particle transport in pellet fueled JET (Jet European Torus) plasmas
[DE90-008077] 13 p1891 N90-20851
SR90, strontium shaped-charge critical ionization velocity experiment
[NASA-CR-186501] 14 p2024 N90-21606
An extended diffusive model for calculating thermal diffusivity from single monopole tokamak heat pulse propagation
[DE90-007958] 14 p2029 N90-21637
Instabilities and vortex dynamics in shear flow of magnetized plasmas
[DE90-009448] 14 p2030 N90-21643
Plasma contactor research, 1989
[NASA-CR-185212] 15 p2168 N90-22389
HF propagation through actively modified ionospheres
[DE90-008931] 16 p2227 N90-22705
A posterior stochastic equation for quantum Brownian motion
[PREPRINT-715] 16 p2315 N90-23194
The large and small scale density structure in the solar corona 16 p2338 N90-23327
Infrared coronal line novae 16 p2339 N90-23328
Evaluation of space plasma data: Effects upon spacecraft materials and predictions of hazardous conditions; polar ARCS
[AD-A219509] 17 p2474 N90-24145
First-principles interatomic potentials for transition metals and their surfaces
[DE90-011233] 18 p2528 N90-24424
AFE dynamic effects in inhomogeneous plasmas
18 p2643 N90-25053
Preliminary results from the quadrupole probe on NEED-1
[FFI-89/7015] 19 p2714 N90-25446
U. radio emission from quiescent filaments
[NASA-CR-186538] 19 p2797 N90-25922
Quantitative spectroscopy of x ray laser plasmas in pulsed power devices
[AD-A221964] 21 p3078 N90-27501
Variation of D-region nitric-oxide density with solar activity and season at the dip equator
22 p3205 N90-28183
On the relation between the electron content of the ionospheric D-region, variations of the riometer absorption, and the H-component of the geomagnetic field
22 p3210 N90-28208
Influence of non-stationary field of magnetospheric convection on the D-region 22 p3210 N90-28209
The stability of the martensitic phases in Cu-Zn-Al at an electron concentration of 1.534
[DE90-628628] 23 p3311 N90-28727
Combined electron cyclotron ray tracing and transport code studies in the compact ignition tokamak
[DE90-014097] 23 p3396 N90-29189
PW Vul: A classical nova with nearly solar abundances
[NASA-CR-185080] 23 p3411 N90-29275
Alfven wave solitons and solar intermediate drift bursts
[MPE-PREPRINT-173] 23 p3413 N90-29287
The II-VI semiconductor superlattices
[AD-A223748] 24 p3553 N90-30101
Subpicosecond Raman study of hot electrons and hot phonons in GaAs
[DE90-015634] 24 p3553 N90-30106

ELECTRON DENSITY PROFILES
Vacuum ultraviolet backgrounds from space - ten years after
[AD-A211353] 03 p0435 N90-12493
Magnetically insulated electron flows in pulsed power systems
[AD-A212748] 04 p0549 N90-13196
An analytic/empirical model of the middle and low latitude ionosphere
[AD-A220004] 17 p2423 N90-23809
Ionospheric equivalent slab thickness and its modeling applications
[AD-A220105] 17 p2424 N90-23811
Ionospheric heating with oblique waves. Volume 2: Applications to high-frequency radio propagation
[AD-A223111] 21 p3025 N90-27202
Electron density profiles in the background of LF absorption during Forbush-decrease and PSE
22 p3208 N90-28199
On the relation between the electron content of the ionospheric D-region, variations of the riometer absorption, and the H-component of the geomagnetic field
22 p3210 N90-28208
Investigation of structure and transport processes in the high latitude ionospheric plasma using ground based and airborne digisondes
[AD-A224397] 24 p3491 N90-29727
A feasibility study for D-region equatorial ionosphere research using VLF radiowaves
[AD-A223685] 24 p3492 N90-29738

ELECTRON DIFFRACTION
Surface roughening of Ge(001) during 200 eV Xe ion bombardment and Ge molecular beam epitaxy
[DE90-000674] 07 p0998 N90-15769
ZELED analysis of aperiodicity and bond lengths in ceramic powders
[DE90-612932] 14 p1955 N90-21193
Retabulation of space group extinctions for electron diffraction
[DE90-612933] 14 p2031 N90-21648
Time-resolved surface structural study by picosecond reflection high-energy electron diffraction
[AD-A218417] 16 p2228 N90-22712
Joint services electronics program
[AD-A220815] 17 p2397 N90-23654
The EISI (Elemental and Interplanar Spacing Index) index: A search/match tool for electron diffraction phase analysis
[DE90-010832] 20 p2830 N90-26097
Scanning tunneling microscopy studies of chemisorbed layers on metal surfaces
[DE90-015623] 24 p3450 N90-29486

ELECTRON DIFFUSION
Anomalous particle diffusion through a magnetic picket fence
[INPE-4841-PRE/1470] 10 p1433 N90-18270
A posterior stochastic equation for quantum Brownian motion
[PREPRINT-715] 16 p2315 N90-23194
Critical behavior of the thermal power near the metal-insulator transition
[PREPRINT-714] 16 p2323 N90-23244
Estimation of minority carrier diffusion lengths in InP/GaAs solar cells
[NASA-TM-103213] 20 p2824 N90-26069
Quasistatic electron diffusion in quantum hadrodynamics
[ETN-90-97297] 22 p3255 N90-28432

ELECTRON DISTRIBUTION
NT ELECTRON DENSITY PROFILES

Physics of high energy photoconductive switches
[AD-A210341] 01 p0060 N90-10345
LABCEDE fluorescence investigations
[AD-A210678] 03 p0370 N90-12114
Development of a numerical solution to the time dependent kinetic equation 03 p0433 N90-12481
Electron heating and static sheath enhancement in front of energized RF antennas
[DE90-001334] 06 p0766 N90-14456
Anisotropy of electron distributions related to the anisotropy and polarization of the continuous emitted x rays 06 p0785 N90-14566
X ray spectrophotometric remote sensing of diffuse auroral ionization
[SD-TR-89-09] 08 p1139 N90-16599
Chemical activation of molecules by metals: Experimental studies of electron distributions and bonding
[DE90-005371] 10 p1428 N90-18238
A numerical solution of the time-dependent Boltzmann equation
[AD-A216397] 10 p1434 N90-18275
Photorefractive damage mechanisms in electro-optic materials
[AD-A219786] 17 p2476 N90-24157

ELECTRON EMISSION
NT FIELD EMISSION
NT PHOTOELECTRIC EMISSION
NT SECONDARY EMISSION
Plasma-anode electron gun research
[AD-A211547] 03 p0312 N90-11773
COSTEP: A comprehensive suprathermal and energetic particle analyzer for SOHO 04 p0568 N90-13314
Particle emission by oblique ion bombardment of gold
[ETN-90-95825] 12 p1711 N90-19827
Correlated electron processes in ion-atom collisions
[DE90-009477] 15 p2165 N90-22370
Plasma contactor research, 1989
[NASA-CR-185212] 15 p2168 N90-22389
Quantum effects in pair cascade models of AGN spectra 19 p2789 N90-25873
Computer simulation of micro-triode performance
[DE90-014191] 23 p3320 N90-28774
Unipolar arcing on the cathode surface of a high voltage diode
[AD-A224122] 23 p3322 N90-28787
Symmetrical layered thin film edge field-emitter-array and method for its production
[AD-D014594] 24 p3464 N90-29569

ELECTRON ENERGY
NT ELECTRON STATES
Physics of high energy photoconductive switches
[AD-A210341] 01 p0060 N90-10345
Global morphology of plasma bubbles in the low latitude ionosphere 02 p0241 N90-11369
Radiative shocks with electron thermal conduction 02 p0293 N90-11670
Calculations of soft x ray emission of REB-heated plasma
[IPPCZ-287] 03 p0407 N90-12329
Structures and energies for small borane compounds: One and two boron compounds
[AD-A212264] 04 p0471 N90-12701
Time evolution of the electron swarm energy distribution function
[AD-A212967] 04 p0557 N90-13247
Some remarks on the working principle of the rocketborne nose tip dc probes in the D-region of the ionosphere 05 p0658 N90-13839
Background electrodynamics measured by EISCAT during the NEED campaign 05 p0660 N90-13851
Towards ab initio calculation of electron energies in semiconductors
[ETN-90-96016] 05 p0704 N90-14121
Electronic energies for Neon dimer dication radiative charge transfer
[AD-A215817] 10 p1429 N90-18244
Numerical simulation of non-inductive current drive for tokamak plasmas with time-varying electron temperatures
[DE90-733144] 10 p1432 N90-18264
A numerical solution of the time-dependent Boltzmann equation
[AD-A216397] 10 p1434 N90-18275
Positron annihilation induced Auger electron spectroscopy 11 p1561 N90-18996
Understanding electronegative effects in core-level electron spectroscopies; application to the high temperature superconductors
[AD-A216728] 11 p1570 N90-19037
Electron stimulated O(-) desorption from O2 condensed on a rare-gas film: Evidence for an indirect Bounce trajectory
[AD-A216725] 12 p1622 N90-19322
Electron energy distributions and vibrational population distributions
[DE90-005550] 12 p1711 N90-19825
The electron momentum-transfer cross sections of tungsten, silicon, and silicon dioxide at energies from 0.1 to 10,000 eV
[DE90-009041] 12 p1712 N90-19833
Production rates for electron beams and swarms in nitrogen
[AD-A218145] 13 p1885 N90-20817
Difference in electron thermal diffusivity and profile between interior and exterior of TFTR L-mode plasmas
[DE90-007479] 13 p1890 N90-20846
Electronic properties of high-temperature superconductors
[AD-A217953] 13 p1898 N90-20892
Experimental study of population inversion and spectral line broadening in a plasma containing a mixture of high Z and low Z ions
[DE90-007552] 14 p2027 N90-21622
A simplified theoretical model for the laser-induced optogalvanic effect
[DE90-613121] 14 p2028 N90-21626
New calculations and measurements of the Coulomb cross-section for the production of direct electron pairs by high energy nuclei
[NASA-TM-101280] 15 p2165 N90-22371
Critical behavior of the thermal power near the metal-insulator transition
[PREPRINT-714] 16 p2323 N90-23244
Electronic structure and lubrication properties of MoS2: A qualitative molecular orbital approach
[AD-A220566] 17 p2380 N90-23557
High resolution electron energy loss spectroscopy studies of chemisorbed species on metal surfaces
[AD-A222272] 21 p2978 N90-26922
On diamond, graphitic and amorphous carbons in primitive extraterrestrial solar system materials 21 p3095 N90-27591
Electron energy spectrum and magnetic interactions in high-T(sub c) superconductors 22 p3149 N90-27857
Temperature-gradient instability induced by conducting end walls
[DE90-014334] 23 p3396 N90-29188
PW Vul: A classical nova with nearly solar abundances
[NASA-CR-185080] 23 p3411 N90-29275
Electrochemistry of metal surfaces
[AD-A224551] 24 p3445 N90-29458
Recent progress in electronic structure calculations for defects in metals
[DE90-016323] 24 p3452 N90-29494

ELECTRON FLUX
U ELECTRONS
U FLUX (RATE)

ELECTRON GAS
Dielectric spectroscopy of semiconductors
[AD-A211989] 04 p0559 N90-13255
Magnetic field generation by acoustic oscillations in solar atmosphere
[DE90-606054] 11 p1594 N90-19180
Exchange and correlation effects in the Visscher-Falicov model for metal intercalated graphite
[DE90-610553] 12 p1627 N90-19349
Quantum ballistic and adiabatic electron transport, studied with quantum point contacts
[ETN-90-97262] 20 p2889 N90-26440

ELECTRON GUNS
Stability requirements of RF linac-driven free-electron lasers
[DE89-016609] 02 p0227 N90-11303
Ion sources, electron guns and beam optics
[DE89-015526] 02 p0274 N90-11562
Plasma-anode electron gun research
[AD-A211547] 03 p0312 N90-11773
Switched power workshop: Introduction and summary
[DE90-000036] 03 p0342 N90-11952
A 2-MeV microwave thermionic gun
[DE89-015640] 04 p0494 N90-12844
Characteristics of an electron-beam rocket pellet accelerator
[DE90-001595] 06 p0729 N90-14252
Electric-gun studies of conductors in high magnetic fields and experiments in dynamic flux compression
[DE90-000815] 06 p0768 N90-14470
Electron-beam phase-only spatial light modulator for matched filtering
[AD-A215026] 09 p1282 N90-17431
Electron assisted glow discharges for conditioning fusion tokamak devices
[DE90-004104] 09 p1284 N90-17445
High voltage pickup plate
[LINO-1989-3] 12 p1654 N90-19510
The impedance of energy efficiency of a coaxial magnetized plasma source used for spheromak formation and sustainment
[DE90-003220] 13 p1889 N90-20841
Thermionic gun control system for the CEBAF injector
[CEBAF-PR-89-028] 19 p2755 N90-25654
Status of the CEBAF injector
[CEBAF-PR-89-027] 19 p2755 N90-25655
Control of nonlinear space-charge emittance growth
[DE90-014752] 23 p3410 N90-29270

ELECTRON IMPACT
Ion formation by electron impact
[AD-A211367] 03 p0403 N90-12305
CANOES 2: Dynamics of atmospheric infrared thermochemical excitation, volume 2
[AD-A213342] 05 p0667 N90-13898
CANOES 2: Dynamics of atmospheric infrared thermochemical excitation, volume 3
[AD-A213343] 05 p0667 N90-13899
CANOES 2: Dynamics of atmospheric infrared thermochemical excitation, volume 4
[AD-A213344] 05 p0667 N90-13900
Model-independent analysis of the Z line shape in e+e- annihilation
[PREPRINT-679] 05 p0698 N90-14089
Theoretical and material studies of thin-film electroluminescent devices
[NASA-CR-186104] 06 p0768 N90-14468
Modeling of runaway electron damage for the design of tokamak plasma facing components
[DE90-000847] 06 p0845 N90-14914
A high spatial resolution study of the thermospheric response to a discrete auroral arc
[NASA-TM-102904] 07 p0961 N90-15559
Electron-impact ionization and electron attachment cross sections of radicals important in transient gaseous discharges
[AD-A217510] 13 p1806 N90-20366
Helium transport in plasma edge regions 14 p2027 N90-21625
Electron-impact spectroscopy 20 p2949 N90-26779

ELECTRON INTERACTIONS
U ELECTRON SCATTERING

ELECTRON IONIZATION
U IONIZATION

ELECTRON IRRADIATION
Metal coordination polymers as potential high-energy lithographic resists
[AD-A216668] 11 p1490 N90-18574
Polymerization of composites
[REPT-892-430-102] 16 p2213 N90-22621
Polymerization of composite materials: A technique developed by Aerospatiale
[REPT-892-430-107] 16 p2213 N90-22623
Effects of large doses of high energy electrons on a YBa2Cu3O6(+)delta high temperature superconductor
[AD-A220423] 17 p2476 N90-24158

ELECTRON MICROSCOPES
A Scanning Photoelectron Microscope (SPEM) at the National Synchrotron Light Source (NSLS)
[DE90-001551] 06 p0780 N90-14537
Surface physics instrumentation
[AD-A220460] 17 p2373 N90-23512
A voltage contrast detector with double channel energy analyzer in a scanning electron microscope
[ISBN-90-6275-568-2] 19 p2694 N90-25330
Scanning electron microscopy by photovoltage contrast imaging
[AD-D014517] 19 p2760 N90-25684
Applications of PC-based digital imaging for storing microscopy images on optical disks
[DE90-011355] 19 p2763 N90-25701
DoD-University research instrumentation program, FY 1986/FY 1987
[AD-A222578] 20 p2859 N90-26263

ELECTRON MICROSCOPY
NT SCANNING TUNNELING MICROSCOPY
Atomic imaging and interfacial analysis
[DE89-015339] 01 p0130 N90-10748
Progress report on grain boundaries
[DE89-015541] 01 p0130 N90-10749
SEM (Scanning Electron Microscope) image analysis of grain growth in microwave-annealed alumina
[DE90-001606] 06 p0746 N90-14339
The design of a computer system for image simulation and image processing of high resolution electron micrographs
[DE90-000179] 06 p0829 N90-14820
High resolution electron microscopy of grain boundaries in nanophase palladium
[DE90-003823] 07 p1002 N90-15800
Direct determination of the morphology, structure and composition of cometary and interstellar ice analogs in the laboratory 08 p1141 N90-16612

Electron beam analysis of particulate cometary material 08 p1141 N90-16613
Mechanical and SEM analysis of artificial comet nucleus samples 08 p1148 N90-16650
Physical chemical characterization of the surface of carbon fibers: Test report
[REPT-49-740/F] 09 p1188 N90-16881
Novel approach for high resolution TEM (Transmission Electron Microscopy) studies of ceramic-ceramic interfaces
[DE90-005272] 09 p1199 N90-16945
Analytical electron microscopy of catalyst preparations
[DE90-008699] 13 p1773 N90-20173
High resolution transmission electron microscopy study of defect structures in mixed-phase YBaCuO
[DE90-007767] 13 p1894 N90-20873
Grain boundary precipitation in Ni3Al based alloys
[AERE-R-13362] 14 p1950 N90-21161
High voltage/high resolution studies of metal and semiconductor interfaces
[DE90-009065] 14 p2032 N90-21656
Simulated image maps for use in experimental high-resolution electron microscopy
[DE90-009176] 14 p2032 N90-21657
An analytical study of tribochemical phases with colloidal additives. Contributions made by energy filtering electron microscopy
[ECL-89-009] 17 p2374 N90-23521
Electron microscopy of interfaces in silicon carbide whisker-reinforced alumina composites
[DE90-010439] 18 p2519 N90-24386
Atomic structure of Ag/Ni interfaces
[DE90-010053] 18 p2618 N90-24914
Au-Ge-Ni-Ti ohmic contacts on gallium arsenide
[DE90-011064] 18 p2625 N90-24960
Atomic scale imaging of the structure and chemistry of semiconductor interfaces
[DE90-011321] 18 p2626 N90-24965
Scanning electron microscopy by photovoltage contrast imaging
[AD-D014517] 19 p2760 N90-25684
The application of HREELS to model catalysts: CO and C2H4 adsorption on Pt/Al2O3
[AD-A222744] 20 p2831 N90-26103
Structures and mechanical properties of near-beta titanium alloys Ti/10Fe2Al3 and Ti/10Cu3Al3
[ONERA-NT-1989-3] 20 p2835 N90-26123
Experiment K-6-06. Morphometric and EM analyses of tibial epiphyseal plates from Cosmos 1887 rats
20 p2893 N90-26460
Microstructural development in HSLA-100 steel weld metals
[AD-A222105] 21 p2982 N90-26944
The column-by-column compositional mapping at semiconductor interfaces using Z-contrast STEM
[DE90-012594] 21 p3081 N90-27516
Nature and origin of interstellar diamond from the Allende CV3 meteorite 21 p3092 N90-27581
Diamonds in detonation soot
21 p3094 N90-27585
Incoherent imaging of materials structure and composition by Z-contrast stem
[DE90-012789] 22 p3155 N90-27888
Technical activities 1989, Electron and Optical Physics Division
[PB90-207267] 23 p3415 N90-29296
Scanning tunneling microscopy studies of chemisorbed layers on metal surfaces
[DE90-015623] 24 p3450 N90-29486
Fractographic analysis of fatigue crack growth under two-blocks loading on 2024-T351 sheet specimens
[LR-628] 24 p3482 N90-29680
Effects of blocks of overloads and underloads on fatigue crack growth in 2024-T351 sheet specimens: Fractographic analysis and crack closure predictions
[LR-629] 24 p3482 N90-29681
Transmission electron microscopy study of ICB Al on Ge and Si(001) substrates
[DE90-015299] 24 p3553 N90-30103
High resolution transmission electron microscopy of aluminophosphates
[DE90-015632] 24 p3553 N90-30105
High resolution transmission electron microscopy of partial states of oxygen order in YBa2Cu3O(z)
[DE90-015637] 24 p3554 N90-30108

ELECTRON MOBILITY
Self-field-induced chaotic electron motion in free electron lasers
[DE90-001710] 06 p0790 N90-14598
Band-to-band transitions in poly (phenyl methyl silane)
[DE90-003575] 07 p0990 N90-15720
Magnetic mechanisms of high temperature superconductivity
[DE90-003625] 07 p1001 N90-15796
Electron scattering by native defects in uniformly and modulation doped semiconductor structures
[DE90-006084] 10 p1437 N90-18296
Anomalous transport in toroidal plasmas
[DE90-006549] 12 p1717 N90-19859
Direct implantation process development and characterization in advanced Hg(1)-(x)Cd(x) Te EPI layers
[AD-A219133] 16 p2324 N90-23252
Spectral structure and generation mechanism of ducted VLF whistler mode sideband waves
24 p3489 N90-29720

ELECTRON MULTIPLIERS
U PHOTOMULTIPLIER TUBES

ELECTRON OPTICS
Failure analysis handbook
[AD-A219747] 17 p2413 N90-23752

ELECTRON ORBITALS
Spin-orbit relaxation rates of Bi(6p(3)) 2D(3/2) following photolysis of Bi(CH3)3 at lambda = 193 nm
[AD-A211792] 03 p0402 N90-12303
General contraction of Gaussian basis sets. Part 2: Atomic natural orbitals and the calculation of atomic and molecular properties
[NASA-CR-186201] 08 p1119 N90-16482
The Hueckel model for small metal clusters. 4: Orbital properties and cohesive energies for model clusters of up to several hundred atoms
[AD-A216161] 10 p1354 N90-17852
Investigation of Schottky barriers
[AD-A218422] 16 p2323 N90-23247

ELECTRON OSCILLATIONS
Free electron laser injection oscillator
[AD-D014180] 21 p3007 N90-27095

ELECTRON PARAMAGNETIC RESONANCE
Magnetic resonance of polymers at surfaces
[AD-A212225] 04 p0480 N90-12753
Electron Spin Resonance (ESR) studies of returned comet nucleus samples 08 p1148 N90-16651
A new approach for the utilization of electron paramagnetic resonance and an investigation of copper oxide superconductors
[AD-A213833] 09 p1277 N90-17404
Spectroscopic techniques for the analysis of CdTe substrates used for the growth of HgCdTe
[AD-A214545] 09 p1288 N90-17466
Dynamics and stabilization of materials possessing high energy content
[AD-A216320] 11 p1489 N90-18570
Photorefractive damage mechanisms in electro-optic materials
[AD-A219786] 17 p2476 N90-24157
Molecular dynamics of physical aging processes in polymer glasses (experiment and theory)
[AD-A222848] 21 p2984 N90-26959
An EPR methodology for measuring the London penetration depth for the ceramic superconductors
22 p3143 N90-27828
An electron spin resonance study of adsorbed gases in ultrahigh vacuum
[ETN-90-97323] 24 p3447 N90-29469

ELECTRON PATHS
U ELECTRON TRAJECTORIES

ELECTRON PHONON INTERACTIONS
A model of the isotope effect of the oxide superconductor
[DE89-635907] 06 p0855 N90-14971
General many-body systems
[DE90-000685] 07 p0982 N90-15670
Tunneling spectroscopy and the electron-phonon interaction in Ba(1-x)K(x)BiO3
[DE90-002842] 07 p0999 N90-15776
Superconductivity in Ba(1-x)BiO3
[DE90-003781] 12 p1718 N90-19869
Modified tight-binding approximation and electron-phonon spectral function for transition metals
[DE90-614022] 14 p1950 N90-21166
Optical phonons and electronic properties in double heterostructures
[AD-A219436] 17 p2475 N90-24153
High resolution electron energy loss spectroscopy studies of chemisorbed species on metal surfaces
[AD-A222272] 21 p2978 N90-26922
Electron-phonon interaction and transport in artificially made semiconductor microstructures
[AD-A223061] 21 p3082 N90-27529
Coupled bipolarons and optical phonons as a model for high-T(sub c) superconductors
22 p3149 N90-27854

ELECTRON PLASMA
High-frequency instability of the sheath-plasma resonance
[NASA-CR-186127] 06 p0844 N90-14910
Modeling of runaway electron damage for the design of tokamak plasma facing components
[DE90-000847] 06 p0845 N90-14914
Possibility of low-frequency electron wave in a beam-plasma system
[DE90-601021] 09 p1284 N90-17441
Generation of axial and lateral magnetic fields in laser produced plasmas
[DE90-607470] 10 p1432 N90-18260
The dynamics of electrons in very intense lasers
[DE90-007246] 11 p1516 N90-18729
Difference in electron thermal diffusivity and profile between interior and exterior of TFTR L-mode plasmas
[DE90-007479] 13 p1890 N90-20846
Cyclotron maser and plasma wave growth in magnetic loops
[NASA-CR-179862] 15 p2170 N90-22402
Millimeter-wave generation via plasma three-wave mixing
[AD-A222010] 22 p3247 N90-28415
High average power CW FELS (Free Electron Laser) for application to plasma heating: Designs and experiments
[DE90-011085] 24 p3474 N90-29633

ELECTRON PRECIPITATION
A study of the spatial scales of discrete polar auroral arcs
[NASA-CR-186806] 19 p2714 N90-25444
A change of mesospheric ozone content under electron precipitation influence 22 p3207 N90-28191

ELECTRON PROBES
Calibration approach to electron probe microanalysis: A study with PWA-1480, a nickel base superalloy
[NASA-TM-102393] 06 p0745 N90-14335
Analysis of particulates of comet nucleus samples: Possible use of olivine as indicator phase
08 p1147 N90-16648

ELECTRON PUMPING
Charge pumping as a measurement method for the characterization of short channel MOSFETS: Review, development, and comparison of measurement process
[ETN-90-95726] 12 p1654 N90-19504
High efficiency flashlamp-pumped titanium: Sapphire laser
[AD-A217598] 13 p1806 N90-20367
Electron beam pumped XeF(C yields A) laser scaling
[AD-A220022] 17 p2409 N90-23728
Research studies on extreme ultraviolet and soft x ray lasers
[AD-A220271] 18 p2562 N90-24621
Towards a quantum pump of electric charges and currents
[AD-A221257] 18 p2607 N90-24851
New discharge pumping method for CO2 lasers
[AD-A220898] 20 p2866 N90-26307

ELECTRON RADIATION
NT BETA PARTICLES
NT ELECTRON BEAMS
NT RELATIVISTIC ELECTRON BEAMS
Assessment of bifacial silicon solar cells for space applications 10 p1342 N90-17779
Research of the interaction between hydrogen and deuterium with atomic eigen defects and dislocations in nickel and iron
[ETN-90-95380] 13 p1776 N90-20195
Stream field measurements of a half spheric cylinder by thin hypersonic stream with the electron radiation technique 18 p2490 N90-24232

ELECTRON RECOMBINATION
NT RADIATIVE RECOMBINATION
Charge pumping as a measurement method for the characterization of short channel MOSFETS: Review, development, and comparison of measurement process
[ETN-90-95726] 12 p1654 N90-19504
Recombination lines of C I and N II in the interstellar medium 15 p2182 N90-22466
New observations of interstellar organic molecules
21 p3094 N90-27587

ELECTRON RING ACCELERATORS
U STORAGE RINGS (PARTICLE ACCELERATORS)

ELECTRON RUNAWAY (PLASMA PHYSICS)
A study of runaway electron confinement and theory of neoclassical MHD turbulence
[DE89-016728] 02 p0277 N90-11584
Analytical theory of the Bunemann instability for electron runaway
[IPF-88-3] 16 p2319 N90-23224

ELECTRON SCATTERING
NT ELECTRON RUNAWAY (PLASMA PHYSICS)
Studies of ultrathin magnetic films and particle-surface interactions with spin-sensitive electron spectroscopies
[DE89-016741] 02 p0273 N90-11556
New theoretical approaches for studying electron collisions with small molecules
[DE89-017543] 02 p0273 N90-11558
Theoretical atomic physics for fusion
[DE89-017363] 02 p0274 N90-11563

Laser production of soft x rays by multiquantum processes and the excitation of atomic inner-shell states
[AD-A211372] 03 p0353 N90-12021
LABCEDE fluorescence investigations
[AD-A210678] 03 p0370 N90-12114
New developments in the ab initio treatment of low energy electron collisions with molecules
[DE89-015294] 03 p0402 N90-12299
Proof of the feasibility of coherent and incoherent schemes for pumping a gamma-ray laser
[AD-A212315] 04 p0506 N90-12921
Exotic Higgs production at e+e- colliders
[PREPRINT-671] 05 p0698 N90-14088
Elastic impurity scattering in double-barrier resonant tunneling structures
[AD-A212850] 05 p0702 N90-14110
Interaction of low-energy electrons and positrons with condensed matter: Stopping powers and inelastic mean free paths from optical data
[DE90-001001] 06 p0840 N90-14882
NIKHEF-K contributions to the 1989 Particle Accelerator Conference
[NIKHEF/AMPS/89/03] 06 p0841 N90-14891
Neutrino oscillations: An essay in honor of Felix Boehm
[DE90-003223] 08 p1121 N90-16491
Q-2 and A dependence of delta (1232) electroexcitation in nuclei
[DE90-003470] 08 p1121 N90-16492
Electron scattering by native defects in uniformly and modulation doped semiconductor structures
[DE90-006084] 10 p1437 N90-18296
Scattering of positrons and electrons by alkali atoms
11 p1556 N90-18959
Elastic scattering of e- and e+ from Rb and Cd
11 p1556 N90-18960
Ab initio R-matrix calculations of e+-molecule scattering 11 p1557 N90-18970
Positronium reflection and positronium beams
11 p1559 N90-18980
Low-energy scattering of electrons and positrons in liquids 11 p1559 N90-18981
Resonances in low-energy positron-alkali scattering
11 p1560 N90-18992
Background studies in gas ionizing x ray detectors
12 p1636 N90-19399
The 41st Annual Gaseous Electronics Conference
[AD-A214540] 12 p1715 N90-19851
Large basis space effects in electron scattering form factors of light nuclei
[DE90-613501] 14 p2025 N90-21609
Inelastic electron scattering from surfaces
[DE90-009365] 14 p2025 N90-21614
Thomson scattering in a magnetic field
14 p2040 N90-21699
Correlated electron processes in ion-atom collisions
[DE90-009477] 15 p2165 N90-22370
Transport properties of anisotropic superconductors
15 p2170 N90-22404
A study of the relation between grain boundary type and sensitisation in a partially-sensitised AISI 304 stainless steel using electron back-scattering patterns
[AERE-R-13327] 16 p2321 N90-23234
Spectral evolution of active galactic nuclei Penrose Compton scattering processes and gamma ray emission from Seyfert galaxies 16 p2337 N90-23317
Ensemble Monte Carlo simulation of electron transport in AlGaAs/GaAs heterostructures
[ISBN-90-9003048-4] 18 p2622 N90-24940
Electromigration in metallic microstructures
[AD-A221208] 18 p2622 N90-24942
Electron-impact spectroscopy
20 p2949 N90-26779
Support for the Forty-Second Annual Gaseous Electronics Conference
[AD-A222881] 21 p3073 N90-27473
New developments in double sided silicon strip detectors 22 p3179 N90-28039
Ground level atmospheric gamma ray flux measurements in the 1 to 6 MeV range
22 p3264 N90-28483
Medium energy nuclear physics research
[DE90-015852] 24 p3544 N90-30042
Subpicosecond Raman study of hot electrons and hot phonons in GaAs
[DE90-015634] 24 p3553 N90-30106

ELECTRON SOURCES

A compact X-ray free electron laser
[DE89-017236] 02 p0226 N90-11297
CANOES 2: Dynamics of atmospheric infrared thermochemical excitation, volume 4
[AD-A213344] 05 p0667 N90-13900
Theory of harmonic radiation using a single-electron source model
[DE90-002412] 06 p0791 N90-14606
Dose analysis of the model 112A Pulserad pulsed x ray generator by its CYLTRAN
[AD-A220372] 17 p2471 N90-24125
Photorefractive damage mechanisms in electro-optic materials
[AD-A219786] 17 p2476 N90-24157

ELECTRON SPECTROSCOPY

Studies of ultrathin magnetic films and particle-surface interactions with spin-sensitive electron spectroscopies
[DE89-016741] 02 p0273 N90-11556
Quantitative interpretation of auger lineshapes and electron/photon stimulated desorption
[AD-A211550] 03 p0324 N90-11842
FORTRAN program for x ray photoelectron spectroscopy data reformatting
[NASA-TP-2957] 03 p0409 N90-12348
Auger and x ray absorption studies of solid molecular oxygen
[DE90-003966] 07 p1006 N90-15825
An Auger electron spectroscopy study of surface-preparation contaminants
[NASA-TP-2972] 09 p1203 N90-16968
Spectroscopic evidence for carbon-carbon bonding in carbide layers on metals
[AD-A216726] 11 p1479 N90-18512
Extracting chemical information form Auger line shapes
[AD-A216729] 11 p1483 N90-18537
Dynamics and stabilization of materials possessing high energy content
[AD-A216320] 11 p1489 N90-18570
Positron annihilation induced Auger electron spectroscopy 11 p1561 N90-18996
Deep level transient spectroscopy in resistive layers
[DE90-008349] 13 p1772 N90-20169
Magnetron sputtered boron films and Ti/B multilayer structures
[DE90-009190] 14 p1948 N90-21153
Surface physics instrumentation
[AD-A220460] 17 p2373 N90-23512
The application of HREELS to model catalysts: CO and C2H4 adsorption on Pt/Al2O3
[AD-A222744] 20 p2831 N90-26103
Ni impurity effects on hydrogen surface chemistry and etching of Si(111)
[AD-A222083] 21 p2977 N90-26921
Face-specific interaction of MoS4(2-) with oriented crystals of (0001) CdX(X = Se, S)
[AD-A222405] 21 p3084 N90-27537
Nature and origin of interstellar diamond from the Allende CV3 meteorite 21 p3092 N90-27581
Use of electron spectroscopies in the tribological evaluation of diamond films
[DE90-014421] 23 p3334 N90-28848
Electrochemistry of metal surfaces
[AD-A224551] 24 p3445 N90-29458

ELECTRON SPIN

Factors affecting electron spin polarization in photosynthetic systems
[DE90-000196] 06 p0819 N90-14764
Aspects of Raman scattering
[AD-A213926] 07 p0992 N90-15736
Theoretical studies of spin-forbidden processes within the Breit-Pauli approximation
[AD-A217778] 13 p1885 N90-20815
Theory of a charged spinning particle in a gravitational and electromagnetic field
[NIKHEF-H/89-4] 15 p2165 N90-22373

ELECTRON SPIN RESONANCE

U ELECTRON PARAMAGNETIC RESONANCE

ELECTRON STATES

Forty-fourth symposium on molecular spectroscopy
[AD-A210752] 02 p0195 N90-11111
Quantitative interpretation of auger lineshapes and electron/photon stimulated desorption
[AD-A211550] 03 p0324 N90-11842
Spin-orbit relaxation rates of Bi(6p(3)) 2D(3/2) following photolysis of Bi(CH3)3 at lambda = 193 nm
[AD-A211792] 03 p0402 N90-12303
A search for the electric dipole of the electron
[DE90-001572] 08 p1120 N90-16484
Electronic properties of GaAs-(Al,Ga)As quasiperiodic
[AD-A214704] 09 p1289 N90-17472
Excited state lifetime measurements of ytterbium in indium phosphide
[AD-A215709] 09 p1291 N90-17483
Density of electronic states in a biased resonant tunneling structure
[AD-A215735] 09 p1291 N90-17486
Dynamics of electronically excited species in gaseous and condensed phase
[AD-A217696] 13 p1884 N90-20812
Electronically metastable molecules of high symmetry
[AD-A217768] 13 p1885 N90-20814
Positron trapping in semiconductors
[PB90-165606] 15 p2172 N90-22410
Reply to coupled S- and D-wave states in the thorium-doped heavy-fermion superconducting UBe13 by H. Pleiner and H. R. Brand
[AD-A220843] 17 p2477 N90-24164
Electronic state and superconductivity of YBa2Cu3-xO7-y (M=Al,Zn and Sn) systems
22 p3146 N90-27842
Research on the structural and electronic properties of defects in amorphous silicon
[DE90-000342] 23 p3312 N90-28730
Interface formation and percusory dynamics
[AD-A224128] 23 p3402 N90-29223
Theory of electronic states and formations energies of defect complexes, interstitial defects, and crystal growth in semiconductors
[AD-A224069] 24 p3551 N90-30093

ELECTRON TELESCOPES

U PARTICLE TELESCOPES

ELECTRON TEMPERATURE

U ELECTRON ENERGY

ELECTRON TRAJECTORIES

Analytical treatment of electron trajectory straightener issues in free-electron lasers
[DE90-002405] 06 p0790 N90-14603
Electron stimulated O(-) desorption from O2 condensed on a rare-gas film: Evidence for an indirect Bounce trajectory
[AD-A216725] 12 p1622 N90-19322

ELECTRON TRANSFER

NMR evidence for a planar arene intermediate in the electron-transfer induced eta 6 to eta 4 hapticity change of a rhodium arene complex
[AD-A210211] 01 p0033 N90-10177
Solvent relaxation in electron-transfer reactions: Comparisons between barrier-crossing dynamics in water and polar aprotic media
[AD-A210212] 01 p0040 N90-10220
A structural basis for electron transfer in bacterial photosynthesis
[DE89-015702] 01 p0120 N90-10687
Solvent dynamical effects in electron transfer: Predicted influences of electron coupling upon the rate-dielectric friction dependence
[AD-A210193] 01 p0120 N90-10690
Solvent effects on intervalence electron-transfer energies for biferrocene cations: Comparisons with molecular models of solvent reorganization
[AD-A210263] 01 p0120 N90-10691
Solvent dynamical effects in electron transfer: Evaluation of electronic matrix coupling elements for metallocene self-exchange reactions
[AD-A210306] 01 p0121 N90-10692
Controlling photoinduced electron transfer rates in donor-spacer-acceptor molecules by changing the electronic properties of the spacer
[DE89-015128] 01 p0128 N90-10735
Investigations of the influence of magnetically long range ordered phases on the electronic charge transport in metallic glasses
[ETN-89-94672] 02 p0202 N90-11155
Electron transfer reactions
[AD-A210711] 02 p0271 N90-11545
Iron (III) initiated autoxidation of 1,2,3,4-tetrahydrocarbazole: An example of electron transfer
[AD-A211857] 03 p0323 N90-11836
Mechanism of electrochemical activation of carbon electrodes: Role of graphite lattice defects
[AD-A211644] 03 p0325 N90-11845
Electron transport in heterojunction superlattices
[AD-A212366] 04 p0560 N90-13265
Reorganization free energy for electron transfers at liquid-liquid and dielectric semiconductor-liquid interfaces
[AD-A212985] 05 p0703 N90-14111
Factors affecting electron spin polarization in photosynthetic systems
[DE90-000196] 06 p0819 N90-14764
Multiple electron capture in close ion-atom collisions
[DE90-001541] 06 p0840 N90-14885
Charge transfer and bond lengths in YBa2Cu(sub 3-x)M(sub x)O(sub 6+y)
[DE90-002241] 06 p0854 N90-14966
Interfacial systems for photochemical energy conversion
[DE90-003181] 07 p0953 N90-15514
Photochemical solar energy conversion utilizing semiconductors localized in membrane mimetic systems
[DE90-003450] 07 p0953 N90-15515
Dynamics of electron transfer for a nonsuperexchange coherent mechanism, 1
[AD-A213450] 07 p0990 N90-15721
Dynamics of electron transfer for a non-superexchange coherent mechanisms. 2: Numerical calculations
[AD-A213511] 07 p0990 N90-15722
Intense REB (Relativistic Electron Beam) transport in a weakly magnetized plasma
[DE90-002978] 07 p0994 N90-15749

Photoinduced electron transfer processes in homogeneous and microheterogeneous solutions
[DE90-006048] 10 p1352 N90-17842
Research on monolithic millimeter-wave devices
[AD-A215771] 10 p1379 N90-17996
Interactions of molecules with surfaces
[DE90-005337] 10 p1428 N90-18237
Surface production of ions
[AD-A216470] 11 p1562 N90-19003
Studies of photochemically and electrochemically driven electron transport in zeolites
[DE90-007659] 12 p1624 N90-19335
Energy transfer and photochemistry in biomimetic solar conversion
[PB90-114562] 12 p1681 N90-19652
Linear free energy relations for multielectron transfer kinetics: A brief look at the Bronsted/Tafel analogy
[AD-A215078] 12 p1710 N90-19823
Ligand-centered electron-transfer redox processes for manganese, iron, and cobalt complexes in relation to selected catalytic systems
[AD-A217957] 13 p1773 N90-20177
Interactions of molecules with surfaces
[DE90-007555] 13 p1883 N90-20806
The development of a simulation program of the anode side for aluminum/air batteries
[PB90-165754] 14 p1970 N90-21286
Modeling and experimental studies of oxide covered metal surfaces
[DE90-009961] 17 p2375 N90-23525
Theoretical studies of electrons and electron transfer processes in fluids
[DE90-008414] 17 p2470 N90-24117
Status of the CEBAF injector
[CEBAF-PR-89-027] 19 p2755 N90-25655
Dynamical solvent effects on electron-transfer processes: Recent progress and perspectives
[AD-A222603] 20 p2830 N90-26101
Ionic atmosphere effects on the energetics of thermal and optical electron-exchange reactions: Application to ferrocenium-ferrocene self exchange
[AD-A222605] 20 p2889 N90-26441
All-optical photochromic spatial light modulators based on photoinduced electron transfer in rigid matrices
[NASA-CASE-NPO-17612-1-CU] 21 p3076 N90-27487
Fundamental electron transfer processes at the single crystal semiconductor/liquid interface
[DE90-011438] 21 p3079 N90-27508
Double layer effects on the enthalpy of activation of heterogeneous electron transfer reactions
[AD-A221934] 22 p3245 N90-28404
Correlated charge changing ion-atom collisions
[DE90-014662] 23 p3393 N90-29171

ELECTRON TRANSITIONS
Forty-fourth symposium on molecular spectroscopy
[AD-A210752] 02 p0195 N90-11111
LABCEDE fluorescence investigations
[AD-A210678] 03 p0370 N90-12114
Quantitative AES and XPS: Determination of the electron spectrometer transmission function and the detector sensitivity energy dependencies for the production of true electron emission spectra in AES and XPS
[NPL-DMA(A)-194] 05 p0623 N90-13634
Atomic structure and spectral perturbations in hot dense plasmas 06 p0785 N90-14567
Determination of hyperfine structures and Rydberg convergence limits of selected optical transitions in Nb-93 using resonance ionization spectroscopy
[PB90-110719] 08 p1122 N90-16498
Electronic energies for Neon dimer dication radiative charge transfer
[AD-A215817] 10 p1429 N90-18244
Threshold photodetachment spectroscopy of the I + HI transition state region
[AD-A218410] 16 p2260 N90-22883

ELECTRON TUBES
NT BACKWARD WAVE TUBES
NT CARCINOTRONS
NT CATHODE RAY TUBES
NT COLD CATHODE TUBES
NT CYCLOTRON RESONANCE DEVICES
NT GAS DISCHARGE TUBES
NT IGNITRONS
NT IMAGE DISSECTOR TUBES
NT IMAGE TUBES
NT KLYSTRONS
NT MAGNETRONS
NT MICROWAVE TUBES
NT PHOTOMULTIPLIER TUBES
NT THERMIONIC DIODES
NT THYRATRONS
NT TRAVELING WAVE TUBES
NT VACUUM TUBES
NT VIDICONS

Low resistivity electrodeless streamer tubes
[PREPRINT-685-89] 05 p0636 N90-13712
Heterodyne characterization of high-speed photomixers for the ultraviolet
[AD-A220914] 18 p2547 N90-24538

ELECTRON TUNNELING
Dwell time and average local speed in a resonant tunneling structure
[AD-A210566] 01 p0133 N90-10764
SIS (Superconductor-Insulator-Superconductor) mixer research
[AD-A211607] 03 p0414 N90-12375
Tunneling microscopy of superconductors and tunneling barriers
[AD-A212120] 04 p0559 N90-13257
Electron transport in heterojunction superlattices
[AD-A212368] 04 p0560 N90-13265
Research on GaAs quantum-coupled structures that can be used as electron devices
[AD-A214015] 07 p0924 N90-15350
Tunnelling effects on low energy fusion cross sections
[AD-A214010] 07 p0997 N90-15762
Tunneling spectroscopy and the electron-phonon interaction in Ba(1-x)K(x)BiO3
[DE90-002842] 07 p0999 N90-15776
Point defects and interfaces in insulating solids
[AD-A214668] 09 p1289 N90-17471
High quality tunnel junction devices using high T(sub c) superconductors
[AD-D014329] 10 p1435 N90-18283
Tunneling microscopy of submonolayer adsorbates on Si3
[AD-A216985] 12 p1719 N90-19876
Design and calibration of a vacuum compatible scanning tunneling microscope
[NASA-TM-102514] 13 p1804 N90-20353
Surface physics instrumentation
[AD-A220460] 17 p2373 N90-23512
Electrical transport through tunnel barriers and thin dielectric layers and physical properties of the high Tc oxide superconductors
[AD-A219860] 17 p2477 N90-24165
Quantum-confined hole states in double-barrier resonant tunneling structures
[AD-A221342] 18 p2623 N90-24946

ELECTRON-ION RECOMBINATION
NT RADIATIVE RECOMBINATION
Dielectronic excitation and recombination in crystal channels
[DE89-016864] 02 p0284 N90-11625
Ion and electron interactions at thermal and suprathermal energies
[AD-A216905] 12 p1622 N90-19323
Femtosecond studies of electron photodetachment of simple ions in liquid water: Solvation and geminate recombination dynamics
[AD-A218520] 16 p2215 N90-22634
A gas-phase high voltage electrical isolator with controlled breakdown
[RAE-TR-78030] 19 p2669 N90-25180

ELECTRON-POSITRON ANNIHILATION
U POSITRON ANNIHILATION

ELECTRON-POSITRON PAIRS
Search for resonances in positron-atom systems 11 p1560 N90-18991
Relativistic processes in active galactic nuclei 14 p2040 N90-21698
The behaviour of the L3 muon chambers in a magnetic field
[ETN-90-96920] 18 p2613 N90-24884
Reacceleration of pairs in compact sources 19 p2787 N90-25859
Electron positron pair winds and the Eddington limit 19 p2791 N90-25888
The origin of the continuum of AGN and the X ray background 19 p2795 N90-25912

ELECTRON-POSITRON PLASMAS
Ultrarelativistic envelope solitons in electron-positron plasma of the pulsar magnetosphere
[DE90-613289] 14 p1967 N90-21264
Nonlinear interaction of photons and phonons in electron-positron plasmas
[DE90-009341] 14 p2030 N90-21640

ELECTRONIC AIRCRAFT
Using simulation to determine a strategy for positively tracking a cruise missile by CMMCA
[AD-A220526] 17 p2362 N90-23448

ELECTRONIC AMPLIFIERS
U AMPLIFIERS

ELECTRONIC CONTROL
Independent Orbiter Assessment (IOA): Assessment of the body flap subsystem FMEA/CIL
[NASA-CR-185575] 02 p0172 N90-10968
Engine controls for the 1990's
[PNR90546] 03 p0308 N90-11748
Apparatus for cooling electronic components in aircraft
[AD-D014207] 05 p0579 N90-13373
Advanced detection, isolation, and accommodation of sensor failures in turbofan engines: Real-time microcomputer implementation
[NASA-TP-2925] 07 p0883 N90-15112
Magnetic coupled current sensing techniques for spacecraft power systems 10 p1335 N90-17725
Signal processing device to control microwave output
[AD-A216931] 11 p1502 N90-18648
The implementation and operation of a variable-response electronic throttle control system for a TF-104G aircraft
[NASA-TM-101696] 13 p1756 N90-20086
Electronic precipitator control
[NASA-CASE-LAR-13273-2] 13 p1798 N90-20320
Human centrifuge controller
[NAL-TM-SE-8901] 14 p1929 N90-21043
Analog electronic control differential transmitter
[AD-D014508] 19 p2685 N90-25272
Impact of end effector technology on telemanipulation performance 19 p2736 N90-25549
The application of intelligent process control to space based systems 21 p3041 N90-27282
Propulsion system-flight control integration and optimization: Flight evaluation and technology transition
[NASA-TM-4207] 23 p3278 N90-28551

ELECTRONIC COUNTERMEASURES
Network analyzer for nonstatic jamming
[AD-A210759] 02 p0212 N90-11216
Research on heating, instabilities, turbulence and RF emission from electric field dominated plasmas
[AD-A212122] 04 p0557 N90-13243
Development of a parallel link model for meteor burst communication
[AD-A215629] 09 p1208 N90-17001
Wideband S band transmitter
[AD-A217620] 13 p1794 N90-20295
Optimizing ECM techniques against monopulse acquisition and tracking radars
[AD-A220036] 17 p2393 N90-23629
Serrodyning by means of a digital phase shifter
[AD-A219593] 17 p2396 N90-23646
HF spread spectrum, an audit of the power requirements and LPI vulnerability 20 p2849 N90-26203
Studies of ECCM improvements for frequency-hopping CPFSK systems
[AD-A222995] 21 p2995 N90-27023

ELECTRONIC EQUIPMENT
NT AVALANCHE DIODES
NT BIPOLAR TRANSISTORS
NT CHARGE COUPLED DEVICES
NT CHARGE FLOW DEVICES
NT CHARGE INJECTION DEVICES
NT CMOS
NT DIODES
NT ELECTRONIC FILTERS
NT ELECTRONIC MODULES
NT ELECTRONIC PACKAGING
NT FIELD EFFECT TRANSISTORS
NT GALLIUM ARSENIDE LASERS
NT GUNN DIODES
NT HETEROJUNCTION DEVICES
NT HIGH ELECTRON MOBILITY TRANSISTORS
NT ITO (SEMICONDUCTORS)
NT JFET
NT JUNCTION DIODES
NT JUNCTION TRANSISTORS
NT LIGHT EMITTING DIODES
NT METAL OXIDE SEMICONDUCTORS
NT MIM (SEMICONDUCTORS)
NT MINIATURE ELECTRONIC EQUIPMENT
NT MIS (SEMICONDUCTORS)
NT MODFETS
NT MOM (SEMICONDUCTORS)
NT PHOTODIODES
NT PHOTOTRANSISTORS
NT PHOTOVOLTAIC CELLS
NT PLASMA DIODES
NT RUBY LASERS
NT SCHOTTKY DIODES
NT SEMICONDUCTOR DEVICES
NT SEMICONDUCTOR DIODES
NT SEMICONDUCTOR LASERS
NT SILICON CONTROLLED RECTIFIERS
NT SILICON TRANSISTORS
NT SIS (SUPERCONDUCTORS)
NT SOI (SEMICONDUCTORS)
NT SOLAR CELLS
NT SOLID STATE DEVICES
NT SOLID STATE LASERS
NT SOS (SEMICONDUCTORS)
NT SPACECRAFT ELECTRONIC EQUIPMENT
NT THERMIONIC DIODES
NT THERMISTORS

NT THYRISTORS
NT TRANSFERRED ELECTRON DEVICES
NT TRANSISTORS
NT VARACTOR DIODES
NT VARISTORS
NT YAG LASERS
Electronic encapsulation using foam with bonded metal covers for a filter pack
[DE89-014010] 01 p0048 N90-10276
Director, Operational Test and Evaluation report FY-88
[AD-A206784] 01 p0135 N90-10778
A comparison of fixed-base and driven-base modal testing of an electronics package
[DE89-016673] 02 p0217 N90-11240
HPW (High Power Microwave) testing of electronic components
[DE89-016682] 02 p0217 N90-11241
Electronic publishing: Guide to selection
[PB89-214753] 02 p0256 N90-11448
Numerical simulation of aeroplane response to a lightning injection
[ETN-89-95271] 03 p0303 N90-11716
Advanced light source master oscillator
[DE90-000123] 03 p0342 N90-11953
Design of scientific payloads and components
[AD-A211819] 03 p0351 N90-12005
Electronic warfare: Reliable equipment needed to test Air Force's electronic warfare systems
[AD-A212952] 05 p0632 N90-13687
Joint Services Electronics Program
[AD-A213015] 05 p0634 N90-13699
Conference Proceedings of the Human-Electronic Crew: Can They Work Together
[AD-A211871] 05 p0676 N90-13936
Modeling of power electronic systems with EMTP
[NASA-TM-102375] 05 p0695 N90-14060
Power factor controller study
[DE89-017655] 06 p0767 N90-14458
Fabrication of NBN based electronic devices with silicon barriers
[AD-D014230] 06 p0767 N90-14463
Human factors evaluation of electroluminescent display Number 1
[DE90-002231] 06 p0822 N90-14777
Design of a custom load cell for a precision assembly application
[DE90-004439] 07 p0923 N90-15340
Research on GaAs quantum-coupled structures that can be used as electron devices
[AD-A214015] 07 p0924 N90-15350
Technology of fast spark gaps
[AD-A214199] 07 p0925 N90-15353
Overview on radiation effects in electronics
[DE90-000841] 07 p0926 N90-15357
An electronic pressure profile display system for aeronautic test facilities
[NASA-TM-102478] 08 p1032 N90-15964
New electronic materials and CO2 reduction
[AD-A214679] 09 p1191 N90-16899
Intrinsically safe 5-V, 4-A rechargeable power supply
[PB90-103235] 09 p1209 N90-17006
A guide to quality assurance indicators for the defense electronics industry
[AD-A215630] 09 p1235 N90-17166
Temperature control and calibration issues in the growth, processing and characterization of electronic materials
10 p1365 N90-17914
Suggestions for designers of navy electronic equipment, 1989 edition, revision B
[AD-A215961] 10 p1380 N90-17998
RADC reliability engineer's TOOLKIT
[AD-A215977] 10 p1394 N90-18058
Reliability assessment using finite element techniques
[AD-A216907] 11 p1502 N90-18647
Preparation and characterization of alumina films prepared by a novel spray pyrolysis method
[AD-A217570] 12 p1625 N90-19339
Influence of the parameters: Charge order, sequence classification, partial sequential circuit, and process regularity of a working charge (Gaussian process) on the lifetime of a component made of 3.1354 T3 and 3.4377 T761
[ETN-90-95378] 12 p1653 N90-19503
Passivating layer for III-V semiconductor materials
[AD-D014321] 12 p1719 N90-19872
Computed tomography of electronics
[AD-A217976] 13 p1797 N90-20314
Environmental projects, volume 11. Environmental assessment: Addition to operations building, Mars site
[NASA-CR-186449] 14 p2003 N90-21479
The CAD/CAM product data standards: IGES/PDES (Initial Graphics Exchange Specification/Product Data Exchange Standards, the present and the future
[DE90-008803] 14 p2015 N90-21549
Pulse-width dependent radiation effects on electronic components
[AD-A219517] 17 p2395 N90-23643
Statistical design of MOS VLSI (Very Large Scale Integrated) circuits with designed experiments
[AD-A219654] 17 p2396 N90-23647
Novel numerical algorithms for sensing, discrimination, and control
[AD-A220805] 17 p2444 N90-23929
Electronics principles inventory, Sheppard Technical Training Center
[AD-A219935] 18 p2547 N90-24534
Facilities for improving evaluations of electromagnetic susceptibilities of weapon systems and electronic equipment
[PB90-155862] 21 p2961 N90-26837
Approaches to orthogonally fused conducting polymers for molecular electronics
[AD-A222546] 22 p3159 N90-27915
Control of a Cossor CSP1250 ionospheric simulator in an automated HF test bed
[AD-A223446] 24 p3461 N90-29549
Proceedings of the 14th Annual Electronics Manufacturing Seminar
[AD-A224276] 24 p3463 N90-29563
Reliability study of TWT output RF window
[AD-A223688] 24 p3465 N90-29574
Transport of nonneutral plasmas
[AD-A223457] 24 p3549 N90-30077
ELECTRONIC EQUIPMENT TESTS
Consumer electronics testing to fast-rise EMP (Electromagnetic Pulse) VEMPS (Vertical Electromagnetic Pulse Simulator) 2 development
[AD-A210505] 01 p0057 N90-10323
A comparison of fixed-base and driven-base modal testing of an electronics package
[DE89-016673] 02 p0217 N90-11240
Built-in generation for CMOS circuits
[IMAG-RR-736-I] 04 p0496 N90-12855
Built in test of folded PLAs
[IMAG-RR-758-I] 08 p1061 N90-16134
Remote use of an Electron Beam Tester (EBT)
[IMAG-RR-760-I] 08 p1077 N90-16233
SINA: A test system for proximity fuses
[FEL-1989-101] 12 p1653 N90-19498
PVDF contact probes
[VTT-RR-623] 20 p2857 N90-26253
Facilities for improving evaluations of electromagnetic susceptibilities of weapon systems and electronic equipment
[PB90-155862] 21 p2961 N90-26837
ELECTRONIC FILTERS
Electronic encapsulation using foam with bonded metal covers for a filter pack
[DE89-014010] 01 p0048 N90-10276
ELECTRONIC LEVELS
U ELECTRON ENERGY
U ENERGY LEVELS
ELECTRONIC MAIL
A formatting style for typesetting and distributing draft international standards
[NPL-DITC-143/89] 04 p0530 N90-13059
Internet protocol handbook. Volume 4: The Domain Name System (DNS) handbook
[AD-A214698] 09 p1296 N90-17512
Technologies for electronic transfer of information: The present state and trends in Europe
15 p2177 N90-22441
Technology for electronic transfer of information: The present and future in North America
15 p2177 N90-22442
Innovations in telecommunications networks
15 p2178 N90-22444
Megatendances 15 p2178 N90-22445
Document delivery via ISDN or satellite networks
15 p2178 N90-22446
Electronic mail systems 15 p2179 N90-22451
Privacy-enhanced electronic mail
[PCS-TR90-150-REV-1] 19 p2683 N90-25261
Communications and media services
22 p3258 N90-28449
ELECTRONIC MODULES
Reusable navigation module 09 p1165 N90-16742
A microprocessor controlled strain gauge calibration module
[AR-005-579] 23 p3329 N90-28821
High frequency bundle protection
[DIGEL-1990-1] 24 p3466 N90-29582
ELECTRONIC PACKAGING
A comparison of fixed-base and driven-base modal testing of an electronics package
[DE89-016673] 02 p0217 N90-11240
MM and T for VHSIC multichip packages
[AD-A213259] 05 p0635 N90-13703
Moisture control in sealed electronic packages
[DE90-008136] 13 p1771 N90-20166
The development of ultraviolet-ozone cleaning as a production process in the packaging of integrated circuits
[DE90-007960] 14 p1959 N90-21220
Severe shock and vibration environments for electronic components
[DE90-007686] 15 p2117 N90-22113
Dynamic response of a complex encapsulated electronic assembly subjected to a severe shock environment
[DE90-007689] 15 p2118 N90-22114
Materials for high-density electronic packaging and interconnection
[NASA-CR-186934] 21 p3000 N90-27049
ELECTRONIC SIGNAL MEASUREMENT
U SIGNAL MEASUREMENT
ELECTRONIC SPECTRA
Quantitative interpretation of auger lineshapes and electron/photon stimulated desorption
[AD-A211550] 03 p0324 N90-11842
Ion formation by electron impact
[AD-A211367] 03 p0403 N90-12305
CANOES 2: Dynamics of atmospheric infrared thermochemical excitation, volume 3
[AD-A213343] 05 p0667 N90-13899
CANOES 2: Dynamics of atmospheric infrared thermochemical excitation, volume 4
[AD-A213344] 05 p0667 N90-13900
The production and spectroscopy of molecular ions isolated in solid neon
[AD-A213723] 07 p0895 N90-15174
Support for the 16th International Conference on the Physics of Electronic and Atomic Collisions
[AD-A218567] 16 p2315 N90-23200
Electronic and structural properties of Si10 cluster
[AD-A222429] 21 p3074 N90-27478
ELECTRONIC STRUCTURE
U ATOMIC STRUCTURE
ELECTRONIC SWITCHES
U SWITCHING CIRCUITS
ELECTRONIC WARFARE
Preliminary report on the feasibility of high power Electronic Warfare (EW) using explosive energy sources
[MRL-TR-89-3] 04 p0483 N90-12775
Electronic warfare: Reliable equipment needed to test Air Force's electronic warfare systems
[AD-A212952] 05 p0632 N90-13687
Event-train restoration via backpropagation neural networks
[AD-A216308] 10 p1420 N90-18189
Application of high-temperature superconducting thin-film devices to electro-optical and electronic warfare systems
[AD-A218805] 16 p2323 N90-23249
Electronic warfare technology: Trends and visions
[AD-A223034] 20 p2856 N90-26246
Overview of requirements and networks for voice communications and speech processing
21 p2992 N90-27007
High temperature superconductivity applications for electronic warfare and microwave systems
[AD-A222972] 21 p3082 N90-27528
ELECTRONS
NT CONDUCTION ELECTRONS
NT FREE ELECTRONS
NT HIGH ENERGY ELECTRONS
NT HOT ELECTRONS
NT PHOTOELECTRONS
NT PI-ELECTRONS
NT POLARONS
NT RELATIVISTIC ELECTRON BEAMS
Solvent dynamical effects in electron transfer: Predicted influences of electron coupling upon the rate-dielectric friction dependence
[AD-A210193] 01 p0120 N90-10690
Auxiliary-field transformations for repulsive potentials: A physical approach
[DE89-016677] 02 p0214 N90-11223
Observations of ionosphere/magnetosphere interactions from the Dynamics Explorer satellites
02 p0242 N90-11376
ANTHEM simulation of the early time magnetic field penetration of the plasma surrounding a high density Z-pinch
[DE89-016980] 02 p0277 N90-11585
Passage of ultrarelativistic electrons through real crystals
[DE89-618624] 02 p0282 N90-11613
Quantitative interpretation of auger lineshapes and electron/photon stimulated desorption
[AD-A211550] 03 p0324 N90-11842
Electron-positron momentum distribution measurements of high-T(sub c) superconductors and related systems
[DE89-017538] 03 p0411 N90-12358
Minimal total cross section for e(+)e(-) yields W(+)W(-)
[NIKHEF-H/88-12] 04 p0553 N90-13222

Local pairing and antiferromagnetism in high-T sub c superconductors
[AD-A213004] 05 p0703 N90-14113
A diagnostic for determining the quality of single-reference electron correlation methods
[NASA-TM-101929] 06 p0838 N90-14874
Interaction of low-energy electrons and positrons with condensed matter: Stopping powers and inelastic mean free paths from optical data
[DE90-001001] 06 p0840 N90-14882
Physical process in MPD plasmas
[AD-A213679] 07 p0896 N90-15761
A search for the electric dipole of the electron
[DE90-001572] 08 p1120 N90-16484
Electron beam induced oxygen in YBa2Cu3O(7-x) superconductors
[DE90-004839] 08 p1133 N90-16565
The effect of electric field on attachment of electrons to solutes in liquid argon
[DE90-003969] 11 p1482 N90-18529
Lower limits on the absolute dissociative electron attachment cross section from O2 condensed on rare-gas films
[AD-A216727] 11 p1483 N90-18536
Strongly coupled one-dimensional system and the polymer
[AD-A216330] 11 p1489 N90-18571
Identification and solution of a charging problem in a high-altitude detector
[DE90-008637] 12 p1616 N90-19296
Effect of electron-excitation on radiation damage in ion-irradiated FCC metals
[DE90-719537] 12 p1626 N90-19344
Causality of plasma permittivity with loss and restoring terms
[NASA-TM-101671] 12 p1645 N90-19453
Preparation and properties of the system Cu(x)Pd(1-x)O (0 less than or equal to x less than or equal to 0.175)
[AD-A217567] 12 p1723 N90-19901
Energy transfer between electrons and ions in collision cascades in solids
[AERE-R-13662] 13 p1883 N90-20801
Electronically metastable molecules of high symmetry
[AD-A217768] 13 p1885 N90-20814
Modified tight-binding approximation and electron-phonon spectral function for transition metals
[DE90-614022] 14 p1950 N90-21166
Polarization: Effects on second harmonic power in light scattering by free electrons
[DE90-612842] 14 p2025 N90-21608
Large basis space effects in electron scattering form factors of light nuclei
[DE90-613501] 14 p2025 N90-21609
Langmuir wave interaction with ion acoustic wave
[DE90-615407] 14 p2027 N90-21624
MHD modes driven by anomalous electron viscosity and their role in fast sawtooth crashes
[DE90-009311] 14 p2029 N90-21639
High energy phenomena during solar flares
[INPE-4961-TDL/390] 14 p2043 N90-21713
A balloon measurement of the isotopic composition of galactic cosmic ray iron 14 p2043 N90-21717
Gas dynamic theory of flight of fast electron flux in plasma
[DE90-618767] 16 p2319 N90-23220
Theoretical studies of electrons and electron transfer processes in fluids
[DE90-008414] 17 p2470 N90-24117
Electronic and ionic transport in processable conducting polymers
[AD-A221045] 18 p2530 N90-24436
Adlayer physics
[AD-A221064] 19 p2673 N90-25203
The charged particle radiation environment for AXAF
[NASA-TM-100405] 20 p2942 N90-26741
Dissociative recombination of molecular ions with electrons 20 p2946 N90-26767
Research on optogalvanic effects
[AD-A221512] 21 p3071 N90-27463
Slow positron beam generator for lifetime studies
[NASA-CASE-LAR-14250-1-SB] 21 p3073 N90-27472
Symmetrical layered thin film edge field-emitter-array and method for its production
[AD-D014594] 24 p3464 N90-29569
New real space correlated-basis-functions approach for the electron correlations of the semiconductor inversion layer
[DE90-627315] 24 p3551 N90-30090

ELECTROPHORESIS
Combined capillary electrophoresis and electrospray ionization mass spectrometry
[DE90-001903] 06 p0743 N90-14322
Capillary electrophoresis ionization-mass spectrometry and tandem mass spectrometry
[DE90-002664] 07 p0892 N90-15158
Fluorescence and elastic scattering from laser dye-filled capillaries
[AD-A217026] 11 p1484 N90-18540
Research in biological separations and cell culture
[NASA-CR-172060] 15 p2135 N90-22202
Suitability of electrodeposition processes for high temperature superconductors
[IAR-89-22] 19 p2760 N90-25685

ELECTROPHYSICS
NT ELECTRO-OPTICS
NT MOLECULAR ELECTRONICS
Physics and materials science of high temperature superconductors
[AD-A211246] 02 p0283 N90-11619
The 41st Annual Gaseous Electronics Conference
[AD-A214540] 12 p1715 N90-19851
Basic research in electronics (JSEP)
[AD-A219931] 17 p2398 N90-23661

ELECTROPHYSIOLOGY
Electroporation: Theory of basic mechanisms
[AD-A210196] 01 p0091 N90-10520
Extrathalamic modulation of cortical function
[AD-A211044] 01 p0094 N90-10535
Seminars of Applied Physics, Materials Physics and Biomedical Engineering, 1989
[PB89-218572] 04 p0548 N90-13192
Laser retinal effects: Electrophysiological determination in visual cortical cells of monkeys and cats
[AD-A218937] 16 p2261 N90-22888
Brain stem evoked responses in altered G environments
[AD-A220097] 17 p2435 N90-23874

ELECTROPLATING
Micromechanisms of surface friction in zinc electrogalvanized steel sheets
[DE89-011819] 01 p0077 N90-10440
Electrolitic deposited ohmic contacts on III-V compound semiconductors: A review
[PB89-217400] 03 p0410 N90-12350
Benefits from combining electroplating and physical vapor deposition technologies
[DE90-002700] 07 p0917 N90-15301
Electroplating simulation
[DE90-003683] 08 p1054 N90-16091
The substitution of IVD (Ion Vapor Deposition) aluminum for cadmium
[AD-A215633] 09 p1195 N90-16921
Reduction of 50 micron thick solar cell weight by selective back contact silver plating 10 p1342 N90-17778
Plating nickel-63 on copper coupons
[DE90-005023] 10 p1356 N90-17862
Surface modification of steels and aluminum alloys to control corrosion and hydrogen embrittlement. Part 1: Chemical methods
[AD-A216272] 10 p1356 N90-17866

ELECTROPOLISHING
A feasibility study of hydrogen dosage estimation in screw threads submitted to surface electrolytic treatment
[CETIM-110110] 04 p0476 N90-12730
An Auger electron spectroscopy study of surface-preparation contaminants
[NASA-TP-2972] 09 p1203 N90-16968
Relationship between microstructure, spinodal-like decomposition and selective electropolishing of irradiated invar-type alloys
[DE90-015293] 24 p3450 N90-29484

ELECTRORHEOLOGICAL FLUIDS
US Army Research Office Workshop on Smart Materials, Structures and Mathematical Issues proceedings
[AD-A218528] 17 p2468 N90-24110

ELECTROSEISMIC EFFECT
U ELECTRIC CURRENT
U SEISMIC WAVES

ELECTROSTATIC BONDING
Direct glassing of silicon solar cells 10 p1341 N90-17769
A concept of a pilot production plant for directly glassed silicon 10 p1341 N90-17770

ELECTROSTATIC CHARGE
Simulation of the EMP (Electromagnetic Pulse) from ESD (Electrostatic Discharge)
[DE89-014484] 03 p0337 N90-11918
The physics of double layers and their role in astrophysics
[TRITA-EPP-89-03] 03 p0421 N90-12421
RF and dc desensitized electroexplosive device
[AD-D014206] 04 p0497 N90-12862
Workshop on ESD (Electrostatic Discharge) Ignition of Composite Solid Propellants
[AD-A218599] 17 p2382 N90-23569
Hazards protection for space suits and spacecraft
[NASA-CASE-MSC-21366-1] 19 p2725 N90-25498
Spacecraft charging effects
[RAE-TM-SPACE-375] 23 p3287 N90-28594

ELECTROSTATIC EROSION
U SPARK MACHINING

ELECTROSTATIC FIELDS
U ELECTRIC FIELDS

ELECTROSTATIC PLASMA
U PLASMAS (PHYSICS)

ELECTROSTATIC PRECIPITATORS
Ambient flow studies and particulate collection measurements: A laminar flow, reduced entrainment electrostatic precipitator
[DE90-001457] 08 p1063 N90-16149

ELECTROSTATIC PROBES
PISCES program plasma-surface interactions research
[DE89-015622] 02 p0276 N90-11578
Some remarks on the working principle of the rocketborne nose tip dc probes in the D-region of the ionosphere 05 p0658 N90-13839
Two possible configurations for the top-hat electrostatic analyzer: A numerical study
[IFSI-88-18] 08 p1077 N90-16229
CIS-2 analyzer derivation of hardware parameters
[IFSI-89-13] 08 p1077 N90-16230
BEAR electrostatic analyzer: Flight results
[DE90-006511] 11 p1498 N90-18625
Computerized analysis of hydrogen plasma in a compact H(sup -) cusp source
[DE90-006881] 11 p1569 N90-19029
Ion and electron interactions at thermal and suprathermal energies
[AD-A216905] 12 p1622 N90-19323

ELECTROSTATIC PROPULSION
NT ION PROPULSION

ELECTROSTATIC WAVES
Low frequency electrostatic waves observed in the vicinity of an auroral arc 02 p0243 N90-11378
Observations of electrostatic hydrogen cyclotron waves and electric field fluctuations near one Hz in auroral acceleration regions 05 p0658 N90-13842
Langmuir wave interaction with ion-sound one. Part 1: Stochastic effects
[DE90-603368] 08 p1118 N90-16474
On condensation driven by electrostatic interactions in macroionic solutions
[DE89-636072] 08 p1120 N90-16487
Nonlinear interaction of electrostatic waves at a narrow inhomogeneous layer of a warm magnetoactive plasma
[DE90-610624] 12 p1717 N90-19857
Langmuir wave interaction with ion acoustic wave
[DE90-615407] 14 p2027 N90-21624
Anomalous decay of Langmuir turbulence. High power, high frequency radiation from beam-plasma interaactions
[AD-A224282] 24 p3547 N90-30065

ELECTROSTATICS
Electrostatically suspended rotor for angular encoder
[NASA-CASE-MFS-28294-1] 01 p0054 N90-10310
New electrodynamic and electrostatic models with applications to antenna theory, superconductor slots, and lasers 01 p0055 N90-10316
A severe human ESD (Electrostatic Discharge) model for safety and high reliability system qualification testing
[DE89-016177] 02 p0216 N90-11233
Empirical models of convection electric fields and electrostatic potential at high latitude from EISCAT observations: Preliminary results 02 p0243 N90-11377
Electrostatic turbulence in the high latitude ionosphere 02 p0246 N90-11392
Molecular dynamics study of the primitive model of 1-3 electrolyte studies
[AD-A211653] 03 p0325 N90-11846
Resistive block methods for electrostatic field solutions with internal elements
[DE89-017535] 03 p0337 N90-11920
Dynamics Explorer-1 satellite study of electrostatic ion cyclotron waves 05 p0702 N90-14105
A numerical model for the axisymmetric equilibrium shape of drops in uniform motion: Effects of external flow, electric field and surface charge 07 p0874 N90-15071
Oblique ionospheric heating and effects on radio propagation
[AD-A214756] 09 p1205 N90-16983
Large-diameter geostationary millimeter wavelength antenna concept 12 p1609 N90-19254
The calculation of hydrogen-bonding properties
[DE90-007534] 13 p1772 N90-20168
The GRADIO spaceborne gravity gradiometer: Development and accommodation 13 p1840 N90-20560
The impedance of energy efficiency of a coaxial magnetized plasma source used for spheromak formation and sustainment
[DE90-003220] 13 p1889 N90-20841
Enhanced pinch effect due to electrostatic potential
[DE90-007088] 13 p1890 N90-20844

Radon concentration over the Brazilian Amazon Basin during the wet season (Belem-Manaus GTE-ABLE-2B flight of April 24, 1987)
[INPE-4892-PRE/1493] 14 p2004 N90-21486
Once more about the sizes of fast-moving objects
[DE90-615204] 14 p2022 N90-21592
XPS studies of doped polypyrrole films
[AD-A219424] 17 p2379 N90-23550
Transient pulse monitor
[AD-A220353] 18 p2508 N90-24335
Relativistic klystron amplifiers driven by modulated intense relativistic electron beams
[AD-A221075] 18 p2607 N90-24849
LEO high voltage solar array arcing response model, continuation 5
[NASA-CR-186505] 19 p2709 N90-25418
Field-induced surface chemistry of NO
[AD-A223007] 21 p2977 N90-26915
Silicon containing electroconductive polymers and structures made therefrom
[NASA-CASE-NPO-17826-1-CU] 21 p2983 N90-26952
Computerized simulation of phenomena in plasma via particles
[INPE-4595-RPE/569] 23 p3397 N90-29194
Electron acoustic and magnetoacoustic modes in a magnetized beam plasma system
[DE90-627473] 23 p3398 N90-29199

ELECTROSTRICTION
Piezoelectric and electrostrictive materials for transducer applications, volume 1
[AD-A223560] 24 p3480 N90-29668
Piezoelectric and electrostrictive materials for transducer applications, volume 2
[AD-A223561] 24 p3480 N90-29669

ELECTROTHERMAL ENGINES
NT ARC JET ENGINES
NT PLASMA ENGINES
NT RESISTOJET ENGINES
Transport properties of plasmas in microwave electrothermal thrusters
[AD-A219408] 16 p2320 N90-23228

ELEMENT ABUNDANCE
U ABUNDANCE

ELEMENTARY EXCITATIONS
NT EXCITONS
NT MAGNONS
NT PHONONS
NT PLASMONS
NT POLARONS
Transport properties of anisotropic superconductors 15 p2170 N90-22404
Electronic theory of solids, surfaces, interfaces, and clusters 16 p2320 N90-23230

ELEMENTARY PARTICLE INTERACTIONS
NT ELECTRON CAPTURE
NT HIGH ENERGY INTERACTIONS
NT MESON-NUCLEON INTERACTIONS
NT NUCLEON-NUCLEON INTERACTIONS
NT STRONG INTERACTIONS (FIELD THEORY)
NT WEAK ENERGY INTERACTIONS
NT WEAK INTERACTIONS (FIELD THEORY)
Exclusive production of p, p-, pi, and pi- in photon photon collisions
[NIKHEF-H/89-9] 15 p2165 N90-22376

ELEMENTARY PARTICLES
NT ALPHA PARTICLES
NT ANTINEUTRINOS
NT ANTINUCLEONS
NT ANTIPARTICLES
NT ANTIPROTONS
NT BARYONS
NT BETA PARTICLES
NT BOSONS
NT COLD NEUTRONS
NT CONDUCTION ELECTRONS
NT DEUTERONS
NT ELECTRON-POSITRON PAIRS
NT ELECTRONS
NT ETA-MESONS
NT FAST NEUTRONS
NT FERMIONS
NT FREE ELECTRONS
NT GLUONS
NT GRAVITONS
NT HADRONS
NT HIGH ENERGY ELECTRONS
NT HOT ELECTRONS
NT HYPERONS
NT LEPTONS
NT MESONS
NT MUONS
NT NEUTRINOS
NT NEUTRONS
NT NUCLEONS
NT PHOTOELECTRONS
NT PHOTONEUTRONS
NT PHOTONS
NT PI-ELECTRONS
NT PIONS
NT POLARONS
NT POSITRONS
NT PROTONS
NT QUARKS
NT RECOIL PROTONS
NT SOLAR NEUTRINOS
NT SOLAR NEUTRONS
NT SOLAR PROTONS
Twistons
[RSRE-MEMO-4234] 04 p0562 N90-13275
Nuclear physics and cosmology
[NASA-CR-186166] 05 p0713 N90-14167
Studies of elementary particles: Proposal
[DE90-001120] 06 p0839 N90-14879
Possible measurement of the gravitational acceleration of molecules, atoms, nuclei, elementary particles, and antiparticles
[DE90-719559] 08 p1121 N90-16490
Elementary particles and cosmology
[DE90-610648] 11 p1591 N90-19177
Current experiments in elementary particle physics
[DE90-008062] 14 p2024 N90-21607
Thermal relics: Do we know their abundances
[NASA-CR-183334] 17 p2485 N90-24213
Activities report of the Werner-Heisenberg Institute for Physics, Munich, Federal Republic of Germany
[ISSN-0173-6256] 21 p3075 N90-27481
Higher order equations of motion
[DE90-627522] 24 p3543 N90-30038

ELEVATION
Height and gradient from shading
[AD-A212338] 04 p0504 N90-12908
Use of beta-splines for digital elevation modeling
[INPE-4941-PRE/1431] 10 p1400 N90-18093
Project Floval: Correction of relief effects in eucalyptus reforestration
[INPE-4814-RPE/590] 11 p1525 N90-18777
Position computation without elevation information for computed centerline operations
[DOT/FAA/CT-TN89/42] 17 p2349 N90-23379
Digital terrain elevation data compact disk-read only memory prototype evaluation
[AD-A218545] 17 p2442 N90-23915
Noise measurements of turboprop airplanes at different overflight elevations 18 p2609 N90-24860

ELEVATION ANGLE
Effects of miniature CRT (Cathode Ray Tube) location upon primary and secondary task performances
[AD-A210223] 01 p0101 N90-10573
Lateral attenuation of military aircraft flight noise
[AD-A218041] 13 p1882 N90-20799

ELEVATIONS (DRAWINGS)
U DRAWINGS

ELEVATORS (CONTROL SURFACES)
Hinge moment coefficient derivatives for trailing-edge controls on wings at subsonic speeds
[ESDU-89009] 06 p0726 N90-14239
Boeing/NASA composite components flight service evaluation
[NASA-CR-181898] 16 p2210 N90-22609
Short period control using angular acceleration feedback: Compensation for first lag servo
[NAL-TM-600] 24 p3435 N90-29399

ELEVATORS (LIFTS)
The space station tethered elevator system
[NASA-CR-186051] 06 p0732 N90-14265

ELEVONS
Independent Orbiter Assessment (IOA): Analysis of the elevon subsystem
[NASA-CR-185576] 02 p0166 N90-10935
Independent Orbiter Assessment (IOA): Analysis of the mechanical actuation subsystem
[NASA-CR-185525] 02 p0168 N90-10944
Independent Orbiter Assessment (IOA): Assessment of the mechanical actuation subsystem, volume 1
[NASA-CR-185527-VOL-1] 02 p0169 N90-10952
Independent Orbiter Assessment (IOA): Assessment of the mechanical actuation subsystem, volume 2
[NASA-CR-185527-VOL-2] 02 p0169 N90-10953
Independent Orbiter Assessment (IOA): Assessment of the elevon actuator subsystem FMEA/CIL
[NASA-CR-185578] 02 p0173 N90-10970

ELLIPSES
A tensor product b-spline method for 3D multi-block elliptic grid generation
[DE89-017440] 06 p0836 N90-14859
Downward continuation of the free-air gravity anomalies to the ellipsoid using the gradient solution and terrain correction: An attempt of global numerical computations 13 p1836 N90-20541
Some ray tracing problems related to circles and ellipses
[AD-A219306] 16 p2318 N90-23217
On Bernstein type inequalities and a weighted Chebyshev approximation problem on ellipses
[NASA-CR-180368] 17 p2456 N90-24011

ELLIPSOIDS
Compact surface in three-dimensional ellipsoid with prescribed mean curvature (I)
[DE89-618381] 02 p0264 N90-11502
Incompressible flow about ellipsoids of revolution
[REPT-88-02] 03 p0302 N90-11713
Flow in the neighborhood of an ellipsoid cylinder of revolution model
[ONERA-RT-22/7252-AN-000A] 04 p0502 N90-12895
Geometric considerations for a waypoint guidance method
[DE90-001803] 07 p0878 N90-15088
Membership-set parameter estimation via optimal bounding ellipsoids
[AD-A213807] 07 p0984 N90-15685
Numerical boundary layer calculations on the DFVLR ellipsoid of revolution 08 p1070 N90-16193
Numerical simulation of laminar hypersonic flows about an ellipsoid 08 p1071 N90-16198
Contribution to the study of three-dimensional separation in turbulent incompressible flow
[ESA-TT-1169] 11 p1510 N90-18697

ELLIPSOMETERS
Novel in situ spectroscopic ellipsometer for real time analysis of CVD diamond films
[AD-A213218] 05 p0644 N90-13762
An ellipsometric measurement of optical properties for InP surfaces
[AD-A217185] 13 p1887 N90-20827
Refractive index profiles of thermally grown and chemically vapor deposited films on silicon
[AD-A217187] 13 p1893 N90-20865
Ellipsometric study of YBa2Cu3O(7-x) laser ablated and co-evaporated films
[NASA-TM-103223] 20 p2932 N90-26682
Spectroscopic ellipsometry in vacuum ultraviolet spectral area
[ETN-90-97317] 22 p3249 N90-28426

ELLIPSOMETRY
Spectroscopic ellipsometry characterization of CVD deposition and doping of polysilicon multilayer structures
[RSRE-MEMO-4258] 04 p0466 N90-12671
Spectral emissivities and optical constants of electromagnetically levitated liquid metals as functions of temperature and wavelength 10 p1364 N90-17907
Semiconductor measurement technology: A software program for aiding the analysis of ellipsometric measurements, simple spectroscopic models
[PB90-216847] 23 p3398 N90-29201

ELLIPTIC DIFFERENTIAL EQUATIONS
On the existence of a maximal weak solution for a semilinear elliptic equation
[REPT-89-06] 04 p0539 N90-13120
Parallel mathematical software
[DE90-002694] 06 p0829 N90-14822
A comparison result and elliptic equations involving subcritical exponents
[DE90-001772] 06 p0834 N90-14850
Iterative methods of domain decomposition with cross-points for the solution of discrete elliptic problems
[DE90-000719] 06 p0835 N90-14854
Mixed singular linear elliptic equations
[DE90-600722] 07 p0982 N90-15674
Harmonic mappings into manifolds with boundary
[DE90-606961] 09 p1277 N90-17402
A parallel iterative method for solving 3-dimensional elliptic partial differential equations
[DE90-005187] 10 p1422 N90-18199
Analysis of linear multigrid methods for elliptic differential equations with discontinuous and anisotropic coefficients
[ETN-90-96269] 11 p1553 N90-18944
A parallel multigrid method for solving elliptic partial differential equations
[DE90-007929] 14 p2021 N90-21584
Fourier analysis of finite element preconditioned collocation schemes
[NASA-CR-182040] 16 p2304 N90-23128
Differential Loran-C using three secondary stations
[AD-A219573] 17 p2350 N90-23381
Bivariate simplicial splines in finite element computations
[MEMO-823] 18 p2600 N90-24797
Numerical analysis
[AD-A221982] 22 p3242 N90-28385
Elliptic grid generation 24 p3471 N90-29612

ELLIPTIC FUNCTIONS
On geometry of inhomogeneous Heisenberg ferromagnet: Nonintegrable case
[MEMO-789] 05 p0691 N90-14030

The p- and h-p versions of the finite element method: An overview
[AD-A216902] 12 p1705 N90-19789
On the equation: Delta u+c=Ke(sup u)
[DE90-612741] 14 p2020 N90-21575

ELLIPTIC INTEGRALS
U ELLIPTIC FUNCTIONS

ELLIPTICAL CYLINDERS
Transversal, longitudinal, and three dimensional eddy currents in cylindrical guides with elliptic diameters
[ETN-90-97302] 22 p3168 N90-27967

ELLIPTICAL GALAXIES
UV observations of NGC 205
[NASA-CR-185975] 02 p0291 N90-11661
Radio and optical observations of nearby active galaxies 06 p0860 N90-15000
Counterrotating cores in elliptical galaxies 16 p2332 N90-23288
Studies in gravitational lensing and numerical hydrodynamics 16 p2332 N90-23290

ELLIPTICAL ORBITS
NT TRANSFER ORBITS
An analytic development of orbit determination for a distant, planetary orbiter 04 p0485 N90-12787
Control and stability of a spinning symmetric satellite in an elliptical orbit
[AD-A216284] 10 p1328 N90-17672
Lightweight EHF communications satellites 21 p3070 N90-27453

ELLIPTICAL POLARIZATION
Semiconductor measurement technology: A software program for aiding the analysis of ellipsometric measurements, simple models
[PB89-235923] 04 p0560 N90-13261
Integrated optics anisotropic waveguides and devices
[AD-A217064] 12 p1715 N90-19849

ELONGATION
Brominated graphitized carbon fibers
[NASA-CASE-LEW-14698-2] 07 p0910 N90-15262
Elastic recovery and polymer-polymer interactions
[AD-A217085] 12 p1633 N90-19384
Experiments at high elongations in DIII-D
[DE90-013217] 21 p3078 N90-27500

ELUTION
The chemical basis for the origin of the genetic code and the process of protein synthesis
[NASA-CR-186590] 15 p2136 N90-22205
Pre-concentration method for inductively coupled plasma-mass spectrometry
[PB90-181348] 19 p2673 N90-25202

ELUTRIATION
U ELUTION

EMANATION
U EMISSION

EMBEDDED COMPUTER SYSTEMS
NT AIRBORNE/SPACEBORNE COMPUTERS
Dynamic embedding of trees in hypercubes with constant dilation and load
[AD-A211884] 03 p0392 N90-12236
Work-preserving emulations of fixed-connection networks
[AD-A211915] 04 p0535 N90-13093
A fault-tolerant software algorithm for a network of transputers
[AD-A213092] 05 p0682 N90-13972
Ada programming guidelines for deterministic storage management
[NASA-CR-181308] 05 p0684 N90-13982
A portable ionosonde in support of reliable communications 06 p0762 N90-14431
Study on advanced information processing system
[NASA-CR-186342] 10 p1415 N90-18154
Proceeding of the Embedded AI Languages Workshop
[AD-A218531] 17 p2442 N90-23914
High performance processing system for embedded control applications in space 18 p2507 N90-24330
Intelligent real-time problem-solving: Issues, concepts and research methodology
[AD-A218868] 18 p2598 N90-24781
Onboard processor technology review 21 p3017 N90-27152
Applications of ISES for vegetation and land use 21 p3018 N90-27158
A model parametric real-time logic
[REPT-90-010] 22 p3241 N90-28381
Concepts of concurrent programming
[AD-A223897] 23 p3382 N90-29110

EMBEDDING
Calibration and de-embedding of microwave measurements using any combination of one- or two-port standards
[PB89-212674] 03 p0337 N90-11916
Optical fibre witnesses of fatigue damage in composite materials 04 p0465 N90-12660
Embedded function methods for compressible high speed turbulent flow
[NASA-CR-186131] 06 p0773 N90-14498
Interaction of hydrogen in palladium as prescribed by the embedded atom method
[DE90-003893] 07 p0907 N90-15244
Effect of vortex circulation on injectant from a single film-cooling hole and a row of film-cooling holes in a turbulent boundary layer. Part 1: Injection beneath the vortex downwash
[AD-A215288] 09 p1218 N90-17063
Strain and dynamic measurements using fiber optic sensors embedded into graphite/epoxy tubes 14 p1937 N90-21090
Structural tailoring of select fiber composite structures
[NASA-TM-102484] 14 p1948 N90-21137
Image simulation of geometric targets for synthetic aperture radar 14 p1964 N90-21245
Feature-associated mesh embedding for complex configurations 15 p2095 N90-21988
Towards a Sarkovski order for the embedding of disks maintaining their orientation
[REPT-89-43] 15 p2151 N90-22289
Instability-related delamination growth of embedded and edge delaminations
[NASA-TM-100655] 17 p2370 N90-23494
Improved self-reduction algorithms for graphs with bounded tree width
[RUU-CS-88-29] 18 p2601 N90-24805
An embedded fibre optic sensor for impact damage detection in composite materials
[UTIAS-332] 20 p2926 N90-26650
Method of forming three-dimensional semiconductor structures
[NASA-CASE-NPO-17835-1-CU] 21 p3081 N90-27518
Development of an expert system embedding pattern recognition techniques for pollution source identification
[PB90-185927] 22 p3197 N90-28139
Using embedded microcontrollers in radar test equipment
[DE90-014997] 23 p3319 N90-28763

EMBRITTLEMENT
Effects of precipitate distribution on 293 K and 77 K properties of 2090-T81 weldments
[DE90-002332] 06 p0747 N90-14349
Embrittlement of laboratory- and reactor-aged CF-3, CF-8, and CF-8M duplex stainless steels
[DE90-002777] 06 p0748 N90-14354
Accelerated aging embrittlement of cast duplex stainless steel: Activation energy for extrapolation
[DE90-001773] 07 p0903 N90-15221
Cast stainless steel aging: Mechanisms and predictions
[DE90-003772] 07 p0907 N90-15241
Microstructural explanation for irradiation embrittlement of V-15Cr-5Ti
[DE90-004112] 08 p1045 N90-16041
Plasma and ion fluorination for chemical hardening of synthetic rubbers
[AD-A216388] 10 p1360 N90-17885
Tellurium embrittlement of type 316 steel
[AERE-R-13440] 13 p1776 N90-20192
Magneto acoustic emission apparatus for testing materials for embrittlement
[NASA-CASE-LAR-13817-1] 14 p1951 N90-21170
Measurements and mechanisms of localized aqueous corrosion in aluminum-lithium alloys 16 p2219 N90-22656
Vanadium alloys with improved resistance to helium embrittlement
[DE90-009811] 17 p2375 N90-23524
Monoenergetic positron beam studies of near-surface phenomena
[ETN-90-96947] 18 p2613 N90-24887
Alloy design of ordered intermetallics
[DE90-016031] 24 p3451 N90-29490
The use of automated ball indentation testing to measure flow properties and estimate fracture toughness in metallic materials
[DE90-015797] 24 p3452 N90-29493

EMBRYOLOGY
Microgravity as a tool in developmental biology
[ESA-SP-1123] 19 p2680 N90-25239
Early mammalian development and possible involvement of gravity 19 p2680 N90-25242
Experimental control of axis polarity in amphibian embryos 19 p2680 N90-25244
The first seven minutes of a Zenopus egg fertilised on a sounding rocket in space 19 p2680 N90-25245
The role of gravity in bird development 19 p2681 N90-25246

EMBRYOS
Polarity establishment, morphogenesis, and cultured plant cells in space 05 p0677 N90-13943
Gravity and animal embryos 05 p0678 N90-13951
Computer aided mechanogenesis of skeletal muscle organs from single cells in vitro
[NASA-CR-187025] 23 p3354 N90-28959

EMERALD
U BERYL

EMERGENCIES
The suitability of diffusion and wind-field techniques for an emergency-response dispersion model
[PB89-190219] 01 p0085 N90-10481
Project AENEAS: A feasibility study for crew emergency return vehicle
[PB89-217020] 03 p0317 N90-11799
A methodology for evaluating heavy gas dispersion models
[AD-A214009] 07 p0887 N90-15131
Aircraft accident report: Delta Air Lines, Inc., Boeing 727-232, N473DA, Dallas-Fort Worth International Airport, Texas, August 31, 1988
[PB89-910406] 08 p1019 N90-15895
Aircraft fire safety in the Canadian Forces 10 p1315 N90-17604
Passenger behaviour in aircraft emergencies involving smoke and fire 10 p1317 N90-17613
Smokehoods donned quickly. The impact of donning smokehoods on evacuation times 10 p1317 N90-17614
Flight crew training for fire fighting 10 p1317 N90-17615
The effects of wearing passenger protective breathing equipment on evacuation times through type 3 and type 4 emergency aircraft exits in clear air and smoke. Phase 1: Evacuations in clear air. Phase 2: Evacuations in smoke
[AD-A216798] 11 p1453 N90-18374
Perspectives on the use of rule-based control 14 p1908 N90-20940
The influence of adjacent seating configurations on egress through a type 3 emergency exit
[AD-A218393] 17 p2348 N90-23371
Project EGRESS: Earthbound guaranteed reentry from space station. The design of an assured crew recovery vehicle for the space station
[NASA-CR-186657] 19 p2664 N90-25162
Orbiter utilization as an ACRV
[NASA-TM-102700] 20 p2817 N90-26032
Preliminary subsystem designs for the Assured Crew Return Vehicle (ACRV), volume 1
[NASA-CR-186677-VOL-1] 20 p2818 N90-26039
Space operations: NASA's communications support for Earth orbiting spacecraft. Report to Chairman, Subcommittee on Space Science and Applications, Committee on Science, Space and Technology, House of Representatives
[GAO/IMTEC-89-41] 20 p2851 N90-26215
Human factors: The human interface with aircraft interiors
[NIAR-90-18] 20 p2900 N90-26496
NASA/USRA University advanced design program
[NASA-CR-186050] 21 p2965 N90-26855
Hermes emergency reentry trajectories consequences on the Ariane 5 trajectories 22 p3127 N90-27747

EMERGENCY BREATHING TECHNIQUES
Arctic cold weather medicine and accidental hypothermia
[AD-A223090] 20 p2899 N90-26487

EMERGENCY LIFE SUSTAINING SYSTEMS
Project AENEAS: A feasibility study for crew emergency return vehicle
[PB89-217020] 03 p0317 N90-11799

EMERGENCY LOCATOR TRANSMITTERS
Feasibility of millimeter-accuracy geodetic positioning and vehicle tracking with repeater satellites
[AD-A214755] 09 p1182 N90-16854

EMISSION
NT ACOUSTIC EMISSION
NT BIOLUMINESCENCE
NT CATHODE GLOW
NT CATHODOLUMINESCENCE
NT CHEMILUMINESCENCE
NT ELECTROLUMINESCENCE
NT ELECTRON EMISSION
NT EXHAUST EMISSION
NT FIELD EMISSION
NT FLUORESCENCE
NT HYDROXYL EMISSION
NT ION EMISSION
NT LASER INDUCED FLUORESCENCE
NT LIGHT EMISSION
NT LUMINESCENCE
NT MICROWAVE EMISSION
NT NEUTRON EMISSION
NT PARTICLE EMISSION
NT PHOSPHORESCENCE
NT PHOTOELECTRIC EMISSION
NT PHOTOIONIZATION
NT PHOTOLUMINESCENCE

NT RADIO BURSTS
NT RADIO EMISSION
NT RESONANCE FLUORESCENCE
NT SECONDARY EMISSION
NT SOLAR RADIO BURSTS
NT SOLAR RADIO EMISSION
NT SPACECRAFT GLOW
NT SPECTRAL EMISSION
NT SPONTANEOUS EMISSION
NT STIMULATED EMISSION
NT THERMAL EMISSION
NT THERMIONIC EMISSION
NT THERMOLUMINESCENCE
NT TYPE 3 BURSTS
NT WATER MASERS
NT X RAY FLUORESCENCE

Global data bases on distribution, characteristics and methane emission of natural wetlands: Documentation of archived data tape
[NASA-TM-4153] 03 p0365 N90-12090

On the role of Coulomb forces in atomic radiative emission
[IRF-PREPRINT-106] 03 p0403 N90-12308

Analysis of high temperature superconductors by means of PIXE and RBS methods
[DE89-630241] 04 p0558 N90-13252

Analysis of acid rain and associated phenomena
[DE90-002555] 06 p0812 N90-14725

Spectral studies of solid propellant combustion. 2: Emission and absorption results for M-30 and HMX1 propellants
[AD-A213857] 07 p0915 N90-15292

Thermal and statistical properties of nuclei and nuclear systems
[DE90-000183] 07 p0990 N90-15717

Comparison of emissions of transit buses using methanol and diesel fuel
[DE90-005652] 10 p1391 N90-18044

Cold fusion research
[DE90-005611] 10 p1433 N90-18267

Effect of barrier layers in burn-through experiments with 351-nm laser illumination
[DE90-006806] 12 p1667 N90-19577

Overview of the methodologies used to compile large scale emissions inventories
[DE90-008518] 13 p1830 N90-20509

Populations of excited states and reaction mechanisms in the emission of complex fragments
[DE90-007481] 13 p1886 N90-20819

A fossil energy perspective on global climate change
[DE90-007894] 14 p2004 N90-21483

Source attribution for tropospheric ozone in the US
[DE90-007994] 14 p2004 N90-21484

Radon concentration over the Brazilian Amazon Basin during the wet season (Belem-Manaus GTE-ABLE-2B flight of April 24, 1987)
[INPE-4892-PRE/1493] 14 p2004 N90-21486

An evaluation of the relationship between the production and use of energy and atmospheric methane emissions
[DE90-007982] 14 p2004 N90-21487

Optical emission from the high inclination X ray transient EXO 0748-676 19 p2779 N90-25809

Astronomy at ultra-high energies: Results from the CYGNUS experiment
[DE90-011979] 20 p2940 N90-26732

Vertical emitting, ring geometry, ultra-low threshold, and ultra-high speed quantum well lasers for optical interconnect
[AD-A222932] 21 p3008 N90-27098

Acid deposition: No such thing as a free launch
[DE90-015085] 23 p3348 N90-28920

EMISSION SPECTRA

X-ray bright points and He I lambda 10830 dark points
01 p0139 N90-10802

Small grains in reflection nebulae: A study of diffuse interstellar bands, elemental depletions and infrared flux
02 p0293 N90-11672

Retrieval of atomic oxygen and temperature in the thermosphere. Part 2: Feasibility of an experiment based on limb emission in the OI lines
[AD-A211807] 03 p0371 N90-12121

Investigation of atmospheric emissions in ultraviolet, vacuum ultraviolet, and extreme ultraviolet wavelength
[AD-A212169] 03 p0371 N90-12123

Electron cyclotron emission and absorption experiment on the CASTOR tokamak
[IPPCZ-285] 03 p0407 N90-12331

Auroral particle acceleration by dc and low frequency electric fields 05 p0658 N90-13841

Mapping of upper electronic reaction surfaces by tuned laser photolysis and by absorption and emission spectroscopies
[DE90-000125] 06 p0741 N90-14314

The formation of metal-oxygen species at low temperatures
[DE90-002298] 06 p0743 N90-14323

Solid-state fluorescence above 1000 C: Application to high-temperature laser thermometry
[DE90-000728] 06 p0789 N90-14594

A study of the infrared emission of galactic supernova remnants 06 p0861 N90-15006

Description of SHARC: The Strategic High-Altitude Radiance Code
[AD-A213806] 07 p0961 N90-15555

ICP/AES (Inductively Coupled Plasma/Atomic Emission Spectroscopy): A modern analytical tool
[DE90-003822] 07 p0997 N90-15765

Spectroscopic and laser properties of Cr:LiCaAlF6 and Cr:LiSrAlF6 crystals
[DE90-000783] 07 p0998 N90-15770

Near-infrared polarimetry and spectroscopy of comets
07 p1011 N90-15857

Natural and man-made emissions at 1.0 to 5.6 MHz measured between 10 and 18 R sub E
[MPE-PREPRINT-146] 08 p1058 N90-16116

Determination of hyperfine structures and Rydberg convergence limits of selected optical transitions in Nb-93 using resonance ionization spectroscopy
[PB90-110719] 08 p1122 N90-16498

Use of the Egret instrument in studies of the origin of the cosmic radiation. 2: Spectral signatures of discrete cosmic-ray sources
[DE90-003595] 08 p1154 N90-16682

Evaluating CO, CO2 and H2O concentration by partial integration of absorption band spectra
[ISL-R-110/88] 09 p1244 N90-17219

Singlet oxygen and iodine monofluoride collisional energy transfer mechanism
[AD-A215711] 09 p1280 N90-17421

Low temperature photoluminescence study of uranium implanted into III-V semiconductors and AlGaAs
[AD-A215710] 09 p1291 N90-17484

Selective excitation luminescence and photoluminescence investigations of ytterbium doped InP, GaAs and AlGaAs
[AD-A215713] 09 p1291 N90-17485

Chemical interactions and light emissions from vented species
[AD-A214130] 10 p1327 N90-17668

Measurement of radiation property of long infrared emitter and examination of infrared radiation heating process
[DE90-741971] 10 p1425 N90-18222

Model of oxygen ions resonant lines emission of REB-heated plasma
[IPPCZ-294] 10 p1432 N90-18261

Solid-state fluorescence above 1000 C: Application to high-temperature laser thermography
[DE90-006422] 11 p1514 N90-18721

Properties and performance of the LiCaAlF6:Cr(3+) laser material
[DE90-007242] 11 p1516 N90-18728

The 2.7/4.3 micron CO2 branching ratio measurement
[AD-A215952] 11 p1534 N90-18830

Studies of atmospheric molecules by multiphoton spectroscopy
[DE90-005829] 11 p1534 N90-18833

GRIS observations of the Galactic Center
11 p1559 N90-18982

Positron annihilation in gamma-ray bursts
11 p1559 N90-18983

Dust continuum spectra from model HII regions
11 p1580 N90-19099

IR line emission from dense photodissociation regions
11 p1580 N90-19100

Airborne observations of the infrared emission bands
11 p1580 N90-19101

IR line emission from supernovae in molecular clouds
11 p1580 N90-19102

An almost total disjunction between emission and absorption dust features: What does it tell us?
11 p1581 N90-19106

Wide-beam balloon observations of the 157.7 microns (CII) line 11 p1581 N90-19108

Mapping and spectroscopy of the 3.3 microns feature in Orion 11 p1582 N90-19112

Infrared line emission from high-velocity outflows in star-forming regions 11 p1582 N90-19116

High resolution infrared spectroscopy of symbiotic stars 11 p1583 N90-19125

A survey of PAH emission in HII regions, planetary and proto-planetary nebulae 11 p1584 N90-19129

H53-alpha emission from M82
11 p1588 N90-19156

Noise behavior of semiconductor lasers by optic feedback
[ETN-90-95728] 12 p1668 N90-19583

Far-ultraviolet spectroscopy of Comet Halley
12 p1736 N90-19979

Spectral solar radiation data base documentation, volume 1
[DE89-009447] 13 p1841 N90-20571

Remote sensing applied to sea water quality researches in coastal regions: A review
[INPE-4935-PRE/1425] 14 p1995 N90-21438

Free-field propagation of high intensity noise
[NASA-CR-186577] 14 p2024 N90-21604

Spectral response of wheat and its relationship with agronomic variables in the tropical region
[INPE-5018-RPE/612] 15 p2122 N90-22138

Field reports on radiometric campaigns of soybeans in the Federal district: Safra 88/89
[INPE-5021-RPE/615] 15 p2122 N90-22139

The emission lines in the ultra-violet spectrum of Beta Lyrae 15 p2183 N90-22474

The diffuse galactic gamma ray emission
16 p2333 N90-23296

Current status of SHARC, the strategic high altitude radiance code, and description of its new auroral module
[AD-A221068] 18 p2580 N90-24698

Space station contamination study: Assessment of contaminant spectral brightness
[NASA-CR-186173] 19 p2666 N90-25169

Emission lines from X ray binaries
19 p2769 N90-25733

X ray observations of SS433 and its jets
19 p2769 N90-25734

Non-thermal radio emission of X ray binaries
19 p2769 N90-25738

A unified model of accretion flows and X ray emission in low mass X ray binary systems
19 p2770 N90-25742

VHE gamma ray emission from Northern Hemisphere X ray binaries 19 p2772 N90-25760

IUE observations of Cyg X-2 and Sco X-1: Accretion disks and the z-shaped curve 19 p2783 N90-25832

The X ray spectra of emission line AGN
19 p2785 N90-25850

Extended line emission in AGN: Looking at the central engine 19 p2788 N90-25870

Detailed non-LTE calculations of the iron emission from NGC 1068 19 p2788 N90-25872

Long term multi-frequency study of 3C 273
19 p2790 N90-25879

X ray polarization of the reprocessed emission from accretion disk in Seyfert galaxies
19 p2792 N90-25892

Variability of the continuum emission of GQ Comae
19 p2793 N90-25903

Detection of hard X ray emission from a type 2 Seyfert galaxy 19 p2794 N90-25905

Digital filtering of plume emission spectra
[NASA-TM-103135] 20 p2824 N90-26070

Carbon chemistry of circumstellar envelopes
21 p3090 N90-27570

FT-IR spectroscopic studies of polycyclic aromatic hydrocarbons 21 p3095 N90-27592

XES studies of density of states of high temperature superconductors 22 p3150 N90-27859

Detection of emission lines from the secondary star in IX Vel (=CPD-48 deg 1577)
[MPE-PREPRINT-172] 22 p3265 N90-28485

The ionization structure of planetary nebulae 10: NGC 2392
[NASA-CR-186960] 23 p3411 N90-29274

Optical emissions from bombarding atmospheric gases with heavy ions
[AD-A223544] 24 p3543 N90-30040

Soft x ray emission spectra from laser-irradiated high-Z targets
[AD-A223552] 24 p3552 N90-30099

EMISSIVITY

Total hemispherical emittance measured at high temperatures by the calorimetric method
[NASA-TM-102322] 01 p0054 N90-10309

Infrared temperature measurement with automatic consideration of emissivity
[ESA-TT-1131] 03 p0351 N90-12008

Three dimensional analysis of the structure of the atmosphere in polar environments by vertical satellite sounding. Interest for the meteorological forecasts at high latitudes
[ETN-90-95506] 05 p0671 N90-13911

The average ion model. Computation of the absorption and emission coefficients in hot plasmas
06 p0785 N90-14569

Evaluation of platinum silicide and indium antimonide as detector materials for space-based remote sensing in the 3.0-to-5.0 micrometer wavelength band
[AD-A216182] 10 p1354 N90-17853

Optical Johnson noise thermometry
10 p1363 N90-17899

Non-contact true temperature measurements in the microgravity environment 10 p1364 N90-17906

Materials thermal and thermoradiative properties/characterization technology
10 p1367 N90-17925

X ray spectra produced by NaF implosions
[AD-A215803] 10 p1429 N90-18243
Interrelationship of spatial and radiometric resolution in the thermal infrared band
[INPE-4860-TDL/371] 11 p1523 N90-18771
Techniques for measurement of the optical properties of materials
[DE90-006902] 11 p1566 N90-19014
Analysis of methods to determine emissivity for ground surface targets in the spectral band 8 to 14 microns
[INPE-4984-TDL/394] 13 p1820 N90-20447
Multiwavelength pyrometry to correct for reflected radiation
[NASA-TM-102578] 17 p2407 N90-23714
Characterizing microwave propagation using the AFGL microwave attenuation/transmittance/brightness temperature code
[AD-A220248] 18 p2543 N90-24513
Properties of cirrus from multispectral AVHRR imagery data 22 p3223 N90-28277
Thermal imaging assessment
[AD-A224400] 24 p3460 N90-29542

EMISSOGRAPHS
U RECORDING INSTRUMENTS

EMITTANCE
Emittance, catalysis, and dynamic oxidation of Ti-14Al-21Nb
[NASA-TP-2955] 01 p0044 N90-10248
Total hemispherical emittance measured at high temperatures by the calorimetric method
[NASA-TM-102322] 01 p0054 N90-10309
Minimized emittance growth with elliptical beam pipes in FEL (Free-Electron Laser)
[DE89-016982] 02 p0228 N90-11305
Extraction induced emittance growth for negative ion sources
[DE89-017586] 02 p0273 N90-11559
An experimental and theoretical study of the aeroacoustics of external-Coanda gas flares 06 p0773 N90-14495
Observation of atomic relaxation near an interface through detection of emitted fluorescence
[AD-A214308] 07 p0991 N90-15725
Principles and formulation of solar reflecting and low infrared emitting coatings for defence use
[MRL-TR-89-2] 10 p1358 N90-17874
Report on the multicolor pyrometry session at the Second NASA Non-Contact Temperature-Measurement Workshop 10 p1367 N90-17926
Experimental investigation of relationship between nonlinear field energy and emittance growth
[AD-A215813] 10 p1430 N90-18246
Thermal radiation characteristics of nonisothermal cylindrical enclosures using a numerical ray tracing technique
[NASA-TM-102527] 14 p1972 N90-21296
Problems in radiative transfer in astrophysics: An escape probability treatment of line overlap and a model of the masers around VX Sgr 14 p2041 N90-21705
Measuring and modeling near-surface reflected and emitted radiation fluxes at the FIFE site
[NASA-CR-180953] 20 p2879 N90-26378
Slow positron beam generator for lifetime studies
[NASA-CASE-LAR-14250-1-SB] 21 p3073 N90-27472
On planetary nebulae as sources of carbon dust: Infrared emission from planetary nebulae of the galactic halo 21 p3093 N90-27583
Direct and remote sensing observations of the effects of ships on clouds 22 p3218 N90-28252
The effects of atomic oxygen on the thermal emittance of high temperature radiator surfaces
[NASA-TM-103224] 23 p3301 N90-28670
Effects and tolerances of injection jitter in the SLC and future linear colliders
[DE90-014805] 23 p3394 N90-29179
Control of nonlinear space-charge emittance growth
[DE90-014752] 23 p3410 N90-29270

EMITTERS
NT THERMIONIC CATHODES
Decision-aid design factors in connection with HF communication and emitter location disciplines 06 p0758 N90-14413
Large-aperture sparse array detector system for multiple emitter location
[AD-D014303] 07 p0925 N90-15355
Measurement of radiation property of long infrared emitter and examination of infrared radiation heating process
[DE90-741971] 10 p1425 N90-18222
Radiation-hard high-efficiency InP space solar cell development
[AD-A216857] 11 p1528 N90-18800
Spectral line shape code for multielectron emitters
[DE90-006526] 13 p1891 N90-20853
Production and analysis by mass spectrometry of beams of polyglycol ions 15 p2066 N90-21835
Field emitter array integrated distributed amplifiers
[AD-D014493] 22 p3166 N90-27958
Emitter and base recombination parameters in solar cells: Measurement process and dependence on temperature and injection
[ETN-90-97305] 22 p3196 N90-28138
Computer simulation of micro-triode performance
[DE90-014191] 23 p3320 N90-28774
Symmetrical layered thin film edge field-emitter-array and method for its production
[AD-D014594] 24 p3464 N90-29569
Optical emissions from bombarding atmospheric gases with heavy ions
[AD-A223544] 24 p3543 N90-30040

EMOTIONAL FACTORS
Excitatory and inhibitory backward conditioning in the rat 15 p2135 N90-22204
Optimism and cardiovascular reactivity to psychological and cold pressor stress
[AD-A223818] 24 p3498 N90-29771
Coping strategies and mood during cold weather training
[AD-A223915] 24 p3498 N90-29773

EMOTIONS
Psychophysiological correlates of human adaptation in antarctica
[AD-A216679] 10 p1412 N90-18142
Ability and metacognitive determinants of skill acquisition and transfer
[AD-A224569] 24 p3499 N90-29776

EMPENNAGE
U TAIL ASSEMBLIES

EMPLOYMENT
Science and technology resources in US industry: Surveys of science resources series, 1975-1986
[PB90-107194] 06 p0756 N90-14401

EMULSIONS
NT NUCLEAR EMULSIONS
Basic research on processing of ceramics for space structures
[AD-A205954] 02 p0199 N90-11139
Correlating microemulsion fuel composition, structure and combustion properties
[DE89-017779] 03 p0333 N90-11898
Chemical and photochemical reactivity in microemulsions and waterless microemulsions
[AD-A211778] 04 p0470 N90-12692
Model filled polymers I. Synthesis of crosslinked monodisperse polystyrene beads
[AD-A213228] 05 p0627 N90-13660
Electromagnetic scale models using emulsions
[AD-A214855] 09 p1211 N90-17022
Theory of microemulsions in a gravitational field 09 p1224 N90-17099
New calculations and measurements of the Coulomb cross-section for the production of direct electron pairs by high energy nuclei
[NASA-TM-101280] 15 p2165 N90-22371
Undercooling and nucleation in rapid solidification rate metal powders using solid in solid emulsification
[AD-A218527] 17 p2375 N90-23526
Solidification of highly undercooled liquid droplets
[AD-A218776] 17 p2376 N90-23529
Criteria for coal tar seal coats on airport pavements. Volume 2: Laboratory and field studies
[AD-A220167] 18 p2498 N90-24277
Toughening of SAN copolymers by an SAN emulsion grafted rubber
[AD-A224213] 24 p3453 N90-29502

ENCAPSULATING
Electronic encapsulation using foam with bonded metal covers for a filter pack
[DE89-014010] 01 p0048 N90-10276
Bulk and shear moduli of epoxy encapsulants
[DE90-000899] 06 p0751 N90-14371
Selection of phase-change and containment materials for thermal energy storage
[NASA-CR-186228] 07 p0952 N90-15506
Object Oriented Programming Systems (OOPS) and frame representations: An investigation of programming paradigms
[NASA-CR-186084] 12 p1699 N90-19758
Ductile alloy encapsulated ceramic armor development
[AD-A217632] 14 p1954 N90-21183
Dynamic response of a complex encapsulated electronic assembly subjected to a severe shock environment
[DE90-007689] 15 p2118 N90-22114
Multi-element spherical shell generation
[NASA-CASE-NPO-17203-1-CU] 17 p2405 N90-23700
Development of microencapsulation techniques
[AD-A223032] 20 p2841 N90-26159
Underwater connect and disconnect plug and receptacle
[AD-D014175] 21 p2998 N90-27039

ENCODERS
U CODERS

ENCODING
U CODING

ENCOUNTERS
Dust environment modelling from encounters with comet P/Halley 17 p2485 N90-24210

END EFFECTORS
Interchangeable end effector tools utilized on the protoflight manipulator arm
[NASA-CR-179374] 01 p0078 N90-10447
Kinematics, special configurations and performance evaluation of serial manipulators 04 p0508 N90-12927
Acceleration sets of planar manipulators. Part 1: Theory
[AD-A213162] 04 p0510 N90-12945
Definition, determination and characterization of acceleration sets for spatial manipulators
[AD-A213366] 05 p0651 N90-13793
On control of manipulators
[ISBN-90-9002789-0] 05 p0652 N90-13804
New approach to the inverse problem of six-link manipulators via the optimization technique
[DE90-710044] 07 p0940 N90-15441
Method and apparatus for positioning a robotic end effector
[NASA-CASE-MSC-21476-1] 09 p1230 N90-17137
Applications of a fingertip sensor for the Salisbury robot hand
[DE90-005002] 09 p1231 N90-17142
Learning-based position control of a closed-kinematic chain robot end-effector
[NASA-CR-186283] 10 p1391 N90-18043
Kinematic control of robotic manipulators with multiple interchangeable wrists 12 p1670 N90-19592
Advanced control schemes and kinematic analysis for a kinematically redundant 7 DOF manipulator
[NASA-CR-186175] 12 p1671 N90-19599
Development of a passive robot-controlled reaction arm 13 p1809 N90-20389
Gripping device
[NASA-CASE-MSC-21365-1] 13 p1812 N90-20408
A robot end effector exchange mechanism for space applications 15 p2113 N90-22088
Modeling of control forces for kinematical constraints in the dynamics of multibody systems: A new approach 16 p2287 N90-23031
Determination of joint drives for stable end-effector motion in flexible robotic systems 16 p2288 N90-23034
Rod gripper, changer, and storage system
[NASA-CR-183154] 17 p2411 N90-23739
NASA/GSFC split-rail parallel gripper 18 p2507 N90-24328
A three fingered multijointed gripper as a working tool for experimental use 18 p2507 N90-24329
Flexible test bed for space telepresence and telemanipulation research 18 p2508 N90-24334
Real time inverse kinematics with joint limits and spatial constraints
[AD-A220462] 18 p2586 N90-24723
Third Annual Workshop on Space Operations Automation and Robotics (SOAR 1989)
[NASA-CP-3059] 19 p2727 N90-25503
Impact of end effector technology on telemanipulation performance 19 p2736 N90-25549
Smart hands for the EVA retriever 19 p2736 N90-25550
Direct drive robotic hand
[NASA-CASE-NPO-17917-1-CU] 20 p2872 N90-26339
Grasping with mechanical intelligence
[NASA-CR-186864] 20 p2900 N90-26498
Space station definitions, design, and development. Task 5: Multiple arm telerobot coordination and control: Manipulator design methodology
[NASA-CR-182043] 20 p2914 N90-26577
Electronics design of the infrared/ultrasonic sensing for a robot gripper
[PB90-160383] 21 p3010 N90-27109
Kinematic functions for the 7 DOF robotics research arm 23 p3363 N90-29003
A fast lightstripe rangefinding system with smart VLSI sensor 23 p3366 N90-29019
Computational neural learning formalisms for manipulator inverse kinematics 23 p3368 N90-29030
Grasp planning under uncertainty 23 p3370 N90-29041
Characterization and control of self-motions in redundant manipulators 23 p3370 N90-29045

Autonomous dexterous end-effectors for space robotics 24 p3501 N90-29788
Design and control of a multi-fingered robot hand provided with tactile feedback 24 p3501 N90-29789
Force/torque and tactile sensors for sensor-based manipulator control 24 p3501 N90-29791
Redundant sensorized arm+hand system for space telerobotized manipulation 24 p3502 N90-29792
Modeling and sensory feedback control for space manipulators 24 p3504 N90-29807
The 3-D vision system integrated dexterous hand 24 p3511 N90-29850
A control approach for robots with flexible links and rigid end-effectors 24 p3516 N90-29879
Integration of a sensor based multiple robot environment for space applications: The Johnson Space Center Teleoperator Branch Robotics Laboratory 24 p3518 N90-29890
Dexterous manipulator flight demonstration 24 p3522 N90-29911

END PLATES
Limit analysis of welded tee end connections for hollow tubes
[PB89-191647] 01 p0079 N90-10452
Double swivel toggle release
[NASA-CASE-MSC-21436-1] 14 p1987 N90-21390

END-TO-END DATA SYSTEMS
Space station technology summary 11 p1474 N90-18482

ENDFIRE ARRAYS
NT YAGI ANTENNAS

ENDOCRINE GLANDS
NT ADRENAL GLAND
NT PINEAL GLAND
NT PITUITARY GLAND
NT TESTES

ENDOCRINE SECRETIONS
NT CORTICOSTEROIDS
NT HORMONES
NT INSULIN
NT PITUITARY HORMONES
NT PROSTAGLANDINS

ENDOCRINOLOGY
USSR Space Life Sciences Digest, issue 23
[NASA-CR-3922(27)] 03 p0378 N90-12154

ENDOTHERMIC FUELS
Production of jet fuels from coal-derived liquids. Volume 11: Production of advanced endothermic fuel blends from Great Plains Gasification Plant naphtha by-product stream
[AD-A210251] 02 p0207 N90-11184

ENERGETIC PARTICLES
NT ARGON PLASMA
NT BETA PARTICLES
NT BOUNDARY LAYER PLASMAS
NT CESIUM PLASMA
NT COLD PLASMAS
NT COLLISIONAL PLASMAS
NT COLLISIONLESS PLASMAS
NT CONDUCTION ELECTRONS
NT COSMIC PLASMA
NT CYLINDRICAL PLASMAS
NT DENSE PLASMAS
NT ELECTRON PLASMA
NT ELECTRON-POSITRON PLASMAS
NT ELECTRONS
NT HEAVY NUCLEI
NT HELIUM PLASMA
NT HIGH ENERGY ELECTRONS
NT HIGH TEMPERATURE PLASMAS
NT HOT ELECTRONS
NT HYDROGEN PLASMA
NT LASER PLASMAS
NT METALLIC PLASMAS
NT NITROGEN PLASMA
NT NONEQUILIBRIUM PLASMAS
NT NONUNIFORM PLASMAS
NT NUCLEI (NUCLEAR PHYSICS)
NT ODD-ODD NUCLEI
NT OXYGEN PLASMA
NT PI-ELECTRONS
NT PLASMA FOCUS
NT PLASMAS (PHYSICS)
NT RELATIVISTIC PLASMAS
NT ROTATING PLASMAS
NT SEMICONDUCTOR PLASMAS
NT SOLAR WIND
NT SPACE PLASMAS
NT SPHERICAL PLASMAS
NT STELLAR WINDS
NT STRONGLY COUPLED PLASMAS
NT THERMAL PLASMAS
NT TOROIDAL PLASMAS
Particle emission and charging effects induced by fracture
[AD-A210215] 01 p0080 N90-10459
Interplanetary energetic particle observations of the March 1989 events 03 p0434 N90-12484
Cosmic strings and ultra-high energy cosmic rays
[NASA-CR-185924] 03 p0435 N90-12492
CELIAS: Charge, element and isotope analysis system for SOHO 04 p0568 N90-13313
COSTEP: A comprehensive suprathermal and energetic particle analyzer for SOHO 04 p0568 N90-13314
ERNE: Energetic and Relativistic Nuclei and Electron experiment 04 p0568 N90-13315
Destabilization of tokamak pressure-gradient driven instabilities by energetic alpha populations
[DE90-003716] 07 p0996 N90-15756
Solar cycle effects on trapped energetic particles
[AD-A215028] 09 p1300 N90-17532
The illusive Geminga: What is it 16 p2335 N90-23307
Investigation of the Saturn dust environment from the analysis of energetic charged particle measurements
[NASA-CR-186727] 20 p2950 N90-26784

ENERGY ABSORPTION
NT ELECTROMAGNETIC ABSORPTION
NT GAMMA RAY ABSORPTION
NT INFRARED ABSORPTION
NT MOLECULAR ABSORPTION
NT MULTIPHOTON ABSORPTION
NT PHOTOABSORPTION
NT POLAR CAP ABSORPTION
NT RADIATION ABSORPTION
NT THERMAL ABSORPTION
NT THERMALIZATION (ENERGY ABSORPTION)
NT ULTRAVIOLET ABSORPTION
NT X RAY ABSORPTION
Density clamping phenomena in electron cyclotron resonance heated plasmas on Heliotron E
[DE90-719523] 09 p1284 N90-17442
Low-energy gamma ray attenuation characteristics of aviation fuels
[NASA-TP-2974] 11 p1543 N90-18882
Optimization of fracture resistance in composites
[AD-A217431] 13 p1768 N90-20144
Low energy ion generator
[DE90-759905] 14 p1955 N90-21195
High power, high sensitivity microwave calorimeter
[AD-D014427] 14 p1982 N90-21355
Formulation of non-reflecting boundary conditions in numerical models of the atmosphere 15 p2129 N90-22175
Aircraft crash survival design guide. Volume 4: Aircraft seats, restraints, litters, and cockpit/cabin delethalization
[AD-A218437] 16 p2198 N90-22548
Theoretical analysis and pressure distribution of thin-walled metal inverbuckle energy absorbing tubes 17 p2414 N90-23758
Operational effects on crashworthy seat attenuators
[AD-A221148] 18 p2495 N90-24259
A review of crashworthiness of composite aircraft structures
[AD-A221555] 22 p3115 N90-27697
Mechanics of impact energy absorption
[PB90-190836] 22 p3190 N90-28101
Crash-impact behavior of graphite/epoxy composite sine wave webs 23 p3300 N90-28667

ENERGY BANDS
NT CONDUCTION BANDS
NT FORBIDDEN BANDS
Composite vs constituent particle aspects of hole motion in the CuO2 plane
[DE89-618864] 04 p0558 N90-13251
The effect of annealing treatments on defect structure and diffusion lengths in n-type GaAs
[AD-A214215] 07 p1005 N90-15817
Theory of the electronic and optical properties of semiconductor heterostructures
[AD-A214132] 08 p1130 N90-16544
Tailorable infrared sensing device with strain layer superlattice structure
[NASA-CASE-NPO-16617-2-CU] 09 p1227 N90-17118
Electronic properties of high-temperature superconductors
[AD-A217953] 13 p1898 N90-20892
Adlayer physics
[AD-A221064] 19 p2673 N90-25203
Mir-Kvant-HEXE hard X ray light curve of SN 1987A 19 p2775 N90-25776
X ray variability of active galactic nuclei 19 p2795 N90-25914

ENERGY BUDGETS
NT ATMOSPHERIC HEAT BUDGET
NT EARTH RADIATION BUDGET
NT HEAT BUDGET
An investigation of satellite sounding products for the remote sensing of the surface energy balance and soil moisture
[NASA-CR-186073] 06 p0801 N90-14664
Improved energy and power balance at Nova targets
[DE90-007260] 13 p1807 N90-20372
Cloud types and the tropical Earth radiation budget, revised
[NASA-CR-180475] 13 p1843 N90-20582
The extension of rapid distortion theory to stratified shear flows 14 p2005 N90-21491
Superheterodyne three-wave detection of gravitation waves
[DE90-620465] 16 p2255 N90-22856
Measuring and modeling near-surface reflected and emitted radiation fluxes at the FIFE site
[NASA-CR-180953] 20 p2879 N90-26378
ERBE and CERES broadband scanning radiometers 21 p3016 N90-27149
A study of the effect of synoptic scale processes in GCM modelling
[NASA-CR-184804] 21 p3021 N90-27175
Downwelled longwave surface irradiance data from five sites for the FIRE/SRB Wisconsin Experiment from October 12 through November 2, 1986
[NASA-TM-102597] 21 p3030 N90-27225
Solar wind and high energy particle effects in the middle atmosphere 22 p3206 N90-28188
Inhomogeneities of stratocumulus liquid water 22 p3213 N90-28228
The radiation budget of stratocumulus clouds measured by tethered balloon instrumentation: Variability of flux measurements 22 p3216 N90-28242
Structural analysis of stratocumulus convection 22 p3216 N90-28243
A case study of cumulus formation beneath a stratocumulus sheet: Its structure and effect on boundary layer budgets 22 p3219 N90-28256
A cloudiness transition in a marine boundary layer 22 p3219 N90-28259
Laboratory experiments on stability and entrainment of oceanic stratocumulus. Part 1: Instability experiment 22 p3220 N90-28263
A scheme for parameterizing cirrus cloud ice water content in general circulation models 22 p3226 N90-28292
Simulation and measurement of the heat exchange between the urban canopy and boundary layers 24 p3486 N90-29702

ENERGY CONSERVATION
Research on ultra low wear materials for energy conservation
[DE89-015096] 01 p0046 N90-10263
Technology applications bulletins
[DE89-017454] 02 p0288 N90-11651
Power factor controller study
[DE89-017655] 06 p0767 N90-14458
How far can the world get on energy efficiency alone
[DE90-001349] 06 p0805 N90-14686
Global energy and the greenhouse issue
[DE90-001394] 06 p0809 N90-14709
US energy use: New technologies and policies in response to global warming
[DE90-002170] 06 p0812 N90-14724
Planning minimum-energy paths in an off-road environment with anisotropic traversal costs and motion constraints
[AD-A214181] 07 p0942 N90-15457
A guide for estimating potential energy savings from increased solar reflectance of a low-sloped roof
[DE90-003720] 07 p0955 N90-15526
Guidelines for evaluating energy analysis software
[AD-A214171] 07 p0976 N90-15640
Federal roles to realize national energy-efficiency opportunities in the 1990s
[DE90-004410] 08 p1096 N90-16348
Proceedings of the Conference on Technology-Based Confidence Building: Energy and Environment
[DE90-003363] 08 p1099 N90-16366
The potential impact of conservation, alternative energy sources, and reduced nonenergy emissions on global warming
[DE90-004494] 09 p1244 N90-17220
Multi-dimensional discrete ordinates solutions to combined mode radiation heat transfer problems and their application to a free-falling particle, direct absorption solar receiver
[DE90-004987] 09 p1300 N90-17531
Office of Industrial Programs research in progress
[DE90-002100] 10 p1440 N90-18311
Energy markets in the 1990's and beyond: A comparison of energy intensity in the United States and Japan
[DE90-005535] 11 p1528 N90-18797
Operational fact-finding report on heat pump systems for industrial use
[DE89-782295] 12 p1658 N90-19527
A preliminary analysis of US CO2 emissions reduction potential from energy conservation and the substitution of natural gas for coal in the period to 2010
[DOE/NBB-0085] 12 p1684 N90-19673

Modeling studies of electrolyte flow and bubble behavior in advanced Hall cells
[DE90-007013] 13 p1795 N90-20303
Energy storage and distribution
[DE89-009487] 13 p1826 N90-20488
Controlling Summer Heat Islands: Proceedings
[DE90-008075] 13 p1830 N90-20508
The impedance of energy efficiency of a coaxial magnetized plasma source used for spheromak formation and sustainment
[DE90-003220] 13 p1889 N90-20841
Nonflammable hydraulic power system for tactical aircraft. Volume 1: Aircraft system definition, design and analysis
[AD-A218493] 17 p2356 N90-23409
Outlook for ceramics in heat engines, 1990 - 2010: A technical and economic assessment based on a worldwide Delphi survey
[DE90-011262] 19 p2679 N90-25234
Opportunities in solar energy research over the next decade
[DE90-012479] 21 p3019 N90-27164
Energy Efficient Engine: Flight propulsion system final design and analysis
[NASA-CR-168219] 23 p3279 N90-28558
Energy Efficient Engine core design and performance report
[NASA-CR-168069] 23 p3279 N90-28559
Energy Efficient Engine integrated core/low spool design and performance report
[NASA-CR-168211] 23 p3280 N90-28561
Energy efficient engine program technology benefit/cost study. Volume 1: Executive summary
[NASA-CR-174766-VOL-1] 23 p3280 N90-28564
Energy Efficient Engine: Control system preliminary definition report
[NASA-CR-179578] 23 p3281 N90-28569
Open cycle heat pump development for local resource use. Phase 2: District heating case study analysis
[DE90-011123] 23 p3345 N90-28904
Transferring building energy technologies by linking government and private-sector programs
[DE90-000346] 23 p3408 N90-29258
The technology transfer process: Background for the national energy strategy
[DE90-015301] 24 p3559 N90-30139

ENERGY CONSUMPTION
Technology applications bulletins
[DE89-017454] 02 p0268 N90-11651
Activities report on KEMA R and D
[ST-REPT-VOL-6-NO-12] 03 p0387 N90-12100
Measurement of mechanical work and energy expenditure in running and bicycling
05 p0675 N90-13935
Characterization of electric vehicle velocity and power profiles using road test data
[DE90-002085] 06 p0795 N90-14630
Laboratory study of the dynamic losses of a single speed, split system air-to-air heat pump having tube and plate fin heat exchangers, 1985 to 1986
[DE90-000970] 07 p0927 N90-15367
Planning minimum-energy paths in an off-road environment with anisotropic traversal costs and motion constraints
[AD-A214181] 07 p0942 N90-15457
Guidelines for evaluating energy analysis software
[AD-A214171] 07 p0976 N90-15640
Overview of photovoltaic and battery applications
[PB90-120536] 09 p1242 N90-17206
The potential impact of conservation, alternative energy sources, and reduced nonenergy emissions on global warming
[DE90-004494] 09 p1244 N90-17220
Cost and energy consumption estimates for the aluminum-air battery anode fuel cycle
[DE90-005810] 11 p1503 N90-18656
Thermal remote sensing in the differentiation of soybean crops (glycine max (L.) merrill) submitted to water deficit
[INPE-4900-PRE/1501] 11 p1522 N90-18782
Energy markets in the 1990's and beyond: A comparison of energy intensity in the United States and Japan
[DE90-005535] 11 p1528 N90-18797
Advanced absorption technology development in the United States
[DE90-001336] 12 p1641 N90-19428
Survey on the possibility of introducing new energy to regional development plans
[DE89-782627] 12 p1681 N90-19654
Analyses of power consumption for two sliding vane type compressors
[AD-A218366] 13 p1812 N90-20406
Energy storage and distribution
[DE89-009487] 13 p1826 N90-20488
Perspectives on solar energy and the environment
[DE90-007680] 13 p1828 N90-20494
The effects of climate change on energy planning and operations in the Pacific Northwest. Volume 1: Overview
[DE90-009464] 17 p2425 N90-23816
T4A thruster starting sequences and the design of an electromagnetic sequencer for cyclic life tests
[RAE-TR-77042] 19 p2669 N90-25179
Comparison of joint space versus task force load distribution optimization for a multiarm manipulator system
24 p3515 N90-29873

ENERGY CONVERSION
NT BIOMASS ENERGY PRODUCTION
NT GEOTHERMAL ENERGY CONVERSION
NT OCEAN THERMAL ENERGY CONVERSION
NT PHOTOTHERMAL CONVERSION
NT PHOTOVOLTAIC CONVERSION
NT SATELLITE SOLAR ENERGY CONVERSION
NT SOLAR ENERGY CONVERSION
NT WATERWAVE ENERGY CONVERSION
Second Beamed Space-Power Workshop
[NASA-CP-3037] 01 p0027 N90-10140
Bidirectional power converter control electronics
[NASA-CR-175070] 01 p0032 N90-10175
An assessment of technology for self-powered gas appliances: A GATC (Gas Appliance Technology Center)
[PB89-219265] 03 p0354 N90-12026
Interfacial systems for photochemical energy conversion
[DE90-003181] 07 p0953 N90-15514
Photochemical solar energy conversion utilizing semiconductors localized in membrane mimetic systems
[DE90-003450] 07 p0953 N90-15515
Organic cathode for a secondary battery
[NASA-CASE-NPO-17604-1-CU]
08 p1059 N90-16124
Mechanoelectric conversion by uniaxial constraint in piezoelectric generators: Optimization of electrical, mechanical, and physico-chemical parameters of materials
[ISAL-89-0020] 08 p1078 N90-16235
Production of jet fuels from coal derived liquids. Volume 10: Jet fuels production by-products, utility, and sulfur emissions control integration study
[AD-A213872] 09 p1200 N90-16951
Copper chloride cathode for a secondary battery
[NASA-CASE-NPO-17640-1-CU]
09 p1210 N90-17011
The 1989 National Convention Record IEE Japan, part 11
[DE89-910083] 09 p1210 N90-17014
Outlook for new energies. Secondary batteries
[DE90-734946] 09 p1210 N90-17017
Overview of photovoltaic and battery applications
[PB90-120536] 09 p1242 N90-17206
Analysis of competition among the kinds of energy at the era of complexed energy: General review
[DE89-910215] 11 p1527 N90-18793
Analysis of inter-energy competition in the age of complex energies
[DE89-910216] 11 p1527 N90-18794
Phase control mechanism for wave energy conversion
[AD-D014354] 12 p1681 N90-19657
Substorms: Their expansion and recovery phases
[DE90-008970] 14 p2042 N90-21712
ECUT: Energy Conversion and Utilization Technologies program. Biocatalysis project
[NASA-CR-186866] 19 p2717 N90-25458
Analysis of a Mars-stationary orbiting microwave power transmission system
[NASA-TM-101344] 20 p2843 N90-26172
Ignition and combustion of liquid propellants
[AD-A224150] 23 p3316 N90-28746

ENERGY CONVERSION EFFICIENCY
High-efficiency CuInSe2 and CuInGaSe2 based cells and materials research
[DE89-009449] 01 p0083 N90-10471
Laser grooved and polycrystalline silicon solar cell research
[DE89-015196] 02 p0237 N90-11347
Analysis of the efficiency of a dielectric solar energy collector
[PB89-212716] 03 p0366 N90-12092
The photovoltaic properties of an Al In As/InP heterojunctions grown by LPE method
[NASA-CR-185996] 05 p0665 N90-13886
The current status of x ray conversion efficiency modeling
[DE90-000931] 06 p0789 N90-14591
Research on high-efficiency, multiple-gap, multijunction, amorphous-silicon-based alloy thin-film solar cells
[DE89-009444] 06 p0803 N90-14673
Research on high-efficiency, single-junction, monolithic, thin-film amorphous silicon solar cells
[DE89-000846] 06 p0805 N90-14687
High-efficiency large-area CdTe modules
[DE89-009498] 06 p0806 N90-14689
Photovoltaic Measurements and Performance Branch
[DE89-009500] 06 p0807 N90-14695
The impact of global warming on the energy system
[DE89-017775] 06 p0810 N90-14712
Propulsion research on the hybrid plume rocket
[AD-A214420] 07 p0887 N90-15132
Research on high-efficiency, single-junction, monolithic, thin-film amorphous silicon solar cells, phase 1
[DE89-009495] 07 p0951 N90-15502
High-efficiency silicon concentrator solar cells for use with prismatic covers
[DE90-002644] 07 p0952 N90-15509
Energy conversion efficiency in high current Raman regime Free Electron Laser (FEL). 1: Single mode analysis
[DE90-719527] 09 p1227 N90-17120
Biomass fuels in the developing countries: An overview
[DE90-002616] 09 p1241 N90-17201
Light-trapping concentrator cells
[DE90-004988] 09 p1242 N90-17205
High-efficiency copper ternary thin film solar cells
[DE89-009470] 09 p1242 N90-17207
Research on amorphous silicon based thin film photovoltaic devices. Phase 2: Research on stable high-efficiency, large area amorphous silicon based submodules
[DE89-009515] 09 p1243 N90-17209
European regenerative fuel cell technology for space use 10 p1333 N90-17709
Ga0.47In0.53As cells for GaAs-stacked photovoltaic tandems 10 p1338 N90-17749
GaAs cells on Si substrates: A new challenge for space photovoltaic applications 10 p1339 N90-17750
GaAs solar cells with V-grooved emitters
10 p1339 N90-17754
AlGaAs/GaAs solar cells with efficiencies greater than 22 percent 10 p1339 N90-17755
Indium phosphide solar cell research in the United States: Comparison with non-photovoltaic sources
10 p1340 N90-17758
Pilot production of 70 micron thin silicon solar cells
10 p1343 N90-17780
GaAs back point contact solar cell simulation
10 p1343 N90-17781
Solar cell electrodynamic characteristics test equipment 10 p1344 N90-17791
Assessment of in-orbit performance data of a bifacial flight experiment 10 p1344 N90-17793
Research relating to crystalline silicon-film on a foreign substrate
[DE90-005720] 11 p1491 N90-18582
Advanced absorption technology development in the United States
[DE90-001336] 12 p1641 N90-19428
Strategies for high efficiency operation of the E-beam excited atomic xenon laser using high-power and high-energy loading
[DE90-005196] 13 p1806 N90-20370
High-efficiency silicon concentrator solar cell research
[DE90-008040] 13 p1827 N90-20490
High-efficiency silicon solar cells for a 22-sun line-focus module
[DE90-010242] 16 p2251 N90-22840
Enhanced ceria solid electrolyte fuel cell development. Reduction of electronic conductivity permits use of a solid ceria electrolyte in high efficiency high power density fuel cells at temperatures compatible with metallic cell hardware
[AD-A219297] 16 p2253 N90-22846
Interdigitated back contact silicon solar cell analysis and design recommendations for space use
[AD-A220414] 17 p2420 N90-23790
Summary results of an assessment of research projects in the national photovoltaics program
[DE90-008222] 18 p2577 N90-24680
Photovoltaic measurements and performance branch
[DE90-000324] 18 p2577 N90-24681
Development of a point-contact solar cell using high-volume processing techniques
[DE90-010330] 18 p2577 N90-24683
Research on design and fabrication of high-efficiency solar cells
[DE90-012010] 19 p2711 N90-25429
Use of high-temperature superconductors in superconducting magnetic energy power sources
[DE90-011119] 19 p2761 N90-25686
Silicon concentrator solar cell development
[DE90-011782] 20 p2880 N90-26386
Megawatt solar power systems for lunar surface operations
[NASA-CR-186509] 20 p2881 N90-26391
Recent technological advances in thin film solar cells
[DE90-000321] 21 p3019 N90-27165

Sandia's CONCEPT-90 photovoltaic concentrator module
[DE90-012243] 22 p3196 N90-28134
Solar electricity and solar fuels
[DE90-796156] 22 p3196 N90-28135
Energy Efficient Engine high pressure turbine component test performance report
[NASA-CR-168289] 23 p3278 N90-28553
Energy Efficient Engine acoustic supporting technology report
[NASA-CR-174834] 23 p3279 N90-28557
Energy Efficient Engine: Flight propulsion system final design and analysis
[NASA-CR-168219] 23 p3279 N90-28558
Energy Efficient Engine program advanced turbofan nacelle definition study
[NASA-CR-174942] 23 p3280 N90-28560
Assessment of battery technologies for electric vehicles. Volume 2, part 2: Appendices
[DE90-014610] 23 p3321 N90-28778
Fuel cells: Their applications, technological status, market and opportunity
[DE90-796158] 23 p3344 N90-28895
Evaluation of the STM4-120 kinematic Stirling engine
[DE90-013836] 23 p3344 N90-28897
A 10kW class molten carbonate fuel cell test: The stack with electrolyte plate prepared with paper-making method
[DE90-507841] 23 p3344 N90-28900
Study of power generation systems for CO2 collection: LNG combined cycle
[DE90-507881] 23 p3345 N90-28901
Performance measurements and energy balance of an SPS V160 Stirling motor at the German Aerospace Research Establishment
[DLR-MITT-90-03] 23 p3345 N90-28903
Research on stable, large-area, amorphous silicon based submodules, phase 3
[DE90-000339] 23 p3399 N90-29204
Basic studies of 3-V high efficiency cell components
[DE90-000360] 24 p3484 N90-29696

ENERGY CONVERTERS
U DIRECT POWER GENERATORS

ENERGY DENSITY
U FLUX DENSITY

ENERGY DISSIPATION
A mechanical power flow capability for the finite element code NASTRAN
[AD-A212202] 04 p0513 N90-12964
Three D flows in turbine blade rows 05 p0641 N90-13739
Damping characteristics of metal matrix composites
[AD-A213712] 07 p0891 N90-15151
Flux parameterization techniques in the atmospheric surface layer 07 p0959 N90-15548
A numerical simulation model for the study of magnetohydrodynamic (MHD) waves in a structured medium 07 p1012 N90-15864
Experimental investigation of a three-dimensional wake. Part 2: Spectral and turbulent energy analysis
[ONERA-RT-32/5025-AYD-PT-2] 08 p1018 N90-15887
Turbulent heat and momentum transfer in recirculating and impinging flows 09 p1215 N90-17043
Energy decay and boundary control for distributed parameter systems with viscoelastic damping
[AD-A216468] 11 p1519 N90-18748
Muzzle shunt augmentation of conventional railguns
[DE90-007505] 12 p1607 N90-19248
Present status of (mu)CF theory
[DE90-007547] 13 p1884 N90-20809
An investigation of secondary flows in nozzle guide vanes 14 p1923 N90-21016
Losses in the tip-leakage flow of a planar cascade of turbine blades 14 p1925 N90-21027
Surface characterization of hydrogen charged and uncharged alpha-2 and gamma titanium aluminide alloys using AES and REELS
[NASA-CR-186561] 14 p1951 N90-21171
The evolution of the supernova remnant IC 443 15 p2186 N90-22486
Test and evaluation of surf forecasting model
[AD-A219580] 17 p2430 N90-23845
Controling, cabling and protection of GTO thyristors in pulse inverters
[ETN-90-96500] 18 p2549 N90-24548
Exploding neutron stars near the minimum mass: The total energy release 19 p2774 N90-25769
The application of HREELS to model catalysts: CO and C2H4 adsorption on Pt/Al2O3
[AD-A222744] 20 p2831 N90-26103
Measurements of energy dispersion at liquid-solid interfaces: Fluorescence quenching of pyrene bound to fumed silica
[AD-A222371] 21 p2978 N90-26926
On diamond, graphitic and amorphous carbons in primitive extraterrestrial solar system materials 21 p3095 N90-27591
Rain-fade simulation and power augmentation for satellite communication systems
[NASA-TM-103134] 23 p3319 N90-28768
Estimation of individual coupling loss factors in a multi-subsystem
[ISVR-TR-184] 23 p3389 N90-29141
Satellite measurements of magnetospheric Poynting flux
[AD-A224391] 24 p3490 N90-29724

ENERGY DISTRIBUTION
NT SPECTRAL ENERGY DISTRIBUTION
Global and local fluctuations in multiplicity and transverse energy for central ultra-relativistic heavy-ion interactions
[LUIP-8903] 02 p0272 N90-11555
Fluctuations in transverse energy and multiplicity, energy densities, and neutral pion spectra in nucleus-nucleus collisions at 200 GeV/nucleon
[DE89-017583] 03 p0402 N90-12302
Time evolution of the electron swarm energy distribution function
[AD-A212967] 04 p0557 N90-13247
Background electrodynamics measured by EISCAT during the NEED campaign 05 p0660 N90-13851
Analysis of catalytically enhanced solar absorption chemical reactors. 2: Predicted characteristics of a 100 kW chemical reactor
[DE89-014743] 07 p0954 N90-15521
Maxwellian cascade model
[DE90-004389] 10 p1427 N90-18235
Electron energy distributions and vibrational population distributions
[DE90-005550] 12 p1711 N90-19825
New calculations and measurements of the Coulomb cross-section for the production of direct electron pairs by high energy nuclei
[NASA-TM-101280] 15 p2165 N90-22371
The high temperature behavior of gallium and indium liquid metal ion sources
[AERE-R-13321] 16 p2217 N90-22647
On the nature of the 1980 outburst of the Be/X ray binary A0535+26=HDE 245770 19 p2778 N90-25803
Excimer laser fragmentation studies of selected oximes: Nascent OH internal energy distributions and the search of H2CN fluorescence
[AD-A222622] 20 p2868 N90-26317
Vacuum deposition by pulsed laser radiation: Plasma composition, deposition techniques, and thin film properties
[ETN-90-97263] 20 p2931 N90-26677

ENERGY EFFICIENCY TRANSPORT PROGRAM
U ACEE PROGRAM

ENERGY EXCHANGE
U ENERGY TRANSFER

ENERGY GAPS (SOLID STATE)
Two photon absorption characterization
[AD-A210508] 01 p0121 N90-10694
Optical dispersion relations for diamondlike carbon films
[NASA-TM-102356] 01 p0129 N90-10738
A fermi liquid electric structure and the nature of the carriers in high-T(sub c) cuprates: A photoemission study
[DE89-016774] 02 p0284 N90-11624
Graded bandgap solar cells
[AD-A211537] 03 p0367 N90-12097
Local pairing and antiferromagnetism in high-T sub c superconductors
[AD-A213004] 05 p0703 N90-14113
Multiband photoconductive detector based on layered semiconductor quantum wells
[AD-D014232] 06 p0849 N90-14936
Molecules with enhanced electronic polarizabilities based on defect-like states in conjugated polymers
[NASA-CASE-NPO-17633-1-CU] 07 p0910 N90-15263
Picosecond photoconductivity using a graded bandgap Al(x)Ga(1-x)As active detecting layer
[DE90-003452] 07 p1000 N90-15786
The effect of annealing treatments on defect structure and diffusion lengths in n-type GaAs
[AD-A214215] 07 p1005 N90-15817
An investigation of narrow-bandgap semiconductors: Devices, circuits, and systems 15 p2171 N90-22406
Direct implantation process development and characterization in advanced Hg(1)-(x)Cd(x) Te EPI layers
[AD-A219133] 16 p2324 N90-23252

ENERGY LEVELS
NT ATOMIC ENERGY LEVELS
NT ELECTRON STATES
NT GROUND STATE
NT INTERMOLECULAR FORCES
NT MOLECULAR ENERGY LEVELS
Quantum chemical investigations of the mechanism of cationic polymerization and theoretical prediction of crystal densities and decomposition pathways of energetic molecules
[AD-A210322] 02 p0200 N90-11143
Prospects for wavelength tunable lasers based on vacancy defects in alkaline-earth oxides
[DE90-001078] 06 p0789 N90-14592
High resolution-angle resolved photoemission studies of high temperature superconductors
[DE89-017691] 06 p0852 N90-14950
Tunnelling effects on low energy fusion cross sections
[AD-A214010] 07 p0997 N90-15762
X ray absorption studies of YBa2Cu3O(6+x), La(2-x)Sr(x)CuO4, and Nd(2-x)Ce(x)CuO4
[DE90-003640] 07 p1002 N90-15797
On the observation of a transition from fusion to multifragmentation in high multiplicity O16 induced reactions
[LUIP-8812] 08 p1119 N90-16481
A computer program to calculate the population numbers of multi-level species
[IFSI-89-15] 08 p1151 N90-16671
Maxwellian cascade model
[DE90-004389] 10 p1427 N90-18235
Coherent state in the roton region of superfluid helium-4
[DE90-610677] 12 p1720 N90-19882
Precompound decay models for medium energy nuclear reactions
[DE90-008352] 13 p1884 N90-20808
Determinations of photon spectra
[AD-A218003] 13 p1885 N90-20816
Surface physics instrumentation
[AD-A220460] 17 p2373 N90-23512
Intersubband transitions in an asymmetric quantum well with a thin barrier of a delta-function potential
[AD-A220723] 17 p2477 N90-24162
New electronic states of NH and ND observed by resonance enhanced multiphoton ionization spectroscopy 20 p2945 N90-26760
Resonance enhanced two-laser infrared multiple photon dissociation of gaseous ions
[AD-A221826] 21 p2970 N90-26879
Research on stable, large-area, amorphous silicon based submodules, phase 3
[DE90-000339] 23 p3399 N90-29204
Monte Carlo simulation of complex spectra for opacity calculations
[DE90-015198] 24 p3561 N90-30147

ENERGY LOSS
U ENERGY DISSIPATION

ENERGY METHODS
NT STRAIN ENERGY METHODS
Solution of the Boltzmann equation using an energy group method
[AD-A213138] 05 p0699 N90-14096
Low energy neutral particle energy analyser by time of flight method
[DE90-719529] 08 p1125 N90-16517
A comparison of flutter calculations based on eigenvalue and energy method 11 p1459 N90-18406
An approximate viscous shock layer method for calculating the hypersonic flow over blunt-nosed bodies 14 p1910 N90-20947
Elastic stability and nonlinear behavior of imperfect shells with initial stresses 15 p2110 N90-22070
Proceedings of a research workshop on Computational Condensed Matter Physics. Total Energy Methods and Physics of III-V Semiconductors
[AD-A219568] 17 p2476 N90-24156
Estimation of individual coupling loss factors in a multi-subsystem
[ISVR-TR-184] 23 p3389 N90-29141

ENERGY POLICY
The Third Pacific Basin Biofuels Workshop: Proceedings
[DE90-002523] 07 p0953 N90-15513
Energy management and recovery 08 p1032 N90-15962
A qualitative architecture for understanding policy responses to global change
[DE90-003936] 08 p1099 N90-16384
Alternative fuels R/D needs: Program directions
[DE90-007053] 11 p1495 N90-18603
Analysis of competition among the kinds of energy at the era of complexed energy: General review
[DE89-910215] 11 p1527 N90-18793

Analysis of inter-energy competition in the age of complex energies
[DE89-910216] 11 p1527 N90-18794
Analysis of competition among kinds of energy at the era of complexed energy. (Report on overseas study)
[DE89-910213] 12 p1680 N90-19650
Pyranometry
[DWD-14] 12 p1682 N90-19661
Perspectives on solar energy and the environment
[DE90-007680] 13 p1828 N90-20494
Activities report in technical-physical research
[ETN-90-96771] 17 p2487 N90-24223
The potential of renewable energy
[DE90-000322] 21 p3019 N90-27163
Responding to the threat of global warming: Options for the Pacific and Asia
[DE90-014756] 23 p3347 N90-28918

ENERGY REQUIREMENTS
Energy management and recovery
08 p1032 N90-15962

ENERGY SOURCES
The 1989 National Convention Record IEE Japan, part 11
[DE89-910083] 09 p1210 N90-17014
The extended equivalent source technique with underdetermined sources
[DE90-006989] 11 p1499 N90-18627
Analysis of competition among the kinds of energy at the era of complexed energy: General review
[DE89-910215] 11 p1527 N90-18793
The high energy source 3C 273
16 p2337 N90-23318
The potential of renewable energy
[DE90-000322] 21 p3019 N90-27163

ENERGY SPECTRA
NT ELECTRONIC SPECTRA
NT NEUTRON SPECTRA
A solar extreme ultraviolet flux model
02 p0296 N90-11686
Wave particle interactions
[DE89-017527] 03 p0407 N90-12335
Evidence for anomalous cosmic ray hydrogen
06 p0861 N90-15005
A large detector for cosmic ray abundance and energy measurements 06 p0867 N90-15037
Characterizing transient vibrations using band limited moments
[DE90-000799] 07 p0945 N90-15473
Substructural dependence of the multiparticle production in relativistic heavy-ion interactions
[LUIP-8904] 07 p0989 N90-15716
Target nucleus fragmentation in O16 + (Ag,Br) interactions at 200 A GeV
[LUIP-8906] 07 p0991 N90-15727
A calculation of energetic proton spectra producedat substorm onset in the fields of the explosive reconnection model 07 p1013 N90-15866
LEAP: A balloon-borne search for low-energy cosmic ray antiprotons 07 p1015 N90-15878
Experimental investigation of a three-dimensional wake. Part 2: Spectral and turbulent energy analysis
[ONERA-RT-32/5025-AYD-PT-2]
08 p1018 N90-15887
PROTEL: Design, fabrication, calibration, testing, and satellite integration of a proton telescope
[AD-A214564] 09 p1183 N90-16861
Background studies in gas ionizing x ray detectors
12 p1636 N90-19399
Cosmic ray composition and muon decoherence at the knee of the all-particle cosmic ray spectrum
12 p1745 N90-20035
Determinations of photon spectra
[AD-A218003] 13 p1885 N90-20816
Gamma-ray production cross section measurements using a white neutron source from 1 to 400 MeV
[DE90-008906] 14 p2025 N90-21610
Long term intensity stability of Auger electron spectrometers: Instructions for the interlaboratory comparison
[NPL-DMM(A)-1] 15 p2102 N90-22027
The modeling of IRAS detections of classical novae and related objects 15 p2185 N90-22482
Spectral determinations for discrete sources with EGRET 16 p2336 N90-23312
What is learned from high energy bursts and flares
16 p2336 N90-23314
Gamma rays from active galactic nuclei
16 p2337 N90-23316
Kinematics under wind waves
[AD-A219541] 17 p2430 N90-23844
Dose analysis of the model 112A Pulserad pulsed x ray generator by its CYLTRAN
[AD-A220372] 17 p2471 N90-24125
Analysis of energy spectra of the ions in the coma of Halley's comet for the evaluation of the production ratio of methane and ammonia
[ETN-90-96489] 18 p2638 N90-25026
Is the hard tail of X rays from GX339-4 a Compton scattering component 19 p2779 N90-25806
High energy X ray observations of GX 1+4 with HEXE
19 p2779 N90-25808
The role of comptonisation in energy spectra of standard QPO-sources 19 p2781 N90-25820
Electron energy spectrum and magnetic interactions in high-T(sub c) superconductors 22 p3149 N90-27857
A search for low energy cosmic ray antiprctons
24 p3564 N90-30161

ENERGY STORAGE
NT ELECTRIC ENERGY STORAGE
NT HEAT STORAGE
NT MAGNETIC ENERGY STORAGE
Capacitive energy storage at cryogenic temperatures, phase 2
[AD-A210366] 01 p0061 N90-10347
Energy storage and distribution program summary. Volume 2: Research summaries, fiscal year 1988
[DE89-000867] 01 p0083 N90-10470
Propagation of normal zones of finite size in large, composite superconductors
[DE89-016866] 02 p0282 N90-11611
Phase change material for spacecraft thermal management
[AD-A211404] 04 p0462 N90-12648
Heat pipe and thermal energy storage and corrosion studies (1988)
[AD-A212655] 04 p0472 N90-12706
Elastomeric impulse energy storage and transfer system
[AD-D014223] 06 p0730 N90-14255
A heat receiver design for solar dynamic space power systems
[NASA-TM-102473] 06 p0735 N90-14283
Energy ratings for metal oxide varistors under repetitively pulsed operation
[DE90-002353] 06 p0770 N90-14480
Performance of the 10-kV, 100-kA pulsed-power modules for the FRX-C magnetic compression experiment
[DE89-014027] 06 p0845 N90-14917
Thermal energy storage
[DE90-000953] 07 p0950 N90-15500
Selection of phase-change and containment materials for thermal energy storage
[NASA-CR-186228] 07 p0952 N90-15506
Satellite thermal storage systems using metallic phase-change materials
[DE89-016872] 07 p0952 N90-15507
Ninth Battery and Electrochemical Contractors' Conference: Extended abstracts
[DE89-016837] 08 p1059 N90-16120
Investigation and study on compressed air storage power generation system, part 2
[DE90-702648] 08 p1097 N90-16354
Modeling energy output of inertial storage devices for the DIII-D tokamak
[DE90-004096] 08 p1126 N90-16524
Space Station Freedom energy storage system design and development 10 p1332 N90-17701
Hydrogen/oxygen SPE (trademark) electrochemical devices for zero-g applications 10 p1333 N90-17710
Water removal studies on high power hydrogen-oxygen fuel cells with alkaline electrolytes
10 p1333 N90-17712
Solid polymer electrolyte water electrolysis as a mean of energy storage for space applications
10 p1334 N90-17713
Nickel hydrogen cell design for space applications
10 p1334 N90-17714
Electron production, electron attachment, and charge recombination process in high pressure gas discharges
[AD-A216301] 10 p1434 N90-18274
Lithium ambient-temperature battery reliability
[DE90-005758] 11 p1502 N90-18650
ARDEC (Armament Research, Development and Engineering Center) electric gun in-house test program
[AD-A217337] 13 p1760 N90-20105
Exploratory battery technology development and testing report for 1988
[DE90-007996] 13 p1794 N90-20297
Energy storage and distribution
[DE89-009487] 13 p1826 N90-20488
Novel electrodes for advanced energy storage systems
[DE90-008667] 13 p1828 N90-20496
Physical performance and carbohydrate consumption in CF commandos during a 5-day field trial
[AD-A217204] 13 p1850 N90-20619
Analysis of thermal energy storage material with change-of-phase volumetric effects
[NASA-TM-102457] 15 p2092 N90-21974
Reactions of N2A3 sigma u + and candidates for short wavelengths lasers
[DE90-009514] 15 p2103 N90-22033
Experimental studies on energy storage
[AD-A219032] 16 p2252 N90-22845
Evaluation of the state of charge of battery electrodes with ac impedance techniques
[AD-A219561] 17 p2420 N90-23789
Lunar orbiting microwave beam power system
[NASA-TM-103211] 19 p2667 N90-25173
Energy storage for a lunar base by the reversible chemical reaction: CaO+H2O reversible reaction Ca(OH)2
[NASA-TM-103145] 19 p2709 N90-25419
The use of hydrogen in energy economy of Finland
[DE90-796180] 20 p2881 N90-26388
A lightweight solid polymer electrolyte fuel cell with stack power density of 3 kW/lb (7kW/kg)
[AD-A223068] 21 p3020 N90-27169
A solar power system for an early Mars expedition
[NASA-TM-103219] 22 p3243 N90-28393
Development of the sodium/sulfur technology for energy storage
[DE90-014329] 23 p3344 N90-28899
Proceedings of the High Energy Density Materials Contractors Conference
[AD-A223793] 24 p3484 N90-29695
Experimental studies leading to energy storage. Spectroscopy and dynamics of polyatomic hydrogen in liquid, solid and gaseous hydrogen plasmas
[AD-A224343] 24 p3547 N90-30066

ENERGY STORAGE DEVICES
U ENERGY STORAGE

ENERGY TECHNOLOGY
NT GEOTHERMAL TECHNOLOGY
Gyrotron development for space power beaming
01 p0028 N90-10148
History and status of beamed power technology and applications at 2.45 Gigahertz 01 p0029 N90-10150
Summaries of the FY 1989 Applied Mathematical Sciences Research program
[DE89-016694] 02 p0267 N90-11521
Technology applications bulletins
[DE89-017454] 02 p0288 N90-11651
Activities report on KEMA R and D
[ST-REPT-VOL-6-NO-12] 03 p0367 N90-12100
FEDIX: An on-line information service for universities and other research organizations: User's guide, version 2.0, release 1
[DE89-016695] 03 p0417 N90-12398
Advanced energy system program
[PB89-235170] 05 p0665 N90-13887
How far can the world get on energy efficiency alone
[DE90-001349] 06 p0805 N90-14686
The impact of global warming on the energy system
[DE89-017775] 06 p0810 N90-14712
Molten carbonate fuel cell technology improvement
[DE90-001934] 07 p0950 N90-15501
The Solar Power Satellite (SPS): Progress so far
07 p1008 N90-15840
SERI (Solar Energy Research Institute) solar radiation resource assessment project
[DE89-009456] 08 p1097 N90-16352
Outlook for new energies. Secondary batteries
[DE90-734946] 09 p1210 N90-17017
The potential impact of conservation, alternative energy sources, and reduced nonenergy emissions on global warming
[DE90-004494] 09 p1244 N90-17220
Hydrogen energy coordinating committee: Summary of DOE hydrogen programs
[DE90-004480] 10 p1361 N90-17891
Energy technology R and D and the greenhouse effect
[DE90-001339] 10 p1406 N90-18107
Office of Industrial Programs research in progress
[DE90-002100] 10 p1440 N90-18311
Progress in thin film solar photovoltaic technologies
[DE89-009513] 11 p1527 N90-18792
Analysis of competition among the kinds of energy at the era of complexed energy: General review
[DE89-910215] 11 p1527 N90-18793
Analysis of inter-energy competition in the age of complex energies
[DE89-910216] 11 p1527 N90-18794
Advanced battery development
[DE90-006073] 11 p1529 N90-18806
Programs in Renewable Energy
[DE89-009489] 11 p1530 N90-18809
Hawaii integrated biofuels research program, phase 1
[DE90-006885] 11 p1530 N90-18811

Operational fact-finding report on heat pump systems for industrial use
[DE89-782295] 12 p1658 N90-19527
Solid oxide fuel cell cogeneration system conceptual design, program 2
[PB90-114968] 12 p1681 N90-19653
A preliminary analysis of US CO2 emissions reduction potential from energy conservation and the substitution of natural gas for coal in the period to 2010
[DOE/NBB-0085] 12 p1684 N90-19673
An evaluation of the relationship between the production and use of energy and atmospheric methane emissions
[DE90-007982] 14 p2004 N90-21487
A theoretical and experimental investigation of an absorption refrigeration system for application with solar energy units 16 p2226 N90-22697
Ocean energy program summary
[DE89-009481] 16 p2251 N90-22836
Geothermal energy program summary
[DE89-009485] 16 p2251 N90-22837
Geothermal energy program summary
[DE89-009486] 16 p2251 N90-22838
Nuclear power in space
[GPO-23-835] 16 p2316 N90-23202
Biofuels program summary. Volume 2: Research summaries
[DE89-009484] 18 p2576 N90-24678
SERI photovoltaic subcontract reports: 1989 abstracts and document control information, March 1, 1987 to February 29, 1988
[DE90-000336] 18 p2577 N90-24682
The use of hydrogen in energy economy of Finland
[DE90-796180] 20 p2881 N90-26388
Energy data base: Subject categories and scope
[DE90-009212] 20 p2936 N90-26706
Hydrogen Energy Coordinating Committee summary of DOE hydrogen programs for FY 1988
[DOE/CE-0242] 21 p2989 N90-26989
The potential of renewable energy
[DE90-000322] 21 p3019 N90-27163
Opportunities in solar energy research over the next decade
[DE90-012479] 21 p3019 N90-27164
The production potential of wind power in Finland
[DE90-796157] 22 p3196 N90-28136
Survey of superconductors for energy applications
[DE90-796181] 22 p3248 N90-28420
Fuel cells: Their applications, technological status, market and opportunity
[DE90-796158] 23 p3344 N90-28895
Solar energy for high temperature technology and applications
[ETN-90-97429] 23 p3345 N90-28902
Transferring building energy technologies by linking government and private-sector programs
[DE90-000346] 23 p3408 N90-29258
Some studies related to a new Hexagonal Compound Parabolic Concentrator (HCPC) as a secondary in tandem with a solar tower
[DLR-FB-90-12] 24 p3485 N90-29700

ENERGY TRANSFER
NT LINEAR ENERGY TRANSFER (LET)
Numerical simulation of detonation transfer between gaseous explosive layers
[MRL-RR-1-89] 01 p0069 N90-10395
The auroral energy deposition over the polar ionosphere during substorms
[AD-A210522] 01 p0086 N90-10490
Energy dependent transport problem with generalized boundary conditions
[DE89-617843] 01 p0118 N90-10676
Particle kinetic simulation of high altitude hypervelocity flight
[NASA-CR-186003] 02 p0147 N90-10840
A severe human ESD (Electrostatic Discharge) model for safety and high reliability system qualification testing
[DE89-016177] 02 p0216 N90-11233
Laser production of soft x rays by multiquantum processes and the excitation of atomic inner-shell states
[AD-A211372] 03 p0353 N90-12021
Quantum-mechanical derivation of the Davydov equations for multi-quanta states
[DE89-015250] 03 p0401 N90-12297
Energy transfer and non-linear optical properties at near ultraviolet wavelengths: Rare earth 4f(yields)5d transitions in crystals and glasses
[DE90-000065] 03 p0405 N90-12321
Rotational and vibrational nonequilibrium effects in rarefied, hypersonic flow
[NASA-CR-182559] 04 p0437 N90-12498
Analysis and simulation of dynamics of spacecraft power systems 04 p0463 N90-12653
A mechanical power flow capability for the finite element code NASTRAN
[AD-A212202] 04 p0513 N90-12964
Time evolution of the electron swarm energy distribution function
[AD-A212967] 04 p0557 N90-13247
Energy exchange of interacting solitons in multidimensions
[PREPRINT-662] 05 p0696 N90-14071
Energy barriers in SK spin-glass model
[PREPRINT-665] 05 p0704 N90-14119
Energy ratings for metal oxide varistors under repetitively pulsed operation
[DE90-002353] 06 p0770 N90-14480
Inductive store opening switch and tests for energy transfer to a load
[DE90-002818] 06 p0770 N90-14482
Energy deposition in low power coaxial plasma thrusters 06 p0844 N90-14911
Kinetic studies following state-selective laser excitation
[DE90-003232] 07 p0935 N90-15415
Determination of stepsize parameters for intermolecular vibrational energy transfer
[DE90-003346] 07 p0990 N90-15719
Rotational energy transfer in metastable states of heteronuclear molecules
[AD-A214425] 08 p1120 N90-16485
Recent progress on the HESS (High Explosive Spheromak Source) experiment
[DE90-003218] 08 p1125 N90-16520
Progress with small, high-magnetic-field spheromaks in CTX
[DE90-003395] 08 p1127 N90-16527
Physical models for supersonic turbulent boundary layer structure
[AD-A215284] 09 p1160 N90-16716
Combustion of hydrogen and hydrocarbons in fluorine
[AD-A214621] 09 p1190 N90-16896
Theory of the dissociation dynamics of small molecules on metal surfaces: Finite temperature studies
[DE90-005217] 09 p1195 N90-16923
Singlet oxygen and iodine monofluoride collisional energy transfer mechanism
[AD-A215711] 09 p1280 N90-17421
Interactions of molecules with surfaces
[DE90-005337] 10 p1428 N90-18237
Scale transformations, the energy-momentum tensor, and the equation of state
[DE90-005372] 10 p1440 N90-18308
Report from magnetospheric science 10 p1444 N90-18334
Energy transfer and photochemistry in biomimetic solar conversion
[PB90-114562] 12 p1681 N90-19652
Energy deposition measurements for E-beam pumped excimer lasers
[DE90-007545] 13 p1806 N90-20365
Solar cyclical trend study of the mid-latitude, quiet-time, meridional, neutral winds at winter solstice conditions
[AD-A217398] 13 p1841 N90-20568
A continued study of optical sound generation and amplification
[AD-A217640] 13 p1882 N90-20796
Energy transfer between electrons and ions in collision cascades in solids
[AERE-R-13662] 13 p1883 N90-20801
Interactions of molecules with surfaces
[DE90-007555] 13 p1883 N90-20806
The numerical simulation of multistage turbomachinery flows 14 p1925 N90-21025
The extension of rapid distortion theory to stratified shear flows 14 p2005 N90-21491
The generally covariant representation of energy-momentum pseudotensor of gravitational field
[DE90-615203] 14 p2034 N90-21669
Incomplete fusion reactors at low and intermediate energies
[KVI-809] 16 p2316 N90-23206
A study of gravity wave variability, saturation, and turbulence generation in the mesosphere and lower thermosphere
[AD-A220018] 17 p2424 N90-23810
Prediction of high-voltage, broadband RF pulse generation from an air gas avalanche switch
[DE90-010183] 18 p2549 N90-24551
IR transition moments and collisional dynamics of vibrationally excited OH radicals via time-resolved laser absorption spectroscopy
[AD-A221005] 18 p2580 N90-24696
Fast plasma mixing: A new excitation method for CW gas lasers
[AD-A220290] 18 p2617 N90-24904
Decay rate and resonance fluorescence spectrum of a molecule near a composite material surface
[AD-A219692] 19 p2671 N90-25192
Rotational and translational effects in collisions of electronically excited diatomic hydrides
[NASA-CR-186770] 20 p2829 N90-26093
Theoretical studies of solar pumped lasers
[NASA-CR-186712] 20 p2867 N90-26308
A closed form solution to HZE propagation
[NASA-TM-103482] 20 p2924 N90-26640
Determination of molecular spectroscopic parameters and energy-transfer rates by double-resonance spectroscopy 20 p2944 N90-26755
Measurements of the methane relaxation times for application to the infrared emission models of the upper atmospheres of outer planets and Titan 20 p2945 N90-26759
Structure and dynamics of excited atoms
[AD-A221973] 21 p3074 N90-27474
Ultra-fast visualization of a turbulent boundary layer by a laser velocimeter
[IMFL-89-37] 22 p3181 N90-28048
Energy deposition of corpuscular radiation in the middle atmosphere 22 p3206 N90-28190
A new calculation of the radiative cooling by carbon dioxide in the middle atmosphere and the lower thermosphere 22 p3210 N90-28211
Energy transmission by means of coherent quasi-mono-chromatic light beams 23 p3392 N90-29163
Theoretical studies of proton beams in solar flare loops 23 p3413 N90-29286
Simulation and measurement of the heat exchange between the urban canopy and boundary layers 24 p3486 N90-29702
Effects of energy, momentum and particle transport in the near-earth solar terrestrial system
[AD-A224393] 24 p3490 N90-29726

ENGINE AIRFRAME INTEGRATION
A supersonic through-flow fan engine airframe integration study
[NASA-CR-185140] 01 p0001 N90-10004
Re-engine with the Rolls-Royce Tay 670, the route to significant noise reduction
[PNR90585] 04 p0455 N90-12606
Space transportation booster engine configuration study. Addendum: Design definition document
[NASA-CR-183854] 09 p1184 N90-16862
A comparison of scramjet engine performances of various cycles
[NAL-TR-1042] 24 p3434 N90-29397
Analysis of scramjet engine characteristics
[NAL-TR-1041] 24 p3434 N90-29398

ENGINE CONTROL
NT ROCKET ENGINE CONTROL
NT TURBOJET ENGINE CONTROL
Full scale technology demonstration of a modern counterrotating unducted fan engine concept. Engine test
[NASA-CR-180869] 01 p0011 N90-10049
Independent Orbiter Assessment (IOA): Analysis of the hydraulics/water spray boiler subsystem
[NASA-CR-185541] 02 p0165 N90-10934
An open-loop transient thermodynamic model of the Couguar turbojet
[AD-A211774] 03 p0307 N90-11745
Engine controls for the 1990's
[PNR90546] 03 p0308 N90-11748
Automatic prestart or post shutoff engine lubricator
[AD-D014259] 08 p1084 N90-16273
Software verification plan for GCS — guidance and control software
[NASA-TM-101668] 10 p1394 N90-18057
The implementation and operation of a variable-response electronic throttle control system for a TF-104G aircraft
[NASA-TM-101696] 13 p1756 N90-20086
Software requirements: Guidance and control software development specification
[NASA-CR-182058] 20 p2906 N90-26527
Propulsion system-flight control integration and optimization: Flight evaluation and technology transition
[NASA-TM-4207] 23 p3278 N90-28551
Smart microsensors for high temperature applications, phase 1
[AD-A224151] 23 p3330 N90-28828

ENGINE COOLANTS
Cooling of rocket thrust chambers with liquid oxygen
[NASA-TM-103146] 16 p2210 N90-22605
Computer code for predicting coolant flow and heat transfer in turbomachinery
[NASA-TP-2985] 22 p3120 N90-27722

ENGINE DESIGN
NT ROCKET ENGINE DESIGN
A supersonic through-flow fan engine airframe integration study
[NASA-CR-185140] 01 p0001 N90-10004
Performance potential of an advanced technology Mach 3 turbojet engine installed on a conceptual high-speed civil transport
[NASA-TM-4144] 01 p0008 N90-10034

Advanced Turbine Technology Applications Project (ATTAP)
[NASA-CR-185133] 01 p0008 N90-10036
Large-scale Advanced Prop-fan (LAP) technology assessment report
[NASA-CR-182142] 01 p0010 N90-10046
Full scale technology demonstration of a modern counterrotating unducted fan engine concept. Design report
[NASA-CR-180867] 01 p0010 N90-10048
Revolutionary opportunities for materials and structures study
[NASA-CR-179642] 01 p0034 N90-10184
Combustor influence on fighter engine operability 01 p0035 N90-10193
Effects of low-frequency instabilities on the operation of Ramjet air inlets 01 p0036 N90-10198
Advanced technologies impact on compressor design and development: A perspective
[NASA-TM-102341] 02 p0156 N90-10891
Automotive Stirling engine development program
[NASA-CR-180839] 02 p0289 N90-11654
Wave combustors for trans-atmospheric vehicles
[NASA-TM-102238] 03 p0307 N90-11742
Advanced technology in military gas turbine design and manufacture
[PNR90545] 03 p0307 N90-11747
Engine controls for the 1990's
[PNR90546] 03 p0308 N90-11748
Future military powerplants — fighter aircraft engines
[PNR90554] 03 p0308 N90-11749
Nuclear closed-cycle gaseous heat engine concept
[DE89-016824] 03 p0404 N90-12313
Advanced clearance control systems — blade tips
[PNR90553] 04 p0454 N90-12601
A vision of the future: The new engine technology
[PNR90566] 04 p0455 N90-12603
Designing for reliable and low maintenance cost aero engines
[PNR90570] 04 p0455 N90-12604
The next generation supersonic transport engine: Critical issues
[PNR90576] 04 p0455 N90-12605
Material requirements for future aeroengines
[PNR90595] 04 p0456 N90-12610
A computer integrated approach to dimensional inspection
[PNR90596] 04 p0456 N90-12611
Gas turbine performance analysis
[PNR90599] 04 p0456 N90-12614
Rolls-Royce and ERCOFTAC
[PNR90600] 04 p0456 N90-12615
Blading design for multi-storage HP compressor
[PNR90602] 04 p0456 N90-12616
NASA/USRA advanced space design program: The laser powered interorbital vehicle
[NASA-CR-186044] 04 p0462 N90-12646
Composite materials for future aeroengines
[PNR90584] 04 p0466 N90-12667
The future of non ferrous metals in aerospace engines
[PNR90572] 04 p0475 N90-12720
Cryostatless high temperature supercurrent bearings for rocket engine turbopumps
[NASA-CR-183807] 04 p0509 N90-12935
The commercial aircraft noise problem
[PNR90577] 04 p0550 N90-13203
Advanced Turbine Technology Applications Project (ATTAP)
[NASA-CR-185109] 05 p0709 N90-14153
SP-100 power system conceptual design for lunar base applications
[NASA-TM-102090] 06 p0866 N90-15030
A study of variable geometry in advanced gas turbines 07 p0881 N90-15104
Ceramic technology for advanced heat engines project
[DE90-001852] 07 p0908 N90-15251
Space shuttle solid rocket booster redesign and testing 09 p1175 N90-16804
Mission-dependent selection of propulsion systems for reusable launch vehicles 09 p1177 N90-16815
High-performance LO2-CH4 engine with ceramic matrix composite materials 09 p1180 N90-16840
Space transportation booster engine configuration study. Addendum: Design definition document
[NASA-CR-183854] 09 p1184 N90-16862
AGARD/SMP Review: Damage Tolerance for Engine Structures. 2: Defects and Quantitative Materials Behaviour — conference
[AGARD-R-769] 11 p1457 N90-18396
Future technology requirements (related to defects and quantitative material behavior to aid in implementation of damage tolerance for design of engine structures) 11 p1459 N90-18403
Compressor performance tests in the compressor research facility 11 p1463 N90-18428
Stall and recovery in multistage axial flow compressors 11 p1464 N90-18429
Stirling engine technologies in Japan
[DE89-782296] 11 p1528 N90-18795
Investigation of SSME alternate high pressure fuel turbopump lift-off seal fluid and structural dynamic interaction 12 p1636 N90-19400
Monostable electrovalve
[INPE-4928-RPE/595] 12 p1651 N90-19487
Low cost Brayton engine for gas-fired cogeneration system, phase 1
[PB90-127457] 12 p1681 N90-19655
Development and fabrication of structural components for a scramjet engine
[NASA-CR-181945] 13 p1757 N90-20088
Analyses of power consumption for two sliding vane type compressors
[AD-A218366] 13 p1812 N90-20406
Supersonic through-flow fan engine and aircraft mission performance
[NASA-TM-102304] 14 p1927 N90-21038
Recent Stirling engine loss-understanding results
[NASA-TM-103122] 14 p1942 N90-21114
Assessment of fundamental materials needs for Thick Thermal Barrier Coatings (TTBC's) for truck diesel engines
[NASA-TM-103130] 17 p2377 N90-23536
Study of the engine bird ingestion experience of the Boeing 737 aircraft (October 1986 to September 1988)
[DOT/FAA/CT-89/29] 19 p2656 N90-25119
From 1959-1989: 30 years of service experience with ramjets
[PNR90677] 19 p2660 N90-25139
Integrated controls and health monitoring for chemical transfer propulsion
[NASA-TM-103185] 19 p2668 N90-25178
Rocket combustion chamber life-enhancing design concepts
[NASA-CR-185257] 19 p2669 N90-25183
Ion thrusters and spacecraft configuration
[RAE-TM-SPACE-206] 19 p2682 N90-25253
Transatmospheric vehicle research
[NASA-CR-186705] 20 p2807 N90-25970
Combustion in the gas turbine. Part 1: Combustor types and design
[CIT/SME/VKI/RS/1] 20 p2810 N90-25986
Combustion in the gas turbine. Part 2: Preliminary design and performance
[CIT/SME/VKI/RS/3] 20 p2810 N90-25987
Combustion in the gas turbine. Part 3: Fuel injection, ignition and stability
[CIT/SME/VKI/RS/4] 20 p2810 N90-25988
Combustor cooling aspects
[CIT/SME/VKI/RS/5] 20 p2810 N90-25989
Supersonic combustor testing 20 p2811 N90-25998
Prediction and measurement of rotor blade/stator vane dynamic characteristics of a modern aero-engine axial compressor
[PNR90667] 20 p2812 N90-26002
The impact and requirements of new materials on aeroengines
[PNR90671] 20 p2812 N90-26003
Research and development of advanced gas turbine
[DE90-503377] 20 p2871 N90-26335
Preliminary designs for 25 kWe advanced Stirling conversion systems for dish electric applications
[NASA-TM-103188] 20 p2940 N90-26729
The composite load spectra project 21 p3047 N90-27323
The role of component testing 22 p3117 N90-27707
Comparative Engine Performance Measurements
[AGARD-LS-169] 22 p3118 N90-27711
Design of the UETP experiment 22 p3118 N90-27712
The basis for facility comparison 22 p3118 N90-27713
Hydrocarbon-fueled scramjet combustor component development tests 22 p3162 N90-27934
Flight set 360H005 (STS-28) seals, volume 4
[NASA-CR-183904] 22 p3181 N90-28051
Energy Efficient Engine combustor test hardware detailed design report
[NASA-CR-168301] 23 p3279 N90-28554
Energy Efficient Engine (E3) combustion system component technology performance report
[NASA-CR-168274] 23 p3279 N90-28555
Energy Efficient Engine exhaust mixer model technology report addendum; phase 3 test program
[NASA-CR-174799] 23 p3279 N90-28556
Energy Efficient Engine: Flight propulsion system final design and analysis
[NASA-CR-168219] 23 p3279 N90-28558
Energy Efficient Engine core design and performance report
[NASA-CR-168069] 23 p3279 N90-28559
Energy Efficient Engine program advanced turbofan nacelle definition study
[NASA-CR-174942] 23 p3280 N90-28560
Energy Efficient Engine: Control system component performance report
[NASA-CR-174651] 23 p3280 N90-28562
NASA/GE Energy Efficient Engine low pressure turbine scaled test vehicle performance report
[NASA-CR-168290] 23 p3280 N90-28563
Energy Efficient Engine integrated core/low spool test hardware design report
[NASA-CR-168137] 23 p3281 N90-28566
Liquid Rocket Booster (LRB) for the Space Transportation System (STS) systems study. Volume 1: Executive summary
[NASA-CR-183822] 23 p3288 N90-28599
Liquid Rocket Booster (LRB) for the Space Transportation System (STS) systems study, volume 2
[NASA-CR-183786] 23 p3288 N90-28600
Liquid Rocket Booster (LRB) for the Space Transportation System (STS) systems study. Appendix F: Performance and trajectory for ALS/LRB launch vehicles
[NASA-CR-183792-APP-F] 23 p3289 N90-28606
The space transportation main engine phase A' study
[NASA-CR-179399] 23 p3290 N90-28610
Advanced Earth-to-orbit propulsion technology program overview: Impact of civil space technology initiative 23 p3290 N90-28612
Oxygen/hydrogen technology test bed status update 23 p3290 N90-28613
Injector element characterization methodology 23 p3294 N90-28634
Variable mixture ratio performance through nitrogen augmentation 23 p3295 N90-28639
High variable mixture ratio oxygen/hydrogen engine 23 p3295 N90-28640
A failure diagnosis system based on a neural network classifier for the space shuttle main engine
[NASA-TM-103607] 23 p3299 N90-28659
Automotive Stirling engine development program
[NASA-CR-180840] 23 p3408 N90-29260

ENGINE FAILURE
Report on an overseas visit, June 1988
[AD-A210374] 01 p0009 N90-10040
X-ray spectroscopy of the SSME plume
[NASA-CR-185308] 01 p0031 N90-10168
Statistics on aircraft gas turbine engine rotor failures that occurred in US commercial aviation during 1986
[DOT/FAA/CT-89/30] 14 p1922 N90-21008
Compendium of fracture mechanics problems
[NASA-TM-100393] 14 p1992 N90-21414
Framework for a space shuttle main engine health monitoring system
[NASA-CR-185224] 15 p2061 N90-21809
Application of neural networks to the F/A-18 engine condition monitoring system
[AD-A219820] 18 p2497 N90-24271
Rocket engine failure detection using system identification techiques
[NASA-CR-185259] 19 p2664 N90-25159
Multi-sensor analysis techniques for SSME safety monitoring
[NASA-CR-185260] 22 p3124 N90-27732
Reliability growth modeling analysis of the space shuttle main engines based upon the Weibull process
[NASA-TM-103511] 22 p3189 N90-28098

ENGINE INLETS
Development of a VSAERO (Vortex Separation Aerodynamics) model of the F/A-18
[AD-A212442] 04 p0448 N90-12566
Engine inlet distortion in a 9.2 percent scale vectored thrust STOVL model in ground effect
[NASA-TM-102358] 10 p1307 N90-17561
Study of bird ingestions into small inlet area, aircraft turbine engines (May 1987 to April 1988)
[DOT/FAA/CT-89/17] 11 p1453 N90-18375
Control of flow separation and mixing by aerodynamic excitation
[NASA-TM-103131] 15 p2047 N90-21733
Finite element elastic-plastic-creep and cyclic life analysis of a cowl lip
[NASA-TM-102342] 16 p2246 N90-22808
Finite element analysis of structural components using viscoplastic models with application to a cowl lip problem
[NASA-CR-185189] 17 p2416 N90-23769
Research and development of advanced gas turbine
[DE90-503377] 20 p2871 N90-26335
Ramjet and ramrocket propulsion systems for missiles 21 p2973 N90-26897
Modeling of supersonic reacting flow fields 21 p2973 N90-26898

Development of advanced combustion technology for medium and high speed natural gas engines
[PB90-198565] 23 p3331 N90-28836

ENGINE MONITORING INSTRUMENTS

X-ray spectroscopy of the SSME plume
[NASA-CR-185308] 01 p0031 N90-10168
A simulation evaluation of the engine monitoring and control system display
[NASA-TP-2960] 11 p1457 N90-18393
Framework for a space shuttle main engine health monitoring system
[NASA-CR-185224] 15 p2061 N90-21809
Preliminary development of an intelligent computer assistant for engine monitoring
[NASA-TM-101702] 15 p2157 N90-22322
Diesel engine condition monitoring: Laser-based diagnostic techniques 17 p2410 N90-23733
Application of neural networks to the F/A-18 engine condition monitoring system
[AD-A219820] 18 p2497 N90-24271
Reusable rocket engine turbopump health monitoring system, part 3
[NASA-CR-182294] 20 p2869 N90-26320
Computer modeling and data processing methods: An essential part of jet engine condition monitoring and fault diagnosis 22 p3104 N90-27626
Experimental identification of helicopter engine dynamics from closed loop data
22 p3104 N90-27627
Advanced algorithms design and implementation in on-board microprocessor systems for engine life usage monitoring 22 p3104 N90-27628
Harrier Information Management System (HIMS): The system and the approach 22 p3105 N90-27630
The role of inflight engine condition monitoring on life cycle management of CF-18/F404 engine components
22 p3118 N90-27706
Multi-sensor analysis techniques for SSME safety monitoring
[NASA-CR-185260] 22 p3124 N90-27732

ENGINE NOISE

Near-field noise predictions of an aircraft in cruise
04 p0443 N90-12538
The 757 NLF glove flight test results
04 p0445 N90-12546
Re-engine with the Rolls-Royce Tay 670, the route to significant noise reduction
[PNR90585] 04 p0455 N90-12606
The commercial aircraft noise problem
[PNR90577] 04 p0550 N90-13203
Evaluation of analysis techniques for low frequency interior noise and vibration of commercial aircraft
[NASA-CR-181851] 06 p0837 N90-14866
A/F32T-9 large turbo fan engine enclosed noise suppressor system (T-9 NSS), exterior far-field and interior noise, McConnell AFB, Kansas
[AD-A220535] 17 p2354 N90-23402
Noise measurements of turboprop airplanes at different overflight elevations 18 p2609 N90-24860
Predicting the audibility and annoyance of unducted fan engines 18 p2610 N90-24869
Stage 2 re-engining: The only way to achieve a real stage 3 aircraft
[PNR90636] 20 p2808 N90-25977
Air Force procedure for predicting aircraft noise around airbases: Airbase operations program (BASEOPS) description
[AD-A223069] 21 p3072 N90-27466
Air Force procedure for predicting aircraft noise around airbases: Noise Exposure Model (NOISEMAP). User's manual
[AD-A223162] 21 p3072 N90-27467
Vibration responses of two house structures during the Edwards Air Force Base phase of the national sonic boom program
[NASA-CR-182089] 23 p3393 N90-29169
Audibility and annoyance of en route noise of unducted fan engines
[AD-A223687] 24 p3543 N90-30035

ENGINE PARTS

Full scale technology demonstration of a modern counterrotating unducted fan engine concept: Component test
[NASA-CR-180868] 01 p0010 N90-10047
Materials for engine applications above 3000 deg F: An overview
[NASA-TM-100169] 01 p0034 N90-10188
Improved silicon carbide for advanced heat engines
[NASA-CR-180831] 01 p0051 N90-10293
Advanced Turbine Technology Applications Program, (ATTAP): A plan for improving the prototype production of ceramic components for the gas turbine engine, 1988--1992
[DE89-015566] 02 p0230 N90-11320
Automotive Stirling engine development program
[NASA-CR-180839] 02 p0289 N90-11654
Effects of a heat cycle on material strength
[NAL-TM-562] 03 p0306 N90-11737
Advanced technology in military gas turbine design and manufacture
[PNR90545] 03 p0307 N90-11747
Aluminium alloy development for aero engines
[PNR90548] 03 p0330 N90-11874
Development of texture analysis and its applications to titanium aero engine components
[PNR90561] 04 p0454 N90-12602
The role of component testing
[PNR90589] 04 p0455 N90-12608
Real-time simulation of an F110/STOVL turbofan engine
[NASA-TM-102409] 04 p0457 N90-12618
The 4th US Army Workshop on Low Heat Rejection Engines
[AD-A212378] 04 p0510 N90-12942
Constitutive modeling for isotropic materials (HOST)
[NASA-CR-179522] 05 p0582 N90-13390
Constitutive modeling for isotropic materials (HOST)
[NASA-CR-174718] 05 p0582 N90-13391
A study of variable geometry in advanced gas turbines
07 p0881 N90-15104
Ceramic technology for advanced heat engines project
[DE90-001852] 07 p0908 N90-15251
Development of an integrated BEM approach for hot fluid structure interaction
[NASA-CR-186214] 07 p0927 N90-15364
Proceedings of the 1988 Structural Integrity Program Conference
[AD-A213545] 07 p0947 N90-15486
Advanced composite polar boss
[AD-D014287] 08 p1037 N90-15994
AGARD/SMP Review: Damage Tolerance for Engine Structures. 2: Defects and Quantitative Materials Behaviour --- conference
[AGARD-R-769] 11 p1457 N90-18396
Defects in monoblock cast turbine wheels
11 p1458 N90-18400
Crack propagation from artificial defects in typical engine disk materials; interpretation of experimental results by means of 3D J integral 11 p1458 N90-18401
Review of modelling methods to take account of material structure and defects 11 p1458 N90-18402
Future technology requirements (related to defects and quantitative material behavior to aid in implementation of damage tolerance for design of engine structures)
11 p1459 N90-18403
The need for a common approach within AGARD --- engine component defects 11 p1459 N90-18404
Transient pressure test article test program
11 p1470 N90-18463
Probability of failure and risk assessment of propulsion structural components 11 p1471 N90-18470
Development of inspection techniques for quantitatively measuring surface contamination on SRM hardware
[NASA-CR-183902] 12 p1673 N90-19608
Compendium of abstracts and viewgraphs.
[AD-A217189] 13 p1767 N90-20140
Attachment of lead wires to thin film thermocouples mounted on high temperature materials using the parallel gap welding process
[NASA-TM-102442] 14 p1983 N90-21361
High-temperature test facility at the NASA Lewis engine components research laboratory
[NASA-TM-103143] 19 p2662 N90-25151
Combustion in the gas turbine. Part 2: Preliminary design and performance
[CIT/SME/VKI/RS/3] 20 p2810 N90-25987
The application of engineering ceramics in gas turbines
[PNR90676] 20 p2812 N90-26005
The role of NDI in the certification of turbine engine components
[PNR90629] 20 p2874 N90-26349
AGARD damage tolerance concepts for engine structures Workshop 3, Component Behaviour and Life Management 22 p3117 N90-27705
The role of component testing
22 p3117 N90-27707
The role of inflight engine condition monitoring on life cycle management of CF-18/F404 engine components
22 p3118 N90-27708
Life management planning 22 p3118 N90-27709
Component behaviour and life management: The need for common AGARD approaches and actions
22 p3118 N90-27710
The role of NDI in the certification of turbine engine components 22 p3184 N90-28069
Critical inspection of high performance turbine engine components: The RFC concept
22 p3185 N90-28073
Energy Efficient Engine: Control system component performance report
[NASA-CR-174851] 23 p3280 N90-28562
A comparison of single-cycle versus multi-cycle proof testing strategies 23 p3296 N90-28646
Evaluation of high temperature protective coatings for gas turbine engines under simulated service conditions
23 p3309 N90-28712
Surface property improvement in titanium alloy gas turbine components through ion implantation
23 p3309 N90-28713
Improved silicon carbide for advanced heat engines
[NASA-CR-182186] 23 p3313 N90-28735

ENGINE RELIGHT (IN-FLIGHT)

U AIR START

ENGINE TESTING LABORATORIES

Test facility and preliminary performance of a 100 kW class MPD thruster 11 p1472 N90-18476

ENGINE TESTS

NT COLD FLOW TESTS
Performance potential of an advanced technology Mach 3 turbojet engine installed on a conceptual high-speed civil transport
[NASA-TM-4144] 01 p0008 N90-10034
Full scale technology demonstration of a modern counterrotating unducted fan engine concept: Component test
[NASA-CR-180868] 01 p0010 N90-10047
Full scale technology demonstration of a modern counterrotating unducted fan engine concept. Engine test
[NASA-CR-180869] 01 p0011 N90-10049
Test and evaluation: Reducing risks to military aircraft from bird collisions. Report to the Chairman, Legislation, and National Security Subcommittee, Committee on Goverment Operations, House of Representatives
[AD-A210670] 02 p0148 N90-10845
The effect of electrode configuration on arcjet performance
[NASA-TM-102346] 02 p0189 N90-11081
Automotive Stirling engine development program
[NASA-CR-180839] 02 p0289 N90-11654
The role of component testing
[PNR90589] 04 p0455 N90-12608
Flight motor set 360L001 (STS-26R). (Reconstructed dynamic loads analysis)
[NASA-CR-183811] 04 p0464 N90-12656
A data acquisition and processing system for six component solid rocket motor testing
[AD-A212200] 04 p0464 N90-12657
Aviation Engine Test Facilities (AETF) fire protection study
[AD-A211483] 04 p0483 N90-12777
Advanced Turbine Technology Applications Project (ATTAP)
[NASA-CR-185109] 05 p0709 N90-14153
AGARD Highlights 89/2 06 p0717 N90-14184
Advanced detection, isolation, and accommodation of sensor failures in turbofan engines: Real-time microcomputer implementation
[NASA-TP-2925] 07 p0883 N90-15112
Space shuttle solid rocket booster redesign and testing 09 p1175 N90-16804
Test facility and preliminary performance of a 100 kW class MPD thruster 11 p1472 N90-18476
The Uniform Engine Test Programme
[AGARD-AR-248] 12 p1604 N90-19232
Iterative procedures for space shuttle main engine performance models 12 p1639 N90-19416
First Vulcain engine test results
[MBB-UK-0054/88-PUB] 19 p2652 N90-25093
Evaluation of various thrust calculation techniques on an F404 engine
[NASA-TP-3001] 19 p2659 N90-25134
Gas Turbine Combustion, volume 2
[VKI-LS-1990-02-VOL-2] 20 p2811 N90-25995
Combustion instrumentation 20 p2811 N90-25996
Subsonic combustor testing 20 p2811 N90-25997
Supersonic combustor testing
20 p2811 N90-25998
Handbook of uncertainty methodology for engine testing at Pyestock (England)
[RAE-TM-P-1179] 20 p2812 N90-26007
QM-8 final performance evaluation report: SEALS, volume 4
[NASA-CR-183958] 20 p2869 N90-26324
Bringing aircraft noise testing down to Earth
[PNR90642] 20 p2924 N90-26637
Advanced Turbine Technology Applications Project (ATTAP)
[NASA-CR-185240] 20 p2939 N90-26728
Comparative evaluation of Allison T56 engine chip detectors
[AD-A221864] 21 p2960 N90-26832

Inductive knowledge acquisition experience with commercial tools for space shuttle main engine testing
21 p3048 N90-27326
AGARD/SMP Review Damage Tolerance for Engine Structures. 3: Component Behaviour and Life Management
[AGARD-R-770] 22 p3117 N90-27704
AGARD damage tolerance concepts for engine structures Workshop 3, Component Behaviour and Life Management 22 p3117 N90-27705
The role of component testing
22 p3117 N90-27707
Component behaviour and life management: The need for common AGARD approaches and actions
22 p3118 N90-27710
Comparative Engine Performance Measurements
[AGARD-LS-169] 22 p3118 N90-27711
Design of the UETP experiment
22 p3118 N90-27712
The basis for facility comparison
22 p3118 N90-27713
Investigation of factors affecting data comparison
22 p3119 N90-27714
Comparison of ground-level test cells and ground-level to altitude test cells 22 p3119 N90-27716
Experience in developing an improved design of experiment (lessons learned) 22 p3120 N90-27718
Experience in developing an improved altitude test capability 22 p3120 N90-27719
Experience in developing an improved ground-level test capability 22 p3120 N90-27720
General test plan 22 p3120 N90-27721
Engine testing of thermographic phosphors
[DE90-013269] 22 p3182 N90-28059
Reliability growth modeling analysis of the space shuttle main engines based upon the Weibull process
[NASA-TM-103511] 22 p3189 N90-28098
The reduction of smoke emissions from Allison T56 engines
[ARL-PROP-R-182] 23 p3277 N90-28547
Energy Efficient Engine: Control system component performance report
[NASA-CR-174651] 23 p3280 N90-28562
Energy Efficient Engine integrated core/low spool test hardware design report
[NASA-CR-168137] 23 p3281 N90-28566
Energy Efficient Engine: Combustor component performance program
[NASA-CR-179533] 23 p3281 N90-28568
Source emission test of gas turbine engine test facility, Kelly AFB, TX
[AD-A223869] 23 p3282 N90-28571
Liquid Rocket Booster (LRB) for the Space Transportation System (STS) systems study. Appendix E: Pressure-fed booster test bed for the liquid rocket booster study
[NASA-CR-183791-APP-E] 23 p3289 N90-28605
Oxygen/hydrogen technology test bed status update
23 p3290 N90-28613
The effects of a compressor rebuild on gas turbine engine performance: Final results
23 p3306 N90-28701
Development of advanced combustion technology for medium and high speed natural gas engines
[PB90-198565] 23 p3331 N90-28836
Evaluation of the STM4-120 kinematic Stirling engine
[DE90-013836] 23 p3344 N90-28897

ENGINEERING
Summary of research academic departments, 1987-1988
[AD-A213252] 05 p0716 N90-14183
Federal Scientists and Engineers: 1988. (Detailed statistical tables)
[PB90-226895] 22 p3256 N90-28437
Procedures for DOE-Navy exchange and approval of engineering information and material management required for production of W88-0/Mk5 RBA (reentry body assembly)
[DE90-014763] 23 p3287 N90-28595

ENGINEERING DEVELOPMENT
U PRODUCT DEVELOPMENT

ENGINEERING DRAWINGS
CRRES (Combined Release and Radiation Effects Satellite) SPACERAD plasma wave experiment
[AD-A210791] 02 p0278 N90-11587
The DAB model of drawing processes
08 p1155 N90-16691
Recognizing three-dimensional objects without the use of models
[AD-A216766] 11 p1540 N90-18862

ENGINEERING MANAGEMENT
The application of quality assurance to engineering management
[DE89-009955] 03 p0416 N90-12386
Program manager's handbook
[AD-A214338] 07 p1009 N90-15844
Systems engineering management guide
[AD-A223168] 21 p3085 N90-27544
OMNI development of an engineering product data management system
[DE90-002407] 21 p3086 N90-27550
Quality function deployment as a mechanism for process characterization and control
[DE90-014755] 23 p3337 N90-28857

ENGINES
NT ADVANCED SOLID ROCKET MOTOR (STS)
NT AIR BREATHING ENGINES
NT APOGEE BOOST MOTORS
NT ARC JET ENGINES
NT ASROC ENGINE
NT BOOSTER ROCKET ENGINES
NT DIESEL ENGINES
NT DUCTED ROCKET ENGINES
NT ELECTRIC ROCKET ENGINES
NT ELECTROTHERMAL ENGINES
NT FREE-PISTON ENGINES
NT GAS TURBINE ENGINES
NT HELICOPTER ENGINES
NT HYBRID PROPELLANT ROCKET ENGINES
NT HYDROGEN ENGINES
NT HYDROGEN OXYGEN ENGINES
NT INTERNAL COMBUSTION ENGINES
NT ION ENGINES
NT JET ENGINES
NT LIQUID PROPELLANT ROCKET ENGINES
NT MERCURY ION ENGINES
NT MICROROCKET ENGINES
NT NUCLEAR ENGINE FOR ROCKET VEHICLES
NT NUCLEAR ROCKET ENGINES
NT ORBIT MANEUVERING ENGINE (SPACE SHUTTLE)
NT OXYGEN-HYDROCARBON ROCKET ENGINES
NT PISTON ENGINES
NT PLASMA ENGINES
NT RAMJET ENGINES
NT RESISTOJET ENGINES
NT REUSABLE ROCKET ENGINES
NT ROCKET ENGINES
NT ROTARY ENGINES
NT SOLID PROPELLANT ROCKET ENGINES
NT SPACE SHUTTLE BOOSTERS
NT SPACE SHUTTLE MAIN ENGINE
NT STIRLING ENGINES
NT SUPERSONIC COMBUSTION RAMJET ENGINES
NT TURBINE ENGINES
NT TURBOFAN ENGINES
NT TURBOJET ENGINES
NT TURBOPROP ENGINES
NT TURBORAMJET ENGINES
NT UPPER STAGE ROCKET ENGINES
Nuclear closed-cycle gaseous heat engine concept
[DE89-016824] 03 p0404 N90-12313
Ultrafine microstructure composites prepared by chemical vapor deposition
[AD-A219650] 17 p2389 N90-23484
Ceramic technology for advanced heat engines project data base
[DE90-011491] 18 p2532 N90-24448
Outlook for ceramics in heat engines, 1990 - 2010: A technical and economic assessment based on a worldwide Delphi survey
[DE90-011262] 19 p2679 N90-25234

ENGLAND
Potential vorticity in extratropical cyclones
07 p0962 N90-15564

ENGLISH LANGUAGE
Terminology strategies for international information exchange
[AD-A214147] 07 p1010 N90-15853
The inside-outside algorithm: Further experiments on three and four letter word spelling and implementation on an array processor
[RSRE-MEMO-4256] 08 p1110 N90-16426
Parrot: The Janus paraphraser
[AD-A214588] 09 p1265 N90-17332
An introduction to Montague grammar
[REPT-89-46] 15 p2147 N90-22266
Proceedings of the 12th Symposium on Signal and Image Processing English-Language Abstracts
[AD-A218806] 17 p2388 N90-23598
Natural language syntax and first order inference
[AD-A219944] 17 p2447 N90-23951
Research in knowledge delivery
[AD-A219920] 17 p2480 N90-24180
The NATO thesaurus project
[NASA-CR-186931] 21 p3087 N90-27552

ENHANCEMENT
U AUGMENTATION

ENLARGING
U EXPANSION

ENO SCHEMES
U ESSENTIALLY NON-OSCILLATORY SCHEMES

ENRICHMENT
Test and evaluation of polymeric membranes for oxygen enrichment of air
[DE90-000555] 06 p0742 N90-14321
Surface enrichment and evaporation in a polymer mixture of long and short chains
[DE90-010073] 18 p2529 N90-24429

ENSTROPHY
U VORTICITY

ENTHALPY
NT GIBBS FREE ENERGY
NT HEAT OF FORMATION
NT LATENT HEAT
Interactive computer program for the generation of enthalpy-entropy and temperature-entropy charts of nitrogen and hydrogen
[DLR-FB-89-27] 04 p0533 N90-13081
Energies of organic compounds
[DE90-003174] 06 p0743 N90-14324
Vapor-liquid equilibria for complex mixtures with special emphasis on the critical region
[PB90-130345] 12 p1622 N90-19324
Wetting of metallic carbides by non-reactive liquid metals
[AERE-M-3759] 13 p1775 N90-20185
The structural basis for fatigue initiation in glassy polymers
[DE90-009342] 14 p1956 N90-21200
The Chemkin Thermodynamic Data Base
[DE90-007953] 14 p2035 N90-21676
Determination of the velocity, density, maximum flux, and enthalpy profiles for a very high temperature arc jet nozzle flow
[AD-A218390] 17 p2402 N90-23682
Extra compressibility terms for Favre-averaged two-equation models of inhomogeneous turbulent flows
[NASA-CR-177556] 17 p2405 N90-23701
High enthalpy hypersonic wind tunnel F4: General description and associated instrumentation
18 p2489 N90-24228
The arc-hot wind tunnel 18 p2489 N90-24230
A theoretical analysis of the acoustic radiation from two-dimensional turbulent mixing layers
18 p2551 N90-24559
Double layer effects on the enthalpy of activation of heterogeneous electron transfer reactions
[AD-A221934] 22 p3245 N90-28404
Thermophysical properties of Helium-4 from 0.8 to 1500 K with pressures to 2000 MPa
[NASA-CR-186992] 23 p3303 N90-28681
Design of an axisymmetric, contoured nozzle for the HEG
[DLR-FB-90-04] 23 p3327 N90-28812

ENTRAINMENT
Saltation thresholds and entrainment of fine particles at Earth and Martian pressures
[NASA-TM-102193] 06 p0860 N90-14997
Ambient Test Rig (ATR) flow studies: A laminar flow, reduced entrainment electrostatic precipitator
[DE90-000144] 08 p1062 N90-16142
Ambient flow studies and particulate collection measurements: A laminar flow, reduced entrainment electrostatic precipitator
[DE90-001457] 08 p1063 N90-16149
Numerical simulations of coherent structures in a jet flame with a noncircular cross section
[AD-A216710] 11 p1483 N90-18535
Leading edge vortex dynamics on a pitching delta wing
[NASA-CR-186327] 12 p1598 N90-19198
A review of models for the analysis of the injection of densely loaded flows into entrained flow gasifiers
[DE90-000453] 12 p1662 N90-19550
An experimental investigation of mixing in buoyant flows 15 p2090 N90-21963
Laser Doppler anemometry measurements of a confined turbulent water jet with a uniform background flow
15 p2092 N90-21971
Fundamental studies on spray combustion and turbulent combustion
[AD-A219840] 18 p2521 N90-24394
On the natural frequencies of a short circular cylinder, including the effects of entrained mass
[LR-602] 19 p2704 N90-25383
Cloud top entrainment instability and cloud top distributions 22 p3214 N90-28231
Structural analysis of stratocumulus convection
22 p3216 N90-28243
Laboratory experiments on stability and entrainment of oceanic stratocumulus. Part 1: Instability experiment
22 p3220 N90-28263
Laboratory experiments on stability and entrainment of oceanic stratocumulus. Part 2: Entrainment experiment
22 p3220 N90-28264
The entrainment rate for a row of turbulent jets
[NASA-CR-185278] 23 p3269 N90-28504

ENTROPY
Estimating functionals related to a density by a class of statistics based on spacings
[REPT-89-11] 03 p0398 N90-12275
Interactive computer program for the generation of enthalpy-entropy and temperature-entropy charts of nitrogen and hydrogen
[DLR-FB-89-27] 04 p0533 N90-13081
An entropy based approach to nonlinear stability
06 p0773 N90-14500
Algorithmic randomness, physical entropy, measurements, and the second law
[DE90-002413] 06 p0830 N90-14823
Dissipative effects in Friedmann universes
[DE89-618838] 08 p1150 N90-16663
Numerical predictions of local entropy generation for an impinging jet
[DE90-004671] 09 p1220 N90-17081
An entropy-based approach to nonlinear stability
[NASA-TM-101086] 09 p1272 N90-17376
A kinetic equation with kinetic entropy functions for scalar conservation laws
[NASA-CR-181985] 09 p1277 N90-17401
Heat capacities of solid polymers (The Advanced THermal Analysis System, ATHAS)
[DE90-007130] 11 p1493 N90-18595
The extended equivalent source technique with underdetermined sources
[DE90-006989] 11 p1499 N90-18627
On metric entropy, Vapnik-Chervonenkis dimension, and learnability for a class of distributions
[AD-A217331] 13 p1876 N90-20759
Experimental feasibility of investigating acoustic waves in Couette flow with entropy and pressure gradients
[NASA-TM-102621] 13 p1882 N90-20795
The measurements of thermoacoustic phenomena using thermoacoustic couples
[AD-A218018] 13 p1882 N90-20798
A Lagrangian formalism for nonequilibrium ensembles
[DE90-612748] 14 p2020 N90-21579
Nonoptimal entropy generation by heat transfer in cryogenic domain
[DE90-007544] 14 p2034 N90-21667
Rapid mass transfer in binary systems
16 p2332 N90-23289
The dynamic instability of adiabatic blastwaves
[NASA-CR-182498] 17 p2401 N90-23679
Adaptive time series analysis using predictive inference and entropy
[AD-A222337] 21 p2997 N90-27033
Entropy wave instability in compact ramjets
22 p3162 N90-27932
Thermophysical properties of Helium-4 from 0.8 to 1500 K with pressures to 2000 MPa
[NASA-CR-186992] 23 p3303 N90-28681
Viscous causal cosmologies
[DE90-627487] 23 p3412 N90-29282

ENTROPY (STATISTICS)
NT MAXIMUM ENTROPY METHOD
Multivariate clustering based on entropy
[PB89-233993] 10 p1439 N90-18303
Selecting multinomial populations
[AD-A219256] 16 p2309 N90-23159
Unification of statistical methods for continuous and discrete data
[AD-A224307] 24 p3540 N90-30017
Time series, statistics, and information
[AD-A224317] 24 p3540 N90-30018

ENUMERATION
The 0-1 multiknapsack problem: Heuristic and reduction methods
[INPE-4894-PRE/1495] 12 p1704 N90-19782

ENVIRONMENT EFFECTS
Hydrazine fate and transformation in natural waters and soils
02 p0204 N90-11165
Methodology of developing a combined environmental stress schedule for reliability growth testing
[AD-A211053] 02 p0231 N90-11326
Potential effects of global climate change on the United States. Executive summary. Draft
[PB89-161046] 02 p0237 N90-11350
Interrelation of experimental exposure and ambient air quality data for comparison of ozone exposure indices and estimating agricultural losses
[PB89-195036] 02 p0238 N90-11353
Coatings for gas turbine compressors
[NLR-MP-88045-U] 03 p0308 N90-11750
Final Environmental Impact Statement for the Galileo Mission (Tier 2)
[NASA-TM-101825] 03 p0367 N90-12102
Global environmental effects of impact-generated aerosols: Results from a general circulation model
[DE89-008033] 03 p0368 N90-12106
The next generation supersonic transport engine: Critical issues
[PNR90576] 04 p0455 N90-12605
Development of an inventory of materials potentially sensitive to ambient atmospheric acidity in the South Coast Air Basin
[PB89-224604] 04 p0516 N90-12982
Optical properties monitor: Experiment definition phase
[NASA-CR-183836] 05 p0899 N90-14092
Engineer's Refractive Effects Prediction System (EREPS)
06 p0758 N90-14411
Proceedings of the US/FRG (Fed. Republic of Germany) research symposium: Effects of Atmospheric Pollutants on the Spruce-Fir Forests of the Eastern United States and the Fed. Republic of Germany
[PB90-107160] 06 p0808 N90-14704
A model for the simulation of the ozone budget in the atmosphere under anthropogenic perturbation
[DE89-636296] 06 p0811 N90-14719
Modelling of the effects of the equatorial electrojet on its environment
[DE89-636298] 06 p0811 N90-14720
Draft Environmental Impact Statement for the Ulysses Mission (Tier 2)
[NASA-TM-102903] 06 p0812 N90-14727
Climate-biosphere interactions scope of work
[PB90-106444] 06 p0814 N90-14734
Long-term worldwide environmental effects caused by acid rain from fossil fuels
[DE90-001534] 07 p0956 N90-15533
Evaluate and characterize mechanisms controlling transport, fate, and effects of army smokes in the aerosol wind tunnel: Transport, transformations, fate, and terrestrial ecological effects of hexachloroethane obscurant smokes
[DE90-002923] 07 p0957 N90-15536
Interconnectedness in nature and in science: The case of climate and climate modeling
[PB90-113986] 08 p1098 N90-16358
Assessment of the importance of acidic fogwater and cloudwater in affecting terrestrial vegetation: Some important case studies
[DE90-002216] 08 p1098 N90-16361
A qualitative architecture for understanding policy responses to global change
[DE90-003936] 08 p1099 N90-16364
Measuring the demand for environmental studies
[PB90-100207] 09 p1244 N90-17214
Environmental impact statement on the US Antarctic program
[DE90-004940] 09 p1245 N90-17221
The use of computer programs to determine environmental compliance, predict performance, and assess impacts
[DE90-005230] 09 p1245 N90-17222
Noise and sonic boom impact technology. Initial development of an Assessment System for Aircraft Noise (ASAN). Volume 1: Executive summary
[AD-A214164] 09 p1278 N90-17410
Noise and sonic boom impact technology. Initial development of an Assessment System for Aircraft Noise (ASAN). Volume 2: System design strategy
[AD-A214454] 09 p1278 N90-17411
A CCIR aeronautical mobile satellite report
10 p1372 N90-17954
Remote sensing: Environmental effects of surface films
[AD-A216190] 10 p1400 N90-18094
Chamber investigations of the fate of diesel emissions in the atmosphere, volume 1, task 3
[PB90-114422] 10 p1405 N90-18103
Environmental impact assessment: Process and implementation
[DE90-004882] 10 p1406 N90-18109
Effects of global climate change on agroecosystems: Scope of work
[PB90-120023] 11 p1531 N90-18813
Tropospheric chemistry of natural hydrocarbons and energy-related pollutants: Biosphere/climate feedbacks
[DE90-005643] 11 p1532 N90-18820
Natural and anthropogenic climate change
[DE90-006488] 11 p1532 N90-18822
Atlantic outer continental shelf: Description of the Mid-Atlantic environment
[PB90-100033] 11 p1537 N90-18849
Sensitivity of ecological landscapes and regions to global climatic change
[PB90-120072] 12 p1684 N90-19674
Final safety analysis report for the Ulysses Mission
[DE90-008690] 14 p1940 N90-21106
MECCA program documentation
[NOAA-TR-NESDIS-46] 14 p2003 N90-21477
Environmental projects, volume 11. Environmental assessment: Addition to operations building, Mars site
[NASA-CR-186449] 14 p2003 N90-21479
Final environmental impact statement for the Galileo Mission (Tier 2)
[NASA-TM-102925] 15 p2124 N90-22147
Draft environmental impact statement for the Galileo Mission (Tier 2)
[NASA-TM-102926] 15 p2124 N90-22148
Site visit to US Antarctic Program (USAP) facilities and the Research Vessel Polar Duke
[DE90-009396] 15 p2126 N90-22159
Uncertainty analysis of the accident effect area of a BLEVE
[REPT-89-49] 15 p2126 N90-22160
Final Environmental Impact Statement for the Ulysses Mission (Tier 2)
[NASA-TM-101104] 15 p2126 N90-22162
International treaties and active experiments in space
[AD-A219368] 16 p2328 N90-23272
Effects of solar ultraviolet radiation on biogeochemical dynamics in aquatic environments
[AD-A221119] 18 p2578 N90-24687
Optical properties monitor: Experiment definition phase
[NASA-CR-4293] 19 p2666 N90-25170
Proceedings of the LDEF Materials Data Analysis Workshop
[NASA-CP-10046] 20 p2826 N90-26075
Characterization of biogenic aerosol particles from the Amazon Basin during dry and wet season
20 p2886 N90-26418
Evaluation of composite components on the Bell 206L and Sikorsky S-76 helicopters
[NASA-TM-4195] 22 p3135 N90-27787
Acid deposition in Maryland: Summary of results through 1989
[PB90-229782] 22 p3200 N90-28160
Chasing a specter: Risk management for global environmental change
[DE90-014455] 23 p3347 N90-28917
Puerto Rico Workshop on Land-Based Sources of Marine Pollution in the Wider Caribbean Region
[PB90-184094] 23 p3348 N90-28921
Natural and anthropogenic climate change
[DE90-015528] 23 p3348 N90-28923
Effects of thruster firings on the shuttle environment 1: Neutral gas composition
[AD-A224404] 24 p3487 N90-29707
Effects of increased CO2 on forest response
[DE90-015406] 24 p3487 N90-29708
Assessment System for Aircraft Noise (ASAN): Development of alpha-test prototype system software
[AD-A223770] 24 p3543 N90-30036

ENVIRONMENT MANAGEMENT
Evaluation of mid-to-long term basic research for environmental restoration
[DE89-015621] 02 p0238 N90-11355
Global climate change and NEPA (National Environmental Policy Act) analyses
[DE90-003704] 07 p0958 N90-15540
Paper on geography in environmental management: Research and new techniques
[INPE-4840-PRE/1469] 11 p1531 N90-18816
Atlantic outer continental shelf: Description of the Mid-Atlantic environment
[PB90-100033] 11 p1537 N90-18849
Managing the global environment
[AD-A218615] 19 p2712 N90-25434
Global Climate Change: Seeking a Global Consensus
[S-HRG-101-842] 24 p3486 N90-29704
Environmental quality, 1970 - 1990
[PB90-214610] 24 p3487 N90-29705

ENVIRONMENT MODELS
The Regional Polar Ice Prediction System, Berents Sea (RPIPS-B): A technical description
[AD-A213159] 04 p0522 N90-13012
Environmental constraints for polar platform design
[RAE-TR-89014] 09 p1181 N90-16849
Comparison of two Navy environmental database models: Generalized Digital Environmental Model and Podeszwa sound speed profile model
[AD-A215848] 11 p1544 N90-18889
Uncertainty analysis of the accident effect area of a BLEVE
[REPT-89-49] 15 p2126 N90-22160
A study of mesoscale acid deposition in the lower Ohio River Valley
16 p2253 N90-22848
Integral and series representation of infinitely divisible processes with applications to their prediction and to their sample path, statistical, and structural properties
[AD-A219625] 17 p2456 N90-24017
An Eulerian transport model for NO(sub x)-compounds
20 p2884 N90-26406
Role of grid-based, reactive air quality modeling in policy analysis: Perspectives and implications, as drawn from a case study
[PB90-187204] 22 p3198 N90-28150
Space station contamination modeling
[NASA-CR-183871] 23 p3286 N90-28590

Perspectives on the Chesapeake Bay, 1990: Advances in estuarine sciences
[PB90-248600] 23 p3354 N90-28954
Building an environment model using depth information 23 p3374 N90-29064
Data Base Analyzer and Parameter Estimator (DBAPE) interactive computer program user's manual
[PB90-193053] 23 p3406 N90-29252

ENVIRONMENT POLLUTION
NT AIR POLLUTION
NT GLOBAL AIR POLLUTION
NT INDOOR AIR POLLUTION
NT WATER POLLUTION
Organic explosives and related compounds. Environmental and health considerations
[AD-A210554] 01 p0054 N90-10306
The Third Conference on the Environmental Chemistry of Hydrazine Fuels
[AD-A197632] 02 p0203 N90-11157
Measurement of hydrazine contamination in soils 02 p0206 N90-11180
Discussions of global environmental problems
[DE90-002747] 06 p0811 N90-14718
Environmental surveillance data
[DE90-001275] 07 p0956 N90-15532
Environmental, health, and safety concerns associated with nonpetroleum fuel use in US transportation
[DE90-004367] 08 p1099 N90-16362
Atlantic outer continental shelf: Description of the Mid-Atlantic environment
[PB90-100033] 11 p1537 N90-18849
Uncertainty analysis of the accident effect area of a BLEVE
[REPT-89-49] 15 p2126 N90-22160
The environmental liabilities of government contractors and agencies 17 p2481 N90-24186
Proposed definition of the term en route in en route aircraft noise 18 p2608 N90-24854
En route noise of two turboprop aircraft
[DLR-MITT-89-18] 18 p2609 N90-24859
US Forest Service and National Park Service Wilderness Aircraft Overflight Study: Sociological background and study plans 18 p2609 N90-24863
The effect of noise-abatement profiles on noise immissions and human annoyance underneath a subsequent climbpath 18 p2610 N90-24865
Problems related to aircraft noise in Switzerland 18 p2611 N90-24871
Survey of applicability of electric vehicles (EVs) in specific regions such as resorts
[DE90-503592] 20 p2871 N90-26336
Subjective-probability-based scenarios for uncertain input parameters: Stratospheric ozone depletion
[N-3140-EPA/JMO/RC] 22 p3199 N90-28157
Environmental quality, 1970 - 1990
[PB90-214610] 24 p3487 N90-29705

ENVIRONMENT PROTECTION
National Climate Program five-year plan, 1989-1993
[PB89-207369] 02 p0252 N90-11426
Environmental Projects. Volume 8: Modifications of wastewater evaporation ponds
[NASA-CR-186099] 06 p0808 N90-14700
Managing marine protected areas: An action plan
[PB89-158778] 06 p0808 N90-14701
International aspects of restrictions of ozone-depleting substances
[DE90-001813] 07 p0957 N90-15534
Environmental Projects. Volume 9: Construction of hazardous materials storage facilities
[NASA-CR-186296] 09 p1244 N90-17216
Proceedings of the 2nd United States/USSR Symposium on Air Pollution Effects on Vegetation Including Forest Ecosystems
[PB90-127119] 12 p1685 N90-19678
HCl Vapor Characterization and Detection. JANNAF Safety and Environmental Protection Subcommittee Workshop
[AD-A216252] 16 p2208 N90-22596
The application of remote sensing techniques for regional planning, environmental studies, and environment maintenance
[BCRS-89-16] 18 p2574 N90-24667
Managing the global environment
[AD-A218615] 19 p2712 N90-25434
Success of EPA's stratospheric ozone engineering research
[PB90-246265] 24 p3487 N90-29706

ENVIRONMENT SIMULATION
NT ACOUSTIC SIMULATION
NT ALTITUDE SIMULATION
NT NEUTRAL BUOYANCY SIMULATION
NT SPACE ENVIRONMENT SIMULATION
NT THERMAL SIMULATION
NT WEIGHTLESSNESS SIMULATION
The Environmental Test Centre at ESTEC (an overview) 02 p0187 N90-11064
The behavior of hydrazine vapor in an environmental chamber under simulated atmospheric conditions 02 p0203 N90-11161
Modeling of hydrazine surface interactions in environmental reaction chambers 02 p0203 N90-11162
Artificial intelligence in process control: Knowledge base for the shuttle ECS model 08 p1156 N90-16697
Analysis of indirect effects of lightning on a metallic A 300 wing: Test report
[REPT-E87/645800] 09 p1162 N90-16726
Simulation of the dynamic environment for missile component testing: Demonstration
[AD-A216979] 11 p1466 N90-18443
The EURAD Model: Structure and First Results
[REPT-61] 12 p1686 N90-19680
Simulation of the propagation of radiactive substances from the example of Chernobyl (USSR) 12 p1686 N90-19685
Fracture mechanical aspects of dust emission processes from a model comet surface 12 p1740 N90-20004
Assessment of crew workload measurement methods, techniques and procedures. Volume 1: Process, methods and results
[AD-A217699] 13 p1855 N90-20647
Proceedings of the 13th International Congress on Instrumentation in Aerospace Simulation Facilities
[EOARD-LR-89-069] 14 p1929 N90-21046
Hubble space telescope six-battery test bed
[NASA-TM-103506] 22 p3124 N90-27731
Ceramic matrix composites in simulated SSME environments 23 p3298 N90-28655

ENVIRONMENT SIMULATORS
NT SOLAR SIMULATORS
NT SPACE SIMULATORS
Aircraft Reply and Interference Environment Simulator (ARIES) hardware principles of operation. Volume 2: Appendixes
[DOT/FAA/CT-TN88/4-2] 04 p0484 N90-12781
Aircraft Reply and Interference Environment Simulator (ARIES) hardware principles of operation, volume 1
[DOT/FAA/CT-TN88/4-1] 04 p0484 N90-12782

ENVIRONMENTAL CHAMBERS
U TEST CHAMBERS

ENVIRONMENTAL CHEMISTRY
NT AEROTHERMOCHEMISTRY
NT ATMOSPHERIC CHEMISTRY
NT BIOGEOCHEMISTRY
NT GEOCHEMISTRY
NT MARINE CHEMISTRY
Characterization and evaluation of acid rain in East Central Florida from 1978 to 1987: Ten year summary report
[NASA-TM-102149] 01 p0084 N90-10478
International Conference on Global and Regional Atmospheric Environmental Chemistry and visit to Hangzhou, China, foreign trip report
[DE90-000099] 06 p0810 N90-14713
Laboratory investigations: Low Earth orbit environment chemistry with spacecraft surfaces 19 p2732 N90-25531

ENVIRONMENTAL CONTROL
DNSS: German/Norwegian work team Space Subsea. Environmental control and life support subsystems (technical matters), phase 2
[ETN-90-95905] 08 p1105 N90-16398
Artificial intelligence in process control: Knowledge base for the shuttle ECS model 08 p1156 N90-16697
Space Station Freedom environmental control and life support system phase 3 simplified integrated test detailed report
[NASA-TM-4204] 16 p2207 N90-22593
The environmental control and life support system advanced automation project. Phase 1: Application evaluation 19 p2730 N90-25523
Scientific guidelines for preservation of samples collected from Mars
[NASA-TM-4184] 19 p2796 N90-25918
Fluid Phase Separation (FPS) experiment for flight on a space shuttle Get Away Special (GAS) canister
[NASA-CR-186830] 20 p2841 N90-26161
Automation of closed environments in space for human comfort and safety
[NASA-CR-186834] 20 p2901 N90-26500

ENVIRONMENTAL ENGINEERING
National Climate Program five-year plan, 1989-1993
[PB89-207369] 02 p0252 N90-11426
A modular habitation unit adapted for service in low earth and geostationary earth orbits
[ILR-MITT-217] 08 p1036 N90-15990
Activities report of the National Electrotechnic Institute Galileo Ferraris
[ETN-90-96178] 08 p1157 N90-16705

ENVIRONMENTAL MONITORING
Meeting Review: Workshop on Airborne Instrumentation
[PB89-174775] 01 p0007 N90-10032
ELF (Extremely Low Frequency) Communications System Ecological Monitoring Program: Electromagnetic field measurements and engineering support, 1988
[AD-A210200] 01 p0056 N90-10321
Characterization and evaluation of acid rain in East Central Florida from 1978 to 1987: Ten year summary report
[NASA-TM-102149] 01 p0084 N90-10478
Spatial characterization of acid rain stress in Canadian Shield Lakes
[NASA-CR-183446] 01 p0084 N90-10479
Geophysical monitoring for climatic change number 16
[PB89-159628] 01 p0087 N90-10494
National Climate Program five-year plan, 1989-1993
[PB89-207369] 02 p0252 N90-11426
Investigation on analyzing computer-aided forest disease classifications
[DFVLR-FB-89-16] 03 p0369 N90-12112
Summary of 1987 and 1988 manatee aerial surveys at Kennedy Space Center
[NASA-TM-102783] 06 p0802 N90-14669
Profile measurements of sulfur dioxide, nitrogen oxides, and nitric acid deposition velocities in California's south coast air basin
[PB90-104001] 06 p0808 N90-14703
Integrated computer-based tools to facilitate environmental monitoring, assessment, and restoration
[DE90-002732] 06 p0811 N90-14717
Environmental surveillance data
[DE90-001275] 07 p0956 N90-15532
Global climate change and NEPA (National Environmental Policy Act) analyses
[DE90-003704] 07 p0958 N90-15540
Operational ozone monitoring with the Global Ozone Monitoring Radiometer (GOMR)
[PB90-114034] 08 p1096 N90-16359
ELF (Extremely Low Frequency) communications system ecological monitoring program: Summary of 1988 progress
[AD-A216153] 10 p1377 N90-17981
Measuring Day-Night Noise Levels (DNL) using the metrosonics db-310 sound level analyzer (Dosimeter)
[AD-A215757] 10 p1427 N90-18230
Remote sensing applied to the monitoring of mineral extraction in the proximity of urban areas: Pros and cons
[INPE-4867-PRE/1478] 11 p1522 N90-18766
ERS-1 European remote sensing satellite: A new tool for global environmental monitoring in the 1990's
[ESA-BR-36] 11 p1526 N90-18782
Application of high performance liquid chromatography/mass spectrometry to environmental analysis
[PB90-116963] 11 p1531 N90-18814
Real time environment monitoring using data from METEOSAT and NOAA imaging satellites
[NLR-MP-87070-U] 12 p1684 N90-19672
Use of environmental monitoring data in evaluation of atmospheric modeling results
[DE90-008607] 13 p1831 N90-20510
Mission to planet Earth 15 p2125 N90-22153
ELF (Extremely Low Frequency) communications systems ecological monitoring program: Wetland studies
[AD-A218632] 16 p2229 N90-22716
Nimbus-7 TOMS Antarctic ozone atlas: August through November, 1989
[NASA-RP-1237] 17 p2428 N90-23837
Development of a consolidated environmental data base
[DE90-009419] 17 p2479 N90-24177
Identifying atmospheric monitoring needs for Space Station Freedom 18 p2628 N90-24977
Solid Earth, gravity field and environment 19 p2708 N90-25412
Operational satellite environmental monitoring for food security by FAO: The ARTEMIS system 19 p2708 N90-25413
Tools for mapping environmental monitoring data
[PB90-129685] 19 p2712 N90-25432
Research programs: Meteorological prediction. Oceanic processes. Climate and global change monitoring. Satellite instrumentation and calibration 19 p2714 N90-25447
Vertical ozone probing with lidar 20 p2885 N90-26416
Investigation of the effects of acid deposition on materials
[PB90-158973] 22 p3197 N90-28143
Laboratory and field evaluations of extrasensitive sulfur dioxide and nitrogen dioxide analyzers for acid deposition monitoring
[PB90-201062] 22 p3199 N90-28153

Environmental radioactivity measurement intercomparison exercise
[NPL-RSA(EXT)-5] 22 p3200 N90-28158
National air quality and emissions trends report, 1988
[PB90-200114] 23 p3346 N90-28909
Atmosphere and water quality monitoring on Space Station Freedom
[NASA-CR-186707] 23 p3378 N90-29084
SamTrack: A sample tracking system for environmental monitoring
[DE90-016026] 24 p3488 N90-29712

ENVIRONMENTAL QUALITY
NT AIR QUALITY
NT WATER QUALITY
Reporting environmental data of known quality
[DE89-016214] 02 p0239 N90-11359
Environmental quality and the shift to alternative fuels: Progress and interim findings of a Department of Energy study of transition in vehicular power systems
[DE90-002178] 06 p0810 N90-14716
The US National Transonic Facility, NTF
08 p1028 N90-15942
Measuring the demand for environmental studies
[PB90-100207] 09 p1244 N90-17214
Synthetic aperture radar imagery of airports and surrounding areas: Philadelphia Airport
[NASA-CR-4280] 11 p1453 N90-18372
Environmental quality, 1970 - 1990
[PB90-214610] 24 p3487 N90-29705

ENVIRONMENTAL RESEARCH SATELLITES
World Weather Watch. Global observing system-satellite sub-system. Information on meteorological and other environmental satellites, second edition
[WMO-411-ED-2] 08 p1103 N90-16386

ENVIRONMENTAL SURVEYS
Stratospheric ozone depletion
[PB89-207476] 02 p0238 N90-11354
Investigation on analyzing computer-aided forest disease classifications
[DFVLR-FB-89-16] 03 p0369 N90-12112
Draft Environmental Impact Statement for the Ulysses Mission (Tier 2)
[NASA-TM-102903] 06 p0812 N90-14727
Global climate change and NEPA (National Environmental Policy Act) analyses
[DE90-003704] 07 p0958 N90-15540
HCl monitor, phase 2
[AD-A213572] 07 p0958 N90-15542
Environmental impact statement on the US Antarctic program
[DE90-004940] 09 p1245 N90-17221
Noise and sonic boom impact technology. Initial development of an Assessment System for Aircraft Noise (ASAN). Volume 1: Executive summary
[AD-A214164] 09 p1278 N90-17410
Noise and sonic boom impact technology. Initial development of an Assessment System for Aircraft Noise (ASAN). Volume 2: System design strategy
[AD-A214454] 09 p1278 N90-17411
Noise and sonic boom impact technology. Initial development of an Assessment System for Aircraft Noise (ASAN). Volume 3: Technical description
[AD-A214455] 09 p1278 N90-17412
Remote sensing: Environmental effects of surface films
[AD-A216190] 10 p1400 N90-18094
Environmental impact assessment: Process and implementation
[DE90-004882] 10 p1406 N90-18109
Photointerpretation with instruments for evaluation of environmental impact: Mata Atlantica in Cubata
[INPE-4910-PRE/1511] 11 p1531 N90-18817
Gaithersburg Nike control and launch area preliminary assessment/site inspection, Gaithersburg, Maryland
[AD-A217791] 14 p2003 N90-21482
Final (Tier 1) environmental impact statement for the Galileo and Ulysses Missions
[NASA-TM-102917] 15 p2056 N90-21779
Final environmental impact statement for the Galileo Mission (Tier 2)
[NASA-TM-102925] 15 p2124 N90-22147
Draft environmental impact statement for the Galileo Mission (Tier 2)
[NASA-TM-102926] 15 p2124 N90-22148
Site visit to US Antarctic Program (USAP) facilities and the Research Vessel Polar Duke
[DE90-009396] 15 p2126 N90-22159
Final Environmental Impact Statement for the Ulysses Mission (Tier 2)
[NASA-TM-101104] 15 p2126 N90-22162
Specification for environmental measurements to assess radar sensors
[AD-A219127] 16 p2250 N90-22833
Assessment System for Aircraft Noise (ASAN) citation database. Volume 3: New citation review procedures
[AD-A219177] 16 p2314 N90-23190
Updating a dosage-effect relationship for the prevalence of annoyance due to general transportation noise
[AD-A219416] 17 p2421 N90-23794
The environmental liabilities of government contractors and agencies 17 p2481 N90-24186
The application of remote sensing techniques for regional planning, environmental studies, and environment maintenance
[BCRS-89-16] 18 p2574 N90-24667
Mapping and monitoring land use and land degradation in part of East Kalimantan, Indonesia, using aerospace remote sensing techniques: A SPOT case study
[BCRS-88-16B] 19 p2705 N90-25394
The transfer of mercury between the atmosphere and lake or soil surfaces 20 p2886 N90-26419
Air Force procedure for predicting aircraft noise around airbases: Airbase operations program (BASEOPS) description
[AD-A223069] 21 p3072 N90-27466
Use of Ni63 overvoltage gap switches in the flight termination systems on boosters launched from US Army Kwajalein Atoll (USAKA)
[AD-A223866] 23 p3299 N90-28661

ENVIRONMENTAL TEMPERATURE
U AMBIENT TEMPERATURE

ENVIRONMENTAL TESTS
NT COLD WEATHER TESTS
NT CORROSION TESTS
NT HIGH TEMPERATURE TESTS
NT LOW TEMPERATURE TESTS
NT NEUTRAL BUOYANCY SIMULATION
Spacecraft Structures and Mechanical Testing
[ESA-SP-289] 02 p0176 N90-10986
Environmental testing: An approach to more cost efficiency 02 p0176 N90-10988
The Environmental Test Centre at ESTEC (an overview) 02 p0187 N90-11084
Methodology of developing a combined environmental stress schedule for reliability growth testing
[AD-A211053] 02 p0231 N90-11326
Air velocity mapping of environmental test chambers
[AD-A212082] 03 p0310 N90-11764
Biology in microgravity: A guide for experimenters
[ESA-TM-02] 04 p0482 N90-12769
Thermal environmental tests on space simulation chamber
[DE90-000927] 06 p0729 N90-14251
A lithium sulphur dioxide cell for deep space applications 10 p1334 N90-17718
Pilot production of 70 micron thin silicon solar cells
10 p1343 N90-17780
Simulation of the dynamic environment for missile component testing: Demonstration
[AD-A216979] 11 p1466 N90-18443
Field evaluation of a passive sampling device for hydrazines in ambient air
[NASA-TM-103456] 18 p2578 N90-24686
The chemical effects of the Martian environment on power system component materials: A theoretical approach
[NASA-TM-103203] 20 p2825 N90-26074
Effect of casting procedures and diesel engine environment on the behavior of aluminum titanate
[AD-A223079] 20 p2835 N90-26126
Soil experiment
[NASA-CR-184927] 20 p2842 N90-26185
Structural and optical properties of DMP-128 holograms during environmental testing
[AD-A221691] 21 p3007 N90-27094
Development of testing and analysis methodology to assess the long term durability of polymeric composites at high temperatures
[NASA-TM-102714] 23 p3339 N90-28871
Effect of environment upon mechanical behavior of structural ceramics for application in the DOE ceramic technology for advanced heat engines project
[DE90-014770] 24 p3453 N90-29500

ENVIRONMENTS
NT AEROSPACE ENVIRONMENTS
NT CHROMOSPHERE
NT CISLUNAR SPACE
NT DEEP SPACE
NT EARTH ENVIRONMENT
NT EARTH MAGNETOSPHERE
NT EARTH ORBITAL ENVIRONMENTS
NT EXTRATERRESTRIAL ENVIRONMENTS
NT GEOMAGNETIC TAIL
NT HIGH ALTITUDE ENVIRONMENTS
NT HIGH TEMPERATURE ENVIRONMENTS
NT ICE ENVIRONMENTS
NT INTERPLANETARY SPACE
NT INTERSTELLAR SPACE
NT JUPITER ATMOSPHERE
NT LOW TEMPERATURE ENVIRONMENTS
NT LUNAR ATMOSPHERE
NT LUNAR ENVIRONMENT
NT MAGNETOSHEATH
NT MARINE ENVIRONMENTS
NT MARS ATMOSPHERE
NT MARS ENVIRONMENT
NT MIDLATITUDE ATMOSPHERE
NT PLANETARY ATMOSPHERES
NT PLANETARY IONOSPHERES
NT PLANETARY MAGNETOSPHERES
NT SATELLITE ATMOSPHERES
NT SATURN ATMOSPHERE
NT SOLAR ATMOSPHERE
NT SPACECRAFT ENVIRONMENTS
NT STELLAR ATMOSPHERES
NT THERMAL ENVIRONMENTS
NT VENUS ATMOSPHERE
NT VENUS CLOUDS
Modeling large-scale vegetation dynamics
[DE90-008883] 14 p2004 N90-21485
Evaluation of VHF intercept and direction finding systems
[AD-A219805] 17 p2350 N90-23382
Earth observation from the interstellar space
[REPT-44/89] 17 p2418 N90-23781

ENZYME ACTIVITY
NT FERMENTATION
Decomposition in Arctic terrestrial environments
[DE90-001198] 06 p0809 N90-14706
Conservation of body calcium by increased dietary intake of potassium: A potential measure to reduce the osteoporosis process during prolonged exposure to microgravity 18 p2631 N90-24993
Experiment K-6-10. Effects of zero gravity on myofibril protein content and isomyosin distribution in rodent skeletal muscle 20 p2894 N90-26464
Experiment K-6-14. Hepatic function in rats after spaceflight 20 p2895 N90-26468

ENZYMES
NT CATALASE
NT CHOLINESTERASE
NT CYTOCHROMES
NT OXIDASE
Biological and biochemical methane reactions
[PB89-232615] 04 p0516 N90-12977
Modern biofuel cells for waste recycling in life support systems
[NASA-CR-185963] 05 p0638 N90-13718
Electronic materials high-T(sub c) superconductivity polymers and composites structural materials surface science and catalysts industry participation
[NASA-CR-186063] 07 p0890 N90-15145
Carbon and hydrogen metabolism of green algae in light and dark
[DE90-008648] 13 p1849 N90-20612
Experiment K-6-21. Effect of microgravity on 1) metabolic enzymes of type 1 and type 2 muscle fibers and on 2) metabolic enzymes, neutransmitter amino acids, and neurotransmitter associated enzymes in motor and somatosensory cerebral cortex. Part 1: Metabolic enzymes of individual muscle fibers; part 2: metabolic enzymes of hippocampus and spinal cord 20 p2896 N90-26474
Computer simulation of chemical reactions in synthetic model compounds and genetically engineered active sites
[AD-A222611] 20 p2898 N90-26483

ENZYMOLOGY
USSR Space Life Sciences Digest, issue 22
[NASA-CR-3922(26)] 03 p0378 N90-12153

EOS
U LANDSAT SATELLITES

EPHEMERIDES
NT PLANET EPHEMERIDES
Fifty year canon of lunar eclipses: 1986-2035
[NASA-RP-1216] 10 p1446 N90-18342
Evaluation of influences of errors involved in orbit propagation of artificial satellites
[INPE-4962-TDL/391] 11 p1466 N90-18441
A satellite simulation program
[AD-A216079] 13 p1764 N90-20124
Establishing a GPS-baseline between Seattle, Washington and Monterey, California
[AD-A220089] 18 p2495 N90-24262
Nongravitational forces by Halley's comet
[ETN-90-96491] 18 p2638 N90-25027

EPHEMERIS TIME
M15:AC211/X2127+119: Optical curve, improved ephemeris, and phasing of EXOSAT X ray data
19 p2771 N90-25749

EPICYCLOIDS
Demonstration epicyclic gearbox
[PNR90567] 04 p0508 N90-12932

EPIDEMIOLOGY
The United States Air Force School of Aerospace Medicine: Special report
[AD-A217740] 13 p1851 N90-20622

Proceedings of a workshop on Carcinogenic Potential of Extremely Low Frequency Magnetic Fields
[DE90-614340] 14 p2010 N90-21520
Symposium on Applied Probability
[AD-A218760] 18 p2605 N90-24838
Bioelectromagnetic effects of the Electromagnetic Pulse (EMP)
[AD-A221552] 21 p3033 N90-27243

EPINEPHRINE
The effects of high intensity cycle exercise on sympatho-adrenal-medullary response patterns
[AD-A217962] 13 p1852 N90-20628
The effects of graded exercise at sea level on plasma proenkephalin peptide F and catecholamine responses
[AD-A218195] 13 p1853 N90-20633

EPITAXY
NT LIQUID PHASE EPITAXY
NT MOLECULAR BEAM EPITAXY
NT VAPOR PHASE EPITAXY
Epitaxial GaAs on SOI wafers
[AD-A209009] 01 p0127 N90-10729
Methods to decrease defect density in GaAs/Si heteroepitaxy
[DE89-016306] 01 p0131 N90-10753
Properties of devices prepared with epitaxial layers on InP
[AD-A210304] 01 p0132 N90-10759
Intergranular and interphase boundaries in ceramics
[DE89-016969] 02 p0202 N90-11154
Proceedings of the Workshop on Compound Semiconductor Devices and Integrated Circuits (13th) held in Cabourg, France on 10-12 May 1989
[AD-A211848] 03 p0343 N90-11954
Development and evaluation of an instrument for rapid electroreflectance of semiconductor materials
[AD-A211690] 03 p0414 N90-12376
The growth of epitaxial GaAs and GaAlAs on silicon substrates by OMVPE
[AD-A212873] 04 p0561 N90-13269
Hydrogen radical enhanced growth of solar cells
[DE89-009497] 06 p0806 N90-14894
Method of sensitizing PB-Salt epitaxial films for Schottky diodes
[AD-D014244] 06 p0850 N90-14937
The influence of the substrate surface on the nucleation and growth of superconducting thin films
[DE90-003649] 06 p0857 N90-14983
Research on GaAs quantum-coupled structures that can be used as electron devices
[AD-A214015] 07 p0924 N90-15350
Epitaxial iron films
[AD-A213551] 07 p1003 N90-15807
Metals and Ceramics Division Materials Sciences Program
[DE90-004371] 08 p1050 N90-16070
Heteroepitaxy of GaAs on Si: Methods to decrease the defect density in the epilayer
[DE90-004028] 08 p1131 N90-16551
The 1MeV-electron irradiation induced defects in epitaxially grown 3C-SiC
[DE90-719574] 08 p1131 N90-16554
Fundamental issues in heteroepitaxy (condensed from the DOE panel report)
[DE90-003980] 08 p1132 N90-16555
Crystallization of nanocomposite glasses made by the SSG process
[AD-A214572] 09 p1197 N90-16933
Growth of epitaxial SiC layers onto on- and off-axis 6H-SiC substrates by ion beam deposition
[DE90-004236] 09 p1267 N90-17459
Carbon doping of compound semiconductor epitaxial layers using carbon tetrachloride
[AD-A215053] 09 p1290 N90-17477
Epitaxial growth of Cr(011) on LiF(001)
[DE90-005635] 09 p1293 N90-17496
Materials processing of diamond: Etching, doping by ion implantation and contact formation
[AD-A216530] 10 p1438 N90-18301
Pulsed laser deposition of high T(sub c) superconducting thin films
[AD-A216507] 11 p1569 N90-19034
In situ growth of epitaxial superconducting YBa2Cu3O(7-x) films on insulating semiconducting and ferroelectric K(Ta, Nb)O3 by pulsed laser ablation
[DE90-006568] 11 p1571 N90-19043
In situ growth of high quality epitaxial YBa2Cu3O(7-x) thin films at moderate temperatures by pulsed laser ablation
[DE90-006629] 11 p1571 N90-19045
Passivating layer for III-V semiconductor materials
[AD-D014321] 12 p1719 N90-19872
Heteroepitaxial growth of germanium films by supersonic free jet chemical beam epitaxy
[DE90-006621] 12 p1720 N90-19877
Growth, characterization and device development in monocrystalline diamond films
[AD-A218211] 13 p1898 N90-20895
Improved Si:As BIBIB (Back-Illuminated Blocked-Impurity-Band) hybrid arrays
14 p1981 N90-21349
Measurement of localized deep levels and wafer non-uniformities at 3-5 semiconductor heterojunctions
[AD-A218547] 16 p2323 N90-23248
New directions in InP solar cell research
[NASA-TM-103160] 17 p2398 N90-23662
Epitaxy of TiO2 thin film on sapphire by MOCVDVD
[DE90-010054] 18 p2618 N90-24915
Deposition of electrooptic thin films
[DE90-010543] 18 p2619 N90-24922
Synthesis of large area, monocrystalline TiC as a substrate for heteroepitaxial growth of beta-SiC
[AD-A221392] 18 p2623 N90-24948
Superconductivity in nonsymmetric epitaxial YBa2Cu3O(sub 7-delta)-PrBa2Cu3O(sub 7-delta) superlattices grown by pulsed laser ablation
[DE90-011637] 19 p2761 N90-25687
Large, orientation-dependent enhancements of critical currents in Y1Ba2Cu3O(7-x) epitaxial thin films: Evidence for intrinsic flux pinning
[DE90-009424] 20 p2929 N90-26666
Critical currents and high temperature superconductors 22 p3142 N90-27823
Microscopic aspects of the initial stages of epitaxial growth. A scanning tunneling microscopy study
[AD-A224325] 24 p3551 N90-30094
Scanning tunneling microscopy of semiconductor surfaces
[AD-A223339] 24 p3552 N90-30095
The II-VI semiconductor superlattices
[AD-A223748] 24 p3553 N90-30101

EPNL
U EFFECTIVE PERCEIVED NOISE LEVELS

EPOCHS
U TIME MEASUREMENT

EPOXIDES
U EPOXY COMPOUNDS

EPOXY COMPOUNDS
NT ETHYLENE OXIDE
NT PROPYLENE OXIDE
Influence of the structure of epoxy network models on the volumetric, mechanical and viscoelastic properties
[ISAL-89-0024] 04 p0466 N90-12666
Structure and properties of polymer interphases
[AD-A212796] 04 p0481 N90-12763
The adhesive bonding of thermoplastic composites
[AD-A213358] 05 p0618 N90-13605
Cellular thermosetting fluorodiepoxide polymers
[NASA-CASE-GSC-13008-2] 09 p1199 N90-16949
Non-destructive characterization of epoxy/dicyandiamide interphases using surface-enhanced Raman scattering
[AD-A215894] 10 p1353 N90-17846
An investigation of the chemistry of silane coupling agents for adhesive bonding of aluminum
[AD-A220797] 17 p2381 N90-23560

EPOXY MATRIX COMPOSITES
Hardening mechanisms and analysis of the structure of the TGDDM/DDS epoxy resin system (tetraglycidyl-4,4' diaminodiphenylmethane/4,4' diaminodiphenylsulfone)
[NOTE-TECHNIQUE-1988-8] 04 p0465 N90-12662
Influence of the structure of epoxy network models on the volumetric, mechanical and viscoelastic properties
[ISAL-89-0024] 04 p0466 N90-12666
A study of progressive cracking damage to carbon-epoxy composites and methods of crack reduction
[REPT-RE-49-324/F] 04 p0467 N90-12676
Some aspects of test frequency influence on the fatigue behavior of ARALL
[LR-549] 05 p0620 N90-13616
Instrumented impact and residual tensile strength testing of eight-ply carbon eopoxy specimens
[NASA-TP-2981] 08 p1040 N90-16007
Effects of moisture on composite materials
09 p1185 N90-16866
Fatigue delamination onset prediction in tapered composite laminates
[NASA-TM-101673] 09 p1236 N90-17177
Compressive strength of carbon/epoxy laminated under multiaxial stress
[DE90-005552] 11 p1478 N90-18505
Calculation of mechanical properties variations depending on matrix parameters in a composite, as a function of the test temperature
[DT-311/88] 11 p1481 N90-18526
Impact of composites in the aerospace industry
[ETN-90-96231] 11 p1481 N90-18527
Cross-sectional examination of the damage zone in impacted specimens of carbon/epoxy and carbon/PEEK composites
[NASA-TM-100391] 14 p1944 N90-21125
Resistivity of pristine and intercalated graphite fiber epoxy composites
[NASA-TM-102576] 14 p1955 N90-21182
Characterization and role of an elastomeric interphase within polyepoxy reinforced glass, both particulate and fibrous
[ISAL-89-0064] 16 p2222 N90-22676
AECM3: Acoustic Emission Conditions for failure prediction of winding carbon structures
[REPT-892-430-115] 18 p2517 N90-24374
Tension fatigue of glass/epoxy and graphite/epoxy tapered laminates
[NASA-TM-102628] 19 p2671 N90-25191
Low velocity instrumented impact testing of four new damage tolerant carbon/epoxy composite systems
[NASA-TP-3029] 19 p2672 N90-25198
Open hole and post-impact compression fatigue of stitched and unstitched carbon/epoxy composites
[NASA-TM-102676] 19 p2701 N90-25370
Strain energy release rate analysis of delamination in a tapered laminate subjected to tension load
[NASA-TM-102592] 20 p2826 N90-26076
Erosion mechanisms in composite materials and ripple formation mechanism in erosion
[IAR-89-4-PT-1] 20 p2826 N90-26078
Elementary characterization of the pre-impregnated carbon/epoxy NCHR 914/155/34 percent-T300F from Brochier after the technical note CEAT number 1/M/87
[CEAT-PV-M7/6211] 22 p3154 N90-27884
Development of an automated ultrasonic inspection system for composite structure on in-service aircraft
22 p3186 N90-28079
Factors influencing the mode I interlaminar fracture resistance of toughened matrix composites
23 p3300 N90-28668
Inelastic analysis of laminated composites
23 p3301 N90-28669
Behavior of aramid/epoxy wounded tubes under uniaxial and biaxial loading
[ETCA-89-R-150] 23 p3339 N90-28873

EPOXY RESINS
NT PHENOLIC EPOXY RESINS
Hardening mechanisms and analysis of the structure of the TGDDM/DDS epoxy resin system (tetraglycidyl-4,4' diaminodiphenylmethane/4,4' diaminodiphenylsulfone)
[NOTE-TECHNIQUE-1988-8] 04 p0465 N90-12662
Behavior of the adhesive A2 submitted to mechanical traction
[CETIM-105290] 04 p0479 N90-12748
Chemical treatment of epoxy resins to reduce moisture sensitivity and to improve the mechanical properties
[AD-A212360] 04 p0481 N90-12758
Bulk and shear moduli of epoxy encapsulants
[DE90-000899] 06 p0751 N90-14371
Mechanistic modeling of epoxy resins
[DE89-015119] 07 p0908 N90-15247
Epoxy-resin cable terminations
[AD-A213789] 07 p0942 N90-15454
Adhesive for composite bonding
[DE90-005663] 09 p1188 N90-16885
Thermoelastic response of an epoxy
[AD-A215639] 09 p1198 N90-16942
Fundamental studies of time-dependent response and fracture of cross-linked polymers
[AD-A216694] 10 p1360 N90-17886
Structural study of thermo-hardenable matrices. Deformation processes of composite matrices as a function of their molecular structure
[ONERA-RT-10/3521-M] 11 p1481 N90-18522
Compression testing of thick-section composite materials
[AD-A217234] 13 p1767 N90-20142
Materials and selection criteria analysis for the compact ignition tokamak toroidal field coil turn-to-turn insulation system: Photographic summary ofllaboratory testing
[DE90-008020] 13 p1891 N90-20850
Criteria for polymer concrete on airport pavements
[DOT/FAA/DS-89/18] 14 p1929 N90-21045
Effect of surface oxygen on adhesion of carbon fiber-reinforced composites
[AD-A220777] 17 p2369 N90-23486
The interface chemistry of phenolic and epoxy adhesives with a model aluminium surface
[MBB-Z-0288-89-PUB] 18 p2531 N90-24441
Mechanisms for solid particle erosion in ductile and brittle materials
[NIAR-90-11] 19 p2675 N90-25210
Fractography of composite delamination
[NASA-CR-181965] 19 p2702 N90-25372
Evolution of structure and viscoelasticity in diethanolamine-cured epoxy
[DE90-011256] 20 p2837 N90-26134
Crash-impact behavior of graphite/epoxy composite sine wave webs 23 p3300 N90-28667

EQUATIONS OF MOTION
NT EULER EQUATIONS OF MOTION
NT HELMHOLTZ VORTICITY EQUATION
NT HYDRODYNAMIC EQUATIONS
NT KINEMATIC EQUATIONS
NT KINETIC EQUATIONS
NT NAVIER-STOKES EQUATION
NT REYNOLDS EQUATION
Two-phase potential flow 01 p0067 N90-10387
The architecture of NEWTON: A general-purpose dynamics simulator
[NASA-CR-185489] 01 p0118 N90-10678
Tangent map analysis of the beam-beam interaction
[DE89-015857] 01 p0120 N90-10689
On the motion equation of an elastically supported two degree of freedon gyro
[NAL-TM-568] 02 p0223 N90-11276
A nonoscillatory, characteristically convected, finite volume scheme for multidimensional convection problems
[NASA-TM-102354] 02 p0263 N90-11497
DMC (Distinct Motion Code): A rigid body motion code for determining the interaction of multiple spherical particles
[DE89-016929] 02 p0270 N90-11543
Stall/spin/flight simulation
[DOT/FAA/CT-88/28] 03 p0310 N90-11765
DART: A simulation code for charged particle beams, revision 1
[DE89-016697] 03 p0404 N90-12312
Non-stationary computer model of the asymptotic region of an electric arc gas heater
[IPPCZ-288] 03 p0407 N90-12330
Corrections to the thin wall approximation in general relativity
[NASA-CR-186078] 04 p0562 N90-13274
Software and hardware description of the helicopter motion equations for VAX computers
[AD-A213248] 05 p0579 N90-13375
Simulation of spacecraft attitude dynamics using TREETOPS and model-specific computer Codes 05 p0587 N90-13419
Optimal trajectories for the Aeroassisted Flight Experiment. Part 1: Equations of motion in an Earth-fixed system
[NASA-CR-186134] 05 p0592 N90-13441
Optimal trajectories for the Aeroassisted Flight Experiment. Part 2: Equations of motion in an inertial system
[NASA-CR-186135] 05 p0592 N90-13442
Attitude and shape control of optimally designed large space structures 05 p0613 N90-13579
AcSim: Aircraft simulation program with application to flight profile generation
[AD-A212466] 06 p0723 N90-14217
Introduction to data items on flight path optimisation
[ESDU-89015] 06 p0723 N90-14221
Multigrid solutions of elliptic fluid flow problems 06 p0775 N90-14507
Chaotic behavior in nonlinear polarization dynamics
[DE89-013453] 06 p0788 N90-14589
Self-field-induced chaotic electron motion in free electron lasers
[DE90-001710] 06 p0790 N90-14598
Stability and dynamics of constrained flexible multibody systems 06 p0791 N90-14609
Design limitations on ultra-high velocity projectile launchers
[DE89-012933] 07 p0885 N90-15118
Introduction to bifurcation theory
[DE90-003319] 07 p0982 N90-15673
Interface phonons in semiconductor double heterostructures
[AD-A213732] 07 p1003 N90-15810
The dynamics of domain walls and strings
[NASA-CR-186255] 07 p1007 N90-15832
Calculation of the flow field of a multiblade helicopter rotor using a Euler method including the wake 08 p1069 N90-16189
Restoring force method and response estimation
[DE90-002394] 08 p1116 N90-16463
Integrable classical systems in higher dimensions
[DE90-600737] 08 p1118 N90-16473
High-order mixture homogenization of fiber-reinforced composites
[AD-A215247] 09 p1187 N90-16876
Reacting flows 10 p1309 N90-17573
Equations of motion of slung load systems with results for dual lift
[NASA-TM-102246] 10 p1322 N90-17641
Satellite motion around an oblate planet: A perturbation solution for all orbital parameters
[AD-A216176] 10 p1326 N90-17661
Investigation of the observability of a satellite cluster in a near circular orbit
[AD-A216224] 10 p1326 N90-17662
Transient elastic waves on anisotropic half-spaces 10 p1396 N90-18074
Construction of second constant of motion for two dimensional classical super systems
[DE90-607046] 10 p1423 N90-18208
Analytical formulation for the interaction problem of dynamic reentry, and effects due to flexibility and vibration in an aerospace vehicle
[INPE-4963-TDL/392] 11 p1467 N90-18448
Using the method of matched asymptotic expansions, analytically investigate the three-dimensional, atmosphere entry problem
[AD-A216287] 11 p1468 N90-18451
Improved computational fluid dynamics for continuum hypersonic flow
[AD-A216981] 11 p1506 N90-18674
System properties from frequency response functions, part 1
[ISVR-TR-166-PT-1] 11 p1520 N90-18754
A vectorized algorithm for 3D dynamics of a tethered satellite 12 p1640 N90-19423
Causality of plasma permittivity with loss and restoring terms
[NASA-TM-101671] 12 p1645 N90-19453
Nonlinear continuum mechanics and applied analysis
[AD-A213629] 12 p1709 N90-19812
ETO (Earth-To-Orbit): A trajectory program for aerospace vehicles
[AD-A218157] 13 p1760 N90-20103
Discrete-time control of a spacecraft with retargetable flexible antennas 13 p1763 N90-20119
Discrete-time control of a spacecraft with retargetable flexible antennas
[AD-A218345] 13 p1764 N90-20125
The invertibility principle for a simple hurricane model
[AD-A218344] 13 p1848 N90-20605
Periodic trajectories for two-dimensional nonintegrable Hamiltonians
[DE90-008082] 13 p1877 N90-20765
Integrability and chaos in nonlinearly coupled optical beams
[DE90-007540] 13 p1888 N90-20834
Parametric resonance in horizontal axis wind turbines 14 p1912 N90-20962
Design of a helicopter automatic flight control system using adaptive control 14 p1928 N90-21040
Modeling and control of flexible space platforms with articulated payloads 14 p1935 N90-21073
United States Air Force Academy get-away-special flexible beam experiment 14 p1937 N90-21088
Notes on the unsteady rectilinear motion of a perfect gas. Part 8: General theory and general waves in a homentropic gas
[PB90-167149] 14 p1974 N90-21309
Development of a dynamic modeling technique and its application to the analysis and control of a high-precision robotic manipulator 14 p1987 N90-21391
A new approach to solve the kinematics resolution of a redundant robot
[DE90-010213] 14 p1988 N90-21397
Flutter of slender bodies under axial stress
[PB90-167024] 14 p1994 N90-21425
The extension of rapid distortion theory to stratified shear flows 14 p2005 N90-21491
Extension of the constraints algebra for the closed string with the fixed topology world sheet
[DE90-612745] 14 p2020 N90-21577
Instabilities and vortex dynamics in shear flow of magnetized plasmas
[DE90-009448] 14 p2030 N90-21643
The dynamics of scalar fields in the early universe 14 p2039 N90-21696
Homogeneous dilute turbulent particle-laden water flows 15 p2090 N90-21965
Mathematical modeling of fluid-solid mixtures
[DE90-009152] 15 p2098 N90-22007
Dynamics of an oscillator with three-degrees-of-freedom in a uniform windfield
[REPT-89-56] 15 p2119 N90-22121
Reynolds stress closure in jet flows using instability wave modeling 16 p2196 N90-22534
Aspects of efficient and reliable multibody system simulation 16 p2279 N90-22991
Systematic generation of multibody equations of motion suitable for recursive and parallel manipulation 16 p2280 N90-22992
Recursive linearization of multibody dynamics equations of motion 16 p2280 N90-22993
An innovations approach to decoupling of multibody dynamics and control 16 p2280 N90-22994
A nearly-linear computational-cost scheme for the forward dynamics of an N-body pendulum 16 p2280 N90-22996
A robot arm simulation with a shared memory multiprocessor machine 16 p2283 N90-23008
Multi-flexible-body dynamics capturing motion-induced stiffness 16 p2284 N90-23013
Nonlinear finite element formulation for the large displacement analysis in multibody system dynamics 16 p2284 N90-23015
Determination of joint drives for stable end-effector motion in flexible robotic systems 16 p2288 N90-23034
Simulation studies using multibody dynamics code DART 16 p2288 N90-23036
Modal identities for multibody elastic spacecraft: An aid to selecting modes for simulation 16 p2296 N90-23075
Multibody dynamics model building using graphical interfaces 16 p2297 N90-23082
Semianalytic satellite theory
[AD-A220744] 17 p2361 N90-23444
Simulation and interdisciplinary design methodology for control-structure interaction systems 17 p2385 N90-23584
Extra compressibility terms for Favre-averaged two-equation models of inhomogeneous turbulent flows
[NASA-CR-177556] 17 p2405 N90-23701
Stability and stability sensitivity by periodically time dependent systems: Hill versus Floquet
[ILR-MITT-221(1989)] 17 p2463 N90-24071
Efficient motion planning for an L-shaped object
[RUU-CS-88-38] 17 p2463 N90-24073
Classical theory of radiating strings
[NASA-CR-186607] 17 p2485 N90-24214
Control of large space structures
[AD-A221216] 18 p2511 N90-24345
Coupled rotor-body equations of motion hover flight
[NASA-CR-186710] 19 p2655 N90-25111
Modeling flexible aircraft for flight control design
[AD-A219123] 19 p2660 N90-25140
Identification of aerodynamic models for maneuvering aircraft
[NASA-CR-186630] 20 p2802 N90-25943
Algorithms to solve nonlinear time dependent problems of engineering and physics
[AD-A221463] 21 p3055 N90-27366
Identification techniques for nonlinear differential equations of motion
[AD-A220895] 21 p3062 N90-27407
On the application of similarity laws to a scaled railway bogie model
[DLR-FB-90-06] 23 p3335 N90-28853
A nonlinear finite element formulation for the large displacement analysis of plates 23 p3338 N90-28867
Tip-position control of a flexible beam: Modeling approaches and experimental verification
[AD-A224249] 24 p3476 N90-29643
Spectral structure and generation mechanism of ducted VLF whistler mode sideband waves 24 p3489 N90-29720
Windshear estimation along the trajectory of an aircraft 24 p3494 N90-29745
Three-dimensional numerical study of thunderstorm downdrafts and associated cutflow boundaries 24 p3494 N90-29746
Recursive multibody dynamics and discrete-time optimal control 24 p3513 N90-29860
The effects of gear reduction on robot dynamics 24 p3513 N90-29861
On equations of motion on complex Grassman manifold
[DE90-628369] 24 p3537 N90-29999
A canonical integration technique of arbitrary order
[DE90-628377] 24 p3541 N90-30025
Higher order equations of motion
[DE90-627522] 24 p3543 N90-30038
Effective actions for bosonic topological defects
[NASA-CR-187271] 24 p3544 N90-30041
Study of a 1-Hz hypocycloidal pinch (HCP) pump for production of ultraviolet lasers
[AD-A224091] 24 p3547 N90-30064

EQUATIONS OF STATE
NT HUGONIOT EQUATION OF STATE
Analysis of a model and sequential numerical method for thermal reservoir simulation
[DE89-015117] 01 p0067 N90-10384
Experimental measurements of shock-induced vaporization in cadmium and lead
[DE89-016877] 02 p0194 N90-11103
Consequence of condensed-phase formation in transient burning of TiHx/KClO in a closed system
[DE89-013922] 02 p0208 N90-11188
Acceleration of metal plates
[DE89-016816] 02 p0209 N90-11197
Irreversible phase transition and wave propagation in silicate geologic materials
[DE89-016031] 02 p0250 N90-11414
Equation-of-state data of synthetic Uranus
[DE89-016509] 02 p0296 N90-11683

Solar opacities constrained by solar neutrinos and solar oscillations
[DE89-016988] 02 p0297 N90-11687
Phase behavior of pure and mixed systems at high pressure
[DE89-017734] 03 p0322 N90-11832
VISAR wave profile measurements in supra-compressed HE
[DE89-017736] 03 p0346 N90-11976
Characteristics of flyer impact for one-dimensional shock-wave study applications
[DE89-017887] 03 p0346 N90-11977
Properties of strongly coupled multi-ionic plasmas
[DE89-017782] 03 p0408 N90-12339
The generalized van der Waals theory of pure fluids and mixtures
[DE90-000504] 06 p0740 N90-14307
Thermodynamic properties and hydrodynamic response of high-density high-temperature C H N O mixtures
[DE90-000836] 06 p0742 N90-14318
The Periodic Law at high pressures
[DE90-000837] 06 p0742 N90-14319
Detonation product equation of state for Baratol
[DE90-001050] 06 p0753 N90-14384
Non-equilibrium effects of slow diffusion controlled reactions on the properties of explosives
[DE90-000822] 06 p0754 N90-14391
General exact solution for homogeneous time-dependent self-gravitating perfect fluids
[DE89-618425] 06 p0776 N90-14514
Perturbations in high-velocity gas flow
[DE90-000539] 06 p0777 N90-14520
A new simulation method for the efficient calculation of benchmarks for detonation products equations of state
[DE90-001837] 06 p0777 N90-14522
Some numerical experiments concerning the equation of state algorithm for multi-material cells in HULL
[DE89-008240] 06 p0830 N90-14827
Equation of state and opacity of dense plasmas
[DE90-002223] 06 p0847 N90-14926
Perturbation methods for the calculation of gravitational waves from slightly non-spherical spacetimes with applications to stellar core collapse
06 p0863 N90-15015
Hydrodynamics code calculations of debris clouds produced by ball-plate impacts
[DE89-015270] 07 p0939 N90-15439
Maximum entropy and equations of state for random cellular structures
[DE90-002840] 07 p1006 N90-15827
Shapes of star-gas waves in spiral galaxies
[NASA-CR-186289] 07 p1011 N90-15859
Equation of state of partially-ionized dense plasmas
[DE90-005246] 09 p1286 N90-17452
Discretization of the steady state semiconductor device equations
[AD-A215807] 10 p1438 N90-18298
Scale transformations, the energy-momentum tensor, and the equation of state
[DE90-005372] 10 p1440 N90-18308
Strange-quark-matter stars
[DE90-006102] 10 p1446 N90-18347
Vapor-liquid equilibria for complex mixtures with special emphasis on the critical region
[PB90-130345] 12 p1622 N90-19324
Numerical modelling of shocks in gases and metals
[MRL-RR-8-89] 12 p1658 N90-19528
Update on the OPAL opacity code
[DE90-009946] 15 p2184 N90-22480
HYPUF upgrade
[AD-A218400] 17 p2379 N90-23547
Nonlocal free energy density functional approximations for the electrical double layer; comparison with Monte Carlo results for 2:1 salt
[AD-A220911] 18 p2521 N90-24395
Encoding of the Burgess metal electrical resistivity model into SESAME format and its adaptation to the metal nickel
[DE90-010816] 18 p2526 N90-24419
The composition and physical properties of the Earth's mantle and core 18 p2579 N90-24689
Nonstandard big bang models
[DE90-625593] 20 p2941 N90-26736
Substitution principle theory for compressible flows
21 p2953 N90-26791
Linear averaged and sampled data models for large signal control of high power factor ac-dc converters
[AD-A221976] 21 p3020 N90-27170
Theoretical thermodynamics: Equation of state and perturbation studies
[PB90-199332] 22 p3255 N90-28430
Estimation of individual coupling loss factors in a multi-subsystem
[ISVR-TR-184] 23 p3389 N90-29141
Rotating neutron stars and the equation of state of dense matter
[DE90-014185] 23 p3410 N90-29269
Statistically designed study of the variables and parameters of carbon dioxide equations of state
[DE90-016196] 24 p3447 N90-29467
Robust design of LQG controllers
24 p3475 N90-29639
Innovative uses of parallel computers
[AD-A223578] 24 p3533 N90-29980
Nucleus-nucleus collisions and the nuclear equation of state
[DE90-015427] 24 p3543 N90-30037

EQUATORIAL ATMOSPHERE
A low-order model of the equatorial ocean-atmosphere system 06 p0813 N90-14730
A feasibility study for D-region equatorial ionosphere research using VLF radiowaves
[AD-A223685] 24 p3492 N90-29738

EQUATORIAL ELECTROJET
Modelling of the effects of the equatorial electrojet on its environment
[DE89-636298] 06 p0811 N90-14720

EQUATORIAL ORBITS
Space operations: NASA's communications support for Earth orbiting spacecraft. Report to Chairman, Subcommittee on Space Science and Applications, Committee on Science, Space and Technology, House of Representatives
[GAO/IMTEC-89-41] 20 p2851 N90-26215

EQUATORIAL REGIONS
Observations and modelling of deep equatorial currents in the central Pacific
[PB89-198139] 03 p0377 N90-12145
Dynamics of the equatorial undercurrent and its termination
[PB89-198147] 03 p0377 N90-12146
Geology of the Venus equatorial region from Pioneer Venus radar imaging 03 p0427 N90-12447
Study of the atmospheric emissions of OI wavelength 557.7 nm and O2 (0,0) wavelength 781.9 nm in the equatorial region utilizing measurement of photometer on-board a rocket
[INPE-4811-TDL/358] 11 p1533 N90-18827
Geology of coronae and domal structures on Venus and models of their origin 15 p2191 N90-22513
Preliminary results of the peak experiment. ALTAIR deep-space measurements
[AD-A218622] 16 p2229 N90-22714
A numerical study of the seasonal variability of the Somali current
[AD-A220708] 17 p2427 N90-23829
Evolution of overlapping spreading centers: A SeaMARC 2 investigation
[AD-A223102] 21 p3025 N90-27200

EQUATORS
NT MAGNETIC EQUATOR

EQUILIBRIUM DIAGRAMS
U PHASE DIAGRAMS

EQUILIBRIUM EQUATIONS
Electromagnetic jets in pulsar magnetospheres and near magnetized accretion disks 02 p0294 N90-11675
Equilibrium solutions of a spherical pendulum with rotating point of suspension and friction
[ESA-TT-1139] 03 p0400 N90-12288
On the extremum electric charge problem of steady electromagnetic equilibria
[TRITA-EPP-89-04] 04 p0489 N90-12809
The free energy of Maxwell-Vlasov equilibria
[DE90-003318] 07 p0988 N90-15705
Compatibility conditions of structural mechanics for finite element analysis
[NASA-TM-102413] 09 p1237 N90-17180
Integrated force method versus displacement method for finite element analysis
[NASA-TP-2937] 10 p1398 N90-18081
Modelling late-time atmospheres of supernovae
15 p2189 N90-22500
Rigorous analysis of low temperature stochastic Ising models: Metastability and exponential approach to equilibrium
[PREPRINT-720] 16 p2312 N90-23175
Derivation of the governing equations of anisotropic conical shells
[LR-609] 19 p2704 N90-25387
Three dimensional studies of helical equilibria and magnetic surface breaking due to the finite beta effect
[DE90-508078] 24 p3548 N90-30071

EQUILIBRIUM FLOW
Multicellular natural convection in a narrow vertical slot
[AD-A216411] 11 p1505 N90-18668
Development of a defect stream function, law of the wall/wake method for compressible turbulent boundary layers
[NASA-CR-4286] 11 p1507 N90-18675
Siphon flows in isolated magnetic flux tubes. 3: The equilibrium path of the flux tube arch
[NASA-CR-186297] 12 p1709 N90-19813
Equilibrium and stability analysis of magnetospheric plasmas 15 p2057 N90-21782

EQUILIBRIUM METHODS
Equilibrium and stability in composite thin shell
02 p0178 N90-10998

EQUIPMENT SPECIFICATIONS
Free-world microelectronic manufacturing equipment
[FASAC-TAR-4070] 02 p0215 N90-11228
A slow strain-rate tensile testing machine
[ARL-MAT-TM-399] 05 p0645 N90-13764
Fundamental results from microgravity cell experiments with possible commericial applications
05 p0676 N90-13940
Do the design concepts used for the space flight hardware directly affect cell structure and/or cell function ground based simulations 05 p0679 N90-13953
Stand Alone Pressure Measurement Device (SAPMD) for the space shuttle Orbiter, part 1
[NASA-CR-172119-PT-1] 08 p1072 N90-16202
Stand Alone Pressure Measurement Device (SAPMD) for the space shuttle Orbiter, part 2
[NASA-CR-172119-PT-2] 08 p1072 N90-16203
Design of a pyrometer for temperature measurements on the solid fuel combustion chamber
[LR-530] 12 p1664 N90-19561
Goes I-M and beyond: Science requirements and technology challenges 14 p1934 N90-21067
Acquisition of an analytical x ray and image analysis system
[AD-A221376] 18 p2593 N90-24756
Earth Sciences Requirements for the Information Sciences Experiment System
[NASA-CP-3072] 21 p3015 N90-27140
SAGE 3: A visible wavelength limb sounder
21 p3016 N90-27147
Some design considerations for small piezo-electrical ceramic transducers
[FEL-1989-68] 22 p3178 N90-28034
Formulation of design guidelines for automated robotic assembly in outerspace 23 p3365 N90-29017

EQUIPOTENTIALS
Sensitivity analysis with a simple charging code
[RAE-TM-SPACE-374] 20 p2929 N90-26882

EQUIVALENCE
Determinism yields (event structure isomorphism equals step sequence equivalence)
[CWI-CS-R8839] 02 p0263 N90-11492
On the equivalence of BS-stability and B-consistency
[CWI-NM-R8815] 02 p0268 N90-11530
Mathematical equivalence in a primitive Ella
[RSRE-MEMO-4225] 04 p0531 N90-13066
Transformations and representations of nonlinear systems
[MEMO-776] 04 p0544 N90-13184
Experimental constraints on metric and non-metric theories of gravity 12 p1730 N90-19948
The Stanford equivalence principle program
12 p1733 N90-19963
Superconducting gravity gradiometer and a test of inverse square law 12 p1735 N90-19975
The gravitational lens effect and its optical equivalents
[DE90-612767] 14 p2035 N90-21673
On the independence of B-splines on unordered knot sets
[MEMO-827] 18 p2600 N90-24800
Proving Boolean equivalence with Prolog
[AD-A221766] 21 p3065 N90-27427
Hydrocarbon-fueled scramjet combustor component development tests 22 p3162 N90-27934

EQUIVALENT CIRCUITS
A general-purpose computer program for the Volterra-series analysis of nonlinear microwave circuits
[AD-A210768] 02 p0216 N90-11236
A new vision to model the parallel resonant converter
10 p1336 N90-17727
Vector circuit theory for multilayered isotropic and chiral structures: Reflection and transmission
[PB90-122474] 12 p1652 N90-19495
Investigation of tapered multiple microstrip lines for VLSI circuits
[AD-A217855] 13 p1797 N90-20310
Analytical and experimental study of high phase order induction motors
[NASA-CR-186580] 15 p2088 N90-21952
Equivalent circuit models for ac impedance data analysis
[NASA-TM-100402] 19 p2686 N90-25277
An experimental system for measuring the wavenumber-frequency response of Timoshenko beams
[AD-A222569] 20 p2878 N90-26374

ER FLUIDS
U ELECTRORHEOLOGICAL FLUIDS

ERBE
U EARTH RADIATION BUDGET EXPERIMENT
ERBIUM
NT ERBIUM ISOTOPES
Microstructures and properties of superconducting Y-Er-BaCu-O thin films obtained from disordered Y-Er-BaF2-Cu films 22 p3147 N90-27848
Laser diode pumped, erbium-doped, solid state laser with high slope efficiency
[AD-D014482] 22 p3179 N90-28040
ERBIUM ALLOYS
Crystal and magnetic structure of Er(2)(Co(sub x)Fe(sub 1-x))(17) compounds
[DE90-004926] 10 p1436 N90-18288
ERBIUM ISOTOPES
Optogalvanic laser spectroscopic and interference spectroscopic experiments of isotope gap and hyperfine structure for spectrum of Europium 1 and Erbium 2
[ETN-90-95358] 12 p1623 N90-19327
ERBIUM 169
U ERBIUM ISOTOPES
ERBIUM 171
U ERBIUM ISOTOPES
ERECTION
U CONSTRUCTION
ERGODIC PROCESS
Radon transform analysis of a probabilistic method for image generation
[AD-A207814] 01 p0123 N90-10702
Stochastic flows in networks
[AD-A211209] 02 p0266 N90-11515
Recurrence and ergodicity for exponential family state-space models
[AD-A213466] 07 p0983 N90-15677
The intrinsic stochasticity of near-integrable Hamiltonian systems
[IPPCZ-282] 15 p2167 N90-22386
On ergodicity and recurrence properties of a Markov chain with an application to an open Jackson network
[TW-89-10] 17 p2467 N90-24099
Strong consistency of the least squares estimator for a non-ergodic threshold autoregressive model
[IMAG-RR-791-M] 20 p2918 N90-26604
ERGONOMICS
U HUMAN FACTORS ENGINEERING
EROSION
NT SOIL EROSION
NT WIND EROSION
Determination of neutral particle concentration at erosion laser plasma expansion into vacuum
[DE89-620128] 02 p0228 N90-11308
PISCES program plasma-surface interactions research
[DE89-015622] 02 p0276 N90-11578
Pipe and bend erosion by pneumatic transport of solids at high temperature
[DE89-015741] 06 p0778 N90-14524
Erosion of ceramic composites by various erodents
[DE90-005650] 09 p1199 N90-16948
Technique for evaluating the erosive properties of ablative internal insulation materials
11 p1471 N90-18466
Fundamental aspects of erosion and impact damage
[DE90-006640] 11 p1492 N90-18587
Erosion monitoring using remote sensing, part 2
[BCRS-89-15] 11 p1526 N90-18785
Evaluation of the response of aluminum alloys to single and multiple particle impacts
[DE90-003689] 12 p1676 N90-19626
Magnetic vapor shield mechanism for protection of material surfaces exposed to high heat load
[AD-A217667] 13 p1780 N90-20217
Advanced electric propulsion research, 1989
[NASA-CR-185237] 15 p2062 N90-21810
Hollow cathode operation at high discharge currents
[NASA-CR-185238] 15 p2088 N90-21953
Characterization of particle impact by quantitative acoustic emission
[AERE-R-13028] 16 p2246 N90-22810
Erosional development of bedrock spur and gully topography in the Valles Marineris, Mars
[NASA-CR-180655] 17 p2424 N90-23813
Fracture toughness and solid-particle erosion of ceramic-matrix whisker-reinforced composites
[DE90-009713] 18 p2517 N90-24376
Subsurface hardening and flow of aluminum during the incubation period of solid particle erosion
[DE90-010141] 18 p2525 N90-24409
Mechanisms for solid particle erosion in ductile and brittle materials
[NIAR-90-11] 19 p2675 N90-25210
Erosion mechanisms in composite materials and ripple formation mechanism in erosion
[IAR-89-4-PT-1] 20 p2826 N90-26078
Erosion mechanisms in composite materials and ripple formation mechanism in erosion
[IAR-89-4-PT-2] 20 p2826 N90-26079
Flight set 360L001 (STS-26) igniter, post flight
[NASA-CR-183957] 20 p2870 N90-26325
Proceedings of US Army Research Office Workshop on US Army Applications for Diamond and Diamondlike Materials
[AD-A224193] 23 p3314 N90-28741
Solid particle erosion in turbulent flows past tube banks
[DE90-015711] 24 p3469 N90-29598
EROSIVE BURNING
Analysis of propulsive powder combustion products and their corrosive effects
[ISL-CO-248/88] 11 p1495 N90-18605
ERROR ANALYSIS
Phase 2 testing and evaluation of low data rate voice CODEC equipment
[ACD-330-PHASE-2] 01 p0055 N90-10315
Inherent bias in nonlinear least squares analysis of first-order kinetic data
[AD-A210677] 01 p0114 N90-10651
The computation and use of the asymptotic covariance matrix for measurement error models
[PB89-215321] 01 p0115 N90-10659
Research in mathematics and computer science: Calculation of the probability of undetected error for certain error detection codes, phase 1
[AD-A210302] 01 p0115 N90-10664
Using self-calibrating thermocouples in industry
[DE89-013539] 02 p0223 N90-11278
Iterative network magnitude estimation and uncertainty assessment with noisy and clipped data
[AD-A210707] 02 p0265 N90-11507
New statistical approaches to galaxy clustering
02 p0294 N90-11674
Discrete filtering techniques applied to sequential GPS range measurements
[NASA-CR-177472] 03 p0305 N90-11730
Convergence results for pseudospectral approximations of hyperbolic systems by a penalty type boundary treatment
[NASA-CR-181929] 03 p0391 N90-12230
The fault monitoring and diagnosis knowledge-based system for space power systems: AMPERES, phase 1
[NASA-CR-185486] 04 p0464 N90-12654
A statistical study of radio-source structure effects on astrometric very long baseline interferometry observations 04 p0485 N90-12788
On the decoder error probability of linear codes
04 p0486 N90-12793
Extended Kalman filter for attitude estimation of the earth radiation budget satellite 05 p0590 N90-13433
Error allocation and accuracy assessment
05 p0603 N90-13501
Choice of a differential method for the attitude restitution in dynamic unbalance
[CNES-CT/DTI/MS/CM/290] 05 p0613 N90-13582
An accurate timing model for fault simulation in MOS circuits
[AD-A213153] 05 p0635 N90-13702
GRADIO: An error analysis of the spaceborne gravity gradiometer
[ETN-90-96010] 05 p0667 N90-13901
An artificial intelligence approach to analog system diagnosis
[AD-A213135] 05 p0686 N90-13992
Methodology for the calibration of and data acquisition with a six-degree-of-freedom acceleration measurement device
[PB89-233597] 06 p0779 N90-14531
Some edge-enhancing operators and their applications to image enhancement and edge detection
06 p0828 N90-14810
Local error estimates for discontinuous solutions of nonlinear hyperbolic equations
[NASA-CR-181960] 06 p0834 N90-14847
Error modeling of bias-type parameters for TOPEX orbit determination 07 p0884 N90-15117
Geosat/ERM altimeter data analysis for the determination of global oceanic mesoscale variability
07 p0949 N90-15492
Analytical techniques for tracking filter implementation
08 p1021 N90-15903
Results of error correction techniques applied on two high accuracy coordinate measuring machines
[DE90-003341] 08 p1112 N90-16439
A statistical study of the surface accuracy of a planar truss beam
[NASA-TM-4161] 09 p1235 N90-17171
Transient fault behavior in a microprocessor: A case study
[NASA-CR-186240] 10 p1320 N90-17633
Lower bounds on multiple-source direction finding in the presence of direction-dependent antenna-array-calibration errors
[AD-A215825] 10 p1376 N90-17979
Binary correlators for optical computing and pattern recognition 10 p1441 N90-18318
An error sensitivity model for Doppler positioning using transit satellites
[AD-A216724] 11 p1455 N90-18381
Evaluation of influences of errors involved in orbit propagation of artificial satellites
[INPE-4962-TDL/391] 11 p1466 N90-18441
Autonomous orbit determination using GPS
[INPE-4815-TDL/361] 11 p1466 N90-18442
Angle estimation in the presence of mainbeam interference
[AD-A216832] 11 p1498 N90-18621
Error analysis of some Galerkin least squares methods for the elasticity equations
[DE90-608611] 12 p1705 N90-19790
Error control techniques for satellite and space communications
[NASA-CR-186221] 13 p1788 N90-20263
Analysis of methods to determine emissivity for ground surface targets in the spectral band 8 to 14 microns
[INPE-4984-TDL/394] 13 p1820 N90-20447
Gravity field determination and error assessment techniques 13 p1832 N90-20517
An improved error assessment for the GEM-T1 gravitational model 13 p1832 N90-20518
Synopsis of early field test results from the gravity gradiometer survey system 13 p1833 N90-20525
The Rapid Geodetic Survey System (RGSS)
13 p1834 N90-20528
Geographically correlated orbit error
13 p1838 N90-20551
Gravity field information from Gravity Probe-B
13 p1839 N90-20554
Local gravity disturbance estimation from multiple-high-single-low satellite-to-satellite tracking
13 p1839 N90-20555
A discussion of observation model, error sources and signal size for spaceborne gravitational gradiometry
13 p1839 N90-20557
Satellite radar altimetry over ice. Volume 1: Processing and corrections of Seasat data over Greenland
[NASA-RP-1233-VOL-1] 13 p1840 N90-20562
Study of possible solar heating effects on thermosonde probes: Error analysis
[AD-A218116] 13 p1903 N90-20917
LDV measurements and the flow analysis in the vortex region of a radial inflow turbine
14 p1922 N90-21007
Foundations of measurement and instrumentation
[NASA-RP-1222] 14 p1981 N90-21351
Engagement analysis study
[DE90-009529] 15 p2163 N90-22359
Pressure and shear stress measurement uncertainty for DARPA SUBOFF experiment
[AD-A219109] 16 p2243 N90-22798
Differential Loran-C using three secondary stations
[AD-A219573] 17 p2350 N90-23381
The effects of wiggler errors on free electron laser performance
[AD-A220421] 17 p2409 N90-23725
Failure analysis and modeling of a multicomputer system
[NASA-CR-186697] 17 p2451 N90-23980
Local and global order reduction of some LOD schemes
[CWI-NM-R8914] 17 p2459 N90-24041
Mean square error behavior for prediction in linear regression models
[AD-A219988] 17 p2466 N90-24092
System analysis of a tactical multi-satellite communication system
[AD-A220344] 18 p2510 N90-24343
A study of effects of instructional modes in a sequence of computer-assisted instruction lessons, with an introduction to computer-aided diagnosis of arithmetic errors 18 p2589 N90-24730
On the use of stability regions in the numerical analysis of stability value problems
[TW-89-07] 18 p2603 N90-24826
Observation of ship movement by aeroplane
[FFI-90/7001] 19 p2657 N90-25124
Handbook of uncertainty methodology for engine testing at Pyestock (England)
[RAE-TM-P-1179] 20 p2812 N90-26007
Continuous on-line link error rate detector
[AD-D014510] 20 p2850 N90-26209
Information content of a single pass of phase-delay data from a short baseline connected element interferometer
20 p2852 N90-26220
Initial results on fault diagnosis of DSN antenna control assemblies using pattern recognition techniques
20 p2854 N90-26228
Video camera system for locating bullet holes in targets at a ballistics tunnel
[NASA-TM-4197] 20 p2865 N90-26296

Self-checking on-line testable static RAM
[NASA-CASE-NPO-17939-1-CU]
20 p2904 N90-26518
Refractive error analysis in the interferometric measurement of 2-D density fields containing strong gradients
[LR-616] 20 p2927 N90-26655
Obtaining consistent models of helicopter flight-data measurement errors using kinematic-compatibility and state-reconstruction methods
[AD-A222533] 21 p2954 N90-26799
Object oriented fault diagnosis system for space shuttle main engine redlines 21 p3046 N90-27315
Numerical methods for shallow water flow
22 p3172 N90-27992
Tutorial on Reed-Solomon error correction coding
[NASA-TM-102162] 22 p3234 N90-28339
Error detection and control for nonlinear shell analysis
[NASA-TM-102723] 23 p3340 N90-28877
Consistency and convergence for numerical radiation conditions
[NASA-TM-103262] 23 p3387 N90-29124
Theoretical specifications of the trajectory estimation for a space navigation system with the function of guidance and control
[NAL-TR-1032] 24 p3439 N90-29420
Robust design of LQG controllers
24 p3475 N90-29639
Analytic least squares
[NPL-DES-86] 24 p3531 N90-29971
A posteriori error estimates for parametrized nonlinear equations
[AD-A224067] 24 p3537 N90-29997
Survey of formal specification techniques for reactive systems
[AD-A223741] 24 p3538 N90-30005
Sensitivity of the error in multivariate statistical interpolation to parameter values
[AD-A224076] 24 p3540 N90-30015
An error estimate for Tremolieres method for the discretization of parabolic variational inequalities
[DE90-627169] 24 p3541 N90-30024

ERROR BAND
U ACCURACY

ERROR CORRECTING CODES
Multi-level bandwidth efficient block modulation codes
[NASA-CR-185484] 01 p0056 N90-10317
Results of error correction techniques applied on two high accuracy coordinate measuring machines
[DE90-003341] 08 p1112 N90-16439
Error detection and correction for a multiple frequency quaternary phase shift keyed signal
[AD-A215706] 09 p1208 N90-17003
An adaptive ARQ (Automatic Repeat Request) strategy for packet switching data communication networks
[AD-A216597] 11 p1497 N90-18615
Fast transform decoding of nonsystematic Reed-Solomon codes 12 p1644 N90-19447
Local area network with fault-checking, priorities, and redundant backup
[NASA-CASE-NPO-16949-1-CU]
12 p1703 N90-19776
Iterative defect correction and multigrid accelerated explicit time stepping schemes for the steady Euler equations
[CWI-NM-R8908] 17 p2459 N90-24039
New multi-level codes over GF(q)
[NASA-CR-186662] 19 p2744 N90-25594
A versatile integrated block codes encoder-decoder
20 p2848 N90-26197
New synchronisation techniques applicable to multi-tone transmission systems 20 p2848 N90-26199
Verification-correction of a program for including uncertainties in the robot automatic programming
[ETN-90-97246] 20 p2915 N90-26588
VLSI architecture for a Reed-Solomon decoder
[NASA-CASE-NPO-17897-1-CU]
21 p2998 N90-27040
Cyclic error correcting block codes for reliability increasing of VLSI networks
[ETN-90-97304] 22 p3168 N90-27968
Analysis of the integrity of the Microwave Landing System (MLS) data functions 24 p3428 N90-29365
Integrating rule-based and neural-net techniques for spectral analysis
[AD-A223517] 24 p3446 N90-29482

ERROR CORRECTING DEVICES
Utilization of the generalized likelihood ratio test for the suppresion of systematic errors in noisy systems
[ETN-89-94656] 02 p0214 N90-11225
Application of an optimal filter for inflatable sphere data processing 05 p0659 N90-13849
Experiences with and error handling in a knowledge base assisted system for payload experiment automation
18 p2504 N90-24306
On the calibration of an autocollimator-comparator guide of a vertical target levelling rod differing from the ABBE's principle
[ISBN-951-754-887-7] 19 p2694 N90-25331

ERROR DETECTION CODES
Research in mathematics and computer science: Calculation of the probability of undetected error for certain error detection codes, phase 1
[AD-A210302] 01 p0115 N90-10864
Utilization of the generalized likelihood ratio test for the suppression of systematic errors in noisy systems
[ETN-89-94656] 02 p0214 N90-11225
Fine resolution errors in secondary surveillance radar altitude reporting amongst aircraft transmitting the conspicuity codes 4321 and 4322
[RSRE-88004] 04 p0490 N90-12816
Non-separate arithmetic codes
[RSRE-MEMO-4215] 04 p0530 N90-13058
Error allocation and accuracy assessment
05 p0603 N90-13501
The compilation of astrometric data
05 p0607 N90-13537
Standard stars and photometric calibration
05 p0607 N90-13539
Multigrid and defect correction for the steady Navier-Stokes equations: Applications to aerodynamics
[ETN-90-96011] 05 p0639 N90-13727
Error detection and correction for a multiple frequency quaternary phase shift keyed signal
[AD-A215706] 09 p1208 N90-17003
SHARP: A multi-mission artificial intelligence system for spacecraft telemetry monitoring and diagnosis
[NASA-CR-186285] 11 p1467 N90-18444
Error detection in data processing devices by means of residue codes
[ETN-90-95370] 12 p1701 N90-19767
Local area network with fault-checking, priorities, and redundant backup
[NASA-CASE-NPO-16949-1-CU]
12 p1703 N90-19776
Detection of bridging faults in DFCMOS combinational gates
[REPT-89-060] 16 p2231 N90-22726
Measurement errors 17 p2359 N90-23426
A formal mechanism for determining redundancy and irrelevance in Hypertext views
[TR-89-9] 17 p2450 N90-23970
Non-linear systems identification using neural networks
[RR-370] 19 p2748 N90-25616
A parallel recursive prediction error algorithm for training layered neural networks
[RR-373] 19 p2748 N90-25617
A comparison of the backpropagation and recursive prediction error algorithms for training neural networks
[RR-379] 19 p2748 N90-25620
Communications and tracking expert systems study
[NASA-CR-185935] 21 p2992 N90-27004
The identification of software failure regions
[AD-A223058] 21 p3052 N90-27352
Computer modeling and data processing methods: An essential part of jet engine condition monitoring and fault diagnosis 22 p3104 N90-27626
Knowledge based diagnosis of jet engines under consideration of model based methods
22 p3105 N90-27631
Analysis and design of algorithm-based fault-tolerant systems
[NASA-CR-186684] 22 p3236 N90-28352
Fault Detection and Isolation (FDI) techniques for guidance and control systems 24 p3428 N90-29366

ERROR FUNCTIONS
On some problems in reliability theory
09 p1233 N90-17155
Asymptotic boundary conditions for dissipative waves: General theory
[NASA-TM-102497] 11 p1551 N90-18927
Some software implementation of the functions sine and cosine
[DE90-010398] 21 p3050 N90-27339

ERROR SIGNALS
Lower bounds on multiple-source direction finding in the presence of direction-dependent antenna-array-calibration errors
[AD-A215825] 10 p1376 N90-17979
Angle estimation in the presence of mainbeam interference
[AD-A216832] 11 p1498 N90-18621
The adaptive line enhancer applied to chirp detection
[DE90-006772] 13 p1789 N90-20268
First-order intensity statistics for non-Rayleigh fading
[AD-A217572] 13 p1841 N90-20569
A parametric detection approach using multichannel processes
[AD-A219328] 17 p2395 N90-23641
Self-checking on-line testable static RAM
[NASA-CASE-NPO-17939-1-CU]
20 p2904 N90-26518
Multistage estimation of received carrier signal parameters under very high dynamic conditions of the receiver
[NASA-CASE-NPO-17911-1-CU]
21 p2994 N90-27016
Modified fast frequency acquisition via adaptive least squares algorithm
[NASA-CASE-NPO-17845-1-CU]
21 p3050 N90-27341

ERRORS
NT INSTRUMENT ERRORS
NT PHASE ERROR
NT PILOT ERROR
NT POSITION ERRORS
NT RANDOM ERRORS
NT RANGE ERRORS
NT ROOT-MEAN-SQUARE ERRORS
NT TRUNCATION ERRORS
Optimal q-Markov COVER for finite precision implementation 01 p0023 N90-10117
Dependency-directed localization of software bugs
[AD-A210837] 01 p0106 N90-10606
Error estimation and self-adaptive mesh refinement for boundary element method 03 p0356 N90-12037
A survey of camera error sources in machine vision systems
[DE89-014072] 03 p0405 N90-12318
A performance comparison between block interleaved and helically interleaved concatenated coding systems
04 p0486 N90-12792
Direction-of-arrival calculations at VLF/LF (Very Low Frequency/Low Frequency)
[AD-A212620] 04 p0493 N90-12833
Optimum data weighting and error calibration for estimation of gravitational parameters
[NASA-TM-100737] 04 p0517 N90-12985
Multiparameter radar estimation of raindrop size distribution
[AD-A212410] 04 p0521 N90-13007
An error estimator for parameter choice in regulating least square problems. Application to regularized deconvolution
[IMAG-RR-744-M] 04 p0540 N90-13125
A frequency domain technique for improving sound field reproduction
[RAE-TM-MM-10] 04 p0551 N90-13205
The effects of seasonal and latitudinal earth infrared radiance variations on ERBS attitude control
05 p0586 N90-13414
Optimum data weighting and error calibration for estimation of gravitational parameters
05 p0591 N90-13437
A laboratory verification sensor
05 p0599 N90-13477
The problem of automation: Inappropriate feedback and interaction, not overautomation
[NASA-CR-186126] 05 p0686 N90-13994
Adaptive canceller limitations caused by I,Q mismatch errors
[AD-A214287] 07 p0919 N90-15318
Formulation and verification of a technique for compensation of pneumatic attenuation errors in airborne pressure sensing devices 09 p1221 N90-17084
Laser wave estimation
[AD-A213867] 09 p1227 N90-17119
Causes of aircrew error in the Royal Air Force
09 p1254 N90-17276
Dynamic response for thermal control and measurement and fast radiation thermometry
10 p1367 N90-17924
Evaluation of two methods for acquisition of training statistics for digital analysis of areas prepared for plowing
[INPE-4901-PRE/1502] 11 p1522 N90-18763
Temporal response of atmospheric turbulence compensation
[DE90-006354] 11 p1535 N90-18837
Determination of Earth orientation using the Global Positioning System 12 p1642 N90-19435
Disturbance torque rejection properties of the NASA/JPL 70-meter antenna axis servos
12 p1644 N90-19450
Marginal test and analysis of DRAM with masked alpha radiation
[RB-4180] 12 p1699 N90-19754
Viscous shock profiles and primitive formulations
[NASA-CR-182029] 13 p1750 N90-20049
A guide to performing and documenting safety analyses
[DE90-008687] 13 p1788 N90-20260
Error control techniques for satellite and space communications
[NASA-CR-186221] 13 p1788 N90-20263

Treatment of geodetic leveling in the integrated geodesy approach 13 p1837 N90-20546
Systematic errors in power measurements made with a dual six-port ANA
[PB90-145160] 14 p1968 N90-21276
Performance evaluation of MSS/LANDSAT data in the estimation of fluvial channel width
[INPE-4906-PRE/1507] 14 p2000 N90-21463
SIGNIF: A C function to compute significant digits
[DE90-009242] 14 p2015 N90-21550
Interpreting meteorological data reports for LOWTRAN Navy aerosol model extinction calculations 15 p2082 N90-21920
Increased stuck-at fault coverage with reduced I(sub DDQ) test sets
[DE90-009509] 16 p2245 N90-22804
Error cancellation in HPBL derivation of elastic hole-pressure error
[AD-A219854] 17 p2417 N90-23771
Stability and error estimates for sinc interpolation
[CWI-AM-R8914] 18 p2599 N90-24790
Direct calculation of Newton steps without accumulating Jacobians
[DE90-009702] 18 p2607 N90-24847
Feasibility study of a synthesis procedure for array feeds to improve radiation performance of large distorted reflector antennas
[NASA-CR-186641] 20 p2851 N90-26213
Preliminary error budget for an optical ranging system: Range, range rate, and differenced range observables 20 p2853 N90-26227
Dallas/Fort Worth simulation, volume 1
[DOT/FAA/CT-TN89/28-VOL-1] 21 p2955 N90-26802
Adaptive optics correction in real-time for dynamic wavefront errors
[AD-A221588] 21 p3077 N90-27495
Sideslip-induced static pressure errors in flight-test measurements
[NASA-TM-102846] 22 p3116 N90-27702
Measurement uncertainty in gas turbine performance determination 22 p3119 N90-27717
Power bounded prolongations and Picard-Lindeloef iteration
[PB90-190877] 22 p3242 N90-28384
Studies in automatic speech recognition and its application in aerospace 23 p3318 N90-28759
Treatment of systematic errors 2: Fusion of ultrasound and visual sensor data
[DE90-014780] 23 p3334 N90-28850
Selective learning algorithm for certain types of learning failure in multilayer perceptrons
[AD-A223982] 23 p3362 N90-28998
Plan recognition for space telerobotics 23 p3369 N90-29036
Performance monitoring, fault detection, fault localization design guidance
[AD-A223619] 24 p3478 N90-29655
Human error classification and data collection
[DE90-631408] 24 p3522 N90-29915

ERS-1 (ESA SATELLITE)
ERS-1 European remote sensing satellite: A new tool for global environmental monitoring in the 1990's
[ESA-BR-36] 11 p1526 N90-18782
The VIERS-1 project. The Delft wind/wave experiment: Experiment and first results, part 1
[BCRS-89-24-PT-1] 17 p2418 N90-23779
Analysis and test interaction in the development of a hold down and release mechanism 18 p2539 N90-24489

ERTS
U LANDSAT SATELLITES

ERYTHROCYTES
Regulation of erythropoiesis in rats during space flight
[NASA-CR-177537] 23 p3378 N90-29086

ESA
U EUROPEAN SPACE AGENCY

ESA SATELLITES
NT ERS-1 (ESA SATELLITE)
NT EUROPEAN COMMUNICATIONS SATELLITE
NT EXOSAT SATELLITE
NT HIPPARCOS SATELLITE
NT INFRARED SPACE OBSERVATORY (ISO)
NT MARECS MARITIME SATELLITES
NT METEOSAT SATELLITE
US Activity with the OLYMPUS satellite 10 p1374 N90-17964
Compendium of meteorological space programs, satellites, and experiments
[NASA-TM-102924] 12 p1607 N90-19243

ESA SPACECRAFT
NT COLUMBUS SPACE STATION
NT ERS-1 (ESA SATELLITE)
NT ESA SATELLITES
NT EUROPEAN COMMUNICATIONS SATELLITE
NT EXOSAT SATELLITE
NT GIOTTO MISSION
NT HIPPARCOS SATELLITE
NT INFRARED SPACE OBSERVATORY (ISO)
NT MARECS MARITIME SATELLITES
NT METEOSAT SATELLITE
The determination of offgassing products from materials and assembled articles to be used in a manned space vehicle crew compartment
[ESA-PSS-01-729-ISSUE-1] 11 p1469 N90-18461
Rosetta/CNSR, ESA's planetary cornerstone mission 12 p1738 N90-19990
ARISTOTELES: A European approach for an Earth gravity field recovery mission 13 p1839 N90-20559

ESCAPE (ABANDONMENT)
The human factors relating to escape and survival from helicopters ditching in water
[AGARD-AG-305(E)] 05 p0576 N90-13358

ESCAPE CAPSULES
Requirements for protective pressure suits for the Hermes spacecrew 13 p1753 N90-20065

ESCAPE SYSTEMS
A preliminary sensitivity analysis of the Generalized Escape System Simulation (GESS) computer program
[DE89-016891] 02 p0148 N90-10844
Crew emergency return vehicle autoland feasibility study
[NASA-CR-181940] 08 p1028 N90-15937
Safety and rescue during STS operations 08 p1034 N90-15975
Assured crew return capability architecture 08 p1034 N90-15977
Supersonic aerodynamic characteristics of a proposed Assured Crew Return Capability (ACRC) lifting-body configuration
[NASA-TM-4136] 10 p1307 N90-17560
Smokehoods donned quickly. The impact of donning smokehoods on evacuation times 10 p1317 N90-17614
Implications of Advanced Technologies for Air and Spacecraft Escape
[AGARD-CP-472] 13 p1751 N90-20054
Development of acceleration exposure limits for advanced escape systems 13 p1751 N90-20055
Development of an ejection seat specification for a new fighter aircraft 13 p1751 N90-20057
Escape systems research at RAE 13 p1751 N90-20058
Fighter escape system: The next step forward 13 p1752 N90-20059
Potential role of avionics in escape systems 13 p1752 N90-20060
Ejection seat training of jet pilots and weapon system officers at the German Air Force School of Aviation Medicine 13 p1752 N90-20061
The USAF Advanced Dynamic Anthropomorphic Manikin (ADAM) 13 p1752 N90-20062
Controllable propulsion for escape systems control 13 p1753 N90-20064
Forward canopy feasibility and Thru-The-Canopy (TTC) ejection system study
[AD-A220360] 18 p2495 N90-24258
Development of a microcomputer based software system for use in crewmember ejection analysis
[AD-A220398] 19 p2656 N90-25117
Orbiter utilization as an ACRV
[NASA-TM-102700] 20 p2817 N90-26032

ESCHERICHIA
The sensory transduction pathways in bacterial chemotaxis 05 p0677 N90-13944

ESRO
U EUROPEAN SPACE AGENCY

ESRO SATELLITES
U ESA SATELLITES

ESSENTIALLY NON-OSCILLATORY SCHEMES
Finite-volume application of high order ENO schemes to multi-dimensional boundary-value problems
[NASA-CR-186917] 22 p3242 N90-28387
Numerical experiments on the accuracy of ENO and modified ENO schemes
[NASA-CR-182083] 23 p3387 N90-29128
Numerical methods for systems of conservation laws of mixed type using flux splitting
[NASA-CR-182084] 23 p3387 N90-29129

ESTERS
NT ACRYLATES
NT ASPARTATES
NT CARBAMATES (TRADENAME)
NT CARBOXYLATES
NT CELLULOSE NITRATE
NT ISOCYANATES
NT LACTATES
NT LEXAN (TRADEMARK)
NT PETN
NT PHTHALATES
NT POLYCARBONATES
NT POLYESTERS
NT POLYETHYLENE TEREPHTHALATE
NT SULFONATES
NT URETHANES
The size of the alkyl group R is the principal factor determining the wettability of surface-functionalized polyethylenes (PE-CONHR and PE-CO2R) by water
[AD-A216007] 10 p1354 N90-17851
Monocoque structure for the SKITTER three-legged walker
[NASA-CR-184635] 18 p2534 N90-24454

ESTIMATES
NT COST ESTIMATES
Minimum-variance reduced-order estimation algorithms from Pontrygin's minimum principle 01 p0021 N90-10105
A unified view of infinitesimal perturbation analysis and likelihood ratios
[AD-A210682] 01 p0114 N90-10652
Studies in estimation theory, applications and implementations
[AD-A210712] 01 p0114 N90-10653
Passive trajectography by azimuth: Improvement of estimation quality 02 p0150 N90-10854
Estimation on nonlinear damping in second order distributed parameter systems
[NASA-CR-181890] 02 p0263 N90-11494
Error estimation and self-adaptive mesh refinement for boundary element method 03 p0356 N90-12037
Likelihood cross-validation bandwidth selection for nonparametric kernel density estimators
[REPT-89-10] 03 p0398 N90-12279
On the application of modified stepwise regression for the estimation of aircraft stability and control parameters
[REPT-8905] 05 p0583 N90-13400
Simultaneous quaternion estimation (QUEST) and bias determination 05 p0587 N90-13417
Error allocation and accuracy assessment 05 p0603 N90-13501
Large deviation estimates in the stochastic quantization of phi sub 2 exp 4
[PREPRINT-686] 05 p0693 N90-14050
Rainfall estimation over Africa using satellite data 06 p0815 N90-14742
Local error estimates for discontinuous solutions of nonlinear hyperbolic equations
[NASA-CR-181960] 06 p0834 N90-14847
Theoretical investigations of the structures and binding energies of Be(sub n) and Mg(sub n) (n = 3-5) clusters
[NASA-TM-101931] 08 p1120 N90-16483
Sensitivity of space system availability predictions to underlying component reliability estimates
[AD-A215535] 09 p1183 N90-16858
Time and spatially-dependent estimates of pollutant trace gas emissions and their effect on tropospheric ozone 09 p1243 N90-17212
Estimates of galactic cosmic ray shielding requirements during solar minimum
[NASA-TM-4167] 09 p1300 N90-17535
Spectral responses of soybeans and their relationship with agronomical parameters
[INPE-4832-PRE/1462] 10 p1398 N90-18084
LANDSAT-TM and agrometeorological data in the wheat crop yield estimation at the farm level
[INPE-4842-PRE/1471] 10 p1400 N90-18091
Stochastic approach to the initiation of pitting corrosion
[AERE-R-13348] 13 p1775 N90-20190
A knowledge-based information based for crop area estimation
[INPE-4990-PRE/1555] 14 p1996 N90-21444
Adaptive frequency estimation by MUSIC (Multiple Signal Classification) method
[PB90-166794] 15 p2086 N90-21943
Efficient estimation in the Clayton-Cuzick model for survival data
[TW-88-06] 15 p2161 N90-22348
Quantifying and reducing uncertainty in the assimilative mapping of ionospheric electrodynamics 16 p2254 N90-22854
A survey on the structured singular value 16 p2281 N90-22998
Sample size for correlation estimates
[AD-A219810] 17 p2465 N90-24085
The 1991 NASA authorization: National Aeronautics and Space Administration fiscal year 1991 authorization request and budget estimates
[GPO-27-291] 17 p2481 N90-24188
National patterns of research and development resources: 1989
[NSF-89-308] 17 p2486 N90-24218
A quantitative technique to estimate microburst wind shear hazard to aircraft 18 p2640 N90-25040
A noncontacting motion monitoring system for an astronaut translation aid
[NASA-TM-102640] 19 p2693 N90-25325

Physical parameterization of snow albedo for use in climate models
[PB90-167313] 19 p2712 N90-25433
Estimation of convective rain volumes utilizing the are-time-integral technique
[NASA-CR-186814] 20 p2890 N90-26449
Variance reduction for quantile estimates in simulations via nonlinear controls
[AD-A222653] 20 p2916 N90-26590
Comparison of overstory canopy cover estimates on forest survey plots
[PB90-159484] 22 p3194 N90-28126
Structure-borne noise estimates for the PTA aircraft
[NASA-CR-4315] 22 p3244 N90-28396
National air pollutant emission estimates, 1940-1988
[PB90-199266] 23 p3346 N90-28908
Estimation and representation of multidimensional mappings
[DLR-MITT-90-06] 24 p3531 N90-29967

ESTIMATING
NT ORBITAL POSITION ESTIMATION
NT PARAMETER IDENTIFICATION
NT SYSTEM IDENTIFICATION
Improved estimation of the disturbance variance in a linear regression model
[AD-A210272] 01 p0112 N90-10641
Studies in estimation theory, applications and implementations
[AD-A210712] 01 p0114 N90-10653
Analytic signals in the damping coefficient estimation 02 p0178 N90-11003
Parameter estimation in functional and partial differential equations
[AD-A211040] 02 p0265 N90-11511
Statistical models for the optimal estimation of oceanic fields
[AD-A211786] 03 p0377 N90-12149
On finding the largest normal mean and estimating the selected mean
[AD-A211628] 03 p0394 N90-12245
Empirical Bayes estimation of binomial parameter with symmetric priors
[AD-A211646] 03 p0394 N90-12246
Splines and equations of nonlinear parameters
[IMAG-RR-750-M] 03 p0395 N90-12257
Fast sampling and stability of nonlinear sampled data systems. Part 2: Sampling rate estimations
[RR-341] 03 p0397 N90-12271
Estimating functionals related to a density by a class of statistics based on spacings
[REPT-89-11] 03 p0398 N90-12275
Estimating the time to fatigue failure of mooring cables
[PB89-220677] 04 p0511 N90-12946
Optimum data weighting and error calibration for estimation of gravitational parameters
[NASA-TM-100737] 04 p0517 N90-12985
Bilinear modeling and nonlinear estimation 05 p0589 N90-13430
Extended Kalman filter for attitude estimation of the earth radiation budget satellite 05 p0590 N90-13433
Estimation of rain rate using spatial and multichannel coherence: Analysis of SSM/I data 05 p0670 N90-13905
Estimation of convolution tail behavior
[MEMO-COSOR-89-04] 05 p0693 N90-14051
Normal force, pitching moment, and side force of forebody-cylinder combinations for angles of attack up to 90 degrees and Mach numbers up to 5
[ESDU-89014] 06 p0718 N90-14192
Example of procedure in calculation of control hinge moments
[ESDU-89010] 06 p0727 N90-14240
The effects of clutter-rejection filtering on estimating weather spectrum parameters
[NASA-CR-186212] 06 p0817 N90-14754
Power spectral estimation algorithms
[NASA-CR-186189] 06 p0828 N90-14812
Estimating methods for counting process intensities: Non-parametric methods
[IMAG-RR-774-M] 06 p0834 N90-14846
A guide for estimating potential energy savings from increased solar reflectance of a low-sloped roof
[DE90-003720] 07 p0955 N90-15526
Estimating departure times from traffic counts using dynamic assignment
[DE89-016259] 07 p0979 N90-15653
Membership-set parameter estimation via optimal bounding ellipsoids
[AD-A213807] 07 p0984 N90-15685
On-line estimation of mechanical nonlinearities in compliant two-link robot manipulators 08 p1085 N90-16280
Estimating water flow through a hillslope using the massively parallel processor 08 p1114 N90-16449
Multiple model adaptive estimation techniques for adaptive model-based robot control
[AD-A215742] 09 p1231 N90-17146
On some problems in reliability theory 09 p1233 N90-17155
Evaluation of the use of flat terrain models versus complex terrain screening models in estimating pollutant transport and deposition in complex terrain
[DE90-005271] 09 p1245 N90-17223
Three position estimation procedures
[AD-A214992] 09 p1276 N90-17395
On the temperature of surfaces 10 p1366 N90-17917
Some applications of model-based parameter estimation in computational electromagnetics 10 p1369 N90-17935
Evaluation of digital classification results of summer cultivation in a test area in the Parana-Ano state harvest 1986-1987
[INPE-4828-PRE/1459] 10 p1399 N90-18085
Estimation in a discrete tail rate family of recapture sampling models
[NASA-CR-180452] 10 p1421 N90-18197
A general method of using prior information in a simultaneous equation system
[NOAA-TR-NESDIS-47] 10 p1423 N90-18209
Attitude estimation procedure for spin stabilized satellites
[INPE-4866-TDL/377] 11 p1467 N90-18449
Methods for trend analysis: Examples with problem/failure data 12 p1635 N90-19396
Survey on the social and economic influences of wide-spreading heat-pump technology
[DE89-782204] 12 p1658 N90-19526
Evaluation of TM/LANDSAT and HRV/SPOT data in the identification of reforested areas in the Mogi-Guacu (SP) region
[INPE-4874-PRE/1485] 13 p1819 N90-20442
Local gravity disturbance estimation from multiple-high-single-low satellite-to-satellite tracking 13 p1839 N90-20555
Analysis of altimetry over inland seas
[NASA-TM-100729] 13 p1840 N90-20566
Systematic errors in power measurements made with a dual six-port ANA
[PB90-145160] 14 p1968 N90-21276
Agricultural yield estimation of sugarcane based on agrometeorological-spectral model
[INPE-5016-RPE/610] 14 p1996 N90-21441
Performance evaluation of MSS/LANDSAT data in the estimation of fluvial channel width
[INPE-4906-PRE/1507] 14 p2000 N90-21463
Exact closed-form expressions for the performance of the split-symbol moments estimator of signal-to-noise ratio 15 p2077 N90-21894
Sliding control of pointing and tracking with operator spline estimation 16 p2281 N90-22997
Parameter estimation in linear filtering
[AD-A218566] 16 p2307 N90-23144
Diode laser satellite systems for beamed power transmission
[NASA-TP-2992] 18 p2556 N90-24585
A Bayesian approach to reliability and confidence 18 p2628 N90-24974
Weight and cost forecasting for advanced manned space vehicles 18 p2632 N90-24998
The effect of aircraft size on cabin floor dynamic pulses
[DOT/FAA/CT-88/15] 19 p2659 N90-25136
An accurate numerical technique for determining flight test rate gyroscope biases prior to takeoff
[AD-A220987] 19 p2660 N90-25138
Effects of simplifying assumptions on optimal trajectory estimation for a high-performance aircraft
[NASA-TM-101721] 19 p2661 N90-25142
Seasonal LAI in slash pine estimated with LANDSAT TM
[NASA-TM-102278] 19 p2706 N90-25397
A novel multireceiver communications system configuration based on optimal estimation theory
[NASA-CR-186847] 20 p2851 N90-26216
Estimation of convective rain volumes utilizing the are-time-integral technique
[NASA-CR-186814] 20 p2890 N90-26449
Multistage estimation of received carrier signal parameters under very high dynamic conditions of the receiver
[NASA-CASE-NPO-17911-1-CU] 21 p2994 N90-27016
Modified fast frequency acquisition via adaptive least squares algorithm
[NASA-CASE-NPO-17845-1-CU] 21 p3050 N90-27341
Modification of the background flow by roll vortices 22 p3219 N90-28258
Structure-borne noise estimates for the PTA aircraft
[NASA-CR-4315] 22 p3244 N90-28396
Estimating the spatial variability of trace gas deposition velocities
[PB90-208570] 23 p3349 N90-28928
Data Base Analyzer and Parameter Estimator (DBAPE) interactive computer program user's manual
[PB90-193053] 23 p3406 N90-29252
Performance analysis of subspace-based parameter estimation algorithms
[AD-A224523] 24 p3463 N90-29566
Windshear estimation along the trajectory of an aircraft 24 p3494 N90-29745

ESTUARIES
Evaluation of the mangrove areas of the Rio Piaui (SE) through remote sensing
[INPE-4909-PRE/1510] 14 p1998 N90-21454
MECCA program documentation
[NOAA-TR-NESDIS-46] 14 p2003 N90-21477
Vertically averaged spectral model for tidal circulation in estuaries. Part 1: Model formulation
[PB90-181678] 22 p3230 N90-28319
Perspectives on the Chesapeake Bay, 1990: Advances in estuarine sciences
[PB90-248600] 23 p3354 N90-28954

ETA-MESONS
Theoretical aspects of electroweak and other interactions in medium energy nuclear physics
[DE90-004015] 08 p1121 N90-16483

ETALONS
An imaging vector magnetograph for the next solar maximum 03 p0435 N90-12489
Fellowship in physics/modern optics and quantum electronics
[AD-A218772] 17 p2469 N90-24111

ETCHING
Scanning tunneling microscopy etching of micrometer level features on p-type GaAs
[AD-A209216] 01 p0058 N90-10328
Characterization of 4/3 technology large-scale integrated circuit on polysilicon processes
[BDX-613-3971] 01 p0059 N90-10335
Custom diffraction gratings
[AD-A211002] 01 p0124 N90-10712
Reactive ion etching of SiC thin films by mixtures of fluorinated gases and oxygen
[AD-A211046] 02 p0195 N90-11113
Electrochemical study of the etching of III to V semiconductors
[ETN-90-96015] 05 p0623 N90-13633
Method of making self-aligned GaAs/AlGaAs FET's
[AD-D014229] 06 p0849 N90-14935
Research on GaAs quantum-coupled structures that can be used as electron devices
[AD-A214015] 07 p0924 N90-15350
Silicon membrane formation
[DE90-003022] 08 p1049 N90-16064
Materials processing of diamond: Etching, doping by ion implantation and contact formation
[AD-A216530] 10 p1438 N90-18301
Metal coordination polymers as potential high-energy lithographic resists
[AD-A216668] 11 p1490 N90-18574
The track-etch detector for the MACRO experiment at the Gran Sasso Laboratory
[DE90-003235] 11 p1594 N90-19182
Oxygenation and possible etching of high T(sub c) superconducting films by oxygen plasma
[DE90-004956] 12 p1719 N90-19871
Mechanisms of reactive etching
[AD-A217679] 13 p1770 N90-20160
In-situ differential reflectance study of the etching of SiO2 films
[AD-A217186] 13 p1893 N90-20864
The investigation of multilayer x ray reflectors as x ray optical elements
[DE90-009044] 14 p2026 N90-21621
Theoretical studies of photochemical methods for semiconductor etching
[AD-A218475] 17 p2475 N90-24151
Molecular beam epitaxial growth of heterostructures to study quantum interference phenomena
[AD-A219442] 17 p2475 N90-24154
Direct writing of microstructures for solid-state electronics
[AD-A220996] 18 p2535 N90-24460
Chlorine reactive-ion-beam etching of InSb and InAs0.15Sb0.85/InSb strained-layer-superlattices
[DE90-010848] 18 p2625 N90-24958
Seamless metal-clad fiber-reinforced organic matrix composite structures and process for their manufacture
[NASA-CASE-LAR-13562-1] 19 p2672 N90-25196
The role of heat transfer during reactive-ion etching of polymer films
[AD-A222072] 21 p2977 N90-26919

Ni impurity effects on hydrogen surface chemistry and etching of Si(111)
[AD-A222083] 21 p2977 N90-26921
Face-specific interaction of MoS4(2-) with oriented crystals of (0001) CdX(X = Se, S)
[AD-A222405] 21 p3084 N90-27537
Optoelectronics Research Center
[AD-A221926] 22 p3246 N90-28410

ETHANE
Thermal stability of the carbon-carbon bond in ethylene adsorbed on Si(100): An isotopic mixing study
[AD-A211591] 04 p0470 N90-12691
Extracting chemical information form Auger line shapes
[AD-A216729] 11 p1483 N90-18537
Substituted 1,1,1-triaryl-2,2,2-trifluoroethanes and processes for their synthesis
[NASA-CASE-LEW-14345-2] 17 p2371 N90-23497
Quantitative determination of 1, 2-ethanediol contamination in used diesel lubricating oils by gas chromatography/mass spectrometry
[AD-A218592] 17 p2371 N90-23498
Laboratory studies, analysis, and interpretation of the spectra of hydrocarbons present in planetary atmospheres including cyanoacetylene, acetylene, propane, and ethane 20 p2943 N90-26748

ETHANE NITRILE
U ACETONITRILE

ETHANOL
U ETHYL ALCOHOL

ETHERS
NT ACETALS
Curable polyether compositions
[AD-D014200] 04 p0468 N90-12679
Polyimides with carbonyl and ether connecting groups between the aromatic rings
[NASA-CASE-LAR-14001-1] 07 p0910 N90-15260
Determination of the thermal stability of perfluoroalkylethers
[NASA-TM-102493] 10 p1358 N90-17875
Experience with synthetic fluorinated fluid lubricants 15 p2114 N90-22095
Imide/arylene ether copolymers
[NASA-CASE-LAR-14159-1-CU] 21 p2983 N90-26953

ETHNIC FACTORS
ONR (Office of Naval Research) summer scholars for the 1989 PREFACE Program
[AD-A217746] 13 p1903 N90-20919
Air Force Officer Qualifying Test (AFOQT): Development of quick score composites for forms P1 and P2
[AD-A223868] 23 p3362 N90-28997

ETHYL ALCOHOL
In-flight evaluations of turbine fuel extenders
[DOT/FAA/CT-89/33] 12 p1633 N90-19387
Turbine fuel alternatives (near term)
[AD-A219405] 16 p2225 N90-22695
Development of a spark assisted direct injection multifuel diesel engine especially for alcohol fuels
[ACTA-POLYTEC-SCAND-ME-94] 17 p2412 N90-23747
CRC low- and intermediate-temperature driveability program using gasoline-alcohol blends
[AD-A221321] 18 p2533 N90-24453
Nature and origin of interstellar diamond from the Allende CV3 meteorite 21 p3092 N90-27581

ETHYL COMPOUNDS
Determination of the minimum energy conformation of alkyl substituted pyrazines
[AD-A216974] 11 p1484 N90-18539
Retention index monitoring of volatile organic compounds using thermal desorption gas chromatography
[AD-A221117] 18 p2521 N90-24397

ETHYLENE
NT VINYLIDENE
Thermal stability of the carbon-carbon bond in ethylene adsorbed on Si(100): An isotopic mixing study
[AD-A211591] 04 p0470 N90-12691
Mechanisms of the electrochemistry of small organic molecules
[PB90-100785] 08 p1040 N90-16012
Extracting chemical information form Auger line shapes
[AD-A216729] 11 p1483 N90-18537
Nonflammable hydraulic power system for tactical aircraft. Volume 1: Aircraft system definition, design and analysis
[AD-A218493] 17 p2356 N90-23409
The application of HREELS to model catalysts: CO and C2H4 adsorption on Pt/Al2O3
[AD-A222744] 20 p2831 N90-26103
Quantitative confirmation of diffusion-limited oxidation theories
[DE90-012997] 20 p2838 N90-26143
Structure and radiation properties of turbulent diffusion flames
[PB90-218777] 22 p3155 N90-27887

ETHYLENE COMPOUNDS
Quantitative determination of 1, 2-ethanediol contamination in used diesel lubricating oils by gas chromatography/mass spectrometry
[AD-A218592] 17 p2371 N90-23498

ETHYLENE OXIDE
Synthesis and physical properties of poly(perfluoroalkylether) urethanes
[AD-A210500] 01 p0050 N90-10287
Plasma modification of poly (p-phenylenebenzobisthiazole)
[AD-A215781] 10 p1433 N90-18272
Durable heat diaphragm from ordered polymer films
[AD-A220794] 17 p2381 N90-23559

ETIOLOGY
Exertional heatstroke: An international perspective. An introduction: The role of exercise in the etiology of exertional heatstroke
[AD-A212242] 04 p0523 N90-13020

ETTINGSHAUSEN COOLERS
U THERMOELECTRIC COOLING

EUCLIDEAN GEOMETRY
NT ANALYTIC GEOMETRY
NT ANGLE OF ATTACK
NT ANGLES (GEOMETRY)
NT BRAGG ANGLE
NT CARTESIAN COORDINATES
NT CIRCLES (GEOMETRY)
NT CIRCUMFERENCES
NT CONICS
NT DESCRIPTIVE GEOMETRY
NT DIHEDRAL ANGLE
NT ELEVATION ANGLE
NT ELLIPSES
NT EPICYCLOIDS
NT FIXED POINTS (MATHEMATICS)
NT GEODESIC LINES
NT GREAT CIRCLES
NT LEADING EDGE SWEEP
NT LINES (GEOMETRY)
NT LOOK ANGLES (ELECTRONICS)
NT OCTAHEDRONS
NT PARABOLAS
NT PARALLELEPIPEDS
NT POINTS (MATHEMATICS)
NT POLYGONS
NT POLYHEDRONS
NT PROJECTIVE GEOMETRY
NT PROLATE SPHEROIDS
NT RADII
NT RECTANGLES
NT RHOMBOIDS
NT SQUARES (MATHEMATICS)
NT SWEEP ANGLE
NT TANGENTS
NT TETRAHEDRONS
NT TORUSES
NT TRAPEZOIDS
NT TRIANGLES
NT TRIGONOMETRY
NT ZERO ANGLE OF ATTACK
On the expected complexity of the three-dimensional Voronoi diagram
[PB89-209332] 01 p0112 N90-10636
On the areas of various bodies in the Euclidean space: The case of irregular convex polygons
[DE89-618377] 02 p0264 N90-11500
Local structure of a 2-codimensional conformally flat submanifold in an Euclidean space R(sup n+2)
[DE89-618379] 02 p0264 N90-11501
A remark on the Kelvin transform and a non-linear partial differential equation
[PB90-165622] 14 p2021 N90-21589
Characteristics consequences of space-time coordinate relativization
[DE90-615201] 14 p2034 N90-21668
Efficient computer algebra algorithms for polynomial matrices in control design 16 p2285 N90-23022
Non-symmetric double well and Euclidean functional integral
[PREPRINT-709] 16 p2305 N90-23133
Effective action for induced gravity on a 2-dimensional manifold
[PREPRINT-712] 16 p2311 N90-23173
New multi-level codes over GF(q)
[NASA-CR-186862] 19 p2744 N90-25594
On Einsteinian 4-submanifolds in E(sup 6)
[DE90-627149] 23 p3402 N90-29226

EUCLIDEAN SPACE
U EUCLIDEAN GEOMETRY

EULER EQUATIONS OF MOTION
Supersonic flow computations over aerospace configurations using an Euler marching solver
[NASA-CR-4085] 01 p0003 N90-10012
Remote control missile model test 01 p0013 N90-10063
Numerical simulation of leading-edge vortex rollup and bursting 02 p0145 N90-10831
The upwind control volume scheme for unstructured triangular grids
[NASA-TM-101664] 03 p0301 N90-11703
Numerical simulation of unsteady rotational flow over propfan configurations
[NASA-CR-186037] 04 p0438 N90-12500
Improvements in the formulations and numerical solution of the Euler problem for swept wings
[RAE-TM-AERO-2139] 04 p0447 N90-12562
Euler equation solutions applied to a helicopter rotor in forward moving flight
[ONERA-RSF-32/1285-AY-346A] 04 p0452 N90-12592
Multigrid solution method for the Euler equations
[PB89-219463] 04 p0539 N90-13116
Block-structured solution of three-dimensional transonic flows using parallel processing
[AD-A212851] 05 p0572 N90-13330
Transonic Euler solutions on mutually interfering finned bodies
[AD-A213395] 05 p0572 N90-13331
Computation of flow fields around propellers and hovering rotors based on the solution of the Euler equations
[DLR-FB-89-37] 05 p0572 N90-13333
Application of an efficient hybrid scheme for aeroelastic analysis of advanced propellers
[NASA-TM-102428] 05 p0576 N90-13355
Gas flows in rocket motors. Volume 3, appendix D: Computer code listings
[AD-A213350] 05 p0616 N90-13593
Multigrid and defect correction for the steady Navier-Stokes equations: Applications to aerodynamics
[ETN-90-96011] 05 p0639 N90-13727
Calculation of flow fields by the solution of the Euler equations using an extended finite volume discretization scheme
[DLR-FB-89-38] 05 p0639 N90-13729
Numerical Methods for Flows in Turbomachinery, volume 1
[VKI-LS-1989-06-VOL-1] 05 p0640 N90-13735
Inviscid 3D solution methods 05 p0640 N90-13736
A dynamic multiblock approach to solving the unsteady Euler equations about complex configurations 06 p0773 N90-14497
Euler and Navier-Stokes computations for two-dimensional geometries using unstructured meshes
[NASA-CR-181977] 08 p1019 N90-15893
Adaptive local grid refinement for the compressible 3-D Euler equations
[FFA-TN-1989-40] 08 p1064 N90-16155
Research on three different Euler's schemes applied to a delta wing with vortical flows 08 p1068 N90-16184
Calculation of two and three dimensional super and hypersonic flows by solving the Euler equations 08 p1070 N90-16197
Definition, transformation-formulae and measurements of tipvane angles
[IW-R510] 08 p1097 N90-16351
On the numerical solution of the dynamically loaded hydrodynamic lubrication of the point contact problem
[NASA-TM-102427] 09 p1220 N90-17076
Computation of compressible viscous flows 10 p1308 N90-17567
Unsteady Euler analysis of the flow field of a propfan at an angle of attack
[NASA-TM-102426] 10 p1426 N90-18229
Numerical investigation of unsteady flow in oscillating turbine and compressor cascades 11 p1459 N90-18407
Implementation of a finite element process for the Euler equations of the gas dynamics
[PREPRINT-500] 12 p1861 N90-19545
Numerical simulations of supersonic flow through oscillating cascade sections
[NASA-TM-103100] 13 p1750 N90-20051
Some aspects of Essentially Nonoscillatory (ENO) formulations for the Euler equations, part 3
[NASA-CR-4285] 14 p1910 N90-20949
Computation of nonequilibrium chemically reacting flows in hypersonic flow field 14 p1911 N90-20954
An evaluation of the two-dimensional Euler and Navier-Stokes calculations based on a flux-vector splitting
[PB90-166778] 14 p1912 N90-20963

Optimization of aerodynamic designs using computational fluid dynamics 14 p1920 N90-20999
Cepstrum analysis and applications to computational fluid dynamic solutions 14 p1973 N90-21302
PROTEUS two-dimensional Navier-Stokes computer code, version 1.0. Volume 1: Analysis description [NASA-TM-102551] 14 p1973 N90-21303
PROTEUS two-dimensional Navier-Stokes computer code, version 1.0. Volume 2: User's guide [NASA-TM-102552] 14 p1973 N90-21306
Adaptive grid embedding for the two-dimensional flux-split Euler equations [NASA-CR-186533] 14 p2019 N90-21571
Applications of Mesh Generation to Complex 3-D Configurations [AGARD-CP-464] 15 p2093 N90-21975
Unsteady Euler solutions on dynamic blocked grids for complex configurations 15 p2094 N90-21982
Grid patching approaches for complex three-dimensional configurations 15 p2094 N90-21985
Feature-associated mesh embedding for complex configurations 15 p2095 N90-21988
Generation and adaptation of 3-D unstructured grids for transient problems 15 p2096 N90-21994
Investigation of advanced counterrotation blade configuration concepts for high speed turboprop systems, task 1: Ducted propfan analysis [NASA-CR-185217] 16 p2202 N90-22567
The development of a system for the numerical simulation of Euler flows 16 p2277 N90-22980
Stable boundary conditions for Cartesian grid calculations [NASA-CR-182048] 16 p2306 N90-23139
Codice ETF-3D: Euler transonic flow user manual [DLC/FLU-INT-TN-006] 17 p2346 N90-23362
Euler code predicted separation at the airfoil trailing edge [FFA-TN-1989-30] 17 p2346 N90-23364
On upwind formulations and non equilibrium chemistry [DLC/FLU-INT-TN-014] 17 p2403 N90-23691
Iterative defect correction and multigrid accelerated explicit time stepping schemes for the steady Euler equations [CWI-NM-R8908] 17 p2459 N90-24039
Code ETF-3D. Euler transonic flow: Theoretical manual [DLC/FLU-INT-TN-005] 18 p2493 N90-24247
Code ETF-3D. Euler transonic flow: Validation manual [DLC/FLU-INT-TN-007] 18 p2493 N90-24248
Notes on the unsteady rectilinear motion of a perfect gas. 9: The expansion to vacuum of a finite mass of uniform homentropic gas [LR-590-9] 19 p2692 N90-25316
A parallel Newton-Euler formulation for fast dynamic simulation of robot manipulators [RR-368] 19 p2748 N90-25614
The role of computational fluids dynamics in missile aerodynamics [NLR-MP-88072-U] 20 p2804 N90-25952
Analysis and mitigation of numerical dissipation in inviscid and viscid computation of vortex-dominated flows [NASA-CR-186887] 20 p2862 N90-26281
Development of a system for the numerical simulation of Euler flows, with results of preliminary 3-D propeller-slipstream/exhaust-jet calculations [NLR-TR-88008-U] 20 p2863 N90-26285
An Eulerian transport model for NO(sub x)-compounds 20 p2884 N90-26406
An approximate method for calculating three-dimensional inviscid hypersonic flow fields [NASA-TP-3018] 21 p3002 N90-27066
Hyperbolic conservation laws and numerical methods 22 p3172 N90-27990
Computational Fluid Dynamics, Volume 2 [VKI-LS-1990-03-VOL-2] 22 p3172 N90-27993
Towards a genuinely multi-dimensional upwind scheme 22 p3172 N90-27995
Efficient solution of the steady Euler equations with a centered implicit method 22 p3173 N90-27999
Solution of Euler equations using finite element method and the kinetic decomposition of the flows: Study of the self-adaptation of the grid and of the calculation field [CERT-1/334700-DERI-GAN] 22 p3176 N90-28020
Solution of Euler equations applied to a rotor of a helicopter in steady flight [ONERA-RSF-1/3731-AY-002A] 23 p3269 N90-28500
Multigrid for hypersonic inviscid flows [NASA-CR-182082] 23 p3387 N90-29125
Transonic 3-D Euler analysis of flows around fanjet engine and TPS (Turbine Powered Simulator). Comparison with wind tunnel experiment, evaluation of TPS testing method and 3-D flow [NAL-TR-1045] 24 p3421 N90-29327
Calculation of flow fields by the solution of the Euler equations using an extended finite volume discretization scheme [ESA-TT-1204] 24 p3470 N90-29605
Recursive Newton-Euler formulation of manipulator dynamics 24 p3513 N90-29862

EULER-LAGRANGE EQUATION
Fluid-structure interaction effects in tank structures due to sloshing and hydrodynamic ram: Coupled Lagangian-Eulerian simulations 02 p0181 N90-11022
Computation of transient three-dimensional interstage flowfields using the arbitrary Lagrangian-Eulerian method 02 p0219 N90-11253
A distributed pipelined architecture of the recursive Lagrangian equations of motion for robot manipulators with VLSI implementation — VLSI (very large scale integration) [RR-353] 03 p0344 N90-11966
Application of Lagrangian blending functions for grid generation around airplane geometries [NASA-CR-186318] 08 p1018 N90-15891
And still, a new beginning: The Galerkin least-squares gradient method [DE89-636435] 08 p1116 N90-16461
A quasi-Lagrangian moving grid technique for investigating compressible flows 14 p1972 N90-21298
Perturbation techniques in the dynamics and control of flexible manipulators [OUEL-1772/89] 15 p2107 N90-22053
Lagrangian model simulation of the turbulent transport of evaporating jet droplets 15 p2128 N90-22168
On the planar translation of two bodies in a uniform flow [AD-A220143] 17 p2404 N90-23698
Skew-symmetric matrices in classical mechanics [MEMO-COSOR-89-23] 17 p2459 N90-24036

EURECA (ESA)
Experiment facilities for materials and fluid sciences embarked on Eureca-1 [ESA-SP-1118] 08 p1053 N90-16088
Eurolaser definition phase, solid state lasers working group: Active medium, laser active crystals [ETN-90-95899] 08 p1083 N90-16266
Design considerations and lessons learned on the European retrievable carrier 10 p1332 N90-17698
Shutter mechanism for controlling the exposure of samples to solar radiation 18 p2540 N90-24498
Mechanism for deployment and retraction of biological samples 18 p2540 N90-24499
Hemispherical pointing mechanism 18 p2541 N90-24502

EUROPE
A history of West European rocketry and space research [AD-A211191] 02 p0297 N90-11690
An atlas of ECMWF analyses (1980-1987). Part 1: First moment quantities [NASA-TM-100747-PT-1] 10 p1408 N90-18120
Investigation report of the investigation commission for interchange of heat pump technology in Europe [DE89-782293] 11 p1505 N90-18666
The EURAD Model: Structure and First Results [REPT-61] 12 p1686 N90-19680
Development and status of the EURAD project 12 p1686 N90-19681
Long range geoid control through the European GPS traverse: Final results 13 p1837 N90-20545
Microgravity science and applications bibliography, 1989 revision [NASA-TM-4192] 14 p1957 N90-21207
The automation plan of the General Directorate 1 (search) of the European Patent Office 15 p2178 N90-22448
The RACE (research and development in advanced technologies for Europe) program: A 1989 update [AD-A218509] 16 p2228 N90-22713
Hypersonic aerodynamics of spacecraft [DLC-EST-TD-032] 17 p2346 N90-23361

EUROPEAN AIRBUS
NT A-300 AIRCRAFT
NT A-310 AIRCRAFT
NT A-320 AIRCRAFT
Properties of Al-Li alloys 07 p0898 N90-15191
Fire hardening of aircraft through upgrades of materials and designs 10 p1315 N90-17605
Software maintenance on Airbus family [REPT-892-111-101] 17 p2444 N90-23931
Aerodynamic development perspective for traffic aeroplanes [DGLR-89-141] 18 p2495 N90-24260
Simulation of transport aeroplanes [MBB-UT-007/89-PUB] 19 p2651 N90-25089

EUROPEAN COMMUNICATIONS SATELLITE
ECS: Sixth year in orbit [ESA-BR-70] 24 p3440 N90-29428

EUROPEAN INCOHERENT SCATTER RADAR
U EISCAT RADAR SYSTEM (EUROPE)

EUROPEAN RETRIEVABLE CARRIER
U EURECA (ESA)

EUROPEAN SPACE AGENCY
European space technology: Celebrating twenty-five years of research and development [ESA-BR-55] 04 p0569 N90-13322
European Rocket and Balloon Programs and Related Research [ESA-SP-291] 05 p0656 N90-13826
An international discussion on research in solar and space physics 06 p0859 N90-14996
From small beginnings... The story of ESRO's sounding rocket programme in celebration of the twenty-fifth anniversary of the first ESRO sounding rocket launch [ESA-BR-60] 08 p1038 N90-15999
Science plan for the Alaska SAR facility program. Phase 1: Data from the first European sensing satellite, ERS-1 [NASA-CR-185028] 08 p1091 N90-16312
ESA/Earthnet 08 p1093 N90-16325
Catalogue of ESA publications in 1987 [ESA-SP-1087] 08 p1137 N90-16590
Focus 88: The activities of the European Space Agency [ESA-BR-43] 08 p1157 N90-16706
Progress in Space Transportation [ESA-SP-293] 09 p1173 N90-16782
The European long-term space plan: A basis for autonomy and cooperation 09 p1173 N90-16784
ESA project to promote and assist technology transfer by industry 11 p1576 N90-19069
ESRIN [ESA-BR-58] 12 p1677 N90-19631
Vision of the Remote Sensing Management Commission on the ESA long term Earth observation program [BCRS-89-11] 17 p2419 N90-23785
ECOS: The ESA Costing Software [ESA-BR-56] 21 p3039 N90-27274
Upcoming planetary missions and the applicability of high temperature superconductor bolometers 22 p3140 N90-27811
ESA's report to the 28th COSPAR meeting [ESA-SP-1124] 24 p3560 N90-30141
Activities report of the Space Science Department [ESA-SP-1126] 24 p3560 N90-30142
Activities report of the European Space Agency [ISSN-0258-025X] 24 p3565 N90-30169

EUROPEAN SPACE PROGRAMS
NT FRENCH SPACE PROGRAM
NT ITALIAN SPACE PROGRAM
NT SWEDISH SPACE PROGRAM
NT U.S.S.R. SPACE PROGRAM
Aeritalia Space Systems Group, Turin, Italy [EOARD-LR-89-041] 02 p0159 N90-10908
Laser sounding from space: Report of the ESA Technology Working Group on Space Laser Sounding and Ranging [ESA-SP-1108] 03 p0354 N90-12024
European space technology: Celebrating twenty-five years of research and development [ESA-BR-55] 04 p0569 N90-13322
The Hipparcos Mission. Prelaunch status. Volume 1: The Hipparcos satellite [ESA-SP-1111-VOL-1] 05 p0603 N90-13499
The Norwegian balloon and sounding rocket program 1989-1992 05 p0656 N90-13829
Large heavy duty balloons in Europe 05 p0661 N90-13858
The Skylark sounding rocket program and future launcher developments by British Aerospace (Space Systems) Ltd. 05 p0662 N90-13871
The German space science program 05 p0662 N90-13873
Comparison of the space program performance of countries with space programs [ILR-MITT-222] 05 p0709 N90-14150
Mission to Mars. Report of the Mars exploration study team [ESA-SP-1117] 08 p1033 N90-15968
Flight experiment hardware for sounding rocket investigations. Materials science and fluid sciences [ESA-SP-1116] 08 p1038 N90-15998
The HERMES development program 08 p1071 N90-16199
ESA/Earthnet 08 p1093 N90-16325
Focus 88: The activities of the European Space Agency [ESA-BR-43] 08 p1157 N90-16706
The European long-term space plan: A basis for autonomy and cooperation 09 p1173 N90-16784
ESA's space transportation programme 09 p1173 N90-16786

The German hypersonic technology programme
09 p1174 N90-16790
Views on the evolution of European space transport: The reference launcher concept EARL 2
09 p1179 N90-16831
The European space effort: An integral part of the construction of Europe 09 p1180 N90-16845
A comparison of European and American microgravity combustion experimental techniques
09 p1202 N90-16966
Packet telemetry standard
[ESA-PSS-04-106-ISSUE-1] 11 p1467 N90-18447
System safety requirements for ESA space systems and associated equipment
[ESA-PSS-01-40-ISSUE-2] 11 p1469 N90-18460
The determination of offgassing products from materials and assembled articles to be used in a manned space vehicle crew compartment
[ESA-PSS-01-729-ISSUE-1] 11 p1469 N90-18461
Configuration management and control for ESA space systems
[ESA-PSS-01-11-ISSUE-1] 11 p1574 N90-19061
Component selection, procurement and control for ESA space systems
[ESA-PSS-01-60-ISSUE-2] 11 p1574 N90-19062
Space technology transfers in Europe
11 p1576 N90-19070
The Infrared Space Observatory
11 p1589 N90-19163
TOPAS preparation study: Summary representation of the study results
[OHB-TN-TOP-011/87] 12 p1607 N90-19244
Project for the European space organization in the area of space debris
[REPT-29/89] 12 p1615 N90-19290
Physics and Mechanics of Cometary Materials
[ESA-SP-302] 12 p1738 N90-19989
Rosetta/CNSR altimeter and sounding radar
12 p1741 N90-20009
First impressions of the comet drilling problem
12 p1743 N90-20021
Center of Gravity: Metallic Solidification
[DFVLR-IB-333-89/3] 13 p1784 N90-20238
German microgravity program and flight opportunities
13 p1784 N90-20239
User center and assitance 13 p1784 N90-20240
Microgravity conditions of a space vehicle
13 p1785 N90-20247
Satellite navigation system projects: European complement to GPS (CE-GPS), NAVSAT
17 p2360 N90-23434
Archimedes mission aspects
[ETN-90-96556] 17 p2361 N90-23442
Land mobile communications from non geostationary orbits (review of Archimedes ESA study)
[REPT-892-440-106] 17 p2392 N90-23624
Research and development: Technical and scientific publications 1989
[ISSN-0931-9751] 19 p2649 N90-25075
Space exploration: Cost, schedule, and performance of NASA's Ulysses Mission to the Sun. Fact sheet for the Chairman, Subcommittee on Science, Technology, and Space, Committee on Commerce, Science, and Transportation, US Senate
[GAO/NSIAD-88-129FS] 20 p2815 N90-26023
An introductory guide preparing to use the ESTEC environmental test facilities
[ESA-TM-05] 24 p3438 N90-29419
ESA's report to the 28th COSPAR meeting
[ESA-SP-1124] 24 p3560 N90-30141
Activities report of the Space Science Department
[ESA-SP-1126] 24 p3560 N90-30142
Some personal reminiscences. The ESRO-ESA space science story: Twenty-five years of European cooperation
[ESA-BR-66] 24 p3565 N90-30168
Activities report of the European Space Agency
[ISSN-0258-025X] 24 p3565 N90-30169

EUROPEAN SPACE RESEARCH ORGANIZATION
U EUROPEAN SPACE AGENCY

EUROPEAN SPACE RESEARCH ORGANIZATION SAT
U ESA SATELLITES

EUROPIUM
NT EUROPIUM ISOTOPES

EUROPIUM ISOTOPES
Optogalvanic laser spectroscopic and interference spectroscopic experiments of isotope gap and hyperfine structure for spectrum of Europium 1 and Erbium 2
[ETN-90-95358] 12 p1623 N90-19327
Examinations of hyperfine structure and isotope displacement of the elements gadolinium and europium with laser fluorescence and two photon spectroscopy
[ETN-90-97312] 24 p3447 N90-29468

EUTECTIC COMPOSITES
Tribological properties of PM212: A high-temperature, self-lubricating, powder metallurgy composite
[NASA-TM-102355] 04 p0465 N90-12659
Microstructural development in HSLA-100 steel weld metals
[AD-A222105] 21 p2982 N90-26944

EUTECTIC DIAGRAMS
U PHASE DIAGRAMS

EUTECTICS
Heat pipe and thermal energy storage and corrosion studies (1988)
[AD-A212655] 04 p0472 N90-12706
Hardening and toughening of ZnS-Ga2S3 ceramics by solid-state reactions
[AD-A213875] 07 p0912 N90-15276
Characterization of the thermal degradation of selected energetic materials and mixtures by Rapid-Scan Fourier Transform Infrared (RSFTIR) spectroscopy
[AD-A214411] 07 p0916 N90-15296
The experimental evaluation and application of high-temperature solid lubricants
[NASA-TM-102476] 09 p1198 N90-16944
Phase properties of the rapid cooled palladium-silicon alloy in the concentration range 40 to 58 at. percent Si
[DE90-719525] 09 p1284 N90-17444
Damping associated with incipient melting in aluminum-indium alloys
[AD-A220241] 18 p2525 N90-24412
Processing and properties of advanced aluminum alloys
[AD-A221292] 18 p2526 N90-24416
The experimental evaluation and application of high temperature solid lubricants 18 p2564 N90-24631
Two-dimensional model of a Space Station Freedom thermal energy storage canister
[NASA-TM-103124] 20 p2862 N90-26279
Effect of protective coatings on mechanical properties of superalloys 23 p3308 N90-28707
Influence of convection on microstructure
[NASA-CR-186506] 24 p3448 N90-29470

EUTROPHICATION
Eutrophication assessment through remote sensing techniques
[INPE-4932-PRE/1422] 10 p1398 N90-18083

EUVE
U EXTREME ULTRAVIOLET EXPLORER SATELLITE

EVA
U EXTRAVEHICULAR ACTIVITY

EVACUATING
Smokehoods donned quickly. The impact of donning smokehoods on evacuation times
10 p1317 N90-17614

EVACUATING (TRANSPORTATION)
Aerospace vehicle design, spacecraft section. Volume 1: Project Groups 3-5
[NASA-CR-186053] 06 p0731 N90-14263
Aerospace vehicle design, spacecraft section. Volume 1: Project Groups 3-5
[NASA-CR-186054] 06 p0731 N90-14264
The effects of wearing passenger protective breathing equipment on evacuation times through type 3 and type 4 emergency aircraft exits in clear air and smoke. Phase 1: Evacuations in clear air. Phase 2: Evacuations in smoke
[AD-A216798] 11 p1453 N90-18374
The influence of adjacent seating configurations on egress through a type 3 emergency exit
[AD-A218393] 17 p2348 N90-23371
Project EGRESS: Earthbound guaranteed reentry from space station. The design of an assured crew recovery vehicle for the space station
[NASA-CR-186657] 19 p2664 N90-25162
Aircraft evacuations: The effect of passenger motivation and cabin configuration adjacent to the exit
[CAA-PAPER-89019] 24 p3423 N90-29336

EVALUATION
NT TRAINING EVALUATION
Director, Operational Test and Evaluation report FY-88
[AD-A206784] 01 p0135 N90-10778
Numerical simulation of aeroplane response to a lightning injection
[ETN-89-95271] 03 p0303 N90-11716
On the Hellinger type distances for filtered experiments
[CWI-MS-R8818] 04 p0542 N90-13146
The infrared spectrograph during the SIRTF pre-definition phase
[NASA-CR-183234] 05 p0644 N90-13759
Measurement of the light flux density patterns from luminaires proposed as photon sources for photosynthesis during space travel
[NASA-CR-186124] 05 p0672 N90-13916
Software dependability growth characterization, modeling and evaluation
[LAAS-89320] 08 p1112 N90-16437
Method of producing a thin silicon-on-insulator layer
[AD-D014330] 09 p1290 N90-17478
First impressions of the comet drilling problem
12 p1743 N90-20021
The advantages and limitations of sputtered molybdenum disulphide as a space lubricant
18 p2537 N90-24471
Evaluation of scintillometer
[FOA-C-30546-3.1] 18 p2555 N90-24578
SOAR 89: Space Station. Space suit test program
19 p2727 N90-25506
A survey of concurrent readers and writers
[CWI-CS-R8936] 19 p2741 N90-25581
Space projects: Improvements needed in selecting future projects for private financing
[GAO/NSIAD-90-147] 22 p3256 N90-28439

EVAPORATION
NT EVAPOTRANSPIRATION
NT TRANSPIRATION
Experimental measurements of shock-induced vaporization in cadmium and lead
[DE89-016877] 02 p0194 N90-11103
Global distribution of moisture, evaporation-precipitation, and diabatic heating rates
03 p0362 N90-12069
High temperature chemistry of complex vaporization/decomposition processes
[DE89-016559] 06 p0740 N90-14306
Propagation prediction for the North Sea environment
06 p0760 N90-14423
Environmental Projects. Volume 8: Modifications of wastewater evaporation ponds
[NASA-CR-186099] 06 p0808 N90-14700
Method of sensitizing PB-Salt epitaxial films for Schottky diodes
[AD-D014244] 06 p0850 N90-14937
Semi-empirical theory of heat-transfer when boiling
[DE89-635418] 06 p0857 N90-14984
Time-dependent free convection in liquid metals
[DE90-000957] 07 p0927 N90-15366
Specification for evaporation duct height calculations
[AD-A213841] 07 p0964 N90-15570
Anomalous absorption by atmospheric water vapor and stabilized water fogs in the infrared and CM-wave regions
[AD-A214202] 07 p0964 N90-15572
The fabrication of YBa2Cu3O7 thin films by thermal coevaporation in oxygen
[DE90-003960] 07 p1006 N90-15824
Externally vaporizing system for turbine combustor
[AD-D014284] 08 p1024 N90-15918
Low-altitude millimeter-wave propagation in the evaporation duct
[AD-A214432] 08 p1057 N90-16108
Droplet vaporisation and combustion in microgravity
09 p1202 N90-16963
Remote sensing of evaporation ducts for Naval warfare
[AD-A214849] 10 p1374 N90-17965
A model for evaporation of freely falling droplets
[PUBL-AIR-QUALITY-6] 10 p1384 N90-18007
Microcomputer enhanced optical investigation of spreading and evaporative processes in ultra thin films
[DE90-006323] 11 p1492 N90-18585
Cloud hole-boring with infrared lasers: Theory and experiment
[DE90-006519] 11 p1515 N90-18723
Thermal remote sensing in the differentiation of soybean crops (glycine max (L.) merrill) submitted to water deficit
[INPE-4900-PRE/1501] 11 p1522 N90-18762
Evaporation duct effects at millimeter wavelengths
15 p2080 N90-21914
Millimetre-wave propagation in the evaporation duct
15 p2084 N90-21929
An experimental investigation of mixing in buoyant flows 15 p2090 N90-21963
From Penman to Makkink: A new method for the calculation of the climatological evaporation numbers
[KNMI-TR-111] 15 p2126 N90-22161
Lagrangian model simulation of the turbulent transport of evaporating jet droplets 15 p2128 N90-22168
The Al-26(rho, gamma)Si-27 reaction: Stellar origins of galactic Al-26 15 p2188 N90-22498
Convergent strand array liquid pumping system
[NASA-CASE-NPO-17301-1-CU]
17 p2385 N90-23587
In-situ processing of epitaxial and textured high (Tc) superconducting HoBa2Cu3O(7-x) thin films by pulsed laser evaporation technique
[DE90-009828] 17 p2474 N90-24148
Surface enrichment and evaporation in a polymer mixture of long and short chains
[DE90-010073] 18 p2529 N90-24429
Radar clutter via waveguide methods
[AD-A220237] 18 p2542 N90-24512

The modeling of drop-containing turbulent eddies
[NASA-CR-186805] 18 p2553 N90-24570
Sequentially evaporated thin film YBa2Cu3O(7-x) superconducting microwave ring resonator
[NASA-TM-103180] 19 p2685 N90-25273
Boiling/evaporative heat transfer from spheres in packed-bed thermal energy storage units
[DE90-012023] 19 p2711 N90-25430
Ellipsometric study of YBa2Cu3O(7-x) laser ablated and co-evaporated films
[NASA-TM-103223] 20 p2932 N90-26682
Physical characteristics of clothing materials with regard to heat transport
[IZF-1989-10] 22 p3233 N90-28336
Calculation of clothing insulation and vapour resistance
[IZF-1989-49] 22 p3234 N90-28338
Transient cooling of a hot surface by droplets evaporation
[PB90-227968] 23 p3325 N90-28799

EVAPORATION RATE
Hydration effects on human physiology and exercise-heat performance
[AD-A217969] 13 p1852 N90-20629

EVAPORATIVE COOLING
NT FILM COOLING
NT SWEAT COOLING
An experimental investigation of mixing in buoyant flows 15 p2090 N90-21963
Laboratory experiments on stability and entrainment of oceanic stratocumulus. Part 2: Entrainment experiment 22 p3220 N90-28264

EVAPOTRANSPIRATION
Evapotranspiration studies for protective barriers: Experimental plans
[DE90-005206] 10 p1405 N90-18106

EVASIVE ACTIONS
A homing missile guidance law based on new target maneuver models
[AD-A220392] 17 p2356 N90-23410
A passive homing missile guidance law based on new target maneuver models
[AD-A220419] 17 p2356 N90-23411

EVECTION
U LUNAR ORBITS
U ORBIT PERTURBATION
U SOLAR GRAVITATION

EVENT HORIZON
Information loss down a black hole
[DE90-627482] 24 p3562 N90-30154

EVENTS
Computational and statistical issues in discrete-event simulation
[AD-A210743] 01 p0116 N90-10668
Determinism yields (event structure isomorphism equals step sequence equivalence)
[CWI-CS-R8839] 02 p0263 N90-11492
A simple definition for parallel composition of prime event structures
[CWI-CS-R8903] 04 p0532 N90-13074

EVOKED RESPONSE (PSYCHOPHYSIOLOGY)
Electrophysiological studies of visual attention and resource allocation
[AD-A212287] 04 p0525 N90-13030
Evaluation of two objective measures of effective auditory stimulus level
[AD-A214669] 09 p1250 N90-17255
Brain activity during tactical decision-making. Part 3: Relationships between probe-evoked potentials, simulation performance, and on-job performance
[AD-A217207] 13 p1854 N90-20638
Mental lapses and event-related potentials
[AD-A219454] 17 p2436 N90-23878

EVOLUTION (DEVELOPMENT)
NT BIOLOGICAL EVOLUTION
NT CHEMICAL EVOLUTION
NT GALACTIC EVOLUTION
NT LUNAR EVOLUTION
NT PLANETARY EVOLUTION
NT STAR FORMATION
NT STELLAR EVOLUTION
NT STELLAR MASS ACCRETION
Evolution of flight commands in Aeritalia design
[ETN-89-95211] 03 p0309 N90-11759
Small scale structure on cosmic strings
[NASA-CR-186075] 04 p0565 N90-13298
US Space Shuttle evolution 09 p1178 N90-16829
Publications of the Exobiology Program for 1988: A special bibliography
[NASA-TM-4169] 09 p1262 N90-17316
Physical models of cometary nuclei: A review 12 p1738 N90-19991
Physical processes in cometary ices inferred from laboratory studies 12 p1739 N90-19996
Laboratory studies of cometary ice analogues 12 p1739 N90-19997
Evolution of ices and carbonaceous materials in the laboratory and in comets 12 p1739 N90-19998
Spectral plane quasars, spectral turn-over, and frequency atlas
[INPE-5011-TDL/399] 16 p2329 N90-23277
Dynamic and photometric evolutionary models of tidal tails and ripples 18 p2637 N90-25024
Evolution of overlapping spreading centers: A SeaMARC 2 investigation
[AD-A223102] 21 p3025 N90-27200
Some aspects of the structure and evolution of oceanic spreading centers 24 p3496 N90-29757

EVOLUTION (LIBERATION)
NT GAS EVOLUTION

EXACTNESS
U PRECISION

EXCHANGING
NT CHARGE EXCHANGE
NT GAS EXCHANGE
NT ION EXCHANGING
NT SPIN EXCHANGE

EXCIMER LASERS
Elements of a 200 watt pulsed excimer laser 02 p0226 N90-11295
Dissociation and vibrational relaxation of XeF by various collision partners
[AD-A210769] 02 p0227 N90-11300
Formation and modification of surface alloys by excimer laser melting and resolidification
[DE89-016968] 03 p0327 N90-11856
Microwave excited excimer laser
[ETN-90-95909] 05 p0648 N90-13781
Qualification of diode foil materials for excimer lasers
[DE90-000602] 06 p0789 N90-14593
Laser mixing of titanium on silicon carbide
[DE90-003216] 07 p0891 N90-15150
Excimer emission from alkali diatomic and alkaline-earth-noble-gas molecules
[AD-A214246] 07 p0896 N90-15179
Kinetic studies following state-selective laser excitation
[DE90-003232] 07 p0935 N90-15415
Development of tunable excimer lasers
[AD-A213521] 07 p0936 N90-15421
Eurolaser. High power excimer laser: Optical crystals
[ETN-90-95901] 08 p1132 N90-16558
Migration of carbon in tempered martensitic steel during excimer laser melting
[DE90-004838] 09 p1195 N90-16922
Development of KrF lasers for fusion
[DE90-007830] 11 p1515 N90-18726
Pulsed laser deposition of high T(sub c) superconducting thin films
[AD-A216507] 11 p1569 N90-19034
Energy deposition measurements for E-beam pumped excimer lasers
[DE90-007545] 13 p1806 N90-20365
Development of a laser fluorosensor for the aircraft supported analysis of maritime toxic agents loads: Definition phase
[ETN-90-95320] 13 p1829 N90-20499
Shaping radiation pattern of excimer laser by means of controllable intracavity mirror 16 p2310 N90-23186
Long pulse narrowband XeCl laser studies
[AD-A219774] 17 p2409 N90-23724
Electron beam pumped XeF(C yields A) laser scaling
[AD-A220022] 17 p2409 N90-23728
Reports from the German Meteorological Service. No. 179: Development, realization and functioning of lidar to evaluate the atmospheric ozone profile
[ISBN-3-88148-252-0] 18 p2578 N90-24685
SiC film deposited by pulsed excimer laser ablation
[DE90-010634] 18 p2622 N90-24938
Superconductivity in nonsymmetric epitaxial YBa2Cu3O(sub 7-delta)-PrBa2Cu3O(sub 7-delta) superlattices grown by pulsed laser ablation
[DE90-011637] 19 p2761 N90-25687
Formation of Titanium-boron surface alloys by excimer laser mixing
[DE90-013172] 20 p2834 N90-26118
Excimer laser fragmentation studies of selected oximes: Nascent OH internal energy distributions and the search of H2CN fluorescence
[AD-A222622] 20 p2868 N90-26317
Raman scattering measurements using UV excimer lasers 21 p2974 N90-26902
Concentration, temperature, and density in a hydrogen-air flame by excimer-induced Raman scattering 21 p2974 N90-26903
Beam combining of excimer lasers by stimulated Raman scattering
[AD-A222973] 21 p3008 N90-27099
Diagnostics for hydrogen atoms and molecules in H-atom sources and beams using VUV laser light
[AD-A222340] 21 p3074 N90-27476
Laser ablated high T(sub c) superconducting thin YBa2Cu3O(7-x) films on substrates suitable for microwave applications 22 p3139 N90-27808

EXCITATION
NT ACOUSTIC EXCITATION
NT ATOMIC EXCITATIONS
NT HARMONIC EXCITATION
NT MOLECULAR EXCITATION
NT SELF EXCITATION
NT WAVE EXCITATION
Radiationless transitions and excited-state absorption of low-field chromium complexes in solids
[AD-A210653] 02 p0194 N90-11105
Symmetry breaking phenomena in liquid Helium-4
[DE89-618886] 04 p0469 N90-12685
Ground states of a two-dimensional charged-boson system
[AD-A212363] 04 p0553 N90-13226
Microwave excited excimer laser
[ETN-90-95909] 05 p0648 N90-13781
CANOES 2: Dynamics of atmospheric infrared thermochemical excitation, volume 1
[AD-A213341] 05 p0667 N90-13897
CANOES 2: Dynamics of atmospheric infrared thermochemical excitation, volume 2
[AD-A213342] 05 p0667 N90-13898
CANOES 2: Dynamics of atmospheric infrared thermochemical excitation, volume 3
[AD-A213343] 05 p0667 N90-13899
Further observations of rotationally excited far infrared OH16 and OH18 emission in Orion-KL: Tighter constraints on the nature of the emitting region
[NASA-CR-186004] 05 p0710 N90-14156
Theoretical and material studies of thin-film electroluminescent devices
[NASA-CR-186104] 06 p0768 N90-14488
Transient response of flexible rotor-bearing systems subjected to combined unbalance and ground excitations 06 p0792 N90-14616
Calculation of two-neutron multiplicity in photonuclear reactions
[NASA-TP-2968] 06 p0841 N90-14890
The effectiveness of vane-aileron excitation in the experimental determination of flutter speed by parameter identification
[NASA-TP-2971] 07 p0880 N90-15100
Kinetic studies following state-selective laser excitation
[DE90-003232] 07 p0935 N90-15415
Phonons and charge-transfer excitations in HTS superconductors
[DE89-016816] 07 p0997 N90-15768
Plasmon excitation in the scattering of electromagnetic waves from good conductors
[AD-A214026] 08 p1056 N90-16107
Q-2 and A dependence of delta (1232) electroexcitation in nuclei
[DE90-003470] 08 p1121 N90-16492
An estimation of the one-loop mass shifts in open superstring theory
[DE90-719578] 08 p1136 N90-16582
Fluorescence from photoexcitation of Cl2 at 50 to 105 nm
[NASA-CR-186206] 09 p1189 N90-16888
Selective excitation luminescence and photoluminescence investigations of ytterbium doped InP, GaAs and AlGaAs
[AD-A215713] 09 p1291 N90-17485
A numerical solution to the Boltzmann equation for use in calculating pumping rates in a CO2 discharge laser
[AD-A216376] 11 p1514 N90-18718
Study of the atmospheric emissions of OI wavelength 557.7 nm and O2 (0,0) wavelength 761.9 nm in the equatorial region utilizing measurement of photometer on-board a rocket
[INPE-4811-TDL/358] 11 p1533 N90-18827
A study of the interaction of light with surfaces of sub-micron dimensions
[DE90-006646] 11 p1571 N90-19048
Time resolved gain/loss studies under low and high power loading for the XeF C-A transition
[DE90-007506] 12 p1655 N90-19517
Goldstone excitation and symmetry breaking mechanism in superfluid He-4
[DE90-610676] 12 p1720 N90-19881
Strategies for high efficiency operation of the E-beam excited atomic xenon laser using high-power and high-energy loading
[DE90-005196] 13 p1806 N90-20370
Energy transfer between electrons and ions in collision cascades in solids
[AERE-R-13662] 13 p1883 N90-20801
Populations of excited states and reaction mechanisms in the emission of complex fragments
[DE90-007481] 13 p1886 N90-20819

Large basis space effects in electron scattering form factors of light nuclei
[DE90-613501] 14 p2025 N90-21609
Vibration analysis of systems with random parametric excitations 15 p2109 N90-22060
Dynamic response of structures with uncertain parameters 15 p2119 N90-22125
The Al-26(rho, gamma)Si-27 reaction: Stellar origins of galactic Al-26 15 p2188 N90-22498
Forced scattering of electromagnetic waves on electron beam in periodically inhomogeneous plasma
[DE90-620705] 16 p2228 N90-22707
Excitation of hypersound at boundary between Type-2 superconductor and a concentrated paramagnetic compound 16 p2310 N90-23164
Theoretical studies of electrons and electron transfer processes in fluids
[DE90-008414] 17 p2470 N90-24117
Rotational and translational effects in collisions of electronically excited diatomic hydrides
[NASA-CR-186770] 20 p2829 N90-26093
A study of the influence of Hg(6(3)P2) population in a low-pressure discharge on mercury ion emission at 194.2 nm 20 p2853 N90-26223
Excimer laser fragmentation studies of selected oximes: Nascent OH internal energy distributions and the search of H2CN fluorescence
[AD-A222622] 20 p2868 N90-26317
Formation and deactivation of vibrationally excited atmospheric molecules
[AD-A222660] 20 p2889 N90-26442
Advanced optical diagnostics in hypersonic research 21 p2975 N90-26905
Structure and dynamics of excited atoms
[AD-A221973] 21 p3074 N90-27474
Surface and defect excitations in covalently bonded solids
[AD-A221995] 23 p3303 N90-28682
Model calculations for a 600 angstrom laser based on photopumping of Mo(sup 6+) by a spectral line of Mo(sup 11+)
[DE90-015202] 24 p3474 N90-29634

EXCITED STATES
U EXCITATION

EXCITONS
Femtosecond dynamics of fluoro-aluminum phthal ocyanine and linear alkane molecules
[AD-A210939] 01 p0133 N90-10766
Nonlinear optical studies of resonant systems
[AD-A211032] 02 p0227 N90-11301
Phonons and charge-transfer excitations in HTS superconductors
[DE89-016616] 07 p0997 N90-15768
Theory of the electronic and optical properties of semiconductor heterostructures
[AD-A214132] 08 p1130 N90-16544
Nonlinear optical studies of the optical and electronic properties of semiconductor heterostructures
[AD-A223408] 24 p3552 N90-30096
Optical nonlinearity due to structure defects and bistability in the band discontinuity area of CdS
[ETN-90-97303] 24 p3554 N90-30112

EXECUTIVE AIRCRAFT
U GENERAL AVIATION AIRCRAFT
U PASSENGER AIRCRAFT

EXECUTIVE SYSTEMS (COMPUTERS)
U OPERATING SYSTEMS (COMPUTERS)

EXERCISE
U PHYSICAL EXERCISE

EXERCISE PHYSIOLOGY
Exertional heatstroke: An international perspective. An introduction: The role of exercise in the etiology of exertional heatstroke
[AD-A212242] 04 p0523 N90-13020
Prediction of thermal stress casualties
[AD-A212356] 04 p0523 N90-13022
Exercise countermeasures for bed rest deconditioning
[NASA-TM-101045] 05 p0674 N90-13926
Temperature regulation during upper body exercise: Able bodied and spinal cord injured
[AD-A215130] 09 p1252 N90-17264
Elevated central venous pressure: A consequence of exercise training-induced hypervolemia
[NASA-TM-102965] 13 p1850 N90-20617
National Aeronautics and Space Administration (NASA)/American Society for Engineering Education (ASEE) Summer Faculty Fellowship Program-1989, volume 1
[NASA-CR-185601-VOL-1] 18 p2627 N90-24972
Overtraining and exercise motivation: A research prospectus 18 p2629 N90-24982
Work enhancement and thermal changes during intermittent work in cool water after carbohydrate loading
[AD-A222877] 21 p3034 N90-27247

EXERTION
U PHYSICAL WORK

EXHAUST CLOUDS
Infrared absorption gas sensor for the detection of HCl in launch vehicle exhaust clouds 16 p2209 N90-22600

EXHAUST DIFFUSERS
Device for the dilution of hot exhaust jets
[ETN-90-97435] 22 p3120 N90-27723

EXHAUST EMISSION
MOBILE4 oxygenated fuels version user's guide
[PB89-230700] 05 p0629 N90-13674
Factors that may influence responses of the US transportation sector to policies for reducing greenhouse gas emissions
[DE90-000704] 07 p0958 N90-15543
Chemical interactions and light emissions from vented species
[AD-A214130] 10 p1327 N90-17668
Chamber investigations of the fate of diesel emissions in the atmosphere, volume 1, task 3
[PB90-114422] 10 p1405 N90-18103
Chamber investigations of the fate of diesel emissions in the atmosphere. Volume 2: AMES assay and GCMS final data reports and gas phase projections
[PB90-114430] 10 p1405 N90-18104
A preliminary analysis of US CO2 emissions reduction potential from energy conservation and the substitution of natural gas for coal in the period to 2010
[DOE/NBB-0085] 12 p1684 N90-19673
A study of mesoscale acid deposition in the lower Ohio River Valley 16 p2253 N90-22848
Pollutants: Production and methods of reduction
[CIT/SME/VKI/RS/6] 20 p2810 N90-25990
Aircraft exhaust emissions: An engine manufacturer's perspective
[PNR90675] 20 p2812 N90-26004
Options for controlling the global warming impact from motor vehicles
[PB90-161688] 22 p3197 N90-28142
Policy options for stabilizing global climate. Volume 2: Chapters 7-9
[PB90-182312] 22 p3198 N90-28147
Compiling air toxics emission inventories, 2nd edition
[PB90-185422] 22 p3198 N90-28148
The reduction of smoke emissions from Allison T56 engines
[ARL-PROP-R-182] 23 p3277 N90-28547
Energy Efficient Engine exhaust mixer model technology report addendum; phase 3 test program
[NASA-CR-174799] 23 p3279 N90-28556
Source emission test of gas turbine engine test facility, Kelly AFB, TX
[AD-A223869] 23 p3282 N90-28571
National air pollutant emission estimates, 1940-1988
[PB90-199266] 23 p3346 N90-28908
National air quality and emissions trends report, 1988
[PB90-200114] 23 p3346 N90-28909

EXHAUST FLOW SIMULATION
NT ATMOSPHERIC ENTRY SIMULATION
Steady and unsteady potential flow around thin annular wings and engines with simulation of jet engine flow
[DFVLR-FB-89-18] 03 p0302 N90-11711
Application of the singularity-separating method to computing problems of solid-propellant combustion in a closed vessel
[PREPRINT-489] 08 p1053 N90-16086
On the direct simulation of vortex shedding
[LR-513] 15 p2048 N90-21743
Analysis of a six-component, flow-through, strain-gage, force balance used for hypersonic wind tunnel models with scramjet exhaust flow simulation
[NASA-CR-186585] 15 p2055 N90-21775
Analysis of internal flow in a ventral nozzle for STOVL aircraft
[NASA-TM-103123] 17 p2355 N90-23404
Device for the dilution of hot exhaust jets
[ETN-90-97435] 22 p3120 N90-27723

EXHAUST GASES
A simulator for a hydrocarbon ramrocket fuel gas generator: First phase development
[AR-005-621] 02 p0189 N90-11080
Effects of atmospheric mix and toxic fumes on military performance
[PB89-223630] 04 p0522 N90-13015
Gas identification system using graded temperature sensor and neural net interpretation
[AD-A213359] 05 p0622 N90-13627
Design and fabricate a metallic hydride heat pump with a cooling capacity of 9000 BTU/H
[AD-A213756] 07 p0931 N90-15388
Factors that may influence responses of the US transportation sector to policies for reducing greenhouse gas emissions
[DE90-000704] 07 p0958 N90-15543
A qualitative architecture for understanding policy responses to global change
[DE90-003936] 08 p1099 N90-16364
Plume flowfield analysis of the shuttle primary Reaction Control System (RCS) rocket engine
[NASA-CR-186315] 10 p1329 N90-17676
Preliminary collection 891 of lectures/papers in Symposium by Society of Automotive Engineers of Japan
[DE90-710449] 10 p1391 N90-18045
Chamber investigations of the fate of diesel emissions in the atmosphere, volume 1, task 3
[PB90-114422] 10 p1405 N90-18103
Chamber investigations of the fate of diesel emissions in the atmosphere. Volume 2: AMES assay and GCMS final data reports and gas phase projections
[PB90-114430] 10 p1405 N90-18104
Estimation of the distribution of SO2 and NOX emission in Europe 12 p1688 N90-19699
Emission data for the EURAD project 12 p1688 N90-19700
An evaluation of the relationship between the production and use of energy and atmospheric methane emissions
[DE90-007982] 14 p2004 N90-21487
Exhaust environment measurements of a turbofan engine equipped with an afterburner and 2D nozzle
[NASA-CR-4289] 15 p2052 N90-21760
CO-oxidation catalysts: Low-temperature CO oxidation over Noble-Metal Reducible Oxide (NMRO) catalysts 18 p2556 N90-24588
Digital filtering of plume emission spectra
[NASA-TM-103135] 20 p2824 N90-26070
Effects of thruster firings on the shuttle environment 1: Neutral gas composition
[AD-A224404] 24 p3487 N90-29707

EXHAUST JETS
U EXHAUST GASES

EXHAUST NOZZLES
NT CONVERGENT-DIVERGENT NOZZLES
NT TURBINE EXHAUST NOZZLES
Investigation of advanced mixer-ejector exhaust system
[AD-A211943] 03 p0301 N90-11705
Altitude testing of the 2D V/STOL ADEN demonstrator on an F404 engine
[NASA-CR-174824] 10 p1321 N90-17638
Static investigation of a two-dimensional convergent-divergent exhaust nozzle with multiaxis thrust-vectoring capability
[NASA-TP-2973] 12 p1597 N90-19193
Exhaust nozzles for propulsion systems with emphasis on supersonic cruise aircraft
[NASA-RP-1235] 14 p1927 N90-21037
Performance characteristics of a one-third-scale, vectorable ventral nozzle for SSTOVL aircraft
[NASA-TM-103120] 15 p2045 N90-21725
Exhaust environment measurements of a turbofan engine equipped with an afterburner and 2D nozzle
[NASA-CR-4289] 15 p2052 N90-21760
Shelf life extension for the lot AAE nozzle severance LSCs
[NASA-CR-183878] 15 p2062 N90-21813
Experimental and analytical study of close-coupled ventral nozzles for ASTOVL aircraft
[NASA-TM-103170] 18 p2496 N90-24273
Analysis and design of optimized truncated scarfed nozzles subject to external flow effects
[NASA-TM-103175] 19 p2654 N90-25106
Hot gas ingestion characteristics and flow visualization of a vectored thrust STOVL concept
[NASA-TM-103212] 20 p2813 N90-26009
Entropy wave instability in compact ramjets 22 p3162 N90-27932
Calibration of the PARC program for propulsion-type flows
[AD-A224253] 24 p3434 N90-29395

EXHAUST SYSTEMS
X-2 limited flight test plan
[AD-A214412] 07 p0880 N90-15099
Experience in developing an improved ground-level test capability 22 p3120 N90-27720

EXHAUST VELOCITY
The effects of magnetic nozzle configurations on plasma thrusters
[NASA-CR-186465] 14 p1941 N90-21109

EXHAUSTION
The effect of caffeine on endurance time to exhaustion at high altitude
[AD-A212069] 03 p0380 N90-12163

EXISTENCE THEOREMS
A general existence and uniqueness theorem for implicit differential-algebraic equations
[AD-A217965] 13 p1878 N90-20770

An existence theorem for periodic solutions and applications to some third order nonlinear differential equations
[DE90-627152] 24 p3536 N90-29992

EXITS (DOORS)
U DOORS

EXOBIOLOGY
Aerospace medicine and biology: A continuing bibliography with indexes (supplement 328)
[NASA-SP-7011(328)] 01 p0092 N90-10524
USSR Space Life Sciences Digest, issue 24
[NASA-CR-3922(28)] 03 p0378 N90-12152
Aerospace medicine and biology: A continuing bibliography with indexes (supplement 329)
[NASA-SP-7011(329)] 03 p0382 N90-12173
Life science research in space
[ESA-SP-1105] 05 p0672 N90-13917
Aerospace medicine and biology: A continuing bibliography with indexes (supplement 330)
[NASA-SP-7011(330)] 05 p0674 N90-13925
USSR Space Life Sciences Digest. Index to issues 21-25
[NASA-CR-3922(30)] 06 p0819 N90-14763
Exploring the living universe: A strategy for space life sciences
[NASA-TM-101891] 06 p0822 N90-14778
Publications of the Exobiology Program for 1988: A special bibliography
[NASA-TM-4169] 09 p1262 N90-17316
Aerospace medicine and biology: A continuing bibliography with indexes (supplement 333)
[NASA-SP-7011(333)] 10 p1411 N90-18136
Aerospace medicine and biology: A continuing bibliography with indexes (supplement 331)
[NASA-SP-7011(331)] 10 p1411 N90-18137
USSR Space Life Sciences Digest, issue 26
[NASA-CR-3922(31)] 14 p2009 N90-21513
USSR Space Life Sciences Digest, issue 25
[NASA-CR-3922(29)] 15 p2135 N90-22203
Aerospace medicine and biology: A continuing bibliography with indexes (supplement 334)
[NASA-SP-7011(334)] 15 p2136 N90-22207
Aerospace medicine and biology: A continuing bibliography with indexes (supplement 335)
[NASA-SP-7011(335)] 15 p2136 N90-22208
Strategic implementation plan
[NASA-TM-102907] 17 p2433 N90-23861
Aerospace medicine and biology: A continuing bibliography with indexes (supplement 336)
[NASA-SP-7011(336)] 17 p2436 N90-23877
USSR space life sciences digest, issue 27
[NASA-CR-3922(32)] 19 p2717 N90-25457
Aerospace medicine and biology: A cumulative index to a continuing bibliography (supplement 332)
[NASA-SP-7011(332)] 19 p2722 N90-25480
Aerospace medicine and biology: A continuing bibliography with indexes (supplement 337)
[NASA-SP-7011(337)] 19 p2722 N90-25481
Aerospace medicine and biology: A continuing bibliography with indexes (supplement 338)
[NASA-SP-7011(338)] 19 p2722 N90-25482
Scientific guidelines for preservation of samples collected from Mars
[NASA-TM-4184] 19 p2796 N90-25918
The US Experiments Flown on the Soviet Biosatellite Cosmos 1887
[NASA-TM-102254] 20 p2891 N90-26452
Aerospace medicine and biology: A continuing bibliography with indexes (supplement 339)
[NASA-SP-7011(339)] 22 p3232 N90-28327
Aerospace medicine and biology: A continuing bibliography with indexes (supplement 340)
[NASA-SP-7011(340)] 23 p3355 N90-28963

EXOSAT SATELLITE
Galactic x ray astronomy with EXOSAT
08 p1139 N90-16597
An atlas of aperiodic variability in HMXB
[MPE-PREPRINT-158] 08 p1140 N90-16605
Recent and future x ray observations of classical novae during the outburst stage
[MPE-PREPRINT-159] 08 p1140 N90-16606
EXOSAT measurements of the pulse period of Vela X-1
[MPE-PREPRINT-157] 08 p1152 N90-16673
Analysis of an observation of the x ray astronomy satellite EXOSAT at the low mass x ray binary star system GX5-1
[ETN-90-95828] 12 p1747 N90-20042
EXOSAT observations of Seyfert type galaxies
13 p1901 N90-20910
EXOSAT observations of Cygnus X-1: Study of the soft x ray excess
17 p2483 N90-24199
EXOSAT observations of the pulse profile of Her X-1 during intermediate intensity states in a 35-day-cycle in 1985
17 p2483 N90-24201
EXOSAT deep exposure of the LMC X-4 region
17 p2483 N90-24203
M15:AC211/X2127+119: Optical curve, improved ephemeris, and phasing of EXOSAT X ray data
19 p2771 N90-25749
The soft X ray spectrum of Cygnus X-1
19 p2771 N90-25751
EXOSAT deep exposure of the LMC X-4 region
19 p2780 N90-25814
EXOSAT observation of the pulsar PSR 1509-58
19 p2782 N90-25829
A search for iron features in the EXOSAT spectral survey sources
19 p2791 N90-25887
X ray spectrum and variability of MRK 509 as observed with EXOSAT and Ginga
19 p2794 N90-25904
ESA's report to the 28th COSPAR meeting
[ESA-SP-1124] 24 p3560 N90-30141

EXOSPHERE
Measurement of optical radiations in spacecraft environments
[AD-A213814] 07 p0950 N90-15497

EXOTHERMIC REACTIONS
Numerical study of diffusion jet flames
12 p1621 N90-19316
Observation of a magic number in the ion distribution of ethene clusters
[AD-A219837] 18 p2521 N90-24393

EXPANDABLE STRUCTURES
NT AIR BAG RESTRAINT DEVICES
NT BALLOONS
NT BEACON EXPLORER A
NT BEACON SATELLITES
NT BELLOWS
NT HIGH ALTITUDE BALLOONS
NT INFLATABLE SPACECRAFT
NT INFLATABLE STRUCTURES
NT TETHERED BALLOONS
Expandable radiator
[AD-D014258] 08 p1063 N90-16147
Collapsible fabric tank testing
[AD-A217861] 14 p1987 N90-21388
Design of a telescoping tube system for access and handling equipment
15 p2116 N90-22102
Failure mechanism of urethane elastomer coated fabric collapsible fuel tanks
[AD-A221033] 18 p2530 N90-24435

EXPANSION
NT GAS EXPANSION
NT SERIES EXPANSION
NT THERMAL EXPANSION
Distribution of a sum of n random variables and a central limit theorem based on moments or on coefficients of polynomial dependence
[IMAG-RR-768-M] 05 p0692 N90-14040
Is the number of photons conserved in an expanding universe
[DE89-618836] 06 p0864 N90-15018
Ring expansion and equilibration in organophosphazenes, and the relationship to polymerization
[AD-A218234] 13 p1782 N90-20230
Expanding ring joint
[AD-D014398] 14 p1986 N90-21384
Stability of compactification during inflation
[NASA-CR-186597] 15 p2189 N90-22502
The theory and simulation of plasmoid formation and propagation
[AD-A222048] 21 p3079 N90-27504

EXPANSION WAVES
U ELASTIC WAVES

EXPEDITIONS
JARE data reports, no. 140 (meteorology 21): Meteorological data at Asuka Camp, Antarctica in 1987
[ISSN-0075-3343] 15 p2132 N90-22188

EXPENDABLE STAGES (SPACECRAFT)
Glavkosmos operational space transportation systems
09 p1174 N90-16791
The development of a complementary expendable launch vehicle interface for an STS deployable payload
15 p2113 N90-22086
IRIS system and future application to expandable launchers
[IAF-89-212] 20 p2818 N90-26035

EXPERIENCE
Target selection in anti-tank operations: Effects of experience
[FOA-C-50073-5.2] 17 p2436 N90-23882
The value of real experience
[PNR90619] 20 p2934 N90-26696
Severe thunderstorm cases of July 1988 through June 1989
[PB90-226424] 22 p3229 N90-28311

EXPERIMENT DESIGN
Conceptual design of liquid droplet radiator shuttle-attached experiment
[NASA-CR-185164] 03 p0318 N90-11805
Conceptual design of liquid droplet radiator shuttle-attached experiment technical requirements document
[NASA-CR-185165] 03 p0318 N90-11806
Cells in Space
[NASA-CP-10034] 05 p0676 N90-13939
Fundamental results from microgravity cell experiments with possible commercial applications
05 p0676 N90-13940
Effects of microgravity on growth hormone concentration and distribution in plants
05 p0678 N90-13947
Gravity receptors and responses
05 p0678 N90-13948
Human factors issues in performing life science experiments in a 0-G environment
05 p0679 N90-13952
Do the design concepts used for the space flight hardware directly affect cell structure and/or cell function ground based simulations
05 p0679 N90-13953
Model system studies with a phase separated membrane bioreactor
05 p0679 N90-13954
Design challenges for space bioreactors
05 p0679 N90-13955
Fermentation and oxygen transfer in microgravity
05 p0679 N90-13956
Shuttle Laser Technology Experiment Facility (LTEF)-to-airplane lasercom experiment: Airplane considerations
[NASA-TM-100749] 06 p0731 N90-14260
Design considerations for space flight hardware
[NASA-TM-102300] 06 p0734 N90-14275
Engineering sciences design. Design and implementation of components for a bioregenerative system for growing higher order plants in space
[NASA-CR-186056] 06 p0819 N90-14761
QUEST/Ada: Query utility environment for software testing of Ada
[NASA-CR-186121] 06 p0823 N90-14787
Physical and Electrical Standards Laboratory general operating procedures
[DE90-003515] 07 p0884 N90-15116
Onorbit electron beam welding experiment definition
[NASA-CR-183847] 07 p0938 N90-15431
Developmental versions of FORTRAN/77 routines for the design and analysis of mixture experiments
[DE90-003513] 07 p0974 N90-15624
Conceptual design of a moving belt radiator shuttle-attached experiments: Technical requirement Document
[NASA-CR-185168] 08 p1038 N90-15996
Method for the evaluation of toxicity of combustion products from aircraft cabin materials: Analysis and results
10 p1316 N90-17612
Materials thermal and thermoradiative properties/characterization technology
10 p1367 N90-17925
Design of a microwave calorimeter for the microwave tokamak experiment
[DE90-004486] 10 p1387 N90-18026
The Advanced Composition Explorer
[DE90-006522] 12 p1737 N90-19987
Experimental proposition aboard the second data collecting satellite-SCD 2 of the MECB
[INPE-4980-RPE/606] 13 p1765 N90-20128
ARISTOTELES: A European approach for an Earth gravity field recovery mission
13 p1839 N90-20559
The GRADIO spaceborne gravity gradiometer: Development and accommodation
13 p1840 N90-20560
High power millimeter wave source development program
15 p2061 N90-21805
Designing good experiments to test bad hypotheses
[AD-A218977] 16 p2263 N90-22900
Conceptual design of a Moving Belt Radiator (MBR) shuttle-attached experiment
[NASA-CR-185169] 17 p2367 N90-23474
Statistical design of MOS VLSI (Very Large Scale Integrated) circuits with designed experiments
[AD-A219654] 17 p2396 N90-23647
National Educators' Workshop: Update 1989 Standard Experiments in Engineering Materials Science and Technology
[NASA-CP-3074] 18 p2513 N90-24350
Experiments and other methods for developing expertise with design of experiments in a classroom setting
18 p2516 N90-24367
SEDS experiment design definition
[NASA-CR-183909] 19 p2665 N90-25165
Integrated support structure
[NASA-CR-186835] 20 p2841 N90-26162
Launching a dream: A teachers guide to a simulated space shuttle mission
[NASA-TM-89715] 20 p2934 N90-26693
Design of the UETP experiment
22 p3118 N90-27712

Experience in developing an improved design of experiment (lessons learned) 22 p3120 N90-27718

EXPERIMENTAL AIRCRAFT
U RESEARCH AIRCRAFT

EXPERIMENTATION
On the Hellinger type distances for filtered experiments
[CWI-MS-R8818] 04 p0542 N90-13146
The processes of scientific research: The strategy of experimentation 06 p0824 N90-14788
Fundamental considerations in testing in cryogenic wind tunnels 08 p1030 N90-15951
Structural alterations in the cornea from exposure to infrared radiation
[AD-A215340] 09 p1253 N90-17269
Microgravity noncontact temperature requirements at NASA Lewis Research Center 10 p1362 N90-17897
Plasma diagnostics generated in the Compact Torus of UNICAMP
[INPE-4862-RPE/593] 10 p1433 N90-18271
Experiments on the unsteady flow in a supersonic compressor stage 11 p1482 N90-18422
Low velocity dust-dust collisions 12 p1741 N90-20011
Microgravity Science and Application Program tasks, 1989 revision
[NASA-TM-4191] 13 p1786 N90-20252
International treaties and active experiments in space
[AD-A219368] 16 p2328 N90-23272
Demo of three ways to use a computer to assist in lab 18 p2515 N90-24364

EXPERT SYSTEMS
Hierarchical damage tolerant controllers for smart structures
[AD-A209422] 01 p0005 N90-10022
Validation of missile simulation 01 p0014 N90-10066
Real-time support for high performance aircraft operation
[NASA-CR-185475] 01 p0015 N90-10075
Knowledge-based machine vision systems for space station automation
[NASA-CR-185710] 01 p0025 N90-10124
A rocket engine design expert system
[NASA-TM-102373] 01 p0032 N90-10172
Development of an expert system supporting short-circuit tests for circuit breakers
[DE89-760384] 01 p0059 N90-10334
An expert system for optimal gear design 01 p0077 N90-10439
Advancing automation and robotics technology for the space station Freedom and for the US economy
[NASA-TM-101561] 01 p0102 N90-10577
Cost metric algorithms for internetwork applications
[AD-A210324] 01 p0105 N90-10597
The applicability and limitations of expert system shells
[AD-A210801] 01 p0110 N90-10625
The development of an expert system for the creative design of mechanisms
[AD-A211115] 01 p0110 N90-10628
An analytical hierarchy process approach to establish the systems analyst's knowledge base for selecting an information requirements determination strategy 01 p0136 N90-10785
Parallel inference based on delta processing
[CWI-CS-R8846] 02 p0261 N90-11482
Applications of artificial intelligence to digital photogrammetry 02 p0262 N90-11486
Nonlinear maneuver autopilot for the F-15 aircraft
[NASA-CR-179442] 02 p0262 N90-11487
Systems analysis considerations in artificial intelligence/expert systems technology applications
[DE89-016847] 02 p0262 N90-11490
Partially specified probability measures in expert systems
[CWI-CS-R8842] 02 p0269 N90-11536
Coupling rule-based and object-oriented programming for the classification of machined features
[DE89-017705] 03 p0334 N90-11903
Reasoning about change and exceptions in automated process planning
[DE89-017706] 03 p0386 N90-12195
Computer-based tutors for explaining and managing the process of diagnostic reasoning
[AD-A211738] 03 p0390 N90-12222
Distributed knowledge-based systems
[AD-A211984] 03 p0418 N90-12401
The fault monitoring and diagnosis knowledge-based system for space power systems: AMPERES, phase 1
[NASA-CR-185486] 04 p0464 N90-12654
Automated monitor and control for deep space network subsystems 04 p0486 N90-12794
Investigation of North Atlantic fog and development of a marine fog forecast system
[AD-A211780] 04 p0519 N90-12999
An expert system for VM performance analysis
[REPT-89-30] 04 p0528 N90-13045
A knowledge-based approach to automated flow-field zoning for computational fluid dynamics
[NASA-TM-101072] 04 p0528 N90-13048
Expert systems as deductive systems
[CWI-CS-R8825] 04 p0532 N90-13073
Expert system for test program set fault candidate selection
[AD-A213338] 04 p0535 N90-13091
Path expression based operating systems
[MEMO-INF-88-68] 04 p0536 N90-13097
Semantics and consistency of rule-based expert systems
[CWI-CS-R8824] 04 p0543 N90-13153
Expert systems for adaptive control of large space structures 05 p0595 N90-13452
A knowledge-based system design/information tool for aircraft flight control systems
[NASA-TM-101704] 05 p0685 N90-13990
Applications of artificial intelligence to space station and automated software techniques: High level robot command language
[NASA-CR-182997] 05 p0686 N90-13991
An artificial intelligence approach to analog system diagnosis
[AD-A213135] 05 p0686 N90-13992
A knowledge-based flight status monitor for real-time application in digital avionics systems
[NASA-TM-101710] 05 p0686 N90-13995
Empirical analysis and refinement of expert system knowledge bases
[AD-A213240] 05 p0707 N90-14143
A portable ionosonde in support of reliable communications 06 p0762 N90-14431
Expert system for fault diagnostics of rotating machines
[DE89-766980] 06 p0793 N90-14621
Knowledge-based reusable software synthesis system 06 p0824 N90-14791
Architectures for reasoning in parallel
[NASA-CR-186237] 06 p0832 N90-14836
The design and implementation of an intelligent interface for information retrieval 06 p0858 N90-14991
Autonomous land navigation in a structured environment
[DE90-001625] 07 p0878 N90-15087
An expert system for quality assurance (a.k.a.) QA Express
[DE90-003887] 07 p0944 N90-15467
Where to from here. Future applications of mental models of complex performance
[DE90-002091] 07 p0967 N90-15586
Knowledge based text generation
[AD-A214273] 07 p0977 N90-15645
Investigation of the applicability of a functional programming model to fault-tolerant parallel processing for knowledge-based systems
[NASA-CR-181938] 07 p0979 N90-15654
Gaze controls with interactions and delays
[AD-A214286] 07 p0981 N90-15667
An intelligence-driven RPV mission planner 08 p1027 N90-15932
Knowledge-based imaging-sensor fusion system 08 p1075 N90-16220
A knowledge-based machine vision system for space station automation 08 p1075 N90-16221
Expert system control of a six-legged walking telerobot
[DE90-004661] 08 p1086 N90-16285
User interaction with self-learning systems
[AD-A214280] 08 p1105 N90-16395
Discrete event simulation tool for analysis of qualitative models of continuous processing systems
[NASA-CASE-MSC-21465-1] 08 p1107 N90-16410
On the efficient exploitation of speculation under data flow paradigms of control
[AD-A214112] 08 p1115 N90-16455
Experiences with knowledge-base and large database integration
[DE90-000686] 08 p1137 N90-16591
Artificial intelligence in process control: Knowledge base for the shuttle ECS model 08 p1156 N90-16697
Advances in Techniques and Technologies for Air Vehicle Navigation and Guidance
[AGARD-CP-455] 09 p1163 N90-16731
NASA/RAE cooperation on a knowledge based flight status monitor 09 p1164 N90-16738
Expert system for Kalman filter supervision: Application to autonomous satellite navigation 09 p1164 N90-16739
Intelligent landmarks recognition in satellites images 09 p1165 N90-16741
Application of model based reasoning to diagnosis of faults in inertial navigation equipment
[AD-A215561] 09 p1166 N90-16750
Knowledge based signal processing
[AD-A214864] 09 p1205 N90-16986
A circuit extraction system and graphical display for VLSI (Very Large Scale Integrated) design
[AD-A215668] 09 p1214 N90-17038
Rule-based systems for visibility forecasts
[AD-A214622] 09 p1248 N90-17239
A knowledge based approach to program debugging
[AD-A214941] 09 p1266 N90-17344
Use of hypermedia as a user interface for an artificial intelligence-based problem solver
[AD-A215551] 09 p1271 N90-17370
Use of semiempirical aerodynamic methods for preliminary design 10 p1304 N90-17546
VULCAIN: An expert system dedicated to fire risk analysis within complex industrial environments 10 p1314 N90-17599
Decision-analytic approach to rule-based expert system development using GPS (Global Positioning System) as the model
[AD-A216179] 10 p1319 N90-17626
Hypercube expert system shell-applying production parallelism
[AD-A215762] 10 p1418 N90-18173
Expert systems development methodology
[AD-A216892] 10 p1421 N90-18191
Application of artificial intelligence control to the vapor-liquid-solid silicon carbide whisker process
[DE90-007835] 11 p1480 N90-18519
Knowledge-based fault detection and analysis for robots: First results for the ROTEX robots
[ESA-TT-1150] 11 p1518 N90-18742
Teleoperator servoloop tuning using an expert system
[DE90-005674] 11 p1542 N90-18876
Knowledge-based extensible natural language interface technology program
[AD-A216664] 11 p1545 N90-18897
User manual for NEXT 1.2: NLR engineering X-pert system toolkit
[NLR-TR-87178-U] 11 p1547 N90-18905
Computation and control with neural nets
[DE90-006460] 11 p1548 N90-18911
Derivation of an efficient rule system pattern matcher
[AD-A216801] 11 p1549 N90-18917
A rule-based paradigm for intelligent adaptive flight control 12 p1605 N90-19238
Artificial intelligence issues related to automated computing operations 12 p1637 N90-19404
Flight crew aiding for recovery from subsystem failures
[NASA-CR-181905] 12 p1696 N90-19741
An expert system for the design of heating, ventilating, and air-conditioning systems
[AD-A218287] 13 p1788 N90-20262
Robot navigation research using the HERMIES mobile robot
[DE90-001952] 13 p1810 N90-20396
Computer simulation of the mathematical modeling involved in constitutive equation development: Via symbolic computations
[NASA-TM-102532] 13 p1816 N90-20428
A system for analysis and interpretation of lineaments in remote sensing images
[INPE-4893-PRE/1494] 13 p1840 N90-20565
A prototype expert system to forecast severe winds in the western Mediterranean Sea
[AD-A218017] 13 p1845 N90-20593
Broadening the interface bandwidth in simulation based training 13 p1859 N90-20666
Hybrid intelligent perception system: Intelligent perception through combining artificial neural networks and an expert system
[DE90-007483] 13 p1874 N90-20746
Investigation of air transportation technology at Princeton University, 1988-1989 14 p1907 N90-20935
An expert system for wind shear avoidance 14 p1908 N90-20938
Rule-based mechanisms of learning for intelligent adaptive flight control 14 p1908 N90-20939
Progress in inverse design and optimization in aerodynamics 14 p1916 N90-20977
Thermal control system corrosion study
[NASA-TM-102220] 14 p1971 N90-21294
A knowledge-based information based for crop area estimation
[INPE-4990-PRE/1555] 14 p1996 N90-21444
Cooperating intelligent systems
[NASA-CR-184982] 14 p2012 N90-21529
Expert systems for automated maintenance of a Mars oxygen production system
[NASA-CR-186209] 15 p2138 N90-22215
Photonic processing at NASA Ames Research Center 15 p2141 N90-22234
The WAVE model for advanced knowledge processing
[OUEL-1803/89] 15 p2151 N90-22291

A knowledge-based approach to improving optimization techniques in system planning 15 p2154 N90-22303
NASA ground terminal communication equipment automated fault isolation expert systems 15 p2154 N90-22305
Autonomous power expert system 15 p2154 N90-22306
Knowledge-based and integrated monitoring and diagnosis in autonomous power systems 15 p2155 N90-22310
The procedure safety system 15 p2155 N90-22311
Using expert systems to implement a semantic data model of a large mass storage system 15 p2156 N90-22315
Adaptive pattern recognition by mini-max neural networks as a part of an intelligent processor 15 p2156 N90-22317
A knowledge-based system with learning for computer communication network design 15 p2157 N90-22319
Evaluation of a proposed expert system development methodology: Two case studies 15 p2157 N00-22320
Preliminary development of an intelligent computer assistant for engine monitoring [NASA-TM-101702] 15 p2157 N90-22322
An expert system for simulating electric loads aboard Space Station Freedom [NASA-TM-103150] 15 p2158 N90-22325
An intelligent interface for the design of optimal control systems [INPE-4917-PRE/1516] 15 p2159 N90-22332
Neural implementation of a method for solving systems of linear algebraic equations [NPL-DITC-155/89] 15 p2162 N90-22356
Facilitating knowledge sharing in organizations: Semiautonomous agents that learn to gather, classify, and distribute environmental scanning knowledge 15 p2176 N90-22435
Knowledge-based semantic query processing: An optimal transformation approach 15 p2176 N90-22437
Knowledge management: An abstraction of knowledge base and database management systems [NASA-CR-4273] 16 p2278 N90-22986
Multidisciplinary Expert-aided Analysis and Design (MEAD) 16 p2291 N90-23050
Neural networks in support of manned space 16 p2298 N90-23088
RF network selection in a rule-based system. NOSC project ZE68: Cost metric algorithms for internetwork applications [AD-A219389] 16 p2301 N90-23116
Application of artificial intelligence in electronic circuit diagnosis 16 p2303 N90-23122
Automated electric power management and control for Space Station Freedom [NASA-TM-103151] 16 p2304 N90-23125
Syntax, semantics, and pragmatism: An integrated focus based on textual linguistic knowledge [INPE-4992-PRE/1554] 16 p2326 N90-23262
Explanation generation in expert systems (a literature review and implementation) [AD-A218741] 16 p2327 N90-23268
Knowledge based system for Hermes orbital operations ground support [REPT-892-440-102] 17 p2361 N90-23443
An expert system for the study of high duty bonded joints in aerospace structures [REPT-892-430-110] 17 p2414 N90-23753
Advancing automation and robotics technology for the Space Station Freedom and for the US economy [NASA-TM-102668] 17 p2439 N90-23899
Memory-based expert systems [AD-A219875] 17 p2440 N90-23907
Generation of expert systems by partial evaluation [AD-A220427] 17 p2443 N90-23920
An expert system to perform on-line controller tuning [NASA-TM-103101] 17 p2453 N90-23991
Northeast Artificial Intelligence Consortium. Volume 3: The Versatile Maintenance Expert System research project [AD-A218716] 17 p2453 N90-23993
Northeast Artificial Intelligence Consortium. Volume 4. Distributed AI for communications network management [AD-A218717] 17 p2453 N90-23994
A viewpoint on the contribution of expert systems of logistics [REPT-892-320-101] 17 p2454 N90-24002
Intelligent, real-time problem solving [AD-A219929] 17 p2455 N90-24006
Experiences with and error handling in a knowledge base assisted system for payload experiment automation 18 p2504 N90-24306
On-board expert system for manned rendezvous operation assistance 18 p2504 N90-24309
Graph structure model [DE90-008945] 18 p2594 N90-24760
Solving problems by interrogating sets of knowledge systems: Toward a theory of multiple knowledge systems 18 p2629 N90-24979
Knowledge-based control of an adaptive interface 18 p2630 N90-24987
Mars Rover imaging systems and directional filtering 18 p2648 N90-25071
Flight-testing of the self-repairing flight control system using the F-15 highly integrated digital electronic control flight research facility [NASA-TM-101725] 19 p2661 N90-25144
Autonomous power expert system [NASA-CR-185263] 19 p2670 N90-25187
Advanced fuel properties, phase 1 [AD-A219788] 19 p2679 N90-25236
Third Annual Workshop on Space Operations Automation and Robotics (SOAR 1989) [NASA-CP-3059] 19 p2727 N90-25503
NASA systems autonomy demonstration project: Advanced automation demonstration of Space Station Freedom thermal control system 19 p2728 N90-25510
StarPlan: A model-based diagnostic system for spacecraft 19 p2728 N90-25511
Solar array automation limitations 19 p2729 N90-25513
Autonomous power expert fault diagnostic system for Space Station Freedom electrical power system testbed 19 p2730 N90-25521
An expert system to advise astronauts during experiments: The protocol manager module 19 p2730 N90-25522
Monitoring and control of spacecraft systems using procedural reasoning 19 p2731 N90-25524
Knowledge representation to support reasoning based on multiple models 19 p2731 N90-25525
CLEAR: Automating control centers with expert system technology 19 p2733 N90-25533
OMS FDIR: Initial prototyping 19 p2738 N90-25562
An intelligent simulation training system 19 p2739 N90-25566
A model for a knowledge-based system's life cycle 19 p2739 N90-25569
ACES: Space shuttle flight software analysis expert system 19 p2739 N90-25571
MEXP: A programming tool for the CESAR programmable systolic array multiprocessor [FFI-89/7020] 19 p2744 N90-25598
Automated angular momentum recoupling algebra [DE90-011988] 19 p2750 N90-25626
Inference and control mechanisms in NEXT 2.0 [NLR-MP-88062-U] 20 p2844 N90-26175
Reusable rocket engine turbopump health monitoring system, part 3 [NASA-CR-182294] 20 p2869 N90-26320
Neural networks for detecting defects in aircraft structures [IAR-90-4] 20 p2873 N90-26345
Robotic-aided system for inspection of aging aircraft [NIAR-90-9] 20 p2873 N90-26346
Application of symbolic computations to the constitutive modeling of structural materials [NASA-TM-103225] 20 p2876 N90-26364
Knowledge-based system for flight information management [NASA-TM-102685] 20 p2903 N90-26511
An expert system based software sizing tool, phase 2 [NASA-CR-186706] 20 p2905 N90-26525
Integrating expert systems with solid modeling through interprocess communications and the applications interface specification [DE90-012996] 20 p2907 N90-26537
Material selection and design: An expert system approach [PNR90611] 20 p2908 N90-26544
Prototyping an in-house business intelligence database [PNR90665] 20 p2937 N90-26709
Proceedings of the 1987 Aircraft/Engine Structural Integrity Program (ASIP/ENSIP) Conference [AD-A198037] 21 p2956 N90-26807
An expert system advisor for damage repair of composite wing skins (repairman) 21 p2956 N90-26810
Communications and tracking expert systems study [NASA-CR-185935] 21 p2992 N90-27004
A regional forecasting model [AD-A221556] 21 p3031 N90-27235
Genetic algorithm based fuzzy control of spacecraft autonomous rendezvous 21 p3041 N90-27281
Artificial intelligence in the materials processing laboratory 21 p3041 N90-27283
An architecture for intelligent task interruption 21 p3041 N90-27284
A knowledge-based approach to configuration layout, justification, and documentation 21 p3041 N90-27286
KIPSE1: A Knowledge-based Interactive Problem Solving Environment for data estimation and pattern classification 21 p3041 N90-27287
An architecture for rule based system explanation 21 p3042 N90-27288
ATS displays: A reasoning visualization tool for expert systems 21 p3042 N90-27290
Expert System Development Methodology (ESDM) 21 p3042 N90-27292
A hybrid approach to space power control 21 p3043 N90-27293
Knowledge-based systems and NASA's software support environment 21 p3043 N90-27296
Graphical explanation in an expert system for Space Station Freedom rack integration 21 p3044 N90-27299
Space station advanced automation 21 p3044 N90-27300
An application of design knowledge captured from multiple sources 21 p3045 N90-27306
The integration of automated knowledge acquisition with computer-aided software engineering for space shuttle expert systems 21 p3045 N90-27307
Artificial Intelligence Software Engineering (AISE) model 21 p3045 N90-27309
The real-time learning mechanism of the Scientific Research Associates Advanced Robotic System (SRAARS) 21 p3046 N90-27312
A model for a space shuttle safing and failure-detection expert 21 p3046 N90-27314
Construction of dynamic stochastic simulation models using knowledge-based techniques 21 p3047 N90-27322
The composite load spectra project 21 p3047 N90-27323
Intelligent tutoring systems for space applications 21 p3048 N90-27324
Documentation and knowledge acquisition 21 p3048 N90-27325
Inductive knowledge acquisition experience with commercial tools for space shuttle main engine testing 21 p3048 N90-27326
VIP: A knowledge-based design aid for the engineering of space systems 21 p3048 N90-27327
Resolution of seven-axis manipulator redundancy: A heuristic issue 21 p3049 N90-27331
Compiling knowledge-based systems from KEE to Ada 21 p3049 N90-27334
Automated unit-level testing with heuristic rules 21 p3049 N90-27335
Ada as an implementation language for knowledge based systems 21 p3050 N90-27337
Producing process plans out of CAD files through AI techniques [ETN-90-97273] 21 p3050 N90-27338
Expert system in software engineering using Structured Analysis and Design Technique (SADT) [AD-A223022] 21 p3052 N90-27351
Knowledge based quality assurance tools [AD-A223064] 21 p3053 N90-27353
Guide for the management of expert systems development [AD-A221847] 21 p3056 N90-27378
Past, present and future: Aircraft integrated monitoring systems: An ever-developing technology 22 p3103 N90-27618
Expert system diagnostics and parts life tracking as applied to the AV-8B aircraft for the USMC 22 p3104 N90-27629
Knowledge based diagnosis of jet engines under consideration of model based methods 22 p3105 N90-27631
On line diagnostics of rotating machinery using expert system technology 22 p3105 N90-27632
Public-sector aviation issues, 1987 to 1988 graduate research award papers [PB90-191206] 22 p3110 N90-27667
Expert system for pilot assistance: The challenge of an intensive prototyping [ETN-90-97274] 22 p3111 N90-27674
Use of acoustic emission for continuous surveillance of aircraft structures 22 p3188 N90-28092
Development of an expert system embedding pattern recognition techniques for pollution source identification [PB90-185927] 22 p3197 N90-28139
Structured analysis of the applicability of A and R technologies in space programs [MBB-UO-0084-90-PUB] 22 p3256 N90-28436
ROSES, a Robot Operating System Expert Scheduler: Methodological framework [DE90-014782] 23 p3334 N90-28851

A survey of planning and scheduling research at the NASA Ames Research Center 23 p3376 N90-29076
Graph structure model
[DE90-014930] 23 p3381 N90-29097
Inference engine for expert systems
[INPE-4565-PRE/1306] 23 p3382 N90-29104
A hardware/software environment to support R/D in intelligent machines and mobile robotic systems
[DE90-014458] 23 p3385 N90-29119
An expert system to perform on-line controller restructuring for abrupt model changes
[NASA-TM-103809] 23 p3385 N90-29121
Model authoring system for fail safe analysis
[NASA-CR-4317] 23 p3389 N90-29142
A knowledge-based system design/information tool
[NASA-CR-4316] 23 p3389 N90-29143
Integrating rule-based and neural-net techniques for spectral analysis
[AD-A223517] 24 p3446 N90-29462
Information management in an integrated space telerobot 24 p3511 N90-29846
Redundancy in sensors, control and planning of a robotic system for space telerobotics 24 p3511 N90-29847
Determining robot actions for tasks requiring sensor interaction 24 p3514 N90-29868
Interset: A natural language interface for teleoperated robotic assembly of the EASE space structure 24 p3517 N90-29885
Multi-level manual and autonomous control superposition for intelligent telerobot 24 p3518 N90-29888
Coordination in a hierarchical multi-actuator controller 24 p3520 N90-29900
Distributed communications and control network for robotic mining 24 p3520 N90-29901
Generic task problem solvers in Soar 24 p3521 N90-29904
Optical symbolic processor for expert system execution
[AD-A224284] 24 p3525 N90-29931
An analysis of the distinction between deep and shallow expert systems
[AD-A224443] 24 p3534 N90-29987
Knowledge-based expert system configurator
[DE90-011711] 24 p3558 N90-30135

EXPLODING CONDUCTOR CIRCUITS
U CIRCUITS
U EXPLODING WIRES

EXPLODING CONDUCTORS
U EXPLODING WIRES

EXPLODING WIRES
Shock pressure determination in detonator wires
[DE89-017756] 03 p0350 N90-12002
Electrothermal response testing more than a quality assurance tool
[DE90-001449] 06 p0780 N90-14536
The fundamentals of metal combustion in composite explosives revealed by high speed microphotography
[DE90-005255] 09 p1192 N90-16910
Excess transit time as a function of burst current in an exploding bridgewire detonator
[DE90-007168] 11 p1512 N90-18708
Qualification test rationale for measuring the resistance of equipment to pyrotechnic shock
[REPT-892-430-117] 16 p2207 N90-22590

EXPLORATION
NT LUNAR EXPLORATION
NT MINERAL EXPLORATION
NT OIL EXPLORATION
NT SPACE EXPLORATION

EXPLORER SATELLITES
NT COSMIC BACKGROUND EXPLORER SATELLITE
NT EXPLORER 20 SATELLITE
NT EXPLORER 31 SATELLITE
NT EXTREME ULTRAVIOLET EXPLORER SATELLITE
NT INTERNATIONAL SUN EARTH EXPLORER 3
Rocket and satellite observations of the local interstellar medium 02 p0292 N90-11668
The Explorer program for astronomy and astrophysics 05 p0712 N90-14159
The Advanced Composition Explorer
[DE90-006522] 12 p1737 N90-19987
Differentiation of three dimensional models of the zodiacal interplanetary dust cloud for experiments with micrometeoroids decay detectors on the space station
[ETN-90-98488] 18 p2637 N90-25025

EXPLORER 20 SATELLITE
Results from Alouette 1, Explorer 20, Alouette 2, and Explorer 31
[NASA-TM-101822] 24 p3483 N90-29690

EXPLORER 31 SATELLITE
Results from Alouette 1, Explorer 20, Alouette 2, and Explorer 31
[NASA-TM-101822] 24 p3483 N90-29690

EXPLOSION SUPPRESSION
Fuel tank explosion protection 08 p1023 N90-15914
Onboard fire- and explosion suppression for fighter aircraft 10 p1315 N90-17602

EXPLOSIONS
NT AERIAL EXPLOSIONS
NT CHEMICAL EXPLOSIONS
NT GAS EXPLOSIONS
NT NUCLEAR EXPLOSIONS
NT THERMONUCLEAR EXPLOSIONS
NT UNDERGROUND EXPLOSIONS
Remarks on certain aspects of solid explosive detonation via small projectile impact
[AD-A210648] 01 p0054 N90-10307
Shock behavior of explosives about the C-J (Chapman-Juget) point
[DE89-007642] 01 p0070 N90-10400
Carbon in detonations
[DE89-016037] 02 p0208 N90-11189
Indexes for the proceedings of the symposia (international) on detonation, 1951 through 1985
[DE89-015178] 03 p0345 N90-11972
Exploding metallic foil fuse modeling at Los Alamos
[DE89-016970] 03 p0350 N90-11998
Expected supernovae rates and gravitational waves detection
[NOTA-INTERNA-933] 05 p0713 N90-14166
Testing and performance of a high-gain flux-compression generator
[DE90-002808] 06 p0772 N90-14492
Safety Status Report for the Ulysses mission. Book 2: Accident analysis-appendices. General purpose heat source radioisotope thermoelectric generator program
[DE90-006830] 12 p1614 N90-19286
Present and future risk of collision of satellites and manned platforms with other space objects and particles in terrestrial orbit
[R-8840] 12 p1615 N90-19288
Modelling late-time atmospheres of supernovae 15 p2189 N90-22500
SPHC (Smooth Particle Hydrodynamics Code) manual
[AD-A220743] 17 p2444 N90-23928
The effects of blast trauma (impulse noise) on hearing: A parametric study source 2
[AD-A221731] 21 p3035 N90-27253
Methods for detecting low-frequency signals in the presence of strong winds
[AD-A223980] 23 p3320 N90-28769
Unipolar arcing on the cathode surface of a high voltage diode
[AD-A224122] 23 p3322 N90-28787

EXPLOSIVE DEVICES
NT BOMBS (ORDNANCE)
NT BOOSTERS (EXPLOSIVES)
NT CAPS (EXPLOSIVES)
NT DETONATORS
NT EXPLODING WIRES
NT INITIATORS (EXPLOSIVES)
NT SHAPED CHARGES
NT TORPEDOES
Test of EED (Electro-Explosive Devices). Part 3: Statistical aspects on the estimation of sensitivity
[FOA-C-20749-2.3-PT-3] 02 p0209 N90-11194
RF and dc desensitized electroexplosive device
[AD-D014206] 04 p0497 N90-12862

EXPLOSIVE FORMING
Metal matrix composites from dynamic consolidation of powder mixtures
[DE90-010951] 18 p2519 N90-24388

EXPLOSIVE GASES
U FLAMMABLE GASES

EXPLOSIVES
NT CELLULOSE NITRATE
NT HMX
NT RDX
NT TATB
NT TRINITROTOLUENE
Effects of binder concentration on the properties of plastic-bonded explosives
[DE89-007744] 01 p0053 N90-10301
Free-expansion experiments and modeling in detonation: Chemistry and hydrodynamics on a laboratory scale
[DE89-007748] 01 p0053 N90-10302
Organic explosives and related compounds. Environmental and health considerations
[AD-A210554] 01 p0054 N90-10306
Shock behavior of explosives about the C-J (Chapman-Juget) point
[DE89-007642] 01 p0070 N90-10400
Laser initiation of secondary explosives
[DE89-010229] 01 p0075 N90-10431
In-situ study of the chemically driven flow fields in initiating homogeneous and heterogeneous nitromethane explosives
[DE89-008415] 02 p0207 N90-11186
Estimation of the C-J pressure of explosives
[DE89-013811] 02 p0208 N90-11187
Laser-driven miniature flyer plates for shock initiation of secondary explosives
[DE89-016587] 02 p0225 N90-11288
Magnetic flux compression
[DE89-016991] 02 p0271 N90-11546
A critical assessment of models available for the shock initiation of heterogeneous explosives
[MRL-TR-89-17] 03 p0333 N90-11896
Sensitivity relationships in energetic materials
[DE89-016967] 03 p0333 N90-11897
Indexes for the proceedings of the symposia (international) on detonation, 1951 through 1985
[DE89-015178] 03 p0345 N90-11972
Lagrangian analysis of MIV (Magnetic Impulse-Velocity) gauge experiments on PBX 9502 using the mass-displacement moment function
[DE89-018612] 03 p0350 N90-12000
Thermal initiation of confined primary explosives with a proton beam
[AD-A212954] 04 p0482 N90-12767
Preliminary report on the feasibility of high power Electronic Warfare (EW) using explosive energy sources
[MRL-TR-89-3] 04 p0483 N90-12775
Nuclear magnetic resonance signatures of nitrogen-containing compounds
[AD-A213375] 05 p0622 N90-13628
Thermodynamic properties and hydrodynamic response of high-density high-temperature C H N O mixtures
[DE90-000836] 06 p0742 N90-14318
Pentafluorothio polynitroaliphatic explosives
[AD-D014221] 06 p0753 N90-14383
Detonation product equation of state for Baratol
[DE90-001050] 06 p0753 N90-14384
Calibration curves for some standard Gap Tests
[DE89-016599] 06 p0754 N90-14389
Non-equilibrium effects of slow diffusion controlled reactions on the properties of explosives
[DE90-000822] 06 p0754 N90-14391
Phase changes in carbon and nitrogen systems: Their effects on the detonation properties of high explosives
[DE90-000829] 06 p0755 N90-14392
Reactive flow measurements and calculations for ZrH2-based composite explosives
[DE90-000831] 06 p0755 N90-14393
Reaction zone structure in supracompressed detonating explosives
[DE90-000832] 06 p0755 N90-14394
Fast transit gas- and condensed-phase chemistry of energetic materials
[DE90-001656] 06 p0755 N90-14395
Simultaneous thermal analysis techniques for characterization of energetic materials
[DE90-003028] 07 p0914 N90-15289
Characterization of the thermal degradation of selected energetic materials and mixtures by Rapid-Scan Fourier Transform Infrared (RSFTIR) spectroscopy
[AD-A214411] 07 p0916 N90-15296
Design of a spheromak compressor driven by high explosives
[DE90-003652] 08 p1088 N90-16283
The fundamentals of metal combustion in composite explosives revealed by high speed microphotography
[DE90-005255] 09 p1192 N90-16910
A preliminary assessment of 3-Nitro-1,2,4-Triazol-5-One (NTO) as an insensitive high explosive
[AD-A215063] 10 p1360 N90-17889
Microconvective heating of granular explosives by a semiconductor bridge
[DE90-005710] 11 p1484 N90-18541
Investigation of the phase stabilizing effect of 4 percent potassium fluoride on ammonium nitrate
[AD-A215313] 11 p1494 N90-18599
A program of fundamental research on explosives at Los Alamos
[DE90-006509] 11 p1495 N90-18602
High-Explosives Applications Facility (HEAF)
[DE90-008122] 13 p1787 N90-20257
An evaluation of metal salts of 3-nitro-1,2,4-triazol-5-one (NTO) as potential primary explosives
[MRL-TN-563] 14 p1956 N90-21202
Determination of detonation parameters of booster explosives at small charge diameters
[MRL-TR-89-45] 14 p1957 N90-21204
Minutes of the 23rd Explosives Safety Seminar, volume 1
[AD-A218264] 14 p1958 N90-21213
Minutes of the 23rd Eplosives Safety Seminar, volume 2
[AD-A218265] 14 p1959 N90-21214

High explosives (PBX9502) characterization using computerized tomography
[DE90-008170] 14 p1990 N90-21404
Ignition testing of low-energy laser diode ignited components
[DE90-009968] 16 p2214 N90-22630
The sensitivity of several explosives to ignition in the launch environment
[AD-A221581] 21 p2990 N90-26993
Diamonds in detonation soot 21 p3094 N90-27585
Shock dynamics in the sub-nanometer femtosecond domain
[DE90-014390] 23 p3304 N90-28689
Unipolar arcing on the cathode surface of a high voltage diode
[AD-A224122] 23 p3322 N90-28787

EXPONENTIAL FUNCTIONS
NT LOGARITHMS
Inherent bias in nonlinear least squares analysis of first-order kinetic data
[AD-A210677] 01 p0114 N90-10651
Recurrence and ergodicity for exponential family state-space models
[AD-A213466] 07 p0983 N90-15677
Strong large deviation and local limit theorems
[AD-A213610] 07 p0986 N90-15698
A further note on generalized hyperexponential distributions
[AD-A214881] 09 p1275 N90-17394
On the exponential convergence of the h-p version for boundary element Galerkin methods on polygons
[AD-A215814] 10 p1423 N90-18210
The h-p version of the boundary element method with geometric mesh on polygonal domains
[AD-A215815] 10 p1423 N90-18211
An algorithm for efficient estimation of superimposed exponential signals
[AD-A217218] 13 p1865 N90-20698
A note on overdispersed exponential families
[AD-A216277] 14 p2018 N90-21565
Characterizing exponential distributions via conditional independence
[AD-A219255] 16 p2309 N90-23158
Approximate interval estimation methods for the reliability of systems using component data with exponential and Weibull distributions
[AD-A219857] 17 p2460 N90-24048
Classical and Bayes-P subset selection procedures for double exponential populations
[AD-A223830] 24 p3538 N90-30006

EXPONENTS
Fluctuations of the Lyapunov exponent in disordered systems
[PREPRINT-690] 05 p0695 N90-14063
A comparison result and elliptic equations involving subcritical exponents
[DE90-001772] 06 p0834 N90-14850

EXPORTS
U INTERNATIONAL TRADE

EXPOSURE
Method and apparatus for maintaining thermal control in plasma conditions
[NASA-CASE-MFS-28368-1] 01 p0125 N90-10717
Occupational safety considerations with hydrazine 02 p0207 N90-11182
Optical properties monitor: Experiment definition phase
[NASA-CR-183836] 05 p0699 N90-14092
Radiation damage and its influence on source requirements for high resolution x ray holography
[DE90-002508] 06 p0781 N90-14540
Biological effects of hyperthermia and potential risk associated with ultrasonic exposure
[PB89-100702] 06 p0820 N90-14768
Variability of cultivar responses to ozone
[PB89-225460] 07 p0956 N90-15528
Fuel resistant coatings for metal and composite fuel tanks 08 p1022 N90-15911
Integral fuel tank certification and test methods 08 p1023 N90-15916
Fracture toughness of ferritic alloys at very high neutron exposures
[DE90-004519] 08 p1046 N90-16046
Short-term bioassays may be useful in evaluating fiber/whisker hazards
[DE90-003707] 08 p1104 N90-16393
Safety evaluation of infrared lamp power output for oculometer eye/head tracker system
[AD-A215809] 10 p1411 N90-18138
Development of acceleration exposure limits for advanced escape systems 13 p1751 N90-20055
Simplified model for solar cosmic ray exposure in manned Earth orbital flights
[NASA-TM-4182] 14 p2043 N90-21715
Studies of 60-Hz exposure effects on human function
[DE90-009473] 15 p2137 N90-22210
The physiological cost of wearing the propellant handler's ensemble at the Kennedy Space Center
[NASA-TM-102786] 16 p2275 N90-22966
High peak power microwave pulses at 2.37 GHz: No effects on vigilance performance in monkeys
[AD-A219570] 17 p2433 N90-23863
Model for predicting the effects of laser exposures and eye protection on vision
[AD-A219697] 17 p2434 N90-23868
Analyses of the predictability of noise-induced sleep disturbance
[AD-A220156] 17 p2435 N90-23876
Dazzling glare: Protection criteria versus visual performance
[AD-A219676] 17 p2438 N90-23889
Improved model for solar cosmic ray exposure in manned Earth orbital flights
[NASA-TP-2987] 18 p2639 N90-25031
Integrated controls and health monitoring for chemical transfer propulsion
[NASA-TM-103185] 19 p2668 N90-25178
The effects of acid fog and dew on materials
[PB90-157496] 19 p2712 N90-25436
Mechanisms of microwave induced damage in biologic materials
[AD-A222454] 21 p3033 N90-27242
Scandia-stabilized zirconia coating for composites
[AD-D014550] 22 p3160 N90-27917
Oxidation, sulfidation, and hot corrosion: Mechanisms and interrelationships 23 p3307 N90-28702
Preliminary exposure study to determine the effects of acid deposition on coated steel substrates
[PB90-201799] 23 p3309 N90-28715
Study of meteorological processes important in the degradation of materials through surface temperature
[PB90-222720] 23 p3336 N90-28856
Evaluation of physiological and psychological impairment of human performance in cold stressed subjects
[AD-A223635] 24 p3498 N90-29769

EXPRESSIONS (MATHEMATICS)
U FORMULAS (MATHEMATICS)

EXPULSION
The nature of cometary materials 08 p1147 N90-16647

EXTARS
U X RAY STARS

EXTENDED DURATION SPACE FLIGHT
U LONG DURATION SPACE FLIGHT

EXTENSOMETERS
Geotechnical instrumentation
[PB89-198675] 07 p0933 N90-15398
New inflight experiments to measure aerodynamics loads
[ETN-90-97276] 21 p2961 N90-26834

EXTERNAL COMBUSTION ENGINES
NT STIRLING ENGINES

EXTERNAL STORE SEPARATION
New test techniques to evaluate near field effects for supersonic store carriage and separation 01 p0013 N90-10062
Marginal release disturbances on advanced missiles 01 p0014 N90-10070
Evaluation of store carriage (and release) environment using flight instrumented stores 02 p0153 N90-10876
Missile Aerodynamics: NEAR Conference on Missile Aerodynamics
[ISBN-0-9620629-1-X] 10 p1303 N90-17540
Application of experimental techniques to store release problems 10 p1304 N90-17545
Prediction methods for store separation 10 p1305 N90-17549
An overlapped grid method for multigrid, finite volume/difference flow solvers: MaGGiE
[NASA-CR-182008] 14 p1911 N90-20953

EXTERNAL STORES
NT PODS (EXTERNAL STORES)
Computation of transonic flow about stores
[AD-A210402] 01 p0002 N90-10009
Evaluation of store carriage (and release) environment using flight instrumented stores 02 p0153 N90-10876
CF 18 480 Gallon External Fuel Tank Stores Clearance Program 02 p0153 N90-10877
The integration of stores on modern tactical aircraft: Where we have been, and what we should do for the future 10 p1305 N90-17552
Water-tunnel investigation of concepts for alleviation of adverse inlet spillage interactions with external stores
[NASA-TM-4181] 12 p1599 N90-19199
Integration of externally carried weapon systems with military helicopters
[AGARD-AR-247] 22 p3115 N90-27696

EXTERNAL SURFACE CURRENTS
The 1984 direct strike lightning data, part 1
[NASA-TM-87690-PT-1] 01 p0089 N90-10505
Scalar Green function method for microstrip antenna analysis based on the exact image theory
[PB89-216838] 04 p0488 N90-12805

EXTERNAL TANKS
Independent Orbiter Assessment (IOA): Analysis of the orbiter main propulsion system
[NASA-CR-185584] 02 p0164 N90-10927
Independent Orbiter Assessment (IOA): Assessment of the mechanical actuation subsystem, volume 1
[NASA-CR-185527-VOL-1] 02 p0169 N90-10952
Independent Orbiter Assessment (IOA): Assessment of the mechanical actuation subsystem, volume 2
[NASA-CR-185527-VOL-2] 02 p0169 N90-10953
Compendium of fracture mechanics problems
[NASA-TM-100393] 14 p1992 N90-21414
Space Shuttle, NASA's major changes to flight hardware: Fact sheet for the Chairman, Committee on Science, Space, and Technology, House of Representatives
[GAO/NSIAD-88-173FS] 15 p2181 N90-22461
Remote measurement of ice thickness on the shuttle external tank surface
[NASA-TM-102667] 18 p2555 N90-24584
Debris/ice/TPS assessment and photographic analysis for shuttle mission STS-31R
[NASA-TM-102790] 20 p2819 N90-26040
QM-8 final performance evaluation report: SEALS, volume 4
[NASA-CR-183958] 20 p2869 N90-26324
The effect of impurity gasses on variable polarity plasma arc welded 2219 aluminum
[NASA-CR-183803] 21 p2980 N90-26935
Debrix/ice/TPS assessment and photographic analysis of Shuttle Mission STS-32R
[NASA-TM-102787] 22 p3124 N90-27733
Autonomous propulsion system requirements for placement of an STS (Space Transportation System) external tank in low Earth orbit
[PB90-183302] 22 p3133 N90-27777

EXTERNALLY BLOWN FLAPS
NT UPPER SURFACE BLOWN FLAPS

EXTINCTION
NT INTERSTELLAR EXTINCTION
Atmospheric horizontal-inhomogeneity effects on the optical depths determined by the double-elevation-angle lidar technique
[AD-A212836] 04 p0493 N90-12839
An investigation of flame spread over shallow liquid pools in microgravity and nonair environments
[NASA-TM-102425] 05 p0630 N90-13680
Effects of flame stretch on the propagation, extinction, and stability of premixed flames 06 p0739 N90-14301
Lidar technique for adjusting aerosol model number densities to existing conditions
[AD-A213846] 08 p1101 N90-16374
Interstellar and cometary dust 08 p1145 N90-16636
The extinction and structure of counterflow premixed flames
[AD-A218106] 13 p1773 N90-20178
Retabulation of space group extinctions for electron diffraction
[DE90-612933] 14 p2031 N90-21648
Interpreting meteorological data reports for LOWTRAN Navy aerosol model extinction calculations 15 p2082 N90-21920
Nonlinear interaction between laser radiation and aerosols
[FOA-C-20768-2.3] 18 p2563 N90-24623
Non-premixed turbulent CO/H2 flames at local extinction conditions 21 p2975 N90-26907
High pulse energy flashlamp pumpable laser dyes
[AD-A223075] 22 p3180 N90-28042
A historical supernova's lower limit to the galactic stellar-collapse rate
[FERMILAB-PUB-90/24-A] 22 p3262 N90-28472

EXTINGUISHERS
U FIRE EXTINGUISHERS

EXTINGUISHING
NT FLAMEOUT
Test method for fire extinguishing powder, Nordtest project 675-87
[PB90-166984] 15 p2073 N90-21874
The computer modeling of the combustion and extinction of methane-air premixed flames by thermally stable gases
[PB90-189432] 21 p2976 N90-26910

EXTRACTION
NT ION EXTRACTION
Measurement of hydrazine contamination in soils 02 p0206 N90-11180

Extraction induced emittance growth for negative ion sources
[DE89-017586] 02 p0273 N90-11559
Isolating contour information from arbitrary images 08 p1074 N90-16217
Injection parameters and beam oscillations during extraction
[NIKHEF-K/AMPS/89-07] 11 p1499 N90-18632
Remote sensing applied to the monitoring of mineral extraction in the proximity of urban areas: Pros and cons
[INPE-4867-PRE/1478] 11 p1522 N90-18766
Digital processing of TM/LANDSAT data in monitoring interior water
[INPE-4956-PRE/1533] 14 p1997 N90-21448
Studies on the use of supercritical ammonia for ceramic nitride synthesis and fabrication
[NASA-TM-102570] 15 p2068 N90-21843
Kinetic and extraction measurements on 12C18O2
[AD-A220417] 17 p2472 N90-24133
Interaction of the large eddy structure in the inner-half of a turbulent boundary layer 18 p2551 N90-24561
Automatic line network extraction from aerial imagery of urban areas through knowledge based image analysis
[AD-A222675] 20 p2880 N90-26385
Automated extraction of knowledge for model-based diagnostics 21 p3047 N90-27318
Using decision-tree classifier systems to extract knowledge from databases 21 p3048 N90-27328

EXTRAGALACTIC LIGHT
U EXTRATERRESTRIAL RADIATION
U LIGHT (VISIBLE RADIATION)

EXTRAGALACTIC MEDIA
U INTERGALACTIC MEDIA

EXTRAGALACTIC RADIO SOURCES
NT RADIO GALAXIES
NT RADIO JETS (ASTRONOMY)
The link to extragalactic objects 05 p0608 N90-13544
A search for the effects of active magnetic fields in extra-galactic radio sources 05 p0712 N90-14161
Short time scale variability of the BL Lac object OJ 287 in the near-infrared
[IFSI-89-3] 08 p1140 N90-16603
Asymmetric depolarization in powerful extragalactic radio sources 22 p3264 N90-28484
Radio outbursts in extragalactic sources 23 p3414 N90-29291

EXTRAPOLATION
Approximate simulation model for analysis and optimization in engineering system design
[NASA-TM-101616] 01 p0054 N90-10308
Sequential design of experiments with physically based models 23
[AD-A211918] 03 p0393 N90-12239
Techniques for accelerating iterative methods for the solution of mathematical problems
[AD-A218272] 13 p1878 N90-20775
Extrapolation of missile flight lines
[ETN-90-96494] 18 p2508 N90-24336
Efficient implementation of minimal polynomial and reduced rank extrapolation methods
[NASA-TM-103240] 20 p2920 N90-26616
Extrapolation procedures at outflow boundaries for the Navier-Stokes equations
[FFA-TN-1990-23] 23 p3327 N90-28811

EXTRATERRESTRIAL ENVIRONMENTS
NT CHROMOSPHERE
NT CISLUNAR SPACE
NT DEEP SPACE
NT EARTH ORBITAL ENVIRONMENTS
NT INTERPLANETARY SPACE
NT INTERSTELLAR SPACE
NT JUPITER ATMOSPHERE
NT LUNAR ATMOSPHERE
NT LUNAR ENVIRONMENT
NT MARS ATMOSPHERE
NT MARS ENVIRONMENT
NT PLANETARY ATMOSPHERES
NT PLANETARY IONOSPHERES
NT PLANETARY MAGNETOSPHERES
NT SATELLITE ATMOSPHERES
NT SATURN ATMOSPHERE
NT SOLAR ATMOSPHERE
NT STELLAR ATMOSPHERES
NT VENUS ATMOSPHERE
NT VENUS CLOUDS
Publications of the Exobiology Program for 1988: A special bibliography
[NASA-TM-4169] 09 p1262 N90-17316
Laser intersatellite transmission experiment spatial acquisition, tracking, and pointing system
[AD-A215934] 10 p1389 N90-18036
Effects of thruster firings on the shuttle environment 1: Neutral gas composition
[AD-A224404] 24 p3487 N90-29707
Re-analysis of data on the space radiation environment above southeast Asia
[AD-A224155] 24 p3564 N90-30162

EXTRATERRESTRIAL INTELLIGENCE
The NASA SETI sky survey: Recent developments 04 p0488 N90-12804

EXTRATERRESTRIAL LIFE
Publications of the Exobiology Program for 1988: A special bibliography
[NASA-TM-4169] 09 p1262 N90-17316
Extraterrestrial life in the universe
[NASA-TM-102363] 15 p2181 N90-22464

EXTRATERRESTRIAL MATTER
NT COSMIC GASES
NT COSMIC PLASMA
NT DARK MATTER
NT INTERSTELLAR GAS
NT INTERSTELLAR MATTER
Skewering the universe with QSO lines of sight: Lyman alpha clouds as probes of large scale structure 16 p2329 N90-23278
Reconstructing primordial density fluctuations 16 p2333 N90-23293

EXTRATERRESTRIAL RADIATION
NT EXTRATERRESTRIAL RADIO WAVES
NT GALACTIC COSMIC RAYS
NT GALACTIC RADIATION
NT GAMMA RAY BURSTS
NT INTERSTELLAR RADIATION
NT PLANETARY RADIATION
NT RADIO BURSTS
NT SOLAR CORPUSCULAR RADIATION
NT SOLAR COSMIC RAYS
NT SOLAR NEUTRINOS
NT SOLAR NEUTRONS
NT SOLAR PROTONS
NT SOLAR RADIATION
NT SOLAR RADIO BURSTS
NT SOLAR RADIO EMISSION
NT SOLAR WIND
NT SOLAR X-RAYS
NT STELLAR RADIATION
NT STELLAR WINDS
NT SUNLIGHT
NT TYPE 3 BURSTS
NT ZODIACAL LIGHT
Radioactivity induced in gamma-ray spectrometers
[RAE-TM-SPACE-363] 04 p0569 N90-13317
Interzodiak 2: Observation of EUV-resonance radiation 05 p0660 N90-13854
A search for the effects of active magnetic fields in extra-galactic radio sources 05 p0712 N90-14161
Environmental constraints for polar platform design
[RAE-TR-89014] 09 p1181 N90-16849
Predicting switched-bias response from steady-state irradiations
[DE90-006770] 18 p2624 N90-24950
Program review: The lifetime effects of space radiation in rhesus monkeys
[AD-A221127] 19 p2716 N90-25454
Active star-forming galaxies in the X ray foreground 19 p2785 N90-25848
Properties of sources that may contribute the other half of the cosmic X ray background 19 p2788 N90-25866
Space radiation studies
[NASA-CR-183991] 19 p2798 N90-25925
The effects of space radiation on thin films of YBa2Cu3O(sub 7-x) 22 p3147 N90-27845
Comparison of dose estimates using the buildup-factor method and a Baryon transport code (BRYNTRN) with Monte Carlo results
[NASA-TP-3021] 23 p3414 N90-29290
Predictions of radiation backgrounds for GRO/OSSE
[RAE-TM-SPACE-372] 23 p3414 N90-29293
Re-analysis of data on the space radiation environment above southeast Asia
[AD-A224155] 24 p3564 N90-30162

EXTRATERRESTRIAL RADIO WAVES
NT RADIO BURSTS
NT SOLAR RADIO BURSTS
NT SOLAR RADIO EMISSION
NT TYPE 3 BURSTS
A search for radio pulsars in globular clusters and transient X ray sources 19 p2772 N90-25755

EXTRATERRESTRIAL RESOURCES
Report of NASA Lunar Energy Enterprise Case Study Task Force
[NASA-TM-101652] 07 p1007 N90-15836
Report of the NASA lunar energy enterprise case study task force 07 p1008 N90-15837
Analysis of the financial factors governing the profitability of lunar helium-3 07 p1008 N90-15838
Lunar power system summary of studies for the lunar enterprise task force NASA-office of exploration 07 p1008 N90-15841
Transportation and operations aspects of space energy systems 07 p1008 N90-15842
Importance of helium-3 for the future 07 p1009 N90-15843

EXTRATERRESTRIAL ROVING VEHICLES
U ROVING VEHICLES

EXTRAVEHICULAR ACTIVITY
Independent Orbiter Assessment (IOA): Analysis of the extravehicular mobility unit
[NASA-CR-185540] 02 p0166 N90-10937
Independent Orbiter Assessment (IOA): Analysis of the crew equipment subsystem
[NASA-CR-185591] 02 p0170 N90-10958
Independent Orbiter Assessment (IOA): Assessment of the crew equipment subsystem
[NASA-CR-185577] 02 p0173 N90-10971
Extravehicular activity welding experiment
[NASA-CR-183848] 06 p0791 N90-14608
EVA space suit. General concepts of design and arrangement 08 p1034 N90-15976
ESA's space transportation programme 09 p1173 N90-16786
Suitport extra-vehicular access facility
[NASA-CASE-ARC-11635-1] 09 p1183 N90-16860
Working on the moon: The Apollo experience
[DE90-003662] 12 p1697 N90-19744
Vision science and technology for supervised intelligent space robots 15 p2139 N90-22221
Second European In-Orbit Operations Technology Symposium
[ESA-SP-297] 18 p2499 N90-24280
Toward the development of COSMO-LAB 18 p2500 N90-24281
On-orbit operations of the Space Station Freedom attached payloads accommodations equipment 18 p2500 N90-24283
Operations considerations in Space Station Freedom assembly 18 p2500 N90-24284
In-orbit operations research and development program of the Toulouse Space Center 18 p2501 N90-24290
The SPIDER robotic system 18 p2501 N90-24291
Flight support system servicing aid tool 18 p2501 N90-24293
Evolution of EVA capabilities for space station construction and maintenance: Soviet and American experience 18 p2502 N90-24295
The European EVA suit: An optimized tool for Hermes/MTFF in-orbit operations 18 p2502 N90-24296
Telerobotic application to EVA 18 p2502 N90-24298
Fourth European Space Mechanisms and Tribology Symposium
[ESA-SP-299] 18 p2535 N90-24462
Mechanisms to assemble space structures in extravehicular environment 18 p2538 N90-24480
The European EVA spacesuit mechanisms 18 p2538 N90-24481
EVA power tool prototype 18 p2538 N90-24482
Electrical connector for operation in space 18 p2541 N90-24507
The use of underwater dynamometry to evaluate two space suits 18 p2632 N90-24995
A direct-interface, fusible heat sink for astronaut cooling
[NASA-TM-102835] 19 p2689 N90-25292
Smart hands for the EVA retriever 19 p2736 N90-25550
Technology for an intelligent, free-flying robot for crew and equipment retrieval in space 19 p2738 N90-25564
Design of a lunar transportation system, volume 2
[NASA-CR-186833-VOL-2] 20 p2871 N90-26333
The challenge of assembling a space station in orbit 22 p3130 N90-27763
In-space construction and dynamics of large space structures 22 p3130 N90-27764
The astronaut and the banana peel: An EVA retriever scenario 24 p3519 N90-29897
Preliminary hazard analysis in design application to EVA space suit
[ETN-90-97585] 24 p3523 N90-29918

EXTRAVEHICULAR MOBILITY UNITS
Independent Orbiter Assessment (IOA): Analysis of the extravehicular mobility unit
[NASA-CR-185540] 02 p0166 N90-10937
Independent Orbiter Assessment (IOA): Assessment of the extravehicular mobility unit, volume 1
[NASA-CR-185536-VOL-1] 02 p0169 N90-10950
Independent Orbiter Assessment (IOA): Assessment of the extravehicular mobility unit, volume 2
[NASA-CR-185536-VOL-2] 02 p0169 N90-10951
Independent Orbiter Assessment (IOA): CIL issues resolution report, volume 2
[NASA-CR-185524-VOL-2] 02 p0170 N90-10955

EVA space suit. General concepts of design and arrangement 08 p1034 N90-15978
EXTREMA
U RANGE (EXTREMES)
EXTREME ULTRAVIOLET EXPLORER SATELLITE
True covariance simulation of the EUVE update filter 05 p0589 N90-13427
Feasibility of using Extreme Ultraviolet Explorer (EUVE) reaction wheels to satisfy Space Infrared Telescope Facility (SIRTF) maneuver requirements
[NASA-TM-100389] 12 p1663 N90-19556
EXTREME ULTRAVIOLET RADIATION
A solar extreme ultraviolet flux model 02 p0296 N90-11686
Investigation of atmospheric emissions in ultraviolet, vacuum ultraviolet, and extreme ultraviolet wavelength
[AD-A212169] 03 p0371 N90-12123
The SOHO mission. Scientific and technical aspects of the instruments
[ESA-SP-1104] 04 p0566 N90-13302
SUMER: Solar Ultraviolet Measurements of Emitted Radiation 04 p0567 N90-13307
CDS: The Coronal Diagnostic Spectrometer 04 p0567 N90-13308
EIT: Solar corona synoptic observations from SOHO with an Extreme-ultraviolet Imaging Telescope 04 p0567 N90-13309
Proof-of-principle experiment for a hot electron pumped XUV amplifier
[DE90-000820] 06 p0787 N90-14586
The ratio of neutral hydrogen to neutral helium in the local interstellar medium 15 p2189 N90-22499
The EUV spectral shape of the big-bump in HS1700+6416 and F9: A genuine difference between Seyfert's and QSO's 19 p2789 N90-25878
EXTREMELY HIGH FREQUENCIES
Effects of rain attenuation on satellite EHF (Extremely High Frequency) communications in the US
[AD-A210517] 01 p0057 N90-10325
Ka-band MMIC beam steered transmitter array 04 p0488 N90-12803
A real-time signal combining system for Ka-band feed arrays using maximum-likelihood weight estimates 15 p2076 N90-21888
EHF heterojunction bipolar transistors
[AD-A220984] 18 p2548 N90-24541
UBVRI-photopolarimetry and the X ray dips of V471 Tau 19 p2775 N90-25781
Optical emission from the high inclination X ray transient EXO 0748-676 19 p2779 N90-25809
Design and performance analysis of the DSS-13 beam waveguide antenna 20 p2853 N90-26225
EXTREMELY LOW FREQUENCIES
ELF (Extremely Low Frequency) Communications System Ecological Monitoring Program: Electromagnetic field measurements and engineering support, 1988
[AD-A210200] 01 p0056 N90-10321
MTX (Microwave Tokamak Experiment)/ELF (Electron Laser Facility) 2 microwave power measurements and calibration for the 2-GW, 140-GHz, ELF 2 Free Electron Laser (FEL)
[DE90-000825] 06 p0846 N90-14922
Introduction to extremely-low-frequency electric and magnetic fields
[DE90-002662] 07 p0966 N90-15578
ELF (Extremely Low Frequency) communications system ecological monitoring program: Summary of 1988 progress
[AD-A216153] 10 p1377 N90-17981
ELF (Extremely Low Frequency) communications system ecological monitoring program: Slime mold studies
[AD-A218623] 16 p2229 N90-22715
ELF (Extremely Low Frequency) communications systems ecological monitoring program: Wetland studies
[AD-A218632] 16 p2229 N90-22716
Exposure of human cells to electromagnetic fields
[AD-A219377] 16 p2261 N90-22889
Microspacecraft and Earth observation: Electrical field (ELF) measurement project
[NASA-CR-186621] 20 p2886 N90-26436
Lightweight EHF communications satellites 21 p3070 N90-27453
Tactical EHF satellite communications for NATO employing non-geostationary orbits 21 p3070 N90-27454
EXTREMELY LOW RADIO FREQUENCIES
HIPAS 1987-88: ULF research and campaign support
[AD-A211720] 03 p0339 N90-11933
ULF/VLF ocean bottom seismo-acoustics
[AD-A218810] 17 p2429 N90-23843
EXTREMUM VALUES
NT LIMITS (MATHEMATICS)
NT MAXIMA
NT MINIMA
On the extremum electric charge problem of steady electromagnetic equilibria
[TRITA-EPP-89-04] 04 p0489 N90-12809
EXTRUDING
NT PULTRUSION
Deformation of Ti-6Al-4V bar and extrusion under superplastic forming conditions
[RAE-TM-MAT/STR-1110] 03 p0330 N90-11875
Deformation of extruded titanium alloys under superplastic conditions
[RAE-TM-MAT/STR-1111] 03 p0330 N90-11876
Process for producing a shaped, extruded product from a crosslinkable polymeric composition
[GB-PATENT-2-201-677-A] 05 p0627 N90-13662
Fabrication of superconductor coils
[DE90-003571] 07 p0922 N90-15338
Micromechanics of an extrusion in high-cycle fatigue with creep
[AD-A213509] 07 p0947 N90-15485
Extrusion of alumina-silicon carbide whisker composites
[DE90-004379] 09 p1186 N90-16869
Deformation and fracture of TiAl + W at elevated temperatures
[DE90-006490] 12 p1628 N90-19356
Novel processing of HTS based conductors
[DE90-005956] 12 p1722 N90-19892
Microstructure and mechanical properties of nickel aluminide powders consolidated by extrusion and hot isostatic pressing
[DE90-009777] 15 p2070 N90-21855
Investigation of metal processing technology
[AD-A218835] 17 p2376 N90-23531
RF surface resistance measurements in the Pb-Bi-Sr-Ca-Cu-O system
[DE90-010412] 18 p2621 N90-24932
Fabrication of intermetallic compounds by solid state reaction of roll-bonded materials
[AD-A221960] 21 p2982 N90-26943
EYE (ANATOMY)
NT CORNEA
NT FOVEA
NT RETINA
Development of a performance-based test of gaze capability: A threshold approach
[AD-A214675] 09 p1259 N90-17301
Attenuating the luminous output of the AN/PVS-5A night vision goggles and its effects on visual acuity
[AD-A214895] 09 p1261 N90-17311
Safety evaluation of infrared lamp power output for oculometer eye/head tracker system
[AD-A215809] 10 p1411 N90-18138
Computing with neural maps: Application to perceptual and cognitive functions
[AD-A216689] 10 p1412 N90-18143
Visual processing of object velocity and acceleration
[AD-A216509] 11 p1539 N90-18858
Biological applications and effects of optical masers
[AD-A217910] 13 p1808 N90-20385
Sampling and noise in vision networks 15 p2138 N90-22217
DURIP-Instrumentation for recording and analyzing multiple input/output saccadic eye movement neurosensory control
[AD-A219905] 17 p2435 N90-23871
Effect of laser glare and aircraft windscreen on visual search performance under low ambient lighting
[AD-A219456] 17 p2437 N90-23888
DURIP: Improved eye movement monitoring capabilities for studies in visual cognition
[AD-A220355] 18 p2586 N90-24722
Nonlinear optical protection against frequency agile lasers
[AD-D014535] 19 p2695 N90-25335
The interaction of chromostereopsis and stereopsis in stereoscopic CRT (Cathode Ray Tubes) displays
[AD-A217906] 23 p3277 N90-28544
EYE MOVEMENTS
NT NYSTAGMUS
NT SACCADIC EYE MOVEMENTS
NT VESTIBULAR NYSTAGMUS
Effects of miniature CRT (Cathode Ray Tube) location upon primary and secondary task performances
[AD-A210223] 01 p0101 N90-10573
Eye movements and spatial pattern vision
[AD-A211650] 03 p0381 N90-12169
Safety evaluation of infrared lamp power output for oculometer eye/head tracker system
[AD-A215809] 10 p1411 N90-18138
Psychological studies of visual cortical function
[AD-A217029] 11 p1541 N90-18872
Visual selective attention
[AD-A219204], 16 p2265 N90-22910
Voluntary presetting of the vestibular ocular reflex permits gaze stabilization despite perturbation of fast head movements 16 p2274 N90-22960
DURIP: Improved eye movement monitoring capabilities for studies in visual cognition
[AD-A220355] 18 p2586 N90-24722
Eye tracking device for the measurement of flight performance in simulators
[AD-A220075] 20 p2898 N90-26484
EYE PROTECTION
Eye/sensor protection against laser irradiation organic nonlinear optical materials
[AD-A210599] 01 p0093 N90-10531
The Si(1-x)Nx Rugate
[AD-A211236] 02 p0275 N90-11572
A review of laser filter materials
[AD-A213134] 05 p0648 N90-13776
Analysis and evaluation of technical data on the photochromic and non-linear optical properties of materials. Appendix: Eye/sensor protection by an optical fuse mirror at a focal plane: Feasibility assessment
[AD-A214051] 07 p0896 N90-15177
Analysis and evaluation of technical data on the photochromic and non-linear optical properties of materials
[AD-A214212] 07 p0896 N90-15178
Analysis and evaluation of technical data on the photochromic and non-linear optical properties of materials
[AD-A214050] 08 p1041 N90-16014
Analysis and evaluation of technical data on the photochromic and non-linear optical properties of materials
[AD-A216124] 10 p1431 N90-18254
Analysis and evaluation of technical data on the photochromic and non-linear optical properties of materials
[AD-A219398] 16 p2318 N90-23219
Laser eye protection
[AD-A219659] 17 p2408 N90-23722
Model for predicting the effects of laser exposures and eye protection on vision
[AD-A219697] 17 p2434 N90-23868
Dazzling glare: Protection criteria versus visual performance
[AD-A219676] 17 p2438 N90-23889
Field evaluation of laser protective eyewear
[AD-A221324] 18 p2586 N90-24725
Characterization of a Ho:Tm:Cr:YAG laser with a Cr:GSAG laser as pumping source 18 p2642 N90-25047
Nonlinear optical protection against frequency agile lasers
[AD-D014535] 19 p2695 N90-25335
A note on the statistics of laser speckle
[AD-A222408] 21 p3009 N90-27103
EYEPIECES
Prescribing spectacles for aviators
[AD-A214830] 09 p1260 N90-17310

F

F CENTERS
U COLOR CENTERS
F DISPLAYS
U F REGION
F LAYER
U F REGION
F REGION
NT F 2 REGION
Simulation of the polar cap F region ionization using an experimental convection electric field 02 p0241 N90-11370
Medium scale structure of the F-region 02 p0241 N90-11372
Polar F layer lacuna irregularities at Dumont d'Urville 02 p0243 N90-11379
Seasonal and geomagnetic response of the thermosphere and ionosphere 02 p0243 N90-11380
Quiet time conductivities of the auroral ionosphere 02 p0244 N90-11383
Auroral and sub-auroral F-layer irregularity studies in the Northern and Southern Hemisphere during the equinox transition study September 16-26, 1984 02 p0246 N90-11393
Examples of meteorological behavior of the ionosphere 02 p0246 N90-11395
Multistation/multiparameter observations with a network of digital ionosondes 02 p0247 N90-11396
Coordinated multi-parameter measurements and predictions of the global-scale ionosphere 02 p0247 N90-11397
An ionospheric model for HF sky-wave backscatter radar 02 p0247 N90-11401
Ionospheric total electron content, and far ultraviolet, near infrared oxygen emission 02 p0249 N90-11410

Role of chemical effects in daytime high latitude trough formation
[AD-A211772] 04 p0518 N90-12989
Auroral and sub-auroral interaction at the F region ionosphere
[AD-A213284] 05 p0666 N90-13896
Scientific investigations of the Space Research Group
[ISBN-0-642-13252-6] 08 p1138 N90-16595
Low latitude F-region dynamical processes from atomic oxygen nightglow emissions
[INPE-4999-PRE/1561] 14 p2006 N90-21494
Plasma instabilities associated with the injection of artificial ion beams into the ionosphere
16 p2254 N90-22851
An analytic/empirical model of the middle and low latitude ionosphere
[AD-A220004] 17 p2423 N90-23809
Evaluation of space plasma data: Effects upon spacecraft materials and predictions of hazardous conditions; polar ARCS
[AD-A219509] 17 p2474 N90-24145
Observations of plasma structure freezing scale at equatorial latitudes
[AD-A222529] 21 p3026 N90-27207
Influence of non-stationary field of magnetospheric convection on the D-region 22 p3210 N90-28209
Investigation of structure and transport processes in the high latitude ionospheric plasma using ground based and airborne digisondes
[AD-A224397] 24 p3491 N90-29727

F STARS
FGK stars and T Tauri stars: Monograph series on nonthermal phenomena in stellar atmospheres
[NASA-SP-502] 10 p1446 N90-18344

F 2 REGION
North-south tropical F2 layer asymmetry at west AFrican and Pacific longitudes 02 p0247 N90-11398
Radio propagation conditions forecast above a low latitude region 02 p0247 N90-11400

F-4 AIRCRAFT
Cost effectiveness of composite materials on the F-15 and F-16 aircrafts
[AD-A216353] 10 p1320 N90-17631

F-8 AIRCRAFT
A comparison of time-optimal interception trajectories for the F-8 and F-15
[NASA-CR-186300] 15 p2050 N90-21753

F-110 AIRCRAFT
U F-4 AIRCRAFT

F-14 AIRCRAFT
F-14 VSTFE and results of the cleanup flight test program 04 p0445 N90-12547
Flutter clearance of the F-14A variable-sweep transition flight experiment airplane, phase 2
[NASA-TM-101717] 19 p2659 N90-25135

F-15 AIRCRAFT
Nonlinear maneuver autopilot for the F-15 aircraft
[NASA-CR-179442] 02 p0262 N90-11487
Cost effectiveness of composite materials on the F-15 and F-16 aircrafts
[AD-A216353] 10 p1320 N90-17631
A comparison of time-optimal interception trajectories for the F-8 and F-15
[NASA-CR-186300] 15 p2050 N90-21753
Dynamic ground-effect measurements on the F-15 STOL and Maneuver Technology Demonstrator (S/MTD) configuration
[NASA-TP-3000] 16 p2195 N90-22531
Visual behavior in the F-15 simulator for air-to-air combat
[AD-A218648] 16 p2262 N90-22893
Flight-testing of the self-repairing flight control system using the F-15 highly integrated digital electronic control flight research facility
[NASA-TM-101725] 19 p2661 N90-25144
Success in tutoring electronic troubleshooting
19 p2739 N90-25568
Effect of tail size reductions on longitudinal aerodynamic characteristics of a three surface F-15 model with nonaxisymmetric nozzles
[NASA-TP-3036] 20 p2802 N90-25938
Application of multifunction inertial reference systems to fighter aircraft 24 p3423 N90-29341
Integrated navigation/flight control for future high performance aircraft 24 p3427 N90-29362

F-16 AIRCRAFT
Terrain-aided navigation and target acquisition on the AFTI/F-16 09 p1166 N90-16747
Cost effectiveness of composite materials on the F-15 and F-16 aircrafts
[AD-A216353] 10 p1320 N90-17631
Stability characteristics of a combat aircraft with control surface failure
[AD-A216196] 10 p1323 N90-17648

F-17 AIRCRAFT
An experimental investigation of support strut interference on a three-percent fighter model at high angles of attack
[AD-A219793] 17 p2345 N90-23353

F-18 AIRCRAFT
Definition and reduction of the F-18 windshield birdstrike hazard
[AD-A210700] 01 p0004 N90-10015
CF 18 480 Gallon External Fuel Tank Stores Clearance Program 02 p0153 N90-10877
Flutter clearance of the F-18 high-angle-of-attack research vehicle with experimental wingtip instrumentation pods
[NASA-TM-4148] 03 p0305 N90-11732
Flow visualization of the effect of pitch rate on the vortex development on the scale model of a F-18 fighter aircraft
[AD-A214244] 07 p0876 N90-15080
Water-tunnel study results of a TF/A-18 and F/A-18 canopy flow visualization
[NASA-TM-101705] 16 p2195 N90-22532
Fighter agility metrics, research, and test
[NASA-CR-186118] 17 p2351 N90-23386
Application of neural networks to the F/A-18 engine condition monitoring system
[AD-A219820] 18 p2497 N90-24271
Predicting F/A-18 fleet replacement squadron performance using an automated battery of performance-based tests
[AD-A223899] 23 p3277 N90-28543
A knowledge-based system design/information tool
[NASA-CR-4316] 23 p3389 N90-29143

F-86 AIRCRAFT
Scientific justification and development plan for a mid-sized jet research aircraft
[PB89-208995] 03 p0305 N90-11731

F-104 AIRCRAFT
Airdata calibration of a high-performance aircraft for measuring atmospheric wind profiles
[NASA-TM-101714] 06 p0725 N90-14228
Sonic boom signature data from cruciform microphone array experiments during the 1966-1967 EAFB national sonic boom evaluation program
[NASA-CR-182027] 14 p2024 N90-21605

F-111 AIRCRAFT
Development of a graphite/bismaleimide leading edge for the F-111 (EF-111A) horizontal stabilizer
21 p2956 N90-26809

FAB (PROGRAMMING LANGUAGE)
U FORTRAN

FABRICATION
NT SPACE MANUFACTURING
PMR graphite engine duct development
[NASA-CR-182228] 01 p0008 N90-10037
The effects of normal annealing cycles during IGFET fabrication on initial and radiation induced gate insulator defects
[AD-A210282] 01 p0049 N90-10278
Preparation and evaluation of composite membranes for zinc/bromine storage batteries
[DE89-009931] 01 p0059 N90-10339
Thin film thermocouples for high temperature measurement
[PB89-209290] 01 p0073 N90-10420
High-efficiency CuInSe2 and CuInGaSe2 based cells and materials research
[DE89-009449] 01 p0083 N90-10471
Alternative fabrication techniques for high-efficiency CuInSe2 and CuInSe2-alloy films and cells
[DE89-009451] 01 p0083 N90-10474
Second-order nonlinear optical devices in poled polymers
[DE89-015842] 01 p0123 N90-10703
Ceramic processing of bulk high-T(sub c) superconductors
[DE89-015703] 01 p0128 N90-10736
CuInSe2 solar cell research by sputter deposition
[DE89-009450] 02 p0236 N90-11345
Novel thin-film CuInSe2 fabrication
[DE89-009440] 02 p0281 N90-11604
Manufacturing and the manufacturing engineer in the year 2000, revision
[DE89-017707] 03 p0335 N90-11904
High gain flux compression generator fabrication issues
[DE89-017888] 03 p0342 N90-11951
Design of scientific payloads and components
[AD-A211819] 03 p0351 N90-12005
Fabrication of modulated vanes for a split-coaxial RFQ
[DE88-757235] 03 p0403 N90-12310
Beam assisted fabrication of 3-5/Si monolithic devices
[AD-A212046] 03 p0412 N90-12367
Scaling of an 85 GHz gyrotron to operate at 94 GHz
[AD-A212756] 04 p0504 N90-12909
Optical clock distribution to VLSI chips
[AD-A212269] 04 p0560 N90-13264
Activities report of the metallic manufacturing industry
[ISSN-0524-7705] 05 p0625 N90-13649
Development and characterization of PdCr temperature-compensated wire resistance strain gage
[NASA-CR-185153] 05 p0644 N90-13761
Computer-aided fabrication system implementation
[AD-A213005] 05 p0682 N90-13969
Sol-gel processing science using a Sol-Gel Optics Research Facility (SGORF)
[AD-A213056] 05 p0699 N90-14095
Retrieving and integrating IC fabrication data from dissimilar databases
[AD-A211890] 05 p0707 N90-14140
Sandia Satellite Program summary of operational procedures
[DE90-000892] 06 p0728 N90-14249
Designing for superplastic alloys
06 p0744 N90-14332
An electroformed nickel-sulfur alloy for a nose cone
[DE90-000866] 06 p0745 N90-14337
Automated glass fiber drawing
[DE90-000894] 06 p0751 N90-14367
Integrating and enhancing tools for ASIC (Application-Specific Integrated Circuits) design using MOSIS (Metal Oxide Semiconductor Implementation Service) fabrication
[DE90-001601] 06 p0769 N90-14475
Practical superconductor development for electrical power applications
[DE90-001804] 06 p0771 N90-14487
Method for fabricating thin film metallic meshes for use as Fabry-Perot interferometer elements, filters and other devices
[AD-D014236] 06 p0779 N90-14529
Results of the 1989 NASA/JPL balloon flight solar cell calibration program
[NASA-CR-186114] 06 p0803 N90-14672
Technology development program for an advanced microsheet glass concentrator
[NASA-TM-102406] 06 p0804 N90-14678
Photovoltaic Measurements and Performance Branch
[DE89-009500] 06 p0807 N90-14695
Design and calibration of an in-stack, low-pressure impactor
[AD-A213531] 07 p0882 N90-15105
Al-Li alloy developed by Pechiney
07 p0897 N90-15186
Fabrication of test-articles from Al-Li 2091 for Fokker 100 07 p0899 N90-15196
Fabrication characteristics of 8090 alloy
07 p0899 N90-15198
Aluminum-lithium: Application of plate and sheet to fighter aircraft 07 p0900 N90-15202
High performance powder metallurgy aluminum alloys: An overview 07 p0900 N90-15204
Short fibre and particulate reinforced metal matrix composites 07 p0901 N90-15207
Superconducting film fabrication by the sol-gel process
[DE90-002069] 07 p0909 N90-15252
Fabrication of superconductor coils
[DE90-003571] 07 p0922 N90-15338
Design of a custom load cell for a precision assembly application
[DE90-004439] 07 p0923 N90-15340
Advanced double layer capacitor
[AD-A213406] 07 p0923 N90-15341
Laser-material interactions
[AD-A214421] 07 p0937 N90-15425
Development of the RAIDS (Remote Atmospheric and Ionospheric Detector System) extreme ultraviolet wedge and strip detector
[AD-A213730] 07 p0949 N90-15495
Research on amorphous silicon-germanium alloys for tandem solar cells
[DE89-009436] 07 p0950 N90-15499
Research on high-efficiency, single-junction, monolithic, thin-film amorphous silicon solar cells, phase 2
[DE89-009496] 07 p0951 N90-15503
High-efficiency silicon concentrator solar cells for use with prismatic covers
[DE90-002644] 07 p0952 N90-15509
Characterization of new cathode materials for molten carbonate fuel cells
[DE90-003547] 07 p0953 N90-15516
Fabrication of porous ceramic electrode structures
[DE90-003548] 07 p0953 N90-15517
Characteristics of CMOS analog integrated structures using MOSIS (Metal Oxide Semiconductor Implementation System)
[DE90-001630] 07 p0998 N90-15773
Thermally stable metal/GaAs contacts
[DE90-002122] 07 p0998 N90-15774

Processing and fabrication of YBa2Cu4O8 and YBa2Cu4O8/YBa2Cu3O(x) composites
[DE90-003559] 07 p1001 N90-15789
Computer-controlled ion beam sputter-deposition of superconducting oxide films
[AD-A213921] 07 p1004 N90-15812
High-temperature ceramic superconductors
[AD-A214251] 07 p1005 N90-15818
The fabrication of YBa2Cu3O7 thin films by thermal coevaporation in oxygen
[DE90-003960] 07 p1006 N90-15824
Materials and techniques for model construction 08 p1030 N90-15954
Some recent developments in materials and techniques for model fabrication 08 p1031 N90-15955
Models for cryogenic wind tunnels 08 p1031 N90-15956
Experience with strain-gage balances for cryogenic wind tunnels 08 p1031 N90-15958
Cryogenic balances for the US NTF 08 p1031 N90-15959
Performance of an Inductively Coupled Plasma-Mass Spectrometer Analyzer system
[DE90-004002] 08 p1043 N90-16025
Synthesis of air-sinterable lanthanum chromite powders
[DE90-004681] 08 p1046 N90-16049
Porous ceramic bodies
[AD-D014277] 08 p1049 N90-16061
Artificially structured superconductors
[DE90-004851] 08 p1134 N90-16567
Sealing L-alloys/FeS(x) cells for a bipolar battery
[DE90-004887] 09 p1214 N90-17040
Heat pipes for wing leading edges of hypersonic vehicles
[NASA-CR-181922] 09 p1216 N90-17055
Light-trapping concentrator cells
[DE90-004988] 09 p1242 N90-17205
Research on amorphous silicon based thin film photovoltaic devices. Phase 2: Research on stable high-efficiency, large area amorphous silicon based submodules
[DE89-009515] 09 p1243 N90-17209
Computer-aided fabrication of integrated circuits
[AD-A215439] 09 p1268 N90-17352
Fabrication of nanometer single crystal metallic CoSi2 structures on Si
[NASA-CASE-NPO-17736-1-CU] 09 p1286 N90-17455
Optical waveguide fabrication by stoichiometric implantation of Ti and O into LiNbO3
[DE90-004238] 09 p1292 N90-17488
HF wire antennas over real ground: Computer simulation and measurement 10 p1370 N90-17937
Characterization and development report for the SA3124, a 15-volt zener diode
[DE90-005711] 10 p1379 N90-17993
Process development and fabrication of space station type aluminum-clad graphite epoxy struts
[NASA-CR-181873] 11 p1468 N90-18454
Electronically Variable Pressure Regulator (EVPR) 11 p1474 N90-18484
Small displacement, long life on-orbit compressor design and fabrication 11 p1475 N90-18489
A statistical evaluation of the variation in laminated composite properties resulting from ply misalignment
[DE90-006371] 11 p1481 N90-18525
Hydrogenated amorphous silicon films prepared by glow discharge of disilane
[DE90-000309] 11 p1491 N90-18581
Performance and modeling of superconducting ring resonators at millimeter-wave frequencies
[NASA-TM-102526] 11 p1500 N90-18634
Cost and energy consumption estimates for the aluminum-air battery anode fuel cycle
[DE90-005810] 11 p1503 N90-18656
Unfurlable, continuous-surface reflector concept 12 p1609 N90-19257
Silicon carbide semiconductor device fabrication and characterization
[NASA-CR-186354] 12 p1719 N90-19873
Development and fabrication of structural components for a scramjet engine
[NASA-CR-181945] 13 p1757 N90-20088
Simple reflection holography
[DE90-008309] 13 p1805 N90-20359
An applicational process for dynamic balancing of turbomachinery shafting
[NASA-TM-102537] 13 p1810 N90-20392
Monolithic solid oxide fuel cell development 13 p1822 N90-20460
The electrochemical generation of useful chemical species from lunar materials 13 p1822 N90-20461
CCST (Center for Compound Semiconductor Technology) research briefs
[DE90-007782] 13 p1895 N90-20874
Reinforcement-matrix interface effects in metal matrix composites
[MRL-TN-562] 14 p1943 N90-21120
The investigation of multilayer x ray reflectors as x ray optical elements
[DE90-009044] 14 p2026 N90-21621
Toughened YBa2Cu3O(sub x)/ZrO2 composites
[DE90-007796] 14 p2031 N90-21645
Contract crystal growth and fabrication services
[AD-A218327] 14 p2031 N90-21646
Shock compression of solids: A tutorial
[DE90-009185] 14 p2032 N90-21659
Advanced manufacturing technology: A Department of Energy technology transfer initiative
[DE90-008601] 14 p2037 N90-21688
Studies on the use of supercritical ammonia for ceramic nitride synthesis and fabrication
[NASA-TM-102570] 15 p2068 N90-21843
Development of the methods and means of precise forming and geometry control of superconducting current-carrying element for the UNR pulsed dipoles
[DE90-620108] 15 p2173 N90-22419
Pultrusion process development for long space boom model
[NASA-TM-4017] 16 p2214 N90-22628
Miniature traveling wave tube and method of making
[NASA-CASE-LEW-14520-1] 16 p2230 N90-22724
Axisymmetric and cylindrically orthotropic analysis of filament winding 16 p2248 N90-22811
Solar Concentrator Advanced Development Program
[NASA-CR-185173] 16 p2250 N90-22834
Composite curing: A new process
[REPT-892-430-114] 17 p2370 N90-23490
Multi-element spherical shell generation
[NASA-CASE-NPO-17203-1-CU] 17 p2405 N90-23700
Using template/hotwire cutting to demonstrate moldless composite fabrication 18 p2515 N90-24361
Mechanical property characterization of fiber-reinforced SiC matrix composites
[DE90-011316] 18 p2520 N90-24390
Development and evaluation of advanced austenitic alloys
[DE90-011315] 18 p2528 N90-24425
Direct writing of microstructures for solid-state electronics
[AD-A220996] 18 p2535 N90-24460
The 30-GHz monolithic receive module
[NASA-CR-180849] 18 p2545 N90-24528
Gallium arsenide pilot line for high performance components
[AD-A220948] 18 p2547 N90-24540
Rapid thermal processing of high temperature superconducting fiber
[NASA-CR-186803] 18 p2626 N90-24964
The Stealth biplane: A proposal in response to a low Reynolds Number station keeping mission
[NASA-CR-186680] 19 p2658 N90-25127
High-temperature test facility at the NASA Lewis engine components research laboratory
[NASA-TM-103143] 19 p2662 N90-25151
Fabricating vanadium sheet to improve symmetry of drawn parts
[DE90-011253] 19 p2682 N90-25257
Fabrication of low frequency structureborne vibration isolation mount
[AD-D014532] 19 p2697 N90-25348
The effects of different diffusion sources on silicon solar cell recombination properties
[DE90-011235] 19 p2710 N90-25426
Research on design and fabrication of high-efficiency solar cells
[DE90-012010] 19 p2711 N90-25429
Sol-gel processing for fiber optic applications
[DE90-012083] 19 p2758 N90-25675
A resistance strain gage with repeatable and cancellable apparent strain for use to 800 C
[NASA-CR-185256] 20 p2823 N90-26063
Carbon-carbon composites: Emerging materials for hypersonic flight
[NASA-TM-103472] 20 p2827 N90-26080
Advanced Turbine Technology Applications Project (ATTAP)
[NASA-CR-185240] 20 p2939 N90-26728
A study on carbon Fiber (long fiber) reinforced copper matrix composite
[AD-A221584] 21 p2972 N90-26891
Fabrication of intermetallic compounds by solid state reaction of roll-bonded materials
[AD-A221960] 21 p2982 N90-26943
Metal chloride cathode for a battery
[NASA-CASE-NPO-17809-1-CU] 21 p2998 N90-27041
Development of a sealed bipolar Li-alloy/FeS2 battery for electric vehicles
[DE90-013650] 21 p2999 N90-27045
The preparation of ACEL thin films
[AD-A222919] 21 p2999 N90-27048
Polar coordinate laser writer for binary optics fabrication
[AD-A222827] 21 p3008 N90-27097
Design of GaAs charge coupled devices
[DE90-012124] 21 p3080 N90-27513
Oxide superconductors under magnetic field 22 p3139 N90-27807
Perspectives on high temperature superconducting electronics 22 p3139 N90-27810
Grain orientation studies in superconductors 22 p3148 N90-27852
Monolithic solid oxide fuel cell technology development, phase 1A
[PB90-183237] 22 p3195 N90-28132
Sandia's CONCEPT-90 photovoltaic concentrator module
[DE90-012243] 22 p3196 N90-28134
Optoelectronics Research Center
[AD-A221926] 22 p3246 N90-28410
Strengthening and toughening mechanisms in ceramic fiber-reinforced glass matrix composites 23 p3300 N90-28666
Fabrication of spherical pressure vessels from composite materials
[INPE-4598-RPE/570] 23 p3302 N90-28675
Zinc-bromine battery development
[DE90-014751] 23 p3321 N90-28781
High temperature superconducting thin film microwave circuits: Fabrication, characterization, and applications
[NASA-TM-103235] 23 p3322 N90-28786
A tandem system of ionization chambers for effective energy determination of unknown X-radiation fields
[DE90-630463] 24 p3436 N90-29405
Studies of surface heat transfer in an arc-heated wind tunnel
[NAL-TR-1048] 24 p3437 N90-29410
Two terminal CuInSe2 based cascade cells
[DE90-000363] 24 p3485 N90-29697
A review of manganin gauge technology for measurements in the gigapascal range
[MRL-TR-90-5] 24 p3541 N90-30026
Practical superconductor development for electrical power applications
[DE90-014836] 24 p3554 N90-30109

FABRICS
NT PARACHUTE FABRICS
NT WOOL
The interlaminar fracture toughness of woven graphite/epoxy composites
[NASA-TP-2950] 01 p0033 N90-10179
Thermoregulatory responses to intermittent exercise are influenced by knit structure of underwear
[AD-A209087] 01 p0095 N90-10541
Design of ceramic fabric heat pipe with water working fluid
[DE89-016565] 02 p0221 N90-11265
New Fabric Development Program
[AD-A211549] 03 p0332 N90-11891
The elastic properties of woven polymeric fabric
[DE89-015391] 07 p0909 N90-15255
The experimental evaluation and application of high-temperature solid lubricants
[NASA-TM-102476] 09 p1198 N90-16944
Some practical advice on cold weather clothing
[AD-A215936] 10 p1414 N90-18148
Instrumented impact testing of fabric-reinforced composite materials
[AD-A216764] 11 p1479 N90-18513
Development and application of nonflammable, high-temperature beta fibers
[NASA-TM-102158] 13 p1855 N90-20645
Collapsible fabric tank testing
[AD-A217861] 14 p1987 N90-21388
Testing carbon fabric for oxidation mass loss 15 p2063 N90-21819
High temperature insulation barrier composite
[NASA-CASE-MFS-29241-1] 17 p2368 N90-23480
Comparison of Goretex laminated and Dermoflex coated fabrics
[AD-A219383] 17 p2368 N90-23481
A preliminary design of interior structure and foundation of an inflatable lunar habitat 18 p2633 N90-24999
Lunar regolith bagging system
[NASA-CR-186652] 19 p2677 N90-25224
Sunlight diffusing tent for lunar worksite
[NASA-CR-186651] 19 p2677 N90-25225
X ray diffraction analysis of control and test fibers
[MTL-TR-89-58] 19 p2678 N90-25233
Device and method for detecting and displaying crossover pattern in precision winding
[AD-D014539] 19 p2685 N90-25276
Open hole and post-impact compression fatigue of stitched and unstitched carbon/epoxy composites
[NASA-TM-102676] 19 p2701 N90-25370

Hazards protection for space suits and spacecraft
[NASA-CASE-MSC-21366-1] 19 p2725 N90-25498
FABRY-PEROT INTERFEROMETERS
Use of depletion edge translation for high-speed modulation and switching of lightwaves
[AD-A211186] 01 p0124 N90-10713
An imaging vector magnetograph for the next solar maximum 03 p0435 N90-12489
Method for fabricating thin film metallic meshes for use as Fabry-Perot interferometer elements, filters and other devices
[AD-D014236] 06 p0779 N90-14529
High resolution Doppler lidar
[NASA-CR-183288] 06 p0781 N90-14542
Spatial imaging using confocal Fabry-Perot interferometers
[DE90-008363] 13 p1807 N90-20378
Design and status of the detector block for the ISO-SWS 14 p1980 N90-21341
Further development of the cryogenic Fabry-Perot interchange mechanism for ISO LWS 18 p2539 N90-24492
Optical techniques for determination of normal shock position in supersonic flows for aerospace applications
[NASA-TM-103201] 19 p2693 N90-25323
High power arcjet
[NASA-CR-183086] 23 p3298 N90-28658
FABRY-PEROT LASERS
U LASERS
FACE CENTERED CUBIC LATTICES
Energetics of BCC-FCC lattice deformation in iron
[AD-A213801] 07 p0905 N90-15233
Full vector wave calculation of photonic band structures in face-centered cubic dielectric media
[AD-A222616] 20 p2933 N90-26686
FACETS
U FLAT SURFACES
FACTOR ANALYSIS
A fan-in algorithm for distributed sparse numerical factorization
[AD-A211569] 04 p0529 N90-13054
The processes of scientific research: The strategy of experimentation 06 p0824 N90-14788
Factor analytic reduction of the carotid-cardiac baroreflex parameters 08 p1155 N90-16693
The effects of wearing passenger protective breathing equipment on evacuation times through type 3 and type 4 emergency aircraft exits in clear air and smoke. Phase 1: Evacuations in clear air. Phase 2: Evacuations in smoke
[AD-A216798] 11 p1453 N90-18374
Explicit modeling of composite plates and beams in the dynamics of multibody systems 16 p2285 N90-23019
FACTORIES
U INDUSTRIAL PLANTS
FACTORIZATION
A matrix factorization and its application to large-scale linear programming
[AD-A211293] 03 p0394 N90-12244
A fan-in algorithm for distributed sparse numerical factorization
[AD-A211569] 04 p0529 N90-13054
Local mode smoothing analysis of various incomplete factorization iterative methods in two dimensions
[REPT-89-36] 04 p0540 N90-13129
NUMVEC FORTRAN library manual chapter: Simultaneous linear equations
[CWI-NM-R8903] 04 p0541 N90-13135
Some remarks on the gap metric
[MEMO-COSOR-88-34] 05 p0690 N90-14029
A block QR factorization algorithm using restricted pivoting
[DE90-001921] 07 p0972 N90-15613
Asymptotically fast triangularization of matrices over rings
[DE90-003161] 08 p1117 N90-16471
Dynamic factorization in large-scale optimization
[AD-A214568] 10 p1416 N90-18161
Factoring symmetric indefinite matrices on high-performance architectures
[NASA-CR-181982] 10 p1421 N90-18195
Orbit determination of artificial Earth satellites through estmation techniques combined with state smoothing techniques
[INPE-4959-TDL/388] 11 p1465 N90-18440
Boolean minimization and algebraic factorization procedures for fully testable sequential machines
[AD-A216779] 11 p1553 N90-18940
Kreim factorization of covariance operators of 2-parameter random fields and application to the likelihood ratio
[MEMO-802] 11 p1555 N90-18953
Euler's theorem for polynomials
[AD-A218148] 13 p1878 N90-20774
UD filtering and smoothing applied to orbit determination
[INPE-4966-PRE/1535] 15 p2189 N90-22501
Spatial operator algebra framework for multibody system dynamics 16 p2279 N90-22989
A nearly-linear computational-cost scheme for the forward dynamics of an N-body pendulum 16 p2280 N90-22996
Efficient computer algebra algorithms for polynomial matrices in control design 16 p2285 N90-23022
An algorithm for the solution of dynamic linear programs 16 p2286 N90-23026
Factoring homomorphisms
[CS-8908] 16 p2299 N90-23096
A fast, preconditioned conjugate gradient Toeplitz solver
[NASA-CR-180367] 18 p2589 N90-24731
Finite element formulations for compressible flows 18 p2632 N90-24996
H-infinity control: An exploratory study
[EUT-88-E-211] 20 p2915 N90-26584
An adaptive blocking strategy for matrix factorizations
[DE90-011108] 21 p3051 N90-27343
A comparison of two central difference schemes for solving the Navier-Stokes equations
[NASA-TM-102815] 22 p3108 N90-27854
Implicit solution of three-dimensional internal turbulent flows
[NASA-TM-103099] 22 p3170 N90-27982
Factorization of the characteristic equation for three layer ducts
[AD-A223867] 23 p3354 N90-28956
FADDEEV EQUATIONS
Some exact solutions of the three-identical-particle problem with S-wave inverse square potentials
[DE89-618402] 02 p0267 N90-11524
FADING
NT SELECTIVE FADING
NT SIGNAL FADING
FAIL-SAFE SYSTEMS
Development of shape memory metal as the actuator of a fail safe mechanism 15 p2112 N90-22081
Model authoring system for fail safe analysis
[NASA-CR-4317] 23 p3389 N90-29142
Software design for high integrity systems
[ETN-90-97517] 24 p3530 N90-29966
FAILURE
NT ENGINE FAILURE
NT STRUCTURAL FAILURE
NT SYSTEM FAILURES
Optimal integral controller with sensor failure accommodation 01 p0024 N90-10123
Failure behavior of PEEK and its short-fiber composite systems
[AD-A210729] 01 p0035 N90-10189
Delayed failure of silver-aided diffusion welds between steel
[DE89-016652] 01 p0045 N90-10252
Limit analysis of welded tee end connections for hollow tubes
[PB89-191647] 01 p0079 N90-10452
Ductile failure
[AD-A212975] 05 p0618 N90-13601
Analytical derivation and verification of zero-gyro control for the IUE satellite
[NASA-TM-100748] 05 p0645 N90-13787
Electrical breakdown in vacuum
[DE90-001623] 06 p0771 N90-14485
Failure probability estimate of Type 304 stainless steel piping
[DE90-000659] 06 p0796 N90-14635
Display interface concepts for automated fault diagnosis
[NASA-TM-101610] 07 p0881 N90-15102
Using small scale tests to estimate the failure diameter of a propellant
[DE90-001166] 07 p0913 N90-15281
Damage evaluation from surface displacement data 07 p0944 N90-15469
Cryogenic engineering and materials 08 p1030 N90-15949
Natural icing re-evaluation of the EH-60A Quick Fix helicopter
[AD-A214728] 09 p1162 N90-16723
Implementing fault-tolerant sensors
[NASA-CR-186269] 09 p1225 N90-17105
Statistical theory of reliability
[AD-A215320] 09 p1234 N90-17161
Internal failures in model elastomeric composites
[AD-A215923] 10 p1348 N90-17818
A study of failure characteristics in thermoplastic composite laminates due to an eccentric circular discontinuity
[AD-A216226] 10 p1349 N90-17827
Development of a progressive failure model for strength of laminated composite structure
[AD-A216966] 11 p1480 N90-18517
Effect of temperature on the storage life of polysulfide aircraft sealants
[MRL-TR-89-31] 12 p1629 N90-19364
Residual stresses: A review of their measurement and interpretation using x ray diffraction
[AERE-R-13005] 13 p1815 N90-20423
Space Station Freedom integrated fault model 13 p1860 N90-20673
On the stability of amorphous silica coatings for high temperature service
[AERE-R-13425] 14 p1953 N90-21179
Double swivel toggle release
[NASA-CASE-MSC-21436-1] 14 p1987 N90-21390
Evaluation of a prototype lighted ball marker for powerline obstructions
[DOT/FAA/CT-TN90/12] 15 p2055 N90-21774
Dynamic response of a complex encapsulated electronic assembly subjected to a severe shock environment
[DE90-007689] 15 p2118 N90-22114
Continued research on the strain to failure of thick-walled cylinders subjected to internal pressure
[DE90-008952] 15 p2118 N90-22115
General purpose heat source radioisotope thermoelectric generator program. Book 1: Accident analysis
[REPT-90SDS4202-BK-1] 15 p2166 N90-22379
General purpose heat source radioisotope thermoelectric generator. Book 2: Accident analysis, appendices
[REPT-90SDS4202-BK-2] 15 p2166 N90-22380
Determination of joint drives for stable end-effector motion in flexible robotic systems 16 p2288 N90-23034
Evaluation of room-temperature chloroaluminate molten salts as electrolytes for high energy density batteries
[AD-A223097] 20 p2860 N90-26267
The response and failure mechanisms of circular metal and composite plates subjected to underwater shock loading
[AD-A222200] 21 p3013 N90-27131
A Protection And Detection Surface (PADS) for damage tolerance
[NASA-TP-3011] 22 p3135 N90-27788
DEPEND: A design environment for prediction and evaluation of system dependability
[NASA-CR-186890] 22 p3189 N90-28094
Nylon and teflon scribe effect on NBR to Chemlok 233 and NBR to NBR bond interfaces
[NASA-CR-184004] 22 p3189 N90-28095
Liquid Rocket Booster (LRB) for the Space Transportation System (STS) systems study. Appendix E: Pressure-fed booster test bed for the liquid rocket booster study
[NASA-CR-183791-APP-E] 23 p3289 N90-28805
Assessment and improvement of aeroengine disc structural integrity 24 p3433 N90-29392
Reliability study of TWT output RF window
[AD-A223688] 24 p3485 N90-29574
FAILURE ANALYSIS
Model 0A wind turbine generator FMEA
[NASA-TM-102378] 03 p0356 N90-12034
RAN (Royal Australian Navy) vibration analysis system operator's guide
[AD-A212441] 04 p0453 N90-12596
SSME structural dynamic model development
[NASA-CR-183671] 04 p0463 N90-12650
Numerical analysis of notch test damage to laminated composite plates submitted to uniaxial traction
[CETIM-107310] 04 p0467 N90-12675
The nature and control of skidding in lightly loaded intershaft bearings
[PNR90591] 04 p0508 N90-12933
Estimating the time to fatigue failure of mooring cables
[PB89-220677] 04 p0511 N90-12946
Thermal barrier coating life prediction model development, phase 1
[NASA-CR-182230] 05 p0581 N90-13388
Re-entry hazards and cosmos 1900
[FOA-C-30535-9.4] 05 p0613 N90-13583
Failure processes in unidirectional composite materials 05 p0617 N90-13598
Constant amplitude fatigue of ARALL-2 laminates
[LR-539] 05 p0620 N90-13615
An investigation of gear mesh failure prediction techniques
[NASA-TM-102340] 05 p0649 N90-13785
Fatigue resistance of pressure vessels in high strength steels effect of some improvement techniques
[CRIF-MT-176] 05 p0652 N90-13799
SRB thermal environments
[NASA-CR-183801] 06 p0734 N90-14276
Cavitation and superplasticity 06 p0744 N90-14329

Numerical and empirical verification of the stress state in a ceramic, button-head, tensile specimen
[DE90-001645] 06 p0752 N90-14375
A laboratory test for fuel injector deposit studies
[DE90-000602] 06 p0795 N90-14629
Evaluation of the improved OV-ID anti-icing system, phase 2
[AD-A213928] 07 p0877 N90-15083
Current launch vehicle reliability practice and data base assessment. Volume 1: Executive summary and report body
[AD-A2 3600] 07 p0885 N90-15121
A study of impact damage in composite laminates
07 p0888 N90-15137
Fatigue properties of SiC/Al composites
07 p0889 N90-15138
Composite activities at Lawrence Livermore National Laboratory
[DE90-002979] 07 p0891 N90-15149
Characterization and in situ testing of diamond films
[DE90-003155] 07 p0911 N90-15265
A paradigm for robust geometric algorithms
[AD-A214324] 07 p0978 N90-15647
Diesel starting system monitor: Prototype development
[DE90-004425] 08 p1084 N90-16276
Cyclic fatigue of hot-isostatic-pressed silicon nitride
[PB90-122649] 08 p1090 N90-16308
Rainflow counting algorithm for the LIFE2 fatigue analysis code
[DE90-002834] 08 p1096 N90-16344
Complex availability problems solved with simulation
[DE89-012610] 08 p1116 N90-16459
Analysis of damaged components from DOE security helicopter N7EG
[DE90-004488] 09 p1162 N90-16729
Failure analysis of a missile locking hook from the F-14 jet
[AD-A214995] 09 p1194 N90-16917
Magellan/Galileo solder joint failure analysis and recommendations
[NASA-CR-186294] 09 p1233 N90-17157
Analysis of composite ring of compression test data
[DE90-004468] 09 p1239 N90-17194
Analysis of the National Transonic Facility mishap
[NASA-TM-101686] 10 p1318 N90-17620
A study of the structural efficiency of fluted core graphite-epoxy panels
[NASA-TM-101681] 10 p1396 N90-18070
Discrete proportional Plus Integral (PI) multivariable control laws for the Control Reconfigurable Combat Aircraft (CRCA)
[AD-A215664] 11 p1484 N90-18431
SHARP: A multi-mission artificial intelligence system for spacecraft telemetry monitoring and diagnosis
[NASA-CR-186285] 11 p1467 N90-18444
Effect of correlation on multi-engine rocket propulsion systems 11 p1471 N90-18467
Probability of failure and risk assessment of propulsion structural components 11 p1471 N90-18470
Electronically Variable Pressure Regulator (EVPR)
11 p1474 N90-18484
Innovative design of composite structures: The use of curvilinear fiber format in structural design of composites
[NASA-CR-186406] 12 p1620 N90-19308
Time-dependent failure of silver-interlayer diffusion bonds between non-deforming base-metals
[DE90-006925] 12 p1628 N90-19357
Methods for trend analysis: Examples with problem/failure data 12 p1635 N90-19396
Evaluation of the heat transfer module (FAHT) of Failure Analysis Nonlinear Thermal And Structural Integrated Code (FANTASTIC) 12 p1637 N90-19407
Space Station Freedom electric power system availability study
[NASA-CR-185181] 13 p1763 N90-20120
innovative design of composite structures: The use of curvilinear fiber format in composite structure design
[NASA-CR-186453] 13 p1766 N90-20136
Fundamental aspects of and failure modes in high-temperature composites
[NASA-TM-102558] 13 p1769 N90-20151
Tellurium embrittlement of type 316 steel
[AERE-R-13440] 13 p1776 N90-20192
Pyrotechnic device technology
[DE90-007683] 13 p1783 N90-20234
A guide to performing and documenting safety analyses
[DE90-008688] 13 p1788 N90-20261
Product assurance technology for procuring reliable, radiation-hard, custom LSI/VLSI electronics
[NASA-CR-185954] 13 p1791 N90-20281
Time-dependent failure of silver interlayer welds
[DE90-008015] 13 p1818 N90-20440
KOH concentration effect on the cycle life of nickel-hydrogen cells. Part 4: Results of failure analyses
13 p1824 N90-20475
GCS plan for software aspects of certification
[NASA-CR-181972] 13 p1864 N90-20694
Using formal methods to develop a paradigm for software design
[DE90-005633] 13 p1866 N90-20703
Effect of KOH concentration on LEO cycle life of IPV nickel-hydrogen flight battery cells
[NASA-TM-103127] 14 p1942 N90-21116
Characterization of failure processes in tungsten copper composites under fatigue loading conditions
[NASA-TM-102371] 14 p1943 N90-21123
Fracture and longevity of composite structures
[AD-A217827] 14 p1944 N90-21127
Compressive behavior of laminated composite structures 14 p1945 N90-21134
Two-dimensional damage models of fiber-reinforced composites 14 p1946 N90-21135
The structural basis for fatigue initiation in glassy polymers
[DE90-009342] 14 p1956 N90-21200
Compendium of fracture mechanics problems
[NASA-TM-100393] 14 p1992 N90-21414
Development of a fracture analysis technique for use with a general-purpose finite element program
14 p1992 N90-21416
Strength in notched and impact-damaged laminates
15 p2064 N90-21820
Review of analysis methods for mechanically fastened joints in composites
[LR-599] 15 p2107 N90-22050
A methodology for knowledge-based restructurable control to accommodate system failures
15 p2109 N90-22058
Elasto-plastic analysis for contact fatigue failure
15 p2112 N90-22078
SPOT 4 space magnetic recorder mechanisms
15 p2112 N90-22082
Knowledge-based and integrated monitoring and diagnosis in autonomous power systems
15 p2155 N90-22310
Computational and experimental investigations of rotating stall in compressor cascades
16 p2201 N90-22565
Damage analysis following slight deformations of composite materials
[RDS-1-007-64] 16 p2212 N90-22618
Elevated temperature crack growth in aluminum alloys: Tensile deformation of 2618 and FVS0812 aluminum alloys 16 p2218 N90-22654
Measurements and mechanisms of localized aqueous corrosion in aluminum-lithium alloys
16 p2219 N90-22656
Thermal/structural analysis of the shaft-disk region of a fan drive system
[NASA-TM-101687] 16 p2245 N90-22807
Ultrafine microstructure composites prepared by chemical vapor deposition
[AD-A219650] 17 p2369 N90-23484
Fracture mechanism maps for advanced structural ceramics. Part 1: Methodology and hot-pressed silicon nitride results
[AD-A220428] 17 p2380 N90-23556
Health management system for rocket engines
[NASA-CR-185223] 17 p2383 N90-23574
Failure analysis handbook
[AD-A219747] 17 p2413 N90-23752
Failure analysis and modeling of a multicomputer system
[NASA-CR-186697] 17 p2451 N90-23980
Columbus onboard FDIR concept
18 p2500 N90-24286
AECM3: Acoustic Emission Conditions for failure prediction of winding carbon structures
[REPT-892-430-115] 18 p2517 N90-24374
Metal matrix composites microfracture: Computational simulation
[NASA-TM-103153] 18 p2518 N90-24383
Abrasion resistant coatings on plastics
18 p2529 N90-24428
Failure mechanism of urethane elastomer coated fabric collapsible fuel tanks
[AD-A221033] 18 p2530 N90-24435
HDTV: A chance to enhance television colorimetry
[BBC-RD-1990/2] 18 p2543 N90-24515
Incorporation of a progressive failure analysis method in the CSM testbed software system
18 p2640 N90-25036
Development of a finite element based delamination analysis for laminates subject to extension, bending, and torsion 18 p2642 N90-25049
Failure of the ERBE scanner instrument aboard NOAA 10 spacecraft and results of failure analysis
[NASA-TM-102661] 19 p2694 N90-25328
Experimental observations and finite element analysis of the initiation of fiber microbuckling in notched composite laminates
[NASA-CR-186207] 19 p2699 N90-25359
Loads analysis and testing of flight configuration solid rocket motor outer boot ring segments
[NASA-TP-3028] 19 p2701 N90-25366
Behavior of composite/metal aircraft structural elements and components under crash type loads: What are they telling us
[NASA-TM-102681] 19 p2701 N90-25368
Open hole and post-impact compression fatigue of stitched and unstitched carbon/epoxy composites
[NASA-TM-102676] 19 p2701 N90-25370
Hardware and software reliability estimation using simulations
[NASA-CR-186637] 19 p2741 N90-25580
GSC configuration management plan
[NASA-CR-182044] 19 p2743 N90-25587
Reliability model generator specification
[NASA-CR-182005] 19 p2752 N90-25638
Study on failure modes of boron fiber reinforced aluminum composite materials by AE method, part 2
[DE90-505522] 20 p2828 N90-26086
A comparison of the post-buckling behavior of metallic and composite plates with centrally located cutouts
[NIAR-90-14] 20 p2875 N90-26356
Design of ceramic components with the NASA/CARES computer program
[NASA-TM-102369] 20 p2875 N90-26359
Scaling effects in the static and dynamic response of graphite-epoxy beam-columns
[NASA-TM-102697] 20 p2876 N90-26363
The response and failure mechanisms of circular metal and composite plates subjected to underwater shock loading
[AD-A222200] 21 p3013 N90-27131
Dynamic test input generation for multiple-fault isolation 21 p3040 N90-27280
Hermes emergency reentry trajectories consequences on the Ariane 5 trajectories 22 p3127 N90-27747
Tolerating failures of continuous-valued sensors
[NASA-CR-187028] 22 p3178 N90-28035
NASCRAC (trademark): A fracture mechanics analysis code 23 p3296 N90-28645
Probabilistic model for fracture mechanics service life analysis 23 p3297 N90-28650
Probability models for the failure of fibres and fibrous composite materials 23 p3300 N90-28665
Molten salt induced high temperature degradation of thermal barrier coatings 23 p3307 N90-28704
Periodic gaits for the CMU ambler
23 p3367 N90-29027
Techniques for autonomous GPS integrity monitoring
24 p3424 N90-29345
A low cost inertial/GPS integrated approach to land navigation 24 p3430 N90-29374
Characterization of unnotched SCS-6/Ti-15-3 metal matrix composites at 650 C
[NASA-TM-102699] 24 p3444 N90-29450
Reliability analysis/assessment of advanced technologies
[AD-A223647] 24 p3465 N90-29573
Fractographic analysis of fatigue failures of airframe equipment parts: Examples of a rod end housing and a rod end cap
[NAL-TR-1047] 24 p3483 N90-29686
Using minimal spanning trees to compare the reliability of network topologies
[NASA-TM-4208] 24 p3539 N90-30014

FAILURE MODES

Independent Orbiter Assessment (IOA): Analysis of the manned maneuvering unit
[NASA-CR-185565] 02 p0161 N90-10913
Independent Orbiter Assessment (IOA): Assessment of the electrical power generation/fuel cell powerplant subsystem FMEA/CIL
[NASA-CR-185562] 02 p0161 N90-10914
Independent Orbiter Assessment (IOA): Analysis of the electrical power generation/fuel cell powerplant subsystem
[NASA-CR-185561] 02 p0161 N90-10915
Independent Orbiter Assessment (IOA): Analysis of the rudder/speed brake subsystem
[NASA-CR-185560] 02 p0161 N90-10916
Independent Orbiter Assessment (IOA): Assessment of the data processing system FMEA/CIL
[NASA-CR-185546] 02 p0162 N90-10917
Independent Orbiter Assessment (IOA): Analysis of the electrical power generation/power reactant storage and distribution subsystem
[NASA-CR-185556] 02 p0162 N90-10918
Independent Orbiter Assessment (IOA): Analysis of the orbital maneuvering system
[NASA-CR-185554] 02 p0162 N90-10919

Independent Orbiter Assessment (IOA): Analysis of the guidance, navigation, and control subsystem
[NASA-CR-185555] 02 p0162 N90-10920
Independent Orbiter Assessment (IOA): Analysis of the nose wheel steering subsystem
[NASA-CR-185548] 02 p0163 N90-10921
Independent Orbiter Assessment (IOA): FMEA/CIL instructions and ground rules
[NASA-CR-185551] 02 p0163 N90-10922
Independent Orbiter Assessment (IOA): Assessment of the electrical power generation/power reactant storage and distribution subsystem FMEA/CIL
[NASA-CR-185545] 02 p0163 N90-10923
Independent Orbiter Assessment (IOA): Analysis of the DPS subsystem
[NASA-CR-185549] 02 p0163 N90-10924
Independent Orbiter Assessment (IOA): Analysis of the atmospheric revitalization pressure control subsystem
[NASA-CR-185593] 02 p0163 N90-10925
Independent Orbiter Assessment (IOA): Analysis of the remote manipulator system
[NASA-CR-185585] 02 p0164 N90-10926
Independent Orbiter Assessment (IOA): Analysis of the orbiter main propulsion system
[NASA-CR-185584] 02 p0164 N90-10927
Independent Orbiter Assessment (IOA): Analysis of the instrumentation subsystem
[NASA-CR-185571] 02 p0164 N90-10928
Independent Orbiter Assessment (IOA): Analysis of the ascent thrust vector control actuator subsystem
[NASA-CR-185579] 02 p0164 N90-10929
Independent Orbiter Assessment (IOA): Analysis of the body flap subsystem
[NASA-CR-185574] 02 p0165 N90-10930
Independent Orbiter Assessment (IOA): Analysis of the auxiliary power unit
[NASA-CR-185568] 02 p0165 N90-10931
Independent Orbiter Assessment (IOA): Analysis of the backup flight system
[NASA-CR-185567] 02 p0165 N90-10932
Independent Orbiter Assessment (IOA): Analysis of the electrical power distribution and control/electrical power generation subsystem
[NASA-CR-185538] 02 p0165 N90-10933
Independent Orbiter Assessment (IOA): Analysis of the hydraulics/water spray boiler subsystem
[NASA-CR-185541] 02 p0165 N90-10934
Independent Orbiter Assessment (IOA): Analysis of the elevon subsystem
[NASA-CR-185576] 02 p0166 N90-10935
Independent Orbiter Assessment (IOA): Analysis of the electrical power distribution and control/remote manipulator system subsystem
[NASA-CR-185526] 02 p0166 N90-10936
Independent Orbiter Assessment (IOA): Analysis of the extravehicular mobility unit
[NASA-CR-185540] 02 p0166 N90-10937
Independent Orbiter Assessment (IOA): Analysis of the reaction control system, volume 1
[NASA-CR-185532-VOL-1] 02 p0166 N90-10938
Independent Orbiter Assessment (IOA): Analysis of the reaction control system, volume 2
[NASA-CR-185532-VOL-2] 02 p0167 N90-10939
Independent Orbiter Assessment (IOA): Analysis of the reaction control system, volume 3
[NASA-CR-185532-VOL-3] 02 p0167 N90-10940
Independent Orbiter Assessment (IOA): Analysis of the electrical power distribution and control subsystem, volume 1
[NASA-CR-185529-VOL-1] 02 p0167 N90-10941
Independent Orbiter Assessment (IOA): Analysis of the electrical power distribution and control subsystem, volume 2
[NASA-CR-185529-VOL-2] 02 p0167 N90-10942
Independent Orbiter Assessment (IOA): Analysis of the landing/deceleration subsystem
[NASA-CR-185569] 02 p0167 N90-10943
Independent Orbiter Assessment (IOA): Analysis of the mechanical actuation subsystem
[NASA-CR-185525] 02 p0168 N90-10944
Independent Orbiter Assessment (IOA): Analysis of the pyrotechnics subsystem
[NASA-CR-185530] 02 p0168 N90-10945
Independent Orbiter Assessment (IOA): Assessment of the pyrotechnics subsystem
[NASA-CR-185531] 02 p0168 N90-10946
Independent Orbiter Assessment (IOA): Assessment of the nose wheel steering subsystem
[NASA-CR-185533] 02 p0168 N90-10947
Independent Orbiter Assessment (IOA): Weibull analysis report
[NASA-CR-185534] 02 p0168 N90-10948
Independent Orbiter Assessment (IOA): Assessment of the purge, vent and drain subsystem
[NASA-CR-185535] 02 p0168 N90-10949
Independent Orbiter Assessment (IOA): Assessment of the extravehicular mobility unit, volume 1
[NASA-CR-185536-VOL-1] 02 p0169 N90-10950
Independent Orbiter Assessment (IOA): Assessment of the extravehicular mobility unit, volume 2
[NASA-CR-185536-VOL-2] 02 p0169 N90-10951
Independent Orbiter Assessment (IOA): Assessment of the mechanical actuation subsystem, volume 1
[NASA-CR-185527-VOL-1] 02 p0169 N90-10952
Independent Orbiter Assessment (IOA): Assessment of the mechanical actuation subsystem, volume 2
[NASA-CR-185527-VOL-2] 02 p0169 N90-10953
Independent Orbiter Assessment (IOA): CIL issues resolution report, volume 1
[NASA-CR-185524-VOL-1] 02 p0169 N90-10954
Independent Orbiter Assessment (IOA): CIL issues resolution report, volume 2
[NASA-CR-185524-VOL-2] 02 p0170 N90-10955
Independent Orbiter Assessment (IOA) CIL issues resolution report, volume 3
[NASA-CR-185524-VOL-3] 02 p0170 N90-10956
Independent Orbiter Assessment (IOA): Assessment of the atmospheric revitalization pressure control subsystem FMEA/CIL
[NASA-CR-185594] 02 p0170 N90-10957
Independent Orbiter Assessment (IOA): Analysis of the crew equipment subsystem
[NASA-CR-185591] 02 p0170 N90-10958
Independent Orbiter Assessment (IOA): Assessment of the ascent thrust vector control actuator subsystem FMEA/CIL
[NASA-CR-185590] 02 p0170 N90-10959
Independent Orbiter Assessment (IOA): FMEA/CIL assessment
[NASA-CR-185589] 02 p0170 N90-10960
Independent Orbiter Assessment (IOA): Assessment of the displays and controls subsystem
[NASA-CR-185588] 02 p0171 N90-10961
Independent Orbiter Assessment (IOA): Assessment of the Orbiter Experiment (OEX) subsystem
[NASA-CR-185587] 02 p0171 N90-10962
Independent Orbiter Assessment (IOA): Analysis of the Orbiter Experiment (OEX) subsystem
[NASA-CR-185586] 02 p0171 N90-10963
Independent Orbiter Assessment (IOA): Assessment of the remote manipulator system FMEA/CIL
[NASA-CR-185592] 02 p0171 N90-10964
Independent Orbiter Assessment (IOA): Assessment of the EPD and C/remote manipulator system FMEA/CIL
[NASA-CR-185583] 02 p0172 N90-10965
Independent Orbiter Assessment (IOA): Assessment of the landing/deceleration (LDG/DEC) subsystem FMEA/CIL
[NASA-CR-185570] 02 p0172 N90-10966
Independent Orbiter Assessment (IOA): Analysis of the communication and tracking subsystem
[NASA-CR-185582] 02 p0172 N90-10967
Independent Orbiter Assessment (IOA): Assessment of the body flap subsystem FMEA/CIL
[NASA-CR-185575] 02 p0172 N90-10968
Independent Orbiter Assessment (IOA): Analysis of the purge, vent and drain subsystem
[NASA-CR-185547] 02 p0172 N90-10969
Independent Orbiter Assessment (IOA): Assessment of the elevon actuator subsystem FMEA/CIL
[NASA-CR-185578] 02 p0173 N90-10970
Independent Orbiter Assessment (IOA): Assessment of the crew equipment subsystem
[NASA-CR-185577] 02 p0173 N90-10971
Independent Orbiter Assessment (IOA): Assessment of instrumental subsystem FMEA/CIL
[NASA-CR-185572] 02 p0173 N90-10972
Independent Orbiter Assessment (IOA): Assessment of the backup flight system FMEA/CIL
[NASA-CR-185566] 02 p0173 N90-10973
Independent Orbiter Assessment (IOA): Assessment of the manned maneuvering unit
[NASA-CR-185564] 02 p0173 N90-10974
Independent Orbiter Assessment (IOA): Assessment of the rudder/speed brake subsystem FMEA/CIL
[NASA-CR-185558] 02 p0174 N90-10975
Independent Orbiter Assessment (IOA): Assessment of the auxiliary power unit
[NASA-CR-185580] 02 p0174 N90-10976
Independent Orbiter Assessment (IOA): Assessment of the life support and airlock support systems, volume 1
[NASA-CR-185581-VOL-1] 02 p0174 N90-10977
Independent Orbiter Assessment (IOA): Assessment of the life support and airlock support systems, volume 2
[NASA-CR-185581-VOL-2] 02 p0174 N90-10978
Independent Orbiter Assessment (IOA): Assessment of the active thermal control system
[NASA-CR-185573] 02 p0174 N90-10979
Failure modes and mechanisms in nickel alloys: Primarily austenitic stainless steel
[DE89-016823] 02 p0198 N90-11132
Independent Orbiter Assessment (IOA): Analysis of the displays and controls subsystem
[NASA-CR-185563] 03 p0312 N90-11774
Independent Orbiter Assessment (IOA): Assessment of the orbiter main propulsion system FMEA/CIL, volume 1
[NASA-CR-185559-VOL-1] 03 p0312 N90-11775
Independent Orbiter Assessment (IOA): Assessment of the main propulsion subsystem FMEA/CIL, volume 2
[NASA-CR-185559-VOL-2] 03 p0313 N90-11776
Independent Orbiter Assessment (IOA): Assessment of the main propulsion subsystem FMEA/CIL, volume 3
[NASA-CR-185559-VOL-3] 03 p0313 N90-11777
Independent Orbiter Assessment (IOA): Assessment of the main propulsion subsystem FMEA/CIL, volume 4
[NASA-CR-185559-VOL-4] 03 p0313 N90-11778
Independent Orbiter Assessment (IOA): Assessment of the electrical power distribution and control subsystem, volume 1
[NASA-CR-185557-VOL-1] 03 p0313 N90-11779
Independent Orbiter Assessment (IOA): Assessment of the electrical power distribution and control subsystem, volume 2
[NASA-CR-185557-VOL-2] 03 p0313 N90-11780
Independent Orbiter Assessment (IOA): Assessment of the electrical power distribution and control subsystem, volume 3
[NASA-CR-185557-VOL-3] 03 p0313 N90-11781
Independent Orbiter Assessment (IOA): Analysis of the active thermal control subsystem
[NASA-CR-185553] 03 p0314 N90-11782
Independent Orbiter Assessment (IOA): FMEA/CIL assessment
[NASA-CR-185550] 03 p0314 N90-11783
Independent Orbiter Assessment (IOA): Assessment of the guidance, navigation, and control subsystem FMEA/CIL
[NASA-CR-185552] 03 p0314 N90-11784
Independent Orbiter Assessment (IOA): Assessment of the Electrical Power Distribution and Control/Electrical Power Generation (EPD and C/EPG) FMEA/CIL
[NASA-CR-185542] 03 p0314 N90-11785
Independent Orbiter Assessment (IOA): Analysis of the life support and airlock support subsystems
[NASA-CR-185539] 03 p0314 N90-11786
Independent Orbiter Assessment (IOA): Assessment of the orbital maneuvering system FMEA/CIL, volume 1
[NASA-CR-185544-VOL-1] 03 p0315 N90-11787
Independent Orbiter Assessment (IOA): Assessment of the orbital maneuvering subsystem, volume 2
[NASA-CR-185544-VOL-2] 03 p0315 N90-11788
Independent Orbiter Assessment (IOA): Assessment of the communication and tracking subsystem, volume 1
[NASA-CR-185528-VOL-1] 03 p0315 N90-11789
Independent Orbiter Assessment (IOA): Assessment of the communication and tracking subsystem, volume 2
[NASA-CR-185528-VOL-2] 03 p0315 N90-11790
Independent Orbiter Assessment (IOA): Assessment of the communication and tracking subsystem, volume 3
[NASA-CR-185528-VOL-3] 03 p0315 N90-11791
Independent Orbiter Assessment (IOA): Assessment of the hydraulics/water spray boiler subsystem
[NASA-CR-185537] 03 p0316 N90-11792
Independent Orbiter Assessment (IOA): Assessment of the reaction control system, volume 1
[NASA-CR-185543-VOL-1] 03 p0316 N90-11793
Independent Orbiter Assessment (IOA): Assessment of the reaction control system, volume 3
[NASA-CR-185543-VOL-3] 03 p0316 N90-11795
Independent Orbiter Assessment (IOA): Assessment of the reaction control system, volume 4
[NASA-CR-185543-VOL-4] 03 p0316 N90-11796
Independent Orbiter Assessment (IOA): Assessment of the reaction control system, volume 5
[NASA-CR-185543-VOL-5] 03 p0316 N90-11797
Model 0A wind turbine generator FMEA
[NASA-TM-102378] 03 p0356 N90-12034
An investigation of gear mesh failure prediction techniques
[NASA-TM-102340] 05 p0649 N90-13785
Zinc/bromine battery evaluation at SNL (Sandia National Laboratory)
[DE89-015847] 06 p0769 N90-14473
Fatigue properties of SiC/Al composites
07 p0889 N90-15138
Fatigue, fracture mechanics and corrosion properties of some aluminium-lithium alloys 07 p0898 N90-15194
Studies on some failure modes in latex barrier films
[PB89-209308] 07 p0908 N90-15246
Discrete event simulation tool for analysis of qualitative models of continuous processing systems
[NASA-CASE-MSC-21465-1] 08 p1107 N90-16410
Validation of an exponentially decreasing failure rate software reliability model
[AD-A215546] 09 p1235 N90-17165

Investigation of failure modes in a ceramic composite under off-axis loading
[AD-A216133] 10 p1348 N90-17820
Review of component defects, their relationship to manufacturing process, and their effect on materials behaviour (for critical rotating parts)
11 p1458 N90-18399
A new broadband pulsed high voltage monitor
[DE90-006264] 11 p1502 N90-18651
Fundamental aspects of and failure modes in high-temperature composites
[NASA-TM-102558] 13 p1769 N90-20151
Pyrotechnic device technology
[DE90-007683] 13 p1783 N90-20234
Nine-year aging behavior of the ceramic flatpack resonator
[DE90-008044] 13 p1813 N90-20412
KOH concentration effect on the cycle life of nickel-hydrogen cells. Part 4: Results of failure analyses
13 p1824 N90-20475
Compressive behavior of laminated composite structures 14 p1945 N90-21134
Resistance mechanics for laminated composite materials
[INPE-4919-RPE/594] 14 p1947 N90-21141
Development of a fracture analysis technique for use with a general-purpose finite element program
14 p1992 N90-21416
Delamination failure in a unidirectional curved composite laminate
[NASA-CR-182018] 14 p1993 N90-21421
Failure and degradation modes in selected solar materials: A review
[DE90-009075] 14 p2002 N90-21476
Framework for a space shuttle main engine health monitoring system
[NASA-CR-185224] 15 p2061 N90-21809
Strength in notched and impact-damaged laminates
15 p2064 N90-21820
Fracture toughness and tensile properties of alloy HT9 in thin sections under high neutron fluences
[DE90-008386] 15 p2069 N90-21851
Failure mechanisms under complex loading of glass-reinforced polyester composites and their matrices: The effect of superposed hydrostatic pressures up to 300 MPa on axial tensile and compressive strengths, and in-plane shear properties of unidirtionally reinforced glass-polyester composites and the relevant polyesters
15 p2110 N90-22072
Expert systems for automated maintenance of a Mars oxygen production system
[NASA-CR-186209] 15 p2138 N90-22215
General purpose heat source radioisotope thermoelectric generator. Book 2: Accident analysis, appendices
[REPT-90SDS4202-BK-2] 15 p2166 N90-22380
Probabilistic structural analysis of aerospace components using NESSUS
[NASA-TM-102324] 16 p2248 N90-22823
Health management system for rocket engines
[NASA-CR-185223] 17 p2383 N90-23574
Fatigue testing apparatus
[NASA-CASE-LEW-14124-1] 17 p2407 N90-23712
Atomic velocity distributions out of hydrogen maser dissociators
[AD-A219500] 17 p2408 N90-23721
Lunar rated fasteners
[NASA-CR-182856] 17 p2411 N90-23737
Failure analysis handbook
[AD-A219747] 17 p2413 N90-23752
An experimental evaluation of software redundancy as a strategy for improving reliability
[NASA-TM-102613] 17 p2448 N90-23958
A decision support system for control and automation of dynamical processes
[AD-A219501] 17 p2454 N90-23995
Failure mechanisms of GaAs transistors: A literature survey
[AD-A221089] 18 p2548 N90-24543
Unique failure behavior of metal/composite aircraft structural components under crash type loads
[NASA-TM-102679] 18 p2572 N90-24660
Development of a finite element based delamination analysis for laminates subject to extension, bending, and torsion 18 p2642 N90-25049
Fatigue analysis of mini-mast space truss
18 p2643 N90-25052
Tension fatigue of glass/epoxy and graphite/epoxy tapered laminates
[NASA-TM-102628] 19 p2671 N90-25191
Failure of the ERBE scanner instrument aboard NOAA 10 spacecraft and results of failure analysis
[NASA-TM-102661] 19 p2694 N90-25328
Reliability model generator specification
[NASA-CR-182005] 19 p2752 N90-25638
Study on failure modes of boron fiber reinforced aluminum composite materials by AE method, part 2
[DE90-505522] 20 p2828 N90-26086
Extension of a noninteractive reliability model for ceramic matrix composites
[NASA-CR-185267] 20 p2838 N90-26142
Study on failure modes of SiC fiber reinforced aluminum composite materials by AE method
[DE90-505518] 21 p2971 N90-26884
Modal interaction in postbuckled plates. Theory
[NASA-TP-2943] 21 p3012 N90-27121
Applications of ISES for the oceans
21 p3017 N90-27156
A model for a space shuttle safing and failure-detection expert 21 p3046 N90-27314
Object oriented fault diagnosis system for space shuttle main engine redlines 21 p3046 N90-27315
SDI satellite autonomy using AI and Ada
21 p3050 N90-27336
DMSP's interactive tactical terminal
21 p3068 N90-27441
Study of failure processes in fiber reinforced composites using acoustic emission techniques
22 p3188 N90-28090
Use of acoustic emission for continuous surveillance of aircraft structures 22 p3188 N90-28092
Ceramics Analysis and Reliability Evaluation of Structures (CARES). Users and programmers manual
[NASA-TP-2916] 22 p3190 N90-28099
Theory of stress transfer in a cross-ply laminate containing a parallel array of transverse cracks
[NPL-DMA(A)-189] 22 p3192 N90-28109
System reliability optimization of aircraft wings
23 p3275 N90-28536
Probabilistic model for fracture mechanics service life analysis 23 p3297 N90-28650
Model authoring system for fail safe analysis
[NASA-CR-4317] 23 p3389 N90-29142

FAINT OBJECT CAMERA
A long look back: ESA's faint object camera. The story of the faint object camera, one of ESA's contributions to the Hubble space telescope
[ESA-BR-67] 19 p2784 N90-25839

FAINT OBJECTS
A high galactic latitude survey of far ultraviolet excess objects 15 p2183 N90-22473

FAIRCHILD MILITARY AIRCRAFT
U MILITARY AIRCRAFT

FAIRINGS
An experimental investigation of helicopter rotor hub fairing drag characteristics
[NASA-TM-102182] 03 p0300 N90-11701
Axial compression buckling test on the H-2 launch vehicle satellite fairing structural element prototype (aluminum surface plate/aluminum honeycomb sandwiched curved surface plate)
[NAL-TM-563] 03 p0356 N90-12039

FALLOUT
The Surface Air Sampling Program
[DE90-014873] 24 p3487 N90-29711

FALSE ALARMS
Severe local storm warning verification: 1988
[PB89-226310] 03 p0374 N90-12134
Long term integration for radar detection of small targets in clutter 09 p1203 N90-16972
Adaptive multiple-band CFAR (Constant-False-Alarm-Rate) detection of an optical pattern with unknown spectral distribution
[AD-A214754] 09 p1281 N90-17429
Differential psychological analysis of a computer-based audio-visual test of vigilance
[ESA-TT-1136] 19 p2724 N90-25494
The variably trimmed mean CFAR detector for nonhomogeneous background
[AD-A222801] 20 p2856 N90-26243
Safety net functions 22 p3113 N90-27685

FAN BLADES
Laser anemometer measurements in a transonic axial-flow fan rotor
[NASA-TP-2879] 02 p0218 N90-11245
Fractographic and microstructural analysis of fatigue crack growth in a Ti-6Al-4V fan disc forging
[NLR-MP-88028-U] 03 p0330 N90-11877
Development of an advanced fan blade containment system
[DOT/FAA/CT-89/20] 05 p0581 N90-13386
Thermal/structural analysis of the shaft-disk region of a fan drive system
[NASA-TM-101687] 16 p2245 N90-22807

FANS
WINCOF-I code for prediction of fan compressor unit with water ingestion
[NASA-CR-185157] 15 p2045 N90-21724

FAR FIELDS
A method to model fuze performance. Part 2: Calculation of target reflections with physical optics
[FEL-1989-21-PT-2] 04 p0491 N90-12822
Calculation of the odd and even integral components of the wave resistance Green's function
[AD-A212384] 04 p0503 N90-12900
Numerical evaluation of the far field wave pattern of the radiation Green's function
[AD-A212839] 04 p0546 N90-13176
Estimation of subsonic far-field jet-mixing noise from single-stream circular nozzles
[ESDU-89041] 09 p1161 N90-16721
Near-field bistatic RCS (Radar Cross-Section) measurements
[AD-A217011] 12 p1646 N90-19458
An injective far-field pattern operator and inverse scattering problem in a finite depth ocean
[PB90-159294] 22 p3230 N90-28318
Theory of planar near-field measurement
[FEL-89-B273] 22 p3244 N90-28395

FAR INFRARED RADIATION
Far infrared, submm and mm spectroscopy of the galactic center: Radio arc and +20/+50 km s (exp -1) clouds
[NASA-CR-185497] 04 p0565 N90-13296
Far-infrared heterodyne receivers
05 p0597 N90-13465
Development of FIR arrays with integrating amplifiers
05 p0598 N90-13473
Further observations of rotationally excited far infrared OH16 and OH18 emission in Orion-KL: Tighter constraints on the nature of the emitting region
[NASA-CR-186004] 05 p0710 N90-14156
A compact, high-powered far-infrared (FIR) laser
[DE89-016786] 06 p0789 N90-14597
Wide-beam balloon observations of the 157.7 microns (CII) line 11 p1581 N90-19108
Herbig Ae/Be stars: Fine structure far-infrared lines
11 p1584 N90-19126
Far-infrared spectroscopy of galaxies
11 p1586 N90-19146
Evolutionary synthesis of the far-infrared emission in starburst galaxies 11 p1587 N90-19152
Far infrared fine structure lines in active galaxies
11 p1588 N90-19157
The correlation between radio and far-infrared emission for disk galaxies 11 p1588 N90-19158
Search for far infrared radiation from optically pumped defect modes
[AD-A216976] 12 p1714 N90-19843
Nuclear activity, morphology, and far infrared properties of spiral galaxies
[ETN-90-95373] 12 p1744 N90-20024
Extrinsic germanium Blocked Impurity Bank (BIB) detectors 14 p1976 N90-21322
Ga:Ge array development 14 p1977 N90-21323
Stressed detector arrays for airborne astronomy
14 p1978 N90-21332
Alternating gradient photodetector
[NASA-CASE-NPO-17235-1-CU]
14 p1982 N90-21358
A compact, high-powered Far-Infrared (FIR) laser
[DE90-009996] 20 p2867 N90-26312
High resolution spectroscopy in the microwave and far infrared 20 p2943 N90-26746
Description of SAFIRE for ISES
21 p3016 N90-27148
Implications of the IRAS data for galactic gamma-ray astronomy and EGRET
[NASA-TM-103452] 22 p3261 N90-28466
Quantifying the FIR interaction enhancement in paired galaxies
[DE90-627485] 23 p3412 N90-29281
Integrated technology in MCT/GaAs and MCT/Si for medium and long wavelength infrared
[AD-A223557] 24 p3552 N90-30100

FAR ULTRAVIOLET RADIATION
NT LYMAN ALPHA RADIATION
Ionospheric total electron content, and far ultraviolet, near infrared oxygen emission 02 p0249 N90-11410
Photolysis of spacecraft contaminants
[AD-A211715] 03 p0317 N90-11801
Investigation of atmospheric emissions in ultraviolet, vacuum ultraviolet, and extreme ultraviolet wavelength
[AD-A212169] 03 p0371 N90-12123
The SMM UV observations of Active Region 5395
03 p0434 N90-12485
Vacuum ultraviolet backgrounds from space - ten years after
[AD-A211353] 03 p0435 N90-12493
Development of the RAIDS (Remote Atmospheric and Ionospheric Detector System) extreme ultraviolet wedge and strip detector
[AD-A213730] 07 p0949 N90-15495

Shock layer vacuum UV spectroscopy in an arc-jet wind tunnel
|NASA-TM-102258| 09 p1226 N90-17112
Photodissociation regions: Observations and theory 11 p1579 N90-19098
Transmission and reflection studies of thin films in the vacuum ultraviolet 12 p1638 N90-19412
Quantum yield of photocathodes in far and extreme ultraviolet wavelength area
|ETN-90-95731| 12 p1654 N90-19505
A high galactic latitude survey of far ultraviolet excess objects 15 p2183 N90-22473
Research studies on extreme ultraviolet and soft x ray lasers
|AD-A220271| 18 p2562 N90-24621
Absolute vacuum ultraviolet photoabsorption cross section studies of atomic and molecular species: Techniques and observational data 20 p2944 N90-26754

FARADAY EFFECT
Sensors for nondestructive testing and evaluation of materials
|DE89-014763| 02 p0223 N90-11279
Effect of electrical double layer on transport limited currents at microelectrodes
|AD-A211586| 03 p0324 N90-11843
Preliminary investigation of Faraday rotation effects and description of polarization measurements on the AFGL high latitude meteor scatter test bed
|AD-A211298| 04 p0488 N90-12806
Development and application of diagnostic instrumentation for measurements of electron density and conductivity
|DE90-004076| 09 p1228 N90-17127
Faraday rotation mapping of mercury cadmium telluride
|AD-A224278| 23 p3311 N90-28729

FARADAY ROTATION
U FARADAY EFFECT

FARM CROPS
NT COTTON
NT LEGUMINOUS PLANTS
NT SOYBEANS
NT SUGAR CANE
NT WHEAT
Assessment of crop response to increases in atmospheric carbon dioxide concentrations: Summary of research progress report, July 1, 1988--June 30, 1989
|DE89-016251| 02 p0239 N90-11360
Evaluation of digital classification results of summer cultivation in a test area in the Parana-Ano state harvest 1986-1987
|INPE-4828-PRE/1459| 10 p1399 N90-18085
LANDSAT-TM and agrometeorological data in the wheat crop yield estimation at the farm level
|INPE-4842-PRE/1471| 10 p1400 N90-18091
Aerial photographs to support the fiscalization process of agriculture loans in the Irece-BA region
|INPE-4839-PRE/1468| 10 p1400 N90-18092
Relationships between spectral parameters and agronomics of wheat and beam crops
|INPE-4791-RPE/584| 11 p1523 N90-18768
Development of the agricultural information system. Characteristics and results of the Distrito Federal model
|INPE-4940-PRE/1430| 11 p1524 N90-18773
Relationship of radiometric field measurements of wheat in the Assis-Safra region, 1988
|INPE-4949-RPE/598| 13 p1819 N90-20443
LANDSAT-5 data in the study of wheat and bean crops
|INPE-4746-RPE/580| 13 p1819 N90-20444
Agricultural yield estimation of sugarcane based on agrometeorological-spectral model
|INPE-5016-RPE/610| 14 p1996 N90-21441
A knowledge-based information based for crop area estimation
|INPE-4990-PRE/1555| 14 p1996 N90-21444
Project CANASATE: Remote sensing applied to sugar cane crop survey
|INPE-4902-PRE/1503| 14 p1997 N90-21446
Aerial photography as an aid for agricultural credit control
|INPE-5019-RPE/613| 14 p1999 N90-21455
Evaluation of classification performance and proportion estimate of the sugar cane crop through PROCEDURE-INPE utilizing LANDSAT data
|INPE-4899-PRE/1500| 14 p1999 N90-21458
Wheat productivity estimate through field radiometry
|INPE-4994-PRE/1556| 14 p2000 N90-21460
A proposal to demonstrate production of salad crops in the space station mockup facility with particular attention to space, energy, and labor constraints
|NASA-CR-186811| 19 p2725 N90-25500
Catching our breath: Next steps for reducing urban ozone
|PB90-130451| 20 p2883 N90-26398
Data Base Analyzer and Parameter Estimator (DBAPE) interactive computer program user's manual
|PB90-193053| 23 p3406 N90-29252

FARMLANDS
Availability of multitemporal LANDSAT data accompanying the variation of water surfaces in the program area of Careiro PDRI/AM
|INPE-4896-PRE/1496| 12 p1677 N90-19634

FAST FOURIER TRANSFORMATIONS
A combined finite element and boundary integral formulation for solution via CGFFT of 2-dimensional scattering problems
|NASA-CR-184781| 01 p0055 N90-10313
Calculation of transient response from time-harmonic spectrum
|AD-A211972| 03 p0393 N90-12241
Dynamics of electron transfer for a non-superexchange coherent mechanisms. 2: Numerical calculations
|AD-A213511| 07 p0990 N90-15722
A combined finite element-boundary element formulation for solution of two-dimensional problems via CGFFT
|NASA-CR-186464| 12 p1620 N90-19309
Fast transform decoding of nonsystematic Reed-Solomon codes 12 p1644 N90-19447
FFT-local gravimetric geoid computation 13 p1835 N90-20536
Performance of FFT methods in local gravity field modelling 13 p1835 N90-20537
Downward continuation of the free-air gravity anomalies to the ellipsoid using the gradient solution and terrain correction: An attempt of global numerical computations 13 p1836 N90-20541
Regional quasigeoid determination in Northern Germany and comparison with GPS 13 p1837 N90-20544
Analysis of gamma squared Velorum photometry from the South Pole 15 p2183 N90-22472
Spectral characteristics of low-angle radar ground clutter
|AD-A220817| 17 p2392 N90-23622
A modified fast Fourier transform
|AD-A220567| 17 p2457 N90-24023
Toeplitz matrices: Algebra and algorithms
|AD-A223174| 21 p3064 N90-27416

FAST NEUTRONS
Microstructural evolution of martensitic steels during fast neutron irradiation
|DE89-016231| 07 p0902 N90-15212
Defect structures in copper and gold irradiated with fast neutrons, 14 MeV neutrons and 600 to 800 MeV protons
|DE90-007529| 12 p1629 N90-19359
An influence of fast neutron irradiation on the properties of p-i-n wide-based diodes
|DE90-611148| 18 p2550 N90-24556
Emission of quick neutrons and non-equilibrium phenomena by central shocks in the reaction 40 Ar + 40 Ca at 20 MeV/u
|ETN-90-97296| 24 p3544 N90-30043

FAST NUCLEAR REACTORS
NT LIQUID METAL FAST BREEDER REACTORS

FASTENERS
NT ANCHORS (FASTENERS)
NT BOLTS
NT LOCKS (FASTENERS)
NT NUTS (FASTENERS)
NT PINS
NT RIVETS
NT SCREWS
Pivotal mono wing cruise missile with wing deployment and fastener mechanism
|AD-D014191| 04 p0452 N90-12594
On the motion of compliantly-connected rigid bodies in contact. Part 1: The motion prediction problem
|AD-A214135| 07 p0948 N90-15489
On the motion of compliantly-connected rigid bodies in contact. Part 2: A system for analyzing designs for assembly
|AD-A214136| 07 p0948 N90-15490
Fatigue of aluminium alloy joints with various fastener systems. Low load transfer
|ESDU-89046| 09 p1239 N90-17193
Fastener design manual
|NASA-RP-1228| 11 p1517 N90-18740
Double swivel toggle release
|NASA-CASE-MSC-21436-1| 14 p1987 N90-21390
Review of analysis methods for mechanically fastened joints in composites
|LR-599| 15 p2107 N90-22050
Lunar rated fasteners
|NASA-CR-182856| 17 p2411 N90-23737
Shape memory alloys for robot grippers and mechanical hands 18 p2536 N90-24466
Clamping device for pressurized module radiator panel 18 p2539 N90-24488
The tetrahedral wedge attachment mechanism 18 p2539 N90-24490
Neural networks for detecting defects in aircraft structures
|IAR-90-4| 20 p2873 N90-26345
B-1B improved windshield development. Volume 2: Magna analysis: Baseline and parametric
|AD-A221501| 21 p2960 N90-26828
Overcenter collet space station truss fastener
|NASA-CASE-MSC-21504-1| 21 p2966 N90-26859
Braided composite fasteners and method for producing same
|NASA-CASE-LAR-14062-1| 21 p3010 N90-27114
Progress in the detection of cracks under installed fasteners using eddy currents 22 p3186 N90-28081
New aspects in aircraft inspection using eddy current methods 22 p3187 N90-28085

FATIGUE (BIOLOGY)
NT FLIGHT FATIGUE
NT MUSCULAR FATIGUE
Human performance in continuous/sustained operations and the demands of extended work/rest schedules: An annotated bibliography, volume 2
|AD-A210504| 01 p0093 N90-10530
Heatstroke pathophysiology: The energy depletion model
|AD-A212156| 03 p0380 N90-12164
Heat exhaustion
|AD-A212128| 04 p0522 N90-13014
The effect of concurrent strength and endurance training on electromechanical delay, maximum voluntary contraction, and rate of force development
|AD-A213316| 04 p0525 N90-13028
Fatigue, pilot deviations and time of day
|NASA-CR-185369| 04 p0526 N90-13035
The development of a model of the human responses to load carriage 06 p0821 N90-14775

FATIGUE (MATERIALS)
NT BENDING FATIGUE
NT METAL FATIGUE
NT STRUCTURAL STRAIN
NT THERMAL FATIGUE
A review of Australian and New Zealand investigations on aeronautical fatigue during the period April 1987 to March 1989
|AD-A210373| 01 p0006 N90-10026
Evaluation of titanium castings for aerospace components 01 p0043 N90-10237
Limit analysis of welded tee end connections for hollow tubes
|PB89-191647| 01 p0079 N90-10452
Porosity and crack initiation during low cycle fatigue
|AD-A210989| 01 p0081 N90-10464
Effects of a heat cycle on material strength
|NAL-TM-562| 03 p0306 N90-11737
Stochastic propagation of an array of parallel cracks: Exploratory work on matrix fatigue damage in composite laminates
|DE89-017837| 03 p0319 N90-11813
Improvement in pre-constraint fatigue resistance of modular ferretic and bainitic steel by shot peening treatments
|CETIM-106370| 04 p0476 N90-12727
Estimating the time to fatigue failure of mooring cables
|PB89-220677| 04 p0511 N90-12946
Proceedings of the Army Symposium on Solid Mechanics, 1989: Mechanics of Engineered Materials and Applications
|AD-A211954| 04 p0511 N90-12951
Nondestructive analysis of aileron fatigue and aging in a Mirage F1
|REPT-M6-594000| 05 p0580 N90-13378
Measuring of the complete stiffness matrix for anisotropic laminated materials
|DLR-MITT-89-11| 05 p0618 N90-13606
Measuring of the complete stiffness matrix for anisotropic laminated materials
|DLR-MITT-89-12| 05 p0618 N90-13607
Some aspects of test frequency influence on the fatigue behavior of ARALL
|LR-549| 05 p0620 N90-13616
An investigation of gear mesh failure prediction techniques
|NASA-TM-102340| 05 p0649 N90-13785
A computer-controlled automated test system for fatigue and fracture testing
|DE90-002931| 06 p0800 N90-14661
Design temperatures for flexible airfield pavement design
|AD-A214141| 07 p0884 N90-15115
Short fibre and particulate reinforced metal matrix composites 07 p0901 N90-15207
Fatigue loading history reconstruction based on the rain-flow technique
|NASA-CR-181942| 07 p0947 N90-15482
Micromechanics of an extrusion in high-cycle fatigue with creep
|AD-A213509| 07 p0947 N90-15485

Review of investigations on aeronautical fatigue in the Federal Republic of Germany
[LBF-S-182] 08 p1089 N90-16302
Rainflow counting algorithm for the LIFE2 fatigue analysis code
[DE90-002834] 08 p1096 N90-16344
Inspection development for T-37 wing spar cap lug
[AD-A214826] 09 p1159 N90-16708
Assessment of strength limiting flaws in ceramic heat exchanger tubes, phase 2
[DE90-004081] 09 p1220 N90-17080
Effect of oxygen on the tear strength of elastomers
[AD-A215845] 10 p1359 N90-17879
AGARD/SMP Review: Damage Tolerance for Engine Structures. 2: Defects and Quantitative Materials Behaviour --- conference
[AGARD-R-769] 11 p1457 N90-18396
Identification of a cast iron alloy containing nonstrategic elements
[NASA-CR-185174] 11 p1487 N90-18559
Life of concentrated contacts in the mixed EHD and boundary film regimes
[AD-A216673] 11 p1517 N90-18738
Biaxial strength and stress rupture of hot-pressed silicon nitride
[AD-A216950] 11 p1519 N90-18750
Security calculations of rip reached construction elements by means of probabilistic breaking mechanics and a Markov process
[ETN-90-95890] 12 p1676 N90-19624
Evaluation of thermal cycling creep-fatigue damage for a molten salt receiver
[DE90-002907] 12 p1684 N90-19670
Fracture mechanical aspects of dust emission processes from a model comet surface 12 p1740 N90-20004
Hydrogen, thermal ageing and the role of carbides in fatigue of a high strength steel
[AERE-R-13599] 13 p1774 N90-20183
Fatigue crack growth in martensitic 2 1/4Cr-1Mo steel at elevated temperatures
[AERE-R-13524] 13 p1776 N90-20191
The diffraction of ultrasound by cracks: Comparison of experiment with theory
[AERE-R-13334] 13 p1813 N90-20410
Through-the-thickness fatigue crack closure behavior in an aluminum alloy
[NASA-TM-102590] 13 p1816 N90-20427
Characterization of failure processes in tungsten copper composites under fatigue loading conditions
[NASA-TM-102371] 14 p1943 N90-21123
Crack stoppers and ARALL laminates
[PB90-166588] 14 p1947 N90-21142
Titanium aluminides: Processing, properties and potential
[AERE-R-13198] 14 p1949 N90-21158
Fatigue crack growth from narrow-band Gaussian spectrum loading in 6063 aluminum alloy
[DE90-008957] 14 p1952 N90-21173
The structural basis for fatigue initiation in glassy polymers
[DE90-009342] 14 p1956 N90-21200
Fatigue damage growth mechanisms in continuous fiber reinforced titanium matrix composites
[NASA-TM-102594] 14 p1991 N90-21409
NASA airframe structural integrity program
[NASA-TM-102637] 14 p1993 N90-21422
An internal/external pressure, tension/compression multiaxial fatigue system
[DE90-009510] 14 p1994 N90-21430
A real time neural net estimator of fatigue life
[NASA-TM-103117] 14 p2018 N90-21564
Development of ultrasonic nondestructive methods for defect and damage characterization in composite materials 15 p2063 N90-21816
Three-dimensional fatigue crack closure behavior of metals 15 p2070 N90-21857
Contact mechanics for three-dimensional geometries 15 p2111 N90-22076
Cycle life machine for AX-5 space suit 15 p2112 N90-22080
Fatigue crack growth in unidirectional metal matrix composite
[NASA-TM-103102] 15 p2118 N90-22117
Fatigue crack growth predictions for variable-amplitude and spectrum loading
[LR-526] 15 p2118 N90-22118
Rotor loading on a three-bladed wind turbine 15 p2123 N90-22145
Cooling of rocket thrust chambers with liquid oxygen
[NASA-TM-103146] 16 p2210 N90-22605
A life prediction model for laminated composite structural components
[NASA-CR-186587] 16 p2212 N90-22614
Fatigue crack growth in a unidirectional SCS-6/Ti-15-3 composite
[NASA-TM-103095] 16 p2217 N90-22646
NASA-UVA light aerospace alloy and structures technology program
[NASA-CR-182607] 16 p2217 N90-22651
Fracture toughness and fatigue crack initiation tests of welded precipitation-hardening stainless steel
[AD-A218745] 16 p2221 N90-22669
Structure-property relations in aluminum-lithium alloys
[AD-A219183] 16 p2222 N90-22672
Fatigue crack growth investigation of a Ti-6Al-4V forging under complex loading conditions: NATO/AGARD supplemental engine disk program
[AD-A220239] 17 p2377 N90-23538
Failure analysis handbook
[AD-A219747] 17 p2413 N90-23752
Wide range stress intensity factor and crack-mouth-opening displacement expressions suitable for short crack fracture testing with arc bend-chord support samples
[AD-A218395] 17 p2415 N90-23761
Corrosion fatigue crack propagation in metals
[NASA-CR-4301] 18 p2524 N90-24405
Processing and properties of advanced aluminum alloys
[AD-A221292] 18 p2526 N90-24416
Fatigue crack propagation in austenitic stainless steels at cryogenic temperatures
[DE90-011597] 18 p2528 N90-24426
Cyclic damage zones ahead of tensile fatigue cracks in ceramic materials
[DE90-008372] 18 p2531 N90-24442
Fatigue crack growth in ceramic materials at ambient and elevated temperatures
[DE90-008418] 18 p2531 N90-24443
Monoenergetic positron beam studies of near-surface phenomena
[ETN-90-96947] 18 p2613 N90-24887
Modeling growth of fatigue cracks which originate at rivet holes 18 p2645 N90-25060
Investigation on sheet material of 8090 and 2091 aluminium-lithium alloy
[MBB-UT-122/89-PUB] 19 p2652 N90-25090
Tension fatigue of glass/epoxy and graphite/epoxy tapered laminates
[NASA-TM-102628] 19 p2671 N90-25191
Study on application of ultrasonic wave measurement to creep-fatigue damage detection
[DE89-782317] 19 p2700 N90-25361
Probabilistic approach to the certification for fatigue durability of composite structures
[DE90-505521] 20 p2828 N90-26085
Small crack growth and its influence in near alpha-titanium alloys
[RAE-TM-P-1171] 20 p2835 N90-26121
Development of creep-fatigue damage detection method of rotor steel by ultrasonic wave measurement
[DE90-503792] 20 p2877 N90-26365
Fatigue life assessment using a short crack growth model
[PNR90663] 20 p2877 N90-26367
Determination of the heat dissipated from a specimen undergoing cyclic plasticity by a hybrid numerical/experimental method
[AD-A221575] 21 p2982 N90-26946
Fracture mechanics analysis for short cracks
[AD-A222170] 21 p3013 N90-27130
Study of failure processes in fiber reinforced composites using acoustic emission techniques 22 p3188 N90-28090
Fatigue crack monitoring from initiation to through cracking in welded thick steel sections
[ARE-TM(UHS)-90203] 22 p3194 N90-28122
Energy efficient engine pin fin and ceramic composite segmented liner combustor sector rig test report
[NASA-CR-179534] 23 p3281 N90-28567
NASCRAC (trademark): A fracture mechanics analysis code 23 p3296 N90-28645
Fretting wear and fretting fatigue at temperatures up to 600 C 23 p3307 N90-28706
Fretting fatigue strength of Ti-6Al-4V at room and elevated temperatures and ways of improving it 23 p3308 N90-28709
Reliability analysis of maintained structural system vulnerable to fatigue and fracture 23 p3338 N90-28868
Evaluation of static and fatigue properties of thin sheets of 8090-T8 aluminum-lithium alloy and observation of its fracture surfaces
[NAL-TR-1039] 24 p3453 N90-29499
Extension of plasma source ion implantation to ion beam enhanced deposition
[AD-A224462] 24 p3454 N90-29506
Fractographic analysis of fatigue crack growth under two-blocks loading on 2024-T351 sheet specimens
[LR-628] 24 p3482 N90-29680
Effects of blocks of overloads and underloads on fatigue crack growth in 2024-T351 sheet specimens: Fractographic analysis and crack closure predictions
[LR-629] 24 p3482 N90-29681
Fatigue, static tensile strength and stress corrosion of aircraft materials and structures. Part 1: Text
[LR-630-PT-1-REV] 24 p3482 N90-29682
Fatigue, static tensile strength and stress corrosion of aircraft materials and structures. Part 2: Figures
[LR-630-PT-2] 24 p3482 N90-29683
Fractographic observations on fatigue crack growth under miniTWIST flight-simulation loading (2024-T3 material)
[LR-631] 24 p3483 N90-29684
Fractographic analysis of fatigue failures of airframe equipment parts: Examples of a rod end housing and a rod end cap
[NAL-TR-1047] 24 p3483 N90-29686

FATIGUE LIFE

A review of Australian and New Zealand investigations on aeronautical fatigue during the period April 1987 to March 1989
[AD-A210373] 01 p0006 N90-10026
Porosity and crack initiation during low cycle fatigue
[AD-A210989] 01 p0081 N90-10464
Study of a gallium arsenide solar cell interconnector 02 p0182 N90-11033
Creep and fracture behavior of heat resistant steels in characteristic cases of variable fatigue loading
[ETN-89-94671] 03 p0326 N90-11855
In service life monitoring system using g-meter readings and mass configuration control
[ETN-89-95218] 03 p0356 N90-12035
Fatigue behavior of silicon carbide Whisker/Aluminum composite
[AD-A213094] 05 p0618 N90-13603
Application of fracture mechanics and half-cycle method to the prediction of fatigue life of B-52 aircraft pylon components
[NASA-TM-88277] 05 p0655 N90-13820
Fatigue analysis and reconstruction of helicopter load spectra 06 p0739 N90-14304
Thermal fatigue durability for advanced propulsion materials
[NASA-TM-102348] 06 p0797 N90-14641
Thermal mechanical fatigue of coated blade materials
[AD-A214258] 07 p0882 N90-15107
Fatigue and fracture behaviour of a PM Al-Li alloy 07 p0899 N90-15195
Isothermal fatigue behavior of Sn-Pb solar joints
[DE90-003280] 07 p0943 N90-15464
Fatigue loading history reconstruction based on the rain-flow technique
[NASA-CR-181942] 07 p0947 N90-15482
Fatigue life estimates for helicopter loading spectra
[NASA-CR-181941] 08 p1088 N90-16294
A transient plasticity study and low cycle fatigue analysis of the Space Station Freedom photovoltaic solar array blanket
[NASA-TM-102516] 12 p1674 N90-19617
Fatigue damage growth mechanisms in continuous fiber reinforced titanium matrix composites
[NASA-TM-102594] 14 p1991 N90-21409
An evaluation of the pressure proof test concept for thin sheet 2024-T3
[NASA-TM-101675] 14 p1994 N90-21424
A real time neural net estimator of fatigue life
[NASA-TM-103117] 14 p2018 N90-21564
Hydrogenation of stainless steels implanted with nitrogen
[DE90-617397] 16 p2221 N90-22666
Fracture toughness and fatigue crack initiation tests of welded precipitation-hardening stainless steel
[AD-A218745] 16 p2221 N90-22669
Surface pitting fatigue life of noninvolute, low-contact-ratio gears
[NASA-TM-103116] 16 p2242 N90-22790
Fracture mechanics assessment of a cracked 16-inch inner diameter 1945 vintage-jacketed pressure vessel
[AD-A219135] 16 p2248 N90-22819
High temperature fatigue behavior of a SiC/Ti-24Al-11Nb composite
[NASA-TM-103157] 16 p2248 N90-22822
About the effect of loading sequence on the fatigue life of notched specimens made from steel and aluminum alloys
[LBF-FB-186(1989)] 18 p2526 N90-24414
Fatigue analysis of mini-mast space truss 18 p2643 N90-25052
Flexural fatigue life prediction of closed hat-section using materially nonlinear axial fatigue characteristics 18 p2645 N90-25062
Scratches and shot peening effects on the fatigue life of aluminum-lithium alloys
[NIAR-90-15] 19 p2674 N90-25208

Surface condition effect on the fatigue behavior of aluminum lithium alloys
[NIAR-90-13] 19 p2674 N90-25209
Cyclic stress strain behavior of an austenitic stainless steel Polarit 778 under variable amplitude loading
[VTT-RR-647] 19 p2675 N90-25215
Open hole and post-impact compression fatigue of stitched and unstitched carbon/epoxy composites
[NASA-TM-102676] 19 p2701 N90-25370
The effect of local thinning on the remaining life of superheater tubes
[VTT-RR-631] 19 p2703 N90-25377
A study of the fatigue behavior in scratched samples of Al-Li alloy (2090-T3)
[IAR-89-24] 20 p2832 N90-26107
Microstructural design for fatigue crack growth resistance in Ni-base alloy
[PNR90632] 20 p2834 N90-26120
Retirement for cause of the F100 engine 21 p2957 N90-26813
Damage tolerance analysis for manned hypervelocity vehicles. Volume 2: Software user's manual
[AD-A222136] 21 p2959 N90-26826
Multichannel on-board load and fatigue monitoring 22 p3103 N90-27621
Life management planning 22 p3118 N90-27709
Methodology of the fatigue under shocks. Experimental results: 7075 T6 and 35 NCD16
[ETCA-89-R-140] 22 p3157 N90-27901
Use of acoustic emission for continuous surveillance of aircraft structures 22 p3188 N90-28092
Constitutive and life modeling of single crystal blade alloys for root attachment analysis 23 p3296 N90-28643
The fatigue damage behavior of a single crystal superalloy 23 p3296 N90-28644
Characterization of unnotched SCS-6/Ti-15-3 metal matrix composites at 650 C
[NASA-TM-102699] 24 p3444 N90-29450

FATIGUE TESTING MACHINES
Contribution to the fatigue behavior study of composite materials reinforced with unidirectional glass fibers
[ECL-88-20] 05 p0619 N90-13612
Fatigue testing apparatus
[AD-D014544] 22 p3192 N90-28108

FATIGUE TESTS
Worked-in holes in three-dimensional reinforced composites 02 p0186 N90-11060
Creep and fracture behavior of heat resistant steels in characteristic cases of variable fatigue loading
[ETN-89-94671] 03 p0326 N90-11855
Effect of fretting on fatigue strength of aluminium alloys
[ESDU-89004] 03 p0329 N90-11870
Determination and description of the long term creep behavior of high temperature gas turbine materials
[ETN-89-94985] 03 p0329 N90-11871
WISPER: A standardized fatigue load sequence for HAWT-blades
[NLR-MP-88029-U] 03 p0359 N90-12055
Optical fibre witnesses of fatigue damage in composite materials 04 p0465 N90-12660
Damage tolerance of CFRP sandwich panels
[FFA-TN-1988-70] 04 p0465 N90-12664
Shear fatigue testing and life prediction of fibre composites
[REPT-8519] 04 p0466 N90-12668
Potential difference applied to the measurement of small fatigue crack growth at notches in Ti-6Al-4V
[FFA-TN-1989-09] 04 p0512 N90-12952
Fatigue behavior of specimens under compression load spectra
[ETN-89-95207] 04 p0512 N90-12954
Fatigue testing of welded steel assemblies with or without finishing treatments
[CETIM-107900] 04 p0513 N90-12961
Some new techniques for aircraft fuselage skin tests
[LR-547] 05 p0580 N90-13379
Study of fatigue degradation mechanisms in unidirectional composite materials. Application to cumulative damage
[ECL-88-12] 05 p0619 N90-13611
Contribution to the fatigue behavior study of composite materials reinforced with unidirectional glass fibers
[ECL-88-20] 05 p0619 N90-13612
Constant amplitude fatigue of ARALL-2 laminates
[LR-539] 05 p0620 N90-13615
Mechanical property characterization of VascoMax T-300
[AD-A212950] 05 p0623 N90-13637
An investigation of gear mesh failure prediction techniques
[NASA-TM-102340] 05 p0649 N90-13785
Fatigue resistance of pressure vessels in high strength steels effect of some improvement techniques
[CRIF-MT-176] 05 p0652 N90-13799
An evaluation of a fatigue crack growth prediction model for variable-amplitude loading (PREFFAS)
[LR-537] 05 p0656 N90-13822
Design temperatures for flexible airfield pavement design
[AD-A214141] 07 p0884 N90-15115
Composite activities at Lawrence Livermore National Laboratory
[DE90-002979] 07 p0891 N90-15149
Fatigue behavior of vertical axis wind turbine airfoils with two weld configurations
[DE90-002628] 07 p0955 N90-15525
Fatigue and impact strength of diffusion bonded titanium alloy joints
[RAE-TM-MAT/STR-1123] 08 p1045 N90-16043
FRAG requirements for control of fatigue testing
[RAE-TM-MAT/STR-1130] 08 p1089 N90-16300
Calibration of a pulsed potential crack monitor for use in fatigue crack growth studies
[RAE-TM-M/S-1126] 08 p1089 N90-16301
Review of investigations on aeronautical fatigue in the Federal Republic of Germany
[LBF-S-182] 08 p1089 N90-16302
Inspection development for T-37 wing spar cap lug
[AD-A214826] 09 p1159 N90-16708
Fatigue delamination onset prediction in tapered composite laminates
[NASA-TM-101673] 09 p1236 N90-17177
The need for a common approach within AGARD --- engine component defects 11 p1459 N90-18404
Interlaminar fracture testing of carbon fibre/PEEK composites validity and applications 11 p1477 N90-18497
Biaxial strength and stress rupture of hot-pressed silicon nitride
[AD-A216950] 11 p1519 N90-18750
Static strength and damage tolerance tests on the Fokker 100 airframe
[NLR-MP-88023-U] 12 p1604 N90-19228
Rolling contact fatigue of surface modified 440C using a 'Ge-Polymet' type disc rod test rig
[NASA-TM-100390] 13 p1777 N90-20200
Strength and microstructure of ceramics
[AD-A217752] 13 p1782 N90-20227
A corrosion fatigue/stress corrosion testing facility at Materials Research Laboratory
[MRL-TN-568] 14 p1929 N90-21044
Fractographic analysis of the crack growth rate and the shear lip development of 2024-T3 specimens under simple variable-amplitude loading
[PB90-167032] 14 p1994 N90-21427
Damage analysis following slight deformations of composite materials
[RDS-1-007-64] 16 p2212 N90-22618
Characterisation of fatigue of aluminium alloys by acoustic emission. Part 1: Identification of source mechanism
[AERE-R-13302-PT-1] 17 p2375 N90-23522
Characterisation of fatigue of aluminium alloys by acoustic emission. Part 2: Discrimination between primary and other emissions
[AERE-R-13303-PT-2] 17 p2375 N90-23523
Fatigue crack growth investigation of a Ti-6Al-4V forging under complex loading conditions: NATO/AGARD supplemental engine disk program
[AD-A220239] 17 p2377 N90-23538
Fatigue testing of glass fibre reinforced epoxy using the WISPER sequence
[FFA-TN-1989-45] 17 p2381 N90-23561
Fatigue testing apparatus
[NASA-CASE-LEW-14124-1] 17 p2407 N90-23712
Brittle torsional fatigue crack initiation in an otherwise ductile environment
[AD-A220858] 17 p2416 N90-23767
Open hole and post-impact compression fatigue of stitched and unstitched carbon/epoxy composites
[NASA-TM-102676] 19 p2701 N90-25370
A study of the fatigue behavior in scratched samples of Al-Li alloy (2090-T3)
[IAR-89-24] 20 p2832 N90-26107
Investigation of crack-closure prediction models for fatigue in aluminium alloy sheet under flight-simulation loading
[LR-619] 20 p2877 N90-26369
Static and fatigue strength of an adhesive bonded CFRP butt-strap joint: The effects of stacking sequence and temperature
[NLR-TR-88036-U] 20 p2877 N90-26370
An aluminum quality breakthrough for aircraft structural reliability 21 p2957 N90-26816
Study of the behavior of Al metallic matrix + SiC composite materials under fatigue tests
[ETCA-89-R-077] 22 p3154 N90-27881
Influence of a surface finishing on the fatigue behavior of a 32CDV13 steel
[ETCA-89-R-164] 22 p3157 N90-27902
Ultrasonic inspection of advanced CFRP structures by computer-controlled, pulse-echo technique 22 p3185 N90-28075
An ultrasonic system for in-service non-destructive inspection of composite structures 22 p3185 N90-28076
Fatigue testing apparatus
[AD-D014544] 22 p3192 N90-28108
Application of advanced coating techniques to rocket engine components 23 p3298 N90-28654
Static and dynamic characterization of the ATR 72 rods made of Ti 10.2.3 titanium alloy
[REPT-49-238] 23 p3310 N90-28722
Microstructure: Property correlation --- multiaxial fatigue damage evolution in waspaloy
[NASA-CR-180406] 23 p3340 N90-28880
Evaluation of static and fatigue properties of thin sheets of 8090-T8 aluminum-lithium alloy and observation of its fracture surfaces
[NAL-TR-1039] 24 p3453 N90-29499
Fractographic observations on fatigue crack growth under miniTWIST flight-simulation loading (2024-T3 material)
[LR-631] 24 p3483 N90-29684

FATS
Measurement of body fat by neutron inelastic scattering: Comments on installation, operation, and error analysis
[DE90-006765] 11 p1540 N90-18868

FATTY ACIDS
NT ACETIC ACID

FAULT MECHANICS
U FRACTURE MECHANICS

FAULT TOLERANCE
Development of pressure containment and damage tolerance technology for composite fuselage structures in large transport aircraft
[NASA-CR-3996] 01 p0034 N90-10186
Documentation of the current fault detection, isolation and reconfiguration software of the AIPS fault-tolerant processor
[NASA-TM-89154] 01 p0106 N90-10602
Applications of the hybrid automated reliability predictor: Revised edition
[NASA-TP-2760-REV] 02 p0257 N90-11454
Experiments in fault tolerant software reliability
[NASA-CR-185927] 02 p0258 N90-11460
An open-loop transient thermodynamic model of the Couguar turbojet
[AD-A211774] 03 p0307 N90-11745
Redundancies and don't cares in sequential logic synthesis
[AD-A211931] 03 p0343 N90-11956
Software fault tolerance
[RSRE-MEMO-4237] 04 p0450 N90-12575
Algorithmic fault tolerance
[RSRE-MEMO-4214] 04 p0530 N90-13057
A fault-tolerant software algorithm for a network of transputers
[AD-A213092] 05 p0682 N90-13972
Laboratory test methodology for evaluating the effects of electromagnetic disturbances on fault-tolerant control systems
[NASA-TM-101665] 05 p0695 N90-14061
NETRA: A parallel architecture for integrated vision systems. 1: Architecture and organization
[NASA-CR-185955] 06 p0832 N90-14839
Implementing fault-tolerant sensors
[NASA-CR-186251] 07 p0933 N90-15400
Integrated approach fault tolerance-current state and future requirements
[AD-A214402] 07 p0944 N90-15465
Investigation of the applicability of a functional programming model to fault-tolerant parallel processing for knowledge-based systems
[NASA-CR-181938] 07 p0979 N90-15654
VLSI integrated circuit tests
[IMAG-RR-763-I] 08 p1061 N90-16135
An empirical comparison of software fault tolerance and fault elimination
[NASA-CR-186313] 08 p1108 N90-16414
Algorithms for fault tolerant distributed systems
[AD-A214447] 08 p1109 N90-16416
Software dependability growth characterization, modeling and evaluation
[LAAS-89320] 08 p1112 N90-16437
Application of model based reasoning to diagnosis of faults in inertial navigation equipment
[AD-A215561] 09 p1166 N90-16750
Implementing fault-tolerant sensors
[NASA-CR-186269] 09 p1225 N90-17105
R/M/T (Reliability, Maintainability, and Testability) design for fault tolerance, technical manager's design implementation guide
[AD-A215531] 09 p1234 N90-17164
RADC fault tolerant system reliability evaluation facility
[AD-A215298] 09 p1267 N90-17348

The use of efficient broadcast protocols in asynchronous distributed systems
[NASA-CR-186272] 09 p1269 N90-17358
Transient fault behavior in a microprocessor: A case study
[NASA-CR-186240] 10 p1320 N90-17633
Study on advanced information processing system
[NASA-CR-186342] 10 p1415 N90-18154
Dynamic reconfiguration and link fault tolerance in a transputer network
[AD-A215105] 12 p1642 N90-19433
Fault simulator evaluation
[AD-A217782] 13 p1796 N90-20308
Approximate evaluation of reliability and related quantities via perturbation techniques
[AD-A218340] 13 p1814 N90-20417
Sensor and actuator selection for fault-tolerant control of flexible structures
[AD-A217364] 13 p1817 N90-20433
Space Station Freedom integrated fault model
13 p1860 N90-20673
Using formal methods to develop a paradigm for software design
[DE90-005633] 13 p1866 N90-20703
Asynchronous design for parallel processing architectures
[AD-A217421] 13 p1872 N90-20734
Neural networks for aircraft control
14 p1908 N90-20937
Double swivel toggle release
[NASA-CASE-MSC-21436-1] 14 p1987 N90-21390
Fault tolerant hypercube computer system architecture
[NASA-CASE-NPO-16859-1-CU]
14 p2012 N90-21527
Exploiting virtual synchrony in distributed systems
[NASA-CR-182855] 14 p2016 N90-21555
The art of fault-tolerant system reliability modeling
[NASA-TM-102623] 15 p2152 N90-22292
The 1990 Goddard Conference on Space Applications of Artificial Intelligence
[NASA-CP-3066] 15 p2152 N90-22294
NASA ground terminal communication equipment automated fault isolation expert systems
15 p2154 N90-22305
Autonomous power expert system
15 p2154 N90-22306
Adaptive pattern recognition by mini-max neural networks as a part of an intelligent processor
15 p2156 N90-22317
Bounded-time fault-tolerant rule-based systems
15 p2157 N90-22318
Detection of bridging faults in DFCMOS combinational gates
[REPT-89-060] 16 p2231 N90-22726
Real-time closed-loop simulation and upset evaluation of control systems in harsh electromagnetic environments 16 p2294 N90-23069
Fault tolerant multiprocessing and development of tools
[AD-A219216] 16 p2301 N90-23110
Interconnection networks for highly parallel supercomputing architectures
[REPT-89-053] 16 p2302 N90-23118
An experimental study of fault propagation in a jet-engine controller
[NASA-CR-181335] 17 p2354 N90-23401
FASTER: The Fault Tolerant Architecture Simulation Tool for Evaluating Reliability, introduction and applications
[AD-A219941] 17 p2414 N90-23755
An experimental evaluation of software redundancy as a strategy for improving reliability
[NASA-TM-102613] 17 p2448 N90-23958
Columbus onboard FDIR concept
18 p2500 N90-24286
Multi-version software reliability through fault-avoidance and fault-tolerance
[NASA-CR-186502] 19 p2742 N90-25584
Technical evaluation report on the Guidance and Control Panel 49th Symposium on Fault Tolerant Design Concepts for Highly Integrated Flight Critical Guidance and Control Systems
[AGARD-AR-281] 20 p2813 N90-26012
Making real-time reactive systems reliable
[NASA-CR-186642] 20 p2873 N90-26344
Adaptive fault-tolerant routing in hypercube multicomputers
[NASA-CR-186781] 20 p2903 N90-26513
Self-checking on-line testable static RAM
[NASA-CASE-NPO-17939-1-CU]
20 p2904 N90-26518
Closed-form solution of decomposable stochastic models
[NASA-TM-103466] 20 p2920 N90-26619
Dynamic test input generation for multiple-fault isolation 21 p3040 N90-27280
The application of intelligent process control to space based systems 21 p3041 N90-27282
A study on diagnosability of space station ECLSS
21 p3043 N90-27294
Attitude Determination and Control System (ADCS) and Maintenance and Diagnostic System (MDS): A maintenance and diagnostic system for Space Station Freedom 21 p3043 N90-27295
Space Station Freedom ECLSS: A step toward autonomous regenerative life support systems
21 p3043 N90-27297
SDI satellite autonomy using AI and Ada
21 p3050 N90-27336
The identification of software failure regions
[AD-A223058] 21 p3052 N90-27352
Recovery in distributed systems using optimistic message logging and checkpointing
[AD-A222104] 21 p3054 N90-27361
Transparent optimistic rollback recovery
[AD-A222102] 21 p3070 N90-27455
Aircraft Integrated Monitoring Systems
[DLR-MITT-90-04] 22 p3103 N90-27617
Tolerating failures of continuous-valued sensors
[NASA-CR-187028] 22 p3178 N90-28035
DEPEND: A design environment for prediction and evaluation of system dependability
[NASA-CR-186890] 22 p3189 N90-28094
Analysis and design of algorithm-based fault-tolerant systems
[NASA-CR-186884] 22 p3236 N90-28352
Fault-tolerance in massively parallel silicon architectures: The case of neural nets
[REPT-90-012] 22 p3240 N90-28375
A single wafer bit-sliced convolver: An optimum statistical solution for the implementation of redundancy
[REPT-89-019] 24 p3466 N90-29584
Formal design and verification of a reliable computing platform for real-time control. Phase 1: Results
[NASA-TM-102716] 24 p3530 N90-29965
Low cost management of replicated data in fault-tolerant distributed systems
[NASA-CR-186370] 24 p3532 N90-29976
Reliable communication in the presence of failures
[NASA-CR-183046] 24 p3533 N90-29977
Fault tolerant design for multistage routing networks
[AD-A224267] 24 p3533 N90-29978

FAULT TREES
An artificial intelligence approach to analog system diagnosis
[AD-A213135] 05 p0686 N90-13992
Fault tree analysis: A tool for battery safety and reliability studies
[DE90-002582] 08 p1086 N90-16287
Safety Status Report for the Ulysses mission. Book 2: Accident analysis-appendices. General purpose heat source radioisotope thermoelectric generator program
[DE90-006830] 12 p1614 N90-19286
CMOS IC I(sub DDQ) testing for the 1990s
[DE90-009508] 17 p2394 N90-23634
Communications and tracking expert systems study
[NASA-CR-185935] 21 p2992 N90-27004
A diagnosis system using object-oriented fault tree models 21 p3046 N90-27313
Techniques for developing a system safety risk assessment model
[AD-A223477] 24 p3477 N90-29654
Using minimal spanning trees to compare the reliability of network topologies
[NASA-TM-4208] 24 p3539 N90-30014

FAULTS
NASA ground terminal communication equipment automated fault isolation expert systems
15 p2154 N90-22305
CLEAR: Automating control centers with expert system technology 19 p2733 N90-25533
Fault Detection and Isolation (FDI) techniques for guidance and control systems 24 p3428 N90-29366

FAUNA
U ANIMALS

FCC LATTICES
U FACE CENTERED CUBIC LATTICES

FEAR
Fear-potentiated startle as a model system for analyzing learning and memory
[AD-A212131] 04 p0525 N90-13029
Passenger behaviour in aircraft emergencies involving smoke and fire 10 p1317 N90-17613

FEASIBILITY
Can ion acceleration by double-cyclotron absorption produce O(+) ion conics
[IRF-PREPRINT-114] 02 p0280 N90-11600
Feasibility of using Extreme Ultraviolet Explorer (EUVE) reaction wheels to satisfy Space Infrared Telescope Facility (SIRTF) maneuver requirements
[NASA-TM-100389] 12 p1663 N90-19556
Remote measurement of ice thickness on the shuttle external tank surface
[NASA-TM-102667] 18 p2555 N90-24584
Studies of surface heat transfer in an arc-heated wind tunnel
[NAL-TR-1048] 24 p3437 N90-29410

FEASIBILITY ANALYSIS
A feasibility assessment of installation, operation and disposal options for nuclear reactor power system concepts for a NASA growth space station
[NASA-TM-89923] 01 p0032 N90-10174
Development of the large spacecraft structure
02 p0180 N90-11020
Transient vibration testing of spacecraft structures. Experience with multiaxial base motion and combined base motion and point force excitation
02 p0183 N90-11039
Advanced Turbine Technology Applications Program, (ATTAP): A plan for improving the prototype production of ceramic components for the gas turbine engine, 1988--1992
[DE89-015566] 02 p0230 N90-11320
Feasibility of graphics voice telephones for the post 2000 era
[FEL-1988-26] 03 p0340 N90-11937
Computer controlled MHD power consolidation and pulse-generation system
[DE89-015600] 03 p0407 N90-12333
A survey of permanently-manned lunar base concepts
[AD-A212575] 04 p0460 N90-12638
Proof of the feasibility of coherent and incoherent schemes for pumping a gamma-ray laser
[AD-A212315] 04 p0506 N90-12921
An air coupled transmission mode acoustic microscope for on-line non-destructive evaluation
[AD-A211416] 04 p0511 N90-12947
What is the balance sheet for investment in automated manufacturing
[CETIM-105490] 04 p0532 N90-13071
Applications of superconductor technologies to transportation
[DE90-000856] 06 p0853 N90-14961
Analysis and evaluation of technical data on the photochromic and non-linear optical properties of materials. Appendix: Eye/sensor protection by an optical fuse mirror at a focal plane: Feasibility assessment
[AD-A214051] 07 p0896 N90-15177
Feasibility study of using industrial robot for ultrasound testing
[DE90-002977] 07 p0943 N90-15461
Spectral sensitivity of device power output for tandem a-Si alloy solar cells
[DE89-009421] 08 p1095 N90-16340
Conceptual design analysis for hybrid-cycle OTEC plants for co-production of electric power and desalinated water
[DE90-003551] 08 p1097 N90-16350
Investigation and study on compressed air storage power generation system, part 2
[DE90-702648] 08 p1097 N90-16354
ATF-2 studies
[DE90-004380] 08 p1124 N90-16510
Remote Manipulator System (RMS)-based Controls-Structures Interaction (CSI) flight experiment feasibility study
[NASA-CR-181952] 09 p1230 N90-17136
A wind tunnel study of a sting-mounted circulation control wing
[AD-A216248] 10 p1310 N90-17577
Surveys concerning the effect to introduce electric vehicles. On the possibility of new technology and introducing measures
[DE90-742057] 10 p1391 N90-18046
Advanced battery development
[DE90-006073] 11 p1529 N90-18806
Feasibility of Mealy design for processor controlpaths
[MEMO-INF-89-53] 11 p1550 N90-18923
Technical and administrative feasibility of microlight remote sensing applications for river boards
[BCRS-89-01] 12 p1679 N90-19643
A technical and economic evaluation of oxygen-enriched combustion in diesel engines using water-emulsified fuels
[DE90-008095] 13 p1810 N90-20394
Testing of an advanced thermochemical conversion reactor system
[DE90-007989] 15 p2123 N90-22141
Human exploration of space: A review of NASA's 90-day study and alternatives
[NASA-CR-186394] 17 p2357 N90-23418
Extreme quantile estimation in binary response models
[AD-A220150] 17 p2466 N90-24093
Forward canopy feasibility and Thru-The-Canopy (TTC) ejection system study
[AD-A220360] 18 p2495 N90-24258

Lunar orbiting microwave beam power system
[NASA-TM-103211] 19 p2667 N90-25173
Feasibility study for the advanced one-dimensional high temperature optical strain measurement system, phase 3
[NASA-CR-185254] 19 p2693 N90-25324
Real-time measurement of mental workload: A feasibility study 19 p2734 N90-25540
Dendritic web silicon photovoltaic cell research
[DE90-011786] 20 p2880 N90-26387
Study of the feasibility of several mixtures
[IMAG-RR-776-M] 21 p3057 N90-27379
Independent research and independent exploratory development programs
[AD-A222690] 21 p3101 N90-27612
Swissair studies on the compressibility of aircraft data 22 p3105 N90-27637
Liquid Rocket Booster (LRB) for the Space Transportation System (STS) systems study. Volume 1: Executive summary
[NASA-CR-183822] 23 p3288 N90-28599
Feasibility of the temperature measurements in hypersonic flow by multibeam coherent Raman anti-Stokes scattering
[ONERA-RF-56/7131-PY] 24 p3419 N90-29312

FEATURE EXTRACTION
U PATTERN RECOGNITION

FECES
Generation rates and chemical compositions of waste streams in a typical crewed space habitat
[NASA-TM-102799] 22 p3233 N90-28333

FEDERAL BUDGETS
Forecasting contracting workload
[AD-A211935] 03 p0416 N90-12387
FY 1990/FY 1991 biennial budget descriptive summaries for the Strategic Defense Initiative Organization
[AD-A211985] 03 p0419 N90-12409
Departments of Veterans Affairs and Housing and Urban Development, and Independent Agencies Appropriations Bill, 1990
[H-REPT-101-150] 04 p0563 N90-13281
National Aeronautics and Space Administration 04 p0563 N90-13282
Fiscal year 1990 authorization request and budget estimates for the National Aeronautics and Space Administration
[GPO-96-945] 04 p0563 N90-13283
Departments of Veterans Affairs and Housing and Urban Development, and Independent Agencies Appropriation Bill, 1990
[S-REPT-101-128] 04 p0563 N90-13284
The 1990 National Aeronautics and Space Administration Authorization
[GPO-98-466] 04 p0563 N90-13285
Department of Veterans Affairs and Housing and Urban Development, and Independent Agencies Appropriations Act, 1990
[HR-2916-PP] 04 p0564 N90-13286
National Aeronautics and Space Administration 04 p0564 N90-13287
National Aeronautics and Space Administration Authorization Act, fiscal year 1990
[S-REPT-101-157] 04 p0564 N90-13288
National Aeronautics and Space Administration Authorization Act, fiscal year 1990
[S-REPT-101-157] 04 p0564 N90-13289
National Aeronautics and Space Administration Multiyear Authorization Act of 1989 05 p0709 N90-14148
National Aeronautics and Space Administration authorization
[S-HRG-101-348] 05 p0709 N90-14149
National Action Plan on Superconductivity Research and Development
[PB89-138512] 12 p1720 N90-19883
Current information technology resource requirements of the Federal government: Major systems acquisitions and planned resources
[PB90-146820] 15 p2177 N90-22439
Space funding: NASA and DOD activities for fiscal years 1981 through 1989. Fact sheet for the Chairman and the Ranking Minority Member, Subcommittee on Science, Technology, and Space, Committee on Commerce, Science, and Transportation, US Senate
[GAO/NSIAD-89-102FS] 17 p2481 N90-24187
The 1991 NASA authorization: National Aeronautics and Space Administration fiscal year 1991 authorization request and budget estimates
[GPO-27-291] 17 p2481 N90-24188
Satellite data archiving: US and foreign activities and plans for environmental information
[GAO/RCED-88-201] 18 p2633 N90-25001
Departments of Veterans Affairs and Housing and Urban Development, and Independent Agencies Appropriations for Fiscal Year 1990, part 2
[S-HRG-101-345-PT-2] 18 p2636 N90-25017
National Aeronautics and Space Administration, 2 May 1989 18 p2636 N90-25018
National Aeronautics and Space Administration, 3 May 1989 18 p2636 N90-25019
Departments of Veterans Affairs and Housing and Urban Development, and independent agencies appropriations for 1991. Part 4: National Aeronautics and Space Administration
[GPO-30-861] 21 p3088 N90-27561
Independent research and independent exploratory development programs
[AD-A222690] 21 p3101 N90-27612
Space program safety: Funding for NASA's safety organizations should be centralized
[GAO/NSIAD-90-187] 22 p3255 N90-28434
Space projects: Improvements needed in selecting future projects for private financing
[GAO/NSIAD-90-147] 22 p3256 N90-28439
Federal R and D funding by budget function: Fiscal years 1989-1991
[PB90-226879] 23 p3404 N90-29237
NASA authorization, 1991, volume 2
[GPO-32-196] 24 p3559 N90-30138

FEDERAL REPUBLIC OF GERMANY
U WEST GERMANY

FEDERATIONS
NT BUREAUS (ORGANIZATIONS)
Navigation programmes: Financial and institutional aspects 17 p2361 N90-23441

FEED SYSTEMS
Thin section casting program. Volume 5: Westinghouse MHD Project
[DE89-009035] 02 p0210 N90-11203
The 1989 JANNAF Propulsion Meeting, volume 1
[CPIA-PUBL-515-VOL-1] 11 p1470 N90-18462
The use of the gas feed system and the vitiator for the solid fuel combustion chamber
[LR-528] 12 p1623 N90-19329
Hybrid propulsion technology program. Volume 1: Conceptional design package
[NASA-CR-183953] 15 p2060 N90-21793
Hybrid propulsion technology program. Volume 2: Technology definition package
[NASA-CR-183954] 15 p2060 N90-21794
Beamforming devices and feed structures for a DBS flat-plate antenna
[BBC-RD-1989/12] 17 p2386 N90-23592
Combustion instability coupling with feed system acoustics 23 p3293 N90-28629

FEEDBACK
NT BIOFEEDBACK
NT NEGATIVE FEEDBACK
NT NONLINEAR FEEDBACK
NT POSITIVE FEEDBACK
NT SENSORY FEEDBACK
Bilateral force reflection for teleoperators with masters and slaves with dissimilar and possibly redundant kinematics
[DE90-004392] 08 p1061 N90-16132
Formulation and verification of a technique for compensation of pneumatic attenuation errors in airborne pressure sensing devices 09 p1221 N90-17084
Feedback effects in computer-based skill learning
[AD-A214560] 09 p1258 N90-17298
Dynamic response for thermal control and measurement and fast radiation thermometry 10 p1367 N90-17924
Electronically Variable Pressure Regulator (EVPR) 11 p1474 N90-18484
Teleoperator servoloop tuning using an expert system
[DE90-005674] 11 p1542 N90-18876
Microwave oscillator with reduced phase noise by negative feedback incorporating microwave signals with suppressed carrier 12 p1643 N90-19437
Aiming control: Theory and applications to dynamic control of space structures
[AD-A217877] 13 p1764 N90-20123
Passive navigation using image irradiance tracking 15 p2141 N90-22232
Single mode communication link
[AD-A219499] 17 p2388 N90-23601
Almost input-output decoupling with stability
[MEMO-819] 18 p2597 N90-24778
Variable force and visual feedback effects on teleoperator man/machine performance 23 p3364 N90-29008
TSC (Tokamak Simulation Code) simulations of Alcator C-MOD discharges 3: Study of axisymmetric stability
[DE90-015386] 23 p3398 N90-29198
Performance constraints and compensation for teleoperation with delay 24 p3517 N90-29881

FEEDBACK AMPLIFIERS
Feedback charge amplifier integrated on the detector wafer
[REPT-89-037] 04 p0496 N90-12852
Image amplification in photoreactive crystals and utilization in optical reaction systems
[ETN-90-97285] 24 p3546 N90-30059

FEEDBACK CIRCUITS
Transfer functions for nonlinear systems via Fourier-Borel transforms
[NASA-TM-100034] 02 p0145 N90-10828

FEEDBACK CONTROL
Structural stability augmentation system design using BODEDIRECT: A quick and accurate approach 01 p0023 N90-10116
Modeling and stabilization of large flexible space stations 01 p0024 N90-10120
Optimal integral controller with sensor failure accommodation 01 p0024 N90-10123
A simple, mass balance model of carbon flow in a controlled ecological life support system
[NASA-TM-102151] 01 p0101 N90-10571
Optimal and on-board near-optimal midcourse guidance 02 p0150 N90-10857
Flight test results of a complex precise digital flight control system 02 p0152 N90-10870
Control of turbulent mixing layers
[AD-A211413] 03 p0301 N90-11708
Adaptive control law design for model uncertainty compensation
[AD-A211712] 03 p0309 N90-11758
Effect of control surface mass unbalance on the stability of a closed-loop active control system
[NASA-TP-2952] 03 p0357 N90-12042
Adaptive feedback linearization: Stability and robustness
[PB89-219497] 03 p0390 N90-12220
Operating experience with the Sandia terminal switching network and fiber optic loop
[DE89-007422] 03 p0404 N90-12317
A robust digital model following controller for helicopters
[ESA-TT-1041] 04 p0457 N90-12621
Wideband phase-locked angular modulator 04 p0487 N90-12798
The M/G/1 processor sharing queue as the almost sure limit of feedback queues
[REPT-89-32] 04 p0528 N90-13044
Impact of tether cutting on onboard navigation during the Tethered Satellite Mission-1 05 p0588 N90-13424
Adaptive strategies for controls of flexible arms
[NASA-CR-185868] 05 p0649 N90-13783
A new approach to control single-link flexible arms. Part 3: Adaptive control of the tip position with payload changes
[AD-A213337] 05 p0650 N90-13792
The problem of automation: Inappropriate feedback and interaction, not overautomation
[NASA-CR-186126] 05 p0686 N90-13994
The quadratic matrix inequality in singular H infinity control with state feedback
[MEMO-COSOR-89-03] 05 p0686 N90-13997
The singular H infinity control problem with dynamic measurement feedback
[MEMO-COSOR-89-14] 05 p0687 N90-14000
Another approach to the local disturbance decoupling problem with stability for nonlinear systems
[MEMO-799] 05 p0691 N90-14033
Turbulence effects of aircraft flight dynamics and control 07 p0871 N90-15055
Effect of modal truncation on derivatives of closed-loop damping ratios in structural control 07 p0882 N90-15109
Advanced detection, isolation, and accommodation of sensor failures in turbofan engines: Real-time microcomputer implementation
[NASA-TP-2925] 07 p0883 N90-15112
Feed back Petrov-Galerkin methods for convection dominated problems
[DE89-636436] 08 p1063 N90-16148
Mathematical model for adaptive control system of ASEA robot at Kennedy Space Center 08 p1157 N90-16701
Feedback control of combustion instabilities: A case study in active adaptive control of complex physical systems
[AD-A215385] 09 p1192 N90-16905
Industrial Modernization Incentives Program: Computer-aided log book
[AD-A214614] 09 p1265 N90-17335
Permanent magnet flux-biased magnetic actuator with flux feedback
[NASA-CASE-LAR-13785-1] 09 p1277 N90-17403
Design of a robust controller for an unstable nonminimum phase guided missile
[AD-A216147] 10 p1323 N90-17645
Linear and non-linear control of high-order converters after reducing the order by appropriate techniques 10 p1336 N90-17733

High speed digital control of high frequency PWM converters 10 p1337 N90-17736
Discrete proportional Plus Integral (PI) multivariable control laws for the Control Reconfigurable Combat Aircraft (CRCA)
[AD-A215664] 11 p1464 N90-18431
Application of variable-gain output feedback for high-alpha control
[NASA-TM-102603] 11 p1464 N90-18434
Energy decay and boundary control for distributed parameter systems with viscoelastic damping
[AD-A216468] 11 p1519 N90-18748
Practical methods for robust multivariable control
[AD-A216937] 11 p1550 N90-18920
Contribution to the study of stability robustness of nonlinear multivariable regulators
[INPE-4801-TDL/356] 11 p1554 N90-18950
Output model-following control synthesis for an oblique-wing aircraft
[NASA-TM-100454] 12 p1606 N90-19241
Advanced topics in structural dynamics: The maneuver of flexible spacecraft, and on-off decentralized control of flexible structures 12 p1612 N90-19274
Design of a telerobotic controller with joint torque sensors
[DE90-008753] 13 p1812 N90-20404
Stochastic robustness of linear control systems 14 p1908 N90-20941
Optimization of the structural and control system for LSS with reduced-order model 14 p1935 N90-21075
Controller reduction for effective interdisciplinary design of active structures 14 p1935 N90-21077
On the continuous dependence with respect to sampling of the linear quadratic regulator problem for distributed parameter systems
[NASA-CR-182012] 14 p2018 N90-21566
Balanced bridge feedback control system
[NASA-CASE-NPO-17430-1-CU] 15 p2088 N90-21951
High order P-G finite elements for convection-dominated problems
[DE90-614743] 15 p2097 N90-21998
A new six-degree-of-freedom force-reflecting hand controller for space telerobotics 15 p2113 N90-22089
Branch point placement
[OUEL-1767/89] 15 p2158 N90-22329
An intelligent interface for the design of optimal control systems
[INPE-4917-PRE/1516] 15 p2159 N90-22332
Engagement analysis study
[DE90-009529] 15 p2163 N90-22359
Limiting performance based structural and control optimization for large vibrating structures 16 p2202 N90-22568
Equipment specifications for launcher guidance using multivariable frequency methods
[REPT-892-422-106] 16 p2205 N90-22582
The elastic-plastic behavior of composite materials 16 p2212 N90-22615
Systematic generation of multibody equations of motion suitable for recursive and parallel manipulation 16 p2280 N90-22992
Algorithms for computing the multivariable stability margin 16 p2291 N90-22999
Robustness analysis for real parametric uncertainty 16 p2281 N90-23000
A disturbance based control/structure design algorithm 16 p2282 N90-23003
Using deflation in the pole assignment problem with output feedback 16 p2282 N90-23004
Efficient computer algebra algorithms for polynomial matrices in control design 16 p2285 N90-23022
Integrated control-system design via generalized LQG (GLQG) theory 16 p2286 N90-23023
An algorithm for the solution of dynamic linear programs 16 p2286 N90-23026
Control of a flexible planar truss using proof mass actuators 16 p2288 N90-23035
Simulation studies using multibody dynamics code DART 16 p2288 N90-23036
Minimal complexity control law synthesis 16 p2292 N90-23057
OPTICON: Pro-Matlab software for large order controlled structure design 16 p2292 N90-23058
Robust fixed order dynamic compensation for large space structure control 16 p2292 N90-23059
Multivariable frequency weighted model order reduction for control synthesis
[AIAA-89-3558] 16 p2292 N90-23060
Man-in-the-control-loop simulation of manipulators 16 p2293 N90-23063
The use of real-time, hardware-in-the-loop simulation in the design and development of the new Hughes HS601 spacecraft attitude control system 16 p2293 N90-23065
Real-time closed-loop simulation and upset evaluation of control systems in harsh electromagnetic environments 16 p2294 N90-23069
Numerical algorithms for computations of feedback laws arising in control of flexible systems 16 p2297 N90-23085
About linear systems robustness: Linear programming approach
[LAAS-89-384] 16 p2303 N90-23123
Helicopter Airborne Laser Positioning System (HALPS)
[NASA-TM-102814] 17 p2354 N90-23399
Fractional state feedback control of undamped and viscoelastically-damped structures
[AD-A220477] 17 p2412 N90-23746
Adaptive control of a system with periodic dynamics: Application of an impulse response method to the helicopter vibration problem 17 p2453 N90-23990
Design and investigation of a dive plane sliding mode compensator for an autonomous underwater vehicle
[AD-A219552] 17 p2454 N90-23997
The discrete time H infinity control problem: The full-information case
[MEMO-COSOR-89-25] 17 p2455 N90-24003
Completion of the squares in the finite horizon H infinity control problem by measurement feedback
[MEMO-COSOR-89-27] 17 p2455 N90-24004
Almost disturbance decoupling by measurement feedback: A frequency domain analysis
[CWI-BS-R8910] 17 p2455 N90-24005
A hierarchical approach to large space structure control
[DE90-010681] 18 p2511 N90-24347
The problem of robust compensation for systems with unmodeled dynamics
[AD-A221246] 18 p2548 N90-24545
Overview on the Hermes in-orbit control system
[MBB-UK-0056/89-PUB] 19 p2652 N90-25094
Modeling flexible aircraft for flight control design
[AD-A219123] 19 p2660 N90-25140
Design and implementation of sensor systems for control of a closed-loop life support system
[NASA-CR-186675] 19 p2725 N90-25497
A control problem for Burgers' equation with bounded input/output
[NASA-CR-182062] 19 p2747 N90-25608
Synthesis and validation of feedback guidance laws for air-to-air interceptions
[LR-615] 19 p2752 N90-25639
Synthesis of individual rotor blade control system for gust alleviation
[NASA-TM-101886] 20 p2807 N90-25972
Robustness evaluation of H2 and H(infinity) control theory as applied to a transport aircraft
[AD-A222795] 20 p2814 N90-26018
ISIS and META projects
[NASA-CR-186645] 20 p2905 N90-26524
On the robust stability of MIMO linear feedback systems
[EUT-88-E-212] 20 p2915 N90-26585
Closed-loop autonomous docking system
[NASA-CASE-MFS-28421-1] 21 p2966 N90-26861
Heat exchanger with oscillating flow
[NASA-CASE-LAR-14033-1] 21 p3004 N90-27072
Generalized interpolation theory for the design and analysis of robust feedback systems
[AD-A222130] 21 p3060 N90-27399
Integrated structural/control design via multiobjective optimization
[AD-A223088] 21 p3071 N90-27459
The instrument pointing system: Precision attitude control in space 22 p3129 N90-27756
Fiber-optic projected-fringe digital interferometry
[NASA-TM-103252] 22 p3178 N90-28033
Algorithmic components in evaluating systems dependability
[REPT-88-044] 22 p3237 N90-28358
Active control of flexible structures 23 p3282 N90-28575
Real time guidance and propulsion control for single-stage-to-orbit airbreathing vehicles 23 p3285 N90-28587
Solutions to the frictional dynamics problem and the reciprocal variable feedback methodology for design and control of robot mechanisms 23 p3333 N90-28846
Kinematics, controls, and path planning results for a redundant manipulator 23 p3363 N90-29005
Adjustable impedance, force feedback and command language aids for telerobotics (parts 1-4 of an 8-part MIT progress report) 23 p3363 N90-29007
The JPL telerobot operator control station. Part 1: Hardware 23 p3371 N90-29049
The JPL telerobot operator control station. Part 2: Software 23 p3371 N90-29050
Implementation and design of a teleoperation system based on a VMEBUS/68020 pipelined architecture 23 p3372 N90-29053
Human machine interaction via the transfer of power and information signals 23 p3372 N90-29054
On the simulation of space based manipulators with contact 23 p3373 N90-29056
Preliminary results on noncollocated torque control of space robot actuators 23 p3373 N90-29057
Portable Dextrous Force Feedback Master for robot telemanipulation (PDMFF) 23 p3373 N90-29058
Robust controller design by contraction of a pole region
[ESA-TT-1042] 23 p3384 N90-29118
An expert system to perform on-line controller restructuring for abrupt model changes
[NASA-TM-103609] 23 p3385 N90-29121
Geometric theory for infinite dimensional systems
[ETN-90-96922] 23 p3389 N90-29144
Control and estimation for aerospace applications with system time delays 24 p3428 N90-29367
A comparison of scramjet engine performances of various cycles
[NAL-TR-1042] 24 p3434 N90-29397
Short period control using angular acceleration feedback: Compensation for first lag servo
[NAL-TM-600] 24 p3435 N90-29399
Sample rate effects on disturbance rejection for digital control systems 24 p3435 N90-29400
A three axis attitude control of a satellite
[NASDA-TR-22] 24 p3439 N90-29421
Suspension systems for ground testing large space structures
[NASA-CR-4325] 24 p3439 N90-29424
Robust design of LQG controllers 24 p3475 N90-29639
Robots, systems, and flexible automation
[DE90-015802] 24 p3476 N90-29649
Design and control of a multi-fingered robot hand provided with tactile feedback 24 p3501 N90-29789
Weighted feature selection criteria for visual servoing of a telerobot 24 p3503 N90-29801
Modeling and sensory feedback control for space manipulators 24 p3504 N90-29807
Experiments in cooperative manipulation: A system perspective 24 p3505 N90-29812
Linear analysis of a force reflective teleoperator 24 p3513 N90-29856
Real-time cartesian force feedback control of a teleoperated robot 24 p3513 N90-29857
Performance constraints and compensation for teleoperation with delay 24 p3517 N90-29881
MacRootLocus: A CAD design tool for feedback control systems
[AD-A223772] 24 p3528 N90-29951

FEEDERS
Plasma gun with coaxial powder feed and adjustable cathode
[NASA-CASE-LEW-14901-1] 01 p0126 N90-10718
Analysis of the 60-Hz power system at KSC: The Orsino substation 08 p1155 N90-16692

FEEDFORWARD CONTROL
A hybrid optimisation strategy for adaptive feed-forward layered networks
[RSRE-MEMO-4193] 03 p0391 N90-12226
One-class generalization in second-order backpropagation networks for image classification
[DE89-015845] 07 p0980 N90-15661
Analog hardware for learning neural networks
[NASA-CASE-NPO-17664-1-CU] 21 p3057 N90-27384
Active control of flexible structures 23 p3282 N90-28575
Manipulators with flexible links: A simple model and experiments 24 p3501 N90-29786
Performance constraints and compensation for teleoperation with delay 24 p3517 N90-29881

FEELINGS
U SENSORY FEEDBACK

FEET (ANATOMY)
Engineering specification and system design for CAD/CAM of custom shoes: UMC project effort
[NASA-CR-186547] 15 p2145 N90-22255

FEMALES
ONR (Office of Naval Research) summer scholars for the 1989 PREFACE Program
[AD-A217746] 13 p1903 N90-20919
A trend analysis of women who hold Federal Aviation Administration certificates: Relationship to the representation of women in collegiate aviation faculty ranks
[IAR-90-3] 19 p2762 N90-25691
Human performance in cockpit-related systems
[NIAR-90-7] 20 p2900 N90-26495

FEMUR
Experiment K-6-01. Distribution and biochemistry of mineral and matrix in the femurs of rats 20 p2892 N90-26455

FENCES
Boundary walls, fences and hoardings: Mean and peak wind loads and overturning moments
[ESDU-89050] 09 p1239 N90-17190
FENCES (BARRIERS)
Energy barriers in SK spin-glass model
[PREPRINT-665] 05 p0704 N90-14119
FERMENTATION
Fermentation and oxygen transfer in microgravity 05 p0679 N90-13956
FERMI LIQUIDS
A fermi liquid electric structure and the nature of the carriers in high-T(sub c) cuprates: A photoemission study
[DE89-016774] 02 p0284 N90-11624
High resolution-angle resolved photoemission studies of high temperature superconductors
[DE89-017691] 06 p0852 N90-14950
The superconducting state of the high-transition temperature superconductors: Experimental basis 22 p3136 N90-27793
Phenomenological theory of the normal and superconductive states of Cu-O and Bi-O metals 22 p3142 N90-27819
Electronic structure Fermi liquid theory of high T(sub c) superconductors: Comparison with experiments 22 p3142 N90-27821
FERMI SURFACES
Tunneling microscopy of superconductors and tunneling barriers
[AD-A212120] 04 p0559 N90-13257
X ray absorption studies of YBa2Cu3O(6 − x), La(2-x)Sr(x)CuO4, and Nd(2-x)Ce(x)CuO4
[DE90-003640] 07 p1002 N90-15797
Electron scattering by native defects in uniformly and modulation doped semiconductor structures
[DE90-006084] 10 p1437 N90-18296
Transport properties of anisotropic superconductors 15 p2170 N90-22404
Fundamental and practical studies of metal contacts on mercury zinc telluride
[AD-A218730] 17 p2376 N90-23528
Electronic structure Fermi liquid theory of high T(sub c) superconductors: Comparison with experiments 22 p3142 N90-27821
FERMIONS
NT ANTINEUTRINOS
NT BARYONS
NT COLD NEUTRONS
NT CONDUCTION ELECTRONS
NT ETA-MESONS
NT FAST NEUTRONS
NT HYPERONS
NT LEPTONS
NT MUONS
NT NEUTRINOS
NT NEUTRONS
NT PHOTONEUTRONS
NT PROTONS
NT RECOIL PROTONS
NT SOLAR NEUTRINOS
NT SOLAR NEUTRONS
NT SOLAR PROTONS
Mixed-valent and heavy fermions and related systems
[DE89-016335] 01 p0129 N90-10743
Quantization of anomalous gauge theories on a lattice
[DE89-010247] 01 p0135 N90-10776
Lattice fields and strong interactions
[DE89-015099] 01 p0135 N90-10777
Studies of novel superconductors
[DE89-016744] 02 p0282 N90-11609
The interacting boson approximation
[KVI-774] 04 p0552 N90-13215
More on the super WZW theory
[NIKHEF-H/88-11] 04 p0562 N90-13273
Lattice QCD estimate of mixing parameters for heavy meson systems
[PREPRINT-687] 05 p0697 N90-14079
A lattice study of semileptonic decays of D-mesons
[PREPRINT-660] 05 p0698 N90-14086
Research in theoretical physics
[DE90-005605] 09 p1294 N90-17500
Superstring field theory
[DE90-007694] 13 p1899 N90-20897
Improving fermion operators
[PREPRINT-710] 16 p2315 N90-23193
Mixing of DIS operators in lattice QCD
[PREPRINT-708] 16 p2323 N90-23243
Searching for heavy fermion materials in Ce intermetallic compounds
[DE90-011809] 20 p2834 N90-26116
Dirac's equation as a geodesic in Riemann space
[DE90-627194] 23 p3390 N90-29152
Anyons and Chern-Simons theory on compact spaces of finite genus
[DE90-627216] 23 p3391 N90-29157
Superconductivity in mixed boson-fermion systems
[DE90-627491] 23 p3401 N90-29216
FERRIC IONS
Reactive atmosphere processing of BaTiO3 and origins of its photorefractive effect
[AD-A215034] 09 p1289 N90-17475
FERRITES
Development of high frequency spice models for ferrite core inductors and transformers
[DE89-015121] 03 p0341 N90-11946
Parametric study of power absorption from electromagnetic waves by small ferrite spheres
[NASA-TP-2949] 03 p0399 N90-12282
Embrittlement of laboratory- and reactor-aged CF-3, CF-8, and CF-8M duplex stainless steels
[DE90-002777] 06 p0748 N90-14354
The effects of Mo2C morphology and strain distribution on the fatigue properties of Fe-C-Mo dual-phase steels 07 p0901 N90-15210
Finite element analysis of propagation in waveguide components with application to ferrite phase shifters
[FOA-C-30529-3.2] 09 p1204 N90-16977
Field theoretical analysis and synthesis of broadband waveguide: Height, plane shunt circulators with multiple layer material insertions
[ETN-90-95360] 12 p1647 N90-19469
Dual-mode latching reciprocal ferrite phase shifter
[FEL-1988-55] 12 p1652 N90-19497
New ferrite-filled waveguiding structures analysed by the averaging method
[PB90-165671] 14 p1967 N90-21269
The effect of aging at 343 C on type 308 stainless steel weldments
[DE90-009232] 15 p2069 N90-21853
A framework to correlate a/W ratio effects on elastic-plastic fracture toughness (J (sub c))
[AD-A222822] 21 p3012 N90-27125
The influence of solidification rate on solute redistribution and second-phase formation in stainless steel alloys
[DE90-015189] 24 p3450 N90-29482
Activities of the Division of Microwave Technology
[FOA-C-30555-3.2] 24 p3459 N90-29537
FERRITIC STAINLESS STEELS
Improvement in pre-constraint fatigue resistance of modular ferretic and bainitic steel by shot peening treatments
[CETIM-106370] 04 p0476 N90-12727
Fusion reactor materials
[DE90-000976] 07 p0994 N90-15744
Three-dimensional Fe analysis of the surface distribution in notched compact samples of 20 MnMoNi 55
[W-1/89] 12 p1676 N90-19625
FERROALLOYS
U IRON ALLOYS
FERROCENES
Solvent relaxation in electron-transfer reactions: Comparisons between barrier-crossing dynamics in water and polar aprotic media
[AD-A210212] 01 p0040 N90-10220
Solvent effects on intervalence electron-transfer energies for biferrocene cations: Comparisons with molecular models of solvent reorganization
[AD-A210263] 01 p0120 N90-10691
Investigation of fuel additive effects on sooting flames
[AD-A212925] 04 p0473 N90-12709
Electrochemistry in near-critical and supercritical fluids. 8: Methyl viologen, decamethylferrocene, Os(bpy)3(sup 2 −) and ferrocene in acetonitrile and the effect of pressure on diffusion coefficients under supercritical conditions
[AD-A213407] 07 p0895 N90-15172
Evaluation of ion intercalation in conducting polymers
[AD-A219423] 17 p2379 N90-23549
Ionic atmosphere effects on the energetics of thermal and optical electron-exchange reactions: Application to ferrocenium-ferrocene self exchange
[AD-A222605] 20 p2889 N90-26441
FERROELECTRICITY
Behaviour of VF(sub 2)/VF(sub 3) piezoelectric copolymers under shock loading
[DE89-016538] 02 p0201 N90-11145
Chevron layer structures in Surface Stabilized Ferroelectric Liquid Crystal (SSFLC) cells filled with a material which exhibits the chiral nematic to smectic C* phase transition
[DE89-016985] 02 p0285 N90-11628
Analysis of the efficiency of a dielectric solar energy collector
[PB89-212716] 03 p0366 N90-12092
Metallo-organic decomposition process for dielectric films
[AD-A211590] 04 p0495 N90-12849
Studies of structure and switching dynamics in ferroelectric crystal and liquid crystal thin films
[AD-A212650] 05 p0702 N90-14109
New devices using ferroelectric thin films
[DE90-000789] 07 p0921 N90-15328
Thermodynamic studies on the ferroelectric phase transition in neutron irradiated (Li(sub x)K(1-x))2SO4 crystals at high temperature
[DE89-635786] 08 p1130 N90-16545
Develop techniques for ion implantation of PLZT for adaptive optics
[AD-A216005] 10 p1431 N90-18253
Piezoelectric polymer PVDF shock gauge: State of the research art
[ISL-CO-207/89] 11 p1512 N90-18705
In situ growth of epitaxial superconducting YBa2Cu3O(7-x) films on insulating semiconducting and ferroelectric K(Ta, Nb)O3 by pulsed laser ablation
[DE90-006568] 11 p1571 N90-19043
A new thermal sensor for x ray microcalorimetry
[DE90-008547] 13 p1805 N90-20360
The study of VF2/VF3 piezoelectric copolymeteres submitted to shocks
[ISL-CO-210/9] 20 p2931 N90-26679
Research on sputtering of ferroelectric thin films
[AD-A221792] 21 p2983 N90-26949
The mechanism of high-T(sub c) superconductivity due to bound hole mediators: Relationship to ferroelectricity 22 p3143 N90-27825
Coupled bipolarons and optical phonons as a model for high-T(sub c) superconductors 22 p3149 N90-27854
The relation between ferroelasticity and superconductivity 22 p3150 N90-27861
FERROMAGNETIC FILMS
Surface magneto-optical studies of ultrathin ferromagnetic films
[DE90-002199] 06 p0856 N90-14980
High speed magneto-resistive random access memory
[NASA-CASE-NPO-17954-1-CU] 20 p2904 N90-26519
FERROMAGNETIC MATERIALS
NT FERROMAGNETIC FILMS
Spin fluctuations and excitations in a 2D xy-ferromagnet: CoCl2 in graphite
[DE89-017600] 02 p0196 N90-11119
Investigations of the influence of magnetically long range ordered phases on the electronic charge transport in metallic glasses
[ETN-89-94672] 02 p0202 N90-11155
On geometry of inhomogeneous Heisenberg ferromagnet: Nonintegrable case
[MEMO-789] 05 p0691 N90-14030
Improved amorphous metal materials for magnetic pulse compression
[DE90-005723] 11 p1486 N90-18555
Crystallographic and magnetic properties of (C6 D11 ND3)CuBr3 and (Zn(1-x)Mn(x))3As2: A neutron scattering study
[ECN-219] 11 p1573 N90-19055
Barkhausen noise analysis and ferromagnetic materials
[AD-A217989] 13 p1881 N90-20792
Superconducting and normal compounds: Some high field/high pressure effects 16 p2320 N90-23229
Microwigglers for submillimeter wavelength free-electron lasers
[AD-A220185] 17 p2409 N90-23730
Method of obtaining current-conducting polymer materials
[AD-A222129] 22 p3159 N90-27914
Systematic approach to critical phenomena by the extended variational method and coherent-anomaly method
[DE90-627320] 23 p3392 N90-29165
Z(6) model: Criticality and break-collape method
[DE90-627323] 23 p3401 N90-29214
Theoretical investigations of Pi-conjugated polyradicals as models for organic magnetic materials
[AD-A223411] 24 p3446 N90-29461
FERROMAGNETISM
Rigorous analysis of low temperature stochastic Ising models: Metastability and exponential approach to equilibrium
[PREPRINT-720] 16 p2312 N90-23175
FERRY SPACECRAFT
The spacebus power conditioning application to the Eutelsat 2 spacecraft 10 p1330 N90-17689
The partnership: Space shuttle, space science, and space station
[NASA-TM-102900] 14 p1930 N90-21050
FERTILIZATION
The first seven minutes of a Zenopus egg fertilised on a sounding rocket in space 19 p2680 N90-25245
Automatic experiment container for fertilisation of frog eggs in space: A multi-purpose piece of classified space hardware 19 p2681 N90-25249
The influence of a sounding rocket flight on sexual activation in Chlamydomonas gametes 19 p2681 N90-25250

FET (TRANSISTORS)
U FIELD EFFECT TRANSISTORS
FEYNMAN DIAGRAMS
Homogeneous chaos, p-forms, scaling and the feynman integral
[AD-A218339] 13 p1879 N90-20777
Characteristics consequences of space-time coordinate relativization
[DE90-615201] 14 p2034 N90-21668
FFT
U FAST FOURIER TRANSFORMATIONS
FIBER COMPOSITES
NT CARBON FIBER REINFORCED PLASTICS
NT GLASS FIBER REINFORCED PLASTICS
Space structures concepts and materials
[NASA-CR-183727] 01 p0025 N90-10128
Mechanics of damping for fiber composite laminates including hygro-thermal effects
[NASA-TM-102329] 01 p0034 N90-10185
Failure behavior of PEEK and its short-fiber composite systems
[AD-A210729] 01 p0035 N90-10189
Field repair of composite materials in Army service: Planning for the future
[AD-A210732] 01 p0035 N90-10190
Zirconia toughened SiC whisker reinforced alumina composites small business innovation research
[NASA-CR-179629] 01 p0052 N90-10294
Hygrothermal deformations of composite shells 02 p0185 N90-11055
Composites reinforced with thermotropic liquid crystal copolyester fibers
[AD-A211226] 02 p0191 N90-11089
Interfacial adsorption and crystallization of polycarbonate in carbon fiber composites
[AD-A211230] 02 p0191 N90-11090
An integrated methodology for optimizing structural composite damping
[NASA-TM-102343] 03 p0319 N90-11808
Interlaminar stress concentration in fiber composites
[ETN-89-94670] 03 p0319 N90-11809
Carbon fiber reinforced glass matrix composites for structural space based applications
[AD-A211682] 03 p0320 N90-11818
Ballistic properties of composite materials for personnel protection
[MRL-TR-89-6] 04 p0465 N90-12661
Shear fatigue testing and life prediction of fibre composites
[REPT-8519] 04 p0466 N90-12668
Biaxial flexing of a fiber-reinforced aluminum composite
[AD-A212742] 04 p0468 N90-12681
Device for inspection of materials by eddy current methods
[AD-D014205] 04 p0511 N90-12948
Orthotropic elasto-plastic behavior of AS4/APC-2 thermoplastic composite in compression
[NASA-CR-186080] 04 p0513 N90-12959
Status of Gr/glass composites technology at UTOS 05 p0596 N90-13459
Failure processes in unidirectional composite materials 05 p0617 N90-13598
Localization of ultrasound in thick composites
[AD-A212994] 05 p0618 N90-13602
Fiber reinforced cementitious composites technology
[PB89-227813] 05 p0619 N90-13608
Impact tests of three composite materials with carbon fiber cores
[REPT-M6-582500] 05 p0619 N90-13610
Impact tests on aluminum 2024 T3, aramid and glass reinforced aluminum laminates and thermoplastic composites
[LR-534] 05 p0619 N90-13613
Constant amplitude fatigue of ARALL-2 laminates
[LR-539] 05 p0620 N90-13615
Oxidation effects on the mechanical properties of SiC fiber-reinforced reaction-bonded silicon nitride matrix composites
[NASA-TM-102360] 06 p0736 N90-14287
Carbon fiber reinforced metal matrix composites
[AD-D014245] 06 p0737 N90-14289
Elasto-plastic analysis of unidirectional fiber-reinforced composites subjected to transverse normal loading using the finite element method 06 p0737 N90-14292
Parametric studies to determine the effect of compliant layers on metal matrix composite systems
[NASA-TM-102465] 06 p0737 N90-14294
Friction and wear of glassy carbon in sliding contact, revision 1
[DE90-000743] 06 p0750 N90-14365
Challenges in processing for polymer composites
[DE90-002224] 06 p0752 N90-14376
A study of impact damage in composite laminates 07 p0888 N90-15137
The mechanical behavior of a fiber-reinforced brittle matrix composite 07 p0889 N90-15139
Composite activities at Lawrence Livermore National Laboratory
[DE90-002979] 07 p0891 N90-15149
Transverse (through-the-thickness) shear stiffnesses of fibre reinforced composite laminated plates (computer program)
[ESDU-89013] 07 p0891 N90-15152
Metal matrix composites with long inorganic fibers 07 p0901 N90-15206
Short fibre and particulate reinforced metal matrix composites 07 p0901 N90-15207
SESAME equation of state for a polymer composite: Phenolic refrasil
[LA-11512-MS] 07 p0910 N90-15264
Toughening behavior and interfacial properties of fiber-reinforced ceramic composites
[DE89-015351] 07 p0913 N90-15279
Probabilistic simulation of uncertainties in composite uniaxial strengths
[NASA-TM-102483] 08 p1040 N90-16008
Two new techniques for predicting delamination growth in laminated plates 09 p1185 N90-16865
Interfaces of organic matrices and graphite fiber composites: A review of the literature
[AD-A214504] 09 p1186 N90-16870
Rapid solidification processing of composites
[AD-A215175] 09 p1187 N90-16875
High-order mixture homogenization of fiber-reinforced composites
[AD-A215247] 09 p1187 N90-16876
Compression testing of carbon fibers
[AD-A215296] 09 p1187 N90-16877
High-order mixture homogenization of periodic nonlinear composites 10 p1347 N90-17814
Damping loss factor determination of glass and graphite fiber composites
[AD-A214535] 10 p1347 N90-17816
Studies on deformation and fracture of viscoelastic composite materials
[AD-A216095] 10 p1348 N90-17819
Effects of elevated temperatures and thermal cycling on ceramic composite materials
[AD-A216242] 10 p1350 N90-17828
Critical field enhancement due to field penetration in fine-filament superconductors
[DE90-005389] 10 p1435 N90-18282
Third European Conference on Composite Materials
[EOARD-LR-89-050] 11 p1476 N90-18494
Modified bismaleimides for carbon fibre composites 11 p1476 N90-18495
Enhanced bonding of fiber reinforcements to thermoset resins 11 p1476 N90-18496
Interlaminar fracture testing of carbon fibre/PEEK composites validity and applications 11 p1477 N90-18497
State of the art and future prospects for high temperature composites 11 p1477 N90-18498
Silicon carbo-nitride ceramic matrix composites by polymer pyrolysis 11 p1477 N90-18499
Ceramic matrix composites, new high performance materials 11 p1477 N90-18500
Sputter deposition of diffusion barrier coatings on SiC monofilaments for use in Ti-based composites 11 p1477 N90-18502
Measuring strain in carbon fibre composite laminates using the Raman optomechanical strain gauge 11 p1477 N90-18503
Theory and verification of the fiber composite damage model implemented in DYNA3D
[AD-A216600] 11 p1479 N90-18511
Heat treatment study of the SiC/Ti-15-3 composite system
[NASA-TP-2970] 12 p1618 N90-19302
Innovative design of composite structures: The use of curvilinear fiber format in structural design of composites
[NASA-CR-186406] 12 p1620 N90-19308
Thermo-oxidative stability studies of PMR-15 polymer matrix composites reinforced with various fibers
[NASA-TM-102439] 12 p1620 N90-19310
The creep behavior of an aramide fiber reinforced wound tow-strap
[LR-546] 12 p1620 N90-19312
Tensile behavior of cylindrical pressure tanks in fiber assembling + metal hybrid structure
[ILR-MITT-213] 12 p1675 N90-19618
Infiltration mechanics in conventional and hybridised fibre reinforced metal matrix composites
[AERE-R-13330] 13 p1766 N90-20134
Composite laminate tailoring with probabilistic constraints and loads
[NASA-TM-102515] 13 p1766 N90-20138
Compression testing of thick-section composite materials
[AD-A217234] 13 p1767 N90-20142
Optimization of fracture resistance in composites
[AD-A217431] 13 p1768 N90-20144
Oxygen concentrations on surfaces of carbon fibers
[AD-A217724] 13 p1769 N90-20152
COMGEN: A computer program for generating finite element models of composite materials at the micro level
[NASA-TM-102556] 13 p1818 N90-20438
Characterization of failure processes in tungsten copper composites under fatigue loading conditions
[NASA-TM-102371] 14 p1943 N90-21123
Use of unbalanced laminates as a screening method for microcracking
[NASA-TM-102517] 14 p1944 N90-21124
Fracture and longevity of composite structures
[AD-A217827] 14 p1944 N90-21127
Multi-objective shape and material optimization of composite structures including damping
[NASA-TM-102579] 14 p1945 N90-21132
Two-dimensional damage models of fiber-reinforced composites 14 p1946 N90-21135
Structural tailoring of select fiber composite structures
[NASA-TM-102484] 14 p1946 N90-21137
High temperature fatigue behavior of tungsten copper composites
[NASA-TM-102404] 14 p1946 N90-21138
Micromechanics analysis of space simulated thermal deformations and stresses in continuous fiber reinforced composites
[NASA-TM-102633] 14 p1946 N90-21140
Fatigue damage growth mechanisms in continuous fiber reinforced titanium matrix composites
[NASA-TM-102594] 14 p1991 N90-21409
Small business innovation research. Abstracts of 1988 phase 1 awards
[NASA-TM-102991] 14 p2036 N90-21680
Interfacial studies in fiber-reinforced thermoplastic-matrix composites 15 p2062 N90-21814
Computational simulation of structural fracture in fiber composites
[NASA-TM-102505] 15 p2064 N90-21821
METCAN verification status
[NASA-TM-103119] 15 p2064 N90-21824
Matrix density effects on the mechanical properties of SiC/RBSN composites
[NASA-TM-103098] 15 p2065 N90-21826
Failure mechanisms under complex loading of glass-reinforced polyester composites and their matrices: The effect of superposed hydrostatic pressures up to 300 MPa on axial tensile and compressive strengths, and in-plane shear properties of unidirtionally reinforced glass-polyester composites and the relevant polyesters 15 p2110 N90-22072
The stress field due to an edge dislocation and some fracture problems for a three-phase composite cylinder model 15 p2120 N90-22126
A study of woven fabric-reinforced composite materials using an invariant-based orthotropic plasticity formulation 16 p2211 N90-22611
Fatigue crack growth in a unidirectional SCS-6/Ti-15-3 composite
[NASA-TM-103095] 16 p2217 N90-22646
Microcracking and toughness of ceramic-fiber/ceramic-matrix composites under high temperature
[AD-A218516] 16 p2223 N90-22680
Computations of weight functions in fracture mechanics 16 p2246 N90-22809
High temperature fatigue behavior of a SiC/Ti-24Al-11Nb composite
[NASA-TM-103157] 16 p2248 N90-22822
MTS high temperature testing system
[AD-A219613] 17 p2369 N90-23483
Effect of surface oxygen on adhesion of carbon fiber-reinforced composites
[AD-A220777] 17 p2369 N90-23486
Composite curing: A new process
[REPT-892-430-114] 17 p2370 N90-23490
Rate dependent constitutive models for fiber reinforced polymer composites
[NASA-TM-102665] 17 p2370 N90-23492
Acousto-ultrasonic nondestructive evaluation of materials using laser beam generation and detection
[NASA-CR-186694] 17 p2398 N90-23664
National Educators' Workshop: Update 1989 Standard Experiments in Engineering Materials Science and Technology
[NASA-CP-3074] 18 p2513 N90-24350
The assessment of metal fiber reinforced polymeric composites 18 p2514 N90-24357
An elastic/viscoplastic constitutive model for fiber-reinforced thermoplastic composites 18 p2516 N90-24371
Stress fields in composite materials by means of a nonclassical approach 18 p2517 N90-24372

Influence of interfacial shear strength on the mechanical properties of SiC fiber reinforced reaction-bonded silicon nitride matrix composites
[NASA-TM-102462] 18 p2518 N90-24382
Simplified design procedures for fiber composite structural components/joints
[NASA-TM-103113] 18 p2519 N90-24384
Mechanical property characterization of fiber-reinforced SiC matrix composites
[DE90-011316] 18 p2520 N90-24390
A creep model for metallic composites based on matrix testing: Application to Kanthal composites
[NASA-TM-103172] 19 p2672 N90-25193
Seamless metal-clad fiber-reinforced organic matrix composite structures and process for their manufacture
[NASA-CASE-LAR-13562-1] 19 p2672 N90-25196
Experimental observations and finite element analysis of the initiation of fiber microbuckling in notched composite laminates
[NASA-CR-186207] 19 p2699 N90-25359
Thermomechanical testing techniques for high-temparature composites: TMF behavior of SiC(SCS-6)/Ti-15-3
[NASA-TM-103171] 19 p2701 N90-25367
Vitreous joining of SiC fiber reinforced SiC composites
[DE90-012951] 20 p2827 N90-26081
The influence of microstructure on the tensile behavior of an aluminum metal matrix composite
[NASA-TM-102694] 20 p2827 N90-26082
Study on failure modes of boron fiber reinforced aluminum composite materials by AE method, part 2
[DE90-505522] 20 p2828 N90-26086
Plate rods and leaf springs with hybrid structure: Cross section optimization following different target criteria
[ILR-MITT-227(1989)] 20 p2877 N90-26366
Reliability analysis of continuous fiber composite laminates
[NASA-CR-185265] 20 p2878 N90-26372
An embedded fibre optic sensor for impact damage detection in composite materials
[UTIAS-332] 20 p2926 N90-26650
Development of a graphite/bismaleimide leading edge for the F-111 (EF-111A) horizontal stabilizer
21 p2956 N90-26809
A study on carbon Fiber (long fiber) reinforced copper matrix composite
[AD-A221584] 21 p2972 N90-26891
Micromechanics of interfaces in high temperature ceramics
[AD-A222027] 21 p2987 N90-26973
The response and failure mechanisms of circular metal and composite plates subjected to underwater shock loading
[AD-A222200] 21 p3013 N90-27131
Nondestructive evaluation of adhesively-bonded joints
22 p3185 N90-28074
Neutron radiography: Applications and systems
22 p3186 N90-28080
Study of failure processes in fiber reinforced composites using acoustic emission techniques
22 p3188 N90-28090
Input-output characterization of fiber reinforced composites by P waves
[NASA-CR-185287] 22 p3189 N90-28097
Micromechanical model of crack growth in fiber reinforced ceramics
[NASA-CR-4321] 22 p3192 N90-28113
Transcrystalline morphology in carbon fibre composites with thermoplastic matrix and its influence on the mechanical properties
[FOA-C-20783-2.1] 22 p3248 N90-28423
Probability models for the failure of fibres and fibrous composite materials 23 p3300 N90-28665
Strengthening and toughening mechanisms in ceramic fiber-reinforced glass matrix composites
23 p3300 N90-28666
Factors influencing the mode I interlaminar fracture resistance of toughened matrix composites
23 p3300 N90-28668
Is there anything of practical value hidden amongst the composite toughening theories. A Jim Mueller prospective
[DE90-014905] 23 p3301 N90-28673
Polymer research
[PB90-246638] 23 p3313 N90-28737
Evaluation of ARALL-4: An aramid fiber reinforced aluminum
[AD-A223502] 24 p3443 N90-29443
Development of dual fiber reinforced glass matrix composites for structural space based applications
[AD-A223801] 24 p3444 N90-29446
Interlaminar shear tests on continuous fiber reinforced thermoplastics: The effects of rubber forming
[LR-621] 24 p3444 N90-29451
Precursor structure-fiber property relationships in polyacrylonitrile-based carbon fibers
[AD-A224246] 24 p3454 N90-29503

FIBER OPTICS

Multimode fiber interferometry and several-mode fiber polarimetry via phase conjugation
[DE89-014226] 01 p0123 N90-10706
Automation of fiber-optic pigtailing process: Laser welding demonstration program
[AD-A210351] 01 p0123 N90-10707
Fiber optic technique for surveillance and control of mine fields
[FOA-C-30526-3.1] 02 p0225 N90-11293
Fiber optics: A brief introduction
[DE89-009337] 02 p0274 N90-11567
Adaptive gigabit fiber optics local area network
[AD-A210794] 02 p0275 N90-11571
In-situ cure monitoring of composites by fiber-optic molecular sensors
[AD-A211495] 03 p0320 N90-11817
High power, solid state RF pulse generators
[AD-D014172] 03 p0341 N90-11941
Operating experience with the Sandia terminal switching network and fiber optic loop
[DE89-007422] 03 p0404 N90-12317
Optical data transmission systems in radiation environment
[DE90-000174] 03 p0405 N90-12322
Small-radius bending loss in single-mode fibers
[AD-A211822] 03 p0405 N90-12323
Silicon-etalon fiber-optic temperature sensor
[NASA-TM-102389] 05 p0580 N90-13381
Fiber-optic sensors for composite cure analysis and lifetime nondestructive evaluation
[DE90-001739] 06 p0738 N90-14296
Method and apparatus to enhance the sensitivity of cylindrical magnetostrictive transducer to magnetic fields
[AD-D014218] 06 p0767 N90-14459
A fiber-fed imaging spectrometer
[DE90-001008] 06 p0781 N90-14538
Simulated Brillouin backscattering in optical fibers: A ring resonator 06 p0783 N90-14556
Spectral contents readout of birefringent sensor
[NASA-CR-179444] 06 p0843 N90-14905
Fly-by-light flight control system technology development plan
[NASA-CR-181953] 07 p0883 N90-15111
Voice Multiplex System (VMS)
[AD-A213902] 07 p0919 N90-15315
A new kind of heterodyne fiber-optic gyroscope
[AD-A213953] 07 p0933 N90-15404
Laser communication system with wide band magnetostrictive modulation
[AD-D014302] 07 p0937 N90-15427
Fiber optic sensing system
[NASA-CASE-LEW-14795-1] 07 p0992 N90-15733
A simple fiber optic autocorrelation tachometer
[ETN-90-96146] 08 p1077 N90-16228
Chromatic dispersion compensation in a Fresnel lens by means of a diffraction grating
[DE90-004030] 08 p1123 N90-16506
Miniature GPS-based guidance package
09 p1163 N90-16736
NASA Laser Light Scattering Advanced Technology Development Workshop, 1988
[NASA-CP-10033] 09 p1221 N90-17085
Laser light scattering review 09 p1221 N90-17086
Design of fiber optic probes for laser light scattering
09 p1222 N90-17090
Improved optics for laser light scattering
09 p1222 N90-17092
Investigation of a magnetostrictive fiber optic interferometric sensor
[AD-A215666] 09 p1226 N90-17111
The Advanced Digital-Optical Control System (ADOCS) user demonstration program
[AD-A215984] 10 p1323 N90-17644
The application of fiber optic technology to flowmeters
[AD-A214389] 10 p1430 N90-18247
Fiber optic transversal filter/variable delay line
[AD-D014328] 10 p1430 N90-18248
A 13-point Thomson scattering system for JFT-2M plasma
[DE90-733140] 10 p1432 N90-18263
Measuring strain in carbon fibre composite laminates using the Raman optomechanical strain gauge
11 p1477 N90-18503
Proceedings of the 38th International Wire and Cable Symposium
[AD-A216023] 11 p1501 N90-18638
Design, implementation and test of an RS-232 compatible bi-directional, full duplex, fiber-optic interface with provision for hardware handshaking on a minimum of fiber-optic lines
[AD-A216604] 11 p1566 N90-19012
Applications of FM-CW laser radar to antenna contour mapping 12 p1611 N90-19270
Apparatus and method for minimizing polarization-induced signal fading in an interferometric fiber-optic sensor using input-polarization modulation
[AD-D014315] 12 p1642 N90-19430
Effect of laser frequency noise on fiber-optic frequency reference distribution 12 p1643 N90-19438
Thermal coefficient of delay for various coaxial and fiber-optic cables 12 p1643 N90-19439
Opto-Em and devices investigation
[AD-A215033] 12 p1709 N90-19814
A space-based optical communication system utilizing fiber optics
[AD-A217333] 13 p1887 N90-20828
Advanced instrumentation for aircraft icing research
[NASA-CR-185225] 14 p1921 N90-21006
Strain and dynamic measurements using fiber optic sensors embedded into graphite/epoxy tubes
14 p1937 N90-21090
Bit-error-rate testing of fiber optic data links for MMIC-based phased array antennas
[NASA-TM-102523] 14 p1966 N90-21261
Intensity to frequency conversion technique in intensity modulated fiber optic sensing systems
[NASA-TM-102562] 14 p1969 N90-21277
Civil air transport: A fresh look at power-by-wire and fly-by-light
[NASA-TM-102574] 14 p1969 N90-21283
A fiber optic sensor for noncontact measurement of shaft speed, torque, and power
[NASA-TM-102481] 14 p1983 N90-21360
Fiber optic void fraction sensor
[DE90-009124] 14 p1983 N90-21366
Passive stabilization of a fiber optic nonlinear interferometric sensor
[AD-D014438] 14 p2026 N90-21620
Microwave Landing System (MLS) multiple system design interoperability interface control report
[DOT/FAA/SA-89/2] 15 p2050 N90-21750
Microwave analog fiber-optic link for use in the deep space network 15 p2075 N90-21883
Optical shutter switching matrix
[NASA-CASE-KSC-11392-1] 15 p2167 N90-22383
Measurement of HCl by near-infrared diode laser absorption 16 p2209 N90-22601
A fiber-optic current sensor for aerospace applications
[NASA-TM-103152] 16 p2239 N90-22773
Vertical emitting, ring geometry, ultra-low threshold, and ultra-high speed quantum well lasers for optical interconnect
[AD-A219946] 17 p2409 N90-23727
Optical links for microwave application
[AD-A220574] 17 p2472 N90-24134
Material evaluation of optical fibers and payout bobbins: An overview
[AD-A220104] 17 p2473 N90-24140
Method and apparatus for determining optical absorption and emission characteristics of a crystal or non-crystalline fiber
[NASA-CASE-LAR-13963-1] 17 p2475 N90-24150
Infrared fiber-optical temperature sensor
[AD-D014519] 19 p2693 N90-25321
Comparison test of droplet sizing instruments used in icing research
[DOT/FAA/CT-TN90/13] 19 p2693 N90-25322
Differential polarimetric fiber optic sensor
[AD-D014501] 19 p2757 N90-25668
Sol-gel processing for fiber optic applications
[DE90-012083] 19 p2758 N90-25675
Design of an optically controlled Ka-band GaAs MMIC phased-array antenna
[NASA-TM-103147] 20 p2857 N90-26250
An embedded fibre optic sensor for impact damage detection in composite materials
[UTIAS-332] 20 p2926 N90-26650
Apparatus and method for minimizing polarization-induced signal fading in an interferometric fiber-optic sensor using input-polarization control
[AD-D014492] 22 p3164 N90-27940
Stand-alone terrestrial and satellite networks for nationwide interoperation of broadband networks
[PB90-172404] 22 p3164 N90-27942
Fiber-optic projected-fringe digital interferometry
[NASA-TM-103252] 22 p3178 N90-28033
Serial interferometric fiber-optic sensor array
[AD-D014466] 22 p3246 N90-28407
Application of integrated optical components in optical fiber communication
[FEL-89-B252] 23 p3395 N90-29183
Engineering and the advancement of human welfare. Ten outstanding achievements 1964-1989
[ISBN-0-309-04185-6] 23 p3415 N90-29297
Inertial grade fiber gyros 24 p3426 N90-29353

Development and evaluation of hermetic laser diode ignited pyrotechnic components
[DE90-015745] 24 p3458 N90-29529
Evaluation of a potential Wave Division Multiplexer (WDM) for use in the IRSTD
[AD-A223945] 24 p3463 N90-29560
High speed bus technology development
[AD-A224486] 24 p3463 N90-29565
Real-time concentration monitoring of large aerodynamic diameter fiber aerosols using the geometric optic inversion technique
[AD-A224167] 24 p3545 N90-30048

FIBER ORIENTATION
Study of fatigue degradation mechanisms in unidirectional composite materials. Application to cumulative damage
[ECL-88-12] 05 p0619 N90-13611
Contribution to the fatigue behavior study of composite materials reinforced with unidirectional glass fibers
[ECL-88-20] 05 p0619 N90-13612
Innovative design of composite structures: The use of curvilinear fiber format in structural design of composites
[NASA-CR-186406] 12 p1620 N90-19308
Innovative design of composite structures: The use of curvilinear fiber format to improve buckling resistance of composite plates with central circular holes
[NASA-CR-186454] 13 p1766 N90-20135
Innovative design of composite structures: The use of curvilinear fiber format in composite structure design
[NASA-CR-186453] 13 p1766 N90-20136
Compression testing of thick-section composite materials
[AD-A217234] 13 p1767 N90-20142
Optimization of laminated composite plates
[AD-A217621] 13 p1768 N90-20146
Resistivity of pristine and intercalated graphite fiber epoxy composites
[NASA-TM-102576] 14 p1955 N90-21192
Fatigue crack growth in unidirectional metal matrix composite
[NASA-TM-103102] 15 p2118 N90-22117
Structural behavior of composites with progressive fracture
[NASA-TM-102370] 17 p2368 N90-23477
Damage states in laminated composite three-point bend specimens: An experimental-analytical correlation study
[NASA-TM-101800] 20 p2827 N90-26083
Creep and creep rupture of strongly reinforced metallic composites
[NASA-CR-185286] 22 p3192 N90-28110
Precursor structure-fiber property relationships in polyacrylonitrile-based carbon fibers
[AD-A224246] 24 p3454 N90-29503

FIBER STRENGTH
Toughening behavior and interfacial properties of fiber-reinforced ceramic composites
[DE89-015351] 07 p0913 N90-15279
The effect of fiber coatings on interfacial shear strength and the mechanical behavior of ceramic composites
[DE90-007574] 12 p1632 N90-19380
Matrix density effects on the mechanical properties of SiC/RBSN composites
[NASA-TM-103098] 15 p2065 N90-21826
Compressive strength of rigid-rod polymer fibers
[AD-A221886] 21 p2989 N90-26987

FIBERGLASS
U GLASS FIBERS

FIBERS
NT BORON FIBERS
NT CARBON FIBERS
NT CERAMIC FIBERS
NT COTTON FIBERS
NT GLASS FIBERS
NT METAL FIBERS
NT NYLON (TRADEMARK)
NT OPTICAL FIBERS
NT RAYON
NT REINFORCING FIBERS
NT SYNTHETIC FIBERS
NT WOOL
Solid fiber Z-pinches: Cold-start computations
[DE89-016768] 02 p0279 N90-11592
Density of intercalated graphite fibers
[NASA-TM-102411] 06 p0750 N90-14362
Experimental study on the filamentary instability in laser-matter interactions at short wave lengths
06 p0782 N90-14547
Composite activities at Lawrence Livermore National Laboratory
[DE90-002979] 07 p0891 N90-15149
Short-term bioassays may be useful in evaluating fiber/whisker hazards
[DE90-003707] 08 p1104 N90-16393
Investigation into the effect of fibre size on the tribological behaviour of semi-metallic brake material
09 p1185 N90-16864
Three-dimensional stress analysis of plain weave composites
[NASA-TM-101672] 10 p1347 N90-17813
Investigation of the failure modes in a metal matrix composite under thermal cycling
[AD-A216195] 10 p1349 N90-17825
The processing and mechanical properties of high temperature/high performance composites. Book 3, section 2: Strength and fracture resistance, part
[AD-A216143] 11 p1478 N90-18508
Damage assessment in composites by acousto-ultrasonic technique
[AD-A216590] 11 p1479 N90-18510
Calculations of braiding parameters
[AD-A216836] 11 p1479 N90-18515
Optical studies of dynamical processes in disordered materials
[DE90-007080] 12 p1631 N90-19372
The effect of fiber coatings on interfacial shear strength and the mechanical behavior of ceramic composites
[DE90-007574] 12 p1632 N90-19380
All-fiber SFPM (Stimulated Four Photon Mixing) amplifier
[AD-D014358] 12 p1713 N90-19841
Fiber pushout test: A three-dimensional finite element computational simulation
[NASA-TM-102565] 14 p1945 N90-21131
Microcracking and toughness of ceramic-fiber/ceramic-matrix composites under high temperature
[AD-A218516] 16 p2223 N90-22680
Composite ceramic superconducting wires for electric motor applications
[AD-A219131] 16 p2224 N90-22689
Rapid thermal processing of high temperature superconducting fiber
[NASA-CR-186803] 18 p2626 N90-24964
Calculation of thick wall fiber binders for rotor components of modern helicopters
[MBB-UD-554/84-PUB] 19 p2660 N90-25137
Alumina reinforced tetragonal zirconia (TZP) composites
[DE90-011871] 19 p2672 N90-25194
X ray diffraction analysis of control and test fibers
[MTL-TR-89-58] 19 p2678 N90-25233
Device and method for detecting and displaying crossover pattern in precision winding
[AD-D014539] 19 p2685 N90-25276
Towards 2000: The composite engine
[PNR90646] 20 p2811 N90-26000
Development of ceramic hybrid combustor: Design and combustion test results
[DE90-503442] 20 p2839 N90-26149
Study on failure modes of SiC fiber reinforced aluminum composite materials by AE method
[DE90-505518] 21 p2971 N90-26884
Manufacturing and mechanical properties of new textile fiber preforms for structural sandwich applications
[MBB-Z-0296-90-PUB] 21 p2972 N90-26895
Probability models for the failure of fibres and fibrous composite materials 23 p3300 N90-28665

FIBROUS MATERIALS
U FIBERS

FIDELITY
U ACCURACY

FIELD ALIGNED CURRENTS
Electrostatic turbulence in the high latitude ionosphere
02 p0246 N90-11392
The auroral current - voltage relationship
05 p0658 N90-13843
On the structure of the tail magnetic field
[IFSI-88-19] 08 p1101 N90-16378
A self-consistent theory of radial transport of field-aligned current by microturbulence
[DE90-007920] 14 p2028 N90-21631

FIELD EFFECT TRANSISTORS
NT CHARGE FLOW DEVICES
NT JFET
NT MODFETS
Vacuum microelectronics for beam power and rectennas 01 p0028 N90-10146
The effects of normal annealing cycles during IGFET fabrication on initial and radiation induced gate insulator defects
[AD-A210282] 01 p0049 N90-10278
Epitaxial GaAs on SOI wafers
[AD-A209009] 01 p0127 N90-10729
Advanced GaAs process modeling, volume 1
[AD-A210385] 01 p0132 N90-10761
The analysis of current-mirror MOSFETs for use in radiation environments
[AD-A212527] 04 p0497 N90-12866
Strong-inversion model of threshold voltage in modulation doped field effect transistors: The role of unintentional acceptors
[AD-A212750] 04 p0498 N90-12870
Dielectric spectroscopy of semiconductors
[AD-A211989] 04 p0559 N90-13255
GaAs gate dynamic memory technology
[AD-A212387] 04 p0560 N90-13266
The growth of epitaxial GaAs and GaAlAs on silicon substrates by OMVPE
[AD-A212873] 04 p0561 N90-13269
Elaboration and characterization of MISFET transistors on InP
[ECL-88-19] 05 p0636 N90-13709
Integrated optoelectronic receivers
[AD-A213376] 05 p0700 N90-14098
Analytical and computer-aided models of InP-based MISFETs and heterojunction devices
[AD-A211861] 05 p0702 N90-14106
Field-effect spectroscopy of interface states
[AD-A212998] 05 p0703 N90-14112
Method of making self-aligned GaAs/AlGaAs FET's
[AD-D014229] 06 p0849 N90-14935
The effects of heavy particle radiation on semiconductor devices
[DE90-001679] 06 p0854 N90-14962
Development of high performance beta-SiC field-effect transistors
[AD-A213885] 07 p0924 N90-15346
Power semiconductor devices for space nuclear power systems
[DE90-001178] 07 p1005 N90-15819
OPFET (Optical Field-Effect Transistor) demodulator-downconverter for detecting microwave modulated optical signals
[AD-D014294] 08 p1060 N90-16128
Optimization of the intermodulation performance of GaAs MESFET small-signal amplifiers
[AD-A215193] 09 p1212 N90-17026
Modeling the gate I/V characteristic of a GaAs MESFET for Volterra-series analysis
[AD-A215314] 09 p1212 N90-17030
Evaluation of doped phthalocyanines and a chemically-sensitive field effect transistor for detecting nitrogen dioxide
[AD-A215662] 09 p1214 N90-17037
The growth of epitaxial GaAs and GaAlAs on silicon substrates by OMVPE
[AD-A214642] 09 p1288 N90-17469
Interfacial and thin film chemistry in electron device fabrication
[AD-A214784] 09 p1289 N90-17473
Thermal characteristics of power MOS-FETS. Results obtained with the IRF-250 10 p1330 N90-17688
An assessment of the use of resonant-mode topologies for high frequency power conversion
10 p1335 N90-17726
Techniques for high frequency power conversion
10 p1336 N90-17729
Innovations in the design and matching of magnetic components and semiconductors up performance and reliability of power converters 10 p1336 N90-17731
Study and implementation of a monolithic photoreceiver integrating a photodiode and a junction field effect transistor in GaInAs with polarization resistance
[IDI-18902] 10 p1379 N90-17990
Charge pumping as a measurement method for the characterization of short channel MOSFETS: Review, development, and comparison of measurement process
[ETN-90-95726] 12 p1654 N90-19504
Field effect transistor structures based on strain induced polarization charges
[DE90-007247] 12 p1655 N90-19515
Silicon carbide semiconductor device fabrication and characterization
[NASA-CR-186354] 12 p1719 N90-19873
Microwave field effect transistor
[NASA-CASE-GSC-12442-2] 13 p1792 N90-20282
InSb DRO array characteristics
14 p1977 N90-21326
Low noise HgCdTe 128 x 128 SWIR FPA for Hubble space telescope 14 p1979 N90-21337
Laboratory and telescope use of the NICMOS2 128 x 128 HgCdTe array 14 p1979 N90-21338
HgCdTe 256x256 NWIR FPA
14 p1981 N90-21348
Improved Si:As BIBIB (Back-Illuminated Blocked-Impurity-Band) hybrid arrays
14 p1981 N90-21349
Problems associated with residual and mismatch stresses in thin film structures 14 p1990 N90-21407
Excess noise, anomalous effects and reliability of high frequency devices (Schottky diodes, MESFET and HEMT)
[LAAS-89-394] 16 p2231 N90-22728
Continued development and characterization of doped layers, contacts, and associated electronic devices in silicon carbide
[AD-A219211] 16 p2232 N90-22737

Continued development and characterization of doped layers, contacts and associated electronic devices in silicon carbide
[AD-A219234] 16 p2232 N90-22738
Development of high performance beta-SiC field-effect transistors
[AD-A218392] 17 p2394 N90-23637
The 30-GHz monolithic receive module
[NASA-CR-180849] 18 p2545 N90-24528
Failure mechanisms of GaAs transistors: A literature survey
[AD-A221089] 18 p2548 N90-24543
Fundamental studies and device development in beta silicon carbide
[AD-A219253] 19 p2676 N90-25220
Neutron and gamma irradiation effects on power semiconductor switches
[NASA-TM-103200] 19 p2686 N90-25278
Subthreshold technique for fixed and interface trapped charge separation in irradiated MOSFETs
[AD-A221861] 21 p3001 N90-27061
Transient annealing characterization of irradiated MOSFETS
[AD-A223877] 23 p3401 N90-29220
High throughput MBE materials for MODFET's
[AD-A223452] 24 p3552 N90-30097
The II-VI semiconductor superlattices
[AD-A223748] 24 p3553 N90-30101
Extended characterization of the damage by hot charge carriers in gate oxide by short channel MOS field effect transistors
[ETN-90-97313] 24 p3555 N90-30114

FIELD EMISSION
Micro-cavity integrable vacuum diodes and triodes
[DE89-016649] 01 p0060 N90-10344
Technology of fast spark gaps
[AD-A214199] 07 p0925 N90-15353
Experimental investigation of relationship between nonlinear field energy and emittance growth
[AD-A215813] 10 p1430 N90-18246
A progress report on the Livermore Miniature Vacuum Tube Project
[DE90-008302] 13 p1794 N90-20299
Amplified spontaneous emission measurements on the aurora large-aperture module
[DE90-004841] 13 p1806 N90-20369
An assessment of the hardness of miniature vacuum tubes to high-voltage transients
[DE90-009541] 15 p2089 N90-21956

FIELD INTENSITY METERS
Gradiometry and gravitomagnetic field detection
12 p1733 N90-19962

FIELD OF VIEW
Field-of-View variations and stripe-texturing effects on assault landing performance in the C-130 weapon system trainer
[AD-A212763] 04 p0459 N90-12634
The baffles 05 p0604 N90-13509
Remote sensing of the aerosol scattering coefficient with a multi-field-of view lidar 06 p0763 N90-14437
Appearance analysis from CAD models
[IMAG-RR-756-I-IMAG-88-LIFIA] 08 p1111 N90-16434
Arrays for space applications
12 p1610 N90-19265
Turbulence spectral widths view angle independence as observed by Doppler radar
[AD-A219169] 16 p2199 N90-22550
Helmet-mounted pilot night vision systems: Human factors issues 16 p2269 N90-22930
Perceived orientation, spatial layout and the geometry of pictures 16 p2269 N90-22933
Wide-angle display developments by computer graphics 16 p2275 N90-22963
Tracking performance and influence of field of view
23 p3360 N90-28988

FIELD STRENGTH
NT ELECTRIC FIELD STRENGTH
NT MAGNETIC FLUX
On canonical quantization of the electromagnetic field in terms of field strengths
[DE89-615389] 01 p0055 N90-10314
The FTZ HF propagation model for use on small computers and its accuracy 06 p0765 N90-14447
Kilometric type III radio bursts and interplanetary transients 06 p0867 N90-15038
Alternative techniques for some typical MIL-STD-461/462 types of measurements
[PB89-235139] 07 p0917 N90-15302
Prediction of VHF/UHF mobile reception in urban areas: Comparison with measurements in London
[BBC-RD-1989/11] 14 p1965 N90-21255
ELF (Extremely Low Frequency) communications system ecological monitoring program: Slime mold studies
[AD-A218623] 16 p2229 N90-22715
ELF (Extremely Low Frequency) communications systems ecological monitoring program: Wetland studies
[AD-A218632] 16 p2229 N90-22716
Dissociation phenomena in electron-beam sustained carbon dioxide lasers 18 p2560 N90-24610
Characterization of a high-intensity, subpicosecond XeCl laser system
[DE90-011970] 20 p2867 N90-26310
Comparative evaluation of Allison T56 engine chip detectors
[AD-A221864] 21 p2960 N90-26832
Sounder update and field strength software modifications for Special Operations Radio Frequency Management System (SORFMS). Volume 1: Program descriptions and testing
[AD-A224510] 24 p3460 N90-29543
Interstellar magnetic fields: An observational perspective 24 p3560 N90-30144

FIELD THEORY (ALGEBRA)
NT QUADRATIC EQUATIONS
Note on p-semisimple BCI-algebras
[DE90-606955] 10 p1423 N90-18206
Operator algebra from fusion rules: The infinite number of Ising theories
[NIKHEF-H/89-7] 15 p2165 N90-22374
Generalized killing equations and symmetries of spinning space
[NIKHEF-H/89-8] 15 p2165 N90-22375
Search of primitive polynomials over finite fields
[IMAG-RR-797-M] 20 p2918 N90-26607
Tutorial on Reed-Solomon error correction coding
[NASA-TM-102162] 22 p3234 N90-28339

FIELD THEORY (PHYSICS)
NT GRAND UNIFIED THEORY
NT QUANTUM CHROMODYNAMICS
NT STRONG INTERACTIONS (FIELD THEORY)
NT WEAK INTERACTIONS (FIELD THEORY)
A theoretical high energy physics program
[DE89-012685] 01 p0121 N90-10696
On some stochastic properties of the infinitely dimensional Hamiltonian systems of classical mechanics
[DE89-618403] 02 p0267 N90-11525
Three level constraints on conformal field theories and string models
[DE89-016942] 02 p0286 N90-11634
Superfiled formulation of Chern-Simons supersymmetry
[DE89-618459] 02 p0286 N90-11636
General action for topological quantum field theories
[DE89-618460] 02 p0286 N90-11637
Moduli spaces and topological quantum field theories
[DE89-016943] 02 p0287 N90-11639
Operator product coefficients in non-diagonal conformal field theories
[PB89-216873] 03 p0399 N90-12283
Bordered surfaces, off-shell amplitudes, sewing, and string field theory
[DE90-000006] 03 p0414 N90-12378
Dimensional reduction at high temperature revisited
[KVI-791] 04 p0549 N90-13194
Operator product coefficients in non-diagonal conformal field theories
[NIKHEF-H/88-19] 04 p0553 N90-13224
Corrections to the thin wall approximation in general relativity
[NASA-CR-186078] 04 p0562 N90-13274
Large deviation estimates in the stochastic quantization of phi sub 2 exp 4
[PREPRINT-686] 05 p0693 N90-14050
Aspects of field theory related to the Zakharov problem 06 p0783 N90-14551
Nonlocality and stochastic quantization of field theory
[DE89-633913] 07 p1007 N90-15833
On averaged force acting on a particle in HF electromagnetic field
[DE90-600984] 08 p1057 N90-16109
The theory of hybrid stochastic algorithms
[DE90-003941] 08 p1109 N90-16421
Multiplet classification of highest weight modules over quantum universal enveloping algebras: The U(sub q)(sl(3,C)) example
[DE90-600720] 08 p1116 N90-16464
The off-shell closed strings as the topological open membranes: Dynamical transmutation of world sheet dimension
[DE89-635721] 08 p1134 N90-16571
Proceedings of the 23rd Annual Seminar on Theoretical Physics
[DE90-601827] 08 p1135 N90-16577
Quantum fields in cosmological space-times: A soluble example
[DE89-618837] 08 p1150 N90-16662
Research in theoretical physics
[DE90-005605] 09 p1294 N90-17500
Research program in elementary particle theory
[DE90-005600] 10 p1428 N90-18241
Solution of a class of conformal quantum field theory models in D-dimensional space
[DE90-607094] 10 p1439 N90-18306
Theoretical and experimental high energy physics
[DE90-006168] 11 p1565 N90-19006
Geometric continuum regularization of quantum field theory
[DE90-006099] 11 p1573 N90-19058
Quantum cosmological origin of large scale structures of the universe
[DE90-610647] 11 p1591 N90-19176
Goldstone excitation and symmetry breaking mechanism in superfluid He-4
[DE90-610676] 12 p1720 N90-19881
Dimensional transition of the universe
[DE90-741461] 12 p1724 N90-19910
Quantum field theory on higher-genus Riemann surfaces
[DE90-741469] 12 p1725 N90-19912
Superstring field theory
[DE90-007694] 13 p1899 N90-20897
Linking numbers and variational method
[DE90-612793] 14 p2020 N90-21582
Fusion algebra and fusing matrices
[DE90-612798] 14 p2021 N90-21583
Rings
[DE90-009035] 14 p2025 N90-21613
Studies in quantum field theory
[DE90-008731] 14 p2035 N90-21677
Theory of a charged spinning particle in a gravitational and electromagnetic field
[NIKHEF-H/89-4] 15 p2165 N90-22373
Replica scaling analysis of interfaces in random media
[PREPRINT-713] 16 p2312 N90-23174
CERC (Center for Energy Research Computation) report: Results of the CERC Project with recommendations for ANL (Argonne National Laboratory) institutional strategies in advanced scientific computing
[DE90-008238] 18 p2594 N90-24759
On null tratorial torsion in vacuum quadratic Poincare gauge field theory
[MATHS-REPT-A-111] 19 p2751 N90-25630
A new class of exact solutions of the vacuum quadratic Poincare gauge field theory
[MATHS-REPT-A-119] 20 p2933 N90-26691
On trivector torsion in vacuum quadratic Poincare gauge field theory
[MATHS-REPT-A-121] 20 p2933 N90-26692
Geologic interpretation of gravity anomalies
[AD-A222910] 21 p3025 N90-27199
Theory of planar near-field measurement
[FEL-89-B273] 22 p3244 N90-28395
Topology of singularities and phase diagram of N=2 superconformal field theories
[DE90-627213] 23 p3391 N90-29155
Brorfelde Geomagnetic Observatory: Magnetic results, 1987
[ISBN-87-7478-297-5] 24 p3496 N90-29756
Higher order equations of motion
[DE90-627522] 24 p3543 N90-30038
On Dirac's conjecture for Hamiltonian systems with first and second class constraints
[DE90-627206] 24 p3555 N90-30116
A new vector-tensor theory and higher-dimensional cosmology
[DE90-507990] 24 p3555 N90-30117
Introductory lectures on conformal field theory and strings
[DE90-627219] 24 p3556 N90-30120

FIGHTER AIRCRAFT
NT F-4 AIRCRAFT
NT F-8 AIRCRAFT
NT F-14 AIRCRAFT
NT F-15 AIRCRAFT
NT F-16 AIRCRAFT
NT F-17 AIRCRAFT
NT F-18 AIRCRAFT
NT F-86 AIRCRAFT
NT F-104 AIRCRAFT
NT F-111 AIRCRAFT
Wind tunnel support system effects on a fighter aircraft model at Mach numbers from 0.6 to 2.0
[AD-A210614] 01 p0002 N90-10010
Problems related to the acquisition, processing and utilization of the modal parameters measured in flight tests in order to obtain the full envelope for flutter
[ETN-89-95210] 03 p0305 N90-11735
Future military powerplants --- fighter aircraft engines
[PNR90554] 03 p0308 N90-11749
Low-speed wind-tunnel study of reaction control-jet effectiveness for hover and transition of a STOVL fighter concept
[NASA-TM-4147] 03 p0308 N90-11751
The aerodynamic experimental center of Aeritalia: Combat aircraft group
[ETN-89-95213] 03 p0311 N90-11766

Estimating the relationships between the state of the art of technology and production cost for the US aircraft
[AD-A212127] 04 p0437 N90-12495
Development and applications of reliability and maintainability design criteria in military aircraft
[ETN-89-95208] 04 p0452 N90-12591
Spatial tests for aviators
[IZF-1988-15] 04 p0527 N90-13041
An experimental investigation of thrust vectoring two-dimensional convergent-divergent nozzles installed in a twin-engine fighter model at high angles of attack
[NASA-TM-4155] 08 p1017 N90-15884
The use of prototypes in selected foreign fighter aircraft development programs: Rafale, EAP, Lavi, and Gripen
[AD-A214500] 09 p1159 N90-16707
Application of multifunction inertial reference systems to fighter aircraft 09 p1164 N90-16740
The integration of stores on modern tactical aircraft: Where we have been, and what we should do for the future 10 p1305 N90-17552
Dynamic derivatives of missiles and fighter-type configurations at high angles of attack 10 p1306 N90-17554
Onboard fire- and explosion suppression for fighter aircraft 10 p1315 N90-17602
The technology challenge of the advanced tactical fighter: A study of the technology transition process
[AD-A216109] 10 p1320 N90-17630
The effects of wind tunnel data uncertainty on aircraft point performance predictions
[AD-A216091] 11 p1456 N90-18387
Influence of forebody geometry on aerodynamic characteristics and a design guide for defining departure/spin resistant forebody configurations
[AD-A216714] 11 p1456 N90-18388
Development of an ejection seat specification for a new fighter aircraft 13 p1751 N90-20057
F-15B high angle-of-attack phenomena and spin prediction using bifurcation analysis
[AD-A217366] 13 p1754 N90-20073
The implementation and operation of a variable-response electronic throttle control system for a TF-104G aircraft
[NASA-TM-101696] 13 p1756 N90-20086
Radar observations of a formation of two fighters: A case study for ISAR imaging 14 p1963 N90-21240
Human factors in fighter software development
[PD-CF-9003] 14 p2011 N90-21522
Preliminary design of a supersonic Short Takeoff and Vertical Landing (STOVL) fighter aircraft
[NASA-CR-186670] 17 p2352 N90-23394
Throughput and delay characteristics for a slow-frequency hopped aircraft-to-aircraft packet radio network
[AD-A220525] 17 p2389 N90-23609
A study of the technology required for advanced vertical take-off aircraft
[ETN-90-96786] 18 p2497 N90-24268
Convex models of malfunction diagnosis in high performance aircraft
[AD-A218514] 19 p2649 N90-25073
Research and development: Technical and scientific publications 1989
[ISSN-0931-9751] 19 p2649 N90-25075
Time-optimal aircraft pursuit-evasion with a weapon envelope constraint
[NASA-CR-186640] 19 p2658 N90-25126
Design of a low cost short takeoff-vertical landing export fighter/attack aircraft
[NASA-CR-186658] 19 p2659 N90-25132
Prevalence of G-induced cervical injury in US Air Force pilots 19 p2717 N90-25460
Qualitative evaluation of a conformal velocity vector display for use at high angles-of-attack in fighter aircraft
[NASA-TM-102629] 20 p2809 N90-25981
Special essays for the 40th anniversary of the revolution: The chief designer discusses the F-8 2 and future fighter planes
[AD-A221587] 21 p2960 N90-26829
Innovative control concepts and component integration for a generic supercruise fighter 23 p3273 N90-28521
A look at tomorrow today 23 p3273 N90-28524
Inflight thrust vectoring: A further degree of freedom in the aerodynamic/flight mechanical design of modern fighter aircraft 23 p3274 N90-28528
Aerodynamic interferences of in-flight thrust reversers in ground effect 23 p3274 N90-28529
Damage tolerance of the fighter aircraft 37 Viggen. Part 1: Analytical assessment
[FFA-TN-1990-12-PT-1] 23 p3276 N90-28538
Damage tolerance of the fighter aircraft 37 Viggen. Part 2: Experimental verification
[FFA-TN-1990-13-PT-2] 23 p3276 N90-28539
Effective optimal control of a fighter aircraft engine 23 p3277 N90-28548
A conceptual framework for fighter flight control systems
[PD-CF-9009] 23 p3283 N90-28577
Fighter agility metrics
[NASA-CR-187289] 24 p3432 N90-29389

FIGURE OF MERIT
An empirically derived figure of merit for the quality of overall task performance 18 p2644 N90-25058

FILAMENT WINDING
Preliminary experiments on filament winding nylon impregnated glass fibers (FIT)
[LR-545] 05 p0628 N90-13669
Filament winding of composite cylinders 14 p1943 N90-21119
Production of a variety of shapes using wrapping and draping techniques
[REPT-892-430-122] 16 p2213 N90-22625
Axisymmetric and cylindrically orthotropic analysis of filament winding 16 p2246 N90-22811
Composite curing: A new process
[REPT-892-430-114] 17 p2370 N90-23490

FILAMENT WOUND CONSTRUCTION
U FILAMENT WINDING

FILAMENTS (SOLAR PHYSICS)
U SOLAR PROMINENCES

FILE MAINTENANCE (COMPUTERS)
Initial flight qualification and operational maintenance of X-29A flight software
[NASA-TM-101703] 01 p0005 N90-10023
SESAME equation of state for a polymer composite: Phenolic refrasil
[LA-11512-MS] 07 p0910 N90-15264
ARGOS (A Research GMMP Operating System): Overvie w and interfaces
[AD-A213871] 07 p0970 N90-15599
UNIX internals. Part 1: Intertask communication in UNIX. Part 2: UNIX file system
[CNES-NT-122-PT-1/2] 08 p1107 N90-16405
The procedures for easy running of the HULL computer code under VMS
[MRL-GD-0023] 10 p1417 N90-18165
Using the K-25 C/TD common file system: A guide to CFSI
[DE90-005815] 11 p1593 N90-19179
A model research archive: Archive and research implications for original records and support documents
[DE90-008246] 13 p1900 N90-20906
Access to supercomputers 16 p2277 N90-22979
Assessment System for Aircraft Noise (ASAN) citation database. Volume 2: Database update manual
[AD-A219176] 16 p2314 N90-23189
Guide for the management of expert systems development
[AD-A221847] 21 p3056 N90-27378

FILLERS
Multi-element spherical shell generation
[NASA-CASE-NPO-17203-1-CU] 17 p2405 N90-23700
Filler metal development for Hastelloy alloy XR
[DE90-791084] 21 p2981 N90-26939
Rheology of filler rubber: Silica-silicone
[AD-A223600] 24 p3455 N90-29511

FILLETS
Effective methods of controlling a junction vortex system in an incompressible, three-dimensional, turbulent flow 15 p2047 N90-21732
Flat plate vibration analysis experimental and numerical fillet study
[AD-A218789] 16 p2247 N90-22818

FILLING
Model filled polymers 3. Rheological behavior of polystyrene containing crosslinked polystyrene beads
[AD-A215867] 11 p1489 N90-18567
Rapidly quantifying the relative distention of a human bladder
[NASA-CASE-LAR-13901-1-NP] 14 p2010 N90-21519

FILM BOILING
Pool boiling from rotating and stationary spheres in liquid nitrogen 23 p3292 N90-28621
Gas-film flow in tubes
[DE90-011526] 23 p3324 N90-28793

FILM COOLING
Effect of vortex circulation on injectant from a single film-cooling hole and a row of film-cooling holes in a turbulent boundary layer. Part 1: Injection beneath the vortex downwash
[AD-A215288] 09 p1218 N90-17063
Turbulence structure resulting from interaction between an embedded vortex and wall jet
[AD-A215702] 10 p1383 N90-18004
Investigation of heat transfer with film cooling to a flat plate in a shock tube
[AD-A216379] 10 p1386 N90-18019
Numerical and experimental analysis of a thin liquid film on a rotating disk related to development of a spacecraft absorption cooling system
[NASA-CR-183457] 12 p1657 N90-19523
Heat transfer near the entrance to a film cooling hole in a gas turbine blade
[AD-A217396] 13 p1757 N90-20089
Gas-jet and tangent-slot film cooling tests of a 12.5 deg cone at Mach number of 6.7
[NASA-TP-2786] 23 p3326 N90-28806
Effect of vortex circulation on injectant from a single film-cooling hole and a row of film-cooling holes in a turbulent boundary layer. Part 2: Injection beneath the vortex upwash
[AD-A223894] 23 p3328 N90-28818
Further studies of turbulence structure resulting from interactions between embedded vortices and wall jets at high blowing ratios
[AD-A223296] 24 p3468 N90-29593

FILM THICKNESS
Calculation on film preparation and film motion of a swirl atomizer
[ESA-TT-1096] 03 p0348 N90-11990
Absolute determination of the wall shear stress by means of an interferometer
[DFVLR-FB-89-13] 03 p0349 N90-11991
A capacitive technique for real-time monitoring polymer coating thickness on carbon filaments during prepregging process
[NASA-TM-101682] 06 p0780 N90-14533
On the numerical solution of the dynamically loaded hydrodynamic lubrication of the point contact problem
[NASA-TM-102427] 09 p1220 N90-17076
Film thickness in lubricated Hertzian contacts. Part 2: Point contacts
[ESDU-89045] 09 p1232 N90-17148
Application of x ray absorption edge spectrometry to the non-destructive determination of element concentrations, coating thickness and areal densities
[AERE-R-13030] 16 p2245 N90-22802
The onset of superconductivity in two-dimensional disordered systems 16 p2321 N90-23232
Tribology of MoS2: Effect of film thickness 18 p2541 N90-24505
Ellipsometric study of YBa2Cu3O(7-x) laser ablated and co-evaporated films
[NASA-TM-103223] 20 p2932 N90-26682

FILTERING
U FILTRATION

FILTERS
Optical excisor modeling
[AD-A219338] 16 p2230 N90-22722

FILTRATION
NT SPATIAL FILTERING
Properties of F-34 (JP-8) fuel for 1988
[AD-A210188] 01 p0053 N90-10303
The fluid mechanics of filters 06 p0773 N90-14499
Predicting the performance of ceramic filters by the use of silt density index
[DE90-001316] 07 p0909 N90-15256
Low cost filter development and control of permeability in high temperature, high pressure ceramic filter elements
[DE90-000403] 11 p1507 N90-18676
Some observations on liquid flow through filters
[AERE-R-13300] 16 p2234 N90-22748
Parameter estimation in linear filtering
[AD-A218566] 16 p2307 N90-23144
Bilateral prediction
[AD-A219564] 17 p2456 N90-24016
Sample holder support for microscopes
[NASA-CASE-MFS-28420-1] 21 p3010 N90-27113
Data analysis techniques 21 p3017 N90-27151
Ozone for trace organic contaminant removal
[PB90-221680] 23 p3347 N90-28916
Effect of particulate fillers on the rheology of polymer melts
[AD-A223601] 24 p3455 N90-29512
Estimation and representation of multidimensional mappings
[DLR-MITT-90-06] 24 p3531 N90-29967

FINANCE
Aerial photographs to support the fiscalization process of agriculture loans in the Irece-BA region
[INPE-4839-PRE/1468] 10 p1400 N90-18092
The bringing to market of the RF alert (a case study in technology transfer) 11 p1576 N90-19073
National patterns of research and development resources: 1989
[NSF-89-308] 17 p2486 N90-24218

FINANCIAL MANAGEMENT
Aerial photography as an aid for agricultural credit control
[INPE-5019-RPE/613] 14 p1999 N90-21455

Financing of large space transportation projects: Research on the financial project for the SSPS
[ILR-MITT-228(1989)] 17 p2363 N90-23436
Space shuttle: Changes to the solid rocket motor contract
[GAO/NSIAD-88-203] 18 p2636 N90-25016
Development of acceptance plans for airport pavement materials. Volume 1: Development
[DOT/FAA/RD-90/15] 23 p3284 N90-28581
Guide to charging for the CCF
[RSRE-89022] 23 p3404 N90-29238

FINE STRUCTURE

Study on edge plasma physics and particle control in the Heliotron E device
[DE90-719524] 09 p1284 N90-17443
IR line emission from dense photodissociation regions 11 p1580 N90-19100
Herbig Ae/Be stars: Fine structure far-infrared lines 11 p1584 N90-19126
Far infrared fine structure lines in active galaxies 11 p1588 N90-19157
Glancing angle XAFS (X ray Absorption Fine Structure) and x ray reflectivity studies of transition-metal/aluminum interfaces
[DE90-005575] 12 p1627 N90-19353
Extended x ray absorption fine structure analysis applied to composite materials
[DE90-008575] 13 p1769 N90-20150
L shell XANES (X ray Absorption Near Edge Structure) for solid metals: Ti, V, Cr, Fe, Ni, Cu
[DE90-008043] 13 p1896 N90-20880
The observed properties of the intermediate-degree gravity modes and their relevance to the solar neutrino paradox 15 p2193 N90-22519
Weak-beam electron microscopy of dislocation splitting in TiAl: Relationship to plasticity
[ESA-TT-1159] 19 p2676 N90-25217
Ultrasensitive laser spectroscopy in solids: Statistical fine structure and single-molecule detection
[AD-A222391] 21 p3074 N90-27477
Fracture-EXAFS: A new method for the study of interfaces in thin films and polycrystalline materials
[DE90-013736] 21 p3081 N90-27521
Nonlinear multi-mode coupling of the solar gravity modes in a rotationally split multiplet 21 p3100 N90-27608
Fifteenth International Conference on X Ray and Inner-Shell Processes
[DE90-013024] 23 p3393 N90-29170
XANES and EXAFS study of Au-substituted YBa2Cu3O(7-delta)
[NASA-TM-103291] 23 p3401 N90-29219

FINGERS

Hand shaping: A paradigm for cognitive/motoric interaction
[AD-A219908] 17 p2437 N90-23885
Rotationally actuated prosthetic helping hand
[NASA-CASE-MFS-28426-1] 21 p3036 N90-27261
Criteria for a recommended standard: Occupational exposure to hand-arm vibration
[PB90-168048] 22 p3233 N90-28331
Response to reflected-force feedback to fingers in teleoperations 24 p3509 N90-29837

FINGERS (ROBOTICS)

U END EFFECTORS

FINITE DIFFERENCE THEORY

Numerically determined transition in separated internal flow 01 p0065 N90-10374
Numerical simulation of turbulent plane channel flows 01 p0067 N90-10382
Numerical simulation of coherent structures in an incompressible mixing layer 01 p0067 N90-10383
IFD (Implicit Finite Difference): Interfaced with Harvard open ocean model forecasts
[AD-A210521] 01 p0090 N90-10517
Tests of various finite difference algorithms applied to a simple water vapor transport problem on a staggered grid
[AD-A210229] 01 p0105 N90-10596
Direct discretization of planar div-curl problems
[NASA-CR-181935] 02 p0263 N90-11498
Effect of electrical double layer on transport limited currents at microelectrodes
[AD-A211586] 03 p0324 N90-11843
Viscous split algorithms for the time dependent incompressible Navier-Stokes equations
[AD-A211592] 03 p0348 N90-11985
An Eigenvalue Analysis of finite-difference approximations for hyperbolic IBVPs
[NASA-TM-102241] 04 p0541 N90-13137
Flux-corrected transport algorithms for two-dimensional compressible magnetohydrodynamics
[AD-A212757] 04 p0557 N90-13246
Computation of viscous incompressible flows
[NASA-TM-101090] 05 p0572 N90-13329
Comparison of integral and finite-difference methods for predicting the turbulent boundary layer on axisymmetric bodies
[ARE-TM(UHA)-88512] 05 p0643 N90-13752
Using Broyden updates to approximate the Jacobian in a semi-implicit backward differentiation code
[AD-A213239] 05 p0688 N90-14010
Computation of unsteady transonic flow about airfoils in frequency domain using the full-potential equation 06 p0719 N90-14198
On the application of subcell resolution to conservation laws with stiff source terms
[NASA-TM-102384] 06 p0833 N90-14844
Iterative methods of domain decomposition with cross-points for the solution of discrete elliptic problems
[DE90-000719] 06 p0835 N90-14854
Finite difference techniques and rotor blade aeroelastic partial differential equations with quasisteady aerodynamics 07 p0875 N90-15075
An examination of helicopter rotor load calculations
[AD-A214295] 07 p0880 N90-15098
Nonlinear maps with competitive interactions: Fixed-points, bifurcations, and chaotic attractors
[DE90-001858] 07 p0986 N90-15695
Physical process in MPD plasmas
[AD-A213679] 07 p0996 N90-15761
Personal computer study of finite-difference methods for the transonic small disturbance equation
[NASA-TM-102582] 08 p1019 N90-15892
Computation of the unsteady facilitated transport of oxygen in hemoglobin
[NASA-TM-102251] 08 p1106 N90-16400
Stochastic simulation of charged particle transport on the massively parallel processor 08 p1114 N90-16448
A review of high-speed, convective, heat-transfer computation methods 10 p1305 N90-17548
Shock-shock boundary layer interactions 10 p1308 N90-17569
Fluid transmission line dynamics for signals of finite amplitude
[AD-A215758] 10 p1385 N90-18014
Dynamics of column stability with partial end restraints
[NASA-TM-101651] 10 p1396 N90-18069
Numerical simulation of the incompressible inhomogeneous turbulence in a plane channel flow
[ONERA-NT-1988-5] 11 p1508 N90-18686
Computation of hypersonic unsteady viscous flow over a cylinder 12 p1597 N90-19194
Three-dimensional viscous rotor flow calculations using a viscous-inviscid interaction approach
[NASA-TM-102235] 12 p1599 N90-19204
Digital determination of the three dimensional flow in turbomachines with the S1-S2 current function process
[ITSM-MITT-30] 12 p1605 N90-19236
A parametric heat transfer study for cryogenic ball bearings in SSME HPOTP 12 p1635 N90-19397
Computational fluid dynamics method for low Reynolds number flow in a precessing/spinning, liquid filled cylinder with rounded endcaps
[AD-A216997] 12 p1659 N90-19531
Computer simulations and experiments to study the fracture of rods by flying plates
[DE90-008308] 13 p1817 N90-20437
Recent advances in 3D finite difference mesh generation using the BRL-CAD package
[DE90-007854] 13 p1866 N90-20704
Cell averaging Chebyshev methods for hyperbolic problems
[NASA-CR-182028] 13 p1877 N90-20768
A fast collocation method for transonic airfoil design 14 p1917 N90-20984
Application of an inverse method to the design of a radial inflow turbine 14 p1918 N90-20989
Numerical method for designing 3D turbomachinery blade rows 14 p1918 N90-20990
Optimization of aerodynamic designs using computational fluid dynamics 14 p1920 N90-20999
PROTEUS two-dimensional Navier-Stokes computer code, version 1.0. Volume 3: Programmer's reference
[NASA-TM-102553] 14 p1974 N90-21307
High accuracy solutions of incompressible Navier-Stokes equations
[NASA-TM-102539] 14 p2018 N90-21567
An upwind-differencing scheme for the incompressible Navier-Stokes equations
[NASA-TM-101051] 15 p2051 N90-21757
Experimental determination of thermal conductance in bolted joint impact in satellites
[INPE-4989-PRE/1551] 15 p2059 N90-21788
Elastic stability and nonlinear behavior of imperfect shells with initial stresses 15 p2110 N90-22070
Numerical solutions of the nonlinear theory of curved beams 15 p2110 N90-22071
An analysis of the finite-differenced, even-parity discrete-ordinates equations in slab geometry
[DE90-006479] 15 p2160 N90-22337
Dynamical approach study of spurious steady-state numerical solutions of nonlinear differential equations. Part 1: The ODE connection and its implications for algorithm development in computational fluid dynamics
[NASA-TM-102820] 15 p2160 N90-22339
Computer simulation of time-dependent spherically symmetric spacetimes containing radiating fluids: Formalism and code tests 15 p2185 N90-22483
Large-scale advanced propeller blade pressure distributions: Prediction and data
[NASA-TM-102316] 16 p2201 N90-22564
Adaptive mesh experiments for hyperbolic partial differential equations
[AD-A219194] 16 p2307 N90-23148
Studies in gravitational lensing and numerical hydrodynamics 16 p2332 N90-23290
The 3-D composite velocity solutions for subsonic/transonic flow over forebodies and afterbodies
[AD-A220370] 17 p2345 N90-23354
Solution of the steady state incompressible Navier-Stokes equations at high Reynolds numbers
[VKI-TN-170] 17 p2404 N90-23692
Large eddy simulation of a fully turbulent plane channel flow
[VKI-TN-171] 17 p2404 N90-23693
Low Prandtl number convection in a rectangular cavity with longitudinal thermal gradient and transverse g-jitters
[REPT-892-430-109] 17 p2404 N90-23695
Cyclotomy and association schemes
[REPT-89-73] 17 p2458 N90-24030
Reduced order models for nonlinear aerodynamics 18 p2492 N90-24244
Personal Computer (PC) thermal analyzer
[AD-A221325] 18 p2548 N90-24546
Stability theory for methods to solve the Navier-Stokes equations, part 1
[FFA-TN-1988-65-PT-1] 19 p2691 N90-25312
Generation of an axisymmetric cylindrical shell element using a shooting method
[ACTA-POLYTEC-SCAND-CI-93] 19 p2700 N90-25362
Adaptive node movement in finite-difference solutions of partial differential equations with applications to gasdynamics, part 1
[UTIAS-333-PT-1] 19 p2750 N90-25622
Adaptive node movement in finite-difference solutions of partial differential equations with applications to gasdynamics, part 2
[UTIAS-333-PT-2] 19 p2750 N90-25623
Trajectory optimization for an asymmetric launch vehicle
[NASA-CR-185630] 20 p2817 N90-26033
Galerkin finite difference Laplacian operators on isolated unstructured triangular meshes by linear combinations
[NASA-TM-103209] 20 p2861 N90-26276
Two-dimensional model of a Space Station Freedom thermal energy storage canister
[NASA-TM-103124] 20 p2862 N90-26279
ARLSUPER version 1.0, program users guide
[AD-A222693] 21 p2953 N90-26793
Determination of the heat dissipated from a specimen undergoing cyclic plasticity by a hybrid numerical/experimental method
[AD-A221575] 21 p2982 N90-26946
Thermal analysis of heat pipe radiators with a rectangular groove wick structure
[AD-A222952] 21 p3004 N90-27074
Proceedings of Workshop on Reliability in Computational Mechanics
[AD-A221694] 21 p3065 N90-27426
A comparison of two central difference schemes for solving the Navier-Stokes equations
[NASA-TM-102815] 22 p3108 N90-27654
A finite difference treatment of Stokes-type flows: Preliminary report
[NASA-CR-186480] 22 p3168 N90-27970
Parallelization of implicit finite difference schemes in computational fluid dynamics
[NASA-CR-182081] 22 p3243 N90-28392
Study of a variable step network and comparison between the radii method and the parabolic equations, applied to the acoustic propagation in the atmosphere
[ONERA-RF-12/3641-PY] 22 p3245 N90-28401
Calculation of temperature distribution in various turbine blades using a boundary-fitted coordinate transformation method 23 p3278 N90-28550
Numerical methods for systems of conservation laws of mixed type using flux splitting
[NASA-CR-182084] 23 p3387 N90-29129
A potential-vorticity decomposition for the boundary integral equation analysis of viscous flows 24 p3417 N90-29301

Numerical simulations of blade-vortex interactions and lifting hovering rotor flows
[AD-A224238] 24 p3417 N90-29302
Finite difference modeling of laser diode ignited components
[DE90-015652] 24 p3474 N90-29635
Parallelization of a method for solving three dimensional Navier-Stokes equations on a distributed memory multiprocessor
[ONERA-RTS-1/3717-CY] 24 p3534 N90-29983

FINITE ELEMENT METHOD

Aeroelastic tailoring procedure for controlling fin hinge moments 01 p0013 N90-10058
A finite element approach for large motion dynamic analysis of multibody structures in space 01 p0019 N90-10093
Enhanced element-specific modal formulations for flexible multibody dynamics 01 p0019 N90-10094
Combustion-driven oscillation in large combustion systems for power generation 01 p0038 N90-10207
A combined finite element and boundary integral formulation for solution via CGFFT of 2-dimensional scattering problems
[NASA-CR-184781] 01 p0055 N90-10313
Iterative performance and an adaptive procedure for viscous flow problems 01 p0069 N90-10397
The MHOST finite element program: 3-D inelastic analysis methods for hot section components. Volume 2: User's manual
[NASA-CR-182235-VOL-2] 01 p0079 N90-10450
The MHOST finite element program: 3-D inelastic analysis methods for hot section components. Volume 3: Systems' manual
[NASA-CR-182236] 01 p0079 N90-10451
Analysis and test of a 16-foot radial rib reflector developmental model
[NASA-TM-101648] 01 p0080 N90-10457
BLOT: A mesh and curve plot program for the output of a finite element analysis
[DE89-013994] 01 p0104 N90-10590
Updating of finite element model by means of normal mode parameters 02 p0177 N90-10992
Parametric identification of conservative self adjoint structures 02 p0177 N90-10994
Employment of modal survey methodologies in dynamic analysis procedures 02 p0179 N90-11006
Experiences using a major FEM package interactively for spacecraft applications 02 p0179 N90-11008
Numerical analysis of nonlinear viscoelastic structures: Application to elastomers and rubber-like materials 02 p0180 N90-11013
Nonlinear collapse simulation of anisotropic plates and corrugated panels 02 p0183 N90-11035
Numerical models for exterior and interior fluid-structure interaction problems 02 p0188 N90-11073
Exploitation of data management facilities for finite element analysis in aerospace structural engineering applications 02 p0188 N90-11078
Accelerated aging of metal matrix composites 02 p0190 N90-11085
On a Taylor Weak Statement for finite element computations in gas dynamics 02 p0219 N90-11251
A finite element formulation for inelastic plates and shells based on a mixed variational principle 02 p0233 N90-11334
An analytical and experimental study of the elastodynamic response characteristics of planar linkage mechanism with bearing clearances 02 p0233 N90-11336
Computational methods for complex flowfields
[AD-A211485] 03 p0347 N90-11983
Efficient finite element solution of Navier-Stokes equations and related topics
[AD-A211647] 03 p0348 N90-11986
A C(Superscript)-Anisoparametric three-node shallow shell element for general shell analysis
[AD-A212094] 03 p0358 N90-12049
Investigation of difficult component effects on finite element model vibration prediction for the Bell AH-1G helicopter. Volume 1: Ground vibration test results
[NASA-CR-181916-VOL-1] 03 p0360 N90-12058
A least-squares finite element method for incompressible Navier-Stokes problems
[NASA-TM-102365] 03 p0392 N90-12231
Numerical solution of acoustic-structure interaction problems
[AD-A211505] 03 p0400 N90-12283
An electromagnetic finite element particle code on an unstructured grid
[DE89-017532] 03 p0407 N90-12336
SSME structural dynamic model development
[NASA-CR-183671] 04 p0463 N90-12650
Surface treatments of carbon fibers in an organic environment. Finite element analysis of pull-out tests
[ONERA-RT-7/3549-M] 04 p0471 N90-12698
A mechanical power flow capability for the finite element code NASTRAN
[AD-A212202] 04 p0513 N90-12964
Constitutive modeling for isotropic materials (HOST)
[NASA-CR-174718] 05 p0582 N90-13391
Review and evaluation of a turbomachinery throughflow finite element code
[AD-A213058] 05 p0650 N90-13787
Probabilistic finite element analysis of dynamic structural response
[AD-A213249] 05 p0650 N90-13789
A study on the sensitivity and simultaneous adjustment of a hoop-column antenna surface
[NASA-TM-101538] 05 p0653 N90-13807
Time domain coupling of the boundary and finite element methods for elastodynamics
[AD-A213243] 05 p0654 N90-13811
Investigation of difficult component effects on finite element model vibration prediction for the Bell AG-1G helicopter. Volume 2: Correlation results
[NASA-CR-181916-VOL-2] 05 p0654 N90-13814
A mixed finite element solution of the linear acoustic equations
[ECL-89-006] 05 p0697 N90-14075
Finite element analysis of laminated composite plates 06 p0737 N90-14291
Elasto-plastic analysis of unidirectional fiber-reinforced composites subjected to transverse normal loading using the finite element method 06 p0737 N90-14292
Finite element analysis of frictional contact problems 06 p0792 N90-14612
Tire modeling by finite elements 06 p0792 N90-14614
Transient response of flexible rotor-bearing systems subjected to combined unbalance and ground excitations 06 p0792 N90-14616
Non-linear vibrations, stability, and dynamics of structures and mechanisms
[AD-A212152] 06 p0796 N90-14839
Parallel eigenanalysis of finite element models in a completely connected architecture
[NASA-CR-185166] 06 p0799 N90-14852
Effects of aeroelastic tailoring on anisotropic composite material beam models of helicopter blades
[AD-A213478] 07 p0879 N90-15095
Solution of potential flow past an elastic body using the boundary element technique
[AD-A213843] 07 p0931 N90-15390
Mesh refinement in finite element analysis by minimization of the stiffness matrix trace
[NASA-CR-185170] 07 p0938 N90-15434
Nonlinear strain-displacement relations for thin axisymmetric shells
[PB89-226013] 07 p0945 N90-15470
Utilization of a PC for finite element modeling
[AD-A214173] 07 p0971 N90-15605
Space shuttle Production Verification Motor 1 (PV-1) static fire
[NASA-CR-183784] 08 p1037 N90-15991
Open-mode delamination stress concentrations in horseshoe and elliptic composite curved bars subjected to end forces
[NASA-TM-4164] 08 p1039 N90-16004
Feed back Petrov-Galerkin methods for convection dominated problems
[DE89-636436] 08 p1063 N90-16148
Extrapolation techniques for finite element approximations of Stokes and Navier-Stokes flow over a backward facing step
[PREPRINT-499] 08 p1065 N90-16160
Finite element calculations for transonic flows taking into account several far field boundary conditions 08 p1069 N90-16188
Dynamic analysis of geared rotors by finite elements
[NASA-TM-102349] 08 p1086 N90-16286
Element-by-element preconditioning techniques for large-scale, vectorized finite element analysis in nonlinear solid and structural mechanics 08 p1087 N90-16291
BAM: German Federal Institute for Materials Research and Testing, Berlin
[DE90-004293] 08 p1090 N90-16307
And still, a new beginning: The Galerkin least-squares gradient method
[DE89-636435] 08 p1116 N90-16461
A new finite element formulation for CFD:8. The Galerkin/least-squares method for advective-diffusive equations
[DE89-636437] 08 p1116 N90-16462
Robustness of a moving-bank multiple model adaptive controller for a large space structure
[AD-A215670] 09 p1183 N90-16859
High-order mixture homogenization of fiber-reinforced composites
[AD-A215247] 09 p1187 N90-16876
A finite element-boundary integral formulation for scattering by three-dimensional cavity-backed apertures
[NASA-CR-186332] 09 p1187 N90-16878
Finite element analysis of propagation in waveguide components with application to ferrite phase shifters
[FOA-C-30529-3.2] 09 p1204 N90-16977
Optimum element density studies for finite-element thermal analysis of hypersonic aircraft structures
[NASA-TM-4163] 09 p1219 N90-17074
Stress analysis in pressure vessels by mixed finite element methods taking into account shear deformation
[DE90-606755] 09 p1233 N90-17152
Eigensolution of finite element problems in a completely connected parallel architecture
[NASA-TM-102450] 09 p1236 N90-17173
Compatibility conditions of structural mechanics for finite element analysis
[NASA-TM-102413] 09 p1237 N90-17180
On the superconvergence of the SBB method
[DE89-635709] 09 p1272 N90-17375
Sampling scattered data onto rectangular grids for volume visualization
[AD-A215533] 09 p1274 N90-17384
Shock-shock boundary layer interactions 10 p1308 N90-17569
Analysis of the National Transonic Facility mishap
[NASA-TM-101686] 10 p1318 N90-17620
Prediction of high temperature metal matrix composite ply properties
[NASA-TM-102490] 10 p1348 N90-17817
Damage mechanisms and indenter size effects in cross plied carbon-carbon composites
[AD-A216413] 10 p1351 N90-17832
A finite element analysis of porosity effects on materials
[AD-A216225] 10 p1359 N90-17884
Finite element modeling and thermal simulations of transistor integrated circuits
[AD-A215928] 10 p1380 N90-17997
Transient finite element computations on the transputer system
[NASA-CR-185199] 10 p1396 N90-18071
A higher-order plate theory with ideal finite element suitability
[AD-A216163] 10 p1397 N90-18075
Finite element investigation of a composite cylindrical shell under transverse load with through thickness shear and snapping
[AD-A216377] 10 p1397 N90-18078
Investigation of collapse characteristics of cylindrical composite panels with large cutouts
[AD-A216378] 10 p1397 N90-18079
Validation of the boundary element method applied to complex fracture mechanics conditions
[AD-A216412] 10 p1398 N90-18080
Integrated force method versus displacement method for finite element analysis
[NASA-TP-2937] 10 p1398 N90-18081
POS2D: A graphic program for analysing axisymmetric and two-dimensional structures
[DE90-608884] 10 p1417 N90-18168
Theory and verification of the fiber composite damage model implemented in DYNA3D
[AD-A216600] 11 p1479 N90-18511
Reliability assessment using finite element techniques
[AD-A216907] 11 p1502 N90-18647
Transient responses of coupled systems
[ONERA-RT-13/3596-RY-070-R] 11 p1509 N90-18687
Development of an experimental space station model for structural dynamics research
[NASA-TM-102601] 11 p1519 N90-18751
Optimization of the reference parameters in the accompanying solar panel dynamics
[INPE-4795-PRE/1449] 11 p1528 N90-18798
The interpretation of crustal dynamics data in terms of plate interactions and active tectonics of the Anatolian plate and surrounding regions in the Middle East
[NASA-CR-186200] 11 p1533 N90-18824
Efficient preconditioning for the p-version finite element method in two dimensions
[AD-A216210] 11 p1551 N90-18928
Research equipment
[AD-A216515] 11 p1552 N90-18937
Three-dimensional structural analyses of reentry vehicles
[DE90-006278] 12 p1615 N90-19291
A combined finite element-boundary element formulation for solution of two-dimensional problems via CGFFT
[NASA-CR-186464] 12 p1620 N90-19309
Practical calculation of the liveload of carbon fiber reinforced plastics by the finite element method
[ETN-90-95867] 12 p1620 N90-19311

Effects of turbulence mixing, variable properties, and vaporization on spray droplet combustion
[NASA-CR-186463] 12 p1623 N90-19326
Finite element approximations of the stokes flow problem based upon various variational principles
[DE90-608612] 12 p1659 N90-19533
Finite element analysis of a quartz rotation sensor
[DE90-006959] 12 p1664 N90-19562
Viscoelastic adherend effects in adhesively bonded composite-to-composite joints 12 p1670 N90-19594
Modeling and analysis of the space shuttle nose-gear tire with semianalytic finite elements
[NASA-TP-2977] 12 p1670 N90-19595
Computational aspects of sensitivity calculations in linear transient structural analysis
[NASA-TM-4156] 12 p1673 N90-19610
Modal analysis of nonprismatic beams: Uniform segment method
[AD-A216952] 12 p1674 N90-19614
PATRAN-STAGS translator (PATSTAGS)
[NASA-TM-100388] 12 p1674 N90-19616
Development of finished beam and shell elements from engineering models for structures under high inelastic deformations
[ETN-90-95377] 12 p1675 N90-19619
Digital treatment of elastic-plastic structures by means of quadratic optimization processes from the finite element method
[ETN-90-95823] 12 p1675 N90-19621
Development of finite beam and shell elements for structures under great inelastic deformations
[ETN-90-95869] 12 p1675 N90-19623
Interlaminar shear stress effects on the postbuckling response of graphite-epoxy panels
[NASA-TM-102626] 12 p1676 N90-19630
Study of the optimization of reference parameters to the dynamic constraints of solar panels
[INPE-4793-TDL/355] 12 p1681 N90-19656
The p- and h-p versions of the finite element method: An overview
[AD-A216902] 12 p1705 N90-19789
Hierarchical basis preconditioners for second order elliptic problems in three dimensions
[DE90-005980] 12 p1706 N90-19793
Finite element mesh generation starting from general geometric models
[REPT-88-93] 12 p1707 N90-19803
A review of the analytical simulation of aircraft crash dynamics
[NASA-TM-102595] 13 p1753 N90-20068
Optimization of laminated composite plates
[AD-A217621] 13 p1768 N90-20146
Fluid dynamics analysis of a rotating axisymmetric part using FIDAP
[DE90-008733] 13 p1802 N90-20340
Parallel algorithms in the finite element approximation of flow problems
[AD-A217729] 13 p1802 N90-20341
A 4-node assumed-stress hybrid shell element with rotational degrees of freedom
[NASA-CR-4279] 13 p1815 N90-20422
Rotordynamic analysis with shell elements for the transfer matrix method
[AD-A217455] 13 p1817 N90-20434
Finite element models to predict the structural response of 120-mm sabot/rods during launch
[DE90-007497] 13 p1817 N90-20436
COMGEN: A computer program for generating finite element models of composite materials at the micro level
[NASA-TM-102556] 13 p1818 N90-20438
Plan, formulate, and discuss a NASTRAN finite element model of the UH-60A helicopter airframe
[NASA-CR-181975] 13 p1818 N90-20439
Time-dependent failure of silver interlayer welds
[DE90-008015] 13 p1818 N90-20440
Automated finite element modeling and simulation 13 p1875 N90-20753
Comparison of C- and O-grid generation methods using a NACA 0012 airfoil
[AD-A216375] 14 p1910 N90-20948
The role of structural analysis in airworthiness certification
[BR112064] 14 p1915 N90-20972
An inverse method for the design of turbomachine blades 14 p1918 N90-20986
A study on secondary flow and spanwise mixing in axial flow compressors 14 p1923 N90-21012
Analysis of the rotor tip leakage flow with tip cooling air ejection 14 p1926 N90-21029
Element-specific modal formulations for large-displacement multibody dynamics 14 p1934 N90-21069
A distributed finite-element modeling and control approach for large flexible structures 14 p1934 N90-21071
Stress analysis of rocket motors with viscoelastic propellant by a mixed finite element model 14 p1941 N90-21112
Numerical simulation model for hydrazine attitude control thrusters. Part 1: Model description
[INPE-4952-RPE/601] 14 p1942 N90-21115
Combined effect of matrix cracking and stress-free edge on delamination
[NASA-TM-102591] 14 p1944 N90-21126
Three-dimensional elastic-plastic analysis of shallow cracks in single-edge-crack-tension specimens
[NASA-TM-102636] 14 p1945 N90-21130
Fiber pushout test: A three-dimensional finite element computational simulation
[NASA-TM-102565] 14 p1945 N90-21131
Micromechanics analysis of space simulated thermal deformations and stresses in continuous fiber reinforced composites
[NASA-TM-102633] 14 p1948 N90-21140
The 4th Annual Review of Progress in Applied Computational Electromagnetics
[AD-A217912] 14 p1966 N90-21257
Analysis and finite element approximation of some optimal control problems associated with the Navier-Stokes equations 14 p1972 N90-21299
Fourier series methods for plates and shells with cracks and inclusions 14 p1990 N90-21406
Problems associated with residual and mismatch stresses in thin film structures 14 p1990 N90-21407
The computational structural mechanics testbed generic structural-element processor manual
[NASA-CR-181728] 14 p1991 N90-21410
Direct formulation of a 4-node hybrid shell element with rotational degrees of freedom
[NASA-CR-4282] 14 p1991 N90-21411
Development of a fracture analysis technique for use with a general-purpose finite element program 14 p1992 N90-21416
Determination of stresses around cutouts in multilayered composite plate and shell structures 14 p1992 N90-21417
Delamination failure in a unidirectional curved composite laminate
[NASA-CR-182018] 14 p1993 N90-21421
A numerical and theoretical study of seismic wave diffraction in complex geologic structure
[AD-A218209] 14 p2005 N90-21490
On the stability of a certain difference scheme
[PB90-165614] 14 p2021 N90-21588
Finite element algorithms for hyperbolic conservation laws with forcing terms
[INPE-5024-RPE/617] 14 p2022 N90-21595
The thermo-mechanical behavior of cometary nuclei 14 p2041 N90-21703
Towards a unified analysis methodology for composite rotor blades 15 p2046 N90-21730
A decentralized linear quadratic control design method for flexible structures 15 p2054 N90-21770
Computational simulation of structural fracture in fiber composites
[NASA-TM-102505] 15 p2064 N90-21821
Modelling of the impact response of fibre-reinforced composites
[OUEL-1784/89] 15 p2065 N90-21827
Failure analysis of woven hybrid composite using a finite element method
[OUEL-1791/89] 15 p2065 N90-21828
Energy release rate analysis of interfacial cracks in composites 15 p2065 N90-21829
Numerical simulation model of hydrazine attitude control thrusters
[INPE-4965-PRE/1534] 15 p2068 N90-21848
Three-dimensional fatigue crack closure behavior of metals 15 p2070 N90-21857
A stress-strength interference approach to fast and delayed fracture reliability analysis for ceramic components 15 p2070 N90-21859
Fracture mechanics of monolithic ceramic materials under small scale microcracking conditions 15 p2070 N90-21860
Applications of Mesh Generation to Complex 3-D Configurations
[AGARD-CP-464] 15 p2093 N90-21975
Automatic grid generation in complex three-dimensional configurations using a frontal system 15 p2096 N90-21992
Unstructured finite element mesh generation and adaptive procedures for CFD 15 p2096 N90-21993
Application of the TRANAIR rectangular grid approach to the aerodynamic analysis of complex configurations 15 p2096 N90-21996
High order P-G finite elements for convection-dominated problems
[DE90-614743] 15 p2097 N90-21998
Practical nonlinear simulation of rotating machinery dynamics with application to turbine blade rubbing 15 p2104 N90-22038
Finite element analysis of elastic contact problems with friction 15 p2105 N90-22040
Natural modes of cracked beams and identification of cracks 15 p2111 N90-22075
Elasto-plastic analysis for contact fatigue failure 15 p2112 N90-22078
On the design and development of a miniature ceramic gimbal bearing 15 p2115 N90-22100
Coordinate systems for plastic yield surfaces stress and strain space theories
[PB90-164765] 15 p2117 N90-22110
Computational methods and plasticity
[LR-583] 15 p2119 N90-22120
Free wave propagation in orthogonally stiffened cylinders 15 p2119 N90-22124
Dynamic response of structures with uncertain parameters 15 p2119 N90-22125
Analysis of a finite two-dimensional solid with an inclined crack and a rigid inclusion 15 p2120 N90-22127
An investigation into the foundations of elastic-plastic fracture mechanics 15 p2120 N90-22130
Three-dimensional finite element formulations for thick and thin laminated plates 15 p2121 N90-22132
Internal fractures in model elastomeric composites 15 p2121 N90-22133
Probabilistic finite elements: Applications to fracture and fatigue 15 p2121 N90-22134
Paving: A new approach to automated quadrilateral mesh generation
[DE90-010244] 15 p2146 N90-22260
The minimum drag profile in laminar flow: A numerical way 16 p2196 N90-22535
Impact damage in graphite/epoxy laminates: Damage characterization, acoustic emission, and finite element simulation, volumes 1 and 2 16 p2211 N90-22610
A study of woven fabric-reinforced composite materials using an invariant-based orthotropic plasticity formulation 16 p2211 N90-22611
Large deformation analysis of laminated composite structures by a continuum-based shell element with transverse deformation 16 p2211 N90-22613
A life prediction model for laminated composite structural components
[NASA-CR-186587] 16 p2212 N90-22614
Design of cryogenic tanks for launch vehicles 16 p2220 N90-22662
The behaviour of mechanically fastened joints in composite structures 16 p2242 N90-22789
Thermal/structural analysis of the shaft-disk region of a fan drive system
[NASA-TM-101687] 16 p2245 N90-22807
Finite element elastic-plastic-creep and cyclic life analysis of a cowl lip
[NASA-TM-102342] 16 p2246 N90-22808
Computations of weight functions in fracture mechanics 16 p2246 N90-22809
Fracture mechanics assessment of a cracked 16-inch inner diameter 1945 vintage-jacketed pressure vessel
[AD-A219135] 16 p2248 N90-22819
Nonlinear finite element formulation for the large displacement analysis in multibody system dynamics 16 p2284 N90-23015
The coupling effects of kinematics and flexibility on the Lagrangian dynamic formulation of open chain deformable links 16 p2284 N90-23018
A finite element based method for solution of optimal control problems 16 p2286 N90-23027
Approximate minimum-time trajectories for 2-link flexible manipulators 16 p2287 N90-23030
On trajectory generation for flexible space crane: Inverse dynamics analysis by LATDYN 16 p2288 N90-23037
Model reduction in the physical coordinate system 16 p2295 N90-23074
Dynamic analysis of flexible mechanical systems using LATDYN 16 p2296 N90-23080
Numerical algorithms for computations of feedback laws arising in control of flexible systems 16 p2297 N90-23085
Mini-mast dynamic analysis using the truss-beam model 16 p2297 N90-23087
Vectors and matrices: Two turbo pascal units for fast program development
[AD-A218917] 16 p2300 N90-23105
Fourier analysis of finite element preconditioned collocation schemes
[NASA-CR-182040] 16 p2304 N90-23128
Numerical studies of the active control of sound transmission through double partitions
[ISVR-TR-183] 16 p2313 N90-23181
Correlation/validation of finite element code analyses for vibration assessment of avionic equipment
[AD-A220393] 17 p2353 N90-23398

Modeling and control of flexible vehicles in space
[AD-A219622] 17 p2365 N90-23465
Development of new methods for predicting the bistatic electromagnetic scattering from absorbing shapes
[AD-A219327] 17 p2388 N90-23600
Algebraic turbulence modeling for unstructured and adaptive meshes
[NASA-CR-182035] 17 p2401 N90-23676
On computing the pressure by the p version of the finite element method for Stokes problem
[AD-A219887] 17 p2404 N90-23697
Non-linear dynamic analysis of geared systems, part 2
[NASA-CR-180495] 17 p2410 N90-23732
Application of finite-element-based solution technologies for viscoplastic structural analyses
[NASA-CR-185196] 17 p2414 N90-23757
Finite element formulations for coupled fluid/structure eigenvalue analysis
[AD-A220793] 17 p2416 N90-23766
STARS: An integrated general-purpose finite element structural, aeroelastic, and aeroservoelastic analysis computer program
[NASA-TM-101709] 17 p2416 N90-23768
Finite element analysis of structural components using viscoplastic models with application to a cowl lip problem
[NASA-CR-185189] 17 p2416 N90-23769
Design of finite element systems for parallel computers 17 p2450 N90-23975
An H(m)sub 0 interpolation result
[AD-A219888] 17 p2461 N90-24051
A fast PC-based solver for simultaneous linear equations
[AD-A220190] 17 p2461 N90-24056
Short time Force and moment measurement System for shock tubes (SFS) for measuring times less than 10 ms 18 p2490 N90-24233
Rotary-Jet thrust augmentor with jet-flapped blades 18 p2492 N90-24243
Metal matrix composites microfracture: Computational simulation
[NASA-TM-103153] 18 p2518 N90-24383
Cyclic damage zones ahead of tensile fatigue cracks in ceramic materials
[DE90-008372] 18 p2531 N90-24442
Personal Computer (PC) thermal analyzer
[AD-A221325] 18 p2548 N90-24546
Eighteenth NASTRAN (R) Users' Colloquium
[NASA-CP-3069] 18 p2568 N90-24637
Accuracy of the QUAD4 thick shell element 18 p2569 N90-24641
Eigenvalue computations with the QUAD4 consistent-mass matrix 18 p2569 N90-24642
Low velocity impact analysis with NASTRAN 18 p2570 N90-24647
Coupled BE/FE/BE approach for scattering from fluid-filled structures 18 p2570 N90-24649
Accuracy improvements in finite element stress analysis 18 p2571 N90-24651
Computational methods and plasticity
[PB90-167917] 18 p2571 N90-24652
A numerical study of plasticity induced closure in short cracks by the finite element method
[AD-A220471] 18 p2571 N90-24654
A vectroized elastic/plastic power law hardening material model including Lueders strain
[DE90-010172] 18 p2572 N90-24655
On the performance of algorithms for large-scale bound constrained problems
[DE90-010084] 18 p2590 N90-24736
Bivariate simplicial splines in finite element computations
[MEMO-823] 18 p2600 N90-24797
Finite element formulations for compressible flows 18 p2632 N90-24996
Dynamic analysis of flexible multibody structures 18 p2642 N90-25048
Development of a finite element based delamination analysis for laminates subject to extension, bending, and torsion 18 p2642 N90-25049
Fatigue analysis of mini-mast space truss 18 p2643 N90-25052
Extension-torsion coupling behavior of advanced composite tilt-rotor blades 18 p2644 N90-25057
Development and application of an optimization procedure for space and aircraft structures
[MBB-FW-522/S/PUB-383] 19 p2650 N90-25078
Hybrid analysis: Coupling of the finite element method with analytical approaches
[MBB-UO-0048/89-PUB] 19 p2650 N90-25079
The application of the finite element method to an aerodynamic problem specific to propeller design
[LR-614] 19 p2656 N90-25116
Calculation of thick wall fiber binders for rotor components of modern helicopters
[MBB-UD-554/84-PUB] 19 p2660 N90-25137
Ground shake test of the UH-60A helicopter airframe and comparison with NASTRAN finite element model predictions
[NASA-CR-181993] 19 p2661 N90-25143
A numerical micromechanics analysis of the mechanical properties of a plain weave composite
[OUEL-1760/89] 19 p2673 N90-25201
Experimental observations and finite element analysis of the initiation of fiber microbuckling in notched composite laminates
[NASA-CR-186207] 19 p2699 N90-25359
Generation of an axisymmetric cylindrical shell element using a shooting method
[ACTA-POLYTEC-SCAND-CI-93] 19 p2700 N90-25362
Free vibrations of thin-walled semicircular graphite-epoxy composite frames
[NASA-TM-102680] 19 p2701 N90-25365
Calculation of flight vibration levels of the AH-1G helicopter and correlation with existing flight vibration measurements
[NASA-CR-182031] 19 p2702 N90-25375
Calculations of welding stresses and deformations by means of finite element method
[VTT-RR-648] 19 p2703 N90-25382
A suitable transverse shear stiffness definition for buckling of laminates and sandwich plates
[LR-603] 19 p2704 N90-25384
Adaptive node movement in finite-difference solutions of partial differential equations with applications to gasdynamics, part 1
[UTIAS-333-PT-1] 19 p2750 N90-25622
Adaptive node movement in finite-difference solutions of partial differential equations with applications to gasdynamics, part 2
[UTIAS-333-PT-2] 19 p2750 N90-25623
An adaptive finite element method for shock developing partial differential equation
[FFI-89/7014] 19 p2751 N90-25632
Computational crash dynamics. Project 1.2: Computational crash dynamics analysis
[IAR-89-19] 20 p2804 N90-25956
Structural analysis and optimization of a propfan blade using a finite element method
[DLR-FB-90-01] 20 p2812 N90-26006
Strain energy release rate analysis of delamination in a tapered laminate subjected to tension load
[NASA-TM-102592] 20 p2826 N90-26076
Determination of the stress distributions in a ceramic: Tensile specimen using numerical techniques
[NASA-TM-101914] 20 p2837 N90-26132
Computer simulation of gear tooth manufacturing processes
[NASA-CR-185200] 20 p2843 N90-26171
A comparison of the post-buckling behavior of metallic and composite plates with centrally located cutouts
[NIAR-90-14] 20 p2875 N90-26356
Design of ceramic components with the NASA/CARES computer program
[NASA-TM-102369] 20 p2875 N90-26359
ANTIPASTO: An interactive mesh generator and preprocessor for two-dimensional analysis programs
[DE90-011755] 20 p2906 N90-26530
Parallel processors and nonlinear structural dynamics algorithms and software
[NASA-CR-186755] 20 p2907 N90-26536
Generation and improvement of meshes for finite elements methods in two and three dimensions
[ETN-90-97249] 20 p2919 N90-26611
Photoelasticity: A cost effective design tool 21 p2958 N90-26819
Finite element models of USAF aircraft structures 21 p2958 N90-26820
B-1B improved windshield development. Volume 2: Magna analysis: Baseline and parametric
[AD-A221501] 21 p2960 N90-26828
Numerical interactive grid generation for 3-D flow calculations
[NLR-MP-88055-U] 21 p3003 N90-27069
Fracture mechanics analysis for short cracks
[AD-A222170] 21 p3013 N90-27130
Load-point compliance for the arc bend-arc support fracture toughness specimen
[AD-A221618] 21 p3014 N90-27134
Proceedings of Workshop on Reliability in Computational Mechanics
[AD-A221694] 21 p3065 N90-27426
Deployment of large flexible space structures 22 p3131 N90-27766
Computational Fluid Dynamics, volume 1
[VKI-LS-1990-03-VOL-1] 22 p3171 N90-27989
The streamline diffusion finite element method for compressible and incompressible fluid flow 22 p3172 N90-27991
Numerical methods for shallow water flow 22 p3172 N90-27992
Fluctuation splitting for multidimensional convection problems: An alternative to finite volume and finite element methods 22 p3173 N90-28000
A finite element method for turbulent incompressible flow 22 p3174 N90-28007
Solution of Euler equations using finite element method and the kinetic decomposition of the flows: Study of the self-adaptation of the grid and of the calculation field
[CERT-1/334700-DERI-GAN] 22 p3176 N90-28020
Numerical study of turbulence in the presence of walls
[ONERA-RSF-15/3419-AY-114A] 22 p3176 N90-28024
Mechanics of impact energy absorption
[PB90-190836] 22 p3190 N90-28101
Parametrical retiming of vibrational models of structures
[ONERA-RT-9/3313-RY-080-R] 22 p3194 N90-28121
Liquid Rocket Booster (LRB) for the Space Transportation System (STS) systems study. Appendix A: Stress analysis report for the pump-fed and pressure-fed liquid rocket booster
[NASA-CR-183787-APP-A] 23 p3288 N90-28601
A hybrid-stress finite element for linear anisotropic elasticity 23 p3290 N90-28614
Probabilistic structural analysis methods development for SSME 23 p3291 N90-28616
Mechanical behavior of thick, curved, laminated composites 23 p3299 N90-28664
Lecture notes on incompressible flow and the finite element method
[DE90-014665] 23 p3326 N90-28805
Vortice-propeller interaction
[LIMSI-89-9] 23 p3326 N90-28809
Finite element analysis of coupled thermoelasticity
[PB90-201211] 23 p3337 N90-28860
Correlation of AH-1G airframe flight vibration data with a coupled rotor-fuselage analysis
[NASA-CR-181974] 23 p3338 N90-28865
Plan, execute, and discuss vibration measurements and correlations to evaluate a NASTRAN finite element model of the AH-64 helicopter airframe
[NASA-CR-181973] 23 p3338 N90-28866
A nonlinear finite element formulation for the large displacement analysis of plates 23 p3338 N90-28867
Application of discrete Fourier series to the finite element stress analysis of axi-symmetric solids
[PB90-231010] 23 p3339 N90-28870
Parametric solution of nonlinear structure problems
[ONERA-RT-21/3542-RY-082-R] 23 p3340 N90-28874
Error detection and control for nonlinear shell analysis
[NASA-TM-102723] 23 p3340 N90-28877
Second order tensor finite element
[NASA-CR-184008] 23 p3386 N90-29122
Large hydrodynamic tunnel: Calculation of the acoustic transparency of the jet stream
[REPT-89/115] 23 p3393 N90-29167
A package for 3-D unstructured grid generation, finite-element flow solution and flow field visualization
[NASA-CR-182090] 24 p3419 N90-29309
Nonlinear static and dynamic modeling of composite rotor blades including warping effects 24 p3431 N90-29382
Assessment and improvement of aeroengine disc structural integrity 24 p3433 N90-29392
Structural testing and analytical research of turbine components
[AD-A223516] 24 p3434 N90-29396
Variational formulation and finite element implementation of Pagano's theory of laminated plates 24 p3442 N90-29437
Reliability study of TWT output RF window
[AD-A223688] 24 p3465 N90-29574
Dual and primal mixed Petrov-Galerkin finite element methods in heat transfer problems
[DE90-627190] 24 p3468 N90-29592
Optimization of tetrahedrical meshes for finite element calculation methods in fluids mechanics
[ETN-90-97560] 24 p3469 N90-29603
Rotordynamic properties of high pressure seals: An experimental approach 24 p3475 N90-29640
Tip-position control of a flexible beam: Modeling approaches and experimental verification
[AD-A224249] 24 p3476 N90-29643
On a generalized laminate theory with application to bending, vibration, and delamination buckling in composite laminates 24 p3478 N90-29659
The ACR-program for automatic finite element model generation for part through cracks
[DE90-631545] 24 p3479 N90-29662
Comparison of crack closure result obtained by 3D elastic-plastic FEM and modified Dugdale model
[FFA-TN-1990-18] 24 p3481 N90-29675

Computer-aided engineering environment for controlled mechanical systems
| AD-A223551 | 24 p3527 N90-29942
A posteriori error estimates for parametrized nonlinear equations
| AD-A224067 | 24 p3537 N90-29997

FINITE IMPULSE RESPONSE FILTERS
U FIR FILTERS

FINITE VOLUME METHOD
Numerical solution of three-dimensional unsteady flows: Application to instability problems 01 p0065 N90-10375
A nonoscillatory, characteristically convected, finite volume scheme for multidimensional convection problems
| NASA-TM-102354 | 02 p0263 N90-11497
Direct discretization of planar div-curl problems
| NASA-CR-181935 | 02 p0263 N90-11498
Computation of flow fields around propellers and hovering rotors based on the solution of the Euler equations
| DLR-FB-89-37 | 05 p0572 N90-13333
Calculation of flow fields by the solution of the Euler equations using an extended finite volume discretization scheme
| DLR-FB-89-38 | 05 p0639 N90-13729
Advanced 3-D CFD algorithm for turbomachinery 06 p0725 N90-14233
A finite volume calculation method for three dimensional, complex flows 08 p1070 N90-16195
High-resolution Euler computations of unsteady transonic flows in cascades 11 p1462 N90-18420
Analysis of unsteady heat transfer by natural convection in a two-dimensional square cavity using a high order finite-volume method 12 p1657 N90-19521
An overlapped grid method for multigrid, finite volume/difference flow solvers: MaGGiE
| NASA-CR-182008 | 14 p1911 N90-20953
A computational design method for shock free transonic cascades and airfoils 14 p1918 N90-20986
Compact finite volume methods for the diffusion equation
| NASA-CR-186477 | 14 p2019 N90-21568
Numerical simulation of hypersonic flow around a space plane. Part 2: Application to high angles of attack flow
| NAL-TR-1011T | 15 p2045 N90-21726
Large-scale advanced propeller blade pressure distributions: Prediction and data
| NASA-TM-102316 | 16 p2201 N90-22564
A computer code for the prediction of aerodynamic characteristics of lifting airfoils at transonic speed
| DLC-EST-TN-030 | 17 p2346 N90-23359
Stability theory for methods to solve the Navier-Stokes equations, part 1
| FFA-TN-1988-65-PT-1 | 19 p2691 N90-25312
The finite analytic method and its applications. Volume 1: Laminar and turbulent flows past two-dimensional and axisymmetric bodies
| AD-A222787 | 20 p2864 N90-26294
FINFLO: A finite-volume based computer program for two-dimensional and axisymmetric compressible flow
| PB90-189473 | 22 p3169 N90-27974
Computation of compressible, vortical flows 22 p3172 N90-27996
Fluctuation splitting for multidimensional convection problems: An alternative to finite volume and finite element methods 22 p3173 N90-28000
The PHOENICS flow-simulation system 22 p3174 N90-28006
Finite-volume application of high order ENO schemes to multi-dimensional boundary-value problems
| NASA-CR-186917 | 22 p3242 N90-28387
Numerical resolution of Navier-Stokes equations using several turbulence models and applications on turbomachines
| ETN-90-97478 | 23 p3326 N90-28808
Calculation of flow fields by the solution of the Euler equations using an extended finite volume discretization scheme
| ESA-TT-1204 | 24 p3470 N90-29605
The fundamentals of adaptive grid movement 24 p3470 N90-29610

FINITE-STATE MACHINES
U TURING MACHINES

FINLAND
Calculated solar radiation incident upon slopes of different orientated surfaces in Finland
| FMI-MP-8 | 03 p0370 N90-12116

FINNED BODIES
Aerodynamic test and analysis of a slender generic missile configuration
| AD-A212522 | 04 p0448 N90-12567
Transonic Euler solutions on mutually interfering finned bodies
| AD-A213395 | 05 p0572 N90-13331
Laminar forced convection inside externally finned tubes
| DE89-636431 | 07 p0928 N90-15373
External flow computations for a finned 60mm ramjet in steady supersonic flight
| AD-A216998 | 12 p1605 N90-19233

FINS
Aeroelastic tailoring procedure for controlling fin hinge moments 01 p0013 N90-10058
Remote control missile model test 01 p0013 N90-10063
Simulation of glancing shock wave and boundary layer interaction
| NASA-TM-102233 | 03 p0345 N90-11970
Additions and corrections to SUPER: A program for calculating steady and oscillatory supersonic flow over a thin wing, tail plane and fin
| AD-A211771 | 04 p0438 N90-12501
Glancing shock-boundary layer interactions 10 p1309 N90-17571
Numerical investigation of some control methods for 3-D turbulent interactions due to sharp fins 15 p2053 N90-21764
Calculation of the aeroelastic blade stabilization with linearized process
| MITT-87-01 | 18 p2497 N90-24272
Yaw fin deployment apparatus for ejection seat
| AD-D014512 | 19 p2656 N90-25118
A computational study of the effectiveness of coating materials for KE projectile fins subjected to the combined effects of inbore and aerodynamic heating
| AD-A222595 | 20 p2840 N90-26155
Damage tolerance of the fighter aircraft 37 Viggen. Part 1: Analytical assessment
| FFA-TN-1990-12-PT-1 | 23 p3276 N90-28538
Damage tolerance of the fighter aircraft 37 Viggen. Part 2: Experimental verification
| FFA-TN-1990-13-PT-2 | 23 p3276 N90-28539
A study of heat and fluid flow phenomena on the gas side of circular-tube plate-fin heat exchangers 23 p3324 N90-28795

FIR FILTERS
Adaptive clutter rejection filters for airborne Doppler weather radar applied to the detection of low altitude windshear
| NASA-CR-186211 | 06 p0766 N90-14453
The effects of clutter-rejection filtering on estimating weather spectrum parameters
| NASA-CR-186212 | 06 p0817 N90-14754

FIRE CONTROL
Algorithm development for SDI weapons system allocation
| AD-A212973 | 04 p0534 N90-13090
China-built airborne synchronous laser ranger the new L-8 jet trainer aircraft
| AD-A213835 | 07 p0936 N90-15422
Diagnostics and firing control for the cylindrical reconnection launcher
| DE90-007677 | 13 p1761 N90-20107
Performance-based measures of merit for tactical situation awareness 23 p3358 N90-28976
Application of multifunction inertial reference systems to fighter aircraft 24 p3423 N90-29341

FIRE DAMAGE
Upward flame spread on vertical walls
| PB89-214787 | 01 p0039 N90-10217
Risk-based fire safety experiment definition for manned spacecraft
| NASA-CR-183835 | 06 p0731 N90-14262
A discussion of fire suppression induced equipment damage and systems impact through an examination of spurious fire suppression actuation incidents
| DE90-000792 | 06 p0756 N90-14402

FIRE EXTINGUISHERS
Aircraft cabin fire suppression by means of an interior water spray system
| CAA-PAPER-88014 | 03 p0303 N90-11719
Advanced spacecraft fire safety: Proposed projects and program plan
| NASA-CR-185147 | 04 p0462 N90-12645
Aviation Engine Test Facilities (AETF) fire protection study
| AD-A211483 | 04 p0483 N90-12777
A discussion of fire suppression induced equipment damage and systems impact through an examination of spurious fire suppression actuation incidents
| DE90-000792 | 06 p0756 N90-14402
Fire safety applications for spacecraft 10 p1314 N90-17595
US Navy aircraft fire protection technology 10 p1315 N90-17603
Preliminary fire extinguishing tests with handheld bottles: A comparison of extinguishing compounds
| DOT/FAA/CT-TN89/60 | 10 p1368 N90-17930
Selective automatic fire extinguisher for computers (SAFECOMP): Developmental test and evaluation/initial operational test and evaluation
| AD-A217790 | 14 p1958 N90-21212
Testing of flame screens and flame arresters as Devices designed to Prevent the Passage of Flame (DPPF) into tanks containing flammable atmospheres according to an IMO standard
| AD-A222566 | 20 p2844 N90-26177
The computer modeling of the combustion and extinction of methane-air premixed flames by thermally stable gases
| PB90-189432 | 21 p2976 N90-26910
Developing air tanker performance guidelines
| PB90-183765 | 22 p3114 N90-27695

FIRE FIGHTING
A discussion of fire suppression induced equipment damage and systems impact through an examination of spurious fire suppression actuation incidents
| DE90-000792 | 06 p0756 N90-14402
Aircraft internal fires 10 p1313 N90-17593
VULCAIN: An expert system dedicated to fire risk analysis within complex industrial environments 10 p1314 N90-17599
Flight crew training for fire fighting 10 p1317 N90-17615
Developing air tanker performance guidelines
| PB90-183765 | 22 p3114 N90-27695

FIRE PREVENTION
Aircraft cabin fire suppression by means of an interior water spray system
| CAA-PAPER-88014 | 03 p0303 N90-11719
Advanced spacecraft fire safety: Proposed projects and program plan
| NASA-CR-185147 | 04 p0462 N90-12645
Aviation Engine Test Facilities (AETF) fire protection study
| AD-A211483 | 04 p0483 N90-12777
Risk-based fire safety experiment definition for manned spacecraft
| NASA-CR-183835 | 06 p0731 N90-14262
Investigation and characteristics of major fire-related accidents in civil air transports over the past ten years 10 p1311 N90-17582
Aircraft fires: A study of transport accidents from 1975 to the present 10 p1311 N90-17583
Development of improved fire safety standards adopted by the Federal Aviation Administration 10 p1312 N90-17585
Fire safety in civil aviation 10 p1312 N90-17586
A review of UK civil aviation fire and cabin safety research 10 p1312 N90-17587
Objectives and results of cabin fire research in Germany 10 p1312 N90-17588
New aircraft cabin and cargo flammability standards for transport category aircraft 10 p1312 N90-17589
Fire prevention in transport airplane passenger cabins 10 p1313 N90-17590
Fire safety applications for spacecraft 10 p1314 N90-17595
Fire science and aircraft safety 10 p1314 N90-17596
Hot surface ignition studies of aviation fluids 10 p1314 N90-17600
Onboard fire- and explosion suppression for fighter aircraft 10 p1315 N90-17602
US Navy aircraft fire protection technology 10 p1315 N90-17603
Aircraft fire safety in the Canadian Forces 10 p1315 N90-17604
Fire hardening of aircraft through upgrades of materials and designs 10 p1315 N90-17605
Fire hardening of an aircraft passenger cabin 10 p1315 N90-17606
Fire resistance and breakdown of composite materials 10 p1316 N90-17607
Advanced materials for interior and equipment related to fire safety in aviation 10 p1316 N90-17608
Heat release rate measurement for evaluating the flammability of aircraft materials 10 p1316 N90-17610
Testing of flame screens and flame arresters as Devices designed to Prevent the Passage of Flame (DPPF) into tanks containing flammable atmospheres according to an IMO standard
| AD-A222566 | 20 p2844 N90-26177

FIRE RESISTANCE
U FLAMMABILITY

FIRE RETARDANTS
U FLAME RETARDANTS

FIREBREAKS
Geographic information system: Coded data of agrocattle-raising projects in the Amazon
| INPE-4978-PRE/1543 | 15 p2180 N90-22457

FIREPROOFING
Aircraft cabin fire suppression by means of an interior water spray system
|CAA-PAPER-88014| 03 p0303 N90-11719
Fire prevention in transport airplane passenger cabins 10 p1313 N90-17590
Onboard fire- and explosion suppression for lighter aircraft 10 p1315 N90-17602

FIRES
NT FOREST FIRES
Aviation Engine Test Facilities (AETF) fire protection study
|AD-A211483| 04 p0483 N90-12777
A discussion of fire suppression induced equipment damage and systems impact through an examination of spurious fire suppression actuation incidents
|DE90-000792| 06 p0756 N90-14402
RAAF Orion aircraft A9-300 oxygen fire
|AD-A215496| 09 p1162 N90-16725
Workshop on the Effects of Combined Fire Products on Human Physiological and Psychological Performance
|AD-A215465| 09 p1253 N90-17270
Aircraft Fire Safety
|AGARD-CP-467| 10 p1311 N90-17581
Aircraft fires: A study of transport accidents from 1975 to the present 10 p1311 N90-17583
Aircraft fire safety: Learning from past accidents 10 p1312 N90-17584
Fire safety in civil aviation 10 p1312 N90-17586
A review of UK civil aviation fire and cabin safety research 10 p1312 N90-17587
Objectives and results of cabin fire research in Germany 10 p1312 N90-17588
Fire prevention in transport airplane passenger cabins 10 p1313 N90-17590
Characteristics of transport, aircraft fires measured by full-scale tests 10 p1313 N90-17591
Full scale study of a cabin fire in an A300 fuselage section 10 p1313 N90-17592
Aircraft internal fires 10 p1313 N90-17593
Fire safety applications for spacecraft 10 p1314 N90-17595
Fire science and aircraft safety 10 p1314 N90-17596
Forced and natural venting of aircraft cabin fires: A numerical simulation 10 p1314 N90-17597
Time development of convection flow patterns in aircraft cabins under post-crash fire exposure 10 p1314 N90-17598
VULCAIN: An expert system dedicated to fire risk analysis within complex industrial environments 10 p1314 N90-17599
Hot surface ignition studies of aviation fluids 10 p1314 N90-17600
The stability of fuel fires 10 p1315 N90-17601
Onboard fire- and explosion suppression for fighter aircraft 10 p1315 N90-17602
US Navy aircraft fire protection technology 10 p1315 N90-17603
Aircraft fire safety in the Canadian Forces 10 p1315 N90-17604
Fire hardening of aircraft through upgrades of materials and designs 10 p1315 N90-17605
Fire hardening of an aircraft passenger cabin 10 p1315 N90-17606
Advanced materials for interior and equipment related to fire safety in aviation 10 p1316 N90-17608
New materials for civil aircraft furnishing 10 p1316 N90-17609
Flammability testing of aircraft cabin materials 10 p1316 N90-17611
Method for the evaluation of toxicity of combustion products from aircraft cabin materials: Analysis and results 10 p1316 N90-17612
Passenger behaviour in aircraft emergencies involving smoke and fire 10 p1317 N90-17613
Flight crew training for fire fighting 10 p1317 N90-17615
The investigation of particulate matter in the lungs of smoke inhalation death victims 10 p1317 N90-17617
The importance of pathophysiological parameters in fire modelling of aircraft accidents 10 p1317 N90-17618
Modelling time to incapacitation and death from toxic and physical hazards in aircraft fires 10 p1318 N90-17619
Preliminary fire extinguishing tests with handheld bottles: A comparison of extinguishing compounds
|DOT/FAA/CT-TN89/60| 10 p1368 N90-17930
The thermal response of generic objects in JP-4 pool fires
|DE90-008503| 13 p1788 N90-20259
Full-scale air transport category fuselage burnthrough tests
|DOT/FAA/CT-TN89/65| 14 p1913 N90-20967
Test method for fire extinguishing powder, Nordtest project 675-87
|PB90-166984| 15 p2073 N90-21874
The influence of large, cold objects on engulfing fire environments
|DE90-003342| 15 p2073 N90-21875
Aircraft crash survival design guide. Volume 5: Aircraft postcrash survival
|AD-A218438| 16 p2198 N90-22549
Fire hazards of aerosol cans in aircraft cargo compartments
|DOT/FAA/CT-89/32| 17 p2347 N90-23389
Flammability of fire resistant, aircraft hydraulic fluid
|DOT/FAA/CT-TN90/19| 19 p2677 N90-25222
Activities report for the IBDF-INPE project SEQE, year 1987
|INPE-4534-RPE/565| 23 p3415 N90-29298

FIREWORKS
U PYROTECHNICS

FIRING (IGNITING)
NT TEST FIRING
An evaluation of ethylene-vinyl acetate copolymers as desensitizers for RDX in insensitive booster compositions prepared by slurry coating technology
|MRL-TR-89-33| 12 p1633 N90-19385
Preparation, characterisation and cookoff behaviour of booster compositions prepared from RDX and acrylic or ethylene-vinyl acetate dispersions
|MRL-TR-89-44| 14 p1957 N90-21203

FIRST AID
What should athletes know about low body temperature (hypothermia)
|AD-A218316| 13 p1854 N90-20637
Arctic cold weather medicine and accidental hypothermia
|AD-A223090| 20 p2899 N90-26487

FISCHER-TROPSCH PROCESS
Natural gas to liquids
|DE89-000982| 03 p0322 N90-11828

FISH
U FISHES

FISHES
Predicting effects of global climate change on reservoir water quality and fish habitat
|DE90-003674| 12 p1689 N90-19704
Transduction of nanovolt signals: Limits of electric-field detection
|AD-A219214| 16 p2312 N90-23177
Outer continental shelf environmental assessment program. Volume 66: Principal investigators
|PB90-194747| 22 p3199 N90-28154
Exogenous and endogenous control of activity behavior and the fitness of fish
|DLR-FB-90-14| 24 p3497 N90-29766

FISHTAILING
U YAW

FISSILE MATERIALS
U FISSIONABLE MATERIALS

FISSION
Activities report of the Joint Research Center
|ETN-89-95757| 04 p0569 N90-13321
Biomodal spontaneous fission
|DE90-001516| 06 p0840 N90-14886
Proceedings of the specialists' meeting on physics and engineering of fission and spallation
|DE90-719706| 08 p1125 N90-16519

FISSION PRODUCTS
Proceedings of the specialists' meeting on physics and engineering of fission and spallation
|DE90-719706| 08 p1125 N90-16519
The Surface Air Sampling Program
|DE90-014873| 24 p3487 N90-29711

FISSIONABLE MATERIALS
The gamma-ray laser project: Proof of the feasibility of coherent and incoherent schemes for pumping a gamma-ray laser
|AD-A216008| 10 p1389 N90-18037
Multimegawatt space nuclear power supply, phase 1. Supplement: D180-30619-8
|DE90-012433| 20 p2926 N90-26647

FITNESS
NT PHYSICAL FITNESS

FITTINGS
Epoxy-resin cable terminations
|AD-A213789| 07 p0942 N90-15454
Space shuttle RCS oxidizer leak repair for STS-26 11 p1474 N90-18485
Underwater connect and disconnect plug and receptacle
|AD-D014175| 21 p2998 N90-27039

FIX
U FIXING

FIXED POINT ARITHMETIC
Fixed points of expansive analytic maps
|AD-A214356| 10 p1421 N90-18194
Finite element analysis of elastic contact problems with friction 15 p2105 N90-22040
Undetermined coefficient problems for quasi-linear parabolic equations
|AD-A218462| 16 p2306 N90-23141
Solution of the Stokes system by boundary integral equations and fixed point iterative schemes
|DE90-627166| 23 p3389 N90-29138

FIXED POINTS (MATHEMATICS)
Fixed point iteration on point-symmetric interference graphs
|MEMO-INF-89-23| 02 p0269 N90-11535
On the differentiable manifold of fixed order stable linear systems
|REPT-88-89| 03 p0394 N90-12250
Nonlinear maps with competitive interactions: Fixed-points, bifurcations, and chaotic attractors
|DE90-001858| 07 p0986 N90-15695
Fixed points of expansive analytic maps
|AD-A214356| 10 p1421 N90-18194
A method for computing the stationary points of a function subject to linear equality constraints
|DE90-610427| 12 p1706 N90-19797
Fixed point theory in multiply ordered spaces
|REPT-89-74| 17 p2458 N90-24031
Explicit fixed points for interpretability logic
|ITLI-ML-89-01| 18 p2603 N90-24820

FIXED WINGS
Preliminary design of a family of three close air support aircraft
|NASA-CR-186070| 09 p1166 N90-16751
Extension of a three-dimensional viscous wing flow analysis
|NASA-CR-182023| 17 p2344 N90-23348

FIXED-WING AIRCRAFT
U AIRCRAFT CONFIGURATIONS
U FIXED WINGS

FIXING
Study of rifampicin fixation on plasma proteins by derivative spectrophotometry
|CERMA-89-25| 11 p1540 N90-18866

FIXTURES
Stress analysis of the Princeton Plasma Physics Laboratory 1/2- x 1/2-inch shear/compression test fixture
|DE90-004401| 08 p1124 N90-16512

FLAME DEFLECTORS
Testing of flame screens and flame arresters as Devices designed to Prevent the Passage of Flame (DPPF) into tanks containing flammable atmospheres according to an IMO standard
|AD-A223536| 20 p2844 N90-26177

FLAME FRONTS
U FLAME PROPAGATION

FLAME INTERACTION
U CHEMICAL REACTIONS
U FLAME PROPAGATION

FLAME IONIZATION
Peak analysis in gas chromatography and the development of new stationary phases for anion chromatography
|DE90-014428| 23 p3304 N90-28687

FLAME PROBES
Investigation of fuel additive effects on sooting flames
|AD-A212925| 04 p0473 N90-12709

FLAME PROPAGATION
Upward flame spread on vertical walls
|PB89-214787| 01 p0039 N90-10217
Premixed turbulent flame propagation
|AD-A211489| 03 p0324 N90-11841
FLIC (FLame with Implicit Convection): A detailed, two-dimensional flame model
|AD-A212953| 04 p0473 N90-12710
Experimental and computational study of combustion limits in natural-gas fueled internal combustion engines
|PB89-235196| 05 p0629 N90-13673
An investigation of flame spread over shallow liquid pools in microgravity and nonair environments
|NASA-TM-102425| 05 p0630 N90-13680
Effects of flame stretch on the propagation, extinction, and stability of premixed flames 06 p0739 N90-14301
Flame acceleration studies in the MINIFLAME facility
|DE90-000041| 06 p0740 N90-14310
A numerical study of thin flame representations
|DE89-017889| 06 p0741 N90-14313
A tomographic study of premixed turbulent stagnation point flames
|DE90-002462| 07 p0892 N90-15156
Fuel tank explosion protection 08 p1023 N90-15914
Assessing the flammability of composite materials
|PB90-112996| 08 p1039 N90-16002
Combustion Experiments During KC-135 Parabolic Flights
|ESA-SP-1113| 09 p1201 N90-16958

Polymer group microgravity combustion experiment
09 p1202 N90-16964
Heterogeneous combustion processes under microgravity conditions 09 p1202 N90-16965
Fire science and aircraft safety
10 p1314 N90-17596
Wick-type liquid-metal combustion
|AD-A216019| 11 p1482 N90-18530
Aerodynamic and kinetic processes in flames
|AD-A217796| 13 p1773 N90-20176
The extinction and structure of counterflow premixed flames
|AD-A218106| 13 p1773 N90-20178
Studies on reactive flows 15 p2066 N90-21831
Fire propagation in concurrent flows
|PB90-151754| 15 p2066 N90-21834
The influence of large, cold objects on engulfing fire environments
|DE90-003342| 15 p2073 N90-21875
Numerical investigation of turbulent flame sheets
|AD-A218553| 16 p2215 N90-22635
Nonlinear spectroscopy of multicomponent droplets and 2- and 3-dimensional measurements in flames
|AD-A218569| 16 p2215 N90-22636
Two-dimensional velocimetry instrumentation
|AD-A218450| 16 p2239 N90-22774
Premixed turbulent flame propagation
|AD-A219834| 17 p2373 N90-23515
Chemistry of combustion processes
20 p2811 N90-25994
Testing of flame screens and flame arresters as Devices designed to Prevent the Passage of Flame (DPPF) into tanks containing flammable atmospheres according to an IMO standard
|AD-A222566| 20 p2844 N90-26177
Asymptotic analysis of dissipative waves with applications to their numerical simulation
|NASA-TM-103231| 20 p2920 N90-26615
Hydrocarbon-fueled scramjet combustor component development tests 22 p3162 N90-27934

FLAME QUENCHING
U EXTINGUISHING
U QUENCHING (COOLING)

FLAME RETARDANTS
Development of improved fire safety standards adopted by the Federal Aviation Administration
10 p1312 N90-17585
Fire resistance and breakdown of composite materials
10 p1316 N90-17607
Development and application of nonflammable, high-temperature beta fibers
|NASA-TM-102158| 13 p1855 N90-20645
Ternary reactions among polymer substrate-organohalogen-antimony oxides under pyrolytic, oxidative and flaming conditions
|PB90-154766| 15 p2071 N90-21861

FLAME SPECTROSCOPY
Study of the hydroxyl radical by DRASC resonance in a high pressure flame --- Diffusion Raman Anti-Stokes Coherence (DRASC)
|ONERA-RS-53/7131-PY| 05 p0622 N90-13632
Spectral studies of solid propellant combustion. 2: Emission and absorption results for M-30 and HMX1 propellants
|AD-A213857| 07 p0915 N90-15292
Measurement of the speed and temperature of ignition gases
|ISL-CO-246/88| 09 p1192 N90-16908
Study of new technique of solid combustible materials to determination of volatile elements by flame atomic absorption spectrophotometry
|DE90-612907| 14 p1947 N90-21147
Nonlinear spectroscopy of multicomponent droplets and 2- and 3-dimensional measurements in flames
|AD-A218569| 16 p2215 N90-22636
Temperature and OH concentrations in a solid propellant flame using absorption techniques
|AD-A222591| 20 p2830 N90-26100
Spectroscopic study of combustion diagnostics on hydroxyl radicals
|NASA-CR-186998| 23 p3305 N90-28694
Spectroscopy of propellant-related flames
|AD-A224068| 24 p3457 N90-29525

FLAME STABILITY
Combustion characteristics of sprays
|AD-A213651| 07 p0895 N90-15173
Swirl-stabilized flames: Fluid dynamics, mixing, and flame stability limits 08 p1040 N90-16009
Premixed flames in microgravity
09 p1201 N90-16959
Electric field-induced flame convection in the absence of gravity 09 p1202 N90-16962
Theoretical investigation of the stabilization of a diffusion flame above a recirculation region
|ESA-TT-1149| 11 p1484 N90-18543
On the use of external burning to reduce aerospace vehicle transonic drag
|NASA-TM-103107| 15 p2052 N90-21762
Flame extinction in compressible flow
21 p2973 N90-26899

FLAME TEMPERATURE
Investigation of fuel additive effects on sooting flames
|AD-A212925| 04 p0473 N90-12709
Measurements of mean and fluctuating temperature in microgravity 09 p1201 N90-16961
Polymer group microgravity combustion experiment
09 p1202 N90-16964
Design of a pyrometer for temperature measurements on the solid fuel combustion chamber
|LR-530| 12 p1664 N90-19561
Chemical kinetic and aerodynamic structures of flames
|AD-A224281| 24 p3445 N90-29455

FLAMEOUT
In flight relight tests on AM-X single engine fly-by-wire aircraft 02 p0152 N90-10869
Application of neural networks to the F/A-18 engine condition monitoring system
|AD-A219820| 18 p2497 N90-24271

FLAMES
NT DIFFUSION FLAMES
NT PREMIXED FLAMES
Flame acceleration studies in the MINIFLAME facility
|DE90-000041| 06 p0740 N90-14310
A numerical study of thin flame representations
|DE89-017889| 06 p0741 N90-14313
Simultaneous multipoint measurements of density gradients and temperature in a flame
|DE90-001719| 07 p0892 N90-15155
Swirl-stabilized flames: Fluid dynamics, mixing, and flame stability limits 08 p1040 N90-16009
An investigation of flow structure, mixing and chemical reaction in combusting turbulent flows
|AD-A216739| 11 p1483 N90-18538
Investigation of methods to produce a uniform cloud of fuel particles in a flame tube
|NASA-TM-102376| 11 p1505 N90-18665
Spatially high-resolution flame diagnosis by means of spontaneous Raman spectroscopy
|ETN-90-95870| 12 p1623 N90-19328
Saturated fluorescence measurements of the hydroxyl radical in laminar high-pressure flames
|NASA-CR-185218| 15 p2101 N90-22022
Premixed turbulent flame propagation
|AD-A219834| 17 p2373 N90-23515
Contributions to the study of parietal flames due to turbulent diffusion
|ECL-89-22| 17 p2374 N90-23519
Structure of monopropellant spray flames at elevated pressures
|AD-A218676| 17 p2383 N90-23570
Periphery camera system
|AD-A221281| 18 p2555 N90-24583
Asymptotic analysis of dissipative waves with applications to their numerical simulation
|NASA-TM-103231| 20 p2920 N90-26615
Concentration, temperature, and density in a hydrogen-air flame by excimer-induced Raman scattering 21 p2974 N90-26903
PDF modeling of chemical nonequilibrium effects in turbulent nonpremixed jet flames
21 p2975 N90-26908
The computer modeling of the combustion and extinction of methane-air premixed flames by thermally stable gases
|PB90-189432| 21 p2976 N90-26910
Ignition and combustion characteristics of metallized propellants
|NASA-CR-186870| 21 p2976 N90-26911
Carbon stardust: From soot to diamonds
21 p3090 N90-27568
Down-to-earth studies of carbon clusters
21 p3091 N90-27573
A unifying picture of gas-phase formation and growth of PAH (Polycyclic Aromatic Hydrocarbons), soot, diamond and graphite 21 p3091 N90-27575
An ionic mechanism of carbon formation in flames
21 p3093 N90-27582
Model of turbulent diffusion flames and nitric oxide generation
|PB90-155557| 22 p3155 N90-27886
Structure and radiation properties of turbulent diffusion flames
|PB90-218777| 22 p3155 N90-27887
CARS spectroscopy and applications
24 p3420 N90-29321

FLAMMABILITY
Flammability, smoke, and dry arc tracking tests of aircraft electrical wire insulations
|DOT/FAA/CT-89/21| 03 p0302 N90-11714
Advanced spacecraft fire safety: Proposed projects and program plan
|NASA-CR-185147| 04 p0462 N90-12645
Experimental and computational study of combustion limits in natural-gas fueled internal combustion engines
|PB89-235196| 05 p0629 N90-13673
Ignitability test method and apparatus
|NASA-CASE-LAR-13996-1-SB|
07 p0893 N90-15161
Assessing the flammability of composite materials
|PB90-112996| 08 p1039 N90-16002
New aircraft cabin and cargo flammability standards for transport category aircraft 10 p1312 N90-17589
Ignitability of jet-A fuel vapors in aircraft fuel tanks
10 p1313 N90-17594
Hot surface ignition studies of aviation fluids
10 p1314 N90-17600
Fire resistance and breakdown of composite materials
10 p1316 N90-17607
Heat release rate measurement for evaluating the flammability of aircraft materials
10 p1316 N90-17610
Flammability testing of aircraft cabin materials
10 p1316 N90-17611
Full-scale air transport category fuselage burnthrough tests
|DOT/FAA/CT-TN89/65| 14 p1913 N90-20967
Information compendium on nonflammable hydraulic fluid and design requirements for its adoption
|AD-A219569| 17 p2380 N90-23554
Thermodynamic calculations for mixtures of environmentally safe refrigerants using the Lee-Kesler-Ploecker equation of state
|DE90-010493| 18 p2542 N90-24509
Flammability of fire resistant, aircraft hydraulic fluid
|DOT/FAA/CT-TN90/19| 19 p2677 N90-25222
Testing of flame screens and flame arresters as Devices designed to Prevent the Passage of Flame (DPPF) into tanks containing flammable atmospheres according to an IMO standard
|AD-A222566| 20 p2844 N90-26177
Toxicity of thermolysis products from the materials of airplane cockpits
|CEAT-PV-M6/5924/02| 22 p3156 N90-27895
Toxicological aspects of fire onboard aircrafts: Role of the pressurization and ventilation in the cockpit
|ETN-90-97452| 22 p3233 N90-28335
Tests for aircraft interior materials in fire accident
|LR-622| 24 p3423 N90-29337
Chemical kinetic and aerodynamic structures of flames
|AD-A224281| 24 p3445 N90-29455

FLAMMABLE GASES
NT GASEOUS FUELS
Fire hazards of aerosol cans in aircraft cargo compartments
|DOT/FAA/CT-89/32| 17 p2347 N90-23369

FLANGES
Flanged joints of aeroengines
|PNR90594| 04 p0455 N90-12609
Flight set 360T004 (STS-30) field joint protection system, volume 7
|NASA-CR-183829| 06 p0735 N90-14280
A study of the vibrational transmission through flanged joints
|ISVR-TR-181| 11 p1520 N90-18755
Quick connect coupling
|NASA-CASE-MSC-21539-1| 21 p3010 N90-27111

FLAP CONTROL
U AIRCRAFT CONTROL
U FLAPS (CONTROL SURFACES)

FLAPPING
Parametric resonance in horizontal axis wind turbines
14 p1912 N90-20962
Synthesis of individual rotor blade control system for gust alleviation
|NASA-TM-101886| 20 p2807 N90-25972

FLAPS (CONTROL SURFACES)
NT JET FLAPS
NT LEADING EDGE FLAPS
NT UPPER SURFACE BLOWN FLAPS
Independent Orbiter Assessment (IOA): Analysis of the body flap subsystem
|NASA-CR-185574| 02 p0165 N90-10930
Independent Orbiter Assessment (IOA): Assessment of the body flap subsystem FMEA/CIL
|NASA-CR-185575| 02 p0172 N90-10968
Validation of a computer code for analysis of subsonic aerodynamic performance of wings with flaps in combination with a canard or horizontal tail and an application to optimization
|NASA-TP-2961| 06 p0717 N90-14187
Calculation of the flap profile flows with separation based on coupled potential and boundary layer solutions
08 p1069 N90-16191

Analysis and numerical solution of flow over airfoil with control flap 10 p1307 N90-17564
The NASA digital VGH program: Exploration of methods and final results. Volume 2: L 1011 data 1978-1979: 1619 hours
[NASA-CR-181909-VOL-2] 13 p1756 N90-20080

FLARE STARS
Analysis of coordinated observations of a giant stellar flare
[NASA-CR-185961] 05 p0715 N90-14176
As observational and theoretical investigation of stellar flares 06 p0862 N90-15012
Flare stars at radio wavelengths
[NASA-CR-186539] 14 p2044 N90-21719

FLARES
Tracking flares
[ISBN-0-642-13583-5] 08 p1052 N90-16080

FLASH BLINDNESS
Model for predicting the effects of laser exposures and eye protection on vision
[AD-A219697] 17 p2434 N90-23868

FLASH LAMPS
High efficiency flashlamp-pumped titanium: Sapphire laser
[AD-A217598] 13 p1806 N90-20367
Flash-pumped titanium laser
[AD-A217599] 13 p1806 N90-20368
High pulse energy flashlamp pumpable laser dyes
[AD-A223075] 22 p3180 N90-28042

FLASH TUBES
U FLASH LAMPS

FLASHOVER
Review of surface flashover theory
[DE90-000806] 06 p0768 N90-14459

FLAT COAXIAL TRANSMISSION LINES
U MICROSTRIP TRANSMISSION LINES

FLAT PLATES
Numerical investigation of the effects of longitudinal vortices on the onset of transition in a flat plate boundary layer 01 p0063 N90-10363
Experimental study of instability modes in a three-dimensional boundary layer 01 p0064 N90-10369
Primary and secondary stability analysis applied to the DFVLR-transition swept-plate experiment 01 p0065 N90-10371
Numerical investigation of transition in 3D boundary layers 01 p0065 N90-10372
Design guide for predicting nonlinear random response (including snap-through) of buckled plates
[NASA-CR-181877] 01 p0118 N90-10681
Linear instability of supersonic plane wakes
[NASA-CR-181911] 02 p0146 N90-10833
Nonprincipal-plane scattering from flat plates: Second-order and corner diffraction and pattern control of horn antennas
[NASA-CR-185485] 02 p0211 N90-11205
Part A: Nonprincipal-plane scattering from flat plates: Second-order and corner diffractions 02 p0211 N90-11206
Effect of roughness on the stability of boundary layers 04 p0440 N90-12518
Unsteady three-dimensional thin-layer Navier Stokes solutions on dynamic blocked grids
[AD-A212377] 04 p0503 N90-12899
Computation of Navier-Stokes equations for three-dimensional flow separation
[NASA-TM-102266] 05 p0575 N90-13353
Numerical investigation of transition control of a flat plate boundary layer 07 p0926 N90-15361
Flow separation in shock wave boundary layer interactions at hypersonic speeds
[NASA-CR-4274] 08 p1017 N90-15885
New mixing-length model for numerical solution of turbulent supersonic flows 09 p1216 N90-17048
Glancing shock-boundary layer interactions 10 p1309 N90-17571
Effects of controlled three-dimensional perturbations on boundary layer transition
[AD-A215080] 10 p1384 N90-18011
Investigation of heat transfer with film cooling to a flat plate in a shock tube
[AD-A216379] 10 p1386 N90-18019
Experimental investigations of the unsteady boundary layer on an oscillating flat plate. Optimization and validation of a code, for calculating the potential flow/boundary layer coupling of a flat plate and of an oscillating profile
[ETN-90-98254] 11 p1508 N90-18682
Transient heat transfer measurements on a flat plate in turbulent flow using an electrical analog
[AD-A216286] 11 p1573 N90-19057
Calculation of excrescence drag magnification due to pressure gradient at high subsonic speeds
[ESDU-87004] 12 p1598 N90-19195
Leading edge vortex dynamics on a pitching delta wing
[NASA-CR-186327] 12 p1598 N90-19198
Numerical simulations of supersonic flow through oscillating cascade sections
[NASA-TM-103100] 13 p1750 N90-20051
User manual for VICONOPT: An exact analysis and optimum design program covering the buckling and vibration of prismatic assemblies of flat in-plane loaded, anisotropic plates, with approximations for discrete supports, and transverse stiffeners
[NASA-CR-181966] 14 p1991 N90-21413
An investigation of turbulence structure in a low Reynolds number incompressible turbulent boundary layer 15 p2091 N90-21966
Flat plate leading edge receptivity to various freestream disturbance structures 16 p2235 N90-22750
Flat plate vibration analysis experimental and numerical fillet study
[AD-A218789] 16 p2247 N90-22818
On the instability of hypersonic flow past a flat plate
[NASA-CR-182051] 18 p2493 N90-24252
Accuracy of the QUAD4 thick shell element 18 p2569 N90-24641
Eigenvalue computations with the QUAD4 consistent-mass matrix 18 p2569 N90-24642
The Helicopter Antenna Radiation Prediction Code (HARP)
[NASA-CR-186925] 22 p3165 N90-27946
Numerical investigation of laminar-turbulent transition in a flat plate wake
[AD-A222462] 22 p3170 N90-27978
The effects of grid-generated turbulence on flat and concave turbulent boundary layers 23 p3324 N90-28797
A planar rocket motor model for visualization of violent reaction due to fragment impact
[AD-A224273] 24 p3441 N90-29431
Bistatic radar cross section of a perfectly conducting rhombus-shaped flat plate
[AD-A223418] 24 p3460 N90-29546

FLAT SURFACES
The multifractal nature of turbulence 16 p2235 N90-22752

FLATNESS
Flatness and roughness metrological tests on the WRA flight unit receiver box and ACPB canister of the RETE experiment
[IFSI-88-20] 10 p1368 N90-17928

FLAVOR (PARTICLE PHYSICS)
Aspects of the physics of the standard model
[PREPRINT-670] 05 p0698 N90-14087

FLAW DETECTION
U NONDESTRUCTIVE TESTS

FLAWS
U DEFECTS

FLEXIBILITY
Flexure strength of advanced ceramics: A round robin exercise
[AD-A212101] 03 p0332 N90-11889
Numerical simulation of unsteady rotational flow over propfan configurations
[NASA-CR-186037] 04 p0438 N90-12500
Analysis of the non-planar response of a cantilever, with the aid of computerized symbolic manipulation
[AD-A212421] 04 p0545 N90-13172
Crazing and degradation of flexure strength in acrylic plates as a function of time
[AD-A212835] 06 p0749 N90-14357
Finite element analysis of frictional contact problems 06 p0792 N90-14612
Flexural and torsional-flexural buckling of thin-walled open section struts
[ESDU-89007] 06 p0797 N90-14643
The dynamics of domain walls and strings
[NASA-CR-186255] 07 p1007 N90-15832
Effects of heat treatment on microstructure and flexural properties of unidirectional carbon-carbon composites
[AD-A214985] 09 p1186 N90-16873
LARC-IA: A flexible backbone polyimide
[NASA-TM-102586] 09 p1196 N90-16926
Copolyimide with a combination of flexibilizing groups
[NASA-CASE-LAR-13821-1] 09 p1199 N90-16950
Analytical formulation for the interaction problem of dynamic reentry, and effects due to flexibility and vibration in an aerospace vehicle
[INPE-4963-TDL/392] 11 p1467 N90-18448
Orbital fluid resupply assessment 11 p1475 N90-18487
A study of the effects of disk flexibility on the rotordynamics of the space shuttle main engine turbo-pumps 12 p1636 N90-19401
Design and implementation of a flexible robot
[AD-A216453] 12 p1671 N90-19601
Control system design of the third flexible joint of PUMA 560 robot
[AD-A218075] 13 p1812 N90-20405
Stabilized determination of geopotential coefficients by the mixed hom-BLUP approach 13 p1832 N90-20520
High gloss corrosion-resistant coatings
[AD-D014403] 14 p1954 N90-21184
End point control of flexible manipulators
[AD-A217319] 14 p1986 N90-21383
New flexible circuit material evaluation
[DE90-008313] 15 p2071 N90-21866
Rotor loading on a three-bladed wind turbine 15 p2123 N90-22145
Relationship between flexibility of closure and success in pilot night vision sensor system training
[AD-A221439] 16 p2261 N90-22890
The coupling effects of kinematics and flexibility on the Lagrangian dynamic formulation of open chain deformable links 16 p2284 N90-23018
Durable heat diaphragm from ordered polymer films
[AD-A220794] 17 p2381 N90-23559
High temperature flexible seal
[NASA-CASE-LEW-14695-1] 17 p2413 N90-23751
Mechanical property characterization of fiber-reinforced SiC matrix composites
[DE90-011316] 18 p2520 N90-24390
Postbuckling response of long thick plates loaded in compression including higher order transverse shearing effects
[NASA-TM-102663] 19 p2700 N90-25363
Control of intelligent robots in space 23 p3365 N90-29013
Structural testing and analytical research of turbine components
[AD-A223516] 24 p3434 N90-29396
Active vibration damping of flexible structures
[DLR-FB-90-03] 24 p3481 N90-29676
Modeling, design, and control of flexible manipulator arms: Status and trends 24 p3500 N90-29782
Dynamical modeling of serial manipulators with flexible links and joints using the method of kinematic influence 24 p3500 N90-29783
Technology and task parameters relating to the effectiveness of the bracing strategy 24 p3500 N90-29785
Experiments in identification and control of flexible-link manipulators 24 p3501 N90-29787
Design and control of a multi-fingered robot hand provided with tactile feedback 24 p3501 N90-29789

FLEXIBLE BODIES
NT FLEXIBLE SPACECRAFT
The application of TSIM software to act design and analysis on flexible aircraft 01 p0018 N90-10086
Modeling and control system design and analysis tools for flexible structures 01 p0018 N90-10090
Lumped mass formulations for modeling flexible body systems 01 p0019 N90-10091
Simulation of flexible structures with impact: Experimental validation 01 p0020 N90-10097
Linearized flexibility models in multibody dynamics and control 01 p0020 N90-10099
A performance comparison of integration algorithms in simulating flexible structures 01 p0021 N90-10101
Flexible robot control: Modeling and experiments 01 p0021 N90-10104
Automated model formulation for time-varying flexible structures 01 p0022 N90-10107
Flexible aircraft dynamic modeling for dynamic analysis and control synthesis 01 p0022 N90-10112
Experimental validation of flexible robot arm modeling and control 01 p0023 N90-10113
Controlling flexible structures: A survey of methods 01 p0023 N90-10114
Aircraft modal supression system: Existing design approach and its shortcomings 01 p0023 N90-10115
Structural stability augmentation system design using BODEDIRECT: A quick and accurate approach 01 p0023 N90-10116
Active vibration mitigation of distributed parameter, smart-type structures using Pseudo-Feedback Optimal Control (PFOC) 01 p0024 N90-10121
A new approach to control single-link flexible arms. Part 1: Modelling and identification in the presence of joint friction
[AD-A210590] 01 p0078 N90-10445
Frequency domain design of robust controllers for space structures
[AD-A211172] 02 p0176 N90-10985
GEMMES: A new tool for dynamic modeling 02 p0179 N90-11005
Use of Lanczos vectors in structural dynamics 02 p0179 N90-11011

Control and optimization for observations of systems governed by controlled partial differential equations
[AD-A211122] 02 p0266 N90-11513
Guaranteed cost control of flexible space structures 02 p0287 N90-11643
Computer-aided design of flexible assembly systems
[PB89-216253] 03 p0354 N90-12025
Adaptive strategies for controls of flexible arms
[NASA-CR-185868] 05 p0649 N90-13783
Manipulation strategies for massive space payloads
[NASA-CR-186081] 06 p0728 N90-14247
Optimal stochastic modeling and control of flexible structures
[AD-A212347] 06 p0733 N90-14269
Stability and dynamics of constrained flexible multibody systems 06 p0791 N90-14609
Transient response of flexible rotor-bearing systems subjected to combined unbalance and ground excitations 06 p0792 N90-14616
On the motion of compliantly-connected rigid bodies in contact. Part 1: The motion prediction problem
[AD-A214135] 07 p0948 N90-15489
Dynamic modeling of flexible bodies in multibody systems 09 p1229 N90-17134
Remote Manipulator System (RMS)-based Controls-Structures Interaction (CSI) flight experiment feasibility study
[NASA-CR-181952] 09 p1230 N90-17136
Dynamic interactions and globally optimal maneuver of distributed systems 09 p1236 N90-17172
Active control of a flexible structure using a modal positive position feedback controller
[NASA-CR-186336] 09 p1272 N90-17371
Optimization of sensors and actuators positioning aimed at obtaining reduced models for the synthesis of optimal control regulators of flexible structures
[INPE-4760-TDL/348] 11 p1468 N90-18450
Experiments in end-point control of a flexible robot with a mini-manipulator 12 p1671 N90-19596
Modified independent modal space control of flexible structures 12 p1671 N90-19597
Sensor and actuator selection for fault-tolerant control of flexible structures
[AD-A217384] 13 p1817 N90-20433
NASA/DOD Controls-Structures Interaction Technology 1989
[NASA-CP-3041] 14 p1933 N90-21062
A survey of experiments and experimental facilities for active control of flexible structures 14 p1936 N90-21079
A decentralized linear quadratic control design method for flexible structures 15 p2054 N90-21770
Robust control of flexible structures 15 p2058 N90-21784
Nonlinear spline operator interpolation and sliding control of deformable maneuvering bodies 15 p2074 N90-21878
Robust control of vibration in flexible structures 16 p2241 N90-22787
Spatial operator algebra framework for multibody system dynamics 16 p2279 N90-22989
Systematic generation of multibody equations of motion suitable for recursive and parallel manipulation 16 p2280 N90-22992
Experimental experience with flexible structures 16 p2281 N90-23002
A disturbance based control/structure design algorithm 16 p2282 N90-23003
Multi-flexible-body dynamics capturing motion-induced stiffness 16 p2284 N90-23013
Nonlinear strain-displacement relations and flexible multibody dynamics 16 p2284 N90-23014
Nonlinear finite element formulation for the large displacement analysis in multibody system dynamics 16 p2284 N90-23015
Frequency response modeling and control of flexible structures: Computational methods 16 p2285 N90-23021
Control of a flexible planar truss using proof mass actuators 16 p2288 N90-23035
A decoupled recursive approach for constrained flexible multibody system dynamics 16 p2289 N90-23042
Substructural controller synthesis 16 p2292 N90-23055
Multibody dynamics: Modeling component flexibility with fixed, free, loaded, constraint, and residual modes 16 p2295 N90-23072
Model reduction in the physical coordinate system 16 p2295 N90-23074
Structural modeling for control design (articulated multibody component representation) 16 p2296 N90-23077
Significance of norms and completeness in variational based methods 16 p2296 N90-23078
Controlling flexible structures with second order actuator dynamics 16 p2297 N90-23083
Analytic semigroups: Applications to inverse problems for flexible structures
[NASA-CR-182047] 16 p2306 N90-23138
Modeling and control of flexible vehicles in space
[AD-A219622] 17 p2365 N90-23465
A theory of control for infinite dimensional systems with application to large scale space structures
[AD-A219937] 17 p2366 N90-23469
Nonlinear dynamics and control of flexible structures
[AD-A218372] 17 p2386 N90-23588
Nonlinear dynamics and control of flexible structures
[AD-A218476] 17 p2386 N90-23589
Numerical optimization, system theoretic and software tools for the integrated design of flexible structures and their control systems
[AD-A219877] 17 p2447 N90-23949
Dynamic modeling and control of a flexible arm holding a non-rigid payload 18 p2507 N90-24331
Control of large space structures
[AD-A221216] 18 p2511 N90-24345
Dynamic analysis of flexible multibody structures 18 p2642 N90-25048
Studies in non-linear unsteady aerodynamics
[AD-A221228] 19 p2654 N90-25108
Modeling flexible aircraft for flight control design
[AD-A219123] 19 p2660 N90-25140
Control structure interaction instrumentation
[AD-A221375] 19 p2693 N90-25320
Robust controller designs for second-order dynamic system: A virtual passive approach
[NASA-TM-102666] 19 p2701 N90-25369
Computer-aided design of advanced control algorithms for industrial robotics: An overview of ESPRIT project SACODY
[REPT-81-DT-89-47] 19 p2744 N90-25596
Design and implementation of robust decentralized control laws for the ACES structure at Marshall Space Flight Center
[NASA-CR-4310] 20 p2820 N90-26046
Intergration of system identification and robust controller designs for flexible structures in space
[NASA-TM-102695] 20 p2876 N90-26362
Increasing the margin of stability of arbitrarily finite modes of flexible large space structures with damping
[AD-A221742] 21 p2967 N90-26867
Suspension mechanism and method
[NASA-CASE-LAR-14142-1] 21 p3011 N90-27116
The effect of nonlinearities on flexible structures
[AD-A222705] 21 p3012 N90-27124
Flexible structure control and rigid body dynamics 22 p3129 N90-27757
Deployment of large flexible space structures 22 p3131 N90-27766
Robust eigensystem assignment for second-order estimators
[NASA-TM-102696] 22 p3191 N90-28103
Active control of flexible structures 23 p3282 N90-28575
The dynamics and control of large flexible space structures - 13
[NASA-CR-186930] 23 p3286 N90-28591
Tip-position control of a flexible beam: Modeling approaches and experimental verification
[AD-A224249] 24 p3476 N90-29643
Research into traveling wave control in flexible structures
[AD-A224504] 24 p3479 N90-29661
Proceedings of Damping '89. Volume 3: Pages ICA-1 through KDC-15
[AD-A223433] 24 p3479 N90-29666

FLEXIBLE SPACECRAFT

Proceedings of the Workshop on Computational Aspects in the Control of Flexible Systems, part 1
[NASA-TM-101578-PT-1] 01 p0017 N90-10080
Additional software developments wanted for modeling and control of flexible space systems 01 p0017 N90-10083
Flexible structure control experiments using a real-time workstation for computer-aided control engineering 01 p0017 N90-10084
A comparison of software for the modeling and control of flexible systems 01 p0019 N90-10092
Enhanced element-specific modal formulations for flexible multibody dynamics 01 p0019 N90-10094
Explicit modeling and computational load distribution for concurrent processing simulation of the space station 01 p0020 N90-10096
Optical processing for distributed sensors in control of flexible spacecraft 01 p0021 N90-10102
Proceedings of the Workshop on Computational Aspects in the Control of Flexible Systems, part 2
[NASA-TM-101578-PT-2] 01 p0021 N90-10103
Control law synthesis and optimization software for large order aeroservoelastic systems 01 p0022 N90-10111
Input-output oriented computation algorithms for the control of large flexible structures 01 p0023 N90-10118
Modeling and stabilization of large flexible space stations 01 p0024 N90-10120
Simulation of spacecraft attitude dynamics using TREETOPS and model-specific computer Codes 05 p0587 N90-13419
Explicit modeling and concurrent processing in the simulation of multibody dynamic systems 05 p0599 N90-13481
The dynamics and control of large flexible space structures - 12, supplement 11
[NASA-CR-185966] 05 p0602 N90-13494
Dynamics and control of flexible spacecraft during and after slewing maneuvers
[NASA-CR-186123] 06 p0733 N90-14270
Baseline experiment for active control of structural vibrations
[AD-A216194] 10 p1397 N90-18076
Advanced topics in structural dynamics: The maneuver of flexible spacecraft, and on-off decentralized control of flexible structures 12 p1612 N90-19274
NASA CSI suspension methods overview 14 p1936 N90-21080
An assessment of multibody simulation tools for articulated spacecraft 16 p2279 N90-22988
Multi-flexible-body dynamics capturing motion-induced stiffness 16 p2284 N90-23013
Simulation studies using multibody dynamics code DART 16 p2288 N90-23036
Enhanced modeling features within TREETOPS 16 p2290 N90-23047
Overview of computational control research at UT Austin 16 p2291 N90-23051
Model reduction for flexible spacecraft with clustered natural frequencies 16 p2291 N90-23054
Issues in CSI analysis for large scale systems 16 p2296 N90-23076
Dynamic analysis of flexible mechanical systems using LATDYN 16 p2296 N90-23080
Neural networks in support of manned space 16 p2298 N90-23088
Theory of filtering and control with application to control of large space structures
[AD-A219936] 17 p2366 N90-23468
Equivalent flexibility modeling: A novel approach towards recursive simulation of flexible spacecraft manipulator dynamics 18 p2505 N90-24316
Dynamic stabilization of large flexible space structures
[ETN-90-96926] 18 p2511 N90-24344
Increasing the margin of stability of arbitrarily finite modes of flexible large space structures with damping
[AD-A221742] 21 p2967 N90-26867

FLEXIBLE WINGS

The active flexible wing aeroservoelastic wind-tunnel test program 01 p0024 N90-10119
Using transonic small disturbance theory for predicting the aeroelastic stability of a flexible wind-tunnel model
[NASA-TM-102617] 13 p1749 N90-20047
Static aeroelastic analysis of a three-dimensional generic wing
[NASA-TM-102231] 13 p1757 N90-20087
Digital-flutter-suppression-system investigations for the active flexible wing wind-tunnel model
[NASA-TM-102618] 13 p1758 N90-20093

FLEXING

Flexure strength of advanced ceramics: A round robin exercise
[AD-A212101] 03 p0332 N90-11889
Biaxial flexing of a fiber-reinforced aluminum composite
[AD-A212742] 04 p0468 N90-12681
Flexural fatigue life prediction of closed hat-section using materially nonlinear axial fatigue characteristics 18 p2645 N90-25062

FLEXURE

U FLEXING

FLIGHT ALTITUDE

Computation of hypersonic low density flows with thermochemical nonequilibrium 13 p1749 N90-20044
High altitude ozone research balloon
[NASA-CR-186653] 19 p2654 N90-25107

FLIGHT CHARACTERISTICS

NT FLIGHT ENVELOPES

Airworthiness and flight characteristics test of the UH-60A Black Hawk helicopter equipped with the XM-139 multiple mine dispensing system (VOLCANO)
[AD-A210271] 01 p0006 N90-10025
Analysis of flight data from a High-Incidence Research Model by system identification methods
[NASA-TP-2940] 01 p0015 N90-10074
GRATE: A new flight test tool for flying qualities evaluation 02 p0152 N90-10868

Unsteady aerodynamics with applications to flight mechanics
[AD-A211944] 03 p0301 N90-11706
Comparison of flying qualities derived from in-flight and ground-based simulators for a jet-transport airplane for the approach and landing pilot tasks
[NASA-TP-2962] 03 p0309 N90-11757
Global stratospheric change: Requirements for a Very-High-Altitude Aircraft for Atmospheric Research
[NASA-CP-10041] 06 p0723 N90-14220
Influence of windshear, downdraft and turbulence on flight safety 07 p0870 N90-15048
A pitch control law for compensation of the phugoid mode induced by windshears 07 p0870 N90-15051
Canard versus aft-tail ride qualities performance and pilot command response 07 p0871 N90-15053
The interference of flightmechanical control laws with those of load alleviation and its influence on structural design 07 p0871 N90-15054
The role of computational fluid dynamics in missile aerodynamics 10 p1304 N90-17547
Longitudinal stability and control characteristics of the Quiet Short-Haul Research Aircraft (QSRA)
[NASA-TP-2965] 10 p1322 N90-17639
Low-speed wind-tunnel investigation of the flight dynamic characteristics of an advanced turboprop business/commuter aircraft configuration
[NASA-TP-2982] 12 p1606 N90-19239
Airworthiness and flight characteristics evaluation of the McDonnell Douglas Helicopter Corporation (MDHC) 530FF helicopter
[AD-A216253] 13 p1755 N90-20076
The Real Time Interactive Display Environment (RTIDE), a display building tool developed by Space Shuttle flight controllers 13 p1857 N90-20654
Flight path reconstruction using extended Kalman filtering techniques
[PD-FC-9001] 14 p1915 N90-20970
Minimum flying qualities. Volume 1: Piloted simulation evaluation of multiple axis flying qualities
[AD-A218560] 16 p2200 N90-22560
Minimum flying qualities. Volume 2: Pilot modeling for flying qualities applications
[AD-A218561] 16 p2201 N90-22561
Minimum flying qualities. Volume 3: Program CC's implementation of the human optimal control model
[AD-A218562] 16 p2201 N90-22562
Development of a least squares time response lower-order equivalent systems technique
[AD-A220527] 17 p2351 N90-23389
Estimating short-period dynamics using an extended Kalman filter
[NASA-TM-101722] 17 p2352 N90-23392
Static wind-tunnel and radio-controlled flight test investigation of a remotely piloted vehicle having a delta wing planform
[NASA-TM-4200] 18 p2491 N90-24238
Aerodynamics and flight mechanics of formation flight
[ETN-90-96497] 19 p2497 N90-24269
H-infinity based integrated flight-propulsion control design for a STOVL aircraft in transition flight
[NASA-TM-103198] 20 p2813 N90-26011
Orbiter utilization as an ACRV
[NASA-TM-102700] 20 p2817 N90-26032
Eye tracking device for the measurement of flight performance in simulators
[AD-A220075] 20 p2898 N90-26484
The SKY SHARK: An RPV designed to investigate the pressure distribution on a lifting surface
[NASA-CR-186222] 21 p2959 N90-26824
Monitoring and controlling flight in windshear 22 p3106 N90-27641
Integration of externally carried weapon systems with military helicopters
[AGARD-AR-247] 22 p3115 N90-27696
Comparison of altitude test cell results 22 p3119 N90-27715
Optimal trajectories for Saenger-type vehicles 22 p3129 N90-27760
Evaluation of composite components on the Bell 206L and Sikorsky S-76 helicopters
[NASA-TM-4195] 22 p3135 N90-27787
Solution of Euler equations applied to a rotor of a helicopter in steady flight
[ONERA-RSF-1/3731-AY-002A] 23 p3269 N90-28500
Aerodynamic parameters of High-Angle-of attack Research Vehicle (HARV) estimated from flight data
[NASA-TM-102692] 23 p3283 N90-28578
Application of multifunction inertial reference systems to fighter aircraft 24 p3423 N90-29341
Fighter agility metrics
[NASA-CR-187289] 24 p3432 N90-29389

FLIGHT CLOTHING
Integrated G-suit/immersion suit
[AD-A212989] 06 p0821 N90-14774
Evaluation of helmet retention systems using a pendulum device
[AD-A215489] 11 p1542 N90-18874

FLIGHT COMPUTERS
U AIRBORNE/SPACEBORNE COMPUTERS

FLIGHT CONDITIONS
A technique for the prediction of aerodynamics and aeroelasticity of rotor blades 05 p0579 N90-13377
Flight in adverse environmental conditions
[AGARD-AR-277] 06 p0723 N90-14218
Frontal clouds and flight conditions in them
[AD-A214250] 07 p0964 N90-15573
A survey of nonuniform inflow models for rotorcraft flight dynamics and control applications
[NASA-TM-102219] 08 p1028 N90-15938
Measurement and prediction of propeller blade surface pressure distributions 14 p1912 N90-20961
The use of numerical optimization for helicopter airfoil and blade design 14 p1919 N90-20995
Data Link Processor (DLP) project transition plan
[DOT/FAA/CT-TN89/68] 14 p1965 N90-21256
Comparison of altitude test cell results 22 p3119 N90-27715
Optimal trajectories for Saenger-type vehicles 22 p3129 N90-27760
Effects of canard position on the aerodynamic characteristics of a close-coupled canard configuration at low speed 23 p3272 N90-28519

FLIGHT CONTROL
NT AUTOMATIC FLIGHT CONTROL
NT FLY BY WIRE CONTROL
NT POINTING CONTROL SYSTEMS
NT THRUST VECTOR CONTROL
Hierarchical damage tolerant controllers for smart structures
[AD-A209422] 01 p0005 N90-10022
Initial flight qualification and operational maintenance of X-29A flight software
[NASA-TM-101703] 01 p0005 N90-10023
Simulation of shuttle flight control system structural interaction with RMS deployed payloads 01 p0020 N90-10100
A320 flight tests: Particularities and innovations 02 p0151 N90-10864
Real-time flight test analysis and display techniques for the X-29A aircraft 02 p0152 N90-10866
Flight test results of a complex precise digital flight control system 02 p0152 N90-10870
An assessment of robustness of flight control systems based on variable structure techniques 02 p0157 N90-10895
Independent Orbiter Assessment (IOA): Analysis of the body flap subsystem
[NASA-CR-185574] 02 p0165 N90-10930
Independent Orbiter Assessment (IOA): Analysis of the backup flight system
[NASA-CR-185567] 02 p0165 N90-10932
Independent Orbiter Assessment (IOA): Analysis of the hydraulics/water spray boiler subsystem
NASA-CR-185541] 02 p0165 N90-10934
Independent Orbiter Assessment (IOA): Assessment of the ascent thrust vector control actuator subsystem FMEA/CIL
[NASA-CR-185590] 02 p0170 N90-10959
Independent Orbiter Assessment (IOA): Assessment of the backup flight system FMEA/CIL
[NASA-CR-185568] 02 p0173 N90-10973
Applications of flight control system methods to an advanced combat rotorcraft
[NASA-TM-101054] 03 p0308 N90-11752
Robust control design for flight control
[AD-A211957] 03 p0309 N90-11756
Comparison of flying qualities derived from in-flight and ground-based simulators for a jet-transport airplane for the approach and landing pilot tasks
[NASA-TP-2962] 03 p0309 N90-11757
Adaptive control law design for model uncertainty compensation
[AD-A211712] 03 p0309 N90-11758
Advanced actuation systems development, volume 1
[AD-A213334] 04 p0458 N90-12624
STOVL aircraft simulation for integrated flight and propulsion control research
[NASA-TM-102419] 05 p0581 N90-13389
A knowledge-based system design/information tool for aircraft flight control systems
[NASA-TM-101704] 05 p0685 N90-13990
A helicopter flight path controller design via a nonlinear transformation technique 06 p0727 N90-14242
Guidance, steering, load relief and control of an asymmetric launch vehicle
[NASA-CR-185598] 06 p0730 N90-14257
Wind shear models for aircraft hazard investigation 07 p0869 N90-15044
How to fly windshear using the fly-by-wire concept 07 p0870 N90-15050
Turbulence effects of aircraft flight dynamics and control 07 p0871 N90-15055
Imaging probabilities, geometry and ergonomics in limited visibility helicopter operations 07 p0872 N90-15060
Fly-by-light flight control system technology development plan
[NASA-CR-181953] 07 p0883 N90-15111
Integrated approach fault tolerance-current state and future requirements
[AD-A214402] 07 p0944 N90-15465
Guidance and Control of Unmanned Air Vehicles
[AGARD-CP-436] 08 p1025 N90-15924
Mirach 100 flight control system 08 p1025 N90-15926
A survey of nonuniform inflow models for rotorcraft flight dynamics and control applications
[NASA-TM-102219] 08 p1028 N90-15938
Advances in Techniques and Technologies for Air Vehicle Navigation and Guidance
[AGARD-CP-455] 09 p1163 N90-16731
Integrated flight guidance system using differential-GPS for landing approach guidance 09 p1163 N90-16735
Parallel processing implementation of a flight controller 09 p1165 N90-16743
Guidance and control considerations for a maneuvering aerial target system 09 p1165 N90-16746
Further development and limited flight testing of the CycloCrane
[AD-A215519] 09 p1167 N90-16754
Formulation and verification of a technique for compensation of pneumatic attenuation errors in airborne pressure sensing devices 09 p1221 N90-17084
Development of an automatic ground collision avoidance system using a digital terrain database
[AD-A216247] 10 p1318 N90-17621
Development of the triplex digital flight control system of the STOL research aircraft ASKA
[NAL-TR-1013] 10 p1322 N90-17640
The Advanced Digital-Optical Control System (ADOCS) user demonstration program
[AD-A215984] 10 p1323 N90-17644
Software verification plan for GCS --- guidance and control software
[NASA-TM-101668] 10 p1394 N90-18057
Discrete proportional Plus Integral (PI) multivariable control laws for the Control Reconfigurable Combat Aircraft (CRCA)
[AD-A215664] 11 p1464 N90-18431
The implications of using integrated software support environment for design of guidance and control systems software
[AGARD-AR-229] 11 p1464 N90-18432
Flexible heat pipe cold plate
[AD-A216053] 11 p1464 N90-18433
Application of variable-gain output feedback for high-alpha control
[NASA-TM-102603] 11 p1464 N90-18434
Practical methods for robust multivariable control
[AD-A216937] 11 p1550 N90-18920
Compensating for pneumatic distortion in pressure sensing devices
[NASA-TM-101716] 12 p1603 N90-19224
A rule-based paradigm for intelligent adaptive flight control 12 p1605 N90-19238
Neurocontrol systems and wing-fluid interactions underlying dragonfly flight 12 p1606 N90-19240
F-15B high angle-of-attack phenomena and spin prediction using bifurcation analysis
[AD-A217366] 13 p1754 N90-20073
Flight termination system battery guidelines
[AD-A217310] 13 p1758 N90-20092
Laboratory implementation of the Continuously Reconfiguring Multi-Microprocessor Flight Control System (CRMMFCS)
[AD-A217730] 13 p1758 N90-20094
Interaction of switch actuation on tracking with a four-axis flight control (cross-coupling)
[AD-A217981] 13 p1758 N90-20095
The Real Time Interactive Display Environment (RTIDE), a display building tool developed by Space Shuttle flight controllers 13 p1857 N90-20654
The Real Time Display Builder (RTDB) 13 p1857 N90-20656
Large screen display for the Mission Control Center 13 p1858 N90-20662
Distributed earth model/orbiter simulation 13 p1860 N90-20671
Optimization of the effective GPS data rate 14 p1907 N90-20932
Investigation of air transportation technology at Princeton University, 1988-1989 14 p1907 N90-20935
Application of stochastic robustness to aircraft control systems 14 p1908 N90-20936

An expert system for wind shear avoidance
14 p1908 N90-20938
Rule-based mechanisms of learning for intelligent adaptive flight control 14 p1908 N90-20939
Civil air transport: A fresh look at power-by-wire and fly-by-light
|NASA-TM-102574| 14 p1969 N90-21283
The insertion of human dynamics models in the flight control loops of V/STOL research aircraft. Appendix 2: The optimal control model of a pilot in V/STOL aircraft control loops
|NASA-CR-186598| 15 p2055 N90-21776
Minimum flying qualities. Volume 1: Piloted simulation evaluation of multiple axis flying qualities
|AD-A218560| 16 p2200 N90-22560
Minimum flying qualities. Volume 2: Pilot modeling for flying qualities applications
|AD-A218561| 16 p2201 N90-22561
Minimum flying qualities. Volume 3: Program CC's implementation of the human optimal control model
|AD-A218562| 16 p2201 N90-22562
Multi-axis control of telemanipulators
16 p2271 N90-22943
Synthetic perspective optical flow: Influence on pilot control tasks 16 p2273 N90-22956
Algorithms for computing the multivariable stability margin 16 p2281 N90-22999
Space station dynamics, attitude control and momentum management 16 p2287 N90-23029
Multidisciplinary Expert-aided Analysis and Design (MEAD) 16 p2291 N90-23050
Six-degree-of-freedom aircraft simulation with mixed-data structure using the applied dynamics simulation language, ADSIM 16 p2294 N90-23067
Prediction of longitudinal pilot induced oscillations using the optimal control model
|AD-A220593| 17 p2356 N90-23412
Miniaturization of flight deflection measurement system
|NASA-CASE-LAR-13628-1| 17 p2406 N90-23707
Development and test of software by safety critical aircraft systems
|MBB-FE-363/S/PUB-384| 19 p2654 N90-25103
DRAG-n-FLY: A proposal in response to a low Reynolds number station keeping mission
|NASA-CR-186666| 19 p2658 N90-25130
Modeling flexible aircraft for flight control design
|AD-A219123| 19 p2660 N90-25140
Flight-testing of the self-repairing flight control system using the F-15 highly integrated digital electronic control flight research facility
|NASA-TM-101725| 19 p2661 N90-25144
ACES: Space shuttle flight software analysis expert system 19 p2739 N90-25571
GCS support/development system configuration document
|NASA-CR-182046| 19 p2743 N90-25589
Reliability model generator specification
|NASA-CR-182005| 19 p2752 N90-25638
Identification of aerodynamic models for maneuvering aircraft
|NASA-CR-186630| 20 p2802 N90-25943
An in-flight interaction of the X-29A canard and flight control system
|NASA-TM-101718| 20 p2807 N90-25973
Technical evaluation report on the Guidance and Control Panel 49th Symposium on Fault Tolerant Design Concepts for Highly Integrated Flight Critical Guidance and Control Systems
|AGARD-AR-281| 20 p2813 N90-26012
Guidance and control strategies for aerospace vehicles
|NASA-CR-186878| 20 p2814 N90-26013
Robustness evaluation of H2 and H(infinity) control theory as applied to a transport aircraft
|AD-A222795| 20 p2814 N90-26018
Software requirements: Guidance and control software development specification
|NASA-CR-182058| 20 p2906 N90-26527
Aerodynamic/dynamic interaction
|AD-A222263| 21 p2954 N90-26798
New inflight experiments to measure aerodynamics loads
|ETN-90-97276| 21 p2961 N90-26834
Daily flight operation monitoring in JAL
22 p3105 N90-27636
Monitoring and controlling flight in windshear
22 p3106 N90-27641
Flight control issues of the next generation space transportation launch vehicles 22 p3126 N90-27742
Space shuttle descent flight verification by simulation: A challenge in implementing flight control system robustness 22 p3127 N90-27748
Advanced transport operating system software upgrade: Flight management/flight controls software description
|NASA-CR-181936| 22 p3239 N90-28366
Aerodynamic and propulsive control development of the STOL and maneuver technology demonstrator
23 p3271 N90-28514
A look at tomorrow today 23 p3273 N90-28524
Validation of the F-18 high alpha research vehicle flight control and avionics systems modifications
|NASA-TM-101723| 23 p3276 N90-28542
Description of the primary flight display and flight guidance system logic in the NASA B-737 transport systems research vehicle
|NASA-TM-102710| 23 p3277 N90-28546
Propulsion system-flight control integration and optimization: Flight evaluation and technology transition
|NASA-TM-4207| 23 p3278 N90-28551
A conceptual framework for fighter flight control systems
|PD-CF-9009| 23 p3283 N90-28577
Model authoring system for fail safe analysis
|NASA-CR-4317| 23 p3389 N90-29142
Flight test engineering with the ATTAS
23 p3391 N90-29160
Analysis, Design and Synthesis Methods for Guidance and Control Systems
|AGARD-AG-314| 24 p3423 N90-29338
Application of multifunction inertial reference systems to fighter aircraft 24 p3423 N90-29341
Integrated navigation/flight control for future high performance aircraft 24 p3427 N90-29362
Fault Detection and Isolation (FDI) techniques for guidance and control systems 24 p3428 N90-29366
Fighter agility metrics
|NASA-CR-187289| 24 p3432 N90-29389
Formal design and verification of a reliable computing platform for real-time control. Phase 1: Results
|NASA-TM-102716| 24 p3530 N90-29965

FLIGHT CREWS

NT SPACECREWS
Task analysis of the UH-60 mission and decision rules for developing a UH-60 workload prediction model. Volume 1: Summary report
|AD-A210763| 02 p0255 N90-11446
Test procedures for the evaluation of helmet and headset mounted active noise reduction systems
|AD-A212991| 05 p0676 N90-13937
Human factors research in aircrew performance and training
|AD-A213285| 05 p0676 N90-13938
Performance evaluation of the Puritan-Bennett crew-member portable protective breathing device as prescribed by portions of FAA action notice A-8150.2
|AD-A211113| 06 p0821 N90-14772
Display interface concepts for automated fault diagnosis
|NASA-TM-101610| 07 p0881 N90-15102
Cockpit resource management: A selected annotated bibliography
|AD-A214272| 07 p0969 N90-15594
Human Behaviour in High Stress Situations in Aerospace Operations
|AGARD-CP-458| 09 p1254 N90-17275
Causes of aircrew error in the Royal Air Force
09 p1254 N90-17276
Psychological reactions of pilots involved in accidents in the Swedish Air Force 09 p1254 N90-17279
The descent from the Olimpus: The effect of accidents on aircrew survivors 09 p1255 N90-17280
Personality assessment in aviation selection
09 p1257 N90-17289
Development of a performance-based test of gaze capability: A threshold approach
|AD-A214675| 09 p1259 N90-17301
Flight crew training for fire fighting
10 p1317 N90-17615
Delivery performance of conventional aircraft by terminal-area, time-based air traffic control: A real-time simulation evaluation
|NASA-TP-2978| 11 p1454 N90-18378
Three input concepts for flight crew interaction with information presented on a large-screen electronic cockpit display
|NASA-TM-4173| 11 p1457 N90-18394
Evaluation of helmet retention systems using a pendulum device
|AD-A215489| 11 p1542 N90-18874
Flight crew aiding for recovery from subsystem failures
|NASA-CR-181905| 12 p1696 N90-19741
Assessment of crew workload measurement methods, techniques and procedures. Volume 2: Guidelines for the use of workload assessment techniques in aircraft certification
|AD-A217067| 12 p1697 N90-19748
Development of acceleration exposure limits for advanced escape systems 13 p1751 N90-20055
Windshear case study: Denver, Colorado, July 11, 1988
|DOT/FAA/DS-89/19| 14 p2008 N90-21509
Personality factors in flight operations. Volume 1: Leader characteristics and crew performance in a full-mission air transport simulation
|NASA-TM-102259| 17 p2348 N90-23370
Effect of laser glare and aircraft windscreen on visual search performance under low ambient lighting
|AD-A219456| 17 p2437 N90-23888
The application of kriging in the statistical analysis of anthropometric data, volume 1
|AD-A220613| 17 p2438 N90-23891
Development of a microcomputer based software system for use in crewmember ejection analysis
|AD-A220398| 19 p2656 N90-25117
Non-ejection neck injuries in high performance aircraft
19 p2717 N90-25461
Radiological investigation of the vertebral column of candidates for military flying training the the Royal Norwegian Air Force 19 p2718 N90-25463
Aircrew neck injuries: A new, or an existing, misunderstood phenomenon 19 p2719 N90-25467
Effects of a time zone shift of 9 hours on the circadian rhythms in cockpit aircrew members on longhaul flights
|ESA-TT-1185| 19 p2722 N90-25485
SHAPA: An interactive software tool for protocol analysis applied to aircrew communications and workload
19 p2734 N90-25541
An analysis of requirements for a P-3 windshear training program
|AD-A222577| 20 p2805 N90-25960
Choosing a pilot subjective workload scale to fit flight operational requirements
|IAR-89-21| 20 p2900 N90-26493
Human factors: The human interface with aircraft interiors
|NIAR-90-18| 20 p2900 N90-26496
Aircrew life support systems enhancement
|AD-A222626| 20 p2902 N90-26505
Military aircrew seating: A human factors engineering approach
|AD-A218049| 23 p3362 N90-28999
Helicopter aircrew helmets and head injury: A protective effect
|AD-A223024| 23 p3377 N90-29080

FLIGHT ENVELOPES

Stability and control derivatives of the De Havilland DHC-2 BEAVER aircraft
|PB89-217525| 03 p0309 N90-11754
Identification of aerodynamic models for maneuvering aircraft
|NASA-CR-186630| 20 p2802 N90-25943
Combat aircraft control requirements
23 p3271 N90-28515
Application of multifunction inertial reference systems to fighter aircraft 24 p3423 N90-29341

FLIGHT FATIGUE

Biochemical and physiological changes in glider pilots during multihour flights
|DLR-FB-89-29| 04 p0523 N90-13018
Psychological mechanisms involved in the disorientation of pilots due to flight conditions
|ETN-89-95014| 04 p0527 N90-13040
Simulator induced sickness in the CP-140 (Aurora) flight deck simulator
|AD-A213096| 05 p0673 N90-13923
Electrocardiogram of military aircraft pilots measured during real flight missions: Study of the variability of the cardiac rhythm in correlation with working stress
|ETN-90-97453| 22 p3231 N90-28324

FLIGHT HAZARDS

NT METEOROID HAZARDS
Effects of lightning on operations of aerospace vehicles 07 p0873 N90-15065
Relative merits of reactive and forward-look detection for wind-shear encounters during landing approach for various microburst escape strategies
|NASA-TM-4158| 07 p0882 N90-15108
Bird impact tests on asymmetric sandwich structures made in Kevlar 49
|CEAT-NT-10/S/83-5| 09 p1152 N90-16727
Bird impact tests on curved structures of the type Sandwich-Kevlar-Nida for normal and angular shooting
|CEAT-NT-10/S/83-4| 09 p1162 N90-16728
Use of clutter residue editing maps during the Denver 1988 Terminal Doppler Weather Radar (TDWR) tests
|AD-A218696| 17 p2426 N90-23822
A quantitative technique to estimate microburst wind shear hazard to aircraft 18 p2640 N90-25040
Development and test of software by safety critical aircraft systems
|MBB-FE-363/S/PUB-384| 19 p2654 N90-25103
Aircraft lightning protection handbook
|AD-A222716| 22 p3110 N90-27668

FLIGHT INSTRUMENTS
NT APPROACH INDICATORS
NT AUTOMATIC PILOTS
NT FLIGHT TEST INSTRUMENTS
NT RADIO ALTIMETERS
Flight simulator evaluation of a head-down display
|NAL-TM-573| 02 p0157 N90-10898
On the motion equation of an elastically supported two degree of freedom gyro
|NAL-TM-568| 02 p0223 N90-11276
Independent Orbiter Assessment (IOA): Analysis of the displays and controls subsystem
|NASA-CR-185563| 03 p0312 N90-11774
Design of scientific payloads and components
|AD-A211819| 03 p0351 N90-12005
Natural icing re-evaluation of the EH-60A Quick Fix helicopter
|AD-A214726| 09 p1162 N90-16723
A simulation evaluation of the engine monitoring and control system display
|NASA-TP-2960| 11 p1457 N90-18393
Flexible heat pipe cold plate
|AD-A216053| 11 p1464 N90-18433
The effect of windscreen bows and HUD pitch ladder format on pilot performance during simulated flight
|AD-A218139| 14 p2011 N90-21523
Space radiation studies
|NASA-CR-183991| 19 p2798 N90-25925
Flight motor set 360L007 (STS-33R)
|NASA-CR-183979| 20 p2824 N90-26067
The interaction of chromostereopsis and stereopsis in stereoscopic CRT (Cathode Ray Tubes) displays
|AD-A217906| 23 p3277 N90-28544

FLIGHT LOAD RECORDERS
Multichannel on-board load and fatigue monitoring
22 p3103 N90-27621

FLIGHT MANAGEMENT SYSTEMS
Navigation experiment NAVEX: The equipment delay times in the Spacelab mission D1
|DFVLR-MITT-89-10| 03 p0304 N90-11728
Development and evaluation at ATCEU of executive and support operations, phase 4A/3D --- ATCEU (Air Traffic Control Evaluation Unit)
|CAA-PAPER-88017| 04 p0449 N90-12572
Operational trial of effect of raising minimum stack level in Heathrow stacks
|CAA-PAPER-89003| 04 p0449 N90-12573
Computer-based tools for assisting air traffic controllers with arrivals flow management
|RSRE-88001| 05 p0577 N90-13366
A knowledge-based system design/information tool for aircraft flight control systems
|NASA-TM-101704| 05 p0685 N90-13990
A knowledge-based flight status monitor for real-time application in digital avionics systems
|NASA-TM-101710| 05 p0686 N90-13995
The development of a low cost data logging system for flight trials based on an IBM compatible PC
|RAE-TM-FM-16| 08 p1023 N90-15917
Checklist reading problems in airplanes equipped with speech recognition systems
|ILR-MITT-223(1989)| 09 p1261 N90-17314
First-order weight corrections for real-time flight path management
|LR-580| 15 p2050 N90-21751
A conflict analysis of 4D descent strategies in a metered, multiple-arrival route environment
|NASA-CR-182019| 15 p2055 N90-21772
The 30th Airlines International Electronics Meeting Proceedings
|ETN-90-96973| 18 p2495 N90-24261
Agenda toward the development of a rational noise descriptor system relevant to human annoyance by en route aircraft noise 18 p2610 N90-24866
Replay and transmission of AIMS-data to mainframe computer using remote transcribers
22 p3105 N90-27634
Flight data replay and analysis system
22 p3105 N90-27635
Daily flight operation monitoring in JAL
22 p3105 N90-27636
Swissair studies on the compressibility of aircraft data
22 p3105 N90-27637
Expert system for pilot assistance: The challenge of an intensive prototyping
|ETN-90-97274| 22 p3111 N90-27674
Integrated Air Traffic Management
|DLR-MITT-89-23| 22 p3112 N90-27676
Air traffic management in Europe: Structure, tasks, potential 22 p3112 N90-27677
On-board planning and control of 4D-trajectories in the TMA 22 p3112 N90-27680
Four-dimensional navigation and Flight Management Systems 22 p3112 N90-27681
On the structure of a future flight operations system
22 p3113 N90-27682
Development of a COMPAS prototype for the ATC Centre at Frankfurt (Fed. Republic of Germany)
22 p3113 N90-27684
Safety net functions 22 p3113 N90-27685
Aspects of data link applications for ATC purposes
22 p3113 N90-27688
Application of a company data link at Lufthansa German Airlines 22 p3113 N90-27689
PHARE: Concept and programme
22 p3114 N90-27690
Integration of flight management and air traffic management systems
|RAE-TM-FM-41| 22 p3114 N90-27693
Advanced transport operating system software upgrade: Flight management/flight controls software description
|NASA-CR-181936| 22 p3239 N90-28366

FLIGHT MECHANICS
Validation of missile simulation
01 p0014 N90-10066
On the development of a basic flight test capability and some related research projects
02 p0155 N90-10885
Realtime processing and display
02 p0155 N90-10886
Flight-mechanical environment on Ariane launch vehicle payloads 02 p0184 N90-11048
Unsteady aerodynamics with applications to flight mechanics
|AD-A211944| 03 p0301 N90-11706
Flight Mechanics/Estimation Theory Symposium, 1989
|NASA-CP-3050| 05 p0586 N90-13413
Optimal trajectories for the Aeroassisted Flight Experiment. Part 1: Equations of motion in an Earth-fixed system
|NASA-CR-186134| 05 p0592 N90-13441
Optimal trajectories for the Aeroassisted Flight Experiment. Part 2: Equations of motion in an inertial system
|NASA-CR-186135| 05 p0592 N90-13442
Flight in adverse environmental conditions
|AGARD-AR-277| 06 p0723 N90-14218
Flight in Adverse Environmental Conditions
|AGARD-CP-470| 07 p0869 N90-15041
Description of atmospheric turbulence
07 p0869 N90-15043
A pitch control law for compensation of the phugoid mode induced by windshears 07 p0870 N90-15051
The interference of flightmechanical control laws with those of load alleviation and its influence on structural design 07 p0871 N90-15054
A study of the effects of Rotating Frame Turbulence (RFT) on helicopter flight mechanics
07 p0872 N90-15058
Optimization and guidance of flight trajectories in the presence of windshear
|NASA-CR-186163| 15 p2049 N90-21747
A comparison of time-optimal interception trajectories for the F-8 and F-15
|NASA-CR-186300| 15 p2050 N90-21753
Aerodynamics and flight mechanics of formation flight
|ETN-90-96497| 18 p2497 N90-24269
The applicability of simple helicopter models for flight mechanics studies
|ETN-90-96962| 20 p2808 N90-25975
Space Vehicle Flight Mechanics
|AGARD-CP-489| 22 p3126 N90-27741
National aero-space plane: Flight mechanics
22 p3129 N90-27759
Flight mechanics applications for tethers in space: Cooperative Italian-US programs
22 p3131 N90-27770
Inflight thrust vectoring: A further degree of freedom in the aerodynamic/flight mechanical design of modern fighter aircraft 23 p3274 N90-28528
Scientific Colloquium in Honor of Prof. Dr. Rer. Nat. Hermann L. Jordan
|ESA-TT-1101| 23 p3391 N90-29159
Flight test engineering with the ATTAS
23 p3391 N90-29160

FLIGHT OPERATIONS
NT CREW PROCEDURES (INFLIGHT)
Independent Orbiter Assessment (IOA): Analysis of the displays and controls subsystem
|NASA-CR-185563| 03 p0312 N90-11774
Research and Technology annual report, 1988
|NASA-TM-101070| 04 p0569 N90-13319
Fuel tank explosion protection
08 p1023 N90-15914
Knowledge representation in space flight operations
13 p1857 N90-20655
Data Link Processor (DLP) project transition plan
|DOT/FAA/CT-TN89/68| 14 p1965 N90-21256
Personality factors in flight operations. Volume 1: Leader characteristics and crew performance in a full-mission air transport simulation
|NASA-TM-102259| 17 p2348 N90-23370
Perspective features of internal automation and robotics for supporting Columbus attached laboratory payload operations 18 p2502 N90-24297
An overview of the joint FAA/NASA aircraft/ground runway friction program
|NASA-TM-103486| 20 p2805 N90-25957
Choosing a pilot subjective workload scale to fit flight operational requirements
|IAR-89-21| 20 p2900 N90-26493
Modeling and analysis of airport and aircraft operations
|PB90-222167| 23 p3271 N90-28511
A FAA Technical Center project transition plan: Mode S
|DOT/FAA/CT-TN90/17| 23 p3319 N90-28765

FLIGHT OPTIMIZATION
Sequential design of experiments with physically based models 23
|AD-A211918| 03 p0393 N90-12239
Induced drag for non-planar wings
|LR-521| 05 p0576 N90-13357
Flight and driving optimization of air breathing aerodynamic space vehicle
|ETN-90-95379| 12 p1607 N90-19246
An approach to on-board optimization of cruise at constant altitude
|LR-581| 15 p2050 N90-21752
Trajectory optimization of a bimodal nuclear powered spacecraft to Mars
|AD-A222974| 21 p2969 N90-26876
Life cycle cost in the conceptual design of subsonic commercial aircraft, volumes 1 and 2
23 p3275 N90-28535

FLIGHT PATHS
NT GLIDE PATHS
The 1987 survey of track keeping and altitudes on Heathrow and Gatwick standard instrument departure routes (DAY)
|CAA-PAPER-88010| 03 p0305 N90-11729
Operational trial of effect of raising minimum stack level in Heathrow stacks
|CAA-PAPER-89003| 04 p0449 N90-12573
FPG2: A flight profile generator program
|AD-A212408| 04 p0453 N90-12595
AcSim: Aircraft simulation program with application to flight profile generation
|AD-A212466| 06 p0723 N90-14217
Introduction to data items on flight path optimisation
|ESDU-89015| 06 p0723 N90-14221
A helicopter flight path controller design via a nonlinear transformation technique 06 p0727 N90-14242
Low level range coverage performance prediction for VHF radar 06 p0763 N90-14439
Geometric considerations for a waypoint guidance method
|DE90-001803| 07 p0878 N90-15088
Reacting flows 10 p1309 N90-17573
Dallas/Fort Worth simulation. Volume 2: Appendixes D, E, and F
|AD-A216613| 11 p1454 N90-18380
Series reversion/inversion of Lambert's time function
|AD-A216243| 12 p1607 N90-19245
Three-dimensional route planning for a cruise missile for minimal detection by observer
|AD-A218336| 13 p1880 N90-20787
Flight path reconstruction using extended Kalman filtering techniques
|PD-FC-9001| 14 p1915 N90-20970
A comparison of time-optimal interception trajectories for the F-8 and F-15
|NASA-CR-186300| 15 p2050 N90-21753
Optimal control of an aircraft flying through a downburst 15 p2053 N90-21765
Dynamic and microphysical characteristics of cirrus clouds as revealed by aircraft, lidar, and other observations during FIRE 15 p2130 N90-22177
Computer vision techniques for rotorcraft low altitude flight 15 p2142 N90-22237
Prediction of longitudinal pilot induced oscillations using the optimal control model
|AD-A220593| 17 p2356 N90-23412
Application of optimal tracking methods to aircraft terrain following
|AD-A221099| 18 p2496 N90-24264
Extrapolation of missile flight lines
|ETN-90-96494| 18 p2508 N90-24336
When propfans cruise, will LDN 65 fly
18 p2610 N90-24864
An aircraft noise study in Norway
18 p2611 N90-24872
Transatmospheric vehicle research
|NASA-CR-186705| 20 p2807 N90-25970
Improving the geometric fidelity of imaging systems employing sensor arrays
|NASA-CASE-NPO-17970-1-CU|
20 p2880 N90-26384

High mountain flying in ski country, USA
|PB90-180316| 22 p3107 N90-27651
R and D aspects of the future operational concept of the BFS 22 p3112 N90-27679
On-board planning and control of 4D-trajectories in the TMA 22 p3112 N90-27680
Four-dimensional navigation and Flight Management Systems 22 p3112 N90-27681
A study of terrain following systems and the creation of flight paths for terrain following vehicles
|FOA-C-20774-2.5| 22 p3114 N90-27691
Ascent and descent trajectory optimization of Ariane 5/Hermes 22 p3126 N90-27743
Optimal trajectories for Saenger-type vehicles 22 p3129 N90-27760
Real time guidance and propulsion control for single-stage-to-orbit airbreathing vehicles 23 p3285 N90-28587

FLIGHT PERFORMANCE
U FLIGHT CHARACTERISTICS

FLIGHT PLANS
Ground and Obstacle Avoidance (GOA) concept of operations
|DOT/FAA/DS-89/08| 02 p0150 N90-10855
National Airspace System flight planning operational concept
|DOT/FAA/DS-89/30| 05 p0577 N90-13362
Control outside of independent surveillance coverage operational concept
|AD-A214163| 07 p0878 N90-15090
The Penguin: A low Reynolds number powered glider for station keeping missions
|NASA-CR-186667| 19 p2658 N90-25129
Enroute flight planning: The design of cooperative planning systems
|NASA-CR-186797| 20 p2806 N90-25964
The potential for digital databases in flight planning and flight aiding for combat aircraft 24 p3429 N90-29371

FLIGHT RECORDERS
Post crash flight analysis: Visualizing flight recorder data
|AD-A212063| 03 p0302 N90-11715
The NASA digital VGH program: Exploration of methods and final results. Volume 2: L 1011 data 1978-1979: 1619 hours
|NASA-CR-181909-VOL-2| 13 p1756 N90-20080
The NASA digital VGH program. Exploration of methods and final results. Volume 1: Development of methods
|NASA-CR-181909-VOL-1| 13 p1756 N90-20081
The NASA digital VGH program. Exploration of methods and final results. Volume 3: B 727 data 1978-1980: 1765 hours
|NASA-CR-181909-VOL-3| 13 p1756 N90-20082
The NASA digital VGH program: Exploration of methods and final results. Volume 4: B 747 data 1978-1980, 1689 hours
|NASA-CR-181909-VOL-4| 13 p1756 N90-20083
The NASA digital VGH program: Exploration of methods and final results. Volume 5: DC 10 data 1981-1982, 129 hours
|NASA-CR-181909-VOL-5| 13 p1756 N90-20084
Windshear case study: Denver, Colorado, July 11, 1988
|DOT/FAA/DS-89/19| 14 p2008 N90-21509
Aircraft Integrated Monitoring Systems
|DLR-MITT-90-04| 22 p3103 N90-27617
The EFA integrated monitoring and recording system: Requirements and concept for implementation 22 p3103 N90-27620
Performance assessment of MIL-STD-1553B on the avionic systems demonstrator rig of British Aerospace 22 p3104 N90-27624
Flight data replay and analysis system 22 p3105 N90-27635
AIMS for helicopters 22 p3106 N90-27639
Monitoring and controlling flight in windshear 22 p3106 N90-27641
The new US flight recorder regulations 22 p3106 N90-27642
The Canadian Aviation Safety Board's flight recorder facility 22 p3106 N90-27643
Australian experience in flight recorder readout and analysis 22 p3106 N90-27644
Automation of the readout, transcription and evaluation of digital flight data at DLR 22 p3106 N90-27645

FLIGHT RULES
NT INSTRUMENT FLIGHT RULES
Development of a standardized three axis sensor for inertial data achievement for future flight rule systems
|ETN-90-96075| 12 p1604 N90-19231
An analysis of GPS as the sole means navigation system in US Navy aircraft 24 p3425 N90-29350

FLIGHT SAFETY
Safer skies with TCAS: Traffic Alert and Collision Avoidance System
|PB89-169221| 01 p0004 N90-10016
See and avoid/cockpit visibility
|DOT/FAA/CT-TN89/18| 02 p0148 N90-10843
The Air Force Flight Test Center Flight Test Safety Program 02 p0153 N90-10872
UK airmisses involving commercial air transport
|CAA-2/88| 03 p0303 N90-11718
Report on orbital debris
|NASA-TM-101855| 04 p0460 N90-12635
National Airspace System airspace management operational concept
|DOT/FAA/DS-89/29| 05 p0577 N90-13361
National Airspace System flight planning operational concept
|DOT/FAA/DS-89/30| 05 p0577 N90-13362
An update to the system safety study of TCAS 2
|DOT/FAA/SA-89/3| 05 p0577 N90-13363
Flight in adverse environmental conditions
|AGARD-AR-277| 06 p0723 N90-14218
Workload induced spatio-temporal distortions and safety of flight
|DE89-016613| 06 p0820 N90-14771
Analysis of severe atmospheric disturbances from airline flight records 07 p0869 N90-15045
Influence of windshear, downdraft and turbulence on flight safety 07 p0870 N90-15048
Ice induced aerodynamic performance degradation of rotorcraft: An overview 07 p0873 N90-15063
Effects of lightning on operations of aerospace vehicles 07 p0873 N90-15065
Aircraft testing in the electromagnetic environment 07 p0873 N90-15066
Turbulence spectral widths view angle independence as observed by Doppler radar
|DOT/FAA/SA-89/2| 07 p0963 N90-15566
Risk assessment and its application to flight safety analysis
|DE90-004985| 09 p1161 N90-16722
Hermes space vehicle: Safety considerations 09 p1178 N90-16825
Aircraft fire safety in the Canadian Forces 10 p1315 N90-17604
Dallas/Fort Worth simulation. Volume 2: Appendixes D, E, and F
|AD-A216613| 11 p1454 N90-18380
System safety requirements for ESA space systems and associated equipment
|ESA-PSS-01-40-ISSUE-2| 11 p1469 N90-18460
Activities report in civil aviation
|ETN-90-95471| 13 p1753 N90-20067
UK airmisses involving commercial air transport, January - April 1989
|ISSN-0951-6301| 16 p2197 N90-22544
Aeronautical decisionmaking for air ambulance program administrators
|DOT/FAA/DS-88/8| 17 p2347 N90-23368
Results of TCAS-2 simulations in reconstructed dangerous encounters (Jul. 1986 to Jun. 1989)
|ETN-90-96474| 17 p2349 N90-23375
Development and test of software by safety critical aircraft systems
|MBB-FE-363/S/PUB-384| 19 p2654 N90-25103
An overview of the joint FAA/NASA aircraft/ground runway friction program
|NASA-TM-103486| 20 p2805 N90-25957
Aviation safety: Serious problems continue to trouble the air traffic control work force. Report to congressional requesters
|GAO/RCED-89-112| 20 p2805 N90-25959
Human factors and safety considerations of night vision systems flight using thermal imaging systems
|AD-A223226| 21 p3037 N90-27263
Daily flight operation monitoring in JAL 22 p3105 N90-27636
Monitoring and controlling flight in windshear 22 p3106 N90-27641
The new US flight recorder regulations 22 p3106 N90-27642
The Canadian Aviation Safety Board's flight recorder facility 22 p3106 N90-27643
High mountain flying in ski country, USA
|PB90-180316| 22 p3107 N90-27651
Air traffic management in Europe: Structure, tasks, potential 22 p3112 N90-27677
Component behaviour and life management: The need for common AGARD approaches and actions 22 p3118 N90-27710
Modeling and analysis of airport and aircraft operations
|PB90-222167| 23 p3271 N90-28511
Spatial disorientation incidents in the RNLAF F16 and F5 aircraft and suggestions for prevention 23 p3357 N90-28973
Workload induced spatio-temporal distortions and safety of flight: An investigation of cognitive intrusions in perceptual processes 23 p3360 N90-28986
Experimental tests on the minimal visual acuity required for safe air crew and air control personnel performance 23 p3360 N90-28987

FLIGHT SIMULATION
Stability and Control of Tactical Missile Systems
|AGARD-CP-451| 01 p0011 N90-10050
Flight Test Techniques
|AGARD-CP-452| 02 p0151 N90-10860
ATTAS flight testing experiences 02 p0151 N90-10862
GRATE: A new flight test tool for flying qualities evaluation 02 p0152 N90-10868
Flight testing of the Tornado Terrain Following System 02 p0153 N90-10875
Identification Friend, Foe or Neutral Joint Test 02 p0154 N90-10881
Flight simulator evaluation of a head-down display
|NAL-TM-573| 02 p0157 N90-10898
Flight simulation test facility: Function and specification of the simulator cockpit system
|NAL-TM-577| 02 p0157 N90-10899
Advanced manned space flight simulation and training: An investigation of simulation host computer system concepts
|NASA-CR-185998| 02 p0160 N90-10911
Stability and control derivatives of the De Havilland DHC-2 BEAVER aircraft
|PB89-217525| 03 p0309 N90-11754
Comparison of flying qualities derived from in-flight and ground-based simulators for a jet-transport airplane for the approach and landing pilot tasks
|NASA-TP-2962| 03 p0309 N90-11757
Stall/spin/flight simulation
|DOT/FAA/CT-88/28| 03 p0310 N90-11765
FPG2: A flight profile generator program
|AD-A212408| 04 p0453 N90-12595
The comparison of the airbase simulation models airbase and sustained
|FEL-1988-66| 04 p0459 N90-12629
Fatigue, pilot deviations and time of day
|NASA-CR-185369| 04 p0526 N90-13035
Psychological mechanisms involved in the disorientation of pilots due to flight conditions
|ETN-89-95014| 04 p0527 N90-13040
Mathematical model identification for flight simulation, based on flight and taxi tests
|LR-550| 05 p0585 N90-13410
The relationship between subjective and objective measures of simulator-induced ataxia
|AD-A213095| 05 p0673 N90-13922
Preliminary study of pharmacological control of space disease
|ETN-90-95015| 05 p0674 N90-13927
Human factors research in aircrew performance and training
|AD-A213285| 05 p0676 N90-13938
AcSim: Aircraft simulation program with application to flight profile generation
|AD-A212466| 06 p0723 N90-14217
Wind shear models for aircraft hazard investigation 07 p0869 N90-15044
A survey of nonuniform inflow models for rotorcraft flight dynamics and control applications
|NASA-TM-102219| 08 p1028 N90-15938
The NASA Langley 0.3-meter transonic cryogenic tunnel 08 p1028 N90-15941
Integrated flight guidance system using differential-GPS for landing approach guidance 09 p1163 N90-16735
Backward transfer and skill acquisition in the AH-1 flight and weapons simulator
|AD-A213432| 09 p1170 N90-16772
Hermes training aircraft 09 p1178 N90-16827
Stress and performance during a simulated flight in a F-16 simulator 09 p1256 N90-17285
Hypersonic nozzle/afterbody performance at low Mach numbers
|AD-A216223| 10 p1309 N90-17575
Time and frequency-domain identification and verification of BO-105 dynamic models
|AD-A216828| 11 p1456 N90-18389
Calculation and optimization of rotor start process
|ETN-90-95894| 12 p1604 N90-19229
Yaw rate control of an air bearing vehicle 12 p1639 N90-19420
Simulator sickness in the CH-47 (Chinook) flight simulator
|AD-A218214| 13 p1853 N90-20634
The Real Time Interactive Display Environment (RTIDE), a display building tool developed by Space Shuttle flight controllers 13 p1857 N90-20654
Efficient utilization of graphics technology for space animation 13 p1859 N90-20663
An early overview of tiltrotor aircraft characteristics and pilot procedures in civil transport applications
|DOT/FAA/DS-89/37| 14 p1921 N90-21003

Stereopsis cueing effects on hover-in-turbulence performance in a simulated rotorcraft
[NASA-TP-2980] 14 p1921 N90-21004
USSR Space Life Sciences Digest, Issue 26
[NASA-CR-3922(31)] 14 p2009 N90-21513
The effect of windscreen bows and HUD pitch ladder format on pilot performance during simulated flight
[AD-A218139] 14 p2011 N90-21523
Aeroelastic simulation of higher harmonic control 15 p2054 N90-21768
Unsteady separated flows produced by complex harmonic motions: Investigation of wing-flow interactions elicited by a mechanical model simulating dragonfly wing kinematics 15 p2100 N90-22018
Minimum flying qualities. Volume 1: Piloted simulation evaluation of multiple axis flying qualities
[AD-A218560] 16 p2200 N90-22560
Minimum flying qualities. Volume 2: Pilot modeling for flying qualities applications
[AD-A218561] 16 p2201 N90-22561
Visual behavior in the F-15 simulator for air-to-air combat
[AD-A218648] 16 p2262 N90-22893
Development of a stereo 3-D pictorial primary flight display 16 p2273 N90-22955
Six-degree-of-freedom aircraft simulation with mixed-data structure using the applied dynamics simulation language, ADSIM 16 p2294 N90-23067
Results of TCAS-2 simulations in reconstructed dangerous encounters (Jul. 1986 to Jun. 1989)
[ETN-90-96474] 17 p2349 N90-23375
Fighter agility metrics, research, and test
[NASA-CR-186118] 17 p2351 N90-23386
Estimating short-period dynamics using an extended Kalman filter
[NASA-TM-101722] 17 p2352 N90-23392
Gamma Ray Observatory (GRO) dynamics simulator requirements and mathematical specifications, revision 1
[NASA-CR-183465] 17 p2362 N90-23447
Real-time simulation clock
[NASA-CASE-LAR-14056-1] 17 p2407 N90-23713
Fractographic observations on fatigue crack growth in 2024-T3 sheet material under flight-simulation loading
[LR-592] 17 p2415 N90-23760
IAPSA 2 small-scale system specification
[NASA-CR-182006] 17 p2467 N90-24103
Helicopter controllability
[AD-A220078] 18 p2498 N90-24275
Simulation of transport aeroplanes
[MBB-UT-007/89-PUB] 19 p2651 N90-25089
Lecture notes on flight simulation techniques
[LR-596] 19 p2662 N90-25153
Usefulness of heart measures in flight simulation 19 p2734 N90-25542
Model following control system design: Preliminary ATTAS in-flight simulation test results
[PD-FC-9003] 20 p2813 N90-26010
Investigation of crack-closure prediction models for fatigue in aluminium alloy sheet under flight-simulation loading
[LR-619] 20 p2877 N90-26369
Launching a dream: A teachers guide to a simulated space shuttle mission
[NASA-TM-89715] 20 p2934 N90-26693
The need for platform motion in modern piloted flight training simulators
[AD-A221720] 21 p2963 N90-26847
Human factors research in aircrew performance and training
[AD-A221657] 21 p3037 N90-27267
Economical graphics display system for flight simulation avionics
[NASA-CR-186886] 22 p3116 N90-27701
Space Vehicle Flight Mechanics
[AGARD-CP-489] 22 p3126 N90-27741
Space shuttle descent flight verification by simulation: A challenge in implementing flight control system robustness 22 p3127 N90-27748
Dallas/Forth Worth simulation. Phase 2: Triple simultaneous parallel Instrument Landing System (ILS) approaches (turbojets)
[DOT/FAA/CT-90/2] 23 p3270 N90-28509
Aerodynamic control design: Experience and results at Aermacchi 23 p3272 N90-28518
An in-flight investigation of ground effect on a forward-swept wing airplane 23 p3275 N90-28533
Real-time aerodynamic heating and surface temperature calculations for hypersonic flight simulation
[NASA-TM-4222] 23 p3327 N90-28815
The effects of acoustic orientation cues on instrument flight performance in a flight simulator 23 p3359 N90-28985
Flight test engineering with the ATTAS 23 p3391 N90-29160
Fighter agility metrics
[NASA-CR-187289] 24 p3432 N90-29389
Workshop on Low Level Flight Training
[AGARD-AR-288] 24 p3436 N90-29404
Terrain visual cue analysis for simulating low-level flight: A multidimensional scaling approach
[AD-A223564] 24 p3436 N90-29407
Fractographic observations on fatigue crack growth under miniTWIST flight-simulation loading (2024-T3 material)
[LR-631] 24 p3483 N90-29684

FLIGHT SIMULATORS
NT COCKPIT SIMULATORS
Advanced manned space flight simulation and training: An investigation of simulation host computer system concepts
[NASA-CR-185998] 02 p0160 N90-10911
A robust digital model following controller for helicopters
[ESA-TT-1041] 04 p0457 N90-12621
Field-of-View variations and stripe-texturing effects on assault landing performance in the C-130 weapon system trainer
[AD-A212763] 04 p0459 N90-12634
Software and hardware description of the helicopter motion equations for VAX computers
[AD-A213248] 05 p0579 N90-13375
Simulator induced sickness in the CP-140 (Aurora) flight deck simulator
[AD-A213096] 05 p0673 N90-13923
Compensatory tracking in disturbance tasks and target following tasks. The influence of cockpit motion on performance and control behavior
[LR-511] 05 p0675 N90-13933
Simulator sickness in the UH-60 (Black Hawk) flight simulator
[AD-A214434] 08 p1104 N90-16392
Hermes training aircraft 09 p1178 N90-16827
Simulator sickness in the CH-47 (Chinook) flight simulator
[AD-A218214] 13 p1853 N90-20634
Inertial navigation system simulator: Behavioral specification, revision
[AD-A219294] 16 p2199 N90-22554
Visual behavior in the F-15 simulator for air-to-air combat
[AD-A218648] 16 p2262 N90-22893
Simulator evaluation of the final approach spacing tool
[NASA-TM-102807] 17 p2348 N90-23374
Voice measures of workload in the advanced flight deck: Additional studies
[NASA-CR-4258] 17 p2437 N90-23887
An object-oriented solution example: A flight simulator electrical system
[AD-A219190] 19 p2661 N90-25145
Evaluation of nonlinear motion-drive algorithms for flight simulators
[UTIAS-TN-272] 19 p2662 N90-25148
Lecture notes on flight simulation techniques
[LR-596] 19 p2662 N90-25153
Eye tracking device for the measurement of flight performance in simulators
[AD-A220075] 20 p2898 N90-26484
Pilot interaction with automated airborne decision making systems
[NASA-CR-186730] 20 p2899 N90-26492
Human performance in cockpit-related systems
[NIAR-90-7] 20 p2900 N90-26495
The need for platform motion in modern piloted flight training simulators
[AD-A221720] 21 p2963 N90-26847
Economical graphics display system for flight simulation avionics
[NASA-CR-186886] 22 p3116 N90-27701
Real-time aerodynamic heating and surface temperature calculations for hypersonic flight simulation
[NASA-TM-4222] 23 p3327 N90-28815
The function of the Interactive Model Assembly Program (IMAP) for a flight simulator
[NAL-TR-1034] 24 p3437 N90-29412

FLIGHT STABILITY TESTS
Airworthiness and flight characteristics test of the UH-60A Black Hawk helicopter equipped with the XM-139 multiple mine dispensing system (VOLCANO)
[AD-A210271] 01 p0006 N90-10025
F-15B high angle-of-attack phenomena and spin prediction using bifurcation analysis
[AD-A217366] 13 p1754 N90-20073
The MANTA: An RPV design to investigate forces and moments on a lifting surface
[NASA-CR-186227] 14 p1915 N90-20971

FLIGHT STRESS (BIOLOGY)
NT SPACE FLIGHT STRESS
Biology in microgravity: A guide for experimenters
[ESA-TM-02] 04 p0482 N90-12769
Effects of a time zone shift of nine hours on the circadian rhythms in cockpit aircrew members on longhaul flights
[DLR-FB-89-31] 04 p0523 N90-13019
Studies on predicting the resynchronization of the circadian system after transmeridian flights
[ESA-TT-1177] 19 p2722 N90-25483
Biochemical and physiological changes in glider pilots during multi-hour flights
[ESA-TT-1183] 19 p2722 N90-25484
Electrocardiogram of military aircraft pilots measured during real flight missions: Study of the variability of the cardiac rhythm in correlation with working stress
[ETN-90-97453] 22 p3231 N90-28324

FLIGHT SURGEONS
The United States Air Force School of Aerospace Medicine: Special report
[AD-A217740] 13 p1851 N90-20622

FLIGHT TECHNICAL ERROR
U PILOT ERROR

FLIGHT TEST INSTRUMENTS
Devices and procedures for the calibration of sensors and measurement: Systems of the flight test support system ATTAS
[DFVLR-MITT-89-06] 03 p0351 N90-12007
Automatic processing of images from the GRATE flight test tool
[DLR-FB-89-28] 04 p0454 N90-12599
Checklist reading problems in airplanes equipped with speech recognition systems
[ILR-MITT-223(1989)] 09 p1261 N90-17314
Continued development and analysis of a new extended Kalman filter for the Completely Integrated Reference Instrumentation System (CIRIS)
[AD-A220106] 17 p2354 N90-23400
Evaluation for DLC-Flap Monitoring System of the VSRA
[NAL-TM-607] 24 p3433 N90-29391

FLIGHT TEST VEHICLES
Development of a flight test methodology for a US Navy half-scale unmanned air vehicle
[AD-A210563] 01 p0006 N90-10029
Initial flight test of half-scale unmanned air vehicle
[AD-A219584] 17 p2351 N90-23388
On-board planning and control of 4D-trajectories in the TMA 22 p3112 N90-27680

FLIGHT TESTS
NT FLIGHT STABILITY TESTS
NT SPACE TRANSPORTATION SYSTEM FLIGHTS
ILS/MLS comparison tests at Miami/Tamiami, Florida Airport
[ACD-330] 01 p0005 N90-10018
Development of a flight test methodology for a US Navy half-scale unmanned air vehicle
[AD-A210563] 01 p0006 N90-10029
Electro-impulse de-icing testing analysis and design
[NASA-CR-4175] 01 p0007 N90-10031
Identification of stability and control parameters of a brilliant ammunition 01 p0014 N90-10065
Marginal release disturbances on advanced missiles 01 p0014 N90-10070
Experience gained in the improvement of the Aspide aerodynamic configuration for the surface to air role 01 p0015 N90-10072
On the interactive computer program IPIS for aircraft parameter identification
[NAL-TR-1000] 01 p0103 N90-10586
Measurement resolution of noise directivity patterns from acoustic flight tests
[NASA-TM-4134] 01 p0118 N90-10679
Flight Test Techniques
[AGARD-CP-452] 02 p0151 N90-10860
US Navy principal site testing concept and the F-18 02 p0151 N90-10861
ATTAS flight testing experiences 02 p0151 N90-10862
P-180 AVANTI: Project and flight test program comprehensive overview 02 p0151 N90-10863
A320 flight tests: Particularities and innovations 02 p0151 N90-10864
The Experimental Aircraft Flight Test Programme 02 p0152 N90-10865
Real-time flight test analysis and display techniques for the X-29A aircraft 02 p0152 N90-10866
Flight test techniques adopted by Avions Marcel Dassault-Breguet Aviation 02 p0152 N90-10867
GRATE: A new flight test tool for flying qualities evaluation 02 p0152 N90-10868
In flight relight tests on AM-X single engine fly-by-wire aircraft 02 p0152 N90-10869
Flight test results of a complex precise digital flight control system 02 p0152 N90-10870
Analysis of flutter tests with the use of a telemetry system 02 p0152 N90-10871
The Air Force Flight Test Center Flight Test Safety Program 02 p0153 N90-10872
Results and practical experience using parameter identification techniques on the AM-X program at Aermacchi 02 p0153 N90-10873

Lessons learned from the integration of flight systems
02 p0153 N90-10874
Flight testing of the Tornado Terrain Following System
02 p0153 N90-10875
Evaluation of store carriage (and release) environment using flight instrumented stores
02 p0153 N90-10876
CF 18 480 Gallon External Fuel Tank Stores Clearance Program
02 p0153 N90-10877
Flow visualization techniques for flight research
02 p0153 N90-10878
Flight testing a newly-designed stand-off weapon dispenser
02 p0154 N90-10880
Flight testing and flight research: From the age of the tower jumper to the age of the astronaut
02 p0154 N90-10882
Flight testing in the Netherlands: An overview
02 p0155 N90-10884
On the development of a basic flight test capability and some related research projects
02 p0155 N90-10885
Flight test instrumentation and data processing at British Aerospace, Warton, U.K.
02 p0155 N90-10887
Heliport surface maneuvering test results
[ACD-330]
02 p0157 N90-10897
Problems related to the acquisition, processing and utilization of the modal parameters measured in flight tests in order to obtain the full envelope for flutter
[ETN-89-95210]
03 p0305 N90-11735
Propfan Test Assessment (PTA): Flight test report
[NASA-CR-182278]
03 p0306 N90-11738
Propfan Test Assessment (PTA)
[NASA-CR-185138]
03 p0306 N90-11739
Devices and procedures for the calibration of sensors and measurement: Systems of the flight test support system ATTAS
[DFVLR-MITT-89-06]
03 p0351 N90-12007
Development flight tests of JetStar LFC leading-edge flight test experiment
04 p0439 N90-12509
The right wing of the LEFT airplane
04 p0439 N90-12510
Performance of laminar-flow leading-edge test articles in cloud encounters
04 p0439 N90-12511
Simulated airline service experience with laminar-flow control leading-edge systems
04 p0439 N90-12512
Flow quality measurements in compressible subsonic flows
04 p0441 N90-12521
Design and test of an NLF wing glove for the variable-sweep transition flight experiment
04 p0444 N90-12544
F-14 VSTFE and results of the cleanup flight test program
04 p0445 N90-12547
Status report on a natural laminar-flow nacelle flight experiment
04 p0445 N90-12550
Pivotal mono wing cruise missile with wing deployment and fastener mechanism
[AD-D014191]
04 p0452 N90-12594
Air Force flight feeding. Volume 1: Evaluation of current system and alternative concepts
[AD-A212789]
04 p0527 N90-13043
UHB demonstrator interior noise control flight tests and analysis
[NASA-CR-181897]
04 p0549 N90-13198
Correlation of Puma airloads: Lifting-line and wake calculation
[NASA-TM-102212]
05 p0572 N90-13327
LORAN C stability integrity assurance
[AD-A212663]
05 p0577 N90-13364
An in-flight investigation of ground effect on a forward-swept wing airplane
[NASA-TM-101708]
06 p0720 N90-14202
An in-flight technique for wind measurement in support of the space shuttle program
[NASA-TM-4154]
06 p0724 N90-14224
Flight evaluation of a pneumatic system for unsteady pressure measurements using conventional sensors
[NASA-TM-4131]
06 p0724 N90-14225
SRB thermal environments
[NASA-CR-183801]
06 p0734 N90-14276
Systems for airborne wind and turbulence measurement
07 p0869 N90-15046
The United States Air Force approach to all-weather testing
07 p0870 N90-15047
NASA's program on icing research and technology
07 p0873 N90-15062
Flight and wind tunnel investigation of aerodynamic effects of aircraft ground deicing/antiicing fluids
07 p0873 N90-15064
Aircraft testing in the electromagnetic environment
07 p0873 N90-15066
Schleicher ASK-21 glider (TG-9) stall and spin
[AD-A213513]
07 p0879 N90-15096
X.2 limited flight test plan
[AD-A214412]
07 p0880 N90-15099
China-built airborne synchronous laser ranger the new L-8 jet trainer aircraft
[AD-A213835]
07 p0936 N90-15422
Mirach 100 flight control system
08 p1025 N90-15926
Navigation and guidance testing of the Lockheed/US Army Aquila remotely piloted vehicle
08 p1027 N90-15935
Pulsed plasma mission endurance test
[AD-A213462]
08 p1037 N90-15993
Risk assessment and its application to flight safety analysis
[DE90-004985]
09 p1161 N90-16722
Natural icing re-evaluation of the EH-60A Quick Fix helicopter
[AD-A214728]
09 p1162 N90-16723
Integrated flight guidance system using differential-GPS for landing approach guidance
09 p1163 N90-16735
NASA/RAE cooperation on a knowledge based flight status monitor
09 p1164 N90-16738
Guidance and control considerations for a maneuvering aerial target system
09 p1165 N90-16746
Terrain-aided navigation and target acquisition on the AFTI/F-16
09 p1166 N90-16747
Further development and limited flight testing of the CycloCrane
[AD-A215519]
09 p1167 N90-16754
Preliminary results from a subsonic high angle-of-attack flush airdata sensing (HI-FADS) system: Design, calibration, and flight test evaluation
[NASA-TM-101713]
09 p1168 N90-16758
Determination of the gravity disturbance on the earth's topographic surface from airborne gravity gradient data
[AD-A214596]
09 p1246 N90-17230
VLA missile development and high angle of attack behavior
10 p1305 N90-17553
Longitudinal stability and control characteristics of the Quiet Short-Haul Research Aircraft (QSRA)
[NASA-TP-2965]
10 p1322 N90-17639
The Advanced Digital-Optical Control System (ADOCS) user demonstration program
[AD-A215984]
10 p1323 N90-17644
Flight survey of the 757 wing noise field and its effects on laminar boundary layer transition. Volume 3: Extended data analysis
[NASA-CR-178419]
10 p1427 N90-18233
Time and frequency-domain identification and verification of BO-105 dynamic models
[AD-A216828]
11 p1456 N90-18389
Wind-tunnel investigation of a flush airdata system at Mach numbers from 0.7 to 1.4
[NASA-TM-101697]
11 p1457 N90-18395
Mission options for an electric propulsion demonstration flight test
11 p1473 N90-18479
Heat transfer measurements from a NACA 0012 airfoil in flight and in the NASA Lewis icing research tunnel
[NASA-CR-4278]
12 p1599 N90-19203
Helicopter flight vibration of large transportation containers: A case for testing tailoring
[DE90-007429]
12 p1601 N90-19215
X-29A aircraft structural loads flight testing
[NASA-TM-101715]
12 p1603 N90-19225
Low-speed wind-tunnel investigation of the flight dynamic characteristics of an advanced turboprop business/commuter aircraft configuration
[NASA-TP-2982]
12 p1606 N90-19239
In-flight evaluations of turbine fuel extenders
[DOT/FAA/CT-89/33]
12 p1633 N90-19387
Sandia National Laboratories' new high level acoustic test facility
[DE90-006810]
12 p1710 N90-19820
A note on an acoustic response during an engine nacelle flight experiment
[NASA-TM-102585]
12 p1710 N90-19821
Airworthiness and flight characteristics evaluation of the McDonnell Douglas Helicopter Corporation (MDHC) 530FF helicopter
[AD-A218253]
13 p1755 N90-20076
Aerodynamic analysis of a US Navy and Marine Corps unmanned air vehicle
[AD-A218282]
13 p1755 N90-20077
Design and performance of a multi-stage cylindrical reconnection launcher
[DE90-007820]
13 p1761 N90-20108
Flight test investigation of certification issues pertaining to general-aviation-type aircraft with natural laminar flow
[NASA-CR-181967]
14 p1911 N90-20952
Severe shock and vibration environments for electronic components
[DE90-007686]
15 p2117 N90-22113
Application of a dynamic stall model to rotor trim and aeroelastic response
16 p2200 N90-22556
Flutter investigations on a Transavia PL12/T-400 aircraft
[AD-A219108]
16 p2203 N90-22570
Boeing/NASA composite components flight service evaluation
[NASA-CR-181898]
16 p2210 N90-22609
Turbine fuel alternatives (near term)
[AD-A219405]
16 p2225 N90-22695
An evaluation of the accuracy of a microwave landing system area navigation system at Miami/Tamiami Florida Airport
[DOT/FAA/CT-TN89/40]
17 p2349 N90-23377
MLS mathematical model validation study using airborne MLS data from Midway Airport engineering flight tests, August 1988
[DOT/FAA/CT-TN90/2]
17 p2349 N90-23378
Fighter agility metrics, research, and test
[NASA-CR-186118]
17 p2351 N90-23386
Preliminary airworthiness evaluation of the RC-12K
[AD-A219545]
17 p2351 N90-23387
Initial flight test of half-scale unmanned air vehicle
[AD-A219584]
17 p2351 N90-23388
Development of a least squares time response lower-order equivalent systems technique
[AD-A220527]
17 p2351 N90-23389
Prediction of longitudinal pilot induced oscillations using the optimal control model
[AD-A220593]
17 p2356 N90-23412
Using simulation to determine a strategy for positively tracking a cruise missile by CMMCA
[AD-A220526]
17 p2362 N90-23448
On the simulation test for the relative motion of separated sub-boosters on M-3S2 with nearly half a model vehicle ST-735 and their motion analyses using inertial sensors output
[ISAS-635]
17 p2366 N90-23471
Static wind-tunnel and radio-controlled flight test investigation of a remotely piloted vehicle having a delta wing planform
[NASA-TM-4200]
18 p2491 N90-24238
Helicopter controllability
[AD-A220078]
18 p2498 N90-24275
En route noise of turboprop aircraft and their acceptability: Report of tests
18 p2609 N90-24858
Realtime simulation at MBB today and future aspects
[MBB-UA-1134/89-PUB]
19 p2653 N90-25098
Video photographic considerations for measuring the proximity of a probe aircraft with a smoke seeded trailing vortex
[NASA-TM-102691]
19 p2657 N90-25120
Evaluation of various thrust calculation techniques on an F404 engine
[NASA-TP-3001]
19 p2659 N90-25134
Flutter clearance of the F-14A variable-sweep transition flight experiment airplane, phase 2
[NASA-TM-101717]
19 p2659 N90-25135
An accurate numerical technique for determining flight test rate gyroscope biases prior to takeoff
[AD-A220987]
19 p2660 N90-25138
Flight-testing of the self-repairing flight control system using the F-15 highly integrated digital electronic control flight research facility
[NASA-TM-101725]
19 p2661 N90-25144
TRENDS: The aeronautical post-test database management system
[NASA-TM-101025]
19 p2662 N90-25149
The 30-kW ammonia arcjet technology
[NASA-CR-186850]
19 p2670 N90-25190
Research at NASA's NFAC wind tunnels
[NASA-TM-102827]
20 p2801 N90-25933
Flight testing of a natural laminar flow airfoil using gliders
[PD-CF-9005]
20 p2801 N90-25936
Model following control system design: Preliminary ATTAS in-flight simulation test results
[PD-FC-9003]
20 p2813 N90-26010
Aeroacoustics of advanced propellers
[NASA-TM-103137]
20 p2923 N90-26635
Obtaining consistent models of helicopter flight-data measurement errors using kinematic-compatibility and state-reconstruction methods
[AD-A222533]
21 p2954 N90-26799
Automated analysis of MXU-553 flight data
21 p2958 N90-26821
The SKY SHARK: An RPV designed to investigate the pressure distribution on a lifting surface
[NASA-CR-186222]
21 p2959 N90-26824
New inflight experiments to measure aerodynamics loads
[ETN-90-97276]
21 p2961 N90-26834
Heliport visual approach surface high temperature and high altitude tests
[DOT/FAA/CT-TN89/34]
22 p3112 N90-27675
Sideslip-induced static pressure errors in flight-test measurements
[NASA-TM-102846]
22 p3116 N90-27702

Flight test investigation of flight director and autopilot functions for helicopter decelerating instrument approaches
|DOT/FAA/CT-TN89/54| 22 p3121 N90-27724
National aero-space plane: Flight mechanics 22 p3129 N90-27759
In-flight flow visualization with pressure measurements at low speeds on the NASA F-18 high alpha research vehicle
|NASA-TM-101726| 23 p3270 N90-28505
Aerodynamic and propulsive control development of the STOL and maneuver technology demonstrator 23 p3271 N90-28514
Control research in the NASA high-alpha technology program 23 p3272 N90-28516
Study of ground effects on flying scaled models 23 p3275 N90-28532
Description of the primary flight display and flight guidance system logic in the NASA B-737 transport systems research vehicle
|NASA-TM-102710| 23 p3277 N90-28546
Development of the electric vehicle analyzer
|AD-A224201| 23 p3323 N90-28788
Flight test engineering with the ATTAS 23 p3391 N90-29160
Vibration responses of two house structures during the Edwards Air Force Base phase of the national sonic boom program
|NASA-CR-182089| 23 p3393 N90-29169
Ring laser gyro principles and techniques 24 p3426 N90-29352
High altitude balloon flight test of the GRAD experiment
|AD-A224398| 24 p3432 N90-29388
Fighter agility metrics
|NASA-CR-187289| 24 p3432 N90-29389
Evaluation for DLC-Flap Monitoring System of the VSRA
|NAL-TM-607| 24 p3433 N90-29391
Procedure for calibrating fly-by-wire control chains of the flying testbed ATTAS
|DLR-MITT-90-02| 24 p3435 N90-29401
Research and development activities at the Goddard Space Flight Center for the flight telerobotic servicer project 24 p3507 N90-29824
Dexterous manipulator flight demonstration 24 p3522 N90-29911
A search for low energy cosmic ray antiprotons 24 p3564 N90-30161

FLIGHT TIME
Series reversion/inversion of Lambert's time function
|AD-A216243| 12 p1607 N90-19245
Four-dimensional navigation and Flight Management Systems 22 p3112 N90-27681

FLIGHT TRAINING
NT SPACE FLIGHT TRAINING
The relationship between subjective and objective measures of simulator-induced ataxia
|AD-A213095| 05 p0673 N90-13922
Simulator sickness in the UH-60 (Black Hawk) flight simulator
|AD-A214434| 08 p1104 N90-16392
Backward transfer and skill acquisition in the AH-1 flight and weapons simulator
|AD-A213432| 09 p1170 N90-16772
Reactions to emergency situations in actual and simulated flight 09 p1255 N90-17283
Prediction of success in flight training by single- and dual-task performance 09 p1257 N90-17293
Flight crew training for fire fighting 10 p1317 N90-17615
Relationship between flexibility of closure and success in pilot night vision sensor system training
|AD-A221439| 16 p2261 N90-22890
Radiological investigation of the vertebral column of candidates for military flying training the the Royal Norwegian Air Force 19 p2718 N90-25463
An analysis of requirements for a P-3 windshear training program
|AD-A222577| 20 p2805 N90-25960
The need for platform motion in modern piloted flight training simulators
|AD-A221720| 21 p2963 N90-26847
Human factors research in aircrew performance and training
|AD-A221657| 21 p3037 N90-27267
Workshop on Low Level Flight Training
|AGARD-AR-288| 24 p3436 N90-29404

FLIGHT VEHICLES
Experimental aeroelasticity history, status and future in brief
|NASA-TM-102651| 14 p1930 N90-21047

FLIP-FLOPS
integrated silicon flip-flop sensors
|ETN-90-96271| 11 p1503 N90-18654

FLIR DETECTORS
Research in computer vision for autonomous systems
|AD-A212420| 04 p0555 N90-13235
Airborne FLIR detection of surface targets 06 p0759 N90-14416
Reduced voltage and restart testing of the 1-watt integral cryogenic cooler (HD-1033B/C/D)
|AD-A215133| 09 p1203 N90-16971
Gabor transforms for forward looking infrared image segmentation
|AD-A215046| 09 p1282 N90-17433
Enhanced tracking of ballistic targets using forward looking infrared measurements with active target illumination
|AD-A215422| 09 p1282 N90-17434
Reliability testing of the Hughes temperature controlled 1/4 watt split cycle cryogenic cooler (HD-1045 (V)/UA)
|AD-A216696| 12 p1641 N90-19426
Helmet-mounted pilot night vision systems: Human factors issues 16 p2269 N90-22930
An assessment of the CD-FLIR as an ARGUS sensor
|AD-A220841| 17 p2473 N90-24137
The effect of random variations of radiosonde data on the predicted FLIR performance calculated by the program UFLR
|AD-A220034| 18 p2615 N90-24896
Nonlinear optical protection against frequency agile lasers
|AD-D014535| 19 p2695 N90-25335
Human factors and safety considerations of night vision systems flight using thermal imaging systems
|AD-A223226| 21 p3037 N90-27263

FLOATING POINT ARITHMETIC
Basic mathematical function libraries for scientific computation
|NASA-TM-102256| 08 p1110 N90-16423
Development of the Kalman filter application and a VHDL model for the AFIT (Air Force Institute of Technology) Floating Point Application Specific Processor (FPASP)
|AD-A215423| 09 p1213 N90-17033
Finite word length considerations in high resolution spectral estimation
|AD-A214684| 09 p1273 N90-17377
Technology development and circuit design for a parallel laser programmable floating point application specific processor
|AD-A215870| 11 p1500 N90-18637
Supercomputers need super arithmetic
|PB90-130253| 15 p2145 N90-22252
ELEFUNT test results under AST FORTRAN V1.8.0 on the sequent symmetry
|DE90-014932| 23 p3387 N90-29127
Formal verification of mathematical software, volume 2
|AD-A223633| 24 p3527 N90-29943

FLOOD CONTROL
Considerations concerning the determination of the most desirable height for sea dikes
|W-8905| 17 p2431 N90-23853

FLOOD DAMAGE
Extreme hurricanes in the nineteenth century
|PB89-201305| 01 p0087 N90-10498

FLOOD PLAINS
Possible use of satellite data for flood plain mapping
|INPE-4968-PRE/1537| 14 p2000 N90-21462

FLOOD PREDICTIONS
Relation of wind field and buoyancy to rainfall inferred from radar
|PB89-208326| 02 p0251 N90-11424
A collection of papers related to heavy precipitation forecasting
|PB89-230833| 05 p0671 N90-13910

FLOODS
Satellite-derived rainfall estimates and propagation characteristics associated with the Mesoscale Convective Systems (MCSs)
|PB89-213417| 03 p0365 N90-12086
Availability of multitemporal LANDSAT data accompanying the variation of water surfaces in the program area of Careiro PDRI/AM
|INPE-4896-PRE/1496| 12 p1677 N90-19634
Performance evaluation of MSS/LANDSAT data in the estimation of fluvial channel width
|INPE-4906-PRE/1507| 14 p2000 N90-21463

FLOORS
Development of improved fire safety standards adopted by the Federal Aviation Administration 10 p1312 N90-17585
Floor pull test of a transport airframe section
|DOT/FAA/CT-TN88/14| 13 p1754 N90-20072
The effect of aircraft size on cabin floor dynamic pulses
|DOT/FAA/CT-88/15| 19 p2659 N90-25136
Evaluation of energy absorption of new concepts of aircraft composite subfloor intersections
|NASA-TP-2951| 21 p2959 N90-26823
A review of research and development in crashworthiness of general aviation aircraft: Seats, restraints and floor structures
|AD-A221557| 22 p3115 N90-27698

FLOQUET THEOREM
A well conditioned formulation for the analysis of multi-layered frequency selective surfaces using a cascaded matrix approach, revised
|RSRE-MEMO-4289-REV| 04 p0496 N90-12858
Stability and stability sensitivity by periodically time dependent systems: Hill versus Floquet
|ILR-MITT-221(1989)| 17 p2463 N90-24071
Stabilization of Taylor-Couette flow due to time-periodic outer cylinder oscillation
|PB90-219130| 23 p3323 N90-28790

FLORA
U PLANTS (BOTANY)

FLORIDA
Catalog of absolutely calibrated, range normalized, wideband, electric field waveforms from located lightning flashes in Florida: July 24 and August 14, 1985 data
|AD-A212708| 04 p0521 N90-13008

FLOW CHARACTERISTICS
NT BOUNDARY LAYER STABILITY
NT FLAME STABILITY
NT FLOW DISTRIBUTION
NT FLOW STABILITY
NT FLOW VELOCITY
NT MAGNETOHYDRODYNAMIC STABILITY
Wall-layer eruptions in turbulent flows
|NASA-TM-102362| 02 p0219 N90-11250
A computational/experimental study of the flow around a body of revolution at angle of attack
|NASA-TM-88329| 02 p0219 N90-11254
Development of an adaptive time of flight system for the measurement of fluid flow velocity 02 p0222 N90-11273
The determination of the aerodynamic characteristics of an ogive-cylinder body in subsonic, curved, incompressible flow, and an assessment of the effect of flow curvature
|REPT-87-13| 03 p0302 N90-11712
Numerical computation of the viscous flow field around a prolate spheroid
|DFVLR-FB-89-22| 03 p0349 N90-11992
An introduction via vorticity dynamics and statistical theory --- turbulent shear flows 05 p0640 N90-13731
Coherent structures in a round jet 05 p0640 N90-13733
Navier-Stokes simulation of the crossflow instability in swept-wing flows
|NASA-CR-186122| 05 p0641 N90-13744
Explicit and implicit calculations of turbulent cavity flows with and without yaw angle
|NASA-CR-186293| 07 p0929 N90-15381
The cryogenic induction tunnel T2 at Toulouse 08 p1029 N90-15946
Automatic control of cryogenic wind tunnels 08 p1031 N90-15957
A numerical simulation of the flow in the diffuser of the NASA Lewis icing research tunnel
|NASA-TM-102480| 08 p1032 N90-15965
A numerical and experimental investigation of multiple shock wave/turbulent boundary layer interactions in a rectangular duct 08 p1062 N90-16141
Study of flow around a sphere in a hydraulic test tunnel
|CERT-1/2313/MES| 08 p1064 N90-16156
Extrapolation techniques for finite element approximations of Stokes and Navier-Stokes flow over a backward facing step
|PREPRINT-499| 08 p1065 N90-16160
Computation of fluid flow and heat transfer in rotating disc-systems 09 p1215 N90-17044
Impingement characteristics of heated plane turbulent jets 09 p1215 N90-17047
Particle resuspension and associated coherent structures in a turbulent boundary layer 09 p1245 N90-17224
Plume flowfield analysis of the shuttle primary Reaction Control System (RCS) rocket engine
|NASA-CR-186315| 10 p1329 N90-17676
Study of the blade/vortice interaction on a one-blade rotor during forward flight (incompressible, non viscous fluid)
|ISL-R-115/88| 11 p1456 N90-18391
Cold flow determination of the internal flow environment around the submerged TVC nozzle for the space shuttle SRM 11 p1470 N90-18465
Calculation of excrescence drag magnification due to pressure gradient at high subsonic speeds
|ESDU-87004| 12 p1598 N90-19195
Measuring flow properties of wicks for heat pipe solar receivers
|DE89-016537| 12 p1683 N90-19664

A method for measuring the material moduli of granular materials: Flow in an orthogonal rheometer
| DE90-007160 | 13 p1801 N90-20339
Aerodynamic optimization by simultaneously updating flow variables and design parameters
14 p1918 N90-20991
LaRC TPI 1500 series polymers
| NASA-CR-181899 | 14 p1945 N90-21129
Experimental and analytical investigations of granular materials: Shear flow and convective heat transfer
15 p2091 N90-21968
Computational and experimental investigations of rotating stall in compressor cascades
16 p2201 N90-22565
Turbulence and complex systems
| ETN-90-96620 | 16 p2236 N90-22758
Experimental study of mixing and combustion processes in a solid-propellant ducted rocket motor
17 p2367 N90-23472
Three-dimensional convection in cylindrical geometry
17 p2399 N90-23668
Boundary conditions for nonlinear hyperbolic systems of conservation laws
| REPT-892-422-101 | 17 p2404 N90-23694
AFE dynamic effects in inhomogeneous plasmas
18 p2643 N90-25053
A review of instability and noise propagation in supersonic flows
| NASA-CR-186800 | 19 p2655 N90-25112
Analysis of turbulent density fluctuations by means of spontaneous Raman diffusion
| ISL-R-103/89 | 20 p2863 N90-26287
Raman scattering measurements using UV excimer lasers
21 p2974 N90-26902
The Langley 14- by 22-foot subsonic tunnel: Description, flow characteristics, and guide for users
| NASA-TP-3008 | 22 p3107 N90-27649
Analysis of vibrational power transmission through a beam system including a flexible section
| ISVR-TR-176 | 23 p3340 N90-28875
Electron-beam fluorescence measurements in hypersonic flows
24 p3420 N90-29318
Determination of density using simultaneous interferometry methods
| IMFL-90/04 | 24 p3547 N90-30061

FLOW CHARTS
Structure flow diagram generator
| PB89-195978 | 01 p0104 N90-10592
Environment for failure region analysis: REACHER - a reachability condition derivation tool
| AD-A214183 | 07 p0977 N90-15641
The semantics of data flow diagrams
| TR-89-16 | 17 p2480 N90-24181

FLOW COEFFICIENTS
NT DISCHARGE COEFFICIENT

FLOW DEFLECTION
Experimental and analytical study of close-coupled ventral nozzles for ASTOVL aircraft
| NASA-TM-103170 | 18 p2498 N90-24273

FLOW DIRECTION INDICATORS
NT WIND VANES
Study for optimization of redundant vane-type flow-direction sensing systems and numerical analysis for design of the systems
| NAL-TM-571 | 02 p0155 N90-10890

FLOW DISTORTION
Compensating for pneumatic distortion in pressure sensing devices
| NASA-TM-101716 | 12 p1603 N90-19224
Wind tunnel investigation of three sonic anemometers
| PB90-149808 | 15 p2046 N90-21729
Theoretical and experimental study of flow-control devices for inlets of indraft wind tunnels
| NASA-TM-100050 | 15 p2056 N90-21778
Fundamental studies on spray combustion and turbulent combustion
| AD-A219840 | 18 p2521 N90-24394
Experience in developing an improved design of experiment (lessons learned) 22 p3120 N90-27718
Experimental study on the dynamic behavior of a revolving blade grill
| REPT-NT-89-CC-18 | 24 p3470 N90-29604

FLOW DISTRIBUTION
A numerical method for solving transonic flow past aircraft in Cartesian coordinates
| NAL-TR-1008 | 01 p0001 N90-10003
Computation of transonic flow about stores
| AD-A210402 | 01 p0002 N90-10009
The present status and the future of missile aerodynamics
01 p0012 N90-10051
Boost-phase discrimination research activities
| NASA-TM-101889 | 01 p0032 N90-10176
Experimental investigation of attachment-line transition in low-speed, high-lift wind-tunnel testing
01 p0062 N90-10358
Stability of a supersonic boundary layer along a swept leading edge 01 p0063 N90-10359
Curvature effects on the stability of three-dimensional laminar boundary layers 01 p0064 N90-10366
Experimental study of instability modes in a three-dimensional boundary layer
01 p0064 N90-10369
A composite velocity procedure for the three-dimensional reduced Navier-Stokes equations
01 p0069 N90-10396
Laminar boundary layer along inviscid surface streamlines over inclined axisymmetric bodies in incompressible flow
| AD-A210202 | 01 p0070 N90-10401
Studies in penetration mechanics
| AD-A210713 | 01 p0079 N90-10448
Numerical simulation of the compressible Orszag-Tang vortex
| AD-A210465 | 01 p0127 N90-10725
Low-Reynolds-number modeling of complex flows with and without density variation 02 p0146 N90-10832
Linear instability of supersonic plane wakes
| NASA-CR-181911 | 02 p0146 N90-10833
User's manual for PEPSIG NASA tip vortex version
| NASA-CR-182178 | 02 p0146 N90-10835
Computation of the tip vortex flowfield for advanced aircraft propellers
| NASA-CR-182179 | 02 p0146 N90-10836
In-situ study of the chemically driven flow fields in initiating homogeneous and heterogeneous nitromethane explosives
| DE89-008415 | 02 p0207 N90-11186
Numerical solutions of turbulent flow with heat transfer over rough surfaces 02 p0218 N90-11246
An experimental investigation of transition in oscillating pipe flow 02 p0218 N90-11249
Method of characteristic studies for rotational flow downstream of a curved shock wave
02 p0219 N90-11252
Computation of transient three-dimensional interstage flowfields using the arbitrary Lagrangian-Eulerian method
02 p0219 N90-11253
Rectangular subsonic jet flow field measurements
| NASA-CR-185962 | 02 p0219 N90-11255
A laser Doppler anemometry investigation of single-phase and particle-laden jet flows
| AD-A210660 | 02 p0220 N90-11261
Questions from the Willmarth Workshop on New Directions in Research on Turbulent Wall-Layer Structures
| AD-A211282 | 02 p0221 N90-11264
A nonoscillatory, characteristically convected, finite volume scheme for multidimensional convection problems
| NASA-TM-102354 | 02 p0263 N90-11497
On transonic flow over segmented slotted wind tunnel wall with mass transfer 02 p0294 N90-11676
The structure of separated flow regions occurring near the leading edge of airfoils - including transition
| NASA-CR-185853 | 03 p0299 N90-11695
Investigation of advanced mixer-ejector exhaust system
| AD-A211943 | 03 p0301 N90-11705
Computation of ramjet internal flowfields
| AD-A212001 | 03 p0307 N90-11743
Analytical studies of three-dimensional combustion processes
| AD-A211903 | 03 p0323 N90-11837
Experimental investigation of a planar shock wave over a double wedge
| AD-A211366 | 03 p0347 N90-11981
Computational methods for complex flowfields
| AD-A211485 | 03 p0347 N90-11983
Three-dimensional, two-phase, transonic, canted nozzle flows
| AD-A211528 | 03 p0347 N90-11984
Experimental research on swept shock Wave/Boundary layer interactions
| AD-A211744 | 03 p0348 N90-11988
Rotational and vibrational nonequilibrium effects in rarefied, hypersonic flow
| NASA-CR-182559 | 04 p0437 N90-12498
Experimental and theoretical investigation of boundary-layer instability mechanisms on a swept leading edge at Mach 3.5 04 p0447 N90-12557
Improved 2D numerical simulation model for strongly coupled heat and fluid flow in a thermal storage
| PB89-218879 | 04 p0500 N90-12878
Investigation of turbulent flow in highly curved ducts with application to turbomachinery components
| NASA-CR-186060 | 04 p0500 N90-12882
Two-phase flow pressure losses in pipeline fittings
| ESDU-89012 | 04 p0500 N90-12883
Reduction of turbulent drag: Boundary layer manipulators
| CERT-RSF-OA-74/2259-AYD |
04 p0501 N90-12889
Numerical evaluation of a solution representing a jet in cross-flow
| RAE-TM-AERO-2137 | 04 p0502 N90-12893
A mechanical power flow capability for the finite element code NASTRAN
| AD-A212202 | 04 p0513 N90-12964
A knowledge-based approach to automated flow-field zoning for computational fluid dynamics
| NASA-TM-101072 | 04 p0528 N90-13048
Multigrid solution method for the Euler equations
| PB89-219463 | 04 p0539 N90-13116
Application of a self-adaptive grid method to complex flows
| NASA-TM-102223 | 05 p0571 N90-13324
Analysis of experimental data for CAST 10-2/DOA 2 supercritical airfoil at low Reynolds numbers and application to high Reynolds number flow
| AD-A211654 | 05 p0571 N90-13326
Study of the integration of wind tunnel and computational methods for aerodynamic configurations
| NASA-TM-102196 | 05 p0572 N90-13332
Computation of flow fields around propellers and hovering rotors based on the solution of the Euler equations
| DLR-FB-89-37 | 05 p0572 N90-13333
Blunt-nose inviscid airflows with coupled nonequilibrium processes 05 p0573 N90-13336
A CFD study of tilt rotor flowfields
| NASA-CR-186116 | 05 p0575 N90-13349
Optimum shape of a blunt forebody in hypersonic flow
| NASA-CR-181955 | 05 p0575 N90-13351
Computation of Navier-Stokes equations for three-dimensional flow separation
| NASA-TM-102266 | 05 p0575 N90-13353
Application of an efficient hybrid scheme for aeroelastic analysis of advanced propellers
| NASA-TM-102428 | 05 p0576 N90-13355
A smoke generator system for aerodynamic flight research
| NASA-TM-4137 | 05 p0578 N90-13372
A planar reacting shear layer system for the study of fluid dynamics-combustion interaction
| NASA-TM-102422 | 05 p0582 N90-13393
A wall interference assessment/correction interface measurement system for the NASA/ARC 12-ft PWT
| NASA-CR-185474 | 05 p0584 N90-13401
Gas flows in rocket motors, volume 1
| AD-A213348 | 05 p0615 N90-13591
SSME LOX post flow analysis/fluid structure interaction. Volume 1: Flow analysis
| NASA-CR-183677 | 05 p0637 N90-13715
Calculation of flow fields by the solution of the Euler equations using an extended finite volume discretization scheme
| DLR-FB-89-38 | 05 p0639 N90-13729
An introduction via vorticity dynamics and statistical theory --- turbulent shear flows
05 p0640 N90-13731
Numerical Methods for Flows in Turbomachinery, volume 1
| VKI-LS-1989-06-VOL-1 | 05 p0640 N90-13735
Unsteady forces induced on finite-span cylinders in a cross-flow 05 p0642 N90-13746
Convective heat transfer measurements from a NACA 0012 airfoil in flight and in the NASA Lewis Icing Research Tunnel
| NASA-TM-102448 | 05 p0642 N90-13750
Computation of nonequilibrium gas flow past blunt bodies
| PREPRINT-488 | 05 p0644 N90-13757
On the topology of three-dimensional viscous flow structures near a plane wall. A classification and non-hyperbolic singularities on the wall
| LR-541 | 05 p0644 N90-13758
An interactive grid generation procedure for axial and radial flow turbomachinery
| NASA-CR-185167 | 05 p0682 N90-13968
Numerical investigations in three-dimensional internal flows
| NASA-CR-186068 | 06 p0718 N90-14189
A computational analysis of the transonic flow field of two-dimensional minimum length nozzles
06 p0718 N90-14194
Navier-Stokes solutions of 2-D transonic flow over unconventional airfoils 06 p0719 N90-14195
Navier-Stokes analysis of airfoils with leading edge ice accretions 06 p0719 N90-14196
Computation of unsteady transonic flow about airfoils in frequency domain using the full-potential equation
06 p0719 N90-14198

An analysis of the viscous flow through a compact radial turbine by the average passage approach
[NASA-TM-102471] 06 p0720 N90-14206
Acoustic-vortical-combustion interaction in a solid fuel ramjet simulator 06 p0726 N90-14234
Effects of flame stretch on the propagation, extinction, and stability of premixed flames
06 p0739 N90-14301
A numerical study of thin flame representations
[DE89-017889] 06 p0741 N90-14313
An experimental and theoretical study of the aeroacoustics of external-Coanda gas flares
06 p0773 N90-14495
Fluid-particle interaction in solid-liquid two-phase grid turbulence 06 p0773 N90-14496
A dynamic multiblock approach to solving the unsteady Euler equations about complex configurations
06 p0773 N90-14497
Numerical solution of the incompressible Navier-Stokes equations 06 p0774 N90-14501
Three-dimensional solution-adaptive grid generation of composite configurations 06 p0775 N90-14509
Spatial evolution of nonlinear acoustic mode instabilities on hypersonic boundary layers
[NASA-TM-102431] 06 p0777 N90-14517
The laminar to slug flow transition in Hele-Shaw flow
[DE90-000636] 06 p0777 N90-14521
An initial look at the dynamics of the microscale flow field within a large wind farm in response to variations in the natural inflow
[DE89-009501] 06 p0804 N90-14682
Unsteady aerodynamics of oscillating and rapidly pitched airfoils 07 p0875 N90-15074
Spatially-resolved, nonintrusive measurements in a nonreacting scramjet combustor using laser-induced iodine fluorescence 07 p0881 N90-15103
Steady flow combustion model for solid-fuel ramjet projectiles
[BRL-TR-2987] 07 p0893 N90-15163
An experimental, analytical, and computational investigation of turbomachinery rotor flow fields
07 p0926 N90-15360
Comments on compressible flow through butterfly valves
[DE89-015730] 07 p0928 N90-15371
A coning motion apparatus for hydrodynamic model testing in a non-planar cross-flow
[AD-A213431] 07 p0930 N90-15383
Reduction of erosion in elbows due to flow modifications, phase 2
[DE89-011702] 07 p0932 N90-15394
Application of a mass-consistent wind model to chinook windstorms
[AD-A213622] 07 p0963 N90-15568
The structure of supersonic turbulent boundary layers subjected to concave surface curvature
08 p1017 N90-15883
Performance of a highly-loaded HP compressor
[RAE-TM-P-1149] 08 p1024 N90-15919
Flow visualization in the cryogenic wind tunnel
08 p1030 N90-15953
Application of the singularity-separating method to computing problems of solid-propellant combustion in a closed vessel
[PREPRINT-489] 08 p1053 N90-16086
Ambient Test Rig (ATR) flow studies: A laminar flow, reduced entrainment electrostatic precipitator
[DE90-000144] 08 p1062 N90-16142
Using the singularity-separating method to study how to decrease the pressure at the end of a tube
[PREPRINT-490] 08 p1065 N90-16158
Numerical analysis of nonstationary fluid flow (a survey)
[PREPRINT-492] 08 p1065 N90-16159
Two-Dimensional Measuring Techniques
[DGLR-PAPERS-88-04] 08 p1078 N90-16236
Coded trajectories for the investigation of strongly unsteady flow fields 08 p1078 N90-16240
Visualization of instability forms of a round free jet using a light sheet method 08 p1079 N90-16241
Visualization of gas flows using the smoke wire technique 08 p1079 N90-16242
Flow field visualization using laser light sheet methods. Quantitative analysis using image processing
08 p1079 N90-16243
Digital image interpretation for optical flow measurement methods: System description and preliminary application examples 08 p1079 N90-16244
The determination of vortex separation frequencies by means of laser light sheet images
[DNW-WTI-88.038] 08 p1079 N90-16245
Flow visualization using the laser light sheet method in vehicle aerodynamics and combustion chamber engineering 08 p1079 N90-16246
Analysis of the measuring range and the accuracy of an existing particle image velocimetry system
08 p1080 N90-16247
Determination of dynamic surface forces using piezoelectric arrays 08 p1080 N90-16249
The use of sublimation methods for the recognition of transition at low speed 08 p1080 N90-16251
Use of the film-of-oil technique for profile measurements in the Transonic Wind tunnel Brunswick (TWB)
08 p1080 N90-16252
Flow visualization of water flows using the crystal violet method 08 p1081 N90-16253
Unsteady heat transfer measurement using thermochromatic liquid crystals as temperature indicators 08 p1081 N90-16254
Surface flow visualization with shear stress sensitivive liquid crystals
[DNW-WTI-88.039] 08 p1081 N90-16255
Quantitative heat transfer measurements using heated liquid crystals 08 p1081 N90-16256
Determination of the heat transfer coefficients in separated flows using an infrared camera
08 p1081 N90-16257
Investigation of ablation phenomena using IR thermography in a hypersonic wind tunnel
08 p1081 N90-16258
Multiple flow regimes in the Northern Hemisphere winter 08 p1100 N90-16372
Controlled vortical flow on delta wings through unsteady leading edge blowing
[NASA-CR-186267] 09 p1160 N90-16712
Flowfield effects of launch on a vertically-launched missile
[AD-A214468] 09 p1160 N90-16714
Measurement of the aerodynamical coefficients related to square section models defined by resemblance to the normalized models AGARD HB1 and HB2 in supersonic flow. Part 2: Incidence up to 25 deg
[ISL-R-108/88-PT-2] 09 p1161 N90-16718
Design manual for microgravity two-phase flow and heat transfer
[AD-A214937] 09 p1201 N90-16957
Flow field observation of a hot He-CO2 jet in microgravity 09 p1201 N90-16960
An experimental study of the effect of streamwise vortices on unsteady turbulent boundary-layer separation
09 p1215 N90-17045
Low-noise nozzle valve
[NASA-CASE-MFS-28383-1] 09 p1216 N90-17051
Capillary flow properties of mesh wicks
[AD-A214769] 09 p1217 N90-17057
Advanced diagnostics for reacting flows
[AD-A215050] 09 p1217 N90-17060
Appendage flow computations using the INS3D computer code
[AD-A215689] 09 p1218 N90-17066
Development of interferometric and holographic techniques in fluid mechanics
[ISL-CO-227/88] 09 p1218 N90-17068
Formation of turbulent layers in the separated region around a body with polygonal cross section at large incidence and rolling
[ISL-R-101/88] 09 p1219 N90-17071
Theoretical study of instabilities in vortices: Applications to hydrodynamics and magnetohydrodynamics
[ETN-90-96103] 09 p1219 N90-17073
Surface acoustic wave sensors and piezoelectric actuators for investigations of transitional and turbulent flows
[AD-A214889] 09 p1279 N90-17415
Advanced diagnostics for reacting flows
[AD-A214795] 09 p1285 N90-17448
Low speed flowfield characterization by infrared measurements of surface temperatures
10 p1306 N90-17556
Time development of convection flow patterns in aircraft cabins under post-crash fire exposure
10 p1314 N90-17598
Viscous three-dimensional analyses for nozzles for hypersonic propulsion
[NASA-CR-185197] 10 p1321 N90-17635
CAST-10-2/DOA 2 Airfoil Studies Workshop Results
[NASA-CP-3052] 10 p1323 N90-17647
Nonlinear transonic Wall-Interference Assessment/Correction (WIAC) procedures and application to cast-10 airfoil results from the NASA 0.3-m TCT 8- by 24-inch Slotted Wall Test Section (SWTS)
10 p1323 N90-17648
Residual interference and wind tunnel wall adaption
10 p1324 N90-17655
Comparison of two- and three-dimensional Navier-Stokes solutions with NASA experimental data for CAST-10 airfoil 10 p1325 N90-17658
Plume flowfield analysis of the shuttle primary Reaction Control System (RCS) rocket engine
[NASA-CR-186315] 10 p1329 N90-17676
FLUSH: A tool for the design of slush hydrogen flow systems
[NASA-TM-102467] 10 p1361 N90-17890
Application of Jameson's type nonlinear artificial dissipation to the two-dimensional Navier-Stokes computation
[NAL-TR-1015T] 10 p1384 N90-18006
Liquid transverse jets in compressible crossflows
10 p1385 N90-18012
Development of an alternative concentration probe calibration method
[AD-A216245] 10 p1388 N90-18031
Experimental investigation of a chemical laser cavity flowfield
[AD-A216398] 10 p1390 N90-18038
Unsteady Euler analysis of the flow field of a propfan at an angle of attack
[NASA-TM-102425] 10 p1426 N90-18229
Computational aerodynamics of ordered vortex flows
[ETN-90-96272] 11 p1452 N90-18368
Test data of flow field of shuttle SRM nozzle joint with bond defects, using unheated air
11 p1470 N90-18464
Experimental flow models for SSME flowfield characterization 11 p1471 N90-18469
Semidiscrete Galerkin modelling of compressible viscous flow past a circular cone at incidence
[NASA-CR-186323] 11 p1505 N90-18664
Multicellular natural convection in a narrow vertical slot
[AD-A216411] 11 p1505 N90-18668
Automation and extension of LDV (Laser-Doppler Velocimetry) measurements of off-design flow in a subsonic cascade wind tunnel
[AD-A216627] 11 p1506 N90-18670
Direct simulation Monte Carlo of shock reflexion on a wedge with boundary layer
[ISL-CO-245/88] 11 p1508 N90-18681
Coronary arterial capacitance and subendocardial vascular patency throughout the cardiac cycle
11 p1538 N90-18855
On the evaluation of aerodynamic influence coefficients
[NLR-MP-87019-U] 12 p1597 N90-19191
Unsteady aerodynamics of delta wings performing maneuvers to high angle of attack
12 p1598 N90-19196
Interaction of an oblique shock wave with supersonic flow over a blunt body 12 p1598 N90-19197
A study of flows over highly-swept wings designed for maneuver at supersonic speeds
[AD-A216837] 12 p1599 N90-19202
A panel process for the calculation of the flow around a wing with front angle damping
[ETN-90-95367] 12 p1600 N90-19207
External flow computations for a finned 60mm ramjet in steady supersonic flight
[AD-A216998] 12 p1605 N90-19233
Experimental and theoretical investigations of flowfields and heat transfer in modern gas turbines
[AD-A217663] 12 p1605 N90-19237
Elastic recovery and polymer-polymer interactions
[AD-A217085] 12 p1633 N90-19384
Separation bubbles at high Reynolds number: Measurement and computation
[CUED/A-AERO/15] 12 p1657 N90-19525
An experimental investigation of the flow field around yawed stranded cables
[AD-A215782] 12 p1658 N90-19529
Flow simulation for aircraft
[NLR-MP-87082-U] 12 p1661 N90-19543
Constructibility limits of multiflow wind turbines with pivots
[ILR-MITT-215] 12 p1682 N90-19662
Spanwise measurements of vertical components of atmospheric turbulence
[NASA-TP-2963] 12 p1692 N90-19718
Siphon flows in isolated magnetic flux tubes. 3: The equilibrium path of the flux tube arch
[NASA-CR-186297] 12 p1709 N90-19813
A storage process of the magnetic energy results from the unsteady plasma flow field in the space active regions and stellar atmosphere
[DE90-610638] 12 p1717 N90-19858
Heat transfer near the entrance to a film cooling hole in a gas turbine blade
[AD-A217396] 13 p1757 N90-20089
A study of low-dimensional models for the wall region of a turbulent boundary layer 13 p1798 N90-20321
Geometric scale of interaction between moving shock and stationary thermal layer
[AD-A217769] 13 p1802 N90-20344
Experimental investigation of the mechanisms underlying vortex kinematics in unsteady separated flows
[AD-A217889] 13 p1802 N90-20348

A sub-cloud layer vorticity budget analysis for two microburst-producing storms from jaws dual-Doppler data
[AD-A218180] 13 p1847 N90-20599
Tools for 3D scientific visualization in computational aerodynamics 13 p1858 N90-20660
Laser-velocimeter-measured flow field around an advanced, swept, eight-blade propeller at Mach 0.8
[NASA-TP-2462] 14 p1909 N90-20942
Users manual for the NASA Lewis Ice Accretion Prediction Code (LEWICE)
[NASA-CR-185129] 14 p1909 N90-20943
On total variation diminishing schemes for transonic turbulent flow computation 14 p1909 N90-20945
Discrete-vortex model for the symmetric-vortex flow on cones
[NASA-TP-2989] 14 p1909 N90-20946
An approximate viscous shock layer method for calculating the hypersonic flow over blunt-nosed bodies 14 p1910 N90-20947
Comparison of C- and O-grid generation methods using a NACA 0012 airfoil
[AD-A216375] 14 p1910 N90-20948
Some aspects of Essentially Nonoscillatory (ENO) formulations for the Euler equations, part 3
[NASA-CR-4285] 14 p1910 N90-20949
Effects of nose bluntness and shock-shock interactions on blunt bodies in viscous hypersonic flows
[NASA-CR-186451] 14 p1910 N90-20950
Computation of nonequilibrium chemically reacting flows in hypersonic flow field 14 p1911 N90-20954
Measurement of lift development on rapidly-accelerated wings 14 p1911 N90-20956
Convergence acceleration of hypersonic flow calculations: A nonlinear relaxation factor 14 p1911 N90-20957
Computation of viscous flow around a propeller-shaft configuration with infinite-pitch rectangular blades 14 p1912 N90-20958
Flow in a forward swept centrifugal fan, volumes 1 and 2 14 p1912 N90-20959
Optimum hypersonic airfoils with attached shocks 14 p1912 N90-20960
An evaluation of the two-dimensional Euler and Navier-Stokes calculations based on a flux-vector splitting
[PB90-166778] 14 p1912 N90-20963
Experimental and numerical investigation of the vortex flow over a sharp edged delta wing; with and without sideslip
[PB90-167131] 14 p1913 N90-20964
Aerodynamic design techniques at DLR Institute for Design Aerodynamics 14 p1916 N90-20979
Aerodynamic design via control theory 14 p1920 N90-20998
Secondary Flows in Turbomachines
[AGARD-CP-469] 14 p1922 N90-21009
Measurement of the flow field in the blade passage and side-wall region of a plane turbine cascade 14 p1924 N90-21019
Centrifugal impeller geometry and its influence on secondary flows 14 p1924 N90-21020
The effect of secondary flow on the redistribution of the total temperature field downstream of a stationary turbine cascade 14 p1926 N90-21033
Supersonic nozzle design of arbitrary cross-section 14 p1927 N90-21035
Subsonic flutter analysis using MSC/NASTRAN
[PB90-166786] 14 p1928 N90-21041
Computer codes for the evaluation of thermodynamic properties, transport properties, and equilibrium constants of an 11-species air model
[NASA-TM-102602] 14 p1972 N90-21297
Analysis and finite element approximation of some optimal control problems associated with the Navier-Stokes equations 14 p1972 N90-21299
The effects of forcing on a single stream shear layer and its parent boundary layer
[NASA-CR-186529] 14 p1973 N90-21301
Flutter of slender bodies under axial stress
[PB90-167024] 14 p1994 N90-21425
Adaptive grid embedding for the two-dimensional flux-split Euler equations
[NASA-CR-186533] 14 p2019 N90-21571
Rectangular subsonic jet flow field measurements
[NASA-CR-181925] 14 p2023 N90-21598
Wind tunnel investigation of three sonic anemometers
[PB90-149808] 15 p2046 N90-21729
Effective methods of controlling a junction vortex system in an incompressible, three-dimensional, turbulent flow 15 p2047 N90-21732
Extension of a streamwise upwind algorithm to a moving grid system
[NASA-TM-102800] 15 p2048 N90-21739
An upwind-differencing scheme for the incompressible Navier-Stokes equations
[NASA-TM-101051] 15 p2051 N90-21757
Numerical investigation of some control methods for 3-D turbulent interactions due to sharp fins 15 p2053 N90-21764
An experimental investigation of the physical mechanisms controlling the asymmetric flow past slender bodies at large angles of attack 15 p2053 N90-21767
Theoretical and experimental study of flow-control devices for inlets of indraft wind tunnels
[NASA-TM-100050] 15 p2056 N90-21778
Prediction of length scales in a Mach reflection flowfield 15 p2089 N90-21959
Interaction of a turbulent round jet with the free surface 15 p2090 N90-21964
Recent developments in grid generation 15 p2093 N90-21976
A structured approach to interactive multiple block grid generation 15 p2094 N90-21983
A discussion on issues relating to multiblock grid generation 15 p2095 N90-21991
Bifurcations in viscous flow fields. On the genesis and development of topologically complicated separated flow structures
[PB90-167156] 15 p2099 N90-22012
The calibration and measuring procedure of a five-hole hemispherical head probe in compressible flow
[LR-585] 15 p2099 N90-22013
Herbig-Haro objects and stellar jets 15 p2186 N90-22487
Water-tunnel study results of a TF/A-18 and F/A-18 canopy flow visualization
[NASA-TM-101705] 16 p2195 N90-22532
Flow visualization in supersonic turbulent boundary layers 16 p2195 N90-22533
The minimum drag profile in laminar flow: A numerical way 16 p2196 N90-22535
Computational and experimental investigations of rotating stall in compressor cascades 16 p2201 N90-22565
Investigation of advanced counterrotation blade configuration concepts for high speed turboprop systems, task 1: Ducted propfan analysis
[NASA-CR-185217] 16 p2202 N90-22567
An investigation of the three-dimensional flow field in a centrifugal compressor 16 p2235 N90-22751
Nonlinear bifurcation study of plane Poiseuille flow
[DLR-FB-89-42] 16 p2236 N90-22756
Holocinematography for studies of turbulent multiphase flow
[AD-A219130] 16 p2237 N90-22765
A numerical study of basic coastal upwelling processes 16 p2259 N90-22878
Numerical flow simulation and supercomputers: More than a digital wind tunnel 16 p2277 N90-22976
The development of a system for the numerical simulation of Euler flows 16 p2277 N90-22980
Extension of a three-dimensional viscous wing flow analysis
[NASA-CR-182023] 17 p2344 N90-23348
Flowfield measurements in the wake of a missile at high angle of attack
[AD-A219645] 17 p2345 N90-23351
Computational analysis of the flowfield of a two-dimensional ejector nozzle
[NASA-CR-185255] 17 p2355 N90-23406
Three-dimensional analysis on flow and temperature distributions for aircraft fuel thermal stability
[AD-A219651] 17 p2383 N90-23571
Experimental study of a three-dimensional shear-driven turbulent boundary layer with streamwise adverse pressure gradient 17 p2399 N90-23669
Computations of a horseshoe vortex around an endwall-mounted cylinder 17 p2400 N90-23673
Equilibrium radiative heating tables for Earth entry
[NASA-TM-102652] 17 p2401 N90-23675
Topology of three-dimensional, variable density flows
[NASA-CR-186622] 17 p2402 N90-23683
Fast grid generation
[AD-D014454] 17 p2402 N90-23685
Composite reduced Navier Stokes procedures for flow problems with strong pressure interactions
[AD-A219621] 17 p2403 N90-23687
Fluid dynamic mechanisms and interactions within separated flows
[AD-A219628] 17 p2403 N90-23689
Thin-layer Navier-Stokes solutions of the asymmetric vortical flow on a tangent ogive body
[AD-A220810] 17 p2403 N90-23690
On the planar translation of two bodies in a uniform flow
[AD-A220143] 17 p2404 N90-23698
Effect of constitutive modeling on the dynamic development of shear bands in viscoplastic materials
[AD-A220443] 17 p2416 N90-23765
PUFFY: A puff diffusion computer model
[FOA-C-40251-4.5] 17 p2421 N90-23796
Stream field measurements of a half spheric cylinder by thin hypersonic stream with the electron radiation technique 18 p2490 N90-24232
Calculation of correction terms for forces and moment measurements in radial flow field of hypersonic spheric nozzles 18 p2490 N90-24234
The interaction of a supersonic streamwise vortex and a normal shock wave 18 p2491 N90-24241
Unsteady potential flow past a propeller blade section
[NASA-CR-4307] 18 p2493 N90-24246
Low-density flow effects for hypervelocity vehicles, phase 2
[AD-A221034] 18 p2493 N90-24249
Experimental and analytical study of close-coupled ventral nozzles for ASTOVL aircraft
[NASA-TM-103170] 18 p2498 N90-24273
A theoretical analysis of the acoustic radiation from two-dimensional turbulent mixing layers 18 p2551 N90-24559
Off-design loss measurements in a compressor cascade
[AD-A220094] 18 p2552 N90-24564
Nonlinear development of Goertler and crossflow vortices and Goertler/Tollmien-Schlichting wave interaction
[AD-A221107] 18 p2553 N90-24571
Characterization of plasma flow through magnetic nozzles
[AD-A221044] 18 p2617 N90-24905
Finite element formulations for compressible flows 18 p2632 N90-24996
AFE dynamic effects in inhomogeneous plasmas 18 p2643 N90-25053
Analysis and design of optimized truncated scarfed nozzles subject to external flow effects
[NASA-TM-103175] 19 p2654 N90-25106
A review of instability and noise propagation in supersonic flows
[NASA-CR-186800] 19 p2655 N90-25112
A lifting surface method for the calculation of steady and unsteady, incompressible propeller aerodynamics
[ESA-TT-1151] 19 p2655 N90-25113
An experimental and theoretical investigation of the flow over plane delta wings with supersonic leading edges
[LR-588] 19 p2655 N90-25114
Investigation of the vortex flow over a sharp-edged delta wing in the transonic speed regime
[LR-594] 19 p2656 N90-25115
LOX manifold tee analysis
[NASA-CR-183994] 19 p2670 N90-25188
Spatially accelerating flow in smooth open channel 19 p2687 N90-25284
Equilibrium radiative heating tables for aerobraking in the Martian atmosphere
[NASA-TM-102659] 19 p2688 N90-25290
Modeling and Applications of Transport Phenomena in Porous Media, volume 1
[VKI-LS-1990-01-VOL-1] 19 p2689 N90-25296
Discrete approach: Percolation theory 19 p2689 N90-25297
Characterization of porous media: Field level 19 p2690 N90-25304
Characterization of fluids in porous media 19 p2690 N90-25305
Boundary conditions for the Navier-Stoke's equations at an artificial boundary intersecting a solid boundary
[FFA-TN-1990-11] 19 p2691 N90-25313
Flow structures around non-hyperbolic singularities on the wall with one vanishing eigenvalue: A discussion of the flow structures and the unfoldings
[LR-586] 19 p2692 N90-25315
Surface dilation and fluid-dynamical behaviour of Newtonian liquids in an overflowing cylinder. 1: Pure liquids
[LR-601] 19 p2692 N90-25317
Identification of aerodynamic models for maneuvering aircraft
[NASA-CR-186630] 20 p2802 N90-25943
Euler analysis comparison with LDV data for an advanced counter-rotation propfan at cruise
[NASA-TM-103249] 20 p2803 N90-25946
Two-dimensional Euler and Navier-Stokes Time accurate simulations of fan rotor flows
[NASA-TM-102402] 20 p2803 N90-25948
Effect of vortex generators on the aerodynamic wing characteristics and body of revolution
[AD-A222813] 20 p2804 N90-25955
Hot gas ingestion characteristics and flow visualization of a vectored thrust STOVL concept
[NASA-TM-103212] 20 p2813 N90-26009

Supersonic reacting internal flow fields
[NASA-TM-103480] 20 p2829 N90-26094
Numerical analysis of three-dimensional particle-laden flow equations
[IAR-90-2] 20 p2860 N90-26268
Measurement of terms and parameters in turbulent models
[NASA-CR-183993] 20 p2860 N90-26271
Frontogenesis in gravity currents: An example with no known applications in oceanography
[MATHS-REPT-A-117] 20 p2863 N90-26284
Computational fluid dynamics 3-D analysis for advanced transonic turbine design
[ETN-90-97282] 20 p2864 N90-26291
Practical developments in holographic interferometry
[PNR90669] 20 p2866 N90-26302
Laser techniques for studying chemical vapor deposition
[DE90-012921] 20 p2867 N90-26311
Aircraft measurements of the turbulence structure in cirrus clouds
[ISSN-0069-5882] 20 p2890 N90-26450
High speed turboprop aeroacoustic study (counterrotation). Volume 1: Model development
[NASA-CR-185241] 20 p2923 N90-26633
Velocity measurements on a lifting rotor/airframe configuration in low speed forward flight
21 p2953 N90-26790
Installation and pretest analysis of DARPA suboff model in the DTRC anechoic wind tunnel
[AD-A221497] 21 p2955 N90-26801
Dallas/Fort Worth simulation, volume 1
[DOT/FAA/CT-TN89/28-VOL-1]
21 p2955 N90-26802
Streamlining algorithms for complete adaptation
21 p2962 N90-26841
Summary of Discussions at the Eleventh Meeting of the Sandia Cooperative Group on the Aerothermochemistry of Turbulent Combustion
[DE89-001846] 21 p2973 N90-26896
Modeling of supersonic reacting flow fields
21 p2973 N90-26898
Development of Planar Laser-Induced Fluorescence (PLIF) techniques for supersonic flows
21 p2974 N90-26900
An approximate method for calculating three-dimensional inviscid hypersonic flow fields
[NASA-TP-3018] 21 p3002 N90-27066
Rotating flow in radial turbomachinery
[AD-A222885] 21 p3004 N90-27073
Inviscid dynamics of unstable shear layers
[AD-A222297] 21 p3004 N90-27077
Parallel numerical simulations of axisymmetric projectile flows using zonal-overlapped grids
[AD-A221711] 21 p3005 N90-27082
Numerical investigation of the incompressible plane shear layer between two gases with different densities
[ETN-90-97315] 21 p3006 N90-27084
Heat and momentum transfer to test samples in the high velocity plasma furnace
[AD-A222182] 21 p3079 N90-27505
Three-dimensional cavity flow fields at subsonic and transonic speeds
[NASA-TM-4209] 22 p3107 N90-27650
Aerodynamics of a linear oscillating cascade
[NASA-TM-103250] 22 p3108 N90-27657
Near-wall modeling of compressible turbulent flows
[NASA-CR-186961] 22 p3109 N90-27658
Jet vortex generators for turbulent flow separation control
[NASA-CR-186959] 22 p3109 N90-27659
Study of the compressibility effects on the turbulence of supersonic drags
[ETN-90-97448] 22 p3109 N90-27661
Computer code for predicting coolant flow and heat transfer in turbomachinery
[NASA-TP-2985] 22 p3120 N90-27722
On computations of the integrated space shuttle flowfield using overset grids
[NASA-CR-186927] 22 p3124 N90-27734
Nonequilibrium radiation and chemistry models for aerocapture vehicle flowfields
[NASA-CR-186728] 22 p3169 N90-27973
Numerical investigation of laminar-turbulent transition in a flat plate wake
[AD-A222462] 22 p3170 N90-27978
Numerical investigation of the thermal stratification in cryogenic tanks subjected to wall heat flux
[NASA-TM-103194] 22 p3171 N90-27984
Flowfield computation of entry vehicles
[NASA-CR-186946] 22 p3171 N90-27986
Analytical resolution of the Oseens differential equation of inclined turning cylinder with gliding
[ETN-90-97316] 22 p3171 N90-27988
Formation of shock waves in a transonic vortex-profile interaction
[MPIS-3/1990] 22 p3174 N90-28010
Nonequilibrium radiation and chemistry models for aerocapture vehicle flowfields
[NASA-CR-186379] 23 p3267 N90-28490
Control of submersible vortex flows
[NASA-TM-102693] 23 p3267 N90-28493
Regular and chaotic motion of uniform elliptical vortices in external linear time dependent velocity fields
23 p3268 N90-28497
In-flight flow visualization with pressure measurements at low speeds on the NASA F-18 high alpha research vehicle
[NASA-TM-101726] 23 p3270 N90-28505
Effects of canard position on the aerodynamic characteristics of a close-coupled canard configuration at low speed
23 p3272 N90-28519
Numerical simulations of flowfields in a central-dump ramjet combustor. 3: Effects of chemistry
[AD-A224145] 23 p3282 N90-28573
On the use of Lagrangian variables in descriptions of unsteady boundary-layer separation
[NASA-CR-182071] 23 p3323 N90-28789
A study of heat and fluid flow phenomena on the gas side of circular-tube plate-fin heat exchangers
23 p3324 N90-28795
An experimental investigation of a single and multiphase confined coaxial jet
23 p3324 N90-28796
Effects of flowfield turbulence on asymmetric vortices over a slender body
[AD-A224139] 23 p3328 N90-28819
Theoretical investigation of non-equilibrium chemistry and optical radiation in hypersonic flow fields
[NASA-CR-186335] 24 p3417 N90-29300
Numerical simulations of blade-vortex interactions and lifting hovering rotor flows
[AD-A224238] 24 p3417 N90-29302
A package for 3-D unstructured grid generation, finite-element flow solution and flow field visualization
[NASA-CR-182090] 24 p3419 N90-29309
Calculation of turbulent air streams in driver cabs
[ETN-90-97320] 24 p3419 N90-29310
Measurement Techniques for Hypersonic Flows
[VKI-LS-1990-05] 24 p3419 N90-29314
Interferometry 24 p3419 N90-29315
Velocity interferometry 24 p3420 N90-29316
Laser velocimetry 24 p3420 N90-29317
Electron-beam fluorescence measurements in hypersonic flows 24 p3420 N90-29318
Applications of LIF to high speed flows
24 p3420 N90-29320
Laser induced fluorescence imaging applications
24 p3420 N90-29322
Laser induced fluorescence: Practical applications
24 p3421 N90-29323
A numerical calculation of hypersonic flow around blunt bodies using upwind difference scheme
[NAL-TR-1025] 24 p3422 N90-29331
Experimental study on the dynamic behavior of a revolving blade grill
[REPT-NT-89-CC-18] 24 p3470 N90-29604
Calculation of flow fields by the solution of the Euler equations using an extended finite volume discretization scheme
[ESA-TT-1204] 24 p3470 N90-29605
Wind tunnel, field, and numerical investigations of plume downwash and dispersion at an arctic industrial site
24 p3489 N90-29721

FLOW EQUATIONS
NT BOUNDARY LAYER EQUATIONS
NT HELMHOLTZ VORTICITY EQUATION
NT NAVIER-STOKES EQUATION
NT REYNOLDS EQUATION
NT VORTICITY EQUATIONS
Boost-phase discrimination research activities
[NASA-TM-101889] 01 p0032 N90-10176
A conforming spectral collocation strategy for Stokes flow through a channel contraction
[NASA-CR-181912] 02 p0263 N90-11495
Direct discretization of planar div-curl problems
[NASA-CR-181935] 02 p0263 N90-11498
A multigrid method combined with defect correction for free convection problems at high Rayleigh numbers
[REPT-89-27] 03 p0396 N90-12264
CFD methods for drag prediction and analysis currently in use in UK
[RAE-TM-AERO-2146] 04 p0448 N90-12563
Surface current and wave modulation measurements over bottom topography: A comparison with theory
[AD-A212469] 04 p0522 N90-13011
Balance laws and centro velocity in dissipative systems
[MEMO-797] 05 p0639 N90-13726
The Eighteenth Conference on Stochastic Processes and their Applications
[AD-A212301] 08 p1040 N90-16010
A new finite element formulation for CFD:8. The Galerkin/least-squares method for advective-diffusive equations
[DE89-636437] 08 p1116 N90-16462
Turbulence models for compressive flows
10 p1308 N90-17568
Conical Euler solution for a highly-swept delta wing undergoing wing-rock motion
[NASA-TM-102609] 12 p1600 N90-19211
Spectral simulation of unsteady compressible flow past a circular cylinder
[NASA-CR-182030] 13 p1750 N90-20050
Composite-grid techniques and adaptive mesh refinement in computational fluid dynamics
[AD-A217383] 13 p1800 N90-20328
Some aspects of Essentially Nonoscillatory (ENO) formulations for the Euler equations, part 3
[NASA-CR-4285] 14 p1910 N90-20949
Multigrid accelerated relaxation solution of transonic full potential flow equation
[PD-CF-8942] 14 p1910 N90-20951
Computation of nonequilibrium chemically reacting flows in hypersonic flow field 14 p1911 N90-20954
Aerodynamic design via control theory
14 p1920 N90-20998
A quasi-Lagrangian moving grid technique for investigating compressible flows
14 p1972 N90-21298
Depth-averaged equations for turbulent free-surface flow
[PB90-164781] 14 p1974 N90-21308
Finite element algorithms for hyperbolic conservation laws with forcing terms
[INPE-5024-RPE/617] 14 p2022 N90-21595
Partial acoustic filtering applied to the equations of compressible flow
[DE90-000673] 15 p2097 N90-22001
Investigation of advanced counterrotation blade configuration concepts for high speed turboprop systems, task 1: Ducted propfan analysis
[NASA-CR-185217] 16 p2202 N90-22567
Gas dynamic theory of flight of fast electron flux in plasma
[DE90-618767] 16 p2319 N90-23220
Numerical modelling of shocks in gases and metals
[AD-A218586] 17 p2402 N90-23684
Modeling studies of the LeeUwin current using a high-resolution primitive equation model
[AD-A219595] 17 p2430 N90-23846
Numerical analysis of three-dimensional particle-laden flow equations
[IAR-90-2] 20 p2860 N90-26268
Computational fluid dynamics for missiles
[RAE-TM-AERO-2171] 20 p2863 N90-26288
The finite analytic method and its applications. Volume 1: Laminar and turbulent flows past two-dimensional and axisymmetric bodies
[AD-A222787] 20 p2864 N90-26294
Two-phase heat transport systems for spacecraft scaling with respect to gravity
[NLR-TP-89127-U] 21 p2965 N90-26857
Rotating flow in radial turbomachinery
[AD-A222885] 21 p3004 N90-27073
Three-dimensional structure of boundary layers in transition to turbulence
[AD-A223242] 21 p3004 N90-27076
FINFLO: A finite-volume based computer program for two-dimensional and axisymmetric compressible flow
[PB90-189473] 22 p3169 N90-27974
Computational Fluid Dynamics, Volume 2
[VKI-LS-1990-03-VOL-2] 22 p3172 N90-27993
On unstructured grids and solvers
22 p3172 N90-27994
Computation of compressible, vortical flows
22 p3172 N90-27996
Efficient solution of the steady Euler equations with a centered implicit method 22 p3173 N90-27999
Fluctuation splitting for multidimensional convection problems: An alternative to finite volume and finite element methods 22 p3173 N90-28000
Computational Fluid Dynamics for Industrial Flows
[VKI-LS-1990-04] 22 p3173 N90-28001
POLYFLOW theoretical background
22 p3173 N90-28005
The PHOENICS flow-simulation system
22 p3174 N90-28006
FLUENT and FLUENT/BFC CFD computer programs
22 p3174 N90-28008
Towards a two dimensional code of anisotropic Godunov type 22 p3175 N90-28018
Vertically averaged spectral model for tidal circulation in estuaries. Part 1: Model formulation
[PB90-181678] 22 p3230 N90-28319

Supersonic/hypersonic aerodynamics and heat transfer for projectile design using viscous-inviscid interaction
| AD-A224354 | 24 p3418 N90-29303
Numerical simulation supersonic free shear layers
| AD-A223771 | 24 p3418 N90-29306
Barotropic mechanisms associated with tropical plume formation 24 p3489 N90-29719

FLOW FIELDS
U FLOW DISTRIBUTION

FLOW GEOMETRY
A composite velocity procedure for the three-dimensional reduced Navier-Stokes equations 01 p0069 N90-10396
A parallel numerical simulation for supersonic flows using zonal overlapped grids and local time steps for common and distributed memory multiprocessors
| DE89-015252 | 02 p0147 N90-10839
Analytical studies of three-dimensional combustion processes
| AD-A211903 | 03 p0323 N90-11837
A theoretical study of ingress for shrouded rotating disk systems with radial outflow
| PNR90586 | 04 p0455 N90-12607
Automatic analysis and exploitation of the flow visualization images
| ETN-89-95712 | 04 p0501 N90-12887
Flow in the neighborhood of an ellipsoid cylinder of revolution model
| ONERA-RT-22/7252-AN-000A | 04 p0502 N90-12895
A knowledge-based approach to automated flow-field zoning for computational fluid dynamics
| NASA-TM-101072 | 04 p0528 N90-13048
Julia-Fatou-Sullivan theory for real one-dimensional dynamics
| REPT-88-100 | 04 p0548 N90-13190
Block-structured solution of three-dimensional transonic flows using parallel processing
| AD-A212851 | 05 p0572 N90-13330
The influence of multiple hot-wire probe geometry on the results of measurements in turbulent flows
| DLR-FB-89-26 | 05 p0639 N90-13724
Numerical Methods for Flows in Turbomachinery, volume 1
| VKI-LS-1989-06-VOL-1 | 05 p0640 N90-13735
Comparison of integral and finite-difference methods for predicting the turbulent boundary layer on axisymmetric bodies
| ARE-TM(UHA)-88512 | 05 p0643 N90-13752
A computational analysis of the transonic flow field of two-dimensional minimum length nozzles 06 p0718 N90-14194
Selection of the energy-efficient enhancement geometry for single-phase turbulent flow inside tubes
| DE89-017690 | 06 p0777 N90-14519
Experimental flow models for SSME flowfield characterization 11 p1471 N90-18469
An experimental investigation of the flow field around yawed stranded cables
| AD-A215782 | 12 p1658 N90-19529
Analytical study of the origin and behavior of asymmetric vortices
| NASA-TM-102796 | 15 p2049 N90-21746
Generation of circumferential velocity contours associated with pulsed point suction on a rotating disk 18 p2646 N90-25065
Instabilities: Miscible and immiscible flows 19 p2689 N90-25298
Effects of forebody geometry on subsonic boundary-layer stability
| NASA-CR-4314 | 20 p2802 N90-25939
The finite analytic method and its applications. Volume 1: Laminar and turbulent flows past two-dimensional and axisymmetric bodies
| AD-A222787 | 20 p2864 N90-26294

FLOW MEASUREMENT
Wide-range fuel flowmeter, phase 2
| AD-A210547 | 01 p0074 N90-10424
Jet-flow from shock tubes
| AD-A210651 | 02 p0220 N90-11260
Development of an adaptive time of flight system for the measurement of fluid flow velocity 02 p0222 N90-11273
Advanced measurement techniques, part 1 04 p0441 N90-12520
Flow quality measurements in compressible subsonic flows 04 p0441 N90-12521
Hot-film system for transition detection in cryogenic wind tunnels 04 p0441 N90-12522
Predicted and hot-film measured Tollmien-Schlichting wave characteristics 04 p0441 N90-12523
Remote detection of boundary-layer transition by an optical system 04 p0441 N90-12524
Three-component laser Doppler velocimeter measurements in a juncture flow 04 p0441 N90-12525
Basic aerodynamic research facility for comparative studies of flow diagnostic techniques 04 p0441 N90-12526
Recent tests at Langley with a University of Tennessee Space Institute (UTSI) skin friction balance 04 p0441 N90-12527
Development of an anti-Stokes coherent Raman diffusion system for measuring hypersonic flow
| ONERA-RSF-1/7301-PY | 04 p0459 N90-12630
Effect of pipe roughness on orifice flow measurement
| PB89-231484 | 04 p0500 N90-12880
Measurements of coefficients of discharge for concentric flange-tapped square-edged orifice meters in water over the Reynolds number range 600 to 2,700,000
| PB89-235147 | 04 p0502 N90-12892
Experimental study of homogeneous turbulence submitted to rotational effects
| ONERA-RSF-10/1145-AY-164A | 04 p0502 N90-12894
Skin friction measurements with hot elements 05 p0574 N90-13345
Pressure measurement techniques in use at the Royal Aerospace Establishment 05 p0574 N90-13347
The influence of multiple hot-wire probe geometry on the results of measurements in turbulent flows
| DLR-FB-89-26 | 05 p0639 N90-13724
On the nonexistence of a strong solution in the boundary problem for a sticky Brownian motion
| CWI-BS-R8901 | 05 p0689 N90-14018
Reactive flow measurements and calculations for ZrH2-based composite explosives
| DE90-000831 | 06 p0755 N90-14393
Rotor induced-inflow-ratio measurements and CAMRAD calculations
| NASA-TP-2946 | 08 p1017 N90-15882
Ambient flow studies and particulate collection measurements: A laminar flow, reduced entrainment electrostatic precipitator
| DE90-001457 | 08 p1063 N90-16149
Measurement of the p, v, T behavior under microgram conditions
| ETN-90-95906 | 08 p1065 N90-16162
Optical flow measuring method using diode lasers, phase coupled arrays, and high frequency pulsed diode lasers 08 p1067 N90-16176
Low flow vortex shedding flowmeter 08 p1156 N90-16700
Optimum location of flow conditioners in a 4-inch orifice meter
| PB90-111675 | 09 p1216 N90-17049
Automation and extension of LDV (Laser-Doppler Velocimetry) measurements of off-design flow in a subsonic cascade wind tunnel
| AD-A216627 | 11 p1506 N90-18670
Transient heat transfer measurements on a flat plate in turbulent flow using an electrical analog
| AD-A216286 | 11 p1573 N90-19057
Nonintrusive optical measurements of turbulence and mixing in a stably stratified fluid 13 p1799 N90-20322
A method for measuring the material moduli of granular materials: Flow in an orthogonal rheometer
| DE90-007160 | 13 p1801 N90-20339
Laser velocimeter measurements of multiphase flow of solids
| DE90-007604 | 14 p1974 N90-21311
The calibration and measuring procedure of a five-hole hemispherical head probe in compressible flow
| LR-585 | 15 p2099 N90-22013
Advanced instrumentation for local measurement of gas-solid suspension flows
| DE90-008498 | 17 p2400 N90-23671
Method of forming a multiple layer dielectric and a hot film sensor therewith
| NASA-CASE-LAR-13678-1 | 17 p2478 N90-24168
Three-dimensional laser velocimeter simultaneity detector
| NASA-CASE-ARC-11876-1 | 19 p2696 N90-25340
Installation and pretest analysis of DARPA suboff model in the DTRC anechoic wind tunnel
| AD-A221497 | 21 p2955 N90-26801
Investigation of factors affecting data comparison 22 p3119 N90-27714
Gas-film flow in tubes
| DE90-011528 | 23 p3324 N90-28793
Measurement Techniques for Hypersonic Flows
| VKI-LS-1990-05 | 24 p3419 N90-29314
Interferometry 24 p3419 N90-29315
Experimental study on the dynamic behavior of a revolving blade grill
| REPT-NT-89-CC-18 | 24 p3470 N90-29604

FLOW PATTERNS
U FLOW DISTRIBUTION

FLOW RATE
U FLOW VELOCITY

FLOW REGULATORS
Bio-reactor chamber
| NASA-CASE-MSC-20929-1 | 09 p1250 N90-17252
The accelerated cooling in GTS plate mill
| ETN-90-97019 | 19 p2682 N90-25256

FLOW RESISTANCE
NT AERODYNAMIC DRAG
NT FRICTION DRAG
NT SUPERSONIC DRAG
NT VISCOUS DRAG
Acquisition and correlation of cryogenic nitrogen mass flow data through a multiple orifice Joule-Thomson device
| NASA-TM-103121 | 16 p2237 N90-22761
Flow resistance and critical shear stress in steep channels 19 p2687 N90-25282
A numerical study of the response of the laminar unsteady separated flow about a circular cylinder to changes of boundary conditions
| DLR-FB-90-10 | 24 p3471 N90-29613

FLOW SEPARATION
U BOUNDARY LAYER SEPARATION
U SEPARATED FLOW

FLOW STABILITY
NT BOUNDARY LAYER STABILITY
NT FLAME STABILITY
NT MAGNETOHYDRODYNAMIC STABILITY
Recent developments in Ramjet pressure oscillation technology 01 p0036 N90-10199
Numerical solution of three-dimensional unsteady flows: Application to instability problems 01 p0065 N90-10375
Wide-range fuel flowmeter, phase 2
| AD-A210547 | 01 p0074 N90-10424
Elimination of spurious eigenvalues in the Chebyshev tau spectral method
| PB89-209282 | 03 p0345 N90-11967
A study of the temporal stability of multiple cell vortices
| NASA-CR-4261 | 03 p0345 N90-11968
Research in Natural Laminar Flow and Laminar-Flow Control, part 1
| NASA-CP-2487-PT-1 | 04 p0438 N90-12503
Long-range LFC transport 04 p0439 N90-12508
Stability theory applications to laminar-flow control 04 p0439 N90-12513
Numerical study of three-dimensional spatial instability of a supersonic flat plate boundary layer
| NASA-CR-181931 | 04 p0499 N90-12874
Effect of suction and cooling on the stability of subsonic and supersonic boundary layers 05 p0642 N90-13745
A note concerning the onset of three dimensionality and time dependence in Goertler vortices
| NASA-CR-181956 | 06 p0718 N90-14193
Effects of flame stretch on the propagation, extinction, and stability of premixed flames 06 p0739 N90-14301
An entropy based approach to nonlinear stability 06 p0773 N90-14500
The stability of Taylor-Couette flow with radial heating 06 p0774 N90-14502
Dynamics of baroclinic instability in rapid cyclogenesis 07 p0962 N90-15563
Detection of flow instabilities at airfoil profiles using piezoelectric arrays 08 p1067 N90-16175
Visualization of instability forms of a round free jet using a light sheet method 08 p1079 N90-16241
Viscous effects on the instability of an axisymmetric jet
| NASA-TM-102396 | 09 p1161 N90-16719
A method for the early detection of instabilities in rotordynamics
| NASA-CR-186307 | 09 p1170 N90-16769
TS - Dean interactions in curved channel flow
| NASA-CR-181983 | 10 p1306 N90-17559
A method for the prediction of supersonic compressor blade performance
| CUED/A-TURBO/TR-126 | 10 p1321 N90-17634
Numerical simulation of unstably stratified sheared flows
| DE90-005396 | 10 p1384 N90-18008
The inviscid stability of supersonic flow past a sharp cone
| NASA-CR-181996 | 11 p1451 N90-18363
Dryout stability and inception at low flowrates
| DE90-006955 | 11 p1509 N90-18692
Turbulent mixing effects in models of thermal blooming
| DE90-007245 | 12 p1667 N90-19580
Amplitude-dependent neutral modes in compressible boundary layer flows
| NASA-TM-102524 | 13 p1799 N90-20326
Analytical study of the origin and behavior of asymmetric vortices
| NASA-TM-102796 | 15 p2049 N90-21746

Modern developments in shear flow control with swirl
[NASA-CR-186586] 15 p2097 N90-22000
A new stability criterion in the shallow-water system for two-dimensional coherent eddies in the atmosphere and oceans 15 p2130 N90-22176
Effect of a crystal-melt interface on Taylor-vortex flow
[NASA-CR-186512] 15 p2171 N90-22408
Reynolds stress closure in jet flows using instability wave modeling 15 p2196 N90-22534
Parallel channel flow excursions
[DE90-009129] 16 p2235 N90-22753
Nonlinear bifurcation study of plane Poiseuille flow
[DLR-FB-89-42] 16 p2236 N90-22756
Numerical study of the onset of instability in the flow past a sphere 17 p2400 N90-23672
Nonlinear interactions in mixing layers and compressible heated round jets
[NASA-CR-186303] 17 p2400 N90-23674
The stability of two-dimensional wakes and shear-layers at high Mach numbers
[NASA-CR-182050] 17 p2401 N90-23676
Unsteady flow phenomena in turbomachines
[AD-A218370] 17 p2402 N90-23680
Generation of circumferential velocity contours associated with pulsed point suction on a rotating disk 18 p2646 N90-25065
A study of non-uniqueness and instability for convex materials
[DE90-012060] 19 p2689 N90-25294
Instabilities: Miscible and immiscible flows 19 p2689 N90-25298
Reaction and transport in porous media 19 p2690 N90-25300
Stability theory for methods to solve the Navier-Stokes equations, part 1
[FFA-TN-1988-65-PT-1] 19 p2691 N90-25312
Experimental investigation of Tollmien-Schlichting instability and transition in similar boundary layer flow in an adverse pressure gradient (Hartree beta = -0.14)
[LR-604] 19 p2692 N90-25318
New discharge pumping method for CO2 lasers
[AD-A220898] 20 p2866 N90-26307
Flow induced nutation instability in spinning solid propellant rockets
[AD-A222504] 21 p2969 N90-26877
Direct numerical simulation of compressible free shear flows 21 p2974 N90-26901
On the linear and nonlinear stability of non-parallel flow 21 p3002 N90-27065
Three-dimensional structure of boundary layers in transition to turbulence
[AD-A223242] 21 p3004 N90-27076
Local and global resonances in heated 2-D jets
[AD-A221671] 21 p3005 N90-27079
Conjugate gradient methods for constrained least squares problems
[AD-A222706] 21 p3063 N90-27411
Aqueous solution properties of ampholytic ionomers
[AD-A222152] 22 p3156 N90-27890
Entropy wave instability in compact ramjets 22 p3162 N90-27932
Solution of the Orr-Sommerfeld equation for three dimensional incompressible flow using Galerkin method and Chebichev polynomials: The COCIP code
[CERT-46/5618-34-DERAT] 22 p3176 N90-28021
Experimental investigations on the stability and vorticity of the vortex breakdown phenomenon above delta wings, measured by the ultrasonic laser method
[ESA-TT-1079] 23 p3268 N90-28498
Secondary instabilities in compressible boundary layers
[NASA-CR-182091] 23 p3269 N90-28502
Stabilization of Taylor-Couette flow due to time-periodic outer cylinder oscillation
[PB90-219130] 23 p3323 N90-28790
Unstable phenomena in mechanical systems
[AD-A223640] 24 p3537 N90-30001

FLOW THEORY
NT MIXING LENGTH FLOW THEORY
Two-phase potential flow 01 p0067 N90-10387
Concepts and experiments on space-time chaos
[ETN-90-96255] 11 p1508 N90-18683
Mathematical modeling of fluid-solid mixtures
[DE90-009152] 15 p2098 N90-22007
Nonstrictly hyperbolic conservation laws
[AD-A218525] 16 p2237 N90-22762
Applications of polyhedral combinatorics to multicommodity flows and compact surfaces
[CWI-BS-R8921] 17 p2462 N90-24060
Short proofs on multicommodity flows and cuts
[CWI-BS-R8922] 17 p2462 N90-24061
On the structure at infinity of a structured system
[CWI-BS-R8918] 17 p2468 N90-24108
An analysis of flow models: From Navier-Stokes to potential flow equations 22 p3173 N90-28002
POLYFLOW theoretical background 22 p3173 N90-28005

FLOW VELOCITY
NT SOLAR WIND VELOCITY
The role of particle collisions in pneumatic transport 01 p0068 N90-10392
A composite velocity procedure for the three-dimensional reduced Navier-Stokes equations 01 p0069 N90-10396
Capillary effects in steady-state flow in heterogeneous cores
[DE89-000758] 01 p0070 N90-10399
Wide-range fuel flowmeter, phase 2
[AD-A210547] 01 p0074 N90-10424
Laser anemometer measurements in a transonic axial-flow fan rotor
[NASA-TP-2879] 02 p0218 N90-11245
The structure of Reynolds stress in the near wall region of a turbulent pipe flow 02 p0218 N90-11247
An experimental study of helicity and related properties in turbulent flows
[DE89-016785] 02 p0220 N90-11259
Gas-phase flowrate effect on disintegrating cryogenic liquid-jets
[NASA-TM-102357] 02 p0223 N90-11277
Some implications of the isotropic momentarily frozen assumptions for the SPAN-MAT program
[NASA-CR-181937] 03 p0301 N90-11704
Air velocity mapping of environmental test chambers
[AD-A212082] 03 p0310 N90-11764
Three-component laser Doppler velocimeter measurements in a juncture flow 04 p0441 N90-12525
Experimental studies on Goertler vortices 04 p0442 N90-12529
Stage effects on stalling and recovery of a high-speed 10-stage axial-flow compressor 04 p0454 N90-12600
Development of an anti-Stokes coherent Raman diffusion system for measuring hypersonic flow
[ONERA-RSF-1/7301-PY] 04 p0459 N90-12630
Measurements of coefficients of discharge for concentric flange-tapped square-edged orifice meters in water over the Reynolds number range 600 to 2,700,000
[PB89-235147] 04 p0502 N90-12892
A new generation of atmospheric tracers: The biological connection
[AD-A212285] 04 p0517 N90-12983
Measurement Techniques in Aerodynamics
[VKI-LS-1989-05] 05 p0573 N90-13339
Practical systems for speckle velocimetry 05 p0574 N90-13341
Laser two focus techniques 05 p0575 N90-13348
Coherent structures in a round jet 05 p0640 N90-13733
Numerical Methods for Flows in Turbomachinery, volume 1
[VKI-LS-1989-06-VOL-1] 05 p0640 N90-13735
Unsteady forces induced on finite-span cylinders in a cross-flow 05 p0642 N90-13746
Fluid flow analysis of the SSME high pressure fuel and oxidizer turbine coolant systems
[NASA-CR-183736] 06 p0734 N90-14277
Fluid-particle interaction in solid-liquid two-phase grid turbulence 06 p0773 N90-14496
Embedded function methods for compressible high speed turbulent flow
[NASA-CR-186131] 06 p0773 N90-14498
Heat transfer to a stationary and moving sphere immersed in a fluidized bed 06 p0774 N90-14503
An experimental investigation of shear layer mixing in supersonic flows 06 p0775 N90-14508
Pipe and bend erosion by pneumatic transport of solids at high temperature
[DE89-015741] 06 p0778 N90-14524
Ion collection by probing objects in flowing magnetized plasmas
[DE90-001711] 06 p0845 N90-14916
Gelled propellant flow: Boundary layer theory for power-law fluids in a converging planar channel
[DE90-000923] 07 p0927 N90-15365
Determination of flow-regime boundaries for cohesive particles
[DE90-001405] 07 p0928 N90-15369
Comments on compressible flow through butterfly valves
[DE89-015730] 07 p0928 N90-15371
Experimental determination of the fluid velocity by spectral analysis of temperature fluctuations
[DE89-636430] 07 p0928 N90-15372
Experimental measurements of the laminar separation bubble on an Eppler 387 airfoil at low Reynolds numbers
[NASA-CR-186263] 07 p0929 N90-15380
Reduction of erosion in elbows due to flow modifications, phase 2
[DE89-011702] 07 p0932 N90-15394
Pipeline vibrations. Fluid transients in non-rigid, unbranched planar piping systems
[ESDU-89030] 07 p0948 N90-15491
Ambient Test Rig (ATR) flow studies: A laminar flow, reduced entrainment electrostatic precipitator
[DE90-000144] 08 p1062 N90-16142
Analysis of the measuring range and the accuracy of an existing particle image velocimetry system 08 p1080 N90-16247
Further development of the PIV method for use in the large wind tunnel 08 p1080 N90-16248
A space-time discretization procedure for wave propagation problems
[NASA-TM-102215] 08 p1105 N90-16399
Low flow vortex shedding flowmeter 08 p1156 N90-16700
Development and application of oxygen flow tagging for velocity measurements and flow visualization in turbulent three-dimensional supersonic flows
[AD-A214491] 09 p1160 N90-16715
Heterogeneous combustion processes under microgravity conditions 09 p1202 N90-16965
Doppler imagery for the visualisation of velocity fields
[ISL-CO-232/88] 09 p1226 N90-17114
Effect of propellant flowrate and purity on carbon deposition in LO2/methane gas generators 11 p1471 N90-18468
Numerical investigations of heat transfer and flow rates in rotating cavities. Simulation of the movement generated by wall temperature gradients, by source-sink mass flows or by the differential rotation of the walls, under the influence or coriolis and centrifugal forces
[ETN-90-96253] 11 p1510 N90-18695
Study on the thermodynamical and mechanical conditions for the generation of high operating pressures with liquefied gases for low and very low flow rates
[ESA-TT-1148] 11 p1510 N90-18696
Study of interfacial behavior in cocurrent gas-liquid flows
[DE90-005988] 12 p1659 N90-19532
Development and utilization of new diagnostics for dense-phase pneumatic transport
[DE90-006787] 12 p1659 N90-19536
Accretion flows in high mass star formation
[DE90-007251] 12 p1744 N90-20027
Nonintrusive optical measurements of turbulence and mixing in a stably stratified fluid 13 p1799 N90-20322
Characterization of fluid flow by digital correlation of scattered light
[NASA-CR-186403] 13 p1799 N90-20324
Relating flow between counter-rotating propellers to aerodynamic interaction noise 14 p1909 N90-20944
LDV measurements and the flow analysis in the vortex region of a radial inflow turbine 14 p1922 N90-21007
SAR image coding 14 p1964 N90-21246
The effects of forcing on a single stream shear layer and its parent boundary layer
[NASA-CR-186529] 14 p1973 N90-21301
Laser velocimeter measurements of multiphase flow of solids
[DE90-007604] 14 p1974 N90-21311
Fire propagation in concurrent flows
[PB90-151754] 15 p2066 N90-21834
Automated analysis of measured turbulent boundary flow
[PB90-147844] 15 p2092 N90-21970
On dual Lagrangian hyperbolic models for one dimensional two phase flow problems
[DE90-007012] 15 p2098 N90-22004
Experimental observations on transition to turbulence in confined coaxial jets and other boundary layer flows
[DE90-008939] 15 p2098 N90-22005
Parallel channel flow excursions
[DE90-009129] 16 p2235 N90-22753
Arcjet load characteristics
[NASA-TM-103190] 19 p2669 N90-25181
Activities report of the Hydraulics Research Laboratory
[ETN-90-96568] 19 p2687 N90-25281
Effect of initial conditions on the development of two-phase jets
[AD-A222621] 20 p2864 N90-26293
Experimental study of an unsteady boundary layer on an oscillating plane plate. Optimization and validation of calculation code for the analysis of the potential flow/boundary layer coupling in the neighborhood of a plane plate and an oscillating profile
[ETN-90-97436] 22 p3175 N90-28013
Experimental study of the Taylor-Goertler instability
[ETN-90-97447] 22 p3175 N90-28014
Towards a two dimensional scheme of anisotropic Godunov type. On the calculation of the velocity of the nodes in the multidimensional Lagrangian codes
[ETN-90-97458] 22 p3175 N90-28017

Towards a two dimensional code of anisotropic Godunov type 22 p3175 N90-28018
On the calculation of the velocity of the nodes in the multidimensional Lagrangian codes 22 p3175 N90-28019
Velocity interferometry 24 p3420 N90-29316
Electron beam for velocity determination 24 p3420 N90-29319
Laser induced fluorescence: Practical applications 24 p3421 N90-29323
Analysis of scramjet engine characteristics [NAL-TR-1041] 24 p3434 N90-29398
Technique for the measurement of noise of the flow associated to the small wave numbers of the turbulence spectra [ETN-90-97558] 24 p3469 N90-29601
Frequency and ventilation: A survey of theoretical and experimental ventilation modelling [LR-625] 24 p3498 N90-29772

FLOW VISUALIZATION
NT NUMERICAL FLOW VISUALIZATION
Flow visualization techniques for flight research 02 p0153 N90-10878
The near-wake flow structure of wake-cylinder interaction and surface loading of cylinder 02 p0218 N90-11248
Application of the wide-field shadowgraph technique to rotor wake visualization [NASA-TM-102222] 03 p0300 N90-11700
Advanced technology in military gas turbine design and manufacture [PNR90545] 03 p0307 N90-11747
Experimental research on swept shock Wave/Boundary layer interactions [AD-A211744] 03 p0348 N90-11988
Advanced measurement techniques, part 1 04 p0441 N90-12520
Recent flow visualization studies in the 0.3-m TCT 04 p0442 N90-12528
Experimental studies on Goertler vortices 04 p0442 N90-12529
Improved 2D numerical simulation model for strongly coupled heat and fluid flow in a thermal storage [PB89-218879] 04 p0500 N90-12878
Study of forces and moments on wing-bodies at high incidence, volumes 1 and 2 05 p0575 N90-13350
A smoke generator system for aerodynamic flight research [NASA-TM-4137] 05 p0578 N90-13372
A vapor generator for transonic flow visualization [NASA-TM-101670] 05 p0584 N90-13403
Visualization of boundary layer transition zone movement on oscillating airfoils with shear-sensitive liquid-crystal coatings [DE89-009570] 06 p0721 N90-14210
Flow visualization of the effect of pitch rate on the vortex development on the scale model of a F-18 fighter aircraft [AD-A214244] 07 p0876 N90-15080
Special Course on Advances in Cryogenic Wind Tunnel Technology [AGARD-R-774] 08 p1028 N90-15939
Flow visualization in the cryogenic wind tunnel 08 p1030 N90-15953
Study of flow around a sphere in a hydraulic test tunnel [CERT-1/2313/MES] 08 p1064 N90-16156
Visualization of 2 and 3 dimensional flows [REPT-1] 08 p1065 N90-16164
Flow field visualization study on a 65 deg delta wing at M = 0.85 08 p1068 N90-16182
Two-Dimensional Measuring Techniques [DGLR-PAPERS-88-04] 08 p1078 N90-16236
Visualization of instability forms of a round free jet using a light sheet method 08 p1079 N90-16241
Visualization of gas flows using the smoke wire technique 08 p1079 N90-16242
Flow field visualization using laser light sheet methods. Quantitative analysis using image processing 08 p1079 N90-16243
Flow visualization using the laser light sheet method in vehicle aerodynamics and combustion chamber engineering 08 p1079 N90-16246
Analysis of the measuring range and the accuracy of an existing particle image velocimetry system 08 p1080 N90-16247
Further development of the PIV method for use in the large wind tunnel 08 p1080 N90-16248
Flow visualization of water flows using the crystal violet method 08 p1081 N90-16253
Surface flow visualization with shear stress sensitivive liquid crystals [DNW-WTI-88.039] 08 p1081 N90-16255
Development and application of oxygen flow tagging for velocity measurements and flow visualization in turbulent three-dimensional supersonic flows [AD-A214491] 09 p1160 N90-16715
Development of flow visualization and nonintrusive velocity measurement in turbulent flow [ETN-90-96077] 09 p1161 N90-16717
Viscous effects on the instability of an axisymmetric jet [NASA-TM-102396] 09 p1161 N90-16719
Advanced diagnostics for reacting flows [AD-A215050] 09 p1217 N90-17060
Effect of vortex circulation on injectant from a single film-cooling hole and a row of film-cooling holes in a turbulent boundary layer. Part 1: Injection beneath the vortex downwash [AD-A215288] 09 p1218 N90-17063
Development of interferometric and holographic techniques in fluid mechanics [ISL-CO-227/88] 09 p1218 N90-17068
Doppler imagery for the visualisation of velocity fields [ISL-CO-232/88] 09 p1226 N90-17114
Sampling scattered data onto rectangular grids for volume visualization [AD-A215533] 09 p1274 N90-17384
A wind tunnel study of a sting-mounted circulation control wing [AD-A216248] 10 p1310 N90-17577
Fluctuating wind forces measured on a bluff body extending from a cavity [AD-A216414] 10 p1386 N90-18020
Aerodynamic testing of a rotating wind turbine blade [DE90-000312] 11 p1451 N90-18362
Supersonic wind tunnel investigation of a tubular projectile [ISL-CO-306/89] 11 p1452 N90-18366
Half model tests on an ONERA calibration model in the transonic wind tunnel Goettingen, Federal Republic of Germany [DLR-MITT-89-20] 11 p1452 N90-18370
A study on deformation and break-up of dispersed particles in elongational flow [ETN-90-96268] 11 p1508 N90-18684
Water-tunnel investigation of concepts for alleviation of adverse inlet spillage interactions with external stores [NASA-TM-4181] 12 p1599 N90-19199
Dynamics of a class of vortex rings [NASA-TM-102257] 12 p1657 N90-19524
An experimental investigation of the flow field around yawed stranded cables [AD-A215782] 12 p1658 N90-19529
Characterization of fluid flow by digital correlation of scattered light [NASA-CR-186403] 13 p1799 N90-20324
Flow visualization studies in a curved rectangular channel with 40 to 1 aspect ratio and a straight channel with bulk flow unsteadiness [AD-A218020] 13 p1803 N90-20348
Tools for 3D scientific visualization in computational aerodynamics 13 p1858 N90-20660
Research on cascade secondary and tip-leakage flows: Periodicity and surface flow visualization 14 p1925 N90-21026
Theoretical study of the flow in a rotating channel. Experimental study through flow visualization in a curved channel 14 p1926 N90-21032
Interaction of a turbulent round jet with the free surface 15 p2090 N90-21964
Experimental observations on transition to turbulence in confined coaxial jets and other boundary layer flows [DE90-008939] 15 p2098 N90-22005
Water-tunnel study results of a TF/A-18 and F/A-18 canopy flow visualization [NASA-TM-101705] 16 p2195 N90-22532
Flow visualization in supersonic turbulent boundary layers 16 p2195 N90-22533
Experimental study of vortex ring interaction with a free surface 16 p2233 N90-22742
A new stochastic model of turbulent dispersion in the convective planetary boundary layer and the results of the Atterbury-87 field study 16 p2254 N90-22853
Natural convection liquid immersion cooling of high density columns of discrete heat sources in a vertical channel [AD-A218388] 17 p2402 N90-23681
Fluid dynamic and acoustic experiments on turbomachine rotors subject to variable flow conditions [AD-A220298] 18 p2552 N90-24565
A laser-induced fluorescence technique for measurement of slot-injected fluid concentration profiles in a plate turbulent boundary layer [AD-A221388] 18 p2553 N90-24572
Ground evaluation of seeding an in-flight wingtip vortex using infrared imaging flow visualization technique 18 p2639 N90-25035
Investigation of the vortex flow over a sharp-edged delta wing in the transonic speed regime [LR-594] 19 p2656 N90-25115
Boiling/evaporative heat transfer from spheres in packed-bed thermal energy storage units [DE90-012023] 19 p2711 N90-25430
Space plane model for visual measurement of aerodynamic heating [DE90-505514] 20 p2803 N90-25949
Hot gas ingestion characteristics and flow visualization of a vectored thrust STOVL concept [NASA-TM-103212] 20 p2813 N90-26009
Informatics aspects of large flow calculations on the SX-2 supercomputer [NLR-MP-88037-U] 20 p2864 N90-26290
Practical developments in holographic interferometry [PNR90669] 20 p2866 N90-26302
Holography and holographic interferometry [PNR90670] 20 p2866 N90-26303
Experiments with unsteady, free surface, three-dimensional vortices in a thermally stable, stratified fluid [AD-A222088] 21 p2954 N90-26796
Flow visualization of dynamic stall on an oscillating airfoil [AD-A222202] 21 p2954 N90-26797
Testing of 3-D models in 2-D adaptive wall test sections 21 p2962 N90-26842
An optical study of the flow start-up process in four convergent-divergent nozzles [AD-A222918] 21 p2963 N90-26846
Study of the structure of the vortices created by the drag of a natched edge by thermal tracing [IMFL-89-26] 22 p3109 N90-27660
Study of missiles in flight [ETN-90-97457] 22 p3109 N90-27662
In-flight flow visualization with pressure measurements at low speeds on the NASA F-18 high alpha research vehicle [NASA-TM-101726] 23 p3270 N90-28505
Free shear layer and swirl flow heat transfer enhancement [PB90-228123] 23 p3325 N90-28798
Experimental investigations on the stability and transition of three-dimensional boundary layers [ESA-TT-1026] 23 p3325 N90-28803
Studies of vortex interactions [AD-A223864] 23 p3328 N90-28817
Applications of LIF to high speed flows 24 p3420 N90-29320
Laser induced fluorescence: Practical applications 24 p3421 N90-29323
Numerical Grid Generation [VKI-LS-1990-06] 24 p3470 N90-29606

FLOWMETERS
NT GAS METERS
NT HOT-WIRE FLOWMETERS
NT RHEOMETERS
Wide-range fuel flowmeter, phase 2 [AD-A210547] 01 p0074 N90-10424
Development of an adaptive time of flight system for the measurement of fluid flow velocity 02 p0222 N90-11273
Measurements of coefficients of discharge for concentric flange-tapped square-edged orifice meters in water over the Reynolds number range 600 to 2,700,000 [PB89-235147] 04 p0502 N90-12892
Low flow vortex shedding flowmeter 08 p1156 N90-16700
The application of fiber optic technology to flowmeters [AD-A214389] 10 p1430 N90-18247
In-situ permeable flow sensor [DE90-008806] 14 p1983 N90-21364
Specifications, tolerances, and other technical requirements for weighing and measuring devices as adopted by the 74th National Conference on Weights and Measures, 1989 (1990 edition) [PB90-184961] 23 p3316 N90-28748

FLUCTUATION
U VARIATIONS

FLUENCE
Improved model for solar cosmic ray exposure in manned Earth orbital flights [NASA-TP-2987] 18 p2639 N90-25031
Departures from plane-wave-like coupling to a Maverick missile in the radiating near-field region of a horn antenna [AD-A222539] 21 p2997 N90-27035

FLUID BOUNDARIES
NT GAS-SOLID INTERFACES
NT LIQUID-LIQUID INTERFACES
NT LIQUID-SOLID INTERFACES
NT LIQUID-VAPOR INTERFACES
Numerical calculations of the collapse of a cavity in the vicinity of a compliant wall [AD-A210489] 01 p0070 N90-10403

On the computation of normal modes of a rotating, viscous, incompressible fluid with a capillary free boundary
[REPT-89-01] 03 p0348 N90-11989
Solution of potential flow past an elastic body using the boundary element technique
[AD-A213843] 07 p0931 N90-15390
Anomalous waves in shock wave - fluid interface collisions
[AD-A213584] 08 p1062 N90-16144
Mass transfer induced convection near gas-liquid interfaces
[ETN-90-96925] 18 p2552 N90-24568
A laser-induced fluorescence technique for measurement of slot-injected fluid concentration profiles in a plate turbulent boundary layer
[AD-A221388] 18 p2553 N90-24572

FLUID DYNAMICS
NT AERODYNAMICS
NT AEROTHERMODYNAMICS
NT COMPUTATIONAL FLUID DYNAMICS
NT ELASTOHYDRODYNAMICS
NT ELECTROHYDRODYNAMICS
NT GAS DYNAMICS
NT HYDRODYNAMICS
NT HYPERSONICS
NT INTERACTIONAL AERODYNAMICS
NT MAGNETOHYDRODYNAMICS
NT RAREFIED GAS DYNAMICS
NT ROTONS
NT ROTOR AERODYNAMICS
NT SUPERSONICS
NT UNSTEADY AERODYNAMICS
NT VORTEX SHEDDING
Quasi-diffusion between phonon and roton gases in two- and three-dimensional liquid helium
[AD-A210565] 02 p0192 N90-11096
Some new algorithms for boundary value problems in smooth particle hydrodynamics
[AD-A211728] 03 p0348 N90-11987
Dynamics of baroclinic wave systems 03 p0362 N90-12072
A least-squares finite element method for incompressible Navier-Stokes problems
[NASA-TM-102385] 03 p0392 N90-12231
A review of quasi-coherent structures in a numerically simulated turbulent boundary layer
[NASA-TM-102191] 05 p0638 N90-13723
Application of multi-grid methods for solving the Navier-Stokes equations
[NASA-TM-102359] 05 p0687 N90-14002
Laser velocimeter and total pressure measurements in circular-to-rectangular transition ducts
[NASA-CR-182286] 06 p0772 N90-14494
An experimental and theoretical study of the aeroacoustics of external-Coanda gas flares 06 p0773 N90-14495
On the application of subcell resolution to conservation laws with stiff source terms
[NASA-TM-102384] 06 p0833 N90-14844
Unsteady three-dimensional thin-layer Navier-Stokes solutions on dynamic blocked grids 07 p0874 N90-15069
Saltation and suspension of particulate matter in air
[AD-A213618] 07 p0960 N90-15552
Numerical methods for parabolic equations and inequalities in very high dimensions
[AD-A214102] 07 p0985 N90-15690
Swirl-stabilized flames: Fluid dynamics, mixing, and flame stability limits 08 p1040 N90-16009
Experiment facilities for materials and fluid sciences embarked on Spacelab
[ESA-SP-1120] 08 p1053 N90-16089
Measurement of the p, v, T behavior under microgram conditions
[ETN-90-95906] 08 p1085 N90-16162
An improvement of convection fidelity in Euler calculations 09 p1159 N90-16709
Unsteadiness of supersonic and hypersonic shock induced turbulent boundary layer separation 10 p1309 N90-17572
Turbulence scale effects on heat transfer in a linear turbine cascade
[AD-A216222] 10 p1321 N90-17637
Microgravity noncontact temperature requirements at NASA Lewis Research Center 10 p1362 N90-17897
Non-Contact Temperature Requirements (NCTM) for drop and bubble physics 10 p1366 N90-17918
Fluid transmission line dynamics for signals of finite amplitude
[AD-A215758] 10 p1385 N90-18014
Modeling the wake as a continuous vortex sheet in a potential-flow solution using vortex panels
[AD-A216220] 10 p1385 N90-18016
Summer Study Program in Geophysical Fluid Dynamics: The Influence of Convection on Large-Scale Circulations, 1988
[AD-A216024] 11 p1535 N90-18840
Proceedings of a contractors meeting on Combustion Rocket Propulsion Diagnostics of Reacting Flow
[AD-A216445] 12 p1617 N90-19297
An experimental investigation of the flow field around yawed stranded cables
[AD-A215782] 12 p1658 N90-19529
Aerodynamic analysis of a US Navy and Marine Corps unmanned air vehicle
[AD-A218282] 13 p1755 N90-20077
Modification and improvement of software for modeling multidimensional reacting fuel flows
[AD-A217789] 13 p1783 N90-20235
A simple multicomponent fluid theory with accurate physics
[DE90-008537] 13 p1801 N90-20334
DURIP optical equipment for high-speed viscous-inviscid interaction research
[AD-A217772] 13 p1802 N90-20345
Spacelab qualified infrared imager for microgravity science experiments
[NASA-TM-102503] 13 p1804 N90-20352
Nonlinear stability in fluid and plasma dynamics
[AD-A217735] 13 p1892 N90-20856
The modelling of heat and mass transfer near solid boundaries and comparison with experimental results
[PB90-167040] 14 p1974 N90-21310
High accuracy solutions of incompressible Navier-Stokes equations
[NASA-TM-102539] 14 p2018 N90-21567
WINCOF-I code for prediction of fan compressor unit with water ingestion
[NASA-CR-185157] 15 p2045 N90-21724
Modeling of vortex-induced oscillations based on indicial response approach
[NASA-CR-186560] 15 p2047 N90-21736
The effects of tortuosity on flow through a natural fracture
[DE90-009193] 15 p2129 N90-22172
Pseudo-steady diffusional growth or collapse of bubbles rising in time dependent pressure fields
[AD-A218825] 16 p2237 N90-22764
Fluid dynamic mechanisms and interactions within separated flows
[AD-A219628] 17 p2403 N90-23689
On upwind formulations and non equilibrium chemistry
[DLC/FLU-INT-TN-014] 17 p2403 N90-23691
Design and manufacturing of an APTF to test fluid behaviour in microgravity environment 18 p2541 N90-24506
Fluid dynamic and acoustic experiments on turbomachine rotors subject to variable flow conditions
[AD-A220298] 18 p2552 N90-24565
Spectral transport model for turbulence
[DE90-011265] 19 p2689 N90-25295
ICASE semiannual report, April 1 - September 30, 1989
[NASA-CR-181988] 19 p2727 N90-25502
Transatmospheric vehicle research
[NASA-CR-186705] 20 p2807 N90-25970
Carbon deposition model for oxygen-hydrocarbon combustion. Task 6: Data analysis and formulation of an empirical model
[NASA-CR-183986] 20 p2829 N90-26095
New findings and instrumentation from the NASA Lewis microgravity facilities
[NASA-TM-103189] 20 p2842 N90-26163
Bubble, Drop and Particle Unit (BDPU): A multi-user microgravity facility
[IAF-89-431] 20 p2842 N90-26164
Low-gravity fluid physics: A program overview
[NASA-TM-103215] 20 p2861 N90-26273
Fluid Dynamics Panel Working Group 12 on Adaptive Wind Tunnel Walls: Technology and Applications
[AGARD-AR-269] 21 p2961 N90-26838
Summary of Discussions at the Eleventh Meeting of the Sandia Cooperative Group on the Aerothermochemistry of Turbulent Combustion
[DE89-001846] 21 p2973 N90-26896
Flux flow and flux dynamics in high-T(sub c) superconductors 22 p3136 N90-27797
Numerical investigation of laminar-turbulent transition in a flat plate wake
[AD-A222462] 22 p3170 N90-27978
Implicit solution of three-dimensional internal turbulent flows
[NASA-TM-103099] 22 p3170 N90-27982
An improved k-epsilon model for near-wall turbulence and comparison with direct numerical simulation
[NASA-TM-103221] 22 p3171 N90-27983
Numerical solution for the velocity-derivative skewness of a low-Reynolds-number decaying Navier-Stokes flow
[NASA-TM-103186] 22 p3171 N90-27985
The reduction of smoke emissions from Allison T56 engines
[ARL-PROP-R-182] 23 p3277 N90-28547
Thermal transfers in unsteady compressible inviscid flow
[ETN-90-97557] 24 p3419 N90-29311
Theoretical study of the interaction between an oblique shock wave and a turbulent boundary layer from a heated wall
[ONERA-RSF-87/7078/AY-100-A] 24 p3419 N90-29313
The development and evaluation of numerical algorithms for MIMD computers
[NASA-TM-101167] 24 p3526 N90-29939

FLUID FILLED SHELLS
NT LIQUID FILLED SHELLS
Coupled BE/FE/BE approach for scattering from fluid-filled structures 18 p2570 N90-24649

FLUID FILMS
NT SQUEEZE FILMS
Structural studies of sputter-deposited MoS2 solid lubricant films
[AD-A212407] 04 p0481 N90-12759
Thickness, velocity, and temperature measurements in falling liquid films
[DE90-004290] 08 p1063 N90-16151
Use of the film-of-oil technique for profile measurements in the Transonic Wind tunnel Brunswick (TWB) 08 p1080 N90-16252
Microcomputer enhanced optical investigation of spreading and evaporative processes in ultra thin films
[DE90-006323] 11 p1492 N90-18585
Life of concentrated contacts in the mixed EHD and boundary film regimes
[AD-A216673] 11 p1517 N90-18738
Numerical and experimental analysis of a thin liquid film on a rotating disk related to development of a spacecraft absorption cooling system
[NASA-CR-183457] 12 p1657 N90-19523
Improved analytical capabilities for foil air bearings, phase 1
[AD-A218071] 14 p1987 N90-21389
A high-speed photography study of cavitation in a dynamically loaded journal bearing
[NASA-TM-103178] 20 p2872 N90-26338
Current research in cavitating fluid films
[NASA-TM-103184] 23 p3323 N90-28791
Gas-film flow in tubes
[DE90-011528] 23 p3324 N90-28793

FLUID FILTERS
NT AIR FILTERS
Some observations on liquid flow through filters
[AERE-R-13300] 16 p2234 N90-22748
Laboratory study of ion-neutral collisions at suprathermal energies
[AD-A222117] 21 p3074 N90-27475

FLUID FLOW
NT ADIABATIC FLOW
NT AIR CURRENTS
NT AIR FLOW
NT AIR JETS
NT ANNULAR FLOW
NT AXIAL FLOW
NT AXISYMMETRIC FLOW
NT BAROTROPIC FLOW
NT BASE FLOW
NT BLASIUS FLOW
NT BLOOD FLOW
NT BOUNDARY LAYER FLOW
NT BOUNDARY LAYER SEPARATION
NT CAPILLARY FLOW
NT CASCADE FLOW
NT CAVITATION FLOW
NT CHANNEL FLOW
NT COAXIAL FLOW
NT COMBUSTIBLE FLOW
NT COMPRESSIBLE FLOW
NT CONICAL FLOW
NT CONTINUUM FLOW
NT CONVECTIVE FLOW
NT COOLING FLOWS (ASTROPHYSICS)
NT CORE FLOW
NT CORNER FLOW
NT COUETTE FLOW
NT COUNTERFLOW
NT CRITICAL FLOW
NT CROSS FLOW
NT DUCTED FLOW
NT EQUILIBRIUM FLOW
NT EQUIPOTENTIALS
NT FREE FLOW
NT FREE MOLECULAR FLOW
NT FUEL FLOW
NT GAS FLOW
NT HARTMANN FLOW
NT HELICAL FLOW

NT HYPERSONIC FLOW
NT INCOMPRESSIBLE FLOW
NT INLET FLOW
NT INVISCID FLOW
NT ISOTHERMAL FLOW
NT JET FLOW
NT JET MIXING FLOW
NT JET STREAMS (METEOROLOGY)
NT KARMAN-BODEWADT FLOW
NT KNUDSEN FLOW
NT LAMINAR FLOW
NT LIQUID FLOW
NT MAGNETOHYDRODYNAMIC FLOW
NT MASS FLOW
NT MERIDIONAL FLOW
NT MOLECULAR FLOW
NT MULTIPHASE FLOW
NT NONEQUILIBRIUM FLOW
NT NONNEWTONIAN FLOW
NT NONUNIFORM FLOW
NT NOZZLE FLOW
NT ONE DIMENSIONAL FLOW
NT OPEN CHANNEL FLOW
NT ORIFICE FLOW
NT OSCILLATING FLOW
NT PARALLEL FLOW
NT PIPE FLOW
NT PLASTIC FLOW
NT POTENTIAL FLOW
NT PROPELLANT TRANSFER
NT RADIAL FLOW
NT RAYLEIGH-BENARD CONVECTION
NT REATTACHED FLOW
NT RECIRCULATIVE FLUID FLOW
NT SECONDARY FLOW
NT SEPARATED FLOW
NT SHEAR FLOW
NT SINGLE-PHASE FLOW
NT SOLIDS FLOW
NT STAGNATION FLOW
NT STEADY FLOW
NT STEAM FLOW
NT STOKES FLOW
NT STRATIFIED FLOW
NT SUBSONIC FLOW
NT SUPERCRITICAL FLOW
NT SUPERSONIC FLOW
NT SUPERSONIC JET FLOW
NT THREE DIMENSIONAL FLOW
NT TRANSITION FLOW
NT TRANSONIC FLOW
NT TURBULENT FLOW
NT TWO DIMENSIONAL FLOW
NT TWO PHASE FLOW
NT UNIFORM FLOW
NT UNSTEADY FLOW
NT VERTICAL AIR CURRENTS
NT VISCOUS FLOW
NT WALL FLOW
NT WATER FLOW
NT WEDGE FLOW

Analysis of a model and sequential numerical method for thermal reservoir simulation
|DE89-015117| 01 p0067 N90-10384

PORFLO-3: A mathematical model for fluid flow, heat, and mass transport in variably saturated geologic media: Users manual, version 1.0
|DE89-013977| 01 p0069 N90-10398

An atmospheric pressure flow reactor: Gas phase kinetics and mechanism in tropospheric conditions without wall effects 02 p0203 N90-11160

On a Taylor Weak Statement for finite element computations in gas dynamics 02 p0219 N90-11251

Development of an adaptive time of flight system for the measurement of fluid flow velocity
02 p0222 N90-11273

Analytical studies of three-dimensional combustion processes
|AD-A211903| 03 p0323 N90-11837

Vortex dynamics
|AD-A212119| 04 p0499 N90-12877

Improved 2D numerical simulation model for strongly coupled heat and fluid flow in a thermal storage
|PB89-218879| 04 p0500 N90-12878

Analysis of high speed pneumatic actuation systems under rotary directional on-off flow control
04 p0507 N90-12926

Application of a self-adaptive grid method to complex flows
|NASA-TM-102223| 05 p0571 N90-13324

SSME LOX post flow analysis/fluid structure interaction. Volume 1: Flow analysis
|NASA-CR-183677| 05 p0637 N90-13715

Fluid flow analysis of the SSME high pressure fuel and oxidizer turbine coolant systems
|NASA-CR-183736| 06 p0734 N90-14277

The fluid mechanics of filters
06 p0773 N90-14499

On the application of subcell resolution to conservation laws with stiff source terms
|NASA-TM-102384| 06 p0833 N90-14844

Single fluid simulations of plasma openings switch behavior
|DE90-002643| 07 p0921 N90-15330

Calibration of seven-hole pressure probes for use in fluid flows with large angularity
|NASA-TM-102200| 07 p0933 N90-15399

Thickness, velocity, and temperature measurements in falling liquid films
|DE90-004290| 08 p1063 N90-16151

Measurement of the p, v, T behavior under microgram conditions
|ETN-90-95906| 08 p1065 N90-16162

Colinear fluctuating wall shear stress and fluctuating pressure transducer
|AD-D014296| 08 p1076 N90-16226

Studies of density distributions in one-dimensional shock-induced debris clouds
|DE90-004089| 08 p1085 N90-16282

Computation of fluid flow and heat transfer in rotating disc-systems 09 p1215 N90-17044

Development of interferometric and holographic techniques in fluid mechanics
|ISL-CO-227/88| 09 p1218 N90-17068

Sampling scattered data onto rectangular grids for volume visualization
|AD-A215533| 09 p1274 N90-17384

The role of computational fluid dynamics in missile aerodynamics 10 p1304 N90-17547

Numerical simulation of unstably stratified sheared flows
|DE90-005396| 10 p1384 N90-18008

Colliding natural convection boundary layer flow in a rectangular enclosure
|DE90-005397| 10 p1384 N90-18009

Spacecraft thermal control design data, volume 4
|ESA-PSS-03-108-ISSUE-1-VOL-4|
11 p1469 N90-18458

Experimental flow models for SSME flowfield characterization 11 p1471 N90-18469

Modeling convective Marangoni flows with void movement in the presence of solid-liquid phase change
|DE90-006474| 11 p1509 N90-18690

Fluidization mechanisms in slurry flow
|DE90-006497| 11 p1509 N90-18691

Numerical and experimental analysis of a thin liquid film on a rotating disk related to development of a spacecraft absorption cooling system
|NASA-CR-183457| 12 p1657 N90-19523

An experimental study of the aeroelastic behaviour of two parallel interfering circular cylinders
12 p1673 N90-19609

Application of natural isotopes in groundwater for solving environmental problems
|DE90-000223| 12 p1689 N90-19703

Modeling studies of electrolyte flow and bubble behavior in advanced Hall cells
|DE90-007013| 13 p1795 N90-20303

Characterization of fluid flow by digital correlation of scattered light
|NASA-CR-186403| 13 p1799 N90-20324

Interior fluid dynamics of liquid-filled projectiles
|AD-A217630| 13 p1800 N90-20330

A simple multicomponent fluid theory with accurate physics
|DE90-006537| 13 p1801 N90-20334

Hydrodynamic interactions and transport coefficients in a suspension of spherical particles
|DE90-008301| 13 p1801 N90-20336

A nonintrusive method for measuring the operating temperature of a solenoid-operated valve
|DE90-007576| 13 p1804 N90-20355

Seismic characterization of fracture properties
|DE90-007759| 13 p1841 N90-20570

Direct sublimation of NaCl salt from carbon matrixes
|DE90-007927| 14 p1946 N90-21139

Apparatus for mixing solutions in low gravity environments
|NASA-CASE-MFS-26047-1| 14 p1958 N90-21209

Mixing of viscous fluids: Behavior of microstructures and chaos
|DE90-008871| 14 p1973 N90-21304

The effect of viscosity on the resistive tearing mode with the presence of shear flow
|DE90-009340| 14 p1974 N90-21312

In-situ permeable flow sensor
|DE90-008806| 14 p1983 N90-21364

Fiber optic void fraction sensor
|DE90-009124| 14 p1983 N90-21366

Instabilities and vortex dynamics in shear flow of magnetized plasmas
|DE90-009448| 14 p2030 N90-21643

A multiblock/multizone code (PAB 3D-v2) for the three-dimensional Navier-Stokes equations: Preliminary applications
|NASA-CR-182032| 15 p2049 N90-21745

Numerical simulation model of hydrazine attitude control thrusters
|INPE-4965-PRE/1534| 15 p2068 N90-21848

Applications of algebraic grid generation
15 p2093 N90-21979

Heat-transfer regimes in nuclear-reactor-pumped gas lasers
|DE90-002904| 15 p2103 N90-22032

Beam propagation in direct nuclear pumped laser amplifiers
|DE90-009613| 15 p2104 N90-22035

The effects of tortuosity on flow through a natural fracture
|DE90-009193| 15 p2129 N90-22172

In-situ fracture stiffness determination
|DE90-009202| 15 p2129 N90-22173

Numerical modelling of shocks in gases and metals
|AD-A218586| 17 p2402 N90-23684

Fast grid generation
|AD-D014454| 17 p2402 N90-23685

Fluid connectors for operation in space
18 p2536 N90-24465

Theoretical studies of non-Newtonian and Newtonian fluid flow through porous media
|DE90-011610| 18 p2554 N90-24576

Heat and fluid flow within the Earth's crust: In situ measurements and mathematical models
18 p2579 N90-24690

Network modeling of fluid flow in porous media
19 p2690 N90-25306

The flow of non Newtonian fluids in porous media
19 p2691 N90-25307

Thermohydraulics of a heat dissipating debris bed
19 p2691 N90-25310

Listening to turbulence: An example of scientific audiolization
|DE90-010637| 19 p2753 N90-25646

Prediction of the ullage gas thermal stratification in a NASP vehicle propellant tank experimental simulation using FLOW-3D
|NASA-TM-103217| 20 p2841 N90-26160

Computational experience with a three-dimensional rotary engine combustion model
|NASA-TM-103104| 20 p2861 N90-26275

Heat exchanger with oscillating flow
|NASA-CASE-LAR-14033-1| 21 p3004 N90-27072

On the spatial eigenvalue approach to high Reynolds number flow in a rotating and nutating cylinder
|AD-A221710| 21 p3005 N90-27081

Flux motion effects in Tl-Ca-Ba-Cu-O thin films
|DE90-012176| 21 p3080 N90-27514

POLYFLOW theoretical background
22 p3173 N90-28005

Solution of Euler equations using finite element method and the kinetic decomposition of the flows: Study of the self-adaptation of the grid and of the calculation field
|CERT-1/334700-DERI-GAN| 22 p3176 N90-28020

A study of heat and fluid flow phenomena on the gas side of circular-tube plate-fin heat exchangers
23 p3324 N90-28795

An experimental investigation of a single and multiphase confined coaxial jet 23 p3324 N90-28796

Laser velocimetry 24 p3420 N90-29317

FLUID INJECTION
NT GAS INJECTION
NT LIQUID INJECTION

Development of a fully automated fluid resupply interface system 18 p2506 N90-24324

FLUID JETS
NT AIR JETS
NT FREE JETS
NT GAS JETS
NT HYDRAULIC JETS

The decay of viscoelastic fluid jets
|ETN-89-94667| 02 p0221 N90-11270

Three component laser Doppler measurements in an axisymmetric jet
|NASA-CR-181908| 03 p0300 N90-11702

Two dimensional orifice array, monodisperse drop source, phase 1
|AD-A211319| 04 p0500 N90-12881

Supercritical fluid chromatography/supersonic jet spectroscopy
|DE90-001378| 06 p0740 N90-14308

Liquid transverse jets in compressible crossflows
10 p1385 N90-18012

UV and VUV spectroscopy and photochemistry of small molecules in a supersonic jet 20 p2947 N90-26771

Supercritical fluid chromatography/supersonic jet spectroscopy
|DE90-015220| 24 p3447 N90-29465

FLUID MANAGEMENT
Evaluation of supercritical cryogen storage and transfer systems for future NASA missions
|NASA-TM-102394| 02 p0160 N90-10912
Evolutionary space station fluids management strategies
|NASA-CR-185137| 02 p0175 N90-10983
Independent Orbiter Assessment (IOA): Assessment of the orbiter main propulsion system FMEA/CIL, volume 1
|NASA-CR-185559-VOL-1| 03 p0312 N90-11775
Independent Orbiter Assessment (IOA): Assessment of the main propulsion subsystem FMEA/CIL, volume 2
|NASA-CR-185559-VOL-2| 03 p0313 N90-11776
Independent Orbiter Assessment (IOA): Assessment of the main propulsion subsystem FMEA/CIL, volume 3
|NASA-CR-185559-VOL-3| 03 p0313 N90-11777
Independent Orbiter Assessment (IOA): Assessment of the main propulsion subsystem FMEA/CIL, volume 4
|NASA-CR-185559-VOL-4| 03 p0313 N90-11778
Vibration isolation technology: Sensitivity of selected classes of space experiments to residual accelerations
|NASA-CR-185443| 04 p0482 N90-12768
CryoTran user's manual, version 1.0
|NASA-TM-102468| 07 p0973 N90-15622
Flight experiment hardware for sounding rocket investigations. Materials science and fluid sciences
|ESA-SP-1116| 08 p1038 N90-15998
Design manual for microgravity two-phase flow and heat transfer
|AD-A214937| 09 p1201 N90-16957
Hydrogen/oxygen SPE (trademark) electrochemical devices for zero-g applications 10 p1333 N90-17710
Spacecraft attitude impacts on COLD-SAT non-vacuum jacketed LH2 supply tank thermal performance
|NASA-TM-103158| 16 p2207 N90-22592
Acquisition and correlation of cryogenic nitrogen mass flow data through a multiple orifice Joule-Thomson device
|NASA-TM-103121| 16 p2237 N90-22761

FLUID MECHANICS
NT AERODYNAMICS
NT AEROTHERMODYNAMICS
NT COMPUTATIONAL FLUID DYNAMICS
NT ELASTOHYDRODYNAMICS
NT ELECTROHYDRODYNAMICS
NT FLUID DYNAMICS
NT GAS DYNAMICS
NT HYDRODYNAMICS
NT HYDROMECHANICS
NT HYDROSTATICS
NT HYPERSONICS
NT INTERACTIONAL AERODYNAMICS
NT MAGNETOHYDRODYNAMICS
NT PNEUMATICS
NT RAREFIED GAS DYNAMICS
NT ROTONS
NT ROTOR AERODYNAMICS
NT SUPERSONICS
NT UNSTEADY AERODYNAMICS
NT VORTEX SHEDDING
Flow visualization techniques for flight research 02 p0153 N90-10878
Numerical analysis, scientific computing and fundamental studies of fluid mechanics
|DE89-017554| 03 p0346 N90-11975
Tank pressure control experiment on the space shuttle
|NASA-TM-102313| 05 p0615 N90-13590
The fluid mechanics of filters 06 p0773 N90-14499
Interfacial area in two-phase flow
|DE90-002210| 06 p0778 N90-14527
Comments on ER (Electrorheological) fluid rheology
|DE90-002892| 07 p0894 N90-15166
A coning motion apparatus for hydrodynamic model testing in a non-planar cross-flow
|AD-A213431| 07 p0930 N90-15383
Test techniques for cryogenic wind tunnels 08 p1030 N90-15952
Absorption fluids data survey: 1989 update
|DE90-003985| 08 p1096 N90-16346
Experimental and theoretical research on the injection of ignition gases into a bed of inert powder
|ISL-CO-251/88| 11 p1485 N90-18547
Analytic solutions for the decay of turbulent swirling flow in a cylinder
|DE90-005744| 11 p1507 N90-18677
Velocity measurement using interferometry
|ISL-CO-221/88| 11 p1512 N90-18709
Multiple versus single scattering of terrestrial infrared longwave radiation in an aerosol-laden planetary boundary layer
|AD-A217709| 13 p1790 N90-20272
Fluid dynamics analysis of a rotating axisymmetric part using FIDAP
|DE90-008733| 13 p1802 N90-20340
Development and application of a generalized dynamic wake theory for lifting rotors 15 p2046 N90-21731
Fundamental studies on hydrology, hydraulics and geometry of river networks
|AD-A218662| 16 p2250 N90-22830
Technical accomplishments of the NASA Lewis Research Center, 1989
|NASA-TM-102296| 17 p2486 N90-24220
An interactive boundary-layer method for unsteady airfoil flows. Part 1: Quasi-steady-state model
|AD-A221220| 18 p2493 N90-24250
Thermodynamic and fluid mechanic analysis of rapid pressurization in a dead-end tube 18 p2631 N90-24990
Optical techniques for determination of normal shock position in supersonic flows for aerospace applications
|NASA-TM-103201| 19 p2693 N90-25323
Fluid Phase Separation (FPS) experiment for flight on a space shuttle Get Away Special (GAS) canister
|NASA-CR-186830| 20 p2841 N90-26161
Isothermal compressibility of SPC/E water
|AD-A222723| 20 p2925 N90-26643
ARLSUPER version 1.0, program users guide
|AD-A222693| 21 p2953 N90-26793
Study of ground effects on flying scaled models 23 p3275 N90-28532
A hybrid perturbation-Galerkin technique for partial differential equations
|NASA-CR-182085| 23 p3327 N90-28814
Rheology of filler rubber: Silica-silicone
|AD-A223600| 24 p3455 N90-29511
Effect of particulate fillers on the rheology of polymer melts
|AD-A223601| 24 p3455 N90-29512
Solid particle erosion in turbulent flows past tube banks
|DE90-015711| 24 p3469 N90-29598

FLUID POWER
Jam resistant fluid power actuator for ballistic-damage tolerant redundant cylinder assemblies
|AD-D014360| 12 p1671 N90-19600
Experiments on liquid immersion natural convection cooling of leadless chip carriers mounted on ceramic substrate
|AD-A219893| 17 p2478 N90-24167

FLUID PRESSURE
NT WATER PRESSURE
Contributions of individual structural modes to the scattered acoustic field
|AD-A219128| 16 p2314 N90-23187
Apparatus to determine the complex mass of a viscous fluid contained in a rigid porous solid from acoustic pressure measurements
|AD-A223709| 24 p3472 N90-29619

FLUID TRANSMISSION LINES
Fluid transmission line dynamics for signals of finite amplitude
|AD-A215758| 10 p1385 N90-18014
Fluid connectors for operation in space 18 p2536 N90-24465
Engineering test results for the Moog Single Line Disconnect
|NASA-TM-100755| 22 p3132 N90-27776

FLUID TRANSPIRATION
U TRANSPIRATION

FLUID-SOLID INTERACTIONS
NT GAS-METAL INTERACTIONS
NT GAS-SOLID INTERACTIONS
Interpretation and modeling of the averaged equations for a fluid-solid flow 01 p0068 N90-10388
Modal analysis of fluid-structure systems by parallel subspace iteration 02 p0181 N90-11024
Numerical models for exterior and interior fluid-structure interaction problems 02 p0188 N90-11073
Fluid-particle interaction in solid-liquid two-phase grid turbulence 06 p0773 N90-14496
Transient responses of coupled systems
|ONERA-RT-13/3596-RY-070-R| 11 p1509 N90-18687

FLUIDICS
Heat exchanger with oscillating flow
|NASA-CASE-LAR-14033-1| 21 p3004 N90-27072

FLUIDIZED BED PROCESSORS
Heat transfer to a stationary and moving sphere immersed in a fluidized bed 06 p0774 N90-14503
Scandia-stabilized zirconia coating for composites
|AD-D014550| 22 p3160 N90-27917

FLUIDS
The generalized van der Waals theory of pure fluids and mixtures
|DE90-000504| 06 p0740 N90-14307
Wide-angle propagation in inhomogeneous fluids and elastic solids using perturbation methods 06 p0837 N90-14868
Computer simulation of time-dependent spherically symmetric spacetimes containing radiating fluids: Formalism and code tests 15 p2185 N90-22483
Fluid-loop reaction system
|NASA-CASE-NPO-17204-1-CU| 20 p2864 N90-26292
Adjustable choke for fluids nozzle
|NASA-CASE-NPO-17625-1-CU| 21 p3003 N90-27070

FLUORESCENCE
NT LASER INDUCED FLUORESCENCE
NT PHOSPHORESCENCE
NT RESONANCE FLUORESCENCE
NT X RAY FLUORESCENCE
Advances in regression: Use of models in spectroscopic data analysis
|AD-A210541| 01 p0116 N90-10665
In-situ cure monitoring of composites by fiber-optic molecular sensors
|AD-A211495| 03 p0320 N90-11817
LABCEDE fluorescence investigations
|AD-A210678| 03 p0370 N90-12114
Comparison of the LOWTRAN 7 code and S3-4 satellite measurements of UV radiance
|AD-A211356| 03 p0372 N90-12124
Development of laser excited atomic fluorescence and ionization spectrometric methods
|DE90-001567| 06 p0742 N90-14320
X ray microprobe for the microcharacterization of materials
|DE89-006038| 06 p0836 N90-14963
Compensation for peak shifts and variable background responses in fluorescence spectroscopy
|DE90-001102| 07 p0892 N90-15154
Sulfur compounds in comets 08 p1143 N90-16627
Fluorescence from photoexcitation of Cl2 at 50 to 105 nm
|NASA-CR-186206| 09 p1189 N90-16888
Fluorescence and elastic scattering from laser dye-filled capillaries
|AD-A217026| 11 p1484 N90-18540
Solid-state fluorescence above 1000 C: Application to high-temperature laser thermography
|DE90-006422| 11 p1514 N90-18721
Fluorescent molecular hydrogen emission from star-forming galaxies 11 p1588 N90-19155
An electrochemical and spectroscopic study of electrode processes
|AD-A217261| 13 p1793 N90-20289
Evaluating thermographic phosphors in an operating turbine engine
|DE90-004874| 15 p2105 N90-22044
Institute for Materials Science and Engineering, nondestructive evaluation: Technical activities
|PB90-132739| 15 p2108 N90-22055
Modeling the lateral diffusion of fluorescent particles within a forest canopy 15 p2121 N90-22136
Spectrum formation in active galactic nuclei and Type 2 supernovae 15 p2187 N90-22490
Sticking coefficient of HCl on aerosols 16 p2208 N90-22598
Human cognitive and motor performance measures under typical cool white fluorescent illumination vs relatively high cool white illuminance/irradiance lighting
|AD-A218445| 16 p2262 N90-22892
Vegetation stress monitoring by fluorescence 19 p2708 N90-25414
Chemical structure and kinetics at liquid/solid interfaces
|AD-A222766| 20 p2831 N90-26105
Dissociative recombination of molecular ions with electrons 20 p2946 N90-26767
Fluorescent probe investigation of a water-soluble polyphosphazene
|AD-A222317| 21 p2978 N90-26925
Measurements of energy dispersion at liquid-solid interfaces: Fluorescence quenching of pyrene bound to fumed silica
|AD-A222371| 21 p2978 N90-26926
Molecular dynamics of physical aging processes in polymer glasses (experiment and theory)
|AD-A222848| 21 p2984 N90-26959
Engine testing of thermographic phosphors
|DE90-013269| 22 p3182 N90-28059
Definition of a near real time microbiological monitor for space vehicles
|NASA-CR-185599| 24 p3441 N90-29430

FLUORESCENT EMISSION
U FLUORESCENCE

FLUORIDES
NT ALUMINUM FLUORIDES
NT BARIUM FLUORIDES
NT BORON FLUORIDES
NT CALCIUM FLUORIDES
NT CHLORINE FLUORIDES

NT CRYOLITE
NT DIFLUORIDES
NT HYDROFLUORIC ACID
NT LANTHANUM FLUORIDES
NT LITHIUM FLUORIDES
NT METAL FLUORIDES
NT NITROGEN FLUORIDES
NT OXYGEN FLUORIDES
NT POLYVINYL FLUORIDE
NT SODIUM FLUORIDES
NT STRONTIUM FLUORIDES
NT SULFUR FLUORIDES

Design and construction of systems for the single-crystals growth of ternary silver halides, alkali halides, and alkaline earth fluorides, and the dielectric investigation of silver halide
|ETN-89-94673| 02 p0286 N90-11632

Synthesis and crystallization behavior of fluoride glasses
|AD-A212142| 04 p0478 N90-12741

Generation of iodine monofluoride in a supersonic multipurpose flowtube facility
|AD-A213082| 05 p0647 N90-13774

Method of making carbon dioxide and chlorine free fluoride-based glass
|AD-D014260| 08 p1048 N90-16060

Group 2 cubic fluorides as dielectrics for III-V compound semiconductors
|AD-A214096| 08 p1129 N90-16542

Multiplexed robotic tactile sensor fabricated from polyvinylidene fluoride film
|AD-A215354| 09 p1231 N90-17145

Feasibility of a super high energy density battery of the Li/BrF3 electrochemical system
|AD-A216794| 11 p1502 N90-18644

FLUORINATION

Reactive ion etching of SiC thin films by mixtures of fluorinated gases and oxygen
|AD-A211046| 02 p0195 N90-11113

Plasma and ion fluorination for chemical hardening of synthetic rubbers
|AD-A216388| 10 p1360 N90-17885

Perfluorinated ligands in organometallic chemistry
|AD-A216415| 11 p1476 N90-18493

Fluorinated graphite fibers as a new engineering material: Promises and challenges
|NASA-TM-102511| 12 p1618 N90-19301

Fluorinated diamond thin films for tribological applications
|AD-A217452| 13 p1779 N90-20214

FLUORINE

The chemistry of hexaazatriphenylene hexanitrile, a polyfunctional heterocycle with potential utility in the formulation of thermostable polymers
|AD-A212353| 04 p0480 N90-12757

Combustion of hydrogen and hydrocarbons in fluorine
|AD-A214621| 09 p1190 N90-16896

Plasma and ion fluorination for chemical hardening of synthetic rubbers
|AD-A216388| 10 p1360 N90-17885

Short-range structure of fluorine-modified phosphate glass
|DE90-013494| 20 p2839 N90-26145

FLUORINE COMPOUNDS

NT ALUMINUM FLUORIDES
NT BARIUM FLUORIDES
NT BORON FLUORIDES
NT CALCIUM FLUORIDES
NT CHLORINE FLUORIDES
NT CRYOLITE
NT DIFLUORIDES
NT DIFLUORO COMPOUNDS
NT FLUORIDES
NT FLUORO COMPOUNDS
NT FLUOROAMINES
NT FLUOROCARBONS
NT FLUOROHYDROCARBONS
NT FLUOROPOLYMERS
NT HYDROFLUORIC ACID
NT LANTHANUM FLUORIDES
NT LITHIUM FLUORIDES
NT METAL FLUORIDES
NT NITROGEN FLUORIDES
NT OXYGEN FLUORIDES
NT POLYTETRAFLUOROETHYLENE
NT POLYVINYL FLUORIDE
NT SODIUM FLUORIDES
NT STRONTIUM FLUORIDES
NT SULFUR FLUORIDES
NT TEFLON (TRADEMARK)
NT TETRAFLUOROHYDRAZINE

Femtosecond dynamics of fluoro-aluminum phthalocyanine and linear alkane molecules
|AD-A210939| 01 p0133 N90-10786

Electrolyte dependence of charge injection processes for electroactive polymer films
|AD-A210787| 02 p0202 N90-11152

Progress in the material development of LiCaAlF(6):Cr(3+) laser crystals
|DE90-009542| 14 p2034 N90-21666

FLUORINE ORGANIC COMPOUNDS

NT FLUOROAMINES
NT FLUOROCARBONS
NT FLUOROHYDROCARBONS
NT FLUOROPOLYMERS
NT POLYVINYL FLUORIDE
NT TEFLON (TRADEMARK)

FLUORO COMPOUNDS

NT CRYOLITE
NT DIFLUORO COMPOUNDS
NT FLUOROAMINES
NT FLUOROCARBONS
NT FLUOROHYDROCARBONS
NT FLUOROPOLYMERS
NT POLYTETRAFLUOROETHYLENE
NT TEFLON (TRADEMARK)
NT TETRAFLUOROHYDRAZINE

Pentafluorothio polynitroaliphatic explosives
|AD-D014221| 06 p0753 N90-14383

Ionic disorder in crystals at high temperatures with emphasis on fluorites
|AERE-R-13544| 13 p1893 N90-20862

Substituted 1,1,1-triaryl-2,2,2-trifluoroethanes and processes for their synthesis
|NASA-CASE-LEW-14345-2| 17 p2371 N90-23497

FLUOROAMINES

Research in energetic compounds
|AD-A214106| 10 p1360 N90-17887

FLUOROCARBONS

Synthesis and chemistry of strained and conjugated fluorocarbons
|AD-A211633| 03 p0324 N90-11844

Potential technologies for collection and destruction of CFCs (Chlorofluorocarbons), halons, and related compounds
|PB89-219968| 03 p0368 N90-12105

Experimental performance of ozone-safe alternative refrigerants: Experimental performance comparisons of R32, R125, R143a, R218, R134a, R152a, R124, R142b, RC318 and R143 in a refrigeration circuit
|DE90-009227| 15 p2073 N90-21876

Success of EPA's stratospheric ozone engineering research
|PB90-246265| 24 p3487 N90-29706

FLUOROHYDROCARBONS

NT POLYTETRAFLUOROETHYLENE
NT TEFLON (TRADEMARK)

Synthesis and chemistry of strained and conjugated fluorocarbons
|AD-A211633| 03 p0324 N90-11844

Studies of Aflas fluoroelastomers
|AD-A213046| 05 p0621 N90-13622

New Condensation polyimides containing 1,1,1-triaryl-2,2,2-trifluoroethane structures
|NASA-CASE-LEW-14346-1| 12 p1618 N90-19300

Reactions of laser-generated free radicals at semiconductor surfaces
|AD-A218552| 16 p2232 N90-22733

FLUOROPLASTICS

U FLUOROPOLYMERS

FLUOROPOLYMERS

NT POLYTETRAFLUOROETHYLENE
NT POLYVINYL FLUORIDE
NT TEFLON (TRADEMARK)

Studies of Aflas fluoroelastomers
|AD-A213046| 05 p0621 N90-13622

The 3F condensation polyimides: Review and update
|NASA-TM-102353| 06 p0750 N90-14363

A novel heat resistant blend produced by compositional quenching: A thermoplastic polyimide impact modified with a fluoroelastomer
|AD-A213724| 07 p0912 N90-15273

Cellular thermosetting fluorodiepoxide polymers
|NASA-CASE-GSC-13008-2| 09 p1199 N90-16949

Electronic and ionic transport in polymers
|AD-A217028| 11 p1491 N90-18579

Development and polarization of ferroelectric polymer gauges, for dynamical acceleration experiments, as those in ballistics shocks
|ISL-R-119/88| 11 p1511 N90-18703

Feasibility of a super high energy density battery of the Li/BrF3 electrochemical system
|AD-A216575| 11 p1528 N90-18799

New Condensation polyimides containing 1,1,1-triaryl-2,2,2-trifluoroethane structures
|NASA-CASE-LEW-14346-1| 12 p1618 N90-19300

Self-calibrating apparatus to find dynamic compressibility of organic solids
|AD-A219780| 17 p2415 N90-23763

A summary of measurements of permittivities and permeabilities of some microwave absorbing materials
|AD-A223221| 21 p2995 N90-27026

The optimum polymer binder for pressable high performance explosives: A preliminary evaluation
|ETN-90-97612| 24 p3457 N90-29524

FLUSHING

Wind-tunnel investigation of a flush airdata system at Mach numbers from 0.7 to 1.4
|NASA-TM-101697| 11 p1457 N90-18395

FLUTING

U GROOVING

FLUTTER

NT SUBSONIC FLUTTER
NT TRANSONIC FLUTTER

Flutter clearance of the F-18 high-angle-of-attack research vehicle with experimental wingtip instrumentation pods
|NASA-TM-4148| 03 p0305 N90-11732

Effect of control surface mass unbalance on the stability of a closed-loop active control system
|NASA-TP-2952| 03 p0357 N90-12042

The effectiveness of vane-aileron excitation in the experimental determination of flutter speed by parameter identification
|NASA-TP-2971| 07 p0880 N90-15100

Unsteady Aerodynamic Phenomena in Turbomachines
|AGARD-CP-468| 11 p1459 N90-18405

A comparison of flutter calculations based on eigenvalue and energy method 11 p1459 N90-18406

Using transonic small disturbance theory for predicting the aeroelastic stability of a flexible wind-tunnel model
|NASA-TM-102617| 13 p1749 N90-20047

Digital-flutter-suppression-system investigations for the active flexible wing wind-tunnel model
|NASA-TM-102618| 13 p1758 N90-20093

An experimental study of tip shape effects on the flutter of aft-swept, flat-plate wings
|NASA-TM-4180| 16 p2199 N90-22555

Flutter clearance of the F-14A variable-sweep transition flight experiment airplane, phase 2
|NASA-TM-101717| 19 p2659 N90-25135

A digital controller for active aeroelastic controls
|NAL-TR-1014| 24 p3435 N90-29402

FLUTTER ANALYSIS

Analysis of flutter tests with the use of a telemetry system 02 p0152 N90-10871

Problems related to the acquisition, processing and utilization of the modal parameters measured in flight tests in order to obtain the full envelope for flutter
|ETN-89-95210| 03 p0305 N90-11735

Experimental transonic flutter characteristics of two 72 deg-sweep delta-wing models
|NASA-TM-101659| 06 p0720 N90-14205

Nonlinear phenomena in computational transonic aeroelasticity 07 p0874 N90-15070

Using transonic small disturbance theory for predicting the aeroelastic stability of a flexible wind-tunnel model
|NASA-TM-102617| 13 p1749 N90-20047

The application of active controls technology to a generic hypersonic aircraft configuration
|NASA-TM-101689| 13 p1754 N90-20071

Subsonic flutter analysis using MSC/NASTRAN
|PB90-186786| 14 p1928 N90-21041

Flutter of slender bodies under axial stress
|PB90-167024| 14 p1994 N90-21425

An experimental study of tip shape effects on the flutter of aft-swept, flat-plate wings
|NASA-TM-4180| 16 p2199 N90-22555

Flutter investigations on a Transavia PL12/T-400 aircraft
|AD-A219108| 16 p2203 N90-22570

Reduced order models for nonlinear aerodynamics 18 p2492 N90-24244

On simplified analytical flutter clearance procedures for light aircraft
|DLR-FB-89-56| 18 p2498 N90-24276

Effects of spoiler surfaces on the aeroelastic behavior of a low-aspect-ratio rectangular wing
|NASA-TM-102622| 22 p3115 N90-27700

Multi-disciplinary optimization of aeroservoelastic systems
|NASA-CR-185931| 24 p3432 N90-29385

FLUX (RATE PER UNIT AREA)

U FLUX DENSITY

FLUX (RATE)

NT HEAT FLUX
NT MAGNETIC FLUX
NT SOLAR FLUX

The inter-outburst behavior of cataclysmic variables
|NASA-CR-186374| 13 p1902 N90-20914

Gas dynamic theory of flight of fast electron flux in plasma
|DE90-618767| 16 p2319 N90-23220

Investigation of plasma density bulge in front of Venus bow shock
[NASA-CR-186937] 22 p3262 N90-28476
Re-analysis of data on the space radiation environment above southeast Asia
[AD-A224155] 24 p3564 N90-30162

FLUX DENSITY
NT CURRENT DENSITY
NT ILLUMINANCE
NT IRRADIANCE
NT LUMINANCE
NT LUMINOUS INTENSITY
NT PARTICLE FLUX DENSITY
NT PHOTON DENSITY
NT PROTON FLUX DENSITY
NT RADIANCE
NT RADIANT FLUX DENSITY
NT SOLAR CONSTANT
NT SOLAR FLUX DENSITY
NT SOUND INTENSITY
NT ZERO SOUND
Assessment of thin film batteries based on polymer electrolytes. Part 1: Energy density
[AD-A212111] 03 p0343 N90-11958
Fluctuations in transverse energy and multiplicity, energy densities, and neutral pion spectra in nucleus-nucleus collisions at 200 GeV/nucleon
[DE89-017583] 03 p0402 N90-12302
Ground states of a two-dimensional charged-boson system
[AD-A212363] 04 p0553 N90-13226
SWAN: A study of solar wind anisotropies 04 p0568 N90-13312
Balance laws and centro velocity in dissipative systems
[MEMO-797] 05 p0639 N90-13726
Measurement of the light flux density patterns from luminaires proposed as photon sources for photosynthesis during space travel
[NASA-CR-186124] 05 p0672 N90-13916
The creation of high energy densities with antimatter beams
[DE90-002383] 06 p0842 N90-14899
Design of a high-gain flux-compression generator
[DE90-002795] 07 p0922 N90-15333
Copper chloride cathode for a secondary battery
[NASA-CASE-NPO-17640-1-CU] 09 p1210 N90-17011
A numerical solution to the Boltzmann equation for use in calculating pumping rates in a CO2 discharge laser
[AD-A216376] 11 p1514 N90-18718
Development of an rf-driven plasma neutralizer for negative ions
[DE90-007298] 11 p1568 N90-19027
Multiple versus single scattering of terrestrial infrared longwave radiation in an aerosol-laden planetary boundary layer
[AD-A217709] 13 p1790 N90-20272
Gamma rays from giant molecular clouds 16 p2334 N90-23298
More data on (possible) gamma ray (point) sources 16 p2335 N90-23309
High frequency, high temperature specific core loss and dynamic B-H hysteresis loop characteristics of soft magnetic alloys
[NASA-TM-103164] 17 p2398 N90-23663
A nonlocal free energy density functional approximation for the electrical double layer
[AD-A220664] 18 p2607 N90-24848
Construction of a hybrid angular velocity reference system for investigation of the dynamic characteristics of strapdown gyros
[ESA-TT-1181] 19 p2694 N90-25332
On the relationship between energy density and net power (intensity) in coupled one-dimensional dynamic systems
[AD-A221071] 19 p2709 N90-25421
Exploding neutron stars near the minimum mass: The total energy release 19 p2774 N90-25769
Apparatus for measuring high-flux heat transfer in radiatively heated compact exchangers
[NASA-CR-186333] 22 p3122 N90-27726
Elliptical flux vortices in polycrystalline YBa2Cu3O7 22 p3136 N90-27795
Ground level atmospheric gamma ray flux measurements in the 1 to 6 MeV range 22 p3264 N90-28483
Ultrasonic verification of five wave fronts in unidirectional graphite epoxy composite
[NASA-CR-185268] 23 p3337 N90-28858
Theoretical studies of proton beams in solar flare loops 23 p3413 N90-29286
Radio outbursts in extragalactic sources 23 p3414 N90-29291
Brorfelde Geomagnetic Observatory: Magnetic results, 1987
[ISBN-87-7478-297-5] 24 p3496 N90-29756

FLUX MAPPING
U FLUX DENSITY
U MAPPING

FLUX PINNING
Pinning of curved flux lines on the boundary between two phases of high temperature superconductors
[DE89-618865] 02 p0283 N90-11614
Flux pinning and microstructure in YBa2Cu3O7
[DE90-001562] 06 p0851 N90-14948
Effects of shock-induced defects on flux pinning in YBa2Cu3O(7-delta)
[DE90-000824] 06 p0853 N90-14959
Shock-induced defects and flux pinning in YBa2Cu3O sub 7-delta + Ag composites
[DE90-000827] 06 p0853 N90-14960
Magnetic flux pinning in YBa2Cu3O7 films
[DE90-003709] 07 p1002 N90-15799
Rotational magnetic processes in YB2Cu3O7
[DE90-000541] 08 p1128 N90-16533
Flux flow, pinning, and resistive behavior in superconducting networks
[DE90-005242] 09 p1293 N90-17493
Materials research issues in superconducting levitation and suspension as applied to magnetic bearings
[DE90-011147] 20 p2929 N90-26667
Magnetic properties of high-T(sub c) superconductors: Rigid levitation, flux pinning, thermal depinning, and fluctuation 22 p3137 N90-27798
Magnetic forces in high-T(sub c) superconducting bearings 22 p3137 N90-27799
Effect of shock pressure on the structure and superconducting properties of Y-Ba-Cu-O in explosively fabricated bulk metal-matrix composites 22 p3138 N90-27804
Comparative study of flux pinning flux creep and critical currents between YBaCuO crystals with and without Y2BaCuO5 inclusions 22 p3152 N90-27869

FLUX QUANTIZATION
Ground level atmospheric gamma ray flux measurements in the 1 to 6 MeV range 22 p3264 N90-28483

FLUX VECTOR SPLITTING
Solution of the thin-layer Navier-Stokes equations for laminar transonic flow
[PB89-221600] 04 p0500 N90-12879
Multigrid solution method for the Euler equations
[PB89-219463] 04 p0539 N90-13116
A dynamic multiblock approach to solving the unsteady Euler equations about complex configurations 06 p0773 N90-14497
An evaluation of the two-dimensional Euler and Navier-Stokes calculations based on a flux-vector splitting
[PB90-166778] 14 p1912 N90-20963
An upwind-differencing scheme for the incompressible Navier-Stokes equations
[NASA-TM-101051] 15 p2051 N90-21757
Calculations of chemically reacting shear flows above solid fuels 22 p3162 N90-27930
Numerical methods for systems of conservation laws of mixed type using flux splitting
[NASA-CR-182084] 23 p3387 N90-29129

FLUXMETERS
U MAGNETIC MEASUREMENT
U MEASURING INSTRUMENTS

FLY ASH
Ambient flow studies and particulate collection measurements: A laminar flow, reduced entrainment electrostatic precipitator
[DE90-001457] 08 p1083 N90-16149

FLY BY WIRE CONTROL
ATTAS flight testing experiences 02 p0151 N90-10862
In flight relight tests on AM-X single engine fly-by-wire aircraft 02 p0152 N90-10869
Engine controls for the 1990's
[PNR90546] 03 p0308 N90-11748
How to fly windshear using the fly-by-wire concept 07 p0870 N90-15050
Applications of modern control theory synthesis to a super-augmented aircraft
[AD-A215431] 09 p1167 N90-16753
Model following control system design: Preliminary ATTAS in-flight simulation test results
[PD-FC-9003] 20 p2813 N90-26010
Start-up built-in test for the DISCUS fault tolerant, fly-by-wire computer system 22 p3104 N90-27625
Space shuttle descent flight verification by simulation: A challenge in implementing flight control system robustness 22 p3127 N90-27748
Procedure for calibrating fly-by-wire control chains of the flying testbed ATTAS
[DLR-MITT-90-02] 24 p3435 N90-29401

FLYBY MISSIONS
NT COMET RENDEZVOUS ASTEROID FLYBY MISSION
NT GIOTTO MISSION
NT GRAND TOURS
NASA Voyager 2 Neptune encounter press kit
[NASA-TM-101851] 01 p0015 N90-10076
Experimental studies of gas trapping in amorphous ice and thermal modelling of comets: Implications for Rosetta 08 p1140 N90-16610
Trajectory-capture cell instrumentation for measurement of dust particle mass, velocity and trajectory, and particle capture 08 p1146 N90-16644

FLYING BEDSTEAD AIRCRAFT
U FLYING PLATFORMS

FLYING PERSONNEL
NT AIRCRAFT PILOTS
NT ASTRONAUTS
NT COSMONAUTS
NT FLIGHT CREWS
NT ORBITAL WORKERS
NT PILOTS (PERSONNEL)
NT SPACECREWS
NT TEST PILOTS

FLYING PLATFORM STABILITY
U AERODYNAMIC STABILITY
U FLYING PLATFORMS

FLYING PLATFORMS
Multiband imaging systems
[AD-A223969] 23 p3343 N90-28893

FLYING QUALITIES
U FLIGHT CHARACTERISTICS

FLYWHEELS
Computer-aided design of flywheel transmission systems 14 p1988 N90-21392

FM (MODULATION)
U FREQUENCY MODULATION

FOAMING
Instantaneously generated foam and its applicability to reduced gravity
[NASA-CR-185208] 13 p1784 N90-20237

FOAMS
Aviation Engine Test Facilities (AETF) fire protection study
[AD-A211483] 04 p0483 N90-12777
The physical properties of microcellular composite foams
[DE90-003658] 08 p1048 N90-16058
Cellular thermosetting fluorodiepoxide polymers
[NASA-CASE-GSC-13008-2] 09 p1199 N90-16949
Instantaneously generated foam and its applicability to reduced gravity
[NASA-CR-185208] 13 p1784 N90-20237
Using template/hotwire cutting to demonstrate moldless composite fabrication 18 p2515 N90-24361
Non-contacting printed circuit waveguide elements
[AD-D014489] 22 p3166 N90-27957
A new low density, high porosity lithium hydride-beryllium hydride foam
[DE90-015150] 23 p3313 N90-28739

FOCAL PLANE ARRAYS
U FOCAL PLANE DEVICES

FOCAL PLANE DEVICES
Laterally stacked Schottky diodes for infrared sensor applications
[NASA-CASE-NPO-17426-1-CU] 01 p0058 N90-10329
A review of focal reducer interferometer systems
[RSRE-MEMO-3486] 04 p0554 N90-13231
Status of direct detector and array development 05 p0596 N90-13464
Advances in SIS receiver technology 05 p0597 N90-13466
Discussion of factors affecting the sensitivity of IR imaging sensors, particularly focal plane mosaic arrays --- staring mosaic arrays
[FOA-C-30536-3.1] 05 p0700 N90-14101
CCD TV focal plane guider development and comparison to SIRTF applications
[NASA-CR-185977] 06 p0842 N90-14900
Focal plane antenna array for millimeter waves
[AD-D014306] 07 p0920 N90-15322
The MPI/AIT X ray Imager (MAXI): High speed PN-CCD's for x ray detection
[MPE-PREPRINT-154] 08 p1077 N90-16234
Enhanced performance IR focal plane arrays using adaptive subtraction
[RSRE-MEMO-4286] 08 p1123 N90-16502
Staring focal plane array system modeling
[AD-A215712] 09 p1283 N90-17438
NRL hybrid reliability. Physics of failure initial study
[AD-A217986] 13 p1898 N90-20893
Study of advanced InSb arrays for SIRTF (Space Infrared Telescope Facility) 14 p1977 N90-21325

Short wavelength HgCdTe staring focal plane for low background astronomy applications
14 p1979 N90-21336
Low noise HgCdTe 128 x 128 SWIR FPA for Hubble space telescope 14 p1979 N90-21337
Future directions for NICMOS arrays
14 p1979 N90-21339
Status of the isophot detector development
14 p1980 N90-21342
HgCdTe 256x256 NWIR FPA
14 p1981 N90-21348
Parallel asynchronous hardware implementation of image processing algorithms 15 p2138 N90-22219
SIRTF: Probing the dark corners of the galaxy
21 p3091 N90-27577

FOCI
NT PLASMA FOCUS
A method of determining a laser-velocimeter focal point and measuring its beam properties using a hot-wire anemometer
|NAL-TR-1043| 24 p3473 N90-29626

FOCUSING
NT DEFOCUSING
NT SELF FOCUSING
Millimeter-wave/infrared rectenna development at Georgia Tech 01 p0028 N90-10147
Nonlinear acoustics: Reflection and refraction, propagation in a periodic waveguide, scattering of sound by sound and ellipsoidal focusing
|AD-A211224| 02 p0271 N90-11550
Near-planar TS waves and longitudinal vortices in channel flow: Nonlinear interaction and focusing
|NASA-CR-181928| 03 p0300 N90-11698
Generation and focusing of pulsed intense ion beams
|DE89-017558| 03 p0408 N90-12338
Electron beam propagation through a magnetic wiggler with random field errors
|AD-A212705| 04 p0498 N90-12867
Catadioptric Optics for laser Doppler velocimeter applications
|NASA-TM-102210| 04 p0504 N90-12904
A Scheiner-principle pocket optometer for self-evaluation and biofeedback accommodation training
|AD-A213171| 04 p0524 N90-13027
Direct computation of 3D shape invariants and the focus of expansion
|AD-A212386| 04 p0549 N90-13195
The phase gradient autofocus algorithm: An optimal estimator of the phase derivative
|DE90-000895| 06 p0828 N90-14814
A scheiner-principle vernier optometer
|AD-D014304| 07 p0934 N90-15405
B-Factory Final Focus System using superconducting quadrupoles
|DE90-004432| 08 p1131 N90-16552
Identification and reduction of Wakefield effects in the wiggler region of the Los Alamos free-electron laser
|DE90-004871| 09 p1228 N90-17128
Improved performance of the Boeing/LANL FEL (Free-Electron Laser) experiment: Extraction efficiency and cavity length detuning effects
|DE90-004872| 09 p1228 N90-17129
Structural and operational aspects of the concentrating SARA-Louver solar generator 10 p1340 N90-17760
Shape from focus
|AD-A215959| 10 p1393 N90-18052
Focused ion beam implantation
|AD-A217987| 13 p1898 N90-20894
Simulated image maps for use in experimental high-resolution electron microscopy
|DE90-009176| 14 p2032 N90-21657
Foil focusing of electron beams
|AD-A219511| 16 p2317 N90-23208
Stability regimes in a rotating quadrupole focusing accelerator
|AD-A219513| 16 p2317 N90-23209
Stability regimes in a helical quadrupole focusing accelerator: Theory and simulation
|AD-A221755| 21 p3079 N90-27507
Target signature modeling and bistatic scattering measurement studies
|NASA-CR-186611| 23 p3319 N90-28766
XMM space telescope: Development plan for the lightweight replicated x ray gratings
|DE90-015620| 24 p3546 N90-30055

FOG
Investigation of North Atlantic fog and development of a marine fog forecast system
|AD-A211780| 04 p0519 N90-12999
Anomalous absorption by atmospheric water vapor and stabilized water fogs in the infrared and CM-wave regions
|AD-A214202| 07 p0964 N90-15572
Assessment of the importance of acidic fogwater and cloudwater in affecting terrestrial vegetation: Some important case studies
|DE90-002216| 08 p1098 N90-16361
Development of an atmospheric diffusion model in fog (1). Literature review of scavenging process by precipitation
|DE89-782318| 12 p1685 N90-19676
The effects of acid fog and dew on materials
|PB90-157496| 19 p2712 N90-25436
Aureole lidar: Ground based measurement
|AD-A223207| 21 p3008 N90-27101
An experiment to make a new design of the Satellite Cloud Information Chart with the combination of visible and infrared data observed by the GMS
21 p3029 N90-27223
Sources of cloud nuclei and development of remote sensing techniques for cloud parameters
|AD-A222464| 21 p3031 N90-27233
Space-base multispectral imagery: Current and future applications and implications to the United States Army
|AD-A224046| 23 p3343 N90-28894

FOG DISPERSAL
Investigation of North Atlantic fog and development of a marine fog forecast system
|AD-A211780| 04 p0519 N90-12999

FOIL BEARINGS
Some problems in hydrodynamic lubrication
09 p1229 N90-17133
Improved analytical capabilities for foil air bearings, phase 1
|AD-A218071| 14 p1987 N90-21389

FOILS (MATERIALS)
NT METAL FOILS
Observation of excited H(sup 0) atoms produced by relativistic H(sup (minus)) ions in carbon and formvar foils
|DE89-015301| 01 p0120 N90-10688
In-situ ion beam measurements of deuterium loading in thin foil electrochemical cells
|DE90-003162| 07 p0952 N90-15511
Design and optimisation of thin foil x ray telescopes
14 p2038 N90-21690
Foil focusing of electron beams
|AD-A219511| 16 p2317 N90-23208

FOKKER AIRCRAFT
Static strength and damage tolerance tests on the Fokker 100 airframe
|NLR-MP-88023-U| 12 p1604 N90-19228
Activities report in aerospace and aerodynamics
|ETN-90-96774| 17 p2487 N90-24224

FOKKER BOND TESTERS
U ADHESION TESTS

FOKKER-PLANCK EQUATION
Development of a numerical solution to the time dependent kinetic equation 03 p0433 N90-12481
Nonlinear interaction of photons and phonons in electron-positron plasmas
|DE90-009341| 14 p2030 N90-21640
Vibration analysis of systems with random parametric excitations 15 p2109 N90-22060

FOLDING
Analysis of photogeologic lineaments in the Ithacare (BA) region: A proposed methodology
|INPE-4855-PRE/1478| 12 p1677 N90-19635

FOLDING STRUCTURES
Test results on conceptual models of the large deployable antenna for mobile communications satellites
02 p0185 N90-11050
A cable-rigidized 3D pantograph
18 p2538 N90-24484
ADELE: Deployment hinge using wraparound strips
18 p2538 N90-24485

FOLDS (GEOLOGY)
Architecture of orogenic belts and convergent zones in Western Ishtar Terra, Venus
03 p0425 N90-12437
Tectonism on Venus: A review
03 p0425 N90-12440

FOLIAGE
Stochastic modelling of EM scattering from foliage
|AD-A213118| 05 p0632 N90-13689
N-port theory applied to backscatter polarimetry and depolarization in foliage penetration
|AD-A213437| 07 p0917 N90-15305
Thermal remote sensing in the differentiation of soybean crops (glycine max (L.) merrill) submitted to water deficit
|INPE-4900-PRE/1501| 11 p1522 N90-18762
Relationships between spectral parameters and agronomics of wheat and beam crops
|INPE-4791-RPE/584| 11 p1523 N90-18768
Millimeter-wave bistatic scattering by terrain
15 p2085 N90-21936

FOOD
Operational satellite environmental monitoring for food security by FAO: The ARTEMIS system
19 p2708 N90-25413

FOOD PROCESSING
NT CANNING
NT PRESERVING
Factors affecting practical application of food irradiation
|DE90-631277| 24 p3522 N90-29914

FOOD PRODUCTION (IN SPACE)
Utilization of non-conventional systems for conversion of biomass to food components
|NASA-CR-177545| 07 p0968 N90-15591

FORBIDDEN BANDS
Near infrared (1-4 micron) spectroscopy of SN1987A
11 p1584 N90-19133

FORBUSH DECREASES
Electron density profiles in the background of LF absorption during Forbush-decrease and PSE
22 p3208 N90-28199

FORBUSH EFFECT
U FORBUSH DECREASES

FORCE DISTRIBUTION
Wind tunnel tests of the influence of aerofoil thickness on the normal force and pitching moment of two slender wings at transonic and supersonic Mach numbers
|ESA-TT-1129| 08 p1018 N90-15889
Force and moment measurements on delta wings in unsteady flow 08 p1068 N90-16185
Optimum spanwise camber for minimum induced drag
|BU-403| 11 p1452 N90-18369
The MANTA: An RPV design to investigate forces and moments on a lifting surface
|NASA-CR-186227| 14 p1915 N90-20971
Analysis of a six-component, flow-through, strain-gage, force balance used for hypersonic wind tunnel models with scramjet exhaust flow simulation
|NASA-CR-186585| 15 p2055 N90-21775
Monitoring of Ritz modal generation
18 p2571 N90-24650
A flight dynamic model of aircraft spinning
|AR-005-600| 23 p3283 N90-28576
Aerodynamic forces acting on a finite rectangular slender body
|NAL-TR-1035| 24 p3421 N90-29329

FORCE FIELDS
U FIELD THEORY (PHYSICS)

FORCED CONVECTION
Laminar forced convection inside externally finned tubes
|DE89-636431| 07 p0928 N90-15373
A model for evaporation of freely falling droplets
|PUBL-AIR-QUALITY-6| 10 p1384 N90-18007
Turbulent thermal convection in rotating cavities, volume 1
|ETN-90-97433| 22 p3174 N90-28011
Turbulent thermal convection in rotating cavities, volume 2
|ETN-90-97434| 22 p3174 N90-28012

FORCED OSCILLATION
U FORCED VIBRATION

FORCED VIBRATION
Active control of the forced and transient response of a finite beam 03 p0357 N90-12040
Dynamic analysis of geared rotors by finite elements
|NASA-TM-102349| 08 p1086 N90-16286
Aerodynamic study on forced vibrations on stator rows of axial compressors 11 p1460 N90-18412
Gust response analysis for cascades operating in nonuniform mean flows 11 p1461 N90-18415
Wave receptance analysis of vibrating beams and stiffened plates 14 p1993 N90-21419
A video-based experimental investigation of wing rock
15 p2054 N90-21771
Experimental investigation of the effect of cavitation on the rotordynamic forces on a whirling centrifugal pump impeller 15 p2105 N90-22039
Elastodynamic scattering and transmission problems in three dimensions by the boundary integral equation method 15 p2111 N90-22077

FORCED VIBRATORY MOTION EQUATIONS
U FORCED VIBRATION

FOREBODIES
NT ABLATIVE NOSE CONES
NT NOSE CONES
NT NOSES (FOREBODIES)
Normal-force-curve and pitching-moment-curve slopes of forebody-cylinder combinations at zero angle of attack for Mach numbers up to 5
|ESDU-89008| 03 p0301 N90-11709
Experimental and numerical analyses of laminar boundary-layer flow stability over an aircraft fuselage forebody 04 p0445 N90-12549
Optimum shape of a blunt forebody in hypersonic flow
|NASA-CR-181955| 05 p0575 N90-13351

Normal force, pitching moment, and side force of forebody-cylinder combinations for angles of attack up to 90 degrees and Mach numbers up to 5
[ESDU-89014] 06 p0718 N90-14192
Static and rotational aerodynamic data from 0 deg to 90 deg angle of attack for a series of basic and altered forebody shapes
[AD-A216582] 11 p1451 N90-18361
Influence of forebody geometry on aerodynamic characteristics and a design guide for defining departure/spin resistant forebody configurations
[AD-A216714] 11 p1456 N90-18388
Effects of nose bluntness and shock-shock interactions on blunt bodies in viscous hypersonic flows
[NASA-CR-186451] 14 p1910 N90-20950
The 3-D composite velocity solutions for subsonic/transonic flow over forebodies and afterbodies
[AD-A220370] 17 p2345 N90-23354
Actuated forebody strakes
[NASA-CASE-LAR-13983-1] 17 p2352 N90-23390
Effects of forebody geometry on subsonic boundary-layer stability
[NASA-CR-4314] 20 p2802 N90-25939
Prediction of subsonic vortex shedding from forebodies with chines
[NASA-CR-4323] 23 p3268 N90-28494
The effects of foreplanes on the static and dynamic characteristics of a combat aircraft model
23 p3273 N90-28520
Development of non-conventional control methods for high angle of attack flight using vortex manipulation
23 p3273 N90-28522

FORECASTING
NT DELPHI METHOD (FORECASTING)
NT NUMERICAL WEATHER FORECASTING
NT PERFORMANCE PREDICTION
NT PREDICTION ANALYSIS TECHNIQUES
NT PROFILE METHOD (FORECASTING)
NT STATISTICAL WEATHER FORECASTING
NT TECHNOLOGICAL FORECASTING
NT WEATHER FORECASTING
IFD (Implicit Finite Difference): Interfaced with Harvard open ocean model forecasts
[AD-A210521] 01 p0090 N90-10517
Joint VHF coherent radar and oblique sounder observations for short term ionosphere forecasting
02 p0247 N90-11399
Radio propagation conditions forecast above a low latitude region 02 p0247 N90-11400
Manufacturing and the manufacturing engineer in the year 2000, revision
[DE89-017707] 03 p0335 N90-11904
Forecasting contracting workload
[AD-A211935] 03 p0416 N90-12387
The Regional Polar Ice Prediction System, Berents Sea (RPIPS-B): A technical description
[AD-A213159] 04 p0522 N90-13012
Operational Decision Aids for Exploiting or Mitigating Electromagnetic Propagation Effects
[AGARD-CP-453] 06 p0757 N90-14405
A forecasting system using the parabolic equation: Application to surface-to-air propagation in the presence of elevated layers 06 p0760 N90-14420
Assessment of anomalous propagation predictions using minisonde refractivity data and the parabolic equation method 06 p0760 N90-14424
A modern trans-ionospheric propagation sensing system 06 p0761 N90-14430
The use of backscatter for modelling ionosphere and jamming in very short term forecasts
06 p0762 N90-14434
A one-dimensional shipboard model for forecasting refractive effects in the planetary boundary layer
06 p0764 N90-14442
Modelling UHF propagation for frequency assignment in radio relay networks 06 p0764 N90-14445
Testing and performance of a high-gain flux-compression generator
[DE90-002808] 06 p0772 N90-14492
Comparison of shock severity measures
[DE90-000790] 06 p0799 N90-14654
Global natural resource monitoring and assessment
[DE90-001294] 06 p0802 N90-14671
Turbulent wind at the equatorial segment of an operating Darrieus wind turbine blade
[DE90-002672] 06 p0807 N90-14698
Application of surface analysis methods to studies of atmospheric deposition in forests
[DE90-000562] 06 p0810 N90-14714
Climate projections with regional resolution
[DE90-000858] 06 p0810 N90-14715
The identification of terrain-induced circulations using principal components
[DE90-001991] 06 p0815 N90-14739
The radar-based short term prediction of the time-space evolution of rain fields
[AD-A213802] 07 p0918 N90-15312
Diesel starting system monitor: Prototype development
[DE90-004425] 08 p1084 N90-16276
A study of the evolution of solar active regions for improving solar flare forecasts
[AD-A216325] 10 p1448 N90-18356
Resource Assessment Project: User needs survey results
[DE89-009502] 11 p1529 N90-18802
Atmospheric Radiation Measurement Program plan
[DE90-006349] 12 p1689 N90-19705
A guide to performing and documenting safety analyses
[DE90-008687] 13 p1788 N90-20260
Energy storage and distribution
[DE89-009487] 13 p1826 N90-20488
Wind Energy Program summary. Volume 1: Overview
[DE89-009479] 13 p1827 N90-20491
Global Warming: A Northwest Perspective
[DE90-008140] 13 p1830 N90-20505
Overview of the methodologies used to compile large scale emissions inventories
[DE90-008518] 13 p1830 N90-20509
An intercomparison of general circulation model predictions of regional climate change
[DE90-008325] 13 p1845 N90-20589
Millimetre-wave propagation in the evaporation duct
15 p2084 N90-21929
Aging characteristics of Li/SO(sub 2) cells
[NASA-CR-180432] 15 p2088 N90-21954
An anomalous wind between valleys: Its characteristics and a proposed explanation
[DE90-008965] 15 p2133 N90-22189
Daytime wind valleys adjacent to the Great Salt Lake
[DE90-008991] 15 p2133 N90-22190
Wind forecasting for utility operations
[DE90-009466] 15 p2133 N90-22193
Forecast of Atlantic seasonal hurricane activity for 1990 15 p2134 N90-22194
FAA (Federal Aviation Administration) aviation forecasts, fiscal years 1990-2001
[AD-A219165] 16 p2195 N90-22530
An interactive method for estimating hailstone size and convectively-driven wind gusts from forecast soundings
[AD-A218499] 16 p2258 N90-22871
Test and evaluation of surf forecasting model
[AD-A219580] 17 p2430 N90-23845
A comparative analysis of work-hour forecasting techniques at the crew level
[AD-A220706] 17 p2438 N90-23894
An interactive life cycle cost forecasting tool
[AD-A220472] 17 p2480 N90-24184
IFR aircraft handled forecast by air route traffic control center: Fiscal years 1990 to 2005
[AD-A220312] 18 p2496 N90-24263
Weight and cost forecasting for advanced manned space vehicles 18 p2632 N90-24998
Estimating the cost of major ongoing cost plus hardware development programs
[NASA-TM-100401] 19 p2764 N90-25705
Study of high-speed civil transports. Summary
[NASA-CR-4236] 20 p2806 N90-25966
Computerized corrosion forecasting model for C-5 aircraft 21 p2957 N90-26815
Study of meteorological processes important in the degradation of materials through surface temperature
[PB90-222720] 23 p3336 N90-28856
Sounder update and field strength software modifications for Special Operations Radio Frequency Management System (SORFMS). Volume 1: Program descriptions and testing
[AD-A224510] 24 p3460 N90-29543

FORECASTS
U FORECASTING

FOREIGN POLICY
NT INTERNATIONAL COOPERATION
NT INTERNATIONAL RELATIONS
NT OUTER SPACE TREATY
Satellite navigation system projects: European complement to GPS (CE-GPS), NAVSAT
17 p2360 N90-23434
Polar prospects: A minerals treaty for Antarctica
[OTA-O-428] 17 p2480 N90-24185

FOREIGN TRADE
U INTERNATIONAL TRADE

FORENSIC SCIENCES
U LAW (JURISPRUDENCE)

FOREST FIRES
Analysis of forest fire smoke using satellite imagery
[AD-A210657] 02 p0236 N90-11339
Rocket-triggered lightning strikes and forest fire ignition 08 p1155 N90-16690
Distribution and movement of smokes from forest fires that occurred along the boundary of the People's Republic of China and the USSR on April-May 1987
21 p3028 N90-27216
Developing air tanker performance guidelines
[PB90-183765] 22 p3114 N90-27695

FOREST MANAGEMENT
NT REFORESTATION
Investigation on analyzing computer-aided forest disease classifications
[DFVLR-FB-89-16] 03 p0369 N90-12112
Proceedings of the US/FRG (Fed. Republic of Germany) research symposium: Effects of Atmospheric Pollutants on the Spruce-Fir Forests of the Eastern United States and the Fed. Republic of Germany
[PB90-107160] 06 p0808 N90-14704
Forest mapping Nuerenberg German national forest with special emphasis on the spectral reflection behavior of pine trees 08 p1093 N90-16328
Use of remote sensing in operational inventory and monitoring agricultural and forestry tasks
08 p1094 N90-16336
Monitoring of reforested areas through digital analysis of TM data
[INPE-4930-PRE/1420] 11 p1522 N90-18764
Multistage forest volume estimation using a sampling system with probability variables
[INPE-4897-PRE/1498] 11 p1523 N90-18769
Proceedings of the 4th European Conference, volume 2
[AD-A216521] 14 p1986 N90-21382
Modeling large-scale vegetation dynamics
[DE90-008883] 14 p2004 N90-21485
Multispectral classification of overlapping classes with applications to forest damage areas
[DLR-FB-89-55] 18 p2574 N90-24666
Inventory and monitoring of extended forest lands by remote sensing 19 p2708 N90-25409

FORESTS
NT RAIN FORESTS
Improvement and extension of a radar forest backscattering model
[NASA-CR-186083] 04 p0515 N90-12973
Global natural resource monitoring and assessment
[DE90-001294] 06 p0802 N90-14671
Proceedings of the US/FRG (Fed. Republic of Germany) research symposium: Effects of Atmospheric Pollutants on the Spruce-Fir Forests of the Eastern United States and the Fed. Republic of Germany
[PB90-107160] 06 p0808 N90-14704
Application of surface analysis methods to studies of atmospheric deposition in forests
[DE90-000562] 06 p0810 N90-14714
Nitrogen deposition to forest trees
[DE90-003285] 06 p0812 N90-14726
Assessment of the importance of acidic fogwater and cloudwater in affecting terrestrial vegetation: Some important case studies
[DE90-002216] 08 p1098 N90-16361
Modeling the effects of air pollution on forest ecosystems: Considerations for applying a model to Southeast Asia
[DE90-004937] 10 p1406 N90-18110
Monitoring of reforested areas through digital analysis of TM data
[INPE-4930-PRE/1420] 11 p1522 N90-18764
Multistage forest volume estimation using a sampling system with probability variables
[INPE-4897-PRE/1498] 11 p1523 N90-18769
Photointerpretation with instruments for evaluation of environmental impact: Mata Atlantica in Cubata
[INPE-4910-PRE/1511] 11 p1531 N90-18817
Some aspects of atmospheric turbulence in forests
[INPE-4951-RPE/600] 11 p1532 N90-18818
Synthesis and analysis of 25 years (1961-1986) of INPE/SRE activities related to the vegetation/forest area
[INPE-4969-RPE/604] 13 p1819 N90-20446
Shade images of forested areas obtained from LANDSAT MSS data
[NASA-TM-102939] 14 p1995 N90-21436
Evolution of remote sensing applied to vegetation and forest at INPE
[INPE-4970-PRE/1538] 14 p1998 N90-21452
Effects of Air Pollution on Western Forests
[PB90-131111] 14 p2003 N90-21481
Millimeter-wave bistatic scattering by terrain
15 p2085 N90-21936
Modeling the lateral diffusion of fluorescent particles within a forest canopy 15 p2121 N90-22136
Cloud chemistry and occurrence in the western United States: A synopsis of current information
[PB90-134248] 15 p2131 N90-22182

A case for archaeological reconnaissance of the Cabo Catoche-Porvenir region of the northeastern Yucatan Peninsula
|NASA-TM-102248| 16 p2249 N90-22827
Seasonal LAI in slash pine estimated with LANDSAT TM
|NASA-TM-102278| 19 p2706 N90-25397
Wideband characterization of forest propagation channels 20 p2846 N90-26188
Catching our breath: Next steps for reducing urban ozone
|PB90-130451| 20 p2883 N90-26398
Measurements of monoterpenes in a coniferous forest 20 p2886 N90-26421
Terpene concentrations and emissions in a Scots pine forest 20 p2886 N90-26422
Comparison of overstory canopy cover estimates on forest survey plots
|PB90-159484| 22 p3194 N90-28126
Evaluation of the role of ozone, acid deposition, and other airborne pollutants in the forests of eastern North America
|PB90-184896| 22 p3197 N90-28140
Climate change and America's forests
|PB90-205477| 22 p3199 N90-28155
A manual for analysis of hemispherical canopy photography
|DE90-014718| 23 p3342 N90-28885
Activities report for the IBDF-INPE project SEQE, year 1987
|INPE-4534-RPE/565| 23 p3415 N90-29298
Effects of increased CO2 on forest response
|DE90-015406| 24 p3487 N90-29708

FORGING
Characterization of the 6242 Si alloy. Centrifugal wheel in conventional forging
|REPT-NT-3967| 10 p1355 N90-17859
Evaluation of material homogeneity as a function of thickness of low-alloy ferritic steel
|DE90-008069| 13 p1777 N90-20202
Investigation of metal processing technology
|AD-A218835| 17 p2376 N90-23531

FORKS
Software to characterize tuning fork resonators used in the Quartz Digital Accelerometer
|DE90-007913| 14 p1983 N90-21363

FORM
U SHAPES

FORM FACTORS
Large basis space effects in electron scattering form factors of light nuclei
|DE90-613501| 14 p2025 N90-21609

FORM PERCEPTION
U SPACE PERCEPTION

FORMALDEHYDE
Structure and properties of resorcinol-formaldehyde gels
|DE90-005201| 10 p1358 N90-17876
The role of clouds in the photochemistry of the background troposphere 12 p1688 N90-19694
Physico-chemical properties of formaldehyde-ice-dust mixtures 12 p1740 N90-20000
Study of the polyoxymethylene and its sputtered fragments: Implications for comets 20 p2949 N90-26781

FORMALISM
The integration of structured and formal methods
|RSRE-MEMO-4293| 04 p0531 N90-13068
Computer oriented methods of multibody dynamics for application in vehicle technology
|DFVLR-FB-89-17| 04 p0533 N90-13080
Corrections to the thin wall approximation in general relativity
|NASA-CR-186078| 04 p0562 N90-13274
Canonical formalism for coupled beam optics
|DE90-003764| 07 p0992 N90-15734
Formalisms for user interface specification and design 08 p1155 N90-16687
Theory of defect process: Basic issues in quantitative understanding
|AERE-R-13661| 13 p1892 N90-20860
A Lagrangian formalism for nonequilibrium ensembles
|DE90-612748| 14 p2020 N90-21579
Problems in radiative transfer in astrophysics: An escape probability treatment of line overlap and a model of the masers around VX Sgr 14 p2041 N90-21705
Incomparable elements in algebraic lattices with applications to formal language theory
|MEMO-INF-89-54| 15 p2148 N90-22269
Processes and formalisms for unbounded choice
|CS-8917| 16 p2305 N90-23135
A process specification formalism based on static COLD
|CWI-CS-R8930| 17 p2448 N90-23960
A formal approach to conformance testing
|MEMO-INF-89-45| 17 p2449 N90-23964
Belief networks in plausible reasoning
|CWI-CS-R8927| 17 p2467 N90-24098
On the relationship between energy density and net power (intensity) in coupled one-dimensional dynamic systems
|AD-A221071| 19 p2709 N90-25421
Formal verification of distributed computing systems: Logic characterization of behaviour equivalence
|LAAS-89386| 20 p2910 N90-26555
High intensity effects in Raman scattering
|DE90-012093| 21 p3076 N90-27486
BRS invariant stochastic quantization of Einstein gravity
|DE90-791126| 21 p3085 N90-27541
An introduction to space trajectories 22 p3127 N90-27749
Study of an environment using formal reasoning. DILOG: State of the art and prototype
|CERT-1/334300-DERI| 22 p3239 N90-28368
Computational neural learning formalisms for manipulator inverse kinematics 23 p3368 N90-29030
Temporal logics meet telerobotics 24 p3521 N90-29905

FORMAT
Robotic vehicle message format
|AD-A210996| 01 p0110 N90-10627
FORTRAN program for x ray photoelectron spectroscopy data reformatting
|NASA-TP-2957| 03 p0409 N90-12348
A formatting style for typesetting and distributing draft international standards
|NPL-DITC-143/89| 04 p0530 N90-13059
Sequential rapid communication visual displays
|AD-D014282| 08 p1056 N90-16106
Executive summary for designing online help systems: Report of year 1 activity
|AD-A214811| 09 p1262 N90-17320
A specification and analysis of the IEEE (Institute of Electrical and Electronic Engineers) token ring protocol
|AD-A214567| 09 p1269 N90-17359
A head up display format for application to V/STOL aircraft approach and landing
|NASA-TM-102216| 10 p1320 N90-17632
Raster Metafile and Raster Metafile Translator
|NASA-TM-102588| 10 p1417 N90-18166
PCI: A PATRAN-NASTRAN model translator 18 p2569 N90-24639
A generic interface between COSMIC/NASTRAN and PATRAN (R) 18 p2569 N90-24640
UEDIT: A full-scale, scrollable APL2 spreadsheet input/output editor
|AD-A222712| 20 p2910 N90-26557
Improved meteorological measurements from buoys and ships (IMET): Preliminary conventions from buoys and standards data and file formats
|PB90-241910| 22 p3229 N90-28312
Distributed database concepts for command and control information systems
|FFI-90/7005| 22 p3260 N90-28462

FORMATES
MHD seed recovery and regeneration
|DE89-002711| 01 p0125 N90-10715

FORMATION HEAT
U HEAT OF FORMATION

FORMIC ACID
New observations of interstellar organic molecules 21 p3094 N90-27587

FORMING TECHNIQUES
NT AUSFORMING
NT CASTING
NT COLD ROLLING
NT COLD WORKING
NT ELECTROFORMING
NT EXPLOSIVE FORMING
NT EXTRUDING
NT FORGING
NT HOT WORKING
NT INJECTION MOLDING
NT METAL DRAWING
NT PRESSING (FORMING)
NT PULTRUSION
NT ROLL FORMING
NT SLIP CASTING
Application of superplastically formed and diffusion bonded aluminum to a laminar flow control leading edge
|NASA-CR-178316| 01 p0007 N90-10030
Superplastic forming and diffusion bonding of rapidly solidified, dispersion strengthened aluminum alloys for elevated temperature structural applications
|NASA-CR-181849| 04 p0474 N90-12718
Superplastic sheet forming 06 p0743 N90-14327
Production of a variety of shapes using wrapping and draping techniques
|REPT-892-430-122| 16 p2213 N90-22625
Dimensional analysis of structures using wrapping techniques
|REPT-892-430-119| 16 p2247 N90-22815
Compression molded polyurethane block copolymers. 1: Thermal and thermomechanical properties
|AD-A220068| 18 p2529 N90-24431
CAD/CAM reinforces the competitive edge of European mouldmakers
|CRIF-MC-88| 20 p2908 N90-26542
Interlaminar shear tests on continuous fiber reinforced thermoplastics: The effects of rubber forming
|LR-621| 24 p3444 N90-29451

FORMULAS (MATHEMATICS)
Process expressions and Hoare's logic
|CWI-CS-R8905| 04 p0532 N90-13076
Jacobi functions as limit cases of q-ultraspherical polynomials
|CWI-PM-R8807| 04 p0541 N90-13139
Index formulas for generalized Wiener-Hopf operators and Boson-Fermion correspondence in 2N dimensions
|CWI-PM-R8811| 04 p0542 N90-13141
The addition formula for little q-Legendre polynomials and the SU(2) quantum group
|CWI-AM-R8906| 04 p0543 N90-13151
Explicit formulas for Hankel norm approximations of infinite-dimensional systems
|TW-289| 04 p0545 N90-13167
A modified Moebius inverse formula and its applications in physics
|DE90-612740| 14 p2022 N90-21594
From Penman to Makkink: A new method for the calculation of the climatological evaporation numbers
|KNMI-TR-111| 15 p2126 N90-22161
Methods of jet calculation
|REPT-892-422-102| 16 p2209 N90-22603

FORMULATIONS
Effective permeability of mixtures
|PB89-218952| 03 p0323 N90-11839
A methodology for formulating a minimal uncertainty model for robust control system design and analysis 16 p2287 N90-23028
Formula scoring: Basic theory and applications
|AD-A218368| 17 p2465 N90-24083
The acute, delayed neurotoxicity evaluation of two jet engine oil formulations
|AD-A222018| 21 p2986 N90-26972
Chiral Maxwell-Garnett mixing formula
|PB90-189143| 23 p3391 N90-29158
An enhanced integrated aerodynamic load/dynamic optimization procedure for helicopter rotor blades
|NASA-CR-4326| 24 p3432 N90-29383

FORTRAN
Manual for Program PSTRESS: Peel stress computation
|NASA-CR-178408| 03 p0321 N90-11822
Calculation of transient response from time-harmonic spectrum
|AD-A211972| 03 p0393 N90-12241
FORTRAN program for x ray photoelectron spectroscopy data reformatting
|NASA-TP-2957| 03 p0409 N90-12348
Subspace iteration algorithms in FORTRAN 77 and FORTRAN 8x
|AD-A212275| 04 p0533 N90-13083
NUMVEC FORTRAN library manual chapter: Simultaneous linear equations
|CWI-NM-R8903| 04 p0541 N90-13135
FORTRAN subroutines for the evaluation of the confluent hypergeometric functions
|AD-A213308| 05 p0689 N90-14012
Developmental versions of FORTRAN/77 routines for the design and analysis of mixture experiments
|DE90-003513| 07 p0974 N90-15624
EZVIDEO, FORTRAN graphics routines for the IBM AT
|DE90-004409| 08 p1109 N90-16422
Lessons learned in the transition to ADA from FORTRAN at NASA/Goddard
|NASA-CR-186458| 12 p1701 N90-19765
Lessons learned in the transition to Ada from FORTRAN at NASA/Goddard
|NASA-TM-103311| 14 p2014 N90-21538
TOODEE: A two-dimensional, time-dependent heat conduction program
|DE90-009631| 15 p2099 N90-22010
FORTRAN coding guidelines
|DE90-009804| 15 p2146 N90-22258
NASTRAN migration to UNIX 18 p2569 N90-24643
A user-friendly, menu-driven, language-free laser characteristics curves graphing program for desk-top IBM PC compatible computers 18 p2644 N90-25056
A simulation code for turbocompound diesel engines
|IAR-89-26| 19 p2697 N90-25348
Interactive grid generation on small computers
|AD-A221234| 19 p2742 N90-25585

LINTERP: A numerical algorithm for interpolating quadrilateral and hexahedral meshes
|DE90-014417| 23 p3379 N90-29090
Software development tools
|PB90-250051| 23 p3381 N90-29103
ELEFUNT test results under AST FORTRAN V1.8.0 on the sequent symmetry
|DE90-014932| 23 p3387 N90-29127
Semiconductor measurement technology. EPROP: An interactive FORTRAN program for computing selected electronic properties of Gallium Arsenide and Silicon
|PB90-222738| 23 p3399 N90-29203

FORWARD LOOKING INFRARED DETECTORS
U FLIR DETECTORS

FORWARD SCATTERING
Droplet sizing instrumentation used for icing research: Operation, calibration, and accuracy
|NASA-CR-182293| 03 p0350 N90-11999
Ion beam analysis of diffusion in polymer glasses
|AD-A212339| 04 p0480 N90-12756
Research on acoustical scattering, diffraction catastrophes, optics of bubbles, acoustical phase conjugation, and wake of an oscillating circular cylinder
|AD-A214168| 07 p0989 N90-15711
CW (Continuous Wave) stimulated Brillouin scattering of long-pulse chemical laser beams
|AD-A216409| 10 p1390 N90-18039
An optical white light speckle process in forward dispersion for measurement of the velocity field in free convective currents
|ETN-90-95913| 12 p1661 N90-19546
Millimeter-wave bistatic scattering by terrain
15 p2085 N90-21936
Comparison test of droplet sizing instruments used in icing research
|DOT/FAA/CT-TN90/13| 19 p2693 N90-25322
Backscatter enhancement in scattering from rough surfaces
|AD-A223110| 21 p2995 N90-27024

FOSSIL FUELS
NT COAL
NT CRUDE OIL
NT NATURAL GAS
NT PEAT
The effect of degree of aromaticity and alkyl substitution of polyaromatic hydrocarbons on instrumental response factors
|DE89-000761| 02 p0196 N90-11117
Activities report on KEMA R and D
|ST-REPT-VOL-6-NO-12| 03 p0367 N90-12100
Long-term worldwide environmental effects caused by acid rain from fossil fuels
|DE90-001534| 07 p0956 N90-15533
Global climate change: A fossil energy perspective
|DE90-003770| 07 p0958 N90-15541
A preliminary analysis of US CO2 emissions reduction potential from energy conservation and the substitution of natural gas for coal in the period to 2010
|DOE/NBB-0085| 12 p1684 N90-19673
A fossil energy perspective on global climate change
|DE90-007894| 14 p2004 N90-21483
Formation kinetics of N2O in the atmosphere
20 p2886 N90-26425
Tropospheric nitrogen: The influence of anthropogenic sources on distributions and deposition
|DE90-015408| 24 p3487 N90-29709

FOSSIL METEORITE CRATERS
U METEORITE CRATERS

FOULING
NT ANTIFOULING
Predicting the performance of ceramic filters by the use of silt density index
|DE90-001316| 07 p0909 N90-15256
Development of a computational fluid dynamics and chemistry model for the fouling of jet fuels
|DE90-005664| 15 p2098 N90-22003
Development of a mathematical model for the thermal decomposition of aviation fuels
|AD-A221673| 21 p2990 N90-26994

FOUNDATIONS
NT PILE FOUNDATIONS

FOURIER ANALYSIS
NT FOURIER SERIES
Data acquisition in aerodynamic research
05 p0574 N90-13340
The initial imperfection data bank at the Delft University of Technology, part 2
|LR-559-PT-2| 05 p0656 N90-13825
Frequency agile synthetic aperture radar
|AD-D014235| 06 p0765 N90-14451
Comparison of shock severity measures
|DE90-000790| 06 p0799 N90-14654
Versatility of the CFR algorithm for limited angle reconstruction
|DE90-001421| 06 p0829 N90-14817
Characterizing transient vibrations using band limited moments
|DE90-000799| 07 p0945 N90-15473
Knowledge based signal processing
|AD-A214864| 09 p1205 N90-16986
Millimeter wave near-field study
|NASA-CR-182014| 14 p1932 N90-21058
A correlation-spectral method for line detection on noisy data
|DE90-007925| 14 p1967 N90-21266
On dual Lagrangian hyperbolic models for one dimensional two phase flow problems
|DE90-007012| 15 p2098 N90-22004
Severe shock and vibration environments for electronic components
|DE90-007686| 15 p2117 N90-22113
Fourier analysis of finite element preconditioned collocation schemes
|NASA-CR-182040| 16 p2304 N90-23128
Frequency domain techniques for analyzing picosecond optical pulses
|AD-A218856| 16 p2318 N90-23214
Two dimensional Fourier analysis of the earth gravitational field using the program package TIM
|ETN-90-96696| 17 p2424 N90-23815
Estimation of noise field directionality: Comparison with Fourier series method
|AD-A220366| 17 p2469 N90-24114
Signal processing on finite groups
|AD-A221129| 18 p2544 N90-24523
A theoretical analysis of the acoustic radiation from two-dimensional turbulent mixing layers
18 p2551 N90-24559
Optical signal processing
|AD-A220332| 18 p2615 N90-24897
Data analysis techniques 21 p3017 N90-27151
Formation of magnetic islands due to field perturbations in toroidal stellarator configurations
|DE90-014789| 23 p3397 N90-29191
Numerical and analytical study of nonlinear bifurcations associated with the morphological stability of two-dimensional single crystals
|PB90-209594| 23 p3398 N90-29200
Numerical simulations of the structure of supersonic shear layers
|AD-A224164| 24 p3467 N90-29587

FOURIER SERIES
Transfer functions for nonlinear systems via Fourier-Borel transforms
|NASA-TM-100034| 02 p0145 N90-10828
Effect of modal truncation on derivatives of closed-loop damping ratios in structural control
07 p0882 N90-15109
Fourier series methods for plates and shells with cracks and inclusions 14 p1990 N90-21406
Analysis of a finite two-dimensional solid with an inclined crack and a rigid inclusion 15 p2120 N90-22127
Dynamic and microphysical characteristics of cirrus clouds as revealed by aircraft, lidar, and other observations during FIRE 15 p2130 N90-22177
Significance of norms and completeness in variational based methods 16 p2296 N90-23078
Stochastic processes as Fourier integrals and dilation of vector measures
|AD-A219413| 16 p2308 N90-23150
Frequency analysis via the method of moment functionals
|NASA-CR-186988| 22 p3239 N90-28367
Stabilization of Taylor-Couette flow due to time-periodic outer cylinder oscillation
|PB90-219130| 23 p3323 N90-28790
Application of discrete Fourier series to the finite element stress analysis of axi-symmetric solids
|PB90-231010| 23 p3339 N90-28870

FOURIER TRANSFORMATION
NT FAST FOURIER TRANSFORMATIONS
An algorithm to calculate the beam momentum distribution from flying wire profiles
|DE89-015587| 01 p0073 N90-10418
Frequency domain aerodynamic analysis of interacting rotating systems 02 p0147 N90-10837
Evaluation of dispersive behavior in periodic structures by discrete Fourier transform 02 p0180 N90-11014
Gridded environmental data compaction: An investigation
|AD-A210580| 02 p0252 N90-11430
Computing the two dimensional fast Fourier transform on a general purpose mesh connected multiprocessor
|DE89-016515| 02 p0266 N90-11518
Implementing the discrete Fourier transform on the hypercube FPS T40
|IMAG-RR-773-I| 05 p0684 N90-13983
Distribution of a sum of n random variables and a central limit theorem based on moments or on coefficients of polynomial dependence
|IMAG-RR-768-M| 05 p0692 N90-14040
Soft x ray microscope using Fourier transform holography
|DE90-002291| 06 p0781 N90-14539
High resolution imaging by phase retrieval and discrimination using speckle, volume 1
|AD-A214243| 07 p0919 N90-15317
A study of a new time-domain method of lines and its application for the characterization of microstrip line and its discontinuities
|AD-A215441| 09 p1213 N90-17034
Testing and data path redesign of a high speed, 16-point Winograd Fourier transform processor
|AD-A215661| 09 p1213 N90-17036
Surface analyses and modelling of rate multiplicity and instabilities
|DE90-005418| 10 p1352 N90-17838
High temperature interaction of SO2 with oxide sorbents
|DE90-000435| 11 p1485 N90-18545
Measurement of spectral emissivity by Fourier transform infrared spectrometer
|DE89-782319| 11 p1510 N90-18698
Mathematical methods of Physics 6: Integral transformation
|INPE-4807-MD/40| 11 p1551 N90-18926
A simulation of optical propagation through atmospheric turbulence using two-dimensional Fourier transform techniques
|AD-A216776| 11 p1566 N90-19013
Signal processing
|DE90-006904| 12 p1647 N90-19464
A technique for convolving unequally spaced samples using fast Fourier transforms
|DE90-006466| 12 p1707 N90-19802
Fourier transform methods in local gravity modeling
13 p1836 N90-20538
Fracture of sandwiched composites
14 p1946 N90-21136
Problems in ISAR processing with range resolution by stepped frequency bursts 14 p1962 N90-21238
Mesooptical Fourier transform microscope: A new device for high energy physics
|DE90-616423| 14 p2026 N90-21615
Propagation of transient acoustic waves in porous media
|ETN-90-96401| 15 p2099 N90-22015
The distribution of molecular clouds in spiral galaxies
15 p2186 N90-22489
Isoplanatic systems in mesooptics
|DE90-009785| 17 p2406 N90-23705
Down-range imaging of radar targets
|AD-A221084| 18 p2544 N90-24521
Renormalized microscopic theory of fluctuations in inhomogeneous magnetized plasmas
|DE90-611307| 18 p2617 N90-24908
Improved processing of ceramic superconductors
|DE90-009721| 18 p2624 N90-24951
Characterization of the surfaces of platinum/tin oxide based catalysts by Fourier transform spectroscopy (FTIR) 18 p2643 N90-25054
Modular arithmetic and randomization for exact matroid problems: Extended abstract
|REPT-89-064| 19 p2751 N90-25628
Methods for probing quasi-periodic oscillations on short time scales 19 p2780 N90-25811
Formation of design envelope criterion in terms of deterministic spectral procedure
|RAE-TM-SS-9| 20 p2804 N90-25953
Application and extension of an analytical model of the confined acoustic beam generated by a transducer
|AD-A222994| 20 p2924 N90-26639
High resolution infrared spectroscopy of planetary molecules using diode lasers and Fourier transform spectrometers 20 p2943 N90-26747
Novel laser gain and time-resolved FTIR studies of photochemistry 20 p2945 N90-26756
Description of SAFIRE for ISES
21 p3016 N90-27148
FT-IR spectroscopic studies of polycyclic aromatic hydrocarbons 21 p3095 N90-27592
Image compression
|AD-A224242| 24 p3537 N90-29998
Adaptive, robust, high-resolution signal processing
|AD-A223728| 24 p3538 N90-30004

FOVEA
The effects of foveal load on peripheral sensitivity in the visual field
|AD-A214872| 09 p1251 N90-17260

FRACTALS
The quantitative analysis of fracture surfaces using fractals
|DE89-015361| 01 p0044 N90-10250
An introduction to fractals and chaos
|AD-A210257| 01 p0117 N90-10675

Configurational statistics of strings, fractals and polymer physics. Part 2: Non Abelian strings
[ROM1F-89-680-PT-2] 05 p0696 N90-14067
Fractal dimension of the fractured surface of materials
[DE89-635764] 07 p0946 N90-15477
A diffusion on a fractal state space
[AD-A213555] 07 p0988 N90-15707
Laser light scattering as a probe of fractal colloid aggregates 09 p1223 N90-17097
Fractal-based image compression
[AD-A215400] 09 p1268 N90-17351
Fractal geometry segmentation of polarimetric synthetic aperture radar images
[AD-A216278] 10 p1377 N90-17982
Chaotic transients, higher dimensional phenomena, and coupled ordinary differential equations
[DE90-006641] 12 p1706 N90-19794
Fractal-based image compression
[AD-A217302] 13 p1865 N90-20699
Low temperature properties of amorphous solids 15 p2171 N90-22405
Applications of dynamical systems theory to fractals: A study of cookie-cutter Cantor sets
[REPT-89-76] 17 p2458 N90-24032
Analogues of the Lebesgue density theorem for fractal sets of reals and integers
[REPT-89-88] 17 p2468 N90-24106
Heterogeneity description using fractal concepts 19 p2690 N90-25299
Particle tracking methods and fractal statistics in groundwater modeling 19 p2691 N90-25309
Fractal structure and fractal time in silica sol-gels
[DE90-013197] 20 p2838 N90-26144
Simple graphical descriptions of natural land profiles and the application of fractal and sub-fractal models to them
[RSRE-MEMO-4305] 22 p3195 N90-28130
A generalised Hubbard Hamiltonian: Influence of temperature and fractality
[DE90-627322] 23 p3400 N90-29213

FRACTIONATION
NT HYDROCRACKING
Thermal stability of jet fuel
[DE90-001160] 06 p0753 N90-14385

FRACTOGRAPHY
The quantitative analysis of fracture surfaces using fractals
[DE89-015361] 01 p0044 N90-10250
Ceramic components in machines, Cologne and Aachen, West Germany; Maastricht, The Netherlands and Brussels, Belgium
[DE89-015831] 01 p0047 N90-10264
Effect of thermal and cyclic loads on silicon carbide yarn reinforced glass matrix composites
[DE89-016554] 02 p0191 N90-11091
A technique to correlate fractography with NDE (Non-Destructive Evaluation) of small samples
[DE89-016904] 02 p0231 N90-11325
Fractographic and microstructural analysis of fatigue crack growth in a Ti-6Al-4V fan disc forging
[NLR-MP-88028-U] 03 p0330 N90-11877
Flexure strength of advanced ceramics: A round robin exercise
[AD-A212101] 03 p0332 N90-11889
Fractography of composite delamination
[NASA-CR-183291] 05 p0617 N90-13599
Fractographic analysis of long rod penetrator-armor ceramic interactions
[AD-A215172] 09 p1197 N90-16938
Comparison of tension, compression, and flexure creep for alumina and silicon nitride ceramics
[DE90-006154] 11 p1492 N90-18586
Fractographic analysis of the crack growth rate and the shear lip development of 2024-T3 specimens under simple variable-amplitude loading
[PB90-167032] 14 p1994 N90-21427
Failure analysis handbook
[AD-A219747] 17 p2413 N90-23752
Fractographic observations on fatigue crack growth in 2024-T3 sheet material under flight-simulation loading
[LR-592] 17 p2415 N90-23760
Fractography of composite delamination
[NASA-CR-181965] 19 p2702 N90-25372
Fractographic analysis of fatigue crack growth under two-blocks loading on 2024-T351 sheet specimens
[LR-628] 24 p3482 N90-29680
Effects of blocks of overloads and underloads on fatigue crack growth in 2024-T351 sheet specimens: Fractographic analysis and crack closure predictions
[LR-629] 24 p3482 N90-29681
Fractographic observations on fatigue crack growth under miniTWIST flight-simulation loading (2024-T3 material)
[LR-631] 24 p3483 N90-29684
Fractographic analysis of fatigue failures of airframe equipment parts: Examples of a rod end housing and a rod end cap
[NAL-TR-1047] 24 p3483 N90-29686

FRACTURE MECHANICS
Failure behavior of PEEK and its short-fiber composite systems
[AD-A210729] 01 p0035 N90-10189
Influence of microstructure and microdamage processes on fracture at high loading rates
[AD-A210307] 01 p0045 N90-10253
Mechanics of the crack path formation
[NASA-CR-185143] 01 p0080 N90-10455
Particle emission and charging effects induced by fracture
[AD-A210215] 01 p0080 N90-10459
Fatigue growth and closure of short cracks
[AD-A210824] 01 p0081 N90-10462
Review of the ESA fracture control policy 02 p0182 N90-11029
A re-evaluation of fatigue threshold test procedures and the simulation and prediction of fatigue crack growth under conditions of low crack closure 02 p0231 N90-11328
Deformation behavior of SiC/2014 Al metal-matrix composite
[AD-A212095] 03 p0320 N90-11816
Fundamental tribological properties of ion-beam-deposited boron nitride films
[NASA-TM-102088] 03 p0331 N90-11881
An application of the J-integral to an incremental analysis of blunting crack behavior
[DE89-016844] 03 p0358 N90-12046
An experimental and analytical program to develop crack tip fracture criteria
[AD-A211565] 03 p0359 N90-12051
Rapid heating tensile tests of high-energy-rate-forged 316L stainless steel charged with hydrogen and tritium
[DE89-017869] 04 p0474 N90-12717
Spall resistance of alumina
[AD-A213213] 04 p0477 N90-12735
Unilateral contact analysis of a crack with friction. Applications
[ETN-89-95511] 04 p0512 N90-12956
The effect of a rigid elliptical inclusion on a straight crack
[AD-A212263] 04 p0513 N90-12965
Ductile failure
[AD-A212975] 05 p0618 N90-13601
Fatigue behavior of silicon carbide Whisker/Aluminum composite
[AD-A213094] 05 p0618 N90-13603
The adhesive bonding of thermoplastic composites
[AD-A213358] 05 p0618 N90-13605
Toughening mechanisms in ceramic composites
[PB89-235907] 05 p0626 N90-13656
Theoretical evaluation of defects in pressure vessels and pipings
[CRIF-MT-174] 05 p0651 N90-13798
Stress intensity factors for cracking metal structures under rapid thermal loading. Volume 2: Theoretical background
[AD-A213297] 05 p0654 N90-13812
Application of fracture mechanics and half-cycle method to the prediction of fatigue life of B-52 aircraft pylon components
[NASA-TM-88277] 05 p0655 N90-13820
Effects of dislocation substructure and prestrain on fracture behavior in aluminum and steel alloys 06 p0745 N90-14334
The effect of hydrogen charging on the mechanical properties of aluminum alloy 2090
[DE90-000129] 06 p0746 N90-14341
Non-linear vibrations, stability, and dynamics of structures and mechanisms
[AD-A212152] 06 p0796 N90-14639
A nonlinear high temperature fracture mechanics basis for strainrange partitioning
[NASA-TM-4133] 06 p0797 N90-14642
Fatigue fracture in the presence of shot peening residual stresses: Initiation, propagation, and relaxation phenomena 06 p0797 N90-14644
Mechanics of interaction of a crack with microcracks 06 p0798 N90-14650
Fracture mechanics of porous materials
[DE90-000023] 06 p0800 N90-14657
Engineering approaches to the application of fracture toughness data in the nuclear industry
[DE90-001596] 06 p0800 N90-14659
An analysis of drilling of composite materials 07 p0889 N90-15142
Fatigue, fracture mechanics and corrosion properties of some aluminium-lithium alloys 07 p0898 N90-15194
Fatigue and fracture behaviour of a PM Al-Li alloy 07 p0899 N90-15195
Hardening and toughening of ZnS-Ga2S3 ceramics by solid-state reactions
[AD-A213875] 07 p0912 N90-15276
On the domain of dominance of the asymptotic elastodynamic crack-tip fields 07 p0944 N90-15468
Experience with J testing of 304/308 stainless steel weldment
[DE90-002046] 07 p0946 N90-15478
Effects of high rate shear on the microstructure and deformation and fracture behavior of two high strength steels
[AD-A214107] 08 p1044 N90-16032
Rainflow counting algorithm for the LIFE2 fatigue analysis code
[DE90-002834] 08 p1096 N90-16344
Effects of heat treatment on microstructure and flexural properties of unidirectional carbon-carbon composites
[AD-A214985] 09 p1186 N90-16873
Assessment of strength limiting flaws in ceramic heat exchanger tubes, phase 2
[DE90-004081] 09 p1220 N90-17080
Analysis of some fracture mechanics test procedures for defence research applications
[MRL-TR-89-11] 09 p1236 N90-17175
Heavy-section steel technology program fracture issues
[DE90-005264] 09 p1240 N90-17195
Studies on deformation and fracture of viscoelastic composite materials
[AD-A216095] 10 p1348 N90-17819
Fundamental studies of time-dependent response and fracture of cross-linked polymers
[AD-A216694] 10 p1360 N90-17886
Validation of the boundary element method applied to complex fracture mechanics conditions
[AD-A216412] 10 p1398 N90-18080
AGARD/SMP Review: Damage Tolerance for Engine Structures. 2: Defects and Quantitative Materials Behaviour --- conference
[AGARD-R-769] 11 p1457 N90-18396
Defects: Their behaviour and related design assumptions 11 p1457 N90-18397
Review of modelling methods to take account of material structure and defects 11 p1458 N90-18402
Compact reinforced composite basic principles
[CBL-41] 11 p1480 N90-18520
Corrosion fatigue of iron-chromium-nickel alloys: Fracture mechanics and chemistry
[DE90-006318] 11 p1487 N90-18556
Identification of a cast iron alloy containing nonstrategic elements
[NASA-CR-185174] 11 p1487 N90-18559
Deformation and fracture of ordered intermetallic compounds
[DE90-007422] 11 p1488 N90-18563
Fundamental aspects of erosion and impact damage
[DE90-006640] 11 p1492 N90-18587
Fracture mechanical aspects of dust emission processes from a model comet surface 12 p1740 N90-20004
Mechanical behavior of whisker reinforced ceramics
[DE90-008758] 13 p1781 N90-20224
Limitations and applications of fracture assessment with R6
[AERE-R-13012] 13 p1815 N90-20425
Computer simulations and experiments to study the fracture of rods by flying plates
[DE90-008308] 13 p1817 N90-20437
A corrosion fatigue/stress corrosion testing facility at Materials Research Laboratory
[MRL-TN-568] 14 p1929 N90-21044
Use of unbalanced laminates as a screening method for microcracking
[NASA-TM-102517] 14 p1944 N90-21124
Fracture and longevity of composite structures
[AD-A217827] 14 p1944 N90-21127
Three-dimensional elastic-plastic analysis of shallow cracks in single-edge-crack-tension specimens
[NASA-TM-102636] 14 p1945 N90-21130
Two-dimensional damage models of fiber-reinforced composites 14 p1946 N90-21135
Shock initiation sensitivity of damaged TP-H1207C composite propellant
[DE90-008509] 14 p1957 N90-21205
Mechanics of interface fracture 14 p1990 N90-21408
Compendium of fracture mechanics problems
[NASA-TM-100393] 14 p1992 N90-21414
Development of a fracture analysis technique for use with a general-purpose finite element program 14 p1992 N90-21416
NASA airframe structural integrity program
[NASA-TM-102637] 14 p1993 N90-21422
An evaluation of the pressure proof test concept for thin sheet 2024-T3
[NASA-TM-101675] 14 p1994 N90-21424

Determination of internal strains in high-temperature superconductor composites by intense pulsed neutron source
[DE90-007799] 14 p2033 N90-21664
The thermo-mechanical behavior of cometary nuclei 14 p2041 N90-21703
Computational simulation of structural fracture in fiber composites
[NASA-TM-102505] 15 p2064 N90-21821
Energy release rate analysis of interfacial cracks in composites 15 p2065 N90-21829
The effect of hydrogen and microstructure on the deformation and fracture behavior of a single crystal nickel-base superalloy
[NASA-CR-185219] 15 p2068 N90-21849
Fracture toughness and tensile properties of alloy HT9 in thin sections under high neutron fluences
[DE90-008386] 15 p2069 N90-21851
Fracture mechanics of monolithic ceramic materials under small scale microcracking conditions 15 p2070 N90-21860
Contact mechanics for three-dimensional geometries 15 p2111 N90-22076
Institute for Materials Science and Engineering, Fracture and Deformation Division: Technical activities, 1989
[PB90-155359] 15 p2116 N90-22106
Nonlinear fracture mechanics using semicircular specimens and tension-softening behavior 15 p2116 N90-22108
Continued research on the strain to failure of thick-walled cylinders subjected to internal pressure
[DE90-008952] 15 p2118 N90-22115
Inclusion of unstable ductile tearing and extrapolated crack-arrest toughness data in PWR vessel integrity assessment
[DE90-009427] 15 p2118 N90-22116
An investigation into the foundations of elastic-plastic fracture mechanics 15 p2120 N90-22130
Probabilistic finite elements: Applications to fracture and fatigue 15 p2121 N90-22134
In-situ fracture stiffness determination
[DE90-009202] 15 p2129 N90-22173
A comprehensive study on microstructure mechanics relationships of ceramic matrix composites
[AD-A219318] 16 p2213 N90-22627
NASA-UVA light aerospace alloy and structures technology program
[NASA-CR-182607] 16 p2217 N90-22651
Elevated temperature crack growth in advanced powder metallurgy aluminum alloys 16 p2218 N90-22653
Elevated temperature crack growth in aluminum alloys: Tensile deformation of 2618 and FVS0812 aluminum alloys 16 p2218 N90-22654
Deformation and fracture of thin sheet aluminum-lithium alloys: The effect of cryogenic temperatures 16 p2218 N90-22655
Deformation and fracture of aluminum-lithium alloys: The effect of dissolved hydrogen 16 p2219 N90-22658
Quantitative characterization of spatial distribution of particles in materials: Application to materials processing 16 p2219 N90-22660
Microcracking and toughness of ceramic-fiber/ceramic-matrix composites under nigh temperature
[AD-A218516] 16 p2223 N90-22680
Computations of weight functions in fracture mechanics 16 p2246 N90-22809
Comparison between data generated from standard fracture toughness specimens and from nonstandard specimens made of a silicon carbide
[DE90-009621] 16 p2247 N90-22814
Material instabilities in solids
[AD-A218451] 16 p2247 N90-22817
Fracture mechanics assessment of a cracked 16-inch inner diameter 1945 vintage-jacketed pressure vessel
[AD-A219135] 16 p2248 N90-22819
Ply cracking in composite laminates 17 p2368 N90-23478
Micro-mechanical modeling of crack growth resistance in a carbon/carbon composite
[DE90-009407] 17 p2368 N90-23479
Controlled crack growth specimen for brittle systems
[NASA-TM-103126] 17 p2378 N90-23543
Failure analysis handbook
[AD-A219747] 17 p2413 N90-23752
Wide range stress intensity factor and crack-mouth-opening displacement expressions suitable for short crack fracture testing with arc bend-chord support samples
[AD-A218395] 17 p2415 N90-23761
Brittle torsional fatigue crack initiation in an otherwise ductile environment
[AD-A220858] 17 p2416 N90-23767
Corrosion fatigue crack propagation in metals
[NASA-CR-4301] 18 p2524 N90-24405
Fracture behavior of surface modified ceramics
[DE90-011552] 18 p2532 N90-24449
Theoretical studies of non-Newtonian and Newtonian fluid flow through porous media
[DE90-011610] 18 p2554 N90-24576
Effect of film adhesion on tribological properties of silver-coated alumina
[DE90-010090] 18 p2564 N90-24632
Use of neutron diffraction in determining strains in high-temperature superconducting composites
[DE90-010404] 18 p2621 N90-24931
Structural zooming research and development of an interactive computer graphical interface for stress analysis of cracks 18 p2641 N90-25042
Deformation and fracture behavior of TiAl
[DE90-012212] 19 p2675 N90-25212
Comparison of two computer codes for crack growth analysis: NASCRAC Versus NASA/FLAGRO
[NASA-TM-100383] 19 p2700 N90-25360
Fractography of composite delamination
[NASA-CR-181965] 19 p2702 N90-25372
ESA fracture control requirements
[ESA-PSS-01-401-ISSUE-1] 19 p2703 N90-25376
Fracture mechanics in integrated design of new, ultra-strong materials and structures
[CBL-REPRINT-21] 19 p2703 N90-25378
Hydrogen induced fracture characteristics of single crystal nickel-based superalloys
[NASA-CR-183992] 20 p2832 N90-26106
Fracture toughness and failure mechanisms in commercial 2091 Al-Li sheet at cryogenic temperatures
[AD-A222803] 20 p2835 N90-26125
Evaluation of fracture strength properties of silicon carbide ceramics under cyclic/static axial loading at ultra-high temperature
[DE90-503402] 20 p2839 N90-26147
Fatigue life assessment using a short crack growth model
[PNR90663] 20 p2877 N90-26367
Retirement for cause of the F100 engine 21 p2957 N90-26813
Damage tolerance analysis for manned hypervelocity vehicles. Volume 2: Software user's manual
[AD-A222136] 21 p2959 N90-26826
Engineering fracture mechanics
[AD-A222699] 21 p3012 N90-27123
Micromechanics of size effect in failure due to distributed cracking
[AD-A223211] 21 p3013 N90-27128
Fracture mechanics analysis for short cracks
[AD-A222170] 21 p3013 N90-27130
Load-point compliance for the arc bend-arc support fracture toughness specimen
[AD-A221618] 21 p3014 N90-27134
On modeling the effect of pore shapes on ductile fracture
[AD-A221774] 21 p3014 N90-27136
Fracture-EXAFS: A new method for the study of interfaces in thin films and polycrystalline materials
[DE90-013736] 21 p3081 N90-27521
The role of component testing 22 p3117 N90-27707
Component behaviour and life management: The need for common AGARD approaches and actions 22 p3118 N90-27710
The role of NDI in the certification of turbine engine components 22 p3184 N90-28069
Damage tolerance analysis for manned hypervelocity vehicles. Volume 1: Final technical report
[AD-A221970] 22 p3191 N90-28106
A comparison of single-cycle versus multiple-cycle proof testing strategies
[NASA-CR-4318] 22 p3193 N90-28115
NASCRAC (trademark): A fracture mechanics analysis code 23 p3296 N90-28645
A comparison of single-cycle versus multi-cycle proof testing strategies 23 p3296 N90-28646
Data base for crack growth properties of materials 23 p3296 N90-28647
Comparison of two computer codes for crack growth analysis: NASCRAC versus NASA/FLAGRO 23 p3297 N90-28648
Probabilistic model for fracture mechanics service life analysis 23 p3297 N90-28650
Crack layer analysis of fatigue fracture of a beta titanium alloy 23 p3338 N90-28864
Assessment and improvement of aeroengine disc structural integrity 24 p3433 N90-29392
Powder processing of aluminides
[DE90-015314] 24 p3444 N90-29447
Surface chemistry and structural effects in the stress corrosion of glass and ceramic materials
[AD-A223305] 24 p3454 N90-29507
Ion-beam-assisted deposition of silver films on zirconia ceramics for improved tribological behavior
[DE90-009706] 24 p3456 N90-29516
The ACR-program for automatic finite element model generation for part through cracks
[DE90-631545] 24 p3479 N90-29662
Studies on crack mechanics
[AD-A223634] 24 p3480 N90-29670
An investigation of crack-tip stress field criteria for predicting cleavage-crack initiation
[DE90-015597] 24 p3480 N90-29672
An investigation of hole-edge crack problem by a combined complex variable and least square method
[LR-626] 24 p3482 N90-29679

FRACTURE RESISTANCE
U FRACTURE STRENGTH

FRACTURE STRENGTH

The interlaminar fracture toughness of woven graphite/epoxy composites
[NASA-TP-2950] 01 p0033 N90-10179
Influence of microstructure and microdamage processes on fracture at high loading rates
[AD-A210307] 01 p0045 N90-10253
Mechanisms of strength and toughness in a microalloyed, precipitation hardened steel
[AD-A210571] 01 p0045 N90-10256
Stress intensity factors and displacements for arc bend samples using collocation
[AD-A210404] 01 p0080 N90-10460
Fracture toughness data base for HT9 and modified 9Cr-1Mo irradiated in several reactors up to approximately 100 dpa
[DE90-000111] 03 p0328 N90-11864
Crack propagation failure of carbon/resin composites
[ONERA-RT-45/7086-M] 04 p0467 N90-12677
Increased fragility of deep pressed thin plates
[CETIM-13-Y-313] 04 p0513 N90-12962
Mechanical property characterization of VascoMax T-300
[AD-A212950] 05 p0623 N90-13637
Toughening mechanisms in ceramic composites
[PB89-235907] 05 p0626 N90-13656
Effects of dislocation substructure and prestrain on fracture behavior in aluminum and steel alloys 06 p0745 N90-14334
The strength-toughness combination of the aluminum-lithium alloys 2090 and 2091 at cryogenic temperatures
[DE90-001425] 06 p0746 N90-14338
The 4.2 K fracture toughness of 304 stainless steel in a magnetic field
[DE90-002083] 06 p0747 N90-14347
Strength and toughness of monolithic and composite silicon nitrides
[NASA-TM-102423] 06 p0751 N90-14368
Engineering approaches to the application of fracture toughness data in the nuclear industry
[DE90-001596] 06 p0800 N90-14659
The mechanical behavior of a fiber-reinforced brittle matrix composite 07 p0889 N90-15139
Empirical and analytical determination of the fracture resistance of a TiB2 particle/SiC matrix composite
[NASA-TM-101940] 07 p0890 N90-15143
Mechanical properties and fracture toughness of 8090-T651 plate and 2091 and 8090 sheet 07 p0897 N90-15188
Investigation on sheet material of 8090 and 2091 aluminium-lithium alloy 07 p0898 N90-15192
Fatigue and fracture behaviour of a PM Al-Li alloy 07 p0899 N90-15195
Directional solidification of superalloys
[NASA-CASE-MFS-28314-1] 07 p0904 N90-15227
Solid-state phase equilibria in the ZnS-Ga2S3 system
[AD-A213944] 07 p0906 N90-15238
Toughening behavior and interfacial properties of fiber-reinforced ceramic composites
[DE89-015351] 07 p0913 N90-15279
Fully articulated four-point-bend loading fixture
[NASA-CASE-LEW-14776-1] 07 p0940 N90-15445
Fractal dimension of the fractured surface of materials
[DE89-635764] 07 p0946 N90-15477
A semiautomated computer-interactive dynamic impact testing system
[DE90-002721] 07 p0946 N90-15479
Method to produce titanium alloy articles with high fatigue and fracture resistance
[AD-D014278] 08 p1043 N90-16029
Fracture toughness of ferritic alloys at very high neutron exposures
[DE90-004519] 08 p1046 N90-16048
Experiences with three-point bending test specimens for determining the crack-arrest fracture toughness K(sub Ia) in low-alloy steel
[DE90-004120] 08 p1089 N90-16306
The effects of hydrogen embrittlement of titanium 08 p1156 N90-16698
Effects of T-tabs and large deflections in DCB specimen tests
[NASA-TM-101677] 09 p1186 N90-16868

The mechanisms of dispersion strengthening and fracture in Al-based XD (TM) alloys
[NASA-CR-4276] 09 p1187 N90-16879
High modulus coatings
[AD-A215448] 09 p1198 N90-16941
Mechanical aspects of interfaces in high performance composites 10 p1347 N90-17812
The processing and mechanical properties of high temperature/high performance composites. Book 1, section 1: Coatings and interfaces
[AD-A216141] 10 p1348 N90-17821
The processing and mechanical properties of high temperature/high performance composites. Book 4, section 3: Flow and creep strength
[AD-A216144] 10 p1349 N90-17822
Environmental embrittlement: A major cause for low ductility of ordered intermetallics
[DE90-006161] 10 p1356 N90-17864
Analysis of ductile fracture under biaxial loading using moire interferometry 10 p1394 N90-18060
Modified bismaleimides for carbon fibre composites 11 p1476 N90-18495
Analysis of whisker-toughened ceramic components: A design engineer's viewpoint
[NASA-TM-102333] 11 p1478 N90-18504
The processing and mechanical properties of high temperature/high performance composites. Book 2, section 2: Strength and fracture resistance
[AD-A216142] 11 p1478 N90-18507
Compact reinforced composite basic principles
[CBL-41] 11 p1480 N90-18520
Biaxial strength and stress rupture of hot-pressed silicon nitride
[AD-A216950] 11 p1519 N90-18750
Identification and development of optimum SiC whiskers for silicon nitride matrix composites
[DE90-006888] 12 p1621 N90-19315
Fracture strength analysis of silicon nitride and silicon carbide ceramics from an international cooperative research program
[DE90-005319] 12 p1630 N90-19368
Optimization of fracture resistance in composites
[AD-A217431] 13 p1768 N90-20144
Effect of heat treatment on the fracture toughness transition properties of an A508 class 3 steel
[AERE-R-13548] 13 p1774 N90-20182
Fatigue crack growth in martensitic 2 1/4Cr-1Mo steel at elevated temperatures
[AERE-R-13524] 13 p1776 N90-20191
Improved toughness alloys based on titanium aluminides
[AD-A218149] 13 p1778 N90-20208
Tensile fracture toughness of ceramic materials: Effects of dynamic loading and elevated temperatures
[DE90-008329] 13 p1781 N90-20223
Strength and microstructure of ceramics
[AD-A217752] 13 p1782 N90-20227
A compendium of sources of fracture toughness and fatigue crack growth data for metallic alloys, part 4
[NASA-TM-102646] 14 p1950 N90-21164
Fracture toughness and crack growth of Zerodur
[NASA-TM-4185] 14 p1954 N90-21187
Research advances in fine ceramics
[DE90-008983] 14 p1956 N90-21197
Fracture toughness and tensile properties of alloy HT9 in thin sections under high neutron fluences
[DE90-008386] 15 p2069 N90-21851
Nonlinear fracture mechanics using semicircular specimens and tension-softening behavior 15 p2116 N90-22108
Elevated temperature crack growth in advanced powder metallurgy aluminum alloys 16 p2218 N90-22653
Fracture toughness and fatigue crack initiation tests of welded precipitation-hardening stainless steel
[AD-A218745] 16 p2221 N90-22669
Comparison between data generated from standard fracture toughness specimens and from nonstandard specimens made of a silicon carbide
[DE90-009621] 16 p2247 N90-22814
The effect of thermal damage on the mechanical properties of polymer regrinds 18 p2515 N90-24363
Fracture toughness and solid-particle erosion of ceramic-matrix whisker-reinforced composites
[DE90-009713] 18 p2517 N90-24376
Fracture-tough, corrosion-resistant bearing steels
[NASA-CR-186796] 19 p2675 N90-25213
Crack bridging processes in toughened ceramics
[DE90-011650] 19 p2678 N90-25231
ESA fracture control requirements
[ESA-PSS-01-401-ISSUE-1] 19 p2703 N90-25376
The effect of manganese on the onset of the stage 2 reaction in an austempered ductile iron matrix
[DE90-011804] 20 p2834 N90-26119
Microstructural design for fatigue crack growth resistance in Ni-base alloy
[PNR90632] 20 p2834 N90-26120
Fracture toughness and failure mechanisms in commercial 2091 Al-Li sheet at cryogenic temperatures
[AD-A222803] 20 p2835 N90-26125
Fracture toughness of polyimide films
[NASA-TM-103473] 20 p2836 N90-26130
Influence of thermal conditioning media on Charpy specimen test temperature
[DE90-012784] 20 p2875 N90-26360
Static and fatigue strength of an adhesive bonded CFRP butt-strap joint: The effects of stacking sequence and temperature
[NLR-TR-88036-U] 20 p2877 N90-26370
Interfacial studies of Chemical Vapor Infiltrated (CVI) ceramic matrix composites
[AD-A221867] 21 p2972 N90-26893
Advanced processing and properties of high performance alloys
[AD-A221776] 21 p2983 N90-26948
Theory of ceramic/zirconia composites: Toughening, strengthening, and synergism
[AD-A222931] 21 p2985 N90-26961
A framework to correlate a/W ratio effects on elastic-plastic fracture toughness (J (sub c))
[AD-A222822] 21 p3012 N90-27125
Load-point compliance for the arc bend-arc support fracture toughness specimen
[AD-A221618] 21 p3014 N90-27134
Plane strain fracture toughness test procedures for particulate metal matrix composites
[NPL-DMM(A)-3] 22 p3153 N90-27873
Development of metastable processing paths for high temperature alloys
[AD-A223144] 22 p3157 N90-27898
Study of the microstructure of a titanium alloy (6246) for turbomachine compressors
[ETN-90-97450] 22 p3157 N90-27900
Influence of a surface finishing on the fatigue behavior of a 32CDV13 steel
[ETCA-89-R-164] 22 p3157 N90-27902
Micromechanical model of crack growth in fiber reinforced ceramics
[NASA-CR-4321] 22 p3192 N90-28113
Damage tolerance of woven graphite-epoxy buffer strip panels
[NASA-TM-102702] 22 p3192 N90-28114
Factors influencing the mode I interlaminar fracture resistance of toughened matrix composites 23 p3300 N90-28668
Micromechanisms of fatigue crack growth and fracture toughness in metal matrix composites
[AD-A223863] 23 p3302 N90-28676
Fretting fatigue strength of Ti-6Al-4V at room and elevated temperatures and ways of improving it 23 p3308 N90-28709
Ascertaining the fracture toughness of ceramic materials by means of bending testpieces of various notch types at ambient and high temperatures
[ESA-TT-992] 23 p3312 N90-28733
Influence of diesel engine exposure on the rupture strength of silicon nitride and partially stabilized zirconia
[DE90-014759] 23 p3334 N90-28849
Mechanical properties and fracture toughness of AAR-TC128 Grade B steel and a micro-alloyed, control-rolled steel, A 8XX grade B, from -80F to +73F
[PB90-207796] 24 p3448 N90-29471
The use of automated ball indentation testing to measure flow properties and estimate fracture toughness in metallic materials
[DE90-015797] 24 p3452 N90-29493

FRACTURE TOUGHNESS
U FRACTURE STRENGTH

FRACTURES (MATERIALS)
NT CRACK TIPS
NT CRACKS
NT MICROCRACKS
NT SHORT CRACKS
NT SURFACE CRACKS
Fracture and three dimensional stress analyses of 7075 aluminum projectile components under spin and inertia load
[AD-A210986] 01 p0081 N90-10463
Review of the ESA fracture control policy 02 p0182 N90-11029
Proceedings of the Army Symposium on Solid Mechanics, 1989: Mechanics of Engineered Materials and Applications
[AD-A211954] 04 p0511 N90-12951
A theory of damage in brittle and cementitious materials, part 1
[AD-A212940] 05 p0627 N90-13658
Theoretical evaluation of defects in pressure vessels and pipings
[CRIF-MT-174] 05 p0651 N90-13798
The Fourth Oxford International Conference on the Mechanical Properties of Materials at High Rates of Strain
[AD-A212293] 05 p0653 N90-13809
BAM: German Federal Institute for Materials Research and Testing, Berlin
[DE90-004293] 08 p1090 N90-16307
Some considerations on resource evaluation of The Geysers
[DE90-002119] 08 p1095 N90-16343
Failure analysis of a missile locking hook from the F-14 jet
[AD-A214995] 09 p1194 N90-16917
Taylor impact testing
[AD-A215018] 09 p1231 N90-17144
Validation of the boundary element method applied to complex fracture mechanics conditions
[AD-A216412] 10 p1398 N90-18080
Spallation and dynamic fracture as an effect of laser induced shock waves in carbon based composite materials
[AD-A216540] 11 p1478 N90-18509
The joint effect of surface microtopography and near-surface structure on microcontact conditions
[DE90-006494] 11 p1493 N90-18591
Summary report of the Summer Conference of the DARPA-Materials Research Council
[AD-A217380] 13 p1767 N90-20143
Fracture of sandwiched composites 14 p1946 N90-21136
A continuum damage model for the quasi-static response of brittle materials
[DE90-007681] 15 p2117 N90-22112
Internal fractures in model elastomeric composites 15 p2121 N90-22133
Surface roughness and the physical properties of fractures
[DE90-006046] 15 p2128 N90-22169
Effects of single fractures on seismic wave propagation
[DE90-009191] 15 p2129 N90-22171
Metal matrix composites microfracture: Computational simulation
[NASA-TM-103153] 18 p2518 N90-24383
Computational investigation of local material strength and toughness on crack growth
[AD-A223189] 21 p3012 N90-27127

FRACTURING
NT CRACKING (FRACTURING)
NT CRUSTAL FRACTURES
NT STRESS CORROSION CRACKING
The quantitative analysis of fracture surfaces using fractals
[DE89-015361] 01 p0044 N90-10250
Review of the ESA fracture control policy 02 p0182 N90-11029
Microstructural effects on spall fracture in 1008 steel
[DE89-016770] 02 p0198 N90-11131
Mechanisms of wear in structural ceramic materials 06 p0749 N90-14360
Critical and subcritical crack-growth behavior along toughened ceramic/metal interfaces 07 p0889 N90-15140
Deformation and fracture of low alloy steels at high temperature
[DE90-001274] 07 p0902 N90-15215
Assessment of strength limiting flaws in ceramic heat exchanger components
[DE90-004086] 08 p1051 N90-16077
Effects of moisture on composite materials 09 p1185 N90-16866
The mechanisms of dispersion strengthening and fracture in Al-based XD (TM) alloys
[NASA-CR-4276] 09 p1187 N90-16879
Studies on deformation and fracture of viscoelastic composite materials
[AD-A216095] 10 p1348 N90-17819
Interlaminar fracture testing of carbon fibre/PEEK composites validity and applications 11 p1477 N90-18497
Spallation and dynamic fracture as an effect of laser induced shock waves in carbon based composite materials
[AD-A216540] 11 p1478 N90-18509
Deformation and fracture of ordered intermetallic compounds
[DE90-007422] 11 p1488 N90-18563
Fracture analysis through photographic imagery of low spatial resolution: A contribution to the study of tectonic evoluation of the Araripe Plateau region
[INPE-4876-PRE/1487] 11 p1520 N90-18756
The patterns of fracture and the conditioning tectonics in the region of the Quadrilatero Ferrifero and part of the Migmatitic-Gnanulitic Complex in Minas Gerais (Brazil)
[INPE-4895-PRE/1496] 11 p1534 N90-18829

Effect of heat treatment on the fracture toughness transition properties of an A508 class 3 steel
[AERE-R-13548] 13 p1774 N90-20182
Ageing effects in welded cast CF3 stainless steel
[AERE-R-13559] 13 p1775 N90-20188
The stress-driven redistribution of point defects in the vicinity of crack-like singularities
[AERE-R-12898] 13 p1815 N90-20424
Acoustic characterisation of an aluminium silicon carbide metal matrix composite
[AERE-R-13273] 14 p1943 N90-21121
A casting and imaging technique for determining void geometry and relative permeability behavior of a single fracture specimen
[DE90-009192] 14 p1989 N90-21403
Contribution for the study of the evolution of part of the Espinhaco supergroup and its foundation through fracture analysis
[INPE-4907-PRE/1508] 14 p1999 N90-21459
The thermo-mechanical behavior of cometary nuclei 14 p2041 N90-21703
Computational simulation of structural fracture in fiber composites
[NASA-TM-102505] 15 p2064 N90-21821
Progression of damage and fracture in composites under dynamic loading
[NASA-TM-103118] 15 p2065 N90-21825
A stress-strength interference approach to fast and delayed fracture reliability analysis for ceramic components 15 p2070 N90-21859
The stress field due to an edge dislocation and some fracture problems for a three-phase composite cylinder model 15 p2120 N90-22126
Probabilistic finite elements: Applications to fracture and fatigue 15 p2121 N90-22134
The effects of tortuosity on flow through a natural fracture
[DE90-009193] 15 p2129 N90-22172
Deformation and fracture of aluminum-lithium alloys: The effect of dissolved hydrogen 16 p2219 N90-22658
Structural behavior of composites with progressive fracture
[NASA-TM-102370] 17 p2368 N90-23477
J-integral and HRR field of a stably growing crack, an experimental analysis
[AD-A220418] 17 p2416 N90-23764
The assessment of metal fiber reinforced polymeric composites 18 p2514 N90-24357
Indentation fracture of brittle materials
[DE90-010709] 18 p2572 N90-24657
Scratches and shot peening effects on the fatigue life of aluminum-lithium alloys
[NIAR-90-15] 19 p2674 N90-25208
Fracture mechanics in integrated design of new, ultra-strong materials and structures
[CBL-REPRINT-21] 19 p2703 N90-25378
Non-ejection neck injuries in high performance aircraft 19 p2717 N90-25461
Hydrogen induced fracture characteristics of single crystal nickel-based superalloys
[NASA-CR-183992] 20 p2832 N90-26108
On modeling the effect of pore shapes on ductile fracture
[AD-A221774] 21 p3014 N90-27136
Impact fracture experiments simulating interstellar grain-grain collisions 21 p3093 N90-27584
Strengthening and toughening mechanisms in ceramic fiber-reinforced glass matrix composites 23 p3300 N90-28666
Characterization of unnotched SCS-6/Ti-15-3 metal matrix composites at 650 C
[NASA-TM-102699] 24 p3444 N90-29450
Mechanical properties and fracture toughness of AAR-TC128 Grade B steel and a micro-alloyed, control-rolled steel, A 8XX grade B, from -80F to +73F
[PB90-207796] 24 p3448 N90-29471
Evaluation of static and fatigue properties of thin sheets of 8090-T8 aluminum-lithium alloy and observation of its fracture surfaces
[NAL-TR-1039] 24 p3453 N90-29499
Some aspects of the structure and evolution of oceanic spreading centers 24 p3496 N90-29757

FRAGMENTATION
Kinetics of diffusion-controlled reactions
[AD-A212161] 03 p0399 N90-12286
Electron attachment and molecular fragmentation in laser-excited plasmas
[AD-A212098] 03 p0409 N90-12343
Spall strength measurements on shockloaded refractory metals
[DE90-000839] 06 p0747 N90-14345
Mechanisms of wear in structural ceramic materials 06 p0749 N90-14360
Hypervelocity impact calculations using CTH: Case studies
[DE90-002891] 06 p0795 N90-14632
Fragmentation statistics from Eulerian hydrocode calculations
[DE90-002906] 07 p0941 N90-15449
Stability and fragmentation of ejecta in hypervelocity impact
[DE90-004087] 08 p1085 N90-16278
On the observation of a transition from fusion to multifragmentation in high multiplicity O16 induced reactions
[LUIP-8812] 08 p1119 N90-16481
A database of fragmentation cross section measurements applicable to cosmic ray propagation calculations
[NASA-CR-186328] 08 p1153 N90-16681
Relationship of fragment size to normalized spall strength for materials
[DE90-004165] 09 p1231 N90-17140
Getting lunar ilmenite: From soils or rocks
[NASA-CR-186498] 12 p1744 N90-20029
Statistics on aircraft gas turbine engine rotor failures that occurred in US commercial aviation during 1986
[DOT/FAA/CT-89/30] 14 p1922 N90-21008
Final safety analysis report for the Ulysses Mission. Volume 2: Accident model document-appendices
[DE90-008695] 14 p1940 N90-21104
Fragmentation of relativistic heavy nuclei with application to cosmic ray propagation 14 p2043 N90-21716
Production and analysis by mass spectrometry of beams of polyglycol ions 15 p2066 N90-21835
Excimer laser fragmentation studies of selected oximes: Nascent OH internal energy distributions and the search of H2CN fluorescence
[AD-A222622] 20 p2868 N90-26317
Study of the polyoxymethylene and its sputtered fragments: Implications for comets 20 p2949 N90-26781
Distributed transitive closure computations: The disconnection set approach
[REPT-90-014] 22 p3259 N90-28459
The formation of globular clusters 23 p3410 N90-29272

FRAGMENTS
Relationship of fragment size to normalized spall strength for materials
[DE90-004165] 09 p1231 N90-17140
Populations of excited states and reaction mechanisms in the emission of complex fragments
[DE90-007481] 13 p1886 N90-20819
Study of the polyoxymethylene and its sputtered fragments: Implications for comets 20 p2949 N90-26781
Nature and origin of interstellar diamond from the Allende CV3 meteorite 21 p3092 N90-27581
A planar rocket motor model for visualization of violent reaction due to fragment impact
[AD-A224273] 24 p3441 N90-29431

FRAME PHOTOGRAPHY
Knowledge based text generation
[AD-A214273] 07 p0977 N90-15645

FRAMES
NT AIRFRAMES
NT CHASSIS
Elastic-plastic instability of plane frames 14 p1992 N90-21415
Graphically-oriented nonlinear analysis of statically loaded plane frames on microcomputers
[PB90-165945] 15 p2144 N90-22248
Free vibrations of thin-walled semicircular graphite-epoxy composite frames
[NASA-TM-102680] 19 p2701 N90-25365
Graphically-oriented linear analysis of plane frames subjected to complex loadings on microcomputers
[PB90-173279] 22 p3190 N90-28102
Lateral buckling of short I-beams under cyclic loading
[PB90-213653] 22 p3191 N90-28104
A neural network for controlling the configuration of frame structure with elastic members 23 p3388 N90-29034

FRAMES (DATA PROCESSING)
Overview of the data acquisition and reductions 05 p0609 N90-13549
Object Oriented Programming Systems (OOPS) and frame representations: An investigation of programming paradigms
[NASA-CR-186084] 12 p1699 N90-19758
Implementing the Canny edge recognizer with datacube image-processing hardware
[OUEL-1786/89] 15 p2148 N90-22272
Multiple inheritance and exceptions in frame systems
[CWI-CS-R8931] 18 p2591 N90-24743
Experiments in variable frame rate analysis for speech recognition
[RSRE-MEMO-4330] 19 p2683 N90-25264
Further experiments in variable frame rate analysis for speech recognition
[RSRE-MEMO-4336] 22 p3165 N90-27951
Direct estimation of structure and motion from multiple frames
[AD-A223903] 24 p3534 N90-29985

FRAMING CAMERAS
Video line processor
[AD-D014198] 04 p0497 N90-12861

FRANCE
Crau 1987: The KNMI contribution --- KNMI (Royal Netherlands Meteorological Institute)
[KNMI-TR-110] 03 p0375 N90-12140
French technological progress in the field of robotics and teleoperation
[DE90-001590] 06 p0794 N90-14626
Terminology strategies for international information exchange
[AD-A214147] 07 p1010 N90-15853
French approach to space technology transfer 11 p1576 N90-19074

FRAUNHOFER LINES
LASCO: A wide-field white light and spectrometric coronagraph for SOHO 04 p0568 N90-13311

FRAUNHOFER REGION
U FAR FIELDS

FREDHOLM EQUATIONS
Index formulas for generalized Wiener-Hopf operators and Boson-Fermion correspondence in 2N dimensions
[CWI-PM-R8811] 04 p0542 N90-13141
Fracture of sandwiched composites 14 p1946 N90-21136
The analysis of stress relaxation on indentation of a rigid punch into a viscoelastic sheet of finite thickness
[NPL-DMA(A)-193] 15 p2162 N90-22357

FREDHOLM OPERATORS
U FREDHOLM EQUATIONS
U OPERATORS (MATHEMATICS)

FREE ATMOSPHERE
Downward continuation of the free-air gravity anomalies to the ellipsoid using the gradient solution and terrain correction: An attempt of global numerical computations 13 p1836 N90-20541
The development of the July 1989 1 deg x 1 deg and 30' x 30' terrestrial mean free-air anomaly data bases
[NASA-CR-186475] 19 p2713 N90-25441

FREE BOUNDARIES
A spectral analysis approach to wave propagation in layered solids 15 p2120 N90-22131
Numerical methods for the problem of the free-boundary plasma equilibrium in a stellarator (torsatron)
[DE90-620580] 16 p2319 N90-23223
Free boundary problems for flow with vorticity
[AD-A218415] 22 p3168 N90-27971

FREE CONVECTION
NT RAYLEIGH-BENARD CONVECTION
Pressure correction splitting methods for the computation of oscillatory free convection in low Pr fluids
[CWI-NM-R8816] 02 p0222 N90-11271
A multigrid method combined with defect correction for free convection problems at high Rayleigh numbers
[REPT-89-27] 03 p0396 N90-12264
Unsteady hydromagnetic flow of a radiating gas in a vertical channel with axial temperature variation
[DE90-600934] 06 p0778 N90-14525
Time-dependent free convection in liquid metals
[DE90-000957] 07 p0927 N90-15366
Time-dependent free convection in low Prandtl number fluids
[DE90-003053] 07 p0929 N90-15377
Simultaneous determination of temperature and velocity fields in a thermal convection flow with non-enclosed liquid crystal tracers 08 p1078 N90-16239
Multicellular natural convection in a narrow vertical slot
[AD-A216411] 11 p1505 N90-18668
Experiments of thermoconvection in a cubic cell
[MPIS-6/1989] 12 p1661 N90-19544
Three-dimensional convection in cylindrical geometry 17 p2399 N90-23668
Modeling turbulent flow with mixed thermal convection transfer
[ECL-89-19] 17 p2405 N90-23704
A line relaxation smoother for the multigrid solution of the Boussinesq equations
[REPT-89-68] 17 p2458 N90-24027
A numerical investigation of thermal convection in highly viscous spherical shells with applications to mantle dynamics in the Earth and other terrestrial planets 18 p2579 N90-24691

FREE ELECTRON LASERS
Technical options for high average power free electron milimeter-wave and laser devices 01 p0029 N90-10151
Laser energy conversion 01 p0029 N90-10152
Shortwavelength coherent radiation: Generation and applications
[AD-A209847] 01 p0074 N90-10427

Biomedical studies with the free electron laser
|AD-A208927| 01 p0091 N90-10519
A compact X-ray free electron laser
|DE89-017236| 02 p0226 N90-11297
Free-electron laser theory
|DE89-620145| 02 p0226 N90-11298
Stability requirements of RF linac-driven free-electron lasers
|DE89-016609| 02 p0227 N90-11303
Minimized emittance growth with elliptical beam pipes in FEL (Free-Electron Laser)
|DE89-016982| 02 p0228 N90-11305
Synchrotron radiation, free electron laser, and nuclear structure
|DE89-017352| 02 p0228 N90-11306
A proposed linac cavity RF drive system for the Los Alamos extreme ultraviolet free-electron laser
|DE89-016614| 03 p0353 N90-12016
Electron beam propagation through a magnetic wiggler with random field errors
|AD-A212705| 04 p0498 N90-12867
Radio frequency linac driven free-electron laser configurations
|AD-A212572| 04 p0507 N90-12922
Cavity eigenmodes for the NIST/NRL (National Institute of Standards and Technology/Naval Research Laboratory) free electron laser
|AD-A212706| 04 p0507 N90-12923
Theoretical and experimental research on a millimeter-wavelength free-electron laser
|AD-A213321| 04 p0507 N90-12925
Ultrafast processes and spectroscopy with free electron lasers
|AD-A212889| 05 p0647 N90-13773
Synchrotron-betatron parametric instability in free-electron lasers
|AD-A213373| 05 p0648 N90-13777
An experimental analysis of the waveguide modes in a high-gain free-electron laser amplifier
05 p0648 N90-13779
Numerical simulations of free-electron laser oscillators
|DE89-003488| 06 p0788 N90-14588
Self-field-induced chaotic electron motion in free electron lasers
|DE90-001710| 06 p0790 N90-14598
Optical design and performance of an XUV FEL (Free-Electron Laser) oscillator
|DE90-002381| 06 p0790 N90-14599
Compact RF-linac free-electron lasers
|DE90-002386| 06 p0790 N90-14600
INEX (Integrated Numerical Experiment) simulations of the Los Alamos HIBAF (High-Brightness Accelerator Free-Electron Laser) free-electron laser MOPA (Master Oscillator Power Amplifier) experiment
|DE90-002387| 06 p0790 N90-14601
Lasing on the third harmonic
|DE90-002389| 06 p0790 N90-14602
Analytical treatment of electron trajectory straightener issues in free-electron lasers
|DE90-002405| 06 p0790 N90-14603
Theory of harmonic radiation using a single-electron source model
|DE90-002412| 06 p0791 N90-14606
Microwave Transport Systems for the MTX (Microwave Tokamak Experiment)
|DE90-000821| 06 p0846 N90-14921
MTX (Microwave Tokamak Experiment)/ELF (Electron Laser Facility) 2 microwave power measurements and calibration for the 2-GW, 140-GHz, ELF 2 Free Electron Laser (FEL)
|DE90-000825| 06 p0846 N90-14922
Precision timing and interlocks systems for FEL (Free-Electron Laser) heating experiments on MTX (Microwave Tokamak Experiment)
|DE90-000833| 06 p0847 N90-14923
Microwave Tokamak Experiment: An overview of the construction and checkout phase
|DE90-000834| 06 p0847 N90-14924
RF superconductivity research and development at Los Alamos National Laboratory
|DE90-002440| 06 p0855 N90-14969
The 17.1-GHz free-electron laser as a microwave source for TeV colliders
|DE90-001506| 07 p0934 N90-15406
Anharmonic betatron motion in free electron lasers
|DE90-001515| 07 p0934 N90-15407
Theory for high gain, high power free electron lasers
|DE90-003024| 07 p0934 N90-15409
Comprehensive, nonintercepting electron-beam diagnostics using spontaneous emission
|DE90-003211| 07 p0935 N90-15414
Initial optical transition radiation measurements of the electron beam for the Boeing free-electron laser experiment
|DE90-003396| 07 p0935 N90-15416
Waveguide effects in superradiant free-electron lasers
|DE90-003605| 07 p0935 N90-15417
A microwiggler Free-Electron Laser at the Brookhaven Accelerator Test Facility
|DE90-003643| 07 p0936 N90-15418
NOISE: A nonlinear optimization induction free-electron laser systems engineering code
|DE90-004438| 07 p0936 N90-15420
Center for X Ray Optics, 1988
|DE90-003300| 07 p0992 N90-15732
Gas optics applicable to free electron laser technology
|AD-A214285| 07 p0993 N90-15741
To construct a linac/storage ring FEL facility
|AD-A214620| 09 p1211 N90-17020
Energy conversion efficiency in high current Raman regime Free Electron Laser (FEL). 1: Single mode analysis
|DE90-719527| 09 p1227 N90-17120
One-dimensional single-mode nonlinear FEL amplification code: User's manual
|DE90-719544| 09 p1227 N90-17121
Identification and reduction of Wakefield effects in the wiggler region of the Los Alamos free-electron laser
|DE90-004871| 09 p1228 N90-17128
Improved performance of the Boeing/LANL FEL (Free-Electron Laser) experiment: Extraction efficiency and cavity length detuning effects
|DE90-004872| 09 p1228 N90-17129
Three-dimensional simulation of free-electron laser harmonics with FRED
|DE90-005253| 09 p1229 N90-17130
Microwave free-electron laser applications for electron cyclotron heating of plasmas
|DE90-005203| 10 p1431 N90-18257
INEX (Integrated Numerical Experiment) simulations of the Boeing FEL system
|DE90-004846| 11 p1513 N90-18712
Theory for high gain, high power free electron lasers
|DE90-005546| 11 p1514 N90-18714
Research on free electron lasers
|AD-A215865| 11 p1514 N90-18715
Resonator modes in high gain free electron lasers
|DE90-006098| 11 p1514 N90-18720
Electron beam and high-speed optical diagnostics for the Los Alamos HIBAF (High Brightness Accelerator FEL) Facility
|DE90-007828| 11 p1515 N90-18725
Hamiltonian analysis and simulation of free electron lasers
|INPE-4785-TDL/351| 11 p1567 N90-19018
Transient and sustained resonance in very slowly varying oscillatory Hamiltonian systems with application to free-electron lasers
|DE90-005984| 12 p1666 N90-19574
Potential biomedical application of the Los Alamos infrared free-electron laser: DNA spectroscopy
|DE90-006505| 12 p1667 N90-19575
On 140 GHz microwave FEL experiments using ELF-2
|DE90-006764| 12 p1667 N90-19576
Results of the PALADIN experiment
|DE90-006776| 12 p1667 N90-19578
First direct observation of FEL (Free-Electron Laser) from lambda=20 to 45 microns
|DE90-007508| 12 p1669 N90-19589
Conference digest: Thirteenth International Conference on Infrared and Millimeter Waves, volume 1039
|AD-A217343| 13 p1793 N90-20291
Harmonic generation mechanisms in short-wavelength free-electron lasers
|DE90-007622| 13 p1807 N90-20374
Picosecond nonlinear studies of complex materials using the free electron laser
|AD-A218215| 13 p1809 N90-20387
SDI (Strategic Defense Initiative): Is its future past
|DE90-008016| 13 p1880 N90-20785
Role of free-electron lasers in strategic defense
|DE90-008028| 13 p1880 N90-20786
Tenth International Free Electron Laser Conference
|DE90-614773| 14 p1985 N90-21376
On storage rings for short wavelength FELs
|DE90-009059| 14 p1985 N90-21379
Proposal for FY86 Lawrence Livermore National Laboratory particle beam research
|DE90-007936| 14 p2026 N90-21617
Free-Space Power Transmission
|NASA-CP-10016| 15 p2060 N90-21795
Free electron lasers driven by linear induction accelerators: High power radiation sources
15 p2060 N90-21800
A free electron laser master oscillator power amplifier experiment
16 p2239 N90-22776
Experimental demonstration of an electromagnetically pumped free-electron laser with cyclotron harmonic idlers
|AD-A218830| 17 p2408 N90-23719
The effects of wiggler errors on free electron laser performance
|AD-A220421| 17 p2409 N90-23725
Microwigglers for submillimeter wavelength free-electron lasers
|AD-A220185| 17 p2409 N90-23730
On using a superconducting linac to drive a short wavelength FEL
|CEBAF-PR-89-019| 19 p2756 N90-25660
OASIS, LLNL version: Software maintenance manual
|DE90-013522| 20 p2868 N90-26313
Free electron laser injection oscillator
|AD-D014180| 21 p3007 N90-27095
Three-dimensional simulations of the generation of one Angstrom radiation by a self-amplified spontaneous emission free-electron laser
|DE90-015032| 23 p3330 N90-28830
Control of nonlinear space-charge emittance growth
|DE90-014752| 23 p3410 N90-29270
Development of an all solid state 6 kHz pulse generator for driving free electron laser amplifiers
|AD-A224105| 24 p3463 N90-29561
High average power CW FELS (Free Electron Laser) for application to plasma heating: Designs and experiments
|DE90-011085| 24 p3474 N90-29633

FREE ELECTRONS
Technology of fast spark gaps
|AD-A214199| 07 p0925 N90-15353
Polarization: Effects on second harmonic power in light scattering by free electrons
|DE90-612842| 14 p2025 N90-21608

FREE ENERGY
NT GIBBS FREE ENERGY
Reorganization free energy for electron transfers at liquid-liquid and dielectric semiconductor-liquid interfaces
|AD-A212985| 05 p0703 N90-14111
Energy barriers in SK spin-glass model
|PREPRINT-665| 05 p0704 N90-14119
Electron theory of long wavelength concentration fluctuations in liquid metal alloys
|DE89-636213| 07 p0904 N90-15225
The free energy of Maxwell-Vlasov equilibria
|DE90-003318| 07 p0988 N90-15705
The free energy principle, negative energy modes, and stability
|DE90-005368| 11 p1573 N90-19056
Linear free energy relations for multielectron transfer kinetics: A brief look at the Bronsted/Tafel analogy
|AD-A215078| 12 p1710 N90-19823
Interaction between implanted ions and intrinsic defects in silica
|DE90-006569| 13 p1892 N90-20858
Nonlocal free energy density functional approximations for the electrical double layer; comparison with Monte Carlo results for 2:1 salt
|AD-A220911| 18 p2521 N90-24395
A nonlocal free energy density functional approximation for the electrical double layer
|AD-A220664| 18 p2607 N90-24848
Thermodynamics and structure of liquid alkali metals from the charged-hard-sphere reference fluid
|DE90-627792| 23 p3311 N90-28725

FREE FALL
A model for evaporation of freely falling droplets
|PUBL-AIR-QUALITY-6| 10 p1384 N90-18007
The Stanford equivalence principle program
12 p1733 N90-19963
Noncontact measurement of high temperature using optical fiber sensors
|NASA-CR-186975| 23 p3329 N90-28825

FREE FLIGHT TEST APPARATUS
Progress in the design of a microgravity facility for in-orbit experiments 18 p2540 N90-24496

FREE FLOW
Direct numerical simulation of turbulent free shear flows
|AD-A210161| 01 p0040 N90-10218
Chemical reactions in turbulent mixing flows
|AD-A211240| 02 p0220 N90-11263
Surface flow and heating distributions on a cylinder in near wake of Aeroassist Flight Experiment (AFE) configuration at incidence in Mach 10 Air
|NASA-TP-2954| 06 p0772 N90-14493
Detailed analysis of the wake and free-flow characteristics at the Goodnoe Hills MOD-2 site
|DE90-002725| 06 p0806 N90-14692
Demonstration of the feasibility of laser induced fluorescence for arc jet flow diagnostics
|NASA-CR-185595| 08 p1040 N90-16013
Turbulence scale effects on heat transfer in a linear turbine cascade
|AD-A216222| 10 p1321 N90-17637
A study of flows over highly-swept wings designed for maneuver at supersonic speeds
|AD-A216837| 12 p1599 N90-19202

An experimental investigation of the flow field around yawed stranded cables
[AD-A215782] 12 p1658 N90-19529
Flat plate leading edge receptivity to various freestream disturbance structures 16 p2235 N90-22750
Flame extinction in compressible flow 21 p2973 N90-26899
Direct numerical simulation of compressible free shear flows 21 p2974 N90-26901
Jet vortex generators for turbulent flow separation control
[NASA-CR-186959] 22 p3109 N90-27659
Calibration of the PARC program for propulsion-type flows
[AD-A224253] 24 p3434 N90-29395
An investigation of the inviscid spatial instability of compressible mixing layers
[AD-A223776] 24 p3468 N90-29596

FREE JETS
Cryogenic free jets
[ESA-TT-1128] 03 p0311 N90-11767
Vapor condensation on liquid surface due to laminar jet-induced mixing: The effects of system parameters
[NASA-TM-102433] 05 p0643 N90-13751
Plume shape optimization of small attitude control thrusters with respect to impingement and thrust
[ISL-CO-220/88] 08 p1064 N90-16153
Visualization of instability forms of a round free jet using a light sheet method 08 p1079 N90-16241
Lecture notes on supersonic molecular beam sources
[MPIS-20/1988] 08 p1121 N90-16494
Theoretical and experimental approach of wave phenomena in free jets
[ISL-CO-247/88] 09 p1219 N90-17069
Tomographic investigations of weakly perturbed supersonic free jets
[MPIS-MITT-91] 12 p1600 N90-19209
Heteroepitaxial growth of germanium films by supersonic free jet chemical beam epitaxy
[DE90-006621] 12 p1720 N90-19877
Interaction of a turbulent round jet with the free surface 15 p2090 N90-21964
Reynolds stress closure in jet flows using instability wave modeling 16 p2196 N90-22534
Modeling of free viscoelastic jets and instability mechanisms
[AD-A221672] 21 p3005 N90-27080
The entrainment rate for a row of turbulent jets
[NASA-CR-185278] 23 p3269 N90-28504

FREE MOLECULAR FLOW
The influence of the gas surface interaction on spacecraft orbital motion 17 p2385 N90-23461

FREE OSCILLATIONS
U FREE VIBRATION

FREE RADICALS
NT HYDROXYL RADICALS
Generation of free radicals during cold injury and rewarming
[AD-A213088] 05 p0672 N90-13915
Atomic hydrogen as a launch vehicle propellant
[NASA-TM-102459] 06 p0735 N90-14284
A measurement of hydroxyl in the daytime mesosphere 06 p0814 N90-14732
Electron Spin Resonance (ESR) studies of returned comet nucleus samples 08 p1148 N90-16651
Laboratory studies of free radical reactions in cloudwater
[DE90-003961] 12 p1694 N90-19730
Infrared absorption spectroscopy and chemical kinetics of free radicals
[DE90-009469] 15 p2067 N90-21837
Reactions of laser-generated free radicals at semiconductor surfaces
[AD-A218552] 16 p2232 N90-22733
Kinetics and thermochemistry of polyatomic free radicals: New results and new understandings 20 p2946 N90-26764
UV and VUV spectroscopy and photochemistry of small molecules in a supersonic jet 20 p2947 N90-26771

FREE STREAM EFFECTS
U FREE FLOW

FREE STREAMS
U FREE FLOW

FREE VIBRATION
Static and free-vibrational response of semi-circular graphite-epoxy frames with thin-walled open sections
[NASA-CR-186097] 05 p0617 N90-13600
On total variation diminishing schemes for transonic turbulent flow computation 14 p1909 N90-20945
Stress analysis of rocket motors with viscoelastic propellant by a mixed finite element model 14 p1941 N90-21112
Wave receptance analysis of vibrating beams and stiffened plates 14 p1993 N90-21419
Free vibrations of thin-walled semicircular graphite-epoxy composite frames
[NASA-TM-102680] 19 p2701 N90-25365
An experimental system for measuring the wavenumber-frequency response of Timoshenko beams
[AD-A222569] 20 p2878 N90-26374
Static and free-vibrational response of semi-circular graphite-epoxy frames with thin-walled open sections
[NASA-CR-4287] 21 p3012 N90-27122

FREE WING AIRCRAFT
An experimental study of tip shape effects on the flutter of aft-swept, flat-plate wings
[NASA-TM-4180] 16 p2199 N90-22555

FREE-PISTON ENGINES
Free-Piston Stirling Engine magnetically coupled heat pump: Critical component evaluation
[DE89-015646] 02 p0229 N90-11316
Dynamic characteristics concerned in the design of a free-piston Stirling engine/magnetic coupling/compressor system
[DE89-015981] 02 p0230 N90-11317

FREEZE DRYING
Processing and fabrication of high temperature oxide superconductors
[AD-A210197] 01 p0131 N90-10755
Bioluminescence for detection of trace compounds
[AD-A219435] 17 p2372 N90-23503

FREEZING
NT ZONE MELTING
Studies on the startup transients and performance of a gas loaded sodium heat pipe
[AD-A211880] 03 p0414 N90-12379
Generation of free radicals during cold injury and rewarming
[AD-A213088] 05 p0672 N90-13915
Soft modes, freezing, and nonlinear response of a dipolar glass
[DE90-003647] 08 p1051 N90-16075
Feasibility of cool storage systems in refrigeration
[DE90-728179] 08 p1054 N90-16093
Thermodynamics of systems with very many components phase equilibrium
[DE90-007345] 11 p1573 N90-19059
Contamination of spacecraft by recontact of dumped liquids 19 p2728 N90-25508

FREEZING POINTS
U MELTING POINTS

FREIGHT
U CARGO

FREIGHT COSTS
Neptune, 2000 plus: Concept of a heavy space freighter for the 21st century
[ILR-MITT-229(1989)] 18 p2509 N90-24338

FREIGHTERS
Neptune, 2000 plus: Concept of a heavy space freighter for the 21st century
[ILR-MITT-229(1989)] 18 p2509 N90-24338

FRENCH SATELLITES
NT SPOT (FRENCH SATELLITE)
Compendium of meteorological space programs, satellites, and experiments
[NASA-TM-102924] 12 p1607 N90-19243

FRENCH SPACE PROGRAM
The French balloon program and related space research 05 p0656 N90-13828
Operational activity in France and a new method of balloon temperature piloting 05 p0660 N90-13857
French studies on advanced space transportation systems 09 p1175 N90-16798

FREON
Composite propellants with high burning rates
[FOA-C-20781-2.1] 23 p3315 N90-28744

FREQUENCIES
NT ACOUSTIC FREQUENCIES
NT AUDIO FREQUENCIES
NT BROADBAND
NT C BAND
NT CARRIER FREQUENCIES
NT CYCLOTRON FREQUENCY
NT EXTREMELY HIGH FREQUENCIES
NT EXTREMELY LOW FREQUENCIES
NT EXTREMELY LOW RADIO FREQUENCIES
NT HIGH FREQUENCIES
NT IONIZATION FREQUENCIES
NT LOW FREQUENCIES
NT MAXIMUM USABLE FREQUENCY
NT MICROWAVE FREQUENCIES
NT NYQUIST FREQUENCIES
NT PLASMA FREQUENCIES
NT RADIO FREQUENCIES
NT RESONANT FREQUENCIES
NT SUPERHIGH FREQUENCIES
NT ULTRAHIGH FREQUENCIES
NT VERY HIGH FREQUENCIES
NT VERY LOW FREQUENCIES
System properties from frequency response functions, part 1
[ISVR-TR-166-PT-1] 11 p1520 N90-18754
Antennas for 20/30 GHz and beyond 12 p1611 N90-19269
An algorithm for efficient estimation of superimposed exponential signals
[AD-A217218] 13 p1865 N90-20698
Adaptive frequency estimation by MUSIC (Multiple Signal Classification) method
[PB90-166794] 15 p2086 N90-21943
Sustained resonance in very slowly varying oscillatory Hamiltonian systems
[DE90-010422] 18 p2598 N90-24783
Frequency doubled operation of a ground state depleted laser using the Nd(3+)(4)F(sub 3/2)-(4)I(sub 9/2) transition in Y2SiO5
[DE90-012089] 19 p2695 N90-25338
The interpretation of nonlinear frequency response functions
[RR-375] 19 p2753 N90-25643
Design of sharp cutoff filters with low quality factors
[AD-A223130] 21 p3000 N90-27051
Intracavity frequency doubling of a Nd:YAG laser with an organic nonlinear optical crystal
[AD-A222392] 21 p3008 N90-27102
Modified fast frequency acquisition via adaptive least squares algorithm
[NASA-CASE-NPO-17845-1-CU] 21 p3050 N90-27341
Auditory processing of complex sounds across frequency channels
[AD-A224147] 23 p3356 N90-28970
Solar oscillation frequency and solar neutrino predictions
[DE90-014918] 23 p3413 N90-29288

FREQUENCY ANALYZERS
An analysis of the time variation of the frequency response of the LMS adaptive line enhancer
[ISVR-TR-175] 08 p1058 N90-16115
Channel selection and control procedures in an automatic HF system 20 p2847 N90-26193
PVDF contact probes
[VTT-RR-623] 20 p2857 N90-26253

FREQUENCY ASSIGNMENT
Modelling UHF propagation for frequency assignment in radio relay networks 06 p0764 N90-14445
Application of heuristic satellite plan synthesis algorithms to requirements of the WARC-88 allotment plan
[NASA-TM-102479] 06 p0835 N90-14856
Numerical Arc Segmentation Algorithm for a Radio Conference-NASARC (version 4.0) technical manual
[NASA-TM-101453] 13 p1788 N90-20264
EINMUF: An HF MUF, FOT, LUF prediction program
[AD-A221577] 21 p3055 N90-27371
Sounder update and field strength software modifications for Special Operations Radio Frequency Management System (SORFMS). Volume 1: Program descriptions and testing
[AD-A224510] 24 p3460 N90-29543

FREQUENCY BANDS
U FREQUENCIES

FREQUENCY CONTROL
NT AUTOMATIC FREQUENCY CONTROL
Efficient nonlinear conversion of laser diode pumped miniature solid state laser sources
[AD-A210708] 01 p0075 N90-10433
Three stages and two systems of visual processing
[AD-A212670] 04 p0525 N90-13032
The 1989 National Convention Record IEE Japan, part 8
[DE89-910081] 09 p1210 N90-17013
Theoretical analysis of microwave and millimeter wave integrated circuits based on magnetic films
[AD-A214772] 09 p1211 N90-17021
Temporal statistics of low-angle ground clutter
[AD-A220816] 17 p2391 N90-23621
Monolithic phase shifter study
[AD-A219859] 18 p2546 N90-24533
The application of SAW devices in expanded frequency spectrum communications
[AD-A222958] 21 p2994 N90-27021

FREQUENCY CONVERSION
U FREQUENCY CONVERTERS

FREQUENCY CONVERTERS
NT DOWN-CONVERTERS
NT FREQUENCY MULTIPLIERS
NT FREQUENCY SYNTHESIZERS
NT UP-CONVERTERS
Design of a power supply system based in two quasi-resonant converters 10 p1336 N90-17728
Intensity to frequency conversion technique in intensity modulated fiber optic sensing systems
[NASA-TM-102562] 14 p1969 N90-21277

Laser physics and laser spectroscopy
[AD-A224379] 24 p3473 N90-29628

FREQUENCY DISTRIBUTION
Observations of fine-scale vertical shear and strain in the upper ocean
[AD-A214476] 10 p1410 N90-18130
Induction motor control
[NASA-TM-102533] 12 p1605 N90-19234
The application of SAW devices in expanded frequency spectrum communications
[AD-A222958] 21 p2994 N90-27021
Ionospheric heating with oblique waves. Volume 2: Applications to high-frequency radio propagation
[AD-A223111] 21 p3025 N90-27202
Jamming performance of frequency-hopped communication systems with nonuniform hopping distributions
[AD-A223419] 24 p3461 N90-29547

FREQUENCY DIVISION MULTIPLEXING
Adaptive gigabit fiber optics local area network
[AD-A210794] 02 p0275 N90-11571
Monochromator configurations for wavelength division multiplexing
[AD-A214833] 09 p1281 N90-17430
Single mode communication link
[AD-A219499] 17 p2388 N90-23601

FREQUENCY HOPPING
Performance of cellular frequency-hopped spread-spectrum radio networks
[AD-A214480] 09 p1204 N90-16978
A real-time rejection circuit to automatically reject multiple interfering hopping signals while passing a lower level desired signal
[AD-D014424] 14 p1965 N90-21251
Joint tactical anti-jam communications: A systems approach
[AD-A219592] 17 p2388 N90-23602
Throughput and delay characteristics for a slow-frequency hopped aircraft-to-aircraft packet radio network
[AD-A220525] 17 p2389 N90-23609
Nonlinear optical protection against frequency agile lasers
[AD-D014535] 19 p2695 N90-25335
New synchronisation techniques applicable to multi-tone transmission systems 20 p2848 N90-26199
New approaches for rapid synchronisation frequency hoppers 20 p2849 N90-26201
Studies of ECCM improvements for frequency-hopping CPFSK systems
[AD-A222995] 21 p2995 N90-27023
Lightweight EHF communications satellites 21 p3070 N90-27453
Jamming performance of frequency-hopped communication systems with nonuniform hopping distributions
[AD-A223419] 24 p3461 N90-29547

FREQUENCY MEASUREMENT
Quantitative methods for waves in space plasmas
[PB89-210256] 02 p0280 N90-11599
Time and frequency in geodesy measuring methods
[SER-C-337] 03 p0365 N90-12087
A well conditioned formulation for the analysis of multi-layered frequency selective surfaces using a cascaded matrix approach, revised
[RSRE-MEMO-4289-REV] 04 p0496 N90-12858
A frequency domain technique for improving sound field reproduction
[RAE-TM-MM-10] 04 p0551 N90-13205
Smooth track generation for target motion analysis
[FEL-1989-83] 04 p0555 N90-13233
Modeling and measurement methods for high speed bipolar transistors
[REPT-11] 05 p0636 N90-13714
Analysis of an R-SQUID noise thermometer
[VTT-PUBL-54] 05 p0645 N90-13769
Detection of a chirping electromagnetic signal
[DE90-002105] 06 p0766 N90-14457
Apparatus for using a time interval counter to measure frequency stability
[NASA-CASE-NPO-17325-1-CU] 09 p1208 N90-17005
Very high frequency measurements of geometric factors in transmission line lead acid cells
[AD-A219463] 17 p2420 N90-23788
Low-frequency measurements of the CMB (Cosmic Microwave Background) spectrum
[DE90-011589] 18 p2639 N90-25033
QPO from the rapid burster 19 p2770 N90-25741
The impacts of Ginga results on QPO models 19 p2770 N90-25744
Electric field strength meters for the HF, VHF, and UHF bands
[BBC-RD-1990/3] 20 p2851 N90-26212

FREQUENCY MODULATION
NT FREQUENCY SHIFT KEYING
Laser dynamics: The system dynamics and network theory of optoelectronic integrated circuit design 02 p0226 N90-11296
Fabrication of modulated vanes for a split-coaxial RFQ
[DE88-757235] 03 p0403 N90-12310
Monolithic laser diode structure for microwave generation
[AD-D014210] 06 p0782 N90-14543
Near real time VHF telemetry of near shore oceanographic data
[AD-A215756] 10 p1327 N90-17666
On the range resolution of point targets with FMCW radar systems
[DLR-FB-89-47] 11 p1499 N90-18629
Auditory perception
[AD-A217012] 11 p1540 N90-18864
Programmable generation of linear frequency modulated pulses 14 p1961 N90-21232
Multiresolution and time-frequency representations of signals
[REPT-89-47] 15 p2087 N90-21946
Monitoring of catalyst performance in CO2 lasers using frequency modulation spectroscopy with diode lasers 18 p2561 N90-24614
Proof of the feasibility of coherent and incoherent schemes for pumping a gamma-ray laser
[AD-A219972] 18 p2562 N90-24620
CORA: A direct sequence spread spectrum radio for voice and data 20 p2848 N90-26195
Direct-sequence spread spectrum system
[AD-A223021] 20 p2856 N90-26245
Phase-sensitive optical detection of ballistic phonon pulses using frequency-modulation spectroscopy and persistent spectral holes
[AD-A221521] 21 p2979 N90-26930
Design of sharp cutoff filters with low quality factors
[AD-A223130] 21 p3000 N90-27051

FREQUENCY MULTIPLIERS
Design, construction and test of a frequency doubler for 183 GHz
[PB89-212591] 03 p0341 N90-11944
High-efficiency Schottky-Varactor frequency multipliers at millimeter waves
[PB90-110701] 09 p1209 N90-17007
Models of intracavity frequency doubled lasers
[AD-A221182] 18 p2563 N90-24628
High frequency, frequency multiplier using parallel gunn diodes
[AD-D014523] 19 p2685 N90-25275

FREQUENCY RANGES
A literature study of wave propagation in the 1-60 GHz range. Application to transportable military communication systems
[FEL-1988-47] 04 p0491 N90-12825
Angle estimation in a multipath environment with an eight element linear array operating at 10.5 GHz
[FEL-1989-15] 04 p0491 N90-12826
Far infrared, submm and mm spectroscopy of the galactic center: Radio arc and +20/+50 km s (exp -1) clouds
[NASA-CR-185497] 04 p0565 N90-13296
Broadband versus narrowband driver/power amplifier: A spectral purity comparison
[DOT/FAA/CT-TN89/73] 10 p1379 N90-17995
A frequency agile 94 GHz pulse-Doppler radar with dual polarisation capability 14 p1960 N90-21226
Nonlinear acoustic interactions in superfluid helium 15 p2164 N90-22367
Obtaining eigensolutions for multiple frequency ranges in a single NASTRAN execution 18 p2570 N90-24644
Short range, close to ground, VHF/UHF propagation: A comparison of measured results with a simple ray-based model
[RSRE-MEMO-4335] 19 p2684 N90-25266
UBVRI-photopolarimetry and the X ray dips of V471 Tau 19 p2775 N90-25781
Multifrequency observation of blazars 19 p2786 N90-25857
Equipment feasibility study: Very high frequency communication equipment (136-137 megahertz)
[DOT/FAA/CT-TN89/72] 20 p2850 N90-26210
Improving the geometric fidelity of imaging systems employing sensor arrays
[NASA-CASE-NPO-17970-1-CU] 20 p2880 N90-26384
Acoustic qualification of an anechoic chamber
[RAE-TM-MAT/STR-1136] 22 p3245 N90-28400

FREQUENCY REGULATION
U FREQUENCY CONTROL

FREQUENCY RESPONSE
Numerically efficient algorithm for model development of high-order systems 01 p0022 N90-10108
Effects of mistuning and matrix structure on the topology of frequency response curves
[NASA-TM-102290] 03 p0357 N90-12041
Review of probabilistic analysis of dynamic response of systems with random parameters
[NASA-CR-186171] 18 p2568 N90-24636

FREQUENCY SCANNING
General multidimensional scanning ratio transformation and its utilization for norm transformation of television signals
[ETN-90-96058] 12 p1648 N90-19470
DURIP theoretical/experimental investigations of highly energetic dication species
[AD-A217771] 13 p1808 N90-20383
A frequency agile 94 GHz pulse-Doppler radar with dual polarisation capability 14 p1960 N90-21226
Low-sidelobe phased array antenna characteristics using the planar near-field Scanning technique: Theory and experiment
[AD-A220611] 17 p2390 N90-23613
Computer-aided mathematical analysis of probability of intercept for ground-based communication intercept system
[AD-A219856] 17 p2392 N90-23627

FREQUENCY SHIFT
Frequency shift induced in laser pulses by plasma density variations
[AD-A214195] 07 p0936 N90-15424
Rotating Doppler frequency shifter
[AD-D014279] 08 p1118 N90-16475
Performance of cellular frequency-hopped spread-spectrum radio networks
[AD-A214480] 09 p1204 N90-16978
Coherent radar measurement of ocean currents from geostationary orbit 12 p1609 N90-19259
Correlation-induced changes of spectra
[AD-A217087] 12 p1669 N90-19591
A neural network based speech recognition system
[AD-A219794] 17 p2389 N90-23606
Synchronization of frequency shift transmission and the effect of oversampling 20 p2848 N90-26200
Control of a Cossor CSP1250 ionospheric simulator in an automated HF test bed
[AD-A223446] 24 p3461 N90-29549

FREQUENCY SHIFT KEYING
Power spectral densities for selected digital phase-continuous MFSK (M-ary Frequency Shift Keying) emissions
[PB90-129990] 12 p1647 N90-19463
Evaluation of a prototype 6 tone modem
[RAE-TM-FM-28] 16 p2228 N90-22708
New synchronisation techniques applicable to multi-tone transmission systems 20 p2848 N90-26199
Combined effects of fast and selective fading on performance of PSK and MSK with coherent detection 20 p2849 N90-26204

FREQUENCY STABILITY
An apparatus for the electrodynamic containment of charged macroparticles 04 p0486 N90-12789
Apparatus for using a time interval counter to measure frequency stability
[NASA-CASE-NPO-17325-1-CU] 09 p1208 N90-17005
Instability investigation for storage mode. Microwave instability (single-bunch instability)
[NIKHEF-K/AMPS/89/05] 11 p1499 N90-18628
Determining the effects of microwave power and C-field setting on the frequency of a cesium atomic frequency standard
[AD-A216599] 11 p1501 N90-18642
Effect of laser frequency noise on fiber-optic frequency reference distribution 12 p1643 N90-19438
Frequency stable high power lasers in space 12 p1734 N90-19969
A review of atomic clock technology, the performance capability of present spaceborne and terrestrial atomic clocks, and a look toward the future 12 p1735 N90-19972
Experiments with a laser interferometric gravitational wave antenna 15 p2184 N90-22476
Design of high-performance negative-feedback oscillators
[ETN-90-96698] 16 p2231 N90-22729
Fundamental studies on spray combustion and turbulent combustion
[AD-A219840] 18 p2521 N90-24394
Stability of laser oscillator systems 18 p2641 N90-25045
Local and global resonances in heated 2-D jets
[AD-A221671] 21 p3005 N90-27079
Structural and optical properties of DMP-128 holograms during environmental testing
[AD-A221691] 21 p3007 N90-27094

FREQUENCY STANDARDS
An apparatus for the electrodynamic containment of charged macroparticles 04 p0486 N90-12789

Determining the effects of microwave power and C-field setting on the frequency of a cesium atomic frequency standard
[AD-A216599] 11 p1501 N90-18642
Thermal coefficient of delay for various coaxial and fiber-optic cables 12 p1643 N90-19439
A review of atomic clock technology, the performance capability of present spaceborne and terrestrial atomic clocks, and a look toward the future 12 p1735 N90-19972
Atomic velocity distributions out of hydrogen maser dissociators
[AD-A219500] 17 p2408 N90-23721
Information content of a single pass of phase-delay data from a short baseline connected element interferometer 20 p2852 N90-26220

FREQUENCY SYNCHRONIZATION
Optimal synchronization of spread spectrum sequenced by nontransferable switching operators 20 p2845 N90-26183

FREQUENCY SYNTHESIZERS
Tunable CW single-frequency source for injection seeding 2-micrometer lasers
[AD-A223979] 23 p3331 N90-28834

FREQUENCY TRANSLATION
U FREQUENCY CONVERTERS

FRESNEL DIFFRACTION
Chromatic dispersion compensation in a Fresnel lens by means of a diffraction grating
[DE90-004030] 08 p1123 N90-16506

FRESNEL INTEGRALS
Infrared reflection-adsorption spectroscopy of the electrode/electrolyte solution interface: Optical considerations
[AD-A221935] 22 p3246 N90-28409

FRESNEL LENSES
Conceptual design study of a 5 kilowatt solar dynamic Brayton power system using a dome Fresnel lens solar concentrator
[NASA-CR-185134] 06 p0735 N90-14281
Chromatic dispersion compensation in a Fresnel lens by means of a diffraction grating
[DE90-004030] 08 p1123 N90-16506
Silicon concentrator solar cell development
[DE90-011782] 20 p2880 N90-26386

FRESNEL REGION
An investigation of the extent of the fresnel region of aperture antennas with attention to superdirectivity
[AD-A217518] 13 p1794 N90-20294

FRESNEL-KIRCHHOFF INTEGRALS
U FRESNEL INTEGRALS

FRETTING
Effect of fretting on fatigue strength of aluminium alloys
[ESDU-89004] 03 p0329 N90-11870
Fretting wear and fretting fatigue at temperatures up to 600 C 23 p3307 N90-28706
Microdamage to ceramic surfaces under sliding conditions 23 p3308 N90-28708
Fretting fatigue strength of Ti-6Al-4V at room and elevated temperatures and ways of improving it 23 p3308 N90-28709
Surface property improvement in titanium alloy gas turbine components through ion implantation 23 p3309 N90-28713

FRICTION
NT AERODYNAMIC DRAG
NT DRY FRICTION
NT FLOW RESISTANCE
NT FRICTION DRAG
NT INTERNAL FRICTION
NT KINETIC FRICTION
NT SKIN FRICTION
NT SLIDING FRICTION
NT SUPERSONIC DRAG
NT VISCOUS DRAG
Friction and wear of oxide-ceramic sliding against IN-718 nickel base alloy at 25 to 800 C in atmospheric air
[NASA-TM-102291] 01 p0046 N90-10262
Research on ultra low wear materials for energy conservation
[DE89-015096] 01 p0046 N90-10263
Micromechanisms of surface friction in zinc electrogalvanized steel sheets
[DE89-011819] 01 p0077 N90-10440
A new approach to control single-link flexible arms. Part 1: Modelling and identification in the presence of joint friction
[AD-A210590] 01 p0078 N90-10445
Solvent dynamical effects in electron transfer: Predicted influences of electron coupling upon the rate-dielectric friction dependence
[AD-A210193] 01 p0120 N90-10690
Morphological aspects of the friction of hot-filament-grown diamond thin films
[DE89-015986] 01 p0130 N90-10750
The effect of twins on critical currents of high Tc superconductors
[AD-A210988] 01 p0133 N90-10768
Analytical study of mistuning/friction/aerodynamics interaction in a bladed disk assembly
[AD-A211139] 02 p0156 N90-10893
Three-dimensional viscoelastic bodies in steady state frictional rolling contact with generalization to Knothe rolling
[REPT-89-23] 03 p0355 N90-12032
A new test machine for measuring friction and wear in controlled atmospheres to 1200 C
[NASA-TM-102405] 04 p0466 N90-12670
Unilateral contact analysis of a crack with friction. Applications
[ETN-89-95511] 04 p0512 N90-12956
A new approach to control single-link flexible arms. Part 3: Adaptive control of the tip position with payload changes
[AD-A213337] 05 p0650 N90-13792
The limiting friction force
[ECL-89-005] 05 p0652 N90-13801
Mechanisms of wear in structural ceramic materials 06 p0749 N90-14360
Finite element analysis of frictional contact problems 06 p0792 N90-14612
Tire modeling by finite elements 06 p0792 N90-14614
Single particle friction tests with cellulose acetate sphere samples
[DE89-017537] 06 p0793 N90-14622
Ion beam modification of metals: Mechanical properties and structure
[AD-A214701] 09 p1194 N90-16915
The experimental evaluation and application of high-temperature solid lubricants
[NASA-TM-102476] 09 p1198 N90-16944
Friction in bearings
[ESDU-89044] 09 p1232 N90-17149
Life of concentrated contacts in the mixed EHD and boundary film regimes
[AD-A216673] 11 p1517 N90-18738
Runaway rubber removal
[AD-A218349] 13 p1759 N90-20100
Numerical simulation model of hydrazine attitude control thrusters
[INPE-4965-PRE/1534] 15 p2068 N90-21848
Finite element analysis of elastic contact problems with friction 15 p2105 N90-22040
Rotor-to-stationary element rub-related vibration phenomena in rotating machinery: Literature survey 15 p2109 N90-22065
Tribomaterial factors in space mechanism brake performance 15 p2114 N90-22096
Active control of bearing preload using piezoelectric translators 15 p2115 N90-22098
Friction and wear of tungsten carbides with nitrogen ion implants
[ECL-89-19] 17 p2371 N90-23496
CVD diamond films for tribological applications
[AD-A220265] 17 p2413 N90-23750
A day in the life of a warm front
[AD-A220373] 17 p2426 N90-23826
Friction and wear of whisker-reinforced ceramic composite bodies
[DE90-011313] 18 p2519 N90-24389
Tribological properties of PVD-applied MoS2 coatings used on space mechanisms 18 p2537 N90-24470
An overview of the joint FAA/NASA aircraft/ground runway friction program
[NASA-TM-103486] 20 p2805 N90-25957
Self-lubricating-diamond like coatings deposition
[AD-A221756] 21 p2988 N90-26983
The effect of tidal friction between galaxies on the formation and development of galactic clusters in the expanding universe
[ETN-90-97314] 21 p3098 N90-27603
Effects of friction and end losses on MHD thruster efficiency
[DE90-013673] 23 p3289 N90-28608
Investigation of maximum achievable body torque for a walking machine with friction cone constraints
[PB90-203175] 23 p3332 N90-28838
Solutions to the frictional dynamics problem and the reciprocal variable feedback methodology for design and control of robot mechanisms 23 p3333 N90-28846
Use of electron spectroscopies in the tribological evaluation of diamond films
[DE90-014421] 23 p3334 N90-28848
Reliability and performance of friction measuring tires and friction equipment correlation
[AD-A223694] 24 p3436 N90-29408
The friction and wear of lubricated Si3N4/SiC(w) composites
[DE90-015790] 24 p3444 N90-29448
Ion-beam-assisted deposition of silver films on zirconia ceramics for improved tribological behavior
[DE90-009706] 24 p3456 N90-29516
Friction, wear and electric characteristics of slip-ring brush materials for space applications. Part 1: Screening by pin-on-disk friction tests
[NAL-TR-1040] 24 p3478 N90-29657
Proceedings of damping '89. Volume 2: Pages FAA-1 through IBD-15
[AD-A223432] 24 p3479 N90-29665

FRICTION COEFFICIENT
U COEFFICIENT OF FRICTION

FRICTION DRAG
NT AERODYNAMIC DRAG
NT SUPERSONIC DRAG
NT VISCOUS DRAG
Control and modification of turbulence 01 p0066 N90-10377
Turbulence management: Application aspects 01 p0066 N90-10378
A brief review of some mechanisms causing boundary layer transition at high speeds
[NASA-TM-102834] 20 p2803 N90-25945

FRICTION FACTOR
Selection of the energy-efficient enhancement geometry for single-phase turbulent flow inside tubes
[DE89-017690] 06 p0777 N90-14519
Finite element analysis of frictional contact problems 06 p0792 N90-14612
Numerical analysis and simulation of frictional particle systems 07 p0937 N90-15430
Investigation into the effect of fibre size on the tribological behaviour of semi-metallic brake material 09 p1185 N90-16864
Incompressible flow friction factors in a simulated heat pipe
[AD-A216288] 10 p1386 N90-18018
Experimentally determined wear behavior of an Al2O3-SiC composite from 25 to 1200 C
[NASA-TM-102549] 13 p1765 N90-20130
Fiber pushout test: A three-dimensional finite element computational simulation
[NASA-TM-102565] 14 p1945 N90-21131
Tribomaterial factors in space mechanism brake performance 15 p2114 N90-22096
AX-5 space suit bearing torque investigation 15 p2115 N90-22101
Bidirectional drive and brake mechanism
[NASA-CASE-MSC-21540-1] 20 p2872 N90-26342
Thermal analysis of the wearing by removal of melted metal during high speed friction
[ETCA-89-R-139] 22 p3183 N90-28067

FRICTION LOSS COEFFICIENT
U FRICTION FACTOR

FRICTION MEASUREMENT
Evaluation of two transport aircraft and several ground test vehicle friction measurements obtained for various runway surface types and conditions. A summary of test results from joint FAA/NASA Runway Friction Program
[NASA-TP-2917] 08 p1021 N90-15902
Investigation of rough elastohydrodynamic contact
[ISAL-89-0029] 08 p1085 N90-16281
Skin friction measurements by laser interferometry in supersonic flows 10 p1306 N90-17557
Elastic and viscoelastic analysis of two multiply layered cylinders rolling over each other with Coulomb friction
[REPT-89-50] 15 p2107 N90-22051
Reliability and performance of friction measuring tires and friction equipment correlation
[AD-A223694] 24 p3436 N90-29408

FRICTION PRESSURE DROP
U SKIN FRICTION

FRICTION REDUCTION
The experimental evaluation and application of high temperature solid lubricants 18 p2564 N90-24631
Hydrodynamic skin-friction reduction
[NASA-CASE-LAR-14078-1-CU] 21 p3003 N90-27071

FRICTION WELDING
The effects of a nearby subsequent fusion weld on the properties of an inertia friction weld
[DE90-007972] 14 p1988 N90-21396

FRINGE PATTERNS
U DIFFRACTION PATTERNS

FROGS
Automatic experiment container for fertilisation of frog eggs in space: A multi-purpose piece of classified space hardware 19 p2681 N90-25249

FRONTAL AREAS (METEOROLOGY)
U FRONTS (METEOROLOGY)

FRONTS
Frontogenesis in gravity currents: An example with no known applications in oceanography
[MATHS-REPT-A-117] 20 p2863 N90-26284

FRONTS (METEOROLOGY)
NT COLD FRONTS
NT WARM FRONTS
Air flow over large scale topography
|AD-A211779| 04 p0519 N90-12998
Identification and quantification of synoptic structure in simulated Tiros N radiance soundings
07 p0959 N90-15546
Frontal clouds and flight conditions in them
|AD-A214250| 07 p0964 N90-15573
Numerical modeling of the atmosphere with an isentropic vertical coordinate 09 p1246 N90-17226
Analysis of significant weather on meso-alpha scales using conventional and remotely sensed data: Exploratory studies
|AD-A214563| 09 p1248 N90-17238
A case study of the 24 August 1986 FLOWS microburst
|AD-A216939| 11 p1537 N90-18847
Structure and dynamics of the Arizona monsoon boundary
|AD-A217378| 13 p1844 N90-20586
Coastal frontogenesis and associated severe weather on 13 March 1986 (GALE IOP 13)
|AD-A217708| 13 p1845 N90-20590
A case study of cloud-to-ground lightning during the GALE program 15 p2132 N90-22185
Tropical squall lines of the Arizona monsoon
16 p2257 N90-22867
A numerical study of the role of meso beta and meso gamma scale vertical exchange processes in the evolution of upper tropospheric frontal systems
|AD-A222057| 21 p3031 N90-27230
Turbulent statistics in the vicinity of an SST front: A north wind case, FASINEX February 16, 1986
22 p3221 N90-28266
The effects of clouds on CO2 forcing
22 p3222 N90-28271
Low-frequency cloud-radiation interactions
22 p3225 N90-28289
Detection and analysis of wind fronts and current shear in digital SAR images
|FFI-89/7016| 24 p3495 N90-29755

FROST
Debris/ice/TPS assessment and photographic analysis for Shuttle Mission STS-28R
|NASA-TM-102152| 01 p0016 N90-10079
Debris/ice/TPS assessment and photographic analysis for Shuttle Mission STS-36
|NASA-TM-102789| 16 p2205 N90-22583

FROST DAMAGE
Definition of research needs to address airport pavement distress in cold regions
|DOT/FAA/DS-89/13| 02 p0157 N90-10896

FROSTBITE
Arctic cold weather medicine and accidental hypothermia
|AD-A223090| 20 p2899 N90-26487

FROZEN SOILS
U PERMAFROST

FUEL CAPSULES
Hydrogen embrittlement of titanium and its alloys
|DE90-602366| 10 p1355 N90-17858
Application of the results of carbon pellet modeling to the problem of plasma penetration
|DE90-012713| 20 p2928 N90-26658

FUEL CELL CATALYSTS
U ELECTROCATALYSTS

FUEL CELL POWER PLANTS
Molten carbonate fuel cell technology improvement
|DE90-001934| 07 p0950 N90-15501
The Hermes fuel cell power plant
10 p1333 N90-17706

FUEL CELLS
NT BIOCHEMICAL FUEL CELLS
NT HYDROGEN OXYGEN FUEL CELLS
NT PHOSPHORIC ACID FUEL CELLS
NT REGENERATIVE FUEL CELLS
Independent Orbiter Assessment (IOA): Assessment of the electrical power generation/fuel cell powerplant subsystem FMEA/CIL
|NASA-CR-185562| 02 p0161 N90-10914
Independent Orbiter Assessment (IOA): Analysis of the electrical power generation/fuel cell powerplant subsystem
|NASA-CR-185561| 02 p0161 N90-10915
Independent Orbiter Assessment (IOA): Analysis of the electrical power generation/power reactant storage and distribution subsystem
|NASA-CR-185556| 02 p0162 N90-10918
Fuel cells for vehicle propulsion applications: A thermodynamic systems analysis
|DE89-017689| 03 p0342 N90-11950
A lightweight solid polymer electrolyte fuel cell with stack power density of 3 kW/lb (7 kW/kg)
|AD-A211542| 03 p0367 N90-12098
Proceedings of the First Annual Fuel Cells Contractors Review Meeting
|DE89-011699| 06 p0803 N90-14675
Heat and mass transfer design issues in PEM fuel cell hardware
|DE89-016779| 06 p0804 N90-14677
Electrode development in monolithic solid oxide fuel cells
|DE90-001910| 06 p0805 N90-14684
Interfacial effects in monolithic solid oxide fuel cells
|DE90-001914| 06 p0806 N90-14690
Solid oxide fuel cells electrodes based on In(sub 2)O(sub 3)-PrO(sub 1.83)-ZrO(sub 2)
|DE90-002666| 06 p0806 N90-14691
Technology Base Research Project for electrochemical energy storage
|DE90-002604| 06 p0806 N90-14693
Molten carbonate fuel cell technology improvement
|DE90-001934| 07 p0950 N90-15501
An assessment and comparison of fuel cells for transportation applications
|DE90-001807| 07 p0952 N90-15508
Oxygen electrode in molten carbonate fuel cells
|DE90-002871| 07 p0952 N90-15510
Characterization of new cathode materials for molten carbonate fuel cells
|DE90-003547| 07 p0953 N90-15516
Fabrication of porous ceramic electrode structures
|DE90-003548| 07 p0953 N90-15517
Synthesis of air-sinterable lanthanum chromite powders
|DE90-004681| 08 p1046 N90-16049
Ninth Battery and Electrochemical Contractors' Conference: Extended abstracts
|DE89-016837| 08 p1059 N90-16120
An approach for testing fuel-cell/battery hybrid power sources for bus applications
|DE90-002090| 08 p1083 N90-16270
Electric and hybrid vehicles: Technical background report for the DOE flexible and alternative fuels study
|DE90-002218| 08 p1084 N90-16271
Development of planar geometry solid oxide fuel cells
|PB90-100769| 08 p1095 N90-16341
The 1989 National Convention Record IEE Japan, part 11
|DE89-910083| 09 p1210 N90-17014
Patents on solid electrolyte fuel cells: Japan
|DE90-702639| 09 p1241 N90-17202
Patents on solid electrolyte fuel cells: US and Britain
|DE90-702640| 09 p1241 N90-17203
Patents on solid electrolyte fuel cells: West Germany, Netherlands and Sweden
|DE90-702641| 09 p1242 N90-17204
Determination of optimum electrolyte composition for molten carbonate fuel cells
|DE90-000410| 09 p1243 N90-17210
The Hermes fuel cell power plant
10 p1333 N90-17706
Advanced space power PEM fuel cell systems
10 p1333 N90-17707
A lightweight solid polymer electrolyte fuel cell with stack power density of 3kW/lb (7 kW/kg)
|AD-A216253| 10 p1401 N90-18100
Cohesive ceramic fabrication
|DE90-007333| 11 p1494 N90-18597
Oxygen electrode in molten carbonate fuel cells
|DE90-005377| 11 p1528 N90-18796
Solid-state proton conductors
|DE90-007595| 11 p1531 N90-18812
Zirconia-based electrodes for solid oxide fuel cells
|DE90-000462| 12 p1655 N90-19513
Solid oxide fuel cell cogeneration system conceptual design, program 2
|PB90-114968| 12 p1681 N90-19653
Life-cycle cost comparisons of advanced storage batteries and fuel cells for utility, stand-alone, and electric vehicle applications
|DE90-008090| 13 p1794 N90-20298
Monolithic solid oxide fuel cell development
13 p1822 N90-20460
Recent advances in solid polymer electrolyte fuel cell technology with low platinum loading electrodes
13 p1823 N90-20465
The application of Dow Chemical's perfluorinated membranes in proton-exchange membrane fuel cells
13 p1823 N90-20466
Hydrogen-oxygen proton-exchange membrane fuel cells and electrolyzers 13 p1823 N90-20467
Electrocatalysis for oxygen electrodes in fuel cells and water electrolyzers for space applications
13 p1823 N90-20468
Oxygen electrodes for rechargeable alkaline fuel cells-II 13 p1823 N90-20469
Non-noble electrocatalysts for alkaline fuel cells
13 p1824 N90-20470
Corrosion testing of candidates for the alkaline fuel cell cathode 13 p1824 N90-20471
Advanced on-site power plant development technology program
|DE90-000443| 13 p1826 N90-20484
Enhanced ceria solid electrolyte fuel cell development. Reduction of electronic conductivity permits use of a solid ceria electrolyte in high efficiency high power density fuel cells at temperatures compatible with metallic cell hardware
|AD-A217840| 13 p1828 N90-20498
Development of planar geometry solid oxide fuel cell technology, phase 2
|PB90-131293| 14 p2001 N90-21467
Alternative materials for solid oxide fuel cells
|DE90-008615| 14 p2001 N90-21468
O2 reduction at the IFC orbiter fuel cell O2 electrode
|NASA-TM-102580| 14 p2001 N90-21469
Catalysts for ultrahigh current density oxygen cathodes for space fuel cell applications
|NASA-CR-180650| 16 p2251 N90-22835
Enhanced ceria solid electrolyte fuel cell development. Reduction of electronic conductivity permits use of a solid ceria electrolyte in high efficiency high power density fuel cells at temperatures compatible with metallic cell hardware
|AD-A219297| 16 p2253 N90-22846
New generation power subsystems for satellites
|AD-A219540| 17 p2365 N90-23464
Selective removal of organics for water reclamation
|NASA-TM-101890| 17 p2421 N90-23797
Megawatt solar power systems for lunar surface operations
|NASA-CR-186509| 20 p2881 N90-26391
A lightweight solid polymer electrolyte fuel cell with stack power density of 3 kW/lb (7kW/kg)
|AD-A223068| 21 p3020 N90-27169
Monolithic solid oxide fuel cell technology development, phase 1A
|PB90-183237| 22 p3195 N90-28132
Fuel cells: Their applications, technological status, market and opportunity
|DE90-796158| 23 p3344 N90-28895
A 10kW class molten carbonate fuel cell test: The stack with electrolyte plate prepared with paper-making method
|DE90-507841| 23 p3344 N90-28900
Electrochemical characteristics of acid electrolytes for fuel cells
|PB90-244385| 24 p3484 N90-29693
Electrochemical evaluation of new fluorosulfonic and fluorophosphonic acids as fuel cell electrolytes
|DE90-016626| 24 p3485 N90-29699

FUEL COMBUSTION
NT NUCLEAR FUEL BURNUP
Revolutionary opportunities for materials and structures study
|NASA-CR-179642| 01 p0034 N90-10184
High energy density solid and liquid hydrocarbon fuels
|AD-A210195| 01 p0053 N90-10304
Turbulent reacting flows in solid-propellant ducted rocket combustors 02 p0189 N90-11079
Evaporation and combustion of dense sprays with a bimodal droplet size distribution
02 p0192 N90-11094
Analysis of opposed jet hydrogen-air counter flow diffusion flame
|NASA-CR-182366| 03 p0321 N90-11825
Correlating microemulsion fuel composition, structure and combustion properties
|DE89-017779| 03 p0333 N90-11898
Two-dimensional analysis of two-phase reacting flow in a firing direct-injection diesel engine
|NASA-TM-102069| 05 p0582 N90-13392
An investigation of flame spread over shallow liquid pools in microgravity and nonair environments
|NASA-TM-102425| 05 p0630 N90-13680
Analysis of rotary engine combustion processes based on unsteady, three-dimensional computations
|NASA-TM-102469| 05 p0642 N90-13749
Comparison of engine knock predictions using a fully-detailed and a reduced chemical kinetic mechanism
|DE90-002805| 07 p0941 N90-15448
Solid fuel combustion chamber
|LR-555| 08 p1038 N90-16001
Investigation into the feasibility of using solid fuel ramjets for high supersonic/low hypersonic tactical missiles
|AD-A214737| 09 p1168 N90-16761
Acquisition of analytical instruments for combustion research
|AD-A214495| 09 p1190 N90-16893
Combustion of hydrogen and hydrocarbons in fluorine
|AD-A214621| 09 p1190 N90-16896

Effect of reduced atmospheric pressure on the performance characteristics of pyrotechnic compositions containing aluminum
[AD-A214473] 09 p1200 N90-16953
Time and spatially dependent estimates of pollutant trace gas emissions and their effect on tropospheric ozone 09 p1243 N90-17212
Full scale catalytic combustion of methane under atmospheric pressure
[DE89-772354] 10 p1351 N90-17835
Alternative fuels R/D needs: Program directions
[DE90-007053] 11 p1495 N90-18603
Investigation of methods to produce a uniform cloud of fuel particles in a flame tube
[NASA-TM-102376] 11 p1505 N90-18665
Effects of turbulence mixing, variable properties, and vaporization on spray droplet combustion
[NASA-CR-186463] 12 p1623 N90-19326
Development and use of an advanced coal-fueled diesel engine cycle simulation with group effects
[DE90-000450] 12 p1672 N90-19607
Structure of model gas flames in nitramines
[AD-A217578] 13 p1770 N90-20159
The modelling of heat and mass transfer near solid boundaries and comparison with experimental results
[PB90-167040] 14 p1974 N90-21310
Detailed mechanism for oxidation of benzene
[NASA-TM-102443] 15 p2067 N90-21842
High speed commercial transport fuels considerations and research needs
[NASA-TM-102535] 15 p2072 N90-21869
Fuel-rich catalytic combustion: A fuel processor for high-speed propulsion
[NASA-TM-103177] 17 p2374 N90-23518
Contributions to the study of parietal flames due to turbulent diffusion
[ECL-89-22] 17 p2374 N90-23519
Combustion of n-butane and isobutane in an internal combustion engine: A comparison of experimental and modeling results
[DE90-005993] 18 p2522 N90-24400
Production and coating of pure boron powders
[AD-A220272] 18 p2533 N90-24452
A low NOx strategy for combusting high nitrogen content fuels
[PB90-155664] 19 p2712 N90-25435
Performance of a supercharged direct-injection stratified-charge rotary combustion engine
[NASA-TM-103105] 20 p2809 N90-25982
Liquid fueled ramjet combustion instability: Acoustical and vortical interactions with burning sprays
[AD-A222752] 20 p2831 N90-26104
A comparison of the contribution of various gases to the greenhouse effect 20 p2885 N90-26414
A theoretical study of flow structure and radiation for multiphase turbulent diffusion flames
[AD-A222934] 21 p2976 N90-26913
Laboratory tests to determine the chemical and physical characteristics of propellant-solvent-fuel oil mixtures
[AD-A222270] 21 p2990 N90-26991
The 26th JANNAF Combustion Meeting, volume 1
[CPIA-PUBL-529-VOL-1] 22 p3161 N90-27927
Regression and combustion characteristics of boron containing fuels for solid fuel ramjets 22 p3161 N90-27928
Pyrolysis and combustion of solid fuels under both subsonic and supersonic conditions 22 p3161 N90-27929
Calculations of chemically reacting shear flows above solid fuels 22 p3162 N90-27930
Calculation of the combustion distribution in a liquid-fuel ramjet 22 p3162 N90-27931
An investigation of solid-fuel, dual-mode combustion ramjets 22 p3162 N90-27933
Hydrocarbon-fueled scramjet combustor component development tests 22 p3162 N90-27934
Modeling of knock in spark-ignition engines
[DE90-010875] 22 p3182 N90-28058
Injector element characterization methodology 23 p3294 N90-28634
Overview on hot gas tests and molten salt corrosion experiments at the DLR 23 p3309 N90-28714
Evaluation of a hybrid kinetics/mixing-controlled combustion model for turbulent premixed and diffusion combustion using KIVA-2
[NASA-TM-103196] 23 p3323 N90-28792
Combustion characteristics of oxygen/hydrogen high pressure preburners for staged combustion cycle rocket engine
[NAL-TR-1044] 24 p3441 N90-29434
Investigation of particulate formation during diesel spray combustion
[DE90-012682] 24 p3446 N90-29464

FUEL CONSERVATION
U FUEL CONSUMPTION

FUEL CONSUMPTION
Results from the second year of operation of the Federal Methanol Fleet at Argonne National Laboratory
[DE89-016935] 02 p0230 N90-11319
View on recent fuel costs in airlines
[NAL-TM-569] 02 p0289 N90-11653
Supersonic boundary-layer transition on the LaRC F-106 and the DFRF F-15 aircraft. Part 1: Transition measurements and stability analysis 04 p0447 N90-12558
Trajectory optimization and guidance for an aerospace plane
[NASA-CR-185884] 05 p0578 N90-13369
Assessment of costs and benefits of flexible and alternative fuel use in the US transportation sector. Technical report three: Methanol production and transportation costs
[DE90-002625] 06 p0755 N90-14396
Guidance analysis of the aeroglide plane change maneuver as a turning point problem
[NASA-TM-101639] 07 p0883 N90-15110
Guidelines for evaluating energy analysis software
[AD-A214171] 07 p0976 N90-15640
Industrial heat pump assessment study
[DE90-004541] 08 p1071 N90-16201
Reducing C130E Hercules operating costs in the Royal Australian Air Force and the United States Air Force by increasing cruise speeds
[AD-A215747] 10 p1319 N90-17629
US Army Methanol-Fueled Administrative Vehicle Demonstration Program
[AD-A216013] 10 p1393 N90-18054
Vehicle acceleration and fuel consumption when operated on JP-8 fuel
[AD-A216275] 10 p1393 N90-18055
Federal methanol fleet update
[DE90-006851] 11 p1517 N90-18741
In-flight evaluations of turbine fuel extenders
[DOT/FAA/CT-89/33] 12 p1633 N90-19387
Civil air transport: A fresh look at power-by-wire and fly-by-light
[NASA-TM-102574] 14 p1969 N90-21283
Computer-aided design of flywheel transmission systems 14 p1988 N90-21392
An approach to on-board optimization of cruise at constant altitude
[LR-581] 15 p2050 N90-21752
Analysis, selection, and implementation of procedures which approve optimal artificial satellite maneuvers
[INPE-5003-TDL/397] 15 p2058 N90-21786
T4A thruster starting sequences and the design of an electromagnetic sequencer for cyclic life tests
[RAE-TR-77042] 19 p2669 N90-25179
Methods and apparatus for providing real-time control of a gaseous propellant rocket propulsion system
[NASA-CASE-MSC-21542-1] 20 p2825 N90-26073
Advanced Turbine Technology Applications Project (ATTAP)
[NASA-CR-185240] 20 p2939 N90-26728
Comparison of altitude test cell results 22 p3119 N90-27715
Comparison of ground-level test cells and ground-level to altitude test cells 22 p3119 N90-27716
General test plan 22 p3120 N90-27721
Energy Efficient Engine acoustic supporting technology report
[NASA-CR-174834] 23 p3279 N90-28557
Energy Efficient Engine core design and performance report
[NASA-CR-168069] 23 p3279 N90-28559
Energy Efficient Engine program advanced turbofan nacelle definition study
[NASA-CR-174942] 23 p3280 N90-28560
Energy Efficient Engine integrated core/low spool design and performance report
[NASA-CR-168211] 23 p3280 N90-28561
Energy efficient engine program technology benefit/cost study, volume 2
[NASA-CR-174766-VOL-2] 23 p3280 N90-28565
Energy Efficient Engine: Combustor component performance program
[NASA-CR-179533] 23 p3281 N90-28568
Energy Efficient Engine: Control system preliminary definition report
[NASA-CR-179578] 23 p3281 N90-28569
Energy Efficient Engine: High-pressure compressor test hardware detailed design report
[NASA-CR-180850] 23 p3281 N90-28570
Results from the fourth year of operation of the Federal Methanol Fleet at Lawrence Berkeley Laboratory
[DE90-014741] 23 p3315 N90-28743
Airline productivity relating on the fuel cost. (2): Fuel consumption values and fuel efficiency
[NAL-TM-604-2] 24 p3422 N90-29333

FUEL CONTROL
Independent Orbiter Assessment (IOA): Assessment of the orbiter main propulsion system FMEA/CIL, volume 1
[NASA-CR-185559-VOL-1] 03 p0312 N90-11775
Independent Orbiter Assessment (IOA): Assessment of the main propulsion subsystem FMEA/CIL, volume 2
[NASA-CR-185559-VOL-2] 03 p0313 N90-11776
Independent Orbiter Assessment (IOA): Assessment of the main propulsion subsystem FMEA/CIL, volume 3
[NASA-CR-185559-VOL-3] 03 p0313 N90-11777
Independent Orbiter Assessment (IOA): Assessment of the main propulsion subsystem FMEA/CIL, volume 4
[NASA-CR-185559-VOL-4] 03 p0313 N90-11778
Guidance and Control strategies for aerospace vehicles
[NASA-CR-186195] 06 p0727 N90-14243

FUEL ELEMENTS (NUCLEAR REACTORS)
U NUCLEAR FUEL ELEMENTS

FUEL FLOW
NT PROPELLANT TRANSFER
Feedback control of combustion instabilities: A case study in active adaptive control of complex physical systems
[AD-A215385] 09 p1192 N90-16905
Numerical study of diffusion jet flames 12 p1621 N90-19316
Comparison of altitude test cell results 22 p3119 N90-27715
Analysis of scramjet engine characteristics
[NAL-TR-1041] 24 p3434 N90-29396

FUEL INJECTION
Experimental study on the stability of small rocket engines with storable liquid propellants 01 p0036 N90-10196
Numerical simulation of unsteady combustion in a dump combustor 01 p0037 N90-10203
Oscillations in non-axisymmetric dump combustors 01 p0037 N90-10205
Two dimensional orifice array, monodisperse drop source, phase 1
[AD-A211319] 04 p0500 N90-12881
Two-dimensional analysis of two-phase reacting flow in a firing direct-injection diesel engine
[NASA-TM-102069] 05 p0582 N90-13392
LOX/hydrocarbon combustion instability investigation
[NASA-CR-182249] 05 p0615 N90-13589
Analysis of rotary engine combustion processes based on unsteady, three-dimensional computations
[NASA-TM-102469] 05 p0642 N90-13749
A laboratory test for fuel injector deposit studies
[DE90-000802] 06 p0795 N90-14629
Extended temperature range rocket injector
[NASA-CASE-LEW-14846-1] 07 p0887 N90-15130
Externally vaporizing system for turbine combustor
[AD-D014284] 08 p1024 N90-15918
Development of a spark assisted direct injection multifuel diesel engine especially for alcohol fuels
[ACTA-POLYTEC-SCAND-ME-94] 17 p2412 N90-23747
A comparison of analytical results for 20 K LOX/hydrogen instabilities
[NASA-TM-103166] 19 p2670 N90-25186
Effect of vane twist on the performance of dome swirlers for gas turbine airblast atomizers
[NASA-TM-103195] 19 p2688 N90-25289
Combustion in the gas turbine. Part 3: Fuel injection, ignition and stability
[CIT/SME/VKI/RS/4] 20 p2810 N90-25988
Calculation of the combustion distribution in a liquid-fuel ramjet 22 p3162 N90-27931
Computer code for the prediction of nozzle admittance 23 p3293 N90-28630
Swirl coaxial injector element characterization for booster engines 23 p3294 N90-28632
Heavy hydrocarbon main injector technology 23 p3294 N90-28633
Evaluation of a hybrid kinetics/mixing-controlled combustion model for turbulent premixed and diffusion combustion using KIVA-2
[NASA-TM-103196] 23 p3323 N90-28792
A comparison of scramjet engine performances of various cycles
[NAL-TR-1042] 24 p3434 N90-29397
Combustion characteristics of oxygen/hydrogen high pressure preburners for staged combustion cycle rocket engine
[NAL-TR-1044] 24 p3441 N90-29434

FUEL OILS
A comparison of the contribution of various gases to the greenhouse effect 20 p2885 N90-26414
Laboratory tests to determine the chemical and physical characteristics of propellant-solvent-fuel oil mixtures
[AD-A222270] 21 p2990 N90-26991

FUEL PRODUCTION
Production of jet fuels from coal-derived liquids. Volume 11: Production of advanced endothermic fuel blends from Great Plains Gasification Plant naphtha by-product stream
|AD-A210251| 02 p0207 N90-11184
Photoconversion of inorganics to methane
|PB89-230643| 06 p0753 N90-14379
Assessment of costs and benefits of flexible and alternative fuel use in the US transportation sector. Technical report three: Methanol production and transportation costs
|DE90-002625| 06 p0755 N90-14396
Photosynthetic water splitting, phase 2
|PB90-132671| 15 p2066 N90-21833
A robotically constructed production and supply base on Phobos
|NASA-CR-186234| 15 p2073 N90-21872
FUEL PUMPS
Compatibility of fuel system components with high density fuel
|AD-A210381| 01 p0006 N90-10027
SSME Alternate Turbopump Development Program: Design verification specification for high-pressure fuel turbopump
|NASA-CR-183676| 01 p0008 N90-10033
FUEL SPRAYS
Theory of droplet. Part 1: Renormalized laws of droplet vaporization in non-dilute sprays 01 p0068 N90-10390
Evaporation and combustion of dense sprays with a bimodal droplet size distribution 02 p0192 N90-11094
Fundamental mechanism of atomization
|AD-A213859| 07 p0915 N90-15293
The stability of fuel fires 10 p1315 N90-17601
Microgravity acoustic mixing for particle cloud combustors
|NASA-CR-185159| 14 p2023 N90-21600
Structure of monopropellant spray flames at elevated pressures
|AD-A218676| 17 p2383 N90-23570
Introducing the VRT gas turbine combustor
|NASA-TM-103176| 17 p2386 N90-23591
The modeling of drop-containing turbulent eddies
|NASA-CR-186805| 18 p2553 N90-24570
Investigation of particulate formation during diesel spray combustion
|DE90-012682| 24 p3446 N90-29464
FUEL SYSTEMS
NT AIRCRAFT FUEL SYSTEMS
Compatibility of fuel system components with high density fuel
|AD-A210381| 01 p0006 N90-10027
Independent Orbiter Assessment (IOA): Assessment of the orbiter main propulsion system FMEA/CIL, volume 1
|NASA-CR-185559-VOL-1| 03 p0312 N90-11775
Independent Orbiter Assessment (IOA): Assessment of the main propulsion subsystem FMEA/CIL, volume 2
|NASA-CR-185559-VOL-2| 03 p0313 N90-11776
Independent Orbiter Assessment (IOA): Assessment of the main propulsion subsystem FMEA/CIL, volume 3
|NASA-CR-185559-VOL-3| 03 p0313 N90-11777
Independent Orbiter Assessment (IOA): Assessment of the main propulsion subsystem FMEA/CIL, volume 4
|NASA-CR-185559-VOL-4| 03 p0313 N90-11778
Fuel resistant coatings for metal and composite fuel tanks 08 p1022 N90-15911
Externally vaporizing system for turbine combustor
|AD-D014284| 08 p1024 N90-15918
Diesel starting system monitor: Prototype development
|DE90-004425| 08 p1084 N90-16276
Low-energy gamma ray attenuation characteristics of aviation fuels
|NASA-TP-2974| 11 p1543 N90-18882
MHD channel development, part 4
|DE90-009552| 15 p2169 N90-22397
Aircraft crash survival design guide. Volume 1: Design criteria and checklists
|AD-A218434| 16 p2198 N90-22545
Aircraft crash survival design guide. Volume 5: Aircraft postcrash survival
|AD-A218438| 16 p2198 N90-22549
Production and coating of pure boron powders
|AD-A220272| 18 p2533 N90-24452
FUEL TANKS
CF 18 480 Gallon External Fuel Tank Stores Clearance Program 02 p0153 N90-10877
Fuel Tank Technology
|AGARD-R-771| 08 p1021 N90-15904
Integral fuel tank sealing practice at British Aerospace (Kingston) 08 p1021 N90-15905
Integral fuel tanks - design, production, aging, repair 08 p1021 N90-15906
Aircraft fuel tank construction and testing experience 08 p1021 N90-15907
The repair of aircraft integral fuel tanks in the RAF: A user's view of fuel tank technology 08 p1022 N90-15908
The effect of primer age on adhesion of polysulphide sealant 08 p1022 N90-15909
Fuel resistant coatings for metal and composite fuel tanks 08 p1022 N90-15911
Spray sealing: A breakthrough in integral fuel tank sealing technology 08 p1022 N90-15912
Design philosophy and construction techniques for integral fuselage fuel tanks 08 p1023 N90-15913
Fuel tank explosion protection 08 p1023 N90-15914
A dynamicist's view of fuel tank skin durability 08 p1023 N90-15915
Integral fuel tank certification and test methods 08 p1023 N90-15916
Linear liquid oscillations in cylindrical containers under zero-gravity
|LRT-WE-9-FB-5(1989)| 08 p1066 N90-16168
Application of experimental techniques to store release problems 10 p1304 N90-17545
Ignitability of jet-A fuel vapors in aircraft fuel tanks 10 p1313 N90-17594
Fuel-elastomer compatibility studies: Results of 80 C/14-day exposure experiments
|AD-A216015| 10 p1361 N90-17893
Inflatable fuel tank buffer
|AD-D014446| 14 p1921 N90-21002
Failure mechanism of urethane elastomer coated fabric collapsible fuel tanks
|AD-A221033| 18 p2530 N90-24435
Laboratory simulation of the effect of rocket thrust on a precessing space vehicle
|NASA-CR-186681| 19 p2669 N90-25182
FUEL TESTS
Development of fuel wear tests using the Cameron-Plint high-frequency reciprocating machine
|AD-A216003| 10 p1361 N90-17892
In-flight evaluations of turbine fuel extenders
|DOT/FAA/CT-89/33| 12 p1633 N90-19387
Turbine fuel alternatives (near term)
|AD-A219405| 16 p2225 N90-22695
Subsonic combustor testing 20 p2811 N90-25997
Comparison of ground-level test cells and ground-level to altitude test cells 22 p3119 N90-27716
FUEL-AIR RATIO
Very-low-frequency oscillations in liquid-fueled ramjets 01 p0037 N90-10204
Investigation of fuel additive effects on sooting flames
|AD-A212925| 04 p0473 N90-12709
A planar reacting shear layer system for the study of fluid dynamics-combustion interaction
|NASA-TM-102422| 05 p0582 N90-13393
Numerical simulations of coherent structures in a jet flame with a noncircular cross section
|AD-A216710| 11 p1483 N90-18535
The modeling of drop-containing turbulent eddies
|NASA-CR-186805| 18 p2553 N90-24570
Development of advanced combustion technology for medium and high speed natural gas engines
|PB90-198565| 23 p3331 N90-28836
FUELING
U REFUELING
FUELS
NT AIRCRAFT FUELS
NT AUTOMOBILE FUELS
NT CHEMICAL FUELS
NT CLEAN FUELS
NT COAL
NT CRUDE OIL
NT DIESEL FUELS
NT ENDOTHERMIC FUELS
NT FOSSIL FUELS
NT FUEL OILS
NT GASEOUS FUELS
NT GASOLINE
NT HIGH ENERGY FUELS
NT HYDROCARBON FUELS
NT HYDROGEN FUELS
NT JET ENGINE FUELS
NT JP-4 JET FUEL
NT JP-8 JET FUEL
NT KEROSENE
NT LIQUID FUELS
NT METAL FUELS
NT MONOPROPELLANTS
NT NATURAL GAS
NT NUCLEAR FUELS
NT PEAT
NT SPENT FUELS
NT SYNTHETIC FUELS
View on recent fuel costs in airlines
|NAL-TM-569| 02 p0289 N90-11653
Methanol fueled vehicles and photochemical models: An evaluation of the state of knowledge
|PB89-214225| 03 p0419 N90-12410
Novel carbamates, their production and their use as fuels additives
|EP-PATENT-0-298-636-A-1| 05 p0629 N90-13676
A laboratory test for fuel injector deposit studies
|DE90-000802| 06 p0795 N90-14629
Products of the hypochlorite oxidation of hydrazine fuels
|AD-A213557| 07 p0915 N90-15291
Improved performance polysulfide based sealant 08 p1022 N90-15910
Alcohol and blends as motor fuels
|DE90-003517| 08 p1053 N90-16085
Improved anode catalysts for coal gas-fueled phosphoric acid fuel cells
|DE90-004016| 08 p1096 N90-16347
Environmental, health, and safety concerns associated with nonpetroleum fuel use in US transportation
|DE90-004367| 08 p1099 N90-16362
Analysis of liquid propellant exposed to elastomeric materials
|AD-A214465| 09 p1200 N90-16952
Hydrogen energy coordinating committee: Summary of DOE hydrogen programs
|DE90-004480| 10 p1361 N90-17891
Fuel-elastomer compatibility studies: Results of 80 C/14-day exposure experiments
|AD-A216015| 10 p1361 N90-17893
US Army Methanol-Fueled Administrative Vehicle Demonstration Program
|AD-A216013| 10 p1383 N90-18054
Office of Industrial Programs research in progress
|DE90-002100| 10 p1440 N90-18311
Hawaii integrated biofuels research program, phase 1
|DE90-006885| 11 p1530 N90-18811
Modification and improvement of software for modeling multidimensional reacting fuel flows
|AD-A217789| 13 p1783 N90-20235
A comparison of the autoignition chemistry of n-butane and isobutane in an internal combustion engine
|DE90-009474| 15 p2067 N90-21838
Method and apparatus for assessing distillate fuel stability by oxygen overpressure
|AD-D014499| 19 p2679 N90-25237
A low NOx strategy for combusting high nitrogen content fuels
|PB90-155664| 19 p2712 N90-25435
Policy options for stabilizing global climate. Volume 2: Chapters 7-9
|PB90-182312| 22 p3198 N90-28147
Analyses of spray and droplet ignition for pure and multicomponent fuels 23 p3304 N90-28688
Fuels research, volume 1
|DE90-015393| 23 p3305 N90-28695
FULL SCALE TESTS
Characteristics of transport, aircraft fires measured by full-scale tests 10 p1313 N90-17591
Full scale study of a cabin fire in an A300 fuselage section 10 p1313 N90-17592
Full-scale air transport category fuselage burnthrough tests
|DOT/FAA/CT-TN89/65| 14 p1913 N90-20967
Numerical study of unsteady flows in large air-driven blast simulators with single and multiple drivers
|UTIAS-334| 17 p2405 N90-23699
QM-6 final performance evaluation report igniter, volume 6
|NASA-CR-184001| 22 p3133 N90-27779
FUMES
Effects of atmospheric mix and toxic fumes on military performance
|PB89-223630| 04 p0522 N90-13015
Method for the evaluation of toxicity of combustion products from aircraft cabin materials: Analysis and results 10 p1316 N90-17612
FUNCTION GENERATORS
A graph-theoretical approach to block-copolymer complexes. Part 3: Loops and cycles
|MEMO-778-PT-3| 04 p0479 N90-12750
FUNCTION SPACE
NT BANACH SPACE
NT HILBERT SPACE
NT SOBOLEV SPACE
Stability and error estimates for sinc interpolation
|CWI-AM-R8914| 18 p2599 N90-24790
FUNCTIONAL ANALYSIS
NT BANACH SPACE
NT CONVOLUTION INTEGRALS
NT FOURIER TRANSFORMATION
NT FREDHOLM EQUATIONS
NT HARMONIC ANALYSIS
NT HILBERT SPACE
NT HILBERT TRANSFORMATION
NT INTEGRAL EQUATIONS

NT INTEGRAL TRANSFORMATIONS
NT J INTEGRAL
NT LAPLACE TRANSFORMATION
NT SINGULAR INTEGRAL EQUATIONS
NT SOBOLEV SPACE
NT VOLTERRA EQUATIONS
NT WIENER HOPF EQUATIONS
NT ZONAL HARMONICS
Discrete-time conversion for simulating finite-horizon Markov processes
|AD-A210683| 01 p0116 N90-10666
Impulse time-integral function and Lagrangian analysis
|DE89-016997| 02 p0221 N90-11268
Visual motion perception
|AD-A210994| 03 p0379 N90-12160
A functional expansion and stability for nonlinear input-output maps
|RR-359| 04 p0539 N90-13121
Flow of harmonic applications of a compact variety on a bordered variety
|DE89-635699| 07 p0985 N90-15692
Pareto optimization design techniques for the AFIT (Air Force Institute of Technology)/AAMRL (Armstrong Aeronautical Medical Research Laboratory) anthropomorphic robotic manipulator
|AD-A216178| 10 p1414 N90-18150
Theory and applications of belief functions
|AD-A217092| 12 p1702 N90-19774
Classical mechanics on superspace
|DE90-608907| 12 p1724 N90-19906
An error estimate for Tremolieres method for the discretization of parabolic variational inequalities
|DE90-627169| 24 p3541 N90-30024

FUNCTIONAL DESIGN SPECIFICATIONS
The development of an expert system for the creative design of mechanisms
|AD-A211115| 01 p0110 N90-10628
Ariane 5 structural design and development 02 p0186 N90-11057
Engineering specification and system design for CAD/CAM of custom shoes. Phase 5: UMC involvement (January 1, 1989 - June 30, 1989)
|NASA-CR-185838| 02 p0257 N90-11456
An update of commercial infrared sensing and imaging instruments 10 p1366 N90-17920
An introduction to selected structured methods
|RSRE-MEMO-4294| 15 p2148 N90-22275
Mechanical design engineering. NASA/university advanced design program: Lunar Bulk Material Transport Vehicle
|NASA-CR-184926| 18 p2534 N90-24455
Integrated controls and health monitoring for chemical transfer propulsion
|NASA-TM-103185| 19 p2668 N90-25178
Contribution to the definition and application of NAUTILE (A new environment for the conception and assembling of integrated circuits)
|ETN-90-97251| 20 p2910 N90-26554
Laboratory and field evaluations of extrasensitive sulfur dioxide and nitrogen dioxide analyzers for acid deposition monitoring
|PB90-201062| 22 p3199 N90-28153
Communications Interface Driver (CID) test plan
|DOT/FAA/CT-TN89/35| 23 p3319 N90-28762
A system architecture for a planetary rover 23 p3365 N90-29015

FUNCTIONAL INTEGRATION
Non-symmetric double well and Euclidean functional integral
|PREPRINT-709| 16 p2305 N90-23133

FUNCTIONALS
Estimating functionals related to a density by a class of statistics based on spacings
|REPT-89-11| 03 p0398 N90-12275

FUNCTIONS (MATHEMATICS)
NT ABEL FUNCTION
NT ANALYTIC FUNCTIONS
NT ASYMPTOTES
NT BOOLEAN FUNCTIONS
NT CONFORMAL MAPPING
NT COORDINATE TRANSFORMATIONS
NT COSINE SERIES
NT DISCRETE FUNCTIONS
NT DISCRIMINANT ANALYSIS (STATISTICS)
NT DISTRIBUTION FUNCTIONS
NT DISTURBING FUNCTIONS
NT ELLIPTIC FUNCTIONS
NT ERROR FUNCTIONS
NT EXPONENTIAL FUNCTIONS
NT FAST FOURIER TRANSFORMATIONS
NT FOURIER TRANSFORMATION
NT FRESNEL INTEGRALS
NT GREEN'S FUNCTIONS
NT HAMILTONIAN FUNCTIONS
NT HANKEL FUNCTIONS
NT HARMONIC FUNCTIONS
NT HYPERBOLIC FUNCTIONS
NT HYPERGEOMETRIC FUNCTIONS
NT KERNEL FUNCTIONS
NT LAGUERRE FUNCTIONS
NT LAPLACE TRANSFORMATION
NT LEGENDRE FUNCTIONS
NT LIAPUNOV FUNCTIONS
NT LINEAR TRANSFORMATIONS
NT LOGARITHMS
NT LORENTZ TRANSFORMATIONS
NT MAXWELL-BOLTZMANN DENSITY FUNCTION
NT MEROMORPHIC FUNCTIONS
NT MODULATION TRANSFER FUNCTION
NT MONOTONE FUNCTIONS
NT NORMAL DENSITY FUNCTIONS
NT ORTHOGONAL FUNCTIONS
NT PENALTY FUNCTION
NT PERIODIC FUNCTIONS
NT POINT SPREAD FUNCTIONS
NT POISSON DENSITY FUNCTIONS
NT PROBABILITY DENSITY FUNCTIONS
NT PROBABILITY DISTRIBUTION FUNCTIONS
NT RAYLEIGH DISTRIBUTION
NT RECURSIVE FUNCTIONS
NT SINE SERIES
NT SPACE-TIME FUNCTIONS
NT SPHERICAL HARMONICS
NT SPLINE FUNCTIONS
NT STEP FUNCTIONS
NT STRESS FUNCTIONS
NT TANGENTS
NT TIME FUNCTIONS
NT TRANSCENDENTAL FUNCTIONS
NT TRANSFER FUNCTIONS
NT TRIGONOMETRIC FUNCTIONS
NT WEIBULL DENSITY FUNCTIONS
NT WEIGHTING FUNCTIONS
An introduction to fractals and chaos
|AD-A210257| 01 p0117 N90-10675
Impulse time-integral function and Lagrangian analysis
|DE89-016997| 02 p0221 N90-11268
Backward analysis on higher order functions
|MEMO-INF-89-19| 02 p0268 N90-11526
An axiomatic theory for partial functions
|MEMO-INF-89-22| 02 p0268 N90-11527
Smooth linearization of hyperbolic fixed points without resonance conditions
|REPT-89-03| 03 p0394 N90-12251
Stable and unstable subspaces of a critical functional differential equation
|PB89-220651| 04 p0538 N90-13115
Parallel projected variable metric algorithms for unconstrained optimization
|NASA-CR-181930| 06 p0833 N90-14842
Classification of modular invariant partition functions for the twisted N=2 superconformal algebra, twisted SU(2) Kac-Moody algebra and D(sub 2K) parafermions
|DE90-600767| 06 p0835 N90-14853
Higher order crossings from a parametric family of linear filters
|AD-A213427| 07 p0983 N90-15676
Fractal-based image compression
|AD-A215400| 09 p1268 N90-17351
Should a function continue
|AD-A216406| 11 p1551 N90-18929
A method for computing the stationary points of a function subject to linear equality constraints
|DE90-610427| 12 p1706 N90-19797
Generalized Herglotz functions and inverse scattering problem in a finite depth ocean
|PB90-150996| 15 p2134 N90-22197
New algorithms for one-loop integrals
|NIKHEF-H/89-17| 15 p2148 N90-22268
Testing of elementary functions in Ada
|CWI-NM-R8909| 17 p2446 N90-23941
Reflexivity, the dual Radon-Nykodym property, and continuity of adjoint semigroups
|CWI-AM-R8908| 17 p2460 N90-24042
On rates of convergence and asymptotic normality in the multiknapsack problem
|CWI-BS-R8912| 17 p2460 N90-24045
Bounding separable recourse functions with limited distribution information
|AD-A219504| 17 p2465 N90-24084
On the notion of currying
|MEMO-INF-89-57| 18 p2592 N90-24749
The performance of wavelets for data compression in selected military applications
|AD-A219230| 18 p2614 N90-24892
The performance of wavelets for data compression in selected military applications. Volume 2: Supplementary tables and graphs
|AD-A219231| 18 p2615 N90-24893
Non-linear systems identification using radial basis functions
|RR-378| 19 p2751 N90-25635
Cartesian closed categories of domains
|ETN-90-97284| 20 p2919 N90-26613
The Second Asilomar Workshop on Progress in Mathematical Programming
|AD-A221986| 21 p3053 N90-27358
Hash functions: A tutorial and status report
|NPL-DITC-151/89| 22 p3238 N90-28361
Local interpolation functions for curve generation with the multi-surface transformation 24 p3470 N90-29608

FUNGI
Air pollution-caused changes in photosynthesis: Effects on plant growth and rhizosphere functions
|DE90-007184| 13 p1829 N90-20501
ELF (Extremely Low Frequency) communications system ecological monitoring program: Slime mold studies
|AD-A218623| 16 p2229 N90-22715

FUNGICIDES
NT CAFFEINE

FUNNELS
Preference numbers and funnel dimension
|REPT-89-57| 15 p2161 N90-22346

FURAN RESINS
NT KEVLAR (TRADEMARK)
NT POLYAMIDE RESINS

FURANS
NT TETRAHYDROFURAN

FURNACES
NT SOLAR FURNACES
Modelling and control of a diffusion/LPCVD furnace
|REPT-88-97| 03 p0336 N90-11910
Temperature profiles in high gradient furnaces 10 p1362 N90-17896
Non-contact temperature measurement requirements 10 p1363 N90-17898
Fusion furnaces for Spacelab 13 p1785 N90-20248
Method of preparing radially homogeneous mercury cadmium telluride crystals
|NASA-CASE-MFS-25786-2| 13 p1898 N90-20896
Activation uniformity dependence of undoped semi-insulating GaAs on post-implant annealing conditions
|ETN-90-96549| 16 p2323 N90-23246
High temperature electric arc furnace and method
|NASA-CASE-MFS-28281-1| 17 p2357 N90-23415
Temperature and melt solid interface control during crystal growth
|NASA-CR-186731| 20 p2929 N90-26664
Heat and momentum transfer to test samples in the high velocity plasma furnace
|AD-A222182| 21 p3079 N90-27505
Scandia-stabilized zirconia coating for composites
|AD-D014550| 22 p3160 N90-27917
Radiative heat transfer
|PB90-247602| 23 p3327 N90-28813

FUSELAGE MOUNTING
U AIRCRAFT PRODUCTION

FUSELAGES
Development of pressure containment and damage tolerance technology for composite fuselage structures in large transport aircraft
|NASA-CR-3996| 01 p0034 N90-10186
Measurements of pressures on the tail and aft fuselage of an airplane model during rotary motions at spin attitudes
|NASA-TP-2939| 02 p0145 N90-10829
Transport composite fuselage technology: Impact dynamics and acoustic transmission
|NASA-CR-4035| 03 p0321 N90-11821
Experimental and numerical analyses of laminar boundary-layer flow stability over an aircraft fuselage forebody 04 p0445 N90-12549
Some new techniques for aircraft fuselage skin tests
|LR-547| 05 p0580 N90-13379
An analytical method for the prediction of unsteady rotor/airframe interactions in forward flight 06 p0724 N90-14223
Investigation on sheet material of 8090 and 2091 aluminium-lithium alloy 07 p0898 N90-15192
Design philosophy and construction techniques for integral fuselage fuel tanks 08 p1023 N90-15913
Full scale study of a cabin fire in an A300 fuselage section 10 p1313 N90-17592
Forced and natural venting of aircraft cabin fires: A numerical simulation 10 p1314 N90-17597
Fuselage design for a specified Mach-sliced area distribution
|NASA-TP-2975| 11 p1455 N90-18385
Floor pull test of a transport airframe section
|DOT/FAA/CT-TN88/14| 13 p1754 N90-20072
Full-scale air transport category fuselage burnthrough tests
|DOT/FAA/CT-TN89/65| 14 p1913 N90-20967

NASA airframe structural integrity program
|NASA-TM-102637| 14 p1993 N90-21422
An evaluation of the pressure proof test concept for thin sheet 2024-T3
|NASA-TM-101675| 14 p1994 N90-21424
Water-tunnel study results of a TF/A-18 and F/A-18 canopy flow visualization
|NASA-TM-101705| 16 p2195 N90-22532
Aircraft crash survival design guide. Volume 3: Aircraft structural crash resistance
|AD-A218436| 16 p2198 N90-22547
Feasibility study for a microwave-powered ozone sniffer aircraft
|NASA-CR-186660| 17 p2353 N90-23397
DRAG-n-FLY: A proposal in response to a low Reynolds number station keeping mission
|NASA-CR-186666| 19 p2658 N90-25130
Design and construction of a wall-climbing robot
|NIAR-90-20| 20 p2870 N90-26327
Asymptotic modal analysis and statistical energy analysis
|NASA-CR-186732| 20 p2923 N90-26634
Correlation of AH-1G airframe flight vibration data with a coupled rotor-fuselage analysis
|NASA-CR-181974| 23 p3338 N90-28865

FUSES
Experimental investigation of a fast-acting exploding metallic foil opening switch
|DE90-001051| 06 p0770 N90-14479

FUSES (ORDNANCE)
Simulation of the dynamic environment for missile component testing: Demonstration
|AD-A216979| 11 p1466 N90-18443
SINA: A test system for proximity fuses
|FEL-1989-101| 12 p1653 N90-19498
The feasibility of detecting corrosion in electric fuzes using the thermal transient technique
|AD-A221385| 18 p2549 N90-24547
Investigation method for AA-proximity fuses
|FEL-89-A194| 24 p3459 N90-29535

FUSIFORM SHAPES
U CONES

FUSION
Activities report of the Joint Research Center
|ETN-89-95757| 04 p0569 N90-13321

FUSION (MELTING)
Thermodynamic principles of the process of the effect of electromagnetic fields on a polymer melt
|AD-A210698| 02 p0201 N90-11149
Center of Gravity: Metallic Solidification
|DFVLR-IB-333-89/3| 13 p1784 N90-20238
Principles of metallic solidification 13 p1784 N90-20241
Supercooling and germ formation 13 p1784 N90-20242
Fusion furnaces for Spacelab 13 p1785 N90-20248
Electromagnetic fusion process and position research 13 p1785 N90-20249
Diffusion and germ formation in glasses 13 p1786 N90-20250
Thermal analysis of the wearing by removal of melted metal during high speed friction
|ETCA-89-R-139| 22 p3183 N90-28067
Aircraft battle damage repair of transparencies
|AD-A224168| 24 p3432 N90-29387

FUSION REACTORS
NT HELIOTRONS
NT SPHEROMAKS
NT STELLARATORS
Fusion reactor materials
|DE90-000976| 07 p0994 N90-15744
Introduction to D-He(3) fusion reactors 07 p1008 N90-15839
Importance of helium-3 for the future 07 p1009 N90-15843
Fourth International Conference on Fusion Reactor Materials
|DE90-006142| 11 p1568 N90-19025
Application of railgun principle to high-velocity hydrogen pellet injection for magnetic fusion reactor refueling
|DE90-008281| 13 p1761 N90-20109
Design of D-3 He commercial tokamak
|DE90-008252| 13 p1891 N90-20852
Fusion technology development
|DE90-007933| 14 p2029 N90-21636
Helium generation in fusion reactor materials
|DE90-013005| 23 p3393 N90-29172
Evaluation of dynamic range for LLNL streak cameras using high contrast pulses and pulse podiatry on the Nova laser system
|DE90-015203| 24 p3472 N90-29620
Accurate calculations of neutron kerma and damage from ENDF/B-VI evaluations for silicon, chromium, iron and nickel, and comparison with ENDF/B-V results
|DE90-016020| 24 p3481 N90-29674
A distributed control and monitor system used in laser fusion research
|DE90-011483| 24 p3549 N90-30078
Overview of advanced fuel fusion
|DE90-015660| 24 p3550 N90-30085

FUSION WELDING
NT ARC WELDING
NT BRAZING
NT ELECTRON BEAM WELDING
NT GAS TUNGSTEN ARC WELDING
NT GAS WELDING
NT PLASMA ARC WELDING
NT ULTRASONIC SOLDERING
The effects of a nearby subsequent fusion weld on the properties of an inertia friction weld
|DE90-007972| 14 p1988 N90-21396
On-line assessment of weld quality using ultrasonics
|AERE-R-13401| 14 p1989 N90-21398

FUZZY SETS
Fuzzy logic and the generalized modus ponens
|REPT-88-92| 03 p0397 N90-12274
RF network selection in a rule-based system. NOSC project ZE68: Cost metric algorithms for internetwork applications
|AD-A219389| 16 p2301 N90-23116
A decision-making aid for multi-layer radar absorbent coverings
|ESA-TT-1173| 19 p2684 N90-25267
Ocean feature recognition using genetic algorithms with fuzzy fitness functions (GA/F3) 19 p2740 N90-25576
Extensions of algebraic image operators: An approach to model-based vision 19 p2741 N90-25577

FUZZY SYSTEMS
Adaptive learning fuzzy control of a mobile robot
|DE90-759898| 14 p2018 N90-21562
Development of probabilistic and possibilistic approaches to approximate reasoning and its applications
|AD-A221945| 21 p3039 N90-27271
Genetic algorithm based fuzzy control of spacecraft autonomous rendezvous 21 p3041 N90-27281

F4H AIRCRAFT
U F-4 AIRCRAFT

F8U AIRCRAFT
U F-8 AIRCRAFT

G

G FORCE
U ACCELERATION (PHYSICS)

G STARS
NT SUN
FGK stars and T Tauri stars: Monograph series on nonthermal phenomena in stellar atmospheres
|NASA-SP-502| 10 p1446 N90-18344
Abundance differences among G and K giants 17 p2484 N90-24208

GADOLINIUM
NT GADOLINIUM ISOTOPES

GADOLINIUM ISOTOPES
Examinations of hyperfine structure and isotope displacement of the elements gadolinium and europium with laser fluorescence and two photon spectroscopy
|ETN-90-97312| 24 p3447 N90-29468

GAGES
U MEASURING INSTRUMENTS

GAIN (AMPLIFICATION)
U AMPLIFICATION

GALACTIC BULGE
Small helium-cooled infrared telescope experiment for Spacelab-2 (IRT)
|NASA-CR-183983| 19 p2765 N90-25708
Identification of galactic bulge X ray bursts with persistent X ray counterparts 19 p2780 N90-25813

GALACTIC CLUSTERS
NT VIRGO GALACTIC CLUSTER
New statistical approaches to galaxy clustering 02 p0294 N90-11674
Far infrared, submm and mm spectroscopy of the galactic center: Radio arc and +20/+50 km s (exp -1) clouds
|NASA-CR-185497| 04 p0565 N90-13296
Cooling flows in clusters of galaxies 06 p0862 N90-15009
Mass functions for eight galactic clusters in the solar neighborhood 08 p1150 N90-16660
A comparison of void distributions in Abell cluster catalogue with numerical simulations
|DE90-610640| 11 p1590 N90-19173
Photometric analyses of abundances in dwarf spheroidal galaxies and globular clusters 12 p1736 N90-19978
Studies of the evolution of the x ray emission of clusters of galaxies
|NASA-CR-186471| 13 p1903 N90-20918
A theoretical scenario for the dynamics of formation and early evolution of globular clusters in galaxies 15 p2187 N90-22494
The mass of the Coma cluster 15 p2188 N90-22496
An astrophysics data program investigation of cluster evolution
|NASA-CR-181296| 15 p2191 N90-22510
A search for additional parameters in the infrared luminosity/21 cm line-width relation for spiral galaxies in clusters of galaxies 16 p2328 N90-23274
Spectroscopic observations of high redshift QSOs: Galaxies and the intergalactic medium at early epochs 16 p2330 N90-23280
The Einstein All-Sky IPC slew survey 19 p2787 N90-25865
The iron abundance gradient in the intracluster medium of Perseus: A galactic wind model. Application to other clusters 19 p2793 N90-25901
Search for large scale extended diffuse X ray emission from the Coma-A1367 supercluster 19 p2794 N90-25906
The effect of tidal friction between galaxies on the formation and development of galactic clusters in the expanding universe
|ETN-90-97314| 21 p3098 N90-27603
Biased clustering in a universe with hot dark matter and cosmic string
|FERMILAB-PUB-90/23-A| 22 p3262 N90-28473
Quasars in galaxy cluster environments 22 p3263 N90-28477

GALACTIC COSMIC RAYS
A large detector for cosmic ray abundance and energy measurements 06 p0867 N90-15037
Galactic cosmic-ray modulation and solar-terrestrial relationships
|IFSI-88-17| 08 p1153 N90-16679
Use of the Egret instrument in studies of the origin of the cosmic radiation. 2: Spectral signatures of discrete cosmic-ray sources
|DE90-003595| 08 p1154 N90-16682
Estimates of galactic cosmic ray shielding requirements during solar minimum
|NASA-TM-4167| 09 p1300 N90-17535
Radiation exposure for manned Mars surface missions
|NASA-TP-2979| 10 p1448 N90-18357
The Advanced Composition Explorer
|DE90-006522| 12 p1737 N90-19987
A balloon measurement of the isotopic composition of galactic cosmic ray iron 14 p2043 N90-21717
The Energetic Gamma-Ray Experiment Telescope (EGRET) Science Symposium
|NASA-CP-3071| 16 p2333 N90-23294
Constraints on the high energy properties of active galactic nuclei 19 p2792 N90-25894
A closed form solution to HZE propagation
|NASA-TM-103482| 20 p2924 N90-26640
The charged particle radiation environment for AXAF
|NASA-TM-100405| 20 p2942 N90-26741
Solar activity, the QBO, and tropospheric responses 22 p3203 N90-28172

GALACTIC EVOLUTION
Research program in theoretical high energy physics
|DE89-013963| 01 p0121 N90-10695
The origin of the universe from quantum chaos: An introduction to current ideas
|AD-A210441| 01 p0141 N90-10813
IRAS observations of the extended galactic objects Cas A and W80 02 p0290 N90-11657
An experiment to search for galactic axions 05 p0710 N90-14158
String correlations and galaxies formation
|ROM1F-89-677| 05 p0713 N90-14170
Non Abelian string correlations and galaxies formation
|ROM1F-89-678| 05 p0714 N90-14171
Des Cloizeaux's law for strings and galaxies formation. Part 2: Non Abelian configurations
|ROM1F-89-682-PT-2| 05 p0714 N90-14173
The grand unified photon spectrum: A coherent view of the diffuse extragalactic background radiation
|NASA-CR-186077| 05 p0715 N90-14180
Cooling flows in clusters of galaxies 06 p0862 N90-15009
The age of the galactic disk
|NASA-CR-186292| 07 p1013 N90-15869
Computer simulation of dust grain evolution 08 p1144 N90-16632
Evolution of carbonaceous chondrite parent bodies: Insights into cometary nuclei 08 p1145 N90-16638
Evolutionary synthesis of the far-infrared emission in starburst galaxies 11 p1587 N90-19152
Studies of the evolution of the x ray emission of clusters of galaxies
|NASA-CR-186471| 13 p1903 N90-20918
The large scale structure of the universe in pancake models of galaxy formation 14 p2040 N90-21701

Search for rapidly star forming galaxies at high redshift 15 p2181 N90-22465
Wind instability as a possible cause of the spiral structure formation in the gaseous subsystem of galaxies with the circular magnetic field
[DE90-618944] 15 p2190 N90-22507
A galaxy formation cookbook: Recipes and utensils 15 p2190 N90-22508
The dynamical evolution of dense clusters of compact stars 16 p2331 N90-23287
Reconstructing primordial density fluctuations 16 p2333 N90-23293
Gravitational collapse, Friedman models and cosmological constant: Does the universe oscillate
[DE90-620792] 16 p2338 N90-23324
Cosmic Background Explorer (COBE) press kit
[P89-10172] 17 p2364 N90-23459
Is AGN spectral evolution needed for the CXB 19 p2786 N90-25856
Constraints on the high energy properties of active galactic nuclei 19 p2792 N90-25894
A research program in theoretical high energy physics
[DE90-013322] 20 p2926 N90-26648
A research program in physics of the early universe
[DE90-013319] 20 p2942 N90-26742
Radio loud far-infrared galaxies
[DE90-012993] 20 p2950 N90-26786
The effect of tidal friction between galaxies on the formation and development of galactic clusters in the expanding universe
[ETN-90-97314] 21 p3098 N90-27603
Optical imaging of IRAS galaxies: The evolution of infrared-bright galaxies 22 p3261 N90-28465
The shock process and light element production in supernovae envelopes
[NASA-CR-182854] 22 p3262 N90-28471
A historical supernova's lower limit to the galactic stellar-collapse rate
[FERMILAB-PUB-90/24-A] 22 p3262 N90-28472
Chemical evolution of dwarf irregular galaxies 22 p3263 N90-28478

GALACTIC MAGNETIC FIELDS
U INTERSTELLAR MAGNETIC FIELDS

GALACTIC MASS
Infrared lines as probes of galactic structure 11 p1585 N90-19139
Complex X ray spectra and thick matter in Seyfert 1 galaxies 19 p2787 N90-25860

GALACTIC NUCLEI
NT ACTIVE GALACTIC NUCLEI
Spectropolarimetry, variability, and the taxonomy of active galactic nuclei 02 p0292 N90-11667
Gamma-ray observations and the distribution of interstellar aluminum-26 08 p1150 N90-16661
Infrared spectroscopy of the central few parsecs of the galaxy 11 p1585 N90-19140
Stellar kinematics in the galactic centre 11 p1586 N90-19141
An infrared imaging Fabry-Perot study of the galactic centre 11 p1586 N90-19142
Near infrared spectroscopy of active galaxies 11 p1586 N90-19143
Spectroscopy of galaxies in the mid-infrared 11 p1586 N90-19145
A search for the CO feature in active galactic nuclei 11 p1587 N90-19151
Infrared (FeII), H and H2 lines in galaxy nuclei 11 p1587 N90-19153
Space telescope searches for black holes in galactic nuclei 12 p1732 N90-19958
The dynamical evolution of dense clusters of compact stars 16 p2331 N90-23287
The accretion disk in the galactic center: An independent indication for a massive central object 19 p2790 N90-25881

GALACTIC RADIATION
NT GALACTIC COSMIC RAYS
Interstellar medium and infrared emission of the galactic disk 05 p0661 N90-13862
Gamma-ray observations and the distribution of interstellar aluminum-26 08 p1150 N90-16661
Gamma ray astronomy and black hole astrophysics
[NASA-CR-186496] 11 p1590 N90-19189
The Energetic Gamma-Ray Experiment Telescope (EGRET) Science Symposium
[NASA-CP-3071] 16 p2333 N90-23294
Spectral evolution of active galactic nuclei Penrose Compton scattering processes and gamma ray emission from Seyfert galaxies 16 p2337 N90-23317
A model for 1/f-type variability in active galactic nuclei 19 p2778 N90-25799
The 23rd ESLAB Symposium on Two Topics in X Ray Astronomy. Volume 2: AGN and the X Ray Background
[ESA-SP-296-VOL-2] 19 p2784 N90-25841
BL Lacs from the EMSS: Number-counts and implications for the luminosity function 19 p2785 N90-25849
The X ray spectra of emission line AGN 19 p2785 N90-25850
The Einstein All-Sky IPC slew survey 19 p2787 N90-25865
Search for large scale extended diffuse X ray emission from the Coma-A1367 supercluster 19 p2794 N90-25906
The origin of the continuum of AGN and the X ray background 19 p2795 N90-25912

GALACTIC ROTATION
A search for additional parameters in the infrared luminosity/21 cm line-width relation for spiral galaxies in clusters of galaxies 16 p2328 N90-23274

GALACTIC STRUCTURE
The mass distribution in the galactic centre estimated from OH/IR stars
[PB89-154884] 02 p0291 N90-11663
Archival research on absorption lines in violently star-forming galaxies
[NASA-CR-185960] 05 p0712 N90-14163
A study of the infrared emission of galactic supernova remnants 06 p0861 N90-15006
The South African Astronomical Observatory
[NASA-CR-186258] 07 p1011 N90-15856
Radio continuum maps at 22 GHz of the H II regions RCW57 and W49
[INPE-4787-TDL/353] 10 p1446 N90-18343
Infrared Spectroscopy in Astronomy
[ESA-SP-290] 11 p1578 N90-19084
Infrared lines as probes of galactic structure 11 p1585 N90-19139
Monte Carlo models and analysis of galactic disk gamma-ray burst distributions 12 p1636 N90-19403
M51's spiral structure
[DE90-007624] 13 p1903 N90-20916
The evolution and geometry of the outer parts of the small Magellanic cloud 14 p2040 N90-21697
Wind instability as a possible cause of the spiral structure formation in the gaseous subsystem of galaxies with the circular magnetic field
[DE90-618944] 15 p2190 N90-22507
The dynamical evolution of dense clusters of compact stars 16 p2331 N90-23287
The Energetic Gamma-Ray Experiment Telescope (EGRET) Science Symposium
[NASA-CP-3071] 16 p2333 N90-23294
Molecular clouds and the large-scale structure of the galaxy 16 p2333 N90-23295
The diffuse galactic gamma ray emission 16 p2333 N90-23296
Very low luminosity AGN 19 p2786 N90-25851
The environmental impact of the X ray flux from active galactic nuclei 19 p2786 N90-25853
Is AGN spectral evolution needed for the CXB 19 p2786 N90-25856
The iron abundance gradient in the intracluster medium of Perseus: A galactic wind model. Application to other clusters 19 p2793 N90-25901
Detection of hard X ray emission from a type 2 Seyfert galaxy 19 p2794 N90-25905

GALAXIES
NT ACTIVE GALAXIES
NT ANDROMEDA GALAXY
NT BARRED GALAXIES
NT DISK GALAXIES
NT DWARF GALAXIES
NT ELLIPTICAL GALAXIES
NT GALACTIC CLUSTERS
NT INTERACTING GALAXIES
NT IRREGULAR GALAXIES
NT MAGELLANIC CLOUDS
NT MILKY WAY GALAXY
NT PECULIAR GALAXIES
NT RADIO GALAXIES
NT SEYFERT GALAXIES
NT SPIRAL GALAXIES
NT STARBURST GALAXIES
NT VIRGO GALACTIC CLUSTER
Archival research on absorption lines in violently star-forming galaxies
[NASA-CR-185960] 05 p0712 N90-14163
Pulsars lost and found: The second Princeton-Arecibo millisecond pulsar search 07 p1013 N90-15865
Galactic x ray astronomy with EXOSAT 08 p1139 N90-16597
Spectroscopy of galaxies in the mid-infrared 11 p1586 N90-19145
Far-infrared spectroscopy of galaxies 11 p1586 N90-19146
Fluorescent molecular hydrogen emission from star-forming galaxies 11 p1588 N90-19155
H53-alpha emission from M82 11 p1588 N90-19156
The optical night sky at low surface brightness: High latitude dust and faint field galaxies 15 p2185 N90-22481
The association of supernovae with regions of recent star formation in late-type galaxies 15 p2188 N90-22497
A galaxy formation cookbook: Recipes and utensils 15 p2190 N90-22508
Gamma rays, cosmic rays, and local molecular clouds 15 p2193 N90-22524
Spectroscopic observations of high redshift QSOs: Galaxies and the intergalactic medium at early epochs 16 p2330 N90-23280
Reconstructing primordial density fluctuations 16 p2333 N90-23293
A model of the diffuse galactic gamma ray emission 16 p2334 N90-23297
Complementary information from mm-wave-, infrared-, and gamma ray astronomy 16 p2334 N90-23299
Implications of the IRAS data for galactic gamma ray astronomy and EGRET 16 p2334 N90-23300
Dipole analysis on EGRET data of extragalactic gamma ray background radiation 16 p2337 N90-23322
Institute of Astronomy 17 p2481 N90-24190
Activities report of the Institute for Astronomy and Astrophysics
[MITT-10] 18 p2636 N90-25020
Multiwavelength constraints on gamma-ray burst sources 18 p2639 N90-25032
Small helium-cooled infrared telescope experiment for Spacelab-2 (IRT)
[NASA-CR-183983] 19 p2765 N90-25708
The 23rd ESLAB Symposium on Two Topics in X Ray Astronomy. Volume 1: X Ray Binaries
[ESA-SP-296-VOL-1] 19 p2765 N90-25711
Astronomy at ultra-high energies: Results from the CYGNUS experiment
[DE90-011979] 20 p2940 N90-26732
SIRTF: Probing the dark corners of the galaxy 21 p3091 N90-27577
Infrared mapping with a two-dimensional infrared array
[AD-A221938] 21 p3096 N90-27596
Optical imaging of IRAS galaxies: The evolution of infrared-bright galaxies 22 p3261 N90-28465
Implications of the IRAS data for galactic gamma-ray astronomy and EGRET
[NASA-TM-103452] 22 p3261 N90-28466
Biased clustering in a universe with hot dark matter and cosmic string
[FERMILAB-PUB-90/23-A] 22 p3262 N90-28473
Quantifying the FIR interaction enhancement in paired galaxies
[DE90-627485] 23 p3412 N90-29281
Gamma ray evidence for cosmic ray sources 23 p3414 N90-29292
An observational study of disk-population globular clusters 24 p3560 N90-30145
Carbon monoxide isotopes and clumping in giant molecular clouds 24 p3562 N90-30151

GALAXY AIRCRAFT
U C-5 AIRCRAFT

GALAXY GROUPS
U GALACTIC CLUSTERS

GALAXY INTERACTION
U INTERACTING GALAXIES

GALERKIN METHOD
Estimation on nonlinear damping in second order distributed parameter systems
[NASA-CR-181890] 02 p0263 N90-11494
Viscous split algorithms for the time dependent incompressible Navier-Stokes equations
[AD-A211592] 03 p0348 N90-11985
Feed back Petrov-Galerkin methods for convection dominated problems
[DE89-636436] 08 p1063 N90-16148
And still, a new beginning: The Galerkin least-squares gradient method
[DE89-636435] 08 p1116 N90-16461
A new finite element formulation for CFD:8. The Galerkin/least-squares method for advective-diffusive equations
[DE89-636437] 08 p1116 N90-16462
Robustness of controllers designed using Galerkin type approximations
[NASA-CR-181986] 10 p1395 N90-18063
On the exponential convergence of the h-p version for boundary element Galerkin methods on polygons
[AD-A215814] 10 p1423 N90-18210
Semidiscrete Galerkin modelling of compressible viscous flow past a circular cone at incidence
[NASA-CR-186323] 11 p1505 N90-18664
Strong source heat transfer simulations based on a GalerKin/gradient least squares method
[DE90-608613] 11 p1507 N90-18678

Implementation of a finite element process for the Euler equations of the gas dynamics
[PREPRINT-500] 12 p1661 N90-19545
Error analysis of some Galerkin least squares methods for the elasticity equations
[DE90-608611] 12 p1705 N90-19790
An approximation theory for the identification of linear thermoelastic systems
[NASA-CR-182015] 13 p1877 N90-20764
Magnetostatic boundary-value problems in the incomplete-nonlinear formulation and methods of their solution
[DE90-615185] 13 p1877 N90-20767
Is Galerkin's method really better
[DE90-008804] 14 p1967 N90-21267
Numerical simulation model of hydrazine attitude control thrusters
[INPE-4965-PRE/1534] 15 p2068 N90-21848
Natural modes of cracked beams and identification of cracks 15 p2111 N90-22075
Application of a dynamic stall model to rotor trim and aeroelastic response 16 p2200 N90-22556
Numerical solution of large Lyapunov equations
[NASA-CR-180359] 17 p2456 N90-24010
Behaviour in the large of numerical solutions to one-dimensional nonlinear viscoelasticity by continuous time Galerkin methods
[AD-A220197] 17 p2461 N90-24057
Galerkin finite difference Laplacian operators on isolated unstructured triangular meshes by linear combinations
[NASA-TM-103209] 20 p2861 N90-26276
Theoretical and computational aspects of turbulence
[AD-A221795] 21 p3005 N90-27083
Solution of Euler equations using finite element method and the kinetic decomposition of the flows: Study of the self-adaptation of the grid and of the calculation field
[CERT-1/334700-DERI-GAN] 22 p3176 N90-28020
Solution of the Orr-Sommerfeld equation for three dimensional incompressible flow using Galerkin method and Chebichev polynomials: The COCIP code
[CERT-46/5618-34-DERAT] 22 p3176 N90-28021
Oscillatory convection
[ESA-TT-890] 23 p3325 N90-28801
A hybrid perturbation-Galerkin technique for partial differential equations
[NASA-CR-182085] 23 p3327 N90-28814
Dual and primal mixed Petrov-Galerkin finite element methods in heat transfer problems
[DE90-627190] 24 p3468 N90-29592
Investigation of the dynamic buckling of liquid-filled tanks 24 p3478 N90-29660

GALILEAN SATELLITES
NT IO

GALILEO MISSION
U GALILEO PROJECT

GALILEO PROJECT
Shuttle Atlantis to deploy Galileo probe toward Jupiter
[NASA-TM-101888] 02 p0175 N90-10982
Final Environmental Impact Statement for the Galileo Mission (Tier 2)
[NASA-TM-101825] 03 p0367 N90-12102
On the development of the power sources for the Ulysses and Galileo missions 10 p1331 N90-17693
Technology update-89
[DE90-005813] 11 p1593 N90-19178
Final (Tier 1) environmental impact statement for the Galileo and Ulysses Missions
[NASA-TM-102917] 15 p2056 N90-21779
Finding the complete path and weight enumerators of convolutional codes 15 p2077 N90-21897
Final environmental impact statement for the Galileo Mission (Tier 2)
[NASA-TM-102925] 15 p2124 N90-22147
Draft environmental impact statement for the Galileo Mission (Tier 2)
[NASA-TM-102926] 15 p2124 N90-22148
Project Galileo: Recognition of the planet Jupiter and its moons
[REPT-42/89] 17 p2486 N90-24216
Space exploration: Cost, schedule, and performance of NASA's Galileo Mission to Jupiter. Fact sheet for the Chairman, Subcommittee on Science, Technology, and Space, Committee on Commerce, Science, and Transportation, US Senate
[GAO/NSIAD-88-138FS] 20 p2816 N90-26025

GALILEO SPACECRAFT
Shuttle Atlantis to deploy Galileo probe toward Jupiter
[NASA-TM-101888] 02 p0175 N90-10982
Safety evaluation report for Galileo: Volume 1
[DE90-003086] 07 p0886 N90-15122
Safety evaluation report for Galileo, volume 2
[DE90-003087] 07 p0886 N90-15123
Safety analysis for the Galileo light-weight radioisotope heater unit
[DE90-007147] 11 p1566 N90-19009
Final (Tier 1) environmental impact statement for the Galileo and Ulysses Missions
[NASA-TM-102917] 15 p2056 N90-21779
Galileo Earth approach navigation using connected-element interferometer phase-delay tracking 15 p2075 N90-21884
A VLSI decomposition of the deBruijn graph 15 p2077 N90-21895
A higher density VLBI catalog for navigating Magellan and Galileo 15 p2078 N90-21904
Final environmental impact statement for the Galileo Mission (Tier 2)
[NASA-TM-102925] 15 p2124 N90-22147
GPHS-RTG response to Challenger type accident 19 p2665 N90-25163
Galileo: Earth avoidance study report
[NASA-CR-186424] 22 p3123 N90-27730

GALLIUM
NT GALLIUM ISOTOPES
Ion beam annealing of Ga-implanted Si
[DE89-016857] 02 p0282 N90-11610
The GALLEX Project
[DE90-005573] 09 p1300 N90-17534
Stressed Ge:Ga photoconductors for space-based astronomy. (Is there life beyond 120 micron) 14 p1975 N90-21315
Extrinsic germanium Blocked Impurity Bank (BIB) detectors 14 p1976 N90-21322
Ga:Ge array development 14 p1977 N90-21323
Initial astronomical results with a new 5-14 micron Si:Ga 58x62 DRO array camera 14 p1978 N90-21334
The high temperature behavior of gallium and indium liquid metal ion sources
[AERE-R-13321] 16 p2217 N90-22647
Enrichment services for chromium isotopes for the GALLEX (gallium experiment) international collaboration experiment on solar neutrino flux
[DE90-014300] 23 p3413 N90-29285

GALLIUM ALLOYS
A critical assessment of thermodynamic and phase diagram data for the Ga-In system
[NPL-DMA(A)-174] 03 p0415 N90-12382

GALLIUM ANTIMONIDES
Secondary ion mass spectrometry characterization of implants into GaAs and GaP for waveguides and integrated optics applications
[AD-A219203] 16 p2324 N90-23254

GALLIUM ARSENIDE LASERS
The III-V semiconductor quantum well lasers and related optoelectronic devices on silicon
[AD-A216980] 12 p1666 N90-19570

GALLIUM ARSENIDES
NT ALUMINUM GALLIUM ARSENIDES
Scanning tunneling microscopy etching of micrometer level features on p-type GaAs
[AD-A209216] 01 p0058 N90-10328
Epitaxial GaAs on SOI wafers
[AD-A209009] 01 p0127 N90-10729
Analysis of the performance of gallium arsenide photoavalanche switches
[DE89-015774] 01 p0129 N90-10739
Lithium compensation of GaAs
[DE89-616080] 01 p0129 N90-10740
Characterization of GaAs/Si/GaAs heterointerfaces
[DE89-016302] 01 p0131 N90-10752
Methods to decrease defect density in GaAs/Si heteroepitaxy
[DE89-016306] 01 p0131 N90-10753
Effects of coherent scattering on infrared absorption in doped semiconductors
[AD-A210224] 01 p0131 N90-10756
Advanced GaAs process modeling, volume 1
[AD-A210385] 01 p0132 N90-10761
High energy neutron irradiation effects in GaAs modulation-Doped Field Effect Transistors (MODFETS): Threshold voltage
[AD-A210502] 01 p0132 N90-10763
Deep traps and sidegating in GaAs devices
[AD-A210740] 01 p0133 N90-10765
Trap gettering by isoelectronic doping of p-GaAs and n-GaAs grown by molecular beam epitaxy
[AD-A211162] 01 p0133 N90-10769
Study of a gallium arsenide solar cell interconnector 02 p0182 N90-11033
Laser altimeter for use over the ocean
[AD-A211252] 02 p0224 N90-11286
Semiconductor quantum well lasers and related optoelectronic devices on silicon, III-V
[AD-A210758] 02 p0227 N90-11299
GaAs ASIC design case study
[DE89-013934] 02 p0258 N90-11461
Thermodynamics, kinetics, and interface morphologies of phase formation reactions between metals and Gallium Arsenide: Bulk vs thin-film studies
[DE89-016469] 02 p0284 N90-11621
Strain and density dependent valence-band masses in InGaAs/GaAs and GaAs/GaAsP strained-layer structures
[DE89-016882] 02 p0285 N90-11627
On-orbit annealing of gallium arsenide solar cell arrays
[AD-A212087] 03 p0334 N90-11900
Ion beam deposition of epitaxial germanium and gallium arsenide layers
[DE89-017439] 03 p0411 N90-12357
Subnanosecond linear GaAs photoconductive switching, revision 1
[DE89-017739] 03 p0412 N90-12363
Development and evaluation of an instrument for rapid electroreflectance of semiconductor materials
[AD-A211690] 03 p0414 N90-12376
Study of the electrical and optical properties of the vanadium and nickel impurities in GaAs
[ISAL-89-0028] 04 p0559 N90-13259
Electron transport in heterojunction superlattices
[AD-A212366] 04 p0560 N90-13265
The growth of epitaxial GaAs and GaAlAs on silicon substrates by OMVPE
[AD-A212873] 04 p0561 N90-13269
Electrochemical study of the etching of III to V semiconductors
[ETN-90-98015] 05 p0623 N90-13633
Development of high gain three terminal devices - at millimeter wave frequencies
[AD-A213089] 05 p0635 N90-13701
Photoelectrochemical behavior of type n of GaAs in concentrated iodide media and realization of an experimental device
[ECL-88-18] 05 p0703 N90-14117
GaAs and GaAs:In: Influence of surface treatments and characterization of homogeneity by photoluminescent imagery
[ECL-88-24] 05 p0704 N90-14118
Characterization of two MMIC GaAs switch matrices at microwave frequencies
[NASA-TM-102449] 06 p0733 N90-14273
Method of making self-aligned GaAs/AlGaAs FET's
[AD-D014229] 06 p0849 N90-14935
Electronic materials high-T(sub c) superconductivity polymers and composites structural materials surface science and catalysts industry participation
[NASA-CR-186063] 07 p0890 N90-15145
Avalanche photoconductive switching
[DE90-002980] 07 p0922 N90-15337
Laser-material interactions
[AD-A214421] 07 p0937 N90-15425
Thermally stable metal/GaAs contacts
[DE90-002122] 07 p0998 N90-15774
The effect of annealing treatments on defect structure and diffusion lengths in n-type GaAs
[AD-A214215] 07 p1005 N90-15817
Radiation resistance of solar cells for space application. 1: Study on the irradiation procedure of electron beams
[DE90-719546] 08 p1096 N90-16349
The influence of residual contamination on the structure and properties of metal/GaAs interfaces
[DE90-000549] 08 p1127 N90-16530
Group 2 cubic fluorides as dielectrics for III-V compound semiconductors
[AD-A214096] 08 p1129 N90-16542
Scanning tunneling microscope studies of surface defects
[AD-A214121] 08 p1130 N90-16543
Heteroepitaxy of GaAs on Si: Methods to decrease the defect density in the epilayer
[DE90-004028] 08 p1131 N90-16551
Optimization of the intermodulation performance of GaAs MESFET small-signal amplifiers
[AD-A215193] 09 p1212 N90-17026
Growth characteristics and electronic behavior of ultrathin epitaxial metallizations
[AD-A214794] 09 p1289 N90-17474
Carbon doping of compound semiconductor epitaxial layers using carbon tetrachloride
[AD-A215053] 09 p1290 N90-17477
Proceedings of the conference on Hot Carriers in Semiconductors
[AD-A215544] 09 p1291 N90-17482
GaAs cells on Si substrates: A new challenge for space photovoltaic applications 10 p1339 N90-17750
Advanced GaAs space solar cells by MOCVD technique 10 p1339 N90-17752
Fabrication of ultra thin GaAs and Ge substrates for high efficiency solar cells 10 p1339 N90-17753
GaAs space solar cells: Pilot production experience using a multi wafer infinite melt liquid phase epitaxy process 10 p1339 N90-17756
Application of gallium arsenide solar cell arrays for long duration low earth orbit missions like Columbus 10 p1340 N90-17759

Ultrasonic and parallel gap welding of GaAs solar cells, experimental and simulation results
10 p1341 N90-17766
GaAs back point contact solar cell simulation
10 p1343 N90-17781
Limits of efficiency of solar cells under AMO-spectrum illumination: Comparison between Si and GaAs cells
10 p1343 N90-17784
Study and implementation of a monolithic photoreceiver integrating a photodiode and a junction field effect transistor in GaInAs with polarization resistance
[IDI-18902] 10 p1379 N90-17990
Integrated optics at Lawrence Livermore National Laboratory
[DE90-003015] 10 p1431 N90-18255
Electron scattering by native defects in uniformly and modulation doped semiconductor structures
[DE90-006084] 10 p1437 N90-18296
A GaAs p-n-p-n thyristor model
[DE90-005757] 11 p1570 N90-19039
CdTe buffered GaAs thin-slab IR waveguide modulators and T/R filter
[AD-A215999] 12 p1651 N90-19488
Heteroepitaxial growth of germanium films by supersonic free jet chemical beam epitaxy
[DE90-006621] 12 p1720 N90-19877
Digital capacity transient spectroscopy of deep structure defects in III-V-Semiconductor structures
[ETN-90-96057] 12 p1722 N90-19890
An electron-beam controlled semiconductor switch
[AD-A217181] 13 p1793 N90-20288
GaAs traveling-wave optical modulators using modulated coplanar electrodes with periodic cross-tie overlays
[AD-A217731] 13 p1888 N90-20835
Differential measurements of the lateral photo effect in GaAs/AlGaAs heterostructures
[AERE-R-13557] 13 p1893 N90-20861
Absolute pressure dependence of the second ionization level of EL2 in GaAs
[DE90-007761] 13 p1894 N90-20872
Peeled film GaAs solar cells for space power
[NASA-TM-103125] 14 p1970 N90-21287
New surface atomic structures for column 5 overlayers on the (110) surfaces of 3-5 compound semiconductors
[DE90-009003] 14 p2033 N90-21663
Development of a unique laboratory standard indium gallium arsenide detector for the 500 to 1700 micron spectral region, phase 2
[NASA-CR-180482] 16 p2238 N90-22767
Acoustoelectronic interaction of surface waves in GaAs-InGaAs superlattices 16 p2310 N90-23163
Optical properties of novel GaAs-based semiconductors 16 p2321 N90-23235
Activation uniformity dependence of undoped semi-insulating GaAs on post-implant annealing conditions
[ETN-90-96549] 16 p2323 N90-23246
Secondary ion mass spectrometry characterization of implants into GaAs and GaP for waveguides and integrated optics applications
[AD-A219203] 16 p2324 N90-23254
Passivation and gating of GaAs and Si surfaces using pseudomorphic structures
[AD-A219351] 16 p2325 N90-23256
Photoreflectance for in-situ characterization of MOCVD growth of semiconductors under micro-gravity conditions
[NASA-CR-186600] 17 p2383 N90-23576
Fundamental and applied aspects of defect engineering in G2As: EL2 and other nonstoichiometric defects
[AD-A218597] 17 p2475 N90-24152
The 30-GHz monolithic receive module
[NASA-CR-180849] 18 p2545 N90-24528
Studies of chemistry and diffusion on silicon and gallium arsenide surfaces using laser-induced thermal desorption
[AD-A220946] 18 p2547 N90-24539
Gallium arsenide pilot line for high performance components
[AD-A220948] 18 p2547 N90-24540
Failure mechanisms of GaAs transistors: A literature survey
[AD-A221089] 18 p2548 N90-24543
HREM defects in GaAs/Ga(1-x)In(x)As strained layer superlattices
[DE90-010610] 18 p2620 N90-24924
Ensemble Monte Carlo simulation of electron transport in AlGaAs/GaAs heterostructures
[ISBN-90-9003048-4] 18 p2622 N90-24940
Au-Ge-Ni-Ti ohmic contacts on gallium arsenide
[DE90-011064] 18 p2625 N90-24960
DURIP: Instrumentation for laser switched power LINAC
[AD-A222629] 20 p2868 N90-26318
Dielectric function of InGaAs in the visible
[NASA-TM-103246] 20 p2932 N90-26683
MBE growth technology for high quality strained III-V layers
[NASA-CASE-NPO-17723-1-CU]
20 p2932 N90-26685
Laser induced surface chemical epitaxy
[AD-A222082] 21 p2977 N90-26920
Integration of picosecond GaAs photoconductive devices with silicon circuits for optical clocking and interconnects
[DE90-012096] 21 p3080 N90-27512
Design of GaAs charge coupled devices
[DE90-012124] 21 p3080 N90-27513
Investigation on the MBE growth and properties of AlGaInAs/InP and InGaAs-InAlAs superlattices
[DE90-012248] 21 p3080 N90-27515
Measurement of deep levels at InGaAs(P)/InP heterojunctions
[AD-A222890] 21 p3082 N90-27526
Defects associated with the incorporation of germanium in gallium arsenide
[AD-A222953] 21 p3082 N90-27527
Semiconductor measurement technology. EPROP: An interactive FORTRAN program for computing selected electronic properties of Gallium Arsenide and Silicon
[PB90-222738] 23 p3399 N90-29203
Innovative techniques for the production of low cost 2D laser diode arrays
[AD-A223575] 24 p3474 N90-29632
Surface photovoltage spectroscopy of real n-type GaAs(110) surfaces
[DE90-627325] 24 p3551 N90-30092
Nonlinear optical studies of the optical and electronic properties of semiconductor heterostructures
[AD-A223408] 24 p3552 N90-30096
Integrated technology in MCT/GaAs and MCT/Si for medium and long wavelength infrared
[AD-A223557] 24 p3552 N90-30100
Subpicosecond Raman study of hot electrons and hot phonons in GaAs
[DE90-015634] 24 p3553 N90-30106
Study of hot carrier relaxation in quantum wells by subpicosecond Raman scattering
[DE90-015635] 24 p3554 N90-30107

GALLIUM COMPOUNDS
NT ALUMINUM GALLIUM ARSENIDES
NT GALLIUM ANTIMONIDES
NT GALLIUM ARSENIDES
NT GALLIUM NITRIDES
NT GALLIUM OXIDES
NT GALLIUM PHOSPHIDES
Phase equilibrium and crystal growth studies on AgGaSe2 and related nonlinear optical materials
[AD-A213650] 07 p1003 N90-15809
The first example of an organogallium compound containing a Ga-Te bond: Synthesis, properties, and molecular structure of ((Me3CCH2)2GaTeph)2
[AD-A219258] 16 p2210 N90-22608

GALLIUM ISOTOPES
The Baksan gallium solar neutrino experiment
[DE89-016036] 03 p0429 N90-12457

GALLIUM NITRIDES
The growth of gallium nitride films via the innovative technique of atomic layer epitaxy
[AD-A210380] 01 p0132 N90-10760

GALLIUM OXIDES
Microstructures of Y123 films on SrTiO3, LaGaO3, and LaAlO3
[DE90-003367] 08 p1129 N90-16537
Growth and characterization of gallium (III) oxide films
[AD-A217568] 12 p1723 N90-19902

GALLIUM PHOSPHIDES
Strain and density dependent valence-band masses in InGaAs/GaAs and GaAs/GaAsP strained-layer structures
[DE89-016882] 02 p0285 N90-11627
Dopant site location in dual-implanted GaP using (111) planar channeling
[DE90-006565] 11 p1571 N90-19042
Annealing group III-V compound doped silicon-germanium alloy for improved thermo-electric conversion efficiency
[NASA-CASE-NPO-17259-1-CU]
12 p1721 N90-19884
Secondary ion mass spectrometry characterization of implants into GaAs and GaP for waveguides and integrated optics applications
[AD-A219203] 16 p2324 N90-23254
Preliminary investigation into the effect of high temperature thermal anneals on the figure of merit of silicon germanium alloys
[AD-A218573] 17 p2375 N90-23527
Negative electron affinity for infrared detection
[AD-A218816] 17 p2395 N90-23639

GALVANIC CELLS
U ELECTROLYTIC CELLS

GALVANIZING
U ZINC COATINGS

GAME THEORY
International Conference on Fixed Point Theory and Applications
[AD-A212369] 04 p0545 N90-13171
The singular zero sum differential game with stability using H infinity control theory
[MEMO-COSOR-89-09] 05 p0687 N90-13999
The activity selection problem: A network and game theoretic approach
[MEMO-794] 05 p0694 N90-14056
A model for comparing game theory and artificial intelligence decision making processes
[AD-A215418] 09 p1271 N90-17369
Defending against a space blockade: CADRE paper
[AD-A215681] 09 p1276 N90-17398
Deterministic differential game solution: The approximate strategy method
[ESA-TT-1158] 11 p1555 N90-18956
Optimal helicopter trajectory planning for terrain following flight
[NASA-CR-186470] 17 p2349 N90-23376
Time-optimal aircraft pursuit-evasion with a weapon envelope constraint
[NASA-CR-186640] 19 p2658 N90-25126
Knowledge and distributed computation
[AD-A223100] 21 p3039 N90-27270
For the definition of two person zero sum games
[ETN-90-97294] 24 p3541 N90-30022

GAMETOCYTES
NT EGGS
NT SPERMATOZOA
The influence of a sounding rocket flight on sexual activation in Chlamydomonas gametes
19 p2681 N90-25250

GAMMA RADIATION
U GAMMA RAYS

GAMMA RAY ABSORPTION
Low-energy gamma ray attenuation characteristics of aviation fuels
[NASA-TP-2974] 11 p1543 N90-18882
The problem of dead layer in gamma ray burst spectra recorded with NaI or CsI crystals
19 p2776 N90-25787

GAMMA RAY ASTRONOMY
Studies of elementary particles
[DE89-014859] 01 p0119 N90-10685
Scientific objectives of solar gamma-ray observations
03 p0430 N90-12463
The Gamma-Ray Observatory: An overview
03 p0430 N90-12464
JPRS Report: Science and technology. USSR: Space. Soviet space program to the year 2000
[JPRS-USP-89-008] 06 p0728 N90-14248
Studies of elementary particles: Proposal
[DE90-001120] 06 p0839 N90-14879
A low-threshold EAS (Extensive-Air-Shower) array for gamma-ray astronomy at Los Alamos
[DE89-016780] 08 p1139 N90-16600
Status of the expansion of the CYGNUS array at Los Alamos
[DE89-016781] 08 p1139 N90-16601
Gamma ray astronomy and black hole astrophysics
[NASA-CR-186496] 11 p1590 N90-19169
Imaging Germanium Telescope Array for Gamma-Rays (IGETAGRAY)
[DE90-006994] 11 p1595 N90-19188
Radial response of the burst and transient source experiment 12 p1637 N90-19408
Astronomy and astrophysics
[REPT-33/89] 12 p1729 N90-19838
Very high energy gamma ray astrophysics
[DE90-006645] 12 p1737 N90-19983
The Energetic Gamma-Ray Experiment Telescope (EGRET) Science Symposium
[NASA-CP-3071] 16 p2333 N90-23294
Complementary information from mm-wave-, infrared-, and gamma ray astronomy 16 p2334 N90-23299
Implications of the IRAS data for galactic gamma ray astronomy and EGRET 16 p2334 N90-23300
Local normal galaxies 16 p2336 N90-23315
Feasibility for EGRET detection of antimatter concentrations in the universe 16 p2338 N90-23323
Gamma Ray Observatory (GRO) dynamics simulator requirements and mathematical specifications, revision 1
[NASA-CR-183465] 17 p2362 N90-23447
The soft gamma ray bursts detected with the APEX experiment: Evidence for a persistent SGR-like activity
19 p2771 N90-25748
VHE gamma ray emission from Southern Hemisphere X ray binaries 19 p2772 N90-25758
Evidence of a 12 ms pulsar in Cygnus X-3
19 p2772 N90-25759
VHE gamma ray emission from Northern Hemisphere X ray binaries 19 p2772 N90-25760

The detection of VHE gamma rays using the atmospheric Cerenkov technique 19 p2773 N90-25761
Constraints on the high energy properties of active galactic nuclei 19 p2792 N90-25894
Implications of the IRAS data for galactic gamma-ray astronomy and EGRET
[NASA-TM-103452] 22 p3261 N90-28466
A study of the sensitivity of an imaging telescope (GRITS) for high energy gamma-ray astronomy
[NASA-CR-186921] 22 p3261 N90-28468

GAMMA RAY BEAMS
Investigations into the influence of the state functions on the cross sections of the direct p,gamma reactions at energies in the 100 keV range, and project of a cascade accelerator for the measurement of the p,gamma capture cross sections
[ETN-89-94662] 02 p0273 N90-11561
Non-random uncertainties in the calibration of protection-level secondary standards
[NPL-RS(EXT)-110] 15 p2166 N90-22378
Derivation of radiation beam non-uniformity corrections for the calibration of large volume ionisation chambers
[NPL-RSA(EXT)-11] 15 p2167 N90-22382

GAMMA RAY BURSTS
The BATSE experiment on the Gamma Ray Observatory: Solar flare hard x ray and gamma-ray capabilities 03 p0431 N90-12469
The solar flare and cosmic gamma-ray burst experiment aboard the Ulysses spacecraft 03 p0431 N90-12470
Relative muon content of UHE showers associated with Hercules X-1
[DE90-000609] 08 p1151 N90-16665
Thermal pair cloud models of MeV gamma ray emissions from Cygnus X-1 and the Galactic Center
[DE90-001168] 09 p1301 N90-17536
Maxwellian cascade model
[DE90-004389] 10 p1427 N90-18235
Positron annihilation in gamma-ray bursts 11 p1559 N90-18983
Monte Carlo models and analysis of galactic disk gamma-ray burst distributions 12 p1636 N90-19403
Radial response of the burst and transient source experiment 12 p1637 N90-19408
The 1989 outburst of V404 Cygni: A very unusual x ray nova
[DE90-008935] 14 p2038 N90-21693
Gamma ray bursts: Current status of observations and theory
[NASA-TM-100398] 15 p2194 N90-22526
Gamma ray bursts: Current status of observations and theory 16 p2336 N90-23313
What is learned from high energy bursts and flares 16 p2336 N90-23314
Cyclotron absorption in gamma ray bursts seen with Ginga 19 p2769 N90-25736
The soft gamma ray bursts detected with the APEX experiment: Evidence for a persistent SGR-like activity 19 p2771 N90-25748
VHE gamma ray emission from Northern Hemisphere X ray binaries 19 p2772 N90-25760
The problem of dead layer in gamma ray burst spectra recorded with NaI or CsI crystals 19 p2776 N90-25787
Gamma ray bursts from magnetospheric plasma oscillations 19 p2779 N90-25805

GAMMA RAY LASERS
Proof of the feasibility of coherent and incoherent schemes for pumping a gamma-ray laser
[AD-A212882] 04 p0507 N90-12924
The gamma-ray laser project: Proof of the feasibility of coherent and incoherent schemes for pumping a gamma-ray laser
[AD-A216008] 10 p1389 N90-18037
Proof of the feasibility of coherent and incoherent schemes for pumping a gamma-ray laser
[AD-A219972] 18 p2562 N90-24620

GAMMA RAY OBSERVATORY
A liquid xenon imaging telescope for 1-30 MeV gamma-ray astrophysics
[NASA-CR-185999] 02 p0291 N90-11662
The Gamma-Ray Observatory: An overview 03 p0430 N90-12464
Capabilities of GRO/OSSE for observing solar flares 03 p0430 N90-12467
The solar gamma ray and neutron capabilities of COMPTEL on the Gamma Ray Observatory 03 p0431 N90-12468
The BATSE experiment on the Gamma Ray Observatory: Solar flare hard x ray and gamma-ray capabilities 03 p0431 N90-12469
Particle transport simulation for spaceborne, NaI gamma-ray spectrometers
[AD-A205150] 04 p0564 N90-13292
A gyroscope calibration analysis for the Gamma Ray Observatory (GRO) 05 p0589 N90-13428
Long-lived space observatories for astronomy and astrophysics
[NASA-CR-185373] 06 p0731 N90-14261
The Energetic Gamma-Ray Experiment Telescope (EGRET) Science Symposium
[NASA-CP-3071] 16 p2333 N90-23294
Molecular clouds and the large-scale structure of the galaxy 16 p2333 N90-23295
Radio pulsar timing observations for GRO 16 p2334 N90-23301
Gamma Ray Observatory (GRO) dynamics simulator requirements and mathematical specifications, revision 1
[NASA-CR-183465] 17 p2362 N90-23447
Predictions of radiation backgrounds for GRO/OSSE
[RAE-TM-SPACE-372] 23 p3414 N90-29293

GAMMA RAY SPECTRA
Gamma radiation background measurements from Spacelab 2
[NASA-CR-183782] 02 p0297 N90-11689
Gamma-ray observations and the distribution of interstellar aluminum-26 08 p1150 N90-16661
Use of the Egret instrument in studies of the origin of the cosmic radiation. 2: Spectral signatures of discrete cosmic-ray sources
[DE90-003595] 08 p1154 N90-16682
GRIS observations of the Galactic Center 11 p1559 N90-18982
Gamma rays from pulsar wind shock acceleration 16 p2336 N90-23311
Radiation-driven evolution of low-mass x ray binaries 18 p2637 N90-25022
Orbitally modulated VHE gamma rays from Cen X-3 19 p2780 N90-25812
Gamma ray evidence for cosmic ray sources 23 p3414 N90-29292

GAMMA RAY SPECTROMETERS
X-ray and gamma-ray spectroscopy of solids under pressure
[DE89-017271] 02 p0196 N90-11118
Capabilities of GRO/OSSE for observing solar flares 03 p0430 N90-12467
A high-speed digital camera system for the observation of rapid H-alpha fluctuations in solar flares 03 p0435 N90-12491
Particle transport simulation for spaceborne, NaI gamma-ray spectrometers
[AD-A205150] 04 p0564 N90-13292
Radioactivity induced in gamma-ray spectrometers
[RAE-TM-SPACE-363] 04 p0569 N90-13317
A fiber-fed imaging spectrometer
[DE90-001008] 06 p0781 N90-14538
A large area, low cost, gamma-ray, imaging spectrometer
[DE90-006993] 11 p1567 N90-19017
Mercuric iodide room temperature gamma-ray detectors
[NASA-TM-103318] 13 p1804 N90-20357
Microchannel photomultipliers in time spectrometer
[DE90-616417] 14 p1982 N90-21356
The problem of dead layer in gamma ray burst spectra recorded with NaI or CsI crystals 19 p2776 N90-25787
Predictions of radiation backgrounds for GRO/OSSE
[RAE-TM-SPACE-372] 23 p3414 N90-29293
New developments in low-energy cosmic gamma-ray detection
[UT-HE-90/07] 24 p3564 N90-30165
Re-analysis of data on the space radiation environment above south-east Asia
[RAE-TR-89048] 24 p3565 N90-30166

GAMMA RAY TELESCOPES
The solar gamma ray and neutron capabilities of COMPTEL on the Gamma Ray Observatory 03 p0431 N90-12468
Solar flare gamma-ray and hard x ray imaging with the GRID-on-a-balloon 03 p0432 N90-12474
Imaging Germanium Telescope Array for Gamma-Rays (IGETAGRAY)
[DE90-006994] 11 p1595 N90-19188
The Energetic Gamma-Ray Experiment Telescope (EGRET) Science Symposium
[NASA-CP-3071] 16 p2333 N90-23294
Implications of the IRAS data for galactic gamma ray astronomy and EGRET 16 p2334 N90-23300
The detection of VHE gamma rays using the atmospheric Cerenkov technique 19 p2773 N90-25761
A study of the sensitivity of an imaging telescope (GRITS) for high energy gamma-ray astronomy
[NASA-CR-186921] 22 p3261 N90-28468

GAMMA RAYS
NT GAMMA RAY BURSTS
Raman spectroscopic study of the rare earth sesquisulfides
[AD-A210610] 01 p0041 N90-10226
MOXE: An X-ray all-sky monitor for Soviet Spectrum-X-Gamma Mission
[NASA-TM-101266] 02 p0223 N90-11280
Airborne gamma radiation snow water equivalent and soil moisture measurements and satellite areal extent of snow cover measuerments: A user's guide, version 3.0
[PB89-177877] 02 p0235 N90-11338
Gamma radiation background measurements from Spacelab 2
[NASA-CR-183782] 02 p0297 N90-11689
An experimental high energy physics program
[DE89-014695] 03 p0403 N90-12311
The hard x rays and gamma-rays from solar flares
[NASA-CR-185982] 03 p0429 N90-12458
The BATSE experiment on the Gamma Ray Observatory: Solar flare hard x ray and gamma-ray capabilities 03 p0431 N90-12469
The solar flare and cosmic gamma-ray burst experiment aboard the Ulysses spacecraft 03 p0431 N90-12470
Proof of the feasibility of coherent and incoherent schemes for pumping a gamma-ray laser
[AD-A212315] 04 p0506 N90-12921
Research in cosmic and gamma ray astrophysics
[NASA-CR-185451] 04 p0569 N90-13316
Gamma ray lines from dark matter annihilation
[DE90-000779] 06 p0864 N90-15021
ROBOCAL (Robotic Calorimetry): An automated NDA (Nondestructive Assay) calorimetry and gamma isotopic system
[DE90-003217] 07 p0894 N90-15168
Coded-aperture imaging in nuclear medicine 08 p1073 N90-16208
The gamma-ray laser project: Proof of the feasibility of coherent and incoherent schemes for pumping a gamma-ray laser
[AD-A216008] 10 p1389 N90-18037
Low-energy gamma ray attenuation characteristics of aviation fuels
[NASA-TP-2974] 11 p1543 N90-18882
Monte Carlo models and analysis of galactic disk gamma-ray burst distributions 12 p1636 N90-19403
Radial response of the burst and transient source experiment 12 p1637 N90-19408
The influence of gamma-radiation on the bandwidth of optical fibres and the reduction of the induced attenuation by bleaching and hardening the fibre
[FEL-1988-62] 12 p1714 N90-19846
Very high energy gamma ray astrophysics
[DE90-006645] 12 p1737 N90-19983
Development of gamma-emitting, receptor-binding radiotracers for imaging the brain and pancreas
[DE90-008314] 13 p1851 N90-20621
The n-p bremsstrahlung in heavy ion collision processes
[DE90-008542] 13 p1886 N90-20823
Gamma-ray production cross section measurements using a white neutron source from 1 to 400 MeV
[DE90-008906] 14 p2025 N90-21610
A search for very high energy gamma rays from the Crab pulsar-nebula 14 p2043 N90-21718
Gamma rays, cosmic rays, and local molecular clouds 15 p2193 N90-22524
Very high energy gamma rays from the Crab nebula and pulsar 15 p2194 N90-22527
Molecular clouds and the large-scale structure of the galaxy 16 p2333 N90-23295
The diffuse galactic gamma ray emission 16 p2333 N90-23296
A model of the diffuse galactic gamma ray emission 16 p2334 N90-23297
Gamma rays from giant molecular clouds 16 p2334 N90-23298
Complementary information from mm-wave-, infrared-, and gamma ray astronomy 16 p2334 N90-23299
Implications of the IRAS data for galactic gamma ray astronomy and EGRET 16 p2334 N90-23300
Radio pulsar timing observations for GRO 16 p2334 N90-23301
Gamma radiation from radio pulsars 16 p2334 N90-23302
Gamma radiation from the Crab and Vela pulsars 16 p2334 N90-23303
Gamma ray pulsars: Models and observations 16 p2335 N90-23304
The sensitivity of EGRET to gamma ray polarization 16 p2335 N90-23305
The illusive Geminga: What is it 16 p2335 N90-23307
COS-B gamma ray sources beyond the predicted diffuse emission 16 p2335 N90-23308
More data on (possible) gamma ray (point) sources 16 p2335 N90-23309
What can gamma rays tell us about binary x ray sources and SNR's 16 p2336 N90-23310
Gamma rays from pulsar wind shock acceleration 16 p2336 N90-23311

Spectral determinations for discrete sources with EGRET 16 p2336 N90-23312
Gamma ray bursts: Current status of observations and theory 16 p2336 N90-23313
What is learned from high energy bursts and flares 16 p2336 N90-23314
Local normal galaxies 16 p2336 N90-23315
Gamma rays from active galactic nuclei 16 p2337 N90-23316
Spectral evolution of active galactic nuclei Penrose Compton scattering processes and gamma ray emission from Seyfert galaxies 16 p2337 N90-23317
The high energy source 3C 273 16 p2337 N90-23318
COMPTEL observations of active galactic nuclei 16 p2337 N90-23319
OSSE observations of active galactic nuclei 16 p2337 N90-23320
Gamma ray cosmology: The extra galactic gamma spectrum and methods to detect the underlying source 16 p2337 N90-23321
Dipole analysis on EGRET data of extragalactic gamma ray background radiation 16 p2337 N90-23322
Feasibility for EGRET detection of antimatter concentrations in the universe 16 p2338 N90-23323
Numerical simulations of x rays and gamma rays from solar flares 16 p2339 N90-23330
Pulse-width dependent radiation effects on electronic components
[AD-A219517] 17 p2395 N90-23643
Proof of the feasibility of coherent and incoherent schemes for pumping a gamma-ray laser
[AD-A219972] 18 p2562 N90-24620
Multiwavelength constraints on gamma-ray burst sources 18 p2639 N90-25032
Neutron and gamma irradiation effects on power semiconductor switches
[NASA-TM-103200] 19 p2686 N90-25278
Cyclotron absorption in gamma ray bursts seen with Ginga 19 p2769 N90-25736
VHE gamma ray emission from Southern Hemisphere X ray binaries 19 p2772 N90-25758
The detection of VHE gamma rays using the atmospheric Cerenkov technique 19 p2773 N90-25761
Nonpotential magnetic fields at sites of gamma ray flares
[NASA-TM-103493] 20 p2950 N90-26785
The effects of space radiation on thin films of YBa2Cu3O(sub 7-x) 22 p3147 N90-27845
Implications of the IRAS data for galactic gamma-ray astronomy and EGRET
[NASA-TM-103452] 22 p3261 N90-28466
A study of the sensitivity of an imaging telescope (GRITS) for high energy gamma-ray astronomy
[NASA-CR-186921] 22 p3261 N90-28468
Ground level atmospheric gamma ray flux measurements in the 1 to 6 MeV range 22 p3264 N90-28483
Some novel sources of x ray beams: Channeling, transition and Cherenkov radiation
[DE90-014442] 23 p3395 N90-29181
Detector to study low-flex hard x ray/gamma ray sources
[UT-HE-90/08] 24 p3564 N90-30164
New developments in low-energy cosmic gamma-ray detection
[UT-HE-90/07] 24 p3564 N90-30165

GANGLIA
Neurocontrol systems and wing-fluid interactions underlying dragonfly flight 12 p1606 N90-19240

GAPS
NT ENERGY GAPS (SOLID STATE)
NT SPARK GAPS

GARMENTS
Garment pressurizing apparatus
[AD-D014451] 22 p3232 N90-28330

GARNETS
NT YTTRIUM-ALUMINUM GARNET
NT YTTRIUM-IRON GARNET

GARP
U GLOBAL ATMOSPHERIC RESEARCH PROGRAM

GAS ANALYSIS
NT OZONOMETRY
The mobile combustion diagnostic fixture and its application to the study of propellant combustion. Part 1: Investigation of the low pressure combustion of LOVA XM39 propellant
[AD-A213272] 05 p0621 N90-13626
HCl monitor, phase 2
[AD-A213572] 07 p0958 N90-15542
Methodology used for gas analysis and control of trace chemical contaminants at a hyperbaric facility. 1: Gas sampling
[AD-A216155] 10 p1325 N90-17659
Device for quickly sensing the amount of O2 in a combustion product gas
[NASA-CASE-LAR-13816-1] 15 p2102 N90-22025
Review of model sensor studies on Pd/SnO2(110) surfaces 18 p2559 N90-24604
Resonance enhanced two-laser infrared multiple photon dissociation of gaseous ions
[AD-A221826] 21 p2970 N90-26879
Requirements for long-life operation of inert gas hollow cathodes: Preliminary report
[NASA-TM-103242] 22 p3134 N90-27783

GAS ATOMIZATION
Spray deposition: A fundamental study of droplet impingement, spreading and consolidation
[AD-A217202] 13 p1787 N90-20255

GAS BEARINGS
Development and testing of a contactless static/dynamic shaft seal with little sealing gas requirement
[KFK-4599] 05 p0652 N90-13802
Some problems in hydrodynamic lubrication 09 p1229 N90-17133
Yaw rate control of an air bearing vehicle 12 p1639 N90-19420
Improved analytical capabilities for foil air bearings, phase 1
[AD-A218071] 14 p1987 N90-21389

GAS CHROMATOGRAPHY
The effect of degree of aromaticity and alkyl substitution of polyaromatic hydrocarbons on instrumental response factors
[DE89-000761] 02 p0196 N90-11117
Analysis of ambient polar volatile organic compounds using chemical ionization-ion trap detector
[PB90-106451] 07 p0956 N90-15529
A gas chromatograph/mass spectrometry method for determining isotopic distributions in organic compounds used in the chemical approach to stable isotope separation
[DE90-005738] 10 p1352 N90-17841
Chamber investigations of the fate of diesel emissions in the atmosphere. Volume 2: AMES assay and GCMS final data reports and gas phase projections
[PB90-114430] 10 p1405 N90-18104
Evaluation of a commercial gas chromatography/matrix isolation-infrared spectrometer for quantitative analysis of priority pollutants
[DE90-006033] 11 p1484 N90-18542
Quantitative determination of 1, 2-ethanediol contamination in used diesel lubricating oils by gas chromatography/mass spectrometry
[AD-A218592] 17 p2371 N90-23498
Retention index monitoring of volatile organic compounds using thermal desorption gas chromatography
[AD-A221117] 18 p2521 N90-24397
Calorimetry, activity, and micro-FTIR analysis of CO chemisorption, titration, and oxidation on supported Pt 18 p2560 N90-24606
Chemisorption studies of Pt/SnO2 catalysts 18 p2560 N90-24609
Proton irradiation of simple gas mixtures: Influence of irradiation parameters 20 p2949 N90-26782
Thermogravimetry-mass spectrometry analysis of gas bubbles in molten glass
[DE90-014116] 23 p3303 N90-28684
Peak analysis in gas chromatography and the development of new stationary phases for anion chromatography
[DE90-014428] 23 p3304 N90-28687

GAS COMPOSITION
NT CARBON DIOXIDE CONCENTRATION
NCAR (National Center for Atmospheric Research) master mechanism of the gas phase chemistry, version 2.0
[PB89-208979] 02 p0249 N90-11413
Profile measurements of sulfur dioxide, nitrogen oxides, and nitric acid deposition velocities in California's south coast air basin
[PB90-104001] 06 p0808 N90-14703
Development and use of a passive technique for measuring nitrogen dioxide in the background atmosphere 16 p2331 N90-23285
The e-beam sustained CO2 laser amplifier 18 p2561 N90-24611
The global consequences of increasing tropospheric ozone concentrations
[NASA-TM-103477] 20 p2883 N90-26401
Results from the IVL TOR Station at Roervik, Sweden. A contribution to the EURATRAC subproject TOR 20 p2885 N90-26415
Structure and radiation properties of turbulent diffusion flames
[PB90-218777] 22 p3155 N90-27887
The vertical ozone distribution during maximum and minimum solar activity 22 p3205 N90-28182
Variation of D-region nitric-oxide density with solar activity and season at the dip equator 22 p3205 N90-28183
Effects of thruster firings on the shuttle environment 1: Neutral gas composition
[AD-A224404] 24 p3487 N90-29707

GAS COOLED REACTORS
NT HIGH TEMPERATURE GAS COOLED REACTORS
Design study of a modular gas-cooled, closed-brayton cycle reactor for marine use
[AD-A213453] 07 p0953 N90-15518

GAS COOLING
Gas flows in rocket motors, volume 1
[AD-A213348] 05 p0615 N90-13591
Gas cooled fuel cell systems technology development program
[DE90-000446] 12 p1683 N90-19668
The modeling of drop-containing turbulent eddies
[NASA-CR-186805] 18 p2553 N90-24570
New discharge pumping method for CO2 lasers
[AD-A220898] 20 p2866 N90-26307

GAS DENSITY
Retrieval of atomic oxygen and temperature in the thermosphere. Part 1: Feasibility of an experiment based on the spectrally resolved 147 micrometer limb emission
[AD-A211987] 04 p0517 N90-12986
A methodology for evaluating heavy gas dispersion models
[AD-A214009] 07 p0887 N90-15131
Shapes of star-gas waves in spiral galaxies
[NASA-CR-186289] 07 p1011 N90-15859
A small, inexpensive apparatus for the determination of the density of powdered materials
[AD-A215393] 09 p1225 N90-17110
Measurement of gas intensity at high dynamic pressures
[ISL-CO-204/89] 11 p1507 N90-18680
Computation of hypersonic low density flows with thermochemical nonequilibrium 13 p1749 N90-20044
Numerical modelling of shocks in gases and metals
[AD-A218586] 17 p2402 N90-23684
A lightweight solid polymer electrolyte fuel cell with stack power density of 3 kW/lb (7kW/kg)
[AD-A223068] 21 p3020 N90-27169
Research on optogalvanic effects
[AD-A221512] 21 p3071 N90-27463

GAS DETECTORS
Independent Orbiter Assessment (IOA): Assessment of the purge, vent and drain subsystem
[NASA-CR-185535] 02 p0168 N90-10949
Independent Orbiter Assessment (IOA): Analysis of the purge, vent and drain subsystem
[NASA-CR-185547] 02 p0172 N90-10969
The Third Conference on the Environmental Chemistry of Hydrazine Fuels
[AD-A197632] 02 p0203 N90-11157
Microsensor and pattern recognition techniques in hydrazine detection 02 p0206 N90-11177
Hydrazine dosimetry 02 p0206 N90-11178
Description of a chemiluminescence detector system specifically designed for monitoring airborne hydrazine and oxidizer propellant vapors 02 p0206 N90-11179
Low ppb level detection of toxic compounds with a fully automated CO2 laser photoacoustic detector 02 p0206 N90-11181
Gas identification system using graded temperature sensor and neural net interpretation
[AD-A213359] 05 p0622 N90-13627
Multisensor technologies for low cost methane detection
[PB89-235188] 05 p0645 N90-13766
Evaluation of doped phthalocyanines and a chemically-sensitive field effect transistor for detecting nitrogen dioxide
[AD-A215862] 09 p1214 N90-17037
Background studies in gas ionizing x ray detectors 12 p1636 N90-19399
Optical paramagnetic/diamagnetic gas sensor
[AD-D014368] 12 p1663 N90-19554
Infrared absorption gas sensor for the detection of HCl in launch vehicle exhaust clouds 16 p2209 N90-22600
Review of model sensor studies on Pd/SnO2(110) surfaces 18 p2559 N90-24604
Requirements for long-life operation of inert gas hollow cathodes: Preliminary report
[NASA-TM-103242] 22 p3134 N90-27783

GAS DIFFUSION
U GASEOUS DIFFUSION

GAS DISCHARGE COUNTERS
U COUNTERS
U GAS DISCHARGE TUBES

GAS DISCHARGE TUBES
NT IGNITRONS
NT THYRATRONS

A composition for the filling of gas-discharge tubes
|AD-A222818| 21 p2999 N90-27047
On the technology for preparation of a HeNe discharge tube for use in a laser gyro
|DLR-MITT-90-01| 24 p3472 N90-29624

GAS DISCHARGES
Electron production, electron attachment, and charge recombination process in high pressure gas discharges
|AD-A216301| 10 p1434 N90-18274
A numerical solution of the time-dependent Boltzmann equation
|AD-A216397| 10 p1434 N90-18275
Electron-impact ionization and electron attachment cross sections of radicals important in transient gaseous discharges
|AD-A217510| 13 p1806 N90-20366
Time-resolved swarm studies in gases with emphasis on electron detachment and ion conversion
|ISBN-90-9003013-1| 18 p2613 N90-24883

GAS DISSOCIATION
An empirical formula for gas switch breakdown delay
|DE89-017233| 03 p0342 N90-11947
Theory of stagnation point heat transfer in dissociated air 05 p0573 N90-13337
Reactions of atmospheric species with clean and H, C, and O implanted species
|AD-A214602| 09 p1244 N90-17218
Lower limits on the absolute dissociative electron attachment cross section from O2 condensed on rare-gas films
|AD-A216727| 11 p1483 N90-18536
Absolute cross-sections for dissociative electron attachment in O2 condensed on Kr films
|AD-A216730| 11 p1570 N90-19038
Dissociation phenomena in electron-beam sustained carbon dioxide lasers 18 p2560 N90-24610
Resonance enhanced two-laser infrared multiple photon dissociation of gaseous ions
|AD-A221826| 21 p2970 N90-26879

GAS DYNAMICS
NT AERODYNAMICS
NT AEROTHERMODYNAMICS
NT HYPERSONICS
NT INTERACTIONAL AERODYNAMICS
NT RAREFIED GAS DYNAMICS
NT ROTOR AERODYNAMICS
NT SUPERSONICS
NT UNSTEADY AERODYNAMICS
Particle kinetic simulation of high altitude hypervelocity flight
|NASA-CR-186003| 02 p0147 N90-10840
On a Taylor Weak Statement for finite element computations in gas dynamics 02 p0219 N90-11251
Method of characteristic studies for rotational flow downstream of a curved shock wave 02 p0219 N90-11252
Gas dynamical processes in the theory of galaxy formation 02 p0294 N90-11673
Enhanced resolution concepts in large scale scientific computing
|AD-A214095| 07 p0932 N90-15393
An entropy-based approach to nonlinear stability
|NASA-TM-101086| 09 p1272 N90-17376
Hypersonic nozzle/afterbody performance at low Mach numbers
|AD-A216223| 10 p1309 N90-17575
Experimental investigation of a chemical laser cavity flowfield
|AD-A216398| 10 p1390 N90-18038
Model calculations for dynamic development of planetary nebulae
|ETN-90-95734| 12 p1744 N90-20025
Spectral simulation of unsteady compressible flow past a circular cylinder
|NASA-CR-182030| 13 p1750 N90-20050
Computation of nonequilibrium chemically reacting flows in hypersonic flow field 14 p1911 N90-20954
Finite element algorithms for hyperbolic conservation laws with forcing terms
|INPE-5024-RPE/617| 14 p2022 N90-21595
Partial acoustic filtering applied to the equations of compressible flow
|DE90-000673| 15 p2097 N90-22001
A galaxy formation cookbook: Recipes and utensils 15 p2190 N90-22508
Gas dynamic theory of flight of fast electron flux in plasma
|DE90-618767| 16 p2319 N90-23220
Hermes preparatory programme: Fluidynamics studies. Activities performed by the Italian researchers
|DLC/COP-HER-TN-002| 17 p2363 N90-23453
Characterization of plasma flow through magnetic nozzles
|AD-A221044| 18 p2617 N90-24905
Project TTA-79: Summary project report
|ETN-90-96773| 19 p2661 N90-25146
Adaptive node movement in finite-difference solutions of partial differential equations with applications to gasdynamics, part 1
|UTIAS-333-PT-1| 19 p2750 N90-25622
Adaptive node movement in finite-difference solutions of partial differential equations with applications to gasdynamics, part 2
|UTIAS-333-PT-2| 19 p2750 N90-25623
Prediction of two-dimensional time-dependent gasdynamic flows for hypersonic studies
|UTIAS-335| 20 p2801 N90-25935
Inviscid dynamics of unstable shear layers
|AD-A222297| 21 p3004 N90-27077
Towards a two dimensional scheme of anisotropic Godunov type. On the calculation of the velocity of the nodes in the multidimensional Lagrangian codes
|ETN-90-97458| 22 p3175 N90-28017
Towards a two dimensional code of anisotropic Godunov type 22 p3175 N90-28018
Finite-volume application of high order ENO schemes to multi-dimensional boundary-value problems
|NASA-CR-186917| 22 p3242 N90-28387
Interferometry 24 p3419 N90-29315

GAS EVOLUTION
Gas evolution and bubble formation on electrodes
|DLR-FB-89-35| 05 p0622 N90-13629
Integrated regenerative fuel cell experimental evaluation
|NASA-CR-185183| 11 p1530 N90-18808

GAS EXCHANGE
Micrometeorological investigation of surface exchange of trace gases: A case study
|PB89-208375| 02 p0249 N90-11412
Canopy stomatal conductance
|DE89-016860| 06 p0809 N90-14711
High-frequency ventilation in dogs with three gases of different densities
|AD-A212862| 06 p0819 N90-14762
Dynamics of carbon dioxide exchange of a wheat community grown in a semi-closed environment 08 p1155 N90-16689
Continuous gas exchange measurements using individual fascicle cuvettes: The tubule system
|DE90-004932| 10 p1405 N90-18105
Effects of high altitude hypoxia on lung and chest wall function during exercise
|AD-A219814| 17 p2434 N90-23869
Carbon dioxide and water exchange rates by a wheat crop in NASA's biomass production chamber: Results from an 86-day study (January to April 1989)
|NASA-TM-102788| 19 p2716 N90-25453
Gas exchange characteristics as indicators of the basic limiting factors in photosynthesis
|DE90-012399| 20 p2898 N90-26481
Rates of vertical mixing, gas exchange, and new productions: Estimates from seasonal gas cycles in the upper ocean near Bermuda
|PB90-244781| 24 p3496 N90-29758

GAS EXPANSION
Notes on the unsteady rectilinear motion of a perfect gas. 9: The expansion to vacuum of a finite mass of uniform homentropic gas
|LR-590-9| 19 p2692 N90-25316
Multicomponent gas sorption Joule-Thomson refrigerator
|NASA-CASE-NPO-17569-1-CU| 20 p2844 N90-26176

GAS EXPLOSIONS
Numerical simulation of detonation transfer between gaseous explosive layers
|MRL-RR-1-89| 01 p0069 N90-10395

GAS FLOW
NT AIR CURRENTS
NT AIR FLOW
NT CONTINUUM FLOW
NT COOLING FLOWS (ASTROPHYSICS)
NT EQUILIBRIUM FLOW
NT FREE MOLECULAR FLOW
NT JET STREAMS (METEOROLOGY)
NT KNUDSEN FLOW
NT MERIDIONAL FLOW
NT MOLECULAR FLOW
NT NONEQUILIBRIUM FLOW
NT PIPE FLOW
NT TRANSITION FLOW
NT VERTICAL AIR CURRENTS
Supersonic flow computations over aerospace configurations using an Euler marching solver
|NASA-CR-4085| 01 p0003 N90-10012
The role of particle collisions in pneumatic transport 01 p0068 N90-10392
Gas-phase flowrate effect on disintegrating cryogenic liquid-jets
|NASA-TM-102357| 02 p0223 N90-11277
Recent progress in research pertaining to estimates of gas-side heat transfer in an aircraft gas turbine
|NASA-TM-102460| 05 p0582 N90-13394
Gas flows in rocket motors. Volume 2, appendix C: Time iterative solution of viscous supersonic flow
|AD-A213349| 05 p0615 N90-13592
Gas flows in rocket motors. Volume 3, appendix D: Computer code listings
|AD-A213350| 05 p0616 N90-13593
Perturbations in high-velocity gas flow
|DE90-000539| 06 p0777 N90-14520
Unsteady hydromagnetic flow of a radiating gas in a vertical channel with axial temperature variation
|DE90-600934| 06 p0778 N90-14525
Isotopic selectivity of surface diffusion: An activated diffusion model
|DE90-003473| 07 p0894 N90-15169
Retractable gas cooled leads for ASTROMAG
|DE90-002679| 07 p0921 N90-15331
Comments on compressible flow through butterfly valves
|DE89-015730| 07 p0928 N90-15371
A brief description of lattice gas models for multiphase flows and magnetohydrodynamics
|DE90-003653| 08 p1062 N90-16143
Visualization of gas flows using the smoke wire technique 08 p1079 N90-16242
Experimental studies of gas trapping in amorphous ice and thermal modelling of comets: Implications for Rosetta 08 p1140 N90-16610
An upwind-biased, point-implicit relaxation algorithm for viscous, compressible perfect-gas flows
|NASA-TP-2953| 09 p1214 N90-17042
Cold flow determination of the internal flow environment around the submerged TVC nozzle for the space shuttle SRM 11 p1470 N90-18465
Three-dimensional structural analyses of reentry vehicles
|DE90-006278| 12 p1615 N90-19291
Development and utilization of new diagnostics for dense-phase pneumatic transport
|DE90-006787| 12 p1659 N90-19536
Determination of flow-regime boundaries for cohesive particles
|DE90-007425| 13 p1800 N90-20332
TiCl4 as a source of TiO2 particles for laser anemometry measurements in hot gas
|NASA-TM-102581| 13 p1805 N90-20358
Notes on the unsteady rectilinear motion of a perfect gas. Part 8: General theory and general waves in a homentropic gas
|PB90-167149| 14 p1974 N90-21309
Numerical simulation of liquid circulation in a bubbly column
|DE90-005226| 15 p2097 N90-22002
On dual Lagrangian hyperbolic models for one dimensional two phase flow problems
|DE90-007012| 15 p2098 N90-22004
Scattered-light scanner measurements of cryogenic liquid-jet breakup
|NASA-TM-102432| 15 p2101 N90-22021
Proceedings of the 9th International Conference on Computing Methods in Applied Science and Engineering
|AD-A219307| 16 p2307 N90-23149
Advanced instrumentation for local measurement of gas-solid suspension flows
|DE90-008498| 17 p2400 N90-23671
Prediction of two-dimensional time-dependent gasdynamic flows for hypersonic studies
|UTIAS-335| 20 p2801 N90-25935
Combustion in the gas turbine. Part 2: Preliminary design and performance
|CIT/SME/VKI/RS/3| 20 p2810 N90-25987
Numerical analysis of three-dimensional particle-laden flow equations
|IAR-90-2| 20 p2860 N90-26268
Optical characterization of clouds of fine liquid-nitrogen particles
|NASA-TM-103208| 20 p2865 N90-26299
An optical study of the flow start-up process in four convergent-divergent nozzles
|AD-A222918| 21 p2963 N90-26846
Flow induced nutation instability in spinning solid propellant rockets
|AD-A222504| 21 p2969 N90-26877
Numerical investigation of the incompressible plane shear layer between two gases with different densities
|ETN-90-97315| 21 p3006 N90-27084
Constitutive laws for discrete velocity models of gas (continued)
|ETN-90-97451| 22 p3175 N90-28016
Development of an integrated BEM for hot fluid-structure interaction 23 p3291 N90-28617
Current research in cavitating fluid films
|NASA-TM-103184| 23 p3323 N90-28791

Gas-film flow in tubes
[DE90-011528] 23 p3324 N90-28793
Velocity interferometry 24 p3420 N90-29316
Electron beam for velocity determination 24 p3420 N90-29319
An investigation of the inviscid spatial instability of compressible mixing layers
[AD-A223776] 24 p3468 N90-29596
Counter-current flow limitation in thin rectangular channels
[DE90-015124] 24 p3469 N90-29599

GAS GENERATOR ENGINES
U ENGINES
U GAS GENERATORS

GAS GENERATORS
Independent Orbiter Assessment (IOA): Weibull analysis report
[NASA-CR-185534] 02 p0168 N90-10948
A simulator for a hydrocarbon ramrocket fuel gas generator: First phase development
[AR-005-621] 02 p0189 N90-11080
Effect of propellant flowrate and purity on carbon deposition in LO2/methane gas generators 11 p1471 N90-18468
Design and operation of an inert gas facility for thermoelectric generator storage
[DE90-007146] 11 p1565 N90-19008
Carbon deposition model for oxygen-hydrocarbon combustion. Task 6: Data analysis and formulation of an empirical model
[NASA-CR-183986] 20 p2829 N90-26095
Renewed aging control of adhesion of inhibitor on the gas generator charges for RB 24
[FOA-C-20780-2.1] 20 p2840 N90-26153
Hybrid propulsion technology program
[NASA-CR-183952] 21 p2968 N90-26870
Design optimization of gas generator hybrid propulsion boosters
[NASA-CR-181096] 23 p3299 N90-28660

GAS GIANT PLANETS
NT JUPITER (PLANET)
NT NEPTUNE (PLANET)
NT SATURN (PLANET)
NT URANUS (PLANET)
Pioneers 10 and 11 deep space missions
[NASA-TM-102269] 10 p1448 N90-18355
Preliminary error budget for an optical ranging system: Range, range rate, and differenced range observables 20 p2853 N90-26227
Measurements of the methane relaxation times for application to the infrared emission models of the upper atmospheres of outer planets and Titan 20 p2945 N90-26759
Chemical kinetics and modeling of planetary atmospheres 20 p2946 N90-26763
Kinetics and thermochemistry of polyatomic free radicals: New results and new understandings 20 p2946 N90-26764
Vapor pressures of acetylene at low temperatures 20 p2949 N90-26777

GAS GUNS
NT LIGHT GAS GUNS
Acceleration of small, light projectiles (including hydrogen isotopes) to high speeds using a two-stage light gas gun
[DE90-002479] 06 p0729 N90-14253

GAS INJECTION
Experimental and theoretical research on the injection of ignition gases into a bed of inert powder
[ISL-CO-251/88] 11 p1485 N90-18547
The use of the gas feed system and the vitiator for the solid fuel combustion chamber
[LR-528] 12 p1623 N90-19329
Construction and characterization of a valve for rapid gas injection
[INPE-4789-RPE/583] 12 p1651 N90-19486
Calibration of the sonic measuring and control cross section in the gas feed installation of the solid fuel combustion chamber
[LR-552] 12 p1661 N90-19548
Analysis of the rotor tip leakage flow with tip cooling air ejection 14 p1926 N90-21029
Analysis of a six-component, flow-through, strain-gage, force balance used for hypersonic wind tunnel models with scramjet exhaust flow simulation
[NASA-CR-186585] 15 p2055 N90-21775

GAS IONIZATION
NT AURORAL IONIZATION
NT FLAME IONIZATION
Laboratory simulations of the solar wind-comet interactions 07 p1015 N90-15875
Photodissociation regions: Observations and theory 11 p1579 N90-19098
Helium transport in plasma edge regions 14 p2027 N90-21625
Polarization effects in ionizing collisions with Ne+(3-P2)- and Ne++(3-D3)-atoms
[ETN-90-96891] 17 p2471 N90-24127

GAS JETS
Gas-phase flowrate effect on disintegrating cryogenic liquid-jets
[NASA-TM-102357] 02 p0223 N90-11277
Swirl-stabilized flames: Fluid dynamics, mixing, and flame stability limits 08 p1040 N90-16009
Application of a three-dimensional Navier-Stokes model for a subsonic jet in a crossflow 13 p1749 N90-20045
Instabilities and subharmonic resonances of subsonic heated round jets, volume 2
[NASA-CR-186058] 15 p2100 N90-22017
Nonlinear interactions in mixing layers and compressible heated round jets
[NASA-CR-186303] 17 p2400 N90-23674
Determination of the velocity, density, maximum flux, and enthalpy profiles for a very high temperature arc jet nozzle flow
[AD-A218390] 17 p2402 N90-23682
A review of instability and noise propagation in supersonic flows
[NASA-CR-186800] 19 p2655 N90-25112
Design of a device to remove lunar dust from space suits for the proposed lunar base
[NASA-CR-186679] 19 p2724 N90-25496
Model of turbulent diffusion flames and nitric oxide generation
[PB90-155557] 22 p3155 N90-27886
Gas-jet and tangent-slot film cooling tests of a 12.5 deg cone at Mach number of 6.7
[NASA-TP-2786] 23 p3326 N90-28806

GAS LASERS
NT CARBON DIOXIDE LASERS
NT CARBON MONOXIDE LASERS
NT EXCIMER LASERS
NT HELIUM-NEON LASERS
NT HF LASERS
NT KRYPTON FLUORIDE LASERS
NT TEA LASERS
NT ULTRAVIOLET LASERS
NT XENON CHLORIDE LASERS
NT XENON FLUORIDE LASERS
Strategies for high efficiency operation of the E-beam excited atomic xenon laser using high-power and high-energy loading
[DE90-005196] 13 p1806 N90-20370
Heat-transfer regimes in nuclear-reactor-pumped gas lasers
[DE90-002904] 15 p2103 N90-22032
Fast plasma mixing: A new excitation method for CW gas lasers
[AD-A220290] 18 p2617 N90-24904
Planar waveguide spectrometer
[DE90-016308] 24 p3546 N90-30057

GAS LIQUEFACTION
U CONDENSING

GAS LUBRICATED BEARINGS
U GAS BEARINGS

GAS MASERS
NT HYDROGEN MASERS

GAS METERS
A new inexpensive electrochemical meter for oxygen in sodium coolant
[DE89-630802] 02 p0194 N90-11104

GAS MIXTURES
NT AIR
NT COMPRESSED AIR
NT DETONABLE GAS MIXTURES
NT HIGH TEMPERATURE AIR
Reactive ion etching of SiC thin films by mixtures of fluorinated gases and oxygen
[AD-A211046] 02 p0195 N90-11113
An empirical formula for gas switch breakdown delay
[DE89-017233] 03 p0342 N90-11947
A nonlinear-optical method for combining high power laser beams
[AD-A211730] 03 p0354 N90-12022
Characterization of nonpremixed turbulent bluff-body burner flames
[PB89-229447] 04 p0469 N90-12689
Properties of Lennard-Jones mixtures at various temperatures and energy ratios with a size ratio of two
[PB89-235204] 04 p0471 N90-12697
Survey of the response of standard limited streamer tubes over the complete range of three-component gas mixtures of isobutane, CO(sub 2), argon
[DE89-016692] 04 p0499 N90-12875
Gas identification system using graded temperature sensor and neural net interpretation
[AD-A213359] 05 p0622 N90-13627
Propagation of sound in vibrationally excited nitrogen and hydrogen gas mixtures
[AD-A213002] 05 p0696 N90-14073
Asymptotic analysis of performance of membrane modules for gas separations
[DE90-000699] 06 p0742 N90-14316
Externally vaporizing system for turbine combustor
[AD-D014284] 08 p1024 N90-15918
Swirl-stabilized flames: Fluid dynamics, mixing, and flame stability limits 08 p1040 N90-16009
New mixing-length model for numerical solution of turbulent supersonic flows 09 p1216 N90-17048
Spectral characteristics of arc-heated low density plasma flows (IV) air and N2-CO2 mixture plasmas
[NAL-TR-1012] 09 p1285 N90-17451
FLUSH: A tool for the design of slush hydrogen flow systems
[NASA-TM-102467] 10 p1361 N90-17890
Electron production, electron attachment, and charge recombination process in high pressure gas discharges
[AD-A216301] 10 p1434 N90-18274
On the dynamics of the combustion process of hydrogen-air and hydrogen-methane-air mixtures
[DLR-FB-89-39] 11 p1485 N90-18548
Molecular theory and computer simulation studies of natural and synthetic gas mixtures
[PB90-130329] 12 p1711 N90-19826
Comets: Dirty snowballs or icy dirtballs 12 p1739 N90-19994
Cometary bodies in the circumstellar disk around beta Pictoris 12 p1741 N90-20010
Multicomponent gas sorption Joule-Thomson refrigerator
[NASA-CASE-NPO-17569-1-CU] 20 p2844 N90-26176
Testing of flame screens and flame arresters as Devices designed to Prevent the Passage of Flame (DPPF) into tanks containing flammable atmospheres according to an IMO standard
[AD-A222566] 20 p2844 N90-26177
Laboratory measurements and modeling of microwave absorption by ammonia in gas mixtures applicable to giant planet atmospheres 20 p2944 N90-26750
Proton irradiation of simple gas mixtures: Influence of irradiation parameters 20 p2949 N90-26782
Concentration, temperature, and density in a hydrogen-air flame by excimer-induced Raman scattering 21 p2974 N90-26903
Investigation of the effects of microalloy constituents, surface treatment and oxidation conditions on the development and breakdown of protective oxide scales
[DE90-015710] 24 p3451 N90-29488

GAS PATH ANALYSIS
Measurement of gas leaks between a projectile and the walls of a tube in a ballistic compressor
[ISL-CO-250/88] 11 p1510 N90-18694

GAS PHASES
U VAPOR PHASES

GAS PIPES
A robot which will investigate the condition of underground pipe
[PB89-230650] 04 p0508 N90-12928
Trailer shield assembly for a welding torch
[NASA-CASE-MFS-29260-1] 12 p1672 N90-19602

GAS PRESSURE
Apparatus and method for monitoring pressure leaks from a sealed system
[AD-D014168] 03 p0349 N90-11995
Neptune's Triton: A moon rich in dry ice and carbon
[NASA-CR-186298] 08 p1152 N90-16675
Two-dimensional calculation of sequential electron layer formation by crossed microwave beams in air at low pressure
[DE90-005254] 09 p1286 N90-17453
Helium permeability through austenitic stainless steel
[DE90-007046] 11 p1488 N90-18562
Construction and calibration of a gas pressure meter with high temporal resolution
[INPE-4953-RPE/602] 11 p1511 N90-18700
Transport of gases through concrete
[AERE-G-4977] 16 p2234 N90-22747
Tests for integrating measurement of gas pressures in flight propellers
[ETN-90-96498] 18 p2494 N90-24253
Garment pressurizing apparatus
[AD-D014451] 22 p3232 N90-28330
Investigation of a heat driven thermoacoustic prime mover
[AD-A223928] 24 p3484 N90-29694

GAS RECOVERY
Study of power generation systems for CO2 collection: LNG combined cycle
[DE90-507881] 23 p3345 N90-28901

GAS SPECTROSCOPY
Forty-fourth symposium on molecular spectroscopy
[AD-A210752] 02 p0195 N90-11111

A gas chromatograph/mass spectrometry method for determining isotopic distributions in organic compounds used in the chemical approach to stable isotope separation
[DE90-005738] 10 p1352 N90-17841
Evaluation of a commercial gas chromatography/matrix isolation-infrared spectrometer for quantitative analysis of priority pollutants
[DE90-006033] 11 p1484 N90-18542

GAS STREAMS
Production of jet fuels from coal derived liquids. Volume 10: Jet fuels production by-products, utility, and sulfur emissions control integration study
[AD-A213872] 09 p1200 N90-16951
Modeling of supersonic reacting flow fields
21 p2973 N90-26898

GAS TEMPERATURE
Gas identification system using graded temperature sensor and neural net interpretation
[AD-A213359] 05 p0622 N90-13627
Unsteady hydromagnetic flow of a radiating gas in a vertical channel with axial temperature variation
[DE90-600934] 06 p0778 N90-14525
Measurement of the speed and temperature of ignition gases
[ISL-CO-246/88] 09 p1192 N90-16908
Overview on hot gas tests and molten salt corrosion experiments at the DLR 23 p3309 N90-28714

GAS TRANSPORT
Transport of gases through concrete
[AERE-G-4977] 16 p2234 N90-22747
Diffusion of penetrants in polymers
[AD-A223217] 21 p2986 N90-26969

GAS TUNGSTEN ARC WELDING
Material properties of 2219-T851 aluminum alloy plasma welded compared to TIG welding
02 p0182 N90-11032
Extravehicular activity welding experiment
[NASA-CR-183848] 06 p0791 N90-14608
BES welding science contractors summary report, 1988 to 1989
[DE90-001004] 06 p0793 N90-14619
Internal wire guide for GTAW welding
[NASA-CASE-MFS-29489-1] 17 p2385 N90-23586
Electrode carrying wire for GTAW welding
[NASA-CASE-MFS-29491-1] 20 p2842 N90-26168

GAS TURBINE ENGINES
NT HYDROGEN ENGINES
NT JET ENGINES
NT RAMJET ENGINES
NT SUPERSONIC COMBUSTION RAMJET ENGINES
NT TURBOFAN ENGINES
NT TURBOJET ENGINES
NT TURBOPROP ENGINES
NT TURBORAMJET ENGINES
Performance potential of an advanced technology Mach 3 turbojet engine installed on a conceptual high-speed civil transport
[NASA-TM-4144] 01 p0008 N90-10034
Advanced Turbine Technology Applications Project (ATTAP)
[NASA-CR-185133] 01 p0008 N90-10036
Report on an overseas visit, June 1988
[AD-A210374] 01 p0009 N90-10040
Combustor influence on fighter engine operability
01 p0035 N90-10193
The MHOST finite element program: 3-D inelastic analysis methods for hot section components. Volume 3: Systems' manual
[NASA-CR-182236] 01 p0079 N90-10451
Advanced technologies impact on compressor design and development: A perspective
[NASA-TM-102341] 02 p0156 N90-10891
Advanced Turbine Technology Applications Program, (ATTAP): A plan for improving the prototype production of ceramic components for the gas turbine engine, 1988--1992
[DE89-015566] 02 p0230 N90-11320
Advanced technology in military gas turbine design and manufacture
[PNR90545] 03 p0307 N90-11747
Gas turbine performance analysis
[PNR90599] 04 p0456 N90-12614
The nature and control of skidding in lightly loaded intershaft bearings
[PNR90591] 04 p0508 N90-12933
Constitutive modeling for isotropic materials (HOST)
[NASA-CR-179522] 05 p0582 N90-13390
Constitutive modeling for isotropic materials (HOST)
[NASA-CR-174718] 05 p0582 N90-13391
Recent progress in research pertaining to estimates of gas-side heat transfer in an aircraft gas turbine
[NASA-TM-102460] 05 p0582 N90-13394
A study of variable geometry in advanced gas turbines
07 p0881 N90-15104
Cycle analysis for helicopter gas turbine engines
[RAE-TM-P-1154] 08 p1025 N90-15921
Low NO(x) potential of gas turbine engines
[NASA-TM-102452] 10 p1321 N90-17636
Study of bird ingestions into small inlet area, aircraft turbine engines (May 1987 to April 1988)
[DOT/FAA/CT-89/17] 11 p1453 N90-18375
AGARD/SMP Review: Damage Tolerance for Engine Structures. 2: Defects and Quantitative Materials Behaviour --- conference
[AGARD-R-769] 11 p1457 N90-18396
Review of modelling methods to take account of material structure and defects 11 p1458 N90-18402
The need for a common approach within AGARD --- engine component defects 11 p1459 N90-18404
Experimental and theoretical investigations of flowfields and heat transfer in modern gas turbines
[AD-A217663] 12 p1605 N90-19237
In-flight evaluations of turbine fuel extenders
[DOT/FAA/CT-89/33] 12 p1633 N90-19387
Heat transfer near the entrance to a film cooling hole in a gas turbine blade
[AD-A217396] 13 p1757 N90-20089
Statistics on aircraft gas turbine engine rotor failures that occurred in US commercial aviation during 1986
[DOT/FAA/CT-89/30] 14 p1922 N90-21008
Evaluating thermographic phosphors in an operating turbine engine
[DE90-004874] 15 p2105 N90-22044
Fatigue crack growth investigation of a Ti-6Al-4V forging under complex loading conditions: NATO/AGARD supplemental engine disk program
[AD-A220239] 17 p2377 N90-23538
Introducing the VRT gas turbine combustor
[NASA-TM-103176] 17 p2386 N90-23591
Processing of advanced ceramics which have potential for use in gas turbine aero engines
[AD-A220988] 19 p2677 N90-25226
Effect of vane twist on the performance of dome swirlers for gas turbine airblast atomizers
[NASA-TM-103195] 19 p2688 N90-25289
Gas Turbine Combustion, volume 1
[VKI-LS-1990-02-VOL-1] 20 p2810 N90-25985
Combustion in the gas turbine. Part 1: Combustor types and design
[CIT/SME/VKI/RS/1] 20 p2810 N90-25986
Combustion in the gas turbine. Part 2: Preliminary design and performance
[CIT/SME/VKI/RS/3] 20 p2810 N90-25987
Combustion in the gas turbine. Part 3: Fuel injection, ignition and stability
[CIT/SME/VKI/RS/4] 20 p2810 N90-25988
Combustor cooling aspects
[CIT/SME/VKI/RS/5] 20 p2810 N90-25989
Pollutants: Production and methods of reduction
[CIT/SME/VKI/RS/6] 20 p2810 N90-25990
Subsonic combustor flow modeling: State of the art of CFD techniques for reacting and combusting flow
20 p2810 N90-25991
Chemistry of combustion processes
20 p2811 N90-25994
Gas Turbine Combustion, volume 2
[VKI-LS-1990-02-VOL-2] 20 p2811 N90-25995
Towards 2000: The composite engine
[PNR90646] 20 p2811 N90-26000
Prediction of rotating disc flow and heat transfer in gas turbine engines
[PNR90650] 20 p2812 N90-26001
Aircraft exhaust emissions: An engine manufacturer's perspective
[PNR90675] 20 p2812 N90-26004
The application of engineering ceramics in gas turbines
[PNR90676] 20 p2812 N90-26005
Elevated temperature crack growth
[NASA-CR-182247] 20 p2875 N90-26355
Advanced Turbine Technology Applications Project (ATTAP)
[NASA-CR-185240] 20 p2939 N90-26728
Retirement for cause of the F100 engine
21 p2957 N90-26813
Comparative evaluation of Allison T56 engine chip detectors
[AD-A221864] 21 p2960 N90-26832
Cost effective technology
[PNR90664] 21 p2991 N90-27002
Self-lubricating surfaces by ion beam processing
[AD-A222489] 21 p3011 N90-27118
Experimental identification of helicopter engine dynamics from closed loop data
22 p3104 N90-27627
AGARD damage tolerance concepts for engine structures Workshop 3, Component Behaviour and Life Management 22 p3117 N90-27705
Life management planning 22 p3118 N90-27709
Experience in developing an improved altitude test capability 22 p3120 N90-27719
The role of NDI in the certification of turbine engine components 22 p3184 N90-28069
Critical inspection of high performance turbine engine components: The RFC concept
22 p3185 N90-28073
Analysis of the T63-A-700 engine used in alcohol turbine fuel extender test
[DOT/FAA/CT-TN90/18] 23 p3278 N90-28549
Calculation of temperature distribution in various turbine blades using a boundary-fitted coordinate transformation method 23 p3278 N90-28550
Energy Efficient Engine exhaust mixer model technology report addendum; phase 3 test program
[NASA-CR-174799] 23 p3279 N90-28556
Energy Efficient Engine integrated core/low spool design and performance report
[NASA-CR-168211] 23 p3280 N90-28561
Energy Efficient Engine integrated core/low spool test hardware design report
[NASA-CR-168137] 23 p3281 N90-28566
Energy Efficient Engine: High-pressure compressor test hardware detailed design report
[NASA-CR-180850] 23 p3281 N90-28570
Source emission test of gas turbine engine test facility, Kelly AFB, TX
[AD-A223869] 23 p3282 N90-28571
The effects of a compressor rebuild on gas turbine engine performance: Final results
23 p3306 N90-28701
Effect of protective coatings on mechanical properties of superalloys 23 p3308 N90-28707
Evaluation of high temperature protective coatings for gas turbine engines under simulated service conditions
23 p3309 N90-28712
Surface property improvement in titanium alloy gas turbine components through ion implantation
23 p3309 N90-28713
Overview on hot gas tests and molten salt corrosion experiments at the DLR 23 p3309 N90-28714
Recommended practices for measurement of gas path pressures and temperatures for performance assessment of aircraft turbine engines and components
[AGARD-AR-245] 24 p3433 N90-29393

GAS TURBINES
Laser energy conversion 01 p0029 N90-10152
Improved silicon carbide for advanced heat engines
[NASA-CR-180831] 01 p0051 N90-10293
Determination and description of the long term creep behavior of high temperature gas turbine materials
[ETN-89-94985] 03 p0329 N90-11871
Studies of gas turbine heat transfer airfoil surfaces and end-wall cooling effects
[AD-A212451] 04 p0457 N90-12620
AGARD Highlights 89/2 06 p0717 N90-14184
Dispersion strengthening of high temperature niobium alloys
[AD-A213829] 07 p0906 N90-15236
Potential applications of structural ceramic composites in gas turbines
[DE90-001273] 07 p0908 N90-15248
Gas turbine regenerators: A method for selecting the optimum plate-finned surface pair for minimum core volume
[AD-A213430] 07 p0930 N90-15382
Analytical study on the decreasing method of thermal stress for ceramic gas turbines
[DE90-734934] 08 p1051 N90-16078
The use of piezofoil sensors for the determination of the unsteady pressure distribution at the surface of a gas turbine blade 08 p1080 N90-16250
Wake interaction effects on the transition process on turbine blades
[AD-A214492] 09 p1168 N90-16759
The development of a T53-L11 engine computer model
[AD-A214533] 09 p1168 N90-16760
Study of the effect of ceramics gas turbine development
[DE90-702638] 09 p1196 N90-16929
Turbulence structure resulting from interaction between an embedded vortex and wall jet
[AD-A215702] 10 p1383 N90-18004
Investigation of heat transfer with film cooling to a flat plate in a shock tube
[AD-A216379] 10 p1386 N90-18019
Aerodynamic superposition principle in vibrating turbine cascades 11 p1460 N90-18410
Development of ceramic combustor for low BTU gases. Design and basic combustion characteristics
[DE89-782287] 12 p1629 N90-19363
Low cost Brayton engine for gas-fired cogeneration system, phase 1
[PB90-127457] 12 p1681 N90-19655

Elastomer compatibility studies
[BR106069] 17 p2378 N90-23542
Advanced gearbox technology
[NASA-CR-179625] 18 p2498 N90-24274
Effect of vane twist on the performance of dome swirlers for gas turbine airblast atomizers
[NASA-TM-103195] 19 p2688 N90-25289
Measurement of velocity and temperature profiles at the exit plane of a tubular gas turbine combustor
[DE90-505519] 20 p2809 N90-25983
Critical evaluation of Jet-A spray combustion using propane chemical kinetics in gas turbine combustion simulated by KIVA-2
[NASA-TM-103173] 20 p2843 N90-26170
Research and development of advanced gas turbine
[DE90-503377] 20 p2871 N90-26335
Comparison of ground-level test cells and ground-level to altitude test cells 22 p3119 N90-27716
Measurement uncertainty in gas turbine performance determination 22 p3119 N90-27717
Reliability analysis of a structural ceramic combustion chamber
[NASA-TM-103264] 22 p3192 N90-28112
Structural response of SSME turbine blade airfoils 23 p3297 N90-28649
Scale adherence effects in oxidation and sulfidation 23 p3307 N90-28703
Study of power generation systems for CO2 collection: LNG combined cycle
[DE90-507881] 23 p3345 N90-28901
Further studies of turbulence structure resulting from interactions between embedded vortices and wall jets at high blowing ratios
[AD-A223296] 24 p3468 N90-29593

GAS VALVES
Zero-G phase detector and separator
[NASA-CASE-LEW-14844-1] 15 p2101 N90-22024

GAS VISCOSITY
Thermophysical properties of benzene. Part 1: The ideal gas and the saturated liquid and vapour
[ESDU-89002-PT-1] 04 p0470 N90-12693
Interfacial viscosity measurements of adsorbed monolayers on metal surfaces
[AD-A221689] 21 p2979 N90-26931

GAS WELDING
NT BRAZING
NT ULTRASONIC SOLDERING
Reduction of residual stress and distortion in HY100 and HY130 high strength steels during welding
[AD-A213532] 07 p0905 N90-15231
Investigation of weld bead cooling rate during startup of gas metal arc welding
[AD-A223567] 24 p3449 N90-29478

GAS-GAS INTERACTIONS
Canopy stomatal conductance
[DE89-016860] 06 p0809 N90-14711
A new model for hydrogen absorption in welds
[AD-A216951] 12 p1626 N90-19347
The 41st Annual Gaseous Electronics Conference
[AD-A214540] 12 p1715 N90-19851

GAS-ION INTERACTIONS
Termolecular associations of ions in gases, recombination and electron-atom collisions
[AD-A217678] 13 p1883 N90-20805

GAS-LIQUID INTERACTIONS
NT AIR WATER INTERACTIONS
Extended inflation from higher dimensional theories
[NASA-CR-180549] 19 p2796 N90-25916
Relic gravitational waves and extended inflation
[NASA-CR-186469] 24 p3493 N90-29740

GAS-METAL INTERACTIONS
A feasibility study of hydrogen dosage estimation in screw threads submitted to surface electrolytic treatment
[CETIM-110110] 04 p0476 N90-12730
Ultrasonic evaluation of porosity in aluminum cast materials
[AD-A213548] 07 p0905 N90-15232
Mechanisms of the electrochemistry of small organic molecules
[PB90-100785] 08 p1040 N90-16012

GAS-SOLID INTERACTIONS
NT GAS-METAL INTERACTIONS
The structure determination of molecular adsorbates with large unit cells or lattice-gas disorder on metal surfaces
[AD-A210926] 01 p0042 N90-10230
The role of particle collisions in pneumatic transport 01 p0068 N90-10392
Scaling and modeling of turbulent suspension flows 01 p0069 N90-10393
Theoretical investigation of gas-surface interactions
[NASA-CR-185492] 02 p0272 N90-11552
Venus volcanism: Rate estimates from laboratory studies of sulfur gas-solid reactions 03 p0422 N90-12428
Modelling of satellite control thruster plumes 05 p0613 N90-13578
Interfacial and thin film chemistry in electron device fabrication
[AD-A214784] 09 p1289 N90-17473
Development and utilization of new diagnostics for dense-phase pneumatic transport
[DE90-006787] 12 p1659 N90-19536
Molecular dynamics and spectroscopy at gas-solid interfaces
[AD-A217743] 13 p1885 N90-20813
The influence of the gas surface interaction on spacecraft orbital motion 17 p2365 N90-23461
Instrumentation for surface reaction dynamics
[AD-A218608] 17 p2406 N90-23708
High resolution electron energy loss spectroscopy studies of chemisorbed species on metal surfaces
[AD-A222272] 21 p2978 N90-26922
Theoretical investigation of gas-surface interactions
[NASA-CR-186881] 22 p3245 N90-28403

GAS-SOLID INTERFACES
Molecular dynamics and spectroscopy at gas-solid interfaces
[AD-A217743] 13 p1885 N90-20813
Laser studies of chemical dynamics at the gas-solid interface
[DE90-008698] 14 p1986 N90-21380

GASDYNAMIC LASERS
Gasdynamic phenomena in nuclear-reactor-pumped lasers
[DE90-005428] 09 p1229 N90-17131

GASEOUS CAVITATION
U CAVITATION FLOW
U GAS FLOW

GASEOUS DIFFUSION
Quasi-diffusion between phonon and roton gases in two- and three-dimensional liquid helium
[AD-A210565] 02 p0192 N90-11096
Computation of the unsteady facilitated transport of oxygen in hemoglobin
[NASA-TM-102251] 08 p1106 N90-16400
Experimental examination of the development behavior of a gaseous body in a steady state and neutral layer turbulent sheet boundary layer with ground asperity
[ETN-90-96067] 12 p1662 N90-19549
Solar and thermic utilization in high temperature area: Research and development
[ETN-90-96062] 12 p1682 N90-19663
Gas diffusion in a cometary crust 12 p1742 N90-20017
The temperature variation of hydrogen diffusion coefficients in metal alloys
[NASA-TM-100397] 15 p2067 N90-21836
Sticking coefficient of HCl on aerosols 16 p2208 N90-22598
Anthropogenic sources of NO(x), SO(x, CO, and CH4: Geographical distribution
[AERONOMICA-ACTA-A-353-1990] 19 p2713 N90-25440

GASEOUS FUELS
NT NATURAL GAS
Gas identification system using graded temperature sensor and neural net interpretation
[AD-A213359] 05 p0622 N90-13627
Photoconversion of inorganics to methane
[PB89-230643] 06 p0753 N90-14379
The conversion of carbonaceous materials to clean carbon and co-product gaseous fuel
[DE90-001561] 06 p0754 N90-14387
Externally vaporizing system for turbine combustor
[AD-D014284] 08 p1024 N90-15918
Production of jet fuels from coal derived liquids. Volume 10: Jet fuels production by-products, utility, and sulfur emissions control integration study
[AD-A213872] 09 p1200 N90-16951
Testing of an advanced thermochemical conversion reactor system
[DE90-007989] 15 p2123 N90-22141
Advanced fuel properties, phase 1
[AD-A219788] 19 p2679 N90-25236

GASEOUS ROCKET PROPELLANTS
Low frequency and high frequency combustion oscillation phenomena inside a rocket combustion chamber fed by liquid or gaseous propellants 01 p0036 N90-10197
Catalytic ignition of hydrogen/oxygen 23 p3293 N90-28627

GASES
NT AIR
NT AMMONIA
NT ARGON
NT CARBON DIOXIDE
NT CARBON MONOXIDE
NT COLD GAS
NT COMPRESSED AIR
NT COMPRESSED GAS
NT COSMIC GASES
NT DETONABLE GAS MIXTURES
NT DEUTERIUM
NT DISSOLVED GASES
NT EXHAUST GASES
NT FLAMMABLE GASES
NT GAS MIXTURES
NT GAS STREAMS
NT GASEOUS FUELS
NT HELIUM
NT HELIUM ISOTOPES
NT HIGH PRESSURE OXYGEN
NT HIGH TEMPERATURE AIR
NT HIGH TEMPERATURE GASES
NT HYDROGEN
NT HYDROGEN ISOTOPES
NT IDEAL GAS
NT INTERSTELLAR GAS
NT IONIZED GASES
NT KRYPTON
NT KRYPTON ISOTOPES
NT KRYPTON 85
NT LIQUEFIED GASES
NT LIQUID HELIUM
NT LIQUID HELIUM 2
NT LIQUID HYDROGEN
NT LIQUID NITROGEN
NT LIQUID OXYGEN
NT MOLECULAR GASES
NT NATURAL GAS
NT NEON
NT NEUTRAL GASES
NT NITROGEN
NT NONCONDENSABLE GASES
NT OXYGEN
NT OXYGEN ISOTOPES
NT OXYGEN 18
NT OZONE
NT RADON
NT RADON ISOTOPES
NT RARE GASES
NT RAREFIED GASES
NT REAL GASES
NT SOLID CRYOGENS
NT SOLIDIFIED GASES
NT TRITIUM
NT XENON
Boost-phase discrimination research activities
[NASA-TM-101889] 01 p0032 N90-10176
Reactive ion etching of SiC thin films by mixtures of fluorinated gases and oxygen
[AD-A211046] 02 p0195 N90-11113
Non-stationary computer model of the asymptotic region of an electric arc gas heater
[IPPCZ-288] 03 p0407 N90-12330
Continuing studies of liquid propellant drops in hot, high-pressure environments
[AD-A212265] 04 p0482 N90-12765
Development of a low noise 10 K J-T refrigeration system
[AD-A213347] 04 p0484 N90-12779
Space station gas compressor technology study program, phase 1
[NASA-CR-183758] 05 p0601 N90-13491
High-frequency ventilation in dogs with three gases of different densities
[AD-A212862] 06 p0819 N90-14762
Gas-liquid-liquid equilibria in mixtures of water, light gases, and hydrocarbons
[DE90-003180] 07 p0894 N90-15167
Gas optics applicable to free electron laser technology
[AD-A214285] 07 p0993 N90-15741
Using inorganic membranes to separate gases: R and D status review
[DE90-004386] 08 p1042 N90-16019
Improved anode catalysts for coal gas-fueled phosphoric acid fuel cells
[DE90-004016] 08 p1096 N90-16347
Kosterlitz-Thouless phase transition in two-dimensional hierarchical Coulomb gases
[DE89-618399] 09 p1189 N90-16890
System for venting gas from a liquid storage tank
[NASA-CASE-MSC-21253-1] 13 p1787 N90-20254
Numerical modelling of shocks in gases and metals
[AD-A218586] 17 p2402 N90-23684
Applications of low temperature CO-oxidation catalysts to breathable gases 18 p2561 N90-24615
Time-resolved swarm studies in gases with emphasis on electron detachment and ion conversion
[ISBN-90-9003013-1] 18 p2613 N90-24883
A lattice gas model for thermohydrodynamics
[DE90-011964] 20 p2933 N90-26690
Laboratory studies of the interaction of ions with condensed gases: Planetary applications 20 p2949 N90-26778
The effect of impurity gasses on variable polarity plasma arc welded 2219 aluminum
[NASA-CR-183803] 21 p2980 N90-26935

Thermochemical data for silicon-containing species from ab initio electronic structure calculations
[DE90-011024] 24 p3446 N90-29463

GASIFICATION
NT COAL GASIFICATION
Production of jet fuels from coal-derived liquids. Volume 11: Production of advanced endothermic fuel blends from Great Plains Gasification Plant naphtha by-product stream
[AD-A210251] 02 p0207 N90-11184
Testing carbon fabric for oxidation mass loss 15 p2063 N90-21819

GASKETS
Improvement of rules relating to clamp calculations
[CETIM-110610] 04 p0509 N90-12939
A study of the vibrational transmission through flanged joints
[ISVR-TR-181] 11 p1520 N90-18755

GASOLINE
MOBILE4 oxygenated fuels version user's guide
[PB89-230700] 05 p0629 N90-13674
US Army Methanol-Fueled Administrative Vehicle Demonstration Program
[AD-A216013] 10 p1393 N90-18054
CRC low- and intermediate-temperature driveability program using gasoline-alcohol blends
[AD-A221321] 18 p2533 N90-24453

GASP
U GLOBAL AIR SAMPLING PROGRAM

GASTROINTESTINAL SYSTEM
NT INTESTINES

GATES (CIRCUITS)
NT THRESHOLD GATES
The effects of normal annealing cycles during IGFET fabrication on initial and radiation induced gate insulator defects
[AD-A210282] 01 p0049 N90-10278
DDN Trusted Guard Gateway: Trusted Guard Gateway (TGG) technology assessment, phase 2
[AD-A210248] 01 p0108 N90-10614
Bias and oxide thickness dependence of trapped charge buildup in MOS devices
[AD-A210264] 01 p0131 N90-10757
A single-phase clocked NOR/NOR CMOS programmable sequential array structure
[AD-A211297] 03 p0387 N90-12203
GaAs gate dynamic memory technology
[AD-A212387] 04 p0560 N90-13266
A counter gating circuit for acoustic emission monitoring of structures cracking under repetitive alternating loads
[ARL-MAT-TM-398] 05 p0653 N90-13808
Method of making self-aligned GaAs/AlGaAs FET's
[AD-D014229] 06 p0849 N90-14935
Integration of a gated microchannel plate detector into the Nova laser system
[DE90-002981] 07 p0935 N90-15413
Modeling the gate I/V characteristic of a GaAs MESFET for Volterra-series analysis
[AD-A215314] 09 p1212 N90-17030
Finite element modeling and thermal simulations of transistor integrated circuits
[AD-A215928] 10 p1380 N90-17997
An overview of radiation-induced interface traps in MOS (Metal-Oxide Semiconductor) structures
[AD-A216101] 10 p1438 N90-18299
A gate array structure for the efficient project of digital circuits: The unit cell array
[ETN-90-95364] 12 p1653 N90-19502
Structured NC
[RUU-CS-89-6] 17 p2452 N90-23989

GAUGE INVARIANCE
D=3 Chern-Simons action, supergravity and quantization
[DE89-617530] 01 p0134 N90-10775
Gauge invariant cosmological perturbations with cold dark matter
[DE89-790940] 02 p0295 N90-11679
Two dimensional conformal supergravity and critical behavior
[DE89-611968] 03 p0420 N90-12414
Multigrid Monte Carlo in an external U(1) gauge field
[NIKHEF-ITFA-88-52] 04 p0538 N90-13114
Chern-Simons theories of symplectic super-diffeomorphisms
[DE89-635700] 07 p0987 N90-15703
Nonlocality and stochastic quantization of field theory
[DE89-633913] 07 p1007 N90-15833
Universe as a topological defect in a higher-dimensional Einstein-Yang-Mills theory
[DE90-719507] 08 p1135 N90-16578
Superstring field theory
[DE90-007694] 13 p1899 N90-20897
Quantization of the N = 2m simple supergravity in d = 2 + 1
[DE90-612765] 14 p2034 N90-21671
Some global problems in gauge theories (variations on a theme of Aharonov and Bohm)
[DE90-009034] 14 p2035 N90-21678

GAUGE THEORY
Quantization of anomalous gauge theories on a lattice
[DE89-010247] 01 p0135 N90-10776
Lattice fields and strong interactions
[DE89-015099] 01 p0135 N90-10777
Homogeneous gravitational fields and limits of gravitational fields 01 p0141 N90-10812
Twistons
[RSRE-MEMO-4234] 04 p0562 N90-13275
Hamiltonian flows, SU(infinity), SO(infinity), USp(infinity), and strings
[DE90-001987] 06 p0835 N90-14851
Designing machines for lattice physics and algorithm investigation
[DE90-003543] 07 p0969 N90-15596
Chern-Simons theories of symplectic super-diffeomorphisms
[DE89-635700] 07 p0987 N90-15703
Abelian gauge theory in topologically non-trivial space
[DE90-710100] 07 p1007 N90-15830
The off-shell closed strings as the topological open membranes: Dynamical transmutation of world sheet dimension
[DE89-635721] 08 p1134 N90-16571
N=2 supergravity in superspace and the BRS symmetry
[DE90-607062] 10 p1439 N90-18305
Research accomplishments and future goals in particle physics
[DE90-007296] 12 p1712 N90-19830
Cosmic string in compactified gauge theory
[DE90-741463] 12 p1738 N90-19988
Chern-Simons superconductivity at finite temperature
[DE90-613393] 14 p2031 N90-21650
Studies in quantum field theory
[DE90-008731] 14 p2035 N90-21677
Some global problems in gauge theories (variations on a theme of Aharonov and Bohm)
[DE90-009034] 14 p2035 N90-21678
Applications of gauge theories to enhance numerical solutions of mixed potential integral equations
[AD-A221520] 21 p3065 N90-27424
Introduction to gauge theories and unification
[DE90-014473] 23 p3402 N90-29225
Higher loop contributions to effective potential of gauge theory at high temperature
[DE90-627208] 23 p3403 N90-29231
Effective actions for bosonic topological defects
[NASA-CR-187271] 24 p3544 N90-30041

GAUSS EQUATION
The fast Gauss transform
[AD-A211287] 02 p0266 N90-11517
A multigrid method for the Navier-Stokes and Boussinesq equations
[REPT-89-17] 04 p0501 N90-12886
Approximations to joint distributions of definite quadratic forms
[AD-A216434] 11 p1551 N90-18930
Local moduli of continuity of some classes of Gaussian processes
[AD-A217692] 13 p1879 N90-20778
Two barriers problem for continuously differentiable processes
[AD-A218564] 16 p2312 N90-23176
Gaussons and states with gaussian Wigner functions are quasi-free states
[DE90-628370] 24 p3556 N90-30121

GAUSS FUNCTION
U GAUSS EQUATION

GAUSS-MARKOV THEOREM
Stochastics realization problems
[CWI-BS-R8920] 17 p2467 N90-24097
Further experiments in variable frame rate analysis for speech recognition
[RSRE-MEMO-4336] 22 p3165 N90-27951
Triphone clustering in the ARM system
[RSRE-MEMO-4357] 22 p3166 N90-27952
Experiments with grand variance in the ARM continuous speech recognition system
[RSRE-MEMO-4359] 22 p3166 N90-27954

GAUSSIAN DISTRIBUTIONS
U NORMAL DENSITY FUNCTIONS

GAUSSIAN ELIMINATION
Efficient computer algebra algorithms for polynomial matrices in control design 16 p2285 N90-23022
Integral and series representation of infinitely divisible processes with applications to their prediction and to their sample path, statistical, and structural properties
[AD-A219625] 17 p2456 N90-24017

GAUSSIAN NOISE
U RANDOM NOISE

GAUSSMETERS
U MAGNETOMETERS

GC-130 AIRCRAFT
U C-130 AIRCRAFT

GCR (REACTORS)
U GAS COOLED REACTORS

GDOP
U GEOMETRIC DILUTION OF PRECISION

GEAR TEETH
Two stage gear tooth dynamics program
[NASA-CR-185110] 01 p0077 N90-10437
Generation and tooth contact analysis of spiral bevel gears with predesigned parabolic functions of transmission errors
[NASA-CR-4259] 03 p0355 N90-12033
Conjugate profiles on mating gear teeth
[MEMO-COSOR-89-01] 05 p0651 N90-13795
Gear noise, vibration, and diagnostic studies at NASA Lewis Research Center
[NASA-TM-102435] 10 p1390 N90-18041
Theory of gearing
[NASA-RP-1212] 12 p1670 N90-19593
A review of gear housing dynamics and acoustics literature
[NASA-CR-185148] 14 p1987 N90-21387
Calculating the time domain average of gear vibration data sampled at less than the Nyquist frequency
[OUEL-1768/89] 15 p2107 N90-22052
Computerized inspection of gear tooth surfaces
[NASA-TM-102395] 15 p2107 N90-22054
Surface pitting fatigue life of noninvolute, low-contact-ratio gears
[NASA-TM-103116] 16 p2242 N90-22790
The curvature of conjugate profiles in points of contract
[MEMO-COSOR-89-18] 16 p2243 N90-22795
Influence of linear profile modification and loading conditions on the dynamic tooth load and stress of high contact ratio gears
[NASA-TM-103136] 16 p2243 N90-22796
Non-linear dynamic analysis of geared systems, part 2
[NASA-CR-180495] 17 p2410 N90-23732
Prediction of gear tooth separation in single-stage gear systems, using numerical techniques
[AD-A220442] 17 p2412 N90-23744
Computer simulation of gear tooth manufacturing processes
[NASA-CR-185200] 20 p2843 N90-26171
Dynamics of multistage gear transmission with effects of gearbox vibrations
[NASA-TM-103109] 22 p3182 N90-28060
Computer-aided design of high-contact-ratio gears for minimum dynamic load and stress
[NASA-TM-103275] 22 p3183 N90-28065

GEARS
An expert system for optimal gear design 01 p0077 N90-10439
Independent Orbiter Assessment (IOA): Weibull analysis report
[NASA-CR-185534] 02 p0168 N90-10948
Generation and tooth contact analysis of spiral bevel gears with predesigned parabolic functions of transmission errors
[NASA-CR-4259] 03 p0355 N90-12033
RAN (Royal Australian Navy) vibration analysis system operator's guide
[AD-A212441] 04 p0453 N90-12596
Demonstration epicyclic gearbox
[PNR90567] 04 p0508 N90-12932
Non linear vibrations in a drive train when coupled to constant torque and constant power loads
[PNR90593] 04 p0508 N90-12934
Vibration transmission through rolling element bearings in geared rotor system, part 1
[NASA-CR-186093] 04 p0509 N90-12936
An investigation of gear mesh failure prediction techniques
[NASA-TM-102340] 05 p0649 N90-13785
Assessment of worm gearing for helicopter transmissions
[NASA-TM-102441] 08 p1025 N90-15923
Continuously variable gear drive transmission
[AD-D014268] 08 p1084 N90-16275
Dynamic analysis of geared rotors by finite elements
[NASA-TM-102349] 08 p1086 N90-16286
Film thickness in lubricated Hertzian contacts. Part 2: Point contacts
[ESDU-89045] 09 p1232 N90-17148
Gear noise, vibration, and diagnostic studies at NASA Lewis Research Center
[NASA-TM-102435] 10 p1390 N90-18041
Life of concentrated contacts in the mixed EHD and boundary film regimes
[AD-A216673] 11 p1517 N90-18738
Theory of gearing
[NASA-RP-1212] 12 p1670 N90-19593
Bearing and gear steels for aerospace applications
[NASA-TM-102529] 13 p1809 N90-20391

Heat engine based on shape memory alloys
[AD-D014400] 14 p1986 N90-21385
A review of gear housing dynamics and acoustics literature
[NASA-CR-185148] 14 p1987 N90-21387
Transmission research activities at NASA Lewis Research Center
[NASA-TM-103132] 14 p1988 N90-21394
Surface pitting fatigue life of noninvolute, low-contact-ratio gears
[NASA-TM-103116] 16 p2242 N90-22790
The curvature of conjugate profiles in points of contract
[MEMO-COSOR-89-18] 16 p2243 N90-22795
Wearing of cryomechanisms at 4 K
[REPT-892-440-103] 17 p2473 N90-24139
Advanced gearbox technology
[NASA-CR-179625] 18 p2498 N90-24274
Computer simulation of gear tooth manufacturing processes
[NASA-CR-185200] 20 p2843 N90-26171
Dynamics of multistage gear transmission with effects of gearbox vibrations
[NASA-TM-103109] 22 p3182 N90-28060
The effects of gear reduction on robot dynamics
24 p3513 N90-29861

GEL PERMEATION CHROMATOGRAPHY
U LIQUID CHROMATOGRAPHY

GELATION
A graph-theoretical approach to block-copolymer complexes. Part 3: Loops and cycles
[MEMO-778-PT-3] 04 p0479 N90-12750

GELLED PROPELLANTS
NT GELLED ROCKET PROPELLANTS

GELLED ROCKET PROPELLANTS
Gelled propellant flow: Boundary layer theory for power-law fluids in a converging planar channel
[DE90-000923] 07 p0927 N90-15365

GELS
NT DOUBLE BASE ROCKET PROPELLANTS
NT SILICA GEL
Applications of NMR spectroscopy to the study of zeolite synthesis
[DE89-015226] 02 p0192 N90-11095
Fifth International Workshop on Glasses and Ceramics from Gels
[DE89-016899] 02 p0201 N90-11147
Bonding aerogels with polyurethanes
[DE90-003050] 07 p0910 N90-15258
Wet spinning of solid polyamic acid fibers
[NASA-CASE-LAR-14162-1] 07 p0910 N90-15259
Crosslinked, flexible, low-molecular-weight polyacrylamide gels for mobility control
[DE90-000202] 07 p0913 N90-15260
Evaluation of a new charge algorithm for a lead-acid battery with gelled electrolyte using a 96V gel cell 4 as a test battery
[DE90-003420] 08 p1061 N90-16133
Development of low density silica aerogel as a capture medium for hyper-velocity particles
[NASA-CR-185930] 08 p1121 N90-16489
Structure and properties of resorcinol-formaldehyde gels
[DE90-005201] 10 p1358 N90-17876
Fractal structure and fractal time in silica sol-gels
[DE90-013197] 20 p2838 N90-26144
Interaction of electromagnetic fields with chondrocytes in gel culture
[AD-A223397] 24 p3497 N90-29765

GENE EXPRESSION
Genetic engineering of enhanced microbial nitrification
[PB89-208334] 03 p0378 N90-12155
Breeding of hydrogen producing anaerobic bacteria. Cellulase secretion from transformed Escherichia coli JM109
[DE90-710739] 10 p1410 N90-18133

GENE REGULATION
U GENE EXPRESSION

GENERAL AVIATION AIRCRAFT
NT DHC 2 AIRCRAFT
The spinning of aircraft: A discussion of spin prediction techniques including a chronological bibliography
[ARL-AERO-R-177] 02 p0155 N90-10888
Census of US civil aircraft
[PB90-120296] 14 p1905 N90-20920
Annual review of aircraft accident data: US general aviation calendar year 1987
[PB90-138066] 14 p1913 N90-20966
The Federal Aviation Administration plan for research, engineering and development. Volume 1: Program plan
[AD-A221263] 19 p2800 N90-25930
The Federal Aviation Administration plan for research, engineering and development. Volume 2: Project descriptions
[AD-A221264] 19 p2800 N90-25931
BASEOPS default profiles for civil aircraft
[AD-A223161] 21 p2959 N90-26825
Annual review of aircraft accident data: US general aviation, calender year 1987
[PB90-138066] 22 p3110 N90-27666
Public-sector aviation issues, 1987 to 1988 graduate research award papers
[PB90-191206] 22 p3110 N90-27667
A review of research and development in crashworthiness of general aviation aircraft: Seats, restraints and floor structures
[AD-A221557] 22 p3115 N90-27698

GENERAL CIRCULATION MODELS (ATMOSPHERIC)
U ATMOSPHERIC GENERAL CIRCULATION MODELS

GENERAL DYNAMICS AIRCRAFT
NT B-58 AIRCRAFT
NT F-111 AIRCRAFT

GENERAL DYNAMICS MILITARY AIRCRAFT
U MILITARY AIRCRAFT

GENERATORS
Back swing phenomenon of synchronous generator. Study on ac-dc power system simulator tests
[DE89-782321] 11 p1500 N90-18635
A digitally controlled system for effecting and presenting a selected electrical resistance
[NASA-CASE-MFS-29149-1] 12 p1652 N90-19492

GENES
Genetic engineering of enhanced microbial nitrification
[PB89-208334] 03 p0378 N90-12155
Biological and biochemical methane reactions
[PB89-232615] 04 p0516 N90-12977
Nomenclature for physical mapping of complex genomes
[DE89-015173] 06 p0859 N90-14994

GENETIC CODE
The chemical basis for the origin of the genetic code and the process of protein synthesis
[NASA-CR-186590] 15 p2136 N90-22205

GENETIC ENGINEERING
Genetic engineering of single-domain magnetic particles
[AD-A210332] 01 p0091 N90-10521
Molecular biology and physiology of methanogenic archaebacteria
[AD-A210399] 01 p0091 N90-10522
Genetic engineering of enhanced microbial nitrification
[PB89-208334] 03 p0378 N90-12155
Breeding of hydrogen producing anaerobic bacteria. Cellulase secretion from transformed Escherichia coli JM109
[DE90-710739] 10 p1410 N90-18133
Human serum albumin crystals and method of preparation
[NASA-CASE-MFS-28234-1] 13 p1850 N90-20616
Artificial life: The coming evolution
[DE90-008860] 14 p2009 N90-21515
Understanding our genetic inheritance. The US Human genome project: The first five years, FY 1991-1995
[DE90-008240] 18 p2584 N90-24718
Engineering and the advancement of human welfare. Ten outstanding achievements 1964-1989
[ISBN-0-309-04185-6] 23 p3415 N90-29297

GENETICS
Molecular biology and physiology of methanogenic archaebacteria
[AD-A210399] 01 p0091 N90-10522
USSR Space Life Sciences Digest, issue 22
[NASA-CR-3922(26)] 03 p0378 N90-12153
Genetic engineering of enhanced microbial nitrification
[PB89-208334] 03 p0378 N90-12155
Life sciences: Lawrence Berkeley Laboratory, 1988
[DE90-008061] 13 p1849 N90-20611
Artificial life: The coming evolution
[DE90-008860] 14 p2009 N90-21515
Understanding our genetic inheritance. The US Human genome project: The first five years, FY 1991-1995
[DE90-008240] 18 p2584 N90-24718
Photosynthesis in intact plants
[DE90-013699] 20 p2898 N90-26482
Computer simulation of chemical reactions in synthetic model compounds and genetically engineered active sites
[AD-A222611] 20 p2898 N90-26483
Japanese molecular biology 1990: An update
[PB90-188707] 23 p3354 N90-28958

GENITOURINARY SYSTEM
NT BLADDER
NT TESTES

GEO ENVIRONMENTS
U EARTH ORBITAL ENVIRONMENTS

GEOASTROPHYSICS
U ASTROPHYSICS
U GEOPHYSICS

GEOBOTANY
Geobotanical remote sensing: A review
[INPE-5026-PRE/1565] 14 p1996 N90-21440

GEOCHEMISTRY
NT BIOGEOCHEMISTRY
Institute of Geophysics and Planetary Physics, 1988
[DE89-014363] 01 p0137 N90-10794
Summaries of the thematic conferences on remote sensing for exploration geology
[NASA-CR-185321] 05 p0664 N90-13880
Earth Sciences Division annual report 1988
[DE90-002617] 06 p0801 N90-14663
Organic geochemical and tectonic evolution of the midcontinent rift system: Organic geochemistry and micropaleontology
[DE89-017561] 06 p0818 N90-14760
Summaries of physical research in the geosciences
[DE90-004993] 08 p1090 N90-16309
Application of natural isotopes in groundwater for solving environmental problems
[DE90-000223] 12 p1689 N90-19703
Geochemical survey on faults overland with alluvial deposits, part 1. Application for the Neodani and the Atera faults survey
[DE89-782326] 12 p1690 N90-19707
Electrochemical phase diagrams for aqueous redox systems
[AD-A217168] 13 p1770 N90-20157
The trace metal geochemistry of suspended oceanic particulate matter
[AD-A218604] 17 p2429 N90-23839
The biogeochemistry of metal cycling
[NASA-CR-4295] 17 p2439 N90-23897
Heat and fluid flow within the Earth's crust: In situ measurements and mathematical models
18 p2579 N90-24690
Proceedings of a workshop on Lunar Volcanic Glasses: Scientific and Resource Potential
[NASA-CR-186631] 20 p2888 N90-26437
Geochemistry and origin of regional dolomites
[DE90-012589] 21 p3024 N90-27196
Geologic studies in Alaska by the US geological survey, 1988
[PB90-180993] 22 p3211 N90-28213

GEOCHRONOLOGY
Fluctuation history of Great Salt Lake, Utah, during the last 13,000 years, part 2
[NASA-CR-185911] 01 p0082 N90-10466
Three ages of Venus 03 p0428 N90-12453
Age constraints for the present fault configuration in the Imperial Valley, California: Evidence for northwestward propagation of the Gulf of California rift system
[NASA-CR-186541] 14 p2006 N90-21493
The 5th International symposium on palaeolimnology
[AD-A219244] 20 p2887 N90-26431

GEOCORONAL EMISSIONS
Interzodiak 2: Observation of EUV-resonance radiation
05 p0660 N90-13854

GEODESIC LINES
Local structure of a 2-codimensional conformally flat submanifold in an Euclidean space R(sup n+2)
[DE89-618379] 02 p0264 N90-11501
Jacobi functions as limit cases of q-ultraspherical polynomials
[CWI-PM-R8807] 04 p0541 N90-13139
On geometry of inhomogeneous Heisenberg ferromagnet: Nonintegrable case
[MEMO-789] 05 p0691 N90-14030
A (2+1)-dimensional pure gravity for an arbitrary closed initial surface
[DE90-701754] 07 p1007 N90-15829
Measurement and analysis of the electromagnetic scattering of a geodesic array of triangular trihedral corner reflectors
[AD-A220457] 17 p2389 N90-23608
On an isospectrality question over compact Riemann surfaces
[DE90-627163] 23 p3390 N90-29147
Dirac's equation as a geodesic in Riemann space
[DE90-627194] 23 p3390 N90-29152
On the relation between the absolute parallelism spaces and spaces having a GL(4) connection
[DE90-627222] 23 p3403 N90-29232

GEODESY
Nonlinear adjustment with or without constraints, applicable to geodetic models
[AD-A210820] 02 p0265 N90-11509
Time and frequency in geodesy measuring methods
[SER-C-337] 03 p0365 N90-12087
Geodetic point positioning with GPS (Global Positioning System) carrier beat phase data from the CASA UNO experiment
[AD-A211955] 04 p0514 N90-12970
Correction of ionospheric effects for the precise orbit determination of satellites 06 p0762 N90-14432
NORDA's pattern analysis laboratory: Current contributions to naval mapping, charting, and geodesy
[AD-A212731] 06 p0801 N90-14665

Superconducting gravity gradiometer mission. Volume 1: Study team executive summary
|NASA-TM-4091-VOL-1| 07 p0959 N90-15545
Integrated geodetic network analysis with stochastic prior information about the gravity field and reference ellipsoid
|SER-C-351| 08 p1091 N90-16317
Focal research effort points of the Institute of Applied Geodesy in the field of digital image processing 08 p1094 N90-16333
Feasibility of millimeter-accuracy geodetic positioning and vehicle tracking with repeater satellites
|AD-A214755| 09 p1182 N90-16854
Charting and Geodetic Services
|PB90-116674| 09 p1240 N90-17196
Enhanced satellite geodesy through the addition of a pseudorange observable
|AD-A214987| 09 p1241 N90-17200
Highly accurate navigation: Integration of navigation and geodesic methods
|SFB-228| 12 p1602 N90-19221
Committee on Geodesy - National Research Council
|AD-A217770| 13 p1821 N90-20452
Gravitational model improvement at the Goddard Space Flight Center 13 p1831 N90-20514
An improved model for the Earth's gravity field 13 p1832 N90-20515
Precise solution for a finite set of spherical coefficients from equiangular gridded data 13 p1833 N90-20522
The Rapid Geodetic Survey System (RGSS) 13 p1834 N90-20528
First year's results and field experience with the latest JILA absolute gravimeter 13 p1834 N90-20529
The role of topography in geodetic gravity field modelling 13 p1835 N90-20534
Performance of FFT methods in local gravity field modelling 13 p1835 N90-20537
Thin-plate spline quadrature of geodetic integrals 13 p1836 N90-20539
Treatment of geodetic leveling in the integrated geodesy approach 13 p1837 N90-20546
Geodynamics and temporal variations in the gravity field 13 p1838 N90-20549
Guidelines, operational procedures, and quality control for the estimation of geodetic point positions from GPS data collected with the TI4100 receiver
|AD-A218460| 16 p2250 N90-22829
The DORIS system 17 p2359 N90-23431
Predicting tidal displacements of the surface of the Earth, volume 1
|ETN-90-96690| 17 p2431 N90-23850
Predicting tidal displacements of the surface of the Earth, volume 2
|ETN-90-96691| 17 p2431 N90-23851
Solid Earth, gravity field and environment 19 p2708 N90-25412
The development of the July 1989 1 deg x 1 deg and 30' x 30' terrestrial mean free-air anomaly data bases
|NASA-CR-186475| 19 p2713 N90-25441
The determination of the orbit of the Japanese satellite Ajisai and the GEM-T1 and GEM-T2 gravity field models
|NASA-TM-100763| 19 p2714 N90-25443
The global positioning system: A new tool for tectonic studies 21 p3014 N90-27137
Observation model and parameter partials for the JPL geodetic (GPS) modeling software 'GPSOMC'
|NASA-CR-186972| 22 p3132 N90-27774
The National Geodetic Survey absolute gravity program
|PB90-156951| 22 p3211 N90-28212
On an isospectrality question over compact Riemann surfaces
|DE90-627163| 23 p3390 N90-29147

GEODETIC ACCURACY
Time and frequency in geodesy measuring methods
|SER-C-337| 03 p0365 N90-12087
Regional height determination using gravimetric and topographical data
|UH-156| 08 p1091 N90-16315
Enhanced satellite geodesy through the addition of a pseudorange observable
|AD-A214987| 09 p1241 N90-17200
Earth model selection for computer simulations
|AD-A216843| 11 p1525 N90-18779
Ambiguity bootstrapping to determine GPS orbits and baselines
|AD-A218206| 14 p1931 N90-21052
Subsystem TM Precision: Progress and perspective
|INPE-5006-PRE/1563| 14 p2000 N90-21461
The GPS-NAVSTAR location and navigation system 17 p2359 N90-23433
Geophysical studies related to geodetic reference frames
|AD-A220249| 18 p2574 N90-24663

GEODETIC COORDINATES
Dynamic analysis of the geodetic networks originating from the Navstar/Global Positioning System (GPS) satellites
|SER-C-346| 08 p1091 N90-16316
Applications of the GPS in photogrammetry
|ETN-90-96004| 12 p1680 N90-19648
Guidelines, operational procedures, and quality control for the estimation of geodetic point positions from GPS data collected with the TI4100 receiver
|AD-A218460| 16 p2250 N90-22829

GEODETIC SATELLITES
NT GEOS 1 SATELLITE
NT GEOS 2 SATELLITE
NT GEOSAT SATELLITES
Feasibility of millimeter-accuracy geodetic positioning and vehicle tracking with repeater satellites
|AD-A214755| 09 p1182 N90-16854
Satellite orbit determination and gravity field recovery from satellite-to-satellite tracking
|LR-605| 19 p2663 N90-25157
The determination of the orbit of the Japanese satellite Ajisai and the GEM-T1 and GEM-T2 gravity field models
|NASA-TM-100763| 19 p2714 N90-25443

GEODETIC SURVEYS
Charting and Geodetic Services
|PB90-116674| 09 p1240 N90-17196
Guidelines, operational procedures, and quality control for the estimation of geodetic point positions from GPS data collected with the TI4100 receiver
|AD-A218460| 16 p2250 N90-22829
Determination of the gravity disturbance by processing the gravity gradiometer surveying system: Processing procedure and results
|AD-A219992| 17 p2423 N90-23808
A survey of equatorial magnetospheric wave activity between 5 and 8 R(sub E)
|AD-A220137| 17 p2424 N90-23812
Solid Earth, gravity field and environment 19 p2708 N90-25412
The National Geodetic Survey absolute gravity program
|PB90-156951| 22 p3211 N90-28212

GEODYNAMICS
Dynamics of mid-ocean ridge systems 07 p0965 N90-15575
The interpretation of crustal dynamics data in terms of plate interactions and active tectonics of the Anatolian plate and surrounding regions in the Middle East
|NASA-CR-186200| 11 p1533 N90-18824
Progress in the Determination of the Earth's Gravity Field
|NASA-CR-185721| 13 p1831 N90-20513
Geodynamics and temporal variations in the gravity field 13 p1838 N90-20549
Age constraints for the present fault configuration in the Imperial Valley, California: Evidence for northwestward propagation of the Gulf of California rift system
|NASA-CR-186541| 14 p2006 N90-21493
NSSDC data listing
|NASA-TM-102989| 15 p2180 N90-22456
Lidar instruments proposed for Eos 21 p3016 N90-27145
Use of geomagnetic data for studies on the Earth's deep interior 21 p3023 N90-27192
NASA geodynamics program: Bibliography
|NASA-TM-4220| 22 p3194 N90-28123

GEOFRACTURES
U GEOLOGICAL FAULTS

GEOGRAPHIC APPLICATIONS PROGRAM
Investigation of the backscatter behavior of selected test areas in two geocoded SEASAT-SAR scenes in greater Bonn (Fed. Republic of Germany) 08 p1094 N90-16331

GEOGRAPHIC INFORMATION SYSTEMS
GRASS/GIS (Geographic Resources Analysis Support System/Geographic Information System) implementation guide
|AD-A214623| 09 p1296 N90-17510
A Geographic Information System (GIS) for the southern Louisiana deltaic environments
|AD-A214676| 09 p1296 N90-17511
Land suitability maps and appropriate land use: An approach using SGI and satellite imagery
|INPE-4827-PRE/1458| 11 p1521 N90-18761
Perspective revision of systematic mapping through orbital imagery
|INPE-4817-PRE/1453| 11 p1524 N90-18775
Thematic coupling between digital images and geographic information systems
|ETN-90-95723| 12 p1679 N90-19646
The mesoscale meteorological model MM4 and its modifications for EURAD 12 p1686 N90-19682
Visibility problems in numerical models of terrain
|INPE-4921-TDL/382| 12 p1726 N90-19919
Analysis and modelling of spatial data proposal of a system for CBERS
|INPE-4911-PRE/1512| 14 p1997 N90-21445
Generation of triangular form models in a microcomputer environment
|INPE-4974-PRE/1539| 14 p1997 N90-21447
Geographic information system: Coded data of agrocattle-raising projects in the Amazon
|INPE-4978-PRE/1543| 15 p2180 N90-22457
Multisensor monitoring of deforestation in the Guinea Highlands of West Africa
|NASA-CR-186709| 19 p2706 N90-25396
Practical applications of remote sensing technology
|NASA-CR-186810| 20 p2879 N90-26377
Hierarchical structure of polygonal data for spatial analysis and representation of cartographical data
|INPE-4986-PRE/1548| 20 p2879 N90-26380
Multiband imaging systems
|AD-A223969| 23 p3343 N90-28893
INPE geographic data base
|INPE-4636-PRE/1348| 23 p3407 N90-29253

GEOGRAPHY
NT OROGRAPHY
Integrated computer-based tools to facilitate environmental monitoring, assessment, and restoration
|DE90-002732| 06 p0811 N90-14717
Paper on geography in environmental management: Research and new techniques
|INPE-4840-PRE/1469| 11 p1531 N90-18816

GEOIDS
Evolution of midplate hotspot swells: Numerical solutions
|NASA-CR-186462| 12 p1691 N90-19713
Progress in the Determination of the Earth's Gravity Field
|NASA-CR-185721| 13 p1831 N90-20513
Progress in the development of high degree potential coefficient models 13 p1832 N90-20516
Geopotential models in the Australian region 13 p1832 N90-20519
FFT-local gravimetric geoid computation 13 p1835 N90-20536
The reduction correction in North America 13 p1836 N90-20540
The geoid in Kenya 13 p1836 N90-20542
GEOID '88: A gravimetric geoid for Canada 13 p1837 N90-20543
Long range geoid control through the European GPS traverse: Final results 13 p1837 N90-20545
A model of the general ocean circulation determined from a joint solution for the Earth's gravity field 13 p1838 N90-20550
Analysis of altimetry over inland seas
|NASA-TM-100729| 13 p1840 N90-20566
The integration of GPS heights into the Australian height datum 19 p2705 N90-25392

GEOLOGICAL FAULTS
NT SAN ANDREAS FAULT
Fracture mechanics of porous materials
|DE90-000023| 06 p0800 N90-14657
Organic geochemical and tectonic evolution of the midcontinent rift system: Organic geochemistry and micropaleontology
|DE89-017561| 06 p0818 N90-14760
Dynamics of mid-ocean ridge systems 07 p0965 N90-15575
Segmentation of topographic profiles of the seafloor based on a self-affine model
|AD-A215938| 10 p1410 N90-18132
Fracture analysis through photographic imagery of low spatial resolution: A contribution to the study of tectonic evoluation of the Araripe Plateau region
|INPE-4876-PRE/1487| 11 p1520 N90-18756
The interpretation of crustal dynamics data in terms of plate interactions and active tectonics of the Anatolian plate and surrounding regions in the Middle East
|NASA-CR-186200| 11 p1533 N90-18824
A system for analysis and interpretation of lineaments in remote sensing images
|INPE-4893-PRE/1494| 13 p1840 N90-20565
Seismic characterization of fracture properties
|DE90-007759| 13 p1841 N90-20570
Characterization of linear structures from remote sensing data; Espinhaco Meridional (MG) sierra
|INPE-4905-PRE/1506| 14 p1997 N90-21449
Geology of Espinhaco Meridional, including the Quadrilatero Ferrifero: Integration through remote sensing data
|INPE-4904-PRE/1505| 14 p1998 N90-21450
Age constraints for the present fault configuration in the Imperial Valley, California: Evidence for northwestward propagation of the Gulf of California rift system
|NASA-CR-186541| 14 p2006 N90-21493
Heat and fluid flow within the Earth's crust: In situ measurements and mathematical models 18 p2579 N90-24690

Evolution of overlapping spreading centers: A SeaMARC 2 investigation
[AD-A223102] 21 p3025 N90-27200
MEVTV Workshop on Tectonic Features on Mars
[NASA-CR-186143] 21 p3100 N90-27609
Some aspects of the structure and evolution of oceanic spreading centers 24 p3496 N90-29757

GEOLOGICAL SURVEYS
Computer-aided boundary delineation of agricultural lands
[NASA-TM-102243] 08 p1091 N90-16313
Determination of the gravity disturbance on the earth's topographic surface from airborne gravity gradient data
[AD-A214596] 09 p1246 N90-17230
Geocoded spaceborne SAR products for geological applications 19 p2708 N90-25410
Land application of imaging spectrometry 19 p2708 N90-25415
Construction of geological and geotechnical information database
[DE90-503417] 20 p2936 N90-26708
Aerial videotape survey of coastal Louisiana, 1986. Louisiana Barrier Island erosion and land loss study: 1985-1990
[PB90-194648] 22 p3195 N90-28128
Geologic studies in Alaska by the US geological survey, 1988
[PB90-180993] 22 p3211 N90-28213
Catalog of strong motion stations in Eastern North America
[PB90-251984] 24 p3490 N90-29722

GEOLOGY
NT CONES (VOLCANOES)
NT GEOCHRONOLOGY
NT GEOMORPHOLOGY
NT GLACIOLOGY
NT HYDROGEOLOGY
NT LITHOLOGY
NT LUNAR GEOLOGY
NT MARS VOLCANOES
NT OROGRAPHY
NT PETROGRAPHY
NT PETROLOGY
NT PHOTOGEOLOGY
NT RADAR GEOLOGY
NT STRUCTURAL PROPERTIES (GEOLOGY)
NT SUBDUCTION (GEOLOGY)
NT TECTONICS
NT VOLCANOES
NT VOLCANOLOGY
National register of research projects, 1986/87. Part 2B: Natural sciences: Physical, engineering and related sciences (new projects)
[DE89-015033] 01 p0143 N90-10826
Summaries of the thematic conferences on remote sensing for exploration geology
[NASA-CR-185321] 05 p0664 N90-13880
Attempt to draw conclusions concerning the geological subsoil from the vegetation using digital image processing of TM data 08 p1093 N90-16329
Orbital remote sensing in the decade of the nineties: New approaches and challenges in geology
[INPE-4838-PRE/1467] 11 p1521 N90-18758
Geological structure of the State of Rio de Janeiro viewed through MSS LANDSAT imagery
[INPE-4826-PRE/1457] 11 p1533 N90-18825
The patterns of fracture and the conditioning tectonics in the region of the Quadrilatero Ferrifero and part of the Migmatitic-Granulitic Complex in Minas Gerais (Brazil)
[INPE-4895-PRE/1496] 11 p1534 N90-18829
Working on the moon: The Apollo experience
[DE90-003662] 12 p1697 N90-19744
Geology, distribution of hot springs and hydrothermal alteration zones of major geothermal areas in Japan
[DE90-753026] 13 p1820 N90-20451
Damage characteristics of time domain histories
[DE90-008787] 13 p1842 N90-20573
JPRS report. Science and technology. USSR: Earth sciences
[JPRS-UES-88-004] 14 p1995 N90-21431
JPRS report. Science and technology. USSR: Earth sciences
[JPRS-UES-89-002] 14 p1995 N90-21432
Results of the Gondwana Project: An example of intercontinental geologic correlation utilizing LANDSAT imagery
[INPE-4870-PRE/1481] 14 p1995 N90-21437
Geobotanical remote sensing: A review
[INPE-5026-PRE/1565] 14 p1996 N90-21440
Geology of Espinhaco Meridional, including the Quadrilatero Ferrifero: Integration through remote sensing data
[INPE-4904-PRE/1505] 14 p1998 N90-21450
Introduction of digital image processing by remote sensors applied to geology
[INPE-5023-RPE/616] 14 p1999 N90-21456
Contribution for the study of the evolution of part of the Espinhaco supergroup and its foundation through fracture analysis
[INPE-4907-PRE/1508] 14 p1999 N90-21459
An anomalous wind between valleys: Its characteristics and a proposed explanation
[DE90-008965] 15 p2133 N90-22189
Natural resources information system for the state of Oklahoma
[DE90-009483] 15 p2180 N90-22458
Geology of coronae and domal structures on Venus and models of their origin 15 p2191 N90-22513
Geoscience and a Lunar Base: A Comprehensive Plan for Lunar Exploration
[NASA-CP-3070] 18 p2638 N90-25030
Micro coring apparatus
[NASA-CR-183072] 20 p2869 N90-26321
Press abstracts of the 21st Lunar and Planetary Science Conference
[NASA-CR-186674] 20 p2941 N90-26738
Applications of ISES for geology 21 p3017 N90-27154
Bibliography of oceanography, meteorology, and geology of Louisiana, Texas, Mississippi, Alabama, and Florida
[PB90-194663] 22 p3194 N90-28124
Aerial videotape survey of coastal Louisiana, 1986. Louisiana Barrier Island erosion and land loss study: 1986-1990
[PB90-194648] 22 p3195 N90-28128

GEOMAGNETIC ANOMALIES
U MAGNETIC ANOMALIES

GEOMAGNETIC CROTCHETS
U SUDDEN IONOSPHERIC DISTURBANCES

GEOMAGNETIC EFFECTS
U MAGNETIC EFFECTS

GEOMAGNETIC EQUATOR
U MAGNETIC EQUATOR

GEOMAGNETIC FIELD
U GEOMAGNETISM

GEOMAGNETIC LATITUDE
An analytic/empirical model of the middle and low latitude ionosphere
[AD-A220004] 17 p2423 N90-23809
Re-analysis of data on the space radiation environment above southeast Asia
[AD-A224155] 24 p3564 N90-30162

GEOMAGNETIC PULSATIONS
The Nurmijarvi Geophysical Observatory 21 p3021 N90-27178
Digital intelligent magnetic recording system DIMARS as the automated workstation at magnetic observatory 21 p3022 N90-27186

GEOMAGNETIC STORMS
U MAGNETIC STORMS

GEOMAGNETIC TAIL
Numerical study of the current sheet and PSBL in a magnetotail model
[NASA-CR-183289] 02 p0293 N90-11669
On the structure of the tail magnetic field
[IFSI-88-19] 08 p1101 N90-16378
The MHD structure of an open magnetotail boundary 15 p2168 N90-22388
On the nature of the plasma sheet boundary layer
[DE90-013158] 20 p2889 N90-26439

GEOMAGNETICALLY TRAPPED PARTICLES
U RADIATION BELTS

GEOMAGNETISM
Short wavelength striations on expanding plasma clouds
[DE89-016585] 02 p0250 N90-11416
HIPAS 1987-88: ULF research and campaign support
[AD-A211720] 03 p0339 N90-11933
Processing of DMSP magnetic data and its use in geomagnetic field modeling
[NASA-TM-100750] 03 p0370 N90-12115
Time-weighted accumulations ap(tau) and Kp(tau)
[RAE-TR-88050] 03 p0421 N90-12422
On the statistics of El Nino occurrences and the relationship of El Nino to volcanic and solar/geomagnetic activity
[NASA-TP-2948] 03 p0429 N90-12456
Spacecraft attitude determination using the earth's magnetic field 05 p0589 N90-13429
Solar-geophysical data number 538, June 1989. Part 1: (Prompt reports). Data for May, April 1989, and late data
[PB89-223838] 06 p0866 N90-15031
On the structure of the tail magnetic field
[IFSI-88-19] 08 p1101 N90-16378
Correlative analyses for geomagnetic indices, cosmic-ray intensities and sunspot numbers recorded since 1937
[IFSI-89-4] 08 p1151 N90-16670
Case studies in data analysis
[AD-A215342] 09 p1248 N90-17241
Report from magnetospheric science 10 p1444 N90-18334
Attitude and spin rate control of a spinning satellite using geomagnetic field
[INPE-4818-NTE/289] 12 p1613 N90-19277
Solar-geophysical data number 541, September 1989. Part 1: (Prompt reports). Data for August, July 1989, and late data
[PB90-122763] 12 p1745 N90-20032
Examination of the background by High Energy X ray Experiment (HEXE) on the space station MIR
[ETN-90-95735] 12 p1746 N90-20041
Measurements of the interaction of high-voltage biassed conductors with the ionosphere
[AD-A218285] 13 p1843 N90-20580
Comparison of quiet time geomagnetic daily variation (Sq) in H component at Eusebio and Cachoeira Paulista
[INPE-4985-PRE/1547] 14 p2043 N90-21714
Solar-geophysical data number 542, October 1989. Part 1: (Prompt reports). Data for September, August 1989, and late data
[PB90-148669] 15 p2193 N90-22520
Godhavn (Greenland) Geophysical Observatory: Magnetic results, 1984
[ISBN-87-7478-289-4] 17 p2423 N90-23807
Proceedings of the International Workshop on Geomagnetic Observatory Data Acquisition and Processing
[GEOPHYSICAL-PUBL-15] 21 p3021 N90-27177
The Nurmijarvi Geophysical Observatory 21 p3021 N90-27178
Coil system for the production of three-component uniform magnetic field at the Nurmijarvi Observatory 21 p3021 N90-27179
Comparisons of the recording instruments. Description of the difference-plots 21 p3022 N90-27181
A new method for the absolute measurement of geomagnetism beginning with DI Flux 21 p3022 N90-27182
Experiences with modern absolute instruments 21 p3022 N90-27183
Institut de Physique du Globe de Paris automatic magnetic observatory 21 p3022 N90-27184
Improvements of automatic magnetic observatories in Italy 21 p3022 N90-27185
Digital intelligent magnetic recording system DIMARS as the automated workstation at magnetic observatory 21 p3022 N90-27186
Proton magnetometers for measurement of the Earth's magnetic field 21 p3023 N90-27188
Some thoughts on data processing 21 p3023 N90-27189
INTERMAGNET 21 p3023 N90-27190
About the derivation of geomagnetic indices from digital data 21 p3023 N90-27191
Use of geomagnetic data for studies on the Earth's deep interior 21 p3023 N90-27192
Use of the method of natural orthogonal components for derivation of S sub R-variation and digital K-indices 21 p3024 N90-27193
Computer production of K-indices by a simple method based on linear elimination 21 p3024 N90-27194
Amplitude and phase scintillation and ionospheric irregularities at sub-auroral latitudes
[AD-A222861] 21 p3025 N90-27198
High-T(sub c) squid application in medicine and geophysics 22 p3139 N90-27806
Intensive MHD-structures penetration in the middle atmosphere initiated in the ionospheric cusp under quiet geomagnetic conditions 22 p3207 N90-28193
Lower thermosphere (80-100 km) dynamics response to solar and geomagnetic activity: Overview 22 p3207 N90-28194
Solar-geophysical data number 544, December 1989. Part 1 (Prompt reports). Data for November, October 1989, and late data
[PB90-171661] 22 p3263 N90-28481
Atmospheric structure and variability
[AD-A223439] 24 p3492 N90-29734
Proceedings of a Workshop on the Geoelectric and Geomagnetic Environment of Continental Margins
[AD-A223743] 24 p3493 N90-29739
A global model of thunderstorm electricity and the prediction of whistler duct formation 24 p3493 N90-29744
Brorfelde Geomagnetic Observatory: Magnetic results, 1987
[ISBN-87-7478-297-5] 24 p3496 N90-29756

GEOMETRIC DILUTION OF PRECISION
Ridge regression processing 14 p1907 N90-20931

GEOMETRIC RECTIFICATION (IMAGERY)
Algorithm for atmospheric corrections of aircraft and satellite imagery
[NASA-TM-100751] 05 p0683 N90-13976

Geocoded spaceborne SAR products for geological applications 19 p2708 N90-25410

GEOMETRICAL ACOUSTICS

An investigation of the diffraction of an acoustic plane wave by a curved surface of finite impedance
[NASA-CR-186069] 04 p0550 N90-13204

GEOMETRICAL HYDROMAGNETICS

U MAGNETOHYDRODYNAMICS

GEOMETRICAL OPTICS

Surface reflection: Physical and geometrical perspectives
[AD-A210592] 01 p0124 N90-10710

Numerical simulation of laser radiation propagation in non-uniform absorbing medium. Geometrical optics approximation
[DE89-632014] 06 p0787 N90-14585

High-frequency asymptotic methods for analyzing the EM scattering by open-ended waveguide cavities
[NASA-CR-186244] 08 p1056 N90-16103

Geometrical optics in inhomogeneous chiral media with application to polarization correction in inhomogeneous lens antennas
[PB90-110669] 08 p1122 N90-16497

Dual-shaped offset reflector antenna designs from solutions of the geometrical optics first-order partial differential equations 15 p2076 N90-21887

The solution of scattering and radiation problems for complex configurations based on 3-D grid and patch models 15 p2096 N90-21997

Research and applications of metallic superlattices, high T(sub c) superconductors, x ray optics, and compact synchrotrons 16 p2311 N90-23170

Intersecting line segments, ray shooting, and other applications of geometric partitioning techniques
[RUU-CS-88-26] 18 p2601 N90-24804

Using the x ray region of the electromagnetic spectrum for alignment: Overview, geometric optics, and design considerations
[DE90-014798] 23 p3317 N90-28752

Polarization correction of Luneburg lens with chiral medium
[PB90-189127] 24 p3544 N90-30046

Real-time concentration monitoring of large aerodynamic diameter fiber aerosols using the geometric optic inversion technique
[AD-A224167] 24 p3545 N90-30048

GEOMETRICAL THEORY OF DIFFRACTION

Constitutive parameter measurements of lossy materials
[NASA-CR-183398] 02 p0281 N90-11603

Chromatic dispersion compensation in a Fresnel lens by means of a diffraction grating
[DE90-004030] 08 p1123 N90-16506

GTD/UTD: Brief history of successive development of theory and recent advances. Applications to antennas on ships and aircraft 10 p1370 N90-17939

Telemetry and telecommand omnidirectional antenna in the short wave band
[ETN-90-96285] 11 p1499 N90-18631

Radar transponder antenna pattern analysis for the space shuttle 12 p1638 N90-19414

Background connection: A necessary object in general relativity
[DE90-620463] 16 p2325 N90-23258

The Helicopter Antenna Radiation Prediction Code (HARP)
[NASA-CR-186925] 22 p3165 N90-27946

GEOMETRODYNAMICS

U RELATIVITY

GEOMETRY

NT ANALYTIC GEOMETRY
NT ANGLE OF ATTACK
NT ANGLES (GEOMETRY)
NT BRAGG ANGLE
NT CARTESIAN COORDINATES
NT CIRCLES (GEOMETRY)
NT CIRCUMFERENCES
NT COMPUTATIONAL GEOMETRY
NT CONICS
NT CRACK GEOMETRY
NT CURL (VECTORS)
NT CURVATURE
NT CURVES (GEOMETRY)
NT DESCRIPTIVE GEOMETRY
NT DIFFERENTIAL GEOMETRY
NT DIHEDRAL ANGLE
NT DUCT GEOMETRY
NT ELEVATION ANGLE
NT ELLIPSES
NT EPICYCLOIDS
NT EUCLIDEAN GEOMETRY
NT FIXED POINTS (MATHEMATICS)
NT FLOW GEOMETRY
NT FRACTALS
NT GEODESIC LINES
NT GREAT CIRCLES
NT HILBERT SPACE
NT HOMOTOPY THEORY
NT INVARIANT IMBEDDINGS
NT LEADING EDGE SWEEP
NT LIE GROUPS
NT LINES (GEOMETRY)
NT LINKS (MATHEMATICS)
NT LOOK ANGLES (ELECTRONICS)
NT METRIC SPACE
NT NOZZLE GEOMETRY
NT OCTAHEDRONS
NT PARABOLAS
NT PARALLELEPIPEDS
NT POINTS (MATHEMATICS)
NT POLYGONS
NT POLYHEDRONS
NT PROJECTIVE GEOMETRY
NT PROLATE SPHEROIDS
NT RADII
NT RECTANGLES
NT RHOMBOIDS
NT RIEMANN MANIFOLD
NT SOBOLEV SPACE
NT SPECIMEN GEOMETRY
NT SPINOR GROUPS
NT SQUARES (MATHEMATICS)
NT SWEEP ANGLE
NT TANGENTS
NT TANK GEOMETRY
NT TENSOR ANALYSIS
NT TETRAHEDRONS
NT TOPOLOGY
NT TORUSES
NT TRAPEZOIDS
NT TRIANGLES
NT TRIGONOMETRY
NT VECTOR ANALYSIS
NT VORTICITY
NT ZERO ANGLE OF ATTACK

Face-specific interaction of MoS4(2-1) with oriented crystals of (0001) CdX (X = Se, S)
[AD-A209519] 01 p0128 N90-10732

Analysis of three- and four-sided uniform waveguides with unusual cross-section/boundary conditions
[AD-A212653] 04 p0493 N90-12834

A new model for the structure of silica glass
[AD-A212972] 05 p0627 N90-13659

Flame acceleration studies in the MINIFLAME facility
[DE90-000041] 06 p0740 N90-14310

Testing and performance of a high-gain flux-compression generator
[DE90-002808] 06 p0772 N90-14492

A study of variable geometry in advanced gas turbines 07 p0881 N90-15104

Application of Lagrangian blending functions for grid generation around airplane geometries
[NASA-CR-186318] 08 p1018 N90-15891

Euler and Navier-Stokes computations for two-dimensional geometries using unstructured meshes
[NASA-CR-181977] 08 p1019 N90-15893

Vorticity amplification in nonorthogonal stagnation flow 08 p1064 N90-16152

Detection of edges using local geometry 08 p1074 N90-16213

Glancing shock-boundary layer interactions 10 p1309 N90-17571

A user's manual for the method of moments Aircraft Modeling Code (AMC)
[NASA-CR-186371] 11 p1456 N90-18390

Probability of failure and risk assessment of propulsion structural components 11 p1471 N90-18470

Study of possible solar heating effects on thermosonde probes: Error analysis
[AD-A218116] 13 p1903 N90-20917

A system for transonic wing design with geometric constraints based on an inverse method 14 p1917 N90-20983

Subsonic and transonic blade design by means of analysis codes 14 p1917 N90-20985

An analysis of the finite-differenced, even-parity discrete-ordinates equations in slab geometry
[DE90-006479] 15 p2160 N90-22337

HYPUF upgrade
[AD-A218400] 17 p2379 N90-23547

Very high frequency measurements of geometric factors in transmission line lead acid cells
[AD-A219463] 17 p2420 N90-23788

Finding minimum area k-gons
[RUU-CS-89-7] 17 p2449 N90-23967

Computational geometry and its application to computer graphics
[RUU-CS-89-8] 17 p2449 N90-23968

Affine polar spaces
[CWI-AM-R8909] 17 p2468 N90-24107

A simple output-sensitive algorithm for hidden surface removal
[RUU-CS-89-26] 18 p2592 N90-24751

Finding complete bipartite subgraphs in bipartite graphs
[RUU-CS-89-30] 18 p2602 N90-24815

Characteristic impedances and loss data for a common stripline pickup geometry
[CEBAF-PR-89-038] 19 p2755 N90-25656

Improving the geometric fidelity of imaging systems employing sensor arrays
[NASA-CASE-NPO-17970-1-CU] 20 p2880 N90-26384

Supersonic jet studies of benzyl alcohols: Minimum energy conformations and torsional motion
[AD-A221815] 21 p2980 N90-26934

Vertical emitting, ring geometry, ultra-low threshold, and ultra-high speed quantum well lasers for optical interconnect
[AD-A222932] 21 p3008 N90-27098

Generalized Voronoi diagrams: Initial results
[IMAG-RR-799-M] 21 p3066 N90-27429

Grid generation and processing for FINFLO flow solver
[PB90-189481] 22 p3169 N90-27975

Geometric theory for infinite dimensional systems
[PB90-190216] 22 p3242 N90-28383

Geometrical properties of an internal local octonionic space in a non-Riemannian manifold
[DE90-627175] 23 p3390 N90-29149

Performance analysis of subspace-based parameter estimation algorithms
[AD-A224523] 24 p3463 N90-29566

GEOMORPHOLOGY

Fluctuation history of Great Salt Lake, Utah, during the last 13,000 years, part 2
[NASA-CR-185911] 01 p0082 N90-10466

ONR/NORDA Workshop on Terrain Analysis and Quantitative Geomorphology
[AD-A210464] 01 p0086 N90-10489

Physiographic and geological setting of the Coastal Engineering Research Center's field research facility
[AD-A210772] 02 p0238 N90-11356

Late quaternary geomorphology of the Great Salt Lake region, Utah, and other hydrographically closed basins in the western United States: A summary of observations
[NASA-CR-185912] 05 p0663 N90-13878

Evolution of overlapping spreading centers: A Sea Mark 2 investigation
[AD-A214278] 07 p0965 N90-15576

Underwater physiography of the continental shelf of Rio Grande do Norte visible through satellite imagery
[INPE-4964-TDL/392] 13 p1820 N90-20448

MEVTV Workshop on Tectonic Features on Mars
[NASA-CR-186143] 21 p3100 N90-27609

GEOPHYSICAL FLUID FLOW CELLS

Laboratory and theoretical models of planetary-scale instabilities and waves 03 p0363 N90-12076

Laboratory and theoretical studies of baroclinic processes 03 p0363 N90-12077

GEOPHYSICAL OBSERVATORIES

NT POGO

Godhavn (Greenland) Geophysical Observatory: Magnetic results, 1984
[ISBN-87-7478-289-4] 17 p2423 N90-23807

The Nurmijarvi Geophysical Observatory 21 p3021 N90-27178

Coil system for the production of three-component uniform magnetic field at the Nurmijarvi Observatory 21 p3021 N90-27179

Institut de Physique du Globe de Paris automatic magnetic observatory 21 p3022 N90-27184

Improvements of automatic magnetic observatories in Italy 21 p3022 N90-27185

Digital intelligent magnetic recording system DIMARS as the automated workstation at magnetic observatory 21 p3022 N90-27186

Improvements in fluxgate magnetometers at Danish Meteorological Institute's Magnetic Observatories 21 p3023 N90-27187

Some thoughts on data processing 21 p3023 N90-27189

INTERMAGNET 21 p3023 N90-27190

GEOPHYSICAL SATELLITES

NT COSMOS SATELLITES
NT POGO

GEOPHYSICS

Kiruna geophysical data: Data Summary 88/7-9, July - September 1988
[PB89-210249] 01 p0086 N90-10487

Institute of Geophysics and Planetary Physics, 1988
[DE89-014363] 01 p0137 N90-10794

Solar-geophysical data number 532, December 1988. Part 1: Data for November, October 1988, and late data
[PB89-152086] 01 p0142 N90-10818

Global atmospheric moisture variability
03 p0361 N90-12062
Dynamics of baroclinic wave systems
03 p0362 N90-12072
Processing of DMSP magnetic data and its use in geomagnetic field modeling
[NASA-TM-100750] 03 p0370 N90-12115
Reports of planetary geology and geophysics program, 1988
[NASA-TM-4130] 03 p0428 N90-12454
The Swedish sounding rocket and balloon program
05 p0657 N90-13830
The thermal behavior of natural backgrounds and its prediction by means of numerical models
06 p0762 N90-14436
Earth Sciences Division annual report 1988
[DE90-002617] 06 p0801 N90-14663
Solar-geophysical data number 539, July 1989. Part 1: (Prompt reports). Data for June, May 1989, and late data
[PB89-235451] 06 p0866 N90-15033
Solar-geophysical data number 539, July 1989. Part 2: (Comprehensive reports). Data for January 1989, and miscellaneous
[PB89-235469] 06 p0866 N90-15034
Space operations: Listing of NASA scientific missions, 1980-2000. Fact sheet for the Chairman, Subcommittee on Space Science and Applications, Committee on Science, Space, and Technology, House of Representatives
[AD-A213493] 07 p1016 N90-15881
Summaries of physical research in the geosciences
[DE90-004993] 08 p1090 N90-16309
Proceedings of the 79th SEGJ Conference
[DE89-760006] 08 p1157 N90-16704
Parameterization of small-scale processes
[AD-A215507] 10 p1398 N90-18082
Processing of DMSP magnetic data: Handbook of programs, tapes, and datasets
[NASA-TM-100757] 10 p1407 N90-18114
Summer Study Program in Geophysical Fluid Dynamics: The Influence of Convection on Large-Scale Circulations, 1988
[AD-A216024] 11 p1535 N90-18840
An analytic model of axisymmetric mantle plume due to thermal and chemical diffusion
[NASA-CR-186461] 12 p1691 N90-19714
Solar-geophysical data number 541, September 1989. Part 2: (Comprehensive reports). Data for March 1989 and miscellaneous
[PB90-122755] 12 p1745 N90-20031
Solar-geophysical data number 541, September 1989. Part 1: (Prompt reports). Data for August, July 1989, and late data
[PB90-122763] 12 p1745 N90-20032
Committee on Geodesy - National Research Council
[AD-A217770] 13 p1821 N90-20452
Progress in the Determination of the Earth's Gravity Field
[NASA-CR-185721] 13 p1831 N90-20513
Gravity field determination and error assessment techniques 13 p1832 N90-20517
Modeling of the Earth's gravity field using the New Global Earth Model (NEWGEM) 13 p1833 N90-20523
Computer processing of multi-channel electromagnetic data from an airborne geophysical survey system
[PB90-138413] 14 p1965 N90-21253
Age constraints for the present fault configuration in the Imperial Valley, California: Evidence for northwestward propagation of the Gulf of California rift system
[NASA-CR-186541] 14 p2006 N90-21493
Topical Conference on the Origin of the Earth
[NASA-CR-185061] 15 p2128 N90-22166
Solar-geophysical data number 542, October 1989. Part 1: (Prompt reports). Data for September, August 1989, and late data
[PB90-148669] 15 p2193 N90-22520
Solar-geophysical data number 542, October 1989. Part 2: (Comprehensive reports). Data for April 1989 and miscellaneous
[PB90-148677] 15 p2193 N90-22521
Quantifying and reducing uncertainty in the assimilative mapping of ionospheric electrodynamics
16 p2254 N90-22854
Proceedings of Workshop on Atmospheric Density and Aerodynamic Drag Models for Air Force Operations, volume 2
[AD-A220382] 17 p2345 N90-23356
The VIERS-1 project. The Delft wind/wave experiment: Experiment and first results, part 1
[BCRS-89-24-PT-1] 17 p2418 N90-23779
The Zenith Z-248 as a scientific workstation
[AD-A219991] 17 p2441 N90-23909
Geoscience and a Lunar Base: A Comprehensive Plan for Lunar Exploration
[NASA-CP-3070] 18 p2638 N90-25030
Spacecraft contamination programs within the Air Force Systems Command Laboratories
19 p2727 N90-25507
Directory of research projects: Planetary geology and geophysics program
[NASA-TM-4211] 20 p2942 N90-26743
Reports of planetary geology and geophysics program, 1989
[NASA-TM-4210] 21 p3100 N90-27606
High-T(sub c) squid application in medicine and geophysics 22 p3139 N90-27806
The National Geodetic Survey absolute gravity program
[PB90-156951] 22 p3211 N90-28212
On estimating scale invariance in stratocumulus cloud fields 22 p3213 N90-28227
Solar-geophysical data number 545, January 1990. Part 2 (Comprehensive reports). Data for July 1989 and miscellaneous
[PB90-182346] 22 p3263 N90-28480
Solar-geophysical data number 544, December 1989. Part 1 (Prompt reports). Data for November, October 1989, and late data
[PB90-171661] 22 p3263 N90-28481
Solar-geophysical data number 544, December 1989. Part 2 (Comprehensive reports). Data for June 1989 and miscellaneous
[PB90-171679] 22 p3264 N90-28482
Geophysical diffraction tomography: A complementary remote sensing technique for hazardous waste site characterization
[DE90-013025] 23 p3341 N90-28882
A radio frequency user's guide to the space environment services center geophysical alert broadcasts
[PB90-240631] 23 p3351 N90-28935
Geophysical turbulence research at NCAR
[AD-A223361] 24 p3492 N90-29732
Proceedings of the 17th Annual Gravity Gradiometer Conference
[AD-A223568] 24 p3492 N90-29735
Proceedings of a Workshop on the Geoelectric and Geomagnetic Environment of Continental Margins
[AD-A223743] 24 p3493 N90-29739

GEOPOTENTIAL
NT GEOPOTENTIAL HEIGHT
Semi-monthly temperature and geopotential anomaly in the upper 500 meters along the Oahu-Farallon Islands great circle from November 15, 1967 through December 15, 1979
[AD-A210640] 01 p0091 N90-10518
Evaluation of 15th- and 30th-order geopotential harmonic coefficients from 26 resonant satellite orbits
[RAE-TR-88045] 04 p0461 N90-12640
The GEM-T2 gravitational model
[NASA-TM-100746] 04 p0517 N90-12984
Climate predictability: A dynamical view
[AERONOMICA-ACTA-A-347-1989] 05 p0671 N90-13909
Error modeling of bias-type parameters for TOPEX orbit determination 07 p0884 N90-15117
Geopotential models in the Australian region 13 p1832 N90-20519
Stabilized determination of geopotential coefficients by the mixed hom-BLUP approach 13 p1832 N90-20520
Geopotential coefficient determination and the gravimetric boundary value problem: A new approach 13 p1833 N90-20521
Regional quasigeoid determination in Northern Germany and comparison with GPS 13 p1837 N90-20544
Treatment of geodetic leveling in the integrated geodesy approach 13 p1837 N90-20546
Spectral analyses of satellite geopotential missions 13 p1838 N90-20552
Gravity field information from Gravity Probe-B 13 p1839 N90-20554
Studies of an orbital gradiometer mission 13 p1839 N90-20558
Determination of the general ocean circulation using satellite altimetry from a simultaneous solution for the Earth's gravity field 16 p2203 N90-22569
Satellite motion in axi-symmetric gravitational field. Part 2: Perturbations due to an arbitrary J(sub l)
[RAE-TR-89022] 16 p2206 N90-22586

GEOPOTENTIAL HEIGHT
Observational studies of low-frequency oscillations in the Southern Hemisphere 02 p0250 N90-11420
An observational study of intramonthly quasi-periodicities in the Northern Hemisphere, extratropical geopotential height field 06 p0813 N90-14729
On mean elements for satellite orbits perturbed by the zonal harmonics of the geopotential
[RAE-TM-SPACE-371] 08 p1033 N90-15971
Multiple flow regimes in the Northern Hemisphere winter 08 p1100 N90-16372
An atlas of ECMWF analyses (1980-1987). Part 1: First moment quantities
[NASA-TM-100747-PT-1] 10 p1408 N90-18120
Long range geoid control through the European GPS traverse: Final results 13 p1837 N90-20545
Structure and dynamics of the Arizona monsoon boundary
[AD-A217378] 13 p1844 N90-20586
Tropopause undulations and the development of extratropical cyclones 15 p2132 N90-22186

GEOPOTENTIAL RESEARCH MISSION
Studies of an orbital gradiometer mission 13 p1839 N90-20558

GEOS 1 SATELLITE
Substorm associated pulsations: A study of plasmaspheric cavity resonance, mid-latitude polarisation and geostationary orbit signatures 02 p0251 N90-11422

GEOS 2 SATELLITE
Substorm associated pulsations: A study of plasmaspheric cavity resonance, mid-latitude polarisation and geostationary orbit signatures 02 p0251 N90-11422

GEOS-B SATELLITE
U GEOS 2 SATELLITE

GEOSAT SATELLITES
Geosat/ERM altimeter data analysis for the determination of global oceanic mesoscale variability 07 p0949 N90-15492
A correlation study of wind speed as measured by the special sensor microwave/imager and the GEOSAT altimeter
[AD-A219841] 18 p2581 N90-24701

GEOSTATIONARY OPERATIONAL ENVIRON SATS
U GOES SATELLITES

GEOSTATIONARY PLATFORMS
U SYNCHRONOUS PLATFORMS

GEOSTATIONARY SATELLITES
U SYNCHRONOUS SATELLITES

GEOSTROPHIC WIND
Tuning of the OSCURS (Ocean Surface Current Simulations) numerical model to ocean surface measurements in the Gulf of Alaska
[PB89-103979] 06 p0818 N90-14759
Precipitation distributions associated with cyclones originating over the Gulf of Mexico and surrounding coastal regions
[AD-A213644] 07 p0963 N90-15569
The Polar Ice Prediction System: A sea ice forecasting system
[AD-A214600] 09 p1249 N90-17246
Synoptic-scale forcing of the low-level jet in developing baroclinic waves 12 p1692 N90-19717
A method for correcting and reducing the pressure data recorded at the PAM 2 stations during GALE
[AD-A218165] 13 p1846 N90-20596
Semigeostrophic flow over orography in a stratified rotating atmosphere 15 p2127 N90-22163
An interactive method for estimating hailstone size and convectively-driven wind gusts from forecast soundings
[AD-A218499] 16 p2258 N90-22871
Modeling studies of the LeeUwin current using a high-resolution primitive equation model
[AD-A219595] 17 p2430 N90-23846
The NASA/MSFC Global Reference Atmospheric Model, 1990 version (GRAM-90)
[NASA-CR-186717] 20 p2888 N90-26435
Modification of the background flow by roll vortices 22 p3219 N90-28258

GEOSYNCHRONOUS EARTH ORBITAL ENVIRONMENTS
U EARTH ORBITAL ENVIRONMENTS

GEOSYNCHRONOUS ORBITS
Geostationary earth science platform concepts 12 p1608 N90-19252
Large space antenna concepts for ESGP 12 p1608 N90-19253
Large-diameter geostationary millimeter wavelength antenna concept 12 p1609 N90-19254
Design of a low-frequency (5-20 GHz), 15-meter-diameter passive radiometer for geostationary earth science platforms 12 p1609 N90-19255
Structures for remotely deployable precision antennas 12 p1609 N90-19256
Coherent radar measurement of ocean currents from geostationary orbit 12 p1609 N90-19259
Synthetic Aperture Interferometric Radiometer (SAIR) 12 p1610 N90-19261
Rain radars for earth science geostationary platforms: Some possibilities 12 p1610 N90-19262
A new concept for high-cycle-life LEO: Rechargeable MnO2-hydrogen 13 p1822 N90-20462
Numerical Arc Segmentation Algorithm for a Radio Conference (NASARC), version 4.0: User's manual
[NASA-TM-101454] 14 p1964 N90-21250

Semianalytic study of high-eccentricity orbit stability and evolution 16 p2204 N90-22574
Plasma interactions and effects for large systems 19 p2735 N90-25545
Texstar: The all-Texas educational satellite system [NASA-CR-186654] 20 p2820 N90-26045
Project SPARC: Space-based aeroassisted reusable craft [NASA-CR-186816] 20 p2821 N90-26051
Reproduction of GMS IR calibration table 21 p3028 N90-27215
Thermal-distortion analysis of an antenna strongback for geostationary high-frequency microwave applications [NASA-TP-3016] 22 p3125 N90-27738
Possible trajectory profiles to achieve the geostationary orbit without any drift phase 22 p3127 N90-27745
Orbit computation 22 p3128 N90-27750
Optimization of the deployment of a pair of satellites in inclined eccentric geosynchronous orbits 22 p3128 N90-27751
Advanced propulsion for LEO and GEO platforms [NASA-TM-103228] 22 p3134 N90-27785

GEOTECHNICAL ENGINEERING
Geotechnical instrumentation [PB89-198675] 07 p0933 N90-15398
Effects of single fractures on seismic wave propagation [DE90-009191] 15 p2129 N90-22171
Construction of geological and geotechnical information database [DE90-503417] 20 p2936 N90-26708
Finite element analysis of coupled thermoelasticity [PB90-201211] 23 p3337 N90-28860

GEOTEMPERATURE
Ozone depletion, greenhouse gases, and climate change [NASA-CR-185323] 03 p0367 N90-12101

GEOTHERMAL ENERGY CONVERSION
Hot dry rock geothermal energy: A renewable energy resource that is ready for development now [DE90-007509] 13 p1826 N90-20485
Geothermal energy program summary [DE89-009485] 16 p2251 N90-22837
Geothermal energy program summary [DE89-009486] 16 p2251 N90-22838
Geothermal fluid genesis in the Great Basin [DE90-014438] 23 p3342 N90-28884

GEOTHERMAL ENERGY UTILIZATION
Investigation report of the investigation commission for interchange of heat pump technology in Europe [DE89-782293] 11 p1505 N90-18666
Hot dry rock geothermal energy: A renewable energy resource that is ready for development now [DE90-007509] 13 p1826 N90-20485
The pressure dilation of a deep, jointed region of the earth [DE90-007537] 15 p2128 N90-22170

GEOTHERMAL RESOURCES
NT GEYSERS
Mid-term report on-the study and development results of the Sunshine Project in fiscal 1987. Study on the evaluation technology of geothermal sources in Japan [DE90-710708] 10 p1400 N90-18095
Geology, distribution of hot springs and hydrothermal alteration zones of major geothermal areas in Japan [DE90-753026] 13 p1820 N90-20451
Hot dry rock geothermal energy: A renewable energy resource that is ready for development now [DE90-007509] 13 p1826 N90-20485
The pressure dilation of a deep, jointed region of the earth [DE90-007537] 15 p2128 N90-22170
Geothermal energy program summary [DE89-009486] 16 p2251 N90-22838
Geothermal fluid genesis in the Great Basin [DE90-014438] 23 p3342 N90-28884

GEOTHERMAL TECHNOLOGY
Mid-term report on-the study and development results of the Sunshine Project in fiscal 1987. Study on the evaluation technology of geothermal sources in Japan [DE90-710708] 10 p1400 N90-18095
The pressure dilation of a deep, jointed region of the earth [DE90-007537] 15 p2128 N90-22170
Geothermal energy program summary [DE89-009485] 16 p2251 N90-22837
Geothermal energy program summary [DE89-009486] 16 p2251 N90-22838
Geothermal fluid genesis in the Great Basin [DE90-014438] 23 p3342 N90-28884

GEOTHERMOMETRY
U GEOTEMPERATURE

GEP TELESCOPES
U PARTICLE TELESCOPES

GERDIEN ARC HEATERS
U ARC HEATING
U HEATING EQUIPMENT

GERMANIUM
High pressure 129I Moessbauer studies of GeI4 molecular crystals [DE89-015269] 02 p0283 N90-11620
High resolution X-ray spectroscopy using germanium microcalorimeters [DE89-017784] 03 p0351 N90-12004
Ion beam deposition of epitaxial germanium and gallium arsenide layers [DE89-017439] 03 p0411 N90-12357
Manufacturing and characterization of insulator-germanium structures [ECL-88-13] 05 p0703 N90-14115
Surface roughening of Ge(001) during 200 eV Xe ion bombardment and Ge molecular beam epitaxy [DE90-000674] 07 p0998 N90-15769
Method of producing a thin silicon-on-insulator layer [AD-D014330] 09 p1290 N90-17478
Imaging Germanium Telescope Array for Gamma-Rays (IGETAGRAY) [DE90-006994] 11 p1595 N90-19188
Heteroepitaxial growth of germanium films by supersonic free jet chemical beam epitaxy [DE90-006621] 12 p1720 N90-19877
Stressed Ge:Ga photoconductors for space-based astronomy. (Is there life beyond 120 micron) 14 p1975 N90-21315
Germanium Blocked Impurity Band (BIB) detectors 14 p1976 N90-21321
Extrinsic germanium Blocked Impurity Bank (BIB) detectors 14 p1976 N90-21322
Ga:Ge array development 14 p1977 N90-21323
Preparation and characterization of Cu2ZnGeS(4-y)Se(y) [AD-A217469] 15 p2171 N90-22407
Rate constant for reaction of atomic hydrogen with germane 20 p2947 N90-26768
Defects associated with the incorporation of germanium in gallium arsenide [AD-A222953] 21 p3082 N90-27527
Kinetic pathway in Stranski-Krastanov growth of Ge on Si(001) [AD-A224324] 24 p3445 N90-29456
Effects of basis set contraction in relativistic calculations on neon, argon, and germanium [AD-A223357] 24 p3446 N90-29460

GERMANIUM ALLOYS
Structure of amorphous silicon alloy films [DE89-009441] 01 p0128 N90-10734
Research on amorphous silicon-germanium alloys for tandem solar cells [DE89-009436] 07 p0950 N90-15499
Annealing group III-V compound doped silicon-germanium alloy for improved thermo-electric conversion efficiency [NASA-CASE-NPO-17259-1-CU] 12 p1721 N90-19884
Preliminary investigation into the effect of high temperature thermal anneals on the figure of merit of silicon germanium alloys [AD-A218573] 17 p2375 N90-23527
Structural and electronic studies of a:SiGe:H alloys [DE90-000313] 19 p2710 N90-25424

GERMANIUM COMPOUNDS
Dislocation behaviour in Ge(x)Si(1-x) epilayers on (001) Si [DE90-007063] 11 p1572 N90-19051
Modified dislocation structures in Ge(x)Si(1-x) double epilayers on (001) Si [DE90-007078] 11 p1572 N90-19052
Advanced gas phase reactor for growth of Ge sub x Si sub 1-x [AD-A219012] 16 p2323 N90-23250
Molecular beam epitaxial growth, characterization, and devices of modulated semiconductor structures [AD-A221545] 21 p3084 N90-27538

GET AWAY SPECIALS (STS)
Control of an experiment to measure acoustic noise in the space shuttle [NPS62-89-022] 06 p0838 N90-14869
Get Away Special: The first ten years [NASA-TM-102921] 09 p1171 N90-16775
Design and test of a compact optics system for the pool boiling experiment [NASA-TM-102530] 13 p1786 N90-20253
United States Air Force Academy get-away-special flexible beam experiment 14 p1937 N90-21088
Consortium for materials development in space [NASA-CR-186534] 17 p2383 N90-23575
Integrated support structure [NASA-CR-186835] 20 p2841 N90-26162

GEYSERS
Some considerations on resource evaluation of The Geysers [DE90-002119] 08 p1095 N90-16343

GIACOBINI-ZINNER COMET
Spectrophotometric observations of comet P/Giacobini-Zinner 08 p1144 N90-16630

GIANT STARS
NT ASYMPTOTIC GIANT BRANCH STARS
NT CARBON STARS
NT RED GIANT STARS
As observational and theoretical investigation of stellar flares 06 p0862 N90-15012
Observations of 40-70 micron bands of ice in IRAS 09371+1212 and other stars 11 p1585 N90-19134

GIBBS FREE ENERGY
SGTE data for pure elements [NPL-DMA(A)-195] 15 p2181 N90-22460
Stress versus temperature dependent activation energies in creep [NASA-TM-103192] 17 p2417 N90-23773
Mechanism of habit change for atmospheric ice crystal growth 24 p3489 N90-29717

GIBBS PHENOMENON
Shock capturing by the spectral viscosity method [NASA-CR-181920] 01 p0112 N90-10639

GIBBS-HELMHOLTZ EQUATIONS
Liquid-vapor equilibrium of multicomponent cryogenic systems 20 p2948 N90-26774

GIMBALS
Internal performance of two nozzles utilizing gimbal concepts for thrust vectoring [NASA-TP-2991] 12 p1599 N90-19200
On the design and development of a miniature ceramic gimbal bearing 15 p2115 N90-22100

GIOTTO MISSION
Hypervelocity impact studies on the Giotto comet Halley mission 06 p0862 N90-15008
Morphology and compositional differentiation of the surface of comets 08 p1143 N90-16624
Organic chemistry of cometary dust as derived from PUMA 1 data 08 p1143 N90-16628
Composition of dust from Comet P/Halley: The mineral fraction 08 p1144 N90-16631
The in-situ cometary particulate size distribution measured for one comet: P/Halley 08 p1145 N90-16637
An 8.4-GHz dual-maser front-end system for Parkes reimplementation 15 p2078 N90-21905
The target pursuit of Giotto camera [ETN-90-96496] 18 p2555 N90-24581
ESA's report to the 28th COSPAR meeting [ESA-SP-1124] 24 p3560 N90-30141
Dust emission by Comet P/Halley 1982i 24 p3563 N90-30159

GLACIERS
Airfields on antarctic glacier ice [AD-A217638] 13 p1759 N90-20097
Surface topography of the Greenland Ice Sheet from satellite radar altimetry [NASA-SP-503] 16 p2253 N90-22850
Ice core studies and the past atmospheric environment of polar regions 20 p2885 N90-26411
Ross Sea oceanographic data, 1983-1987: USCGC GLACIER, January-February 1983; USCGC POLAR SEA, January-February 1984; USCGC POLAR STAR, February 1984; USCGC POLAR SEA, February 1987 [PB90-243932] 23 p3354 N90-28955
Satellite image atlas of glaciers of the world: Irian Jaya, Indonesia, and New Zealand [PB90-230095] 24 p3483 N90-29691

GLACIOLOGY
Ice core studies and the past atmospheric environment of polar regions 20 p2885 N90-26411
The Renland ice core (Greenland): A source for climatic studies over 100,000 years 20 p2885 N90-26412
Proceedings of a Workshop on Antarctic Meteorite Stranding Surfaces [NASA-CR-186575] 20 p2942 N90-26739

GLANDS (ANATOMY)
NT ADRENAL GLAND
NT PINEAL GLAND
NT PITUITARY GLAND
NT TESTES

GLARE
Model for predicting the effects of laser exposures and eye protection on vision [AD-A219697] 17 p2434 N90-23868
Effect of laser glare and aircraft windscreen on visual search performance under low ambient lighting [AD-A219456] 17 p2437 N90-23888
Dazzling glare: Protection criteria versus visual performance [AD-A219676] 17 p2438 N90-23889

The measurement of dark adaptation level in the presence of glare
[PB90-155987] 22 p3231 N90-28323

GLASS
NT BOROSILICATE GLASS
NT E GLASS
NT GLASS FIBERS
NT METALLIC GLASSES
NT S GLASS
NT SILICA GLASS
NT SPIN GLASS

Effect of thermal and cyclic loads on silicon carbide yarn reinforced glass matrix composites
[DE89-016554] 02 p0191 N90-11091
Fifth International Workshop on Glasses and Ceramics from Gels
[DE89-016899] 02 p0201 N90-11147
Electrolyte dependence of charge injection processes for electroactive polymer films
[AD-A210787] 02 p0202 N90-11152
Basic investigations of cutting machinability of inorganic glasses using single-point tools
[W-15/87] 02 p0210 N90-11204
Acoustic studies of new materials: Quasicrystals, low-loss glasses and high Tc superconductors
[AD-A211281] 02 p0272 N90-11551
Carbon fiber reinforced glass matrix composites for structural space based applications
[AD-A211682] 03 p0320 N90-11818
Current research in advanced materials
[DE89-017466] 03 p0331 N90-11884
Linear (passive) and non-linear guided and studies in glass
[AD-A211693] 03 p0406 N90-12325
Project, implementation, and utilization of composite structures
[ETN-89-95209] 04 p0466 N90-12665
Synthesis and high temperature chemistry of methylsilsesquioxane polymers produced by titanium catalyzed redistribution of methylhydridooligo- and polysiloxanes
[AD-A212000] 04 p0477 N90-12736
Synthesis and crystallization behavior of fluoride glasses
[AD-A212142] 04 p0478 N90-12741
Synthesis of inorganic polymers as glass precursors and for other uses. Preceramic block or graft copolymers as potential precursors to nanocomposite materials
[AD-A211978] 05 p0626 N90-13655
Preparation of 110K (Bi, Pb)-Sr-Ca-Cu-O superconductor from glass precursor
[NASA-CR-185162] 05 p0702 N90-14108
Dynamical structure of liquid and amorphous metals
[DE90-003805] 07 p0905 N90-15229
Development of glass-ceramic lasers
[AD-A214146] 07 p0936 N90-15423
Advanced study in solid transport: Rheological behavior of dense suspension
[DE90-003369] 07 p0947 N90-15483
Soft modes, freezing, and nonlinear response of a dipolar glass
[DE90-003647] 08 p1051 N90-16075
Basic studies on separative glass
[DE90-702436] 09 p1196 N90-16928
The preparation and characterisation of oxynitride glasses and glass-ceramics
[AD-A214783] 09 p1197 N90-16935
Superconducting Bi1.5Pb0.5Sr2Ca2Cu3O(x) ceramics by rapid melt quenching and glass crystallization
[NASA-CR-185184] 09 p1288 N90-17465
Solar cell coverglasses with enhanced thermal and mechanical properties 10 p1343 N90-17785
Structural and fast ion transport properties of glassy and amorphous materials
[DE90-005587] 10 p1356 N90-17877
Reflectance modulation with electrochromic Li(sub x)WO(3) films
[DE90-004571] 10 p1435 N90-18279
Evaluating a glass surface produced by ductile grinding
[DE90-006782] 11 p1496 N90-18608
Elimination of platinum inclusions in phosphate laser glasses
[DE90-004479] 12 p1629 N90-19361
Optical studies of dynamical processes in disordered materials
[DE90-007080] 12 p1631 N90-19372
Crystallization behavior and properties of BaO-Al2O3-2SiO2 glass matrices
[NASA-CR-185209] 12 p1631 N90-19374
Radiation-induced density changes and creep in surface layers of glass
[DE90-006112] 12 p1633 N90-19383
Instantaneously generated foam and its applicability to reduced gravity
[NASA-CR-185208] 13 p1784 N90-20237
The structural basis for fatigue initiation in glassy polymers
[DE90-009342] 14 p1956 N90-21200
High resolution stimulated Raman-Brillouin spectroscopy in gases and solids
[DE90-009535] 15 p2067 N90-21840
Brillouin gain spectroscopy in glasses and crystals
[DE90-009536] 15 p2067 N90-21841
Homogeneous dilute turbulent particle-laden water flows 15 p2090 N90-21965
Synthesis and characterization of aromatic polyester and polysiloxane containing block copolymers: Multiphase transparent atomic oxygen resistant damping materials, liquid crystal films, and toughening components of sol/gel glasses
[AD-A218871] 16 p2224 N90-22685
Simulation of inelastic deformation in glassy polypropylene and polycarbonate
[AD-A218891] 16 p2224 N90-22686
Investigation of atomistic simulation of structural and dynamic differences in glassy and liquid states of atactic poly(propylene)
[AD-A218896] 16 p2224 N90-22687
Material instabilities in solids
[AD-A218451] 16 p2247 N90-22817
Dielectric determination of the glass transition temperature (T sub g) 18 p2513 N90-24352
Indentation fracture of brittle materials
[DE90-010709] 18 p2572 N90-24657
Nucleation kinetics in undercooled, class-forming metallic melts
[ESA-TT-1186] 19 p2676 N90-25218
Sol-gel processing for fiber optic applications
[DE90-012083] 19 p2758 N90-25675
Vitreous joining of SiC fiber reinforced SiC composites
[DE90-012951] 20 p2827 N90-26081
Short-range structure of fluorine-modified phosphate glass
[DE90-013494] 20 p2839 N90-26145
Proceedings of a workshop on Lunar Volcanic Glasses: Scientific and Resource Potential
[NASA-CR-186631] 20 p2888 N90-26437
Diffusion of penetrants in polymers
[AD-A223217] 21 p2986 N90-26969
Processing Bi-Pb-Sr-Ca-Cu-O superconductors from amorphous state 22 p3150 N90-27860
Thermogravimetry-mass spectrometry analysis of gas bubbles in molten glass
[DE90-014116] 23 p3303 N90-28684
Surface chemistry and structural effects in the stress corrosion of glass and ceramic materials
[AD-A223305] 24 p3454 N90-29507
Lapping: Polishing and shear mode grinding
[DE90-015188] 24 p3458 N90-29533
A viscoelastic material model for computing stresses in glass
[DE90-014851] 24 p3481 N90-29673
Two terminal CuInSe2 based cascade cells
[DE90-000363] 24 p3485 N90-29697

GLASS COATINGS
Superconducting ceramics in the Bi1.5SrCaCu2O sub x system by melt quenching technique
[NASA-CR-185139] 02 p0281 N90-11606
Direct glassing of silicon solar cells
10 p1341 N90-17769
A concept of a pilot production plant for directly glassed silicon 10 p1341 N90-17770
Solar cell coverglasses with enhanced thermal and mechanical properties 10 p1343 N90-17785
Preparation and characterization of thin films based on sol-gel technique and development of spectroscopic probe for film formation and characterization
[AD-A221762] 21 p2988 N90-26984
Development of dual fiber reinforced glass matrix composites for structural space based applications
[AD-A223801] 24 p3444 N90-29446

GLASS FIBER REINFORCED PLASTICS
The high-frequency dielectric properties of glass fibre reinforced plastic and honeycomb layers
[AD-A210581] 01 p0051 N90-10289
Study of fatigue degradation mechanisms in unidirectional composite materials. Application to cumulative damage
[ECL-88-12] 05 p0619 N90-13611
Contribution to the fatigue behavior study of composite materials reinforced with unidirectional glass fibers
[ECL-88-20] 05 p0619 N90-13612
Preliminary experiments on filament winding nylon impregnated glass fibers (FIT)
[LR-545] 05 p0628 N90-13669
An analysis of drilling of composite materials
07 p0889 N90-15142
New materials and structural concepts for space transportation systems 09 p1179 N90-16837
Pressure air tightness tests of laminated panels for wing leading edge heat shields
[INFORME-I-377/89] 10 p1358 N90-17873
Enhanced bonding of fiber reinforcements to thermoset resins 11 p1476 N90-18496
Failure analysis of woven hybrid composite using a finite element method
[OUEL-1791/89] 15 p2065 N90-21828
Rheology of injection mould filling with DMCs
[NPL-DMA(A)-196] 16 p2222 N90-22675
Fatigue testing of glass fibre reinforced epoxy using the WISPER sequence
[FFA-TN-1989-45] 17 p2381 N90-23561
Tension fatigue of glass/epoxy and graphite/epoxy tapered laminates
[NASA-TM-102628] 19 p2671 N90-25191
Strain energy release rate analysis of delamination in a tapered laminate subjected to tension load
[NASA-TM-102592] 20 p2826 N90-26076
Erosion mechanisms in composite materials and ripple formation mechanism in erosion
[IAR-89-4-PT-1] 20 p2826 N90-26078
An examination of impact damage in glass-phenolic and aluminum honeycomb core composite panels
[NASA-TP-3042] 22 p3153 N90-27876
Study of an impact on organic matrix and long fibers composite plates (thermal aspect)
[ETCA-89-R-155] 22 p3154 N90-27882

GLASS FIBERS
Y-Si-Al-O-N glass fibers
[AD-A211170] 02 p0190 N90-11088
Automated glass fiber drawing
[DE90-000894] 06 p0751 N90-14367
Damping loss factor determination of glass and graphite fiber composites
[AD-A214535] 10 p1347 N90-17816
Damping loss factor determination of glass and graphite epoxy laminated composites using vertically oriented cantilever beams
[AD-A216529] 10 p1351 N90-17833
Thermal analysis of polymer composites
[AD-A216947] 11 p1490 N90-18578
Lunar regolith bagging system
[NASA-CR-186683] 19 p2677 N90-25223
Preparation and characterization of properties of oxynitride glasses and fibers
[AD-A221334] 19 p2677 N90-25227
The response and failure mechanisms of circular metal and composite plates subjected to underwater shock loading
[AD-A222200] 21 p3013 N90-27131
Development of dual fiber reinforced glass matrix composites for structural space based applications
[AD-A223801] 24 p3444 N90-29446

GLASS LASERS
Overview of laser concepts 01 p0029 N90-10154
Advanced source development and applications. Laser-produced plasmas: A compact soft x ray source with high peak brightness
[AD-A212677] 04 p0557 N90-13245
Ultrahigh-brightness lasers and their applications
[DE90-000877] 06 p0789 N90-14596
Laser glass (1989)
[DE90-002754] 07 p0909 N90-15257
Development of glass-ceramic lasers
[AD-A214146] 07 p0936 N90-15423
Spallation and dynamic fracture as an effect of laser induced shock waves in carbon based composite materials
[AD-A216540] 11 p1478 N90-18509
Generation of ultrashort laser pulses from neodymium glass oscillator and regenerative amplifier
14 p1984 N90-21373

GLASS TRANSITION TEMPERATURE
The 3F condensation polyimides: Review and update
[NASA-TM-102353] 06 p0750 N90-14363
Soft modes, freezing, and nonlinear response of a dipolar glass
[DE90-003647] 08 p1051 N90-16075
The preparation and characterisation of oxynitride glasses and glass-ceramics
[AD-A214783] 09 p1197 N90-16935
Thermomechanical properties of polymeric materials and related stresses
[NASA-TM-100758] 15 p2071 N90-21864
Dielectric determination of the glass transition temperature (T sub g) 18 p2513 N90-24352
Dynamic mechanical analysis of polymeric materials
18 p2513 N90-24353
Vitreous joining of SiC fiber reinforced SiC composites
[DE90-012951] 20 p2827 N90-26081

Composite materials with improved properties in compression: Copolymerization of 1,1-dimethyl-1-Silacyclopent-3-ene and 1,1-diphenyl-1-Silacyclopent-3-ene. Characterization of copolymer microstructures by H1, C13, and Si29 NMR spectroscopy
[AD-A221686] 21 p2972 N90-26892

GLASSWARE
Low temperature properties of glasses
02 p0200 N90-11141

GLASSY CARBON
Friction and wear of glassy carbon in sliding contact, revision 1
[DE90-000743] 06 p0750 N90-14365
Morphology changes due to oxidative treatment of glassy carbon electrodes and its applications
[AD-A219425] 17 p2371 N90-23501
Survival of carbon grains in shocks
21 p3090 N90-27567

GLAUBER THEORY
Positron collisions with alkali-metal atoms
11 p1556 N90-18962

GLAUERT COEFFICIENT
U AERODYNAMIC FORCES
U MACH NUMBER

GLIDE ANGLES
U GLIDE PATHS

GLIDE LANDINGS
Landing tests for Buran shuttle with jet engine-equipped mock-up
02 p0158 N90-10904

GLIDE PATHS
ILS mathematical modeling study of the effects of proposed hangar construction at the Orlando International Airport, Runway 17R, Orlando, Florida
[DOT/FAA/CT-TN89/52] 03 p0310 N90-11762

GLIDE SLOPES
U GLIDE PATHS

GLIDERS
Biochemical and physiological changes in glider pilots during multihour flights
[DLR-FB-89-29] 04 p0523 N90-13018
Schleicher ASK-21 glider (TG-9) stall and spin
[AD-A213513] 07 p0879 N90-15096
PLATO: A European plateform orbiter concept
[MBB-UO-0061/89-PUB] 19 p2652 N90-25095
The Penguin: A low Reynolds number powered glider for station keeping missions
[NASA-CR-186667] 19 p2658 N90-25129
Biochemical and physiological changes in glider pilots during multi-hour flights
[ESA-TT-1183] 19 p2722 N90-25484
Flight testing of a natural laminar flow airfoil using gliders
[PD-CF-9005] 20 p2801 N90-25936

GLINT
Analysis of phase retrieval in active imaging
[AD-A221080] 18 p2563 N90-24626
Laser radar angular tracking
[AD-A222741] 20 p2869 N90-26319

GLOBAL AIR POLLUTION
A preliminary analysis of US CO2 emissions reduction potential from energy conservation and the substitution of natural gas for coal in the period to 2010
[DOE/NBB-0085] 12 p1684 N90-19673

GLOBAL AIR SAMPLING PROGRAM
Airborne chemistry measurements
19 p2707 N90-25405

GLOBAL ATMOSPHERIC RESEARCH PROGRAM
Dynamics and energetics of the South Pacific Convergence Zone during FGGE SOP-1 and South Pacific Convergence Zone and global-scale
03 p0361 N90-12065
Guide on the global observing system
[WMO-488-REV] 08 p1103 N90-16385
The role of an upstream cyclone and corresponding synoptic/planetary-scale interactions during the development of a blocking anticyclone
08 p1150 N90-16659
Numerical simulations of the rapid cyclogenesis over Canada and evolution of a cold front observed on 25-26 April 1979 (SESAME-AVE-3)
09 p1247 N90-17234

GLOBAL POSITIONING SYSTEM
Guidance simulation and test support for differential GPS flight experiment
[NASA-CR-177471] 01 p0005 N90-10021
A high performance airborne INS/GPS Integrated Navigation System
02 p0149 N90-10850
High accuracy coordinate determination using the global positioning system
02 p0150 N90-10858
STS-GPS (Space Transportation System - Global Positioning System) tracking experiment for gravitation estimation: Feasibility study
[AD-A211265] 02 p0150 N90-10859
Sentinel satellite positional precision derived from the NAVSTAR global positioning system
[AD-A211876] 03 p0303 N90-11720
Discrete filtering techniques applied to sequential GPS range measurements
[NASA-CR-177472] 03 p0305 N90-11730
On the precision and reliability of GPS networks computed using the double difference observable
[ETN-89-95719] 04 p0449 N90-12571
Stable Kalman filters for processing clock measurement data
04 p0487 N90-12801
Geodetic point positioning with GPS (Global Positioning System) carrier beat phase data from the CASA UNO experiment
[AD-A211955] 04 p0514 N90-12970
Realization of a different NAVSTAR global positioning system for hydrographic surveying
[ETN-89-95720] 04 p0515 N90-12972
Test network Delft
[ETN-90-96009] 05 p0577 N90-13365
Geodetic network adjustment using GPS triple difference observations and a priori stochastic information
[TR-1-1987] 05 p0577 N90-13367
Processing of undifferences GPS carrier beat phase measurements and adjustment computations
[TR-5-1988] 05 p0578 N90-13368
Supplementing geodetic data with prior information for crustal deformation in the Imperial Valley, California
[TR-6-1988] 05 p0668 N90-13904
Advances in techniques and technologies for air vehicle navigation and guidance
[AGARD-AR-276] 08 p1020 N90-15899
GPS network analysis: The influence of stochastic prior information of orbital elements on ground station position measures
[TR-4-1988] 08 p1020 N90-15901
Regional height determination using gravimetric and topographical data
[UH-156] 08 p1091 N90-16315
Dynamic analysis of the geodetic networks originating from the Navstar/Global Positioning System (GPS) satellites
[SER-C-346] 08 p1091 N90-16316
Advances in Techniques and Technologies for Air Vehicle Navigation and Guidance
[AGARD-CP-455] 09 p1163 N90-16731
Recent developments in TERPROM
09 p1163 N90-16732
Integrated flight guidance system using differential-GPS for landing approach guidance
09 p1163 N90-16735
Miniature GPS-based guidance package
09 p1163 N90-16736
Modeling the effects of the use of GPS (Global Positioning System) derived altitude indication in the C-17A airdrop system
[AD-A215366] 09 p1166 N90-16748
Decision-analytic approach to rule-based expert system development using GPS (Global Positioning System) as the model
[AD-A216179] 10 p1319 N90-17626
The Fourteenth Biennial Guidance Test Symposium, volume 1
[AD-A216925] 11 p1455 N90-18383
Autonomous orbit determination using GPS
[INPE-4815-TDL/361] 11 p1466 N90-18442
The interpretation of crustal dynamics data in terms of plate interactions and active tectonics of the Anatolian plate and surrounding regions in the Middle East
[NASA-CR-186200] 11 p1533 N90-18824
Accuracy of global positioning system broadcast orbits for relative surveys
[PB90-125428] 12 p1602 N90-19218
Calculation of ionospheric corrections for single frequency GPS observations: Investigation of two models
[ETN-90-95450] 12 p1602 N90-19219
Carin and GPS: The combination of dead reckoning, map matching and satellite navigation in a hybrid automobile navigation system
[ETN-90-95451] 12 p1602 N90-19220
The global positioning system
[AD-A217266] 12 p1602 N90-19222
Interoperability issues in the use of satellite-based navigation systems for civil aviation purposes
[AD-A217279] 12 p1602 N90-19223
Determination of Earth orientation using the Global Positioning System
12 p1642 N90-19435
Applications of the GPS in photogrammetry
[ETN-90-96004] 12 p1680 N90-19648
GPS-aided gravimetry at 30 km altitude from a balloon-borne platform
13 p1834 N90-20530
Regional quasigeoid determination in Northern Germany and comparison with GPS
13 p1837 N90-20544
Long range geoid control through the European GPS traverse: Final results
13 p1837 N90-20545
Refinement of Earth's gravity field with Topex GPS measurements
13 p1838 N90-20553
Local gravity disturbance estimation from multiple-high-single-low satellite-to-satellite tracking
13 p1839 N90-20555
Satellite-to-satellite tracking experiment for global gravity field mapping
13 p1839 N90-20556
Ridge regression processing
14 p1907 N90-20931
Optimization of the effective GPS data rate
14 p1907 N90-20932
Sole means navigation and integrity through hybrid Loran-C and NAVSTAR GPS
14 p1907 N90-20933
Autonomous integrated GPS/INS navigation experiment for OMV, Phase 1: Feasibility study
[NASA-CR-4267] 14 p1914 N90-20969
Ambiguity bootstrapping to determine GPS orbits and baselines
[AD-A218206] 14 p1931 N90-21052
Precise estimation of tropospheric path delays with GPS techniques
15 p2074 N90-21881
Apparatus for and a method of determining compass headings
[AD-D014436] 16 p2199 N90-22551
The development of a real-time decimeter-level positioning system using Global Positioning System (GPS) technology
[AD-A218695] 16 p2199 N90-22552
Guidelines, operational procedures, and quality control for the estimation of geodetic point positions from GPS data collected with the TI4100 receiver
[AD-A218460] 16 p2250 N90-22829
Three approximate methods for estimating the best subset of GPS satellites for satellite position calculations
[AD-A220380] 17 p2350 N90-23383
Continued development and analysis of a new extended Kalman filter for the Completely Integrated Reference Instrumentation System (CIRIS)
[AD-A220106] 17 p2354 N90-23400
Satellite orbitography
17 p2359 N90-23432
The GPS-NAVSTAR location and navigation system
17 p2359 N90-23433
Satellite navigation system projects: European complement to GPS (CE-GPS), NAVSAT
17 p2360 N90-23434
Navigation programmes: Financial and institutional aspects
17 p2361 N90-23441
Orbit recovery of a low Earth orbiter from GPS and ground tracking stations
[FFI-89/7012] 17 p2361 N90-23446
Autonomous low earth orbit navigation
[REPT-892-440-101] 17 p2364 N90-23458
The use of additional Global Positioning System (GPS) observations in large scale photogrammetry
[ETN-90-96693] 17 p2418 N90-23778
Establishing a GPS-baseline between Seattle, Washington and Monterey, California
[AD-A220069] 18 p2495 N90-24262
GPS navigational performance in space rendezvous operations
18 p2504 N90-24310
The integration of GPS heights into the Australian height datum
19 p2705 N90-25392
Proceedings of the Second Symposium on GPS Applications in space, volume 1
[AD-A219978] 20 p2806 N90-25962
Proceedings of the Second Symposium on GPS Applications in Space, volume 2
[AD-A219979] 20 p2806 N90-25963
A reduced-dynamic technique for precise orbit determination
20 p2852 N90-26219
FAA Loran early implementation project
[AD-A221866] 21 p2956 N90-26805
Multistage estimation of received carrier signal parameters under very high dynamic conditions of the receiver
[NASA-CASE-NPO-17911-1-CU]
21 p2994 N90-27016
The global positioning system: A new tool for tectonic studies
21 p3014 N90-27137
Global positioning system overview/status
21 p3069 N90-27446
Future applications of GPS to conventional weapons
21 p3069 N90-27447
Potential new tactical applications of the Global Positioning System (GPS)
21 p3069 N90-27449
Report from GPS MANPACK tests in Spitsbergen area (Norway)
[FFI-90/7007] 22 p3114 N90-27692
Observation model and parameter partials for the JPL geodetic (GPS) modeling software 'GPSOMC'
[NASA-CR-186972] 22 p3132 N90-27774
Analysis, Design and Synthesis Methods for Guidance and Control Systems
[AGARD-AG-314] 24 p3423 N90-29338
GPS integrity requirements for use by civil aviation
24 p3423 N90-29339
Integration of GPS and strapdown inertial subsystems into a single unit
24 p3423 N90-29340

Combining LORAN and GPS: The best of both worlds
24 p3424 N90-29343
Techniques for autonomous GPS integrity monitoring
24 p3424 N90-29345
Modular digital GPS receivers
24 p3424 N90-29346
Integration of GPS/INS with partitioned filters
24 p3425 N90-29347
The 2-D and 3-D characterizations of GPS navigation service
24 p3425 N90-29348
Applications of differential GPS
24 p3425 N90-29349
An analysis of GPS as the sole means navigation system in US Navy aircraft
24 p3425 N90-29350
The determination of PDOP (Position Dilution of Precision) in GPS
24 p3425 N90-29351
Independent ground monitor coverage of Global Positioning System (GPS) satellites for use by civil aviation
24 p3428 N90-29364
Fault Detection and Isolation (FDI) techniques for guidance and control systems
24 p3428 N90-29366
A low cost inertial/GPS integrated approach to land navigation
24 p3430 N90-29374
An integrated system for land navigation
24 p3430 N90-29377

GLOBAL TRACKING NETWORK
World Weather Watch: Implementation
[WMO-714] 03 p0375 N90-12139

GLOBAL WARMING
Sensitivity of a regional oxidant model to variations in climate parameters, volume 1 and 2
[PB89-224943] 04 p0516 N90-12981
National Science Foundation
04 p0569 N90-13320
The impact of global warming on the energy system
[DE89-017775] 06 p0810 N90-14712
Climate projections with regional resolution
[DE90-000858] 06 p0810 N90-14715
Discussions of global environmental problems
[DE90-002747] 06 p0811 N90-14718
Carbon dioxide and climate: Summaries of research in FY 1989
[DE90-001791] 06 p0812 N90-14723
US energy use: New technologies and policies in response to global warming
[DE90-002170] 06 p0812 N90-14724
Responding to the threat of global warming: Options for the Pacific and Asia
[DE90-003553] 07 p0957 N90-15539
Global climate change and NEPA (National Environmental Policy Act) analyses
[DE90-003704] 07 p0958 N90-15540
Global climate change: A fossil energy perspective
[DE90-003770] 07 p0958 N90-15541
Scientific linkages in global change
[PB90-112608] 08 p1098 N90-16356
Prospect of new energy. Global warming (1988)
[DE90-702486] 09 p1244 N90-17217
The potential impact of conservation, alternative energy sources, and reduced nonenergy emissions on global warming
[DE90-004494] 09 p1244 N90-17220
Effects of global climate change on agroecosystems: Scope of work
[PB90-120023] 11 p1531 N90-18813
Atmospheric Radiation Measurement Program Plan
[DE90-008108] 13 p1829 N90-20504
Global Warming: A Northwest Perspective
[DE90-008140] 13 p1830 N90-20505
Draft global warming study
[DE90-008446] 13 p1830 N90-20507
Proceedings of the Conference on Technology-Based Confidence Building: Energy and Environment
[CNSS-PAPERS-22] 15 p2125 N90-22152
Options for controlling the global warming impact from motor vehicles
[PB90-161688] 22 p3197 N90-28142
Policy options for stabilizing global climate. Volume 1: Chapters 1-6
[PB90-182304] 22 p3198 N90-28146
Responding to the threat of global warming: Options for the Pacific and Asia
[DE90-014756] 23 p3347 N90-28918

GLOBULAR CLUSTERS
Effects of main-sequence mass loss on the turnoff ages of globular clusters
[DE89-016784] 02 p0295 N90-11678
Deep detection of hot star populations at balloon ultraviolet wavelengths
05 p0661 N90-13865
Ultraviolet properties of hot stars in globular clusters
06 p0862 N90-15007
The age of the galactic disk
[NASA-CR-186292] 07 p1013 N90-15869
Recent progress in understanding the eruptions of classical novae
[NASA-CR-186280] 07 p1014 N90-15870
Photometric analyses of abundances in dwarf spheroidal galaxies and globular clusters
12 p1736 N90-19978
A theoretical scenario for the dynamics of formation and early evolution of globular clusters in galaxies
15 p2187 N90-22494
Globular cluster X ray binaries
19 p2768 N90-25729
Optical observations of LMXB AC211(M15): Solving the puzzle
19 p2768 N90-25731
A search for radio pulsars in globular clusters and transient X ray sources
19 p2772 N90-25755
The formation of globular clusters
23 p3410 N90-29272
An observational study of disk-population globular clusters
24 p3560 N90-30145
The evolution of horizontal branch stars and the calibration of globular cluster ages
24 p3562 N90-30152

GLOBULINS
Characterization of biopolymer surfaces using scanning microscopies
[AD-A216572] 11 p1490 N90-18572

GLOSSARIES
U DICTIONARIES

GLOTRAC (TRACKING NETWORK)
U GLOBAL TRACKING NETWORK

GLOVES
Concepts for microgravity experiments utilizing gloveboxes
[NASA-TM-100378] 02 p0209 N90-11195
Studies on some failure modes in latex barrier films
[PB89-209308] 07 p0908 N90-15246
Handling and analysis of ices in cryostats and glove boxes in view of cometary samples
08 p1146 N90-16643
Ballast system for maintaining constant pressure in a glove box
[NASA-CASE-NPO-17786-1-CU]
09 p1224 N90-17104
Comparison of light duty gloves with natural and synthetic materials under wet and dry conditions
[AD-A218119] 13 p1856 N90-20649

GLOW
U LUMINESCENCE

GLOW DISCHARGES
Advances and directions of ion nitriding/carburizing
[NASA-TM-102398] 03 p0334 N90-11902
Development of laser excited atomic fluorescence and ionization spectrometric methods
[DE90-001567] 06 p0742 N90-14320
Study of microcrystalline, silicon-carbon p-layers prepared by photo-CVD and glow discharge
[DE89-009438] 06 p0850 N90-14939
Electron assisted glow discharges for conditioning fusion tokamak devices
[DE90-004104] 09 p1284 N90-17445
Hydrogenated amorphous silicon films prepared by glow discharge of disilane
[DE90-000309] 11 p1491 N90-18581
The 41st Annual Gaseous Electronics Conference
[AD-A214540] 12 p1715 N90-19851
The glow discharge as an atomization and ionization source
[DE90-007693] 13 p1771 N90-20163
Diagnostics of glow discharges used to produce hydrogenated amorphous silicon films
[DE90-000329] 18 p2522 N90-24402
Pulsed-discharge carbon dioxide lasers
18 p2556 N90-24587

GLUCOSE
Amperometric biosensors for glucose, lactate, and glycolate based on oxidases and redox-modified siloxane polymers
[DE90-002301] 06 p0781 N90-14541

GLUCOSIDES
Cellular and molecular mechanisms of high pressure inotropy in cardiac muscle
[AD-A211695] 03 p0381 N90-12170

GLUES
Design of glued joints, elastoplastic adhesives
[DRIC-T-8168] 03 p0333 N90-11894

GLUONS
Measurement of the fractional momentum carried by the gluons in the low Q squared photon-gluon fusion events at the ep HERA collider
[NOTA-INTERNA-937] 05 p0698 N90-14083

GLYCINE
Thermal expansion of LATGS crystals
[DE89-636239] 08 p1130 N90-16546

GLYCOLS
Synthesis and physical properties of poly(perfluoroalkylether) urethanes
[AD-A210500] 01 p0050 N90-10287
Thickness, velocity, and temperature measurements in falling liquid films
[DE90-004290] 08 p1063 N90-16151
Production and analysis by mass spectrometry of beams of polyglycol ions
15 p2066 N90-21835
Quantitative determination of 1, 2-ethanediol contamination in used diesel lubricating oils by gas chromatography/mass spectrometry
[AD-A218592] 17 p2371 N90-23498

GLYCOLYSIS
Heatstroke pathophysiology: The energy depletion model
[AD-A212156] 03 p0380 N90-12164

GLYCOSIDES
U GLUCOSIDES

GNEISS
Stored mafic/ultramafic crust and early Archean mantle depletion
[NASA-CR-186460] 12 p1691 N90-19715

GOALS
PISCES program plasma-surface interactions research
[DE89-015622] 02 p0276 N90-11578
Requirements of IR space astronomy
14 p1975 N90-21314
Langley aerospace test highlights, 1989
[NASA-TM-102631] 17 p2487 N90-24221
Making it happen: Project management
[PNR90618] 20 p2934 N90-26695

GODDARD EXPERIMENT PACKAGE TELESCOPE
U PARTICLE TELESCOPES

GODDARD TRAJECTORY DETERMINATION SYSTEM
Lifetime predictions for the Solar Maximum Mission (SMM) and San Marco spacecraft
05 p0591 N90-13440

GOERTLER INSTABILITY
Goertler instability on an airfoil: Comparison of marching solution with experimental observations
01 p0063 N90-10364
Stability theory applications to laminar-flow control
04 p0439 N90-12513
Interaction of Tollmien-Schlichting waves and Goertler vortices
04 p0440 N90-12515
Goertler instability on an airfoil
04 p0440 N90-12517
Experimental studies on Goertler vortices
04 p0442 N90-12529
Goertler vortices in growing boundary layers: The leading edge receptivity problem, linear growth and the nonlinear breakdown stage
[NASA-CR-181962] 10 p1306 N90-17555
On the instability of Goertler vortices to nonlinear travelling waves
[NASA-CR-181994] 14 p1970 N90-21289
On the receptivity problem for Goertler vortices: Vortex motions induced by wall roughness
[NASA-CR-182036] 19 p2654 N90-25109
Experimental study of the Taylor-Goertler instability
[ETN-90-97447] 22 p3175 N90-28014

GOES SATELLITES
NT GOES 4
GOES-I/M ascent maneuvers from transfer orbit to station
05 p0587 N90-13421
Data reduction of GOES (Geostationary Operational Environmental Satellite) information from DCP (Data Collection Platform) networks
[AD-A215844] 12 p1678 N90-19637
Research programs: Meteorological prediction, Oceanic processes, Climate and global change monitoring, Satellite instrumentation and calibration
19 p2714 N90-25447
Solar-geophysical data number 545, January 1990. Part 2 (Comprehensive reports). Data for July 1989 and miscellaneous
[PB90-182346] 22 p3263 N90-28480
Solar-geophysical data number 544, December 1989. Part 2 (Comprehensive reports). Data for June 1989 and miscellaneous
[PB90-171679] 22 p3264 N90-28482

GOES 4
The 27-28 October 1986 FIRE IFO cirrus case study: Cirrus parameter relationships derived from satellite and lidar data
[NASA-TM-103469] 20 p2890 N90-26447

GOGGLES
Night sky radiometric measurements during follow-on-evaluation testing of AN/PVS-7 (A, B) at Fort Benning, Georgia
[AD-A211273] 02 p0276 N90-11574
Visual acuity and stereopsis with night vision goggles
[AD-A211552] 03 p0381 N90-12167
Attenuating the luminous output of the AN/PVS-5A night vision goggles and its effects on visual acuity
[AD-A214895] 09 p1261 N90-17311
Human factors engineering testing of aircraft cockpit lighting systems
[AD-A216853] 12 p1697 N90-19743
The application of kriging in the statistical analysis of anthropometric data, volume 1
[AD-A220613] 17 p2438 N90-23891

The application of kriging in the statistical analysis of anthropometric data, volume 2
[AD-A220614] 17 p2438 N90-23892
The application of kriging in the statistical analysis of anthropometric data, volume 3
[AD-A220615] 17 p2438 N90-23893
Field evaluation of laser protective eyewear
[AD-A221324] 18 p2586 N90-24725

GOLD
NT GOLD ISOTOPES
Multiple internal reflection Fourier transform infrared spectroscopy studies of thiocyanate adsorption on silver and gold
[AD-A210245] 01 p0041 N90-10223
X ray diffraction patterns of metal aurocyanides
[DE89-015188] 03 p0326 N90-11851
The effects of trace anions on the voltammetry of single crystal gold surfaces
[AD-A211886] 04 p0558 N90-13254
Rapidity densities and their fluctuations in central 200 A GeV S32 interations with Au and Ag,Br nuclei
[LUIP-8905] 07 p0989 N90-15715
Fundamental studies of surface processes and trace analysis using solid electrodes
[AD-A216538] 11 p1483 N90-18533
Defect structures in copper and gold irradiated with fast neutrons, 14 MeV neutrons and 600 to 800 MeV protons
[DE90-007529] 12 p1629 N90-19359
Particle emission by oblique ion bombardment of gold
[ETN-90-95825] 12 p1711 N90-19327
Infrared and X ray photoelectron spectroscopy studies of the polyimide/metal interface
[AD-A218249] 13 p1773 N90-20179
Compatibility of Au base thick films with solder alloys: Solid state growth of intermetallics
[DE90-009285] 14 p1952 N90-21175
Microstructure of Au/Nb multilayers
[DE90-008722] 14 p2033 N90-21662
Lateral spreading of Au contacts on InP
[NASA-TM-103133] 16 p2252 N90-22843
Modes of attachment of pyridine to gold surfaces
[AD-A219519] 17 p2372 N90-23504
An examination of the relationship between SERS intensities and surface concentration for pyridine adsorbed at the gold/aqueous solution interface
[AD-A219520] 17 p2372 N90-23505
An analysis of the contact sintering process in III-V solar cells
[NASA-TM-103179] 19 p2709 N90-25420
Analysis of strain relaxation in Au/Ni multilayers by x ray diffraction
[IAR-89-25] 20 p2875 N90-26357
Synthesis and structural chemistry of Au(III)-substituted Ba2YCu3O(7-delta)
[NASA-TM-103292] 23 p3305 N90-28696
XANES and EXAFS study of Au-substituted YBa2Cu3O(7-delta)
[NASA-TM-103291] 23 p3401 N90-29219

GOLD COATINGS
Wear of gold-plated contacts: Microscopic aspects, role of oxygen 18 p2538 N90-24479

GOLD ISOTOPES
Strangeness enhancement in 14.6 A GeV/c Si–Au interactions?
[DE90-008826] 14 p2026 N90-21616
Studies of central interactions of Si ions at 14.5 x A GeV/c in Au and Cu
[DE90-015095] 23 p3397 N90-29195

GOLD PLATE
U GOLD COATINGS

GONADS
NT TESTES

GOODNESS OF FIT
Computer problems in goodness-of-fit
[AD-A211411] 03 p0397 N90-12268
Theory of goodness of fit tests and scanning innovation martingales
[CWI-BS-R8904] 05 p0693 N90-14046

GOSS (SUPPORT SYSTEM)
U GROUND OPERATIONAL SUPPORT SYSTEM

GOVERNMENT PROCUREMENT
Congressional involvement and relations: A guide for Department of Defense acquisition managers
[AD-A214408] 07 p1011 N90-15855
Defense Small Business Innovation Research (SBIR) Program: Program solicitation 90.1, FY-1990
[AD-A215350] 09 p1294 N90-17503
Current information technology resource requirements of the Federal government: Major systems acquisitions and planned resources
[PB90-146820] 15 p2177 N90-22439
Small business innovation research program solicitation: Closing date July 16, 1990
[NASA-TM-101798] 17 p2479 N90-24173
Aircraft modifications cost analysis. Volume 1: Overview of the study
[AD-A220764] 19 p2649 N90-25074
Space transportation: NASA has no firm need for increasingly costly orbital maneuvering vehicle
[GAO/NSIAD-90-192] 20 p2819 N90-26041
Space shuttle: Follow-up evaluation of NASA's solid rocket motor procurement. Report to the Chairman, Committee on Government Operations, House of Representatives
[GAO/NSIAD-89-89] 20 p2824 N90-26066
Multivariate model building and model identification
[AD-A221619] 21 p3067 N90-27435

GOVERNMENT/INDUSTRY RELATIONS
Small business innovation research: Program solicitation
[NASA-TM-101869] 05 p0705 N90-14126
Accessing Japanese technical information: A group of essays extracted from the NTIS (National Technical Information Service) Directory of Japanese Technical Resources in the United States for 1987 and 1988
[PB90-100165] 06 p0858 N90-14992
DOD (Department of Defense) Freedom of Information Act Program (incorporating changes 1 and 2)
[PB90-104753] 06 p0859 N90-14993
Report of NASA Lunar Energy Enterprise Case Study Task Force
[NASA-TM-101652] 07 p1007 N90-15836
Report of the NASA lunar energy enterprise case study task force 07 p1008 N90-15837
Defense Small Business Innovation Research (SBIR) Program: Program solicitation 90.1, FY-1990
[AD-A215350] 09 p1294 N90-17503
Promotion of European Space Technology Transfer
[ESA-SP-1122] 11 p1575 N90-19068
DTE and space technology transfer 11 p1576 N90-19071
Introductory remarks for the panel discussions on technology transfer 11 p1576 N90-19075
Problems on transfer of space technology to non-space areas and solutions: Legal aspects 11 p1577 N90-19077
The improvement of technology transfer from space to industry 11 p1577 N90-19079
Small business innovation research program solicitation: Closing date July 16, 1990
[NASA-TM-101798] 17 p2479 N90-24173
Enhancing US competitiveness through Federal scientific and technical information: Issues and opportunities 22 p3258 N90-28450
Goverment's role in standards-related activities: Analysis of comments
[PB90-215534] 23 p3404 N90-29239
State science and technology indicators: An exploratory profile and analysis
[PB90-246711] 23 p3408 N90-29259

GOVERNMENTS
The transfer and diffusion of new technologies: A review of the economics literature
[DE89-015671] 02 p0290 N90-11655
Congressional involvement and relations: A guide for Department of Defense acquisition managers
[AD-A214408] 07 p1011 N90-15855
Federal roles to realize national energy-efficiency opportunities in the 1990s
[DE90-004410] 08 p1096 N90-16348
Study on the measures to promote the use of photovoltaic power generating system overseas
[DE90-742056] 11 p1530 N90-18807
The essence of spacepower: Important influences on the evolution of national spacepower
[AD-A217498] 13 p1879 N90-20781
The influence of adjacent seating configurations on egress through a type 3 emergency exit
[AD-A218393] 17 p2348 N90-23371
Federal Scientists and Engineers: 1988. (Detailed statistical tables)
[PB90-226895] 22 p3256 N90-28437
Goverment's role in standards-related activities: Analysis of comments
[PB90-215534] 23 p3404 N90-29239
FEDIX: An on-line information service for universities and other research organizations: User's guide
[DE90-014835] 24 p3559 N90-30137

GOVERNORS
U SPEED REGULATORS

GRABENS
U GEOLOGICAL FAULTS

GRADIENTS
NT ELECTRON DENSITY PROFILES
NT POTENTIAL GRADIENTS
NT PRESSURE GRADIENTS
NT TEMPERATURE GRADIENTS
NT THERMOCLINES
A unified view of infinitesimal perturbation analysis and likelihood ratios
[AD-A210682] 01 p0114 N90-10652
Height and gradient from shading
[AD-A212338] 04 p0504 N90-12908
The phase gradient autofocus algorithm: An optimal estimator of the phase derivative
[DE90-000895] 06 p0828 N90-14814
Gradient projection techniques for large-scale optimization problems
[DE90-001986] 07 p0973 N90-15618
And still, a new beginning: The Galerkin least-squares gradient method
[DE89-636435] 08 p1116 N90-16461
Optimal iteration steps by stochastic approximation processes for the solution of optimization problems with twice differentiable functions
[ETN-90-95887] 12 p1708 N90-19809
Alternating gradient photodetector
[NASA-CASE-NPO-17235-1-CU] 14 p1982 N90-21358
Electromagnetic inverse profiling of stratified media
[ETN-90-96402] 15 p2087 N90-21947
Determination of the gravity disturbance by processing the gravity gradiometer surveying system: Processing procedure and results
[AD-A219992] 17 p2423 N90-23808
Gradient microphone for measurement of the vectorial sound velocity
[MBB-Z-0259/89-PUB] 19 p2650 N90-25080
A decision-making aid for multi-layer radar absorbent coverings
[ESA-TT-1173] 19 p2684 N90-25267
Automated sensitivity analysis with the Gradient Enhanced Software System (GRESS)
[DE90-011291] 20 p2906 N90-26529
Algorithms to solve nonlinear time dependent problems of engineering and physics
[AD-A221463] 21 p3055 N90-27366
Probing the possibility of a C-12/C-13 galactic abundance gradient 21 p3094 N90-27586

GRADIOMETERS
Terrestrial gravity instrumentation in the 20th Century: A brief review 13 p1834 N90-20527
A discussion of observation model, error sources and signal size for spaceborne gravitational gradiometry 13 p1839 N90-20557
Studies of an orbital gradiometer mission 13 p1839 N90-20558

GRADUATION
U CALIBRATING

GRAFTING
Graft copolymers of rigid-rod poly(p-phenylenebenzobisimidazole)
[AD-A220369] 17 p2380 N90-23555

GRAIN BOUNDARIES
Progress report on grain boundaries
[DE89-015541] 01 p0130 N90-10749
Grain boundary chemistry in irradiated stainless steel and its influence on environmental degradation
[DE89-016827] 02 p0197 N90-11125
Deformation induced microstructural and microchemical changes during thermomechanical treatment
[DE89-017266] 02 p0197 N90-11127
Influence of core-shell grains on the internal stress state and permittivity response of zirconia modified barium titanate
[AD-A211245] 02 p0202 N90-11153
Intergranular and interphase boundaries in ceramics
[DE89-016969] 02 p0202 N90-11154
Kinetics and mechanisms of primary and steady state creep in B- and Al-containing alpha silicon carbide
[AD-A210739] 02 p0283 N90-11616
Elevated temperature aluminum-titanium alloy by powder metallurgy process
[AD-D014165] 03 p0326 N90-11852
Kinetic processes in advanced alloys
[AD-A212049] 03 p0329 N90-11867
Characterization of the Structure and Chemistry of Defects in Materials: Proceedings, volume 138
[DE89-014796] 03 p0410 N90-12352
Effects of grain boundary chemistry on critical current density in oxide superconductors
[DE89-017780] 03 p0412 N90-12365
SEM (Scanning Electron Microscope) image analysis of grain growth in microwave-annealed alumina
[DE90-001606] 06 p0746 N90-14339
Elastic softening in nanocrystalline silicon
[DE90-002268] 06 p0752 N90-14377
Characterization of nanophase materials by x ray diffraction and computer simulation
[DE90-002270] 06 p0752 N90-14378
The feasibility of welding of irradiated materials
[DE90-002200] 06 p0795 N90-14631
Atomic matching across internal interfaces
[DE90-002266] 06 p0841 N90-14889

Anisotropy of oxygen tracer diffusion in YBa2Cu3O7-delta single crystals
[DE90-001931] 06 p0856 N90-14979
Quasicrystals and grain boundaries
[DE90-002213] 06 p0857 N90-14981
High resolution electron microscopy of grain boundaries in nanophase palladium
[DE90-003823] 07 p1002 N90-15800
Computer simulation of electromigration in thin films
[AD-A216382] 10 p1357 N90-17867
The electronic structure of sigma 5 grain boundaries in Cu
[DE90-005999] 10 p1437 N90-18294
A micromechanical viscoplastic stress-strain model with grain boundary sliding
[DE90-006013] 10 p1437 N90-18295
Evaluation of radiation-induced sensitization using electrochemical potentiokinetic reactivation technique for austenitic stainless steels
[DE90-002708] 12 p1627 N90-19352
Glancing angle XAFS (X ray Absorption Fine Structure) and x ray reflectivity studies of transition-metal/aluminum interfaces
[DE90-005575] 12 p1627 N90-19353
The effects of gradients on boundary stability
[DE90-007428] 12 p1722 N90-19894
Tellurium embrittlement of type 316 steel
[AERE-R-13440] 13 p1776 N90-20192
Dynamics of the solidification front
13 p1785 N90-20243
Enhanced ceria solid electrolyte fuel cell development. Reduction of electronic conductivity permits use of a solid ceria electrolyte in high efficiency high power density fuel cells at temperatures compatible with metallic cell hardware
[AD-A217840] 13 p1828 N90-20498
Characterization of failure processes in tungsten copper composites under fatigue loading conditions
[NASA-TM-102371] 14 p1943 N90-21123
A STEM study of changing grain boundary chemistry during the sensitisation of AISI 304 stainless steel
[AERE-R-13418] 14 p1949 N90-21157
Current fluctuations associated with localised corrosion: Mechanistic studies of the early stages of pitting and stress corrosion cracking of stainless steel
[AERE-R-13531] 14 p1950 N90-21159
Mathematical modelling of intergranular attack in stainless steels: A preliminary study
[AERE-M-3698] 14 p1950 N90-21160
Grain boundary precipitation in Ni3Al based alloys
[AERE-R-13362] 14 p1950 N90-21161
Grain boundary chemistry effects on irradiation-assisted stress corrosion cracking
[DE90-008623] 14 p1951 N90-21167
Anisotropy of grain growth in alumina
[DE90-009045] 14 p2032 N90-21655
High voltage/high resolution studies of metal and semiconductor interfaces
[DE90-009065] 14 p2032 N90-21656
Simulated image maps for use in experimental high-resolution electron microscopy
[DE90-009176] 14 p2032 N90-21657
Grain boundary intermetallic phases in alloy 718
[DE90-009812] 15 p2173 N90-22417
A study of the relation between grain boundary type and sensitisation in a partially-sensitised AISI 304 stainless steel using electron back-scattering patterns
[AERE-R-13327] 16 p2321 N90-23234
Ultrahigh carbon steels and their laminates
[AD-A218780] 17 p2376 N90-23530
Cyclic damage zones ahead of tensile fatigue cracks in ceramic materials
[DE90-008372] 18 p2531 N90-24442
Investigations of ultrasonic wave interactions at imperfect boundaries separating anisotropic materials
[DE90-010661] 18 p2612 N90-24875
Electromigration in metallic microstructures
[AD-A221208] 18 p2622 N90-24942
Microstructural dependence of the cavitation damage function in FCC materials
[DE90-012898] 20 p2833 N90-26113
Densification studies of refractory materials using Hot Isostatic Pressing (HIP) and tantalum containment
[DE90-013481] 20 p2833 N90-26114
Diffusion-accommodated grain boundary sliding in a polycrystal
[DE90-012727] 20 p2930 N90-26668
Molecular dynamics simulations of grain-boundary diffusion for varying tilt angle geometries
[DE90-012919] 20 p2930 N90-26669
Fracture-EXAFS: A new method for the study of interfaces in thin films and polycrystalline materials
[DE90-013736] 21 p3081 N90-27521
Effects of grain size and grain boundary on critical current density of high T(sub c) superconducting oxides
22 p3146 N90-27843
High-temperature deformation and microstructural analysis for Si3N4-Sc2O3
[NASA-TM-103239] 23 p3314 N90-28740
Interface formation and percusory dynamics
[AD-A224128] 23 p3402 N90-29223
Processability and high temperature behavior of emerging aerospace alloys
[AD-A224285] 24 p3448 N90-29475
Alloy design of ordered intermetallics
[DE90-016031] 24 p3451 N90-29490
Atomistic studies of grain boundaries in alloys and compounds
[DE90-012401] 24 p3452 N90-29492

GRAIN SIZE
Fatigue crack initiation mechanics of metal aircraft structures
[AD-A210567] 01 p0045 N90-10255
The measurement of infrared spectra of dense ceramics by specular reflectance spectroscopy
[AD-A210609] 01 p0051 N90-10291
Preparation, purification and densification of zinc sulfide powder from organometallics
[AD-A210943] 01 p0052 N90-10298
Influence of grain refining on the casting, physical, mechanical, and electrochemical properties of technical aluminum
[ETN-89-94661] 02 p0199 N90-11135
Investigation of commercial Al-Ti and Al-Ti-B master alloys and development of a new grain refining agent based on carbides for aluminum and aluminum alloys
[ETN-89-94663] 02 p0199 N90-11136
Kinetic processes in advanced alloys
[AD-A212049] 03 p0329 N90-11867
Carbonitrition response of steel plates not destined for heat treatments
[CETIM-106960] 04 p0476 N90-12728
Metallo-organic decomposition process for dielectric films
[AD-A211590] 04 p0495 N90-12849
Irradition-induced grain growth: Role of dislocations
[DE90-003565] 07 p1001 N90-15792
Effect of heat treatment on the fracture toughness transition properties of an A508 class 3 steel
[AERE-R-13548] 13 p1774 N90-20182
Processing, fabrication, characterization and device demonstration of high temperature superconducting ceramics
[AD-A218330] 13 p1782 N90-20231
A systematic study of the effects of metal substitutions for Cu in YBa(sub 2) (Cu(sub 1-x) M(sub x))3 O(sub 7-rho), M=Fe, Co, Al, Ga, Cr, Ni, and Zn
[DE90-003957] 13 p1892 N90-20857
Methods for improving the flowability of a percussion primer composition
[MRL-TR-89-32] 14 p1956 N90-21201
Structure-property relations in aluminum-lithium alloys
[AD-A219183] 16 p2222 N90-22672
Grain growth and phase formation in ion irradiated/annealed thin Ni-Al alloys films
[DE90-010409] 18 p2525 N90-24407
Grain-size distribution and armoring in gravel-bed rivers: A case study 19 p2687 N90-25285
Strengthening in heavily cold worked Cu-20 vol. percent Fe in situ composites
[DE90-011741] 22 p3135 N90-27790
Effects of grain size and grain boundary on critical current density of high T(sub c) superconducting oxides
22 p3146 N90-27843
The affect of gravity on particle collection in inertial impactors
[DE90-013372] 23 p3393 N90-29173
Microstructure of alpha-Al base matrix/SiC particulate composites
[DE90-014894] 24 p3444 N90-29449
Processing of nanocrystalline ceramics
[DE90-015700] 24 p3456 N90-29520

GRAINS (FOOD)
NT WHEAT

GRAMMARS
Computer generation of a tutorial dialogue
[AD-A211976] 03 p0380 N90-12162
Augmentations of grammatical categories in distributional-algebraic models of natural languages
[REPT-89-24] 03 p0396 N90-12262
Abstract grammars based on transductions
[MEMO-INF-89-7-REV] 04 p0531 N90-13063
A table-driven approach to fast context-free parsing
[AD-A212210] 04 p0533 N90-13082
The inside-outside algorithm: Further experiments on three and four letter word spelling and implementation on an array processor
[RSRE-MEMO-4256] 08 p1110 N90-16426
Computational structure of GPSG (Generalized Phrase Structure Grammar) models: Revised generalized phrase structure grammar
[AD-A216803] 11 p1553 N90-18941
An introduction to Montague grammar
[REPT-89-46] 15 p2147 N90-22266
Some remarks on treatment of be in Montague's PTQ --- Proper Treatment of Quantification (PTQ)
[REPT-89-40] 15 p2147 N90-22267
Learning artificial grammars with competitive chunking
[AD-A219270] 16 p2265 N90-22911
Research in knowledge delivery
[AD-A219920] 17 p2480 N90-24180
Higher order attribute grammars
[RUU-CS-89-4] 18 p2590 N90-24735
Modular parser generation
[CWI-CS-R8933] 18 p2592 N90-24745
ATN design tool
[AD-A223030] 20 p2911 N90-26559
Grammar, punctuation, and capitalization: A handbook for technical writers and editors
[NASA-SP-7084] 20 p2937 N90-26710
Short encodings of evolving structures
[AD-A223641] 24 p3527 N90-29944

GRAND TOURS
The Gevaltig: An inertial fusion powered manned spacecraft design for outer solar system missions
[NASA-CR-185163] 08 p1036 N90-15985

GRAND UNIFIED THEORY
The track-etch detector for the MACRO experiment at the Gran Sasso Laboratory
[DE90-003235] 11 p1594 N90-19182
Feasibility for EGRET detection of antimatter concentrations in the universe 16 p2338 N90-23323
Microwave background distortions from domain walls
[NASA-CR-187272] 24 p3462 N90-29556

GRANTS
Energy storage and distribution program summary. Volume 2: Research summaries, fiscal year 1988
[DE89-000867] 01 p0083 N90-10470
NSF Tokyo reports. Twenty-one new areas added for support under Monbusho's priority research area grants
[PB90-199589] 22 p3265 N90-28488

GRANULAR MATERIALS
A numerical laboratory for granular solids
[DE89-016367] 03 p0358 N90-12045
Fractional charging and reentrance in granular superconductors 04 p0557 N90-13248
Statistical model for particle-void deformation kinetics in granular materials during shock wave propagation
[DE89-017729] 07 p0946 N90-15476
A method for measuring the material moduli of granular materials: Flow in an orthogonal rheometer
[DE90-007160] 13 p1801 N90-20339
Experimental and analytical investigations of granular materials: Shear flow and convective heat transfer
15 p2091 N90-21988

GRAPH THEORY
On the 2-extendability of planar graphs
[AD-A210289] 01 p0112 N90-10642
Extending matchings in planar graphs 4
[AD-A210315] 01 p0113 N90-10643
A graph-theoretical approach to block-copolymer complexes. Part 3: Loops and cycles
[MEMO-778-PT-3] 04 p0479 N90-12750
Placing mirrors in grids
[CWI-CS-R8906] 04 p0543 N90-13154
Long dominating cycles and paths in graphs with large neighborhood unions
[MEMO-769] 04 p0544 N90-13157
Novel graph searching methods for image analysis
[AD-A213065] 05 p0682 N90-13971
On smallest nonhamiltonian regular rough graphs
[MEMO-788] 05 p0687 N90-14003
Hamiltonian properties of graphs with large neighborhood unions
[MEMO-779] 05 p0689 •N90-14013
A graph theoretic characterization for the rank of the transfer matrix of a structured system
[CWI-OS-R8819] 05 p0695 N90-14064
Overview and extensions of a system for routing directed graphs on SIMD architectures 08 p1113 N90-16444
Matching extension in regular graphs
[AD-A214757] 09 p1266 N90-17339
A theory for graph-based language specification, analysis, and mapping with application to the development of parallel software
[AD-A214910] 09 p1266 N90-17342
Faster scaling algorithms for general graph matching problems
[AD-A215112] 10 p1417 N90-18163
Theoretical and experimental analyses of parallel combinatorial algorithms
[AD-A216407] 10 p1420 N90-18186
Long path connectivity of regular graphs
[AD-A216477] 11 p1552 N90-18933
Finding critical independent sets and critical vertex subsets are polynomial problems
[AD-A216547] 11 p1552 N90-18938

Minimum cycle covering and integer flows
[AD-A216546] 12 p1705 N90-19785
Panconnectivity of locally connected K(1,3)-free graphs
[AD-A216548] 12 p1705 N90-19786
Almost-optimum parallel speed-ups of algorithms for bipartite matching and related problems
[AD-A215111] 13 p1871 N90-20728
On the existence of local times: A geometric study
[AD-A218337] 13 p1879 N90-20776
A VLSI decomposition of the deBruijn graph
15 p2077 N90-21895
Clustering and uniqueness in mathematical models of percolation phenomena
[ETN-90-96400] 15 p2163 N90-22358
Coloring a graph optimally with two colors
[MEMO-820] 17 p2449 N90-23961
Remarks on Hamiltonian properties of claw-free graphs
[MEMO-829] 17 p2462 N90-24065
Graph representation in a special family of infinite graphs
[MEMO-831] 17 p2463 N90-24067
A general approach to dominance in the plane
[RUU-CS-88-35] 17 p2463 N90-24072
On the structure at infinity of a structured system
[CWI-BS-R8918] 17 p2468 N90-24108
Knowledge graphs and natural language
[MEMO-811] 18 p2592 N90-24746
Construct analysis in knowledge graphs
[MEMO-815] 18 p2599 N90-24794
Achromatic number is NP-complete for cographs and interval graphs
[RUU-CS-88-25] 18 p2600 N90-24803
Ranking intervals under visibility constraints
[RUU-CS-89-18] 18 p2602 N90-24812
A RUTCOR project in discrete applied mathematics
[AD-A221191] 18 p2604 N90-24831
Around three lemmas in Hamiltonian graph theory
[MEMO-816] 18 p2606 N90-24846
Process and representation in graphical displays
19 p2740 N90-25574
Combinatorial problems using a hypercube and Hamming graphs
[ETN-90-97240] 20 p2919 N90-26609
Maintenance of a minimum spanning forest in a dynamic planar graph
[AD-A221425] 21 p3054 N90-27362
Graph structure model
[DE90-014930] 23 p3381 N90-29097
Using minimal spanning trees to compare the reliability of network topologies
[NASA-TM-4208] 24 p3539 N90-30014

GRAPHIC ARTS
NT COMPUTER ANIMATION
Post crash flight analysis: Visualizing flight recorder data
[AD-A212063] 03 p0302 N90-11715
The employment of SITIM-150 as an instructional objective for training in remote sensing
[INPE-4833-PRE/1463] 10 p1440 N90-18310
Graphics mini manual
[NASA-TM-87622-REV] 15 p2144 N90-22247
Cognitive efficiency considerations for good graphic design
[AD-A218976] 16 p2263 N90-22899
A task-analytic approach to the automated design of information graphics
[AD-A219271] 16 p2265 N90-22912
Pictorial communication: Pictures and the synthetic universe 16 p2267 N90-22919
Synesthetic art through 3-D projection: The requirements of a computer-based supermedium
16 p2274 N90-22962
Wide-angle display developments by computer graphics 16 p2275 N90-22963
An abstract data model for the IDEF sub 0 graphical analysis language
[AD-A219855] 17 p2446 N90-23948
Computer-Aided Structural Engineering (CASE) project. User's guide: A Three-Dimensional Stability Analysis/Design Program (3DSAD). Report 2: General loads module
[AD-A220331] 18 p2591 N90-24742
Perspective transformation for wide-view sky scenes
[AD-A222694] 21 p3007 N90-27093
Multi-user facility for high performance optical recording of brain activity (DURIP)
[AD-A223491] 24 p3498 N90-29768
Computer-Aided Structural Engineering (CASE) project: Investigation and design of U-frame structures using program CUFRBC. Volume A: Program criteria and documentation
[AD-A224387] 24 p3525 N90-29934

GRAPHITE
NT PYROLYTIC GRAPHITE
PMR graphite engine duct development
[NASA-CR-182228] 01 p0008 N90-10037
Development of graphite-magnesium composites for space applications 02 p0185 N90-11054
Modifications to the aerotherm charring material thermal response and ablation program (CMA) for carbon ablation analysis
[AD-A211069] 02 p0195 N90-11115
Spin fluctuations and excitations in a 2D xy-ferromagnet: CoCl2 in graphite
[DE89-017600] 02 p0196 N90-11119
Carbon in detonations
[DE89-016037] 02 p0208 N90-11189
Calculation of the refractive index change in dissociating shocked benzene
[DE89-017737] 03 p0322 N90-11833
Analysis of carbon fiber's x ray microscopic structure
[AD-A212215] 04 p0480 N90-12752
An investigation of diamond film deposition in a premixed oxyacetylene flame
[AD-A212595] 04 p0561 N90-13268
Implementation and analysis of adhesion in multimaterials of the type Al(Si)-ZrO2 and graphite, metal or ceramics
[ECL-89-004] 05 p0628 N90-13667
Density of intercalated graphite fibers
[NASA-TM-102411] 06 p0750 N90-14362
Kinetics of the graphite/oxygen reaction in the in-pore diffusion controlled regime. Part 3: Influence of boundary layer diffusion in kinetic experiments at temperatures 970K to 1170K
[JUEL-2284-PT-3] 08 p1042 N90-16024
Interfaces of organic matrices and graphite fiber composites: A review of the literature
[AD-A214504] 09 p1186 N90-16870
Damping loss factor determination of glass and graphite fiber composites
[AD-A214535] 10 p1347 N90-17816
Extracting chemical information form Auger line shapes
[AD-A216729] 11 p1483 N90-18537
Fluorinated graphite fibers as a new engineering material: Promises and challenges
[NASA-TM-102511] 12 p1618 N90-19301
Exchange and correlation effects in the Visscher-Falicov model for metal intercalated graphite
[DE90-610553] 12 p1627 N90-19349
The role of polarity on the stability of graphitic compounds
[DE90-006528] 13 p1780 N90-20218
Resistivity of pristine and intercalated graphite fiber epoxy composites
[NASA-TM-102576] 14 p1955 N90-21192
Morphological control of inter-penetrating polymer networks 18 p2642 N90-25046
Electronic and molecular structure of carbon grains
21 p3091 N90-27574
A unifying picture of gas-phase formation and growth of PAH (Polycyclic Aromatic Hydrocarbons), soot, diamond and graphite 21 p3091 N90-27575
NPL absorbed dose graphite calorimeter correction for the effect of the gaps around the core
[NPL-RSA(EXT)-12] 22 p3178 N90-28032
Crash-impact behavior of graphite/epoxy composite sine wave webs 23 p3300 N90-28667

GRAPHITE-EPOXY COMPOSITES
The interlaminar fracture toughness of woven graphite/epoxy composites
[NASA-TP-2950] 01 p0033 N90-10179
Space environment effects on carbon/epoxy materials
02 p0185 N90-11056
Delamination tests under static compression loading
02 p0186 N90-11061
A study of progressive cracking damage to carbon-epoxy composites and methods of crack reduction
[REPT-RE-49-324/F] 04 p0467 N90-12676
Lightweight composite reflector panels
05 p0596 N90-13462
Static and free-vibrational response of semi-circular graphite-epoxy frames with thin-walled open sections
[NASA-CR-186097] 05 p0617 N90-13600
Gravimetric measurements of materials outgassing applied to graphite-epoxy laminates
[NASA-TM-100753] 05 p0619 N90-13609
Measurement of damping of graphite epoxy composite materials and structural joints
[NASA-CR-183802] 06 p0736 N90-14286
An analysis of drilling of composite materials
07 p0889 N90-15142
Probabilistic simulation of uncertainties in composite uniaxial strengths
[NASA-TM-102483] 08 p1040 N90-16008
Review of investigations on aeronautical fatigue in the Federal Republic of Germany
[LBF-S-182] 08 p1089 N90-16302
The effect of loading on the laser ablation of graphite/epoxy composite material
[AD-A216209] 10 p1349 N90-17826
The behavior of a composite material in compression
[AD-A216324] 10 p1350 N90-17829
Impact damage tolerance of composite cylindrical panels
[AD-A216401] 10 p1350 N90-17830
Eccentricity effects of square cutouts on the natural frequencies and mode shapes of curved rectangular composite panels
[AD-A216410] 10 p1350 N90-17831
Damping loss factor determination of glass and graphite epoxy laminated composites using vertically oriented cantilever beams
[AD-A216529] 10 p1351 N90-17833
Low cost tooling material and process for graphite and Kevlar composites
[NASA-CR-179427] 10 p1351 N90-17834
A study of the structural efficiency of fluted core graphite-epoxy panels
[NASA-TM-101681] 10 p1396 N90-18070
Finite element investigation of a composite cylindrical shell under transverse load with through thickness shear and snapping
[AD-A216377] 10 p1397 N90-18078
Process development and fabrication of space station type aluminum-clad graphite epoxy struts
[NASA-CR-181873] 11 p1468 N90-18454
Damage in a perforated graphite-epoxy composite plate under monotonic and cyclic biaxial loading
[ESA-TT-1117] 11 p1480 N90-18521
Low-energy impact resistance of graphite-epoxy plates and ALS honeycomb sandwich panels
12 p1637 N90-19405
Viscoelastic adherend effects in adhesively bonded composite-to-composite joints 12 p1670 N90-19594
Interlaminar shear stress effects on the postbuckling response of graphite-epoxy panels
[NASA-TM-102626] 12 p1676 N90-19630
Strain and dynamic measurements using fiber optic sensors embedded into graphite/epoxy tubes
14 p1937 N90-21090
Filament winding of composite cylinders
14 p1943 N90-21119
Relevance of impacter shape to nonvisible damage and residual tensile strength of a thick graphite/epoxy laminate
[NASA-TM-102599] 14 p1943 N90-21122
Development of ultrasonic nondestructive methods for defect and damage characterization in composite materials 15 p2063 N90-21816
Energy release rate analysis of interfacial cracks in composites 15 p2065 N90-21829
The controlled-damage concept in design of laminated composites 15 p2065 N90-21830
Boeing/NASA composite components flight service evaluation
[NASA-CR-181898] 16 p2210 N90-22609
Impact damage in graphite/epoxy laminates: Damage characterization, acoustic emission, and finite element simulation, volumes 1 and 2 16 p2211 N90-22610
Ultrasonic detection of critical damage in carbon-epoxy composite materials
[ONERA-RT-5/7256-RY-081-R]
16 p2212 N90-22616
Composite integrity monitoring
[AD-A220813] 17 p2369 N90-23487
Dynamic mechanical analysis of polymeric materials
18 p2513 N90-24353
Tension fatigue of glass/epoxy and graphite/epoxy tapered laminates
[NASA-TM-102628] 19 p2671 N90-25191
An approach for relating the results of quantitative nondestructive evaluation to intrinsic properties of high-performance materials
[NASA-CR-186484] 19 p2699 N90-25355
Free vibrations of thin-walled semicircular graphite-epoxy composite frames
[NASA-TM-102680] 19 p2701 N90-25365
Summary of a study to determine low-velocity impact damage and residual tension strength for a thick graphite/epoxy motor case
[NASA-TM-102678] 19 p2702 N90-25374
Buckling and postbuckling behavior of square compression-loaded graphite-epoxy plates with circular cutouts
[NASA-TP-3007] 20 p2826 N90-26077
A comparison of the post-buckling behavior of metallic and composite plates with centrally located cutouts
[NIAR-90-14] 20 p2875 N90-26356
Scaling effects in the static and dynamic response of graphite-epoxy beam-columns
[NASA-TM-102697] 20 p2876 N90-26363

Reliability analysis of continuous fiber composite laminates
[NASA-CR-185265] 20 p2878 N90-26372
Characterization of impact damage in composites
21 p2957 N90-26811
Static and free-vibrational response of semi-circular graphite-epoxy frames with thin-walled open sections
[NASA-CR-4287] 21 p3012 N90-27122
Improved transverse crack detection in composites
[NASA-TM-103261] 22 p3153 N90-27875
An examination of impact damage in glass-phenolic and aluminum honeycomb core composite panels
[NASA-TP-3042] 22 p3153 N90-27876
Damage tolerance of woven graphite-epoxy buffer strip panels
[NASA-TM-102702] 22 p3192 N90-28114
Crash-impact behavior of graphite/epoxy composite sine wave webs 23 p3300 N90-28667
Ultrasonic verification of five wave fronts in unidirectional graphite epoxy composite
[NASA-CR-185288] 23 p3337 N90-28858

GRAPHITIZATION
Brominated graphitized carbon fibers
[NASA-CASE-LEW-14698-2] 07 p0910 N90-15262
Fluorinated graphite fibers as a new engineering material: Promises and challenges
[NASA-TM-102511] 12 p1618 N90-19301
Surface reactions of the TA6V titanium alloy under laser irradiation
[ETCA-90-R-012] 22 p3158 N90-27904

GRAPHS (CHARTS)
NT BOND GRAPHS
The 1984 direct strike lightning data, part 2
[NASA-TM-87690-PT-2] 01 p0089 N90-10506
The 1984 direct strike lightning data, part 3
[NASA-TM-87690-PT-3] 01 p0089 N90-10507
Extending matchings in planar graphs 4
[AD-A210315] 01 p0113 N90-10643
Parallel graph contraction
[AD-A211916] 03 p0386 N90-12199
Long dominating cycles and paths in graphs with large neighborhood unions
[MEMO-769] 04 p0544 N90-13157
Compression of bitmapped graphic data
[AD-A213141] 05 p0683 N90-13974
On smallest nonhamiltonian regular rough graphs
[MEMO-788] 05 p0687 N90-14003
Hamiltonian properties of graphs with large neighborhood unions
[MEMO-779] 05 p0689 N90-14013
On the performance of on-line algorithms for partition problems
[MEMO-784] 05 p0689 N90-14015
Linear groups and distance-transitive graphs
[CWI-PM-R8805] 05 p0691 N90-14036
On distance-transitive graphs and involutions
[CWI-PM-R8808] 05 p0691 N90-14037
Matching extension in regular graphs
[AD-A214757] 09 p1266 N90-17339
Basic graphics routine technical manual
[AD-A219409] 16 p2302 N90-23117
Conceptual dependency graphs and DJ
[REPT-89-62] 17 p2445 N90-23933
Coloring a graph optimally with two colors
[MEMO-820] 17 p2449 N90-23961
Applications of polyhedral combinatorics to multicommodity flows and compact surfaces
[CWI-BS-R8921] 17 p2462 N90-24060
Short proofs on multicommodity flows and cuts
[CWI-BS-R8922] 17 p2462 N90-24061
Disjoint homotopic paths and trees in a planar graph
[CWI-BS-R8923] 17 p2462 N90-24062
A generalization of Ore's theorem involving neighborhood unions
[MEMO-825] 17 p2462 N90-24064
Remarks on Hamiltonian properties of claw-free graphs
[MEMO-829] 17 p2462 N90-24065
Graph representation in a special family of infinite graphs
[MEMO-831] 17 p2463 N90-24067
On a problem of F. Ruskey
[MEMO-832] 17 p2463 N90-24068
The semantics of data flow diagrams
[TR-89-16] 17 p2480 N90-24181
Exact coloring algorithm for weighted graphs applied to timetabling problems with lectures of different lengths
[MEMO-814] 18 p2592 N90-24747
Construct analysis in knowledge graphs
[MEMO-815] 18 p2599 N90-24794
Achromatic number is NP-complete for cographs and interval graphs
[RUU-CS-88-25] 18 p2600 N90-24803
Improved self-reduction algorithms for graphs with bounded tree width
[RUU-CS-88-29] 18 p2601 N90-24805
Finding complete bipartite subgraphs in bipartite graphs
[RUU-CS-89-30] 18 p2602 N90-24815
Process and representation in graphical displays
19 p2740 N90-25574
Large sets of block designs
[ETN-90-97212] 20 p2918 N90-26602

GRASSES
Measuring and modeling near-surface reflected and emitted radiation fluxes at the FIFE site
[NASA-CR-180953] 20 p2879 N90-26378

GRASSLANDS
Evaluation of the pasture potential in the dry areas of Kenya using combined Earth reconnaissance
08 p1093 N90-16327
Study of anomalies in transition vegetation in Alto Xingo-NT, through remote sensing techniques
[INPE-4601-TDL/334] 23 p3343 N90-28891

GRASSMANN ALGEBRA
U VECTOR SPACES

GRATINGS (SPECTRA)
Design of grazing incidence monochromators involving unconventional gratings
[DE89-016341] 01 p0123 N90-10704
Custom diffraction gratings
[AD-A211002] 01 p0124 N90-10712
A nonlinear-optical method for combining high power laser beams
[AD-A211730] 03 p0354 N90-12022
Real-time sensing of optical alignment
05 p0599 N90-13479
Non-linear optical studies of adsorbates: Spectroscopy and dynamics
[DE90-001543] 06 p0741 N90-14312
A sampled-grating model of moire patterns from digital imaging
[AD-A213364] 06 p0843 N90-14902
Binary optics technology: The theory and design of multi-level diffractive optical elements
[AD-A213404] 07 p0992 N90-15735
Chromatic dispersion compensation in a Fresnel lens by means of a diffraction grating
[DE90-004030] 08 p1123 N90-16506
Transmission micro-grids for shift analysis of x ray frequencies
[MPE-216] 09 p1283 N90-17439
Temperature dependence of photon-gated persistent spectral hole-burning for the meso-tetra-p-tolyl Zn-tetrabenzoporphyrin/chloroform system in poly(methylmethacrylate)
[AD-A216086] 11 p1482 N90-18531
An advanced cooled grating spectrometer for UKIRT-CGS4 11 p1589 N90-19165
Optically tunable gratings for optical interconnects
[AD-A216978] 12 p1714 N90-19844
Production of diffraction gratings using holographic interferometry
[DE90-612841] 14 p1983 N90-21362
Multiwave diffraction analysis of transmission phase gratings
[RSRE-MEMO-4325] 15 p2087 N90-21948
The super-gratings: How to improve the limiting resolution of grating spectrometers
[PREPRINT-695] 16 p2204 N90-22577
High performance holographic elements and media
[AD-A218999] 16 p2239 N90-22775
Fast acting optical beam deflection system
[AD-A220186] 17 p2473 N90-24141
Atom interferometry progress
[AD-A220875] 18 p2613 N90-24882
Advanced multilayer x ray optics
[DE90-008228] 18 p2616 N90-24902
Monolithic arrays of grating-surface-emitting diode lasers and quantum well modulators for optical communications
[NASA-CR-186772] 19 p2758 N90-25674
Spectral signatures of X ray photoionized nebulae
19 p2778 N90-25800
Integrated optics interdigitated-electrode switches
[AD-A223245] 21 p3076 N90-27490
Evaluation of a potential Wave Division Multiplexer (WDM) for use in the IRSTD
[AD-A223945] 24 p3463 N90-29560
XMM space telescope: Development plan for the lightweight replicated x ray gratings
[DE90-015620] 24 p3546 N90-30055
Planar waveguide spectrometer
[DE90-016308] 24 p3546 N90-30057

GRAVIMETERS
GRADIO: An error analysis of the spaceborne gravity gradiometer
[ETN-90-98010] 05 p0667 N90-13901
Determination of the gravity disturbance on the earth's topographic surface from airborne gravity gradient data
[AD-A214596] 09 p1246 N90-17230
Earth tidal analysis based on gravimeter observations and the influence of ocean tides
[ETN-90-95721] 12 p1695 N90-19734
Geopotential coefficient determination and the gravimetric boundary value problem: A new approach
13 p1833 N90-20521
First year's results and field experience with the latest JILA absolute gravimeter 13 p1834 N90-20529
GPS-aided gravimetry at 30 km altitude from a balloon-borne platform 13 p1834 N90-20530
The inverse gravimetric problem in gravity modelling
13 p1835 N90-20535
FFT-local gravimetric geoid computation
13 p1835 N90-20536
The geoid in Kenya 13 p1836 N90-20542
GEOID '88: A gravimetric geoid for Canada
13 p1837 N90-20543
Absolute measurements of gravity
[AD-A222731] 20 p2922 N90-26629

GRAVIMETRY
Standard method for measurement of nonvolatile residue on surfaces
[AD-A213324] 04 p0474 N90-12714
The GEM-T2 gravitational model
[NASA-TM-100746] 04 p0517 N90-12984
Gravimetric measurements of materials outgassing applied to graphite-epoxy laminates
[NASA-TM-100753] 05 p0619 N90-13609
A study of the difference between gravimetric and gamma-gamma density near the surface in northern Yucca Flat
[DE89-017886] 06 p0814 N90-14737
Mid-Oceanic Ridge: A Dynamic Global System
[PB89-198691] 06 p0818 N90-14758
Absolute measurements of gravity
[AD-A222731] 20 p2922 N90-26629
The National Geodetic Survey absolute gravity program
[PB90-156951] 22 p3211 N90-28212

GRAVIRECEPTORS
NT OTOLITH ORGANS
Gravity receptors and responses
05 p0678 N90-13948

GRAVITATION
NT EARTH GRAVITATION
NT GRAVITY ANOMALIES
NT REDUCED GRAVITY
NT SOLAR GRAVITATION
NT STELLAR GRAVITATION
Are there causal vacuum solutions with the symmetries of the Goedel universe in higher-derivative gravity
[DE89-611966] 01 p0134 N90-10770
Partial gravity habitat study: With application to lunar base design
[NASA-CR-186048] 06 p0732 N90-14267
General exact solution for homogeneous time-dependent self-gravitating perfect fluids
[DE89-618425] 06 p0776 N90-14514
Vector fields and gravity on the lattice
[DE89-633885] 06 p0836 N90-14860
Black-hole decay and topological stability in quantum gravity
[DE89-618785] 06 p0863 N90-15017
Classical approach to higher-derivative gravity
[DE89-631649] 06 p0864 N90-15019
SL(2,R) current algebra in two-dimensional conformal quantum gravity
[DE90-600755] 07 p0983 N90-15675
Non Newtonian gravity creeping flow
[DE90-600816] 07 p1006 N90-15828
A (2+1)-dimensional pure gravity for an arbitrary closed initial surface
[DE90-701754] 07 p1007 N90-15829
A numerical simulation model for the study of magnetohydrodynamic (MHD) waves in a structured medium 07 p1012 N90-15864
Continuous spontaneous reduction model involving gravity
[DE90-600730] 08 p1135 N90-16573
The (2+1)-dimensional quantum gravity
[DE90-719556] 08 p1136 N90-16580
Research in theoretical physics
[DE90-005605] 09 p1294 N90-17500
BRS current and related anomalies in two-dimensional gravity and string theories
[DE90-733095] 10 p1440 N90-18307
Streaming gravity mode instability
[DE90-610619] 11 p1535 N90-18835
TOPAS preparation study: Summary representation of the study results
[OHB-TN-TOP-011/87] 12 p1607 N90-19244
Uniqueness of closure of the constraint algebra for quantum gravity
[DE90-610476] 12 p1691 N90-19712

On Einsteinization of background curved space in the induced quantum gravity
[DE90-610477] 12 p1724 N90-19907
Dimensional transition of the universe
[DE90-741461] 12 p1724 N90-19910
Reparametrization BRS cohomology in two-dimensional gravity and non-critical string theories
[DE90-741468] 12 p1725 N90-19911
High stability radio links 12 p1734 N90-19970
Progress in the Determination of the Earth's Gravity Field
[NASA-CR-185721] 13 p1831 N90-20513
Gravitational model improvement at the Goddard Space Flight Center 13 p1831 N90-20514
The 2 + 1 dimensional quantum gravity and the Braid group
[DE90-009036] 14 p2035 N90-21679
Stability of compactification during inflation
[NASA-CR-186597] 15 p2189 N90-22502
Determination of the gravity disturbance by processing the gravity gradiometer surveying system: Processing procedure and results
[AD-A219992] 17 p2423 N90-23808
Out-reach in-space technology experiments program: Control of flexible robot manipulators in zero gravity, experiment definition phase
[NASA-CR-183849] 19 p2696 N90-25343
The determination of the orbit of the Japanese satellite Ajisai and the GEM-T1 and GEM-T2 gravity field models
[NASA-TM-100763] 19 p2714 N90-25443
Extended inflation from higher dimensional theories
[NASA-CR-180549] 19 p2796 N90-25916
Application of inertial instruments for DSN antenna pointing and tracking 20 p2853 N90-26224
Absolute measurements of gravity
[AD-A222731] 20 p2922 N90-26629
Robot dynamics in reduced gravity environment
21 p3049 N90-27333
BRS invariant stochastic quantization of Einstein gravity
[DE90-791126] 21 p3085 N90-27541
Nonlinear multi-mode coupling of the solar gravity modes in a rotationally split multiplet 21 p3100 N90-27608
NASA geodynamics program: Bibliography
[NASA-TM-4220] 22 p3194 N90-28123
Quantum gravity in two dimensions and the SL(2,R) current algebra
[DE90-627215] 23 p3391 N90-29156
Viscous causal cosmologies
[DE90-627487] 23 p3412 N90-29282
A new vector-tensor theory and higher-dimensional cosmology
[DE90-507990] 24 p3555 N90-30117

GRAVITATION THEORY
NT SUPERGRAVITY
Homogeneous gravitational fields and limits of gravitational fields 01 p0141 N90-10812
An exact solution for a thick domain wall in general relativity
[NASA-CR-185013] 07 p1006 N90-15826
Simplicial lattices in classical and quantum gravity: Mathematical structure and application
10 p1439 N90-18304
Experimental constraints on metric and non-metric theories of gravity 12 p1730 N90-19946
Ultra-sensitive inertial sensors via neutral-atom interferometry 12 p1735 N90-19977
Studies in quantum field theory
[DE90-008731] 14 p2035 N90-21677
Generalized killing equations and symmetries of spinning space
[NIKHEF-H/89-8] 15 p2165 N90-22375

GRAVITATIONAL COLLAPSE
Correlation among gravitational wave and neutrino detectors data during SN1987A
[NOTA-INTERNA-932] 05 p0713 N90-14165
Sources of gravitational waves
12 p1730 N90-19942
Gravitational radiation from rotating gravitational collapse 12 p1730 N90-19944
Optical interferometer in space
12 p1731 N90-19953
Accretion flows in high mass star formation
[DE90-007251] 12 p1744 N90-20027
Gravitational effects of global textures
[NASA-CR-186596] 15 p2189 N90-22503
Ultrahigh-energy particle flux from cosmic strings
[NASA-CR-186592] 15 p2194 N90-22525
Gravitational collapse, Friedman models and cosmological constant: Does the universe oscillate
[DE90-620792] 16 p2338 N90-23324
Numerical treatment of shell crossing singularities in the spherically symmetric gravitational collapse
[ETN-90-96967] 20 p2917 N90-26598

GRAVITATIONAL CONSTANT
False vacuum decay in Jordan-Brans-Dicke cosmologies
[NASA-CR-186257] 09 p1293 N90-17497
Small Mercury Relativity Orbiter
12 p1733 N90-19965

GRAVITATIONAL EFFECTS
NT GRAVITATIONAL LENSES
NT LAGRANGIAN EQUILIBRIUM POINTS
A high precision gravity compensation system for the deployment test of the ERS-1 SAR antenna
02 p0183 N90-11038
Effects of gravity on equilibrium crystal shapes
02 p0281 N90-11602
USSR Space Life Sciences Digest, issue 22
[NASA-CR-3922(26)] 03 p0378 N90-12153
Orbit determination and analysis for Cosmos 236 at 15th-order resonance
[RAE-TR-88058] 04 p0461 N90-12641
Cardiovascular, renal, electrolyte, and hormonal changes in man during gravitational stress, weightlessness, and simulated weightlessness: Lower body positive pressure applied by the antigravity suit
[NASA-TM-102232] 04 p0522 N90-13013
Optimum data weighting and error calibration for estimation of gravitational parameters
05 p0591 N90-13437
Facilities for microgravity combustion research
[NASA-TM-102014] 05 p0630 N90-13679
Cells in Space
[NASA-CP-10034] 05 p0676 N90-13939
Fundamental results from microgravity cell experiments with possible commericial applications
05 p0676 N90-13940
Polarity establishment, morphogenesis, and cultured plant cells in space 05 p0677 N90-13943
How to detect when cells in space perceive gravity
05 p0678 N90-13946
Effects of microgravity on growth hormone concentration and distribution in plants 05 p0678 N90-13947
Free swimming organisms: Microgravity as an investigative tool 05 p0678 N90-13949
Human factors issues in performing life science experiments in a 0-G environment
05 p0679 N90-13952
Countermeasures to microgravity
05 p0680 N90-13957
Mid-Oceanic Ridge: A Dynamic Global System
[PB89-198691] 06 p0818 N90-14758
Shapes of star-gas waves in spiral galaxies
[NASA-CR-186289] 07 p1011 N90-15859
Data compression for the microgravity experiments
08 p1074 N90-16212
Effects of gravity waves on the polar O2 and OH airglow 08 p1101 N90-16373
Possible measurement of the gravitational acceleration of molecules, atoms, nuclei, elementary particles, and antiparticles
[DE90-719559] 08 p1121 N90-16490
Protein crystal growth in microgravity
09 p1224 N90-17102
The 1988-1989 NASA space/gravitational biology accomplishments
[NASA-TM-4160] 09 p1250 N90-17251
Non-contact temperature measurements in support of microgravity combustion experiments
10 p1363 N90-17900
A new approach to active vibration isolation for microgravity space experiments
[NASA-TM-102470] 10 p1368 N90-17929
Techniques for studying the effects of microgravity on model particle/cell systems 12 p1640 N90-19424
Design and implementation of a flexible robot
[AD-A216453] 12 p1671 N90-19601
Earth tidal analysis based on gravimeter observations and the influence of ocean tides
[ETN-90-95721] 12 p1695 N90-19734
Gravitational radiation as a test of relativistic gravity
12 p1730 N90-19941
Toward higher order tests of the gravitational interaction 12 p1731 N90-19948
The inverse-square law and quantum gravity
12 p1731 N90-19949
Earth-orbiting resonant-mass gravitational wave detectors 12 p1731 N90-19954
Gradiometry and gravitomagnetic field detection
12 p1733 N90-19962
Secondary arm coarsening and microsegregation in superalloy PWA-1480 single crystals: Effect of low gravity
[NASA-TM-102445] 13 p1776 N90-20194
Instantaneously generated foam and its applicability to reduced gravity
[NASA-CR-185208] 13 p1784 N90-20237
Spacelab qualified infrared imager for microgravity science experiments
[NASA-TM-102503] 13 p1804 N90-20352
The +Gz protection in the future: Review of scientific literature
[AD-A217887] 13 p1851 N90-20623
Toward quantum corrections in black hole thermodynamics 14 p2040 N90-21702
Thermomechanically-induced convective motion and natural convection in confined gaseous helium subjected to boundary heating 15 p2089 N90-21960
A robot end effector exchange mechanism for space applications 15 p2113 N90-22088
Gravitational effects of global textures
[NASA-CR-186596] 15 p2189 N90-22503
Optical, gravitational, and kinesthetic determinants of judged eye level 16 p2274 N90-22959
The effect of elevated gravity on the crystallization of the MFI zeolites, ZSM-5, and silicalite
16 p2320 N90-23231
The dynamical evolution of dense clusters of compact stars 16 p2331 N90-23287
Solidification of dilute alloys under fluctuating residual gravity
[REPT-892-430-112] 17 p2377 N90-23535
Space station based Microacceleration Experiment Platform
[NASA-CR-186659] 19 p2666 N90-25167
The role of gravity on macrosegregation in alloys
[NASA-CR-186530] 19 p2679 N90-25238
Microgravity as a tool in developmental biology
[ESA-SP-1123] 19 p2680 N90-25239
Microgravity and mammalian cells
19 p2680 N90-25240
Early mammalian development and possible involvement of gravity 19 p2680 N90-25242
Microgravity effects on insect development and aging
19 p2680 N90-25243
Experimental control of axis polarity in amphibian embryos 19 p2680 N90-25244
The first seven minutes of a Zenopus egg fertilised on a sounding rocket in space 19 p2680 N90-25245
The role of gravity in bird development
19 p2681 N90-25246
The influence of a sounding rocket flight on sexual activation in Chlamydomonas gametes
19 p2681 N90-25250
Lens and limb regeneration in newt during and after 13-day long spaceflight 19 p2681 N90-25252
Neck Injury in Advanced Military Aircraft Environments
[AGARD-CP-471] 19 p2717 N90-25459
Neck injury prevention possibilities in a high-G-enviroment experience with high sustained +G(sub z) training of pilots in the GAF IAM human centrifuge
19 p2720 N90-25474
New findings and instrumentation from the NASA Lewis microgravity facilities
[NASA-TM-103189] 20 p2842 N90-26163
Soil experiment
[NASA-CR-184927] 20 p2842 N90-26165
Natural melting within a spherical shell
[NASA-TM-102822] 20 p2861 N90-26274
The US Experiments Flown on the Soviet Biosatellite Cosmos 1887
[NASA-TM-102254] 20 p2891 N90-26452
Effects of microgravity on rat muscle
20 p2891 N90-26453
Experiment K-6-01. Distribution and biochemistry of mineral and matrix in the femurs of rats
20 p2892 N90-26455
Experiment K-6-03. Gravity and skeletal growth, part 1. Part 2: Morphology and histochemistry of bone cells and vasculature of the tibia; Part 3: Nuclear volume analysis of osteoblast histogenesis in periodontal ligament cells; Part 4: Intervertebral disc swelling pressure associated with microgravity 20 p2892 N90-26457
Experiment K-6-04. Trace element balance in rats during spaceflight 20 p2892 N90-26458
Experiment K-6-05. The maturaton of bone and dentin matrices in rats flown on Cosmos 1887
20 p2893 N90-26459
Experiment K-6-06. Morphometric and EM analyses of tibial epiphyseal plates from Cosmos 1887 rats
20 p2893 N90-26460
Experiment K-6-08. Biochemical and histochemical observations of vastus medialis
20 p2893 N90-26462
Experiment K-6-10. Effects of zero gravity on myofibril protein content and isomyosin distribution in rodent skeletal muscle 20 p2894 N90-26464

Experiment K-6-21. Effect of microgravity on 1) metabolic enzymes of type 1 and type 2 muscle fibers and on 2) metabolic enzymes, neutransmitter amino acids, and neurotransmitter associated enzymes in motor and somatosensory cerebral cortex. Part 1: Metabolic enzymes of individual muscle fibers; part 2: metabolic enzymes of hippocampus and spinal cord 20 p2896 N90-26474
Experiment K-6-22. Growth hormone regulation, synthesis and secretion in microgravity. Part 1: Somatotroph physiology. Part 2: Immunohistochemical analysis of hypothalamic hormones. Part 3: Plasma analysis 20 p2896 N90-26475
Refractive error analysis in the interferometric measurement of 2-D density fields containing strong gradients
[LR-616] 20 p2927 N90-26655
Reentry trajectory optimization and control 22 p3127 N90-27746
Influence of gravito-inertial force on vestibular nystagmus in man
[IZF-1989-24] 22 p3231 N90-26325
Optical imaging of IRAS galaxies: The evolution of infrared-bright galaxies 22 p3261 N90-28465
Development and approach to low-frequency microgravity isolation systems
[NASA-TP-2984] 23 p3317 N90-28754
The affect of gravity on particle collection in inertial impactors
[DE90-013372] 23 p3393 N90-29173
Satellite motion in an axi-symmetric gravitational field. Part 1: Perturbations due to J2 (second order) and J3
[RAE-TR-88068] 24 p3440 N90-29429

GRAVITATIONAL FIELDS

On analytic modeling of lunar perturbations of artificial satellites of the earth
[AD-A210440] 01 p0016 N90-10078
Homogeneous gravitational fields and limits of gravitational fields 01 p0141 N90-10812
STS-GPS (Space Transportation System - Global Positioning System) tracking experiment for gravitation estimation: Feasibility study
[AD-A211265] 02 p0150 N90-10859
Gravitational nonminimally coupled electromagnetic fields: A possible solution to some idiosincrasies of Einstein-Maxwell theory
[DE89-618430] 02 p0286 N90-11635
The thermal stability between rotating cylinders in a radially symmetrical gravitational field
[DE89-618548] 02 p0287 N90-11638
The GEM-T2 gravitational model
[NASA-TM-100746] 04 p0517 N90-12984
GRADIO: An error analysis of the spaceborne gravity gradiometer
[ETN-90-96010] 05 p0667 N90-13901
A study of the difference between gravimetric and gamma-gamma density near the surface in northern Yucca Flat
[DE89-017886] 06 p0814 N90-14737
Physics with ultra-low energy antiprotons
[DE90-002397] 06 p0840 N90-14888
Shapes of star-gas waves in spiral galaxies
[NASA-CR-186289] 07 p1011 N90-15859
Gravitational lens effect on the cosmic background radiation due to nonlinear inhomogeneities
[DE90-701753] 07 p1013 N90-15868
Integrated geodetic network analysis with stochastic prior information about the gravity field and reference ellipsoid
[SER-C-351] 08 p1091 N90-16317
The (2+1)-dimensional quantum gravity
[DE90-719556] 08 p1136 N90-16580
Double-periodic wormholes in theories with global symmetries
[DE90-719575] 08 p1136 N90-16581
On quantum effects near a black hole singularity
[DE90-600754] 08 p1151 N90-16668
Theory of microemulsions in a gravitational field 09 p1224 N90-17099
Activities report of the Institute of Interplanetary Stellar Physics
[IFSI-89-8] 09 p1298 N90-17520
Report on scientific activity and funds management for 1988
[IFSI-89-9] 09 p1298 N90-17521
Activites report of the Institute of Interplanetary Stellar Physics
[IFSI-88-22] 10 p1445 N90-18339
Scientific activity programs for 1988-1990
[IFSI-88-23] 10 p1445 N90-18340
Scientific activity program for 1989
[IFSI-89-10] 10 p1445 N90-18341
Streaming gravity mode instability
[DE90-610619] 11 p1535 N90-18835
On Einsteinization of background curved space in the induced quantum gravity
[DE90-610477] 12 p1724 N90-19907
Linearized analysis of (2+1)-dimensional Einstein-Maxwell theory
[DE90-741470] 12 p1725 N90-19913
On the Langevin equation for stochastic quantization of gravity
[DE90-750024] 12 p1725 N90-19914
Gravitational radiation as a test of relativistic gravity 12 p1730 N90-19941
Gravitational consequences of modern field theories 12 p1730 N90-19947
LAGEOS 3 and the gravitomagnetic field 12 p1733 N90-19961
Gradiometry and gravitomagnetic field detection 12 p1733 N90-19962
The Stanford equivalence principle program 12 p1733 N90-19963
Icarus lander 12 p1733 N90-19964
Small Mercury Relativity Orbiter 12 p1733 N90-19965
Drag-free satellite control 12 p1735 N90-19974
Superconducting gravity gradiometer and a test of inverse square law 12 p1735 N90-19975
Progress in the Determination of the Earth's Gravity Field
[NASA-CR-185721] 13 p1831 N90-20513
Gravitational model improvement at the Goddard Space Flight Center 13 p1831 N90-20514
An improved model for the Earth's gravity field 13 p1832 N90-20515
Progress in the development of high degree potential coefficient models 13 p1832 N90-20516
Gravity field determination and error assessment techniques 13 p1832 N90-20517
Modeling of the Earth's gravity field using the New Global Earth Model (NEWGEM) 13 p1833 N90-20523
A framework for modelling kinematic measurements in gravity field applications 13 p1833 N90-20524
Gravity field of the Western Weddell Sea: Comparison of airborne gravity and Geosat derived gravity 13 p1833 N90-20526
Critique of the vertical gradient of gravity 13 p1834 N90-20531
Methods for local gravity field approximation 13 p1834 N90-20532
The use of high-resolution terrain data in gravity field prediction 13 p1835 N90-20533
The role of topography in geodetic gravity field modelling 13 p1835 N90-20534
The inverse gravimetric problem in gravity modelling 13 p1835 N90-20535
Performance of FFT methods in local gravity field modelling 13 p1835 N90-20537
Fourier transform methods in local gravity modeling 13 p1836 N90-20538
The reduction correction in North America 13 p1836 N90-20540
Geodynamics and temporal variations in the gravity field 13 p1838 N90-20549
A model of the general ocean circulation determined from a joint solution for the Earth's gravity field 13 p1838 N90-20550
Geographically correlated orbit error 13 p1838 N90-20551
Refinement of Earth's gravity field with Topex GPS measurements 13 p1838 N90-20553
Gravity field information from Gravity Probe-B 13 p1839 N90-20554
ARISTOTELES: A European approach for an Earth gravity field recovery mission 13 p1839 N90-20559
Conserved integral characteristics of the gravitational field
[DE90-615205] 13 p1899 N90-20898
A measurement of the gravitational acceleration of the antiproton
[DE90-008903] 14 p2025 N90-21612
The generally covariant representation of energy-momentum pseudotensor of gravitational field
[DE90-615203] 14 p2034 N90-21669
Theory of a charged spinning particle in a gravitational and electromagnetic field
[NIKHEF-H/89-4] 15 p2165 N90-22373
Numerical investigations of nonlinear behavior in the Einstein equations 15 p2175 N90-22427
Gravitational effects of global textures
[NASA-CR-186596] 15 p2189 N90-22503
Gravitational couplings of the inflation in extended inflation
[NASA-CR-186595] 15 p2190 N90-22504
Determination of the general ocean circulation using satellite altimetry from a simultaneous solution for the Earth's gravity field 16 p2203 N90-22569
Effective action for induced gravity on a 2-dimensional manifold
[PREPRINT-712] 16 p2311 N90-23173
Quantum mechanics in Riemannian space-time
[DE90-620448] 16 p2325 N90-23257
Two dimensional Fourier analysis of the earth gravitational field using the program package TIM
[ETN-90-96696] 17 p2424 N90-23815
Satellite orbit determination and gravity field recovery from satellite-to-satellite tracking
[LR-605] 19 p2663 N90-25157
The determination of the orbit of the Japanese satellite Ajisai and the GEM-T1 and GEM-T2 gravity field models
[NASA-TM-100763] 19 p2714 N90-25443
Accretion onto neutron stars: Radiative transfer in a strong gravitational field 19 p2776 N90-25784
Important experiments to test for longer-ranged new gravitational forces
[DE90-012102] 20 p2888 N90-26434
Geologic interpretation of gravity anomalies
[AD-A222910] 21 p3025 N90-27199
BRS invariant stochastic quantization of Einstein gravity
[DE90-791126] 21 p3085 N90-27541
Unexpected properties of the centrifugal force
[DE90-627197] 23 p3392 N90-29164
Measurement of gravitational acceleration of antimatter
[DE90-627464] 23 p3403 N90-29233
Proceedings of the 17th Annual Gravity Gradiometer Conference
[AD-A223568] 24 p3492 N90-29735

GRAVITATIONAL LENSES

Gravitational lens effect on the cosmic background radiation due to nonlinear inhomogeneities
[DE90-701753] 07 p1013 N90-15868
The gravitational lens effect and its optical equivalents
[DE90-612767] 14 p2035 N90-21673
An astrophysics data program investigation of cluster evolution
[NASA-CR-181296] 15 p2191 N90-22510
Studies in gravitational lensing and numerical hydrodynamics 16 p2332 N90-23290

GRAVITATIONAL PHYSIOLOGY

Cardiovascular, renal, electrolyte, and hormonal changes in man during gravitational stress, weightlessness, and simulated weightlessness: Lower body positive pressure applied by the antigravity suit
[NASA-TM-102232] 04 p0522 N90-13013
Cells in Space
[NASA-CP-10034] 05 p0676 N90-13939
How to detect when cells in space perceive gravity 05 p0678 N90-13946
Gravity receptors and responses 05 p0678 N90-13948
Do the design concepts used for the space flight hardware directly affect cell structure and/or cell function ground based simulations 05 p0679 N90-13953
The 1988-1989 NASA space/gravitational biology accomplishments
[NASA-TM-4160] 09 p1250 N90-17251
National Aeronautics and Space Administration (NASA)/American Society for Engineering Education (ASEE) Summer Faculty Fellowship Program-1989, volume 2
[NASA-CR-185601-VOL-2] 18 p2630 N90-24985
Conservation of body calcium by increased dietary intake of potassium: A potential measure to reduce the osteoporosis process during prolonged exposure to microgravity 18 p2631 N90-24993
Epidermal Growth Factor (EGF) induced signal transduction in A431 cells is sensitive to gravity 19 p2680 N90-25241
The US Experiments Flown on the Soviet Biosatellite Cosmos 1887
[NASA-TM-102254] 20 p2891 N90-26452
Effects of microgravity on rat bone, cartilage and connective tissues 20 p2891 N90-26454
Experiment K-6-01. Distribution and biochemistry of mineral and matrix in the femurs of rats 20 p2892 N90-26455
Experiment K-6-02. Biomedical, biochemical and morphological alterations of muscle and dense, fibrous connective tissues during 14 days of spaceflight 20 p2892 N90-26456
Experiment K-6-03. Gravity and skeletal growth, part 1. Part 2: Morphology and histochemistry of bone cells and vasculature of the tibia; Part 3: Nuclear volume analysis of osteoblast histogenesis in periodontal ligament cells; Part 4: Intervertebral disc swelling pressure associated with microgravity 20 p2892 N90-26457
Experiment K-6-04. Trace element balance in rats during spaceflight 20 p2892 N90-26458
Experiment K-6-05. The maturaton of bone and dentin matrices in rats flown on Cosmos 1887 20 p2893 N90-26459
Experiment K-6-06. Morphometric and EM analyses of tibial epiphyseal plates from Cosmos 1887 rats 20 p2893 N90-26460

Experiment K-6-08: Biochemical and histochemical observations of vastus medialis
20 p2893 N90-26462
Experiment K-6-09: Morphological and biochemical investigation of microgravity-induced nerve and muscle breakdown. Part 1: Investigation of nerve and muscle breakdown during spaceflight; Part 2: Biochemical analysis of EDL and PLT muscles 20 p2893 N90-26463
Experiment K-6-12: Morphometric studies of atrial or granules and hepatocytes. Part 1: Morphometric study of the liver; Part 2: The atrial granular accumulations
20 p2894 N90-26466
Experiment K-6-13: Morphological and biochemical examination of heart tissue. Part 1: Effects of microgravity on the myocardial fine structure of rats flown on Cosmos 1887. Ultrastructure studies. Part 2: Cellular distribution of cyclic ampdependent protein kinase regulatory subunits in heart muscle of rats flown on Cosmos 1887
20 p2894 N90-26467
Experiment K-6-14: Hepatic function in rats after spaceflight 20 p2895 N90-26468
Experiment K-6-21: Effect of microgravity on 1) metabolic enzymes of type 1 and type 2 muscle fibers and on 2) metabolic enzymes, neutransmitter amino acids, and neurotransmitter associated enzymes in motor and somatosensory cerebral cortex. Part 1: Metabolic enzymes of individual muscle fibers; part 2: metabolic enzymes of hippocampus and spinal cord 20 p2896 N90-26474
Experiment K-6-22: Growth hormone regulation, synthesis and secretion in microgravity. Part 1: Somatotroph physiology. Part 2: Immunohistochemical analysis of hypothalamic hormones. Part 3: Plasma analysis 20 p2896 N90-26475

GRAVITATIONAL POTENTIAL
U GRAVITATIONAL FIELDS

GRAVITATIONAL RADIATION
U GRAVITATIONAL WAVES

GRAVITATIONAL WAVE ANTENNAS
Expected supernovae rates and gravitational waves detection
|NOTA-INTERNA-933| 05 p0713 N90-14166
Earth-orbiting resonant-mass gravitational wave detectors 12 p1731 N90-19954
Frequency stable high power lasers in space
12 p1734 N90-19969

GRAVITATIONAL WAVES
Correlation among gravitational wave and neutrino detectors data during SN1987A
|NOTA-INTERNA-932| 05 p0713 N90-14165
Detectable gravitational waves by supernova SN 1987 A pulsar relic
|PREPRINT-658| 05 p0714 N90-14174
Perturbation methods for the calculation of gravitational waves from slightly non-spherical spacetimes with applications to stellar core collapse
06 p0863 N90-15015
Are gravitons windows to higher dimensions
|DE90-600756| 08 p1101 N90-16376
Relativistic Gravitational Experiments in Space
|NASA-CP-3046| 12 p1730 N90-19940
Gravitational radiation as a test of relativistic gravity
12 p1730 N90-19941
Sources of gravitational waves
12 p1730 N90-19942
Detecting gravity waves from binary black holes
12 p1730 N90-19943
Gravitational radiation from rotating gravitational collapse 12 p1730 N90-19944
The pregalactic cosmic gravitational wave background
12 p1730 N90-19945
Gravitational consequences of modern field theories
12 p1730 N90-19947
Toward higher order tests of the gravitational interaction 12 p1731 N90-19948
The inverse-square law and quantum gravity
12 p1731 N90-19949
Advanced Doppler tracking experiments
12 p1731 N90-19951
The space microwave interferometer and the search for cosmic background gravitational wave radiation
12 p1731 N90-19952
Optical interferometer in space
12 p1731 N90-19953
Pulsar timing and gravitational waves
12 p1732 N90-19955
X ray timing observations and gravitational physics
12 p1732 N90-19956
Gravitational experiments on a solar probe mission: Scientific objectives and technology considerations
12 p1733 N90-19966
New tests with old data 12 p1734 N90-19968
Improved ranging systems 12 p1735 N90-19973
Superconducting gravity gradiometer and a test of inverse square law 12 p1735 N90-19975
Ultra-sensitive inertial sensors via neutral-atom interferometry 12 p1735 N90-19977
On the creation of gravitational wave by photon in external electromagnetic field
|DE90-613366| 14 p1967 N90-21265
The synergism of analytic and numerical techniques in general relativity: Calculation of radiative spacetimes
15 p2174 N90-22425
Experiments with a laser interferometric gravitational wave antenna 15 p2184 N90-22476
Gravitational radiation produced by high energy accelerators and high power lasers
|PREPRINT-701| 16 p2240 N90-22782
Superheterodyne three-wave detection of gravitation waves
|DE90-620465| 16 p2255 N90-22856
Radiation-driven evolution of low-mass x ray binaries
18 p2637 N90-25022
Frontogenesis in gravity currents: An example with no known applications in oceanography
|MATHS-REPT-A-117| 20 p2863 N90-26284
Propagation of electromagnetic radiation in a random field of gravitational waves and space radio interferometry
|DE90-627196| 23 p3319 N90-28764
Relic gravitational waves and extended inflation
|NASA-CR-186469| 24 p3493 N90-29740

GRAVITONS
Are gravitons windows to higher dimensions
|DE90-600756| 08 p1101 N90-16376

GRAVITROPISM
Gravitropism in plants: Hydraulics and wall growth properties of responding cells 05 p0678 N90-13950

GRAVITY
U GRAVITATION

GRAVITY ANOMALIES
A study of the difference between gravimetric and gamma-gamma density near the surface in northern Yucca Flat
|DE89-017886| 06 p0814 N90-14737
An improved model for the Earth's gravity field
13 p1832 N90-20515
Progress in the development of high degree potential coefficient models 13 p1832 N90-20516
Geopotential models in the Australian region
13 p1832 N90-20519
Geopotential coefficient determination and the gravimetric boundary value problem: A new approach
13 p1833 N90-20521
Precise solution for a finite set of spherical coefficients from equiangular gridded data 13 p1833 N90-20522
Synopsis of early field test results from the gravity gradiometer survey system 13 p1833 N90-20525
Downward continuation of the free-air gravity anomalies to the ellipsoid using the gradient solution and terrain correction: An attempt of global numerical computations
13 p1836 N90-20541
Determination of mean gravity anomalies in the Taiwan Island 13 p1837 N90-20547
Very accurate upward continuation to low heights in a test of non-Newtonian theory 13 p1837 N90-20548
Refinement of Earth's gravity field with Topex GPS measurements 13 p1838 N90-20553
ARISTOTELES: A European approach for an Earth gravity field recovery mission 13 p1839 N90-20559
Analysis of altimetry over inland seas
|NASA-TM-100729| 13 p1840 N90-20566
User's guide: Programs for processing altimeter data over inland seas
|NASA-TM-100730| 13 p1841 N90-20572
The observed properties of the intermediate-degree gravity modes and their relevance to the solar neutrino paradox 15 p2193 N90-22519
Determination of the gravity disturbance by processing the gravity gradiometer surveying system: Processing procedure and results
|AD-A219992| 17 p2423 N90-23808
The development of the July 1989 1 deg x 1 deg and 30' x 30' terrestrial mean free-air anomaly data bases
|NASA-CR-186475| 19 p2713 N90-25441
The determination of the orbit of the Japanese satellite Ajisai and the GEM-T1 and GEM-T2 gravity field models
|NASA-TM-100763| 19 p2714 N90-25443
Geologic interpretation of gravity anomalies
|AD-A222910| 21 p3025 N90-27199
The role of the topography in gravity gradiometer reductions and in the solution of the geodetic boundary value problem using analytical downward continuation
|AD-A223107| 21 p3025 N90-27201

GRAVITY ASSIST TRAJECTORIES
U SWINGBY TECHNIQUE

GRAVITY GRADIENT SATELLITES
NT ATS

GRAVITY GRADIOMETERS
Superconducting gravity gradiometer mission. Volume 1: Study team executive summary
|NASA-TM-4091-VOL-1| 07 p0959 N90-15545
Gradiometry and gravitomagnetic field detection
12 p1733 N90-19962
Superconducting gravity gradiometer and a test of inverse square law 12 p1735 N90-19975
Inertial corrections by dynamic estimation
12 p1735 N90-19976
Synopsis of early field test results from the gravity gradiometer survey system 13 p1833 N90-20525
The GRADIO spaceborne gravity gradiometer: Development and accommodation
13 p1840 N90-20560
High resolution analysis of satellite gradiometry
13 p1840 N90-20561
Determination of the gravity disturbance by processing the gravity gradiometer surveying system: Processing procedure and results
|AD-A219992| 17 p2423 N90-23808
The role of the topography in gravity gradiometer reductions and in the solution of the geodetic boundary value problem using analytical downward continuation
|AD-A223107| 21 p3025 N90-27201
Proceedings of the 17th Annual Gravity Gradiometer Conference
|AD-A223568| 24 p3492 N90-29735

GRAVITY PROBE B
The gravity probe B relativity gyroscope program
12 p1732 N90-19960
Gravity field information from Gravity Probe-B
13 p1839 N90-20554

GRAVITY WAVES
NT BAROCLINIC WAVES
Non-linear wave-equations for low-frequency acoustic gravity waves 02 p0240 N90-11365
Medium scale structure of the F-region
02 p0241 N90-11372
On the influence of ionospheric conductivity on dispersion of acoustic gravity waves
02 p0244 N90-11386
Atmospheric gravity waves in the auroral source region of TIDs, studied with the EISCAT CP2-data
02 p0244 N90-11387
Effects on electromagnetic wave propagation and rocket vapor trails of intense turbulence generated by breaking internal gravity waves
|AD-A211755| 03 p0373 N90-12130
Fundamentals of middle atmospheric dynamics
|AD-A211747| 04 p0518 N90-12988
A numerical study of rain-induced surface gravity wave attenuation
|AD-A212762| 04 p0549 N90-13197
The effects of gravity waves on horizontal layers: Simulation and interpretation 05 p0660 N90-13852
Polar mesosphere summer echoes and associated atmospheric gravity waves 05 p0660 N90-13856
Effects of gravity waves on the polar O2 and OH airglow 08 p1101 N90-16373
The COBE cosmic 3 K anisotropy experiment: A gravity wave and cosmic string probe 12 p1732 N90-19959
Tropospheric monitoring technology for gravity wave experiments 12 p1734 N90-19971
Formulation of non-reflecting boundary conditions in numerical models of the atmosphere
15 p2129 N90-22175
A theoretical investigation of gravity-wave-generated stress and vorticity in the planetary boundary layer
15 p2191 N90-22512
Gravity wave and turbulence studies using a high-resolution ST radar
|AD-A218877| 16 p2255 N90-22860
Meteor radar studies of the mesopause region and nonlinear atmospheric waves 17 p2421 N90-23799
Nonlinear internal gravity wave critical layers
17 p2422 N90-23801
A study of gravity wave variability, saturation, and turbulence generation in the mesosphere and lower thermosphere
|AD-A220018| 17 p2424 N90-23810
Gravity wave initiated convection
|NASA-CR-186868| 23 p3350 N90-28933
Relic gravitational waves and extended inflation
|NASA-CR-186469| 24 p3493 N90-29740
Tests of initialization procedures with the NRL limited area numerical weather prediction model
|AD-A223549| 24 p3495 N90-29750

GRAVSAT SATELLITES
U GEOPOTENTIAL RESEARCH MISSION

GRAY SCALE
Post script code for grey-scaled displays
|AD-A223099| 21 p3053 N90-27354

GRAZING FLOW
Parametric studies of acoustic duct attenuation ofperforated-plate-on-honeycomb absorber
|NAL-TM-603| 24 p3542 N90-30030

GRAZING INCIDENCE
Design of grazing incidence monochromators involving unconventional gratings
|DE89-016341| 01 p0123 N90-10704
Glancing angle x ray studies of oxide films
|DE89-017828| 06 p0852 N90-14953
Full surface interferometric testing of grazing incidence mirrors
|AD-A213590| 09 p1281 N90-17425
Some considerations on cohesive forces in sun-grazing comets 12 p1742 N90-20015
Full surface interferometric testing of grazing incidence mirrors
|AD-A219394| 16 p2318 N90-23218
GRAZING INCIDENCE TELESCOPES
Soft X-ray astronomy using grazing incidence optics 01 p0138 N90-10797
The design and evaluation of grazing incidence relay optics 01 p0138 N90-10799
Advances in photographic X-ray imaging for solar astronomy 01 p0139 N90-10803
GRAZING LANDS
U GRASSLANDS
GREASES
Molybdenum disulfide-molybdenum oxide lubricants
|AD-D014253| 08 p1048 N90-16059
Flight set 360H005 (STS-28) seals, volume 4
|NASA-CR-183904| 22 p3181 N90-28051
GREAT BASIN (US)
Geothermal fluid genesis in the Great Basin
|DE90-014438| 23 p3342 N90-28884
GREAT BRITAIN
U UNITED KINGDOM
GREAT CIRCLES
The great circle reductions 05 p0609 N90-13553
Great circle interactions: Attitude smoothing and grid-step inconsistencies 05 p0609 N90-13554
General and numerical approach to the sphere solution in FAST 05 p0610 N90-13555
Astrometric parameter determination in FAST 05 p0610 N90-13556
The sphere solution and astrometric parameter determination in NDAC 05 p0610 N90-13557
Great circle reductions: Implementation and simulations 05 p0611 N90-13569
Implementation and simulations of the sphere solution in FAST 05 p0612 N90-13570
Experiments towards a global sphere solution 05 p0612 N90-13576
Geometric considerations for a waypoint guidance method
|DE90-001803| 07 p0878 N90-15088
Small and great circle routines
|AD-A217652| 13 p1820 N90-20449
GREAT LAKES (NORTH AMERICA)
NT LAKE MICHIGAN
Environmental Research Laboratories programs and plans. FY-1989 and FY-1990 plans
|PB90-169988| 22 p3197 N90-28144
GREAT SALT LAKE (UT)
Daytime wind valleys adjacent to the Great Salt Lake
|DE90-008991| 15 p2133 N90-22190
GREEN THEOREM
U GREEN'S FUNCTIONS
GREEN'S FUNCTIONS
Spectral-domain analysis of finite frequency selective surfaces
|AD-A211669| 03 p0339 N90-11932
Scalar Green function method for microstrip antenna analysis based on the exact image theory
|PB89-218838| 04 p0488 N90-12805
Calculation of the odd and even integral components of the wave resistance Green's function
|AD-A212384| 04 p0503 N90-12900
The effect of a rigid elliptical inclusion on a straight crack
|AD-A212263| 04 p0513 N90-12965
Time-domain Green function corresponding to a time-harmonic point source in complex space
|PB89-218846| 04 p0539 N90-13117
Numerical evaluation of the far field wave pattern of the radiation Green's function
|AD-A212839| 04 p0546 N90-13176
Characteristic impedance of microstrip lines
|NASA-TM-101581| 05 p0633 N90-13694
Numerical analysis of scattering by interface flaws
|AD-A212996| 05 p0654 N90-13810
Towards ab initio calculation of electron energies in semiconductors
|ETN-90-96016| 05 p0704 N90-14121
Theoretical models of earthquake phenomena and the physical significance of seismic moment tensor expansions
|AD-A213813| 07 p0961 N90-15556
Simple proof of renormalization group equation in the minimal subtraction scheme
|DE90-600758| 08 p1115 N90-16457
Techniques for analyzing the dynamic response of structural systems using computer-derived Green's functions
|AD-A214523| 09 p1237 N90-17181
Solution of a class of conformal quantum field theory models in D-dimensional space
|DE90-607094| 10 p1439 N90-18306
Numerical Green's functions in optical potential calculations for positron scattering from argon and neon 11 p1557 N90-18971
Green's functions for a theoretical model of an aperture fed stacked-patch microstrip antenna
|AD-A216280| 12 p1645 N90-19455
A comparison between the propagators method and the decomposition method for nonlinear equations
|DE90-005783| 12 p1704 N90-19781
Self-consistant calculation of point and pair structure defects in silicium
|ETN-90-96059| 12 p1722 N90-19891
Investigation of tapered multiple microstrip lines for VLSI circuits
|AD-A217855| 13 p1797 N90-20310
Green's functions for the elastic annulus and their application to various crack problems 15 p2120 N90-22129
Numerical methods for the problem of the free-boundary plasma equilibrium in a stellarator (torsatron)
|DE90-620580| 16 p2319 N90-23223
Applications of cone theory to boundary value problems
|AD-A220939| 18 p2603 N90-24828
A closed form solution to HZE propagation
|NASA-TM-103482| 20 p2924 N90-26640
Computer modeling wave propagation with a variation of the Helmholtz-Kirchhoff relation
|AD-A222746| 20 p2927 N90-26657
Green's functions for dislocations in bonded strips and related crack problems
|NASA-CR-185291| 23 p3340 N90-28878
GREENHOUSE EFFECT
International impacts of global climate change: Testimony to House Appropriations Subcommittee on Foreign Operations, Export Financing and Related Programs
|DE89-014004| 01 p0085 N90-10482
Potential effects of global climate change on the United States. Executive summary. Draft
|PB89-161046| 02 p0237 N90-11350
Potential effects of global climate change on the United States. Volume 1: Regional studies. Draft
|PB89-161053| 02 p0238 N90-11351
Potential effects of global climate change on the United States. Volume 2: National studies. Draft
|PB89-161061| 02 p0238 N90-11352
Assessment of crop response to increases in atmospheric carbon dioxide concentrations: Summary of research progress report, July 1, 1988--June 30, 1989
|DE89-016251| 02 p0239 N90-11360
Ozone depletion, greenhouse gases, and climate change
|NASA-CR-185323| 03 p0367 N90-12101
Policies to encourage private sector responses to potential climate change
|DE89-017244| 03 p0368 N90-12107
Ozone depletion, greenhouse gases, and climate change
|PB89-216097| 03 p0369 N90-12110
Sensitivity of a regional oxidant model to variations in climate parameters, volume 1 and 2
|PB89-224943| 04 p0516 N90-12981
Global energy and the greenhouse issue
|DE90-001394| 06 p0809 N90-14709
On the mitigation of non-CO2 greenhouse gases
|DE89-016659| 06 p0809 N90-14710
The impact of global warming on the energy system
|DE89-017775| 06 p0810 N90-14712
Climate projections with regional resolution
|DE90-000858| 06 p0810 N90-14715
Discussions of global environmental problems
|DE90-002747| 06 p0811 N90-14718
Quantifying the link between change in radiative balance and atmospheric temperature
|DE90-000819| 06 p0811 N90-14721
Strategy for monitoring the effects of land use change on atmospheric CO2 concentrations
|DE90-001635| 06 p0812 N90-14722
Carbon dioxide and climate: Summaries of research in FY 1989
|DE90-001791| 06 p0812 N90-14723
US energy use: New technologies and policies in response to global warming
|DE90-002170| 06 p0812 N90-14724
Greenhouse gases: Changing the global climate
|DE90-002788| 07 p0957 N90-15535
Research project on CO2-induced climate change
|DE90-003531| 07 p0957 N90-15538
Responding to the threat of global warming: Options for the Pacific and Asia
|DE90-003553| 07 p0957 N90-15539
Global climate change: A fossil energy perspective
|DE90-003770| 07 p0958 N90-15541
Factors that may influence responses of the US transportation sector to policies for reducing greenhouse gas emissions
|DE90-000704| 07 p0958 N90-15543
Scientific linkages in global change
|PB90-112608| 08 p1098 N90-16356
Proceedings of the Conference on Technology-Based Confidence Building: Energy and Environment
|DE90-003363| 08 p1099 N90-16366
Biomass fuels in the developing countries: An overview
|DE90-002616| 09 p1241 N90-17201
Prospect of new energy. Global warming (1988)
|DE90-702486| 09 p1244 N90-17217
Energy technology R and D and the greenhouse effect
|DE90-001339| 10 p1406 N90-18107
Effects of global climate change on agroecosystems: Scope of work
|PB90-120023| 11 p1531 N90-18813
Tropospheric chemistry of natural hydrocarbons and energy-related pollutants: Biosphere/climate feedbacks
|DE90-005643| 11 p1532 N90-18820
Natural and anthropogenic climate change
|DE90-006488| 11 p1532 N90-18822
Atmospheric Radiation Measurement Program plan
|DE90-006349| 12 p1689 N90-19705
Atmospheric Radiation Measurement Program Plan
|DE90-008108| 13 p1829 N90-20504
Global Warming: A Northwest Perspective
|DE90-008140| 13 p1830 N90-20505
United States Historical Climatology Network (HCN) serial temperature and precipitation data
|DE90-008029| 13 p1830 N90-20506
Draft global warming study
|DE90-008446| 13 p1830 N90-20507
An intercomparison of general circulation model predictions of regional climate change
|DE90-008325| 13 p1845 N90-20589
A fossil energy perspective on global climate change
|DE90-007894| 14 p2004 N90-21483
Experimental performance of ozone-safe alternative refrigerants: Experimental performance comparisons of R32, R125, R143a, R218, R134a, R152a, R124, R142b, RC318 and R143 in a refrigeration circuit
|DE90-009227| 15 p2073 N90-21876
Global and hemispheric annual temperature variations between 1861 and 1988
|DE90-007993| 16 p2257 N90-22869
Effects of air temperature on atmospheric CO2-plant growth relationships
|DE90-010159| 17 p2420 N90-23793
The effects of climate change on energy planning and operations in the Pacific Northwest. Volume 1: Overview
|DE90-009464| 17 p2425 N90-23816
The effects of climate change on energy planning and operations in the Pacific Northwest. Volume 2: Technical background
|DE90-009465| 17 p2425 N90-23817
A proposal to demonstrate production of salad crops in the space station mockup facility with particular attention to space, energy, and labor constraints
|NASA-CR-186811| 19 p2725 N90-25500
Nordic Symposium on Atmospheric Chemistry
|CM-78| 20 p2883 N90-26403
A comparison of the contribution of various gases to the greenhouse effect 20 p2885 N90-26414
Opportunities in solar energy research over the next decade
|DE90-012479| 21 p3019 N90-27164
Policy options for stabilizing global climate. Volume 1: Chapters 1-6
|PB90-182304| 22 p3198 N90-28146
Policy options for stabilizing global climate. Volume 2: Chapters 7-9
|PB90-182312| 22 p3198 N90-28147
Global climate change: A proposed gas industry program on global climate issues
|PB90-219296| 22 p3199 N90-28156
Inhomogeneities of stratocumulus liquid water 22 p3213 N90-28228
Cirrus clouds and climate feedback: Is the sky falling and should we go tell the king 22 p3225 N90-28288
Chasing a specter: Risk management for global environmental change
|DE90-014455| 23 p3347 N90-28917

Responding to the threat of global warming: Options for the Pacific and Asia
[DE90-014756] 23 p3347 N90-28918
Acid deposition: No such thing as a free launch
[DE90-015085] 23 p3348 N90-28920
Tropospheric nitrogen: The influence of anthropogenic sources on distributions and deposition, executive summary
[DE90-015401] 23 p3348 N90-28922
Natural and anthropogenic climate change
[DE90-015528] 23 p3348 N90-28923
Atmospheric methane data for the period 1983-1985 from the NOAA/GMCC global cooperative flask sampling network
[PB90-208588] 24 p3486 N90-29701
Global Climate Change: Seeking a Global Consensus
[S-HRG-101-842] 24 p3486 N90-29704
Effects of increased CO2 on forest response
[DE90-015406] 24 p3487 N90-29708
Tropospheric nitrogen: The influence of anthropogenic sources on distributions and deposition
[DE90-015408] 24 p3487 N90-29709
Grassland/atmosphere response to changing climate: Coupling regional and local scales
[DE90-015814] 24 p3487 N90-29710

GREENHOUSES
Greenhouse design for a Martian colony: Structural, solar collection and light distribution systems
[NASA-CR-186818] 20 p2901 N90-26501

GREENLAND
Satellite radar altimetry over ice. Volume 1: Processing and corrections of Seasat data over Greenland
[NASA-RP-1233-VOL-1] 13 p1840 N90-20562
Satellite radar altimetry over ice. Volume 2: Users' guide for Greenland elevation data from Seasat
[NASA-RP-1233-VOL-2] 13 p1840 N90-20563
Calculation of IR propagation statistics in the eastern Atlantic for surveillance system performance assessment 15 p2085 N90-21938
Surface topography of the Greenland Ice Sheet from satellite radar altimetry
[NASA-SP-503] 16 p2253 N90-22850

GREGORIAN ANTENNAS
Dual-shaped offset reflector antenna designs from solutions of the geometrical optics first-order partial differential equations 15 p2076 N90-21887

GRENADES
Magnetic flux leakage versus ultrasonic correlation
[AD-A222112] 21 p3071 N90-27462

GRID GENERATION (MATHEMATICS)
Computation of transonic flow about stores
[AD-A210402] 01 p0002 N90-10009
BLOT: A mesh and curve plot program for the output of a finite element analysis
[DE89-013994] 01 p0104 N90-10590
Grid generation procedure using the integral equation method
[NAL-TR-1009] 01 p0111 N90-10630
A high-order Lagrangian-decoupling method for the incompressible Navier-Stokes equations
[NASA-CR-181903] 01 p0111 N90-10631
International conference on numerical grid generation in computational fluid dynamics
[AD-A211082] 02 p0220 N90-11262
A knowledge-based approach to automated flow-field zoning for computational fluid dynamics
[NASA-TM-101072] 04 p0528 N90-13048
A cell-centered multigrid method for three-dimensional anisotropic-diffusion and interface problems
[REPT-89-35] 04 p0540 N90-13128
A moving-grid interface for systems of one-dimensional time-dependent partial differential equations
[CWI-NM-R8904] 04 p0541 N90-13136
Transonic Euler solutions on mutually interfering finned bodies
[AD-A213395] 05 p0572 N90-13331
The initial-boundary value problem for the Davey-Stewartson 1 equation; how to generate and drive localized coherent structures in multidimensions
[PREPRINT-684] 05 p0643 N90-13756
An interactive grid generation procedure for axial and radial flow turbomachinery
[NASA-CR-185167] 05 p0682 N90-13968
Three-dimensional solution-adaptive grid generation of composite configurations 06 p0775 N90-14509
User's guide to PMESH: A grid-generation program for single-rotation and counterrotation advanced turboprops
[NASA-CR-185156] 06 p0823 N90-14783
A tensor product b-spline method for 3D multi-block elliptic grid generation
[DE89-017440] 06 p0836 N90-14859
Mesh refinement in finite element analysis by minimization of the stiffness matrix trace
[NASA-CR-185170] 07 p0938 N90-15434
Application of Lagrangian blending functions for grid generation around airplane geometries
[NASA-CR-186318] 08 p1018 N90-15891
FRAC-IN-THE-BOX utilization
[DE90-003648] 08 p1108 N90-16412
Domain decomposition with local mesh refinement
[AD-A215806] 10 p1418 N90-18175
A simple algebraic grid adaptation scheme with applications to two- and three-dimensional flow problems
[NASA-TM-102446] 11 p1505 N90-18667
Evaluation of the heat transfer module (FAHT) of Failure Analysis Nonlinear Thermal And Structural Integrated Code (FANTASTIC) 12 p1637 N90-19407
A tensor product B-spline method for numerical grid generation
[DE90-005979] 12 p1705 N90-19792
Composite-grid techniques and adaptive mesh refinement in computational fluid dynamics
[AD-A217383] 13 p1800 N90-20328
Evaluation of an adaptive unstructured remeshing technique for integrated fluid-thermal-structural analysis
[NASA-TM-102611] 13 p1815 N90-20426
Recent advances in 3D finite difference mesh generation using the BRL-CAD package
[DE90-007854] 13 p1866 N90-20704
GRID2D/3D: A computer program for generating grid systems in complex-shaped two- and three-dimensional spatial domains. Part 2: User's manual and program listing
[NASA-TM-102454] 13 p1867 N90-20708
Automated finite element modeling and simulation 13 p1875 N90-20753
A time-accurate adaptive grid method and the numerical simulation of a shock-vortex interaction
[NASA-TP-2998] 14 p2011 N90-21524
Applications of Mesh Generation to Complex 3-D Configurations
[AGARD-CP-464] 15 p2093 N90-21975
Recent developments in grid generation 15 p2093 N90-21976
General structured grid generation systems 15 p2093 N90-21977
Algebraic block-structured grid generation based on a macro-block concept 15 p2093 N90-21978
Applications of algebraic grid generation 15 p2093 N90-21979
Geometry and grids of complex configurations for aerodynamic calculation 15 p2093 N90-21980
Mesh generation for flow computation in turbomachine 15 p2094 N90-21981
A structured approach to interactive multiple block grid generation 15 p2094 N90-21983
Grid patching approaches for complex three-dimensional configurations 15 p2094 N90-21985
Multiblock topology specification and grid generation for complete aircraft configurations 15 p2094 N90-21986
Three-dimensional adaptive grids with limited skewness 15 p2095 N90-21987
On the way to an integrated mesh generation system for industrial applications 15 p2095 N90-21989
Generation, optimization, and adaptation of multidomain meshes around complex configurations 15 p2095 N90-21990
A discussion on issues relating to multiblock grid generation 15 p2095 N90-21991
Automatic grid generation in complex three-dimensional configurations using a frontal system 15 p2096 N90-21992
Unstructured finite element mesh generation and adaptive procedures for CFD 15 p2096 N90-21993
Generation and adaptation of 3-D unstructured grids for transient problems 15 p2096 N90-21994
Unstructured mesh generation by a generalized Delaunay algorithm 15 p2096 N90-21995
GRID2D/3D: A computer program for generating grid systems in complex-shaped two- and three-dimensional spatial domains. Part 1: Theory and method
[NASA-TM-102453] 15 p2147 N90-22262
Supersonic flow computations for an ASTOVL aircraft configuration, phase 2, part 2
[NASA-CR-4284] 16 p2234 N90-22746
Stable boundary conditions for Cartesian grid calculations
[NASA-CR-182048] 16 p2306 N90-23139
Algebraic turbulence modeling for unstructured and adaptive meshes
[NASA-CR-182035] 17 p2401 N90-23676
Fast grid generation
[AD-D014454] 17 p2402 N90-23685
A network flow model for load balancing in circuit-switched multicomputers
[NASA-CR-182049] 17 p2451 N90-23977
The implementation of the graphics of program EAGLE: A numerical grid generation code on NASA Langley SNS computer system 18 p2642 N90-25050
Interactive grid generation on small computers
[AD-A221234] 19 p2742 N90-25585
ANTIPASTO: An interactive mesh generator and preprocessor for two-dimensional analysis programs
[DE90-011755] 20 p2906 N90-26530
Generation and improvement of meshes for finite elements methods in two and three dimensions
[ETN-90-97249] 20 p2919 N90-26611
Grid generation and processing for FINFLO flow solver
[PB90-189481] 22 p3169 N90-27975
On unstructured grids and solvers 22 p3172 N90-27994
A package for 3-D unstructured grid generation, finite-element flow solution and flow field visualization
[NASA-CR-182090] 24 p3419 N90-29309
Optimization of tetrahedrical meshes for finite element calculation methods in fluids mechanics
[ETN-90-97560] 24 p3469 N90-29603
Numerical Grid Generation
[VKI-LS-1990-06] 24 p3470 N90-29606
Grid generation 24 p3470 N90-29607
Local interpolation functions for curve generation with the multi-surface transformation 24 p3470 N90-29608
The control point form of algebraic grid generation 24 p3470 N90-29609
The fundamentals of adaptive grid movement 24 p3470 N90-29610
Unstructured mesh methods for CFD 24 p3470 N90-29611
Elliptic grid generation 24 p3471 N90-29612

GRIDS (MATHEMATICS)
U COMPUTATIONAL GRIDS

GRIFFITH CRACK
Elastic indentation fractures
[ETCA-88-R-116] 04 p0512 N90-12955
Computations of weight functions in fracture mechanics 16 p2246 N90-22809

GRINDING
Lapping: Polishing and shear mode grinding
[DE90-015188] 24 p3458 N90-29533

GRINDING (MATERIAL REMOVAL)
NT METAL GRINDING
Evaluating a glass surface produced by ductile grinding
[DE90-006782] 11 p1496 N90-18608

GRINDING MACHINES
Kinematic design NC optical generator 03 p0404 N90-12316

GROOVES
NT RIBLETS
NT V GROOVES
Thermal analysis of heat pipe radiators with a rectangular groove wick structure
[AD-A222952] 21 p3004 N90-27074
Quick connect coupling
[NASA-CASE-MSC-21539-1] 21 p3010 N90-27111
Free shear layer and swirl flow heat transfer enhancement
[PB90-228123] 23 p3325 N90-28798

GROOVING
Custom diffraction gratings
[AD-A211002] 01 p0124 N90-10712
GaAs solar cells with V-grooved emitters 10 p1339 N90-17754

GROUND BASED CONTROL
NT AIR TRAFFIC CONTROL
NT AUTOMATED EN ROUTE ATC
NT RADAR APPROACH CONTROL
Program VSAERO theory document: A computer program for calculating nonlinear aerodynamic characteristics of arbitrary configurations
[NASA-CR-4023] 06 p0720 N90-14200
Prototype software reuse environment at Goddard Space Flight Center 06 p0825 N90-14794
Mathematical modelling and expert system for battery management 10 p1332 N90-17703
A method for determination of control pixels for LANSAT using a reflector
[INPE-4884-PRE/1491] 12 p1677 N90-19632
Large screen display for the Mission Control Center 13 p1858 N90-20662
Improvement of clutter rejection by scanning motion compensation in ground-based monopulse radar
[ETN-90-96550] 16 p2228 N90-22711
Knowledge based system for Hermes orbital operations ground support
[REPT-892-440-102] 17 p2361 N90-23443
IFR aircraft handled forecast by air route traffic control center: Fiscal years 1990 to 2005
[AD-A220312] 18 p2496 N90-24263

CLEAR: Automating control centers with expert system technology 19 p2733 N90-25533
Process and information integration via hypermedia 19 p2733 N90-25534
Possible trajectory profiles to achieve the geostationary orbit without any drift phase 22 p3127 N90-27745

GROUND CLOUDS
U EXHAUST CLOUDS

GROUND EFFECT (AERODYNAMICS)
Wind effect on sound wave propagation at ground vicinity
|CSTB-2-87-008| 04 p0550 N90-13201
An in-flight investigation of ground effect on a forward-swept wing airplane
|NASA-TM-101708| 06 p0720 N90-14202
Engine inlet distortion in a 9.2 percent scale vectored thrust STOVL model in ground effect
|NASA-TM-102358| 10 p1307 N90-17561
Calculation and optimization of rotor start process
|ETN-90-95894| 12 p1604 N90-19229
Prediction of forces and moments for flight vehicle control effectors. Part 2: An analysis of delta wing aerodynamic control effectiveness in ground effect
|NASA-CR-186572| 15 p2047 N90-21735
Dynamic ground-effect measurements on the F-15 STOL and Maneuver Technology Demonstrator (S/MTD) configuration
|NASA-TP-3000| 16 p2195 N90-22531
Aerodynamic performance of a 0.27-scale model of an AH-64 helicopter with baseline and alternate rotor blade sets
|NASA-TM-4201| 18 p2491 N90-24237
The Langley 14- by 22-foot subsonic tunnel: Description, flow characteristics, and guide for users
|NASA-TP-3008| 22 p3107 N90-27649
A two dimensional study of rotor/airfoil interaction in hover
|NASA-CR-183272| 22 p3114 N90-27694
Aerodynamics of Combat Aircraft Controls and of Ground Effects
|AGARD-CP-465| 23 p3271 N90-28513
Aerodynamic interferences of in-flight thrust reversers in ground effect 23 p3274 N90-28529
Study of the ground effects in the CEAT aerohydrodynamic tunnel: Using the results 23 p3274 N90-28530
Dynamic ground effects 23 p3275 N90-28531
Study of ground effects on flying scaled models 23 p3275 N90-28532
An in-flight investigation of ground effect on a forward-swept wing airplane 23 p3275 N90-28533
Determination of the ground effect on the characteristics of the A320 aircraft 23 p3275 N90-28534

GROUND EFFECT (COMMUNICATIONS)
Ground effects on multipath fading
|TELECOM-PARIS-88-E017| 04 p0489 N90-12812
Algorithms for optimal processing of polarimetric radar data
|AD-A217330| 13 p1876 N90-20758
Use of clutter residue editing maps during the Denver 1988 Terminal Doppler Weather Radar (TDWR) tests
|AD-A218696| 17 p2426 N90-23822

GROUND EFFECT MACHINES
NT HOVERCRAFT GROUND EFFECT MACHINES

GROUND HANDLING
An overview of the joint FAA/NASA aircraft/ground runway friction program
|NASA-TM-103486| 20 p2805 N90-25957

GROUND OPERATIONAL SUPPORT SYSTEM
Independent Orbiter Assessment (IOA): Assessment of the electrical power generation/power reactant storage and distribution subsystem FMEA/CIL
|NASA-CR-185545| 02 p0163 N90-10923
The Hipparcos Mission. Prelaunch status. Volume 2: The input catalog
|ESA-SP-1111-VOL-2| 05 p0606 N90-13529
Ground-based astrometric measurements 05 p0607 N90-13536
New ground-based photometric measurements 05 p0607 N90-13538
The link to extragalactic objects 05 p0608 N90-13544
On-ground attitude determination 05 p0609 N90-13552
Tactical UK military satellite ground terminals: A research and development review
|RSRE-MEMO-4262| 08 p1033 N90-15972
Hermes ground operation concepts 09 p1178 N90-16826
Space station Simulation Computer System (SCS) study for NASA/MSFC. Volume 2: Concept document
|NASA-CR-183841| 13 p1762 N90-20114
Harrier Information Management System (HIMS): The system and the approach 22 p3105 N90-27630

GROUND SPEED
Characterization of electric vehicle velocity and power profiles using road test data
|DE90-002085| 06 p0795 N90-14630

GROUND STATE
Computational modeling of pi-conjugated polyradicals
|AD-A210573| 01 p0113 N90-10648
Ground states of a two-dimensional charged-boson system
|AD-A212383| 04 p0553 N90-13226
Generation of iodine monofluoride in a supersonic multipurpose flowtube facility
|AD-A213082| 05 p0647 N90-13774
Contribution to the study of order effects in the Ising model framework: Ground states and phase diagrams
|ESA-TT-1118| 08 p1132 N90-16557
CW ultraviolet laser excited with an electron beam
|AD-A214928| 09 p1227 N90-17123
Electronic energies for Neon dimer dication radiative charge transfer
|AD-A215817| 10 p1429 N90-18244
VUV (Vacuum Ultraviolet) laser diagnostics of H(-) ion sources
|DE90-006072| 11 p1514 N90-18719
Positronium formation in e+ plus H- collisions 11 p1561 N90-18993
Positron-molecule bound states and positive ion production 11 p1561 N90-18994
A ground state depleted laser in neodymium doped yttrium orthosilicate
|DE90-006773| 12 p1668 N90-19586
Characterization of ground state neutral and ion transport during laser ablation of 1:2:3 superconductors by transient optical absorption spectroscopy
|DE90-006623| 12 p1720 N90-19878
Present status of (mu)CF theory
|DE90-007547| 13 p1884 N90-20809
Convergence of hyperspherical adiabatic expansion for helium-like systems
|DE90-620526| 16 p2214 N90-22631
Intersubband transitions in an asymmetric quantum well with a thin barrier of a delta-function potential
|AD-A220723| 17 p2477 N90-24162
Use of ab initio theory in studying various chemical systems
|AD-A220913| 18 p2521 N90-24396
Ground states of semi-linear diffusion equations
|DE90-010419| 18 p2598 N90-24785
Frequency doubled operation of a ground state depleted laser using the Nd(3+)(4)F(sub 3/2)-(4)I(sub 9/2) transition in Y2SiO5
|DE90-012089| 19 p2695 N90-25338
Fast pulsars, strange stars
|DE90-011631| 19 p2765 N90-25710
Supersonic jet studies of benzyl alcohols: Minimum energy conformations and torsional motion
|AD-A221815| 21 p2980 N90-26934
The mechanism of high-T(sub c) superconductivity due to bound hole mediators: Relationship to ferroelectricity 22 p3143 N90-27826
Moessbauer Effect applications using intense radioactive ion beams
|DE90-014981| 23 p3394 N90-29175
Evidence for a coherence gap in Ce3Bi4Pt3
|DE90-014925| 23 p3399 N90-29207
Sigma and pi interactions of the pyrrolic ligand sandwich-like lanthanide phthalocyanines determined from magnetic susceptibility and ligand-field theory
|AD-A223609| 24 p3443 N90-29444
Theoretical investigations of Pi-conjugated polyradicals as models for organic magnetic materials
|AD-A223411| 24 p3446 N90-29481
On a calculation of the ground-state energy in quantum mechanics
|DE90-627182| 24 p3555 N90-30119

GROUND STATIONS
NT EARTH TERMINALS
NT INTEGRATED MISSION CONTROL CENTER
NT POLYSTATION DOPPLER TRACKING SYSTEM
NT SPACE DETECTION AND TRACKING SYSTEM
Omega system performance assessment
|AD-A210342| 01 p0056 N90-10322
Discrete filtering techniques applied to sequential GPS range measurements
|NASA-CR-177472| 03 p0305 N90-11730
The Telecommunications and Data Acquisition Report
|NASA-CR-185093| 04 p0485 N90-12786
Test network Delft
|ETN-90-96009| 05 p0577 N90-13365
GPS network analysis: The influence of stochastic prior information of orbital elements on ground station position measures
|TR-4-1988| 08 p1020 N90-15901
Satellite systems integrated with the terrestrial cellular network for mobile communications
|ESA-STR-228| 08 p1057 N90-16113
Navigation experiment NAVEX data storage and processing
|ESA-TT-1175| 11 p1467 N90-18445
Synchronization of the ground station atomic clocks using three weighted transportable cesium time standards in the Navex navigation experiment
|ESA-TT-1153| 11 p1512 N90-18711
Measurements of the D/H ratio in planetary atmospheres by ground based infrared spectroscopy 11 p1578 N90-19088
The Telecommunications and Data Acquisition Report
|NASA-CR-185033| 12 p1642 N90-19434
ESRIN
|ESA-BR-58| 12 p1677 N90-19631
Environmental projects, volume 10. Environmental assessment: New 34-meter antenna at Apollo site
|NASA-CR-186448| 14 p2003 N90-21480
System analysis of a tactical multi-satellite communication system
|AD-A220344| 18 p2510 N90-24343
Space operations: NASA's communications support for Earth orbiting spacecraft. Report to Chairman, Subcommittee on Space Science and Applications, Committee on Science, Space and Technology, House of Representatives
|GAO/IMTEC-89-41| 20 p2851 N90-26215
Goldstone intracomplex connected element interferometry 20 p2852 N90-26218
Microspacecraft and Earth observation: Electrical field (ELF) measurement project
|NASA-CR-186821| 20 p2888 N90-26436
Bringing aircraft noise testing down to Earth
|PNR90642| 20 p2924 N90-26637
Brief state-of-the-art review on optical communications for the NASA ISES workshop 21 p3017 N90-27153
Applications of ISES for the atmospheric sciences 21 p3017 N90-27155
New features of JAL's ground station 22 p3105 N90-27633
An aeronautical mobile satellite experiment
|NASA-CR-186971| 23 p3287 N90-28593
Independent ground monitor coverage of Global Positioning System (GPS) satellites for use by civil aviation 24 p3428 N90-29364

GROUND SUPPORT EQUIPMENT
NT GROUND OPERATIONAL SUPPORT SYSTEM
Design of a final approach spacing tool for TRACON air traffic control
|NASA-TM-102229| 02 p0147 N90-10841
Design of scientific payloads and components
|AD-A211819| 03 p0351 N90-12005
Electrical testing 05 p0605 N90-13520
The in-orbit initialization phase 05 p0606 N90-13525
Andoya rocket range: New installations, future plans, and investments 05 p0661 N90-13859
Tactical UK military satellite ground terminals: A research and development review
|RSRE-MEMO-4262| 08 p1033 N90-15972
RETE experiment activity at the TSS-1 POCC
|IFSI-89-12| 08 p1036 N90-15988
X-band atmospheric attenuation for an Earth terminal measurement system
|PB90-100736| 08 p1056 N90-16101
Hermes ground operation concepts 09 p1178 N90-16826
System safety requirements for ESA space systems and associated equipment
|ESA-PSS-01-40-ISSUE-2| 11 p1469 N90-18460
The 24th Aerospace Mechanisms Symposium
|NASA-CP-3062| 15 p2112 N90-22079
Design of a telescoping tube system for access and handling equipment 15 p2116 N90-22102
NASA ground terminal communication equipment automated fault isolation expert systems 15 p2154 N90-22305
Replay and transmission of AIMS-data to mainframe computer using remote transcribers 22 p3105 N90-27634
Four-dimensional planner: A ground based planning system for time accurate approach guidance 22 p3113 N90-27683

GROUND SUPPORT SYSTEMS
The role of the ground segment 05 p0606 N90-13527
The DYANA campaign 1990 05 p0662 N90-13870
Esrange 05 p0663 N90-13876
Delta 181 sensor module command center
|AD-A214868| 09 p1182 N90-16855
Environmental projects, volume 11. Environmental assessment: Addition to operations building, Mars site
|NASA-CR-186449| 14 p2003 N90-21479
Environmental projects, volume 10. Environmental assessment: New 34-meter antenna at Apollo site
|NASA-CR-186448| 14 p2003 N90-21480

GROUND TESTS
NT COLD FLOW TESTS
NT PRELAUNCH TESTS
Full scale technology demonstration of a modern counterrotating unducted fan engine concept. Engine test
[NASA-CR-180869] 01 p0011 N90-10049
Acoustic-thermal environment for USB flap structure. Report 1: Ground simulation test results
[NAL-TM-567] 03 p0300 N90-11697
Helicopter rotor test rig (RoTeSt) in DNW: Application and results
[RAE-TRANS-2171] 05 p0585 N90-13408
On-ground photometric calibration 05 p0605 N90-13523
Introductory testimony: Hearing on nuclear power in space
[DE90-001137] 06 p0842 N90-14897
The United States Air Force approach to all-weather testing 07 p0870 N90-15047
NASA's program on icing research and technology 07 p0873 N90-15062
Evaluation of two transport aircraft and several ground test vehicle friction measurements obtained for various runway surface types and conditions. A summary of test results from joint FAA/NASA Runway Friction Program
[NASA-TP-2917] 08 p1021 N90-15902
NASA/DOD Controls-Structures Interaction Technology 1989
[NASA-CP-3041] 14 p1933 N90-21062
An air-bearing weight offload system for ground test of heavy LSS structures 14 p1936 N90-21081
CSI technology validation on an LSS ground experiment facility 14 p1937 N90-21089
Dynamic ground-effect measurements on the F-15 STOL and Maneuver Technology Demonstrator (S/MTD) configuration
[NASA-TP-3000] 16 p2195 N90-22531
Quantifying and reducing uncertainty in the assimilative mapping of ionospheric electrodynamics 16 p2254 N90-22854
National emissions standards for hazardous air pollutants application for approval of construction SP-100 ground engineering system test site
[DE90-007985] 16 p2316 N90-23203
Helicopter Airborne Laser Positioning System (HALPS)
[NASA-TM-102814] 17 p2354 N90-23399
En route noise: NASA propfan test aircraft (corrected data - simplified procedure)
[DOT-TSC-FA953-LR4] 18 p2608 N90-24856
Ground shake test of the UH-60A helicopter airframe and comparison with NASTRAN finite element model predictions
[NASA-CR-181993] 19 p2661 N90-25143
Laboratory simulation of the effect of rocket thrust on a precessing space vehicle
[NASA-CR-186681] 19 p2669 N90-25182
Artificial intelligence for multi-mission planetary operations 19 p2732 N90-25532
General test plan 22 p3120 N90-27721
National aero-space plane: Flight mechanics 22 p3129 N90-27759
Flight motor set 360L001 (STS-26R). Volume 1: System overview, revision A
[NASA-CR-183995] 22 p3133 N90-27778
Control research in the NASA high-alpha technology program 23 p3272 N90-28516
Evaluation for DLC-Flap Monitoring System of the VSRA
[NAL-TM-607] 24 p3433 N90-29391
Suspension systems for ground testing large space structures
[NASA-CR-4325] 24 p3439 N90-29424
An intelligent, free-flying robot 24 p3522 N90-29912

GROUND TRACKS
A comparison of two neural network schemes for navigation 18 p2631 N90-24991

GROUND TRUTH
Evaluation of the mangrove areas of the Rio Piaui (SE) through remote sensing
[INPE-4909-PRE/1510] 14 p1998 N90-21454
Comparison of surface-derived and ISCCP cloud optical properties 22 p3224 N90-28282
A system for recording physical properties of clouds 22 p3227 N90-28301

GROUND WATER
Hydrazine fate and transformation in natural waters and soils 02 p0204 N90-11165
Numerical simulation of hydrazine transport in a sandy soil 02 p0205 N90-11172
Use of ground penetrating radar to define recharge areas in the Central Sand Plain
[PB89-224885] 04 p0490 N90-12814
Image processing of LANDSAT MSS data for buried valley detection in northern Indiana 06 p0802 N90-14668
LANDSAT Thematic Mapper for hydrogeological mapping in Egypt
[BCRS-89-28] 11 p1527 N90-18791
Application of natural isotopes in groundwater for solving environmental problems
[DE90-000223] 12 p1689 N90-19703
Final safety analysis report for the Ulysses Mission. Volume 3 (Book 2): Nuclear risk analysis document-appendices
[DE90-008692] 14 p1939 N90-21102
Corrosion behavior of mild steel ih high pH aqueous media
[PB90-131152] 14 p1950 N90-21162
In-situ permeable flow sensor
[DE90-008806] 14 p1983 N90-21364
United States Air Force research initiation program for 1988, volume 4
[AD-A223126] 21 p3102 N90-27616
Development of an expert system embedding pattern recognition techniques for pollution source identification
[PB90-185927] 22 p3197 N90-28139
A computerized data-base system for land-use and land-cover data collected at ground-water sampling sites in the pilot national water-quality assessment program
[PB90-181868] 22 p3258 N90-28453
Study and analysis of leaking underground storage tank remediation techniques incorporated in states in EPA Region 6
[PB90-214834] 23 p3333 N90-28847
Computer program for converting rectangular coordinates to latitude-longitude coordinates
[PB90-231796] 23 p3342 N90-28883

GROUND WAVE PROPAGATION
A calibrated, omnidirectional, LF loop antenna for GWEN (Ground Wave Emergency Network)
[AD-A211264] 02 p0213 N90-11221
Practical applications of Loran-C for land mobile use or the possibility to use Loran-C as a vehicle-location or vehicle-navigation system
[ETN-90-96265] 11 p1455 N90-18384
Broadband analysis of ground wave propagation at a50 to 400 MHz 20 p2846 N90-26185

GROUND WIND
Central Sudan surface wind data and climate characteristic
[KNMI-WR-88-01] 04 p0520 N90-13000
Atlas of tropical sea surface temperature and surface winds
[PB89-223598] 04 p0521 N90-13009
Application of a mass-consistent wind model to chinook windstorms
[AD-A213622] 07 p0963 N90-15568
Multiparameter scatterometer for remote sensing (RADSER). Project Scatter: State-of-the-art and future applications
[INPE-4871-PRE/1482] 11 p1511 N90-18701
A method for correcting and reducing the pressure data recorded at the PAM 2 stations during GALE
[AD-A218165] 13 p1846 N90-20596
Aeolian removal of dust from radiator surfaces on Mars
[NASA-TM-103205] 20 p2824 N90-26068

GROUND-AIR-GROUND COMMUNICATION
Aircraft Reply and Interference Environment Simulator (ARIES) hardware principles of operation. Volume 2: Appendixes
[DOT/FAA/CT-TN88/4-2] 04 p0484 N90-12781
Aircraft Reply and Interference Environment Simulator (ARIES) hardware principles of operation, volume 1
[DOT/FAA/CT-TN88/4-1] 04 p0484 N90-12782
National airspace system air-ground communications operational concept
[DOT/FAA/DS-90/2] 14 p1964 N90-21249
New features of JAL's ground station 22 p3105 N90-27633
Integrated Air Traffic Management
[DLR-MITT-89-23] 22 p3112 N90-27676
Airline requirements for a future air traffic management system 22 p3112 N90-27678
Aspects of data link applications for ATC purposes 22 p3113 N90-27688

GROUND-TO-AIR MISSILES
U SURFACE TO AIR MISSILES

GROUP BEHAVIOR
U GROUP DYNAMICS

GROUP DYNAMICS
Parallel processing and learning in simple systems
[AD-A210225] 01 p0108 N90-10612
A theory of collective induction
[AD-A210553] 01 p0135 N90-10780
Grouping for recognition
[AD-A216716] 11 p1549 N90-18915
Unsteady group behavior of droplet clouds in swirling flows 16 p2233 N90-22743
Personality factors in flight operations. Volume 1: Leader characteristics and crew performance in a full-mission air transport simulation
[NASA-TM-102259] 17 p2348 N90-23370
The effects of management support on the successful implementation of group decision support systems
[AD-A224473] 23 p3404 N90-29241

GROUP THEORY
NT AUTOMORPHISMS
NT HOMOMORPHISMS
NT SUBGROUPS
The organization of permutation architectures with bussed interconnections
[AD-A210832] 01 p0061 N90-10352
Boolean functions, invariance groups and parallel complexity
[CWI-CS-R8836] 02 p0260 N90-11472
Representations of the twisted SU(2) quantum group and some q-hypergeometric orthogonal polynomials
[CWI-PM-R8809] 04 p0541 N90-13140
The addition formula for little q-Legendre polynomials and the SU(2) quantum group
[CWI-AM-R8906] 04 p0543 N90-13151
Group-kinetic theory and modeling of atmospheric turbulence
[NASA-CR-183776] 06 p0813 N90-14728
Simple proof of renormalization group equation in the minimal subtraction scheme
[DE90-600758] 08 p1115 N90-16457
Multiplet classification of highest weight modules over quantum universal enveloping algebras: The U(sub q)(sl(3,C)) example
[DE90-600720] 08 p1116 N90-16464
On pure radical in semigroups with zero
[DE90-606954] 10 p1422 N90-18205
Minimal prime ideals in semigroups without nilpotent elements
[DE90-606957] 10 p1423 N90-18207
New aspects in bifurcation with symmetry
[AD-A216506] 11 p1552 N90-18935
On free products of torsion free abelian groups
[AD-A218146] 13 p1878 N90-20773
Projective cohomology over a chain complex
[DE90-606958] 13 p1880 N90-20788
The 2 + 1 dimensional quantum gravity and the Braid group
[DE90-009036] 14 p2035 N90-21679
Analytic semigroups: Applications to inverse problems for flexible structures
[NASA-CR-182047] 16 p2306 N90-23138
Gevrey spaces related to Lie algebras of operators
[ETN-90-96892] 17 p2468 N90-24109
Signal processing on finite groups
[AD-A221129] 18 p2544 N90-24523
Formal groups and differential equations
[ETN-90-96924] 18 p2603 N90-24825
Effective Hamiltonians and the theory of invariants
[DE90-611035] 18 p2605 N90-24836
A number-theoretic approach to subgroups of dihedral groups
[AD-A222857] 21 p3063 N90-27413
Gaussons and states with gaussian Wigner functions are quasi-free states
[DE90-628370] 24 p3556 N90-30121

GROUP VELOCITY
Development of an ultra-bright laser and an application to multi-photon ionization 14 p1984 N90-21372
Normal-mode and phase-integral methods for determining phase and group velocities in simple underwater acoustic ducts
[AD-A221393] 18 p2612 N90-24877

GROUP 2A COMPOUNDS
U ALKALINE EARTH COMPOUNDS

GROUP 7A COMPOUNDS
U HALOGEN COMPOUNDS

GROUP 3A COMPOUNDS
Chemiluminescent ion-molecule reactions of group-3 ions with halogens: New optical spectra and reaction dynamics
[MPIS-18/1988] 02 p0196 N90-11120

GROWTH
NT CROP GROWTH
NT CRYSTAL GROWTH
NT CZOCHRALSKI METHOD
NT DIRECTIONAL SOLIDIFICATION (CRYSTALS)
NT EPITAXY
NT LIQUID PHASE EPITAXY
NT MOLECULAR BEAM EPITAXY
NT PROTEIN CRYSTAL GROWTH
NT VAPOR PHASE EPITAXY
NT VEGETATION GROWTH
Evaluation of the mangrove areas of the Rio Piaui (SE) through remote sensing
[INPE-4909-PRE/1510] 14 p1998 N90-21454

Spectral response of wheat and its relationship with agronomic variables in the tropical region
|INPE-5018-RPE/612| 15 p2122 N90-22138
Field reports on radiometric campaigns of soybeans in the Federal district: Safra 88/89
|INPE-5021-RPE/615| 15 p2122 N90-22139
On the statistical analysis of growth
|ETN-90-96923| 18 p2606 N90-24841
Experiment K-6-06. Morphometric and EM analyses of tibial epiphyseal plates from Cosmos 1887 rats
20 p2893 N90-26460
Experiment K-6-22. Growth hormone regulation, synthesis and secretion in microgravity. Part 1: Somatotroph physiology. Part 2: Immunohistochemical analysis of hypothalamic hormones. Part 3: Plasma analysis 20 p2896 N90-26475
Experiment K-6-27. Analysis of radiographs and biosamples from primate studies
20 p2897 N90-26478

GRUMMAN AIRCRAFT
NT F-14 AIRCRAFT
NT F-111 AIRCRAFT

GRUNEISEN CONSTANT
Nonlinearity parameters of polymers
15 p2164 N90-22369

GTDS
U GODDARD TRAJECTORY DETERMINATION SYSTEM

GUARDS (SHIELDS)
Trailer shield assembly for a welding torch
|NASA-CASE-MFS-29260-1| 12 p1672 N90-19602

GUIDANCE (MOTION)
NT AIRCRAFT GUIDANCE
NT INERTIAL GUIDANCE
NT LASER GUIDANCE
NT MAP MATCHING GUIDANCE
NT MIDCOURSE GUIDANCE
NT RENDEZVOUS GUIDANCE
NT SPACECRAFT GUIDANCE
NT STRAPDOWN INERTIAL GUIDANCE
NT TERMINAL GUIDANCE
Rethinking synthesis of fine-motion strategies
|DE89-016671| 02 p0230 N90-11322
Optimal control of aero-assisted orbit transfer vehicles
06 p0727 N90-14241
Guidance and Control strategies for aerospace vehicles
|NASA-CR-186195| 06 p0727 N90-14243
Guidance, steering, load relief and control of an asymmetric launch vehicle
|NASA-CR-185598| 06 p0730 N90-14257
Geometric considerations for a waypoint guidance method
|DE90-001803| 07 p0878 N90-15088
Navigation and guidance testing of the Lockheed/US Army Aquila remotely piloted vehicle
08 p1027 N90-15935
Singular perturbation analysis of AOTV-related trajectory optimization problems
|NASA-CR-186202| 08 p1027 N90-15936
Miniature GPS-based guidance package
09 p1163 N90-16736
Estimation and control of nonlinear and hybrid systems with applications to air-to-air guidance
|AD-A214542| 09 p1170 N90-16770
Software verification plan for GCS --- guidance and control software
|NASA-TM-101668| 10 p1394 N90-18057
The implications of using integrated software support environment for design of guidance and control systems software
|AGARD-AR-229| 11 p1464 N90-18432
Suboptimal period design for a maneuvering missile to evade tracking filters 12 p1650 N90-19479
A homing missile guidance law based on new target maneuver models
|AD-A220392| 17 p2356 N90-23410
A passive homing missile guidance law based on new target maneuver models
|AD-A220419| 17 p2356 N90-23411
Material evaluation of optical fibers and payout bobbins: An overview
|AD-A220104| 17 p2473 N90-24140
A Communications Antenna Pointing System (CAPS): A modular approach 18 p2537 N90-24474
ACES: Space shuttle flight software analysis expert system 19 p2739 N90-25571
Software quality assurance plan for GCS
|NASA-CR-182045| 19 p2743 N90-25588
Synthesis and validation of feedback guidance laws for air-to-air interceptions
|LR-615| 19 p2752 N90-25639
Guidance and control system for an autonomous underwater vehicle
|AD-A222709| 20 p2873 N90-26343

GUIDANCE SENSORS
Evaluation test of CCD area sensor for star sensor
|NAL-TM-570| 02 p0274 N90-11566
CCD TV focal plane guider development and comparison to SIRTF applications
|NASA-CR-185977| 06 p0842 N90-14900

GUIDE VANES
NT JET VANES
Unsteady aerodynamic phenomena in a simulated wake and shock wave passing experiment
11 p1461 N90-18414
LDV measurements and the flow analysis in the vortex region of a radial inflow turbine
14 p1922 N90-21007
An investigation of secondary flows in nozzle guide vanes 14 p1923 N90-21016
Secondary flow predictions for a transonic nozzle guide vane 14 p1924 N90-21017
Secondary flow in a turbine guide vane with low aspect ratio 14 p1924 N90-21018
Detailed heat transfer measurements in nozzle guide vane passages in linear and annular cascades in the presence of secondary flows 14 p1926 N90-21030
Theoretical and experimental study of flow-control devices for inlets of indraft wind tunnels
|NASA-TM-100050| 15 p2056 N90-21778

GULF OF MEXICO
Precipitation distributions associated with cyclones originating over the Gulf of Mexico and surrounding coastal regions
|AD-A213644| 07 p0963 N90-15569
Development of a computer model to predict platform station keeping requirements in the Gulf of Mexico using remote sensing data
|NASA-CR-186678| 19 p2663 N90-25155
Bibliography of oceanography, meteorology, and geology of Louisiana, Texas, Mississippi, Alabama, and Florida
|PB90-194663| 22 p3194 N90-28124

GULF STREAM
A compilation of digitized satellite imagery of the Gulf Stream (1982, 1983, and 1985)
|AD-A210243| 01 p0082 N90-10467
IFD (Implicit Finite Difference): Interfaced with Harvard open ocean model forecasts
|AD-A210521| 01 p0090 N90-10517
An application of ocean wave-current refraction to the gulf stream using SEASAT SAR data
|AD-A216769| 11 p1537 N90-18851
Gulfcasting: Dynamical forecast experiments for G ulf Stream rings and meanders
|AD-A221482| 21 p3032 N90-27238

GULFS
NT GULF OF MEXICO

GUM VULCANIZATES
U VULCANIZED ELASTOMERS

GUMBEL THEORY
U RANGE (EXTREMES)

GUN LAUNCHERS
A superconducting quenchgun for delivering lunar derived oxygen to lunar orbit
|NASA-CR-185161| 15 p2061 N90-21806

GUN PROPELLANTS
Study of new materials for gun propellant formulations
|DE89-015285| 06 p0754 N90-14388
Analysis of liquid propellant exposed to elastomeric materials
|AD-A214465| 09 p1200 N90-16952
Analysis of propulsive powder combustion products and ther corrosive effects
|ISL-CO-248/88| 11 p1495 N90-18605
Microcalometric studies of gun propellant KKR 8
|FOA-C-20770-2.1| 11 p1495 N90-18606
Acute oral toxicity of DIGL-RP solid propellant in Sprague-Dawley rats
|AD-A217712| 13 p1849 N90-20614
A comparison between experiment and simulation for concept VIC regenerative liquid propellant guns. Part 1: 30 mm
|AD-A218556| 16 p2225 N90-22692
Methods for evaluation of thermally induced reactions in liquid propellants
|AD-A218750| 16 p2225 N90-22694
Diffusion in the thermal degradation of NC base propellants
|AD-A219831| 17 p2383 N90-23572
An evaluation of imbedded thermocouples as a solid-propellant combustion diagnostic
|AD-A219947| 17 p2406 N90-23711
The 26th JANNAF Combustion Meeting, volume 1
|CPIA-PUBL-529-VOL-1| 22 p3161 N90-27927
Ignition and combustion of liquid propellants
|AD-A224150| 23 p3316 N90-28746
Electrical ignition of HAN-based liquid propellants
|AD-A223272| 24 p3458 N90-29528

GUN TURRETS
Scientific and technical report voice activated gun turrent control
|AD-A210350| 01 p0110 N90-10623

GUNN DIODES
NT TRANSFERRED ELECTRON DEVICES
Research on monolithic millimeter-wave devices
|AD-A215771| 10 p1379 N90-17996
Focused ion beam implantation
|AD-A217987| 13 p1898 N90-20894
Indium phosphide planar Gunn diode
|AD-A219337| 16 p2233 N90-22740
High frequency, frequency multiplier using parallel gunn diodes
|AD-D014523| 19 p2685 N90-25275

GUNN EFFECT
High frequency, frequency multiplier using parallel gunn diodes
|AD-D014523| 19 p2685 N90-25275

GUNNERY TRAINING
Human factors research in aircrew performance and training
|AD-A213285| 05 p0676 N90-13938

GUNPOWDER
U GUN PROPELLANTS

GUNS (ORDNANCE)
NT ARTILLERY
Elastic-plastic analysis of a thick-walled composite tube subjected to internal pressure
|AD-A215258| 09 p1238 N90-17187
A comparison between experiment and simulation for concept VIC regenerative liquid propellant guns. Part 1: 30 mm
|AD-A218556| 16 p2225 N90-22692

GUST ALLEVIATORS
Active control system for gust load allevation and structural damping 07 p0871 N90-15056
Synthesis of individual rotor blade control system for gust alleviation
|NASA-TM-101886| 20 p2807 N90-25972

GUST LOADS
Active control system for gust load allevation and structural damping 07 p0871 N90-15056
Gust response analysis for cascades operating in nonuniform mean flows 11 p1461 N90-18415

GUSTATORY PERCEPTION
U TASTE

GUSTS
Turbulence effects of aircraft flight dynamics and control 07 p0871 N90-15055
Laser wave estimation
|AD-A213867| 09 p1227 N90-17119
Report on meteorological assessment of Bald Hills incidents, phase 1
|AD-A216201| 10 p1408 N90-18123
Spanwise measurements of vertical components of atmospheric turbulence
|NASA-TP-2963| 12 p1692 N90-19718
Flat plate leading edge receptivity to various freestream disturbance structures 16 p2235 N90-22750
An interactive method for estimating hailstone size and convectively-driven wind gusts from forecast soundings
|AD-A218499| 16 p2258 N90-22871
Development of a linearized unsteady aerodynamic analysis for cascade gust response predictions
|NASA-CR-4308| 22 p3108 N90-27655

GUT
U GRAND UNIFIED THEORY

GYMNASTICS
U PHYSICAL EXERCISE

GYRATION
NT COUNTER ROTATION
NT EARTH ROTATION
NT MOLECULAR ROTATION
NT MUON SPIN ROTATION
NT PRECESSION
NT PROTON PRECESSION
NT QUENCHING (ATOMIC PHYSICS)
NT REVOLVING
NT ROTATION
NT SATELLITE ROTATION
NT SOLAR ROTATION
NT STELLAR ROTATION
Extension to Eulers's theorem to n-dimensional spaces 05 p0589 N90-13431
Construction of a hybrid angular velocity reference system for investigation of the dynamic characteristics of strapdown gyros
|ESA-TT-1181| 19 p2694 N90-25332

GYRATORS
NT MICROWAVE FILTERS

GYROFREQUENCY
On the possibility of producing artificial ionization and polar aurora in the ionosphere by radio-waves emitted from the ground 02 p0245 N90-11388

GYROMAGNETISM
NT GYROFREQUENCY
GYROPLANES
U HELICOPTERS
GYROS
U GYROSCOPES
GYROSCOPES
NT ATTITUDE GYROS
NT CONTROL MOMENT GYROSCOPES
NT LASER GYROSCOPES
NT NUCLEAR GYROSCOPES
NT OPTICAL GYROSCOPES
NT ROTARY GYROSCOPES
On the motion equation of an elastically supported two degree of freedon gyro
|NAL-TM-568| 02 p0223 N90-11276
A gyroscope calibration analysis for the Gamma Ray Observatory (GRO) 05 p0589 N90-13428
Analytical derivation and verification of zero-gyro control for the IUE satellite
|NASA-TM-100748| 05 p0645 N90-13767
A new kind of heterodyne fiber-optic gyroscope
|AD-A213953| 07 p0933 N90-15404
The gravity probe B relativity gyroscope program 12 p1732 N90-19960
Design and testing of a noninteracting control loop for the dynamically tuned dry gyro
|NAL-TR-1017| 13 p1803 N90-20350
Kalman filter formulations for transfer alignment of strapdown inertial units 24 p3424 N90-29342
GYROSCOPIC COUPLING
Bilinear modeling and nonlinear estimation 05 p0589 N90-13430
GYROSCOPIC DRIFT
U GYROSCOPES
U GYROSCOPIC STABILITY
GYROSCOPIC STABILITY
True covariance simulation of the EUVE update filter 05 p0589 N90-13427
A gyroscope calibration analysis for the Gamma Ray Observatory (GRO) 05 p0589 N90-13428
Spacecraft attitude determination using the earth's magnetic field 05 p0589 N90-13429
Extended Kalman filter for attitude estimation of the earth radiation budget satellite 05 p0590 N90-13433
A new kind of heterodyne fiber-optic gyroscope
|AD-A213953| 07 p0933 N90-15404
The anatomy of the gyroscope, part 3
|AGARD-AG-313| 14 p1982 N90-21359
An accurate numerical technique for determining flight test rate gyroscope biases prior to takeoff
|AD-A220987| 19 p2660 N90-25138
GYROSTATS
U GYROSCOPES
GYROTRONS
U CYCLOTRON RESONANCE DEVICES

H

H ALPHA LINE
Fast spectroscopic variations on rapidly-rotating, cool dwarfs. 3: Masses of circumstellar absorbing clouds on AB Doradus
|NASA-CR-186563| 15 p2184 N90-22479
Be/X ray binaries 19 p2766 N90-25715
NASA Marshall Space Flight Center Solar Observatory report, January - June 1990
|NASA-TM-103512| 23 p3409 N90-29268
H BETA LINE
Optical FeII emission and the BLR structure in QSOs 19 p2793 N90-25899
H I REGIONS
Chemical evolution of dwarf irregular galaxies 22 p3263 N90-28478
Star formation and the distribution of HI and infrared emission in M51
|NASA-CR-186928| 23 p3408 N90-29262
H II REGIONS
Orion B: Anatomy of a star-forming region 05 p0710 N90-14155
Radio continuum maps at 22 GHz of the H II regions RCW57 and W49
|INPE-4787-TDL/353| 10 p1446 N90-18343
Dust continuum spectra from model HII regions 11 p1580 N90-19099
Airborne observations of the infrared emission bands 11 p1580 N90-19101
Polycyclic aromatic hydrocarbons in the infrared spectra of IRAS sources 11 p1581 N90-19105
Mapping and spectroscopy of the 3.3 microns feature in Orion 11 p1582 N90-19112
Molecular hydrogen in the HII region G333.6-0.2 11 p1583 N90-19121
A survey of PAH emission in HII regions, planetary and proto-planetary nebulae 11 p1584 N90-19129
Infrared lines as probes of galactic structure 11 p1585 N90-19139
Spectroscopy of galaxies in the mid-infrared 11 p1586 N90-19145
Infrared (FeII), H and H2 lines in galaxy nuclei 11 p1587 N90-19153
Recombination lines of C I and N II in the interstellar medium 15 p2182 N90-22466
Interactions of massive stars with the interstellar medium: Bow shocks and superbubbles 15 p2186 N90-22485
The evolution of the supernova remnant IC 443 15 p2186 N90-22486
The association of supernovae with regions of recent star formation in late-type galaxies 15 p2188 N90-22497
The effect of a stellar wind on an expanding H II region 16 p2333 N90-23292
Spectral measurements of the cosmic microwave background 16 p2340 N90-23334
Molecular gas in S106: Morphology, kinematics, and chemistry of a star forming region 17 p2484 N90-24209
Chemical evolution of dwarf irregular galaxies 22 p3263 N90-28478
Star formation and the distribution of HI and infrared emission in M51
|NASA-CR-186928| 23 p3408 N90-29262
A plasma diagnostic study of two wind-blown shell nebulae: NGC 7635 and NGC 2359 23 p3410 N90-29271
H LINES
NT H ALPHA LINE
NT H BETA LINE
Optical observations of LMXB AC211(M15): Solving the puzzle 19 p2768 N90-25731
H-53 HELICOPTER
Application of damage tolerance 21 p2958 N90-26817
Individual Helicopter Tracking Program (IHTP) for the MH-53J helicopter 21 p2958 N90-26818
HABITABILITY
Space station wardroom habitability and equipment study
|NASA-CR-4246| 09 p1260 N90-17308
Genesis lunar outpost criteria and design
|NASA-CR-186831| 20 p2901 N90-26499
HABITATS
Partial gravity habitat study: With application to lunar base design
|NASA-CR-186048| 06 p0732 N90-14267
Predicting effects of global climate change on reservoir water quality and fish habitat
|DE90-003674| 12 p1689 N90-19704
A preliminary design of interior structure and foundation of an inflatable lunar habitat 18 p2633 N90-24999
Terrapin technologies manned Mars mission proposal
|NASA-CR-186838| 20 p2816 N90-26027
Genesis lunar outpost criteria and design
|NASA-CR-186831| 20 p2901 N90-26499
Generation rates and chemical compositions of waste streams in a typical crewed space habitat
|NASA-TM-102799| 22 p3233 N90-28333
Flora and threatened and endangered plants of John F. Kennedy Space Center, Florida
|NASA-TM-102791| 23 p3349 N90-28925
HABITS
Demonstration of replicable dimensions of health behaviors
|AD-A211920| 03 p0380 N90-12161
Effectiveness of progressive resistance training for increasing maximal repetitive lifting capacity
|AD-A215286| 09 p1252 N90-17267
Minimal sleep to maintain performance: Search for sleep quantum in sustained operations
|AD-A223815| 24 p3498 N90-29770
HADRONS
NT BARYONS
NT MESONS
NT MUONS
Elements of a relativistic microscopic theory of hadronic matter in equilibrium and non-equilibrium
|KVI-796| 04 p0552 N90-13218
Measurement of the fractional momentum carried by the glutons in the low Q squared photon-gluon fusion events at the ep HERA collider
|NOTA-INTERNA-937| 05 p0698 N90-14083
Aspects of the physics of the standard model
|PREPRINT-670| 05 p0698 N90-14087
Model-independent analysis of the Z line shape in e + e- annihilation
|PREPRINT-679| 05 p0698 N90-14089
Big Bang nucleosynthesis and the Quark-Hadron transition
|NASA-CR-186169| 05 p0713 N90-14168
Proceedings of the 23rd Annual Seminar on Theoretical Physics
|DE90-601827| 08 p1135 N90-16577
Digital integrator
|DIGEL-1989-2| 12 p1654 N90-19508
Algorithms for calorimeter simulation with parameterized showers by example of H1 detectors
|MPI-PAE/EXP.EL-200| 12 p1711 N90-19828
Quasistatic electron diffusion in quantum hadrodynamics
|ETN-90-97297| 22 p3255 N90-28432
HAFNIUM
Dehydrogenative polymerization of silanes to polysilanes: A monomeric copper(2) siloxide
|AD-A218550| 16 p2223 N90-22681
HAFNIUM ALLOYS
Experimental evaluation of new alloy coatings
|AD-A214922| 09 p1194 N90-16916
HAFNIUM COMPOUNDS
NT HAFNIUM OXIDES
HAFNIUM OXIDES
ZrO2 sintered compact and method for its production
|DE90-004125| 08 p1039 N90-16006
HAIL
Radar polarimetric studies based on the MAYPOLE 1983 and 1984 field experiments
|AD-A212226| 04 p0492 N90-12830
An estimation of rainfall amounts using radar-derived Z-R relationships
|AD-A217950| 13 p1845 N90-20591
Hail growth in a highly-glaciated central high plains multi-cellular hailstorm 15 p2131 N90-22184
An interactive method for estimating hailstone size and convectively-driven wind gusts from forecast soundings
|AD-A218499| 16 p2258 N90-22871
HAILSTONES
U HAIL
HAILSTORMS
Hail growth in a highly-glaciated central high plains multi-cellular hailstorm 15 p2131 N90-22184
Program on development of basic understanding of severe weather phenomena
|PB90-226564| 23 p3352 N90-28943
HAIRPIN VORTICES
U HORSESHOE VORTICES
HALF CONES
Stability of a supersonic boundary layer on a sharp cone at a small angle of attack 06 p0775 N90-14510
HALF LIFE
Cosmic ray half life of (54)Mn
|DE90-000134| 07 p1016 N90-15880
Cosmic ray half life of Ni-56
|DE90-000132| 08 p1153 N90-16680
Measurement of cross sections: New needs and possibilities
|DE90-007248| 12 p1711 N90-19829
HALF PLANES
Elasto-plastic analysis for contact fatigue failure 15 p2112 N90-22078
HALF SPACES
Transient elastic waves on anisotropic half-spaces 10 p1396 N90-18074
Binary space partitioning trees and their uses 13 p1857 N90-20657
Elastodynamic scattering and transmission problems in three dimensions by the boundary integral equation method 15 p2111 N90-22077
Scattering of waves by inclusions in a nonhomogeneous elastic half space solved by boundary element methods
|PB90-145699| 15 p2116 N90-22107
HALIDES
NT ALKALI HALIDES
NT ALUMINUM CHLORIDES
NT ALUMINUM FLUORIDES
NT BARIUM FLUORIDES
NT BORON CHLORIDES
NT BORON FLUORIDES
NT BROMIDES
NT CALCIUM CHLORIDES
NT CALCIUM FLUORIDES
NT CARBON TETRACHLORIDE
NT CESIUM IODIDES
NT CHLORIDES
NT CHLORINE FLUORIDES
NT COPPER CHLORIDES
NT DIFLUORIDES
NT FLUORIDES
NT HYDROCHLORIC ACID
NT HYDROFLUORIC ACID
NT HYDROGEN CHLORIDES
NT IRON CHLORIDES
NT LANTHANUM FLUORIDES
NT LITHIUM CHLORIDES
NT LITHIUM FLUORIDES
NT METAL HALIDES
NT NITROGEN FLUORIDES

NT OXYGEN FLUORIDES
NT SILVER HALIDES
NT SODIUM CHLORIDES
NT SODIUM FLUORIDES
NT SODIUM IODIDES
NT STRONTIUM FLUORIDES
NT SULFUR FLUORIDES
NT TITANIUM CHLORIDES
Studies on the use of supercritical ammonia for ceramic nitride synthesis and fabrication
[NASA-TM-102570] 15 p2068 N90-21843
Stibathiolanes: Synthesis, solid state structure, and solution behavior
[AD-A223255] 20 p2933 N90-26688

HALL COEFFICIENT
U HALL EFFECT

HALL CURRENTS
U ELECTRIC CURRENT
U HALL EFFECT

HALL EFFECT
Superconductivity and magnetic scattering in the Nd(sub 2-x)Ce(sub x)CuO(sub 4-delta)
[DE89-016524] 03 p0410 N90-12354
Theoretical reversed field pinch studies
[DE90-002114] 06 p0848 N90-14929
Magnetotransport studies of epitaxial Cr thin films
[DE90-001930] 06 p0856 N90-14975
Single fluid simulations of plasma openings switch behavior
[DE90-002643] 07 p0921 N90-15330
Magnetohydrodynamic modeling of plasma opening switches and gas puff plasmas
[DE90-005825] 11 p1569 N90-19028
Superconducting materials
[DE90-007419] 11 p1573 N90-19054
Spectrally selective tinoxide and indiumoxide coatings
[ISBN-90-9003138-3] 17 p2382 N90-23567
Rapid annealing of iron implanted Hg(1-x)Cd(x)Te
[AD-A222777] 21 p3082 N90-27524
Preparation and characteristics of superconducting cuprate thin films: Nd(2-x)Ce(x)CuO4 and substituted Bi-system 22 p3140 N90-27813
Thermal and electric properties of Nd(1.85)Ce(0.15)CuO(4-y) and Pr(1.85)Ce(0.15)CuO(4-y) 22 p3141 N90-27816
Workshop on Low-Dimensional Quantum Field Theory and its Applications
[DE90-508071] 24 p3555 N90-30118

HALLEY'S COMET
Hypervelocity impact studies on the Giotto comet Halley mission 06 p0862 N90-15008
Near-infrared polarimetry and spectroscopy of comets 07 p1011 N90-15857
Morphology and compositional differentiation of the surface of comets 08 p1143 N90-16624
Organic chemistry of cometary dust as derived from PUMA 1 data 08 p1143 N90-16628
Composition of dust from Comet P/Halley: The mineral fraction 08 p1144 N90-16631
Solar nebula condensates and the composition of comets 08 p1144 N90-16634
The in-situ cometary particulate size distribution measured for one comet: P/Halley 08 p1145 N90-16637
Far-ultraviolet spectroscopy of Comet Halley 12 p1736 N90-19979
Comet Halley: An optical continuum study 12 p1736 N90-19981
Comets: Dirty snowballs or icy dirtballs 12 p1739 N90-19994
Hot OH and CN: Evidence for organic molecules close to the nucleus of comet Halley 12 p1742 N90-20012
The composition of cometary nuclei 12 p1743 N90-20022
The production and spatial distribution of neutral and ionized water vapor in Comet P/Halley 15 p2185 N90-22484
Analysis of energy spectra of the ions in the coma of Halley's comet for the evaluation of the production ratio of methane and ammonia
[ETN-90-96489] 18 p2638 N90-25026
Nongravitational forces by Halley's comet
[ETN-90-96491] 18 p2638 N90-25027
Carbon in comet dust 21 p3089 N90-27564
Carbon-rich particles in Comet Halley 21 p3089 N90-27565

HALOCARBONS
NT CHLOROCARBONS
NT FLUOROCARBONS
Ultraviolet absorption cross-sections of bromoform in the temperature range 295-240 K
[AERONOMICA-ACTA-A-348-1989] 05 p0622 N90-13630

HALOE
U HALOGEN OCCULTATION EXPERIMENT

HALOGEN COMPOUNDS
NT ALKALI HALIDES
NT ALUMINUM CHLORIDES
NT ALUMINUM FLUORIDES
NT AMMONIUM PERCHLORATES
NT BARIUM FLUORIDES
NT BORON CHLORIDES
NT BORON FLUORIDES
NT BROMIDES
NT BROMINE COMPOUNDS
NT CALCIUM CHLORIDES
NT CALCIUM FLUORIDES
NT CARBON TETRACHLORIDE
NT CESIUM IODIDES
NT CHLORIDES
NT CHLORINE COMPOUNDS
NT CHLORINE FLUORIDES
NT CHLOROCARBONS
NT COPPER CHLORIDES
NT CRYOLITE
NT DIFLUORIDES
NT DIFLUORO COMPOUNDS
NT FLUORIDES
NT FLUORINE COMPOUNDS
NT FLUORO COMPOUNDS
NT FLUOROAMINES
NT FLUOROCARBONS
NT FLUOROHYDROCARBONS
NT FLUOROPOLYMERS
NT HALIDES
NT HALOCARBONS
NT HYDROCHLORIC ACID
NT HYDROFLUORIC ACID
NT HYDROGEN CHLORIDES
NT IODIDES
NT IODINE COMPOUNDS
NT IRON CHLORIDES
NT LANTHANUM FLUORIDES
NT LITHIUM CHLORIDES
NT LITHIUM FLUORIDES
NT LITHIUM IODATES
NT LITHIUM PERCHLORATES
NT METAL FLUORIDES
NT METAL HALIDES
NT NITROGEN FLUORIDES
NT OXYGEN FLUORIDES
NT PERCHLORATES
NT POLYTETRAFLUOROETHYLENE
NT POLYVINYL FLUORIDE
NT POTASSIUM PERCHLORATES
NT SILVER HALIDES
NT SODIUM CHLORIDES
NT SODIUM FLUORIDES
NT SODIUM IODIDES
NT STRONTIUM FLUORIDES
NT SULFUR FLUORIDES
NT TEFLON (TRADEMARK)
NT TETRAFLUOROHYDRAZINE
NT TITANIUM CHLORIDES
Vapour pressures and critical points of liquids. Halogenated hydrocarbons
[ESDU-89006] 03 p0325 N90-11848
Inorganic halogen oxidizers
[AD-A213990] 07 p0915 N90-15294
Rotational energy transfer in metastable states of heteronuclear molecules
[AD-A214425] 08 p1120 N90-16485

HALOGEN OCCULTATION EXPERIMENT
The retrieval of the concentrations of nitric oxide and nitrogen dioxide from satellite solar occultation measurements at sunset and sunrise 06 p0814 N90-14733

HALOGENATION
NT BROMINATION
NT FLUORINATION
Nonflammable hydraulic power system for tactical aircraft. Volume 1: Aircraft system definition, design and analysis
[AD-A218493] 17 p2356 N90-23409

HALOGENS
NT BROMINE
NT CHLORINE
NT FLUORINE
NT IODINE
NT IODINE ISOTOPES
Chemiluminescent ion-molecule reactions of group-3 ions with halogens: New optical spectra and reaction dynamics
[MPIS-18/1988] 02 p0196 N90-11120
Extraterrestrial halogen and sulfur content of the stratosphere
[DE89-017623] 06 p0815 N90-14738

HALOS
An experiment to search for galactic axions 05 p0710 N90-14158
The disk-halo connection and the nature of the interstellar medium
[NASA-CR-186286] 07 p1012 N90-15860
X rays from the accretion column of compact objects: A Monte Carlo study 19 p2775 N90-25777
On planetary nebulae as sources of carbon dust: Infrared emission from planetary nebulae of the galactic halo 21 p3093 N90-27583

HAMILTON-JACOBI EQUATION
The nonconvex multi-dimensional Riemann problem for Hamilton-Jacobi equations
[NASA-CR-181887] 03 p0384 N90-12182
Symplectic numerical integration of Hamiltonian systems
[DE90-002380] 06 p0835 N90-14855
Perturbations of test mass motion in the Schwarzschild spacetime using the method of Hamilton and Jacobi 11 p1577 N90-19083
High order essentially non-oscillatory schemes for Hamilton-Jacobi equations
[NASA-CR-181995] 16 p2305 N90-23137
Theoretical principles of the FHP-GA trajectory calculation program
[FB-10-89] 19 p2663 N90-25156

HAMILTONIAN FUNCTIONS
Periodic solutions of spatially periodic Hamiltonian systems
[AD-A210645] 01 p0113 N90-10649
Subharmonic solutions near an equilibrium point for Hamiltonian systems
[AD-A210558] 02 p0263 N90-11496
On some stochastic properties of the infinitely dimensional Hamiltonian systems of classical mechanics
[DE89-618403] 02 p0267 N90-11525
Ground-state coding in partially connected neural networks
[NASA-TM-102239] 03 p0391 N90-12227
Homoclinic orbits for a class of Hamiltonian systems
[AD-A210562] 03 p0391 N90-12229
Long dominating cycles and paths in graphs with large neighborhood unions
[MEMO-769] 04 p0544 N90-13157
Periodic solutions of Hamiltonian systems of 3-body type
[AD-A212891] 05 p0687 N90-14005
Hamiltonian properties of graphs with large neighborhood unions
[MEMO-779] 05 p0689 N90-14013
Using the physical structure of a system for control: An illustration
[MEMO-782] 05 p0689 N90-14014
On a new integrable Hamiltonian system with nearest neighbors interaction
[PREPRINT-667] 05 p0692 N90-14043
A unified algebraic approach to integral and discrete evolution equations
[PREPRINT-668] 05 p0692 N90-14044
R-matrices and higher Poisson brackets for integrable systems
[PREPRINT-669] 05 p0696 N90-14069
Hamiltonian flows, SU(infinity), SO(infinity), USp(infinity), and strings
[DE90-001987] 06 p0835 N90-14851
Symplectic numerical integration of Hamiltonian systems
[DE90-002380] 06 p0835 N90-14855
Spectral properties of one dimensional quasi-crystals
[PREPRINT-659] 06 p0850 N90-14938
Hamiltonian chaos in a nonlinear polarized optical beam
[DE90-002437] 07 p0934 N90-15408
The application of optimal control theory for analysis of human jumping and pedaling 07 p0968 N90-15590
Some results on connecting orbits for a class of Hamiltonian systems
[AD-A213536] 07 p0983 N90-15679
Nijenhuis tensor and integrable models
[DE90-001403] 07 p0987 N90-15702
Theory of singular Lagrangians
[DE90-600735] 08 p1115 N90-16456
On gauge fixing and quantization of constrained Hamiltonian systems
[DE90-600732] 08 p1135 N90-16574
KAM: Automatic planning and interpretation of numerical experiments using geometrical methods
[AD-A216805] 11 p1546 N90-18900
System theory and mechanics
[MEMO-807] 11 p1550 N90-18922
Long path connectivity of regular graphs
[AD-A216477] 11 p1552 N90-18933
Hamiltonian analysis and simulation of free electron lasers
[INPE-4785-TDL/351] 11 p1567 N90-19018

Perturbations of test mass motion in the Schwarzschild spacetime using the method of Hamilton and Jacobi
11 p1577 N90-19083

Transient and sustained resonance in very slowly varying oscillatory Hamiltonian systems with application to free-electron lasers
[DE90-005984] 12 p1666 N90-19574

Panconnectivity of locally connected K(1,3)-free graphs
[AD-A216548] 12 p1705 N90-19786

Periodic trajectories for two-dimensional nonintegrable Hamiltonians
[DE90-008082] 13 p1877 N90-20765

Integrability and chaos in nonlinearly coupled optical beams
[DE90-007540] 13 p1888 N90-20834

Periodic solutions for Hamiltonian systems in a nonconvex potential well
[DE90-612752] 14 p2020 N90-21580

The intrinsic stochasticity of near-integrable Hamiltonian systems
[IPPCZ-282] 15 p2167 N90-22386

A proof of the isoenergetic KAM: Theorem from the ordinary one
[W-8906] 16 p2305 N90-23136

Excitation of hypersound at boundary between Type-2 superconductor and a concentrated paramagnetic compound 16 p2310 N90-23164

What is going on in the La2CuO4 superconductors
16 p2311 N90-23171

Efficient smoothing for boundary value models
[AD-A218484] 17 p2456 N90-24014

Discrete mathematics for communication systems
[AD-A220430] 17 p2457 N90-24022

A variational approach to heteroclinic orbits for a class of Hamiltonian systems
[AD-A219853] 17 p2460 N90-24047

A generalization of Ore's theorem involving neighborhood unions
[MEMO-825] 17 p2462 N90-24064

Remarks on Hamiltonian properties of claw-free graphs
[MEMO-829] 17 p2462 N90-24065

Optical phonons and electronic properties in double heterostructures
[AD-A219436] 17 p2475 N90-24153

Sustained resonance in very slowly varying oscillatory Hamiltonian systems
[DE90-010422] 18 p2598 N90-24783

Effective Hamiltonians and the theory of invariants
[DE90-611035] 18 p2605 N90-24836

Around three lemmas in Hamiltonian graph theory
[MEMO-816] 18 p2606 N90-24846

Perturbation methods in the theory of waves and bifurcation phenomena 20 p2916 N90-26593

BRS invariant stochastic quantization of Einstein gravity
[DE90-791126] 21 p3085 N90-27541

An introduction to space trajectories
22 p3127 N90-27749

Anyons and Chern-Simons theory on compact spaces of finite genus
[DE90-627216] 23 p3391 N90-29157

A generalised Hubbard Hamiltonian: Influence of temperature and fractality
[DE90-627322] 23 p3400 N90-29213

Dissipative quantum maps
[DE90-627179] 23 p3402 N90-29227

Quantum chaos and dissipation: Lyapunov exponents
[DE90-627180] 23 p3403 N90-29228

Adiabatic invariance and transient resonance in very slowly varying oscillatory Hamiltonian systems
[DE90-016118] 24 p3538 N90-30007

A canonical integration technique of arbitrary order
[DE90-628377] 24 p3541 N90-30025

Symmetry and island structure of the standard map
[DE90-508076] 24 p3548 N90-30069

Theory of electronic states and formations energies of defect complexes, interstitial defects, and crystal growth in semiconductors
[AD-A224069] 24 p3551 N90-30093

On Dirac's conjecture for Hamiltonian systems with first and second class constraints
[DE90-627206] 24 p3555 N90-30116

HAND (ANATOMY)
NT FINGERS

Hand shaping: A paradigm for cognitive/motoric interaction
[AD-A219908] 17 p2437 N90-23885

Criteria for a recommended standard: Occupational exposure to hand-arm vibration
[PB90-168048] 22 p3233 N90-28331

HANDBOOKS
NT USER MANUALS (COMPUTER PROGRAMS)

Metric handbook for Federal officials: Recommendations of the Interagency Committee on Metric Policy
[PB89-226922] 06 p0756 N90-14400

Program manager's handbook
[AD-A214338] 07 p1009 N90-15844

Processing of DMSP magnetic data: Handbook of programs, tapes, and datasets
[NASA-TM-100757] 10 p1407 N90-18114

Spacecraft thermal control design data, volume 1
[ESA-PSS-03-108-ISSUE-1-VOL-1] 11 p1468 N90-18455

Spacecraft thermal control design data, volume 2
[ESA-PSS-03-108-ISSUE-1-VOL-2] 11 p1469 N90-18456

Spacecraft thermal control design data, volume 3
[ESA-PSS-03-108-ISSUE-1-VOL-3] 11 p1469 N90-18457

Spacecraft thermal control design data, volume 4
[ESA-PSS-03-108-ISSUE-1-VOL-4] 11 p1469 N90-18458

Composites design handbook for space structure applications
[ESA-PSS-03-1101-ISSUE-1-REV-1] 11 p1469 N90-18459

Methods for trend analysis: Examples with problem/failure data 12 p1635 N90-19396

User's guide to the 1.6 x 2.0 square m high speed wind tunnel HST, part 1
[ETN-90-98772] 17 p2357 N90-23414

Space Station Freedom media handbook
[NASA-TM-102901] 17 p2364 N90-23460

Failure analysis handbook
[AD-A219747] 17 p2413 N90-23752

Wright Research and Development Center test facilities handbook
[AD-A222582] 20 p2815 N90-26020

Grammar, punctuation, and capitalization: A handbook for technical writers and editors
[NASA-SP-7084] 20 p2937 N90-26710

Liquid Rocket Booster (LRB) for the Space Transportation System (STS) systems study, volume 2
[NASA-CR-183786] 23 p3288 N90-28600

Specifications, tolerances, and other technical requirements for weighing and measuring devices as adopted by the 74th National Conference on Weights and Measures, 1989 (1990 edition)
[PB90-184961] 23 p3316 N90-28748

HANDLES
Releasable clamping apparatus
[NASA-CASE-MFS-28192-1] 09 p1233 N90-17154

The relationship of isometric grip strength, optimal dynamometer settings, and certain anthropometric factors
[AD-A222046] 21 p3037 N90-27264

HANDLING EQUIPMENT
NT CRANES

Spoken commands control robot that handles radioactive materials
[DE89-012632] 02 p0262 N90-11488

Handling and analysis of ices in cryostats and glove boxes in view of cometary samples
08 p1146 N90-16643

Knowledge-based robotic grasping
[DE90-007216] 13 p1811 N90-20402

HANDLING QUALITIES
U CONTROLLABILITY

HANDS (ROBOTICS)
U END EFFECTORS

HANGARS
ILS (Instrument Landing System) mathematical modeling study on the effects of proposed hangar construction west of runway 18R on localizer performance at Dallas-Fort Worth International Airport
[AD-A210631] 01 p0005 N90-10019

ILS mathematical modeling study of the effects of proposed hangar construction at the Orlando International Airport, Runway 17R, Orlando, Florida
[DOT/FAA/CT-TN89/52] 03 p0310 N90-11762

HANKEL FUNCTIONS
Explicit formulas for Hankel norm approximations of infinite-dimensional systems
[TW-289] 04 p0545 N90-13167

Elastic solutions in a semi-infinite solid with an ellipsoidal inclusion
[AD-A217063] 12 p1625 N90-19338

A frame approach to the H-infinity super-optimal solution
[OUEL-1761/89] 15 p2158 N90-22327

The analysis of stress relaxation on indentation of a rigid punch into a viscoelastic sheet of finite thickness
[NPL-DMA(A)-193] 15 p2162 N90-22357

H-infinity control: An exploratory study
[EUT-88-E-211] 20 p2915 N90-26584

HARDENERS
Materials and selection criteria analysis for the compact ignition tokamak toroidal field coil turn-to-turn insulation system: Photographic summary ofiaboratory testing
[DE90-008020] 13 p1891 N90-20850

HARDENING
Hardening mechanisms and analysis of the structure of the TGDDM/DDS epoxy resin system (tetraglycidyl-4,4' diaminodiphenylmethane/4,4' diaminodiphenylsulfone)
[NOTE-TECHNIQUE-1988-8] 04 p0465 N90-12662

HARDENING (MATERIALS)
NT CARBURIZING
NT COLD HARDENING
NT HOT ISOSTATIC PRESSING
NT HOT PRESSING
NT NITRIDING
NT PRECIPITATION HARDENING
NT SHOT PEENING
NT STRAIN HARDENING
NT WORK HARDENING

Structural study of thermo-hardenable matrices. Deformation processes of composite matrices as a function of their molecular structure
[ONERA-RT-10/3521-M] 11 p1481 N90-18522

Comparison between the damage modes of thermo-hardenable and thermo-plastic composite matrices
[ONERA-RT-47/7086-M] 11 p1481 N90-18523

Study of the dynamical behavior of copper in a shock wave
[ISL-R-123/88] 11 p1507 N90-18679

Development and construction of external laser components for hardening and coating
[MT-15/87] 13 p1806 N90-20364

Elasto-plastic analysis for contact fatigue failure
15 p2112 N90-22078

Approximate analysis for the formation of adiabatic shear bands
[AD-A218751] 16 p2221 N90-22670

Surface reactions in the space environment
[AD-A221767] 21 p2979 N90-26932

A theoretical investigation into the inelastic behavior of metal-matrix composites
[AD-A223973] 23 p3302 N90-28677

HARDENING (SYSTEMS)
Design concepts for hardened communications structures
[AD-A221233] 19 p2683 N90-25260

HARDNESS
NT KNOOP HARDNESS
NT MICROHARDNESS

Structure-mechanical property relationships in ion implanted ceramics
[DE89-010129] 01 p0048 N90-10274

Improving snow roads and airstrips in Antarctica
[AD-A211588] 03 p0335 N90-11907

Quench sensitivity in Al-Cu-Li alloys
[AD-A213055] 05 p0624 N90-13639

Engineering approaches to the application of fracture toughness data in the nuclear industry
[DE90-001596] 06 p0800 N90-14659

Nickel beryllides and their properties
[DE90-001736] 07 p0903 N90-15220

Hardening and toughening of ZnS-Ga2S3 ceramics by solid-state reactions
[AD-A213875] 07 p0912 N90-15276

The mechanism, measurement, and influence of properties on the galling of metals
[DE90-006533] 11 p1487 N90-18558

Evaluation of the response of aluminum alloys to single and multiple particle impacts
[DE90-003689] 12 p1676 N90-19626

Crustal strength of different model comet materials
12 p1740 N90-20003

Ageing effects in welded cast CF3 stainless steel
[AERE-R-13559] 13 p1775 N90-20188

Time-dependent failure of silver interlayer welds
[DE90-008015] 13 p1818 N90-20440

Strengthening mechanisms of tungsten powder reinforced uranium
[DE90-009331] 14 p1947 N90-21144

Mechanical properties of carbon-implanted niobium
[DE90-009864] 15 p2064 N90-21823

Ultrahigh carbon steels and their laminates
[AD-A218780] 17 p2376 N90-23530

The mechanical properties of Cu/TiB2 multilayer structures
[DE90-010608] 18 p2517 N90-24378

The influence of ion implantation on the near-surface mechanical properties of ceramics
[DE90-010139] 18 p2531 N90-24444

TEM, positron lifetime, and hardness measurements of irradiated, cold-worked, and annealed Zr-1 percent Nb
[VTT-RR-650] 19 p2676 N90-25216

Mechanical properties of silica coatings
[DE90-012721] 20 p2837 N90-26138

The effect of crystal orientation on damage accumulation in chromium-implanted Al2O3
[DE90-012294] 20 p2931 N90-26674
Status and applications of diamond and diamond-like materials: An emerging technology
[NASA-CR-186935] 21 p2985 N90-26963
Mechanical properties testing of diamond and diamond-like films by ultra-low load indentation
[DE90-014456] 23 p3337 N90-28861
Effects of low Chromium(3) concentration in electrodeposition of low contraction chromium
[AD-A223338] 24 p3449 N90-29477
Dynamic consolidation of super hard materials
[AD-A224460] 24 p3454 N90-29505

HARDNESS TESTS
Worked-in holes in three-dimensional reinforced composites 02 p0186 N90-11060
Thermomechanical contact phenomena and wear of sliding components
[AD-A211290] 03 p0355 N90-12028
High temperature microhardness tester
[AD-A219567] 17 p2380 N90-23553
Evaluation of static and fatigue properties of thin sheets of 8090-T8 aluminum-lithium alloy and observation of its fracture surfaces
[NAL-TR-1039] 24 p3453 N90-29499

HARDWARE
High volume data storage architecture analysis
[NASA-CR-186239] 06 p0823 N90-14784
Columbus: A user's introduction
[ESA-BR-62] 08 p1036 N90-15989
The NODEN hardware description language
[RSRE-89011] 08 p1111 N90-16431
The algebra of the NODEN analyser
[RSRE-89012] 08 p1111 N90-16432
CESAR LOCAL BUS
[FFI-89/7011] 17 p2440 N90-23903
IAPSA 2 small-scale system specification
[NASA-CR-182006] 17 p2467 N90-24103
Development of a postprocessing and 3D graphical imaging facility
[AD-A221212] 18 p2593 N90-24755
Estimating the cost of major ongoing cost plus hardware development programs
[NASA-TM-100401] 19 p2764 N90-25705

HARMONIC ANALYSIS
NT ZONAL HARMONICS
Processing of DMSP magnetic data and its use in geomagnetic field modeling
[NASA-TM-100750] 03 p0370 N90-12115
First-order Bragg SAR imagery of Kelvin wakes and moving internal wave fields
[AD-A213361] 05 p0633 N90-13691
The initial imperfection data bank at the Delft University of Technology, part 2
[LR-559-PT-2] 05 p0656 N90-13825
Earth tidal analysis based on gravimeter observations and the influence of ocean tides
[ETN-90-95721] 12 p1695 N90-19734
Parametric resonance in horizontal axis wind turbines 14 p1912 N90-20962
Applications of gauge theories to enhance numerical solutions of mixed potential integral equations
[AD-A221520] 21 p3065 N90-27424

HARMONIC CONTROL
Active control of the forced and transient response of a finite beam 03 p0357 N90-12040
Aeroelastic simulation of higher harmonic control 15 p2054 N90-21768

HARMONIC EXCITATION
Low temperature properties of glasses 02 p0200 N90-11141
Modal interactions in shell dynamics 13 p1814 N90-20418
Active control of the forced and transient response of a finite beam
[NASA-CR-181957] 13 p1816 N90-20430
Response of a liquid column to one-sided axial excitation in zero-gravity
[LRT-WE-9-FB-3(1989)] 21 p2991 N90-26996
Non-linear axial vibrations of a cylindrical liquid column in zero-gravity
[LRT-WE-9-FB-4(1989)] 21 p2991 N90-26997
Response of a liquid column to counter-directional excitation under zero-gravity
[LRT-WE-9-FB-6(1989)] 21 p2991 N90-26998
Response of a liquid column to unequal counter-directional excitation under zero-gravity
[LRT-WE-9-FB-7(1989)] 21 p2991 N90-26999
Response of a spinning liquid column to axial excitation
[LRT-WE-9-FB-10(1988)] 21 p3006 N90-27085
Liquid sloshing response in a spinning container due to axial excitation
[LRT-WE-9-FB-9(1989)] 21 p3006 N90-27087
Oscillatory response of a liquid column to counter rotational excitation
[LRT-WE-9-FB-12(1989)] 21 p3006 N90-27088

HARMONIC FUNCTIONS
Orbit determination and analysis for Cosmos 236 at 15th-order resonance
[RAE-TR-88058] 04 p0461 N90-12641
Discretization of the steady state semiconductor device equations
[AD-A215807] 10 p1438 N90-18298
A remark on the Kelvin transform and a non-linear partial differential equation
[PB90-165622] 14 p2021 N90-21589
Annual and interannual variations of Earth-emitted radiation based on a 10-year data set
[NASA-TM-103465] 20 p2887 N90-26432

HARMONIC GENERATIONS
Theory of harmonic radiation using a single-electron source model
[DE90-002412] 06 p0791 N90-14606
Conformation, orientation and interaction in molecular monolayers: A surface second harmonic and sum frequency generation study
[DE90-003108] 08 p1128 N90-16536
Harmonic generation mechanisms in short-wavelength free-electron lasers
[DE90-007622] 13 p1807 N90-20374
Development and applications of a coupled cavity sodium-chloride laser 15 p2102 N90-22029

HARMONIC GENERATORS
CO2 laser plus optimization for harmonic generation
[AD-D014341] 12 p1665 N90-19565
The nonlinear interaction of intense laser pulses in plasmas
[AD-A217604] 12 p1718 N90-19867
Nonlinear optical responses and laser damage thresholds of films of a polarized stilbene side chain liquid crystal polymer and a phthalocyanine
[AD-A219462] 17 p2408 N90-23720
Apparatus for the efficient wavelength conversion of laser radiation
[AD-D014506] 20 p2866 N90-26305
Intracavity frequency doubling of a Nd:YAG laser with an organic nonlinear optical crystal
[AD-A222392] 21 p3008 N90-27102
Design of organic nonlinear optical materials
[AD-A222400] 21 p3084 N90-27536
Tunable CW single-frequency source for injection seeding 2-micrometer lasers
[AD-A223979] 23 p3331 N90-28834

HARMONIC MOTION
Unsteady separated flows produced by complex harmonic motions: Investigation of wing-flow interactions elicited by a mechanical model simulating dragonfly wing kinematics 15 p2100 N90-22018
Application and extension of an analytical model of the confined acoustic beam generated by a transducer
[AD-A222994] 20 p2924 N90-26639

HARMONIC OSCILLATION
Vibrational spectroscopy of boron nitride at high temperatures and pressures
[DE90-008633] 13 p1772 N90-20172
An interactive boundary-layer method for unsteady airfoil flows. Part 1: Quasi-steady-state model
[AD-A221220] 18 p2493 N90-24250

HARMONIC OSCILLATORS
Analysis of a system of two weakly nonlinear coupled harmonic oscillators arising from the field of wind-induced vibrations
[REPT-89-22] 03 p0396 N90-12261
Anharmonic betatron motion in free electron lasers
[DE90-001515] 07 p0934 N90-15407
Development of a small signal theory for the harmonic gyroklystron
[AD-A216274] 10 p1380 N90-17999
On a calculation of the ground-state energy in quantum mechanics
[DE90-627182] 24 p3555 N90-30119

HARMONIC RADIATION
Theory of harmonic radiation using a single-electron source model
[DE90-002412] 06 p0791 N90-14606
The nonlinear interaction of intense laser pulses in plasmas
[AD-A217604] 12 p1718 N90-19867

HARMONICS
NT HARMONIC EXCITATION
NT HARMONIC GENERATIONS
NT HARMONIC OSCILLATION
NT SPHERICAL HARMONICS
NT ZONAL HARMONICS
Subharmonic solutions near an equilibrium point for Hamiltonian systems
[AD-A210558] 02 p0263 N90-11496
Homoclinic orbits for a class of Hamiltonian systems
[AD-A210562] 03 p0391 N90-12229
Calculation of transient response from time-harmonic spectrum
[AD-A211972] 03 p0393 N90-12241
Strong Langmuir turbulence and second harmonics in laser-matter interactions 06 p0782 N90-14548
Lasing on the third harmonic
[DE90-002389] 06 p0790 N90-14602
An examination of helicopter rotor load calculations
[AD-A214295] 07 p0880 N90-15098
Flow of harmonic applications of a compact variety on a bordered variety
[DE89-635699] 07 p0985 N90-15692
Modeling the gate I/V characteristic of a GaAs MESFET for Volterra-series analysis
[AD-A215314] 09 p1212 N90-17030
Angle of arrival detection through analysis of optical fiber intensity patterns
[AD-A215421] 09 p1218 N90-17065
Three-dimensional simulation of free-electron laser harmonics with FRED
[DE90-005253] 09 p1229 N90-17130
Output performance of idealized microwave power amplifiers
[AD-A216797] 11 p1502 N90-18645
Quiet mode for nonlinear rotor models
[NASA-TM-102236] 15 p2051 N90-21758
Nonlinearity parameters of polymers 15 p2164 N90-22369
Analysis of gamma squared Velorum photometry from the South Pole 15 p2183 N90-22472
Spectral methods for electromagnetic propagation and diffraction
[AD-A220291] 17 p2393 N90-23632
Nonlinear interactions in mixing layers and compressible heated round jets
[NASA-CR-186303] 17 p2400 N90-23674
Experimental demonstration of an electromagnetically pumped free-electron laser with cyclotron harmonic idlers
[AD-A218830] 17 p2408 N90-23719
Nonlinear development of Goertler and crossflow vortices and Goertler/Tollmien-Schlichting wave interaction
[AD-A221107] 18 p2553 N90-24571
Inviscid dynamics of unstable shear layers
[AD-A222297] 21 p3004 N90-27077
Wideband impedance transformer for UHF power transistor time domain waveform measurement system
[PB90-210642] 22 p3167 N90-27962

HARNESSES
Human factors: The human interface with aircraft interiors
[NIAR-90-18] 20 p2900 N90-26496

HARTMANN FLOW
On the theory of Heiser and Shercliff experiment. Part 1: MHD flow in an open channel in strong uniform magnetic field
[QUEL-1804/89-PT-1] 15 p2170 N90-22400
On the theory of Heiser and Shercliff experiment. Part 2: MHD flow between two cylinders in strong radical magnetic field
[QUEL-1805/89-PT-2] 15 p2170 N90-22401

HARTREE APPROXIMATION
Atomic effects of beta decay in astrophysics and in elementary particle physics 01 p0141 N90-10811
Structural peculiarities and molecular properties of charge complexes formed on positive ion injection into dense inert gas media
[DE89-633953] 06 p0839 N90-14877
Large scale calculations of the structure and dynamics of dense matter
[DE90-003654] 07 p0991 N90-15726
Dissipation mechanism of the large-amplitude collective motion. Dynamical evolution of a collective bundle of trajectories in the TDHF phase space for a simple soluble model
[DE90-719557] 08 p1118 N90-16477
Large basis space effects in electron scattering form factors of light nuclei
[DE90-613501] 14 p2025 N90-21609
Quasistatic electron diffusion in quantum hadrodynamics
[ETN-90-97297] 22 p3255 N90-28432
Rotating neutron stars and the equation of state of dense matter
[DE90-014185] 23 p3410 N90-29269
On hydrogen chemisorption on metals: The electron correlation effects
[DE90-627318] 24 p3448 N90-29473
On equations of motion on complex Grassman manifold
[DE90-628369] 24 p3537 N90-29999

HARTREE-APPLETON APPROXIMATION
U HARTREE APPROXIMATION

HARTREE-FOCK APPROXIMATION
U HARTREE APPROXIMATION

HASTELLOY (TRADEMARK)
Filler metal development for Hastelloy alloy XR
[DE90-791084] 21 p2981 N90-26939
A welding metallurgy study of Hastelloy Alloys B-2 and W
[DE90-011910] 24 p3449 N90-29481
HATCHES
Independent Orbiter Assessment (IOA): Analysis of the mechanical actuation subsystem
[NASA-CR-185525] 02 p0168 N90-10944
Independent Orbiter Assessment (IOA): Assessment of the mechanical actuation subsystem, volume 1
[NASA-CR-185527-VOL-1] 02 p0169 N90-10952
Independent Orbiter Assessment (IOA): Assessment of the mechanical actuation subsystem, volume 2
[NASA-CR-185527-VOL-2] 02 p0169 N90-10953
Hatch cover
[NASA-CASE-MSC-21356-1] 12 p1613 N90-19278
HAULING
Transportation monitoring unit qualification
[NASA-CR-183930] 14 p1932 N90-21060
HAWAII
Characteristics of cumulus bandclouds off the east coast of Hawaii 15 p2130 N90-22178
HAZ (METALLURGY)
U HEAT AFFECTED ZONE
HAZARDS
NT AIRCRAFT HAZARDS
NT FLIGHT HAZARDS
NT METEOROID HAZARDS
NT RADIATION HAZARDS
NT TOXIC HAZARDS
Definition and reduction of the F-18 windshield birdstrike hazard
[AD-A210700] 01 p0004 N90-10015
Measurement of hydrazine contamination in soils 02 p0206 N90-11180
Base level management of radio frequency radiation protection program
[AD-A211787] 03 p0381 N90-12171
Base level management of radio frequency radiation protection program
[AD-A211759] 04 p0523 N90-13017
Re-entry hazards and cosmos 1900
[FOA-C-30535-9.4] 05 p0613 N90-13583
Environmental Projects. Volume 8: Modifications of wastewater evaporation ponds
[NASA-CR-186099] 06 p0808 N90-14700
Safety and cryogenic wind tunnels 08 p1032 N90-15960
MANPRINT (Manpower and Personnel Integration) evaluation: AN/TRC-170 digital troposcatter radio system
[AD-A211799] 08 p1055 N90-16100
Short-term bioassays may be useful in evaluating fiber/whisker hazards
[DE90-003707] 08 p1104 N90-16393
Polycarbonate article with chemical resistant coating
[NASA-CASE-MSC-21503-1] 09 p1195 N90-16925
Characteristics of transport, aircraft fires measured by full-scale tests 10 p1313 N90-17591
Ignitability of jet-A fuel vapors in aircraft fuel tanks 10 p1313 N90-17594
Fire science and aircraft safety 10 p1314 N90-17596
Advanced materials for interior and equipment related to fire safety in aviation 10 p1316 N90-17608
Flammability testing of aircraft cabin materials 10 p1316 N90-17611
The research program at the Civil Aeromedical Institute concerning protective breathing equipment for use by crew and passengers in an aviation smoke/fume environment 10 p1317 N90-17616
The investigation of particulate matter in the lungs of smoke inhalation death victims 10 p1317 N90-17617
Modelling time to incapacitation and death from toxic and physical hazards in aircraft fires 10 p1318 N90-17619
Safety status report for the Ulysses mission. Book 2: Risk analysis. General purpose heat source radioisotope thermoelectric generator program
[DE90-006827] 12 p1614 N90-19283
The pollution hazard assessment system: Documentation and users manual
[AD-A217108] 12 p1689 N90-19706
High-Explosives Applications Facility (HEAF)
[DE90-008122] 13 p1787 N90-20257
The Terrain-Responsive Atmospheric Code (TRAC) project plan: Development of a hazardous materials dispersion modeling capability with application to ambient air monitoring network design
[DE90-007293] 13 p1829 N90-20502
Workshop on ESD (Electrostatic Discharge) Ignition of Composite Solid Propellants
[AD-A218599] 17 p2382 N90-23569
Evaluation of the head injury hazard during military parachuting
[AD-A220724] 17 p2434 N90-23870
A survey of cervical pain in pilots of a Belgian F-16 Air Defence Wing 19 p2718 N90-25462
Hazards protection for space suits and spacecraft
[NASA-CASE-MSC-21366-1] 19 p2725 N90-25498
Space program: Space debris a potential threat to Space Station and shuttle
[GAO/IMTEC-90-18] 20 p2815 N90-26024
Space shuttle: Follow-up evaluation of NASA's solid rocket motor procurement. Report to the Chairman, Committee on Government Operations, House of Representatives
[GAO/NSIAD-89-89] 20 p2824 N90-26066
Rings of Earth detected by orbital debris radar 20 p2854 N90-26232
Analysis and improved design considerations for airborne pulse Doppler radar signal processing in the detection of hazardous windshear
[NASA-CR-186792] 20 p2890 N90-26448
Space Propulsion Hazards Analysis Manual (SPHAM), volume 1
[AD-A219607] 21 p2969 N90-26874
Space Propulsion Hazards Analysis Manual (SPHAM), volume 2
[AD-A219608] 21 p2969 N90-26875
Hazard classification testing of liquid propellants
[AD-A222070] 21 p2990 N90-26990
Bioelectromagnetic effects of the Electromagnetic Pulse (EMP)
[AD-A221552] 21 p3033 N90-27243
Geophysical diffraction tomography: A complementary remote sensing technique for hazardous waste site characterization
[DE90-013025] 23 p3341 N90-28882
Techniques for developing a system safety risk assessment model
[AD-A223477] 24 p3477 N90-29654
Preliminary hazard analysis in design application to EVA space suit
[ETN-90-97585] 24 p3523 N90-29918
HAZE
Investigation of North Atlantic fog and development of a marine fog forecast system
[AD-A211780] 04 p0519 N90-12999
An illustrated guide of optical characteristics of aircraft transparencies
[AD-A214565] 09 p1167 N90-16752
HC-1 HELICOPTER
U CH-47 HELICOPTER
HD-1 GROUND EFFECT MACHINES
U HOVERCRAFT GROUND EFFECT MACHINES
HEAD (ANATOMY)
Guidelines for safe human exposure to impact acceleration, update A
[AD-A215287] 09 p1253 N90-17268
Evaluation of the head injury hazard during military parachuting
[AD-A220724] 17 p2434 N90-23870
An investigation into techniques for landmark identification of 3D images of human subjects, phase 1
[AD-A218614] 18 p2583 N90-24713
Rheoencephalography in simulated aviation environmental stress
[AD-A221150] 18 p2584 N90-24716
Omni-directional human head-neck response
[SAE-861893] 19 p2721 N90-25478
Measurement techniques, evaluation criteria and injury probability assessment methodologies developed for Navy ejection and crashworthy seat evaluations 19 p2721 N90-25479
Helicopter aircrew helmets and head injury: A protective effect
[AD-A223024] 23 p3377 N90-29080
HEAD DOWN TILT
Interactions of form and orientation 16 p2274 N90-22958
Hemodynamic and ADH responses to central blood volume shifts in cardiac-denervated humans
[NASA-TM-103471] 20 p2898 N90-26485
Joint US/USSR study: Comparison of effects of horizontal and head-down bed rest
[NASA-TP-3037] 23 p3355 N90-28965
HEAD MOVEMENT
Voluntary presetting of the vestibular ocular reflex permits gaze stabilization despite perturbation of fast head movements 18 p2274 N90-22960
Dynamical modifications to the head, load factors from additional weight 19 p2720 N90-25472
Mobility of the head and load effects: Experimental approach in a centrifuge 19 p2720 N90-25473
A helmet mounted display to adapt the telerobotic environment to human vision 19 p2737 N90-25555
Helmet-mounted head restraint
[AD-D014536] 20 p2899 N90-26491
HEAD-UP DISPLAYS
Automatic processing of images from the GRATE flight test tool
[DLR-FB-89-28] 04 p0454 N90-12599
A head up display format for application to V/STOL aircraft approach and landing
[NASA-TM-102216] 10 p1320 N90-17632
Development of the triplex digital flight control system of the STOL research aircraft ASKA
[NAL-TR-1013] 10 p1322 N90-17640
The effect of windscreen bows and HUD pitch ladder format on pilot performance during simulated flight
[AD-A218139] 14 p2011 N90-21523
The eyes prefer real images 16 p2270 N90-22938
A real-time optical 6D tracker for head-mounted display systems
[AD-A222884] 21 p3036 N90-27262
HEADSETS
U EARPHONES
HEALTH
NT HEALTH PHYSICS
NT MENTAL HEALTH
NT PUBLIC HEALTH
Organic explosives and related compounds. Environmental and health considerations
[AD-A210554] 01 p0054 N90-10306
Managing human exposure and health risks: An integrated approach and the role of uncertainty
[DE89-008611] 01 p0092 N90-10525
Evaluation of rocket motor exhaust and liner combustion by-products
[AD-A210747] 02 p0189 N90-11083
MANPRINT (Manpower and Personnel Integration) evaluation: AN/TRC-170 digital troposcatter radio system
[AD-A211799] 08 p1055 N90-16100
Environmental, health, and safety concerns associated with nonpetroleum fuel use in US transportation
[DE90-004367] 08 p1099 N90-16362
A review of the literature on the toxicity of rare-earth metals as it pertains to the engineering demonstration system surrogate testing
[DE90-008049] 13 p1851 N90-20620
Boeing 727-100 test project (high energy radiated field tests)
[DOT/FAA/CT-88/33] 14 p1964 N90-21247
The global consequences of increasing tropospheric ozone concentrations
[NASA-TM-103477] 20 p2883 N90-26401
Bioelectromagnetic effects of the Electromagnetic Pulse (EMP)
[AD-A221552] 21 p3033 N90-27243
Atmospheric Sciences Research in the US EPA climate program
[PB90-221870] 22 p3212 N90-28219
HEALTH PHYSICS
NT PUBLIC HEALTH
Biological effects of power frequency electric and magnetic fields: Background paper
[PB89-209985] 02 p0254 N90-11439
Final Environmental Impact Statement for the Galileo Mission (Tier 2)
[NASA-TM-101825] 03 p0367 N90-12102
Risk analysis: Fundamental concepts, regulatory toxicology, and relative comparisons from radiation biology
[DE90-002466] 11 p1538 N90-18856
HEAO
NT HEAO 1
NT HEAO 2
The softest Einstein AGN (Active Galactic Nuclei)
[DE89-009389] 06 p0864 N90-15020
HEAO A
U HEAO 1
HEAO B
U HEAO 2
HEAO 1
HEAO-1 and IR observations of the X ray pulsar 1E2259+586 19 p2774 N90-25773
HEAO 2
Einstein SSS and MPC observations of Aql X-1 and 4U1820-30 19 p2777 N90-25790
Einstein IPC observations of the 1 to 3 keV X ray background 19 p2785 N90-25846
The Einstein All-Sky IPC slew survey 19 p2787 N90-25865
The dependence of the soft X ray spectral slope with radio property, luminosity, and redshift, for a large sample of AGN from the Einstein IPC data base 19 p2789 N90-25876
Spatial and spectral features of soft diffuse X ray background seen by the Einstein observatory 19 p2792 N90-25895
Einstein SSS+MPC observations of Seyfert type galaxies 19 p2795 N90-25913

HEARING
NT BINAURAL HEARING
Adaptive information processing in auditory cortex
|AD-A211294| 03 p0380 N90-12166
The effects of hearing protectors on speech communication and the perception of warning signals
|AD-A212521| 04 p0492 N90-12832
Shape instabilities of plate-like structures. 1: Experimental observations in heavily cold worked in situ composites
|AD-A212251| 04 p0523 N90-13021
Application of active noise reduction for hearing protection and speech intelligibility improvement
|IZF-1988-21| 04 p0527 N90-13042
The effects of noise on speech and warning signals
|AD-A212520| 04 p0551 N90-13210
Speech reception in quiet and in noisy conditions by individuals with noise-induced hearing loss in relation to their audiogram
|IZF-1989-11| 05 p0633 N90-13692
Evaluation of speech intelligibility through a bone conduction stimulator
|AD-A212002| 05 p0673 N90-13919
A prototype microprocessor based audiometer for use by the CF (Canadian Forces) medical services for periodic hearing tests
|AD-A212990| 05 p0673 N90-13921
Recognition of environmental sounds
|AD-A214942| 09 p1259 N90-17302
Perception of complex auditory patterns
|AD-A219626| 17 p2434 N90-23867
The integration of complex information from auditory and visual channels under stress
|AD-A222686| 21 p3033 N90-27245
The effects of blast trauma (impulse noise) on hearing: A parametric study source 2
|AD-A221731| 21 p3035 N90-27253
Auditory processing of complex sounds across frequency channels
|AD-A224147| 23 p3356 N90-28970
Attention, imagery, and memory: A neuromagnetic investigation
|AD-A224560| 24 p3499 N90-29775

HEART
NT MYOCARDIUM
Cellular and molecular mechanisms of high pressure inotropy in cardiac muscle
|AD-A211695| 03 p0381 N90-12170
Monitoring chaos of cardiac rhythms
|DE90-000692| 07 p0966 N90-15580
Arginine vasopressin lowers pulmonary artery pressure in hypoxic rats by releasing artrial natriuretic peptide
|AD-A215986| 10 p1410 N90-18134
Usefulness of heart measures in flight simulation
19 p2734 N90-25542
Experiment K-6-13. Morphological and biochemical examination of heart tissue. Part 1: Effects of microgravity on the myocardial fine structure of rats flown on Cosmos 1887. Ultrastructure studies. Part 2: Cellular distribution of cyclic ampdependent protein kinase regulatory subunits in heart muscle of rats flown on Cosmos 1887
20 p2894 N90-26467

HEART DISEASES
Prevalence of hypertension among active duty personnel
|AD-A223892| 23 p3356 N90-28968

HEART FUNCTION
Effect of fluid countermeasures of varying osmolarity on cardiovascular responses to orthostatic stress
18 p2628 N90-24978

HEART RATE
The effect of caffeine on endurance time to exhaustion at high altitude
|AD-A212069| 03 p0380 N90-12163
Monitoring chaos of cardiac rhythms
|DE90-000692| 07 p0966 N90-15580
Stress and performance during a simulated flight in a F-16 simulator 09 p1256 N90-17285
The role of blood volume in determining the cardiovascular adjustments to exercise
11 p1538 N90-18854
Effects of a time zone shift of 9 hours on the circadian rhythms in cockpit aircrew members on longhaul flights
|ESA-TT-1185| 19 p2722 N90-25485
Usefulness of heart measures in flight simulation
19 p2734 N90-25542
Hemodynamic and ADH responses to central blood volume shifts in cardiac-denervated humans
|NASA-TM-103471| 20 p2898 N90-26485
Adjustment and validation of the mathematical prediction model for sweat rate, heart rate, and body temperature under outdoor conditions
|AD-A222599| 20 p2898 N90-26486

HEAT
NT DRY HEAT
NT ENTHALPY
NT GIBBS FREE ENERGY
NT HEAT OF COMBUSTION
NT HEAT OF FORMATION
NT LATENT HEAT
NT NUCLEAR HEAT
NT SPECIFIC HEAT
Control of thermoregulatory sweating during exercise in the heat
|AD-A206001| 01 p0092 N90-10523
Heat exhaustion
|AD-A212128| 04 p0522 N90-13014
Ceramic technology for advanced heat engines project
|DE90-001852| 07 p0908 N90-15251
Cold fusion research
|DE90-005611| 10 p1433 N90-18267
Field assessment of wet bulb globe temperature: Present and future
|AD-A218224| 13 p1853 N90-20635
Ceramic technology for advanced heat engines project data base
|DE90-011491| 18 p2532 N90-24448
Preconditioned time-differencing for the parallel solution of the heat equation
|DE90-010636| 18 p2590 N90-24737

HEAT ACCLIMATIZATION
Exertional heatstroke: An international perspective. An introduction: The role of exercise in the etiology of exertional heatstroke
|AD-A212242| 04 p0523 N90-13020

HEAT AFFECTED ZONE
Ageing effects in welded cast CF3 stainless steel
|AERE-R-13559| 13 p1775 N90-20188

HEAT BALANCE
The effect of moisture absorption in clothing on the human heat balance
|AD-A217899| 13 p1852 N90-20626

HEAT BUDGET
NT ATMOSPHERIC HEAT BUDGET
Moisture and heat budgets of a cirrus cloud from aircraft measurements during FIRE 22 p3223 N90-28279

HEAT CAPACITY
U SPECIFIC HEAT

HEAT CONDUCTION
U CONDUCTIVE HEAT TRANSFER

HEAT CONTENT
U ENTHALPY

HEAT DISSIPATION
U COOLING

HEAT DISSIPATION CHILLING
U COOLING

HEAT EFFECTS
U TEMPERATURE EFFECTS

HEAT EQUATIONS
U THERMODYNAMICS

HEAT EXCHANGERS
NT TUBE HEAT EXCHANGERS
High temperature VSCF (Variable Speed Constant Frequency) generator system
|AD-A210823| 01 p0061 N90-10351
Application of process integration to utilities, combined heat and power, and heat pumps
|ESDU-89001| 03 p0335 N90-11909
An introduction to effectiveness: NTU relationships
|ESDU-89016| 03 p0415 N90-12381
A closed-cycle refrigerator for cooling maser amplifiers below 4 Kelvin 04 p0487 N90-12797
High-temperature corrosion of heat exchanger materials
|DE90-001963| 06 p0748 N90-14352
Thermal design of a 10-kW helium refrigerator
|DE90-701785| 06 p0756 N90-14403
Field testing of a ceramic heat exchanger for heat recovery application
|DE90-002082| 06 p0778 N90-14523
Solid lubrication of ceramic surfaces by IAD (Ion-Assisted Deposition)-silver coatings for heat engine applications
|DE90-002860| 07 p0909 N90-15253
Gas turbine regenerators: A method for selecting the optimum plate-finned surface pair for minimum core volume
|AD-A213430| 07 p0930 N90-15382
Reflux condensation in vertical tubes
|ESDU-89038| 07 p0932 N90-15397
Cycle analysis for helicopter gas turbine engines
|RAE-TM-P-1154| 08 p1025 N90-15921
Assessment of strength limiting flaws in ceramic heat exchanger components
|DE90-004086| 08 p1051 N90-16077
Thickness, velocity, and temperature measurements in falling liquid films
|DE90-004290| 08 p1063 N90-16151
Assessment of ground-coupled heat pumps
|DE90-003977| 09 p1220 N90-17079
Assessment of strength limiting flaws in ceramic heat exchanger tubes, phase 2
|DE90-004081| 09 p1220 N90-17080
Spacecraft thermal control design data, volume 4
|ESA-PSS-03-108-ISSUE-1-VOL-4| 11 p1469 N90-18458
Condensation fluid dynamics and heat transfer on rotating spherical surfaces in a microgravitational field
|DE90-005540| 11 p1495 N90-18607
Experimental investigation of condensation of steam in the presence of noncondensable gases using plate heat exchangers
|DE90-002251| 12 p1682 N90-19659
Evaluation of industrial magnetic heat pump/refrigerator concepts that utilize superconducting magnets
|DE90-008093| 13 p1787 N90-20258
Advanced on-site power plant development technology program
|DE90-000443| 13 p1826 N90-20484
Ice-making heat exchanger evaluation and test plan
|DE90-008824| 14 p1959 N90-21218
An experimental evaluation of two nonazeotropic refrigerant mixtures in a water-to-water breadboard heat pump
|DE90-009016| 14 p1973 N90-21305
Pressurized bellows flat contact heat exchanger interface
|NASA-CASE-MSC-21271-1| 15 p2097 N90-21999
High temperature ceramic-tubed reformer
|DE90-009617| 16 p2236 N90-22755
NDE (NonDestructive Evaluation) of ceramic heat exchangers
|DE90-010977| 18 p2554 N90-24575
A parametric study of counterflow heat exchanger transients
|IAR-89-10| 19 p2689 N90-25293
Two-dimensional model of a Space Station Freedom thermal energy storage canister
|NASA-TM-103124| 20 p2862 N90-26279
Heat exchanger with oscillating flow
|NASA-CASE-LAR-14033-1| 21 p3004 N90-27072
Apparatus for measuring high-flux heat transfer in radiatively heated compact exchangers
|NASA-CR-186333| 22 p3122 N90-27726
Numerical investigation of the thermal stratification in cryogenic tanks subjected to wall heat flux
|NASA-TM-103194| 22 p3171 N90-27984
A study of heat and fluid flow phenomena on the gas side of circular-tube plate-fin heat exchangers
23 p3324 N90-28795
Free shear layer and swirl flow heat transfer enhancement
|PB90-228123| 23 p3325 N90-28798
Open cycle heat pump development for local resource use. Phase 2: District heating case study analysis
|DE90-011123| 23 p3345 N90-28904

HEAT FLOW
U HEAT TRANSMISSION

HEAT FLUX
Heat transfer to throat tubes in a square-chambered rocket engine at the NASA Lewis Research Center
|NASA-TM-102336| 02 p0189 N90-11082
Low level remote sensing: Orographic winds
03 p0361 N90-12066
Description of a software library for the calculation of surface fluxes
|KNMI-TR-112| 03 p0375 N90-12141
Thermal loads on tokamak plasma facing components during normal operation and disruptions
|DE90-000794| 06 p0846 N90-14919
Calculation of surface heat transfer parameters during quenching from surface thermocouple signals
|DE89-011620| 07 p0904 N90-15224
High power density spray cooling
|AD-A213575| 07 p0930 N90-15386
Radial heat flux limits in potassium heat pipes: An experimental and analytical investigation
|DE90-002655| 07 p0932 N90-15396
Flux parameterization techniques in the atmospheric surface layer 07 p0959 N90-15548
Potential vorticity in extratropical cyclones
07 p0962 N90-15564
The response of the atmospheric convective boundary layer to surface inhomogeneities
08 p1100 N90-16369
Thermal modelling of various thermal barrier coatings in a high heat flux rocket engine
|NASA-TM-102418| 09 p1193 N90-16911
Design manual for microgravity two-phase flow and heat transfer
|AD-A214937| 09 p1201 N90-16957

Multi-dimensional discrete ordinates solutions to combined mode radiation heat transfer problems and their application to a free-falling particle, direct absorption solar receiver
|DE90-004987| 09 p1300 N90-17531
Effects of heating/cooling on changes in sea surface temperature: Consequences for computation of surface advection from satellite images
|AD-A214125| 10 p1409 N90-18129
Improved computational fluid dynamics for continuum hypersonic flow
|AD-A216981| 11 p1506 N90-18674
Dryout stability and inception at low flowrates
|DE90-006955| 11 p1509 N90-18692
Radiative transport models for solar thermal receiver/reactors
|DE90-000303| 12 p1683 N90-19665
Evolution of midplate hotspot swells: Numerical solutions
|NASA-CR-186462| 12 p1691 N90-19713
Magnetic vapor shield mechanism for protection of material surfaces exposed to high heat load
|AD-A217667| 13 p1780 N90-20217
Effective calibration of heat flux transducers for experimental use
|AD-A218262| 13 p1853 N90-20636
Principles of the radiosity method for canopy reflectance modeling
|DE90-008943| 14 p2001 N90-21466
Flow boiling with enhancement devices for cold plate coolant channel design
|NASA-CR-186358| 15 p2089 N90-21961
An anomalous wind between valleys: Its characteristics and a proposed explanation
|DE90-008965| 15 p2133 N90-22189
Monthly surface thermal forcing in the tropical Pacific from 1980 to 1983
|NASA-CR-183033| 16 p2259 N90-22877
Experimental investigations concerning the propagation of second-sound pulses at critical heat flux
|MPIS-12/1989| 16 p2313 N90-23182
Experiments on the breakdown of heat transfer in liquid helium 2
|MPIS-13/1989| 16 p2326 N90-23259
Natural convection form an array of rectangular protrusions in an enclosure filled with dielectric fluid: Effects of boundary conditions, fluid Prandtl number, and selective powering
|AD-A219819| 18 p2552 N90-24563
Thermal and orbital analysis of Earth monitoring Sun-synchronous space experiments
|NASA-TM-101630| 19 p2666 N90-25168
Calibration technique for heat flux sensors used in fire experiments and standard fire tests
|DOT/FAA/CT-89/26| 19 p2694 N90-25329
Measuring and modeling near-surface reflected and emitted radiation fluxes at the FIFE site
|NASA-CR-180953| 20 p2879 N90-26378
Numerical method for calculating indoor airflows using a turbulence model
|PB90-162009| 21 p3003 N90-27067
Heat exchanger with oscillating flow
|NASA-CASE-LAR-14033-1| 21 p3004 N90-27072
Vandenberg Boundary Layer Survey (VBLS): Results
|AD-A222517| 21 p3031 N90-27234
Apparatus for measuring high-flux heat transfer in radiatively heated compact exchangers
|NASA-CR-186333| 22 p3122 N90-27726
Numerical investigation of the thermal stratification in cryogenic tanks subjected to wall heat flux
|NASA-TM-103194| 22 p3171 N90-27984
The skin temperature of mountain slopes and the determination of the sensible heat flux
|DLR-FB-90-07| 24 p3495 N90-29754

HEAT GAIN
U HEATING

HEAT GENERATION
Influence of theobromine on heat production and body temperatures in cold-exposed humans: A preliminary report
|AD-A217203| 13 p1850 N90-20618
Determination of the heat dissipated from a specimen undergoing cyclic plasticity by a hybrid numerical/experimental method
|AD-A221575| 21 p2982 N90-26946
Evolution and use of combined mechanical and thermal codes for cryogenic turbopump bearings
23 p3291 N90-28618

HEAT ISLANDS
Wind tunnel design of heat island turbulent boundary layer
|IHW-ET/50| 12 p1660 N90-19542
Controlling Summer Heat Islands: Proceedings
|DE90-008075| 13 p1830 N90-20508

HEAT MEASUREMENT
Studies of gas turbine heat transfer airfoil surfaces and end-wall cooling effects
|AD-A212451| 04 p0457 N90-12620
Heat capacities of 1-methyl-3-ethylimidazolium chloride-aluminum chloride molten salts
|AD-A212790| 04 p0472 N90-12707
Heat capacities of solid polymers (The Advanced THermal Analysis System, ATHAS)
|DE90-007130| 11 p1493 N90-18595
Microcalometric studies of gun propellant KKR 8
|FOA-C-20770-2.1| 11 p1495 N90-18606
Thermodynamic properties of supercritical mixtures
|DE90-006720| 12 p1724 N90-19909
Interfacial studies in fiber-reinforced thermoplastic-matrix composites
15 p2062 N90-21814
Natural convection liquid immersion cooling of high density columns of discrete heat sources in a vertical channel
|AD-A218388| 17 p2402 N90-23681
Calorimetry, activity, and micro-FTIR analysis of CO chemisorption, titration, and oxidation on supported Pt
18 p2560 N90-24606
Low-temperature specific heat measurements on metals: Application to high-T(sub c) superconductors
|DE90-011612| 18 p2626 N90-24966
Determination of the SSME high pressure oxidizer turbopump bearing temperature
23 p3291 N90-28619
Simulation and measurement of the heat exchange between the urban canopy and boundary layers
24 p3486 N90-29702

HEAT OF COMBUSTION
High energy density solid and liquid hydrocarbon fuels
|AD-A210195| 01 p0053 N90-10304
Flammability testing of aircraft cabin materials
10 p1316 N90-17611

HEAT OF FORMATION
Convection of a pattern of vorticity through a reacting shock wave
|NASA-CR-181921| 01 p0102 N90-10576
The heat of formation of CN radicals and radiative lifetimes of the A 1 Sigma - state of C2N2
20 p2946 N90-26765

HEAT PIPES
Application of formal optimization techniques in thermal/structural design of a heat-pipe-cooled panel for a hypersonic vehicle
|NASA-TM-89131| 01 p0071 N90-10409
Design of ceramic fabric heat pipe with water working fluid
|DE89-016565| 02 p0221 N90-11265
Studies on the startup transients and performance of a gas loaded sodium heat pipe
|AD-A211880| 03 p0414 N90-12379
Heat pipe and thermal energy storage and corrosion studies (1988)
|AD-A212655| 04 p0472 N90-12706
Heat pipes for sodium-sulfur batteries
|AD-A212523| 04 p0497 N90-12865
Analysis of the performance of heat pipes and phase-change materials with multiple localized heat sources for space applications
|AD-A212232| 04 p0503 N90-12898
An improved algorithm for the modeling of vapor flow in heat pipes
|NASA-CR-185179| 05 p0642 N90-13748
Design and demonstration of heat pipe cooling for NASP and evaluation of heating methods at high heating rates
|DE89-016995| 06 p0724 N90-14227
A heat receiver design for solar dynamic space power systems
|NASA-TM-102473| 06 p0735 N90-14283
Radial heat flux limits in potassium heat pipes: An experimental and analytical investigation
|DE90-002655| 07 p0932 N90-15396
Niobium 1 percent zirconium/potassium and titanium/potassium life-test heat pipe design and testing
|DE90-002430| 07 p0954 N90-15522
Low risk low power heat pipe/thermoelectric space power supply
|DE89-014817| 08 p1095 N90-16342
Heat pipes for wing leading edges of hypersonic vehicles
|NASA-CR-181922| 09 p1216 N90-17055
Capillary flow properties of mesh wicks
|AD-A214769| 09 p1217 N90-17057
Incompressible flow friction factors in a simulated heat pipe
|AD-A216288| 10 p1386 N90-18018
Flexible heat pipe cold plate
|AD-A216053| 11 p1464 N90-18433
Spacecraft thermal control design data, volume 3
|ESA-PSS-03-108-ISSUE-1-VOL-3|
11 p1469 N90-18457
Analytical and experimental investigation of miniature heat pipes, phase 2
|AD-A216945| 11 p1506 N90-18673
Measuring flow properties of wicks for heat pipe solar receivers
|DE89-016537| 12 p1683 N90-19664
Reusable high-temperature heat pipes and heat pipe panels
|NASA-CASE-LAR-13761-1| 13 p1799 N90-20323
Ceramic heat pipe wick
|NASA-CASE-GSC-13199-1| 17 p2378 N90-23541
Transient characteristics of a grooved water heat pipe with variable heat load
|NASA-CR-185280| 20 p2861 N90-26272
Thermal analysis of heat pipe radiators with a rectangular groove wick structure
|AD-A222952| 21 p3004 N90-27074

HEAT PUMPS
Free-Piston Stirling Engine magnetically coupled heat pump: Critical component evaluation
|DE89-015646| 02 p0229 N90-11316
Dynamic characteristics concerned in the design of a free-piston Stirling engine/magnetic coupling/compressor system
|DE89-015981| 02 p0230 N90-11317
System design and performance prediction of a free-piston Stirling engine/magnetic coupling/compressor assembly in a gas residential heat pump
|DE89-016070| 06 p0807 N90-14696
Heat transfer of buried pipe for heat pump application
|DE90-000580| 06 p0807 N90-14697
New heating and cooling technology: Regenerative heat pump according to the Vuilleumier principle
|DE90-002701| 06 p0807 N90-14699
Feasibility analysis of reciprocating magnetic heat pumps
|NASA-CR-186205| 07 p0927 N90-15363
Laboratory study of the dynamic losses of a single speed, split system air-to-air heat pump having tube and plate fin heat exchangers, 1985 to 1986
|DE90-000970| 07 p0927 N90-15367
Recent advances in magnetic heat pump technology
|DE89-013289| 07 p0928 N90-15370
Design and fabricate a metallic hydride heat pump with a cooling capacity of 9000 BTU/H
|AD-A213756| 07 p0931 N90-15388
Annual summary of basic research in thermoacoustic heat transport
|AD-A214185| 07 p1007 N90-15834
Industrial heat pump assessment study
|DE90-004541| 08 p1071 N90-16201
Rotary absorption heat pump sensitivity analysis
|DE90-002877| 09 p1216 N90-17053
Assessment of ground-coupled heat pumps
|DE90-003977| 09 p1220 N90-17079
Hydride heat pumps for upgrading spacecraft waste heat
10 p1385 N90-18013
Energy technology R and D and the greenhouse effect
|DE90-001339| 10 p1406 N90-18107
Investigation report of the investigation commission for interchange of heat pump technology in Europe
|DE89-782293| 11 p1505 N90-18666
Transfer of heat pump technology
|DE90-007373| 11 p1509 N90-18693
Stirling engine technologies in Japan
|DE89-782296| 11 p1528 N90-18795
Advanced absorption technology development in the United States
|DE90-001336| 12 p1641 N90-19428
Survey on the social and economic influences of wide-spreading heat-pump technology
|DE89-782294| 12 p1658 N90-19526
Operational fact-finding report on heat pump systems for industrial use
|DE89-782295| 12 p1658 N90-19527
Evaluation of industrial magnetic heat pump/refrigerator concepts that utilize superconducting magnets
|DE90-008093| 13 p1787 N90-20258
Phase 1 supplemental development of a kinematic Stirling/Rankine commercial gas-fired heat pump system
|PB90-129974| 13 p1825 N90-20483
An experimental evaluation of two nonazeotropic refrigerant mixtures in a water-to-water breadboard heat pump
|DE90-009016| 14 p1973 N90-21305
Ceramic heat pipe wick
|NASA-CASE-GSC-13199-1| 17 p2378 N90-23541
Convergent strand array liquid pumping system
|NASA-CASE-NPO-17301-1-CU|
17 p2385 N90-23587
Boiling/evaporative heat transfer from spheres in packed-bed thermal energy storage units
|DE90-012023| 19 p2711 N90-25430
Advanced heat pump
|AD-D014560| 22 p3170 N90-27979

Open cycle heat pump development for local resource use. Phase 2: District heating case study analysis
[DE90-011123] 23 p3345 N90-28904

HEAT RADIATORS
NT SPACECRAFT RADIATORS
Independent Orbiter Assessment (IOA): Analysis of the active thermal control subsystem
[NASA-CR-185553] 03 p0314 N90-11782
Clamping device for pressurized module radiator panel 18 p2539 N90-24488
Progress in the design of a microgravity facility for in-orbit experiments 18 p2540 N90-24496
Aeolian removal of dust from radiator surfaces on Mars
[NASA-TM-103205] 20 p2824 N90-26068
Thermal analysis of heat pipe radiators with a rectangular groove wick structure
[AD-A222952] 21 p3004 N90-27074
The effects of atomic oxygen on the thermal emittance of high temperature radiator surfaces
[NASA-TM-103224] 23 p3301 N90-28670

HEAT REGULATION
U TEMPERATURE CONTROL

HEAT REJECTION DEVICES
U HEAT RADIATORS

HEAT RESISTANCE
U THERMAL RESISTANCE

HEAT RESISTANT ALLOYS
NT MOLYBDENUM ALLOYS
NT NIOBIUM ALLOYS
NT REFRACTORY METAL ALLOYS
NT TUNGSTEN ALLOYS
NT UDIMET ALLOYS
NT WASPALOY
New structural materials
[AD-A209425] 01 p0044 N90-10246
Development of metastable processing paths for high temperature alloys
[AD-A210550] 01 p0045 N90-10254
Creep and fracture behavior of heat resistant steels in characteristic cases of variable fatigue loading
[ETN-89-94671] 03 p0326 N90-11855
Determination and description of the long term creep behavior of high temperature gas turbine materials
[ETN-89-94985] 03 p0329 N90-11871
An investigation of the irradiation swelling mechanisms in refractory metals at high temperatures
[AD-A211406] 04 p0474 N90-12719
Constitutive modeling for isotropic materials (HOST)
[NASA-CR-179522] 05 p0582 N90-13390
Constitutive modeling for isotropic materials (HOST)
[NASA-CR-174718] 05 p0582 N90-13391
Joint Services Electronics Program
[AD-A213015] 05 p0634 N90-13699
Calibration approach to electron probe microanalysis: A study with PWA-1480, a nickel base superalloy
[NASA-TM-102393] 06 p0745 N90-14335
Thermal fatigue durability for advanced propulsion materials
[NASA-TM-102348] 06 p0797 N90-14641
Deformation and fracture of low alloy steels at high temperature
[DE90-001274] 07 p0902 N90-15215
A review of the effects of microalloying constituents on the formation and breakdown of protective oxide scales on high-temperature alloys at temperatures below 700 C
[DE90-001277] 07 p0902 N90-15216
Directional solidification of superalloys
[NASA-CASE-MFS-28314-1] 07 p0904 N90-15227
Dispersion strengthening of high temperature niobium alloys
[AD-A213829] 07 p0906 N90-15236
Method to produce titanium alloy articles with high fatigue and fracture resistance
[AD-D014278] 08 p1043 N90-16029
Metal matrix composite: Strengthening mechanisms
[AD-A214843] 09 p1186 N90-16871
Heat-resistant steels containing 8 pct Cr
[PB90-108796] 09 p1193 N90-16912
Crack propagation from artificial defects in typical engine disk materials; interpretation of experimental results by means of 3D J integral 11 p1458 N90-18401
An attempt of improving high-temperature fatigue properties of Ni-Cr-W superalloys in HTGR helium
[DE90-741482] 12 p1627 N90-19350
Secondary arm coarsening and microsegregation in superalloy PWA-1480 single crystals: Effect of low gravity
[NASA-TM-102445] 13 p1776 N90-20194
Attachment of lead wires to thin film thermocouples mounted on high temperature materials using the parallel gap welding process
[NASA-TM-102442] 14 p1983 N90-21361
Preliminary investigation into the effect of high temperature thermal anneals on the figure of merit of silicon germanium alloys
[AD-A218573] 17 p2375 N90-23527
Investigation of metal processing technology
[AD-A218835] 17 p2376 N90-23531
Hydrogen induced fracture characteristics of single crystal nickel-based superalloys
[NASA-CR-183992] 20 p2832 N90-26108
Development of metastable processing paths for high temperature alloys
[AD-A223144] 22 p3157 N90-27898
Micromechanics of cyclic deformation in SSME turbopump blade materials 23 p3295 N90-28641
High temperature fatigue behavior of Haynes 188 23 p3295 N90-28642
Constitutive and life modeling of single crystal blade alloys for root attachment analysis 23 p3296 N90-28643
The fatigue damage behavior of a single crystal superalloy 23 p3296 N90-28644
Developments in test procedures for hot-salt corrosion of superalloys 23 p3306 N90-28700
Effect of protective coatings on mechanical properties of superalloys 23 p3308 N90-28707
Processability and high temperature behavior of emerging aerospace alloys
[AD-A224285] 24 p3448 N90-29475
The stress and temperature dependence of creep in an Al-2.0 wt percent Li alloy
[AD-A223676] 24 p3449 N90-29480

HEAT SHIELDING
NT REENTRY SHIELDING
NT REUSABLE HEAT SHIELDING
Preliminary design of a large tetrahedral truss/hexagonal heatshield panel aerobrake
[NASA-TM-101612] 01 p0025 N90-10127
Pressure air tightness tests of laminated panels for wing leading edge heat shields
[INFORME-I-377/89] 10 p1358 N90-17873
Three-dimensional structural analyses of reentry vehicles
[DE90-006278] 12 p1615 N90-19291
Magnetic vapor shield mechanism for protection of material surfaces exposed to high heat load
[AD-A217667] 13 p1780 N90-20217
Mechanistic model for catalytic recombination during aerobraking maneuvers
[NASA-CR-185611] 14 p1932 N90-21059
Carbon-carbon composites: Emerging materials for hypersonic flight
[NASA-TM-103472] 20 p2827 N90-26080

HEAT SINKS
Thermal model for double-drift IMPATT diodes on diamond heat sinks
[AD-A211746] 03 p0415 N90-12380
Flexible heat pipe cold plate
[AD-A216053] 11 p1464 N90-18433
Heat sink effects on weld bead: VPPA process 12 p1639 N90-19418
Development of a point-contact solar cell using high-volume processing techniques
[DE90-010330] 18 p2577 N90-24683
A direct-interface, fusible heat sink for astronaut cooling
[NASA-TM-102835] 19 p2689 N90-25292
Heat sink effects on weld bead: VPPA process
[NASA-CR-186723] 19 p2697 N90-25349
Reliability study of TWT output RF window
[AD-A223688] 24 p3465 N90-29574

HEAT SOURCES
NT GEOTHERMAL RESOURCES
NT GEYSERS
Analysis of the performance of heat pipes and phase-change materials with multiple localized heat sources for space applications
[AD-A212232] 04 p0503 N90-12898
Design and fabricate a metallic hydride heat pump with a cooling capacity of 9000 BTU/H
[AD-A213756] 07 p0931 N90-15388
Expandable radiator
[AD-D014258] 08 p1063 N90-16147
Investigation report of the investigation commission for interchange of heat pump technology in Europe
[DE89-782293] 11 p1505 N90-18666
Operational fact-finding report on heat pump systems for industrial use
[DE89-782295] 12 p1658 N90-19527
General purpose heat source radioisotope thermoelectric generator program. Book 1: Accident analysis
[REPT-90SDS4202-BK-1] 15 p2166 N90-22379
General purpose heat source radioisotope thermoelectric generator. Book 2: Accident analysis, appendices
[REPT-90SDS4202-BK-2] 15 p2166 N90-22380
High temperature electric arc furnace and method
[NASA-CASE-MFS-28281-1] 17 p2357 N90-23415
Natural convection liquid immersion cooling of high density columns of discrete heat sources in a vertical channel
[AD-A218388] 17 p2402 N90-23681
Titanium-boron mixtures as variable heat sources
[DE90-009729] 18 p2522 N90-24401
GPHS-RTG response to Challenger type accident 19 p2665 N90-25163
A study of mixed convection in large baffled rectangular chambers with and without internal heat sources
[AD-A223158] 22 p3169 N90-27977

HEAT STORAGE
Potential industrial applications for composite phase-change materials as thermal energy storage media
[DE89-015170] 02 p0237 N90-11346
Improved 2D numerical simulation model for strongly coupled heat and fluid flow in a thermal storage
[PB89-218879] 04 p0500 N90-12878
A heat receiver design for solar dynamic space power systems
[NASA-TM-102473] 06 p0735 N90-14283
Thermal energy storage
[DE90-000953] 07 p0950 N90-15500
Selection of phase-change and containment materials for thermal energy storage
[NASA-CR-186228] 07 p0952 N90-15506
An experimental and analytical examination of stratified thermal storage 09 p1215 N90-17046
Optimized sensible heat storage systems for application to solar dynamic power generation 10 p1334 N90-17719
Development of a high temperature storage unit for integration with solar dynamic systems 10 p1335 N90-17720
Phase-Change Thermal Energy Storage
[DE89-009426] 11 p1529 N90-18801
Mechanical properties of pure nickel alloys after long term exposures to LiOH and vacuum at 775 K
[NASA-TM-102403] 13 p1774 N90-20181
Thermal decay of an initially hot isothermal water body with application to thermal energy storage
[DE90-614742] 14 p2035 N90-21675
Analysis of thermal energy storage material with change-of-phase volumetric effects
[NASA-TM-102457] 15 p2092 N90-21974
Boiling/evaporative heat transfer from spheres in packed-bed thermal energy storage units
[DE90-012023] 19 p2711 N90-25430
Two-dimensional model of a Space Station Freedom thermal energy storage canister
[NASA-TM-103124] 20 p2862 N90-26279

HEAT STROKE
Heatstroke pathophysiology: The energy depletion model
[AD-A212156] 03 p0380 N90-12164
Exertional heatstroke: An international perspective. An introduction: The role of exercise in the etiology of exertional heatstroke
[AD-A212242] 04 p0523 N90-13020
Heat exhaustion in a rat model: Lithium as a biochemical probe
[AD-A219361] 16 p2260 N90-22884

HEAT TESTS
U HIGH TEMPERATURE TESTS

HEAT TOLERANCE
Heat exhaustion in a rat model: Lithium as a biochemical probe
[AD-A219361] 16 p2260 N90-22884
Physiological reactions to heat stress; quantifying the effects of individual parameters
[IZF-1989-30] 22 p3232 N90-28326

HEAT TRANSFER
NT AERODYNAMIC HEAT TRANSFER
NT CONDUCTIVE HEAT TRANSFER
NT CONVECTIVE HEAT TRANSFER
NT LAMINAR HEAT TRANSFER
NT RADIATIVE HEAT TRANSFER
NT TURBULENT HEAT TRANSFER
Heat transfer characteristics of igniter output plumes
[DE89-011449] 01 p0059 N90-10340
PORFLO-3: A mathematical model for fluid flow, heat, and mass transport in variably saturated geologic media: Users manual, version 1.0
[DE89-013977] 01 p0069 N90-10398
Global existence and asymptotic stability for a nonlinear integrodifferential equation modeling heat flow
[AD-A210647] 01 p0071 N90-10408
Thermoregulatory responses to intermittent exercise are influenced by knit structure of underwear
[AD-A209087] 01 p0095 N90-10541
Energy dependent transport problem with generalized boundary conditions
[DE89-617843] 01 p0118 N90-10676

Heat transfer to throat tubes in a square-chambered rocket engine at the NASA Lewis Research Center
|NASA-TM-102336| 02 p0189 N90-11082

Thin section casting program. Volume 4: Static cast product bending, straightening, and rolling
|DE89-009034| 02 p0210 N90-11202

Design of ceramic fabric heat pipe with water working fluid
|DE89-016565| 02 p0221 N90-11265

The 3-D heat transfer computer calculations of th e performance of the IAEA's air-bath calorimeters
|DE89-016908| 02 p0224 N90-11283

Advanced Turbine Technology Applications Program, (ATTAP)
|DE89-016067| 02 p0230 N90-11318

Application of process integration to utilities, combined heat and power, and heat pumps
|ESDU-89001| 03 p0335 N90-11909

Convective heat transfer in hypobaric environments
|AD-A212060| 03 p0347 N90-11979

Prediction of the thermal environment and thermal response of simple panels exposed to radiant heat
|NASA-TM-101660| 03 p0400 N90-12292

An introduction to effectiveness: NTU relationships
|ESDU-89016| 03 p0415 N90-12381

Phase change material for spacecraft thermal management
|AD-A211404| 04 p0462 N90-12648

South Pole surface radiation balance measurements, April 1986 to February 1988
|PB89-224018| 04 p0519 N90-12993

A fast algorithm for the evaluation of heat potentials
|AD-A211316| 04 p0529 N90-13052

An Introduction to Hypersonic Aerodynamics
|VKI-LS-1989-01| 05 p0573 N90-13334

Theory of stagnation point heat transfer in dissociated air 05 p0573 N90-13337

On catalytic recombination rates in hypersonic stagnation heat transfer 05 p0573 N90-13338

Recent progress in research pertaining to estimates of gas-side heat transfer in an aircraft gas turbine
|NASA-TM-102460| 05 p0582 N90-13394

Metal transfer in gas metal arc welding
|AD-A213390| 05 p0624 N90-13642

Design and demonstration of heat pipe cooling for NASP and evaluation of heating methods at high heating rates
|DE89-016995| 06 p0724 N90-14227

Surface flow and heating distributions on a cylinder in near wake of Aeroassist Flight Experiment (AFE) configuration at incidence in Mach 10 Air
|NASA-TP-2954| 06 p0772 N90-14493

Heat transfer to a stationary and moving sphere immersed in a fluidized bed 06 p0774 N90-14503

Heat transfer in convective boundary layer and channel flows 06 p0774 N90-14505

Selection of the energy-efficient enhancement geometry for single-phase turbulent flow inside tubes
|DE89-017690| 06 p0777 N90-14519

Field testing of a ceramic heat exchanger for heat recovery application
|DE90-002082| 06 p0778 N90-14523

Course A: Numerical modeling of two-phase flows for presentation at Ecole d'Ete d'Analyse Numerique
|DE90-002074| 06 p0778 N90-14526

Interfacial area in two-phase flow
|DE90-002210| 06 p0778 N90-14527

Heat and mass transfer design issues in PEM fuel cell hardware
|DE89-016779| 06 p0804 N90-14677

Heat transfer of buried pipe for heat pump application
|DE90-000580| 06 p0807 N90-14697

New heating and cooling technology: Regenerative heat pump according to the Vuilleumier principle
|DE90-002701| 06 p0807 N90-14699

Program CICC flow and heat transfer in Cable-In-Conduit Conductors
|DE90-001519| 06 p0829 N90-14818

Starlight: A stationary inertial-confinement-fusion reactor with nonvaporizing walls
|DE90-002315| 06 p0847 N90-14927

Semi-empirical theory of heat-transfer when boiling
|DE89-635418| 06 p0857 N90-14984

Calculation of surface heat transfer parameters during quenching from surface thermocouple signals
|DE89-011620| 07 p0904 N90-15224

Critical temperature analysis for a hemispherical charge of a binary explosive
|DE90-001447| 07 p0913 N90-15282

RF transistor thermal/electrical characterization
|DE90-001427| 07 p0920 N90-15326

High power density spray cooling
|AD-A213575| 07 p0930 N90-15386

Radial heat flux limits in potassium heat pipes: An experimental and analytical investigation
|DE90-002655| 07 p0932 N90-15396

Reflux condensation in vertical tubes
|ESDU-89038| 07 p0932 N90-15397

Thermal energy storage
|DE90-000953| 07 p0950 N90-15500

Pulsed EMAT (Electromagnetic Acoustic Transducer) acoustic measurements on a horizontal continuous caster for internal temperature determination
|DE90-002735| 07 p0988 N90-15709

Annual summary of basic research in thermoacoustic heat transport
|AD-A214185| 07 p1007 N90-15834

Aerodynamic and heat transfer measurements on blading for a high rim-speed transonic turbine
|RAE-TM-P-1151| 08 p1024 N90-15920

Conceptual design of a moving belt radiator shuttle-attached experiments: Technical requirement Document
|NASA-CR-185168| 08 p1038 N90-15996

The onset of boiling of the liquid alkali metals
|DE90-002276| 08 p1044 N90-16036

Selection of corrosion-resistant materials for use in molten nitrate salts
|DE90-004351| 08 p1046 N90-16048

Electroplating simulation
|DE90-003683| 08 p1054 N90-16091

Expandable radiator
|AD-D014258| 08 p1063 N90-16147

Thickness, velocity, and temperature measurements in falling liquid films
|DE90-004290| 08 p1063 N90-16151

Modeling a self-calibrating thermocouple for use in a smart temperature measurement system
|DE90-003697| 08 p1081 N90-16259

Thermal histories of the samples of two KOSI comet nucleus simulation experiments 08 p1147 N90-16645

Wake interaction effects on the transition process on turbine blades
|AD-A214492| 09 p1168 N90-16759

The fundamentals of metal combustion in composite explosives revealed by high speed microphotography
|DE90-005255| 09 p1192 N90-16910

Thermal modelling of various thermal barrier coatings in a high heat flux rocket engine
|NASA-TM-102418| 09 p1193 N90-16911

Design manual for microgravity two-phase flow and heat transfer
|AD-A214937| 09 p1201 N90-16957

Turbulent heat and momentum transfer in recirculating and impinging flows 09 p1215 N90-17043

Computation of fluid flow and heat transfer in rotating disc-systems 09 p1215 N90-17044

An experimental and analytical examination of stratified thermal storage 09 p1215 N90-17046

Impingement characteristics of heated plane turbulent jets 09 p1215 N90-17047

Rotary absorption heat pump sensitivity analysis
|DE90-002877| 09 p1216 N90-17053

Nonlinear heat transfer and wave motion
|AD-A214911| 09 p1217 N90-17058

Effect of vortex circulation on injectant from a single film-cooling hole and a row of film-cooling holes in a turbulent boundary layer. Part 1: Injection beneath the vortex downwash
|AD-A215288| 09 p1218 N90-17063

Assessment of ground-coupled heat pumps
|DE90-003977| 09 p1220 N90-17079

A numerical study of the formation of mesoscale convective complexes 09 p1245 N90-17225

Shock-shock boundary layer interactions 10 p1308 N90-17569

Axial flow in corners at supersonic and hypersonic speeds 10 p1308 N90-17570

Glancing shock-boundary layer interactions 10 p1309 N90-17571

Heat release rate measurement for evaluating the flammability of aircraft materials 10 p1316 N90-17610

Viscous three-dimensional analyses for nozzles for hypersonic propulsion
|NASA-CR-185197| 10 p1321 N90-17635

Turbulence scale effects on heat transfer in a linear turbine cascade
|AD-A216222| 10 p1321 N90-17637

The effect of loading on the laser ablation of graphite/epoxy composite material
|AD-A216209| 10 p1349 N90-17826

Colliding natural convection boundary layer flow in a rectangular enclosure
|DE90-005397| 10 p1384 N90-18009

Spacecraft thermal control design data, volume 4
|ESA-PSS-03-108-ISSUE-1-VOL-4| 11 p1469 N90-18458

Microcomputer enhanced optical investigation of spreading and evaporative processes in ultra thin films
|DE90-006323| 11 p1492 N90-18585

Strong source heat transfer simulations based on a GalerKin/gradient least squares method
|DE90-608613| 11 p1507 N90-18678

Modeling convective Marangoni flows with void movement in the presence of solid-liquid phase change
|DE90-006474| 11 p1509 N90-18690

Transfer of heat pump technology
|DE90-007373| 11 p1509 N90-18693

Numerical investigations of heat transfer and flow rates in rotating cavities. Simulation of the movement generated by wall temperature gradients, by source-sink mass flows or by the differential rotation of the walls, under the influence or coriolis and centrifugal forces
|ETN-90-96253| 11 p1510 N90-18695

Experimental and theoretical investigations of flowfields and heat transfer in modern gas turbines
|AD-A217663| 12 p1605 N90-19237

Evaluation of the heat transfer module (FAHT) of Failure Analysis Nonlinear Thermal And Structural Integrated Code (FANTASTIC) 12 p1637 N90-19407

The influence of a wall function on turbine blade heat transfer prediction 12 p1640 N90-19421

Heat transfer definitions and equations
|ESDU-89022| 12 p1657 N90-19522

Numerical and experimental analysis of a thin liquid film on a rotating disk related to development of a spacecraft absorption cooling system
|NASA-CR-183457| 12 p1657 N90-19523

Swept shock/boundary layer interaction experiments in support of CFD code validation
|NASA-CR-186397| 12 p1659 N90-19535

Theoretical and experimental examination of the beginning of turbulence in a heated laminar conduit flow
|ETN-90-95369| 12 p1660 N90-19541

Experimental investigation of condensation of steam in the presence of noncondensable gases using plate heat exchangers
|DE90-002251| 12 p1682 N90-19659

Radiative transport models for solar thermal receiver/reactors
|DE90-000303| 12 p1683 N90-19665

Thermal conductivities and diffusivities of porous ice samples at low pressures and temperatures and possible modes of heat transfer in near surface layers of comets 12 p1739 N90-19999

Design and test of a compact optics system for the pool boiling experiment
|NASA-TM-102530| 13 p1786 N90-20253

The thermal response of generic objects in JP-4 pool fires
|DE90-008503| 13 p1788 N90-20259

Core cooling studies at LLNL (Lawrence Livermore National Laboratory) and Sandia
|DE90-008303| 13 p1795 N90-20300

Area Over Length (AOL): A program for the calculation of effective two-dimensional thermal conductance through an arbitrarily shaped region
|DE90-008005| 13 p1801 N90-20335

The effect of moisture absorption in clothing on the human heat balance
|AD-A217899| 13 p1852 N90-20626

The measurements of thermoacoustic phenomena using thermoacoustic couples
|AD-A218018| 13 p1882 N90-20798

An experimental investigation of the thermal conductivity of porous adsorbents
|AD-A217854| 13 p1899 N90-20899

Ultrasonic techniques for aircraft ice accretion measurement 14 p1906 N90-20926

Users manual for the NASA Lewis Ice Accretion Prediction Code (LEWICE)
|NASA-CR-185129| 14 p1909 N90-20943

Secondary Flows in Turbomachines
|AGARD-CP-469| 14 p1922 N90-21009

Detailed heat transfer measurements in nozzle guide vane passages in linear and annular cascades in the presence of secondary flows 14 p1926 N90-21030

Effects of secondary flow on heat transfer in rotating passages 14 p1926 N90-21031

Theoretical study of the flow in a rotating channel. Experimental study through flow visualization in a curved channel 14 p1926 N90-21032

Surface-cooling effects on compressible boundary-layer instability
|NASA-CR-182003| 14 p1971 N90-21290

Compact scheme for systems of equations applied to fundamental problems of mechanics of continua
|NASA-CR-186494| 14 p1971 N90-21292

Navier-Stokes analysis of turbine blade heat transfer
|NASA-TM-102496| 14 p1972 N90-21300

An experimental evaluation of two nonazeotropic refrigerant mixtures in a water-to-water breadboard heat pump
|DE90-009016| 14 p1973 N90-21305

The modelling of heat and mass transfer near solid boundaries and comparison with experimental results
|PB90-167040| 14 p1974 N90-21310
ULTRA-SHARP nonoscillatory convection schemes for high-speed steady multidimensional flow
|NASA-TM-102568| 14 p2019 N90-21570
Program CICC: Flow and heat transfer in Cable In Conduit Conductors, user's manual
|DE90-007924| 14 p2033 N90-21661
Nonoptimal entropy generation by heat transfer in cryogenic domain
|DE90-007544| 14 p2034 N90-21667
WINCOF-I code for prediction of fan compressor unit with water ingestion
|NASA-CR-185157| 15 p2045 N90-21724
Development and integration of the capillary pumped loop GAS and Hitchhiker flight experiments
|NASA-TM-100756| 15 p2059 N90-21790
Numerical simulation model of hydrazine attitude control thrusters
|INPE-4965-PRE/1534| 15 p2068 N90-21848
Flow boiling with enhancement devices for cold plate coolant channel design
|NASA-CR-186358| 15 p2089 N90-21961
Pressurized bellows flat contact heat exchanger interface
|NASA-CASE-MSC-21271-1| 15 p2097 N90-21999
On dual Lagrangian hyperbolic models for one dimensional two phase flow problems
|DE90-007012| 15 p2098 N90-22004
TOODEE: A two-dimensional, time-dependent heat conduction program
|DE90-009631| 15 p2099 N90-22010
Heat-transfer regimes in nuclear-reactor-pumped gas lasers
|DE90-002904| 15 p2103 N90-22032
Testing of an advanced thermochemical conversion reactor system
|DE90-007989| 15 p2123 N90-22141
Dynamic and microphysical characteristics of cirrus clouds as revealed by aircraft, lidar, and other observations during FIRE 15 p2130 N90-22177
A linear analysis of monsoon base states associated with banded convection 15 p2130 N90-22179
Heat leak measurements in superconducting dipole magnet supports
|DE90-620109| 15 p2173 N90-22420
Modeling of combustion processes in a solid fuel particle
|DE90-009140| 16 p2214 N90-22629
Parallel channel flow excursions
|DE90-009129| 16 p2235 N90-22753
Ocean energy program summary
|DE89-009481| 16 p2251 N90-22836
Geothermal energy program summary
|DE89-009486| 16 p2251 N90-22838
Heat transfer and pressure measurements for the SSME fuel-side turbopump
|NASA-CR-184928| 17 p2355 N90-23405
The effects of Reynolds number, rotor incidence angle, and surface roughness on the heat transfer distribution in a large-scale turbine rotor passage
|NASA-CR-183891| 17 p2410 N90-23731
Titanium-boron mixtures as variable heat sources
|DE90-009729| 18 p2522 N90-24401
Thermodynamic calculations for mixtures of environmentally safe refrigerants using the Lee-Kesler-Ploecker equation of state
|DE90-010493| 18 p2542 N90-24509
Multichip packaging technology with laser-patterned interconnects
|DE90-010743| 18 p2549 N90-24552
Dynamic optimisation of thermal energy systems
|ETN-90-96900| 18 p2576 N90-24676
Ocean energy program summary. Volume 2: Research summaries
|DE89-009482| 18 p2576 N90-24677
Gas production and behavior in the coolant of the SP-100 space nuclear power system
|DE90-010674| 18 p2614 N90-24890
A direct-interface, fusible heat sink for astronaut cooling
|NASA-TM-102835| 19 p2689 N90-25292
Boiling/evaporative heat transfer from spheres in packed-bed thermal energy storage units
|DE90-012023| 19 p2711 N90-25430
NASA systems autonomy demonstration project: Advanced automation demonstration of Space Station Freedom thermal control system 19 p2728 N90-25510
Performance of a supercharged direct-injection stratified-charge rotary combustion engine
|NASA-TM-103105| 20 p2809 N90-25982
Combustor cooling aspects
|CIT/SME/VKI/RS/5| 20 p2810 N90-25989
Prediction of rotating disc flow and heat transfer in gas turbine engines
|PNR90650| 20 p2812 N90-26001
Prediction of the ullage gas thermal stratification in a NASP vehicle propellant tank experimental simulation using FLOW-3D
|NASA-TM-103217| 20 p2841 N90-26160
Transient characteristics of a grooved water heat pipe with variable heat load
|NASA-CR-185280| 20 p2861 N90-26272
Natural melting within a spherical shell
|NASA-TM-102822| 20 p2861 N90-26274
Two-dimensional model of a Space Station Freedom thermal energy storage canister
|NASA-TM-103124| 20 p2862 N90-26279
Structural Mechanics Division research and technology plans for FY 1990 and accomplishments for FY 1989
|NASA-TM-102654| 20 p2878 N90-26361
Thermal management of an accelerator system in space
|DE90-013153| 20 p2922 N90-26627
Mathematical simulation of heat exchanges and thermoelastic constraints in Czochralski crystal growth
|ETN-90-97242| 20 p2931 N90-26680
A lattice gas model for thermohydrodynamics
|DE90-011964| 20 p2933 N90-26690
Preliminary designs for 25 kWe advanced Stirling conversion systems for dish electric applications
|NASA-TM-103188| 20 p2940 N90-26729
A heat transfer analysis for rough turbine airfoils
|AD-A221942| 21 p2960 N90-26831
Two-phase heat transport systems for spacecraft scaling with respect to gravity
|NLR-TP-89127-U| 21 p2965 N90-26857
The role of heat transfer during reactive-ion etching of polymer films
|AD-A222072| 21 p2977 N90-26919
Hydrodynamic skin-friction reduction
|NASA-CASE-LAR-14078-1-CU| 21 p3003 N90-27071
Heat exchanger with oscillating flow
|NASA-CASE-LAR-14033-1| 21 p3004 N90-27072
Thermal analysis of heat pipe radiators with a rectangular groove wick structure
|AD-A222952| 21 p3004 N90-27074
A study of the effect of synoptic scale processes in GCM modelling
|NASA-CR-184804| 21 p3021 N90-27175
The scalability of OTR (Out-of-core Thermionic Reactor) space nuclear power systems
|DE90-013553| 21 p3075 N90-27485
Heat and momentum transfer to test samples in the high velocity plasma furnace
|AD-A222182| 21 p3079 N90-27505
Computer code for predicting coolant flow and heat transfer in turbomachinery
|NASA-TP-2985| 22 p3120 N90-27722
Advanced heat pump
|AD-D014560| 22 p3170 N90-27979
Numerical investigation of the thermal stratification in cryogenic tanks subjected to wall heat flux
|NASA-TM-103194| 22 p3171 N90-27984
The mathematical modeling of arc welding operation
|DE90-013700| 22 p3183 N90-28064
Physical characteristics of clothing materials with regard to heat transport
|IZF-1989-10| 22 p3233 N90-28336
Calculation of clothing insulation and vapour resistance
|IZF-1989-49| 22 p3234 N90-28338
Development of an integrated BEM for hot fluid-structure interaction 23 p3291 N90-28617
A study of heat and fluid flow phenomena on the gas side of circular-tube plate-fin heat exchangers 23 p3324 N90-28795
Gas-jet and tangent-slot film cooling tests of a 12.5 deg cone at Mach number of 6.7
|NASA-TP-2786| 23 p3326 N90-28806
A hybrid perturbation-Galerkin technique for partial differential equations
|NASA-CR-182085| 23 p3327 N90-28814
Effect of vortex circulation on injectant from a single film-cooling hole and a row of film-cooling holes in a turbulent boundary layer. Part 2: Injection beneath the vortex upwash
|AD-A223894| 23 p3328 N90-28818
Laboratory for Laser Energetics review
|DE90-014666| 23 p3330 N90-28829
Evaluation of the STM4-120 kinematic Stirling engine
|DE90-013836| 23 p3344 N90-28897
Studies of surface heat transfer in an arc-heated wind tunnel
|NAL-TR-1048| 24 p3437 N90-29410
A cost-effective realization of environmental temperature control
|DE90-011651| 24 p3458 N90-29532
Spectral measurements of the wall shear stress and wall pressure in a turbulent boundary layer: Theory
|AD-A224070| 24 p3466 N90-29586
Dual and primal mixed Petrov-Galerkin finite element methods in heat transfer problems
|DE90-627190| 24 p3468 N90-29592
Counter-current flow limitation in thin rectangular channels
|DE90-015124| 24 p3469 N90-29599
Finite difference modeling of laser diode ignited components
|DE90-015652| 24 p3474 N90-29635
Simulation and measurement of the heat exchange between the urban canopy and boundary layers 24 p3486 N90-29702

HEAT TRANSFER COEFFICIENTS

Modelling and control of a diffusion/LPCVD furnace
|REPT-88-97| 03 p0336 N90-11910
Convective heat transfer measurements from a NACA 0012 airfoil in flight and in the NASA Lewis Icing Research Tunnel
|NASA-TM-102448| 05 p0642 N90-13750
Heat transfer to a stationary and moving sphere immersed in a fluidized bed 06 p0774 N90-14503
Heat transfer in condensation of lithium vapors
|DE90-002081| 07 p0929 N90-15375
Unsteady heat transfer measurement using thermochromatic liquid crystals as temperature indicators 08 p1081 N90-16254
Quantitative heat transfer measurements using heated liquid crystals 08 p1081 N90-16256
Determination of the heat transfer coefficients in separated flows using an infrared camera 08 p1081 N90-16257
Measurements of heat-transfer coefficients in the interaction regions between oblique shock waves and turbulent boundary layers with a multi-layered thin film heat transfer gauge
|DE90-004123| 09 p1216 N90-17054
Investigation of heat transfer with film cooling to a flat plate in a shock tube
|AD-A216379| 10 p1386 N90-18019
Dryout stability and inception at low flowrates
|DE90-006955| 11 p1509 N90-18692
Heat transfer definitions and equations
|ESDU-89022| 12 p1657 N90-19522
Ultrasonic techniques for aircraft ice accretion measurement 14 p1906 N90-20926
Thermohydraulics of a heat dissipating debris bed 19 p2691 N90-25310
Turbine blade heat transfer coefficient evaluation by modified version of STAN5. Comparison with experimental data
|ETN-90-97283| 20 p2813 N90-26008
Pool boiling from rotating and stationary spheres in liquid nitrogen 23 p3292 N90-28621
A study of heat and fluid flow phenomena on the gas side of circular-tube plate-fin heat exchangers 23 p3324 N90-28795
Supersonic/hypersonic aerodynamics and heat transfer for projectile design using viscous-inviscid interaction
|AD-A224354| 24 p3418 N90-29303

HEAT TRANSMISSION

NT AERODYNAMIC HEAT TRANSFER
NT CONDUCTIVE HEAT TRANSFER
NT CONVECTIVE HEAT TRANSFER
NT HEAT TRANSFER
NT LAMINAR HEAT TRANSFER
NT RADIATIVE HEAT TRANSFER
NT TURBULENT HEAT TRANSFER
Studies of gas turbine heat transfer airfoil surfaces and end-wall cooling effects
|AD-A212451| 04 p0457 N90-12620
A theoretical method for the mechanical calculation of heat exchangers with sliding heads, phase 1 study
|CETIM-110240-PHASE-1| 04 p0502 N90-12896
Analysis of the performance of heat pipes and phase-change materials with multiple localized heat sources for space applications
|AD-A212232| 04 p0503 N90-12898
Time-dependent free convection in low Prandtl number fluids
|DE90-003053| 07 p0929 N90-15377
Experiments on the breakdown of heat transfer in liquid helium 2
|MPIS-13/1989| 16 p2326 N90-23259
Natural convection liquid immersion cooling of high density columns of discrete heat sources in a vertical channel
|AD-A218388| 17 p2402 N90-23681
Heat and fluid flow within the Earth's crust: In situ measurements and mathematical models 18 p2579 N90-24690
Study of an impact on organic matrix and long fibers composite plates (thermal aspect)
|ETCA-89-R-155| 22 p3154 N90-27882

Thermal transfers in unsteady compressible inviscid flow
| ETN-90-97557 | 24 p3419 N90-29311

HEAT TREATMENT
NT ANNEALING
NT LASER ANNEALING
NT NITRIDING
NT STRESS RELIEVING
NT TEMPERING

Development of metastable processing paths for high temperature alloys
| AD-A210550 | 01 p0045 N90-10254
Strain aging in tungsten-heavy alloys
| AD-A211166 | 01 p0046 N90-10259
Composites reinforced with thermotropic liquid crystal copolyester fibers
| AD-A211226 | 02 p0191 N90-11089
An experimental and analytical program to develop crack tip fracture criteria
| AD-A211565 | 03 p0359 N90-12051
The relationship between the mechanical properties of materials after press forming and their in-service properties
| CETIM-101530 | 04 p0475 N90-12723
The effects of heat treatment after welding on the functional properties of assemblies of CrMo alloys. Heat treatment of a mixed assembly of A48 and 10CD9.10 alloys
| CETIM-104320 | 04 p0475 N90-12724
How the common practice of heating plates of austenitic stainless steel during cooling affects their mechanical properties
| CETIM-104500 | 04 p0476 N90-12725
Graduate fellowships in the field of hard magnetic materials
| AD-A212303 | 04 p0477 N90-12733
Stability conditions for steady shearing. Stability conditions for simple shear under mixed thermal boundary conditions 04 p0499 N90-12873
Increased fragility of deep pressed thin plates
| CETIM-13-Y-313 | 04 p0513 N90-12962
Method for growing patterned thin films of superconductors
| AD-D014195 | 04 p0560 N90-13262
Quench sensitivity in Al-Cu-Li alloys
| AD-A213055 | 05 p0624 N90-13639
Practical superconductor development for electrical power applications
| DE90-001804 | 06 p0771 N90-14487
Heat treatment investigation of 4330 vanadium-modified steel
| AD-A214290 | 07 p0906 N90-15239
Phase equilibrium and crystal growth studies on AgGaSe2 and related nonlinear optical materials
| AD-A213650 | 07 p1003 N90-15809
Silicon-based coatings on niobium metal
| DE90-003651 | 08 p1048 N90-16057
Structural stability of heat treated W/B4C multilayers
| DE90-005322 | 09 p1188 N90-16884
Advanced tribological coatings for high specific strength alloys
| AD-A214061 | 09 p1196 N90-16930
Characterization of the 6242 Si alloy. Centrifugal wheel in conventional forging
| REPT-NT-3967 | 10 p1355 N90-17859
Processing of advanced ceramics using microwaves thermal treatments
| DE90-606349 | 12 p1629 N90-19362
Crystallization behavior and properties of BaO-Al2O3-2SiO2 glass matrices
| NASA-CR-185209 | 12 p1631 N90-19374
Influence of heat treating on the mechanical values and the stability of heat barrier coatings
| ETN-90-95902 | 12 p1631 N90-19375
Effect of heat treatment on the fracture toughness transition properties of an A508 class 3 steel
| AERE-R-13548 | 13 p1774 N90-20182
The ageing effect of the matrix-reinforcement interface on the ageing response of an aluminium 6061 alloy reinforced with 20vol percent SiC particulates
| AERE-R-13361 | 13 p1776 N90-20193
Positron annihilation spectroscopy: A nondestructive, submicroscopic characterization technique for structural polymers
| AD-A217748 | 13 p1782 N90-20226
Energy beam treatment for improved adhesion of coatings to surfaces
| AD-D014449 | 14 p1954 N90-21190
A comparison of CuAlNi and other high damping alloys for the purpose of naval ship silencing applications
| AD-A218801 | 16 p2221 N90-22671
Ultrahigh carbon steels and their laminates
| AD-A218780 | 17 p2376 N90-23530
Processing and properties of advanced aluminum alloys
| AD-A221292 | 18 p2526 N90-24416
Rapid thermal processing: A study of the silicon oxidation and of the implanted boron activation
| LAAS-90051 | 20 p2932 N90-26681
Solidification processing of alloys using an applied electric field
| NASA-CASE-MFS-26083-1-CU | 21 p2981 N90-26940
Preparation and characterization of thin films based on sol-gel technique and development of spectroscopic probe for film formation and characterization
| AD-A221762 | 21 p2988 N90-26984

HEATERS
Prediction of the thermal environment and thermal response of simple panels exposed to radiant heat
| NASA-TM-101660 | 03 p0400 N90-12292
Flight set 360T004 (STS-30) field joint protection system, volume 7
| NASA-CR-183829 | 06 p0735 N90-14280
Safety analysis for the Galileo light-weight radioisotope heater unit
| DE90-007147 | 11 p1566 N90-19009
Determination of fundamental thermodynamic properties of constituent materials and performance screening of candidate systems
| AD-A218089 | 13 p1769 N90-20153
Space environment simulation of the SCD-01 satellite through heating plates
| INPE-4988-PRE/1550 | 14 p1940 N90-21105
Flight motor set 360L008 (STS-32R). Volume 1: System overview
| NASA-CR-184010 | 23 p3289 N90-28609

HEATING
NT AERODYNAMIC HEATING
NT ARC HEATING
NT ATMOSPHERIC HEATING
NT ELECTRON CYCLOTRON HEATING
NT GLOBAL WARMING
NT INDUCTION HEATING
NT IONOSPHERIC HEATING
NT KINETIC HEATING
NT LASER HEATING
NT PLASMA HEATING
NT RADIANT HEATING
NT RADIO FREQUENCY HEATING
NT RESISTANCE HEATING
NT SHOCK HEATING
NT SOLAR HEATING
NT SPACE HEATING (BUILDINGS)
NT STRATOSPHERIC WARMING
NT SUPERHEATING
NT TRANSIENT HEATING
NT WATER HEATING

Attenuation of reheat buzz by active control 01 p0036 N90-10201
Microwave Tokamak Experiment (MTX) ohmic heating system
| DE89-017892 | 03 p0408 N90-12340
Application of sound and temperature to control boundary-layer transition 04 p0443 N90-12537
Rapid heating tensile tests of high-energy-rate-forged 316L stainless steel charged with hydrogen and tritium
| DE89-017869 | 04 p0474 N90-12717
Thermal initiation of confined primary explosives with a proton beam
| AD-A212954 | 04 p0482 N90-12767
Rapid heating tensile tests of hydrogen-charged high-energy-rate-forged 316L stainless steel
| DE90-000591 | 06 p0746 N90-14342
The stability of Taylor-Couette flow with radial heating 06 p0774 N90-14502
New heating and cooling technology: Regenerative heat pump according to the Vuilleumier principle
| DE90-002701 | 06 p0807 N90-14699
Surface thermometry of energetic materials by laser-induced fluorescence
| AD-A214423 | 07 p0916 N90-15297
Numerical investigation of transition control of a flat plate boundary layer 07 p0926 N90-15361
Submerged arc welding consumables for HSLA (High Strength Low Alloy)-100 steel
| AD-A213433 | 07 p0941 N90-15452
Hot air heat gun
| AD-D014312 | 09 p1217 N90-17061
Effects of heating/cooling on changes in sea surface temperature: Consequences for computation of surface advection from satellite images
| AD-A214125 | 10 p1409 N90-18129
Microconvective heating of granular explosives by a semiconductor bridge
| DE90-005710 | 11 p1484 N90-18541
Measurement of spectral emissivity by Fourier transform infrared spectrometer
| DE89-782319 | 11 p1510 N90-18698
An expert system for the design of heating, ventilating, and air-conditioning systems
| AD-A218287 | 13 p1788 N90-20262
Boron-containing organosilane polymers and ceramic materials thereof
| NASA-CASE-ARC-11649-2-SB | 14 p1952 N90-21177
Acoustic convective system
| NASA-CASE-NPO-17278-1-CU | 14 p1959 N90-21215
Thermomechanically-induced convective motion and natural convection in confined gaseous helium subjected to boundary heating 15 p2089 N90-21960
Experimental and computational study of the viscoplastic response of high temperature structures 16 p2220 N90-22663
Convergent strand array liquid pumping system
| NASA-CASE-NPO-17301-1-CU | 17 p2385 N90-23587
Aerodynamic pressure and heating-rate distributions in tile gaps around chine regions with pressure gradients at a Mach number of 6.6
| NASA-TP-2988 | 17 p2400 N90-23670
Equilibrium radiative heating tables for Earth entry
| NASA-TM-102652 | 17 p2401 N90-23675
A day in the life of a warm front
| AD-A220373 | 17 p2426 N90-23826
A numerical investigation of thermal convection in highly viscous spherical shells with applications to mantle dynamics in the Earth and other terrestrial planets 18 p2579 N90-24691
Equilibrium radiative heating tables for aerobraking in the Martian atmosphere
| NASA-TM-102659 | 19 p2688 N90-25290
Thermomechanical testing techniques for high-temparature composites: TMF behavior of SiC(SCS-6)/Ti-15-3
| NASA-TM-103171 | 19 p2701 N90-25367
Solid rocket propellant initiation via particle beam heating
| AD-A221900 | 21 p2969 N90-26878
Determination of the heat dissipated from a specimen undergoing cyclic plasticity by a hybrid numerical/experimental method
| AD-A221575 | 21 p2982 N90-26946
Advanced heat pump
| AD-D014560 | 22 p3170 N90-27979
The roles of strain and reheating interval in continuous recrystallization during the thermomechanical processing by warm rolling of an Al-Mg alloy
| AD-A223673 | 24 p3449 N90-29479
A cost-effective realization of environmental temperature control
| DE90-011651 | 24 p3458 N90-29532

HEATING EQUIPMENT
NT BOILERS
NT FURNACES
NT OVENS
NT SOLAR FURNACES
NT VAPORIZERS

Non-stationary computer model of the asymptotic region of an electric arc gas heater
| IPPCZ-288 | 03 p0407 N90-12330
Qualification of improved joint heaters
| NASA-CR-183827 | 05 p0616 N90-13594
Electric field-induced flame convection in the absence of gravity 09 p1202 N90-16962
Hot air heat gun
| AD-D014312 | 09 p1217 N90-17061
Performance predictions for passive solar water heating systems. Report 1: Performance monitoring to validate site-specific estimates of passive solar water heaters. Report 2: Laboratory report. Passive solar water heater tests
| DE90-002879 | 10 p1401 N90-18096
The use of the gas feed system and the vitiator for the solid fuel combustion chamber
| LR-528 | 12 p1623 N90-19329

HEAVY COSMIC RAY PRIMARIES
U HEAVY NUCLEI

HEAVY IONS
Global and local fluctuations in multiplicity and transverse energy for central ultra-relativistic heavy-ion interactions
| LUIP-8903 | 02 p0272 N90-11555
Fluctuations in transverse energy and multiplicity, energy densities, and neutral pion spectra in nucleus-nucleus collisions at 200 GeV/nucleon
| DE89-017583 | 03 p0402 N90-12302
Heating and acceleration of coronal and chromospheric ions during solar flares 03 p0433 N90-12479
Exploring asymmetric heavy-ion reactions at the KX-ray method: The Ne20 + Tb159 reaction at 15 MeV/unit
| KVI-777 | 04 p0552 N90-13216
A study of recoil protons in ultra-relativistic nucleus-nucleus collisions
| LUIP-8907 | 06 p0838 N90-14873

String models for ultrarelativistic heavy ion collisions: Lund model versus color exchange models
[DE88-015856] 06 p0840 N90-14881
Heavy ion interactions
[DE90-001410] 06 p0840 N90-14884
Substructural dependence of the multiparticle production in relativistic heavy-ion interactions
[LUIP-8904] 07 p0989 N90-15716
Heavy ion inelastic scattering with a 4(pi) gamma detector
[DE90-002709] 08 p1120 N90-16488
Lower limit for the average angular momentum leading to fusion
[DE90-004027] 08 p1126 N90-16523
PROTEL: Design, fabrication, calibration, testing, and satellite integration of a proton telescope
[AD-A214564] 09 p1183 N90-16861
Interaction of minor ions with fast and slow shocks
[NASA-CR-186372] 11 p1594 N90-19181
Searching for existing nuclear data
[DE90-007535] 12 p1727 N90-19925
Nuclear interactions of high energy heavy ions and applications in astrophysics
[DE90-006691] 12 p1737 N90-19984
A drift chamber telescope for high-Z particles
[NASA-CR-186497] 12 p1746 N90-20040
Software quality assurance and software safety in the biomed control system
[DE90-008072] 13 p1866 N90-20706
The n-p bremsstrahlung in heavy ion collision processes
[DE90-008542] 13 p1886 N90-20823
Burnout thresholds and cross section of power MOS transistors with heavy ions
[AD-A218998] 16 p2232 N90-22736
Plasma instabilities associated with the injection of artificial ion beams into the ionosphere
16 p2254 N90-22851
Solar flares and magnetospheric particles: Investigations based upon the ONR-602 and ONR-604 experiments
[AD-A218844] 16 p2340 N90-23332
One dimensional heavy ion beam transport: Energy independent model
[NASA-CR-186722] 19 p2754 N90-25650
Heavy ion tests on programmable VLSI
[ETN-90-97254] 20 p2822 N90-26057
A closed form solution to HZE propagation
[NASA-TM-103482] 20 p2924 N90-26640
Ion divergence and the stability of magnetically insulated diodes
[DE90-014565] 23 p3321 N90-28777
Optical emissions from bombarding atmospheric gases with heavy ions
[AD-A223544] 24 p3543 N90-30040

HEAVY LIFT LAUNCH VEHICLES
Definition of avionics concepts for a heavy lift cargo vehicle, appendix A
[NASA-CR-183817] 05 p0580 N90-13380
Definition of avionics concepts for a heavy lift cargo vehicle. Volume 1: Executive summary
[NASA-CR-183818] 06 p0725 N90-14229
Definition of avionics concepts for a heavy lift cargo vehicle, volume 2
[NASA-CR-183819] 06 p0725 N90-14230
Shuttle-C utilization for assembly of the rephased Freedom configuration
[NASA-TM-101658] 07 p0885 N90-15120
Assembly vs. direct launch of transfer vehicles
[NASA-TM-102686] 19 p2797 N90-25921

HEAVY NUCLEI
Compressibility of heavy nuclei at high temperatures
[KVI-792] 04 p0552 N90-13217
Fragmentation of relativistic heavy nuclei with application to cosmic ray propagation 14 p2043 N90-21716

HEAVY WATER
A preliminary investigation of cold fusion by electrolysis of heavy water
[DE90-004383] 09 p1285 N90-17447
An attempt to measure cold-fusion effects
[DE90-613248] 14 p2031 N90-21649

HEF (HIGH ENERGY FUELS)
U HIGH ENERGY FUELS

HEIGHT
NT SCALE HEIGHT
Height and gradient from shading
[AD-A212338] 04 p0504 N90-12908
Specification for evaporation duct height calculations
[AD-A213841] 07 p0964 N90-15570
A technique for the generation of range-height-angle charts
[AD-A214534] 09 p1204 N90-16979
Laser wave estimation
[AD-A213867] 09 p1227 N90-17119
The reduction correction in North America
13 p1836 N90-20540
Analysis of altimetry over inland seas
[NASA-TM-100729] 13 p1840 N90-20566
The integration of GPS heights into the Australian height datum 19 p2705 N90-25392
The 27-28 October 1986 FIRE IFO cirrus case study: Cirrus parameter relationships derived from satellite and lidar data
[NASA-TM-103469] 20 p2890 N90-26447

HEINKEL AIRCRAFT
On the occasion of the 100th birthday of Ernst Heinkel
[MBB/LW/3015/S/PUB/321] 03 p0436 N90-12494

HEISENBERG THEORY
Meixner-Pollaczek polynomials and the Heisenberg algebra
[CWI-PM-R8806] 04 p0541 N90-13138
On geometry of inhomogeneous Heisenberg ferromagnet: Nonintegrable case
[MEMO-789] 05 p0691 N90-14030
Parity violation and superconductivity in doped Mott insulators
[DE90-627493] 23 p3401 N90-29217

HELICAL FLOW
An experimental study of helicity and related properties in turbulent flows
[DE89-016785] 02 p0220 N90-11259

HELICAL WINDINGS
The ANU (Australian National University) Heliac Program
[DE90-006620] 13 p1890 N90-20843

HELICOPTER ATTITUDE INDICATORS
U HELICOPTERS

HELICOPTER CONTROL
Preliminary airworthiness evaluation of the AH-64A equipped with the Air To Air Stinger (ATAS) missile system
[AD-A213030] 05 p0579 N90-13374
A helicopter flight path controller design via a nonlinear transformation technique 06 p0727 N90-14242
Airworthiness and flight characteristics evaluation of the McDonnell Douglas Helicopter Corporation (MDHC) 530FF helicopter
[AD-A218253] 13 p1755 N90-20076
Interaction of switch actuation on tracking with a four-axis flight control (cross-coupling)
[AD-A217981] 13 p1758 N90-20095
Design of a helicopter automatic flight control system using adaptive control 14 p1928 N90-21040
ROSAR (Helicopter-Rotor based Synthetic Aperture Radar) 14 p1961 N90-21229
Aeroelastic simulation of higher harmonic control
15 p2054 N90-21768
Adaptive control of a system with periodic dynamics: Application of an impulse response method to the helicopter vibration problem 17 p2453 N90-23990
Helicopter controllability
[AD-A220078] 18 p2498 N90-24275
Coupled rotor-body equations of motion hover flight
[NASA-CR-186710] 19 p2655 N90-25111
AIMS for helicopters 22 p3106 N90-27639

HELICOPTER DESIGN
Controller design for active vibration suppression of a helicopter
[DFVLR-FB-89-20] 03 p0310 N90-11760
Integrated multidisciplinary optimization of rotorcraft: A plan for development
[NASA-TM-101617] 04 p0450 N90-12580
General approach and scope --- rotor blade design optimization 04 p0451 N90-12581
Rotor blade aerodynamic design
04 p0451 N90-12582
Airframe design considerations: Overview --- rotor design optimization 04 p0451 N90-12586
Validation of the procedures --- integrated multidisciplinary optimization of rotorcraft
04 p0451 N90-12587
Appendix: Results obtained to date --- integrated multidisciplinary optimization of rotorcraft
04 p0451 N90-12588
Euler equation solutions applied to a helicopter rotor in forward moving flight
[ONERA-RSF-32/1285-AY-346A]
04 p0452 N90-12592
Calculation of flight vibration levels of the AH-1G helicopter and correlation with existing flight vibration measurements
[NASA-CR-181923] 11 p1518 N90-18743
Activities report in German aerospace
[ISSN-0070-3966] 11 p1595 N90-19189
Design of a helicopter automatic flight control system using adaptive control 14 p1928 N90-21040
Scenario 2000
[MBB-UD-500/89-PUB] 19 p2652 N90-25092
Research at NASA's NFAC wind tunnels
[NASA-TM-102827] 20 p2801 N90-25933
Development of a method to design helicopter rotors
[REPT-100-30-03] 21 p2960 N90-26830
Design of helicopter components in metal matrix composites
[REPT-100-20-55] 21 p2972 N90-26894

HELICOPTER ENGINES
An appraisal of a number of power assessment procedures being proposed for use in Chinook-Lycoming T55 engine
[AD-A210482] 01 p0009 N90-10041
Coatings for gas turbine compressors
[NLR-MP-88045-U] 03 p0308 N90-11750
Cycle analysis for helicopter gas turbine engines
[RAE-TM-P-1154] 08 p1025 N90-15921
Preliminary airworthiness evaluation of the Woodward hydromechanical unit installed on T700-GE-700 engines in the UH-60A helicopter
[AD-A216751] 11 p1464 N90-18430
Experimental identification of helicopter engine dynamics from closed loop data
22 p3104 N90-27627

HELICOPTER IMPULSIVE NOISE
U BLADE SLAP NOISE

HELICOPTER PERFORMANCE
Airworthiness and flight characteristics test of the UH-60A Black Hawk helicopter equipped with the XM-139 multiple mine dispensing system (VOLCANO)
[AD-A210271] 01 p0006 N90-10025
Helicopter Visual Segment Approach Lighting System (HALS)
[ACD-330] 02 p0150 N90-10856
Heliport surface maneuvering test results
[ACD-330] 02 p0157 N90-10897
Correlation of Puma airloads: Lifting-line and wake calculation
[NASA-TM-102212] 05 p0572 N90-13327
Preliminary airworthiness evaluation of the AH-64A equipped with the Air To Air Stinger (ATAS) missile system
[AD-A213030] 05 p0579 N90-13374
Software and hardware description of the helicopter motion equations for VAX computers
[AD-A213248] 05 p0579 N90-13375
Fatigue life estimates for helicopter loading spectra
[NASA-CR-181941] 08 p1088 N90-16294
Helicopter flight vibration of large transportation containers: A case for testing tailoring
[DE90-007429] 12 p1601 N90-19215
Airworthiness and flight characteristics evaluation of the McDonnell Douglas Helicopter Corporation (MDHC) 530FF helicopter
[AD-A218253] 13 p1755 N90-20076
Performance data from a wind-tunnel test of two main-rotor blade designs for a utility-class helicopter
[NASA-TM-4183] 14 p1916 N90-20974
An early overview of tiltrotor aircraft characteristics and pilot procedures in civil transport applications
[DOT/FAA/DS-89/37] 14 p1921 N90-21003
Indianapolis Downtown Heliport: Operations analysis and marketing history
[REPT-90RR-13] 14 p1930 N90-21049
Aeronautical decisionmaking for air ambulance program administrators
[DOT/FAA/DS-88/8] 17 p2347 N90-23368
Aerodynamic performance of a 0.27-scale model of an AH-64 helicopter with baseline and alternate rotor blade sets
[NASA-TM-4201] 18 p2491 N90-24237
Helicopter controllability
[AD-A220078] 18 p2498 N90-24275
Agusta methodology for pitch link loads prediction in preliminary design phase
[ETN-90-97270] 20 p2808 N90-25978
Obtaining consistent models of helicopter flight-data measurement errors using kinematic-compatibility and state-reconstruction methods
[AD-A222533] 21 p2954 N90-26799
Heliport visual approach surface high temperature and high altitude tests
[DOT/FAA/CT-TN89/34] 22 p3112 N90-27675
Flight test investigation of flight director and autopilot functions for helicopter decelerating instrument approaches
[DOT/FAA/CT-TN89/54] 22 p3121 N90-27724
Evaluation of composite components on the Bell 206L and Sikorsky S-76 helicopters
[NASA-TM-4195] 22 p3135 N90-27787

HELICOPTER PROPELLER DRIVE
Efficiency study comparing two helicopter planetary reduction stages
[NASA-TM-103106] 20 p2871 N90-26334

HELICOPTER ROTORS
U ROTARY WINGS

HELICOPTER TAIL ROTORS
A model suitable for predicting the noise associated with the ducted tail rotor of a helicopter
[ECL-88-09] 05 p0697 N90-14074
The applicability of simple helicopter models for flight mechanics studies
[ETN-90-96962] 20 p2808 N90-25975
HELICOPTER WAKES
Application of the wide-field shadowgraph technique to rotor wake visualization
[NASA-TM-102222] 03 p0300 N90-11700
Analysis of heliport environmental data: Indianapolis downtown heliport, Wall Street heliport. Volume 2: Wall Street heliport data plots
[DOT/FAA/CT-TN87/54-VOL-2] 03 p0310 N90-11761
Rotor induced-inflow-ratio measurements and CAMRAD calculations
[NASA-TP-2946] 08 p1017 N90-15882
Calculation of the flow field of a multiblade helicopter rotor using a Euler method including the wake 08 p1069 N90-16189
Analysis of heliport environmental data: Indianapolis downtown heliport, Wall Street heliport. Volume 3: Indianapolis downtown heliport data plots
[AD-A217412] 13 p1829 N90-20500
The Second ARO Workshop on Rotorcraft Interactional Aerodynamics
[AD-A223310] 24 p3418 N90-29304
HELICOPTERS
NT AH-1G HELICOPTER
NT AH-64 HELICOPTER
NT CH-47 HELICOPTER
NT H-53 HELICOPTER
NT LIGHT HELICOPTERS
NT MILITARY HELICOPTERS
NT UH-1 HELICOPTER
NT UH-60A HELICOPTER
Scientific and technical report voice activated gun turrent control
[AD-A210350] 01 p0110 N90-10623
An experimental investigation of helicopter rotor hub fairing drag characteristics
[NASA-TM-102182] 03 p0300 N90-11701
Sequential design of experiments with physically based models 23
[AD-A211918] 03 p0393 N90-12239
Rotorcraft low altitude CNS benefit/cost analysis: Rotorcraft operations data
[DOT/FAA/DS-89/9] 03 p0419 N90-12406
RAN (Royal Australian Navy) vibration analysis system operator's guide
[AD-A212441] 04 p0453 N90-12596
A robust digital model following controller for helicopters
[ESA-TT-1041] 04 p0457 N90-12621
The human factors relating to escape and survival from helicopters ditching in water
[AGARD-AG-305(E)] 05 p0576 N90-13358
Helicopter rotor test rig (RoTeSt) in DNW: Application and results
[RAE-TRANS-2171] 05 p0585 N90-13408
Human factors research in aircrew performance and training
[AD-A213285] 05 p0676 N90-13938
Effect of blade planform variation on a small-scale hovering rotor
[NASA-TM-4146] 06 p0717 N90-14186
An experimental investigation of the interaction between a model rotor and airframe in forward flight 06 p0723 N90-14219
An analytical method for the prediction of unsteady rotor/airframe interactions in forward flight 06 p0724 N90-14223
A helicopter flight path controller design via a nonlinear transformation technique 06 p0727 N90-14242
Fatigue analysis and reconstruction of helicopter load spectra 06 p0739 N90-14304
A two dimensional power spectral estimate for some nonstationary processes
[NASA-CR-186100] 06 p0833 N90-14843
A study of the effects of Rotating Frame Turbulence (RFT) on helicopter flight mechanics 07 p0872 N90-15058
Imaging probabilities, geometry and ergonomics in limited visibility helicopter operations 07 p0872 N90-15060
Effects of aeroelastic tailoring on anisotropic composite material beam models of helicopter blades
[AD-A213478] 07 p0879 N90-15095
An examination of helicopter rotor load calculations
[AD-A214295] 07 p0880 N90-15098
Adaptive control of helicopter vibrations via the impulse response method
[AD-A213728] 07 p0883 N90-15113
Uses and properties of Al-Li on the new EH101 helicopter 07 p0900 N90-15201
Design of a bounded wave EMP (Electromagnetic Pulse) simulator
[AD-A214137] 07 p0919 N90-15316
Assessment of worm gearing for helicopter transmissions
[NASA-TM-102441] 08 p1025 N90-15923
Natural icing re-evaluation of the EH-60A Quick Fix helicopter
[AD-A214728] 09 p1162 N90-16723
Analysis of damaged components from DOE security helicopter N7EG
[DE90-004488] 09 p1162 N90-16729
Low air speed computation for helicopters: A new approach 09 p1165 N90-16744
Preliminary design of a family of three close air support aircraft
[NASA-CR-186070] 09 p1166 N90-16751
Airborne electromagnetic sensing of sea ice thickness
[AD-A214460] 09 p1240 N90-17198
Equations of motion of slung load systems with results for dual lift
[NASA-TM-102246] 10 p1322 N90-17641
Force determination sensitivities study for full-scale helicopter ground vibration testing
[AD-A215983] 10 p1322 N90-17643
The Advanced Digital-Optical Control System (ADOCS) user demonstration program
[AD-A215984] 10 p1323 N90-17644
Time and frequency-domain identification and verification of BO-105 dynamic models
[AD-A216828] 11 p1456 N90-18389
Life of concentrated contacts in the mixed EHD and boundary film regimes
[AD-A216673] 11 p1517 N90-18738
Heli/SITAN: A terrain referenced navigation algorithm for helicopters
[DE90-005193] 12 p1602 N90-19217
Comparison of oculometer and head-fixed reticle with voice or switch and touch panel for data entry on a generic tactical air combat display
[AD-A217231] 13 p1855 N90-20646
The use of numerical optimization for helicopter airfoil and blade design 14 p1919 N90-20995
Multi-axis control of telemanipulators 16 p2271 N90-22943
Optimal helicopter trajectory planning for terrain following flight
[NASA-CR-186470] 17 p2349 N90-23376
Helicopter Airborne Laser Positioning System (HALPS)
[NASA-TM-102814] 17 p2354 N90-23399
Target selection in anti-tank helicopter operations: Relative weight of cues in target evaluation judgements
[FOA-C-50072-5.2] 17 p2436 N90-23881
Target selection in anti-tank operations: Effects of experience
[FOA-C-50073-5.2] 17 p2436 N90-23882
Mode of presentation of cues in policy capturing: A comparison between verbal and pictorial presentation of targets in judgement of probability to fire
[FOA-C-50074-5.2] 17 p2436 N90-23883
Adaptive control of a system with periodic dynamics: Application of an impulse response method to the helicopter vibration problem 17 p2453 N90-23990
Operational effects on crashworthy seat attenuators
[AD-A221148] 18 p2495 N90-24259
Evaluation of speech recognizers for use in advanced combat helicopter crew station research and development
[NASA-CR-177547] 18 p2496 N90-24265
HPLC analysis of helicopter rotor blade materials
[AD-A221121] 18 p2497 N90-24270
Helicopter controllability
[AD-A220078] 18 p2498 N90-24275
Extension-torsion coupling behavior of advanced composite tilt-rotor blades 18 p2644 N90-25057
Coupled rotor-body equations of motion hover flight
[NASA-CR-186710] 19 p2655 N90-25111
Computation of viscous aerodynamic characteristics of 2-D airfoils for helicopter applications
[NLR-MP-88052-U] 20 p2804 N90-25951
Flow visualization of dynamic stall on an oscillating airfoil
[AD-A222202] 21 p2954 N90-26797
Rotorcraft aeromechanical stability-methodology assessment. Phase 2: Workshop
[NASA-TM-102272] 21 p2955 N90-26800
Device for the dilution of hot exhaust jets
[ETN-90-97435] 22 p3120 N90-27723
The Helicopter Antenna Radiation Prediction Code (HARP)
[NASA-CR-186925] 22 p3165 N90-27946
Solution of Euler equations applied to a rotor of a helicopter in steady flight
[ONERA-RSF-1/3731-AY-002A] 23 p3269 N90-28500
Velocity filtering applied to optical flow calculations
[NASA-TM-102802] 23 p3271 N90-28512
Analysis of heliport environmental data, Intracoastal City
[DOT/FAA/CT-TN89/43] 23 p3284 N90-28584
Helicopter aircrew helmets and head injury: A protective effect
[AD-A223024] 23 p3377 N90-29080
FAA Rotorcraft Research, Engineering, and Development Bibliography 1962-1989
[AD-A224256] 24 p3417 N90-29299
HELIOMAGNETISM
U SOLAR MAGNETIC FIELD
HELIOMETERS
NT PYROHELIOMETERS
HELIOMETRY
U PYROHELIOMETERS
HELIOSEISMOLOGY
The SOHO mission. Scientific and technical aspects of the instruments
[ESA-SP-1104] 04 p0566 N90-13302
SOHO: An observatory to study the solar interior and the solar atmosphere 04 p0566 N90-13303
VIRGO: The solar monitor experiment on SOHO 04 p0567 N90-13305
SOI: The Solar Oscillations Imager on SOHO 04 p0567 N90-13306
Optimization of the reference parameters in the accompanying solar panel dynamics
[INPE-4795-PRE/1449] 11 p1528 N90-18798
Application of solar seismology to study of the convection zone
[AD-A221975] 21 p3101 N90-27610
HELIOSPHERE
An implementation plan for priorities in solar-system space physics
[NASA-CR-185375] 05 p0710 N90-14154
Eleventh European Cosmic Ray Symposium
[DE90-611424] 19 p2798 N90-25927
Space exploration: Cost, schedule, and performance of NASA's Ulysses Mission to the Sun. Fact sheet for the Chairman, Subcommittee on Science, Technology, and Space, Committee on Commerce, Science, and Transportation, US Senate
[GAO/NSIAD-88-129FS] 20 p2815 N90-26023
Activities report of the Space Science Department
[ESA-SP-1126] 24 p3560 N90-30142
HELIOSTATS
Stretched-membrane heliostats for solar central-receiver power plants
[DE89-016034] 01 p0084 N90-10476
Status of stretched-membrane heliostats
[DE90-000801] 12 p1683 N90-19689
Selection and design of a stretched-membrane heliostat for today's markets
[DE90-007997] 13 p1828 N90-20495
Design and demonstration of an improved stretched-membrane heliostat
[DE90-007904] 14 p2001 N90-21470
An assessment of second-generation stretched-membrane mirror modules
[DE90-010243] 16 p2252 N90-22841
Solar thermal program summary. Volume 2: Research summaries
[DE89-009476] 18 p2576 N90-24674
HELIOTRONS
Second harmonic electron cyclotron heating in low and over density plasmas in Heliotron DR
[DE90-719519] 08 p1125 N90-16515
In situ measurement of neutral beam components using the Doppler-shifted H(sub alpha) emissions in Heliotron E
[DE90-719521] 08 p1125 N90-16516
Density clamping phenomena in electron cyclotron resonance heated plasmas on Heliotron E
[DE90-719523] 09 p1284 N90-17442
Study on edge plasma physics and particle control in the Heliotron E device
[DE90-719524] 09 p1284 N90-17443
HELIPORTS
Heliport surface maneuvering test results
[ACD-330] 02 p0157 N90-10897
Analysis of heliport environmental data: Indianapolis downtown heliport, Wall Street heliport. Volume 2: Wall Street heliport data plots
[DOT/FAA/CT-TN87/54-VOL-2] 03 p0310 N90-11761
Analysis of heliport environmental data: Indianapolis downtown heliport, Wall Street heliport. Volume 3: Indianapolis downtown heliport data plots
[AD-A217412] 13 p1829 N90-20500

Indianapolis Downtown Heliport: Operations analysis and marketing history
[REPT-90RR-13] 14 p1930 N90-21049
Analysis of distributions of Visual Meteorological Conditions (VMC) heliport data
[DOT/FAA/CT-TN89/67] 14 p2008 N90-21508
Heliport visual approach surface high temperature and high altitude tests
[DOT/FAA/CT-TN89/34] 22 p3112 N90-27675
Analysis of heliport environmental data, Intracoastal City
[DOT/FAA/CT-TN89/43] 23 p3284 N90-28584
FAA Rotorcraft Research, Engineering, and Development Bibliography 1962-1989
[AD-A224256] 24 p3417 N90-29299

HELIUM
NT HELIUM ISOTOPES
NT LIQUID HELIUM
NT LIQUID HELIUM 2
X-ray bright points and He I lambda 10830 dark points 01 p0139 N90-10802
Independent Orbiter Assessment (IOA): Assessment of the reaction control system, volume 1
[NASA-CR-185543-VOL-1] 03 p0316 N90-11793
Independent Orbiter Assessment (IOA): Assessment of the reaction control system, volume 2
[NASA-CR-185543-VOL-2] 03 p0316 N90-11794
Independent Orbiter Assessment (IOA): Assessment of the reaction control system, volume 3
[NASA-CR-185543-VOL-3] 03 p0316 N90-11795
Independent Orbiter Assessment (IOA): Assessment of the reaction control system, volume 4
[NASA-CR-185543-VOL-4] 03 p0316 N90-11796
Independent Orbiter Assessment (IOA): Assessment of the reaction control system, volume 5
[NASA-CR-185543-VOL-5] 03 p0316 N90-11797
High pressure studies of planetary matter
[DE89-017738] 03 p0428 N90-12455
An investigation of the irradiation swelling mechanisms in refractory metals at high temperatures
[AD-A211406] 04 p0474 N90-12719
Thermal design of a 10-kW helium refrigerator
[DE90-701785] 06 p0756 N90-14403
Hydrogen radical enhanced growth of solar cells
[DE89-009497] 06 p0806 N90-14694
Helium-induced weld cracking in irradiated 304 stainless steel
[DE90-001312] 07 p0903 N90-15219
Rayleigh-Taylor instability in compressible fluids
[DE90-003027] 07 p0929 N90-15376
Large scale calculations of the structure and dynamics of dense matter
[DE90-003654] 07 p0991 N90-15726
Report of NASA Lunar Energy Enterprise Case Study Task Force
[NASA-TM-101652] 07 p1007 N90-15836
Report of the NASA lunar energy enterprise case study task force 07 p1008 N90-15837
Analysis of the financial factors governing the profitability of lunar helium-3 07 p1008 N90-15838
Introduction to D-He(3) fusion reactors 07 p1008 N90-15839
Helium permeability through austenitic stainless steel
[DE90-007046] 11 p1488 N90-18582
Differential elastic scattering cross sections for 54.9eV positrons incident on helium 11 p1558 N90-18975
Double ionization of helium by particle impact 11 p1558 N90-18979
An attempt of improving high-temperature fatigue properties of Ni-Cr-W superalloys in HTGR helium
[DE90-741482] 12 p1627 N90-19350
Thermomechanically-induced convective motion and natural convection in confined gaseous helium subjected to boundary heating 15 p2089 N90-21960
Analysis of gamma squared Velorum photometry from the South Pole 15 p2183 N90-22472
The ratio of neutral hydrogen to neutral helium in the local interstellar medium 15 p2189 N90-22499
Rapid mass transfer in binary systems 16 p2332 N90-23289
Optical observations of LMXB AC211(M15): Solving the puzzle 19 p2768 N90-25731
Transients in turbulent convective heat transfer to a flow of supercritical helium
[ETN-90-97217] 20 p2863 N90-26286
Helium generation in fusion reactor materials
[DE90-013005] 23 p3393 N90-29172
Isotopic tailoring and other techniques used to study helium effects in austenitic alloys
[DE90-016344] 24 p3452 N90-29495
The effect of helium on microstructural evolution in austenitic steels as determined by spectral tailoring experiments
[DE90-016360] 24 p3452 N90-29496
Investigation of a heat driven thermoacoustic prime mover
[AD-A223928] 24 p3484 N90-29694

HELIUM ATOMS
Total cross sections for positrons scattered elastically from helium based on new measurements of total ionization cross sections 11 p1558 N90-18976

HELIUM IONS
Optical observations of interplanetary pick-up ions: The experiment Helly 05 p0661 N90-13863
Ion-irradiation effects in Tl2Ca2Ba2Cu3O10 superconductors
[DE90-003840] 07 p1002 N90-15802

HELIUM ISOTOPES
Flare-in texture in rotating superfluid (3)He-B
[PB89-218994] 03 p0412 N90-12368
Resonant quasiparticle-ion scattering in anisotropic superfluid (3)He
[PB89-221618] 03 p0413 N90-12369
Collective-mode spectroscopy of textures in superfluid (3)He-B
[PB89-221634] 03 p0413 N90-12370
Symmetry breaking phenomena in liquid Helium-4
[DE89-618886] 04 p0469 N90-12685
Improved method for determination of helium-4 in helium-3 by mass spectrometry
[PB89-201404] 04 p0469 N90-12686
Persistent current, NMR, and ion transmission experiments in rotating He-3 superfluids --- Nuclear Magnetic Resonance (NMR)
[ISBN-952-90056-1-X] 04 p0553 N90-13221
Superfluid phase slippage in (3)He-B flow through a narrow channel
[PB89-218986] 04 p0559 N90-13258
A four channel He-3 cooled balloon-borne bolometer radiometer 05 p0597 N90-13469
Construction of the rotating cryostat ROTA2, its use for zero sound experiments in (3)He-B, and calculations of ion mobility in (3)He-A and (3)He-P
[ISBN-952-90091-3-5] 05 p0645 N90-13765
The effective (3)He-nucleon force in a microscopic DWBA approach to the (3)He,t charge exchange reaction --- Distorted Wave-Borne Approximation (DWBA)
[KVI-763] 05 p0697 N90-14077
Cold fusion: Alchemist's dream
[DE90-000865] 06 p0847 N90-14925
Transportation and operations aspects of space energy systems 07 p1008 N90-15842
Importance of helium-3 for the future 07 p1009 N90-15843
Superflow induced phase transition in the axial vortex-free texture of rotating superfluid He-3-B
[PB90-110388] 08 p1127 N90-16531
Results of an attempt to measure increased rates of the reaction D-2 + D-2 yields He-3 + n in a nonelectrochemical cold fusion experiment
[NASA-TM-102430] 09 p1280 N90-17424
Nuclear driving of stellar oscillations and their coupling to convection 10 p1446 N90-18345
Research and development of a helium-4 based solar neutrino detector
[DE90-005416] 10 p1447 N90-18353
Particle detection via rotons in helium-4 superfluid
[DE90-005417] 10 p1448 N90-18354
Nucleation of vortices in superfluid helium-4
[DE90-610675] 12 p1720 N90-19880
Goldstone excitation and symmetry breaking mechanism in superfluid He-4
[DE90-610676] 12 p1720 N90-19881
Coherent state in the roton region of superfluid helium-4
[DE90-610677] 12 p1720 N90-19882
Design of D-3 He commercial tokamak
[DE90-008252] 13 p1891 N90-20852
BASG thermomechanical pump helium 2 transfer tests
[NASA-CR-177541] 14 p1939 N90-21097
Relativistic corrections to He-3 photodisintegration sum rules
[NOTA-INTERNA-942] 16 p2315 N90-23197
An effective He-3 nucleon force for the He-3, t) charge exchange reaction
[KVI-813] 16 p2315 N90-23198
On the technology for preparation of a HeNe discharge tube for use in a laser gyro
[DLR-MITT-90-01] 24 p3472 N90-29624
Overview of advanced fuel fusion
[DE90-015660] 24 p3550 N90-30085

HELIUM PLASMA
Helium transport in plasma edge regions 14 p2027 N90-21625
Detection of emission lines from the secondary star in IX Vel (=CPD-48 deg 1577)
[MPE-PREPRINT-172] 22 p3265 N90-28485
Control of helium accumulation
[DE90-015658] 24 p3550 N90-30084

HELIUM STARS
U B STARS

HELIUM 2
U HELIUM ISOTOPES
U LIQUID HELIUM

HELIUM 3
U HELIUM ISOTOPES

HELIUM 4
U HELIUM ISOTOPES

HELIUM-NEON LASERS
Zeeman interferometry
[DE89-015296] 03 p0352 N90-12012
Comparison of I2-stabilized HE-NE lasers
[PB89-219844] 03 p0352 N90-12014
Laser gyros and field diagnostics
[AD-A220832] 17 p2406 N90-23709
On the technology for preparation of a HeNe discharge tube for use in a laser gyro
[DLR-MITT-90-01] 24 p3472 N90-29624

HELIX TUBES
U TRAVELING WAVE TUBES

HELMET MOUNTED DISPLAYS
On the geometry of a general three-camera headmounted system
[AD-A214790] 09 p1225 N90-17108
Helmet-mounted pilot night vision systems: Human factors issues 16 p2269 N90-22930
Neck Injury in Advanced Military Aircraft Environments
[AGARD-CP-471] 19 p2717 N90-25459
Aircrew neck injuries: A new, or an existing, misunderstood phenomenon 19 p2719 N90-25467
Effects of head mounted devices on head-neck dynamic response to +G(sub z) accelerations 19 p2720 N90-25471
Measurement techniques, evaluation criteria and injury probability assessment methodologies developed for Navy ejection and crashworthy seat evaluations 19 p2721 N90-25479
A helmet mounted display to adapt the telerobotic environment to human vision 19 p2737 N90-25555
Helmet-mounted head restraint
[AD-D014536] 20 p2899 N90-26491
A real-time optical 3D tracker for head-mounted display systems
[AD-A222747] 20 p2902 N90-26508
Tracking a head-mounted display in a room-sized environment with head-mounted cameras
[AD-A222545] 21 p3037 N90-27266
Human factors and safety considerations of night vision systems flight
[USAARL-89-12] 22 p3233 N90-28332
Target acquisition under load factors: Advantages and disadvantages of a helmet mounted sight 23 p3359 N90-28983
Tracking performance and influence of field of view 23 p3360 N90-28988
Head-mounted spatial instruments II: Synthetic reality or impossible dream 24 p3508 N90-29828
Visual processing: Implications for helmet mounted displays
[AD-A223488] 24 p3522 N90-29916

HELMETS
Ballistic properties of composite materials for personnel protection
[MRL-TR-89-6] 04 p0465 N90-12661
Test procedures for the evaluation of helmet and headset mounted active noise reduction systems
[AD-A212991] 05 p0676 N90-13937
Polycarbonate article with chemical resistant coating
[NASA-CASE-MSC-21503-1] 09 p1195 N90-16925
Safety evaluation of infrared lamp power output for oculometer eye/head tracker system
[AD-A215809] 10 p1411 N90-18138
Evaluation of helmet retention systems using a pendulum device
[AD-A215489] 11 p1542 N90-18874
Evaluation of the head injury hazard during military parachuting
[AD-A220724] 17 p2434 N90-23870
Field evaluation of laser protective eyewear
[AD-A221324] 18 p2586 N90-24725
A survey of cervical pain in pilots of a Belgian F-16 Air Defence Wing 19 p2718 N90-25462
Aircrew neck injuries: A new, or an existing, misunderstood phenomenon 19 p2719 N90-25467
Analysis of the biomechanic and ergonomic aspects of the cervical spine under load 19 p2719 N90-25470
A computer simulation model for studying cervical spine injury prevention 19 p2721 N90-25476
Human factors and safety considerations of night vision systems flight using thermal imaging systems
[AD-A223226] 21 p3037 N90-27263
Helicopter aircrew helmets and head injury: A protective effect
[AD-A223024] 23 p3377 N90-29080

HELMHOLTZ RESONATORS
Digital beam position regulation of the superconducting accelerator at Darmstadt
[ETN-90-97293] 22 p3246 N90-28406
HELMHOLTZ VORTICITY EQUATION
Solving time harmonic wave problems on vector processors
[DE90-003956] 08 p1119 N90-16480
Transversal, longitudinal, and three dimensional eddy currents in cylindrical guides with elliptic diameters
[ETN-90-97302] 22 p3168 N90-27967
HELOS (SATELLITE)
U EXOSAT SATELLITE
HEMATOPOIETIC SYSTEM
The effects of simulated hypogravity on murine bone marrow cells 18 p2631 N90-24989
HEMODYNAMIC RESPONSES
Temperature regulation during upper body exercise: Able bodied and spinal cord injured
[AD-A215130] 09 p1252 N90-17264
Psychological and physiological responses of blacks and caucasians to hand cooling
[AD-A215646] 09 p1253 N90-17272
A program for the study of skeletal muscle catabolism following physical trauma
[AD-A216569] 11 p1539 N90-18859
Hydration effects on human physiology and exercise-heat performance
[AD-A217969] 13 p1852 N90-20629
Hemodynamic and ADH responses to central blood volume shifts in cardiac-denervated humans
[NASA-TM-103471] 20 p2898 N90-26485
Fluid and electrolyte homeostasis during spaceflight: Elucidation of mechanisms in a primate
[NASA-CR-177548] 23 p3378 N90-29085
Renal response to seven days of lower body positive pressure in the squirrel monkey
[NASA-CR-183355] 24 p3497 N90-29761
HEMODYNAMICS
NT LOWER BODY NEGATIVE PRESSURE
HEMOGLOBIN
NT CARBOXYHEMOGLOBIN
Human health studies of carbon monoxide (CO) under conditions of military weapons systems crewman exposures. Protocol 1: Formation of COHb
[AD-A210344] 01 p0092 N90-10528
Carboxyalkylated hemoglobin as a potential blood substitute
[AD-A213886] 07 p0966 N90-15582
Computation of the unsteady facilitated transport of oxygen in hemoglobin
[NASA-TM-102251] 08 p1106 N90-16400
HERBIG-HARO OBJECTS
Herbig Ae/Be stars: Fine structure far-infrared lines 11 p1584 N90-19126
Herbig-Haro objects and stellar jets 15 p2186 N90-22487
HERCULES AIRCRAFT
U C-130 AIRCRAFT
HERCULES NOVA
Relative muon content of UHE showers associated with Hercules X-1
[DE90-000609] 08 p1151 N90-16685
HERMES MANNED SPACEPLANE
Thermal and structural analysis of Hermes 02 p0186 N90-11058
Hermes plasma wind tunnel. Preliminary study, phase A1: Annexes, tables, figures
[DVG-HER-TN-002-PT-2] 04 p0459 N90-12632
RVD scenari and interfaces between Hermes and space station 08 p1035 N90-15982
Flows with Separation
[DGLR-PAPERS-88-05] 08 p1066 N90-16169
The HERMES development program 08 p1071 N90-16199
DNSS: German/Norwegian work team Space Subsea. Environmental control and life support subsystems (technical matters), phase 2
[ETN-90-95905] 08 p1105 N90-16398
Progress in Space Transportation
[ESA-SP-293] 09 p1173 N90-16782
Keynote address 09 p1173 N90-16783
ESA's space transportation programme 09 p1173 N90-16786
The Hermes system: Its design objectives and solutions 09 p1177 N90-16821
Aeronautical aspects of Hermes re-entry: Question marks and prospects 09 p1178 N90-16822
Hermes propulsion system 09 p1178 N90-16823
Overview of the Hermes in-orbit control system 09 p1178 N90-16824
Hermes space vehicle: Safety considerations 09 p1178 N90-16825
Hermes ground operation concepts 09 p1178 N90-16826
Hermes training aircraft 09 p1178 N90-16827
The DLR technology programme on space transportation 09 p1180 N90-16841
Aerodynamic simulation conditions in arc heated wind tunnels 09 p1180 N90-16843
The Hermes power system 10 p1330 N90-17682
The Hermes fuel cell power plant 10 p1333 N90-17706
Water removal studies on high power hydrogen-oxygen fuel cells with alkaline electrolytes 10 p1333 N90-17712
SIMOUN: An optimized supersonic high temperature wind tunnel for testing construction materials to be used on the spaceplane
[REPT-892-430-111] 16 p2203 N90-22572
Knowledge based system for Hermes orbital operations ground support
[REPT-892-440-102] 17 p2361 N90-23443
Conceptual work at Aerospatiale on air-breathing and non-air-breathing recoverable launchers
[REPT-892-422-104] 17 p2362 N90-23450
Prediction methods of launcher aeroelastic stability. Application to the Ariane 5/Hermes vehicle. Comparison with test results
[REPT-892-422-107] 17 p2362 N90-23451
Hermes preparatory programme: Fluidynamics studies. Activities performed by the Italian researchers
[DLC/COP-HER-TN-002] 17 p2363 N90-23453
The European EVA suit: An optimized tool for Hermes/MTFF in-orbit operations 18 p2502 N90-24296
HERA and EVA co-operation scenarios 18 p2502 N90-24299
The Hermes robot arm teleoperation and control concept 18 p2503 N90-24301
HERA teleoperation test facility 18 p2503 N90-24303
Hermes rendezvous and navigation system 18 p2504 N90-24308
Docking berthing systems: Functions and simulation 18 p2505 N90-24313
The real-time Hermes robot arm simulator: HSF-P 18 p2506 N90-24319
The Hermes robot arm: System description 18 p2507 N90-24327
Concept design for Hermes docking/berthing mechanism 18 p2536 N90-24464
Overview on the Hermes in-orbit control system
[MBB-UK-0056/89-PUB] 19 p2652 N90-25094
Ascent and descent trajectory optimization of Ariane 5/Hermes 22 p3126 N90-27743
Hermes rendezvous with the space station 22 p3128 N90-27753
HERMES SATELLITE
U COMMUNICATIONS TECHNOLOGY SATELLITE
HERMETIC SEALS
Development and testing of a contactless static/dynamic shaft seal with little sealing gas requirement
[KFK-4599] 05 p0652 N90-13802
Electrical resistance measurements of connector-panel interfaces
[AD-A221431] 21 p3001 N90-27057
Development and evaluation of hermetic laser diode ignited pyrotechnic components
[DE90-015745] 24 p3458 N90-29529
A viscoelastic material model for computing stresses in glass
[DE90-014851] 24 p3481 N90-29673
HERMITIAN POLYNOMIAL
The fast Gauss transform
[AD-A211287] 02 p0266 N90-11517
Distribution of a sum of n random variables and a central limit theorem based on moments or on coefficients of polynomial dependence
[IMAG-RR-768-M] 05 p0692 N90-14040
On induced Hermitian metrics for holomorphic vector bundles
[DE90-612737] 14 p2019 N90-21572
A fast, preconditioned conjugate gradient Toeplitz solver
[NASA-CR-180367] 18 p2589 N90-24731
Casimir effect in a D-dimensional flat spacetime and the cut-off method
[DE90-627177] 23 p3390 N90-29151
HERTZSPRUNG-RUSSELL DIAGRAM
Pulsations of delta Scuti stars
[DE90-003213] 08 p1139 N90-16598
HESSIAN MATRICES
Application of symbolic computations to the constitutive modeling of structural materials
[NASA-TM-103225] 20 p2876 N90-26364
HETEROCYCLIC COMPOUNDS
NT ADENOSINE TRIPHOSPHATE
NT ATROPINE
NT AZOLES
NT AZULENE
NT CAFFEINE
NT ETHYLENE OXIDE
NT HMX
NT NICOTINIC ACID
NT PHTHALOCYANIN
NT PYRIDINES
NT PYRROLES
NT RDX
NT TETRAHYDROFURAN
NT TRYPTOPHAN
The synthesis and structure of stibaindoles
[AD-A222990] 21 p2976 N90-26914
HETERODYNING
NT OPTICAL HETERODYNING
The investigation of the fundamental limits of heterodyne holographic interferometry with the application of imaging laser generated lamb waves
[AD-A211048] 02 p0224 N90-11285
Limitations in the growing of a plasma wave produced by heterodyning two lasers due to modulations and decay instabilities 06 p0783 N90-14552
Deferred electronic heterodyne moire deflectometry: A method for transient density fields measurement
[NASA-CR-182982] 06 p0843 N90-14907
A new kind of heterodyne fiber-optic gyroscope
[AD-A213953] 07 p0933 N90-15404
Feasibility of using frequency offset on very high frequency air/ground voice channels
[DOT/FAA/CT-TN89/71] 14 p1964 N90-21248
Use of the Xybion ISG-camera in the RETRA-1000 TV-Holography unit
[AD-A219842] 18 p2554 N90-24577
RF control system development at CEBAF
[CEBAF-PR-89-026] 19 p2755 N90-25853
Laser radar angular tracking
[AD-A222741] 20 p2869 N90-26319
Absolute wind measurements in the lower thermosphere of Venus using infrared heterodyne spectroscopy
[NASA-CR-4290] 21 p3100 N90-27605
Adaptive polarization diversity detection scheme for coherent communications and interferometric fiber sensors
[AD-D014479] 22 p3163 N90-27938
Noncontact laser thermomechanical nondestructive evaluation for advanced coatings 22 p3187 N90-28087
HETEROGENEITY
Capillary effects in steady-state flow in heterogeneous cores
[DE89-000758] 01 p0070 N90-10399
Tools for application development in heterogeneous distributed environments
[AD-A210238] 01 p0108 N90-10613
Densification of particulate ceramic composites: The role of heterogeneities
[DE90-000177] 03 p0331 N90-11886
Heterogeneous composite and method of making
[AD-D014337] 12 p1619 N90-19306
Heterogeneity description using fractal concepts 19 p2690 N90-25299
Double layer effects on the enthalpy of activation of heterogeneous electron transfer reactions
[AD-A221934] 22 p3245 N90-28404
Regional phase propagation in three dimensionally heterogeneous media
[AD-A223279] 24 p3491 N90-29731
HETEROJUNCTION DEVICES
NT HIGH ELECTRON MOBILITY TRANSISTORS
NT MODFETS
The photovoltaic properties of an Al In As/InP heterojunctions grown by LPE method
[NASA-CR-185996] 05 p0665 N90-13886
Analytical and computer-aided models of InP-based MISFETs and heterojunction devices
[AD-A211861] 05 p0702 N90-14106
Group 2 cubic fluorides as dielectrics for III-V compound semiconductors
[AD-A214096] 08 p1129 N90-16542
Ensemble Monte Carlo simulation of electron transport in AlGaAs/GaAs heterostructures
[ISBN-90-9003048-4] 18 p2622 N90-24940
HETEROJUNCTIONS
High energy neutron irradiation effects in GaAs modulation-Doped Field Effect Transistors (MODFETS): Threshold voltage
[AD-A210502] 01 p0132 N90-10763
CuInSe2 solar cell research by sputter deposition
[DE89-009450] 02 p0236 N90-11345
International workshop on Beam Injection Assessment of Defects in Semiconductors
[AD-A210842] 02 p0283 N90-11617
Graded bandgap solar cells
[AD-A211537] 03 p0367 N90-12097
Development and evaluation of an instrument for rapid electroreflectance of semiconductor materials
[AD-A211690] 03 p0414 N90-12376

Electron transport in heterojunction superlattices
[AD-A212366] 04 p0560 N90-13265
Thin film cadmium telluride, zinc telluride, and mercury zinc telluride solar cells
[DE89-009499] 06 p0804 N90-14681
Interface phonons in semiconductor double heterostructures
[AD-A213732] 07 p1003 N90-15810
Theory of the electronic and optical properties of semiconductor heterostructures
[AD-A214132] 08 p1130 N90-16544
Proceedings of the conference on Hot Carriers in Semiconductors
[AD-A215544] 09 p1291 N90-17482
The III-V semiconductor quantum well lasers and related optoelectronic devices on silicon
[AD-A216980] 12 p1686 N90-19570
Workshop on the Physics and Chemistry of Mercury Cadmium Telluride and Related II-VI compounds
[AD-A217496] 13 p1894 N90-20867
Measurement of localized deep levels and wafer non-uniformities at 3-5 semiconductor heterojunctions
[AD-A218547] 16 p2323 N90-23248
Molecular beam epitaxial growth of heterostructures to study quantum interference phenomena
[AD-A219442] 17 p2475 N90-24154
EHF heterojunction bipolar transistors
[AD-A220984] 18 p2548 N90-24541
Application of InAlAs/GaAs superlattice alloys to GaAs solar cells
[DE90-013070] 20 p2881 N90-26389
Measurement of deep levels at InGaAs(P)/InP heterojunctions
[AD-A222890] 21 p3082 N90-27526
Electron-phonon interaction and transport in artificially made semiconductor microstructures
[AD-A223061] 21 p3082 N90-27529
Nonlinear optical studies of the optical and electronic properties of semiconductor heterostructures
[AD-A223408] 24 p3552 N90-30096

HEURISTIC METHODS
Application of a hybrid generation/utility assessment heuristic to a class of scheduling problems
[NASA-TM-102367] 01 p0117 N90-10674
Procedures for separations within batches of values, 1. The orderly tool kit and some heuristics
[AD-A210652] 02 p0268 N90-11531
Premixed turbulent flame propagation
[AD-A211489] 03 p0324 N90-11841
Reasoning about change and exceptions in automated process planning
[DE89-017706] 03 p0386 N90-12195
On the role of Coulomb forces in atomic radiative emission
[IRF-PREPRINT-106] 03 p0403 N90-12308
Iterative methods for linear complementary and related problems
[AD-A212848] 04 p0534 N90-13089
Vision-based navigation and parallel computing
[AD-A214481] 09 p1264 N90-17327
Representing knowledge intelligently: Production rules, frames, and transitional networks
[AD-A215098] 09 p1271 N90-17368
A model for comparing game theory and artificial intelligence decision making processes
[AD-A215418] 09 p1271 N90-17369
A computer simulation study of a sensor-based heuristic navigation for three-dimensional rough terrain with obstacles
[AD-A215115] 10 p1318 N90-17622
An exact algorithm for the problem of p-medians
[INPE-4924-TDL/384] 11 p1544 N90-18885
Optimum and heuristic algorithms for finite state machine decomposition and partitioning
[AD-A216778] 11 p1546 N90-18899
Iterative procedures for space shuttle main engine performance models 12 p1639 N90-19416
The 0-1 multiknapsack problem: Heuristic and reduction methods
[INPE-4894-PRE/1495] 12 p1704 N90-19782
Trajectory optimization in the presence of constraints
[AD-A218271] 13 p1760 N90-20104
An approach to rescheduling activities based on determination of priority and disruptivity
15 p2153 N90-22299
Space communications scheduler: A rule-based approach to adaptive deadline scheduling
15 p2153 N90-22300
Knowledge-based semantic query processing: An optimal transformation approach
15 p2176 N90-22437
Designing good experiments to test bad hypotheses
[AD-A218977] 16 p2263 N90-22900
Laboratory replication of scientific discovery processes
[AD-A219273] 16 p2266 N90-22913
Scientific discovery as problem solving
[AD-A218887] 16 p2307 N90-23145
Computational aspects of adaptive dimensional reduction for nonlinear boundary value problems
[AD-A219889] 17 p2461 N90-24052
Some convergence results for probabilistic Tabu search
[MEMO-822] 18 p2605 N90-24840
An expert system to advise astronauts during experiments: The protocol manager module
19 p2730 N90-25522
Ocean feature recognition using genetic algorithms with fuzzy fitness functions (GA/F3)
19 p2740 N90-25576
Applications of different design methodologies in navigation systems and development at JPL
20 p2852 N90-26221
Investigation of automated task learning, decomposition and scheduling
[NASA-CR-186791] 20 p2899 N90-26488
An engineering approach to automatic programming
21 p3046 N90-27317
Resolution of seven-axis manipulator redundancy: A heuristic issue 21 p3049 N90-27331
Automated unit-level testing with heuristic rules
21 p3049 N90-27335
Real-time adaptive aircraft scheduling
[NASA-CR-177558] 22 p3110 N90-27669
DEPEND: A design environment for prediction and evaluation of system dependability
[NASA-CR-186890] 22 p3189 N90-28094
Dynamic load-sharing using predicted process resource requirements
[NASA-CR-186891] 22 p3255 N90-28433
Robot Acting on Moving Bodies (RAMBO): Interaction with tumbling objects 23 p3366 N90-29022
Focus of attention in an activity-based scheduler
23 p3369 N90-29039
A Boltzmann machine for the organization of intelligent machines 23 p3370 N90-29040
Efficient mapping algorithms for scheduling robot inverse dynamics computation on a multiprocessor system
23 p3375 N90-29071
Automatic recognition of tractability in inference relations
[AD-A223698] 24 p3538 N90-30003

HEWLETT-PACKARD COMPUTERS
Off-design loss measurements in a compressor cascade
[AD-A220094] 18 p2552 N90-24564

HEXANITROSTILBENE
A shock initiation model for fine-grained hexanitrostilbene
[DE89-007641] 02 p0207 N90-11185

HEXOSES
NT GLUCOSE

HF LASERS
Coupled multiline CW HF lasers: Experimental performance
[AD-A210844] 01 p0075 N90-10434
Master oscillator with power amplifiers: Performance of a two-element CW HF phased-laser array
[AD-A211141] 01 p0076 N90-10435

HHX HELICOPTER
U H-53 HELICOPTER

HIERARCHIES
NT DICHOTOMIES
Hierarchical structure in polymeric solids and its influence on properties
[AD-A210918] 01 p0052 N90-10297
An analytical hierarchy process approach to establish the systems analyst's knowledge base for selecting an information requirements determination strategy
01 p0136 N90-10785
A transformational method for verifying safety properties in real time systems
[AD-A211925] 04 p0529 N90-13051
Communication Overview Program (COP)
06 p0762 N90-14435
Supersymmetric dark matter above the W mass
[NASA-CR-186168] 08 p0863 N90-15016
Hierarchical process composition: Dynamic maintenance of structure in a distributed environment
[AD-A214325] 07 p0978 N90-15648
Connectionist model-based stereo vision for telerobotics 08 p1076 N90-16224
Source hierarchy list. Volume 1: A through D
[AD-A216050] 10 p1442 N90-18321
Source hierarchy list. Volume 2: E through N
[AD-A216051] 10 p1442 N90-18322
Source hierarchy list. Volume 3: O through Z
[AD-A216052] 10 p1442 N90-18323
An approach centered in production rules for a partition of environment and planning in a visual navigation system (SNV)
[INPE-4813-TDL/360] 11 p1517 N90-18737
Object Oriented Programming Systems (OOPS) and frame representations: An investigation of programming paradigms
[NASA-CR-186084] 12 p1699 N90-19758
Fault tolerant hypercube computer system architecture
[NASA-CASE-NPO-16859-1-CU] 14 p2012 N90-21527
A tool for aiding in the reuse of software
[INPE-4981-PRE/1545] 16 p2298 N90-23091
Detecting black holes in packet-radio networks (SRNTN-56)
[AD-A219636] 17 p2389 N90-23604
A parallel algorithm for global routing
[NASA-CR-186152] 17 p2448 N90-23959
Distributed hierarchical routing
[RUU-CS-89-5] 17 p2452 N90-23986
Arithmetic classification of perfect models of stratified programs (extended version)
[CWI-CS-R8928] 17 p2462 N90-24063
Experiences with and error handling in a knowledge base assisted system for payload experiment automation
18 p2504 N90-24306
Automated control of hierarchical systems using value-driven methods 19 p2735 N90-25547
Behavioral networks as a model for intelligent agents
19 p2738 N90-25561
Hierarchical structure of polygonal data for spatial analysis and representation of cartographical data
[INPE-4986-PRE/1548] 20 p2879 N90-26380
Effect of organizational structure on performance of decision making teams
[AD-A223160] 20 p2934 N90-26697
Local design methodologies for a hierarchic control architecture
[AD-A222006] 21 p2966 N90-26862
A 17 degree of freedom anthropomorphic manipulator
23 p3362 N90-29001
Methods and strategies of object localization
23 p3366 N90-29020
Techniques and potential capabilities of multi-resolutional information (knowledge) processing
23 p3374 N90-29062
Design of a structural and functional hierarchy for planning and control of telerobotic systems
24 p3506 N90-29820
An algebraic hierarchical basis preconditioner
[DE90-015875] 24 p3538 N90-30008

HIGH ACCELERATION
Rheoencephalography in simulated aviation environmental stress
[AD-A221150] 18 p2584 N90-24716
Effects of head mounted devices on head-neck dynamic response to +G(sub z) accelerations
19 p2720 N90-25471

HIGH ALTITUDE
Particle kinetic simulation of high altitude hypervelocity flight
[NASA-CR-186003] 02 p0147 N90-10840
Comparison of protective breathing equipment performance at ground level and 8,000 feet altitude using parameters prescribed by portions of FAA action notice A-8150.2
[AD-A212852] 06 p0821 N90-14773
SCATHA (Spacecraft Charging at High Altitudes) atlas data base, volume 1
[AD-A214204] 07 p0886 N90-15127
SCATHA (Spacecraft Charging At High Altitudes) atlas data base, volume 2
[AD-A214205] 07 p0887 N90-15128
Description of SHARC: The Strategic High-Altitude Radiance Code
[AD-A213806] 07 p0961 N90-15555
On the HEMP (High-Altitude Electromagnetic Pulse) response of protective relays
[DE90-003718] 08 p1061 N90-16138
Effect of reduced atmospheric pressure on the performance characteristics of pyrotechnic compositions containing aluminum
[AD-A214473] 09 p1200 N90-16953
Improved computational fluid dynamics for continuum hypersonic flow
[AD-A216981] 11 p1506 N90-18674
Nonlinear mechanics of unstable plasmas as related to high altitude aerodynamics
[AD-A215126] 12 p1716 N90-19852
GPS-aided gravimetry at 30 km altitude from a balloon-borne platform 13 p1834 N90-20530
Hypobaric hypoxia (380 torr) decreases intracellular and total body water in goats
[AD-A218192] 13 p1849 N90-20615
NASA/USRA high altitude reconnaissance aircraft
[NASA-CR-186685] 18 p2496 N90-24266
Global Sentry: NASA/USRA high altitude reconnaissance aircraft design, volume 2
[NASA-CR-186820-VOL-2] 20 p2807 N90-25971

Lightweight EHF communications satellites
21 p3070 N90-27453

HIGH ALTITUDE BALLOONS
Three-meter balloon-borne telescope
05 p0601 N90-13490
Kestrel 3 Program
[DE90-001796] 06 p0721 N90-14209
High altitude ozone research balloon
[NASA-CR-186653] 19 p2654 N90-25107
High altitude balloon flight test of the GRAD experiment
[AD-A224398] 24 p3432 N90-29388

HIGH ALTITUDE BREATHING
The effect of caffeine on endurance time to exhaustion at high altitude
[AD-A212069] 03 p0380 N90-12163

HIGH ALTITUDE ENVIRONMENTS
Metacognition and retrieval from long-term memory at Mount Everest
[AD-A211629] 03 p0382 N90-12177

HIGH ALTITUDE FLIGHT
U HIGH ALTITUDE

HIGH ALTITUDE PRESSURE
Effects of high altitude hypoxia on lung and chest wall function during exercise
[AD-A219814] 17 p2434 N90-23869

HIGH ASPECT RATIO
Aeroelastic characteristics of aircraft with circulation control wings 13 p1754 N90-20070

HIGH ASPECT RATIO WINGS
U SLENDER WINGS

HIGH CURRENT
Commercial high current ignitron development
[DE89-015077] 01 p0058 N90-10331
Collective ion acceleration in high current relativistic electron beams
[DE90-008328] 13 p1886 N90-20821
Method of making a long life high current density cathode from tungsten and iridium powders using a quarternary compound as the impregnant
[AD-D014425] 14 p1958 N90-21211
Gas-puff z-pinch experiment
[IPPCZ-286] 15 p2167 N90-22385
The beta limit in the DIII-D tokamak
[DE90-011896] 19 p2759 N90-25677

HIGH ECCENTRIC LUNAR OCCULTATION SATELLITE
U EXOSAT SATELLITE

HIGH ELECTRON MOBILITY TRANSISTORS
NT MODFETS
Experimental investigations of transport and optical properties of 3-5 quantum well structures grown via molecular beam epitaxy under optimal growth conditions
[AD-A210269] 01 p0132 N90-10758
Development of high gain three terminal devices - at millimeter wave frequencies
[AD-A213089] 05 p0635 N90-13701
The 22 GHz Radioastron receiver: Development of prototype components during the year 1988
[PB89-212583] 07 p0920 N90-15323
Computer aided design of monolithic microwave and millimeter wave integrated circuits and subsystems
[AD-A213656] 07 p0923 N90-15343
The 32-GHz performance of the DSS-14 70-meter antenna: 1989 configuration 12 p1645 N90-19452
Proceedings of the Joint NOSC/NRL (Naval Ocean Systems Center/Naval Research Laboratory) InP Microwave/Millimeter Wave Technology Workshop
[AD-A218216] 14 p1966 N90-21259
Excess noise, anomalous effects and reliability of high frequency devices (Schottky diodes, MESFET and HEMT)
[LAAS-89-394] 16 p2231 N90-22728

HIGH ENERGY ASTRONOMY OBSERVATORIES
U HEAO

HIGH ENERGY ASTRONOMY OBSERVATORY A
U HEAO 1

HIGH ENERGY ASTRONOMY OBSERVATORY B
U HEAO 2

HIGH ENERGY ASTRONOMY OBSERVATORY 1
U HEAO 1

HIGH ENERGY ASTRONOMY OBSERVATORY 2
U HEAO 2

HIGH ENERGY ELECTRONS
NT RELATIVISTIC ELECTRON BEAMS
Physics of high energy photoconductive switches
[AD-A210341] 01 p0060 N90-10345
SCATHA (Spacecraft Charging at High Altitudes) atlas data base, volume 1
[AD-A214204] 07 p0886 N90-15127
SCATHA (Spacecraft Charging At High Altitudes) atlas data base, volume 2
[AD-A214205] 07 p0887 N90-15128
Algorithms for calorimeter simulation with parameterized showers by example of H1 detectors
[MPI-PAE/EXP.EL-200] 12 p1711 N90-19828
High energy phenomena during solar flares
[INPE-4961-TDL/390] 14 p2043 N90-21713
Effects of large doses of high energy electrons on a YBa2Cu3O6(+)delta high temperature superconductor
[AD-A220423] 17 p2476 N90-24158
Hot carrier in subpicosecond photoconductive experiments
[AD-A219874] 17 p2477 N90-24166
LEP and CEBAF polarimeters
[CEBAF-PR-89-010] 19 p2757 N90-25667
Solar wind and high energy particle effects in the middle atmosphere 22 p3206 N90-28188
Energy deposition of corpuscular radiation in the middle atmosphere 22 p3206 N90-28190

HIGH ENERGY FUELS
High energy density solid and liquid hydrocarbon fuels
[AD-A210195] 01 p0053 N90-10304

HIGH ENERGY INTERACTIONS
NT STRONG INTERACTIONS (FIELD THEORY)
Studies of elementary particles
[DE89-014859] 01 p0119 N90-10685
Research program in theoretical high energy physics
[DE89-013963] 01 p0121 N90-10695
A theoretical high energy physics program
[DE89-012685] 01 p0121 N90-10696
Plasma-anode electron gun research
[AD-A211547] 03 p0312 N90-11773
An experimental high energy physics program
[DE89-014695] 03 p0403 N90-12311
Experimental research in high energy physics
[DE90-000061] 03 p0408 N90-12342
A study of recoil protons in ultra-relativistic nucleus-nucleus collisions
[LUIP-8907] 06 p0838 N90-14873
The ultimate structure of matter: The US High Energy Physics Program from the 1950s through the 1980s
[DE90-001784] 06 p0840 N90-14887
Rapidity densities and their fluctuations in central 200 A GeV S32 interations with Au and Ag,Br nuclei
[LUIP-8905] 07 p0989 N90-15715
Substructural dependence of the multiparticle production in relativistic heavy-ion interactions
[LUIP-8904] 07 p0989 N90-15716
Elementary particle physics: Experimental
[DE90-005973] 10 p1429 N90-18242
Research on free electron lasers
[AD-A215865] 11 p1514 N90-18715
Theoretical and experimental high energy physics
[DE90-006168] 11 p1565 N90-19006
Research accomplishments and future goals in particle physics
[DE90-007296] 12 p1712 N90-19830
Experimental and theoretical high energy physics
[DE90-005974] 12 p1712 N90-19834
Studies of high energy phenomena using muons
[DE90-008272] 13 p1886 N90-20820
The design of a large aperture high field dipole
[DE90-007910] 14 p1970 N90-21285
Mesooptical Fourier transform microscope: A new device for high energy physics
[DE90-616423] 14 p2026 N90-21615
A search for very high energy gamma rays from the Crab pulsar-nebula 14 p2043 N90-21718
Hyperon production at 200 and 900 GeV cm energy
[USIP-89-02] 17 p2471 N90-24126
Eleventh European Cosmic Ray Symposium
[DE90-611424] 19 p2798 N90-25927
Important experiments to test for longer-ranged new gravitational forces
[DE90-012102] 20 p2888 N90-26434
A research program in theoretical high energy physics
[DE90-013322] 20 p2926 N90-26648
High energy physics at Tufts University
[DE90-014664] 23 p3394 N90-29174

HIGH ENERGY PROPELLANTS
Shock-wave characterization of energetic booster-rocket propellant WAK-2 and its simulant UGS
[DE90-002633] 07 p0914 N90-15285
Crystal structure of Tetra-Ammonium Adamantyl Tetra-Nitrate (TAATN): High energy/density fuel candidate for liquid propellant
[AD-A215684] 09 p1201 N90-16955
High energy-density liquid rocket fuel performance
[NASA-CR-185279] 23 p3315 N90-28742

HIGH FREQUENCIES
Study of high frequency water vapor absorption parameters
[AD-A210676] 02 p0194 N90-11108
An ionospheric model for HF sky-wave backscatter radar 02 p0247 N90-11401
Accurate measurements of the total angle of arrival of HF skywaves 02 p0248 N90-11402
Ionospheric limitations to the accuracy of SSL estimates of HF transmitter locations 02 p0248 N90-11403
A new approach to HF (High Frequency) channel modeling and simulation. Part 1: Deterministic model
[PB89-203962] 03 p0336 N90-11913
Development of high frequency spice models for ferrite core inductors and transformers
[DE89-015121] 03 p0341 N90-11946
Hybrid PE-ray-mode formulation of high frequency propagation in a bilinear tropospheric surface duct 06 p0759 N90-14417
Wind speed dependence of acoustic ambient vertical directional spectra at high frequency
[AD-A214293] 07 p0989 N90-15712
Use of an HF active monitoring array in the presence of high level interference
[BBC-RD-1989/7] 08 p1055 N90-16096
Optical flow measuring method using diode lasers, phase coupled arrays, and high frequency pulsed diode lasers 08 p1067 N90-16176
High frequency pulsed diode lasers and phase-coupled diode arrays for aerodynamics 08 p1078 N90-16238
Specification for HF Maximum Usable Frequency (MUF) model
[AD-A214996] 09 p1206 N90-16990
An assessment of the use of resonant-mode topologies for high frequency power conversion 10 p1335 N90-17726
Techniques for high frequency power conversion 10 p1336 N90-17729
HF wire antennas over real ground: Computer simulation and measurement 10 p1370 N90-17937
Activities report in DLR research field communication engineering and reconnaissance
[ISSN-0173-0118] 11 p1525 N90-18781
High power, high frequency component test facility
[NASA-TM-102500] 12 p1650 N90-19484
Use of chaotic and random vibrations to generate high frequency test inputs. Part 2: Chaotic vibrations
[DE90-007153] 12 p1676 N90-19627
Use of chaotic and random vibrations to generate high frequency test inputs
[DE90-007412] 12 p1676 N90-19628
Joint services electronics program
[AD-A217961] 13 p1797 N90-20311
Feasibility of using frequency offset on very high frequency air/ground voice channels
[DOT/FAA/CT-TN89/71] 14 p1964 N90-21248
An introduction to high frequency radioteletype systems
[PB90-145533] 14 p1965 N90-21252
Report on STC/Technische Universiteit (TU) Delft Extremely High Frequency (EHF) radio relay study 15 p2081 N90-21915
Survey of instrumental methods for the determination of the high frequency wave spectrum
[IOS-267] 15 p2135 N90-22200
Excess noise, anomalous effects and reliability of high frequency devices (Schottky diodes, MESFET and HEMT)
[LAAS-89-394] 16 p2231 N90-22728
Frequency assignments for HFDF receivers in a search and rescue network
[AD-A220529] 17 p2390 N90-23610
A model of electromagnetic leakage through joints at radio frequencies
[BAE-WES-RP-GEN-EMC-049-T2.2] 17 p2392 N90-23626
High frequency, high temperature specific core loss and dynamic B-H hysteresis loop characteristics of soft magnetic alloys
[NASA-TM-103164] 17 p2398 N90-23663
Utilization of higher frequencies for satellite communications: Determination of atmospheric effects using experiments and models
[DLR-FB-89-46] 18 p2544 N90-24518
Light-millimeter wave interactions in semiconductor devices
[AD-A221214] 18 p2623 N90-24943
High frequency, frequency multiplier using parallel gunn diodes
[AD-D014523] 19 p2685 N90-25275
Analytic study of the high-frequency impedance
[CEBAF-PR-89-014] 19 p2757 N90-25665
Progress and remaining issues in the development of a wideband HF channel model and simulation 20 p2845 N90-26182
Channel selection and control procedures in an automatic HF system 20 p2847 N90-26193
An experimental medium speed wideband modem 20 p2847 N90-26194
Synchronization of frequency shift transmission and the effect of oversampling 20 p2848 N90-26200
Equipment feasibility study: Very high frequency communication equipment (136-137 megahertz)
[DOT/FAA/CT-TN89/72] 20 p2850 N90-26210

Software set-up for data processing of depolarization due to rain and ice crystals in the Olympus project
[EUT-89-E-218] 20 p2855 N90-26240
Specification for HF Lowest Usable Frequency (LUF) model
[AD-A222114] 21 p2996 N90-27031
Improved high power/high frequency inductor
[NASA-CASE-NPO-17830-1-CU] 21 p2998 N90-27042
Higher order diffusion model for a bipolar transistor
[PB90-190901] 22 p3167 N90-27960
Acoustic qualification of an anechoic chamber
[RAE-TM-MAT/STR-1136] 22 p3245 N90-28400
New approach to HF channel modeling and simulation. Part 2: Stochastic model
[PB90-200338] 23 p3317 N90-28755
Sounder update and field strength software modifications for Special Operations Radio Frequency Management System (SORFMS). Volume 1: Program descriptions and testing
[AD-A224510] 24 p3460 N90-29543
Control of a Cossor CSP1250 ionospheric simulator in an automated HF test bed
[AD-A223446] 24 p3461 N90-29549
High frequency bundle protection
[DIGEL-1990-1] 24 p3466 N90-29582

HIGH GAIN
Development of high gain three terminal devices - at millimeter wave frequencies
[AD-A213089] 05 p0635 N90-13701
Testing and performance of a high-gain flux-compression generator
[DE90-002808] 06 p0772 N90-14492
Resonator modes in high gain free electron lasers
[DE90-006098] 11 p1514 N90-18720

HIGH INTENSITY LASERS
U HIGH POWER LASERS

HIGH LATITUDES
U POLAR REGIONS

HIGH LEVEL LANGUAGES
NT ADA (PROGRAMMING LANGUAGE)
NT C (PROGRAMMING LANGUAGE)
Mathematical equivalence in a primitive Ella
[RSRE-MEMO-4225] 04 p0531 N90-13066
Applications of artificial intelligence to space station and automated software techniques: High level robot command language
[NASA-CR-182997] 05 p0686 N90-13991
Architecture and language for a layered relational database 05 p0707 N90-14146
A graphically oriented specification language for automatic code generation. GRASP/Ada: A Graphical Representation of Algorithms, Structure, and Processes for Ada, phase 1
[NASA-CR-183212] 06 p0828 N90-14813
High level language memory management on parallel architectures
[DE89-015018] 07 p0971 N90-15609
An overview of lynx
[AD-A213714] 07 p0975 N90-15631
Research and development in natural language understanding as part of the Strategic Computing Program
[AD-A214587] 09 p1264 N90-17331
A microcode compiler that runs on the IBM AT and supports cascadable microcomputers, part 2
[AD-A215889] 10 p1415 N90-18155
A microcode compiler that runs on the IBM AT and supports cascadable microcomputers, part 1
[AD-A215888] 11 p1542 N90-18877
L: A language for solution of incremental systems in a parallel processing environment
[INPE-4816-TDL/362] 11 p1543 N90-18884
OOPS it's happening, part 1
[AD-A220498] 17 p2443 N90-23922
Language support for parallel computation
[AD-A223072] 20 p2911 N90-26560
Integrating planning and reactive control 23 p3377 N90-29077

HIGH MELTING COMPOUNDS
U REFRACTORY MATERIALS

HIGH POLYMERS
Determinations of molecular weight and molecular weight distribution of high polymers by the rheological properties
[NASA-CR-186450] 14 p1953 N90-21180

HIGH POWER LASERS
NT NOVA LASER SYSTEM
A nonlinear-optical method for combining high power laser beams
[AD-A211730] 03 p0354 N90-12022
Ultra high speed compound semiconductors and real time signal processing
[AD-A211394] 03 p0413 N90-12372
Laser Induced Damage in Optical Materials: 1987
[PB89-221162] 04 p0505 N90-12913
Tunable Solid State Lasers conference edition: Tunable Solid State Lasers Topical Meeting
[AD-A212292] 04 p0506 N90-12920
Proceedings of the High Energy Density Matter (HEDM) Conference
[AD-A212314] 05 p0629 N90-13670
A compact, high-powered far-infrared (FIR) laser
[DE89-016786] 06 p0789 N90-14597
Excimer emission from alkali diatomic and alkaline-earth-noble-gas molecules
[AD-A214246] 07 p0896 N90-15179
Optical properties and laser damage measurements of inorganic polymer films
[DE90-003633] 07 p0911 N90-15267
Theory for high gain, high power free electron lasers
[DE90-003024] 07 p0934 N90-15409
Diffraction limited dichroic combiner diode laser
[AD-D014291] 08 p1082 N90-16263
Ground-based deep-space LADAR for satellite detection: A parametric study
[AD-A215673] 09 p1228 N90-17126
CW (Continuous Wave) stimulated Brillouin scattering of long-pulse chemical laser beams
[AD-A216409] 10 p1390 N90-18039
Electron production, electron attachment, and charge recombination process in high pressure gas discharges
[AD-A216301] 10 p1434 N90-18274
Experimental results of aging and thermal effects in high-power laser diodes
[DE90-005955] 12 p1666 N90-19573
High power semiconductor laser arrays by metalorganic chemical vapor deposition 13 p1805 N90-20363
Laser controlled semiconductor armature for electromagnetic launchers
[AD-D014435] 14 p1931 N90-21055
High intensity laser beam interactions with single droplets 15 p2083 N90-21924
High power CO2 laser instability and its corrections 15 p2102 N90-22028
Direct solar-pumped iodine laser amplifier
[NASA-CR-186442] 15 p2103 N90-22030
Development of mid-infrared solid state lasers for spaceborne lidar
[NASA-CR-185095] 15 p2103 N90-22031
Linear, nonlinear, and tunable guided wave modes for high-power (GaAl)As semiconductor lasers 15 p2104 N90-22036
Beam combining by phase transition nonlinear media
[AD-A219301] 16 p2233 N90-22739
Gravitational radiation produced by high energy accelerators and high power lasers
[PREPRINT-701] 16 p2240 N90-22782
Nonlinear interaction between laser radiation and aerosols
[FOA-C-20768-2.3] 18 p2563 N90-24623
Mode-medium instability and its correction with a Gaussian reflectivity mirror
[NASA-TP-3023] 19 p2758 N90-25673
Ultra precision machining
[AD-A222422] 21 p2991 N90-27003
Laser induced damage in optical materials: 1988
[PB90-185570] 22 p3179 N90-28041
High pulse energy flashlamp pumpable laser dyes
[AD-A223075] 22 p3180 N90-28042
Titanium-doped sapphire lasers with high energy pumping
[RSRE-MEMO-4290] 22 p3181 N90-28050
Innovative techniques for the production of low cost 2D laser diode arrays
[AD-A223575] 24 p3474 N90-29632
Proceedings of the High Energy Density Materials Contractors Conference
[AD-A223793] 24 p3484 N90-29695

HIGH PRESSURE
SSME Alternate Turbopump Development Program: Design verification specification for high-pressure fuel turbopump
[NASA-CR-183676] 01 p0008 N90-10033
Chemistry of nitromethane at very high pressure
[DE89-008016] 01 p0039 N90-10215
Institute of Geophysics and Planetary Physics, 1988
[DE89-014363] 01 p0137 N90-10794
High pressure 129I Moessbauer studies of GeI4 molecular crystals
[DE89-015289] 02 p0283 N90-11620
Cellular and molecular mechanisms of high pressure inotropy in cardiac muscle
[AD-A211695] 03 p0381 N90-12170
High pressure studies of planetary matter
[DE89-017738] 03 p0428 N90-12455
Advanced actuation systems development, volume 1
[AD-A213334] 04 p0458 N90-12624
Thermophysical properties of benzene. Part 2: Thermodynamic properties at elevated pressures
[ESDU-89003-PT-2] 04 p0470 N90-12694
Continuing studies of liquid propellant drops in hot, high-pressure environments
[AD-A212265] 04 p0482 N90-12765
Thermophysical properties of isopropyl alcohol. Part 2: Thermodynamic properties at elevated pressures
[ESDU-89020-PT-2] 06 p0739 N90-14300
The Periodic Law at high pressures
[DE90-000837] 06 p0742 N90-14319
High-temperature/high-pressure x ray diffraction: Recent developments
[DE89-015255] 06 p0851 N90-14949
High-pressure promoted combustion chamber
[NASA-CASE-MSC-21470-1] 09 p1170 N90-16771
Summary of a decade of railgun development for high-pressure research
[DE90-005247] 09 p1172 N90-16780
High pressure waterjet cutting industrial needs survey
[AD-A214952] 10 p1368 N90-17927
Efficiency measurement of high pressure cryogenic rocket pumps
[NAL-TR-1022] 10 p1391 N90-18042
Study on the thermodynamical and mechanical conditions for the generation of high operating pressures with liquefied gases for low and very low flow rates
[ESA-TT-1148] 11 p1510 N90-18696
Piezoelectric polymer PVDF shock gauge: State of the research art
[ISL-CO-207/89] 11 p1512 N90-18705
A parametric heat transfer study for cryogenic ball bearings in SSME HPOTP 12 p1635 N90-19397
Investigation of SSME alternate high pressure fuel turbopump lift-off seal fluid and structural dynamic interaction 12 p1636 N90-19400
A study of the effects of disk flexibility on the rotordynamics of the space shuttle main engine turbo-pumps 12 p1636 N90-19401
Superconducting and normal compounds: Some high field/high pressure effects 16 p2320 N90-23229
Nonflammable hydraulic power system for tactical aircraft. Volume 1: Aircraft system definition, design and analysis
[AD-A218493] 17 p2356 N90-23409
Aerodynamic pressure and heating-rate distributions in tile gaps around chine regions with pressure gradients at a Mach number of 6.6
[NASA-TP-2988] 17 p2400 N90-23670
The effects of Reynolds number, rotor incidence angle, and surface roughness on the heat transfer distribution in a large-scale turbine rotor passage
[NASA-CR-183891] 17 p2410 N90-23731
The hypersonic vacuum wind tunnels: Status, research, and necessary developments 18 p2490 N90-24231
Performance evaluation of LE-7 high pressure pumps
[DE90-505523] 20 p2817 N90-26034
Combustion characteristics of oxygen/hydrogen high pressure preburners for staged combustion cycle rocket engine
[NAL-TR-1044] 24 p3441 N90-29434
Rotordynamic properties of high pressure seals: An experimental approach 24 p3475 N90-29640

HIGH PRESSURE OXYGEN
RAAF Orion aircraft A9-300 oxygen fire
[AD-A215496] 09 p1162 N90-16725

HIGH Q
U Q FACTORS

HIGH RESOLUTION
HDTV displays: Subjective effects of scanning standards and domestic picture sizes
[BBC-RD-1989/9] 02 p0211 N90-11208
High temperature and high resolution UV photoelectron spectroscopy using supersonic molecular beams
[DE90-000176] 03 p0323 N90-11835
Television systems with enhanced image quality for new broadband channels
[ETN-89-94622] 03 p0340 N90-11936
High resolution X-ray spectroscopy using germanium microcalorimeters
[DE89-017784] 03 p0351 N90-12004
Visualization of high-resolution digital terrain
[AD-A212149] 04 p0515 N90-12971
Reflection indicatrices of natural surfaces for AVHRR channels 1 and 2
[DLR-MITT-89-16] 05 p0664 N90-13882
High resolution, wide band Chirp-Z signal analyzer
[AD-D014240] 06 p0768 N90-14465
An image compression algorithm for a high-resolution digital still camera
[NASA-CR-185079] 06 p0780 N90-14532
Radiation damage and its influence on source requirements for high resolution x ray holography
[DE90-002508] 06 p0781 N90-14540
Very high resolution radio observations of molecular cloud cores 06 p0863 N90-15013
Classification of high resolution imagery using texture attributes
[INPE-4888-TDL/379] 11 p1525 N90-18778

The environment of young stellar objects studied by high-resolution infrared spectroscopy
11 p1583 N90-19120
JCMT observations of the circumstellar envelope IRC+10216
11 p1585 N90-19138
Spatially high-resolution flame diagnosis by means of spontaneous Raman spectroscopy
[ETN-90-95870] 12 p1623 N90-19328
A high resolution automatic image measuring system
[WISS-ARB-VERMESSUNGSWESEN-154] 12 p1663 N90-19559
Regional climate change predictions from the Goddard Institute for Space Studies high resolution GCM
[NASA-CR-186375] 12 p1693 N90-19725
High resolution radar target modeling using ARMA (Autoregressive Moving Average) models
[AD-A218212] 13 p1791 N90-20278
The use of high-resolution terrain data in gravity field prediction 13 p1835 N90-20533
Studies of an orbital gradiometer mission
13 p1839 N90-20558
High resolution analysis of satellite gradiometry
13 p1840 N90-20561
Biological soft x ray contact microscopy: Imaging living CHO-SC1 cells and other biological materials
[DE90-007560] 13 p1849 N90-20610
High resolution transmission electron microscopy study of defect structures in mixed-phase YBaCuO
[DE90-007767] 13 p1894 N90-20873
High-resolution Brillouin gain spectroscopy in solids
[DE90-009475] 14 p1949 N90-21155
Application of superresolution methods for airborne radar 14 p1961 N90-21227
HDTV bandwidth reduction using motion compensation and DATV
[BBC-RD-1989/10] 14 p1965 N90-21254
High resolution imaging of the Venus night side using a Rockwell 128x128 HgCdTe array
14 p1978 N90-21330
Simulated image maps for use in experimental high-resolution electron microscopy
[DE90-009176] 14 p2032 N90-21657
Contributions to the development of SLM TEA CO2 laser sources for high resolution molecular spectroscopy
16 p2240 N90-22778
High-resolution radar imaging
[AD-A220809] 17 p2391 N90-23620
Spectral characteristics of low-angle radar ground clutter
[AD-A220817] 17 p2392 N90-23622
The Zenith Z-248 as a scientific workstation
[AD-A219991] 17 p2441 N90-23909
Shape discrimination research using an IBM PC
[AD-A219993] 17 p2447 N90-23953
Spectral feature design in high dimensional multispectral data
[NASA-CR-186647] 18 p2574 N90-24664
Use of high-dimensional spectral data to evaluate organic matter, reflectance relationships in soils
[NASA-CR-186650] 18 p2574 N90-24665
Atomic structure of Ag/Ni interfaces
[DE90-010053] 18 p2618 N90-24914
A comparison of select image-compression algorithms for an electronic still camera 18 p2632 N90-24994
Feasibility of a synthetic aperture Radar with Rotative Antennas (ROSAR)
[MBB-S/PUB-0385] 19 p2651 N90-25088
Concepts for high resolution space based SAR/ISAR systems
[MBB-UK-0057/89-PUB] 19 p2652 N90-25096
Simulations of high-resolution X ray spectra of AGNs
19 p2791 N90-25885
The application of HREELS to model catalysts: CO and C2H4 adsorption on Pt/Al2O3
[AD-A222744] 20 p2831 N90-26103
HIRIS performance study
[NASA-CR-186649] 20 p2878 N90-26375
The interstellar D1 line at high resolution
[NASA-CR-184915] 20 p2941 N90-26737
High resolution spectroscopy in the microwave and far infrared 20 p2943 N90-26746
High resolution infrared spectroscopy of planetary molecules using diode lasers and Fourier transform spectrometers 20 p2943 N90-26747
Recent high resolution laboratory determinations of line broadening and intensity parameters: PH3, CH3D, and CO2 20 p2944 N90-26751
High resolution, low temperature photoabsorption cross-section of C2H2 with application to Saturn's atmosphere 20 p2945 N90-26757
High resolution exponential modeling of fully polarized radar returns
[AD-A221432] 21 p2997 N90-27036
Multispectral variable magnification glancing incidence x ray telescope
[NASA-CASE-MFS-28013-4] 21 p3096 N90-27595
High resolution optical imaging through the atmosphere
[AD-A221913] 21 p3097 N90-27599
High resolution technique and instrument for measuring lattice parameters in single crystals
[AD-D014549] 22 p3177 N90-28029
Intercomparison of standard resolution and high resolution TOVS soundings with radiosonde, lidar, and surface temperature/humidity data
22 p3228 N90-28306
High range resolution radar cross-section profiles: A preliminary analysis
[AD-A223448] 24 p3461 N90-29550
Adaptive, robust, high-resolution signal processing
[AD-A223728] 24 p3538 N90-30004

HIGH REYNOLDS NUMBER
A study of high-lift airfoils at high Reynolds numbers in the Langley low-turbulence pressure tunnel
[NASA-TM-89125] 01 p0001 N90-10002
An investigation of end-wall vortex cavitation in a high Reynolds number axial-flow pump
[AD-A211426] 03 p0347 N90-11982
Design and test of a natural laminar flow/large Reynolds number airfoil with a high design cruise lift coefficient
04 p0444 N90-12543
The cryogenic induction tunnel T2 at Toulouse
08 p1029 N90-15946
Separation bubbles at high Reynolds number: Measurement and computation
[CUED/A-AERO/15] 12 p1657 N90-19525
Low speed testing of a laminar flow airfoil in an adaptive wall wind tunnel
[FFA-TN-1989-08] 17 p2346 N90-23363
Algebraic turbulence modeling for unstructured and adaptive meshes
[NASA-CR-182035] 17 p2401 N90-23676
The stability of two-dimensional wakes and shear-layers at high Mach numbers
[NASA-CR-182050] 17 p2401 N90-23678
Solution of the steady state incompressible Navier-Stokes equations at high Reynolds numbers
[VKI-TN-170] 17 p2404 N90-23692
Vortex-induced boundary layer separation
[AD-A221564] 21 p3005 N90-27078
On the spatial eigenvalue approach to high Reynolds number flow in a rotating and nutating cylinder
[AD-A221710] 21 p3005 N90-27081

HIGH SPEED
Large-scale Advanced Prop-fan (LAP) high speed wind tunnel test report
[NASA-CR-182125] 01 p0010 N90-10045
High-speed machining of aluminum
[DE89-014011] 01 p0077 N90-10441
Analysis of high speed pneumatic actuation systems under rotary directional on-off flow control
04 p0507 N90-12926
High speed quantum-well optoelectronic devices by MBE
[AD-A212585] 04 p0555 N90-13237
Modeling and measurement methods for high speed bipolar transistors
[REPT-11] 05 p0636 N90-13714
Efficient real gas Navier-Stokes computations of high speed flows using an LU scheme
[NASA-TM-102429] 06 p0720 N90-14203
High speed transfer switch with 50 kA and 50 kV ratings
[DE90-002448] 06 p0770 N90-14481
Embedded function methods for compressible high speed turbulent flow
[NASA-CR-186131] 06 p0773 N90-14498
The High-Speed Channel (HSC) and ultra-speed networks
[DE89-015283] 06 p0829 N90-14819
A review of high-speed, convective, heat-transfer computation methods 10 p1305 N90-17548
High speed imaging with a tapped solid state sensor
[DE90-006116] 11 p1511 N90-18702
High speed modem
[AD-D014319] 12 p1698 N90-19750
Aerofoil design techniques 14 p1916 N90-20978
High speed civil transport
[NASA-CR-186661] 17 p2353 N90-23396
Fuel-rich catalytic combustion: A fuel processor for high-speed propulsion
[NASA-TM-103177] 17 p2374 N90-23518
Flow studies in impeller passages
18 p2551 N90-24558
A few modeling and rendering techniques for computer graphics and their implementation on ultra hardware
18 p2640 N90-25038
Optical high-speed parallel backplane
[AD-D014504] 19 p2757 N90-25670
Study of high-speed civil transports. Summary
[NASA-CR-4236] 20 p2808 N90-25966
High speed magneto-resistive random access memory
[NASA-CASE-NPO-17954-1-CU] 20 p2904 N90-26519
Development of advanced combustion technology for medium and high speed natural gas engines
[PB90-198565] 23 p3331 N90-28836

HIGH SPEED CAMERAS
NT FRAMING CAMERAS
Spark camera annotation and control system for the BRL (Ballistic Research Laboratory) Transonic Range Facility
[AD-A212266] 04 p0459 N90-12633
Regression and combustion characteristics of boron containing fuels for solid fuel ramjets
22 p3161 N90-27928
Method to image high speed events using a standard video camera
[AD-D014556] 22 p3177 N90-28030

HIGH SPEED FLIGHT
U HIGH SPEED

HIGH SPEED PHOTOGRAPHY
Interferometry and high speed photography of laser-driven flyer plates
[DE89-016990] 02 p0225 N90-11290
Debris/ice/TPS assessment and photographic analysis for Shuttle Mission STS-33R
[NASA-TM-102785] 09 p1180 N90-16846
Debris/ice/TPS assessment and photographic analysis for Shuttle Mission STS-36
[NASA-TM-102789] 16 p2205 N90-22583
Debris/ice/TPS assessment and photographic analysis for shuttle mission STS-31R
[NASA-TM-102790] 20 p2819 N90-26040
A high-speed photography study of cavitation in a dynamically loaded journal bearing
[NASA-TM-103178] 20 p2872 N90-26338
Debrix/ice/TPS assessment and photographic analysis of Shuttle Mission STS-32R
[NASA-TM-102787] 22 p3124 N90-27733
Analysis of pyrotechnic devices by laser-illuminated high speed photography
[DE90-015741] 24 p3458 N90-29530

HIGH SPEED TRANSPORTATION
U RAPID TRANSIT SYSTEMS

HIGH STRENGTH
The manufacture of superplastic alloys
06 p0745 N90-14333
Current status of the application of conventional aluminium-lithium alloys and the potential for future developments 07 p0900 N90-15203
The processing and mechanical properties of high temperature/high performance composites. Book 2, section 2: Strength and fracture resistance
[AD-A216142] 11 p1478 N90-18507
The processing and mechanical properties of high temperature/high performance composites. Book 3, section 2: Strength and fracture resistance, part
[AD-A216143] 11 p1478 N90-18508
Energy beam treatment for improved adhesion of coatings to surfaces
[AD-D014449] 14 p1954 N90-21190

HIGH STRENGTH ALLOYS
NT HIGH STRENGTH STEELS
NT MARAGING STEELS
Strain aging in tungsten-heavy alloys
[AD-A211166] 01 p0046 N90-10259
Precipitation strengthened high strength, high conductivity Cu-Cr-Nb alloys produced by chill block melt spinning
[NASA-CR-185144] 03 p0326 N90-11853
The effect of composition and aging treatment on the microstructure and mechanical properties of aluminum-lithium-titanium alloys
[AD-A213144] 05 p0624 N90-13640
Designing for superplastic alloys
06 p0744 N90-14332
Fatigue properties of Al-Li alloys
07 p0898 N90-15189
Evaluation of a diffusion/trapping model for hydrogen ingress in high strength alloys
[AD-A215528] 09 p1194 N90-16920
Advanced tribological coatings for high specific strength alloys
[AD-A214061] 09 p1196 N90-16930
MATE (Materials for Advanced Turbine Engines) Program, Project 3. Volume 2: Design, fabrication and evaluation of an oxide dispersion strengthened sheet alloy combustor liner
[NASA-CR-180892] 10 p1357 N90-17868
A numerical study of plasticity induced closure in short cracks by the finite element method
[AD-A220471] 18 p2571 N90-24654

HIGH STRENGTH STEELS
NT MARAGING STEELS

Mechanisms of strength and toughness in a microalloyed, precipitation hardened steel
[AD-A210571] 01 p0045 N90-10256
Fatigue resistance of pressure vessels in high strength steels effect of some improvement techniques
[CRIF-MT-176] 05 p0652 N90-13799
Deformation and fracture of low alloy steels at high temperature
[DE90-001274] 07 p0902 N90-15215
Reduction of residual stress and distortion in HY100 and HY130 high strength steels during welding
[AD-A213532] 07 p0905 N90-15231
Heat treatment investigation of 4330 vanadium-modified steel
[AD-A214290] 07 p0906 N90-15239
Submerged arc welding consumables for HSLA (High Strength Low Alloy)-100 steel
[AD-A213433] 07 p0941 N90-15452
Effects of high rate shear on the microstructure and deformation and fracture behavior of two high strength steels
[AD-A214107] 08 p1044 N90-16032
Failure analysis of a missile locking hook from the F-14 jet
[AD-A214995] 09 p1194 N90-16917
Effect of heat treatment on the fracture toughness transition properties of an A508 class 3 steel
[AERE-R-13548] 13 p1774 N90-20182
Hydrogen, thermal ageing and the role of carbides in fatigue of a high strength steel
[AERE-R-13599] 13 p1774 N90-20183
Spray deposition: A fundamental study of droplet impingement, spreading and consolidation
[AD-A217202] 13 p1787 N90-20255
Mechanistic modeling of corrosion fatigue crack growth of steels in aqueous solutions 18 p2524 N90-24404
Statistical treatment of slow strain rate data for assessment of hydrogen embrittlement in low alloy high strength steel
[ARL-MAT-R-122] 20 p2832 N90-26106
Processing and characterization of high strength, high ductility Hadfield steel
[AD-A221769] 21 p2982 N90-26947

HIGH TEMPERATURE

Materials for engine applications above 3000 deg F: An overview
[NASA-TM-100169] 01 p0034 N90-10188
Thin film thermocouples for high temperature measurement
[PB89-209290] 01 p0073 N90-10420
Fluctuating pressures measured beneath a high-temperature, turbulent boundary layer on a flat plate at Mach number of 5
[NASA-TP-2947] 01 p0118 N90-10680
High-temperature ceramic superconductors
[AD-A211070] 02 p0283 N90-11618
High temperature and high resolution UV photoelectron spectroscopy using supersonic molecular beams
[DE90-000176] 03 p0323 N90-11835
Elevated temperature aluminum-titanium alloy by powder metallurgy process
[AD-D014165] 03 p0326 N90-11852
Laser probe vaporization/oxidation testing of high temperature composites
[AD-A211410] 04 p0465 N90-12663
Synthesis and high temperature chemistry of methylsilsesquioxane polymers produced by titanium catalyzed redistribution of methylhydridooligo- and polysiloxanes
[AD-A212000] 04 p0477 N90-12736
High temperature insulators
[AD-D014193] 04 p0479 N90-12751
Dimensional reduction at high temperature revisited
[KVI-791] 04 p0549 N90-13194
Compressibility of heavy nuclei at high temperatures
[KVI-792] 04 p0552 N90-13217
High temperature capacitive strain gage
[NASA-CR-4266] 05 p0644 N90-13760
Stress intensity factors for cracking metal structures under rapid thermal loading. Volume 2: Theoretical background
[AD-A213297] 05 p0654 N90-13812
Thermodynamic properties and hydrodynamic response of high-density high-temperature C H N O mixtures
[DE90-000836] 06 p0742 N90-14318
Pentafluorothio polynitroaliphatic explosives
[AD-D014221] 06 p0753 N90-14383
Electrical properties of materials for high temperature strain gage applications
[NASA-CR-186192] 06 p0780 N90-14534
High-temperature/high-pressure x ray diffraction: Recent developments
[DE89-015255] 06 p0851 N90-14949
High temperature chemistry of aromatic hydrocarbons
[DE90-003664] 07 p0888 N90-15133
Mechanical behavior of laminated composites at elevated temperatures 07 p0889 N90-15141
High-temperature gel-permeation chromatography of poly(4-methyl-1-pentene)
[DE90-002967] 07 p0893 N90-15159
Microstructural evolution of martensitic steels during fast neutron irradiation
[DE89-016231] 07 p0902 N90-15212
Deformation and fracture of low alloy steels at high temperature
[DE90-001274] 07 p0902 N90-15215
High power density spray cooling
[AD-A213575] 07 p0930 N90-15386
High temperature, flexible, thermal barrier seal
[NASA-CASE-LEW-14672-1] 07 p0940 N90-15444
The influence of carbide precipitation on the creep rupture behavior of high temperature alloys
[JUEL-2211] 08 p1046 N90-16044
The application of a computer data acquisition system for a new high temperature tribometer
[NASA-TM-102508] 10 p1347 N90-17811
Prediction of high temperature metal matrix composite ply properties
[NASA-TM-102490] 10 p1348 N90-17817
The processing and mechanical properties of high temperature/high performance composites. Book 1, section 1: Coatings and interfaces
[AD-A216141] 10 p1348 N90-17821
The processing and mechanical properties of high temperature/high performance composites. Book 4, section 3: Flow and creep strength
[AD-A216144] 10 p1349 N90-17822
The processing and mechanical properties of high temperature/high performance composites. Book 6, section 4: Processing: Matrices and composites, part 2
[AD-A216146] 10 p1349 N90-17824
Temperature profiles in high gradient furnaces 10 p1362 N90-17896
Analysis of biaxial stress fields in plates cracking at elevated temperatures
[AD-A216271] 10 p1397 N90-18077
Experiments on large single crystals of the superconducting oxides YBa2Cu3O7, La sub 2-xBa sub xCuO4, and Bi-Ca-Sr-O
[AD-A215283] 10 p1435 N90-18284
State of the art and future prospects for high temperature composites 11 p1477 N90-18498
Processing and elevated temperature ductility of aluminum alloy 7475
[AD-A216840] 11 p1486 N90-18554
Solid-state fluorescence above 1000 C: Application to high-temperature laser thermography
[DE90-006422] 11 p1514 N90-18721
Deformation and fracture of TiAl + W at elevated temperatures
[DE90-006490] 12 p1628 N90-19356
Demonstration of capabilities of high temperature composites analyzer code HITCAN
[NASA-TM-102560] 12 p1676 N90-19629
Solar and thermic utilization in high temperature area: Research and development
[ETN-90-96062] 12 p1682 N90-19663
Symposium on High Temperature and Materials Chemistry
[DE90-008047] 13 p1768 N90-20148
Fundamental aspects of and failure modes in high-temperature composites
[NASA-TM-102558] 13 p1769 N90-20151
Determination of fundamental thermodynamic properties of constituent materials and performance screening of candidate systems
[AD-A218089] 13 p1769 N90-20153
Vibrational spectroscopy of boron nitride at high temperatures and pressures
[DE90-008633] 13 p1772 N90-20172
Advanced high-temperature batteries 13 p1825 N90-20480
Ionic disorder in crystals at high temperatures with emphasis on fluorites
[AERE-R-13544] 13 p1893 N90-20862
Bis(4-(3,4-dimethylenepyrrolidyl)-phenyl) methane
[NASA-CASE-LAR-13965-1-CU] 14 p1942 N90-21118
High temperature fatigue behavior of tungsten copper composites
[NASA-TM-102404] 14 p1946 N90-21138
Pressure rig for repetitive casting
[NASA-CASE-LAR-14050-1] 14 p1959 N90-21216
Fracture toughness and tensile properties of alloy HT9 in thin sections under high neutron fluences
[DE90-008386] 15 p2069 N90-21851
High-temperature deformation of mechanically-alloyed aluminum IN90211 16 p2216 N90-22645
Elevated temperature crack growth in advanced powder metallurgy aluminum alloys 16 p2218 N90-22653
Elevated temperature crack growth in aluminum alloys: Tensile deformation of 2618 and FVS0812 aluminum alloys 16 p2218 N90-22654
Experimental and computational study of the viscoplastic response of high temperature structures 16 p2220 N90-22663
Microcracking and toughness of ceramic-fiber/ceramic-matrix composites under high temperature
[AD-A218516] 16 p2223 N90-22680
High temperature ceramic-tubed reformer
[DE90-009617] 16 p2236 N90-22755
High temperature insulation barrier composite
[NASA-CASE-MFS-29241-1] 17 p2368 N90-23480
MTS high temperature testing system
[AD-A219613] 17 p2369 N90-23483
High frequency, high temperature specific core loss and dynamic B-H hysteresis loop characteristics of soft magnetic alloys
[NASA-TM-103164] 17 p2398 N90-23663
High temperature flexible seal
[NASA-CASE-LEW-14695-1] 17 p2413 N90-23751
High temperature oxidation of Ni3Al composites
[DE90-010145] 18 p2517 N90-24373
Fatigue crack growth in ceramic materials at ambient and elevated temperatures
[DE90-008418] 18 p2531 N90-24443
Rapid thermal processing of high temperature superconducting fiber
[NASA-CR-186803] 18 p2626 N90-24964
Feasibility study for the advanced one-dimensional high temperature optical strain measurement system, phase 3
[NASA-CR-185254] 19 p2693 N90-25324
Thermomechanical testing techniques for high-temparature composites: TMF behavior of SiC(SCS-6)/Ti-15-3
[NASA-TM-103171] 19 p2701 N90-25367
High-temperature creep under a nonuniform temperature distribution
[ATR-88(3728-02)-1] 19 p2702 N90-25373
Carbon-carbon composites: Emerging materials for hypersonic flight
[NASA-TM-103472] 20 p2827 N90-26080
Extension of a noninteractive reliability model for ceramic matrix composites
[NASA-CR-185267] 20 p2838 N90-26142
Elevated temperature crack growth
[NASA-CR-182247] 20 p2875 N90-26355
Application of symbolic computations to the constitutive modeling of structural materials
[NASA-TM-103225] 20 p2876 N90-26364
A tough high performance composite matrix
[NASA-CASE-LAR-14338-1] 21 p2970 N90-26881
High temperature strength of SiC whisker-reinforced silicon nitride composites
[DE90-013822] 21 p2970 N90-26883
The thermal radiative properties of metals at high temperature
[DE90-012468] 21 p2981 N90-26938
Braided composite fasteners and method for producing same
[NASA-CASE-LAR-14062-1] 21 p3010 N90-27114
Fabrication of composite high temperature superconductor wires from Ag/YBa2Cu3O(sub x) powder produced by AgNO3 decomposition
[AD-A221936] 21 p3083 N90-27532
Synthesis of Y1Ba2Cu3O(sub x) superconducting powders by intermediate phase reaction 22 p3149 N90-27855
Development of polysilsesquioxane composites
[NASA-CR-180263] 22 p3152 N90-27872
High-temperature, corrosion-preventive coating
[AD-D014557] 22 p3160 N90-27918
High-temperature deformation of silicon
[DE90-013628] 22 p3160 N90-27919
Progress in high temperature speckle-shift strain measurement system
[NASA-TM-103255] 22 p3177 N90-28031
Engine testing of thermographic phosphors
[DE90-013269] 22 p3182 N90-28059
Analysis of the T63-A-700 engine used in alcohol turbine fuel extender test
[DOT/FAA/CT-TN90/18] 23 p3278 N90-28549
The effects of atomic oxygen on the thermal emittance of high temperature radiator surfaces
[NASA-TM-103224] 23 p3301 N90-28670
High Temperature Surface Interactions
[AGARD-CP-461] 23 p3306 N90-28698
High temperature surface interactions: Overview 23 p3306 N90-28699
Molten salt induced high temperature degradation of thermal barrier coatings 23 p3307 N90-28704
High temperature oxidation of Al-Li alloys 23 p3307 N90-28705
High temperature protective coatings: Recent trends 23 p3308 N90-28710

Evaluation of high temperature protective coatings for gas turbine engines under simulated service conditions
23 p3309 N90-28712
Surface property improvement in titanium alloy gas turbine components through ion implantation
23 p3309 N90-28713
Mechanical testing activities related to high-performance structural ceramics
[DE90-014299] 23 p3313 N90-28734
Improved silicon carbide for advanced heat engines
[NASA-CR-182186] 23 p3313 N90-28735
High-temperature deformation and microstructural analysis for Si3N4-Sc2O3
[NASA-TM-103239] 23 p3314 N90-28740
High temperature superconducting thin film microwave circuits: Fabrication, characterization, and applications
[NASA-TM-103235] 23 p3322 N90-28786
Noncontact measurement of high temperature using optical fiber sensors
[NASA-CR-186975] 23 p3329 N90-28825
Dynamical information for Fe doped YBa2Cu3O7 superconducting oxides obtained from high temperature Moessbauer studies
[DE90-627871] 23 p3401 N90-29218
Higher loop contributions to effective potential of gauge theory at high temperature
[DE90-627208] 23 p3403 N90-29231
Multiaxial fatigue criterion for 2-1/4 Cr-1 Mo steel for use in high-temperature structural design
[DE90-016039] 24 p3452 N90-29491
The investigation and production of titanium-tantalum junctions diffusion bonded at high temperature (855 C to 920 C): The influence of temperature, time pressure and roughness on the mechanical properties, and the optimisation of the bonded conditions
[BR114894] 24 p3476 N90-29646
Two terminal CuInSe2 based cascade cells
[DE90-000363] 24 p3485 N90-29697
Advanced materials and electrochemical processes in high-temperature solid electrolytes
[DE90-015552] 24 p3553 N90-30104

HIGH TEMPERATURE AIR
Aging of CFRP due to longterm storage in heated air
[ESA-TT-1124] 03 p0333 N90-11893
Hot air heat gun
[AD-D014312] 09 p1217 N90-17061

HIGH TEMPERATURE ALLOYS
U HEAT RESISTANT ALLOYS

HIGH TEMPERATURE ENVIRONMENTS
High temperature VSCF (Variable Speed Constant Frequency) generator system
[AD-A210823] 01 p0061 N90-10351
Reusable high-temperature heat pipes and heat pipe panels
[NASA-CASE-LAR-13761-1] 13 p1799 N90-20323
Review of the state of the technology for joining ceramics for high-temperature structural applications
[DE90-009224] 14 p1956 N90-21199
Interfacial studies of Chemical Vapor Infiltrated (CVI) ceramic matrix composites
[AD-A221867] 21 p2972 N90-26893
Evolution and use of combined mechanical and thermal codes for cryogenic turbopump bearings
23 p3291 N90-28618
Investigation of the effects of microalloy constituents, surface treatment and oxidation conditions on the development and breakdown of protective oxide scales
[DE90-015710] 24 p3451 N90-29488

HIGH TEMPERATURE FLUIDS
NT HIGH TEMPERATURE AIR
NT HIGH TEMPERATURE GASES
Studies on the startup transients and performance of a gas loaded sodium heat pipe
[AD-A211880] 03 p0414 N90-12379

HIGH TEMPERATURE GAS COOLED REACTORS
A review of gas-cooled reactor concepts for SDI (Strategic Defense Initiative)
[DE89-016962] 06 p0842 N90-14898
An attempt of improving high-temperature fatigue properties of Ni-Cr-W superalloys in HTGR helium
[DE90-741482] 12 p1627 N90-19350

HIGH TEMPERATURE GASES
NT HIGH TEMPERATURE AIR
Reactive ion etching of sputtered silicon carbide and tungsten thin films for device applications
[AD-A211711] 03 p0325 N90-11847
The disk-halo connection and the nature of the interstellar medium
[NASA-CR-186286] 07 p1012 N90-15860
Measurement of the speed and temperature of ignition gases
[ISL-CO-246/88] 09 p1192 N90-16908
Depressurization test on hot gas duct
[DE90-710058] 09 p1236 N90-17176
Proceedings of Air Force Office of Scientific Research workshop on Laser Propulsion
[AD-A216563] 12 p1666 N90-19569
TiCl4 as a source of TiO2 particles for laser anemometry measurements in hot gas
[NASA-TM-102581] 13 p1805 N90-20358
Development of high performance beta-SiC field-effect transistors
[AD-A218392] 17 p2394 N90-23637
Determination of the velocity, density, maximum flux, and enthalpy profiles for a very high temperature arc jet nozzle flow
[AD-A218390] 17 p2402 N90-23682
Evaluation of water cooled supersonic temperature and pressure probes for application to 2000 F flows
[NASA-TM-102612] 19 p2753 N90-25645
Hot gas ingestion characteristics and flow visualization of a vectored thrust STOVL concept
[NASA-TM-103212] 20 p2813 N90-26009
Development of an integrated BEM for hot fluid-structure interaction 23 p3291 N90-28617
Overview on hot gas tests and molten salt corrosion experiments at the DLR 23 p3309 N90-28714

HIGH TEMPERATURE LUBRICANTS
Development of a high temperature FZG-Ryder gear lubricant load capacity machine
[AD-A210799] 01 p0079 N90-10449
The experimental evaluation and application of high-temperature solid lubricants
[NASA-TM-102476] 09 p1198 N90-16944
The experimental evaluation and application of high temperature solid lubricants 18 p2564 N90-24631

HIGH TEMPERATURE MATERIALS
U REFRACTORY MATERIALS

HIGH TEMPERATURE NUCLEAR REACTORS
NT HIGH TEMPERATURE GAS COOLED REACTORS

HIGH TEMPERATURE PLASMAS
Research on heating, instabilities, turbulence and RF emission from electric field dominated plasmas
[AD-A212122] 04 p0557 N90-13243
Atomic structure and spectral perturbations in hot dense plasmas 06 p0785 N90-14567
The average ion model. Computation of the absorption and emission coefficients in hot plasmas
06 p0785 N90-14569
Spectroscopic diagnostics of high temperature plasmas
[DE90-003912] 08 p1126 N90-16522
Advanced diagnostics for reacting flows
[AD-A214795] 09 p1285 N90-17448
Results of the H-mode experiments with JT-60 outer and lower divertors
[DE90-733146] 10 p1432 N90-18265
Measurement of the space potential of a high-temperature plasma by fast atomic beam scattering on an ion probe beam
[DE90-006118] 11 p1567 N90-19020
Atomic processes in high temperature plasmas
[DE90-008873] 14 p2028 N90-21632
The intrinsic stochasticity of near-integrable Hamiltonian systems
[IPPCZ-282] 15 p2167 N90-22386
Studies of Io's atmosphere and plasma torus
16 p2338 N90-23326
Characterization of plasma flow through magnetic nozzles
[AD-A221044] 18 p2617 N90-24905
Heat and momentum transfer to test samples in the high velocity plasma furnace
[AD-A222182] 21 p3079 N90-27505
Damage resistant optical coatings prepared using high temperature, plasma chemical-vapor-deposition
[DE90-015042] 23 p3313 N90-28738

HIGH TEMPERATURE PROPELLANTS
Extraction of recovery of plasticizers from solid propellants and munitions
[AD-D014433] 15 p2072 N90-21868

HIGH TEMPERATURE RESEARCH
The Materials Division: A case study
[NASA-TM-102380] 05 p0617 N90-13597
The position of carbon/carbon composites among high temperature composites
[REPT-892-430-126] 16 p2213 N90-22626

HIGH TEMPERATURE SUPERCONDUCTORS
Study of deposition of YBa2Cu3O7-x on cubic zirconia
[NASA-TM-102350] 01 p0128 N90-10737
Magnetic correlations in high T(sub c) oxides in the superconducting state
[DE89-016421] 01 p0130 N90-10746
Processing and fabrication of high temperature oxide superconductors
[AD-A210197] 01 p0131 N90-10755
The effect of twins on critical currents of high Tc superconductors
[AD-A210988] 01 p0133 N90-10768
Acoustic studies of new materials: Quasicrystals, low-loss glasses and high Tc superconductors
[AD-A211281] 02 p0272 N90-11551
Adaptation of the theory of superconductivity to the behavior of oxides
[DE89-016518] 02 p0282 N90-11608
Studies of novel superconductors
[DE89-016744] 02 p0282 N90-11609
Pinning of curved flux lines on the boundary between two phases of high temperature superconductors
[DE89-618865] 02 p0283 N90-11614
High-temperature ceramic superconductors
[AD-A211070] 02 p0283 N90-11618
Physics and materials science of high temperature superconductors
[AD-A211246] 02 p0283 N90-11619
Origins of high-temperature superconductivity in the new copper oxide based ceramic superconductors
[DE89-016543] 02 p0284 N90-11622
A fermi liquid electric structure and the nature of the carriers in high-T(sub c) cuprates: A photoemission study
[DE89-016774] 02 p0284 N90-11624
Neutron scattering experiments on high-temperature superconducting materials: Foreign trip report, September 13, 1988--October 4, 1988
[DE89-017451] 02 p0285 N90-11630
Superconducting switch program
[AD-A211580] 03 p0344 N90-11964
Characterizations of electrical properties of highT(sub c) superconducting materials
[NASA-TM-100380] 03 p0409 N90-12345
RF performance of polycrystalline high-T(sub c) superconductors
[DE89-017671] 03 p0411 N90-12359
Anomalous ion-channeling behavior across the superconducting transition in high-T(sub c) materials
[DE89-017677] 03 p0411 N90-12360
High-temperature superconducting current leads for cryogenic apparatus
[DE89-017680] 03 p0411 N90-12361
Preparation and characterization of single phase Ba(1-x)KxBiO3
[DE89-017735] 03 p0411 N90-12362
Effects of grain boundary chemistry on critical current density in oxide superconductors
[DE89-017780] 03 p0412 N90-12365
Surface, interface, and bulk properties of high T(sub c) superconductors
[AD-A211490] 03 p0413 N90-12373
High temperature superconducting compounds
[AD-A211511] 03 p0413 N90-12374
Resistivity measurements of superconducting materials
[PB89-225700] 04 p0496 N90-12856
Seminars of Applied Physics, Materials Physics and Biomedical Engineering, 1989
[PB89-218572] 04 p0548 N90-13192
Analysis of high temperature superconductors by means of PIXE and RBS methods
[DE89-630241] 04 p0558 N90-13252
Microwave microstrip resonator measurements of Y1Ba2Cu3O(7-x) and Bi2Sr2Ca1Cu2O(8-y) thin films
[NASA-TM-102159] 05 p0635 N90-13704
Construction of a SQUID magnetometer for investigation of screening properties of high-T(sub c) superconductors
[FOA-C-20765-2.2] 05 p0645 N90-13768
Preparation of 110K (Bi, Pb)-Sr-Ca-Cu-O superconductor from glass precursor
[NASA-CR-185162] 05 p0702 N90-14108
Local pairing and antiferromagnetism in high-T sub c superconductors
[AD-A213004] 05 p0703 N90-14113
Application of neutron diffraction NDE to high-temperature superconducting composites
[DE90-002184] 06 p0738 N90-14295
Practical superconductor development for electrical power applications
[DE90-001804] 06 p0771 N90-14487
Static and dynamic magnetization properties of Y1Ba2Cu3O(sub z) thin films
[DE89-017584] 06 p0850 N90-14940
Ion beam analysis and modification of thin-film, high-temperature superconductors
[DE90-000918] 06 p0850 N90-14941
Flux pinning and microstructure in YBa2Cu3O7
[DE90-001562] 06 p0851 N90-14948
High resolution-angle resolved photoemission studies of high temperature superconductors
[DE89-017691] 06 p0852 N90-14950
Oxygen stoichiometry, structural transitions, and thermodynamic behavior of the YBa2Cu3O(x) system
[DE89-017694] 06 p0852 N90-14951
A simple figure of merit for high temperature superconducting switches
[DE90-000610] 06 p0852 N90-14955

Microwave characterization of high-temperature superconductors
[DE90-002408] 06 p0854 N90-14968
RF superconductivity research and development at Los Alamos National Laboratory
[DE90-002440] 06 p0855 N90-14969
Macroscopic persistent currents in high temperature ceramic superconductors
[DE89-636232] 06 p0855 N90-14973
Electronic materials high-T(sub c) superconductivity polymers and composites structural materials surface science and catalysts industry participation
[NASA-CR-186063] 07 p0890 N90-15145
Preparation and properties of icosahedral borides
[DE90-003574] 07 p0896 N90-15180
Composite ceramic superconducting wires for electric motor applications
[AD-A213742] 07 p0912 N90-15274
Theoretical studies on the electronic structure of high-temperature superconductors
[DE90-001301] 07 p0998 N90-15771
Tunneling spectroscopy and the electron-phonon interaction in Ba(1-x)K(x)BiO3
[DE90-002842] 07 p0999 N90-15776
Linear electron-hole-electron pair model of high-temperature superconductivity in La(2-x)M(x)CuO4 and YBa2Cu3O(7-y): Part 2. Dependence of the superconducting transition temperatures on pressure and on hole concentration
[DE90-003012] 07 p0999 N90-15779
Electron-positron momentum distribution measurements of high-T superconductors and related systems
[DE90-002974] 07 p0999 N90-15780
Magnetic mechanisms of high temperature superconductivity
[DE90-003625] 07 p1001 N90-15796
Bulk wave characterization of high T(sub c) superconductors
[AD-A214030] 07 p1004 N90-15813
High-temperature ceramic superconductors
[AD-A214251] 07 p1005 N90-15818
The modified Ginzburg-Landau theory for anisotropic high temperature superconductors
[DE89-635909] 08 p1128 N90-16532
La(sub 2)MO(sub 4 + delta) (M = Cu, Ni, Co): Phase separation and superconductivity resulting from excess oxygen defects
[DE90-001988] 08 p1128 N90-16534
Phonon anomaly at T(sub c) in (Y/ER)Ba2Cu3O(7-delta)
[DE90-003562] 08 p1129 N90-16539
Structure-property correlations in the design of organic metals and superconductors: An overview
[DE90-003794] 08 p1131 N90-16550
Neutron experiments on high-temperature superconductors
[DE90-003978] 08 p1132 N90-16559
Magnetic interactions in Sn-119 substituted for Cu in antiferromagnetic and superconducting lamellar cuprates
[DE90-003661] 08 p1132 N90-16560
Magnetic penetration depth and intragrain critical current density in gain-aligned Tl2Ca2Ba2Cu3O10 superconductor
[DE90-004245] 08 p1133 N90-16562
Artificially structured superconductors
[DE90-004851] 08 p1134 N90-16567
High temperature neutron diffraction study of the formation reaction of bismuth superconductors
[DE90-004883] 08 p1134 N90-16568
Subtle porosity variation in the YBa2Cu3O(7-x) high-temperature superconductor revealed by ultrasonic imaging
[NASA-TM-102130] 09 p1235 N90-17167
A new approach for the utilization of electron paramagnetic resonance and an investigation of copper oxide superconductors
[AD-A213833] 09 p1277 N90-17404
Diffusion and processing of YBa2Cu3O(x)
[DE90-003569] 09 p1286 N90-17457
Electrical transport dissipation effects in epitaxial Y1Ba2Cu3O(7-x) thin films
[DE90-004301] 09 p1287 N90-17461
Review of new energy. Superconductivity
[DE90-734947] 09 p1287 N90-17464
JSEP (Joint Services Electronics Program)
[AD-A215051] 09 p1290 N90-17476
International Conference on Materials and Mechanisms of Superconductivity: High Temperature Superconductors
[AD-A215343] 09 p1290 N90-17480
Flux flow, pinning, and resistive behavior in superconducting networks
[DE90-005242] 09 p1293 N90-17493
Flux lattice melting in the high Tc superconductors
10 p1366 N90-17915
Influence of ion beam mixing on the growth of high temperature oxide superconducting thin film
[DE90-004837] 10 p1435 N90-18280
Critical field enhancement due to field penetration in fine-filament superconductors
[DE90-005389] 10 p1435 N90-18282
High quality tunnel junction devices using high T(sub c) superconductors
[AD-D014329] 10 p1435 N90-18283
High temperature superconductivity
[AD-A215491] 10 p1436 N90-18286
Microwave radiation absorption by Ho(Y)-Ba-Cu-O superconducting ceramics
[DE90-610665] 11 p1492 N90-18588
Luminescence from defects and impurity centers in yttrium oxide
[DE90-004842] 11 p1569 N90-19030
Understanding electronegative effects in core-level electron spectroscopies; application to the high temperature superconductors
[AD-A216728] 11 p1570 N90-19037
What influences order parameters across the superconducting phase boundary
[DE90-610663] 11 p1572 N90-19047
Spectral functions from Quantum Monte Carlo
[DE90-004870] 11 p1572 N90-19050
Laser mass spectrometric studies of high temperature superconductor ablation
[DE90-006518] 12 p1668 N90-19585
Characterization of ground state neutral and ion transport during laser ablation of 1:2:3 superconductors by transient optical absorption spectroscopy
[DE90-006623] 12 p1720 N90-19878
Neutron scattering measurements of the magnetic excitations of high-temperature superconducting materials
[DE90-006567] 12 p1721 N90-19885
Novel processing of HTS based conductors
[DE90-005956] 12 p1722 N90-19892
Band electronic structures and crystal packing forces
[DE90-007669] 12 p1723 N90-19898
High-temperature ceramic superconductors
[AD-A218347] 13 p1783 N90-20233
Copper and oxygen NMR studies on the magnetic properties of YBa2Cu3O(7-y)
[DE90-007889] 13 p1893 N90-20863
High temperature chemistry of oxide superconductors
[DE90-007821] 13 p1895 N90-20875
Stabilization of high (Tc) superconductivity in cadmium sulfide
[DE90-008249] 13 p1896 N90-20881
The electronic properties of high (Tc) superconductors probed by positron annihilation
[DE90-008354] 13 p1896 N90-20883
Systematics in positron annihilation lifetime analysis of high (Tc) superconducting transitions
[DE90-008361] 13 p1896 N90-20884
Electronic properties of high-temperature superconductors
[AD-A217953] 13 p1898 N90-20892
Determination of internal strains in high-temperature superconductor composites by intense pulsed neutron source
[DE90-007799] 14 p2033 N90-21664
Modeling high-temperature superconductors and metallic alloys on the Intel IPSC/860
[DE90-009402] 14 p2033 N90-21665
Assessment of High Temperature Superconducting (HTS) electric motors for rotorcraft propulsion
[NASA-CR-185222] 15 p2052 N90-21761
JETC (Japanese Technology Evaluation Center) Panel Report on High Temperature Superconductivity in Japan
[NASA-CR-180413] 15 p2172 N90-22409
Pulsed laser processing of high temperature superconducting thin films
[DE90-008928] 15 p2172 N90-22413
Overview of current bulk and thick film high temperature superconductor processing strategies
[DE90-008949] 15 p2172 N90-22414
In-situ pulsed laser deposition of high-T(sub c) YBa(sub 2)Cu(sub 3)O(sub 7) superconducting thin films on (100) LaAlO3 substrates
[DE90-009861] 15 p2173 N90-22418
Composite ceramic superconducting wires for electric motor applications
[AD-A219131] 16 p2224 N90-22689
ONR Far East Scientific Information Bulletin, Volume 13, No. 4
[ONRFE-SCI-INFO-BULL-13(4)88]
16 p2311 N90-23168
High temperature superconducting thin films in Japan
16 p2311 N90-23169
Research and applications of metallic superlattices, high T(sub c) superconductors, x ray optics, and compact synchrotrons
16 p2311 N90-23170
What is going on in the La2CuO4 superconductors
16 p2311 N90-23171
Superconducting and normal compounds: Some high field/high pressure effects 16 p2320 N90-23229
Thermal phenomena in high-Tc thin film superconductors 16 p2321 N90-23233
Single crystal NMR of high temperature superconductors 16 p2321 N90-23236
Influence of high energy radiation on critical parameters of superconducting ceramics YBa2Cu3O7
[DE90-620562] 16 p2322 N90-23239
A (inu)SR-investigation of the mixed state of the high-Tc superconductor HoBa2Cu3O7-delta
[DE90-620802] 16 p2322 N90-23241
Application of high-temperature superconducting thin-film devices to electro-optical and electronic warfare systems
[AD-A218805] 16 p2323 N90-23249
In-situ processing of epitaxial and textured high (Tc) superconducting HoBa2Cu3O(7-x) thin films by pulsed laser evaporation technique
[DE90-009826] 17 p2474 N90-24148
High temperature superconductivity
[AD-A219483] 17 p2476 N90-24155
Effects of large doses of high energy electrons on a YBa2Cu3O6(+)delta high temperature superconductor
[AD-A220423] 17 p2476 N90-24158
Electrical transport through tunnel barriers and thin dielectric layers and physical properties of the high Tc oxide superconductors
[AD-A219860] 17 p2477 N90-24165
Stability projections for high temperature superconductors
[AD-A218945] 18 p2618 N90-24913
Magnetic and resistive measurements of the upper critical field in intwinned single crystals of YBa2Cu3O(7-delta)
[DE90-010083] 18 p2619 N90-24918
The defect structure of ion and neutron irradiated YBa2Cu3O(7-delta) single crystals
[DE90-010100] 18 p2619 N90-24920
Cation and anion tracer diffusion in YBa(sub 2)Cu(sub 3)O(sub 7-delta)
[DE90-009708] 18 p2620 N90-24927
Thermal and phase analysis of YBa2Cu3O(7-x) powder compacts with organic acid additives
[DE90-010142] 18 p2620 N90-24930
Use of neutron diffraction in determining strains in high-temperature superconducting composites
[DE90-010404] 18 p2621 N90-24931
Studies on ion scattering and sputtering processes in ion beam sputter-deposition of high Tc superconducting films: The optimization of deposition parameters
[DE90-010538] 18 p2621 N90-24936
Preparation of high Tc superconducting ceramic materials of the Y-Ba-Cu-oxide type
[FOA-C-30550-3.2] 18 p2622 N90-24939
Development of elements of a high Tc superconducting cable
[AD-A221300] 18 p2623 N90-24945
High-temperature superconductors for space power transmission lines
[NASA-TM-103459] 18 p2624 N90-24952
Transverse- and zero-field muon SR investigation of magnetism and superconductivity in (Y(1-x)Pr(x)Ba2Cu3O7)
[DE90-010597] 18 p2624 N90-24953
Protons and lattice defects in perovskite-related oxides
[DE90-010957] 18 p2624 N90-24955
Practical superconductor development for electrical power applications
[DE90-010262] 18 p2625 N90-24957
In-situ growth of superconducting films of Bi-Sr-Ca-Cu-O using magnetron sputtering
[DE90-011161] 18 p2626 N90-24962
Effect of Cu(2+) magnetic moments on the superconductivity of YBa2Cu3O7: The origin of the linear term in the specific heat; the volume fraction of superconductivity
[DE90-011214] 18 p2626 N90-24963
Low-temperature specific heat measurements on metals: Application to high-T(sub c) superconductors
[DE90-011612] 18 p2626 N90-24966
Preparation and properties of superconducting thin films by excimer laser ablation
[DE90-011929] 18 p2626 N90-24967
RF properties of high temperature superconductors: Cavity methods
[DE90-011961] 18 p2627 N90-24969
Sequentially evaporated thin film YBa2Cu3O(7-x) superconducting microwave ring resonator
[NASA-TM-103180] 19 p2685 N90-25273
Surface wave characterization of high T(sub c) superconductors
[AD-A221077] 19 p2760 N90-25683

Suitability of electrodeposition processes for high temperature superconductors
[IAR-89-22] 19 p2760 N90-25685
Use of high-temperature superconductors in superconducting magnetic energy power sources
[DE90-011119] 19 p2761 N90-25686
Pressure dependence of thermoelectric power of high T(sub c) 123 compound
[PD-MT-9001] 20 p2829 N90-26092
Materials research issues in superconducting levitation and suspension as applied to magnetic bearings
[DE90-011147] 20 p2929 N90-26667
NDE (Nondestructive evaluation) of critical currents in high T(sub c) superconductors
[DE90-012953] 20 p2930 N90-26670
Studies on ion scattering and sputtering processes relevant to ion beam sputter deposition of multicomponent thin films
[DE90-010071] 20 p2931 N90-26675
Critical current density, flux creep, and microstructure in a Bi-Sr-Ca-Cu-O system
[DE90-010457] 20 p2931 N90-26676
Passivation of high temperature superconductors
[NASA-CASE-NPO-17949-1-CU] 20 p2932 N90-26684
Fabrication of microwave guides using high Tc superconductors
[AD-A221560] 21 p3001 N90-27059
The effect of processing, deformation and annealing on the microstructure of Y1Ba2Cu3O7-(sub delta)
[DE90-011731] 21 p3079 N90-27510
Pulsed laser deposition of high (Tc) superconducting thin films: Present and future
[DE90-011950] 21 p3080 N90-27511
Flux motion effects in Tl-Ca-Ba-Cu-O thin films
[DE90-012176] 21 p3080 N90-27514
Fabrication of composite high temperature superconductor wires from Ag/YBa2Cu3O(sub x) powder produced by AgNO3 decomposition
[AD-A221936] 21 p3083 N90-27532
A silver-bearing, High-Temperature, Superconducting (HTS) paint
[AD-A221616] 21 p3084 N90-27539
High temperature ceramic superconductors
[AD-A221743] 21 p3084 N90-27540
AMSAHTS 1990: Advances in Materials Science and Applications of High Temperature Superconductors
[NASA-CP-10043] 22 p3136 N90-27792
The superconducting state of the high-transition temperature superconductors: Experimental basis
22 p3136 N90-27793
Pinning, flow and plastic deformation of flux vortices in high T(sub c) superconductors 22 p3136 N90-27796
Flux flow and flux dynamics in high-T(sub c) superconductors 22 p3136 N90-27797
Magnetic properties of high-T(sub c) superconductors: Rigid levitation, flux pinning, thermal depinning, and fluctuation 22 p3137 N90-27798
Magnetic forces in high-T(sub c) superconducting bearings 22 p3137 N90-27799
Oxygen stabilization induced enhancement in J(sub c) and T(sub c) of superconducting oxides
22 p3137 N90-27800
Laser ablated high T(sub c) superconducting thin YBa2Cu3O(7-x) films on substrates suitable for microwave applications 22 p3139 N90-27808
Laser surface interactions of high-T(sub c) superconductors 22 p3139 N90-27809
Perspectives on high temperature superconducting electronics 22 p3139 N90-27810
Upcoming planetary missions and the applicability of high temperature superconductor bolometers
22 p3140 N90-27811
Energetics and crystal chemistry of Ruddlesden-Popper type structures in high T(sub c) ceramic superconductors
22 p3141 N90-27814
Kinetics and thermodynamics of ceramic/metal interface reactions related to high T(sub c) superconducting applications 22 p3141 N90-27815
Thermal and electric properties of Nd(1.85)Ce(0.15)CuO(4-y) and Pr(1.85)Ce(0.15)CuO(4-y)
22 p3141 N90-27816
Effect of oxygen stoichiometry on T(sub c) of Bi-based superconductors 22 p3142 N90-27818
Charge transfer polarisation wave and carrier pairing in the high T(sub c) copper oxides
22 p3142 N90-27820
Electronic structure Fermi liquid theory of high T(sub c) superconductors: Comparison with experiments
22 p3142 N90-27821
An explanation for the rise in T(sub c) in the Tl- and Bi-based high temperature superconductors
22 p3142 N90-27822
Critical currents and high temperature superconductors 22 p3142 N90-27823
Study of local structure and magnetism in high-T(sub c) copper oxide superconductors
22 p3143 N90-27824
Dynamics of the iron spins in superconducting YBa2(Cu(1-x)Fe(x))O7 22 p3143 N90-27825
The mechanism of high-T(sub c) superconductivity due to bound hole mediators: Relationship to ferroelectricity
22 p3143 N90-27826
An EPR methodology for measuring the London penetration depth for the ceramic superconductors
22 p3143 N90-27828
Magnetism and superconductivity of some Tl-Cu oxides 22 p3143 N90-27829
The color of polarization in cuprate superconductors
22 p3144 N90-27830
Stabilization of high T(sub c) phase in bismuth cuprate superconductor by lead doping
22 p3144 N90-27832
Structure and superconducting properties of ((Ln(1-x)Ln*(x) 1/2 (Ba(1-y)Sr(y) 1/3 Ce 1/6) 8Cu6O(z)
22 p3144 N90-27833
Phase compatibilities of YBa2Cu3O(9-delta) type structure in quintenary systems Y-Ba-Cu-O-X (impurity)
22 p3145 N90-27834
Progress of research of high-T(sub c) superconductors
22 p3145 N90-27835
The NASA high temperature superconductivity program 22 p3145 N90-27836
Navy superconductivity efforts
22 p3145 N90-27837
Thermal response of large area high temperature superconducting YBaCuO infrared bolometer
22 p3146 N90-27839
Superconducting film on metallic wire
22 p3146 N90-27840
Effects of grain size and grain boundary on critical current density of high T(sub c) superconducting oxides
22 p3146 N90-27843
Microwave conductivity of laser ablated YBaCuO superconducting films and its relation to microstrip transmission line 22 p3147 N90-27844
Superconductivity in 2-2-3 Y2Ba2Cu3O(sub 8+ delta)
22 p3147 N90-27847
In-situ integrated processing and characterization of thin films of high temperature superconductors, dielectrics and semiconductors by MOCVD 22 p3148 N90-27851
Localization effects in radiationally disordered high-temperature superconductors: Theoretical interpretation 22 p3148 N90-27853
Coupled bipolarons and optical phonons as a model for high-T(sub c) superconductors
22 p3149 N90-27854
Electron energy spectrum and magnetic interactions in high-T(sub c) superconductors 22 p3149 N90-27857
Crystal chemical and quantum chemical studies of Ba(Sr)-Nb oxide compounds 22 p3150 N90-27858
XES studies of density of states of high temperature superconductors 22 p3150 N90-27859
The relation between ferroelasticity and superconductivity 22 p3150 N90-27861
Study of the superconducting properties of the Bi-Ca-Sr-Cu-O system 22 p3151 N90-27866
Magnetic properties of the 110K superconducting phase in Pb-doped Bi-Sr-Ca-Cu-O thin films
22 p3151 N90-27868
In Situ deposition of YBCO high-T(sub c) superconducting thin films by MOCVD and PE-MOCVD
22 p3152 N90-27871
Analysis of microstrip lines with alternative implementation of conductors and superconductors
[NASA-TM-103182] 22 p3167 N90-27966
High T(sub c) copper-oxide superconductors
[AD-D014483] 22 p3247 N90-28416
Synthesis and structural chemistry of Au(III)-substituted Ba2YCu3O(7-delta)
[NASA-TM-103292] 23 p3305 N90-28696
Electron microscopy of transition-metal doped BiCaSrCuO
[DE90-014184] 23 p3398 N90-29202
XANES and EXAFS study of Au-substituted YBa2Cu3O(7-delta)
[NASA-TM-103291] 23 p3401 N90-29219
Investigation of YBa2Cu3O(7-sigma) by NMR and construction of an ultra low temperature cryostat
24 p3550 N90-30088
Practical superconductor development for electrical power applications
[DE90-014836] 24 p3554 N90-30109
Superconductivity and information exchange
[DE90-015767] 24 p3554 N90-30110
Workshop on Low-Dimensional Quantum Field Theory and its Applications
[DE90-508071] 24 p3555 N90-30118

HIGH TEMPERATURE TESTS

Total hemispherical emittance measured at high temperatures by the calorimetric method
[NASA-TM-102322] 01 p0054 N90-10309
Liquid infiltrated C/SiC: An alternative material for hot space structures 02 p0182 N90-11030
Static tensile and tensile creep testing of four boron nitride coated ceramic fibers at elevated temperatures
[NASA-CR-184999] 03 p0318 N90-11807
A new test machine for measuring friction and wear in controlled atmospheres to 1200 C
[NASA-TM-102405] 04 p0486 N90-12670
Thermal characteristics of power MOS-FETS. Results obtained with the IRF-250 10 p1330 N90-17688
Biaxial strength and stress rupture of hot-pressed silicon nitride
[AD-A216950] 11 p1519 N90-18750
Mechanical properties of pure nickel alloys after long term exposures to LiOH and vacuum at 775 K
[NASA-TM-102403] 13 p1774 N90-20181
Performance of Y-TZP materials between 800 C and 1200 C
[AD-A217723] 13 p1897 N90-20890
Uncertainty evaluation in an automated high temperature environmental simulation oven
[REPT-892-430-103] 16 p2203 N90-22571
Qualification test rationale for measuring the resistance of equipment to pyrotechnic shock
[REPT-892-430-117] 16 p2207 N90-22590
Investigation of metal processing technology
[AD-A218835] 17 p2376 N90-23531
High temperature microhardness tester
[AD-A219567] 17 p2380 N90-23553
Study of ball bearings for space use
18 p2537 N90-24477
High-temperature test facility at the NASA Lewis engine components research laboratory
[NASA-TM-103143] 19 p2662 N90-25151
High-temperature materials. Coating, welding, and service tests
[VTT-RR-645] 19 p2675 N90-25214
High temperature multiaxiale creep testing of Nimonic 115
[RAE-TM-P-1182] 20 p2835 N90-26122
Ascertaining the fracture toughness of ceramic materials by means of bending testpieces of various notch types at ambient and high temperatures
[ESA-TT-992] 23 p3312 N90-28733

HIGH VACUUM

Determination of neutral particle concentration at erosion laser plasma expansion into vacuum
[DE89-620128] 02 p0228 N90-11308
KIVA reactive hydrodynamics code applied to detonations in high vacuum
[DE89-016979] 03 p0346 N90-11974
Thermal environmental tests on space simulation chamber
[DE90-000927] 06 p0729 N90-14251
Development of a quadrupole-based Secondary-Ion Mass Spectrometry (SIMS) system at Lewis Research Center
[NASA-TM-102531] 17 p2367 N90-23476

HIGH VOLTAGES

Electrical safety in the high voltage laboratory
[DE90-003026] 08 p1060 N90-16130
Low noise, high voltage supply for carcinotron backward wave oscillators 10 p1338 N90-17742
Intrinsic properties of high voltage wires that may cause sporadic discharges in space vacuum
10 p1338 N90-17743
Analysis and design of a HV dc/dc series resonant converter using a multi-stage voltage multiplier
10 p1338 N90-17746
Outline of high voltage solar array experiment using SFU platform 10 p1345 N90-17801
Solar arrays in the LEO-plasma environment: A model for leakage current phenomena deduced from experimental and theoretical studies
10 p1345 N90-17802
Micrometeoroid impacts on silver bus bar targets at elevated voltages 10 p1346 N90-17805
A new broadband pulsed high voltage monitor
[DE90-006264] 11 p1502 N90-18651
Lightning protection apparatus for RF equipment and the like
[AD-D014336] 12 p1650 N90-19483
High voltage pickup plate
[LINO-1989-3] 12 p1654 N90-19510
Measurements of the interaction of high-voltage biassed conductors with the ionosphere
[AD-A218285] 13 p1843 N90-20580
Evaluation of a prototype lighted ball marker for powerline obstructions
[DOT/FAA/CT-TN90/12] 15 p2055 N90-21774

Conceptual definition of a high voltage power supply test facility
[NASA-CR-185216] 19 p2666 N90-25172
A gas-phase high voltage electrical isolator with controlled breakdown
[RAE-TR-78030] 19 p2669 N90-25180
LEO high voltage solar array arcing response model, continuation 5
[NASA-CR-186505] 19 p2709 N90-25418
On travelling-wave-based protection of high-voltage networks
[ISBN-90-9002955-9] 20 p2858 N90-26260
Direct drive robotic hand
[NASA-CASE-NPO-17917-1-CU] 20 p2872 N90-26339
A 6.4 kV pulse generator with transformers
[DIGEL-1989-1] 21 p3002 N90-27063
L-SWITCH: A PC-program for computing transient voltages and currents during switching off three-phase inductances
[PB90-191412] 22 p3167 N90-27961
PBFA 2 applied B ion diode beam characteristics at high voltages
[DE90-014419] 23 p3396 N90-29190
High voltage picosecond pulse generation using avalanche diodes
[DE90-015194] 24 p3465 N90-29577

HIGHER ORDER LANGUAGES
U HIGH LEVEL LANGUAGES

HIGHLANDS
Multisensor monitoring of deforestation in the Guinea Highlands of West Africa
[NASA-CR-186709] 19 p2706 N90-25396

HIGHWAYS
GRAFIN: GRAFIX interactive manual
[PB89-232136] 06 p0827 N90-14809

HIJACKING
U AIR PIRACY

HILBERT SPACE
NT SOBOLEV SPACE
Numerical optimization in Hilbert space using inexact function and gradient evaluations
[NASA-CR-181926] 01 p0112 N90-10640
Periodic solutions of spatially periodic Hamiltonian systems
[AD-A210645] 01 p0113 N90-10649
D=3 Chern-Simons action, supergravity and quantization
[DE89-617530] 01 p0134 N90-10775
S7 without any construction of Lie group
[DE89-618380] 02 p0269 N90-11539
Markov processes in Hilbert space and continuous spontaneous localization of systems of identical particles
[DE89-618396] 02 p0270 N90-11540
Well posedness of triples of operators (in the sense of linear systems theory)
[TW-292] 04 p0545 N90-13168
On the sum of two maximal monotone operators
[REPT-89-31] 07 p0982 N90-15669
General many-body systems
[DE90-000685] 07 p0982 N90-15670
On functional integral representations in the lower Hubbard band based on generalized coherent states
[DE90-602936] 07 p1003 N90-15804
On gauge fixing and quantization of constrained Hamiltonian systems
[DE90-600732] 08 p1135 N90-16574
Approximation method for nonlinear integral equations of Hammerstein type
[DE90-600727] 09 p1272 N90-17372
Asymptotic behaviour of solutions of a degenerate quasilinear hyperbolic equation
[DE89-635713] 09 p1276 N90-17400
On mean value iterations with application to variational inequality problems
[DE90-005556] 10 p1422 N90-18200
Fixed points by Ishikawa iterations
[DE90-005557] 10 p1424 N90-18219
Iteration methods for solving nonlinear equations in Frechet spaces
[DE90-610429] 12 p1706 N90-19799
Linearized analysis of (2+1)-dimensional Einstein-Maxwell theory
[DE90-741470] 12 p1725 N90-19913
An approximation theory for the identification of linear thermoelastic systems
[NASA-CR-182015] 13 p1877 N90-20764
Local moduli of continuity of some classes of Gaussian processes
[AD-A217692] 13 p1879 N90-20778
A monotone complementarity problem in Hilbert space
[DE90-009755] 14 p2022 N90-21590
Quantization of the N = 2m simple supergravity in d = 2 + 1
[DE90-612765] 14 p2034 N90-21671
A generalized complementarity problem in Hilbert space
[DE90-009576] 15 p2163 N90-22360
Estimation of Hilbert space valued parameters by the method of sieves
[AD-A218565] 16 p2306 N90-23143
A monotone complementarity problem in Hilbert space
[AD-A220819] 17 p2468 N90-24105
Stability and error estimates for sinc interpolation
[CWI-AM-R8914] 18 p2599 N90-24790
Multi-Hilbertian spaces and their duals
[AD-A222344] 21 p3064 N90-27421
Accurate quantum chemical calculations
[NASA-TM-101932] 23 p3303 N90-28680
Old and new ideas in the theory of quantum measurement
[DE90-627181] 23 p3403 N90-29229
An error estimate for Tremolieres method for the discretization of parabolic variational inequalities
[DE90-627169] 24 p3541 N90-30024
Introductory lectures on conformal field theory and strings
[DE90-627219] 24 p3556 N90-30120

HILBERT TRANSFORMATION
Analytic signals in the damping coefficient estimation 02 p0178 N90-11003
Inf-convolution splines
[IMAG-RR-749-M] 03 p0395 N90-12256
Asymptotic law of the orthogonal empirical functions and applications, part 2
[IMAG-RR-792-M-PT-2] 20 p2918 N90-26605
Alternative solutions for Hilbert filtering in a pulse compression radar
[FEL-89-C226] 22 p3165 N90-27950

HILL CURVES
U HILL METHOD

HILL METHOD
Stability and stability sensitivity by periodically time dependent systems: Hill versus Floquet
[ILR-MITT-221(1989)] 17 p2463 N90-24071

HILLER MILITARY AIRCRAFT
U MILITARY AIRCRAFT

HINDRANCE
U CONSTRAINTS

HINGE MOMENTS
U TORQUE

HINGED ROTOR BLADES
U HINGES
U ROTARY WINGS

HINGELESS ROTORS
U RIGID ROTORS

HINGES
The third generation rigid solar array GSR3 02 p0180 N90-11017
Effect of unshielded and shielded horn balances on hinge moment coefficients for controls at low speeds
[ESDU-89003-A] 06 p0726 N90-14238
Hinge moment coefficient derivatives for trailing-edge controls on wings at subsonic speeds
[ESDU-89009] 06 p0726 N90-14239
Example of procedure in calculation of control hinge moments
[ESDU-89010] 06 p0727 N90-14240
The GSR3: A new approach for solar array deployments 10 p1340 N90-17762
Development of the CLAES instrument aperture door system 15 p2112 N90-22083
Dynamic analysis of flexible mechanical systems using LATDYN 16 p2296 N90-23080
ADELE: Deployment hinge using wraparound strips 18 p2538 N90-24485
Some remarks on a hinge actuator for large spot antenna arm deployers 18 p2539 N90-24486
Hitching mechanism for lunar dump train
[NASA-CR-183034] 19 p2697 N90-25344

HIP (PROCESS)
U HOT ISOSTATIC PRESSING

HIPPARCOS SATELLITE
Aeritalia Space Systems Group, Turin, Italy
[EOARD-LR-89-041] 02 p0159 N90-10908
Report on ESA's scientific satellites
[ESA-SP-1110] 04 p0463 N90-12649
The Hipparcos Mission. Prelaunch status. Volume 1: The Hipparcos satellite
[ESA-SP-1111-VOL-1] 05 p0603 N90-13499
Operating principle 05 p0603 N90-13500
Overview of the Hipparcos satellite 05 p0603 N90-13502
Overview of the Hipparcos payload 05 p0603 N90-13503
The telescope mirrors 05 p0603 N90-13504
Payload thermal control 05 p0604 N90-13511
The spacecraft structure 05 p0604 N90-13512
Spacecraft thermal control 05 p0604 N90-13513
Data handling and telecommunications 05 p0604 N90-13514
The attitude and orbit control system 05 p0605 N90-13516
The apogee boost motor 05 p0605 N90-13517
On-board software 05 p0605 N90-13518
Assembly, integration, and verification 05 p0605 N90-13519
Mechanical and thermal testing 05 p0605 N90-13521
Product assurance 05 p0605 N90-13522
On-ground photometric calibration 05 p0605 N90-13523
Launch and early orbit 05 p0606 N90-13524
The in-orbit initialization phase 05 p0606 N90-13525
The role of the ground segment 05 p0606 N90-13527
The interface with the data reduction consortia 05 p0606 N90-13528
The Hipparcos Mission. Prelaunch status. Volume 2: The input catalog
[ESA-SP-1111-VOL-2] 05 p0608 N90-13529
From scientific proposals to the Inca data base 05 p0606 N90-13530
The Inca data base 05 p0607 N90-13531
Mission simulations 05 p0607 N90-13532
Proximity effects on adjacent and multiple stars 05 p0607 N90-13533
Successive iterations of the input catalog 05 p0607 N90-13534
Ground-based astrometric measurements 05 p0607 N90-13536
The compilation of astrometric data 05 p0607 N90-13537
New ground-based photometric measurements 05 p0607 N90-13538
Standard stars and photometric calibration 05 p0607 N90-13539
Double stars 05 p0608 N90-13540
Variable stars 05 p0608 N90-13541
The choice of stars in open clusters 05 p0608 N90-13542
The choice of stars in the Magellanic clouds 05 p0608 N90-13543
The link to extragalactic objects 05 p0608 N90-13544
Minor planets and other solar system objects 05 p0608 N90-13545
The catalogs produced by the Inca consortium 05 p0608 N90-13546
The Hipparcos Mission. Prelaunch status. Volume 3: The data reductions
[ESA-SP-1111-VOL-3] 05 p0609 N90-13548
Validation of the Hipparcos catalog 05 p0611 N90-13564
Linking Hipparcos to a quasi-inertial system 05 p0611 N90-13565
Accuracy and characteristics of the Hipparcos catalog 05 p0611 N90-13566
The first-look data analysis at Utrecht 05 p0612 N90-13571
Modeling of the Hipparcos optical system 05 p0612 N90-13572
Signature objects: Preliminaries for the satellite project HIPPARCOS/TYCHO
[ETN-90-95730] 12 p1729 N90-19934
ESA's report to the 28th COSPAR meeting
[ESA-SP-1124] 24 p3560 N90-30141

HISS
A survey of equatorial magnetospheric wave activity between 5 and 8 R(sub E)
[AD-A220137] 17 p2424 N90-23812

HISTOCHEMICAL ANALYSIS
Experiment K-6-03. Gravity and skeletal growth, part 1. Part 2: Morphology and histochemistry of bone cells and vasculature of the tibia; Part 3: Nuclear volume analysis of osteoblast histogenesis in periodontal ligament cells; Part 4: Intervertebral disc swelling pressure associated with microgravity 20 p2892 N90-26457
Experiment K-6-08. Biochemical and histochemical observations of vastus medialis 20 p2893 N90-26462

HISTOLOGY
The investigation of particulate matter in the lungs of smoke inhalation death victims 10 p1317 N90-17617
The effects of blast trauma (impulse noise) on hearing: A parametric study source 2
[AD-A221731] 21 p3035 N90-27253

HISTORIES
NT CASE HISTORIES
Encyclopedia of US Air Force aircraft and missile systems. Volume 2: Post-World War 2 bombers, 1945-1973
[AD-A209273] 01 p0001 N90-10001

Flight testing and flight research: From the age of the tower jumper to the age of the astronaut
02 p0154 N90-10882
The astronomy of Andean myth: The history of a cosmology
02 p0291 N90-11660
A history of West European rocketry and space research
[AD-A211191] 02 p0297 N90-11690
The fuel cell in space: Yesterday, today and tomorrow
[NASA-TM-102366] 03 p0318 N90-11804
LFC: A maturing concept
[DOUGLAS-PAPER-7878] 04 p0438 N90-12505
Current launch vehicle reliability practice and data base assessment. Volume 1: Executive summary and report body
[AD-A213600] 07 p0885 N90-15121
Fatigue loading history reconstruction based on the rain-flow technique
[NASA-CR-181942] 07 p0947 N90-15482
Understanding developments in computer technology: A pragmatic and synthetic interpretation
07 p0971 N90-15608
The NASA Langley 0.3-meter transonic cryogenic tunnel
08 p1028 N90-15941
A foundation for the design of an astronautics specification system based on dynamic motivation analysis
[ILR-MITT-220] 08 p1033 N90-15969
The development of over-the-horizon radar in Australia
[ISBN-0-642-13561-4] 08 p1055 N90-16099
Transistor and solid-state technology: A historical development
[AD-A218141] 13 p1798 N90-20317
Terrestrial gravity instrumentation in the 20th Century: A brief review
13 p1834 N90-20527
History of visual systems in the Systems Engineering Simulator
13 p1862 N90-20681
The anatomy of the gyroscope, part 3
[AGARD-AG-313] 14 p1982 N90-21359
Space Station Freedom media handbook
[NASA-TM-102901] 17 p2364 N90-23460
On the early history of intuitionistic logic
[ITLI-LP-89-04] 17 p2440 N90-23900
The lessons of Varsovian's reconnaissance
[NASA-TM-103207] 20 p2951 N90-26789
The aims and history of adaptive wall wind tunnels
21 p2962 N90-26839
A historical supernova's lower limit to the galactic stellar-collapse rate
[FERMILAB-PUB-90/24-A] 22 p3262 N90-28472
A look at tomorrow today
23 p3273 N90-28524
Textual regularities applicable to full text searching: The case of family history literature
24 p3557 N90-30125

HLLV
U HEAVY LIFT LAUNCH VEHICLES

HMX
Effects of binder concentration on the properties of plastic-bonded explosives
[DE89-007744] 01 p0053 N90-10301
Particle size effects in the initiation of explosives containing reactive and nonreactive continuous phases
[DE90-000786] 06 p0754 N90-14390
Using small scale tests to estimate the failure diameter of a propellant
[DE90-001166] 07 p0913 N90-15281
Burning rates of two cast nitramine explosives using a hybrid closed bomb-strand burner
[DE90-002785] 07 p0914 N90-15286
Spectral studies of solid propellant combustion. 2: Emission and absorption results for M-30 and HMX1 propellants
[AD-A213857] 07 p0915 N90-15292
Ignition of HMX (cyclotetramethylenetetranitramine) using low energy laser diodes
[DE90-007637] 12 p1624 N90-19334
Condensed phase kinetic deuterium isotope effects in high energy phenomena: Mechanistic investigations and relationships
[AD-A217161] 13 p1770 N90-20156
Temperature measurements through a solid-propellant combustion wave using imbedded fine wire thermocouples
[AD-A218642] 16 p2225 N90-22693
Nitramine composite solid propellant modelling
[AD-A220198] 17 p2383 N90-23573
Study of the induction time in isothermal decomposition of explosives
[DE90-014906] 23 p3315 N90-28745
The optimum polymer binder for pressable high performance explosives: A preliminary evaluation
[ETN-90-97612] 24 p3457 N90-29524

HNST
U HEXANITROSTILBENE

HODOGRAPHS
Crack problems for elastic-plastic materials under antiplane shear loadings
06 p0799 N90-14651

HOGBACKS
U RIDGES

HOHLRAUMS
Total hemispherical emittance measured at high temperatures by the calorimetric method
[NASA-TM-102322] 01 p0054 N90-10309

HOHMANN TRAJECTORIES
U ELLIPTICAL ORBITS
U TRANSFER ORBITS

HOHMANN TRANSFER ORBITS
U ELLIPTICAL ORBITS
U TRANSFER ORBITS

HOLDERS
New tool-holding concept
[DE90-000880] 06 p0794 N90-14624
Ignitability test method and apparatus
[NASA-CASE-LAR-13996-1-SB]
07 p0893 N90-15161
Gripping device
[NASA-CASE-MSC-21365-1] 13 p1812 N90-20408
Sample holder support for microscopes
[NASA-CASE-MFS-28420-1] 21 p3010 N90-27113

HOLE BURNING
Temperature dependence of photon-gated persistent spectral hole-burning for the meso-tetra-p-tolyl Zn-tetrabenzoporphyrin/chloroform system in poly(methylmethacrylate)
[AD-A216086] 11 p1482 N90-18531
Persistant spectral hole-burning: Photon-gating and fundamental statistical limits
[AD-A216084] 11 p1501 N90-18640
Cloud hole-boring with infrared lasers: Theory and experiment
[DE90-006519] 11 p1515 N90-18723

HOLE MOBILITY
Transport properties of thermally grown Cr2O3
[DE89-016703] 02 p0284 N90-11623

HOLES (ELECTRON DEFICIENCIES)
Trap gettering by isoelectronic doping of p-GaAs and n-GaAs grown by molecular beam epitaxy
[AD-A211162] 01 p0133 N90-10769
Quantitative interpretation of auger lineshapes and electron/photon stimulated desorption
[AD-A211550] 03 p0324 N90-11842
Energy relaxation of light holes in InAs(.15)Sb(.85)/InSb multiple quantum wells
[DE89-016035] 03 p0409 N90-12349
Local pairing and antiferromagnetism in high-T sub c superconductors
[AD-A213004] 05 p0703 N90-14113
Linear electron-hole-electron pair model of high-temperature superconductivity in La(2-x)M(x)CuO4 and YBa2Cu3O(7-y): Part 2. Dependence of the superconducting transition temperatures on pressure and on hole concentration
[DE90-003012] 07 p0999 N90-15779
Defect control and denuded trap zones in the 3-5 semiconductors
[AD-A214099] 07 p1004 N90-15814
Chemical-like behavior of electrons and holes in polymeric conductors
[AD-A214496] 09 p1196 N90-16931
Point defects and interfaces in insulating solids
[AD-A214668] 09 p1289 N90-17471
Self-consistant calculation of point and pair structure defects in silicium
[ETN-90-96059] 12 p1722 N90-19891
Positron trapping in semiconductors
[PB90-165606] 15 p2172 N90-22410
Photorefractive damage mechanisms in electro-optic materials
[AD-A219786] 17 p2476 N90-24157
Hot carrier in subpicosecond photoconductive experiments
[AD-A219874] 17 p2477 N90-24166
Quantum-confined hole states in double-barrier resonant tunneling structures
[AD-A221342] 18 p2623 N90-24946
The mechanism of high-T(sub c) superconductivity due to bound hole mediators: Relationship to ferroelectricity
22 p3143 N90-27826
The color of polarization in cuprate superconductors
22 p3144 N90-27830
Spin bipolaron in the framework of emery model for high-T(sub c) copper oxide superconductors
22 p3149 N90-27856
Parity violation and superconductivity in doped Mott insulators
[DE90-627493] 23 p3401 N90-29217

HOLES (MECHANICS)
Influence of hole surface finish, cyclic frequency and spectrum severity on the fatigue behavior of thick section aluminum alloy pin joints
[ARL-STRUC-R-430] 06 p0745 N90-14336
Heat transfer near the entrance to a film cooling hole in a gas turbine blade
[AD-A217396] 13 p1757 N90-20089
Innovative design of composite structures: The use of curvilinear fiber format to improve buckling resistance of composite plates with central circular holes
[NASA-CR-186454] 13 p1766 N90-20135
Innovative design of composite structures: The use of curvilinear fiber format in composite structure design
[NASA-CR-186453] 13 p1766 N90-20136
Modeling growth of fatigue cracks which originate at rivet holes
18 p2645 N90-25080
Open hole and post-impact compression fatigue of stitched and unstitched carbon/epoxy composites
[NASA-TM-102676] 19 p2701 N90-25370
A finite width plate with a single crack at the edge of a central hole. The K-value of the crack and sigma peak at the other side of the hole
[LR-608] 19 p2704 N90-25386
A comparison of the post-buckling behavior of metallic and composite plates with centrally located cutouts
[NIAR-90-14] 20 p2875 N90-26356
A technique for rapid inspection of composite aircraft structure for impact damage
22 p3185 N90-28077
Progress in the detection of cracks under installed fasteners using eddy currents
22 p3186 N90-28081

HOLLAND
U NETHERLANDS

HOLLOW CATHODES
Hollow-cathode experiments to support electrodynamic tether applications
[IFSI-89-5] 08 p1036 N90-15986
Advanced electric propulsion research, 1989
[NASA-CR-185237] 15 p2062 N90-21810
Hollow cathode operation at high discharge currents
[NASA-CR-185238] 15 p2088 N90-21953
Plasma contactor research, 1989
[NASA-CR-185212] 15 p2168 N90-22389
Requirements for long-life operation of inert gas hollow cathodes: Preliminary report
[NASA-TM-103242] 22 p3134 N90-27783

HOLMIUM
Resistivity measurements of superconducting materials
[PB89-225700] 04 p0496 N90-12856
A (mu)SR-investigation of the mixed state of the high-Tc superconductor HoBa2Cu3O7-delta
[DE90-620802] 16 p2322 N90-23241
In-situ processing of epitaxial and textured high (Tc) superconducting HoBa2Cu3O(7-x) thin films by pulsed laser evaporation technique
[DE90-009828] 17 p2474 N90-24148
Characterization of a Ho:Tm:Cr:YAG laser with a Cr:GSAG laser as pumping source
18 p2642 N90-25047

HOLOGRAMMETRY
A numerical simulation of the quasi-heterodyne technique for double-pulsed holographic vibration measurements
[PNR90622] 20 p2865 N90-26301

HOLOGRAPHIC INTERFEROMETRY
The investigation of the fundamental limits of heterodyne holographic interferometry with the application of imaging laser generated lamb waves
[AD-A211048] 02 p0224 N90-11285
Materials characterization using holographic mapping of transient lamb waves
[AD-A211414] 03 p0358 N90-12050
Quantative interferometry
08 p1078 N90-16237
Nondestructive control of composite materials by holographic interferometry
[ISL-CO-244/88] 09 p1188 N90-16882
Development of interferometric and holographic techniques in fluid mechanics
[ISL-CO-227/88] 09 p1218 N90-17068
Non-Fourier computer generated holography for 3-D display
[AD-A215369] 09 p1225 N90-17109
Self compensation of rigid displacements in holographic interferometry
[ISL-CO-219/88] 09 p1226 N90-17113
Eccentricity effects of square cutouts on the natural frequencies and mode shapes of curved rectangular composite panels
[AD-A216410] 10 p1350 N90-17831
Full field visualization of surface and bulk acoustic waves using heterodyne holographic interferometry
[AD-A214353] 10 p1387 N90-18023
Production of diffraction gratings using holographic interferometry
[DE90-612841] 14 p1983 N90-21362

Practical developments in holographic interferometry
[PNR90669] 20 p2866 N90-26302
Holography and holographic interferometry
[PNR90670] 20 p2866 N90-26303
Coherent optical techniques for industrial inspection
[PNR90605] 20 p2927 N90-26654

HOLOGRAPHIC SUBTRACTION
Reduced size holography
[PREPRINT-707] 16 p2239 N90-22771

HOLOGRAPHY
NT ACOUSTICAL HOLOGRAPHY
NT WHITE LIGHT HOLOGRAPHY
Optical processing for distributed sensors in control of flexible spacecraft 01 p0021 N90-10102
Materials characterization using holographic mapping of transient lamb waves
[AD-A211414] 03 p0358 N90-12050
Real-time sensing of optical alignment
05 p0599 N90-13479
Soft x ray microscope using Fourier transform holography
[DE90-002291] 06 p0781 N90-14539
Radiation damage and its influence on source requirements for high resolution x ray holography
[DE90-002508] 06 p0781 N90-14540
The development of coherent x ray lasers for x ray holography
[DE90-000784] 06 p0789 N90-14595
Non-Fourier computer generated holography for 3-D display
[AD-A215369] 09 p1225 N90-17109
Studies of optical matrix multiplication and reconfigurable optical interconnect concepts
[AD-A214645] 09 p1281 N90-17427
Inspection of carbon/epoxy and aluminum honeycomb paraboloidal components by HNDT
[AD-A216796] 11 p1479 N90-18514
Problems of the micro-holographic image analysis
[ISL-CO-201/89] 11 p1511 N90-18704
Computational and visible light experiments for x ray laser holography
[DE90-006774] 11 p1512 N90-18707
Cinehology: A relation between the coherence length of the laser and the object velocity
[ISL-CO-234/88] 11 p1515 N90-18724
X ray microimaging by diffractive techniques
[DE90-008444] 13 p1804 N90-20356
Simple reflection holography
[DE90-008309] 13 p1805 N90-20359
Method for holographic correction of beams of coherent light
[AD-D014406] 14 p1981 N90-21353
Phase-only holographic filters and their applications
[PB90-166802] 14 p1984 N90-21368
Holocinematography for studies of turbulent multiphase flow
[AD-A219130] 16 p2237 N90-22765
Reduced size holography
[PREPRINT-707] 16 p2239 N90-22771
High performance holographic elements and media
[AD-A218999] 16 p2239 N90-22775
Hybrid diffractive-refractive telescope
[AD-A219241] 16 p2318 N90-23216
Implementation of image action plus software for image analysis of solid propellant combustion holograms
[AD-A219644] 17 p2372 N90-23508
Isoplanatic systems in mesooptics
[DE90-009785] 17 p2406 N90-23705
Multiple beam optical processing
[AD-A219048] 17 p2471 N90-24129
Optical computing strategies
[AD-A219433] 17 p2472 N90-24131
Use of the Xybion ISG-camera in the RETRA-1000 TV-Holography unit
[AD-A219842] 18 p2554 N90-24577
A numerical simulation of the quasi-heterodyne technique for double-pulsed holographic vibration measurements
[PNR90622] 20 p2865 N90-26301
Holography and holographic interferometry
[PNR90670] 20 p2866 N90-26303
Optical wavefront computer for stabilizing large space structures
[AD-A221707] 21 p2967 N90-26866
Two-dimensional signal processing and storage, and theory and applications of electromagnetic measurements
[AD-A222984] 21 p2995 N90-27022
Structural and optical properties of DMP-128 holograms during environmental testing
[AD-A221691] 21 p3007 N90-27094
Tracking a head-mounted display in a room-sized environment with head-mounted cameras
[AD-A222545] 21 p3037 N90-27266
All-optical photochromic spatial light modulators based on photoinduced electron transfer in rigid matrices
[NASA-CASE-NPO-17612-1-CU]
21 p3076 N90-27487
Compact 4-D optical neural network architecture
[AD-A222160] 22 p3241 N90-28379
Photoinduced and holographically reinforced light diffusion in electrooptic crystals
[ETN-90-97321] 24 p3547 N90-30060

HOLOMORPHISM
U ANALYTIC FUNCTIONS

HOMEOSTASIS
Effect of low air velocities on thermal homeostasis and comfort during exercise at space station operational temperature and humidity 18 p2628 N90-24975
Fluid and electrolyte homeostasis during spaceflight: Elucidation of mechanisms in a primate
[NASA-CR-177548] 23 p3378 N90-29085

HOMING
Suboptimal period design for a maneuvering missile to evade tracking filters 12 p1650 N90-19479
A homing missile guidance law based on new target maneuver models
[AD-A220392] 17 p2356 N90-23410
A passive homing missile guidance law based on new target maneuver models
[AD-A220419] 17 p2356 N90-23411

HOMING DEVICES
Alternative polar homing strategies
01 p0013 N90-10059
The Swedish defense research needs: For surveillance and seeker applications
[FOA-C-30520-3.3] 02 p0298 N90-11691
Activities of the division of surveillance and seeker systems
[FOA-C-30549] 19 p2684 N90-25269

HOMODYNE RECEPTION
A dual-wavelength passive homodyne detection unit for fiber-coupled white-light interferometers
[ETN-90-97036] 20 p2927 N90-26653

HOMOGENEITY
The rewrite rule machine project
[AD-A210528] 01 p0109 N90-10617
Homogeneous gravitational fields and limits of gravitational fields 01 p0141 N90-10812
An extension of Cochran's test for homogeneity of variances
[AD-A211054] 02 p0269 N90-11534
Atmospheric horizontal-inhomogeneity effects on the optical depths determined by the double-elevation-angle lidar technique
[AD-A212836] 04 p0493 N90-12839
Numerical analysis of scattering by interface flaws
[AD-A212996] 05 p0654 N90-13810
Evaluation of material homogeneity as a function of thickness of low-alloy ferritic steel
[DE90-008069] 13 p1777 N90-20202
Methods for evaluation of thermally induced reactions in liquid propellants
[AD-A218750] 16 p2225 N90-22694
Estimation of noise field directionality: Comparison with Fourier series method
[AD-A220366] 17 p2469 N90-24114
G2-continuity in homogeneous co-ordinates
[MATHS-REPT-A-110] 20 p2917 N90-26599

HOMOGENEOUS TURBULENCE
Application of two-point closures to subgrid scale modeling for homogeneous, 3D turbulence
05 p0640 N90-13732
Large eddy simulation of homogeneous turbulence undergoing shear and thermal gradients. Application to one point closing models
[ECL-88-23] 05 p0643 N90-13754
The analysis and modeling of dilatational terms in compressible turbulence
[NASA-CR-181959] 06 p0776 N90-14513
Modeling the pressure-strain correlation of turbulence: An invariant dynamical systems approach
[NASA-CR-181979] 10 p1383 N90-18003
Analytical methods for the development of Reynolds stress closures in turbulence
[NASA-CR-182017] 12 p1660 N90-19538
Turbulence and complex systems
[ETN-90-96620] 16 p2236 N90-22758
A theoretical study of flow structure and radiation for multiphase turbulent diffusion flames
[AD-A222934] 21 p2976 N90-26913
Experimental study of homogeneous turbulence under rotation and deformation modes
[ONERA-RSF-12/1145-AY-170A]
22 p3176 N90-28023
Experimental study of the effects of rotation on the homogeneous turbulence. Comparison with the EDQNM model
[ONERA-RSF-11/1145-AY-166A]
22 p3176 N90-28025

HOMOGENIZATION
U HOMOGENIZING

HOMOGENIZING
High-order mixture homogenization of fiber-reinforced composites
[AD-A215247] 09 p1187 N90-16876
High-order mixture homogenization of periodic nonlinear composites 10 p1347 N90-17814

HOMOJUNCTIONS
On-orbit results of the LIPS 3/InP homojunction solar cell experiment 10 p1344 N90-17794

HOMOLOGY
Reparametrization BRS cohomology in two-dimensional gravity and non-critical string theories
[DE90-741468] 12 p1725 N90-19911
Projective cohomology over a chain complex
[DE90-606958] 13 p1880 N90-20788

HOMOMORPHISMS
NT AUTOMORPHISMS
NT SUBGROUPS
Modular specifications in process algebra with curious queues
[CWI-CS-R8821] 04 p0543 N90-13152
Note on p-semisimple BCI-algebras
[DE90-606955] 10 p1423 N90-18206
Factoring homomorphisms
[CS-8908] 16 p2299 N90-23096
Processes and formalisms for unbounded choice
[CS-8917] 16 p2305 N90-23135
An algebric approach to infinite data structures
[CS-8909] 16 p2327 N90-23265
Hyperbolic Hjelmslev groups
[ETN-90-97298] 24 p3538 N90-30009

HOMOPOLAR GENERATORS
ARDEC (Armament Research, Development and Engineering Center) electric gun in-house test program
[AD-A217337] 13 p1760 N90-20105

HOMOTOPY THEORY
Finding isolated zero points of complex polynomial mappings
[DE89-617523] 01 p0111 N90-10633
A homotopy approach to the solutions of minimum-fuel space-flight rendezvous problems
14 p1931 N90-21053
H2, fixed architecture, control design for large scale systems
[NASA-CR-180471] 16 p2226 N90-22698
Combined control-structure optimization
16 p2282 N90-23005
Disjoint homotopic paths and trees in a planar graph
[CWI-BS-R8923] 17 p2462 N90-24062

HONEYCOMB CORES
Axial compression buckling test on the H-2 launch vehicle satellite fairing structural element prototype (aluminum surface plate/aluminum honeycomb sandwiched curved surface plate)
[NAL-TM-563] 03 p0356 N90-12039
Stress analysis and minimum weight design of honeycomb sandwich plates 14 p1992 N90-21418
An examination of impact damage in glass-phenolic and aluminum honeycomb core composite panels
[NASA-TP-3042] 22 p3153 N90-27876
Parametric studies of acoustic duct attenuation ofperforated-plate-on-honeycomb absorber
[NAL-TM-603] 24 p3542 N90-30030

HONEYCOMB STRUCTURES
NT HONEYCOMB CORES
The high-frequency dielectric properties of glass fibre reinforced plastic and honeycomb layers
[AD-A210581] 01 p0051 N90-10289
Low-energy impact resistance of graphite-epoxy plates and ALS honeycomb sandwich panels
12 p1637 N90-19405
Stress analysis and minimum weight design of honeycomb sandwich plates 14 p1992 N90-21418
Accuracy of the QUAD4 thick shell element
18 p2569 N90-24641
Development of ceramic fiber type combustor: Improvement of combustor and combustion test results
[DE90-503441] 20 p2839 N90-26148
Manufacturing and mechanical properties of new textile fiber preforms for structural sandwich applications
[MBB-Z-0296-90-PUB] 21 p2972 N90-26895
Development of an automated ultrasonic inspection system for composite structure on in-service aircraft
22 p3186 N90-28079
A low cost shadow moire device for the nondestructive evaluation of impact damage in composite laminates
[AD-A223451] 24 p3443 N90-29442

HOOKS
Lunar crane hook
[NASA-CR-184921] 17 p2384 N90-23579

HOOP COLUMN ANTENNAS
A study on the sensitivity and simultaneous adjustment of a hoop-column antenna surface
[NASA-TM-101538] 05 p0653 N90-13807

HORIZONTAL BRANCH STARS
The evolution of horizontal branch stars and the calibration of globular cluster ages
24 p3562 N90-30152
HORIZONTAL FLIGHT
Three-dimensional viscous rotor flow calculations using a viscous-inviscid interaction approach
[NASA-TM-102235] 12 p1599 N90-19204
Velocity measurements on a lifting rotor/airframe configuration in low speed forward flight
21 p2953 N90-26790
HORIZONTAL POLARIZED SHEAR WAVES
U SH WAVES
HORIZONTAL STABILIZERS
U STABILIZERS (FLUID DYNAMICS)
HORIZONTAL TAIL SURFACES
Validation of a computer code for analysis of subsonic aerodynamic performance of wings with flaps in combination with a canard or horizontal tail and an application to optimization
[NASA-TP-2961] 06 p0717 N90-14187
Installed tailplane lift-curve slope at subsonic speeds
[ESDU-89029] 07 p0876 N90-15081
HORIZONTALLY POLARIZED SHEAR WAVES
U SH WAVES
HORMONES
NT CORTICOSTEROIDS
NT PITUITARY HORMONES
NT PROSTAGLANDINS
Cardiovascular, renal, electrolyte, and hormonal changes in man during gravitational stress, weightlessness, and simulated weightlessness: Lower body positive pressure applied by the antigravity suit
[NASA-TM-102232] 04 p0522 N90-13013
Effects of microgravity on growth hormone concentration and distribution in plants 05 p0678 N90-13947
Peripheral nervous velocity of conduction in fighter pilots 09 p1256 N9C-17287
Alterations in the metabolic and sympathetic response to cold exposure after cold air acclimation
[AD-A216817] 10 p1412 N90-18144
The effects of high intensity cycle exercise on sympatho-adrenal-medullary response patterns
[AD-A217962] 13 p1852 N90-20628
Experiment K-6-20. The effect of spaceflight on pituitary oxytocin and vasopressin content of rats
20 p2896 N90-26473
HORN ANTENNAS
Nonprincipal-plane scattering from flat plates: Second-order and corner diffraction and pattern control of horn antennas
[NASA-CR-185485] 02 p0211 N90-11205
Part B: Pattern control of horn antennas
02 p0211 N90-11207
Scattering from coated structures and antenna pattern control using impedance surfaces, part A/B
[NASA-CR-186871] 20 p2854 N90-26233
Departures from plane-wave-like coupling to a Maverick missile in the radiating near-field region of a horn antenna
[AD-A222539] 21 p2997 N90-27035
Near-field gain of pyramidal horns from 18 to 40 GHz
[PB90-155854] 22 p3164 N90-27941
HORSESHOE VORTICES
Appendage flow computations using the INS3D computer code
[AD-A215689] 09 p1218 N90-17066
Effective methods of controlling a junction vortex system in an incompressible, three-dimensional, turbulent flow
15 p2047 N90-21732
Computations of a horseshoe vortex around an endwall-mounted cylinder 17 p2400 N90-23673
HOSES
Thermodynamic and fluid mechanic analysis of rapid pressurization in a dead-end tube
18 p2631 N90-24990
HOT AIR
U HIGH TEMPERATURE AIR
HOT CORROSION
Effects of hot corrosion on the room temperature strength of structural ceramics
[AD-A212568] 04 p0481 N90-12762
A review of the effects of microalloying constituents on the formation and breakdown of protective oxide scales on high-temperature alloys at temperatures below 700 C
[DE90-001277] 07 p0902 N90-15216
Analysis of propulsive powder combustion products and their corrosive effects
[ISL-CO-248/88] 11 p1495 N90-18605
The oxidation and corrosion of ODS alloys
[NASA-TM-102555] 19 p2675 N90-25211
High temperature surface interactions: Overview
23 p3306 N90-28699
Developments in test procedures for hot-salt corrosion of superalloys 23 p3306 N90-28700
Oxidation, sulfidation, and hot corrosion: Mechanisms and interrelationships 23 p3307 N90-28702
Molten salt induced high temperature degradation of thermal barrier coatings 23 p3307 N90-28704
Evaluation of high temperature protective coatings for gas turbine engines under simulated service conditions
23 p3309 N90-28712
Overview on hot gas tests and molten salt corrosion experiments at the DLR 23 p3309 N90-28714
HOT ELECTRONS
Theoretical and material studies of thin-film electroluminescent devices
[NASA-CR-186104] 06 p0768 N90-14468
Fast electrons in a laser generated plasma
06 p0782 N90-14545
Proof-of-principle experiment for a hot electron pumped XUV amplifier
[DE90-000820] 06 p0787 N90-14586
Subpicosecond Raman study of hot electrons and hot phonons in GaAs
[DE90-015634] 24 p3553 N90-30106
Extended characterization of the damage by hot charge carriers in gate oxide by short channel MOS field effect transistors
[ETN-90-97313] 24 p3555 N90-30114
HOT EXTRUDING
U EXTRUDING
HOT FORMING
U HOT WORKING
HOT GAS SYSTEMS
U HIGH TEMPERATURE GASES
HOT GASES
U HIGH TEMPERATURE GASES
HOT ISOSTATIC PRESSING
Improved process for HIP canning of composites
[NASA-CASE-LEW-14990-1-CU]
07 p0890 N90-15147
Cyclic fatigue of hot-isostatic-pressed silicon nitride
[PB90-122649] 08 p1090 N90-16308
Microstructure and mechanical properties of nickel aluminide powders consolidated by extrusion and hot isostatic pressing
[DE90-009777] 15 p2070 N90-21855
One step HIP canning of powder metallurgy composites
[NASA-CASE-LEW-14719-1] 17 p2370 N90-23493
Processing of advanced ceramics which have potential for use in gas turbine aero engines
[AD-A220988] 19 p2677 N90-25226
Densification studies of refractory materials using Hot Isostatic Pressing (HIP) and tantalum containment
[DE90-013481] 20 p2833 N90-26114
HOT JET EXHAUST
U HIGH TEMPERATURE GASES
U JET EXHAUST
HOT JETS
U JET FLOW
HOT PLASMAS
U HIGH TEMPERATURE PLASMAS
HOT PRESSING
NT HOT ISOSTATIC PRESSING
Processing and characterization of alumina platelet-reinforced mullite composites
[DE90-000057] 03 p0320 N90-11814
Photolithography: A new tool for ceramic science
[DE90-000135] 03 p0331 N90-11885
Production and processing of Cu-Cr-Nb alloys
[NASA-TM-102495] 08 p1047 N90-16053
Biaxial strength and stress rupture of hot-pressed silicon nitride
[AD-A216950] 11 p1519 N90-18750
Crystallization behavior and properties of BaO-Al2O3-2SiO2 glass matrices
[NASA-CR-185209] 12 p1631 N90-19374
Microstructure and mechanical properties of nickel aluminide powders consolidated by extrusion and hot isostatic pressing
[DE90-009777] 15 p2070 N90-21855
Investigation of metal processing technology
[AD-A218835] 17 p2376 N90-23531
Fracture mechanism maps for advanced structural ceramics. Part 1: Methodology and hot-pressed silicon nitride results
[AD-A220428] 17 p2380 N90-23556
A study on carbon Fiber (long fiber) reinforced copper matrix composite
[AD-A221584] 21 p2972 N90-26891
Application of microdesigned interfaces to studies of ceramic processing
[DE90-011633] 21 p2983 N90-26951
Micromechanics analysis of power consolidation in manufacturing particulate-reinforced MMCs (metal matrix composites)
[DE90-014448] 23 p3299 N90-28663
Strengthening and toughening mechanisms in ceramic fiber-reinforced glass matrix composites
23 p3300 N90-28666
Powder processing of aluminides
[DE90-015314] 24 p3444 N90-29447
HOT STARS
NT A STARS
NT B STARS
NT BLUE STARS
NT O STARS
NT WHITE DWARF STARS
NT WOLF-RAYET STARS
Ultraviolet properties of hot stars in globular clusters
06 p0862 N90-15007
The emission lines in the ultra-violet spectrum of Beta Lyrae 15 p2183 N90-22474
Axions and SN 1987A: Axion trapping
[NASA-CR-186604] 18 p2612 N90-24881
Kappa effect pulsational instability for hot extreme helium stars
[DE90-014920] 23 p3411 N90-29277
HOT SURFACES
Hot surface ignition studies of aviation fluids
10 p1314 N90-17600
The stability of fuel fires 10 p1315 N90-17601
High-temperature, corrosion-preventive coating
[AD-D014557] 22 p3160 N90-27918
Transient cooling of a hot surface by droplets evaporation
[PB90-227968] 23 p3325 N90-28799
HOT WORKING
NT AUSFORMING
Thin section casting program. Volume 2: Horizontal TSC (Thin-Section Casting) approach
[DE89-009031] 02 p0210 N90-11199
Thin section casting program. Volume 2-A: Appendix to volume 2
[DE89-009032] 02 p0210 N90-11200
Thin section casting program. Volume 4: Static cast product bending, straightening, and rolling
[DE89-009034] 02 p0210 N90-11202
A study of the hot workability of Al-8.5 wt pct Mg alloys for armor plate applications
[AD-A211680] 03 p0329 N90-11868
An implicit time-integration procedure for a set of internal variable constitutive equations for isotropic elasto-viscoplasticity
[PB90-121302] 08 p1117 N90-16470
Constitutive data acquisition and modelling in aluminium 2014 alloy
[AERE-R-13651] 13 p1775 N90-20186
Behavior of Al-Mg alloys in hot working and superplasticity
[DE90-015193] 23 p3310 N90-28723
HOT-FILM ANEMOMETERS
Advanced measurement techniques, part 1
04 p0441 N90-12520
Hot-film system for transition detection in cryogenic wind tunnels 04 p0441 N90-12522
Predicted and hot-film measured Tollmien-Schlichting wave characteristics 04 p0441 N90-12523
Relating flow between counter-rotating propellers to aerodynamic interaction noise 14 p1909 N90-20944
Method of forming a multiple layer dielectric and a hot film sensor therewith
[NASA-CASE-LAR-13678-1] 17 p2478 N90-24168
HOT-WIRE ANEMOMETERS
Flow quality measurements in compressible subsonic flows 04 p0441 N90-12521
Basic aerodynamic research facility for comparative studies of flow diagnostic techniques
04 p0441 N90-12526
Experimental study of homogeneous turbulence submitted to rotational effects
[ONERA-RSF-10/1145-AY-164A]
04 p0502 N90-12894
Low speed hot and cold wire techniques for unsteady flow 05 p0574 N90-13342
Hot and cold wire applications in supersonic flows: Introductory notes 05 p0574 N90-13343
The influence of multiple hot-wire probe geometry on the results of measurements in turbulent flows
[DLR-FB-89-26] 05 p0639 N90-13724
Development of an alternative concentration probe calibration method
[AD-A216245] 10 p1388 N90-18031
Experimental study of homogeneous turbulence under rotation and deformation modes
[ONERA-RSF-12/1145-AY-170A]
22 p3176 N90-28023
A method of determining a laser-velocimeter focal point and measuring its beam properties using a hot-wire anemometer
[NAL-TR-1043] 24 p3473 N90-29626

HOT-WIRE FLOWMETERS
Low speed hot and cold wire techniques for unsteady flow 05 p0574 N90-13342
Hot and cold wire applications in supersonic flows: Introductory notes 05 p0574 N90-13343
A process for the measurement of the unsteady three dimensional stream vectors in turbomachines
[MITT-89-01] 17 p2405 N90-23702
HOT-WIRE TURBULENCE METERS
U HOT-WIRE FLOWMETERS
U TURBULENCE METERS
HOTOL LAUNCH VEHICLE
HOTOL: A future launcher for Europe 09 p1175 N90-16800
Cost optimisation of reusable aerospaceplane transportation systems 09 p1175 N90-16803
Aerodynamic and structural design challenges of a reusable single stage to orbit air-breathing launch vehicle 09 p1177 N90-16814
HOTSHOT WIND TUNNELS
High enthalpy hypersonic wind tunnel F4: General description and associated instrumentation 18 p2489 N90-24228
HOUSEHOLDER TRANSFORMATIONS
A block QR factorization algorithm using restricted pivoting
[DE90-001921] 07 p0972 N90-15613
HOUSEKEEPING (SPACECRAFT)
On the wings of a dream: The Space Shuttle
[NASA-EP-269] 05 p0593 N90-13446
HOUSINGS
NT COWLINGS
NT RADOMES
The application of cast SiC/Al to rotary engine components
[NASA-CR-179610] 05 p0581 N90-13385
RSRM nozzle fixed housing cooldown test
[NASA-CR-183741] 05 p0614 N90-13587
Gear noise, vibration, and diagnostic studies at NASA Lewis Research Center
[NASA-TM-102435] 10 p1390 N90-18041
A review of gear housing dynamics and acoustics literature
[NASA-CR-185148] 14 p1987 N90-21387
Fractographic analysis of fatigue failures of airframe equipment parts: Examples of a rod end housing and a rod end cap
[NAL-TR-1047] 24 p3483 N90-29686
HOVERCRAFT GROUND EFFECT MACHINES
Design of a new control system for hovercrafts
[ETN-90-96230] 11 p1485 N90-18435
A two dimensional study of rotor/airfoil interaction in hover
[NASA-CR-183272] 22 p3114 N90-27694
HOVERING
Low-speed wind-tunnel study of reaction control-jet effectiveness for hover and transition of a STOVL fighter concept
[NASA-TM-4147] 03 p0308 N90-11751
Effect of blade planform variation on a small-scale hovering rotor
[NASA-TM-4146] 06 p0717 N90-14186
X-2 limited flight test plan
[AD-A214412] 07 p0880 N90-15099
Three-dimensional viscous rotor flow calculations using a viscous-inviscid interaction approach
[NASA-TM-102235] 12 p1599 N90-19204
Analysis of small-scale rotor hover performance data
[NASA-TM-102271] 13 p1799 N90-20325
Stereopsis cueing effects on hover-in-turbulence performance in a simulated rotorcraft
[NASA-TP-2980] 14 p1921 N90-21004
Coupled rotor-body equations of motion hover flight
[NASA-CR-186710] 19 p2655 N90-25111
Model tilt-rotor hover performance and surface pressure measurement
[AD-A222535] 21 p2959 N90-26827
Hover position sensing system 21 p3069 N90-27448
A two dimensional study of rotor/airfoil interaction in hover
[NASA-CR-183272] 22 p3114 N90-27694
The effects of structural flap-lag and pitch-lag coupling on soft inplane hingeless rotor stability in hover
[NASA-TP-3002] 23 p3269 N90-28503
Numerical simulations of blade-vortex interactions and lifting hovering rotor flows
[AD-A224238] 24 p3417 N90-29302
HOVERING STABILITY
Airworthiness and flight characteristics test of the UH-60A Black Hawk helicopter equipped with the XM-139 multiple mine dispensing system (VOLCANO)
[AD-A210271] 01 p0006 N90-10025
The effects of structural flap-lag and pitch-lag coupling on soft inplane hingeless rotor stability in hover
[NASA-TP-3002] 23 p3269 N90-28503
HR DIAGRAM
U HERTZSPRUNG-RUSSELL DIAGRAM
HTGR
U HIGH TEMPERATURE GAS COOLED REACTORS
HTPB PROPELLANTS
Pyrolysis and combustion of solid fuels under both subsonic and supersonic conditions 22 p3161 N90-27929
HU-1 HELICOPTER
U UH-1 HELICOPTER
HUBBLE SPACE TELESCOPE
Space telescope solar array: Nonlinear test and analysis effects 02 p0185 N90-11051
STSA-Space Telescope solar array interconnectors: From simple approaches to complex modeling. A case study of the necessity of complex analysis 02 p0188 N90-11076
Derivation of improved load transformation matrices for launchers-spacecraft coupled analysis, and direct computation of margins of safety 02 p0188 N90-11077
The link to extragalactic objects 05 p0608 N90-13544
Long-lived space observatories for astronomy and astrophysics
[NASA-CR-185373] 06 p0731 N90-14261
Artificial intelligence approaches to astronomical observation scheduling
[NASA-CR-186277] 07 p1012 N90-15862
Automated telescope scheduling
[NASA-CR-186279] 07 p1012 N90-15863
Information reconstruction from speckle interferograms
[ETN-90-95918] 12 p1729 N90-19939
Space telescope searches for black holes in galactic nuclei 12 p1732 N90-19958
Proceedings of the Third Infrared Detector Technology Workshop
[NASA-TM-102209] 14 p1975 N90-21313
Low noise HgCdTe 128 x 128 SWIR FPA for Hubble space telescope 14 p1979 N90-21337
Laboratory and telescope use of the NICMOS2 128 x 128 HgCdTe array 14 p1979 N90-21338
Future directions for NICMOS arrays 14 p1979 N90-21339
Compendium of fracture mechanics problems
[NASA-TM-100393] 14 p1992 N90-21414
Spike: Artificial intelligence scheduling for Hubble space telescope 21 p3040 N90-27277
An application of design knowledge captured from multiple sources 21 p3045 N90-27306
Hubble space telescope six-battery test bed
[NASA-TM-103506] 22 p3124 N90-27731
Minimum weight design of a leaf spring tapered in thickness and width for the Hubble Space Telescope-space support equipment
[NASA-TM-4233] 23 p3340 N90-28879
State-based scheduling: An architecture for telescope observation scheduling 23 p3369 N90-29038
A survey of planning and scheduling research at the NASA Ames Research Center 23 p3376 N90-29076
HUBS
An experimental investigation of helicopter rotor hub fairing drag characteristics
[NASA-TM-102182] 03 p0300 N90-11701
HUGHES AIRCRAFT
NT AH-64 HELICOPTER
HUGHES MILITARY AIRCRAFT
U MILITARY AIRCRAFT
HUGONIOT ADIABAT
U HUGONIOT EQUATION OF STATE
HUGONIOT EQUATION OF STATE
Shock induced dissociation of polyethylene
[DE89-016983] 02 p0221 N90-11267
Hugoniot measurements with the LLNL electric gun facility
[DE90-002809] 07 p0885 N90-15119
SESAME equation of state for a polymer composite: Phenolic refrasil
[LA-11512-MS] 07 p0910 N90-15264
Shock-wave characterization of energetic booster-rocket propellant WAK-2 and its simulant UGS
[DE90-002633] 07 p0914 N90-15285
HUGOFIT and HUGOPLOT: Computer codes for plane shock wave analysis with materials that have non-simple Hugoniots
[DE90-010284] 18 p2594 N90-24761
HULLS (STRUCTURES)
NT SHIP HULLS
A review of the theory and methods for determining dynamic pulse buckling of cylindrical shells
[AD-A214764] 09 p1238 N90-17185
HUMAN BEHAVIOR
Active participation in highly automated systems: Turning the wrong stuff into the right stuff
[AD-A210218] 01 p0101 N90-10572
Demonstration of replicable dimensions of health behaviors
[AD-A211920] 03 p0380 N90-12161
Fear-potentiated startle as a model system for analyzing learning and memory
[AD-A212131] 04 p0525 N90-13029
A guide to reasoning under uncertainty
[REPT-72/87/R486U] 05 p0675 N90-13932
Cognitive and Neural Sciences Division 1989 programs
[AD-A212634] 06 p0820 N90-14769
Human behavior
[PB90-780008] 07 p0967 N90-15584
Pre-treatment with tyrosine reverses hypothermia induced behavioral depression
[AD-A215211] 09 p1252 N90-17265
Sensations of temperature and humidity during intermittent exercise and the influence of underwear knit structure
[AD-A215285] 09 p1252 N90-17266
Human Behaviour in High Stress Situations in Aerospace Operations
[AGARD-CP-458] 09 p1254 N90-17275
Performance recovery following startle: A laboratory approach to the study of behavioral response to sudden aircraft emergencies 09 p1256 N90-17286
Personality assessment in aviation selection 09 p1257 N90-17289
Activation: Positive and negative effects of the alarm system in the brain 09 p1257 N90-17290
The insertion of human dynamics models in the flight control loops of V/STOL research aircraft. Appendix 2: The optimal control model of a pilot in V/STOL aircraft control loops
[NASA-CR-186598] 15 p2055 N90-21776
Human performance models
[FFI-90/7002] 20 p2901 N90-26502
Rule acquisition events in the discovery of problem solving strategies
[AD-A222428] 21 p3037 N90-27265
HUMAN BEINGS
Thermoregulatory responses to intermittent exercise are influenced by knit structure of underwear
[AD-A209087] 01 p0095 N90-10541
Individual differences in associative learning and forgetting
[AD-A212765] 04 p0526 N90-13034
Computational and psychophysical study of human vision using neural networks
[AD-A213290] 05 p0674 N90-13924
Spatiotemporal characteristics of visual localization, phase 2
[AD-A212934] 05 p0674 N90-13929
An architectural model of visual motion understanding
[AD-A214327] 07 p0967 N90-15589
Psychophysiological correlates of human adaptation in antarctica
[AD-A216679] 10 p1412 N90-18142
Alterations in the metabolic and sympathetic response to cold exposure after cold air acclimation
[AD-A216817] 10 p1412 N90-18144
Visual processing of object velocity and acceleration
[AD-A216509] 11 p1539 N90-18858
The computation of color
[AD-A216531] 11 p1548 N90-18914
The pollution hazard assessment system: Documentation and users manual
[AD-A217108] 12 p1689 N90-19706
Influence of theobromine on heat production and body temperatures in cold-exposed humans: A preliminary report
[AD-A217203] 13 p1850 N90-20618
A review of the literature on the toxicity of rare-earth metals as it pertains to the engineering demonstration system surrogate testing
[DE90-008049] 13 p1851 N90-20620
Networks for image acquisition, processing and display 15 p2138 N90-22218
Human motion perception: Higher-order organization 15 p2140 N90-22226
Brain stem evoked responses in altered G environments
[AD-A220097] 17 p2435 N90-23874
An investigation into techniques for landmark identification of 3D images of human subjects, phase 1
[AD-A218614] 18 p2583 N90-24713
Rheoencephalography in simulated aviation environmental stress
[AD-A221150] 18 p2584 N90-24716
Acquiring generalizations to organize human databases
[AD-A219835] 18 p2634 N90-25004
Effect of organizational structure on performance of decision making teams
[AD-A223160] 20 p2934 N90-26697

Effects of protracted ionizing radiation dosage on humans and animals: A brief review of selected investigations
[AD-A222240] 21 p3033 N90-27241

HUMAN BODY

A severe human ESD (Electrostatic Discharge) model for safety and high reliability system qualification testing
[DE89-016177] 02 p0216 N90-11233
Methodology for the calibration of and data acquisition with a six-degree-of-freedom acceleration measurement device
[PB89-233597] 06 p0779 N90-14531
Introduction to extremely-low-frequency electric and magnetic fields
[DE90-002662] 07 p0966 N90-15578
The application of optimal control theory for analysis of human jumping and pedaling
07 p0968 N90-15590
Guidelines for safe human exposure to impact acceleration, update A
[AD-A215287] 09 p1253 N90-17268
Measurement of body fat by neutron inelastic scattering: Comments on installation, operation, and error analysis
[DE90-006765] 11 p1540 N90-18868
Reliability of equivalent sphere model in blood-forming organ dose estimation
[NASA-TM-4178] 12 p1746 N90-20036
The USAF Advanced Dynamic Anthropomorphic Manikin (ADAM) 13 p1752 N90-20062
Kinematic and kinetic analyses of drop landings
14 p2010 N90-21517
Circumferential pressure probe
[NASA-CASE-LAR-13775-1] 17 p2406 N90-23706
Noninvasive estimation of fluid shifts between body compartments by measurement of bioelectric characteristics 18 p2628 N90-24976
Quantitative assessment of human motion using video motion analysis 19 p2730 N90-25518
Biodynamic simulations of an aircraft pilot/passenger in various crash environments
[NIAR-90-6] 20 p2900 N90-26494
An algorithm for automated surface modelling in unigraphics
[AD-A223219] 21 p3053 N90-27355
Microscopic models for electromagnetic wave propagation in highly dispersive media
[AD-A224382] 24 p3460 N90-29540

HUMAN CENTRIFUGES

Human centrifuge controller
[NAL-TM-SE-8901] 14 p1929 N90-21043
Neck injury prevention possibilities in a high-G-enviroment experience with high sustained + G(sub z) training of pilots in the GAF IAM human centrifuge
19 p2720 N90-25474

HUMAN ENGINEERING

U HUMAN FACTORS ENGINEERING

HUMAN FACTORS ENGINEERING

NT MOTION SIMULATION
Classification and reduction of pilot error
[NASA-CR-181867] 01 p0004 N90-10014
Addressing user display requirements from a large and diverse user community
[DE89-011403] 01 p0103 N90-10582
See and avoid/cockpit visibility
[DOT/FAA/CT-TN89/18] 02 p0148 N90-10843
NASA/NBS (National Aeronautics and Space Administration/National Bureau of Standards) standard reference model for telerobot control system architecture (NASREM)
[NASA-CR-185078] 02 p0228 N90-11310
Techniques for optimizing human-machine information transfer related to real-time interactive display systems
[NASA-TM-100450] 02 p0254 N90-11441
Selective removal of organics for water reclamation
[NASA-CR-185959] 02 p0255 N90-11445
Task analysis of the UH-60 mission and decision rules for developing a UH-60 workload prediction model. Volume 1: Summary report
[AD-A210763] 02 p0255 N90-11446
Human Operator Simulator (HOS) 4 user's guide
[AD-A212007] 03 p0310 N90-11783
Project AENEAS: A feasibility study for crew emergency return vehicle
[PB89-217020] 03 p0317 N90-11799
New Fabric Development Program
[AD-A211549] 03 p0332 N90-11891
Wrist orientation effect on grip strength and endurance
[PB89-200935] 03 p0383 N90-12179
Integration of a centralized multiplexed control unit into the cockpit of an aircraft
[F6150-DT410-1-88329] 04 p0458 N90-12622
Psychological mechanisms involved in the disorientation of pilots due to flight conditions
[ETN-89-95014] 04 p0527 N90-13040
The human factors relating to escape and survival from helicopters ditching in water
[AGARD-AG-305(E)] 05 p0576 N90-13358
Software and hardware description of the helicopter motion equations for VAX computers
[AD-A213248] 05 p0579 N90-13375
Human factors research in aircrew performance and training
[AD-A213285] 05 p0676 N90-13938
Human factors issues in performing life science experiments in a 0-G environment
05 p0679 N90-13952
Project Argo: The design and analysis of an all-propulsive and an aeroassisted version of a manned space transportation vehicle
[NASA-CR-186047] 06 p0732 N90-14266
Human factors aspects of decision support systems
06 p0757 N90-14408
Extravehicular activity welding experiment
[NASA-CR-183848] 06 p0791 N90-14608
MIPs and BIPs are megaflops: Limits of unidimensional assessments
[DE89-015707] 06 p0820 N90-14770
Human factors survey of advanced instrumentation and controls
[DE90-002477] 06 p0821 N90-14776
Human factors evaluation of electroluminescent display Number 1
[DE90-002231] 06 p0822 N90-14777
Solution bias in complex systems modeling
[DE90-002001] 06 p0836 N90-14858
The human element: The key to safe, civil operations in adverse weather 07 p0869 N90-15042
Imaging probabilities, geometry and ergonomics in limited visibility helicopter operations
07 p0872 N90-15060
See and avoid/cockpit visibility
[AD-A214214] 07 p0877 N90-15084
Task-oriented display design: Concept and example
[NASA-TM-101685] 07 p0881 N90-15101
An expert system for quality assurance (a.k.a.) QA Express
[DE90-003887] 07 p0944 N90-15467
Model for measuring complex performance in an aviation environment
[DE90-002055] 07 p0967 N90-15585
Architectural study of the design and operation of advanced force feedback manual controllers
[NASA-CR-185948] 07 p0981 N90-15664
MANPRINT (Manpower and Personnel Integration) evaluation: AN/TRC-170 digital troposcatter radio system
[AD-A211799] 08 p1055 N90-16100
Electrical safety in the high voltage laboratory
[DE90-003026] 08 p1060 N90-16130
Assessment of visual function in aerospace medicine
[BMVG-FBWM-89-5] 08 p1105 N90-16397
Human factors in the naval environment: A review of motion sickness and biodynamic problems
[AD-A214733] 09 p1251 N90-17258
Space station wardroom habitability and equipment study
[NASA-CR-4246] 09 p1260 N90-17308
Proximity compatibility and information display: The effects of space and color on the analysis of aircraft stall conditions
[AD-A214488] 09 p1260 N90-17309
Prescribing spectacles for aviators
[AD-A214830] 09 p1260 N90-17310
Attenuating the luminous output of the AN/PVS-5A night vision goggles and its effects on visual acuity
[AD-A214895] 09 p1261 N90-17311
Physiological evaluation of men wearing three different toxicological protective systems
[AD-A215527] 09 p1261 N90-17313
A review of UK civil aviation fire and cabin safety research 10 p1312 N90-17587
New aircraft cabin and cargo flammability standards for transport category aircraft 10 p1312 N90-17589
Full scale study of a cabin fire in an A300 fuselage section 10 p1313 N90-17592
Forced and natural venting of aircraft cabin fires: A numerical simulation 10 p1314 N90-17597
An intelligent tool for the design of presentations: A system identification study
[AD-A215770] 10 p1418 N90-18174
The effects of wearing passenger protective breathing equipment on evacuation times through type 3 and type 4 emergency aircraft exits in clear air and smoke. Phase 1: Evacuations in clear air. Phase 2: Evacuations in smoke
[AD-A216798] 11 p1453 N90-18374
Space orientation and orbital technology
[ISBN-3-89100-015-4] 11 p1465 N90-18437
Anthropometry of a fit test sample used in evaluating the current and improved MCU-2/P masks
[AD-A215173] 11 p1541 N90-18873
Evaluation of helmet retention systems using a pendulum device
[AD-A215489] 11 p1542 N90-18874
Human factors issues in aircraft maintenance and inspection
[AD-A215724] 11 p1542 N90-18875
Architecture for a human-robot symbiotic system
[DE90-005670] 11 p1550 N90-18921
A human factors experimental comparison of two database query languages 11 p1574 N90-19064
Human factors engineering testing of aircraft cockpit lighting systems
[AD-A216853] 12 p1697 N90-19743
A human factors testbed for ground-vehicle telerobotics research
[DE90-006618] 12 p1697 N90-19746
The USAF Advanced Dynamic Anthropomorphic Manikin (ADAM) 13 p1752 N90-20062
Controllable propulsion for escape systems control
13 p1753 N90-20064
Spacecraft escape 13 p1753 N90-20066
A guide to performing and documenting safety analyses
[DE90-008687] 13 p1788 N90-20260
A guide to performing and documenting safety analyses
[DE90-008688] 13 p1788 N90-20261
Using an instrumented manikin for Space Station Freedom analysis 13 p1861 N90-20675
Human task animation from performance models and natural language input 13 p1861 N90-20678
Investigation of air transportation technology at the Massachusetts Institute of Technology, 1988-1989
14 p1905 N90-20922
Human factors in fighter software development
[PD-CF-9003] 14 p2011 N90-21522
The effect of windscreen bows and HUD pitch ladder format on pilot performance during simulated flight
[AD-A218139] 14 p2011 N90-21523
The insertion of human dynamics models in the flight control loops of V/STOL research aircraft. Appendix 2: The optimal control model of a pilot in V/STOL aircraft control loops
[NASA-CR-186598] 15 p2055 N90-21776
Insights into complex human performance
[DE90-006957] 15 p2137 N90-22214
Pyramid image codes 15 p2143 N90-22243
NASA Information Sciences and Human Factors Program
[NASA-TM-4190] 15 p2194 N90-22529
Helmet-mounted pilot night vision systems: Human factors issues 16 p2269 N90-22930
Preliminary evaluation of a small wearable display
[AD-A219867] 17 p2350 N90-23385
Space Station Freedom media handbook
[NASA-TM-102901] 17 p2364 N90-23460
A comparative analysis of work-hour forecasting techniques at the crew level
[AD-A220706] 17 p2438 N90-23894
Evaluation of speech recognizers for use in advanced combat helicopter crew station research and development
[NASA-CR-177547] 18 p2496 N90-24265
Telerobotic architecture for an on-orbit servicer
18 p2503 N90-24302
HERA teleoperation test facility
18 p2503 N90-24303
Teleoperation of a force controlled robot manipulator without force feedback to a human operator
18 p2503 N90-24305
A survey of human factors methodologies and models for improving the maintainability design of emerging Army aviation systems
[AD-A221159] 18 p2586 N90-24724
Knowledge-based control of an adaptive interface
18 p2630 N90-24987
Neck Injury in Advanced Military Aircraft Environments
[AGARD-CP-471] 19 p2717 N90-25459
The role of attention in information processing implications for the design of displays
[AD-A219252] 19 p2723 N90-25486
Third Annual Workshop on Space Operations Automation and Robotics (SOAR 1989)
[NASA-CP-3059] 19 p2727 N90-25503
CREW CHIEF: A computer graphics simulation of an aircraft maintenance technician
19 p2729 N90-25515
Modeling strength data for CREW CHIEF
19 p2729 N90-25516
The use of PLAID in the Space Station Freedom viewing analysis 19 p2729 N90-25517
The human factors of workstation telepresence
19 p2732 N90-25528

Human factors issues in telerobotic systems for Space Station Freedom servicing 19 p2737 N90-25556
Test bed experiments for various telerobotic system characteristics and configurations 19 p2740 N90-25572
A human factors review of data entry devices [DE90-012009] 19 p2763 N90-25703
Literature concerning control and display technology applicable to the Orbital Maneuvering Vehicle (OMV) [NASA-CR-186790] 20 p2820 N90-26048
Pilot interaction with automated airborne decision making systems [NASA-CR-186730] 20 p2899 N90-26492
Choosing a pilot subjective workload scale to fit flight operational requirements [IAR-89-21] 20 p2900 N90-26493
Human factors: The human interface with aircraft interiors [NIAR-90-18] 20 p2900 N90-26496
Motion sickness, visual displays, and armored vehicle design [AD-A222678] 20 p2902 N90-26506
The need for platform motion in modern piloted flight training simulators [AD-A221720] 21 p2963 N90-26847
Human factors and safety considerations of night vision systems flight using thermal imaging systems [AD-A223226] 21 p3037 N90-27263
Human factors research in aircrew performance and training [AD-A221657] 21 p3037 N90-27267
PHARE: Concept and programme 22 p3114 N90-27690
The dynamics of orbital maneuvering: Design and evaluation of a visual display aid for human controllers 22 p3131 N90-27767
Human factors and safety considerations of night vision systems flight [USAARL-89-12] 22 p3233 N90-28332
Development of a methodology for icon evaluation [NPL-DITC-159/90] 22 p3235 N90-28345
A conceptual framework for fighter flight control systems [PD-CF-9009] 23 p3283 N90-28577
Quality function deployment as a mechanism for process characterization and control [DE90-014755] 23 p3337 N90-28857
Techniques and applications for binaural sound manipulation in human-machine interfaces [NASA-TM-102279] 23 p3362 N90-28996
Military aircrew seating: A human factors engineering approach [AD-A218049] 23 p3362 N90-28999
Human factors model concerning the man-machine interface of mining crewstations 23 p3364 N90-29011
Development of a flexible test-bed for robotics, telemanipulation and servicing research 23 p3364 N90-29012
Human factors evaluation and validation criteria for quality training programs: Development, presentation, and assessment [DE90-014724] 23 p3377 N90-29081
Construction and demonstration of a 9-string 6 DOF force reflecting joystick for telerobotics 24 p3509 N90-29836
Response to reflected-force feedback to fingers in teleoperations 24 p3509 N90-29837
A procedure concept for local reflex control of grasping 24 p3509 N90-29839
The telerobot workstation testbed for the shuttle aft flight deck: A project plan for integrating human factors into system design 24 p3518 N90-29887
Information processing and perceptual characteristics of display design: The role of emergent features and objects [AD-A223683] 24 p3558 N90-30133

HUMAN FACTORS LABORATORIES
Psychological mechanisms involved in the disorientation of pilots due to flight conditions [ETN-89-95014] 04 p0527 N90-13040

HUMAN PERFORMANCE
NT ASTRONAUT PERFORMANCE
NT OPERATOR PERFORMANCE
NT PILOT PERFORMANCE
Human performance in continuous/sustained operations and the demands of extended work/rest schedules: An annotated bibliography, volume 2 [AD-A210504] 01 p0093 N90-10530
Daytime sleepiness, performance, mood, nocturnal sleep: The effect of benzodiazepine and caffeine on their relationship [AD-A210915] 01 p0093 N90-10533
Learning to make decisions: When incentives help and hinder [AD-A210185] 01 p0135 N90-10779
USSR Space Life Sciences Digest, issue 24 [NASA-CR-3922(28)] 03 p0378 N90-12152
USSR Space Life Sciences Digest, issue 23 [NASA-CR-3922(27)] 03 p0378 N90-12154
Adaptive information processing in auditory cortex [AD-A211294] 03 p0380 N90-12166
Effects of atmospheric mix and toxic fumes on military performance [PB89-223630] 04 p0522 N90-13015
Effects of serial wet-dry-wet cold exposure: Thermal balance, physical activity, and cognitive performance [AD-A212704] 04 p0524 N90-13025
The effects of noise on performance [AD-A212519] 04 p0551 N90-13209
Cognitive and Neural Sciences Division 1989 programs [AD-A212634] 06 p0820 N90-14769
MIPs and BIPs are megaflops: Limits of unidimensional assessments [DE89-015707] 06 p0820 N90-14770
Dual task performance with LPC (Linear Predictive Coding) degraded speech in a sentence verification task [AD-A214298] 07 p0920 N90-15320
A comparative evaluation and analysis of end-user search performance in an academic environment 07 p1009 N90-15845
A review of circadian effects on selected human information processing tasks [AD-A214673] 09 p1251 N90-17256
Identifying the circadian cycle in human information processing data using periodicity analysis: A synopsis [AD-A214674] 09 p1251 N90-17257
Human factors in the naval environment: A review of motion sickness and biodynamic problems [AD-A214733] 09 p1251 N90-17258
Effectiveness of progressive resistance training for increasing maximal repetitive lifting capacity [AD-A215286] 09 p1252 N90-17267
Workshop on the Effects of Combined Fire Products on Human Physiological and Psychological Performance [AD-A215465] 09 p1253 N90-17270
Human Behaviour in High Stress Situations in Aerospace Operations [AGARD-CP-458] 09 p1254 N90-17275
The descent from the Olimpus: The effect of accidents on aircrew survivors 09 p1255 N90-17280
Leader personality and crew effectiveness: Factors influencing performance in full-mission air transport simulation 09 p1255 N90-17282
Activation: Positive and negative effects of the alarm system in the brain 09 p1257 N90-17290
Standardized tests for research with environmental stressors: The AGARD STRES battery 09 p1258 N90-17295
Feedback effects in computer-based skill learning [AD-A214560] 09 p1258 N90-17298
Physical performance and carbohydrate consumption in CF commandos during a 5-day field trial [AD-A217204] 13 p1850 N90-20619
Hydration effects on human physiology and exercise-heat performance [AD-A217969] 13 p1852 N90-20629
Information gathering and decisionmaking under stress [AD-A218233] 13 p1854 N90-20643
Human task animation from performance models and natural language input 13 p1861 N90-20678
Development of microcomputer-based mental acuity tests for repeated-measures studies [NASA-CR-185607] 14 p2010 N90-21521
Insights into complex human performance [DE90-006957] 15 p2137 N90-22214
Networks for image acquisition, processing and display 15 p2138 N90-22218
Stanford/NASA-Ames Center of Excellence in model-based human performance 15 p2143 N90-22241
Aeronautical decisionmaking for air ambulance program administrators [DOT/FAA/DS-88/8] 17 p2347 N90-23368
Personality factors in flight operations. Volume 1: Leader characteristics and crew performance in a full-mission air transport simulation [NASA-TM-102259] 17 p2348 N90-23370
Effect of extraneous color-coded targets on identification of targets on CRT displays [AD-A219473] 17 p2436 N90-23879
Effect of laser glare and aircraft windscreen on visual search performance under low ambient lighting [AD-A219456] 17 p2437 N90-23888
Overtraining and exercise motivation: A research prospectus 18 p2629 N90-24982
Research in human performance related to space: A compilation of three projects/proposals 18 p2629 N90-24983
Development of a meta-analytic technique to assess stress effects [AD-A220468] 19 p2723 N90-25487
TOM: Test of multiple task performance, user manual [DLR-FB-89-60] 19 p2723 N90-25490
Quantitative assessment of human motion using video motion analysis 19 p2730 N90-25518
Performance-based workload assessment: Allocation strategy and added task sensitivity 19 p2734 N90-25539
Neural networks for detecting defects in aircraft structures [IAR-90-4] 20 p2873 N90-26345
Robotic-aided system for inspection of aging aircraft [NIAR-90-9] 20 p2873 N90-26346
Human performance models [FFI-90/7002] 20 p2901 N90-26502
Effect of organizational structure on performance of decision making teams [AD-A223160] 20 p2934 N90-26697
Content effects in mathematics problem solving [AD-A222436] 21 p3065 N90-27423
Categorization and identification of simultaneous targets [IZF-1989-22] 22 p3234 N90-28337
Variable force and visual feedback effects on teleoperator man/machine performance 23 p3364 N90-29008
Evaluation of physiological and psychological impairment of human performance in cold stressed subjects [AD-A223635] 24 p3498 N90-29769
Minimal sleep to maintain performance: Search for sleep quantum in sustained operations [AD-A223815] 24 p3498 N90-29770
Robotic tele-existence 24 p3502 N90-29796
Human error classification and data collection [DE90-631408] 24 p3522 N90-29915

HUMAN REACTIONS
Psychological reactions of pilots involved in accidents in the Swedish Air Force 09 p1254 N90-17279
The descent from the Olimpus: The effect of accidents on aircrew survivors 09 p1255 N90-17280
Reactions to emergency situations in actual and simulated flight 09 p1255 N90-17283
Performance recovery following startle: A laboratory approach to the study of behavioral response to sudden aircraft emergencies 09 p1256 N90-17286
Activation: Positive and negative effects of the alarm system in the brain 09 p1257 N90-17290
An adaptive human response mechanism controlling the V/STOL aircraft. Appendix 3: The adaptive control model of a pilot in V/STOL aircraft control loops [NASA-CR-166599] 15 p2056 N90-21777
Field-of-view assessment of low-level flight and an airdrop in the C-130 Weapon System Trainer (WST) [AD-A218504] 16 p2200 N90-22559
Human response research update 18 p2611 N90-24873
Omni-directional human head-neck response [SAE-861893] 19 p2721 N90-25478
Study of the application of a stress reactivity test in personnel selection [DLR-FB-89-54] 19 p2723 N90-25489

HUMAN RELATIONS
Leader personality and crew effectiveness: Factors influencing performance in full-mission air transport simulation 09 p1255 N90-17282

HUMAN RESOURCES
Science and technology resources in US industry: Surveys of science resources series, 1975-1986 [PB90-107194] 06 p0756 N90-14401
Project summaries [PB90-103987] 08 p1118 N90-16472
Profiles-aeronautical/astronautical engineering: Human resources and funding [PB90-103888] 09 p1203 N90-16969
National patterns of research and development resources: 1989 [NSF-89-308] 17 p2486 N90-24218

HUMAN TOLERANCES
Biomedical influences on spinal cord function [AD-A210311] 01 p0092 N90-10527
Heat exhaustion [AD-A212128] 04 p0522 N90-13014
Psychophysiological correlates of human adaptation in antarctica [AD-A216679] 10 p1412 N90-18142
Studies of 60-Hz exposure effects on human function [DE90-009473] 15 p2137 N90-22210
Model for predicting the effects of laser exposures and eye protection on vision [AD-A219697] 17 p2434 N90-23868
Effect of laser glare and aircraft windscreen on visual search performance under low ambient lighting [AD-A219456] 17 p2437 N90-23888

Neck injury prevention possibilities in a high-G-enviroment experience with high sustained +G(sub z) training of pilots in the GAF IAM human centrifuge
19 p2720 N90-25474

Annoyance caused by advanced turboprop aircraft flyover noise: Counter-rotating-propeller configuration
[NASA-TP-3027] 23 p3392 N90-29166

HUMAN WASTES
NT FECES
NT URINE

Proposal for a zero-gravity toilet facility for the space station
[NASA-CR-183151] 04 p0526 N90-13036

Electrochemical incineration of wastes
[NASA-CR-187033] 23 p3317 N90-28753

HUMAN-COMPUTER INTERFACE
U MAN-COMPUTER INTERFACE

HUMIDITY

A study of the impact of simulated 183 GHz water vapor retrievals on numerical weather prediction
[AD-A210431] 01 p0088 N90-10504

Measurement of respiratory air temperatures and calculation of respiratory heat loss when working at various ambient temperatures
[AD-A210378] 01 p0093 N90-10529

Methodology of developing a combined environmental stress schedule for reliability growth testing
[AD-A211053] 02 p0231 N90-11326

Test and evaluation of polymeric membranes for oxygen enrichment of air
[DE90-000555] 06 p0742 N90-14321

Climatology of Lawrence Livermore National Laboratory
[DE90-000905] 06 p0818 N90-14756

Effects of moisture on composite materials
09 p1185 N90-16866

Sensations of temperature and humidity during intermittent exercise and the influence of underwear knit structure
[AD-A215285] 09 p1252 N90-17266

Lagrangian model simulation of the turbulent transport of evaporating jet droplets
15 p2128 N90-22168

Mechanisms add foldability to ROSAT solar panels
18 p2538 N90-24483

Effect of low air velocities on thermal homeostasis and comfort during exercise at space station operational temperature and humidity
18 p2628 N90-24975

A LOWTRAN7 sensitivity study in the 8-12 and 3-5 micron bands: Includes comparison with LOWTRAN6 results
[AD-A222094] 21 p3031 N90-27231

Study of the mechanical behavior of composites under complex stress systems
[ETN-90-97455] 22 p3154 N90-27879

Evaluation of EDR-3 vibration, shock, temperature, and humidity recording unit
[NASA-CR-184006] 22 p3177 N90-28028

Mesoscale variability of free tropospheric humidity near San Nicolas Island during FIRE
22 p3214 N90-28234

Structural analysis of stratocumulus convection
22 p3216 N90-28243

Diurnal variation in the turbulent structure of the cloudy marine boundary layer during FIRE 1987
22 p3217 N90-28248

HUMIDITY MEASUREMENT

Survey of the CLUSE main experiment Grand-CLUSE, May 1 - June 15, 1988 --- Humidity Exchange Over the Sea (HEXOS) experiment
[FEL-1988-43] 04 p0518 N90-12991

Infrared water vapor continuum absorption: New atmospheric electrical measurements and theory
[AD-A212594] 04 p0519 N90-12994

Humidity local measurements in the middle atmosphere
05 p0657 N90-13833

Long duration balloon flights in the middle stratosphere
05 p0663 N90-13874

Impact of a unified DMSP meteorological sensor retrieval methodology on global numerical weather prediction
[AD-A220306] 18 p2581 N90-24703

Radio refractivity profiles deduced from lidar measurements
[AD-A221727] 21 p3026 N90-27208

Integrated radiometric profiler for atmospheric humidity and temperature measurements
[AD-A221931] 21 p3032 N90-27237

HURRICANES

Extreme hurricanes in the nineteenth century
[PB89-201305] 01 p0087 N90-10498

Hurricane Research Division fiscal year 1988 programs, fiscal year 1989 projections
[PB89-152268] 02 p0250 N90-11418

The effect of latent heat release on synoptic-to-planetary scale wave interactions: Observational study
03 p0362 N90-12074

Comparison of analytical methods for calculation of wind loads
[NASA-TM-102782] 05 p0654 N90-13813

Summary of 1989 Atlantic tropical cyclone activity and seasonal forecast verification
06 p0815 N90-14743

The dynamics of simulated convective storms in hurricane environments
06 p0816 N90-14747

Forecasters handbook for Central America and adjacent waters
[AD-A216752] 11 p1536 N90-18845

The invertibility principle for a simple hurricane model
[AD-A218344] 13 p1848 N90-20605

Tropical cyclone track predictability and the adjoint method of data assimilation
[AD-A218324] 14 p2007 N90-21505

Forecast of Atlantic seasonal hurricane activity for 1990
15 p2134 N90-22194

Coastal field data collection program. Hurricane Gilbert storm surge data
[AD-A218752] 17 p2426 N90-23823

A Kalman filter with smoothing for hurricane tracking and prediction
[AD-A220413] 17 p2426 N90-23827

Tropical cyclones, 1989: Central north Pacific
[PB90-182536] 17 p2428 N90-23836

The role of eddy fluxes of momentum in hurricane formation
[AD-A219417] 18 p2581 N90-24700

Mariners Weather Log, volume 33, number 3, Summer 1989
[PB90-146846] 20 p2889 N90-26444

HUSTLER AIRCRAFT
U B-58 AIRCRAFT

HYBRID CIRCUITS

Performance of a 300 Mbps 1:16 serial/parallel optoelectronic receiver module
[NASA-TM-103110] 13 p1795 N90-20302

An investigation of narrow-bandgap semiconductors: Devices, circuits, and systems
15 p2171 N90-22406

Reliability analysis/assessment of advanced technologies
[AD-A223647] 24 p3485 N90-29573

HYBRID COMBUSTION
U HYBRID PROPELLANT ROCKET ENGINES

HYBRID COMPUTERS

Hybrid intelligent perception system: Intelligent perception through combining artificial neural networks and an expert system
[DE90-007483] 13 p1874 N90-20746

HYBRID NAVIGATION SYSTEMS

Carin and GPS: The combination of dead reckoning, map matching and satellite navigation in a hybrid automobile navigation system
[ETN-90-95451] 12 p1602 N90-19220

Sole means navigation and integrity through hybrid Loran-C and NAVSTAR GPS
14 p1907 N90-20933

HYBRID PROPELLANT ROCKET ENGINES

Performance integration of a reusable launch vehicle with hybrid airbreathing rocket propulsion
09 p1177 N90-16820

HYBRID PROPELLANTS

Tripropellant combustion process
23 p3293 N90-28631

HYBRID PROPULSION

Investigation into the feasibility of using solid fuel ramjets for high supersonic/low hypersonic tactical missiles
[AD-A214737] 09 p1168 N90-16761

Hybrid propulsion technology program. Volume 1: Conceptional design package
[NASA-CR-183953] 15 p2060 N90-21793

Hybrid propulsion technology program. Volume 2: Technology definition package
[NASA-CR-183954] 15 p2060 N90-21794

Project LOCOST: Laser or Chemical Hybrid Orbital Space Transport
[NASA-CR-186822] 20 p2819 N90-26042

Hybrid propulsion technology program
[NASA-CR-183952] 21 p2968 N90-26870

Design optimization of gas generator hybrid propulsion boosters
[NASA-CR-181096] 23 p3299 N90-28660

HYBRID STRUCTURES

Tensile behavior of cylindrical pressure tanks in fiber assembling + metal hybrid structure
[ILR-MITT-213] 12 p1675 N90-19618

Plate rods and leaf springs with hybrid structure: Cross section optimization following different target criteria
[ILR-MITT-227(1989)] 20 p2877 N90-26366

Reinforcing fibers and technology development for resin composites. Consequences for aircraft structures
[FOA-C-20777-2.5] 22 p3154 N90-27883

HYBRIDS (BIOLOGY)
U GENETIC ENGINEERING

HYDRATION

Computational solution of chemistry problems
[NASA-CR-186000] 05 p0620 N90-13618

Energies of organic compounds
[DE90-003174] 06 p0743 N90-14324

An electrochemical and spectroscopic study of electrode processes
[AD-A217261] 13 p1793 N90-20289

HYDRAULIC ACTUATORS
U ACTUATORS
U HYDRAULIC EQUIPMENT

HYDRAULIC CONTROL

Independent Orbiter Assessment (IOA): Assessment of the hydraulics/water spray boiler subsystem
[NASA-CR-185537] 03 p0316 N90-11792

HYDRAULIC EQUIPMENT

Independent Orbiter Assessment (IOA): Analysis of the hydraulics/water spray boiler subsystem
[NASA-CR-185541] 02 p0165 N90-10934

Independent Orbiter Assessment (IOA): Analysis of the elevon subsystem
[NASA-CR-185576] 02 p0166 N90-10935

Independent Orbiter Assessment (IOA): Analysis of the landing/deceleration subsystem
[NASA-CR-185569] 02 p0167 N90-10943

Independent Orbiter Assessment (IOA): Weibull analysis report
[NASA-CR-185534] 02 p0168 N90-10948

Independent Orbiter Assessment (IOA): Assessment of the hydraulics/water spray boiler subsystem
[NASA-CR-185537] 03 p0316 N90-11792

Review and evaluation of a turbomachinery throughflow finite element code
[AD-A213058] 05 p0650 N90-13787

Power system modeling for a six legged walking vehicle
09 p1221 N90-17083

Flexible heat pipe cold plate
[AD-A216053] 11 p1464 N90-18433

Experimental adaptive control of a hydraulic robot
16 p2303 N90-23121

Nonflammable hydraulic power system for tactical aircraft. Volume 1: Aircraft system definition, design and analysis
[AD-A218493] 17 p2356 N90-23409

Lunar stone saw
[NASA-CR-182438] 17 p2412 N90-23741

Evaluation of abrasion-resistant metallized coatings for civil works applications
[AD-A221078] 18 p2530 N90-24438

Simulated dynamic response of a servovalve controlled hydraulic actuator
[NASA-TM-101644] 20 p2842 N90-26167

Computer-aided engineering environment for controlled mechanical systems
[AD-A223551] 24 p3527 N90-29942

HYDRAULIC FLUIDS
NT SKYDROL (TRADEMARK)

Test and evaluation: Reducing risks to military aircraft from bird collisions. Report to the Chairman, Legislation, and National Security Subcommittee, Committee on Goverment Operations, House of Representatives
[AD-A210670] 02 p0148 N90-10845

Analysis of hydraulic fluids and lubricating oils for the formation of Trimethylolpropane Phosphate (TMP-P)
[AD-A215188] 09 p1198 N90-16939

Information compendium on nonflammable hydraulic fluid and design requirements for its adoption
[AD-A219569] 17 p2380 N90-23554

Compatibility of elastomeric seal compounds with MIL-H-6083 and MIL-H-46170 hydraulic fluid
[AD-A224248] 24 p3454 N90-29504

HYDRAULIC HEATING SOURCES
U HEAT SOURCES
U HYDRAULIC EQUIPMENT

HYDRAULIC JETS

High pressure waterjet cutting industrial needs survey
[AD-A214952] 10 p1368 N90-17927

Laser Doppler anemometry measurements of a confined turbulent water jet with a uniform background flow
15 p2092 N90-21971

Large hydrodynamic tunnel: Calculation of the acoustic transparency of the jet stream
[REPT-89/115] 23 p3393 N90-29167

HYDRAULIC PUMPS
U HYDRAULIC EQUIPMENT
U PUMPS

HYDRAULIC SYSTEMS
U HYDRAULIC EQUIPMENT

HYDRAULIC TEST TUNNELS

Liquid water content and droplet size calibration of the NASA Lewis Icing Research Tunnel
[NASA-TM-102447] 05 p0651 N90-13797

Study of flow around a sphere in a hydraulic test tunnel
[CERT-1/2313/MES] 08 p1064 N90-16156

Prediction of rotor blade-vortex interaction noise from 2-D aerodynamic calculations and measurements
[ISL-CO-243/88] 11 p1451 N90-18365

Experiments with unsteady, free surface, three-dimensional vortices in a thermally stable, stratified fluid
[AD-A222088] 21 p2954 N90-26796
Experimental study of the Taylor-Goertler instability
[ETN-90-97447] 22 p3175 N90-28014
Acoustic confinement in the large hydrodynamic tunnel: Identification of the acoustic charateristics with a one-directional source
[REPT-8228-88] 22 p3244 N90-28399
Large hydrodynamic tunnel: Calculation of the acoustic transparency of the jet stream
[REPT-89/115] 23 p3393 N90-29167

HYDRAULIC VALVES
U HYDRAULIC EQUIPMENT
U VALVES

HYDRAULICS
Gravitropism in plants: Hydraulics and wall growth properties of responding cells 05 p0678 N90-13950

HYDRAZINES
NT DIMETHYLHYDRAZINES
NT METHYLHYDRAZINE
NT TETRAFLUOROHYDRAZINE
The Third Conference on the Environmental Chemistry of Hydrazine Fuels
[AD-A197632] 02 p0203 N90-11157
Surface-catalyzed air oxidation of hydrazines: Environmental chamber studies 02 p0203 N90-11159
An atmospheric pressure flow reactor: Gas phase kinetics and mechanism in tropospheric conditions without wall effects 02 p0203 N90-11160
The behavior of hydrazine vapor in an environmental chamber under simulated atmospheric conditions 02 p0203 N90-11161
Modeling of hydrazine surface interactions in environmental reaction chambers 02 p0203 N90-11162
Trace metal catalysis of hydrazine decomposition: The role of chromium 02 p0204 N90-11163
Interactions of hydrazines with colloidal constituents of soils 02 p0204 N90-11164
Hydrazine fate and transformation in natural waters and soils 02 p0204 N90-11165
Vibrational spectroscopic study of the kaolinite-hydrazine intercalation complex 02 p0204 N90-11166
Surface-catalyzed air oxidation reactions of hydrazines: Tubular reactor studies 02 p0204 N90-11167
A matrix-isolation FT-IR study of hydrazine 02 p0204 N90-11168
Low temperature spectroscope of hydrazine and ammonia complexes 02 p0205 N90-11169
A diffuse reflectance infrared Fourier transform spectroscopic study of adsorbed hydrazines 02 p0205 N90-11170
Numerical simulation of hydrazine transport in a sandy soil 02 p0205 N90-11172
The chemistry of the hypochlorite neutralization of hydrazine fuels 02 p0205 N90-11173
Modeling the ozonolysis of hydrazines wastewater 02 p0205 N90-11175
Fuel neutralization by ozone oxidation 02 p0206 N90-11176
Microsensor and pattern recognition techniques in hydrazine detection 02 p0206 N90-11177
Hydrazine dosimetry 02 p0206 N90-11178
Description of a chemiluminescence detector system specifically designed for monitoring airborne hydrazine and oxidizer propellant vapors 02 p0206 N90-11179
Measurement of hydrazine contamination in soils 02 p0206 N90-11180
Occupational safety considerations with hydrazine 02 p0207 N90-11182
Arcjet thruster research and technology. Phase 1: Executive summary
[NASA-CR-182106] 06 p0734 N90-14278
Products of the hypochlorite oxidation of hydrazine fuels
[AD-A213557] 07 p0915 N90-15291
Study of hydrazine metabolism and toxicity
[AD-A217103] 12 p1695 N90-19736
Numerical simulation model for hydrazine attitude control thrusters. Part 1: Model description
[INPE-4952-RPE/601] 14 p1942 N90-21115
Numerical simulation model of hydrazine attitude control thrusters
[INPE-4965-PRE/1534] 15 p2068 N90-21848
Arcjet load characteristics
[NASA-TM-103190] 19 p2669 N90-25181
Advanced propulsion for LEO and GEO platforms
[NASA-TM-103228] 22 p3134 N90-27785

HYDRIDES
NT AMINO RADICAL
NT BERYLLIUM HYDRIDES
NT BORANES
NT BORON HYDRIDES
NT CARBORANE
NT LITHIUM HYDRIDES
NT METAL HYDRIDES
NT PHOSPHINES
NT SILANES
NT ZIRCONIUM HYDRIDES
Extended basis set calculations of atomization energies: Comparison of isogyric and direct results
[AD-A212268] 04 p0471 N90-12702
Rotational and translational effects in collisions of electronically excited diatomic hydrides
[NASA-CR-186770] 20 p2829 N90-26093

HYDROACOUSTICS
U UNDERWATER ACOUSTICS

HYDROAEROMECHANICS
U AERODYNAMICS

HYDROBALLISTICS
Proceedings of a Workshop on the Geoelectric and Geomagnetic Environment of Continental Margins
[AD-A223743] 24 p3493 N90-29739

HYDROBAROPHONES
U HYDROPHONES

HYDROCARBON COMBUSTION
Computation of ramjet internal flowfields
[AD-A212001] 03 p0307 N90-11743
Kinetics and mechanism of soot formation in hydrocarbon combustion
[NASA-CR-186162] 06 p0740 N90-14305
Tropospheric chemistry of natural hydrocarbons and energy-related pollutants: Biosphere/climate feedbacks
[DE90-005643] 11 p1532 N90-18820

HYDROCARBON FUEL PRODUCTION
Correlating microemulsion fuel composition, structure and combustion properties
[DE89-017779] 03 p0333 N90-11898

HYDROCARBON FUELS
NT CRUDE OIL
NT DIESEL FUELS
NT FOSSIL FUELS
NT GASOLINE
NT JET ENGINE FUELS
NT JP-4 JET FUEL
NT JP-8 JET FUEL
NT NATURAL GAS
High energy density solid and liquid hydrocarbon fuels
[AD-A210195] 01 p0053 N90-10304
A simulator for a hydrocarbon ramrocket fuel gas generator: First phase development
[AR-005-621] 02 p0189 N90-11080
Combustion of hydrogen and hydrocarbons in fluorine
[AD-A214621] 09 p1190 N90-16896
Booster propulsion/vehicle impact study, 2
[NASA-CR-179313] 10 p1346 N90-17809
Dual-fuel, dual-mode rocket engine
[NASA-CASE-LAR-13773-1] 12 p1617 N90-19298
Hydrocarbon-fuel/combustion-chamber-liner materials compatibility
[NASA-CR-185203] 14 p1950 N90-21165
Hybrid propulsion technology program. Volume 1: Conceptional design package
[NASA-CR-183953] 15 p2060 N90-21793
Oxidation and ignition characteristics of hydrocarbon fuels
[AD-A218666] 16 p2215 N90-22637
The effect of catalysts on gas-phase hydrocarbon ignition
[AD-A218775] 17 p2371 N90-23499
Regenerative Cu La zeolite supported desulfurizing sorbents
[NASA-CASE-NPO-17480-1-CU] 20 p2830 N90-26098
Flame extinction in compressible flow 21 p2973 N90-28899
Heavy hydrocarbon main injector technology 23 p3294 N90-28633
High energy-density liquid rocket fuel performance
[NASA-CR-185279] 23 p3315 N90-28742

HYDROCARBONS
NT ACETYLENE
NT ALIPHATIC HYDROCARBONS
NT ALKANES
NT ALKENES
NT BENZENE
NT BUTADIENE
NT BUTANES
NT BUTENES
NT CUBANE
NT CYANOACETYLENE
NT CYCLIC HYDROCARBONS
NT CYCLOBUTANE
NT CYCLOHEXANE
NT DIENES
NT ETHANE
NT ETHYLENE
NT METHANE
NT METHYLENE
NT NAPHTHALENE
NT NATURAL GAS
NT OCTANES
NT OXYACETYLENE
NT PHENANTHRENE
NT POLYBUTADIENE
NT PROPANE
NT PROPYLENE
NT PYRENES
NT STILBENE
NT TOLUENE
NT VINYLIDENE
The effect of degree of aromaticity and alkyl substitution of polyaromatic hydrocarbons on instrumental response factors
[DE89-000761] 02 p0196 N90-11117
Conversion of methane to liquid hydrocarbons
[DE89-017547] 03 p0322 N90-11831
Vapour pressures and critical points of liquids. Halogenated hydrocarbons
[ESDU-89006] 03 p0325 N90-11848
Summaries of the thematic conferences on remote sensing for exploration geology
[NASA-CR-185321] 05 p0664 N90-13880
Orthobaric densities and molar volumes of liquids. Aromatic hydrocarbons
[ESDU-89019] 06 p0738 N90-14299
On the mitigation of non-CO2 greenhouse gases
[DE89-016659] 06 p0809 N90-14710
High temperature chemistry of aromatic hydrocarbons
[DE90-003664] 07 p0888 N90-15133
Gas-liquid-liquid equilibria in mixtures of water, light gases, and hydrocarbons
[DE90-003180] 07 p0894 N90-15167
Production of high density aviation fuels via novel zeolite catalyst routes
[AD-A216444] 11 p1494 N90-18601
Tropospheric chemistry of natural hydrocarbons and energy-related pollutants: Biosphere/climate feedbacks
[DE90-005643] 11 p1532 N90-18820
Polycyclic aromatic hydrocarbons in the infrared spectra of IRAS sources 11 p1581 N90-19105
Unidentified infrared features in proto-planetary nebulae 11 p1584 N90-19130
The calculation of hydrogen-bonding properties
[DE90-007534] 13 p1772 N90-20168
Fire hazards of aerosol cans in aircraft cargo compartments
[DOT/FAA/CT-89/32] 17 p2347 N90-23369
Some 1-(diorganooxyphosphonyl)methyl-2,4- and -2,6-dinitro-benzenes
[NASA-CASE-ARC-11425-3] 17 p2367 N90-23475
Carbon deposition model for oxygen-hydrocarbon combustion. Task 6: Data analysis and formulation of an empirical model
[NASA-CR-183986] 20 p2829 N90-26095
Results from the IVL TOR Station at Roervik, Sweden. A contribution to the EURATRAC subproject TOR 20 p2885 N90-26415
Workshop minutes on Remote Sensing of Hydrocarbons and Toxic Pollutants
[PB90-186370] 22 p3194 N90-28127

HYDROCHLORIC ACID
Observations of stratospheric HCl: 1975-1985
[AERONOMICA-ACTA-A-349-1989] 05 p0666 N90-13892
HCl monitor, phase 2
[AD-A213572] 07 p0958 N90-15542
Study of metal corrosion using ac impedance techniques in the STS launch environment 08 p1155 N90-16688
HCl monitor 16 p2209 N90-22599
Infrared absorption gas sensor for the detection of HCl in launch vehicle exhaust clouds 16 p2209 N90-22600
Measurement of HCl by near-infrared diode laser absorption 16 p2209 N90-22601

HYDROCLIMATOLOGY
Frequency distributions and hydroclimatic characteristics of heavy rainstorms in Illinois
[PB89-203988] 02 p0252 N90-11427
Global lake-level variations from 18,000 to 0 years ago: A palaeoclimate analysis
[DE90-000998] 07 p0956 N90-15531

HYDROCRACKING
Production of high density aviation fuels via novel zeolite catalyst routes
[AD-A216444] 11 p1494 N90-18601

HYDROCYANIC ACID
Effects of atmospheric mix and toxic fumes on military performance
[PB89-223630] 04 p0522 N90-13015
The interstellar medium of a starburst galaxy; millimeter interferometric observations of M82 16 p2329 N90-23276

Role of the methylene amidogen (H2CN) radical in the atmospheres of Titan and Jupiter
20 p2947 N90-26769

HYDRODYNAMIC COEFFICIENTS
Hydrodynamic interactions and transport coefficients in a suspension of spherical particles
[DE90-008301] 13 p1801 N90-20336
Design and construction of a packed column simulator operating under atmospheric and reduced pressure
[ISAL-89-60] 16 p2236 N90-22757

HYDRODYNAMIC EQUATIONS
NT HELMHOLTZ VORTICITY EQUATION
A numerical study of thin flame representations
[DE89-017889] 06 p0741 N90-14313
Modelling of the effects of the equatorial electrojet on its environment
[DE89-636298] 06 p0811 N90-14720
Determination of flow-regime boundaries for cohesive particles
[DE90-001405] 07 p0928 N90-15369
MESA 3-D calculations of armor penetration by projectiles with combined obliquity and yaw
[DE89-015265] 07 p0939 N90-15438
Turbulent mixing effects in models of thermal blooming
[DE90-007245] 12 p1667 N90-19580
Boundary layer parameterization in CTM and MM4
12 p1688 N90-19697
Modeling turbulent flow with mixed thermal convection transfer
[ECL-89-19] 17 p2405 N90-23704
Electron positron pair winds and the Eddington limit
19 p2791 N90-25888
Study of the ocean tides by the assimilation of marigraphic and altimetric satellite data in a hydrodynamic model
[ETN-90-97460] 22 p3231 N90-28320
Unstable phenomena in mechanical systems
[AD-A223640] 24 p3537 N90-30001

HYDRODYNAMIC RAM EFFECT
Fluid-structure interaction effects in tank structures due to sloshing and hydrodynamic ram: Coupled Lagangian-Eulerian simulations
02 p0181 N90-11022
Inflatable fuel tank buffer
[AD-D014446] 14 p1921 N90-21002

HYDRODYNAMIC STABILITY
U FLOW STABILITY

HYDRODYNAMIC TUNNELS
U PLASMA JET WIND TUNNELS

HYDRODYNAMICS
NT ELASTOHYDRODYNAMICS
NT ELECTROHYDRODYNAMICS
NT MAGNETOHYDRODYNAMICS
Free-expansion experiments and modeling in detonation: Chemistry and hydrodynamics on a laboratory scale
[DE89-007748] 01 p0053 N90-10302
Electronic and ionic transport in polymers
[AD-A210654] 02 p0201 N90-11148
Carbon in detonations
[DE89-016037] 02 p0208 N90-11189
Acceleration of metal plates
[DE89-016816] 02 p0209 N90-11197
A critical assessment of models available for the shock initiation of heterogeneous explosives
[MRL-TR-89-17] 03 p0333 N90-11896
KIVA reactive hydrodynamics code applied to detonations in high vacuum
[DE89-016979] 03 p0346 N90-11974
Some new algorithms for boundary value problems in smooth particle hydrodynamics
[AD-A211728] 03 p0348 N90-11987
Corrections for non-ideal effects in reflected shock waves at low Mach numbers
[DE90-002192] 06 p0721 N90-14208
Thermodynamic properties and hydrodynamic response of high-density high-temperature C H N O mixtures
[DE90-000836] 06 p0742 N90-14318
Detonation product equation of state for Baratol
[DE90-001050] 06 p0753 N90-14384
Reaction zone structure in supracompressed detonating explosives
[DE90-000832] 06 p0755 N90-14394
Granular flow: Numerical simulation of dry granular flows and calculation of hydrodynamic interactions in suspensions
[DE89-017544] 06 p0777 N90-14518
Hypervelocity impact calculations using CTH: Case studies
[DE90-002891] 06 p0795 N90-14632
Perturbation methods for the calculation of gravitational waves from slightly non-spherical spacetimes with applications to stellar core collapse
06 p0863 N90-15015
Irreversible processes from reversible mechanics
[DE90-001057] 07 p0927 N90-15368
Rayleigh-Taylor instability in compressible fluids
[DE90-003027] 07 p0929 N90-15376
A coning motion apparatus for hydrodynamic model testing in a non-planar cross-flow
[AD-A213431] 07 p0930 N90-15383
Hydrodynamics code calculations of debris clouds produced by ball-plate impacts
[DE89-015270] 07 p0939 N90-15439
Comparison of multidimensional calculations of long-rod impacts on oblique plates
[DE89-015275] 07 p0939 N90-15440
Development of a three-dimensional local scale atmospheric model with turbulence closure model
[DE90-710045] 07 p0960 N90-15551
Brownian trail rectified
[DE90-003339] 07 p0988 N90-15706
Recent progress in understanding the eruptions of classical novae
[NASA-CR-186280] 07 p1014 N90-15870
Thickness, velocity, and temperature measurements in falling liquid films
[DE90-004290] 08 p1063 N90-16151
Material responses to incident x rays
[DE89-015366] 08 p1089 N90-16305
On the numerical solution of the dynamically loaded hydrodynamic lubrication of the point contact problem
[NASA-TM-102427] 09 p1220 N90-17076
Some problems in hydrodynamic lubrication
09 p1229 N90-17133
The effect of the virtual mass force term on the stability of transient two-phase flow analysis
[DE90-733142] 10 p1384 N90-18010
Oblique impact of two cylinders in a uniform flow
[AD-A215933] 10 p1385 N90-18015
Scuffing modelling and experiments for heavily loaded elastohydrodynamic lubrication contacts
10 p1391 N90-18047
The procedures for easy running of the HULL computer code under VMS
[MRL-GD-0023] 10 p1417 N90-18165
Concepts and experiments on space-time chaos
[ETN-90-96255] 11 p1508 N90-18683
Applications of frequency and wavenumber nonlinear digital signal processing to nonlinear hydrodynamics research
[AD-A216259] 12 p1658 N90-19530
Laser-matter interaction at intensities of 10(sup 12) W/cm(sup 2) and below
[DE90-007536] 12 p1669 N90-19590
Direct absorption receiver
[DE90-000311] 12 p1683 N90-19667
Application of natural isotopes in groundwater for solving environmental problems
[DE90-000223] 12 p1689 N90-19703
Time-dependent two-dimensional radiation hydrodynamics of accreting matter onto highly magnetized neutron stars
[DE90-006927] 12 p1737 N90-19985
Enhancement of mass transfer to a rotating cylinder electrode by inert particles suspended in the electrolyte
[DE90-008054] 13 p1771 N90-20165
The viscoelasticity of curing thermosets
[DE90-006535] 13 p1781 N90-20221
Hydrodynamic interactions and transport coefficients in a suspension of spherical particles
[DE90-008301] 13 p1801 N90-20336
Computer simulations and experiments to study the fracture of rods by flying plates
[DE90-008308] 13 p1817 N90-20437
LLE review
[DE90-008958] 14 p1985 N90-21378
The large scale structure of the universe in pancake models of galaxy formation 14 p2040 N90-21701
Computer simulation of time-dependent spherically symmetric spacetimes containing radiating fluids: Formalism and code tests 15 p2185 N90-22483
Interactions of massive stars with the interstellar medium: Bow shocks and superbubbles
15 p2186 N90-22485
The evolution of the supernova remnant IC 443
15 p2186 N90-22486
A galaxy formation cookbook: Recipes and utensils
15 p2190 N90-22508
Fundamental hydrodynamics research
[AD-A219179] 16 p2238 N90-22786
Studies in gravitational lensing and numerical hydrodynamics 16 p2332 N90-23290
On the planar translation of two bodies in a uniform flow
[AD-A220143] 17 p2404 N90-23698
SPHC (Smooth Particle Hydrodynamics Code) manual
[AD-A220743] 17 p2444 N90-23928
Effects of X radiation on the LAMPSHADE orbital debris satellite shield, 2
[DE90-008214] 18 p2510 N90-24341
Rheology and microstructure of concentrated suspensions
[DE90-009976] 18 p2520 N90-24391
Activities report of the Hydraulics Research Laboratory
[ETN-90-96568] 19 p2687 N90-25281
Radiative shock oscillations in AM Her cataclysmic binaries 19 p2783 N90-25834
A lattice gas model for thermohydrodynamics
[DE90-011964] 20 p2933 N90-26690
An optical study of the flow start-up process in four convergent-divergent nozzles
[AD-A222918] 21 p2963 N90-26846
Hydrodynamic skin-friction reduction
[NASA-CASE-LAR-14078-1-CU] 21 p3003 N90-27071
X ray laser program report for FY 1989
[AD-A221818] 21 p3009 N90-27107
Experimental investigation of the hydrodynamic forces on the shroud of a centrifugal pump impeller
[NASA-CR-186952] 21 p3009 N90-27108
Reduced distribution functions and nonequilibrium thermodynamics of single component fluids
[PB90-189119] 22 p3254 N90-28428
Effects of friction and end losses on MHD thruster efficiency
[DE90-013673] 23 p3289 N90-28608
Three functions that model empirically measured unfrozen water content data and predict relative hydraulic conductivity
[AD-A223875] 23 p3343 N90-28892
The formation of globular clusters
23 p3410 N90-29272
Innovative uses of parallel computers
[AD-A223578] 24 p3533 N90-29980
Unstable phenomena in mechanical systems
[AD-A223640] 24 p3537 N90-30001

HYDROELASTICITY
Analysis of an elastohydrodynamic lubricated point contact: User's manual
[AD-A214257] 07 p0943 N90-15459
Hydroelastic problems in space flight vehicles
[LRT-WE-9-FB-11(1989)] 21 p2967 N90-26868

HYDROELECTRICITY
The 1989 National Convention Record IEE Japan, part 8
[DE89-910081] 09 p1210 N90-17013
Draft global warming study
[DE90-008446] 13 p1830 N90-20507

HYDROFLUORIC ACID
Theoretical Hugoniot of liquid hydrogen fluoride
[DE89-016504] 02 p0193 N90-11099
A high level Ab initio study of the anionic hydrogen-bonded complexes FH-CN-, FH-NC-, H2O-CN- and H2O-NC- 02 p0272 N90-11553

HYDROGEN
NT DEUTERIUM
NT HYDROGEN ISOTOPES
NT LIQUID HYDROGEN
NT TRITIUM
A laser-driven source of polarized hydrogen and deuterium
[DE89-015130] 01 p0075 N90-10429
Hydrogen-silicon carbide interactions
[NASA-TM-102382] 02 p0200 N90-11144
High pressure studies of planetary matter
[DE89-017738] 03 p0428 N90-12455
A high-speed digital camera system for the observation of rapid H-alpha fluctuations in solar flares
03 p0435 N90-12491
Rapid heating tensile tests of high-energy-rate-forged 316L stainless steel charged with hydrogen and tritium
[DE89-017869] 04 p0474 N90-12717
Interactive computer program for the generation of enthalpy-entropy and temperature-entropy charts of nitrogen and hydrogen
[DLR-FB-89-27] 04 p0533 N90-13081
Unsteady diffusion from a hemispherical pit
[NPL-DMA(A)-190] 04 p0553 N90-13220
Effect of adsorbed arsenic on the decomposition rate of nickel hydride
[AD-A213245] 05 p0621 N90-13624
Propagation of sound in vibrationally excited nitrogen and hydrogen gas mixtures
[AD-A213002] 05 p0696 N90-14073
Dynamics Explorer-1 satellite study of electrostatic ion cyclotron waves 05 p0702 N90-14105
The effect of hydrogen charging on the mechanical properties of aluminum alloy 2090
[DE90-000129] 06 p0746 N90-14341
Hydrogen radical enhanced growth of solar cells
[DE89-009497] 06 p0806 N90-14694
Evidence for anomalous cosmic ray hydrogen
06 p0861 N90-15005

Interaction of hydrogen in palladium as prescribed by the embedded atom method
[DE90-003893] 07 p0907 N90-15244
Annual operating plan for fiscal year 1990 for chemical/hydrogen energy systems program
[DE90-003964] 07 p0955 N90-15527
Transition state spectroscopy of hydrogen transfer reactions
[AD-A215041] 09 p1191 N90-16901
Evaluation of a diffusion/trapping model for hydrogen ingress in high strength alloys
[AD-A215528] 09 p1194 N90-16920
Reactions of atmospheric species with clean and H, C, and O implanted species
[AD-A214602] 09 p1244 N90-17218
Improved performance in co-processing through fundamental and mechanistic studies in hydrogen transfer and catalysis
[DE90-004794] 10 p1352 N90-17839
Hydrogen sulfide effect on hydrogen entry into iron: A mechanistic study
[AD-A216214] 10 p1354 N90-17854
Characterization of tetrahydrogen via state-selected excitation of H2
[AD-A216239] 10 p1355 N90-17855
FLUSH: A tool for the design of slush hydrogen flow systems
[NASA-TM-102467] 10 p1361 N90-17890
Hydrogen energy coordinating committee: Summary of DOE hydrogen programs
[DE90-004480] 10 p1361 N90-17891
Breeding of hydrogen producing anaerobic bacteria. Cellulase secretion from transformed Escherichia coli JM109
[DE90-710739] 10 p1410 N90-18133
Results of the H-mode experiments with JT-60 outer and lower divertors
[DE90-733146] 10 p1432 N90-18265
The excitation of molecular hydrogen and its significance 11 p1582 N90-19117
High-excitation lines of molecular hydrogen: A discriminant between shock models 11 p1582 N90-19118
Molecular hydrogen in the HII region G333.6-0.2 11 p1583 N90-19121
Infrared spectroscopy of star formation in galaxies: Extreme conditions and very short time scales 11 p1586 N90-19147
H-alpha emission lines in high redshift quasars 11 p1587 N90-19149
A new model for hydrogen absorption in welds
[AD-A216951] 12 p1626 N90-19347
Electron energy distributions and vibrational population distributions
[DE90-005550] 12 p1711 N90-19825
Supercomputer applications for materials science: Ordering effects of hydrogen in palladium
[DE90-004664] 12 p1718 N90-19870
Application of railgun principle to high-velocity hydrogen pellet injection for magnetic fusion reactor refueling
[DE90-008281] 13 p1761 N90-20109
The calculation of hydrogen-bonding properties
[DE90-007534] 13 p1772 N90-20168
Research of the interaction between hydrogen and deuterium with atomic eigen defects and dislocations in nickel and iron
[ETN-90-95380] 13 p1776 N90-20195
Evaluation of industrial magnetic heat pump/refrigerator concepts that utilize superconducting magnets
[DE90-008093] 13 p1787 N90-20258
Impedance studies of Ni/Cd and Ni/H2 cells using the cell case as a reference electrode 13 p1824 N90-20473
Neutron autoradiography of hydrogen
[DE90-612930] 14 p1948 N90-21148
Surface characterization of hydrogen charged and uncharged alpha-2 and gamma titanium aluminide alloys using AES and REELS
[NASA-CR-186561] 14 p1951 N90-21171
On the use of external burning to reduce aerospace vehicle transonic drag
[NASA-TM-103107] 15 p2052 N90-21762
Photosynthetic water splitting, phase 2
[PB90-132671] 15 p2066 N90-21833
The temperature variation of hydrogen diffusion coefficients in metal alloys
[NASA-TM-100397] 15 p2067 N90-21836
The effect of hydrogen and microstructure on the deformation and fracture behavior of a single crystal nickel-base superalloy
[NASA-CR-185219] 15 p2068 N90-21849
The ratio of neutral hydrogen to neutral helium in the local interstellar medium 15 p2189 N90-22499
Deformation and fracture of aluminum-lithium alloys: The effect of dissolved hydrogen 16 p2219 N90-22658
H2, fixed architecture, control design for large scale systems
[NASA-CR-180471] 16 p2226 N90-22698
Molecular evolution in astrophysical environments 16 p2332 N90-23291
Effects of internal hydrogen on the vacancy loop formation probability in Al
[DE90-011114] 18 p2527 N90-24422
ISS and TPD study of the adsorption and interaction of CO and H2 on polycrystalline Pt 18 p2559 N90-24602
Mars in situ propellants: Carbon monoxide and oxygen ignition experiments
[NASA-TM-103202] 20 p2823 N90-26065
Hydrogen induced fracture characteristics of single crystal nickel-based superalloys
[NASA-CR-183992] 20 p2832 N90-26108
Isothermal compressibility of SPC/E water
[AD-A222723] 20 p2925 N90-26643
Rate constant for reaction of atomic hydrogen with germane 20 p2947 N90-26768
Concentration, temperature, and density in a hydrogen-air flame by excimer-induced Raman scattering 21 p2974 N90-26903
Disk mass densities in edge-on spiral galaxies 21 p3097 N90-27600
Hydrogen in palladium alloys: Experiments, models and simulations
[PB90-200429] 22 p3156 N90-27896
Catalytic ignition of hydrogen/oxygen 23 p3293 N90-28627
Tripropellant combustion process 23 p3293 N90-28631
On hydrogen chemisorption on metals: The electron correlation effects
[DE90-627318] 24 p3448 N90-29473
Formation of hydrogen line and continuum emission in young stellar objects 24 p3562 N90-30150

HYDROGEN AIR FUEL CELLS
U HYDROGEN OXYGEN FUEL CELLS

HYDROGEN ATOMS
Spin-orbit relaxation rates of Bi(6p(3)) 2D(3/2) following photolysis of Bi(CH3)3 at lambda = 193 nm
[AD-A211792] 03 p0402 N90-12303
Atomic hydrogen as a launch vehicle propellant
[NASA-TM-102459] 06 p0735 N90-14284
Interaction of hydrogen in palladium as prescribed by the embedded atom method
[DE90-003893] 07 p0907 N90-15244
Hydrogen desorption from the monohydride phase on Si(100)
[AD-A215237] 09 p1191 N90-16903
VUV (Vacuum Ultraviolet) laser diagnostics of H(-) ion sources
[DE90-006072] 11 p1514 N90-18719
Positron scattering by atomic hydrogen using optical potentials and with positronium formation 11 p1557 N90-18966
The calculation of the contributions to low energy e+H2 scattering from sigma u+ and Pion u symmetries using the Kohn variational method 11 p1557 N90-18969
Ionisation of atomic hydrogen by positron impact 11 p1558 N90-18977
Hydrogen assay foil counting system
[DE90-007415] 12 p1624 N90-19332
Interaction of atomic hydrogen with pico- and femtosecond laser pulses
[AD-A218426] 16 p2241 N90-22785
Use of ab initio theory in studying various chemical systems
[AD-A220913] 18 p2521 N90-24396
Diagnostics for hydrogen atoms and molecules in H-atom sources and beams using VUV laser light
[AD-A222340] 21 p3074 N90-27476
Experimental studies leading to energy storage. Spectroscopy and dynamics of polyatomic hydrogen in liquid, solid and gaseous hydrogen plasmas
[AD-A224343] 24 p3547 N90-30066
On a calculation of the ground-state energy in quantum mechanics
[DE90-627182] 24 p3555 N90-30119

HYDROGEN BONDS
Theoretical Hugoniot of liquid hydrogen fluoride
[DE89-016504] 02 p0193 N90-11099
Theoretical investigation of gas-surface interactions
[NASA-CR-185492] 02 p0272 N90-11552
A high level Ab initio study of the anionic hydrogen-bonded complexes FH-CN-, FH-NC-, H2O-CN- and H2O-NC- 02 p0272 N90-11553
Report of the Specialists' Workshop on Phase Transition Studies on Hydrogen-Bonded Crystals by Neutron and X-ray Diffractometries
[DE89-906638] 02 p0285 N90-11631
Low frequency polarized and depolarized light scattering in H-bonded liquids: CH3(CH2)n-1OH (n = 1,...5)
[PREPRINT-693] 05 p0700 N90-14100
Chemistry of large molecules
[DE90-000813] 06 p0751 N90-14366
Determination of the minimum energy conformation of alkyl substituted pyrazines
[AD-A216974] 11 p1484 N90-18539
The calculation of hydrogen-bonding properties
[DE90-007534] 13 p1772 N90-20168
Use of ab initio theory in studying various chemical systems
[AD-A220913] 18 p2521 N90-24396
Miscibility and phase behavior of poly (enaminonitrile)/PEO blends
[AD-A222255] 21 p2987 N90-26975
Design of organic nonlinear optical materials
[AD-A222400] 21 p3084 N90-27536
Solid-state N15 NMR of N15-labeled nylon 6 and nylon 11
[AD-A223271] 24 p3446 N90-29459
Mechanism of habit change for atmospheric ice crystal growth 24 p3489 N90-29717

HYDROGEN CHLORIDES
NT HYDROCHLORIC ACID
Reactions of hydrogen chloride and boron trichloride with trimethylsilylamino groups
[AD-A209006] 01 p0038 N90-10209
HCl monitor, phase 2
[AD-A213572] 07 p0958 N90-15542
HCl Vapor Characterization and Detection. JANNAF Safety and Environmental Protection Subcommittee Workshop
[AD-A216252] 16 p2208 N90-22596
The HCl/aerosol problem 16 p2208 N90-22597
Viscosity, density and conductivity of ImCl(HCl) sub 1.3
[AD-A218902] 16 p2216 N90-22641

HYDROGEN CLOUDS
NT H I REGIONS
NT H II REGIONS
NT ORION NEBULA
Planetary nebulae 11 p1583 N90-19122
Fluorescent molecular hydrogen emission from star-forming galaxies 11 p1588 N90-19155
Near infrared spectroscopy and spectroscopic imaging of NGC253 11 p1588 N90-19159

HYDROGEN COMPOUNDS
NT AMINO RADICAL
NT BERYLLIUM HYDRIDES
NT BORANES
NT BORON HYDRIDES
NT CARBORANE
NT DEUTERIUM COMPOUNDS
NT HEAVY WATER
NT HYDRIDES
NT HYDROCYANIC ACID
NT HYDROGEN PEROXIDE
NT HYDROGEN SULFIDE
NT LITHIUM HYDRIDES
NT METAL HYDRIDES
NT PHOSPHINES
NT SILANES
NT ZIRCONIUM HYDRIDES
A comparison of photospheric and circumstellar (HCN)/(CO)-ratios for bright carbon stars
[PB90-151101] 15 p2184 N90-22477
Optical properties and transport properties of hydrogenated amorphous silicon
[ETN-90-97215] 20 p2927 N90-26656

HYDROGEN CYANIDES
U HYDROCYANIC ACID

HYDROGEN DEUTERIUM OXIDE
U HEAVY WATER

HYDROGEN EMBRITTLEMENT
Determination of the gaseous hydrogen ductile-brittle transition in copper-nickel alloys
[NASA-TM-86494] 04 p0474 N90-12715
A feasibility study of hydrogen dosage estimation in screw threads submitted to surface electrolytic treatment
[CETIM-110110] 04 p0476 N90-12730
Rapid heating tensile tests of hydrogen-charged high-energy-rate-forged 316L stainless steel
[DE90-000591] 06 p0746 N90-14342
Acoustic emission during intergranular stress corrosion cracking
[DE90-002894] 06 p0749 N90-14355
The effects of hydrogen embrittlement of titanium 08 p1156 N90-16698
Hydrogen sulfide effect on hydrogen entry into iron: A mechanistic study
[AD-A216214] 10 p1354 N90-17854
A review of the mechanism and kinetics of electrochemical hydrogen entry and degradation of metallic systems
[AD-A216671] 10 p1355 N90-17857
Hydrogen embrittlement of titanium and its alloys
[DE90-602366] 10 p1355 N90-17858

Environmental embrittlement: A major cause for low ductility of ordered intermetallics
[DE90-006161] 10 p1356 N90-17864
Response of unirradiated and neutron-irradiated vanadium alloys to Charpy-impact loading
[DE90-004878] 11 p1486 N90-18551
Hydrogen, thermal ageing and the role of carbides in fatigue of a high strength steel
[AERE-R-13599] 13 p1774 N90-20183
Statistical treatment of slow strain rate data for assessment of hydrogen embrittlement in low alloy high strength steel
[ARL-MAT-R-122] 20 p2832 N90-26106

HYDROGEN ENGINES
Development of high-activity para- to ortho-hydrogen conversion catalysts, volume 2
[AD-A218700] 16 p2215 N90-22638
Gas Turbine Combustion, volume 2
[VKI-LS-1990-02-VOL-2] 20 p2811 N90-25995
Supersonic combustor testing
20 p2811 N90-25998
A comparison of scramjet engine performances of various cycles
[NAL-TR-1042] 24 p3434 N90-29397

HYDROGEN FLUORIDE LASERS
U HF LASERS

HYDROGEN FLUORIDES
U HYDROFLUORIC ACID

HYDROGEN FUELS
Thermal protection systems for reentry and hypersonic flight
[DLR-MITT-89-14] 05 p0613 N90-13577
Slush Hydrogen (SLH2) technology development for application to the National Aerospace Plane (NASP)
[NASA-TM-102315] 06 p0732 N90-14268
Dual-fuel, dual-mode rocket engine
[NASA-CASE-LAR-13773-1] 12 p1617 N90-19298
Photosynthetic water splitting, phase 2
[PB90-132671] 15 p2066 N90-21833
The use of hydrogen in energy economy of Finland
[DE90-796180] 20 p2881 N90-26388

HYDROGEN IONS
Observation of excited H(sup 0) atoms produced by relativistic H(sup (minus)) ions in carbon and formvar foils
[DE89-015301] 01 p0120 N90-10688
Atomic and molecular surface and volume processes in the analysis of negative hydrogen discharges
[DE89-015705] 03 p0401 N90-12294
Orion B: Anatomy of a star-forming region
05 p0710 N90-14155
Relativistic self-consistent field studies of atoms and molecules
[AD-A214101] 07 p0991 N90-15724
Generation of H-, H2v(double prime), and H atoms by H2+ and H3+ ions incident upon barium surfaces
[DE90-005549] 09 p1280 N90-17423
Positronium formation in e+ plus H- collisions
11 p1561 N90-18993
Merged beam studies into the mechanisms of hydrogen molecular ion recombination
[AD-A216469] 11 p1562 N90-19002
Surface production of ions
[AD-A216470] 11 p1562 N90-19003
Convergence of hyperspherical adiabatic expansion for helium-like systems
[DE90-620526] 16 p2214 N90-22631
Proceedings of the High Energy Density Materials Contractors Conference
[AD-A223793] 24 p3484 N90-29695
Experimental studies leading to energy storage. Spectroscopy and dynamics of polyatomic hydrogen in liquid, solid and gaseous hydrogen plasmas
[AD-A224343] 24 p3547 N90-30066

HYDROGEN ISOTOPES
NT DEUTERIUM
NT TRITIUM
Acceleration of small, light projectiles (including hydrogen isotopes) to high speeds using a two-stage light gas gun
[DE90-002479] 06 p0729 N90-14253
Interaction of hydrogen isotopes with metals: Deuterium trapped at lattice defects in palladium
[DE90-000811] 06 p0747 N90-14344
Hydrogen desorption from the monohydride phase on Si(100)
[AD-A215237] 09 p1191 N90-16903

HYDROGEN MASERS
Atomic velocity distributions out of hydrogen maser dissociators
[AD-A219500] 17 p2408 N90-23721

HYDROGEN METABOLISM
Carbon and hydrogen metabolism of green algae in light and dark
[DE90-008648] 13 p1849 N90-20612

HYDROGEN OXYGEN ENGINES
Cycle analysis of scramjet engines
[NAL-TR-1002] 01 p0008 N90-10035
A rocket engine design expert system
[NASA-TM-102373] 01 p0032 N90-10172
Heat transfer to throat tubes in a square-chambered rocket engine at the NASA Lewis Research Center
[NASA-TM-102336] 02 p0189 N90-11082
The Pathfinder chemical transfer propulsion program
11 p1471 N90-18471
Advanced APS impacts on vehicle payloads
11 p1472 N90-18472
A comparison of analytical results for 20 K LOX/hydrogen instabilities
[NASA-TM-103166] 19 p2670 N90-25186
Performance evaluation of LE-7 high pressure pumps
[DE90-505523] 20 p2817 N90-26034
Noncoplanar orbit transfer optimization for an aeroassisted sortie vehicle 22 p3128 N90-27752
Oxygen/hydrogen technology test bed status update
23 p3290 N90-28613
High/variable mixture ratio oxygen/hydrogen engines
23 p3295 N90-28637
High/variable mixture ratio O2/H2 engine
23 p3295 N90-28638
Variable mixture ratio performance through nitrogen augmentation 23 p3295 N90-28639
High variable mixture ratio oxygen/hydrogen engine
23 p3295 N90-28640
Investigation of fluid dynamic performance of LE-7 liquid oxygen pump
[NAL-TR-1020] 24 p3476 N90-29650

HYDROGEN OXYGEN FUEL CELLS
Long endurance underwater power system
[AD-A211386] 03 p0366 N90-12096
Hydrogen/oxygen SPE (trademark) electrochemical devices for zero-g applications 10 p1333 N90-17710
Water removal studies on high power hydrogen-oxygen fuel cells with alkaline electrolytes
10 p1333 N90-17712
Integrated regenerative fuel cell experimental evaluation
[NASA-CR-185183] 11 p1530 N90-18808
Space Electrochemical Research and Technology (SERT), 1989
[NASA-CP-3056] 13 p1821 N90-20454
Hydrogen-oxygen proton-exchange membrane fuel cells and electrolyzers 13 p1823 N90-20467
A solar power system for an early Mars expedition
[NASA-TM-103219] 22 p3243 N90-28393

HYDROGEN PEROXIDE
A thermochemical analysis of proposed working fluids for electrothermal guns
[AD-A210661] 02 p0159 N90-10910
Lifetime of singlet oxygen in aqueous hydrogen peroxide (BHP)
[AD-A211545] 03 p0403 N90-12306
Measurement and correlation of the solubility and diffusion coefficient for oxygen and chlorine in basic hydrogen peroxide
[AD-A212348] 04 p0472 N90-12703
Destruction of peroxy radical by Cu ion catalysed reactions on atmospheric particles
20 p2887 N90-26429
Enhanced bioreclamation of jet fuels: A full-scale test at Eglin AFB, Florida
[AD-A222348] 21 p2990 N90-26992

HYDROGEN PLASMA
Hydrogen-assisted thermal donor formation in silicon
[DE89-016809] 02 p0279 N90-11594
Observations of electrostatic hydrogen cyclotron waves and electric field fluctuations near one Hz in auroral acceleration regions 05 p0658 N90-13842
Workshop on Hydrogen Effects in InP and Related Compounds
[AD-A215197] 09 p1290 N90-17479
Model of oxygen ions resonant lines emission of REB-heated plasma
[IPPCZ-294] 10 p1432 N90-18261
Computerized analysis of hydrogen plasma in a compact H(sup -) cusp source
[DE90-006881] 11 p1569 N90-19029
Growth, characterization and device development in monocrystalline diamond films
[AD-A218211] 13 p1898 N90-20895
Characterization of plasma flow through magnetic nozzles
[AD-A221044] 18 p2617 N90-24905
Experimental studies leading to energy storage. Spectroscopy and dynamics of polyatomic hydrogen in liquid, solid and gaseous hydrogen plasmas
[AD-A224343] 24 p3547 N90-30066

HYDROGEN PRODUCTION
Development and evaluation of a process to produce hydrogen from coal
[DE90-003937] 08 p1052 N90-16084
Antihydrogen formation in collisions of positronium with antiprotons 11 p1560 N90-18988
IEA (International Energy Agency) implementing agreement for a program of research and development on the production of hydrogen from water. Task 9: Hydrogen production
[DE90-007354] 12 p1625 N90-19337
Photosynthetic water splitting, phase 2
[PB90-132671] 15 p2066 N90-21833
Impact of low gravity on water electrolysis operation
[NASA-CR-185521] 15 p2072 N90-21870
Hydrogen Energy Coordinating Committee summary of DOE hydrogen programs for FY 1988
[DOE/CE-0242] 21 p2989 N90-26989
Detection of vibrationally excited H2(v double prime) for H(-) production
[AD-A222560] 22 p3180 N90-28044

HYDROGEN RECOMBINATIONS
Predictions of infrared recombinations lines in stellar winds of hot stars 11 p1585 N90-19136
Infrared (FeII), H and H2 lines in galaxy nuclei
11 p1587 N90-19153
H53-alpha emission from M82
11 p1588 N90-19156
Few-body collisions in a weakly interacting Bose gas
[ETN-90-96893] 18 p2613 N90-24886

HYDROGEN SULFIDE
Growth and characterization of zinc sulfide films by conversion of zinc oxide films with H2S
[AD-A213345] 04 p0561 N90-13271
The continuous crystallization of sulfur formed by the liquid-phase reaction of hydrogen sulfide and sulfur dioxide
[DE90-003991] 08 p1041 N90-16018
Hydrogen sulfide effect on hydrogen entry into iron: A mechanistic study
[AD-A216214] 10 p1354 N90-17854
A review of the mechanism and kinetics of electrochemical hydrogen entry and degradation of metallic systems
[AD-A216671] 10 p1355 N90-17857

HYDROGEN 2
U DEUTERIUM

HYDROGEN 3
U TRITIUM

HYDROGEN-BASED ENERGY
On the dynamics of the combustion process of hydrogen-air and hydrogen-methane-air mixtures
[DLR-FB-89-39] 11 p1485 N90-18548
Hydrogen Energy Coordinating Committee summary of DOE hydrogen programs for FY 1988
[DOE/CE-0242] 21 p2989 N90-26989

HYDROGENATION
Catalogic hydrogenation of carbon monoxide
[DE89-017813] 03 p0323 N90-11834
Energy concentration induced by phase transitions in hydrogenated metals
[PREPRINT-672] 05 p0625 N90-13650
Method for refining microstructures on prealloyed titanium powder compacts
[AD-D014280] 08 p1043 N90-16030
Improved performance in co-processing through fundamental and mechanistic studies in hydrogen transfer and catalysis
[DE90-004794] 10 p1352 N90-17839
Hydrogenated amorphous silicon films prepared by glow discharge of disilane
[DE90-000309] 11 p1491 N90-18581
Morphological consequences of catalytic hydrogenation of polymers in the bulk
[DE90-007276] 11 p1494 N90-18598
Hydrous metal oxide-supported catalysts. Part 2: Catalytic properties and applications
[DE90-008098] 12 p1625 N90-19336
Hydrogenation of stainless steels implanted with nitrogen
[DE90-617397] 16 p2221 N90-22666
Methods for evaluation of thermally induced reactions in liquid propellants
[AD-A218750] 16 p2225 N90-22694
Diagnostics of glow discharges used to produce hydrogenated amorphous silicon films
[DE90-000329] 18 p2522 N90-24402
Structural and electronic studies of a:SiGe:H alloys
[DE90-000313] 19 p2710 N90-25424
Mass spectrometry of poly(methyl methacrylate)s of low molecular weight 20 p2829 N90-26091

HYDROGENOLYSIS
NT HYDROCRACKING
Correlations between surface structure and catalytic activity/selectivity
[DE90-003755] 07 p0896 N90-15181

HYDROGEOLOGY
Physiographic and geological setting of the Coastal Engineering Research Center's field research facility
[AD-A210772] 02 p0238 N90-11356

Evolution of overlapping spreading centers: A Sea Mark 2 investigation
[AD-A214278] 07 p0965 N90-15576
LANDSAT Thematic Mapper for hydrogeological mapping in Egypt
[BCRS-89-28] 11 p1527 N90-18791
Evolution of overlapping spreading centers: A SeaMARC 2 investigation
[AD-A223102] 21 p3025 N90-27200
Study and analysis of leaking underground storage tank remediation techniques incorporated in states in EPA Region 6
[PB90-214834] 23 p3333 N90-28847

HYDROGRAPHY
Realization of a different NAVSTAR global positioning system for hydrographic surveying
[ETN-89-95720] 04 p0515 N90-12972
Current velocity and hydrographic observations in the southwestern North Atlantic Ocean: Subtropical Atlantic Climate Studies (STACS), 1988
[PB89-230825] 04 p0521 N90-13010
Comparison of circulation obtained through the trajectory of a drifting buoy tracked by satellite and hydrographic data in the Bransfield Strait
[INPE-4946-TDL/387] 11 p1537 N90-18850
The development of a real-time decimeter-level positioning system using Global Positioning System (GPS) technology
[AD-A218695] 16 p2199 N90-22552
Coastal field data collection program. Hurricane Gilbert storm surge data
[AD-A218752] 17 p2426 N90-23823
Efficient representation of the hydrographic structure of the north atlantic ocean and aspects of the circulation from objective methods
[AD-A218606] 17 p2429 N90-23841
Determination of tide heights from airborne bathymetric data
[AD-A220412] 17 p2430 N90-23848
A range-dependent analysis of acoustic transmission across a cold filament in the California current
[AD-A220175] 18 p2583 N90-24709

HYDROKINETICS
U HYDROMECHANICS

HYDROLOGICAL CYCLE
Low-frequency cloud-radiation interactions
22 p3225 N90-28289

HYDROLOGY
NT HYDROGEOLOGY
Earth Sciences Division annual report 1988
[DE90-002617] 06 p0801 N90-14663
Utilization of remote sensing in geoscientific development and projects 08 p1094 N90-16334
Hypotheses testing of watershed/landscape dynamics in northern Alaska using digital analysis
[DE90-006721] 13 p1820 N90-20450
In-situ fracture stiffness determination
[DE90-009202] 15 p2129 N90-22173
Fundamental studies on hydrology, hydraulics and geometry of river networks
[AD-A218662] 16 p2250 N90-22830

HYDROLOGY MODELS
Support of hydrological models calculations by satellite data 08 p1094 N90-16337
Remote sensing and run-off modelling in the Lake Victoria Basin, Kenya
[BCRS-89-19] 11 p1526 N90-18788
Computer program for converting rectangular coordinates to latitude-longitude coordinates
[PB90-231796] 23 p3342 N90-28883

HYDROLYSIS
Analysis of surface modified colloidal silicas
[DE89-015849] 01 p0047 N90-10267
Preparation, purification and densification of zinc sulfide powder from organometallics
[AD-A210943] 01 p0052 N90-10298
Polyelectrolyte-diffused zinc phosphate conversion coatings and polyacid coupling primers for corrosion protection of steel and aluminum, and alkali-catalyzed hydrolysis of polyimide-based materials
[AD-A212240] 04 p0480 N90-12754
Energies of organic compounds
[DE90-003174] 06 p0743 N90-14324
Synthesis of tetrafluorohydrazine
[AD-D014281] 08 p1052 N90-16083
Hydrous metal oxide-supported catalysts. Part 1: Preparation chemistry and physical and chemical properties
[DE90-007607] 13 p1771 N90-20161
Polysiloxanes derived from the controlled hydrolysis of tetraethoxysilane as precursors to silica for use in ceramic processing
[NASA-TM-102489] 15 p2070 N90-21858
Surface structure and chemistry of high surface area silica gels
[DE90-007684] 15 p2071 N90-21865
Kinetics and structure of silicate sol-gels
[DE90-015702] 24 p3456 N90-29521

HYDROMAGNETIC FLOW
U MAGNETOHYDRODYNAMIC FLOW

HYDROMAGNETIC STABILITY
U MAGNETOHYDRODYNAMIC STABILITY

HYDROMAGNETIC WAVES
U MAGNETOHYDRODYNAMIC WAVES

HYDROMAGNETICS
U MAGNETOHYDRODYNAMICS

HYDROMAGNETISM
U MAGNETOHYDRODYNAMICS

HYDROMECHANICS
NT ELASTOHYDRODYNAMICS
NT ELECTROHYDRODYNAMICS
NT HYDRODYNAMICS
NT HYDROSTATICS
NT MAGNETOHYDRODYNAMICS
Preliminary airworthiness evaluation of the Woodward hydromechanical unit installed on T700-GE-700 engines in the UH-60A helicopter
[AD-A216751] 11 p1464 N90-18430
Modeling towed cable system dynamics
[AD-A223610] 24 p3476 N90-29644

HYDROMETEOROLOGY
NT MARINE METEOROLOGY
Data reduction of GOES (Geostationary Operational Environmental Satellite) information from DCP (Data Collection Platform) networks
[AD-A215844] 12 p1678 N90-19637

HYDROMETERS
Humidity local measurements in the middle atmosphere 05 p0657 N90-13833

HYDROPHONES
Hydrophone investigations of earthquakes and explosion generated high-frequency seismic phases
[AD-A212055] 03 p0371 N90-12122
In situ investigation of sea surface noise from a depth of one meter
[AD-A220158] 17 p2432 N90-23857
Diffraction about acoustically soft panels
[AD-A220850] 17 p2469 N90-24115
Some design considerations for small piezo-electrical ceramic transducers
[FEL-1989-68] 22 p3178 N90-28034
Piezoelectric and electrostrictive materials for transducer applications, volume 1
[AD-A223560] 24 p3480 N90-29868

HYDROPONICS
Continuous hydroponic wheat production using a recirculating system
[NASA-TM-102784] 11 p1538 N90-18853
Utilization of the water soluable fraction of wheat straw as a plant nutrient source
[NASA-TM-103497] 19 p2716 N90-25455

HYDROSTATIC PRESSURE
Cellular and molecular mechanisms of high pressure inotropy in cardiac muscle
[AD-A211695] 03 p0381 N90-12170
Piezoelectric polymer PVDF shock gauge: State of the research art
[ISL-CO-207/89] 11 p1512 N90-18705
On computing the pressure by the p version of the finite element method for Stokes problem
[AD-A219887] 17 p2404 N90-23697
Pressure in the study of organic superconductors
[DE90-011049] 18 p2625 N90-24959
Pressure dependence of thermoelectric power of high T(sub c) 123 compound
[PD-MT-9001] 20 p2829 N90-26092

HYDROSTATICS
As observational and theoretical investigation of stellar flares 06 p0862 N90-15012
Assessment of worm gearing for helicopter transmissions
[NASA-TM-102441] 08 p1025 N90-15923
Coherent phase transformation under nonhydrostatic stress-wave loading
[DE90-005719] 10 p1396 N90-18072
The +Gz protection in the future: Review of scientific literature
[AD-A217887] 13 p1851 N90-20623
Failure mechanisms under complex loading of glass-reinforced polyester composites and their matrices: The effect of superposed hydrostatic pressures up to 300 MPa on axial tensile and compressive strengths, and in-plane shear properties of unidirtionally reinforced glass-polyester composites and the relevant polyesters
15 p2110 N90-22072
A study of creep damage using microradiography and continuum damage mechanics 15 p2117 N90-22109
Semigeostrophic flow over orography in a stratified rotating atmosphere 15 p2127 N90-22163
Pseudo-steady diffusional growth or collapse of bubbles rising in time dependent pressure fields
[AD-A218825] 16 p2237 N90-22764
Evolutionary models of the rotating sun and implications for other low mass stars 16 p2339 N90-23329
Integrated controls and health monitoring fiberoptic shaft monitor
[NASA-CR-185210] 24 p3472 N90-29622

HYDROTHERMAL STRESS ANALYSIS
Hygrothermal effects on the complex moduli of composite laminates 01 p0033 N90-10182
Hygrothermal deformations of composite shells
02 p0185 N90-11055

HYDROX ENGINES
U HYDROGEN OXYGEN ENGINES

HYDROXIDES
NT LITHIUM HYDROXIDES
NT POTASSIUM HYDROXIDES
Cycle-life improvement of Zn/NiOOH cells by the addition of Ca(OH)2 to the zinc electrode
[DE90-004040] 08 p1062 N90-16139

HYDROXYL COMPOUNDS
NT ALCOHOLS
NT ETHYL ALCOHOL
NT GLYCOLS
NT ISOPROPYL ALCOHOL
NT METHYL ALCOHOL
NT PHENOLS
NT POLYVINYL ALCOHOL

HYDROXYL EMISSION
Further observations of rotationally excited far infrared OH16 and OH18 emission in Orion-KL: Tighter constraints on the nature of the emitting region
[NASA-CR-186004] 05 p0710 N90-14156
A measurement of hydroxyl in the daytime mesosphere 06 p0814 N90-14732
Effects of gravity waves on the polar O2 and OH airglow 08 p1101 N90-16373
Simultaneous observations of the emissions OI (5577), O2A(0,1), NaD(5893) and OH(9,4) and the rotational temperatures TO2 and TOH in the upper atmosphere
[INPE-4851-TDL/366] 10 p1407 N90-18113
A three-year study of the OH masers in Orion-KL and a study of the (3,2) transition of ammonia
15 p2183 N90-22471
Kinematic models of cometary comae
15 p2188 N90-22495
Global changes in tropospheric chemistry
19 p2708 N90-25411
Temperature and OH concentrations in a solid propellant flame using absorption techniques
[AD-A222591] 20 p2830 N90-26100

HYDROXYL RADICALS
Study of the hydroxyl radical by DRASC resonance in a high pressure flame --- Diffusion Raman Anti-Stokes Coherence (DRASC)
[ONERA-RS-53/7131-PY] 05 p0622 N90-13632
Analysis of liquid propellant exposed to elastomeric materials
[AD-A214465] 09 p1200 N90-16952
Chemical interactions and light emissions from vented species
[AD-A214130] 10 p1327 N90-17668
Control of the RADM chemistry mechanism of the gas phase 12 p1687 N90-19690
The role of clouds in the photochemistry of the background troposphere 12 p1688 N90-19694
Saturated fluorescence measurements of the hydroxyl radical in laminar high-pressure flames
[NASA-CR-185218] 15 p2101 N90-22022
Kinematic models of cometary comae
15 p2188 N90-22495
Supersonic jet studies of benzyl alcohols: Minimum energy conformations and torsional motion
[AD-A221815] 21 p2980 N90-26934
Radical homopolymerization of a trisubstituted alkene: 1-cyclobutenecarboxylic acid and its polymer
[AD-A223188] 21 p2986 N90-26968
Tropospheric sounders 21 p3016 N90-27150
Study of the radical OH in a high pressure flame by resonant DRASC
[ONERA-RF-57/7131-PY] 23 p3305 N90-28692
Spectroscopic study of combustion diagnostics on hydroxyl radicals
[NASA-CR-186998] 23 p3305 N90-28694
Spectroscopy of propellant-related flames
[AD-A224068] 24 p3457 N90-29525

HYGIENE
On the wings of a dream: The Space Shuttle
[NASA-EP-269] 05 p0593 N90-13446
Environmental quality and occupational health Special Emphasis Area Plan (SEAP)
[AD-A214738] 09 p1251 N90-17259
Identifying atmospheric monitoring needs for Space Station Freedom 18 p2628 N90-24977
Generation rates and chemical compositions of waste streams in a typical crewed space habitat
[NASA-TM-102799] 22 p3233 N90-28333

HYGRAL PROPERTIES
Hygrothermal effects on the complex moduli of composite laminates
01 p0033 N90-10182
Mechanics of damping for fiber composite laminates including hygro-thermal effects
[NASA-TM-102329] 01 p0034 N90-10185
HYPERBARIC CHAMBERS
Methodology used for gas analysis and control of trace chemical contaminants at a hyperbaric facility. 1: Gas sampling
[AD-A216155] 10 p1325 N90-17659
Field calibration of two types of microphones in hyperbaric air
[AD-A219477] 17 p2395 N90-23642
HYPERBOLIC COORDINATES
Similarity solutions that give rise to hyperbolicity and change of type in steady flow of a viscoelastic fluid
[AD-A210920] 01 p0072 N90-10410
Smooth linearization of hyperbolic fixed points without resonance conditions
[REPT-89-03] 03 p0394 N90-12251
Graphs of the state of stress at rounded corners
[MEMT-1] 15 p2119 N90-22122
HYPERBOLIC DIFFERENTIAL EQUATIONS
Global existence and asymptotic stability for a nonlinear integrodifferential equation modeling heat flow
[AD-A210647] 01 p0071 N90-10408
An iterative method for systems of nonlinear hyperbolic equations
[NASA-CR-181919] 01 p0112 N90-10638
Domain decomposition for partial differential equations
[DE89-016669] 02 p0267 N90-11519
Iterated theta method for hyperbolic equations
[CWI-NM-R8809] 04 p0540 N90-13132
An Eigenvalue Analysis of finite-difference approximations for hyperbolic IBVPs
[NASA-TM-102241] 04 p0541 N90-13137
Local error estimates for discontinuous solutions of nonlinear hyperbolic equations
[NASA-CR-181960] 06 p0834 N90-14847
Unsteady three-dimensional thin-layer Navier-Stokes solutions on dynamic blocked grids
07 p0874 N90-15069
Asymptotic behaviour of solutions of a degenerate quasilinear hyperbolic equation
[DE89-635713] 09 p1276 N90-17400
Implementation of a finite element process for the Euler equations of the gas dynamics
[PREPRINT-500] 12 p1661 N90-19545
Cell averaging Chebyshev methods for hyperbolic problems
[NASA-CR-182028] 13 p1877 N90-20768
Fourier analysis of finite element preconditioned collocation schemes
[NASA-CR-182040] 16 p2304 N90-23128
High order essentially non-oscillatory schemes for Hamilton-Jacobi equations
[NASA-CR-181995] 16 p2305 N90-23137
Adaptive mesh experiments for hyperbolic partial differential equations
[AD-A219194] 16 p2307 N90-23148
The CFL condition for spectral approximations to hyperbolic initial-boundary value problems
[NASA-CR-182053] 18 p2604 N90-24833
Shock-layer bounds for a singularly perturbed equation
[NASA-CR-182080] 22 p3243 N90-28391
HYPERBOLIC FUNCTIONS
Convergence results for pseudospectral approximations of hyperbolic systems by a penalty type boundary treatment
[NASA-CR-181929] 03 p0391 N90-12230
High order filtering methods for approximating hyperbolic systems of conservation laws
[NASA-CR-182016] 13 p1856 N90-20650
Some aspects of Essentially Nonoscillatory (ENO) formulations for the Euler equations, part 3
[NASA-CR-4285] 14 p1910 N90-20949
Boundary conditions for nonlinear hyperbolic systems of conservation laws
[REPT-892-422-101] 17 p2404 N90-23694
Computational Fluid Dynamics, volume 1
[VKI-LS-1990-03-VOL-1] 22 p3171 N90-27989
Hyperbolic conservation laws and numerical methods
22 p3172 N90-27990
Computational Fluid Dynamics, Volume 2
[VKI-LS-1990-03-VOL-2] 22 p3172 N90-27993
Difference methods for hyperbolic problems with emphasis on space-centered approximations
22 p3172 N90-27998
Hyperbolic Hjelmslev groups
[ETN-90-97298] 24 p3538 N90-30009
HYPERBOLIC NAVIGATION
NT LORAN
NT LORAN C
HYPERBOLIC SPACE
U HYPERBOLIC COORDINATES
HYPERCUBE MULTIPROCESSORS
A low-cost hypercube load-balance algorithm
[DE89-015739] 01 p0104 N90-10589
Shared memory versus message passing architectures: An application based study
[AD-A210312] 01 p0108 N90-10615
Efficient diagnosis of multiprocessor systems under probabilistic models
[NASA-CR-185965] 03 p0388 N90-12212
Parallel implementation and evaluation of motion estimation system algorithms on a distributed memory multiprocessor using knowledge based mappings
[NASA-CR-185984] 03 p0389 N90-12213
Novel techniques for data decomposition and load balancing for parallel processing of vision systems: Implementation and evaluation using a motion estimation system
[NASA-CR-185991] 03 p0389 N90-12214
Dynamic embedding of trees in hypercubes with constant dilation and load
[AD-A211884] 03 p0392 N90-12236
Four vector-matrix primitives
[AD-A211889] 03 p0392 N90-12237
Fast computation using faulty hypercubes
[AD-A211910] 03 p0393 N90-12238
Work-preserving emulations of fixed-connection networks
[AD-A211915] 04 p0535 N90-13093
Formal calculations and parallelism. Solving linear systems
[ETN-89-95499] 04 p0536 N90-13098
Definition of avionics concepts for a heavy lift cargo vehicle, appendix A
[NASA-CR-183817] 05 p0580 N90-13380
Implementing the discrete Fourier transform on the hypercube FPS T40
[IMAG-RR-773-I] 05 p0684 N90-13983
A multilevel parallel solver for block tridiagonal and banded linear systems
[AD-A213151] 05 p0688 N90-14008
A radar simulation program for a 1024-processor hypercube
[DE89-014494] 06 p0766 N90-14455
Spanning trees of hypercubes with a maximum of sixteen peaks
[IMAG-RR-755-I] 08 p1107 N90-16406
Design and implementation of a multi-sensor fusion algorithm on a hypercube computer architecture
[DE90-003682] 08 p1112 N90-16438
Hypercube expert system shell-applying production parallelism
[AD-A215762] 10 p1418 N90-18173
Distributed decomposition of block-angular linear programs on a hypercube computer
[AD-A216433] 11 p1545 N90-18893
An optimized algorithm for solving the nodal diffusion method on shared memory multiprocessors
[DE90-002703] 12 p1700 N90-19762
Parallel neural net path-planner on hypercube and transputer
[DE90-006324] 12 p1703 N90-19777
Design of a simulation interface for a parellel computing environment
[DE90-008497] 13 p1873 N90-20737
Implementation of a hypercube database system
[DE90-008440] 13 p1900 N90-20905
Fault tolerant hypercube computer system architecture
[NASA-CASE-NPO-16859-1-CU] 14 p2012 N90-21527
Molecular dynamics simulations of short-range force systems on 1024-node hypercubes
[DE90-009833] 15 p2146 N90-22259
Communication overhead on the Intel iPSC-860 hypercube
[NASA-CR-182055] 16 p2278 N90-22982
Algorithmic considerations of integrated design for CSI on a hypercube architecture 16 p2289 N90-23043
Fault tolerant multiprocessing and development of tools
[AD-A219216] 16 p2301 N90-23110
A network flow model for load balancing in circuit-switched multicomputers
[NASA-CR-182049] 17 p2451 N90-23977
Input/output algorithm for M-dimensional rectangular domain decompositions on N-dimensional hypercube multicomputers
[DE90-010494] 18 p2594 N90-24762
Computing Boolean functions on anonymous networks
[CWI-CS-R8935] 18 p2602 N90-24818
Adaptive fault-tolerant routing in hypercube multicomputers
[NASA-CR-186781] 20 p2903 N90-26513
A parallel algorithm for surface plane intersection
[IMAG-RR-794-M] 20 p2909 N90-26549
Parallelization of an annealing simulation applied to improving tetrahedric grids
[IMAG-RR-796-M] 20 p2913 N90-26570
Implementation of algorithms used in calculating the tensor product of matrices on a distributed memory machine
[IMAG-RR-786-I] 20 p2913 N90-26572
Multilayered neural networks: Learning algorithms, implementation on hypercube machines, applications
[ETN-90-97255] 20 p2913 N90-26574
Performance of the Intel iPSC/860 hypercube
[DE90-014697] 22 p3235 N90-28346
Concurrent Image Processing Executive (CIPE). Volume 1: Design overview
[NASA-CR-186853] 22 p3236 N90-28348
Concurrent Image Processing Executive (CIPE). Volume 2: Programmer's guide
[NASA-CR-186854] 22 p3236 N90-28349
Concurrent Image Processing Executive (CIPE). Volume 3: User's guide
[NASA-CR-186848] 22 p3236 N90-28350
Efficient mapping algorithms for scheduling robot inverse dynamics computation on a multiprocessor system
23 p3375 N90-29071
Workshop on Neural Networks
[DE90-014794] 23 p3385 N90-29120
Parallelization of a method for solving three dimensional Navier-Stokes equations on a distributed memory multiprocessor
[ONERA-RTS-1/3717-CY] 24 p3534 N90-29983
HYPERFINE STRUCTURE
Determination of hyperfine structures and Rydberg convergence limits of selected optical transitions in Nb-93 using resonance ionization spectroscopy
[PB90-110719] 08 p1122 N90-16498
The interstellar D1 line at high resolution
[NASA-CR-184915] 20 p2941 N90-26737
Examinations of hyperfine structure and isotope displacement of the elements gadolinium and europium with laser fluorescence and two photon spectroscopy
[ETN-90-97312] 24 p3447 N90-29468
HYPERGEOMETRIC FUNCTIONS
Meixner-Pollaczek polynomials and the Heisenberg algebra
[CWI-PM-R8806] 04 p0541 N90-13138
Jacobi functions as limit cases of q-ultraspherical polynomials
[CWI-PM-R8807] 04 p0541 N90-13139
Representations of the twisted SU(2) quantum group and some q-hypergeometric orthogonal polynomials
[CWI-PM-R8809] 04 p0541 N90-13140
The addition formula for little q-Legendre polynomials and the SU(2) quantum group
[CWI-AM-R8906] 04 p0543 N90-13151
FORTRAN subroutines for the evaluation of the confluent hypergeometric functions
[AD-A213308] 05 p0689 N90-14012
Some comments on the solvable Chiral Potts model
[PREPRINT-673] 05 p0696 N90-14070
On some integral relations involving a generalized hypergeometric polynomial
[DE90-600729] 06 p0835 N90-14852
Some remarks on solutions of Fermats last equation in terms of Wright's hypergeometric function
[AD-A218066] 13 p1878 N90-20771
On a third q-Bessel function
[REPT-89-48] 15 p2161 N90-22344
Polynomial asymptotic estimates of Gegenbauer, Laguerre, and Jacobi polynomials
[CWI-AM-R8911] 17 p2460 N90-24043
The CFL condition for spectral approximations to hyperbolic initial-boundary value problems
[NASA-CR-182053] 18 p2604 N90-24833
Product integration rules at Clenshaw-Curtis and related points: A robust implementation
[DE90-627158] 23 p3382 N90-29106
HYPERGEOMETRY
U HYPERSPACES
HYPERGOLIC ROCKET PROPELLANTS
Coaxial injection technology for hypergolic propellants
09 p1180 N90-16839
Atmospheric dispersion of solid and liquid rocket propellants
[AD-A221293] 21 p3020 N90-27173
HYPERONS
An experimental high energy physics program
[DE89-014695] 03 p0403 N90-12311
Hyperon production at 200 and 900 GeV cm energy
[USIP-89-02] 17 p2471 N90-24126
HYPERPLANES
Affine polar spaces
[CWI-AM-R8909] 17 p2468 N90-24107
HYPERSONIC AIRCRAFT
Keynote address
09 p1173 N90-16783
The German hypersonic technology programme
09 p1174 N90-16790

Progress in Saenger space transportation system definition 09 p1175 N90-16799
HOTOL: A future launcher for Europe 09 p1175 N90-16800
National aero-spaceplane status and plans 09 p1175 N90-16801
Optimum element density studies for finite-element thermal analysis of hypersonic aircraft structures [NASA-TM-4163] 09 p1219 N90-17074
A computational model for thickening boundary layers with mass addition for hypersonic engine inlet testing [AD-A216246] 10 p1310 N90-17576
Investigation of the failure modes in a metal matrix composite under thermal cycling [AD-A216195] 10 p1349 N90-17825
Tracking a hypersonic aircraft from a space platform [AD-A216399] 10 p1377 N90-17984
The application of active controls technology to a generic hypersonic aircraft configuration [NASA-TM-101689] 13 p1754 N90-20071
Prediction of forces and moments for flight vehicle control effectors. Part 1: Validation of methods for predicting hypersonic vehicle controls forces and moments [NASA-CR-186571] 15 p2047 N90-21734
Prediction of forces and moments for flight vehicle control effectors. Part 2: An analysis of delta wing aerodynamic control effectiveness in ground effect [NASA-CR-186572] 15 p2047 N90-21735
Experimental aerothermodynamic research of hypersonic aircraft [NASA-CR-186903] 20 p2804 N90-25954
Maneuvering by means of lateral jets [ISL-CO-255/88] 20 p2814 N90-26015
Active control of aerothermoelastic effects for a conceptual hypersonic aircraft [NASA-TM-102713] 22 p3122 N90-27725

HYPERSONIC BOUNDARY LAYER

Leading edge transition by contamination in hypersonic flow 01 p0063 N90-10360
Hypersonic boundary layers. Viscous effects within the shock layer [CERT-RSF-OA-25/5005-AYD] 04 p0438 N90-12502
Investigation of the development of laminar boundary-layer instabilities along a cooled-wall hollow cylinder at Mach number 8 [AD-A217672] 13 p1800 N90-20331
On the instability of hypersonic flow past a flat plate [NASA-CR-182051] 18 p2493 N90-24252
Boundary layer and shock layer in hypersonic flows [CERT-31/5005-22-DERAT] 22 p3110 N90-27664

HYPERSONIC COMBUSTION

Critical reaction rates in hypersonic combustion chemistry [DE89-014278] 02 p0156 N90-10892
Homogeneous catalysts in hypersonic combustion [DE89-015258] 02 p0193 N90-11098
Wave combustors for trans-atmospheric vehicles [NASA-TM-102238] 03 p0307 N90-11742

HYPERSONIC FLIGHT

The NASA experience in aeronautical R and D: Three case studies with analysis [AD-A211486] 04 p0437 N90-12496
Thermal protection systems for reentry and hypersonic flight [DLR-MITT-89-14] 05 p0613 N90-13577
Thermal/structural analyses of several hydrogen-cooled leading-edge concepts for hypersonic flight vehicles [NASA-TM-102391] 06 p0775 N90-14511
Progress in Saenger space transportation system definition 09 p1175 N90-16799
HOTOL: A future launcher for Europe 09 p1175 N90-16800
National aero-spaceplane status and plans 09 p1175 N90-16801
A computational model for thickening boundary layers with mass addition for hypersonic engine inlet testing [AD-A216246] 10 p1310 N90-17576
Viscous three-dimensional analyses for nozzles for hypersonic propulsion [NASA-CR-185197] 10 p1321 N90-17635
Possible piloting techniques at hypersonic speeds [ISL-CO-216/88] 11 p1456 N90-18392
Transpiration cooling in hypersonic flight [NASA-CR-186435] 13 p1750 N90-20052
Analysis of flow-, thermal-, and structural-interaction of hypersonic structures subjected to severe aerodynamic heating [AD-A217882] 13 p1750 N90-20053
Thermal protection systems for reentry and hypersonic flight [ESA-TT-1179] 19 p2667 N90-25177
Transatmospheric vehicle research [NASA-CR-186705] 20 p2807 N90-25970
Carbon-carbon composites: Emerging materials for hypersonic flight [NASA-TM-103472] 20 p2827 N90-26080
Real-time aerodynamic heating and surface temperature calculations for hypersonic flight simulation [NASA-TM-4222] 23 p3327 N90-28815
Optimal trajectories for hypervelocity flight 24 p3430 N90-29378

HYPERSONIC FLOW

Low-speed, high-lift aerodynamic characteristics of slender, hypersonic accelerator-type configurations [NASA-TP-2945] 02 p0145 N90-10830
Homogeneous catalysts in hypersonic combustion [DE89-015258] 02 p0193 N90-11098
Gas-accelerated plate stability study [DE89-016880] 02 p0225 N90-11289
Rotational and vibrational nonequilibrium effects in rarefied, hypersonic flow [NASA-CR-182559] 04 p0437 N90-12498
Basic research on methods of calculating supersonic and hypersonic flow [ONERA-RSF-19/1123-AY-234A] 04 p0448 N90-12565
Development of an anti-Stokes coherent Raman diffusion system for measuring hypersonic flow [ONERA-RSF-1/7301-PY] 04 p0459 N90-12630
An Introduction to Hypersonic Aerodynamics [VKI-LS-1989-01] 05 p0573 N90-13334
Hypersonic aerodynamics 05 p0573 N90-13335
On catalytic recombination rates in hypersonic stagnation heat transfer 05 p0573 N90-13338
Optimum shape of a blunt forebody in hypersonic flow [NASA-CR-181955] 05 p0575 N90-13351
Measured and predicted aerodynamic coefficients and shock shapes for Aeroassist Flight Experiment (AFE) configuration [NASA-TP-2956] 06 p0717 N90-14185
Efficient real gas Navier-Stokes computations of high speed flows using an LU scheme [NASA-TM-102429] 06 p0720 N90-14203
Spatial evolution of nonlinear acoustic mode instabilities on hypersonic boundary layers [NASA-TM-102431] 06 p0777 N90-14517
Calculation of two and three dimensional super and hypersonic flows by solving the Euler equations 08 p1070 N90-16197
Numerical simulation of laminar hypersonic flows about an ellipsoid 08 p1071 N90-16198
Aerodynamic simulation conditions in arc heated wind tunnels 09 p1180 N90-16843
An upwind-biased, point-implicit relaxation algorithm for viscous, compressible perfect-gas flows [NASA-TP-2953] 09 p1214 N90-17042
Special Course on Three-Dimensional Supersonic/Hypersonic Flows Including Separation [AGARD-R-764] 10 p1308 N90-17565
Opportunities for improved understanding of supersonic and hypersonic flows 10 p1308 N90-17566
Unsteadiness of supersonic and hypersonic shock induced turbulent boundary layer separation 10 p1309 N90-17572
Reacting flows 10 p1309 N90-17573
Hypersonic nozzle/afterbody performance at low Mach numbers [AD-A216223] 10 p1309 N90-17575
Improved computational fluid dynamics for continuum hypersonic flow [AD-A216981] 11 p1506 N90-18674
Computation of hypersonic unsteady viscous flow over a cylinder 12 p1597 N90-19194
Computation of hypersonic low density flows with thermochemical nonequilibrium 13 p1749 N90-20044
An approximate viscous shock layer method for calculating the hypersonic flow over blunt-nosed bodies 14 p1910 N90-20947
Effects of nose bluntness and shock-shock interactions on blunt bodies in viscous hypersonic flows [NASA-CR-186451] 14 p1910 N90-20950
Computation of nonequilibrium chemically reacting flows in hypersonic flow field 14 p1911 N90-20954
Convergence acceleration of hypersonic flow calculations: A nonlinear relaxation factor 14 p1911 N90-20957
Optimum hypersonic airfoils with attached shocks 14 p1912 N90-20960
Numerical simulation of hypersonic flow around a space plane. Part 2: Application to high angles of attack flow [NAL-TR-1011T] 15 p2045 N90-21726
The aerodynamic characteristics of power-law bodies in continuum and transitional hypersonic flow [RAE-TM-AERO-2164] 16 p2196 N90-22537
Proceedings of the 9th International Conference on Computing Methods in Applied Science and Engineering [AD-A219307] 16 p2307 N90-23149
The stability of two-dimensional wakes and shear-layers at high Mach numbers [NASA-CR-182050] 17 p2401 N90-23678
On the instability of hypersonic flow past a flat plate [NASA-CR-182051] 18 p2493 N90-24252
NSFLEX: An implicit relaxation method for the Navier-Stokes equations for a wide range of Mach numbers [MBB-FE-122/S/PUB-366] 19 p2651 N90-25086
Boundary conditions for the Navier-Stoke's equations at an artificial boundary intersecting a solid boundary [FFA-TN-1990-11] 19 p2691 N90-25313
Prediction of two-dimensional time-dependent gasdynamic flows for hypersonic studies [UTIAS-335] 20 p2801 N90-25935
Particle simulation of hypersonic flow [AD-A222704] 21 p2954 N90-26794
Advanced optical diagnostics in hypersonic research 21 p2975 N90-26905
An approximate method for calculating three-dimensional inviscid hypersonic flow fields [NASA-TP-3018] 21 p3002 N90-27066
Progress and challenges in modeling turbulent aerodynamic flows [NASA-TM-102811] 22 p3170 N90-27981
Hypersonic Arbitrary-Body Aerodynamics (HABA) for conceptual design [DE90-014750] 23 p3268 N90-28495
Multigrid for hypersonic inviscid flows [NASA-CR-182082] 23 p3387 N90-29125
Theoretical investigation of non-equilibrium chemistry and optical radiation in hypersonic flow fields [NASA-CR-186335] 24 p3417 N90-29300
Supersonic/hypersonic aerodynamics and heat transfer for projectile design using viscous-inviscid interaction [AD-A224354] 24 p3418 N90-29303
Feasibility of the temperature measurements in hypersonic flow by multibeam coherent Raman anti-Stokes scattering [ONERA-RF-56/7131-PY] 24 p3419 N90-29312
Measurement Techniques for Hypersonic Flows [VKI-LS-1990-05] 24 p3419 N90-29314
Electron-beam fluorescence measurements in hypersonic flows 24 p3420 N90-29318
Applications of LIF to high speed flows 24 p3420 N90-29320
Numerical simulation of hypersonic viscous flow for the design of H-2 orbiting plane (HOPE) [NAL-TR-1028] 24 p3422 N90-29330
A numerical calculation of hypersonic flow around blunt bodies using upwind difference scheme [NAL-TR-1025] 24 p3422 N90-29331

HYPERSONIC FORCES

Possible piloting techniques at hypersonic speeds [ISL-CO-216/88] 11 p1456 N90-18392

HYPERSONIC INLETS

Computational modeling and validation for hypersonic inlets [NASA-TM-103111] 15 p2099 N90-22011
Finite element analysis of structural components using viscoplastic models with application to a cowl lip problem [NASA-CR-185189] 17 p2416 N90-23769
Prediction of two-dimensional time-dependent gasdynamic flows for hypersonic studies [UTIAS-335] 20 p2801 N90-25935

HYPERSONIC NOZZLES

Hypersonic nozzle design [NASA-CR-186261] 07 p0876 N90-15077
Experimental investigation of a chemical laser cavity flowfield [AD-A216398] 10 p1390 N90-18038
Calculation of correction terms for forces and moment measurements in radial flow field of hypersonic spheric nozzles 18 p2490 N90-24234

HYPERSONIC REENTRY

NT UNCONTROLLED REENTRY (SPACECRAFT)
Thermal protection systems for reentry and hypersonic flight [DLR-MITT-89-14] 05 p0613 N90-13577
AFE dynamic effects in inhomogeneous plasmas 18 p2643 N90-25053

HYPERSONIC SHOCK

Hypersonic boundary layers. Viscous effects within the shock layer [CERT-RSF-OA-25/5005-AYD] 04 p0438 N90-12502
Hypersonic aerodynamics 05 p0573 N90-13335
Unsteadiness of supersonic and hypersonic shock induced turbulent boundary layer separation 10 p1309 N90-17572
Optimum hypersonic airfoils with attached shocks 14 p1912 N90-20960

HYPERSONIC SPEED
Particle kinetic simulation of high altitude hypervelocity flight
[NASA-CR-186003] 02 p0147 N90-10840
Flow separation in shock wave boundary layer interactions at hypersonic speeds
[NASA-CR-4274] 08 p1017 N90-15885
Axial flow in corners at supersonic and hypersonic speeds 10 p1308 N90-17570
Hypersonic nozzle/afterbody performance at low Mach numbers
[AD-A216223] 10 p1309 N90-17575
Flow visualization in supersonic turbulent boundary layers 16 p2195 N90-22533
Aerodynamic pressure and heating-rate distributions in tile gaps around chine regions with pressure gradients at a Mach number of 6.6
[NASA-TP-2988] 17 p2400 N90-23670
On the instability of hypersonic flow past a flat plate
[NASA-CR-182051] 18 p2493 N90-24252
An investigation of solid-fuel, dual-mode combustion ramjets 22 p3162 N90-27933

HYPERSONIC TEST APPARATUS
Test and Measurement Technique in Hypersonics
[ILR-MITT-225(1989)] 18 p2489 N90-24225
The gun tunnel of the Brunswick Institute for Fluid Mechanics: Current development status 18 p2489 N90-24227

HYPERSONIC VEHICLES
NT HYPERSONIC AIRCRAFT
Application of formal optimization techniques in thermal/structural design of a heat-pipe-cooled panel for a hypersonic vehicle
[NASA-TM-89131] 01 p0071 N90-10409
Adaptive control law design for model uncertainty compensation
[AD-A211712] 03 p0309 N90-11758
Rotational and vibrational nonequilibrium effects in rarefied, hypersonic flow
[NASA-CR-182559] 04 p0437 N90-12498
Measured and predicted aerodynamic coefficients and shock shapes for Aeroassist Flight Experiment (AFE) configuration
[NASA-TP-2956] 06 p0717 N90-14185
Thermal/structural analyses of several hydrogen-cooled leading-edge concepts for hypersonic flight vehicles
[NASA-TM-102391] 06 p0775 N90-14511
Manned spacecraft
[AD-A214218] 07 p0887 N90-15129
Aerodynamic and structural design challenges of a reusable single stage to orbit air-breathing launch vehicle 09 p1177 N90-16814
Saenger propulsion system options 09 p1177 N90-16818
Verification of aerothermodynamic codes by means of a winged experimental re-entry vehicle 09 p1180 N90-16842
Heat pipes for wing leading edges of hypersonic vehicles
[NASA-CR-181922] 09 p1216 N90-17055
Aeroservoelasticity
[NASA-TM-102620] 12 p1603 N90-19227
Rapid near-optimal trajectory generation and guidance law development for single-stage-to-orbit airbreathing vehicles
[NASA-CR-186299] 12 p1612 N90-19275
Hypersonic waverider configurations for trans-atmospheric vehicles
[AD-A217925] 13 p1755 N90-20074
Low-density flow effects for hypervelocity vehicles, phase 2
[AD-A221034] 18 p2493 N90-24249
Transatmospheric vehicle research
[NASA-CR-186705] 20 p2807 N90-25970
PDWAP: A preliminary design and weights analysis program for aerospace vehicles
[AD-A222614] 20 p2808 N90-25979
Supersonic reacting internal flow fields
[NASA-TM-103480] 20 p2829 N90-26094
Photo-sensitized ignition of hydrogen/oxygen mixtures for hypersonic flight vehicles 22 p3163 N90-27935
Damage tolerance analysis for manned hypervelocity vehicles. Volume 1: Final technical report
[AD-A221970] 22 p3191 N90-28106
Real-time aerodynamic heating and surface temperature calculations for hypersonic flight simulation
[NASA-TM-4222] 23 p3327 N90-28815

HYPERSONIC WIND TUNNELS
NT HOTSHOT WIND TUNNELS
NT PLASMA JET WIND TUNNELS
Design and fabrication requirements for low noise supersonic/hypersonic wind tunnels 04 p0446 N90-12555
Hypersonic nozzle design
[NASA-CR-186261] 07 p0876 N90-15077
Investigation of ablation phenomena using IR thermography in a hypersonic wind tunnel 08 p1081 N90-16258
Quantitative surface temperature measurement using two-color thermographic phosphors and video equipment
[NASA-CASE-LAR-13740-1] 16 p2238 N90-22770
Determination of the velocity, density, maximum flux, and enthalpy profiles for a very high temperature arc jet nozzle flow
[AD-A218390] 17 p2402 N90-23682
Mission of LARVE 18 p2489 N90-24229
The arc-hot wind tunnel 18 p2489 N90-24230
The hypersonic vacuum wind tunnels: Status, research, and necessary developments 18 p2490 N90-24231
Stream field measurements of a half spheric cylinder by thin hypersonic stream with the electron radiation technique 18 p2490 N90-24232
Infrared thermography at hypersonic channel H2K 18 p2490 N90-24235
Infrared thermography 24 p3421 N90-29325

HYPERSONICS
Hypersonic nozzle design
[NASA-CR-186261] 07 p0876 N90-15077
Improved tangent-cone method for the Aerodynamic Preliminary Analysis System (APAS) version of the hypersonic arbitrary-body program
[NASA-TM-4165] 08 p1018 N90-15890
NASA aerodynamics program
[NASA-TM-4175] 09 p1247 N90-17235
High performance missiles of the future 10 p1305 N90-17550
Hypersonic nozzle/afterbody performance at low Mach numbers
[AD-A216223] 10 p1309 N90-17575
Structures and materials technology for hypersonic aerospacecraft
[NASA-TM-102583] 11 p1519 N90-18752
Computation of hypersonic unsteady viscous flow over a cylinder 12 p1597 N90-19194
Prediction of forces and moments for flight vehicle control effectors. Part 1: Validation of methods for predicting hypersonic vehicle controls forces and moments
[NASA-CR-186571] 15 p2047 N90-21734
Excitation of hypersound at boundary between Type-2 superconductor and a concentrated paramagnetic compound 16 p2310 N90-23164
Test and Measurement Technique in Hypersonics
[ILR-MITT-225(1989)] 18 p2489 N90-24225
The wind tunnel of the Ruhr University, Bochum, Federal Republic of Germany for examination of compressible streams until M=6 18 p2489 N90-24226
High enthalpy hypersonic wind tunnel F4: General description and associated instrumentation 18 p2489 N90-24228
Prediction of two-dimensional time-dependent gasdynamic flows for hypersonic studies
[UTIAS-335] 20 p2801 N90-25935
Summary of Discussions at the Eleventh Meeting of the Sandia Cooperative Group on the Aerothermochemistry of Turbulent Combustion
[DE89-001846] 21 p2973 N90-26896
Advanced optical diagnostics in hypersonic research 21 p2975 N90-26905
Noncoplanar orbit transfer optimization for an aeroassisted sortie vehicle 22 p3128 N90-27752
Flight mechanics applications for tethers in space: Cooperative Italian-US programs 22 p3131 N90-27770
Hypersonic Arbitrary-Body Aerodynamics (HABA) for conceptual design
[DE90-014750] 23 p3268 N90-28495

HYPERSPACES
On a third q-Bessel function
[REPT-89-48] 15 p2161 N90-22344
Affine polar spaces
[CWI-AM-R8909] 17 p2468 N90-24107
Formal groups and differential equations
[ETN-90-96924] 18 p2603 N90-24825

HYPERTENSION
Factor analytic reduction of the carotid-cardiac baroreflex parameters 08 p1155 N90-16693
Prevalence of hypertension among active duty personnel
[AD-A223892] 23 p3356 N90-28968

HYPERTHERMIA
Heatstroke pathophysiology: The energy depletion model
[AD-A212156] 03 p0380 N90-12164
Exertional heatstroke: An international perspective. An introduction: The role of exercise in the etiology of exertional heatstroke
[AD-A212242] 04 p0523 N90-13020
Seminars of Applied Physics, Materials Physics and Biomedical Engineering, 1989
[PB89-218572] 04 p0548 N90-13192
Biological effects of hyperthermia and potential risk associated with ultrasonic exposure
[PB89-100702] 06 p0820 N90-14768

HYPERTROPHY
U GROWTH

HYPERVELOCITY ACCELERATORS
U HYPERVELOCITY GUNS

HYPERVELOCITY CRATERING
U HYPERVELOCITY PROJECTILES
U PROJECTILE CRATERING

HYPERVELOCITY GUNS
A thermochemical analysis of proposed working fluids for electrothermal guns
[AD-A210661] 02 p0159 N90-10910
Current management for improved railgun performance
[AD-A212887] 05 p0593 N90-13445
Hugoniot measurements with the LLNL electric gun facility
[DE90-002809] 07 p0885 N90-15119
Progress with small, high-magnetic-field spheromaks in CTX
[DE90-003395] 08 p1127 N90-16527
ARDEC (Armament Research, Development and Engineering Center) electric gun in-house test program
[AD-A217337] 13 p1760 N90-20105
Laser controlled semiconductor armature for electromagnetic launchers
[AD-D014435] 14 p1931 N90-21055

HYPERVELOCITY IMPACT
Orbital debris research at NASA Johnson Space Center, 1986-1988
[NASA-TM-102155] 01 p0138 N90-10795
On protection of Freedom's solar dynamic radiator from the orbital debris environment. Part 1: Preliminary analyses and testing
[NASA-TM-102458] 06 p0736 N90-14285
Hypervelocity impact calculations using CTH: Case studies
[DE90-002891] 06 p0795 N90-14632
Some numerical experiments concerning the equation of state algorithm for multi-material cells in HULL
[DE89-008240] 06 p0830 N90-14827
Hypervelocity impact studies on the Giotto comet Halley mission 06 p0862 N90-15008
Stand-off shields for hypervelocity particles
[DE89-016182] 07 p0939 N90-15437
Effects of parametric variations of complex targets on damage from projectile impact
[DE90-003214] 07 p0941 N90-15450
Stability and fragmentation of ejecta in hypervelocity impact
[DE90-004087] 08 p1085 N90-16278
Hypervelocity acceleration and impact experiments with the LLNL electric gun
[DE90-006924] 10 p1326 N90-17664
Spallation and dynamic fracture as an effect of laser induced shock waves in carbon based composite materials
[AD-A216540] 11 p1478 N90-18509
Global nonlinear optimization of spacecraft protective structures design
[NASA-TM-100387] 14 p1938 N90-21095
Large-scale simulations of monolithic and segmented projectiles impacting spaced armor
[AD-A219374] 16 p2244 N90-22800
Space program: Space debris a potential threat to Space Station and shuttle
[GAO/IMTEC-90-18] 20 p2815 N90-26024
Hypervelocity impact shield
[NASA-CASE-MSC-21420-1] 21 p2966 N90-26858

HYPERVELOCITY LAUNCHERS
Design and commissioning test results for the hypervelocity launcher research complex battery power supply
[AD-A211320] 04 p0495 N90-12848
Performance characteristics of a three-stage railgun
[DE90-002533] 06 p0729 N90-14254
Design limitations on ultra-high velocity projectile launchers
[DE89-012933] 07 p0885 N90-15118
The use of hypervelocity launchers to explore previously inaccessible states of matter
[DE90-004088] 08 p1034 N90-15973
Analysis of near-surface flow physics in a two-stage, 10 km/s, electromagnetic launcher
[DE90-013292] 21 p2964 N90-26852

HYPERVELOCITY PROJECTILES
Design limitations on ultra-high velocity projectile launchers
[DE89-012933] 07 p0885 N90-15118
Stand-off shields for hypervelocity particles
[DE89-016182] 07 p0939 N90-15437

Effects of parametric variations of complex targets on damage from projectile impact
[DE90-003214] 07 p0941 N90-15450
Studies of density distributions in one-dimensional shock-induced debris clouds
[DE90-004089] 08 p1085 N90-16282

HYPERVELOCITY WIND TUNNELS
NT HOTSHOT WIND TUNNELS
NT PLASMA JET WIND TUNNELS
Design of an axisymmetric, contoured nozzle for the HEG
[DLR-FB-90-04] 23 p3327 N90-28812
Applications of LIF to high speed flows
24 p3420 N90-29320

HYPERVENTILATION
Effects of high altitude hypoxia on lung and chest wall function during exercise
[AD-A219814] 17 p2434 N90-23869

HYPERVOLEMIA
Elevated central venous pressure: A consequence of exercise training-induced hypervolemia
[NASA-TM-102965] 13 p1850 N90-20617

HYPNOSIS
Use of self-induced hypnosis to modify thermal balance during cold water immersion
[AD-A216156] 10 p1412 N90-18140

HYPOBARIC ATMOSPHERES
Convective heat transfer in hypobaric environments
[AD-A212060] 03 p0347 N90-11979
Hypobaric hypoxia (380 torr) decreases intracellular and total body water in goats
[AD-A218192] 13 p1849 N90-20615

HYPOKINESIA
Joint US/USSR study: Comparison of effects of horizontal and head-down bed rest
[NASA-TP-3037] 23 p3355 N90-28965

HYPOPHYSIS
U PITUITARY GLAND

HYPOTENSION
Niacin ingested at night causes severe hypotension
[AD-A217896] 13 p1851 N90-20624

HYPOTHERMIA
Radio frequency (13.56 MHz) energy enhances rewarming from mild hypothermia
[AD-A212703] 04 p0524 N90-13024
Generation of free radicals during cold injury and rewarming
[AD-A213088] 05 p0672 N90-13915
Integrated G-suit/immersion suit
[AD-A212989] 06 p0821 N90-14774
Temperature regulation during upper body exercise: Able bodied and spinal cord injured
[AD-A215130] 09 p1252 N90-17264
Pre-treatment with tyrosine reverses hypothermia induced behavioral depression
[AD-A215211] 09 p1252 N90-17265
Alterations in the metabolic and sympathetic response to cold exposure after cold air acclimation
[AD-A216817] 10 p1412 N90-18144
Influence of theobromine on heat production and body temperatures in cold-exposed humans: A preliminary report
[AD-A217203] 13 p1850 N90-20618
What should athletes know about low body temperature (hypothermia)
[AD-A218316] 13 p1854 N90-20637
Field management of accidental hypothermia during diving
[AD-A219560] 17 p2434 N90-23866
Arctic cold weather medicine and accidental hypothermia
[AD-A223090] 20 p2899 N90-26487

HYPOTHESES
NT NULL HYPOTHESIS
On optimal distributed decision architectures in a hypothesis testing environment
[AD-A217824] 13 p1790 N90-20274
Designing good experiments to test bad hypotheses
[AD-A218977] 16 p2263 N90-22900
Explanation and the theory of expert problem solving
[AD-A220861] 17 p2444 N90-23930
An investigation into techniques for landmark identification of 3D images of human subjects, phase 1
[AD-A218614] 18 p2583 N90-24713
The retrieval of information from secondary memory: A review and new findings
[AD-A222760] 20 p2899 N90-26489
Approximate equations for heat conduction in multi-layered cylindrical shells
[NAL-TR-1049] 24 p3471 N90-29614

HYPOXIA
Effects of atmospheric mix and toxic fumes on military performance
[PB89-223630] 04 p0522 N90-13015
Arginine vasopressin lowers pulmonary artery pressure in hypoxic rats by releasing artrial natriuretic peptide
[AD-A215986] 10 p1410 N90-18134
Hypobaric hypoxia (380 torr) decreases intracellular and total body water in goats
[AD-A218192] 13 p1849 N90-20615
The kinetics of dark adaptation in hypoxic subjects
[AD-A218641] 16 p2260 N90-22885
Effects of high altitude hypoxia on lung and chest wall function during exercise
[AD-A219814] 17 p2434 N90-23869
Decompression sickness presenting as a viral syndrome
[AD-A223880] 23 p3356 N90-28967
Evaluation of the performance capability of the aviator under hypoxic conditions operational experience
23 p3361 N90-28991
Oxygen deficiency monitor system
[DE90-014866] 24 p3523 N90-29917

HYSTERESIS
Circuit level modeling of inductive elements
[DE89-015122] 01 p0032 N90-10173
Analysis of spurt phenomena for a non-Newtonian fluid
[AD-A210560] 01 p0071 N90-10405
Development of high frequency spice models for ferrite core inductors and transformers
[DE89-015121] 03 p0341 N90-11946
Parametric study of power absorption from electromagnetic waves by small ferrite spheres
[NASA-TP-2949] 03 p0399 N90-12282
Analysis of new phenomena in shear flow of non-Newtonian fluids
[AD-A212893] 05 p0638 N90-13721
Multiple martensitic transformations, incommensurate/commensurate phases, and charge-density-wave states in plutonium metal: Their consequences
[DE90-001235] 06 p0748 N90-14350
On-line system to measure magnetic characteristics of steel samples
[DE89-633443] 06 p0836 N90-14861
Stall and recovery in multistage axial flow compressors 11 p1464 N90-18429
Ac loss measurements of two multifilamentary NbTi composite strands
[DE90-005388] 12 p1619 N90-19304
High frequency, high temperature specific core loss and dynamic B-H hysteresis loop characteristics of soft magnetic alloys
[NASA-TM-103164] 17 p2398 N90-23663
The magnetization process: Hysteresis
18 p2515 N90-24365
Critical current density, flux creep, and microstructure in a Bi-Sr-Ca-Cu-O system
[DE90-010457] 20 p2931 N90-26676
Determination of the heat dissipated from a specimen undergoing cyclic plasticity by a hybrid numerical/experimental method
[AD-A221575] 21 p2982 N90-26948
Flux flow and flux dynamics in high-T(sub c) superconductors 22 p3136 N90-27797
Magnetic forces in high-T(sub c) superconducting bearings 22 p3137 N90-27799
Development of standards for superconductors
[PB90-196536] 22 p3248 N90-28418
Nonlinear modeling of joint dominated structures
[NASA-CR-4324] 24 p3439 N90-29423

I

I BEAMS
Lateral buckling of short I-beams under cyclic loading
[PB90-213653] 22 p3191 N90-28104

IAPETUS
Optical constraints of kerogen from 0.15 to 40 microns: Comparison with meteoritic organics
20 p2948 N90-26776

IBM COMPUTERS
The development of an Ada programming support environment database: SEAD (Software Engineering and Ada Database), user's manual
[NASA-CR-181219] 06 p0828 N90-14811
The development of a low cost data logging system for flight trials based on an IBM compatible PC
[RAE-TM-FM-16] 08 p1023 N90-15917
Interim Design Database (IDDB) CADAM drawing retrieval program user's manual for the IBM 3081
[DE90-004491] 09 p1269 N90-17356
Shape discrimination research using an IBM PC
[AD-A219993] 17 p2447 N90-23953

ICBM (MISSILES)
U INTERCONTINENTAL BALLISTIC MISSILES

ICE
NT GLACIERS
NT ICE FLOES
NT ICEBERGS
NT LAKE ICE
NT LAND ICE
NT SEA ICE
Debris/ice/TPS assessment and photographic analysis for Shuttle Mission STS-28R
[NASA-TM-102152] 01 p0016 N90-10079
Ice runways near the South Pole
[AD-A211606] 03 p0335 N90-11908
High pressure studies of planetary matter
[DE89-017738] 03 p0428 N90-12455
Estimation of time to maximum supercooling during dynamic frazil ice formation
[AD-A212204] 04 p0471 N90-12699
Debris/ice/TPS assessment and photographic analysis for Shuttle Mission STS-34
[NASA-TM-102153] 05 p0594 N90-13447
Recognition and distinction of clouds, snow, and ice using AVHRR data 08 p1092 N90-16322
Workshop on Analysis of Returned Comet Nucleus Samples
[NASA-CR-184821] 08 p1140 N90-16607
The origin, composition and history of cometary ices from spectroscopic studies 08 p1140 N90-16609
Experimental studies of gas trapping in amorphous ice and thermal modelling of comets: Implications for Rosetta 08 p1140 N90-16610
Direct determination of the morphology, structure and composition of cometary and interstellar ice analogs in the laboratory 08 p1141 N90-16612
Modifications of comet materials by the sublimation process: Results from simulation experiments
08 p1142 N90-16621
Interstellar and cometary dust
08 p1145 N90-16636
Handling and analysis of ices in cryostats and glove boxes in view of cometary samples
08 p1146 N90-16643
Analysis of particulates of comet nucleus samples: Possible use of olivine as indicator phase
08 p1147 N90-16646
The nature of cometary materials
08 p1147 N90-16647
Electron Spin Resonance (ESR) studies of returned comet nucleus samples 08 p1148 N90-16651
Ion bombardment experiments suggesting an origin for organic particles in pre-cometary and cometary ices
08 p1148 N90-16652
Refractory solids in chondrites and comets: How similar 08 p1148 N90-16654
Neptune's Triton: A moon rich in dry ice and carbon
[NASA-CR-186298] 08 p1152 N90-16675
Intermittent Solar Ammonia Absorption Cycle (ISAAC) refrigeration for lesser developed countries
[DE90-006700] 11 p1496 N90-18610
Studies of cubic ice crystals
[AD-A216574] 11 p1534 N90-18832
Spectroscopy and physico-chemistry of CO:H2O and CO2:H2O ices 11 p1581 N90-19111
Ice grains in the dust disk of the bipolar nebula M 1-92 11 p1584 N90-19127
Observations of 40-70 micron bands of ice in IRAS 09371+1212 and other stars 11 p1585 N90-19134
Petrographic working model of the Rosetta sampling and modelling subgroup for a comet nucleus
12 p1738 N90-19992
Physical processes in cometary ices inferred from laboratory studies 12 p1739 N90-19996
Laboratory studies of cometary ice analogues
12 p1739 N90-19997
Evolution of ices and carbonaceous materials in the laboratory and in comets 12 p1739 N90-19998
Physico-chemical properties of formaldehyde-ice-dust mixtures 12 p1740 N90-20000
Introduction to drilling technology
12 p1740 N90-20002
Possible targeting of particle emission by mechanical stress and penetration of sublimating ice-dust-surfaces
12 p1742 N90-20016
Airfields on antarctic glacier ice
[AD-A217638] 13 p1759 N90-20097
Satellite radar altimetry over ice. Volume 1: Processing and corrections of Seasat data over Greenland
[NASA-RP-1233-VOL-1] 13 p1840 N90-20562
Satellite radar altimetry over ice. Volume 2: Users' guide for Greenland elevation data from Seasat
[NASA-RP-1233-VOL-2] 13 p1840 N90-20563
Satellite radar altimetry over ice. Volume 4: Users' guide for Antarctica elevation data from Seasat
[NASA-RP-1233-VOL-4] 13 p1840 N90-20564
Modeling of surface roughness effects on glaze ice accretion 14 p1905 N90-20925

Ultrasonic techniques for aircraft ice accretion measurement 14 p1906 N90-20926
Investigation of surface water behavior during glaze ice accretion 14 p1906 N90-20927
The influence of ice accretion physics on the forecasting of aircraft icing conditions 14 p1906 N90-20928
Ice-making heat exchanger evaluation and test plan [DE90-008824] 14 p1959 N90-21218
Debris/ice/TPS assessment and photographic analysis for Shuttle Mission STS-36 [NASA-TM-102789] 16 p2205 N90-22583
Remote measurement of ice thickness on the shuttle external tank surface [NASA-TM-102667] 18 p2555 N90-24584
Environmental measurements and analysis: Arctic acoustics experiments in the marginal ice zone [AD-A220509] 18 p2582 N90-24708
Contamination of spacecraft by recontact of dumped liquids 19 p2728 N90-25508
Lunar polar coring lander [NASA-CR-186684] 19 p2796 N90-25917
The 27-28 October 1986 FIRE IFO Cirrus case study: Comparison of radiative transfer theory with observations by satellite and aircraft [NASA-TM-103468] 20 p2890 N90-26446
Proceedings of a Workshop on Antarctic Meteorite Stranding Surfaces [NASA-CR-186575] 20 p2942 N90-26739
Photon sputtering of H2O ices: A preliminary report 20 p2949 N90-26783
Guidance document for selecting antiskid materials applied to ice- and snow-covered roadways [PB90-183658] 21 p2983 N90-26950
Applications of ISES for snow, ice, and sea state 21 p3018 N90-27159
Interstellar grain chemistry and organic molecules 21 p3090 N90-27569
Laboratory simulation of interstellar grain chemistry and the production of complex organic molecules 21 p3092 N90-27580
Carbon in the outer solar system 21 p3096 N90-27593
The October 27-28, 1986, FIRE cirrus case study: Cloud microstructure 22 p3224 N90-28283
Three functions that model empirically measured unfrozen water content data and predict relative hydraulic conductivity [AD-A223875] 23 p3343 N90-28892

ICE CLOUDS
Inclusion of clouds and rain in atmospheric slant path calculations 15 p2083 N90-21925
The October 27-28, 1986, FIRE cirrus case study: Cloud microstructure 22 p3224 N90-28283

ICE ENVIRONMENTS
The sea ice margins: A summary of physical phenomena [PB89-212328] 02 p0253 N90-11436
Decomposition in Arctic terrestrial environments [DE90-001198] 06 p0809 N90-14706
SeaRISE: A Multidisciplinary Research Initiative to Predict Rapid Changes in Global Sea Level Caused by Collapse of Marine Ice Sheets [NASA-CP-3075] 16 p2249 N90-22824

ICE FLOES
Ice floe identification in satellite images using mathematical morphology and clustering about principal curves [AD-A213854] 08 p1090 N90-16311
Parallel algorithm for determining motion vectors in ice floe images by matching edge features 08 p1114 N90-16451
Estimating sea ice thickness using time-of-flight data from impulse radar soundings [AD-A218736] 16 p2250 N90-22831

ICE FORMATION
NT CLOUD GLACIATION
Remote sensing techniques of the Wave Propagation Laboratory for the measurement of supercooled liquid water: Applications to aircraft icing [PB89-208102] 02 p0148 N90-10842
Estimation of time to maximum supercooling during dynamic frazil ice formation [AD-A212204] 04 p0471 N90-12699
The Regional Polar Ice Prediction System, Berents Sea (RPIPS-B): A technical description [AD-A213159] 04 p0522 N90-13012
Preparation of binary ice layers by condensation from gas phase [JUEL-2248] 05 p0622 N90-13631
Convective heat transfer measurements from a NACA 0012 airfoil in flight and in the NASA Lewis Icing Research Tunnel [NASA-TM-102448] 05 p0642 N90-13750
Liquid water content and droplet size calibration of the NASA Lewis Icing Research Tunnel [NASA-TM-102447] 05 p0651 N90-13797
Navier-Stokes analysis of airfoils with leading edge ice accretions 06 p0719 N90-14196
Comparison of two droplet sizing systems in an icing wind tunnel [NASA-TM-102456] 06 p0793 N90-14617
Flight in Adverse Environmental Conditions [AGARD-CP-470] 07 p0869 N90-15041
NASA's program on icing research and technology 07 p0873 N90-15062
Ice induced aerodynamic performance degradation of rotorcraft: An overview 07 p0873 N90-15063
Flight and wind tunnel investigation of aerodynamic effects of aircraft ground deicing/antiicing fluids 07 p0873 N90-15064
Evaluation of the improved OV-ID anti-icing system, phase 2 [AD-A213928] 07 p0877 N90-15083
A numerical simulation of the flow in the diffuser of the NASA Lewis icing research tunnel [NASA-TM-102480] 08 p1032 N90-15965
Natural icing re-evaluation of the EH-60A Quick Fix helicopter [AD-A214728] 09 p1162 N90-16723
The collection of non-conus aircraft icing data along with an identification of the geographical areas of potential severe icing and a study of a method of remote determining atmospheric icing data [AD-A215055] 09 p1162 N90-16724
Comparison of drop size distributions from two droplet sizing systems [NASA-TM-102520] 09 p1232 N90-17147
The Polar Ice Prediction System: A sea ice forecasting system [AD-A214600] 09 p1249 N90-17246
The signals of an ice warning device in dependence on total water content and normalized icing degree [DLR-FB-89-52] 11 p1454 N90-18377
Studies of cubic ice crystals [AD-A216574] 11 p1534 N90-18832
Heat transfer measurements from a NACA 0012 airfoil in flight and in the NASA Lewis icing research tunnel [NASA-CR-4278] 12 p1599 N90-19203
Investigation of air transportation technology at the Massachusetts Institute of Technology, 1988-1989 14 p1905 N90-20922
Modeling of surface roughness effects on glaze ice accretion 14 p1905 N90-20925
Ultrasonic techniques for aircraft ice accretion measurement 14 p1906 N90-20926
Investigation of surface water behavior during glaze ice accretion 14 p1906 N90-20927
The influence of ice accretion physics on the forecasting of aircraft icing conditions 14 p1906 N90-20928
Users manual for the NASA Lewis Ice Accretion Prediction Code (LEWICE) [NASA-CR-185129] 14 p1909 N90-20943
Advanced instrumentation for aircraft icing research [NASA-CR-185225] 14 p1921 N90-21006
Swept wing ice accretion modeling [NASA-TM-103114] 15 p2046 N90-21727
On the effectiveness of the production of antarctic bottom water in the Weddell and Ross Seas [AD-A218873] 16 p2259 N90-22880
NASA Lewis icing research tunnel user manual [NASA-TM-102319] 17 p2355 N90-23407
Ice conditions along the Illinois waterway as observed on LANDSAT images, 1972 to 1985 [AD-A219745] 17 p2418 N90-23775
Comparison test of droplet sizing instruments used in icing research [DOT/FAA/CT-TN90/13] 19 p2693 N90-25322
A NASA/university/industry consortium for research on aircraft ice protection [IAR-89-18] 20 p2807 N90-25969
The signals of an ice warning device in dependence on total water content and normalized icing degree [ESA-TT-1207] 24 p3484 N90-29692
Mechanism of habit change for atmospheric ice crystal growth 24 p3489 N90-29717
A documentation of icing-relevant cloud physical parameters on vertical soundings of stratiform clouds [DLR-MITT-90-07] 24 p3495 N90-29753

ICE MAPPING
Coastal subsea permafrost and bedrock observations using dc resistivity [AD-A210784] 02 p0253 N90-11435
Remote sensing data acquisition, analysis and archival [PB89-142566] 03 p0365 N90-12085
The Regional Polar Ice Prediction System, Berents Sea (RPIPS-B): A technical description [AD-A213159] 04 p0522 N90-13012
ERS-1 European remote sensing satellite: A new tool for global environmental monitoring in the 1990's [ESA-BR-36] 11 p1526 N90-18782
Surface topography of the Greenland Ice Sheet from satellite radar altimetry [NASA-SP-503] 16 p2253 N90-22850
Snow and land ice in the climate system: Research problems and possibilities of remote sensing 19 p2707 N90-25407

ICE NUCLEI
Preparation of binary ice layers by condensation from gas phase [JUEL-2248] 05 p0622 N90-13631
Sources of cloud nuclei and development of remote sensing techniques for cloud parameters [AD-A222464] 21 p3031 N90-27233
ETO lidar studies of cirrostratus altocumulogenitus: Another role for supercooled liquid water in cirrus cloud formation 22 p3221 N90-28269
Cirrus microphysics and radiative transfer: Cloud field study on October 28, 1986 22 p3224 N90-28284
The 27-28 October 1986 FIRE IFO cirrus case study: Comparison of satellite and aircraft derived particle size 22 p3224 N90-28285
Cirrus radiative characteristics and the radiative impact of small particles 22 p3224 N90-28286
Cirrus clouds and climate feedback: Is the sky falling and should we go tell the king 22 p3225 N90-28288
Microphysical fundamentals governing cirrus cloud growth: Modeling studies 22 p3225 N90-28291
A scheme for parameterizing cirrus cloud ice water content in general circulation models 22 p3226 N90-28292
The Colorado/Missouri 1989 cirrus mini IFO 22 p3227 N90-28299
The 1973-1974 lidar observations of cirrus clouds at Kwajalein 22 p3227 N90-28303

ICE OBSERVATION
U ICE REPORTING

ICE PACKS
U SEA ICE

ICE PREVENTION
NASA's program on icing research and technology 07 p0873 N90-15062
Flight and wind tunnel investigation of aerodynamic effects of aircraft ground deicing/antiicing fluids 07 p0873 N90-15064
Evaluation of the improved OV-ID anti-icing system, phase 2 [AD-A213928] 07 p0877 N90-15083
Modeling of surface roughness effects on glaze ice accretion 14 p1905 N90-20925

ICE REPORTING
The signals of an ice warning device in dependence on total water content and normalized icing degree [DLR-FB-89-52] 11 p1454 N90-18377

ICE SHELVES
U LAND ICE

ICEBERGS
Mariners Weather Log, volume 33, number 2, Spring 1989 [PB90-146838] 20 p2889 N90-26443

ICELAND
Analysis of radar images of the active volcanic zone at Krafla, Iceland: The effects of look azimuth biasing 03 p0424 N90-12434

ICING
U ICE FORMATION

ICY SATELLITES
NT IAPETUS
NT RHEA (ASTRONOMY)
NT TITANIA

IDEAL FLUIDS
General exact solution for homogeneous time-dependent self-gravitating perfect fluids [DE89-618425] 06 p0776 N90-14514

IDEAL GAS
Computation of transient three-dimensional interstage flowfields using the arbitrary Lagrangian-Eulerian method 02 p0219 N90-11253
Thermophysical properties of benzene. Part 1: The ideal gas and the saturated liquid and vapour [ESDU-89002-PT-1] 04 p0470 N90-12693
Thermophysical properties of isopropyl alcohol. Part 1: The ideal gas and the saturated liquid and vapour [ESDU-89017-PT-1] 06 p0738 N90-14297
Thermal conductivity of gaseous aliphatic hydrocarbons. Part 1: Alkanes [ESDU-89035-PT-1] 07 p0897 N90-15183
Numerical modelling of shocks in gases and metals [MRL-RR-8-89] 12 p1658 N90-19528
Notes on the unsteady rectilinear motion of a perfect gas. Part 8: General theory and general waves in a homentropic gas [PB90-167149] 14 p1974 N90-21309
Partial acoustic filtering applied to the equations of compressible flow [DE90-000673] 15 p2097 N90-22001

IDENTIFY FRIEND OR FOE
U IFF SYSTEMS (IDENTIFICATION)
IDENTIFYING
NT CROP IDENTIFICATION
NT IFF SYSTEMS (IDENTIFICATION)
NT PARAMETER IDENTIFICATION
NT SYSTEM IDENTIFICATION
NT TIMBER IDENTIFICATION
Stimulus-response compatibility in spatial precuing and symbolic identification: Effects of coding practice, retention, and transfer
[AD-A210745] 02 p0255 N90-11443
Experimental research in high energy physics
[DE90-000061] 03 p0408 N90-12342
Gas identification system using graded temperature sensor and neural net interpretation
[AD-A213359] 05 p0622 N90-13627
Identification of impulsive interference channels
[AD-A213154] 05 p0688 N90-14009
The development of two-dimensional object identification techniques
[NASA-CR-186203] 08 p1107 N90-16408
Identifying the circadian cycle in human information processing data using periodicity analysis: A synopsis
[AD-A214674] 09 p1251 N90-17257
Effective techniques for the identification and accommodation of disturbances
14 p1934 N90-21072
The intensity dependent spread model and color constancy 15 p2140 N90-22228
Industrial plastics waste: Identification and segregation 18 p2513 N90-24351
An investigation into techniques for landmark identification of 3D images of human subjects, phase 1
[AD-A218614] 18 p2583 N90-24713
Expansion and orthogonalization of measured modes for structure identification 18 p2647 N90-25068
Ecological study of peat landforms in Canada and Alaska
[NASA-CR-184923] 19 p2705 N90-25391
Ocean feature recognition using genetic algorithms with fuzzy fitness functions (GA/F3)
19 p2740 N90-25576
Identification of tetragonal and cubic structures of zirconia
[AD-A222373] 21 p3083 N90-27535
Development of an expert system embedding pattern recognition techniques for pollution source identification
[PB90-185927] 22 p3197 N90-28139
Nondestructive material characterization
[DE90-015176] 24 p3477 N90-29652
Submicron particle analyzer
[AD-A223558] 24 p3545 N90-30050
Tokamak plasma shape identification with a Legendre-Fourier expansion of the vacuum poloidal flux function in the toroidal coordinates
[DE90-508031] 24 p3548 N90-30068
IDENTITIES
Item identities and their related observables
[AD-A219559] 17 p2468 N90-24104
IDLERS
Experimental demonstration of an electromagnetically pumped free-electron laser with cyclotron harmonic idlers
[AD-A218830] 17 p2408 N90-23719
IFF SYSTEMS (IDENTIFICATION)
Identification Friend, Foe or Neutral Joint Test
02 p0154 N90-10881
IFR (RULES)
U INSTRUMENT FLIGHT RULES
IGFET
U FIELD EFFECT TRANSISTORS
IGNEOUS ROCKS
NT BASALT
NT OBSIDIAN
Geology of Espinhaco Meridional, including the Quadrilatero Ferrifero: Integration through remote sensing data
[INPE-4904-PRE/1505] 14 p1998 N90-21450
IGNIMBRITE
U IGNEOUS ROCKS
IGNITERS
NT BOOSTERS (EXPLOSIVES)
NT CAPS (EXPLOSIVES)
NT DETONATORS
NT EXPLODING WIRES
NT INITIATORS (EXPLOSIVES)
Heat transfer characteristics of igniter output plumes
[DE89-011449] 01 p0059 N90-10340
Evaluation of selected computer models for modeling pyrotechnic and propellant devices
[AD-A213003] 05 p0629 N90-13671
Flight set 360T004 (STS-30) field joint protection system, volume 7
[NASA-CR-183829] 06 p0735 N90-14280
Devices and methods for in-situ combustion ignition
[DE89-000766] 06 p0740 N90-14309
Experimental and theoretical research on the injection of ignition gases into a bed of inert powder
[ISL-CO-251/88] 11 p1485 N90-18547
Flight set 360L001 (STS-26) igniter, post flight
[NASA-CR-183957] 20 p2870 N90-26325
QM-6 final performance evaluation report igniter, volume 6
[NASA-CR-184001] 22 p3133 N90-27779
Igniter adapter-to-igniter chamber deflection test
[NASA-CR-184002] 22 p3133 N90-27780
Electrical ignition of HAN-based liquid propellants
[AD-A223272] 24 p3458 N90-29528
IGNITION
NT ELECTRIC IGNITION
NT SOLID PROPELLANT IGNITION
NT SPARK IGNITION
Heat transfer characteristics of igniter output plumes
[DE89-011449] 01 p0059 N90-10340
Pyrotechnic ignition studies using a gun tunnel
[DE89-012496] 01 p0060 N90-10341
Ignition and burn criteria for D3He tokamak and spherical torus reactors
[DE89-015059] 01 p0125 N90-10716
Powder morphology effects in the ignition of titanium-based pyrotechnics
[DE89-017229] 02 p0208 N90-11191
Laser initiated ignition of liquid propellant
[AD-A212342] 04 p0482 N90-12766
Systems tunnel linear shaped charge lightning strike
[NASA-CR-183832] 05 p0584 N90-13404
The mobile combustion diagnostic fixture and its application to the study of propellant combustion. Part 1: Investigation of the low pressure combustion of LOVA XM39 propellant
[AD-A213272] 05 p0621 N90-13626
Evaluation of selected computer models for modeling pyrotechnic and propellant devices
[AD-A213003] 05 p0629 N90-13671
Devices and methods for in-situ combustion ignition
[DE89-000766] 06 p0740 N90-14309
Flame acceleration studies in the MINIFLAME facility
[DE90-000041] 06 p0740 N90-14310
Ignitability test method and apparatus
[NASA-CASE-LAR-13996-1-SB] 07 p0893 N90-15161
Shock tube ignition of octanes
[DE90-001167] 07 p0893 N90-15164
Using small scale tests to estimate the failure diameter of a propellant
[DE90-001166] 07 p0913 N90-15281
Critical temperature analysis for a hemispherical charge of a binary explosive
[DE90-001447] 07 p0913 N90-15282
The Gevaltig: An inertial fusion powered manned spacecraft design for outer solar system missions
[NASA-CR-185163] 08 p1036 N90-15985
Assessing the flammability of composite materials
[PB90-112996] 08 p1039 N90-16002
Multidimensional numerical simulation of large caliber ignition processes
[ISL-CO-233/88] 08 p1042 N90-16021
Very low energy ignition of pyrotechnics using a Semiconductor Bridge (SCB)
[DE90-002645] 08 p1052 N90-16082
Automatic prestart or post shutoff engine lubricator
[AD-D014259] 08 p1084 N90-16273
Rocket-triggered lightning strikes and forest fire ignition 08 p1155 N90-16690
RAAF Orion aircraft A9-300 oxygen fire
[AD-A215496] 09 p1162 N90-16725
Measurement of the speed and temperature of ignition gases
[ISL-CO-246/88] 09 p1192 N90-16908
The fundamentals of metal combustion in composite explosives revealed by high speed microphotography
[DE90-005255] 09 p1192 N90-16910
Ignitability of jet-A fuel vapors in aircraft fuel tanks
10 p1313 N90-17594
Hot surface ignition studies of aviation fluids
10 p1314 N90-17600
Microconvective heating of granular explosives by a semiconductor bridge
[DE90-005710] 11 p1484 N90-18541
Ignition of HMX (cyclotetramethylenetetranitramine) using low energy laser diodes
[DE90-007637] 12 p1624 N90-19334
A comparison of the autoignition chemistry of n-butane and isobutane in an internal combustion engine
[DE90-009474] 15 p2067 N90-21838
Detailed mechanism for oxidation of benzene
[NASA-TM-102443] 15 p2067 N90-21842
Ignition testing of low-energy laser diode ignited components
[DE90-009968] 16 p2214 N90-22630
Oxidation and ignition characteristics of hydrocarbon fuels
[AD-A218666] 16 p2215 N90-22637
DURIP: Spontaneous Raman system for the study of enhanced combustion and non-thermal plasmas
[AD-A221410] 18 p2564 N90-24629
T4A thruster starting sequences and the design of an electromagnetic sequencer for cyclic life tests
[RAE-TR-77042] 19 p2669 N90-25179
Flammability of fire resistant, aircraft hydraulic fluid
[DOT/FAA/CT-TN90/19] 19 p2677 N90-25222
RSRM-9 (360L009): Ballistics mass properties
[NASA-CR-183944] 20 p2823 N90-26064
Mars in situ propellants: Carbon monoxide and oxygen ignition experiments
[NASA-TM-103202] 20 p2823 N90-26065
Flight motor set 360L007 (STS-33R)
[NASA-CR-183979] 20 p2824 N90-26067
Critical evaluation of Jet-A spray combustion using propane chemical kinetics in gas turbine combustion simulated by KIVA-2
[NASA-TM-103173] 20 p2843 N90-26170
Ignition and combustion characteristics of metallized propellants
[NASA-CR-186870] 21 p2976 N90-26911
The sensitivity of several explosives to ignition in the launch environment
[AD-A221581] 21 p2990 N90-26993
Photo-sensitized ignition of hydrogen/oxygen mixtures for hypersonic flight vehicles 22 p3163 N90-27935
Analyses of spray and droplet ignition for pure and multicomponent fuels 23 p3304 N90-28688
Ignition and combustion of liquid propellants
[AD-A224150] 23 p3316 N90-28746
Ignition and burn control characteristics of thermonuclear plasmas
[DE90-015385] 23 p3398 N90-29197
Investigation of particulate formation during diesel spray combustion
[DE90-012682] 24 p3446 N90-29464
Electrical ignition of HAN-based liquid propellants
[AD-A223272] 24 p3458 N90-29528
Development and evaluation of hermetic laser diode ignited pyrotechnic components
[DE90-015745] 24 p3458 N90-29529
IGNITION LIMITS
Experimental and computational study of combustion limits in natural-gas fueled internal combustion engines
[PB89-235196] 05 p0629 N90-13673
Investigation into the feasibility of using solid fuel ramjets for high supersonic/low hypersonic tactical missiles
[AD-A214737] 09 p1168 N90-16761
IGNITION SYSTEMS
Cold starting a neat methanol (M100) vehicle with long duration spark ignition
[PB89-230692] 06 p0792 N90-14613
Pyrotechnic materials ignited using lasers. High energy photopyrotechnic chains
[REPT-892-430-121] 16 p2225 N90-22691
Optimization of a pulsed air core transformer for low impedance inductive ignition
[AD-A218748] 16 p2232 N90-22734
Combustion in the gas turbine. Part 3: Fuel injection, ignition and stability
[CIT/SME/VKI/RS/4] 20 p281^ N90-25988
Ignition and combustion characteristics of metallized propellants
[NASA-CR-186870] 21 p2976 N90-26911
Igniter adapter-to-igniter chamber deflection test
[NASA-CR-184002] 22 p3133 N90-27780
Catalytic ignition of hydrogen/oxygen
23 p3293 N90-28627
IGNITION TEMPERATURE
Ignition characteristics of the nickel-based alloy UNS N07718 in pressurized oxygen
[NASA-CR-185932] 03 p0326 N90-11850
Oxidation and ignition characteristics of hydrocarbon fuels
[AD-A218666] 16 p2215 N90-22637
Titanium-boron mixtures as variable heat sources
[DE90-009729] 18 p2522 N90-24401
Finite difference modeling of laser diode ignited components
[DE90-015652] 24 p3474 N90-29635
IGNITRONS
Commercial high current ignitron development
[DE89-015077] 01 p0058 N90-10331
ILLINOIS
The interaction and variation of waves and turbulence from MST radar data
[AD-A212849] 05 p0670 N90-13906
Ice conditions along the Illinois waterway as observed on LANDSAT images, 1972 to 1985
[AD-A219745] 17 p2418 N90-23775

ILLUMINANCE
Three-dimensional motion estimation using shading information in multiple frames
[AD-A216804] 11 p1549 N90-18919
Human cognitive and motor performance measures under typical cool white fluorescent illumination vs relatively high cool white illuminance/irradiance lighting
[AD-A218445] 16 p2262 N90-22892

ILLUMINATING
Improved lighting of taxiway/taxiway intersections for Instrument Flight Rules (IFR) operations
[DOT/FAA/CT-TN89/64] 07 p0878 N90-15089
Human factors engineering testing of aircraft cockpit lighting systems
[AD-A216853] 12 p1697 N90-19743
Modified touchdown zone lighting
[DOT/FAA/CT-TN89/70] 14 p1929 N90-21042
Factors affecting the perception of transparent motion 15 p2141 N90-22233
Effect of laser glare and aircraft windscreen on visual search performance under low ambient lighting
[AD-A219456] 17 p2437 N90-23888
Greenhouse design for a Martian colony: Structural, solar collection and light distribution systems
[NASA-CR-186818] 20 p2901 N90-26501

ILLUSIONS
NT OCULOGRAVIC ILLUSIONS
NT OPTICAL ILLUSION
A comparison of two subject-controlled attitude measures during somatogravic illusion exposure
[AD-A212528] 04 p0525 N90-13031
Spatial disorientation incidents in the RNLAF F16 and F5 aircraft and suggestions for prevention 23 p3357 N90-28973

ILMENITE
Getting lunar ilmenite: From soils or rocks
[NASA-CR-186498] 12 p1744 N90-20029
Ilmenite exsolution schemes in Apollo-17 high-Ti basalts
[DE90-011992] 21 p2976 N90-26912

ILS (LANDING SYSTEMS)
U INSTRUMENT LANDING SYSTEMS

IMAGE ANALYSIS
Image-based terrain modeling with thematic mapper applied to resolving the limit of Holocene Lake expansion in the Great Salt Lake Desert, Utah, part 1
[NASA-CR-185913] 01 p0082 N90-10465
Soft X-ray astronomy using grazing incidence optics 01 p0138 N90-10797
The design and evaluation of grazing incidence relay optics 01 p0138 N90-10799
The correspondence between small-scale coronal structures and the evolving solar magnetic field 01 p0138 N90-10800
Spatial and temporal short range total cloud cover estimation by metric analysis of composite imagery 02 p0251 N90-11423
ANIMA: Image analyzer applied to remote sensing
[INPE-4766-PRE/1435] 02 p0256 N90-11447
Characteristics, distribution and geologic/terrain associations of small dome-like hills on Venus 03 p0422 N90-12425
Potential for observing and discriminating impact craters and comparable volcanic landforms on Magellan radar images 03 p0423 N90-12429
Contrasting landform perception with varied radar illumination geometries and at simulated resolutions of Venera and Magellan 03 p0423 N90-12430
Venus surface properties deduced from radar and radiometry 03 p0423 N90-12431
A morphologic study of Venus Ridge belts 03 p0423 N90-12432
Evidence for volcanism in NW Ishtar Terra, Venus 03 p0424 N90-12433
Analysis of radar images of the active volcanic zone at Krafla, Iceland: The effects of look azimuth biasing 03 p0424 N90-12434
Radar scattering mechanisms within the meteor crater ejecta blanket: Geologic implications and relevance to Venus 03 p0424 N90-12435
Aeolian processes on Venus 03 p0425 N90-12436
Architecture of orogenic belts and convergent zones in Western Ishtar Terra, Venus 03 p0425 N90-12437
Tectonism on Venus: A review 03 p0425 N90-12440
Crater identification and resolution of lunar radar images 03 p0426 N90-12441
Radar scattering from desert terrains, Pisgah/Lavic Region, California: Implications for Magellan 03 p0426 N90-12443
Lakshmi Planum: A distinctive highland volcanic province 03 p0426 N90-12444
Impact cratering and the surface age of Venus: The Pre-Magellan controversy 03 p0426 N90-12446
Geology of the Venus equatorial region from Pioneer Venus radar imaging 03 p0427 N90-12447
Venus and the Archean Earth: Thermal considerations 03 p0427 N90-12448
Eastern Ishtar Terra: Tectonic evolution derived from recognized features 03 p0428 N90-12451
Stress distribution and topography of Tellus Regio, Venus 03 p0428 N90-12452
Conception and results of the DLR realtime azimuth processor for the E-SAR system
[DLR-FB-89-30] 04 p0492 N90-12827
A hybrid architecture for feature labelling of oceanographic satellite images
[AD-A212236] 04 p0515 N90-12975
The algebraic basis of mathematical morphology. Part 2: Openings and closings
[CWI-AM-R8904-PT-2] 04 p0543 N90-13150
A review of focal reducer interferometer systems
[RSRE-MEMO-3486] 04 p0554 N90-13231
Analysis of the image dissector tube data 05 p0609 N90-13550
Analysis of the star mapper data 05 p0609 N90-13551
Overview of the Tycho data analysis 05 p0610 N90-13558
Novel graph searching methods for image analysis
[AD-A213065] 05 p0682 N90-13971
An editor for 3D-models for image analysis
[FOA-C-30534-3.4] 05 p0684 N90-13986
SEM (Scanning Electron Microscope) image analysis of grain growth in microwave-annealed alumina
[DE90-001606] 06 p0746 N90-14339
A knowledge-based machine vision system for space station automation 08 p1075 N90-16221
Digital image interpretation for optical flow measurement methods: System description and preliminary application examples 08 p1079 N90-16244
Quantitative evaluation of object-changes in multitemporal AGRISAR imagery
[FIM-195] 08 p1091 N90-16314
Image segmentation by iterative parallel region growing with application to data compression and image analysis 08 p1114 N90-16452
AOIPS 3 user's guide. Volume 2: Program descriptions
[NASA-TM-100725] 09 p1247 N90-17236
Gabor transforms for forward looking infrared image segmentation
[AD-A215046] 09 p1282 N90-17433
Evaluation of digital classification results of summer cultivation in a test area in the Parana-Ano state harvest 1986-1987
[INPE-4828-PRE/1459] 10 p1399 N90-18085
Problems of the micro-holographic image analysis
[ISL-CO-201/89] 11 p1511 N90-18704
Evaluation of TM/LANDSAT and HRV/SPOT data in reforested areas
[INPE-4575-RPE/567] 11 p1524 N90-18772
Classification of high resolution imagery using texture attributes
[INPE-4888-TDL/379] 11 p1525 N90-18778
Comparisons between the RTNEPH (Real-Time Nephanalysis) and AFGL cloud layer analysis algorithms
[AD-A216637] 11 p1536 N90-18844
Application of wavefront analysis techniques to restoring of images degraded by atmospheric turbulence
[ONERA-PUBL-1989-1] 11 p1589 N90-19168
A high resolution automatic image measuring system
[WISS-ARB-VERMESSUNGSWESEN-154] 12 p1663 N90-19559
Possible applications of remote sensing satellite pictures for the water quality management of the Frisian lakes, Netherlands
[BCRS-88-17] 12 p1679 N90-19641
Thematic coupling between digital images and geographic information systems
[ETN-90-95723] 12 p1679 N90-19646
Using image analysis to determine petrophysical properties of reservoir rocks
[DE90-000222] 12 p1680 N90-19649
Thermal infrared scene simulation
[DE90-006900] 12 p1714 N90-19845
Laboratory techniques for the characterisation of snow structures 12 p1741 N90-20007
A system for analysis and interpretation of lineaments in remote sensing images
[INPE-4893-PRE/1494] 13 p1840 N90-20565
Three-dimensional medical image analysis using local dynamic algorithm selection on a multiple-instruction, multiple-data architecture
[AD-A218024] 13 p1852 N90-20630
Texture segmentation using localized spatial filtering
[AD-A218064] 13 p1869 N90-20722
Results of the Gondwana Project: An example of intercontinental geologic correlation utilizing LANDSAT imagery
[INPE-4870-PRE/1481] 14 p1995 N90-21437
Evaluation of classification performance and proportion estimate of the sugar cane crop through PROCEDURE-INPE utilizing LANDSAT data
[INPE-4899-PRE/1500] 14 p1999 N90-21458
Performance evaluation of MSS/LANDSAT data in the estimation of fluvial channel width
[INPE-4906-PRE/1507] 14 p2000 N90-21463
Performance evaluation of morphological edge detectors
[INPE-4975-PRE/1540] 14 p2000 N90-21464
Multiresolution and time-frequency representations of signals
[REPT-89-47] 15 p2087 N90-21946
A study of creep damage using microradiography and continuum damage mechanics 15 p2117 N90-22109
Algorithms and architectures for robot vision 15 p2141 N90-22236
Satellite image analysis using neural networks 15 p2157 N90-22321
Analysis of nonlinear internal waves observed by LANDSAT-TM
[PREPRINT-704] 16 p2249 N90-22828
Spatial Displays and Spatial Instruments
[NASA-CP-10032] 16 p2267 N90-22918
Pictorial communication: Pictures and the synthetic universe 16 p2267 N90-22919
The perception of three-dimensionality across continuous surfaces 16 p2268 N90-22924
The effects of viewpoint on the virtual space of pictures 16 p2269 N90-22932
Perceived orientation, spatial layout and the geometry of pictures 16 p2269 N90-22933
The eyes prefer real images 16 p2270 N90-22938
Spatial issues in user interface design from a graphic design perspective 16 p2270 N90-22939
Quantum-limited image recognition
[AD-A218425] 16 p2299 N90-23101
Classification techniques for quantum-limited and classical-intensity images
[AD-A218693] 16 p2317 N90-23212
Implementation of image action plus software for image analysis of solid propellant combustion holograms
[AD-A219644] 17 p2372 N90-23508
EXOSAT deep exposure of the LMC X-4 region 17 p2483 N90-24203
Acquisition of an analytical x ray and image analysis system
[AD-A221376] 18 p2593 N90-24756
Analysis of camera movement based on a sequence of images
[TELECOM-PARIS-89-D-008] 18 p2616 N90-24901
System for shooting of video images in realtime
[MBB-UM-0009/89-PUB] 19 p2653 N90-25097
Video photographic considerations for measuring the proximity of a probe aircraft with a smoke seeded trailing vortex
[NASA-TM-102691] 19 p2657 N90-25120
Mapping and monitoring land use and land degradation in part of East Kalimantan, Indonesia, using aerospace remote sensing techniques: A SPOT case study
[BCRS-88-16B] 19 p2705 N90-25394
Ocean feature recognition using genetic algorithms with fuzzy fitness functions (GA/F3) 19 p2740 N90-25576
Extensions of algebraic image operators: An approach to model-based vision 19 p2741 N90-25577
A hard X ray observation of the Coma Cluster 19 p2789 N90-25875
Automatic line network extraction from aerial imagery of urban areas through knowledge based image analysis
[AD-A222675] 20 p2880 N90-26385
An experiment to make a new design of the Satellite Cloud Information Chart with the combination of visible and infrared data observed by the GMS 21 p3029 N90-27223
Evaluation of the wake effects on plume dispersion using video image analysis
[PB90-186354] 22 p3169 N90-27972
Concurrent Image Processing Executive (CIPE). Volume 3: User's guide
[NASA-CR-186848] 22 p3236 N90-28350
On-line object feature extraction for multispectral scene representation
[NASA-CR-187006] 23 p3342 N90-28888
Detection of ocean inner waves by synthetic aperture radar: Observations at Gibraltar pass
[ETN-90-97477] 23 p3353 N90-28953
Techniques and potential capabilities of multi-resolutional information (knowledge) processing 23 p3374 N90-29062
National Archives preservation research priorities: Past and present
[PB90-206210] 23 p3405 N90-29242
A global approach to image texture analysis
[AD-A223532] 24 p3527 N90-29941

A manual for microcomputer image analysis
[DE90-015629] 24 p3529 N90-29958
Determination of density using simultaneous interferometry methods
[IMFL-90/04] 24 p3547 N90-30061

IMAGE CONTRAST
Image enhancement software for underwater recovery operations: User's manual
[AD-A212943] 05 p0699 N90-14094
Shade images of forested areas obtained from LANDSAT MSS data
[NASA-TM-102939] 14 p1995 N90-21436
Scanning electron microscopy by photovoltage contrast imaging
[AD-D014517] 19 p2760 N90-25684
Image fusion through multi-resolution contrast decomposition
[IZF-1989-19] 22 p3247 N90-28412

IMAGE CONVERTERS
NT IMAGE TUBES

IMAGE CORRELATORS
Digital processing of TM/LANDSAT data in monitoring interior water
[INPE-4956-PRE/1533] 14 p1997 N90-21448
An acousto-optic image correlator with a throughput rate of 1000 templates per second
[DE90-009323] 15 p2144 N90-22249
A compact real-time acousto-optic image correlator
[DE90-015564] 24 p3548 N90-30054

IMAGE DISSECTOR TUBES
The relay lens systems 05 p0603 N90-13506
The detectors 05 p0604 N90-13507
Analysis of the image dissector tube data 05 p0609 N90-13550

IMAGE ENHANCEMENT
Enhancement of infrared thermographic imagery: Local smoothing and time-based interpolation
[ONERA-RT-8/7254-SN] 04 p0555 N90-13232
Image enhancement software for underwater recovery operations: User's manual
[AD-A212943] 05 p0699 N90-14094
Real time image enhancement during underwater recovery operations
[AD-A213139] 05 p0700 N90-14097
Some edge-enhancing operators and their applications to image enhancement and edge detection 06 p0828 N90-14810
Image enhancement using the IRAS (Infrared Astronomy Satellite) survey data
[AD-A213811] 07 p0950 N90-15496
Order filters, median recursive filter: Analysis and evaluation of performance in image processing
[ISAL-89-0017] 08 p1123 N90-16505
DSS 15, 45, and 65 34-meter high efficiency antenna radio frequency performance enhancement by tilt added to the subreflector during elevation angle changes 20 p2854 N90-26229
Robot Acting on Moving Bodies (RAMBO): Interaction with tumbling objects 23 p3366 N90-29022

IMAGE FILTERS
Image preprocessing by modified median filter
[AD-D014199] 04 p0492 N90-12828
The lidar experiment at Andoya, Norway, during the Summer of 1988
[BONN-IR-89-16] 08 p1058 N90-16117
Order filters, median recursive filter: Analysis and evaluation of performance in image processing
[ISAL-89-0017] 08 p1123 N90-16505
Image smoothing and differentiation with minimal-curvature filters
[AD-A215184] 09 p1273 N90-17382
Mars Rover imaging systems and directional filtering 18 p2648 N90-25071
Automatic line network extraction from aerial imagery of urban areas through knowledge based image analysis
[AD-A222675] 20 p2880 N90-26385
Spatial cross-correlation of Antarctic Sea ice and seabed topography
[NASA-CR-186815] 20 p2891 N90-26451
A reduced-order extended Kalman filter for moving images
[AD-A223742] 24 p3541 N90-30028

IMAGE INTENSIFIERS
Cockpit lighting compatibility with image intensification night imaging systems: Issues and answers
[AD-A210503] 01 p0006 N90-10028
Night sky radiometric measurements during follow-on-evaluation testing of AN/PVS-7 (A, B) at Fort Benning, Georgia
[AD-A211273] 02 p0276 N90-11574
A microchannel plate intensified, subnanosecond, X-ray imaging camera
[DE89-017781] 03 p0350 N90-12003
A validation of the proposed NATO standard method to determine target acquisition distances with image intensifiers
[IZF-1988-8] 04 p0554 N90-13230
Attenuating the luminous output of the AN/PVS-5A night vision goggles and its effects on visual acuity
[AD-A214895] 09 p1261 N90-17311
Optical amplification in 45 deg - cut BaTiO3
[AD-A216043] 11 p1566 N90-19011
Automated segmentation and extraction of area terrain features from radar imagery
[AD-A221096] 18 p2544 N90-24522
Use of the Xybion ISG-camera in the RETRA-1000 TV-Holography unit
[AD-A219842] 18 p2554 N90-24577
Nonlinear optical protection against frequency agile lasers
[AD-D014535] 19 p2695 N90-25335
PHIND, an analytical model to predict target acquisition distance with image intensifiers
[IZF-1989-45] 19 p2724 N90-25493
Stenopic radiography: A non-destructive test without contact 22 p3187 N90-28086
Noise performance of microchannel plate imaging systems
[DE90-015037] 23 p3322 N90-28785

IMAGE MOTION COMPENSATION
GOES I/M image navigation and registration 05 p0588 N90-13422
Self compensation of rigid displacements in holographic interferometry
[ISL-CO-219/88] 09 p1226 N90-17113
The perceptual buildup of three-dimensional structure from motion
[AD-A214640] 09 p1259 N90-17300
A motion compensation study for the PHARUS project 14 p1962 N90-21235
A solution for real time motion compensation for SAR without using inertial navigation systems 14 p1962 N90-21236
The 1D-ISAR imaging of manoeuvering aircraft 14 p1963 N90-21241
Passive navigation using image irradiance tracking 15 p2141 N90-22232

IMAGE PROCESSING
NT GEOMETRIC RECTIFICATION (IMAGERY)
Optical processing for distributed sensors in control of flexible spacecraft 01 p0021 N90-10102
Satellite Data Processing System (SDPS) users manual V1.0
[NASA-CR-183054] 01 p0082 N90-10468
Regulation of nonlinear and generalized linear systems
[AD-A207725] 01 p0109 N90-10619
Robot vehicle video image compression, phase 1
[AD-A210974] 01 p0110 N90-10626
Tellurium-118/antimony-118 generator
[DE89-015225] 01 p0122 N90-10698
Radon transform analysis of a probabilistic method for image generation
[AD-A207814] 01 p0123 N90-10702
A comparison of real-time optical correlators for pattern recognition
[DE89-016416] 01 p0123 N90-10705
Utilization of photorefractive crystals in optical image processing
[ISBN-3-923560-06-0] 02 p0225 N90-11292
Filling or outlining shapes with color: The effects on a visual search task
[AD-A211067] 02 p0255 N90-11444
Computing the two dimensional fast Fourier transform on a general purpose mesh connected multiprocessor
[DE89-016515] 02 p0266 N90-11518
Video imaging systems: A survey
[DE89-016920] 03 p0337 N90-11919
Analysis of two-pass Modified Hough Transform (MHT) technique for the detection of wake like signals
[AD-A211982] 03 p0338 N90-11924
Fast and objective MRTD measurement
[FEL-1988-24] 03 p0351 N90-12006
Discriminating rigid from nonrigid motion
[AD-A211794] 03 p0383 N90-12180
Basic program for raster scan display unit
[NAL-TM-560] 03 p0384 N90-12185
Parallel implementation and evaluation of motion estimation system algorithms on a distributed memory multiprocessor using knowledge based mappings
[NASA-CR-185984] 03 p0389 N90-12213
Novel techniques for data decomposition and load balancing for parallel processing of vision systems: Implementation and evaluation using a motion estimation system
[NASA-CR-185991] 03 p0389 N90-12214
Parallel architectures and parallel algorithms for integrated vision systems
[NASA-CR-185990] 03 p0389 N90-12215
Parallel processing on transputer arrays for the recognition of objects in infrared images
[RSRE-MEMO-4197] 03 p0389 N90-12217
A survey of camera error sources in machine vision systems
[DE89-014072] 03 p0405 N90-12318
Investigation of active regions at high resolution by balloon flights of the Solar Optical Universal Polarimeter (SOUP) 03 p0434 N90-12487
An imaging vector magnetograph for the next solar maximum 03 p0435 N90-12489
On a fast two-dimensional radar imaging process for rotating targets, and an analysis of its image quality
[ESA-TT-1142] 04 p0489 N90-12808
Conception and results of the DLR realtime azimuth processor for the E-SAR system
[DLR-FB-89-30] 04 p0492 N90-12827
Image preprocessing by modified median filter
[AD-D014199] 04 p0492 N90-12828
Video line processor
[AD-D014198] 04 p0497 N90-12861
Readout and signal conditioning for a linear pyroelectric array
[RSRE-MEMO-4102] 04 p0504 N90-12905
A two-dimensional hybrid experimental-numerical technique for elastic-plastic stress analysis 04 p0511 N90-12949
Removing stripes in GOES (Geostationary Operational Environmental Satellites) images by matching empirical distribution functions
[PB89-213359] 04 p0514 N90-12968
An attempt to draw conclusions from the vegetation to the geological underground in the area of Amberg (Germany, F.R.) by means of digital image processing of TM data
[DFVLR-FB-89-24] 04 p0515 N90-12974
Three stages and two systems of visual processing
[AD-A212670] 04 p0525 N90-13032
Visual perception processing in a hierarchical control system: Level 1
[PB89-221188] 04 p0536 N90-13101
The algebraic basis of mathematical morphology. Part 2: Openings and closings
[CWI-AM-R8904-PT-2] 04 p0543 N90-13150
Effect of central obscuration on the LDR point spread function 05 p0598 N90-13475
The Hipparcos Mission. Prelaunch status. Volume 2: The input catalog
[ESA-SP-1111-VOL-2] 05 p0606 N90-13529
From scientific proposals to the Inca data base 05 p0606 N90-13530
Analysis of the image dissector tube data 05 p0609 N90-13550
Photometry: Main mission and Tycho 05 p0610 N90-13560
Double star reductions in FAST 05 p0611 N90-13562
Summaries of the thematic conferences on remote sensing for exploration geology
[NASA-CR-185321] 05 p0664 N90-13880
Estimation of rain rate using spatial and multichannel coherence: Analysis of SSM/I data 05 p0670 N90-13905
Implementation issues in source coding
[NASA-CR-185327] 05 p0681 N90-13963
Novel graph searching methods for image analysis
[AD-A213065] 05 p0682 N90-13971
Algorithm for atmospheric corrections of aircraft and satellite imagery
[NASA-TM-100751] 05 p0683 N90-13976
The algebraic basis of mathematical morphology. Part 1: Dilations and erosions
[CWI-AM-R8807] 05 p0695 N90-14065
Optics and opto-electronics systems
[AD-A212340] 05 p0699 N90-14093
Image enhancement software for underwater recovery operations: User's manual
[AD-A212943] 05 p0699 N90-14094
Real time image enhancement during underwater recovery operations
[AD-A213139] 05 p0700 N90-14097
Automated glass fiber drawing
[DE90-000894] 06 p0751 N90-14367
An image compression algorithm for a high-resolution digital still camera
[NASA-CR-185079] 06 p0780 N90-14532
The development of coherent x ray lasers for x ray holography
[DE90-000784] 06 p0789 N90-14595
NORDA's pattern analysis laboratory: Current contributions to naval mapping, charting, and geodesy
[AD-A212731] 06 p0801 N90-14665
A rough transform technique for extracting lead features from sea ice imagery
[AD-A212758] 06 p0801 N90-14666

Image processing of LANDSAT MSS data for buried valley detection in northern Indiana
06 p0802 N90-14668
X ray microimaging for the life sciences
[DE90-002613] 06 p0819 N90-14766
The phase gradient autofocus algorithm: An optimal estimator of the phase derivative
[DE90-000895] 06 p0828 N90-14814
The design of a computer system for image simulation and image processing of high resolution electron micrographs
[DE90-000179] 06 p0829 N90-14820
Interactive multidimensional data analysis and understanding
[DE90-001794] 06 p0830 N90-14824
Generalization in backpropagation networks: An empirical study using image data
[DE89-012658] 06 p0832 N90-14835
Design of incoherent imaging arrays
[DE90-000861] 06 p0844 N90-14909
Document preservation by electronic imaging. Volume 2: System and experiment description
[PB89-226534] 06 p0858 N90-14988
Document preservation by electronic imaging. Volume 3: Appendices
[PB89-226542] 06 p0858 N90-14989
Component presence-absence detection for automated visual inspection of hybrid microcircuits
[KCP-613-4050] 07 p0922 N90-15335
Sensor integration using concurrent computing on-board the ORNL mobile robot
[DE89-008740] 07 p0939 N90-15436
Image enhancement using the IRAS (Infrared Astronomy Satellite) survey data
[AD-A213811] 07 p0950 N90-15496
Identification and quantification of synoptic structure in simulated Tiros N radiance soundings
07 p0959 N90-15546
Vision in dynamic environments
[AD-A213434] 07 p0967 N90-15587
The role of attention in visual processing
[AD-A214158] 07 p0967 N90-15588
Scry: A distributed image handling system, version 1.1
[DE90-003105] 07 p0973 N90-15621
Evaluation of a simple algorithm for estimating infrared signatures from multi-pixel to sub-pixel targets applied to AGA thermovision imagery
[AD-A214103] 07 p0976 N90-15639
A renormalization group approach to image processing: A new computational method for three-dimensional shapes in robot vision, and the computation complexity of the cooling algorithms
[AD-A214247] 07 p0977 N90-15643
One-class generalization in second-order backpropagation networks for image classification
[DE89-015845] 07 p0980 N90-15661
Design and implementation of two concurrent multi-sensor integration algorithms for mobile robots
[DE90-003041] 07 p0981 N90-15663
Systolic algorithms for imaging from space
[AD-A213870] 07 p0987 N90-15701
Optimal focal-plane restoration
08 p1073 N90-16207
Detection of edges using local geometry
08 p1074 N90-16213
Image processing by Intensity-Dependent Spread (IDS)
08 p1074 N90-16215
From primal sketches to the recovery of intensity and reflectance representations
08 p1074 N90-16216
Parallel asynchronous systems and image processing algorithms
08 p1075 N90-16218
Neural networks for data compression and invariant image recognition
08 p1075 N90-16219
Two-Dimensional Measuring Techniques
[DGLR-PAPERS-88-04] 08 p1078 N90-16236
Quantative interferometry
08 p1078 N90-16237
Flow field visualization using laser light sheet methods. Quantitative analysis using image processing
08 p1079 N90-16243
Digital image interpretation for optical flow measurement methods: System description and preliminary application examples
08 p1079 N90-16244
End-on soft x ray imaging of Field-Reversed Configurations (FRCs) on the Field-Reversal-C (FRX-C)/Large Scale Modification (LSM) experiment
[DE90-004863] 08 p1082 N90-16260
Science plan for the Alaska SAR facility program. Phase 1: Data from the first European sensing satellite, ERS-1
[NASA-CR-185028] 08 p1091 N90-16312
Computer-aided boundary delineation of agricultural lands
[NASA-TM-102243] 08 p1091 N90-16313
Proceedings of the 5th User Seminar of the German Remote Sensing Data Center of the DFVLR
[DFVLR-MITT-89-04] 08 p1092 N90-16318
The Interactive System Meteorology and its use in meteorology and oceanography
08 p1092 N90-16320
Satellite image sequences for motion analysis and change detection
08 p1092 N90-16323
Attempt to draw conclusions concerning the geological subsoil from the vegetation using digital image processing of TM data
08 p1093 N90-16329
The determination of subscale structures in thermal images
08 p1093 N90-16330
Focal research effort points of the Institute of Applied Geodesy in the field of digital image processing
08 p1094 N90-16333
Utilization of remote sensing in geoscientific development and projects
08 p1094 N90-16334
Digital image coding and compression
[PB90-110958] 08 p1107 N90-16409
Alvey MMI007. Object identification from 2D images: The RSRE contribution
[RSRE-MEMO-4277] 08 p1110 N90-16428
Parallel algorithm for determining motion vectors in ice floe images by matching edge features
08 p1114 N90-16451
Order filters, median recursive filter: Analysis and evaluation of performance in image processing
[ISAL-89-0017] 08 p1123 N90-16505
Plant features measurements for robotics
08 p1156 N90-16695
Advances in Techniques and Technologies for Air Vehicle Navigation and Guidance
[AGARD-CP-455] 09 p1163 N90-16731
Position fixing by detection of roads and rivers
09 p1163 N90-16733
Autonomous automatic landing through computer vision
09 p1163 N90-16734
Simulation of synthetic aperture radar 2: Simulating SAR (Synthetic Aperture Radar) using the advanced visual technology system
[AD-A213659] 09 p1204 N90-16976
Advanced diagnostics for reacting flows
[AD-A215050] 09 p1217 N90-17060
Identification and reduction of Wakefield effects in the wiggler region of the Los Alamos free-electron laser
[DE90-004871] 09 p1228 N90-17128
Stimulus familiarity determines recognition strategy for novel 3-D objects
[AD-A215274] 09 p1260 N90-17305
Vision-based navigation and parallel computing
[AD-A214481] 09 p1264 N90-17327
Computer perception of three-dimensional objects
[AD-A215058] 09 p1267 N90-17345
Two adaptive techniques let progressive refinement outperform the traditional radiosity algorithm
[AD-A215174] 09 p1267 N90-17347
Speckle imaging through the atmosphere
[AD-A214652] 09 p1281 N90-17428
Adaptive multiple-band CFAR (Constant-False-Alarm-Rate) detection of an optical pattern with unknown spectral distribution
[AD-A214754] 09 p1281 N90-17429
Hybrid optical/digital architecture for distortion invariant pattern recognition
[AD-A215628] 09 p1282 N90-17435
A vision system for robotic inspection and manipulation
[DE90-005412] 09 p1283 N90-17440
Advanced diagnostics for reacting flows
[AD-A214795] 09 p1285 N90-17448
GRASS/GIS (Geographic Resources Analysis Support System/Geographic Information System) implementation guide
[AD-A214623] 09 p1296 N90-17510
Contribution to the study of design methods for numerical filters with finite pulse response and applications to image processing
[TELECOM-89-E-007] 10 p1376 N90-17974
Fractal geometry segmentation of polarimetric synthetic aperture radar images
[AD-A216278] 10 p1377 N90-17982
A new technique for imaging the logic state of passivated conductors: Biased resistive contrast imaging
[DE90-000686] 10 p1380 N90-18000
Shape from focus
[AD-A215959] 10 p1393 N90-18052
Software for image treatment of the FORCE system operating at the IFSI --- Ist. di Fisica dello Spazio Interplanetario (IFSI)
[IFSI-88-15] 10 p1417 N90-18164
Raster Metafile and Raster Metafile Translator
[NASA-TM-102588] 10 p1417 N90-18166
Decomposition for optimal synthesis in a parallel computing environment
10 p1419 N90-18184
Optical anti-aliasing filters
[AD-A215826] 10 p1430 N90-18251
High speed imaging with a tapped solid state sensor
[DE90-006116] 11 p1511 N90-18702
Problems of the micro-holographic image analysis
[ISL-CO-201/89] 11 p1511 N90-18704
Geometric correction models for HRV-SPOT images
[INPE-5001-TDL/395] 11 p1521 N90-18757
Orbital remote sensing in the decade of the nineties: New approaches and challenges in geology
[INPE-4838-PRE/1467] 11 p1521 N90-18758
Evaluation of selection techniques for multispectral bands employed in the discrimination of carbonatic rocks
[INPE-4850-TDL/365] 11 p1522 N90-18765
Evaluation of TM/LANDSAT and HRV/SPOT data in reforested areas
[INPE-4575-RPE/567] 11 p1524 N90-18772
Remote sensing for the classification and quantification of vegetation in Spring staging areas of Brent geese on the Frisian Islands (Netherlands)
[BCRS-89-27] 11 p1527 N90-18790
Temporal response of atmospheric turbulence compensation
[DE90-006354] 11 p1535 N90-18837
Visual processing of object velocity and acceleration
[AD-A216509] 11 p1539 N90-18858
Recognizing three-dimensional objects without the use of models
[AD-A216766] 11 p1540 N90-18862
Techniques for measurement of the optical properties of materials
[DE90-006902] 11 p1566 N90-19014
Highly accurate navigation: Integration of navigation and geodesic methods
[SFB-228] 12 p1602 N90-19221
Signal processing
[DE90-006904] 12 p1647 N90-19464
Single antenna interferometry
[DE90-008120] 12 p1648 N90-19474
The microchannel plate camera as a detector at high resolution spectrographs: Experiments for velocity distribution in planetary nebulae
[ETN-90-95733] 12 p1664 N90-19560
Selection of optimal textural features for maximum likelihood image classification
[DE90-006901] 12 p1678 N90-19638
Development of software routines for remote sensing digital image processing
[ETN-90-95452] 12 p1679 N90-19640
Segmentation of Side-Looking Airborne Radar (SLAR) images using a priori knowledge
[BCRS-89-03] 12 p1679 N90-19644
Visual processing in texture segregation
[AD-A216539] 12 p1696 N90-19737
Digital production of perspective images
[SER-C-347] 12 p1701 N90-19768
Image manipulation in the SIGGRAPH Interactive Proceedings
[DE90-007542] 12 p1702 N90-19771
Hybrid neural network and rule-based pattern recognition system capable of self-modification
[DE90-007482] 12 p1703 N90-19779
Processing infrared images for target detection: A literature study
[IZF-1988-12] 12 p1715 N90-19847
Structural experiments of planetary nebulae: Charge-coupled devices, image reduction under MIDAS, information representation, and development of an evolution classification for PN's
[ETN-90-95736] 12 p1744 N90-20026
Experimental validation of extended image reconstruction using bispectral speckle interferometry
[DE90-008545] 13 p1772 N90-20171
Characterization of fluid flow by digital correlation of scattered light
[NASA-CR-186403] 13 p1799 N90-20324
Estimation of modeled object pose from monocular images
[DE90-001678] 13 p1804 N90-20354
X ray microimaging by diffractive techniques
[DE90-008444] 13 p1804 N90-20356
Simple reflection holography
[DE90-008309] 13 p1805 N90-20359
Spatial imaging using confocal Fabry-Perot interferometers
[DE90-008363] 13 p1807 N90-20378
Robust performance of multiple tasks by a mobile robot
[DE90-001953] 13 p1811 N90-20397
Knowledge-based robotic grasping
[DE90-007216] 13 p1811 N90-20402
Nine-year aging behavior of the ceramic flatpack resonator
[DE90-008044] 13 p1813 N90-20412
Three-dimensional medical image analysis using local dynamic algorithm selection on a multiple-instruction, multiple-data architecture
[AD-A218024] 13 p1852 N90-20630

A real-time parallel pipelined data-flow image-processing system
[DE90-008324] 13 p1864 N90-20691
Fractal-based image compression
[AD-A217302] 13 p1865 N90-20699
ISLE (Image and Signal Processing LISP Environment) reference manual
[DE90-007858] 13 p1866 N90-20705
Mathematics and physics studies: Multi-project support
[AD-A218208] 13 p1869 N90-20723
Robotic mobility system: Road following algorithms
[AD-A218107] 13 p1874 N90-20748
Placement of multiple apertures for imaging telescopes
[DE90-006991] 13 p1888 N90-20833
A fast ISAR-imaging process and its inherent degrading effects on image quality 14 p1963 N90-21239
Automatic classification of images
[AD-D014437] 14 p1966 N90-21260
A correlation-spectral method for line detection on noisy data
[DE90-007925] 14 p1967 N90-21266
Absolute multilayer characterization at high spatial resolution via real-time soft x ray imaging
[DE90-009181] 14 p1984 N90-21371
A casting and imaging technique for determining void geometry and relative permeability behavior of a single fracture specimen
[DE90-009192] 14 p1989 N90-21403
High explosives (PBX9502) characterization using computerized tomography
[DE90-008170] 14 p1990 N90-21404
Monitoring of agrocattle-raising projects through visual/digital analysis of LANDSAT-TM imagery south of Para state
[INPE-4982-PRE/1542] 14 p1996 N90-21442
A knowledge-based information based for crop area estimation
[INPE-4990-PRE/1555] 14 p1996 N90-21444
Digital processing of TM/LANDSAT data in monitoring interior water
[INPE-4956-PRE/1533] 14 p1997 N90-21448
Introduction of digital image processing by remote sensors applied to geology
[INPE-5023-RPE/616] 14 p1999 N90-21456
Principles of the radiosity method for canopy reflectance modeling
[DE90-008943] 14 p2001 N90-21466
NETRA: A parallel architecture for integrated vision systems 2: Algorithms and performance evaluation
[NASA-CR-186510] 14 p2017 N90-21557
Mesooptical Fourier transform microscope: A new device for high energy physics
[DE90-616423] 14 p2026 N90-21615
Simulated image maps for use in experimental high-resolution electron microscopy
[DE90-009176] 14 p2032 N90-21657
Applications of remote sensing to studies of oceanic upper mixed layer dynamics 15 p2122 N90-22137
Vision Science and Technology at NASA: Results of a Workshop
[NASA-TM-102214-REV-1] 15 p2138 N90-22216
Networks for image acquisition, processing and display 15 p2138 N90-22218
Parallel asynchronous hardware implementation of image processing algorithms 15 p2138 N90-22219
Computation and parallel implementation for early vision 15 p2139 N90-22222
Intensity dependent spread theory 15 p2139 N90-22223
Image gathering, coding, and processing: End-to-end optimization for efficient and robust acquisition of visual information 15 p2139 N90-22224
Hybrid vision activities at NASA Johnson Space Center 15 p2139 N90-22225
Two-dimensional shape recognition using sparse distributed memory 15 p2140 N90-22227
The intensity dependent spread model and color constancy 15 p2140 N90-22228
Motion detection in astronomical and ice floe images 15 p2140 N90-22231
Photonic processing at NASA Ames Research Center 15 p2141 N90-22234
Instrumentation and robotic image processing using top-down model control 15 p2142 N90-22239
Computer vision research at Marshall Space Flight Center 15 p2142 N90-22240
Ames vision group research overview 15 p2143 N90-22242
Pyramid image codes 15 p2143 N90-22243
Intensity dependent spread processor and workstation 15 p2143 N90-22244
Space environment robot vision system 15 p2143 N90-22245
An acousto-optic image correlator with a throughput rate of 1000 templates per second
[DE90-009323] 15 p2144 N90-22249
Symbolic pattern processing system for planar spatial structures
[DE90-001598] 15 p2146 N90-22256
Edge recognition using image-processing hardware
[OUEL-1777/89] 15 p2148 N90-22271
Implementing the Canny edge recognizer with datacube image-processing hardware
[OUEL-1786/89] 15 p2148 N90-22272
Satellite image analysis using neural networks 15 p2157 N90-22321
Low order FIR and IIR filters in dynamic vision
[OUEL-1785/89] 15 p2167 N90-22384
Experimental study of vortex ring interaction with a free surface 16 p2233 N90-22742
ALVINN: An Autonomous Land Vehicle In a Neural Network
[AD-A218975] 16 p2243 N90-22797
The visibility diagram: A data structure for visibility and motion planning problems. Part 1: Application to the visibility polygon query problem
[CS-8913-PT-1] 16 p2299 N90-23098
Transactions of the Seventh Army Conference on Applied Mathematics and Computing
[AD-A219220] 16 p2309 N90-23160
Image segmentation with detection of highlights and inter-reflections using color
[AD-A218710] 16 p2317 N90-23213
Looking at large data sets using binned data plots
[DE90-008206] 16 p2326 N90-23263
Implementation of image action plus software for image analysis of solid propellant combustion holograms
[AD-A219644] 17 p2372 N90-23508
Proceedings of the 12th Symposium on Signal and Image Processing English-Language Abstracts
[AD-A218806] 17 p2388 N90-23598
Research on statistical techniques for signal processing
[AD-A218811] 17 p2388 N90-23599
Atmospheric correction of satellite pictures in the framework of the project Friese Fronten
[BCRS-89-12] 17 p2419 N90-23786
Polar BEAR UV imaging of airglow and aurora-image processing and results
[AD-A219480] 17 p2422 N90-23802
A case study of explosive cyclogenesis in the eastern Pacific Ocean 14 to 17 December 1987
[AD-A219543] 17 p2426 N90-23824
Neuromorphic optical signal processing and image understanding for automated target recognition
[AD-A219827] 17 p2437 N90-23884
A PC-based imaging system for the Naval Postgraduate School Infrared Search and Target Designation (NPS-IRSTD) system
[AD-A220109] 17 p2448 N90-23955
Optical neural nets for scene analysis
[AD-A220657] 17 p2472 N90-24135
Remote optical sensing
[AD-A220780] 17 p2473 N90-24136
Automated segmentation and extraction of area terrain features from radar imagery
[AD-A221096] 18 p2544 N90-24522
The target pursuit of Giotto camera
[ETN-90-96496] 18 p2555 N90-24581
Laser range camera modeling
[DE90-008220] 18 p2562 N90-24618
Analysis of phase retrieval in active imaging
[AD-A221080] 18 p2563 N90-24626
Multispectral classification of overlapping classes with applications to forest damage areas
[DLR-FB-89-55] 18 p2574 N90-24666
An investigation into techniques for landmark identification of 3D images of human subjects, phase 1
[AD-A218614] 18 p2583 N90-24713
Acquisition of an analytical x ray and image analysis system
[AD-A221376] 18 p2593 N90-24756
Parallel algorithmic methods for volumetric rendering
[DE90-011326] 18 p2594 N90-24764
The performance of wavelets for data compression in selected military applications
[AD-A219230] 18 p2614 N90-24892
Image of the angle by partially coherent lighting: Calculations and experiments
[ETN-90-96505] 18 p2616 N90-24900
Concepts for high resolution space based SAR/ISAR systems
[MBB-UK-0057/89-PUB] 19 p2652 N90-25096
Depth buffer shadow algorithms
[DE90-012070] 19 p2744 N90-25595
On the design of a concurrent image analysis system
[DE90-011388] 19 p2746 N90-25605
All-optical device and method for remapping images
[AD-D014540] 19 p2758 N90-25672
Applications of PC-based digital imaging for storing microscopy images on optical disks
[DE90-011355] 19 p2763 N90-25701
Fast classification of ROSAT sources on objective prism plates 19 p2788 N90-25871
Multiple target tracking in a wide-field-of-view camera system
[DE90-013488] 20 p2865 N90-26300
Pattern classification of textura by moment and distance autocorrelation function
[INPE-4976-PRE/1541] 20 p2879 N90-26379
Classification regions in remote sensing imagery utilizing spatial characteristics
[INPE-4913-PRE/1514] 20 p2879 N90-26381
Automatic line network extraction from aerial imagery of urban areas through knowledge based image analysis
[AD-A222675] 20 p2880 N90-26385
Segmentation before and after reconstruction of 3-D surfaces in depth imagery
[RR-788-I-IMAG-97-LIFIA] 20 p2909 N90-26551
Color image processing for navigation: Two road trackers
[AD-A222667] 20 p2916 N90-26591
Applications of digital image processing in testing and evaluation of composite materials
[AD-A222939] 21 p2971 N90-26887
Simulation of synthetic aperture radar 4: Summary and recommendations
[AD-A221822] 21 p2997 N90-27038
Applications of ISES for vegetation and land use 21 p3018 N90-27158
Applications of ISES for snow, ice, and sea state 21 p3018 N90-27159
Application of automatic method to estimating high-level cloud motion wind in operational system and the characteristics of the resultant wind vectors 21 p3028 N90-27218
Detecting perceptual groupings in textures by continuity considerations 21 p3045 N90-27310
A plan for scientific visualization at ANL
[DE90-013565] 21 p3051 N90-27344
Post script code for grey-scaled displays
[AD-A223099] 21 p3053 N90-27354
A programming environment for parallel vision algorithms
[AD-A221486] 21 p3055 N90-27368
Soviet image pattern recognition research
[DE90-010912] 21 p3059 N90-27396
Status report on image information systems and image data base technology
[AD-A221488] 21 p3087 N90-27556
Method to image high speed events using a standard video camera
[AD-D014556] 22 p3177 N90-28030
Engine testing of thermographic phosphors
[DE90-013269] 22 p3182 N90-28059
Development and application of Computed Tomography (CT) for inspection of aerospace components 22 p3187 N90-28083
Integration of multispectral SPOT imagery and panchromatic aerial photography for study in urban land use
[INPE-4967-PRE/1536] 22 p3194 N90-28125
Concurrent Image Processing Executive (CIPE). Volume 1: Design overview
[NASA-CR-186853] 22 p3236 N90-28348
Concurrent Image Processing Executive (CIPE). Volume 2: Programmer's guide
[NASA-CR-186854] 22 p3236 N90-28349
Concurrent Image Processing Executive (CIPE). Volume 3: User's guide
[NASA-CR-186848] 22 p3236 N90-28350
Local spatial frequency analysis for computer vision
[NASA-CR-186990] 22 p3237 N90-28356
START: A module for image processing to IMAGE-BASE
[FOA-C-30551-8.3] 22 p3238 N90-28363
Image fusion through multi-resolution contrast decomposition
[IZF-1989-19] 22 p3247 N90-28412
Simulation of long range atmosphere effects in short range thermal infrared and CCD images
[IZF-1989-27] 22 p3247 N90-28413
Target signature modeling and bistatic scattering measurement studies
[NASA-CR-186611] 23 p3319 N90-28766
Treatment of systematic errors 2: Fusion of ultrasound and visual sensor data
[DE90-014780] 23 p3334 N90-28850
A manual for analysis of hemispherical canopy photography
[DE90-014718] 23 p3342 N90-28885
Digital geometric correction for MSS-LANDSAT imagery
[INPE-4627-PRE/1345] 23 p3342 N90-28886

A tesselated probabilistic representation for spatial robot perception and navigation 23 p3376 N90-29075
Who's who in scientific visualization at LLNL [DE90-014720] 23 p3379 N90-29091
Computer vision and its potential applications in Brazil [INPE-4666-NTE/283] 23 p3381 N90-29100
Fast interactive image generation of line and surface oriented objects in raster systems [ETN-90-97290] 23 p3381 N90-29102
Recognition of infrared images. Part 3: The effect of image processing with a size-contrast box filter on observation performance [IZF-1989-39] 23 p3395 N90-29182
New Voyager radio spectrograms of Uranus [NASA-CR-180381] 23 p3412 N90-29284
A land navigation demonstration vehicle with a color map display for tactical use 24 p3430 N90-29375
Electro-optics engineering support for the integrated launch and recovery television surveillance system [AD-A223450] 24 p3436 N90-29406
AutoPAVER: A software package for automated pavement evaluation [AD-A224176] 24 p3458 N90-29531
Modeling and reconstruction algorithms for detection, location, and identification of subsurface anomalies [AD-A224358] 24 p3459 N90-29539
Long-term flat-field behavior in LLNL streak cameras: Preliminary results [DE90-015615] 24 p3472 N90-29621
Detection and analysis of wind fronts and current shear in digital SAR images [FFI-89/7016] 24 p3495 N90-29755
The 3D model control of image processing 24 p3503 N90-29800
Weighted feature selection criteria for visual servoing of a telerobot 24 p3503 N90-29801
Trinocular stereovision using figural continuity, dealing with curved objects 24 p3503 N90-29802
A fast 3-D object recognition algorithm for the vision system of a special-purpose dexterous manipulator 24 p3503 N90-29803
Visual processing: Implications for helmet mounted displays [AD-A223488] 24 p3522 N90-29916
Digital color representation [DE90-014580] 24 p3524 N90-29924
Parallel architectures and algorithms for image understanding [AD-A223479] 24 p3526 N90-29940
A global approach to image texture analysis [AD-A223532] 24 p3527 N90-29941
A comparison of hardware implementations for low-level vision algorithms [AD-A223699] 24 p3527 N90-29945
Bispectral-based optimization algorithms for speckle imaging [DE90-015610] 24 p3529 N90-29957
A manual for microcomputer image analysis [DE90-015629] 24 p3529 N90-29958
Handbook of data compression algorithms [ESA-TM-06] 24 p3531 N90-29969
Direct estimation of structure and motion from multiple frames [AD-A223903] 24 p3534 N90-29985
Image compression [AD-A224242] 24 p3537 N90-29998
A compact real-time acousto-optic image correlator [DE90-015564] 24 p3546 N90-30054

IMAGE RECONSTRUCTION

Parallel and deterministic algorithms from MRF (Markov Random Fields): Surface reconstruction and integration [AD-A212457] 04 p0533 N90-13084
Faster Phong shading via angular interpolation [CWI-CS-R8909] 04 p0543 N90-13156
Image segmentation for the stereoscopic vision of a mobile robot [ONERA-RT-1/3692-SY] 05 p0652 N90-13800
Versatility of the CFR algorithm for limited angle reconstruction [DE90-001421] 06 p0829 N90-14817
Studies of quantitative methods for imaging from scattered fields [AD-A214047] 07 p0976 N90-15638
A renormalization group approach to image processing: A new computational method for three-dimensional shapes in robot vision, and the computation complexity of the cooling algorithms [AD-A214247] 07 p0977 N90-15643
Visual Information Processing for Television and Telerobotics [NASA-CP-3053] 08 p1072 N90-16204
Linear digital imaging system fidelity analysis 08 p1072 N90-16205
Context dependent anti-aliasing image reconstruction 08 p1073 N90-16209
Image gathering and coding for digital restoration: Information efficiency and visual quality 08 p1073 N90-16211
Application of holography to behavior simulators [ISL-R-111/88] 09 p1226 N90-17115
Problems of the micro-holographic image analysis [ISL-CO-201/89] 11 p1511 N90-18704
Application of wavefront analysis techniques to restoring of images degraded by atmospheric turbulence [ONERA-PUBL-1989-1] 11 p1589 N90-19168
Object detection and amplitude estimation based on maximum a posteriori reconstructions [DE90-007511] 12 p1701 N90-19770
Experimental validation of extended image reconstruction using bispectral speckle interferometry [DE90-008545] 13 p1772 N90-20171
Tomographic processing of synthetic aperture radar signals for enhanced resolution [AD-A217178] 13 p1789 N90-20265
Problems in ISAR processing with range resolution by stepped frequency bursts 14 p1962 N90-21238
Comparison of the algebraic reconstruction technique with the maximum entropy reconstruction technique for a variety of detection tasks [DE90-008933] 14 p2021 N90-21587
Reduced size holography [PREPRINT-707] 16 p2239 N90-22771
Fields, particles, groups: Bertel Laurents 60th Anniversary Symposium [ETN-90-96596] 17 p2478 N90-24170
Analysis of phase retrieval in active imaging [AD-A221080] 18 p2563 N90-24626
The performance of wavelets for data compression in selected military applications [AD-A219230] 18 p2614 N90-24892
National Aeronautics and Space Administration (NASA)/American Society for Engineering Education (ASEE) Summer Faculty Fellowship Program-1989, volume 2 [NASA-CR-185601-VOL-2] 18 p2630 N90-24985
A comparison of select image-compression algorithms for an electronic still camera 18 p2632 N90-24994
Surface reconstruction based on critical contours in a multi-image context [RR-784-I-IMAG-94-LIFIA] 20 p2880 N90-26383
Segmentation before and after reconstruction of 3-D surfaces in depth imagery [RR-788-I-IMAG-97-LIFIA] 20 p2909 N90-26551
Massively parallel architecture: Integrated cell network for image reconstruction [ETN-90-97257] 20 p2913 N90-26575
One way imaging and amplification through an aberrator [AD-A221640] 21 p3009 N90-27106
High resolution optical imaging through the atmosphere [AD-A221913] 21 p3097 N90-27599
Modeling and reconstruction algorithms for detection, location, and identification of subsurface anomalies [AD-A224358] 24 p3459 N90-29539

IMAGE RESOLUTION

HDTV displays: Subjective effects of scanning standards and domestic picture sizes [BBC-RD-1989/9] 02 p0211 N90-11208
Definition of imaging performance for satellite surveillance, models, and simulations [FOA-C-30493-9.4] 02 p0236 N90-11341
Television systems with enhanced image quality for new broadband channels [ETN-89-94622] 03 p0340 N90-11936
Fast and objective MRTD measurement [FEL-1988-24] 03 p0351 N90-12006
The telescope mirrors 05 p0603 N90-13504
The relay lens systems 05 p0603 N90-13506
Astrometric parameter determination in FAST 05 p0610 N90-13556
Double star reductions in NDAC 05 p0610 N90-13561
Data simulations in the fast consortium 05 p0612 N90-13573
Data simulations in the NDAC consortium 05 p0612 N90-13574
Image enhancement using the IRAS (Infrared Astronomy Satellite) survey data [AD-A213811] 07 p0950 N90-15496
Model-based quantification of image quality 08 p1072 N90-16206
Context dependent anti-aliasing image reconstruction 08 p1073 N90-16209
Context dependent prediction and category encoding for DPCM image compression 08 p1073 N90-16210
Isolating contour information from arbitrary images 08 p1074 N90-16217
Distance measurement using laser diodes [ETN-90-96144] 08 p1082 N90-16264
The development of an airborne synthetic aperture radar motion compensation system 09 p1165 N90-16745
Broadband incoherent imaging using multiple aperture optics [AD-A215708] 09 p1282 N90-17437
Staring focal plane array system modeling [AD-A215712] 09 p1283 N90-17438
A new technique for imaging the logic state of passivated conductors: Biased resistive contrast imaging [DE90-000666] 10 p1380 N90-18000
Problems of the micro-holographic image analysis [ISL-CO-201/89] 11 p1511 N90-18704
Optical amplification in 45 deg - cut BaTiO3 [AD-A216043] 11 p1586 N90-19011
Precision segmented reflector, figure verification sensor 12 p1611 N90-19272
A high resolution automatic image measuring system [WISS-ARB-VERMESSUNGSWESEN-154] 12 p1663 N90-19559
Design and performance analysis of adaptive optical telescopes using laser guide stars [AD-A218025] 13 p1902 N90-20913
Application of superresolution methods for airborne radar 14 p1961 N90-21227
A fast ISAR-imaging process and its inherent degrading effects on image quality 14 p1963 N90-21239
The 1D-ISAR imaging of manoeuvering aircraft 14 p1963 N90-21241
InSb DRO array characteristics 14 p1977 N90-21326
Polar BEAR UV imaging of airglow and aurora-image processing and results [AD-A219480] 17 p2422 N90-23802
Down-range imaging of radar targets [AD-A221084] 18 p2544 N90-24521
In-situ topographical imaging of electrode surfaces using high resolution phase-measurement interferometric microscopy [AD-A221021] 18 p2548 N90-24542
Depth buffer shadow algorithms [DE90-012070] 19 p2744 N90-25595
A topological image matcher [OUEL-1798/89] 19 p2744 N90-25600
One way imaging and amplification through an aberrator [AD-A221640] 21 p3009 N90-27106
SAR processing methods [FEL-1989-131] 22 p3165 N90-27948

IMAGE TRANSDUCERS

The investigation of the fundamental limits of heterodyne holographic interferometry with the application of imaging laser generated lamb waves [AD-A211048] 02 p0224 N90-11285

IMAGE TUBES

A large area, low cost, gamma-ray, imaging spectrometer [DE90-006993] 11 p1567 N90-19017
Reliability testing of the Hughes temperature controlled 1/4 watt split cycle cryogenic cooler (HD-1045 (V)/UA) [AD-A216696] 12 p1641 N90-19426

IMAGE VELOCITY SENSORS

The automatic detection of anti-collision lights [RSRE-MEMO-4272] 08 p1019 N90-15896
Innovative techniques for high-resolution imaging and precision tracking [AD-A221380] 18 p2616 N90-24899
Analysis of camera movement based on a sequence of images [TELECOM-PARIS-89-D-008] 18 p2616 N90-24901

IMAGERY

NT ACOUSTICAL HOLOGRAPHY
NT AERIAL PHOTOGRAPHY
NT ALL SKY PHOTOGRAPHY
NT ASTRONOMICAL PHOTOGRAPHY
NT AUTORADIOGRAPHY
NT CINEMATOGRAPHY
NT COLOR PHOTOGRAPHY
NT COMPUTER AIDED TOMOGRAPHY
NT HOLOGRAPHY
NT INFRARED IMAGERY
NT INFRARED PHOTOGRAPHY
NT MICROWAVE IMAGERY
NT NEUTRON RADIOGRAPHY
NT PHOTOMICROGRAPHY
NT PIXELS
NT RADAR IMAGERY
NT RADIOGRAPHY
NT REPRODUCTION (COPYING)
NT SATELLITE IMAGERY
NT SATELLITE-BORNE PHOTOGRAPHY
NT SCHLIEREN PHOTOGRAPHY
NT SHADOWGRAPH PHOTOGRAPHY
NT SPACEBORNE PHOTOGRAPHY
NT STEREOPHOTOGRAPHY
NT STEREOSCOPY

NT TOMOGRAPHY
NT WHITE LIGHT HOLOGRAPHY
NT X RAY IMAGERY
Faster Phong shading via angular interpolation
[CWI-CS-R8909] 04 p0543 N90-13156
SAS graphics in DCF
[PNR90563] 06 p0756 N90-14399
Image processing of LANDSAT MSS data for buried valley detection in northern Indiana 06 p0802 N90-14668
A logic for the pixel assignment step of imagery classification predicated on class structure 07 p0949 N90-15493
Context dependent anti-aliasing image reconstruction 08 p1073 N90-16209
Context dependent prediction and category encoding for DPCM image compression 08 p1073 N90-16210
Fracture analysis through photographic imagery of low spatial resolution: A contribution to the study of tectonic evoluation of the Araripe Plateau region
[INPE-4876-PRE/1487] 11 p1520 N90-18756
Computer vision techniques for rotorcraft low altitude flight 15 p2142 N90-22237
Atmospheric autorotating imaging device
[NASA-CASE-NPO-17390-1-CU] 16 p2238 N90-22769
Surface reconstruction based on critical contours in a multi-image context
[RR-784-I-IMAG-94-LIFIA] 20 p2880 N90-26383
Space-base multispectral imagery: Current and future applications and implications to the United States Army
[AD-A224046] 23 p3343 N90-28894
The function of the Interactive Model Assembly Program (IMAP) for a flight simulator
[NAL-TR-1034] 24 p3437 N90-29412
Attention, imagery, and memory: A neuromagnetic investigation
[AD-A224560] 24 p3499 N90-29775

IMAGES
NT RETINAL IMAGES
Raman characterization of high temperature materials using an imaging detector
[DE89-016308] 01 p0040 N90-10219
A compilation of digitized satellite imagery of the Gulf Stream (1982, 1983, and 1985)
[AD-A210243] 01 p0082 N90-10467
Robust spatial calibration of a planar positron camera
[AD-A210773] 02 p0224 N90-11284
A technique to correlate fractography with NDE (Non-Destructive Evaluation) of small samples
[DE89-016904] 02 p0231 N90-11325
Analysis of forest fire smoke using satellite imagery
[AD-A210657] 02 p0236 N90-11339
Vision-based navigation for autonomous ground vehicles
[AD-A211584] 03 p0304 N90-11725
A high-speed digital camera system for the observation of rapid H-alpha fluctuations in solar flares 03 p0435 N90-12491
Performance of the image statistics decoder in conjunction with the Goldstone-VLA array 04 p0487 N90-12796
Video line processor
[AD-D014198] 04 p0497 N90-12861
Direct computation of 3D shape invariants and the focus of expansion
[AD-A212386] 04 p0549 N90-13195
Computational and psychophysical study of human vision using neural networks
[AD-A213290] 05 p0674 N90-13924
Spatiotemporal characteristics of visual localization, phase 2
[AD-A212934] 05 p0674 N90-13929
Functional decor in the International Space Station: Body orientation cues and picture perception
[NASA-TM-102242] 05 p0675 N90-13931
SAND DEVIL: A digital video link for telemetry applications
[DE90-001879] 06 p0730 N90-14259
Surface thermometry of energetic materials by laser-induced fluorescence
[AD-A214423] 07 p0916 N90-15297
An architectural model of visual motion understanding
[AD-A214327] 07 p0967 N90-15589
Center for X Ray Optics, 1988
[DE90-003300] 07 p0992 N90-15732
High compression image and image sequence coding 08 p1074 N90-16214
From primal sketches to the recovery of intensity and reflectance representations 08 p1074 N90-16216
Reflection technique for thermal mapping of semiconductors
[AD-D014263] 08 p1129 N90-16541
Development of a performance-based test of gaze capability: A threshold approach
[AD-A214675] 09 p1259 N90-17301
Speckle imaging through the atmosphere
[AD-A214652] 09 p1281 N90-17428
Shape from focus
[AD-A215959] 10 p1393 N90-18052
Using image analysis to determine petrophysical properties of reservoir rocks
[DE90-000222] 12 p1680 N90-19649
A technique for convolving unequally spaced samples using fast Fourier transforms
[DE90-006466] 12 p1707 N90-19802
Computer image generation: Reconfigurability as a strategy in high fidelity space applications 13 p1862 N90-20682
Fractal-based image compression
[AD-A217302] 13 p1865 N90-20699
HDTV bandwidth reduction using motion compensation and DATV
[BBC-RD-1989/10] 14 p1965 N90-21254
Automatic classification of images
[AD-D014437] 14 p1966 N90-21260
Sampling and noise in vision networks 15 p2138 N90-22217
Computation and parallel implementation for early vision 15 p2139 N90-22222
Image gathering, coding, and processing: End-to-end optimization for efficient and robust acquisition of visual information 15 p2139 N90-22224
Motion detection in astronomical and ice floe images 15 p2140 N90-22231
Passive navigation using image irradiance tracking 15 p2141 N90-22232
Factors affecting the perception of transparent motion 15 p2141 N90-22233
Ice conditions along the Illinois waterway as observed on LANDSAT images, 1972 to 1985
[AD-A219745] 17 p2418 N90-23775
Parallel algorithmic methods for volumetric rendering
[DE90-011326] 18 p2594 N90-24764
X ray optics
[AD-A221218] 18 p2616 N90-24898
Process of three dimensional lithography in amorphous polymers
[AD-D014500] 19 p2676 N90-25221
All-optical device and method for remapping images
[AD-D014540] 19 p2758 N90-25672
Post script code for grey-scaled displays
[AD-A223099] 21 p3053 N90-27354
Status report on image information systems and image data base technology
[AD-A221488] 21 p3087 N90-27556
Method to image high speed events using a standard video camera
[AD-D014556] 22 p3177 N90-28030
A sensor stabilization/tracking system for unmanned air vehicles
[AD-A224008] 23 p3283 N90-28579
Comparison of methods of space color transformations for enhancement of colored images
[INPE-4977-PRE/1542] 23 p3341 N90-28881
Attention, imagery, and memory: A neuromagnetic investigation
[AD-A224560] 24 p3499 N90-29775
Ray traced scalar fields with shaded polygonal output
[DE90-011023] 24 p3529 N90-29955

IMAGING RADAR
Flashlight radar: A three-dimensional imaging radar
[AD-A213439] 07 p0918 N90-15307
Atmospheric wind measurements using a 50 MHz imaging Doppler Interferometer radar
[AD-A218277] 13 p1847 N90-20601
Real-time adaptive radiometric correction for imaging radars systems 14 p1962 N90-21233
Down-range imaging of radar targets
[AD-A221084] 18 p2544 N90-24521

IMAGING SPECTROMETERS
A fiber-fed imaging spectrometer
[DE90-001008] 06 p0781 N90-14538
Evaluation of the airborne visible-infrared imaging spectrometer for mapping subtle lithological variation
[NASA-CR-186213] 06 p0802 N90-14670
The visible channel of OMEGA-VIMS
[IFSI-89-14] 08 p1077 N90-16231
A large area, low cost, gamma-ray, imaging spectrometer
[DE90-006993] 11 p1567 N90-19017
Spectral feature design in high dimensional multispectral data
[NASA-CR-186647] 18 p2574 N90-24664
Use of high-dimensional spectral data to evaluate organic matter, reflectance relationships in soils
[NASA-CR-186650] 18 p2574 N90-24665
Land application of imaging spectrometry 19 p2708 N90-25415
X ray observations of the LMC field by the TTM instrument onboard the Kvant module: November 1988 to June 1989 19 p2782 N90-25825
TTM-Kvant observations of the galactic plane 19 p2783 N90-25836
Modeling, simulation, and analysis of optical remote sensing systems
[NASA-CR-186648] 20 p2878 N90-26376
Eos visible imagers 21 p3016 N90-27146
Characteristics of pushbroom scanning type radiometer utilizing linear sensors
[NAL-TR-1024] 24 p3472 N90-29625

IMAGING TECHNIQUES
NT RASTER SCANNING
Raman characterization of high temperature materials using an imaging detector
[DE89-016308] 01 p0040 N90-10219
Low-cost three-dimensional stereoscopic display technique for computer-aided design
[DE89-011635] 01 p0104 N90-10594
Negative-working electron beam resist based on poly(methyl methacrylate)
[AD-A207834] 01 p0128 N90-10733
Atomic imaging and interfacial analysis
[DE89-015339] 01 p0130 N90-10748
The investigation of the fundamental limits of heterodyne holographic interferometry with the application of imaging laser generated lamb waves
[AD-A211048] 02 p0224 N90-11285
Definition of imaging performance for satellite surveillance, models, and simulations
[FOA-C-30493-9.4] 02 p0236 N90-11341
Video imaging systems: A survey
[DE89-016920] 03 p0337 N90-11919
The Owens Valley solar array 03 p0435 N90-12490
On a fast two-dimensional radar imaging process for rotating targets, and an analysis of its image quality
[ESA-TT-1142] 04 p0489 N90-12808
An air coupled transmission mode acoustic microscope for on-line non-destructive evaluation
[AD-A211416] 04 p0511 N90-12947
An attempt to draw conclusions from the vegetation to the geological underground in the area of Amberg (Germany, F.R.) by means of digital image processing of TM data
[DFVLR-FB-89-24] 04 p0515 N90-12974
Faster Phong shading via angular interpolation
[CWI-CS-R8909] 04 p0543 N90-13156
Proceedings of the 10 May 1989 Antiproton Technology Workshop: Addendum
[AD-A212804] 04 p0554 N90-13227
A review of focal reducer interferometer systems
[RSRE-MEMO-3486] 04 p0554 N90-13231
Liquid and solid ion plasmas
[AD-A212415] 04 p0557 N90-13244
Image segmentation for the stereoscopic vision of a mobile robot
[ONERA-RT-1/3692-SY] 05 p0652 N90-13800
The effects of gravity waves on horizontal layers: Simulation and interpretation 05 p0660 N90-13852
ALIS: An Auroral Large Imaging System in northern Scandinavia 05 p0663 N90-13877
Study of surface uniformity of semiconductors 3 to 5 by photoluminescence imagery
[ECL-88-15] 05 p0703 N90-14116
GaAs and GaAs:In: Influence of surface treatments and characterization of homogeneity by photoluminescent imagery
[ECL-88-24] 05 p0704 N90-14118
Data compression techniques applied to high resolution high frame rate video technology
[NASA-CR-4263] 06 p0765 N90-14452
A fiber-fed imaging spectrometer
[DE90-001008] 06 p0781 N90-14538
Tomographic imagery by multislot coding applied to x ray diagnostics of laser plasmas: Implementation of a direct electronic detection camera 06 p0787 N90-14579
Laboratory x ray lasers
[DE90-000879] 06 p0788 N90-14590
X ray microimaging for the life sciences
[DE90-002613] 06 p0819 N90-14766
A sampled-grating model of moire patterns from digital imaging
[AD-A213364] 06 p0843 N90-14902
Realtime tracking system for wide-field-of-view telescope
[DE90-001147] 06 p0843 N90-14908
Design of incoherent imaging arrays
[DE90-000861] 06 p0844 N90-14909
MERLIN and VLBI observations of the radio galaxy Virgo A 06 p0860 N90-15001
Development of NMR (Nuclear Magnetic Resonance) imaging probes for advanced ceramics
[DE90-003812] 07 p0911 N90-15269
High resolution imaging by phase retrieval and discrimination using speckle, volume 1
[AD-A214243] 07 p0919 N90-15317

Focal plane antenna array for millimeter waves
[AD-D014306] 07 p0920 N90-15322
Studies of quantitative methods for imaging from scattered fields
[AD-A214047] 07 p0976 N90-15638
Systolic algorithms for imaging from space
[AD-A213870] 07 p0987 N90-15701
Navigation of autonomous air vehicles by passive imaging sensors 08 p1026 N90-15927
Electro-optic sensors for surveillance and target acquisition 08 p1026 N90-15929
Visual Information Processing for Television and Telerobotics
[NASA-CP-3053] 08 p1072 N90-16204
Linear digital imaging system fidelity analysis 08 p1072 N90-16205
Model-based quantification of image quality 08 p1072 N90-16206
Optimal focal-plane restoration 08 p1073 N90-16207
Coded-aperture imaging in nuclear medicine 08 p1073 N90-16208
Image gathering and coding for digital restoration: Information efficiency and visual quality 08 p1073 N90-16211
Data compression for the microgravity experiments 08 p1074 N90-16212
Image processing by Intensity-Dependent Spread (IDS) 08 p1074 N90-16215
Knowledge-based imaging-sensor fusion system 08 p1075 N90-16220
A programmable image compression system 08 p1076 N90-16222
The MPI/AIT X ray Imager (MAXI): High speed PN-CCD's for x ray detection
[MPE-PREPRINT-154] 08 p1077 N90-16234
Science plan for the Alaska SAR facility program. Phase 1: Data from the first European sensing satellite, ERS-1
[NASA-CR-185028] 08 p1091 N90-16312
Quantitative evaluation of object-changes in multitemporal AGRISAR imagery
[FIM-195] 08 p1091 N90-16314
Apparatus for imaging deep arterial and coronary lesions
[NASA-CASE-NPO-17439-1-CU] 08 p1104 N90-16391
Digital image coding and compression
[PB90-110958] 08 p1107 N90-16409
Image segmentation by iterative parallel region growing with application to data compression and image analysis 08 p1114 N90-16452
Proposed concept for the visible/infrared imaging radiometer for second generation Meteosat
[ETN-90-96145] 08 p1123 N90-16503
Plant features measurements for robotics 08 p1156 N90-16695
Intelligent landmarks recognition in satellites images 09 p1165 N90-16741
Development of interferometric and holographic techniques in fluid mechanics
[ISL-CO-227/88] 09 p1218 N90-17068
Doppler imagery for the visualisation of velocity fields
[ISL-CO-232/88] 09 p1226 N90-17114
Noncontact temperature pattern measuring device
[NASA-CASE-NPO-17824-1-CU] 09 p1229 N90-17132
Subtle porosity variation in the YBa2Cu3O(7-x) high-temperature superconductor revealed by ultrasonic imaging
[NASA-TM-102130] 09 p1235 N90-17167
Projection techniques for image restoration 09 p1263 N90-17322
Speckle imaging through the atmosphere
[AD-A214652] 09 p1281 N90-17428
Low speed flowfield characterization by infrared measurements of surface temperatures 10 p1306 N90-17556
A potential nuclear magnetic resonance imaging approach for noncontact temperature measurement 10 p1364 N90-17908
Combustion process science and technology 10 p1366 N90-17916
An update of commercial infrared sensing and imaging instruments 10 p1366 N90-17920
Development of an infrared imaging system for the surface tension driven convection experiment 10 p1367 N90-17922
Evaluation of a delay-Doppler imaging algorithm based on the Wigner-Ville distribution
[AD-A215827] 10 p1377 N90-17980
A new technique for imaging the logic state of passivated conductors: Biased resistive contrast imaging
[DE90-000666] 10 p1380 N90-18000
First test results with a CCD camera developed by INPE
[INPE-4873-PRE/1484] 10 p1388 N90-18029
Eutrophication assessment through remote sensing techniques
[INPE-4932-PRE/1422] 10 p1398 N90-18083
Proposition for an airborne remote sensing system
[INPE-4872-PRE/1483] 10 p1399 N90-18090
Simulation and quantification of high-resolution Z-contrast imaging of semiconductor interfaces
[DE90-006159] 10 p1438 N90-18297
Report from ionospheric science 10 p1444 N90-18333
High speed imaging with a tapped solid state sensor
[DE90-006116] 11 p1511 N90-18702
Interrelationship of spatial and radiometric resolution in the thermal infrared band
[INPE-4860-TDL/371] 11 p1523 N90-18771
Operational requirements and the geostationary platform 12 p1608 N90-19250
Synthetic Aperture Interferometric Radiometer (SAIR) 12 p1610 N90-19261
General multidimensional scanning ratio transformation and its utilization for norm transformation of television signals
[ETN-90-96058] 12 p1648 N90-19470
Parallel distributed networks for image smoothing and segmentation in analog VSLI
[AD-A216780] 12 p1651 N90-19491
A method for determination of control pixels for LANSAT using a reflector
[INPE-4884-PRE/1491] 12 p1677 N90-19632
Availability of multitemporal LANDSAT data accompanying the variation of water surfaces in the program area of Careiro PDRI/AM
[INPE-4896-PRE/1496] 12 p1677 N90-19634
Automated visibility and cloud cover measurements with a solid-state imaging system
[AD-A216906] 12 p1693 N90-19724
NMR (Nuclear Magnetic Resonance) imaging development for the study of solids
[AD-A217073] 12 p1723 N90-19899
Very high energy gamma ray astrophysics
[DE90-006645] 12 p1737 N90-19983
Meteor observations using the 50 MHz MENTOR imaging Doppler interferometer
[AD-A217908] 13 p1790 N90-20276
Design and calibration of a vacuum compatible scanning tunneling microscope
[NASA-TM-102514] 13 p1804 N90-20353
Spatial imaging using confocal Fabry-Perot interferometers
[DE90-008363] 13 p1807 N90-20378
Utilization of LANDSAT-5 and NOAA-9 satellite imagery in the identification of physical-chemical parameters of the water in the Guanabara Bay
[INPE-4761-TDL/349] 13 p1819 N90-20445
Hypotheses testing of watershed/landscape dynamics in northern Alaska using digital analysis
[DE90-006721] 13 p1820 N90-20450
Development of gamma-emitting, receptor-binding radiotracers for imaging the brain and pancreas
[DE90-008314] 13 p1851 N90-20621
Real-time graphics for the Space Station Freedom cupola, developed in the Systems Engineering Simulator 13 p1862 N90-20683
High-resolution acoustical imaging 13 p1881 N90-20793
Placement of multiple apertures for imaging telescopes
[DE90-006991] 13 p1888 N90-20833
Bibliography of spatial interferometry in optical astronomy
[NASA-TM-100754] 13 p1901 N90-20911
SAR and ISAR imagery of marine targets 14 p1962 N90-21237
Image simulation of geometric targets for synthetic aperture radar 14 p1964 N90-21245
Ga:Ge array development 14 p1977 N90-21323
Reduction and analysis techniques for infrared imaging data 14 p1977 N90-21328
High resolution imaging of the Venus night side using a Rockwell 128x128 HgCdTe array 14 p1978 N90-21330
Infrared ground-based astronomy with the Hughes 256 X 256 PtSi array 14 p1978 N90-21331
Initial astronomical results with a new 5-14 micron Si:Ga 58x62 DRO array camera 14 p1978 N90-21334
SOFIA: Stratospheric Observatory for Infrared Astronomy 14 p1980 N90-21346
HgCdTe 256x256 NWIR FPA 14 p1981 N90-21348
Ultrasonic and radiographic evaluation of advanced aerospace materials: Ceramic composites
[NASA-TM-102540] 14 p1989 N90-21401
Cirrus cloud optical properties measured with the University of Wisconsin high spectral resolution and volume imaging lidars 15 p2084 N90-21932
Institute for Materials Science and Engineering, nondestructive evaluation: Technical activities
[PB90-132739] 15 p2108 N90-22055
A study of creep damage using microradiography and continuum damage mechanics 15 p2117 N90-22109
Kalman filter based range estimation for autonomous navigation using imaging sensors 15 p2142 N90-22238
Object detection using structural matching
[INPE-4954-PRE/1532] 15 p2159 N90-22333
An investigation of narrow-bandgap semiconductors: Devices, circuits, and systems 15 p2171 N90-22406
A high galactic latitude survey of far ultraviolet excess objects 15 p2183 N90-22473
The optical night sky at low surface brightness: High latitude dust and faint field galaxies 15 p2185 N90-22481
The production and spatial distribution of neutral and ionized water vapor in Comet P/Halley 15 p2185 N90-22484
Scanning laser photocurrent spectroscopy of electrochemically grown bismuth sulphide films
[AERE-M-3709] 16 p2217 N90-22649
Quantitative surface temperature measurement using two-color thermographic phosphors and video equipment
[NASA-CASE-LAR-13740-1] 16 p2238 N90-22770
Reduced size holography
[PREPRINT-707] 16 p2239 N90-22771
Recent advances in nondestructive evaluation made possible by novel uses of video systems
[NASA-TM-102491] 16 p2244 N90-22801
Spaceborne radar observations: A guide for Magellan radar-image analysis
[NASA-CR-184998] 16 p2249 N90-22826
The eyes prefer real images 16 p2270 N90-22938
Volumetric visualization of 3D data 16 p2275 N90-22964
Studies in gravitational lensing and numerical hydrodynamics 16 p2332 N90-23290
TeV radiation from the Crab nebula and other matters 16 p2335 N90-23306
Proceedings of the 12th Symposium on Signal and Image Processing English-Language Abstracts
[AD-A218806] 17 p2388 N90-23598
High-resolution radar imaging
[AD-A220809] 17 p2391 N90-23620
Diagnosis of auroral dynamics using global auroral imaging with emphasis on large-scale evolutions
[NASA-CR-186623] 17 p2422 N90-23804
A PC-based imaging system for the Naval Postgraduate School Infrared Search and Target Designation (NPS-IRSTD) system
[AD-A220109] 17 p2448 N90-23955
In-situ topographical imaging of electrode surfaces using high resolution phase-measurement interferometric microscopy
[AD-A221021] 18 p2548 N90-24542
Analysis of phase retrieval in active imaging
[AD-A221080] 18 p2563 N90-24626
On the G1 smooth connection between triangular Bernstein-Bezier patches. Part 1: Around and N-patch corner
[TELECOM-PARIS-89-D-012] 18 p2575 N90-24671
On the G1 smooth connection between triangular Bernstein-Bezier patches. Part 2: In a piecewise representation
[TELECOM-PARIS-89-D-013] 18 p2575 N90-24672
Free-form surface modelling using tensor product Bezier patches: A review with new solutions
[TELECOM-PARIS-89-D-014] 18 p2575 N90-24673
Development of a postprocessing and 3D graphical imaging facility
[AD-A221212] 18 p2593 N90-24755
Innovative techniques for high-resolution imaging and precision tracking
[AD-A221380] 18 p2616 N90-24899
Atomic scale imaging of the structure and chemistry of semiconductor interfaces
[DE90-011321] 18 p2626 N90-24965
A comparison of select image-compression algorithms for an electronic still camera 18 p2632 N90-24994
Ground evaluation of seeding an in-flight wingtip vortex using infrared imaging flow visualization technique 18 p2639 N90-25035
Mars Rover imaging systems and directional filtering 18 p2648 N90-25071
Vegetation stress monitoring by fluorescence 19 p2708 N90-25414
Scanning electron microscopy by photovoltage contrast imaging
[AD-D014517] 19 p2760 N90-25684
Applications of PC-based digital imaging for storing microscopy images on optical disks
[DE90-011355] 19 p2763 N90-25701

Einstein IPC observations of the 1 to 3 keV X ray background 19 p2785 N90-25846
The Einstein All-Sky IPC slew survey 19 p2787 N90-25865
Improving the geometric fidelity of imaging systems employing sensor arrays [NASA-CASE-NPO-17970-1-CU] 20 p2880 N90-26384
Segmentation before and after reconstruction of 3-D surfaces in depth imagery [RR-788-I-IMAG-97-LIFIA] 20 p2909 N90-26551
Experiments on superconductor imaging surface magnetometry [DE90-008925] 20 p2929 N90-26665
Development of Planar Laser-Induced Fluorescence (PLIF) techniques for supersonic flows 21 p2974 N90-26900
One way imaging and amplification through an aberrator [AD-A221640] 21 p3009 N90-27106
Eos visible imagers 21 p3016 N90-27146
Human factors and safety considerations of night vision systems flight using thermal imaging systems [AD-A223226] 21 p3037 N90-27263
Detecting perceptual groupings in textures by continuity considerations 21 p3045 N90-27310
SIRTF: Probing the dark corners of the galaxy 21 p3091 N90-27577
Variable magnification variable dispersion glancing incidence imaging x ray spectroscopic telescope [NASA-CASE-MFS-28013-3] 21 p3096 N90-27594
Multispectral variable magnification glancing incidence x ray telescope [NASA-CASE-MFS-28013-4] 21 p3096 N90-27595
High resolution optical imaging through the atmosphere [AD-A221913] 21 p3097 N90-27599
Spatial conductivity measurements on high T(sub c) superconducting films 22 p3148 N90-27849
Incoherent imaging of materials structure and composition by Z-contrast stem [DE90-012789] 22 p3155 N90-27888
Evaluation of the wake effects on plume dispersion using video image analysis [PB90-186354] 22 p3169 N90-27972
In-service inspection of composite components on aircraft at depot and field levels 22 p3186 N90-28078
Analysis of ER-2 radiometer and lidar observations from the 1987 marine stratus experiment 22 p3216 N90-28241
Summary of results and conclusions based on analysis of volume imaging and high spectral resolution lidar data acquired during FIRE phase 1, part 1 22 p3223 N90-28278
Summary of results and conclusions based on analysis of volume imaging and high spectral resolution lidar data acquired during FIRE phase 1, part 2 22 p3227 N90-28300
Concurrent Image Processing Executive (CIPE). Volume 1: Design overview [NASA-CR-186853] 22 p3236 N90-28348
START: A module for image processing to IMAGE-BASE [FOA-C-30551-8.3] 22 p3238 N90-28363
Simulation of long range atmosphere effects in short range thermal infrared and CCD images [IZF-1989-27] 22 p3247 N90-28413
Optical imaging of IRAS galaxies: The evolution of infrared-bright galaxies 22 p3261 N90-28465
A study of the sensitivity of an imaging telescope (GRITS) for high energy gamma-ray astronomy [NASA-CR-186921] 22 p3261 N90-28468
Spatial interferometry in optical astronomy [NASA-RP-1245] 22 p3262 N90-28470
Noncontact measurement of high temperature using optical fiber sensors [NASA-CR-186975] 23 p3329 N90-28825
Comparison of methods of space color transformations for enhancement of colored images [INPE-4977-PRE/1542] 23 p3341 N90-28881
Multiband imaging systems [AD-A223969] 23 p3343 N90-28893
Tropospheric wind profiling using radar interferometry: A feasibility study of a compact mobile system [PB90-217068] 23 p3351 N90-28939
Laser induced fluorescence imaging applications 24 p3420 N90-29322
Bispectral-based optimization algorithms for speckle imaging [DE90-015610] 24 p3529 N90-29957

IMBEDDINGS (MATHEMATICS)
NT INVARIANT IMBEDDINGS

IMCC (CONTROL CENTER)
U INTEGRATED MISSION CONTROL CENTER

IMIDES
NT BISMALEIMIDE
Viscosity, density and conductivity of ImCl(HCl) sub 1.3 [AD-A218002] 16 p2216 N90-22641
Acetylene terminated aspartimides and resins therefrom [NASA-CASE-LAR-14188-1] 17 p2379 N90-23545
Imide/arylene ether copolymers [NASA-CASE-LAR-14159-1-CU] 21 p2983 N90-26953

IMINES
Copolymer-like structures of nematic nitroimine dimers [AD-A217574] 13 p1780 N90-20215

IMMISCIBILITY
U SOLUBILITY

IMMITTANCE
U ELECTRICAL IMPEDANCE

IMMUNE SYSTEMS
Reciprocal relationships between the immune and central nervous system [AD-A221259] 18 p2583 N90-24712

IMMUNITY
Reciprocal relationships between the immune and central nervous system [AD-A221259] 18 p2583 N90-24712

IMMUNOLOGY
Response of lymphocytes to a mitogenic stimulus during spaceflight 05 p0677 N90-13942
Experiment K-6-23. Effect of spaceflight on levels and function of immune cells 20 p2897 N90-26476

IMPACT
NT ECONOMIC IMPACT
NT ELECTRON IMPACT
NT HYPERVELOCITY IMPACT
NT ION IMPACT
NT PROTON IMPACT
Definition and reduction of the F-18 windshield birdstrike hazard [AD-A210700] 01 p0004 N90-10015
Method and apparatus for determining time, direction and composition of impacting space particles [NASA-CASE-LAR-13392-1-CU] 01 p0026 N90-10132
Transient response of a cylindrical shell of finite length to transverse impact [OUEL-1780/89] 15 p2119 N90-22123
Numerical simulation of semi-infinite target penetration by continuous and segmented rods [AD-A219437] 17 p2412 N90-23743
Mechanics of impact energy absorption [PB90-190836] 22 p3190 N90-28101
Evaluation of ARALL-4: An aramid fiber reinforced aluminum [AD-A223502] 24 p3443 N90-29443

IMPACT ACCELERATION
Guidelines for safe human exposure to impact acceleration, update A [AD-A215287] 09 p1253 N90-17268
Omni-directional human head-neck response [SAE-861893] 19 p2721 N90-25478

IMPACT DAMAGE
NT METEORITIC DAMAGE
Simulation of flexible structures with impact: Experimental validation 01 p0020 N90-10097
Aircraft live fire testing 02 p0154 N90-10879
Fractography of composite delamination [NASA-CR-183291] 05 p0617 N90-13599
Impact tests of three composite materials with carbon fiber cores [REPT-M6-582500] 05 p0619 N90-13610
Modeling of runaway electron damage for the design of tokamak plasma facing components [DE90-000847] 06 p0845 N90-14914
A study of impact damage in composite laminates 07 p0888 N90-15137
Effects of parametric variations of complex targets on damage from projectile impact [DE90-003214] 07 p0941 N90-15450
Noise and sonic boom impact technology. Sonic boom damage to conventional structures [AD-A213594] 09 p1237 N90-17178
Noise and sonic boom impact technology. Effects of aircraft noise and sonic booms on structures: An assessment of the current state-of-knowledge [AD-A213919] 09 p1278 N90-17409
Impact damage tolerance of composite cylindrical panels [AD-A216401] 10 p1350 N90-17830
Instrumented impact testing of fabric-reinforced composite materials [AD-A216764] 11 p1479 N90-18513
Fundamental aspects of erosion and impact damage [DE90-006840] 11 p1492 N90-18587
Effects of oblique impact on hypervelocity shield performance [DE90-006936] 11 p1517 N90-18739
Evaluation of repeated impact damage in composite structures 12 p1619 N90-19303
Evaluation of the response of aluminum alloys to single and multiple particle impacts [DE90-003689] 12 p1676 N90-19626
Optimization of fracture resistance in composites [AD-A217431] 13 p1768 N90-20144
Relevance of impacter shape to nonvisible damage and residual tensile strength of a thick graphite/epoxy laminate [NASA-TM-102599] 14 p1943 N90-21122
A computational model of the perforation of multi-layer metallic laminates [MRL-RR-9-89] 14 p1944 N90-21128
Development of ultrasonic nondestructive methods for defect and damage characterization in composite materials 15 p2063 N90-21816
Impact tolerant material [NASA-CASE-LAR-12887-3] 15 p2064 N90-21822
The controlled-damage concept in design of laminated composites 15 p2065 N90-21830
Impact damage in graphite/epoxy laminates: Damage characterization, acoustic emission, and finite element simulation, volumes 1 and 2 16 p2211 N90-22610
Bird impact tests on structures made of Kevlar 49. Monolithic plates under straight-on impact [REPT-S3-4273-PARTIAL-1] 16 p2213 N90-22620
Characterization of particle impact by quantitative acoustic emission [AERE-R-13028] 16 p2246 N90-22810
Astronaut's guide to terrestrial impact craters [NASA-TM-102902] 17 p2421 N90-23798
Unique failure behavior of metal/composite aircraft structural components under crash type loads [NASA-TM-102679] 18 p2572 N90-24660
Low velocity instrumented impact testing of four new damage tolerant carbon/epoxy composite systems [NASA-TP-3029] 19 p2672 N90-25198
X ray diffraction analysis of control and test fibers [MTL-TR-89-58] 19 p2678 N90-25233
Summary of a study to determine low-velocity impact damage and residual tension strength for a thick graphite/epoxy motor case [NASA-TM-102678] 19 p2702 N90-25374
A photoelastic analysis of the strain field around impact damage in a graphite fibre reinforced panel subjected to compression loads [FFA-TN-1989-48] 19 p2703 N90-25379
Space program: Space debris a potential threat to Space Station and shuttle [GAO/IMTEC-90-18] 20 p2815 N90-26024
An embedded fibre optic sensor for impact damage detection in composite materials [UTIAS-332] 20 p2926 N90-26650
Characterization of impact damage in composites 21 p2957 N90-26811
Semi-active orbital debris sweeper [NASA-CASE-MSC-21534-1] 21 p2966 N90-26860
A Protection And Detection Surface (PADS) for damage tolerance [NASA-TP-3011] 22 p3135 N90-27788
An examination of impact damage in glass-phenolic and aluminum honeycomb core composite panels [NASA-TP-3042] 22 p3153 N90-27876
A technique for rapid inspection of composite aircraft structure for impact damage 22 p3185 N90-28077
A low cost shadow moire device for the nondestructive evaluation of impact damage in composite laminates [AD-A223451] 24 p3443 N90-29442

IMPACT DECELERATION
U DECELERATION
U IMPACT ACCELERATION

IMPACT LOADS
Shock compression and release in high-strength ceramics [DE89-013995] 01 p0047 N90-10265
Remarks on certain aspects of solid explosive detonation via small projectile impact [AD-A210648] 01 p0054 N90-10307
EPIC-2 calculated impact loading histories of thin plates [AD-A210557] 01 p0081 N90-10461
Techniques for recovery of shock-loaded samples [DE89-016881] 02 p0233 N90-11337
Irreversible phase transition and wave propagation in silicate geologic materials [DE89-016031] 02 p0250 N90-11414
Performance characteristics of a three-stage railgun [DE90-002533] 06 p0729 N90-14254
Propagation of detonation waves from an impact region [DE90-001184] 06 p0776 N90-14515

Microstructure induced by laser shock in an austenitic steel
06 p0784 N90-14558
Dynamic sintering of metallic powders by laser shock
06 p0784 N90-14559
Projectile impact Hugoniot parameters for selected materials
[DE90-000891] 06 p0793 N90-14618
Hypervelocity impact calculations using CTH: Case studies
[DE90-002891] 06 p0795 N90-14632
Implications and origins of shock structure in solids
[DE90-000846] 06 p0800 N90-14658
Critical time step estimation for three-dimensional explicit impact analysis
[DE90-002187] 06 p0801 N90-14662
Effects of parametric variations of complex targets on damage from projectile impact
[DE90-003214] 07 p0941 N90-15450
Location of interior impact source in randomly excited structures
[DE90-001092] 07 p0945 N90-15474
Stability and fragmentation of ejecta in hypervelocity impact
[DE90-004087] 08 p1085 N90-16278
Test component attachment effects on resonant plate pyrotechnic shock simulation
[DE90-006478] 12 p1662 N90-19551
A review of the analytical simulation of aircraft crash dynamics
[NASA-TM-102595] 13 p1753 N90-20068
Full-scale birdstrike testing of in-service aged F-111 ADBIRT windshield transparencies
[AD-A218035] 13 p1754 N90-20069
Runaway rubber removal
[AD-A218349] 13 p1759 N90-20100
Final safety analysis report for the Ulysses Mission. Volume 2: Accident model document-appendices
[DE90-008695] 14 p1940 N90-21104
Shock initiation sensitivity of damaged TP-H1207C composite propellant
[DE90-008509] 14 p1957 N90-21205
Martensitic transformation induced by stress pulses
[DE90-009534] 15 p2069 N90-21854
A dynamic motion simulator for future European docking systems
15 p2113 N90-22085
Severe shock and vibration environments for electronic components
[DE90-007686] 15 p2117 N90-22113
Dynamic response of a complex encapsulated electronic assembly subjected to a severe shock environment
[DE90-007689] 15 p2118 N90-22114
Aircraft crash survival design guide. Volume 2: Aircraft design crash impact conditions and human tolerance
[AD-A218435] 16 p2198 N90-22546
Effects of X radiation on the LAMPSHADE orbital debris satellite shield, 2
[DE90-008214] 18 p2510 N90-24341
Collision forces for compliant projectiles
[NASA-TM-4203] 22 p3192 N90-28111

IMPACT PREDICTION

Remarks on certain aspects of solid explosive detonation via small projectile impact
[AD-A210648] 01 p0054 N90-10307
Impact response of orthotropic composite plates predicted by a one-parameter differential equation
[FFA-TN-1989-07] 17 p2369 N90-23488
Space program: Space debris a potential threat to Space Station and shuttle
[GAO/IMTEC-90-18] 20 p2815 N90-26024

IMPACT PRESSURES

U IMPACT LOADS

IMPACT RESISTANCE

The 2.5D- and 3D-fabrics for delamination resistant composite laminates and sandwich structures
02 p0186 N90-11063
Transport composite fuselage technology: Impact dynamics and acoustic transmission
[NASA-CR-4035] 03 p0321 N90-11821
Ballistic properties of composite materials for personnel protection
[MRL-TR-89-6] 04 p0465 N90-12661
Spall resistance of alumina
[AD-A213213] 04 p0477 N90-12735
Development of an elastomeric additive to improve the impact resistance of unsaturated polyester networks
[ISAL-89-0006] 08 p1050 N90-16073
Bird impact tests on a Kevlar 49 structure. Monolithic plates. Oblique-angled impact
[REPT-S3-4273] 11 p1454 N90-18376
Low-energy impact resistance of graphite-epoxy plates and ALS honeycomb sandwich panels
12 p1637 N90-19405
Determination of the NDT temperature and Charpy V-notch impact properties of AAR TC128 grades B steel and A 8XX grade B steel
[PB90-207804] 23 p3309 N90-28716

IMPACT SENSITIVITY

U IMPACT RESISTANCE

IMPACT STRENGTH

Definition and reduction of the F-18 windshield birdstrike hazard
[AD-A210700] 01 p0004 N90-10015
Conference on Aerospace Transparent Materials and Enclosures (15th) 16-20 January 1989. Volume 2: Sessions 6-9
[AD-A210201] 01 p0006 N90-10024
Damage tolerance of CFRP sandwich panels
[FFA-TN-1988-70] 04 p0465 N90-12664
A study of the impact of a ball bearing on a long fiber composite plate with a carbon matrix, part 2
[ETCA-88-R-088-PT-2] 04 p0467 N90-12673
Hypervelocity impact calculations using CTH: Case studies
[DE90-002891] 06 p0795 N90-14632
Hydrodynamics code calculations of debris clouds produced by ball-plate impacts
[DE89-015270] 07 p0939 N90-15439
Instrumented impact and residual tensile strength testing of eight-ply carbon eopoxy specimens
[NASA-TP-2981] 08 p1040 N90-16007
Fatigue and impact strength of diffusion bonded titanium alloy joints
[RAE-TM-MAT/STR-1123] 08 p1045 N90-16043
Impact damage tolerance of composite cylindrical panels
[AD-A216401] 10 p1350 N90-17830
Improved toughness alloys based on titanium aluminides
[AD-A218149] 13 p1778 N90-20208
Ultrahigh carbon steels and their laminates
[AD-A218780] 17 p2376 N90-23530
The effect of thermal damage on the mechanical properties of polymer regrinds 18 p2515 N90-24363
Determination of the NDT temperature and Charpy V-notch impact properties of AAR TC128 grades B steel and A 8XX grade B steel
[PB90-207804] 23 p3309 N90-28716

IMPACT TESTS

NT CHARPY IMPACT TEST
Alternative test methodology for ballistic performance ranking of armor ceramics
[AD-A210587] 01 p0051 N90-10290
Numerical simulation of micrometeroids and debris hypervelocity impacts on Columbus pressurized modules
02 p0188 N90-11075
Damage tolerance of CFRP sandwich panels
[FFA-TN-1988-70] 04 p0465 N90-12664
A study of the impact of a ball bearing on a long fiber composite plate with a carbon matrix, part 2
[ETCA-88-R-088-PT-2] 04 p0467 N90-12673
Mathematical simulation of dynamic compression tests using the Hopkinson bar method
[ISL-R-128/87] 04 p0513 N90-12960
Fatigue testing of welded steel assemblies with or without finishing treatments
[CETIM-107900] 04 p0513 N90-12961
Impact tests of three composite materials with carbon fiber cores
[REPT-M6-582500] 05 p0619 N90-13610
Impact tests on aluminum 2024 T3, aramid and glass reinforced aluminum laminates and thermoplastic composites
[LR-534] 05 p0619 N90-13613
On protection of Freedom's solar dynamic radiator from the orbital debris environment. Part 1: Preliminary analyses and testing
[NASA-TM-102458] 06 p0736 N90-14285
Evaluation of shock isolation techniques for a piezoresistive accelerometer
[DE89-014496] 06 p0780 N90-14535
Some numerical experiments concerning the equation of state algorithm for multi-material cells in HULL
[DE89-008240] 06 p0830 N90-14827
Instrumented impact and residual tensile strength testing of eight-ply carbon eopoxy specimens
[NASA-TP-2981] 08 p1040 N90-16007
Studies of density distributions in one-dimensional shock-induced debris clouds
[DE90-004089] 08 p1085 N90-16282
Taylor impact testing
[AD-A215018] 09 p1231 N90-17144
Hypervelocity acceleration and impact experiments with the LLNL electric gun
[DE90-006924] 10 p1326 N90-17664
The 59th Shock and Vibration Symposium, volume 2
[AD-A214579] 10 p1395 N90-18065
Bird impact tests on a Kevlar 49 structure. Monolithic plates. Oblique-angled impact
[REPT-S3-4273] 11 p1454 N90-18376
Instrumented impact testing of fabric-reinforced composite materials
[AD-A216764] 11 p1479 N90-18513
Liquid oxygen LOX compatibility evaluations of aluminum lithium (Al-Li) alloys: Investigation of the Alcoa 2090 and MMC weldalite 049 alloys 12 p1636 N90-19398
Use of chaotic and random vibrations to generate high frequency test inputs. Part 2: Chaotic vibrations
[DE90-007153] 12 p1676 N90-19627
Simple light gas guns for hypervelocity studies
[DE90-008907] 14 p1931 N90-21056
Cross-sectional examination of the damage zone in impacted specimens of carbon/epoxy and carbon/PEEK composites
[NASA-TM-100391] 14 p1944 N90-21125
Bird impact tests on Kevlar 29 and 49 sandwich structures under straight-on and glancing impact
[REPT-S3-4273-PARTIAL-6] 16 p2212 N90-22617
Bird impact tests on Kevlar plates. Sandwich Kevlar-nida submitted to straight-on and glancing impact
[REPT-S3-4273-PARTIAL-3] 16 p2212 N90-22619
Bird impact tests on structures made of Kevlar 49. Monolithic plates under straight-on impact
[REPT-S3-4273-PARTIAL-1] 16 p2213 N90-22620
The assessment of metal fiber reinforced polymeric composites 18 p2514 N90-24357
Fracture toughness and solid-particle erosion of ceramic-matrix whisker-reinforced composites
[DE90-009713] 18 p2517 N90-24376
The effect of aircraft size on cabin floor dynamic pulses
[DOT/FAA/CT-88/15] 19 p2659 N90-25136
Low velocity instrumented impact testing of four new damage tolerant carbon/epoxy composite systems
[NASA-TP-3029] 19 p2672 N90-25198
Fractography of composite delamination
[NASA-CR-181965] 19 p2702 N90-25372
An embedded fibre optic sensor for impact damage detection in composite materials
[UTIAS-332] 20 p2926 N90-26650
Study of an impact on organic matrix and long fibers composite plates (thermal aspect)
[ETCA-89-R-155] 22 p3154 N90-27882
Collision forces for compliant projectiles
[NASA-TM-4203] 22 p3192 N90-28111
Crash-impact behavior of graphite/epoxy composite sine wave webs 23 p3300 N90-28667
A planar rocket motor model for visualization of violent reaction due to fragment impact
[AD-A224273] 24 p3441 N90-29431
The use of automated ball indentation testing to measure flow properties and estimate fracture toughness in metallic materials
[DE90-015797] 24 p3452 N90-29493

IMPACT TOLERANCES

Biomedical influences on spinal cord function
[AD-A210311] 01 p0092 N90-10527
Aircraft crash survival design guide. Volume 2: Aircraft design crash impact conditions and human tolerance
[AD-A218435] 16 p2198 N90-22546

IMPACTORS

Design and calibration of an in-stack, low-pressure impactor
[AD-A213531] 07 p0882 N90-15105
Instrumentation of pendulum impactor using metal foil strain gauges
[PB90-122656] 10 p1387 N90-18024
Low velocity impact analysis with NASTRAN
18 p2570 N90-24647
Collision forces for compliant projectiles
[NASA-TM-4203] 22 p3192 N90-28111
The affect of gravity on particle collection in inertial impactors
[DE90-013372] 23 p3393 N90-29173

IMPATT DIODES

U AVALANCHE DIODES

IMPEDANCE

NT ACOUSTIC IMPEDANCE
NT CONTACT RESISTANCE
NT ELECTRICAL IMPEDANCE
NT ELECTRICAL RESISTANCE
NT REACTANCE
NT TRANSCONDUCTANCE
Impedance analysis of ionic transport in polypyrrole-polyazulene copolymer and its charge-discharge characteristics
[AD-A210979] 01 p0052 N90-10299
The theory of ac impedance of rough electrode-electrolyte interfaces
[DE89-017474] 02 p0217 N90-11243
Capacitive behavior in conducting polymers
[AD-A212448] 04 p0481 N90-12760
Advanced actuation systems development, volume 2
[AD-A213378] 05 p0583 N90-13398
Application of ac impedance method for diagnosis of lithium secondary battery degradation. Preliminary study with AA size Li/MoS2 cells
[DE90-702474] 08 p1061 N90-16137

Measurement of reflection and impedance in a beam by the structural intensity technique
[DE90-728212] 08 p1088 N90-16299
Experimental evaluation of impedance control for robotic aircraft refueling
[AD-A215532] 09 p1167 N90-16755
Changes in impedance of Ni electrodes upon standing and cycling
[NASA-TM-102438] 10 p1401 N90-18097
Microwave field effect transistor
[NASA-CASE-GSC-12442-2] 13 p1792 N90-20282
Recent improvements to the electromagnetic surface patch code
[AD-A217479] 13 p1794 N90-20293
Impedance studies of Ni/Cd and Ni/H2 cells using the cell case as a reference electrode
13 p1824 N90-20473
Nickel-hydrogen capacity loss on storage
13 p1825 N90-20478
The impedance of energy efficiency of a coaxial magnetized plasma source used for spheromak formation and sustainment
[DE90-003220] 13 p1889 N90-20841
Systematic errors in power measurements made with a dual six-port ANA
[PB90-145160] 14 p1968 N90-21276
Low frequency gyrotron amplifier investigation, phase 2
[AD-A217096] 14 p1981 N90-21352
A simplified theoretical model for the laser-induced optogalvanic effect
[DE90-613121] 14 p2028 N90-21626
Linear and nonlinear electrical response of condensed matter: Ionic, dielectric, and mixed-conduction materials
[AD-A218771] 16 p2215 N90-22639
Nonintrusive method and apparatus for monitoring the cure of polymeric materials
[NASA-CASE-LAR-13465-1] 17 p2378 N90-23544
Evaluation of the state of charge of battery electrodes with ac impedance techniques
[AD-A219561] 17 p2420 N90-23789
RF properties of high temperature superconductors: Cavity methods
[DE90-011961] 18 p2627 N90-24969
Equivalent circuit models for ac impedance data analysis
[NASA-TM-100402] 19 p2686 N90-25277
Impedance and wakefields beyond cutoff
[CEBAF-PR-89-016] 19 p2756 N90-25663
Analytic study of the high-frequency impedance
[CEBAF-PR-89-014] 19 p2757 N90-25665
Scattering from coated structures and antenna pattern control using impedance surfaces, part A/B
[NASA-CR-186871] 20 p2854 N90-26233
Spatial conductivity measurements on high T(sub c) superconducting films 22 p3148 N90-27849
Wideband impedance transformer for UHF power transistor time domain waveform measurement system
[PB90-210642] 22 p3167 N90-27962
Electromagnetic scattering from two-dimensional thick material junctions
[NASA-CR-186468] 23 p3319 N90-28767
Adjustable impedance, force feedback and command language aids for telerobotics (parts 1-4 of an 8-part MIT progress report) 23 p3363 N90-29007
Impedance hand controllers for increasing efficiency in teleoperations 24 p3502 N90-29793

IMPEDANCE MATCHING
A study of loaded microstrip antennas and their applications to arrays
[AD-A214857] 09 p1205 N90-16985
Research into traveling wave control in flexible structures
[AD-A224504] 24 p3479 N90-29661

IMPEDANCE MEASUREMENT
Impedance studies of the cell Pt/Ag+ conducting glass/Ag beta-alumina/Pt
[AD-A209820] 01 p0038 N90-10210
Analysis of coaxial wire measurement of longitudinal coupling impedance
[DE89-015748] 02 p0215 N90-11230
Measurement of reflection and impedance in a beam by the structural intensity technique
[DE90-728212] 08 p1088 N90-16299
Silicon hybrid wafer scale integration interconnect evaluation
[AD-A215353] 09 p1212 N90-17031
The 120 VDC test bed for Columbus power system
10 p1329 N90-17679
Impedance studies of Ni/Cd and Ni/H2 cells using the cell case as a reference electrode
13 p1824 N90-20473
Characterization by means of electrochemical impedance measurement and optoelectrochemical analysis of electrolytic, insulating, and semiconducting solution structures. Development of a cartographic analysis method for optoelectrochemical impedance
[ECL-89-15] 17 p2474 N90-24144
Metallurgical analysis of leaking tray packs
[AD-A223157] 22 p3157 N90-27899
Acoustic confinement in the large hydrodynamic tunnel: Identification of the acoustic charateristics with a one-directional source
[REPT-8228-88] 22 p3244 N90-28399
Apparatus to determine the complex mass of a viscous fluid contained in a rigid porous solid from acoustic pressure measurements
[AD-A223709] 24 p3472 N90-29619

IMPELLER BLADES
U ROTOR BLADES (TURBOMACHINERY)

IMPELLERS
NT PUMP IMPELLERS
SSME structural dynamic model development
[NASA-CR-183671] 04 p0463 N90-12650
A three-dimensional potential flow analysis of dynamic fluid forces acting on a whirling centrifugal impeller bounded by a volute 05 p0637 N90-13717
MM and T advanced balancing/machining
[AD-A213103] 05 p0648 N90-13775
Flow in a forward swept centrifugal fan, volumes 1 and 2 14 p1912 N90-20959
Application of an inverse method to the design of a radial inflow turbine 14 p1918 N90-20989
Centrifugal impeller geometry and its influence on secondary flows 14 p1924 N90-21020
Flow studies in impeller passages
18 p2551 N90-24558
Turbomachinery rotor forces
[NASA-CR-183779] 23 p3334 N90-28852

IMPERFECTIONS
U DEFECTS

IMPERIAL VALLEY (CA)
Supplementing geodetic data with prior information for crustal deformation in the Imperial Valley, California
[TR-6-1988] 05 p0668 N90-13904

IMPINGEMENT
NT JET IMPINGEMENT
Modelling of satellite control thruster plumes
05 p0613 N90-13578
An experimental investigation of the interaction between a model rotor and airframe in forward flight
06 p0723 N90-14219
Turbulent heat and momentum transfer in recirculating and impinging flows 09 p1215 N90-17043
Numerical predictions of local entropy generation for an impinging jet
[DE90-004671] 09 p1220 N90-17081
Spray deposition: A fundamental study of droplet impingement, spreading and consolidation
[AD-A217202] 13 p1787 N90-20255

IMPLANTATION
NT ION IMPLANTATION
Method of producing a thin silicon-on-insulator layer
[AD-D014330] 09 p1290 N90-17478
Workshop on Hydrogen Effects in InP and Related Compounds
[AD-A215197] 09 p1290 N90-17479
Luminescence of lanthanides and actinides implanted into binary III-V semiconductors and AlGaAs
[AD-A215759] 11 p1569 N90-19031
The interaction of polymeric materials with ceramic surfaces with special reference to the behaviour of bioceramics 20 p2836 N90-26127
Defects associated with the incorporation of germanium in gallium arsenide
[AD-A222953] 21 p3082 N90-27527

IMPLOSIONS
Apparatus and method for monitoring pressure leaks from a sealed system
[AD-D014168] 03 p0349 N90-11995
Advanced concepts theory
[AD-A211665] 03 p0409 N90-12344
X ray shadowscopy in implosion experiments
06 p0784 N90-14563
Trapezoidal crystal in the six beam implosion
06 p0786 N90-14577
Design of a spheromak compressor driven by high explosives
[DE90-003652] 08 p1086 N90-16283
Scaling Z-pinch plasmas with atomic number for a given K-shell emission
[AD-A215703] 09 p1285 N90-17450
X ray spectra produced by NaF implosions
[AD-A215803] 10 p1429 N90-18243
Advanced concepts theory annual report, 1989
[AD-A220768] 17 p2474 N90-24146

IMPREGNATING
Raman spectroscopic analysis of impregnated cathodes
[AD-A214559] 09 p1190 N90-16895
Method of making a long life high current density cathode from tungsten and iridium powders using a quarternary compound as the impregnant
[AD-D014425] 14 p1958 N90-21211

IMPROVED TIROS OPERATIONAL SATELLITES
U ITOS SATELLITES

IMPROVEMENT
Blue upconversion thulium laser
[DE90-006517] 12 p1668 N90-19584
Aviation security: Corrective actions underway, but better inspection guidance still needed. Report to the Chairwoman, Government Activities and Transportation Subcommittee, Committee on Government Operations, House of Representatives
[GAO/RCED-88-160] 17 p2347 N90-23367
Transonic wing charge improvements by passive shock boundary layer interference control: Development status and prospects
[ETN-90-96463] 18 p2496 N90-24267
Further development of the cryogenic Fabry-Perot interchange mechanism for ISO LWS
18 p2539 N90-24492
Modifications of the DUTSCAT system
[BCRS-89-33] 18 p2555 N90-24582
Improved silicon carbide for advanced heat engines
[NASA-CR-182186] 23 p3313 N90-28735

IMPULSE GENERATORS
Lightweight, broadband, pulsed, frequency agile, self-screening jammer for airborne deployment
[AD-D014468] 22 p3163 N90-27937

IMPULSES
Impulse time-integral function and Lagrangian analysis
[DE89-016997] 02 p0221 N90-11268
Adaptive control of helicopter vibrations via the impulse response method
[AD-A213728] 07 p0883 N90-15113
Improvement of impulse breakdown strength of an XLPE cable by modifing semiconducting layer
[DE90-734942] 09 p1287 N90-17463
Adaptive control of a system with periodic dynamics: Application of an impulse response method to the helicopter vibration problem 17 p2453 N90-23990
Estimation of the impulse response of a broadband mobile radio channel in suburbia at 910 MHz
20 p2846 N90-26187

IMPURITIES
Two photon absorption characterization
[AD-A210508] 01 p0121 N90-10694
Dynamics of nucleation at electrochemical interfaces via surface EXAFS and standing wave measurements
[AD-A210733] 02 p0195 N90-11109
Ozonation of hydrazines and their associated impurities 02 p0205 N90-11174
PISCES program plasma-surface interactions research
[DE89-015622] 02 p0276 N90-11578
The effects of trace anions on the voltammetry of single crystal gold surfaces
[AD-A211886] 04 p0558 N90-13254
Study of the electrical and optical properties of the vanadium and nickel impurities in GaAs
[ISAL-89-0028] 04 p0559 N90-13259
Elastic impurity scattering in double-barrier resonant tunneling structures
[AD-A212850] 05 p0702 N90-14110
Survey on synthesis technologies of methanol as an alternative fuel
[DE89-901303] 07 p0914 N90-15284
Pairs of chalcogen impurities in silicon
[DE89-635767] 08 p1049 N90-16063
Synthesis of tetrafluorohydrazine
[AD-D014281] 08 p1052 N90-16083
Determination of iron in chromium plating and polishing solutions by atomic absorption spectrometry
[AD-A214467] 09 p1189 N90-16892
Study on edge plasma physics and particle control in the Heliotron E device
[DE90-719524] 09 p1284 N90-17443
Structural instabilities, impurities, and defects in electronic materials
[AD-A215384] 09 p1290 N90-17481
Luminescence from defects and impurity centers in yttrium oxide
[DE90-004842] 11 p1569 N90-19030
Improved Si:As BIBIB (Back-Illuminated Blocked-Impurity-Band) hybrid arrays
14 p1981 N90-21349
Impurity control in toroidal devices
[DE90-618585] 15 p2170 N90-22399
A low temperature calorimetric study of several high-T(sub c) superconductors 16 p2322 N90-23237
Negative electron affinity for infrared detection
[AD-A218816] 17 p2395 N90-23639

Preparation of ultra-pure metal halides
[AD-D014529] 19 p2674 N90-25204
Role of surface passivation in the integrated processing of MOS structures
[AD-A222630] 20 p2859 N90-26264
Ni impurity effects on hydrogen surface chemistry and etching of Si(111)
[AD-A222083] 21 p2977 N90-26921
The effect of impurity gasses on variable polarity plasma arc welded 2219 aluminum
[NASA-CR-183803] 21 p2980 N90-26935
Defects associated with the incorporation of germanium in gallium arsenide
[AD-A222953] 21 p3082 N90-27527
Effects of grain size and grain boundary on critical current density of high T(sub c) superconducting oxides
22 p3146 N90-27843
Studies of iron impurities in YxPr1-xBa2Cu3O7-delta
22 p3151 N90-27865
Microstructure and impurity effects on tungsten heavy alloys
[AD-A224220] 23 p3311 N90-28728
Semiconductor measurement technology. EPROP: An interactive FORTRAN program for computing selected electronic properties of Gallium Arsenide and Silicon
[PB90-222738] 23 p3399 N90-29203
Recent progress in electronic structure calculations for defects in metals
[DE90-016323] 24 p3452 N90-29494

IN-FLIGHT MONITORING
Flight Motor Set 360L003 (STS-29R)
[NASA-CR-183739-VOL-1] 01 p0031 N90-10170
Independent Orbiter Assessment (IOA): Assessment of the Orbiter Experiment (OEX) subsystem
[NASA-CR-185587] 02 p0171 N90-10962
Independent Orbiter Assessment (IOA): Analysis of the Orbiter Experiment (OEX) subsystem
[NASA-CR-185586] 02 p0171 N90-10963
Independent Orbiter Assessment (IOA): Assessment of instrumental subsystem FMEA/CIL
[NASA-CR-185572] 02 p0173 N90-10972
Measurement effects on the calculation of in-flight thrust for an F404 turbofan engine
[NASA-TM-4140] 03 p0307 N90-11741
A knowledge-based flight status monitor for real-time application in digital avionics systems
[NASA-TM-101710] 05 p0686 N90-13995
An in-flight investigation of ground effect on a forward-swept wing airplane
[NASA-TM-101708] 06 p0720 N90-14202
An in-flight technique for wind measurement in support of the space shuttle program
[NASA-TM-4154] 06 p0724 N90-14224
Systems for airborne wind and turbulence measurement 07 p0869 N90-15046
Direct measurement of laminar instability amplification factors in flight 08 p1067 N90-16178
NASA/RAE cooperation on a knowledge based flight status monitor 09 p1164 N90-16738
Assessment of in-orbit performance data of a bifacial flight experiment 10 p1344 N90-17793
On-orbit results of the LIPS 3/InP homojunction solar cell experiment 10 p1344 N90-17794
SPOT 1 solar array: Three years in orbit performance evaluation 10 p1344 N90-17795
Optimization of the effective GPS data rate
14 p1907 N90-20932
Preliminary development of an intelligent computer assistant for engine monitoring
[NASA-TM-101702] 15 p2157 N90-22322
Calculation of flight vibration levels of the AH-1G helicopter and correlation with existing flight vibration measurements
[NASA-CR-182031] 19 p2702 N90-25375
An automated calibration laboratory for flight research instrumentation: Requirements and a proposed design approach
[NASA-TM-101719] 20 p2912 N90-26564
New inflight experiments to measure aerodynamics loads
[ETN-90-97276] 21 p2961 N90-26834
The EFA integrated monitoring and recording system: Requirements and concept for implementation
22 p3103 N90-27620
Start-up built-in test for the DISCUS fault tolerant, fly-by-wire computer system 22 p3104 N90-27625
Expert system diagnostics and parts life tracking as applied to the AV-8B aircraft for the USMC
22 p3104 N90-27629
Harrier Information Management System (HIMS): The system and the approach 22 p3105 N90-27630
New features of JAL's ground station
22 p3105 N90-27633
Daily flight operation monitoring in JAL
22 p3105 N90-27636
AIMS for helicopters 22 p3106 N90-27639
Monitoring and controlling flight in windshear
22 p3106 N90-27641
The role of inflight engine condition monitoring on life cycle management of CF-18/F404 engine components
22 p3118 N90-27708
An in-flight investigation of ground effect on a forward-swept wing airplane 23 p3275 N90-28533
In-flight investigation of shuttle tile pressure orifice installations
[NASA-TM-4219] 23 p3328 N90-28820
Evaluation for DLC-Flap Monitoring System of the VSRA
[NAL-TM-607] 24 p3433 N90-29391

IN-FLIGHT STARTING
U AIR START

INACTIVATION
U DEACTIVATION

INCENTIVES
NT CONTRACT INCENTIVES
Learning to make decisions: When incentives help and hinder
[AD-A210185] 01 p0135 N90-10779
The effect of incentives on the reliability and validity of cognitive speed tests
[AD-A211346] 03 p0383 N90-12181
Technology transfer: Implementation status of the Federal Technology Transfer Act of 1986. Report to Congressional requesters
[GAO/RCED-89-154] 19 p2764 N90-25707

INCIDENCE
NT GRAZING INCIDENCE
Semidiscrete Galerkin modelling of compressible viscous flow past a circular cone at incidence
[NASA-CR-186323] 11 p1505 N90-18664
The effects of compressor endwall flow on airfoil incidence and deviation 14 p1922 N90-21011
Mechanical paint removal techniques for aircraft structures
[IAR-89-23] 19 p2682 N90-25254
Study of missiles in flight
[ETN-90-97457] 22 p3109 N90-27662
High power oblique incidence HF ionospheric modification
[AD-A224402] 24 p3491 N90-29729

INCIDENT RADIATION
Reflection from layered media with special attention to the microwave region
[ESA-TT-1155] 08 p1057 N90-16111

INCLUSIONS
The effect of a rigid elliptical inclusion on a straight crack
[AD-A212263] 04 p0513 N90-12965
Crack tip toughening by inclusions with pairs of shear transformations
[DE89-007845] 07 p0909 N90-15254
Variations in volatiles in magma bodies based on studies of melt inclusions
[DE90-006272] 11 p1532 N90-18821
Elastic solutions in a semi-infinite solid with an ellipsoidal inclusion
[AD-A217063] 12 p1625 N90-19338
Elimination of platinum inclusions in phosphate laser glasses
[DE90-004479] 12 p1629 N90-19361
P-T condition fo deformation from fluid inclusions in mylonites
[NASA-CR-186377] 12 p1690 N90-19710
Fourier series methods for plates and shells with cracks and inclusions 14 p1990 N90-21406
Scattering of waves by inclusions in a nonhomogeneous elastic half space solved by boundary element methods
[PB90-145699] 15 p2116 N90-22107
Comparative study of flux pinning flux creep and critical currents between YBaCuO crystals with and without Y2BaCuO5 inclusions 22 p3152 N90-27869

INCOHERENCE
Proof of the feasibility of coherent and incoherent schemes for pumping a gamma-ray laser
[AD-A212315] 04 p0506 N90-12921
Effects of temporal and induced spatial incoherence on parametric instabilities in laser plasma interactions
06 p0782 N90-14549
Design of incoherent imaging arrays
[DE90-000861] 06 p0844 N90-14909
An x ray source for lithography
[AD-D014596] 24 p3473 N90-29630

INCOHERENT SCATTER RADAR
NT EISCAT RADAR SYSTEM (EUROPE)
Doppler spectra from incoherent backscatter: Principles and examples for application for POLDIRAD
[DLR-FB-89-48] 11 p1499 N90-18630

INCOHERENT SCATTERING
Doppler spectra from incoherent backscatter: Principles and examples for application for POLDIRAD
[DLR-FB-89-48] 11 p1499 N90-18630
Evaluation of space plasma data: Effects upon spacecraft materials and predictions of hazardous conditions; polar ARCS
[AD-A219509] 17 p2474 N90-24145
On the explanation of anomalies in inelastic neutron scattering by high-T(sub c) superconductors
[DE90-620561] 17 p2475 N90-24149
Ion neutral gas coupling in the polar atmosphere: Use of EISCAT for the calculation of thermospheric parameters
[ETN-90-96490] 18 p2580 N90-24694
Simple graphical descriptions of natural land profiles and the application of fractal and sub-fractal models to them
[RSRE-MEMO-4305] 22 p3195 N90-28130

INCOMPRESSIBILITY
Nonlinear stability in fluid and plasma dynamics
[AD-A217735] 13 p1892 N90-20856

INCOMPRESSIBLE BOUNDARY LAYER
Primary and secondary stability analysis applied to the DFVLR-transition swept-plate experiment
01 p0065 N90-10371
Numerical simulation of coherent structures in an incompressible mixing layer 01 p0067 N90-10383
An investigation of turbulence structure in a low Reynolds number incompressible turbulent boundary layer
15 p2091 N90-21966
Flat plate leading edge receptivity to various freestream disturbance structures 16 p2235 N90-22750

INCOMPRESSIBLE FLOW
NT STOKES FLOW
Numerical investigation of the effects of longitudinal vortices on the onset of transition in a flat plate boundary layer 01 p0063 N90-10363
Numerical simulation of turbulent plane channel flows
01 p0067 N90-10382
Effect of particle velocity fluctuations on the inertia coupling in two-phase flow 01 p0068 N90-10391
Laminar boundary layer along inviscid surface streamlines over inclined axisymmetric bodies in incompressible flow
[AD-A210202] 01 p0070 N90-10401
Two counter-rotating vortices approaching a free surface in a viscous fluid
[AD-A210495] 01 p0070 N90-10404
Stability of discontinuous shearing motions of a non-Newtonian fluid
[AD-A210643] 01 p0071 N90-10406
Stability of discontinuous steady states in shearing motion of a non-Newtonian fluid
[AD-A210644] 01 p0071 N90-10407
A high-order Lagrangian-decoupling method for the incompressible Navier-Stokes equations
[NASA-CR-181903] 01 p0111 N90-10631
Numerical simulation of the compressible Orszag-Tang vortex
[AD-A210465] 01 p0127 N90-10725
Steady and unsteady potential flow around thin annular wings and engines with simulation of jet engine flow
[DFVLR-FB-89-18] 03 p0302 N90-11711
Incompressible flow about ellipsoids of revolution
[REPT-88-02] 03 p0302 N90-11713
Efficient finite element solution of Navier-Stokes equations and related topics
[AD-A211647] 03 p0348 N90-11986
A least-squares finite element method for incompressible Navier-Stokes problems
[NASA-TM-102385] 03 p0392 N90-12231
Numerical algorithms for steady and unsteady incompressible Navier-Stokes equations
[NASA-CR-186039] 04 p0437 N90-12499
Numerical evaluation of a solution representing a jet in cross-flow
[RAE-TM-AERO-2137] 04 p0502 N90-12893
Computation of viscous incompressible flows
[NASA-TM-101090] 05 p0572 N90-13329
Computational investigation of incompressible airfoil flows at high angles of attack
[AD-A205885] 06 p0720 N90-14201
Numerical solution of the incompressible Navier-Stokes equations 06 p0774 N90-14501
A numeric analysis of incompressible, viscous flow around a symmetrical body of revolution
[ISL-CO-215/87] 08 p1064 N90-16157
A solution method for the time-dependent Navier-Stokes equations for laminar, incompressible flow
[FFA-146] 09 p1219 N90-17075
Pressure losses in flow through a sudden contraction of duct area
[ESDU-89040] 09 p1220 N90-17077
The evolution of linearized perturbations of parallel flows
[DE90-005978] 09 p1221 N90-17082
Incompressible flow friction factors in a simulated heat pipe
[AD-A216288] 10 p1386 N90-18018

Conditions at the downstream boundary for simulations of viscous incompressible flow
[NASA-TM-102510] 10 p1422 N90-18198
Numerical simulation of the incompressible inhomogeneous turbulence in a plane channel flow
[ONERA-NT-1988-5] 11 p1508 N90-18686
Numerical simulation of the vortex breakdown
[ONERA-RSF-4/4368-AY-004A] 11 p1509 N90-18689
Modeling convective Marangoni flows with void movement in the presence of solid-liquid phase change
[DE90-006474] 11 p1509 N90-18690
Computational fluid dynamics method for low Reynolds number flow in a precessing/spinning, liquid filled cylinder with rounded endcaps
[AD-A216997] 12 p1659 N90-19531
Numerical simulation methods of incompressible flows and an application to the space shuttle main engine
[NASA-TM-100038] 13 p1800 N90-20333
Parallel algorithms in the finite element approximation of flow problems
[AD-A217729] 13 p1802 N90-20341
High accuracy solutions of incompressible Navier-Stokes equations
[NASA-TM-102539] 14 p2018 N90-21567
ULTRA-SHARP nonoscillatory convection schemes for high-speed steady multidimensional flow
[NASA-TM-102568] 14 p2019 N90-21570
Transition from resistive-g to eta-i driven turbulence in stellarator systems
[DE90-009382] 14 p2030 N90-21641
Effective methods of controlling a junction vortex system in an incompressible, three-dimensional, turbulent flow 15 p2047 N90-21732
Modeling of vortex-induced oscillations based on indicial response approach
[NASA-CR-186560] 15 p2047 N90-21736
An upwind-differencing scheme for the incompressible Navier-Stokes equations
[NASA-TM-101051] 15 p2051 N90-21757
Plane Stokes flow driven by capillarity on a free surface: Overview and status
[DE90-009166] 15 p2098 N90-22008
An unsteady time asymptotic flow in the square driven cavity
[NASA-TM-103141] 15 p2099 N90-22016
Fundamental hydrodynamics research
[AD-A219179] 16 p2238 N90-22766
Computations of a horseshoe vortex around an endwall-mounted cylinder 17 p2400 N90-23673
Center for Analysis of Heterogeneous and Nonlinear Media
[AD-A219627] 17 p2403 N90-23688
Solution of the steady state incompressible Navier-Stokes equations at high Reynolds numbers
[VKI-TN-170] 17 p2404 N90-23692
On the planar translation of two bodies in a uniform flow
[AD-A220143] 17 p2404 N90-23698
Nonlinear development of Goertler and crossflow vortices and Goertler/Tollmien-Schlichting wave interaction
[AD-A221107] 18 p2553 N90-24571
Spectral transport model for turbulence
[DE90-011265] 19 p2689 N90-25295
Turbulization of shear flows in astrophysics 19 p2773 N90-25763
Three-dimensional structure of boundary layers in transition to turbulence
[AD-A223242] 21 p3004 N90-27076
Numerical investigation of the incompressible plane shear layer between two gases with different densities
[ETN-90-97315] 21 p3006 N90-27084
Numerical solution for the velocity-derivative skewness of a low-Reynolds-number decaying Navier-Stokes flow
[NASA-TM-103186] 22 p3171 N90-27985
The discretization of the three dimensional boundary layer equations
[ETN-90-97292] 22 p3171 N90-27987
The streamline diffusion finite element method for compressible and incompressible fluid flow 22 p3172 N90-27991
Discretization methods for the incompressible Navier-Stokes equations 22 p3173 N90-28003
A finite element method for turbulent incompressible flow 22 p3174 N90-28007
Calculation of unsteady two dimensional viscous incompressible flows by spectral methods
[ETN-90-97449] 22 p3175 N90-28015
Calculation of surface free three dimensional flows
[ONERA-RSF-5/4368-AY-002A] 22 p3176 N90-28022
Regular and chaotic motion of uniform elliptical vortices in external linear time dependent velocity fields 23 p3268 N90-28497
Development of comprehensive numerical schemes for predicting evaporating gas-droplets flow processes of a liquid-fueled combustor
[NASA-CR-187018] 23 p3305 N90-28693
Lecture notes on incompressible flow and the finite element method
[DE90-014665] 23 p3326 N90-28805
Development of turbulence models for the analysis of compressible or incompressible unsteady flow
[ETN-90-97486] 23 p3326 N90-28810
An investigation of chaotic Kolmogorov flows
[NASA-CR-182079] 23 p3328 N90-28816
A potential-vorticity decomposition for the boundary integral equation analysis of viscous flows 24 p3417 N90-29301

INCOMPRESSIBLE FLUIDS
Pressure correction splitting methods for the computation of oscillatory free convection in low Pr fluids
[CWI-NM-R8816] 02 p0222 N90-11271
On the computation of normal modes of a rotating, viscous, incompressible fluid with a capillary free boundary
[REPT-89-01] 03 p0348 N90-11989
A multigrid algorithm for the incompressible Navier-Stokes equation
[GMD-374] 03 p0349 N90-11993
Numerical investigation of transition control of a flat plate boundary layer 07 p0926 N90-15361
The invertibility principle for a simple hurricane model
[AD-A218344] 13 p1848 N90-20605
Hydroelastic problems in space flight vehicles
[LRT-WE-9-FB-11(1989)] 21 p2967 N90-26868
Response of a liquid column to one-sided axial excitation in zero-gravity
[LRT-WE-9-FB-3(1989)] 21 p2991 N90-26996
Non-linear axial vibrations of a cylindrical liquid column in zero-gravity
[LRT-WE-9-FB-4(1989)] 21 p2991 N90-26997
Response of a liquid column to counter-directional excitation under zero-gravity
[LRT-WE-9-FB-6(1989)] 21 p2991 N90-26998
Response of differently axially excited viscous liquid bridges in zero-gravity
[LRT-WE-9-FB-14(1989)] 21 p2991 N90-27001
Response of a liquid column with respect to oscillatory rotational top- and bottom excitation
[LRT-WE-9-FB-8(1989)] 21 p3006 N90-27086
Liquid sloshing response in a spinning container due to axial excitation
[LRT-WE-9-FB-9(1989)] 21 p3006 N90-27087
Oscillatory response of a liquid column to counter rotational excitation
[LRT-WE-9-FB-12(1989)] 21 p3006 N90-27088
Response of a liquid bridge with rotationally excited bottom
[LRT-WE-9-FB-13(1989)] 21 p3006 N90-27089

INCONEL (TRADEMARK)
Threshold for fatigue crack propagation
[DLR-FB-89-33] 05 p0655 N90-13815
The influence of carbide precipitation on the creep rupture behavior of high temperature alloys
[JUEL-2211] 08 p1046 N90-16044
Grain boundary intermetallic phases in alloy 718
[DE90-009612] 15 p2173 N90-22417
The assessment of metal fiber reinforced polymeric composites 18 p2514 N90-24357

INDENTATION
Elastic indentation fractures
[ETCA-88-R-116] 04 p0512 N90-12955
High temperature microhardness tester
[AD-A219567] 17 p2380 N90-23553
Indentation fracture of brittle materials
[DE90-010709] 18 p2572 N90-24657
The use of automated ball indentation testing to measure flow properties and estimate fracture toughness in metallic materials
[DE90-015797] 24 p3452 N90-29493

INDEPENDENT VARIABLES
NT LATTICE PARAMETERS
Interpretation and manipulation of Edgeworth expansions
[MEMO-775] 04 p0544 N90-13163
Fast algorithms for estimating mixture parameters
[AD-A213869] 07 p0976 N90-15636
Nonparametric selection, ranking and testing
[AD-A219254] 19 p2752 N90-25636
Queing networks with finite capacities
[AD-A221547] 21 p3065 N90-27425

INDEXES (DOCUMENTATION)
Space station systems: A bibliography with indexes (supplement 8)
[NASA-SP-7056(08)] 01 p0026 N90-10131
Aerospace medicine and biology: A continuing bibliography with indexes (supplement 328)
[NASA-SP-7011(328)] 01 p0092 N90-10524
NASA scientific and technical publications: A catalog of special publications, reference publications, conference publications, and technical papers, 1988
[NASA-SP-7063(03)] 01 p0136 N90-10782
Aeronautical engineering: A continuing bibliography with indexes (supplement 243)
[NASA-SP-7037(243)] 03 p0299 N90-11693
Aeronautical engineering: A continuing bibliography with indexes (supplement 244)
[NASA-SP-7037(244)] 03 p0299 N90-11694
Indexes for the proceedings of the symposia (international) on detonation, 1951 through 1985
[DE89-015178] 03 p0345 N90-11972
Earth resources: A continuing bibliography with indexes (issue 63)
[NASA-SP-7041(63)] 03 p0366 N90-12091
Aerospace medicine and biology: A continuing bibliography with indexes (supplement 329)
[NASA-SP-7011(329)] 03 p0382 N90-12173
Criss-cross directory of NASA N numbers and DOD AD numbers. Volume 2, part 1: AD to N, 1979-1986. N to AD, 1962-1986
[NASA-TM-101814] 03 p0416 N90-12388
Criss-cross directory of NASA N numbers and DOD AD numbers. Volume 2, part 2: AD to N, 1979-1986. N to AD, 1962-1986
[NASA-TM-101815] 03 p0416 N90-12389
Aeronautical engineering: A continuing bibliography with indexes (supplement 245)
[NASA-SP-7037(245)] 04 p0437 N90-12497
A summary of 30 years of space launches
[AERONOMICA-ACTA-F-39-1989] 05 p0585 N90-13411
Space station systems: A bibliography with indexes (supplement 9)
[NASA-SP-7056(09)] 05 p0613 N90-13580
Aerospace medicine and biology: A continuing bibliography with indexes (supplement 330)
[NASA-SP-7011(330)] 05 p0674 N90-13925
AFOSR technical report summaries
[AD-A213148] 05 p0707 N90-14142
Publications of the Jet Propulsion Laboratory, 1988
[NASA-CR-185956] 06 p0859 N90-14995
Aeronautical engineering: A continuing bibliography with indexes (supplement 246)
[NASA-SP-7037(246)] 07 p0874 N90-15068
Bibliography of Lewis Research Center technical publications announced in 1988
[NASA-TM-102034] 07 p1009 N90-15846
AGARD index of publications, 1986-1988
[AGARD-INDEX-86-88] 08 p1136 N90-16585
JSC document index
[NASA-TM-102923] 08 p1137 N90-16589
Aeronautical engineering: A continuing bibliography with indexes (supplement 247)
[NASA-SP-7037(247)] 10 p1303 N90-17537
Aerospace medicine and biology: A continuing bibliography with indexes (supplement 333)
[NASA-SP-7011(333)] 10 p1411 N90-18136
Aerospace medicine and biology: A continuing bibliography with indexes (supplement 331)
[NASA-SP-7011(331)] 10 p1411 N90-18137
Source hierarchy list. Volume 3: O through Z
[AD-A216052] 10 p1442 N90-18323
Aeronautical engineering: A continuing bibliography with indexes (supplement 249)
[NASA-SP-7037(249)] 12 p1597 N90-19190
Free indexation: Combinatorial analysis and a compositional algorithm
[AD-A218219] 13 p1869 N90-20724
Bibliography of spatial interferometry in optical astronomy
[NASA-TM-100754] 13 p1901 N90-20911
Aeronautical engineering: A continuing bibliography with indexes (supplement 250)
[NASA-SP-7037(250)] 15 p2045 N90-21722
European network of interest in the measurement and analysis of mean sea levels from tide gauge records
[PB90-151929] 15 p2134 N90-22196
Aerospace medicine and biology: A continuing bibliography with indexes (supplement 334)
[NASA-SP-7011(334)] 15 p2136 N90-22207
Aerospace medicine and biology: A continuing bibliography with indexes (supplement 335)
[NASA-SP-7011(335)] 15 p2136 N90-22208
Index to NASA news releases and speeches, 1986
[NASA-TM-101899] 15 p2175 N90-22430
Index to NASA news releases and speeches, 1987
[NASA-TM-101900] 15 p2175 N90-22431
Index to NASA news releases and speeches, 1988
[NASA-TM-101901] 15 p2175 N90-22432
NASA Thesaurus supplement: A four part cumulative supplement to the 1988 edition of the NASA Thesaurus (supplement 3)
[NASA-SP-7064-SUPPL-3] 15 p2177 N90-22438
Aircraft drawings index 17 p2343 N90-23340

Aeronautical engineering: A continuing bibliography with indexes (supplement 251)
[NASA-SP-7037(251)] 17 p2343 N90-23344
Aeronautical engineering: A continuing bibliography with indexes (supplement 252)
[NASA-SP-7037(252)] 17 p2343 N90-23345
Aerospace medicine and biology: A continuing bibliography with indexes (supplement 336)
[NASA-SP-7011(336)] 17 p2436 N90-23877
Index of FAA office of aviation medicine reports: 1961 through 1989
[AD-A221414] 18 p2635 N90-25011
Aeronautical engineering: A cumulative index to a continuing bibliography (supplement 248)
[NASA-SP-7037(248)] 19 p2649 N90-25072
Aeronautical engineering: A continuing bibliography with indexes (supplement 253)
[NASA-SP-7037(253)] 19 p2654 N90-25105
Space station systems: A bibliography with indexes (supplement 10)
[NASA-SP-7056(10)] 19 p2666 N90-25171
Aerospace medicine and biology: A cumulative index to a continuing bibliography (supplement 332)
[NASA-SP-7011(332)] 19 p2722 N90-25480
Aerospace medicine and biology: A continuing bibliography with indexes (supplement 337)
[NASA-SP-7011(337)] 19 p2722 N90-25481
Aerospace medicine and biology: A continuing bibliography with indexes (supplement 338)
[NASA-SP-7011(338)] 19 p2722 N90-25482
The EISI (Elemental and Interplanar Spacing Index) index: A search/match tool for electron diffraction phase analysis
[DE90-010832] 20 p2830 N90-26097
The NATO thesaurus project
[NASA-CR-186931] 21 p3087 N90-27552
Aeronautical engineering: A continuing bibliography with indexes (supplement 254)
[NASA-SP-7037(254)] 22 p3107 N90-27647
Aeronautical engineering: A continuing bibliography with indexes (supplement 255)
[NASA-SP-7037(255)] 22 p3107 N90-27648
Aerospace medicine and biology: A continuing bibliography with indexes (supplement 339)
[NASA-SP-7011(339)] 22 p3232 N90-28327
Air University Library index to military periodicals. Cumulative issue: January to March 1989, Volume 40, Number 1
[PB90-182296] 22 p3258 N90-28452
Aerospace medicine and biology: A continuing bibliography with indexes (supplement 340)
[NASA-SP-7011(340)] 23 p3355 N90-28963
Efficiency and effectiveness of deep structure-based subject indexing languages: PRECIS vs. DSIS
23 p3406 N90-29248
FAA Rotorcraft Research, Engineering, and Development Bibliography 1962-1989
[AD-A224256] 24 p3417 N90-29299
Data catalog series for space science and applications flight missions. Volume 6: Master index volume
[NASA-TM-101913] 24 p3438 N90-29416

INDEXES (RATIOS)
NT KP INDEX
Index formulas for generalized Wiener-Hopf operators and Boson-Fermion correspondence in 2N dimensions
[CWI-PM-R8811] 04 p0542 N90-13141

INDIAN OCEAN
Use of microwave satellite data to study variations in rainfall over the Indian Ocean
[NASA-CR-186408] 14 p2007 N90-21501
US Navy regional climatic study of southern African waters
[AD-A218792] 16 p2258 N90-22874
A numerical study of the seasonal variability of the Somali current
[AD-A220708] 17 p2427 N90-23829

INDIAN SPACE PROGRAM
Comparison of the space program performance of countries with space programs
[ILR-MITT-222] 05 p0709 N90-14150

INDIAN SPACECRAFT
Compendium of meteorological space programs, satellites, and experiments
[NASA-TM-102924] 12 p1607 N90-19243

INDICATING INSTRUMENTS
NT APPROACH INDICATORS
NT CLOUD HEIGHT INDICATORS
NT COMPASSES
NT FLOW DIRECTION INDICATORS
NT MICROBALANCES
NT POSITION INDICATORS
NT RADIO DIRECTION FINDERS
NT SMOKE DETECTORS
NT SPEED INDICATORS
NT STRAIN GAGE BALANCES
NT TACHOMETERS
NT WIND VANES
Reflection indicatrices of natural surfaces for AVHRR channels 1 and 2
[DLR-MITT-89-16] 05 p0664 N90-13882
Recent leak telescope development
[DE90-004101] 09 p1225 N90-17106

INDIUM
Trap gettering by isoelectronic doping of p-GaAs and n-GaAs grown by molecular beam epitaxy
[AD-A211162] 01 p0133 N90-10769
Digital capacity transient spectroscopy of deep structure defects in III-V-Semiconductor structures
[ETN-90-96057] 12 p1722 N90-19890
CuInSe2 and CdTe: Scale-up for manufacturing
[DE89-009503] 13 p1827 N90-20489
The high temperature behavior of gallium and indium liquid metal ion sources
[AERE-R-13321] 16 p2217 N90-22647
Spectrally selective tinoxide and indiumoxide coatings
[ISBN-90-9003138-3] 17 p2382 N90-23567

INDIUM ALLOYS
A critical assessment of thermodynamic and phase diagram data for the Ga-In system
[NPL-DMA(A)-174] 03 p0415 N90-12382
Damping associated with incipient melting in aluminum-indium alloys
[AD-A220241] 18 p2525 N90-24412
Damping capacity of aluminum 6061-indium alloys
[AD-A222802] 20 p2835 N90-26124

INDIUM ANTIMONIDES
Energy relaxation of light holes in InAs(.15)Sb(.85)/InSb multiple quantum wells
[DE89-016035] 03 p0409 N90-12349
Evaluation of platinum silicide and indium antimonide as detector materials for space-based remote sensing in the 3.0-to-5.0 micrometer wavelength band
[AD-A216182] 10 p1354 N90-17853
Current status of InAsSb strained layer superlattice infrared detectors: Demonstration of a high detectivity, 10 micron photodiode
[DE90-000800] 10 p1434 N90-18276
Study of advanced InSb arrays for SIRTF (Space Infrared Telescope Facility) 14 p1977 N90-21325
Secondary ion mass spectrometry characterization of implants into GaAs and GaP for waveguides and integrated optics applications
[AD-A219203] 16 p2324 N90-23254
Tin doping of InSb grown by MOCVD using tetraethyltin
[DE90-009727] 18 p2620 N90-24929
Improving the performance of InAs(1-x)Sb(x)/InSb infrared detectors grown by metal organic chemical vapor deposition
[DE90-009743] 18 p2625 N90-24956
Chlorine reactive-ion-beam etching of InSb and InAs0.15Sb0.85/InSb strained-layer-superlattices
[DE90-010848] 18 p2625 N90-24958
Radiation effects in InAsSb strained-layer superlattice photodiodes induced by dose-rate and transient x ray environments
[DE90-015000] 23 p3400 N90-29208

INDIUM ARSENIDES
Strain and density dependent valence-band masses in InGaAs/GaAs and GaAs/GaAsP strained-layer structures
[DE89-016882] 02 p0285 N90-11627
Development of high gain three terminal devices - at millimeter wave frequencies
[AD-A213089] 05 p0635 N90-13701
Current status of InAsSb strained layer superlattice infrared detectors: Demonstration of a high detectivity, 10 micron photodiode
[DE90-000800] 10 p1434 N90-18276
Development of a unique laboratory standard indium gallium arsenide detector for the 500 to 1700 micron spectral region, phase 2
[NASA-CR-180482] 16 p2238 N90-22767
Acoustoelectronic interaction of surface waves in GaAs-InGaAs superlattices 16 p2310 N90-23163
Secondary ion mass spectrometry characterization of implants into GaAs and GaP for waveguides and integrated optics applications
[AD-A219203] 16 p2324 N90-23254
Improving the performance of InAs(1-x)Sb(x)/InSb infrared detectors grown by metal organic chemical vapor deposition
[DE90-009743] 18 p2625 N90-24956
Chlorine reactive-ion-beam etching of InSb and InAs0.15Sb0.85/InSb strained-layer-superlattices
[DE90-010848] 18 p2625 N90-24958
Application of InAlAs/GaAs superlattice alloys to GaAs solar cells
[DE90-013070] 20 p2881 N90-26389
Measurement of deep levels at InGaAs(P)/InP heterojunctions
[AD-A222890] 21 p3082 N90-27526
Radiation effects in InAsSb strained-layer superlattice photodiodes induced by dose-rate and transient x ray environments
[DE90-015000] 23 p3400 N90-29208

INDIUM COMPOUNDS
NT INDIUM ANTIMONIDES
NT INDIUM ARSENIDES
NT INDIUM PHOSPHIDES
Electrochemical study of the etching of III to V semiconductors
[ETN-90-96015] 05 p0623 N90-13633
GaAs and GaAs:In: Influence of surface treatments and characterization of homogeneity by photoluminescent imagery
[ECL-88-24] 05 p0704 N90-14118
Solid oxide fuel cells electrodes based on In(sub 2)O(sub 3)-PrO(sub 1.83)-ZrO(sub 2)
[DE90-002666] 06 p0806 N90-14691
Investigations of CuInSe2 thin films and contacts
[DE90-000301] 12 p1721 N90-19886
HREM defects in GaAs/Ga(1-x)In(x)As strained layer superlattices
[DE90-010610] 18 p2620 N90-24924
Dielectric function of InGaAs in the visible
[NASA-TM-103246] 20 p2932 N90-26683

INDIUM PHOSPHIDES
Properties of devices prepared with epitaxial layers on InP
[AD-A210304] 01 p0132 N90-10759
Beam assisted fabrication of 3-5/Si monolithic devices
[AD-A212046] 03 p0412 N90-12367
Elaboration and characterization of MISFET transistors on InP
[ECL-88-19] 05 p0636 N90-13709
Analytical and computer-aided models of InP-based MISFETs and heterojunction devices
[AD-A211861] 05 p0702 N90-14106
Field-effect spectroscopy of interface states
[AD-A212998] 05 p0703 N90-14112
Study of metal-insulator-semiconductor structures on indium phosphide, implemented by anodic oxidation
[ECL-88-10] 05 p0703 N90-14114
Hydrogen radical enhanced growth of solar cells
[DE89-009497] 06 p0806 N90-14694
Excited state lifetime measurements of ytterbium in indium phosphide
[AD-A215709] 09 p1291 N90-17483
Radiation effects in ITO/InP solar cells
10 p1340 N90-17757
Indium phosphide solar cell research in the United States: Comparison with non-photovoltaic sources
10 p1340 N90-17758
On-orbit results of the LIPS 3/InP homojunction solar cell experiment 10 p1344 N90-17794
Opto-Em and devices investigation
[AD-A215033] 12 p1709 N90-19814
Electron beam induced damage in PECVD Si3N4 and SiO2 films on InP
[NASA-TM-102544] 13 p1810 N90-20393
An ellipsometric measurement of optical properties for InP surfaces
[AD-A217185] 13 p1887 N90-20827
Indium phosphide planar Gunn diode
[AD-A219337] 16 p2233 N90-22740
Lateral spreading of Au contacts on InP
[NASA-TM-103133] 16 p2252 N90-22843
Secondary ion mass spectrometry characterization of implants into GaAs and GaP for waveguides and integrated optics applications
[AD-A219203] 16 p2324 N90-23254
New directions in InP solar cell research
[NASA-TM-103160] 17 p2398 N90-23662
Radiation-hard-high-efficiency InP space solar cell development
[AD-A220500] 17 p2420 N90-23791
An analysis of the contact sintering process in III-V solar cells
[NASA-TM-103179] 19 p2709 N90-25420
Investigation on the MBE growth and properties of AlGaInAs/InP and InGaAs-InAlAs superlattices
[DE90-012248] 21 p3080 N90-27515
Measurement of deep levels at InGaAs(P)/InP heterojunctions
[AD-A222890] 21 p3082 N90-27526

INDIUM-TIN-OXIDE SEMICONDUCTORS
U ITO (SEMICONDUCTORS)

INDOLES
NT TRYPTOPHAN

INDONESIA
Project TTA-79: Summary project report
[ETN-90-96773] 19 p2661 N90-25146

Mapping and monitoring land use and land degradation in part of East Kalimantan, Indonesia, using aerospace remote sensing techniques: A SPOT case study
[BCRS-88-16B] 19 p2705 N90-25394
Satellite image atlas of glaciers of the world: Irian Jaya, Indonesia, and New Zealand
[PB90-230095] 24 p3483 N90-29691

INDOOR AIR POLLUTION
Pilot investigation of indoor-outdoor and personal PM10 (thoracic) and associated ionic compounds and mutagenic activity
[PB89-222723] 05 p0673 N90-13920
Atmosphere and water quality monitoring on Space Station Freedom
[NASA-CR-186707] 23 p3378 N90-29084

INDUCED FLUID FLOW
U FLUID FLOW

INDUCTANCE
The design of low inductance electrical circuits for slapper detonator systems
[AD-A214981] 09 p1212 N90-17024
Gas-puff z-pinch experiment
[IPPCZ-286] 15 p2167 N90-22385
Very high frequency measurements of geometric factors in transmission line lead acid cells
[AD-A219463] 17 p2420 N90-23788
L-SWITCH: A PC program for computing transient voltages and currents during switching off three-phase inductances
[EUT-89-E-221] 20 p2858 N90-26257
Application of a rechargeable, small caliber railgun power supply
[AD-A224207] 24 p3438 N90-29418

INDUCTION
Free electron lasers driven by linear induction accelerators: High power radiation sources
15 p2060 N90-21800
Induction-type metal detector with increased scanning area capability
[NASA-CASE-KSC-11386-1] 15 p2101 N90-22023
A knowledge-based system with learning for computer communication network design
15 p2157 N90-22319

INDUCTION (MATHEMATICS)
A theory of collective induction
[AD-A210553] 01 p0135 N90-10780
Completeness of resolution by transfinite induction
[CWI-CS-R8837] 02 p0260 N90-11473
Kolmogorov complexity and its applications
[CWI-CS-R8901] 04 p0548 N90-13191
Inductive reasoning and Kolmogorov complexity (preliminary version)
[CWI-CS-R8915] 05 p0695 N90-14062
Induction on a continuous variable
[DE90-606952] 10 p1422 N90-18203
Efficient specialization of relational concepts
[AD-A218889] 16 p2262 N90-22894

INDUCTION HEATING
Electromagnetic fusion process and position research
13 p1785 N90-20249
Aircraft battle damage repair of transparencies
[AD-A224168] 24 p3432 N90-29387

INDUCTION MOTORS
Adjustable speed drive study, part 1
[DE89-017654] 03 p0342 N90-11948
Mathematical models for the linear induction motor
[RR-WB-88-17] 04 p0496 N90-12853
Induction motor control
[NASA-TM-102533] 12 p1605 N90-19234
Aerospace induction motor actuators driven from a 20-kHz power link
[NASA-TM-102482] 13 p1756 N90-20085
Electromechanical actuation for thrust vector control applications
[NASA-TM-102548] 14 p1968 N90-21272
Analytical and experimental study of high phase order induction motors
[NASA-CR-186580] 15 p2088 N90-21952
Field oriented control of induction motors
[NASA-TM-103154] 16 p2231 N90-22731
Identification method for estimation of electrical parameters of induction motors
[ETN-90-97306] 22 p3168 N90-27969

INDUCTION SYSTEMS
U INTAKE SYSTEMS

INDUCTORS
Circuit level modeling of inductive elements
[DE89-015122] 01 p0032 N90-10173
Development of high frequency spice models for ferrite core inductors and transformers
[DE89-015121] 03 p0341 N90-11946
Improved high power/high frequency inductor
[NASA-CASE-NPO-17830-1-CU]
21 p2998 N90-27042

INDUSTRIAL ENERGY
Potential industrial applications for composite phase-change materials as thermal energy storage media
[DE89-015170] 02 p0237 N90-11346
Office of Industrial Programs research in progress
[DE90-002100] 10 p1440 N90-18311

INDUSTRIAL MANAGEMENT
NT ENGINEERING MANAGEMENT
NT INVENTORY MANAGEMENT
NT PERSONNEL MANAGEMENT
Internal technology transfer 11 p1577 N90-19080
Operational fact-finding report on heat pump systems for industrial use
[DE89-782295] 12 p1658 N90-19527
Making it happen: Project management
[PNR90618] 20 p2934 N90-26695

INDUSTRIAL PLANTS
The effects of noise on performance
[AD-A212519] 04 p0551 N90-13209
Retrieving and integrating IC fabrication data from dissimilar databases
[AD-A211890] 05 p0707 N90-14140
Industrial heat pump assessment study
[DE90-004541] 08 p1071 N90-16201
The use of technology transfer centers by department of defense industrial facilities
[AD-A216863] 10 p1443 N90-18328

INDUSTRIAL SAFETY
Human performance in continuous/sustained operations and the demands of extended work/rest schedules: An annotated bibliography, volume 2
[AD-A210504] 01 p0093 N90-10530
Electrical safety in the high voltage laboratory
[DE90-003026] 08 p1060 N90-16130
Environmental quality and occupational health Special Emphasis Area Plan (SEAP)
[AD-A214738] 09 p1251 N90-17259
A review of the literature on the toxicity of rare-earth metals as it pertains to the engineering demonstration system surrogate testing
[DE90-008049] 13 p1851 N90-20620
Space shuttle: Follow-up evaluation of NASA's solid rocket motor procurement. Report to the Chairman, Committee on Government Operations, House of Representatives
[GAO/NSIAD-89-89] 20 p2824 N90-26066

INDUSTRIAL WASTES
Industrial plastics waste: Identification and segregation
18 p2513 N90-24351

INDUSTRIES
NT AEROSPACE INDUSTRY
NT AIRCRAFT INDUSTRY
NT DEFENSE INDUSTRY
NT WEAPONS INDUSTRY
Using self-calibrating thermocouples in industry
[DE89-013539] 02 p0223 N90-11278
Centers for the commercial development of space
[NASA-PAM-525] 05 p0709 N90-14151
NASA commercial programs
[NASA-TM-101853] 05 p0709 N90-14152
Microgravity Science and Application Program tasks, 1989 revision
[NASA-TM-4191] 13 p1786 N90-20252
Photovoltaic energy
[DE89-009473] 13 p1826 N90-20486
Technology for electronic transfer of information: The present and future in North America
15 p2177 N90-22442
Langley aerospace test highlights, 1989
[NASA-TM-102631] 17 p2487 N90-24221
Preparing technicians for engineering materials technology 18 p2516 N90-24369
Future automotive materials: Evolution or revolution
18 p2516 N90-24370
Enhancing US competitiveness through Federal scientific and technical information: Issues and opportunities 22 p3258 N90-28450
Industrial patent activity in the US. Part 1: Time series profile by company and country of origin, 1969-1989
[PB90-214404] 22 p3259 N90-28454
Scientists, engineers, and technicians in nonmanufacturing industries: 1987. (Detailed statistical tables)
[PB90-226903] 23 p3404 N90-29235
Industrial patent activity in the US. Part 2: Alphabetical listing by company, 1969-1989
[PB90-214412] 23 p3405 N90-29246
Success of EPA's stratospheric ozone engineering research
[PB90-246265] 24 p3487 N90-29706

INELASTIC BODIES
U RIGID STRUCTURES

INELASTIC COLLISIONS
Interaction of low-energy electrons and positrons with condensed matter: Stopping powers and inelastic mean free paths from optical data
[DE90-001001] 06 p0840 N90-14882
Investigations of the interactions of radiation with matter
[AD-A213554] 07 p0991 N90-15723
Inelastic collisions of positrons with one-valence-electron targets 11 p1556 N90-18963
Determination of molecular spectroscopic parameters and energy-transfer rates by double-resonance spectroscopy 20 p2944 N90-26755

INELASTIC SCATTERING
Neutron scattering studies of amorphous Invar alloys
[DE89-016868] 02 p0197 N90-11126
Detailed photonuclear cross-section calculations and astrophysical applications
[DE89-017531] 03 p0421 N90-12419
A theoretical perspective on neutrino physics
[DE90-000759] 06 p0839 N90-14878
Solid State Division
[DE90-000979] 06 p0851 N90-14945
Magnetic excitations in thulium metal
[DE90-002475] 06 p0855 N90-14970
Structure and dynamics of disordered systems
[DE90-001408] 07 p0990 N90-15718
Heavy ion inelastic scattering with a 4(pi) gamma detector
[DE90-002709] 08 p1120 N90-16488
Elementary particle physics: Experimental
[DE90-005973] 10 p1429 N90-18242
Measurement of body fat by neutron inelastic scattering: Comments on installation, operation, and error analysis
[DE90-006765] 11 p1540 N90-18868
Inelastic scattering of positrons with sodium
11 p1556 N90-18961
Theoretical survey on positronium formation and ionisation in positron atom scattering
11 p1556 N90-18965
Positron scattering by atomic hydrogen using optical potentials and with positronium formation
11 p1557 N90-18966
Background studies in gas ionizing x ray detectors
12 p1636 N90-19399
Transverse spin observables in chromodynamics
[DE90-005638] 12 p1711 N90-19824
Bose condensate in superfluid (sup 4)He and momentum distributions by deep inelastic scattering
[DE90-007541] 12 p1712 N90-19832
The electron momentum-transfer cross sections of tungsten, silicon, and silicon dioxide at energies from 0.1 to 10,000 eV
[DE90-009041] 12 p1712 N90-19833
Large-angle elastic and inelastic scattering of Pi+ and Pi- from Si28 and Ca40
[AD-A218163] 13 p1885 N90-20818
US-Japan Workshop on Atomic Collisions in Solids: Abstracts of lectures
[DE90-008979] 14 p2025 N90-21611
Inelastic electron scattering from surfaces
[DE90-009365] 14 p2025 N90-21614
QCD Compton scattering at HERA energy
[NIKHEF-H/89-3] 15 p2165 N90-22372
Low temperature properties of amorphous solids
15 p2171 N90-22405
On the explanation of anomalies in inelastic neutron scattering by high-T(sub c) superconductors
[DE90-620561] 17 p2475 N90-24149

INELASTIC STRESS
A finite element formulation for inelastic plates and shells based on a mixed variational principle
02 p0233 N90-11334

INEQUALITIES
NT SCHWARTZ INEQUALITY
The quadratic matrix inequality in singular H infinity control with state feedback
[MEMO-COSOR-89-03] 05 p0686 N90-13997
A basic theorem of complementarity for the generalized variational-like inequality problem
[DE90-003102] 07 p0973 N90-15620
Two basic partial orderings for distributions derived from Schur functions and majorization
[AD-A213703] 07 p0984 N90-15682
On mean value iterations with application to variational inequality problems
[DE90-005556] 10 p1422 N90-18200
Generalized quasi-variational inequality and implicit complementarity problems
[AD-A215191] 13 p1875 N90-20755
On Bernstein type inequalities and a weighted Chebyshev approximation problem on ellipses
[NASA-CR-180368] 17 p2456 N90-24011
Structure of linear-quadratic control
[ETN-90-96894] 18 p2602 N90-24819

Weighted norm inequalities for Riemann-Liouville fractional integral
[DE90-627153] 23 p3388 N90-29132

INERT GASES
U RARE GASES

INERTIA
NT INERTIA PRINCIPLE
NT MACH INERTIA PRINCIPLE
Effect of particle velocity fluctuations on the inertia coupling in two-phase flow 01 p0068 N90-10391
Fracture and three dimensional stress analyses of 7075 aluminum projectile components under spin and inertia load
[AD-A210986] 01 p0081 N90-10463
Effect of control surface mass unbalance on the stability of a closed-loop active control system
[NASA-TP-2952] 03 p0357 N90-12042
On the identification of local minimizers in inertia-controlling methods for quadratic programming
[AD-A212514] 04 p0534 N90-13086
On the identification of local minimizers in inertia-controlling methods for quadratic programming
[DE89-017330] 07 p0973 N90-15616
Robot vibration control using inertial damping forces
[NASA-CR-186808] 19 p2698 N90-25352
Influence of gravito-inertial force on vestibular nystagmus in man
[IZF-1989-24] 22 p3231 N90-28325
Parallel algorithms for computation of the manipulator inertia matrix 23 p3376 N90-29072

INERTIA MOMENTS
U MOMENTS OF INERTIA

INERTIA PRINCIPLE
NT MACH INERTIA PRINCIPLE
Inertial corrections by dynamic estimation 12 p1735 N90-19976
Ultra-sensitive inertial sensors via neutral-atom interferometry 12 p1735 N90-19977

INERTIA WHEELS
U COUNTER-ROTATING WHEELS
U REACTION WHEELS

INERTIAL CONFINEMENT FUSION
NTES laser facility for physics experiments: Building 381 high bay option
[DE89-014326] 01 p0074 N90-10428
Pulsed-power switching for inertial confinement fusion with light ion beams
[DE89-016810] 02 p0279 N90-11595
Starlight: A stationary inertial-confinement-fusion reactor with nonvaporizing walls
[DE90-002315] 06 p0847 N90-14927
The search for solid state fusion lasers
[DE89-012301] 07 p0934 N90-15410
The Gevaltig: An inertial fusion powered manned spacecraft design for outer solar system missions
[NASA-CR-185163] 08 p1036 N90-15985
Light ion beam drivers for inertial confinement fusion
[DE90-004196] 08 p1127 N90-16528
Overview of defense applications of ICF (Inertial Confinement Fusion)
[DE90-005745] 10 p1433 N90-18269
Development of KrF lasers for fusion
[DE90-007830] 11 p1515 N90-18726
Energy deposition measurements for E-beam pumped excimer lasers
[DE90-007545] 13 p1806 N90-20365
Shaped pulses from Nova for inertial confinement fusion experiments
[DE90-007261] 13 p1807 N90-20373
Laser Program of the Lawrence Livermore National Laboratory
[DE90-008198] 16 p2240 N90-22779
Chemical and laser sciences division
[DE90-013532] 21 p3101 N90-27611
Ion divergence and the stability of magnetically insulated diodes
[DE90-014565] 23 p3321 N90-28777
Laboratory for Laser Energetics review
[DE90-014666] 23 p3330 N90-28829
Characterization of electron flow in positive-polarity linear-induction accelerators
[DE90-014998] 23 p3394 N90-29177
A review of self generated B-field in ICF corona
[DE90-627479] 24 p3547 N90-30063
UCD-LLNL collaboration on basic plasma physics research in inertial confinement fusion
[DE90-015771] 24 p3549 N90-30081

INERTIAL FORCES
U INERTIA

INERTIAL FUSION (REACTOR)
Development of KrF lasers for fusion
[DE90-007830] 11 p1515 N90-18726
Laboratory for Laser Energetics review
[DE90-014666] 23 p3330 N90-28829

INERTIAL GUIDANCE
NT STRAPDOWN INERTIAL GUIDANCE
The development of mission-specific advanced inertially-based avionics system 02 p0149 N90-10851
Guidance and Control Panel Symposium on Guidance and Control of Unmanned Air Vehicles
[AGARD-AR-260] 04 p0458 N90-12623
Development of a superconducting six-axis accelerometer
[AD-A215948] 10 p1319 N90-17625
Guidance and targeting for the strategic target system
[DE90-005239] 20 p2817 N90-26031
Ring laser gyro principles and techniques 24 p3426 N90-29352

INERTIAL MEASURING UNITS
U INERTIAL PLATFORMS

INERTIAL NAVIGATION
Design of a Kalman filter for transfer alignment 02 p0149 N90-10848
Development of the integrated all-weather navigation system for Tornado 02 p0149 N90-10849
A high performance airborne INS/GPS Integrated Navigation System 02 p0149 N90-10850
Case study on rapid software prototyping and automated software generation: An inertial navigation system
[AD-A212272] 04 p0450 N90-12578
RTSIN1: A model of a strapdown INS on a two-axis rate table
[AD-A212406] 04 p0450 N90-12579
FPG2: A flight profile generator program
[AD-A212408] 04 p0453 N90-12595
Shuttle tethered operations: The effect on orbital trajectory and inertial navigation 05 p0588 N90-13425
Advances in techniques and technologies for air vehicle navigation and guidance
[AGARD-AR-276] 08 p1020 N90-15899
Recent developments in TERPROM 09 p1163 N90-16732
SINS1: A model of a strapdown inertial navigation system
[AD-A215495] 09 p1166 N90-16749
Application of model based reasoning to diagnosis of faults in inertial navigation equipment
[AD-A215561] 09 p1166 N90-16750
Development of a superconducting six-axis accelerometer
[AD-A215948] 10 p1319 N90-17625
Optimization of the effective GPS data rate 14 p1907 N90-20932
Autonomous integrated GPS/INS navigation experiment for OMV. Phase 1: Feasibility study
[NASA-CR-4267] 14 p1914 N90-20969
Passive navigation using image irradiance tracking 15 p2141 N90-22232
Inertial navigation system simulator: Behavioral specification, revision
[AD-A219294] 16 p2199 N90-22554
Continued development and analysis of a new extended Kalman filter for the Completely Integrated Reference Instrumentation System (CIRIS)
[AD-A220106] 17 p2354 N90-23400
Laser gyros and field diagnostics
[AD-A220832] 17 p2406 N90-23709
Construction of a hybrid angular velocity reference system for investigation of the dynamic characteristics of strapdown gyros
[ESA-TT-1181] 19 p2694 N90-25332
Integration of GPS/INS with partitioned filters 24 p3425 N90-29347
Inertial grade fiber gyros 24 p3426 N90-29353
Use of a three-axis monolithic ring laser gyro and digital signal processor in an inertial sensor element 24 p3426 N90-29354
Ring laser gyro marine inertial navigation systems 24 p3426 N90-29355
JTIDS relative navigation: Principles, architecture, and inertial mixing 24 p3426 N90-29357
Integrated navigation/flight control for future high performance aircraft 24 p3427 N90-29362
State estimation for systems moving through random fields 24 p3429 N90-29373
A low cost inertial/GPS integrated approach to land navigation 24 p3430 N90-29374
A land navigation demonstration vehicle with a color map display for tactical use 24 p3430 N90-29375
An integrated system for land navigation 24 p3430 N90-29377
Inertial navigation system simulator program: Top-level design
[AD-A223762] 24 p3431 N90-29379
Proceedings of the 17th Annual Gravity Gradiometer Conference
[AD-A223568] 24 p3492 N90-29735

INERTIAL PLATFORMS
STS-GPS (Space Transportation System - Global Positioning System) tracking experiment for gravitation estimation: Feasibility study
[AD-A211265] 02 p0150 N90-10859
A gyroscope calibration analysis for the Gamma Ray Observatory (GRO) 05 p0589 N90-13428
The Rapid Geodetic Survey System (RGSS) 13 p1834 N90-20528

INERTIAL REFERENCE SYSTEMS
Hybrid angular velocity reference system for the investigation of dynamic properties of strapdown gryos
[DFVLR-FB-89-25] 04 p0450 N90-12577
Application of multifunction inertial reference systems to fighter aircraft 09 p1164 N90-16740
Application of multifunction inertial reference systems to fighter aircraft 24 p3423 N90-29341

INERTIAL UPPER STAGE
Atmospheric dispersion of solid and liquid rocket propellants
[AD-A221293] 21 p3020 N90-27173

INFERENCE
Parallel inference based on delta processing
[CWI-CS-R8846] 02 p0261 N90-11482
Doppler statistics of ocean velocity variability
[AD-A211687] 03 p0377 N90-12148
Illustration of Bayesian inference in normal data models using Gibbs sampling
[AD-A212630] 04 p0547 N90-13187
Kolmogorov complexity and its applications
[CWI-CS-R8901] 04 p0548 N90-13191
Inductive reasoning and Kolmogorov complexity (preliminary version)
[CWI-CS-R8915] 05 p0695 N90-14062
Optimization of monotonic inference algorithms in propositional and first order logic
[LAAS-89204] 08 p1111 N90-16436
A theory of quantitative inference for artifact sets applied to a mechanical design compiler
[AD-A216535] 11 p1545 N90-18896
Theory and applications of belief functions
[AD-A217092] 12 p1702 N90-19774
Time and truth in plans 14 p1906 N90-20930
Analyzing spacecraft configurations through specialization and default reasoning 15 p2155 N90-22308
Knowledge structure representation and automated updates in intelligent information management systems 15 p2156 N90-22316
Connectionism and compositional semantics
[AD-A219029] 16 p2264 N90-22904
Bayesian nonparametric prediction and statistical inference
[AD-A218473] 16 p2308 N90-23154
Statistical inference from sampled data
[AD-A218731] 16 p2309 N90-23156
Bayesian learning
[NASA-CR-181528] 17 p2465 N90-24082
Explanation of Bayesian conditioning for decision support systems 18 p2633 N90-25002
Inference and control mechanisms in NEXT 2.0
[NLR-MP-88062-U] 20 p2844 N90-26175
Adaptive time series analysis using predictive inference and entropy
[AD-A222337] 21 p2997 N90-27033
ATS displays: A reasoning visualization tool for expert systems 21 p3042 N90-27290
A knowledge base architecture for distributed knowledge agents 21 p3044 N90-27302
Preference relations, Chisini-de Finetti means and Bayesian inference in retrieval-system modelling
[ESA-STR-230] 22 p3260 N90-28461
Inference engine for expert systems
[INPE-4565-PRE/1306] 23 p3382 N90-29104
Systems reliability and inference: Summary of accomplishments 1988-1990
[AD-A224433] 24 p3477 N90-29653
What kind of computation is intelligence. A framework for integrating different kinds of expertise 24 p3506 N90-29817
Strategies for tutoring multiple bugs
[AD-A223921] 24 p3524 N90-29927
An analysis of the distinction between deep and shallow expert systems
[AD-A224443] 24 p3534 N90-29987
Saddlepoint approximations in conditional inference
[AD-A223280] 24 p3537 N90-30000
Automatic recognition of tractability in inference relations
[AD-A223698] 24 p3538 N90-30003

INFILTRATION
Investigations into the infiltration kinetics, wettability, and interfacial bond strength of Al/SiC composites
[AD-A211924] 03 p0320 N90-11815

Computer synthesis of ceramic preforms for molten-metal infiltration
[DE90-000826] 06 p0751 N90-14370
A cure process model for resin transfer molding of advanced composites
[NASA-CR-186247] 09 p1185 N90-16867
Infiltration mechanics in conventional and hybridised fibre reinforced metal matrix composites
[AERE-R-13330] 13 p1766 N90-20134
Characterization of ceramic matrix composites fabricated by chemical vapor infiltration
[DE90-008409] 13 p1768 N90-20149

INFINITY
Realization theoretic solution of two analytic matrix equations with applications to stabilization of infinite-dimensional systems
[AD-A211118] 02 p0265 N90-11512
The quadratic matrix inequality in singular H infinity control with state feedback
[MEMO-COSOR-89-03] 05 p0686 N90-13997
The singular zero sum differential game with stability using H infinity control theory
[MEMO-COSOR-89-09] 05 p0687 N90-13999
The singular H infinity control problem with dynamic measurement feedback
[MEMO-COSOR-89-14] 05 p0687 N90-14000
A frame approach to the H-infinity super-optimal solution
[OUEL-1761/89] 15 p2158 N90-22327
On the structure at infinity of a structured system
[CWI-BS-R8918] 17 p2468 N90-24108

INFLATABLE DEVICES
U INFLATABLE STRUCTURES

INFLATABLE SPACECRAFT
NT BEACON EXPLORER A
NT BEACON SATELLITES
Structural concepts for very large (400-meter-diameter) solar concentrators 01 p0029 N90-10153
Structural problems of accurate inflatable surfaces 02 p0184 N90-11044

INFLATABLE STRUCTURES
NT AIR BAG RESTRAINT DEVICES
NT BALLOONS
NT BEACON EXPLORER A
NT BEACON SATELLITES
NT HIGH ALTITUDE BALLOONS
NT INFLATABLE SPACECRAFT
NT TETHERED BALLOONS
Ballast system for maintaining constant pressure in a glove box
[NASA-CASE-NPO-17786-1-CU] 09 p1224 N90-17104
Advances in large inflatable reflectors 12 p1609 N90-19258
Inflatable fuel tank buffer
[AD-D014446] 14 p1921 N90-21002
Free-Space Power Transmission
[NASA-CP-10016] 15 p2060 N90-21795
Inflatable antennas for microwave pwoer transmission 15 p2060 N90-21799
A preliminary design of interior structure and foundation of an inflatable lunar habitat 18 p2633 N90-24999

INFLATING
Gravitational couplings of the inflation in extended inflation
[NASA-CR-186595] 15 p2190 N90-22504
Anisotropic inflation 16 p2331 N90-23286
Baryogenesis in extended inflation. Part 1: Baryogenesis via production and decay of supermassive bosons
[NASA-CR-180615] 17 p2470 N90-24120
Wind tunnel tests of a 20-gore disk-gap-band parachute
[AD-A221326] 18 p2493 N90-24251

INFLUENCE COEFFICIENT
On the evaluation of aerodynamic influence coefficients
[NLR-MP-87019-U] 12 p1597 N90-19191

INFORMATION
Polymorphism and information loss in Martin-Loef's type theory
[CS-8814] 04 p0533 N90-13079
Isolating contour information from arbitrary images 08 p1074 N90-16217
Information capacity of the matched Gaussian channel with jamming. 1: Finite-dimensional channel
[AD-A214782] 09 p1205 N90-16984
Information capacity of dimension-limited channels
[AD-A215238] 09 p1207 N90-16996
A review of circadian effects on selected human information processing tasks
[AD-A214673] 09 p1251 N90-17256
Identifying the circadian cycle in human information processing data using periodicity analysis: A synopsis
[AD-A214674] 09 p1251 N90-17257
United States Department of Energy stategic defense initiative: New and innovative concepts program
[DE90-005006] 09 p1276 N90-17399
Applications to the aerospace and defense R and D community: The DOD computer-aided acquisition and logistics support (CALS) initiative 15 p2179 N90-22453
Information content of a single pass of phase-delay data from a short baseline connected element interferometer 20 p2852 N90-26220
Capacity for patterns and sequences in Kanerva's SDM as compared to other associative memory models
[NASA-CR-180701] 20 p2905 N90-26522

INFORMATION DISSEMINATION
NT MESSAGES
NT SELECTIVE DISSEMINATION OF INFORMATION
Toward a national research network
[PB89-198709] 02 p0287 N90-11644
The transfer and diffusion of new technologies: A review of the economics literature
[DE89-015671] 02 p0290 N90-11655
National Library of Medicine DOCLINE (tradename) manual
[PB89-188676] 03 p0416 N90-12390
Activities report of the Kernfysisch Versneller Instituut
[ETN-89-95752] 04 p0553 N90-13219
Activities report of the Joint Research Center
[ETN-89-95757] 04 p0569 N90-13321
Activities report of the World Meteorological Organization
[WMO-713] 05 p0671 N90-13912
Federal scientific and technical information in an electronic age: Opportunities and challenges
[PB90-114414] 09 p1295 N90-17505
Research Reports: 1989 NASA/ASEE Summer Faculty Fellowship Program
[NASA-CR-183837] 12 p1634 N90-19390
High performance computing and networking for science
[PB90-131228] 14 p2011 N90-21526
Facilitating knowledge sharing in organizations: Semiautonomous agents that learn to gather, classify, and distribute environmental scanning knowledge 15 p2176 N90-22435
Technologies for electronic transfer of information: The present state and trends in Europe 15 p2177 N90-22441
Technology for electronic transfer of information: The present and future in North America 15 p2177 N90-22442
Space Station Freedom media handbook
[NASA-TM-102901] 17 p2364 N90-23460
NASA/American Society for Engineering Education (ASEE) Summer Faculty Fellowship Program 1989
[NASA-CR-181894] 18 p2639 N90-25034
Conceptual design for aerospace vehicles 18 p2641 N90-25043
NASA's experience in the international exchange of scientific and technical information in the aerospace field
[NASA-TM-103093] 19 p2764 N90-25704
Technology transfer: Implementation status of the Federal Technology Transfer Act of 1986. Report to Congressional requesters
[GAO/RCED-89-154] 19 p2764 N90-25707
NASA project status reports: Congressional requirements can be met, but reliability must be ensured
[GAO/NSIAD-90-40] 20 p2843 N90-26169
MTP: An atomic multicast transport protocol
[NASA-CR-186716] 20 p2858 N90-26254
International standards for text preparation and interchange
[DE90-011868] 20 p2935 N90-26699
Information resources management, 1984-1989: A bibliography with indexes
[NASA-SP-7079] 21 p3086 N90-27548
Government Information Quarterly. Volume 7, no. 2: National Aeronautics and Space Administration Scientific and Technical Information Programs. Special issue
[ISSN-0740-624X] 22 p3257 N90-28440
Introduction to National Aeronautics and Space Administration's scientific and technical information programs 22 p3257 N90-28441
Management of information in a research and development agency 22 p3257 N90-28442
Scientific and technical information management 22 p3257 N90-28444
Enhancing US competitiveness through Federal scientific and technical information: Issues and opportunities 22 p3258 N90-28450
Distributed database concepts for command and control information systems
[FFI-90/7005] 22 p3260 N90-28462
Procedures for DOE-Navy exchange and approval of engineering information and material management required for production of W88-0/Mk5 RBA (reentry body assembly)
[DE90-014763] 23 p3287 N90-28595
Transferring building energy technologies by linking government and private-sector programs
[DE90-000346] 23 p3408 N90-29258
Overview of Omega signal coverage 24 p3429 N90-29368
External information sources and aerospace R/D: The use and importance of technical reports by US Aerospace engineers and scientists
[NASA-TM-101232] 24 p3558 N90-30132
FEDIX: An on-line information service for universities and other research organizations: User's guide
[DE90-014835] 24 p3559 N90-30137

INFORMATION FLOW
A signal processing language for coarse grain data flow multiprocessors
[AD-A213863] 07 p0976 N90-15635
Communication-efficient arbitration models for low-resolution data flow computing
[AD-A214768] 09 p1262 N90-17319
Strategies for concurrent processing of complex algorithms in data driven architectures
[NASA-CR-186515] 14 p2013 N90-21535
Information technology applications: A British Aerospace Military Aircraft Ltd view 15 p2180 N90-22455
Interdisciplinary research: Promoting collaboration between the life sciences and medicine and the physical sciences and engineering 17 p2478 N90-24171
Behavioral networks as a model for intelligent agents 19 p2738 N90-25561
Theft of information in the take-grant protection model
[NASA-CR-186638] 19 p2763 N90-25702

INFORMATION MANAGEMENT
NT RECORDS MANAGEMENT
Extreme hurricanes in the nineteenth century
[PB89-201305] 01 p0087 N90-10498
Meteorological support: Descriptions of application programs for accessing and displaying data
[PB89-194625] 01 p0088 N90-10500
Waveform generator signal processing software
[PB89-192660] 01 p0103 N90-10587
Weeding policy and procedures: Information services
[AD-A210568] 01 p0137 N90-10790
Development of Information Quality Engineering (IQE) methodology for information resource management
[AD-A210615] 01 p0137 N90-10791
Reporting environmental data of known quality
[DE89-016214] 02 p0239 N90-11359
Techniques for optimizing human-machine information transfer related to real-time interactive display systems
[NASA-TM-100450] 02 p0254 N90-11441
Electronic publishing: Guide to selection
[PB89-214753] 02 p0256 N90-11448
A methodology for the design of continuous-dataflow synchronous systems
[PB89-184360] 02 p0274 N90-11564
Micro-based fact collection tool user's manual
[NASA-CR-180414] 05 p0684 N90-13981
Integrated computer-based tools to facilitate environmental monitoring, assessment, and restoration
[DE90-002732] 06 p0811 N90-14717
High volume data storage architecture analysis
[NASA-CR-186239] 06 p0823 N90-14784
Introduction to the framework and tasks of the DFD — German Remote Sensing Data Center (DFD)
08 p1092 N90-16319
FY 1989 update to the Information Resources Management review plan
[DE90-004185] 08 p1138 N90-16593
Integrated IMA (Information Mission Areas) IC (Information Center) guide
[AD-A216944] 11 p1547 N90-18903
Information management systems for integrating the technical data and regulatory requirements of environmental restoration activities
[DE90-008622] 13 p1831 N90-20511
Using expert systems to implement a semantic data model of a large mass storage system 15 p2156 N90-22315
Knowledge structure representation and automated updates in intelligent information management systems 15 p2156 N90-22316
Managing Federal information resources
[PB90-100173] 15 p2175 N90-22429
How to get it: A guide to defense-related information resources
[AD-A201600] 15 p2176 N90-22433
Electronic mail systems 15 p2179 N90-22451
Language in action
[ITLI-LP-89-04] 17 p2480 N90-24182
Automatic speech recognition in air-ground data link 18 p2640 N90-25037

Technical guide on documentation requirements for open market contract acquisitions of information resources
[NASA-TM-102650] 19 p2762 N90-25695
Knowledge-based system for flight information management
[NASA-TM-102685] 20 p2903 N90-26511
International standards for text preparation and interchange
[DE90-011868] 20 p2935 N90-26699
IRDS prototyping with applications to the representation of EA/RA models
[NASA-CR-186066] 21 p3039 N90-27273
Context propagation truth maintenance system
[RR-779-I] 21 p3057 N90-27380
Information resources management, 1984-1989: A bibliography with indexes
[NASA-SP-7079] 21 p3086 N90-27548
Helping America compete: The role of Federal scientific and technical information
[OTA-CIT-454] 21 p3086 N90-27549
The role of the US government technical report in aeronautics: An exploratory study
[NASA-TM-893470] 21 p3087 N90-27553
Flight data replay and analysis system 22 p3105 N90-27635
Swissair studies on the compressibility of aircraft data 22 p3105 N90-27637
Aspects of data link applications for ATC purposes 22 p3113 N90-27688
A technology assessment of alternative communications systems for the space exploration initiative
[NASA-TM-103243] 22 p3125 N90-27736
Government Information Quarterly. Volume 7, no. 2: National Aeronautics and Space Administration Scientific and Technical Information Programs. Special issue
[ISSN-0740-624X] 22 p3257 N90-28440
Introduction to National Aeronautics and Space Administration's scientific and technical information programs 22 p3257 N90-28441
Management of information in a research and development agency 22 p3257 N90-28442
Scientific and technical information management 22 p3257 N90-28444
NASA scientific and technical information for the 1990s 22 p3257 N90-28445
Enhancing US competitiveness through Federal scientific and technical information: Issues and opportunities 22 p3258 N90-28450
Information management directions: The integration challenge
[PB90-219866] 23 p3405 N90-29245
Information management in an integrated space telerobot 24 p3511 N90-29846

INFORMATION PROCESSING (BIOLOGY)

Extrathalamic modulation of cortical function
[AD-A211044] 01 p0094 N90-10535
Integration of neurobiological and computational analyses of the neural network essentials for conditioned taste aversions
[AD-A210228] 01 p0094 N90-10537
Models of mental functioning
[AD-A210456] 01 p0094 N90-10538
Adaptive information processing in auditory cortex
[AD-A211294] 03 p0380 N90-12166
Metacognition and retrieval from long-term memory at Mount Everest
[AD-A211629] 03 p0382 N90-12177
Electrophysiological studies of visual attention and resource allocation
[AD-A212287] 04 p0525 N90-13030
Visual perception processing in a hierarchical control system: Level 1
[PB89-221188] 04 p0536 N90-13101
Role of retinocortical processing in spatial vision
[AD-A210995] 05 p0672 N90-13918
Gravity receptors and responses 05 p0678 N90-13948
The application of queuing theory to the modelling of CP-140 aircraft communications
[AD-A213479] 07 p0918 N90-15310
The components of scientific visualization
[DE90-001992] 07 p0972 N90-15614
Numerical facility: Convergence of cognitive and factor analytic models
[AD-A213627] 07 p0983 N90-15680
Training and selecting individuals for high levels of information processing load 09 p1256 N90-17288
Prediction of success in flight training by single- and dual-task performance 09 p1257 N90-17293
The role of chaos in hemispheric process and attention
[AD-A217674] 13 p1854 N90-20639
The boundaries of hemispheric processing in visual pattern recognition
[AD-A217675] 13 p1854 N90-20640
The perceptual interaction of graphical attributes in thirteen bivariate displays
[AD-A217980] 13 p1868 N90-20720
CEREBRAL WEEVIL: A machine learning model for hemispheric categorization of complex visual patterns
[AD-A218143] 13 p1874 N90-20749
A preliminary analysis of the SOAR architecture as a basis for general intelligence
[AD-A218913] 16 p2262 N90-22896
Cognitive efficiency considerations for good graphic design
[AD-A218976] 16 p2263 N90-22899
Information processing approaches to cognitive development
[AD-A219200] 16 p2265 N90-22908
A task-analytic approach to the automated design of information graphics
[AD-A219271] 16 p2265 N90-22912
Laboratory replication of scientific discovery processes
[AD-A219273] 16 p2266 N90-22913
An instructable Connectionist/Control architecture: Using rule-based instructions to accomplish connectionist learning in a human time scale
[AD-A219274] 16 p2266 N90-22914
How to reinforce perception of depth in single two-dimensional pictures 16 p2270 N90-22937
Process and representation in graphical displays 19 p2740 N90-25574
Collective computation of neural network
[AD-A221848] 21 p3061 N90-27405
Effects of organizational structure on performance: Experimental results
[AD-A222871] 21 p3085 N90-27543
Categorization and identification of simultaneous targets
[IZF-1989-22] 22 p3234 N90-28337
Research in command and control for the Dutch Army Corps (1NL)
[IZF-1989-28] 23 p3318 N90-28760
A methodology for the objective measurement of pilot situation awareness 23 p3357 N90-28974
Situational Awareness Rating Technique (SART): The development of a tool for aircrew systems design 23 p3357 N90-28975
Evaluation of the Situational Awareness Rating Technique (SART) as a tool for aircrew systems design 23 p3358 N90-28977
Attention gradients in situation awareness 23 p3358 N90-28978
Towards a future cockpit: The prototyping and pilot integration of the Mission Management Aid (MMA) 23 p3358 N90-28979
The simulation of localized sounds for improved situational awareness 23 p3359 N90-28984
Neurophysiological correlates of information processing abilities during divided attention situations in air traffic controllers 23 p3360 N90-28989
IEEE Conference on Neural Information Processing Systems, Natural and Synthetic
[AD-A223611] 24 p3461 N90-29552
A layered abduction model of perception: Integrating bottom-up and top-down processing in a multi-sense agent 24 p3512 N90-29851

INFORMATION RETRIEVAL

The impact of recovery on concurrency control
[AD-A210828] 01 p0106 N90-10603
Online support for the intellectual activity of browsing 01 p0136 N90-10784
Experimental database retrieval system DARTS (Handling Manual)
[DE89-906473] 02 p0289 N90-11652
Program distribution for unclassified scientific and technical reports: Instructions and category scope notes, revision 75
[DE89-005395] 03 p0416 N90-12391
Problem of incomplete information in relational databases
[PB89-217533] 03 p0417 N90-12393
Interoperability of heterogeneous information systems: The COST 11(ter) Project
[PB89-217541] 03 p0417 N90-12394
Retrieving and integrating IC fabrication data from dissimilar databases
[AD-A211890] 05 p0707 N90-14140
AFOSR technical report summaries
[AD-A213148] 05 p0707 N90-14142
Automated reuseable components system study results 06 p0824 N90-14790
The design and implementation of an intelligent interface for information retrieval 06 p0858 N90-14991
Identification and quantification of synoptic structure in simulated TIROS N radiance soundings
[AD-A213729] 07 p0960 N90-15553
Reconfigurable N-dimensional computer memory
[AD-D014309] 07 p0971 N90-15607
A comparative evaluation and analysis of end-user search performance in an academic environment 07 p1009 N90-15845
Alternative representations for database responses 07 p1009 N90-15847
Procurement of an optical disk information storage and retrieval system
[DE90-001372] 07 p1010 N90-15849
Interim Design Database (IDDB) CADAM drawing retrieval program user's manual for the IBM 3081
[DE90-004491] 09 p1269 N90-17356
The real-time roll-back and recovery of transactions in database systems
[AD-A214471] 09 p1295 N90-17506
A hybrid model for document retrieval systems 10 p1441 N90-18315
Source hierarchy list. Volume 1: A through D
[AD-A216050] 10 p1442 N90-18321
Source hierarchy list. Volume 2: E through N
[AD-A216051] 10 p1442 N90-18322
Source hierarchy list. Volume 3: O through Z
[AD-A216052] 10 p1442 N90-18323
A human factors experimental comparison of two database query languages 11 p1574 N90-19064
The expression of syntagmatic relationships in frame-based indexing 12 p1726 N90-19917
CRISP (Computer Retrieval of Information on Scientific Projects) thesauras, fiscal year 1990
[PB90-138652] 12 p1726 N90-19922
Transaction processing in a quality control laboratory
[DE90-004655] 13 p1813 N90-20414
A model research archive: Archive and research implications for original records and support documents
[DE90-008246] 13 p1900 N90-20906
A formal approach to user models in data retrieval
[PB90-124728] 14 p2036 N90-21682
How to get it: A guide to defense-related information resources
[AD-A201600] 15 p2176 N90-22433
NASA Thesaurus supplement: A four part cumulative supplement to the 1988 edition of the NASA Thesaurus (supplement 3)
[NASA-SP-7064-SUPPL-3] 15 p2177 N90-22438
Desk top publishing: What you need to know 15 p2178 N90-22449
Electronic transfer of information applications in the Societe Aerospatiale 15 p2179 N90-22454
Assessment System for Aircraft Noise (ASAN) citation database. Volume 1: User's manual
[AD-A219175] 16 p2314 N90-23188
Assessment System for Aircraft Noise (ASAN) citation database. Volume 2: Database update manual
[AD-A219176] 16 p2314 N90-23189
Assessment System for Aircraft Noise (ASAN) citation database. Volume 3: New citation review procedures
[AD-A219177] 16 p2314 N90-23190
Satellite data archiving: US and foreign activities and plans for environmental information
[GAO/RCED-88-201] 18 p2633 N90-25001
The EISI (Elemental and Interplanar Spacing Index) index: A search/match tool for electron diffraction phase analysis
[DE90-010832] 20 p2830 N90-26097
The retrieval of information from secondary memory: A review and new findings
[AD-A222760] 20 p2899 N90-26489
Energy data base: Subject categories and scope
[DE90-009212] 20 p2936 N90-26706
Automatic information processing and high performance skills: Application to training
[AD-A221709] 21 p3036 N90-27259
Automatic information processing and high performance skills: Acquisition, transfer, and retention
[AD-A221744] 21 p3036 N90-27260
A theoretical model of optimistic recovery in distributed systems
[AD-A222055] 21 p3054 N90-27359
Finding the maximum recoverable system state in optimistic rollback recovery methods
[AD-A222338] 21 p3064 N90-27419
Information resources management, 1984-1989: A bibliography with indexes
[NASA-SP-7079] 21 p3086 N90-27548
Helping America compete: The role of Federal scientific and technical information
[OTA-CIT-454] 21 p3086 N90-27549
Further research on heading in text
[AD-A221511] 21 p3087 N90-27557
Advanced retrieval assistance for the DGIS gateway
[AD-A221592] 21 p3087 N90-27558
Computer modeling and data processing methods: An essential part of jet engine condition monitoring and fault diagnosis 22 p3104 N90-27626
CUIS user's manual
[ESA-TM-03] 22 p3132 N90-27775

Appendix A: NASA information services
22 p3258 N90-28451
Preference relations, Chisini-de Finetti means and Bayesian inference in retrieval-system modelling
[ESA-STR-230] 22 p3260 N90-28461
The SPECIALIST: Natural language processing system
[PB90-240029] 23 p3381 N90-29098
Efficiency and effectiveness of deep structure-based subject indexing languages: PRECIS vs. DSIS
23 p3406 N90-29248
Textual regularities applicable to full text searching: The case of family history literature
24 p3557 N90-30125
Search strategies for computer-stored information: A microcomputer tutorial 24 p3557 N90-30126

INFORMATION SYSTEMS
NT GEOGRAPHIC INFORMATION SYSTEMS
NT INTEGRATED LIBRARY SYSTEMS
NT MANAGEMENT INFORMATION SYSTEMS
NT NUMERICAL DATA BASES

Satellite Data Processing System (SDPS) users manual V1.0
[NASA-CR-183054] 01 p0082 N90-10468
Planning an Integrated On-line Library System (IOLS)
[AD-A209406] 01 p0136 N90-10783
Online support for the intellectual activity of browsing
01 p0136 N90-10784
Motivating the notion of generic design within information processing theory: The design problem space
[AD-A210266] 01 p0136 N90-10786
Weeding policy and procedures: Information services
[AD-A210568] 01 p0137 N90-10790
Development of Information Quality Engineering (IQE) methodology for information resource management
[AD-A210615] 01 p0137 N90-10791
Defense Technical Information Center cataloging guidelines
[AD-A211000] 01 p0137 N90-10792
Techniques for optimizing human-machine information transfer related to real-time interactive display systems
[NASA-TM-100450] 02 p0254 N90-11441
Electronic publishing: Guide to selection
[PB89-214753] 02 p0256 N90-11448
Performance reports for EIM (Engineering Information Management) computer systems: A managerial perspective
[DE89-015194] 02 p0256 N90-11449
Considerations for a design and operations knowledge support system for Space Station Freedom
[NASA-TM-102156] 02 p0256 N90-11451
Operating experience with the Sandia terminal switching network and fiber optic loop
[DE89-007422] 03 p0404 N90-12317
Program distribution for unclassified scientific and technical reports: Instructions and category scope notes, revision 75
[DE89-005395] 03 p0416 N90-12391
Role of conceptual models in the design and use of information systems
[PB89-217376] 03 p0416 N90-12392
Interoperability of heterogeneous information systems: The COST 11(ter) Project
[PB89-217541] 03 p0417 N90-12394
Building a user-friendly data dictionary system in ORACLE
[DE89-014878] 03 p0417 N90-12397
FEDIX: An on-line information service for universities and other research organizations: User's guide, version 2.0, release 1
[DE89-016695] 03 p0417 N90-12398
DOD Gateway Information System (DGIS) common command language: A retrospective on the introduction of prolog as the development tool
[AD-A211941] 03 p0418 N90-12400
Access to Max '91 information via computer networks
03 p0430 N90-12466
Telescience Testbed Pilot Program
[NASA-CR-184997] 04 p0528 N90-13047
Fellowships in information and stochastic systems
[AD-A212385] 04 p0563 N90-13280
Executive overview and introduction to the SMAP information system life-cycle and documentation standards
[NASA-TM-101765] 05 p0706 N90-14134
Information system life-cycle and documentation standards, volume 1
[NASA-TM-101856] 05 p0706 N90-14135
Management plan documentation standard and Data Item Descriptions (DID). Volume of the information system life-cycle and documentation standards, volume 2
[NASA-TM-101857] 05 p0706 N90-14136
Product specification documentation standard and Data Item Descriptions (DID). Volume of the information system life-cycle and documentation standards, volume 3
[NASA-TM-101858] 05 p0706 N90-14137
Assurance specification documentation standard and Data Item Descriptions (DID). Volume of the information system life-cycle and documentation standards, volume 4
[NASA-TM-101859] 05 p0706 N90-14138
Management control and status reports documentation standard and Data Item Descriptions (DID). Volume of the information system life-cycle and documentation standards, volume 5
[NASA-TM-101860] 05 p0706 N90-14139
The DOD Gateway Information System: Operational prototype and transition period 1987-1988
[AD-A213044] 05 p0707 N90-14141
AFOSR technical report summaries
[AD-A213148] 05 p0707 N90-14142
ERIS: Engineering Resource Information System
[AD-A213357] 05 p0707 N90-14144
Integrated computer-based tools to facilitate environmental monitoring, assessment, and restoration
[DE90-002732] 06 p0811 N90-14717
JPL reuse program 06 p0825 N90-14795
Level 2 software reuse study
06 p0826 N90-14800
AdaNET services 06 p0827 N90-14806
DOCTORD Database System user's guide, June 1989: dBase 3 PLUS Physician/(Part B Medicare): Personal computer reference system and user's guide
[PB90-100181] 07 p0966 N90-15579
Statistical information system for cultivation of the soil. Use of remote sensing in official statistics
08 p1095 N90-16338
Database design using NIAM (Nijssen Information Analysis Method) modeling
[DE89-014831] 08 p1138 N90-16592
FY 1989 update to the Information Resources Management review plan
[DE90-004185] 08 p1138 N90-16593
Proximity compatibility and information display: The effects of space and color on the analysis of aircraft stall conditions
[AD-A214488] 09 p1260 N90-17309
Automated information systems plan
[AD-A214982] 09 p1296 N90-17514
Definition of a management information system to support performance risk assessment
[AD-A215464] 09 p1297 N90-17516
Proceedings of Colloquium 110 of the International Astronomical Union on Library and Information Services in Astronomy
[AD-A215612] 09 p1298 N90-17523
NASA Propagation Information Center
10 p1371 N90-17946
Study on advanced information processing system
[NASA-CR-186342] 10 p1415 N90-18154
A hybrid model for document retrieval systems
10 p1441 N90-18315
Source header list. Volume 1: A through K
[AD-A216000] 10 p1442 N90-18319
Source header list. Volume 2: L through Z
[AD-A216001] 10 p1442 N90-18320
An analysis of the impacts of computer-based information systems on research and development organizations
[AD-A216283] 10 p1442 N90-18324
Development of the agricultural information system. Characteristics and results of the Distrito Federal model
[INPE-4940-PRE/1430] 11 p1524 N90-18773
Paper on geography in environmental management: Research and new techniques
[INPE-4840-PRE/1469] 11 p1531 N90-18816
DoD manual for standard data elements
[AD-A216441] 11 p1575 N90-19066
Low earth orbiting satellite for international information exchange system
[DE90-007186] 12 p1615 N90-19292
Augmenting and updating NASA spacelink electronic information system 12 p1634 N90-19392
ESRIN
[ESA-BR-58] 12 p1677 N90-19631
Executive information systems for providing next generation strategic information: An evaluation of EIS (Executive Information System) software and recommended applicability within the FAA computing environment
[AD-A216672] 12 p1726 N90-19920
National Technical Information Service 1989 Users Conference proceedings
[PB90-142563] 12 p1726 N90-19921
Information management systems for integrating the technical data and regulatory requirements of environmental restoration activities
[DE90-008622] 13 p1831 N90-20511
Software quality assurance and software safety in the biomed control system
[DE90-008072] 13 p1866 N90-20706
A model research archive: Archive and research implications for original records and support documents
[DE90-008246] 13 p1900 N90-20906
Investigation of air transportation technology at the Massachusetts Institute of Technology, 1988-1989
14 p1905 N90-20922
A knowledge-based information based for crop area estimation
[INPE-4990-PRE/1555] 14 p1996 N90-21444
A formal approach to user models in data retrieval
[PB90-124728] 14 p2036 N90-21682
Army War College final prototype optical disk system testing and evaluation report
[DE90-008852] 14 p2036 N90-21685
The ultimate CASE tool
[DE90-009351] 14 p2037 N90-21687
Managing Federal information resources
[PB90-100173] 15 p2175 N90-22429
Current information technology resource requirements of the Federal government: Major systems acquisitions and planned resources
[PB90-146820] 15 p2177 N90-22439
Electronic Transfer of Information and its Impact on Aerospace and Defence Research and Development
[AGARD-CP-466] 15 p2177 N90-22440
Innovations in telecommunications networks
15 p2178 N90-22444
Megatendances 15 p2178 N90-22445
The Weapons Laboratory technical library: Automating with STILAS 15 p2178 N90-22447
The automation plan of the General Directorate 1 (search) of the European Patent Office
15 p2178 N90-22448
Electronic transfer of information applications in the Societe Aerospatiale 15 p2179 N90-22454
Information technology applications: A British Aerospace Military Aircraft Ltd view 15 p2180 N90-22455
NSSDC data listing
[NASA-TM-102989] 15 p2180 N90-22456
Natural resources information system for the state of Oklahoma
[DE90-009483] 15 p2180 N90-22458
BTOS database evaluation
[AD-A219304] 16 p2328 N90-23271
Activities report of the Division of Informations Systems (FOA 37)
[FOA-C-30552-3.4] 17 p2480 N90-24178
Towards elegant design of highly interactive information systems using an object-oriented approach
[REPT-89-75] 17 p2480 N90-24179
Ceramic technology for advanced heat engines project data base
[DE90-011491] 18 p2532 N90-24448
Enhancing a relational database: Stepwise, bottom-up design
[DE90-010834] 18 p2635 N90-25012
Process and information integration via hypermedia
19 p2733 N90-25534
Object-oriented design: Deriving conceptual solutions to large-scale information processing problems
[DE90-011189] 19 p2763 N90-25699
Applications of PC-based digital imaging for storing microscopy images on optical disks
[DE90-011355] 19 p2763 N90-25701
Energy data base: Subject categories and scope
[DE90-009212] 20 p2936 N90-26706
VISTA (Vertical Integration of Science, Technology, and Applications) user interface software study
[DE90-010003] 20 p2936 N90-26707
Modernization of PRC meteorological service
[AD-A221761] 21 p3032 N90-27236
Information resources management, 1984-1989: A bibliography with indexes
[NASA-SP-7079] 21 p3086 N90-27548
Representing processes in the extended entity-relationship model
[DE90-013350] 21 p3086 N90-27551
The role of the US government technical report in aeronautics: An exploratory study
[NASA-TM-893470] 21 p3087 N90-27553
Interim status and recommendations for the Engineering Information System (EIS) program
[AD-A222060] 21 p3087 N90-27555
Status report on image information systems and image data base technology
[AD-A221488] 21 p3087 N90-27556
Advanced retrieval assistance for the DGIS gateway
[AD-A221592] 21 p3087 N90-27558
CUIS user's manual
[ESA-TM-03] 22 p3132 N90-27775
Government Information Quarterly. Volume 7, no. 2: National Aeronautics and Space Administration Scientific and Technical Information Programs. Special issue
[ISSN-0740-624X] 22 p3257 N90-28440

Introduction to National Aeronautics and Space Administration's scientific and technical information programs 22 p3257 N90-28441
Management of information in a research and development agency 22 p3257 N90-28442
The new space and Earth science information systems at NASA's archive 22 p3257 N90-28443
Scientific and technical information management 22 p3257 N90-28444
NASA scientific and technical information for the 1990s 22 p3257 N90-28445
Communications and media services 22 p3258 N90-28449
Appendix A: NASA information services 22 p3258 N90-28451
Providing dynamic sorting and searching capabilities using SQL*Forms
[DE90-012735] 22 p3259 N90-28456
Relational databases with NIAM models bid so long to top-down designs
[DE90-013496] 22 p3259 N90-28457
Distributed database concepts for command and control information systems
[FFI-90/7005] 22 p3260 N90-28462
Evaluation of existing aircraft operator data bases
[DOT/FAA/CT-90/18] 22 p3260 N90-28463
The personal computer: An untapped source for the United States Army War College
[AD-A223976] 23 p3379 N90-29087
A comparison of password techniques for multilevel authentication mechanisms
[AD-A224245] 23 p3379 N90-29089
Object database management systems: Concepts and features
[PB90-216813] 23 p3405 N90-29243
Automated information system life-cycle management manual
[PB90-219288] 23 p3405 N90-29244
International aircraft operator data base master requirements and implementation plan
[DOT/FAA/CT-90/17] 23 p3405 N90-29247
Crossroads of Information Technology Standards
[PB90-239732] 23 p3406 N90-29251
Optical storage technology
[AD-A224028] 23 p3407 N90-29254
Time-based competition for competitive advantage: An information technology perspective
[AD-A224474] 23 p3407 N90-29255
Data catalog series for space science and applications flight missions. Volume 5A: Descriptions of astronomy, astrophysics, and solar physics spacecraft and investigations. Volume 5B: Descriptions of data sets from astronomy, astrophysics, and solar physics spacecraft and investigations
[NASA-TM-101908] 24 p3437 N90-29413
Data catalog series for space science and applications flight flight missions. Volume 2B: Descriptions of data sets from geostationary and high-altitude scientific spacecraft and investigations
[NASA-TM-101909] 24 p3437 N90-29414
Data catalog series for space science and applications flight missions. Volume 1A: Descriptions of planetary and heliocentric spacecraft and investigations, second edition
[NASA-TM-101910] 24 p3438 N90-29415
Data catalog series for space science and applications flight missions. Volume 6: Master index volume
[NASA-TM-101913] 24 p3438 N90-29416
Results from Alouette 1, Explorer 20, Alouette 2, and Explorer 31
[NASA-TM-101822] 24 p3483 N90-29690
The worldwide ionospheric data base
[NASA-TM-101823] 24 p3488 N90-29714
Tele-autonomous systems: New methods for projecting and coordinating intelligent action at a distance 24 p3502 N90-29794
Data catalog series for space science and applications flight missions. Volume 4B: Descriptions of data sets from meteorological and terrestrial applications spacecraft and investigations
[NASA-TM-101880] 24 p3556 N90-30123
External information sources and aerospace R/D: The use and importance of technical reports by US Aerospace engineers and scientists
[NASA-TM-101232] 24 p3558 N90-30132
Integration of information systems components
[DE90-011761] 24 p3559 N90-30136
FEDIX: An on-line information service for universities and other research organizations: User's guide
[DE90-014835] 24 p3559 N90-30137
Data catalog series for space science and applications flight missions. Volume 3B: Descriptions of data sets from low- and medium-altitude scientific spacecraft and investigations
[NASA-TM-89680] 24 p3560 N90-30140
Data catalog series for space science and applications flight missions. Volume 1B: Descriptions of data sets from planetary and heliocentric spacecraft and investigations
[NASA-TM-89695] 24 p3561 N90-30148
Interplanetary medium data book, supplement 4, 1985-1988
[NASA-TM-101867] 24 p3561 N90-30149
A guide to the National Space Science Data Center
[NASA-TM-89637] 24 p3565 N90-30167

INFORMATION THEORY

Motivating the notion of generic design within information processing theory: The design problem space
[AD-A210266] 01 p0136 N90-10786
Completeness of resolution by transfinite induction
[CWI-CS-R8837] 02 p0260 N90-11473
Summaries of the FY 1989 Applied Mathematical Sciences Research program
[DE89-016694] 02 p0267 N90-11521
Geodetic network adjustment using GPS triple difference observations and a priori stochastic information
[TR-1-1987] 05 p0577 N90-13367
Inductive reasoning and Kolmogorov complexity (preliminary version)
[CWI-CS-R8915] 05 p0695 N90-14062
Assessment of the efficiency of nondestructive techniques in materials testing studies based on the information criterion
[DE89-635444] 06 p0796 N90-14834
Solution bias in complex systems modeling
[DE90-002001] 06 p0836 N90-14858
High compression image and image sequence coding 08 p1074 N90-16214
Information capacity of the matched Gaussian channel with jamming. 1: Finite-dimensional channel
[AD-A214782] 09 p1205 N90-16984
Coding capacity for a class of additive channels
[AD-A215054] 09 p1206 N90-16993
Information capacity of dimension-limited channels
[AD-A215238] 09 p1207 N90-16996
Computation at the edge of chaos: Phase transition and emergent computation
[DE90-007488] 12 p1708 N90-19811
A paradoxical result in unconditionally secure authentication codes, and an explanation
[DE90-008529] 13 p1867 N90-20710
Spectral analytic methods for the estimation of number of signals and directions of arrival
[AD-A217219] 13 p1876 N90-20757
The ultimate CASE tool
[DE90-009351] 14 p2037 N90-21687
Vision science and technology for supervised intelligent space robots 15 p2139 N90-22221
Image gathering, coding, and processing: End-to-end optimization for efficient and robust acquisition of visual information 15 p2139 N90-22224
How to get it: A guide to defense-related information resources
[AD-A201600] 15 p2176 N90-22433
Current information technology resource requirements of the Federal government: Major systems acquisitions and planned resources
[PB90-146820] 15 p2177 N90-22439
A formal mechanism for determining redundancy and irrelevance in Hypertext views
[TR-89-9] 17 p2450 N90-23970
Modal logic as a theory of information
[ITLI-LP-89-05] 17 p2480 N90-24183
The role of the US government technical report in aeronautics: An exploratory study
[NASA-TM-893470] 21 p3087 N90-27553
Using information to measure software complexity
[REPT-89-022] 22 p3238 N90-28359
An environment to support problem solving
[ISBN-90-9003151-0] 22 p3259 N90-28458
A Boltzmann machine for the organization of intelligent machines 23 p3370 N90-29040
The effect of software reusability on information theory based software metrics
[AD-A224472] 24 p3526 N90-29936

INFORMATION TRANSFER

An introduction to input/output automata
[AD-A210831] 01 p0106 N90-10604
User's guide to the Space Environment Services Center geophysical alert broadcasts
[PB89-194617] 02 p0249 N90-11411
FEDIX: An on-line information service for universities and other research organizations: User's guide, version 2.0, release 1
[DE89-016695] 03 p0417 N90-12398
DOD Gateway Information System (DGIS) common command language: A retrospective on the introduction of prolog as the development tool
[AD-A211941] 03 p0418 N90-12400
Research in optical interconnection techniques
[AD-A214028] 07 p0993 N90-15739
Investigation of IGES for CAD/CAE data transfer 08 p1157 N90-16702
Federal scientific and technical information in an electronic age: Opportunities and challenges
[PB90-114414] 09 p1295 N90-17505
An adaptive ARQ (Automatic Repeat Request) strategy for packet switching data communication networks
[AD-A216597] 11 p1497 N90-18615
Low earth orbiting satellite for international information exchange system
[DE90-007186] 12 p1615 N90-19292
High throughput data communication system
[AD-D014342] 12 p1642 N90-19432
High speed modem
[AD-D014319] 12 p1698 N90-19750
Weather data dissemination to aircraft 14 p1907 N90-20934
Electronic transfer of information applications in the Societe Aerospatiale 15 p2179 N90-22454
NASA's experience in the international exchange of scientific and technical information in the aerospace field
[NASA-TM-103093] 19 p2764 N90-25704
Minimization of the cost of information transfer in HF spread spectrum transmission 20 p2848 N90-26198
Helping America compete: The role of Federal scientific and technical information
[OTA-CIT-454] 21 p3086 N90-27549
The role of the US government technical report in aeronautics: An exploratory study
[NASA-TM-893470] 21 p3087 N90-27553
Advanced retrieval assistance for the DGIS gateway
[AD-A221592] 21 p3087 N90-27558
Technology utilization: Managing the transfer of NASA aerospace technology to other industries 22 p3257 N90-28446
Multisensor evaluation framework
[AD-A224271] 24 p3522 N90-29913

INFORMATION TRANSMISSION

U DATA TRANSMISSION

INFRARED ABSORPTION

Effects of coherent scattering on infrared absorption in doped semiconductors
[AD-A210224] 01 p0131 N90-10756
Infrared water vapor continuum absorption: New atmospheric electrical measurements and theory
[AD-A212594] 04 p0519 N90-12994
Infrared diagnostics for interstellar solid state chemistry 11 p1580 N90-19103
Infrared absorption study of zinc-doped silicon
[DE90-007779] 13 p1771 N90-20164
Infrared absorption spectroscopy and chemical kinetics of free radicals
[DE90-009469] 15 p2067 N90-21837
A temperature-dependent regular infrared band model for absorption and dispersion 15 p2083 N90-21927
Infrared absorption gas sensor for the detection of HCl in launch vehicle exhaust clouds 16 p2209 N90-22600
FT-IR spectroscopic studies of polycyclic aromatic hydrocarbons 21 p3095 N90-27592

INFRARED ASTRONOMY

Analysis of nearly simultaneous X-ray and optical observations of active galactic nuclei 01 p0139 N90-10806
Automatic classification of spectra from the Infrared Astronomical Satellite (IRAS)
[NASA-RP-1217] 01 p0140 N90-10807
Aspects of the development of a 1-5 micron infrared camera for astronomy 02 p0290 N90-11656
Integrating detectors and their application to infrared astronomy 02 p0290 N90-11659
Three-meter balloon-borne telescope 05 p0601 N90-13490
Interstellar medium and infrared emission of the galactic disk 05 p0661 N90-13862
Interplanetary dust close to the Sun (F corona): Its observation in the visible and infrared by a rocket-borne coronagraph 05 p0661 N90-13864
Activities report of the Institute of Interplanetary Stellar Physics
[IFSI-89-8] 09 p1298 N90-17520
Report on scientific activity and funds management for 1988
[IFSI-89-9] 09 p1298 N90-17521
Activities report of the Institute of Interplanetary Stellar Physics
[IFSI-88-22] 10 p1445 N90-18339
Scientific activity programs for 1988-1990
[IFSI-88-23] 10 p1445 N90-18340
Scientific activity program for 1989
[IFSI-89-10] 10 p1445 N90-18341
Detecting extended solar system structures with COBE (Cosmic Background Explorer)
[AD-A216380] 10 p1447 N90-18349
Infrared Spectroscopy in Astronomy
[ESA-SP-290] 11 p1578 N90-19084

Interstellar extinction in the infrared
11 p1579 N90-19095
Infrared diagnostics for interstellar solid state chemistry
11 p1580 N90-19103
Molecular hydrogen in the HII region G333.6-0.2
11 p1583 N90-19121
Infrared spectroscopy of novae and related objects
11 p1583 N90-19123
Infrared spectroscopy of supernova 1987A
11 p1583 N90-19124
High resolution infrared spectroscopy of symbiotic stars
11 p1583 N90-19125
Ice grains in the dust disk of the bipolar nebula M 1-92
11 p1584 N90-19127
Dust in planetary nebulae: IRSPEC observations in the 3.0 micron-3.8 micron range
11 p1584 N90-19132
JCMT observations of the circumstellar envelope IRC+10216
11 p1585 N90-19138
Mathematics and physics studies: Multi-project support
[AD-A218208] 13 p1869 N90-20723
Mark 3 interferometer
[AD-A217188] 13 p1902 N90-20912
Proceedings of the Third Infrared Detector Technology Workshop
[NASA-TM-102209] 14 p1975 N90-21313
Discovery of low mass objects in Taurus
14 p1978 N90-21329
Infrared ground-based astronomy with the Hughes 256 X 256 PtSi array
14 p1978 N90-21331
Stressed detector arrays for airborne astronomy
14 p1978 N90-21332
Preliminary results on two-dimensional interferometry of HL Tau
14 p1979 N90-21335
Short wavelength HgCdTe staring focal plane for low background astronomy applications
14 p1979 N90-21336
Introduction to the Infrared Space Observatory (ISO)
14 p1979 N90-21340
SIRTF in high earth orbit
14 p1980 N90-21345
SOFIA: Stratospheric Observatory for Infrared Astronomy
14 p1980 N90-21346
Ultraviolet and infrared studies of Be stars
16 p2329 N90-23275
Complementary information from mm-wave-, infrared-, and gamma ray astronomy
16 p2334 N90-23299
Dipole analysis on EGRET data of extragalactic gamma ray background radiation
16 p2337 N90-23322
Multifrequency observation of blazars
19 p2786 N90-25857
Recent high resolution laboratory determinations of line broadening and intensity parameters: PH3, CH3D, and CO2
20 p2944 N90-26751
SIRTF: Probing the dark corners of the galaxy
21 p3091 N90-27577
Infrared mapping with a two-dimensional infrared array
[AD-A221938] 21 p3096 N90-27596
Infrared observations of the solar system in support of Large Aperture Infrared Telescope (LARITS): Calibration
[AD-A222222] 21 p3097 N90-27597
Infrared observations of the solar system in support of Large Aperture Infrared Telescope (LARITS): Calibration. Appendices
[AD-A222245] 21 p3097 N90-27598
Quantifying the FIR interaction enhancement in paired galaxies
[DE90-627485] 23 p3412 N90-29281

INFRARED ASTRONOMY SATELLITE
Telescope structure for cryogenic application
02 p0180 N90-11019
IRAS observations of the extended galactic objects Cas A and W80
02 p0290 N90-11657
Image enhancement using the IRAS (Infrared Astronomy Satellite) survey data
[AD-A213811] 07 p0950 N90-15496
Outflows in high mass star-forming regions
08 p1149 N90-16657
Polycyclic aromatic hydrocarbons in the infrared spectra of IRAS sources
11 p1581 N90-19105
IRAS LRS spectra of extended objects: The Crab nebula
11 p1581 N90-19107
AFGL ten micron mosaic array spectrometer: Recent results
14 p1978 N90-21333
The molecular cloud content of early type galaxies. 2: A molecular ring in NGC 404
[PB90-124348] 14 p2039 N90-21695
Implications of the IRAS data for galactic gamma ray astronomy and EGRET
16 p2334 N90-23300
On planetary nebulae as sources of carbon dust: Infrared emission from planetary nebulae of the galactic halo
21 p3093 N90-27583
Optical imaging of IRAS galaxies: The evolution of infrared-bright galaxies
22 p3261 N90-28465
Implications of the IRAS data for galactic gamma-ray astronomy and EGRET
[NASA-TM-103452] 22 p3261 N90-28466
An infrared sky model based on the IRAS point source data
[NASA-CR-177526] 23 p3409 N90-29265

INFRARED DETECTORS
NT FLIR DETECTORS
NT INFRARED RADIOMETERS
Laterally stacked Schottky diodes for infrared sensor applications
[NASA-CASE-NPO-17426-1-CU]
01 p0058 N90-10329
Offaxis radiance studies for infrared sensors
[AD-A210790] 02 p0275 N90-11570
Integrating detectors and their application to infrared astronomy
02 p0290 N90-11659
Improved pattern recognition techniques for real time operation
[AD-A211395] 03 p0324 N90-11840
Vanadium dioxide protective devices
[AD-A212018] 03 p0332 N90-11887
Infrared detector array
[AD-D014170] 03 p0350 N90-11997
Infrared temperature measurement with automatic consideration of emissivity
[ESA-TT-1131] 03 p0351 N90-12008
Development of microstructured DH diode lasers and detectors for the near and medium IR spectral domain using molecular beam epitaxy
[IPM-15/1988] 03 p0354 N90-12023
Readout and signal conditioning for a linear pyroelectric array
[RSRE-MEMO-4102] 04 p0504 N90-12905
Photoelectron pumped phosphors
[AD-A213202] 04 p0505 N90-12912
Status of direct detector and array development
05 p0596 N90-13464
The infrared spectrograph during the SIRTF pre-definition phase
[NASA-CR-183234] 05 p0644 N90-13759
Discussion of factors affecting the sensitivity of IR imaging sensors, particularly focal plane mosaic arrays --- staring mosaic arrays
[FOA-C-30536-3.1] 05 p0700 N90-14101
Determination of the heat transfer coefficients in separated flows using an infrared camera
08 p1081 N90-16257
Enhanced performance IR focal plane arrays using adaptive subtraction
[RSRE-MEMO-4286] 08 p1123 N90-16502
Ground-based deep-space LADAR for satellite detection: A parametric study
[AD-A215673] 09 p1228 N90-17126
Adaptive multiple-band CFAR (Constant-False-Alarm-Rate) detection of an optical pattern with unknown spectral distribution
[AD-A214754] 09 p1281 N90-17429
Infrared target detection: Signal and noise sensitivity analysis
[AD-A215707] 09 p1282 N90-17436
Spectroscopic techniques for the analysis of CdTe substrates used for the growth of HgCdTe
[AD-A214545] 09 p1288 N90-17466
An update of commercial infrared sensing and imaging instruments
10 p1366 N90-17920
Current status of InAsSb strained layer superlattice infrared detectors: Demonstration of a high detectivity, 10 micron photodiode
[DE90-000800] 10 p1434 N90-18276
Performance parameter characterisation of various types of IR single element detectors
11 p1586 N90-19161
Contact formation on (Hg,Cd) Te
[AD-A217088] 12 p1723 N90-19900
Modification, testing, and calibration of infrared search and target designator hardware received from NSWC
[AD-A217920] 13 p1889 N90-20837
NRL hybrid reliability. Physics of failure initial study
[AD-A217986] 13 p1898 N90-20893
Proceedings of the Third Infrared Detector Technology Workshop
[NASA-TM-102209] 14 p1975 N90-21313
The potential for high performance HgCdTe arrays at 4 microns
14 p1976 N90-21320
Extrinsic germanium Blocked Impurity Bank (BIB) detectors
14 p1976 N90-21322
Common source cascode amplifiers for integrating IR-FPA applications
14 p1977 N90-21324
Reduction and analysis techniques for infrared imaging data
14 p1977 N90-21328
Stressed detector arrays for airborne astronomy
14 p1978 N90-21332
Design and status of the detector block for the ISO-SWS
14 p1980 N90-21341
SOFIA: Stratospheric Observatory for Infrared Astronomy
14 p1980 N90-21346
Laboratory characterization of direct readout Si:Sb and Si:Ga infrared detector arrays
14 p1980 N90-21347
Improved Si:As BIBIB (Back-Illuminated Blocked-Impurity-Band) hybrid arrays
14 p1981 N90-21349
HCl Vapor Characterization and Detection. JANNAF Safety and Environmental Protection Subcommittee Workshop
[AD-A216252] 16 p2208 N90-22596
Direct implantation process development and characterization in advanced Hg(1)-(x)Cd(x) Te EPI layers
[AD-A219133] 16 p2324 N90-23252
Negative electron affinity for infrared detection
[AD-A218816] 17 p2395 N90-23639
A PC-based imaging system for the Naval Postgraduate School Infrared Search and Target Designation (NPS-IRSTD) system
[AD-A220109] 17 p2448 N90-23955
Improving the performance of InAs(1-x)Sb(x)/InSb infrared detectors grown by metal organic chemical vapor deposition
[DE90-009743] 18 p2625 N90-24956
Infrared fiber-optical temperature sensor
[AD-D014519] 19 p2693 N90-25321
Optical motion detector detecting visible and near infrared light
[AD-D014515] 19 p2758 N90-25671
Multicolor infrared photodetector
[AD-D014511] 20 p2865 N90-26297
Reproduction of GMS IR calibration table
21 p3026 N90-27215
Infrared mapping with a two-dimensional infrared array
[AD-A221938] 21 p3096 N90-27596
Infrared observations of the solar system in support of Large Aperture Infrared Telescope (LARITS): Calibration
[AD-A222222] 21 p3097 N90-27597
Infrared observations of the solar system in support of Large Aperture Infrared Telescope (LARITS): Calibration. Appendices
[AD-A222245] 21 p3097 N90-27598
Quantum well infrared detectors 1: Some calculations of their optical properties
[RSRE-MEMO-4363] 24 p3547 N90-30062
Integrated technology in MCT/GaAs and MCT/Si for medium and long wavelength infrared
[AD-A223557] 24 p3552 N90-30100

INFRARED FILTERS
CdTe buffered GaAs thin-slab IR waveguide modulators and T/R filter
[AD-A215999] 12 p1651 N90-19488

INFRARED HORIZON SCANNERS
U INFRARED SCANNERS

INFRARED IMAGERY
A compilation of digitized satellite imagery of the Gulf Stream (1982, 1983, and 1985)
[AD-A210243] 01 p0082 N90-10467
Adaptive tracking of maneuvering targets based on IR image data
02 p0149 N90-10853
Parallel processing on transputer arrays for the recognition of objects in infrared images
[RSRE-MEMO-4197] 03 p0389 N90-12217
Enhancement of infrared thermographic imagery: Local smoothing and time-based interpolation
[ONERA-RT-8/7254-SN] 04 p0555 N90-13232
Discussion of factors affecting the sensitivity of IR imaging sensors, particularly focal plane mosaic arrays --- staring mosaic arrays
[FOA-C-30536-3.1] 05 p0700 N90-14101
A rough transform technique for extracting lead features from sea ice imagery
[AD-A212758] 06 p0801 N90-14666
Rainfall estimation over Africa using satellite data
06 p0815 N90-14742
High resolution imaging by phase retrieval and discrimination using speckle, volume 1
[AD-A214243] 07 p0919 N90-15317
Measurement of optical radiations in spacecraft environments
[AD-A213814] 07 p0950 N90-15497
Evaluation of a simple algorithm for estimating infrared signatures from multi-pixel to sub-pixel targets applied to AGA thermovision imagery
[AD-A214103] 07 p0976 N90-15639
Investigation of ablation phenomena using IR thermography in a hypersonic wind tunnel
08 p1081 N90-16258
Simulation of synthetic aperture radar 2: Simulating SAR (Synthetic Aperture Radar) using the advanced visual technology system
[AD-A213659] 09 p1204 N90-16976
Adaptive multiple-band CFAR (Constant-False-Alarm-Rate) detection of an optical pattern with unknown spectral distribution
[AD-A214754] 09 p1281 N90-17429
Staring focal plane array system modeling
[AD-A215712] 09 p1283 N90-17438

Low speed flowfield characterization by infrared measurements of surface temperatures
10 p1306 N90-17556
Proceedings of the Second Noncontact Temperature Measurement Workshop
[NASA-CR-181289] 10 p1362 N90-17894
Use of anomolous thermal imaging effects for multi-mode systems control during crystal growth
10 p1365 N90-17910
An update of commercial infrared sensing and imaging instruments 10 p1366 N90-17920
Development of an infrared imaging system for the surface tension driven convection experiment
10 p1367 N90-17922
NCTM workshop splinter session, IR thermal measurement instruments 10 p1367 N90-17923
Infrared spectroscopy and imaging of supernova remnants 11 p1580 N90-19104
IRCAM observations of the Reipurth 50 IR source
11 p1583 N90-19119
An infrared imaging Fabry-Perot study of the galactic centre 11 p1586 N90-19142
Reliability testing of the Hughes temperature controlled 1/4 watt split cycle cryogenic cooler (HD-1045 (V)/UA)
[AD-A216696] 12 p1641 N90-19426
The utilization of an infrared imaging system as a cooling slot blockage detector in the inspection of a transpiration cooled nozzle
[NASA-TM-102608] 12 p1663 N90-19555
ARGUS/LLNL IR camera calibration and characterization
[AD-A217076] 12 p1664 N90-19563
Processing infrared images for target detection: A literature study
[IZF-1988-12] 12 p1715 N90-19847
Correlation of AVHRR imagery with sub-surface features in California current
[AD-A218184] 13 p1848 N90-20607
Proceedings of the 13th International Congress on Instrumentation in Aerospace Simulation Facilities
[EOARD-LR-89-069] 14 p1929 N90-21046
Reduction and analysis techniques for infrared imaging data 14 p1977 N90-21328
An assessment of the CD-FLIR as an ARGUS sensor
[AD-A220841] 17 p2473 N90-24137
Infrared thermography at hypersonic channel H2K
18 p2490 N90-24235
Ground evaluation of seeding an in-flight wingtip vortex using infrared imaging flow visualization technique
18 p2639 N90-25035
HEAO-1 and IR observations of the X ray pulsar 1E2259+586 19 p2774 N90-25773
Meteorological Satellite Center Technical Note, no. 17, 1988
[ISSN-0388-9653] 21 p3028 N90-27213
Dust clouds Kosa from the east Asian dust storms in 1982-1988 as observed by the GMS satellite
21 p3028 N90-27214
Distribution and movement of smokes from forest fires that occurred along the boundary of the People's Republic of China and the USSR on April-May 1987
21 p3028 N90-27216
An experiment to make a new design of the Satellite Cloud Information Chart with the combination of visible and infrared data observed by the GMS
21 p3029 N90-27223
Gulfcasting: Dynamical forecast experiments for G ulf Stream rings and meanders
[AD-A221482] 21 p3032 N90-27238
Human factors and safety considerations of night vision systems flight using thermal imaging systems
[AD-A223226] 21 p3037 N90-27263
Infrared mapping with a two-dimensional infrared array
[AD-A221938] 21 p3096 N90-27596
Recognition of infrared images. Part 3: The effect of image processing with a size-contrast box filter on observation performance
[IZF-1989-39] 23 p3395 N90-29182
Thermal imaging assessment
[AD-A224400] 24 p3460 N90-29542

INFRARED INSPECTION

Temperature measurement during welding of solar cells and calibration of finite element models
10 p1342 N90-17774

INFRARED INSTRUMENTS

NT FLIR DETECTORS
NT INFRARED DETECTORS
NT INFRARED INTERFEROMETERS
NT INFRARED RADIOMETERS
NT INFRARED SCANNERS
NT INFRARED SPECTROMETERS
Solid-state phase equilibria in the ZnS-Ga2S3 system
[AD-A213944] 07 p0906 N90-15238
IRCAM observations of the Reipurth 50 IR source
11 p1583 N90-19119
Calculation of IR propagation statistics in the eastern Atlantic for surveillance system performance assessment 15 p2085 N90-21938
Atmospheric modelling studies: A modelling comparison between IR and millimetric atmospheric propagation
15 p2086 N90-21941
Conceptual design study for Infrared Limb Experiment (IRLE)
[NASA-CR-186950] 21 p2968 N90-26869
Electronics design of the infrared/ultrasonic sensing for a robot gripper
[PB90-180383] 21 p3010 N90-27109
Tracking a head-mounted display in a room-sized environment with head-mounted cameras
[AD-A222545] 21 p3037 N90-27266

INFRARED INTERFEROMETERS

An infrared imaging Fabry-Perot study of the galactic centre 11 p1586 N90-19142
Mark 3 interferometer
[AD-A217188] 13 p1902 N90-20912
An analysis of the characteristics of atmospheric profiles obtained with the High resolution Interferometer Sounder (HIS) 24 p3488 N90-29716

INFRARED LASERS

Development of microstructured DH diode lasers and detectors for the near and medium IR spectral domain using molecular beam epitaxy
[IPM-15/1988] 03 p0354 N90-12023
Tunable Solid State Lasers conference edition: Tunable Solid State Lasers Topical Meeting
[AD-A212292] 04 p0506 N90-12920
Development of X diagnostics with 1 Gw laser pulses
06 p0786 N90-14578
A compact, high-powered far-infrared (FIR) laser
[DE89-016786] 06 p0789 N90-14597
Laser detection and discrimination system
[AD-D014301] 07 p0937 N90-15426
Development of a solar-powered infrared injection laser microminiature transmitting system
[DE90-005672] 10 p1389 N90-18034
Cloud hole-boring with infrared lasers: Theory and experiment
[DE90-006519] 11 p1515 N90-18723
Potential biomedical application of the Los Alamos infrared free-electron laser: DNA spectroscopy
[DE90-006505] 12 p1667 N90-19575
Laser enhanced chemical reactions
[DE90-008273] 13 p1807 N90-20377
Development of mid-infrared solid state lasers for spaceborne lidar
[NASA-CR-185095] 15 p2103 N90-22031
A compact, high-powered Far-Infrared (FIR) laser
[DE90-009996] 20 p2867 N90-26312
Laser diagnostics of plasma thrusters
[AD-A221682] 21 p3079 N90-27506

INFRARED MASERS

U INFRARED LASERS

INFRARED PHOTOGRAPHY

ARGUS/LLNL IR camera calibration and characterization
[AD-A217076] 12 p1664 N90-19563
Investigation of air transportation technology at the Massachusetts Institute of Technology, 1988-1989
14 p1905 N90-20922
National mapping program. Fact sheet: Black and white photographs. NHAP (National High Altitude Photography Program)
[PB90-185042] 21 p3015 N90-27139
Infrared mapping with a two-dimensional infrared array
[AD-A221938] 21 p3096 N90-27596

INFRARED PHOTOMETRY

Short time scale variability of the BL Lac object OJ 287 in the near-infrared
[IFSI-89-3] 08 p1140 N90-16603
Tailorable infrared sensing device with strain layer superlattice structure
[NASA-CASE-NPO-16617-2-CU]
09 p1227 N90-17118
Photometry of variable AFGL sources
[AD-A216938] 11 p1594 N90-19185
An optical and infrared study of blazars
12 p1728 N90-19930
Photometric monitoring of early type emission line stars 15 p2184 N90-22478

INFRARED RADAR

Front range lidar, aircraft, and balloon experiment
[PB90-225301] 22 p3212 N90-28218
On the use of IR lidar and K(sub a)-band radar for observing cirrus clouds 22 p3228 N90-28305

INFRARED RADIATION

NT FAR INFRARED RADIATION
NT NEAR INFRARED RADIATION
Millimeter-wave/infrared rectenna development at Georgia Tech 01 p0028 N90-10147
Biomedical studies with the free electron laser
[AD-A208927] 01 p0091 N90-10519
Infrared temperature measurement with automatic consideration of emissivity
[ESA-TT-1131] 03 p0351 N90-12008
Infrared backscattering 03 p0364 N90-12083
Mark-3 interferometer
[AD-A213155] 04 p0505 N90-12911
The effects of seasonal and latitudinal earth infrared radiance variations on ERBS attitude control
05 p0586 N90-13414
Development of mid-infrared solid state lasers for spaceborne lidar
[NASA-CR-183290] 05 p0647 N90-13772
CANOES 2: Dynamics of atmospheric infrared thermochemical excitation, volume 1
[AD-A213341] 05 p0867 N90-13897
CANOES 2: Dynamics of atmospheric infrared thermochemical excitation, volume 2
[AD-A213342] 05 p0667 N90-13898
CANOES 2: Dynamics of atmospheric infrared thermochemical excitation, volume 3
[AD-A213343] 05 p0867 N90-13899
CANOES 2: Dynamics of atmospheric infrared thermochemical excitation, volume 4
[AD-A213344] 05 p0667 N90-13900
Weather satellite and computer modeling approaches to assessing propagation over marine environments
06 p0764 N90-14443
Solid-state phase equilibria in the ZnS-Ga2S3 system
[AD-A213944] 07 p0906 N90-15238
Description of SHARC: The Strategic High-Altitude Radiance Code
[AD-A213806] 07 p0961 N90-15555
Anomalous absorption by atmospheric water vapor and stabilized water fogs in the infrared and CM-wave regions
[AD-A214202] 07 p0964 N90-15572
A statistical model of the infrared signature of a wind roughened sea
[AD-A214531] 09 p1249 N90-17245
Structural alterations in the cornea from exposure to infrared radiation
[AD-A215340] 09 p1253 N90-17269
Principles and formulation of solar reflecting and low infrared emitting coatings for defence use
[MRL-TR-89-2] 10 p1358 N90-17874
Infrared thermal imaging figures of merit
10 p1364 N90-17904
IR optical fiber-based noncontact pyrometer for drop tube instrumentation 10 p1365 N90-17909
NCTM workshop splinter session, IR thermal measurement instruments 10 p1367 N90-17923
Safety evaluation of infrared lamp power output for oculometer eye/head tracker system
[AD-A215809] 10 p1411 N90-18138
Measurement of radiation property of long infrared emitter and examination of infrared radiation heating process
[DE90-741971] 10 p1425 N90-18222
Reflectance modulation with electrochromic Li(sub x)WO(3) films
[DE90-004571] 10 p1435 N90-18279
Interrelationship of spatial and radiometric resolution in the thermal infrared band
[INPE-4860-TDL/371] 11 p1523 N90-18771
Proceedings of the 6th Conference on Hot Carriers in Semiconductors
[AD-A215978] 11 p1589 N90-19032
An advanced cooled grating spectrometer for UKIRT-CGS4 11 p1589 N90-19165
Photometry of variable AFGL sources
[AD-A216938] 11 p1594 N90-19185
Development of the blackbody probe type pyrometer, part 1. Experimental study on the fundamental characteristics
[DE89-782288] 12 p1663 N90-19553
Atmospheric Radiation Measurement Program plan
[DE90-006349] 12 p1689 N90-19705
Thermal infrared scene simulation
[DE90-006900] 12 p1714 N90-19845
Conference digest: Thirteenth International Conference on Infrared and Millimeter Waves, volume 1039
[AD-A217343] 13 p1793 N90-20291
Study of new technique of solid combustible materials to determination of volatile elements by flame atomic absorption spectrophotometry
[DE90-612907] 14 p1947 N90-21147
Common source cascode amplifiers for integrating IR-FPA applications 14 p1977 N90-21324
Experience with the UKIRT InSb array camera
14 p1977 N90-21327
High resolution imaging of the Venus night side using a Rockwell 128x128 HgCdTe array
14 p1978 N90-21330
Infrared ground-based astronomy with the Hughes 256 X 256 PtSi array 14 p1978 N90-21331

Short wavelength HgCdTe staring focal plane for low background astronomy applications
14 p1979 N90-21336
New water vapor masers in the Southern Hemisphere
[INPE-4844-PRE/1473] 14 p2037 N90-21689
Atmospheric Propagation in the UV, Visible, IR, and mm-Wave Region and Related Systems Aspects
[AGARD-CP-454] 15 p2079 N90-21907
The Mediterranean marine environment and its effects on aerosols and infrared transmission
15 p2079 N90-21909
Millimetric, infrared, and optical propagation studies over a 500 m path 15 p2080 N90-21913
LOWTRAN 7: Status, review, and impact for short-to-long-wavelength infrared applications
15 p2081 N90-21917
Infrared propagation in the air-sea boundary layer
15 p2083 N90-21926
Technique for selecting an aerosol model useful for infrared atmospheric transmittance calculations
15 p2085 N90-21934
Fast method for computing infrared transmission, computation examples 15 p2086 N90-21942
The calculation of infrared limb emission by ozone in the terrestrial middle atmosphere
15 p2125 N90-22151
The modeling of IRAS detections of classical novae and related objects 15 p2185 N90-22482
A search for additional parameters in the infrared luminosity/21 cm line-width relation for spiral galaxies in clusters of galaxies 16 p2328 N90-23274
Infrared coronal line novae 16 p2339 N90-23328
Cosmic Background Explorer (COBE) press kit
[P89-10172] 17 p2364 N90-23459
Transmission of infrared radiation through the Australian atmosphere: Predictions using the LOWTRAN model
[AD-A220340] 17 p2428 N90-23835
IR and millimeter waves: Properties, models, and examples of ground target applications
[FOA-C-30541-3.3] 18 p2543 N90-24516
Reports from the German Meteorological Service. No. 178: Climatological research about the atmospheric counter radiation and comparison of calculation processes by means of measurements in the Upper Rhine Valley (Fed. Republic of Germany) during a year
[ISBN-3-88148-249-0] 18 p2582 N90-24704
Feasibility of using lasers and infrared heaters as UNREP icing countermeasures
[AD-A219031] 19 p2695 N90-25333
Satellite material contaminant optical properties
19 p2732 N90-25529
The 27-28 October 1986 FIRE IFO cirrus case study: Cirrus parameter relationships derived from satellite and lidar data
[NASA-TM-103469] 20 p2890 N90-26447
Implementation of sensor and control designs for bioregenerative systems
[NASA-CR-186655] 20 p2897 N90-26479
Development of eye-safe lidar for aerosol measurements
[NASA-CR-186905] 20 p2901 N90-26503
Infrared line parameters at low temperatures relevant to planetary atmospheres 20 p2944 N90-26753
Conceptual design study for Infrared Limb Experiment (IRLE)
[NASA-CR-186950] 21 p2968 N90-26869
Description of SAFIRE for ISES
21 p3016 N90-27148
An outline for the RTNEPH infrared atmospheric water vapor attenuation study
[AD-A221753] 21 p3027 N90-27209
The possible presence of interstellar PAHs in meteorites and interplanetary dust particles
21 p3092 N90-27579
Laboratory simulation of interstellar grain chemistry and the production of complex organic molecules
21 p3092 N90-27580
On planetary nebulae as sources of carbon dust: Infrared emission from planetary nebulae of the galactic halo
21 p3093 N90-27583
FT-IR spectroscopic studies of polycyclic aromatic hydrocarbons 21 p3095 N90-27592
Infrared observations of the solar system in support of Large Aperture Infrared Telescope (LARITS): Calibration
[AD-A222222] 21 p3097 N90-27597
Thermal response of large area high temperature superconducting YBaCuO infrared bolometer
22 p3146 N90-27839
The application of infrared thermography to the nondestructive testing of composite materials
22 p3187 N90-28084
Spatial scales of cirrus cloud properties
22 p3222 N90-28275
Interpretation of cirrus cloud properties using coincident satellite and lidar data during the FIRE cirrus IFO
22 p3223 N90-28276
A comparative study of infrared radiance measurements by an ER-2 based radiometer and the LANDSAT 5 Thematic Mapper (TM-6) 22 p3226 N90-28294
Radiative properties of cirrus clouds inferred from broadband measurements during FIRE
22 p3226 N90-28295
Transient cooling of a hot surface by droplets evaporation
[PB90-227968] 23 p3325 N90-28799
Star formation and the distribution of HI and infrared emission in M51
[NASA-CR-186928] 23 p3408 N90-29262
On the infrared behaviour of some non-Minkowskian quantum fields 23 p3410 N90-29273
Pointing control system for the Teal Ruby experiment
24 p3429 N90-29370
Theoretical and experimental comparison of infrared and visible laser scattering from a variety of surface types
[RSRE-MEMO-4348] 24 p3474 N90-29636
Measurements of the high altitude infrared characteristics of the atmosphere
[AD-A224401] 24 p3491 N90-29728

INFRARED RADIOMETERS
NT ADVANCED VERY HIGH RESOLUTION RADIOMETER
Proposed concept for the visible/infrared imaging radiometer for second generation Meteosat
[ETN-90-96145] 08 p1123 N90-16503
The utilization of an infrared imaging system as a cooling slot blockage detector in the inspection of a transpiration cooled nozzle
[NASA-TM-102608] 12 p1663 N90-19555
ARGUS/LLNL IR camera calibration and characterization
[AD-A217076] 12 p1664 N90-19583
HgCdTe 256x256 NWIR FPA
14 p1981 N90-21348
IR and millimeter waves: Properties, models, and examples of ground target applications
[FOA-C-30541-3.3] 18 p2543 N90-24516
Calibration of the visible and near-infrared channels of the LANDSAT-5 Thematic Mapper using high-altitude aircraft measurements
[NASA-TM-102185] 21 p3015 N90-27138
High resolution infrared measurements
22 p3221 N90-28265
Infrared thermography 24 p3421 N90-29325

INFRARED SCANNERS
Debris/ice/TPS assessment and photographic analysis for shuttle mission STS-31R
[NASA-TM-102790] 20 p2819 N90-26040
Resonant coupling through a slot to a loaded cylindrical cavity: Experimental results
[AD-A223000] 20 p2922 N90-26631

INFRARED SIGNATURES
Thermal radiation from terrain: Measurements and first results
[FOA-C-30525-3.1] 02 p0236 N90-11342
Design and tests of simple, inexpensive optical beacon for use on small satellites
[AD-A213325] 04 p0555 N90-13238
Evaluation of a simple algorithm for estimating infrared signatures from multi-pixel to sub-pixel targets applied to AGA thermovision imagery
[AD-A214103] 07 p0976 N90-15639
A statistical model of the infrared signature of a wind roughened sea
[AD-A214531] 09 p1249 N90-17245
Adaptive multiple-band CFAR (Constant-False-Alarm-Rate) detection of an optical pattern with unknown spectral distribution
[AD-A214754] 09 p1281 N90-17429
Mathematics and physics studies: Multi-project support
[AD-A218208] 13 p1869 N90-20723
Search of the optical counterpart of the X rays source 1H 0521+373 19 p2780 N90-25815

INFRARED SOURCES (ASTRONOMY)
NT INFRARED STARS
Short time scale variability of the BL Lac object OJ 287 in the near-infrared
[IFSI-89-3] 08 p1140 N90-16603
Outflows in high mass star-forming regions
08 p1149 N90-16657
Photometry of variable AFGL sources
[AD-A216938] 11 p1594 N90-19185
Multiwavelength observations of BL Lacertae
19 p2791 N90-25886

INFRARED SPACE OBSERVATORY (ISO)
Telescope structure for cryogenic application
02 p0180 N90-11019
The service module structure of the IOS spacecraft development and qualification program
02 p0181 N90-11021
Report on ESA's scientific satellites
[ESA-SP-1110] 04 p0463 N90-12649
The ISO solar generator: Solar cells and OSR mixed
10 p1341 N90-17767
Design development and qualification of a solar array with OSRs (SSM) bonded to the ISO spacecraft rigid sunshield 10 p1341 N90-17768
Infrared diagnostics for interstellar solid state chemistry 11 p1580 N90-19103
The ISO short wavelength spectrometer
11 p1589 N90-19162
The Infrared Space Observatory
11 p1589 N90-19163
Spectrophotometry of dust with Isophot
11 p1589 N90-19164
Isophot-S, a low resolution 2.5 to 12 microns spectrometer for ISO 11 p1589 N90-19167
Proceedings of the Third Infrared Detector Technology Workshop
[NASA-TM-102209] 14 p1975 N90-21313
Introduction to the Infrared Space Observatory (ISO)
14 p1979 N90-21340
Design and status of the detector block for the ISO-SWS 14 p1980 N90-21341
Status of the isophot detector development
14 p1980 N90-21342
ISO/LWS: Detector status 14 p1980 N90-21343
ISO camera array development status
14 p1980 N90-21344
ISO attitude and orbit control subsystem
[REPT-892-440-104] 17 p2366 N90-23467
Wearing of cryomechanisms at 4 K
[REPT-892-440-103] 17 p2473 N90-24139
Wearing of cryomechanisms at 4 K
18 p2537 N90-24476
Further development of the cryogenic Fabry-Perot interchange mechanism for ISO LWS
18 p2539 N90-24492

INFRARED SPECTRA
Multiple internal reflection Fourier transform infrared spectroscopy studies of thiocyanate adsorption on silver and gold
[AD-A210245] 01 p0041 N90-10223
Automatic classification of spectra from the Infrared Astronomical Satellite (IRAS)
[NASA-RP-1217] 01 p0140 N90-10807
Vibrational spectroscopic study of the kaolinite-hydrazine intercalation complex
02 p0204 N90-11166
Infrared spectrometry of aerosols
[AD-A213303] 04 p0473 N90-12713
A high-resolution atlas of the infrared spectrum of the Sun and the Earth atmosphere from space: A compilation of ATMOS spectra of the region from 650 to 4800 cm (2.3 to 16 micron). Volume 1: The Sun
[NASA-RP-1224-VOL-1] 05 p0666 N90-13893
Propagation of sound in vibrationally excited nitrogen and hydrogen gas mixtures
[AD-A213002] 05 p0696 N90-14073
A study of the infrared emission of galactic supernova remnants 06 p0861 N90-15006
Cloud phase discrimination by near-infrared remote sensing 08 p1090 N90-16310
Development of a solar-powered infrared injection laser microminiature transmitting system
[DE90-005672] 10 p1389 N90-18034
The 2.7/4.3 micron CO2 branching ratio measurement
[AD-A215952] 11 p1534 N90-18830
Techniques for measurement of the optical properties of materials
[DE90-006902] 11 p1566 N90-19014
A unified model for the 3.28 micron and 3.4 micron spectral feature in the interstellar medium and in comets
11 p1579 N90-19092
Interpretation of the 10 micron and 20 micron absorption bands in comets, the interstellar medium, and in an external galaxy 11 p1579 N90-19093
Interstellar extinction in the infrared
11 p1579 N90-19095
Spectropolarimetry as a diagnostic of the interstellar medium 11 p1579 N90-19096
Airborne observations of the infrared emission bands
11 p1580 N90-19101
Polycyclic aromatic hydrocarbons in the infrared spectra of IRAS sources 11 p1581 N90-19105
IRAS LRS spectra of extended objects: The Crab nebula 11 p1581 N90-19107
Wide-beam balloon observations of the 157.7 microns (CII) line 11 p1581 N90-19108
A coal model for the carriers of the unidentified IR bands 11 p1581 N90-19110
Spectroscopy and physico-chemistry of CO:H2O and CO2:H2O ices 11 p1581 N90-19111
Mapping and spectroscopy of the 3.3 microns feature in Orion 11 p1582 N90-19112
An implication of the IR identification of PAHs: The heating of the diffuse is gas 11 p1582 N90-19113

The infrared spectral signature of star formation
11 p1582 N90-19114
Infrared diagnostics of interstellar shocks
11 p1582 N90-19115
Infrared line emission from high-velocity outflows in star-forming regions 11 p1582 N90-19116
The excitation of molecular hydrogen and its significance 11 p1582 N90-19117
High-excitation lines of molecular hydrogen: A discriminant between shock models
11 p1582 N90-19118
Ice grains in the dust disk of the bipolar nebula M 1-92 11 p1584 N90-19127
IR spectrophotometry of bright carbon stars
11 p1584 N90-19131
Carbon monoxide in supernova 1987A
11 p1585 N90-19135
Predictions of infrared recombinations lines in stellar winds of hot stars 11 p1585 N90-19136
Infrared lines as probes of galactic structure
11 p1585 N90-19139
Evolutionary synthesis of the far-infrared emission in starburst galaxies 11 p1587 N90-19152
Infrared properties of five spiral galaxies
11 p1587 N90-19154
Far infrared fine structure lines in active galaxies
11 p1588 N90-19157
The optical properties of beryllium
[DE90-006372] 12 p1715 N90-19848
Evolution of ices and carbonaceous materials in the laboratory and in comets 12 p1739 N90-19998
Infrared absorption study of zinc-doped silicon
[DE90-007779] 13 p1771 N90-20164
Bibliography of spatial interferometry in optical astronomy
[NASA-TM-100754] 13 p1901 N90-20911
On the substitution of Sr ions at Y sites in YB(suba2)Cu3O(sub7-d)
[DE90-613395] 14 p2031 N90-21652
Experimental investigations of low-energy (4 to 40 eV) collisions of O(-)(P2) ions and O(P3) atoms with surfaces
19 p2732 N90-25530
Measurements of CH4, N2O, CO, H2O and O3 in the middle atmosphere by the ATMOS experiment on Spacelab 3
[NASA-TM-103476] 20 p2883 N90-26400
Infrared spectra of van de Waals complexes of importance in planetary atmospheres
20 p2943 N90-26749
Novel laser gain and time-resolved FTIR studies of photochemistry 20 p2945 N90-26756
Gaussian quadrature exponential sum modeling of near infrared methane laboratory spectra obtained at temperatures from 106 to 297 K
20 p2945 N90-26758
Measurements of the methane relaxation times for application to the infrared emission models of the upper atmospheres of outer planets and Titan
20 p2945 N90-26759
Resonance enhanced two-laser infrared multiple photon dissociation of gaseous ions
[AD-A221826] 21 p2970 N90-26879
SIRTF: Probing the dark corners of the galaxy
21 p3091 N90-27577
Laboratory simulation of interstellar grain chemistry and the production of complex organic molecules
21 p3092 N90-27580
Four techniques to measure complex refractive indices of liquids and solids at carbon dioxide laser wavelengths in the infrared spectral region
[AD-A222007] 22 p3180 N90-28043
Remote sounding through semi-transparent cirrus cloud 22 p3226 N90-28296
IR spectral characteristics of cirrus clouds
22 p3226 N90-28297
Infrared reflection-adsorption spectroscopy of the electrode/electrolyte solution interface: Optical considerations
[AD-A221935] 22 p3246 N90-28409
Spatial interferometry in optical astronomy
[NASA-RP-1245] 22 p3262 N90-28470
An infrared sky model based on the IRAS point source data
[NASA-CR-177526] 23 p3409 N90-29265
An analysis of the characteristics of atmospheric profiles obtained with the High resolution Interferometer Sounder (HIS) 24 p3488 N90-29716
Measurements of the high altitude infrared characteristics of the atmosphere
[AD-A224401] 24 p3491 N90-29728

INFRARED SPECTROMETERS

Improved pattern recognition techniques for real time operation
[AD-A211395] 03 p0324 N90-11840
Infrared spectrometry of aerosols
[AD-A213303] 04 p0473 N90-12713
The infrared spectrograph during the SIRTF pre-definition phase
[NASA-CR-183234] 05 p0644 N90-13759
Evaluation of the airborne visible-infrared imaging spectrometer for mapping subtle lithological variation
[NASA-CR-186213] 06 p0802 N90-14670
The visible channel of OMEGA-VIMS
[IFSI-89-14] 08 p1077 N90-16231
Evaluation of a commercial gas chromatography/matrix isolation-infrared spectrometer for quantitative analysis of priority pollutants
[DE90-006033] 11 p1484 N90-18542
Measurement of spectral emissivity by Fourier transform infrared spectrometer
[DE89-782319] 11 p1510 N90-18698
The ISO short wavelength spectrometer
11 p1589 N90-19162
The Infrared Space Observatory
11 p1589 N90-19163
An advanced cooled grating spectrometer for UKIRT-CGS4 11 p1589 N90-19165
Isophot-S, a low resolution 2.5 to 12 microns spectrometer for ISO 11 p1589 N90-19167
Infrared heterodyne spectroscopy of polyatomic molecules in circumstellar envelopes
12 p1736 N90-19980
Proceedings of the Third Infrared Detector Technology Workshop
[NASA-TM-102209] 14 p1975 N90-21313
High resolution imaging of the Venus night side using a Rockwell 128x128 HgCdTe array
14 p1978 N90-21330
Low noise HgCdTe 128 x 128 SWIR FPA for Hubble space telescope 14 p1979 N90-21337
Laboratory and telescope use of the NICMOS2 128 x 128 HgCdTe array 14 p1979 N90-21338
Future directions for NICMOS arrays
14 p1979 N90-21339
IR transition moments and collisional dynamics of vibrationally excited OH radicals via time-resolved laser absorption spectroscopy
[AD-A221005] 18 p2580 N90-24696
HIRIS performance study
[NASA-CR-186649] 20 p2878 N90-26375
Eos visible imagers 21 p3016 N90-27146
Absolute wind measurements in the lower thermosphere of Venus using infrared heterodyne spectroscopy
[NASA-CR-4290] 21 p3100 N90-27605
Workshop minutes on Remote Sensing of Hydrocarbons and Toxic Pollutants
[PB90-186370] 22 p3194 N90-28127

INFRARED SPECTROSCOPY

Attenuated total reflection FTIR spectroscopy for measuring interfacial reaction kinetics at silica surfaces
[AD-A210314] 01 p0041 N90-10224
Characterization of diamond films by thermogravimetric analysis and infrared spectroscopy
[AD-A210564] 01 p0050 N90-10288
Real-time observations of aerosol composition changes
[DE89-012382] 01 p0073 N90-10422
Forty-fourth symposium on molecular spectroscopy
[AD-A210752] 02 p0195 N90-11111
Atmospheric chemistry of the fuel hydrazines
02 p0203 N90-11158
A matrix-isolation FT-IR study of hydrazine
02 p0204 N90-11168
Low temperature spectroscope of hydrazine and ammonia complexes 02 p0205 N90-11169
Integrating detectors and their application to infrared astronomy 02 p0290 N90-11659
Improved pattern recognition techniques for real time operation
[AD-A211395] 03 p0324 N90-11840
Infrared spectrometry of aerosols
[AD-A213303] 04 p0473 N90-12713
Semiconductor measurement technology: Database for and statistical analysis of the interlaboratory determination of the conversion coefficient for the measurement of the interstitial oxygen content of silicon by infrared absorption
[PB89-221170] 04 p0558 N90-13253
Observations of stratospheric HCl: 1975-1985
[AERONOMICA-ACTA-A-349-1989]
05 p0666 N90-13892
Outlier detection in multivariate calibration
[DE90-001502] 07 p0982 N90-15672
Infrared Spectroscopy in Astronomy
[ESA-SP-290] 11 p1578 N90-19084
IR spectroscopy of planets and satellites; Venus, Mars, giant planets, and Titan 11 p1578 N90-19085
Infrared cometary spectroscopy
11 p1578 N90-19086
Measurements of the D/H ratio in planetary atmospheres by ground based infrared spectroscopy
11 p1578 N90-19088
The unidentified IR bands in laboratory, in interstellar medium, and in comets 11 p1578 N90-19089
Observations of CO on Mars in the infrared and millimetre range 11 p1578 N90-19090
Near infrared spectroscopy of Mars: Study of the surface mineralogy 11 p1579 N90-19091
A unified model for the 3.28 micron and 3.4 micron spectral feature in the interstellar medium and in comets
11 p1579 N90-19092
Infrared spectroscopy of dust
11 p1579 N90-19094
Chemistry on interstellar grains and implications for infrared spectroscopy 11 p1579 N90-19097
Dust continuum spectra from model HII regions
11 p1580 N90-19099
IR line emission from dense photodissociation regions
11 p1580 N90-19100
IR line emission from supernovae in molecular clouds
11 p1580 N90-19102
Infrared spectroscopy and imaging of supernova remnants 11 p1580 N90-19104
An almost total disjunction between emission and absorption dust features: What does it tell us?
11 p1581 N90-19106
Near infrared spectroscopy of the supernova remnant RCW103 11 p1581 N90-19109
Infrared line emission from high-velocity outflows in star-forming regions 11 p1582 N90-19116
The environment of young stellar objects studied by high-resolution infrared spectroscopy
11 p1583 N90-19120
Molecular hydrogen in the HII region G333.6-0.2
11 p1583 N90-19121
Planetary nebulae 11 p1583 N90-19122
Infrared spectroscopy of novae and related objects
11 p1583 N90-19123
Infrared spectroscopy of supernova 1987A
11 p1583 N90-19124
High resolution infrared spectroscopy of symbiotic stars 11 p1583 N90-19125
CO infrared bands in atmospheres of long-period variables 11 p1584 N90-19128
A survey of PAH emission in HII regions, planetary and proto-planetary nebulae 11 p1584 N90-19129
Unidentified infrared features in proto-planetary nebulae 11 p1584 N90-19130
Dust in planetary nebulae: IRSPEC observations in the 3.0 micron-3.8 micron range 11 p1584 N90-19132
Near infrared (1-4 micron) spectroscopy of SN1987A
11 p1584 N90-19133
Infrared spectroscopy of the central few parsecs of the galaxy 11 p1585 N90-19140
Stellar kinematics in the galactic centre
11 p1586 N90-19141
Near infrared spectroscopy of active galaxies
11 p1586 N90-19143
Near-infrared spectroscopy of starburst and interacting galaxies 11 p1586 N90-19144
Spectroscopy of galaxies in the mid-infrared
11 p1586 N90-19145
Far-infrared spectroscopy of galaxies
11 p1586 N90-19146
Infrared spectroscopy of star formation in galaxies: Extreme conditions and very short time scales
11 p1586 N90-19147
A search for the CO feature in active galactic nuclei
11 p1587 N90-19151
Infrared (FeII), H and H2 lines in galaxy nuclei
11 p1587 N90-19153
Near infrared spectroscopy and spectroscopic imaging of NGC253 11 p1588 N90-19159
Infrared heterodyne spectroscopy of polyatomic molecules in circumstellar envelopes
12 p1736 N90-19980
Infrared and X ray photoelectron spectroscopy studies of the polyimide/metal interface
[AD-A218249] 13 p1773 N90-20179
Application of novel data processing techniques to the analysis of Ion Mobility Spectrometry (IMS) data
[AD-A219976] 17 p2374 N90-23516
In situ analysis of CO during chemisorption and oxidation on graphite: Supported Pt by FTIR-microspectrometry
18 p2559 N90-24605
Calorimetry, activity, and micro-FTIR analysis of CO chemisorption, titration, and oxidation on supported Pt
18 p2560 N90-24606
Characterization of the surfaces of platinum/tin oxide based catalysts by Fourier Transform Infrared Spectroscopy (FTIR) 18 p2560 N90-24608
High resolution infrared spectroscopy of planetary molecules using diode lasers and Fourier transform spectrometers 20 p2943 N90-26747
FT-IR spectroscopic studies of polycyclic aromatic hydrocarbons 21 p3095 N90-27592

Absolute wind measurements in the lower thermosphere of Venus using infrared heterodyne spectroscopy
[NASA-CR-4290] 21 p3100 N90-27605
Infrared spectroscopic measurements on planetary atmospheric gases 23 p3412 N90-29283
Experimental studies leading to energy storage. Spectroscopy and dynamics of polyatomic hydrogen in liquid, solid and gaseous hydrogen plasmas
[AD-A224343] 24 p3547 N90-30066
Absolute wind measurements in the lower thermosphere of Venus using infrared heterodyne spectroscopy 24 p3561 N90-30146

INFRARED STARS
The mass distribution in the galactic centre estimated from OH/IR stars
[PB89-154884] 02 p0291 N90-11663
Cometary bodies in the circumstellar disk around beta Pictoris 12 p1741 N90-20010
Investigation of the late stages of stellar evolution: Mass loss from evolved stars 15 p2187 N90-22492

INFRARED TELESCOPES
NT LARGE DEPLOYABLE REFLECTOR
NT SPACE INFRARED TELESCOPE FACILITY
Telescope structure for cryogenic application 02 p0180 N90-11019
Diffraction, chopping, and background subtraction for LDR 05 p0598 N90-13476
The infrared spectrograph during the SIRTF pre-definition phase
[NASA-CR-183234] 05 p0644 N90-13759
The Infrared Space Observatory 11 p1589 N90-19163
Spectrophotometry of dust with Isophot 11 p1589 N90-19164
An advanced cooled grating spectrometer for UKIRT-CGS4 11 p1589 N90-19165
Feasibility of using Extreme Ultraviolet Explorer (EUVE) reaction wheels to satisfy Space Infrared Telescope Facility (SIRTF) maneuver requirements
[NASA-TM-100389] 12 p1663 N90-19556
Requirements of IR space astronomy 14 p1975 N90-21314
A 100 micro Kelvin bolometer system for SIRTF 14 p1976 N90-21317
Study of advanced InSb arrays for SIRTF (Space Infrared Telescope Facility) 14 p1977 N90-21325
Experience with the UKIRT InSb array camera 14 p1977 N90-21327
Laboratory characterization of direct readout Si:Sb and Si:Ga infrared detector arrays 14 p1980 N90-21347
Small helium-cooled infrared telescope experiment for Spacelab-2 (IRT)
[NASA-CR-183983] 19 p2765 N90-25708
Research and facilities handbook 1989
[ISSN-0267-6281] 19 p2784 N90-25840
SIRTF: Probing the dark corners of the galaxy 21 p3091 N90-27577
Infrared observations of the solar system in support of Large Aperture Infrared Telescope (LARITS): Calibration
[AD-A222222] 21 p3097 N90-27597
Infrared observations of the solar system in support of Large Aperture Infrared Telescope (LARITS): Calibration. Appendices
[AD-A222245] 21 p3097 N90-27598

INFRARED TRACKING
The design and implementation of a position measuring system for a remotely controlled video camera
[AD-A218077] 13 p1805 N90-20362
Modification, testing, and calibration of infrared search and target designator hardware received from NSWC
[AD-A217920] 13 p1889 N90-20837

INFRARED WINDOWS
Preparation, properties, and development of calcium lanthanum sulfide as an 8- to 12-micrometer transmitting ceramic
[AD-A220200] 17 p2382 N90-23565
Properties of cirrus from multispectral AVHRR imagery data 22 p3223 N90-28277
The 27-28 October 1986 FIRE IFO cirrus case study: Comparison of satellite and aircraft derived particle size 22 p3224 N90-28285
Infrared reflection-adsorption spectroscopy of the electrode/electrolyte solution interface: Optical considerations
[AD-A221935] 22 p3246 N90-28409

INGESTION (BIOLOGY)
NT DRINKING
NT EATING
The pollution hazard assessment system: Documentation and users manual
[AD-A217108] 12 p1689 N90-19706
Niacin ingested at night causes severe hypotension
[AD-A217896] 13 p1851 N90-20624

INGESTION (ENGINES)
Study of the engine bird ingestion experience of the Boeing 737 aircraft
[DOT/FAA/CT-89/16] 05 p0576 N90-13360
Study of bird ingestions into small inlet area, aircraft turbine engines (May 1987 to April 1988)
[DOT/FAA/CT-89/17] 11 p1453 N90-18375

INGOTS
Experimental and numerical investigations of the crack arrest behavior of steels and cast iron materials
[MPA-TWB-88-03] 05 p0623 N90-13635
Constitutive data acquisition and modelling in aluminium 2014 alloy
[AERE-R-13651] 13 p1775 N90-20186
Oxidation characteristics of Ti-14Al-21Nb ingot alloy
[NASA-TP-3012] 19 p2674 N90-25206

INHALATION
U RESPIRATION

INHIBITION (PSYCHOLOGY)
Excitatory and inhibitory backward conditioning in the rat 15 p2135 N90-22204

INHIBITORS
Polypeptide inhibitors of mineral scaling and corrosion
[AD-A210507] 01 p0041 N90-10225
Acetylcholinesterase inhibition and information processing in the auditory cortex
[AD-A216092] 10 p1411 N90-18139

INHOMOGENEITY
Electromagnetic wave propagation through circular waveguides containing radially inhomogeneous lossy media
[AD-A213062] 05 p0632 N90-13688
On geometry of inhomogeneous Heisenberg ferromagnet: Nonintegrable case
[MEMO-789] 05 p0691 N90-14030
Transversal inhomogeneity and radiative transfer in plasmas obtained by laser impact 06 p0785 N90-14568
The response of the atmospheric convective boundary layer to surface inhomogeneities 08 p1100 N90-16369
Associated distributions in the analysis of two-dimensional random walks
[CWI-BS-R8917] 17 p2486 N90-24095
A Markov chain identity and monotonicity of the diffusion constants for a random walk in a heterogeneous environment
[CWI-AM-R8917] 18 p2605 N90-24839
Renormalized microscopic theory of fluctuations in inhomogeneous magnetized plasmas
[DE90-611307] 18 p2617 N90-24908

INITIAL VALUE PROBLEMS
U BOUNDARY VALUE PROBLEMS

INITIATION
Laser initiation of secondary explosives
[DE89-010229] 01 p0075 N90-10431
Shock initiation of LX-17 as a function of its initial temperature
[DE89-017730] 02 p0208 N90-11192
Thermal initiation of confined primary explosives with a proton beam
[AD-A212954] 04 p0482 N90-12767
Particle size effects in the initiation of explosives containing reactive and nonreactive continuous phases
[DE90-000786] 06 p0754 N90-14390
Initiation precursors and initiators in laser-induced copolymerization of styrene and maleic anhydride in acetone
[NASA-TM-4166] 10 p1346 N90-17810
An evaluation of metal salts of 3-nitro-1,2,4-triazol-5-one (NTO) as potential primary explosives
[MRL-TN-563] 14 p1956 N90-21202

INITIATORS (EXPLOSIVES)
NT BOOSTERS (EXPLOSIVES)
NT CAPS (EXPLOSIVES)
NT DETONATORS
NT EXPLODING WIRES
A shock initiation model for fine-grained hexanitrostilbene
[DE89-007641] 02 p0207 N90-11185
Test of EED (Electro-Explosive Devices). Part 3: Statistical aspects on the estimation of sensitivity
[FOA-C-20749-2.3-PT-3] 02 p0209 N90-11194
Means for protecting electroexplosive devices which are subject to a wide variety of radio frequency
[AD-D014219] 06 p0753 N90-14382
Pyrotechnic materials ignited using lasers. High energy photopyrotechnic chains
[REPT-892-430-121] 16 p2225 N90-22691

INJECTION
NT CARRIER INJECTION
NT FLUID INJECTION
NT FUEL INJECTION
NT GAS INJECTION
NT ION INJECTION
NT LIQUID INJECTION
Thin-film integrated injection logic
[AD-D014190] 04 p0497 N90-12860
Acceleration of small, light projectiles (including hydrogen isotopes) to high speeds using a two-stage light gas gun
[DE90-002479] 06 p0729 N90-14253
Coaxial injection technology for hypergolic propellants 09 p1180 N90-16839
Effect of vortex circulation on injectant from a single film-cooling hole and a row of film-cooling holes in a turbulent boundary layer. Part 1: Injection beneath the vortex downwash
[AD-A215288] 09 p1218 N90-17063
Low NO(x) potential of gas turbine engines
[NASA-TM-102452] 10 p1321 N90-17636
Diode pumped monolithic Nd:YLF 1.053 micron mini-laser and its application to injection seeding
[DE90-005323] 10 p1390 N90-18040
Development of an rf-driven plasma neutralizer for negative ions
[DE90-007298] 11 p1568 N90-19027
A review of models for the analysis of the injection of densely loaded flows into entrained flow gasifiers
[DE90-000453] 12 p1662 N90-19550
Application of railgun principle to high-velocity hydrogen pellet injection for magnetic fusion reactor refueling
[DE90-008281] 13 p1761 N90-20109
A laser-induced fluorescence technique for measurement of slot-injected fluid concentration profiles in a plate turbulent boundary layer
[AD-A221388] 18 p2553 N90-24572
Effect of vortex circulation on injectant from a single film-cooling hole and a row of film-cooling holes in a turbulent boundary layer. Part 2: Injection beneath the vortex upwash
[AD-A223894] 23 p3328 N90-28818
Tunable CW single-frequency source for injection seeding 2-micrometer lasers
[AD-A223979] 23 p3331 N90-28834
Effects and tolerances of injection jitter in the SLC and future linear colliders
[DE90-014805] 23 p3394 N90-29179

INJECTION CARBURETORS
U FUEL INJECTION

INJECTION LASERS
Development of a solar-powered infrared injection laser microminiature transmitting system
[DE90-005672] 10 p1389 N90-18034
High power semiconductor laser arrays by metalorganic chemical vapor deposition 13 p1805 N90-20363
Apparatus for the efficient wavelength conversion of laser radiation
[AD-D014506] 20 p2866 N90-26305
Free electron laser injection oscillator
[AD-D014180] 21 p3007 N90-27095
Tunable CW single-frequency source for injection seeding 2-micrometer lasers
[AD-A223979] 23 p3331 N90-28834

INJECTION LOCKING
Linear, nonlinear, and tunable guided wave modes for high-power (GaAl)As semiconductor lasers 15 p2104 N90-22036

INJECTION MOLDING
Improved silicon carbide for advanced heat engines
[NASA-CR-180831] 01 p0051 N90-10293
A cure process model for resin transfer molding of advanced composites
[NASA-CR-186247] 09 p1185 N90-16867
Rapid prototyping of tools
[AD-A215956] 10 p1392 N90-18050
Improved silicon carbide for advanced heat engines
[NASA-CR-182186] 23 p3313 N90-28735

INJECTORS
NT VORTEX INJECTORS
A rocket engine design expert system
[NASA-TM-102373] 01 p0032 N90-10172
Cold starting a neat methanol (M100) vehicle with long duration spark ignition
[PB89-230692] 06 p0792 N90-14613
A laboratory test for fuel injector deposit studies
[DE90-000802] 06 p0795 N90-14629
Extended temperature range rocket injector
[NASA-CASE-LEW-14846-1] 07 p0887 N90-15130
Railgun performance with a two-stage light-gas gun injector
[DE90-009183] 14 p1932 N90-21057
Status of the CEBAF injector
[CEBAF-PR-89-027] 19 p2755 N90-25855
High repetition rate kickers for linear colliders
[CEBAF-PR-89-020] 19 p2756 N90-25661
Subsonic combustor testing 20 p2811 N90-25997
The structural dynamics analysis of the main injector LOX inlet tee and its redesign
[NASA-CR-186764] 20 p2875 N90-26358
Modeling of supersonic reacting flow fields 21 p2973 N90-26898

Injector element characterization methodology
23 p3294 N90-28634

INJURIES
NT BURNS (INJURIES)
NT EJECTION INJURIES
NT FROSTBITE
NT LESIONS
NT PARACHUTING INJURY
NT PARALYSIS
NT RADIATION INJURIES
NT WHIPLASH INJURIES
Biomedical influences on spinal cord function
[AD-A210311] 01 p0092 N90-10527
Exertional heatstroke: An international perspective. An introduction: The role of exercise in the etiology of exertional heatstroke
[AD-A212242] 04 p0523 N90-13020
Generation of free radicals during cold injury and rewarming
[AD-A213088] 05 p0672 N90-13915
Guidelines for safe human exposure to impact acceleration, update A
[AD-A215287] 09 p1253 N90-17268
Windblast protection for advanced ejection seats
13 p1752 N90-20063
Field assessment of wet bulb globe temperature: Present and future
[AD-A218224] 13 p1853 N90-20635
Kinematic and kinetic analyses of drop landings
14 p2010 N90-21517
Economic values for evaluation of Federal Aviation Administration investment and regulatory programs
[AD-A219882] 17 p2343 N90-23343
Evaluation of the head injury hazard during military parachuting
[AD-A220724] 17 p2434 N90-23870
Neck Injury in Advanced Military Aircraft Environments
[AGARD-CP-471] 19 p2717 N90-25459
Prevalence of G-induced cervical injury in US Air Force pilots 19 p2717 N90-25460
Non-ejection neck injuries in high performance aircraft
19 p2717 N90-25461
A survey of cervical pain in pilots of a Belgian F-16 Air Defence Wing 19 p2718 N90-25462
Radiological investigation of the vertebral column of candidates for military flying training the the Royal Norwegian Air Force 19 p2718 N90-25463
Electronystagmographic findings following cervical injuries 19 p2718 N90-25466
Aircrew neck injuries: A new, or an existing, misunderstood phenomenon 19 p2719 N90-25467
Flexion, extension and lateral bending responses of the cervical spine 19 p2719 N90-25468
A kinematic/dynamic model for prediction of neck injury during impact acceleration 19 p2719 N90-25469
Neck injury prevention possibilities in a high-G-enviroment experience with high sustained +G(sub z) training of pilots in the GAF IAM human centrifuge
19 p2720 N90-25474
A computer simulation model for studying cervical spine injury prevention 19 p2721 N90-25476
Measurement techniques, evaluation criteria and injury probability assessment methodologies developed for Navy ejection and crashworthy seat evaluations
19 p2721 N90-25479
Helicopter aircrew helmets and head injury: A protective effect
[AD-A223024] 23 p3377 N90-29080

INLAND WATERS
NT GROUND WATER
Ice conditions along the Illinois waterway as observed on LANDSAT images, 1972 to 1985
[AD-A219745] 17 p2418 N90-23775

INLET FLOW
A computational analysis of the transonic flow field of two-dimensional minimum length nozzles
06 p0718 N90-14194
Rotor induced-inflow-ratio measurements and CAMRAD calculations
[NASA-TP-2946] 08 p1017 N90-15882
A method for the prediction of supersonic compressor blade performance
[CUED/A-TURBO/TR-126] 10 p1321 N90-17634
Research on a two-dimensional inlet for a supersonic V/STOL propulsion system. Appendix A
[NASA-CR-174945] 11 p1451 N90-18364
Water-tunnel investigation of concepts for alleviation of adverse inlet spillage interactions with external stores
[NASA-TM-4181] 12 p1599 N90-19199
Application of an inverse method to the design of a radial inflow turbine 14 p1918 N90-20989
LDV measurements and the flow analysis in the vortex region of a radial inflow turbine
14 p1922 N90-21007
Control of flow separation and mixing by aerodynamic excitation
[NASA-TM-103131] 15 p2047 N90-21733
Theoretical and experimental study of flow-control devices for inlets of indraft wind tunnels
[NASA-TM-100050] 15 p2056 N90-21778
Computational modeling and validation for hypersonic inlets
[NASA-TM-103111] 15 p2099 N90-22011
Aerodynamics of a linear oscillating cascade
[NASA-TM-103250] 22 p3108 N90-27657
Experience in developing an improved design of experiment (lessons learned) 22 p3120 N90-27718
Experience in developing an improved altitude test capability 22 p3120 N90-27719

INLET NOZZLES
Computer code for the prediction of nozzle admittance
23 p3293 N90-28630

INLET TEMPERATURE
A parametric study of counterflow heat exchanger transients
[IAR-89-10] 19 p2689 N90-25293
Research and development of advanced gas turbine
[DE90-503377] 20 p2871 N90-26335
High/variable mixture ratio oxygen/hydrogen engines
23 p3295 N90-28637

INLETS (DEVICES)
U INTAKE SYSTEMS

INOCULATION
Ground evaluation of seeding an in-flight wingtip vortex using infrared imaging flow visualization technique
18 p2639 N90-25035

INORGANIC CHEMISTRY
Cloud chemistry and occurrence in the western United States: A synopsis of current information
[PB90-134248] 15 p2131 N90-22182
Diluted magnetic semiconductors
[AD-A220444] 17 p2476 N90-24159
Synthesis, structure, and properties of Ca2ZnN2
[AD-A222012] 21 p3083 N90-27533

INORGANIC COATINGS
NT ANODIC COATINGS
NT CERAMIC COATINGS
Laboratory for the processing and evaluation of inorganic matrix composites
[AD-A216881] 11 p1480 N90-18516

INORGANIC COMPOUNDS
NT AMMONIA
Photoconversion of inorganics to methane
[PB89-230643] 06 p0753 N90-14379
Ceramic processing using inorganic polymers
[DE90-003638] 07 p0911 N90-15268

INORGANIC MATERIALS
Inorganic composite materials in Japan: Status and trends
[PB90-174392] 22 p3135 N90-27789

INORGANIC NITRATES
NT AMMONIUM NITRATES
NT SILVER NITRATES

INORGANIC PEROXIDES
NT HYDROGEN PEROXIDE

INORGANIC SULFIDES
NT BISMUTH SULFIDES
NT CADMIUM SULFIDES
NT CALCIUM SULFIDES
NT HYDROGEN SULFIDE
NT MOLYBDENUM DISULFIDES
NT MOLYBDENUM SULFIDES
NT POLYSULFIDES
NT ZINC SULFIDES

INPUT
Computer availability impact on the archiving of scientific and technical reports
[AD-A210283] 01 p0136 N90-10787
LEXER: A tool for lexical analysis of program input
[DE89-016924] 02 p0288 N90-11649
Three input concepts for flight crew interaction with information presented on a large-screen electronic cockpit display
[NASA-TM-4173] 11 p1457 N90-18394
A human factors review of data entry devices
[DE90-012009] 19 p2763 N90-25703

INPUT/OUTPUT ROUTINES
An introduction to input/output automata
[AD-A210831] 01 p0106 N90-10604
Rational expansion for nonlinear input-output maps
[RR-348] 03 p0394 N90-12248
A functional expansion and stability for nonlinear input-output maps
[RR-359] 04 p0539 N90-13121
A test matrix sequencer for research test facility automation
[NASA-TM-103108] 17 p2357 N90-23416
Input/output algorithm for M-dimensional rectangular domain decompositions on N-dimensional hypercube multicomputers
[DE90-010494] 18 p2594 N90-24762
An input-size/output-size trade-off in the time-complexity of rectilinear hidden surface removal
[RUU-CS-89-24] 18 p2602 N90-24814
The basis system
[DE90-012077] 19 p2743 N90-25591
A search routine for optimization in a wind power system with variable speed
[FOA-C-20779-2.1] 20 p2882 N90-26395
UEDIT: A full-scale, scrollable APL2 spreadsheet input/output editor
[AD-A222712] 20 p2910 N90-26557
The system matrix characterisation of input-output equivalence
[MATHS-REPT-A-112] 20 p2918 N90-26600
The need for headers: An impossibility result for communication over unreliable channels
[AD-A222823] 21 p2994 N90-27018

INSAT SATELLITES
U INDIAN SPACECRAFT

INSECTICIDES
NT CARBAMATES (TRADENAME)
NT URETHANES

INSECTS
NT COCKROACHES
NT DROSOPHILA
Visual processing of object velocity and acceleration
[AD-A216509] 11 p1539 N90-18858
Multitemporal analysis of LANDSAT/TM digital imagery in the detection of areas affected by caterpillar (sibine fusca) attack in the dende (elais guineensis) palm plantation
[INPE-4979-PRE/1544] 14 p1999 N90-21457
Unsteady separated flows produced by complex harmonic motions: Investigation of wing-flow interactions elicited by a mechanical model simulating dragonfly wing kinematics 15 p2100 N90-22018

INSENSITIVITY
U SENSITIVITY

INSERTION LOSS
Evaluation of a thermistior power measurement system for use on the NPL antenna extrapolation range
[NPL-DES-89] 24 p3466 N90-29583

INSERTS
Application of high-rate cutting tools
[AD-A214644] 09 p1203 N90-16970

INSOLATION
SERI (Solar Energy Research Institute) solar radiation resource assessment project
[DE89-009456] 08 p1097 N90-16352

INSOMNIA
Psychophysiological correlates of human adaptation in antarctica
[AD-A216679] 10 p1412 N90-18142

INSPECTION
NT INFRARED INSPECTION
NT X RAY INSPECTION
Generic system components of the Thiokol ultrasonic RSRM case-to-insulation bondline inspection system
[NASA-CR-183738] 01 p0031 N90-10171
The creation of quality: New directions in the production of aeronautics castings 01 p0043 N90-10241
Stochastic propagation of an array of parallel cracks: Exploratory work on matrix fatigue damage in composite laminates
[DE89-017837] 03 p0319 N90-11813
A computer integrated approach to dimensional inspection
[PNR90596] 04 p0456 N90-12611
A robot which will investigate the condition of underground pipe
[PB89-230650] 04 p0508 N90-12928
NDI (Nondestructive Inspection) oriented corrosion control for Army aircraft. Phase 1: Inspection methods
[AD-A213368] 05 p0576 N90-13359
Considerations about the acceptance inspection of HS fasteners intended for controlled tightening
[CRIF-MT-175] 05 p0653 N90-13806
Component presence-absence detection for automated visual inspection of hybrid microcircuits
[KCP-613-4050] 07 p0922 N90-15335
Back to basics
[DE90-002734] 07 p0943 N90-15463
Inspection development for T-37 wing spar cap lug
[AD-A214826] 09 p1159 N90-16708
Human factors issues in aircraft maintenance and inspection
[AD-A215724] 11 p1542 N90-18875
VLSI implementation of moment invariants for automated inspection
[DE90-005318] 12 p1652 N90-19493

Development of inspection techniques for quantitatively measuring surface contamination on SRM hardware
[NASA-CR-183902] 12 p1673 N90-19608
Shaping the insonifying pulse to optimise B-scans obtained in austenite
[AERE-R-13518] 13 p1775 N90-20187
A guide to performing and documenting safety analyses
[DE90-008688] 13 p1788 N90-20261
Research and development quality assurance planning
[DE90-003687] 13 p1813 N90-20413
High explosives (PBX9502) characterization using computerized tomography
[DE90-008170] 14 p1990 N90-21404
Compendium of fracture mechanics problems
[NASA-TM-100393] 14 p1992 N90-21414
Computerized inspection of gear tooth surfaces
[NASA-TM-102395] 15 p2107 N90-22054
The JPL/KSC telerobotic inspection demonstration 15 p2155 N90-22312
Debris/ice/TPS assessment and photographic analysis for Shuttle Mission STS-36
[NASA-TM-102789] 16 p2205 N90-22583
Aviation security: Corrective actions underway, but better inspection guidance still needed. Report to the Chairwoman, Government Activities and Transportation Subcommittee, Committee on Government Operations, House of Representatives
[GAO/RCED-88-160] 17 p2347 N90-23367
Method of radiographic inspection of wooden members
[NASA-CASE-LAR-13724-1] 17 p2414 N90-23756
Supervisory controlled telemanipulation and vision systems for inspection and maintenance operations 18 p2508 N90-24333
Modeling growth of fatigue cracks which originate at rivet holes 18 p2645 N90-25060
Eddy current inspection at the nuclear power plants
[VTT-RR-653] 19 p2699 N90-25357
Inspection of welds with eddy current
[TTR-RR-644] 19 p2699 N90-25358
The Flight Telerobotic Servicer (FTS) NASA's first operational robotic system 19 p2733 N90-25537
Debris/ice/TPS assessment and photographic analysis for shuttle mission STS-31R
[NASA-TM-102790] 20 p2819 N90-26040
Acousto-optic signature analysis for inspection of the orbiter thermal protection tile bonds
[DE90-013089] 20 p2819 N90-26043
Design and construction of a wall-climbing robot
[NIAR-90-20] 20 p2870 N90-26327
Neural networks for detecting defects in aircraft structures
[IAR-90-4] 20 p2873 N90-26345
Robotic-aided system for inspection of aging aircraft
[NIAR-90-9] 20 p2873 N90-26346
Field experience in using laser acoustic sensing for inspection
[DE90-012954] 20 p2873 N90-26347
NDT in aerospace: The next decade (1990's)
[PNR90628] 20 p2874 N90-26348
The role of NDI in the certification of turbine engine components
[PNR90629] 20 p2874 N90-26349
Characterization of inspection performance
[NLR-MP-88068-U] 20 p2874 N90-26350
Coherent optical techniques for industrial inspection
[PNR90605] 20 p2927 N90-26654
A general discussion of the retirement for cause inspection system 21 p2957 N90-26814
Individual Helicopter Tracking Program (IHTP) for the MH-53J helicopter 21 p2958 N90-26818
Magnetic flux leakage versus ultrasonic correlation
[AD-A222112] 21 p3071 N90-27462
Debrix/ice/TPS assessment and photographic analysis of Shuttle Mission STS-32R
[NASA-TM-102787] 22 p3124 N90-27733
Flight motor set 360L001 (STS-26R). Volume 1: System overview, revision A
[NASA-CR-183995] 22 p3133 N90-27778
Flight motor set 360L006 (STS-34). Volume 1: System overview
[NASA-CR-184007] 22 p3133 N90-27781
Impact of Emerging NDE-NDI Methods on Aircraft Design, Manufacture, and Maintenance
[AGARD-CP-462] 22 p3184 N90-28068
The role of NDI in the certification of turbine engine components 22 p3184 N90-28069
NDI-concept for composites in future military aircraft 22 p3184 N90-28070
Assessment and demonstration of the capabilities of NDI processes, equipment, and personnel 22 p3184 N90-28071
Inspection reliability 22 p3184 N90-28072
Critical inspection of high performance turbine engine components: The RFC concept 22 p3185 N90-28073
Ultrasonic inspection of advanced CFRP structures by computer-controlled, pulse-echo technique 22 p3185 N90-28075
An ultrasonic system for in-service non-destructive inspection of composite structures 22 p3185 N90-28076
A technique for rapid inspection of composite aircraft structure for impact damage 22 p3185 N90-28077
In-service inspection of composite components on aircraft at depot and field levels 22 p3186 N90-28078
Development of an automated ultrasonic inspection system for composite structure on in-service aircraft 22 p3186 N90-28079
Neutron radiography: Applications and systems 22 p3186 N90-28080
Development and application of Computed Tomography (CT) for inspection of aerospace components 22 p3187 N90-28083
New aspects in aircraft inspection using eddy current methods 22 p3187 N90-28085
Inspection system for in-situ inspection of aircraft composite structures 22 p3188 N90-28091
Use of acoustic emission for continuous surveillance of aircraft structures 22 p3188 N90-28092
Impact of NDE-NDI methods on aircraft design, manufacture, and maintenance, from the fundamental point of view 22 p3189 N90-28093
Guidelines for pressure vessel safety assessment
[PB90-219619] 23 p3316 N90-28749
An improved method for choosing sampling points for the inspection of complex surfaces in a computer-aided manufacturing environment 23 p3380 N90-29093
A low cost shadow moire device for the nondestructive evaluation of impact damage in composite laminates
[AD-A223451] 24 p3443 N90-29442
Fractographic analysis of fatigue failures of airframe equipment parts: Examples of a rod end housing and a rod end cap
[NAL-TR-1047] 24 p3483 N90-29686

INSTABILITY
U STABILITY

INSTALLATION
U INSTALLING

INSTALLING
Epoxy-resin cable terminations
[AD-A213789] 07 p0942 N90-15454
Antenna installation on aircraft: Theory and practice 10 p1371 N90-17941
Thiokol/Wasatch installation evaluation of the redesigned field joint protection system (concepts 1 and 3)
[NASA-CR-183860] 13 p1785 N90-20127
Development of high performance beta-SiC field-effect transistors
[AD-A218392] 17 p2394 N90-23637
Lunar rated fasteners
[NASA-CR-182856] 17 p2411 N90-23737
Performance of battery charge controllers
[DE90-011413] 19 p2686 N90-25279
In-flight investigation of shuttle tile pressure orifice installations
[NASA-TM-4219] 23 p3328 N90-28820

INSTITUTIONS
NT BUREAUS (ORGANIZATIONS)
Activities report of the Institute for Communication Technology
[ETN-90-95383] 12 p1747 N90-20043

INSTRUCTION SETS (COMPUTERS)
User manual of the force structure model scenario editor SCENE
[FEL-1988-101] 04 p0531 N90-13069
Modular specifications in process algebra with curious queues
[CWI-CS-R8821] 04 p0543 N90-13152
Design of a specification language by abstract syntax engineering
[CWI-CS-R8934] 18 p2599 N90-24789

INSTRUCTIONS
U EDUCATION

INSTRUCTORS
Elementary and middle school science improvement project
[NASA-CR-183768] 05 p0705 N90-14125
Backward transfer and skill acquisition in the AH-1 flight and weapons simulator
[AD-A213432] 09 p1170 N90-16772
Research Reports: 1989 NASA/ASEE Summer Faculty Fellowship Program
[NASA-CR-183837] 12 p1634 N90-19390

INSTRUMENT APPROACH
Flight test investigation of flight director and autopilot functions for helicopter decelerating instrument approaches
[DOT/FAA/CT-TN89/54] 22 p3121 N90-27724
Dallas/Forth Worth simulation. Phase 2: Triple simultaneous parallel Instrument Landing System (ILS) approaches (turbojets)
[DOT/FAA/CT-90/2] 23 p3270 N90-28509

INSTRUMENT COMPENSATION
NT TEMPERATURE COMPENSATION
A high precision gravity compensation system for the deployment test of the ERS-1 SAR antenna 02 p0183 N90-11038

INSTRUMENT DRIFT
U DRIFT (INSTRUMENTATION)

INSTRUMENT ERRORS
A gyroscope calibration analysis for the Gamma Ray Observatory (GRO) 05 p0589 N90-13428
Identification and solution of a charging problem in a high-altitude detector
[DE90-008637] 12 p1616 N90-19296
Measurement errors 17 p2359 N90-23426
Rheometer strain and strain-rate errors
[DE90-013845] 23 p3329 N90-28824

INSTRUMENT FLIGHT RULES
Improved lighting of taxiway/taxiway intersections for Instrument Flight Rules (IFR) operations
[DOT/FAA/CT-TN89/64] 07 p0878 N90-15089
IFR aircraft handled forecast by air route traffic control center: Fiscal years 1990 to 2005
[AD-A220312] 18 p2496 N90-24263

INSTRUMENT LANDING SYSTEMS
ILS/MLS comparison tests at Miami/Tamiami, Florida Airport
[ACD-330] 01 p0005 N90-10018
ILS (Instrument Landing System) mathematical modeling study on the effects of proposed hangar construction west of runway 18R on localizer performance at Dallas-Fort Worth International Airport
[AD-A210631] 01 p0005 N90-10019
ILS mathematical modeling study of the effects of proposed hangar construction at the Orlando International Airport, Runway 17R, Orlando, Florida
[DOT/FAA/CT-TN89/52] 03 p0310 N90-11762
An evaluation of the accuracy of a microwave landing system area navigation system at Miami/Tamiami Florida Airport
[DOT/FAA/CT-TN89/40] 17 p2349 N90-23377
Dallas/Forth Worth simulation. Phase 2: Triple simultaneous parallel Instrument Landing System (ILS) approaches (turbojets)
[DOT/FAA/CT-90/2] 23 p3270 N90-28509

INSTRUMENT RECEIVERS
CRRES (Combined Release and Radiation Effects Satellite) SPACERAD plasma wave experiment
[AD-A210791] 02 p0278 N90-11587

INSTRUMENTAL ANALYSIS
U AUTOMATION

INSTRUMENTATION
U INSTRUMENTS

INSTRUMENTS
National Science Foundation 04 p0569 N90-13320

INSULATING MATERIALS
U INSULATION

INSULATION
NT ELECTRICAL INSULATION
NT MULTILAYER INSULATION
NT THERMAL INSULATION
Deep traps and sidegating in GaAs devices
[AD-A210740] 01 p0133 N90-10765
The 4th US Army Workshop on Low Heat Rejection Engines
[AD-A212379] 04 p0510 N90-12943
Magnetically insulated electron flows in pulsed power systems
[AD-A212746] 04 p0549 N90-13196
Temperature stable ceramic dielectric compositions
[AD-D014209] 06 p0749 N90-14358
Resultant forces and moments in completely restrained plates subjected to a recovery temperature varying linearly with time
[ESDU-89024] 07 p0947 N90-15480
Thermal stresses in unrestrained plates subjected to a recovery temperature varying linearly with time
[ESDU-89025] 07 p0947 N90-15481
Theoretical and computational studies of magnetic insulation and other plasma-opening-switch phenomena
[DE90-004421] 07 p0996 N90-15757
Temperatures in plates subjected to a recovery temperature varying linearly with time
[ESDU-89023] 07 p1007 N90-15831
Energy management and recovery 08 p1032 N90-15962

Command operated liquid metal opening switch
[AD-D014262] 08 p1060 N90-16126
The 1989 JANNAF Propulsion Meeting, volume 1
[CPIA-PUBL-515-VOL-1] 11 p1470 N90-18462
Technique for evaluating the erosive properties of ablative internal insulation materials
11 p1471 N90-18466
Heterogeneous composite and method of making
[AD-D014337] 12 p1619 N90-19306
Pressure rig for repetitive casting
[NASA-CASE-LAR-14050-1] 14 p1959 N90-21216
Airborne sound insulation of slits, joints, and sealing stripes
[PB90-128976] 14 p2023 N90-21599
Qualification of the RSRM case membrane case-to-insulation bondline inspection using the Thiokol Corporation ultrasonic RSRM bondline inspection system
[NASA-CR-183940] 16 p2209 N90-22602
Qualification of the RSRM field joint CF case-to-insulation bondline inspection using the Thiokol Corporation ultrasonic RSRM bondline inspection system
[NASA-CR-183931] 16 p2242 N90-22788
High temperature insulation barrier composite
[NASA-CASE-MFS-29241-1] 17 p2368 N90-23480
Comparison of currents predicted by NASCAP/LEO model simulations with elementary Langmuir-type bare probe models for an insulated cable containing a single pinhole
[NASA-TM-102486] 20 p2821 N90-26054
Flight motor set 360L007 (STS-33R)
[NASA-CR-183979] 20 p2824 N90-26067
Flight motor set 360L001 (STS-26R). Volume 1: System overview, revision A
[NASA-CR-183995] 22 p3133 N90-27778
Flight set 360H005 (STS-28) seals, volume 4
[NASA-CR-183904] 22 p3181 N90-28051
Nylon and teflon scribe effect on NBR to Chemlok 233 and NBR to NBR bond interfaces
[NASA-CR-184004] 22 p3189 N90-28095

INSULATORS

The effects of normal annealing cycles during IGFET fabrication on initial and radiation induced gate insulator defects
[AD-A210282] 01 p0049 N90-10278
High temperature insulators
[AD-D014193] 04 p0479 N90-12751
Manufacturing and characterization of insulator-germanium structures
[ECL-88-13] 05 p0703 N90-14115
Fabrication of superconductor coils
[DE90-003571] 07 p0922 N90-15338
Development of a diamond insulator for thermionic applications
[DE90-002849] 08 p1048 N90-16055
Process for lowering the dielectric constant of polyimides using diamic acid additives
[NASA-CASE-LAR-13902-1] 17 p2379 N90-23546
Solar array arcing in plasmas
19 p2737 N90-25558
Parity violation and superconductivity in doped Mott insulators
[DE90-627493] 23 p3401 N90-29217

INSULIN

Insulin and insulin-like growth factor-1 induce pronounced hypertrophy of skeletal myofibers in tissue culture
[NASA-CR-187026] 23 p3354 N90-28960

INSURANCE (CONTRACTS)

Launch insurance: Its role in the future development of commerce in space 09 p1174 N90-16795
Damage responsibility and liability in space stations
20 p2937 N90-26714

INTAKE SYSTEMS

NT ENGINE INLETS
NT HYPERSONIC INLETS
NT INTERNAL COMPRESSION INLETS
NT SUPERSONIC INLETS
Analysis of results from wind tunnel tests of inlets for an advanced turboprop nacelle installation
[NASA-CR-174937] 01 p0003 N90-10011
Effects of low-frequency instabilities on the operation of Ramjet air inlets 01 p0036 N90-10198
Recent developments in Ramjet pressure oscillation technology 01 p0036 N90-10199
Structural vibration and shock isolator
[AD-D014202] 04 p0509 N90-12940
Inflatable fuel tank buffer
[AD-D014446] 14 p1921 N90-21002
Unsteady flow phenomena in turbomachines
[AD-A218370] 17 p2402 N90-23680
The structural dynamics analysis of the main injector LOX inlet tee and its redesign
[NASA-CR-186764] 20 p2875 N90-26358
A heat transfer analysis for rough turbine airfoils
[AD-A221942] 21 p2960 N90-26831
Flow coupling between a rotor and a stator in turbomachinery
[AD-A223882] 23 p3282 N90-28572
Numerical simulations of flowfields in a central-dump ramjet combustor. 3: Effects of chemistry
[AD-A224145] 23 p3282 N90-28573
The equipment for mass flow measurements in the low-speed wind tunnel at DFVLR in Brunswick (Federal Republic of Germany)
[ESA-TT-1125] 23 p3285 N90-28585
Development of advanced combustion technology for medium and high speed natural gas engines
[PB90-198565] 23 p3331 N90-28836

INTEGERS

Basic mathematical function libraries for scientific computation
[NASA-TM-102256] 08 p1110 N90-16423
An exact algorithm for the problem of p-medians
[INPE-4924-TDL/384] 11 p1544 N90-18885
Minimum cycle covering and integer flows
[AD-A216546] 12 p1705 N90-19785
Boron-containing organosilane polymers and ceramic materials thereof
[NASA-CASE-ARC-11649-2-SB]
14 p1952 N90-21177
A new second-order integration algorithm for simulating mechanical dynamic systems 16 p2293 N90-23064
Supercongruences
[CWI-AM-R8918] 18 p2599 N90-24791
On parallel hashing and integer sorting
[AD-A221569] 21 p3058 N90-27390
The center of the enveloping algebra of the semidirect product of the Heisenberg lie algebra h(sub n) and a reductive Lie algebra S the rank of which is equal to 1 or 2
[DE90-627155] 23 p3388 N90-29133

INTEGRAL CALCULUS

Programs for numerical integration of piece-wise smooth functions
[DE89-620449] 02 p0258 N90-11464
Hausdorff measure and boundary behavior of analytic functions
[ETN-90-96501] 18 p2605 N90-24835

INTEGRAL EQUATIONS

NT FREDHOLM EQUATIONS
NT J INTEGRAL
NT SINGULAR INTEGRAL EQUATIONS
NT VOLTERRA EQUATIONS
NT WIENER HOPF EQUATIONS
Grid generation procedure using the integral equation method
[NAL-TR-1009] 01 p0111 N90-10630
An evaluation of the Chaboche and Bodner-Partom viscoplastic constitutive theories for strain rate sensitive materials 02 p0232 N90-11330
On the numerical solution of two-point boundary value problems
[AD-A211244] 02 p0266 N90-11516
Some exact solutions of the three-identical-particle problem with S-wave inverse square potentials
[DE89-618402] 02 p0267 N90-11524
Microscopic approach to the generator coordinate method
[DE89-016701] 03 p0392 N90-12233
Mapping nonlinear integro-differential equations into the frequency domain
[RR-366] 03 p0394 N90-12249
Numerical analysis of scattering by interface flaws
[AD-A212996] 05 p0654 N90-13810
A unified algebraic approach to integral and discrete evolution equations
[PREPRINT-668] 05 p0692 N90-14044
On some integral relations involving a generalized hypergeometric polynomial
[DE90-600729] 06 p0835 N90-14852
An alternative derivation for an integral equation for linearized subsonic flow over a wing
[AD-A214140] 07 p0876 N90-15079
Simple proof of renormalization group equation in the minimal subtraction scheme
[DE90-600758] 08 p1115 N90-16457
Modeling antennas and scatterers of arbitrary shape embedded in layered dielectric media
[AD-A214902] 09 p1211 N90-17023
Approximation method for nonlinear integral equations of Hammerstein type
[DE90-600727] 09 p1272 N90-17372
A selective survey of computational electromagnetics for antenna applications 10 p1369 N90-17933
A comparison between the propagators method and the decomposition method for nonlinear equations
[DE90-005783] 12 p1704 N90-19781
On a non classical oblique derivative problem for parabolic singular integro-differential operators
[DE90-612739] 14 p2020 N90-21574
Elastodynamic scattering and transmission problems in three dimensions by the boundary integral equation method 15 p2111 N90-22077
On approximation of nonlinear boundary integral equations for the combined method
[DE90-009784] 16 p2305 N90-23130
Hypersingular integrals and the two dimensional Helmholtz equation
[DE90-009821] 17 p2456 N90-24012
A comparison of the K-pulse and E-pulse techniques for aspect independent radar target identification
[AD-A220172] 18 p2542 N90-24511
Integral-equation methods in steady and unsteady subsonic, transonic and supersonic aerodynamics for interdisciplinary design
[NASA-TM-102677] 19 p2655 N90-25110
Estimation of convective rain volumes utilizing the are-time-integral technique
[NASA-CR-186814] 20 p2890 N90-26449
Applications of gauge theories to enhance numerical solutions of mixed potential integral equations
[AD-A221520] 21 p3065 N90-27424

INTEGRAL TRANSFORMATIONS

NT FAST FOURIER TRANSFORMATIONS
NT FOURIER TRANSFORMATION
NT HILBERT TRANSFORMATION
NT LAPLACE TRANSFORMATION
Mathematical methods of Physics 6: Integral transformation
[INPE-4807-MD/40] 11 p1551 N90-18926
Numerical solutions to steady-state problems with discontinuities
[AD-A222205] 21 p3064 N90-27418

INTEGRALS

NT CONVOLUTION INTEGRALS
Evaluation of integrals related to the Debye function
[DE89-016930] 02 p0264 N90-11499
Calculation of the odd and even integral components of the wave resistance Green's function
[AD-A212384] 04 p0503 N90-12900
Integrable classical systems in higher dimensions
[DE90-600737] 08 p1118 N90-16473
Conserved integral characteristics of the gravitational field
[DE90-615205] 13 p1899 N90-20898
New algorithms for one-loop integrals
[NIKHEF-H/89-17] 15 p2148 N90-22268
Stochastic processes as Fourier integrals and dilation of vector measures
[AD-A219413] 16 p2308 N90-23150
Incomplete integrals of cylindrical functions
[AD-A219512] 16 p2310 N90-23161
Hypersingular integrals and the two dimensional Helmholtz equation
[DE90-009821] 17 p2456 N90-24012
A general method for approximating improper integrals
[AD-A221153] 18 p2604 N90-24830
Elevated temperature crack growth
[NASA-CR-182247] 20 p2875 N90-26355
Product integration rules at Clenshaw-Curtis and related points: A robust implementation
[DE90-627158] 23 p3382 N90-29106
Weighted norm inequalities for Riemann-Liouville fractional integral
[DE90-627153] 23 p3388 N90-29132
Asymptotics of Laplace-Dirichlet integrals
[DE90-627165] 23 p3388 N90-29137
Trapezoidal stratified Monte Carlo integration
[AD-A223565] 24 p3540 N90-30021

INTEGRATED CIRCUITS

NT APPLICATION SPECIFIC INTEGRATED CIRCUITS
NT LARGE SCALE INTEGRATION
NT LINEAR INTEGRATED CIRCUITS
NT VERY LARGE SCALE INTEGRATION
NT VHSIC (CIRCUITS)
Circuit level modeling of inductive elements
[DE89-015122] 01 p0032 N90-10173
Micro-cavity integrable vacuum diodes and triodes
[DE89-016649] 01 p0060 N90-10344
Focused ion beam implantation
[AD-A210977] 01 p0133 N90-10767
Free-world microelectronic manufacturing equipment
[FASAC-TAR-4070] 02 p0215 N90-11228
A new semicustom integrated bipolar amplifier for silicon strip detectors
[DE89-015585] 02 p0215 N90-11229
Laser dynamics: The system dynamics and network theory of optoelectronic integrated circuit design
02 p0226 N90-11296
Optical coherence multiplexing for interprocessor communications
[DE89-016186] 02 p0275 N90-11568

Proceedings of the Workshop on Compound Semiconductor Devices and Integrated Circuits (13th) held in Cabourg, France on 10-12 May 1989
[AD-A211848] 03 p0343 N90-11954
Nearly optimal algorithms and bounds for multilayer channel routing
[AD-A211913] 03 p0343 N90-11955
Linear (passive) and non-linear guided and studies in glass
[AD-A211693] 03 p0406 N90-12325
Niobium and niobium nitride contacts on semiconducting material
[AD-D014177] 03 p0409 N90-12347
Beam assisted fabrication of 3-5/Si monolithic devices
[AD-A212046] 03 p0412 N90-12367
Ka-band MMIC beam steered transmitter array
04 p0488 N90-12803
A 2d-1 lower bound 2-layer knock-knee channel routing
[AD-A211948] 04 p0495 N90-12847
Research on the controllability of integrated circuits by means of electron beams
[ETN-90-95710] 05 p0636 N90-13708
Computer-aided fabrication system implementation
[AD-A213005] 05 p0682 N90-13969
Integrated optoelectronic receivers
[AD-A213376] 05 p0700 N90-14098
Characterization of two MMIC GaAs switch matrices at microwave frequencies
[NASA-TM-102449] 06 p0733 N90-14273
Integrating and enhancing tools for ASIC (Application-Specific Integrated Circuits) design using MOSIS (Metal Oxide Semiconductor Implementation Service) fabrication
[DE90-001601] 06 p0769 N90-14475
The effects of heavy particle radiation on semiconductor devices
[DE90-001679] 06 p0854 N90-14962
Computer aided design of monolithic microwave and millimeter wave integrated circuits and subsystems
[AD-A213656] 07 p0923 N90-15343
Research on GaAs quantum-coupled structures that can be used as electron devices
[AD-A214015] 07 p0924 N90-15350
VLSI theory and parallel supercomputing
[AD-A214035] 07 p0925 N90-15351
A study of Inter-Injection-Locked phased arrays
[AD-A214097] 07 p0925 N90-15352
Characteristics of CMOS analog integrated structures using MOSIS (Metal Oxide Semiconductor Implementation System)
[DE90-001630] 07 p0996 N90-15773
Solid state research
[AD-A213405] 07 p1003 N90-15806
CAE (Computer-Aided Engineering) tools' limitations case study: An SSI (Small Scale Integrated) design to an ASIC (Application Specific Integrated Circuit)
[DE90-002902] 08 p1109 N90-16418
Spacecraft environmental anomalies handbook
[NASA-CR-186331] 09 p1182 N90-16852
Universal nondestructive MM-wave integrated circuit test fixture
[NASA-CASE-LEW-14746-1] 09 p1209 N90-17009
Development of the Kalman filter application and a VHDL model for the AFIT (Air Force Institute of Technology) Floating Point Application Specific Processor (FPASP)
[AD-A215423] 09 p1213 N90-17033
Evaluation of doped phthalocyanines and a chemically-sensitive field effect transistor for detecting nitrogen dioxide
[AD-A215662] 09 p1214 N90-17037
Computer-aided fabrication of integrated circuits
[AD-A215439] 09 p1268 N90-17352
Study and implementation of a monolithic photoreceiver integrating a photodiode and a junction field effect transistor in GaInAs with polarization resistance
[IDI-18902] 10 p1379 N90-17990
Research on monolithic millimeter-wave devices
[AD-A215771] 10 p1379 N90-17996
A new technique for imaging the logic state of passivated conductors: Biased resistive contrast imaging
[DE90-000666] 10 p1380 N90-18000
Reconfigurable antennas, monolithic microwave integrated circuits with feeding networks for microstrip antennas
[AD-A216916] 11 p1498 N90-18622
DANCIR (device and circuit simulator): A three dimensional steady-state semiconductor device simulator
[DE90-006370] 11 p1504 N90-18658
A virtual zero-time, monolithic systolic sorting array
[DE90-001000] 12 p1698 N90-19753
CCST (Center for Compound Semiconductor Technology) research briefs
[DE90-006446] 12 p1721 N90-19887
Processing, fabrication, characterization and device demonstration of high temperature superconducting ceramics
[AD-A218330] 13 p1782 N90-20231
Radiation-hardened wafer scale integration
[AD-A217332] 13 p1793 N90-20290
Fault simulator evaluation
[AD-A217782] 13 p1796 N90-20308
The design of high-performance circuits for digital signal processing
[AD-A217786] 13 p1796 N90-20309
Transistor and solid-state technology: A historical development
[AD-A218141] 13 p1798 N90-20317
Identification of defects in SOI (Silicon-On-Insulator) wafers
[DE90-006020] 13 p1895 N90-20879
The development of ultraviolet-ozone cleaning as a production process in the packaging of integrated circuits
[DE90-007960] 14 p1959 N90-21220
Coplanar waveguide fed phased array antenna
[NASA-TM-102522] 14 p1968 N90-21273
Optical control of an 8-element Ka-band phased array using a high-speed optoelectronic interconnect
[NASA-TM-102550] 14 p1968 N90-21275
CMOS IC I(sub DDQ) testing for the 1990s
[DE90-009508] 17 p2394 N90-23634
Statistical design of MOS VLSI (Very Large Scale Integrated) circuits with designed experiments
[AD-A219654] 17 p2396 N90-23647
Test diagnostics of RF effects in integrated circuits
[AD-A219737] 17 p2396 N90-23648
Circuit recognition of VLSI layouts
[AD-A219806] 17 p2396 N90-23649
Integrated silicon flow sensors
[ETN-90-96906] 17 p2407 N90-23715
Report of research activity at the Research Laboratory of Electronics 17 p2486 N90-24217
Direct writing of microstructures for solid-state electronics
[AD-A220998] 18 p2535 N90-24460
Workshop on III-V Integrated Optoelectronics
[AD-A218759] 18 p2546 N90-24529
Monolithic phase shifter study
[AD-A219859] 18 p2546 N90-24533
Development of an all silicon integrated optical modulator for high speed data communications and sensor applications
[AD-A220270] 18 p2547 N90-24535
Analysis and applications of the crosstie-overlay slow-wave structure
[AD-A220286] 18 p2547 N90-24537
Multichip packaging technology with laser-patterned interconnects
[DE90-010743] 18 p2549 N90-24552
Center for Space Microelectronics Technology 1988-1989 technical report
[NASA-CR-186849] 19 p2753 N90-25642
Monolithic Optical Programmable Spectrograph (MOPS)
[AD-D014502] 19 p2757 N90-25669
Design of an optically controlled Ka-band GaAs MMIC phased-array antenna
[NASA-TM-103147] 20 p2857 N90-26250
LASER: A Layout Sensitivity Explorer. Report and user's manual
[EUT-89-E-216] 20 p2908 N90-26545
Massively parallel architecture: Integrated cell network for image reconstruction
[ETN-90-97257] 20 p2913 N90-26575
Field emitter array integrated distributed amplifiers
[AD-D014493] 22 p3166 N90-27958
Fault-tolerance in massively parallel silicon architectures: The case of neural nets
[REPT-90-012] 22 p3240 N90-28375
Reliability analysis/assessment of advanced technologies
[AD-A223647] 24 p3465 N90-29573
A single wafer bit-sliced convolver: An optimum statistical solution for the implementation of redundancy
[REPT-89-019] 24 p3466 N90-29584
MUSE: A systolic array for adaptive nulling with 64 degrees of freedom, using Givens transformations and wafer scale integration
[AD-A223812] 24 p3529 N90-29953

INTEGRATED LIBRARY SYSTEMS
National Library of Medicine DOCLINE (tradename) manual
[PB89-188676] 03 p0416 N90-12390

INTEGRATED MISSION CONTROL CENTER
The cosmic radiation effects and activation monitor
[RAE-TM-SPACE-364] 04 p0569 N90-13318
Prototype software reuse environment at Goddard Space Flight Center 06 p0825 N90-14794
RETE experiment activity at the TSS-1 POCC
[IFSI-89-12] 08 p1036 N90-15988
Large screen display for the Mission Control Center
13 p1858 N90-20662
CLEAR: Automating control centers with expert system technology 19 p2733 N90-25533
Process and information integration via hypermedia
19 p2733 N90-25534

INTEGRATED OPTICS
Novel physical effects in intersecting optical waveguides 02 p0274 N90-11565
Growth and characterization of zinc sulfide films by conversion of zinc oxide films with H2S
[AD-A213345] 04 p0561 N90-13271
Integrated optics at Lawrence Livermore National Laboratory
[DE90-003015] 10 p1431 N90-18255
All-fiber SFPM (Stimulated Four Photon Mixing) amplifier
[AD-D014358] 12 p1713 N90-19841
Integrated optics anisotropic waveguides and devices
[AD-A217084] 12 p1715 N90-19849
Direct writing of microstructures for solid-state electronics
[AD-A220998] 18 p2535 N90-24460
Integrated optics interdigitated-electrode switches
[AD-A223245] 21 p3076 N90-27490
Application of integrated optical components in optical fiber communication
[FEL-89-B252] 23 p3395 N90-29183
Planar waveguide spectrometer
[DE90-016308] 24 p3546 N90-30057

INTEGRATION (REAL VARIABLES)
U MEASURE AND INTEGRATION

INTEGRATORS
NT DIGITAL INTEGRATORS
Interference rejection and detection performance of the smallest of circuit
[AD-A215153] 09 p1212 N90-17025

INTEGRITY
NT COMPUTER PROGRAM INTEGRITY
Fuel Tank Technology
[AGARD-R-771] 08 p1021 N90-15904
Mechanical strain isolator mount
[NASA-CASE-LAR-13580-1] 08 p1084 N90-16272
GPS integrity requirements for use by civil aviation
24 p3423 N90-29339
Analysis of the integrity of the Microwave Landing System (MLS) data functions 24 p3428 N90-29365

INTEGRODIFFERENTIAL EQUATIONS
U DIFFERENTIAL EQUATIONS
U INTEGRAL EQUATIONS

INTELLECT
A guide to reasoning under uncertainty
[REPT-72/87/R486U] 05 p0675 N90-13932
Numerical facility: Convergence of cognitive and factor analytic models
[AD-A213627] 07 p0983 N90-15680

INTELLIGENCE
NT ARTIFICIAL INTELLIGENCE
NT EXPERT SYSTEMS
NT EXTRATERRESTRIAL INTELLIGENCE
NT INTELLECT
The components of scientific visualization
[DE90-001992] 07 p0972 N90-15614
Development of microcomputer-based mental acuity tests for repeated-measures studies
[NASA-CR-185607] 14 p2010 N90-21521
Tele-autonomous systems: New methods for projecting and coordinating intelligent action at a distance
24 p3502 N90-29794

INTELLIGENT STRUCTURES
U SMART STRUCTURES

INTELLIGIBILITY
NT SPEECH RECOGNITION
Attention and vigilance in speech perception
[AD-A210493] 01 p0095 N90-10539
Removal of noise from noise-degraded speech signals
[AD-A212876] 04 p0493 N90-12840
The effects of noise on speech and warning signals
[AD-A212520] 04 p0551 N90-13210
Evaluation of speech intelligibility through a bone conduction stimulator
[AD-A212002] 05 p0673 N90-13919
Test procedures for the evaluation of helmet and headset mounted active noise reduction systems
[AD-A212991] 05 p0676 N90-13937
Dual task performance with LPC (Linear Predictive Coding) degraded speech in a sentence verification task
[AD-A214296] 07 p0920 N90-15320
Current methods of digital speech processing
21 p2993 N90-27010
Quality evaluation of speech processing systems
21 p2993 N90-27012

RADC/EEV diagnostic rhyme test system improvements
[AD-A223187] 21 p2995 N90-27025
Comparison of speech intelligibility in cockpit noise using SPH-4 flight helmet with and without active noise reduction
[NASA-CR-177564] 23 p3271 N90-28510

INTELSAT SATELLITES
Advances in design and testing of spacecraft structures 02 p0180 N90-11018

INTENSIFICATION
U AMPLIFICATION

INTENSIFIER TUBES
U IMAGE INTENSIFIERS

INTENSIFIERS
NT IMAGE INTENSIFIERS

INTERACTING GALAXIES
Near-infrared spectroscopy of starburst and interacting galaxies 11 p1586 N90-19144
The strengths of the 2.3 micron CO band in luminous interacting and merging galaxies 11 p1587 N90-19148
Optical imaging of IRAS galaxies: The evolution of infrared-bright galaxies 22 p3261 N90-28465

INTERACTIONAL AERODYNAMICS
Frequency domain aerodynamic analysis of interacting rotating systems 02 p0147 N90-10837
A model suitable for predicting the noise associated with the ducted tail rotor of a helicopter
[ECL-88-09] 05 p0697 N90-14074
Body effect on wing angle of attack and pitching moment at zero lift at low speeds
[ESDU-89042] 09 p1167 N90-16757
Application of a three-dimensional Navier-Stokes model for a subsonic jet in a crossflow 13 p1749 N90-20045
A two dimensional study of rotor/airfoil interaction in hover
[NASA-CR-183272] 22 p3114 N90-27694
The Second ARO Workshop on Rotorcraft Interactional Aerodynamics
[AD-A223310] 24 p3418 N90-29304

INTERACTIONS
Three-dimensional unsteady transonic viscous-inviscid interaction 01 p0001 N90-10005
NASA'S controls-structures interaction program 01 p0017 N90-10081
Lumped mass formulations for modeling flexible body systems 01 p0019 N90-10091
Computer simulation of plasma interactions near Titan 01 p0142 N90-10816
On the interaction of a pulsar with the ambient medium utilizing x ray images of the Crab nebula
[MPE-215] 08 p1140 N90-16604
Detection of potential space station control/structure interaction with CO-ST-IN 14 p1935 N90-21074
Optimization of the structural and control system for LSS with reduced-order model 14 p1935 N90-21075
Computational architecture for integrated controls and structures design 14 p1935 N90-21076
Controller reduction for effective interdisciplinary design of active structures 14 p1935 N90-21077
Recent experience in simultaneous control-structure optimization 14 p1936 N90-21078
A survey of experiments and experimental facilities for active control of flexible structures 14 p1936 N90-21079
NASA CSI suspension methods overview 14 p1936 N90-21080
ASCIE: An integrated experiment to study CSI in large segmented optical systems 14 p1936 N90-21082
CSI sensing and control: Analytical and experimental results 14 p1936 N90-21083
Experimental evaluation of active-member control of precision structures 14 p1936 N90-21084
Controls, Astrophysics, and Structures Experiment in Space (CASES) 14 p1937 N90-21085
CSI technology validation on an LSS ground experiment facility 14 p1937 N90-21089
Initial operational capability of the ASTREX large space structures test bed 14 p1938 N90-21091
Numerical investigation of some control methods for 3-D turbulent interactions due to sharp fins 15 p2053 N90-21764

INTERACTIVE CONTROL
Adaptive structures to meet future requirements for large precision structures 02 p0178 N90-11001
System and performance analysis of a low density actively controlled mirror for astronomic observation 02 p0178 N90-11002
Experiences using a major FEM package interactively for spacecraft applications 02 p0179 N90-11008
MSP: Modeling of concurrent processes. Version 1.00 General introduction and directions for use
[REPT-88-88] 02 p0260 N90-11477
Spoken commands control robot that handles radioactive materials
[DE89-012632] 02 p0262 N90-11488
Manual for Program PSTRESS: Peel stress computation
[NASA-CR-178408] 03 p0321 N90-11822
Design mechanism for interactive graphics mechanism design
[PB89-219513] 03 p0387 N90-12202
ANDECS-PERLUDE 2.0: A databased, interactive system of control software user's guide
[DFVLR-MITT-89-07] 03 p0418 N90-12404
On modeling resources in multiprocessor systems
[MEMO-INF-88-33] 04 p0535 N90-13095
An interactive method for the flow calculation of airfoils with local separation regions 08 p1069 N90-16190
The Interactive System Meteorology and its use in meteorology and oceanography 08 p1092 N90-16320
Applications of algebraic grid generation 15 p2093 N90-21979
Iterative defect correction and multigrid accelerated explicit time stepping schemes for the steady Euler equations
[CWI-NM-R8908] 17 p2459 N90-24039
Criteria for device selection: A comparison between a mouse and a touchscreen as an input device for interactive video
[NPL-DITC-158/90] 22 p3235 N90-28344

INTERACTIVE GRAPHICS
U COMPUTER GRAPHICS

INTERATOMIC FORCES
First-principles interatomic potentials in transition metals: Multi-ion interactions and their analytic representation
[DE90-001990] 06 p0748 N90-14353
Helium transport in plasma edge regions 14 p2027 N90-21625
First-principles interatomic potentials for transition metals and their surfaces
[DE90-011233] 18 p2528 N90-24424

INTERCALATION
Density of intercalated graphite fibers
[NASA-TM-102411] 06 p0750 N90-14362
Cell performance of ultra-thin polymer cathode systems. Part 1: Anion intercalating polymer cathode
[AD-A216037] 11 p1501 N90-18639
Exchange and correlation effects in the Visscher-Falicov model for metal intercalated graphite
[DE90-610553] 12 p1627 N90-19349
Feasibility of intercalated graphite railgun armatures
[NASA-TM-102546] 14 p1953 N90-21181
Resistivity of pristine and intercalated graphite fiber epoxy composites
[NASA-TM-102576] 14 p1955 N90-21192

INTERCEPTION
Optimal, impulsive, time-fixed orbital rendezvous and interception with path constraints 13 p1760 N90-20102
Power transmission device
[AD-D014430] 14 p1969 N90-21281
A comparison of time-optimal interception trajectories for the F-8 and F-15
[NASA-CR-186300] 15 p2050 N90-21753
Evaluation of VHF intercept and direction finding systems
[AD-A219805] 17 p2350 N90-23382
A theoretical model for airborne radars
[AD-A220735] 17 p2390 N90-23615
Computer-aided mathematical analysis of probability of intercept for ground-based communication intercept system
[AD-A219856] 17 p2392 N90-23627
Synthesis and validation of feedback guidance laws for air-to-air interceptions
[LR-615] 19 p2752 N90-25639

INTERCEPTOR AIRCRAFT
U FIGHTER AIRCRAFT

INTERCONNECTION
U JOINING

INTERCONTINENTAL BALLISTIC MISSILES
Complex availability problems solved with simulation
[DE89-012610] 08 p1116 N90-16459

INTERFACE STABILITY
Synthesis and interfacial properties of new generation polyurethane systems
[AD-A210446] 01 p0050 N90-10286
Fabrication of NBN based electronic devices with silicon barriers
[AD-D014230] 06 p0767 N90-14463
Anomalous waves in shock wave - fluid interface collisions
[AD-A213584] 08 p1062 N90-16144
Study of interfacial behavior in cocurrent gas-liquid flows
[DE90-005988] 12 p1659 N90-19532
Microstructure and stability of TiB2 and Cu multilayers
[DE90-011955] 18 p2627 N90-24968
Interfacial studies of Chemical Vapor Infiltrated (CVI) ceramic matrix composites
[AD-A221867] 21 p2972 N90-26893
Polycrystalline thin film cadmium telluride n-i-p solar cells
[DE90-000351] 21 p3019 N90-27167
Two terminal CuInSe2 based cascade cells
[DE90-000363] 24 p3485 N90-29697

INTERFACES
NT FLUID BOUNDARIES
NT GAS-SOLID INTERFACES
NT LIQUID-LIQUID INTERFACES
NT LIQUID-SOLID INTERFACES
NT LIQUID-VAPOR INTERFACES
NT SOLID-SOLID INTERFACES
Attenuated total reflection FTIR spectroscopy for measuring interfacial reaction kinetics at silica surfaces
[AD-A210314] 01 p0041 N90-10224
Delayed failure of silver-aided diffusion welds between steel
[DE89-016652] 01 p0045 N90-10252
Atomic imaging and interfacial analysis
[DE89-015339] 01 p0130 N90-10748
Characterization of GaAs/Si/GaAs heterointerfaces
[DE89-016302] 01 p0131 N90-10752
Interfacial adsorption and crystallization of polycarbonate in carbon fiber composites
[AD-A211230] 02 p0191 N90-11090
Intergranular and interphase boundaries in ceramics
[DE89-016969] 02 p0202 N90-11154
An integrated distributed processing interface for supercomputers and workstations
[DE89-016769] 02 p0260 N90-11478
Human Operator Simulator (HOS) 4 user's guide
[AD-A212007] 03 p0310 N90-11763
Short period multilayers: Interface dominated structures
[DE89-017536] 03 p0319 N90-11812
Power up modification for video switcher microprocessor interface for sensor system processing system
[AD-A211543] 03 p0344 N90-11962
Structure and properties of polymer interphases
[AD-A212796] 04 p0481 N90-12763
Stress waves through projectile joints and interfaces
[AD-A212201] 04 p0513 N90-12963
State of the art of human/machine dialog tool prototypes
[TELECOM-PARIS-89-H001] 04 p0527 N90-13038
A cell-centered multigrid method for three-dimensional anisotropic-diffusion and interface problems
[REPT-89-35] 04 p0540 N90-13128
A moving-grid interface for systems of one-dimensional time-dependent partial differential equations
[CWI-NM-R8904] 04 p0541 N90-13136
Development of a shuttle plume radiation heating indicator
[NASA-CR-183679] 05 p0614 N90-13584
Transport phenomena and interfacial kinetics in multiphase combustion systems
[AD-A212932] 05 p0621 N90-13620
Unified model of charge build up and annealing of oxide charge and interface states in SiO2 due to stress
[HMI-B-465] 05 p0704 N90-14120
Database interfaces on NASA's heterogeneous distributed database system
[NASA-CR-185420] 05 p0706 N90-14133
SAS graphics in DCF
[PNR90563] 06 p0756 N90-14399
Nondestructive evaluation of flaw clusters and thin layer interfaces 06 p0795 N90-14633
The development of an Ada programming support environment database: SEAD (Software Engineering and Ada Database), user's manual
[NASA-CR-181219] 06 p0828 N90-14811
Atomic matching across internal interfaces
[DE90-002266] 06 p0841 N90-14889
Magnetic and electrical properties
[DE90-002183] 06 p0856 N90-14977
The design and implementation of an intelligent interface for information retrieval 06 p0858 N90-14991
Display interface concepts for automated fault diagnosis
[NASA-TM-101610] 07 p0881 N90-15102
Rayleigh-Taylor instability in compressible fluids
[DE90-003027] 07 p0929 N90-15376
Laser-material interactions
[AD-A214421] 07 p0937 N90-15425
High temperature, flexible, thermal barrier seal
[NASA-CASE-LEW-14672-1] 07 p0940 N90-15444
Interfacial systems for photochemical energy conversion
[DE90-003181] 07 p0953 N90-15514

Interface phonons in semiconductor double heterostructures
[AD-A213732] 07 p1003 N90-15810
RVD scenari and interfaces between Hermes and space station 08 p1035 N90-15982
A generic fine-grained parallel C 08 p1115 N90-16454
Interfaces of organic matrices and graphite fiber composites: A review of the literature
[AD-A214504] 09 p1186 N90-16870
Novel approach for high resolution TEM (Transmission Electron Microscopy) studies of ceramic-ceramic interfaces
[DE90-005272] 09 p1199 N90-16945
Light-trapping concentrator cells
[DE90-004988] 09 p1242 N90-17205
A guide to IRUS-2 application development
[AD-A214758] 09 p1266 N90-17340
Surface-enhanced Raman scattering
[AD-A215976] 10 p1353 N90-17849
Numerical model of bond strength measurements
[DE90-006000] 10 p1396 N90-18073
KAPSE Interface Team (KIT) public report, volume 7
[AD-A215838] 10 p1418 N90-18176
Simulation and quantification of high-resolution Z-contrast imaging of semiconductor interfaces
[DE90-006159] 10 p1438 N90-18297
An overview of radiation-induced interface traps in MOS (Metal-Oxide Semiconductor) structures
[AD-A216101] 10 p1438 N90-18299
Design, implementation and test of an RS-232 compatible bi-directional, full duplex, fiber-optic interface with provision for hardware handshaking on a minimum of fiber-optic lines
[AD-A216604] 11 p1566 N90-19012
Nanolayer reactions in aluminum-metal interfaces
[DE90-004955] 12 p1626 N90-19342
Interface science in deformation processing of ceramics
[DE90-008424] 13 p1780 N90-20219
Modeling studies of electrolyte flow and bubble behavior in advanced Hall cells
[DE90-007013] 13 p1795 N90-20303
RenderMan design principles 13 p1857 N90-20653
The use of graphics in the design of the human-telerobot interface 13 p1860 N90-20670
Magnetic properties of surfaces and interfaces
[DE90-007348] 13 p1880 N90-20789
An investigation of the dislocation structure of the Ni/Ag phase boundary
[DE90-008428] 13 p1895 N90-20876
High voltage/high resolution studies of metal and semiconductor interfaces
[DE90-009065] 14 p2032 N90-21656
Scalable coherent interface
[DE90-008011] 15 p2149 N90-22277
Comparison of location systems 17 p2360 N90-23437
Analysis of regional phases using three-component data
[AD-A219482] 17 p2422 N90-23803
Northeast Artificial Intelligence Consortium. Volume 3: The Versatile Maintenance Expert System research project
[AD-A218716] 17 p2453 N90-23993
Optical phonons and electronic properties in double heterostructures
[AD-A219436] 17 p2475 N90-24153
Characterization of solid state bonding between Coors AD-999 alumina and niobium
[DE90-010653] 18 p2518 N90-24379
Electron microscopy of interfaces in silicon carbide whisker-reinforced alumina composites
[DE90-010439] 18 p2519 N90-24386
Surface and interface studies by Auger electron spectroscopy
[ETN-90-98948] 18 p2522 N90-24398
Dynamics of bulk and surface-adsorbed polyacrylates
[AD-A221046] 18 p2530 N90-24437
A generic interface between COSMIC/NASTRAN and PATRAN (R) 18 p2569 N90-24640
Investigations of ultrasonic wave interactions at imperfect boundaries separating anisotropic materials
[DE90-010661] 18 p2612 N90-24875
Realtime simulation at MBB today and future aspects
[MBB-UA-1134/89-PUB] 19 p2653 N90-25098
An approach to a real-time distribution system 19 p2733 N90-25535
QATT: A natural language interface for QPE
[UIUCDCS-R-89-1535] 19 p2743 N90-25590
The effect of interfacial characteristics on the mechanical performance of ceramic-ceramic composites
[AD-A223031] 20 p2829 N90-26090
Structured electrode interfaces
[AD-A222763] 20 p2859 N90-26265
Role of interfaces and interphases in the evolution mechanics of material systems
[AD-A222702] 21 p2971 N90-26885
Probing interfacial structure and composition with x ray standing waves
[AD-A223071] 21 p2977 N90-26916
Interfacial viscosity measurements of adsorbed monolayers on metal surfaces
[AD-A221689] 21 p2979 N90-26931
Application of microdesigned interfaces to studies of ceramic processing
[DE90-011633] 21 p2983 N90-26951
Micromechanics of interfaces in high temperature ceramics
[AD-A222027] 21 p2987 N90-26973
The operational feature exchange language
[AD-A222497] 21 p3060 N90-27401
The column-by-column compositional mapping at semiconductor interfaces using Z-contrast STEM
[DE90-012594] 21 p3081 N90-27516
Fracture-EXAFS: A new method for the study of interfaces in thin films and polycrystalline materials
[DE90-013736] 21 p3081 N90-27521
Surfaces and interfaces of ceramics and metals
[DE90-014381] 22 p3160 N90-27920
UV-induced degradation of the Si-SiO2 interface: Applications to the point contact solar cell
[DE90-013843] 23 p3344 N90-28898
Elastic interfaces
[REPT-90-003] 24 p3493 N90-29742
Graphic interface for attribute-based data language queries from a personal computer to the multi-lingual, multi-model, multi-backend database system over an Ethernet network
[AD-A223738] 24 p3528 N90-29948

INTERFACIAL ENERGY
Atomic structure of Ag/Ni interfaces
[DE90-010053] 18 p2618 N90-24914
Interface formation and percusory dynamics
[AD-A224128] 23 p3402 N90-29223

INTERFACIAL STRAIN
U INTERFACIAL TENSION

INTERFACIAL TENSION
Characterization of polymeric surfaces and interfaces
[AD-A210227] 01 p0049 N90-10277
Analytic theory for the selection of Saffman-Taylor fingers in the presence of thin film effects
[NASA-CR-181910] 01 p0118 N90-10677
Thermocapillary migration of liquid droplets in a temperature gradient in a density matched system
[NASA-CR-185178] 06 p0776 N90-14512
Development of an elastomeric additive to improve the impact resistance of unsaturated polyester networks
[ISAL-89-0006] 08 p1050 N90-16073
Determination of dynamic surface forces using piezoelectric arrays 08 p1080 N90-16249
A quantitative analysis of slip phenomena along a dry contact surface between two bodies in comparison to interfacial crack propagation
[ISAL-89-0032] 08 p1089 N90-16304
Elastic-plastic analysis of a thick-walled composite tube subjected to internal pressure
[AD-A215258] 09 p1238 N90-17187
On the temperature of surfaces 10 p1366 N90-17917
Development of an infrared imaging system for the surface tension driven convection experiment 10 p1367 N90-17922
NCTM workshop splinter session, IR thermal measurement instruments 10 p1367 N90-17923
Studies of the structure and properties of organic monolayers, multilayers and superlattices
[DE90-008330] 13 p1765 N90-20129
Spacelab qualified infrared imager for microgravity science experiments
[NASA-TM-102503] 13 p1804 N90-20352
Energy release rate analysis of interfacial cracks in composites 15 p2065 N90-21829
VAMAS project on variable weld penetration: Surface tension of the steels
[NPL-DMA(A)-188] 15 p2070 N90-21856
Development of a device for surface tension measurement and phenomenological rheology
[ECL-89-12] 17 p2382 N90-23568
Convergent strand array liquid pumping system
[NASA-CASE-NPO-17301-1-CU] 17 p2385 N90-23587
Fundamental studies on spray combustion and turbulent combustion
[AD-A219640] 18 p2521 N90-24394
Interface tribology and space conditions 18 p2536 N90-24469
Microstructure and stability of TiB2 and Cu multilayers
[DE90-011955] 18 p2627 N90-24968
Approximate natural damped frequencies of a finite viscous floating-zone under zero-gravity condition
[LRT-WE-9-FB-8(1988)] 21 p2990 N90-26995
Strength under various modes of deformation
[AD-A222412] 21 p3013 N90-27132
Effects of low bond number liquid motions on spacecraft attitude 22 p3131 N90-27768
Design of a CO2 laser power control system for a Spacelab microgravity experiment
[NASA-TM-103112] 23 p3331 N90-28833

INTERFERENCE
Residual interference assessment in adaptive wall wind tunnels
[NASA-CR-181896] 04 p0458 N90-12625
Use of an HF active monitoring array in the presence of high level interference
[BBC-RD-1989/7] 08 p1055 N90-16096

INTERFERENCE DRAG
Wind tunnel support system effects on a fighter aircraft model at Mach numbers from 0.6 to 2.0
[AD-A210614] 01 p0002 N90-10010
An experimental investigation of helicopter rotor hub fairing drag characteristics
[NASA-TM-102182] 03 p0300 N90-11701
Slotted-wall research with disk and parachute models in a low-speed wind tunnel
[DE90-002989] 15 p2048 N90-21737
Subsonic sting interference on the aerodynamic characteristics of a family of slanted-base ogive-cylinders
[NASA-CR-4299] 18 p2492 N90-24242
Sting-support interference on afterbody drag at transonic speeds
[NAL-TM-EA-8902] 23 p3267 N90-28492

INTERFERENCE FIT
Internal rotor friction instability
[NASA-CR-183942] 14 p1988 N90-21395
Cryogenic anti-friction bearing with inner race
[NASA-CASE-MFS-28384-1] 21 p3010 N90-27112

INTERFERENCE GRATING
Atom interferometry progress
[AD-A220875] 18 p2613 N90-24882

INTERFERENCE IMMUNITY
Radio interference in the near-earth environment
[NASA-CR-180479] 11 p1498 N90-18623

INTERFERENCE MONOCHROMATIZATION
U DIFFRACTION

INTERFEROGRAMS
U INTERFEROMETRY

INTERFEROMETERS
NT ETALONS
NT FABRY-PEROT INTERFEROMETERS
NT INFRARED INTERFEROMETERS
NT MACH-ZEHNDER INTERFEROMETERS
NT MICHELSON INTERFEROMETERS
NT MICROWAVE INTERFEROMETERS
NT RADIO INTERFEROMETERS
Absolute determination of the wall shear stress by means of an interferometer
[DFVLR-FB-89-13] 03 p0349 N90-11991
Mark-3 interferometer
[AD-A213155] 04 p0505 N90-12911
A review of focal reducer interferometer systems
[RSRE-MEMO-3486] 04 p0554 N90-13231
LASCO: A wide-field white light and spectrometric coronagraph for SOHO 04 p0568 N90-13311
Fiber-optic sensors for composite cure analysis and lifetime nondestructive evaluation
[DE90-001739] 06 p0738 N90-14296
Fiber optic sensing system
[NASA-CASE-LEW-14795-1] 07 p0992 N90-15733
Full surface interferometric testing of grazing incidence mirrors
[AD-A213590] 09 p1281 N90-17425
Development and test of power amplifiers for the driving of low-voltage piezo-actuators in multistable interferometers
[DLR-MITT-89-19] 11 p1504 N90-18662
Meteor observations using the 50 MHz MENTOR imaging Doppler interferometer
[AD-A217908] 13 p1790 N90-20276
Optimization of digital filters for a short-scan interferometer
[AD-A217997] 13 p1798 N90-20315
Atmospheric wind measurements using a 50 MHz imaging Doppler interferometer radar
[AD-A218277] 13 p1847 N90-20601
A spaceborne optical interferometer: The JPL CSI mission focus 14 p1933 N90-21063
Preliminary results on two-dimensional interferometry of HL Tau 14 p1979 N90-21335
Passive stabilization of a fiber optic nonlinear interferometric sensor
[AD-D014438] 14 p2026 N90-21620

The investigation of multilayer x ray reflectors as x ray optical elements
[DE90-009044] 14 p2026 N90-21621
Galileo Earth approach navigation using connected-element interferometer phase-delay tracking 15 p2075 N90-21884
Using connected-element interferometer phase-delay data for Magellan navigation in Venus orbit 15 p2075 N90-21885
Full surface interferometric testing of grazing incidence mirrors
[AD-A219394] 16 p2318 N90-23218
Information content of a single pass of phase-delay data from a short baseline connected element interferometer 20 p2852 N90-26220
Absolute measurements of gravity
[AD-A222731] 20 p2922 N90-26629
A dual-wavelength passive homodyne detection unit for fiber-coupled white-light interferometers
[ETN-90-97036] 20 p2927 N90-26653
Analysis of cirrus optical properties with data from NASA ER2 High-resolution Interferometer Sounder (HIS)
[NASA-CR-186365] 21 p3030 N90-27227
Equal path, phase shifting, sample point interferometer for monitoring the configuration of surfaces
[NASA-CASE-NPO-17913-1-CU] 21 p3076 N90-27488
Carbon chemistry of circumstellar envelopes 21 p3090 N90-27570
Fiber-optic projected-fringe digital interferometry
[NASA-TM-103252] 22 p3178 N90-28033
Serial interferometric fiber-optic sensor array
[AD-D014466] 22 p3246 N90-28407
Tropospheric wind profiling using radar interferometry: A feasibility study of a compact mobile system
[PB90-217068] 23 p3351 N90-28939
Determination of density using simultaneous interferometry methods
[IMFL-90/04] 24 p3547 N90-30061

INTERFEROMETRY
NT DIFFERENTIAL INTERFEROMETRY
NT HOLOGRAPHIC INTERFEROMETRY
NT LASER INTERFEROMETRY
NT MOIRE INTERFEROMETRY
NT SPECKLE INTERFEROMETRY
NT VERY LONG BASE INTERFEROMETRY
Master oscillator with power amplifiers: Performance of a two-element CW HF phased-laser array
[AD-A211141] 01 p0076 N90-10435
An interferometric strain-displacement measurement system
[NASA-TM-101638] 01 p0080 N90-10454
Multimode fiber interferometry and several-mode fiber polarimetry via phase conjugation
[DE89-014226] 01 p0123 N90-10706
Simultaneous multiple frequency interferometry: An application of homodyne phase measurement
[DE89-013975] 01 p0126 N90-10719
Project Radioastron 02 p0158 N90-10901
Interferometry and high speed photography of laser-driven flyer plates
[DE89-016990] 02 p0225 N90-11290
Synthetic Aperture Interferometric Radiometer (SAIR) 12 p1610 N90-19261
Apparatus and method for minimizing polarization-induced signal fading in an interferometric fiber-optic sensor using input-polarization modulation
[AD-D014315] 12 p1642 N90-19430
Single antenna interferometry
[DE90-008120] 12 p1648 N90-19474
Bibliography of spatial interferometry in optical astronomy
[NASA-TM-100754] 13 p1901 N90-20911
The anatomy of the gyroscope, part 3
[AGARD-AG-313] 14 p1982 N90-21359
Passive stabilization of a fiber optic nonlinear interferometric sensor
[AD-D014438] 14 p2026 N90-21620
Full surface interferometric testing of grazing incidence mirrors
[AD-A219394] 16 p2318 N90-23218
The interstellar medium of a starburst galaxy; millimeter interferometric observations of M82 16 p2329 N90-23276
Anderson Mesa, Arizona as a site for an optical interferometric array 16 p2330 N90-23281
Evaluation and representation of two and three dimensional data fields from optical stream measurements
[MPIS-18/1989] 17 p2474 N90-24143
In-situ topographical imaging of electrode surfaces using high resolution phase-measurement interferometric microscopy
[AD-A221021] 18 p2548 N90-24542
Atom interferometry progress
[AD-A220875] 18 p2613 N90-24882
Goldstone intracomplex connected element interferometry 20 p2852 N90-26218
Refractive error analysis in the interferometric measurement of 2-D density fields containing strong gradients
[LR-616] 20 p2927 N90-26655
Equal path, phase shifting, sample point interferometer for monitoring the configuration of surfaces
[NASA-CASE-NPO-17913-1-CU] 21 p3076 N90-27488
Infrared mapping with a two-dimensional infrared array
[AD-A221938] 21 p3096 N90-27596
Adaptive polarization diversity detection scheme for coherent communications and interferometric fiber sensors
[AD-D014479] 22 p3163 N90-27938
Apparatus and method for minimizing polarization-induced signal fading in an interferometric fiber-optic sensor using input-polarization control
[AD-D014492] 22 p3164 N90-27940
Fiber-optic projected-fringe digital interferometry
[NASA-TM-103252] 22 p3178 N90-28033
Tropospheric wind profiling using radar interferometry: A feasibility study of a compact mobile system
[PB90-217068] 23 p3351 N90-28939
Velocity interferometry 24 p3420 N90-29316
Determination of density using simultaneous interferometry methods
[IMFL-90/04] 24 p3547 N90-30061

INTERFERON
Reciprocal relationships between the immune and central nervous system
[AD-A221259] 18 p2583 N90-24712

INTERGALACTIC MEDIA
The link to extragalactic objects 05 p0608 N90-13544
Cooling flows in clusters of galaxies 06 p0862 N90-15009
Interpretation of the 10 micron and 20 micron absorption bands in comets, the interstellar medium, and in an external galaxy 11 p1579 N90-19093
Skewering the universe with QSO lines of sight: Lyman alpha clouds as probes of large scale structure 16 p2329 N90-23278
Spectroscopic observations of high redshift QSOs: Galaxies and the intergalactic medium at early epochs 16 p2330 N90-23280

INTERGRANULAR CORROSION
Failure modes and mechanisms in nickel alloys: Primarily austenitic stainless steel
[DE89-016823] 02 p0198 N90-11132
A STEM study of changing grain boundary chemistry during the sensitisation of AISI 304 stainless steel
[AERE-R-13418] 14 p1949 N90-21157
The initiation of intergranular stress corrosion-cracking on sensitized stainless steel in dilute thiosulphate solutions
[AERE-R-13317] 16 p2217 N90-22648
Corrosion of aluminum alloys by IRFNA
[AD-A223011] 22 p3157 N90-27897

INTERIM STAGES (SPACECRAFT)
NT INERTIAL UPPER STAGE
Aeritalia Space Systems Group, Turin, Italy
[EOARD-LR-89-041] 02 p0159 N90-10908

INTERIM UPPER STAGE (STS)
U INERTIAL UPPER STAGE

INTERIOR BALLISTICS
Multidimensional numerical simulation of large caliber ignition processes
[ISL-CO-233/88] 08 p1042 N90-16021
Measurement of gas leaks between a projectile and the walls of a tube in a ballistic compressor
[ISL-CO-250/88] 11 p1510 N90-18694

INTERLAYERS
NT MULTILAYER INSULATION
Evaluation of a neoprene latex modified SAMI (Stress Absorbing Membrane Interlayer)
[PB89-226435] 05 p0628 N90-13665
Time-dependent failure of silver interlayer welds
[DE90-008015] 13 p1818 N90-20440

INTERLOCKING
U LOCKING

INTERMETALLICS
New structural materials
[AD-A209425] 01 p0044 N90-10246
Development of metastable processing paths for high temperature alloys
[AD-A210550] 01 p0045 N90-10254
Electronic structure of transition metal alloys and intermetallics: Charge transfer and its implications for Moessbauer effect measurements
[DE89-017603] 03 p0327 N90-11860
Deformation and defects in Laves-phase intermetallic compounds
[DE89-017798] 03 p0328 N90-11862
Carbon fiber reinforced metal matrix composites
[AD-D014245] 06 p0737 N90-14289
Advances and future directions in superplastic materials 06 p0744 N90-14328
Phases in lanthanum-nickel-aluminum intermetallic alloys
[DE90-000651] 06 p0746 N90-14343
Practical limitations of ALCHEMI measurements on ordered intermetallic alloys
[DE90-000700] 06 p0853 N90-14957
Exchange coupling in metals as understood then and now
[DE90-001271] 07 p0902 N90-15214
Selection of phase-change and containment materials for thermal energy storage
[NASA-CR-186228] 07 p0952 N90-15506
Deformation twinning in ordered intermetallic compounds
[DE89-014779] 07 p0997 N90-15767
Molecular-dynamics study of the amorphization of CuTi
[DE90-003563] 07 p1001 N90-15791
Design of coupled or uncoupled multifilamentary SSC-type strands with almost zero retained magnetization at fields near 0.3 T
[DE90-005391] 08 p1047 N90-16052
Metals and Ceramics Division Materials Sciences Program
[DE90-004371] 08 p1050 N90-16070
Development of a reliable fabrication technique to produce intermetallic compounds
[AD-A215004] 09 p1194 N90-16918
Hardness-damage correlations in Ta implanted single crystal Ni3Al
[DE90-005270] 09 p1293 N90-17494
The processing and mechanical properties of high temperature/high performance composites. Book 5, section 4: Processing: Matrices and composites, part 1
[AD-A216145] 10 p1349 N90-17823
The processing and mechanical properties of high temperature/high performance composites. Book 6, section 4: Processing: Matrices and composites, part 2
[AD-A216146] 10 p1349 N90-17824
Environmental embrittlement: A major cause for low ductility of ordered intermetallics
[DE90-006161] 10 p1356 N90-17864
The processing and mechanical properties of high temperature/high performance composites. Book 3, section 2: Strength and fracture resistance, part
[AD-A216143] 11 p1478 N90-18508
Deformation and fracture of ordered intermetallic compounds
[DE90-007422] 11 p1488 N90-18563
Irradiation-induced amorphization and elastic shear instability in intermetallic compounds
[DE90-004845] 12 p1625 N90-19341
Creep behavior of alloys based on TiAl containing TiB2 and TiN particulates
[DE90-006489] 12 p1628 N90-19355
An introduction to nickel aluminide alloy
[DE90-008565] 13 p1778 N90-20207
Lecture on ordered intermetallic alloys
[DE90-009011] 14 p1951 N90-21169
Compatibility of Au base thick films with solder alloys: Solid state growth of intermetallics
[DE90-009285] 14 p1952 N90-21175
Controlled production and characterization of metastable intermetallics
[DE90-009384] 14 p1952 N90-21176
Welding behavior and welding metallurgy of ductile intermetallic alloys
[DE90-008908] 15 p2069 N90-21852
Grain boundary intermetallic phases in alloy 718
[DE90-009812] 15 p2173 N90-22417
High temperature fatigue behavior of a SiC/Ti-24Al-11Nb composite
[NASA-TM-103157] 16 p2248 N90-22822
Reply to coupled S- and D-wave states in the thorium-doped heavy-fermion superconducting UBe13 by H. Pleiner and H. R. Brand
[AD-A220843] 17 p2477 N90-24164
Ta and Nb reinforced MoSi2
[DE90-010596] 18 p2517 N90-24377
Vibrational and optical properties of amorphous metals
[DE90-011427] 18 p2522 N90-24403
The effects of cooling rate XD (trademark) TiAl weld microstructure
[DE90-011975] 18 p2528 N90-24427
Deformation and fracture behavior of TiAl
[DE90-012212] 19 p2675 N90-25212
Oxide thermal stability on gamma titanium aluminide
[DE90-012054] 19 p2678 N90-25232
Searching for heavy fermion materials in Ce intermetallic compounds
[DE90-011809] 20 p2834 N90-26116

Fundamental studies of strongly magnetic rare earth-transition metal alloys
[DE90-012458] 21 p2980 N90-26937
Antiferromagnetism and enhanced heat in CeM2Sn (M = Ni, Ir, Cu, Rh, Pd, and Pt
[DE90-014924] 23 p3399 N90-29206
Powder processing of aluminides
[DE90-015314] 24 p3444 N90-29447
Alloy design of ordered intermetallics
[DE90-016031] 24 p3451 N90-29490
Atomistic studies of grain boundaries in alloys and compounds
[DE90-012401] 24 p3452 N90-29492
Fundamental studies on intermetallic compounds
[ONERA-RT-4/1855-M] 24 p3453 N90-29497

INTERMITTENCY
The multifractal nature of turbulence
16 p2235 N90-22752

INTERMODULATION
Optimization of the intermodulation performance of GaAs MESFET small-signal amplifiers
[AD-A215193] 09 p1212 N90-17026

INTERMOLECULAR FORCES
Phase behavior of pure and mixed systems at high pressure
[DE89-017734] 03 p0322 N90-11832
Molecular dynamics of lipid bilayers
[AD-A211492] 04 p0552 N90-13214
Theoretical studies of electrons and electron transfer processes in fluids
[DE90-008414] 17 p2470 N90-24117

INTERMONTANE FLOORS
U VALLEYS

INTERNAL COMBUSTION ENGINES
NT DIESEL ENGINES
NT GAS TURBINE ENGINES
NT HELICOPTER ENGINES
NT HYDROGEN ENGINES
NT JET ENGINES
NT RAMJET ENGINES
NT ROTARY ENGINES
NT SUPERSONIC COMBUSTION RAMJET ENGINES
NT TURBOFAN ENGINES
NT TURBOJET ENGINES
NT TURBOPROP ENGINES
NT TURBORAMJET ENGINES
The 4th US Army Workshop on Low Heat Rejection Engines
[AD-A212378] 04 p0510 N90-12942
The 4th US Army Workshop on Low Heat Rejection Engines
[AD-A212379] 04 p0510 N90-12943
Experimental and computational study of combustion limits in natural-gas fueled internal combustion engines
[PB89-235196] 05 p0629 N90-13673
Comparison of engine knock predictions using a fully-detailed and a reduced chemical kinetic mechanism
[DE90-002805] 07 p0941 N90-15448
Multi-dimensional modeling of convective heat transfer with application to I.C. engines
[DE90-003245] 07 p0941 N90-15451
Results from the third year of operation of the Federal Methanol Fleet at Lawrence Berkeley Laboratory
[DE90-003306] 08 p1084 N90-16277
Preliminary collection 891 of lectures/papers in Symposium by Society of Automotive Engineers of Japan
[DE90-710449] 10 p1391 N90-18045
Federal methanol fleet update
[DE90-006851] 11 p1517 N90-18741
Lightweight piston architecture
[NASA-CASE-LAR-13926-1] 15 p2105 N90-22042
Contributions to the study of parietal flames due to turbulent diffusion
[ECL-89-22] 17 p2374 N90-23519
Combustion of n-butane and isobutane in an internal combustion engine: A comparison of experimental and modeling results
[DE90-005993] 18 p2522 N90-24400
Critical evaluation of Jet-A spray combustion using propane chemical kinetics in gas turbine combustion simulated by KIVA-2
[NASA-TM-103173] 20 p2843 N90-26170
Modeling of knock in spark-ignition engines
[DE90-010875] 22 p3182 N90-28058
Results from the fourth year of operation of the Federal Methanol Fleet at Lawrence Berkeley Laboratory
[DE90-014741] 23 p3315 N90-28743
Smart microsensors for high temperature applications, phase 1
[AD-A224151] 23 p3330 N90-28828
Development of advanced combustion technology for medium and high speed natural gas engines
[PB90-198565] 23 p3331 N90-28836

INTERNAL COMPRESSION INLETS
Numerical investigations in three-dimensional internal flows
[NASA-CR-186068] 06 p0718 N90-14189

INTERNAL ENERGY
Supersonic jet studies of benzyl alcohols: Minimum energy conformations and torsional motion
[AD-A221815] 21 p2980 N90-26934
Determination of the heat dissipated from a specimen undergoing cyclic plasticity by a hybrid numerical/experimental method
[AD-A221575] 21 p2982 N90-26946
Thermophysical properties of Helium-4 from 0.8 to 1500 K with pressures to 2000 MPa
[NASA-CR-186992] 23 p3303 N90-28681

INTERNAL FRICTION
Internal rotor friction instability
[NASA-CR-183942] 14 p1988 N90-21395

INTERNAL PRESSURE
Blow-out of rubber blocks due to internal heating
[AD-A215730] 09 p1198 N90-16943
Elastic-plastic analysis of a thick-walled composite tube subjected to internal pressure
[AD-A215258] 09 p1238 N90-17187
Continued research on the strain to failure of thick-walled cylinders subjected to internal pressure
[DE90-008952] 15 p2118 N90-22115
The yield and post-yield behavior of high-density polyethylene
[NASA-CR-186574] 19 p2676 N90-25219

INTERNAL STRESS
U RESIDUAL STRESS

INTERNAL WAVES
NT PLANETARY WAVES
Non-linear wave-equations for low-frequency acoustic gravity waves
02 p0240 N90-11365
Effects on electromagnetic wave propagation and rocket vapor trails of intense turbulence generated by breaking internal gravity waves
[AD-A211755] 03 p0373 N90-12130
First-order Bragg SAR imagery of Kelvin wakes and moving internal wave fields
[AD-A213361] 05 p0633 N90-13691
Measurement of fluctuations in the tilt of Arctic ice at the CEAREX Oceanography Camp: Experiment review, data catalog, and preliminary results
[AD-A215059] 09 p1249 N90-17249
Formulation of non-reflecting boundary conditions in numerical models of the atmosphere
15 p2129 N90-22175
Nonlinear internal gravity wave critical layers
17 p2422 N90-23801
The browse file of NASA/JPL quick-look radar images from the Loch Linnhe 1989 experiment
[NASA-CR-186855] 20 p2935 N90-26701

INTERNATIONAL COMETARY EXPLORER
U INTERNATIONAL SUN EARTH EXPLORER 3

INTERNATIONAL COOPERATION
NT OUTER SPACE TREATY
Meeting of intercosmos space physics group
02 p0158 N90-10902
USSR and international cooperation in space
02 p0158 N90-10905
Globalization of Technology: International Perspectives. Proceedings of the 6th Convocation of the Council of Academies of Engineering and Technological Sciences
[PB89-198840] 02 p0288 N90-11645
Wider horizons: Potential contributions by space systems to socio-economic advancement in developing countries
[ESA-SP-1106] 04 p0562 N90-13276
Technology transfer to the United States: The MIT (Massachusetts Institute of Technology) Japan Science and Technology Program. A background paper of OTA's (Office of Technology Assessment's) assessment on technology, innovation, and US trade
[PB89-224711] 04 p0564 N90-13291
The SIMBAD data base 05 p0608 N90-13547
Swiss scientific balloon and sounding rocket experiments 1987-1989 05 p0656 N90-13827
AGARD Highlights 89/2 06 p0717 N90-14184
Discussions of global environmental problems
[DE90-002747] 06 p0811 N90-14718
An international discussion on research in solar and space physics 06 p0859 N90-14996
International aspects of restrictions of ozone-depleting substances
[DE90-001813] 07 p0957 N90-15534
Prospects for space arms control
[DE90-003392] 07 p0987 N90-15700
Crew Safety and Rescue in Space: An International Approach
[ESA-SP-300] 08 p1034 N90-15974
Systems interoperability approach Apollo/Soyuz test project 08 p1035 N90-15979
Crew safety and rescue aids
08 p1035 N90-15980
Guide on the global observing system
[WMO-488-REV] 08 p1103 N90-16385
Glavkosmos U.S.S.R. and the basic objectives of its activity 09 p1174 N90-16788
The DLR technology programme on space transportation 09 p1180 N90-16841
The European space effort: An integral part of the construction of Europe 09 p1180 N90-16845
A comparison of European and American microgravity combustion experimental techniques
09 p1202 N90-16966
Long term planning for space flight activities within the DFVLR
[DFVLR-IB-303-88/2] 11 p1465 N90-18438
ESA project to promote and assist technology transfer by industry 11 p1576 N90-19069
Proceedings of the Conference on Technology-Based Confidence Building: Energy and Environment
[CNSS-PAPERS-22] 15 p2125 N90-22152
Mission to planet Earth 15 p2125 N90-22153
The International Space University
[NASA-TM-103163] 16 p2209 N90-22604
International cooperation for Mars exploration and sample return
[NASA-CR-186511] 17 p2358 N90-23419
Navigation programmes: Financial and institutional aspects 17 p2361 N90-23441
Space Station Freedom media handbook
[NASA-TM-102901] 17 p2364 N90-23460
Polar prospects: A minerals treaty for Antarctica
[OTA-O-428] 17 p2480 N90-24185
National Aeronautics and Space Administration, 3 May 1989 18 p2636 N90-25019
NASA's experience in the international exchange of scientific and technical information in the aerospace field
[NASA-TM-103093] 19 p2764 N90-25704
Technology transfer: US and foreign participation in R and D at Federal laboratories
[GAO/RCED-88-203BR] 19 p2764 N90-25706
Second Meeting of the Space Agency Forum on the International Space Year (SAFISY)
[ESA-SP-1115] 19 p2800 N90-25932
Space exploration: Cost, schedule, and performance of NASA's Ulysses Mission to the Sun. Fact sheet for the Chairman, Subcommittee on Science, Technology, and Space, Committee on Commerce, Science, and Transportation, US Senate
[GAO/NSIAD-88-129FS] 20 p2815 N90-26023
Manned Space Stations: Legal Issues
[ESA-SP-305] 20 p2937 N90-26711
The US/International Space Station: Legal aspects of space objects and jurisdiction and control
20 p2937 N90-26713
MIR: A Soviet Space Station. Some legal aspects of international cooperation 20 p2938 N90-26715
The International Space Station: The legal framework
20 p2938 N90-26716
The partnership concept and international management 20 p2938 N90-26717
The International Space Station: Conditions of access and use 20 p2938 N90-26718
Human work in space: The astronaut's legal status. Introduction 20 p2938 N90-26719
The manned national space station: international legal considerations 20 p2938 N90-26720
The astronauts' legal status: The International Space Station 20 p2938 N90-26721
Crossborder movements: Goods, personnel and technologies 20 p2939 N90-26722
Space Station intellectual property rights and US patent law 20 p2939 N90-26723
Possible solutions 20 p2939 N90-26726
Space law put to the test by the International Space Station 20 p2939 N90-26727
INTERMAGNET 21 p3023 N90-27190
ECOS: The ESA Costing Software
[ESA-BR-56] 21 p3039 N90-27274
Integrated Air Traffic Management
[DLR-MITT-89-23] 22 p3112 N90-27676
Airline requirements for a future air traffic management system 22 p3112 N90-27678
PHARE: Concept and programme
22 p3114 N90-27690
Goverment's role in standards-related activities: Analysis of comments
[PB90-215534] 23 p3404 N90-29239
Global Climate Change: Seeking a Global Consensus
[S-HRG-101-842] 24 p3486 N90-29704
Success of EPA's stratospheric ozone engineering research
[PB90-246265] 24 p3487 N90-29706

Some personal reminiscences. The ESRO-ESA space science story: Twenty-five years of European cooperation
[ESA-BR-66] 24 p3565 N90-30168

INTERNATIONAL LAW
NT SPACE LAW

INTERNATIONAL RELATIONS
NT INTERNATIONAL COOPERATION
NT OUTER SPACE TREATY
Technology transfer and the FSX: Effects on the United States/Japanese relationship
[AD-A216348] 10 p1443 N90-18327
International treaties and active experiments in space
[AD-A219368] 16 p2328 N90-23272
Brazil, the United States, and the missile technology control regime
[AD-A220551] 17 p2362 N90-23449
Department of Energy Strategic Defense Initiative programs: Potential programmatic and facility impacts due to a prospective defense and space treaty
[DE90-012717] 21 p3067 N90-27437

INTERNATIONAL SOLAR POLAR MISSION
U ULYSSES MISSION

INTERNATIONAL SUN EARTH EXPLORER 3
Spectrophotometric observations of comet P/Giacobini-Zinner 08 p1144 N90-16630

INTERNATIONAL SUN EARTH EXPLORERS
NT INTERNATIONAL SUN EARTH EXPLORER 3

INTERNATIONAL SYSTEM OF UNITS
Metric handbook for Federal officials: Recommendations of the Interagency Committee on Metric Policy
[PB89-226922] 06 p0756 N90-14400

INTERNATIONAL TRADE
COCOM (Coordinating Committee for Multilateral Exports), technology transfer and its impact on national security
[AD-A214569] 09 p1297 N90-17519

INTERNATIONAL ULTRAVIOLET EXPLORER
U IUE

INTERORBITAL TRAJECTORIES
Shuttle tethered operations: The effect on orbital trajectory and inertial navigation
05 p0588 N90-13425
Interactive orbital proximity operations planning system 16 p2273 N90-22953

INTERPERSONAL RELATIONS
U HUMAN RELATIONS

INTERPLANETARY DUST
NT ZODIACAL DUST
Interplanetary dust close to the Sun (F corona): Its observation in the visible and infrared by a rocket-borne coronagraph 05 p0661 N90-13864
Extraterrestrial halogen and sulfur content of the stratosphere
[DE89-017623] 06 p0815 [illegible]90-14738
A model of the thermal and electrical properties of cosmic dust particles 06 p0863 N90-15014
Solar-geophysical data number 540, August 1989. Part 2: (Comprehensive reports). Data for February 1989
[PB89-108598] 06 p0867 N90-15039
Near-infrared polarimetry and spectroscopy of comets
07 p1011 N90-15857
Identification of solar nebula condensates in interplanetary dust particles and unequilibrated ordinary chondrites 08 p1144 N90-16629
What if chondritic porous interplanetary dust particles are not the real McCoy 08 p1146 N90-16642
Isotopic microanalysis of returned comet nucleus samples 08 p1149 N90-16655
The measurement of trace elements in interplanetary dust and cometary particles by ultra-high sensitivity INAA
08 p1149 N90-16656
Analogies between cometary, interplanetary, and interstellar matter 11 p1578 N90-19087
Infrared spectroscopy of dust
11 p1579 N90-19094
Interstellar extinction in the infrared
11 p1579 N90-19095
Spectropolarimetry as a diagnostic of the interstellar medium 11 p1579 N90-19096
Dust continuum spectra from model HII regions
11 p1580 N90-19099
Infrared diagnostics for interstellar solid state chemistry 11 p1580 N90-19103
An almost total disjunction between emission and absorption dust features: What does it tell us?
11 p1581 N90-19106
Planetary nebulae 11 p1583 N90-19122
Ice grains in the dust disk of the bipolar nebula M 1-92 11 p1584 N90-19127
Dust in planetary nebulae: IRSPEC observations in the 3.0 micron-3.8 micron range 11 p1584 N90-19132
Porosity and ice-dust mixtures in cometary particles
12 p1743 N90-20018
Mechanical properties of fluffy agglomerates consisting of core-mantle-particles 12 p1743 N90-20019
Carbon in the Galaxy: Studies from Earth and Space
[NASA-CP-3061] 21 p3089 N90-27562
Carbon in comet dust 21 p3089 N90-27564
Astronomical observations of solid phase carbon
21 p3089 N90-27566
Carbon stardust: From soot to diamonds
21 p3090 N90-27568
The possible presence of interstellar PAHs in meteorites and interplanetary dust particles
21 p3092 N90-27579
Raman spectroscopic studies of carbon in extra-terrestrial materials 21 p3095 N90-27589
On diamond, graphitic and amorphous carbons in primitive extraterrestrial solar system materials
21 p3095 N90-27591

INTERPLANETARY FLIGHT
JPRS Report: Science and Technology. USSR: Space
[JPRS-USP-89-007] 02 p0158 N90-10900
Manned spacecraft
[AD-A214218] 07 p0887 N90-15129
Reports of planetary astronomy, 1986
[NASA-TM-100776] 08 p1138 N90-16596
Mars in this century: The Olympia Project
[DE90-008356] 14 p2042 N90-21709
A spring-actuated spin and eject device for interplanetary missions 18 p2540 N90-24493

INTERPLANETARY MAGNETIC FIELDS
Studies of time-dependent polar cap convection patterns 02 p0251 N90-11421
Rotation of the photospheric magnetic fields: A north-south asymmetry
[NASA-CR-186159] 05 p0715 N90-14177
Kilometric type III radio bursts and interplanetary transients 06 p0867 N90-15038
Laboratory simulations of the solar wind-comet interactions 07 p1015 N90-15875
Polar cusps latitudinal shift and its relation to the IMF-By component
[IFSI-88-14] 08 p1101 N90-16377
Some properties of so-called magnetic cloud structures in the solar wind
[IFSI-88-16] 08 p1153 N90-16678
Quantifying and reducing uncertainty in the assimilative mapping of ionospheric electrodynamics
[AD-A218057] 13 p1842 N90-20577
A study of auroral activity in the nightside polar cap
16 p2254 N90-22852
Evaluation of space plasma data: Effects upon spacecraft materials and predictions of hazardous conditions; polar ARCS
[AD-A219509] 17 p2474 N90-24145
Electrodynamics of the high latitude ionosphere
[AD-A223229] 21 p3026 N90-27203
Relationship between solar activities and thunderstorm activities in the Beijing area and the northeast region of China 22 p3208 N90-28197
The influence of IMF on the lower ionosphere plasma in high and middle latitudes 22 p3208 N90-28200
Solar or meteorological control of lower ionospheric fluctuations (2-15 and 27 days) in middle latitudes
22 p3209 N90-28202
Interplanetary medium data book, supplement 4, 1985-1988
[NASA-TM-101867] 24 p3561 N90-30149

INTERPLANETARY MEDIUM
NT INTERPLANETARY DUST
NT ZODIACAL DUST
Interzodiak 2: Observation of EUV-resonance radiation
05 p0660 N90-13854
Interstellar medium and infrared emission of the galactic disk 05 p0661 N90-13862
Optical observations of interplanetary pick-up ions: The experiment Helly 05 p0661 N90-13863
Project Supernova 1987 05 p0662 N90-13866
Activities report of the Institute of Interplanetary Stellar Physics
[IFSI-89-8] 09 p1298 N90-17520
Report on scientific activity and funds management for 1988
[IFSI-89-9] 09 p1298 N90-17521
Activities report of the Institute of Interplanetary Stellar Physics
[IFSI-88-22] 10 p1445 N90-18339
Scientific activity programs for 1988-1990
[IFSI-88-23] 10 p1445 N90-18340
Scientific activity program for 1989
[IFSI-89-10] 10 p1445 N90-18341
Interplanetary medium data book, supplement 4, 1985-1988
[NASA-TM-101867] 24 p3561 N90-30149

INTERPLANETARY NAVIGATION
The effect of interplanetary trajectory options on a manned Mars aerobrake configuration
[NASA-TP-3019] 20 p2818 N90-26036

INTERPLANETARY PROPULSION
U INTERPLANETARY SPACECRAFT
U ROCKET ENGINES

INTERPLANETARY SPACE
MHD (magnetohydrodynamic) modeling of solar and interplanetary processes
[PB89-215461] 03 p0420 N90-12416
Interplanetary energetic particle observations of the March 1989 events 03 p0434 N90-12484
Stochastic simulation of charged particle transport on the massively parallel processor
08 p1114 N90-16448
MHD (Magnetohydrodynamic) slow shocks in coronal and interplanetary space
[AD-A214725] 09 p1299 N90-17527
Zodiacal dust bands: Their relation to asteroid families
[AD-A216025] 11 p1590 N90-19170
Solar flares and magnetospheric particles: Investigations based upon the ONR-602 and ONR-604 experiments
[AD-A218844] 16 p2340 N90-23332
Data catalog series for space science and applications flight missions. Volume 5A: Descriptions of astronomy, astrophysics, and solar physics spacecraft and investigations. Volume 5B: Descriptions of data sets from astronomy, astrophysics, and solar physics spacecraft and investigations
[NASA-TM-101908] 24 p3437 N90-29413
Data catalog series for space science and applications flight flight missions. Volume 2B: Descriptions of data sets from geostationary and high-altitude scientific spacecraft and investigations
[NASA-TM-101909] 24 p3437 N90-29414
Data catalog series for space science and applications flight missions. Volume 1A: Descriptions of planetary and heliocentric spacecraft and investigations, second edition
[NASA-TM-101910] 24 p3438 N90-29415
Data catalog series for space science and applications flight missions. Volume 6: Master index volume
[NASA-TM-101913] 24 p3438 N90-29416
Data catalog series for space science and applications flight missions. Volume 4B: Descriptions of data sets from meteorological and terrestrial applications spacecraft and investigations
[NASA-TM-101880] 24 p3556 N90-30123
Data catalog series for space science and applications flight missions. Volume 3B: Descriptions of data sets from low- and medium-altitude scientific spacecraft and investigations
[NASA-TM-89680] 24 p3560 N90-30140
Data catalog series for space science and applications flight missions. Volume 1B: Descriptions of data sets from planetary and heliocentric spacecraft and investigations
[NASA-TM-89695] 24 p3561 N90-30148

INTERPLANETARY SPACECRAFT
NT GALILEO SPACECRAFT
NT JUPITER PROBES
NT MAGELLAN SPACECRAFT (NASA)
NT MARS OBSERVER
NT PIONEER VENUS SPACECRAFT
NT PIONEER VENUS 1 SPACECRAFT
NT PIONEER 10 SPACE PROBE
NT PIONEER 11 SPACE PROBE
NT VIKING LANDER SPACECRAFT
NT VOYAGER 1 SPACECRAFT
NT VOYAGER 2 SPACECRAFT
USSR and international cooperation in space
02 p0158 N90-10905
Preliminary investigation of parameter sensitivities for atmospheric entry and aerobraking at Mars
[NASA-TM-101607] 10 p1327 N90-17667
The importance of batteries in unmanned missions
13 p1821 N90-20456
System control of an autonomous planetary mobile spacecraft 15 p2155 N90-22313
Data catalog series for space science and applications flight missions. Volume 5A: Descriptions of astronomy, astrophysics, and solar physics spacecraft and investigations. Volume 5B: Descriptions of data sets from astronomy, astrophysics, and solar physics spacecraft and investigations
[NASA-TM-101908] 24 p3437 N90-29413
Data catalog series for space science and applications flight flight missions. Volume 2B: Descriptions of data sets from geostationary and high-altitude scientific spacecraft and investigations
[NASA-TM-101909] 24 p3437 N90-29414
Data catalog series for space science and applications flight missions. Volume 1A: Descriptions of planetary and heliocentric spacecraft and investigations, second edition
[NASA-TM-101910] 24 p3438 N90-29415
Data catalog series for space science and applications flight missions. Volume 6: Master index volume
[NASA-TM-101913] 24 p3438 N90-29416

Data catalog series for space science and applications flight missions. Volume 4B: Descriptions of data sets from meteorological and terrestrial applications spacecraft and investigations
[NASA-TM-101880] 24 p3556 N90-30123
Data catalog series for space science and applications flight missions. Volume 3B: Descriptions of data sets from low- and medium-altitude scientific spacecraft and investigations
[NASA-TM-89680] 24 p3560 N90-30140
Data catalog series for space science and applications flight missions. Volume 1B: Descriptions of data sets from planetary and heliocentric spacecraft and investigations
[NASA-TM-89695] 24 p3561 N90-30148

INTERPLANETARY TRAJECTORIES
Nongravitational forces by Halley's comet
[ETN-90-96491] 18 p2638 N90-25027
The effect of interplanetary trajectory options on a manned Mars aerobrake configuration
[NASA-TP-3019] 20 p2818 N90-26036
Trajectory optimization of a bimodal nuclear powered spacecraft to Mars
[AD-A222974] 21 p2969 N90-26876

INTERPOLATION
Thermodynamic and dynamic processes in the updraft region of GALE (Genesis of Atlantic Lows Experiment) IOP (Intensive Observation Period) 9
[AD-A208139] 01 p0087 N90-10496
On two polynomial spaces associated with a box spline
[AD-A210559] 01 p0113 N90-10646
Numerical treatment of the thermo-structural-dynamic problems: The interpolation techniques
02 p0180 N90-11016
An interpolation theorem in equational logic
[CWI-CS-R8838] 02 p0268 N90-11528
Alias-free Wigner distribution function and complex ambiguity function for discrete-time samples
[AD-A211050] 02 p0269 N90-11533
Operational measures of central tendency
[DE89-016959] 03 p0392 N90-12234
Calculation of transient response from time-harmonic spectrum
[AD-A211972] 03 p0393 N90-12241
Inf-convolution splines
[IMAG-RR-749-M] 03 p0395 N90-12256
A theory of networks for approximation and learning
[AD-A212359] 04 p0538 N90-13110
Faster Phong shading via angular interpolation
[CWI-CS-R8909] 04 p0543 N90-13156
Enhancement of infrared thermographic imagery: Local smoothing and time-based interpolation
[ONERA-RT-8/7254-SN] 04 p0555 N90-13232
Feature modeling: The incorporation of a front and eddy map into optimum interpolation-based thermal analysis
[AD-A213253] 05 p0672 N90-13914
Thermophysical properties of isopropyl alcohol. Part 2: Thermodynamic properties at elevated pressures
[ESDU-89020-PT-2] 06 p0739 N90-14300
Rainfall estimation over Africa using satellite data
06 p0815 N90-14742
Modified Chebyshev pseudospectral method with O(N exp -1) time step restriction
[NASA-CR-181958] 06 p0834 N90-14848
Application of Lagrangian blending functions for grid generation around airplane geometries
[NASA-CR-186318] 08 p1018 N90-15891
Context dependent anti-aliasing image reconstruction
08 p1073 N90-16209
Image smoothing and differentiation with minimal-curvature filters
[AD-A215184] 09 p1273 N90-17382
Inverse scattering and tomography
[AD-A216456] 11 p1551 N90-18932
Analysis and design of symmetrical airfoils
[PD-CF-8943] 12 p1601 N90-19213
Analysis of unsteady heat transfer by natural convection in a two-dimensional square cavity using a high order finite-volume method 12 p1657 N90-19521
Calculation of nonlinear viscoelastic processes for plastic layer textile membranes
[ETN-90-95868] 12 p1675 N90-19622
Initialization of EURAD, part 2
12 p1688 N90-19696
A technique for convolving unequally spaced samples using fast Fourier transforms
[DE90-006466] 12 p1707 N90-19802
A linear filtering technique for removal of low-frequency noise
[DE90-006183] 13 p1794 N90-20296
An overlapped grid method for multigrid, finite volume/difference flow solvers: MaGGiE
[NASA-CR-182008] 14 p1911 N90-20953
Quiet mode for nonlinear rotor models
[NASA-TM-102236] 15 p2051 N90-21758
Nonlinear spline operator interpolation and sliding control of deformable maneuvering bodies
15 p2074 N90-21878
Inclusion of clouds and rain in atmospheric slant path calculations 15 p2083 N90-21925
Algebraic block-structured grid generation based on a macro-block concept 15 p2093 N90-21976
Motion detection in astronomical and ice floe images
15 p2140 N90-22231
An algorithm and computer program for the calculation of envelope curves
[PB90-155409] 15 p2145 N90-22254
Multiprocessing on supercomputers for computational aerodynamics
[NASA-TM-102806] 17 p2347 N90-23366
PUFFY: A puff diffusion computer model
[FOA-C-40251-4.5] 17 p2421 N90-23796
An H(m)sub 0 interpolation result
[AD-A219888] 17 p2461 N90-24051
Application of frequency interpolation to acoustic-structure interaction problems
[AD-A219330] 17 p2469 N90-24113
Stability and error estimates for sinc interpolation
[CWI-AM-R8914] 18 p2599 N90-24790
Characterization of porous media: Field level
19 p2690 N90-25304
Interactive grid generation on small computers
[AD-A221234] 19 p2742 N90-25585
A topological image matcher
[OUEL-1798/89] 19 p2744 N90-25600
Modular arithmetic and randomization for exact matroid problems: Extended abstract
[REPT-89-064] 19 p2751 N90-25628
Comment on high resolution simulations of cosmic strings. 1: Network evoloution
[NASA-CR-186606] 20 p2941 N90-26734
Gulfcasting: Dynamical forecast experiments for G ulf Stream rings and meanders
[AD-A221482] 21 p3032 N90-27238
Generalized interpolation theory for the design and analysis of robust feedback systems
[AD-A222130] 21 p3060 N90-27399
LINTERP: A numerical algorithm for interpolating quadrilateral and hexahedral meshes
[DE90-014417] 23 p3379 N90-29090
Local interpolation functions for curve generation with the multi-surface transformation
24 p3470 N90-29608
Estimation and representation of multidimensional mappings
[DLR-MITT-90-06] 24 p3531 N90-29967
Sensitivity of the error in multivariate statistical interpolation to parameter values
[AD-A224076] 24 p3540 N90-30015

INTERPOLATORS
U REPEATERS

INTERPROCESSOR COMMUNICATION
DDN Trusted Guard Gateway: Trusted Guard Gateway (TGG) technology assessment, phase 2
[AD-A210248] 01 p0108 N90-10614
An integrated distributed processing interface for supercomputers and workstations
[DE89-016769] 02 p0260 N90-11478
Optical coherence multiplexing for interprocessor communications
[DE89-016186] 02 p0275 N90-11568
On the communication complexity of solving a polynomial equation
[AD-A211945] 03 p0393 N90-12240
DOD Gateway Information System (DGIS) common command language: A retrospective on the introduction of prolog as the development tool
[AD-A211941] 03 p0418 N90-12400
An implementation-oriented specification of the TUMULT communication primitives
[MEMO-INF-88-34] 04 p0536 N90-13098
Implementing the discrete Fourier transform on the hypercube FPS T40
[IMAG-RR-773-I] 05 p0684 N90-13983
Fast serial communication module
[DE89-633753] 06 p0766 N90-14454
UNIX internals. Part 1: Intertask communication in UNIX. Part 2: UNIX file system
[CNES-NT-122-PT-1/2] 08 p1107 N90-16405
Algorithms for fault tolerant distributed systems
[AD-A214447] 08 p1109 N90-16416
A specification and analysis of the IEEE (Institute of Electrical and Electronic Engineers) token ring protocol
[AD-A214567] 09 p1269 N90-17359
Parallel functional computation
[AD-A214627] 09 p1269 N90-17360
Merlin: A superglue for multicomputer systems
[NASA-CR-186330] 09 p1271 N90-17366
Flosolver Mk1B: An eight processor parallel machine
[PD-CF-8941] 12 p1699 N90-19755
Express cubes: Improving the performance of k-ary n-cube interconnection networks
[AD-A217117] 13 p1793 N90-20287
A scheme for supporting automatic data migration on multicomputers
[NASA-CR-182038] 16 p2276 N90-22973
Communication overhead on the Intel iPSC-860 hypercube
[NASA-CR-182055] 16 p2278 N90-22982
Durra: A task-level description language reference manual, version 2
[AD-A219293] 16 p2301 N90-23114
Locality in parallel computation
[AD-A218733] 16 p2302 N90-23120
Control of randomly sampled robotic systems
[AD-A218948] 16 p2309 N90-23157
Simulation and analysis of a MFQPSK signal transmitted through an acoustic medium
[AD-A220345] 17 p2393 N90-23633
Applications for the scalable coherent interface
[DE90-011795] 20 p2903 N90-26514
Integrating expert systems with solid modeling through interprocess communications and the applications interface specification
[DE90-012996] 20 p2907 N90-26537
A parallel algorithm for surface plane intersection
[IMAG-RR-794-M] 20 p2909 N90-26549
Implementation of algorithms used in calculating the tensor product of matrices on a distributed memory machine
[IMAG-RR-786-I] 20 p2913 N90-26572
Supercomputer workstation communication
[AD-A222466] 21 p3039 N90-27272
Interconnection networks and parallel processing
[FEL-1989-112] 22 p3240 N90-28376
On the stability of robotic systems with random communication rates 24 p3514 N90-29865
Reliable communication in the presence of failures
[NASA-CR-183046] 24 p3533 N90-29977

INTERROGATION
A parallel algorithm for surface plane intersection
[IMAG-RR-794-M] 20 p2909 N90-26549

INTERSECTIONS
Improved lighting of taxiway/taxiway intersections for instrument Flight Rules (IFR) operations
[DOT/FAA/CT-TN89/64] 07 p0878 N90-15089

INTERSTELLAR CHEMISTRY
Rocket and satellite observations of the local interstellar medium 02 p0292 N90-11668
Non-equilibrium chemistry in the solar nebula and early solar system: Implications for the chemistry of comets
08 p1142 N90-16618
Interstellar HCN, HNC and HCO+: Stability experiments with acoustooptic spectrometers
[ETN-90-96495] 18 p2638 N90-25028
Carbon in the Galaxy: Studies from Earth and Space
[NASA-CP-3061] 21 p3089 N90-27562
Interstellar grain chemistry and organic molecules
21 p3090 N90-27569
Carbon chemistry of circumstellar envelopes
21 p3090 N90-27570
Carbon chemistry in dense molecular clouds: Theory and observational constraints 21 p3090 N90-27571
Laboratory simulation of interstellar grain chemistry and the production of complex organic molecules
21 p3092 N90-27580
The ionization structure of planetary nebulae 10: NGC 2392
[NASA-CR-186960] 23 p3411 N90-29274

INTERSTELLAR EXTINCTION
Interstellar extinction in the infrared
11 p1579 N90-19095
Comet Halley: An optical continuum study
12 p1736 N90-19981
Probing the possibility of a C-12/C-13 galactic abundance gradient 21 p3094 N90-27586
An observational study of disk-population globular clusters 24 p3560 N90-30145

INTERSTELLAR GAS
Rocket and satellite observations of the local interstellar medium 02 p0292 N90-11668
Role of dust to gas production rate ratio in cometary physics 08 p1143 N90-16625
Infrared diagnostics of interstellar shocks
11 p1582 N90-19115
The excitation of molecular hydrogen and its significance 11 p1582 N90-19117
Interactions of massive stars with the interstellar medium: Bow shocks and superbubbles
15 p2186 N90-22485
The environmental impact of the X ray flux from active galactic nuclei 19 p2786 N90-25853
Search for interstellar methane
21 p3094 N90-27588

Strong associated C 4 absorption in low redshift quasars
[NASA-CR-186936] 22 p3262 N90-28469

INTERSTELLAR MAGNETIC FIELDS
The interaction of supernovae and pulsars with the circumstellar environment 02 p0293 N90-11671
Interstellar magnetic fields: An observational perspective 24 p3560 N90-30144

INTERSTELLAR MASERS
Very high resolution radio observations of molecular cloud cores 06 p0863 N90-15013
A three-year study of the OH masers in Orion-KL and a study of the (3,2) transition of ammonia 15 p2183 N90-22471
Investigation of the late stages of stellar evolution: Mass loss from evolved stars 15 p2187 N90-22492

INTERSTELLAR MATTER
NT DARK MATTER
NT INTERSTELLAR GAS
IRAS observations of the extended galactic objects Cas A and W80 02 p0290 N90-11657
Rocket and satellite observations of the local interstellar medium 02 p0292 N90-11668
Small grains in reflection nebulae: A study of diffuse interstellar bands, elemental depletions and infrared flux 02 p0293 N90-11672
Nonequilibrium ionization in supernova remnants: The case of Tycho
[MPE-PREPRINT-153] 04 p0565 N90-13295
Properties of evolved star circumstellar grains 06 p0861 N90-15003
Evidence for anomalous cosmic ray hydrogen 06 p0861 N90-15005
The disk-halo connection and the nature of the interstellar medium
[NASA-CR-186286] 07 p1012 N90-15860
The volatile composition of comets
[NASA-CR-186281] 07 p1014 N90-15871
Workshop on Analysis of Returned Comet Nucleus Samples
[NASA-CR-184821] 08 p1140 N90-16607
Direct determination of the morphology, structure and composition of cometary and interstellar ice analogs in the laboratory 08 p1141 N90-16612
The carbon chemistry of meteorites: Relationships to comets 08 p1141 N90-16615
Analysis of organic compounds in returned comet nucleus samples 08 p1142 N90-16617
From interstellar dust to comets 08 p1142 N90-16620
Comments on comet shapes and aggregation processes 08 p1142 N90-16622
Computer simulation of dust grain evolution 08 p1144 N90-16632
Solar nebula condensates and the composition of comets 08 p1144 N90-16634
Interstellar and cometary dust 08 p1145 N90-16636
Metamorphism of cosmic dust: Processing from circumstellar outflows to the cometary regolith 08 p1146 N90-16641
Gamma-ray observations and the distribution of interstellar aluminum-26 08 p1150 N90-16661
Turbulent stripping of interstellar clouds by interaction with supernova remnants
[DE90-003622] 08 p1152 N90-16674
Analogies between cometary, interplanetary, and interstellar matter 11 p1578 N90-19087
The unidentified IR bands in laboratory, in interstellar medium, and in comets 11 p1578 N90-19089
A unified model for the 3.28 micron and 3.4 micron spectral feature in the interstellar medium and in comets 11 p1579 N90-19092
Interpretation of the 10 micron and 20 micron absorption bands in comets, the interstellar medium, and in an external galaxy 11 p1579 N90-19093
Spectropolarimetry as a diagnostic of the interstellar medium 11 p1579 N90-19096
Chemistry on interstellar grains and implications for infrared spectroscopy 11 p1579 N90-19097
A coal model for the carriers of the unidentified IR bands 11 p1581 N90-19110
An implication of the IR identification of PAHs: The heating of the diffuse is gas 11 p1582 N90-19113
Hydrodynamical simulations of collisions between interstellar clouds
[DE90-006921] 11 p1590 N90-19172
A test of the interstellar dust model of comets 12 p1739 N90-19995
Recombination lines of C I and N II in the interstellar medium 15 p2182 N90-22466
The optical night sky at low surface brightness: High latitude dust and faint field galaxies 15 p2185 N90-22481
The evolution of the supernova remnant IC 443 15 p2186 N90-22486
The Al-26(rho, gamma)Si-27 reaction: Stellar origins of galactic Al-26 15 p2188 N90-22498
The ratio of neutral hydrogen to neutral helium in the local interstellar medium 15 p2189 N90-22499
The interstellar medium of a starburst galaxy; millimeter interferometric observations of M82 16 p2329 N90-23276
The effect of a stellar wind on an expanding H II region 16 p2333 N90-23292
The interstellar D1 line at high resolution
[NASA-CR-184915] 20 p2941 N90-26737
Carbon in primitive meteorites 21 p3089 N90-27563
CI, CII, and CO as tracers of gas phase carbon 21 p3091 N90-27572
A unifying picture of gas-phase formation and growth of PAH (Polycyclic Aromatic Hydrocarbons), soot, diamond and graphite 21 p3091 N90-27575
The formation and structure of circumstellar and interstellar dust 21 p3091 N90-27576
SIRTF: Probing the dark corners of the galaxy 21 p3091 N90-27577
Laboratory simulation of interstellar grain chemistry and the production of complex organic molecules 21 p3092 N90-27580
Nature and origin of interstellar diamond from the Allende CV3 meteorite 21 p3092 N90-27581
New observations of interstellar organic molecules 21 p3094 N90-27587
Can the chirality of the ISM be measured 21 p3095 N90-27590
On diamond, graphitic and amorphous carbons in primitive extraterrestrial solar system materials 21 p3095 N90-27591
Star formation and the distribution of HI and infrared emission in M51
[NASA-CR-186928] 23 p3408 N90-29262
Near-infrared speckle observations of T Tauri stars and a multi-wavelength study of the prototype star T Tauri 23 p3409 N90-29264
A plasma diagnostic study of two wind-blown shell nebulae: NGC 7635 and NGC 2359 23 p3410 N90-29271

INTERSTELLAR MICROWAVE SPECTRA
U INTERSTELLAR RADIATION
U MICROWAVE SPECTRA

INTERSTELLAR RADIATION
Laboratory simulation of interstellar grain chemistry and the production of complex organic molecules 21 p3092 N90-27580

INTERSTELLAR REDDENING
U INTERSTELLAR EXTINCTION

INTERSTELLAR SPACE
IRAS observations of the extended galactic objects Cas A and W80 02 p0290 N90-11657
Earth observation from the interstellar space
[REPT-44/89] 17 p2418 N90-23781

INTERSTITIALS
Interstitial formation, non-equilibrium and macroscopic processes in mercury cadmium telluride
[AD-A212412] 04 p0561 N90-13267
Theory of electronic states and formations energies of defect complexes, interstitial defects, and crystal growth in semiconductors
[AD-A224069] 24 p3551 N90-30093

INTERSYMBOLIC INTERFERENCE
Numerical analysis of chaotic symbol sequences generated by parabolic and triangle maps of the interval
[MPIS-22/1987] 04 p0539 N90-13124

INTERVALS
Small sample theory for steady state confidence intervals
[AD-A212097] 03 p0393 N90-12242
Apparatus for using a time interval counter to measure frequency stability
[NASA-CASE-NPO-17325-1-CU] 09 p1208 N90-17005
Ranking intervals under visibility constraints
[RUU-CS-89-18] 18 p2602 N90-24812
The roles of strain and reheating interval in continuous recrystallization during the thermomechanical processing by warm rolling of an Al-Mg alloy
[AD-A223673] 24 p3449 N90-29479

INTESTINES
Experiment K-6-17. Structural changes and cell turnover in the rats small intestine induced by spaceflight 20 p2895 N90-26470

INTRAVEHICULAR ACTIVITY
Toward the development of COSMO-LAB 18 p2500 N90-24281
Flight support system servicing aid tool 18 p2501 N90-24293

INTRUSION
Micromechanics of an extrusion in high-cycle fatigue with creep
[AD-A213509] 07 p0947 N90-15485
Predicting the audibility and annoyance of unducted fan engines 18 p2610 N90-24869

INVALIDITY
U ERRORS

INVARIANCE
NT GAUGE INVARIANCE
Boolean functions, invariance groups and parallel complexity
[CWI-CS-R8836] 02 p0260 N90-11472
Some 1(sub p) invariant probability measures
[REPT-88-91] 03 p0397 N90-12273
Classification of modular invariant partition functions for the twisted N=2 superconformal algebra, twisted SU(2) Kac-Moody algebra and D(sub 2K) parafermions
[DE90-600767] 06 p0835 N90-14853
Modular invariants for theta-functions with characteristics and the twisted N=2 superconformal and SU(2) Kac-Moody algebras
[DE89-635701] 07 p0982 N90-15671
Modeling the pressure-strain correlation of turbulence: An invariant dynamical systems approach
[NASA-CR-181979] 10 p1383 N90-18003
Fractal-based image compression
[AD-A217302] 13 p1865 N90-20699
Local supersymmetry in non-relativistic systems
[DE90-612751] 14 p2034 N90-21670
Conserved conformal currents in curved space-time
[DE90-612766] 14 p2034 N90-21672
Hopf bifurcation with nonsemisimple 1:1 resonance e
[MEMO-808] 15 p2161 N90-22347
Symmetry in the dynamics of a polarized fluid
[ETN-90-96896] 18 p2552 N90-24567
A Lyapunov bound for solutions of Poisson's equation
[AD-A220223] 18 p2599 N90-24787
Effective Hamiltonians and the theory of invariants
[DE90-611035] 18 p2605 N90-24836
BRS invariant stochastic quantization of Einstein gravity
[DE90-791126] 21 p3085 N90-27541
On estimating scale invariance in stratocumulus cloud fields 22 p3213 N90-28227
Geometric theory for infinite dimensional systems
[PB90-190216] 22 p3242 N90-28383
Asymptotic behavior of solutions of diffusion-like partial differential equations invariant to a family of affine groups
[DE90-014792] 23 p3388 N90-29130
Adiabatic invariance and transient resonance in very slowly varying oscillatory Hamiltonian systems
[DE90-016118] 24 p3538 N90-30007
Spatial structure of particle-orbit loss regions in l=2 helical systems
[DE90-508080] 24 p3548 N90-30073

INVARIANT IMBEDDINGS
Geometric theory for infinite dimensional systems
[ETN-90-96922] 23 p3389 N90-29144

INVENTIONS
Crosslinkable polymer
[GB-PATENT-2-205-846-A] 05 p0628 N90-13663
Invention and innovation: Alternative mechanisms for enhancing organizational competitiveness
[DE89-015858] 08 p1136 N90-16584
A new type of radioluminescent light source
[DE90-004294] 09 p1210 N90-17015
From invention to innovation: Commercialization of new technology by independent and small business inventors
[DE90-006944] 12 p1727 N90-19927
Production activities in space: The problems of protection 20 p2939 N90-26725
Possible solutions 20 p2939 N90-26726

INVENTORIES
NT CROP INVENTORIES
NT TIMBER INVENTORY
Air Force flight feeding. Volume 1: Evaluation of current system and alternative concepts
[AD-A212789] 04 p0527 N90-13043
NAPAP (National Acid Precipitation Assessment Program) emissions inventory: Overview of allocation factors, 1985
[PB90-126012] 12 p1685 N90-19679
Overview of the methodologies used to compile large scale emissions inventories
[DE90-008518] 13 p1830 N90-20509
Inventory of program packages related to the project SIMONA
[ETN-90-96397] 15 p2148 N90-22270
Electronics principles inventory, Sheppard Technical Training Center
[AD-A219935] 18 p2547 N90-24534
Compiling air toxics emission inventories, 2nd edition
[PB90-185422] 22 p3198 N90-28148
World jet airplane inventory at year-end 1989
[PB90-207218] 23 p3267 N90-28489

INVENTORY MANAGEMENT
Study of the feasibility of several mixtures
[IMAG-RR-776-M] 21 p3057 N90-27379

INVERSE KINEMATICS
Kinematic control of robotic manipulators with multiple interchangeable wrists 12 p1670 N90-19592
Dynamics and control of robot manipulators with closed-kinematic chain mechanism 12 p1671 N90-19598
The development of computational algorithms for manipulator inverse kinematics [DE90-759877] 14 p2017 N90-21561
An inverse kinematics algorithm for a highly redundant variable-geometry-truss manipulator 16 p2288 N90-23033
Real time inverse kinematics with joint limits and spatial constraints [AD-A220462] 18 p2586 N90-24723
Kinematics, controls, and path planning results for a redundant manipulator 23 p3363 N90-29005
A complete analytical solution for the inverse instantaneous kinematics of a spherical-revolute-spherical (7R) redundant manipulator 23 p3363 N90-29006
Computational neural learning formalisms for manipulator inverse kinematics 23 p3368 N90-29030
Kinematics and control algorithm development and simulation for a redundant two-arm robotic manipulator system 24 p3516 N90-29877

INVERSE SCATTERING
The initial-boundary value problem for the Davey-Stewartson 1 equation; how to generate and drive localized coherent structures in multidimensions [PREPRINT-684] 05 p0643 N90-13756
Nonlinear wave propagation [AD-A215500] 10 p1375 N90-17968
On the quantum inverse problem for a new type of nonlinear Schroedinger equation for Alfven waves in plasma [DE90-607469] 10 p1431 N90-18259
Direct and inverse scattering problem associated with the elliptic Sinh-Gordon equation [AD-A216455] 11 p1551 N90-18931
Inverse scattering and tomography [AD-A216456] 11 p1551 N90-18932
Generalized Herglotz functions and inverse scattering problem in a finite depth ocean [PB90-150996] 15 p2134 N90-22197
The effects of caustics in acoustic inverse scattering experiments [AD-A218454] 16 p2313 N90-23185
Nonlinear waves and inverse scattering [AD-A218483] 17 p2387 N90-23597
Sparse approximations of inverse matrices [ETN-90-98904] 17 p2464 N90-24074
An injective far-field pattern operator and inverse scattering problem in a finite depth ocean [PB90-159294] 22 p3230 N90-28318

INVERSIONS
NT POPULATION INVERSION
NT TEMPERATURE INVERSIONS
Batch LCAP2-linear control analysis, version 2.0: User's manual [AD-A211670] 04 p0461 N90-12643
Three dimensional analysis of the structure of the atmosphere in polar environments by vertical satellite sounding. Interest for the meteorological forecasts at high latitudes [ETN-90-95506] 05 p0671 N90-13911
Variational problems in astrophysics 09 p1298 N90-17524
Nonlinear wave propagation [AD-A215500] 10 p1375 N90-17968
An application of ocean wave-current refraction to the gulf stream using SEASAT SAR data [AD-A216769] 11 p1537 N90-18851
Multiple versus single scattering of terrestrial infrared longwave radiation in an aerosol-laden planetary boundary layer [AD-A217709] 13 p1790 N90-20272
Characteristics of cumulus bandclouds off the east coast of Hawaii 15 p2130 N90-22178
A three-year study of the OH masers in Orion-KL and a study of the (3,2) transition of ammonia 15 p2183 N90-22471
Program inversion: More than fun [CS-8903] 16 p2299 N90-23095
Inverting the flow of computation [TR-89-10] 17 p2450 N90-23971
Aureole lidar: Ground based measurement [AD-A223207] 21 p3008 N90-27101
Improving the accuracy of inverse iteration [AD-A221846] 21 p3056 N90-27377
July 16, 1987 revisited: Lessons for modelers 22 p3214 N90-28232
The above-inversion moisture structure observed during FIRE 22 p3215 N90-28235
On the dynamic and thermodynamic structures of marine stratocumulus 22 p3216 N90-28244
Turbulence structure in clear and cloudy regions of the 7 July 1987 Electra mission 22 p3217 N90-28247
Diurnal variation in the turbulent structure of the cloudy marine boundary layer during FIRE 1987 22 p3217 N90-28248
Laboratory experiments on stability and entrainment of oceanic stratocumulus. Part 1: Instability experiment 22 p3220 N90-28263
Hitting lines with two-dimensional Brownian motion [AD-A223595] 24 p3541 N90-30027
Real-time concentration monitoring of large aerodynamic diameter fiber aerosols using the geometric optic inversion technique [AD-A224167] 24 p3545 N90-30048

INVERTEBRATES
NT COCKROACHES
NT DROSOPHILA
NT INSECTS

INVERTERS
Utilization criteria for transistors of diverse technology in pulse inverters with high switching frequency [ETN-90-95359] 12 p1653 N90-19500
MHD channel development, part 3 [DE90-009551] 15 p2169 N90-22396
An ultrasonic-switching three phase current source inverter with insulated gate bipolar transistors [EMV-89-11] 17 p2399 N90-23666
Controling, cabling and protection of GTO thyristors in pulse inverters [ETN-90-96500] 18 p2549 N90-24548
Electrical characterization of a Mapham inverter using pulse testing techniques [NASA-TM-103254] 22 p3134 N90-27784

INVESTIGATION
NT ACCIDENT INVESTIGATION
NT AIRCRAFT ACCIDENT INVESTIGATION

INVESTMENTS
The economic impact of automation technology [AD-A213363] 05 p0630 N90-13682
The impact of global warming on the energy system [DE89-017775] 06 p0810 N90-14712
Using goal programming to determine the optimal engine mix for UH-1 helicopters [AD-A214893] 09 p1168 N90-16762

INVISCID FLOW
NT STAGNATION FLOW
Three-dimensional unsteady transonic viscous-inviscid interaction 01 p0001 N90-10005
A three-dimensional linear stability approach to transition on wings at incidence 01 p0065 N90-10373
Effect of particle velocity fluctuations on the inertia coupling in two-phase flow 01 p0068 N90-10391
Laminar boundary layer along inviscid surface streamlines over inclined axisymmetric bodies in incompressible flow [AD-A210202] 01 p0070 N90-10401
Calculation on film preparation and film motion of a swirl atomizer [ESA-TT-1096] 03 p0348 N90-11990
Supersonic boundary-layer transition on the LaRC F-106 and the DFRF F-15 aircraft. Part 2: Aerodynamic predictions 04 p0447 N90-12559
Numerical evaluation of a solution representing a jet in cross-flow [RAE-TM-AERO-2137] 04 p0502 N90-12893
Computation of flow fields around propellers and hovering rotors based on the solution of the Euler equations [DLR-FB-89-37] 05 p0572 N90-13333
Hypersonic aerodynamics 05 p0573 N90-13335
Blunt-nose inviscid airflows with coupled nonequilibrium processes 05 p0573 N90-13336
Gas flows in rocket motors. Volume 3, appendix D: Computer code listings [AD-A213350] 05 p0616 N90-13593
Inviscid 3D solution methods 05 p0640 N90-13736
Inviscid 2D solutions on unstructured, adaptive grids 05 p0640 N90-13737
Three-dimensional solution-adaptive grid generation of composite configurations 06 p0775 N90-14509
Dynamics of a class of vortex rings 07 p0926 N90-15362
The precise calculation of the inviscid leading edge flow on a laminar airfoil using simple methods and verification by measurements on the TLF pilot model 08 p1068 N90-16180
An improvement of convection fidelity in Euler calculations 09 p1159 N90-16709
Oblique impact of two cylinders in a uniform flow [AD-A215933] 10 p1385 N90-18015
The inviscid stability of supersonic flow past a sharp cone [NASA-CR-181996] 11 p1451 N90-18363
Calculation of the unsteady two-dimensional, inviscid, compressible flow around a strongly cambered oscillating single blade 11 p1460 N90-18409
Numerical modelling of shocks in gases and metals [MRL-RR-8-89] 12 p1658 N90-19528
DURIP optical equipment for high-speed viscous-inviscid interaction research [AD-A217772] 13 p1802 N90-20345
Numerical modeling of airblast [AD-A217993] 13 p1803 N90-20347
Numerical method for designing 3D turbomachinery blade rows 14 p1918 N90-20990
Surface-cooling effects on compressible boundary-layer instability [NASA-CR-182003] 14 p1971 N90-21290
Prediction of length scales in a Mach reflection flowfield 15 p2089 N90-21959
Stable boundary conditions for Cartesian grid calculations [NASA-CR-182048] 16 p2306 N90-23139
The stability of two-dimensional wakes and shear-layers at high Mach numbers [NASA-CR-182050] 17 p2401 N90-23678
Thin-layer Navier-Stokes solutions of the asymmetric vortical flow on a tangent ogive body [AD-A220810] 17 p2403 N90-23690
Fluid oscillations in an open, flexible container [REPT-89-69] 17 p2404 N90-23696
Flow studies in impeller passages 18 p2551 N90-24558
Vortex-induced boundary-layer separation 18 p2551 N90-24560
On the receptivity problem for Goertler vortices: Vortex motions induced by wall roughness [NASA-CR-182036] 19 p2654 N90-25109
Integral-equation methods in steady and unsteady subsonic, transonic and supersonic aerodynamics for interdisciplinary design [NASA-TM-102677] 19 p2655 N90-25110
Analysis and mitigation of numerical dissipation in inviscid and viscid computation of vortex-dominated flows [NASA-CR-186887] 20 p2862 N90-26281
Computational fluid dynamics 3-D analysis for advanced transonic turbine design [ETN-90-97282] 20 p2864 N90-26291
An approximate method for calculating three-dimensional inviscid hypersonic flow fields [NASA-TP-3018] 21 p3002 N90-27066
Inviscid dynamics of unstable shear layers [AD-A222297] 21 p3004 N90-27077
Vortex-induced boundary layer separation [AD-A221564] 21 p3005 N90-27078
On computations of the integrated space shuttle flowfield using overset grids [NASA-CR-186927] 22 p3124 N90-27734
Effects of low bond number liquid motions on spacecraft attitude 22 p3131 N90-27768
Model of turbulent diffusion flames and nitric oxide generation [PB90-155557] 22 p3155 N90-27886
Free boundary problems for flow with vorticity [AD-A218415] 22 p3168 N90-27971
FINFLO: A finite-volume based computer program for two-dimensional and axisymmetric compressible flow [PB90-189473] 22 p3169 N90-27974
Do inviscid vortex sheets roll-up [PD-CF-9010] 23 p3267 N90-28491
Regular and chaotic motion of uniform elliptical vortices in external linear time dependent velocity fields 23 p3268 N90-28497
An investigation of the steady and unsteady near wake and its effect on a laminar boundary layer 23 p3324 N90-28794
Multigrid for hypersonic inviscid flows [NASA-CR-182082] 23 p3387 N90-29125
Supersonic/hypersonic aerodynamics and heat transfer for projectile design using viscous-inviscid interaction [AD-A224354] 24 p3418 N90-29303
An investigation of the inviscid spatial instability of compressible mixing layers [AD-A223776] 24 p3468 N90-29596

INVISIBILITY
U VISIBILITY

IO
Ion bombardment of Io and Mercury 02 p0296 N90-11682
Ultraviolet observations of the atmosphere of Io and the plasma torus 12 p1728 N90-19929
Sulphur silicate interactions on the Jovian satellite Io 15 p2192 N90-22515
Studies of Io's atmosphere and plasma torus 16 p2338 N90-23326

IODATES
NT LITHIUM IODATES

IODIDES
NT CESIUM IODIDES
NT SODIUM IODIDES
Mercuric iodide room temperature gamma-ray detectors
[NASA-TM-103318] 13 p1804 N90-20357
Determinations of photon spectra
[AD-A218003] 13 p1885 N90-20816
IODINE
NT IODINE ISOTOPES
Measurement of pressure fluctuations in a resonant chamber with laser-induced iodine fluorescence
[ESA-TT-1123] 03 p0406 N90-12326
Spatially-resolved, nonintrusive measurements in a nonreacting scramjet combustor using laser-induced iodine fluorescence 07 p0881 N90-15103
Injection-seeded Nd:YAG laser linewidth measurement using saturation spectroscopy in iodine
[DE90-009537] 15 p2103 N90-22034
Threshold photodetachment spectroscopy of the I + HI transition state region
[AD-A218410] 16 p2260 N90-22883
Electrochemical control of iodine disinfectant for space transportation system and space station potable water 18 p2629 N90-24981
IODINE COMPOUNDS
NT CESIUM IODIDES
NT IODIDES
NT LITHIUM IODATES
NT SODIUM IODIDES
Generation of iodine monofluoride in a supersonic multipurpose flowtube facility
[AD-A213082] 05 p0647 N90-13774
Singlet oxygen and iodine monofluoride collisional energy transfer mechanism
[AD-A215711] 09 p1280 N90-17421
Thermal conductivity of quasi-one dimensional conductors
[DE90-004844] 10 p1435 N90-18281
IODINE ISOTOPES
High pressure 129I Moessbauer studies of GeI4 molecular crystals
[DE89-015269] 02 p0283 N90-11620
IODINE LASERS
Earth orbit laser systems 01 p0030 N90-10162
Beamed laser power in support of near-earth missions 01 p0031 N90-10167
Microwave excitation of oxygen O2 (delta 1) for an oxygen-iodine laser
[DFVLR-FB-89-23] 04 p0506 N90-12919
Direct solar-pumped iodine laser amplifier
[NASA-CR-186442] 15 p2103 N90-22030
ION ACCELERATORS
Ion divergence and the stability of magnetically insulated diodes
[DE90-014565] 23 p3321 N90-28777
ION ACOUSTIC WAVES
Langmuir wave interaction with ion-sound one. Part 1: Stochastic effects
[DE90-603368] 08 p1118 N90-16474
Langmuir wave interaction with ion acoustic wave
[DE90-615407] 14 p2027 N90-21624
ION BEAMS
Custom diffraction gratings
[AD-A211002] 01 p0124 N90-10712
Focused ion beam implantation
[AD-A210977] 01 p0133 N90-10787
Reactive ion etching of SiC thin films by mixtures of fluorinated gases and oxygen
[AD-A211046] 02 p0195 N90-11113
Simulation of an axially symmetric ion-optical system
[DE89-620129] 02 p0273 N90-11560
Ion sources, electron guns and beam optics
[DE89-015526] 02 p0274 N90-11562
The Si(1-x)Nx Rugate
[AD-A211236] 02 p0275 N90-11572
Pulsed-power switching for inertial confinement fusion with light ion beams
[DE89-016810] 02 p0279 N90-11595
Ion beam annealing of Ga-implanted Si
[DE89-016857] 02 p0282 N90-11610
Ion bombardment of Io and Mercury 02 p0296 N90-11682
Reactive ion etching of sputtered silicon carbide and tungsten thin films for device applications
[AD-A211711] 03 p0325 N90-11847
Fundamental tribological properties of ion-beam-deposited boron nitride films
[NASA-TM-102088] 03 p0331 N90-11881
Ion-assisted deposition of high-temperature lubricious surfaces
[DE89-012397] 03 p0331 N90-11883
Photolithography: A new tool for ceramic science
[DE90-000135] 03 p0331 N90-11885
Advances and directions of ion nitriding/carburizing
[NASA-TM-102398] 03 p0334 N90-11902
Beam dynamics of a liquid metal ion source
[DE89-015856] 03 p0401 N90-12295
Generation and focusing of pulsed intense ion beams
[DE89-017558] 03 p0408 N90-12338
Anomalous ion-channeling behavior across the superconducting transition in high-T(sub c) materials
[DE89-017677] 03 p0411 N90-12360
Current limiting mechanisms in electron and ion beams experiments
[AD-A212295] 04 p0460 N90-12637
Mechanisms in reactive ion etching of silicon carbide thin films
[AD-A213018] 05 p0634 N90-13700
Structure-property relationships in surface-modified ceramics. NATO Advanced Science Institutes, series E: Applied Sciences, volume 170
[AD-A212939] 06 p0749 N90-14359
Ion beam analysis and modification of thin-film, high-temperature superconductors
[DE90-000918] 06 p0850 N90-14941
Ion beam processing of advanced electronic materials
[DE89-017342] 06 p0851 N90-14944
Surface modification of metals by ion beams
[DE90-001285] 07 p0903 N90-15218
Surface roughening of Ge(001) during 200 eV Xe ion bombardment and Ge molecular beam epitaxy
[DE90-000674] 07 p0998 N90-15769
Computer-controlled ion beam sputter-deposition of superconducting oxide films
[AD-A213921] 07 p1004 N90-15812
Structure-property relationships in ion-beam surface-modified ceramics: Theory and applications
[AD-A212785] 08 p1047 N90-16054
Effect of carbon on ion beam mixing of Fe-Ti bilayers
[DE90-003650] 08 p1048 N90-16056
Silicon-based coatings on niobium metal
[DE90-003651] 08 p1048 N90-16057
Light ion beam drivers for inertial confinement fusion
[DE90-004196] 08 p1127 N90-16528
Effects of ion dose on the morphology and crystallization of amorphous germanium
[DE90-003564] 08 p1130 N90-16547
Ion beam annealing of Si co-implanted with Ga and As
[DE90-004297] 08 p1132 N90-16556
Ion beam modification of metals: Mechanical properties and structure
[AD-A214701] 09 p1194 N90-16915
Adhesion of silver films to ion-bombarded alumina
[DE90-005642] 09 p1199 N90-16947
Growth of epitaxical SiC layers onto on- and off-axis 6H-SiC substrates by ion beam deposition
[DE90-004236] 09 p1287 N90-17459
Influence of ion beam mixing on the growth of high temperature oxide superconducting thin film
[DE90-004837] 10 p1435 N90-18280
Materials processing of diamond: Etching, doping by ion implantation and contact formation
[AD-A216530] 10 p1438 N90-18301
Microstructural variations in aluminum oxide coatings deposited using a dual beam ion system
[DE90-006040] 11 p1491 N90-18583
Merged beam studies into the mechanisms of hydrogen molecular ion recombination
[AD-A216469] 11 p1562 N90-19002
Development of an rf-driven plasma neutralizer for negative ions
[DE90-007298] 11 p1568 N90-19027
International conference on Surface Modification of Metals by Ion Beams
[AD-A215872] 12 p1626 N90-19345
The TISOL facility at TRIUMF
[DE90-006682] 12 p1713 N90-19837
Ion mixing and surface modification in metal-semiconductor systems
[DE90-007557] 12 p1723 N90-19897
Physical sputtering of metallic systems by charged-particle impact
[DE90-007803] 13 p1777 N90-20201
Software quality assurance and software safety in the biomed control system
[DE90-008072] 13 p1866 N90-20706
Collective ion acceleration in high current relativistic electron beams
[DE90-006328] 13 p1886 N90-20821
Focused ion beam implantation
[AD-A217987] 13 p1898 N90-20894
Low energy ion generator
[DE90-759905] 14 p1955 N90-21195
The high temperature behavior of gallium and indium liquid metal ion sources
[AERE-R-13321] 16 p2217 N90-22647
Amorphization of metals by ion implantation and ion beam mixing
[DE90-620571] 16 p2221 N90-22667
Plasma instabilities associated with the injection of artificial ion beams into the ionosphere 16 p2254 N90-22851
Intense electron beam propagation across a magnetic field
[DE90-009993] 16 p2316 N90-23204
Grain growth and phase formation in ion irradiated/annealed thin Ni-Al alloys films
[DE90-010409] 18 p2525 N90-24407
Deposition of electrooptic thin films
[DE90-010543] 18 p2619 N90-24922
Computer-controlled ion beam sputter deposition of multicomponent oxides
[DE90-010544] 18 p2619 N90-24923
Chlorine reactive-ion-beam etching of InSb and InAs0.15Sb0.85/InSb strained-layer-superlattices
[DE90-010848] 18 p2625 N90-24958
One dimensional heavy ion beam transport: Energy independent model
[NASA-CR-186722] 19 p2754 N90-25650
A closed form solution to HZE propagation
[NASA-TM-103482] 20 p2924 N90-26640
Studies on ion scattering and sputtering processes relevant to ion beam sputter deposition of multicomponent thin films
[DE90-010071] 20 p2931 N90-26675
Application of microdesigned interfaces to studies of ceramic processing
[DE90-011633] 21 p2983 N90-26951
Self-lubricating-diamond like coatings deposition
[AD-A221756] 21 p2988 N90-26983
Ion beam processing of diamond
[AD-A221475] 21 p3001 N90-27058
High current metal ion implantation
[AD-A223098] 21 p3083 N90-27530
Ion divergence and the stability of magnetically insulated diodes
[DE90-014565] 23 p3321 N90-28777
Moessbauer Effect applications using intense radioactive ion beams
[DE90-014981] 23 p3394 N90-29175
PBFA 2 applied B ion diode beam characteristics at high voltages
[DE90-014419] 23 p3396 N90-29190
Electron beam for velocity determination 24 p3420 N90-29319
Extension of plasma source ion implantation to ion beam enhanced deposition
[AD-A224462] 24 p3454 N90-29506
Adhesion of silver films to ion-bombarded zirconia
[DE90-010088] 24 p3456 N90-29517
Ion-beam mixing of Fe/B layers for tribological applications
[DE90-010091] 24 p3456 N90-29518
Prospects for nuclear astrophysics with intense radioactive ion beams
[DE90-015616] 24 p3544 N90-30044
ION CHAMBERS
U IONIZATION CHAMBERS
ION CURRENTS
NT ION BEAMS
Solid state voltammetry and sensors in solids and gases
[DE90-003234] 08 p1129 N90-16538
Structural and fast ion transport properties of glassy and amorphous materials
[DE90-005587] 10 p1358 N90-17877
Electronic and ionic transport in processable conducting polymers
[AD-A218093] 13 p1782 N90-20229
Evaluation of ion intercalation in conducting polymers
[AD-A219423] 17 p2379 N90-23549
Microelectronic device reliability
[AD-A218774] 17 p2394 N90-23638
Electronic conduction in molten cryolite saturated with alumina
[DE90-015090] 23 p3400 N90-29211
ION CYCLOTRON RADIATION
Can ion acceleration by double-cyclotron absorption produce O(+) ion conics
[IRF-PREPRINT-114] 02 p0280 N90-11600
Dynamics Explorer-1 satellite study of electrostatic ion cyclotron waves 05 p0702 N90-14105
ION DENSITY (CONCENTRATION)
NT IONOSPHERIC ION DENSITY
Determination of neutral particle concentration at erosion laser plasma expansion into vacuum
[DE89-620128] 02 p0228 N90-11308
ANTHEM simulation of the early time magnetic field penetration of the plasma surrounding a high density Z-pinch
[DE89-016980] 02 p0277 N90-11585
A double focusing mass-spectrometer for simultaneous ion measurements in the stratosphere 05 p0659 N90-13848

Modification of ionic population by non-Maxwellian effects 06 p0785 N90-14565
A double focussing mass-spectrometer for simultaneous ion measurements in the stratosphere
[AERONOMICA-ACTA-A-350-1989] 08 p1102 N90-16379
Characterization of ground state neutral and ion transport during laser ablation of 1:2:3 superconductors by transient optical absorption spectroscopy
[DE90-006623] 12 p1720 N90-19878
The production and spatial distribution of neutral and ionized water vapor in Comet P/Halley 15 p2185 N90-22484
The importance of adiabatic variations in trapped particle distributions observed by the SCATHA satellite
[AD-A220859] 17 p2423 N90-23806
An analytic/empirical model of the middle and low latitude ionosphere
[AD-A220004] 17 p2423 N90-23809
Analysis of energy spectra of the ions in the coma of Halley's comet for the evaluation of the production ratio of methane and ammonia
[ETN-90-96489] 18 p2638 N90-25026
An assessment of the application of in situ ion-density data from DMSP to modeling of transionospheric scintillation
[AD-A222695] 24 p3491 N90-29730

ION DISTRIBUTION
Dynamics Explorer-1 satellite study of electrostatic ion cyclotron waves 05 p0702 N90-14105
A computer program to calculate the population numbers of multi-level species
[IFSI-89-15] 08 p1151 N90-16671
Determination of solar flare accelerated ion angular distributions from SMM gamma ray and neutron measurements and determination of the He-3/H ratio in the solar photosphere from SMM gamma ray measurements
[NASA-CR-186038] 08 p1153 N90-16676
The importance of adiabatic variations in trapped particle distributions observed by the SCATHA satellite
[AD-A220859] 17 p2423 N90-23806
Observation of a magic number in the ion distribution of ethene clusters
[AD-A219837] 18 p2521 N90-24393
Nondestructive one- and two-dimensional doping profiling by inverse methods
[ETN-90-97264] 20 p2874 N90-26351
Background effects in ESDIAD measurements on Si(111)-(7x7)
[AD-A222242] 21 p3001 N90-27056
Studies of ionospheric dynamics utilizing data from DMSP
[AD-A223370] 24 p3492 N90-29733
A study of water vapor, electrical parameters, and radio propagation
[AD-A223582] 24 p3492 N90-29736

ION EMISSION
COSTEP: A comprehensive suprathermal and energetic particle analyzer for SOHO 04 p0568 N90-13314
RAIDS: An orbiting observatory for ionospheric remote sensing from space
[AD-A213717] 07 p0949 N90-15494
Reactions of atmospheric species with clean and H, C, and O implanted species
[AD-A214602] 09 p1244 N90-17218
Surface production of ions
[AD-A216470] 11 p1562 N90-19003
A study of the influence of Hg(6(3)P2) population in a low-pressure discharge on mercury ion emission at 194.2 nm 20 p2853 N90-26223
Laser diode pumped, erbium-doped, solid state laser with high slope efficiency
[AD-D014482] 22 p3179 N90-28040

ION ENGINES
NT MERCURY ION ENGINES
Power processing unit for 20mN-class ion engine system 10 p1336 N90-17732
TFE verification program
[DE90-008227] 18 p2614 N90-24891
Ion thrusters and spacecraft configuration
[RAE-TM-SPACE-206] 19 p2682 N90-25253

ION EXCHANGE MEMBRANE ELECTROLYTES
An assessment and comparison of fuel cells for transportation applications
[DE90-001807] 07 p0952 N90-15508
Advanced space power PEM fuel cell systems 10 p1333 N90-17707
Regenerative fuel cell systems for project pathfinder 10 p1333 N90-17708
European regenerative fuel cell technology for space use 10 p1333 N90-17709
Electrocatalysis for oxygen electrodes in fuel cells and water electrolyzers for space applications 13 p1823 N90-20468
The development and characterization of ion exchange membranes for selected electrochemical power sources
[DE90-009741] 20 p2857 N90-26251

ION EXCHANGING
Long endurance underwater power system
[AD-A211386] 03 p0366 N90-12096
Linear (passive) and non-linear guided and studies in glass
[AD-A211693] 03 p0406 N90-12325
Photochemical observation of ion flows in membrane channels
[AD-A212449] 04 p0472 N90-12705
Electronic and ionic transport in polymers
[AD-A217028] 11 p1491 N90-18579
Hydrous metal oxide-supported catalysts. Part 2: Catalytic properties and applications
[DE90-008098] 12 p1625 N90-19336
Improvements in macroreticular particles for ion-exchange and gel-permeation chromatography
[DE90-003717] 18 p2522 N90-24399
Research on optogalvanic effects
[AD-A221512] 21 p3071 N90-27463

ION EXTRACTION
Ion formation by electron impact
[AD-A211367] 03 p0403 N90-12305
Investigation of boundary for the negative ion extraction in the sheet-plasma negative ion source
[DE90-719532] 09 p1286 N90-17458
Pulsed field sample neutralization
[DE90-015131] 24 p3445 N90-29452

ION GAGES
U IONIZATION GAGES

ION IMPACT
Plasma-anode electron gun research
[AD-A211547] 03 p0312 N90-11773
Ion formation by electron impact
[AD-A211367] 03 p0403 N90-12305
Multiple-ionization of xenon atoms by positron impact 11 p1558 N90-18978
Surface production of ions
[AD-A216470] 11 p1562 N90-19003
Physical sputtering of metallic systems by charged-particle impact
[DE90-007803] 13 p1777 N90-20201

ION IMPLANTATION
Structure-mechanical property relationships in ion implanted ceramics
[DE89-010129] 01 p0048 N90-10274
Photoreflectance study of boron ion-implanted (100) cadmium telluride
[SD-TR-88-89] 01 p0053 N90-10300
Advanced GaAs process modeling, volume 1
[AD-A210365] 01 p0132 N90-10761
Focused ion beam implantation
[AD-A210977] 01 p0133 N90-10767
Ion implantation of two titanium alloys
[DE89-016958] 02 p0198 N90-11133
Hydrogen-assisted thermal donor formation in silicon
[DE89-016809] 02 p0279 N90-11594
Ion beam annealing of Ga-implanted Si
[DE89-016857] 02 p0282 N90-11610
Characterization of the Structure and Chemistry of Defects in Materials: Proceedings, volume 138
[DE89-014796] 03 p0410 N90-12352
Ion beam deposition of epitaxial germanium and gallium arsenide layers
[DE89-017439] 03 p0411 N90-12357
Structure-property relationships in surface-modified ceramics. NATO Advanced Science Institutes, series E: Applied Sciences, volume 170
[AD-A212939] 06 p0749 N90-14359
Ion beam analysis and modification of thin-film, high-temperature superconductors
[DE90-000918] 06 p0850 N90-14941
Ion beam processing of advanced electronic materials
[DE89-017342] 06 p0851 N90-14944
Surface engineering by high energy beams
[DE90-001296] 07 p0908 N90-15250
Effect of carbon on ion beam mixing of Fe-Ti bilayers
[DE90-003650] 08 p1048 N90-16056
Characterization of B and N implanted fused silica
[DE90-004198] 08 p1050 N90-16069
Metals and Ceramics Division Materials Sciences Program
[DE90-004371] 08 p1050 N90-16070
Ion beam annealing of Si co-implanted with Ga and As
[DE90-004297] 08 p1132 N90-16556
Strengthening of aluminum by oxygen implantation: Experimental results and mechanical modeling
[DE90-005960] 09 p1195 N90-16924
Low temperature photoluminescence study of uranium implanted into III-V semiconductors and AlGaAs
[AD-A215710] 09 p1291 N90-17484
Hardness-damage correlations in Ta implanted single crystal Ni3Al
[DE90-005270] 09 p1293 N90-17494
Effects of O2 ion bombardment of Y-BaCu-oxide during thin film growth
[DE90-005315] 09 p1293 N90-17495
Strain induced amorphization of aluminium by manganese implantation
[DE90-607259] 10 p1356 N90-17863
Develop techniques for ion implantation of PLZT for adaptive optics
[AD-A216005] 10 p1431 N90-18253
Materials processing of diamond: Etching, doping by ion implantation and contact formation
[AD-A216530] 10 p1438 N90-18301
Ion implantation-induced amorphization of ceramic oxides
[DE90-006564] 11 p1571 N90-19041
Dopant site location in dual-implanted GaP using (111) planar channeling
[DE90-006565] 11 p1571 N90-19042
International conference on Surface Modification of Metals by Ion Beams
[AD-A215872] 12 p1626 N90-19345
Modification of surface mechanical properties of high-chromium tool steel by carbon-implanted codeposited Fe-Ti films
[DE90-007502] 12 p1628 N90-19358
Particle emission by oblique ion bombardment of gold
[ETN-90-95825] 12 p1711 N90-19827
Silicon carbide semiconductor device fabrication and characterization
[NASA-CR-186354] 12 p1719 N90-19873
Rolling contact fatigue of surface modified 440C using a 'Ge-Polymet' type disc rod test rig
[NASA-TM-100390] 13 p1777 N90-20200
Radiation disorder and aperiodicity in irradiated ceramics
[DE90-008253] 13 p1781 N90-20222
Interaction between implanted ions and intrinsic defects in silica
[DE90-006569] 13 p1892 N90-20858
Workshop on the Physics and Chemistry of Mercury Cadmium Telluride and Related II-VI compounds
[AD-A217496] 13 p1894 N90-20867
Focused ion beam implantation
[AD-A217987] 13 p1898 N90-20894
Formation of subsurface aluminum layers in beryllium by ion implantation and post-implant annealing
[DE90-007975] 14 p1951 N90-21172
Energy beam treatment for improved adhesion of coatings to surfaces
[AD-D014449] 14 p1954 N90-21190
Proceedings of the Joint NOSC/NRL (Naval Ocean Systems Center/Naval Research Laboratory) InP Microwave/Millimeter Wave Technology Workshop
[AD-A218216] 14 p1966 N90-21259
Mechanical properties of carbon-implanted niobium
[DE90-009864] 15 p2064 N90-21823
Improved high temperature oxidation behavior of alloys by ion implantation
[AERE-R-13309] 16 p2217 N90-22650
Hydrogenation of stainless steels implanted with nitrogen
[DE90-617397] 16 p2221 N90-22666
Amorphization of metals by ion implantation and ion beam mixing
[DE90-620571] 16 p2221 N90-22667
Direct implantation process development and characterization in advanced Hg(1)-(x)Cd(x) Te EPI layers
[AD-A219133] 16 p2324 N90-23252
Secondary ion mass spectrometry characterization of implants into GaAs and GaP for waveguides and integrated optics applications
[AD-A219203] 16 p2324 N90-23254
Friction and wear of tungsten carbides with nitrogen ion implants
[ECL-89-19] 17 p2371 N90-23496
The influence of ion implantation on the near-surface mechanical properties of ceramics
[DE90-010139] 18 p2531 N90-24444
The effect of crystal orientation on damage accumulation in chromium-implanted Al2O3
[DE90-012294] 20 p2931 N90-26674
Rapid thermal processing: A study of the silicon oxidation and of the implanted boron activation
[LAAS-90051] 20 p2932 N90-26681
Passive mechanisms of surfaces produced by ion beam mixing and ion implantation
[AD-A222432] 21 p2982 N90-26945
Status and applications of diamond and diamond-like materials: An emerging technology
[NASA-CR-186935] 21 p2985 N90-26963

Development of a multi-purpose, pulsed-laser system for solar cell processing applications
[DE90-012181] 21 p3008 N90-27096
Self-lubricating surfaces by ion beam processing
[AD-A222489] 21 p3011 N90-27118
Rapid annealing of iron implanted Hg(1-x)Cd(x)Te
[AD-A222777] 21 p3082 N90-27524
High current metal ion implantation
[AD-A223098] 21 p3083 N90-27530
Fretting wear and fretting fatigue at temperatures up to 600 C 23 p3307 N90-28706
Surface property improvement in titanium alloy gas turbine components through ion implantation 23 p3309 N90-28713
Moessbauer Effect applications using intense radioactive ion beams
[DE90-014981] 23 p3394 N90-29175
Extension of plasma source ion implantation to ion beam enhanced deposition
[AD-A224462] 24 p3454 N90-29506

ION INJECTION
Structural peculiarities and molecular properties of charge complexes formed on positive ion injection into dense inert gas media
[DE89-633953] 06 p0839 N90-14877

ION IRRADIATION
NT DEUTERON IRRADIATION
NT PROTON IRRADIATION
Defect structures preceding amorphization by ion irradiations in YBa2Cu3O(7-delta)
[DE89-016905] 02 p0282 N90-11612
Ion-irradiation effects in Tl2Ca2Ba2Cu3O10 superconductors
[DE90-003840] 07 p1002 N90-15802
Structure-property relationships in ion-beam surface-modified ceramics: Theory and applications
[AD-A212785] 08 p1047 N90-16054
Mass loss during x ray microanalysis
[DE90-003954] 08 p1049 N90-16067
Ion bombardment experiments suggesting an origin for organic particles in pre-cometary and cometary ices 08 p1148 N90-16652
Electronic structure and lubrication properties of MoS2: A qualitative molecular orbital approach
[AD-A220566] 17 p2380 N90-23557
Cascade collapse in copper and nickel
[DE90-011115] 18 p2527 N90-24423
Optical emissions from bombarding atmospheric gases with heavy ions
[AD-A223544] 24 p3543 N90-30040

ION MOTION
Direction-dependent stopping power and beam deflection in anisotropic solids
[DE90-001076] 06 p0840 N90-14883
Quartz crystal microbalance studies: Solvent effects in conducting polymer films
[AD-A219426] 17 p2372 N90-23502

ION OSCILLATION
U PLASMA OSCILLATIONS

ION PLATING
Ion-assisted deposition of high-temperature lubricious surfaces
[DE89-012397] 03 p0331 N90-11883

ION PROBES
Isotopic microanalysis of returned comet nucleus samples 08 p1149 N90-16655
Measurement of the space potential of a high-temperature plasma by fast atomic beam scattering on an ion probe beam
[DE90-006118] 11 p1567 N90-19020
Y1Ba2Cu3O(7-x) laser-ablation plume dynamics measurement by nanosecond response ion probe: Comparison with optical measurements
[DE90-007658] 13 p1807 N90-20375
Development of a quadrupole-based Secondary-Ion Mass Spectrometry (SIMS) system at Lewis Research Center
[NASA-TM-102531] 17 p2367 N90-23476
Fluorescent probe investigation of a water-soluble polyphosphazene
[AD-A222317] 21 p2978 N90-26925
Preparation and characterization of thin films based on sol-gel technique and development of spectroscopic probe for film formation and characterization
[AD-A221762] 21 p2988 N90-26984

ION PRODUCTION RATES
Atomic and molecular surface and volume processes in the analysis of negative hydrogen discharges
[DE89-015705] 03 p0401 N90-12294
Positron-molecule bound states and positive ion production 11 p1561 N90-18994
Initial results of positron ionization mass spectrometry 11 p1561 N90-18995
Advanced electric propulsion research, 1989
[NASA-CR-185237] 15 p2062 N90-21810

ION PROPULSION
Propulsion research on the hybrid plume rocket
[AD-A214420] 07 p0887 N90-15132
Performance of large area xenon ion thrusters for orbit transfer missions 11 p1472 N90-18475
Mission options for an electric propulsion demonstration flight test 11 p1473 N90-18479
Viability study of ionic microthruster tests on MECB satellite
[INPE-4973-RPE/605] 11 p1475 N90-18490
Experimental proposition aboard the second data collecting satellite-SCD 2 of the MECB
[INPE-4980-RPE/606] 13 p1765 N90-20128
Advanced electric propulsion research, 1989
[NASA-CR-185237] 15 p2062 N90-21810
Hollow cathode operation at high discharge currents
[NASA-CR-185238] 15 p2088 N90-21953

ION RECOMBINATION
Atomic and molecular surface and volume processes in the analysis of negative hydrogen discharges
[DE89-015705] 03 p0401 N90-12294
Merged beam studies into the mechanisms of hydrogen molecular ion recombination
[AD-A216469] 11 p1562 N90-19002
Dissociative recombination of molecular ions with electrons 20 p2946 N90-26767

ION SCATTERING
Resonant quasiparticle-ion scattering in anisotropic superfluid (3)He
[PB89-221618] 03 p0413 N90-12369
Heavy ion inelastic scattering with a 4(pi) gamma detector
[DE90-002709] 08 p1120 N90-16488
Computer simulation of ionospheric radio frequency heating
[DE90-009478] 15 p2087 N90-21944
Studies on ion scattering and sputtering processes in ion beam sputter-deposition of high Tc superconducting films: The optimization of deposition parameters
[DE90-010538] 18 p2621 N90-24936
Studies on ion scattering and sputtering processes relevant to ion beam sputter deposition of multicomponent thin films
[DE90-010071] 20 p2931 N90-26675
Structure of metal overlayers by low energy alkali ion scattering: Cu/Ru(0001) and Sn/Pt(111)
[DE90-014453] 23 p3310 N90-28718

ION SOURCES
Determination of neutral particle concentration at erosion laser plasma expansion into vacuum
[DE89-620128] 02 p0228 N90-11308
Extraction induced emittance growth for negative ion sources
[DE89-017586] 02 p0273 N90-11559
Simulation of an axially symmetric ion-optical system
[DE89-620129] 02 p0273 N90-11560
Ion sources, electron guns and beam optics
[DE89-015526] 02 p0274 N90-11562
Beam dynamics of a liquid metal ion source
[DE89-015856] 03 p0401 N90-12295
Generation and focusing of pulsed intense ion beams
[DE89-017558] 03 p0408 N90-12338
Ion beam deposition of epitaxial germanium and gallium arsenide layers
[DE89-017439] 03 p0411 N90-12357
Broad-beam multi-ampere metal ion source
[DE90-003106] 08 p1059 N90-16123
In situ measurement of neutral beam components using the Doppler-shifted H(sub alpha) emissions in Heliotron E
[DE90-719521] 08 p1125 N90-16516
Investigation of boundary for the negative ion extraction in the sheet-plasma negative ion source
[DE90-719532] 09 p1286 N90-17458
VUV (Vacuum Ultraviolot) laser diagnostics of H(-) ion sources
[DE90-006072] 11 p1514 N90-18719
Surface production of ions
[AD-A216470] 11 p1562 N90-19003
Computerized analysis of hydrogen plasma in a compact H(sup -) cusp source
[DE90-006881] 11 p1569 N90-19029
The TISOL facility at TRIUMF
[DE90-006882] 12 p1713 N90-19837
The high temperature behavior of gallium and indium liquid metal ion sources
[AERE-R-13321] 16 p2217 N90-22647
Diagnostics for hydrogen atoms and molecules in H-atom sources and beams using VUV laser light
[AD-A222340] 21 p3074 N90-27476
Detection of vibrationally excited H2(v double prime) for H(-) production
[AD-A222560] 22 p3180 N90-28044
Ion divergence and the stability of magnetically insulated diodes
[DE90-014565] 23 p3321 N90-28777
PBFA 2 applied B ion diode beam characteristics at high voltages
[DE90-014419] 23 p3396 N90-29190

ION SPECTROMETERS
U MASS SPECTROMETERS

ION TEMPERATURE
Ion temperature gradient instability
[DE89-016574] 02 p0277 N90-11580
Background electrodynamics measured by EISCAT during the NEED campaign 05 p0660 N90-13851
Ion collection by probing objects in flowing magnetized plasmas
[DE90-001711] 06 p0845 N90-14916
Interaction of minor ions with fast and slow shocks
[NASA-CR-186372] 11 p1594 N90-19181
Helium transport in plasma edge regions 14 p2027 N90-21625

ION TRAPS (INSTRUMENTATION)
State-resolved reaction dynamics
[AD-A211613] 03 p0403 N90-12307
An apparatus for the electrodynamic containment of charged macroparticles 04 p0486 N90-12789
Analysis of ambient polar volatile organic compounds using chemical ionization-ion trap detector
[PB90-106451] 07 p0956 N90-15529
Simple analytic potentials for linear ion traps 12 p1642 N90-19436
Traps for neutral atoms
[AD-A220925] 18 p2613 N90-24885

ION-GAS INTERACTIONS
U GAS-ION INTERACTIONS

IONIC COLLISIONS
Exploring asymmetric heavy-ion reactions at the KX-ray method: The Ne20 + Tb159 reaction at 15 MeV/unit
[KVI-777] 04 p0552 N90-13216
An explicit partition of the fusion-like cross section
[KVI-797] 04 p0553 N90-13225
String models for ultrarelativistic heavy ion collisions: Lund model versus color exchange models
[DE88-015856] 06 p0840 N90-14881
Heavy ion interactions
[DE90-001410] 06 p0840 N90-14884
Generation of H-, H2v(double prime), and H atoms by H2+ and H3+ ions incident upon barium surfaces
[DE90-005549] 09 p1280 N90-17423
DURIP theoretical/experimental investigations of highly energetic dication species
[AD-A217771] 13 p1808 N90-20383
Atomic processes in high temperature plasmas
[DE90-008873] 14 p2028 N90-21632
Production and analysis by mass spectrometry of beams of polyglycol ions 15 p2066 N90-21835
Support for the 16th International Conference on the Physics of Electronic and Atomic Collisions
[AD-A218567] 16 p2315 N90-23200
Experimental investigations of low-energy (4 to 40 eV) collisions of O(-)(P2) ions and O(P3) atoms with surfaces 19 p2732 N90-25530
Ion-heated thermal comptonization models and X ray spectral correlations in active galactic nuclei 19 p2790 N90-25880
A research program in physics of the early universe
[DE90-013319] 20 p2942 N90-26742
Correlated charge changing ion-atom collisions
[DE90-014662] 23 p3393 N90-29171

IONIC CONDUCTIVITY
U ION CURRENTS

IONIC CRYSTALS
Coupled magnetoplasmon-phonon modes at the surface of a semi-infinite semiconductor superlattice
[DE90-612904] 14 p2031 N90-21647

IONIC DIFFUSION
The rapid inward diffusion of cold ions in tokamaks and their effect on ion transport
[DE90-006863] 11 p1568 N90-19022
Use of microelectrode arrays to directly measure diffusion of ions in solid electrolytes: Physical diffusion of Ag(+) in a solid polymer electrolyte
[AD-A222026] 22 p3159 N90-27913

IONIC MOBILITY
Construction of the rotating cryostat ROTA2, its use for zero sound experiments in (3)He-B, and calculations of ion mobility in (3)He-A and (3)He-P
[ISBN-952-90091-3-5] 05 p0645 N90-13765
Transport processes through monomolecular films
[AD-A213609] 07 p0923 N90-15342

IONIC PROPELLANTS
U ION ENGINES

IONIC REACTIONS
Searching for existing nuclear data
[DE90-007535] 12 p1727 N90-19925
Ionic atmosphere effects on the energetics of thermal and optical electron-exchange reactions: Application to ferrocenium-ferrocene self exchange
[AD-A222605] 20 p2889 N90-26441

State-to-state ion-molecule reaction dynamics at thermal energies
[AD-A221589] 21 p3074 N90-27479
An ionic mechanism of carbon formation in flames 21 p3093 N90-27582

IONIZATION
NT AURORAL IONIZATION
NT FLAME IONIZATION
NT GAS IONIZATION
NT ION PRODUCTION RATES
NT NONEQUILIBRIUM IONIZATION
NT PHOTOIONIZATION
Improved propagation models for discrete random media
[AD-A211085] 01 p0057 N90-10327
Simulation of the polar cap F region ionization using an experimental convection electric field 02 p0241 N90-11370
On the possibility of producing artificial ionization and polar aurora in the ionosphere by radio-waves emitted from the ground 02 p0245 N90-11388
Laser ionization mass spectroscopy
[DE89-008039] 03 p0352 N90-12015
Polymer characterization by electrohydrodynamic ionization mass spectrometry
[AD-A212130] 04 p0478 N90-12739
Development of laser excited atomic fluorescence and ionization spectrometric methods
[DE90-001567] 06 p0742 N90-14320
Combined capillary electrophoresis and electrospray ionization mass spectrometry
[DE90-001903] 06 p0743 N90-14322
Nonresonant and resonant multiphoton ionization of (NO)(sub n) and Ar(sub n)NO clusters with picosecond laser pulses
[DE89-016853] 06 p0791 N90-14607
Improved performance of low-T(sub c) superconductors for detection of minimum-ionizing particles
[DE90-001985] 06 p0856 N90-14976
Analysis of ambient polar volatile organic compounds using chemical ionization-ion trap detector
[PB90-106451] 07 p0956 N90-15529
Upper atmosphere research
[ISBN-0-642-13582-7] 08 p1100 N90-16368
Chemical-like behavior of electrons and holes in polymeric conductors
[AD-A214496] 09 p1196 N90-16931
Two-dimensional, long-pulse simulation of microwave-induced electron layer evolution in low-pressure air
[DE90-005180] 09 p1208 N90-17004
Equation of state of partially-ionized dense plasmas
[DE90-005246] 09 p1286 N90-17452
PRPSIM: A FORTRAN code to calculate properties of radio wave propagation in a structured ionized medium. Volume 2: Theory and models
[AD-A216299] 10 p1377 N90-17983
Chemical activation of molecules by metals: Experimental studies of electron distributions and bonding
[DE90-005371] 10 p1428 N90-18238
Model of oxygen ions resonant lines emission of REB-heated plasma
[IPPCZ-294] 10 p1432 N90-18261
Research on sliding spark preionization in a TEA CO2 laser
[ISL-R-113/88] 11 p1516 N90-18732
Proceedings of the 6th Conference on Hot Carriers in Semiconductors
[AD-A215978] 11 p1569 N90-19032
Two-dimensional, long-pulse computer calculation of microwave-induced electron layer formation in low-pressure air
[DE90-005994] 12 p1646 N90-19459
Radiation of electromagnetic waves by an accelerated charged particle in medium
[DE90-610458] 12 p1646 N90-19461
Electron energy distributions and vibrational population distributions
[DE90-005550] 12 p1711 N90-19825
Model calculations for dynamic development of planetary nebulae
[ETN-90-95734] 12 p1744 N90-20025
The glow discharge as an atomization and ionization source
[DE90-007693] 13 p1771 N90-20163
DURIP FTIR studies of solid state reaction dynamics
[AD-A217713] 13 p1773 N90-20174
Interactions of molecules with surfaces
[DE90-007555] 13 p1883 N90-20806
Time-resolved spectroscopy of nonequilibrium ionization in laser-produced plasmas
[DE90-008663] 13 p1891 N90-20854
Absolute pressure dependence of the second ionization level of EL2 in GaAs
[DE90-007761] 13 p1894 N90-20872
Alternating gradient photodetector
[NASA-CASE-NPO-17235-1-CU] 14 p1982 N90-21358
Development of an ultra-bright laser and an application to multi-photon ionization 14 p1984 N90-21372
LLE review
[DE90-008958] 14 p1985 N90-21378
SR90, strontium shaped-charge critical ionization velocity experiment
[NASA-CR-186501] 14 p2024 N90-21606
Atomic processes in high temperature plasmas
[DE90-008873] 14 p2028 N90-21632
Molecular evolution in astrophysical environments 16 p2332 N90-23291
HYPUF upgrade
[AD-A218400] 17 p2379 N90-23547
Ionization effects in the radiative driving of stellar winds in massive X ray binary systems 19 p2781 N90-25823
New electronic states of NH and ND observed by resonance enhanced multiphoton ionization spectroscopy 20 p2945 N90-26760
UV and VUV spectroscopy and photochemistry of small molecules in a supersonic jet 20 p2947 N90-26771
Crossed-microwave-beam air ionization laboratory experiments
[DE90-012056] 21 p3024 N90-27195
Structure and dynamics of excited atoms
[AD-A221973] 21 p3074 N90-27474
The dynamic electric microfield in ionic and polar media
[AD-A222534] 22 p3156 N90-27891
Pulsations of the white dwarf component in V471 tauri-like binaries
[DE90-014921] 23 p3409 N90-29267
The ionization structure of planetary nebulae 10: NGC 2392
[NASA-CR-186960] 23 p3411 N90-29274
Optical emissions from bombarding atmospheric gases with heavy ions
[AD-A223544] 24 p3543 N90-30040

IONIZATION CHAMBERS
NT BUBBLE CHAMBERS
NT PROPORTIONAL COUNTERS
The RAP unit: A remote autoranging picoammeter
[DE90-007711] 14 p1982 N90-21357
Derivation of radiation beam non-uniformity corrections for the calibration of large volume ionisation chambers
[NPL-RSA(EXT)-11] 15 p2167 N90-22382
A tandem system of ionization chambers for effective energy determination of unknown X-radiation fields
[DE90-630463] 24 p3436 N90-29405

IONIZATION COUNTERS
U IONIZATION CHAMBERS
U RADIATION COUNTERS

IONIZATION CROSS SECTIONS
Ion formation by electron impact
[AD-A211367] 03 p0403 N90-12305
Investigations of the interactions of radiation with matter
[AD-A213554] 07 p0991 N90-15723
Lower limits on the absolute dissociative electron attachment cross section from O2 condensed on rare-gas films
[AD-A216727] 11 p1483 N90-18536
Theoretical survey on positronium formation and ionisation in positron atom scattering 11 p1556 N90-18965
Total cross sections for positrons scattered elastically from helium based on new measurements of total ionization cross sections 11 p1558 N90-18976
Ionisation of atomic hydrogen by positron impact 11 p1558 N90-18977
Multiple-ionization of xenon atoms by positron impact 11 p1558 N90-18978
Double ionization of helium by particle impact 11 p1558 N90-18979
Absolute cross-sections for dissociative electron attachment in O2 condensed on Kr films
[AD-A216730] 11 p1570 N90-19038
An implication of the IR identification of PAHs: The heating of the diffuse is gas 11 p1582 N90-19113
Current and future uses of accelerators in particle astrophysics
[DE90-006667] 11 p1595 N90-19186
Electron-impact ionization and electron attachment cross sections of radicals important in transient gaseous discharges
[AD-A217510] 13 p1806 N90-20366

IONIZATION FREQUENCIES
An experimental study of microwave transmission through a decaying plasma
[AD-A210586] 01 p0127 N90-10726

IONIZATION GAGES
Construction and calibration of a gas pressure meter with high temporal resolution
[INPE-4953-RPE/602] 11 p1511 N90-18700

IONIZATION POTENTIALS
Positron scattering by atomic hydrogen using optical potentials and with positronium formation 11 p1557 N90-18966
New parameter-free polarization potentials in low-energy positron collisions 11 p1557 N90-18968
Theoretical studies of electrons and electron transfer processes in fluids
[DE90-008414] 17 p2470 N90-24117
Ion/molecule reactions of arsenic and phosphorus cluster ions: Ionization potentials and novel reaction pathways
[AD-A222019] 21 p2977 N90-26918

IONIZED GASES
Properties of strongly coupled multi-ionic plasmas
[DE89-017782] 03 p0408 N90-12339
Sound waves in weakly ionized gas
[DE90-620704] 16 p2313 N90-23180
Molecular gas in S106: Morphology, kinematics, and chemistry of a star forming region 17 p2484 N90-24209

IONIZED PLASMAS
U PLASMAS (PHYSICS)

IONIZING RADIATION
NT ALPHA PARTICLES
NT BETA PARTICLES
NT COSMIC RAY SHOWERS
NT COSMIC RAYS
NT COSMIC X RAYS
NT EXTREME ULTRAVIOLET RADIATION
NT FAR ULTRAVIOLET RADIATION
NT GALACTIC COSMIC RAYS
NT GAMMA RAY BEAMS
NT GAMMA RAY BURSTS
NT GAMMA RAYS
NT LYMAN ALPHA RADIATION
NT NEAR ULTRAVIOLET RADIATION
NT SECONDARY COSMIC RAYS
NT SOLAR COSMIC RAYS
NT SOLAR X-RAYS
NT ULTRAVIOLET RADIATION
NT X RAYS
Process for crosslinking methylene-containing aromatic polymers with ionizing radiation
[NASA-CASE-LAR-13448-1] 14 p1956 N90-21198
Ga:Ge array development 14 p1977 N90-21323
Effects of protracted ionizing radiation dosage on humans and animals: A brief review of selected investigations
[AD-A222240] 21 p3033 N90-27241
Effects of ionizing radiation on the performance of selected tactical combat crews
[AD-A222680] 21 p3034 N90-27248
Activities of the Division of Microwave Technology
[FOA-C-30555-3.2] 24 p3459 N90-29537

IONOGRAMS
New perspectives for the inversion of backscatter ionograms 06 p0761 N90-14427

IONOSONDES
Multistation/multiparameter observations with a network of digital ionosondes 02 p0247 N90-11396
A portable ionosonde in support of reliable communications 06 p0762 N90-14431
An analytic/empirical model of the middle and low latitude ionosphere
[AD-A220004] 17 p2423 N90-23809
Bermuda ionosonde tests in support of OTH-B
[NASA-TM-89359] 19 p2713 N90-25442
Investigation of structure and transport processes in the high latitude ionospheric plasma using ground based and airborne digisondes
[AD-A224397] 24 p3491 N90-29727

IONOSPHERE EXPLORER A
U EXPLORER 20 SATELLITE

IONOSPHERE-MAGNETOSPHERE COUPLING
U MAGNETOSPHERE-IONOSPHERE COUPLING

IONOSPHERES
Computer simulation of plasma interactions near Titan 01 p0142 N90-10816

IONOSPHERIC ABSORPTION
U ELECTROMAGNETIC ABSORPTION
U IONOSPHERIC PROPAGATION

IONOSPHERIC COMPOSITION
Investigations into the properties, conditions, and effects of the ionosphere
[AD-A217807] 14 p2005 N90-21489

IONOSPHERIC CONDUCTIVITY
On the influence of ionospheric conductivity on dispersion of acoustic gravity waves 02 p0244 N90-11386

New approach to omega PPCs (Propagation Corrections)
[AD-A215610] 09 p1207 N90-17000

IONOSPHERIC CURRENTS
NT AURORAL ELECTROJETS
NT ELECTROJETS
NT EQUATORIAL ELECTROJET
HIPAS 1987-88: ULF research and campaign support
[AD-A211720] 03 p0339 N90-11933
Equilibrium and stability analysis of magnetospheric plasmas 15 p2057 N90-21782

IONOSPHERIC DISTURBANCES
NT IONOSPHERIC STORMS
NT SUDDEN IONOSPHERIC DISTURBANCES
Plasma theory and simulation
[AD-A207952] 01 p0125 N90-10714
Atmospheric gravity waves in the auroral source region of TIDs, studied with the EISCAT CP2-data 02 p0244 N90-11387
Ionospheric irregularities due to powerful HF radio transmissions 02 p0245 N90-11389
A review on radio studies of auroral E-region ionospheric irregularities 02 p0245 N90-11390
Ionospheric irregularities and their effects on electromagnetic waves propagating through them 02 p0245 N90-11391
Electrostatic turbulence in the high latitude ionosphere 02 p0246 N90-11392
Examples of meteorological behavior of the ionosphere 02 p0246 N90-11395
North-south tropical F2 layer asymmetry at west African and Pacific longitudes 02 p0247 N90-11398
Oblique ionospheric heating and effects on radio propagation
[AD-A214756] 09 p1205 N90-16983
Chemical interactions and light emissions from vented species
[AD-A214130] 10 p1327 N90-17668
ACIRF user's guide: Theory and examples
[AD-A216436] 11 p1496 N90-18613
Calculation of ionospheric corrections for single frequency GPS observations: Investigation of two models
[ETN-90-95450] 12 p1602 N90-19219
Ionospheric heating with oblique waves. Volume 1: Electron density perturbations
[AD-A216260] 12 p1690 N90-19709
Center of excellence in theoretical geoplasma research
[AD-A215035] 14 p2005 N90-21488
Radar detection during scintillation
[AD-A220099] 17 p2393 N90-23630
The importance of adiabatic variations in trapped particle distributions observed by the SCATHA satellite
[AD-A220859] 17 p2423 N90-23806
Evaluation of space plasma data: Effects upon spacecraft materials and predictions of hazardous conditions; polar ARCS
[AD-A219509] 17 p2474 N90-24145
Experimental analysis of the HF linkage 20 p2845 N90-26181
System factors to be considered in assessing propagation effects on modern digital satellite communications systems 20 p2850 N90-26208
Amplitude and phase scintillation and ionospheric irregularities at sub-auroral latitudes
[AD-A222861] 21 p3025 N90-27198
Electrodynamics of the high latitude ionosphere
[AD-A223229] 21 p3026 N90-27203
Ionospheric irregularities: Source, structure, plasma processes and effects on sensor systems
[AD-A223908] 24 p3490 N90-29723

IONOSPHERIC DRIFT
Investigation of structure and transport processes in the high latitude ionospheric plasma using ground based and airborne digisondes
[AD-A224397] 24 p3491 N90-29727

IONOSPHERIC ELECTRON DENSITY
Global ionospheric dynamics: A review 02 p0241 N90-11367
A fully analytic, low and middle latitude ionospheric model 02 p0241 N90-11368
Global morphology of plasma bubbles in the low latitude ionosphere 02 p0241 N90-11369
The middle and high latitude ionosphere at approximately 550 km altitude 02 p0242 N90-11374
Modelling ionospheric density structures 02 p0242 N90-11375
Quiet time conductivities of the auroral ionosphere 02 p0244 N90-11383
Electrostatic turbulence in the high latitude ionosphere 02 p0246 N90-11392
Examples of meteorological behavior of the ionosphere 02 p0246 N90-11395
Ionospheric total electron content, and far ultraviolet, near infrared oxygen emission 02 p0249 N90-11410
Enhanced electron density layers in the high-latitude lower ionosphere 05 p0657 N90-13832
Scientific investigations of the Space Research Group
[ISBN-0-642-13252-6] 08 p1138 N90-16595
Ionospheric heating with oblique waves. Volume 2: Applications to high-frequency radio propagation
[AD-A223111] 21 p3025 N90-27202

IONOSPHERIC F-SCATTER PROPAGATION
Measurement errors 17 p2359 N90-23426

IONOSPHERIC HEATING
HIPAS 1987-88: ULF research and campaign support
[AD-A211720] 03 p0339 N90-11933
Coherency properties of strong Langmuir turbulence
[DE89-009290] 03 p0371 N90-12119
Oblique ionospheric heating and effects on radio propagation
[AD-A214756] 09 p1205 N90-16983
Ionospheric heating with oblique waves. Volume 1: Electron density perturbations
[AD-A216260] 12 p1690 N90-19709
Center of excellence in theoretical geoplasma research
[AD-A215035] 14 p2005 N90-21488
Computer simulation of ionospheric radio frequency heating
[DE90-009478] 15 p2087 N90-21944
Ionospheric heating with oblique waves. Volume 2: Applications to high-frequency radio propagation
[AD-A223111] 21 p3025 N90-27202

IONOSPHERIC ION DENSITY
Dynamics of cavitons in strong Langmuir turbulence
[DE90-008918] 14 p2029 N90-21633
Actions of magnetospheres on planetary atmospheres
[IRF-SR-203] 17 p2486 N90-24215
An assessment of the application of in situ ion-density data from DMSP to modeling of transionospheric scintillation
[AD-A224392] 24 p3490 N90-29725

IONOSPHERIC NOISE
NT WHISTLERS
NRL/VOA modifications to IONCAP as of 12 July 1988
[AD-A211546] 03 p0338 N90-11929

IONOSPHERIC PROPAGATION
NT IONOSPHERIC F-SCATTER PROPAGATION
Atmospheric gravity waves in the auroral source region of TIDs, studied with the EISCAT CP2-data 02 p0244 N90-11387
On the possibility of producing artificial ionization and polar aurora in the ionosphere by radio-waves emitted from the ground 02 p0245 N90-11388
Influence of ionospheric variations on high-reliability HF systems utilizing large bases 02 p0248 N90-11404
NRL/VOA modifications to IONCAP as of 12 July 1988
[AD-A211546] 03 p0338 N90-11929
The use of backscatter for modelling ionosphere and jamming in very short term forecasts 06 p0762 N90-14434
Effects of strong scattering on transionospheric propagation
[AD-A216708] 11 p1497 N90-18617
Calculation of ionospheric corrections for single frequency GPS observations: Investigation of two models
[ETN-90-95450] 12 p1602 N90-19219
HF propagation through actively modified ionospheres
[DE90-008931] 16 p2227 N90-22705
Effects of ionospheric modification on system performance 20 p2849 N90-26202
EINMUF: An HF MUF, FOT, LUF prediction program
[AD-A221577] 21 p3055 N90-27371
An assessment of the application of in situ ion-density data from DMSP to modeling of transionospheric scintillation
[AD-A224392] 24 p3490 N90-29725
An assessment of the application of in situ ion-density data from DMSP to modeling of transionospheric scintillation
[AD-A222695] 24 p3491 N90-29730

IONOSPHERIC REFLECTION
U IONOSPHERIC PROPAGATION

IONOSPHERIC SOUNDING
First results from HF (High-Frequency) oblique backscatter soundings to the northwest of College, Alaska using a modified ULCAR digisonde D-256
[AD-A214931] 09 p1206 N90-16987
The worldwide ionospheric data base
[NASA-TM-101823] 24 p3488 N90-29714

IONOSPHERIC STORMS
NT SUDDEN IONOSPHERIC DISTURBANCES
Average diurnal and seasonal profiles of ionospheric storms 02 p0241 N90-11371
Stormtime coupling of the neutral and ionized upper atmosphere at middle latitudes 02 p0243 N90-11381
Diagnosis of auroral dynamics using global auroral imaging with emphasis on large-scale evolutions
[NASA-CR-186623] 17 p2422 N90-23804

IONOSPHERICS
NT HISS

IONS
NT ANIONS
NT CATIONS
NT CESIUM IONS
NT DEUTERONS
NT FERRIC IONS
NT HEAVY IONS
NT HELIUM IONS
NT HYDROGEN IONS
NT LIGHT IONS
NT METAL IONS
NT MOLECULAR IONS
NT NEGATIVE IONS
NT NITROGEN IONS
NT OXYGEN IONS
NT POSITIVE IONS
NT RECOIL IONS
NT TRITONS
NT TRIVALENT IONS
Electronic and ionic transport in polymers
[AD-A210654] 02 p0201 N90-11148
Computer simulations of electromagnetic ion instabilities in the plasma sheet boundary layer
[DE89-016596] 02 p0278 N90-11588
The multivalent beta'-aluminas
[AD-A212103] 04 p0478 N90-12738
Liquid and solid ion plasmas
[AD-A212415] 04 p0557 N90-13244
Pilot investigation of indoor-outdoor and personal PM10 (thoracic) and associated ionic compounds and mutagenic activity
[PB89-222723] 05 p0673 N90-13920
Use of a krypton isotope for rapid ion changeover at the Lawrence Berkeley Laboratory 88-inch cyclotron
[NASA-CR-186107] 05 p0698 N90-14084
Studies of neutral and ion transport during laser ablation of 1:2:3 superconductors by optical absorption spectroscopy
[DE90-001968] 06 p0790 N90-14604
Multiple electron capture in close ion-atom collisions
[DE90-001541] 06 p0840 N90-14885
Toroidal rotation retardation and ion anomalous transport by drift waves in a tokamak
[DE89-634427] 06 p0844 N90-14913
Electronic and ionic transport in polymers
[AD-A217028] 11 p1491 N90-18579
Interaction of minor ions with fast and slow shocks
[NASA-CR-186372] 11 p1594 N90-19181
Energy transfer between electrons and ions in collision cascades in solids
[AERE-R-13662] 13 p1883 N90-20801
Ionic equilibrium between octahedral and tetrahedral complexes in liquid aluminium-sodium fluoride mixtures
[DE90-613690] 14 p1948 N90-21150
X ray laser with enhanced x ray gain through photodepopulation
[AD-D014448] 14 p1985 N90-21375
Production and analysis by mass spectrometry of beams of polyglycol ions 15 p2066 N90-21835
Hollow cathode operation at high discharge currents
[NASA-CR-185238] 15 p2088 N90-21953
Application of novel data processing techniques to the analysis of Ion Mobility Spectrometry (IMS) data
[AD-A219976] 17 p2374 N90-23516
Electronic and ionic transport in processable conducting polymers
[AD-A221045] 18 p2530 N90-24436
Laboratory studies of the interaction of ions with condensed gases: Planetary applications 20 p2949 N90-26778
Ion/molecule reactions of arsenic and phosphorus cluster ions: Ionization potentials and novel reaction pathways
[AD-A222019] 21 p2977 N90-26918
The role of heat transfer during reactive-ion etching of polymer films
[AD-A222072] 21 p2977 N90-26919
Laboratory study of ion-neutral collisions at suprathermal energies
[AD-A222117] 21 p3074 N90-27475
An ionic mechanism of carbon formation in flames 21 p3093 N90-27582
Use of microelectrode arrays to directly measure diffusion of ions in solid electrolytes: Physical diffusion of Ag(+) in a solid polymer electrolyte
[AD-A222026] 22 p3159 N90-27913
New resonantly photo-pumped x ray laser scheme
[DE90-015044] 23 p3331 N90-28831

IP (IMPACT PREDICTION)
U COMPUTERIZED SIMULATION

IRAS
U INFRARED ASTRONOMY SATELLITE
IRAS-ARAKI-ALCOCK COMET
Sulfur compounds in comets
08 p1143 N90-16627
IRASERS
U INFRARED LASERS
IRIDIUM
Monomers, polymers and transition metal complexes based upon carboranes
[AD-A210226] 01 p0040 N90-10221
Thermodynamics, kinetics, and interface morphologies of phase formation reactions between metals and Gallium Arsenide: Bulk vs thin-film studies
[DE89-016469] 02 p0284 N90-11621
Luminescence in applied magnetic fields
[AD-A211551] 03 p0399 N90-12287
Experimental evaluation of new alloy coatings
[AD-A214922] 09 p1194 N90-16916
Method of making a long life high current density cathode from tungsten and iridium powders using a quarternary compound as the impregnant
[AD-D014425] 14 p1958 N90-21211
Antiferromagnetism and enhanced heat in CeM2Sn (M = Ni, Ir, Cu, Rh, Pd, and Pt
[DE90-014924] 23 p3399 N90-29206
IRIS SATELLITES
IRIS system and future application to expandable launchers
[IAF-89-212] 20 p2818 N90-26035
IRON
NT IRON ISOTOPES
Genetic engineering of single-domain magnetic particles
[AD-A210332] 01 p0091 N90-10521
Iron (III) initiated autoxidation of 1,2,3,4-tetrahydrocarbazole: An example of electron transfer
[AD-A211857] 03 p0323 N90-11836
High pressure studies of planetary matter
[DE89-017738] 03 p0428 N90-12455
Experimental and numerical investigations of the crack arrest behavior of steels and cast iron materials
[MPA-TWB-88-03] 05 p0623 N90-13635
Internal and external nitriding and nitrocarburizing of iron and iron-based alloys
[ETN-90-96012] 05 p0625 N90-13646
A theory of damage in brittle and cementitious materials, part 1
[AD-A212940] 05 p0627 N90-13658
Metal film coatings on amorphous metallic alloys
[AD-D014308] 07 p0907 N90-15240
Two-dimensional magnetic phase transition of ultrathin iron films on Pd(100)
[DE90-003555] 07 p1000 N90-15788
Epitaxial iron films
[AD-A213551] 07 p1003 N90-15807
Determination of iron in chromium plating and polishing solutions by atomic absorption spectrometry
[AD-A214467] 09 p1189 N90-16892
Mechanics of iron, its stability and phase transformation
[DE89-636210] 09 p1193 N90-16913
Photoelectron spectroscopic study of the interaction of thin Fe films with the MoS2(0001) surface
[AD-A214348] 10 p1351 N90-17836
Hydrogen sulfide effect on hydrogen entry into iron: A mechanistic study
[AD-A216214] 10 p1354 N90-17854
Infrared (FeII), H and H2 lines in galaxy nuclei
11 p1587 N90-19153
Near infrared spectroscopy and spectroscopic imaging of NGC253
11 p1588 N90-19159
The preparation and properties of iron doped II-VI chalcogenides
[AD-A217569] 12 p1724 N90-19903
Ligand-centered electron-transfer redox processes for manganese, iron, and cobalt complexes in relation to selected catalytic systems
[AD-A217957] 13 p1773 N90-20177
L shell XANES (X ray Absorption Near Edge Structure) for solid metals: Ti, V, Cr, Fe, Ni, Cu
[DE90-008043] 13 p1896 N90-20680
Studies of mechano-chemical interactions in the tribological behavior of materials
[NASA-TM-102545] 14 p1953 N90-21182
A balloon measurement of the isotopic composition of galactic cosmic ray iron
14 p2043 N90-21717
Tribological and mechanical properties of Fe/Ti multilayered films
[DE90-011949] 18 p2565 N90-24635
Iron K-shell lines from relativistic accretion disks
19 p2766 N90-25714
Spectral variability of LMC X-4
19 p2766 N90-25717
Detailed non-LTE calculations of the iron emission from NGC 1068
19 p2788 N90-25872
Iron lines from X ray illuminated accretion discs in AGN
19 p2790 N90-25884
A search for iron features in the EXOSAT spectral survey sources
19 p2791 N90-25887
The X ray spectrum of MCG-6-30-15
19 p2793 N90-25898
Optical FeII emission and the BLR structure in QSOs
19 p2793 N90-25899
The iron abundance gradient in the intracluster medium of Perseus: A galactic wind model. Application to other clusters
19 p2793 N90-25901
Studies of iron impurities in YxPr1-xBa2Cu3O7-delta
22 p3151 N90-27865
Effects of Al substitution by Fe in CeAl2
[DE90-627843] 23 p3311 N90-28726
Helium generation in fusion reactor materials
[DE90-013005] 23 p3393 N90-29172
Ion-beam mixing of Fe/B layers for tribological applications
[DE90-010091] 24 p3456 N90-29518
IRON ALLOYS
NT AUSTENITIC STAINLESS STEELS
NT BAINITIC STEEL
NT CARBON STEELS
NT CHROMIUM STEELS
NT FERRITIC STAINLESS STEELS
NT HIGH STRENGTH STEELS
NT LOW CARBON STEELS
NT MARAGING STEELS
NT MARTENSITIC STAINLESS STEELS
NT NICKEL STEELS
NT STAINLESS STEELS
NT STEELS
Establishment and initial operation of a resource facility for RSR (Rapid Solidification Rate) processed alloys in pilot quantities
[AD-A210369] 01 p0050 N90-10283
Internal and external nitriding and nitrocarburizing of iron and iron-based alloys
[ETN-90-96012] 05 p0625 N90-13646
The effects of alloying and thermal factors on the solidification and mechanical properties of gray iron
[VTT-619] 05 p0625 N90-13651
Energetics of BCC-FCC lattice deformation in iron
[AD-A213801] 07 p0905 N90-15233
Fracture toughness of ferritic alloys at very high neutron exposures
[DE90-004519] 08 p1046 N90-16046
Effect of carbon on ion beam mixing of Fe-Ti bilayers
[DE90-003650] 08 p1048 N90-16056
Anisotropy and microstructure of high coercivity rare earth iron permanent magnets, list of papers published
[AD-A214160] 08 p1118 N90-16476
Corrosion fatigue of iron-chromium-nickel alloys: Fracture mechanics and chemistry
[DE90-006318] 11 p1487 N90-18556
Identification of a cast iron alloy containing nonstrategic elements
[NASA-CR-185174] 11 p1487 N90-18559
Corrosion properties of Fe3Al in H2S-H2-H2O mixtures
[DE90-004936] 13 p1772 N90-20167
On the stability of amorphous silica coatings for high temperature service
[AERE-R-13425] 14 p1953 N90-21179
Martensitic transformation induced by stress pulses
[DE90-009534] 15 p2069 N90-21854
Pulsed and modulated passage NMRON studies of cobalt-iron alloys
17 p2470 N90-24118
A study of the phase decomposition of Fe-Ni-Al-Mo alloys
[DE90-010143] 18 p2524 N90-24406
Studies on phosphorus segregation in austenite
[ISBN-952-90-1488-0] 18 p2526 N90-24417
Morphological and structural characterization of the spinodal decomposition of Fe-Cr alloys
[DE90-010496] 18 p2526 N90-24418
The effect of manganese on the onset of the stage 2 reaction in an austempered ductile iron matrix
[DE90-011804] 20 p2834 N90-28119
Strengthening in heavily cold worked Cu-20 vol. percent Fe in situ composites
[DE90-011741] 22 p3135 N90-27790
Investigation of the effects of microalloy constituents, surface treatment and oxidation conditions on the development and breakdown of protective oxide scales
[DE90-015710] 24 p3451 N90-29488
Isotopic tailoring and other techniques used to study helium effects in austenitic alloys
[DE90-016344] 24 p3452 N90-29495
The effect of helium on microstructural evolution in austenitic steels as determined by spectral tailoring experiments
[DE90-016360] 24 p3452 N90-29496
IRON CHLORIDES
Modeling of sodium/metal chloride batteries
[DE89-017685] 06 p0770 N90-14478
IRON COMPOUNDS
NT FERRITES
NT FERROCENES
NT ILMENITE
NT IRON CHLORIDES
Electrochemistry in near-critical and supercritical fluids. Part 7: SO2
[AD-A208207] 01 p0039 N90-10214
Sealing L-alloys/FeS(x) cells for a bipolar battery
[DE90-004887] 09 p1214 N90-17040
Metallaboranes as precursors to metallic glasses
[AD-A216946] 11 p1490 N90-18577
Improvement study of iron disilicide thermoelectric materials
[AD-A218946] 16 p2252 N90-22844
Dynamics of the iron spins in superconducting YBa2(Cu(1-x)Fe(x))O7
22 p3143 N90-27825
IRON ISOTOPES
Dynamical information for Fe doped YBa2Cu3O7 superconducting oxides obtained from high temperature Moessbauer studies
[DE90-627871] 23 p3401 N90-29218
IRON METEORITES
An atom probe study of phase decomposition in three iron meteorites
[DE89-017581] 03 p0421 N90-12420
Meteoritic basalts
[NASA-CR-185949] 06 p0861 N90-15004
IRON OXIDES
NT ILMENITE
IROQUOIS HELICOPTER
U UH-1 HELICOPTER
IRRADIANCE
NT ILLUMINANCE
NT SOLAR CONSTANT
An anisotropic shadowband correction for parameterized sky conditions and geometry
[DE89-014916] 01 p0085 N90-10485
Solar radiation in Linkoeping (Sweden): Variations over half a year in irradiance and spectral composition in the interval 400-1000 nm
[FOA-C-30521-3.1] 02 p0250 N90-11417
Solar-geophysical data number 538, June 1989. Part 2: (Comprehensive reports). Data for December 1988 and miscellaneous
[PB89-223846] 06 p0866 N90-15032
Measurement system of spectral irradiance in the near infrared
11 p1588 N90-19160
Analysis of methods to determine emissivity for ground surface targets in the spectral band 8 to 14 microns
[INPE-4984-TDL/394] 13 p1820 N90-20447
Downward shortwave surface irradiance from 17 sites for the FIRE/SRB Wisconsin experiment
[NASA-TM-102596] 13 p1844 N90-20583
Measurement of the reflectance ratio of natural light in the sea
[IOS-265] 15 p2135 N90-22199
Passive navigation using image irradiance tracking
15 p2141 N90-22232
Downwelled longwave surface irradiance data from five sites for the FIRE/SRB Wisconsin Experiment from October 12 through November 2, 1986
[NASA-TM-102597] 21 p3030 N90-27225
Observed solar near UV variability: A contribution to variations of the solar constant
22 p3201 N90-28163
Impact of cirrus on the surface radiative environment at the FIRE ETLA Palisades, NY site
22 p3221 N90-28270
IRRADIATION
NT AURORAL IRRADIATION
NT DEUTERON IRRADIATION
NT ELECTRON IRRADIATION
NT ION IRRADIATION
NT NEUTRON IRRADIATION
NT PROTON IRRADIATION
NT X RAY IRRADIATION
Eye/sensor protection against laser irradiation organic nonlinear optical materials
[AD-A210599] 01 p0093 N90-10531
Generation of 3/2 omega sub o radiation in inhomogeneous plasmas under the irradiation of intense electromagnetic waves
[DE89-015723] 01 p0126 N90-10722
Grain boundary chemistry in irradiated stainless steel and its influence on environmental degradation
[DE89-016827] 02 p0197 N90-11125
Fracture toughness data base for HT9 and modified 9Cr-1Mo irradiated in several reactors up to approximately 100 dpa
[DE90-000111] 03 p0328 N90-11864

An investigation of the irradiation swelling mechanisms in refractory metals at high temperatures
[AD-A211406] 04 p0474 N90-12719
Nuclear magnetic resonance signatures of nitrogen-containing compounds
[AD-A213375] 05 p0622 N90-13628
Optical properties monitor: Experiment definition phase
[NASA-CR-183836] 05 p0699 N90-14092
The feasibility of welding of irradiated materials
[DE90-002200] 06 p0795 N90-14631
The effects of heavy particle radiation on semiconductor devices
[DE90-001679] 06 p0854 N90-14962
Microstructural evolution of martensitic steels during fast neutron irradiation
[DE89-016231] 07 p0902 N90-15212
Helium-induced weld cracking in irradiated 304 stainless steel
[DE90-001312] 07 p0903 N90-15219
Optical properties and laser damage measurements of inorganic polymer films
[DE90-003633] 07 p0911 N90-15267
Fusion reactor materials
[DE90-000976] 07 p0994 N90-15744
Irradition-induced grain growth: Role of dislocations
[DE90-003565] 07 p1001 N90-15792
Defense to laser light irradiation
[AD-D014286] 08 p1036 N90-15984
Evaluation of potential cold x ray shield materials tested on Proto II
[DE90-004348] 08 p1039 N90-16003
Microstructural explanation for irradiation embrittlement of V-15Cr-5Ti
[DE90-004112] 08 p1045 N90-16041
Phase evolution during neutron irradiation of commercial Fe-Cr-Mn alloys
[DE90-004113] 08 p1045 N90-16042
Irradiation creep and swelling of annealed type 304L stainless steel at approximately 390 C and high neutron fluence
[DE90-004521] 08 p1046 N90-16047
Modeling dislocation evolution in irradiated alloys
[DE90-004921] 08 p1047 N90-16051
Structure-property relationships in ion-beam surface-modified ceramics: Theory and applications
[AD-A212785] 08 p1047 N90-16054
Metals and Ceramics Division Materials Sciences Program
[DE90-004371] 08 p1050 N90-16070
Radiation resistance of solar cells for space application. 1: Study on the irradiation procedure of electron beams
[DE90-719546] 08 p1096 N90-16349
Mechanisms of microwave induced damage in biologic materials
[AD-A213480] 08 p1104 N90-16390
Atomic processes in plasmas under ultra-intense laser irradiation
[DE90-003221] 08 p1126 N90-16521
Effects of ion dose on the morphology and crystallization of amorphous germanium
[DE90-003564] 08 p1130 N90-16547
The 1MeV-electron irradiation induced defects in epitaxially grown 3C-SiC
[DE90-719574] 08 p1131 N90-16554
Heavy-section steel technology program fracture issues
[DE90-005264] 09 p1240 N90-17195
Optical nutation in polymers irradiated by ultrashort laser pulses
[AD-A212927] 10 p1357 N90-17869
Electron-beam induced damage in thin insulating films on compound semiconductors
[NASA-CR-185177] 10 p1378 N90-17987
Nonlinear optical processes in one-dimensional polymers
[AD-A216103] 11 p1489 N90-18568
Polymerization of nitro compounds on silver surfaces during surface-enhanced Raman scattering
[AD-A216116] 11 p1489 N90-18569
Irradiation-induced amorphization and elastic shear instability in intermetallic compounds
[DE90-004845] 12 p1625 N90-19341
Effect of electron-excitation on radiation damage in ion-irradiated FCC metals
[DE90-719537] 12 p1626 N90-19344
Defect structures in copper and gold irradiated with fast neutrons, 14 MeV neutrons and 600 to 800 MeV protons
[DE90-007529] 12 p1629 N90-19359
Electron beam induced damage in PECVD Si3N4 and SiO2 films on InP
[NASA-TM-102544] 13 p1810 N90-20393
The stress-driven redistribution of point defects in the vicinity of crack-like singularities
[AERE-R-12898] 13 p1815 N90-20424
Grain boundary chemistry effects on irradiation-assisted stress corrosion cracking
[DE90-008623] 14 p1951 N90-21167
Low energy ion generator
[DE90-759905] 14 p1955 N90-21195
Ga:Ge array development 14 p1977 N90-21323
A simplified theoretical model for the laser-induced optogalvanic effect
[DE90-613121] 14 p2028 N90-21626
Fracture toughness and tensile properties of alloy HT9 in thin sections under high neutron fluences
[DE90-008386] 15 p2069 N90-21851
High intensity laser beam interactions with single droplets 15 p2083 N90-21924
Producing dense plasmas with x rays
[DE90-009539] 15 p2169 N90-22393
Photovoltaic advanced research and development project: Solar radiation research
[DE90-000302] 16 p2251 N90-22839
A study of low level laser retinal damage
[AD-A218919] 16 p2261 N90-22887
Influence of high energy radiation on critical parameters of superconducting ceramics YBa2Cu3O7
[DE90-620562] 16 p2322 N90-23239
Gamma rays from giant molecular clouds 16 p2334 N90-23298
Laser eye protection
[AD-A219659] 17 p2408 N90-23722
High peak power microwave pulses at 2.37 GHz: No effects on vigilance performance in monkeys
[AD-A219570] 17 p2433 N90-23863
The mechanical properties of Cu/TiB2 multilayer structures
[DE90-010608] 18 p2517 N90-24378
Grain growth and phase formation in ion irradiated/annealed thin Ni-Al alloys films
[DE90-010409] 18 p2525 N90-24407
Irradiation effects on impact behavior of 12Cr-1MoVW and 2 1/4Cr-1Mo steels
[DE90-011075] 18 p2527 N90-24421
Irradiation assisted stress corrosion cracking
[DE90-010629] 18 p2572 N90-24656
In vitro photoreactivation of transforming DNA of bacillus subtilis spores after irradiation with UV light
[DLR-FB-89-45] 18 p2583 N90-24710
Monoenergetic positron beam studies of near-surface phenomena
[ETN-90-96947] 18 p2613 N90-24887
TFE verification program
[DE90-008227] 18 p2614 N90-24891
The defect structure of ion and neutron irradiated YBa2Cu3O(7-delta) single crystals
[DE90-010100] 18 p2619 N90-24920
Predicting switched-bias response from steady-state irradiations
[DE90-006770] 18 p2624 N90-24950
Neutron and gamma irradiation effects on power semiconductor switches
[NASA-TM-103200] 19 p2686 N90-25278
SERI solar radiation resource assessment project
[DE90-000307] 19 p2711 N90-25428
A study of the influence of Hg(6(3)P2) population in a low-pressure discharge on mercury ion emission at 194.2 nm 20 p2853 N90-26223
Excimer laser fragmentation studies of selected oximes: Nascent OH internal energy distributions and the search of H2CN fluorescence
[AD-A222622] 20 p2868 N90-26317
Surface reactions in the space environment
[AD-A221767] 21 p2979 N90-26932
Subthreshold technique for fixed and interface trapped charge separation in irradiated MOSFETs
[AD-A221861] 21 p3001 N90-27061
Effects of protracted ionizing radiation dosage on humans and animals: A brief review of selected investigations
[AD-A222240] 21 p3033 N90-27241
Radiation-curable prepreg composites
[DE90-629740] 23 p3301 N90-28674
Density changes of generation 1.5 and 2.0 copper alloys irradiated at 411 to 414 C and 529 C in FFTF-MOTA
[DE90-015291] 23 p3311 N90-28724
Transient annealing characterization of irradiated MOSFETS
[AD-A223877] 23 p3401 N90-29220
Relationship between microstructure, spinodal-like decomposition and selective electropolishing of irradiated invar-type alloys
[DE90-015293] 24 p3450 N90-29484
Tensile behavior and swelling of ternary austenitic alloys irradiated in different neutron spectra
[DE90-015295] 24 p3450 N90-29485
The effect of helium on microstructural evolution in austenitic steels as determined by spectral tailoring experiments
[DE90-016360] 24 p3452 N90-29496
Factors affecting practical application of food irradiation
[DE90-631277] 24 p3522 N90-29914
High resolution transmission electron microscopy of partial states of oxygen order in YBa2Cu3O(z)
[DE90-015637] 24 p3554 N90-30108

IRREGULAR GALAXIES
Chemical evolution of dwarf irregular galaxies 22 p3263 N90-28478

IRREGULARITIES
Localized vibrations of nearly periodic structures with irregularities 06 p0798 N90-14648
Low latitude F-region dynamical processes from atomic oxygen nightglow emissions
[INPE-4999-PRE/1561] 14 p2006 N90-21494
The initial imperfection databank at the Delft University of Technology, part 3
[LR-568] 15 p2057 N90-21783

IRREVERSIBLE PROCESSES
Electrolyte dependence of charge injection processes for electroactive polymer films
[AD-A210787] 02 p0202 N90-11152
Irreversible phase transition and wave propagation in silicate geologic materials
[DE89-016031] 02 p0250 N90-11414
Irreversible processes from reversible mechanics
[DE90-001057] 07 p0927 N90-15368
Nonlinear wave propagation
[AD-A215500] 10 p1375 N90-17968

IRROTATIONAL FLOW
U POTENTIAL FLOW

IRS (INDIAN SPACECRAFT)
U INDIAN SPACECRAFT

ISCHEMIA
Generation of free radicals during cold injury and rewarming
[AD-A213088] 05 p0672 N90-13915

ISENTROPE
A description of tropical cyclone recurvature in terms of isentropic potential vorticity
[AD-A218482] 17 p2425 N90-23821

ISING MODEL
Energy barriers in SK spin-glass model
[PREPRINT-665] 05 p0704 N90-14119
Surface magneto-optical studies of ultrathin ferromagnetic films
[DE90-002199] 06 p0856 N90-14980
Contribution to the study of order effects in the Ising model framework: Ground states and phase diagrams
[ESA-TT-1118] 08 p1132 N90-16557
Solution of a class of conformal quantum field theory models in D-dimensional space
[DE90-607094] 10 p1439 N90-18306
The renormalization group and lattice QCD
[DE90-004860] 12 p1724 N90-19905
Electronic structure, alloy phase stability, and phase diagrams
[DE90-008306] 13 p1778 N90-20203
Magnetic properties of surfaces and interfaces
[DE90-007348] 13 p1880 N90-20789
The geometry of disorder: Report 1987 to 1990
[DE90-008250] 13 p1896 N90-20882
Operator algebra from fusion rules: The infinite number of Ising theories
[NIKHEF-H/89-7] 15 p2165 N90-22374
Rigorous analysis of low temperature stochastic Ising models: Metastability and exponential approach to equilibrium
[PREPRINT-720] 16 p2312 N90-23175
Systematic approach to critical phenomena by the extended variational method and coherent-anomaly method
[DE90-627320] 23 p3392 N90-29165

ISIS SATELLITES
NT ALOUETTE 2 SATELLITE

ISLANDS
NT GREENLAND
NT HAWAII
NT ICELAND
NT INDONESIA
NT JAPAN
NT MALAGASY REPUBLIC
NT MERRITT ISLAND (FL)
NT NEW ZEALAND
Evolution of midplate hotspot swells: Numerical solutions
[NASA-CR-186462] 12 p1691 N90-19713
A day-to-day comparison study of Seasat scatterometer winds with winds observed from islands in the tropical Pacific
[NASA-CR-186696] 22 p3212 N90-28223

ISOBUTANE
U BUTANES

ISOBUTYLENE
U BUTENES

ISOCHROMATICS
Isoplanatic systems in mesooptics
[DE90-009785] 17 p2406 N90-23705
ISOCYANATES
An investigation of the degradation and stabilization of polymer systems
[AD-A210362] 01 p0049 N90-10282
Chemical treatment of epoxy resins to reduce moisture sensitivity and to improve the mechanical properties
[AD-A212360] 04 p0481 N90-12758
Informal conference on the Chemistry of Energetic Azides, Isocyanates, and Related Species
[AD-A219825] 17 p2373 N90-23514
ISOENERGETIC PROCESSES
The interaction of a supersonic streamwise vortex and a normal shock wave 18 p2491 N90-24241
ISOLATION
Documentation of the current fault detection, isolation and reconfiguration software of the AIPS fault-tolerant processor
[NASA-TM-89154] 01 p0106 N90-10602
Vibration isolation technology: Sensitivity of selected classes of space experiments to residual accelerations
[NASA-CR-185443] 04 p0482 N90-12768
Structural vibration and shock isolator
[AD-D014202] 04 p0509 N90-12940
Ballast system for maintaining constant pressure in a glove box
[NASA-CASE-NPO-17786-1-CU] 09 p1224 N90-17104
Structural vibration and shock isolation in a high pressure environment
[AD-D014311] 09 p1238 N90-17186
Psychophysiological correlates of human adaptation in antarctica
[AD-A216679] 10 p1412 N90-18142
Elastomeric electrical isolation membrane
[AD-D014365] 12 p1651 N90-19490
Vibration isolation versus vibration compensation on multiple payload platforms 14 p1933 N90-21066
ISOLATORS
NT VIBRATION ISOLATORS
Mechanical strain isolator mount
[NASA-CASE-LAR-13580-1] 08 p1084 N90-16272
A gas-phase high voltage electrical isolator with controlled breakdown
[RAE-TR-78030] 19 p2669 N90-25180
High performance millimeter-wave microstrip circulators and isolators
[NASA-CR-186276] 19 p2685 N90-25270
Luminescence from electroformed metal-isolator-metal-structures
[ETN-90-97295] 22 p3249 N90-28425
ISOMERIZATION
NT ORTHO PARA CONVERSION
ISOMERS
NT ISOPROPYL ALCOHOL
NT PHENANTHRENE
The chemical basis for the origin of the genetic code and the process of protein synthesis
[NASA-CR-186590] 15 p2136 N90-22205
ISOMORPHISM
Banach C*-algebras not containing a subspace isomorphic to C(sub 0)
[DE90-610428] 12 p1706 N90-19796
Graph representation in a special family of infinite graphs
[MEMO-831] 17 p2463 N90-24067
ISOPARAMETRIC FINITE ELEMENTS
Elastodynamic scattering and transmission problems in three dimensions by the boundary integral equation method 15 p2111 N90-22077
ISOPLETHS
U NOMOGRAPHS
ISOPROPYL ALCOHOL
Equation-of-state data of synthetic Uranus
[DE89-016509] 02 p0296 N90-11683
Thermophysical properties of isopropyl alcohol. Part 2: Thermodynamic properties at elevated pressures
[ESDU-89020-PT-2] 06 p0739 N90-14300
ISOPROPYL COMPOUNDS
NT ISOPROPYL ALCOHOL
ISOTHERMAL FLOW
Scalar dissipation measurements in the developing region of a jet 21 p2976 N90-26909
ISOTHERMAL PROCESSES
Vibration isolation technology: Sensitivity of selected classes of space experiments to residual accelerations
[NASA-CR-185443] 04 p0482 N90-12768
The mechanisms of dispersion strengthening and fracture in Al-based XD (TM) alloys
[NASA-CR-4276] 09 p1187 N90-16879
ISOTHERMS
A seasonal isotherm depth climatology for the eastern tropical Pacific
[PB89-193577] 01 p0090 N90-10512
Self-calibrating apparatus to find dynamic compressibility of organic solids
[AD-A219780] 17 p2415 N90-23763
The composition and physical properties of the Earth's mantle and core 18 p2579 N90-24689
ISOTOPE EFFECT
A model of the isotope effect of the oxide superconductor
[DE89-635907] 06 p0855 N90-14971
Superconductivity in Ba(1-x)BiO3
[DE90-003781] 12 p1718 N90-19869
Stable isotope studies of cometary analogue materials 12 p1740 N90-20001
Condensed phase kinetic deuterium isotope effects in high energy phenomena: Mechanistic investigations and relationships
[AD-A217161] 13 p1770 N90-20156
Towards a Sarkovski order for the embedding of disks maintaining their orientation
[REPT-89-43] 15 p2151 N90-22289
Combined effect of isotopic substitution, temperature, and magnetic field on the lifetimes of triplet biradicals
[AD-A219711] 17 p2372 N90-23509
Probing the possibility of a C-12/C-13 galactic abundance gradient 21 p3094 N90-27586
ISOTOPE SEPARATION
Isotopic selectivity of surface diffusion: An activated diffusion model
[DE90-003473] 07 p0894 N90-15169
Isotope driven critical scattering and phase separation from mixtures of deuterated and protonated polymers
[DE90-003976] 08 p1051 N90-16076
A gas chromatograph/mass spectrometry method for determining isotopic distributions in organic compounds used in the chemical approach to stable isotope separation
[DE90-005738] 10 p1352 N90-17841
Helium permeability through austenitic stainless steel
[DE90-007046] 11 p1488 N90-18562
The TISOL facility at TRIUMF
[DE90-006882] 12 p1713 N90-19837
Enrichment services for chromium isotopes for the GALLEX (gallium experiment) international collaboration experiment on solar neutrino flux
[DE90-014300] 23 p3413 N90-29285
ISOTOPE SHIFT
U ISOTOPE EFFECT
ISOTOPES
NT ALUMINUM ISOTOPES
NT ALUMINUM 26
NT AMERICIUM
NT ANTIMONY ISOTOPES
NT BORON ISOTOPES
NT CALCIUM ISOTOPES
NT CARBON ISOTOPES
NT CARBON 12
NT CARBON 13
NT CARBON 14
NT CESIUM VAPOR
NT CHROMIUM ISOTOPES
NT COBALT ISOTOPES
NT COBALT 60
NT COPPER ISOTOPES
NT CURIUM
NT DEUTERIUM
NT ERBIUM ISOTOPES
NT EUROPIUM ISOTOPES
NT GADOLINIUM ISOTOPES
NT GALLIUM ISOTOPES
NT GOLD ISOTOPES
NT HELIUM ISOTOPES
NT HYDROGEN ISOTOPES
NT IODINE ISOTOPES
NT IRON ISOTOPES
NT KRYPTON ISOTOPES
NT KRYPTON 85
NT LANTHANUM ISOTOPES
NT LEAD ISOTOPES
NT LITHIUM ISOTOPES
NT MAGNESIUM ISOTOPES
NT MANGANESE ISOTOPES
NT MERCURY ISOTOPES
NT NICKEL ISOTOPES
NT NIOBIUM ISOTOPES
NT OXYGEN ISOTOPES
NT OXYGEN 18
NT PLUTONIUM
NT POLONIUM ISOTOPES
NT RADIOACTIVE ISOTOPES
NT RADON ISOTOPES
NT SILICON ISOTOPES
NT TELLURIUM
NT TELLURIUM ISOTOPES
NT TIN ISOTOPES
NT TRITIUM
NT URANIUM ISOTOPES
CELIAS: Charge, element and isotope analysis system for SOHO 04 p0568 N90-13313
Nonpotential scattering for the density matrix and quantum gravity
[PREPRINT-688] 05 p0697 N90-14080
Phases in lanthanum-nickel-aluminum intermetallic alloys
[DE90-000651] 06 p0746 N90-14343
Heavy ion interactions
[DE90-001410] 06 p0840 N90-14884
On the free carrier-negative U center interacting model for the high-T(sub c) oxide superconductor
[DE89-635908] 07 p0998 N90-15775
Isotope driven critical scattering and phase separation from mixtures of deuterated and protonated polymers
[DE90-003976] 08 p1051 N90-16076
On the isotope analysis of cometary dust 08 p1141 N90-16611
Isotopic microanalysis of returned comet nucleus samples 08 p1149 N90-16655
Quality control programs for isotope dilution mass spectrometry
[DE90-004259] 09 p1189 N90-16891
Safety analysis for the Galileo light-weight radioisotope heater unit
[DE90-007147] 11 p1566 N90-19009
Application of natural isotopes in groundwater for solving environmental problems
[DE90-000223] 12 p1689 N90-19703
Fragmentation of relativistic heavy nuclei with application to cosmic ray propagation 14 p2043 N90-21716
A balloon measurement of the isotopic composition of galactic cosmic ray iron 14 p2043 N90-21717
Pre-concentration method for inductively coupled plasma-mass spectrometry
[PB90-181348] 19 p2673 N90-25202
Carbon monoxide isotopes and clumping in giant molecular clouds 24 p3562 N90-30151
ISOTOPIC LABELING
Tellurium-118/antimony-118 generator
[DE89-015225] 01 p0122 N90-10698
The Renland ice core (Greenland): A source for climatic studies over 100,000 years 20 p2885 N90-26412
Geothermal fluid genesis in the Great Basin
[DE90-014438] 23 p3342 N90-28884
ISOTOPIC SPIN
Theoretical studies in nuclear physics
[DE90-005981] 11 p1565 N90-19005
ISOTROPIC MEDIA
The initial imperfection data bank at the Delft University of Technology, part 2
[LR-559-PT-2] 05 p0356 N90-13825
Viscoplasticity: A thermodynamic formulation
[NASA-TM-102388] 06 p0797 N90-14640
Defects: Their behaviour and related design assumptions 11 p1457 N90-18397
Generalized WKB approximation for stratified isotropic chiral structures
[PB90-165689] 14 p1967 N90-21270
Input-output characterization of fiber reinforced composites by P waves
[NASA-CR-185287] 22 p3189 N90-28097
ISOTROPIC TURBULENCE
Evaluation of the near-wall k-epsilon turbulence model by comparison with direct simulations of turbulent channel flow
[AD-A212674] 04 p0503 N90-12903
Spectral study of a compressible isotropic turbulence
[ECL-88-16] 05 p0643 N90-13753
The analysis and modeling of dilatational terms in compressible turbulence
[NASA-CR-181959] 06 p0776 N90-14513
Application of a Reynolds stress turbulence model to the compressible shear layer
[NASA-CR-182002] 12 p1660 N90-19537
The extension of rapid distortion theory to stratified shear flows 14 p2005 N90-21491
The analysis and simulation of compressible turbulence
[NASA-CR-181997] 16 p2197 N90-22539
Turbulence and complex systems
[ETN-90-96620] 16 p2236 N90-22758
ISOTROPY
NT ISOTROPIC MEDIA
Some implications of the isotropic momentarily frozen assumptions for the SPAN-MAT program
[NASA-CR-181937] 03 p0301 N90-11704
A thermoelastic transversely isotropic thick walled cylinder/disk application: An analytical solution and study
[NASA-TM-102320] 04 p0511 N90-12950
A generalized thermomechanical constitutive model for metal matrix composites with plastic strain and damage 06 p0737 N90-14293
Fluid-particle interaction in solid-liquid two-phase grid turbulence 06 p0773 N90-14496

Turbulence spectral widths view angle independence as observed by Doppler radar
[DOT/FAA/SA-89/2] 07 p0963 N90-15566
An objective time-integration procedure for isotropic rate-independent and rate-dependent elastic-plastic constitutive equations
[PB90-121245] 11 p1550 N90-18925
Background studies in gas ionizing x ray detectors 12 p1636 N90-19399
Anisotropic inflation 16 p2331 N90-23286
A viscoplastic model with application to LiF-22 percent CaF2 hypereutectic salt
[NASA-TM-103181] 17 p2417 N90-23770
Multiwavelength constraints on gamma-ray burst sources 18 p2639 N90-25032
A creep model for metallic composites based on matrix testing: Application to Kanthal composites
[NASA-TM-103172] 19 p2672 N90-25193
The yield and post-yield behavior of high-density polyethylene
[NASA-CR-186574] 19 p2676 N90-25219
Theory of biaxial graded-index optical fiber
[NASA-CR-186882] 20 p2927 N90-26652
Observations of plasma structure freezing scale at equatorial latitudes
[AD-A222529] 21 p3026 N90-27207
Elliptical flux vortices in polycrystalline YBa2Cu3O7 22 p3136 N90-27795
Dissipation of mechanical work and temperature rise in AS4/PEEK thermoplastic composite
[NASA-CR-186893] 23 p3302 N90-28678

ITALIAN SPACE PROGRAM
The ITALSAT experiment 10 p1374 N90-17962
The Italian approach to small satellites for low cost access to space developments
[ETN-90-96552] 16 p2206 N90-22587

ITERATION
NT CONJUGATE GRADIENT METHOD
NT ITERATIVE SOLUTION
NT NEWTON METHODS
NT PREDICTOR-CORRECTOR METHODS
Numerical optimization in Hilbert space using inexact function and gradient evaluations
[NASA-CR-181926] 01 p0112 N90-10640
An introduction to fractals and chaos
[AD-A210257] 01 p0117 N90-10675
Modal analysis of fluid-structure systems by parallel subspace iteration 02 p0181 N90-11024
Asynchronous integration of ordinary differential equations on multiprocessors
[DE89-014169] 02 p0263 N90-11493
Fixed point iteration on point-symmetric interference graphs
[MEMO-INF-89-23] 02 p0269 N90-11535
Multiplicative iterative algorithms for convex programming
[CWI-AM-R8808] 04 p0532 N90-13072
Iterative methods for linear complementary and related problems
[AD-A212848] 04 p0534 N90-13089
Local mode smoothing analysis of various incomplete factorization iterative methods in two dimensions
[REPT-89-36] 04 p0540 N90-13129
Iterated theta method for hyperbolic equations
[CWI-NM-R8809] 04 p0540 N90-13132
An iterative method to solve the nonlinear Poisson's equation in the case of plasma tangential discontinuities
[AERONOMICA-ACTA-A-346-1989] 05 p0692 N90-14045
A study of incremental-iterative strategies for nonlinear analyses
[PB89-226005] 06 p0798 N90-14646
An iterative Bayes procedure for reliability assessment
[DE90-002106] 07 p0944 N90-15466
Tensor methods for unconstrained optimization using second derivatives
[AD-A213642] 07 p0983 N90-15681
Parameter estimation of linear systems in the presence of process noise using the maximum liklihood method
[ESDU-89032] 07 p0985 N90-15693
Improved solution techniques for the eigenstructure of fractional order systems
[AD-A213844] 08 p1088 N90-16295
A monotone surrogate algorithm for the 0-1 Multiknapsack problem
[INPE-4933-PRE/1423] 10 p1417 N90-18169
Domain decomposition with local mesh refinement
[AD-A215806] 10 p1418 N90-18175
Numerical algorithms for parallel computers
[AD-A216812] 10 p1419 N90-18181
On mean value iterations with application to variational inequality problems
[DE90-005556] 10 p1422 N90-18200
Fixed points by Ishikawa iterations
[DE90-005557] 10 p1424 N90-18219
Optimum and heuristic algorithms for finite state machine decomposition and partitioning
[AD-A216778] 11 p1546 N90-18899
Iterative procedures for space shuttle main engine performance models 12 p1639 N90-19416
Convergence properties of iterative algorithms for solving the nodal diffusion equations
[DE89-016859] 12 p1707 N90-19804
Optimal iteration steps by stochastic approximation processes for the solution of optimization problems with twice differentiable functions
[ETN-90-95887] 12 p1708 N90-19809
Integrated optics anisotropic waveguides and devices
[AD-A217064] 12 p1715 N90-19849
Investigation of tapered multiple microstrip lines for VLSI circuits
[AD-A217855] 13 p1797 N90-20310
A time stepping algorithm for parallel computers
[DE90-008163] 13 p1873 N90-20738
A model and implementation of multigrid for massively parallel computers
[DE90-008165] 13 p1873 N90-20739
Techniques for accelerating iterative methods for the solution of mathematical problems
[AD-A218272] 13 p1878 N90-20775
A two-dimensional unsteady analysis for transonic and supersonic cascade flows 14 p1911 N90-20955
Convergence acceleration of hypersonic flow calculations: A nonlinear relaxation factor 14 p1911 N90-20957
Application of an inverse method to the design of a radial inflow turbine 14 p1918 N90-20989
Computational prediction and measurement of the flow in axial turbine cascades and stages 14 p1925 N90-21028
Multigrid on massively parallel computers
[DE90-008999] 14 p2017 N90-21560
High accuracy solutions of incompressible Navier-Stokes equations
[NASA-TM-102539] 14 p2018 N90-21567
A parallel multigrid method for solving elliptic partial differential equations
[DE90-007929] 14 p2021 N90-21584
Towards a unified analysis methodology for composite rotor blades 15 p2046 N90-21730
Analysis, selection, and implementation of procedures which approve optimal artificial satellite maneuvers
[INPE-5003-TDL/397] 15 p2058 N90-21786
Passive shape control of space antennas with determinate truss support structures 15 p2087 N90-21949
Optimal 3-dimensional methods for linear programming
[PB90-155391] 15 p2145 N90-22253
Incomparable elements in algebraic lattices with applications to formal language theory
[MEMO-INF-89-54] 15 p2148 N90-22269
A nearly-linear computational-cost scheme for the forward dynamics of an N-body pendulum 16 p2280 N90-22996
Parallel processing of real-time dynamic systems simulation on OSCAR (Optimally SCheduled Advanced multiprocessoR) 16 p2282 N90-23006
Minimal complexity control law synthesis 16 p2292 N90-23057
Fourier analysis of finite element preconditioned collocation schemes
[NASA-CR-182040] 16 p2304 N90-23128
Undetermined coefficient problems for quasi-linear parabolic equations
[AD-A218462] 16 p2306 N90-23141
Chebyshev polynomials are not always optimal
[NASA-CR-181465] 17 p2455 N90-24008
Iterative defect correction and multigrid accelerated explicit time stepping schemes for the steady Euler equations
[CWI-NM-R8908] 17 p2459 N90-24039
Majority voting: Characterization and algorithms
[RUU-CS-88-32] 18 p2592 N90-24750
On the statistical analysis of growth
[ETN-90-96923] 18 p2606 N90-24841
Neuromorphic learning of continuous-valued mappings from noise-corrupted data. Application to real-time adaptive control
[NASA-TM-4176] 19 p2747 N90-25607
Run-time parallelization and scheduling of loops
[NASA-CR-182039] 20 p2902 N90-26509
A build-up interior method for linear programming: Affine scaling form
[AD-A221802] 21 p3056 N90-27375
Improving the accuracy of inverse iteration
[AD-A221846] 21 p3056 N90-27377
Design of robust multivariable controllers
[AD-A222096] 21 p3060 N90-27397
Investigations on improved iterative methods for solving sparse systems of linear equations
[AD-A221980] 21 p3064 N90-27417
Parallel performance of domain-decomposed preconditioned Krylov methods for PDEs with adaptive refinement
[AD-A222339] 21 p3064 N90-27420
A Bayesian derivation of an iterative autofocus/super-resolution algorithm
[RSRE-MEMO-4337] 22 p3239 N90-28371
Power bounded prolongations and Picard-Lindeloef iteration
[PB90-190877] 22 p3242 N90-28384
Peak analysis in gas chromatography and the development of new stationary phases for anion chromatography
[DE90-014428] 23 p3304 N90-28687
Piecewise linear models of processor utilization
[DE90-014774] 23 p3384 N90-29115
Nonlinear static and dynamic modeling of composite rotor blades including warping effects 24 p3431 N90-29382
Fast algorithms for parallel architectures
[AD-A223731] 24 p3528 N90-29947
Image compression
[AD-A224242] 24 p3537 N90-29998

ITERATIVE NETWORKS
Iterative network magnitude estimation and uncertainty assessment with noisy and clipped data
[AD-A210707] 02 p0265 N90-11507
Frequency assignments for HFDF receivers in a search and rescue network
[AD-A220529] 17 p2390 N90-23610

ITERATIVE SOLUTION
Iterative performance and an adaptive procedure for viscous flow problems 01 p0089 N90-10397
The MHOST finite element program: 3-D inelastic analysis methods for hot section components. Volume 3: Systems' manual
[NASA-CR-182236] 01 p0079 N90-10451
An iterative method for systems of nonlinear hyperbolic equations
[NASA-CR-181919] 01 p0112 N90-10638
Numerical solutions of turbulent flow with heat transfer over rough surfaces 02 p0218 N90-11246
Variable step iteration of high-order Runge-Kutta methods on parallel computers
[CWI-NM-R8817] 02 p0260 N90-11476
Particle simulation in curvilinear coordinate systems
[DE89-016727] 02 p0277 N90-11583
On the computation of normal modes of a rotating, viscous, incompressible fluid with a capillary free boundary
[REPT-89-01] 03 p0348 N90-11989
Some observations on the convergence behavior of GMRES
[REPT-89-09] 03 p0395 N90-12252
The convergence behavior of some iterative solution methods
[REPT-89-19] 03 p0396 N90-12260
A long time tail for random walk in random scenery
[REPT-89-08] 03 p0398 N90-12278
Solution of the thin-layer Navier-Stokes equations for laminar transonic flow
[PB89-221600] 04 p0500 N90-12879
A linearized surface condition in low speed hydrodynamics
[REPT-89-04] 04 p0501 N90-12885
Subspace iteration algorithms in FORTRAN 77 and FORTRAN 8x
[AD-A212275] 04 p0533 N90-13083
Iterative methods for linear complementary and related problems
[AD-A212848] 04 p0534 N90-13089
Multigrid solution method for the Euler equations
[PB89-219463] 04 p0539 N90-13116
Gas flows in rocket motors. Volume 2, appendix C: Time iterative solution of viscous supersonic flow
[AD-A213349] 05 p0615 N90-13592
An iterative method to solve the nonlinear Poisson's equation in the case of plasma tangential discontinuities
[AERONOMICA-ACTA-A-346-1989] 05 p0692 N90-14045
Some quick and efficient methods for bearing-only target motion analysis
[IMAG-RR-762-M] 05 p0693 N90-14049
Program VSAERO theory document: A computer program for calculating nonlinear aerodynamic characteristics of arbitrary configurations
[NASA-CR-4023] 06 p0720 N90-14200
Approximate methods for dynamic plastic deformation of structures
[DE90-002214] 06 p0800 N90-14660
Krylov methods preconditioned with incompletely factored matrices on the CM-2
[NASA-CR-181961] 06 p0822 N90-14779

Versatility of the CFR algorithm for limited angle reconstruction
[DE90-001421] 06 p0829 N90-14817
Iterative methods of domain decomposition with cross-points for the solution of discrete elliptic problems
[DE90-000719] 06 p0835 N90-14854
Structure properties of confined systems. Hard spheres between ideal walls
[DE90-600818] 07 p0929 N90-15378
Element-by-element preconditioning techniques for large-scale, vectorized finite element analysis in nonlinear solid and structural mechanics 08 p1087 N90-16291
Fractal-based image compression
[AD-A215400] 09 p1268 N90-17351
An iterative solution to aeroelastic effects in potential flow
[AD-A216291] 10 p1310 N90-17580
A parallel iterative method for solving 3-dimensional elliptic partial differential equations
[DE90-005187] 10 p1422 N90-18199
Iterative methods for nonlinear set-valued operators of the monotone type with applications to operator equations
[DE90-606950] 10 p1422 N90-18202
KAM: Automatic planning and interpretation of numerical experiments using geometrical methods
[AD-A216805] 11 p1546 N90-18900
Waveform methods for ordinary differential equations
[DE90-006593] 11 p1553 N90-18943
Hierarchical basis preconditioners for second order elliptic problems in three dimensions
[DE90-005960] 12 p1706 N90-19793
Iteration methods for solving nonlinear equations in Frechet spaces
[DE90-610429] 12 p1706 N90-19799
Projection-iteration methods for solving nonlinear operator equations
[DE90-610433] 12 p1707 N90-19801
Techniques for accelerating iterative methods for the solution of mathematical problems
[AD-A218272] 13 p1878 N90-20775
The parallel algorithm for solving the three-dimensional integral magnetostatic equations
[DE90-616529] 14 p2015 N90-21547
Local mode smoothing analysis for various incomplete factorization iterative methods in three dimensions
[REPT-89-38] 15 p2147 N90-22263
Performance of the IMP array processing algorithm: First results
[RSRE-MEMO-4291] 15 p2148 N90-22274
The incorporation of a multigrid method into the orthogonal curvilinear coordinate version of the Rolls-Royce PACE computer program
[TT-8804] 19 p2751 N90-25627
Using implicit ODE methods with iterative linear equation solvers in spectral methods
[FFI-89/7017] 19 p2751 N90-25633
Efficient implementation of minimal polynomial and reduced rank extrapolation methods
[NASA-TM-103240] 20 p2920 N90-26616
Investigations on improved iterative methods for solving sparse systems of linear equations
[AD-A221980] 21 p3064 N90-27417
Power bounded prolongations and Picard-Lindeloef iteration
[PB90-190877] 22 p3242 N90-28384
Parallelization of implicit finite difference schemes in computational fluid dynamics
[NASA-CR-182081] 22 p3243 N90-28392
An asymptotically induced domain decomposition method for parabolic boundary layer problems
[DE90-014620] 23 p3326 N90-28804
Error detection and control for nonlinear shell analysis
[NASA-TM-102723] 23 p3340 N90-28877
Solution of the Stokes system by boundary integral equations and fixed point iterative schemes
[DE90-627166] 23 p3389 N90-29138
Solution of nonlinear eigenvalue problems via parallel shooting
[LR-587] 24 p3539 N90-30013

ITO (SEMICONDUCTORS)
Radiation effects in ITO/InP solar cells
10 p1340 N90-17757
Indium phosphide solar cell research in the United States: Comparison with non-photovoltaic sources
10 p1340 N90-17758

ITOS SATELLITES
Research programs: Meteorological prediction. Oceanic processes. Climate and global change monitoring. Satellite instrumentation and calibration
19 p2714 N90-25447

IUE
Analytical derivation and verification of zero-gyro control for the IUE satellite
[NASA-TM-100748] 05 p0645 N90-13767
Archival research on absorption lines in violently star-forming galaxies
[NASA-CR-185960] 05 p0712 N90-14163
Sulfur compounds in comets
08 p1143 N90-16627
Observations of Cygnus X-2 with IUE: Ultraviolet results from a multiwavelength campaign
17 p2482 N90-24193
IUE observations of Cyg X-2 and Sco X-1: Accretion disks and the z-shaped curve 19 p2783 N90-25832
ESA's report to the 28th COSPAR meeting
[ESA-SP-1124] 24 p3560 N90-30141
The impact of IUE on studies of the nova outburst: 1985-1990
[DE90-014915] 24 p3563 N90-30156
IUE-ULDA access guide no. 2. International Ultraviolet Explorer-Uniform Low Dispersion Archive: Comets
[ESA-SP-1134] 24 p3563 N90-30157

IUS
U INERTIAL UPPER STAGE

IZSAK ELLIPSOID
U ELLIPSOIDS
U GEODESY

J

J INTEGRAL
An application of the J-integral to an incremental analysis of blunting crack behavior
[DE89-016844] 03 p0358 N90-12046
Experience with J testing of 304/308 stainless steel weldment
[DE90-002046] 07 p0946 N90-15478
Limitations and applications of fracture assessment with R6
[AERE-R-13012] 13 p1815 N90-20425
Nonlinear fracture mechanics using semicircular specimens and tension-softening behavior
15 p2116 N90-22108
J-integral and HRR field of a stably growing crack, an experimental analysis
[AD-A220418] 17 p2416 N90-23764
A framework to correlate a/W ratio effects on elastic-plastic fracture toughness (J (sub c))
[AD-A222822] 21 p3012 N90-27125
Mechanical properties and fracture toughness of AAR-TC128 Grade B steel and a micro-alloyed, control-rolled steel, A 8XX grade B, from -80F to +73F
[PB90-207796] 24 p3448 N90-29471

JACKS (ELECTRICAL)
U ELECTRIC CONNECTORS

JACOBI INTEGRAL
Direct calculation of Newton steps without accumulating Jacobians
[DE90-009702] 18 p2607 N90-24847

JACOBI MATRIX METHOD
Distributed VLSI architecture for fast Jacobian and inverse Jacobian formulations
[RR-346] 03 p0390 N90-12218
Integrated optics anisotropic waveguides and devices
[AD-A217064] 12 p1715 N90-19849
On a method for computing eigenvalues and eigenfunctions of linear differential operators
[PREPRINT-706] 17 p2456 N90-24013

JACOBI POLYNOMIALS
U HYPERGEOMETRIC FUNCTIONS

JAMMERS
Lightweight, broadband, pulsed, frequency agile, self-screening jammer for airborne deployment
[AD-D014468] 22 p3163 N90-27937

JAMMING
Network analyzer for nonstatic jamming
[AD-A210759] 02 p0212 N90-11216
Performance analysis of hybrid ARQ protocols in a slotted code division multiple-access network
[AD-A211078] 02 p0213 N90-11219
Preliminary report on the feasibility of high power Electronic Warfare (EW) using explosive energy sources
[MRL-TR-89-3] 04 p0483 N90-12775
Performance analysis of large adaptive sidelobe canceller arrays with reused elements
[AD-A212888] 04 p0494 N90-12841
Automated Steerable Nulling Antenna Processor (SNAP) model
[PB89-231740] 04 p0509 N90-12937
Fellowships in information and stochastic systems
[AD-A212385] 04 p0563 N90-13280
The use of backscatter for modelling ionosphere and jamming in very short term forecasts
06 p0762 N90-14434
Method for eliminating self-screening noise jamming in radar systems
[AD-D014271] 08 p1056 N90-16105
Modeling the response of a monopulse radar to impulsive jamming signals using the Block Oriented System Simulator (BOSS)
[AD-A215560] 10 p1375 N90-17969
Packet radio networks under dynamic jamming
[AD-A217094] 12 p1648 N90-19475
Performance of adaptive nulling antennas in a jamming environment
[AD-A219305] 16 p2230 N90-22720
Joint tactical anti-jam communications: A systems approach
[AD-A219592] 17 p2388 N90-23602
A theoretical model for airborne radars
[AD-A220735] 17 p2390 N90-23615
Optimizing ECM techniques against monopulse acquisition and tracking radars
[AD-A220036] 17 p2393 N90-23629
Serrodyning by means of a digital phase shifter
[AD-A219593] 17 p2396 N90-23646
Tracking performance of a combined Costas/AFC-loop under noisy Rayleigh/Rician channel conditions with additive Gaussian noise jamming
[ETN-90-98964] 20 p2855 N90-26237
Electronic warfare technology: Trends and visions
[AD-A223034] 20 p2856 N90-26246
Dynamic jamming of networks
[AD-A223044] 20 p2856 N90-26247
A novel communication network simulator
[AD-A223045] 20 p2857 N90-26248
Studies of ECCM improvements for frequency-hopping CPFSK systems
[AD-A222995] 21 p2995 N90-27023
Measured effects of repeater jamming on direct-sequence spread spectrum receivers that use envelope detectors
[AD-A222231] 21 p2996 N90-27032
Tactical uses of the DSCS 3 communications system
21 p3069 N90-27450
Lightweight EHF communications satellites
21 p3070 N90-27453
Lightweight, broadband, pulsed, frequency agile, self-screening jammer for airborne deployment
[AD-D014468] 22 p3163 N90-27937
Modular digital GPS receivers
24 p3424 N90-29346
PLRS: A new spread spectrum position location reporting system 24 p3427 N90-29358
Jamming performance of frequency-hopped communication systems with nonuniform hopping distributions
[AD-A223419] 24 p3461 N90-29547
An experimental study of voice communication over a bandlimited channel using variable bit width delta modulation
[AD-A223445] 24 p3461 N90-29548

JAPAN
Japanese structural ceramics research and development 01 p0048 N90-10272
Technology transfer to the United States: The MIT (Massachusetts Institute of Technology) Japan Science and Technology Program. A background paper of OTA's (Office of Technology Assessment's) assessment on technology, innovation, and US trade
[PB89-224711] 04 p0564 N90-13291
Automation and robotics in construction: Japanese research and development
[AD-A214170] 07 p0942 N90-15456
Lightning observations on Japan Sea coast in winter
[DE90-702485] 08 p1103 N90-16387
Study of the effect of ceramics gas turbine development
[DE90-702638] 09 p1196 N90-16929
Preliminary collection 891 of lectures/papers in Symposium by Society of Automotive Engineers of Japan
[DE90-710449] 10 p1391 N90-18045
Technology transfer and the FSX: Effects on the United States/Japanese relationship
[AD-A216348] 10 p1443 N90-18327
Optimal planning method of underground distribution system, part 2. Application to various types of system configurations
[DE89-782323] 11 p1500 N90-18636
Energy markets in the 1990's and beyond: A comparison of energy intensity in the United States and Japan
[DE90-005535] 11 p1528 N90-18797
Survey on the possibility of introducing new energy to regional development plans
[DE89-782627] 12 p1681 N90-19654
Geology, distribution of hot springs and hydrothermal alteration zones of major geothermal areas in Japan
[DE90-753026] 13 p1820 N90-20451
Microgravity science and applications bibliography, 1989 revision
[NASA-TM-4192] 14 p1957 N90-21207

Japanese magnetic confinement fusion research
15 p2169 N90-22392
Technologies for electronic transfer of information: The present state and trends in Japan
15 p2177 N90-22443
Research and applications of metallic superlattices, high T(sub c) superconductors, x ray optics, and compact synchrotrons
16 p2311 N90-23170
Current Japanese supercomputers for computational fluid dynamics applications
16 p2311 N90-23172
NSF Tokyo reports. The 1989 survey of research and development in Japan
[PB90-199340] 22 p3265 N90-28487
NSF Tokyo reports. Twenty-one new areas added for support under Monbusho's priority research area grants
[PB90-199589] 22 p3265 N90-28488
Japanese molecular biology 1990: An update
[PB90-188707] 23 p3354 N90-28958
Numerical simulation of hypersonic viscous flow for the design of H-2 orbiting plane (HOPE)
[NAL-TR-1028] 24 p3422 N90-29330
Some topics in computational transonic aerodynamics: Revision
[NAL-TR-1018T] 24 p3422 N90-29332

JAPANESE SPACE PROGRAM
Comparison of the space program performance of countries with space programs
[ILR-MITT-222] 05 p0709 N90-14150
NASDA's approach to the interoperability of safety and rescue in space
08 p1035 N90-15981
Overview of Japan's current and future space transportation programmes
09 p1174 N90-16789
Development status of Japan's new launch vehicle: H-2 rocket
09 p1176 N90-16807
HOPE: Its concept and technical features
09 p1179 N90-16835
Japanese experiment module electrical power system
10 p1329 N90-17680
The solar array of Japanese solar observatory satellite Solar-A
10 p1345 N90-17798
Ginga observations of QPO
19 p2769 N90-25739
Ginga observations of dipping low mass X ray binaries
19 p2781 N90-25821
Constraints on the SS433 system from the Ginga observations
19 p2784 N90-25838
Ginga observations of the X ray spectra of AGN
19 p2786 N90-25854
X ray spectrum and variability of MRK 509 as observed with EXOSAT and Ginga
19 p2794 N90-25904

JAPANESE SPACECRAFT
Overview of Japan's current and future space transportation programmes
09 p1174 N90-16789
On the simulation test for the relative motion of separated sub-boosters on M-3S2 with nearly half a model vehicle ST-735 and their motion analyses using inertial sensors output
[ISAS-635] 17 p2366 N90-23471

JARRING
U MECHANICAL SHOCK

JC-130 AIRCRAFT
U C-130 AIRCRAFT

JEEPS
U AUTOMOBILES

JET AIRCRAFT
NT A-300 AIRCRAFT
NT A-310 AIRCRAFT
NT A-320 AIRCRAFT
NT B-52 AIRCRAFT
NT B-58 AIRCRAFT
NT B-70 AIRCRAFT
NT BOEING 727 AIRCRAFT
NT BOEING 737 AIRCRAFT
NT BOEING 747 AIRCRAFT
NT BOEING 757 AIRCRAFT
NT C-5 AIRCRAFT
NT C-130 AIRCRAFT
NT C-135 AIRCRAFT
NT C-140 AIRCRAFT
NT C-141 AIRCRAFT
NT CONCORDE AIRCRAFT
NT DC 10 AIRCRAFT
NT DHC 2 AIRCRAFT
NT EUROPEAN AIRBUS
NT F-4 AIRCRAFT
NT F-8 AIRCRAFT
NT F-14 AIRCRAFT
NT F-15 AIRCRAFT
NT F-16 AIRCRAFT
NT F-17 AIRCRAFT
NT F-18 AIRCRAFT
NT F-86 AIRCRAFT
NT F-104 AIRCRAFT
NT F-111 AIRCRAFT
NT L-1011 AIRCRAFT
NT P-3 AIRCRAFT
NT TURBOFAN AIRCRAFT
NT TURBOPROP AIRCRAFT
NT U-2 AIRCRAFT
Modifying high-order aeroelastic math model of a jet transport using maximum likelihood estimation
01 p0021 N90-10106
Comparison of flying qualities derived from in-flight and ground-based simulators for a jet-transport airplane for the approach and landing pilot tasks
[NASA-TP-2962] 03 p0309 N90-11757
Inspection development for T-37 wing spar cap lug
[AD-A214826] 09 p1159 N90-16708
Throughput and delay characteristics for a slow-frequency hopped aircraft-to-aircraft packet radio network
[AD-A220525] 17 p2389 N90-23609
Forward canopy feasibility and Thru-The-Canopy (TTC) ejection system study
[AD-A220360] 18 p2495 N90-24258
Special essays for the 40th anniversary of the revolution: The chief designer discusses the F-8 2 and future fighter planes
[AD-A221587] 21 p2960 N90-26829
World jet airplane inventory at year-end 1989
[PB90-207218] 23 p3267 N90-28489
Predicting F/A-18 fleet replacement squadron performance using an automated battery of performance-based tests
[AD-A223899] 23 p3277 N90-28543
Engineering and the advancement of human welfare. Ten outstanding achievements 1964-1989
[ISBN-0-309-04185-6] 23 p3415 N90-29297

JET AIRCRAFT NOISE
What should be done with those noisy old aircraft
[PNR90562] 04 p0452 N90-12593
Re-engine with the Rolls-Royce Tay 670, the route to significant noise reduction
[PNR90585] 04 p0455 N90-12606
The commercial aircraft noise problem
[PNR90577] 04 p0550 N90-13203
Dynamics of a class of vortex rings
07 p0926 N90-15362
Noise levels from a VSTOL aircraft measured at ground level and at 1.2 m above the ground
[NPL-RSA(EXT)-009] 11 p1562 N90-18999
Exhaust environment measurements of a turbofan engine equipped with an afterburner and 2D nozzle
[NASA-CR-4289] 15 p2052 N90-21760
En route noise annoyance laboratory test: Preliminary results
18 p2611 N90-24870

JET AIRSTREAMS
U JET STREAMS (METEOROLOGY)

JET AUGMENTED WING FLAPS
U JET FLAPS

JET BLAST EFFECTS
Jet-flow from shock tubes
[AD-A210651] 02 p0220 N90-11260

JET CONTROL
The use of lateral jet control at Aerospatiale
10 p1305 N90-17551
Maneuvering by means of lateral jets
[ISL-CO-255/88] 20 p2814 N90-26015

JET DAMPING
U DAMPING

JET DRIVE
U JET PROPULSION

JET ENGINE FUELS
NT JP-4 JET FUEL
NT JP-8 JET FUEL
Compatibility of fuel system components with high density fuel
[AD-A210381] 01 p0006 N90-10027
Wide-range fuel flowmeter, phase 2
[AD-A210547] 01 p0074 N90-10424
Production of jet fuels from coal-derived liquids. Volume 11: Production of advanced endothermic fuel blends from Great Plains Gasification Plant naphtha by-product stream
[AD-A210251] 02 p0207 N90-11184
The prediction of middle distillate fuel properties using liquid chromatography-proton nuclear magnetic resonance spectroscopy data
[AD-A211879] 03 p0334 N90-11899
Thermal stability of jet fuel
[DE90-001160] 06 p0753 N90-14385
Thermal stability of jet fuel
[DE90-002760] 07 p0914 N90-15288
Fundamental mechanism of atomization
[AD-A213859] 07 p0915 N90-15293
Production of jet fuels from coal derived liquids. Volume 10: Jet fuels production by-products, utility, and sulfur emissions control integration study
[AD-A213872] 09 p1200 N90-16951
Development of fuel wear tests using the Cameron-Plint high-frequency reciprocating machine
[AD-A216003] 10 p1361 N90-17892
Concentric layer ramjet fuel
[AD-D014443] 14 p1941 N90-21111
Development of a computational fluid dynamics and chemistry model for the fouling of jet fuels
[DE90-005864] 15 p2098 N90-22003
Turbine fuel alternatives (near term)
[AD-A219405] 16 p2225 N90-22695
Three-dimensional analysis on flow and temperature distributions for aircraft fuel thermal stability
[AD-A219651] 17 p2383 N90-23571
Enhanced bioreclamation of jet fuels: A full-scale test at Eglin AFB, Florida
[AD-A222348] 21 p2990 N90-26992
Production of jet fuels from coal-derived liquids. Volume 13: Evaluation of storage and thermal stability of jet fuels derived from coal liquids
[AD-A224576] 24 p3457 N90-29527

JET ENGINES
NT RAMJET ENGINES
NT SUPERSONIC COMBUSTION RAMJET ENGINES
NT TURBOFAN ENGINES
NT TURBOJET ENGINES
NT TURBOPROP ENGINES
NT TURBORAMJET ENGINES
Effects of a heat cycle on material strength
[NAL-TM-562] 03 p0306 N90-11737
The RB199: An in-service success
[PNR90544] 03 p0307 N90-11746
Coatings for gas turbine compressors
[NLR-MP-88045-U] 03 p0308 N90-11750
Aluminium alloy development for aero engines
[PNR90548] 03 p0330 N90-11874
Dynamic tip clearance measurements in axial flow compressors
[PNR90597] 04 p0456 N90-12612
Characterization of chemicals on engine exhaust particles
[AD-A213566] 07 p0882 N90-15106
Research programs in aeronautical engineering, solid state physics, and materials science at Technion-Israel Institute of Technology, Haifa, Israel
[EOARD-LR-89-068] 14 p2044 N90-21720
WINCOF-I code for prediction of fan compressor unit with water ingestion
[NASA-CR-185157] 15 p2045 N90-21724
A/F32T-9 large turbo fan engine enclosed noise suppressor system (T-9 NSS), exterior far-field and interior noise, McConnell AFB, Kansas
[AD-A220535] 17 p2354 N90-23402
Joint services electronics program
[AD-A220815] 17 p2397 N90-23654
The jet engine: 1932
[ISBN-3-922010-49-0] 19 p2670 N90-25189
Knowledge based diagnosis of jet engines under consideration of model based methods
22 p3105 N90-27631

JET EXHAUST
Methods of jet calculation
[REPT-892-422-102] 16 p2209 N90-22603
Numerical resolution of Navier-Stokes equations using several turbulence models and applications on turbomachines
[ETN-90-97478] 23 p3326 N90-28808

JET FLAMES
U FLAMES
U JET FLOW

JET FLAPS
Rotary-Jet thrust augmentor with jet-flapped blades
18 p2492 N90-24243

JET FLIGHT
U JET AIRCRAFT

JET FLOW
NT AIR JETS
NT SUPERSONIC JET FLOW
Symmetry breaking bifurcations and the growth of chaos in a rotating fluid
[AD-A210969] 01 p0072 N90-10411
Rectangular subsonic jet flow field measurements
[NASA-CR-185962] 02 p0219 N90-11255
Steady and unsteady potential flow around thin annular wings and engines with simulation of jet engine flow
[DFVLR-FB-89-18] 03 p0302 N90-11711
Low-speed wind-tunnel study of reaction control-jet effectiveness for hover and transition of a STOVL fighter concept
[NASA-TM-4147] 03 p0308 N90-11751
Cryogenic free jets
[ESA-TT-1128] 03 p0311 N90-11767
Numerical evaluation of a solution representing a jet in cross-flow
[RAE-TM-AERO-2137] 04 p0502 N90-12893
Coherent structures in a round jet
05 p0640 N90-13733
Numerical solutions of the complete Navier-Stokes equations
[NASA-CR-186102] 05 p0642 N90-13747

Model and computation of three-dimensional turbulent jets in a crossflow
[ECL-89-007] 05 p0643 N90-13755
Swirl-stabilized flames: Fluid dynamics, mixing, and flame stability limits 08 p1040 N90-16009
Demonstration of the feasibility of laser induced fluorescence for arc jet flow diagnostics
[NASA-CR-185595] 08 p1040 N90-16013
Viscous effects on the instability of an axisymmetric jet
[NASA-TM-102396] 09 p1161 N90-16719
Experimental study of velocity fields and turbulence in a turbojet engine
[ISL-CO-231/88] 09 p1169 N90-16766
Coaxial injection technology for hypergolic propellants 09 p1180 N90-16839
Flow field observation of a hot He-CO2 jet in microgravity 09 p1201 N90-16960
Theoretical and experimental approach of wave phenomena in free jets
[ISL-CO-247/88] 09 p1219 N90-17069
Numerical predictions of local entropy generation for an impinging jet
[DE90-004671] 09 p1220 N90-17081
Liquid transverse jets in compressible crossflows 10 p1385 N90-18012
Numerical simulations of coherent structures in a jet flame with a noncircular cross section
[AD-A216710] 11 p1483 N90-18535
Numerical study of diffusion jet flames 12 p1621 N90-19316
System for venting gas from a liquid storage tank
[NASA-CASE-MSC-21253-1] 13 p1787 N90-20254
Rectangular subsonic jet flow field measurements
[NASA-CR-181925] 14 p2023 N90-21598
Interaction of a turbulent round jet with the free surface 15 p2090 N90-21964
Herbig-Haro objects and stellar jets 15 p2186 N90-22487
Methods of jet calculation
[REPT-892-422-102] 16 p2209 N90-22603
Temperature determination of shock layer using spectroscopic techniques 18 p2628 N90-24973
Non-premixed turbulent CO/H2 flames at local extinction conditions 21 p2975 N90-26907
Scalar dissipation measurements in the developing region of a jet 21 p2976 N90-26909
Local and global resonances in heated 2-D jets
[AD-A221671] 21 p3005 N90-27079
Modeling of free viscoelastic jets and instability mechanisms
[AD-A221672] 21 p3005 N90-27080
Jet vortex generators for turbulent flow separation control
[NASA-CR-186959] 22 p3109 N90-27659
Model of turbulent diffusion flames and nitric oxide generation
[PB90-155557] 22 p3155 N90-27886
Applications of LIF to high speed flows 24 p3420 N90-29320
Calibration of the PARC program for propulsion-type flows
[AD-A224253] 24 p3434 N90-29395

JET FUELS
U JET ENGINE FUELS

JET IMPINGEMENT
Plume shape optimization of small attitude control thrusters with respect to impingement and thrust
[ISL-CO-220/88] 08 p1084 N90-16153
Impingement characteristics of heated plane turbulent jets 09 p1215 N90-17047
A wind tunnel study of a sting-mounted circulation control wing
[AD-A216248] 10 p1310 N90-17577

JET LAG
Effects of a time zone shift of nine hours on the circadian rhythms in cockpit aircrew members on longhaul flights
[DLR-FB-89-31] 04 p0523 N90-13019
A laboratory study of the effects of diet and bright light countermeasures to jet lag
[AD-A220148] 17 p2435 N90-23875
Melatonin, light and, circadian cycles
[AD-A223196] 21 p3035 N90-27256

JET MIXING FLOW
Characterization of nonpremixed turbulent bluff-body burner flames
[PB89-229447] 04 p0469 N90-12689
Buoyancy effects on the vapor condensation rate on a horizontal liquid surface
[NASA-TM-102437] 05 p0629 N90-13675
Vapor condensation on liquid surface due to laminar jet-induced mixing: The effects of system parameters
[NASA-TM-102433] 05 p0643 N90-13751
Estimation of subsonic far-field jet-mixing noise from single-stream circular nozzles
[ESDU-89041] 09 p1161 N90-16721
An investigation of flow structure, mixing and chemical reaction in combusting turbulent flows
[AD-A216739] 11 p1483 N90-18538
The effects of compressibility on a supersonic mixing layer
[AD-A219315] 16 p2197 N90-22543

JET NOISE
U JET AIRCRAFT NOISE

JET NOZZLES
The effect of electrode configuration on arcjet performance
[NASA-TM-102346] 02 p0189 N90-11081

JET PILOTS
U AIRCRAFT PILOTS

JET PROPULSION
STOVL aircraft simulation for integrated flight and propulsion control research
[NASA-TM-102419] 05 p0581 N90-13389

JET PUMPS
An experimental investigation of a single and multiphase confined coaxial jet 23 p3324 N90-28796

JET STAR AIRCRAFT
U C-140 AIRCRAFT

JET STREAMS (METEOROLOGY)
Investigations of polar air stream cyclogenesis based on numerical simulations with a mesoscale model
[PB89-214563] 03 p0373 N90-12132
Diagnostic and kinematic fields associated with curved and straight jet streaks using a two-layer primitive equation model 08 p1100 N90-16371
Analysis of significant weather on meso-alpha scales using conventional and remotely sensed data: Exploratory studies
[AD-A214563] 09 p1248 N90-17238
Synoptic-scale forcing of the low-level jet in developing baroclinic waves 12 p1692 N90-19717
Correlation of atmospheric optical turbulence and meteorological measurements
[AD-A218019] 13 p1842 N90-20576
Atmospheric turbulence measurements in support of adaptive optics technology
[AD-A220445] 17 p2423 N90-23805
An observational study of the circulation in the Southern Hemisphere stratosphere 24 p3488 N90-29715

JET THRUST
High power arcjet
[NASA-CR-183086] 23 p3298 N90-28658

JET VANES
Investigations of thrust vector control for high-alpha pitchover 01 p0014 N90-10067

JETAVATORS
U GUIDE VANES

JETTISON SYSTEMS
On the selection of crewmember rescue means for manned space launch systems 08 p1035 N90-15978

JETTISONING
Independent Orbiter Assessment (IOA): Analysis of the electrical power distribution and control/remote manipulator system subsystem
[NASA-CR-185526] 02 p0166 N90-10936

JFET
The potential for high performance HgCdTe arrays at 4 microns 14 p1976 N90-21320
Burnout thresholds and cross section of power MOS transistors with heavy ions
[AD-A218998] 16 p2232 N90-22736
An electronic spirit level tilt sensor
[ETN-90-96697] 17 p2406 N90-23710
Polycrystalline diamond Junction Field Effect Transistors (JFETS)
[AD-A222238] 21 p3083 N90-27534
Polycrystalline diamond Junction Field Effect Transistors (JFETS)
[AD-A223784] 24 p3465 N90-29576

JITTER
U VIBRATION

JOBS
U TASKS

JOINED WINGS
Application of the joined wing to tiltrotor aircraft
[NASA-CR-177543] 07 p0879 N90-15093

JOINING
The organization of permutation architectures with bussed interconnections
[AD-A210832] 01 p0061 N90-10352
Study of a gallium arsenide solar cell interconnector 02 p0182 N90-11033
Development of an aluminium solar cell interconnector technology 10 p1341 N90-17771

JOINTS (ANATOMY)
NT WRIST
Control of human arm movement via optimization 15 p2159 N90-22334
Decompression sickness affecting the temporomandibular joint
[AD-A220959] 18 p2584 N90-24715

JOINTS (JUNCTIONS)
NT BOLTED JOINTS
NT BUTT JOINTS
NT INTERFERENCE FIT
NT METAL JOINTS
NT RIVETED JOINTS
NT SOLDERED JOINTS
NT WELDED JOINTS
Flight set 360T004 (STS-30) insulation component, interim release, volume 3
[NASA-CR-183746] 01 p0031 N90-10169
Modeling and simulation of spatial robotic manipulators with flexible links and joint drives for control strategies implementation and evaluation 02 p0228 N90-11311
An analytical and experimental study of the elastodynamic response characteristics of planar linkage mechanism with bearing clearances 02 p0233 N90-11336
Investigations into the infiltration kinetics, wettability, and interfacial bond strength of Al/SiC composites
[AD-A211924] 03 p0320 N90-11815
Stress waves through projectile joints and interfaces
[AD-A212201] 04 p0513 N90-12963
Effects of joints in truss structures 05 p0600 N90-13486
Joints in deployable space truss structures 05 p0601 N90-13489
QM-8 field joint protection system, volume 7
[NASA-CR-183748] 05 p0614 N90-13586
Qualification of improved joint heaters
[NASA-CR-183827] 05 p0616 N90-13594
The adhesive bonding of thermoplastic composites
[AD-A213358] 05 p0618 N90-13605
Measurement of damping of graphite epoxy composite materials and structural joints
[NASA-CR-183802] 06 p0736 N90-14286
The stress analysis of thin-walled screwed tubular joints 06 p0796 N90-14637
An investigation of elastic guided waves for ceramic joint evaluation
[DE90-004400] 08 p1050 N90-16071
Mechanical aspects of interfaces in high performance composites 10 p1347 N90-17812
Test data of flow field of shuttle SRM nozzle joint with bond defects, using unheated air 11 p1470 N90-18464
Threaded joint design for composites
[DE90-005553] 11 p1478 N90-18506
Preliminary evaluation of the strength of pin-joints in laminated composite materials
[DE90-006353] 11 p1481 N90-18524
A global approach for the identification of structural connection properties
[NASA-TM-102502] 11 p1518 N90-18745
A study of the vibrational transmission through flanged joints
[ISVR-TR-181] 11 p1520 N90-18755
Thermo-oxidative stability studies of PMR-15 polymer matrix composites reinforced with various fibers
[NASA-TM-102439] 12 p1620 N90-19310
Viscoelastic adherend effects in adhesively bonded composite-to-composite joints 12 p1670 N90-19594
Thiokol/Wasatch installation evaluation of the redesigned field joint protection system (concepts 1 and 3)
[NASA-CR-183860] 13 p1765 N90-20127
The CMU Reconfigurable Modular Manipulator System
[CMU-RI-TR-88-7] 13 p1809 N90-20388
Control system design of the third flexible joint of PUMA 560 robot
[AD-A218075] 13 p1812 N90-20405
Heavily loaded joints for assembling aerobrake support trusses
[NASA-CR-181992] 14 p1939 N90-21099
Fiber pushout test: A three-dimensional finite element computational simulation
[NASA-TM-102585] 14 p1945 N90-21131
Expanding ring joint
[AD-D014398] 14 p1986 N90-21384
The development of computational algorithms for manipulator inverse kinematics
[DE90-759877] 14 p2017 N90-21561
Definition of large components assembled on-orbit and robot compatible mechanical joints
[NASA-TM-100395] 15 p2105 N90-22043
Cycle life machine for AX-5 space suit 15 p2112 N90-22080
AX-5 space suit bearing torque investigation 15 p2115 N90-22101
Circularity measuring system: A shape gauge designed especially for use on large objects 15 p2116 N90-22104

Study and sizing of bonded joints in space structures
[REPT-892-430-124] 16 p2207 N90-22591
An alternate interconnect method for joining flexible circuits using conductive adhesives
[DE90-008194] 16 p2222 N90-22674
Evaluation of joints bonded with elastoplastic adhesives
[REPT-892-430-120] 16 p2247 N90-22816
A nearly-linear computational-cost scheme for the forward dynamics of an N-body pendulum
16 p2280 N90-22996
Determination of joint drives for stable end-effector motion in flexible robotic systems
16 p2288 N90-23034
A model of electromagnetic leakage through joints at radio frequencies
[BAE-WES-RP-GEN-EMC-049-T2.2]
17 p2392 N90-23626
An expert system for the study of high duty bonded joints in aerospace structures
[REPT-892-430-110] 17 p2414 N90-23753
A compact joint for the ROTEX manipulator
18 p2536 N90-24467
The tetrahedral wedge attachment mechanism
18 p2539 N90-24490
Free-form surface modelling using tensor product Bezier patches: A review with new solutions
[TELECOM-PARIS-89-D-014] 18 p2575 N90-24673
Real time inverse kinematics with joint limits and spatial constraints
[AD-A220462] 18 p2586 N90-24723
Method of insetting predesigned disbond areas into composite laminates
[NASA-CASE-LAR-13225-1] 19 p2672 N90-25197
Vitreous joining of SiC fiber reinforced SiC composites
[DE90-012951] 20 p2827 N90-26081
Accuracy analysis of the space shuttle solid rocket motor profile measuring device
[NASA-TM-101131] 21 p2968 N90-26871
Environmental integrity of coating/metal interface
[AD-A222426] 21 p2987 N90-26978
An interdisciplinary approach to the predictive modeling of structural adhesive bonding
[AD-A221703] 21 p2988 N90-26982
Effects of low bond number liquid motions on spacecraft attitude 22 p3131 N90-27768
Evaluation of EA-934NA with 2.5 percent Cab-O-Sil
[NASA-CR-184005] 22 p3158 N90-27909
Approaches to orthogonally fused conducting polymers for molecular electronics
[AD-A222546] 22 p3159 N90-27915
Guidelines for threaded fasteners
[ESA-PSS-03-208-ISSUE-1] 22 p3182 N90-28061
Nondestructive evaluation of adhesively-bonded joints
22 p3185 N90-28074
Advanced NDE techniques for quantitative characterization of aircraft 22 p3188 N90-28088
Nylon and teflon scribe effect on NBR to Chemlok 233 and NBR to NBR bond interfaces
[NASA-CR-184004] 22 p3189 N90-28095
Flight motor set 360L008 (STS-32R). Volume 1: System overview
[NASA-CR-184010] 23 p3289 N90-28609
Solutions to the frictional dynamics problem and the reciprocal variable feedback methodology for design and control of robot mechanisms 23 p3333 N90-28846
Nonlinear modeling of joint dominated structures
[NASA-CR-4324] 24 p3439 N90-29423
Dynamical modeling of serial manipulators with flexible links and joints using the method of kinematic influence
24 p3500 N90-29783
Traction-drive force transmission for telerobotic joints
24 p3501 N90-29790

JORDAN FORM
JOE: Jordan Optimized Eigensolver. A step toward a numerical Jordan form analyzer for control and interactive thermo-structural-dynamic applications
02 p0184 N90-11047
Simplified linear-time Jordan sorting and polygon clipping
[AD-A215110] 13 p1864 N90-20693
Algorithms and evaluation for regulation of linear, time-independent difference systems under position value limitation
[ETN-90-97308] 22 p3238 N90-28364

JOSEPHSON JUNCTIONS
Fabrication of NBN based electronic devices with silicon barriers
[AD-D014230] 06 p0767 N90-14463
Theory of strongly fluctuating superconductivity
[DE90-001073] 06 p0850 N90-14942
Flux flow, pinning, and resistive behavior in superconducting networks
[DE90-005242] 09 p1293 N90-17493
Nonlinear dynamics of domain walls and vortices in two-dimensional systems
[DE90-004840] 10 p1425 N90-18221
High quality tunnel junction devices using high T(sub c) superconductors
[AD-D014329] 10 p1435 N90-18283
Novel processing of HTS based conductors
[DE90-005956] 12 p1722 N90-19892
An ultra-small capacitance Josephson junction
[DE90-613396] 14 p2032 N90-21653
A refrigerated Dewar for the Josephson array voltage calibration system
[DE90-005237] 15 p2172 N90-22412
Construction of a 345 gigahertz receiver based on superconducting tunnel junctions
[AD-A218781] 16 p2232 N90-22735
Electrical transport through tunnel barriers and thin dielectric layers and physical properties of the high Tc oxide superconductors
[AD-A219860] 17 p2477 N90-24165
Dynamical properties of two-dimensional Josephson junction arrays
[AD-A223965] 23 p3402 N90-29221

JOULE HEATING
U OHMIC DISSIPATION
U RESISTANCE HEATING

JOULE-THOMSON EFFECT
Development of a low noise 10 K J-T refrigeration system
[AD-A213347] 04 p0484 N90-12779
Acquisition and correlation of cryogenic nitrogen mass flow data through a multiple orifice Joule-Thomson device
[NASA-TM-103121] 16 p2237 N90-22761
Multicomponent gas sorption Joule-Thomson refrigerator
[NASA-CASE-NPO-17569-1-CU]
20 p2844 N90-26176

JOURNAL BEARINGS
Transient response of flexible rotor-bearing systems subjected to combined unbalance and ground excitations 06 p0792 N90-14616
Thermal analysis of fixed and tilting pad journal bearings including cross-film viscosity variations and deformations
07 p0937 N90-15429
Some problems in hydrodynamic lubrication
09 p1229 N90-17133
On the performance of algorithms for large-scale bound constrained problems
[DE90-010084] 18 p2590 N90-24736
A high-speed photography study of cavitation in a dynamically loaded journal bearing
[NASA-TM-103178] 20 p2872 N90-26338
Current research in cavitating fluid films
[NASA-TM-103184] 23 p3323 N90-28791
Rotordynamic properties of high pressure seals: An experimental approach 24 p3475 N90-29640

JOURNALS (DOCUMENTS)
U PERIODICALS

JOURNALS (SHAFTS)
U SHAFTS (MACHINE ELEMENTS)

JP-4 JET FUEL
In-flight evaluations of turbine fuel extenders
[DOT/FAA/CT-89/33] 12 p1633 N90-19387
The thermal response of generic objects in JP-4 pool fires
[DE90-008503] 13 p1788 N90-20259
Equilibrium swelling of elastomeric materials in solvent environments
[DE90-010164] 18 p2529 N90-24430

JP-8 JET FUEL
Properties of F-34 (JP-8) fuel for 1988
[AD-A210188] 01 p0053 N90-10303
Vehicle acceleration and fuel consumption when operated on JP-8 fuel
[AD-A216275] 10 p1393 N90-18055

JUDGMENTS
Effects of stress on judgment and decision making in dynamic tasks
[AD-A210605] 01 p0135 N90-10781
Metacognition and retrieval from long-term memory at Mount Everest
[AD-A211629] 03 p0382 N90-12177
Systematicity as a selection constraint in analogical mapping
[AD-A216029] 11 p1541 N90-18869
Target selection in anti-tank helicopter operations: Relative weight of cues in target evaluation judgements
[FOA-C-50072-5.2] 17 p2436 N90-23881
Target selection in anti-tank operations: Effects of experience
[FOA-C-50073-5.2] 17 p2436 N90-23882
Mode of presentation of cues in policy capturing: A comparison between verbal and pictorial presentation of targets in judgement of probability to fire
[FOA-C-50074-5.2] 17 p2436 N90-23883
Hand shaping: A paradigm for cognitive/motoric interaction
[AD-A219908] 17 p2437 N90-23885
Conference on The Perception of Structure Program and Abstracts
[AD-A222437] 22 p3232 N90-28328
Information processing and perceptual characteristics of display design: The role of emergent features and objects
[AD-A223683] 24 p3558 N90-30133

JUNCTION DIODES
Contact formation on (Hg,Cd) Te
[AD-A217088] 12 p1723 N90-19900
Characterization of a solid-state microelectrochemical diode employing a poly(vinyl alcohol)/phosphoric acid solid-state electrolyte: Rectification at junctions between WO3 and polyaniline
[AD-A222025] 21 p3000 N90-27054

JUNCTION FIELD EFFECT TRANSISTORS
U JFET

JUNCTION TRANSISTORS
NT JFET
Neutron and gamma irradiation effects on power semiconductor switches
[NASA-TM-103200] 19 p2686 N90-25278

JUNGLES
U TROPICAL REGIONS

JUPITER (PLANET)
Upper ionosphere and magnetospheric-ionospheric coupling
[DE89-619727] 02 p0250 N90-11415
A dynamical study of Jupiter's Great Red Spot
02 p0295 N90-11681
Ion bombardment of Io and Mercury
02 p0296 N90-11682
Technology update-89
[DE90-005813] 11 p1593 N90-19178
Equilibrium and stability analysis of magnetospheric plasmas 15 p2057 N90-21782
Jupiter's drifting decametric bursts with the changing time scale
[DE90-618870] 15 p2192 N90-22517
Auroral ultraviolet darkening on the outer planets
15 p2192 N90-22518
Studies of Io's atmosphere and plasma torus
16 p2338 N90-23326
Project Galileo: Recognition of the planet Jupiter and its moons
[REPT-42/89] 17 p2486 N90-24216
NASA/USRA university advanced design program at the University of Illinois for the 1989-1990 academic year
[NASA-CR-186829] 20 p2821 N90-26049
Carbon in the outer solar system
21 p3096 N90-27593

JUPITER ATMOSPHERE
A dynamical study of Jupiter's Great Red Spot
02 p0295 N90-11681
Project Galileo: Recognition of the planet Jupiter and its moons
[REPT-42/89] 17 p2486 N90-24216
Space exploration: Cost, schedule, and performance of NASA's Galileo Mission to Jupiter. Fact sheet for the Chairman, Subcommittee on Science, Technology, and Space, Committee on Commerce, Science, and Transportation, US Senate
[GAO/NSIAD-88-138FS] 20 p2816 N90-26025
Rate constant for reaction of atomic hydrogen with germane 20 p2947 N90-26768
Role of the methylene amidogen (H2CN) radical in the atmospheres of Titan and Jupiter
20 p2947 N90-26769

JUPITER PROBES
NT GALILEO SPACECRAFT
Space exploration: Cost, schedule, and performance of NASA's Galileo Mission to Jupiter. Fact sheet for the Chairman, Subcommittee on Science, Technology, and Space, Committee on Commerce, Science, and Transportation, US Senate
[GAO/NSIAD-88-138FS] 20 p2816 N90-26025

JUPITER RED SPOT
A dynamical study of Jupiter's Great Red Spot
02 p0295 N90-11681

JUPITER SATELLITES
NT IO
Project Galileo: Recognition of the planet Jupiter and its moons
[REPT-42/89] 17 p2486 N90-24216
Space exploration: Cost, schedule, and performance of NASA's Galileo Mission to Jupiter. Fact sheet for the Chairman, Subcommittee on Science, Technology, and Space, Committee on Commerce, Science, and Transportation, US Senate
[GAO/NSIAD-88-138FS] 20 p2816 N90-26025
Laboratory studies of the interaction of ions with condensed gases: Planetary applications
20 p2949 N90-26778

K

K BAND
U EXTREMELY HIGH FREQUENCIES

K LINES
Iron K-shell lines from relativistic accretion disks
19 p2766 N90-25714
Emission lines from X ray binaries
19 p2769 N90-25733
The X ray spectra of emission line AGN
19 p2785 N90-25850
Detailed non-LTE calculations of the iron emission from NGC 1068
19 p2788 N90-25872
Iron lines from X ray illuminated accretion discs in AGN
19 p2790 N90-25884
The X ray spectrum of MCG-6-30-15
19 p2793 N90-25898

K STARS
The winds of high luminosity late-type bright stars
[NASA-CR-182961] 05 p0712 N90-14160
FGK stars and T Tauri stars: Monograph series on nonthermal phenomena in stellar atmospheres
[NASA-SP-502] 10 p1446 N90-18344
Abundance differences among G and K giants
17 p2484 N90-24206

K-EPSILON TURBULENCE MODEL
Turbulent reacting flows in solid-propellant ducted rocket combustors
02 p0189 N90-11079
Investigation of turbulent flow in highly curved ducts with application to turbomachinery components
[NASA-CR-186060] 04 p0500 N90-12882
Evaluation of the near-wall k-epsilon turbulence model by comparison with direct simulations of turbulent channel flow
[AD-A212674] 04 p0503 N90-12903
Multigrid calculations of 3-D turbulent viscous flows
[NASA-CR-185154] 05 p0571 N90-13323
Depth-averaged equations for turbulent free-surface flow
[PB90-164781] 14 p1974 N90-21308
Numerical study of laminar and turbulent flows past two-dimensional and axisymmetric bodies
15 p2100 N90-22020
The computation of turbulent thin shear flows associated with flow around multielement aerofoils
18 p2491 N90-24240
A critical evaluation of two-equation models for near wall turbulence
[NASA-CR-182068] 20 p2860 N90-26270
Calculation of 3D turbulent jets in crossflow with a multigrid method and a second-moment closure model
[NASA-TM-103159] 20 p2862 N90-26282
A theoretical study of flow structure and radiation for multiphase turbulent diffusion flames
[AD-A222934] 21 p2976 N90-26913
Near-wall modelling of compressible turbulent flows
[NASA-CR-186961] 22 p3109 N90-27658
Modeling of near-wall turbulence
[NASA-TM-103222] 22 p3174 N90-28009
Turbulent thermal convection in rotating cavities, volume 1
[ETN-90-97433] 22 p3174 N90-28011
Turbulent thermal convection in rotating cavities, volume 2
[ETN-90-97434] 22 p3174 N90-28012
Development of comprehensive numerical schemes for predicting evaporating gas-droplets flow processes of a liquid-fueled combustor
[NASA-CR-187018] 23 p3305 N90-28693
Vortice-propeller interaction
[LIMSI-89-9] 23 p3326 N90-28809
Wind tunnel, field, and numerical investigations of plume downwash and dispersion at an arctic industrial site
24 p3489 N90-29721

KA BAND
U EXTREMELY HIGH FREQUENCIES

KALMAN FILTERS
Guidance simulation and test support for differential GPS flight experiment
[NASA-CR-177471] 01 p0005 N90-10021
Kalman Filter Integration of Modern Guidance and Navigation Systems
[AGARD-LS-166] 02 p0148 N90-10847
Design of a Kalman filter for transfer alignment
02 p0149 N90-10848
Development of the integrated all-weather navigation system for Tornado
02 p0149 N90-10849
A high performance airborne INS/GPS Integrated Navigation System
02 p0149 N90-10850
The development of mission-specific advanced inertially-based avionics system
02 p0149 N90-10851
Development of a marine integrated navigation system
02 p0149 N90-10852
Adaptive tracking of maneuvering targets based on IR image data
02 p0149 N90-10853
Discrete filtering techniques applied to sequential GPS range measurements
[NASA-CR-177472] 03 p0305 N90-11730
Stable Kalman filters for processing clock measurement data
04 p0487 N90-12801
True covariance simulation of the EUVE update filter
05 p0589 N90-13427
Bilinear modeling and nonlinear estimation
05 p0589 N90-13430
Extended Kalman filter for attitude estimation of the earth radiation budget satellite
05 p0590 N90-13433
On-line range prediction system, part 2
[NASA-CR-185889] 05 p0647 N90-13771
Centralized and decentralized Kalman filter techniques for tracking, navigation, and control
[AD-A214245] 07 p0878 N90-15091
Expert system for Kalman filter supervision: Application to autonomous satellite navigation
09 p1164 N90-16739
Development of the Kalman filter application and a VHDL model for the AFIT (Air Force Institute of Technology) Floating Point Application Specific Processor (FPASP)
[AD-A215423] 09 p1213 N90-17033
Nonparametric estimation of trends in linear stochastic systems
[AD-A213741] 09 p1272 N90-17374
Investigation of the observability of a satellite cluster in a near circular orbit
[AD-A216224] 10 p1326 N90-17662
Tracking a hypersonic aircraft from a space platform
[AD-A216399] 10 p1377 N90-17984
An error sensitivity model for Doppler positioning using transit satellites
[AD-A216724] 11 p1455 N90-18381
Orbit determination of artificial Earth satellites through estimation techniques combined with state smoothing techniques
[INPE-4959-TDL/388] 11 p1465 N90-18440
Self-tuning control techniques, implicit and explicit, with parameter estimation in Kalman filters, applied to artificial satellite attitude
[INPE-4857-TDL/368] 12 p1613 N90-19276
Suboptimal period design for a maneuvering missile to evade tracking filters
12 p1650 N90-19479
An improved airborne wind measurement technique for the NAE (National Aeronautical Establishment) Twin Otter
[AD-A217978] 13 p1842 N90-20575
Autonomous integrated GPS/INS navigation experiment for OMV. Phase 1: Feasibility study
[NASA-CR-4267] 14 p1914 N90-20969
Flight path reconstruction using extended Kalman filtering techniques
[PD-FC-9001] 14 p1915 N90-20970
An adaptive human response mechanism controlling the V/STOL aircraft. Appendix 3: The adaptive control model of a pilot in V/STOL aircraft control loops
[NASA-CR-186599] 15 p2056 N90-21777
Kalman filter based range estimation for autonomous navigation using imaging sensors
15 p2142 N90-22238
UD filtering and smoothing applied to orbit determination
[INPE-4966-PRE/1535] 15 p2189 N90-22501
An innovations approach to decoupling of multibody dynamics and control
16 p2280 N90-22994
On a fallacious conjecture about the stabilizability properties of solutions of the Riccati difference equation
[REPT-89-007] 16 p2305 N90-23132
Estimating short-period dynamics using an extended Kalman filter
[NASA-TM-101722] 17 p2352 N90-23392
A passive homing missile guidance law based on new target maneuver models
[AD-A220419] 17 p2356 N90-23411
Signal processing: Kalman filtering
17 p2359 N90-23428
A Kalman filter with smoothing for hurricane tracking and prediction
[AD-A220413] 17 p2426 N90-23827
Comparison of batch means and independent replications techniques to applications of the Kalman filter for simulation output analysis
[AD-A220656] 17 p2444 N90-23925
Computational tools for multi-linked flexible structures
[NASA-CR-186139] 17 p2462 N90-24058
Observation of ship movement by aeroplane
[FFI-90/7001] 19 p2657 N90-25124
Obtaining consistent models of helicopter flight-data measurement errors using kinematic-compatibility and state-reconstruction methods
[AD-A222533] 21 p2954 N90-26799
Control of orbiting large space structural systems with discrete time observational data and random measurement noise
[AD-A222476] 21 p2967 N90-26863
Multistage estimation of received carrier signal parameters under very high dynamic conditions of the receiver
[NASA-CASE-NPO-17911-1-CU]
21 p2994 N90-27016
Noise adaptation and correlated maneuver gating of an extended Kalman filter
[AD-A221713] 21 p3001 N90-27060
Kalman filter formulations for transfer alignment of strapdown inertial units
24 p3424 N90-29342
Integration of GPS/INS with partitioned filters
24 p3425 N90-29347
Observability of relative navigation using range-only measurements
24 p3427 N90-29360
State estimation for systems moving through random fields
24 p3429 N90-29373
Direct estimation of structure and motion from multiple frames
[AD-A223903] 24 p3534 N90-29985
A reduced-order extended Kalman filter for moving images
[AD-A223742] 24 p3541 N90-30028

KAOLINITE
Vibrational spectroscopic study of the kaolinite-hydrazine intercalation complex
02 p0204 N90-11166

KAPPA-EPSILON TURBULENCE MODEL
U K-EPSILON TURBULENCE MODEL

KAPTON (TRADEMARK)
A study of physical properties of ODPA-p-PDA polyimide films
[NASA-TM-102625] 13 p1766 N90-20137
Evaluations of new polyimide films for flexible circuit applications at EG and G Mound Applied Technologies
[DE90-014117] 23 p3312 N90-28731

KARMAN VORTEX STREET
Flat plate leading edge receptivity to various freestream disturbance structures
16 p2235 N90-22750

KARMAN-BODEWADT FLOW
Prediction of rotating disc flow and heat transfer in gas turbine engines
[PNR90650] 20 p2812 N90-26001

KC-130 AIRCRAFT
U C-130 AIRCRAFT

KC-135 AIRCRAFT
U C-135 AIRCRAFT

KENYA
Evaluation of the pasture potential in the dry areas of Kenya using combined Earth reconnaissance
08 p1093 N90-16327
Remote sensing and run-off modelling in the Lake Victoria Basin, Kenya
[BCRS-89-19] 11 p1526 N90-18788
The geoid in Kenya
13 p1836 N90-20542

KEPLER LAWS
Calculation of double-lunar swingby trajectories: I. Keplerian foundation
05 p0590 N90-13435
The hyperbolic Kepler's equation, and the elliptic equation revisited
[RAE-TM-SPACE-369] 09 p1274 N90-17388
On universal elements, and conversion procedures to and from position and velocity
[RAE-TM-SPACE-370] 09 p1277 N90-17406
Forbidden tangential orbit transfers between intersecting Keplerian orbits
[NASA-TP-3031] 20 p2816 N90-26028

KERNEL FUNCTIONS
Boundary kernel estimation of the two sample comparison density function
[AD-A210757] 02 p0268 N90-11532
Likelihood cross-validation bandwidth selection for nonparametric kernel density estimators
[REPT-89-10] 03 p0398 N90-12279
A kernel approach to estimation of the sphere radius density in Wicksell's corpuscle problem
[CWI-MS-R8809] 04 p0542 N90-13142
Optimal focal-plane restoration
08 p1073 N90-16207
A distributed kernel for simulation of the VHSIC hardware description language
[AD-A215419] 09 p1213 N90-17032
Temporal response of atmospheric turbulence compensation
[DE90-006354] 11 p1535 N90-18837
DARK (Distributed Ada Real-Time Kernel) porting and extension guide Kernel version 3.0
[AD-A219291] 16 p2301 N90-23112
Version description and installation guide Kernel version 3.0
[AD-A219292] 16 p2301 N90-23113
Kernel architecture manual
[AD-A219295] 16 p2301 N90-23115
Anisotropic inflation
16 p2331 N90-23286
Applications of non-parametric density estimation
[AD-A220206] 17 p2466 N90-24094

The interpretation of nonlinear frequency response functions
[RR-375] 19 p2753 N90-25643

KEROGEN
Optical constraints of kerogen from 0.15 to 40 microns: Comparison with meteoritic organics
20 p2948 N90-26776

KEROSENE
The measurement, modeling, and prediction of traction for rocket propellant 1
[NASA-CR-185186] 12 p1633 N90-19386

KERR MAGNETOOPTICAL EFFECT
Laser physics and laser techniques
[AD-A211117] 02 p0227 N90-11302

KEVLAR (TRADEMARK)
Project, implementation, and utilization of composite structures
[ETN-89-95209] 04 p0466 N90-12665
Bird impact tests on asymmetric sandwich structures made in Kevlar 49
[CEAT-NT-10/S/83-5] 09 p1162 N90-16727
Bird impact tests on curved structures of the type Sandwich-Kevlar-Nida for normal and angular shooting
[CEAT-NT-10/S/83-4] 09 p1162 N90-16728
Impact damage tolerance of composite cylindrical panels
[AD-A216401] 10 p1350 N90-17830
Low cost tooling material and process for graphite and Kevlar composites
[NASA-CR-179427] 10 p1351 N90-17834
Bird impact tests on a Kevlar 49 structure. Monolithic plates. Oblique-angled impact
[REPT-S3-4273] 11 p1454 N90-18376
Bird impact tests on Kevlar 29 and 49 sandwich structures under straight-on and glancing impact
[REPT-S3-4273-PARTIAL-6] 16 p2212 N90-22617
Bird impact tests on Kevlar plates. Sandwich Kevlar-nida submitted to straight-on and glancing impact
[REPT-S3-4273-PARTIAL-3] 16 p2212 N90-22619
Bird impact tests on structures made of Kevlar 49. Monolithic plates under straight-on impact
[REPT-S3-4273-PARTIAL-1] 16 p2213 N90-22620
Lunar regolith bagging system
[NASA-CR-186652] 19 p2677 N90-25224
Compressive strength of rigid-rod polymer fibers
[AD-A221886] 21 p2989 N90-26987
ARALL (ARamid ALuminum Laminate), a literature survey
[FOA-C-20782-2.5] 23 p3301 N90-28671
Behavior of aramid/epoxy wounded tubes under uniaxial and biaxial loading
[ETCA-89-R-150] 23 p3339 N90-28873

KEYING
NT FREQUENCY SHIFT KEYING
NT PHASE SHIFT KEYING

KINEMATIC EQUATIONS
The architecture of NEWTON: A general-purpose dynamics simulator
[NASA-CR-185489] 01 p0118 N90-10678
Dynamic robot models using the Manutec r3 as an example
[ESA-TT-1132] 04 p0458 N90-12626
Dynamics and control of robot manipulators with closed-kinematic chain mechanism
12 p1671 N90-19598
Flight path reconstruction using extended Kalman filtering techniques
[PD-FC-9001] 14 p1915 N90-20970
Systematic generation of multibody equations of motion suitable for recursive and parallel manipulation
16 p2280 N90-22992
The coupling effects of kinematics and flexibility on the Lagrangian dynamic formulation of open chain deformable links 16 p2284 N90-23018
Dynamical modeling of serial manipulators with flexible links and joints using the method of kinematic influence
24 p3500 N90-29783
Design and control of a multi-fingered robot hand provided with tactile feedback 24 p3501 N90-29789

KINEMATICS
NT BODY KINEMATICS
NT INVERSE KINEMATICS
Winged versus wingless airframes
01 p0015 N90-10073
Lumped mass formulations for modeling flexible body systems 01 p0019 N90-10091
Efficiency and capabilities of multi-body simulations
01 p0019 N90-10095
Shape control of high degree-of-freedom variable geometry trusses 01 p0024 N90-10122
Relating tolerances and kinematic behavior
[AD-A211125] 01 p0055 N90-10311
The generalized drift flux approach: Identification of the void-drift closure law 01 p0067 N90-10386
Studies in penetration mechanics
[AD-A210713] 01 p0079 N90-10448
The development of an expert system for the creative design of mechanisms
[AD-A211115] 01 p0110 N90-10628
Kinematic design NC optical generator
03 p0404 N90-12316
Kinematics, special configurations and performance evaluation of serial manipulators
04 p0508 N90-12927
SSME LOX post flow analysis/fluid structure interaction. Volume 2: Fluid structure interaction
[NASA-CR-183678] 05 p0637 N90-13716
Tire modeling by finite elements
06 p0792 N90-14614
High-frequency ventilation in dogs with three gases of different densities
[AD-A212862] 06 p0819 N90-14762
New approach to the inverse problem of six-link manipulators via the optimization technique
[DE90-710044] 07 p0940 N90-15441
Spatial dynamics of deformable multibody systems with variable kinematic structure
[AD-A214098] 07 p0942 N90-15455
Architectural study of the design and operation of advanced force feedback manual controllers
[NASA-CR-185948] 07 p0981 N90-15664
Bilateral force reflection for teleoperators with masters and slaves with dissimilar and possibly redundant kinematics
[DE90-004392] 08 p1061 N90-16132
Diagnostic and kinematic fields associated with curved and straight jet streaks using a two-layer primitive equation model 08 p1100 N90-16371
Finite element investigation of a composite cylindrical shell under transverse load with through thickness shear and snapping
[AD-A216377] 10 p1397 N90-18078
On the kinematic behavior of robots while executing general robot level commands
[PB90-120965] 11 p1517 N90-18735
Preliminary design of a pointer for movement of a solar simulator
[INPE-4864-TDL/375] 11 p1517 N90-18736
Kinematic control of robotic manipulators with multiple interchangeable wrists 12 p1670 N90-19592
Theory of gearing
[NASA-RP-1212] 12 p1670 N90-19593
Advanced control schemes and kinematic analysis for a kinematically redundant 7 DOF manipulator
[NASA-CR-186175] 12 p1671 N90-19599
Experimental investigation of the mechanisms underlying vortex kinematics in unsteady separated flows
[AD-A217889] 13 p1802 N90-20346
The CMU Reconfigurable Modular Manipulator System
[CMU-RI-TR-88-7] 13 p1809 N90-20388
Model development in viscoplastic ratchetting
[NASA-TM-102509] 13 p1816 N90-20431
Phase 1 supplemental development of a kinematic Stirling/Rankine commercial gas-fired heat pump system
[PB90-129974] 13 p1825 N90-20483
A framework for modelling kinematic measurements in gravity field applications 13 p1833 N90-20524
Coastal frontogenesis and associated severe weather on 13 March 1986 (GALE IOP 13)
[AD-A217708] 13 p1845 N90-20590
Derivation of kinematic fields using wind profiler data from the 1985 pre-storm experiment
[AD-A217952] 13 p1845 N90-20592
A case study of a quasi-stationary tropical convective line
[AD-A218325] 13 p1847 N90-20604
The development of the Canadian Mobile Servicing System Kinematic Simulation Facility
13 p1861 N90-20676
Software systems for modeling articulated figures
13 p1861 N90-20677
Development of a dynamic modeling technique and its application to the analysis and control of a high-precision robotic manipulator 14 p1987 N90-21391
A new approach to solve the kinematics resolution of a redundant robot
[DE90-010213] 14 p1988 N90-21397
Elastic-plastic instability of plane frames
14 p1992 N90-21415
Kinematic and kinetic analyses of drop landings
14 p2010 N90-21517
Direct inversion of rigid-body rotational dynamics
[NASA-TM-102798] 15 p2055 N90-21773
Unsteady separated flows produced by complex harmonic motions: Investigation of wing-flow interactions elicited by a mechanical model simulating dragonfly wing kinematics 15 p2100 N90-22018
An alternative method to solving the kinematics of a redundant robot
[DE90-006892] 15 p2106 N90-22045
Elasto-plastic analysis for contact fatigue failure
15 p2112 N90-22078
Control of human arm movement via optimization
15 p2159 N90-22334
Kinematic models of cometary comae
15 p2188 N90-22495
Systematic generation of multibody equations of motion suitable for recursive and parallel manipulation
16 p2280 N90-22992
Recursive linearization of multibody dynamics equations of motion 16 p2280 N90-22993
Efficient dynamic simulation for multiple chain robotic mechanisms 16 p2280 N90-22995
A nearly-linear computational-cost scheme for the forward dynamics of an N-body pendulum
16 p2280 N90-22996
Nonlinear finite element formulation for the large displacement analysis in multibody system dynamics
16 p2284 N90-23015
The coupling effects of kinematics and flexibility on the Lagrangian dynamic formulation of open chain deformable links 16 p2284 N90-23018
Modeling of control forces for kinematical constraints in the dynamics of multibody systems: A new approach
16 p2287 N90-23031
Characterization of robotics parallel algorithms and mapping onto a reconfigurable SIMD machine
16 p2289 N90-23039
Counterrotating cores in elliptical galaxies
16 p2332 N90-23288
Spectral evolution of active galactic nuclei Penrose Compton scattering processes and gamma ray emission from Seyfert galaxies 16 p2337 N90-23317
A viscoplastic model with application to LiF-22 percent CaF2 hypereutectic salt
[NASA-TM-103181] 17 p2417 N90-23770
Initiation and propagation of thunderstorm mesocyclones 17 p2428 N90-23838
Kinematics under wind waves
[AD-A219541] 17 p2430 N90-23844
Molecular gas in S106: Morphology, kinematics, and chemistry of a star forming region
17 p2484 N90-24209
Three legged walking mobile platform: Kinematic and dynamic analysis and simulation
[NASA-CR-184929] 18 p2535 N90-24457
New liquid cathode electrolytes in high rate cells
[AD-A219822] 18 p2546 N90-24531
Kinematic Weyl space-time models
[ETN-90-96508] 18 p2627 N90-24971
Some kinematic relations of thin elastic shells
[LR-612] 19 p2704 N90-25388
Neck injury in Advanced Military Aircraft Environments
[AGARD-CP-471] 19 p2717 N90-25459
A kinematic/dynamic model for prediction of neck injury during impact acceleration 19 p2719 N90-25469
Analysis of the biomechanic and ergonomic aspects of the cervical spine under load 19 p2719 N90-25470
Omni-directional human head-neck response
[SAE-861893] 19 p2721 N90-25478
A global approach for using kinematic redundancy to minimize base reactions of manipulators
[NASA-CR-186825] 19 p2725 N90-25499
Kinematically redundant arm formulations for coordinated multiple arm implementations
19 p2736 N90-25551
Polarization observables in deuteron photo- and electro-disintegration
[CEBAF-PR-89-022] 19 p2756 N90-25659
Control strategy for cooperating disparate manipulators
[NASA-CR-186809] 20 p2870 N90-26328
Analysis of strain relaxation in Au/Ni multilayers by x ray diffraction
[IAR-89-25] 20 p2875 N90-26357
Biodynamic simulations of an aircraft pilot/passenger in various crash environments
[NIAR-90-6] 20 p2900 N90-26494
Position control of redundant manipulators using an adaptive error-based control scheme
[NASA-CR-186812] 20 p2914 N90-26578
Mobility studies in multiloop spatial linkages
20 p2922 N90-26628
Method and apparatus for configuration control of redundant robots
[NASA-CASE-NPO-17801-1-CU]
21 p3010 N90-27110
Development of an integrated mobile robot system at Carnegie-Mellon University
[AD-A222494] 21 p3011 N90-27119
Multiple arm manipulation
[PB90-199506] 22 p3182 N90-28056
Lateral buckling of short I-beams under cyclic loading
[PB90-213653] 22 p3191 N90-28104

A theoretical investigation into the inelastic behavior of metal-matrix composites
[AD-A223973] 23 p3302 N90-28677
Motion coordination for mobile robots in unstructured environments
[PB90-199498] 23 p3332 N90-28837
Evaluation of the STM4-120 kinematic Stirling engine
[DE90-013836] 23 p3344 N90-28897
A new approach to global control of redundant manipulators 23 p3363 N90-29002
Kinematic functions for the 7 DOF robotics research arm 23 p3363 N90-29003
Cartesian control of redundant robots 23 p3363 N90-29004
Kinematics, controls, and path planning results for a redundant manipulator 23 p3363 N90-29005
Grasp planning under uncertainty 23 p3370 N90-29041
Characterization and control of self-motions in redundant manipulators 23 p3370 N90-29045
Multiple cooperating manipulators: The case of kinematically redundant arms 23 p3371 N90-29046
Reflexive obstacle avoidance for kinematically-redundant manipulators 23 p3371 N90-29047
On the simulation of space based manipulators with contact 23 p3373 N90-29056
Parallel algorithms for computation of the manipulator inertia matrix 23 p3376 N90-29072
A method for modeling kinematic hardening and cyclic strain effects
[ONERA-RT-77/1765-RY-089-R] 24 p3481 N90-29677
Windshear estimation along the trajectory of an aircraft 24 p3494 N90-29745
How to push a block along a wall 24 p3511 N90-29848
Recursive multibody dynamics and discrete-time optimal control 24 p3513 N90-29860
Kinematic sensitivity of robot manipulators 24 p3513 N90-29863
Kinematics and control algorithm development and simulation for a redundant two-arm robotic manipulator system 24 p3516 N90-29877
Inverse dynamics of a 3 degree of freedom spatial flexible manipulator 24 p3516 N90-29878
A spatial operator algebra for manipulator modeling and control 24 p3519 N90-29894

KINESTHESIA
Telepresence for space: The state of the concept 19 p2731 N90-25526

KINESTHESIS
U PROPRIOCEPTION

KINETIC ENERGY
The structure determination of molecular adsorbates with large unit cells or lattice-gas disorder on metal surfaces
[AD-A210926] 01 p0042 N90-10230
Turbulence kinetic energy equation for dilute suspensions 01 p0069 N90-10394
Studies in penetration mechanics
[AD-A210713] 01 p0079 N90-10448
Davydov solutions at 300 Kelvin: The final search
[DE89-015248] 03 p0401 N90-12296
Synchrotron-radiation experiments with recoil ions
[DE89-017579] 03 p0402 N90-12301
Solution of the Boltzmann equation using an energy group method
[AD-A213138] 05 p0699 N90-14096
Elastomeric impulse energy storage and transfer system
[AD-D014223] 06 p0730 N90-14255
Biomodal spontaneous fission
[DE90-001516] 06 p0840 N90-14886
Flux parameterization techniques in the atmospheric surface layer 07 p0959 N90-15548
Stability and fragmentation of ejecta in hypervelocity impact
[DE90-004087] 08 p1085 N90-16278
An experimental study of the effect of streamwise vortices on unsteady turbulent boundary-layer separation 09 p1215 N90-17045
Interactions of molecules with surfaces
[DE90-005337] 10 p1428 N90-18237
Experimental investigation of relationship between nonlinear field energy and emittance growth
[AD-A215813] 10 p1430 N90-18246
Scale transformations, the energy-momentum tensor, and the equation of state
[DE90-005372] 10 p1440 N90-18308
Antiproton-matter interactions in antiproton applications 11 p1560 N90-18989
Two-meter laser material response impulse measurements
[AD-A215834] 12 p1685 N90-19567
The atmospheric energy cycle of stationary and transient waves
[ISSN-0069-5882] 12 p1694 N90-19728
Theoretical modeling studies of the marine planetary
[AD-A217200] 13 p1841 N90-20567
SDI (Strategic Defense Initiative): Is its future past
[DE90-008016] 13 p1880 N90-20785
Role of free-electron lasers in strategic defense
[DE90-008028] 13 p1880 N90-20786
Polyatomic reaction dynamics
[DE90-008668] 13 p1884 N90-20811
Secondary flow calculations for axial and radial compressors 14 p1925 N90-21024
Scaling of nonnuclear kinetic-energy antisatellites
[DE90-009758] 15 p2059 N90-21791
Test and evaluation of surf forecasting model
[AD-A219580] 17 p2430 N90-23845
A computational study of the effectiveness of coating materials for KE projectile fins subjected to the combined effects of inbore and aerodynamic heating
[AD-A222595] 20 p2840 N90-26155
An improved k-epsilon model for near-wall turbulence and comparison with direct numerical simulation
[NASA-TM-103221] 22 p3171 N90-27983
Turbulence spectra of the FIRE stratocumulus-topped boundary layers 22 p3217 N90-28246
A case study of cumulus formation beneath a stratocumulus sheet: Its structure and effect on boundary layer budgets 22 p3219 N90-28256
On the dynamics of severe thunderstorms
[DE90-627922] 23 p3353 N90-28950
A search for low energy cosmic ray antiprotons 24 p3564 N90-30161

KINETIC EQUATIONS
NT HELMHOLTZ VORTICITY EQUATION
NT HYDRODYNAMIC EQUATIONS
NT KINEMATIC EQUATIONS
Kinetics of diffusion-controlled reactions
[AD-A212161] 03 p0399 N90-12286
The behavior of beams of relativistic non-thermal electrons under the influence of collisions and synchrotron losses
[NASA-CR-185983] 03 p0401 N90-12298
Stellarator transport theory
[DE89-016371] 03 p0406 N90-12328
Development of a numerical solution to the time dependent kinetic equation 03 p0433 N90-12481
Kinetics and mechanism of soot formation in hydrocarbon combustion
[NASA-CR-186162] 06 p0740 N90-14305
Group-kinetic theory and modeling of atmospheric turbulence
[NASA-CR-183776] 06 p0813 N90-14728
Ion collection by probing objects in flowing magnetized plasmas
[DE90-001711] 06 p0845 N90-14916
A kinetic equation with kinetic entropy functions for scalar conservation laws
[NASA-CR-181985] 09 p1277 N90-17401
Longitudinal traveling waves bifurcating from Vlasov plasma equilibria 12 p1715 N90-19850
Reaction and transport in porous media 19 p2690 N90-25300
Nonlinear supersonic motions of magnetized plasma flow with mass loading
[AERONOMICA-ACTA-A-354-1990] 19 p2760 N90-25681
Applied mathematics of transport theory
[DE90-014627] 23 p3387 N90-29126

KINETIC FRICTION
NT SLIDING FRICTION
Equilibrium solutions of a spherical pendulum with rotating point of suspension and friction
[ESA-TT-1139] 03 p0400 N90-12288
Thermal analysis of the wearing by removal of melted metal during high speed friction
[ETCA-89-R-139] 22 p3183 N90-28067
Blade tip rubbing stress prediction 23 p3290 N90-28615

KINETIC HEATING
NT AERODYNAMIC HEATING
NT SHOCK HEATING
Kinetic effects in Alfven wave heating. Part 2: Propagation and absorption with a single minority species
[DE89-016619] 01 p0126 N90-10724

KINETIC THEORY
NT MIXING LENGTH FLOW THEORY
NT TRANSPORT THEORY
Energy dependent transport problem with generalized boundary conditions
[DE89-617843] 01 p0118 N90-10676
Time evolution of the electron swarm energy distribution function
[AD-A212967] 04 p0557 N90-13247
Group-kinetic theory and modeling of atmospheric turbulence
[NASA-CR-183776] 06 p0813 N90-14728
Kinetic relations and the propagation of phase boundaries in solids
[AD-A215881] 11 p1519 N90-18747
Kinetic theory of low-frequency nonlinear structures in magnetized plasmas
[DE90-611306] 18 p2617 N90-24907

KINETICS
NT KINETIC ENERGY
NT NEWTON THEORY
NT REACTION KINETICS
NT VARIABLE MASS SYSTEMS
Lumped mass formulations for modeling flexible body systems 01 p0019 N90-10091
Hierarchical structure in polymeric solids and its influence on properties
[AD-A210918] 01 p0052 N90-10297
Inherent bias in nonlinear least squares analysis of first-order kinetic data
[AD-A210677] 01 p0114 N90-10651
Particle kinetic simulation of high altitude hypervelocity flight
[NASA-CR-186003] 02 p0147 N90-10840
Enhanced oxidation and solovolysis reactions in chemically inert microheterogeneous systems
[AD-A210748] 02 p0195 N90-11110
An atmospheric pressure flow reactor: Gas phase kinetics and mechanism in tropospheric conditions without wall effects 02 p0203 N90-11160
Numerical simulation of hydrazine transport in a sandy soil 02 p0205 N90-11172
Kinetics and mechanisms of primary and steady state creep in B- and Al-containing alpha silicon carbide
[AD-A210739] 02 p0283 N90-11616
Photolysis of spacecraft contaminants
[AD-A211715] 03 p0317 N90-11801
Investigations into the infiltration kinetics, wettability, and interfacial bond strength of Al/SiC composites
[AD-A211924] 03 p0320 N90-11815
Photodissociation of XeF2 (xenon difluoride) at 193 nm
[AD-A211663] 04 p0506 N90-12916
RTM user's guide
[NASA-CR-186091] 04 p0531 N90-13065
Laboratory x ray lasers
[DE90-000879] 06 p0788 N90-14590
Hypervelocity impact calculations using CTH: Case studies
[DE90-002891] 06 p0795 N90-14632
Critical temperature analysis for a hemispherical charge of a binary explosive
[DE90-001447] 07 p0913 N90-15282
Statistical model for particle-void deformation kinetics in granular materials during shock wave propagation
[DE89-017729] 07 p0946 N90-15476
The continuous crystallization of sulfur formed by the liquid-phase reaction of hydrogen sulfide and sulfur dioxide
[DE90-003991] 08 p1041 N90-16018
Theoretical studies of chemisorption and surface reactions on nickel and silicon
[DE90-004849] 08 p1047 N90-16050
Bilateral force reflection for teleoperators with masters and slaves with dissimilar and possibly redundant kinematics
[DE90-004392] 08 p1061 N90-16132
MHD Integrated topping cycle project
[DE90-004141] 08 p1126 N90-16525
Use of computer simulations to analyze limitations of kinetic models for recrystallization
[DE90-003618] 08 p1130 N90-16548
Hydride heat pumps for upgrading spacecraft waste heat 10 p1385 N90-18013
Electrochemical investigations of novel solid redox polymerization electrodes
[DE90-006087] 11 p1492 N90-18584
A numerical solution to the Boltzmann equation for use in calculating pumping rates in a CO2 discharge laser
[AD-A216376] 11 p1514 N90-18718
Evaluation of radiation-induced sensitization using electrochemical potentiokinetic reactivation technique for austenitic stainless steels
[DE90-002708] 12 p1627 N90-19352
Nonlinear continuum mechanics and applied analysis
[AD-A213629] 12 p1709 N90-19812
Linear free energy relations for multielectron transfer kinetics: A brief look at the Bronsted/Tafel analogy
[AD-A215078] 12 p1710 N90-19823
Condensed phase kinetic deuterium isotope effects in high energy phenomena: Mechanistic investigations and relationships
[AD-A217161] 13 p1770 N90-20156
Aerodynamic and kinetic processes in flames
[AD-A217796] 13 p1773 N90-20176

Spallation of oxide scales from 20 percent Cr/25 percent Ni/Nb stainless steel
[AERE-R-13464] 13 p1775 N90-20189
The stress-driven redistribution of point defects in the vicinity of crack-like singularities
[AERE-R-12898] 13 p1815 N90-20424
The electrochemical generation of useful chemical species from lunar materials 13 p1822 N90-20461
In-situ differential reflectance study of the etching of SiO2 films
[AD-A217186] 13 p1893 N90-20864
Center of excellence in theoretical geoplasma research
[AD-A215035] 14 p2005 N90-21488
The development of computational algorithms for manipulator inverse kinematics
[DE90-759877] 14 p2017 N90-21561
Anisotropy of grain growth in alumina
[DE90-009045] 14 p2032 N90-21655
Development of a computational fluid dynamics and chemistry model for the fouling of jet fuels
[DE90-005664] 15 p2098 N90-22003
Sticking coefficient of HCl on aerosols 16 p2208 N90-22598
The effects of zinc addition on the environmental stability of Al-Li alloys 16 p2219 N90-22657
The kinetics of dark adaptation in hypoxic subjects
[AD-A218641] 16 p2260 N90-22885
Pulsed-discharge carbon dioxide lasers 18 p2556 N90-24587
Rare-isotope and kinetic studies of Pt/SnO2 catalysts 18 p2558 N90-24598
Nucleation kinetics in undercooled, class-forming metallic melts
[ESA-TT-1186] 19 p2676 N90-25218
Formation and deactivation of vibrationally excited atmospheric molecules
[AD-A222660] 20 p2889 N90-26442
Novel laser gain and time-resolved FTIR studies of photochemistry 20 p2945 N90-26756
Summary of Discussions at the Eleventh Meeting of the Sandia Cooperative Group on the Aerothermochemistry of Turbulent Combustion
[DE89-001846] 21 p2973 N90-26896
Four-step kinetics for methane and implications for turbulent combustion 21 p2975 N90-26906
Measurements of energy dispersion at liquid-solid interfaces: Fluorescence quenching of pyrene bound to fumed silica
[AD-A222371] 21 p2978 N90-26926
POLYFLOW theoretical background 22 p3173 N90-28005
Solution of Euler equations using finite element method and the kinetic decomposition of the flows: Study of the self-adaptation of the grid and of the calculation field
[CERT-1/334700-DERI-GAN] 22 p3176 N90-28020
Numerical and analytical study of nonlinear bifurcations associated with the morphological stability of two-dimensional single crystals
[PB90-209594] 23 p3398 N90-29200
Investigation of the effects of microalloy constituents, surface treatment and oxidation conditions on the development and breakdown of protective oxide scales
[DE90-015710] 24 p3451 N90-29488

KIRCHHOFF LAW OF NETWORKS
Parametric version of structural vibration models
[ONERA-RT-9/3313-RY-080-R] 09 p1238 N90-17188

KIRCHHOFF LAW OF RADIATION
Computer modeling wave propagation with a variation of the Helmholtz-Kirchhoff relation
[AD-A222746] 20 p2927 N90-26657

KIRCHHOFF-HELMHOLTZ FLOW
U PIPE FLOW

KIRCHHOFF-HUYGENS PRINCIPLE
U DIFFRACTION
U WAVE PROPAGATION

KITE BALLOONS
U TETHERED BALLOONS

KITS
An expert system advisor for damage repair of composite wing skins (repairman) 21 p2956 N90-26810

KLEIN-GORDON EQUATION
Quantum fields in cosmological space-times: A soluble example
[DE89-618837] 08 p1150 N90-16662

KLYSTRONS
Modification of MEA modulator-klystron units enabling short pulse injection into a pulse-stretcher ring 06 p0841 N90-14894
Performance and modification of the MEA RF drive system 06 p0842 N90-14895
Recent progress in relativistic klystron research
[DE90-000942] 08 p1059 N90-16121
Megawatt-klystron amplifiers in L-band
[DE90-004864] 10 p1379 N90-17992
Development of a small signal theory for the harmonic gyroklystron
[AD-A216274] 10 p1380 N90-17999
Digital to position converter
[DIGEL-1984-4] 12 p1654 N90-19509
Relativistic klystron afterburner simulation techniques
[DE90-008539] 13 p1796 N90-20305
Radar RFI at Goldstone DSS 12 and DSS 16 15 p2078 N90-21900
Millimeter-wave gyroklystron amplifier experiment using a relativistic electron beam
[AD-A221209] 18 p2548 N90-24544
Relativistic klystron amplifiers driven by modulated intense relativistic electron beams
[AD-A221075] 18 p2607 N90-24849
RF power generation for future linear colliders
[DE90-014804] 23 p3394 N90-29178
High power microwaves for defense and accelerator applications
[AD-A223550] 24 p3464 N90-29572

KNIGHT SHIFT
U NUCLEAR MAGNETIC RESONANCE

KNOOP HARDNESS
Small screw study: Fastener tensile strength and optimum thread depth
[DE90-005001] 09 p1231 N90-17141

KNOWLEDGE
NT PHILOSOPHY
Designing and designing knowledge in engineering and architecture
[PB89-219521] 03 p0415 N90-12383
Knowledge-based reusable software synthesis system 06 p0824 N90-14791
Representing knowledge intelligently: Production rules, frames, and transitional networks
[AD-A215098] 09 p1271 N90-17368
The formation and use of knowledge structures in problem solving domains
[AD-A216512] 11 p1552 N90-18936
Solving problems by interrogating sets of knowledge systems: Toward a theory of multiple knowledge systems 18 p2629 N90-24979
Knowledge and distributed computation
[AD-A223100] 21 p3039 N90-27270

KNOWLEDGE BASED SYSTEMS
U EXPERT SYSTEMS

KNOWLEDGE BASES (ARTIFICIAL INTELLIGENCE)
Knowledge-based machine vision systems for space station automation
[NASA-CR-185710] 01 p0025 N90-10124
Considerations for a design and operations knowledge support system for Space Station Freedom
[NASA-TM-102156] 02 p0256 N90-11451
Parallel implementation and evaluation of motion estimation system algorithms on a distributed memory multiprocessor using knowledge based mappings
[NASA-CR-185984] 03 p0389 N90-12213
Computer-based tutors for explaining and managing the process of diagnostic reasoning
[AD-A211738] 03 p0390 N90-12222
Interoperability of heterogeneous information systems: The COST 11(ter) Project
[PB89-217541] 03 p0417 N90-12394
Detailed description of the knowledge-based system for physical database design, volume 2
[PB89-229033] 03 p0417 N90-12395
Distributed knowledge-based systems
[AD-A211984] 03 p0418 N90-12401
A knowledge-based approach to automated flow-field zoning for computational fluid dynamics
[NASA-TM-101072] 04 p0528 N90-13048
Expert systems for adaptive control of large space structures 05 p0595 N90-13452
A knowledge-based system design/information tool for aircraft flight control systems
[NASA-TM-101704] 05 p0685 N90-13990
A knowledge-based flight status monitor for real-time application in digital avionics systems
[NASA-TM-101710] 05 p0686 N90-13995
Empirical analysis and refinement of expert system knowledge bases
[AD-A213240] 05 p0707 N90-14143
Experiences with knowledge-base and large database integration
[DE90-000686] 08 p1137 N90-16591
Artificial intelligence in process control: Knowledge base for the shuttle ECS model 08 p1156 N90-16697
Rule-based systems for visibility forecasts
[AD-A214622] 09 p1248 N90-17239
Representing knowledge intelligently: Production rules, frames, and transitional networks
[AD-A215098] 09 p1271 N90-17368
Knowledge-based fault detection and analysis for robots: First results for the ROTEX robots
[ESA-TT-1150] 11 p1518 N90-18742
User manual for NEXT 1.2: NLR engineering X-pert system toolkit
[NLR-TR-87178-U] 11 p1547 N90-18905
Cooperating intelligent systems
[NASA-CR-184982] 14 p2012 N90-21529
A methodology for knowledge-based restructurable control to accommodate system failures 15 p2109 N90-22058
PLAN-IT-2: The next generation planning and scheduling tool 15 p2153 N90-22298
SURE (Science User Resource Expert): A science planning and scheduling assistant for a resource based environment 15 p2153 N90-22302
A knowledge-based approach to improving optimization techniques in system planning 15 p2154 N90-22303
Knowledge-based and integrated monitoring and diagnosis in autonomous power systems 15 p2155 N90-22310
Knowledge management: An abstraction of knowledge base and database management systems
[NASA-CR-4273] 16 p2278 N90-22986
Solving problems by interrogating sets of knowledge systems: Toward a theory of multiple knowledge systems 18 p2629 N90-24979
National Aeronautics and Space Administration (NASA)/American Society for Engineering Education (ASEE) Summer Faculty Fellowship Program-1989, volume 2
[NASA-CR-185601-VOL-2] 18 p2630 N90-24985
Knowledge-based control of an adaptive interface 18 p2630 N90-24987
Using integrity constraints to control search in knowledge base systems
[AD-A221291] 18 p2634 N90-25009
Third Annual Workshop on Space Operations Automation and Robotics (SOAR 1989)
[NASA-CP-3059] 19 p2727 N90-25503
StarPlan: A model-based diagnostic system for spacecraft 19 p2728 N90-25511
Autonomous power expert fault diagnostic system for Space Station Freedom electrical power system testbed 19 p2730 N90-25521
Knowledge representation to support reasoning based on multiple models 19 p2731 N90-25525
A model for a knowledge-based system's life cycle 19 p2739 N90-25569
Knowledge-Based Systems (KBS) development standards: A maintenance perspective 19 p2739 N90-25570
Knowledge-based system for flight information management
[NASA-TM-102685] 20 p2903 N90-26511
Fifth Conference on Artificial Intelligence for Space Applications
[NASA-CP-3073] 21 p3040 N90-27275
A knowledge-based approach to configuration layout, justification, and documentation 21 p3041 N90-27286
KIPSE1: A Knowledge-based Interactive Problem Solving Environment for data estimation and pattern classification 21 p3041 N90-27287
An architecture for rule based system explanation 21 p3042 N90-27288
Knowledge-based systems and NASA's software support environment 21 p3043 N90-27296
Graphical explanation in an expert system for Space Station Freedom rack integration 21 p3044 N90-27299
Space station advanced automation 21 p3044 N90-27300
A development framework for artificial intelligence based distributed operations support systems 21 p3044 N90-27301
A knowledge base architecture for distributed knowledge agents 21 p3044 N90-27302
Artificial Intelligence Software Engineering (AISE) model 21 p3045 N90-27309
Automated extraction of knowledge for model-based diagnostics 21 p3047 N90-27318
Documentation and knowledge acquisition 21 p3048 N90-27325
VIP: A knowledge-based design aid for the engineering of space systems 21 p3048 N90-27327
DEB: A Diagnostic Experience Browser using similarity networks 21 p3048 N90-27329
Expert system in software engineering using Structured Analysis and Design Technique (SADT)
[AD-A223022] 21 p3052 N90-27351
Proceedings of the Conference on Artificial Intelligence in the Department of Energy Complex
[DE90-011634] 22 p3241 N90-28378
Techniques and potential capabilities of multi-resolutional information (knowledge) processing 23 p3374 N90-29062
Perceptual telerobotics 23 p3374 N90-29063

Graph structure model
[DE90-014930] 23 p3381 N90-29097
Model authoring system for fail safe analysis
[NASA-CR-4317] 23 p3389 N90-29142
A knowledge-based system design/information tool
[NASA-CR-4316] 23 p3389 N90-29143
Reactive behavior, learning, and anticipation
24 p3521 N90-29908
Knowledge base refinement as improving an incorrect and incomplete domain theory
[AD-A224441] 24 p3526 N90-29935
Knowledge-based expert system configurator
[DE90-011711] 24 p3558 N90-30135

KNOWLEDGE REPRESENTATION
Toward a theory of representation design
[AD-A210885] 01 p0116 N90-10670
A survey of research methods to study design
[AD-A211213] 02 p0262 N90-11491
The Knowledge Representation Project
[AD-A211288] 02 p0288 N90-11650
The fault monitoring and diagnosis knowledge-based system for space power systems: AMPERES, phase 1
[NASA-CR-185486] 04 p0464 N90-12654
Expert systems as deductive systems
[CWI-CS-R8825] 04 p0532 N90-13073
Conceptual dependency theory and robot programming
[REPT-89-20] 04 p0537 N90-13106
Semantics and consistency of rule-based expert systems
[CWI-CS-R8824] 04 p0543 N90-13153
Advanced Software Development Workstation Project
06 p0827 N90-14807
Principles and algorithms for causal reasoning with uncertainty
[AD-A214248] 07 p0977 N90-15644
A structured connectionist approach to direct inferences and figurative adjective-noun combinations
[AD-A214326] 07 p0978 N90-15649
Optimization of monotonic inference algorithms in propositional and first order logic
[LAAS-89204] 08 p1111 N90-16436
Research and development in natural language understanding as part of the Strategic Computing Program
[AD-A214586] 09 p1264 N90-17330
Knowledge representation in space flight operations
13 p1857 N90-20655
Joint Japanese-American Workshop on Future Trends in Logic Programming
[DE90-008343] 13 p1867 N90-20709
Knowledge structure representation and automated updates in intelligent information management systems
15 p2156 N90-22316
Syntax, semantics, and pragmatism: An integrated focus based on textual linguistic knowledge
[INPE-4992-PRE/1554] 16 p2326 N90-23262
Formal methods in knowledge representation
[TR-89-11] 17 p2450 N90-23972
A viewpoint on the contribution of expert systems of logistics
[REPT-892-320-101] 17 p2454 N90-24002
Belief networks in plausible reasoning
[CWI-CS-R8927] 17 p2467 N90-24098
Research in knowledge delivery
[AD-A219920] 17 p2480 N90-24180
Multiple inheritance and exceptions in frame systems
[CWI-CS-R8931] 18 p2591 N90-24743
Knowledge graphs and natural language
[MEMO-811] 18 p2592 N90-24746
Construct analysis in knowledge graphs
[MEMO-815] 18 p2599 N90-24794
Knowledge representation to support reasoning based on multiple models 19 p2731 N90-25525
Knowledge and inhibition in asynchronous distributed systems
[TR-90-1139] 20 p2935 N90-26703
Knowledge representation for commonality
21 p3041 N90-27285
ATS displays: A reasoning visualization tool for expert systems 21 p3042 N90-27290
A knowledge base architecture for distributed knowledge agents 21 p3044 N90-27302
Capturing design knowledge 21 p3045 N90-27305
A diagnosis system using object-oriented fault tree models 21 p3046 N90-27313
Knowledge representation in PARKA
[AD-A221471] 21 p3055 N90-27367
Multiresolutional models of uncertainty generation and reduction 23 p3370 N90-29043
A survey of planning and scheduling research at the NASA Ames Research Center 23 p3376 N90-29076
Integrating planning, execution, and learning
23 p3377 N90-29079
Designing intelligent computer aided instruction systems with integrated knowledge representation schemes
[AD-A224178] 23 p3383 N90-29113
Temporal logics meet telerobotics
24 p3521 N90-29905
Knowledge base refinement as improving an incorrect and incomplete domain theory
[AD-A224441] 24 p3526 N90-29935
Machine recognition as representation and search
[AD-A223700] 24 p3528 N90-29946
An analysis of the distinction between deep and shallow expert systems
[AD-A224443] 24 p3534 N90-29987

KNUDSEN FLOW
Gas diffusion in a cometary crust
12 p1742 N90-20017

KNUDSEN NUMBER
U KNUDSEN FLOW

KOLMOGOROFF THEORY
Nonlinear systems and Kolmogorov's representation theorem
[RR-363] 04 p0508 N90-12931
Kolmogorov complexity and its applications
[CWI-CS-R8901] 04 p0548 N90-13191

KONDO EFFECT
Effects of Al substitution by Fe in CeAl2
[DE90-627843] 23 p3311 N90-28726
Evidence for a coherence gap in Ce3Bi4Pt3
[DE90-014925] 23 p3399 N90-29207

KORTEWEG-DEVRIES EQUATION
Analysis of nonlinear internal waves observed by LANDSAT-TM
[PREPRINT-704] 16 p2249 N90-22828
Efficient numerical methods for evolution partial differential equations
[AD-A219790] 17 p2457 N90-24020

KP INDEX
About the derivation of geomagnetic indices from digital data 21 p3023 N90-27191
Use of the method of natural orthogonal components for derivation of S sub R-variation and digital K-indices
21 p3024 N90-27193
Computer production of K-indices by a simple method based on linear elimination 21 p3024 N90-27194

KRIGING
The application of kriging in the statistical analysis of anthropometric data, volume 1
[AD-A220613] 17 p2438 N90-23891
The application of kriging in the statistical analysis of anthropometric data, volume 2
[AD-A220614] 17 p2438 N90-23892
The application of kriging in the statistical analysis of anthropometric data, volume 3
[AD-A220615] 17 p2438 N90-23893

KRONECKER PRODUCT
U ORTHOGONALITY

KRYPTON
NT KRYPTON ISOTOPES
NT KRYPTON 85
Lower limits on the absolute dissociative electron attachment cross section from O2 condensed on rare-gas films
[AD-A216727] 11 p1483 N90-18536
Absolute cross-sections for dissociative electron attachment in O2 condensed on Kr films
[AD-A216730] 11 p1570 N90-19038
A composition for the filling of gas-discharge tubes
[AD-A222818] 21 p2999 N90-27047

KRYPTON FLUORIDE LASERS
Air breakdown photography in the picosecond domain
[DE89-016775] 03 p0322 N90-11830
Development of KrF lasers for fusion
[DE90-007830] 11 p1515 N90-18726
Anode plasma formation as a possible mechanism for an electrical stress limit in cold cathode diodes
[DE90-007503] 12 p1655 N90-19516

KRYPTON ISOTOPES
NT KRYPTON 85
Use of a krypton isotope for rapid ion changeover at the Lawrence Berkeley Laboratory 88-inch cyclotron
[NASA-CR-186107] 05 p0698 N90-14084

KRYPTON 85
Simulation of global Kr-85 and (14)CO2 distribution by means of a time-dependent, two dimensional model of the atmosphere
[ETN-90-95376] 12 p1689 N90-19702

KU BAND
U SUPERHIGH FREQUENCIES

KUTTA-JOUKOWSKI CONDITION
Experimental study of validity of the unstationary Kutta condition, with high Strouhal numbers
[ETN-90-95914] 12 p1661 N90-19547
Euler code predicted separation at the airfoil trailing edge
[FFA-TN-1989-30] 17 p2346 N90-23364

L

L BAND
U ULTRAHIGH FREQUENCIES

L-1011 AIRCRAFT
The NASA digital VGH program: Exploration of methods and final results. Volume 2: L 1011 data 1978-1979: 1619 hours
[NASA-CR-181909-VOL-2] 13 p1756 N90-20080
The NASA digital VGH program. Exploration of methods and final results. Volume 1: Development of methods
[NASA-CR-181909-VOL-1] 13 p1756 N90-20081

LABELING (MARKING)
U MARKING

LABOR
A comparative analysis of work-hour forecasting techniques at the crew level
[AD-A220706] 17 p2438 N90-23894

LABORATORIES
NT ENGINE TESTING LABORATORIES
NT HUMAN FACTORS LABORATORIES
NT LONG DURATION EXPOSURE FACILITY
NT MANNED ORBITAL LABORATORIES
NT SKYLAB 1
NT SPACE LABORATORIES
NT SPACELAB
Research and test facilities for development of technologies and experiments with commercial applications
[NASA-TM-101789] 02 p0159 N90-10909
Lawrence Livermore National Laboratory (LLNL) research on cold fusion
[DE90-000930] 06 p0845 N90-14915
FRAG requirements for control of fatigue testing
[RAE-TM-MAT/STR-1130] 08 p1089 N90-16300
Activities report of the National Electrotechnic Institute Galileo Ferraris
[ETN-90-96178] 08 p1157 N90-16705
Total quality management: An application in a research and development laboratory
[AD-A215808] 10 p1440 N90-18312
Space-based radar simulation laboratory
[AD-A216722] 11 p1497 N90-18618
Life sciences: Lawrence Berkeley Laboratory, 1988
[DE90-008061] 13 p1849 N90-20611
The United States Air Force School of Aerospace Medicine: Special report
[AD-A217740] 13 p1851 N90-20622
Analytical sciences
[DE90-007965] 14 p1948 N90-21152
Regional remote sensing laboratory
[INPE-4922-PRE/1519] 14 p2001 N90-21465
International science and technology policies: Testimony before the Subcommittee on International Scientific Cooperation, Committee on Science, Space, and Technology, United States House of Representatives
[DE90-009416] 15 p2181 N90-22463
The role of automation and robotics in the Lunar-Based Chemical Analysis Laboratory
[DE90-009401] 15 p2192 N90-22516
Demo of three ways to use a computer to assist in lab
18 p2515 N90-24364
Project TTA-79: Summary project report
[ETN-90-96773] 19 p2661 N90-25146
Artificial intelligence within AFSC
19 p2727 N90-25504
An automated calibration laboratory for flight research instrumentation: Requirements and a proposed design approach
[NASA-TM-101719] 20 p2912 N90-26564
Development of standards for superconductors
[PB90-196536] 22 p3248 N90-28418
Educational and research activities of the Dig ital Systems Laboratory at Helsinki University of Technology
[PB90-190893] 22 p3265 N90-28486
The MTL Torsional Split-Hopkinson bar
[AD-A223278] 24 p3479 N90-29663
Oxygen deficiency monitor system
[DE90-014866] 24 p3523 N90-29917

LABORATORY EQUIPMENT
Interlaboratory comparison of two types of line-source thermal-conductivity apparatus measuring five insulating materials
[PB89-218325] 02 p0200 N90-11142
Hanging drop crystal growth apparatus and method
[NASA-CASE-MFS-28206-1-SB]
16 p2322 N90-23242

LABYRINTH
NT OTOLITH ORGANS
NT SEMICIRCULAR CANALS
NT VESTIBULES

LACTATES
Amperometric biosensors for glucose, lactate, and glycolate based on oxidases and redox-modified siloxane polymers
[DE90-002301] 06 p0781 N90-14541

The effects of graded exercise at sea level on plasma proenkephalin peptide F and catecholamine responses
[AD-A218195] 13 p1853 N90-20633

LAG (DELAY)
U TIME LAG

LAGEOS (SATELLITE)
LAGEOS 3 and the gravitomagnetic field
12 p1733 N90-19961

LAGRANGE COORDINATES
XRAD: A one dimensional Lagrangian code with radiative transport 06 p0785 N90-14570
A complete description of robot manipulator dynamics based on Lagrangian mechanics
[DE90-741467] 12 p1672 N90-19603
On the planar translation of two bodies in a uniform flow
[AD-A220143] 17 p2404 N90-23698
An angular weighting approach for calculating gradients and divergences
[DE90-013164] 20 p2908 N90-26539
On the use of Lagrangian variables in descriptions of unsteady boundary-layer separation
[NASA-CR-182071] 23 p3323 N90-28789
Deterministic transport on an arbitrarily-connected grid
[DE90-015148] 23 p3388 N90-29131

LAGRANGE EQUATIONS OF MOTION
U EULER-LAGRANGE EQUATION

LAGRANGE MULTIPLIERS
On the construction of the scattering matrix for locally-noncommutative interactions of relativistic fields
[DE89-630138] 02 p0287 N90-11640
Semi-Lagrangian, semi-implicit solutions of the shallow water equations in one dimension
[AD-A212658] 04 p0503 N90-12902
A moving-grid interface for systems of one-dimensional time-dependent partial differential equations
[CWI-NM-R8904] 04 p0541 N90-13136
Neural network models for linear programming
[DE89-015974] 07 p0979 N90-15651
Theory of singular Lagrangians
[DE90-600735] 08 p1115 N90-16456
Suboptimal and hybrid numerical solution schemes for orbit transfer manoeuvres
[INPE-4991-PRE/1556] 14 p1931 N90-21054
Determination of the heat dissipated from a specimen undergoing cyclic plasticity by a hybrid numerical/experimental method
[AD-A221575] 21 p2982 N90-26946

LAGRANGIAN EQUILIBRIUM POINTS
Multiple solutions for Lagrangian systems in T superscript n
[AD-A210646] 01 p0113 N90-10650
On a rate of convergence of the multiknapsack value function
[CWI-MS-R8812] 04 p0542 N90-13144
Intermittency and multifractality in magnetic dynamos
[PREPRINT-702] 16 p2319 N90-23226

LAGUERRE FUNCTIONS
A simple proof of a differential equation for generalizations of Laguerre polynomials
[REPT-89-15] 03 p0395 N90-12253
Generalizations of Laguerre polynomials
[REPT-89-25] 03 p0396 N90-12263
A generalization of Moak's q-Laguerre polynomials
[REPT-89-21] 04 p0540 N90-13126
Meixner-Pollaczek polynomials and the Heisenberg algebra
[CWI-PM-R8806] 04 p0541 N90-13138
Computational aspects of pseudospectral Laguerre approximations
[NASA-CR-181934] 05 p0691 N90-14038
Distribution of a sum of n random variables and a central limit theorem based on moments or on coefficients of polynomial dependence
[IMAG-RR-768-M] 05 p0692 N90-14040
Generalizations of a q-analogue of Laguerre polynomials
[REPT-89-51] 15 p2161 N90-22345
Polynomial asymptotic estimates of Gegenbauer, Laguerre, and Jacobi polynomials
[CWI-AM-R8911] 17 p2460 N90-24043

LAKE BEDS
U BEDS (GEOLOGY)

LAKE ICE
NT ICE FLOES
Ice conditions along the Illinois waterway as observed on LANDSAT images, 1972 to 1985
[AD-A219745] 17 p2418 N90-23775

LAKE MICHIGAN
Organic geochemical and tectonic evolution of the midcontinent rift system: Organic geochemistry and micropaleontology
[DE89-017561] 06 p0818 N90-14760
An aircraft investigation of a convective boundary layer over Lake Michigan
[AD-A218175] 13 p1846 N90-20598
Ice conditions along the Illinois waterway as observed on LANDSAT images, 1972 to 1985
[AD-A219745] 17 p2418 N90-23775

LAKES
NT GREAT LAKES (NORTH AMERICA)
NT GREAT SALT LAKE (UT)
NT LAKE MICHIGAN
Spatial characterization of acid rain stress in Canadian Shield Lakes
[NASA-CR-183446] 01 p0084 N90-10479
Late quaternary geomorphology of the Great Salt Lake region, Utah, and other hydrographically closed basins in the western United States: A summary of observations
[NASA-CR-185912] 05 p0663 N90-13878
Steady state model to determine lake resources at risk to acid deposition in the Sierra Nevada, California
[PB89-103995] 06 p0809 N90-14705
Global lake-level variations from 18,000 to 0 years ago: A palaeoclimate analysis
[DE90-000998] 07 p0956 N90-15531
Remote sensing and run-off modelling in the Lake Victoria Basin, Kenya
[BCRS-89-19] 11 p1526 N90-18788
Possible applications of remote sensing satellite pictures for the water quality management of the Frisian lakes, Netherlands
[BCRS-88-17] 12 p1679 N90-19641
Activities report of the Hydraulics Research Laboratory
[ETN-90-96568] 19 p2687 N90-25281
A two layer model for the simulation of internal linear and nonlinear waves in Lake Geneva (Switzerland)
19 p2687 N90-25286
Study of seasonal variation of mixing phenomena in the hypolimnion of Lake Geneva (Switzerland)
19 p2688 N90-25287
On the fine-scale mixing in the metalimnion and the seasonal thermocline of the Leman (Lake Geneva, Switzerland) 19 p2688 N90-25288
The transfer of mercury between the atmosphere and lake or soil surfaces 20 p2886 N90-26419
The 5th International symposium on palaeolimnology
[AD-A219244] 20 p2887 N90-26431

LAMB WAVES
The investigation of the fundamental limits of heterodyne holographic interferometry with the application of imaging laser generated lamb waves
[AD-A211048] 02 p0224 N90-11285
Materials characterization using holographic mapping of transient lamb waves
[AD-A211414] 03 p0358 N90-12050
The propagation of time harmonic Rayleigh-Lamb waves in a bimaterial plate
[AD-A216834] 11 p1519 N90-18749

LAMINAR BOUNDARY LAYER
Curvature effects on the stability of three-dimensional laminar boundary layers 01 p0064 N90-10366
Control and modification of turbulence
01 p0066 N90-10377
Laminar boundary layer along inviscid surface streamlines over inclined axisymmetric bodies in incompressible flow
[AD-A210202] 01 p0070 N90-10401
Research in Natural Laminar Flow and Laminar-Flow Control, part 1
[NASA-CP-2487-PT-1] 04 p0438 N90-12503
Laminar flow: Challenge and potential
04 p0438 N90-12504
LFC: A maturing concept
[DOUGLAS-PAPER-7878] 04 p0438 N90-12505
Lockheed laminar-flow control systems development and applications 04 p0438 N90-12506
Laminar flow: The Cessna perspective
04 p0439 N90-12507
Long-range LFC transport 04 p0439 N90-12508
Development flight tests of JetStar LFC leading-edge flight test experiment 04 p0439 N90-12509
The right wing of the LEFT airplane
04 p0439 N90-12510
Performance of laminar-flow leading-edge test articles in cloud encounters 04 p0439 N90-12511
Simulated airline service experience with laminar-flow control leading-edge systems 04 p0439 N90-12512
Stability theory applications to laminar-flow control
04 p0439 N90-12513
Nonparallel stability of boundary layers
04 p0440 N90-12514
Goertler instability on an airfoil
04 p0440 N90-12517
Effect of roughness on the stability of boundary layers
04 p0440 N90-12518
Research in Natural Laminar Flow and Laminar-Flow Control, part 2
[NASA-CP-2487-PT-2] 04 p0440 N90-12519
Advanced measurement techniques, part 1
04 p0441 N90-12520
Flow quality measurements in compressible subsonic flows 04 p0441 N90-12521
Predicted and hot-film measured Tollmien-Schlichting wave characteristics 04 p0441 N90-12523
Experimental studies on Goertler vortices
04 p0442 N90-12529
An experimental evaluation of slots versus porous strips for laminar-flow applications 04 p0442 N90-12530
Results of LFC experiment on slotted swept supercritical airfoil in Langley's 8-foot transonic pressure tunnel
04 p0442 N90-12531
Boundary-layer stability analysis of Langley Research Center 8-foot LFC experimental data
04 p0442 N90-12532
Sensitivity of LFC techniques in the non-linear regime
04 p0442 N90-12533
Numerical solutions of the compressible 3-D boundary-layer equations for aerospace configurations with emphasis on LFC 04 p0443 N90-12534
Theoretical methods and design studies for NLF and HLFC swept wings at subsonic and supersonic speeds
04 p0443 N90-12535
Near-field noise predictions of an aircraft in cruise
04 p0443 N90-12538
Design and test of an NLF wing glove for the variable-sweep transition flight experiment
04 p0444 N90-12544
Experimental and numerical analyses of laminar boundary-layer flow stability over an aircraft fuselage forebody 04 p0445 N90-12549
Status report on a natural laminar-flow nacelle flight experiment 04 p0445 N90-12550
Nacelle aerodynamic performance
04 p0446 N90-12552
Supersonic laminar-flow control
04 p0446 N90-12554
Multiple paths to subharmonic laminar breakdown in a boundary layer
[NASA-CR-181948] 05 p0638 N90-13722
Numerical investigations in three-dimensional internal flows
[NASA-CR-186068] 06 p0718 N90-14189
Stability of a supersonic boundary layer on a sharp cone at a small angle of attack 06 p0775 N90-14510
Unsteady three-dimensional thin-layer Navier-Stokes solutions on dynamic blocked grids
07 p0874 N90-15069
A direct-inverse method for transonic and separated flows about airfoils
[NASA-CR-4270] 07 p0875 N90-15072
Experimental measurements of the laminar separation bubble on an Eppler 387 airfoil at low Reynolds numbers
[NASA-CR-186263] 07 p0929 N90-15380
Experiments on the laminar-turbulent transition on swept wings 08 p1066 N90-16170
Direct measurement of laminar instability amplification factors in flight 08 p1067 N90-16178
Numerical studies on laminar-turbulent transition in boundary layers 10 p1383 N90-18001
Flight survey of the 757 wing noise field and its effects on laminar boundary layer transition. Volume 3: Extended data analysis
[NASA-CR-178419] 10 p1427 N90-18233
Experimental and theoretical aerodynamic characteristics of a high-lift semispan wing model
[NASA-TP-2990] 13 p1749 N90-20046
Investigation of the development of laminar boundary-layer instabilities along a cooled-wall hollow cylinder at Mach number 8
[AD-A217672] 13 p1800 N90-20331
An analytic study of nonsteady two-phase laminar boundary layer around an airfoil
18 p2643 N90-25051
Interactive calculation procedures for mixed compression inlets
[NASA-CR-186581] 20 p2801 N90-25934
Effects of forebody geometry on subsonic boundary-layer stability
[NASA-CR-4314] 20 p2802 N90-25939
Application of laminar flow control to supersonic transport configurations
[NASA-CR-181917] 20 p2803 N90-25944
Experimental study on the vortices generated by the body of a missile during flight. Part 1: Laminar boundary layer
[ONERA-RT-40/1147-AY-130A-PT-1]
22 p3110 N90-27665
An investigation of the steady and unsteady near wake and its effect on a laminar boundary layer
23 p3324 N90-28794
Transition of the boundary layer
[DERAT-RSF-50/5018-37] 24 p3469 N90-29600

LAMINAR BOUNDARY LAYER SEPARATION
U BOUNDARY LAYER SEPARATION
U LAMINAR BOUNDARY LAYER

LAMINAR FLAMES
U FLAMES
U LAMINAR FLOW
LAMINAR FLOW
NT BLASIUS FLOW
NT HARTMANN FLOW
NT STRATIFIED FLOW
Application of superplastically formed and diffusion bonded aluminum to a laminar flow control leading edge
[NASA-CR-178316] 01 p0007 N90-10030
Laminar flow control perforated wing panel development
[NASA-CR-178166] 01 p0034 N90-10187
Bifurcations in Poiseuille flow and wall turbulence
01 p0065 N90-10370
Numerically determined transition in separated internal flow 01 p0065 N90-10374
Elimination of spurious eigenvalues in the Chebyshev tau spectral method
[PB89-209282] 03 p0345 N90-11967
Numerical analysis, scientific computing and fundamental studies of fluid mechanics
[DE89-017554] 03 p0346 N90-11975
Numerical algorithms for steady and unsteady incompressible Navier-Stokes equations
[NASA-CR-186039] 04 p0437 N90-12499
Research in Natural Laminar Flow and Laminar-Flow Control, part 1
[NASA-CP-2487-PT-1] 04 p0438 N90-12503
Laminar flow: Challenge and potential
04 p0438 N90-12504
LFC: A maturing concept
[DOUGLAS-PAPER-7878] 04 p0438 N90-12505
Research in Natural Laminar Flow and Laminar-Flow Control, part 2
[NASA-CP-2487-PT-2] 04 p0440 N90-12519
Research in Natural Laminar Flow and Laminar-Flow Control, part 3
[NASA-CP-2487-PT-3] 04 p0443 N90-12539
The design of an airfoil for a high-altitude, long-endurance remotely piloted vehicle
04 p0445 N90-12545
F-14 VSTFE and results of the cleanup flight test program 04 p0445 N90-12547
Variable-Sweep Transition Flight Experiment (VSTFE): Stability code development and clean-up glove data analysis 04 p0445 N90-12548
Nacelle aerodynamic performance
04 p0446 N90-12552
Effects of acoustic sources 04 p0446 N90-12553
Supersonic laminar-flow control
04 p0446 N90-12554
Supersonic boundary-layer transition on the LaRC F-106 and the DFRF F-15 aircraft. Part 1: Transition measurements and stability analysis
04 p0447 N90-12558
Supersonic boundary-layer transition on the LaRC F-106 and the DFRF F-15 aircraft. Part 2: Aerodynamic predictions 04 p0447 N90-12559
Asymptotic analyses of the structures and characteristics of flames 04 p0468 N90-12683
A computationally efficient modelling of laminar separation bubbles
[NASA-CR-185854] 04 p0499 N90-12872
Solution of the thin-layer Navier-Stokes equations for laminar transonic flow
[PB89-221600] 04 p0500 N90-12879
Transition in surface boundary layers
[CERT-RSF-OA-43/5018-AYD]
04 p0502 N90-12897
Seminars of Applied Physics, Materials Physics and Biomedical Engineering, 1989
[PB89-218572] 04 p0548 N90-13192
Generalized similarity solutions for three dimensional, laminar, steady, compressible boundary layer flows on swept profile cylinders
[DLR-FB-89-34] 05 p0639 N90-13725
Numerical simulation of transition in three-dimensional boundary layers
[DLR-FB-89-12] 05 p0639 N90-13728
Application of multi-grid methods for solving the Navier-Stokes equations
[NASA-TM-102359] 05 p0687 N90-14002
Numerical solution of the incompressible Navier-Stokes equations 06 p0774 N90-14501
The laminar to slug flow transition in Hele-Shaw flow
[DE90-000636] 06 p0777 N90-14521
Laminar forced convection inside externally finned tubes
[DE89-636431] 07 p0928 N90-15373
Time-dependent free convection in low Prandtl number fluids
[DE90-003053] 07 p0929 N90-15377
Ambient Test Rig (ATR) flow studies: A laminar flow, reduced entrainment electrostatic precipitator
[DE90-000144] 08 p1062 N90-16142
Numerical simulation of the laminar and turbulent three dimensional flow on a delta wing with sharp leading edge 08 p1069 N90-16186
Numerical simulation of laminar hypersonic flows about an ellipsoid 08 p1071 N90-16198
An experimental investigation of viscous aspects of propeller blade flow 09 p1159 N90-16711
Viscous effects on the instability of an axisymmetric jet
[NASA-TM-102396] 09 p1161 N90-16719
A solution method for the time-dependent Navier-Stokes equations for laminar, incompressible flow
[FFA-146] 09 p1219 N90-17075
The evolution of linearized perturbations of parallel flows
[DE90-005978] 09 p1221 N90-17082
Simulated-airline-service flight tests of laminar-flow control with perforated-surface suction system
[NASA-TP-2966] 10 p1319 N90-17627
Effects of controlled three-dimensional perturbations on boundary layer transition
[AD-A215080] 10 p1384 N90-18011
Numerical investigations of heat transfer and flow rates in rotating cavities. Simulation of the movement generated by wall temperature gradients, by source-sink mass flows or by the differential rotation of the walls, under the influence or coriolis and centrifugal forces
[ETN-90-96253] 11 p1510 N90-18695
Computation of hypersonic unsteady viscous flow over a cylinder 12 p1597 N90-19194
Spatially high-resolution flame diagnosis by means of spontaneous Raman spectroscopy
[ETN-90-95870] 12 p1623 N90-19328
Method and apparatus for detecting laminar flow separation and reattachment
[NASA-CASE-LAR-13952-1-SB]
12 p1659 N90-19534
Conforming Chebyshev spectral collocation methods for the solution of laminar flow in a constricted channel
[NASA-CR-182011] 12 p1660 N90-19539
Theoretical and experimental examination of the beginning of turbulence in a heated laminar conduit flow
[ETN-90-95369] 12 p1660 N90-19541
A note on an acoustic response during an engine nacelle flight experiment
[NASA-TM-102585] 12 p1710 N90-19821
Modification and improvement of software for modeling multidimensional reacting fuel flows
[AD-A217789] 13 p1783 N90-20235
Flight test investigation of certification issues pertaining to general-aviation-type aircraft with natural laminar flow
[NASA-CR-181967] 14 p1911 N90-20952
An experimental investigation of the physical mechanisms controlling the asymmetric flow past slender bodies at large angles of attack
15 p2053 N90-21767
European research on viscous flow (EuroVisc)
[NLR-TP-89077-U] 15 p2099 N90-22014
Saturated fluorescence measurements of the hydroxyl radical in laminar high-pressure flames
[NASA-CR-185218] 15 p2101 N90-22022
The laminar flow element: Its use as a flow standard
[PB90-129677] 15 p2126 N90-22157
The minimum drag profile in laminar flow: A numerical way 16 p2196 N90-22535
Some observations on liquid flow through filters
[AERE-R-13300] 16 p2234 N90-22748
Nonlinear bifurcation study of plane Poiseuille flow
[DLR-FB-89-42] 16 p2236 N90-22756
Prediction of aerodynamic performance of airfoils in low Reynolds number flows
[DLC-EST-TN-031] 17 p2346 N90-23360
Low speed testing of a laminar flow airfoil in an adaptive wall wind tunnel
[FFA-TN-1989-08] 17 p2346 N90-23363
The stability of two-dimensional wakes and shear-layers at high Mach numbers
[NASA-CR-182050] 17 p2401 N90-23678
Thin-layer Navier-Stokes solutions of the asymmetric vortical flow on a tangent ogive body
[AD-A220810] 17 p2403 N90-23690
Method of forming a multiple layer dielectric and a hot film sensor therewith
[NASA-CASE-LAR-13678-1] 17 p2478 N90-24168
Flutter clearance of the F-14A variable-sweep transition flight experiment airplane, phase 2
[NASA-TM-101717] 19 p2659 N90-25135
Chemistry of combustion processes
20 p2811 N90-25994
The finite analytic method and its applications. Volume 1: Laminar and turbulent flows past two-dimensional and axisymmetric bodies
[AD-A222787] 20 p2864 N90-26294
Effects of 2 Hz imposed bulk flow unsteadiness on laminar-turbulent transition in a straight channel
[AD-A223028] 20 p2864 N90-26295
Four-step kinetics for methane and implications for turbulent combustion 21 p2975 N90-26906
Thermal transfers in unsteady compressible inviscid flow
[ETN-90-97557] 24 p3419 N90-29311
A boundary-layer transition model for the Navier-Stokes computation for a natural-laminar-flow airfoil
[NAL-TR-1038T] 24 p3421 N90-29328
Effects of 1 Hz imposed bulk flow unsteadiness on laminar/turbulent transition in a straight channel
[AD-A223396] 24 p3468 N90-29594
Frequency and ventilation: A survey of theoretical and experimental ventilation modelling
[LR-625] 24 p3498 N90-29772
LAMINAR FLOW AIRFOILS
Dynamics and control of turbulent shear flows
[AD-A210396] 01 p0070 N90-10402
Research in Natural Laminar Flow and Laminar-Flow Control, part 1
[NASA-CP-2487-PT-1] 04 p0438 N90-12503
Laminar flow: Challenge and potential
04 p0438 N90-12504
Laminar flow: The Cessna perspective
04 p0439 N90-12507
Long-range LFC transport 04 p0439 N90-12508
Development flight tests of JetStar LFC leading-edge flight test experiment 04 p0439 N90-12509
The right wing of the LEFT airplane
04 p0439 N90-12510
Performance of laminar-flow leading-edge test articles in cloud encounters 04 p0439 N90-12511
Simulated airline service experience with laminar-flow control leading-edge systems 04 p0439 N90-12512
Boundary-layer receptivity and laminar-flow airfoil design 04 p0440 N90-12516
Goertler instability on an airfoil
04 p0440 N90-12517
Research in Natural Laminar Flow and Laminar-Flow Control, part 2
[NASA-CP-2487-PT-2] 04 p0440 N90-12519
Predicted and hot-film measured Tollmien-Schlichting wave characteristics 04 p0441 N90-12523
Results of LFC experiment on slotted swept supercritical airfoil in Langley's 8-foot transonic pressure tunnel
04 p0442 N90-12531
Boundary-layer stability analysis of Langley Research Center 8-foot LFC experimental data
04 p0442 N90-12532
Theoretical methods and design studies for NLF and HLFC swept wings at subsonic and supersonic speeds
04 p0443 N90-12535
Research in Natural Laminar Flow and Laminar-Flow Control, part 3
[NASA-CP-2487-PT-3] 04 p0443 N90-12539
Design of the low-speed NLF(1)-0414F and the high-speed HSNLF(1)-0213 airfoils with high-lift systems
04 p0444 N90-12540
Wind tunnel results of the low-speed NLF(1)-0414F airfoil 04 p0444 N90-12541
Wind tunnel results of the high-speed NLF(1)-0213 airfoil 04 p0444 N90-12542
Design and test of a natural laminar flow/large Reynolds number airfoil with a high design cruise lift coefficient
04 p0444 N90-12543
The 757 NLF glove flight test results
04 p0445 N90-12546
Nacelle design 04 p0446 N90-12551
Transition in surface boundary layers
[CERT-RSF-OA-43/5018-AYD]
04 p0502 N90-12897
Unsteady three-dimensional thin-layer Navier Stokes solutions on dynamic blocked grids
[AD-A212377] 04 p0503 N90-12899
Semi-empirical transition criteria for the design of laminar profiles 08 p1067 N90-16174
The precise calculation of the inviscid leading edge flow on a laminar airfoil using simple methods and verification by measurements on the TLF pilot model
08 p1068 N90-16180
Design of a natural laminar flow airfoil for an unmanned aircraft
[PD-CF-9004] 14 p1916 N90-20975
Aerofoil design techniques 14 p1916 N90-20978
Low speed testing of a laminar flow airfoil in an adaptive wall wind tunnel
[FFA-TN-1989-08] 17 p2346 N90-23363
Composite reduced Navier Stokes procedures for flow problems with strong pressure interactions
[AD-A219621] 17 p2403 N90-23687
Flight testing of a natural laminar flow airfoil using gliders
[PD-CF-9005] 20 p2801 N90-25936
LAMINAR FLOW CONTROL
U BOUNDARY LAYER CONTROL
U LAMINAR BOUNDARY LAYER

LAMINAR HEAT TRANSFER
Studies of gas turbine heat transfer airfoil surfaces and end-wall cooling effects
[AD-A212451] 04 p0457 N90-12620
Time-dependent free convection in liquid metals
[DE90-000957] 07 p0927 N90-15366
Study of vortex arrays induced artificially and from centrifugal instabilities
[AD-A216499] 11 p1506 N90-18669
Dryout stability and inception at low flowrates
[DE90-006955] 11 p1509 N90-18692
Turbine blade heat transfer coefficient evaluation by modified version of STAN5. Comparison with experimental data
[ETN-90-97283] 20 p2813 N90-26008
Gas-film flow in tubes
[DE90-011528] 23 p3324 N90-28793

LAMINAR JETS
U JET FLOW
U LAMINAR FLOW

LAMINAR MIXING
Premixed turbulent flame propagation
[AD-A211489] 03 p0324 N90-11841
Buoyancy effects on the vapor condensation rate on a horizontal liquid surface
[NASA-TM-102437] 05 p0629 N90-13675
Vapor condensation on liquid surface due to laminar jet-induced mixing: The effects of system parameters
[NASA-TM-102433] 05 p0643 N90-13751
Chaos and turbulence
[AD-A215310] 09 p1294 N90-17499
Aerodynamic and kinetic processes in flames
[AD-A217796] 13 p1773 N90-20176
Mixing of viscous fluids: Behavior of microstructures and chaos
[DE90-008871] 14 p1973 N90-21304
Experimental observations on transition to turbulence in confined coaxial jets and other boundary layer flows
[DE90-008939] 15 p2098 N90-22005
A study of mixed convection in large baffled rectangular chambers with and without internal heat sources
[AD-A223158] 22 p3169 N90-27977
Chemical kinetic and aerodynamic structures of flames
[AD-A224281] 24 p3445 N90-29455

LAMINAR WAKES
Numerical investigation of laminar-turbulent transition in a flat plate wake
[AD-A222462] 22 p3170 N90-27978

LAMINATED MATERIALS
U LAMINATES

LAMINATES
Mechanics of damping for fiber composite laminates including hygro-thermal effects
[NASA-TM-102329] 01 p0034 N90-10185
Analysis of delamination growth
02 p0183 N90-11036
Delamination tests under static compression loading
02 p0186 N90-11061
The 2.5D- and 3D-fabrics for delamination resistant composite laminates and sandwich structures
02 p0186 N90-11063
Intrinsic damage and strength criteria for advanced composite laminates in space applications
02 p0187 N90-11071
Interlaminar stress concentration in fiber composites
[ETN-89-94670] 03 p0319 N90-11809
Short period multilayers: Interface dominated structures
[DE89-017536] 03 p0319 N90-11812
Stochastic propagation of an array of parallel cracks: Exploratory work on matrix fatigue damage in composite laminates
[DE89-017837] 03 p0319 N90-11813
Aging of CFRP due to longterm storage in heated air
[ESA-TT-1124] 03 p0333 N90-11893
Spectroscopic ellipsometry characterization of CVD deposition and doping of polysilicon multilayer structures
[RSRE-MEMO-4258] 04 p0466 N90-12671
Nonlinear theories concerning laminated composites under compression with delamination
[ONERA-RT-19/3542-RY-081-R] 04 p0467 N90-12672
Numerical analysis of notch test damage to laminated composite plates submitted to uniaxial traction
[CETIM-107310] 04 p0467 N90-12675
Analysis of carbon fiber's x ray microscopic structure
[AD-A212215] 04 p0480 N90-12752
Rolling of ARALL laminates (an alternative method for post-stretching ARALL laminates)
[LR-560] 04 p0484 N90-12778
Measuring of the complete stiffness matrix for anisotropic laminated materials
[DLR-MITT-89-11] 05 p0618 N90-13606
Measuring of the complete stiffness matrix for anisotropic laminated materials
[DLR-MITT-89-12] 05 p0618 N90-13607
Impact tests on aluminum 2024 T3, aramid and glass reinforced aluminum laminates and thermoplastic composites
[LR-534] 05 p0619 N90-13613
Buckling of delaminations in ARALL laminates
[LR-535] 05 p0619 N90-13614
Constant amplitude fatigue of ARALL-2 laminates
[LR-539] 05 p0620 N90-13615
Optical modulators based on polymers
[EP-PATENT-0-294-061-A1] 05 p0700 N90-14099
Finite element analysis of laminated composite plates
06 p0737 N90-14291
Effects of aeroelastic tailoring on anisotropic composite material beam models of helicopter blades
[AD-A213478] 07 p0879 N90-15095
A study of impact damage in composite laminates
07 p0888 N90-15137
Mechanical behavior of laminated composites at elevated temperatures 07 p0889 N90-15141
Transverse (through-the-thickness) shear stiffnesses of fibre reinforced composite laminated plates (computer program)
[ESDU-89013] 07 p0891 N90-15152
Two dimensional laminated shell theory including parabolic transverse shear
[AD-A213817] 07 p0948 N90-15487
Reflection from layered media with special attention to the microwave region
[ESA-TT-1155] 08 p1057 N90-16111
Two new techniques for predicting delamination growth in laminated plates 09 p1185 N90-16865
A cure process model for resin transfer molding of advanced composites
[NASA-CR-186247] 09 p1185 N90-16867
Rapid solidification processing of composites
[AD-A215175] 09 p1187 N90-16875
Fatigue delamination onset prediction in tapered composite laminates
[NASA-TM-101673] 09 p1236 N90-17177
Generslized pulse equations for through-transmission evaluation of arbitrary multilayered structures
[NASA-TM-100752] 09 p1278 N90-17407
Three-dimensional stress analysis of plain weave composites
[NASA-TM-101672] 10 p1347 N90-17813
High-order mixture homogenization of periodic nonlinear composites 10 p1347 N90-17814
Damping loss factor determination of glass and graphite fiber composites
[AD-A214535] 10 p1347 N90-17816
Studies on deformation and fracture of viscoelastic composite materials
[AD-A216095] 10 p1348 N90-17819
A study of failure characteristics in thermoplastic composite laminates due to an eccentric circular discontinuity
[AD-A216226] 10 p1349 N90-17827
Impact damage tolerance of composite cylindrical panels
[AD-A216401] 10 p1350 N90-17830
Damage mechanisms and indenter size effects in cross plied carbon-carbon composites
[AD-A216413] 10 p1351 N90-17832
Damping loss factor determination of glass and graphite epoxy laminated composites using vertically oriented cantilever beams
[AD-A216529] 10 p1351 N90-17833
Finite element investigation of a composite cylindrical shell under transverse load with through thickness shear and snapping
[AD-A216377] 10 p1397 N90-18078
Measuring strain in carbon fibre composite laminates using the Raman optomechanical strain gauge
11 p1477 N90-18503
Compressive strength of carbon/epoxy laminated under multiaxial stress
[DE90-005552] 11 p1478 N90-18505
Threaded joint design for composites
[DE90-005553] 11 p1478 N90-18508
Damage assessment in composites by acousto-ultrasonic technique
[AD-A216590] 11 p1479 N90-18510
Theory and verification of the fiber composite damage model implemented in DYNA3D
[AD-A216600] 11 p1479 N90-18511
Instrumented impact testing of fabric-reinforced composite materials
[AD-A216764] 11 p1479 N90-18513
Development of a progressive failure model for strength of laminated composite structure
[AD-A216966] 11 p1480 N90-18517
A statistical evaluation of the variation in laminated composite properties resulting from ply misalignment
[DE90-006371] 11 p1481 N90-18525
Evaluation of repeated impact damage in composite structures 12 p1619 N90-19303
Steady state temperatures and thermal stresses in a spherical or cylindrical laminated shell
[ESDU-89027] 12 p1674 N90-19612
Compendium of abstracts and viewgraphs.
[AD-A217189] 13 p1767 N90-20140
Through-thickness strain response of thick composites in compression
[AD-A217233] 13 p1767 N90-20141
Compression testing of thick-section composite materials
[AD-A217234] 13 p1767 N90-20142
Optimization of laminated composite plates
[AD-A217621] 13 p1768 N90-20146
Postbuckling behavior of laminated specially orthotropic plates by affine transformation 13 p1814 N90-20420
Relevance of impacter shape to nonvisible damage and residual tensile strength of a thick graphite/epoxy laminate
[NASA-TM-102599] 14 p1943 N90-21122
Use of unbalanced laminates as a screening method for microcracking
[NASA-TM-102517] 14 p1944 N90-21124
Combined effect of matrix cracking and stress-free edge on delamination
[NASA-TM-102591] 14 p1944 N90-21126
A computational model of the perforation of multi-layer metallic laminates
[MRL-RR-9-89] 14 p1944 N90-21128
Compressive behavior of laminated composite structures 14 p1945 N90-21134
Resistance mechanics for laminated composite materials
[INPE-4919-RPE/594] 14 p1947 N90-21141
Crack stoppers and ARALL laminates
[PB90-166588] 14 p1947 N90-21142
Determination of stresses around cutouts in multilayered composite plate and shell structures
14 p1992 N90-21417
Delamination failure in a unidirectional curved composite laminate
[NASA-CR-182018] 14 p1993 N90-21421
Residual stresses in laminated thermoplastic matrix composites 15 p2063 N90-21815
Strength in notched and impact-damaged laminates
15 p2064 N90-21820
Computational simulation of structural fracture in fiber composites
[NASA-TM-102505] 15 p2064 N90-21821
Modelling of the impact response of fibre-reinforced composites
[OUEL-1784/89] 15 p2065 N90-21827
Failure analysis of woven hybrid composite using a finite element method
[OUEL-1791/89] 15 p2065 N90-21828
The controlled-damage concept in design of laminated composites 15 p2065 N90-21830
Institute for Materials Science and Engineering, nondestructive evaluation: Technical activities
[PB90-132739] 15 p2108 N90-22055
Three-dimensional finite element formulations for thick and thin laminated plates 15 p2121 N90-22132
Large deformation analysis of laminated composite structures by a continuum-based shell element with transverse deformation 16 p2211 N90-22613
A life prediction model for laminated composite structural components
[NASA-CR-186587] 16 p2212 N90-22614
Explicit modeling of composite plates and beams in the dynamics of multibody systems
16 p2285 N90-23019
Ply cracking in composite laminates
17 p2368 N90-23478
Instability-related delamination growth of embedded and edge delaminations
[NASA-TM-100655] 17 p2370 N90-23494
An orthotropic theory of viscoplasticity based on overstress for thermomechanical deformation and its application to laminated metal matrix composites
17 p2415 N90-23759
Method of forming a multiple layer dielectric and a hot film sensor therewith
[NASA-CASE-LAR-13678-1] 17 p2478 N90-24168
Novel pulsed plasma treatment and coating process: Multilayer structures for optical computing applications
[AD-A220737] 18 p2615 N90-24894
Development of a finite element based delamination analysis for laminates subject to extension, bending, and torsion 18 p2642 N90-25049
An approach for design and analysis of composite rotor blades
[AD-A219257] 19 p2657 N90-25125

Calculation of thick wall fiber binders for rotor components of modern helicopters
[MBB-UD-554/84-PUB] 19 p2660 N90-25137
Tension fatigue of glass/epoxy and graphite/epoxy tapered laminates
[NASA-TM-102628] 19 p2671 N90-25191
Method of inserting predesigned disbond areas into composite laminates
[NASA-CASE-LAR-13225-1] 19 p2672 N90-25197
Experimental observations and finite element analysis of the initiation of fiber microbuckling in notched composite laminates
[NASA-CR-186207] 19 p2699 N90-25359
Innovative design of composite structures: Axisymmetric deformations of unsymmetrically laminated cylinders loaded in axial compression
[NASA-CR-186635] 19 p2700 N90-25364
Fractography of composite delamination
[NASA-CR-181965] 19 p2702 N90-25372
A suitable transverse shear stiffness definition for buckling of laminates and sandwich plates
[LR-603] 19 p2704 N90-25384
Strain energy release rate analysis of delamination in a tapered laminate subjected to tension load
[NASA-TM-102592] 20 p2826 N90-26076
Damage states in laminated composite three-point bend specimens: An experimental-analytical correlation study
[NASA-TM-101800] 20 p2827 N90-26083
Fracture toughness and failure mechanisms in commercial 2091 Al-Li sheet at cryogenic temperatures
[AD-A222803] 20 p2835 N90-26125
The blunt notch behaviour of metal laminates: ARALL and GLARE
[LR-617] 20 p2877 N90-26368
Reliability analysis of continuous fiber composite laminates
[NASA-CR-185265] 20 p2878 N90-26372
Evaluation of energy absorption of new concepts of aircraft composite subfloor intersections
[NASA-TP-2951] 21 p2959 N90-26823
Study of the mechanical behavior of composites under complex stress systems
[ETN-90-97455] 22 p3154 N90-27879
Theory of stress transfer in a cross-ply laminate containing a parallel array of transverse cracks
[NPL-DMA(A)-189] 22 p3192 N90-28109
Experimental analysis of the buckling of composite plates under compression loads
[IMFL-89-28] 22 p3193 N90-28119
Mechanical behavior of thick, curved, laminated composites 23 p3299 N90-28664
Inelastic analysis of laminated composites 23 p3301 N90-28669
ARALL (ARamid ALuminum Laminate), a literature survey
[FOA-C-20782-2.5] 23 p3301 N90-28671
Aircraft battle damage repair of transparencies
[AD-A224168] 24 p3432 N90-29387
Variational formulation and finite element implementation of Pagano's theory of laminated plates 24 p3442 N90-29437
A low cost shadow moire device for the nondestructive evaluation of impact damage in composite laminates
[AD-A223451] 24 p3443 N90-29442
Prediction and control of processing-induced residual stresses in composites. Part 2: AS4/PEEK composite
[AD-A223696] 24 p3443 N90-29445
Interlaminar shear tests on continuous fiber reinforced thermoplastics: The effects of rubber forming
[LR-621] 24 p3444 N90-29451
On a generalized laminate theory with application to bending, vibration, and delamination buckling in composite laminates 24 p3478 N90-29659

LAMINATIONS
U LAMINATES

LAMPS
U LUMINAIRES

LAN (COMPUTER NETWORKS)
U LOCAL AREA NETWORKS

LAND
NT COASTAL PLAINS
NT DESERTS
NT FARMLANDS
NT FLOOD PLAINS
NT GRASSLANDS
NT MARSHLANDS
NT MOJAVE DESERT (CA)
NT NATIONAL PARKS
NT PLAINS
NT SAHARA DESERT (AFRICA)
NT WETLANDS

LAND ICE

Snow and land ice in the climate system: Research problems and possibilities of remote sensing 19 p2707 N90-25407

LAND MANAGEMENT

Use of remote sensing data for land and building statistics 08 p1094 N90-16335
Possible applications of remote sensing in the preparatory phase of a land management project
[BCRS-88-19] 12 p1679 N90-19642

LAND MOBILE SATELLITE SERVICE

Satellite systems integrated with the terrestrial cellular network for mobile communications
[ESA-STR-228] 08 p1057 N90-16113
Proceedings of the Thirteenth NASA Propagation Experimenters Meeting (NAPEX 13)
[NASA-CR-186062] 10 p1371 N90-17945
The Australian experiment with ETS-V 10 p1372 N90-17949
LMSS drive simulator for multipath propagation 10 p1372 N90-17950
Japanese propagation experiments with ETS-5 10 p1372 N90-17951
LMSS modeling status report 10 p1372 N90-17953
The GEOSTAR location and messaging system 17 p2360 N90-23435
LOCSTAR: A satellite radiodetermination system for Europe 17 p2360 N90-23436
Land mobile communications from non geostationary orbits (review of Archimedes ESA study)
[REPT-892-440-106] 17 p2392 N90-23624

LAND USE

Wider horizons: Potential contributions by space systems to socio-economic advancement in developing countries
[ESA-SP-1106] 04 p0562 N90-13278
Aircraft/airport compatibility: Some strategic, tactical, and operational issues
[TT-8902] 05 p0585 N90-13409
Strategy for monitoring the effects of land use change on atmospheric CO2 concentrations
[DE90-001635] 06 p0812 N90-14722
Computer-aided boundary delineation of agricultural lands
[NASA-TM-102243] 08 p1091 N90-16313
Support of hydrological models calculations by satellite data 08 p1094 N90-16337
TM land use classification of a region. Utilization for planning and statistics 08 p1095 N90-16339
Land suitability maps and appropriate land use: An approach using SGI and satellite imagery
[INPE-4827-PRE/1458] 11 p1521 N90-18761
Development of the agricultural information system. Characteristics and results of the Distrito Federal model
[INPE-4940-PRE/1430] 11 p1524 N90-18773
Improvement of classification results from satellite imagery to update and differentiate land use classes on topographic maps
[BCRS-89-17] 11 p1526 N90-18786
Photointerpretation with instruments for evaluation of environmental impact: Mata Atlantica in Cubata
[INPE-4910-PRE/1511] 11 p1531 N90-18817
The potential of combined use of satellite data with topographic TM information for manual/visual and digital updating of land use
[NLR-MP-88021-U] 12 p1678 N90-19639
Survey of land use through remote sensing
[INPE-5032-MD/042] 14 p1996 N90-21443
Digital processing of TM/LANDSAT data in monitoring interior water
[INPE-4956-PRE/1533] 14 p1997 N90-21448
Aerial photography as an aid for agricultural credit control
[INPE-5019-RPE/613] 14 p1999 N90-21455
Operational digital land use map 1:50,000; investigation of a multiple automatic classification based on SPOT and LANDSAT Thematic Mapper satellite pictures
[BCRS-89-10] 17 p2419 N90-23784
Mapping and monitoring land use and land degradation in part of East Kalimantan, Indonesia, using aerospace remote sensing techniques: A SPOT case study
[BCRS-88-16B] 19 p2705 N90-25394
Multisensor monitoring of deforestation in the Guinea Highlands of West Africa
[NASA-CR-186709] 19 p2706 N90-25396
Practical applications of remote sensing technology
[NASA-CR-186810] 20 p2879 N90-26377
Applications of ISES for vegetation and land use 21 p3018 N90-27158
Integration of multispectral SPOT imagery and panchromatic aerial photography for study in urban land use
[INPE-4967-PRE/1536] 22 p3194 N90-28125
The production potential of wind power in Finland
[DE90-796157] 22 p3196 N90-28136
A computerized data-base system for land-use and land-cover data collected at ground-water sampling sites in the pilot national water-quality assessment program
[PB90-181868] 22 p3258 N90-28453

LANDAU FACTOR

High temperature x ray diffraction and Landau theory investigations of order-disorder transition in defect NaCl-type solids
[DE90-011807] 20 p2930 N90-26673

LANDAU-GINZBURG EQUATIONS

Critical magnetic fields (H(sub c2), H(sub c1)) and kappa in YBa2(Cu0.98M0.02)3O(7+delta), M=Ni, Al, and Cu
[DE89-016412] 01 p0130 N90-10745
Singularity theory and N = 2 superconformal field theories
[DE89-016582] 02 p0269 N90-11538
Large deviation estimates in the stochastic quantization of phi sub 2 exp 4
[PREPRINT-686] 05 p0693 N90-14050
The modified Ginzburg-Landau theory for anisotropic high temperature superconductors
[DE89-635909] 08 p1128 N90-16532
Propagation of chaos and the McKean-Vlasov equation in duals of nuclear spaces
[AD-A224431] 24 p3543 N90-30039

LANDFORMS
NT BEDS (GEOLOGY)
NT CANALS
NT CONES (VOLCANOES)
NT GREAT BASIN (US)
NT GREENLAND
NT HAWAII
NT ICELAND
NT INDONESIA
NT ISLANDS
NT JAPAN
NT MALAGASY REPUBLIC
NT MARS VOLCANOES
NT MASSIFS
NT MERRITT ISLAND (FL)
NT MOUNTAINS
NT NEW ZEALAND
NT PENINSULAS
NT RIVER BASINS
NT ROCKY MOUNTAINS (NORTH AMERICA)
NT SIERRA NEVADA MOUNTAINS (CA)
NT STRUCTURAL BASINS
NT TERRACES (LANDFORMS)
NT VOLCANOES
NT WATERSHEDS

Acoustical effects of a large ridge on low-frequency sound propagation in stationary and moving atmospheres
[NASA-CR-186001] 03 p0400 N90-12290
Contrasting landform perception with varied radar illumination geometries and at simulated resolutions of Venera and Magellan 03 p0423 N90-12430
A morphologic study of Venus Ridge belts 03 p0423 N90-12432
Dynamics of mid-ocean ridge systems 07 p0965 N90-15575
Quantification of structural field data in the Rio Grande do Norte basin and neighborhood
[INPE-4821-RPE/591] 11 p1533 N90-18826
Ecological study of peat landforms in Canada and Alaska
[NASA-CR-184923] 19 p2705 N90-25391
MEVTV Workshop on Tectonic Features on Mars
[NASA-CR-186143] 21 p3100 N90-27609

LANDING
NT AIRCRAFT LANDING
NT CRASH LANDING
NT DITCHING (LANDING)
NT GLIDE LANDINGS
NT LUNAR LANDING
NT MARS LANDING
NT SPACECRAFT LANDING
NT TOUCHDOWN
NT VERTICAL LANDING
NT WATER LANDING

Relative merits of reactive and forward-look detection for wind-shear encounters during landing approach for various microburst escape strategies
[NASA-TM-4158] 07 p0882 N90-15108
Crew emergency return vehicle autoland feasibility study
[NASA-CR-181940] 08 p1028 N90-15937
Kinematic and kinetic analyses of drop landings 14 p2010 N90-21517
Replication of NASPAC Dallas/Fort Worth study
[DOT/FAA/CT-TN90/26] 19 p2657 N90-25123
BASEOPS default profiles for civil aircraft
[AD-A223161] 21 p2959 N90-26825

LANDING AIDS
NT APPROACH INDICATORS
NT DISCRETE ADDRESS BEACON SYSTEM
NT INSTRUMENT LANDING SYSTEMS
NT MICROWAVE LANDING SYSTEMS
NT RUNWAY LIGHTS

Modified touchdown zone lighting
[DOT/FAA/CT-TN89/70] 14 p1929 N90-21042
Preliminary Subsystem Designs for the Assured Crew Return Vehicle (ACRV), volumes 1-3
[NASA-CR-186662] 17 p2363 N90-23455
Preliminary subsystem designs for the Assured Crew Return Vehicle (ACRV), volume 1
[NASA-CR-186677-VOL-1] 20 p2818 N90-26039
Four-dimensional navigation and Flight Management Systems 22 p3112 N90-27681
Approach towards a future integrated airport surface traffic management 22 p3113 N90-27686

LANDING GEAR
Independent Orbiter Assessment (IOA): Analysis of the landing/deceleration subsystem
[NASA-CR-185569] 02 p0167 N90-10943
Independent Orbiter Assessment (IOA): Assessment of the landing/deceleration (LDG/DEC) subsystem FMEA/CIL
[NASA-CR-185570] 02 p0172 N90-10966
Modeling and analysis of the space shuttle nose-gear tire with semianalytic finite elements
[NASA-TP-2977] 12 p1670 N90-19595
Advances in optimal active control techniques for aerospace systems; application to aircraft active landing gear 15 p2054 N90-21769

LANDING INSTRUMENTS
NT APPROACH INDICATORS

LANDING MODULES
NT LUNAR LANDING MODULES
NT LUNAR MODULE

LANDING SIMULATION
Route data representation for ATC simulation experiments
[RSRE-MEMO-4133] 04 p0450 N90-12576
Wind shear models for aircraft hazard investigation 07 p0869 N90-15044
Hermes training aircraft 09 p1178 N90-16827
Vibration responses of two house structures during the Edwards Air Force Base phase of the national sonic boom program
[NASA-CR-182089] 23 p3393 N90-29169

LANDING SITES
NT LUNAR LANDING SITES
Improving snow roads and airstrips in Antarctica
[AD-A211588] 03 p0335 N90-11907
Ice runways near the South Pole
[AD-A211606] 03 p0335 N90-11908
Quantitative studies of the Martian south polar region using spacecraft images 15 p2191 N90-22514
Mars landing site catalog
[NASA-RP-1238] 21 p3100 N90-27607

LANDING SYSTEMS
U LANDING AIDS

LANDMARKS
An investigation into techniques for landmark identification of 3D images of human subjects, phase 1
[AD-A218614] 18 p2583 N90-24713

LANDSAT SATELLITES
NT LANDSAT 5
The use of LANDSAT-TM data for the management of pine forestations in central Chile
[DLR-FB-89-44] 05 p0664 N90-13881
Image processing of LANDSAT MSS data for buried valley detection in northern Indiana 06 p0802 N90-14668
Evaluation of the pasture potential in the dry areas of Kenya using combined Earth reconnaissance 08 p1093 N90-16327
Image segmentation by iterative parallel region growing with application to data compression and image analysis 08 p1114 N90-16452
Adaptive multiple-band CFAR (Constant-False-Alarm-Rate) detection of an optical pattern with unknown spectral distribution
[AD-A214754] 09 p1281 N90-17429
Wheat yield estimation at the farm level using LANDSAT TM and agrometeorological data
[INPE-5017-RPE/611] 14 p1996 N90-21439
Monitoring vegetation of Brazil: Potentialities of multi-sensors approach
[INPE-4993-PRE/1555] 14 p1998 N90-21451
Development of remote sensing techniques for the investigation of neotectonic activity, eastern transverse ranges and vicinity, southern California 18 p2573 N90-24662
Ecological study of peat landforms in Canada and Alaska
[NASA-CR-184923] 19 p2705 N90-25391
Seasonal LAI in slash pine estimated with LANDSAT TM
[NASA-TM-102278] 19 p2706 N90-25397
The 27-28 October 1986 FIRE IFO Cirrus case study: Comparison of radiative transfer theory with observations by satellite and aircraft
[NASA-TM-103468] 20 p2890 N90-26446
Satellite image atlas of glaciers of the world: Irian Jaya, Indonesia, and New Zealand
[PB90-230095] 24 p3483 N90-29691

LANDSAT 5
Atmospheric correction of thematic mapping measurements about seabeds of the German Bay
[GKSS-89/E/47] 20 p2816 N90-26029
Calibration of the visible and near-infrared channels of the LANDSAT-5 Thematic Mapper using high-altitude aircraft measurements
[NASA-TM-102185] 21 p3015 N90-27138

LANDSCAPE
U TERRAIN
U TOPOGRAPHY

LANES
U PATHS

LANGEVIN FORMULA
On the Langevin equation for stochastic quantization of gravity
[DE90-750024] 12 p1725 N90-19914

LANGMUIR PROBES
U ELECTROSTATIC PROBES

LANGUAGE PROGRAMMING
A common distributed language approach to software integration
[NASA-CR-185499] 01 p0103 N90-10584
Specification of Viper1 in Z
[RSRE-MEMO-4195] 04 p0490 N90-12817
Specification of Viper2 in Z
[RSRE-MEMO-4217] 04 p0490 N90-12819
LOTOS tools based on the Cornell synthesizer generator
[MEMO-INF-89-5] 04 p0530 N90-13062
A Z specification of the MaCHO interface editor
[RSRE-MEMO-4247] 04 p0531 N90-13067
Research and development in natural language understanding as part of the Strategic Computing Program
[AD-A214587] 09 p1264 N90-17331
Research and development in natural language understanding as part of the strategic computing program
[AD-A214611] 09 p1265 N90-17333
Incomparable elements in algebraic lattices with applications to formal language theory
[MEMO-INF-89-54] 15 p2148 N90-22269
Automatic compiler construction
[AD-A218777] 16 p2278 N90-22983
The semantics of TRIDL
[TR-89-17] 17 p2450 N90-23973
Design of a specification language by abstract syntax engineering
[CWI-CS-R8934] 18 p2599 N90-24789
Outline and realization of a polymorphic language extension for ELAN
[TR-89-23] 19 p2743 N90-25592
Language and system support for concurrent programming
[AD-A223760] 24 p3528 N90-29949

LANGUAGES
NT ADA (PROGRAMMING LANGUAGE)
NT ALGOL
NT APL (PROGRAMMING LANGUAGE)
NT ASSEMBLY LANGUAGE
NT BASIC (PROGRAMMING LANGUAGE)
NT C (PROGRAMMING LANGUAGE)
NT COMMAND LANGUAGES
NT CONTEXT FREE LANGUAGES
NT ENGLISH LANGUAGE
NT FORTRAN
NT HIGH LEVEL LANGUAGES
NT LISP (PROGRAMMING LANGUAGE)
NT NATURAL LANGUAGE (COMPUTERS)
NT PASCAL (PROGRAMMING LANGUAGE)
NT PROGRAMMING LANGUAGES
NT PROLOG (PROGRAMMING LANGUAGE)
NT QUERY LANGUAGES
NT SENTENCES
NT WORDS (LANGUAGE)
Augmentations of grammatical categories in distributional-algebraic models of natural languages
[REPT-89-24] 03 p0396 N90-12262
Process expressions and Hoare's logic
[CWI-CS-R8905] 04 p0532 N90-13076
Anaphoric trees and an extension of the model of anaphora resolution
[REPT-89-37] 04 p0540 N90-13130
Connected digit recognition in a multilingual environment
[AD-A196150] 10 p1371 N90-17942
Compound sets in mathematical programming modeling languages
[MEMO-834] 17 p2449 N90-23963
Non-interactive zero knowledge
[AD-A222698] 21 p3052 N90-27347
Efficiency and effectiveness of deep structure-based subject indexing languages: PRECIS vs. DSIS 23 p3406 N90-29248

LANTHANIDE SERIES METALS
U RARE EARTH ELEMENTS

LANTHANUM
NT LANTHANUM ISOTOPES
Develop techniques for ion implantation of PLZT for adaptive optics
[AD-A216005] 10 p1431 N90-18253
Growth and patterning of laser ablated superconducting YBa2Cu3O7 films on LaAlO3 substrates
[NASA-TM-102436] 15 p2173 N90-22421
Preparation, properties, and development of calcium lanthanum sulfide as an 8- to 12-micrometer transmitting ceramic
[AD-A220200] 17 p2382 N90-23565

LANTHANUM ALLOYS
Phases in lanthanum-nickel-aluminum intermetallic alloys
[DE90-000651] 06 p0746 N90-14343

LANTHANUM COMPOUNDS
NT LANTHANUM FLUORIDES
NT LANTHANUM OXIDES
On the photoemission spectrum and optical gap in La2CuO4
[DE89-015281] 02 p0281 N90-11605
Linear electron-hole-electron pair model of high-temperature superconductivity in La(2-x)M(x)CuO4 and YBa2Cu3O(7-y): Part 2. Dependence of the superconducting transition temperatures on pressure and on hole concentration
[DE90-003012] 07 p0999 N90-15779
Synthesis of air-sinterable lanthanum chromite powders
[DE90-004681] 08 p1046 N90-16049
Structural, magnetic and electrical properties of La(sub 2-x) Ba(sub x) NiO4
[AD-A214347] 10 p1434 N90-18278
On the explanation of anomalies in inelastic neutron scattering by high-T(sub c) superconductors
[DE90-620561] 17 p2475 N90-24149
Sigma and pi interactions of the pyrrolic ligand sandwich-like lanthanide phthalocyanines determined from magnetic susceptibility and ligand-field theory
[AD-A223609] 24 p3443 N90-29444

LANTHANUM FLUORIDES
Microstructure of thin films
[AD-A219262] 16 p2324 N90-23255

LANTHANUM ISOTOPES
Magnetic correlations in La(2-x)Sr(x)CuO4 from NQR relaxation and specific heat 22 p3143 N90-27827

LANTHANUM OXIDES
Magnetic correlations in high T(sub c) oxides in the superconducting state
[DE89-016421] 01 p0130 N90-10746
La(sub 2)MO(sub 4 + delta) (M = Cu, Ni, Co): Phase separation and superconductivity resulting from excess oxygen defects
[DE90-001988] 08 p1128 N90-16534
Microstructures of Y123 films on SrTiO3, LaGaO3, and LaAlO3
[DE90-003367] 08 p1129 N90-16537
Superconducting and semiconducting thin films of La(sub 123) and Y(sub 123) and their superlattices
[DE90-009565] 15 p2173 N90-22416
In-situ pulsed laser deposition of high-T(sub c) YBa(sub 2)Cu(sub 3)O(sub 7) superconducting thin films on (100) LaAlO3 substrates
[DE90-009861] 15 p2173 N90-22418
What is going on in the La2CuO4 superconductors 16 p2311 N90-23171

LANTHANUM 140
U LANTHANUM ISOTOPES

LAPLACE OPERATORS
U LAPLACE TRANSFORMATION

LAPLACE TRANSFORMATION
Some 1(sub p) invariant probability measures
[REPT-88-91] 03 p0397 N90-12273
Self-decomposable distributions and branching processes
[MEMO-COSOR-89-06] 05 p0693 N90-14052
Propagation of transient acoustic waves in porous media
[ETN-90-96401] 15 p2099 N90-22015
The analysis of stress relaxation on indentation of a rigid punch into a viscoelastic sheet of finite thickness
[NPL-DMA(A)-193] 15 p2162 N90-22357
On ergodicity and recurrence properties of a Markov chain with an application to an open Jackson network
[TW-89-10] 17 p2467 N90-24099
Solution of exterior acoustic problems by the boundary element method 18 p2611 N90-24874
Galerkin finite difference Laplacian operators on isolated unstructured triangular meshes by linear combinations
[NASA-TM-103209] 20 p2861 N90-26276

Power bounded prolongations and Picard-Lindeloef iteration
[PB90-190877] 22 p3242 N90-28384
Classical and Bayes-P subset selection procedures for double exponential populations
[AD-A223830] 24 p3538 N90-30006

LARGE DEPLOYABLE REFLECTOR
Report of the Asilomar 3 LDR Workshop
[NASA-CR-184656] 05 p0594 N90-13449
Introduction to the report of the Asilomar 3 LDR workshop 05 p0594 N90-13450
A figure control sensor for the Large Deployable Reflector (LDR) 05 p0594 N90-13451
Pointing control for LDR 05 p0595 N90-13453
Space telescope pointing control 05 p0595 N90-13454
Wavefront error sensing for LDR 05 p0595 N90-13455
Segment alignment control system 05 p0595 N90-13457
Composite panel development at JPL 05 p0595 N90-13458
Large Deployable Reflector (LDR) thermal characteristics 05 p0596 N90-13460
Advanced composite materials for precision segmented reflectors 05 p0596 N90-13461
Lightweight composite reflector panels 05 p0596 N90-13462
Low temperature optical testing of CFRP telescope panels 05 p0596 N90-13463
Status of direct detector and array development 05 p0596 N90-13464
Cryogenic systems for the large deployable reflector 05 p0597 N90-13470
Cryogenics for LDR 05 p0598 N90-13471
LDR cryogenics 05 p0598 N90-13472
Development of FIR arrays with integrating amplifiers 05 p0598 N90-13473
Effect of central obscuration on the LDR point spread function 05 p0598 N90-13475
Diffraction, chopping, and background subtraction for LDR 05 p0598 N90-13476
Effects of joints in truss structures 05 p0600 N90-13486
Support trusses for large precision segmented reflectors: Preliminary design and analysis
[NASA-TM-101560] 11 p1468 N90-18453
Unfurlable, continuous-surface reflector concept 12 p1609 N90-19257
Millimeter radiometer system technology 12 p1610 N90-19260

LARGE SCALE INTEGRATION
Characterization of 4/3 technology large-scale integrated circuit on polysilicon processes
[BDX-613-3971] 01 p0059 N90-10335
Product assurance technology for procuring reliable, radiation-hard, custom LSI/VLSI electronics
[NASA-CR-185954] 13 p1791 N90-20281
Statistical design of MOS VLSI (Very Large Scale Integrated) circuits with designed experiments
[AD-A219654] 17 p2396 N90-23647
Multiple target tracking in a wide-field-of-view camera system
[DE90-013488] 20 p2865 N90-26300

LARGE SPACE STRUCTURES
Flexible structure control experiments using a real-time workstation for computer-aided control engineering 01 p0017 N90-10084
A finite element approach for large motion dynamic analysis of multibody structures in space 01 p0019 N90-10093
Proceedings of the Workshop on Computational Aspects in the Control of Flexible Systems, part 2
[NASA-TM-101578-PT-2] 01 p0021 N90-10103
Use of the quasilinearization algorithm for the simulation of LSS slewing 01 p0022 N90-10110
Input-output oriented computation algorithms for the control of large flexible structures 01 p0023 N90-10118
Modeling and stabilization of large flexible space stations 01 p0024 N90-10120
Active vibration mitigation of distributed parameter, smart-type structures using Pseudo-Feedback Optimal Control (PFOC) 01 p0024 N90-10121
System identification for large space structures 01 p0025 N90-10126
Preliminary design of a large tetrahedral truss/hexagonal heatshield panel aerobrake
[NASA-TM-101612] 01 p0025 N90-10127
Space structures concepts and materials
[NASA-CR-183727] 01 p0025 N90-10128
Technology for large space systems: A bibliography with indexes (supplement 21)
[NASA-SP-7046(21)] 01 p0026 N90-10130
Structural concepts for very large (400-meter-diameter) solar concentrators 01 p0029 N90-10153
Wave-mode coordinate analysis of L junction in LSS
[AD-A211116] 02 p0176 N90-10984
Frequency domain design of robust controllers for space structures
[AD-A211172] 02 p0176 N90-10985
A contribution to the stability analysis of large space structures 02 p0177 N90-10997
Adaptive structures to meet future requirements for large precision structures 02 p0178 N90-11001
Thermoelastic behavior of large space structures: Modeling and control 02 p0179 N90-11012
Evaluation of dispersive behavior in periodic structures by discrete Fourier transform 02 p0180 N90-11014
Development of the large spacecraft structure 02 p0180 N90-11020
Basic research on processing of ceramics for space structures
[AD-A205954] 02 p0199 N90-11139
Guaranteed cost control of flexible space structures 02 p0287 N90-11643
A closed-cycle refrigerator for cooling maser amplifiers below 4 Kelvin 04 p0487 N90-12797
Report of the Asilomar 3 LDR Workshop
[NASA-CR-184656] 05 p0594 N90-13449
Expert systems for adaptive control of large space structures 05 p0595 N90-13452
Real-time sensing of optical alignment 05 p0599 N90-13479
Assembly considerations for large reflectors 05 p0599 N90-13480
Explicit modeling and concurrent processing in the simulation of multibody dynamic systems 05 p0599 N90-13481
Initial test results for the mini-mast 05 p0600 N90-13482
LDR structural experiment definition 05 p0600 N90-13483
Control of optical systems 05 p0600 N90-13484
Hybrid deployable support truss designs for LDR 05 p0600 N90-13485
PACOSS program 05 p0601 N90-13487
LDR structural technology activities at JPL 05 p0601 N90-13488
Joints in deployable space truss structures 05 p0601 N90-13489
The dynamics and control of large flexible space structures - 12, supplement 11
[NASA-CR-185966] 05 p0602 N90-13494
Attitude and shape control of optimally designed large space structures 05 p0613 N90-13579
Dynamics and control of flexible spacecraft during and after slewing maneuvers
[NASA-CR-186123] 06 p0733 N90-14270
Screening actuator locations for static shape control
[NASA-CR-181970] 09 p1182 N90-16851
Robustness of a moving-bank multiple model adaptive controller for a large space structure
[AD-A215670] 09 p1183 N90-16859
Remote Manipulator System (RMS)-based Controls-Structures Interaction (CSI) flight experiment feasibility study
[NASA-CR-181952] 09 p1230 N90-17136
Earth Science Geostationary Platform Technology
[NASA-CP-3040] 12 p1608 N90-19249
Science requirements for passive microwave sensors on earth science geostationary platforms 12 p1608 N90-19251
Structures for remotely deployable precision antennas 12 p1609 N90-19256
Advances in large inflatable reflectors 12 p1609 N90-19258
Large antenna measurement and compensation techniques 12 p1610 N90-19263
Application of attachment modes in the control of large space structures
[NASA-CR-185604] 12 p1613 N90-19280
Modified independent modal space control of flexible structures 12 p1671 N90-19597
Component count and preliminary assembly considerations for large space truss structures
[NASA-TM-102604] 13 p1763 N90-20121
Aiming control: Theory and applications to dynamic control of space structures
[AD-A217877] 13 p1764 N90-20123
NASA/DOD Controls-Structures Interaction Technology 1989
[NASA-CP-3041] 14 p1933 N90-21062
PACOSS program status and results 14 p1933 N90-21065
Controlled multibody dynamics simulation for large space structures 14 p1934 N90-21068
Nonlinear and distributed parameter models of the mini-mast truss 14 p1934 N90-21070
Optimization of the structural and control system for LSS with reduced-order model 14 p1935 N90-21075
An air-bearing weight offload system for ground test of heavy LSS structures 14 p1936 N90-21081
Controls, Astrophysics, and Structures Experiment in Space (CASES) 14 p1937 N90-21085
LACE flight dynamics experiment 14 p1937 N90-21086
Space truss zero gravity dynamics 14 p1937 N90-21087
CSI technology validation on an LSS ground experiment facility 14 p1937 N90-21089
Strain and dynamic measurements using fiber optic sensors embedded into graphite/epoxy tubes 14 p1937 N90-21090
Initial operational capability of the ASTREX large space structures test bed 14 p1938 N90-21091
In-house experiments in large space structures at the Air Force Wright Aeronautical Laboratories Flight Dynamics Laboratory 14 p1938 N90-21092
Preliminary design approach for large high precision segmented reflectors
[NASA-TM-102605] 14 p1938 N90-21096
Large space systems antenna technology 15 p2060 N90-21798
Inflatable antennas for microwave power transmission 15 p2060 N90-21799
Definition of large components assembled on-orbit and robot compatible mechanical joints
[NASA-TM-100395] 15 p2105 N90-22043
The 24th Aerospace Mechanisms Symposium
[NASA-CP-3062] 15 p2112 N90-22079
Pultrusion process development for long space boom model
[NASA-TM-4017] 16 p2214 N90-22628
The effect of mechanical deformation on the radiation patterns of large space-based arrays
[AD-A219288] 16 p2230 N90-22719
Experimental experience with flexible structures 16 p2281 N90-23002
Simulation studies using multibody dynamics code DART 16 p2288 N90-23036
On trajectory generation for flexible space crane: Inverse dynamics analysis by LATDYN 16 p2288 N90-23037
Robust fixed order dynamic compensation for large space structure control 16 p2292 N90-23059
Mini-mast dynamic analysis using the truss-beam model 16 p2297 N90-23087
Modeling and control of flexible vehicles in space
[AD-A219622] 17 p2365 N90-23465
Theory of filtering and control with application to control of large space structures
[AD-A219936] 17 p2366 N90-23468
A theory of control for infinite dimensional systems with application to large scale space structures
[AD-A219937] 17 p2366 N90-23469
Dynamic stabilization of large flexible space structures
[ETN-90-96926] 18 p2511 N90-24344
Control of large space structures
[AD-A221216] 18 p2511 N90-24345
A hierarchical approach to large space structure control
[DE90-010681] 18 p2511 N90-24347
Review of probabilistic analysis of dynamic response of systems with random parameters
[NASA-CR-186171] 18 p2568 N90-24636
Dynamic analysis of space-related linear and non-linear structures
[NASA-TM-103490] 19 p2687 N90-25174
Discharge transient coupling in large space power systems 19 p2735 N90-25544
Design and implementation of robust decentralized control laws for the ACES structure at Marshall Space Flight Center
[NASA-CR-4310] 20 p2820 N90-26046
Technology for large space systems: A bibliography with indexes (supplement 22)
[NASA-SP-7046(22)] 20 p2822 N90-26056
Structures for remotely deployable precision antennas
[NASA-CR-182065] 20 p2822 N90-26061
Feasibility study of a synthesis procedure for array feeds to improve radiation performance of large distorted reflector antennas
[NASA-CR-186641] 20 p2851 N90-26213
Intergration of system identification and robust controller designs for flexible structures in space
[NASA-TM-102695] 20 p2876 N90-26362
Computational methods for problems in aerodynamics using parallel and vector architecture
[AD-A221979] 21 p2954 N90-26795
Local design methodologies for a hierarchic control architecture
[AD-A222006] 21 p2966 N90-26862
Control of orbiting large space structural systems with discrete time observational data and random measurement noise
[AD-A222476] 21 p2967 N90-26863

Optical wavefront computer for stabilizing large space structures
[AD-A221707] 21 p2967 N90-26866
Increasing the margin of stability of arbitrarily finite modes of flexible large space structures with damping
[AD-A221742] 21 p2967 N90-26867
Flexible structure control and rigid body dynamics 22 p3129 N90-27757
In-space construction and dynamics of large space structures 22 p3130 N90-27764
Deployment of large flexible space structures 22 p3131 N90-27766
The dynamics and control of large flexible space structures - 13
[NASA-CR-186930] 23 p3286 N90-28591
Transformational part-count in layered octahedral-tetrahedral truss configurations
[NASA-TM-102635] 23 p3287 N90-28598
Suspension systems for ground testing large space structures
[NASA-CR-4325] 24 p3439 N90-29424

LARGE SPACE TELESCOPE
U HUBBLE SPACE TELESCOPE

LASER ALTIMETERS
Laser altimeter for use over the ocean
[AD-A211252] 02 p0224 N90-11286
The recovery of orbital and geophysical parameters using a spaceborne laser ranging system 02 p0226 N90-11294
Lidar instruments proposed for Eos 21 p3016 N90-27145

LASER ANEMOMETERS
Laser anemometer measurements in a transonic axial-flow fan rotor
[NASA-TP-2879] 02 p0218 N90-11245
Near wall, three-dimensional turbulence measurements: A challenge for laser velocimetry
[NASA-TM-102252] 03 p0346 N90-11978
Flow in the neighborhood of an ellipsoid cylinder of revolution model
[ONERA-RT-22/7252-AN-000A] 04 p0502 N90-12895
Laser two focus techniques 05 p0575 N90-13348
Experimental study of velocity fields and turbulence in a turbojet engine
[ISL-CO-231/88] 09 p1169 N90-16766
Measurement of the speed and temperature of ignition gases
[ISL-CO-246/88] 09 p1192 N90-16908
Miniature instrumentation for laser light scattering experiments 09 p1222 N90-17088
Experimental investigations of the unsteady boundary layer on an oscillating flat plate. Optimization and validation of a code, for calculating the potential flow/boundary layer coupling of a flat plate and of an oscillating profile
[ETN-90-96254] 11 p1508 N90-18682
TiCl4 as a source of TiO2 particles for laser anemometry measurements in hot gas
[NASA-TM-102581] 13 p1805 N90-20358
Laser Doppler anemometry measurements of a confined turbulent water jet with a uniform background flow 15 p2092 N90-21971
Multi-axis, 3-D, scanning LDA (Laser Doppler Anemometer) system for unsteady aerodynamics
[AD-A218571] 16 p2197 N90-22541
Effect of initial conditions on the development of two-phase jets
[AD-A222621] 20 p2864 N90-26293

LASER ANNEALING
Novel thin-film CuInSe2 fabrication
[DE89-009440] 02 p0281 N90-11604
Pulsed laser processing of high temperature superconducting thin films
[DE90-008928] 15 p2172 N90-22413
Direct implantation process development and characterization in advanced Hg(1)-(x)Cd(x) Te EPI layers
[AD-A219133] 16 p2324 N90-23252

LASER APPLICATIONS
NT LASER CUTTING
NT LASER FUSION
New energy conversion techniques in space, applicable to propulsion
[AIAA-79-1338] 01 p0028 N90-10145
Technical options for high average power free electron milimeter-wave and laser devices 01 p0029 N90-10151
Overview of laser concepts 01 p0029 N90-10154
Laser-powered lunar base 01 p0029 N90-10156
Laser-powered Martian rover 01 p0029 N90-10157
Beamed laser power in support of near-earth missions 01 p0031 N90-10167
New electrodynamic and electrostatic models with applications to antenna theory, superconductor slots, and lasers 01 p0055 N90-10316
A laser-driven source of polarized hydrogen and deuterium
[DE89-015130] 01 p0075 N90-10429
Laser initiation of secondary explosives
[DE89-010229] 01 p0075 N90-10431
Precision materials characterization in the near millimeter and submillimeter wavelength range
[AD-A210655] 02 p0194 N90-11106
Laser physics and laser techniques
[AD-A211117] 02 p0227 N90-11302
LAWS simulation: Sampling strategies and wind computation algorithms 03 p0364 N90-12081
Volumetric analysis by spontaneous Raman diffusion in a supersonic wind tunnel
[ISL-R-109/88] 04 p0448 N90-12564
Vibration intensity. Evaluation of a remote measuring system
[CETIM-110430] 04 p0504 N90-12907
Design and performance of an on-satellite laser diagnostic system for a free space optical heterodyne frequency-shift-keyed communication system
[AD-A211986] 04 p0505 N90-12915
Lectures on x ray lasers
[ETN-89-95516] 04 p0506 N90-12917
Liquid and solid ion plasmas
[AD-A212415] 04 p0557 N90-13244
Measurement Techniques in Aerodynamics
[VKI-LS-1989-05] 05 p0573 N90-13339
Laser applications in supersonic unsteady flow 05 p0574 N90-13344
Laser two focus techniques 05 p0575 N90-13348
Optimum data weighting and error calibration for estimation of gravitational parameters 05 p0591 N90-13437
Development of mid-infrared solid state lasers for spaceborne lidar
[NASA-CR-183290] 05 p0647 N90-13772
MM and T advanced balancing/machining
[AD-A213103] 05 p0648 N90-13775
Quantitative non-destructive evaluation using laser generated ultrasonic pulses 05 p0653 N90-13805
Precision of semi-geometrically determined SLR baselines vs. site occupation time
[ETN-90-96007] 05 p0665 N90-13885
Shuttle Laser Technology Experiment Facility (LTEF)-to-airplane lasercom experiment: Airplane considerations
[NASA-TM-100749] 06 p0731 N90-14260
Development of laser excited atomic fluorescence and ionization spectrometric methods
[DE90-001567] 06 p0742 N90-14320
Laser activities 06 p0786 N90-14576
Assessment of research needs for laser technologies applied to advanced spectrographic methods
[DE90-001154] 06 p0788 N90-14587
Laboratory x ray lasers
[DE90-000879] 06 p0788 N90-14590
Solid-state fluorescence above 1000 C: Application to high-temperature laser thermometry
[DE90-000728] 06 p0789 N90-14594
Noncontacting laser ultrasonic generation and detection at the surface of molten metal
[DE90-002020] 06 p0791 N90-14605
Laser mixing of titanium on silicon carbide
[DE90-003216] 07 p0891 N90-15150
China-built airborne synchronous laser ranger the new L-8 jet trainer aircraft
[AD-A213835] 07 p0936 N90-15422
Gas optics applicable to free electron laser technology
[AD-A214285] 07 p0993 N90-15741
Electro-optic sensors for surveillance and target acquisition 08 p1026 N90-15929
The first year's work of race project 1036 WTDM broadband customer premises network
[BBC-RD-1989/6] 08 p1055 N90-16097
Backscattering effects in DIAL due to water vapor
[SER-WISS-ABHANDL-89] 08 p1082 N90-16265
Shock thickness measurements with laser beams
[MPIS-7/1989] 08 p1083 N90-16267
Results of error correction techniques applied on two high accuracy coordinate measuring machines
[DE90-003341] 08 p1112 N90-16439
Resonance enhanced Raman studies of as-grown and laser-processed HgCdTe
[AD-A213855] 08 p1129 N90-16540
Nondestructive control of composite materials by holographic interferometry
[ISL-CO-244/88] 09 p1188 N90-16882
Noncontact temperature pattern measuring device
[NASA-CASE-NPO-17824-1-CU] 09 p1229 N90-17132
Simulation of micrometeoroid impacts by laser pulses 10 p1346 N90-17806
Initiation precursors and initiators in laser-induced copolymerization of styrene and maleic anhydride in acetone
[NASA-TM-4166] 10 p1346 N90-17810
Solid state lasers for use in non-contact temperature measurements 10 p1363 N90-17901
Analysis and test of a wide angle spectrometer
[AD-A215819] 10 p1388 N90-18030
Microwave free-electron laser applications for electron cyclotron heating of plasmas
[DE90-005203] 10 p1431 N90-18257
Technology development and circuit design for a parallel laser programmable floating point application specific processor
[AD-A215870] 11 p1500 N90-18637
Performance of a 500 watt Nd:GGG zigzag slab oscillator
[DE90-006263] 11 p1503 N90-18657
Solid-state fluorescence above 1000 C: Application to high-temperature laser thermography
[DE90-006422] 11 p1514 N90-18721
Fast algorithms for calculating laser wavefront phase compensation given noisy measurements of phase gradient
[DE90-006357] 11 p1515 N90-18727
Stark and Zeeman effects on laser cooling of positronium 11 p1560 N90-18986
Laser Technology Center
[PB90-115387] 12 p1665 N90-19564
Potential biomedical application of the Los Alamos infrared free-electron laser: DNA spectroscopy
[DE90-006505] 12 p1667 N90-19575
FWP executive summaries: Basic energy sciences materials sciences programs
[DE90-008373] 12 p1722 N90-19893
Determination of fundamental thermodynamic properties of constituent materials and performance screening of candidate systems
[AD-A218089] 13 p1769 N90-20153
Isotope exchange in oxide-containing catalyst
[NASA-CASE-LAR-13542-2-SB] 13 p1769 N90-20154
Development and construction of external laser components for hardening and coating
[MT-15/87] 13 p1806 N90-20364
Robotic mobility system: Road following algorithms
[AD-A218107] 13 p1874 N90-20748
Laser-produced plasmas in medicine
[DE90-007623] 13 p1891 N90-20849
Differential measurements of the lateral photo effect in GaAs/AlGaAs heterostructures
[AERE-R-13557] 13 p1893 N90-20861
Ultra-high brightness laser research at LLNL (Lawrence Livermore National Laboratory)
[DE90-008366] 13 p1896 N90-20885
Production of diffraction gratings using holographic interferometry
[DE90-612841] 14 p1983 N90-21362
Some recent applications of laser ultrasound to the characterisation of materials
[AERE-R-13438] 14 p1985 N90-21374
New corrosion resistant ceramic coatings by laser processing
[AERE-R-13166] 15 p2071 N90-21863
Reactions of N2A3 sigma u + and candidates for short wavelengths lasers
[DE90-009514] 15 p2103 N90-22033
Ignition testing of low-energy laser diode ignited components
[DE90-009968] 16 p2214 N90-22630
Pyrotechnic materials ignited using lasers. High energy photopyrotechnic chains
[REPT-892-430-121] 16 p2225 N90-22691
Applications of laser ultrasound
[AERE-R-13106] 16 p2239 N90-22777
JPRS report: Science and technology. USSR: Physics and mathematics
[JPRS-UPM-89-001] 16 p2310 N90-23162
Natural convection liquid immersion cooling of high density columns of discrete heat sources in a vertical channel
[AD-A218388] 17 p2402 N90-23681
Laser eye protection
[AD-A219659] 17 p2408 N90-23722
Diesel engine condition monitoring: Laser-based diagnostic techniques 17 p2410 N90-23733
Direct writing of microstructures for solid-state electronics
[AD-A220996] 18 p2535 N90-24460
Potential technology transfers of research on low-temperature carbon monoxide-oxygen recombination catalysts 18 p2562 N90-24616
Laser range camera modeling
[DE90-008220] 18 p2562 N90-24618
X ray optics
[AD-A221218] 18 p2616 N90-24898

Possibilities of Nd: YAG laser utilization in medicine
[MBB-UE-0002/88-PUB] 19 p2653 N90-25100
Laser ultrasonic measurements on ceramic materials with rough surfaces
[DE90-012961] 20 p2838 N90-26141
Laser techniques for studying chemical vapor deposition
[DE90-012921] 20 p2867 N90-26311
Field experience in using laser acoustic sensing for inspection
[DE90-012954] 20 p2873 N90-26347
Ellipsometric study of YBa2Cu3O(7-x) laser ablated and co-evaporated films
[NASA-TM-103223] 20 p2932 N90-26682
Diagnostics for hydrogen atoms and molecules in H-atom sources and beams using VUV laser light
[AD-A222340] 21 p3074 N90-27476
Laser spectroscopy of plasmas
[AD-A221978] 21 p3078 N90-27502
Microwave conductivity of laser ablated YBaCuO superconducting films and its relation to microstrip transmission line 22 p3147 N90-27844
Laser diode pumped, erbium-doped, solid state laser with high slope efficiency
[AD-D014482] 22 p3179 N90-28040
Detection of vibrationally excited H2(v double prime) for H(-) production
[AD-A222560] 22 p3180 N90-28044
A tunable, continuous wave, thulium-doped, solid state laser cross-reference to related application
[AD-D014558] 22 p3180 N90-28045
Compact 4-D optical neural network architecture
[AD-A222160] 22 p3241 N90-28379
Engineering and the advancement of human welfare. Ten outstanding achievements 1964-1989
[ISBN-0-309-04185-6] 23 p3415 N90-29297
Investigation of laser diagnostics of PACVO (Plasma Assisted Chemical Vapor Deposition) processes for depositing hard face coatings
[DE90-016209] 24 p3457 N90-29522
Proceedings of the 14th Annual Electronics Manufacturing Seminar
[AD-A224276] 24 p3463 N90-29563

LASER BEAM DEFOCUSING
U THERMAL BLOOMING

LASER BEAMS
Stimulated rotational Raman scattering
[DE89-016427] 01 p0075 N90-10430
Efficient nonlinear conversion of laser diode pumped miniature solid state laser sources
[AD-A210708] 01 p0075 N90-10433
Coupled multiline CW HF lasers: Experimental performance
[AD-A210844] 01 p0075 N90-10434
Eye/sensor protection against laser irradiation organic nonlinear optical materials
[AD-A210599] 01 p0093 N90-10531
Study of deposition of YBa2Cu3O7-x on cubic zirconia
[NASA-TM-102350] 01 p0128 N90-10737
Comparison of laser and neutral particle beam discrimination
[DE89-017786] 03 p0353 N90-12018
A nonlinear-optical method for combining high power laser beams
[AD-A211730] 03 p0354 N90-12022
Laser initiated ignition of liquid propellant
[AD-A212342] 04 p0482 N90-12766
Catadioptric Optics for laser Doppler velocimeter applications
[NASA-TM-102210] 04 p0504 N90-12904
B factory via conversion of 1 TeV electron beams into 1 TeV photon beams
[DE89-017692] 04 p0505 N90-12914
Laser two focus techniques 05 p0575 N90-13348
Field evaluation of a Nissan laser collision avoidance system
[PB90-105602] 06 p0722 N90-14215
Statistics of two-color laser beam propagation in the turbulent atmosphere (spectral correlation)
[PB89-236699] 06 p0787 N90-14581
Laboratory x ray lasers
[DE90-000879] 06 p0788 N90-14590
The current status of x ray conversion efficiency modeling
[DE90-000931] 06 p0789 N90-14591
Analysis and evaluation of technical data on the photochromic and non-linear optical properties of materials. Appendix: Eye/sensor protection by an optical fuse mirror at a focal plane: Feasibility assessment
[AD-A214051] 07 p0896 N90-15177
Analysis and evaluation of technical data on the photochromic and non-linear optical properties of materials
[AD-A214212] 07 p0896 N90-15178
Surface engineering by high energy beams
[DE90-001296] 07 p0908 N90-15250
High resolution imaging by phase retrieval and discrimination using speckle, volume 1
[AD-A214243] 07 p0919 N90-15317
Frequency shift induced in laser pulses by plasma density variations
[AD-A214195] 07 p0936 N90-15424
Aerosol heating and vaporization of high-flux laser beams
[DE90-003471] 07 p0937 N90-15428
Microfluctuations of plasma density in a theta-pinch and spatial coherency of a probing laser beam
[DE90-603347] 07 p0996 N90-15760
Analysis and evaluation of technical data on the photochromic and non-linear optical properties of materials
[AD-A214050] 08 p1041 N90-16014
Flow field visualization using laser light sheet methods. Quantitative analysis using image processing 08 p1079 N90-16243
The determination of vortex separation frequencies by means of laser light sheet images
[DNW-WTI-88.038] 08 p1079 N90-16245
Flow visualization using the laser light sheet method in vehicle aerodynamics and combustion chamber engineering 08 p1079 N90-16246
Statistics of a reflected laser beam in the turbulent atmosphere (path correlation)
[PB90-113994] 08 p1082 N90-16261
Diffraction limited dichroic combiner diode laser
[AD-D014291] 08 p1082 N90-16263
High speed signal extraction using electro-optic techniques
[AD-A214446] 08 p1122 N90-16500
NASA Laser Light Scattering Advanced Technology Development Workshop, 1988
[NASA-CP-10033] 09 p1221 N90-17085
Laser light scattering review 09 p1221 N90-17086
Critical fluid light scattering 09 p1222 N90-17087
Miniature instrumentation for laser light scattering experiments 09 p1222 N90-17088
Design of fiber optic probes for laser light scattering 09 p1222 N90-17090
Maximum likelihood techniques in QELS 09 p1222 N90-17091
Improved optics for laser light scattering 09 p1222 N90-17092
Advanced instrumentation for QELS experiments 09 p1223 N90-17093
Enhanced resolution particle size distributions by multiple angle photon correlation spectroscopy 09 p1223 N90-17094
Online submicron particle sizing by dynamic light scattering using autodilution 09 p1223 N90-17095
Light scattering instrumentation for micro gravity research 09 p1223 N90-17096
Laser light scattering as a probe of fractal colloid aggregates 09 p1223 N90-17097
Proposed uses of laser light scattering instruments for polymerization studies 09 p1224 N90-17100
Polymer solution phase separation: Microgravity simulation 09 p1224 N90-17101
CW ultraviolet laser excited with an electron beam
[AD-A214928] 09 p1227 N90-17123
Ground-based deep-space LADAR for satellite detection: A parametric study
[AD-A215673] 09 p1228 N90-17126
Laser cooling of neutral atoms
[AD-A214440] 09 p1279 N90-17418
Enhanced tracking of ballistic targets using forward looking infrared measurements with active target illumination
[AD-A215422] 09 p1282 N90-17434
Optical Johnson noise thermometry 10 p1363 N90-17899
Laser diffraction particle sizing: Instrument probe volume relocation and elongation
[NASA-TM-102512] 10 p1387 N90-18025
Two dimensional modifications of Gaussian laser light bundles
[AD-A215207] 10 p1389 N90-18033
Numeric model of a CO2 laser amplifier
[AD-A215818] 10 p1389 N90-18035
CW (Continuous Wave) stimulated Brillouin scattering of long-pulse chemical laser beams
[AD-A216409] 10 p1390 N90-18039
Electron production, electron attachment, and charge recombination process in high pressure gas discharges
[AD-A216301] 10 p1434 N90-18274
Temperature dependence of photon-gated persistent spectral hole-burning for the meso-tetra-p-tolyl Zn-tetrabenzoporphyrin/chloroform system in poly(methylmethacrylate)
[AD-A216086] 11 p1482 N90-18531
Nonlinear optical processes in one-dimensional polymers
[AD-A216103] 11 p1489 N90-18568
Theory for high gain, high power free electron lasers
[DE90-005546] 11 p1514 N90-18714
Ultrafast chemical dynamics of reactions in beams
[AD-A216319] 11 p1514 N90-18717
A study of the interaction of light with surfaces of sub-micron dimensions
[DE90-006646] 11 p1571 N90-19046
Linear theory of thermal blooming in turbulence
[DE90-007243] 12 p1667 N90-19579
Correlation-induced changes of spectra
[AD-A217087] 12 p1669 N90-19591
Atmospheric thermal blooming and beam clearing by aerosol vaporization
[DE90-006271] 12 p1690 N90-19711
The nonlinear interaction of intense laser pulses in plasmas
[AD-A217604] 12 p1718 N90-19867
Multi-dimensional LADAR tracking and adaptive grasping for spaceborne assembly of SDI (Strategic Defense Initiative) platforms
[AD-A218236] 13 p1791 N90-20279
Development and construction of external laser components for hardening and coating
[MT-15/87] 13 p1806 N90-20364
Shaped pulses from Nova for inertial confinement fusion experiments
[DE90-007261] 13 p1807 N90-20373
Measurement of the stimulated thermal Rayleigh scattering instability
[DE90-007849] 13 p1807 N90-20376
Picosecond laser study of polyatomic molecules
[DE90-008647] 13 p1808 N90-20381
Short wavelength laser/materials interactions
[AD-A218015] 13 p1808 N90-20386
Power transmission device
[AD-D014430] 14 p1969 N90-21281
New corrosion resistant ceramic coatings by laser processing
[AERE-R-13166] 15 p2071 N90-21863
High intensity laser beam interactions with single droplets 15 p2083 N90-21924
High power CO2 laser instability and its corrections 15 p2102 N90-22028
Beam combining by phase transition nonlinear media
[AD-A219301] 16 p2233 N90-22739
Measurements and simulation of controlled beamfront motion in the Laser Controlled Collective Accelerator
[DE90-009992] 16 p2240 N90-22780
Comparison of solar pumped Nd:YAG and Nd:Cr:GSGG lasers at liquid nitrogen and room temperature
[DLR-FB-89-41] 16 p2240 N90-22781
A study of low level laser retinal damage
[AD-A218919] 16 p2261 N90-22887
Laser retinal effects: Electrophysiological determination in visual cortical cells of monkeys and cats
[AD-A218937] 16 p2261 N90-22888
Acousto-ultrasonic nondestructive evaluation of materials using laser beam generation and detection
[NASA-CR-186694] 17 p2398 N90-23664
Heterodyne characterization of high-speed photomixers for the ultraviolet
[AD-A220914] 18 p2547 N90-24538
Use of the Xybion ISG-camera in the RETRA-1000 TV-Holography unit
[AD-A219842] 18 p2554 N90-24577
Models of intracavity frequency doubled lasers
[AD-A221182] 18 p2563 N90-24628
An investigation into techniques for landmark identification of 3D images of human subjects, phase 1
[AD-A218614] 18 p2583 N90-24713
Mode-medium instability and its correction with a Gaussian reflectivity mirror
[NASA-TP-3023] 19 p2758 N90-25673
Apparatus for the efficient wavelength conversion of laser radiation
[AD-D014506] 20 p2866 N90-26305
Theoretical studies of solar pumped lasers
[NASA-CR-186712] 20 p2867 N90-26308
DURIP: Instrumentation for laser switched power LINAC
[AD-A222629] 20 p2868 N90-26318
Beam rider for an Articulated Robot Manipulator (ARM) accurate positioning of long flexible manipulators
[NASA-CR-185151] 20 p2914 N90-26581
State-to-state ion-molecule reaction dynamics at thermal energies
[AD-A221589] 21 p3074 N90-27479
Sintering of ceramics by laser irradiation
[ETCA-89-R-134] 22 p3161 N90-27926
Improved compact optical RF spectrum analyzer
[AD-D014481] 22 p3177 N90-28026
Noncontact laser thermomechanical nondestructive evaluation for advanced coatings 22 p3187 N90-28087

Velocity Interferometer System for Any Reflector (VISAR): Displacement mode data reduction
[DE90-015027] 23 p3395 N90-29184
Control and estimation for aerospace applications with system time delays 24 p3428 N90-29367
Evaluation of dynamic range for LLNL streak cameras using high contrast pulses and pulse podiatry on the Nova laser system
[DE90-015203] 24 p3472 N90-29620
A method of determining a laser-velocimeter focal point and measuring its beam properties using a hot-wire anemometer
[NAL-TR-1043] 24 p3473 N90-29626
Laser beam stop
[AD-D014595] 24 p3473 N90-29629
Soft x ray emission spectra from laser-irradiated high-Z targets
[AD-A223552] 24 p3552 N90-30099
Subpicosecond Raman study of hot electrons and hot phonons in GaAs
[DE90-015634] 24 p3553 N90-30106

LASER CAVITIES

NTES laser facility for physics experiments: Building 381 high bay option
[DE89-014326] 01 p0074 N90-10428
Coupled multiline CW HF lasers: Experimental performance
[AD-A210844] 01 p0075 N90-10434
A proposed linac cavity RF drive system for the Los Alamos extreme ultraviolet free-electron laser
[DE89-016614] 03 p0353 N90-12016
Cavity eigenmodes for the NIST/NRL (National Institute of Standards and Technology/Naval Research Laboratory) free electron laser
[AD-A212706] 04 p0507 N90-12923
A compact, high-powered far-infrared (FIR) laser
[DE89-016786] 06 p0789 N90-14597
Gas optics applicable to free electron laser technology
[AD-A214285] 07 p0993 N90-15741
Theoretical and experimental investigation of coupled Ar-ion lasers
[AD-A214908] 09 p1227 N90-17122
Improved performance of the Boeing/LANL FEL (Free-Electron Laser) experiment: Extraction efficiency and cavity length detuning effects
[DE90-004872] 09 p1228 N90-17129
Numeric model of a CO2 laser amplifier
[AD-A215818] 10 p1389 N90-18035
Experimental investigation of a chemical laser cavity flowfield
[AD-A216398] 10 p1390 N90-18038
CO2 laser plus optimization for harmonic generation
[AD-D014341] 12 p1665 N90-19565
Narrow-bandwidth unstable laser resonator
[AD-D014362] 12 p1665 N90-19568
Development and applications of a coupled cavity sodium-chloride laser 15 p2102 N90-22029
Contributions to the development of SLM TEA CO2 laser sources for high resolution molecular spectroscopy 16 p2240 N90-22778
Electron beam pumped XeF(C yields A) laser scaling
[AD-A220022] 17 p2409 N90-23728
Models of intracavity frequency doubled lasers
[AD-A221182] 18 p2563 N90-24628
An investigation of a mathematical model of an optically pumped Ti(3+):Al2O3 laser system 18 p2646 N90-25063
Free electron laser injection oscillator
[AD-D014180] 21 p3007 N90-27095
Potential of solar-simulator-pumped alexandrite lasers
[NASA-TM-102701] 22 p3180 N90-28046

LASER COMMUNICATION

U OPTICAL COMMUNICATION

LASER CUTTING

Characterization of surfaces cut with a laser beam and thermal model of the process
[ISAL-89-0008] 05 p0648 N90-13780
Precision laser cutting
[DE90-009949] 17 p2407 N90-23717

LASER DAMAGE

Treatment of laser-induced retinal injuries
[AD-A210284] 01 p0092 N90-10526
Laser Induced Damage in Optical Materials: 1987
[PB89-221162] 04 p0505 N90-12913
Analysis and evaluation of technical data on the photochromic and non-linear optical properties of materials. Appendix: Eye/sensor protection by an optical fuse mirror at a focal plane: Feasibility assessment
[AD-A214051] 07 p0896 N90-15177
Analysis and evaluation of technical data on the photochromic and non-linear optical properties of materials
[AD-A214212] 07 p0896 N90-15178
Optical properties and laser damage measurements of inorganic polymer films
[DE90-003633] 07 p0911 N90-15267
Laser-induced surface ablation and optical damage of ZnS crystals caused by single- and multiple-pulse laser-irradiation
[DE90-003807] 07 p0936 N90-15419
Analysis and evaluation of technical data on the photochromic and non-linear optical properties of materials
[AD-A214050] 08 p1041 N90-16014
Structural alterations in the cornea from exposure to infrared radiation
[AD-A215340] 09 p1253 N90-17269
Spallation and dynamic fracture as an effect of laser induced shock waves in carbon based composite materials
[AD-A216540] 11 p1478 N90-18509
Effect of barrier layers in burn-through experiments with 351-nm laser illumination
[DE90-006806] 12 p1667 N90-19577
A study of low level laser retinal damage
[AD-A218919] 16 p2261 N90-22887
Laser retinal effects: Electrophysiological determination in visual cortical cells of monkeys and cats
[AD-A218937] 16 p2261 N90-22888
Nonlinear optical responses and laser damage thresholds of films of a polarized stilbene side chain liquid crystal polymer and a phthalocyanine
[AD-A219462] 17 p2408 N90-23720
Laser eye protection
[AD-A219659] 17 p2408 N90-23722
Model for predicting the effects of laser exposures and eye protection on vision
[AD-A219697] 17 p2434 N90-23868
Effect of laser glare and aircraft windscreen on visual search performance under low ambient lighting
[AD-A219456] 17 p2437 N90-23888
Dazzling glare: Protection criteria versus visual performance
[AD-A219676] 17 p2438 N90-23889
Field evaluation of laser protective eyewear
[AD-A221324] 18 p2586 N90-24725
Nonlinear optical protection against frequency agile lasers
[AD-D014535] 19 p2695 N90-25335
Expanded damage test facilities at LLNL
[DE90-011466] 19 p2695 N90-25336
Damage measurements on optical materials for use in high-peak-power lasers
[DE90-013489] 20 p2868 N90-26314
Laser damage database at 1064 nm
[DE90-013490] 20 p2868 N90-26315
Nonlinear material response to very rapid energy deposition
[AD-A221932] 21 p2989 N90-26988
A note on the statistics of laser speckle
[AD-A222408] 21 p3009 N90-27103
Laser induced damage in optical materials: 1988
[PB90-185570] 22 p3179 N90-28041

LASER DIODES

U SEMICONDUCTOR LASERS

LASER DOPPLER VELOCIMETERS

Advances in instrumentation for experimental stress and vibration analysis and its applications 02 p0187 N90-11069
A laser Doppler anemometry investigation of single-phase and particle-laden jet flows
[AD-A210660] 02 p0220 N90-11261
Three component laser Doppler measurements in an axisymmetric jet
[NASA-CR-181908] 03 p0300 N90-11702
Three-component laser Doppler velocimeter measurements in a juncture flow 04 p0441 N90-12525
Basic aerodynamic research facility for comparative studies of flow diagnostic techniques 04 p0441 N90-12526
Experimental studies on Goertler vortices 04 p0442 N90-12529
Catadioptric Optics for laser Doppler velocimeter applications
[NASA-TM-102210] 04 p0504 N90-12904
Practical systems for speckle velocimetry 05 p0574 N90-13341
Laser applications in supersonic unsteady flow 05 p0574 N90-13344
The 3D LDA techniques in vortex studies and boundary layer surveys 05 p0574 N90-13346
Reaction zone structure in supracompressed detonating explosives
[DE90-000832] 06 p0755 N90-14394
Laser velocimeter and total pressure measurements in circular-to-rectangular transition ducts
[NASA-CR-182286] 06 p0772 N90-14494
Solid fuel combustion chamber
[LR-555] 08 p1038 N90-16001
Miniature laser Doppler anemometer with a diode laser
[ISL-CO-224/88] 08 p1077 N90-16232
High frequency pulsed diode lasers and phase-coupled diode arrays for aerodynamics 08 p1078 N90-16238
Laser velocimeter seed particle sizing by the whisker particle collector and laser aerosol spectrometer methods
[PB90-111287] 09 p1224 N90-17103
Automation and extension of LDV (Laser-Doppler Velocimetry) measurements of off-design flow in a subsonic cascade wind tunnel
[AD-A216627] 11 p1506 N90-18670
Measurement of gas intensity at high dynamic pressures
[ISL-CO-204/89] 11 p1507 N90-18680
Laser-velocimeter-measured flow field around an advanced, swept, eight-blade propeller at Mach 0.8
[NASA-TP-2462] 14 p1909 N90-20942
LDV measurements and the flow analysis in the vortex region of a radial inflow turbine 14 p1922 N90-21007
Laser velocimeter measurements of multiphase flow of solids
[DE90-007604] 14 p1974 N90-21311
The optical measurement of acoustic velocity fields 14 p2023 N90-21601
Multi-axis, 3-D, scanning LDA (Laser Doppler Anemometer) system for unsteady aerodynamics
[AD-A218571] 16 p2197 N90-22541
An investigation of the three-dimensional flow field in a centrifugal compressor 16 p2235 N90-22751
Two-dimensional velocimetry instrumentation
[AD-A218450] 16 p2239 N90-22774
Three-dimensional laser velocimeter simultaneity detector
[NASA-CASE-ARC-11876-1] 19 p2696 N90-25340
Euler analysis comparison with LDV data for an advanced counter-rotation propfan at cruise
[NASA-TM-103249] 20 p2803 N90-25946
Combustion instrumentation 20 p2811 N90-25996
Ultra-fast visualization of a turbulent boundary layer by a laser velocimeter
[IMFL-89-37] 22 p3181 N90-28048
The effects of grid-generated turbulence on flat and concave turbulent boundary layers 23 p3324 N90-28797
Laser velocimetry 24 p3420 N90-29317
A method of determining a laser-velocimeter focal point and measuring its beam properties using a hot-wire anemometer
[NAL-TR-1043] 24 p3473 N90-29626

LASER FUSION

Microwave excitation of oxygen O2 (delta 1) for an oxygen-iodine laser
[DFVLR-FB-89-23] 04 p0506 N90-12919
The 17th AINSE Plasma Physics Conference: Conference handbook
[DE90-600936] 07 p0996 N90-15759
Development of KrF lasers for fusion
[DE90-007830] 11 p1515 N90-18726
Surface reactions of the TA6V titanium alloy under laser irradiation
[ETCA-90-R-012] 22 p3158 N90-27904
Sintering of ceramics by laser irradiation
[ETCA-89-R-134] 22 p3161 N90-27926
Evaluation of dynamic range for LLNL streak cameras using high contrast pulses and pulse podiatry on the Nova laser system
[DE90-015203] 24 p3472 N90-29620
A distributed control and monitor system used in laser fusion research
[DE90-011483] 24 p3549 N90-30078

LASER GEODYNAMIC SATELLITE

U LAGEOS (SATELLITE)

LASER GUIDANCE

A new technique for guiding of electron beams
[DE90-008660] 13 p1886 N90-20824
Design and performance analysis of adaptive optical telescopes using laser guide stars
[AD-A218025] 13 p1902 N90-20913

LASER GYROSCOPES

Miniaturized triaxial laser gyro 01 p0013 N90-10061
Hybrid angular velocity reference system for the investigation of dynamic properties of strapdown gryos
[DFVLR-FB-89-25] 04 p0450 N90-12577
The anatomy of the gyroscope, part 3
[AGARD-AG-313] 14 p1982 N90-21359
Laser gyros and field diagnostics
[AD-A220832] 17 p2406 N90-23709
Angle measurements using the laser gyro GG 1342
[DLR-FB-89-50] 18 p2555 N90-24579

Construction of a hybrid angular velocity reference system for investigation of the dynamic characteristics of strapdown gyros
[ESA-TT-1181] 19 p2694 N90-25332
Ring laser gyro principles and techniques
24 p3426 N90-29352
Use of a three-axis monolithic ring laser gyro and digital signal processor in an inertial sensor element
24 p3426 N90-29354
Ring laser gyro marine inertial navigation systems
24 p3426 N90-29355
Novel approaches to sensitivity enhancement of ring laser gyros
[AD-A224335] 24 p3471 N90-29617
On the technology for preparation of a HeNe discharge tube for use in a laser gyro
[DLR-MITT-90-01] 24 p3472 N90-29624

LASER HEATING
Lectures on x ray lasers
[ETN-89-95516] 04 p0506 N90-12917
Numerical simulation of the preheating by x rays in spherical plasmas 06 p0784 N90-14564
Migration of carbon in tempered martensitic steel during excimer laser melting
[DE90-004836] 09 p1195 N90-16922
Feasibility of using lasers and infrared heaters as UNREP icing countermeasures
[AD-A219031] 19 p2695 N90-25333
Nonlinear material response to very rapid energy deposition
[AD-A221932] 21 p2989 N90-26988
Unipolar arcing on the cathode surface of a high voltage diode
[AD-A224122] 23 p3322 N90-28787
Study of a 1-Hz hypocycloidal pinch (HCP) pump for production of ultraviolet lasers
[AD-A224091] 24 p3547 N90-30064

LASER INDUCED FLUORESCENCE
State-resolved reaction dynamics
[AD-A211613] 03 p0403 N90-12307
Measurement of pressure fluctuations in a resonant chamber with laser-induced iodine fluorescence
[ESA-TT-1123] 03 p0406 N90-12326
Fiber-optic sensors for composite cure analysis and lifetime nondestructive evaluation
[DE90-001739] 06 p0738 N90-14296
Solid-state fluorescence above 1000 C: Application to high-temperature laser thermometry
[DE90-000728] 06 p0789 N90-14594
Spatially-resolved, nonintrusive measurements in a nonreacting scramjet combustor using laser-induced iodine fluorescence 07 p0881 N90-15103
Surface thermometry of energetic materials by laser-induced fluorescence
[AD-A214423] 07 p0916 N90-15297
Kinetic studies following state-selective laser excitation
[DE90-003232] 07 p0935 N90-15415
Observation of atomic relaxation near an interface through detection of emitted fluorescence
[AD-A214308] 07 p0991 N90-15725
Demonstration of the feasibility of laser induced fluorescence for arc jet flow diagnostics
[NASA-CR-185595] 08 p1040 N90-16013
Advanced diagnostics for reacting flows
[AD-A215050] 09 p1217 N90-17060
Advanced diagnostics for reacting flows
[AD-A214795] 09 p1285 N90-17448
An investigation of flow structure, mixing and chemical reaction in combusting turbulent flows
[AD-A216739] 11 p1483 N90-18538
Fluorescence and elastic scattering from laser dye-filled capillaries
[AD-A217026] 11 p1484 N90-18540
Time resolved gain/loss studies under low and high power loading for the XeF C-A transition
[DE90-007506] 12 p1655 N90-19517
Development and utilization of new diagnostics for dense-phase pneumatic transport
[DE90-006787] 12 p1659 N90-19536
Development of a receiver for a space-based laser radar system
[AD-A215079] 12 p1665 N90-19566
Definition study of Laser Experimental Active Fluorsensor (LEAF)
[BCRS-88-18] 12 p1668 N90-19582
Development of a laser fluorosensor for the aircraft supported analysis of maritime toxic agents loads: Definition phase
[ETN-90-95320] 13 p1829 N90-20499
Reactive and anisotropic elastic scattering of highly laser-vibration-excited diatomic molecules
[MPIS-19/1988] 13 p1883 N90-20804
Saturated fluorescence measurements of the hydroxyl radical in laminar high-pressure flames
[NASA-CR-185218] 15 p2101 N90-22022
The 18th Informal Conference on Photochemistry
[AD-A219779] 17 p2373 N90-23510
A laser-induced fluorescence technique for measurement of slot-injected fluid concentration profiles in a plate turbulent boundary layer
[AD-A221388] 18 p2553 N90-24572
Temperature determination of shock layer using spectroscopic techniques 18 p2628 N90-24973
Excimer laser fragmentation studies of selected oximes: Nascent OH internal energy distributions and the search of H2CN fluorescence
[AD-A222622] 20 p2868 N90-26317
Development of Planar Laser-Induced Fluorescence (PLIF) techniques for supersonic flows
21 p2974 N90-26900
Advanced optical diagnostics in hypersonic research
21 p2975 N90-26905
Spectroscopy of ions and their clusters
[AD-A223109] 21 p2977 N90-26917
Experimental study of the Taylor-Goertler instability
[ETN-90-97447] 22 p3175 N90-28014
High pulse energy flashlamp pumpable laser dyes
[AD-A223075] 22 p3180 N90-28042
Detection of vibrationally excited H2(v double prime) for H(-) production
[AD-A222560] 22 p3180 N90-28044
A study of catalysts and mechanisms in synthesis reactions
[DE90-015064] 23 p3304 N90-28691
Study of the radical OH in a high pressure flame by resonant DRASC
[ONERA-RF-57/7131-PY] 23 p3305 N90-28692
Studies of vortex interactions
[AD-A223864] 23 p3328 N90-28817
Electron-beam fluorescence measurements in hypersonic flows 24 p3420 N90-29318
Applications of LIF to high speed flows
24 p3420 N90-29320
Laser induced fluorescence imaging applications
24 p3420 N90-29322
Laser induced fluorescence: Practical applications
24 p3421 N90-29323
Laser beam stop
[AD-D014595] 24 p3473 N90-29629
Pyrromethene-BF2 complexes as laser dyes
[AD-A223562] 24 p3473 N90-29631

LASER INTERFEROMETRY
Shortwavelength coherent radiation: Generation and applications
[AD-A209847] 01 p0074 N90-10427
Zeeman interferometry
[DE89-015296] 03 p0352 N90-12012
Remote detection of boundary-layer transition by an optical system 04 p0441 N90-12524
Doppler imagery for the visualisation of velocity fields
[ISL-CO-232/88] 09 p1226 N90-17114
Skin friction measurements by laser interferometry in supersonic flows 10 p1306 N90-17557
Optical interferometer in space
12 p1731 N90-19953
Optical interferometers for tests of relativistic gravity in space 12 p1734 N90-19967
Frequency stable high power lasers in space
12 p1734 N90-19969
Study on rotating plasma with submillimeter laser interferometer
[DE90-615387] 14 p2027 N90-21623
Experiments with a laser interferometric gravitational wave antenna 15 p2184 N90-22476
Analysis of phase retrieval in active imaging
[AD-A221080] 18 p2563 N90-24626
Coherent optical techniques for industrial inspection
[PNR90605] 20 p2927 N90-26654
Laser diagnostics of plasma thrusters
[AD-A221682] 21 p3079 N90-27506
Serial interferometric fiber-optic sensor array
[AD-D014466] 22 p3246 N90-28407
Velocity Interferometer System for Any Reflector (VISAR): Displacement mode data reduction
[DE90-015027] 23 p3395 N90-29184

LASER MATERIALS
New laser materials
[DE89-017524] 03 p0353 N90-12017
Development of microstructured DH diode lasers and detectors for the near and medium IR spectral domain using molecular beam epitaxy
[IPM-15/1988] 03 p0354 N90-12023
Tunable Solid State Lasers conference edition: Tunable Solid State Lasers Topical Meeting
[AD-A212292] 04 p0506 N90-12920
A review of laser filter materials
[AD-A213134] 05 p0648 N90-13776
Qualification of diode foil materials for excimer lasers
[DE90-000602] 06 p0789 N90-14593
Development of glass-ceramic lasers
[AD-A214146] 07 p0936 N90-15423
Host materials for transition-metal ions
[AD-A213605] 07 p1003 N90-15808
Spallation and dynamic fracture as an effect of laser induced shock waves in carbon based composite materials
[AD-A216540] 11 p1478 N90-18509
Properties and performance of the LiCaAlF6:Cr(3+) laser material
[DE90-007242] 11 p1516 N90-18728
Elimination of platinum inclusions in phosphate laser glasses
[DE90-004479] 12 p1629 N90-19361
Performance of zig-zag slab regenerative ring amplifier laser system
[DE90-006995] 13 p1806 N90-20371
Direct solar-pumped iodine laser amplifier
[NASA-CR-186442] 15 p2103 N90-22030
Beam combining by phase transition nonlinear media
[AD-A219301] 16 p2233 N90-22739
Comparison of solar pumped Nd:YAG and Nd:Cr:GSGG lasers at liquid nitrogen and room temperature
[DLR-FB-89-41] 16 p2240 N90-22781
Optical spectroscopy of Ti(3+) doped YAlO3
[AD-A219043] 16 p2324 N90-23251
Advanced technology in welding, materials processing and evaluation
[DE90-010799] 19 p2697 N90-25347
Theoretical studies of solar pumped lasers
[NASA-CR-186712] 20 p2867 N90-26308
Laser physics and laser spectroscopy
[AD-A224379] 24 p3473 N90-29628

LASER MODE LOCKING
Picosecond Laser Facility
[AD-A217784] 13 p1808 N90-20384
Development and applications of a coupled cavity sodium-chloride laser 15 p2102 N90-22029

LASER MODES
Energy conversion efficiency in high current Raman regime Free Electron Laser (FEL). 1: Single mode analysis
[DE90-719527] 09 p1227 N90-17120

LASER OUTPUTS
Laser initiation of secondary explosives
[DE89-010229] 01 p0075 N90-10431
Multiline multimode CW chemical laser performance
[AD-A210613] 01 p0075 N90-10432
Master oscillator with power amplifiers: Performance of a two-element CW HF phased-laser array
[AD-A211141] 01 p0076 N90-10435
Semiconductor quantum well lasers and related optoelectronic devices on silicon, III-V
[AD-A210758] 02 p0227 N90-11299
Acceleration of thin foil targets using fiber-coupled optical pulses
[DE89-016526] 02 p0275 N90-11569
Propagation of an elliptical laser beam through the turbulent atmosphere (vertical beams)
[PB89-208680] 03 p0352 N90-12010
Comparison of I2-stabilized HE-NE lasers
[PB89-219844] 03 p0352 N90-12014
Tunable Solid State Lasers conference edition: Tunable Solid State Lasers Topical Meeting
[AD-A212292] 04 p0506 N90-12920
Activities report in laser matter interactions
[ETN-90-95515] 06 p0782 N90-14544
The 17.1-GHz free-electron laser as a microwave source for TeV colliders
[DE90-001506] 07 p0934 N90-15406
Fiber optic sensing system
[NASA-CASE-LEW-14795-1] 07 p0992 N90-15733
Aspects of Raman scattering
[AD-A213926] 07 p0992 N90-15736
Defense to laser light irradiation
[AD-D014286] 08 p1036 N90-15984
Atomic processes in plasmas under ultra-intense laser irradiation
[DE90-003221] 08 p1126 N90-16521
Design principles of the LVT-2 model laser instrument for the measurement of visual characteristics
[AD-A214951] 09 p1228 N90-17124
Two dimensional modifications of Gaussian laser light bundles
[AD-A215207] 10 p1389 N90-18033
Long laser-pulse method of producing Y-Ba-Cu-O superconducting films
[DE90-005202] 10 p1436 N90-18289
A numerical solution to the Boltzmann equation for use in calculating pumping rates in a CO2 discharge laser
[AD-A216376] 11 p1514 N90-18718
Study of discharge mechanisms and the stability of transverse electric discharges in the gas mixtures
[ISL-R-114/88] 11 p1516 N90-18733
Narrow-bandwidth unstable laser resonator
[AD-D014362] 12 p1665 N90-19568
High power semiconductor laser arrays by metalorganic chemical vapor deposition 13 p1805 N90-20363

Strategies for high efficiency operation of the E-beam excited atomic xenon laser using high-power and high-energy loading
[DE90-005196] 13 p1806 N90-20370
Y1Ba2Cu3O(7-x) laser-ablation plume dynamics measurement by nanosecond response ion probe: Comparison with optical measurements
[DE90-007658] 13 p1807 N90-20375
Spatial imaging using confocal Fabry-Perot interferometers
[DE90-008363] 13 p1807 N90-20378
X ray laser with enhanced x ray gain through photodepopulation
[AD-D014448] 14 p1985 N90-21375
Cloud hole-boring with long pulse CO2 lasers
[DE90-008946] 14 p1985 N90-21377
Effect of atmospheric turbulence on electro-optical systems 15 p2086 N90-21940
Development of mid-infrared solid state lasers for spaceborne lidar
[NASA-CR-185095] 15 p2103 N90-22031
Experimental study of vortex ring interaction with a free surface 16 p2233 N90-22742
A free electron laser master oscillator power amplifier experiment 16 p2239 N90-22776
Contributions to the development of SLM TEA CO2 laser sources for high resolution molecular spectroscopy 16 p2240 N90-22778
Dynamics and instabilities in homogeneously broadened lasers
[AD-A218427] 16 p2241 N90-22786
The effects of wiggler errors on free electron laser performance
[AD-A220421] 17 p2409 N90-23725
Spectral properties of a 1.3-micrometers InGaAsP diode laser under modulation
[AD-A220066] 17 p2409 N90-23729
Proof of the feasibility of coherent and incoherent schemes for pumping a gamma-ray laser
[AD-A219972] 18 p2562 N90-24620
A user-friendly, menu-driven, language-free laser characteristics curves graphing program for desk-top IBM PC compatible computers 18 p2644 N90-25056
An investigation of a mathematical model of an optically pumped Ti(3+):Al2O3 laser system 18 p2646 N90-25063
A study of the influence of Hg(6(3)P2) population in a low-pressure discharge on mercury ion emission at 194.2 nm 20 p2853 N90-26223
DURIP: Instrumentation for laser switched power LINAC
[AD-A222629] 20 p2868 N90-26318
Novel laser gain and time-resolved FTIR studies of photochemistry 20 p2945 N90-26756
Beam combining of excimer lasers by stimulated Raman scattering
[AD-A222973] 21 p3008 N90-27099
Laser diode pumped, erbium-doped, solid state laser with high slope efficiency
[AD-D014482] 22 p3179 N90-28040
Design of a CO2 laser power control system for a Spacelab microgravity experiment
[NASA-TM-103112] 23 p3331 N90-28833

LASER PLASMA INTERACTIONS

Generation of 3/2 omega sub o radiation in inhomogeneous plasmas under the irradiation of intense electromagnetic waves
[DE89-015723] 01 p0126 N90-10722
Electron attachment and molecular fragmentation in laser-excited plasmas
[AD-A212098] 03 p0409 N90-12343
Lectures on x ray lasers
[ETN-89-95516] 04 p0506 N90-12917
Activities report in laser matter interactions
[ETN-90-95515] 06 p0782 N90-14544
Fast electrons in a laser generated plasma 06 p0782 N90-14545
Production of homogeneous plasmas for laser-plasma interaction experiments 06 p0782 N90-14546
Experimental study on the filamentary instability in laser-matter interactions at short wave lengths 06 p0782 N90-14547
Strong Langmuir turbulence and second harmonics in laser-matter interactions 06 p0782 N90-14548
Effects of temporal and induced spatial incoherence on parametric instabilities in laser plasma interactions 06 p0782 N90-14549
The supersonic anisotropic collapse of Langmuir waves 06 p0783 N90-14550
Aspects of field theory related to the Zakharov problem 06 p0783 N90-14551
Limitations in the growing of a plasma wave produced by heterodyning two lasers due to modulations and decay instabilities 06 p0783 N90-14552
Interaction of a low flux laser beam with a solid target 06 p0783 N90-14554
Box experiments. Nonlinear effects at plasma resonance 06 p0783 N90-14555
Experimental study of the shock waves generated by high energy laser pulses 06 p0784 N90-14557
Measurement of the high density zone of a plasma target by absorption spectroscopy 06 p0784 N90-14560
Time integrated study of spectral emission in the X-UV domain at the outlet of a laser shock, at the back of single or double foil targets 06 p0784 N90-14561
Measurement of the X-UV emission from the back face of thin foils illuminated by an A4 omega laser 06 p0784 N90-14562
X ray shadowscopy in implosion experiments 06 p0784 N90-14563
Modification of ionic population by non-Maxwellian effects 06 p0785 N90-14565
Atomic structure and spectral perturbations in hot dense plasmas 06 p0785 N90-14567
The average ion model. Computation of the absorption and emission coefficients in hot plasmas 06 p0785 N90-14569
XRAD: A one dimensional Lagrangian code with radiative transport 06 p0785 N90-14570
Population inversions calculated for lithium-like ions in a plasma 06 p0786 N90-14571
Study of lithium-like ions for amplifying radiation below 100 angstroms. Experiment at the Rutherford Appleton Laboratory 06 p0786 N90-14572
Single beam interactions for the study of x ray lasers 06 p0786 N90-14573
X-UV amplification in a plasma column of five centimeters. Five beams experiment 06 p0786 N90-14574
Characteristics of an x ray source created by a laser plasma 06 p0786 N90-14575
Laser activities 06 p0786 N90-14576
Development of X diagnostics with 1 Gw laser pulses 06 p0786 N90-14578
Tomographic imagery by multislot coding applied to x ray diagnostics of laser plasmas: Implementation of a direct electronic detection camera 06 p0787 N90-14579
Computer simulation of laser plasma interaction
[DE90-002828] 07 p0994 N90-15748
Laser-matter interaction at intensities of 10(sup 12) W/cm(sup 2) and below
[DE90-007536] 12 p1669 N90-19590
The 41st Annual Gaseous Electronics Conference
[AD-A214540] 12 p1715 N90-19851
Activities report of the Institute for Plasma Research
[ETN-90-96467] 16 p2319 N90-23225
Unipolar arcing on the cathode surface of a high voltage diode
[AD-A224122] 23 p3322 N90-28787
Studies of central interactions of Si ions at 14.5 x A GeV/c in Au and Cu
[DE90-015095] 23 p3397 N90-29195
Experimental studies leading to energy storage. Spectroscopy and dynamics of polyatomic hydrogen in liquid, solid and gaseous hydrogen plasmas
[AD-A224343] 24 p3547 N90-30066
Experimental observations of nonlinear effects in laser-plasma interactions
[DE90-015195] 24 p3549 N90-30079

LASER PLASMAS

X-ray lithography studies of polysilane using a laser plasma X-ray source
[DE89-015390] 01 p0047 N90-10266
Shortwavelength coherent radiation: Generation and applications
[AD-A209847] 01 p0074 N90-10427
Generation of 3/2 omega sub o radiation in inhomogeneous plasmas under the irradiation of intense electromagnetic waves
[DE89-015723] 01 p0126 N90-10722
Determination of neutral particle concentration at erosion laser plasma expansion into vacuum
[DE89-620128] 02 p0228 N90-11308
Switched power workshop: Introduction and summary
[DE90-000036] 03 p0342 N90-11952
Temporal and spatial filtering remedies for dispersion in electromagnetic particle codes
[DE89-017534] 03 p0408 N90-12337
Liquid and solid ion plasmas
[AD-A212415] 04 p0557 N90-13244
Activities report in laser matter interactions
[ETN-90-95515] 06 p0782 N90-14544
Fast electrons in a laser generated plasma 06 p0782 N90-14545
Production of homogeneous plasmas for laser-plasma interaction experiments 06 p0782 N90-14546
Experimental study on the filamentary instability in laser-matter interactions at short wave lengths 06 p0782 N90-14547
Strong Langmuir turbulence and second harmonics in laser-matter interactions 06 p0782 N90-14548
Effects of temporal and induced spatial incoherence on parametric instabilities in laser plasma interactions 06 p0782 N90-14549
The supersonic anisotropic collapse of Langmuir waves 06 p0783 N90-14550
Aspects of field theory related to the Zakharov problem 06 p0783 N90-14551
Limitations in the growing of a plasma wave produced by heterodyning two lasers due to modulations and decay instabilities 06 p0783 N90-14552
Use of plasmas for the acceleration of particles to very high energy 06 p0783 N90-14553
Interaction of a low flux laser beam with a solid target 06 p0783 N90-14554
Box experiments. Nonlinear effects at plasma resonance 06 p0783 N90-14555
Measurement of the high density zone of a plasma target by absorption spectroscopy 06 p0784 N90-14560
Time integrated study of spectral emission in the X-UV domain at the outlet of a laser shock, at the back of single or double foil targets 06 p0784 N90-14561
Measurement of the X-UV emission from the back face of thin foils illuminated by an A4 omega laser 06 p0784 N90-14562
X ray shadowscopy in implosion experiments 06 p0784 N90-14563
Numerical simulation of the preheating by x rays in spherical plasmas 06 p0784 N90-14564
Modification of ionic population by non-Maxwellian effects 06 p0785 N90-14565
Anisotropy of electron distributions related to the anisotropy and polarization of the continuous emitted x rays 06 p0785 N90-14566
Transversal inhomogeneity and radiative transfer in plasmas obtained by laser impact 06 p0785 N90-14568
The average ion model. Computation of the absorption and emission coefficients in hot plasmas 06 p0785 N90-14569
XRAD: A one dimensional Lagrangian code with radiative transport 06 p0785 N90-14570
Population inversions calculated for lithium-like ions in a plasma 06 p0786 N90-14571
Study of lithium-like ions for amplifying radiation below 100 angstroms. Experiment at the Rutherford Appleton Laboratory 06 p0786 N90-14572
Single beam interactions for the study of x ray lasers 06 p0786 N90-14573
X-UV amplification in a plasma column of five centimeters. Five beams experiment 06 p0786 N90-14574
Characteristics of an x ray source created by a laser plasma 06 p0786 N90-14575
Laser activities 06 p0786 N90-14576
Trapezoidal crystal in the six beam implosion 06 p0786 N90-14577
Development of X diagnostics with 1 Gw laser pulses 06 p0786 N90-14578
Tomographic imagery by multislot coding applied to x ray diagnostics of laser plasmas: Implementation of a direct electronic detection camera 06 p0787 N90-14579
Development of X diagnostics around the pulse 1 laser 06 p0787 N90-14580
The search for solid state fusion lasers
[DE89-012301] 07 p0934 N90-15410
Computer simulation of laser plasma interaction
[DE90-002828] 07 p0994 N90-15748
Atomic processes in plasmas under ultra-intense laser irradiation
[DE90-003221] 08 p1126 N90-16521
Workshop on Hydrogen Effects in InP and Related Compounds
[AD-A215197] 09 p1290 N90-17479
Generation of axial and lateral magnetic fields in laser produced plasmas
[DE90-607470] 10 p1432 N90-18260
Proceedings of a contractors meeting on Combustion Rocket Propulsion Diagnostics of Reacting Flow
[AD-A216445] 12 p1617 N90-19297
Two-meter laser material response impulse measurements
[AD-A215834] 12 p1665 N90-19567
The 41st Annual Gaseous Electronics Conference
[AD-A214540] 12 p1715 N90-19851
Characterization of ground state neutral and ion transport during laser ablation of 1:2:3 superconductors by transient optical absorption spectroscopy
[DE90-006623] 12 p1720 N90-19878
Laser-produced plasmas in medicine
[DE90-007623] 13 p1891 N90-20849
Time-resolved spectroscopy of nonequilibrium ionization in laser-produced plasmas
[DE90-008663] 13 p1891 N90-20854
X ray laser with enhanced x ray gain through photodepopulation
[AD-D014448] 14 p1985 N90-21375

Experimental study of population inversion and spectral line broadening in a plasma containing a mixture of high Z and low Z ions
[DE90-007552] 14 p2027 N90-21622
Nonlinear spectroscopy of multicomponent droplets and 2- and 3-dimensional measurements in flames
[AD-A218567] 16 p2215 N90-22636
System analysis and project of a laser-moved spaceship
[ILR-MITT-232(1989)] 18 p2513 N90-24348
DURIP: Spontaneous Raman system for the study of enhanced combustion and non-thermal plasmas
[AD-A221410] 18 p2564 N90-24629
Soft x ray resist characterization: Studies with a laser plasma x ray source
[DE90-013493] 20 p2928 N90-26661
Support for the Forty-Second Annual Gaseous Electronics Conference
[AD-A222881] 21 p3073 N90-27473
Quantitative spectroscopy of x ray laser plasmas in pulsed power devices
[AD-A221964] 21 p3078 N90-27501
Laser diagnostics of plasma thrusters
[AD-A221682] 21 p3079 N90-27506
Unipolar arcing on the cathode surface of a high voltage diode
[AD-A224122] 23 p3322 N90-28787
Studies of central interactions of Si ions at 14.5 x A GeV/c in Au and Cu
[DE90-015095] 23 p3397 N90-29195
Study of a 1-Hz hypocycloidal pinch (HCP) pump for production of ultraviolet lasers
[AD-A224091] 24 p3547 N90-30064
Experimental observations of nonlinear effects in laser-plasma interactions
[DE90-015195] 24 p3549 N90-30079
UCD-LLNL collaboration on basic plasma physics research in inertial confinement fusion
[DE90-015771] 24 p3549 N90-30081
Soft x ray contact imaging of biological specimens using a laser-produced plasma as an x ray source
[DE90-016098] 24 p3549 N90-30082
Soft x ray emission spectra from laser-irradiated high-Z targets
[AD-A223552] 24 p3552 N90-30099

LASER POWER BEAMING
Second Beamed Space-Power Workshop
[NASA-CP-3037] 01 p0027 N90-10140
Power beaming options 01 p0027 N90-10142
New energy conversion techniques in space, applicable to propulsion
[AIAA-79-1338] 01 p0028 N90-10145
Laser energy conversion 01 p0029 N90-10152
Overview of laser concepts 01 p0029 N90-10154
Laser-powered lunar base 01 p0029 N90-10156
Laser-powered Martian rover 01 p0029 N90-10157
Low-earth-orbit to low-lunar-orbit laser freighter 01 p0030 N90-10160
Earth orbit laser systems 01 p0030 N90-10162
Laser diode array and transmission optics 01 p0030 N90-10163
Laser thruster 01 p0030 N90-10164
The Solar Power Satellite (SPS): Progress so far 07 p1008 N90-15840
Solar-pumped laser for free space power transmission 15 p2061 N90-21604
Diode laser satellite systems for beamed power transmission
[NASA-TP-2992] 18 p2556 N90-24585
Characterization of a high-intensity, subpicosecond XeCl laser system
[DE90-011970] 20 p2867 N90-26310
Potential of solar-simulator-pumped alexandrite lasers
[NASA-TM-102701] 22 p3180 N90-28046

LASER PROPULSION
Second Beamed Space-Power Workshop
[NASA-CP-3037] 01 p0027 N90-10140
Power beaming options 01 p0027 N90-10142
Laser propulsion to earth orbit. Has its time come? 01 p0028 N90-10143
Laser energy conversion 01 p0029 N90-10152
Overview of laser concepts 01 p0029 N90-10154
Low-earth-orbit to low-lunar-orbit laser freighter 01 p0030 N90-10160
Laser propulsion option 01 p0030 N90-10161
Earth orbit laser systems 01 p0030 N90-10162
Laser thruster 01 p0030 N90-10164
NASA/USRA advanced space design program: The laser powered interorbital vehicle
[NASA-CR-186044] 04 p0462 N90-12646
Proceedings of the High Energy Density Matter (HEDM) Conference
[AD-A212314] 05 p0629 N90-13670
Laser-supported detonation waves and pulsed laser propulsion
[DE90-002753] 07 p0935 N90-15412
Proceedings of Air Force Office of Scientific Research workshop on Laser Propulsion
[AD-A216563] 12 p1666 N90-19569
Project LOCOST: Laser or Chemical Hybrid Orbital Space Transport
[NASA-CR-186822] 20 p2819 N90-26042
Aspects of acoustic noise generation by a laser-propelled vehicle
[DE90-012087] 21 p2964 N90-26851

LASER PUMPING
Overview of laser concepts 01 p0029 N90-10154
Efficient nonlinear conversion of laser diode pumped miniature solid state laser sources
[AD-A210708] 01 p0075 N90-10433
Photodissociation of XeF2 (xenon difluoride) at 193 nm
[AD-A211663] 04 p0506 N90-12916
Tunable Solid State Lasers conference edition: Tunable Solid State Lasers Topical Meeting
[AD-A212292] 04 p0506 N90-12920
Proof of the feasibility of coherent and incoherent schemes for pumping a gamma-ray laser
[AD-A212882] 04 p0507 N90-12924
Development of mid-infrared solid state lasers for spaceborne lidar
[NASA-CR-183290] 05 p0647 N90-13772
An experimental analysis of the waveguide modes in a high-gain free-electron laser amplifier 05 p0648 N90-13779
Eurolaser CO2 laser
[ETN-90-95907] 06 p0787 N90-14582
Optical nutation in polymers irradiated by ultrashort laser pulses
[AD-A212927] 10 p1357 N90-17869
The gamma-ray laser project: Proof of the feasibility of coherent and incoherent schemes for pumping a gamma-ray laser
[AD-A216008] 10 p1389 N90-18037
Diode pumped monolithic Nd:YLF 1.053 micron mini-laser and its application to injection seeding
[DE90-005323] 10 p1390 N90-18040
High efficiency flashlamp-pumped titanium: Sapphire laser
[AD-A217598] 13 p1806 N90-20367
Flash-pumped titanium laser
[AD-A217599] 13 p1806 N90-20368
Picosecond Laser Facility
[AD-A217784] 13 p1808 N90-20384
Picosecond nonlinear studies of complex materials using the free electron laser
[AD-A218215] 13 p1809 N90-20387
Crystallography, spectroscopic analysis, and lasing properties of Nd3+:Y3Sc2Al3O12
[AD-A217792] 13 p1897 N90-20891
Progress in the material development of LiCaAlF(6):Cr(3+) laser crystals
[DE90-009542] 14 p2034 N90-21666
Direct solar-pumped iodine laser amplifier
[NASA-CR-186442] 15 p2103 N90-22030
Development of mid-infrared solid state lasers for spaceborne lidar
[NASA-CR-185095] 15 p2103 N90-22031
Modeling of thermal lensing in side and end-pumped finite solid-state laser rods
[NASA-CR-4300] 17 p2407 N90-23716
Characterization of a Ho:Tm:Cr:YAG laser with a Cr:GSAG laser as pumping source 18 p2642 N90-25047
Diode laser-pumped solid-state lasers: A breakthrough in modern laser technology
[MBB-Z-0276/89-PUB] 19 p2649 N90-25077
A room-temperature, laser diode-pumped, Q-switched, 2 micron, thulium-doped, solid state laser
[AD-D014527] 19 p2695 N90-25334
Diode laser pumped single mode 1.3 microns Nd:YALO microlaser
[AD-A223036] 21 p3008 N90-27100
A solid-state multiple-pass amplifier for diode pumped coherent laser radar systems
[AD-A222537] 21 p3009 N90-27104
Study of short-lived unstable nuclei by means of laser optical pumping
[AD-A222561] 21 p3009 N90-27105
Laser diode pumped, erbium-doped, solid state laser with high slope efficiency
[AD-D014482] 22 p3179 N90-28040
High pulse energy flashlamp pumpable laser dyes
[AD-A223075] 22 p3180 N90-28042
A tunable, continuous wave, thulium-doped, solid state laser cross-reference to related application
[AD-D014558] 22 p3180 N90-28045

LASER RADAR
U OPTICAL RADAR

LASER RADIATION
U LASER BEAMS

LASER RANGE FINDERS
The 1988 year end report for road following at Carnegie-Mellon
[NASA-CR-185967] 01 p0078 N90-10446
The recovery of orbital and geophysical parameters using a spaceborne laser ranging system 02 p0226 N90-11294
Calibration of a visioceilometer, a hand held lidar system
[FEL-1988-73] 03 p0374 N90-12137
A closer look at the visioceilometer
[FEL-1989-80] 03 p0374 N90-12138
China-built airborne synchronous laser ranger the new L-8 jet trainer aircraft
[AD-A213835] 07 p0936 N90-15422
Lidar instruments proposed for Eos 21 p3016 N90-27145
Eos visible imagers 21 p3016 N90-27146
HERMIES-3: A step toward autonomous mobility, manipulation, and perception 23 p3374 N90-29065

LASER RANGER/TRACKER
On-line range prediction system, part 2
[NASA-CR-185889] 05 p0647 N90-13771
Outline on the future Italian transportable laser ranging station
[CISE-4845] 05 p0649 N90-13782

LASER SPECTROMETERS
Forty-fourth symposium on molecular spectroscopy
[AD-A210752] 02 p0195 N90-11111
Far-infrared heterodyne receivers 05 p0597 N90-13465
Laser velocimeter seed particle sizing by the whisker particle collector and laser aerosol spectrometer methods
[PB90-111287] 09 p1224 N90-17103
Fluorescence and elastic scattering from laser dye-filled capillaries
[AD-A217026] 11 p1484 N90-18540
A laser spectrometer and wavemeter for pulsed lasers
[NASA-CR-181731] 23 p3331 N90-28832
Infrared spectroscopic measurements on planetary atmospheric gases 23 p3412 N90-29283

LASER SPECTROSCOPY
NT OPTOGALVANIC SPECTROSCOPY
Laser Raman spectroscopy: A literature review
[FOA-C-20753-2.3] 02 p0196 N90-11121
Nonlinear optical studies of resonant systems
[AD-A211032] 02 p0227 N90-11301
Growth and characterization of materials for tunable lasers in the near infrared spectral region
[NASA-CR-185832] 03 p0352 N90-12009
Laser ionization mass spectroscopy
[DE89-008039] 03 p0352 N90-12015
Laser Raman spectroscopy in studies of corrosion and electrocatalysis
[DE90-001414] 06 p0741 N90-14311
Mapping of upper electronic reaction surfaces by tuned laser photolysis and by absorption and emission spectroscopies
[DE90-000125] 06 p0741 N90-14314
Studies of neutral and ion transport during laser ablation of 1:2:3 superconductors by optical absorption spectroscopy
[DE90-001968] 06 p0790 N90-14604
The production and spectroscopy of molecular ions isolated in solid neon
[AD-A213723] 07 p0895 N90-15174
Determination of the minimum energy conformation of alkyl substituted pyrazines
[AD-A216974] 11 p1484 N90-18539
Persistant spectral hole-burning: Photon-gating and fundamental statistical limits
[AD-A216084] 11 p1501 N90-18640
Ultrasensitive laser spectroscopy in solids: Single-molecule detection
[AD-A216085] 11 p1514 N90-18716
VUV (Vacuum Ultraviolet) laser diagnostics of H(-) ion sources
[DE90-006072] 11 p1514 N90-18719
Generation of intensive UV laser radiation and utilization in high resolution spectroscopy of SO2
[ETN-90-95361] 12 p1668 N90-19581
Definition study of Laser Experimental Active Fluorsensor (LEAF)
[BCRS-88-18] 12 p1668 N90-19582
A ground state depleted laser in neodymium doped yttrium orthosilicate
[DE90-006773] 12 p1668 N90-19586
Assessment of research needs for laser technologies applied to advanced spectroscopic methods
[DE90-007402] 12 p1669 N90-19588

Characterization of ground state neutral and ion transport during laser ablation of 1:2:3 superconductors by transient optical absorption spectroscopy
[DE90-006623] 12 p1720 N90-19878
Pulsed laser photothermal spectroscopy of liquids and solids
[DE90-008642] 13 p1808 N90-20380
Picosecond laser study of polyatomic molecules
[DE90-008647] 13 p1808 N90-20381
Transient effects in Brillouin gain spectroscopy in solids
[DE90-009476] 15 p2067 N90-21839
Reactions of N2A3 sigma u + and candidates for short wavelengths lasers
[DE90-009514] 15 p2103 N90-22033
Injection-seeded Nd:YAG laser linewidth measurement using saturation spectroscopy in iodine
[DE90-009537] 15 p2103 N90-22034
Evaluating thermographic phosphors in an operating turbine engine
[DE90-004874] 15 p2105 N90-22044
Scanning laser photocurrent spectroscopy of electrochemically grown bismuth sulphide films
[AERE-M-3709] 16 p2217 N90-22649
Time-resolved surface structural study by picosecond reflection high-energy electron diffraction
[AD-A218417] 16 p2228 N90-22712
Informal conference on the Chemistry of Energetic Azides, Isocyanates, and Related Species
[AD-A219825] 17 p2373 N90-23514
Monitoring of catalyst performance in CO2 lasers using frequency modulation spectroscopy with diode lasers
18 p2561 N90-24614
IR transition moments and collisional dynamics of vibrationally excited OH radicals via time-resolved laser absorption spectroscopy
[AD-A221005] 18 p2580 N90-24696
A study of the influence of Hg(6(3)P2) population in a low-pressure discharge on mercury ion emission at 194.2 nm 20 p2853 N90-26223
Novel laser gain and time-resolved FTIR studies of photochemistry 20 p2945 N90-26756
Methane overtone absorption by intracavity laser spectroscopy 20 p2946 N90-26762
Ultrasensitive laser spectroscopy in solids: Statistical fine structure and single-molecule detection
[AD-A222391] 21 p3074 N90-27477
Laser spectroscopy of plasmas
[AD-A221978] 21 p3078 N90-27502
Optoelectronics Research Center
[AD-A221926] 22 p3246 N90-28410
Proceedings of the 45th Ohio State University Symposium on Molecular Spectroscopy
[AD-A224349] 24 p3445 N90-29457
Examinations of hyperfine structure and isotope displacement of the elements gadolinium and europium with laser fluorescence and two photon spectroscopy
[ETN-90-97312] 24 p3447 N90-29468
Laser physics and laser spectroscopy
[AD-A224379] 24 p3473 N90-29628
Pyrromethene-BF2 complexes as laser dyes
[AD-A223562] 24 p3473 N90-29631
Proceedings of the High Energy Density Materials Contractors Conference
[AD-A223793] 24 p3484 N90-29695

LASER STABILITY

Effect of a random wind field on thermal blooming instabilities
[DE90-007241] 11 p1532 N90-18823
Noise behavior of semiconductor lasers by optic feedback
[ETN-90-95728] 12 p1668 N90-19583
Electronic and ionic transport in processable conducting polymers
[AD-A218093] 13 p1782 N90-20229
Measurement of the stimulated thermal Rayleigh scattering instability
[DE90-007849] 13 p1807 N90-20376
Laser line transport with refraction
[DE90-008683] 13 p1808 N90-20382
Experiments with a laser interferometric gravitational wave antenna 15 p2184 N90-22476
Dynamics and instabilities in homogeneously broadened lasers
[AD-A218427] 16 p2241 N90-22786
Electron beam pumped XeF(C yields A) laser scaling
[AD-A220022] 17 p2409 N90-23728
Stability of laser oscillator systems
18 p2641 N90-25045
Mode-medium instability and its correction with a Gaussian reflectivity mirror
[NASA-TP-3023] 19 p2758 N90-25673

LASER TARGET INTERACTIONS

Experimental study of the shock waves generated by high energy laser pulses 06 p0784 N90-14557
Effects produced by pulsed CO2 lasers
[ISL-R-112/88] 11 p1516 N90-18731
Two-meter laser material response impulse measurements
[AD-A215834] 12 p1665 N90-19567
Short wavelength laser/materials interactions
[AD-A218015] 13 p1808 N90-20386

LASER TARGETS

Activities report in laser matter interactions
[ETN-90-95515] 06 p0782 N90-14544
Fast electrons in a laser generated plasma
06 p0782 N90-14545
Production of homogeneous plasmas for laser-plasma interaction experiments 06 p0782 N90-14546
Experimental study on the filamentary instability in laser-matter interactions at short wave lengths
06 p0782 N90-14547
Strong Langmuir turbulence and second harmonics in laser-matter interactions 06 p0782 N90-14548
Effects of temporal and induced spatial incoherence on parametric instabilities in laser plasma interactions
06 p0782 N90-14549
Interaction of a low flux laser beam with a solid target
06 p0783 N90-14554
Experimental study of the shock waves generated by high energy laser pulses 06 p0784 N90-14557
Microstructure induced by laser shock in an austenitic steel 06 p0784 N90-14558
Dynamic sintering of metallic powders by laser shock
06 p0784 N90-14559
Measurement of the high density zone of a plasma target by absorption spectroscopy 06 p0784 N90-14560
Time integrated study of spectral emission in the X-UV domain at the outlet of a laser shock, at the back of single or double foil targets 06 p0784 N90-14561
Measurement of the X-UV emission from the back face of thin foils illuminated by an A4 omega laser
06 p0784 N90-14562
X ray shadowscopy in implosion experiments
06 p0784 N90-14563
Modification of ionic population by non-Maxwellian effects 06 p0785 N90-14565
Transversal inhomogeneity and radiative transfer in plasmas obtained by laser impact
06 p0785 N90-14568
The average ion model. Computation of the absorption and emission coefficients in hot plasmas
06 p0785 N90-14569
Population inversions calculated for lithium-like ions in a plasma 06 p0786 N90-14571
Study of lithium-like ions for amplifying radiation below 100 angstroms. Experiment at the Rutherford Appleton Laboratory 06 p0786 N90-14572
Single beam interactions for the study of x ray lasers
06 p0786 N90-14573
X-UV amplification in a plasma column of five centimeters. Five beams experiment
06 p0786 N90-14574
Characteristics of an x ray source created by a laser plasma 06 p0786 N90-14575
Development of X diagnostics with 1 Gw laser pulses
06 p0786 N90-14578
NTES (Nuclear Test and Experimental Sciences) program laser facility for physics experiments Building 391 High Bay Option
[DE90-001795] 07 p0935 N90-15411
Studies of density distributions in one-dimensional shock-induced debris clouds
[DE90-004089] 08 p1085 N90-16282
Effect of barrier layers in burn-through experiments with 351-nm laser illumination
[DE90-006806] 12 p1667 N90-19577
Improved energy and power balance at Nova targets
[DE90-007260] 13 p1807 N90-20372
Shaped pulses from Nova for inertial confinement fusion experiments
[DE90-007261] 13 p1807 N90-20373
LLE review
[DE90-008958] 14 p1985 N90-21378
Experimental study of population inversion and spectral line broadening in a plasma containing a mixture of high Z and low Z ions
[DE90-007552] 14 p2027 N90-21622
Laser Program of the Lawrence Livermore National Laboratory
[DE90-008198] 16 p2240 N90-22779
Effect of laser glare and aircraft windscreen on visual search performance under low ambient lighting
[AD-A219456] 17 p2437 N90-23888
Analysis of phase retrieval in active imaging
[AD-A221080] 18 p2563 N90-24626
High pulse energy flashlamp pumpable laser dyes
[AD-A223075] 22 p3180 N90-28042
Soft x ray emission spectra from laser-irradiated high-Z targets
[AD-A223552] 24 p3552 N90-30099

LASER WEAPONS

Stimulated rotational Raman scattering
[DE89-016427] 01 p0075 N90-10430
Laser techniques for ground to air applications
[FOA-C-30524-3.1] 02 p0228 N90-11309
Assessment of space power related measurement requirements of the Strategic Defense Initiative
[PB89-209357] 02 p0236 N90-11343
Overview of defense applications of ICF (Inertial Confinement Fusion)
[DE90-005745] 10 p1433 N90-18269
Field evaluation of laser protective eyewear
[AD-A221324] 18 p2586 N90-24725

LASER WELDING

NT BRAZING
NT FUSION WELDING
NT GAS WELDING
Automation of fiber-optic pigtailing process: Laser welding demonstration program
[AD-A210351] 01 p0123 N90-10707
Heat treatment of pulsed Nd: YAG laser welds in a Ti-14.8 wt pct Al-21.3 wt pct Nb titanium aluminide
[DE90-003484] 07 p0905 N90-15228
Power beam technology at Los Alamos: A review of research and development activities
[DE90-009002] 22 p3182 N90-28057

LASERS

NT AIRBORNE LASERS
NT ARGON LASERS
NT ATMOSPHERIC LASERS
NT CARBON DIOXIDE LASERS
NT CARBON LASERS
NT CARBON MONOXIDE LASERS
NT CHEMICAL LASERS
NT CONTINUOUS WAVE LASERS
NT DISTRIBUTED FEEDBACK LASERS
NT DYE LASERS
NT EXCIMER LASERS
NT FREE ELECTRON LASERS
NT GALLIUM ARSENIDE LASERS
NT GAMMA RAY LASERS
NT GAS LASERS
NT GASDYNAMIC LASERS
NT GLASS LASERS
NT HELIUM-NEON LASERS
NT HF LASERS
NT HIGH POWER LASERS
NT INFRARED LASERS
NT INJECTION LASERS
NT IODINE LASERS
NT KRYPTON FLUORIDE LASERS
NT METAL VAPOR LASERS
NT NEODYMIUM LASERS
NT NOVA LASER SYSTEM
NT NUCLEAR PUMPED LASERS
NT ORGANIC LASERS
NT PULSED LASERS
NT Q SWITCHED LASERS
NT RAMAN LASERS
NT RARE GAS-HALIDE LASERS
NT RING LASERS
NT RUBY LASERS
NT SEMICONDUCTOR LASERS
NT SOLAR-PUMPED LASERS
NT SOLID STATE LASERS
NT SPACEBORNE LASERS
NT TEA LASERS
NT TUNABLE LASERS
NT ULTRASHORT PULSED LASERS
NT ULTRAVIOLET LASERS
NT WAVEGUIDE LASERS
NT X RAY LASERS
NT XENON CHLORIDE LASERS
NT XENON FLUORIDE LASERS
NT YAG LASERS
NTES laser facility for physics experiments: Building 381 high bay option
[DE89-014326] 01 p0074 N90-10428
Custom diffraction gratings
[AD-A211002] 01 p0124 N90-10712
Laser grooved and polycrystalline silicon solar cell research
[DE89-015196] 02 p0237 N90-11347
International workshop on Beam Injection Assessment of Defects in Semiconductors
[AD-A210842] 02 p0283 N90-11617
Apollo lightcraft project
[NASA-CR-186055] 04 p0464 N90-12655
Monolithic laser diode structure for microwave generation
[AD-D014210] 06 p0782 N90-14543
Numerical simulation of laser radiation propagation in non-uniform absorbing medium. Geometrical optics approximation
[DE89-632014] 06 p0787 N90-14585

Laser probing non-cylindrical Z-pinch in near-isolator region of a discharged chamber
[DE89-632018] 06 p0844 N90-14912
Starlight: A stationary inertial-confinement-fusion reactor with nonvaporizing walls
[DE90-002315] 06 p0847 N90-14927
High power density spray cooling
[AD-A213575] 07 p0930 N90-15386
NTES (Nuclear Test and Experimental Sciences) program laser facility for physics experiments Building 391 High Bay Option
[DE90-001795] 07 p0935 N90-15411
Optical guiding by plasma waves in the plasma beat wave accelerator
[AD-A214288] 07 p0997 N90-15763
Innovative optoelectronic materials and structures using OMVPE
[AD-A214192] 07 p1004 N90-15815
Interfacial and thin film chemistry in electron device fabrication
[AD-A214784] 09 p1289 N90-17473
Design of a power supply system based in two quasi-resonant converters 10 p1306 N90-17728
Laser diffraction particle sizing: Instrument probe volume relocation and elongation
[NASA-TM-102512] 10 p1387 N90-18025
Diode pumped monolithic Nd:YLF 1.053 micron mini-laser and its application to injection seeding
[DE90-005323] 10 p1390 N90-18040
Performance and modeling of superconducting ring resonators at millimeter-wave frequencies
[NASA-TM-102526] 11 p1500 N90-18634
A high optical density measuring spectrometer
[AD-D014331] 12 p1621 N90-19318
Effect of barrier layers in burn-through experiments with 351-nm laser illumination
[DE90-006806] 12 p1667 N90-19577
Atmospheric thermal blooming and beam clearing by aerosol vaporization
[DE90-006271] 12 p1690 N90-19711
High efficiency flashlamp-pumped titanium: Sapphire laser
[AD-A217598] 13 p1806 N90-20367
Laser line transport with refraction
[DE90-008683] 13 p1808 N90-20382
Observation of nonlinear reflectivity from InSb surface and optical switching application
[AD-A217184] 13 p1887 N90-20826
Apparatus and method for locating the axis of symmetry (center of circular cross section) of three dimensional objects
[AD-D014407] 14 p1982 N90-21354
LLE review
[DE90-008958] 14 p1985 N90-21378
Laser studies of chemical dynamics at the gas-solid interface
[DE90-008698] 14 p1986 N90-21380
Space power generation and distribution
[DE90-008678] 14 p2002 N90-21474
JPRS report: Science and technology. USSR: Physics and mathematics
[JPRS-UPM-90-002] 14 p2022 N90-21593
A simplified theoretical model for the laser-induced optogalvanic effect
[DE90-613121] 14 p2028 N90-21626
Relativistic stimulated Brillouin and Raman scattering in a laser-produced plasma
[DE90-613123] 14 p2028 N90-21627
Army War College final prototype optical disk system testing and evaluation report
[DE90-008852] 14 p2036 N90-21685
Research programs in aeronautical engineering, solid state physics, and materials science at Technion-Israel Institute of Technology, Haifa, Israel
[EOARD-LR-89-068] 14 p2044 N90-21720
Growth and patterning of laser ablated superconducting YBa2Cu3O7 films on LaAlO3 substrates
[NASA-TM-102436] 15 p2173 N90-22421
International science and technology policies: Testimony before the Subcommittee on International Scientific Cooperation, Committee on Science, Space, and Technology, United States House of Representatives
[DE90-009416] 15 p2181 N90-22463
Faster simulation plots 16 p2295 N90-23071
Fellowship in physics/modern optics and quantum electronics
[AD-A218772] 17 p2469 N90-24111
MIT (Massachusetts Institute of Technology) short-wavelength laser project
[DE90-008975] 18 p2562 N90-24619
Phase locking of two HIQ resonators
[AD-A221123] 18 p2563 N90-24627
Light-millimeter wave interactions in semiconductor devices
[AD-A221214] 18 p2623 N90-24943
A user-friendly, menu-driven, language-free laser characteristics curves graphing program for desk-top IBM PC compatible computers 18 p2644 N90-25056
Lunar orbiting microwave beam power system
[NASA-TM-103211] 19 p2667 N90-25173
Expanded damage test facilities at LLNL
[DE90-011466] 19 p2695 N90-25336
Frequency doubled operation of a ground state depleted laser using the Nd(3+)(4)F(sub 3/2)-(4)I(sub 9/2) transition in Y2SiO5
[DE90-012089] 19 p2695 N90-25338
Three-dimensional laser velocimeter simultaneity detector
[NASA-CASE-ARC-11876-1] 19 p2696 N90-25340
SDIO/IST ultrashort wavelength laser: Novel experimental schemes for observing the Moessbauer effect in long-lived nuclear levels and nuclear coherent states
[AD-A222607] 20 p2868 N90-26316
Field experience in using laser acoustic sensing for inspection
[DE90-012954] 20 p2873 N90-26347
Development of eye-safe lidar for aerosol measurements
[NASA-CR-186905] 20 p2901 N90-26503
Non-premixed turbulent CO/H2 flames at local extinction conditions 21 p2975 N90-26907
Polar coordinate laser writer for binary optics fabrication
[AD-A222827] 21 p3008 N90-27097
Near-field gain of pyramidal horns from 18 to 40 GHz
[PB90-155854] 22 p3164 N90-27941
Laser induced damage in optical materials: 1988
[PB90-185570] 22 p3179 N90-28041
Engine testing of thermographic phosphors
[DE90-013269] 22 p3182 N90-28059
Noncontact laser thermomechanical nondestructive evaluation for advanced coatings 22 p3187 N90-28087
Experimental investigations on the stability and vorticity of the vortex breakdown phenomenon above delta wings, measured by the ultrasonic laser method
[ESA-TT-1079] 23 p3268 N90-28498
Wind lidar for BEST
[CNES-NT-125] 23 p3353 N90-28947
A laser tracking dynamic robot metrology instrument 23 p3366 N90-29021
Model calculations for a 600 angstrom laser based on photopumping of Mo(sup 6+) by a spectral line of Mo(sup 11+)
[DE90-015202] 24 p3474 N90-29634

LASING
Development of mid-infrared solid state lasers for spaceborne lidar
[NASA-CR-183290] 05 p0647 N90-13772
Lasing on the third harmonic
[DE90-002389] 06 p0790 N90-14602
Two-meter laser material response impulse measurements
[AD-A215834] 12 p1665 N90-19567
Generation of intensive UV laser radiation and utilization in high resolution spectroscopy of SO2
[ETN-90-95361] 12 p1668 N90-19581
First direct observation of FEL (Free-Electron Laser) from lambda = 20 to 45 microns
[DE90-007508] 12 p1669 N90-19589
Generation of ultrashort laser pulses from neodymium glass oscillator and regenerative amplifier 14 p1984 N90-21373
Tenth International Free Electron Laser Conference
[DE90-614773] 14 p1985 N90-21376
Solar-pumped laser for free space power transmission 15 p2061 N90-21804
High power CO2 laser instability and its corrections 15 p2102 N90-22028
High-order mode dependencies in gain-guided twin-stripe laser diode arrays
[AD-A220868] 18 p2562 N90-24617
Characterization of a Ho:Tm:Cr:YAG laser with a Cr:GSAG laser as pumping source 18 p2642 N90-25047
Frequency doubled operation of a ground state depleted laser using the Nd(3+)(4)F(sub 3/2)-(4)I(sub 9/2) transition in Y2SiO5
[DE90-012089] 19 p2695 N90-25338
Mode-medium instability and its correction with a Gaussian reflectivity mirror
[NASA-TP-3023] 19 p2758 N90-25673
Theoretical studies of solar pumped lasers
[NASA-CR-186712] 20 p2867 N90-26308
A compact, high-powered Far-Infrared (FIR) laser
[DE90-009996] 20 p2867 N90-26312
Potential of solar-simulator-pumped alexandrite lasers
[NASA-TM-102701] 22 p3180 N90-28046

LASV
U F-111 AIRCRAFT

LATCH-UP
The effects of heavy particle radiation on semiconductor devices
[DE90-001679] 06 p0854 N90-14962
Dual-mode latching reciprocal ferrite phase shifter
[FEL-1988-55] 12 p1652 N90-19497
A gate array structure for the efficient project of digital circuits: The unit cell array
[ETN-90-95364] 12 p1653 N90-19502

LATCHES
Independent Orbiter Assessment (IOA): Analysis of the electrical power distribution and control/remote manipulator system subsystem
[NASA-CR-185526] 02 p0166 N90-10936
Mechanized fluid connector and assembly tool system
[NASA-CASE-MSC-21434-1] 09 p1230 N90-17138
A robot end effector exchange mechanism for space applications 15 p2113 N90-22088
Relatchable launch restraint mechanism for deployable booms 15 p2114 N90-22091
Driving and latching of the Starlab pointing mirror doors 15 p2114 N90-22093
Orbital Maneuvering Vehicle (OMV) three-point docking latch 15 p2114 N90-22094
SKITTER/implement mechanical interface
[NASA-CR-184920] 17 p2384 N90-23578

LATE STARS
NT CARBON STARS
NT COOL STARS
NT FLARE STARS
NT K STARS
NT M STARS
NT MIRA VARIABLES
The winds of high luminosity late-type bright stars
[NASA-CR-182961] 05 p0712 N90-14160
CO infrared bands in atmospheres of long-period variables 11 p1584 N90-19128
Stellar kinematics in the galactic centre 11 p1586 N90-19141
Magnetic fields in late-type dwarfs: Preliminary results from a multiline approach
[SER-C-PREPUB-FASC-31] 12 p1728 N90-19928

LATENT HEAT
The effect of latent heat release on synoptic-to-planetary wave interactions and its implication for satellite observations: Theoretical modeling 03 p0362 N90-12073
The effect of latent heat release on synoptic-to-planetary scale wave interactions: Observational study 03 p0362 N90-12074
Cloud parameterization in EURAD and its future development 12 p1687 N90-19692
Applications of microwave radiometric measurements to infer tropical cyclone intensity and strength
[AD-A218273] 13 p1847 N90-20600
Monthly surface thermal forcing in the tropical Pacific from 1980 to 1983
[NASA-CR-183033] 16 p2259 N90-22877

LATERAL CONTROL
Periodic-disturbance accommodating control of the space station for asymptotic momentum management 05 p0586 N90-13416
Synthesis of control law, on a RPV, in order to minimize the number of sensors 08 p1025 N90-15925
Results of aircraft open-loop tests of an experimental magnetic leader cable system for guidance during roll-out and turnoff
[NASA-TM-4135] 09 p1169 N90-16767
Design of integrated pitch axis for autopilot/autothrottle and integrated lateral axis for autopilot/yaw damper for NASA TSRV airplane using integral LQG methodology
[NASA-CR-4268] 09 p1169 N90-16768
The use of lateral jet control at Aerospatiale 10 p1305 N90-17551
Fighter agility metrics, research, and test
[NASA-CR-186118] 17 p2351 N90-23386
Lateral-directional stability and control characteristics of the Quiet Short-Haul Research Aircraft (QSRA)
[NASA-TM-102250] 17 p2356 N90-23413
Maneuvering by means of lateral jets
[ISL-CO-255/88] 20 p2814 N90-26015

LATERAL STABILITY
Lateral-directional stability and control characteristics of the Quiet Short-Haul Research Aircraft (QSRA)
[NASA-TM-102250] 17 p2356 N90-23413
The effects of foreplanes on the static and dynamic characteristics of a combat aircraft model 23 p3273 N90-28520

LATERALITY
U LATERAL STABILITY

LATERALIZATION
U LATERAL CONTROL

LATEX
Studies on some failure modes in latex barrier films
[PB89-209308] 07 p0908 N90-15246

LATITUDE
NT GEOMAGNETIC LATITUDE
The effects of seasonal and latitudinal earth infrared radiance variations on ERBS attitude control
05 p0586 N90-13414
Polar cusps latitudinal shift and its relation to the IMF-By component
[IFSI-88-14] 08 p1101 N90-16377
On the relationship between the phases of 27-day total ozone and solar activity indices in different latitudinal zones 22 p3205 N90-28180
The vertical ozone distribution during maximum and minimum solar activity 22 p3205 N90-28182
Computer program for converting rectangular coordinates to latitude-longitude coordinates
[PB90-231796] 23 p3342 N90-28883
LATTICE IMPERFECTIONS
U CRYSTAL DEFECTS
LATTICE PARAMETERS
Thermal expansion and phase transformation studies on some materials by high temperature X-ray powder diffractometry
[DE89-631032] 02 p0198 N90-11130
Improving fermion operators
[PREPRINT-710] 16 p2315 N90-23193
Lattice field theory
[PREPRINT-719] 16 p2323 N90-23245
Atomic structure of Ag/Ni interfaces
[DE90-010053] 18 p2618 N90-24914
High resolution technique and instrument for measuring lattice parameters in single crystals
[AD-D014549] 22 p3177 N90-28029
Synthesis and structural chemistry of Au(III)-substituted Ba2YCu3O(7-delta)
[NASA-TM-103292] 23 p3305 N90-28696
LATTICE VIBRATIONS
Study of disorder and strain in semiconductor heterostructures and superlattices by Raman scattering
02 p0280 N90-11601
Strongly coupled one-dimensional system and the polymer
[AD-A216330] 11 p1489 N90-18571
Structure and vibrational excitations of reconstructed semiconductor surfaces
[DE90-006589] 11 p1571 N90-19044
Ionic disorder in crystals at high temperatures with emphasis on fluorites
[AERE-R-13544] 13 p1893 N90-20862
Modified tight-binding approximation and electron-phonon spectral function for transition metals
[DE90-614022] 14 p1950 N90-21166
Mixing of DIS operators in lattice QCD
[PREPRINT-708] 16 p2323 N90-23243
LATTICES
Vector fields and gravity on the lattice
[DE89-633885] 06 p0836 N90-14860
LATTICES (MATHEMATICS)
NT BOOLEAN ALGEBRA
NT BOOLEAN FUNCTIONS
Stochastic quantization
[AD-A210942] 01 p0117 N90-10671
A long time tail for random walk in random scenery
[REPT-89-08] 03 p0398 N90-12278
The algebraic basis of mathematical morphology. Part 2: Openings and closings
[CWI-AM-R8904-PT-2] 04 p0543 N90-13150
The algebraic basis of mathematical morphology. Part 1: Dilations and erosions
[CWI-AM-R8807] 05 p0695 N90-14065
A lattice study of semileptonic decays of D-mesons
[PREPRINT-660] 05 p0698 N90-14086
Designing machines for lattice physics and algorithm investigation
[DE90-003543] 07 p0969 N90-15596
A nonlinear vortex-lattice method for the calculation of interference effects between free vortex sheets and wings 08 p1068 N90-16183
Simplicial lattices in classical and quantum gravity: Mathematical structure and application
10 p1439 N90-18304
Incomparable elements in algebraic lattices with applications to formal language theory
[MEMO-INF-89-54] 15 p2148 N90-22269
Diffusion in lattices with anisotropic scatterers
[CWI-AM-R8921] 18 p2599 N90-24792
LAUE METHOD
New approach to the dynamical diffraction theory in the case of three-dimensional perfect crystal
[DE90-620563] 16 p2322 N90-23240
LAUNCH CLOUDS
U EXHAUST CLOUDS
LAUNCH COMPLEXES
U LAUNCHING BASES
LAUNCH DATES
A summary of 30 years of space launches
[AERONOMICA-ACTA-F-39-1989]
05 p0585 N90-13411
Space exploration: Cost, schedule, and performance of NASA's Galileo Mission to Jupiter. Fact sheet for the Chairman, Subcommittee on Science, Technology, and Space, Committee on Commerce, Science, and Transportation, US Senate
[GAO/NSIAD-88-138FS] 20 p2816 N90-26025
LAUNCH TIME
U LAUNCH WINDOWS
LAUNCH VEHICLE CONFIGURATIONS
Ariane 5 structural design and development
02 p0186 N90-11057
Low Earth Orbit Raider (LER) winged air launch vehicle concept
[NASA-CR-186057] 04 p0452 N90-12590
Qualification of the 4th stage propulsor of the Brazilian launcher. SLV: A new sounding rocket
05 p0661 N90-13860
Comparison between horizontally launched air-breathing single and two-stage to orbit space vehicles
09 p1175 N90-16802
Development status of Japan's new launch vehicle: H-2 rocket 09 p1176 N90-16807
Parametric assessment of propulsion system mass for airbreathing launcher configurations
09 p1177 N90-16819
Operational drivers for launcher architectures
09 p1178 N90-16828
Advanced launch vehicle configurations and performance trades 22 p3126 N90-27744
LAUNCH VEHICLES
NT ARIANE LAUNCH VEHICLE
NT HEAVY LIFT LAUNCH VEHICLES
NT HOTOL LAUNCH VEHICLE
NT PEGASUS AIR-LAUNCHED BOOSTER
NT RECOVERABLE LAUNCH VEHICLES
NT REUSABLE LAUNCH VEHICLES
NT SINGLE STAGE TO ORBIT VEHICLES
NT TITAN LAUNCH VEHICLES
Liquid rocket booster study. Volume 2, book 5, appendix 9: LRB alternate applications and evolutionary growth
[NASA-CR-183604] 01 p0026 N90-10134
Liquid rocket booster study. Volume 2, book 6, appendix 10: Vehicle systems effects
[NASA-CR-183605] 01 p0027 N90-10138
Low Earth Orbit Raider (LER) winged air launch vehicle concept
[NASA-CR-186057] 04 p0452 N90-12590
Apollo lightcraft project
[NASA-CR-186055] 04 p0464 N90-12655
Guidance, steering, load relief and control of an asymmetric launch vehicle
[NASA-CR-185598] 06 p0730 N90-14257
Atomic hydrogen as a launch vehicle propellant
[NASA-TM-102459] 06 p0735 N90-14284
Current launch vehicle reliability practice and data base assessment. Volume 1: Executive summary and report body
[AD-A213600] 07 p0885 N90-15121
Aerodynamic and structural design challenges of a reusable single stage to orbit air-breathing launch vehicle 09 p1177 N90-16814
Operational drivers for launcher architectures
09 p1178 N90-16828
Views on the evolution of European space transport: The reference launcher concept EARL 2
09 p1179 N90-16831
The joint DOD/NASA Advanced Launch System (ALS) programme 09 p1179 N90-16832
Booster propulsion/vehicle impact study, 2
[NASA-CR-179313] 10 p1346 N90-17809
Advanced launch vehicle propulsion at the NASA Lewis Research Center
[NASA-TM-103096] 13 p1761 N90-20110
Advanced Launch System (ALS): Electrical actuation and power systems improve operability and cost picture
[NASA-TM-102547] 14 p1968 N90-21271
The development of a complementary expendable launch vehicle interface for an STS deployable payload
15 p2113 N90-22086
US access to space: Launch vehicle choices for 1990 to 2010 16 p2205 N90-22579
Earth-to-orbit vehicle providing a reusable orbital stage
[NASA-CASE-LAR-13486-1] 16 p2206 N90-22584
Infrared absorption gas sensor for the detection of HCl in launch vehicle exhaust clouds
16 p2209 N90-22600
Design of cryogenic tanks for launch vehicles
16 p2220 N90-22662
Study to identify future cryogen payload elements/users for space shuttle launch during period 1990 to 2000
[NASA-CR-186311] 17 p2363 N90-23452
On the simulation test for the relative motion of separated sub-boosters on M-3S2 with nearly half a model vehicle ST-735 and their motion analyses using inertial sensors output
[ISAS-635] 17 p2366 N90-23471
Neptune, 2000 plus: Concept of a heavy space freighter for the 21st century
[ILR-MITT-229(1989)] 18 p2509 N90-24338
Assembly vs. direct launch of transfer vehicles
[NASA-TM-102686] 19 p2797 N90-25921
PDWAP: A preliminary design and weights analysis program for aerospace vehicles
[AD-A222614] 20 p2808 N90-25979
Guidance and targeting for the strategic target system
[DE90-005239] 20 p2817 N90-26031
Trajectory optimization for an asymmetric launch vehicle
[NASA-CR-185630] 20 p2817 N90-26033
IRIS system and future application to expandable launchers
[IAF-89-212] 20 p2818 N90-26035
Report of the Defense Science Board 1989 summer study on national space launch strategy
[AD-A222419] 21 p2963 N90-26848
Hybrid propulsion technology program
[NASA-CR-183952] 21 p2968 N90-26870
Space Propulsion Hazards Analysis Manual (SPHAM), volume 1
[AD-A219607] 21 p2969 N90-26874
Space Propulsion Hazards Analysis Manual (SPHAM), volume 2
[AD-A219608] 21 p2969 N90-26875
Affordable spacecraft: Design and launch alternatives. Background paper 22 p3125 N90-27737
Flight control issues of the next generation space transportation launch vehicles 22 p3126 N90-27742
Ascent and descent optimizations of an air-breathing launch vehicle 22 p3130 N90-27761
Global optimization of air breathing launch vehicle trajectories 22 p3130 N90-27762
Liquid Rocket Booster (LRB) for the Space Transportation System (STS) systems study. Appendix F: Performance and trajectory for ALS/LRB launch vehicles
[NASA-CR-183792-APP-F] 23 p3289 N90-28606
Summary of booster propulsion/vehicle impact study results 23 p3294 N90-28635
Operational cost drivers 23 p3294 N90-28636
Investigation of fluid dynamic performance of LE-7 liquid oxygen pump
[NAL-TR-1020] 24 p3476 N90-29650
LAUNCH WINDOWS
Space exploration: Cost, schedule, and performance of NASA's Galileo Mission to Jupiter. Fact sheet for the Chairman, Subcommittee on Science, Technology, and Space, Committee on Commerce, Science, and Transportation, US Senate
[GAO/NSIAD-88-138FS] 20 p2816 N90-26025
Atmospheric environment for space shuttle (STS-33) launch
[NASA-TM-100399] 22 p3200 N90-28159
LAUNCHERS
NT GUN LAUNCHERS
NT HYPERVELOCITY LAUNCHERS
NT MISSILE LAUNCHERS
NT ROCKET LAUNCHERS
The Brazilian space program: Actual state of the art
05 p0661 N90-13861
The Skylark sounding rocket program and future launcher developments by British Aerospace (Space Systems) Ltd. 05 p0662 N90-13871
From small beginnings... The story of ESRO's sounding rocket programme in celebration of the twenty-fifth anniversary of the first ESRO sounding rocket launch
[ESA-BR-60] 08 p1038 N90-15999
Design of JT-60U ICRF launcher
[DE90-733145] 10 p1326 N90-17663
Dual frequency launcher for circularly polarized antenna
[AD-D014361] 12 p1645 N90-19456
A 10-stage reconnection demonstration launcher
[DE90-007653] 13 p1760 N90-20106
Diagnostics and firing control for the cylindrical reconnection launcher
[DE90-007677] 13 p1761 N90-20107
Design and performance of a multi-stage cylindrical reconnection launcher
[DE90-007820] 13 p1761 N90-20108
Laser controlled semiconductor armature for electromagnetic launchers
[AD-D014435] 14 p1931 N90-21055
Control of surface melting and ablation in electromagnetic launchers via the magnetic vapor shielding mechanism
[AD-A219035] 16 p2204 N90-22578

Multivariate analysis of launcher guidance robustness
[REPT-892-422-105] 16 p2205 N90-22581
Equipment specifications for launcher guidance using multivariable frequency methods
[REPT-892-422-106] 16 p2205 N90-22582

LAUNCHING
NT AIR LAUNCHING
NT LIFTOFF (LAUNCHING)
NT LUNAR LAUNCH
NT ORBITAL LAUNCHING
NT ROCKET LAUNCHING
NT SEA LAUNCHING
NT SPACECRAFT LAUNCHING
Stress waves through projectile joints and interfaces
[AD-A212201] 04 p0513 N90-12963
Current management for improved railgun performance
[AD-A212887] 05 p0593 N90-13445
Guidance, steering, load relief and control of an asymmetric launch vehicle
[NASA-CR-185598] 06 p0730 N90-14257
Shuttle-C utilization for assembly of the rephased Freedom configuration
[NASA-TM-101658] 07 p0885 N90-15120
Laser-supported detonation waves and pulsed laser propulsion
[DE90-002753] 07 p0935 N90-15412
Mechanical design of the inside launch system for electron cyclotron heating in D3-D
[DE90-003292] 07 p0995 N90-15751
Flowfield effects of launch on a vertically-launched missile
[AD-A214468] 09 p1160 N90-16714
Finite element models to predict the structural response of 120-mm sabot/rods during launch
[DE90-007497] 13 p1817 N90-20436
NASA's Advanced Communications Technology Satellite (ACTS): Will it benefit commercial/military satellites
[AD-A217710] 14 p1939 N90-21100
Current management for improved railgun performance 15 p2057 N90-21781
Flight motor set 360L007 (STS-33R)
[NASA-CR-183979] 20 p2824 N90-26067
The SKY SHARK: An RPV designed to investigate the pressure distribution on a lifting surface
[NASA-CR-186222] 21 p2959 N90-26824
Debrix/ice/TPS assessment and photographic analysis of Shuttle Mission STS-32R
[NASA-TM-102787] 22 p3124 N90-27733
Affordable spacecraft: Design and launch alternatives. Background paper
[PB90-203225] 22 p3126 N90-27740
Flight motor set 360L001 (STS-26R). Volume 1: System overview, revision A
[NASA-CR-183995] 22 p3133 N90-27778
Flight motor set 360L006 (STS-34). Volume 1: System overview
[NASA-CR-184007] 22 p3133 N90-27781
Electro-optics engineering support for the integrated launch and recovery television surveillance system
[AD-A223450] 24 p3436 N90-29406
Lubrication characteristics of rolling bearings lubricated by self-lubricating composite retainers. Part 1: Selection of bearings for Earth sensors
[NAL-TR-1019] 24 p3477 N90-29651

LAUNCHING BASES
NT CAPE KENNEDY LAUNCH COMPLEX
Andoya rocket range: New installations, future plans, and investments 05 p0661 N90-13859
Esrange 05 p0663 N90-13876

LAUNCHING DEVICES
U LAUNCHERS

LAUNCHING PADS
TOPAS preparation study: Summary representation of the study results
[OHB-TN-TOP-011/87] 12 p1607 N90-19244
Soil stabilization mat for lunar launch/landing site
[NASA-CR-186690] 20 p2836 N90-26128
A transient response analysis of the space shuttle vehicle during liftoff
[NASA-TM-103505] 22 p3125 N90-27735

LAUNCHING SITES
NT LAUNCHING PADS
From small beginnings... The story of ESRO's sounding rocket programme in celebration of the twenty-fifth anniversary of the first ESRO sounding rocket launch
[ESA-BR-60] 08 p1038 N90-15999
The Ariane-5 Programme 09 p1176 N90-16808
Gaithersburg Nike control and launch area preliminary assessment/site inspection, Gaithersburg, Maryland
[AD-A217791] 14 p2003 N90-21482
Space shuttle: The future of the Vandenberg launch site needs to be determined
[GAO/NSIAD-88-158] 18 p2509 N90-24337
Soil stabilization mat for lunar launch/landing site
[NASA-CR-186690] 20 p2836 N90-26128

LAW (JURISPRUDENCE)
NT LEGAL LIABILITY
NT SPACE LAW
Congressional involvement and relations: A guide for Department of Defense acquisition managers
[AD-A214408] 07 p1011 N90-15855
Introductory remarks for the panel discussions on technology transfer 11 p1576 N90-19075
Problems on transfer of space technology to non-space areas and solutions: Legal aspects
11 p1577 N90-19077
Copyright and home copying: Technology challenges the law
[PB90-151309] 21 p3086 N90-27547
Legal ramifications of intellectual property
22 p3258 N90-28448

LAWS
NT CHILD-LANGMUIR LAW
NT CLOSURE LAW
NT CONSERVATION LAWS
NT KEPLER LAWS
NT KIRCHHOFF LAW OF RADIATION
NT RADIATION LAWS
NT SCALING LAWS
NT SNELLS LAW
The environmental liabilities of government contractors and agencies 17 p2481 N90-24186

LAY-UP
Transverse (through-the-thickness) shear stiffnesses of fibre reinforced composite laminated plates (computer program)
[ESDU-89013] 07 p0891 N90-15152
Nylon and teflon scribe effect on NBR to Chemlok 233 and NBR to NBR bond interfaces
[NASA-CR-184004] 22 p3189 N90-28095

LAYOUTS
A 2d-1 lower bound 2-layer knock-knee channel routing
[AD-A211948] 04 p0495 N90-12847
Optimal layout via Boolean satisfiability
[AD-A216777] 12 p1705 N90-19787
Circuit recognition of VLSI layouts
[AD-A219806] 17 p2396 N90-23649
Gemini2: A second generation layout validation program
[AD-A220731] 17 p2444 N90-23926
Space station based Microacceleration Experiment Platform
[NASA-CR-186659] 19 p2666 N90-25167

LDEF
U LONG DURATION EXPOSURE FACILITY

LDR (TELESCOPE)
U LARGE DEPLOYABLE REFLECTOR

LEAD (METAL)
NT LEAD ISOTOPES
Experimental measurements of shock-induced vaporization in cadmium and lead
[DE89-016877] 02 p0194 N90-11103
Review of the national ambient air quality standards for lead: Exposure analysis methodology and validation
[PB89-207914] 03 p0368 N90-12104
Method of sensitizing PB-Salt epitaxial films for Schottky diodes
[AD-D014244] 06 p0850 N90-14937
Develop techniques for ion implantation of PLZT for adaptive optics
[AD-A216005] 10 p1431 N90-18253
Fundamental studies of surface processes and trace analysis using solid electrodes
[AD-A216538] 11 p1483 N90-18533
The performance of PTFE, lead, and MoS2 as lubricant films for ball bearings operating in vacuum at 20 K
18 p2540 N90-24495
Stabilization of high T(sub c) phase in bismuth cuprate superconductor by lead doping
22 p3144 N90-27832

LEAD ACID BATTERIES
Laboratory testing of Sonnenschein DF6V180 6 volt traction battery
[DE90-002080] 06 p0771 N90-14486
Status and results of ANL life evaluation of valve-regulated lead-acid load-leveling batteries
[DE90-001918] 07 p0921 N90-15329
Life evaluation of valve-regulated lead-acid batteries for load-leveling applications
[DE90-002188] 07 p0922 N90-15336
Evaluation of a new charge algorithm for a lead-acid battery with gelled electrolyte using a 96V gel cell 4 as a test battery
[DE90-003420] 08 p1061 N90-16133
Investigation of a photovoltaic/battery hybrid system for powering the high arctic data communications system
[AD-A218353] 13 p1798 N90-20319
Very high frequency measurements of geometric factors in transmission line lead acid cells
[AD-A219463] 17 p2420 N90-23788
Application of ultracapacitors in electric vehicle propulsion systems
[DE90-010884] 18 p2550 N90-24554
The INEL battery data base
[DE90-010914] 18 p2550 N90-24555
Life evaluation of valve regulated lead-acid batteries for cycling applications
[DE90-013649] 21 p2999 N90-27044

LEAD ALLOYS
Primary arm spacing in directionally solidified Pb-10 wt percent Sn alloys
[NASA-CR-185190] 06 p0756 N90-14398
Isothermal fatigue behavior of Sn-Pb solar joints
[DE90-003280] 07 p0943 N90-15464
The metallurgical mechanisms of solder fatigue
[DE90-008390] 13 p1778 N90-20206
Phase equilibria and solution thermodynamics of bismuth-lead alloys
[PB90-138421] 14 p1950 N90-21163

LEAD COMPOUNDS
NT LEAD OXIDES
NT LEAD TELLURIDES
NT LEAD TITANATES
Catalysts for ultrahigh current density oxygen cathodes for space fuel cell applications
[NASA-CR-180650] 16 p2251 N90-22835
Piezoelectric and electrostrictive materials for transducer applications, volume 1
[AD-A223560] 24 p3480 N90-29668

LEAD ISOTOPES
Cyclic deformation of Sn-60 to Pb-40 solder joints during thermomechanical fatigue
[DE90-004197] 09 p1237 N90-17179
The long-term variation of lead-210 in relation to particle-bound sulphur in surface air in Finland
20 p2884 N90-26407

LEAD OXIDES
Chemically prepared PZT films doped with niobium
[DE90-006811] 13 p1892 N90-20859
Selective electrocatalysis of anodic oxygen-transfer reactions at chemically modified, thin-film lead dioxide electrodes
[DE90-011747] 20 p2857 N90-26252

LEAD TELLURIDES
Bridgman crystal growth
[NASA-CR-186204] 07 p0997 N90-15766

LEAD TITANATES
Synthesis and microstructure of highly oriented PbTiO3 thin films prepared by a sol-gel method
[AD-A211735] 03 p0414 N90-12377

LEAD ZIRCONATE TITANATES
New mechanism for toughening ceramic materials
[AD-A211651] 03 p0332 N90-11892
Special purpose spatial light modulators
[AD-A223794] 24 p3545 N90-30052

LEADERSHIP
Human behavior
[PB90-780008] 07 p0967 N90-15584
Leader personality and crew effectiveness: Factors influencing performance in full-mission air transport simulation 09 p1255 N90-17282
Personality factors in flight operations. Volume 1: Leader characteristics and crew performance in a full-mission air transport simulation
[NASA-TM-102259] 17 p2348 N90-23370
Comparative assessment of world research efforts on magnetic confinement fusion 19 p2759 N90-25680

LEADING EDGE FLAPS
Navier-Stokes analysis of airfoils with leading edge ice accretions 06 p0719 N90-14196

LEADING EDGE SWEEP
Stability of a supersonic boundary layer along a swept leading edge 01 p0063 N90-10359
Direct numerical study of leading-edge contamination
01 p0063 N90-10361
Computational design of low aspect ratio wing-winglet configurations for transonic wind-tunnel tests
[NASA-CR-181939] 10 p1303 N90-17539

LEADING EDGES
NT BLUNT LEADING EDGES
NT SHARP LEADING EDGES
Application of superplastically formed and diffusion bonded aluminum to a laminar flow control leading edge
[NASA-CR-178316] 01 p0007 N90-10030
Laminar flow control perforated wing panel development
[NASA-CR-178166] 01 p0034 N90-10187
Leading edge transition by contamination in hypersonic flow 01 p0063 N90-10360
Experimental study of transition and leading edge contamination on swept wings 01 p0063 N90-10362
Numerical simulation of leading-edge vortex rollup and bursting 02 p0145 N90-10831

The structure of separated flow regions occurring near the leading edge of airfoils - including transition
[NASA-CR-185853] 03 p0299 N90-11695
The right wing of the LEFT airplane 04 p0439 N90-12510
Performance of laminar-flow leading-edge test articles in cloud encounters 04 p0439 N90-12511
Simulated airline service experience with laminar-flow control leading-edge systems 04 p0439 N90-12512
Experimental and theoretical investigation of boundary-layer instability mechanisms on a swept leading edge at Mach 3.5 04 p0447 N90-12557
Stall/spin aerodynamic data project
[DOT/FAA/CT-88/29] 06 p0723 N90-14222
Thermal/structural analyses of several hydrogen-cooled leading-edge concepts for hypersonic flight vehicles
[NASA-TM-102391] 06 p0775 N90-14511
The precise calculation of the inviscid leading edge flow on a laminar airfoil using simple methods and verification by measurements on the TLF pilot model 08 p1068 N90-16180
Controlled vortical flow on delta wings through unsteady leading edge blowing
[NASA-CR-186267] 09 p1160 N90-16712
Heat pipes for wing leading edges of hypersonic vehicles
[NASA-CR-181922] 09 p1216 N90-17055
Goertler vortices in growing boundary layers: The leading edge receptivity problem, linear growth and the nonlinear breakdown stage
[NASA-CR-181962] 10 p1306 N90-17555
Simulated-airline-service flight tests of laminar-flow control with perforated-surface suction system
[NASA-TP-2966] 10 p1319 N90-17627
Unsteady viscous calculation method for cascades with leading edge induced separation 11 p1459 N90-18408
Leading edge vortex dynamics on a pitching delta wing
[NASA-CR-186327] 12 p1598 N90-19198
Large-scale advanced propeller blade pressure distributions: Prediction and data
[NASA-TM-102316] 16 p2201 N90-22564
Flat plate leading edge receptivity to various freestream disturbance structures 16 p2235 N90-22750
Finite element elastic-plastic-creep and cyclic life analysis of a cowl lip
[NASA-TM-102342] 16 p2246 N90-22808
Computational modeling of three-dimensional compressible leading edge vortices
[AD-A221022] 18 p2553 N90-24569
An experimental and theoretical investigation of the flow over plane delta wings with supersonic leading edges
[LR-588] 19 p2655 N90-25114
Experimental study on vortex and shock wave development on a 65 deg delta wing
[NLR-MP-88033-U] 20 p2804 N90-25950
Development of a graphite/bismaleimide leading edge for the F-111 (EF-111A) horizontal stabilizer 21 p2956 N90-26809
Genesis of bow echoes: A rear-inflow induced meso-convective structure
[PB90-209776] 23 p3349 N90-28926

LEAKAGE

Hydrazine fate and transformation in natural waters and soils 02 p0204 N90-11165
Apparatus and method for monitoring pressure leaks from a sealed system
[AD-D014168] 03 p0349 N90-11995
Long endurance underwater power system
[AD-A211386] 03 p0366 N90-12096
Flows with tip leakage 05 p0641 N90-13740
Fuel Tank Technology
[AGARD-R-771] 08 p1021 N90-15904
Integral fuel tank sealing practice at British Aerospace (Kingston) 08 p1021 N90-15905
Integral fuel tanks - design, production, aging, repair 08 p1021 N90-15906
Aircraft fuel tank construction and testing experience 08 p1021 N90-15907
The repair of aircraft integral fuel tanks in the RAF: A user's view of fuel tank technology 08 p1022 N90-15908
Spray sealing: A breakthrough in integral fuel tank sealing technology 08 p1022 N90-15912
Design philosophy and construction techniques for integral fuselage fuel tanks 08 p1023 N90-15913
A dynamicist's view of fuel tank skin durability 08 p1023 N90-15915
Integral fuel tank certification and test methods 08 p1023 N90-15916
Recent leak telescope development
[DE90-004101] 09 p1225 N90-17106
Investigations on hot spots effects in reverse biased spatial solar cells 10 p1344 N90-17789
Space shuttle RCS oxidizer leak repair for STS-26 11 p1474 N90-18485
Superfluid helium orbital resupply coupling 11 p1475 N90-18488
Evaluation of the Scott aviation portable protective breathing device for contaminant leakage as prescribed by FAA Action Notice A-8150.2. Phase 1: Original tests of the portable protective breathing device. Phase 2: Tests of the redesigned portable protective breathing device
[AD-A216799] 12 p1601 N90-19214
Technology evaluation for space station atmospheric leakage
[DE90-007844] 12 p1616 N90-19294
Research on cascade secondary and tip-leakage flows: Periodicity and surface flow visualization 14 p1925 N90-21026
Losses in the tip-leakage flow of a planar cascade of turbine blades 14 p1925 N90-21027
Analysis of the rotor tip leakage flow with tip cooling air ejection 14 p1926 N90-21029
Heat leak measurements in superconducting dipole magnet supports
[DE90-620109] 15 p2173 N90-22420
A model of electromagnetic leakage through joints at radio frequencies
[BAE-WES-RP-GEN-EMC-049-T2.2] 17 p2392 N90-23626
High temperature flexible seal
[NASA-CASE-LEW-14695-1] 17 p2413 N90-23751
Spacecraft external molecular contamination analysis 19 p2730 N90-25520
Experimental investigation of the hydrodynamic forces on the shroud of a centrifugal pump impeller
[NASA-CR-186952] 21 p3009 N90-27108
Magnetic flux leakage versus ultrasonic correlation
[AD-A222112] 21 p3071 N90-27462
Requirements for long-life operation of inert gas hollow cathodes: Preliminary report
[NASA-TM-103242] 22 p3134 N90-27783
Garment pressurizing apparatus
[AD-D014451] 22 p3232 N90-28330
Study and analysis of leaking underground storage tank remediation techniques incorporated in states in EPA Region 6
[PB90-214834] 23 p3333 N90-28847
Leak detection aid
[DE90-014678] 24 p3471 N90-29616

LEARNING

NT ASTRONAUT TRAINING
NT CONDITIONING (LEARNING)
NT MAZE LEARNING
NT TRANSFER OF TRAINING
On learning from exercises
[AD-A210593] 01 p0101 N90-10574
Parallel processing and learning in simple systems
[AD-A210225] 01 p0108 N90-10612
Some results on learning
[AD-A210591] 01 p0110 N90-10624
Learning to make decisions: When incentives help and hinder
[AD-A210185] 01 p0135 N90-10779
Synaptic plasticity and memory formation
[AD-A211368] 03 p0379 N90-12158
Adaptive information processing in auditory cortex
[AD-A211294] 03 p0380 N90-12166
Fear-potentiated startle as a model system for analyzing learning and memory
[AD-A212131] 04 p0525 N90-13029
Effects of type of responding on memory/visual search: Responding just yes or just no can lead to inflexible performance
[AD-A212764] 04 p0526 N90-13033
Feedback effects in computer-based skill learning
[AD-A214560] 09 p1258 N90-17298
Job planning and execution monitoring for a human-robot symbiotic system
[DE90-004464] 09 p1261 N90-17315
Teaching a new methodology for designing relational data bases: An experiment testing the effectiveness of an intelligent tutoring system on cognitive skill acquisition (volumes 1 and 2) 11 p1574 N90-19063
An approach to elemental task learning
[DE90-006614] 12 p1697 N90-19745
Role of cognitive factors in the acquisition of cognitive skill
[AD-A218069] 13 p1854 N90-20642
A long-term retention advantage for spatial information learned naturally and in the laboratory
[AD-A218268] 13 p1855 N90-20644
On metric entropy, Vapnik-Chervonenkis dimension, and learnability for a class of distributions
[AD-A217331] 13 p1876 N90-20759
Towards the knowledge level in SOAR: The role of the architecture in the use of knowledge
[NASA-CR-186615] 16 p2262 N90-22897
Rules and maps in connectionist symbol processing
[AD-A219028] 16 p2264 N90-22903
Cognitive architectures and rational analysis: Comment
[AD-A219199] 16 p2264 N90-22907
Learning artificial grammars with competitive chunking
[AD-A219270] 16 p2265 N90-22911
Laboratory replication of scientific discovery processes
[AD-A219273] 16 p2266 N90-22913
An instructable Connectionist/Control architecture: Using rule-based instructions to accomplish connectionist learning in a human time scale
[AD-A219274] 16 p2266 N90-22914
Learning environment for neural networks and transient acoustics
[AD-A219000] 16 p2314 N90-23186
DURIP: Computational modeling of cognitive processes
[AD-A219934] 17 p2437 N90-23886
Analysis of neural systems involved in modulation of memory storage
[AD-A220230] 18 p2584 N90-24714
Acquiring generalizations to organize human databases
[AD-A219835] 18 p2634 N90-25004
United States Naval Academy summary of Research, Academic Departments, 1989-1990
[AD-A221219] 19 p2800 N90-25929
Mathematical problem-solving transfer: The effects of cognitive load and attention a schema acquisition and rule automation 20 p2917 N90-26594
Rule acquisition events in the discovery of problem solving strategies
[AD-A222428] 21 p3037 N90-27265
The effects of training on errors of perceived direction in perspective displays
[NASA-TM-102792] 22 p3232 N90-28329
Selective learning algorithm for certain types of learning failure in multilayer perceptrons
[AD-A223982] 23 p3362 N90-28998
Designing intelligent computer aided instruction systems with integrated knowledge representation schemes
[AD-A224178] 23 p3383 N90-29113
Integrating rule-based and neural-net techniques for spectral analysis
[AD-A223517] 24 p3446 N90-29462

LEARNING CURVES

A comparative analysis of work-hour forecasting techniques at the crew level
[AD-A220706] 17 p2438 N90-23894
Extensions to the learning curve: An analysis of factors influence unit cost of weapon systems
[AD-A224119] 23 p3407 N90-29256

LEARNING MACHINES

U MACHINE LEARNING

LEARNING THEORY

Biological investigations of adaptive networks: Neuronal control of conditioned responses
[AD-A211043] 01 p0094 N90-10534
Inferring data base requirements from examples in forms 02 p0288 N90-11646
A theory of networks for approximation and learning
[AD-A212359] 04 p0538 N90-13110
Measuring learning ability by dynamic testing
[AD-A215273] 09 p1259 N90-17304
Structural understanding in problem solving
[AD-A214776] 09 p1273 N90-17379
Symposium on air traffic control training for tomorrow's technology
[PB90-127325] 12 p1601 N90-19216
On metric entropy, Vapnik-Chervonenkis dimension, and learnability for a class of distributions
[AD-A217331] 13 p1876 N90-20759
What makes some problems hard: Explorations in the problem space of difficulty
[AD-A219002] 16 p2263 N90-22901
Discovering problem solving strategies: What humans do and machines don't (yet)
[AD-A219008] 16 p2263 N90-22902
Learning events in the acquisition of three skills
[AD-A219038] 16 p2264 N90-22905
Non-LIFO (Last-In-First-Out) execution of cognitive procedures
[AD-A219277] 16 p2266 N90-22916
Practical issues in the complexity of neural networks
[AD-A221420] 21 p3058 N90-27389
A user modelling approach for computer-based critiquing
[AD-A224042] 23 p3379 N90-29088
Learning in tele-autonomous systems using Soar 24 p3506 N90-29819
Knowledge base refinement as improving an incorrect and incomplete domain theory
[AD-A224441] 24 p3526 N90-29935
Search strategies for computer-stored information: A microcomputer tutorial 24 p3557 N90-30126

LEAST SQUARES METHOD
A FORTRAN program for the calculation of the calibration coefficients of a six-component strain gauge balance
[AD-A210375] 01 p0105 N90-10599
Inherent bias in nonlinear least squares analysis of first-order kinetic data
[AD-A210677] 01 p0114 N90-10651
Advances in regression: Use of models in spectroscopic data analysis
[AD-A210541] 01 p0116 N90-10665
Robust spatial calibration of a planar positron camera
[AD-A210773] 02 p0224 N90-11284
Iterative network magnitude estimation and uncertainty assessment with noisy and clipped data
[AD-A210707] 02 p0265 N90-11507
Nonlinear adjustment with or without constraints, applicable to geodetic models
[AD-A210820] 02 p0265 N90-11509
Two enhancements of the logarithmic least-squares method for analyzing subjective comparisons
[AD-A211192] 02 p0266 N90-11514
An improved algorithm for the determination of the system paramters of a visual binary by least squares
02 p0290 N90-11658
A least-squares finite element method for incompressible Navier-Stokes problems
[NASA-TM-102385] 03 p0392 N90-12231
Asymptotic bias of autoregressive estimators
[IMAG-RR-745-M] 03 p0395 N90-12255
Orthogonal least squares methods and their application to nonlinear system identification
[RR-343] 03 p0395 N90-12259
Self-tuning control of nonlinear Armax models --- Autoregressive Moving Average with eXogeneous (ARMAX) inputs
[RR-362] 04 p0508 N90-12930
An error estimator for parameter choice in regulating least square problems. Application to regularized deconvolution
[IMAG-RR-744-M] 04 p0540 N90-13125
NUMVEC FORTRAN library manual chapter: Simultaneous linear equations
[CWI-NM-R8903] 04 p0541 N90-13135
Exponential modeling using combined forward and backward prediction
[AD-A212317] 04 p0545 N90-13169
Outlier detection in multivariate calibration
[DE90-001502] 07 p0982 N90-15672
And still, a new beginning: The Galerkin least-squares gradient method
[DE89-636435] 08 p1116 N90-16461
A new finite element formulation for CFD:8. The Galerkin/least-squares method for advective-diffusive equations
[DE89-636437] 08 p1116 N90-16462
Implementation of adaptive arrays in the block oriented systems simulator
[AD-A215545] 09 p1171 N90-16774
Adaptive vibration control of vibration isolation mounts, using an LMS-based control algorithm
[AD-A214386] 10 p1394 N90-18061
Strong source heat transfer simulations based on a GalerKin/gradient least squares method
[DE90-608613] 11 p1507 N90-18678
Self-tuning control techniques, implicit and explicit, with parameter estimation in Kalman filters, applied to artificial satellite attitude
[INPE-4857-TDL/368] 12 p1613 N90-19276
Application of adaptive least-squares algorithm to multi-element array signal reconstruction
12 p1644 N90-19448
Error analysis of some Galerkin least squares methods for the elasticity equations
[DE90-608611] 12 p1705 N90-19790
Swing-free movement of simply suspended objects employing parameter estimation
[DE90-002238] 13 p1811 N90-20398
Methods for local gravity field approximation
13 p1834 N90-20532
Treatment of geodetic leveling in the integrated geodesy approach 13 p1837 N90-20546
Quantifying and reducing uncertainty in the assimilative mapping of ionospheric electrodynamics
[AD-A216057] 13 p1842 N90-20577
A note on overdispersed exponential families
[AD-A216277] 14 p2018 N90-21565
The use of local polynomial approximations in a knot-placement strategy for least squares spline fitting
[NPL-DITC-148/89] 15 p2162 N90-22355
Quantifying and reducing uncertainty in the assimilative mapping of ionospheric electrodynamics
16 p2254 N90-22854
The application of a non-linear least squares method to predicting seat transmissibility
[ISVR-TR-173] 16 p2275 N90-22967
Analytic semigroups: Applications to inverse problems for flexible structures
[NASA-CR-182047] 16 p2306 N90-23138
Transfer matrices for multimode optical fiber systems
[AD-A218459] 16 p2317 N90-23210
Development of a least squares time response lower-order equivalent systems technique
[AD-A220527] 17 p2351 N90-23389
Adaptive control of a system with periodic dynamics: Application of an impulse response method to the helicopter vibration problem 17 p2453 N90-23990
Application of optimal tracking methods to aircraft terrain following
[AD-A221099] 18 p2496 N90-24264
Accuracy improvements in finite element stress analysis 18 p2571 N90-24651
Equivalent circuit models for ac impedance data analysis
[NASA-TM-100402] 19 p2686 N90-25277
Minimum variance control of nonlinear systems
[RR-369] 19 p2748 N90-25615
Variance reduction for quantile estimates in simulations via nonlinear controls
[AD-A222653] 20 p2916 N90-26590
Strong consistency of the least squares estimator for a non-ergodic threshold autoregressive model
[IMAG-RR-791-M] 20 p2918 N90-26604
A study of the asymptotic properties of least square estimators for multiple phase regression problems
[ETN-90-97244] 20 p2921 N90-26620
Gaussian quadrature exponential sum modeling of near infrared methane laboratory spectra obtained at temperatures from 106 to 297 K
20 p2945 N90-26758
Computer production of K-indices by a simple method based on linear elimination 21 p3024 N90-27194
Modified fast frequency acquisition via adaptive least squares algorithm
[NASA-CASE-NPO-17845-1-CU]
21 p3050 N90-27341
ROBFIT: A code for the analysis of histogram spectra with nonlinear regression and robust estimation
[AD-A221527] 21 p3055 N90-27369
Projection methods for solving nonlinear systems of equations
[NASA-TM-101878] 21 p3063 N90-27409
Frequency analysis via the method of moment functionals
[NASA-CR-186988] 22 p3239 N90-28367
Robust circle and sphere fitting by least squares
[NPL-DITC-153/89] 22 p3243 N90-28389
Macromolecular calculations for the XTAL-system of crystallographic programs
[AD-A222345] 22 p3248 N90-28421
Recursive least-squares learning algorithms for neural networks
[DE90-014926] 23 p3380 N90-29096
An investigation of hole-edge crack problem by a combined complex variable and least square method
[LR-626] 24 p3482 N90-29679
A parallel least squares collocation conjugate gradient approach for the advection diffusion equation
[DE90-015965] 24 p3530 N90-29961
Analytic least squares
[NPL-DES-86] 24 p3531 N90-29971

LEAVES
LANDSAT-5 data in the study of wheat and bean crops
[INPE-4746-RPE/580] 13 p1819 N90-20444
Seasonal LAI in slash pine estimated with LANDSAT TM
[NASA-TM-102278] 19 p2706 N90-25397

LEBESGUE THEOREM
Analogues of the Lebesgue density theorem for fractal sets of reals and integers
[REPT-89-88] 17 p2468 N90-24106
The axiomatization of randomness
[ITLI-ML-89-06] 18 p2603 N90-24824

LECTURES
Preliminary collection 891 of lectures/papers in Symposium by Society of Automotive Engineers of Japan
[DE90-710449] 10 p1391 N90-18045
The employment of SITIM-150 as an instructional objective for training in remote sensing
[INPE-4833-PRE/1463] 10 p1440 N90-18310
Index to NASA news releases and speeches, 1986
[NASA-TM-101899] 15 p2175 N90-22430
Index to NASA news releases and speeches, 1987
[NASA-TM-101900] 15 p2175 N90-22431
Index to NASA news releases and speeches, 1988
[NASA-TM-101901] 15 p2175 N90-22432
Texstar: The all-Texas educational satellite system
[NASA-CR-186654] 20 p2820 N90-26045

LED (DIODES)
U LIGHT EMITTING DIODES

LEG (ANATOMY)
NT FEET (ANATOMY)
Neural networks for real-time sensory data processing and sensorimotor control
[AD-A223096] 20 p2916 N90-26592

LEGAL LIABILITY
Legal aspects of commercial space transportation
09 p1175 N90-16796
The environmental liabilities of government contractors and agencies 17 p2481 N90-24186
Damage responsibility and liability in space stations
20 p2937 N90-26714
The astronauts' legal status: The International Space Station 20 p2938 N90-26721

LEGENDRE CODE
U COMPUTER PROGRAMMING
U NEUTRON SCATTERING

LEGENDRE FUNCTIONS
The 16-O photodisintegration at low energies
[NOTA-INTERNA-941] 16 p2315 N90-23196
Notes on the unsteady rectilinear motion of a perfect gas. 9: The expansion to vacuum of a finite mass of uniform homentropic gas
[LR-590-9] 19 p2692 N90-25316

LEGENDRE POLYNOMIALS
U LEGENDRE FUNCTIONS

LEGENDRE TRANSFORMATION
U LEGENDRE FUNCTIONS

LEGUMINOUS PLANTS
NT SOYBEANS
Variability of cultivar responses to ozone
[PB89-225460] 07 p0956 N90-15528
Radiometric study of wheat and bean crops in three types of latossolo
[INPE-4843-PRE/1472] 11 p1523 N90-18767

LEM (LUNAR MODULE)
U LUNAR MODULE

LEMMAS
U THEOREMS

LENGTH
NT DIFFUSION LENGTH
Comparison of I2-stabilized HE-NE lasers
[PB89-219844] 03 p0352 N90-12014
On the scale of diffusion lengths observable by neutron reflection: Application to polymers
[DE90-005645] 10 p1358 N90-17878

LENNARD-JONES GAS
Properties of Lennard-Jones mixtures at various temperatures and energy ratios with a size ratio of two
[PB89-235204] 04 p0471 N90-12697

LENNARD-JONES POTENTIAL
Molecular theory of fluid phase equilioria
[PB90-131277] 15 p2066 N90-21832

LENS ANTENNAS
Frequency independent constant beamwidth directional lens antenna for very wideband and multi-channel electromagnetic communications
[AD-D014214] 06 p0765 N90-14449
Geometrical optics in inhomogeneous chiral media with application to polarization correction in inhomogeneous lens antennas
[PB90-110669] 08 p1122 N90-16497
Polarization correction of Luneburg lens with chiral medium
[PB90-189127] 24 p3544 N90-30048

LENS DESIGN
Catadioptric Optics for laser Doppler velocimeter applications
[NASA-TM-102210] 04 p0504 N90-12904
Conceptual design study of a 5 kilowatt solar dynamic Brayton power system using a dome Fresnel lens solar concentrator
[NASA-CR-185134] 06 p0735 N90-14281
Binary optics technology: The theory and design of multi-level diffractive optical elements
[AD-A213404] 07 p0992 N90-15735

LENSES
NT FRESNEL LENSES
NT GRAVITATIONAL LENSES
NT MAGNETIC LENSES
NT WIDE ANGLE LENSES
NT WIRE GRID LENSES
The modulating grid 05 p0603 N90-13505
The relay lens systems 05 p0603 N90-13506
A scheiner-principle vernier optometer
[AD-D014304] 07 p0934 N90-15405
Binary optics technology: The theory and design of multi-level diffractive optical elements
[AD-A213404] 07 p0992 N90-15735
Gas optics applicable to free electron laser technology
[AD-A214285] 07 p0993 N90-15741
Monochromator configurations for wavelength division multiplexing
[AD-A214833] 09 p1281 N90-17430

Laser diffraction particle sizing: Instrument probe volume relocation and elongation
[NASA-TM-102512] 10 p1387 N90-18025
Narrow-bandwidth unstable laser resonator
[AD-D014362] 12 p1665 N90-19568
Simple reflection holography
[DE90-008309] 13 p1805 N90-20359
Hybrid diffractive-refractive telescope
[AD-A219241] 16 p2318 N90-23216
Modeling of thermal lensing in side and end-pumped finite solid-state laser rods
[NASA-CR-4300] 17 p2407 N90-23716
Tracking a head-mounted display in a room-sized environment with head-mounted cameras
[AD-A222545] 21 p3037 N90-27266

LEO ENVIRONMENTS
U EARTH ORBITAL ENVIRONMENTS

LEPTONS
NT ANTINEUTRINOS
NT CONDUCTION ELECTRONS
NT ELECTRONS
NT MUONS
NT NEUTRINOS
NT POSITRONS
NT SOLAR NEUTRINOS
A lattice study of semileptonic decays of D-mesons
[PREPRINT-660] 05 p0698 N90-14086
The AMY Experiment
[DE90-001153] 06 p0839 N90-14880
Dissipative effects in Friedmann universes
[DE89-618838] 08 p1150 N90-16663
Cosmological baryon and lepton number in the presence of electroweak fermion-number violation
[NASA-CR-186609] 17 p2470 N90-24123

LESIONS
Apparatus for imaging deep arterial and coronary lesions
[NASA-CASE-NPO-17439-1-CU] 08 p1104 N90-16391
Dazzling glare: Protection criteria versus visual performance
[AD-A219676] 17 p2438 N90-23889
Experiment K-6-22. Growth hormone regulation, synthesis and secretion in microgravity. Part 1: Somatotroph physiology. Part 2: Immunohistochemical analysis of hypothalamic hormones. Part 3: Plasma analysis 20 p2896 N90-26475
DNA damage and repair in human skin: Pathways and questions
[DE90-015126] 23 p3356 N90-28966

LETHALITY
Modelling time to incapacitation and death from toxic and physical hazards in aircraft fires 10 p1318 N90-17619
Acute oral toxicity of DIGL-RP solid propellant in Sprague-Dawley rats
[AD-A217712] 13 p1849 N90-20614

LETTERS (SYMBOLS)
U SYMBOLS

LEUKOCYTES
NT LYMPHOCYTES
Reciprocal relationships between the immune and central nervous system
[AD-A221259] 18 p2583 N90-24712

LEVEL (HORIZONTAL)
NT LIQUID LEVELS

LEVEL (QUANTITY)
NT ATOMIC ENERGY LEVELS
NT EFFECTIVE PERCEIVED NOISE LEVELS
NT ELECTRON STATES
NT ENERGY LEVELS
NT GROUND STATE
NT INTERMOLECULAR FORCES
NT MOLECULAR ENERGY LEVELS

LEVELING
The effect of leveling coatings on the atomic oxygen durability of solar concentrator surfaces
[NASA-TM-102557] 14 p1941 N90-21110

LEVITATION
NT ACOUSTIC LEVITATION
Spectral emissivities and optical constants of electromagnetically levitated liquid metals as functions of temperature and wavelength 10 p1364 N90-17907
The NASA, Marshall Space Flight Center drop tube user's manual
[NASA-TM-100392] 13 p1786 N90-20251
Materials research issues in superconducting levitation and suspension as applied to magnetic bearings
[DE90-011147] 20 p2929 N90-26667
Magnetic properties of high-T(sub c) superconductors: Rigid levitation, flux pinning, thermal depinning, and fluctuation 22 p3137 N90-27798
Magnetic forces in high-T(sub c) superconducting bearings 22 p3137 N90-27799

LEVITATION MELTING
Containerless Processing of Metals: Undercooling and Solidification
[DLR-MITT-89-15] 05 p0625 N90-13645
Electromagnetic fusion process and position research 13 p1785 N90-20249

LEXAN (TRADEMARK)
Positron annihilation spectroscopy: A nondestructive, submicroscopic characterization technique for structural polymers
[AD-A217748] 13 p1782 N90-20226

LIABILITIES
NT LEGAL LIABILITY

LIAPUNOV FUNCTIONS
Can perceptrons find Lyapunov functions: An algorithmic approach to systems stability
[RR-365] 03 p0391 N90-12224
Fluctuations of the Lyapunov exponent in disordered systems
[PREPRINT-690] 05 p0695 N90-14063
Contribution to the study of stability robustness of nonlinear multivariable regulators
[INPE-4801-TDL/356] 11 p1554 N90-18950
Nonlinear stability analysis and control of dynamical robotic systems 15 p2104 N90-22037
A new stability criterion in the shallow-water system for two-dimensional coherent eddies in the atmosphere and oceans 15 p2130 N90-22176
About linear systems robustness: Linear programming approach
[LAAS-89-384] 16 p2303 N90-23123
Intermittency and multifractality in magnetic dynamos
[PREPRINT-702] 16 p2319 N90-23226
Numerical solution of large Lyapunov equations
[NASA-CR-180359] 17 p2456 N90-24010
A Lyapunov bound for solutions of Poisson's equation
[AD-A220223] 18 p2599 N90-24787
Lyapunov-based control for switched power converters
[AD-A221974] 21 p3000 N90-27053
Dissipative quantum maps
[DE90-627179] 23 p3402 N90-29227
Quantum chaos and dissipation: Lyapunov exponents
[DE90-627180] 23 p3403 N90-29228

LIBRARIES
Planning an Integrated On-line Library System (IOLS)
[AD-A209406] 01 p0136 N90-10783
Weeding policy and procedures: Information services
[AD-A210568] 01 p0137 N90-10790
Automated reuseable components system study results 06 p0824 N90-14790
Knowledge-based reusable software synthesis system 06 p0824 N90-14791
Reuse at the Software Productivity Consortium 06 p0825 N90-14798
Level 2 software reuse study 06 p0826 N90-14800
An SSE approach to reusability 06 p0826 N90-14801
Support for life-cycle product reuse in NASA's SSE 06 p0826 N90-14802
AdaNET services 06 p0827 N90-14806
Proceedings of the Conference on Application of Scanning Methodologies in Libraries
[PB89-233415] 06 p0858 N90-14990
The StarLite project
[AD-A214193] 07 p0977 N90-15642
Computer-Aided Design for Built-In-Test (CADBIT). Volume 2: BIT Library
[AD-A215738] 09 p1268 N90-17354
Proceedings of Colloquium 110 of the International Astronomical Union on Library and Information Services in Astronomy
[AD-A215612] 09 p1298 N90-17523
Hypercluster parallel processing library user's manual
[NASA-CR-185231] 14 p2016 N90-21552
Medical subject headings: Annotated alphabetic list, 1990
[PB90-100009] 14 p2036 N90-21683
Appendix A: NASA information services 22 p3258 N90-28451
Digital geometric correction for MSS-LANDSAT imagery
[INPE-4627-PRE/1345] 23 p3342 N90-28886

LIBRATION
A lunar far-side very low frequency array
[NASA-CP-3039] 01 p0139 N90-10805

LICENSING
Methodology panel 11 p1576 N90-19076

LIDAR
U OPTICAL RADAR

LIE GROUPS
NT SPINOR GROUPS
Extended Weyl group for Kac-Moody algebras
[DE89-617525] 01 p0111 N90-10634
N=1,2 supergravities in 2+1 dimensions as Chern-Simons theories
[DE89-612006] 01 p0134 N90-10771
S7 without any construction of Lie group
[DE89-618380] 02 p0269 N90-11539
Global linear representations of nonlinear systems and the adjoint map
[RR-347] 03 p0394 N90-12247
Lie-algebraic aspects of the classical nonrelativistic Calogero-Moser models
[CWI-AM-R8901] 04 p0542 N90-13148
R-matrices and higher Poisson brackets for integrable systems
[PREPRINT-669] 05 p0696 N90-14069
Hamiltonian flows, SU(infinity), SO(infinity), USp(infinity), and strings
[DE90-001987] 06 p0835 N90-14851
Continuum analogues of contragredient Lie algebras: Lie algebras with a Cartan operator and nonlinear dynamical systems
[DE89-635698] 07 p0985 N90-15691
Nijenhuis tensor and integrable models
[DE90-001403] 07 p0987 N90-15702
Lefschetz trace formula and BRST
[DE89-635705] 07 p1007 N90-15835
Multiplet classification of highest weight modules over quantum universal enveloping algebras: The U(sub q)(sl(3,C)) example
[DE90-600720] 08 p1116 N90-16464
Quantum sl(2) enveloping algebra and representations of braid group
[DE90-607044] 09 p1275 N90-17389
New aspects in bifurcation with symmetry
[AD-A216506] 11 p1552 N90-18935
Calculation of Lie algebra cohomology by computer
[MEMO-833] 17 p2449 N90-23962
Gevrey spaces related to Lie algebras of operators
[ETN-90-96892] 17 p2468 N90-24109
Effective Hamiltonians and the theory of invariants
[DE90-611035] 18 p2605 N90-24836
From Lie group transformation to the generalized Koiter initial postbuckling theory of perfect shells
[LR-613] 19 p2704 N90-25389
Nonlinear systems, the Lie series, and the left shift operator: Application to nonlinear optimal control
[RR-376] 19 p2748 N90-25619
Limit cycles and bifurcation in piecewise-linear and piecewise-analytic systems. 1: General theory
[RR-372] 19 p2751 N90-25634
The center of the enveloping algebra of the semidirect product of the Heisenberg lie algebra h(sub n) and a reductive Lie algebra S the rank of which is equal to 1 or 2
[DE90-627155] 23 p3388 N90-29133
The combinatorics computation for Casimir operators of the symplectic Lie algebra and the application for determining the center of the enveloping algebra of a semidirect product
[DE90-627161] 23 p3388 N90-29136
Trees, bialgebras and intrinsic numerical algorithms
[NASA-CR-187031] 24 p3524 N90-29925

LIF (FLUORESCENCE)
U LASER INDUCED FLUORESCENCE

LIFE (BIOLOGY)
U LIFE SCIENCES

LIFE (DURABILITY)
NT CARRIER LIFETIME
NT FATIGUE LIFE
NT HALF LIFE
NT PLASMA LIFETIME
NT SATELLITE LIFETIME
NT SERVICE LIFE
NT STORAGE STABILITY
US Air Force certification of castings 01 p0042 N90-10232
Aerospace system unified life cycle engineering producibility measurement issues
[AD-A210937] 01 p0106 N90-10607
The use of damage characterization for life prediction methodologies 02 p0185 N90-11053
Lifetime testing of commercially available 3.0 (mu)f, 100 kV pulsed-power capacitors
[DE89-017230] 02 p0217 N90-11242
A re-evaluation of fatigue threshold test procedures and the simulation and prediction of fatigue crack growth under conditions of low crack closure 02 p0231 N90-11328
Shear fatigue testing and life prediction of fibre composites
[REPT-8519] 04 p0466 N90-12668
The quality of vacuum deposited surface treatments
[CETIM-107040] 04 p0476 N90-12729
Atmospheric drag model calibrations for spacecraft lifetime prediction 05 p0591 N90-13439

Lifetime predictions for the Solar Maximum Mission (SMM) and San Marco spacecraft
05 p0591 N90-13440
Cryogenic systems for the large deployable reflector
05 p0597 N90-13470
Mean stress and the exhaustion of fatigue-damage resistance
[NASA-TM-101311] 05 p0655 N90-13819
Advanced Turbine Technology Applications Project (ATTAP)
[NASA-CR-185109] 05 p0709 N90-14153
Predictive aging of elastomers in air: The importance of understanding diffusion-limited oxidation effects
[DE90-001385] 06 p0751 N90-14372
Sodium/sulfur evaluation at SNL
[DE89-015846] 06 p0769 N90-14472
Zinc/bromine battery evaluation at SNL (Sandia National Laboratory)
[DE89-015847] 06 p0769 N90-14473
Support for life-cycle product reuse in NASA's SSE
06 p0826 N90-14802
Status and results of ANL life evaluation of valve-regulated lead-acid load-leveling batteries
[DE90-001918] 07 p0921 N90-15329
Fuel Tank Technology
[AGARD-R-771] 08 p1021 N90-15904
The effect of primer age on adhesion of polysulphide sealant 08 p1022 N90-15909
Long term creep strength of silver alloyed copper
[DE90-602367] 08 p1045 N90-16039
Assessment of strength limiting flaws in ceramic heat exchanger components
[DE90-004086] 08 p1051 N90-16077
Assessment of strength limiting flaws in ceramic heat exchanger tubes, phase 2
[DE90-004081] 09 p1220 N90-17080
AGARD/SMP Review: Damage Tolerance for Engine Structures. 2: Defects and Quantitative Materials Behaviour — conference
[AGARD-R-769] 11 p1457 N90-18396
Review of modelling methods to take account of material structure and defects 11 p1458 N90-18402
Life of concentrated contacts in the mixed EHD and boundary film regimes
[AD-A216673] 11 p1517 N90-18738
Effect of temperature on the storage life of polysulfide aircraft sealants
[MRL-TR-89-31] 12 p1629 N90-19364
Influence of the parameters: Charge order, sequence classification, partial sequential circuit, and process regularity of a working charge (Gaussian process) on the lifetime of a component made of 3.1354 T3 and 3.4377 T761
[ETN-90-95378] 12 p1653 N90-19503
Bearing and gear steels for aerospace applications
[NASA-TM-102529] 13 p1809 N90-20391
The importance of batteries in unmanned missions
13 p1821 N90-20456
A new concept for high-cycle-life LEO: Rechargeable MnO2-hydrogen 13 p1822 N90-20462
Characterization testing of a 40 AHR bipolar nickel-hydrogen battery 13 p1822 N90-20463
The application of electrochemical impedance spectroscopy for characterizing the degradation of Ni(OH)2/NiOOH electrodes 13 p1824 N90-20474
KOH concentration effect on the cycle life of nickel-hydrogen cells. Part 4: Results of failure analyses
13 p1824 N90-20475
Effect of KOH concentration on LEO cycle life of IPV nickel-hydrogen flight battery cells
[NASA-TM-103127] 14 p1942 N90-21116
Method of making a long life high current density cathode from tungsten and iridium powders using a quarternary compound as the impregnant
[AD-D014425] 14 p1958 N90-21211
Electrochemical impregnation and cycle life of lightweight nickel electrodes for nickel-hydrogen cells
[NASA-TM-103140] 15 p2068 N90-21844
Practical nonlinear simulation of rotating machinery dynamics with application to turbine blade rubbing
15 p2104 N90-22038
A life prediction model for laminated composite structural components
[NASA-CR-186587] 16 p2212 N90-22614
Finite element elastic-plastic-creep and cyclic life analysis of a cowl lip
[NASA-TM-102342] 16 p2246 N90-22808
Corrosion fatigue crack propagation in metals
[NASA-CR-4301] 18 p2524 N90-24405
Evaluation of abrasion-resistant metallized coatings for civil works applications
[AD-A221078] 18 p2530 N90-24438
Study of ball bearings for space use
18 p2537 N90-24477
Phillips CO-oxidation catalyts for long-lived CO2 lasers: Activity and initial characterization studies
18 p2557 N90-24592
Advanced tube-bundle rocket thrust chamber
[NASA-TM-103139] 19 p2670 N90-25185
A model for a knowledge-based system's life cycle
19 p2739 N90-25569
Proceedings of the LDEF Materials Data Analysis Workshop
[NASA-CP-10046] 20 p2826 N90-26075
NDT in aerospace: The next decade (1990's)
[PNR90628] 20 p2874 N90-26348
Fatigue life assessment using a short crack growth model
[PNR90663] 20 p2877 N90-26367
Multimegawatt space nuclear power supply, phase 1. Volume 3: Annotated outline of preliminary safety assessment D180-30619-7
[DE90-012432] 20 p2926 N90-26646
Lessons learned for composite aircraft structures qualification 21 p2956 N90-26808
An aluminum quality breakthrough for aircraft structural reliability 21 p2957 N90-26816
Peak identification techniques
21 p2959 N90-26822
Role of interfaces and interphases in the evolution mechanics of material systems
[AD-A222702] 21 p2971 N90-26885
Block 6: The future DMSP space systems
21 p3068 N90-27443
Expert system diagnostics and parts life tracking as applied to the AV-8B aircraft for the USMC
22 p3104 N90-27629
Harrier Information Management System (HIMS): The system and the approach 22 p3105 N90-27630
Requirements for long-life operation of inert gas hollow cathodes: Preliminary report
[NASA-TM-103242] 22 p3134 N90-27783
Assessment and demonstration of the capabilities of NDI processes, equipment, and personnel
22 p3184 N90-28071
Damage tolerance of the fighter aircraft 37 Viggen. Part 1: Analytical assessment
[FFA-TN-1990-12-PT-1] 23 p3276 N90-28538
Damage tolerance of the fighter aircraft 37 Viggen. Part 2: Experimental verification
[FFA-TN-1990-13-PT-2] 23 p3276 N90-28539
Development of an integrated BEM for hot fluid-structure interaction 23 p3291 N90-28617
Structural response of SSME turbine blade airfoils
23 p3297 N90-28649
Thermal analysis of thermal barrier coatings in a high heat flux environment 23 p3297 N90-28652
Application of advanced coating techniques to rocket engine components 23 p3298 N90-28654
Ceramic matrix composites in simulated SSME environments 23 p3298 N90-28655
Automated information system life-cycle management manual
[PB90-219288] 23 p3405 N90-29244

LIFE CYCLE COSTS
Compatibility of fuel system components with high density fuel
[AD-A210381] 01 p0006 N90-10027
Aerospace system unified life cycle engineering producibility measurement issues
[AD-A210937] 01 p0106 N90-10607
Terrestrial nickel/hydrogen battery development at Johnson Controls, Inc.
[DE89-015843] 06 p0769 N90-14471
Cost optimisation of reusable aerospaceplane transportation systems 09 p1175 N90-16803
Validation of an exponentially decreasing failure rate software reliability model
[AD-A215546] 09 p1235 N90-17165
Cost effectiveness of composite materials on the F-15 and F-16 aircrafts
[AD-A216353] 10 p1320 N90-17631
Life-cycle cost comparisons of advanced storage batteries and fuel cells for utility, stand-alone, and electric vehicle applications
[DE90-008090] 13 p1794 N90-20298
Preliminary design of a supersonic Short Takeoff and Vertical Landing (STOVL) fighter aircraft
[NASA-CR-186670] 17 p2352 N90-23394
An interactive life cycle cost forecasting tool
[AD-A220472] 17 p2480 N90-24184
Operations and support cost modeling using Markov chains 18 p2648 N90-25070
Retirement for cause of the F100 engine
21 p2957 N90-26813
Systems engineering management guide
[AD-A223168] 21 p3085 N90-27544
Computer support for conducting supportability trade-offs in a team setting
[AD-A222002] 22 p3237 N90-28355
Life cycle cost in the conceptual design of subsonic commercial aircraft, volumes 1 and 2
23 p3275 N90-28535
Operational cost drivers 23 p3294 N90-28636

LIFE RAFTS
Sweep width determination for HU-25B airborne radars: Life raft and recreational boat targets
[AD-A221362] 18 p2545 N90-24524

LIFE SCIENCES
NT EXTRATERRESTRIAL LIFE
NT MOLECULAR BIOLOGY
USSR Space Life Sciences Digest, issue 24
[NASA-CR-3922(28)] 03 p0378 N90-12152
Life science research in space
[ESA-SP-1105] 05 p0672 N90-13917
Human factors issues in performing life science experiments in a 0-G environment
05 p0679 N90-13952
USSR Space Life Sciences Digest. Index to issues 21-25
[NASA-CR-3922(30)] 06 p0819 N90-14783
X ray microimaging for the life sciences
[DE90-002613] 06 p0819 N90-14786
Exploring the living universe: A strategy for space life sciences
[NASA-TM-101891] 06 p0822 N90-14778
Space operations: Listing of NASA scientific missions, 1980-2000. Fact sheet for the Chairman, Subcommittee on Space Science and Applications, Committee on Science, Space, and Technology, House of Representatives
[AD-A213493] 07 p1016 N90-15881
Life sciences: Lawrence Berkeley Laboratory, 1988
[DE90-008061] 13 p1849 N90-20611
USSR Space Life Sciences Digest, issue 26
[NASA-CR-3922(31)] 14 p2009 N90-21513
USSR Space Life Sciences Digest, issue 25
[NASA-CR-3922(29)] 15 p2135 N90-22203
Strategic implementation plan
[NASA-TM-102907] 17 p2433 N90-23861
USSR space life sciences digest, issue 27
[NASA-CR-3922(32)] 19 p2717 N90-25457
JPRS report: Science and technology. USSR: Earth sciences
[JPRS-UES-90-004] 24 p3483 N90-29688
JPRS report: Science and technology. USSR: Earth sciences
[JPRS-UES-90-003] 24 p3483 N90-29689
JPRS Report: Science and technology. USSR: Life sciences
[JPRS-ULS-90-007] 24 p3497 N90-29762
JPRS report: Science and technology. USSR: Life sciences
[JPRS-ULS-90-004] 24 p3497 N90-29763

LIFE SUPPORT SYSTEMS
NT CLOSED ECOLOGICAL SYSTEMS
NT EMERGENCY LIFE SUSTAINING SYSTEMS
Independent Orbiter Assessment (IOA): Analysis of the extravehicular mobility unit
[NASA-CR-185540] 02 p0166 N90-10937
Independent Orbiter Assessment (IOA): CIL issues resolution report, volume 1
[NASA-CR-185524-VOL-1] 02 p0169 N90-10954
Independent Orbiter Assessment (IOA): Assessment of the atmospheric revitalization pressure control subsystem FMEA/CIL
[NASA-CR-185594] 02 p0170 N90-10957
Independent Orbiter Assessment (IOA): Assessment of the life support and airlock support systems, volume 1
[NASA-CR-185581-VOL-1] 02 p0174 N90-10977
Independent Orbiter Assessment (IOA): Assessment of the life support and airlock support systems, volume 2
[NASA-CR-185581-VOL-2] 02 p0174 N90-10978
Selective removal of organics for water reclamation
[NASA-CR-185959] 02 p0255 N90-11445
Independent Orbiter Assessment (IOA): Analysis of the life support and airlock support subsystems
[NASA-CR-185539] 03 p0314 N90-11786
USSR Space Life Sciences Digest, issue 24
[NASA-CR-3922(28)] 03 p0378 N90-12152
USSR Space Life Sciences Digest, issue 23
[NASA-CR-3922(27)] 03 p0378 N90-12154
The human factors relating to escape and survival from helicopters ditching in water
[AGARD-AG-305(E)] 05 p0576 N90-13358
CIS-lunar space infrastructure lunar technologies: Executive summary
[NASA-CR-186220] 06 p0865 N90-15029
DNSS: German/Norwegian work team Space Subsea. Environmental control and life support subsystems (technical matters), phase 2
[ETN-90-95905] 08 p1105 N90-16398
Suitport extra-vehicular access facility
[NASA-CASE-ARC-11635-1] 09 p1183 N90-16860
Hydrogen/oxygen SPE (trademark) electrochemical devices for zero-g applications 10 p1333 N90-17710

Regulation of nitrogen uptake and assimilation: Effects of nitrogen source, root-zone pH, and aerial CO2 concentration on growth and productivity of soybeans
[NASA-CR-177546] 10 p1413 N90-18147
Implications of Advanced Technologies for Air and Spacecraft Escape
[AGARD-CP-472] 13 p1751 N90-20054
Publications of the NASA Controlled Ecological Life Support System (CELSS) Program, 1979-1989
[NASA-CR-4297] 15 p2051 N90-21754
Space Station Freedom environmental control and life support system phase 3 simplified integrated test detailed report
[NASA-TM-4204] 16 p2207 N90-22593
Project WISH: The Emerald City
[NASA-CR-186692] 17 p2366 N90-23470
Identifying atmospheric monitoring needs for Space Station Freedom 18 p2628 N90-24977
A direct-interface, fusible heat sink for astronaut cooling
[NASA-TM-102835] 19 p2689 N90-25292
Utilization of the water soluable fraction of wheat straw as a plant nutrient source
[NASA-TM-103497] 19 p2716 N90-25455
Design and implementation of sensor systems for control of a closed-loop life support system
[NASA-CR-186675] 19 p2725 N90-25497
The environmental control and life support system advanced automation project. Phase 1: Application evaluation 19 p2730 N90-25523
Fluid Phase Separation (FPS) experiment for flight on a space shuttle Get Away Special (GAS) canister
[NASA-CR-186830] 20 p2841 N90-26161
Automation of closed environments in space for human comfort and safety
[NASA-CR-186834] 20 p2901 N90-26500
Development of membrane process for carbon dioxide separation from diving atmosphere
[AD-A222606] 20 p2901 N90-26504
Aircrew life support systems enhancement
[AD-A222626] 20 p2902 N90-26505
Lunar lander conceptual design
[NASA-CR-186233] 21 p2965 N90-26856
Space Station Freedom ECLSS: A step toward autonomous regenerative life support systems 21 p3043 N90-27297
Generation rates and chemical compositions of waste streams in a typical crewed space habitat
[NASA-TM-102799] 22 p3233 N90-28333
A solar power system for an early Mars expedition
[NASA-TM-103219] 22 p3243 N90-28393
Automated simulation as part of a design workstation
[NASA-TM-102852] 23 p3378 N90-29083
A lunar space station
[NASA-CR-186223] 24 p3563 N90-30158

LIFETIME (DURABILITY)
U LIFE (DURABILITY)

LIFT
NT ZERO LIFT
Experimental investigation of attachment-line transition in low-speed, high-lift wind-tunnel testing 01 p0062 N90-10358
Low-speed, high-lift aerodynamic characteristics of slender, hypersonic accelerator-type configurations
[NASA-TP-2945] 02 p0145 N90-10830
Wind tunnel results of the low-speed NLF(1)-0414F airfoil 04 p0444 N90-12541
Powered-lift aircraft technology
[NASA-SP-501] 04 p0452 N90-12589
Correlation of Puma airloads: Lifting-line and wake calculation
[NASA-TM-102212] 05 p0572 N90-13327
Induced drag for non-planar wings
[LR-521] 05 p0576 N90-13357
A direct-inverse method for transonic and separated flows about airfoils
[NASA-CR-4270] 07 p0875 N90-15072
The maximum lift coefficient of plain wings at subsonic speeds
[ESDU-89034] 07 p0876 N90-15082
Serrated trailing edges for improving lift and drag characteristics of lifting surfaces
[NASA-CASE-LAR-13870-1] 07 p0879 N90-15094
Using the method of matched asymptotic expansions, analytically investigate the three-dimensional, atmosphere entry problem
[AD-A216287] 11 p1468 N90-18451
Measurement of lift development on rapidly-accelerated wings 14 p1911 N90-20956
Application of a dynamic stall model to rotor trim and aeroelastic response 16 p2200 N90-22556
Unsteady potential flow past a propeller blade section
[NASA-CR-4307] 18 p2493 N90-24246
Hermes emergency reentry trajectories consequences on the Ariane 5 trajectories 22 p3127 N90-27747
Study of the ground effects in the CEAT aerohydrodynamic tunnel: Using the results 23 p3274 N90-28530
Numerical simulations of blade-vortex interactions and lifting hovering rotor flows
[AD-A224238] 24 p3417 N90-29302

LIFT COEFFICIENTS
U AERODYNAMIC COEFFICIENTS
U LIFT

LIFT DEVICES
Wind tunnel results of the high-speed NLF(1)-0213 airfoil 04 p0444 N90-12542
Aeroelastic control of composite lifting surfaces: Integrated aeroelastic control optimization 05 p0583 N90-13396
Installed tailplane lift-curve slope at subsonic speeds
[ESDU-89029] 07 p0876 N90-15081
The maximum lift coefficient of plain wings at subsonic speeds
[ESDU-89034] 07 p0876 N90-15082
Serrated trailing edges for improving lift and drag characteristics of lifting surfaces
[NASA-CASE-LAR-13870-1] 07 p0879 N90-15094
The SKY SHARK: An RPV designed to investigate the pressure distribution on a lifting surface
[NASA-CR-186222] 21 p2959 N90-26824

LIFT DISTRIBUTION
U FORCE DISTRIBUTION
U LIFT

LIFT DRAG RATIO
Design and test of a natural laminar flow/large Reynolds number airfoil with a high design cruise lift coefficient 04 p0444 N90-12543
Measurement of the aerodynamical coefficients related to square section models defined by resemblance to the normalized models AGARD HB1 and HB2 in supersonic flow. Part 2: Incidence up to 25 deg
[ISL-R-108/88-PT-2] 09 p1161 N90-16718
Hypersonic wavorider configurations for trans-atmospheric vehicles
[AD-A217925] 13 p1755 N90-20074
An aerodynamic tradeoff study of the scissor wing configuration
[NASA-CR-186576] 14 p1913 N90-20965

LIFT FORCES
U LIFT

LIFTING BODIES
NT LIFTING REENTRY VEHICLES
Unsteady aerodynamics of oscillating and rapidly pitched airfoils 07 p0875 N90-15074
Supersonic aerodynamic characteristics of a proposed Assured Crew Return Capability (ACRC) lifting-body configuration
[NASA-TM-4136] 10 p1307 N90-17560
Equations of motion of slung load systems with results for dual lift
[NASA-TM-102246] 10 p1322 N90-17641
Studies in non-linear unsteady aerodynamics
[AD-A221228] 19 p2654 N90-25108
A lifting surface method for the calculation of steady and unsteady, incompressible propeller aerodynamics
[ESA-TT-1151] 19 p2655 N90-25113
Aerodynamics of bodies in shear flow 23 p3268 N90-28496

LIFTING REENTRY VEHICLES
Optimum ascent performance of winged two-stage vehicles 09 p1177 N90-16816

LIFTING ROTORS
An analytical method for the prediction of unsteady rotor/airframe interactions in forward flight 06 p0724 N90-14223
Performance of an optimized rotor blade at off-design flight conditions
[NASA-CR-4288] 12 p1603 N90-19226
Development and application of a generalized dynamic wake theory for lifting rotors 15 p2046 N90-21731
Numerical simulations of blade-vortex interactions and lifting hovering rotor flows
[AD-A224238] 24 p3417 N90-29302

LIFTING SURFACES
U LIFT DEVICES
U LIFTING BODIES
U SURFACES

LIFTOFF (LAUNCHING)
Flight motor set 360L001 (STS-26R). (Reconstructed dynamic loads analysis)
[NASA-CR-183811] 04 p0464 N90-12656
A transient response analysis of the space shuttle vehicle during liftoff
[NASA-TM-103505] 22 p3125 N90-27735

LIFTS
Investigation of the effects of external supports on manual lifting
[PB90-103367] 09 p1260 N90-17307

LIGAMENTS
Non-ejection neck injuries in high performance aircraft 19 p2717 N90-25461
Experiment K-6-03. Gravity and skeletal growth, part 1. Part 2: Morphology and histochemistry of bone cells and vasculature of the tibia; Part 3: Nuclear volume analysis of osteoblast histogenesis in periodontal ligament cells; Part 4: Intervertebral disc swelling pressure associated with microgravity 20 p2892 N90-26457

LIGANDS
Electron density modulation of catalytic metal centers by substituted aryl-isocyanide ligands
[AD-A212875] 04 p0473 N90-12708
Electrochemical parameterization of metal complex redox potentials, using the ruthenium(III)/ruthenium(II) couple to generate a ligand electrochemical series
[AD-A214439] 08 p1041 N90-16015
The physical-organic chemistry of surfaces, and its relevance to molecular recognition
[AD-A215987] 10 p1354 N90-17850
Perfluorinated ligands in organometallic chemistry
[AD-A216415] 11 p1476 N90-18493
Ligand-centered electron-transfer redox processes for manganese, iron, and cobalt complexes in relation to selected catalytic systems
[AD-A217957] 13 p1773 N90-20177
Metal alkoxides: Models for metal oxides. Alkoxide ligands in early transition metal organometallic chemistry
[DE90-007523] 13 p1894 N90-20869
Theoretical studies of silicon chemistry
[AD-A219232] 16 p2225 N90-22690
Sigma and pi interactions of the pyrrolic ligand sandwich-like lanthanide phthalocyanines determined from magnetic susceptibility and ligand-field theory.
[AD-A223609] 24 p3443 N90-29444

LIGHT (VISIBLE RADIATION)
NT AIRGLOW
NT COHERENT LIGHT
NT GEOCORONAL EMISSIONS
NT NIGHTGLOW
NT POLARIZED LIGHT
NT SKY RADIATION
NT SUNLIGHT
NT ZODIACAL LIGHT
Raman characterization of high temperature materials using an imaging detector
[DE89-016308] 01 p0040 N90-10219
Turbulence effects on reflected optical patterns (atmosphere and structure)
[PB89-208094] 03 p0404 N90-12315
The visible channel of OMEGA-VIMS
[IFSI-89-14] 08 p1077 N90-16231
Attenuating the luminous output of the AN/PVS-5A night vision goggles and its effects on visual acuity
[AD-A214895] 09 p1261 N90-17311
New type of optical bistability in polymers mediated by phonons
[AD-A216102] 10 p1359 N90-17882
Investigation of multiple scattering in aqueous suspensions of non-absorbing polystrene microspheres using spectrophotometry
[BCRS-89-09] 11 p1485 N90-18549
Correlation-induced changes of spectra
[AD-A217087] 12 p1669 N90-19591
Speckle interferometry for high resolution pictures of astronomical objects
[ETN-90-95827] 12 p1729 N90-19936
Biological applications and effects of optical masers
[AD-A217910] 13 p1808 N90-20385
Microwave transmission line and method of modulating the phase of a signal passed through said line
[AD-D014457] 17 p2395 N90-23640
A laboratory study of the effects of diet and bright light countermeasures to jet lag
[AD-A220148] 17 p2435 N90-23875
Hot carrier in subpicosecond photoconductive experiments
[AD-A219874] 17 p2477 N90-24166
The low mass X ray binaries in the LMC 19 p2768 N90-25730
Optical observations of GS2000+25 19 p2773 N90-25762
Unusual counterparts of the soft X ray transients 4U 1543-47 and 4U 2129+47 in quiescence: Interlopers or third stars 19 p2773 N90-25764
XB 1905+00: A very compact low-mass X ray binary viewed at low inclination 19 p2773 N90-25765
QSO optical counts and constraints on the X ray background 19 p2789 N90-25877
Phase-sensitive optical detection of ballistic phonon pulses using frequency-modulation spectroscopy and persistent spectral holes
[AD-A221521] 21 p2979 N90-26930
Melatonin, light and, circadian cycles
[AD-A223196] 21 p3035 N90-27256

Serial interferometric fiber-optic sensor array
[AD-D014466] 22 p3246 N90-28407
Small angle generating apparatus
[AD-D014467] 22 p3246 N90-28408
Theoretical and experimental comparison of infrared and visible laser scattering from a variety of surface types
[RSRE-MEMO-4348] 24 p3474 N90-29636
Exogenous and endogenous control of activity behavior and the fitness of fish
[DLR-FB-90-14] 24 p3497 N90-29766

LIGHT ABSORPTION
U ELECTROMAGNETIC ABSORPTION

LIGHT ADAPTATION
Exogenous and endogenous control of activity behavior and the fitness of fish
[DLR-FB-90-14] 24 p3497 N90-29766

LIGHT AIRCRAFT
NT LIGHT HELICOPTERS
The effect of higher education variables on cadet performance during 1987 light aircraft training
[AD-A210199] 01 p0094 N90-10536
On simplified analytical flutter clearance procedures for light aircraft
[DLR-FB-89-56] 18 p2498 N90-24276

LIGHT ALLOYS
NT ALUMINUM ALLOYS
NT BERYLLIUM ALLOYS
NT MAGNESIUM ALLOYS
The evolution of light alloys in the aerospace industry
[ETN-89-95216] 03 p0329 N90-11872
NASA-UVA light aerospace alloy and structures technology program
[NASA-CR-182607] 16 p2217 N90-22651

LIGHT AMPLIFIERS
All-fiber SFPM (Stimulated Four Photon Mixing) amplifier
[AD-D014358] 12 p1713 N90-19841
Direct solar-pumped iodine laser amplifier
[NASA-CR-186442] 15 p2103 N90-22030
Beam propagation in direct nuclear pumped laser amplifiers
[DE90-009613] 15 p2104 N90-22035
Use of the Xybion ISG-camera in the RETRA-1000 TV-Holography unit
[AD-A219842] 18 p2554 N90-24577
The e-beam sustained CO2 laser amplifier
18 p2561 N90-24611
Performance of alumina-supported Pt catalysts in an electron-beam-sustained CO2 laser amplifier
18 p2561 N90-24613
Development of an all solid state 6 kHz pulse generator for driving free electron laser amplifiers
[AD-A224105] 24 p3463 N90-29561

LIGHT BEAMS
NT LASER BEAMS
Two dimensional modifications of Gaussian laser light bundles
[AD-A215207] 10 p1389 N90-18033
Thermal modulation of light beams
[AD-D014322] 12 p1713 N90-19840
Integrability and chaos in nonlinearly coupled optical beams
[DE90-007540] 13 p1888 N90-20834
Diamond: A high power optical material
[DE90-008941] 14 p1955 N90-21196
Method for holographic correction of beams of coherent light
[AD-D014406] 14 p1981 N90-21353
Relativistic light bending near neutron stars
19 p2779 N90-25810
Energy transmission by means of coherent quasi-mono-chromatic light beams
23 p3392 N90-29163

LIGHT BULBS
U LUMINAIRES

LIGHT COMMUNICATION
U OPTICAL COMMUNICATION

LIGHT CURVE
Pre-pulses: Signature of a trigger process in short (less than 60 secs) solar hard x ray flares
03 p0432 N90-12476
Variable stars 05 p0606 N90-13541
Mir-Kvant-Hexe hard x ray light curve of SN 1987A
17 p2482 N90-24197
The pulsed light curve of Vela X-1
17 p2483 N90-24202
Fast pulsars, strange stars
[DE90-011631] 19 p2765 N90-25710
The bright X ray transient GS2023+338 (=V404 Cyg) in optical outburst and decline 19 p2767 N90-25724
The low mass X ray binaries in the LMC
19 p2768 N90-25730
M15:AC211/X2127+119: Optical curve, improved ephemeris, and phasing of EXOSAT X ray data
19 p2771 N90-25749
X ray nova GS 2000+25 = Nova Vul 1988: X ray and optical light curves, spectra, and model
19 p2772 N90-25757
Optical observations of GS2000+25
19 p2773 N90-25762
Is KO Vel (E1013-477) an intermediate polar
19 p2773 N90-25766
Variability of the X ray sources in M31
19 p2773 N90-25768
Observations of black hole candidates with the Mir-Kvant HEXE 19 p2774 N90-25774
Mir-Kvant-HEXE hard X ray light curve of SN 1987A
19 p2775 N90-25776
The long-term optical behaviour of X Per = 3U 0352+30 19 p2776 N90-25783
The X ray dip source 4U 1624-49
19 p2776 N90-25786
Einstein SSS and MPC observations of Aql X-1 and 4U1820-30 19 p2777 N90-25790
The 3S0114+65 and its peculiar companion
19 p2777 N90-25792
Properties of circumstellar matter in GX301-2 observed by Tenma 19 p2778 N90-25798
The optical light curve of Cygnus X-1
19 p2778 N90-25801
A shell ejection model for optical light variations in Be stars: Application to Be/X ray binaries
19 p2779 N90-25804
Optical emission from the high inclination X ray transient EXO 0748-676 19 p2779 N90-25809
Search of the optical counterpart of the X rays source 1H 0521+373 19 p2780 N90-25815
The pulsed light curve of Vela X-1
19 p2781 N90-25819
A new transient X ray burst source near GX 1+4
19 p2782 N90-25826
Optical light curves of HZ Her in the model of freely precessing neutron star 19 p2783 N90-25831
Rapid X ray variability in BL Lacertae objects
19 p2787 N90-25862
Long timescale X ray variability in AGN
19 p2788 N90-25868
The interstellar D1 line at high resolution
[NASA-CR-184915] 20 p2941 N90-26737

LIGHT DURATION
U PULSE DURATION

LIGHT ELEMENTS
The shock process and light element production in supernovae envelopes
[NASA-CR-182854] 22 p3262 N90-28471

LIGHT EMISSION
NT BIOLUMINESCENCE
NT CATHODE GLOW
NT CATHODOLUMINESCENCE
NT CHEMILUMINESCENCE
NT ELECTROLUMINESCENCE
NT FLUORESCENCE
NT LASER INDUCED FLUORESCENCE
NT LUMINESCENCE
NT PHOSPHORESCENCE
NT PHOTOLUMINESCENCE
NT RESONANCE FLUORESCENCE
NT SPACECRAFT GLOW
NT THERMOLUMINESCENCE
NT X RAY FLUORESCENCE
Interplanetary dust close to the Sun (F corona): Its observation in the visible and infrared by a rocket-borne coronagraph 05 p0661 N90-13864
VLA and VLBI observations of core dominated quasars 06 p0860 N90-15002
Spacecraft optical contamination environment
[AD-A218088] 13 p1889 N90-20838
Extended optical emission in 3CR radio galaxies
15 p2193 N90-22523
Method and apparatus for determining optical absorption and emission characteristics of a crystal or non-crystalline fiber
[NASA-CASE-LAR-13963-1] 17 p2475 N90-24150
Multiwavelength constraints on gamma-ray burst sources 18 p2639 N90-25032
Experiments on initial behaviour of corona generated with electrical pulses superimposed on DC bias
[EUT-89-E-226] 20 p2858 N90-26259
Laser induced fluorescence imaging applications
24 p3420 N90-29322

LIGHT EMITTING DIODES
Fiber optic sensing system
[NASA-CASE-LEW-14795-1] 07 p0992 N90-15733
Liquid level measurement system for analog and digital readout
[AD-D014297] 08 p1076 N90-16227
Light source for dynamic testing of photo detectors
[FEL-1989-69] 22 p3247 N90-28414

LIGHT GAS GUNS
Solving the blow-by problem in a two-stage gun
[DE90-000842] 06 p0728 N90-14246
Acceleration of small, light projectiles (including hydrogen isotopes) to high speeds using a two-stage light gas gun
[DE90-002479] 06 p0729 N90-14253
Design limitations on ultra-high velocity projectile launchers
[DE89-012933] 07 p0885 N90-15118
Simple light gas guns for hypervelocity studies
[DE90-008907] 14 p1931 N90-21056
Railgun performance with a two-stage light-gas gun injector
[DE90-009183] 14 p1932 N90-21057

LIGHT HELICOPTERS
Hover position sensing system
21 p3069 N90-27448

LIGHT INTENSITY
U LUMINOUS INTENSITY

LIGHT IONS
Pulsed-power switching for inertial confinement fusion with light ion beams
[DE89-016810] 02 p0279 N90-11595
Light ion beam drivers for inertial confinement fusion
[DE90-004196] 08 p1127 N90-16528
Impedance characteristics of terawatt ion diodes
[DE90-006276] 12 p1652 N90-19494
Emission of quick neutrons and non-equilibrium phenomena by central shocks in the reaction 40 Ar + 40 Ca at 20 MeV/u
[ETN-90-97296] 24 p3544 N90-30043

LIGHT MODULATION
Characterization of liquid crystal displays for optical signal processing applications
[AD-A212832] 04 p0505 N90-12910
Optical modulators based on polymers
[EP-PATENT-0-294-061-A1] 05 p0700 N90-14099
Research on materials and components for opto-electronic signal processing and computing
[AD-A213740] 07 p1003 N90-15811
Electron-beam phase-only spatial light modulator for matched filtering
[AD-A215026] 09 p1282 N90-17431
Hybrid optical/digital architecture for distortion invariant pattern recognition
[AD-A215628] 09 p1282 N90-17435
Apparatus and method for minimizing polarization-induced signal fading in an interferometric fiber-optic sensor using input-polarization modulation
[AD-D014315] 12 p1642 N90-19430
Development of an all silicon integrated optical modulator for high speed data communications and sensor applications
[AD-A220270] 18 p2547 N90-24535
Optical calculation of correlation filters for a robotic vision system 18 p2630 N90-24986
Scanning electron microscopy by photovoltage contrast imaging
[AD-D014517] 19 p2760 N90-25684
Studies of the possible X ray triple 4U1915-05
19 p2768 N90-25727
All-optical photochromic spatial light modulators based on photoinduced electron transfer in rigid matrices
[NASA-CASE-NPO-17612-1-CU]
21 p3076 N90-27487
Effects and control of the correlation properties of light sources
[AD-A224539] 24 p3545 N90-30049
Optical signal computing
[AD-A223624] 24 p3545 N90-30051
Special purpose spatial light modulators
[AD-A223794] 24 p3545 N90-30052

LIGHT PRESSURE
U ILLUMINANCE

LIGHT PROBES
U LIGHT BEAMS

LIGHT SCATTERING
NT HALOS
An anisotropic shadowband correction for parameterized sky conditions and geometry
[DE89-014916] 01 p0085 N90-10485
The interaction of supernovae and pulsars with the circumstellar environment 02 p0293 N90-11671
Droplet sizing instrumentation used for icing research: Operation, calibration, and accuracy
[NASA-CR-182293] 03 p0350 N90-11999
Small particle scattering and absorption
[AD-A213168] 04 p0473 N90-12711
Semiconductor measurement technology: A software program for aiding the analysis of ellipsometric measurements, simple models
[PB89-235923] 04 p0560 N90-13261
Low frequency polarized and depolarized light scattering in H-bonded liquids: CH3(CH2)n-1OH (n=1,...5)
[PREPRINT-693] 05 p0700 N90-14100
Simulated Brillouin backscattering in optical fibers: A ring resonator 06 p0783 N90-14556

Research on acoustical scattering, diffraction catastrophes, optics of bubbles, acoustical phase conjugation, and wake of an oscillating circular cylinder
[AD-A214168] 07 p0989 N90-15711
SBS (Stimulated Brillouin Scattering) pulse distortion in multimode optical fibers: Preliminary results
[DE90-003023] 07 p0992 N90-15731
The middle Martian atmosphere
07 p1014 N90-15874
The determination of vortex separation frequencies by means of laser light sheet images
[DNW-WTI-88.038] 08 p1079 N90-16245
NASA Laser Light Scattering Advanced Technology Development Workshop, 1988
[NASA-CP-10033] 09 p1221 N90-17085
Laser light scattering review 09 p1221 N90-17086
Critical fluid light scattering 09 p1222 N90-17087
Miniature instrumentation for laser light scattering experiments 09 p1222 N90-17088
Design of fiber optic probes for laser light scattering
09 p1222 N90-17090
Maximum likelihood techniques in QELS
09 p1222 N90-17091
Improved optics for laser light scattering
09 p1222 N90-17092
Advanced instrumentation for QELS experiments
09 p1223 N90-17093
Enhanced resolution particle size distributions by multiple angle photon correlation spectroscopy
09 p1223 N90-17094
Online submicron particle sizing by dynamic light scattering using autodilution 09 p1223 N90-17095
Light scattering instrumentation for micro gravity research 09 p1223 N90-17096
Laser light scattering as a probe of fractal colloid aggregates 09 p1223 N90-17097
Proposed uses of laser light scattering instruments for polymerization studies 09 p1224 N90-17100
Polymer solution phase separation: Microgravity simulation 09 p1224 N90-17101
Magnetostatic wave device characterization by Brillouin light scattering
[AD-A213798] 09 p1281 N90-17426
On the temperature of surfaces
10 p1366 N90-17917
Fluorescence and elastic scattering from laser dye-filled capillaries
[AD-A217026] 11 p1484 N90-18540
Optical amplification in 45 deg - cut BaTiO3
[AD-A216043] 11 p1566 N90-19011
Light-scattering measurements of CVD (Chemical Vapor Deposition) silicon carbide
[DE90-007885] 12 p1632 N90-19382
Electronic and ionic transport in processable conducting polymers
[AD-A218093] 13 p1782 N90-20229
Characterization of fluid flow by digital correlation of scattered light
[NASA-CR-186403] 13 p1799 N90-20324
Stress field near crack tip: An experimental evaluation of the three dimensional variation
[AD-A217878] 13 p1818 N90-20441
Experimental and theoretical studies of light scattering by small particles
[AD-A217432] 13 p1888 N90-20831
Determinations of molecular weight and molecular weight distribution of high polymers by the rheological properties
[NASA-CR-186450] 14 p1953 N90-21180
Polarization: Effects on second harmonic power in light scattering by free electrons
[DE90-612842] 14 p2025 N90-21608
Large basis space effects in electron scattering form factors of light nuclei
[DE90-613501] 14 p2025 N90-21609
Brillouin gain spectroscopy in glasses and crystals
[DE90-009536] 15 p2067 N90-21841
Measurement of the reflectance ratio of natural light in the sea
[IOS-265] 15 p2135 N90-22199
Phase Doppler droplet sizing: Scattering angle effects
[DE90-009571] 16 p2236 N90-22754
Microstructure of thin films
[AD-A219262] 16 p2324 N90-23255
Optical properties of cometary dust
[AD-A218790] 16 p2338 N90-23325
Nondestructive measurement of residual stresses in aircraft transparencies
[AD-A218680] 17 p2415 N90-23762
Decay rate and resonance fluorescence spectrum of a molecule near a composite material surface
[AD-A219692] 19 p2671 N90-25192
Interaction of electromagnetic signals with particulate clouds
[AD-A222804] 20 p2856 N90-26244
Optical characterization of clouds of fine liquid-nitrogen particles
[NASA-TM-103208] 20 p2865 N90-26299
Investigations of polarized light scattering from rough surfaces
[AD-A221943] 21 p3076 N90-27491
Particle size distribution determined from measured scattered light
[MPIS-5/1990] 21 p3077 N90-27497
Scattering of CO2-laser radiation by water droplets
[FOA-C-20776-2.3] 22 p3181 N90-28049
The spatial scalar structure of premixed turbulent stagnation point flames
[DE90-014189] 23 p3303 N90-28686
Near-angle scattering and binary optics
[AD-A224140] 23 p3396 N90-29186
Definition of a near real time microbiological monitor for space vehicles
[NASA-CR-185599] 24 p3441 N90-29430
Submicron particle analyzer
[AD-A223558] 24 p3545 N90-30050
Light scattering from surface and sub-surface defects
[DE90-016311] 24 p3546 N90-30058
Photoinduced and holographically reinforced light diffusion in electrooptic crystals
[ETN-90-97321] 24 p3547 N90-30060

LIGHT SCATTERING METERS

Particle size distribution determined from measured scattered light
[MPIS-5/1990] 21 p3077 N90-27497

LIGHT SOURCES

Cockpit lighting compatibility with image intensification night imaging systems: Issues and answers
[AD-A210503] 01 p0006 N90-10028
Advanced light source master oscillator
[DE90-000123] 03 p0342 N90-11953
The national synchrotron light source and its applications
[DE89-017605] 03 p0405 N90-12320
A Scanning Photoelectron Microscope (SPEM) at the National Synchrotron Light Source (NSLS)
[DE90-001551] 06 p0780 N90-14537
Interferometric surface distortion detector
[AD-D014211] 06 p0842 N90-14901
Liquid level measurement system for analog and digital readout
[AD-D014297] 08 p1076 N90-16227
A new type of radioluminescent light source
[DE90-004294] 09 p1210 N90-17015
Research on stable high-efficiency, large area, amorphous silicon-based solar cells, phase 2
[DE89-009491] 09 p1242 N90-17208
Attenuating the luminous output of the AN/PVS-5A night vision goggles and its effects on visual acuity
[AD-A214895] 09 p1261 N90-17311
Research investigation directed toward extending the useful range of the electromagnetic spectrum
[AD-A217460] 13 p1789 N90-20267
Railgun performance with a two-stage light-gas gun injector
[DE90-009183] 14 p1932 N90-21057
Status of the advanced light source
[DE90-015636] 23 p3395 N90-29185
Effects and control of the correlation properties of light sources
[AD-A224539] 24 p3545 N90-30049

LIGHT TRANSMISSION

NT HALOS
NT LIGHT SCATTERING
Coherent multilchannel techniques for integrated broadband communications subscriber lines
[AD-A209323] 01 p0055 N90-10312
Improved propagation models for discrete random media
[AD-A211085] 01 p0057 N90-10327
Turbulence effects on reflected optical patterns (atmosphere and structure)
[PB89-208094] 03 p0404 N90-12315
Probability density function of optical scintillations (scintillation distribution)
[PB89-103912] 06 p0843 N90-14906
Solid-state phase equilibria in the ZnS-Ga2S3 system
[AD-A213944] 07 p0906 N90-15238
Nonlinear optical material studies
[AD-A213938] 07 p0993 N90-15737
Light-trapping concentrator cells
[DE90-004988] 09 p1242 N90-17205
Optical transmission through clouds
[AD-A214765] 09 p1248 N90-17240
Diamond: A high power optical material
[DE90-008941] 14 p1955 N90-21196
Differential polarimetric fiber optic sensor
[AD-D014501] 19 p2757 N90-25668
An embedded fibre optic sensor for impact damage detection in composite materials
[UTIAS-332] 20 p2926 N90-26650
Optical transmission through a polarization preserving single mode optical fiber at two Ar(+) laser wavelengths
[NASA-TM-103475] 20 p2926 N90-26651

LIGHTING

U ILLUMINATING

LIGHTING EQUIPMENT

NT AIRCRAFT LIGHTS
NT FLASH LAMPS
NT LUMINAIRES
NT RUNWAY LIGHTS
Cockpit lighting compatibility with image intensification night imaging systems: Issues and answers
[AD-A210503] 01 p0006 N90-10028
Human factors engineering testing of aircraft cockpit lighting systems
[AD-A216853] 12 p1697 N90-19743
Effect of laser glare and aircraft windscreen on visual search performance under low ambient lighting
[AD-A219456] 17 p2437 N90-23888

LIGHTNING

Varistor-particle lightning arrestor connector performance under simulated extreme lightning currents
[DE89-012663] 01 p0060 N90-10342
National Severe Storms Laboratory, fiscal year 1988
[PB89-156145] 01 p0087 N90-10493
Data processing in lightning warning systems
[DE89-012495] 01 p0088 N90-10502
The 1984 direct strike lightning data, part 1
[NASA-TM-87690-PT-1] 01 p0089 N90-10505
The 1984 direct strike lightning data, part 2
[NASA-TM-87690-PT-2] 01 p0089 N90-10506
The 1984 direct strike lightning data, part 3
[NASA-TM-87690-PT-3] 01 p0089 N90-10507
Internal voltages and currents in well-shielded cylindrical objects due to simulated direct-strike lightning
[DE89-012664] 02 p0215 N90-11231
Performance of transient limiters under laboratory, simulated, and rocket-triggered lightning conditions
[DE89-015773] 02 p0216 N90-11238
Numerical simulation of aeroplane response to a lightning injection
[ETN-89-95271] 03 p0303 N90-11716
Lightning and surge protection of photovoltaic installations: Two case histories, Vulcano and Kythnos
[PB89-229058] 03 p0374 N90-12135
Lightning data study in conjunction with geostationary satellite data
[NASA-CR-179286] 03 p0375 N90-12142
Long wave atmospheric noise model, phase 1. Volume 1: Lightning occurrence rates and propagation theory
[AD-A212794] 04 p0493 N90-12836
Catalog of absolutely calibrated, range normalized, wideband, electric field waveforms from located lightning flashes in Florida: July 24 and August 14, 1985 data
[AD-A212708] 04 p0521 N90-13008
Systems tunnel linear shaped charge lightning strike
[NASA-CR-183832] 05 p0584 N90-13404
Evaluation of the indirect effects of lightning on a system: Double transfer function method
[RAE-TRANS-2172] 06 p0721 N90-14211
JPS heater and sensor lightning qualification
[NASA-CR-183830] 06 p0779 N90-14530
Effects of lightning on operations of aerospace vehicles 07 p0873 N90-15065
Principal characteristics of lightning on aircraft
07 p0874 N90-15067
Characteristics of electromagnetic wave forms with lightning in winter season
[DE89-901256] 07 p0963 N90-15567
Lightning observations on Japan Sea coast in winter
[DE90-702485] 08 p1103 N90-16387
Characteristics of electromagnetic wave forms with lightning in winter season (2): Characteristics in frequency domain
[DE90-734989] 08 p1103 N90-16388
Rocket-triggered lightning strikes and forest fire ignition 08 p1155 N90-16690
Analysis of indirect effects of lightning on a metallic A 300 wing: Test report
[REPT-E87/645800] 09 p1162 N90-16726
Study on lightning parameters in the light of long gap discharge phenomena
[DE90-734987] 09 p1248 N90-17237
Continuing current in cloud-to-ground lightning
[DE90-741969] 10 p1408 N90-18119
The 1985 and 1986 direct strike lightning data, part 1
[NASA-TM-100533-PT-1] 10 p1409 N90-18125
The 1985 and 1986 direct strike lightning data, part 2
[NASA-TM-100533-PT-2] 10 p1409 N90-18126
Lightning surge characteristics of transmission towers. Lightning surge characteristics of 15-meter-high scale model tower
[DE89-782322] 12 p1692 N90-19721
Simulation fidelity in lightning penetration studies
[DE90-006367] 12 p1694 N90-19731

The 41st Annual Gaseous Electronics Conference
[AD-A214540] 12 p1715 N90-19851
Radar detection of lightning and electric fields
[AD-A217894] 13 p1842 N90-20574
Second National Winter Weather Workshop Conducted by the National Weather Service
[PB90-147414] 15 p2131 N90-22183
A case study of cloud-to-ground lightning during the GALE program 15 p2132 N90-22185
Tropical squall lines of the Arizona monsoon 16 p2257 N90-22867
A comparison of lightning network data with surface weather observations
[AD-A220003] 17 p2427 N90-23832
Evaluation of correlations between meteorological measurements and observations of lightning activity using artificial neural systems
[AD-A222659] 21 p3030 N90-27229
Climate of the Kennedy Space Center and vicinity
[NASA-TM-103498] 22 p3228 N90-28307
Size, duration, and rate of growth of nocturnal lightning events appearing on space shuttle video tapes
[NASA-CR-4313] 22 p3229 N90-28310
Study of the relationships between radar structure and the electrical activity of clouds
[ETN-90-97488] 23 p3352 N90-28946
Mesoscale Lightning Experiment (MLE): A view of lightning as seen from space during the STS-26 mission
[NASA-TM-103513] 23 p3353 N90-28951
Numerical simulation of the lightning return stroke 24 p3493 N90-29743

LIGHTNING SUPPRESSION
Varistor-particle lightning arrestor connector performance under simulated extreme lightning currents
[DE89-012663] 01 p0060 N90-10342
Performance of transient limiters under laboratory, simulated, and rocket-triggered lightning conditions
[DE89-015773] 02 p0216 N90-11238
Cable coupling lightning transient qualification
[NASA-CR-183826] 05 p0584 N90-13405
Lightning protection apparatus for RF equipment and the like
[AD-D014336] 12 p1650 N90-19483
Aircraft lightning protection handbook
[AD-A222716] 22 p3110 N90-27668

LIGHTS
U LUMINAIRES

LIGNIN
Assessment of biobased materials
[DE90-000300] 13 p1780 N90-20220

LIKELIHOOD RATIO
Utilization of the generalized likelihood ratio test for the suppression of systematic errors in noisy systems
[ETN-89-94656] 02 p0214 N90-11225
Software development for avionics SSME control and diagnostics
[NASA-CR-184894] 05 p0681 N90-13964
Likelihood ratio derivative estimators for stochastic systems
[AD-A213787] 07 p0984 N90-15684
Results on the detection of signals in spherically invariant random noise
[AD-A214933] 09 p1206 N90-16988
Kreim factorization of covariance operators of 2-parameter random fields and application to the likelihood ratio
[MEMO-802] 11 p1555 N90-18953
A hypothesis test of cumulative sums of multinomial parameters
[AD-A221466] 21 p3067 N90-27434

LIMB BRIGHTENING
The calculation of infrared limb emission by ozone in the terrestrial middle atmosphere 15 p2125 N90-22151

LIMBS (ANATOMY)
NT ARM (ANATOMY)
NT FEET (ANATOMY)
NT FINGERS
NT HAND (ANATOMY)
NT LEG (ANATOMY)

LIME
U CALCIUM OXIDES

LIMEN
Effect of contralateral masking parameters on difference limen for intensity
[AD-A214169] 10 p1411 N90-18135

LIMESTONE
Organic geochemical and tectonic evolution of the midcontinent rift system: Organic geochemistry and micropaleontology
[DE89-017561] 06 p0818 N90-14760
Geochemistry and origin of regional dolomites
[DE90-012589] 21 p3024 N90-27196

LIMITATIONS
U CONSTRAINTS

LIMITER AMPLIFIERS
Compression phenomena in hard-saturated microwave amplifiers
[AD-A214546] 09 p1204 N90-16980

LIMITER CIRCUITS
Current limiting mechanisms in electron and ion beams experiments
[AD-A212295] 04 p0460 N90-12637
Proposal of arc driving type fault current limiter
[DE89-782290] 12 p1650 N90-19485

LIMITERS (FUSION REACTORS)
Thermal loads on tokamak plasma facing components during normal operation and disruptions
[DE90-000794] 06 p0846 N90-14919
First pump limiter experiments in TORE SUPRA
[DE90-004968] 10 p1432 N90-18266
Particle transport in pellet fueled JET (Jet European Torus) plasmas
[DE90-008077] 13 p1891 N90-20851
Temperature-gradient instability induced by conducting end walls
[DE90-014334] 23 p3396 N90-29188
Overview of advanced fuel fusion
[DE90-015660] 24 p3550 N90-30085

LIMITS (MATHEMATICS)
Limit analysis of welded tee end connections for hollow tubes
[PB89-191647] 01 p0079 N90-10452
Domain of attraction of an operator between supremum and sum
[REPT-89-05] 04 p0539 N90-13119
Jacobi functions as limit cases of q-ultraspherical polynomials
[CWI-PM-R8807] 04 p0541 N90-13139
Convergence of one-leg multistep methods for stiff nonlinear initial value problems
[CWI-NM-R8911] 17 p2459 N90-24040
Hausdorff measure and boundary behavior of analytic functions
[ETN-90-96501] 18 p2605 N90-24835
The existence of smooth densities for the prediction filtering and smoothing problems
[AD-A222108] 21 p3066 N90-27432

LIMNOLOGY
Remote sensing of interior water: Perspectives
[INPE-4875-PRE/1486] 11 p1531 N90-18815
Activities report of the Hydraulics Research Laboratory
[ETN-90-96568] 19 p2687 N90-25281
A two layer model for the simulation of internal linear and nonlinear waves in Lake Geneva (Switzerland) 19 p2687 N90-25286
On the fine-scale mixing in the metalimnion and the seasonal thermocline of the Leman (Lake Geneva, Switzerland) 19 p2688 N90-25288
The 5th International symposium on palaeolimnology
[AD-A219244] 20 p2887 N90-26431

LINE CURRENT
Voltage source ac-to-dc converters for high-power transmitters 15 p2075 N90-21886

LINE OF SIGHT
LAWS simulation: Sampling strategies and wind computation algorithms 03 p0364 N90-12081
A Scheiner-principle pocket optometer for self-evaluation and biofeedback accommodation training
[AD-A213171] 04 p0524 N90-13027
An approach to optical structures control 05 p0595 N90-13456
The moving platform simulator 2: A networked real-time visual simulator with distributed processing and line-of-sight displays
[AD-A214936] 09 p1266 N90-17343
User-friendly software for the design of digital line-of-sight radio links
[PB90-118472] 12 p1700 N90-19760
Field-of-view assessment of low-level flight and an airdrop in the C-130 Weapon System Trainer (WST)
[AD-A218504] 16 p2200 N90-22559
Skewering the universe with QSO lines of sight: Lyman alpha clouds as probes of large scale structure 16 p2329 N90-23278
Evaluation of Stochastic models for estimating the persistence probability of cloud-free lines-of-sight
[AD-A220283] 18 p2581 N90-24702

LINE SHAPE
Model-independent analysis of the Z line shape in e + e- annihilation
[PREPRINT-679] 05 p0698 N90-14089
Extracting chemical information form Auger line shapes
[AD-A216729] 11 p1483 N90-18537
Spectral line shape code for multielectron emitters
[DE90-008526] 13 p1891 N90-20853

LINE SPECTRA
NT BALMER SERIES
NT ELECTRONIC SPECTRA
NT FRAUNHOFER LINES
NT H ALPHA LINE
NT H BETA LINE
NT H LINES
NT K LINES
NT LYMAN SPECTRA
NT RYDBERG SERIES
X-ray bright points and He I lambda 10830 dark points 01 p0139 N90-10802
Nonlinear optical studies of resonant systems
[AD-A211032] 02 p0227 N90-11301
The Si(1-x)Nx Rugate
[AD-A211236] 02 p0275 N90-11572
Quantitative interpretation of auger lineshapes and electron/photon stimulated desorption
[AD-A211550] 03 p0324 N90-11842
Far infrared, submm and mm spectroscopy of the galactic center: Radio arc and +20/+50 km s (exp -1) clouds
[NASA-CR-185497] 04 p0565 N90-13296
Far-infrared heterodyne receivers 05 p0597 N90-13465
Archival research on absorption lines in violently star-forming galaxies
[NASA-CR-185960] 05 p0712 N90-14163
Gamma ray lines from dark matter annihilation
[DE90-000779] 06 p0864 N90-15021
The upper main sequence of OB associations. Part 2: The single-lined O stars: Spectral classification of northern stars and lines of C and N
[SER-C-PREPUBL-FASC-39] 08 p1139 N90-16602
Temperature dependence of photon-gated persistent spectral hole-burning for the meso-tetra-p-tolyl Zn-tetrabenzoporphyrin/chloroform system in poly(methylmethacrylate)
[AD-A216086] 11 p1482 N90-18531
Millimeter-wave propagation in the mesosphere
[PB90-119868] 11 p1496 N90-18612
Ultrasensitive laser spectroscopy in solids: Single-molecule detection
[AD-A216085] 11 p1514 N90-18716
GRIS observations of the Galactic Center 11 p1559 N90-18982
Positron annihilation in gamma-ray bursts 11 p1559 N90-18983
IR line emission from dense photodissociation regions 11 p1580 N90-19100
Near infrared spectroscopy of the supernova remnant RCW103 11 p1581 N90-19109
High-excitation lines of molecular hydrogen: A discriminant between shock models 11 p1582 N90-19118
Planetary nebulae 11 p1583 N90-19122
Observations of 40-70 micron bands of ice in IRAS 09371+1212 and other stars 11 p1585 N90-19134
Predictions of infrared recombinations lines in stellar winds of hot stars 11 p1585 N90-19136
JCMT observations of the circumstellar envelope IRC+10216 11 p1585 N90-19138
Infrared lines as probes of galactic structure 11 p1585 N90-19139
An infrared imaging Fabry-Perot study of the galactic centre 11 p1586 N90-19142
The strengths of the 2.3 micron CO band in luminous interacting and merging galaxies 11 p1587 N90-19148
H-alpha emission lines in high redshift quasars 11 p1587 N90-19149
Infrared (FeII), H and H2 lines in galaxy nuclei 11 p1587 N90-19153
Power spectral densities for selected digital phase-continuous MFSK (M-ary Frequency Shift Keying) emissions
[PB90-129990] 12 p1647 N90-19463
Definition study of Laser Experimental Active Fluorsensor (LEAF)
[BCRS-88-18] 12 p1668 N90-19582
Correlation-induced changes of spectra
[AD-A217087] 12 p1669 N90-19591
Far-ultraviolet spectroscopy of Comet Halley 12 p1736 N90-19979
O-star parameters from line profiles of wind-blanketed model atmospheres 12 p1736 N90-19982
The adaptive line enhancer applied to chirp detection
[DE90-006772] 13 p1789 N90-20268
Spectral line shape code for multielectron emitters
[DE90-008526] 13 p1891 N90-20853
Zones of feasibility for retrieval of surface pressure from observations of absorption in the A band of oxygen
[DAR-TP-19] 14 p2006 N90-21495
Experimental study of population inversion and spectral line broadening in a plasma containing a mixture of high Z and low Z ions
[DE90-007552] 14 p2027 N90-21622
Problems in radiative transfer in astrophysics: An escape probability treatment of line overlap and a model of the masers around VX Sgr 14 p2041 N90-21705

Injection-seeded Nd:YAG laser linewidth measurement using saturation spectroscopy in iodine
[DE90-009537] 15 p2103 N90-22034
Improved crystal bending techniques applied to the LLNL dual-arm Johann mounting x ray spectrometer
[DE90-009528] 15 p2173 N90-22415
Kinematic models of cometary comae 15 p2188 N90-22495
High spatial resolution isotopic CO and CS observations of M17 SW: The clumpy structure of the molecular cloud core
[MPE-PREPRINT-161] 16 p2330 N90-23283
Infrared coronal line novae 16 p2339 N90-23328
An intensity expression organising spectral line intensity data
[IRF-SR-202] 17 p2373 N90-23513
Spectral variability of LMC X-4 17 p2483 N90-24204
X ray spectra of OVV QSOs 19 p2787 N90-25863
Extended line emission in AGN: Looking at the central engine 19 p2788 N90-25870
A search for iron features in the EXOSAT spectral survey sources 19 p2791 N90-25887
Infrared line parameters at low temperatures relevant to planetary atmospheres 20 p2944 N90-26753
Line identification studies using traditional techniques and wavelength coincidence statistics
[NASA-CR-186901] 22 p3261 N90-28467

LINEAMENT
U STRUCTURAL PROPERTIES (GEOLOGY)

LINEAR ACCELERATORS
A battery-powered, solid state magnetic compressor with applications for high PRF accelerators and lasers
[DE89-015770] 01 p0058 N90-10332
A proposed linac cavity RF drive system for the Los Alamos extreme ultraviolet free-electron laser
[DE89-016614] 03 p0353 N90-12016
Use of the NPL linac for x ray dosimetry --- linear accelerator (linac)
[NPL-RSA(EXT)-6] 03 p0404 N90-12314
Radio frequency linac driven free-electron laser configurations
[AD-A212572] 04 p0507 N90-12922
Compact RF-linac free-electron lasers
[DE90-002386] 06 p0790 N90-14600
An Energy Spectrum Compressor system (ESC) for the Amsterdam pulse stretcher (AmPS) 06 p0842 N90-14896
The 17.1-GHz free-electron laser as a microwave source for TeV colliders
[DE90-001506] 07 p0934 N90-15406
Proposal for a study of laser acceleration of electrons using micrograting structures at ATF
[DE90-003699] 08 p1082 N90-16262
To construct a linac/storage ring FEL facility
[AD-A214620] 09 p1211 N90-17020
Electron beam and high-speed optical diagnostics for the Los Alamos HIBAF (High Brightness Accelerator FEL) Facility
[DE90-007828] 11 p1515 N90-18725
On 140 GHz microwave FEL experiments using ELF-2
[DE90-006764] 12 p1667 N90-19576
Fifth-order aberrations in magnetic quadrupole-octupole systems
[DE90-007489] 12 p1712 N90-19831
Gamma-ray production cross section measurements using a white neutron source from 1 to 400 MeV
[DE90-008906] 14 p2025 N90-21610
Free electron lasers driven by linear induction accelerators: High power radiation sources 15 p2060 N90-21800
Foil focusing of electron beams
[AD-A219511] 16 p2317 N90-23208
Pulse-width dependent radiation effects on electronic components
[AD-A219517] 17 p2395 N90-23643
Use of the TACL system at CEBAF for control of the cryogenic test facility
[CEBAF-PR-89-024] 19 p2755 N90-25652
The CEBAF instrumentation and control system
[CEBAF-PR-89-037] 19 p2755 N90-25657
Design of CEBAF's RF separator and results of cold tests
[CEBAF-PR-89-021] 19 p2756 N90-25658
On using a superconducting linac to drive a short wavelength FEL
[CEBAF-PR-89-019] 19 p2756 N90-25660
High repetition rate kickers for linear colliders
[CEBAF-PR-89-020] 19 p2756 N90-25661
Requirements for longitudinal HOM damping in superconducting recirculating linacs
[CEBAF-PR-89-018] 19 p2756 N90-25662
A simple beam position monitor system for CEBAF
[CEBAF-PR-89-015] 19 p2757 N90-25664
DURIP: Instrumentation for laser switched power LINAC
[AD-A222629] 20 p2868 N90-26318
A beauty factory using an SRF linac and a storage ring
[CEBAF-PR-89-017] 20 p2925 N90-26644
Characterization of electron flow in positive-polarity linear-induction accelerators
[DE90-014998] 23 p3394 N90-29177
RF power generation for future linear colliders
[DE90-014804] 23 p3394 N90-29178
Effects and tolerances of injection jitter in the SLC and future linear colliders
[DE90-014805] 23 p3394 N90-29179
Long pulse diode experiments
[DE90-016218] 24 p3465 N90-29578
Medium energy nuclear physics research
[DE90-015852] 24 p3544 N90-30042

LINEAR ARRAYS
NT YAGI ANTENNAS
Angle estimation in a multipath environment with an eight element linear array operating at 10.5 GHz
[FEL-1989-15] 04 p0491 N90-12826
First test results with a CCD camera developed by INPE
[INPE-4873-PRE/1484] 10 p1388 N90-18029
Navigation software for the MPL vertical line array
[AD-A220166] 17 p2432 N90-23860
Estimation of noise field directionality: Comparison with Fourier series method
[AD-A220366] 17 p2469 N90-24114
Development of a hybrid adaptive beamformer
[AD-A219652] 17 p2471 N90-24128
An L-band antenna array with integrated phase shifters
[DLR-FB-89-63] 18 p2544 N90-24519
Optical high-speed parallel backplane
[AD-D014504] 19 p2757 N90-25670
A laser spectrometer and wavemeter for pulsed lasers
[NASA-CR-181731] 23 p3331 N90-28832
Block Lanczos algorithm
[AD-A224011] 23 p3383 N90-29111
Performance analysis of subspace-based parameter estimation algorithms
[AD-A224523] 24 p3463 N90-29566
Characteristics of pushbroom scanning type radiometer utilizing linear sensors
[NAL-TR-1024] 24 p3472 N90-29625

LINEAR ENERGY TRANSFER (LET)
Linear free energy relations for multielectron transfer kinetics: A brief look at the Bronsted/Tafel analogy
[AD-A215078] 12 p1710 N90-19823
On the relationship between energy density and net power (intensity) in coupled one-dimensional dynamic systems
[AD-A221071] 19 p2709 N90-25421
An advanced single event upset tester
[AD-A223613] 24 p3564 N90-30163

LINEAR EQUATIONS
NT LINEAR EVOLUTION EQUATIONS
NT RICCATI EQUATION
A study of the asymptotic behavior of linear difference equations with polynomial coefficients
[IMAG-RR-743-M] 03 p0395 N90-12254
The convergence behavior of some iterative solution methods
[REPT-89-19] 03 p0396 N90-12260
Kinematics, special configurations and performance evaluation of serial manipulators 04 p0508 N90-12927
Solution of the Boltzmann equation using an energy group method
[AD-A213138] 05 p0699 N90-14096
Group implicit concurrent algorithms in nonlinear structural dynamics
[NASA-CR-185950] 06 p0796 N90-14638
Krylov methods preconditioned with incompletely factored matrices on the CM-2
[NASA-CR-181961] 06 p0822 N90-14779
Mixed singular linear elliptic equations
[DE90-600722] 07 p0982 N90-15674
Projection techniques for image restoration 09 p1263 N90-17322
Studies in statistical signal processing
[AD-A214490] 09 p1275 N90-17393
A method for computing the stationary points of a function subject to linear equality constraints
[DE90-610427] 12 p1706 N90-19797
Observer based compensators for nonlinear systems
[AD-A217426] 13 p1876 N90-20760
Modal identities for multibody elastic spacecraft: An aid to selecting modes for simulation 16 p2296 N90-23075
An intensity expression organising spectral line intensity data
[IRF-SR-202] 17 p2373 N90-23513
On the parallel solution of parabolic equations
[NASA-CR-180363] 17 p2455 N90-24009
Progress in the polynomial solution of the standard H-infinity optimal control problem
[MEMO-817] 18 p2597 N90-24777
An approach to systematic phase-lock loop design
[ETN-90-96905] 19 p2686 N90-25280
Using implicit ODE methods with iterative linear equation solvers in spectral methods
[FFI-89/7017] 19 p2751 N90-25633
Asymptotic optimality of the fast randomized versions of GCV and C(sub L) in ridge regression and regularization
[IMAG-RR-793-M] 20 p2918 N90-26606
Contribution to the study of differential equations and to the differences in the complex field
[ETN-90-97250] 20 p2919 N90-26612
Efficient implementation of minimal polynomial and reduced rank extrapolation methods
[NASA-TM-103240] 20 p2920 N90-26616
Applied mathematical modules for use in a linear algebra service course
[AD-A222814] 20 p2920 N90-26618
Linear algebra on a CRAY X-MP
[AD-A221780] 21 p3056 N90-27374
Investigations on improved iterative methods for solving sparse systems of linear equations
[AD-A221980] 21 p3064 N90-27417
Particle size distribution determined from measured scattered light
[MPIS-5/1990] 21 p3077 N90-27497
Linear iterative solvers for implicit ODE methods
[NASA-CR-182074] 22 p3242 N90-28386
Parallel algorithms for computation of the manipulator inertia matrix 23 p3376 N90-29072

LINEAR EVOLUTION EQUATIONS
Control and stabilization of linear and nonlinear distributed systems
[AD-A216446] 11 p1547 N90-18908
The synergism of analytic and numerical techniques in general relativity: Calculation of radiative spacetimes 15 p2174 N90-22425

LINEAR FILTERS
NT KALMAN FILTERS
On the Hellinger type distances for filtered experiments
[CWI-MS-R8818] 04 p0542 N90-13146
Higher order crossings from a parametric family of linear filters
[AD-A213427] 07 p0983 N90-15676
An analysis of the time variation of the frequency response of the LMS adaptive line enhancer
[ISVR-TR-175] 08 p1058 N90-16115
Parameter estimation in linear filtering
[AD-A218566] 16 p2307 N90-23144
Filter process for parasitic suppression for reception of spectrally separated emission signals
[ETN-90-96506] 18 p2545 N90-24526

LINEAR INTEGRATED CIRCUITS
Rigorous calculations of lumped electrical parameters for a microstrip interdigitated electrode structure
[AD-A215337] 10 p1378 N90-17989

LINEAR OPERATORS
Well posedness of triples of operators (in the sense of linear systems theory)
[TW-292] 04 p0545 N90-13168
Some remarks on the gap metric
[MEMO-COSOR-88-34] 05 p0690 N90-14029
Completion of the squares in the finite horizon H infinity control problem by measurement feedback
[MEMO-COSOR-89-27] 17 p2455 N90-24004
On a method for computing eigenvalues and eigenfunctions of linear differential operators
[PREPRINT-706] 17 p2456 N90-24013
A spatial operator algebra for manipulator modeling and control 24 p3519 N90-29894

LINEAR POLARIZATION
VLA and VLBI observations of core dominated quasars 06 p0860 N90-15002
The sensitivity of EGRET to gamma ray polarization 16 p2335 N90-23305
Equal path, phase shifting, sample point interferometer for monitoring the configuration of surfaces
[NASA-CASE-NPO-17913-1-CU] 21 p3076 N90-27488
Robust controller design by contraction of a pole region
[ESA-TT-1042] 23 p3384 N90-29118

LINEAR PREDICTION
The convergence behavior of some iterative solution methods
[REPT-89-19] 03 p0396 N90-12260
Dual task performance with LPC (Linear Predictive Coding) degraded speech in a sentence verification task
[AD-A214298] 07 p0920 N90-15320
Speech coding 21 p2992 N90-27009

Toeplitz matrices: Algebra and algorithms
[AD-A223174] 21 p3064 N90-27416

LINEAR PROGRAMMING
Primal barrier methods for linear programming
[AD-A210501] 01 p0105 N90-10600
Partially specified probability measures in expert systems
[CWI-CS-R8842] 02 p0269 N90-11536
A polynomial method of approximate weighted centers for linear programming
[REPT-89-13] 03 p0388 N90-12210
A matrix factorization and its application to large-scale linear programming
[AD-A211293] 03 p0394 N90-12244
Iterative methods for linear complementary and related problems
[AD-A212848] 04 p0534 N90-13089
Monte Carlo (importance) sampling within a Benders' decomposition algorithm for stochastic linear programs
[AD-A212854] 04 p0548 N90-13189
Stopping rules for a class of random methods for detecting necessary linear inequality constraints
[MEMO-777] 05 p0683 N90-13977
Description and manipulation of convex polygons using polarity
[IMAG-RR-771-M] 05 p0692 N90-14041
The parallel decomposition of linear programs
[DE90-003538] 07 p0974 N90-15625
Neural network models for linear programming
[DE89-015974] 07 p0979 N90-15651
A neural network for bounded linear programming
[DE89-015975] 07 p0979 N90-15652
Polynomial transfer lot sizing techniques for batch processing on consecutive machines
[AD-A214198] 07 p0980 N90-15660
Numerical optimization
[AD-A213758] 07 p0984 N90-15683
Using goal programming to determine the optimal engine mix for UH-1 helicopters
[AD-A214893] 09 p1168 N90-16762
Piecewise linear-quadratic programming and its applications
[AD-A214489] 09 p1264 N90-17328
Dynamic factorization in large-scale optimization
[AD-A214568] 10 p1416 N90-18161
Faster scaling algorithms for general graph matching problems
[AD-A215112] 10 p1417 N90-18163
Nonprocedural implementation of mathematical programming algorithms
[AD-A216039] 10 p1419 N90-18179
Optimum spanwise camber for minimum induced drag
[BU-403] 11 p1452 N90-18369
Vertical migration in operational system nucleus
[INPE-4879-RPE/593] 11 p1543 N90-18883
Distributed decomposition of block-angular linear programs on a hypercube computer
[AD-A216433] 11 p1545 N90-18893
Recurrence conditions for average and Blackwell optimality in denumerable state Markov decision chains
[TW-89-02] 11 p1555 N90-18952
Computational methods and plasticity
[LR-583] 15 p2119 N90-22120
Optimal 3-dimensional methods for linear programming
[PB90-155391] 15 p2145 N90-22253
Symbolic pattern processing system for planar spatial structures
[DE90-001598] 15 p2146 N90-22256
Long steps with the logarithmic penalty barrier function in linear programming
[REPT-89-44] 15 p2147 N90-22265
Contractivity in the maximum norm for Runge-Kutta methods
[TW-89-06] 15 p2162 N90-22352
Linear programming tools for integer programming
[AD-A219013] 16 p2300 N90-23106
About linear systems robustness: Linear programming approach
[LAAS-89-384] 16 p2303 N90-23123
A survey of search directions in interior point methods for linear programming
[REPT-89-65] 17 p2445 N90-23934
An O(square root of n) complexity reduction for the long-step path-following algorithm for linear programming
[REPT-89-85] 17 p2445 N90-23940
On linear time minor tests and depth first search
[RUU-CS-89-1] 17 p2446 N90-23944
A vectorization algorithm for the solution of large, sparse triangular systems of equations
[AD-A219850] 17 p2446 N90-23947
Adaptive filtering and control
[AD-A219556] 17 p2454 N90-23998
A solution for the variance-penalized Markov decision problem based on parametric linear programming
[TW-90-02] 17 p2467 N90-24100
Collision detection using linear programming
18 p2507 N90-24326
A block-LU update for large-scale linear programming
[AD-A219849] 18 p2590 N90-24738
Adaptive and comparative studies of optimization algorithms: Implementations and applications
[ETN-90-97243] 20 p2910 N90-26553
Computer assisted analysis and modelling of structured problems
[AD-A222991] 21 p3052 N90-27350
The Second Asilomar Workshop on Progress in Mathematical Programming
[AD-A221986] 21 p3053 N90-27358
A build-up interior method for linear programming: Affine scaling form
[AD-A221802] 21 p3056 N90-27375
Study of the feasibility of several mixtures
[IMAG-RR-776-M] 21 p3057 N90-27379
Numerical solutions to steady-state problems with discontinuities
[AD-A222205] 21 p3064 N90-27418
Investigation of maximum achievable body torque for a walking machine with friction cone constraints
[PB90-203175] 23 p3332 N90-28838
Workshop on Neural Networks
[DE90-014794] 23 p3385 N90-29120
Time optimal movement of cooperating robots
24 p3505 N90-29815
New approaches to linear and nonlinear programming
[AD-A224328] 24 p3525 N90-29932

LINEAR QUADRATIC GAUSSIAN CONTROL
Modelling and control of a diffusion/LPCVD furnace
[REPT-88-97] 03 p0336 N90-11910
Nongaussian linear filtering, identification of linear systems, and the symplectic group
[CWI-PM-R8810] 04 p0547 N90-13184
The totally singular linear quadratic problem with indefinite cost
[MEMO-COSOR-89-05] 05 p0687 N90-13998
Crew emergency return vehicle autoland feasibility study
[NASA-CR-181940] 08 p1028 N90-15937
Design of integrated pitch axis for autopilot/autothrottle and integrated lateral axis for autopilot/yaw damper for NASA TSRV airplane using integral LQG methodology
[NASA-CR-4268] 09 p1169 N90-16768
Experiments in end-point control of a flexible robot with a mini-manipulator 12 p1671 N90-19596
H2, fixed architecture, control design for large scale systems
[NASA-CR-180471] 16 p2226 N90-22698
Combined control-structure optimization
16 p2282 N90-23005
Integrated control-system design via generalized LQG (GLQG) theory 16 p2286 N90-23023
Overview of computational control research at UT Austin 16 p2291 N90-23051
Substructural controller synthesis
16 p2292 N90-23055
Approximation in LQG control of a thermoelastic rod
16 p2297 N90-23084
Real time adaptive control of an Autonomous Underwater Vehicle (AUV)
[AD-A219544] 17 p2454 N90-23996
Control of orbiting large space structural systems with discrete time observational data and random measurement noise
[AD-A222476] 21 p2967 N90-26863
Optimal control law phenomena in certain adaptive second-order observation systems
[AD-A224274] 24 p3534 N90-29986

LINEAR QUADRATIC REGULATOR
NT LINEAR QUADRATIC GAUSSIAN CONTROL
Autonomous spacecraft attitude control using magnetic torquing only 05 p0586 N90-13415
The algebraic Riccati equation and singular optimal control
[MEMO-COSOR-88-31] 05 p0690 N90-14028
An interactive system applied to the linear quadratic problem
[INPE-4945-TDL/386] 11 p1548 N90-18913
Contribution to the study of stability robustness of nonlinear multivariable regulators
[INPE-4801-TDL/356] 11 p1554 N90-18950
Integrated control/structure optimization by multilevel decomposition
[NASA-TM-102619] 12 p1613 N90-19281
Discrete-time control of a spacecraft with retargetable flexible antennas 13 p1763 N90-20119
Discrete-time control of a spacecraft with retargetable flexible antennas
[AD-A218345] 13 p1764 N90-20125
On the continuous dependence with respect to sampling of the linear quadratic regulator problem for distributed parameter systems
[NASA-CR-182012] 14 p2018 N90-21566
A decentralized linear quadratic control design method for flexible structures 15 p2054 N90-21770
Combined control-structure optimization
16 p2282 N90-23005
An algorithm for the solution of dynamic linear programs 16 p2286 N90-23026
A priori results in linear-quadratic optimal control theory (extended version)
[MEMO-COSOR-89-17] 16 p2304 N90-23124
Simulation and interdisciplinary design methodology for control-structure interaction systems
17 p2385 N90-23584
Linear-quadratic problems and the Riccati equation
[MEMO-COSOR-89-26] 17 p2459 N90-24037
Structure of linear-quadratic control
[ETN-90-96894] 18 p2602 N90-24819
Approximations of thermoelastic and viscoelastic control systems
[NASA-CR-182054] 18 p2604 N90-24834
An LQR controller design approach for a Large Gap Magnetic Suspension System (LGMSS)
[NASA-TM-101606] 23 p3316 N90-28751

LINEAR REGULATOR
U LINEAR QUADRATIC REGULATOR

LINEAR SYSTEMS
Regulation of nonlinear and generalized linear systems
[AD-A207725] 01 p0109 N90-10619
Studies in estimation theory, applications and implementations
[AD-A210712] 01 p0114 N90-10653
Adaptive feedback linearization: Stability and robustness
[PB89-219497] 03 p0390 N90-12220
A dynamic proof of the Frobenius-Perron theorem for Metzler matrices
[AD-A211839] 03 p0392 N90-12235
On the differentiable manifold of fixed order stable linear systems
[REPT-88-89] 03 p0394 N90-12250
Some observations on the convergence behavior of GMRES
[REPT-89-09] 03 p0395 N90-12252
The convergence behavior of some iterative solution methods
[REPT-89-19] 03 p0396 N90-12260
Advanced actuation systems development, volume 1
[AD-A213334] 04 p0458 N90-12624
Solving three dimensional block bidiagonal linear systems on vector computers
[REPT-89-14] 04 p0530 N90-13056
Solving 3D block bidiagonal linear systems on vector computers
[CWI-NM-R8819] 04 p0530 N90-13061
Formal calculations and parallesism. Solving linear systems
[ETN-89-95499] 04 p0536 N90-13098
Well posedness of triples of operators (in the sense of linear systems theory)
[TW-292] 04 p0545 N90-13168
Exponential modeling using combined forward and backward prediction
[AD-A212317] 04 p0545 N90-13169
Nongaussian linear filtering, identification of linear systems, and the symplectic group
[CWI-PM-R8810] 04 p0547 N90-13184
Advanced actuation systems development, volume 2
[AD-A213378] 05 p0583 N90-13398
A transient response method for linear coupled substructures
[NASA-TP-2926] 05 p0592 N90-13444
Model reduction of weakly damped mechanical systems
[MEMO-798] 05 p0686 N90-13993
The output-stabilizable subspace and linear optimal control
[MEMO-COSOR-89-15] 05 p0687 N90-14001
A multilevel parallel solver for block tridiagonal and banded linear systems
[AD-A213151] 05 p0688 N90-14008
The regular indefinite linear quadratic problem with linear endpoint constraints
[MEMO-COSOR-88-15] 05 p0690 N90-14022
Stabilizability and detectability of discrete-time time-varying systems
[MEMO-COSOR-88-16] 05 p0690 N90-14023
A graph theoretic characterization for the rank of the transfer matrix of a structured system
[CWI-OS-R8819] 05 p0695 N90-14064
A mixed finite element solution of the linear acoustic equations
[ECL-89-006] 05 p0697 N90-14075

Optimal stochastic modeling and control of flexible structures
|AD-A212347| 06 p0733 N90-14269
Parameter estimation of linear systems in the presence of process noise using the maximum liklihood method
|ESDU-89032| 07 p0985 N90-15693
Linear digital imaging system fidelity analysis 08 p1072 N90-16205
Element-by-element preconditioning techniques for large-scale, vectorized finite element analysis in nonlinear solid and structural mechanics 08 p1087 N90-16291
Uniform stability for time-varying infinite-dimensional discrete linear systems
|DE89-635712| 08 p1116 N90-16460
Nonparametric estimation of trends in linear stochastic systems
|AD-A213741| 09 p1272 N90-17374
Domain decomposition with local mesh refinement
|AD-A215806| 10 p1418 N90-18175
Numerical algorithms for parallel computers
|AD-A216812| 10 p1419 N90-18181
Control and stabilization of linear and nonlinear distributed systems
|AD-A216446| 11 p1547 N90-18908
Adaptive state estimation and sampling rate analysis for invariant linear dynamic systems in time
|INPE-4960-TDL/389| 11 p1554 N90-18951
Simple analytic potentials for linear ion traps 12 p1642 N90-19436
Computational aspects of sensitivity calculations in linear transient structural analysis
|NASA-TM-4156| 12 p1673 N90-19610
Parallel algorithms for boundary value problems
|NASA-TM-102498| 12 p1704 N90-19783
A linear systems theory approach to the range-independent acoustic channel
|AD-A216551| 12 p1710 N90-19817
An approximation theory for the identification of linear thermoelastic systems
|NASA-CR-182015| 13 p1877 N90-20764
Stochastic robustness of linear control systems 14 p1908 N90-20941
Dynamic response of structures with uncertain parameters 15 p2119 N90-22125
A nearly-linear computational-cost scheme for the forward dynamics of an N-body pendulum 16 p2280 N90-22996
A survey on the structured singular value 16 p2281 N90-22998
Robustness analysis for real parametric uncertainty 16 p2281 N90-23000
H(2)- and H(infinity)-design tools for linear time-invariant systems 16 p2286 N90-23025
About linear systems robustness: Linear programming approach
|LAAS-89-384| 16 p2303 N90-23123
Fractional state feedback control of undamped and viscoelastically-damped structures
|AD-A220477| 17 p2412 N90-23746
Bit-optimal election in synchronous rings
|RUU-CS-89-2| 17 p2446 N90-23945
Almost disturbance decoupling by measurement feedback: A frequency domain analysis
|CWI-BS-R8910| 17 p2455 N90-24005
Structure of linear-quadratic control
|ETN-90-96894| 18 p2602 N90-24819
Analog electronic control differential transmitter
|AD-D014508| 19 p2685 N90-25272
On two transformations in the generalized theory of linear systems
|MATHS-REPT-A-109| 19 p2751 N90-25629
Limit cycles and bifurcation in piecewise-linear and piecewise-analytic systems. 1: General theory
|RR-372| 19 p2751 N90-25634
Inhomogeneous electric field effects in a linear RF quadruple trap 20 p2853 N90-26222
On output deadbeat control of discrete-time multivariable systems
|MATHS-REPT-A-122| 20 p2915 N90-26583
On the robust stability of MIMO linear feedback systems
|EUT-88-E-212| 20 p2915 N90-26585
Parallel/distributed direct method for solving linear systems
|NASA-TM-103229| 20 p2919 N90-26614
Some remarks on the generalised Bareiss and Levinson algorithms
|AD-A221957| 21 p3053 N90-27357
Algorithms and evaluation for regulation of linear, time-independent difference systems under position value limitation
|ETN-90-97308| 22 p3238 N90-28364
Frequency analysis via the method of moment functionals
|NASA-CR-186988| 22 p3239 N90-28367
Control and estimation for aerospace applications with system time delays 24 p3428 N90-29367
Robust design of LQG controllers 24 p3475 N90-29639
Modeling towed cable system dynamics
|AD-A223610| 24 p3476 N90-29644
Systems reliability and inference: Summary of accomplishments 1988-1990
|AD-A224433| 24 p3477 N90-29653
On the stability of robotic systems with random communication rates 24 p3514 N90-29865
Computer-aided engineering environment for controlled mechanical systems
|AD-A223551| 24 p3527 N90-29942
Some overdetermined systems of complex partial differential equations
|DE90-627162| 24 p3536 N90-29995

LINEAR TRANSFORMATIONS
Global linear representations of nonlinear systems and the adjoint map
|RR-347| 03 p0394 N90-12247
Minimal complexity control law synthesis 16 p2292 N90-23057
Compensatability and optimal compensation of systems with stochastic parameters
|REPT-89-61| 17 p2457 N90-24024
A Bayesian proportional model for software reliability
|IMAG-RR-795-M| 20 p2874 N90-26353
Asymptotic law of the orthogonal empirical functions and applications, part 2
|IMAG-RR-792-M-PT-2| 20 p2918 N90-26605
Improved front-end analysis in the ARM system: Linear transformations of SRUbank
|RSRE-MEMO-4358| 22 p3166 N90-27953

LINEAR VIBRATION
Analysis of nonlinear systems using ARMA (Autoregressive Moving Average) models
|DE90-002395| 08 p1088 N90-16297

LINEARITY
Improved estimation of the disturbance variance in a linear regression model
|AD-A210272| 01 p0112 N90-10641
Convective heat transfer in hypobaric environments
|AD-A212060| 03 p0347 N90-11979
On the existence of a maximal weak solution for a semilinear elliptic equation
|REPT-89-06| 04 p0539 N90-13120
Linear groups and distance-transitive graphs
|CWI-PM-R8805| 05 p0691 N90-14036
Fluid transmission line dynamics for signals of finite amplitude
|AD-A215758| 10 p1385 N90-18014
On detecting influential data and selecting regression variables
|AD-A216387| 10 p1423 N90-18213
Computational aspects of adaptive dimensional reduction for nonlinear boundary value problems
|AD-A219889| 17 p2461 N90-24052
M-estimators in linear models with long range dependent errors
|AD-A219921| 17 p2461 N90-24053
On a problem of F. Ruskey
|MEMO-832| 17 p2463 N90-24068

LINEARIZATION
Parameter identification for an abstract Cauchy problem by quasilinearization
|NASA-CR-181933| 03 p0385 N90-12192
Smooth linearization of hyperbolic fixed points without resonance conditions
|REPT-89-03| 03 p0394 N90-12251
Towards a complete local solution of the nonlinear model matching problem
|MEMO-781| 04 p0545 N90-13166
Another approach to the local disturbance decoupling problem with stability for nonlinear systems
|MEMO-799| 05 p0691 N90-14033
Computational aerodynamics of ordered vortex flows
|ETN-90-96272| 11 p1452 N90-18368
Nonlinear model matching: A local solution and two worked examples
|MEMO-809| 11 p1554 N90-18948
Recursive linearization of multibody dynamics equations of motion 16 p2280 N90-22993
A control problem for Burgers' equation with bounded input/output
|NASA-CR-182062| 19 p2747 N90-25608
Analysis and design methods for nonlinear control systems
|AD-A221621| 21 p3061 N90-27404
The discretization of the three dimensional boundary layer equations
|ETN-90-97292| 22 p3171 N90-27987

LINERS
U LININGS

LINES (GEOMETRY)
NT GEODESIC LINES
Intersecting line segments, ray shooting, and other applications of geometric partitioning techniques
|RUU-CS-88-26| 18 p2601 N90-24804
Counting and reporting intersections in arrangements of line segments
|RUU-CS-89-12| 18 p2601 N90-24808
Hierarchical structure of polygonal data for spatial analysis and representation of cartographical data
|INPE-4986-PRE/1548| 20 p2879 N90-26380

LING-TEMCO-VOUGHT AIRCRAFT
NT F-8 AIRCRAFT

LINGUISTICS
NT MACHINE TRANSLATION
NT PHONEMES
NT SEMANTICS
NT SENTENCES
NT SYNTAX
NT WORDS (LANGUAGE)
Augmentations of grammatical categories in distributional-algebraic models of natural languages
|REPT-89-24| 03 p0396 N90-12262
Some techniques for anaphora resolution in algebraic linguistics
|REPT-89-28| 03 p0396 N90-12265
Self-organizing semantic maps
|PB89-212609| 04 p0529 N90-13049
Anaphoric trees and an extension of the model of anaphora resolution
|REPT-89-37| 04 p0540 N90-13130
Knowledge based text generation
|AD-A214273| 07 p0977 N90-15645
Research and development in natural language understanding as part of the strategic computing program
|AD-A214611| 09 p1265 N90-17333
Approaches tc the planning of coherent text
|AD-A216463| 11 p1545 N90-18895
Knowledge-based extensible natural language interface technology program
|AD-A216664| 11 p1545 N90-18897
Computational structure of GPSG (Generalized Phrase Structure Grammar) models: Revised generalized phrase structure grammar
|AD-A216803| 11 p1553 N90-18941
Rules and maps in connectionist symbol processing
|AD-A219028| 16 p2264 N90-22903
Sentence comprehension: A parallel distributed processing approach
|AD-A218886| 16 p2300 N90-23104
Syntax, semantics, and pragmatism: An integrated focus based on textual linguistic knowledge
|INPE-4992-PRE/1554| 16 p2326 N90-23262
Rhetorical structure theory and text analysis
|AD-A222655| 20 p2941 N90-26733
Knowledge and distributed computation
|AD-A223100| 21 p3039 N90-27270
Efficiency and effectiveness of deep structure-based subject indexing languages: PRECIS vs. DSIS 23 p3406 N90-29248
Statement of research objectives and summary of research efforts
|RLE-PR-132| 23 p3415 N90-29295

LININGS
NT ROCKET LININGS
Steam cooled rich-burn combustor liner
|NASA-CASE-LEW-13609-1| 03 p0321 N90-11824
Elasticity effects on cavitation in a squeeze film damper undergoing noncentered circular whirl
|NASA-TM-102392| 05 p0649 N90-13786
MATE (Materials for Advanced Turbine Engines) Program, Project 3. Volume 2: Design, fabrication and evaluation of an oxide dispersion strengthened sheet alloy combustor liner
|NASA-CR-180892| 10 p1357 N90-17868
Hydrocarbon-fuel/combustion-chamber-liner materials compatibility
|NASA-CR-185203| 14 p1950 N90-21165
Internal wire guide for GTAW welding
|NASA-CASE-MFS-29489-1| 17 p2385 N90-23586
Thermodynamic and fluid mechanic analysis of rapid pressurization in a dead-end tube 18 p2631 N90-24990
Experiment K-6-17. Structural changes and cell turnover in the rats small intestine induced by spaceflight 20 p2895 N90-26470
Energy efficient engine pin fin and ceramic composite segmented liner combustor sector rig test report
|NASA-CR-179534| 23 p3281 N90-28567
Development of improved self lubricating cages for SSME HPOTP bearings 23 p3292 N90-28623
Cage stability analysis for SSME HPOTP bearings 23 p3292 N90-28625
Parametric studies of acoustic duct attenuation ofperforated-plate-on-honeycomb absorber
|NAL-TM-603| 24 p3542 N90-30030

LINKAGES
Shape control of high degree-of-freedom variable geometry trusses
01 p0024 N90-10122
Modeling and simulation of spatial robotic manipulators with flexible links and joint drives for control strategies implementation and evaluation
02 p0228 N90-11311
An analytical and experimental study of the elastodynamic response characteristics of planar linkage mechanism with bearing clearances
02 p0233 N90-11336
A procedure for force-balancing planar linkages using counterweights
[ESDU-89028] 07 p0940 N90-15446
Skin friction balance
[NASA-CASE-LAR-13710-1] 09 p1226 N90-17117
A comparison of techniques for balancing planar linkages
[ESDU-89043] 09 p1232 N90-17150
Releasable clamping apparatus
[NASA-CASE-MFS-28192-1] 09 p1233 N90-17154
Cycle life machine for AX-5 space suit
15 p2112 N90-22080
The coupling effects of kinematics and flexibility on the Lagrangian dynamic formulation of open chain deformable links
16 p2284 N90-23018
Core sample extractor
[NASA-CR-182864] 17 p2411 N90-23740
Mobility studies in multiloop spatial linkages
20 p2922 N90-26628
Dynamical modeling of serial manipulators with flexible links and joints using the method of kinematic influence
24 p3500 N90-29783

LINKING
U JOINING

LINKS
Computer conferencing: Minds meeting anywhere anytime
15 p2179 N90-22452

LINKS (MATHEMATICS)
On rectilinear link distance
[RUU-CS-89-13] 18 p2634 N90-25008

LIOUVILLE EQUATIONS
Modeling Doppler broadening in Raman propagation
[DE90-008042] 13 p1789 N90-20269
A Lagrangian formalism for nonequilibrium ensembles
[DE90-612748] 14 p2020 N90-21579
Convergence of hyperspherical adiabatic expansion for helium-like systems
[DE90-620526] 16 p2214 N90-22631
Weighted norm inequalities for Riemann-Liouville fractional integral
[DE90-627153] 23 p3388 N90-29132

LIPIDS
NT CASTOR OIL
NT CORTICOSTEROIDS
NT FATS
NT PROSTAGLANDINS
Electrical field dependence of protein conformation and channel function in lipid membranes of different compositions
[AD-A210236] 01 p0040 N90-10222
Membrane fusion: The role of polyphosphatidylinositol
[AD-A211289] 03 p0379 N90-12156
Molecular dynamics of lipid bilayers
[AD-A211492] 04 p0552 N90-13214
Transport processes through monomolecular films
[AD-A213609] 07 p0923 N90-15342
Influence of theobromine on heat production and body temperatures in cold-exposed humans: A preliminary report
[AD-A217203] 13 p1850 N90-20618
A new class of lubricants derived from archaebacterial lipids
[AD-D014429] 14 p1954 N90-21185

LIQUEFACTION
NT COAL LIQUEFACTION
Evaluation of industrial magnetic heat pump/refrigerator concepts that utilize superconducting magnets
[DE90-008093] 13 p1787 N90-20258

LIQUEFIED GASES
NT LIQUID HELIUM
NT LIQUID HELIUM 2
NT LIQUID HYDROGEN
NT LIQUID NITROGEN
NT LIQUID OXYGEN
Study on the thermodynamical and mechanical conditions for the generation of high operating pressures with liquefied gases for low and very low flow rates
[ESA-TT-1148] 11 p1510 N90-18696
High speed commercial transport fuels considerations and research needs
[NASA-TM-102535] 15 p2072 N90-21869
Performance evaluation of LE-7 high pressure pumps
[DE90-505523] 20 p2817 N90-26034

LIQUID ALLOYS
Solidification of dilute alloys under fluctuating residual gravity
[REPT-892-430-112] 17 p2377 N90-23535

LIQUID ATOMIZATION
Survey of the CLUSE main experiment Grand-CLUSE, May 1 - June 15, 1988 --- Humidity Exchange Over the Sea (HEXOS) experiment
[FEL-1988-43] 04 p0518 N90-12991
Scattered-light scanner measurements of cryogenic liquid-jet breakup
[NASA-TM-102432] 15 p2101 N90-22021
Fundamental studies on spray combustion and turbulent combustion
[AD-A219840] 18 p2521 N90-24394

LIQUID CHROMATOGRAPHY
A new method for the characterization of solutes and solvent phases using solvatochromic parameters
[AD-A211238] 02 p0196 N90-11118
The prediction of middle distillate fuel properties using liquid chromatography-proton nuclear magnetic resonance spectroscopy data
[AD-A211879] 03 p0334 N90-11899
Research and Development Opportunities in Supercritical Fluid Technology
[DE89-015320] 04 p0469 N90-12684
Supercritical fluid chromatography/supersonic jet spectroscopy
[DE90-001378] 06 p0740 N90-14308
Compensation for peak shifts and variable background responses in fluorescence spectroscopy
[DE90-001102] 07 p0892 N90-15154
High-temperature gel-permeation chromatography of poly(4-methyl-1-pentene)
[DE90-002967] 07 p0893 N90-15159
Application of high performance liquid chromatography/mass spectrometry to environmental analysis
[PB90-116963] 11 p1531 N90-18814
Determinations of molecular weight and molecular weight distribution of high polymers by the rheological properties
[NASA-CR-186450] 14 p1953 N90-21180
HPLC analysis of helicopter rotor blade materials
[AD-A221121] 18 p2497 N90-24270
Improvements in macroreticular particles for ion-exchange and gel-permeation chromatography
[DE90-003717] 18 p2522 N90-24399
Construction of a UV cell for micro-liquid chromatography
[PML-1989-B] 22 p3156 N90-27894
Supercritical fluid chromatography/supersonic jet spectroscopy
[DE90-015220] 24 p3447 N90-29465

LIQUID COOLED REACTORS
NT PATHFINDER NUCLEAR REACTOR
NT ZERO POWER REACTORS

LIQUID COOLING
NT FILM COOLING
Modification, testing, and calibration of infrared search and target designator hardware received from NSWC
[AD-A217920] 13 p1889 N90-20837
Experiments on liquid immersion natural convection cooling of leadless chip carriers mounted on ceramic substrate
[AD-A219893] 17 p2478 N90-24167
Natural convection form an array of rectangular protrusions in an enclosure filled with dielectric fluid: Effects of boundary conditions, fluid Prandtl number, and selective powering
[AD-A219819] 18 p2552 N90-24563
Thermal protection systems for reentry and hypersonic flight
[ESA-TT-1179] 19 p2667 N90-25177
Evaluation of water cooled supersonic temperature and pressure probes for application to 2000 F flows
[NASA-TM-102612] 19 p2753 N90-25645
Work enhancement and thermal changes during intermittent work in cool water after carbohydrate loading
[AD-A222877] 21 p3034 N90-27247

LIQUID CRYSTALS
Mechanical properties, solubilities, and processabilities in the design of the first super-strong liquid-crystalline polymers
[DE89-009252] 01 p0048 N90-10273
Flow visualization techniques for flight research
02 p0153 N90-10878
Composites reinforced with thermotropic liquid crystal copolyester fibers
[AD-A211226] 02 p0191 N90-11089
Chevron layer structures in Surface Stabilized Ferroelectric Liquid Crystal (SSFLC) cells filled with a material which exhibits the chiral nematic to smectic C* phase transition
[DE89-016985] 02 p0285 N90-11628
Advanced measurement techniques, part 1
04 p0441 N90-12520
Characterization of liquid crystal displays for optical signal processing applications
[AD-A212832] 04 p0505 N90-12910
Studies of structure and switching dynamics in ferroelectric crystal and liquid crystal thin films
[AD-A212650] 05 p0702 N90-14109
Visualization of boundary layer transition zone movement on oscillating airfoils with shear-sensitive liquid-crystal coatings
[DE89-009570] 06 p0721 N90-14210
The structure and properties of liquid crystal polymers
06 p0749 N90-14356
Optical solitons in liquid crystals
[DE90-000694] 07 p0991 N90-15728
Simultaneous determination of temperature and velocity fields in a thermal convection flow with non-enclosed liquid crystal tracers
08 p1078 N90-16239
Unsteady heat transfer measurement using thermochromatic liquid crystals as temperature indicators
08 p1081 N90-16254
Surface flow visualization with shear stress sensitivive liquid crystals
[DNW-WTI-88.039] 08 p1081 N90-16255
Quantitative heat transfer measurements using heated liquid crystals
08 p1081 N90-16256
Conformation, orientation and interaction in molecular monolayers: A surface second harmonic and sum frequency generation study
[DE90-003108] 09 p1128 N90-16536
Structures instabilities in filament liquid crystals
[ETN-90-95916] 12 p1721 N90-19888
Rigid rod molecules as liquid crystal thermosets
[AD-A217573] 13 p1770 N90-20158
Copolymer-like structures of nematic nitroimine dimers
[AD-A217574] 13 p1780 N90-20215
Polymer liquid crystals with side chain discogens
[AD-A218013] 13 p1782 N90-20228
LLE review
[DE90-008958] 14 p1985 N90-21378
Synthesis and properties of a thermotropic copolyester based on 4,4 prime-dihydroxy-a,a prime-dimethylbenzalazine
[AD-A218803] 16 p2223 N90-22682
Processing of thermotropic liquid crystalline polymers and their blends
[AD-A218804] 16 p2223 N90-22683
Synthesis and characterization of aromatic polyester and polysiloxane containing block copolymers: Multiphase transparent atomic oxygen resistant damping materials, liquid crystal films, and toughening components of sol/gel glasses
[AD-A218871] 16 p2224 N90-22685
Characterization and processing of blends of polyethylene terephthalate with several liquid crystalline polymers
[AD-A219565] 17 p2380 N90-23552
Nonlinear optical responses and laser damage thresholds of films of a polarized stilbene side chain liquid crystal polymer and a phthalocyanine
[AD-A219462] 17 p2408 N90-23720
NMR and optical studies of piezoelectric polymers
[DE90-012459] 20 p2837 N90-26137
Elastomers and other organic composites
[AD-A222772] 21 p2984 N90-26958
Liquid crystalline polymers
[NASA-CR-186949] 21 p2986 N90-26971
Novel side-chain liquid cyrstalline polymers
[AD-A221998] 22 p3159 N90-27911
Structure and dynamic properties of combined polymeric main-chain/side-chain liquid crystals
[ETN-90-97299] 22 p3160 N90-27921
Electric properties of highly oriented rigid chain, polymeric liquid crystals
[ETN-90-97287] 22 p3248 N90-28424
Use of liquid crystals for qualitative and quantitative 2-D studies of transition and skin friction
[RAE-TM-AERO-2159] 23 p3325 N90-28800

LIQUID DROPS
U DROPS (LIQUIDS)

LIQUID FILLED SHELLS
Computational fluid dynamics method for low Reynolds number flow in a precessing/spinning, liquid filled cylinder with rounded endcaps
[AD-A216997] 12 p1659 N90-19531
Interior fluid dynamics of liquid-filled projectiles
[AD-A217630] 13 p1800 N90-20330
On the spatial eigenvalue approach to high Reynolds number flow in a rotating and nutating cylinder
[AD-A221710] 21 p3005 N90-27081
Investigation of the dynamic buckling of liquid-filled tanks
24 p3478 N90-29660

LIQUID FLOW
NT OPEN CHANNEL FLOW
NT WATER FLOW

Analysis of new phenomena in shear flow of non-Newtonian fluids
[AD-A212893] 05 p0638 N90-13721
Pipeline vibrations. Fluid transients in non-rigid, unbranched planar piping systems
[ESDU-89030] 07 p0948 N90-15491
Command operated liquid metal opening switch
[AD-D014262] 08 p1060 N90-16126
Some observations on liquid flow through filters
[AERE-R-13300] 16 p2234 N90-22748
The role of gravity on macrosegregation in alloys
[NASA-CR-186530] 19 p2679 N90-25238
Effect of a crystal-melt interface on Taylor-Vortex flow with buoyancy
[PB90-244401] 24 p3551 N90-30089

LIQUID FUELS
NT AIRCRAFT FUELS
NT AUTOMOBILE FUELS
NT DIESEL FUELS
NT GASOLINE
NT HYDROGEN FUELS
NT JET ENGINE FUELS
NT JP-4 JET FUEL
NT JP-8 JET FUEL
NT KEROSENE
Very-low-frequency oscillations in liquid-fueled ramjets 01 p0037 N90-10204
High energy density solid and liquid hydrocarbon fuels
[AD-A210195] 01 p0053 N90-10304
Crystal structure of Tetra-Ammonium Adamantyl Tetra-Nitrate (TAATN): High energy/density fuel candidate for liquid propellant
[AD-A215684] 09 p1201 N90-16955
Optimum catalytic process for alcohol fuels from syngas
[DE90-005290] 11 p1494 N90-18600
Electrochemical phase diagrams for aqueous redox systems
[AD-A217168] 13 p1770 N90-20157
A comparison between experiment and simulation for concept VIC regenerative liquid propellant guns. Part 1: 30 mm
[AD-A218556] 16 p2225 N90-22692
Fundamental studies on spray combustion and turbulent combustion
[AD-A219840] 18 p2521 N90-24394
The jet engine: 1932
[ISBN-3-922010-49-0] 19 p2670 N90-25189
Liquid fueled ramjet combustion instability: Acoustical and vortical interactions with burning sprays
[AD-A222752] 20 p2831 N90-26104
Calculation of the combustion distribution in a liquid-fuel ramjet 22 p3162 N90-27931
Ignition and combustion of liquid propellants
[AD-A224150] 23 p3316 N90-28746

LIQUID HELIUM
NT LIQUID HELIUM 2
Quasi-diffusion between phonon and roton gases in two- and three-dimensional liquid helium
[AD-A210565] 02 p0192 N90-11096
Symmetry breaking phenomena in liquid Helium-4
[DE89-618886] 04 p0469 N90-12685
Persistent current, NMR, and ion transmission experiments in rotating He-3 superfluids --- Nuclear Magnetic Resonance (NMR)
[ISBN-952-90056-1-X] 04 p0553 N90-13221
Construction of the rotating cryostat ROTA2, its use for zero sound experiments in (3)He-B, and calculations of ion mobility in (3)He-A and (3)He-P
[ISBN-952-90091-3-5] 05 p0645 N90-13765
Path integral simulations of liquid helium
[DE90-001171] 06 p0836 N90-14862
Design and testing of a superfluid liquid helium cooling loop
[NASA-CR-182776] 09 p1216 N90-17050
Nonlinear acoustic interactions in superfluid helium 15 p2164 N90-22367
Millimeter-wave acoustic transducers
[AD-A221402] 18 p2612 N90-24878
Spacecraft thermal control design data, volume 5. Section R: Cryogenic cooling. Section S: Existing satellites
[ESA-PSS-03-108-ISSUE-1-VOL-5] 22 p3132 N90-27772

LIQUID HELIUM 2
Design and testing of a superfluid liquid helium cooling loop
[NASA-CR-182776] 09 p1216 N90-17050
Superfluid helium orbital resupply coupling 11 p1475 N90-18488
Mechano-caloric cooling device
[NASA-CR-186316] 12 p1662 N90-19552
BASG thermomechanical pump helium 2 transfer tests
[NASA-CR-177541] 14 p1939 N90-21097
Experiments on the breakdown of heat transfer in liquid helium 2
[MPIS-13/1989] 16 p2326 N90-23259
Thermophysical properties of Helium-4 from 0.8 to 1500 K with pressures to 2000 MPa
[NASA-CR-186992] 23 p3303 N90-28681

LIQUID HYDROGEN
Liquid rocket booster study. Volume 2, book 1
[NASA-CR-183600] 01 p0026 N90-10133
Program for high speed computation of physical properties of propellants and combustion gas of an LH2/LOX rocket engine
[NAL-TM-564] 03 p0318 N90-11803
Spacecraft attitude impacts on COLD-SAT non-vacuum jacketed LH2 supply tank thermal performance
[NASA-TM-103158] 16 p2207 N90-22592
Initial experimentation on the nonvented fill of a 0.14m3 (5 ft. 3) dewar with nitrogen and hydrogen
[NASA-TM-103155] 20 p2862 N90-26278

LIQUID INJECTION
Electrolyte dependence of charge injection processes for electroactive polymer films
[AD-A210787] 02 p0202 N90-11152
The evaluation of a metered mixer for RTV silicone for RSRM nozzle backfill operations
[NASA-CR-183831] 05 p0645 N90-13763
Liquid Transfer Cryogenic Test Facility: Initial hydrogen and nitrogen no-vent fill data
[NASA-TM-102572] 14 p1972 N90-21295

LIQUID LEVELS
Liquid level measurement system for analog and digital readout
[AD-D014297] 08 p1076 N90-16227

LIQUID LITHIUM
Wick-type liquid-metal combustion
[AD-A216019] 11 p1482 N90-18530

LIQUID MERCURY
U MERCURY (METAL)

LIQUID METAL FAST BREEDER REACTORS
Static pressure distribution in an angular channel with helicoidal wire
[DE89-636474] 07 p0928 N90-15374

LIQUID METALS
NT LIQUID LITHIUM
NT LIQUID SODIUM
NT MERCURY (METAL)
Beam dynamics of a liquid metal ion source
[DE89-015856] 03 p0401 N90-12295
Computer synthesis of ceramic preforms for molten-metal infiltration
[DE90-000826] 06 p0751 N90-14370
Electron theory of long wavelength concentration fluctuations in liquid metal alloys
[DE89-636213] 07 p0904 N90-15225
Dynamical structure of liquid and amorphous metals
[DE90-003805] 07 p0905 N90-15229
Time-dependent free convection in liquid metals
[DE90-000957] 07 p0927 N90-15366
Time-dependent free convection in low Prandtl number fluids
[DE90-003053] 07 p0929 N90-15377
The onset of boiling of the liquid alkali metals
[DE90-002276] 08 p1044 N90-16036
Command operated liquid metal opening switch
[AD-D014262] 08 p1060 N90-16126
Development of a wet vapor homogeneous liquid metal MHD power system
[DE90-001468] 08 p1124 N90-16508
Spectral emissivities and optical constants of electromagnetically levitated liquid metals as functions of temperature and wavelength 10 p1364 N90-17907
Magnetohydrodynamic liquid-metal flows in a rectangular channel with an axial magnetic field, a moving conducting wall, and free surfaces
[AD-A216276] 10 p1425 N90-18223
Particle emission by oblique ion bombardment of gold
[ETN-90-95825] 12 p1711 N90-19827
Wetting of metallic carbides by non-reactive liquid metals
[AERE-M-3759] 13 p1775 N90-20185
The high temperature behavior of gallium and indium liquid metal ion sources
[AERE-R-13321] 16 p2217 N90-22647
A theoretical study of flow structure and radiation for multiphase turbulent diffusion flames
[AD-A222934] 21 p2976 N90-26913
Thermodynamics and structure of liquid alkali metals from the charged-hard-sphere reference fluid
[DE90-627792] 23 p3311 N90-28725

LIQUID NITROGEN
Acquisition and correlation of cryogenic nitrogen mass flow data through a multiple orifice Joule-Thomson device
[NASA-TM-103121] 16 p2237 N90-22761
Comparison of solar pumped Nd:YAG and Nd:Cr:GSGG lasers at liquid nitrogen and room temperature
[DLR-FB-89-41] 16 p2240 N90-22781
Initial experimentation on the nonvented fill of a 0.14m3 (5 ft. 3) dewar with nitrogen and hydrogen
[NASA-TM-103155] 20 p2862 N90-26278
Optical characterization of clouds of fine liquid-nitrogen particles
[NASA-TM-103208] 20 p2865 N90-26299
Pool boiling from rotating and stationary spheres in liquid nitrogen 23 p3292 N90-28621
Variable mixture ratio performance through nitrogen augmentation 23 p3295 N90-28639

LIQUID OXYGEN
Liquid rocket booster study. Volume 2, book 1
[NASA-CR-183600] 01 p0026 N90-10133
Program for high speed computation of physical properties of propellants and combustion gas of an LH2/LOX rocket engine
[NAL-TM-564] 03 p0318 N90-11803
SSME LOX post flow analysis/fluid structure interaction. Volume 1: Flow analysis
[NASA-CR-183677] 05 p0637 N90-13715
SSME LOX post flow analysis/fluid structure interaction. Volume 2: Fluid structure interaction
[NASA-CR-183678] 05 p0637 N90-13716
High-performance LO2-CH4 engine with ceramic matrix composite materials 09 p1180 N90-16840
Liquid oxygen LOX compatibility evaluations of aluminum lithium (Al-Li) alloys: Investigation of the Alcoa 2090 and MMC weldalite 049 alloys 12 p1636 N90-19398
A superconducting quenchgun for delivering lunar derived oxygen to lunar orbit
[NASA-CR-185161] 15 p2061 N90-21806
Cooling of rocket thrust chambers with liquid oxygen
[NASA-TM-103146] 16 p2210 N90-22605
The structural dynamics analysis of the main injector LOX inlet tee and its redesign
[NASA-CR-186764] 20 p2875 N90-26358
Rocketdyne LOX bearing tester program 23 p3293 N90-28626
Oxygen/methane combustion stability investigation 23 p3293 N90-28628
Investigation of fluid dynamic performance of LE-7 liquid oxygen pump
[NAL-TR-1020] 24 p3476 N90-29650

LIQUID OXYGEN HYDROCARBON ROCKET ENGINES
U OXYGEN-HYDROCARBON ROCKET ENGINES

LIQUID PHASE EPITAXY
The photovoltaic properties of an Al In As/InP heterojunctions grown by LPE method
[NASA-CR-185996] 05 p0665 N90-13886
Integrated optoelectronic receivers
[AD-A213376] 05 p0700 N90-14098
Advanced GaAs space solar cells by MOCVD technique 10 p1339 N90-17752
AlGaAs/GaAs solar cells with efficiencies greater than 22 percent 10 p1339 N90-17755
GaAs space solar cells: Pilot production experience using a multi wafer infinite melt liquid phase epitaxy process 10 p1339 N90-17756
Diluted magnetic semiconductors
[AD-A220444] 17 p2476 N90-24159
Manufacturing and characterization of liquid-phase epitaxy layers with atomic levels at the crystal surface and at the hetero limit surfaces in the system GaAs-AlGaAs
[ETN-90-97310] 24 p3554 N90-30113

LIQUID PHASES
Survey on synthesis technologies of methanol as an alternative fuel
[DE89-901303] 07 p0914 N90-15284
Statistical mechanical models for liquid and amorphous structure in covalently bonded systems
[DE90-607233] 10 p1428 N90-18240
Low-energy scattering of electrons and positrons in liquids 11 p1559 N90-18981
Systems with a miscibility gap in the liquid state 13 p1785 N90-20245
Dynamics of electronically excited species in gaseous and condensed phase
[AD-A217696] 13 p1884 N90-20812
Molecular theory of fluid phase equilibria
[PB90-131277] 15 p2066 N90-21832
The HCl/aerosol problem 16 p2208 N90-22597
Fluid Phase Separation (FPS) experiment for flight on a space shuttle Get Away Special (GAS) canister
[NASA-CR-186830] 20 p2841 N90-26161
Two-dimensional model of a Space Station Freedom thermal energy storage canister
[NASA-TM-103124] 20 p2862 N90-26279
Optical constants of solid methane 20 p2948 N90-26775
Solidification processing of alloys using an applied electric field
[NASA-CASE-MFS-26083-1-CU] 21 p2981 N90-26940

Response of a liquid column to one-sided axial excitation in zero-gravity
[LRT-WE-9-FB-3(1989)] 21 p2991 N90-26996
Non-linear axial vibrations of a cylindrical liquid column in zero-gravity
[LRT-WE-9-FB-4(1989)] 21 p2991 N90-26997
Response of a liquid column to counter-directional excitation under zero-gravity
[LRT-WE-9-FB-6(1989)] 21 p2991 N90-26998
Response of a liquid column to unequal counter-directional excitation under zero-gravity
[LRT-WE-9-FB-7(1989)] 21 p2991 N90-26999
Response of differently axially excited viscous liquid bridges in zero-gravity
[LRT-WE-9-FB-14(1989)] 21 p2991 N90-27001
Response of a liquid column with respect to oscillatory rotational top- and bottom excitation
[LRT-WE-9-FB-8(1989)] 21 p3006 N90-27086
Oscillatory response of a liquid column to counter rotational excitation
[LRT-WE-9-FB-12(1989)] 21 p3006 N90-27088
Response of a liquid bridge with rotationally excited bottom
[LRT-WE-9-FB-13(1989)] 21 p3006 N90-27089
Response of a viscous liquid column to various pitch-excitations
[LRT-WE-9-FB-15(1989)] 21 p3006 N90-27090
Response of differently axial-excited spinning liquid columns
[LRT-WE-9-FB-16(1989)] 21 p3006 N90-27091
Nonlinear axisymmetric free vibrations of a liquid in a cylindrical tank with an elastic bottom
[LRT-WE-9-FB-17(1989)] 21 p3006 N90-27092
Phase diagram and thermodynamic data for the Am-Pu system
[NPL-DMM(A)-5] 22 p3255 N90-28431
Ignition and combustion of liquid propellants
[AD-A224150] 23 p3316 N90-28746
An experimental investigation of a single and multiphase confined coaxial jet 23 p3324 N90-28796

LIQUID PROPELLANT ROCKET ENGINES
NT HYDROGEN OXYGEN ENGINES
NT OXYGEN-HYDROCARBON ROCKET ENGINES
NT SPACE SHUTTLE MAIN ENGINE
Liquid rocket booster study. Volume 2, book 1
[NASA-CR-183600] 01 p0026 N90-10133
Liquid rocket booster study. Volume 2, book 5, appendix 9: LRB alternate applications and evolutionary growth
[NASA-CR-183604] 01 p0026 N90-10134
Liquid rocket booster study. Volume 2, book 4, appendices 6-8: Reports of Rocketdyne, Pratt and Whitney, and TRW
[NASA-CR-183603] 01 p0027 N90-10135
Liquid rocket booster study. Volume 2, book 2, appendix 1: Trades studies
[NASA-CR-183601] 01 p0027 N90-10136
Liquid rocket booster study. Volume 1: Executive summary
[NASA-CR-183599] 01 p0027 N90-10137
Liquid rocket booster study. Volume 2, book 6, appendix 10: Vehicle systems effects
[NASA-CR-183605] 01 p0027 N90-10138
Liquid rocket booster study. Volume 2, book 3, appendices 2-5: PPIP, transition plan, AMOS plan, and environmental analysis
[NASA-CR-183602] 01 p0027 N90-10139
A rocket engine design expert system
[NASA-TM-102373] 01 p0032 N90-10172
Combustion Instabilities in Liquid-Fuelled Propulsion Systems
[AGARD-CP-450] 01 p0035 N90-10191
Experimental study on the stability of small rocket engines with storable liquid propellants
01 p0036 N90-10196
Numerical simulation model for hydrazine attitude control thrusters. Part 1: Model description
[INPE-4952-RPE/601] 14 p1942 N90-21115
Cooling of rocket thrust chambers with liquid oxygen
[NASA-TM-103146] 16 p2210 N90-22605
Development of high-activity para- to ortho-hydrogen conversion catalysts, volume 2
[AD-A218700] 16 p2215 N90-22638
Noncoplanar orbit transfer optimization for an aeroassisted sortie vehicle 22 p3128 N90-27752
Liquid Rocket Booster (LRB) for the Space Transportation System (STS) systems study. Volume 1: Executive summary
[NASA-CR-183822] 23 p3288 N90-28599
Advanced Earth-to-Orbit Propulsion Technology 1988, volume 1
[NASA-CP-3012-VOL-1] 23 p3290 N90-28611
Spectroscopic study of combustion diagnostics on hydroxyl radicals
[NASA-CR-186998] 23 p3305 N90-28694

LIQUID ROCKET PROPELLANTS
NT CRYOGENIC ROCKET PROPELLANTS
NT GELLED ROCKET PROPELLANTS
NT HYPERGOLIC ROCKET PROPELLANTS
NT MONOPROPELLANTS
NT RP-1 ROCKET PROPELLANTS
NT SLURRY PROPELLANTS
NT SLUSH HYDROGEN
Liquid rocket booster study. Volume 2, book 4, appendices 6-8: Reports of Rocketdyne, Pratt and Whitney, and TRW
[NASA-CR-183603] 01 p0027 N90-10135
Combustion Instabilities in Liquid-Fuelled Propulsion Systems
[AGARD-CP-450] 01 p0035 N90-10191
Combustion instabilities in liquid-fueled propulsion systems: An overview 01 p0035 N90-10192
Low frequency and high frequency combustion oscillation phenomena inside a rocket combustion chamber fed by liquid or gaseous propellants
01 p0036 N90-10197
The Third Conference on the Environmental Chemistry of Hydrazine Fuels
[AD-A197632] 02 p0203 N90-11157
Surface-catalyzed air oxidation of hydrazines: Environmental chamber studies
02 p0203 N90-11159
Modeling the ozonolysis of hydrazines wastewater
02 p0205 N90-11175
Fuel neutralization by ozone oxidation
02 p0206 N90-11176
Description of a chemiluminescence detector system specifically designed for monitoring airborne hydrazine and oxidizer propellant vapors 02 p0206 N90-11179
Measurement of hydrazine contamination in soils
02 p0206 N90-11180
Continuing studies of liquid propellant drops in hot, high-pressure environments
[AD-A212265] 04 p0482 N90-12765
Extended temperature range rocket injector
[NASA-CASE-LEW-14846-1] 07 p0887 N90-15130
The liquid rocket booster and its potential for the STS
09 p1179 N90-16833
Orbital fluid resupply assessment
11 p1475 N90-18487
Methods and apparatus for providing real-time control of a gaseous propellant rocket propulsion system
[NASA-CASE-MSC-21542-1] 20 p2825 N90-26073
Hazard classification testing of liquid propellants
[AD-A222070] 21 p2990 N90-26990
Atmospheric dispersion of solid and liquid rocket propellants
[AD-A221293] 21 p3020 N90-27173
Advanced propulsion for LEO and GEO platforms
[NASA-TM-103228] 22 p3134 N90-27785
Liquid Rocket Booster (LRB) for the Space Transportation System (STS) systems study, volume 2
[NASA-CR-183786] 23 p3288 N90-28600
Liquid Rocket Booster (LRB) for the Space Transportation System (STS) systems study. Appendix B: Liquid rocket booster acoustic and thermal environments
[NASA-CR-183788-APP-B] 23 p3288 N90-28602
Liquid Rocket Booster (LRB) for the Space Transportation System (STS) systems study. Appendix F: Performance and trajectory for ALS/LRB launch vehicles
[NASA-CR-183792-APP-F] 23 p3289 N90-28606
Advanced Earth-to-Orbit Propulsion Technology 1988, volume 1
[NASA-CP-3012-VOL-1] 23 p3290 N90-28611
High energy-density liquid rocket fuel performance
[NASA-CR-185279] 23 p3315 N90-28742

LIQUID ROTATION
U ROTATING LIQUIDS

LIQUID SLOSHING
Fluid-structure interaction effects in tank structures due to sloshing and hydrodynamic ram: Coupled Lagangian-Eulerian simulations
02 p0181 N90-11022
Modeling of liquid sloshing effects in multibody systems 02 p0181 N90-11023
Small amplitude liquid oscillations in a rectangular container under zero-gravity
[LRT-WE-9-FB-2(1989)] 08 p1066 N90-16167
Linear liquid oscillations in cylindrical containers under zero-gravity
[LRT-WE-9-FB-5(1989)] 08 p1066 N90-16168
Investigation of liquid sloshing in spin-stabilized satellites
[AD-A214730] 09 p1182 N90-16853
Laboratory simulation of the effect of rocket thrust on a precessing space vehicle
[NASA-CR-186681] 19 p2669 N90-25182
Liquid sloshing response in a spinning container due to axial excitation
[LRT-WE-9-FB-9(1989)] 21 p3006 N90-27087

LIQUID SODIUM
Studies on the startup transients and performance of a gas loaded sodium heat pipe
[AD-A211880] 03 p0414 N90-12379

LIQUID SURFACES
NT MENISCI
Characterization of polymeric surfaces and interfaces
[AD-A210227] 01 p0049 N90-10277
Self-assembled organic monolayer films
[AD-A212006] 03 p0323 N90-11838
Response of a rotating finite annular liquid layer to axial excitation
[LRT-WE-9-FB-15(1988)] 08 p1053 N90-16090
Interior fluid dynamics of liquid-filled projectiles
[AD-A217630] 13 p1800 N90-20330
Inflatable fuel tank buffer
[AD-D014446] 14 p1921 N90-21002
Experiments on liquid immersion natural convection cooling of leadless chip carriers mounted on ceramic substrate
[AD-A219893] 17 p2478 N90-24167
Chemical structure and kinetics at liquid/solid interfaces
[AD-A222766] 20 p2831 N90-26105
Exact results for the structured liquid-solid interface
[AD-A222762] 20 p2922 N90-26630
Approximate natural damped frequencies of a finite viscous floating-zone under zero-gravity condition
[LRT-WE-9-FB-8(1988)] 21 p2990 N90-26995
Response of a viscous liquid column to pitching- and roll-excitation in zero-gravity environment
[LRT-WE-9-FB-10(1989)] 21 p2991 N90-27000
Response of differently axially excited viscous liquid bridges in zero-gravity
[LRT-WE-9-FB-14(1989)] 21 p2991 N90-27001
Response of a spinning liquid column to axial excitation
[LRT-WE-9-FB-10(1988)] 21 p3006 N90-27085
Liquid sloshing response in a spinning container due to axial excitation
[LRT-WE-9-FB-9(1989)] 21 p3006 N90-27087
Response of differently axial-excited spinning liquid columns
[LRT-WE-9-FB-16(1989)] 21 p3006 N90-27091
Investigations of polarized light scattering from rough surfaces
[AD-A221943] 21 p3076 N90-27491

LIQUID WASTES
NT URINE
NT WASTE WATER

LIQUID-GAS MIXTURES
NT AEROSOLS
NT FOG
Preparation of binary ice layers by condensation from gas phase
[JUEL-2248] 05 p0622 N90-13631
Gas-liquid-liquid equilibria in mixtures of water, light gases, and hydrocarbons
[DE90-003180] 07 p0894 N90-15167
Study of interfacial behavior in cocurrent gas-liquid flows
[DE90-005988] 12 p1659 N90-19532
An experimental investigation of the physical mechanisms controlling the asymmetric flow past slender bodies at large angles of attack
15 p2053 N90-21767

LIQUID-LIQUID INTERFACES
Reorganization free energy for electron transfers at liquid-liquid and dielectric semiconductor-liquid interfaces
[AD-A212985] 05 p0703 N90-14111
Interfacial area in two-phase flow
[DE90-002210] 06 p0778 N90-14527
Gas-liquid-liquid equilibria in mixtures of water, light gases, and hydrocarbons
[DE90-003180] 07 p0894 N90-15167

LIQUID-SOLID INTERFACES
Interpretation and modeling of the averaged equations for a fluid-solid flow 01 p0068 N90-10388
Hybrid particle-fluid approach to low-frequency turbulence in magnetically confined plasmas
[DE89-015904] 02 p0277 N90-11579
Self-assembled organic monolayer films
[AD-A212006] 03 p0323 N90-11838
Interactive computer program for the generation of enthalpy-entropy and temperature-entropy charts of nitrogen and hydrogen
[DLR-FB-89-27] 04 p0533 N90-13081
Reorganization free energy for electron transfers at liquid-liquid and dielectric semiconductor-liquid interfaces
[AD-A212985] 05 p0703 N90-14111
Principles of metallic solidification
13 p1784 N90-20241
Supercooling and germ formation
13 p1784 N90-20242
Dynamics of the solidification front
13 p1785 N90-20243

Dispersion reinforced materials
13 p1785 N90-20244
Chemical structure and kinetics at liquid/solid interfaces
[AD-A222766] 20 p2831 N90-26105
Exact results for the structured liquid-solid interface
[AD-A222762] 20 p2922 N90-26630
Measurements of energy dispersion at liquid-solid interfaces: Fluorescence quenching of pyrene bound to fumed silica
[AD-A222371] 21 p2978 N90-26926
Variable length-scale studies at interfaces with X ray standing waves
[AD-A223043] 21 p3004 N90-27075
Fundamental electron transfer processes at the single crystal semiconductor/liquid interface
[DE90-011438] 21 p3079 N90-27508

LIQUID-VAPOR EQUILIBRIUM
Vapor-liquid equilibrium of binary mixtures in the extended critical region. Part 1: Thermodynamic model
[PB89-218374] 04 p0469 N90-12687
Gas-liquid-liquid equilibria in mixtures of water, light gases, and hydrocarbons
[DE90-003180] 07 p0894 N90-15167
Vapor-liquid equilibria for complex mixtures with special emphasis on the critical region
[PB90-130345] 12 p1622 N90-19324
Liquid-vapor equilibrium of multicomponent cryogenic systems 20 p2948 N90-26774
Theoretical thermodynamics: Equation of state and perturbation studies
[PB90-199332] 22 p3255 N90-28430

LIQUID-VAPOR INTERFACES
Buoyancy effects on the vapor condensation rate on a horizontal liquid surface
[NASA-TM-102437] 05 p0629 N90-13675
Vapor condensation on liquid surface due to laminar jet-induced mixing: The effects of system parameters
[NASA-TM-102433] 05 p0643 N90-13751
Model system studies with a phase separated membrane bioreactor 05 p0679 N90-13954
Interfacial area in two-phase flow
[DE90-002210] 06 p0778 N90-14527
Transport processes through monomolecular films
[AD-A213609] 07 p0923 N90-15342
On condensation driven by electrostatic interactions in macroionic solutions
[DE89-636072] 08 p1120 N90-16487
Analytical and experimental investigation of miniature heat pipes, phase 2
[AD-A216945] 11 p1506 N90-18673
Study of interfacial behavior in cocurrent gas-liquid flows
[DE90-005988] 12 p1659 N90-19532
Molecular theory and computer simulation studies of natural and synthetic gas mixtures
[PB90-130329] 12 p1711 N90-19826
Numerical simulation of liquid circulation in a bubbly column
[DE90-005226] 15 p2097 N90-22002
Mass transfer induced convection near gas-liquid interfaces
[ETN-90-96925] 18 p2552 N90-24568

LIQUIDS
NT CRYOGENIC FLUIDS
NT FERMI LIQUIDS
NT HYDRAULIC FLUIDS
NT LIQUEFIED GASES
NT LIQUID HELIUM
NT LIQUID HELIUM 2
NT LIQUID HYDROGEN
NT LIQUID LITHIUM
NT LIQUID METALS
NT LIQUID NITROGEN
NT LIQUID OXYGEN
NT LIQUID SODIUM
NT MERCURY (METAL)
NT MERCURY ISOTOPES
NT ORGANIC LIQUIDS
NT POTABLE WATER
NT ROTATING LIQUIDS
NT SKYDROL (TRADEMARK)
Theoretical and experimental investigation of nonlinear optoacoustics in liquids
[AD-A210427] 01 p0124 N90-10708
Natural gas to liquids
[DE89-000982] 03 p0322 N90-11828
Conversion of methane to liquid hydrocarbons
[DE89-017547] 03 p0322 N90-11831
Shock-induced reaction in several liquids
[DE89-016594] 03 p0346 N90-11973
Thermophysical properties of buta-1,3-diene
[ESDU-89005] 05 p0620 N90-13619
Thermophysical properties of isopropyl alcohol. Part 1: The ideal gas and the saturated liquid and vapour
[ESDU-89017-PT-1] 06 p0738 N90-14297
Orthobaric densities and molar volumes of liquids. Introduction to data items issued after July 1989
[ESDU-89018] 06 p0738 N90-14298
Orthobaric densities and molar volumes of liquids. Aromatic hydrocarbons
[ESDU-89019] 06 p0738 N90-14299
Structure properties of confined systems. Hard spheres between ideal walls
[DE90-600818] 07 p0929 N90-15378
Thickness, velocity, and temperature measurements in falling liquid films
[DE90-004290] 08 p1063 N90-16151
Diffraction studies of the structure of glasses and liquids
[DE90-007662] 12 p1632 N90-19381
Chemical and electrochemical studies in ionic liquids
[AD-A217742] 13 p1773 N90-20175
Pulsed laser photothermal spectroscopy of liquids and solids
[DE90-008642] 13 p1808 N90-20380
A solution level indicator system
[DE90-007939] 14 p1948 N90-21151
Laser velocimeter measurements of multiphase flow of solids
[DE90-007604] 14 p1974 N90-21311
A weak formulation for phase-change problems with bulk movement due to unequal densities
[DE90-009398] 15 p2163 N90-22361
Femtosecond studies of electron photodetachment of simple ions in liquid water: Solvation and geminate recombination dynamics
[AD-A218520] 16 p2215 N90-22634
Side moment exerted by a spinning, coning, highly viscous liquid payload
[AD-A218746] 16 p2237 N90-22763
Contamination of spacecraft by recontact of dumped liquids 19 p2728 N90-25508
Dynamics of fluids in bulk and near a vertical wall: Studied by photoncorrelation spectroscopy
[PB90-200452] 22 p3169 N90-27976
Four techniques to measure complex refractive indices of liquids and solids at carbon dioxide laser wavelengths in the infrared spectral region
[AD-A222007] 22 p3180 N90-28043
Estimation of liquid heat capacities. 1: Review and evaluation of Missenard method
[AD-A224161] 24 p3445 N90-29454

LISP (PROGRAMMING LANGUAGE)
Parallel execution of LISP programs
[AD-A219623] 17 p2451 N90-23978
Ada as an implementation language for knowledge based systems 21 p3050 N90-27337

LISTS
Source header list. Volume 1: A through K
[AD-A216000] 10 p1442 N90-18319
Source header list. Volume 2: L through Z
[AD-A216001] 10 p1442 N90-18320
Source hierarchy list. Volume 1: A through D
[AD-A216050] 10 p1442 N90-18321
Source hierarchy list. Volume 2: E through N
[AD-A216051] 10 p1442 N90-18322
Source hierarchy list. Volume 3: O through Z
[AD-A216052] 10 p1442 N90-18323
Medical subject headings: Annotated alphabetic list, 1990
[PB90-100009] 14 p2036 N90-21683

LITERATURE
NT BIOGRAPHY
NT DOCUMENTATION
Origin and effect of pores in aluminum welded joints
[REPT-87M/43/05720/SCP/GRF] 12 p1675 N90-19620
Processing infrared images for target detection: A literature study
[IZF-1988-12] 12 p1715 N90-19847
Literature file on fast kickers and SEPTA: Components for deflection and separation of particle beams
[LINO-162] 12 p1727 N90-19924
The Moon has set
[REPT-89-07] 12 p1728 N90-19933
Chemistry within molecular clusters
[AD-A219836] 18 p2520 N90-24392
Impact of the whole national economy of defense spending and space in the US: A literature analysis
[ISSN-0342-0787] 22 p3260 N90-28464

LITHERGOLIC PROPELLANTS
U HYBRID PROPELLANTS

LITHIUM
NT LIQUID LITHIUM
NT LITHIUM ISOTOPES
The use of lithium batteries in biomedical devices
[AD-A210789] 01 p0061 N90-10350
Lithium compensation of GaAs
[DE89-616080] 01 p0129 N90-10740
New secondary batteries utilizing electronically conductive polymer cathodes
[NASA-CR-185885] 02 p0215 N90-11227
Research in X-ray optics with the ultimate aim of constructing a synchrotron radiation pumped soft X-ray lithium laser
[DE89-016788] 02 p0227 N90-11304
Carbon isotope ratios and lithium abundances in open cluster giants 02 p0292 N90-11684
Assessment of thin film batteries based on polymer electrolytes. Part 1: Energy density
[AD-A212111] 03 p0343 N90-11958
The use of lithium batteries in biomedical devices
[AD-A212187] 04 p0497 N90-12863
Population inversions calculated for lithium-like ions in a plasma 06 p0786 N90-14571
Heat transfer in condensation of lithium vapors
[DE90-002081] 07 p0929 N90-15375
Research and development of lithium/polyaniline battery, part 2
[DE90-734985] 09 p1211 N90-17018
Determination of optimum electrolyte composition for molten carbonate fuel cells
[DE90-000410] 09 p1243 N90-17210
Lithium ambient-temperature battery reliability
[DE90-005758] 11 p1502 N90-18650
Feasibility of a super high energy density battery of the Li/BrF3 electrochemical system
[AD-A216575] 11 p1528 N90-18799
Positronium formation in Ss state in e+-Li scattering 11 p1557 N90-18967
Optimizing superplastic response in navalite, a lithium containing aluminum-magnesium alloy
[AD-A216552] 12 p1626 N90-19346
Advanced high-temperature batteries 13 p1825 N90-20480
Advances in ambient temperature secondary lithium cells 13 p1825 N90-20481
Active primary lithium thionyl chloride battery for artillery applications
[DE90-009511] 15 p2089 N90-21955
Heat exhaustion in a rat model: Lithium as a biochemical probe
[AD-A219361] 16 p2260 N90-22884
Laser temperature-jump kinetic studies of fast reactions in nonaqueous solutions
[AD-A218819] 17 p2371 N90-23500

LITHIUM ALLOYS
Quench sensitivity in Al-Cu-Li alloys
[AD-A213055] 05 p0624 N90-13639
The effect of composition and aging treatment on the microstructure and mechanical properties of aluminum-lithium-titanium alloys
[AD-A213144] 05 p0624 N90-13640
Advances and future directions in superplastic materials 06 p0744 N90-14328
The strength-toughness combination of the aluminum-lithium alloys 2090 and 2091 at cryogenic temperatures
[DE90-001425] 06 p0746 N90-14338
New Light Alloys
[AGARD-CP-444] 07 p0897 N90-15185
Al-Li alloy developed by Pechiney 07 p0897 N90-15186
The microstructure and properties of aluminum-lithium alloys 07 p0897 N90-15187
Mechanical properties and fracture toughness of 8090-T651 plate and 2091 and 8090 sheet 07 p0897 N90-15188
Fatigue properties of Al-Li alloys 07 p0898 N90-15189
Corrosion and stress corrosion of aluminium-lithium alloys 07 p0898 N90-15190
Properties of Al-Li alloys 07 p0898 N90-15191
Investigation on sheet material of 8090 and 2091 aluminium-lithium alloy 07 p0898 N90-15192
Aluminum lithium alloys for Navy aircraft 07 p0898 N90-15193
Fatigue, fracture mechanics and corrosion properties of some aluminium-lithium alloys 07 p0898 N90-15194
Fatigue and fracture behaviour of a PM Al-Li alloy 07 p0899 N90-15195
Fabrication of test-articles from Al-Li 2091 for Fokker 100 07 p0899 N90-15196
Putting alloy 2091 to work 07 p0899 N90-15197
Fabrication characteristics of 8090 alloy 07 p0899 N90-15198
Superplastic performance and properties of the Lital Alloys 07 p0899 N90-15199
Point of view of a civil aircraft manufacturer on Al-Li alloy 07 p0899 N90-15200
Uses and properties of Al-Li on the new EH101 helicopter 07 p0900 N90-15201
Aluminum-lithium: Application of plate and sheet to fighter aircraft 07 p0900 N90-15202

Current status of the application of conventional aluminium-lithium alloys and the potential for future developments 07 p0900 N90-15203
Rechargable molten-electrolyte lithium batteries
[DE90-003774] 07 p0923 N90-15339
Lithium cobalt oxide thin film and its electrochromism
[DE90-004570] 08 p1133 N90-16564
Comparative analysis between the mechanical properties of conventional alloys and Al-Li
[INFORME-DT-317/89] 10 p1356 N90-17861
Effect of a single overload upon fatigue crack growth in an aluminum-lithium alloy
[AD-A216183] 10 p1356 N90-17865
Optimizing superplastic response in navalite, a lithium containing aluminum-magnesium alloy
[AD-A216552] 12 p1626 N90-19348
Liquid oxygen LOX compatibility evaluations of aluminum lithium (Al-Li) alloys: Investigation of the Alcoa 2090 and MMC weldalite 049 alloys 12 p1636 N90-19398
Evaluation of 2090-T8E48 aluminum-lithium plates
[AD-A217262] 13 p1776 N90-20196
Determination of Li-Al alloy extent in tubular aluminum elements by small source neutron radiology
[DE90-009142] 14 p1952 N90-21174
Deformation and fracture of thin sheet aluminum-lithium alloys: The effect of cryogenic temperatures 16 p2218 N90-22655
Measurements and mechanisms of localized aqueous corrosion in aluminum-lithium alloys 16 p2219 N90-22656
The effects of zinc addition on the environmental stability of Al-Li alloys 16 p2219 N90-22657
Deformation and fracture of aluminum-lithium alloys: The effect of dissolved hydrogen 16 p2219 N90-22658
The lithium concentration dependence of creep in binary aluminum-lithium alloys
[AD-A218706] 16 p2221 N90-22668
Structure-property relations in aluminum-lithium alloys
[AD-A219183] 16 p2222 N90-22672
Electronic structure and phase stability properties of Al-Li alloys
[DE90-010632] 18 p2525 N90-24410
Precipitation on dislocations in Al-Li-Cc-Mg-Zr
[AD-A221124] 18 p2526 N90-24415
Investigation on sheet material of 8090 and 2091 aluminium-lithium alloy
[MBB-UT-122/89-PUB] 19 p2652 N90-25090
Scratches and shot peening effects on the fatigue life of aluminum-lithium alloys
[NIAR-90-15] 19 p2674 N90-25208
Surface condition effect on the fatigue behavior of aluminum lithium alloys
[NIAR-90-13] 19 p2674 N90-25209
A study of the fatigue behavior in scratched samples of Al-Li alloy (2090-T3)
[IAR-89-24] 20 p2832 N90-26107
Fracture toughness and failure mechanisms in commercial 2091 Al-Li sheet at cryogenic temperatures
[AD-A222803] 20 p2835 N90-26125
Corrosion protection of metal matrix composites
[AD-A222951] 21 p2971 N90-26888
Weldment mechanical properties of aluminum-copper-lithium alloy, 2090, at ambient and cryogenic temperatures
[DE90-014178] 21 p2981 N90-26941
Development of a sealed bipolar Li-alloy/FeS2 battery for electric vehicles
[DE90-013650] 21 p2999 N90-27045
Characterization of the pitting corrosion of aluminum-lithium alloys
[ETCA-89-R-176] 22 p3157 N90-27903
High temperature oxidation of Al-Li alloys 23 p3307 N90-28705
The stress and temperature dependence of creep in an Al-2.0 wt percent Li alloy
[AD-A223676] 24 p3449 N90-29480
Evaluation of static and fatigue properties of thin sheets of 8090-T8 aluminum-lithium alloy and observation of its fracture surfaces
[NAL-TR-1039] 24 p3453 N90-29499

LITHIUM BORATES
Polarization matrices of lithium tetraborate
[AD-A210774] 02 p0195 N90-11112
Temperature and coupling behavior of resonators and transducers of lithium tetraborate driven by lateral and thickness fields
[AD-A219548] 17 p2395 N90-23644

LITHIUM CHLORIDES
The effect of carbon type and processing on high rate thionyl chloride cathode collectors
[AD-A219823] 18 p2546 N90-24532

LITHIUM COMPOUNDS
NT LITHIUM BORATES
NT LITHIUM CHLORIDES
NT LITHIUM FLUORIDES
NT LITHIUM HYDRIDES
NT LITHIUM HYDROXIDES
NT LITHIUM IODATES
NT LITHIUM NIOBATES
NT LITHIUM OXIDES
NT LITHIUM PERCHLORATES
NT LITHIUM SULFATES
A thermochemical analysis of proposed working fluids for electrothermal guns
[AD-A210661] 02 p0159 N90-10910
Polarization matrices of lithium tetraborate
[AD-A210774] 02 p0195 N90-11112
Spectroscopic and laser properties of Cr:LiCaAlF6 and Cr:LiSrAlF6 crystals
[DE90-000783] 07 p0998 N90-15770
Ternary reciprocal system of lithium and potassium fluorides and bromides
[DE90-004938] 10 p1352 N90-17840
Performance of superconductive oxides as cathodes for lithium rechargeable batteries
[AD-A216030] 10 p1401 N90-18098
Application of polymer electrolytes to lithium batteries
[AD-A216038] 10 p1401 N90-18099
Integrated optics at Lawrence Livermore National Laboratory
[DE90-003015] 10 p1431 N90-18255
Properties and performance of the LiCaAlF6:Cr(3+) laser material
[DE90-007242] 11 p1516 N90-18728

LITHIUM FLUORIDES
Epitaxial growth of Cr(011) on LiF(001)
[DE90-005635] 09 p1293 N90-17496
Development of a high temperature storage unit for integration with solar dynamic systems 10 p1335 N90-17720
Hot filament technique for measuring the thermal conductivity of molten lithium fluoride
[NASA-TM-102506] 12 p1631 N90-19373
A viscoplastic model with application to LiF-22 percent CaF2 hypereutectic salt
[NASA-TM-103181] 17 p2417 N90-23770

LITHIUM HYDRIDES
A new low density, high porosity lithium hydride-beryllium hydride foam
[DE90-015150] 23 p3313 N90-28739

LITHIUM HYDROXIDES
Mechanical properties of pure nickel alloys after long term exposures to LiOH and vacuum at 775 K
[NASA-TM-102403] 13 p1774 N90-20181

LITHIUM IODATES
One way imaging and amplification through an aberrator
[AD-A221640] 21 p3009 N90-27106

LITHIUM ISOTOPES
Investigation of correlations in nuclei with the (e,e'X) reaction
[ETN-90-96398] 15 p2166 N90-22377
The shock process and light element production in supernovae envelopes
[NASA-CR-182854] 22 p3262 N90-28471

LITHIUM NIOBATES
Electron-beam phase-only spatial light modulator for matched filtering
[AD-A215026] 09 p1282 N90-17431
Modeling and realization of plane acousto-optic unilateral band modulators
[ETN-90-95824] 12 p1710 N90-19818
Secondary ion mass spectrometry characterization of implants into GaAs and GaP for waveguides and integrated optics applications
[AD-A219203] 16 p2324 N90-23254
Photorefractive damage mechanisms in electro-optic materials
[AD-A219786] 17 p2476 N90-24157
Analysis and realization of integrated optical polarizers and absorbers on LiNbO3
[ETN-90-96504] 18 p2623 N90-24949
Photoinduced and holographically reinforced light diffusion in electrooptic crystals
[ETN-90-97321] 24 p3547 N90-30060

LITHIUM OXIDES
Synthetic polypeptide composites for sensor applications
[AD-A210797] 01 p0052 N90-10296
Lithium polymer electrolyte battery, electrochemical behavior of cathode materials
[AD-A210755] 02 p0216 N90-11235
Lithium cobalt oxide thin film and its electrochromism
[DE90-004570] 08 p1133 N90-16564
Optical waveguide fabrication by stoichiometric implantation of Ti and O into LiNbO3
[DE90-004238] 09 p1292 N90-17488
Preliminary study of rechargeable lithium cells for space applications 10 p1334 N90-17717
Reflectance modulation with electrochromic Li(sub x)WO(3) films
[DE90-004571] 10 p1435 N90-18279

LITHIUM PERCHLORATES
Rechargeable lithium/polymer cathode batteries
[AD-A210978] 01 p0062 N90-10354

LITHIUM SULFATES
Thermodynamic studies on the ferroelectric phase transition in neutron irradiated (Li(sub x)K(1-x))2SO4 crystals at high temperature
[DE89-635786] 08 p1130 N90-16545

LITHIUM SULFUR BATTERIES
Polarization of Li/SOCl2 cells
[DE90-000883] 06 p0804 N90-14680
Novel high-rate, all solid-state, sodium and lithium/organosulfur batteries
[DE90-001014] 07 p0920 N90-15325
Application of ac impedance method for diagnosis of lithium secondary battery degradation. Preliminary study with AA size Li/MoS2 cells
[DE90-702474] 08 p1061 N90-16137
Evaluation of a prototype lithium molybdenum disulfide secondary battery for load conditioner: Characteristics and performance of 70Wh class BC cell
[DE90-702460] 09 p1210 N90-17016
Sealing L-alloys/FeS(x) cells for a bipolar battery
[DE90-004887] 09 p1214 N90-17040
A lithium sulphur dioxide cell for deep space applications 10 p1334 N90-17718
All-solid-state thin-film rechargeable lithium batteries using solid redox polymerization electrodes
[DE90-008665] 13 p1796 N90-20306
Novel electrodes for advanced energy storage systems
[DE90-008667] 13 p1828 N90-20496
Aging characteristics of Li/SO(sub 2) cells
[NASA-CR-180432] 15 p2088 N90-21954
Development of a sealed bipolar Li-alloy/FeS2 battery for electric vehicles
[DE90-013650] 21 p2999 N90-27045

LITHIUM 4
U LITHIUM ISOTOPES

LITHIUM 6
U LITHIUM ISOTOPES

LITHOGRAPHY
NT PHOTOLITHOGRAPHY
X-ray lithography studies of polysilane using a laser plasma X-ray source
[DE89-015390] 01 p0047 N90-10266
A compact X-ray lithography lattice using superferric magnets
[DE89-013947] 01 p0127 N90-10728
X-ray lithography sources: A review
[DE89-017610] 02 p0271 N90-11547
Inspection of carbon/epoxy and aluminum honeycomb paraboloidal components by HNDT
[AD-A216796] 11 p1479 N90-18514
Metal coordination polymers as potential high-energy lithographic resists
[AD-A216668] 11 p1490 N90-18574
Research project in microelectronic engineering and imaging science
[DE90-006907] 11 p1503 N90-18653
Biological soft x ray contact microscopy: Imaging living CHO-SC1 cells and other biological materials
[DE90-007560] 13 p1849 N90-20610
In-situ differential reflectance study of the etching of SiO2 films
[AD-A217186] 13 p1893 N90-20864
Extrinsic germanium Blocked Impurity Bank (BIB) detectors 14 p1976 N90-21322
Report on the fifth workshop on synchrotron x ray lithography
[DE90-007903] 15 p2172 N90-22411
Modified maleic anhydride copolymers as e-beam resists
[AD-A218470] 16 p2223 N90-22679
Molecular beam epitaxial growth of heterostructures to study quantum interference phenomena
[AD-A219442] 17 p2475 N90-24154
Process of three dimensional lithography in amorphous polymers
[AD-D014500] 19 p2676 N90-25221
The role of heat transfer during reactive-ion etching of polymer films
[AD-A222072] 21 p2977 N90-26919
An x ray source for lithography
[AD-D014596] 24 p3473 N90-29630

LITHOLOGY
Physiographic and geological setting of the Coastal Engineering Research Center's field research facility
[AD-A210772] 02 p0238 N90-11356
Evaluation of the airborne visible-infrared imaging spectrometer for mapping subtle lithological variation
[NASA-CR-186213] 06 p0802 N90-14670
Development of remote sensing techniques for the investigation of neotectonic activity, eastern transverse ranges and vicinity, southern California 18 p2573 N90-24662

LITHOSPHERE
NT EARTH CORE
NT EARTH CRUST
NT EARTH MANTLE
NT EARTH SURFACE
Dynamics of mid-ocean ridge systems
07 p0965 N90-15575
Evolution of midplate hotspot swells: Numerical solutions
[NASA-CR-186462] 12 p1691 N90-19713
An analytic model of axisymmetric mantle plume due to thermal and chemical diffusion
[NASA-CR-186461] 12 p1691 N90-19714
Stored mafic/ultramafic crust and early Archean mantle depletion
[NASA-CR-186460] 12 p1691 N90-19715
LIVER
Study of hydrazine metabolism and toxicity
[AD-A217103] 12 p1695 N90-19736
Experiment K-6-12. Morphometric studies of atrial or granules and hepatocytes. Part 1: Morphometric study of the liver; Part 2: The atrial granular accumulations
20 p2894 N90-26466
Experiment K-6-14. Hepatic function in rats after spaceflight 20 p2895 N90-26468
LMFBR
U LIQUID METAL FAST BREEDER REACTORS
LOAD DISTRIBUTION (FORCES)
A new test procedure for a wing made with carbon fiber composites
[ETN-89-95220] 03 p0320 N90-11820
Chordwise loading and camber for two-dimensional thin sections
[AD-A213318] 04 p0448 N90-12568
Fatigue life estimates for helicopter loading spectra
[NASA-CR-181941] 08 p1088 N90-16294
Studies on deformation and fracture of viscoelastic composite materials
[AD-A216095] 10 p1348 N90-17819
Application of attachment modes in the control of large space structures
[NASA-CR-185604] 12 p1613 N90-19280
Innovative design of composite structures: The use of curvilinear fiber format to improve buckling resistance of composite plates with central circular holes
[NASA-CR-186454] 13 p1766 N90-20135
Stress analysis and minimum weight design of honeycomb sandwich plates 14 p1992 N90-21418
Numerical solutions of the nonlinear theory of curved beams 15 p2110 N90-22071
Composite integrity monitoring
[AD-A220813] 17 p2369 N90-23487
A lifting surface method for the calculation of steady and unsteady, incompressible propeller aerodynamics
[ESA-TT-1151] 19 p2655 N90-25113
Computer-aided design of high-contact-ratio gears for minimum dynamic load and stress
[NASA-TM-103275] 22 p3183 N90-28065
LOAD FACTORS
U LOADS (FORCES)
LOAD TESTING MACHINES
Development of a high temperature FZG-Ryder gear lubricant load capacity machine
[AD-A210799] 01 p0079 N90-10449
Fully articulated four-point-bend loading fixture
[NASA-CASE-LEW-14776-1] 07 p0940 N90-15445
Cycle life machine for AX-5 space suit
15 p2112 N90-22080
A dynamic motion simulator for future European docking systems 15 p2113 N90-22085
Evaluating Statistical Process Control (SPC) techniques and computing the uncertainty of force calibrations
18 p2631 N90-24992
LOAD TESTS
Fatigue crack initiation mechanics of metal aircraft structures
[AD-A210567] 01 p0045 N90-10255
Development of a high temperature FZG-Ryder gear lubricant load capacity machine
[AD-A210799] 01 p0079 N90-10449
Fracture and three dimensional stress analyses of 7075 aluminum projectile components under spin and inertia load
[AD-A210986] 01 p0081 N90-10463
STS payload design load evolution
02 p0176 N90-10989
Equilibrium and stability in composite thin shell
02 p0178 N90-10998
Multi-axis transient testing: Experimental investigations
02 p0184 N90-11042
A new test procedure for a wing made with carbon fiber composites
[ETN-89-95220] 03 p0320 N90-11820
WISPER: A standardized fatigue load sequence for HAWT-blades
[NLR-MP-88029-U] 03 p0359 N90-12055
Flight motor set 360L001 (STS-26R). (Reconstructed dynamic loads analysis)
[NASA-CR-183811] 04 p0464 N90-12656
Fatigue testing of welded steel assemblies with or without finishing treatments
[CETIM-107900] 04 p0513 N90-12961
Failure processes in unidirectional composite materials
05 p0617 N90-13598
Static and free-vibrational response of semi-circular graphite-epoxy frames with thin-walled open sections
[NASA-CR-186097] 05 p0617 N90-13600
General buckling tests with thin-walled shells
[DLR-MITT-89-13] 05 p0655 N90-13816
Elasto-plastic analysis of unidirectional fiber-reinforced composites subjected to transverse normal loading using the finite element method 06 p0737 N90-14292
Characterization and in situ testing of diamond films
[DE90-003155] 07 p0911 N90-15265
Analysis and testing of axial compression in imperfect slender truss struts
[NASA-TM-4174] 08 p1087 N90-16292
Effects of T-tabs and large deflections in DCB specimen tests
[NASA-TM-101677] 09 p1186 N90-16868
Hydrogen embrittlement of titanium and its alloys
[DE90-602366] 10 p1355 N90-17858
Compressive strength of carbon/epoxy laminated under multiaxial stress
[DE90-005552] 11 p1478 N90-18505
Floor pull test of a transport airframe section
[DOT/FAA/CT-TN88/14] 13 p1754 N90-20072
Measurements and mechanisms of localized aqueous corrosion in aluminum-lithium alloys
16 p2219 N90-22656
Fatigue testing of glass fibre reinforced epoxy using the WISPER sequence
[FFA-TN-1989-45] 17 p2381 N90-23561
Study of ball bearings for space use
18 p2537 N90-24477
Static and free-vibrational response of semi-circular graphite-epoxy frames with thin-walled open sections
[NASA-CR-4287] 21 p3012 N90-27122
Calculation of service life of turbomachine components 22 p3117 N90-27706
The role of component testing
22 p3117 N90-27707
Characterization of the CP 214 T851. Dissection of a cast flat bar for a standard spar
[CEAT-PV-M4/462200] 22 p3158 N90-27905
Characterization of the 7175 T7352. Dissection of a die casting standard spar
[CEAT-PV-M5/528900] 22 p3158 N90-27906
Characterization of the 7010 T73651. Dissection of a sheet billet for a standard spar
[CEAT-PV-M5/521700] 22 p3158 N90-27908
Damage tolerance of woven graphite-epoxy buffer strip panels
[NASA-TM-102702] 22 p3192 N90-28114
Behavior of aramid/epoxy wounded tubes under uniaxial and biaxial loading
[ETCA-89-R-150] 23 p3339 N90-28873
LOADING FORCES
U LOADS (FORCES)
LOADING MOMENTS
Computer-Aided Structural Engineering (CASE) project: Investigation and design of U-frame structures using program CUFRBC. Volume A: Program criteria and documentation
[AD-A224387] 24 p3525 N90-29934
LOADING OPERATIONS
Classification and simulation of single and multi-degree-of-freedom motions
[AD-A214925] 09 p1231 N90-17143
LOADING RATE
Influence of microstructure and microdamage processes on fracture at high loading rates
[AD-A210307] 01 p0045 N90-10253
An evaluation of a fatigue crack growth prediction model for variable-amplitude loading (PREFFAS)
[LR-537] 05 p0656 N90-13822
The effect of loading on the laser ablation of graphite/epoxy composite material
[AD-A216209] 10 p1349 N90-17826
LOADING WAVES
U ELASTIC WAVES
U LOADS (FORCES)
LOADS (FORCES)
NT AERODYNAMIC LOADS
NT AXIAL COMPRESSION LOADS
NT AXIAL LOADS
NT BLAST LOADS
NT COMPRESSION LOADS
NT CONTACT LOADS
NT CRITICAL LOADING
NT CYCLIC LOADS
NT DYNAMIC LOADS
NT EDGE LOADING
NT GUST LOADS
NT IMPACT LOADS
NT ROLLING CONTACT LOADS
NT SHOCK LOADS
NT STATIC LOADS
NT THRUST LOADS
NT TRANSIENT LOADS
NT VIBRATORY LOADS
NT WING LOADING
A comparison of wind turbulence simulation models for stochastic loads analysis for horizontal-axis wind turbines
[DE89-009442] 01 p0083 N90-10473
Overview of actual buckling calculation methods for space vehicle structures 02 p0177 N90-10995
Key structures mechanical issues of the European Space Station and platform program Columbus
02 p0188 N90-11072
Derivation of improved load transformation matrices for launchers-spacecraft coupled analysis, and direct computation of margins of safety
02 p0188 N90-11077
Planar sliding of a rigid body with dry friction: Limit surfaces and dynamics of motion
02 p0229 N90-11314
The dynamic performance of robot manipulators under different operating conditions
[RR-345] 03 p0355 N90-12031
Multilayer theory for delamination analysis of a composite curved bar subjected to end forces and end moments
[NASA-TM-4139] 04 p0466 N90-12669
Fatigue behavior of specimens under compression load spectra
[ETN-89-95207] 04 p0512 N90-12954
Study of forces and moments on wing-bodies at high incidence, volumes 1 and 2 05 p0575 N90-13350
A transient response method for linear coupled substructures
[NASA-TP-2926] 05 p0592 N90-13444
Cryogenic systems for the large deployable reflector
05 p0597 N90-13470
Initial test results for the mini-mast
05 p0600 N90-13482
Normal force, pitching moment, and side force of forebody-cylinder combinations for angles of attack up to 90 degrees and Mach numbers up to 5
[ESDU-89014] 06 p0718 N90-14192
Fatigue analysis and reconstruction of helicopter load spectra 06 p0739 N90-14304
Influence of hole surface finish, cyclic frequency and spectrum severity on the fatigue behavior of thick section aluminum alloy pin joints
[ARL-STRUC-R-430] 06 p0745 N90-14336
Inductive store opening switch and tests for energy transfer to a load
[DE90-002818] 06 p0770 N90-14482
The stress analysis of thin-walled screwed tubular joints 06 p0796 N90-14637
A theoretical investigation of the column behavior of cold-formed square hollow sections
[PB89-225981] 06 p0797 N90-14645
A study of incremental-iterative strategies for nonlinear analyses
[PB89-226005] 06 p0798 N90-14646
The development of a model of the human responses to load carriage 06 p0821 N90-14775
Thermal loads on tokamak plasma facing components during normal operation and disruptions
[DE90-000794] 06 p0846 N90-14919
Design of a custom load cell for a precision assembly application
[DE90-004439] 07 p0923 N90-15340
Investigation of loads generated by temperature transients in pipes
[DE89-636433] 07 p0932 N90-15395
Single element magnetic suspension actuator
[NASA-CASE-LAR-13981-1] 07 p0940 N90-15442
A procedure for force-balancing planar linkages using counterweights
[ESDU-89028] 07 p0940 N90-15446
Fatigue loading history reconstruction based on the rain-flow technique
[NASA-CR-181942] 07 p0947 N90-15482
An examination of the fatigue meter records from the RAAF Orion P-3C fleet
[AD-A214000] 10 p1319 N90-17628
Equations of motion of slung load systems with results for dual lift
[NASA-TM-102246] 10 p1322 N90-17641
Investigation of failure modes in a ceramic composite under off-axis loading
[AD-A216133] 10 p1348 N90-17820
Transient elastic waves on anisotropic half-spaces
10 p1396 N90-18074

Finite element investigation of a composite cylindrical shell under transverse load with through thickness shear and snapping
[AD-A216377] 10 p1397 N90-18078
Integrated force method versus displacement method for finite element analysis
[NASA-TP-2937] 10 p1398 N90-18081
A comparison of flutter calculations based on eigenvalue and energy method 11 p1459 N90-18406
Blade row interaction effects on compressor measurements 11 p1452 N90-18419
Fastener design manual
[NASA-RP-1228] 11 p1517 N90-18740
Temperature compensated crystal oscillator (TCXO) with improved temperature compensation
[AD-D014334] 12 p1650 N90-19482
Floor pull test of a transport airframe section
[DOT/FAA/CT-TN88/14] 13 p1754 N90-20072
Experimentally determined wear behavior of an Al2O3-SiC composite from 25 to 1200 C
[NASA-TM-102549] 13 p1765 N90-20130
Innovative design of composite structures: The use of curvilinear fiber format in composite structure design
[NASA-CR-186453] 13 p1766 N90-20136
Composite laminate tailoring with probabilistic constraints and loads
[NASA-TM-102515] 13 p1766 N90-20138
COMGEN: A computer program for generating finite element models of composite materials at the micro level
[NASA-TM-102556] 13 p1818 N90-20438
Heavily loaded joints for assembling aerobrake support trusses
[NASA-CR-181992] 14 p1939 N90-21099
Passive shape control of space antennas with determinate truss support structures
15 p2087 N90-21949
Nonlinear fracture mechanics using semicircular specimens and tension-softening behavior
15 p2116 N90-22108
ANILISA: Computational module for Koiter's imperfection sensitivity theory
[LR-582] 15 p2119 N90-22119
Adaptive control of a flexible manipulator with unknown changing loads 15 p2152 N90-22293
An expert system for simulating electric loads aboard Space Station Freedom
[NASA-TM-103150] 15 p2158 N90-22325
Experimental verification of dynamic simulation
16 p2285 N90-23020
Modeling of control forces for kinematical constraints in the dynamics of multibody systems: A new approach
16 p2287 N90-23031
Fatigue testing apparatus
[NASA-CASE-LEW-14124-1] 17 p2407 N90-23712
Physiological and perceptual responses to prolonged treadmill load carriage
[AD-A218809] 17 p2433 N90-23865
A network flow model for load balancing in circuit-switched multicomputers
[NASA-CR-182049] 17 p2451 N90-23077
About the effect of loading sequence on the fatigue life of notched specimens made from steel and aluminum alloys
[LBF-FB-186(1989)] 18 p2526 N90-24414
Unique failure behavior of metal/composite aircraft structural components under crash type loads
[NASA-TM-102679] 18 p2572 N90-24660
Evaluating Statistical Process Control (SPC) techniques and computing the uncertainty of force calibrations
18 p2631 N90-24992
Arcjet load characteristics
[NASA-TM-103190] 19 p2669 N90-25181
An analysis of space power system masses
[NASA-TM-103199] 19 p2669 N90-25184
Postbuckling response of long thick plates loaded in compression including higher order transverse shearing effects
[NASA-TM-102663] 19 p2700 N90-25363
Behavior of composite/metal aircraft structural elements and components under crash type loads: What are they telling us
[NASA-TM-102681] 19 p2701 N90-25368
A study on ultrasonic detection and characterization of partially closed fatigue cracks
[DE90-011748] 19 p2702 N90-25371
Radiological investigation of the vertebral column of candidates for military flying training the the Royal Norwegian Air Force 19 p2718 N90-25463
Analysis of the biomechanic and ergonomic aspects of the cervical spine under load 19 p2719 N90-25470
Effects of head mounted devices on head-neck dynamic response to +G(sub z) accelerations
19 p2720 N90-25471
Dynamical modifications to the head, load factors from additional weight 19 p2720 N90-25472
Mobility of the head and load effects: Experimental approach in a centrifuge 19 p2720 N90-25473
Omni-directional human head-neck response
[SAE-861893] 19 p2721 N90-25478
An unsteady lifting surface method for single rotation propellers
[NASA-CR-4302] 20 p2802 N90-25940
Strain energy release rate analysis of delamination in a tapered laminate subjected to tension load
[NASA-TM-102592] 20 p2826 N90-26076
QM-8 final performance evaluation report: SEALS, volume 4
[NASA-CR-183958] 20 p2869 N90-26324
Power saw
[NASA-CASE-MSC-21469-1] 20 p2872 N90-26340
Experiment K-6-07. Metabolic and morphologic properties of muscle fibers after spaceflight
20 p2893 N90-26461
Application of damage tolerance
21 p2958 N90-26817
Load-point compliance for the arc bend-arc support fracture toughness specimen
[AD-A221618] 21 p3014 N90-27134
Wind loads and local pressure distributions on parabolic dish solar collectors
[DE90-000328] 21 p3019 N90-27166
The composite load spectra project
21 p3047 N90-27323
SDI satellite autonomy using AI and Ada
21 p3050 N90-27336
Motion translator
[AD-D014452] 22 p3181 N90-28053
Graphically-oriented linear analysis of plane frames subjected to complex loadings on microcomputers
[PB90-173279] 22 p3190 N90-28102
The effect of rapid spoiler deployment on the transient forces on an aerofoil 23 p3274 N90-28527
Energy Efficient Engine high pressure turbine component test performance report
[NASA-CR-168289] 23 p3278 N90-28553
Liquid Rocket Booster (LRB) for the Space Transportation System (STS) systems study. Appendix E: Pressure-fed booster test bed for the liquid rocket booster study
[NASA-CR-183791-APP-E] 23 p3289 N90-28605
Probabilistic structural analysis methods development for SSME 23 p3291 N90-28616
Mechanical behavior of thick, curved, laminated composites 23 p3299 N90-28664
Target acquisition under load factors: Advantages and disadvantages of a helmet mounted sight
23 p3359 N90-28983
Variable force and visual feedback effects on teleoperator man/machine performance
23 p3364 N90-29008
Measurement of hand dynamics in a microsurgery environment: Preliminary data in the design of a bimanual telemicro-operation test bed 23 p3364 N90-29010
Multiple cooperating manipulators: The case of kinematically redundant arms 23 p3371 N90-29046
An enhanced integrated aerodynamic load/dynamic optimization procedure for helicopter rotor blades
[NASA-CR-4326] 24 p3432 N90-29383
Estimation of power spectral density of runway roughness
[NAL-TR-1037] 24 p3437 N90-29411
Friction, wear and electric characteristics of slip-ring brush materials for space applications. Part 1: Screening by pin-on-disk friction tests
[NAL-TR-1040] 24 p3478 N90-29657
Fatigue, static tensile strength and stress corrosion of aircraft materials and structures. Part 1: Text
[LR-630-PT-1-REV] 24 p3482 N90-29682
Fatigue, static tensile strength and stress corrosion of aircraft materials and structures. Part 2: Figures
[LR-630-PT-2] 24 p3482 N90-29683
Communications Interface Driver (CID) software principles of operation
[DOT/FAA/CT-TN89/46] 24 p3526 N90-29937

LOCAL AREA NETWORKS
Adaptive gigabit fiber optics local area network
[AD-A210794] 02 p0275 N90-11571
Spacelab system analysis Marshall Avionics System Testbed (MAST)
[NASA-CR-183804] 03 p0317 N90-11802
Spacelab system analysis: The modified free access protocol: An access protocol for communication systems with periodic and Poisson traffic
[NASA-CR-183805] 05 p0602 N90-13497
On stability of queueing models of local area networks with slotted ring protocols
[MEMO-795] 05 p0694 N90-14057
Analysis of a queueing model for slotted ring networks
[MEMO-796] 05 p0694 N90-14058
Dynamic workload modeling of high speed token rings in a metropolitan area network
[MEMO-INF-89-21] 05 p0694 N90-14059
MIPs and BIPs are megaflops: Limits of unidimensional assessments
[DE89-015707] 06 p0820 N90-14770
The Aerospace Energy Systems Laboratory: A BITBUS networking application
[NASA-TM-4149] 06 p0831 N90-14829
Multiple crossbar network: A switched high-speed local network
[DE90-001839] 06 p0831 N90-14833
Voice Multiplex System (VMS)
[AD-A213902] 07 p0919 N90-15315
LLNL's plan for a prototype circuit switch, a potential gigabit LAN of the future
[DE90-003614] 07 p0969 N90-15597
Issues and approaches for electronic document approval and transmittal using digital signatures and text authentication: Prototype documentation
[DE90-003382] 08 p1058 N90-16119
Computer viruses and related threats: A management guide
[PB90-111683] 11 p1543 N90-18881
Random access transmission algorithms for data local area networks
[AD-A216443] 12 p1700 N90-19761
Local area network with fault-checking, priorities, and redundant backup
[NASA-CASE-NPO-16949-1-CU]
12 p1703 N90-19776
Traffic placement policies for a multi-band network
15 p2149 N90-22279
Fairness problems at the media access level for high-speed networks 15 p2151 N90-22287
Access to supercomputers 16 p2277 N90-22979
Use of optical storage devices as shared resources in local area networks
[AD-A219198] 16 p2327 N90-23269
The design of a local area network configuration management system for the Naval Postgraduate School Administrative Sciences Department
[AD-A219643] 17 p2451 N90-23979
ISDN in the local environment: The CISLAN project
[MEMO-INF-89-70] 17 p2452 N90-23985
AIRNET: A real-time comunications network for aircraft
[NASA-CR-186140] 18 p2543 N90-24514
Construction of an Ethernet model with the PROMISE simulation tool
[NLR-MP-88047-U] 18 p2593 N90-24757
Performance analysis of local area networks
[NASA-CR-186639] 18 p2595 N90-24767
Results of the REALAN project: Replacing the Ethernet access mechanism by the real-time access mechanism of Twentenet
[MEMO-INF-89-55] 18 p2596 N90-24768
Analysis of a queueing model of the Orwell slotted ring
[MEMO-812] 18 p2606 N90-24843
An automated calibration laboratory for flight research instrumentation: Requirements and a proposed design approach
[NASA-TM-101719] 20 p2912 N90-26564
Efficient network topologies for extensible massively parallel computers
[ETN-90-97220] 20 p2912 N90-26568
Applications of ISES for geology
21 p3017 N90-27154
Development of a COMPAS prototype for the ATC Centre at Frankfurt (Fed. Republic of Germany)
22 p3113 N90-27684
High speed bus technology development
[AD-A224486] 24 p3463 N90-29565
Turbo pascal implementation of a distributed processing network of MS-DOS microcomputers connected in a master-slave configuration
[AD-A223925] 24 p3525 N90-29928
Working implementation agreements for open systems interconnection protocols
[PB90-197948] 24 p3557 N90-30127

LOCAL GROUP (ASTRONOMY)
NT MILKY WAY GALAXY

LOCALIZATION
U POSITION (LOCATION)

LOCATES SYSTEM
General introduction to location and navigation capabilities 17 p2358 N90-23421

LOCATION
U POSITION (LOCATION)

LOCATION OF AIR TRAFFIC SATELLITES
U LOCATES SYSTEM

LOCKHEED AIRCRAFT
NT C-5 AIRCRAFT
NT C-130 AIRCRAFT
NT C-140 AIRCRAFT

NT C-141 AIRCRAFT
NT F-104 AIRCRAFT
NT L-1011 AIRCRAFT
NT P-3 AIRCRAFT
NT U-2 AIRCRAFT
LOCKHEED C-5 AIRCRAFT
U C-5 AIRCRAFT
LOCKHEED U-2 AIRCRAFT
U U-2 AIRCRAFT
LOCKING
NT LASER MODE LOCKING
A real-time locking protocol
[AD-A211514] 03 p0418 N90-12403
Phase control mechanism for wave energy conversion
[AD-D014354] 12 p1681 N90-19657
Quick connect coupling
[NASA-CASE-MSC-21539-1] 21 p3010 N90-27111
LOCKS (FASTENERS)
Quick disconnect duct coupler
[AD-D014265] 08 p1084 N90-16274
Expanding ring joint
[AD-D014398] 14 p1986 N90-21384
LOCOMOTION
NT ASTRONAUT LOCOMOTION
NT WALKING
Planning systems for autonomous legged vehicles
[AD-A214242] 07 p0942 N90-15458
Periodic gaits for the CMU ambler
23 p3367 N90-29027
First results in terrain mapping for a roving planetary explorer 23 p3375 N90-29066
Exogenous and endogenous control of activity behavior and the fitness of fish
[DLR-FB-90-14] 24 p3497 N90-29766
LOCOMOTIVES
Heat engines
[DE90-000485] 20 p2882 N90-26393
LOGARITHMS
The weighted sum of two S-units being a square
[MEMO-792] 05 p0691 N90-14031
Solving a specific Thue-Mahler equation
[MEMO-793] 05 p0691 N90-14032
Long steps with the logarithmic penalty barrier function in linear programming
[REPT-89-44] 15 p2147 N90-22265
An intensity expression organising spectral line intensity data
[IRF-SR-202] 17 p2373 N90-23513
An O(square root of n) complexity reduction for the long-step path-following algorithm for linear programming
[REPT-89-85] 17 p2445 N90-23940
Converses for write-unidirectional memories
[EUT-89-E-220] 20 p2909 N90-26546
LOGIC
Temporal logics meet telerobotics
24 p3521 N90-29905
An efficient temporal logic for robotic task planning
24 p3521 N90-29906
LOGIC CIRCUITS
NT THRESHOLD GATES
Northeast Artificial Intelligence Consortium annual report for 1987. Volume 7, part A: Time oriented problem solving
[AD-A210331] 01 p0110 N90-10622
Redundancies and don't cares in sequential logic synthesis
[AD-A211931] 03 p0343 N90-11956
Optical arithmetic logic using the modified signed-digit redundant number representation
[AD-D014176] 03 p0384 N90-12186
A single-phase clocked NOR/NOR CMOS programmable sequential array structure
[AD-A211297] 03 p0387 N90-12203
Delay test generation for synchronous sequential circuits
[AD-A211917] 05 p0634 N90-13697
Fault tree analysis: A tool for battery safety and reliability studies
[DE90-002582] 08 p1086 N90-16287
Algorithms for fault tolerant distributed systems
[AD-A214447] 08 p1109 N90-16416
The NODEN hardware description language
[RSRE-89011] 08 p1111 N90-16431
The algebra of the NODEN analyser
[RSRE-89012] 08 p1111 N90-16432
A circuit extraction system and graphical display for VLSI (Very Large Scale Integrated) design
[AD-A215668] 09 p1214 N90-17038
A unified approach to the synthesis of fully testable sequential machines
[AD-A217120] 13 p1863 N90-20687
Irredundant sequential machines via optimal logic synthesis
[AD-A217119] 13 p1873 N90-20742
An investigation of narrow-bandgap semiconductors: Devices, circuits, and systems 15 p2171 N90-22406
An instructable Connectionist/Control architecture: Using rule-based instructions to accomplish connectionist learning in a human time scale
[AD-A219274] 16 p2266 N90-22914
Long period pseudo random number sequence generator
[NASA-CASE-NPO-17241-1-CU]
17 p2394 N90-23636
On axiomatizations for propositional logics of programs
[RUU-CS-88-34] 17 p2449 N90-23966
Structured NC
[RUU-CS-89-6] 17 p2452 N90-23989
Gallium arsenide pilot line for high performance components
[AD-A220948] 18 p2547 N90-24540
Highest integration in microelectronics: Development of digital ASICs for PARS3-LR
[MBB-UA-1151/89-PUB] 19 p2653 N90-25099
Implementation of an algorithm for travelling-wave-based directional detection
[EUT-89-E-214] 20 p2855 N90-26239
On the design and analysis of multiple-storage elements
[AD-A223095] 20 p2859 N90-26266
Conception of a reconfigurable microprocessor
[ETN-90-97248] 20 p2904 N90-26517
Formal verification of the JANUS on-line multiplier
[IMAG-RR-785-I] 20 p2909 N90-26550
Development of probabilistic and possibilistic approaches to approximate reasoning and its applications
[AD-A221945] 21 p3039 N90-27271
Genetic algorithm based fuzzy control of spacecraft autonomous rendezvous 21 p3041 N90-27281
Basic properties and limits of integrated arrays of dissipative circuit and logic elements
[AD-A224533] 24 p3464 N90-29567
A VHDL interface for Altera design files
[AD-A224476] 24 p3523 N90-29920
Optical signal computing
[AD-A223624] 24 p3545 N90-30051
LOGIC DESIGN
An axiomatic theory for partial functions
[MEMO-INF-89-22] 02 p0268 N90-11527
An interpolation theorem in equational logic
[CWI-CS-R8838] 02 p0268 N90-11528
Constructing a calculus of programs
[CWI-CS-R8914] 05 p0683 N90-13979
A logic for the pixel assignment step of imagery classification predicated on class structure
07 p0949 N90-15493
Principles and algorithms for causal reasoning with uncertainty
[AD-A214248] 07 p0977 N90-15644
Designing distributed algorithms by means of formal sequentially phased reasoning
[TR-89-8] 17 p2449 N90-23969
Sequentiality in orthogonal term rewriting systems
[CWI-CS-R8932] 18 p2592 N90-24744
On the use of equational type logic for software engineering and protocol design
[MEMO-INF-89-52] 18 p2592 N90-24748
The bit full-decomposition of sequential machines
[EUT-89-E-223] 20 p2904 N90-26516
The full-decomposition of sequential machines with the separate realization of the next-state and output functions
[EUT-89-E-222] 20 p2909 N90-26547
MINAS: An algorithm for systematic state assignment of sequential machines: Computational aspects and results
[EUT-89-E-217] 20 p2912 N90-26566
LOGIC NETWORKS
U LOGIC CIRCUITS
LOGIC PROGRAMMING
Applications of algebraic logic and universal algebra to computer science
[AD-A210556] 01 p0113 N90-10645
An axiomatic theory for partial functions
[MEMO-INF-89-22] 02 p0268 N90-11527
An interpolation theorem in equational logic
[CWI-CS-R8838] 02 p0268 N90-11528
Multiplicative iterative algorithms for convex programming
[CWI-AM-R8808] 04 p0532 N90-13072
Expert systems as deductive systems
[CWI-CS-R8825] 04 p0532 N90-13073
Process expressions and Hoare's logic
[CWI-CS-R8905] 04 p0532 N90-13076
Characterizing termination of logic problems with level mappings
[CWI-CS-R8912] 04 p0532 N90-13077
On the safe approximation of PROLOG programs
[CWI-CS-R8913] 05 p0683 N90-13978
Program transformation with abstract relation algebras
[AD-A213270] 05 p0688 N90-14011
Strand: A practical parallel programming language
[DE90-002861] 06 p0830 N90-14825
Research in mathematics and computer science at Argonne
[DE90-000975] 07 p0969 N90-15595
D3-D cryogenic control system upgrade
[DE90-003290] 08 p1054 N90-16092
Built in test of folded PLAs
[IMAG-RR-758-I] 08 p1061 N90-16134
Efficient algorithms for dilated mappings of binary trees
[NASA-CR-181980] 09 p1262 N90-17317
A knowledge based approach to program debugging
[AD-A214941] 09 p1266 N90-17344
Parallel logic programming and parallel systems software and hardware
[AD-A214635] 09 p1270 N90-17361
Logical architecture
[INPE-4792-RPE/585] 10 p1418 N90-18171
Joint Japanese-American Workshop on Future Trends in Logic Programming
[DE90-008343] 13 p1867 N90-20709
Exact algorithms for output encoding, state assignment and four-level Boolean minimization
[AD-A217121] 13 p1876 N90-20756
VLSI binary updown counter
[NASA-CASE-NPO-17205-1-CU]
14 p2011 N90-21525
An introduction to selected structured methods
[RSRE-MEMO-4294] 15 p2148 N90-22275
Conceptual modeling via logic programming
[AD-A219785] 17 p2442 N90-23919
The LORE-interpreter: Notes on the implementation
[REPT-89-60] 17 p2445 N90-23932
The Delfi3-interpreter: Notes on the implementation
[REPT-89-72] 17 p2445 N90-23935
On axiomatizations for propositional logics of programs
[RUU-CS-88-34] 17 p2449 N90-23966
Multiple inheritance and exceptions in frame systems
[CWI-CS-R8931] 18 p2591 N90-24743
On the use of equational type logic for software engineering and protocol design
[MEMO-INF-89-52] 18 p2592 N90-24748
Using integrity constraints to control search in knowledge base systems
[AD-A221291] 18 p2634 N90-25009
MINAS: An algorithm for systematic state assignment of sequential machines: Computational aspects and results
[EUT-89-E-217] 20 p2912 N90-26566
Derivation of sorting programs
21 p3047 N90-27319
Logic level data conversion system
[AD-D014545] 22 p3167 N90-27963
Integrating mono-valued functions in deductive databases: A recursive extension of MILANT
[REPT-90-018] 22 p3239 N90-28370
A model parametric real-time logic
[REPT-90-010] 22 p3241 N90-28381
Evaluating recursive queries in distributed databases
[REPT-90-015] 22 p3260 N90-28460
LOGIC UNITS
U ARITHMETIC AND LOGIC UNITS
LOGICAL ELEMENTS
ATS displays: A reasoning visualization tool for expert systems 21 p3042 N90-27290
Basic properties and limits of integrated arrays of dissipative circuit and logic elements
[AD-A224533] 24 p3464 N90-29567
LOGISTICS
NT SPACE LOGISTICS
US Navy principal site testing concept and the F-18
02 p0151 N90-10861
A survey of permanently-manned lunar base concepts
[AD-A212575] 04 p0460 N90-12638
Total quality management plan: Technical and logistics services
[AD-A212864] 05 p0705 N90-14128
International conference management
08 p1136 N90-16583
Experimental evaluation of impedance control for robotic aircraft refueling
[AD-A215532] 09 p1167 N90-16755
RADC fault tolerant system reliability evaluation facility
[AD-A215298] 09 p1267 N90-17348
Orbital fluid resupply assessment
11 p1475 N90-18487
Electronic publishing with Standard Generalized Markup Language (SGML) 15 p2179 N90-22450

Applications to the aerospace and defense R and D community: The DOD computer-aided acquisition and logistics support (CALS) initiative
15 p2179 N90-22453
Environmental effects upon cross-servicing of aircraft in NATO
[AD-A218374] 17 p2343 N90-23341
Peacetime replacement and crash damage factors for army aircraft
[AD-A218544] 17 p2348 N90-23372
A viewpoint on the contribution of expert systems of logistics
[REPT-892-320-101] 17 p2454 N90-24002
A survey of human factors methodologies and models for improving the maintainability design of emerging Army aviation systems
[AD-A221159] 18 p2586 N90-24724
Acquisition of an analytical x ray and image analysis system
[AD-A221376] 18 p2593 N90-24756
The 30-kW ammonia arcjet technology
[NASA-CR-186850] 19 p2670 N90-25190
A research program in computer technology
[AD-A221184] 19 p2746 N90-25606
Planning for Space Station Freedom laboratory payload integration
[NASA-CR-186751] 20 p2820 N90-26047
Retirement for cause of the F100 engine
21 p2957 N90-26813
NASA/USRA University advanced design program
[NASA-CR-186050] 21 p2965 N90-26855
Space Station attached payloads
21 p3015 N90-27141
Advanced robotics for Air Force operations
[PB90-157009] 22 p3182 N90-28055
Airborne target detection, acquisition, and tracking devices
[AD-A223852] 24 p3462 N90-29555
Performance monitoring, fault detection, fault localization design guidance
[AD-A223619] 24 p3478 N90-29655
Multi-user facility for high performance optical recording of brain activity (DURIP)
[AD-A223491] 24 p3498 N90-29768
Software development: A product life-cycle perspective
[AD-A223783] 24 p3528 N90-29952

LOGISTICS MANAGEMENT
NT INVENTORY MANAGEMENT
Program manager's handbook
[AD-A214338] 07 p1009 N90-15844
Manufacturing control: A basis for analysis
[PNR90639] 20 p2844 N90-26174
Systems engineering management guide
[AD-A223168] 21 p3085 N90-27544

LONG DURATION EXPOSURE FACILITY
Syncom 4 deploy, LDEF retrieval highlight 10-day Columbia flight
[NASA-NEWS-RELEASE-89-180]
05 p0594 N90-13448
Experiment facilities for materials and fluid sciences embarked on Eureca-1
[ESA-SP-1118] 08 p1053 N90-16088
Proceedings of the LDEF Materials Data Analysis Workshop
[NASA-CP-10046] 20 p2826 N90-26075
Heavy Nucleus Collector (HNC) project for the NASA Long Duration Exposure Facility (LDEF)
[NASA-CR-182094] 24 p3544 N90-30045

LONG DURATION SPACE FLIGHT
Space Station Freedom: A foothold on the future
[NASA-NP-107/10-88] 02 p0159 N90-10907
Science and applications on the space station: A strategic vision
[NASA-TM-101863] 05 p0601 N90-13493
Bone mineral measurement using dual energy x ray densitometry 05 p0680 N90-13958
JPRS Report: Science and technology. USSR: Space. Soviet space program to the year 2000
[JPRS-USP-89-008] 06 p0728 N90-14248
Autonomous electrical power supply subsystem for the Vesta mission 10 p1331 N90-17692
A lithium sulphur dioxide cell for deep space applications 10 p1334 N90-17718
Application of gallium arsenide solar cell arrays for long duration low earth orbit missions like Columbus
10 p1340 N90-17759
The solar array design of the Vesta small bodies spacecraft 10 p1345 N90-17799
The International Space University
[NASA-TM-103163] 16 p2209 N90-22604
Effects of microgravity on rat muscle
20 p2891 N90-26453
Generation rates and chemical compositions of waste streams in a typical crewed space habitat
[NASA-TM-102799] 22 p3233 N90-28333

LONG PERIOD VARIABLES
U MIRA VARIABLES

LONG RANGE NAVIGATION
U LORAN

LONG TERM EFFECTS
Background of the workshop
10 p1444 N90-18330
Long term intensity stability of Auger electron spectrometers: Instructions for the interlaboratory comparison
[NPL-DMM(A)-1] 15 p2102 N90-22027
A study of concept options for the evolution of Space Station Freedom
[NASA-TM-102675] 19 p2663 N90-25154
Development of testing and analysis methodology to assess the long term durability of polymeric composites at high temperatures
[NASA-TM-102714] 23 p3339 N90-28871

LONG WAVE RADIATION
Proof of the feasibility of coherent and incoherent schemes for pumping a gamma-ray laser
[AD-A212882] 04 p0507 N90-12924
Relationship between the longwave cloud radiative forcing at the surface and the top of the atmosphere
22 p3222 N90-28273

LONG WAVES (METEOROLOGY)
U PLANETARY WAVES

LONGITUDE
Computer program for converting rectangular coordinates to latitude-longitude coordinates
[PB90-231796] 23 p3342 N90-28883

LONGITUDINAL CONTROL
The active control of an unstable canard aircraft
02 p0156 N90-10894
An experimental investigation of thrust vectoring two-dimensional convergent-divergent nozzles installed in a twin-engine fighter model at high angles of attack
[NASA-TM-4155] 08 p1017 N90-15884
Design of integrated pitch axis for autopilot/autothrottle and integrated lateral axis for autopilot/yaw damper for NASA TSRV airplane using integral LQG methodology
[NASA-CR-4268] 09 p1169 N90-16768
Longitudinal stability and control characteristics of the Quiet Short-Haul Research Aircraft (QSRA)
[NASA-TP-2965] 10 p1322 N90-17639
Development of a preliminary high-angle-of-attack nose-down pitch control requirement for high-performance aircraft
[NASA-TM-101684] 12 p1600 N90-19206
Feasibility study for a microwave-powered ozone sniffer aircraft
[NASA-CR-186660] 17 p2353 N90-23397
Short period control using angular acceleration feedback: Compensation for first lag servo
[NAL-TM-600] 24 p3435 N90-29399

LONGITUDINAL STABILITY
Prediction of dynamic derivatives
01 p0012 N90-10055
Dynamic derivatives of missiles and fighter-type configurations at high angles of attack
10 p1306 N90-17554
Longitudinal stability and control characteristics of the Quiet Short-Haul Research Aircraft (QSRA)
[NASA-TP-2965] 10 p1322 N90-17639
Stability of hollow beams in longitudinal phase space
[DE90-004284] 10 p1427 N90-18234

LONGITUDINAL WAVES
NT PLANE WAVES
On strongly nonlinear vortex/wave interactions in boundary-layer transition
[NASA-CR-181963] 07 p0876 N90-15078
Longitudinal traveling waves bifurcating from Vlasov plasma equilibria 12 p1715 N90-19850

LOOK ANGLES (ELECTRONICS)
Analysis of radar images of the active volcanic zone at Krafla, Iceland: The effects of look azimuth biasing
03 p0424 N90-12434

LOOP ANTENNAS
A calibrated, omnidirectional, LF loop antenna for GWEN (Ground Wave Emergency Network)
[AD-A211264] 02 p0213 N90-11221
Characteristics of electromagnetic wave forms with lightning in winter season
[DE89-901256] 07 p0963 N90-15567

LOOPS
Des Cloizeaux's law for strings and galaxies formation. Part 2: Non Abelian configurations
[ROM1F-89-682-PT-2] 05 p0714 N90-14173
Portable digital pressure indicator for calibrating magnetic tape recorders
[NASA-TM-101650] 07 p0933 N90-15401
Design and testing of a superfluid liquid helium cooling loop
[NASA-CR-182776] 09 p1216 N90-17050
Majority voting: Characterization and algorithms
[RUU-CS-88-32] 18 p2592 N90-24750
An approach to systematic phase-lock loop design
[ETN-90-96905] 19 p2686 N90-25280
A new scheme for identification and control
[EUT-88-E-213] 20 p2915 N90-26586
Mobility studies in multiloop spatial linkages
20 p2922 N90-26628

LORAN
NT LORAN C
FAA Loran early implementation project
[AD-A221866] 21 p2956 N90-26805
Combining LORAN and GPS: The best of both worlds
24 p3424 N90-29343

LORAN C
LORAN C stability integrity assurance
[AD-A212663] 05 p0577 N90-13364
Loran C monitor: Facilities Central Processing Unit (FCPU) port evaluation
[DOT/FAA/CT-TN89/57] 10 p1318 N90-17623
Practical applications of Loran-C for land mobile use or the possibility to use Loran-C as a vehicle-location or vehicle-navigation system
[ETN-90-96265] 11 p1455 N90-18384
Sole means navigation and integrity through hybrid Loran-C and NAVSTAR GPS 14 p1907 N90-20933
Differential Loran-C using three secondary stations
[AD-A219573] 17 p2350 N90-23381

LORENTZ FORCE
On the influence of ionospheric conductivity on dispersion of acoustic gravity waves
02 p0244 N90-11386
Testing results of the MIT Probe
[DE89-016679] 02 p0278 N90-11590
Command operated liquid metal opening switch
[AD-D014262] 08 p1060 N90-16126
Analysis of near-surface flow physics in a two-stage, 10 km/s, electromagnetic launcher
[DE90-013292] 21 p2964 N90-26852

LORENTZ TRANSFORMATIONS
Quantum effects in pair cascade models of AGN spectra 19 p2789 N90-25873
Relativistic effects in low energy nucleon-nucleon scattering
[CEBAF-PR-89-025] 21 p3075 N90-27483

LOSS OF COOLANT
Thermal analyses of power subsystem components
[NASA-CR-186314] 24 p3474 N90-29637

LOSSES
Analysis of loss mechanisms in polycrystalline thin-film solar cells
[DE89-009454] 03 p0366 N90-12093
Effects of main-sequence mass loss on the turnoff ages of population 1 clusters
[DE89-016755] 03 p0421 N90-12417
Polymorphism and information loss in Martin-Loef's type theory
[CS-8814] 04 p0533 N90-13079
Speech reception in quiet and in noisy conditions by individuals with noise-induced hearing loss in relation to their audiogram
[IZF-1989-11] 05 p0633 N90-13692
Forward scatter propagation path loss testing using surrogate terrain in the 100 to 1500 MHz region
06 p0760 N90-14425
FLUSH: A tool for the design of slush hydrogen flow systems
[NASA-TM-102467] 10 p1361 N90-17890
Ac loss measurements of two multifilamentary NbTi composite strands
[DE90-005388] 12 p1619 N90-19304
Quantization effects in Viterbi decoding rate 1/n convolutional codes 12 p1644 N90-19445
Nickel-hydrogen capacity loss on storage
13 p1825 N90-20478
A comparison of the mechanisms of cold- and microgravity-induced fluid loss
[AD-A218098] 13 p1852 N90-20631
Testing carbon fabric for oxidation mass loss
15 p2063 N90-21819
High frequency, high temperature specific core loss and dynamic B-H hysteresis loop characteristics of soft magnetic alloys
[NASA-TM-103164] 17 p2398 N90-23663
Off-design loss measurements in a compressor cascade
[AD-A220094] 18 p2552 N90-24564
Aircrew neck injuries: A new, or an existing, misunderstood phenomenon 19 p2719 N90-25467
Characteristic impedances and loss data for a common stripline pickup geometry
[CEBAF-PR-89-038] 19 p2755 N90-25656
Decay of secondary flow and the associated loss variation downstream of an annual turbine stator cascade
[DE90-505520] 20 p2809 N90-25984
Regulation of erythropoiesis in rats during space flight
[NASA-CR-177537] 23 p3378 N90-29086

Spatial structure of particle-orbit loss regions in l=2 helical systems
[DE90-508080] 24 p3548 N90-30073
High resolution transmission electron microscopy of partial states of oxygen order in YBa2Cu3O(z)
[DE90-015637] 24 p3554 N90-30108

LOSSLESS MATERIALS
Implementation issues in source coding
[NASA-CR-185327] 05 p0681 N90-13963
Millimeter wave filter design with suspended stripline
[AD-A219582] 17 p2395 N90-23645

LOSSY MEDIA
Part B: Pattern control of horn antennas
02 p0211 N90-11207
Constitutive parameter measurements of lossy materials
[NASA-CR-183398] 02 p0281 N90-11603
Electromagnetic wave propagation through circular waveguides containing radially inhomogeneous lossy media
[AD-A213062] 05 p0632 N90-13688
Implementation issues in source coding
[NASA-CR-185327] 05 p0681 N90-13963
Annular slot antenna radiating into lossy material
[NPL-DITC-152/89] 22 p3165 N90-27945

LOUDNESS
On categorizing sounds
[AD-A216417] 10 p1427 N90-18232

LOUISIANA
A Geographic Information System (GIS) for the southern Louisiana deltaic environments
[AD-A214676] 09 p1296 N90-17511

LOUVERS
Spacecraft thermal control design data, volume 3
[ESA-PSS-03-108-ISSUE-1-VOL-3]
11 p1469 N90-18457

LOVE WAVES
Investigations of Eurasian seismic sources and upper mantle structure
[AD-A211806] 03 p0371 N90-12120

LOW ALLOY STEELS
U HIGH STRENGTH STEELS

LOW ALTITUDE
Rotorcraft low altitude CNS benefit/cost analysis: Rotorcraft operations data
[DOT/FAA/DS-89/9] 03 p0419 N90-12406
Low-altitude millimeter-wave propagation in the evaporation duct
[AD-A214432] 08 p1057 N90-16108
Sparse breakdown and statistical sneakthrough effects in low-altitude microwave propagation
[DE90-007252] 12 p1648 N90-19473
Computer vision techniques for rotorcraft low altitude flight 15 p2142 N90-22237
System analysis of a tactical multi-satellite communication system
[AD-A220344] 18 p2510 N90-24343

LOW ASPECT RATIO
Secondary flow in a turbine guide vane with low aspect ratio 14 p1924 N90-21018

LOW ASPECT RATIO WINGS
NT DELTA WINGS
Experimental transonic flutter characteristics of two 72 deg-sweep delta-wing models
[NASA-TM-101659] 06 p0720 N90-14205
Computational design of low aspect ratio wing-winglet configurations for transonic wind-tunnel tests
[NASA-CR-181939] 10 p1303 N90-17539
Effects of spoiler surfaces on the aeroelastic behavior of a low-aspect-ratio rectangular wing
[NASA-TM-102622] 22 p3115 N90-27700

LOW CARBON STEELS
Mechanisms of strength and toughness in a microalloyed, precipitation hardened steel
[AD-A210571] 01 p0045 N90-10256
Preliminary exposure study to determine the effects of acid deposition on coated steel substrates
[PB90-201799] 23 p3309 N90-28715

LOW CONCENTRATIONS
Effects of low Chromium(3) concentration in electrodeposition of low contraction chromium
[AD-A223338] 24 p3449 N90-29477

LOW CONDUCTIVITY
Development of low thermal conductivity pan-based carbon fibers for solid rocket motor nozzle applications
15 p2063 N90-21818
High temperature insulation barrier composite
[NASA-CASE-MFS-29241-1] 17 p2368 N90-23480

LOW COST
Network of dedicated processors for finding lowest-cost map path
[NASA-CASE-NPO-17716-1-CU]
01 p0107 N90-10608
Low cost tooling material and process for graphite and Kevlar composites
[NASA-CR-179427] 10 p1351 N90-17834
The design and analysis of algorithm and data structure for efficient solutions of minimum-cost network flow problems on MISD and MIMD 10 p1441 N90-18313
A large area, low cost, gamma-ray, imaging spectrometer
[DE90-006993] 11 p1567 N90-19017
Low-cost small satellites for astrophysical missions
[DE90-007625] 12 p1616 N90-19293
Fighter escape system: The next step forward
13 p1752 N90-20059
Low cost station keeping maneuvers for a small-satellites constellation in tundra orbits
[ETN-90-96553] 16 p2206 N90-22588
Low cost processing routes leading to high-performance ceramic tiles
[AD-A219034] 16 p2224 N90-22688
Orbit control strategy for a constellation of three satellites in tundra orbits
[AAS-89-411] 17 p2361 N90-23445
Creature co-op: Achieving robust remote operations with a community of low-cost robots
21 p3044 N90-27303
A low cost inertial/GPS integrated approach to land navigation 24 p3430 N90-29374

LOW DENSITY FLOW
Spectral characteristics of arc-heated low density plasma flows (IV) air and N2-CO2 mixture plasmas
[NAL-TR-1012] 09 p1285 N90-17451
Computation of hypersonic low density flows with thermochemical nonequilibrium
13 p1749 N90-20044
Low-density flow effects for hypervelocity vehicles, phase 2
[AD-A221034] 18 p2493 N90-24249

LOW DENSITY GASES
U RAREFIED GASES

LOW DENSITY MATERIALS
Polymer group microgravity combustion experiment
09 p1202 N90-16964
A new low density, high porosity lithium hydride-beryllium hydride foam
[DE90-015150] 23 p3313 N90-28739
Percolation and low density materials: Theory and applications
[AD-A224237] 24 p3442 N90-29438

LOW DENSITY WIND TUNNELS
Spectral characteristics of arc-heated low density plasma flows (IV) air and N2-CO2 mixture plasmas
[NAL-TR-1012] 09 p1285 N90-17451
Experimental techniques in the field of low density aerodynamics
[AGARD-AG-318(FR)] 21 p2953 N90-26792

LOW EARTH ORBITAL ENVIRONMENTS
U EARTH ORBITAL ENVIRONMENTS

LOW FREQUENCIES
NT VERY LOW FREQUENCIES
Acoustical effects of a large ridge on low-frequency sound propagation in stationary and moving atmospheres
[NASA-CR-186001] 03 p0400 N90-12290
Auroral particle acceleration by dc and low frequency electric fields 05 p0658 N90-13841
Low frequency polarized and depolarized light scattering in H-bonded liquids: CH3(CH2)n-1OH (n=1,...5)
[PREPRINT-693] 05 p0700 N90-14100
Possibility of low-frequency electron wave in a beam-plasma system
[DE90-601021] 09 p1284 N90-17441
South Pacific OMEGA validation analysis
[AD-A215916] 10 p1319 N90-17624
Trends in VLF/LF (Very Low Frequency/Low Frequency) modem performance testing
[AD-A216576] 11 p1497 N90-18614
Design of a low-frequency (5-20 GHz), 15-meter-diameter passive radiometer for geostationary earth science platforms 12 p1609 N90-19255
A linear filtering technique for removal of low-frequency noise
[DE90-006183] 13 p1794 N90-20296
Proceedings of a workshop on Carcinogenic Potential of Extremely Low Frequency Magnetic Fields
[DE90-614340] 14 p2010 N90-21520
Kinetic theory of low-frequency nonlinear structures in magnetized plasmas
[DE90-611306] 18 p2617 N90-24907
Low-frequency oscillations in vlasov plasmas: The quadratic polarization approximation
[DE90-611309] 18 p2617 N90-24910
Low-frequency measurements of the CMB (Cosmic Microwave Background) spectrum
[DE90-011589] 18 p2639 N90-25033
Fabrication of low frequency structureborne vibration isolation mount
[AD-D014532] 19 p2697 N90-25346
The behaviour of SS433 and Cygnus X-3 at low frequency 19 p2772 N90-25758
Proceedings of the US-Japan Fusion Cooperation Program Exchange P148 Workshop on Advanced Current Drive Concepts
[IPPJ-REV-4] 21 p3078 N90-27498
Low-frequency cloud-radiation interactions
22 p3225 N90-28289
Acoustic qualification of an anechoic chamber
[RAE-TM-MAT/STR-1136] 22 p3245 N90-28400

LOW FREQUENCY BANDS
NT VERY LOW FREQUENCIES

LOW GRAVITY
U REDUCED GRAVITY

LOW GRAVITY MANUFACTURING
Concepts for microgravity experiments utilizing gloveboxes
[NASA-TM-100378] 02 p0209 N90-11195
Protein crystal growth in low gravity
[NASA-CR-186082] 04 p0483 N90-12770
Containerless Processing of Metals: Undercooling and Solidification
[DLR-MITT-89-15] 05 p0625 N90-13645
Materials processing in low gravity
[NASA-CR-183733] 06 p0755 N90-14397
Polymeric materials science in the microgravity environment 10 p1365 N90-17913
Microgravity science and applications: Apparatus and facilities
[NASA-TM-101892] 23 p3285 N90-28588

LOW LATITUDES
U TROPICAL REGIONS

LOW MASS
U MASS

LOW MOLECULAR WEIGHTS
Crosslinked, flexible, low-molecular-weight polyacrylamide gels for mobility control
[DE90-000202] 07 p0913 N90-15280
Mass spectrometry of poly(methyl methacrylate)s of low molecular weight 20 p2829 N90-26091

LOW NOISE
Design and fabrication requirements for low noise supersonic/hypersonic wind tunnels
04 p0446 N90-12555
Development of a low noise 10 K J-T refrigeration system
[AD-A213347] 04 p0484 N90-12779
Design and realization of a two stage C-band low noise amplifier
[FEL-89-B265] 23 p3322 N90-28783

LOW PASS FILTERS
Adaptive canceller limitations caused by I,Q mismatch errors
[AD-A214287] 07 p0919 N90-15318
Aggregate filter
[AD-A215029] 09 p1282 N90-17432
Hybrid (optical/electronic) computing and digital optical computing
[AD-A214502] 10 p1416 N90-18160

LOW PRESSURE
NT HIGH ALTITUDE PRESSURE
Effect of reduced atmospheric pressure on the performance characteristics of pyrotechnic compositions containing aluminum
[AD-A214473] 09 p1200 N90-16953
Two-dimensional calculation of sequential electron layer formation by crossed microwave beams in air at low pressure
[DE90-005254] 09 p1286 N90-17453
Two-dimensional, long-pulse computer calculation of microwave-induced electron layer formation in low-pressure air
[DE90-005994] 12 p1646 N90-19459
Synthesis of ceramic superconductors under low oxygen pressure
[DE90-010415] 18 p2621 N90-24933
Technology for low pressure plasma processes, a new approach: The plasma box concept
[MBB-UE-0003/89-PUB] 19 p2653 N90-25101
A study of the influence of Hg(6(3)P2) population in a low-pressure discharge on mercury ion emission at 194.2 nm 20 p2853 N90-26223
NASA/GE Energy Efficient Engine low pressure turbine scaled test vehicle performance report
[NASA-CR-168290] 23 p3280 N90-28563

LOW PRESSURE CHAMBERS
U VACUUM CHAMBERS

LOW REYNOLDS NUMBER
Low-Reynolds-number modeling of complex flows with and without density variation 02 p0146 N90-10832
Computational fluid dynamics method for low Reynolds number flow in a precessing/spinning, liquid filled cylinder with rounded endcaps
[AD-A216997] 12 p1659 N90-19531
The effect of adverse pressure gradient on turbulent burst structure in low-Reynolds number equilibrium boundary layers
[AD-A217308] 13 p1799 N90-20327

An investigation of turbulence structure in a low Reynolds number incompressible turbulent boundary layer
15 p2091 N90-21966
Prediction of aerodynamic performance of airfoils in low Reynolds number flows
[DLC-EST-TN-031] 17 p2346 N90-23360
The Stealth biplane: A proposal in response to a low Reynolds Number station keeping mission
[NASA-CR-186680] 19 p2658 N90-25127
Project Dawdler: A proposal in response to a low Reynolds number station keeping mission
[NASA-CR-186668] 19 p2658 N90-25128
The Penguin: A low Reynolds number powered glider for station keeping missions
[NASA-CR-186667] 19 p2658 N90-25129
DRAG-n-FLY: A proposal in response to a low Reynolds number station keeping mission
[NASA-CR-186666] 19 p2658 N90-25130
The FX/90: A proposal in response to a low Reynolds Number station keeping mission
[NASA-CR-186665] 19 p2659 N90-25131
The Screem-J4D: A proposal in response to a low Reynolds number station keeping mission
[NASA-CR-186664] 20 p2807 N90-25968
Experimental techniques in the field of low density aerodynamics
[AGARD-AG-318(FR)] 21 p2953 N90-26792
Numerical solution for the velocity-derivative skewness of a low-Reynolds-number decaying Navier-Stokes flow
[NASA-TM-103186] 22 p3171 N90-27985

LOW SPEED
Mathematical models for the linear induction motor
[RR-WB-88-17] 04 p0496 N90-12853
Low air speed computation for helicopters: A new approach 09 p1165 N90-16744
Low speed flowfield characterization by infrared measurements of surface temperatures
10 p1306 N90-17556
Study on the thermodynamical and mechanical conditions for the generation of high operating pressures with liquefied gases for low and very low flow rates
[ESA-TT-1148] 11 p1510 N90-18696
Space mechanism of low velocity for an array of solar panels: Analysis and design of an experimental model; dimensions of bearings
[INPE-4859-TDL/370] 13 p1809 N90-20390
Low velocity impact analysis with NASTRAN
18 p2570 N90-24647
Low velocity instrumented impact testing of four new damage tolerant carbon/epoxy composite systems
[NASA-TP-3029] 19 p2672 N90-25198
Summary of a study to determine low-velocity impact damage and residual tension strength for a thick graphite/epoxy motor case
[NASA-TM-102678] 19 p2702 N90-25374
Velocity measurements on a lifting rotor/airframe configuration in low speed forward flight
21 p2953 N90-26790
Effects of canard position on the aerodynamic characteristics of a close-coupled canard configuration at low speed 23 p3272 N90-28519

LOW SPEED STABILITY
Low-speed wind tunnel investigation of the static stability and control characteristics of an advanced turboprop configuration with the propellers placed over the tail
[NASA-CR-186900] 20 p2814 N90-26017

LOW SPEED WIND TUNNELS
NT SUBSONIC WIND TUNNELS
Comparison of the results of tests on A300 aircraft in the RAE 5 metre and ONERA F1 wind tunnels
[RAE-TM-AERO-2130] 03 p0311 N90-11768
The use of sublimation methods for the recognition of transition at low speed 08 p1080 N90-16251
The DFVLR 3-m x 3-m low speed wind tunnel (NWG) in Goettingen
[ESA-TT-1156] 11 p1465 N90-18436
Comparison between design and installed acoustic characteristics of NASA Lewis 9- by 15-foot low-speed wind tunnel acoustic treatment
[NASA-TP-2996] 12 p1606 N90-19242
Design of a high angle of attack robotic sting mount for tests in a low speed wind tunnel
[AD-A218105] 13 p1759 N90-20099
Static wind-tunnel and radio-controlled flight test investigation of a remotely piloted vehicle having a delta wing planform
[NASA-TM-4200] 18 p2491 N90-24236
The low-speed wind tunnel at DFVLR in Brunswick (status 1988)
[ESA-TT-1163] 19 p2662 N90-25152
Innovative control concepts and component integration for a generic supercruise fighter
23 p3273 N90-28521
The equipment for mass flow measurements in the low-speed wind tunnel at DFVLR in Brunswick (Federal Republic of Germany)
[ESA-TT-1125] 23 p3285 N90-28585
A microprocessor controlled strain gauge calibration module
[AR-005-579] 23 p3329 N90-28821

LOW TEMPERATURE
NT CRYOGENIC TEMPERATURE
Reactions of hydrogen chloride and boron trichloride with trimethylsilylamino groups
[AD-A209006] 01 p0038 N90-10209
Low temperature processing of reaction sintered silicon nitride
[DE89-017455] 02 p0191 N90-11092
Low temperature properties of glasses
02 p0200 N90-11141
Low temperature spectroscope of hydrazine and ammonia complexes 02 p0205 N90-11169
Thermal model for double-drift IMPATT diodes on diamond heat sinks
[AD-A211746] 03 p0415 N90-12380
An approach to low temperature high strain rate superplasticity in aluminum alloy 2090
[AD-A212271] 04 p0476 N90-12731
Synthesis and properties of NdNiO(3) prepared by low temperature methods
[AD-A212117] 04 p0559 N90-13256
Analysis of an R-SQUID noise thermometer
[VTT-PUBL-54] 05 p0645 N90-13769
Operational activity in France and a new method of balloon temperature piloting 05 p0660 N90-13857
The formation of metal-oxygen species at low temperatures
[DE90-002298] 06 p0743 N90-14323
Cold starting a neat methanol (M100) vehicle with long duration spark ignition
[PB89-230692] 06 p0792 N90-14613
Investigation of low temperature multilevel dielectrics for application for radiation tolerant, submicron-scaled IC technology
[AD-A216114] 10 p1433 N90-18273
Low temperature specific heat and magnetic susceptibility of NbTi and NbTiMn alloys
[DE90-005390] 11 p1486 N90-18552
Low temperature elastic and dielectric properties of incommensurate barium sodium niobate
[AD-A216969] 12 p1709 N90-19815
Physical processes in cometary ices inferred from laboratory studies 12 p1739 N90-19996
A comparison of the mechanisms of cold- and microgravity-induced fluid loss
[AD-A218098] 13 p1852 N90-20631
The influence of large, cold objects on engulfing fire environments
[DE90-003342] 15 p2073 N90-21875
Low temperature properties of amorphous solids
15 p2171 N90-22405
A low temperature calorimetric study of several high-T(sub c) superconductors 16 p2322 N90-23237
Low-Temperature CO-Oxidation Catalysts for Long-Life CO2 Lasers
[NASA-CP-3076] 18 p2556 N90-24586
Effect of pretreatment on a platinized tin oxide catalyst used for low-temperature CO-oxidation
18 p2558 N90-24599
Applications of low temperature CO-oxidation catalysts to breathable gases 18 p2561 N90-24615
Potential technology transfers of research on low-temperature carbon monoxide-oxygen recombination catalysts 18 p2562 N90-24616
Sputtered superconducting films of Bi2Sr2CaCu2O(x) made by low-temperature, in-situ growth
[DE90-010092] 18 p2619 N90-24919
Traps for neutral atoms
[AD-A221331] 19 p2754 N90-25649
Infrared line parameters at low temperatures relevant to planetary atmospheres 20 p2944 N90-26753
High resolution, low temperature photoabsorption cross-section of C2H2 with application to Saturn's atmosphere 20 p2945 N90-26757
Vapor pressures of acetylene at low temperatures
20 p2949 N90-26777
Physics and techniques for the investigation of the properties of ultra small systems
[AD-A221985] 21 p3071 N90-27461
Modeling of carbon monoxide oxidation kinetics over NASA carbon dioxide laser catalysts
[NASA-CR-186356] 22 p3155 N90-27885
Mode competition in the quasioptical gyrotron
[AD-A222181] 23 p3329 N90-28823
Evaluation of physiological and psychological impairment of human performance in cold stressed subjects
[AD-A223635] 24 p3498 N90-29769
Investigation of YBa2Cu3O(7-sigma) by NMR and construction of an ultra low temperature cryostat
24 p3550 N90-30088

LOW TEMPERATURE ENVIRONMENTS
Effective calibration of heat flux transducers for experimental use
[AD-A218262] 13 p1853 N90-20636
What should athletes know about low body temperature (hypothermia)
[AD-A218316] 13 p1854 N90-20637

LOW TEMPERATURE PHYSICS
Highlights of papers presented at the workshop on Cold Fusion Phenomena
[DE89-016956] 03 p0407 N90-12334
Record of forum on cold fusion
[DE90-749883] 12 p1717 N90-19863
Study to identify future cryogen payload elements/users for space shuttle launch during period 1990 to 2000
[NASA-CR-186311] 17 p2363 N90-23452

LOW TEMPERATURE PLASMAS
U COLD PLASMAS

LOW TEMPERATURE TESTS
Low temperature optical testing of CFRP telescope panels 05 p0596 N90-13463
SPOT 4 magnetic tape recorder mechanisms
18 p2540 N90-24500
Materials studies for magnetic fusion energy applications at low temperatures, volume 12
[PB90-157553] 22 p3248 N90-28417

LOW THRUST
A trajectory generation and system characterization model for cislunar low-thrust spacecraft. Volume 2: Technical manual
[NASA-CR-185172] 15 p2061 N90-21807
Low thrust rocket test facility
[NASA-TM-103206] 19 p2663 N90-25158

LOW THRUST PROPULSION
NT ELECTROMAGNETIC PROPULSION
NT ION PROPULSION
NT PLASMA PROPULSION
Advanced onboard propulsion benefits and status
[NASA-TM-103174] 22 p3134 N90-27786

LOW TURBULENCE
Turbulence and complex systems
[ETN-90-96620] 16 p2236 N90-22758

LOW VELOCITY
U LOW SPEED

LOW VISIBILITY
Flight in Adverse Environmental Conditions
[AGARD-CP-470] 07 p0869 N90-15041
Modified touchdown zone lighting
[DOT/FAA/CT-TN89/70] 14 p1929 N90-21042

LOW VOLTAGE
Reduced voltage and restart testing of the 1-watt integral cryogenic cooler (HD-1033B/C/D)
[AD-A215133] 09 p1203 N90-16971
Development and test of power amplifiers for the driving of low-voltage piezo-actuators in multistable interferometers
[DLR-MITT-89-19] 11 p1504 N90-18662
Radiation-hard-high-efficiency InP space solar cell development
[AD-A220500] 17 p2420 N90-23791

LOW WEIGHT
Low weight variable GRV power supply as part of the injector electronics to be developed for the electron accelerator MEA
[DIGEL-1989-6] 11 p1504 N90-18661

LOWER ATMOSPHERE
NT TROPOPAUSE
NT TROPOSPHERE
Correspondence between solar fine-scale structures in the corona, transition region, and lower atmosphere from collaborative observations 01 p0139 N90-10804
Environmental Research Laboratories programs and plans. FY-1989 and FY-1990 plans
[PB90-169988] 22 p3197 N90-28144

LOWER BODY NEGATIVE PRESSURE
Preliminary study of pharmacological control of space disease
[ETN-90-95015] 05 p0674 N90-13927
Use of lower body negative pressure as a countermeasure to negative Gz acceleration
[AD-A213927] 07 p0967 N90-15583
Strategies to sustain and enhance performance in stressful environments
[AD-A221224] 18 p2583 N90-24711
Cardiovascular deconditioning of cosmonauts: Role, importance and applications of the lower body negative pressure
[ETN-90-97507] 23 p3355 N90-28964
Joint US/USSR study: Comparison of effects of horizontal and head-down bed rest
[NASA-TP-3037] 23 p3355 N90-28965

LOWER IONOSPHERE
NT D REGION

Solar cosmic ray effects in the lower ionosphere
22 p3208 N90-28201
Solar or meteorological control of lower ionospheric fluctuations (2-15 and 27 days) in middle latitudes
22 p3209 N90-28202
Post-flare effects in the lower ionosphere of middle latitudes
22 p3209 N90-28205

LOX (OXYGEN)
U LIQUID OXYGEN

LOX-HYDROCARBON ROCKET ENGINES
U OXYGEN-HYDROCARBON ROCKET ENGINES

LOX-HYDROGEN ENGINES
U HYDROGEN OXYGEN ENGINES

LQG CONTROL
U LINEAR QUADRATIC GAUSSIAN CONTROL

LQR
U LINEAR QUADRATIC REGULATOR

LRV (VEHICLE)
U LUNAR ROVING VEHICLES

LSI
U LARGE SCALE INTEGRATION

LST
U HUBBLE SPACE TELESCOPE

LUBRICANT TESTS
Development of a high temperature FZG-Ryder gear lubricant load capacity machine
[AD-A210799] 01 p0079 N90-10449
Characterization of self-lubricating surface materials
[CETIM-108060] 04 p0479 N90-12749
Cold press lubrication: Fine tuning of the CETIM Forgelub test
[CETIM-105160] 04 p0509 N90-12938
Evaluation of newly formulated Dow Corning 321 dry film lubricant
[NASA-CR-183828] 05 p0627 N90-13661
Development of fuel wear tests using the Cameron-Plint high-frequency reciprocating machine
[AD-A216003] 10 p1361 N90-17892
The performance of PTFE, lead, and MoS2 as lubricant films for ball bearings operating in vacuum at 20 K
18 p2540 N90-24495
Micro separometer and ball-on-cylinder lubricity evaluator tests or corrosion inhibitor/lubricity improver additives
[AD-A221339] 19 p2678 N90-25228

LUBRICANTS
NT HIGH TEMPERATURE LUBRICANTS
NT LUBRICATING OILS
NT SOLID LUBRICANTS
Plasma-deposited amorphous hydrogenated carbon films and their tribological properties
[NASA-TM-102379] 03 p0331 N90-11880
Analysis of hydraulic fluids and lubricating oils for the formation of Trimethylolpropane Phosphate (TMP-P)
[AD-A215188] 09 p1198 N90-16939
Traction modeling of military lubricants
[AD-A213866] 09 p1230 N90-17139
Film thickness in lubricated Hertzian contacts. Part 2: Point contacts
[ESDU-89045] 09 p1232 N90-17148
Life of concentrated contacts in the mixed EHD and boundary film regimes
[AD-A216673] 11 p1517 N90-18738
Tribological properties of boric acid and boric-acid-forming surfaces. Part 2: Formation and self-lubrication mechanisms of boric acid films on boron- and boric-oxide-containing surfaces
[DE90-005632] 13 p1811 N90-20400
A new class of lubricants derived from archaebacterial lipids
[AD-D014429] 14 p1954 N90-21185
Improved Thermo-Oxidative-Deposition screening tests for turbine lubricants
[AD-A217795] 14 p1954 N90-21188
Influence of the deposition conditions on radiofrequency magnetron sputtered MoS2 films
[NASA-TP-2994] 14 p1958 N90-21210
Improved analytical capabilities for foil air bearings, phase 1
[AD-A218071] 14 p1987 N90-21389
Self-lubricating polymer composites and polymer transfer film lubrication for space applications
[NASA-TM-102492] 15 p2071 N90-21862
Bearing elastohydrodynamic lubrication: A complex calculation made simple
[NASA-TM-102575] 15 p2105 N90-22041
Experience with synthetic fluorinated fluid lubricants
15 p2114 N90-22095
AX-5 space suit bearing torque investigation
15 p2115 N90-22101
Elastomer compatibility studies
[BR106069] 17 p2378 N90-23542
Development of a device for surface tension measurement and phenomenological rheology
[ECL-89-12] 17 p2382 N90-23568
Effect of film adhesion on tribological properties of silver-coated alumina
[DE90-010090] 18 p2564 N90-24632
A high-speed photography study of cavitation in a dynamically loaded journal bearing
[NASA-TM-103178] 20 p2872 N90-26338
Use of electron spectroscopies in the tribological evaluation of diamond films
[DE90-014421] 23 p3334 N90-28848
Scale effects in steady-state friction
[DE90-012943] 24 p3476 N90-29647

LUBRICATING OILS
Development of a high temperature FZG-Ryder gear lubricant load capacity machine
[AD-A210799] 01 p0079 N90-10449
Automatic prestart or post shutoff engine lubricator
[AD-D014259] 08 p1084 N90-16273
Analysis of hydraulic fluids and lubricating oils for the formation of Trimethylolpropane Phosphate (TMP-P)
[AD-A215188] 09 p1198 N90-16939
Experience with synthetic fluorinated fluid lubricants
15 p2114 N90-22095
Positive lubrication system 15 p2115 N90-22097
Quantitative determination of 1, 2-ethanediol contamination in used diesel lubricating oils by gas chromatography/mass spectrometry
[AD-A218592] 17 p2371 N90-23498
The acute, delayed neurotoxicity evaluation of two jet engine oil formulations
[AD-A222018] 21 p2986 N90-26972
Liquid lubrication in space
[NASA-RP-1240] 22 p3183 N90-28063

LUBRICATION
NT BOUNDARY LUBRICATION
NT SELF LUBRICATION
NT SPACECRAFT LUBRICATION
Efficient numerical method for computation of thermohydrodynamics of laminar lubricating films
[NASA-CR-185136] 02 p0219 N90-11256
Tribological properties of ceramic/Ti3Al-Nb sliding couples for use as candidate seal materials to 700 deg C
[NASA-TM-102401] 04 p0464 N90-12658
Solid lubrication of ceramic surfaces by IAD (ion-Assisted Deposition)-silver coatings for heat engine applications
[DE90-002860] 07 p0909 N90-15253
Analysis of an elastohydrodynamic lubricated point contact: User's manual
[AD-A214257] 07 p0943 N90-15459
Automatic prestart or post shutoff engine lubricator
[AD-D014259] 08 p1084 N90-16273
Investigation of rough elastohydrodynamic contact
[ISAL-89-0029] 08 p1085 N90-16281
On the numerical solution of the dynamically loaded hydrodynamic lubrication of the point contact problem
[NASA-TM-102427] 09 p1220 N90-17076
Some problems in hydrodynamic lubrication
09 p1229 N90-17133
Film thickness in lubricated Hertzian contacts. Part 2: Point contacts
[ESDU-89045] 09 p1232 N90-17148
Development of fuel wear tests using the Cameron-Plint high-frequency reciprocating machine
[AD-A216003] 10 p1361 N90-17892
Scuffing modelling and experiments for heavily loaded elastohydrodynamic lubrication contacts
10 p1391 N90-18047
In-line wear monitor
[AD-A217799] 13 p1757 N90-20091
Space mechanism of low velocity for an array of solar panels: Analysis and design of an experimental model; dimensions of bearings
[INPE-4859-TDL/370] 13 p1809 N90-20390
Bearing elastohydrodynamic lubrication: A complex calculation made simple
[NASA-TM-102575] 15 p2105 N90-22041
An analytical study of tribochemical phases with colloidal additives. Contributions made by energy filtering electron microscopy
[ECL-89-009] 17 p2374 N90-23521
Investigation of metal processing technology
[AD-A218835] 17 p2376 N90-23531
Electronic structure and lubrication properties of MoS2: A qualitative molecular orbital approach
[AD-A220566] 17 p2380 N90-23557
Interface tribology and space conditions
18 p2536 N90-24469
The performance of PTFE, lead, and MoS2 as lubricant films for ball bearings operating in vacuum at 20 K
18 p2540 N90-24495
Thick and compact MoS2 coatings
18 p2541 N90-24501
The experimental evaluation and application of high temperature solid lubricants 18 p2564 N90-24631
Liquid lubrication in space
[NASA-RP-1240] 22 p3183 N90-28063
Pratt and Whitney cryogenic turbopump bearing experience 23 p3292 N90-28624
Current research in cavitating fluid films
[NASA-TM-103184] 23 p3323 N90-28791
The friction and wear of lubricated Si3N4/SiC(w) composites
[DE90-015790] 24 p3444 N90-29448
Lubrication characteristics of rolling bearings lubricated by self-lubricating composite retainers. Part 1: Selection of bearings for Earth sensors
[NAL-TR-1019] 24 p3477 N90-29651

LUBRICATION SYSTEMS
Structural studies of sputter-deposited MoS2 solid lubricant films
[AD-A212407] 04 p0481 N90-12759
Life of concentrated contacts in the mixed EHD and boundary film regimes
[AD-A216673] 11 p1517 N90-18738
Positive lubrication system 15 p2115 N90-22097
Liquid lubrication in space
[NASA-RP-1240] 22 p3183 N90-28063

LUCITE (TRADEMARK)
U POLYMETHYL METHACRYLATE

LUDER BANDS
U PLASTIC DEFORMATION
U YIELD POINT

LUGS
Influence of hole surface finish, cyclic frequency and spectrum severity on the fatigue behavior of thick section aluminum alloy pin joints
[ARL-STRUC-R-430] 06 p0745 N90-14336
Inspection development for T-37 wing spar cap lug
[AD-A214826] 09 p1159 N90-16708

LUMBERING AREAS
U FORESTS

LUMINAIRES
NT AIRCRAFT LIGHTS
NT FLASH LAMPS
NT RUNWAY LIGHTS
Apparatus and method for monitoring pressure leaks from a sealed system
[AD-D014168] 03 p0349 N90-11995
Measurement of the light flux density patterns from luminaires proposed as photon sources for photosynthesis during space travel
[NASA-CR-186124] 05 p0672 N90-13916
Improved lighting of taxiway/taxiway intersections for Instrument Flight Rules (IFR) operations
[DOT/FAA/CT-TN89/64] 07 p0878 N90-15089
Safety evaluation of infrared lamp power output for oculometer eye/head tracker system
[AD-A215809] 10 p1411 N90-18138

LUMINANCE
Three stages and two systems of visual processing
[AD-A212670] 04 p0525 N90-13032
The effects of luminance boundaries on color perception
[AD-A216741] 11 p1539 N90-18860
The computation of color
[AD-A216531] 11 p1548 N90-18914
Tunable XeCl-laser featuring high spectral luminance
16 p2311 N90-23167
HDTV: A chance to enhance television colorimetry
[BBC-RD-1990/2] 18 p2543 N90-24515
The effects of luminance boundaries on color perception
[AD-A221544] 21 p3034 N90-27251
Simulation of long range atmosphere effects in short range thermal infrared and CCD images
[IZF-1989-27] 22 p3247 N90-28413

LUMINESCENCE
NT BIOLUMINESCENCE
NT CATHODE GLOW
NT CATHODOLUMINESCENCE
NT CHEMILUMINESCENCE
NT ELECTROLUMINESCENCE
NT FLUORESCENCE
NT LASER INDUCED FLUORESCENCE
NT PHOSPHORESCENCE
NT PHOTOLUMINESCENCE
NT RESONANCE FLUORESCENCE
NT SPACECRAFT GLOW
NT THERMOLUMINESCENCE
NT X RAY FLUORESCENCE
A new type of radioluminescent light source
[DE90-004294] 09 p1210 N90-17015
Luminescence probe studies of ionomers. Part 3: Distribution of decay rate constants for tris bipyridyl Ruthenium(II) in Nafion membranes
[AD-A215885] 10 p1359 N90-17880
Luminescence from defects and impurity centers in yttrium oxide
[DE90-004842] 11 p1569 N90-19030

Photorefractive damage mechanisms in electro-optic materials
[AD-A219786] 17 p2476 N90-24157
Molecular studies of dense cores
17 p2484 N90-24207
Dissociation phenomena in electron-beam sustained carbon dioxide lasers 18 p2560 N90-24610
Experimental investigations of low-energy (4 to 40 eV) collisions of O(-)(P2) ions and O(P3) atoms with surfaces
19 p2732 N90-25530
Electronic and photonic power applications
[DE90-015567] 24 p3485 N90-29698

LUMINESCENT INTENSITY
U LUMINOUS INTENSITY

LUMINOSITY
NT STELLAR LUMINOSITY
The process e(-)p giving gamma e(-)p as a fast luminosity for the HERA collider
[NIKHEF-H/88-13] 04 p0553 N90-13223
Soft x ray emission from classical novae in outburst
[DE90-006480] 11 p1595 N90-19187
Nearly simultaneous optical, ultraviolet, and x ray observations of three PG quasars
[NASA-CR-186355] 12 p1728 N90-19932
Studies of the evolution of the x ray emission of clusters of galaxies
[NASA-CR-186471] 13 p1903 N90-20918
Discovery of low mass objects in Taurus
14 p1978 N90-21329
Recent advances in the studies of the nova outburst
[DE90-008936] 14 p2038 N90-21691
Multi-wavelength observations of novae in outburst
[DE90-008934] 14 p2038 N90-21692
Search for rapidly star forming galaxies at high redshift
15 p2181 N90-22465
Extended optical emission in 3CR radio galaxies
15 p2193 N90-22523
A search for additional parameters in the infrared luminosity/21 cm line-width relation for spiral galaxies in clusters of galaxies 16 p2328 N90-23274
Spectral plane quasars, spectral turn-over, and frequency atlas
[INPE-5011-TDL/399] 16 p2329 N90-23277
Gamma rays from pulsar wind shock acceleration
16 p2336 N90-23311
The high energy source 3C 273
16 p2337 N90-23318
Axions and SN 1987A: Axion trapping
[NASA-CR-186604] 18 p2612 N90-24881
The optical characteristics of a sample of soft X ray selected active galactic nuclei 19 p2784 N90-25843
BL Lacs from the EMSS: Number-counts and implications for the luminosity function
19 p2785 N90-25849
Very low luminosity AGN 19 p2786 N90-25851
X ray constraints on the beaming hypothesis for BL Lacertae objects 19 p2793 N90-25900
Detection of hard X ray emission from a type 2 Seyfert galaxy 19 p2794 N90-25905
Pulsations of B star models by an opacity mechanism
[DE90-014923] 23 p3412 N90-29279

LUMINOUS FLUX DENSITY
U LUMINOUS INTENSITY

LUMINOUS INTENSITY
NT ILLUMINANCE
NT LUMINANCE
Luminescence in applied magnetic fields
[AD-A211551] 03 p0399 N90-12287
Design and tests of simple, inexpensive optical beacon for use on small satellites
[AD-A213325] 04 p0555 N90-13238
Proximity effects on adjacent and multiple stars
05 p0607 N90-13533
Attenuating the luminous output of the AN/PVS-5A night vision goggles and its effects on visual acuity
[AD-A214895] 09 p1261 N90-17311
Interdigitated back contact silicon solar cell analysis and design recommendations for space use
[AD-A220414] 17 p2420 N90-23790
Optical motion detector detecting visible and near infrared light
[AD-D014515] 19 p2758 N90-25871
Human factors and safety considerations of night vision systems flight using thermal imaging systems
[AD-A223226] 21 p3037 N90-27263
Electro-optics engineering support for the integrated launch and recovery television surveillance system
[AD-A223450] 24 p3436 N90-29406

LUMPED PARAMETER SYSTEMS
Nonlinear mechanics of unstable plasmas as related to high altitude aerodynamics
[AD-A215126] 12 p1716 N90-19852

LUNAR ATMOSPHERE
Design of a lunar transportation system, volume 2
[NASA-CR-186833-VOL-2] 20 p2871 N90-26333

LUNAR BASES
Second Beamed Space-Power Workshop
[NASA-CP-3037] 01 p0027 N90-10140
Office of exploration overview
01 p0027 N90-10141
Laser-powered lunar base 01 p0029 N90-10156
Power for the moon: Is microwave power beaming an option? 01 p0030 N90-10158
Low-earth-orbit to low-lunar-orbit laser freighter
01 p0030 N90-10160
Laser propulsion option 01 p0030 N90-10161
Laser thruster 01 p0030 N90-10164
A lunar far-side very low frequency array
[NASA-CP-3039] 01 p0139 N90-10805
A survey of permanently-manned lunar base concepts
[AD-A212575] 04 p0460 N90-12638
Partial gravity habitat study: With application to lunar base design
[NASA-CR-186048] 06 p0732 N90-14267
SP-100 power system conceptual design for lunar base applications
[NASA-TM-102090] 06 p0866 N90-15030
Lunar construction utility vehicle
[NASA-CR-186231] 07 p0939 N90-15435
Lunar power system summary of studies for the lunar enterprise task force NASA-office of exploration
07 p1008 N90-15841
Transportation and operations aspects of space energy systems 07 p1008 N90-15842
A quasi-economic role for lunar science
[DE90-000679] 07 p1015 N90-15876
The first 1000 days of a future lunar base
[ILR-MITT-224] 08 p1033 N90-15970
Extending terrestrial mobile robotics to a proposed lunar base
[DE89-016179] 12 p1672 N90-19806
Space power generation and distribution
[DE90-008676] 14 p2002 N90-21474
Mars in this century: The Olympia Project
[DE90-008356] 14 p2042 N90-21709
The role of automation and robotics in the Lunar-Based Chemical Analysis Laboratory
[DE90-009401] 15 p2192 N90-22516
Lunar base 2 (the second thousand days of a base on the Moon)
[ILR-MITT-230(1989)] 16 p2275 N90-22968
Design of an unmanned lunar cargo lander that reconfigures into a shelter for a habitation module or disassembles into parts useful to a permanent manned lunar base
[NASA-CR-186687] 17 p2363 N90-23454
Lunar crane hook
[NASA-CR-184921] 17 p2384 N90-23579
Three legged walking mobile platform: Kinematic and dynamic analysis and simulation
[NASA-CR-184929] 18 p2535 N90-24457
Design of an autonomous teleoperated cargo transporting vehicle for lunar base operations
[NASA-CR-186686] 18 p2565 N90-24633
Geoscience and a Lunar Base: A Comprehensive Plan for Lunar Exploration
[NASA-CP-3070] 18 p2638 N90-25030
Design of a thermal and micrometeorite protection system for an unmanned lunar cargo lander
[NASA-CR-186682] 19 p2664 N90-25161
Lunar regolith bagging system
[NASA-CR-186652] 19 p2677 N90-25224
Self-contained robotic arm manipulator
[NASA-CR-184925] 19 p2696 N90-25342
Energy storage for a lunar base by the reversible chemical reaction: CaO+H2O reversible reaction Ca(OH)2
[NASA-TM-103145] 19 p2709 N90-25419
Man-machine interface for the control of a lunar transport machine
[NASA-CR-184935] 19 p2724 N90-25495
Design of a device to remove lunar dust from space suits for the proposed lunar base
[NASA-CR-186679] 19 p2724 N90-25496
Lunar polar coring lander
[NASA-CR-186684] 19 p2796 N90-25917
Figure of merit studies of beam power concepts for advanced space exploration
[NASA-CR-186720] 20 p2854 N90-26234
Design of an autonomous Lunar construction utility vehicle
[NASA-CR-186832] 20 p2870 N90-26330
Design of a lunar transportation system, volume 2
[NASA-CR-186833-VOL-2] 20 p2871 N90-26333
Genesis lunar outpost criteria and design
[NASA-CR-186831] 20 p2901 N90-26499
Lunar lander conceptual design
[NASA-CR-186233] 21 p2965 N90-26856

LUNAR COMPOSITION
Ilmenite exsolution schemes in Apollo-17 high-Ti basalts
[DE90-011992] 21 p2976 N90-26912

LUNAR CRATERS
Crater identification and resolution of lunar radar images 03 p0426 N90-12441

LUNAR DUST
Design of a device to remove lunar dust from space suits for the proposed lunar base
[NASA-CR-186679] 19 p2724 N90-25496

LUNAR ECLIPSES
Fifty year canon of lunar eclipses: 1986-2035
[NASA-RP-1216] 10 p1446 N90-18342

LUNAR EFFECTS
On analytic modeling of lunar perturbations of artificial satellites of the earth
[AD-A210440] 01 p0016 N90-10078

LUNAR ENVIRONMENT
NT LUNAR ATMOSPHERE
Lunar rated fasteners
[NASA-CR-182856] 17 p2411 N90-23737
Rod gripper, changer, and storage system
[NASA-CR-183154] 17 p2411 N90-23739
Design of a thermal and micrometeorite protection system for an unmanned lunar cargo lander
[NASA-CR-186682] 19 p2664 N90-25161
Soil experiment
[NASA-CR-184927] 20 p2842 N90-26165

LUNAR EVOLUTION
Office of exploration overview
01 p0027 N90-10141

LUNAR EXPLORATION
Applicability of the beamed power concept to lunar rovers, construction, mining, explorers and other mobile equipment 01 p0030 N90-10159
Workshop on Moon in Transition: Apollo 14, KREEP, and Evolved Lunar Rocks
[NASA-CR-186153] 06 p0865 N90-15026
CIS-lunar space infrastructure lunar technologies: Executive summary
[NASA-CR-186220] 06 p0865 N90-15029
Science exploration opportunities for manned missions to the Moon, Mars, Phobos, and an asteroid
[NASA-CR-186295] 09 p1171 N90-16776
Human exploration of space: A review of NASA's 90-day study and alternatives
[NASA-CR-186394] 17 p2357 N90-23418
Design of a rotary stepped auger for a lunar environment
[NASA-CR-184919] 17 p2384 N90-23577
SKITTER/implement mechanical interface
[NASA-CR-184920] 17 p2384 N90-23578
Tubular space truss structure for SKITTER 2 robot
[NASA-CR-184922] 17 p2384 N90-23580
Lunar hand tools
[NASA-CR-184924] 17 p2384 N90-23581
Proof of principal for staircase auger chip removal theory
[NASA-CR-184934] 17 p2385 N90-23583
Two wheeled lunar dumptruck
[NASA-CR-182840] 17 p2410 N90-23734
Lunar robotic maintenance module
[NASA-CR-183071] 17 p2411 N90-23735
Lunar drill and test apparatus
[NASA-CR-183052] 17 p2411 N90-23736
Lunar drill footplate and casing
[NASA-CR-183153] 17 p2411 N90-23738
Core sample extractor
[NASA-CR-182864] 17 p2411 N90-23740
Lunar stone saw
[NASA-CR-182438] 17 p2412 N90-23741
Geoscience and a Lunar Base: A Comprehensive Plan for Lunar Exploration
[NASA-CP-3070] 18 p2638 N90-25030
United States planetary rover status: 1989
[NASA-CR-186843] 19 p2698 N90-25353
Micro coring apparatus
[NASA-CR-183072] 20 p2869 N90-26321

LUNAR FLIGHT
Technology development, demonstration, and orbital support requirements for manned lunar and Mars missions
[NASA-TM-101666] 10 p1447 N90-18350

LUNAR FLYING VEHICLES
Design of a lunar transportation system, volume 2
[NASA-CR-186833-VOL-2] 20 p2871 N90-26333

LUNAR GEOLOGY
Workshop on Moon in Transition: Apollo 14, KREEP, and Evolved Lunar Rocks
[NASA-CR-186153] 06 p0865 N90-15026
The Apollo 15 coarse fines (4-10 mm)
[NASA-TM-101934] 06 p0865 N90-15027

LUNAR IONOSPHERE
U LUNAR ATMOSPHERE

LUNAR LANDING
Proposal for a lunar landing pod for SKITTER
[NASA-CR-184933] 18 p2510 N90-24340
Lunar lander conceptual design
[NASA-CR-186233] 21 p2965 N90-26856
Engineering and the advancement of human welfare. Ten outstanding achievements 1964-1989
[ISBN-0-309-04185-6] 23 p3415 N90-29297
LUNAR LANDING MODULES
NT LUNAR MODULE
Design of an unmanned lunar cargo lander that reconfigures into a shelter for a habitation module or disassembles into parts useful to a permanent manned lunar base
[NASA-CR-186687] 17 p2363 N90-23454
Proposal for a lunar landing pod for SKITTER
[NASA-CR-184933] 18 p2510 N90-24340
LUNAR LANDING SITES
Soil stabilization mat for lunar launch/landing site
[NASA-CR-186690] 20 p2836 N90-26128
LUNAR LAUNCH
Soil stabilization mat for lunar launch/landing site
[NASA-CR-186690] 20 p2836 N90-26128
LUNAR MANTLE
Proceedings of a workshop on Lunar Volcanic Glasses: Scientific and Resource Potential
[NASA-CR-186631] 20 p2888 N90-26437
LUNAR MARIA
Proceedings of a workshop on Lunar Volcanic Glasses: Scientific and Resource Potential
[NASA-CR-186631] 20 p2888 N90-26437
LUNAR MODULE
Soil Transport Implement
[NASA-CR-184931] 17 p2385 N90-23582
LUNAR OBSERVATORIES
Human exploration mission studies
13 p1821 N90-20457
Design of a Lunar farside observatory
[NASA-CR-186671] 19 p2765 N90-25709
Genesis lunar outpost criteria and design
[NASA-CR-186831] 20 p2901 N90-26499
LUNAR ORBITS
Gyrotron development for space power beaming
01 p0028 N90-10148
Low-earth-orbit to low-lunar-orbit laser freighter
01 p0030 N90-10160
Laser propulsion option 01 p0030 N90-10161
Earth orbit laser systems 01 p0030 N90-10162
A superconducting quenchgun for delivering lunar derived oxygen to lunar orbit
[NASA-CR-185161] 15 p2061 N90-21806
LUNAR PERTURBATION
U LUNAR EFFECTS
LUNAR PHASES
Tidal and lunar data for Point Mugu, San Nicolas Island, and the Barking Sands Area during 1990
[AD-A214828] 09 p1249 N90-17248
LUNAR PROGRAMS
Lunar construction utility vehicle
[NASA-CR-186231] 07 p0939 N90-15435
LUNAR RANGEFINDING
Determination of parameters of the Earth-Moon system: A contribution to model extension, evaluation, results
[SER-C-353] 22 p3263 N90-28479
LUNAR ROCKS
Workshop on Moon in Transition: Apollo 14, KREEP, and Evolved Lunar Rocks
[NASA-CR-186153] 06 p0865 N90-15026
The Apollo 15 coarse fines (4-10 mm)
[NASA-TM-101934] 06 p0865 N90-15027
Lunar stone saw
[NASA-CR-182438] 17 p2412 N90-23741
Lunar regolith bagging system
[NASA-CR-186683] 19 p2677 N90-25223
Lunar regolith bagging system
[NASA-CR-186652] 19 p2677 N90-25224
LUNAR ROVING VEHICLES
Applicability of the beamed power concept to lunar rovers, construction, mining, explorers and other mobile equipment 01 p0030 N90-10159
CIS-lunar space infrastructure lunar technologies: Executive summary
[NASA-CR-186220] 06 p0865 N90-15029
Lunar surface mobility studies, past and future
[AD-A216451] 10 p1393 N90-18056
Mechanical design engineering. NASA/university advanced design program: Lunar Bulk Material Transport Vehicle
[NASA-CR-184926] 18 p2534 N90-24455
Micro coring apparatus
[NASA-CR-183072] 20 p2869 N90-26321
Design of a lunar transportation system, volume 2
[NASA-CR-186833-VOL-2] 20 p2871 N90-26333
LUNAR SATELLITES
NT ORBITING LUNAR STATIONS
LUNAR SCATTERING
U DIFFUSE RADIATION
LUNAR SHELTERS
Lunar shelter
[ILR-MITT-233(1989)] 17 p2439 N90-23896
LUNAR SOIL
NT LUNAR DUST
Report of NASA Lunar Energy Enterprise Case Study Task Force
[NASA-TM-101652] 07 p1007 N90-15836
Report of the NASA lunar energy enterprise case study task force 07 p1008 N90-15837
Importance of helium-3 for the future
07 p1009 N90-15843
Lunar surface mobility studies, past and future
[AD-A216451] 10 p1393 N90-18056
Getting lunar ilmenite: From soils or rocks
[NASA-CR-186498] 12 p1744 N90-20029
The electrochemical generation of useful chemical species from lunar materials 13 p1822 N90-20461
Soil Transport Implement
[NASA-CR-184931] 17 p2385 N90-23582
Mechanical design engineering. NASA/university advanced design program: Lunar Bulk Material Transport Vehicle
[NASA-CR-184926] 18 p2534 N90-24455
Lunar material transport vehicle
[NASA-CR-185929] 18 p2534 N90-24456
Lunar regolith bagging system
[NASA-CR-186652] 19 p2677 N90-25224
Energy storage for a lunar base by the reversible chemical reaction: CaO+H2O reversible reaction Ca(OH)2
[NASA-TM-103145] 19 p2709 N90-25419
Lunar polar coring lander
[NASA-CR-186684] 19 p2796 N90-25917
Soil stabilization mat for lunar launch/landing site
[NASA-CR-186690] 20 p2836 N90-26128
Soil experiment
[NASA-CR-184927] 20 p2842 N90-26165
LUNAR SPACECRAFT
NT LUNAR LANDING MODULES
NT LUNAR MODULE
NT ORBITING LUNAR STATIONS
LUNAR SURFACE
Report of NASA Lunar Energy Enterprise Case Study Task Force
[NASA-TM-101652] 07 p1007 N90-15836
Report of the NASA lunar energy enterprise case study task force 07 p1008 N90-15837
Analysis of the financial factors governing the profitability of lunar helium-3 07 p1008 N90-15838
Transportation and operations aspects of space energy systems 07 p1008 N90-15842
Lunar surface mobility studies, past and future
[AD-A216451] 10 p1393 N90-18056
Lunar rated fasteners
[NASA-CR-182856] 17 p2411 N90-23737
Proposal for a lunar landing pod for SKITTER
[NASA-CR-184933] 18 p2510 N90-24340
Vertically reciprocating auger
[NASA-CR-182822] 18 p2535 N90-24458
Conceptual design and analysis of roads and road construction machinery for initial lunar base operations
[NASA-CR-186673] 18 p2535 N90-24459
Design of a thermal and micrometeorite protection system for an unmanned lunar cargo lander
[NASA-CR-186682] 19 p2664 N90-25161
Sunlight diffusing tent for lunar worksite
[NASA-CR-186651] 19 p2677 N90-25225
Self-contained robotic arm manipulator
[NASA-CR-184925] 19 p2696 N90-25342
Man-machine interface for the control of a lunar transport machine
[NASA-CR-184935] 19 p2724 N90-25495
Lunar deep drill apparatus
[NASA-CR-182756] 20 p2869 N90-26322
Lunar articulated remote transportation system
[NASA-CR-186817-VOL-1] 20 p2871 N90-26332
Design of a lunar transportation system, volume 2
[NASA-CR-186833-VOL-2] 20 p2871 N90-26333
Megawatt solar power systems for lunar surface operations
[NASA-CR-186509] 20 p2881 N90-26391
Proceedings of a workshop on Lunar Volcanic Glasses: Scientific and Resource Potential
[NASA-CR-186631] 20 p2888 N90-26437
Genesis lunar outpost criteria and design
[NASA-CR-186831] 20 p2901 N90-26499
LUNAR SURFACE VEHICLES
NT LUNAR ROVING VEHICLES
Lunar construction utility vehicle
[NASA-CR-186231] 07 p0939 N90-15435
Extending terrestrial mobile robotics to a proposed lunar base
[DE89-016179] 12 p1672 N90-19606
SKITTER/implement mechanical interface
[NASA-CR-184920] 17 p2384 N90-23578
Tubular space truss structure for SKITTER 2 robot
[NASA-CR-184922] 17 p2384 N90-23580
Two wheeled lunar dumptruck
[NASA-CR-182840] 17 p2410 N90-23734
Rod gripper, changer, and storage system
[NASA-CR-183154] 17 p2411 N90-23739
Proposal for a lunar landing pod for SKITTER
[NASA-CR-184933] 18 p2510 N90-24340
Mechanical design engineering. NASA/university advanced design program: Lunar Bulk Material Transport Vehicle
[NASA-CR-184926] 18 p2534 N90-24455
Lunar material transport vehicle
[NASA-CR-185929] 18 p2534 N90-24456
Three legged walking mobile platform: Kinematic and dynamic analysis and simulation
[NASA-CR-184929] 18 p2535 N90-24457
Conceptual design and analysis of roads and road construction machinery for initial lunar base operations
[NASA-CR-186673] 18 p2535 N90-24459
Design of an autonomous teleoperated cargo transporting vehicle for lunar base operations
[NASA-CR-186686] 18 p2565 N90-24633
Hitching mechanism for lunar dump train
[NASA-CR-183034] 19 p2697 N90-25344
Man-machine interface for the control of a lunar transport machine
[NASA-CR-184935] 19 p2724 N90-25495
Proof of principle model for a lunar dumptruck
[NASA-CR-182557] 20 p2869 N90-26323
Design of an autonomous Lunar construction utility vehicle
[NASA-CR-186832] 20 p2870 N90-26330
LUNAR TOPOGRAPHY
Crater identification and resolution of lunar radar images 03 p0426 N90-12441
Lunar surface mobility studies, past and future
[AD-A216451] 10 p1393 N90-18056
Analysis of alternative concepts for transport systems on the Moon surface
[ETN-90-95727] 12 p1672 N90-19605
LUNAR TRAJECTORIES
NT EARTH-MOON TRAJECTORIES
LUNEBERG LENSES
U RADAR CORNER REFLECTORS
LUNGS
The investigation of particulate matter in the lungs of smoke inhalation death victims
10 p1317 N90-17617
L x ray spectrometry in vivo with a Si(Li)-NaI(Tl)
[DE90-005649] 10 p1387 N90-18028
Arginine vasopressin lowers pulmonary artery pressure in hypoxic rats by releasing artrial natriuretic peptide
[AD-A215986] 10 p1410 N90-18134
Effects of high altitude hypoxia on lung and chest wall function during exercise
[AD-A219814] 17 p2434 N90-23869
Frequency and ventilation: A survey of theoretical and experimental ventilation modelling
[LR-625] 24 p3498 N90-29772
LYAPUNOV FUNCTIONS
U LIAPUNOV FUNCTIONS
LYMAN ALPHA RADIATION
Design and technical aspects of the Solly instrument
05 p0659 N90-13847
Observation of the solar Lyman-alpha line
05 p0662 N90-13868
The low-ion QSO absorption-line systems
05 p0712 N90-14162
H-alpha emission lines in high redshift quasars
11 p1587 N90-19149
Skewering the universe with QSO lines of sight: Lyman alpha clouds as probes of large scale structure
16 p2329 N90-23278
Onboard detection of intrinsic Ly alpha radiation from a neutral particle beam
[DE90-010341] 18 p2511 N90-24346
The mesospheric responses to short-term solar ultraviolet variability 22 p3204 N90-28174
The 27-day versus 13.5-day variations in the solar Lyman-alpha radiation and the radio wave absorption in the lower ionosphere over Europe
22 p3209 N90-28203
LYMAN SPECTRA
The low-ion QSO absorption-line systems
05 p0712 N90-14162
Optical FeII emission and the BLR structure in QSOs
19 p2793 N90-25899
LYMPHOCYTES
Response of lymphocytes to a mitogenic stimulus during spaceflight 05 p0677 N90-13942
LYOPHILS
U COLLOIDS

LYRA CONSTELLATION
The emission lines in the ultra-violet spectrum of Beta Lyrae 15 p2183 N90-22474

M

M STARS
The winds of high luminosity late-type bright stars [NASA-CR-182961] 05 p0712 N90-14160
Properties of evolved star circumstellar grains 06 p0861 N90-15003
Observations of 40-70 micron bands of ice in IRAS 09371+1212 and other stars 11 p1585 N90-19134
A new interpretation of the feature of SiO maser spectra associated with M-type star [DE90-610641] 11 p1590 N90-19174
M WINGS
U VARIABLE SWEEP WINGS
MAARS
U CRATERS
MACH INERTIA PRINCIPLE
Estimation of extra drag force on a circular cylinder due to the presence of solid particles in subsonic compressible flow [AD-A218635] 16 p2197 N90-22542
MACH NUMBER
A study of high-lift airfoils at high Reynolds numbers in the Langley low-turbulence pressure tunnel [NASA-TM-89125] 01 p0001 N90-10002
Wind tunnel support system effects on a fighter aircraft model at Mach numbers from 0.6 to 2.0 [AD-A210614] 01 p0002 N90-10010
Fluctuating pressures measured beneath a high-temperature, turbulent boundary layer on a flat plate at Mach number of 5 [NASA-TP-2947] 01 p0118 N90-10680
Normal-force-curve and pitching-moment-curve slopes of forebody-cylinder combinations at zero angle of attack for Mach numbers up to 5 [ESDU-89008] 03 p0301 N90-11709
Experimental and theoretical investigation of boundary-layer instability mechanisms on a swept leading edge at Mach 3.5 04 p0447 N90-12557
Transition in surface boundary layers [CERT-RSF-OA-43/5018-AYD] 04 p0502 N90-12897
Normal force, pitching moment, and side force of forebody-cylinder combinations for angles of attack up to 90 degrees and Mach numbers up to 5 [ESDU-89014] 06 p0718 N90-14192
Corrections for non-ideal effects in reflected shock waves at low Mach numbers [DE90-002192] 06 p0721 N90-14208
Fuselage design for a specified Mach-sliced area distribution [NASA-TP-2975] 11 p1455 N90-18385
A numerical investigation of the compressible mixing layer [AD-A217738] 13 p1802 N90-20343
Instabilities and subharmonic resonances of subsonic heated round jets, volume 2 [NASA-CR-186058] 15 p2100 N90-22017
The effects of compressibility on a supersonic mixing layer [AD-A219315] 16 p2197 N90-22543
Computation of low Mach number compressible flow 17 p2344 N90-23346
Destabilization of supersonic free shear layers by parametric excitation using Mach waves generated by a wavy wall [AD-A219655] 17 p2345 N90-23352
The stability of two-dimensional wakes and shear-layers at high Mach numbers [NASA-CR-182050] 17 p2401 N90-23678
The wind tunnel of the Ruhr University, Bochum, Federal Republic of Germany for examination of compressible streams until M=6 18 p2489 N90-24226
The gun tunnel of the Brunswick Institute for Fluid Mechanics: Current development status 18 p2489 N90-24227
Calculation of the aeroelastic blade stabilization with linearized process [MITT-87-01] 18 p2497 N90-24272
MACH REFLECTION
Prediction of length scales in a Mach reflection flowfield 15 p2089 N90-21959
MACH-ZEHNDER INTERFEROMETERS
Interferometry 24 p3419 N90-29315
MACHINE LEARNING
User interaction with self-learning systems [AD-A214280] 08 p1105 N90-16395
A genetic adaptive system for image understanding and learning research [AD-A214810] 09 p1271 N90-17367
The strength of weak learnability [AD-A216389] 10 p1420 N90-18190
Concept formation and generalization based on experimentation by an autonomous mobile robot [DE90-001731] 13 p1810 N90-20395
CEREBRAL WEEVIL: A machine learning model for hemispheric categorization of complex visual patterns [AD-A218143] 13 p1874 N90-20749
Rule-based mechanisms of learning for intelligent adaptive flight control 14 p1908 N90-20939
Adaptive learning fuzzy control of a mobile robot [DE90-759898] 14 p2018 N90-21562
Efficient specialization of relational concepts [AD-A218889] 16 p2262 N90-22894
Discovering problem solving strategies: What humans do and machines don't (yet) [AD-A219008] 16 p2263 N90-22902
Learning events in the acquisition of three skills [AD-A219038] 16 p2264 N90-22905
Adaptive Resonance Theory 1 [AD-A219044] 16 p2304 N90-23126
Generation of expert systems by partial evaluation [AD-A220427] 17 p2443 N90-23920
Bayesian learning [NASA-CR-181528] 17 p2465 N90-24082
Multilayered neural networks: Learning algorithms, implementation on hypercube machines, applications [ETN-90-97255] 20 p2913 N90-26574
Rule acquisition events in the discovery of problem solving strategies [AD-A222428] 21 p3037 N90-27265
The real-time learning mechanism of the Scientific Research Associates Advanced Robotic System (SRAARS) 21 p3046 N90-27312
Using decision-tree classifier systems to extract knowledge from databases 21 p3048 N90-27328
Neural network with dynamically adaptable neurons [NASA-CASE-NPO-17803-1-CU] 21 p3057 N90-27385
A neural network for feature extraction [AD-A223059] 21 p3058 N90-27387
Learning binary relations and total orders [AD-A221643] 21 p3059 N90-27392
Genetic algorithms: The state of the art and some research proposals [REPT-89-058] 22 p3241 N90-28380
Multi-layer neural networks for robot control 23 p3368 N90-29031
A Boltzmann machine for the organization of intelligent machines 23 p3370 N90-29040
Multiresolutional models of uncertainty generation and reduction 23 p3370 N90-29043
How do robots take two parts apart 23 p3374 N90-29061
A survey of planning and scheduling research at the NASA Ames Research Center 23 p3376 N90-29076
Learning in stochastic neural networks for constraint satisfaction problems 23 p3377 N90-29078
Integrating planning, execution, and learning 23 p3377 N90-29079
Recursive least-squares learning algorithms for neural networks [DE90-014926] 23 p3380 N90-29096
An improved adaptive control for repetitive motion of robots 24 p3508 N90-29831
Instruction dialogues: Teaching new skills to a robot 24 p3517 N90-29884
Reactive behavior, learning, and anticipation 24 p3521 N90-29908
Machine learning [AD-A223732] 24 p3534 N90-29988
MACHINE LIFE
U SERVICE LIFE
MACHINE RECOGNITION
U ARTIFICIAL INTELLIGENCE
MACHINE STORAGE
U COMPUTER STORAGE DEVICES
MACHINE TOOLS
NT BORING MACHINES
NT GRINDING MACHINES
NT MILLING MACHINES
The quality of vacuum deposited surface treatments [CETIM-107040] 04 p0476 N90-12729
Electrode/workpiece combinations [DE90-003919] 08 p1054 N90-16095
Computerized inspection of gear tooth surfaces [NASA-TM-102395] 15 p2107 N90-22054
Underwater connect and disconnect plug and receptacle [AD-D014175] 21 p2998 N90-27039
MACHINE TRANSLATION
Inductive reasoning and Kolmogorov complexity (preliminary version) [CWI-CS-R8915] 05 p0695 N90-14062
Technologies for electronic transfer of information: The present state and trends in Japan 15 p2177 N90-22443
MACHINE VISION
U COMPUTER VISION
MACHINERY
Elements of active vibration control for rotating machinery [NASA-TM-102368] 16 p2227 N90-22703
MACHINING
NT CHEMICAL MACHINING
NT MILLING (MACHINING)
NT SPARK MACHINING
High-speed machining of aluminum [DE89-014011] 01 p0077 N90-10441
Basic investigations of cutting machinability of inorganic glasses using single-point tools [W-15/87] 02 p0210 N90-11204
Engineering specification and system design for CAD/CAM of custom shoes. Phase 5: UMC involvement (January 1, 1989 - June 30, 1989) [NASA-CR-185838] 02 p0257 N90-11456
Fabrication of modulated vanes for a split-coaxial RFQ [DE88-757235] 03 p0403 N90-12310
MM and T advanced balancing/machining [AD-A213103] 05 p0648 N90-13775
New tool-holding concept [DE90-000880] 06 p0794 N90-14624
An analysis of drilling of composite materials 07 p0889 N90-15142
Nondestructive testing of ceramics by acoustic microscopy [AERE-R-13350] 13 p1813 N90-20411
Advanced manufacturing technology: A Department of Energy technology transfer initiative [DE90-008601] 14 p2037 N90-21688
Data and conclusions from tests on small screws [DE90-007500] 15 p2106 N90-22046
Machining of new materials at Aerospatiale [REPT-892-430-104] 16 p2213 N90-22622
Integrating expert systems with solid modeling through interprocess communications and the applications interface specification [DE90-012996] 20 p2907 N90-26537
Ultra precision machining [AD-A222422] 21 p2991 N90-27003
Plastic superconductor bearings any size, any shape, 77 k and up 22 p3145 N90-27838
Quality function deployment as a mechanism for process characterization and control [DE90-014755] 23 p3337 N90-28857
A cost-effective realization of environmental temperature control [DE90-011651] 24 p3458 N90-29532
Non-contact contour gage [DE90-014672] 24 p3475 N90-29642
MACROCLIMATE
U CLIMATE
MACROMOLECULES
Improvements in macroreticular particles for ion-exchange and gel-permeation chromatography [DE90-003717] 18 p2522 N90-24399
Workshop on High-Field NMR and Biological Applications [DE90-010002] 18 p2614 N90-24889
Magnetic resonance elucidation of molecule/macromolecule interaction stereochemistry [AD-A221444] 21 p2979 N90-26928
MACROPHAGES
Reciprocal relationships between the immune and central nervous system [AD-A221259] 18 p2583 N90-24712
MACROSCOPIC EQUATIONS
Quantum non-demolition stroboscopic observables and multipumping back-action evasion schemes [PREPRINT-699] 16 p2326 N90-23260
Are quantum measurements on macroscopic bodies feasible [PREPRINT-700] 16 p2326 N90-23261
Continuum approach and contaminant transport in ground water flows 19 p2690 N90-25301
MACULAR VISION
U VISION
MADAGASCAR
U MALAGASY REPUBLIC
MAGAZINES (SUPPLY CHAMBERS)
Minutes of the 23rd Explosives Safety Seminar, volume 1 [AD-A218264] 14 p1958 N90-21213
MAGELLAN PROJECT (NASA)
Using connected-element interferometer phase-delay data for Magellan navigation in Venus orbit 15 p2075 N90-21885

Space exploration: Cost, schedule, and performance of NASA's Magellan Mission to Venus. Fact sheet for the Chairman, Subcommittee on Science, Technology, and Space, Committee on Commerce, Science, and Transportation, US Senate
[GAO/NSIAD-88-130FS] 20 p2815 N90-26022
The Magellan Venus explorer's guide
[NASA-CR-186968] 23 p3286 N90-28592

MAGELLAN SPACECRAFT (NASA)
A higher density VLBI catalog for navigating Magellan and Galileo 15 p2078 N90-21904
The Magellan Venus explorer's guide
[NASA-CR-186968] 23 p3286 N90-28592

MAGELLANIC CLOUDS
The choice of stars in the Magellanic clouds 05 p0608 N90-13543
The South African Astronomical Observatory
[NASA-CR-186258] 07 p1011 N90-15856
The evolution and geometry of the outer parts of the small Magellanic cloud 14 p2040 N90-21697
A theoretical scenario for the dynamics of formation and early evolution of globular clusters in galaxies 15 p2187 N90-22494
Local normal galaxies 16 p2336 N90-23315
The low mass X ray binaries in the LMC 19 p2768 N90-25730
EXOSAT deep exposure of the LMC X-4 region 19 p2780 N90-25814
On the problem of the supernova expansion law in the large Magellanic cloud 19 p2781 N90-25818
X ray observations of the LMC field by the TTM instrument onboard the Kvant module: November 1988 to June 1989 19 p2782 N90-25825
Nova LMC (Large Magellanic Cloud) 1990 no. 1: The first extragalactic neon nova
[NASA-CR-180409] 23 p3411 N90-29276

MAGMA
Variations in volatiles in magma bodies based on studies of melt inclusions
[DE90-006272] 11 p1532 N90-18821
Stored mafic/ultramafic crust and early Archean mantle depletion
[NASA-CR-186460] 12 p1691 N90-19715
Geology of Espinhaco Meridional, including the Quadrilatero Ferrifero: Integration through remote sensing data
[INPE-4904-PRE/1505] 14 p1998 N90-21450
Sulphur silicate interactions on the Jovian satellite Io 15 p2192 N90-22515
Proceedings of a workshop on Lunar Volcanic Glasses: Scientific and Resource Potential
[NASA-CR-186631] 20 p2888 N90-26437

MAGNESIUM
NT MAGNESIUM ISOTOPES
Development of graphite-magnesium composites for space applications 02 p0185 N90-11054

MAGNESIUM ALLOYS
The improved corrosion resistance of ultra high purity magnesium alloy castings 01 p0044 N90-10245
A study of the hot workability of Al-8.5 wt pct Mg alloys for armor plate applications
[AD-A211680] 03 p0329 N90-11868
New Light Alloys
[AGARD-CP-444] 07 p0897 N90-15185
Magnesium alloy technology for aerospace applications 07 p0901 N90-15209
Cryogenic mechanical properties of low density superplastic Al-Mg-Sc alloys
[DE90-002120] 07 p0904 N90-15222
A fundamental understanding of the effect of alloying elements on the corrosion resistance of rapidly solidified Mg alloys
[AD-A216767] 11 p1486 N90-18553
Processing and elevated temperature ductility of aluminum alloy 7475
[AD-A216840] 11 p1486 N90-18554
Optimizing superplastic response in navalite, a lithium containing aluminum-magnesium alloy
[AD-A216552] 12 p1626 N90-19346
Precipitation on dislocations in Al-Li-Cc-Mg-Zr
[AD-A221124] 18 p2526 N90-24415
Behavior of Al-Mg alloys in hot working and superplasticity
[DE90-015193] 23 p3310 N90-28723
The roles of strain and reheating interval in continuous recrystallization during the thermomechanical processing by warm rolling of an Al-Mg alloy
[AD-A223673] 24 p3449 N90-29479

MAGNESIUM COMPOUNDS
NT CHLOROPHYLLS
NT DOLOMITE (MINERAL)
NT MAGNESIUM OXIDES
Chemistry-structure-properly interrelationships for calcareous deposits as stand-alone coatings
[AD-A216031] 10 p1359 N90-17881

MAGNESIUM ISOTOPES
Plasma centrifuge with vacuum arc discharge applied to the separation of stable isotopes
[INPE-4925-TDL/385] 12 p1716 N90-19854
The Al-26(rho, gamma)Si-27 reaction: Stellar origins of galactic Al-26 15 p2188 N90-22498

MAGNESIUM OXIDES
Prospects for wavelength tunable lasers based on vacancy defects in alkaline-earth oxides
[DE90-001078] 06 p0789 N90-14592
Processing and properties of nanophase oxides
[DE90-003826] 07 p0895 N90-15171
Laser detection and discrimination system
[AD-D014301] 07 p0937 N90-15426
Edge geometry superconducting tunnel junctions utilizing an NbN/MgO/NbN thin film structure
[NASA-CASE-NPO-17812-1-CU] 09 p1286 N90-17456
Biaxial strength and stress rupture of hot-pressed silicon nitride
[AD-A216950] 11 p1519 N90-18750
Resistivity measurements of halide-salt/MgO separators for thermal cells
[DE90-009740] 18 p2550 N90-24553
Microstructure of sputtered superconducting films of Bi2Sr2CaCu2O(x) made by low-temperature, in situ growth
[DE90-010067] 18 p2618 N90-24916
Development of a sealed bipolar Li-alloy/FeS2 battery for electric vehicles
[DE90-013650] 21 p2999 N90-27045
Surfaces and interfaces of ceramics and metals
[DE90-014381] 22 p3160 N90-27920

MAGNESYN (TRADEMARK)
U SERVOMOTORS

MAGNET COILS
Testing results of the MIT Probe
[DE89-016679] 02 p0278 N90-11590
Retractable gas cooled leads for ASTROMAG
[DE90-002679] 07 p0921 N90-15331
Fabrication of superconductor coils
[DE90-003571] 07 p0922 N90-15338
Modeling energy output of inertial storage devices for the DIII-D tokamak
[DE90-004096] 08 p1126 N90-16524
Materials and selection criteria analysis for the compact ignition tokamak toroidal field coil turn-to-turn insulation system: Photographic summary oflaboratory testing
[DE90-008020] 13 p1891 N90-20850

MAGNETIC ABSORPTION
U ELECTROMAGNETIC ABSORPTION

MAGNETIC ANOMALIES
New approach to omega PPCs (Propagation Corrections)
[AD-A215610] 09 p1207 N90-17000
Proceedings of the International Workshop on Geomagnetic Observatory Data Acquisition and Processing
[GEOPHYSICAL-PUBL-15] 21 p3021 N90-27177
Proceedings of a Workshop on the Geoelectric and Geomagnetic Environment of Continental Margins
[AD-A223743] 24 p3493 N90-29739
Some aspects of the structure and evolution of oceanic spreading centers 24 p3496 N90-29757
Re-analysis of data on the space radiation environment above southeast Asia
[AD-A224155] 24 p3564 N90-30162

MAGNETIC BEARINGS
Cryostatless high temperature supercurrent bearings for rocket engine turbopumps
[NASA-CR-183807] 04 p0509 N90-12935
Materials research issues in superconducting levitation and suspension as applied to magnetic bearings
[DE90-011147] 20 p2929 N90-26667

MAGNETIC CHARGE DENSITY
Electrodynamics of the high latitude ionosphere
[AD-A223229] 21 p3026 N90-27203

MAGNETIC CLOUDS
Some properties of so-called magnetic cloud structures in the solar wind
[IFSI-88-16] 08 p1153 N90-16678
Interstellar magnetic fields: An observational perspective 24 p3560 N90-30144

MAGNETIC COILS
NT MAGNET COILS
Coil system for the production of three-component uniform magnetic field at the Nurmijarvi Observatory 21 p3021 N90-27179
Measuring sensitivities and orthogonalities of magnetometer sensors in the Nurmijarvi coil hut 21 p3022 N90-27180
Comparisons of the recording instruments. Description of the difference-plots 21 p3022 N90-27181

MAGNETIC COMPRESSION
A battery-powered, solid state magnetic compressor with applications for high PRF accelerators and lasers
[DE89-015770] 01 p0058 N90-10332
High gain flux compression generator fabrication issues
[DE89-017888] 03 p0342 N90-11951
Performance of the 10-kV, 100-kA pulsed-power modules for the FRX-C magnetic compression experiment
[DE89-014027] 06 p0845 N90-14917
Design of a high-gain flux-compression generator
[DE90-002795] 07 p0922 N90-15333
The 17th AINSE Plasma Physics Conference: Conference handbook
[DE90-600936] 07 p0996 N90-15759
Improved amorphous metal materials for magnetic pulse compression
[DE90-005723] 11 p1486 N90-18555
Advances in spheromak understanding and parameters
[DE90-012052] 19 p2759 N90-25678
Stellarator status, 1989
[DE90-014791] 23 p3397 N90-29192

MAGNETIC CONTROL
Autonomous spacecraft attitude control using magnetic torquing only 05 p0586 N90-13415
Spacecraft attitude determination using the earth's magnetic field 05 p0589 N90-13429
Results of aircraft open-loop tests of an experimental magnetic leader cable system for guidance during roll-out and turnoff
[NASA-TM-4135] 09 p1169 N90-16767
Ignition and burn control characteristics of thermonuclear plasmas
[DE90-015385] 23 p3398 N90-29197

MAGNETIC COOLING
Thermodynamic principles of the process of the effect of electromagnetic fields on a polymer melt
[AD-A210698] 02 p0201 N90-11149
Feasibility analysis of reciprocating magnetic heat pumps
[NASA-CR-186205] 07 p0927 N90-15363
Laser cooling of neutral atoms
[AD-A214440] 09 p1279 N90-17418
A 100 micro Kelvin bolometer system for SIRTF 14 p1976 N90-21317
Improved processing of ceramic superconductors
[DE90-009721] 18 p2624 N90-24951

MAGNETIC CORES
Thin film magnetic memory elements
[AD-D014178] 03 p0398 N90-12281
Tuned-circuit Johnson noise thermometry
[DE89-016221] 07 p0925 N90-15356
Core cooling studies at LLNL (Lawrence Livermore National Laboratory) and Sandia
[DE90-008303] 13 p1795 N90-20300
Modeling tape-wound magnetic switches
[DE90-015121] 23 p3322 N90-28782

MAGNETIC DIFFUSION
Intermittency and multifractality in magnetic dynamos
[PREPRINT-702] 16 p2319 N90-23226
Improved processing of ceramic superconductors
[DE90-009721] 18 p2624 N90-24951

MAGNETIC DIPOLES
The effect of flux creep on the magnetization field in the SSC diopole magnets
[DE90-000124] 03 p0399 N90-12284
Acoustic emission diagnostic techniques for high-field high current-density super inducting poles
[DE90-007400] 11 p1562 N90-19000
Mechanical disturbances in high-performance superconducting dipoles
[DE90-006237] 11 p1570 N90-19040
The design of a large aperture high field dipole
[DE90-007910] 14 p1970 N90-21285
Characterization of the plasma in magnetic multidipole discharges
[DE90-613219] 14 p2028 N90-21628
Heat leak measurements in superconducting dipole magnet supports
[DE90-620109] 15 p2173 N90-22420
Advanced artificial dielectric materials for millimeter wavelength applications, part A
[AD-A220221] 17 p2469 N90-24112
Experiments on superconductor imaging surface magnetometry
[DE90-008925] 20 p2929 N90-26665
Quasi-static analysis of scattering from a chiral sphere
[PB90-189135] 22 p3164 N90-27943

MAGNETIC DISKS
Evaluation of optical storage technology for decision support databases 15 p2176 N90-22436
Wear mechanisms of amorphous carbon and zirconia coatings on rigid disk magnetic recording media
[DE90-011053] 20 p2837 N90-26133

Modification of a cam facility
[AD-A221828] 21 p3056 N90-27376
MAGNETIC DISTURBANCES
NT MAGNETIC STORMS
User's guide to the Space Environment Services Center geophysical alert broadcasts
[PB89-194617] 02 p0249 N90-11411
Solar-geophysical data number 536, part 1. Data for March, Febuary 1989 and late data
[PB89-194716] 02 p0296 N90-11684
The 10.7-cm microwave observations of AR 5395 and related terrestrial effects 03 p0433 N90-12483
Comparisons of the recording instruments. Description of the difference-plots 21 p3022 N90-27181
Use of the method of natural orthogonal components for derivation of S sub R-variation and digital K-indices 21 p3024 N90-27193
Intensive MHD-structures penetration in the middle atmosphere initiated in the ionospheric cusp under quiet geomagnetic conditions 22 p3207 N90-28193
MAGNETIC EFFECTS
Investigation of resonant ac-dc magnetic field effects
[AD-A211612] 03 p0379 N90-12159
The 10.7-cm microwave observations of AR 5395 and related terrestrial effects 03 p0433 N90-12483
Magnetic interactions in Sn-119 substituted for Cu in antiferromagnetic and superconducting lamellar cuprates
[DE90-003661] 08 p1132 N90-16560
The effects of magnetic nozzle configurations on plasma thrusters
[NASA-CR-186465] 14 p1941 N90-21109
Current drive in a supernova 15 p2187 N90-22491
High Intensity Electro-Magnetic and Ultrasonic Effects on Inorganic Materials Behavior and Processing Workshop
[AD-A218884] 18 p2215 N90-22640
Dynamics of motion charged particles in a field of two electromagnetic waves
[DE90-620690] 16 p2228 N90-22706
Superconducting and normal compounds: Some high field/high pressure effects 16 p2320 N90-23229
Combined effect of isotopic substitution, temperature, and magnetic field on the lifetimes of triplet biradicals
[AD-A219711] 17 p2372 N90-23509
The effect of magnetic field on the critical current density of bulk superconducting wires
[DE90-010458] 18 p2621 N90-24934
Structure and superconducting properties of ((Ln(1-x)Ln*(x) 1/2 (Ba(1-y)Sr(y) 1/3 Ce 1/6) 8Cu8O(z) 22 p3144 N90-27833
Electron energy spectrum and magnetic interactions in high-T(sub c) superconductors 22 p3149 N90-27857
Studies of iron impurities in YxPr1-xBa2Cu3O7-delta 22 p3151 N90-27865
Comparative study of flux pinning flux creep and critical currents between YBaCuO crystals with and without Y2BaCuO5 inclusions 22 p3152 N90-27869
Three dimensional studies of helical equilibria and magnetic surface breaking due to the finite beta effect
[DE90-508078] 24 p3548 N90-30071
MAGNETIC ENERGY STORAGE
Surveys concerning the effect to introduce electric vehicles. On the possibility of new technology and introducing measures
[DE90-742057] 10 p1391 N90-18046
Use of high-temperature superconductors in superconducting magnetic energy power sources
[DE90-011119] 19 p2761 N90-25686
Parametric design studies of toroidal magnetic energy storage units
[DE90-013086] 20 p2881 N90-26390
Survey of superconductors for energy applications
[DE90-796181] 22 p3248 N90-28420
MAGNETIC EQUATOR
A survey of equatorial magnetospheric wave activity between 5 and 8 R(sub E)
[AD-A220137] 17 p2424 N90-23812
MAGNETIC FIELD CONFIGURATIONS
Compact torus configurations with high frequency driven currents
[ETN-89-94674] 02 p0280 N90-11598
Studies of plasma performance and transport in the Advanced Toroidal Facility (ATF)
[DE90-001737] 07 p0994 N90-15746
Initial results from FRC (Field-Reversed Configuration) compression experiments on FRX-C/LSM
[DE90-003390] 07 p0995 N90-15754
End-on soft x ray imaging of Field-Reversed Configurations (FRCs) on the Field-Reversal-C (FRX-C)/Large Scale Modification (LSM) experiment
[DE90-004863] 08 p1082 N90-16260
On the structure of the tail magnetic field
[IFSI-88-19] 08 p1101 N90-16378
Terrestrial magnetosphere magnetic field models
[REPT-89/CT/DTI/MS/AS/154] 08 p1102 N90-16380
Recent progress on the HESS (High Explosive Spheromak Source) experiment
[DE90-003218] 08 p1125 N90-16520
Investigation of a magnetostrictive fiber optic interferometric sensor
[AD-A215666] 09 p1226 N90-17111
Magnetohydrodynamic liquid-metal flows in a rectangular channel with an axial magnetic field, a moving conducting wall, and free surfaces
[AD-A216276] 10 p1425 N90-18223
Generation of axial and lateral magnetic fields in laser produced plasmas
[DE90-607470] 10 p1432 N90-18260
Crystal and magnetic structure of Er(2)(Co(sub x)Fe(sub 1-x))(17) compounds
[DE90-004926] 10 p1436 N90-18288
Hollow cathode operation at high discharge currents
[NASA-CR-185238] 15 p2088 N90-21953
Accretion induced collapse and field decay 19 p2783 N90-25833
The plasma wave signature of a 'magnetic hole' in the vicinity of the magnetopause
[NASA-CR-187027] 22 p3212 N90-28220
Formation of magnetic islands due to field perturbations in toroidal stellarator configurations
[DE90-014789] 23 p3397 N90-29191
MAGNETIC FIELD INTENSITY
U MAGNETIC FLUX
MAGNETIC FIELD RECONNECTION
The observation of possible reconnection events in the boundary changes of solar coronal holes 01 p0138 N90-10801
Spontaneous magnetic reconnection in a turbulent plasma 13 p1889 N90-20840
Experimental study of vortex ring interaction with a free surface 16 p2233 N90-22742
On the nature of the plasma sheet boundary layer
[DE90-013158] 20 p2889 N90-26439
A study of magnetic field reconnection and plasma processes in the magnetosphere
[DE90-016117] 24 p3493 N90-29741
MAGNETIC FIELDS
NT BIOMAGNETISM
NT GEOMAGNETISM
NT INTERPLANETARY MAGNETIC FIELDS
NT INTERSTELLAR MAGNETIC FIELDS
NT MAGNETIC CLOUDS
NT MAGNETOSTATIC FIELDS
NT NONUNIFORM MAGNETIC FIELDS
NT PLANETARY MAGNETIC FIELDS
NT SOLAR MAGNETIC FIELD
NT STELLAR MAGNETIC FIELDS
NT TRAPPED MAGNETIC FIELDS
On canonical quantization of the electromagnetic field in terms of field strengths
[DE89-615389] 01 p0055 N90-10314
The 1984 direct strike lightning data, part 1
[NASA-TM-87690-PT-1] 01 p0089 N90-10505
Observations of azimuthal asymmetry for certain FRC operating regimes
[DE89-015300] 01 p0126 N90-10721
Mixed-valent and heavy fermions and related systems
[DE89-016335] 01 p0129 N90-10743
Critical magnetic fields (H(sub c2), H(sub c1)) and kappa in YBa2(Cu0.98M0.02)3O(7+delta), M=Ni, Al, and Cu
[DE89-016412] 01 p0130 N90-10745
Magnetic correlations in high T(sub c) oxides in the superconducting state
[DE89-016421] 01 p0130 N90-10746
Substorm associated pulsations: A study of plasmaspheric cavity resonance, mid-latitude polarisation and geostationary orbit signatures 02 p0251 N90-11422
Extraction induced emittance growth for negative ion sources
[DE89-017586] 02 p0273 N90-11559
Boundary effects on the MHD dynamo in laboratory plasmas
[DE89-015207] 02 p0276 N90-11576
ANTHEM simulation of the early time magnetic field penetration of the plasma surrounding a high density Z-pinch
[DE89-016980] 02 p0277 N90-11585
Launched electrons in plasma opening switches
[DE89-016886] 02 p0279 N90-11596
Physics and materials science of high temperature superconductors
[AD-A211246] 02 p0283 N90-11619
The stability of magnetohydrodynamic shock waves in molecular clouds 02 p0292 N90-11665
Development of high frequency spice models for ferrite core inductors and transformers
[DE89-015121] 03 p0341 N90-11946
Periodic permanent magnet structures
[AD-D014173] 03 p0398 N90-12280
Luminescence in applied magnetic fields
[AD-A211551] 03 p0399 N90-12287
Stellarator transport theory
[DE89-016371] 03 p0406 N90-12328
Superconductivity and magnetic scattering in the Nd(sub 2-x)Ce(sub x)CuO(sub 4-delta)
[DE89-016524] 03 p0410 N90-12354
Direction-of-arrival calculations at VLF/LF (Very Low Frequency/Low Frequency)
[AD-A212620] 04 p0493 N90-12833
Electron beam propagation through a magnetic wiggler with random field errors
[AD-A212705] 04 p0498 N90-12867
A survey of the current state-of-the-art in high-energy-product permanent magnets
[AD-A211761] 04 p0549 N90-13193
Three-dimensional equilibria and Mercier stability calculations
[DE89-015907] 04 p0556 N90-13239
Magneto-elastic interactions in conducting structures in transient magnetic fields 05 p0632 N90-13686
A solvable self-similar model of the sausage instability in a resistive Z-pinch
[AD-A213137] 05 p0688 N90-14006
A search for the effects of active magnetic fields in extra-galactic radio sources 05 p0712 N90-14161
High power transducers
[AD-D014225] 06 p0767 N90-14461
Electric-gun studies of conductors in high magnetic fields and experiments in dynamic flux compression
[DE90-000815] 06 p0768 N90-14470
Use of superconducting plates and shells to deflect magnetic noise fields: Application to MEG
[DE89-012592] 06 p0803 N90-14676
Two-dimensional behavior of Megagauss-field-confined solid fiber Z-pinches
[DE90-000684] 06 p0845 N90-14918
Theoretical reversed field pinch studies
[DE90-002114] 06 p0848 N90-14929
Macroscopic persistent currents in high temperature ceramic superconductors
[DE89-636232] 06 p0855 N90-14973
SCATHA (Spacecraft Charging at High Altitudes) atlas data base, volume 1
[AD-A214204] 07 p0886 N90-15127
SCATHA (Spacecraft Charging At High Altitudes) atlas data base, volume 2
[AD-A214205] 07 p0887 N90-15128
Exchange coupling in metals as understood then and now
[DE90-001271] 07 p0902 N90-15214
Anharmonic betatron motion in free electron lasers
[DE90-001515] 07 p0934 N90-15407
Theory of interacting plasmas in space 07 p0993 N90-15742
Simulation of radial expansion of an electron beam injected into a background plasma
[NASA-CR-186188] 07 p0994 N90-15743
Intense REB (Relativistic Electron Beam) transport in a weakly magnetized plasma
[DE90-002978] 07 p0994 N90-15749
Initial results from FRC (Field-Reversed Configuration) compression experiments on FRX-C/LSM
[DE90-003390] 07 p0995 N90-15754
Theoretical and computational studies of magnetic insulation and other plasma-opening-switch phenomena
[DE90-004421] 07 p0996 N90-15757
Near-surface sputtered particle transport for an oblique incidence magnetic field plasma
[DE90-004422] 07 p0996 N90-15758
A numerical simulation model for the study of magnetohydrodynamic (MHD) waves in a structured medium 07 p1012 N90-15864
Design of coupled or uncoupled multifilamentary SSC-type strands with almost zero retained magnetization at fields near 0.3 T
[DE90-005391] 08 p1047 N90-16052
Terrestrial magnetosphere magnetic field models
[REPT-89/CT/DTI/MS/AS/154] 08 p1102 N90-16380
Geometrical optics in inhomogeneous chiral media with application to polarization correction in inhomogeneous lens antennas
[PB90-110669] 08 p1122 N90-16497
Toroidal magnetic fields in terms of field-line invariants
[DE89-016610] 08 p1123 N90-16507
Magnetic penetration depth and intragrain critical current density in gain-aligned Tl2Ca2Ba2Cu3O10 superconductor
[DE90-004245] 08 p1133 N90-16562
The dynamics of dust in planetary magnetospheres 08 p1149 N90-16658

Nonlinear modulational stability and propagation of an electromagnetic pulse in a two-component, neutral plasma
[AD-A215131] 09 p1207 N90-16994
The 1989 National Convention Record IEE Japan, part 7
[DE89-910080] 09 p1210 N90-17012
Energy conversion efficiency in high current Raman regime Free Electron Laser (FEL). 1: Single mode analysis
[DE90-719527] 09 p1227 N90-17120
Preliminary evaluation of space station transmission line in a ring configuration
[NASA-TM-102461] 10 p1329 N90-17677
Processing of DMSP magnetic data: Handbook of programs, tapes, and datasets
[NASA-TM-100757] 10 p1407 N90-18114
Magnetohydrodynamic liquid-metal flows in a rectangular channel with an axial magnetic field, a moving conducting wall, and free surfaces
[AD-A216276] 10 p1425 N90-18223
Generation of axial and lateral magnetic fields in laser produced plasmas
[DE90-607470] 10 p1432 N90-18260
Anomalous particle diffusion through a magnetic picket fence
[INPE-4841-PRE/1470] 10 p1433 N90-18270
Alfven wave stability in D III-D
[DE90-005555] 10 p1437 N90-18291
Microwave radiation absorption by Ho(Y)-Ba-Cu-O superconducting ceramics
[DE90-610665] 11 p1492 N90-18588
Streaming gravity mode instability
[DE90-610619] 11 p1535 N90-18835
Development of an rf-driven plasma neutralizer for negative ions
[DE90-007298] 11 p1568 N90-19027
Green's functions for a theoretical model of an aperture fed stacked-patch microstrip antenna
[AD-A216280] 12 p1645 N90-19455
Impedance characteristics of terawatt ion diodes
[DE90-006276] 12 p1652 N90-19494
Numerical simulation of cross field amplifiers
[DE90-006459] 12 p1652 N90-19496
Theoretical and experimental studies of a brushless disk rotor motor with permanent magnetic excitation and gap windings
[ETN-90-96056] 12 p1655 N90-19512
Overview of recent results from the Advanced Toroidal Facility
[DE90-005673] 12 p1716 N90-19853
Nonlinear interaction of electrostatic waves at a narrow inhomogeneous layer of a warm magnetoactive plasma
[DE90-610624] 12 p1717 N90-19857
Critical current density and transition temperature measurements of Y-Ba-Cu-O rods
[AD-A216695] 12 p1719 N90-19875
High energy x ray observations on the Crab nebula and the double star source GX 1+4
[ETN-90-95829] 12 p1729 N90-19937
LAGEOS 3 and the gravitomagnetic field
12 p1733 N90-19961
Gradiometry and gravitomagnetic field detection
12 p1733 N90-19962
Time-dependent two-dimensional radiation hydrodynamics of accreting matter onto highly magnetized neutron stars
[DE90-006927] 12 p1737 N90-19985
Disturbance structures and its magnetic field features in plasma comet tail
[DE90-610636] 12 p1737 N90-19986
Magnetic hardening studies and novel techniques for preparation of high performance magnets
[AD-A217737] 13 p1881 N90-20790
Enhanced pinch effect due to electrostatic potential
[DE90-007088] 13 p1890 N90-20844
The effects of magnetic nozzle configurations on plasma thrusters
[NASA-CR-186465] 14 p1941 N90-21109
Generalized WKB approximation for stratified isotropic chiral structures
[PB90-165689] 14 p1967 N90-21270
A 100 micro Kelvin bolometer system for SIRTF
14 p1976 N90-21317
The parallel algorithm for solving the three-dimensional integral magnetostatic equations
[DE90-616529] 14 p2015 N90-21547
Relativistic stimulated Brillouin and Raman scattering in a laser-produced plasma
[DE90-613123] 14 p2028 N90-21627
On the relativistic Vlasov equation in guiding-center coordinates
[DE90-613241] 14 p2028 N90-21629
MHD modes driven by anomalous electron viscosity and their role in fast sawtooth crashes
[DE90-009311] 14 p2029 N90-21639
Coupled magnetoplasmon-phonon modes at the surface of a semi-infinite semiconductor superlattice
[DE90-612904] 14 p2031 N90-21647
Recent advances in the studies of the nova outburst
[DE90-008936] 14 p2038 N90-21691
Thomson scattering in a magnetic field
14 p2040 N90-21699
Magnetic turbulence versus safety factor in the Tokapole 2 tokamak
15 p2168 N90-22391
On the theory of Heiser and Shercliff experiment. Part 1: MHD flow in an open channel in strong uniform magnetic field
[OUEL-1804/89-PT-1] 15 p2170 N90-22400
On the theory of Heiser and Shercliff experiment. Part 2: MHD flow between two cylinders in strong radical magnetic field
[OUEL-1805/89-PT-2] 15 p2170 N90-22401
A theoretical scenario for the dynamics of formation and early evolution of globular clusters in galaxies
15 p2187 N90-22494
Wind instability as a possible cause of the spiral structure formation in the gaseous subsystem of galaxies with the circular magnetic field
[DE90-618944] 15 p2190 N90-22507
Dynamics of motion charged particles in a field of two electromagnetic waves
[DE90-620690] 16 p2228 N90-22706
Intense electron beam propagation across a magnetic field
[DE90-009993] 16 p2316 N90-23204
Intermittency and multifractality in magnetic dynamos
[PREPRINT-702] 16 p2319 N90-23226
Single crystal NMR of high temperature superconductors
16 p2321 N90-23236
A (mu)SR-investigation of the mixed state of the high-Tc superconductor HoBa2Cu3O7-delta
[DE90-620802] 16 p2322 N90-23241
Nonreciprocal components in the 140 and 220 GHz bands utilizing magnetoplasmons on semiconducting substrates
[AD-A219136] 16 p2324 N90-23253
What is learned from high energy bursts and flares
16 p2336 N90-23314
Local normal galaxies
16 p2336 N90-23315
The effects of wiggler errors on free electron laser performance
[AD-A220421] 17 p2409 N90-23725
Preparation and properties of iron doped II-VI chalcogenides
[AD-A220802] 17 p2477 N90-24163
Models of the external source contribution to magnetospheric magnetic fields for CRRES data analysis
[AD-A221059] 18 p2580 N90-24697
The behaviour of the L3 muon chambers in a magnetic field
[ETN-90-96920] 18 p2613 N90-24884
Renormalized microscopic theory of fluctuations in inhomogeneous magnetized plasmas
[DE90-611307] 18 p2617 N90-24908
RF surface resistance measurements in the Pb-Bi-Sr-Ca-Cu-O system
[DE90-010412] 18 p2621 N90-24932
The effect of magnetic field on the critical current density of bulk superconducting wires
[DE90-010458] 18 p2621 N90-24934
A study of the spatial scales of discrete polar auroral arcs
[NASA-CR-186806] 19 p2714 N90-25444
Interactions between the Space Station and the environment: A preliminary assessment of EMI
19 p2737 N90-25557
Terbium-dysprosium magnetostrictive high power transducers
[AD-D014509] 19 p2753 N90-25641
The beta limit in the DIII-D tokamak
[DE90-011896] 19 p2759 N90-25677
Formation of magnetic islands due to field perturbations in toroidal stellarators
[DE90-012132] 19 p2759 N90-25679
Space exploration: Cost, schedule, and performance of NASA's Galileo Mission to Jupiter. Fact sheet for the Chairman, Subcommittee on Science, Technology, and Space, Committee on Commerce, Science, and Transportation, US Senate
[GAO/NSIAD-88-138FS] 20 p2816 N90-26025
Confinement of nonneutral plasma in unconventional geometries
[DE90-013048] 20 p2928 N90-26659
Characterization of NbTi multifilamentary superconducting wires
[DE90-626245] 20 p2930 N90-26672
Free electron laser injection oscillator
[AD-D014180] 21 p3007 N90-27095
Observations of plasma structure freezing scale at equatorial latitudes
[AD-A222529] 21 p3026 N90-27207
Evaluation of magnetospheric internal magnetic field models and existing software
[AD-A221816] 21 p3027 N90-27210
Nonlogarithmic magnetization relaxation at the initial time intervals and magnetic field dependence of the flux creep rate in Bi2Sr2Ca(sub I)Cu2Ox single crystals
22 p3137 N90-27801
Oxide superconductors under magnetic field
22 p3139 N90-27807
Studies of iron impurities in YxPr1-xBa2Cu3O7-delta
22 p3151 N90-27865
A YBCO RF-SQUID magnetometer and its applications
22 p3151 N90-27867
Quasi-static analysis of scattering from a chiral sphere
[PB90-189135] 22 p3164 N90-27943
Further studies of 60 Hz exposure effects on human function
[DE90-014377] 23 p3355 N90-28962
Physics of the L to H transition in DIII-D
[DE90-014120] 23 p3396 N90-29137
Electron microscopy of transition-metal doped BiCaSrCuO
[DE90-014184] 23 p3398 N90-29202
Vlasov-Maxwell equilibria of solar coronal loops
[DE90-015025] 23 p3414 N90-29289
Theoretical and experimental examinations of brushless monophase direct current motors
[ETN-90-97301] 24 p3466 N90-29580
A review of self generated B-field in ICF corona
[DE90-627479] 24 p3547 N90-30063
Tokamak plasma shape identification with a Legendre-Fourier expansion of the vacuum poloidal flux function in the toroidal coordinates
[DE90-508031] 24 p3548 N90-30068
Structure of magnetic field in tokamaks
[DE90-628904] 24 p3549 N90-30075
Magnetic surfaces in tokamaks
[DE90-628905] 24 p3549 N90-30076
Lectures in plasma diagnostics
[DE90-015825] 24 p3550 N90-30086
Compact toroid research
[DE90-016123] 24 p3550 N90-30087

MAGNETIC FILMS

Studies of ultrathin magnetic films and particle-surface interactions with spin-sensitive electron spectroscopies
[DE89-016741] 02 p0273 N90-11556
Thin film magnetic memory elements
[AD-D014178] 03 p0398 N90-12281
Epitaxial iron films
[AD-A213551] 07 p1003 N90-15807

MAGNETIC FLUX

Gaussmeter determination of 302 stainless steel material condition
[BDX-613-3941] 01 p0044 N90-10249
Magnetic flux compression
[DE89-016991] 02 p0271 N90-11546
Pinning of curved flux lines on the boundary between two phases of high temperature superconductors
[DE89-618865] 02 p0283 N90-11614
High gain flux compression generator fabrication issues
[DE89-017888] 03 p0342 N90-11951
Investigation of resonant ac-dc magnetic field effects
[AD-A211612] 03 p0379 N90-12159
Investigation of active regions at high resolution by balloon flights of the Solar Optical Universal Polarimeter (SOUP)
03 p0434 N90-12487
Shear-induced inflation of coronal magnetic fields
[NASA-CR-186103] 05 p0715 N90-14178
Testing and performance of a high-gain flux-compression generator
[DE90-002808] 06 p0772 N90-14492
Design of a high-gain flux-compression generator
[DE90-002795] 07 p0922 N90-15333
Magnetic flux pinning in YBa2Cu3O7 films
[DE90-003709] 07 p1002 N90-15799
Effects of non-linearity in the variation of pinning potential with current-density on magnetic flux creep in high and low T(sub c) superconductors
[DE90-003952] 07 p1005 N90-15822
Analysis of the CUK converter in delta V mode by charge and flux balances
10 p1337 N90-17738
Flux lattice melting in the high Tc superconductors
10 p1366 N90-17915
Report from solar physics
10 p1445 N90-18335
Siphon flows in isolated magnetic flux tubes. 3: The equilibrium path of the flux tube arch
[NASA-CR-186297] 12 p1709 N90-19813
Overview of recent results from the Advanced Toroidal Facility
[DE90-005673] 12 p1716 N90-19853
The MHD structure of an open magnetotail boundary
15 p2168 N90-22388

High frequency, high temperature specific core loss and dynamic B-H hysteresis loop characteristics of soft magnetic alloys
[NASA-TM-103164] 17 p2398 N90-23663
U. radio emission from quiescent filaments
[NASA-CR-186538] 19 p2797 N90-25922
Materials research issues in superconducting levitation and suspension as applied to magnetic bearings
[DE90-011147] 20 p2929 N90-26667
A new method for the absolute measurement of geomagnetism beginning with DI Flux 21 p3022 N90-27182
Improvements in fluxgate magnetometers at Danish Meteorological Institute's Magnetic Observatories 21 p3023 N90-27187
Magnetic flux leakage versus ultrasonic correlation
[AD-A222112] 21 p3071 N90-27462
Elliptical flux vortices in polycrystalline YBa2Cu3O7 22 p3136 N90-27795
Flux flow and flux dynamics in high-T(sub c) superconductors 22 p3136 N90-27797
Magnetic properties of high-T(sub c) superconductors: Rigid levitation, flux pinning, thermal depinning, and fluctuation 22 p3137 N90-27798
Nonlogarithmic magnetization relaxation at the initial time intervals and magnetic field dependence of the flux creep rate in Bi2Sr2Ca(sub l)Cu2Ox single crystals 22 p3137 N90-27801
Scaling behaviour of relaxation dependencies in metaloxide superconductors 22 p3138 N90-27802
Effect of shock pressure on the structure and superconducting properties of Y-Ba-Cu-O in explosively fabricated bulk metal-matrix composites 22 p3138 N90-27804
Interstellar magnetic fields: An observational perspective 24 p3560 N90-30144

MAGNETIC INDUCTION
Correlation between microstructure and magnetic properties of porous sintered iron and porous iron containing composites
[KFK-4522] 05 p0625 N90-13647
Electron beam sensitive devices for controllability
[IMAG-RR-761-I] 05 p0636 N90-13707
Optimization of a pulsed air core transformer for low impedance inductive ignition
[AD-A218748] 16 p2232 N90-22734

MAGNETIC INDUCTION PROBES
U MAGNETIC PROBES

MAGNETIC LENSES
Transmission micro-grids for shift analysis of x ray frequencies
[MPE-216] 09 p1283 N90-17439

MAGNETIC LEVITATION VEHICLES
Magnetically levitated micro-robotics 02 p0270 N90-11542
California air transportation study: A transportation system for the California Corridor of the year 2010
[NASA-CR-186219] 06 p0722 N90-14212
Markets for high-speed intercity Maglev technology: A systems analysis approach
[DE89-017683] 06 p0794 N90-14623
Applications of superconductor technologies to transportation
[DE90-000856] 06 p0853 N90-14961
Magnetic suspension railway systems based on space technology 11 p1577 N90-19081

MAGNETIC MATERIALS
NT FERROMAGNETIC FILMS
NT FERROMAGNETIC MATERIALS
Genetic engineering of single-domain magnetic particles
[AD-A210332] 01 p0091 N90-10521
Effective permeability of mixtures
[PB89-216952] 03 p0323 N90-11839
Graduate fellowships in the field of hard magnetic materials
[AD-A212303] 04 p0477 N90-12733
Magnetic excitations in thulium metal
[DE90-002475] 06 p0855 N90-14970
Electron Spin Resonance (ESR) studies of returned comet nucleus samples 08 p1148 N90-16651
Activities report of the National Electrotechnic Institute Galileo Ferraris
[ETN-90-96178] 08 p1157 N90-16705
New electronic materials and CO2 reduction
[AD-A214679] 09 p1191 N90-16899
Fundamental studies of new magnetic heterostructures: Their growth, crystallographic structure, magnetic, and electronic properties
[DE90-007381] 11 p1572 N90-19053
Neutron scattering measurements of the magnetic excitations of high-temperature superconducting materials
[DE90-006567] 12 p1721 N90-19885
Diluted magnetic semiconductors
[AD-A220444] 17 p2476 N90-24159
The magnetization process: Hysteresis 18 p2515 N90-24365
Fundamental studies of strongly magnetic rare earth-transition metal alloys
[DE90-012458] 21 p2980 N90-26937
A summary of measurements of permittivities and permeabilities of some microwave absorbing materials
[AD-A223221] 21 p2995 N90-27026
Quasi-static analysis of scattering from a chiral sphere
[PB90-189135] 22 p3164 N90-27943
Optical storage technology
[AD-A224028] 23 p3407 N90-29254
Organic polyradical models for organic magnetic materials
[AD-A223691] 24 p3442 N90-29435
Theoretical investigations and attempted synthesis of organic magnetic polymers and oligomers
[AD-A223409] 24 p3455 N90-29509
Some aspects of the structure and evolution of oceanic spreading centers 24 p3496 N90-29757

MAGNETIC MEASUREMENT
On-line system to measure magnetic characteristics of steel samples
[DE89-633443] 06 p0836 N90-14861
High frequency, high temperature specific core loss and dynamic B-H hysteresis loop characteristics of soft magnetic alloys
[NASA-TM-103164] 17 p2398 N90-23663
Godhavn (Greenland) Geophysical Observatory: Magnetic results, 1984
[ISBN-87-7478-289-4] 17 p2423 N90-23807
Magnetic and resistive measurements of the upper critical field in intwinned single crystals of YBa2Cu3O(7-delta)
[DE90-010083] 18 p2619 N90-24918
The use of curium as a rare Earth substitute in high T(sub c)-related compounds
[DE90-009724] 18 p2620 N90-24928
Experiments on superconductor imaging surface magnetometry
[DE90-008925] 20 p2929 N90-26665
The Nurmijarvi Geophysical Observatory 21 p3021 N90-27178
Preparation and magnetic measurements of single crystal Tl2Ba2CaCu2O8
[DE90-013657] 21 p3081 N90-27519
Magnetic forces in high-T(sub c) superconducting bearings 22 p3137 N90-27799
Operation and calibration of MRL permeameter for measurement of DC magnetic properties of materials under stress
[MRL-TN-574] 23 p3338 N90-28863
Proceedings of a Workshop on the Geoelectric and Geomagnetic Environment of Continental Margins
[AD-A223743] 24 p3493 N90-29739

MAGNETIC MEMORIES
U MAGNETIC STORAGE

MAGNETIC METALS
U MAGNETIC MATERIALS
U METALS

MAGNETIC MIRRORS
NT TANDEM MIRRORS
Magnetic mirror confinement concepts system studies
[DE90-003667] 07 p0995 N90-15753
Spectroscopic diagnostics of high temperature plasmas
[DE90-003912] 08 p1126 N90-16522

MAGNETIC MOMENTS
Attitude and spin rate control of a spinning satellite using geomagnetic field
[INPE-4818-NTE/289] 12 p1613 N90-19277
Anomalous transport in toroidal plasmas
[DE90-006549] 12 p1717 N90-19859
Theoretical investigations in elementary particle physics
[DE90-007178] 13 p1883 N90-20802
Effect of Cu(2+) magnetic moments on the superconductivity of YBa2Cu3O7: The origin of the linear term in the specific heat; the volume fraction of superconductivity
[DE90-011214] 18 p2626 N90-24963
Low-temperature specific heat measurements on metals: Application to high-T(sub c) superconductors
[DE90-011612] 18 p2626 N90-24966
Study of short-lived unstable nuclei by means of laser optical pumping
[AD-A222561] 21 p3009 N90-27105
Localization effects in radiationally disordered high-temperature superconductors: Theoretical interpretation 22 p3148 N90-27853
Electron energy spectrum and magnetic interactions in high-T(sub c) superconductors 22 p3149 N90-27857

MAGNETIC PERMEABILITY
Multiple martensitic transformations, incommensurate/commensurate phases, and charge-density-wave states in plutonium metal: Their consequences
[DE90-001235] 06 p0748 N90-14350
Critical field enhancement due to field penetration in fine-filament superconductors
[DE90-005389] 10 p1435 N90-18282
Low temperature specific heat and magnetic susceptibility of NbTi and NbTiMn alloys
[DE90-005390] 11 p1486 N90-18552
Theoretical and experimental studies of a brushless disk rotor motor with permanent magnetic excitation and gap windings
[ETN-90-96056] 12 p1655 N90-19512
A low temperature calorimetric study of several high-T(sub c) superconductors 16 p2322 N90-23237
Searching for heavy fermion materials in Ce intermetallic compounds
[DE90-011809] 20 p2834 N90-26116
Synthesis, structure, and properties of a new ternary metal nitride, Ca3CrN3
[AD-A222274] 21 p2978 N90-26924
Thermal and electric properties of Nd(1.85)Ce(0.15)CuO(4-y) and Pr(1.85)Ce(0.15)CuO(4-y) 22 p3141 N90-27816
Magnetic correlations in La(2-x)Sr(x)CuO4 from NQR relaxation and specific heat 22 p3143 N90-27827
Systematic approach to critical phenomena by the extended variational method and coherent-anomaly method
[DE90-627320] 23 p3392 N90-29165
Sigma and pi interactions of the pyrrolic ligand sandwich-like lanthanide phthalocyanines determined from magnetic susceptibility and ligand-field theory
[AD-A223609] 24 p3443 N90-29444

MAGNETIC PROBES
Measuring the thickness of austenitic weld deposits on carbon steel walls using a magnetic method
[DE89-635446] 06 p0794 N90-14628
Development of NMR (Nuclear Magnetic Resonance) imaging probes for advanced ceramics
[DE90-003812] 07 p0911 N90-15269
Magnetic coupled current sensing techniques for spacecraft power systems 10 p1335 N90-17725

MAGNETIC PROPERTIES
NT ANTIFERROMAGNETISM
NT BIOMAGNETISM
NT DIAMAGNETISM
NT FERROMAGNETISM
NT GEOMAGNETISM
NT GYROFREQUENCY
NT MAGNETIC EFFECTS
NT MAGNETIC FIELD RECONNECTION
NT MAGNETIC INDUCTION
NT MAGNETIC MOMENTS
NT MAGNETIC PERMEABILITY
NT MAGNETIC SUSPENSION
NT MAGNETOACOUSTICS
NT MAGNETORESISTIVITY
NT MAGNETOSTRICTION
NT PARAMAGNETISM
NT POLARIZATION CHARACTERISTICS
NT RELUCTANCE
NT SPIN-LATTICE RELAXATION
NT THERMOMAGNETIC EFFECTS
Neutron scattering studies of amorphous Invar alloys
[DE89-016868] 02 p0197 N90-11126
Investigations of the influence of magnetically long range ordered phases on the electronic charge transport in metallic glasses
[ETN-89-94672] 02 p0202 N90-11155
Studies of ultrathin magnetic films and particle-surface interactions with spin-sensitive electron spectroscopies
[DE89-016741] 02 p0273 N90-11556
Graduate fellowships in the field of hard magnetic materials
[AD-A212303] 04 p0477 N90-12733
Synthesis and properties of NdNiO(3) prepared by low temperature methods
[AD-A212117] 04 p0559 N90-13256
On-line system to measure magnetic characteristics of steel samples
[DE89-633443] 06 p0836 N90-14861
Solid State Division
[DE90-000979] 06 p0851 N90-14945
Muon SR investigation of magnetism and superconductivity in (Y(1-x)Pr(x))Ba2Cu3O7
[DE90-000689] 06 p0852 N90-14956
Magnetic excitations in thulium metal
[DE90-002475] 06 p0855 N90-14970
Magnetotransport studies of epitaxial Cr thin films
[DE90-001930] 06 p0856 N90-14975
Magnetic and electrical properties
[DE90-002183] 06 p0856 N90-14977

Surface magneto-optical studies of ultrathin ferromagnetic films
[DE90-002199] 06 p0856 N90-14980
Magnetic behavior of curium and americium-curium alloys
[DE89-017808] 07 p0902 N90-15213
Magnetic viscosity in Ni/Cu compositionally-modulated alloys
[DE90-002303] 07 p0904 N90-15223
Magnetic and electronic correlations in YBa2Cu3O(sub 6+x)
[DE89-017604] 07 p1000 N90-15785
Two-dimensional magnetic phase transition of ultrathin iron films on Pd(100)
[DE90-003555] 07 p1000 N90-15788
Magnetic mechanisms of high temperature superconductivity
[DE90-003625] 07 p1001 N90-15796
Effects of non-linearity in the variation of pinning potential with current-density on magnetic flux creep in high and low T(sub c) superconductors
[DE90-003952] 07 p1005 N90-15822
Properties and design of multifilamentary NbTi composite superconductors
[DE90-004904] 08 p1134 N90-16569
Magnetic studies of proximity-effect coupling in a very closely spaced fine-filament NbTi/CuMn composite superconductor
[DE90-005387] 08 p1134 N90-16570
A new approach for the utilization of electron paramagnetic resonance and an investigation of copper oxide superconductors
[AD-A213833] 09 p1277 N90-17404
Structural, magnetic and electrical properties of La(sub 2-x) Ba(sub x) NiO4
[AD-A214347] 10 p1434 N90-18278
Improved amorphous metal materials for magnetic pulse compression
[DE90-005723] 11 p1486 N90-18555
Modern theory of magnetism
[DE90-007374] 11 p1561 N90-18998
Fundamental studies of new magnetic heterostructures: Their growth, crystallographic structure, magnetic, and electronic properties
[DE90-007381] 11 p1572 N90-19053
Crystallographic and magnetic properties of (C6 D11 ND3)CuBr3 and (Zn(1-x)Mn(x))3As2: A neutron scattering study
[ECN-219] 11 p1573 N90-19055
Neutron scattering measurements of the magnetic excitations of high-temperature superconducting materials
[DE90-006567] 12 p1721 N90-19885
Preparation and properties of the system Cu(x)Pd(1-x)O (0 less than or equal to x less than or equal to 0.175)
[AD-A217567] 12 p1723 N90-19901
The preparation and properties of iron doped II-VI chalcogenides
[AD-A217569] 12 p1724 N90-19903
Magnetic hardening studies and novel techniques for preparation of high performance magnets
[AD-A217737] 13 p1881 N90-20790
Stabilization of high (Tc) superconductivity in cadmium sulfide
[DE90-008249] 13 p1896 N90-20881
Technology assessment of superconductivity
[AD-A217697] 13 p1897 N90-20889
Preparation and characterization of Cu2ZnGeS(4-y)Se(y)
[AD-A217469] 15 p2171 N90-22407
Investigation of optical nonlinearities, conductivity and magnetism in organometallic materials
[AD-A218548] 16 p2317 N90-23211
Preparation and properties of iron doped II-VI chalcogenides
[AD-A220802] 17 p2477 N90-24163
Synthesis, structure, electric, and magnetic properties of CaNiN
[AD-A222273] 21 p2978 N90-26923
Fundamental studies of strongly magnetic rare earth-transition metal alloys
[DE90-012458] 21 p2980 N90-26937
Preparation and magnetic measurements of single crystal Tl2Ba2CaCu2O8
[DE90-013657] 21 p3081 N90-27519
Magnetic properties of high-T(sub c) superconductors: Rigid levitation, flux pinning, thermal depinning, and fluctuation 22 p3137 N90-27798
Microstructure and magnetization of doped Y-Ba-Ca-O materials prepared by melt quench and post annealing method 22 p3138 N90-27803
The NASA high temperature superconductivity program 22 p3145 N90-27836
Magnetic properties of the 110K superconducting phase in Pb-doped Bi-Sr-Ca-Cu-O thin films 22 p3151 N90-27868
Surface and defect excitations in covalently bonded solids
[AD-A221995] 23 p3303 N90-28682
Operation and calibration of MRL permeameter for measurement of DC magnetic properties of materials under stress
[MRL-TN-574] 23 p3338 N90-28863
Antiferromagnetism and enhanced heat in CeM2Sn (M = Ni, Ir, Cu, Rh, Pd, and Pt
[DE90-014924] 23 p3399 N90-29206
Investigation of the application in the simulation program 'PSpice' of the Jiles-Atherton model for nonlinear magnetic materials in order to predict the degaussing of magnets
[LINO-1990-1] 24 p3541 N90-30029

MAGNETIC PUMPING
Gordon Conference on Atomic Physics
[AD-A211946] 03 p0402 N90-12304

MAGNETIC RECORDING
Portable digital pressure indicator for calibrating magnetic tape recorders
[NASA-TM-101650] 07 p0933 N90-15401
SPOT 4 space magnetic recorder mechanisms 15 p2112 N90-22082
SPOT 4 magnetic tape recorder mechanisms 18 p2540 N90-24500
Wear mechanisms of amorphous carbon and zirconia coatings on rigid disk magnetic recording media
[DE90-011053] 20 p2837 N90-26133
Measuring sensitivities and orthogonalities of magnetometer sensors in the Nurmijarvi coil hut 21 p3022 N90-27180
Digital intelligent magnetic recording system DIMARS as the automated workstation at magnetic observatory 21 p3022 N90-27186

MAGNETIC RELAXATION
NT SPIN-LATTICE RELAXATION

MAGNETIC RESONANCE
NT ELECTRON PARAMAGNETIC RESONANCE
NT NUCLEAR MAGNETIC RESONANCE
NT PROTON MAGNETIC RESONANCE
NT PROTON RESONANCE
Solvent relaxation in electron-transfer reactions: Comparisons between barrier-crossing dynamics in water and polar aprotic media
[AD-A210212] 01 p0040 N90-10220
Surface cooled, vacuum impregnated superconducting magnet systems: Design, construction, applications
[ETN-90-96014] 05 p0696 N90-14072
Medium energy nuclear physics research
[DE90-015852] 24 p3544 N90-30042

MAGNETIC SHIELDING
Measuring the shielding effectiveness of superconductive composites
[DE89-015164] 01 p0033 N90-10180
On the HEMP (High-Altitude Electromagnetic Pulse) response of protective relays
[DE90-003718] 08 p1061 N90-16138
Magnetic vapor shield mechanism for protection of material surfaces exposed to high heat load
[AD-A217667] 13 p1780 N90-20217
Control of surface melting and ablation in electromagnetic launchers via the magnetic vapor shielding mechanism
[AD-A219035] 16 p2204 N90-22578
Analysis of three-dimensional eddy current field. Application to calculation of magnetic screening effect of the damper system in a model superconducting generator
[DE90-507869] 23 p3321 N90-28779

MAGNETIC SIGNALS
HIPAS 1987-88: ULF research and campaign support
[AD-A211720] 03 p0339 N90-11933

MAGNETIC SIGNATURES
Magnetograph group summary 03 p0429 N90-12461
An imaging vector magnetograph for the next solar maximum 03 p0435 N90-12489
NASA Marshall Space Flight Center solar observatory report, January to December 1989
[NASA-TM-100404] 19 p2797 N90-25923
The plasma wave signature of a 'magnetic hole' in the vicinity of the magnetopause
[NASA-CR-187027] 22 p3212 N90-28220
NASA Marshall Space Flight Center Solar Observatory report, January - June 1990
[NASA-TM-103512] 23 p3409 N90-29268

MAGNETIC SPECTROSCOPY
Spectroscopic diagnostics of high temperature plasmas
[DE90-003912] 08 p1126 N90-16522
Coulomb-dissociation of 156 MeV 6Li-projectiles
[KFK-4691] 21 p3075 N90-27482
Lectures in plasma diagnostics
[DE90-015825] 24 p3550 N90-30086

MAGNETIC STARS
Accretion shock geometries in the magnetic variables
[NASA-CR-186290] 08 p1150 N90-16664
Gamma ray bursts: Current status of observations and theory
[NASA-TM-100398] 15 p2194 N90-22526
Gamma ray bursts: Current status of observations and theory 16 p2336 N90-23313
Linearly extended cyclotron emission regions in AM Herculis systems 19 p2775 N90-25778

MAGNETIC STORAGE
NT MAGNETIC DISKS
Thin film magnetic memory elements
[AD-D014178] 03 p0398 N90-12281
Space operations: NASA is not properly safeguarding valuable data from past missions
[GAO/IMTEC-90-1] 20 p2936 N90-26704
Bloch-line memory element and RAM memory
[AD-D014488] 22 p3234 N90-28340
Storage allocation in Ada
[NPL-DITC-156/90] 22 p3235 N90-28343
Theoretical investigations of Pi-conjugated polyradicals as models for organic magnetic materials
[AD-A223411] 24 p3446 N90-29461

MAGNETIC STORMS
The auroral energy deposition over the polar ionosphere during substorms
[AD-A210522] 01 p0086 N90-10490
Magnetospheric substorms as a signature of the solar terrestrial interaction 02 p0240 N90-11363
Stormtime coupling of the neutral and ionized upper atmosphere at middle latitudes 02 p0243 N90-11381
Auroral and sub-auroral F-layer irregularity studies in the Northern and Southern Hemisphere during the equinox transition study September 16-26, 1984 02 p0246 N90-11393
Radio propagation conditions forecast above a low latitude region 02 p0247 N90-11400
Substorm associated pulsations: A study of plasmaspheric cavity resonance, mid-latitude polarisation and geostationary orbit signatures 02 p0251 N90-11422
Numerical study of the current sheet and PSBL in a magnetotail model
[NASA-CR-183289] 02 p0293 N90-11669
Distribution of auroral precipitation at midnight during a magnetic storm
[PB89-213136] 03 p0370 N90-12118
Some of the terrestrial effects of AR 5395 03 p0433 N90-12482
Auroral and sub-auroral interaction at the F region ionosphere
[AD-A213284] 05 p0666 N90-13896
A calculation of energetic proton spectra producedat substorm onset in the fields of the explosive reconnection model 07 p1013 N90-15866
Kiruna geophysical data
[PB90-123985] 09 p1247 N90-17232
A current disruption mechanism in the neutral sheet for triggering substorm expansions
[NASA-CR-186260] 09 p1298 N90-17525
Active probing of space plasmas
[AD-A216867] 12 p1716 N90-19855
Substorms: Their expansion and recovery phases
[DE90-008970] 14 p2042 N90-21712
Diagnosis of auroral dynamics using global auroral imaging with emphasis on large-scale evolutions
[NASA-CR-186623] 17 p2422 N90-23804
Lower thermosphere (80-100 km) dynamics response to solar and geomagnetic activity: Overview 22 p3207 N90-28194
Ionospheric effects of the extreme solar activity of February 1986 22 p3210 N90-28207
Atmospheric structure and variability
[AD-A223439] 24 p3492 N90-29734

MAGNETIC SUBSTORMS
U MAGNETIC STORMS

MAGNETIC SURVEYS
Proceedings of the 79th SEGJ Conference
[DE89-760006] 08 p1157 N90-16704
Proceedings of the International Workshop on Geomagnetic Observatory Data Acquisition and Processing
[GEOPHYSICAL-PUBL-15] 21 p3021 N90-27177

MAGNETIC SUSCEPTIBILITY
U MAGNETIC PERMEABILITY

MAGNETIC SUSPENSION
An experimental investigation of the aerodynamic characteristics of slanted base ogive cylinders using magnetic suspension technology
[NASA-CR-181708] 02 p0146 N90-10834
Magnetically levitated micro-robotics 02 p0270 N90-11542

Techniques for extreme attitude suspension of a wind tunnel model in a magnetic suspension and balance system
[NASA-CR-181895] 06 p0728 N90-14245
Opportunities and prospects for Maglev in North America
[DE90-002190] 06 p0794 N90-14627
Single element magnetic suspension actuator
[NASA-CASE-LAR-13981-1] 07 p0940 N90-15442
A linearly controlled direct-current power source for high-current inductive loads in a magnetic suspension wind tunnel
[NASA-TM-4198] 19 p2692 N90-25319
Materials research issues in superconducting levitation and suspension as applied to magnetic bearings
[DE90-011147] 20 p2929 N90-26667
An LQR controller design approach for a Large Gap Magnetic Suspension System (LGMSS)
[NASA-TM-101606] 23 p3316 N90-28751

MAGNETIC SWITCHING
Innovations in the design and matching of magnetic components and semiconductors up performance and reliability of power converters 10 p1336 N90-17731
Free electron lasers driven by linear induction accelerators: High power radiation sources 15 p2060 N90-21800
Investigations into the use of dielectric coatings in magnetic switches
[DE90-014331] 23 p3321 N90-28776
Modeling tape-wound magnetic switches
[DE90-015121] 23 p3322 N90-28782

MAGNETIC TAPE RECORDERS
U MAGNETIC RECORDING
U TAPE RECORDERS

MAGNETIC TAPE TRANSPORTS
SPOT 4 magnetic tape recorder mechanisms 18 p2540 N90-24500

MAGNETIC TAPES
NT COMPUTER COMPATIBLE TAPES
A signal realization data base generated by the multiple phase-screen method
[AD-A214004] 07 p1010 N90-15852
Space operations: NASA is not properly safeguarding valuable data from past missions
[GAO/IMTEC-90-1] 20 p2936 N90-26704

MAGNETIC VARIATIONS
NT GEOMAGNETIC PULSATIONS
A solvable self-similar model of the sausage instability in a resistive Z-pinch
[AD-A213137] 05 p0688 N90-14006
Physical process in MPD plasmas
[AD-A213679] 07 p0996 N90-15761
Magnetohydrodynamic liquid-metal flows in a rectangular channel with an axial magnetic field, a moving conducting wall, and free surfaces
[AD-A216276] 10 p1425 N90-18223
Comparison of quiet time geomagnetic daily variation (Sq) in H component at Eusebio and Cachoeira Paulista
[INPE-4985-PRE/1547] 14 p2043 N90-21714
Improvements of automatic magnetic observatories in Italy 21 p3022 N90-27185
Use of the method of natural orthogonal components for derivation of S sub R-variation and digital K-indices 21 p3024 N90-27193
Computer production of K-indices by a simple method based on linear elimination 21 p3024 N90-27194
On the relation between the electron content of the ionospheric D-region, variations of the riometer absorption, and the H-component of the geomagnetic field 22 p3210 N90-28208
Satellite measurements of magnetospheric Poynting flux
[AD-A224391] 24 p3490 N90-29724

MAGNETICALLY TRAPPED PARTICLES
NT RADIATION BELTS

MAGNETIZATION
Effects of shock-modification on superconductivity in Tl2Ca2Ba2Cu3Oy and Bi2CaSr2Cu2Ox
[DE89-017231] 02 p0285 N90-11629
The effect of flux creep on the magnetization field in the SSC diopole magnets
[DE90-000124] 03 p0399 N90-12284
Preparation and characterization of single phase Ba(1-x)KxBiO3
[DE89-017735] 03 p0411 N90-12362
Static and dynamic magnetization properties of Y1Ba2Cu3O(sub z) thin films
[DE89-017584] 06 p0850 N90-14940
Design of coupled or uncoupled multifilamentary SSC-type strands with almost zero retained magnetization at fields near 0.3 T
[DE90-005391] 08 p1047 N90-16052
Rotational magnetic processes in YB2Cu3O7
[DE90-000541] 08 p1128 N90-16533
Magnetic studies of proximity-effect coupling in a very closely spaced fine-filament NbTi/CuMn composite superconductor
[DE90-005387] 08 p1134 N90-16570
Finite element analysis of propagation in waveguide components with application to ferrite phase shifters
[FOA-C-30529-3.2] 09 p1204 N90-16977
Anisotropy and dimensionality in untwinned crystals of YBa2Cu3O(7-delta)
[DE90-004890] 10 p1436 N90-18287
A computer control system for the alternating gradient magnetometer 12 p1636 N90-19402
Center of excellence in theoretical geoplasma research
[AD-A215035] 14 p2005 N90-21488
The magnetization process: Hysteresis 18 p2515 N90-24365
Flux flow and flux dynamics in high-T(sub c) superconductors 22 p3136 N90-27797
Nonlogarithmic magnetization relaxation at the initial time intervals and magnetic field dependence of the flux creep rate in Bi2Sr2Ca(sub l)Cu2Ox single crystals 22 p3137 N90-27801
Scaling behaviour of relaxation dependencies in metaloxide superconductors 22 p3138 N90-27802
Microstructure and magnetization of doped Y-Ba-Ca-O materials prepared by melt quench and post annealing method 22 p3138 N90-27803
Study of local structure and magnetism in high-T(sub c) copper oxide superconductors 22 p3143 N90-27824
Measurement of H(sub c1) in a single crystal of YBa2Cu3O7 with low pinning 22 p3151 N90-27864
Effects of Al substitution by Fe in CeAl2
[DE90-627843] 23 p3311 N90-28726
Modeling tape-wound magnetic switches
[DE90-015121] 23 p3322 N90-28782
Investigation of YBa2Cu3O(7-sigma) by NMR and construction of an ultra low temperature cryostat 24 p3550 N90-30089

MAGNETO-OPTICS
Two photon absorption characterization
[AD-A210508] 01 p0121 N90-10694
Surface magneto-optical studies of ultrathin ferromagnetic films
[DE90-002199] 06 p0856 N90-14980
Laser glass (1989)
[DE90-002754] 07 p0909 N90-15257
Hybrid optical/digital architecture for distortion invariant pattern recognition
[AD-A215628] 09 p1282 N90-17435
Polymeric aluminasilazane precursors for aluminosilicon nitride
[AD-A222755] 20 p2841 N90-26158
Linear laser diode arrays for improvement in optical disk recording for space stations
[NASA-CR-4322] 22 p3180 N90-28047

MAGNETOACOUSTIC WAVES
Scattering of an ICRF magnetosonic wave by plasma density turbulence
[DE89-015223] 01 p0126 N90-10720
Magneto acoustic emission apparatus for testing materials for embrittlement
[NASA-CASE-LAR-13817-1] 14 p1951 N90-21170
Theoretical studies of proton beams in solar flare loops 23 p3413 N90-29286

MAGNETOACOUSTICS
Electron acoustic and magnetoacoustic modes in a magnetized beam plasma system
[DE90-627473] 23 p3398 N90-29199

MAGNETOACTIVITY
NT MAGNETIC FIELD RECONNECTION
NT MAGNETORESISTIVITY

MAGNETOCARDIOGRAPHY
High-T(sub c) squid application in medicine and geophysics 22 p3139 N90-27806

MAGNETOELASTIC WAVES
NT MAGNETOACOUSTIC WAVES

MAGNETOELASTICITY
U MAGNETOSTRICTION

MAGNETOGASDYNAMICS
U MAGNETOHYDRODYNAMICS

MAGNETOGRAMS
U MAGNETIC SIGNATURES

MAGNETOHYDRODYNAMIC ACCELERATION
U PLASMA ACCELERATION

MAGNETOHYDRODYNAMIC FLOW
Computer simulation of plasma interactions near Titan 01 p0142 N90-10816
Hermes plasma wind tunnel. Preliminary study, phase A1: Annexes, tables, figures
[DVG-HER-TN-002-PT-2] 04 p0459 N90-12632
Unsteady hydromagnetic flow of a radiating gas in a vertical channel with axial temperature variation
[DE90-600934] 06 p0778 N90-14525
Ion collection by probing objects in flowing magnetized plasmas
[DE90-001711] 06 p0845 N90-14916
On the thermal stability of flow of a radiating two-component plasma in a porous medium between two rotating cylinders
[DE89-636426] 06 p0847 N90-14928
User's manual for MGMHD: A multigrid three-dimensional computer code for the analysis of magnetohydrodynamic generators and diffusers
[DE90-004453] 08 p1127 N90-16526
Magnetohydrodynamic liquid-metal flows in a rectangular channel with an axial magnetic field, a moving conducting wall, and free surfaces
[AD-A216276] 10 p1425 N90-18223
Interaction of minor ions with fast and slow shocks
[NASA-CR-186372] 11 p1594 N90-19181
A storage process of the magnetic energy results from the unsteady plasma flow field in the space active regions and stellar atmosphere
[DE90-610638] 12 p1717 N90-19858
The effects of magnetic nozzle configurations on plasma thrusters
[NASA-CR-186465] 14 p1941 N90-21109
On the theory of Heiser and Sherciiff experiment. Part 1: MHD flow in an open channel in strong uniform magnetic field
[OUEL-1804/89-PT-1] 15 p2170 N90-22400
On the theory of Heiser and Sherciiff experiment. Part 2: MHD flow between two cylinders in strong radical magnetic field
[OUEL-1805/89-PT-2] 15 p2170 N90-22401
Multipole moments in general relativity and dynamical perturbations of black-hole magnetospheres 15 p2190 N90-22509
Intermittency and multifractality in magnetic dynamos
[PREPRINT-702] 16 p2319 N90-23226
Characterization of plasma flow through magnetic nozzles
[AD-A221044] 18 p2617 N90-24905
Nonlinear supersonic motions of magnetized plasma flow with mass loading
[AERONOMICA-ACTA-A-354-1990] 19 p2760 N90-25681
Heat and momentum transfer to test samples in the high velocity plasma furnace
[AD-A222182] 21 p3079 N90-27505

MAGNETOHYDRODYNAMIC GENERATORS
Laser energy conversion 01 p0029 N90-10152
Computer controlled MHD power consolidation and pulse-generation system
[DE89-015600] 03 p0407 N90-12333
Preliminary report on the feasibility of high power Electronic Warfare (EW) using explosive energy sources
[MRL-TR-89-3] 04 p0483 N90-12775
Development of a wet vapor homogeneous liquid metal MHD power system
[DE90-001468] 08 p1124 N90-16508
MHD Integrated topping cycle project
[DE90-004141] 08 p1126 N90-16525
User's manual for MGMHD: A multigrid three-dimensional computer code for the analysis of magnetohydrodynamic generators and diffusers
[DE90-004453] 08 p1127 N90-16526
MHD channel development, part 1
[DE90-009549] 15 p2169 N90-22394
MHD channel development, part 2
[DE90-009550] 15 p2169 N90-22395
MHD channel development, part 3
[DE90-009551] 15 p2169 N90-22396
MHD channel development, part 4
[DE90-009552] 15 p2169 N90-22397
Direct conversion technology
[NASA-CR-186795] 18 p2576 N90-24675
Effects of friction and end losses on MHD thruster efficiency
[DE90-013673] 23 p3289 N90-28608
Diagnostic development and support of MHD test facilities
[DE90-015403] 24 p3550 N90-30083

MAGNETOHYDRODYNAMIC STABILITY
Low frequency electrostatic waves observed in the vicinity of an auroral arc 02 p0243 N90-11378
A review on radio studies of auroral E-region ionospheric irregularities 02 p0245 N90-11390
Short wavelength striations on expanding plasma clouds
[DE89-016585] 02 p0250 N90-11416
Ion temperature gradient instability
[DE89-016574] 02 p0277 N90-11580
Computer simulations of electromagnetic ion instabilities in the plasma sheet boundary layer
[DE89-016596] 02 p0278 N90-11588
Three-dimensional equilibria and Mercier stability calculations
[DE89-015907] 04 p0556 N90-13239

Preliminary results of the rocket and scatter experiments ROSE: Measurements with the newly designed spherical probe
05 p0659 N90-13850
A solvable self-similar model of the sausage instability in a resistive Z-pinch
[AD-A213137] 05 p0688 N90-14006
Experimental study on the filamentary instability in laser-matter interactions at short wave lengths
06 p0782 N90-14547
Effects of temporal and induced spatial incoherence on parametric instabilities in laser plasma interactions
06 p0782 N90-14549
Limitations in the growing of a plasma wave produced by heterodyning two lasers due to modulations and decay instabilities
06 p0783 N90-14552
Use of plasmas for the acceleration of particles to very high energy
06 p0783 N90-14553
High-frequency instability of the sheath-plasma resonance
[NASA-CR-186127] 06 p0844 N90-14910
Two-dimensional behavior of Megagauss-field-confined solid fiber Z-pinches
[DE90-000684] 06 p0845 N90-14918
Stability of the Global Alfven Eigenmode in the presence of fusion alpha particles in an ignited tokamak plasma
[DE89-016618] 06 p0848 N90-14930
Theory of interacting plasmas in space
07 p0993 N90-15742
Destabilization of tokamak pressure-gradient driven instabilities by energetic alpha populations
[DE90-003716] 07 p0996 N90-15756
Microfluctuations of plasma density in a theta-pinch and spatial coherency of a probing laser beam
[DE90-603347] 07 p0996 N90-15760
MHD stable high beta spheromak equilibrium
[DE90-004873] 08 p1127 N90-16529
Theoretical study of instabilities in vortices: Applications to hydrodynamics and magnetohydrodynamics
[ETN-90-96103] 09 p1219 N90-17073
Possibility of low-frequency electron wave in a beam-plasma system
[DE90-601021] 09 p1284 N90-17441
A current disruption mechanism in the neutral sheet for triggering substorm expansions
[NASA-CR-186260] 09 p1298 N90-17525
Dissipative trapped electron modes in ell equals 2 torsatrons
[DE90-004919] 10 p1431 N90-18256
Results of the H-mode experiments with JT-60 outer and lower divertors
[DE90-733146] 10 p1432 N90-18265
Alfven wave stability in D III-D
[DE90-005555] 10 p1437 N90-18291
Particle simulations in magnetospheric plasmas
[AD-A216256] 11 p1534 N90-18831
Streaming gravity mode instability
[DE90-610619] 11 p1535 N90-18835
Direct and inverse scattering problem associated with the elliptic Sinh-Gordon equation
[AD-A216455] 11 p1551 N90-18931
The lower hybrid drift instability and the evolution of plasma gradients
[DE90-006521] 11 p1568 N90-19021
The free energy principle, negative energy modes, and stability
[DE90-005368] 11 p1573 N90-19056
Nonlinear mechanics of unstable plasmas as related to high altitude aerodynamics
[AD-A215126] 12 p1716 N90-19852
Overview of recent results from the Advanced Toroidal Facility
[DE90-005673] 12 p1716 N90-19853
Theory of field reversed configurations
[DE90-006702] 12 p1717 N90-19860
Plasma simulation on magnetohydrodynamic time scales
[DE90-007490] 12 p1718 N90-19865
Spontaneous magnetic reconnection in a turbulent plasma
13 p1889 N90-20840
High elongation plasmas
[DE90-007575] 13 p1891 N90-20848
Nonlinear stability in fluid and plasma dynamics
[AD-A217735] 13 p1892 N90-20856
The effect of viscosity on the resistive tearing mode with the presence of shear flow
[DE90-009340] 14 p1974 N90-21312
Fusion burn dynamics in Dense Z-Pinch (DZP)
[DE90-007976] 14 p2029 N90-21638
MHD modes driven by anomalous electron viscosity and their role in fast sawtooth crashes
[DE90-009311] 14 p2029 N90-21639
Transition from resistive-g to eta-i driven turbulence in stellarator systems
[DE90-009382] 14 p2030 N90-21641
Instabilities and vortex dynamics in shear flow of magnetized plasmas
[DE90-009448] 14 p2030 N90-21643
Solar flares and dynamics of Langmuir waves in current-carrying plasmas
[IPPCZ-291] 14 p2042 N90-21710
Equilibrium and stability analysis of magnetospheric plasmas
15 p2057 N90-21782
Magnetic turbulence versus safety factor in the Tokapole 2 tokamak
15 p2168 N90-22391
Wind instability as a possible cause of the spiral structure formation in the gaseous subsystem of galaxies with the circular magnetic field
[DE90-618944] 15 p2190 N90-22507
Jupiter's drifting decametric bursts with the changing time scale
[DE90-618870] 15 p2192 N90-22517
Plasma instabilities associated with the injection of artificial ion beams into the ionosphere
16 p2254 N90-22851
Resonant MHD modes with toroidal coupling
[DE90-010077] 16 p2319 N90-23222
Analytical theory of the Bunemann instability for electron runaway
[IPF-88-3] 16 p2319 N90-23224
Finite amplitude surface waves in cooled plasmas with smeared interface
[DE90-611308] 18 p2617 N90-24909
Advances in spheromak understanding and parameters
[DE90-012052] 19 p2759 N90-25678
Proceedings of the US-Japan Fusion Cooperation Program Exchange P148 Workshop on Advanced Current Drive Concepts
[IPPJ-REV-4] 21 p3078 N90-27498
Experiments at high elongations in DIII-D
[DE90-013217] 21 p3078 N90-27500
Temperature-gradient instability induced by conducting end walls
[DE90-014334] 23 p3396 N90-29188
Nonlinear tearing mode: Rutherford regime and global characteristics
[DE90-015003] 23 p3397 N90-29193
Resonant MHD modes with toroidal coupling
[DE90-015185] 23 p3397 N90-29196
TSC (Tokamak Simulation Code) simulations of Alcator C-MOD discharges 3: Study of axisymmetric stability
[DE90-015386] 23 p3398 N90-29198
Ionospheric irregularities: Source, structure, plasma processes and effects on sensor systems
[AD-A223908] 24 p3490 N90-29723
Unstable phenomena in mechanical systems
[AD-A223640] 24 p3537 N90-30001
Transport of nonneutral plasmas
[AD-A223457] 24 p3549 N90-30077
Control of helium accumulation
[DE90-015658] 24 p3550 N90-30084

MAGNETOHYDRODYNAMIC TURBULENCE

NT PLASMA TURBULENCE

Numerical simulation of the compressible Orszag-Tang vortex
[AD-A210465] 01 p0127 N90-10725
A study of runaway electron confinement and theory of neoclassical MHD turbulence
[DE89-016728] 02 p0277 N90-11584
The stability of magnetohydrodynamic shock waves in molecular clouds
02 p0292 N90-11665

MAGNETOHYDRODYNAMIC WAVES

NT ELECTROSTATIC WAVES
NT PLASMA WAVES

Kinetic effects in Alfven wave heating. Part 2: Propagation and absorption with a single minority species
[DE89-016619] 01 p0126 N90-10724
Theory of high-n toroidicity-induced shear Alfven eigenmode in tokamaks
[DE89-016726] 02 p0277 N90-11582
The stability of magnetohydrodynamic shock waves in molecular clouds
02 p0292 N90-11665
HIPAS 1987-88: ULF research and campaign support
[AD-A211720] 03 p0339 N90-11933
Stability of the Global Alfven Eigenmode in the presence of fusion alpha particles in an ignited tokamak plasma
[DE89-016618] 06 p0848 N90-14930
Experiments on linear high beta helical axis stellarators to study simulated toroidal effects and Alfven-wave heating
[DE90-001704] 07 p0994 N90-15745
The 17th AINSE Plasma Physics Conference: Conference handbook
[DE90-600936] 07 p0996 N90-15759
A numerical simulation model for the study of magnetohydrodynamic (MHD) waves in a structured medium
07 p1012 N90-15864
On the quantum inverse problem for a new type of nonlinear Schroedinger equation for Alfven waves in plasma
[DE90-607469] 10 p1431 N90-18259
Alfven wave stability in D III-D
[DE90-005555] 10 p1437 N90-18291
Thermonuclear instability of global-type shear Alfven modes
[DE90-007087] 11 p1568 N90-19026
Slow shocks in coronal mass ejections
[NASA-CR-186578] 15 p2193 N90-22522
Gamma rays, cosmic rays, and local molecular clouds
15 p2193 N90-22524
Intensive MHD-structures penetration in the middle atmosphere initiated in the ionospheric cusp under quiet geomagnetic conditions
22 p3207 N90-28193
Theoretical studies of proton beams in solar flare loops
23 p3413 N90-29286
Alfven wave solitons and solar intermediate drift bursts
[MPE-PREPRINT-173] 23 p3413 N90-29287

MAGNETOHYDRODYNAMICS

MHD seed recovery and regeneration
[DE89-002711] 01 p0125 N90-10715
Thin section casting program. Volume 1: Executive summary and overview
[DE89-009030] 02 p0209 N90-11198
Thin section casting program. Volume 2: Horizontal TSC (Thin-Section Casting) approach
[DE89-009031] 02 p0210 N90-11199
Thin section casting program. Volume 5: Westinghouse MHD Project
[DE89-009035] 02 p0210 N90-11203
Boundary effects on the MHD dynamo in laboratory plasmas
[DE89-015207] 02 p0276 N90-11576
Solid fiber Z-pinches: Cold-start computations
[DE89-016768] 02 p0279 N90-11592
Exploding metallic foil fuse modeling at Los Alamos
[DE89-016970] 03 p0350 N90-11998
Non-stationary computer model of the asymptotic region of an electric arc gas heater
[IPPCZ-288] 03 p0407 N90-12330
Advanced concepts theory
[AD-A211665] 03 p0409 N90-12344
MHD (magnetohydrodynamic) modeling of solar and interplanetary processes
[PB89-215461] 03 p0420 N90-12416
Flux-corrected transport algorithms for two-dimensional compressible magnetohydrodynamics
[AD-A212757] 04 p0557 N90-13246
Modelling of the effects of the equatorial electrojet on its environment
[DE89-636298] 06 p0811 N90-14720
Computer controlled MHD power consolidation and pulse-generation system
[DE90-001224] 07 p0981 N90-15662
A numerical simulation model for the study of magnetohydrodynamic (MHD) waves in a structured medium
07 p1012 N90-15864
A brief description of lattice gas models for multiphase flows and magnetohydrodynamics
[DE90-003653] 08 p1062 N90-16143
Development of a wet vapor homogeneous liquid metal MHD power system
[DE90-001468] 08 p1124 N90-16508
MHD integrated topping cycle project
[DE90-004141] 08 p1126 N90-16525
User's manual for MGMHD: A multigrid three-dimensional computer code for the analysis of magnetohydrodynamic generators and diffusers
[DE90-004453] 08 p1127 N90-16526
Development and application of diagnostic instrumentation for measurements of electron density and conductivity
[DE90-004076] 09 p1228 N90-17127
MHD (Magnetohydrodynamic) slow shocks in coronal and interplanetary space
[AD-A214725] 09 p1299 N90-17527
Magnetohydrodynamic liquid-metal flows in a rectangular channel with an axial magnetic field, a moving conducting wall, and free surfaces
[AD-A216276] 10 p1425 N90-18223
Cohesive ceramic fabrication
[DE90-007333] 11 p1494 N90-18597
Magnetohydrodynamic modeling of plasma opening switches and gas puff plasmas
[DE90-005825] 11 p1569 N90-19028
A storage process of the magnetic energy results from the unsteady plasma flow field in the space active regions and stellar atmosphere
[DE90-610638] 12 p1717 N90-19858
Plasma simulation on magnetohydrodynamic time scales
[DE90-007490] 12 p1718 N90-19865

Diagnostic development and support of MHD (Magnetohydrodynamics) test facilities
[DE90-004969] 13 p1890 N90-20845
Numerical code AEOLUS-E1 for analysing free-boundary resistive MHD mode
[DE90-759903] 14 p2026 N90-21630
The MHD structure of an open magnetotail boundary
15 p2168 N90-22388
MHD channel development, part 1
[DE90-009549] 15 p2169 N90-22394
MHD channel development, part 2
[DE90-009550] 15 p2169 N90-22395
MHD channel development, part 3
[DE90-009551] 15 p2169 N90-22396
MHD channel development, part 4
[DE90-009552] 15 p2169 N90-22397
Advanced concepts theory annual report, 1989
[AD-A220768] 17 p2474 N90-24146
Advances in spheromak understanding and parameters
[DE90-012052] 19 p2759 N90-25678
Time-dependent two dimensional radiation hydrodynamics of accreting matter onto highly magnetized neutron stars 19 p2767 N90-25722
Three dimensional accretion disk simulation with external magnetic field 19 p2772 N90-25754
A theory of the rapid burster (MXB1730-335)
19 p2775 N90-25782
Analytical studies of magnetospheric pulsations
[AD-A222275] 21 p3026 N90-27205
United States Air Force research initiation program for 1988, volume 1
[AD-A223123] 21 p3101 N90-27613
Resonant MHD modes with toroidal coupling
[DE90-015185] 23 p3397 N90-29196
Solar oscillation frequency and solar neutrino predictions
[DE90-014918] 23 p3413 N90-29288
Vlasov-Maxwell equilibria of solar coronal loops
[DE90-015025] 23 p3414 N90-29289
Satellite measurements of magnetospheric Poynting flux
[AD-A224391] 24 p3490 N90-29724
Beam and plasma physics research
[AD-A224452] 24 p3548 N90-30067
Transformation group methods in plasma physics
[DE90-628755] 24 p3548 N90-30074

MAGNETOIONIC PLASMA
U PLASMAS (PHYSICS)

MAGNETOMETERS
NT VARIOMETERS
Gaussmeter determination of 302 stainless steel material condition
[BDX-613-3941] 01 p0044 N90-10249
CRRES (Combined Release and Radiation Effects Satellite) SPACERAD plasma wave experiment
[AD-A210791] 02 p0278 N90-11587
HIPAS 1987-88: ULF research and campaign support
[AD-A211720] 03 p0339 N90-11933
Construction of a SQUID magnetometer for investigation of screening properties of high-T(sub c) superconductors
[FOA-C-20765-2.2] 05 p0845 N90-13768
High precision rocket attitude reconstruction using star sensor and magnetometer data
05 p0659 N90-13844
A computer control system for the alternating gradient magnetometer 12 p1636 N90-19402
NASA Marshall Space Flight Center solar observatory report, January to December 1989
[NASA-TM-100404] 19 p2797 N90-25923
Experiments on superconductor imaging surface magnetometry
[DE90-008925] 20 p2929 N90-26665
The Nurmijarvi Geophysical Observatory
21 p3021 N90-27178
Coil system for the production of three-component uniform magnetic field at the Nurmijarvi Observatory
21 p3021 N90-27179
Measuring sensitivities and orthogonalities of magnetometer sensors in the Nurmijarvi coil hut
21 p3022 N90-27180
Comparisons of the recording instruments. Description of the difference-plots 21 p3022 N90-27181
A new method for the absolute measurement of geomagnetism beginning with DI Flux
21 p3022 N90-27182
Experiences with modern absolute instruments
21 p3022 N90-27183
Institut de Physique du Globe de Paris automatic magnetic observatory 21 p3022 N90-27184
Proton magnetometers for measurement of the Earth's magnetic field 21 p3023 N90-27188
Some thoughts on data processing
21 p3023 N90-27189
High-T(sub c) squid application in medicine and geophysics 22 p3139 N90-27806
A YBCO RF-SQUID magnetometer and its applications 22 p3151 N90-27867
Brorfelde Geomagnetic Observatory: Magnetic results, 1987
[ISBN-87-7478-297-5] 24 p3496 N90-29756

MAGNETOMETRY
U MAGNETIC MEASUREMENT

MAGNETOPLASMADYNAMICS
Physical process in MPD plasmas
[AD-A213679] 07 p0996 N90-15761
Design of a thrust stand for high power electric propulsion devices
[NASA-TM-102372] 08 p1037 N90-15992
Effects of scaling on the performance of magnetoplasmadynamic thrusters
[AD-A215690] 09 p1184 N90-16863
Test facility and preliminary performance of a 100 kW class MPD thruster 11 p1472 N90-18476
Advanced solar-propelled cargo spacecraft for Mars missions
[NASA-CR-186218] 19 p2665 N90-25164
Geometric effects in applied-field MPD thrusters
[NASA-TM-103259] 22 p3134 N90-27782

MAGNETOPLASMAS
U PLASMAS (PHYSICS)

MAGNETORESISTIVITY
Magnetotransport studies of epitaxial Cr thin films
[DE90-001930] 06 p0856 N90-14975
Diluted magnetic semiconductors
[AD-A220444] 17 p2476 N90-24159
Use of geomagnetic data for studies on the Earth's deep interior 21 p3023 N90-27192

MAGNETOSHEATH
Plasma waves in the earth's foreshock, bow shock, and magnetosheath 01 p0086 N90-10486
The MHD structure of an open magnetotail boundary
15 p2168 N90-22388

MAGNETOSPHERE-IONOSPHERE COUPLING
Ionospheric Structure and Variability on a Global Scale and Interactions with Atmosphere and Magnetosphere
[AGARD-CP-441] 02 p0239 N90-11361
Magnetospheric substorms as a signature of the solar terrestrial interaction 02 p0240 N90-11363
Observations of ionosphere/magnetosphere interactions from the Dynamics Explorer satellites
02 p0242 N90-11376
Quiet time conductivities of the auroral ionosphere
02 p0244 N90-11383
Upper ionosphere and magnetospheric-ionospheric coupling
[DE89-619727] 02 p0250 N90-11415

MAGNETOSPHERES
Multipole moments in general relativity and dynamical perturbations of black-hole magnetospheres
15 p2190 N90-22509

MAGNETOSPHERIC ELECTRON DENSITY
Electron populations above the nightside auroral oval during magnetic quiet times
[IRF-PREPRINT-116] 19 p2714 N90-25445

MAGNETOSPHERIC INSTABILITY
Particle simulations in magnetospheric plasmas
[AD-A216256] 11 p1534 N90-18831

MAGNETOSTATIC FIELDS
Finite element analysis of propagation in waveguide components with application to ferrite phase shifters
[FOA-C-30529-3.2] 09 p1204 N90-16977

MAGNETOSTATICS
Magnetostatic wave device characterization by Brillouin light scattering
[AD-A213798] 09 p1281 N90-17426
Magnetostatic boundary-value problems in the incomplete-nonlinear formulation and methods of their solution
[DE90-615185] 13 p1877 N90-20767
The parallel algorithm for solving the three-dimensional integral magnetostatic equations
[DE90-616529] 14 p2015 N90-21547
Magnetostatic wave transducers, resonators and dispersion control
[AD-A223437] 24 p3464 N90-29571

MAGNETOSTRICTION
Magnetostrictive torque sensor
[AD-D014169] 03 p0349 N90-11996
Magneto-elastic interactions in conducting structures in transient magnetic fields 05 p0632 N90-13686
Method and apparatus to enhance the sensitivity of cylindrical magnetostrictive transducer to magnetic fields
[AD-D014218] 06 p0767 N90-14459
Investigation of a magnetostrictive fiber optic interferometric sensor
[AD-A215666] 09 p1226 N90-17111
Terbium-dysprosium magnetostrictive high power transducers
[AD-D014509] 19 p2753 N90-25641
Magnetostrictive direct drive motors
[NASA-CR-186895] 23 p3335 N90-28855

MAGNETOTELLURIC PROFILING
U MAGNETIC SURVEYS

MAGNETOVARIOGRAPHS
U VARIOMETERS

MAGNETRON SPUTTERING
Synthesis and study of materials for superconducting electronics
[AD-A212966] 04 p0561 N90-13270
Metal film coatings on amorphous metallic alloys
[AD-D014308] 07 p0907 N90-15240
Negative ion surface plasma source development for plasma trap injectors in Novosibirsk
[DE90-006082] 12 p1716 N90-19856
Magnetron sputtered boron films and Ti/B multilayer structures
[DE90-009190] 14 p1948 N90-21153
Influence of the deposition conditions on radiofrequency magnetron sputtered MoS2 films
[NASA-TP-2994] 14 p1958 N90-21210
Effects of microstructure and adhesion on performance of sputter-deposited MoS2 solid lubricant coatings
[AD-A220900] 18 p2530 N90-24434
Thick and compact MoS2 coatings
18 p2541 N90-24501
In-situ growth of superconducting films of Bi-Sr-Ca-Cu-O using magnetron sputtering
[DE90-011161] 18 p2626 N90-24962
Research on sputtering of ferroelectric thin films
[AD-A221782] 21 p2983 N90-26949
Preparation and characteristics of superconducting cuprate thin films: Nd(2-x)Ce(x)CuO4 and substituted Bi-system 22 p3140 N90-27813
Special purpose spatial light modulators
[AD-A223794] 24 p3545 N90-30052

MAGNETRONS
Alternative fabrication techniques for high-efficiency CuInSe2 and CuInSe2-alloy films and cells
[DE89-009451] 01 p0083 N90-10474
Massachusetts Institute of Technology Plasma Fusion Center
[DE89-016050] 01 p0126 N90-10723
Numerical simulation of cross field amplifiers
[DE90-006459] 12 p1652 N90-19496
Measurement of gravitational acceleration of antimatter
[DE90-627464] 23 p3403 N90-29233
High power microwaves for defense and accelerator applications
[AD-A223550] 24 p3464 N90-29572

MAGNETS
NT ELECTROMAGNETS
NT PERMANENT MAGNETS
NT SUPERCONDUCTING MAGNETS
NT WIGGLER MAGNETS
Free-Piston Stirling Engine magnetically coupled heat pump: Critical component evaluation
[DE89-015646] 02 p0229 N90-11316
Plasma separation process: Magnet move to Oak Ridge National Laboratory
[DE89-017457] 04 p0556 N90-13242
Further studies of transverse stress effects in cable-in-conduit conductors
[DE90-001517] 06 p0771 N90-14484
Nonlinear dynamics of domain walls and vortices in two-dimensional systems
[DE90-004840] 10 p1425 N90-18221

MAGNIFICATION
Calculation of excrescence drag magnification due to pressure gradient at high subsonic speeds
[ESDU-87004] 12 p1598 N90-19195
Shaping radiation pattern of excimer laser by means of controllable intracavity mirror
16 p2310 N90-23166
Variable magnification variable dispersion glancing incidence imaging x ray spectroscopic telescope
[NASA-CASE-MFS-28013-3] 21 p3096 N90-27594
Multispectral variable magnification glancing incidence x ray telescope
[NASA-CASE-MFS-28013-4] 21 p3096 N90-27595

MAGNIFIERS
U MAGNIFICATION

MAGNITUDE
NT STELLAR MAGNITUDE

MAGNONS
Spin fluctuations and excitations in a 2D xy-ferromagnet: CoCl2 in graphite
[DE89-017600] 02 p0196 N90-11119

MAGNUS EFFECT
Internal Magnus effects in superfluid 3He-A
[PB89-212617] 03 p0410 N90-12351

MAIN SEQUENCE STARS
NT DWARF NOVAE
NT DWARF STARS
NT FLARE STARS
NT SUN

Effects of main-sequence mass loss on the turnoff ages of globular clusters
[DE89-016784] 02 p0295 N90-11678
Effects of main-sequence mass loss on the turnoff ages of population 1 clusters
[DE89-016755] 03 p0421 N90-12417
The age of the galactic disk
[NASA-CR-186292] 07 p1013 N90-15869
Outflows in high mass star-forming regions
08 p1149 N90-16657
Evolutionary models of the rotating sun and implications for other low mass stars 16 p2339 N90-23329

MAINTAINABILITY
The RB199: An in-service success
[PNR90544] 03 p0307 N90-11746
Development and applications of reliability and maintainability design criteria in military aircraft
[ETN-89-95208] 04 p0452 N90-12591
A new view of weapon system reliability and maintainability
[AD-A213281] 05 p0580 N90-13382
Electronic warfare: Reliable equipment needed to test Air Force's electronic warfare systems
[AD-A212952] 05 p0632 N90-13687
The repair of aircraft integral fuel tanks in the RAF: A user's view of fuel tank technology
08 p1022 N90-15908
Spray sealing: A breakthrough in integral fuel tank sealing technology 08 p1022 N90-15912
Complex availability problems solved with simulation
[DE89-012610] 08 p1116 N90-16459
Sensitivity of space system availability predictions to underlying component reliability estimates
[AD-A215535] 09 p1183 N90-16858
Basic research in reliability for real systems
[AD-A214536] 09 p1234 N90-17158
Project management in successful reliability and maintainability improvement programs
[AD-A215424] 09 p1234 N90-17162
R/M/T (Reliability, Maintainability, and Testability) design for fault tolerance, technical manager's design implementation guide
[AD-A215531] 09 p1234 N90-17164
Space Station Freedom electric power system availability study
[NASA-CR-185181] 13 p1763 N90-20120
A survey of human factors methodologies and models for improving the maintainability design of emerging Army aviation systems
[AD-A221159] 18 p2586 N90-24724
The Army/Air Force RAMCAD (Reliability And Maintainability Computer-Aided Design) program
[AD-A220923] 18 p2593 N90-24753
Design and construction of a wall-climbing robot
[NIAR-90-20] 20 p2870 N90-26327
STOVL fighter propulsion reliability, maintainability, and supportability characterization
[AD-A224221] 23 p3282 N90-28574
Reliability analysis of maintained structural system vulnerable to fatigue and fracture
23 p3338 N90-28868
Application of multifunction inertial reference systems to fighter aircraft 24 p3423 N90-29341
Performance monitoring, fault detection, fault localization design guidance
[AD-A223619] 24 p3478 N90-29655

MAINTENANCE
NT AIRCRAFT MAINTENANCE
NT FILE MAINTENANCE (COMPUTERS)
NT SPACE MAINTENANCE
NT SPACECRAFT MAINTENANCE
A review of Australian and New Zealand investigations on aeronautical fatigue during the period April 1987 to March 1989
[AD-A210373] 01 p0006 N90-10026
Field repair of composite materials in Army service: Planning for the future
[AD-A210732] 01 p0035 N90-10190
Results from the second year of operation of the Federal Methanol Fleet at Argonne National Laboratory
[DE89-016935] 02 p0230 N90-11319
Improving snow roads and airstrips in Antarctica
[AD-A211588] 03 p0335 N90-11907
DSEP (Dual Shaft Electric Propulsion) operation and maintenance manual for the NVH and TB-2 vehicles: Advanced Dual Shaft Electric Propulsion System technology development program
[DE89-017549] 03 p0420 N90-12411
Evaluation of a damaged F/A-18 horizontal stabilator
[AD-A212573] 04 p0453 N90-12597
Designing for reliable and low maintenance cost aero engines
[PNR90570] 04 p0455 N90-12604
A new view of weapon system reliability and maintainability
[AD-A213281] 05 p0580 N90-13382
A new view of weapon system reliability and maintainability: Executive summary
[AD-A213282] 05 p0580 N90-13383
The US space station and its electric power system
[NASA-TM-101974] 05 p0616 N90-13596
Electronic warfare: Reliable equipment needed to test Air Force's electronic warfare systems
[AD-A212952] 05 p0632 N90-13687
Life evaluation of valve-regulated lead-acid batteries for load-leveling applications
[DE90-002188] 07 p0922 N90-15336
MANPRINT methods monograph: Aiding the development of manned system performance criteria
[AD-A213543] 07 p0968 N90-15593
Tools for simulation-based training
[AD-A214307] 07 p0978 N90-15646
Hierarchical process composition: Dynamic maintenance of structure in a distributed environment
[AD-A214325] 07 p0978 N90-15648
Fuel Tank Technology
[AGARD-R-771] 08 p1021 N90-15904
Integral fuel tank sealing practice at British Aerospace (Kingston) 08 p1021 N90-15905
The effect of primer age on adhesion of polysulphide sealant 08 p1022 N90-15909
Fuel tank explosion protection
08 p1023 N90-15914
New optimization techniques in database access and maintenance 08 p1137 N90-16586
An illustrated guide of optical characteristics of aircraft transparencies
[AD-A214565] 09 p1167 N90-16752
High-pressure promoted combustion chamber
[NASA-CASE-MSC-21470-1] 09 p1170 N90-16771
Space shuttle RCS oxidizer leak repair for STS-26
11 p1474 N90-18485
Brake performance of the McDonnell Douglas DC-10-30/40 during high speed, high energy rejected takeoffs
[PB90-917004] 14 p1920 N90-21000
Vibration isolation versus vibration compensation on multiple payload platforms 14 p1933 N90-21066
Thermal control system corrosion study
[NASA-TM-102220] 14 p1971 N90-21294
Maintenance = reuse-oriented software development
[NASA-CR-186455] 14 p2012 N90-21531
Microwave Landing System (MLS) remote monitoring subsystem/remote maintenance monitoring system
[DOT/FAA/PS-89/2] 15 p2050 N90-21749
Advances in optimal active control techniques for aerospace systems; application to aircraft active landing gear 15 p2054 N90-21769
Reliability importance measures and their calculation
[DE90-620391] 15 p2108 N90-22057
Expert systems for automated maintenance of a Mars oxygen production system
[NASA-CR-186209] 15 p2138 N90-22215
Lunar robotic maintenance module
[NASA-CR-183071] 17 p2411 N90-23735
Software maintenance on Airbus family
[REPT-892-111-101] 17 p2444 N90-23931
Northeast Artificial Intelligence Consortium. Volume 3: The Versatile Maintenance Expert System research project
[AD-A218716] 17 p2453 N90-23993
Supervisory controlled telemanipulation and vision systems for inspection and maintenance operations
18 p2508 N90-24333
Space shuttle: The future of the Vandenberg launch site needs to be determined
[GAO/NSIAD-88-158] 18 p2509 N90-24337
Self-contained robotic arm manipulator
[NASA-CR-184925] 19 p2696 N90-25342
Performance of a self-aligning solar array tracking controller
[DE90-011184] 19 p2698 N90-25350
Crystalline photovoltaic cell research, status, and future direction
[DE90-011478] 19 p2710 N90-25427
Smart built-in test 19 p2728 N90-25512
Autonomous power expert fault diagnostic system for Space Station Freedom electrical power system testbed
19 p2730 N90-25521
OMS FDIR: Initial prototyping
19 p2738 N90-25562
Knowledge-Based Systems (KBS) development standards: A maintenance perspective
19 p2739 N90-25570
OASIS, LLNL version: Software maintenance manual
[DE90-013522] 20 p2868 N90-26313
An expert system advisor for damage repair of composite wing skins (repairman) 21 p2956 N90-26810
Maintenance of a minimum spanning forest in a dynamic planar graph
[AD-A221425] 21 p3054 N90-27362
A hypothesis test of cumulative sums of multinomial parameters
[AD-A221466] 21 p3067 N90-27434
DMSP's interactive tactical terminal
21 p3068 N90-27441
CUIS user's manual
[ESA-TM-03] 22 p3132 N90-27775
Advanced robotics for Air Force operations
[PB90-157009] 22 p3182 N90-28055
Impact of Emerging NDE-NDI Methods on Aircraft Design, Manufacture, and Maintenance
[AGARD-CP-462] 22 p3184 N90-28068
Neutron radiography: Applications and systems
22 p3186 N90-28080
Development and testing of rapid repair methods for war damaged runways
[AD-A223970] 23 p3285 N90-28586
Results from the fourth year of operation of the Federal Methanol Fleet at Lawrence Berkeley Laboratory
[DE90-014741] 23 p3315 N90-28743
Reliability analysis of maintained structural system vulnerable to fatigue and fracture
23 p3338 N90-28868
The NASA/OAST telerobot testbed architecture
23 p3365 N90-29016
Aircraft battle damage repair of transparencies
[AD-A224168] 24 p3432 N90-29387
Estimation of power spectral density of runway roughness
[NAL-TR-1037] 24 p3437 N90-29411
Oxygen deficiency monitor system
[DE90-014866] 24 p3523 N90-29917

MAINTENANCE TRAINING
Tools for simulation-based training
[AD-A214307] 07 p0978 N90-15646
An exploration of issues related to future space logisticians
[AD-A215374] 09 p1276 N90-17397
Report of the First Annual Airborne Weapons Training Technology Review
[DE90-007189] 12 p1697 N90-19747

MALAGASY REPUBLIC
US Navy regional climatic study of the Mozambique channel and adjacent waters
[AD-A218793] 16 p2258 N90-22875

MALES
Human performance in cockpit-related systems
[NIAR-90-7] 20 p2900 N90-26495

MALFUNCTIONS
Rotor-to-stationary element rub-related vibration phenomena in rotating machinery: Literature survey
15 p2109 N90-22065
Convex models of malfunction diagnosis in high performance aircraft
[AD-A218514] 19 p2649 N90-25073
Monitoring and control of spacecraft systems using procedural reasoning 19 p2731 N90-25524
The sensitivity of several explosives to ignition in the launch environment
[AD-A221581] 21 p2990 N90-26993
A model for a space shuttle safing and failure-detection expert 21 p3048 N90-27314

MAMMALS
NT HUMAN BEINGS
NT MANATEES
NT MICE
NT MONKEYS
NT PRIMATES
NT RATS
NT RODENTS
Sound Localization by Human Observers symposium proceedings
[AD-A212877] 04 p0524 N90-13026
Microgravity and mammalian cells
19 p2680 N90-25240
Early mammalian development and possible involvement of gravity 19 p2680 N90-25242
The effects of blast trauma (impulse noise) on hearing: A parametric study source 2
[AD-A221731] 21 p3035 N90-27253

MAN
U HUMAN BEINGS

MAN ENVIRONMENT INTERACTIONS
Evaluation of mid-to-long term basic research for environmental restoration
[DE89-015621] 02 p0238 N90-11355
A model for the simulation of the ozone budget in the atmosphere under anthropogenic perturbation
[DE89-636294] 06 p0811 N90-14719
Natural and anthropogenic climate change
[DE90-006488] 11 p1532 N90-18822
Overview of the methodologies used to compile large scale emissions inventories
[DE90-008518] 13 p1830 N90-20509
Global changes in tropospheric chemistry
19 p2708 N90-25411

Anthropogenic sources of NO(x), SO()x, CO, and CH4: Geographical distribution
[AERONOMICA-ACTA-A-353-1990] 19 p2713 N90-25440
Measurements of tropospheric nitric acid over the Western United States and Northeastern Pacific Ocean
[NASA-TM-103470] 20 p2883 N90-26399
Applications of ISES for coastal zone studies 21 p3018 N90-27157
The influence of continental sources of aerosols on the marine stratocumulus during FIRE IFO-1 22 p3218 N90-28250
Observations of anthropogenic cloud condensation nuclei 22 p3218 N90-28251
Natural and anthropogenic climate change
[DE90-015528] 23 p3348 N90-28923

MAN MACHINE SYSTEMS
NT MAN-COMPUTER INTERFACE
CONSOLE: A CAD tandem for optimization-based design interacting with user-supplied simulators 01 p0017 N90-10085
Addressing user display requirements from a large and diverse user community
[DE89-011403] 01 p0103 N90-10582
Independent Orbiter Assessment (IOA): Assessment of the remote manipulator system FMEA/CIL
[NASA-CR-185592] 02 p0171 N90-10964
Techniques for optimizing human-machine information transfer related to real-time interactive display systems
[NASA-TM-100450] 02 p0254 N90-11441
Filling or outlining shapes with color: The effects on a visual search task
[AD-A211067] 02 p0255 N90-11444
Task analysis of the UH-60 mission and decision rules for developing a UH-60 workload prediction model. Volume 1: Summary report
[AD-A210763] 02 p0255 N90-11446
USSR Space Life Sciences Digest, issue 24
[NASA-CR-3922(28)] 03 p0378 N90-12152
Waiting times in polling systems with Markovian server routing
[CWI-BS-R8905] 05 p0685 N90-13989
The problem of automation: Inappropriate feedback and interaction, not overautomation
[NASA-CR-186126] 05 p0686 N90-13994
Task-oriented display design: Concept and example
[NASA-TM-101685] 07 p0881 N90-15101
Automation and robotics in construction: Japanese research and development
[AD-A214170] 07 p0942 N90-15456
SIMON (SuperIntelligent Mobile Observing Navigator): A high-reliability robot for a radiation environment
[DE90-003888] 07 p0943 N90-15460
Model for measuring complex performance in an aviation environment
[DE90-002055] 07 p0967 N90-15585
Architectural study of the design and operation of advanced force feedback manual controllers
[NASA-CR-185948] 07 p0981 N90-15664
Distribution of hardware and software elements in unmanned air vehicle systems 08 p1027 N90-15933
Formalisms for user interface specification and design 08 p1155 N90-16687
FAA air traffic control operations concepts. Volume 7: ATCT (Airport Traffic Control Towers) tower controllers
[AD-A210455] 09 p1163 N90-16730
Advances in navigation support systems based on operational pilot's heuristics 09 p1164 N90-16737
Proximity compatibility and information display: The effects of space and color on the analysis of aircraft stall conditions
[AD-A214488] 09 p1260 N90-17309
Job planning and execution monitoring for a human-robot symbiotic system
[DE90-004464] 09 p1261 N90-17315
Three input concepts for flight crew interaction with information presented on a large-screen electronic cockpit display
[NASA-TM-4173] 11 p1457 N90-18394
Assessment of crew workload measurement methods, techniques and procedures. Volume 2: Guidelines for the use of workload assessment techniques in aircraft certification
[AD-A217067] 12 p1697 N90-19748
Aiding the decision maker: Perceptual and cognitive issues at the human-machine interface
[AD-A217862] 13 p1855 N90-20648
Graphics Technology in Space Applications (GTSA 1989)
[NASA-CP-3045] 13 p1856 N90-20651
The use of graphics in the design of the human-telerobot interface 13 p1860 N90-20670
Simulator comparison of thumball, thumb switch, and touch screen input concepts for interaction with a large screen cockpit display format
[NASA-TM-102587] 14 p1921 N90-21005
An adaptive human response mechanism controlling the V/STOL aircraft. Appendix 3: The adaptive control model of a pilot in V/STOL aircraft control loops
[NASA-CR-186599] 15 p2056 N90-21777
Insights into complex human performance
[DE90-006957] 15 p2137 N90-22214
Hybrid vision activities at NASA Johnson Space Center 15 p2139 N90-22225
Model-based method for terrain-following display design
[AD-A219302] 16 p2201 N90-22563
Telepresence, time delay, and adaptation 16 p2271 N90-22944
Visual enhancements in pick-and-place tasks: Human operators controlling a simulated cylindrical manipulator 16 p2271 N90-22946
Lunar regolith bagging system
[NASA-CR-186683] 19 p2677 N90-25223
Man-machine interface for the control of a lunar transport machine
[NASA-CR-184935] 19 p2724 N90-25495
NASA systems autonomy demonstration project: Advanced automation demonstration of Space Station Freedom thermal control system 19 p2728 N90-25510
Telepresence for space: The state of the concept 19 p2731 N90-25526
Telepresence and Space Station Freedom workstation operations 19 p2731 N90-25527
The human factors of workstation telepresence 19 p2732 N90-25528
Human factors issues in telerobotic systems for Space Station Freedom servicing 19 p2737 N90-25556
The JPL telerobot operator control station: Operational experiences 19 p2738 N90-25565
Qualitative evaluation of a conformal velocity vector display for use at high angles-of-attack in fighter aircraft
[NASA-TM-102629] 20 p2809 N90-25981
Human performance models
[FFI-90/7002] 20 p2901 N90-26502
Psychophysiological assessment of pilot workload in an applied setting
[AD-A222707] 20 p2902 N90-26507
Speech Analysis and Synthesis and Man-Machine Speech Communications for Air Operations
[AGARD-LS-170] 21 p2992 N90-27006
Speech recognition based on pattern recognition techniques 21 p2993 N90-27011
A vision-based telerobotic control station 21 p3046 N90-27311
A conceptual framework for fighter flight control systems
[PD-CF-9009] 23 p3283 N90-28577
Experiments in the dynamic and strategic control of cooperating manipulators 23 p3333 N90-28845
Techniques and applications for binaural sound manipulation in human-machine interfaces
[NASA-TM-102279] 23 p3362 N90-28998
Proceedings of the NASA Conference on Space Telerobotics, volume 1
[NASA-CR-186856] 23 p3362 N90-29000
Adjustable impedance, force feedback and command language aids for telerobotics (parts 1-4 of an 8-part MIT progress report) 23 p3363 N90-29007
Variable force and visual feedback effects on teleoperator man/machine performance 23 p3364 N90-29008
Teleoperator comfort and psychometric stability: Criteria for limiting master-controller forces of operation and feedback during telemanipulation 23 p3364 N90-29009
Human factors model concerning the man-machine interface of mining crewstations 23 p3364 N90-29011
The NASA/OAST telerobot testbed architecture 23 p3365 N90-29016
Proceedings of the NASA Conference on Space Telerobotics, volume 2
[NASA-CR-186857] 23 p3370 N90-29044
The JPL telerobot operator control station. Part 1: Hardware 23 p3371 N90-29049
The JPL telerobot operator control station. Part 2: Software 23 p3371 N90-29050
Implementation and design of a teleoperation system based on a VMEBUS/68020 pipelined architecture 23 p3372 N90-29053
Human machine interaction via the transfer of power and information signals 23 p3372 N90-29054
Proceedings of the NASA Conference on Space Telerobotics, volume 3
[NASA-CR-186858] 24 p3500 N90-29780
A design strategy for autonomous systems 24 p3508 N90-29818
Use of graphics in decision aids for telerobotic control: (Parts 5-8 of an 8-part MIT progress report) 24 p3508 N90-29829
Proceedings of the NASA Conference on Space Telerobotics, volume 4
[NASA-CR-186859] 24 p3508 N90-29830
Global models: Robot sensing, control, and sensory-motor skills 24 p3511 N90-29849
Proceedings of the NASA Conference on Space Telerobotics, volume 5
[NASA-CR-186860] 24 p3516 N90-29874
The telerobot workstation testbed for the shuttle aft flight deck: A project plan for integrating human factors into system design 24 p3518 N90-29887
Next generation space robot 24 p3520 N90-29899
An intelligent, free-flying robot 24 p3522 N90-29912
Graphic interface for attribute-based data language queries from a personal computer to the multi-lingual, multi-model, multi-backend database system over an Ethernet network
[AD-A223738] 24 p3528 N90-29948

MAN TENDED FREE FLYERS
Key structures mechanical issues of the European Space Station and platform program Columbus 02 p0188 N90-11072
The European EVA suit: An optimized tool for Hermes/MTFF in-orbit operations 18 p2502 N90-24296
Docking berthing systems: Functions and simulation 18 p2505 N90-24313
Concept synthesis of an equipment manipulation and transportation system EMATS 24 p3510 N90-29844

MAN-COMPUTER INTERFACE
Northeast Artificial Intelligence Consortium annual report for 1987. Volume 5: Building an intelligent assistant: The acquisition, integration and maintenance of complex distributed tasks
[AD-A210330] 01 p0109 N90-10821
Filling or outlining shapes with color: The effects on a visual search task
[AD-A211067] 02 p0255 N90-11444
ISI's (Information Sciences Institute) SDI architecture simulator: An experiment in adding new software to the system
[AD-A211314] 03 p0387 N90-12204
Visualization of high-resolution digital terrain
[AD-A212149] 04 p0515 N90-12971
State of the art of human/machine dialog tool prototypes
[TELECOM-PARIS-89-H001] 04 p0527 N90-13038
ISI's (Information Sciences Institute) SDI architecture simulator: Initial prototype user interface
[AD-A211325] 04 p0529 N90-13053
Conceptual dependency theory and robot programming
[REPT-89-20] 04 p0537 N90-13106
Flight deck automation: Promises and realities
[NASA-CP-10036] 05 p0580 N90-13384
Conference Proceedings of the Human-Electronic Crew: Can They Work Together
[AD-A211871] 05 p0676 N90-13936
Workloads and waiting times in single-server systems with multiple customer classes
[CWI-BS-R8906] 05 p0689 N90-14020
Action languages: Dimensions, effects
[NASA-CR-183388] 05 p0716 N90-14181
MIPs and BIPs are megaflops: Limits of unidimensional assessments
[DE89-015707] 06 p0820 N90-14770
Development of a robotics system for automated chemical analysis of sediment, sludges, and soils
[DE90-003637] 07 p0895 N90-15170
The components of scientific visualization
[DE90-001992] 07 p0972 N90-15614
User interaction with self-learning systems
[AD-A214280] 08 p1105 N90-16395
NASA/ASEE Summer Faculty Fellowship Program
[NASA-CR-166837] 08 p1154 N90-16686
Formalisms for user interface specification and design 08 p1155 N90-16687
Checklist reading problems in airplanes equipped with speech recognition systems
[ILR-MITT-223(1989)] 09 p1261 N90-17314
Executive summary for designing online help systems: Report of year 1 activity
[AD-A214811] 09 p1262 N90-17320
Access to multiple underlying systems in Janus
[AD-A214585] 09 p1264 N90-17329
Parrot: The Janus paraphraser
[AD-A214588] 09 p1265 N90-17332
IRUS-II user manual
[AD-A214612] 09 p1265 N90-17334
A theory for graph-based language specification, analysis, and mapping with application to the development of parallel software
[AD-A214910] 09 p1266 N90-17342

Help design software project
[AD-A214883] 09 p1270 N90-17362
The Columbus power system simulation programme 10 p1330 N90-17686
An intelligent tool for the design of presentations: A system identification study
[AD-A215770] 10 p1418 N90-18174
Knowledge-based extensible natural language interface technology program
[AD-A216664] 11 p1545 N90-18897
A human factors experimental comparison of two database query languages 11 p1574 N90-19064
Design and architecture of fourth and fifth generation software engineering environments
[ETN-90-95365] 12 p1698 N90-19752
Queuing theory approach to modelling the dynamics of the human-computer interface
[AD-A216870] 12 p1705 N90-19788
Comparison of oculometer and head-fixed reticle with voice or switch and touch panel for data entry on a generic tactical air combat display
[AD-A217231] 13 p1855 N90-20646
The development of the Canadian Mobile Servicing System Kinematic Simulation Facility 13 p1861 N90-20676
Design of a simulation interface for a parellel computing environment
[DE90-008497] 13 p1873 N90-20737
Understanding the computing system domain of advanced computing with microcomputers
[DE90-009825] 15 p2145 N90-22251
The application of connectionism to query planning/scheduling in intelligent user interfaces 15 p2152 N90-22295
Spatial issues in user interface design from a graphic design perspective 16 p2270 N90-22939
A computer graphics system for visualizing spacecraft in orbit 16 p2272 N90-22952
Interactive orbital proximity operations planning system 16 p2273 N90-22953
Experiences in teleoperation of land vehicles 16 p2273 N90-22954
Multimedia system control
[AD-A219392] 16 p2276 N90-22971
Automatic compiler construction
[AD-A218777] 16 p2278 N90-22983
Graphics equipment for data analysis
[AD-A218983] 16 p2278 N90-22985
Multibody dynamics model building using graphical interfaces 16 p2297 N90-23082
Natural language processing: A tutorial
[AD-A219096] 16 p2300 N90-23108
Learning environment for neural networks and transient acoustics
[AD-A219000] 16 p2314 N90-23186
Telerobotic application to EVA 18 p2502 N90-24298
Telerobotic architecture for an on-orbit servicer 18 p2503 N90-24302
Interconnection of the graphics language for database system to the multi-lingual, multi-model, multi-backend database system over an Ethernet network
[AD-A220081] 18 p2591 N90-24739
National Aeronautics and Space Administration (NASA)/American Society for Engineering Education (ASEE) Summer Faculty Fellowship Program-1989, volume 2
[NASA-CR-185601-VOL-2] 18 p2630 N90-24985
Knowledge-based control of an adaptive interface 18 p2630 N90-24987
Development and test of software by safety critical aircraft systems
[MBB-FE-363/S/PUB-384] 19 p2654 N90-25103
The human factors of workstation telepresence 19 p2732 N90-25528
Listening to turbulence: An example of scientific audiolization
[DE90-010637] 19 p2753 N90-25646
VISTA (Vertical Integration of Science, Technology, and Applications) user interface software study
[DE90-010003] 20 p2936 N90-26707
A real-time optical 6D tracker for head-mounted display systems
[AD-A222884] 21 p3036 N90-27262
An application of design knowledge captured from multiple sources 21 p3045 N90-27306
A model for a space shuttle safing and failure-detection expert 21 p3046 N90-27314
A structure for maturing intelligent tutoring system student models 21 p3047 N90-27320
Intelligent tutoring systems for space applications 21 p3048 N90-27324
Artificial intelligence techniques for modeling database user behavior 21 p3049 N90-27330
On the structure of a future flight operations system 22 p3113 N90-27682
Four-dimensional planner: A ground based planning system for time accurate approach guidance 22 p3113 N90-27683
Development of a COMPAS prototype for the ATC Centre at Frankfurt (Fed. Republic of Germany) 22 p3113 N90-27684
Criteria for device selection: A comparison between a mouse and a touchscreen as an input device for interactive video
[NPL-DITC-158/90] 22 p3235 N90-28344
Development of a methodology for icon evaluation
[NPL-DITC-159/90] 22 p3235 N90-28345
Building a user interface using SQL*Forms and an intermediate table
[DE90-012729] 22 p3259 N90-28455
Providing dynamic sorting and searching capabilities using SQL*Forms
[DE90-012735] 22 p3259 N90-28456
A user modelling approach for computer-based critiquing
[AD-A224042] 23 p3379 N90-29088
Graphic interface for attribute-based data language queries from a personal computer to the multi-lingual, multi-model, multi-backend database system over an Ethernet network
[AD-A223738] 24 p3528 N90-29948
Unstructured mesh relaxation
[DE90-015614] 24 p3534 N90-29989

MANAGEMENT
NT CONFIGURATION MANAGEMENT
NT CONTRACT MANAGEMENT
NT DATA MANAGEMENT
NT ENGINEERING MANAGEMENT
NT ENVIRONMENT MANAGEMENT
NT FINANCIAL MANAGEMENT
NT FOREST MANAGEMENT
NT INDUSTRIAL MANAGEMENT
NT INFORMATION MANAGEMENT
NT INVENTORY MANAGEMENT
NT LAND MANAGEMENT
NT LOGISTICS MANAGEMENT
NT PERSONNEL MANAGEMENT
NT PROCUREMENT MANAGEMENT
NT PRODUCTION MANAGEMENT
NT PROJECT MANAGEMENT
NT RECORDS MANAGEMENT
NT REFORESTATION
NT RESEARCH MANAGEMENT
NT RESOURCES MANAGEMENT
NT SAFETY MANAGEMENT
NT SYSTEMS MANAGEMENT
NT WATER MANAGEMENT
Technical communications in aeronautics: Results of an exploratory study. An analysis of managers' and nonmanagers' responses
[NASA-TM-101625] 02 p0288 N90-11647
Base level management of radio frequency radiation protection program
[AD-A211759] 04 p0523 N90-13017
Invention and innovation: Alternative mechanisms for enhancing organizational competitiveness
[DE89-015858] 08 p1136 N90-16584
Preliminary fire extinguishing tests with handheld bottles: A comparison of extinguishing compounds
[DOT/FAA/CT-TN89/60] 10 p1368 N90-17930
Object orientated simulation on transputer arrays using time warp
[AD-A219795] 17 p2389 N90-23607
Management: A bibliography for NASA managers
[NASA-SP-7500(24)] 17 p2479 N90-24174
Airport capacity enhancement plan 1989
[PB90-197997] 23 p3270 N90-28507
Total quality management: A recipe for success
[AD-A223287] 24 p3556 N90-30122

MANAGEMENT ANALYSIS
A guide to reasoning under uncertainty
[REPT-72/87/R486U] 05 p0675 N90-13932
America's shuttle returns to space 09 p1174 N90-16792
Middle management of research
[NASA-TM-102417] 13 p1899 N90-20901
The design of a local area network configuration management system for the Naval Postgraduate School Administrative Sciences Department
[AD-A219643] 17 p2451 N90-23979

MANAGEMENT INFORMATION SYSTEMS
The Hipparcos Mission. Prelaunch status. Volume 2: The input catalog
[ESA-SP-1111-VOL-2] 05 p0606 N90-13529
Project ORION microcomputer management system
[AD-A212945] 05 p0680 N90-13959
Management control and status reports documentation standard and Data Item Descriptions (DID). Volume of the information system life-cycle and documentation standards, volume 5
[NASA-TM-101860] 05 p0706 N90-14139
GRAFIN: GRAFIX interactive manual
[PB89-232136] 06 p0827 N90-14809
A dynamic systems engineering methodology research study. Phase 2: Evaluating methodologies, tools, and techniques for applicability to NASA's systems projects
[NASA-CR-181319] 06 p0857 N90-14985
Validity of empirical studies of information system effectiveness
[AD-A214474] 09 p1295 N90-17507
Definition of a management information system to support performance risk assessment
[AD-A215464] 09 p1297 N90-17516
Integrated IMA (Information Mission Areas) IC (Information Center) guide
[AD-A216944] 11 p1547 N90-18903
Defense Technical Information Center Executive Information System: Documentation and user's manual
[AD-A216235] 11 p1575 N90-19065
An empirical test of a comprehensive model for predicting successful information systems implementation
[AD-A218124] 13 p1900 N90-20908
Knowledge-based semantic query processing: An optimal transformation approach 15 p2176 N90-22437
The design of a local area network configuration management system for the Naval Postgraduate School Administrative Sciences Department
[AD-A219643] 17 p2451 N90-23979
Symbolic reasoning in model-based diagnosis: Efficient and effective information processing
[MEMO-INF-89-03] 17 p2452 N90-23984
NASA project status reports: Congressional requirements can be met, but reliability must be ensured
[GAO/NSIAD-90-40] 20 p2843 N90-26169
The value of real experience
[PNR90619] 20 p2934 N90-26696
Prototyping an in-house business intelligence database
[PNR90665] 20 p2937 N90-26709
Computer support for conducting supportability trade-offs in a team setting
[AD-A222002] 22 p3237 N90-28355
Optical storage technology
[AD-A224028] 23 p3407 N90-29254

MANAGEMENT METHODS
NT DELPHI METHOD (FORECASTING)
NT PROFILE METHOD (FORECASTING)
The Air Force Flight Test Center Flight Test Safety Program 02 p0153 N90-10872
Issues in NASA program and project management
[NASA-SP-6101(02)] 04 p0562 N90-13277
Space Station Engineering Design Issues
[NASA-CR-185978] 05 p0601 N90-13492
Management control and status reports documentation standard and Data Item Descriptions (DID). Volume of the information system life-cycle and documentation standards, volume 5
[NASA-TM-101860] 05 p0706 N90-14139
How far can the world get on energy efficiency alone
[DE90-001349] 06 p0805 N90-14686
DOCTORD Database System user's guide, June 1989: dBase 3 PLUS Physician/(Part B Medicare): Personal computer reference system and user's guide
[PB90-100181] 07 p0966 N90-15579
Guidelines for evaluating energy analysis software
[AD-A214171] 07 p0976 N90-15640
Discrete event simulation tool for analysis of qualitative models of continuous processing systems
[NASA-CASE-MSC-21465-1] 08 p1107 N90-16410
International conference management 08 p1136 N90-16583
FY 1989 update to the Information Resources Management review plan
[DE90-004185] 08 p1138 N90-16593
R/M/T (Reliability, Maintainability, and Testability) design for fault tolerance, technical manager's design implementation guide
[AD-A215531] 09 p1234 N90-17164
Supporting tools of solar-terrestrial science 10 p1444 N90-18331
Integrated IMA (Information Mission Areas) IC (Information Center) guide
[AD-A216944] 11 p1547 N90-18903
On optimal distributed decision architectures in a hypothesis testing environment
[AD-A217824] 13 p1790 N90-20274
Current management for improved railgun performance 15 p2057 N90-21781
Electronic publishing with Standard Generalized Markup Language (SGML) 15 p2179 N90-22450
Information technology applications: A British Aerospace Military Aircraft Ltd view 15 p2180 N90-22455
Sensor performance analysis
[NASA-RP-1241] 17 p2418 N90-23780

Northeast Artificial Intelligence Consortium. Volume 4. Distributed AI for communications network management
[AD-A218717] 17 p2453 N90-23994
Management: A bibliography for NASA managers
[NASA-SP-7500(24)] 17 p2479 N90-24174
Recent experiences and future expectations in data storage technology
[DE90-011488] 18 p2589 N90-24729
The basis system
[DE90-012077] 19 p2743 N90-25591
The value of real experience
[PNR90619] 20 p2934 N90-26696
The composite load spectra project
21 p3047 N90-27323
Assessment and demonstration of the capabilities of NDI processes, equipment, and personnel
22 p3184 N90-28071
Towards a future cockpit: The prototyping and pilot integration of the Mission Management Aid (MMA)
23 p3358 N90-28979
Information management directions: The integration challenge
[PB90-219866] 23 p3405 N90-29245
Transferring building energy technologies by linking government and private-sector programs
[DE90-000346] 23 p3408 N90-29258
AutoPAVER: A software package for automated pavement evaluation
[AD-A224176] 24 p3458 N90-29531

MANAGEMENT PLANNING
NT PRODUCTION PLANNING
NT PROJECT PLANNING
Structure flow diagram generator
[PB89-195978] 01 p0104 N90-10592
Preference propagation in temporal/capacity constraint graphs
[AD-A210668] 02 p0264 N90-11506
Development and evaluation at ATCEU of executive and support operations, phase 4A/3D — ATCEU (Air Traffic Control Evaluation Unit)
[CAA-PAPER-88017] 04 p0449 N90-12572
The interface with the data reduction consortia
05 p0606 N90-13528
Long-range plan for management and use of the radio spectrum by agencies and establishments of the Federal Government
[PB89-232367] 05 p0633 N90-13693
Project ORION microcomputer management system
[AD-A212945] 05 p0680 N90-13959
Total quality management implementation strategy: Directorate of Quality Assurance
[AD-A212863] 05 p0705 N90-14127
Total quality management plan: Technical and logistics services
[AD-A212864] 05 p0705 N90-14128
Total quality management implementing plan: Office of small and disadvantaged business utilization
[AD-A212865] 05 p0705 N90-14129
Total quality management plan: Office of Congressional Affairs
[AD-A212866] 05 p0705 N90-14130
Total quality management: Directorate of Contract Management master plan
[AD-A212867] 05 p0705 N90-14131
Total quality management plan: Office of Public Affairs
[AD-A212868] 05 p0705 N90-14132
Program manager's handbook
[AD-A214338] 07 p1009 N90-15844
International conference management
08 p1136 N90-16583
US Space Shuttle evolution 09 p1178 N90-16829
Toward an electrical power utility for space exploration
10 p1329 N90-17681
The Hermes fuel cell power plant
10 p1333 N90-17706
National airspace system plan: Facilities, equipment, associated development and other capital needs
[AD-A215882] 11 p1453 N90-18373
The Pathfinder chemical transfer propulsion program
11 p1471 N90-18471
An integrative research review of the relationship between technology and structure: A meta-analytic synthesis
[AD-A218115] 13 p1899 N90-20903
Quality at a glance
[AD-A217297] 14 p1989 N90-21400
Software Management Environment (SME) concepts and architecture
[NASA-TM-103306] 14 p2014 N90-21543
Management: A bibliography for NASA managers
[NASA-SP-7500(24)] 17 p2479 N90-24174
Agenda toward the development of a rational noise descriptor system relevant to human annoyance by en route aircraft noise 18 p2610 N90-24866
GSC configuration management plan
[NASA-CR-182044] 19 p2743 N90-25587
Making it happen: Project management
[PNR90618] 20 p2934 N90-26695
The value of real experience
[PNR90619] 20 p2934 N90-26696
Agent independent task planning
21 p3040 N90-27276
Study of the feasibility of several mixtures
[IMAG-RR-776-M] 21 p3057 N90-27379
Flight service automation system, model 1 full capacity, NAS operational test and evaluation integration test plan
[DOT/FAA/CT-TN90/4] 22 p3111 N90-27672
Aerial videotape survey of coastal Louisiana, 1986. Louisiana Barrier Island erosion and land loss study: 1986-1990
[PB90-194648] 22 p3195 N90-28128
Grasp planning under uncertainty
23 p3370 N90-29041
The effects of management support on the successful implementation of group decision support systems
[AD-A224473] 23 p3404 N90-29241
International aircraft operator data base master requirements and implementation plan
[DOT/FAA/CT-90/17] 23 p3405 N90-29247
AutoPAVER: A software package for automated pavement evaluation
[AD-A224176] 24 p3458 N90-29531
Total quality management: A recipe for success
[AD-A223287] 24 p3556 N90-30122

MANAGEMENT SYSTEMS
NT FLIGHT MANAGEMENT SYSTEMS
NT MANAGEMENT INFORMATION SYSTEMS
Preference propagation in temporal/capacity constraint graphs
[AD-A210668] 02 p0264 N90-11506
Artificial intelligence for communication prospects
[FEL-1989-1] 04 p0537 N90-13107
Level 2 software reuse study
06 p0826 N90-14800
An SSE approach to reusability
06 p0826 N90-14801
Mathematical modelling and expert system for battery management 10 p1332 N90-17703
Superfluid helium orbital resupply coupling
11 p1475 N90-18488
Information management systems for integrating the technical data and regulatory requirements of environmental restoration activities
[DE90-008622] 13 p1831 N90-20511
Detection of potential space station control/structure interaction with CO-ST-IN 14 p1935 N90-21074
Integrating automated support for a software management cycle into the TAME system
[NASA-CR-186457] 14 p2013 N90-21532
Automated electric power management and control for Space Station Freedom
[NASA-TM-103151] 16 p2304 N90-23125
Health management system for rocket engines
[NASA-CR-185223] 17 p2383 N90-23574
The design of a local area network configuration management system for the Naval Postgraduate School Administrative Sciences Department
[AD-A219643] 17 p2451 N90-23979
OMS FDIR: Initial prototyping
19 p2738 N90-25562
Making real-time reactive systems reliable
[NASA-CR-186642] 20 p2873 N90-26344
OMNI development of an engineering product data management system
[DE90-002407] 21 p3086 N90-27550
Real-time adaptive aircraft scheduling
[NASA-CR-177558] 22 p3110 N90-27669
The effects of management support on the successful implementation of group decision support systems
[AD-A224473] 23 p3404 N90-29241
Automated information system life-cycle management manual
[PB90-219288] 23 p3405 N90-29244
Sounder update and field strength software modifications for Special Operations Radio Frequency Management System (SORFMS). Volume 1: Program descriptions and testing
[AD-A224510] 24 p3460 N90-29543

MANATEES
Summary of 1987 and 1988 manatee aerial surveys at Kennedy Space Center
[NASA-TM-102783] 06 p0802 N90-14689

MANDRELS
Calculations of braiding parameters
[AD-A216836] 11 p1479 N90-18515
Axisymmetric and cylindrically orthotropic analysis of filament winding 16 p2246 N90-22811

MANEUVERABILITY
Vortex induced characteristics of missiles in unsteady maneuvers 01 p0012 N90-10057
Winged versus wingless airframes
01 p0015 N90-10073
Centralized and decentralized Kalman filter techniques for tracking, navigation, and control
[AD-A214245] 07 p0878 N90-15091
High performance missiles of the future
10 p1305 N90-17550
Possible piloting techniques at hypersonic speeds
[ISL-CO-216/88] 11 p1456 N90-18392
Discrete proportional Plus Integral (PI) multivariable control laws for the Control Reconfigurable Combat Aircraft (CRCA)
[AD-A215664] 11 p1464 N90-18431
Design of a new control system for hovercrafts
[ETN-90-96230] 11 p1465 N90-18435
Nonlinear continuum mechanics and applied analysis
[AD-A213629] 12 p1709 N90-19812
OMV (Orbital Maneuvering Vehicle) payload support concept for Pegasus boosted payloads
[AD-A218371] 17 p2365 N90-23463
Studies in non-linear unsteady aerodynamics
[AD-A221228] 19 p2654 N90-25108
Identification of aerodynamic models for maneuvering aircraft
[NASA-CR-186630] 20 p2802 N90-25943
Combat aircraft control requirements for agility
23 p3272 N90-28517
Analysis of dynamic transient response and postflutter behavior of super-maneuvering airplane
[AD-A224126] 24 p3432 N90-29386
Fighter agility metrics
[NASA-CR-187289] 24 p3432 N90-29389

MANEUVERABLE REENTRY BODIES
NT LIFTING REENTRY VEHICLES
Singular perturbation analysis of AOTV-related trajectory optimization problems
[NASA-CR-186202] 08 p1027 N90-15936
Generating optimally evasive MaRV trajectories
[DE90-004496] 10 p1328 N90-17671

MANEUVERABLE SPACECRAFT
NT AEROSPACE PLANES
NT ASTRO VEHICLE
NT FERRY SPACECRAFT
NT HOTOL LAUNCH VEHICLE
Project Argo: The design and analysis of an all-propulsive and an aeroassisted version of a manned space transportation vehicle
[NASA-CR-186047] 06 p0732 N90-14266
Cooperative control of two active spacecraft during proximity operations
[NASA-CR-185596] 09 p1172 N90-16778

MANEUVERS
NT AIRCRAFT MANEUVERS
NT EVASIVE ACTIONS
NT HOVERING
NT ORBITAL MANEUVERS
NT ORBITAL RENDEZVOUS
NT SIDESLIP
NT SPACECRAFT DOCKING
NT SPACECRAFT MANEUVERS
Passive trajectography by azimuth: Improvement of estimation quality 02 p0150 N90-10854
Guidance and control considerations for a maneuvering aerial target system 09 p1165 N90-16746
Dynamic interactions and globally optimal maneuver of distributed systems 09 p1236 N90-17172
High performance missiles of the future
10 p1305 N90-17550
The use of lateral jet control at Aerospatiale
10 p1305 N90-17551
VLA missile development and high angle of attack behavior 10 p1305 N90-17553
Suboptimal period design for a maneuvering missile to evade tracking filters 12 p1650 N90-19479
Potential role of avionics in escape systems
13 p1752 N90-20060
Optimal and near-optimal medium range air-to-air missile guidance against maneuvering targets
15 p2053 N90-21766
Nonlinear spline operator interpolation and sliding control of deformable maneuvering bodies
15 p2074 N90-21878
Sliding control of pointing and tracking with operator spline estimation 16 p2281 N90-22997
Identification of aerodynamic models for maneuvering aircraft
[NASA-CR-186630] 20 p2802 N90-25943
Maneuvering by means of lateral jets
[ISL-CO-255/88] 20 p2814 N90-26015

MANGANESE
NT MANGANESE ISOTOPES
Influence of the composition of the metal deposited on carbon manganese welds on the work properties of the melted area depending on the operating mode of the weld
[CETIM-104530] 04 p0476 N90-12726

Strain induced amorphization of aluminium by manganese implantation
[DE90-607259] 10 p1356 N90-17863
Ligand-centered electron-transfer redox processes for manganese, iron, and cobalt complexes in relation to selected catalytic systems
[AD-A217957] 13 p1773 N90-20177
The effect of manganese on the onset of the stage 2 reaction in an austempered ductile iron matrix
[DE90-011804] 20 p2834 N90-26119

MANGANESE ALLOYS
NT MANGANIN (TRADEMARK)
An investigation of the sensitization behavior of Fe-Mn-Cr austenitic steels
[DE90-002719] 07 p0904 N90-15226
Phase stability of a manganese-stabilized low-activation martensitic steel
[DE90-004114] 09 p1193 N90-16914
Effect of manganese additions on the physical and superconducting properties of Nb-46.5Ti
[DE90-005393] 10 p1436 N90-18290
Low temperature specific heat and magnetic susceptibility of NbTi and NbTiMn alloys
[DE90-005390] 11 p1486 N90-18552

MANGANESE COMPOUNDS
NT MANGANESE OXIDES

MANGANESE ISOTOPES
Cosmic ray half life of (54)Mn
[DE90-000134] 07 p1016 N90-15880

MANGANESE OXIDES
Sintering studies on high field varistors
[DE90-002626] 07 p0926 N90-15359

MANGANESE 53
U MANGANESE ISOTOPES

MANGANESE 54
U MANGANESE ISOTOPES

MANGANESE 56
U MANGANESE ISOTOPES

MANGANIN (TRADEMARK)
A review of manganin gauge technology for measurements in the gigapascal range
[MRL-TR-90-5] 24 p3541 N90-30026

MANIFOLDS
Extended temperature range rocket injector
[NASA-CASE-LEW-14846-1] 07 p0887 N90-15130
LOX manifold tee analysis
[NASA-CR-183994] 19 p2670 N90-25188
Development of advanced combustion technology for medium and high speed natural gas engines
[PB90-198565] 23 p3331 N90-28836

MANIFOLDS (MATHEMATICS)
NT RIEMANN MANIFOLD
Finding isolated zero points of complex polynomial mappings
[DE89-617523] 01 p0111 N90-10633
Local structure of a 2-codimensional conformally flat submanifold in an Euclidean space R(sup n+2)
[DE89-618379] 02 p0264 N90-11501
Analytic manifolds in uniform algebras
[DE89-618384] 02 p0264 N90-11505
Some notes on perturbations of differential-algebraic equations
[PB89-218564] 03 p0393 N90-12243
Global linear representations of nonlinear systems and the adjoint map
[RR-347] 03 p0394 N90-12247
Chern-Simons theories of symplectic super-diffeomorphisms
[DE89-635700] 07 p0987 N90-15703
Stochastic action of dynamical systems on curved manifolds. The isokinetic developing map on trajectories
[PREPRINT-666] 08 p1117 N90-16466
Dynamics of a class of vortex rings
[NASA-TM-102257] 12 p1657 N90-19524
The monad construction and Hermetian-Einstein metrics
[DE90-612738] 14 p2019 N90-21573
On a non classical oblique derivative problem for parabolic singular integro-differential operators
[DE90-612739] 14 p2020 N90-21574
Linking numbers and variational method
[DE90-612793] 14 p2020 N90-21582
Theoretical and computational aspects of turbulence
[AD-A221795] 21 p3005 N90-27083
The structure of random discrete spacetime
[NASA-CR-182841] 22 p3255 N90-28429
On Einsteinian 4-submanifolds in E(sup 6)
[DE90-627149] 23 p3402 N90-29226
On equations of motion on complex Grassman manifold
[DE90-628369] 24 p3537 N90-29999

MANIPULATION
U MANIPULATORS

MANIPULATORS
NT REMOTE MANIPULATOR SYSTEM
Simulation and control problems in elastic robots
01 p0020 N90-10098
Flexible robot control: Modeling and experiments
01 p0021 N90-10104
Experimental validation of flexible robot arm modeling and control
01 p0023 N90-10113
Shape control of high degree-of-freedom variable geometry trusses
01 p0024 N90-10122
Autonomous mobile robot research using the HERMIES-3 robot
[DE89-015916] 01 p0078 N90-10443
Interchangeable end effector tools utilized on the protoflight manipulator arm
[NASA-CR-179374] 01 p0078 N90-10447
Optimized resolved rate control of seven-degree-of-freedom Laboratory Telerobotic Manipulator (LTM) with application to three-dimensional graphics simulation
[NASA-TP-2938] 01 p0109 N90-10618
Independent Orbiter Assessment (IOA): Assessment of the EPD and C/remote manipulator system FMEA/CIL
[NASA-CR-185583] 02 p0172 N90-10965
Modeling and simulation of spatial robotic manipulators with flexible links and joint drives for control strategies implementation and evaluation 02 p0228 N90-11311
Rethinking synthesis of fine-motion strategies
[DE89-016671] 02 p0230 N90-11322
Telescience Testbed Pilot Program
[NASA-CR-184594] 02 p0257 N90-11455
Magnetically levitated micro-robotics
02 p0270 N90-11542
A distributed pipelined architecture of the recursive Lagrangian equations of motion for robot manipulators with VLSI implementation --- VLSI (very large scale integration)
[RR-353] 03 p0344 N90-11966
An optimum trajectory planner for robot manipulators in joint-space and under physical constraints
[RR-349] 03 p0355 N90-12029
On the complexity analysis of the coriolis and centripetal effects of a 6 DOF robot manipulator --- Degrees of Freedom (DOF)
[RR-344] 03 p0355 N90-12030
The dynamic performance of robot manipulators under different operating conditions
[RR-345] 03 p0355 N90-12031
Navigation of robotic systems
[DE89-017507] 03 p0390 N90-12219
Fast forward dynamics algorithm for robot arms using multiprocessing
[RR-367] 03 p0391 N90-12225
Kinematics, special configurations and performance evaluation of serial manipulators
04 p0508 N90-12927
Acceleration sets of planar manipulators. Part 1: Theory
[AD-A213162] 04 p0510 N90-12945
Visual perception processing in a hierarchical control system: Level 1
[PB89-221188] 04 p0536 N90-13101
Identification of robot dynamics: A parallel processing approach
[RR-361] 04 p0537 N90-13103
Real-time robot motion: The VLSI implementation via transputers
[RR-364] 04 p0537 N90-13104
Assembly considerations for large reflectors
05 p0599 N90-13480
Adaptive strategies for controls of flexible arms
[NASA-CR-185868] 05 p0649 N90-13783
Design and control of a two-degree-of-freedom lightweight flexible arm
[AD-A213335] 05 p0650 N90-13790
Acceleration sets of planar manipulators. Part 2: Applications and experiments
[AD-A213336] 05 p0650 N90-13791
Definition, determination and characterization of acceleration sets for spatial manipulators
[AD-A213366] 05 p0651 N90-13793
Performance evaluation of a six-axis generalized force-reflecting teleoperator
[NASA-CR-186106] 05 p0651 N90-13796
On control of manipulators
[ISBN-90-9002789-0] 05 p0652 N90-13804
Manipulation strategies for massive space payloads
[NASA-CR-186081] 06 p0728 N90-14247
Controller design for a robotic manipulator
06 p0792 N90-14615
Results of the manipulator test test stand study: Comparison of manipulators and evaluation of equipment items
[DE90-000977] 06 p0794 N90-14625
French technological progress in the field of robotics and teleoperation
[DE90-001590] 06 p0794 N90-14626
Control of mechanical manipulators
07 p0938 N90-15432
On the analysis and optimization of a platform manipulator 07 p0938 N90-15433
New approach to the inverse problem of six-link manipulators via the optimization technique
[DE90-710044] 07 p0940 N90-15441
Base reaction optimization of redundant manipulators for space applications
[NASA-CR-186274] 07 p0941 N90-15447
Spatial dynamics of deformable multibody systems with variable kinematic structure
[AD-A214098] 07 p0942 N90-15455
Feasibility study of using industrial robot for ultrasound testing
[DE90-002977] 07 p0943 N90-15461
Bilateral force reflection for teleoperators with masters and slaves with dissimilar and possibly redundant kinematics
[DE90-004392] 08 p1061 N90-16132
On-line estimation of mechanical nonlinearities in compliant two-link robot manipulators
08 p1085 N90-16280
Examples of robots and teleoperators at the Savannah River Site
[DE90-004659] 08 p1086 N90-16284
Mathematical model for adaptive control system of ASEA robot at Kennedy Space Center
08 p1157 N90-16701
Dynamic modeling of flexible bodies in multibody systems 09 p1229 N90-17134
Applications of a fingertip sensor for the Salisbury robot hand
[DE90-005002] 09 p1231 N90-17142
Classification and simulation of single and multi-degree-of-freedom motions
[AD-A214925] 09 p1231 N90-17143
Multiple model adaptive estimation techniques for adaptive model-based robot control
[AD-A215742] 09 p1231 N90-17146
Payload invariant control via neural networks: Development and experimental evaluation
[AD-A215740] 09 p1260 N90-17306
A vision system for robotic inspection and manipulation
[DE90-005412] 09 p1283 N90-17440
Pareto optimization design techniques for the AFIT (Air Force Institute of Technology)/AAMRL (Armstrong Aeronautical Medical Research Laboratory) anthropomorphic robotic manipulator
[AD-A216178] 10 p1414 N90-18150
On the kinematic behavior of robots while executing general robot level commands
[PB90-120965] 11 p1517 N90-18735
Preliminary design of a pointer for movement of a solar simulator
[INPE-4864-TDL/375] 11 p1517 N90-18736
Teleoperator servoloop tuning using an expert system
[DE90-005674] 11 p1542 N90-18876
Architecture for a human-robot symbiotic system
[DE90-005670] 11 p1550 N90-18921
Kinematic control of robotic manipulators with multiple interchangeable wrists 12 p1670 N90-19592
Experiments in end-point control of a flexible robot with a mini-manipulator 12 p1671 N90-19596
Dynamics and control of robot manipulators with closed-kinematic chain mechanism
12 p1671 N90-19598
Advanced control schemes and kinematic analysis for a kinematically redundant 7 DOF manipulator
[NASA-CR-186175] 12 p1671 N90-19599
A complete description of robot manipulator dynamics based on Lagrangian mechanics
[DE90-741467] 12 p1672 N90-19603
Multi-dimensional LADAR tracking and adaptive grasping for spaceborne assembly of SDI (Strategic Defense Initiative) platforms
[AD-A218236] 13 p1791 N90-20279
The CMU Reconfigurable Modular Manipulator System
[CMU-RI-TR-88-7] 13 p1809 N90-20388
Development of a passive robot-controlled reaction arm 13 p1809 N90-20389
Resolved motion rate and resolved acceleration servo-control of wheeled mobile robots
[DE90-002585] 13 p1811 N90-20399
Knowledge-based robotic grasping
[DE90-007216] 13 p1811 N90-20402
Dynamic damping control: Implementation issues and simulation results
[DE90-007687] 13 p1812 N90-20403
Design of a telerobotic controller with joint torque sensors
[DE90-008753] 13 p1812 N90-20404
Control system design of the third flexible joint of PUMA 560 robot
[AD-A218075] 13 p1812 N90-20405

Gripping device
[NASA-CASE-MSC-21365-1] 13 p1812 N90-20408
Graphical programming and the use of simulation for space-based manipulators 13 p1861 N90-20674
Using an instrumented manikin for Space Station Freedom analysis 13 p1861 N90-20675
Boundary equations of configuration obstacles for manipulators
[DE90-002101] 13 p1874 N90-20745
Modeling elastomer displacements for tactile sensing applications
[DE90-007959] 14 p1984 N90-21370
End point control of flexible manipulators
[AD-A217319] 14 p1986 N90-21383
Development of a dynamic modeling technique and its application to the analysis and control of a high-precision robotic manipulator 14 p1987 N90-21391
Application of optimization in design and motion control of robot manipulators 14 p1988 N90-21393
The development of computational algorithms for manipulator inverse kinematics
[DE90-759877] 14 p2017 N90-21561
Nonlinear stability analysis and control of dynamical robotic systems 15 p2104 N90-22037
The Shock and Vibration Digest, volume 21, no. 3 15 p2109 N90-22064
Development of a multipurpose hand controller for JEMRMS 15 p2113 N90-22087
The resupply interface mechanism RMS compatibility test 15 p2113 N90-22090
Vision science and technology for supervised intelligent space robots 15 p2139 N90-22221
Instrumentation and robotic image processing using top-down model control 15 p2142 N90-22239
Adaptive control of a flexible manipulator with unknown changing loads 15 p2152 N90-22293
The JPL/KSC telerobotic inspection demonstration 15 p2155 N90-22312
Visual enhancements in pick-and-place tasks: Human operators controlling a simulated cylindrical manipulator 16 p2271 N90-22946
Displays for telemanipulation 16 p2272 N90-22948
Recursive linearization of multibody dynamics equations of motion 16 p2280 N90-22993
An innovations approach to decoupling of multibody dynamics and control 16 p2280 N90-22994
A robot arm simulation with a shared memory multiprocessor machine 16 p2283 N90-23008
Parallel algorithms and architecture for computation of manipulator forward dynamics 16 p2283 N90-23010
Development of efficient computer program for dynamic simulation of telerobotic manipulation 16 p2284 N90-23017
Experimental verification of dynamic simulation 16 p2285 N90-23020
Approximate minimum-time trajectories for 2-link flexible manipulators 16 p2287 N90-23030
An inverse kinematics algorithm for a highly redundant variable-geometry-truss manipulator 16 p2288 N90-23033
Determination of joint drives for stable end-effector motion in flexible robotic systems 16 p2288 N90-23034
Parallel conjugate gradient algorithms for manipulator dynamic simulation 16 p2290 N90-23045
Man-in-the-control-loop simulation of manipulators 16 p2293 N90-23063
Control of randomly sampled robotic systems
[AD-A218948] 16 p2309 N90-23157
Adaptive control methods for mechanical manipulators: A comparative study
[AD-A219965] 17 p2413 N90-23749
HERA and EVA co-operation scenarios 18 p2502 N90-24299
HERA teleoperation test facility 18 p2503 N90-24303
A flexible teleoperation test bed for human factors experimentation 18 p2503 N90-24304
Experiences with and error handling in a knowledge base assisted system for payload experiment automation 18 p2504 N90-24306
Robotic simulation support to systems development 18 p2505 N90-24315
Equivalent flexibility modeling: A novel approach towards recursive simulation of flexible spacecraft manipulator dynamics 18 p2505 N90-24316
ROSED: Robotic Servicing Demonstrator 18 p2505 N90-24318
The real-time Hermes robot arm simulator: HSF-P 18 p2506 N90-24319
Collision detection using linear programming 18 p2507 N90-24326
The Hermes robot arm: System description 18 p2507 N90-24327
NASA/GSFC split-rail parallel gripper 18 p2507 N90-24328
Dynamics and control of free-flying inspection and maintenance vehicle with manipulators 18 p2508 N90-24332
Supervisory controlled telemanipulation and vision systems for inspection and maintenance operations 18 p2508 N90-24333
Flexible test bed for space telepresence and telemanipulation research 18 p2508 N90-24334
A compact joint for the ROTEX manipulator 18 p2536 N90-24467
Self-contained robotic arm manipulator
[NASA-CR-184925] 19 p2696 N90-25342
Out-reach in-space technology experiments program: Control of flexible robot manipulators in zero gravity, experiment definition phase
[NASA-CR-183849] 19 p2696 N90-25343
A global approach for using kinematic redundancy to minimize base reactions of manipulators
[NASA-CR-186825] 19 p2725 N90-25499
Third Annual Workshop on Space Operations Automation and Robotics (SOAR 1989)
[NASA-CP-3059] 19 p2727 N90-25503
Telepresence and Space Station Freedom workstation operations 19 p2731 N90-25527
The Flight Telerobotic Servicer (FTS) NASA's first operational robotic system 19 p2733 N90-25537
The telerobot testbed: An architecture for remote servicing 19 p2734 N90-25538
A task control architecture for autonomous robots 19 p2735 N90-25546
Impact of end effector technology on telemanipulation performance 19 p2736 N90-25549
Numerical approach of collision avoidance and optimal control on robotic manipulators 19 p2736 N90-25552
Technology for an intelligent, free-flying robot for crew and equipment retrieval in space 19 p2738 N90-25564
A laboratory breadboard system for dual-arm teleoperation 19 p2740 N90-25573
Adaptive tracking for complex systems using reduced-order models
[NASA-CR-183464] 19 p2747 N90-25609
Trajectory planning and control of a 6 DOF manipulator with Stewart platform-based mechanism
[NASA-CR-186813] 19 p2747 N90-25610
A parallel Newton-Euler formulation for fast dynamic simulation of robot manipulators
[RR-368] 19 p2748 N90-25614
Adaptive robot control using artificial neural networks: An application in the theory of cognition
[RR-374] 19 p2748 N90-25618
Control strategy for cooperating disparate manipulators
[NASA-CR-186809] 20 p2870 N90-26328
An inverse dynamic method yielding flexible manipulator state trajectories
[NASA-CR-186807] 20 p2870 N90-26329
Space station definitions, design, and development. Task 5: Multiple arm telerobot coordination and control: Manipulator design methodology
[NASA-CR-182043] 20 p2914 N90-26577
Position control of redundant manipulators using an adaptive error-based control scheme
[NASA-CR-186812] 20 p2914 N90-26578
Beam rider for an Articulated Robot Manipulator (ARM) accurate positioning of long flexible manipulators
[NASA-CR-185151] 20 p2914 N90-26581
Method and apparatus for configuration control of redundant robots
[NASA-CASE-NPO-17801-1-CU] 21 p3010 N90-27110
Agent independent task planning 21 p3040 N90-27276
Simulation-based intelligent robotic agent for Space Station Freedom 21 p3043 N90-27298
A vision-based telerobotic control station 21 p3046 N90-27311
Resolution of seven-axis manipulator redundancy: A heuristic issue 21 p3049 N90-27331
Robot dynamics in reduced gravity environment 21 p3049 N90-27333
Development, implementation, and validation of control algorithms for the dual-arm robotic manipulation of a single object
[AD-A222502] 21 p3060 N90-27402
Multiple arm manipulation
[PB90-199506] 22 p3182 N90-28056
Reaction-compensation technology for microgravity laboratory robots
[NASA-TM-103271] 22 p3183 N90-28062
Motion coordination for mobile robots in unstructured environments
[PB90-199498] 23 p3332 N90-28837
Motion coordination for a mobile manipulator system
[PB90-203076] 23 p3332 N90-28839
Dynamic modeling and payload-adaptation control of a flexible one-link manipulator 23 p3333 N90-28843
Experiments in the dynamic and strategic control of cooperating manipulators 23 p3333 N90-28845
Proceedings of the NASA Conference on Space Telerobotics, volume 1
[NASA-CR-186856] 23 p3362 N90-29000
A 17 degree of freedom anthropomorphic manipulator 23 p3362 N90-29001
A new approach to global control of redundant manipulators 23 p3363 N90-29002
Kinematic functions for the 7 DOF robotics research arm 23 p3363 N90-29003
Kinematics, controls, and path planning results for a redundant manipulator 23 p3363 N90-29005
A complete analytical solution for the inverse instantaneous kinematics of a spherical-revolute-spherical (7R) redundant manipulator 23 p3363 N90-29006
Development of a flexible test-bed for robotics, telemanipulation and servicing research 23 p3364 N90-29012
Modularity in robotic systems 23 p3365 N90-29014
Computational neural learning formalisms for manipulator inverse kinematics 23 p3368 N90-29030
Multi-layer neural networks for robot control 23 p3368 N90-29031
A neural network for controlling the configuration of frame structure with elastic members 23 p3368 N90-29034
Proceedings of the NASA Conference on Space Telerobotics, volume 2
[NASA-CR-186857] 23 p3370 N90-29044
Characterization and control of self-motions in redundant manipulators 23 p3370 N90-29045
Multiple cooperating manipulators: The case of kinematically redundant arms 23 p3371 N90-29046
Reflexive obstacle avoidance for kinematically-redundant manipulators 23 p3371 N90-29047
Preliminary study of a serial-parallel redundant manipulator 23 p3371 N90-29048
Design of a monitor and simulation terminal (master) for space station telerobotics and telescience 23 p3372 N90-29051
Performance evaluation of a 6 axis high fidelity generalized force reflecting teleoperator 23 p3372 N90-29052
Human machine interaction via the transfer of power and information signals 23 p3372 N90-29054
On the simulation of space based manipulators with contact 23 p3373 N90-29056
Preliminary results on noncollocated torque control of space robot actuators 23 p3373 N90-29057
Portable Dextrous Force Feedback Master for robot telemanipulation (PDMFF) 23 p3373 N90-29058
Experiences with the JPL telerobot testbed: Issues and insights 23 p3373 N90-29059
The KALI multi-arm robot programming and control environment 23 p3373 N90-29060
How do robots take two parts apart 23 p3374 N90-29061
HERMIES-3: A step toward autonomous mobility, manipulation, and perception 23 p3374 N90-29065
Robotic sampling system for an unmanned Mars mission 23 p3375 N90-29070
Efficient mapping algorithms for scheduling robot inverse dynamics computation on a multiprocessor system 23 p3375 N90-29071
Parallel algorithms for computation of the manipulator inertia matrix 23 p3376 N90-29072
Planning robot actions under position and shape uncertainty 23 p3376 N90-29073
A hardware/software environment to support R/D in intelligent machines and mobile robotic systems
[DE90-014458] 23 p3385 N90-29119
Quick-connect coupler for remote manipulation
[DE90-015352] 24 p3476 N90-29648
Robots, systems, and flexible automation
[DE90-015802] 24 p3476 N90-29649
Modeling, design, and control of flexible manipulator arms: Status and trends 24 p3500 N90-29782
Dynamical modeling of serial manipulators with flexible links and joints using the method of kinematic influence 24 p3500 N90-29783
Capture of free-flying payloads with flexible space manipulators 24 p3500 N90-29784
Technology and task parameters relating to the effectiveness of the bracing strategy 24 p3500 N90-29785
Manipulators with flexible links: A simple model and experiments 24 p3501 N90-29786

Experiments in identification and control of flexible-link manipulators 24 p3501 N90-29787
Autonomous dexterous end-effectors for space robotics 24 p3501 N90-29788
Traction-drive force transmission for telerobotic joints 24 p3501 N90-29790
Force/torque and tactile sensors for sensor-based manipulator control 24 p3501 N90-29791
Redundant sensorized arm+hand system for space telerobotized manipulation 24 p3502 N90-29792
Impedance hand controllers for increasing efficiency in teleoperations 24 p3502 N90-29793
Tele-autonomous systems: New methods for projecting and coordinating intelligent action at a distance 24 p3502 N90-29794
An advanced telerobotic system for shuttle payload changeout room processing applications 24 p3502 N90-29795
Robotic tele-existence 24 p3502 N90-29796
Redundancy of space manipulator on free-flying vehicle and its nonholonomic path planning 24 p3502 N90-29797
Telepresence system development for application to the control of remote robotic systems 24 p3503 N90-29799
The 3D model control of image processing 24 p3503 N90-29800
Use of 3D vision for fine robot motion 24 p3503 N90-29804
Telerobotic workstation design aid 24 p3504 N90-29805
Modeling and sensory feedback control for space manipulators 24 p3504 N90-29807
Autonomous sensor-based dual-arm satellite grappling 24 p3504 N90-29809
Stability analysis of multiple-robot control systems 24 p3505 N90-29811
Experiments in cooperative manipulation: A system perspective 24 p3505 N90-29812
On the manipulability of dual cooperative robots 24 p3505 N90-29813
Controlling multiple manipulators using RIPS 24 p3505 N90-29814
Research and development activities at the Goddard Space Flight Center for the flight telerobotic servicer project 24 p3507 N90-29824
The Goddard Space Flight Center (GSFC) robotics technology testbed 24 p3507 N90-29825
Proceedings of the NASA Conference on Space Telerobotics, volume 4 [NASA-CR-186859] 24 p3508 N90-29830
An improved adaptive control for repetitive motion of robots 24 p3508 N90-29831
Direct adaptive control of a PUMA 560 industrial robot 24 p3508 N90-29832
Model based manipulator control 24 p3509 N90-29833
Discrete-time adaptive control of robot manipulators 24 p3509 N90-29834
A discrete decentralized variable structure robotic controller 24 p3509 N90-29835
Construction and demonstration of a 9-string 6 DOF force reflecting joystick for telerobotics 24 p3509 N90-29836
The JAU-JPL anthropomorphic telerobot 24 p3509 N90-29838
Performance limitations of bilateral force reflection imposed by operator dynamic characteristics 24 p3510 N90-29840
Sensor-based fine telemanipulation for space robotics 24 p3510 N90-29841
ROTEX-TRIIFEX: Proposal for a joint FRG-USA telerobotic flight experiment 24 p3510 N90-29842
Test and training simulator for ground-based teleoperated in-orbit servicing 24 p3510 N90-29843
Concept synthesis of an equipment manipulation and transportation system EMATS 24 p3510 N90-29844
Force-reflective teleoperated system with shared and compliant control capabilities 24 p3510 N90-29845
Redundancy in sensors, control and planning of a robotic system for space telerobotics 24 p3511 N90-29847
How to push a block along a wall 24 p3511 N90-29848
The 3-D vision system integrated dexterous hand 24 p3511 N90-29850
Linear analysis of a force reflective teleoperator 24 p3513 N90-29856
Real-time cartesian force feedback control of a teleoperated robot 24 p3513 N90-29857
Assembly of objects with not fully predefined shapes 24 p3513 N90-29859
The effects of gear reduction on robot dynamics 24 p3513 N90-29861
Recursive Newton-Euler formulation of manipulator dynamics 24 p3513 N90-29862
Kinematic sensitivity of robot manipulators 24 p3513 N90-29863
Efficient conjugate gradient-algorithms for computation of the manipulator forward dynamics 24 p3514 N90-29864
Determining robot actions for tasks requiring sensor interaction 24 p3514 N90-29868
The laboratory telerobotic manipulator program 24 p3515 N90-29869
Robotic control of the seven-degree-of-freedom NASA laboratory telerobotic manipulator 24 p3515 N90-29870
The control of space manipulators subject to spacecraft attitude control saturation limits 24 p3515 N90-29871
Comparison of joint space versus task force load distribution optimization for a multiarm manipulator system 24 p3515 N90-29873
Proceedings of the NASA Conference on Space Telerobotics, volume 5 [NASA-CR-186860] 24 p3516 N90-29874
Telerobotic activities at Johnson Space Center 24 p3516 N90-29875
Application of recursive manipulator dynamics to hybrid software/hardware simulation 24 p3516 N90-29876
Kinematics and control algorithm development and simulation for a redundant two-arm robotic manipulator system 24 p3516 N90-29877
Inverse dynamics of a 3 degree of freedom spatial flexible manipulator 24 p3516 N90-29878
A control approach for robots with flexible links and rigid end-effectors 24 p3516 N90-29879
Multi-level manual and autonomous control superposition for intelligent telerobot 24 p3518 N90-29888
An alternative control structure for telerobotics 24 p3518 N90-29889
The JPL telerobotic Manipulator Control and Mechanization (MCM) subsystem 24 p3519 N90-29892
On discrete control of nonlinear systems with applications to robotics 24 p3519 N90-29893
A spatial operator algebra for manipulator modeling and control 24 p3519 N90-29894
Flight experiments in telerobotics-Orbiter middeck concept 24 p3519 N90-29895
Experimental study on two-dimensional free-flying robot satellite model 24 p3519 N90-29896
The astronaut and the banana peel: An EVA retriever scenario 24 p3519 N90-29897
Computed torque control of a free-flying cooperat ing-arm robot 24 p3520 N90-29898
Computer simulation and design of a three degree-of-freedom shoulder module 24 p3520 N90-29902
A collision avoidance system for a spaceplane manipulator arm 24 p3521 N90-29903
A comparison of the Shuttle remote manipulator system and the Space Station Freedom mobile servicing center 24 p3522 N90-29910
An intelligent, free-flying robot 24 p3522 N90-29912

MANNED AERODYNAMIC REUSABLE SPACESHIP
U MARS (MANNED REUSABLE SPACECRAFT)

MANNED MANEUVERING UNITS
Independent Orbiter Assessment (IOA): Analysis of the manned maneuvering unit [NASA-CR-185565] 02 p0161 N90-10913
Independent Orbiter Assessment (IOA): Assessment of the manned maneuvering unit [NASA-CR-185564] 02 p0173 N90-10974
TALON and CRADLE: Systems for the rescue of tumbling spacecraft and astronauts, a preliminary design 09 p1181 N90-16847
Technology for an intelligent, free-flying robot for crew and equipment retrieval in space 19 p2738 N90-25564

MANNED MARS MISSIONS
Aerobraking characteristics for several potential manned Mars entry vehicles [NASA-TM-101669] 06 p0733 N90-14272
Preliminary investigation of parameter sensitivities for atmospheric entry and aerobraking at Mars [NASA-TM-101607] 10 p1327 N90-17667
Radiation exposure for manned Mars surface missions [NASA-TP-2979] 10 p1448 N90-18357
Mars in this century: The Olympia Project [DE90-008356] 14 p2042 N90-21709
Project Exodus [NASA-CR-186836] 20 p2816 N90-26026
Terrapin technologies manned Mars mission proposal [NASA-CR-186838] 20 p2816 N90-26027
The effect of interplanetary trajectory options on a manned Mars aerobrake configuration [NASA-TP-3019] 20 p2818 N90-26036
Possible applications of tethered systems to Mars exploration missions [IAF-89-489] 20 p2822 N90-26060
A solar power system for an early Mars expedition [NASA-TM-103219] 22 p3243 N90-28393

MANNED ORBITAL LABORATORIES
NT SKYLAB 1
NT SPACELAB
A modular habitation unit adapted for service in low earth and geostationary earth orbits [ILR-MITT-217] 08 p1036 N90-15990
Space Station Workshop: Commercial Missions and User Requirements [NASA-TM-102912] 15 p2175 N90-22428

MANNED ORBITAL SPACE STATIONS
U SPACE STATIONS

MANNED SPACE FLIGHT
NT APOLLO 15 FLIGHT
NT SPACE SHUTTLE MISSION 41-G
NT SPACE SHUTTLE MISSION 51-J
NT SPACE SHUTTLE MISSION 51-L
NT SPACE SHUTTLE MISSION 61-A
NT SPACE SHUTTLE MISSION 61-B
NT SPACE SHUTTLE MISSION 61-C
NT SPACE SHUTTLE MISSION 61-E
NT SPACE SHUTTLE MISSIONS
JPRS Report: Science and Technology. USSR: Space [JPRS-USP-89-007] 02 p0158 N90-10900
USSR and international cooperation in space 02 p0158 N90-10905
Advanced manned space flight simulation and training: An investigation of simulation host computer system concepts [NASA-CR-185998] 02 p0160 N90-10911
Cells in Space [NASA-CP-10034] 05 p0676 N90-13939
Countermeasures to microgravity 05 p0680 N90-13957
The Gevaltig: An inertial fusion powered manned spacecraft design for outer solar system missions [NASA-CR-185163] 08 p1036 N90-15985
Science exploration opportunities for manned missions to the Moon, Mars, Phobos, and an asteroid [NASA-CR-186295] 09 p1171 N90-16776
Advanced manned launch systems 09 p1175 N90-16797
Transportation systems for manned space missions 09 p1176 N90-16805
Estimates of galactic cosmic ray shielding requirements during solar minimum [NASA-TM-4167] 09 p1300 N90-17535
Present and future risk of satellite and manned platforms collisions with other space objects and particles on earth orbits [R-8841] 12 p1815 N90-19287
Augmenting and updating NASA spacelink electronic information system 12 p1634 N90-19392
A robotically constructed production and supply base on Phobos [NASA-CR-186234] 15 p2073 N90-21872
Aeronautics and space report of the President: 1987 activities 15 p2181 N90-22462
Neural networks in support of manned space 16 p2298 N90-23088
The European EVA spacesuit mechanisms 18 p2538 N90-24481
Lunar polar coring lander [NASA-CR-186684] 19 p2796 N90-25917

MANNED SPACECRAFT
NT AEROSPACE PLANES
NT ASTRO VEHICLE
NT ATLANTIS (ORBITER)
NT BURAN SPACE SHUTTLE
NT CHALLENGER (ORBITER)
NT COLUMBIA (ORBITER)
NT COLUMBUS SPACE STATION
NT FERRY SPACECRAFT
NT HERMES MANNED SPACEPLANE
NT HOTOL LAUNCH VEHICLE
NT LUNAR MODULE
NT MAN TENDED FREE FLYERS
NT MANNED ORBITAL LABORATORIES
NT MARS (MANNED REUSABLE SPACECRAFT)
NT MIR SPACE STATION
NT SKYLAB 1
NT SPACE SHUTTLE ORBITERS
NT SPACE SHUTTLES
NT SPACELAB
A survey of permanently-manned lunar base concepts [AD-A212575] 04 p0460 N90-12638
Apollo lightcraft project [NASA-CR-186055] 04 p0464 N90-12655
Risk-based fire safety experiment definition for manned spacecraft [NASA-CR-183835] 06 p0731 N90-14262

Project Argo: The design and analysis of an all-propulsive and an aeroassisted version of a manned space transportation vehicle
[NASA-CR-186047] 06 p0732 N90-14266
Manned spacecraft
[AD-A214218] 07 p0887 N90-15129
Systems interoperability approach Apollo/Soyuz test project 08 p1035 N90-15979
Transportation systems for manned space missions 09 p1176 N90-16805
Hatch cover
[NASA-CASE-MSC-21356-1] 12 p1613 N90-19278
Weight and cost forecasting for advanced manned space vehicles 18 p2632 N90-24998
The astronauts' legal status: The International Space Station 20 p2938 N90-26721

MANPOWER
NT SCIENTISTS
MANPRINT (Manpower and Personnel Integration) evaluation: AN/TRC-170 digital troposcatter radio system
[AD-A211799] 08 p1055 N90-16100
A survey of human factors methodologies and models for improving the maintainability design of emerging Army aviation systems
[AD-A221159] 18 p2586 N90-24724
A measurement of the effectiveness of the Airway Science Program to meet Federal Aviation Administration work force needs
[NIAR-90-5] 20 p2934 N90-26694
Federal Scientists and Engineers: 1988. (Detailed statistical tables)
[PB90-226895] 22 p3256 N90-28437

MANTLE (EARTH STRUCTURE)
U EARTH MANTLE

MANUAL CONTROL
NT VISUAL CONTROL
Architectural study of the design and operation of advanced force feedback manual controllers
[NASA-CR-185948] 07 p0981 N90-15664
Development of a multipurpose hand controller for JEMRMS 15 p2113 N90-22087
A new six-degree-of-freedom force-reflecting hand controller for space telerobotics 15 p2113 N90-22089
Minimum flying qualities. Volume 3: Program CC's implementation of the human optimal control model
[AD-A218562] 16 p2201 N90-22562
Adapting to variable prismatic displacement 16 p2271 N90-22945
Direction of movement effects under transformed visual/motor mappings 16 p2272 N90-22947
Man-machine interface for the control of a lunar transport machine
[NASA-CR-184935] 19 p2724 N90-25495
The relationship of isometric grip strength, optimal dynamometer settings, and certain anthropometric factors
[AD-A222046] 21 p3037 N90-27264
Tele-Autonomous control involving contact — object localization
[NASA-CR-187004] 23 p3335 N90-28854
Interset: A natural language interface for teleoperated robotic assembly of the EASE space structure 24 p3517 N90-29885
Multi-level manual and autonomous control superposition for intelligent telerobot 24 p3518 N90-29888
The JPL telerobotic Manipulator Control and Mechanization (MCM) subsystem 24 p3519 N90-29892

MANUALS
NT USER MANUALS (COMPUTER PROGRAMS)
Manual of regulations and procedures for federal radio frequency management, May 1986 edition: Revisions for January 1989
[PB89-193791] 01 p0056 N90-10320
Defense Technical Information Center cataloging guidelines
[AD-A211000] 01 p0137 N90-10792
Transport systems research vehicle color display system operations manual
[NASA-TM-101577] 03 p0306 N90-11736
DSEP (Dual Shaft Electric Propulsion) operation and maintenance manual for the NVH and TB-2 vehicles: Advanced Dual Shaft Electric Propulsion System technology development program
[DE89-017549] 03 p0420 N90-12411
User's manual for the ride motion simulator
[AD-A212855] 05 p0584 N90-13402
Columbus: A user's introduction
[ESA-BR-62] 08 p1036 N90-15989
Spark source mass spectrometry software documentation and verification
[DE90-004463] 09 p1192 N90-16909
Fastener design manual
[NASA-RP-1228] 11 p1517 N90-18740
DoD manual for standard data elements
[AD-A216441] 11 p1575 N90-19066
The NASA, Marshall Space Flight Center drop tube user's manual
[NASA-TM-100392] 13 p1786 N90-20251
Software Engineering Laboratory (SEL) database organization and user's guide
[NASA-TM-103304] 14 p2015 N90-21545
FORTRAN coding guidelines
[DE90-009804] 15 p2146 N90-22258
Lunar crane hook
[NASA-CR-184921] 17 p2384 N90-23579
The environmental liabilities of government contractors and agencies 17 p2481 N90-24186
Launching a dream: A teachers guide to a simulated space shuttle mission
[NASA-TM-89715] 20 p2934 N90-26693
Animated computer-generated video-tape instruction using DIGLIB (Device Independent Graphics Library)
[DE90-015360] 23 p3382 N90-29105

MANUFACTURING
NT COMPUTER AIDED MANUFACTURING
NT LOW GRAVITY MANUFACTURING
NT SPACE MANUFACTURING
Using computer design and simulation to improve manufacturing productivity
[AD-A210338] 01 p0105 N90-10598
Study of the application of automation to composites manufacture
[AD-A211049] 02 p0190 N90-11087
Free-world microelectronic manufacturing equipment
[FASAC-TAR-4070] 02 p0215 N90-11228
Coupling rule-based and object-oriented programming for the classification of machined features
[DE89-017705] 03 p0334 N90-11903
Manufacturing and the manufacturing engineer in the year 2000, revision
[DE89-017707] 03 p0335 N90-11904
Application of dimensional analysis to statistical process modeling
[AD-A211881] 03 p0335 N90-11905
Reasoning about change and exceptions in automated process planning
[DE89-017706] 03 p0386 N90-12195
Proceedings of the DOD Workshop on the Manufacturing/Producibility of Organic Matrix Composites
[AD-A212577] 04 p0468 N90-12680
Activities report of the metallic manufacturing industry
[ISSN-0524-7705] 05 p0625 N90-13649
The economic impact of automation technology
[AD-A213363] 05 p0630 N90-13682
Evolution of the EPR procedure for polycrystalline Si ribbon drawing for photovoltaic cell manufacturing
[ISAL-89-0027] 05 p0665 N90-13888
Study of metal-insulator-semiconductor structures on indium phosphide, implemented by anodic oxidation
[ECL-88-10] 05 p0703 N90-14114
Retrieving and integrating IC fabrication data from dissimilar databases
[AD-A211890] 05 p0707 N90-14140
Superplasticity
[AGARD-LS-158] 06 p0743 N90-14325
Superplasticity: An overview 06 p0743 N90-14326
The manufacture of superplastic alloys 06 p0745 N90-14333
A strategy for concurrent product and process design of aerospace components
[DE90-002926] 07 p0916 N90-15299
Back to basics
[DE90-002734] 07 p0943 N90-15463
Aircraft fuel tank construction and testing experience 08 p1021 N90-15907
Method of making carbon dioxide and chlorine free fluoride-based glass
[AD-D014260] 08 p1048 N90-16060
Advanced GaAs space solar cells by MOCVD technique 10 p1339 N90-17752
GaAs space solar cells: Pilot production experience using a multi wafer infinite melt liquid phase epitaxy process 10 p1339 N90-17756
Ultrasonic and parallel gap welding of GaAs solar cells, experimental and simulation results 10 p1341 N90-17766
A concept of a pilot production plant for directly glassed silicon 10 p1341 N90-17770
Manufacture and testing of a solar panel assembly comprising bifacial solar cells (AMOC-SPA) 10 p1342 N90-17773
Assessment of solar cell quality criteria 10 p1342 N90-17776
Pilot production of 70 micron thin silicon solar cells 10 p1343 N90-17780
Study of defect distribution in manufacturing test E8 No. 2 (program A-330/340)
[INFORME-I-366/89] 10 p1358 N90-17872
Defects: Their behaviour and related design assumptions 11 p1457 N90-18397
Review of component defects, their relationship to manufacturing process, and their effect on materials behaviour (for critical rotating parts) 11 p1458 N90-18399
Process development and fabrication of space station type aluminum-clad graphite epoxy struts
[NASA-CR-181873] 11 p1468 N90-18454
Ion chromatography in the manufacture of multilayer circuit boards
[DE90-005560] 11 p1503 N90-18652
Cost and energy consumption estimates for the aluminum-air battery anode fuel cycle
[DE90-005810] 11 p1503 N90-18656
Operational fact-finding report on heat pump systems for industrial use
[DE89-782295] 12 p1658 N90-19527
Statistical equipment modeling for VLSI manufacturing
[DE90-008527] 13 p1795 N90-20304
Phase 1 supplemental development of a kinematic Stirling/Rankine commercial gas-fired heat pump system
[PB90-129974] 13 p1825 N90-20483
CuInSe2 and CdTe: Scale-up for manufacturing
[DE89-009503] 13 p1827 N90-20489
Filament winding of composite cylinders 14 p1943 N90-21119
JPRS report: Science and technology. USSR: Electronics and electrical engineering
[JPRS-UEE-90-002] 14 p1970 N90-21284
High explosives (PBX9502) characterization using computerized tomography
[DE90-008170] 14 p1990 N90-21404
Design and demonstration of an improved stretched-membrane heliostat
[DE90-007904] 14 p2001 N90-21470
Advanced manufacturing technology: A Department of Energy technology transfer initiative
[DE90-008601] 14 p2037 N90-21688
Aging characteristics of Li/SO(sub 2) cells
[NASA-CR-180432] 15 p2088 N90-21954
Laboratory testing of Saft SEH-5-200 6 volt traction battery
[DE90-009787] 15 p2089 N90-21958
Data and conclusions from tests on small screws
[DE90-007500] 15 p2106 N90-22046
The surprising possibilities of wrapping
[REPT-892-430-108] 16 p2213 N90-22624
Rheology of injection mould filling with DMCs
[NPL-DMA(A)-196] 16 p2222 N90-22675
Increased stuck-at fault coverage with reduced I(sub DDQ) test sets
[DE90-009509] 16 p2245 N90-22804
Recent implementations on ceramic composites and thermostructural materials
[REPT-892-430-106] 17 p2370 N90-23489
CMOS IC I(sub DDQ) testing for the 1990s
[DE90-009508] 17 p2394 N90-23634
National Educators' Workshop: Update 1989 Standard Experiments in Engineering Materials Science and Technology
[NASA-CP-3074] 18 p2513 N90-24350
Manual and computer-aided materials selection for industrial production: An exercise in decision making 18 p2516 N90-24368
Future automotive materials: Evolution or revolution 18 p2516 N90-24370
State of the art and future prospects for high temperature composites
[REPT-892-430-125] 18 p2517 N90-24375
Multichip packaging technology with laser-patterned interconnects
[DE90-010743] 18 p2549 N90-24552
Photovoltaic concentrator technology development
[DE90-011479] 18 p2577 N90-24684
Strut-node joint conjugates for the assembly of semi-permanent or reusable truss structures 18 p2640 N90-25039
Performance of battery charge controllers
[DE90-011413] 19 p2686 N90-25279
The photovoltaic concentrator initiative
[DE90-011228] 19 p2710 N90-25425
Towards 2000: The composite engine
[PNR90648] 20 p2811 N90-26000
Influence of the manufacturing conditions on the microstructure and mechanical properties of the silicon nitride
[ISAL-90-0008] 20 p2840 N90-26154
Computer simulation of gear tooth manufacturing processes
[NASA-CR-185200] 20 p2843 N90-26171
Manufacturing control: A basis for analysis
[PNR90639] 20 p2844 N90-26174

NDT in aerospace: The next decade (1990's)
[PNR90628] 20 p2874 N90-26348
Conception of a reconfigurable microprocessor
[ETN-90-97248] 20 p2904 N90-26517
New core design for use with precision composite reflectors
[NASA-CASE-NPO-17858-1-CU]
21 p2970 N90-26880
Manufacturing and mechanical properties of new textile fiber preforms for structural sandwich applications
[MBB-Z-0296-90-PUB] 21 p2972 N90-26895
Cost effective technology
[PNR90664] 21 p2991 N90-27002
Polycrystalline thin film cadmium telluride n-i-p solar cells
[DE90-000351] 21 p3019 N90-27167
Scandia-stabilized zirconia coating for composites
[AD-D014550] 22 p3160 N90-27917
Impact of Emerging NDE-NDI Methods on Aircraft Design, Manufacture, and Maintenance
[AGARD-CP-462] 22 p3184 N90-28068
Impact of NDE-NDI methods on aircraft design, manufacture, and maintenance, from the fundamental point of view 22 p3189 N90-28093
Optoelectronics Research Center
[AD-A221926] 22 p3246 N90-28410
Life cycle cost in the conceptual design of subsonic commercial aircraft, volumes 1 and 2
23 p3275 N90-28535
Radiation-curable prepreg composites
[DE90-629740] 23 p3301 N90-28674
Realization of equipment for manufacturing titanium alloy electrodes for first step melting
[ONERA-RT-15/3578-M] 24 p3453 N90-29498
Proceedings of the 14th Annual Electronics Manufacturing Seminar
[AD-A224276] 24 p3463 N90-29563
Vacuum mechatronics 24 p3512 N90-29854

MANY BODY PROBLEM

Modeling of liquid sloshing effects in multibody systems 02 p0181 N90-11023
GALAX: A two-dimensional N-body code for disk galaxy dynamics
[PB89-217780] 03 p0420 N90-12415
Towards a parallel algorithm for the many body problem
[CS-8813] 04 p0533 N90-13078
Elements of a relativistic microscopic theory of hadronic matter in equilibrium and non-equilibrium
[KVI-796] 04 p0552 N90-13218
Periodic solutions of Hamiltonian systems of 3-body type
[AD-A212891] 05 p0687 N90-14005
Irreversible processes from reversible mechanics
[DE90-001057] 07 p0927 N90-15368
General many-body systems
[DE90-000685] 07 p0982 N90-15670
Relativistic self-consistent field studies of atoms and molecules
[AD-A214101] 07 p0991 N90-15724
Stable orbits about the Martian moons
[AD-A216400] 10 p1447 N90-18352
Multibody modeling and verification
12 p1640 N90-19422
Periodic trajectories for two-dimensional nonintegrable Hamiltonians
[DE90-008082] 13 p1877 N90-20765
Controlled multibody dynamics simulation for large space structures 14 p1934 N90-21068
Element-specific modal formulations for large-displacement multibody dynamics
14 p1934 N90-21069
The large scale structure of the universe in pancake models of galaxy formation 14 p2040 N90-21701
The distribution of molecular clouds in spiral galaxies
15 p2186 N90-22489
Proceedings of the 3rd Annual Conference on Aerospace Computational Control, volume 1
[NASA-CR-186446] 16 p2279 N90-22987
A nearly-linear computational-cost scheme for the forward dynamics of an N-body pendulum
16 p2280 N90-22996
Modeling of control forces for kinematical constraints in the dynamics of multibody systems: A new approach
16 p2287 N90-23031
About the order of Appel's algorithm
[CS-8910] 16 p2299 N90-23097
Time-dependent density-functional theory
[AD-A220993] 18 p2604 N90-24829
Dynamic analysis of flexible multibody structures
18 p2642 N90-25048
Molecular interactions and properties with many-body methods
[AD-A222631] 20 p2924 N90-26642
Effects of basis set contraction in relativistic calculations on neon, argon, and germanium
[AD-A223357] 24 p3446 N90-29460

MANY PARTICLE THEORY

U MANY BODY PROBLEM

MAP MATCHING GUIDANCE

Navigation up-date using radar mapping: Assessment and optimisation simulation tool
08 p1026 N90-15928
Carin and GPS: The combination of dead reckoning, map matching and satellite navigation in a hybrid automobile navigation system
[ETN-90-95451] 12 p1602 N90-19220
Position finding and ground target direction finding by an aircraft with a gimballed video camera
[DLR-FB-89-62] 22 p3111 N90-27673

MAPPING

NT CADASTRAL MAPPING
NT COMPUTER AIDED MAPPING
NT ICE MAPPING
NT PHOTOMAPPING
NT PLANETARY MAPPING
NT SOIL MAPPING
NT THEMATIC MAPPING
NT THERMAL MAPPING
The 1988 year end report for road following at Carnegie-Mellon
[NASA-CR-185967] 01 p0078 N90-10446
Network of dedicated processors for finding lowest-cost map path
[NASA-CASE-NPO-17716-1-CU]
01 p0107 N90-10608
Air velocity mapping of environmental test chambers
[AD-A212082] 03 p0310 N90-11764
Mapping nonlinear integro-differential equations into the frequency domain
[RR-366] 03 p0394 N90-12249
Height and gradient from shading
[AD-A212338] 04 p0504 N90-12908
A robot which will investigate the condition of underground pipe
[PB89-230650] 04 p0508 N90-12928
Visualization of high-resolution digital terrain
[AD-A212149] 04 p0515 N90-12971
A mapping for converting Mascot designs to Ada programs
[RSRE-MEMO-4244] 04 p0531 N90-13070
Julia-Fatou-Sullivan theory for real one-dimensional dynamics
[REPT-88-100] 04 p0548 N90-13190
Definition, determination and characterization of acceleration sets for spatial manipulators
[AD-A213366] 05 p0651 N90-13793
Extended memory library for AFOS (Automation of Field Operations and Services) applications
[PB89-230858] 05 p0708 N90-14147
Orion B: Anatomy of a star-forming region
05 p0710 N90-14155
Low level range coverage performance prediction for VHF radar 06 p0763 N90-14439
NORDA's pattern analysis laboratory: Current contributions to naval mapping, charting, and geodesy
[AD-A212731] 06 p0801 N90-14665
Evaluation of the airborne visible-infrared imaging spectrometer for mapping subtle lithological variation
[NASA-CR-186213] 06 p0802 N90-14670
Nomenclature for physical mapping of complex genomes
[DE89-015173] 06 p0859 N90-14994
Surface thermometry of energetic materials by laser-induced fluorescence
[AD-A214423] 07 p0916 N90-15297
China-built airborne synchronous laser ranger the new L-8 jet trainer aircraft
[AD-A213835] 07 p0936 N90-15422
SIMON (SuperIntelligent Mobile Observing Navigator): A high-reliability robot for a radiation environment
[DE90-003888] 07 p0943 N90-15460
Evolution of overlapping spreading centers: A Sea Mark 2 investigation
[AD-A214278] 07 p0965 N90-15576
Parallel algorithms for interactive manipulation of digital terrain models 08 p1113 N90-16445
Scientific investigations of the Space Research Group
[ISBN-0-642-13252-6] 08 p1138 N90-16595
Charting and Geodetic Services
[PB90-116674] 09 p1240 N90-17196
Mission report on the Orbiter Camera Payload System (OCPS) Large Format Camera (LFC) and Attitude Reference System (ARS)
[NASA-CR-186273] 09 p1240 N90-17197
An analysis of scatter decomposition
[NASA-CR-181978] 09 p1276 N90-17396
Harmonic mappings into manifolds with boundary
[DE90-606961] 09 p1277 N90-17402
Use of beta-splines for digital elevation modeling
[INPE-4941-PRE/1431] 10 p1400 N90-18093
Fixed points of expansive analytic maps
[AD-A214356] 10 p1421 N90-18194
Structured analysis tool interface to the strategic defense initiative architecture dataflow modeling technique
[AD-A216281] 10 p1424 N90-18218
Fixed points by Ishikawa iterations
[DE90-005557] 10 p1424 N90-18219
Radio continuum maps at 22 GHz of the H II regions RCW57 and W49
[INPE-4787-TDL/353] 10 p1446 N90-18343
An evaluation of an airborne laser profiling system for high precision terrain mapping
[AD-A217025] 11 p1525 N90-18780
Systematicity as a selection constraint in analogical mapping
[AD-A216029] 11 p1541 N90-18869
Using special-purpose computing to examine chaotic behavior in nonlinear mappings
[AD-A216800] 11 p1549 N90-18916
A method for determination of control pixels for LANSAT using a reflector
[INPE-4884-PRE/1491] 12 p1677 N90-19632
Synthesis and analysis of 25 years (1961-1986) of INPE/SRE activities related to the vegetation/forest area
[INPE-4969-RPE/604] 13 p1819 N90-20446
Progress in the Determination of the Earth's Gravity Field
[NASA-CR-185721] 13 p1831 N90-20513
Gravity field of the Western Weddell Sea: Comparison of airborne gravity and Geosat derived gravity
13 p1833 N90-20526
Geodynamics and temporal variations in the gravity field 13 p1838 N90-20549
Gravity field information from Gravity Probe-B
13 p1839 N90-20554
Local gravity disturbance estimation from multiple-high-single-low satellite-to-satellite tracking
13 p1839 N90-20555
Monitoring of agrocattle-raising projects through visual/digital analysis of LANDSAT-TM imagery south of Para state
[INPE-4982-PRE/1542] 14 p1996 N90-21442
Project CANASATE: Remote sensing applied to sugar cane crop survey
[INPE-4902-PRE/1503] 14 p1997 N90-21446
Possible use of satellite data for flood plain mapping
[INPE-4968-PRE/1537] 14 p2000 N90-21462
A monotone complementarity problem in Hilbert space
[DE90-009755] 14 p2022 N90-21590
Simulated image maps for use in experimental high-resolution electron microscopy
[DE90-009176] 14 p2032 N90-21657
STORM: A statistical object representation model
[DE90-009048] 14 p2036 N90-21686
A three-year study of the OH masers in Orion-KL and a study of the (3,2) transition of ammonia
15 p2183 N90-22471
Calculation of 3-dimensional synthetic seismograms on the connection machine
[AD-A218472] 16 p2255 N90-22857
Displays, instruments, and the multi-dimensional world of cartography 16 p2271 N90-22942
Characterization of robotics parallel algorithms and mapping onto a reconfigurable SIMD machine
16 p2289 N90-23039
Line simplification and digital cartographic databases
[DE90-010194] 18 p2634 N90-25003
CNES space programmes related to climate
19 p2706 N90-25400
Tools for mapping environmental monitoring data
[PB90-129685] 19 p2712 N90-25432
All-optical device and method for remapping images
[AD-D014540] 19 p2758 N90-25672
Automatic line network extraction from aerial imagery of urban areas through knowledge based image analysis
[AD-A222675] 20 p2880 N90-26385
Converses for write-unidirectional memories
[EUT-89-E-220] 20 p2909 N90-26548
Solubility characteristics of a methacrylate copolymer
[AD-A222938] 21 p2985 N90-26962
National mapping program. Fact sheet: Black and white photographs, NHAP (National High Altitude Photography Program)
[PB90-185042] 21 p3015 N90-27139
The column-by-column compositional mapping at semiconductor interfaces using Z-contrast STEM
[DE90-012594] 21 p3081 N90-27516
Infrared mapping with a two-dimensional infrared array
[AD-A221938] 21 p3096 N90-27596
Aerial videotape survey of coastal Louisiana, 1986. Louisiana Barrier Island erosion and land loss study: 1986-1990
[PB90-194648] 22 p3195 N90-28128

Map learning with indistinguishable locations
23 p3367 N90-29025
Exploiting map plans as resources for action
23 p3367 N90-29028
First results in terrain mapping for a roving planetary explorer 23 p3375 N90-29066
Satellite image atlas of glaciers of the world: Irian Jaya, Indonesia, and New Zealand
[PB90-230095] 24 p3483 N90-29691
Proceedings of the 17th Annual Gravity Gradiometer Conference
[AD-A223568] 24 p3492 N90-29735
Symmetry and island structure of the standard map
[DE90-508076] 24 p3548 N90-30069

MAPS
NT ASTRONOMICAL MAPS
NT METEOROLOGICAL CHARTS
NT PHOTOMAPS
NT RADAR CLUTTER MAPS
NT RADAR MAPS
NT RELIEF MAPS
Linkoeping's A.I. Consortium (LAIC) for plan guided systems. Review of the first 18 months
[FOA-C-30528-3.4] 02 p0269 N90-11537
Effects of the advanced map interpretation and terrain analysis course on contour-level navigation performance
[AD-A212163] 03 p0304 N90-11723
Problem-dependent transformations of 3D terrain elevation maps into cost precursor maps
[PB89-218127] 04 p0514 N90-12969
Self-organizing semantic maps
[PB89-212609] 04 p0529 N90-13049
Julia-Fatou-Sullivan theory for real one-dimensional dynamics
[REPT-88-100] 04 p0548 N90-13190
Direct computation of 3D shape invariants and the focus of expansion
[AD-A212386] 04 p0549 N90-13195
Feature modeling: The incorporation of a front and eddy map into optimum interpolation-based thermal analysis
[AD-A213253] 05 p0672 N90-13914
Nonlinear maps with competitive interactions: Fixed-points, bifurcations, and chaotic attractors
[DE90-001858] 07 p0986 N90-15895
Atlas of albedo and absorbed solar radiation derived from Nimbus 7 Earth radiation budget data set, November 1978 to October 1985
[NASA-RP-1231] 09 p1247 N90-17233
A split-and-merge method for creating polygonal homogeneous-vegetation regions from digitized terrain data
[AD-A218080] 13 p1821 N90-20453
Displays, instruments, and the multi-dimensional world of cartography 16 p2271 N90-22942
Atlas/data abstract for the United States and selected areas, fiscal year 1989
[AD-A219289] 16 p2327 N90-23270
Ice conditions along the Illinois waterway as observed on LANDSAT images, 1972 to 1985
[AD-A219745] 17 p2418 N90-23775
Astronaut's guide to terrestrial impact craters
[NASA-TM-102902] 17 p2421 N90-23798
US Navy hindcast spectral ocean wave model climatic atlas: Mediterranean Sea
[AD-A219755] 17 p2426 N90-23825
Line simplification and digital cartographic databases
[DE90-010194] 18 p2634 N90-25003
Anthropogenic sources of NO(x), SO()x, CO, and CH4: Geographical distribution
[AERONOMICA-ACTA-A-353-1990]
19 p2713 N90-25440
The main products and their distribution of FY-1 meteorological satellite
[AD-A221582] 21 p2967 N90-26865
Simple graphical descriptions of natural land profiles and the application of fractal and sub-fractal models to them
[RSRE-MEMO-4305] 22 p3195 N90-28130

MARAGING STEELS
Mechanical property characterization of VascoMax T-300
[AD-A212950] 05 p0623 N90-13637
Brittle torsional fatigue crack initiation in an otherwise ductile environment
[AD-A220858] 17 p2416 N90-23767

MARANGONI CONVECTION
Design challenges for space bioreactors
05 p0679 N90-13955
Modeling convective Marangoni flows with void movement in the presence of solid-liquid phase change
[DE90-006474] 11 p1509 N90-18690
Mass transfer induced convection near gas-liquid interfaces
[ETN-90-96925] 18 p2552 N90-24568

MARECS MARITIME SATELLITES
Field measurements in MSAT-X
10 p1371 N90-17947

MARIA
NT LUNAR MARIA

MARINE BIOLOGY
Biochemical cycling and fluxes between the deep euphotic zone and other oceanic realms
[PB89-152458] 01 p0089 N90-10509
Adaptation and resistance of ecosystems to stress
[AD-A212999] 05 p0665 N90-13889
Modeling the upper ocean and its interaction with the atmosphere
[DE90-008980] 14 p2008 N90-21511
Effects of solar ultraviolet radiation on biogeochemical dynamics in aquatic environments
[AD-A221119] 18 p2578 N90-24687

MARINE CHEMISTRY
On the applicability of CAESAR for the remote sensing of bottom depth and bottom composition of shallow waters: A model study
[BCRS-89-13] 11 p1526 N90-18783
The trace metal geochemistry of suspended oceanic particulate matter
[AD-A218604] 17 p2429 N90-23839

MARINE ENVIRONMENTS
International Conference on Aerosols and Background Pollution Abstracts
[AD-A210970] 01 p0085 N90-10483
Weather satellite and computer modeling approaches to assessing propagation over marine environments
06 p0764 N90-14443
Managing marine protected areas: An action plan
[PB89-158778] 06 p0808 N90-14701
MF/HF multistatic mid-ocean radar experiments in support of SWOTHR (Surface-Wave Over-The-Horizon Radar)
[AD-A213830] 07 p0919 N90-15314
Further research on dynamics of marine atmospheres in tropical cyclones
[AD-A213882] 07 p0964 N90-15571
Potential impact of stratospheric ozone depletion on marine ecosystems
[PB90-112616] 08 p1098 N90-16360
Remote sensing of evaporation ducts for Naval warfare
[AD-A214849] 10 p1374 N90-17965
Effect of marine atmosphere on performance of electrooptical systems
[AD-A215947] 10 p1430 N90-18252
Sounding and surface meteorological data from the Land/Sea Breeze Experiment (LASBEX)
[AD-A216269] 11 p1536 N90-18842
Research and development on enhanced degradable plastics
[AD-A217180] 13 p1779 N90-20212
Theoretical modeling studies of the marine planetary
[AD-A217200] 13 p1841 N90-20567
US Navy regional climatic study of the Central East Asian coast and associated waters
[AD-A217448] 13 p1844 N90-20587
SAR and ISAR imagery of marine targets
14 p1962 N90-21237
The Mediterranean marine environment and its effects on aerosols and infrared transmission
15 p2079 N90-21909
On the effectiveness of the production of antarctic bottom water in the Weddell and Ross Seas
[AD-A218873] 16 p2259 N90-22880
Vertical directionality measurements of ambient noise in the NE Pacific
[AD-A220007] 17 p2432 N90-23856
Effects of solar ultraviolet radiation on biogeochemical dynamics in aquatic environments
[AD-A221119] 18 p2578 N90-24687
A correlation study of wind speed as measured by the special sensor microwave/imager and the GEOSAT altimeter
[AD-A219841] 18 p2581 N90-24701
Environmental measurements and analysis: Arctic acoustics experiments in the marginal ice zone
[AD-A220509] 18 p2582 N90-24708
Mariners Weather Log, volume 33, number 2, Spring 1989
[PB90-146838] 20 p2889 N90-26443
Mariners Weather Log, volume 33, number 3, Summer 1989
[PB90-146846] 20 p2889 N90-26444
Mariners Weather Log, volume 33, number 4, Fall 1989
[PB90-146853] 20 p2890 N90-26445
Corrosion protection of metal matrix composites
[AD-A222951] 21 p2971 N90-26888
Cloud reflectance characteristics in the presence of variable Dimethylsulfide (DMS) sources
[AD-A222806] 21 p3024 N90-27197
Specification for a standard electromagnetic propagation model
[AD-A223556] 24 p3461 N90-29551

MARINE MAMMALS
NT MANATEES

MARINE METEOROLOGY
Mariners Weather Log, volume 32, number 3, Summer 1988
[PB88-248075] 01 p0086 N90-10491
US Navy regional climatic study of the United States Atlantic Coast and associated waters
[AD-A210198] 01 p0088 N90-10503
Hydrophone investigations of earthquakes and explosion generated high-frequency seismic phases
[AD-A212055] 03 p0371 N90-12122
Airborne profiles taken near San Nicolas Island, California, during Operation FIRE (First ISCCP (International Satellite Cloud Climatology Project) regional experiment) (1987): Aerosol size distributions, air and surface temperatures, cloud top temperatures, and relative humidities
[AD-A211664] 03 p0374 N90-12136
Compendium of marine meteorological and oceanographic products of the Ocean Products Center, revision 1
[PB89-230684] 04 p0514 N90-12967
Investigation of North Atlantic fog and development of a marine fog forecast system
[AD-A211780] 04 p0519 N90-12999
Physical models for aerosol in the marine mixed-layer
06 p0763 N90-14438
The chemistry and dynamics of marine stratocumulus
08 p1102 N90-16381
US Navy regional climatic study of the Central East Asian coast and associated waters
[AD-A217448] 13 p1844 N90-20587
Coastal frontogenesis and associated severe weather on 13 March 1986 (GALE IOP 13)
[AD-A217708] 13 p1845 N90-20590
A modeling study of the cloud-topped marine boundary layer
[AD-A218103] 13 p1846 N90-20594
Numerical simulations of the cloud-capped marine boundary layer 14 p2008 N90-21506
A survey of the maritime-aerosol data collected at South Uist and the implications for the LOWTRAN maritime aerosol model 15 p2079 N90-21908
The Mediterranean marine environment and its effects on aerosols and infrared transmission
15 p2079 N90-21909
The naval oceanic vertical aerosol model
15 p2082 N90-21921
Infrared propagation in the air-sea boundary layer
15 p2083 N90-21926
Aerosol separator for use in aircraft
[PB90-142217] 15 p2125 N90-22155
Impact of marine boundary layer parameterization on a numerical simulation of cyclogenesis during a cold air outbreak event 16 p2256 N90-22864
US Navy regional climatic study of southern African waters
[AD-A218792] 16 p2258 N90-22874
US Navy regional climatic study of the Mozambique channel and adjacent waters
[AD-A218793] 16 p2258 N90-22875
Coastal field data collection program. Hurricane Gilbert storm surge data
[AD-A218752] 17 p2426 N90-23823
US Navy hindcast spectral ocean wave model climatic atlas: Mediterranean Sea
[AD-A219755] 17 p2426 N90-23825
A correlation study of wind speed as measured by the special sensor microwave/imager and the GEOSAT altimeter
[AD-A219841] 18 p2581 N90-24701
Boundary layer parameterization for use in a limited area forecast model 21 p3029 N90-27224
FIRE Science Results 1989
[NASA-CP-3079] 22 p3213 N90-28224
Comparative climatology of four marine stratocumulus regimes 22 p3213 N90-28225
Large-scale variability in marine stratocumulus clouds defined from simultaneous aircraft and satellite measurements 22 p3213 N90-28226
Inhomogeneities of stratocumulus liquid water
22 p3213 N90-28228
Intercomparisons of GOES-derived cloud parameters and surface observations over San Nicolas Island
22 p3214 N90-28229
July 16, 1987 revisited: Lessons for modelers
22 p3214 N90-28232
An eight-month climatology of marine stratocumulus cloud fraction, albedo, and integrated liquid water
22 p3214 N90-28233
Mesoscale variability of free tropospheric humidity near San Nicolas Island during FIRE
22 p3214 N90-28234
Reflectivities of uniform and broken stratiform clouds: An update 22 p3215 N90-28236

Spectral absorption of marine stratocumulus clouds derived from in situ cloud radiation measurements
22 p3215 N90-28238
Cloud optical parameters as derived from the multispectral cloud radiometer 22 p3215 N90-28239
Satellite-derived cloud and radiation fields over the marine stratocumulus IFO 22 p3216 N90-28240
Analysis of ER-2 radiometer and lidar observations from the 1987 marine stratus experiment
22 p3216 N90-28241
The radiation budget of stratocumulus clouds measured by tethered balloon instrumentation: Variability of flux measurements 22 p3216 N90-28242
On the dynamic and thermodynamic structures of marine stratocumulus 22 p3216 N90-28244
Turbulence structure in clear and cloudy regions of the 7 July 1987 Electra mission 22 p3217 N90-28247
Diurnal variation in the turbulent structure of the cloudy marine boundary layer during FIRE 1987
22 p3217 N90-28248
The influence of continental sources of aerosols on the marine stratocumulus during FIRE IFO-1
22 p3218 N90-28250
Optical properties of marine stratocumulus clouds modified by ship track effluents
22 p3218 N90-28253
Stratus: An interactive steady state mixed layer model for personal computers 22 p3219 N90-28255
A case study of cumulus formation beneath a stratocumulus sheet: Its structure and effect on boundary layer budgets 22 p3219 N90-28256
Verification of the naval oceanic vertical aerosol model during FIRE 22 p3219 N90-28257
A cloudiness transition in a marine boundary layer
22 p3219 N90-28259
Analysis of marine stratocumulus clearing events during FIRE 22 p3220 N90-28260
FIRE aircraft observations of horizontal and vertical transport in marine stratocumulus
22 p3220 N90-28261
Vertical-velocity skewness in the marine stratus-topped boundary layer 22 p3220 N90-28262
Laboratory experiments on stability and entrainment of oceanic stratocumulus. Part 1: Instability experiment
22 p3220 N90-28263
Laboratory experiments on stability and entrainment of oceanic stratocumulus. Part 2: Entrainment experiment
22 p3220 N90-28264

MARINE NAVIGATION
U SURFACE NAVIGATION

MARINE PROPULSION
Copolymers for drag reduction in marine propulsion: New molecular structures with enhanced effectiveness
[AD-A214444] 08 p1049 N90-16062
Computation of viscous flow around a propeller-shaft configuration with infinite-pitch rectangular blades
14 p1912 N90-20958
Vortice-propeller interaction
[LIMSI-89-9] 23 p3326 N90-28809

MARINE TECHNOLOGY
NRL (Naval Research Laboratory) Review
[AD-A212886] 05 p0716 N90-14182
Summary of research academic departments, 1987-1988
[AD-A213252] 05 p0716 N90-14183
NORDA's pattern analysis laboratory: Current contributions to naval mapping, charting, and geodesy
[AD-A212731] 06 p0801 N90-14665
Design study of a modular gas-cooled, closed-brayton cycle reactor for marine use
[AD-A213453] 07 p0953 N90-15518
Maritime safety information in the year 2000: Listen up, Navy, the times they are a changin'
[AD-A220563] 17 p2390 N90-23611
Independent research and independent exploratory development programs
[AD-A222690] 21 p3101 N90-27612

MARINE TRANSPORTATION
Observation of ship movement by aeroplane
[FFI-90/7001] 19 p2657 N90-25124
Combining LORAN and GPS: The best of both worlds
24 p3424 N90-29343
Ring laser gyro marine inertial navigation systems
24 p3426 N90-29355

MARITIME SATELLITES
NT ERS-1 (ESA SATELLITE)
NT MARECS MARITIME SATELLITES

MARKERS
Frame synchronization methods based on channel symbol measurements 04 p0486 N90-12795
Evaluation of a prototype lighted ball marker for powerline obstructions
[DOT/FAA/CT-TN90/12] 15 p2055 N90-21774
Experiment K-6-18. Study of muscarinic and gaba (benzodiazepine) receptors in the sensory-motor cortex, hippcampus and spinal code 20 p2895 N90-26471

MARKET RESEARCH
California air transportation study: A transportation system for the California Corridor of the year 2010
[NASA-CR-186219] 06 p0722 N90-14212
Markets for high-speed intercity Maglev technology: A systems analysis approach
[DE89-017683] 06 p0794 N90-14623
The international space transportation market: A European perspective 09 p1173 N90-16785
An assessment of potential markets for small satellites
[NASA-TM-101943] 09 p1181 N90-16848
The bringing to market of the RF alert (a case study in technology transfer) 11 p1576 N90-19073
Introductory remarks for the panel discussions on technology transfer 11 p1576 N90-19075
Indianapolis Downtown Heliport: Operations analysis and marketing history
[REPT-90RR-13] 14 p1930 N90-21049
Technology for electronic transfer of information: The present and future in North America
15 p2177 N90-22442
Space projects: Improvements needed in selecting future projects for private financing
[GAO/NSIAD-90-147] 22 p3256 N90-28439
The nuclear battery
[DE90-630400] 24 p3462 N90-29559

MARKETING
Japanese structural ceramics research and development 01 p0048 N90-10272
Consumer Ozone Protection Act of 1989
[S-HRG-101-377] 06 p0809 N90-14708
Methodology panel 11 p1576 N90-19076
Identification of and response to market demand
11 p1577 N90-19078
From invention to innovation: Commercialization of new technology by independent and small business inventors
[DE90-006944] 12 p1727 N90-19927
Indianapolis Downtown Heliport: Operations analysis and marketing history
[REPT-90RR-13] 14 p1930 N90-21049
Photovoltaic concentrator technology development
[DE90-011479] 18 p2577 N90-24684
Scenario 2000
[MBB-UD-500/89-PUB] 19 p2652 N90-25092
Outlook for ceramics in heat engines, 1990 - 2010: A technical and economic assessment based on a worldwide Delphi survey
[DE90-011262] 19 p2679 N90-25234

MARKING
NT ISOTOPIC LABELING
Method of marking titanium alloy articles having distinct microstructural regions corresponding to high creep and fatigue resistance
[AD-D014283] 08 p1043 N90-16031
Does DNA cytometry have a place in the clinical laboratory
[DE90-007652] 14 p2009 N90-21512
Conference on Instrumental Activation Analysis: IAA 89
[DE90-615661] 19 p2694 N90-25327

MARKOV CHAINS
Markov chain moment formulas for regenerative simulation
[AD-A210684] 01 p0116 N90-10667
Likelihood ratio derivative estimators for stochastic systems
[AD-A213787] 07 p0984 N90-15684
A further note on generalized hyperexponential distributions
[AD-A214881] 09 p1275 N90-17394
An algorithm for finding characteristic roots of quasi-triangular Markov chains
[AD-A215490] 10 p1421 N90-18196
Recurrence conditions for average and Blackwell optimality in denumerable state Markov decision chains
[TW-89-02] 11 p1555 N90-18952
The existence of sensitive optimal policies in two multi-dimensional queueing models
[TW-89-11] 17 p2464 N90-24080
Note on the optimality of the generalized shortest queue policy
[TW-90-01] 17 p2464 N90-24081
The M/G/1 queue with permanent customers
[CWI-BS-R8919] 17 p2467 N90-24096
On ergodicity and recurrence properties of a Markov chain with an application to an open Jackson network
[TW-89-10] 17 p2467 N90-24099
Synchronously parallel Boltzmann machines: A mathematical model
[MEMO-COSOR-89-21] 18 p2590 N90-24732
A Markov chain identity and monotonicity of the diffusion constants for a random walk in a heterogeneous environment
[CWI-AM-R8917] 18 p2605 N90-24839
Solving problems by interrogating sets of knowledge systems: Toward a theory of multiple knowledge systems 18 p2629 N90-24979
Operations and support cost modeling using Markov chains 18 p2648 N90-25070

MARKOV PROCESSES
NT MARKOV CHAINS
Optimal q-Markov COVER for finite precision implementation 01 p0023 N90-10117
Discrete-time conversion for simulating finite-horizon Markov processes
[AD-A210683] 01 p0116 N90-10666
Radon transform analysis of a probabilistic method for image generation
[AD-A207814] 01 p0123 N90-10702
Markov processes in Hilbert space and continuous spontaneous localization of systems of identical particles
[DE89-618396] 02 p0270 N90-11540
A unified framework for simulating Markovian models of highly dependable systems
[AD-A212164] 03 p0396 N90-12267
Parallel and deterministic algorithms from MRF (Markov Random Fields): Surface reconstruction and integration
[AD-A212457] 04 p0533 N90-13084
Extended performability modeling using dynamic queing networks
[MEMO-INF-89-15] 04 p0536 N90-13099
Note on the convergence of simulated annealing algorithms
[MEMO-774] 04 p0544 N90-13162
Explicit modelling of state duration correlations in hidden Markov models --- speech recognition
[RSRE-MEMO-4152] 04 p0546 N90-13178
Random truncation models and Markov processes
[CWI-MS-R8817] 04 p0547 N90-13181
Stochastic process models in device physics
[AD-A212284] 04 p0547 N90-13185
Random Markov processes and uniform martingales
[CWI-BS-R8908] 05 p0690 N90-14021
The theory of hybrid stochastic algorithms
[DE90-003941] 08 p1109 N90-16421
Stochastic models in reliability
[AD-A215479] 09 p1234 N90-17163
System identification and filtering of nonlinear controlled Markov processes by canonical variate analysis
[AD-A214873] 09 p1273 N90-17381
Influence of the parameters: Charge order, sequence classification, partial sequential circuit, and process regularity of a working charge (Gaussian process) on the lifetime of a component made of 3.1354 T3 and 3.4377 T761
[ETN-90-95378] 12 p1653 N90-19503
Security calculations of rip reached construction elements by means of probabilistic breaking mechanics and a Markov process
[ETN-90-95890] 12 p1676 N90-19624
Modeling and classification of acoustic transients by speech recognition techniques
[AD-A218070] 13 p1791 N90-20277
Approximate evaluation of reliability and related quantities via perturbation techniques
[AD-A218340] 13 p1814 N90-20417
A solution for the variance-penalized Markov decision problem based on parametric linear programming
[TW-90-02] 17 p2467 N90-24100
Evaluation of Stochastic models for estimating the persistence probability of cloud-free lines-of-sight
[AD-A220283] 18 p2581 N90-24702
A Lyapunov bound for solutions of Poisson's equation
[AD-A220223] 18 p2599 N90-24787
Uniform limit theorems for synchronous processes with applications to queues
[AD-A220224] 18 p2599 N90-24788
Some convergence results for probabilistic Tabu search
[MEMO-822] 18 p2605 N90-24840
The development of the time-delayed neural network architecture
[AD-A221540] 21 p3061 N90-27403
Consequences of monotonicity for Markov transition functions
[AD-A222852] 21 p3063 N90-27412
IEEE Conference on Neural Information Processing Systems, Natural and Synthetic
[AD-A223611] 24 p3461 N90-29552

MARS (MANNED REUSABLE SPACECRAFT)
Advanced manned launch systems
09 p1175 N90-16797

MARS (PLANET)
Office of exploration overview
01 p0027 N90-10141
Laser-powered Martian rover
01 p0029 N90-10157
Soviet Mars program 02 p0158 N90-10903
Sagdeyev discusses space missions, policy, Mars plans 02 p0159 N90-10906

Design of a solar sail mission to Mars
[NASA-CR-186045] 03 p0311 N90-11771
Stable orbits about the Martian moons
[AD-A216400] 10 p1447 N90-18352
Observations of CO on Mars in the infrared and millimetre range 11 p1578 N90-19090
Near infrared spectroscopy of Mars: Study of the surface mineralogy 11 p1579 N90-19091
A robotically constructed production and supply base on Phobos
[NASA-CR-186234] 15 p2073 N90-21872
Quantitative studies of the Martian south polar region using spacecraft images 15 p2191 N90-22514
Human exploration of space: A review of NASA's 90-day study and alternatives
[NASA-CR-186394] 17 p2357 N90-23418
A numerical investigation of thermal convection in highly viscous spherical shells with applications to mantle dynamics in the Earth and other terrestrial planets 18 p2579 N90-24691
Mars in this decade: The great exploration
[DE90-011232] 19 p2797 N90-25920
Greenhouse design for a Martian colony: Structural, solar collection and light distribution systems
[NASA-CR-186818] 20 p2901 N90-26501
Press abstracts of the 21st Lunar and Planetary Science Conference
[NASA-CR-186874] 20 p2941 N90-26738
MECA Workshop on Dust on Mars 3
[NASA-CR-185065] 21 p3100 N90-27604
Mars landing site catalog
[NASA-RP-1238] 21 p3100 N90-27607

MARS ATMOSPHERE
Saltation thresholds and entrainment of fine particles at Earth and Martian pressures
[NASA-TM-102193] 06 p0860 N90-14997
The middle Martian atmosphere 07 p1014 N90-15874
An investigation of long term orbits about the planet Mars using a dynamic atmosphere model
[AD-A216111] 10 p1447 N90-18351
Radiation exposure for manned Mars surface missions
[NASA-TP-2979] 10 p1448 N90-18357
Use of random Martian atmosphere to evaluate potential entry guidance schemes
[NASA-TM-102606] 13 p1784 N90-20122
Preliminary design of a long-endurance Mars aircraft
[NASA-CR-185243] 15 p2052 N90-21763
Expert systems for automated maintenance of a Mars oxygen production system
[NASA-CR-186209] 15 p2139 N90-22215
Equilibrium radiative heating tables for aerobraking in the Martian atmosphere
[NASA-TM-102659] 19 p2688 N90-25290
Space exploration: Cost, schedule, and performance of NASA's Mars Observer Mission. Fact sheet for the Chairman, Subcommittee on Science, Technology, and Space, Committee on Commerce, Science, and Transportation, US Senate
[GAO/NSIAD-88-137FS] 20 p2815 N90-26021
Mars in situ propellants: Carbon monoxide and oxygen ignition experiments
[NASA-TM-103202] 20 p2823 N90-26065
The chemical effects of the Martian environment on power system component materials: A theoretical approach
[NASA-TM-103203] 20 p2825 N90-26074
Infrared spectra of van de Waals complexes of importance in planetary atmospheres 20 p2943 N90-26749
MECA Workshop on Dust on Mars 3
[NASA-CR-185065] 21 p3100 N90-27604

MARS ENVIRONMENT
NT MARS ATMOSPHERE
M.I.N.G., Mars Investment for a New Generation: Robotic construction of a permanently manned Mars base
[NASA-CR-186224] 06 p0865 N90-15028
Aeolian removal of dust from photovoltaic surfaces on Mars
[NASA-TM-102507] 12 p1617 N90-19299
Space exploration: Cost, schedule, and performance of NASA's Mars Observer Mission. Fact sheet for the Chairman, Subcommittee on Science, Technology, and Space, Committee on Commerce, Science, and Transportation, US Senate
[GAO/NSIAD-88-137FS] 20 p2815 N90-26021

MARS GEOSCIENCE CLIMATOLOGY ORBITER
U MARS OBSERVER

MARS LANDING
Mars landing site catalog
[NASA-RP-1238] 21 p3100 N90-27607

MARS OBSERVER
Mission to Mars. Report of the Mars exploration study team
[ESA-SP-1117] 08 p1033 N90-15968
Space exploration: Cost, schedule, and performance of NASA's Mars Observer Mission. Fact sheet for the Chairman, Subcommittee on Science, Technology, and Space, Committee on Commerce, Science, and Transportation, US Senate
[GAO/NSIAD-88-137FS] 20 p2815 N90-26021

MARS PHOTOGRAPHS
Quantitative studies of the Martian south polar region using spacecraft images 15 p2191 N90-22514

MARS PROBES
NT MARS OBSERVER
NT VIKING LANDER SPACECRAFT

MARS ROVER SAMPLE RETURN MISSION
U MARS SAMPLE RETURN MISSIONS

MARS SAMPLE RETURN MISSIONS
Mission to Mars. Report of the Mars exploration study team
[ESA-SP-1117] 08 p1033 N90-15968
Preliminary investigation of parameter sensitivities for atmospheric entry and aerobraking at Mars
[NASA-TM-101607] 10 p1327 N90-17667
International cooperation for Mars exploration and sample return
[NASA-CR-186511] 17 p2358 N90-23419
Mars Rover imaging systems and directional filtering 18 p2648 N90-25071
Robotic sampling system for an unmanned Mars mission 23 p3375 N90-29070

MARS SATELLITES
NT DEIMOS
NT PHOBOS

MARS SURFACE
Mission to Mars. Report of the Mars exploration study team
[ESA-SP-1117] 08 p1033 N90-15968
Radiation exposure for manned Mars surface missions
[NASA-TP-2979] 10 p1448 N90-18357
Aeolian removal of dust from photovoltaic surfaces on Mars
[NASA-TM-102507] 12 p1617 N90-19299
Quantitative studies of the Martian south polar region using spacecraft images 15 p2191 N90-22514
Erosional development of bedrock spur and gully topography in the Valles Marineris, Mars
[NASA-CR-180655] 17 p2424 N90-23813
Evaluation of off-road terrain with static stereo and monoscopic displays 19 p2740 N90-25575
Space exploration: Cost, schedule, and performance of NASA's Mars Observer Mission. Fact sheet for the Chairman, Subcommittee on Science, Technology, and Space, Committee on Commerce, Science, and Transportation, US Senate
[GAO/NSIAD-88-137FS] 20 p2815 N90-26021
Terrapin technologies manned Mars mission proposal
[NASA-CR-186838] 20 p2816 N90-26027
Aeolian removal of dust from radiator surfaces on Mars
[NASA-TM-103205] 20 p2824 N90-26068
The chemical effects of the Martian environment on power system component materials: A theoretical approach
[NASA-TM-103203] 20 p2825 N90-26074
Analysis of a Mars-stationary orbiting microwave power transmission system
[NASA-TM-101344] 20 p2843 N90-26172
University of Maryland walking robot: A design project for undergraduate students
[NASA-CR-186839] 20 p2870 N90-26331
Autoplan: A self-processing network model for an extended blocks world planning environment
[NASA-CR-186733] 20 p2905 N90-26526
Press abstracts of the 21st Lunar and Planetary Science Conference
[NASA-CR-186874] 20 p2941 N90-26738
MECA Workshop on Dust on Mars 3
[NASA-CR-185065] 21 p3100 N90-27604
MEVTV Workshop on Tectonic Features on Mars
[NASA-CR-186143] 21 p3100 N90-27609
Satellite-map position estimation for the Mars rover 23 p3375 N90-29069
Robotic sampling system for an unmanned Mars mission 23 p3375 N90-29070
The flight telerobotic servicer: NASA's first operational space robot 24 p3500 N90-29781

MARS SURFACE SAMPLES
International cooperation for Mars exploration and sample return
[NASA-CR-186511] 17 p2358 N90-23419
Scientific guidelines for preservation of samples collected from Mars
[NASA-TM-4184] 19 p2796 N90-25918

MARS VOLCANOES
MEVTV Workshop on Early Tectonic and Volcanic Evolution of Mars
[NASA-CR-186098] 21 p3021 N90-27176
MEVTV Workshop on Tectonic Features on Mars
[NASA-CR-186143] 21 p3100 N90-27609

MARSHES
U MARSHLANDS

MARSHLANDS
A case for archaeological reconnaissance of the Cabo Catoche-Porvenir region of the northeastern Yucatan Peninsula
[NASA-TM-102248] 16 p2249 N90-22827
Ecological study of peat landforms in Canada and Alaska
[NASA-CR-184923] 19 p2705 N90-25391

MARTENSITE
Use of overlapped reflection for determining the retained austenite by X-ray diffraction
[DE89-615450] 02 p0198 N90-11128
Martensite transformation in NiTi alloys induced by tensile stress pulses
[DE90-001832] 06 p0747 N90-14346
Microstructural evolution of martensitic steels during fast neutron irradiation
[DE89-016231] 07 p0902 N90-15212
Heat treatment investigation of 4330 vanadium-modified steel
[AD-A214290] 07 p0906 N90-15239
Twin boundaries, interfaces and modulated structures in martensites
[DE90-012899] 20 p2833 N90-26111
Microstructural development in HSLA-100 steel weld metals
[AD-A222105] 21 p2982 N90-26944
The stability of the martensitic phases in Cu-Zn-Al at an electron concentration of 1.534
[DE90-628628] 23 p3311 N90-28727

MARTENSITIC STAINLESS STEELS
Phase stability of a manganese-stabilized low-activation martensitic steel
[DE90-004114] 09 p1193 N90-16914
Migration of carbon in tempered martensitic steel during excimer laser melting
[DE90-004838] 09 p1195 N90-16922
Fatigue crack growth in martensitic 2 1/4Cr-1Mo steel at elevated temperatures
[AERE-R-13524] 13 p1776 N90-20191
Rolling contact fatigue of surface modified 440C using a 'Ge-Polymet' type disc rod test rig
[NASA-TM-100390] 13 p1777 N90-20200

MARTENSITIC TRANSFORMATION
Martensite transformation in NiTi alloys induced by tensile stress pulses
[DE90-001832] 06 p0747 N90-14346
Multiple martensitic transformations, incommensurate/commensurate phases, and charge-density-wave states in plutonium metal: Their consequences
[DE90-001235] 06 p0748 N90-14350
Theory of the energetics and nonclassical nucleation for martensitic transformations from partially soft lattice modes
[DE90-002182] 06 p0854 N90-14964
Energetics of BCC-FCC lattice deformation in iron
[AD-A213801] 07 p0905 N90-15233
Heat-resistant steels containing 8 pct Cr
[PB90-108796] 09 p1193 N90-16912
Martensitic transformation induced by stress pulses
[DE90-009534] 15 p2069 N90-21854
The stability of the martensitic phases in Cu-Zn-Al at an electron concentration of 1.534
[DE90-628628] 23 p3311 N90-28727

MARTINGALES
On the smooth fit boundary conditions in the optimal stopping problem for semimartingales
[CWI-MS-R8819] 04 p0542 N90-13147
Random Markov processes and uniform martingales
[CWI-BS-R8908] 05 p0690 N90-14021
Theory of goodness of fit tests and scanning innovation martingales
[CWI-BS-R8904] 05 p0693 N90-14046
Bilateral prediction
[AD-A219564] 17 p2456 N90-24016
The existence of smooth densities for the prediction filtering and smoothing problems
[AD-A222108] 21 p3066 N90-27432

MARYLAND
Acid deposition in Maryland: Summary of results through 1989
[PB90-229782] 22 p3200 N90-28160

MASER OUTPUTS
Spin-lattice relaxation and the calculation of gain, pump power, and noise temperature in ruby 04 p0486 N90-12790

MASER PUMPING
Spin-lattice relaxation and the calculation of gain, pump power, and noise temperature in ruby 04 p0486 N90-12790

MASER RESONATORS
U MASERS
MASERS
NT HYDROGEN MASERS
NT INTERSTELLAR MASERS
NT TRAVELING WAVE MASERS
NT WATER MASERS
A closed-cycle refrigerator for cooling maser amplifiers below 4 Kelvin 04 p0487 N90-12797
Research on heating, instabilities, turbulence and RF emission from electric field dominated plasmas [AD-A212122] 04 p0557 N90-13243
Nonlinear quantum effects in the Maser model: A large N scaling behaviour [DE89-631631] 06 p0787 N90-14584
Squeezing of many-atom radiation in an optical cavity [AD-A215736] 09 p1280 N90-17422
A new interpretation of the feature of SiO maser spectra associated with M-type star [DE90-610641] 11 p1590 N90-19174
Biological applications and effects of optical masers [AD-A217910] 13 p1808 N90-20385
Operation of a step tunable megawatt gyrotron 15 p2061 N90-21802
The 10-100 kW submillimeter gyrotron 15 p2061 N90-21803
An 8.4-GHz dual-maser front-end system for Parkes reimplementation 15 p2078 N90-21905
Cyclotron maser and plasma wave growth in magnetic loops [NASA-CR-179862] 15 p2170 N90-22402
Gravitational radiation produced by high energy accelerators and high power lasers [PREPRINT-701] 16 p2240 N90-22782
Potential of solar-simulator-pumped alexandrite lasers [NASA-TM-102701] 22 p3180 N90-28046
An x ray source for lithography [AD-D014596] 24 p3473 N90-29630
MASKING
Effect of contralateral masking parameters on difference limen for intensity [AD-A214169] 10 p1411 N90-18135
Method for maintaining precise suction strip porosities [NASA-CASE-LAR-13638-1] 12 p1641 N90-19427
Binaural masking: An analysis of models [AD-A221668] 21 p3035 N90-27252
MASKS
Anthropometry of a fit test sample used in evaluating the current and improved MCU-2/P masks [AD-A215173] 11 p1541 N90-18873
MASS
NT CENTER OF MASS
NT CRITICAL MASS
NT GALACTIC MASS
NT PARTICLE MASS
NT STELLAR MASS
Estimation of the C-J pressure of explosives [DE89-013811] 02 p0208 N90-11187
Effects of main-sequence mass loss on the turnoff ages of population 1 clusters [DE89-016755] 03 p0421 N90-12417
Black-hole decay and topological stability in quantum gravity [DE89-618785] 06 p0863 N90-15017
Mass loss during x ray microanalysis [DE90-003954] 08 p1049 N90-16067
Some theoretical aspects of cold fusion: A report [DE90-601098] 08 p1125 N90-16514
Quartz crystal resonator mass loading [AD-A215199] 09 p1212 N90-17028
Development of a mass averaging temperature probe 11 p1461 N90-18418
Cepheid masses for models with enhanced opacities [DE90-014919] 23 p3409 N90-29266
MASS DISTRIBUTION
Theoretical statistics of zero-age cataclysmic variables 01 p0141 N90-10810
Effect of control surface mass unbalance on the stability of a closed-loop active control system [NASA-TP-2952] 03 p0357 N90-12042
Biomodal spontaneous fission [DE90-001516] 06 p0840 N90-14886
A procedure for force-balancing planar linkages using counterweights [ESDU-89028] 07 p0940 N90-15446
Agglomeration of ceramic powders 09 p1223 N90-17098
The effect of loading on the laser ablation of graphite/epoxy composite material [AD-A216209] 10 p1349 N90-17826
Evaluation of helmet retention systems using a pendulum device [AD-A215489] 11 p1542 N90-18874
Mapping and spectroscopy of the 3.3 microns feature in Orion 11 p1582 N90-19112
Inclusion of clouds and rain in atmospheric slant path calculations 15 p2083 N90-21925
The mass of the Coma cluster 15 p2188 N90-22496
An astrophysics data program investigation of cluster evolution [NASA-CR-181296] 15 p2191 N90-22510
Dust environment modelling from encounters with comet P/Halley 17 p2485 N90-24210
Neptune, 2000 plus: Concept of a heavy space freighter for the 21st century [ILR-MITT-229(1989)] 18 p2509 N90-24338
Multiwavelength constraints on gamma-ray burst sources 18 p2639 N90-25032
A kinematic/dynamic model for prediction of neck injury during impact acceleration 19 p2719 N90-25469
Nonlinear supersonic motions of magnetized plasma flow with mass loading [AERONOMICA-ACTA-A-354-1990] 19 p2760 N90-25681
The accretion disk in the galactic center: An independent indication for a massive central object 19 p2790 N90-25881
The iron abundance gradient in the intracluster medium of Perseus: A galactic wind model. Application to other clusters 19 p2793 N90-25901
Neutral column density and soft excesses in active galactic nuclei 19 p2794 N90-25908
Near-infrared speckle observations of T Tauri stars and a multi-wavelength study of the prototype star T Tauri 23 p3409 N90-29264
MASS FILTERS
U FLUID FILTERS
MASS FLOW
A simple, mass balance model of carbon flow in a controlled ecological life support system [NASA-TM-102151] 01 p0101 N90-10571
Physical process in MPD plasmas [AD-A213679] 07 p0996 N90-15761
Geometric scale of interaction between moving shock and stationary thermal layer [AD-A217769] 13 p1802 N90-20344
The equipment for mass flow measurements in the low-speed wind tunnel at DFVLR in Brunswick (Federal Republic of Germany) [ESA-TT-1125] 23 p3285 N90-28585
Specifications, tolerances, and other technical requirements for weighing and measuring devices as adopted by the 74th National Conference on Weights and Measures, 1989 (1990 edition) [PB90-184961] 23 p3316 N90-28748
MASS FLOW FACTORS
Annual summary of basic research in thermoacoustic heat transport [AD-A214185] 07 p1007 N90-15834
MASS FLOW RATE
Two-phase flow pressure losses in pipeline fittings [ESDU-89012] 04 p0500 N90-12883
Acquisition and correlation of cryogenic nitrogen mass flow data through a multiple orifice Joule-Thomson device [NASA-TM-103121] 16 p2237 N90-22761
The entrainment rate for a row of turbulent jets [NASA-CR-185278] 23 p3269 N90-28504
The equipment for mass flow measurements in the low-speed wind tunnel at DFVLR in Brunswick (Federal Republic of Germany) [ESA-TT-1125] 23 p3285 N90-28585
MASS RATIOS
NT MASS TO LIGHT RATIOS
Theoretical statistics of zero-age cataclysmic variables 01 p0141 N90-10810
MASS SPECTRA
Time-resolved mass spectrometry technique for studying fast transient CHNO explosive decomposition kinetics [DE89-016540] 02 p0193 N90-11101
Initial results of positron ionization mass spectrometry 11 p1561 N90-18995
Study of the polyoxymethylene and its sputtered fragments: Implications for comets 20 p2949 N90-26781
Composite materials with improved properties in compression. Appendix 1: Cyclopropanation of poly(1-methyl 1-phenyl 1-sila-cis-pent-3-ene). Synthesis and characterization of poly(1-methyl 3,4-methylene-1-phenyl 1-sila-cis-pent-3-ene) [AD-A221494] 21 p2971 N90-26889
Spectroscopy of ions and their clusters [AD-A223109] 21 p2977 N90-26917
Studies of central interactions of Si ions at 14.5 x A GeV/c in Au and Cu [DE90-015095] 23 p3397 N90-29195
Emission of quick neutrons and non-equilibrium phenomena by central shocks in the reaction 40 Ar + 40 Ca at 20 MeV/u [ETN-90-97296] 24 p3544 N90-30043
MASS SPECTROMETERS
Ion detector on the basis of microchannel plates for a high-sensitive mass spectrometer [DE89-620335] 02 p0225 N90-11291
Experimental research in high energy physics [DE90-000061] 03 p0408 N90-12342
A double focusing mass-spectrometer for simultaneous ion measurements in the stratosphere 05 p0659 N90-13848
Neutral air turbulence in the middle and upper atmosphere observed during the MAC/EPSILON campaign 05 p0660 N90-13855
Strategic characteristics of Dynamics Explorer 1 retarding ion mass spectrometer and the consequences for core plasma measurements [AD-A214013] 07 p0886 N90-15125
Performance of an Inductively Coupled Plasma-Mass Spectrometer Analyzer system [DE90-004002] 08 p1043 N90-16025
A double focussing mass-spectrometer for simultaneous ion measurements in the stratosphere [AERONOMICA-ACTA-A-350-1989] 08 p1102 N90-16379
The in-situ cometary particulate size distribution measured for one comet: P/Halley 08 p1145 N90-16637
Acquisition of analytical instruments for combustion research [AD-A214495] 09 p1190 N90-16893
Spark source mass spectrometry software documentation and verification [DE90-004463] 09 p1192 N90-16909
Development of a quadrupole-based Secondary-Ion Mass Spectrometry (SIMS) system at Lewis Research Center [NASA-TM-102531] 17 p2367 N90-23476
Surface physics instrumentation [AD-A220460] 17 p2373 N90-23512
Pre-concentration method for inductively coupled plasma-mass spectrometry [PB90-181348] 19 p2673 N90-25202
Thermogravimetry-mass spectrometry analysis of gas bubbles in molten glass [DE90-014116] 23 p3303 N90-28684
Reflection Mass Spectrometry (REMS) during 3/5 MBE [DE90-014568] 23 p3304 N90-28690
MASS SPECTROMETRY
U MASS SPECTROSCOPY
MASS SPECTROSCOPY
The effect of degree of aromaticity and alkyl substitution of polyaromatic hydrocarbons on instrumental response factors [DE89-000761] 02 p0196 N90-11117
Laser ionization mass spectroscopy [DE89-008039] 03 p0352 N90-12015
Improved method for determination of helium-4 in helium-3 by mass spectrometry [PB89-201404] 04 p0469 N90-12686
Polymer characterization by electrohydrodynamic ionization mass spectrometry [AD-A212130] 04 p0478 N90-12739
Combined capillary electrophoresis and electrospray ionization mass spectrometry [DE90-001903] 06 p0743 N90-14322
Capillary electrophoresis ionization-mass spectrometry and tandem mass spectrometry [DE90-002664] 07 p0892 N90-15158
Analysis of ambient polar volatile organic compounds using chemical ionization-ion trap detector [PB90-106451] 07 p0956 N90-15529
Organic chemistry of cometary dust as derived from PUMA 1 data 08 p1143 N90-16628
Composition of dust from Comet P/Halley: The mineral fraction 08 p1144 N90-16631
Quality control programs for isotope dilution mass spectrometry [DE90-004259] 09 p1189 N90-16891
Kinetics of boron hydride interconversion reactions [AD-A215386] 09 p1192 N90-16906
A gas chromatograph/mass spectrometry method for determining isotopic distributions in organic compounds used in the chemical approach to stable isotope separation [DE90-005738] 10 p1352 N90-17841
Chamber investigations of the fate of diesel emissions in the atmosphere. Volume 2: AMES assay and GCMS final data reports and gas phase projections [PB90-114430] 10 p1405 N90-18104
Evaluation of a commercial gas chromatography/matrix isolation-infrared spectrometer for quantitative analysis of priority pollutants [DE90-006033] 11 p1484 N90-18542

Application of high performance liquid chromatography/mass spectrometry to environmental analysis
[PB90-116963] 11 p1531 N90-18814
Laser mass spectrometric studies of high temperature superconductor ablation
[DE90-006518] 12 p1668 N90-19585
CCST (Center for Compound Semiconductor Technology) research briefs
[DE90-006446] 12 p1721 N90-19887
Production and analysis by mass spectrometry of beams of polyglycol ions 15 p2066 N90-21835
Development of a quadrupole-based Secondary-Ion Mass Spectrometry (SIMS) system at Lewis Research Center
[NASA-TM-102531] 17 p2367 N90-23476
Monitoring of catalyst performance in CO2 lasers using frequency modulation spectroscopy with diode lasers 18 p2561 N90-24614
Mass spectrometry of poly(methyl methacrylate)s of low molecular weight 20 p2829 N90-26091
Laboratory study of ion-neutral collisions at suprathermal energies
[AD-A222117] 21 p3074 N90-27475
Chemical and laser sciences division
[DE90-013532] 21 p3101 N90-27611
Mass spectrometric analysis of hydrogen isotopes in metals and metal hydrides
[DE90-014118] 23 p3303 N90-28685
Reflection Mass Spectrometry (REMS) during 3/5 MBE
[DE90-014568] 23 p3304 N90-28690
Study of the induction time in isothermal decomposition of explosives
[DE90-014906] 23 p3315 N90-28745
Proceedings of a discussion meeting on Thermodynamics of Alloys
[AD-A224336] 24 p3449 N90-29476
Production of NO, NO2 and N2O in air by breakdown with high power microwaves: A preliminary report
[AD-A223297] 24 p3495 N90-29749

MASS TO LIGHT RATIOS

On the mass to light ratios of dwarf spheroidal galaxies
[DE90-610645] 11 p1591 N90-19175

MASS TRANSFER

PORFLO-3: A mathematical model for fluid flow, heat, and mass transport in variably saturated geologic media: Users manual, version 1.0
[DE89-013977] 01 p0069 N90-10398
On transonic flow over segmented slotted wind tunnel wall with mass transfer 02 p0294 N90-11676
A lightweight solid polymer electrolyte fuel cell with stack power density of 3 kW/lb (7 kW/kg)
[AD-A211542] 03 p0367 N90-12098
Human body regional convective heat transfer determination using sublimating naphthalene disks
[AD-A212170] 03 p0380 N90-12165
Studies of gas turbine heat transfer airfoil surfaces and end-wall cooling effects
[AD-A212451] 04 p0457 N90-12620
Heat and mass transfer design issues in PEM fuel cell hardware
[DE89-016779] 06 p0804 N90-14677
Advanced study in solid transport: Rheological behavior of dense suspension
[DE90-003369] 07 p0947 N90-15483
Thermal histories of the samples of two KOSI comet nucleus simulation experiments 08 p1147 N90-16645
Evaluation of the use of flat terrain models versus complex terrain screening models in estimating pollutant transport and deposition in complex terrain
[DE90-005271] 09 p1245 N90-17223
A model for evaporation of freely falling droplets
[PUBL-AIR-QUALITY-6] 10 p1384 N90-18007
Dose assessment during complex meteorology in the Texas Panhandle
[DE90-006026] 10 p1408 N90-18118
Oxygen electrode in molten carbonate fuel cells
[DE90-005377] 11 p1528 N90-18796
Perspectives on aerosol deposition to natural surfaces
[DE90-003398] 11 p1532 N90-18819
Enhancement of mass transfer to a rotating cylinder electrode by inert particles suspended in the electrolyte
[DE90-008054] 13 p1771 N90-20165
Mass transfer from a sphere in an oscillating flow with zero mean velocity
[NASA-TM-102566] 13 p1801 N90-20338
Solar cyclical trend study of the mid-latitude, quiet-time, meridional, neutral winds at winter solstice conditions
[AD-A217398] 13 p1841 N90-20568
Numerical simulation model for hydrazine attitude control thrusters. Part 1: Model description
[INPE-4952-RPE/601] 14 p1942 N90-21115
The modelling of heat and mass transfer near solid boundaries and comparison with experimental results
[PB90-167040] 14 p1974 N90-21310
WINCOF-I code for prediction of fan compressor unit with water ingestion
[NASA-CR-185157] 15 p2045 N90-21724
Investigation of the late stages of stellar evolution: Mass loss from evolved stars 15 p2187 N90-22492
The association of supernovae with regions of recent star formation in late-type galaxies 15 p2188 N90-22497
Sticking coefficient of HCl on aerosols 16 p2208 N90-22598
Rapid mass transfer in binary systems 16 p2332 N90-23289
Numerical and physical modelling of bubbly flow phenomena
[DE90-009837] 17 p2401 N90-23677
Precision laser cutting
[DE90-009949] 17 p2407 N90-23717
Improvements in macroreticular particles for ion-exchange and gel-permeation chromatography
[DE90-003717] 18 p2522 N90-24399
Mass transfer induced convection near gas-liquid interfaces
[ETN-90-96925] 18 p2552 N90-24568
Radiation-driven evolution of low-mass x ray binaries 18 p2637 N90-25022
Large scale structure and microwave background anisotropies in cosmological models and stellar photometry techniques with the wide field/planetary camera of the Hubble space telescope 18 p2637 N90-25023
Hard X rays with a power law spectrum from a neutron star accreting through the relativistic gap 19 p2777 N90-25793
Photon sputtering of H2O ices: A preliminary report 20 p2949 N90-26783
The mathematical modeling of arc welding operation
[DE90-013700] 22 p3183 N90-28064
Gas-film flow in tubes
[DE90-011528] 23 p3324 N90-28793

MASSIFS

Satellite image atlas of glaciers of the world: Irian Jaya, Indonesia, and New Zealand
[PB90-230095] 24 p3483 N90-29691

MASSIVELY PARALLEL PROCESSORS

The rewrite rule machine project
[AD-A210528] 01 p0109 N90-10617
The upwind control volume scheme for unstructured triangular grids
[NASA-TM-101664] 03 p0301 N90-11703
Krylov methods preconditioned with incompletely factored matrices on the CM-2
[NASA-CR-181961] 06 p0822 N90-14779
High performance parallel architectures
[DE90-001055] 06 p0823 N90-14782
Paralation views: Abstractions for efficient scientific computing on the connection machine
[AD-A213935] 07 p0971 N90-15604
How to cluster in parallel with neural networks 08 p1113 N90-16443
Parallel algorithms for interactive manipulation of digital terrain models 08 p1113 N90-16445
Stochastic simulation of charged particle transport on the massively parallel processor 08 p1114 N90-16448
Estimating water flow through a hillslope using the massively parallel processor 08 p1114 N90-16449
Scan line graphics generation on the massively parallel processor 08 p1114 N90-16450
BLITZEN: A highly integrated massively parallel machine 08 p1115 N90-16453
A generic fine-grained parallel C 08 p1115 N90-16454
Parallelizing the SDI ACCESS algorithm for the Connection Machine-2
[DE90-006382] 11 p1548 N90-18909
Massively-parallel computational fluid dynamics
[AD-A217732] 13 p1802 N90-20342
Parallel computer graphics algorithms for the connection machine
[AD-A217300] 13 p1872 N90-20733
A model and implementation of multigrid for massively parallel computers
[DE90-008165] 13 p1873 N90-20739
Implementation of midcourse tracking and correlation on massively parallel computers
[DE90-008166] 13 p1873 N90-20740
Performance bounds on parallel self-initiating discrete-event
[NASA-CR-182010] 14 p2016 N90-21556
Multigrid on massively parallel computers
[DE90-008999] 14 p2017 N90-21560
Calculation of 3-dimensional synthetic seismograms on the connection machine
[AD-A218472] 16 p2255 N90-22857
Computational chaos in massively parallel neural networks 16 p2283 N90-23012
Potential performance of methods for parallelism across time in ODEs
[DE90-010992] 18 p2596 N90-24774
Efficient network topologies for extensible massively parallel computers
[ETN-90-97220] 20 p2912 N90-26568
Massively parallel architecture: Integrated cell network for image reconstruction
[ETN-90-97257] 20 p2913 N90-26575
An even-parity/odd-parity formulation for deterministic transport calculations on massively parallel computers
[DE90-015036] 23 p3384 N90-29116
Overcoming rule-based rigidity and connectionist limitations through massively-parallel case-based reasoning
[NASA-CR-186963] 23 p3384 N90-29117
Fault tolerant design for multistage routing networks
[AD-A224267] 24 p3533 N90-29978

MASTICATION

Decompression sickness affecting the temporomandibular joint
[AD-A220959] 18 p2584 N90-24715

MATCHED FILTERS

Analysis of two-pass Modified Hough Transform (MHT) technique for the detection of wake like signals
[AD-A211982] 03 p0338 N90-11924
Efficient detection of small moving objects
[AD-A213314] 05 p0632 N90-13690
Electron-beam phase-only spatial light modulator for matched filtering
[AD-A215026] 09 p1282 N90-17431
Neurobeamformer 2: Further exploration of adaptive beamforming via neural networks
[AD-A215118] 10 p1426 N90-18226
High-resolution acoustical imaging 13 p1881 N90-20793
Phase-only holographic filters and their applications
[PB90-166802] 14 p1984 N90-21368
Quantum-limited image recognition
[AD-A218425] 16 p2299 N90-23101
Laser radar angular tracking
[AD-A222741] 20 p2869 N90-26319

MATCHING

Extending matchings in planar graphs 4
[AD-A210315] 01 p0113 N90-10643
Optimal matching of 3-D convex polyhedra
[TELECOM-PARIS-89C003] 03 p0395 N90-12258
Towards a complete local solution of the nonlinear model matching problem
[MEMO-781] 04 p0545 N90-13166
Conjugate profiles on mating gear teeth
[MEMO-COSOR-89-01] 05 p0651 N90-13795
An editor for 3D-models for image analysis
[FOA-C-30534-3.4] 05 p0684 N90-13986
Matching extension in regular graphs
[AD-A214757] 09 p1266 N90-17339
Derivation of an efficient rule system pattern matcher
[AD-A216801] 11 p1549 N90-18917
Conjugate field approaches for active array compensation 12 p1610 N90-19266
On the verification of hypothesized matches in model-based recognition
[AD-A214718] 12 p1699 N90-19759
Almost-optimum parallel speed-ups of algorithms for bipartite matching and related problems
[AD-A215111] 13 p1871 N90-20728
Robust adaptive nonlinear control under extended matching conditions
[AD-A217684] 13 p1874 N90-20744
Object detection using structural matching
[INPE-4954-PRE/1532] 15 p2159 N90-22333
Development of a least squares time response lower-order equivalent systems technique
[AD-A220527] 17 p2351 N90-23389
A topological image matcher
[OUEL-1798/89] 19 p2744 N90-25600
The image of weighted combinatorial problems
[REPT-88-017] 21 p3057 N90-27382

MATERIAL ABSORPTION

Phase equilibrium and crystal growth studies on AgGaSe2 and related nonlinear optical materials
[AD-A213650] 07 p1003 N90-15809
Plasma cloaking: Air chemistry, broadband absorption, and plasma generation
[AD-A222044] 21 p3078 N90-27503
Laser diode pumped, erbium-doped, solid state laser with high slope efficiency
[AD-D014482] 22 p3179 N90-28040

MATERIAL BALANCE

NT WATER BALANCE

MATERIAL REMOVAL (MACHINING)
U MACHINING
MATERIAL STRENGTH
U MECHANICAL PROPERTIES
MATERIALS
Material evaluation of optical fibers and payout bobbins: An overview
[AD-A220104] 17 p2473 N90-24140
MATERIALS HANDLING
NT GROUND HANDLING
NT PROPELLANT TRANSFER
NT REMOTE HANDLING
Plasma separation process: Magnet move to Oak Ridge National Laboratory
[DE89-017457] 04 p0556 N90-13242
Examples of robots and teleoperators at the Savannah River Site
[DE90-004659] 08 p1086 N90-16284
Handling and analysis of ices in cryostats and glove boxes in view of cometary samples
08 p1146 N90-16643
Effectiveness of progressive resistance training for increasing maximal repetitive lifting capacity
[AD-A215286] 09 p1252 N90-17267
RF modal quantity gaging 11 p1474 N90-18483
Knowledge-based robotic grasping
[DE90-007216] 13 p1811 N90-20402
RIPE: An object-oriented Robot Independent Programming Environment
[DE90-008501] 13 p1866 N90-20707
Application of optimization in design and motion control of robot manipulators 14 p1988 N90-21393
Technical accomplishments of the NASA Lewis Research Center, 1989
[NASA-TM-102296] 17 p2486 N90-24220
Modeling strength data for CREW CHIEF
19 p2729 N90-25516
Very low height drop test. Conditioning and tandem dropping of two loads conditioned in two PC6 platforms assembled by rigid structures
[REPT-89/07] 22 p3193 N90-28116
Very low height drop test. Conditioning and tandem dropping of two loads conditioned in two PC6 platforms assembled by one PD9 platform and rigid structures
[REPT-89/04] 22 p3193 N90-28117
Very low height drop test. Conditioning and tandem dropping of two loads conditionned in two PC6 platforms assembled by rigid structures
[REPT-89/08] 22 p3193 N90-28118
MATERIALS RECOVERY
NT NUCLEAR FUEL REPROCESSING
NT SOLVOLYSIS
NT WATER RECLAMATION
Correlating microemulsion fuel composition, structure and combustion properties
[DE89-017779] 03 p0333 N90-11898
Research and Development Opponunities in Supercritical Fluid Technology
[DE89-015320] 04 p0469 N90-12684
Managing the waste stream: Background information for planning source separation programs
[PB90-100223] 07 p0956 N90-15530
Enhanced bioreclamation of jet fuels: A full-scale test at Eglin AFB, Florida
[AD-A222348] 21 p2990 N90-26992
Study of power generation systems for CO2 collection: LNG combined cycle
[DE90-507881] 23 p3345 N90-28901
MATERIALS SCIENCE
Flight experiment hardware for sounding rocket investigations. Materials science and fluid sciences
[ESA-SP-1116] 08 p1038 N90-15998
Solid state research
[NASA-CR-186699] 17 p2476 N90-24160
Solid state research
[NASA-CR-186700] 17 p2477 N90-24161
Future automotive materials: Evolution or revolution
18 p2516 N90-24370
MATERIALS TESTS
Research and test facilities for development of technologies and experiments with commercial applications
[NASA-TM-101789] 02 p0159 N90-10909
Tests for aircraft interior materials in fire accident
[LR-622] 24 p3423 N90-29337
MATHEMATICAL ANALYSIS
U APPLICATIONS OF MATHEMATICS
MATHEMATICAL LOGIC
NT ALGORITHMS
NT AXIOMS
NT BOOLEAN ALGEBRA
NT BOOLEAN FUNCTIONS
NT EQUIVALENCE
NT FORMULAS (MATHEMATICS)
NT LATTICES (MATHEMATICS)
NT PARSING ALGORITHMS
NT SET THEORY
NT SIMPLEX METHOD
Applications of algebraic logic and universal algebra to computer science
[AD-A210556] 01 p0113 N90-10845
A digital model for level-clocked circuitry
[AD-A211937] 03 p0343 N90-11957
Optical arithmetic logic using the modified signed-digit redundant number representation
[AD-D014176] 03 p0384 N90-12186
Some techniques for anaphora resolution in algebraic linguistics
[REPT-89-28] 03 p0396 N90-12265
Fuzzy logic and the generalized modus ponens
[REPT-88-92] 03 p0397 N90-12274
Anaphoric trees and an extension of the model of anaphora resolution
[REPT-89-37] 04 p0540 N90-13130
Optimization of monotonic inference algorithms in propositional and first order logic
[LAAS-89204] 08 p1111 N90-16436
Job planning and execution monitoring for a human-robot symbiotic system
[DE90-004464] 09 p1261 N90-17315
Research and development in natural language understanding as part of the Strategic Computing Program
[AD-A214586] 09 p1264 N90-17330
Induction on a continuous variable
[DE90-606952] 10 p1422 N90-18203
Joint Japanese-American Workshop on Future Trends in Logic Programming
[DE90-008343] 13 p1867 N90-20709
A paradoxical result in unconditionally secure authentication codes, and an explanation
[DE90-008529] 13 p1867 N90-20710
OTTER (Organized Techniques for Theorem-proving and Effective Research) 2.0 users guide
[DE90-007978] 14 p2018 N90-21563
Some remarks on treatment of be in Montague's PTQ --- Proper Treatment of Quantification (PTQ)
[REPT-89-40] 15 p2147 N90-22267
Increased stuck-at fault coverage with reduced I(sub DDQ) test sets
[DE90-009509] 16 p2245 N90-22804
CMOS IC I(sub DDQ) testing for the 1990s
[DE90-009508] 17 p2394 N90-23634
On the early history of intuitionistic logic
[ITLI-LP-89-04] 17 p2440 N90-23900
Remarks on intuitionism and the philosophy of mathematics
[ITLI-LP-88-05] 17 p2440 N90-23901
Explanation and the theory of expert problem solving
[AD-A220861] 17 p2444 N90-23930
On models for propositional dynamic logic
[RUU-CS-89-3] 17 p2460 N90-24046
Arithmetic classification of perfect models of stratified programs (extended version)
[CWI-CS-R8928] 17 p2462 N90-24063
The fine-structure of categorial semantics
[ITLI-LP-89-01] 17 p2464 N90-24075
Dynamic predicate logic: Towards a compositional, non-representational semantics of discourse
[ITLI-LP-89-02] 17 p2464 N90-24076
Two-dimensional modal logics for relational algebras and temporal logic of intervals
[ITLI-LP-89-03] 17 p2464 N90-24077
Intensional Lambek calculi: Theory and application
[ITLI-LP-89-06] 17 p2464 N90-24078
Language in action
[ITLI-LP-89-04] 17 p2480 N90-24182
Modal logic as a theory of information
[ITLI-LP-89-05] 17 p2480 N90-24183
Explicit fixed points for interpretability logic
[ITLI-ML-89-01] 18 p2603 N90-24820
Rosser orderings and free variables
[ITLI-ML-89-03] 18 p2603 N90-24822
Sigma-completeness and bounded arithmetic
[ITLI-ML-89-05] 18 p2603 N90-24823
Formal verification of distributed computing systems: Logic characterization of behaviour equivalence
[LAAS-89386] 20 p2910 N90-26555
Study of an environment using formal reasoning. DILOG: State of the art and prototype
[CERT-1/334300-DERI] 22 p3239 N90-28368
MATHEMATICAL MODELS
NT ANALOG SIMULATION
NT BIOLOGICAL MODELS (MATHEMATICS)
NT DIGITAL SIMULATION
NT K-EPSILON TURBULENCE MODEL
NT PETRI NETS
NT TURBULENCE MODELS
ILS (Instrument Landing System) mathematical modeling study on the effects of proposed hangar construction west of runway 18R on localizer performance at Dallas-Fort Worth International Airport
[AD-A210631] 01 p0005 N90-10019
The addition of Bendix MLS (Microwave Landing System) antenna patterns to MLS mathematical model
[AD-A210633] 01 p0005 N90-10020
Compatibility of fuel system components with high density fuel
[AD-A210381] 01 p0006 N90-10027
The measurement of boundary layers on a compressor blade in cascade. Volume 1: Experimental technique, analysis and results
[NASA-CR-185118-VOL-1] 01 p0009 N90-10038
Missile Datcom: Enhancements for design applications
01 p0012 N90-10054
Aeroelastic tailoring procedure for controlling fin hinge moments 01 p0013 N90-10058
Identification of stability and control parameters of a brilliant ammunition 01 p0014 N90-10065
On analytic modeling of lunar perturbations of artificial satellites of the earth
[AD-A210440] 01 p0016 N90-10078
DYSCO: A software system for modeling general dynamic systems 01 p0018 N90-10089
Lumped mass formulations for modeling flexible body systems 01 p0019 N90-10091
Explicit modeling and computational load distribution for concurrent processing simulation of the space station
01 p0020 N90-10096
Simulation and control problems in elastic robots
01 p0020 N90-10098
Linearized flexibility models in multibody dynamics and control 01 p0020 N90-10099
Flexible robot control: Modeling and experiments
01 p0021 N90-10104
Modifying high-order aeroelastic math model of a jet transport using maximum likelihood estimation
01 p0021 N90-10106
Automated model formulation for time-varying flexible structures 01 p0022 N90-10107
Numerically efficient algorithm for model development of high-order systems 01 p0022 N90-10108
On modelling nonlinear damping in distributed parameter systems 01 p0022 N90-10109
Flexible aircraft dynamic modeling for dynamic analysis and control synthesis 01 p0022 N90-10112
Aircraft modal supression system: Existing design approach and its shortcomings
01 p0023 N90-10115
Modeling and stabilization of large flexible space stations 01 p0024 N90-10120
System identification for large space structures
01 p0025 N90-10126
Boost-phase discrimination research activities
[NASA-TM-101889] 01 p0032 N90-10176
Dynamic instability characteristics of aircraft turbine engine combustors 01 p0036 N90-10195
Very-low-frequency oscillations in liquid-fueled ramjets
01 p0037 N90-10204
Combustion-driven oscillation in large combustion systems for power generation 01 p0038 N90-10207
Reaction of oxygen with allene
[DE89-015219] 01 p0039 N90-10216
Direct numerical simulation of turbulent free shear flows
[AD-A210161] 01 p0040 N90-10218
Approximate simulation model for analysis and optimization in engineering system design
[NASA-TM-101616] 01 p0054 N90-10308
New electrodynamic and electrostatic models with applications to antenna theory, superconductor slots, and lasers 01 p0055 N90-10316
Improved propagation models for discrete random media
[AD-A211085] 01 p0057 N90-10327
Statistical modeling of electrical components
[BDX-613-3939] 01 p0059 N90-10336
Experimental study of instability modes in a three-dimensional boundary layer
01 p0064 N90-10369
Constitutive Relationships and Models in Continuum Theories of Multiphase Flows --- conferences
[NASA-CP-3047] 01 p0067 N90-10385
Iterative performance and an adaptive procedure for viscous flow problems 01 p0069 N90-10397
PORFLO-3: A mathematical model for fluid flow, heat, and mass transport in variably saturated geologic media: Users manual, version 1.0
[DE89-013977] 01 p0069 N90-10398
Global existence and asymptotic stability for a nonlinear integrodifferential equation modeling heat flow
[AD-A210647] 01 p0071 N90-10408

Similarity solutions that give rise to hyperbolicity and change of type in steady flow of a viscoelastic fluid
[AD-A210920] 01 p0072 N90-10410
Symmetry breaking bifurcations and the growth of chaos in a rotating fluid
[AD-A210969] 01 p0072 N90-10411
Design and operating characteristics of a CW relevant quasi-optical gyrotron with variable mirror separation
[AD-A210611] 01 p0074 N90-10425
The MHOST finite element program: 3-D inelastic analysis methods for hot section components. Volume 2: User's manual
[NASA-CR-182235-VOL-2] 01 p0079 N90-10450
Global/local stress analysis of composite structures
[NASA-TM-101640] 01 p0080 N90-10456
Analysis and test of a 16-foot radial rib reflector developmental model
[NASA-TM-101648] 01 p0080 N90-10457
Image-based terrain modeling with thematic mapper applied to resolving the limit of Holocene Lake expansion in the Great Salt Lake Desert, Utah, part 1
[NASA-CR-185913] 01 p0082 N90-10465
Evaluation of the North Atlantic seasonal nitrogen model, version 2
[DE89-016157] 01 p0090 N90-10515
Surface wave ray tracing and Ms:yield determination in a laterally heterogeneous earth
[AD-A210241] 01 p0090 N90-10516
Managing human exposure and health risks: An integrated approach and the role of uncertainty
[DE89-008611] 01 p0092 N90-10525
Tracking performance evaluation
[AD-A210499] 01 p0095 N90-10540
A simple, mass balance model of carbon flow in a controlled ecological life support system
[NASA-TM-102151] 01 p0101 N90-10571
Tests of various finite difference algorithms applied to a simple water vapor transport problem on a staggered grid
[AD-A210229] 01 p0105 N90-10596
Adaptive robust control 01 p0109 N90-10620
Numerical optimization in Hilbert space using inexact function and gradient evaluations
[NASA-CR-181926] 01 p0112 N90-10640
On lower confidence for PCS in truncated location parameter models
[AD-A210274] 01 p0115 N90-10661
A unified approach to estimating tail behavior
[AD-A210961] 01 p0117 N90-10672
Analytic theory for the selection of Saffman-Taylor fingers in the presence of thin film effects
[NASA-CR-181910] 01 p0118 N90-10677
A symplectic coherent beam-beam model
[DE89-015386] 01 p0122 N90-10701
Numerical simulation of the compressible Orszag-Tang vortex
[AD-A210465] 01 p0127 N90-10725
Effects of stress on judgment and decision making in dynamic tasks
[AD-A210605] 01 p0135 N90-10781
Low-Reynolds-number modeling of complex flows with and without density variation 02 p0146 N90-10832
A preliminary sensitivity analysis of the Generalized Escape System Simulation (GESS) computer program
[DE89-016691] 02 p0148 N90-10844
Results and practical experience using parameter identification techniques on the AM-X program at Aermacchi 02 p0153 N90-10873
On the development of a basic flight test capability and some related research projects
02 p0155 N90-10885
Environmental testing: An approach to more cost efficiency 02 p0176 N90-10988
STS payload design load evolution
02 p0176 N90-10989
A review of the Error of Matrix Method (EMM) for structural dynamic model comparison
02 p0177 N90-10993
Parametric identification of conservative self adjoint structures 02 p0177 N90-10994
A contribution to the stability analysis of large space structures 02 p0177 N90-10997
A super element for multibody dynamics
02 p0178 N90-11004
GEMMES: A new tool for dynamic modeling
02 p0179 N90-11005
Use of Lanczos vectors in structural dynamics
02 p0179 N90-11011
Evaluation of dispersive behavior in periodic structures by discrete Fourier transform 02 p0180 N90-11014
A direct two response approach for updating analytical dynamic models of structures with emphasis on uniqueness 02 p0182 N90-11028
Study of a gallium arsenide solar cell interconnector
02 p0182 N90-11033
Analysis of delamination growth
02 p0183 N90-11036
Induced shock loads during the separation of the Ariane 5 VEB structure 02 p0184 N90-11045
Mathematical model and predictions for static and dynamic behavior of solar array structure
02 p0184 N90-11049
Space telescope solar array: Nonlinear test and analysis effects 02 p0185 N90-11051
Hygrothermal deformations of composite shells
02 p0185 N90-11055
Numerical models for exterior and interior fluid-structure interaction problems 02 p0188 N90-11073
STSA-Space Telescope solar array interconnectors: From simple approaches to complex modeling. A case study of the necessity of complex analysis
02 p0188 N90-11076
Thermochemical model for shock-induced chemical reactions in porous thermite: The heat detonation model
[DE89-016528] 02 p0193 N90-11100
Modeling of hydrazine surface interactions in environmental reaction chambers
02 p0203 N90-11162
Numerical simulation of hydrazine transport in a sandy soil 02 p0205 N90-11172
Nitramine composite solid propellant modeling
02 p0207 N90-11183
A shock initiation model for fine-grained hexanitrostilbene
[DE89-007641] 02 p0207 N90-11185
Estimation of the C-J pressure of explosives
[DE89-013811] 02 p0208 N90-11187
Sharp shock model for propagating detonation waves
[DE89-016772] 02 p0221 N90-11266
Modeling and simulation of spatial robotic manipulators with flexible links and joint drives for control strategies implementation and evaluation 02 p0228 N90-11311
An evaluation of the Chaboche and Bodner-Partom viscoplastic constitutive theories for strain rate sensitive materials 02 p0232 N90-11330
The dynamic stability of an axially loaded beam with lateral elastic support and damping
02 p0232 N90-11331
An improved beam model for the vibrations of rotor blades 02 p0232 N90-11333
Empirical models of convection electric fields and electrostatic potential at high latitude from EISCAT observations: Preliminary results
02 p0243 N90-11377
Studies of time-dependent polar cap convection patterns 02 p0251 N90-11421
DOE/CEC Workshop on Critical Evaluation of Radiobiological Data to Biophysical Modeling
[DE89-015214] 02 p0254 N90-11437
Computer symbiosis: Emergence of symbiotic behavior through evolution
[DE89-015247] 02 p0256 N90-11450
Control and optimization for observations of systems governed by controlled partial differential equations
[AD-A211122] 02 p0266 N90-11513
Summaries of the FY 1989 Applied Mathematical Sciences Research program
[DE89-016694] 02 p0267 N90-11521
Partially specified probability measures in expert systems
[CWI-CS-R8842] 02 p0269 N90-11536
Singularity theory and N = 2 superconformal field theories
[DE89-016582] 02 p0269 N90-11538
Hybrid particle-fluid approach to low-frequency turbulence in magnetically confined plasmas
[DE89-015904] 02 p0277 N90-11579
Propagation of normal zones of finite size in large, composite superconductors
[DE89-016866] 02 p0282 N90-11611
General covariance and strings
[DE89-016505] 02 p0286 N90-11633
The upwind control volume scheme for unstructured triangular grids
[NASA-TM-101664] 03 p0301 N90-11703
Robust control design for flight control
[AD-A211957] 03 p0309 N90-11756
ILS mathematical modeling study of the effects of proposed hangar construction at the Orlando International Airport, Runway 17R, Orlando, Florida
[DOT/FAA/CT-TN89/52] 03 p0310 N90-11762
An integrated methodology for optimizing structural composite damping
[NASA-TM-102343] 03 p0319 N90-11808
Analysis of opposed jet hydrogen-air counter flow diffusion flame
[NASA-CR-182366] 03 p0321 N90-11825
International seminar on the inelastic behavior of solids: Models and utilization
[DE89-017420] 03 p0327 N90-11858
A rate-dependent constitutive model for Be
[DE89-017755] 03 p0327 N90-11861
A critical assessment of models available for the shock initiation of heterogeneous explosives
[MRL-TR-89-17] 03 p0333 N90-11896
Application of dimensional analysis to statistical process modeling
[AD-A211881] 03 p0335 N90-11905
Modelling and control of a diffusion/LPCVD furnace
[REPT-88-97] 03 p0336 N90-11910
Recent advances to NEC (Numerical Electromagnetics Code): Applications and validation
[DE89-009231] 03 p0337 N90-11917
Clutter models for subsurface electromagnetic applications
[PB89-229678] 03 p0338 N90-11925
Modeling of diffraction reflection and clutter loss in UHF radio wave propagation
[FEL-1988-28] 03 p0340 N90-11938
A digital model for level-clocked circuitry
[AD-A211937] 03 p0343 N90-11957
KIVA reactive hydrodynamics code applied to detonations in high vacuum
[DE89-016979] 03 p0346 N90-11974
Exploding metallic foil fuse modeling at Los Alamos
[DE89-016970] 03 p0350 N90-11998
An experimental and analytical program to develop crack tip fracture criteria
[AD-A211565] 03 p0359 N90-12051
Disturbances in the Arizona Monsoon
03 p0362 N90-12071
The effect of latent heat release on synoptic-to-planetary wave interactions and its implication for satellite observations: Theoretical modeling
03 p0362 N90-12073
The effect of latent heat release on synoptic-to-planetary scale wave interactions: Observational study
03 p0362 N90-12074
Use of satellite data and modeling to asses the influence of stratospheric processes on the troposphere
03 p0363 N90-12075
Laboratory and theoretical models of planetary-scale instabilities and waves 03 p0363 N90-12076
Laboratory and theoretical studies of baroclinic processes 03 p0363 N90-12077
A lightweight solid polymer electrolyte fuel cell with stack power density of 3 kW/lb (7 kW/kg)
[AD-A211542] 03 p0367 N90-12098
Evaluation and sensitivity analyses results of the MESOPUFF 2 model with CAPTEX (Cross-Appalachian Tracer Experiment) measurements
[PB89-198253] 03 p0368 N90-12103
Review of the national ambient air quality standards for lead: Exposure analysis methodology and validation
[PB89-207914] 03 p0368 N90-12104
Processing of DMSP magnetic data and its use in geomagnetic field modeling
[NASA-TM-100750] 03 p0370 N90-12115
Investigations of Eurasian seismic sources and upper mantle structure
[AD-A211806] 03 p0371 N90-12120
Seismic wave attenuation and yield determination at regional distances
[AD-A211548] 03 p0372 N90-12128
The conditional-event approach to distributed simulation
[NASA-CR-185890] 03 p0387 N90-12200
Efficient diagnosis of multiprocessor systems under probabilistic models
[NASA-CR-185965] 03 p0388 N90-12212
Sequential design of experiments with physically based models 23
[AD-A211918] 03 p0393 N90-12239
Mapping nonlinear integro-differential equations into the frequency domain
[RR-366] 03 p0394 N90-12249
Augmentations of grammatical categories in distributional-algebraic models of natural languages
[REPT-89-24] 03 p0396 N90-12262
On the asymptotic optimality of certain empirical Bayes simultaneous testing procedures
[AD-A211649] 03 p0397 N90-12270
Modeling and analysis of nonlinear time series
[RR-355] 03 p0397 N90-12272
Numerical solution of acoustic-structure interaction problems
[AD-A211505] 03 p0400 N90-12293
Non-stationary computer model of the asymptotic region of an electric arc gas heater
[IPPCZ-288] 03 p0407 N90-12330
Role of conceptual models in the design and use of information systems
[PB89-217376] 03 p0416 N90-12392
Problem of incomplete information in relational databases
[PB89-217533] 03 p0417 N90-12393

Flare model sensitivity of the Balmer spectrum
03 p0432 N90-12477
Basic research on methods of calculating supersonic and hypersonic flow
[ONERA-RSF-19/1123-AY-234A]
04 p0448 N90-12565
Euler equation solutions applied to a helicopter rotor in forward moving flight
[ONERA-RSF-32/1285-AY-346A]
04 p0452 N90-12592
Dynamic robot models using the Manutec r3 as an example
[ESA-TT-1132] 04 p0458 N90-12626
Phase change material for spacecraft thermal management
[AD-A211404] 04 p0462 N90-12648
SSME structural dynamic model development
[NASA-CR-183671] 04 p0463 N90-12650
Modeling of the dielectric behavior of composite materials
[CERT-1/1398-MO] 04 p0467 N90-12674
Vapor-liquid equilibrium of binary mixtures in the extended critical region. Part 1: Thermodynamic model
[PB89-218374] 04 p0469 N90-12687
FLIC (FLame with Implicit Convection): A detailed, two-dimensional flame model
[AD-A212953] 04 p0473 N90-12710
Vibration isolation technology: Sensitivity of selected classes of space experiments to residual accelerations
[NASA-CR-185443] 04 p0482 N90-12768
Aircraft SAR simulation Sargen 1.0
[FEL-1989-44] 04 p0491 N90-12823
Long wave atmospheric noise model, phase 1. Volume 1: Lightning occurrence rates and propagation theory
[AD-A212794] 04 p0493 N90-12836
Long wave atmospheric noise model, phase 1. Volume 2: Mode parameters
[AD-A212795] 04 p0493 N90-12837
Wire grid modeling of the linear tapered slot antenna
[AD-A212977] 04 p0494 N90-12842
Mathematical models for the linear induction motor
[RR-WB-88-17] 04 p0496 N90-12853
A computationally efficient modelling of laminar separation bubbles
[NASA-CR-185854] 04 p0499 N90-12872
A theoretical method for the mechanical calculation of heat exchangers with sliding heads, phase 1 study
[CETIM-110240-PHASE-1] 04 p0502 N90-12896
Evaluation of the near-wall k-epsilon turbulence model by comparison with direct simulations of turbulent channel flow
[AD-A212674] 04 p0503 N90-12903
Automated Steerable Nulling Antenna Processor (SNAP) model
[PB89-231740] 04 p0509 N90-12937
Mathematical simulation of dynamic compression tests using the Hopkinson bar method
[ISL-R-128/87] 04 p0513 N90-12960
Modeling the temperature rise at the tip of a fast crack
[AD-A212418] 04 p0514 N90-12966
Geodetic point positioning with GPS (Global Positioning System) carrier beat phase data from the CASA UNO experiment
[AD-A211955] 04 p0514 N90-12970
Improvement and extension of a radar forest backscattering model
[NASA-CR-186083] 04 p0515 N90-12973
Analysis and modeling of summertime convective cloud and precipitation structure over the Southeastern United States
[NASA-CR-185436] 04 p0519 N90-12996
NTRFACE for MAGIC
[AD-A212858] 04 p0538 N90-13112
A new decision rule for model structure identification of a class of nonlinear dynamic systems
[RR-360] 04 p0539 N90-13122
Lie-algebraic aspects of the classical nonrelativistic Calogero-Moser models
[CWI-AM-R8901] 04 p0542 N90-13148
The algebraic basis of mathematical morphology. Part 2: Openings and closings
[CWI-AM-R8904-PT-2] 04 p0543 N90-13150
Semantics and consistency of rule-based expert systems
[CWI-CS-R8824] 04 p0543 N90-13153
Remarks on the control of discrete time nonlinear systems
[MEMO-770] 04 p0544 N90-13158
The discrete-time single-server queueing model
[MEMO-780] 04 p0544 N90-13165
Towards a complete local solution of the nonlinear model matching problem
[MEMO-781] 04 p0545 N90-13166
Exponential modeling using combined forward and backward prediction
[AD-A212317] 04 p0545 N90-13169
Explicit modelling of state duration correlations in hidden Markov models --- speech recognition
[RSRE-MEMO-4152] 04 p0546 N90-13178
Random truncation models and Markov processes
[CWI-MS-R8817] 04 p0547 N90-13181
Different notions of uncertainty in quasi-probabilistic models
[CWI-CS-R8847] 04 p0547 N90-13182
Stochastic process models in device physics
[AD-A212284] 04 p0547 N90-13185
Corrections to the thin wall approximation in general relativity
[NASA-CR-186078] 04 p0562 N90-13274
Strings, p-branes and Skyrmions in curved space
04 p0565 N90-13293
Test network Delft
[ETN-90-96009] 05 p0577 N90-13365
Thermal barrier coating life prediction model development, phase 1
[NASA-CR-182230] 05 p0581 N90-13388
Constitutive modeling for isotropic materials (HOST)
[NASA-CR-179522] 05 p0582 N90-13390
Constitutive modeling for isotropic materials (HOST)
[NASA-CR-174718] 05 p0582 N90-13391
Discretization and model reduction for a class of nonlinear systems 05 p0583 N90-13397
Mathematical model identification for flight simulation, based on flight and taxi tests
[LR-550] 05 p0585 N90-13410
GOES I/M image navigation and registration
05 p0588 N90-13422
Bilinear modeling and nonlinear estimation
05 p0589 N90-13430
Atmospheric drag model calibrations for spacecraft lifetime prediction 05 p0591 N90-13439
A transient response method for linear coupled substructures
[NASA-TP-2926] 05 p0592 N90-13444
Large Deployable Reflector (LDR) thermal characteristics 05 p0596 N90-13460
Advanced composite materials for precision segmented reflectors 05 p0596 N90-13461
Explicit modeling and concurrent processing in the simulation of multibody dynamic systems
05 p0599 N90-13481
Initial test results for the mini-mast
05 p0600 N90-13482
A practical approach for minimum time control of the Spacecraft Control Laboratory Experiment (SCOLE), appendix A
[NASA-CR-186008] 05 p0602 N90-13495
Tycho astrometry 05 p0610 N90-13559
Modeling of the Hipparcos optical system
05 p0612 N90-13572
Modelling of satellite control thruster plumes
05 p0613 N90-13578
Fractography of composite delamination
[NASA-CR-183291] 05 p0617 N90-13599
A new model for the structure of silica glass
[AD-A212972] 05 p0627 N90-13659
Evaluation of selected computer models for modeling pyrotechnic and propellant devices
[AD-A213003] 05 p0629 N90-13671
Magneto-elastic interactions in conducting structures in transient magnetic fields 05 p0632 N90-13686
Stochastic modelling of EM scattering from foliage
[AD-A213118] 05 p0632 N90-13689
A three-dimensional potential flow analysis of dynamic fluid forces acting on a whirling centrifugal impeller bounded by a volute 05 p0637 N90-13717
Quadratic dynamical systems describing shear flow of non-Newtonian fluids
[AD-A212892] 05 p0638 N90-13720
An improved algorithm for the modeling of vapor flow in heat pipes
[NASA-CR-185179] 05 p0642 N90-13748
Large eddy simulation of homogeneous turbulence undergoing shear and thermal gradients. Application to one point closing models
[ECL-88-23] 05 p0643 N90-13754
Model and computation of three-dimensional turbulent jets in a crossflow
[ECL-89-007] 05 p0643 N90-13755
A stochastic model for the calculation of multiple scattered lidar returns
[DLR-FB-89-36] 05 p0648 N90-13778
Characterization of surfaces cut with a laser beam and thermal model of the process
[ISAL-89-0008] 05 p0648 N90-13780
The limiting friction force
[ECL-89-005] 05 p0652 N90-13801
Quantitative non-destructive evaluation using laser generated ultrasonic pulses 05 p0653 N90-13805
A study on the sensitivity and simultaneous adjustment of a hoop-column antenna surface
[NASA-TM-101538] 05 p0653 N90-13807
An evaluation of a fatigue crack growth prediction model for variable-amplitude loading (PREFFAS)
[LR-537] 05 p0656 N90-13822
Buckling load analysis for imperfect cylindrical shells, part 1
[LR-543-PT-1] 05 p0656 N90-13823
Design and evaluation of a new biaxial testing method for sheet material (SUPERBAT)
[LR-548] 05 p0656 N90-13824
The use of a deformation model for sampling digitalized stereoscopic images
[IMAG-RR-753-I] 05 p0664 N90-13884
Precision of semi-geometrically determined SLR baselines vs. site occupation time
[ETN-90-96007] 05 p0665 N90-13885
Strain accumulation and surface deformation along the San Andreas, California
[NASA-CR-185893] 05 p0666 N90-13894
The structural memory: A network model for human perception of serial objects
[CWI-CS-R8829] 05 p0675 N90-13930
Model reduction of weakly damped mechanical systems
[MEMO-798] 05 p0686 N90-13993
A solvable self-similar model of the sausage instability in a resistive Z-pinch
[AD-A213137] 05 p0688 N90-14006
Why stochastic modeling is essential in analyzing interdicted transportation network performance
[AD-A213140] 05 p0688 N90-14007
Using the physical structure of a system for control: An illustration
[MEMO-782] 05 p0689 N90-14014
Analysis of three approaches to qualitative simulation
[MEMO-INF-89-32] 05 p0691 N90-14035
A unified algebraic approach to integral and discrete evolution equations
[PREPRINT-668] 05 p0692 N90-14044
Self-decomposable distributions and branching processes
[MEMO-COSOR-89-06] 05 p0693 N90-14052
On stability of queueing models of local area networks with slotted ring protocols
[MEMO-795] 05 p0694 N90-14057
Analysis of a queueing model for slotted ring networks
[MEMO-796] 05 p0694 N90-14058
Modeling of power electronic systems with EMTP
[NASA-TM-102375] 05 p0695 N90-14060
Some comments on the solvable Chiral Potts model
[PREPRINT-673] 05 p0696 N90-14070
Analytical and computer-aided models of InP-based MISFETs and heterojunction devices
[AD-A211861] 05 p0702 N90-14106
Shear-induced inflation of coronal magnetic fields
[NASA-CR-186103] 05 p0715 N90-14178
Efficient real gas Navier-Stokes computations of high speed flows using an LU scheme
[NASA-TM-102429] 06 p0720 N90-14203
Risk-based fire safety experiment definition for manned spacecraft
[NASA-CR-183835] 06 p0731 N90-14262
Slush Hydrogen (SLH2) technology development for application to the National Aerospace Plane (NASP)
[NASA-TM-102315] 06 p0732 N90-14268
Optimal stochastic modeling and control of flexible structures
[AD-A212347] 06 p0733 N90-14269
A generalized thermomechanical constitutive model for metal matrix composites with plastic strain and damage
06 p0737 N90-14293
Investigation of combustion instability in ramjet combustors 06 p0739 N90-14303
Kinetics and mechanism of soot formation in hydrocarbon combustion
[NASA-CR-186162] 06 p0740 N90-14305
A numerical study of thin flame representations
[DE89-017889] 06 p0741 N90-14313
The thermally induced gas-phase reactions of methane and oxygen: A comparison of experimental and computational results
[DE90-000785] 06 p0742 N90-14317
RPE: A parabolic equation radio assessment model
06 p0759 N90-14419
A forecasting system using the parabolic equation: Application to surface-to-air propagation in the presence of elevated layers 06 p0760 N90-14420
Propagation modeling for some horizontally varying tropospheric ducts 06 p0760 N90-14422
Propagation prediction for the North Sea environment
06 p0760 N90-14423
Forward scatter propagation path loss testing using surrogate terrain in the 100 to 1500 MHz region
06 p0760 N90-14425

Improved reliability prediction for HF digital voice transmission 06 p0761 N90-14429
The thermal behavior of natural backgrounds and its prediction by means of numerical models 06 p0762 N90-14436
Low level range coverage performance prediction for VHF radar 06 p0763 N90-14439
Weather satellite and computer modeling approaches to assessing propagation over marine environments 06 p0764 N90-14443
The FTZ HF propagation model for use on small computers and its accuracy 06 p0765 N90-14447
Electron heating and static sheath enhancement in front of energized RF antennas
[DE90-001334] 06 p0766 N90-14456
Modeling of sodium/metal chloride batteries
[DE89-017685] 06 p0770 N90-14478
The fluid mechanics of filters 06 p0773 N90-14499
Granular flow: Numerical simulation of dry granular flows and calculation of hydrodynamic interactions in suspensions
[DE89-017544] 06 p0777 N90-14518
Pipe and bend erosion by pneumatic transport of solids at high temperature
[DE89-015741] 06 p0778 N90-14524
Course A: Numerical modeling of two-phase flows for presentation at Ecole d'Ete d'Analyse Numerique
[DE90-002074] 06 p0778 N90-14526
Electrothermal response testing more than a quality assurance tool
[DE90-001449] 06 p0780 N90-14536
Theoretical studies of solar lasers and converters
[NASA-CR-186194] 06 p0787 N90-14583
The current status of x ray conversion efficiency modeling
[DE90-000931] 06 p0789 N90-14591
Theory of harmonic radiation using a single-electron source model
[DE90-002412] 06 p0791 N90-14606
Tire modeling by finite elements 06 p0792 N90-14614
BES welding science contractors summary report, 1988 to 1989
[DE90-001004] 06 p0793 N90-14619
Thermal fatigue durability for advanced propulsion materials
[NASA-TM-102348] 06 p0797 N90-14641
Comparison of shock severity measures
[DE90-000790] 06 p0799 N90-14654
Implications and origins of shock structure in solids
[DE90-000846] 06 p0800 N90-14658
Critical time step estimation for three-dimensional explicit impact analysis
[DE90-002187] 06 p0801 N90-14662
Earth Sciences Division annual report 1988
[DE90-002617] 06 p0801 N90-14663
Heat transfer of buried pipe for heat pump application
[DE90-000580] 06 p0807 N90-14697
Turbulent wind at the equatorial segment of an operating Darrieus wind turbine blade
[DE90-002672] 06 p0807 N90-14698
A model for the simulation of the ozone budget in the atmosphere under anthropogenic perturbation
[DE89-636294] 06 p0811 N90-14719
Quantifying the link between change in radiative balance and atmospheric temperature
[DE90-000819] 06 p0811 N90-14721
Extraterrestrial halogen and sulfur content of the stratosphere
[DE89-017623] 06 p0815 N90-14738
Meteorological monitoring for environmental/dose assessment and emergency response modeling: How much is enough
[DE90-002726] 06 p0818 N90-14757
Factors affecting electron spin polarization in photosynthetic systems
[DE90-000196] 06 p0819 N90-14784
The development of a model of the human responses to load carriage 06 p0821 N90-14775
Program CICC flow and heat transfer in Cable-In-Conduit Conductors
[DE90-001519] 06 p0829 N90-14818
Symmetry breaking bifurcations of a current sheet
[DE90-601005] 06 p0837 N90-14864
Wide-angle propagation in inhomogeneous fluids and elastic solids using perturbation methods 06 p0837 N90-14868
Particle simulations in magnetospheric plasmas
[NASA-CR-186238] 06 p0848 N90-14934
REFLECT: A computer program for the x ray reflectivity of bent perfect crystals
[DE90-001266] 06 p0851 N90-14946
Developing integrated parametric planning models for budgeting and managing complex projects
[NASA-CR-186006] 06 p0857 N90-14986
A model of the thermal and electrical properties of cosmic dust particles 06 p0863 N90-15014
Dark matter and the solar neutrino problem: Can particle physics provide a single solution
[DE90-001827] 06 p0864 N90-15024
Analysis of severe atmospheric disturbances from airline flight records 07 p0869 N90-15045
Systems for airborne wind and turbulence measurement 07 p0869 N90-15046
A pitch control law for compensation of the phugoid mode induced by windshears 07 p0870 N90-15051
Aircraft response and pilot behaviour during a wake vortex encounter perpendicular to the vortex axis 07 p0871 N90-15057
A numerical model for the axisymmetric equilibrium shape of drops in uniform motion: Effects of external flow, electric field and surface charge 07 p0874 N90-15071
Numerical simulation of the unsteady two-dimensional flow in a time-dependent doubly-connected domain 07 p0875 N90-15073
Modeling and control of the rapid deployment of towed airborne devices 07 p0879 N90-15092
Error modeling of bias-type parameters for TOPEX orbit determination 07 p0884 N90-15117
Propulsion research on the hybrid plume rocket
[AD-A214420] 07 p0887 N90-15132
A tomographic study of premixed turbulent stagnation point flames
[DE90-002462] 07 p0892 N90-15156
Steady flow combustion model for solid-fuel ramjet projectiles
[BRL-TR-2987] 07 p0893 N90-15163
Shock tube ignition of octanes
[DE90-001167] 07 p0893 N90-15164
Isotopic selectivity of surface diffusion: An activated diffusion model
[DE90-003473] 07 p0894 N90-15169
The effects of Mo2C morphology and strain distribution on the fatigue properties of Fe-C-Mo dual-phase steels 07 p0901 N90-15210
Ceramic technology for advanced heat engines project
[DE90-001852] 07 p0908 N90-15251
The elastic properties of woven polymeric fabric
[DE89-015391] 07 p0909 N90-15255
More efficient sensitivity testing
[DE90-002639] 07 p0916 N90-15298
A strategy for concurrent product and process design of aerospace components
[DE90-002926] 07 p0916 N90-15299
The application of queuing theory to the modelling of CP-140 aircraft communications
[AD-A213479] 07 p0918 N90-15310
Design of a high-gain flux-compression generator
[DE90-002795] 07 p0922 N90-15333
Numerical investigation of transition control of a flat plate boundary layer 07 p0926 N90-15361
Development of an integrated BEM approach for hot fluid structure interaction
[NASA-CR-186214] 07 p0927 N90-15364
Determination of flow-regime boundaries for cohesive particles
[DE90-001405] 07 p0928 N90-15369
An algebraic turbulence model for flow separation caused by forward and backward facing steps
[AD-A213800] 07 p0931 N90-15389
Aerosol heating and vaporization of high-flux laser beams
[DE90-003471] 07 p0937 N90-15428
Control of mechanical manipulators 07 p0938 N90-15432
Comparison of engine knock predictions using a fully-detailed and a reduced chemical kinetic mechanism
[DE90-002805] 07 p0941 N90-15448
Multi-dimensional modeling of convective heat transfer with application to I.C. engines
[DE90-003245] 07 p0941 N90-15451
Development of a rate independent plasticity theory for general cyclic loading 07 p0945 N90-15471
Parametric identification of discrete time series models for structural response prediction 07 p0945 N90-15472
Characterizing transient vibrations using band limited moments
[DE90-000799] 07 p0945 N90-15473
Statistical model for particle-void deformation kinetics in granular materials during shock wave propagation
[DE89-017729] 07 p0946 N90-15476
Analysis of catalytically enhanced solar absorption chemical reactors: 1 - numerical model description
[DE89-014742] 07 p0951 N90-15505
Prediction of stochastic blade loads for three-bladed, rigid-hub rotors
[DE89-009508] 07 p0954 N90-15520
Calculation of source and structure parameters at regional and teleseismic distances
[AD-A214297] 07 p0961 N90-15558
Further research on dynamics of marine atmospheres in tropical cyclones
[AD-A213882] 07 p0964 N90-15571
The application of optimal control theory for analysis of human jumping and pedaling 07 p0968 N90-15590
CryoTran user's manual, version 1.0
[NASA-TM-102468] 07 p0973 N90-15622
Knowledge based text generation
[AD-A214273] 07 p0977 N90-15645
Neural network models for linear programming
[DE89-015974] 07 p0979 N90-15651
Recurrence and ergodicity for exponential family state-space models
[AD-A213466] 07 p0983 N90-15677
Numerical facility: Convergence of cognitive and factor analytic models
[AD-A213627] 07 p0983 N90-15680
Queues with negative arrivals
[AD-A213860] 07 p0984 N90-15687
Use of the linear variate method of Monte Carlo for estimating uncertainty in thermal-hydraulic codes
[DE89-017871] 07 p0985 N90-15694
Theory of interacting plasmas in space 07 p0993 N90-15742
Progress in LTE and non-LTE transport calculations
[DE90-003394] 07 p0997 N90-15764
Bridgman crystal growth
[NASA-CR-186204] 07 p0997 N90-15766
A numerical simulation model for the study of magnetohydrodynamic (MHD) waves in a structured medium 07 p1012 N90-15864
Rotor induced-inflow-ratio measurements and CAMRAD calculations
[NASA-TP-2946] 08 p1017 N90-15882
Assessment of computational prediction of tail buffeting
[NASA-TM-101613] 08 p1018 N90-15886
Euler and Navier-Stokes computations for two-dimensional geometries using unstructured meshes
[NASA-CR-181977] 08 p1019 N90-15893
Automatic control of KKK: Requirements, sensors, actuators, and control performance results 08 p1029 N90-15944
The continuous crystallization of sulfur formed by the liquid-phase reaction of hydrogen sulfide and sulfur dioxide
[DE90-003991] 08 p1041 N90-16018
Elastic moduli of copper: Electronic structure contributions from pseudopotentials and full-potential linear muffin-tin orbital band structure calculations
[DE90-004423] 08 p1044 N90-16037
Modeling dislocation evolution in irradiated alloys
[DE90-004921] 08 p1047 N90-16051
Piezoelectric ceramic modeling and characterization at high levels of mechanical activity
[ISAL-89-0030] 08 p1051 N90-16074
On averaged force acting on a particle in HF electromagnetic field
[DE90-600984] 08 p1057 N90-16109
A brief description of lattice gas models for multiphase flows and magnetohydrodynamics
[DE90-003653] 08 p1062 N90-16143
Vorticity amplification in nonorthogonal stagnation flow 08 p1064 N90-16152
Calculation of turbulent choppy flow mixing
[ETN-90-95929] 08 p1065 N90-16165
Grid-independent wall layer turbulence model for complex flow calculations
[DE90-003500] 08 p1071 N90-16200
Improved solution techniques for the eigenstructure of fractional order systems
[AD-A213844] 08 p1088 N90-16295
Analysis of nonlinear systems using ARMA (Autoregressive Moving Average) models
[DE90-002395] 08 p1088 N90-16297
Integrated geodetic network analysis with stochastic prior information about the gravity field and reference ellipsoid
[SER-C-351] 08 p1091 N90-16317
Some considerations on resource evaluation of The Geysers
[DE90-002119] 08 p1095 N90-16343
Mesoscale analysis by numerical modelling coupled with satellite-based sounding 08 p1100 N90-16370
Diagnostic and kinematic fields associated with curved and straight jet streaks using a two-layer primitive equation model 08 p1100 N90-16371
Terrestrial magnetosphere magnetic field models
[REPT-89/CT/DTI/MS/AS/154] 08 p1102 N90-16380

Stochastic model of the NASA/MSFC ground facility for large space structures with uncertain parameters: The maximum entropy approach, part 2
[NASA-CR-186009] 08 p1107 N90-16407
Discrete event simulation tool for analysis of qualitative models of continuous processing systems
[NASA-CASE-MSC-21465-1] 08 p1107 N90-16410
Dissipation mechanism of the large-amplitude collective motion. Dynamical evolution of a collective bundle of trajectories in the TDHF phase space for a simple soluble model
[DE90-719557] 08 p1118 N90-16477
On the observation of a transition from fusion to multifragmentation in high multiplicity O16 induced reactions
[LUIP-8812] 08 p1119 N90-16481
Development of a wet vapor homogeneous liquid metal MHD power system
[DE90-001468] 08 p1124 N90-16508
Fracto-fusion. Mechanism of cold fusion
[DE90-719573] 08 p1125 N90-16518
Continuous spontaneous reduction model involving gravity
[DE90-600730] 08 p1135 N90-16573
Modeling the near acoustic field of a rocket during launch 08 p1156 N90-16694
Mathematical model for adaptive control system of ASEA robot at Kennedy Space Center 08 p1157 N90-16701
A method for the early detection of instabilities in rotordynamics
[NASA-CR-186307] 09 p1170 N90-16769
Effects of scaling on the performance of magnetoplasmadynamic thrusters
[AD-A215690] 09 p1184 N90-16863
High-order mixture homogenization of fiber-reinforced composites
[AD-A215247] 09 p1187 N90-16876
An engineering approach to two-phase flow modeling in reduced gravity
[DE90-005539] 09 p1202 N90-16967
Upper semicontinuous global attractors for viscous flow
[NASA-CR-181976] 09 p1217 N90-17056
Nonlinear heat transfer and wave motion
[AD-A214911] 09 p1217 N90-17058
Optimum element density studies for finite-element thermal analysis of hypersonic aircraft structures
[NASA-TM-4163] 09 p1219 N90-17074
Numerical predictions of local entropy generation for an impinging jet
[DE90-004671] 09 p1220 N90-17081
Agglomeration of ceramic powders 09 p1223 N90-17098
Laser wave estimation
[AD-A213867] 09 p1227 N90-17119
Traction modeling of military lubricants
[AD-A213866] 09 p1230 N90-17139
Chemical effect of fuel composition changes on emissions from a DI Diesel engine
[DE90-004466] 09 p1232 N90-17151
Validation of an exponentially decreasing failure rate software reliability model
[AD-A215546] 09 p1235 N90-17165
Eigensolution of finite element problems in a completely connected parallel architecture
[NASA-TM-102450] 09 p1236 N90-17173
A summary of the Bodner-Stouffer constitutive model
[AD-A214532] 09 p1237 N90-17182
The 59th Shock and Vibration Symposium, volume 1
[AD-A214578] 09 p1238 N90-17183
Parametric version of structural vibration models
[ONERA-RT-9/3313-RY-080-R] 09 p1238 N90-17188
The potential impact of conservation, alternative energy sources, and reduced nonenergy emissions on global warming
[DE90-004494] 09 p1244 N90-17220
The use of computer programs to determine environmental compliance, predict performance, and assess impacts
[DE90-005230] 09 p1245 N90-17222
Evaluation of the use of flat terrain models versus complex terrain screening models in estimating pollutant transport and deposition in complex terrain
[DE90-005271] 09 p1245 N90-17223
Distribution and seasonal variations of diffuse fraction
[DE90-601303] 09 p1246 N90-17228
Observing systems simulation experiments: Their role in meteorology
[AD-A215705] 09 p1248 N90-17243
A statistical model of the infrared signature of a wind roughened sea
[AD-A214531] 09 p1249 N90-17245
Statistically based decompression tables 5: Haldane-Vann models for air diving
[AD-A214934] 09 p1251 N90-17261
Training and selecting individuals for high levels of information processing load 09 p1256 N90-17288
A model for visual attention
[AD-A214505] 09 p1258 N90-17297
Piecewise linear-quadratic programming and its applications
[AD-A214489] 09 p1264 N90-17328
Active control of a flexible structure using a modal positive position feedback controller
[NASA-CR-186336] 09 p1272 N90-17371
Staring focal plane array system modeling
[AD-A215712] 09 p1283 N90-17438
VHSIC/VHSIC-Like reliability prediction modeling
[AD-A214601] 09 p1288 N90-17468
False vacuum decay in Jordan-Brans-Dicke cosmologies
[NASA-CR-186257] 09 p1293 N90-17497
Chaos and turbulence
[AD-A215310] 09 p1294 N90-17499
Multi-dimensional discrete ordinates solutions to combined mode radiation heat transfer problems and their application to a free-falling particle, direct absorption solar receiver
[DE90-004987] 09 p1300 N90-17531
TS - Dean interactions in curved channel flow
[NASA-CR-181983] 10 p1306 N90-17559
A computational model for thickening boundary layers with mass addition for hypersonic engine inlet testing
[AD-A216246] 10 p1310 N90-17576
A review of UK civil aviation fire and cabin safety research 10 p1312 N90-17587
Forced and natural venting of aircraft cabin fires: A numerical simulation 10 p1314 N90-17597
Time development of convection flow patterns in aircraft cabins under post-crash fire exposure 10 p1314 N90-17598
The importance of pathophysiological parameters in fire modelling of aircraft accidents 10 p1317 N90-17618
Modelling time to incapacitation and death from toxic and physical hazards in aircraft fires 10 p1318 N90-17619
Analysis of the National Transonic Facility mishap
[NASA-TM-101686] 10 p1318 N90-17620
An examination of the fatigue meter records from the RAAF Orion P-3C fleet
[AD-A214000] 10 p1319 N90-17628
A method for the prediction of supersonic compressor blade performance
[CUED/A-TURBO/TR-126] 10 p1321 N90-17634
Simulation of shading in synthetic surfaces
[INPE-4869-PRE/1480] 10 p1326 N90-17660
New power system modelling approaches on the basis of equivalent state variables 10 p1330 N90-17687
Electrical battery model for LEO application based on absolute instantaneous state of charge 10 p1332 N90-17702
Mathematical modelling and expert system for battery management 10 p1332 N90-17703
Optimized sensible heat storage systems for application to solar dynamic power generation 10 p1334 N90-17719
New models and techniques for predicting radiation effects on solar array performances 10 p1344 N90-17790
Solar arrays in the LEO-plasma environment: A model for leakage current phenomena deduced from experimental and theoretical studies 10 p1345 N90-17802
High-order mixture homogenization of periodic nonlinear composites 10 p1347 N90-17814
Prediction of high temperature metal matrix composite ply properties
[NASA-TM-102490] 10 p1348 N90-17817
The processing and mechanical properties of high temperature/high performance composites. Book 5, section 4: Processing: Matrices and composites, part 1
[AD-A216145] 10 p1349 N90-17823
The processing and mechanical properties of high temperature/high performance composites. Book 6, section 4: Processing: Matrices and composites, part 2
[AD-A216146] 10 p1349 N90-17824
Surface analyses and modelling of rate multiplicity and instabilities
[DE90-005418] 10 p1352 N90-17838
A finite element analysis of porosity effects on materials
[AD-A216225] 10 p1359 N90-17884
FLUSH: A tool for the design of slush hydrogen flow systems
[NASA-TM-102467] 10 p1361 N90-17890
A selective survey of computational electromagnetics for antenna applications 10 p1369 N90-17933
Recent advances to NEC: Applications and validation 10 p1369 N90-17934
Some applications of model-based parameter estimation in computational electromagnetics 10 p1369 N90-17935
Measurement and computer simulation of antennas on ships and aircraft for results of operational reliability 10 p1369 N90-17936
HF wire antennas over real ground: Computer simulation and measurement 10 p1370 N90-17937
LMSS modeling status report 10 p1372 N90-17953
Rain attenuation measurements: Variability and data quality assessment 10 p1373 N90-17955
Unsteady two level models
[TELECOM-89-E-006] 10 p1375 N90-17973
A model for evaporation of freely falling droplets
[PUBL-AIR-QUALITY-6] 10 p1384 N90-18007
Numerical simulation of unstably stratified sheared flows
[DE90-005396] 10 p1384 N90-18008
Colliding natural convection boundary layer flow in a rectangular enclosure
[DE90-005397] 10 p1384 N90-18009
Fluid transmission line dynamics for signals of finite amplitude
[AD-A215758] 10 p1385 N90-18014
Numerical simulation of compressible vortices
[AD-A216221] 10 p1385 N90-18017
Steady-state and transient Zener parameters in viscoplasticity: Drag strength versus yield strength
[NASA-TM-102487] 10 p1395 N90-18064
Numerical model of bond strength measurements
[DE90-006000] 10 p1396 N90-18073
Evapotranspiration studies for protective barriers: Experimental plans
[DE90-005206] 10 p1405 N90-18106
Modeling the effects of air pollution on forest ecosystems: Considerations for applying a model to Southeast Asia
[DE90-004937] 10 p1406 N90-18110
Assessment of the theory and hypotheses of the acidification of watersheds
[DE90-005528] 10 p1406 N90-18111
Self-similar growth of three-dimensional fault
[DE90-608162] 10 p1407 N90-18112
Dose assessment during complex meteorology in the Texas Panhandle
[DE90-006026] 10 p1408 N90-18118
Some problems in oceanic radiative transfer
[AD-A215935] 10 p1410 N90-18131
Pareto optimization design techniques for the AFIT (Air Force Institute of Technology)/AAMRL (Armstrong Aeronautical Medical Research Laboratory) anthropomorphic robotic manipulator
[AD-A216178] 10 p1414 N90-18150
A general method of using prior information in a simultaneous equation system
[NOAA-TR-NESDIS-47] 10 p1423 N90-18209
On detecting influential data and selecting regression variables
[AD-A216387] 10 p1423 N90-18213
User's guide to OPUS (Optimal Preferential Utility and Strategies)
[AD-A214384] 10 p1424 N90-18217
An approximate model for the performance and acoustic predictions of counterrotating propeller configurations
[NASA-CR-180667] 10 p1426 N90-18228
Maxwellian cascade model
[DE90-004389] 10 p1427 N90-18235
Statistical mechanical models for liquid and amorphous structure in covalently bonded systems
[DE90-607233] 10 p1428 N90-18240
A micromechanical viscoplastic stress-strain model with grain boundary sliding
[DE90-006013] 10 p1437 N90-18295
Solution of a class of conformal quantum field theory models in D-dimensional space
[DE90-607094] 10 p1439 N90-18306
A hybrid model for document retrieval systems 10 p1441 N90-18315
Nuclear driving of stellar oscillations and their coupling to convection 10 p1446 N90-18345
The inviscid stability of supersonic flow past a sharp cone
[NASA-CR-181996] 11 p1451 N90-18363
Computational aerodynamics of ordered vortex flows
[ETN-90-96272] 11 p1452 N90-18368
Review of modelling methods to take account of material structure and defects 11 p1458 N90-18402
Unsteady viscous calculation method for cascades with leading edge induced separation 11 p1459 N90-18408
Aerodynamic study on forced vibrations on stator rows of axial compressors 11 p1460 N90-18412

Unsteady blade loads due to wake influence
11 p1460 N90-18413
Asymptotic analysis of transonic flow through oscillating cascades
11 p1462 N90-18421
Modelling unsteady transition and its effects on profile loss
11 p1462 N90-18423
Stall and recovery in multistage axial flow compressors
11 p1464 N90-18429
Autonomous orbit determination using GPS
[INPE-4815-TDL/361] 11 p1466 N90-18442
Experimental flow models for SSME flowfield characterization
11 p1471 N90-18469
The processing and mechanical properties of high temperature/high performance composites. Book 2, section 2: Strength and fracture resistance
[AD-A216142] 11 p1478 N90-18507
The processing and mechanical properties of high temperature/high performance composites. Book 3, section 2: Strength and fracture resistance, part
[AD-A216143] 11 p1478 N90-18508
Development of a progressive failure model for strength of laminated composite structure
[AD-A216966] 11 p1480 N90-18517
Experimental and theoretical research on the injection of ignition gases into a bed of inert powder
[ISL-CO-251/88] 11 p1485 N90-18547
Analytical and experimental investigation of miniature heat pipes, phase 2
[AD-A216945] 11 p1506 N90-18673
Dryout stability and inception at low flowrates
[DE90-006955] 11 p1509 N90-18692
INEX (Integrated Numerical Experiment) simulations of the Boeing FEL system
[DE90-004846] 11 p1513 N90-18712
Theory for high gain, high power free electron lasers
[DE90-005546] 11 p1514 N90-18714
Research on free electron lasers
[AD-A215865] 11 p1514 N90-18715
Development of an experimental space station model for structural dynamics research
[NASA-TM-102601] 11 p1519 N90-18751
Geometric correction models for HRV-SPOT images
[INPE-5001-TDL/395] 11 p1521 N90-18757
TVI: A mathematical model for global estimation of Brazilian cerrado phytomass
[INPE-4836-PRE/1465] 11 p1521 N90-18759
Earth model selection for computer simulations
[AD-A216843] 11 p1525 N90-18779
Variations in volatiles in magma bodies based on studies of melt inclusions
[DE90-006272] 11 p1532 N90-18821
Effect of a random wind field on thermal blooming instabilities
[DE90-007241] 11 p1532 N90-18823
L: A language for solution of incremental systems in a parallel processing environment
[INPE-4816-TDL/362] 11 p1543 N90-18884
An integrated vision on methodologies and environments for modeling and simulation assisted by computer
[INPE-4861-TDL/372] 11 p1544 N90-18886
An objective time-integration procedure for isotropic rate-independent and rate-dependent elastic-plastic constitutive equations
[PB90-121245] 11 p1550 N90-18925
Computational structure of GPSG (Generalized Phrase Structure Grammar) models: Revised generalized phrase structure grammar
[AD-A216803] 11 p1553 N90-18941
Analysis of linear multigrid methods for elliptic differential equations with discontinuous and anisotropic coefficients
[ETN-90-96269] 11 p1553 N90-18944
Can the square law be validated
[DE90-007112] 11 p1553 N90-18945
Using dynamic queueing networks as a tool for specifying performability models
[MEMO-INF-89-51] 11 p1554 N90-18949
Adaptive state estimation and sampling rate analysis for invariant linear dynamic systems in time
[INPE-4960-TDL/389] 11 p1554 N90-18951
A model of incomplete chromatic adaptation for calculating corresponding colors
[DE90-006905] 11 p1567 N90-19016
Magnetohydrodynamic modeling of plasma opening switches and gas puff plasmas
[DE90-005825] 11 p1569 N90-19028
Mechanical disturbances in high-performance superconducting dipoles
[DE90-006237] 11 p1570 N90-19040
Calculation of ionospheric corrections for single frequency GPS observations: Investigation of two models
[ETN-90-95450] 12 p1602 N90-19219
Calculation and optimization of rotor start process
[ETN-90-95894] 12 p1604 N90-19229
Muzzle shunt augmentation of conventional railguns
[DE90-007505] 12 p1607 N90-19248
Self-tuning control techniques, implicit and explicit, with parameter estimation in Kalman filters, applied to artificial satellite attitude
[INPE-4857-TDL/368] 12 p1613 N90-19276
Application of attachment modes in the control of large space structures
[NASA-CR-185604] 12 p1613 N90-19280
Safety Status Report for the Ulysses mission. Book 1: Accident analysis. General purpose heat source radioisotope thermoelectric generator program
[DE90-006829] 12 p1614 N90-19285
Numerical study of diffusion jet flames
12 p1621 N90-19316
Effects of nonuniform potential and current distributions in electrochemical systems
[DE90-007349] 12 p1623 N90-19325
The measurement, modeling, and prediction of traction for rocket propellant 1
[NASA-CR-185186] 12 p1633 N90-19386
A PBL-radiation model for application to regional numerical weather prediction
12 p1635 N90-19394
A parametric heat transfer study for cryogenic ball bearings in SSME HPOTP
12 p1635 N90-19397
A study of the effects of disk flexibility on the rotordynamics of the space shuttle main engine turbo-pumps
12 p1636 N90-19401
Monte Carlo models and analysis of galactic disk gamma-ray burst distributions
12 p1636 N90-19403
Analytical optical scattering in clouds
12 p1638 N90-19413
Multibody modeling and verification
12 p1640 N90-19422
A vectorized algorithm for 3D dynamics of a tethered satellite
12 p1640 N90-19423
Simple analytic potentials for linear ion traps
12 p1642 N90-19436
Performance of the all-digital data-transition tracking loop in the advanced receiver
12 p1643 N90-19440
Costas loop lock detection in the advanced receiver
12 p1643 N90-19441
Green's functions for a theoretical model of an aperture fed stacked-patch microstrip antenna
[AD-A216280] 12 p1645 N90-19455
Signal processing
[DE90-006904] 12 p1647 N90-19464
Numerical modelling of shocks in gases and metals
[MRL-RR-8-89] 12 p1658 N90-19528
Conforming Chebyshev spectral collocation methods for the solution of laminar flow in a constricted channel
[NASA-CR-182011] 12 p1660 N90-19539
Flow simulation for aircraft
[NLR-MP-87082-U] 12 p1661 N90-19543
A review of models for the analysis of the injection of densely loaded flows into entrained flow gasifiers
[DE90-000453] 12 p1662 N90-19550
Turbulent mixing effects in models of thermal blooming
[DE90-007245] 12 p1667 N90-19580
Modeling and analysis of the space shuttle nose-gear tire with semianalytic finite elements
[NASA-TP-2977] 12 p1670 N90-19595
A complete description of robot manipulator dynamics based on Lagrangian mechanics
[DE90-741467] 12 p1672 N90-19603
PATRAN-STAGS translator (PATSTAGS)
[NASA-TM-100388] 12 p1674 N90-19616
Development of finished beam and shell elements from engineering models for structures under high inelastic deformations
[ETN-90-95377] 12 p1675 N90-19619
Use of chaotic and random vibrations to generate high frequency test inputs. Part 2: Chaotic vibrations
[DE90-007153] 12 p1676 N90-19627
Use of chaotic and random vibrations to generate high frequency test inputs
[DE90-007412] 12 p1676 N90-19628
Selection of optimal textural features for maximum likelihood image classification
[DE90-006901] 12 p1678 N90-19638
Study of the optimization of reference parameters to the dynamic constraints of solar panels
[INPE-4793-TDL/355] 12 p1681 N90-19656
An analytic model of axisymmetric mantle plume due to thermal and chemical diffusion
[NASA-CR-186461] 12 p1691 N90-19714
Status of a nonlinear water surge model in February 1988
[KNMI-WR-88-03] 12 p1695 N90-19735
Positioning control of highest accuracy for very dynamic coupled system
[ETN-90-95893] 12 p1701 N90-19769
Finite element mesh generation starting from general geometric models
[REPT-88-93] 12 p1707 N90-19803
Numerical simulation of acoustic scatter from subsurface bubble clouds
[AD-A217068] 12 p1710 N90-19822
A simple model for the determination of L(sub 0), D and tau in a semiconductor and their temperature dependence
[DE90-610564] 12 p1720 N90-19879
Construction of four-dimensional open superstrings
[DE90-006484] 12 p1724 N90-19908
Visibility problems in numerical models of terrain
[INPE-4921-TDL/382] 12 p1726 N90-19919
Reliability of equivalent sphere model in blood-forming organ dose estimation
[NASA-TM-4178] 12 p1746 N90-20036
Using transonic small disturbance theory for predicting the aeroelastic stability of a flexible wind-tunnel model
[NASA-TM-102617] 13 p1749 N90-20047
Development of acceleration exposure limits for advanced escape systems
13 p1751 N90-20055
Aeroelastic characteristics of aircraft with circulation control wings
13 p1754 N90-20070
A video-based experimental investigation of wing rock
[AD-A218244] 13 p1755 N90-20075
Component count and preliminary assembly considerations for large space truss structures
[NASA-TM-102604] 13 p1763 N90-20121
Use of random Martian atmosphere to evaluate potential entry guidance schemes
[NASA-TM-102606] 13 p1764 N90-20122
Summary report of the Summer Conference of the DARPA-Materials Research Council
[AD-A217380] 13 p1767 N90-20143
Structure of model gas flames in nitramines
[AD-A217578] 13 p1770 N90-20159
Moisture control in sealed electronic packages
[DE90-008136] 13 p1771 N90-20166
Spallation of oxide scales from 20 percent Cr/25 percent Ni/Nb stainless steel
[AERE-R-13464] 13 p1775 N90-20189
Stochastic approach to the initiation of pitting corrosion
[AERE-R-13348] 13 p1775 N90-20190
Secondary arm coarsening and microsegregation in superalloy PWA-1480 single crystals: Effect of low gravity
[NASA-TM-102445] 13 p1776 N90-20194
A unified integrated model for sputter coating uniformity
[DE90-008322] 13 p1778 N90-20205
Magnetic vapor shield mechanism for protection of material surfaces exposed to high heat load
[AD-A217667] 13 p1780 N90-20217
Modification and improvement of software for modeling multidimensional reacting fuel flows
[AD-A217789] 13 p1783 N90-20235
Modelling Doppler broadening in Raman propagation
[DE90-008042] 13 p1789 N90-20269
High resolution radar target modeling using ARMA (Autoregressive Moving Average) models
[AD-A218212] 13 p1791 N90-20278
Statistical equipment modeling for VLSI manufacturing
[DE90-008527] 13 p1795 N90-20304
Amplitude-dependent neutral modes in compressible boundary layer flows
[NASA-TM-102524] 13 p1799 N90-20326
Geometric scale of interaction between moving shock and stationary thermal layer
[AD-A217769] 13 p1802 N90-20344
Harmonic generation mechanisms in short-wavelength free-electron lasers
[DE90-007622] 13 p1807 N90-20374
Laser-induced shock waves effects in materials
[DE90-007626] 13 p1807 N90-20379
Laser line transport with refraction
[DE90-008683] 13 p1808 N90-20382
The diffraction of ultrasound by cracks: Comparison of experiment with theory
[AERE-R-13334] 13 p1813 N90-20410
Computer simulation of the mathematical modeling involved in constitutive equation development: Via symbolic computations
[NASA-TM-102532] 13 p1816 N90-20428
Model development in viscoplastic ratchetting
[NASA-TM-102509] 13 p1816 N90-20431
Computational simulation of damping in composite structures
[NASA-TM-102567] 13 p1817 N90-20432
COMGEN: A computer program for generating finite element models of composite materials at the micro level
[NASA-TM-102556] 13 p1818 N90-20438
Plan, formulate, and discuss a NASTRAN finite element model of the UH-60A helicopter airframe
[NASA-CR-181975] 13 p1818 N90-20439

Analysis of methods to determine emissivity for ground surface targets in the spectral band 8 to 14 microns
[INPE-4984-TDL/394] 13 p1820 N90-20447
Simulation of landscape disturbances and the effect of climatic change
[DE90-007565] 13 p1829 N90-20503
Atmospheric Radiation Measurement Program Plan
[DE90-008108] 13 p1829 N90-20504
Overview of the methodologies used to compile large scale emissions inventories
[DE90-008518] 13 p1830 N90-20509
Use of environmental monitoring data in evaluation of atmospheric modeling results
[DE90-008607] 13 p1831 N90-20510
Processes of community development and responses of ecosystems to climate change
[DE90-008640] 13 p1831 N90-20512
Progress in the Determination of the Earth's Gravity Field
[NASA-CR-185721] 13 p1831 N90-20513
Gravitational model improvement at the Goddard Space Flight Center 13 p1831 N90-20514
An improved model for the Earth's gravity field
13 p1832 N90-20515
Progress in the development of high degree potential coefficient models 13 p1832 N90-20516
Gravity field determination and error assessment techniques 13 p1832 N90-20517
An improved error assessment for the GEM-T1 gravitational model 13 p1832 N90-20518
Geopotential models in the Australian region
13 p1832 N90-20519
Stabilized determination of geopotential coefficients by the mixed hom-BLUP approach
13 p1832 N90-20520
Precise solution for a finite set of spherical coefficients from equiangular gridded data 13 p1833 N90-20522
Modeling of the Earth's gravity field using the New Global Earth Model (NEWGEM) 13 p1833 N90-20523
A framework for modelling kinematic measurements in gravity field applications 13 p1833 N90-20524
The use of high-resolution terrain data in gravity field prediction 13 p1835 N90-20533
The role of topography in geodetic gravity field modelling 13 p1835 N90-20534
The inverse gravimetric problem in gravity modelling
13 p1835 N90-20535
FFT-local gravimetric geoid computation
13 p1835 N90-20536
Performance of FFT methods in local gravity field modelling 13 p1835 N90-20537
Fourier transform methods in local gravity modeling
13 p1836 N90-20538
Downward continuation of the free-air gravity anomalies to the ellipsoid using the gradient solution and terrain correction: An attempt of global numerical computations
13 p1836 N90-20541
The geoid in Kenya 13 p1836 N90-20542
GEOID '88: A gravimetric geoid for Canada
13 p1837 N90-20543
Regional quasigeoid determination in Northern Germany and comparison with GPS 13 p1837 N90-20544
Treatment of geodetic leveling in the integrated geodesy approach 13 p1837 N90-20546
Determination of mean gravity anomalies in the Taiwan Island 13 p1837 N90-20547
Very accurate upward continuation to low heights in a test of non-Newtonian theory 13 p1837 N90-20548
Geodynamics and temporal variations in the gravity field 13 p1838 N90-20549
Geographically correlated orbit error
13 p1838 N90-20551
Spectral analyses of satellite geopotential missions
13 p1838 N90-20552
Local gravity disturbance estimation from multiple-high-single-low satellite-to-satellite tracking
13 p1839 N90-20555
Satellite-to-satellite tracking experiment for global gravity field mapping 13 p1839 N90-20556
A discussion of observation model, error sources and signal size for spaceborne gravitational gradiometry
13 p1839 N90-20557
Studies of an orbital gradiometer mission
13 p1839 N90-20558
Theoretical modeling studies of the marine planetary
[AD-A217200] 13 p1841 N90-20567
Seismic characterization of fracture properties
[DE90-007759] 13 p1841 N90-20570
Damage characteristics of time domain histories
[DE90-008787] 13 p1842 N90-20573
A modeling study of the cloud-topped marine boundary layer
[AD-A218103] 13 p1846 N90-20594
The invertibility principle for a simple hurricane model
[AD-A218344] 13 p1848 N90-20605
Space Station Freedom integrated fault model
13 p1860 N90-20673
Computing mean responses in nonlinear models
[AD-A217642] 13 p1865 N90-20700
Computational complexity of random access models
[AD-A217685] 13 p1865 N90-20701
Automated finite element modeling and simulation
13 p1875 N90-20753
Spectral analytic methods for the estimation of number of signals and directions of arrival
[AD-A217219] 13 p1876 N90-20757
Observer based compensators for nonlinear systems
[AD-A217426] 13 p1876 N90-20760
Micro SAINT programs for numerical methods of integration and differential equations
[AD-A218097] 13 p1878 N90-20772
Slepian models and regression approximations in crossing and extreme value theory
[AD-A218338] 13 p1879 N90-20779
The n-p bremsstrahlung in heavy ion collision processes
[DE90-008542] 13 p1886 N90-20823
Spectral line shape code for multielectron emitters
[DE90-008526] 13 p1891 N90-20853
The electronic properties of high (Tc) superconductors probed by positron annihilation
[DE90-008354] 13 p1896 N90-20883
Systematics in positron annihilation lifetime analysis of high (Tc) superconducting transitions
[DE90-008361] 13 p1896 N90-20884
Growth, characterization and device development in monocrystalline diamond films
[AD-A218211] 13 p1898 N90-20895
An empirical test of a comprehensive model for predicting successful information systems implementation
[AD-A218124] 13 p1900 N90-20908
EXOSAT observations of Seyfert type galaxies
13 p1901 N90-20910
Discrete-vortex model for the symmetric-vortex flow on cones
[NASA-TP-2989] 14 p1909 N90-20946
A two-dimensional unsteady analysis for transonic and supersonic cascade flows 14 p1911 N90-20955
Parametric resonance in horizontal axis wind turbines
14 p1912 N90-20962
An efficient airfoil design method using the Navier-Stokes equations 14 p1917 N90-20981
An intensive procedure for the design of pressure-specified three-dimensional configurations at subsonic and supersonic speeds by means of a higher-order panel method 14 p1917 N90-20982
Subsonic and transonic blade design by means of analysis codes 14 p1917 N90-20985
Inverse computation of transonic internal flows with application for multi-point-design of supercritical compressor blades 14 p1918 N90-20987
Numerical method for designing 3D turbomachinery blade rows 14 p1918 N90-20990
Constrained spanload optimization for minimum drag of multi-lifting-surface configurations
14 p1919 N90-20992
Secondary flows and radial mixing predictions in axial compressors 14 p1922 N90-21010
A study on secondary flow and spanwise mixing in axial flow compressors 14 p1923 N90-21012
Parabolized calculations of turbulent three dimensional flows in a turbine duct 14 p1923 N90-21013
Experimental and numerical study on basic phenomena of secondary flows in turbines 14 p1923 N90-21014
Secondary flow calculations for axial and radial compressors 14 p1925 N90-21024
The numerical simulation of multistage turbomachinery flows 14 p1925 N90-21025
Research on cascade secondary and tip-leakage flows: Periodicity and surface flow visualization
14 p1925 N90-21026
Analysis of the rotor tip leakage flow with tip cooling air ejection 14 p1926 N90-21029
Experimental and theoretical investigation of optimal control methods with model reduction
14 p1928 N90-21039
Design of a helicopter automatic flight control system using adaptive control 14 p1928 N90-21040
Subsonic flutter analysis using MSC/NASTRAN
[PB90-166786] 14 p1928 N90-21041
NASA/DOD Controls-Structures Interaction Technology 1989
[NASA-CP-3041] 14 p1933 N90-21062
Element-specific modal formulations for large-displacement multibody dynamics
14 p1934 N90-21069
Nonlinear and distributed parameter models of the mini-mast truss 14 p1934 N90-21070
A distributed finite-element modeling and control approach for large flexible structures
14 p1934 N90-21071
Modeling and control of flexible space platforms with articulated payloads 14 p1935 N90-21073
Optimization of the structural and control system for LSS with reduced-order model 14 p1935 N90-21075
Recent experience in simultaneous control-structure optimization 14 p1936 N90-21078
CSI sensing and control: Analytical and experimental results 14 p1936 N90-21083
Experimental evaluation of active-member control of precision structures 14 p1936 N90-21084
LACE flight dynamics experiment
14 p1937 N90-21086
Stress analysis of rocket motors with viscoelastic propellant by a mixed finite element model
14 p1941 N90-21112
A computational model of the perforation of multi-layer metallic laminates
[MRL-RR-9-89] 14 p1944 N90-21128
Resistance mechanics for laminated composite materials
[INPE-4919-RPE/594] 14 p1947 N90-21141
Mathematical modelling of intergranular attack in stainless steels: A preliminary study
[AERE-M-3698] 14 p1950 N90-21160
Intensity to frequency conversion technique in intensity modulated fiber optic sensing systems
[NASA-TM-102562] 14 p1969 N90-21277
Numerical simulation of vortex breakdown
14 p1970 N90-21288
Computer codes for the evaluation of thermodynamic properties, transport properties, and equilibrium constants of an 11-species air model
[NASA-TM-102602] 14 p1972 N90-21297
PROTEUS two-dimensional Navier-Stokes computer code, version 1.0. Volume 1: Analysis description
[NASA-TM-102551] 14 p1973 N90-21303
PROTEUS two-dimensional Navier-Stokes computer code, version 1.0. Volume 2: User's guide
[NASA-TM-102552] 14 p1973 N90-21306
PROTEUS two-dimensional Navier-Stokes computer code, version 1.0. Volume 3: Programmer's reference
[NASA-TM-102553] 14 p1974 N90-21307
Near contact phenomena and transient effects in far infrared photoconductors 14 p1976 N90-21316
Modeling elastomer displacements for tactile sensing applications
[DE90-007959] 14 p1984 N90-21370
On-line assessment of weld quality using ultrasonics
[AERE-R-13401] 14 p1989 N90-21398
Elastic-plastic instability of plane frames
14 p1992 N90-21415
Development of a fracture analysis technique for use with a general-purpose finite element program
14 p1992 N90-21416
Thermomechanical deformation testing and modeling in the presence of metallurgical instabilities
[NASA-CR-185188] 14 p1993 N90-21420
A numerical model for the determination of periodic solutions of pipes subjected to non-conservative loads
[DE90-614756] 14 p1993 N90-21423
A modification of a low-order Reissner-Mindlin plate bending element
[PB90-165630] 14 p1994 N90-21428
Possible use of satellite data for flood plain mapping
[INPE-4968-PRE/1537] 14 p2000 N90-21462
Modeling large-scale vegetation dynamics
[DE90-008883] 14 p2004 N90-21485
The influence of lateral boundary conditions, fixed surface forcings, and synoptic situations upon predictability estimates using limited area numerical models
14 p2005 N90-21492
Theory and application of nonlinear normal mode initialization
[PB90-166000] 14 p2006 N90-21497
Numerical simulations of the cloud-capped marine boundary layer 14 p2008 N90-21506
Extension of the constraints algebra for the closed string with the fixed topology world sheet
[DE90-612745] 14 p2020 N90-21577
Stability of a solitary wave solution to a set of coupled Boussinesq-like equations
[DE90-008927] 14 p2021 N90-21586
US-Japan Workshop on Atomic Collisions in Solids: Abstracts of lectures
[DE90-008979] 14 p2025 N90-21611
A simplified theoretical model for the laser-induced optogalvanic effect
[DE90-613121] 14 p2028 N90-21626
An extended diffusive model for calculating thermal diffusivity from single monopole tokamak heat pulse propagation
[DE90-007958] 14 p2029 N90-21637

Transition from resistive-g to eta-i driven turbulence in stellarator systems
[DE90-009382] 14 p2030 N90-21641
Model atmospheres for novae during the early stages
[NASA-CR-180498] 14 p2038 N90-21694
The dynamics of scalar fields in the early universe
14 p2039 N90-21696
A theoretical study of circumstellar dust around Ae/Be stars 14 p2040 N90-21700
Small scale structures and density of star-forming regions 14 p2041 N90-21706
Substorms: Their expansion and recovery phases
[DE90-008970] 14 p2042 N90-21712
Simplified model for solar cosmic ray exposure in manned Earth orbital flights
[NASA-TM-4182] 14 p2043 N90-21715
A balloon measurement of the isotopic composition of galactic cosmic ray iron 14 p2043 N90-21717
Development and application of a generalized dynamic wake theory for lifting rotors 15 p2046 N90-21731
Modeling of vortex-induced oscillations based on indicial response approach
[NASA-CR-186560] 15 p2047 N90-21736
Analytical study of the origin and behavior of asymmetric vortices
[NASA-TM-102796] 15 p2049 N90-21746
Conceptual design optimization study
[NASA-CR-4298] 15 p2051 N90-21755
Quiet mode for nonlinear rotor models
[NASA-TM-102236] 15 p2051 N90-21758
A decentralized linear quadratic control design method for flexible structures 15 p2054 N90-21770
A conflict analysis of 4D descent strategies in a metered, multiple-arrival route environment
[NASA-CR-182019] 15 p2055 N90-21772
The insertion of human dynamics models in the flight control loops of V/STOL research aircraft. Appendix 2: The optimal control model of a pilot in V/STOL aircraft control loops
[NASA-CR-186598] 15 p2055 N90-21776
Strength in notched and impact-damaged laminates
15 p2064 N90-21820
Studies on reactive flows 15 p2066 N90-21831
Numerical simulation model of hydrazine attitude control thrusters
[INPE-4965-PRE/1534] 15 p2068 N90-21848
Nonlinear spline operator interpolation and sliding control of deformable maneuvering bodies
15 p2074 N90-21878
Evaporation duct effects at millimeter wavelengths
15 p2080 N90-21914
Lidar measurement of concentration and turbulence in battlefield obscurants 15 p2084 N90-21931
Modelling UV-visible radiation observed from space
15 p2085 N90-21937
Computation of broad spectral band electro-optical system transmittance response characteristics to military smokes and obscurants using field test data from transmissometer system measurements
15 p2086 N90-21939
Effect of atmospheric turbulence on electro-optical systems 15 p2086 N90-21940
Passive shape control of space antennas with determinate truss support structures
15 p2087 N90-21949
Experimental and analytical investigations of granular materials: Shear flow and convective heat transfer
15 p2091 N90-21968
Numerical simulation of liquid circulation in a bubbly column
[DE90-005226] 15 p2097 N90-22002
Mathematical modeling of fluid-solid mixtures
[DE90-009152] 15 p2098 N90-22007
Nonlinear stability analysis and control of dynamical robotic systems 15 p2104 N90-22037
Practical nonlinear simulation of rotating machinery dynamics with application to turbine blade rubbing
15 p2104 N90-22038
An alternative method to solving the kinematics of a redundant robot
[DE90-006892] 15 p2106 N90-22045
Computerized inspection of gear tooth surfaces
[NASA-TM-102395] 15 p2107 N90-22054
The Shock and Vibration Digest, volume 21, no. 2
15 p2109 N90-22059
Contact mechanics for three-dimensional geometries
15 p2111 N90-22076
A continuum damage model for the quasi-static response of brittle materials
[DE90-007681] 15 p2117 N90-22112
Severe shock and vibration environments for electronic components
[DE90-007686] 15 p2117 N90-22113
The stress field due to an edge dislocation and some fracture problems for a three-phase composite cylinder model 15 p2120 N90-22126
Analysis of a finite two-dimensional solid with an inclined crack and a rigid inclusion 15 p2120 N90-22127
The mechanics of shear band formation in thermal viscoplastic materials at high rates of loading
15 p2120 N90-22128
Three-dimensional finite element formulations for thick and thin laminated plates 15 p2121 N90-22132
The interpretation of SAGE 2 ozone measurements in the lower mesosphere 15 p2124 N90-22149
The calculation of infrared limb emission by ozone in the terrestrial middle atmosphere
15 p2125 N90-22151
Mission to planet Earth 15 p2125 N90-22153
Formulation of non-reflecting boundary conditions in numerical models of the atmosphere
15 p2129 N90-22175
Second National Winter Weather Workshop Conducted by the National Weather Service
[PB90-147414] 15 p2131 N90-22183
The effects of linear acceleration on perception and nystagmus 15 p2136 N90-22209
The art of fault-tolerant system reliability modeling
[NASA-TM-102623] 15 p2152 N90-22292
Object detection using structural matching
[INPE-4954-PRE/1532] 15 p2159 N90-22333
Efficient estimation in the Clayton-Cuzick model for survival data
[TW-88-06] 15 p2161 N90-22348
Clustering and uniqueness in mathematical models of percolation phenomena
[ETN-90-96400] 15 p2163 N90-22358
On the structure of Mandelbrot's percolation process and other random Cantor sets
[REPT-89-54] 15 p2163 N90-22362
Diffraction of light by ultrasonic pulses
15 p2164 N90-22366
An investigation of the generation and radiation of aerodynamic noise in real piping systems
15 p2164 N90-22368
Hybrid modeling of plasmas and applications to fusion and space physics 15 p2168 N90-22387
Impurity control in toroidal devices
[DE90-618585] 15 p2170 N90-22399
Optical bistability in semiconducting material
15 p2174 N90-22424
The evolution of the supernova remnant IC 443
15 p2186 N90-22486
Modelling late-time atmospheres of supernovae
15 p2189 N90-22500
Stability of compactification during inflation
[NASA-CR-186597] 15 p2189 N90-22502
Gravitational couplings of the inflation in extended inflation
[NASA-CR-186595] 15 p2190 N90-22504
Soft inflation
[NASA-CR-186593] 15 p2190 N90-22506
Geology of coronae and domal structures on Venus and models of their origin 15 p2191 N90-22513
Reynolds stress closure in jet flows using instability wave modeling 16 p2196 N90-22534
Application of a dynamic stall model to rotor trim and aeroelastic response 16 p2200 N90-22556
Model-based method for terrain-following display design
[AD-A219302] 16 p2201 N90-22563
A modeling technique for STOVL ejector and volume dynamics
[NASA-TM-103167] 16 p2202 N90-22566
A study of woven fabric-reinforced composite materials using an invariant-based orthotropic plasticity formulation
16 p2211 N90-22611
A life prediction model for laminated composite structural components
[NASA-CR-186587] 16 p2212 N90-22614
A comprehensive study on microstructure mechanics relationships of ceramic matrix composites
[AD-A219316] 16 p2213 N90-22627
Calcium carbonate scale dissolution in water stabilized by carbon dioxide treatment
[AD-A218502] 16 p2214 N90-22633
Numerical investigation of turbulent flame sheets
[AD-A218553] 16 p2215 N90-22635
Design of cryogenic tanks for launch vehicles
16 p2220 N90-22662
HF propagation through actively modified ionospheres
[DE90-008931] 16 p2227 N90-22705
Qualitative aspects of signal processing through dynamical neural networks
[PREPRINT-711] 16 p2228 N90-22709
Optical excisor modeling
[AD-A219338] 16 p2230 N90-22722
Optimization of a pulsed air core transformer for low impedance inductive ignition
[AD-A218748] 16 p2232 N90-22734
An investigation of the three-dimensional flow field in a centrifugal compressor 16 p2235 N90-22751
Nonstrictly hyperbolic conservation laws
[AD-A218525] 16 p2237 N90-22762
Modelling and computer control of a mechanical system
[W-8908] 16 p2243 N90-22794
Axisymmetric and cylindrically orthotropic analysis of filament winding 16 p2246 N90-22811
Localization of vibration in disordered nearly cyclic structures 16 p2246 N90-22812
Comparison between data generated from standard fracture toughness specimens and from nonstandard specimens made of a silicon carbide
[DE90-009621] 16 p2247 N90-22814
Fundamental studies on hydrology, hydraulics and geometry of river networks
[AD-A218662] 16 p2250 N90-22830
A new stochastic model of turbulent dispersion in the convective planetary boundary layer and the results of the Atterbury-87 field study 16 p2254 N90-22853
Tropical squall lines of the Arizona monsoon
16 p2257 N90-22867
Evidence for self-refraction in a convergence zone: NPE (Nonlinear progressive wave equation) model results
[AD-A218546] 16 p2259 N90-22879
Stochastic interactive activation and the effect of context on perception
[AD-A218929] 16 p2262 N90-22898
Sensory conflict in motion sickness: An observer theory approach 16 p2273 N90-22957
Experimental experience with flexible structures
16 p2281 N90-23002
A finite element based method for solution of optimal control problems 16 p2286 N90-23027
A methodology for formulating a minimal uncertainty model for robust control system design and analysis
16 p2287 N90-23028
Modeling of control forces for kinematical constraints in the dynamics of multibody systems: A new approach
16 p2287 N90-23031
Concurrent processing simulation of the space station
16 p2289 N90-23041
Enhanced modeling features within TREETOPS
16 p2290 N90-23047
Modal identities for multibody elastic spacecraft: An aid to selecting modes for simulation
16 p2296 N90-23075
Factoring homomorphisms
[CS-8908] 16 p2299 N90-23096
Index and consistency analysis for DAE (Differential Algebraic Equation) systems for Stefan-Maxwell diffusion-reaction problems
[DE90-008188] 16 p2304 N90-23129
Periodic ARMA models: Optimal prediction and minimum-phase condition
[REPT-89-006] 16 p2305 N90-23131
On a fallacious conjecture about the stabilizability properties of solutions of the Riccati difference equation
[REPT-89-007] 16 p2305 N90-23132
Processes and formalisms for unbounded choice
[CS-8917] 16 p2305 N90-23135
Proceedings of the 9th International Conference on Computing Methods in Applied Science and Engineering
[AD-A219307] 16 p2307 N90-23149
Selecting multinomial populations
[AD-A219256] 16 p2309 N90-23159
Time-varying filter modelling and time-frequency characterisation of nonstationary sound fields due to a moving source 16 p2312 N90-23178
Looking at large data sets using binned data plots
[DE90-008206] 16 p2326 N90-23263
Towards a calculus of data refinement
[CS-8902] 16 p2326 N90-23264
Studies of Io's atmosphere and plasma torus
16 p2338 N90-23326
A study of supermanuever aerodynamics
[AD-A218378] 17 p2344 N90-23349
A computer code for the prediction of aerodynamic characteristics of lifting airfoils at transonic speed
[DLC-EST-TN-030] 17 p2345 N90-23359
MLS mathematical model validation study using airborne MLS data from Midway Airport engineering flight tests, August 1988
[DOT/FAA/CT-TN90/2] 17 p2349 N90-23378
Modelling and control of a balloon borne stabilized platform 17 p2355 N90-23408
Experimental study of mixing and combustion processes in a solid-propellant ducted rocket motor
17 p2367 N90-23472
Ply cracking in composite laminates
17 p2368 N90-23478
Rate dependent constitutive models for fiber reinforced polymer composites
[NASA-TM-102665] 17 p2370 N90-23492
Numerical simulation of turbulent combustion using vortex methods
[AD-A219624] 17 p2372 N90-23507

Reactions of silane in active nitrogen
[AD-A220371] 17 p2373 N90-23511
HYPUF upgrade
[AD-A218400] 17 p2379 N90-23547
Soil Transport Implement
[NASA-CR-184931] 17 p2385 N90-23582
Qualitative models for space system engineering
[NASA-CR-180682] 17 p2385 N90-23585
Nonlinear dynamics and control of flexible structures
[AD-A218372] 17 p2386 N90-23588
Unfairness caused by quadratic backoff in a packet-radio network
[AD-A219635] 17 p2388 N90-23603
Artificial dielectrics
[AD-A219671] 17 p2389 N90-23605
A model of electromagnetic leakage through joints at radio frequencies
[BAE-WES-RP-GEN-EMC-049-T2.2] 17 p2392 N90-23626
Study and simulation of the behavior of a high frequency transformer
[ECL-89-008] 17 p2399 N90-23667
Numerical and physical modelling of bubbly flow phenomena
[DE90-009637] 17 p2401 N90-23677
Numerical modelling of shocks in gases and metals
[AD-A218586] 17 p2402 N90-23684
Numerical study of unsteady flows in large air-driven blast simulators with single and multiple drivers
[UTIAS-334] 17 p2405 N90-23699
Modeling of thermal lensing in side and end-pumped finite solid-state laser rods
[NASA-CR-4300] 17 p2407 N90-23716
Non-linear dynamic analysis of geared systems, part 2
[NASA-CR-180495] 17 p2410 N90-23732
Numerical simulation of semi-infinite target penetration by continuous and segmented rods
[AD-A219437] 17 p2412 N90-23743
A viscoplastic model with application to LiF-22 percent CaF2 hypereutectic salt
[NASA-TM-103181] 17 p2417 N90-23770
Strain softening in viscoelasticity of the rate type
[AD-A219915] 17 p2417 N90-23772
An analytic/empirical model of the middle and low latitude ionosphere
[AD-A220004] 17 p2423 N90-23809
Ionospheric equivalent slab thickness and its modeling applications
[AD-A220105] 17 p2424 N90-23811
The Very Long Baseline Interferometry (VLBI) functional model and the relation with tectonic motions
[ETN-90-96694] 17 p2424 N90-23814
US Navy hindcast spectral ocean wave model climatic atlas: Mediterranean Sea
[AD-A219755] 17 p2426 N90-23825
A day in the life of a warm front
[AD-A220373] 17 p2426 N90-23826
Test and evaluation of surf forecasting model
[AD-A219580] 17 p2430 N90-23845
Modeling studies of the LeeUwin current using a high-resolution primitive equation model
[AD-A219595] 17 p2430 N90-23846
A numerical study of wind forcing in the eastern boundary current system off Portugal
[AD-A219596] 17 p2430 N90-23847
Predicting tidal displacements of the surface of the Earth, volume 1
[ETN-90-96690] 17 p2431 N90-23850
Predicting tidal displacements of the surface of the Earth, volume 2
[ETN-90-96691] 17 p2431 N90-23851
Model for predicting the effects of laser exposures and eye protection on vision
[AD-A219697] 17 p2434 N90-23868
DURIP: Computational modeling of cognitive processes
[AD-A219934] 17 p2437 N90-23886
The cost of conservative synchronization in parallel discrete event simulations
[NASA-CR-182034] 17 p2441 N90-23912
Conceptual modeling via logic programming
[AD-A219785] 17 p2442 N90-23919
Design and investigation of a dive plane sliding mode compensator for an autonomous underwater vehicle
[AD-A219552] 17 p2454 N90-23997
Efficient smoothing for boundary value models
[AD-A218484] 17 p2456 N90-24014
Analytic parabolic equation solutions
[AD-A218588] 17 p2456 N90-24015
A uniform representation scheme for freeform geometric modeling
[REPT-89-70] 17 p2458 N90-24028
An H(m)sub 0 interpolation result
[AD-A219888] 17 p2461 N90-24051
M-estimators in linear models with long range dependent errors
[AD-A219921] 17 p2461 N90-24053
A general approach to dominance in the plane
[RUU-CS-88-35] 17 p2463 N90-24072
Formula scoring: Basic theory and applications
[AD-A218368] 17 p2465 N90-24083
Mean square error behavior for prediction in linear regression models
[AD-A219988] 17 p2466 N90-24092
Extreme quantile estimation in binary response models
[AD-A220150] 17 p2466 N90-24093
Stochastics realization problems
[CWI-BS-R8920] 17 p2467 N90-24097
Cosmological baryon and lepton number in the presence of electroweak fermion-number violation
[NASA-CR-186609] 17 p2470 N90-24123
Proceedings of a research workshop on Computational Condensed Matter Physics. Total Energy Methods and Physics of III-V Semiconductors
[AD-A219568] 17 p2476 N90-24156
Dust environment modelling from encounters with comet P/Halley 17 p2485 N90-24210
The computation of turbulent thin shear flows associated with flow around multielement aerofoils 18 p2491 N90-24240
Reduced order models for nonlinear aerodynamics 18 p2492 N90-24244
Groundbased simulations of in-orbit operations 18 p2505 N90-24314
Equivalent flexibility modeling: A novel approach towards recursive simulation of flexible spacecraft manipulator dynamics 18 p2505 N90-24316
Dynamic stabilization of large flexible space structures
[ETN-90-96926] 18 p2511 N90-24344
An elastic/viscoplastic constitutive model for fiber-reinforced thermoplastic composites 18 p2516 N90-24371
Metal matrix composites microfracture: Computational simulation
[NASA-TM-103153] 18 p2518 N90-24383
Encoding of the Burgess metal electrical resistivity model into SESAME format and its adaptation to the metal nickel
[DE90-010816] 18 p2526 N90-24419
Understanding tropscatter propagation
[AD-A220969] 18 p2544 N90-24520
The problem of robust compensation for systems with unmodeled dynamics
[AD-A221246] 18 p2548 N90-24545
Mass transfer induced convection near gas-liquid interfaces
[ETN-90-96925] 18 p2552 N90-24568
Computational modeling of three-dimensional compressible leading edge vortices
[AD-A221022] 18 p2553 N90-24569
NDE (NonDestructive Evaluation) of ceramic heat exchangers
[DE90-010977] 18 p2554 N90-24575
Theoretical studies of non-Newtonian and Newtonian fluid flow through porous media
[DE90-011610] 18 p2554 N90-24576
Laser range camera modeling
[DE90-008220] 18 p2562 N90-24618
Obtaining an equivalent beam 18 p2570 N90-24646
Accuracy improvements in finite element stress analysis 18 p2571 N90-24651
Analysis of shell-type structures subjected to time-dependent mechanical and thermal loading
[NASA-CR-185077] 18 p2571 N90-24653
A vectroized elastic/plastic power law hardening material model including Lueders strain
[DE90-010172] 18 p2572 N90-24655
Modelling and synergism: Optical and microwave remote sensing. Partial report 1: Preliminary study
[BCRS-89-23] 18 p2575 N90-24668
On the G1 smooth connection between triangular Bernstein-Bezier patches. Part 1: Around and N-patch corner
[TELECOM-PARIS-89-D-012] 18 p2575 N90-24671
Dynamic optimisation of thermal energy systems
[ETN-90-96900] 18 p2576 N90-24676
A direct absorber reactor/receiver for solar thermal applications
[DE90-006280] 18 p2577 N90-24679
Heat and fluid flow within the Earth's crust: In situ measurements and mathematical models 18 p2579 N90-24690
A numerical investigation of thermal convection in highly viscous spherical shells with applications to mantle dynamics in the Earth and other terrestrial planets 18 p2579 N90-24691
Evaluation of Stochastic models for estimating the persistence probability of cloud-free lines-of-sight
[AD-A220283] 18 p2581 N90-24702
Synchronously parallel Boltzmann machines: A mathematical model
[MEMO-COSOR-89-21] 18 p2590 N90-24732
A comparison of variance-controlled and non-controlled principal components
[AD-A220530] 18 p2598 N90-24782
Uniform limit theorems for synchronous processes with applications to queues
[AD-A220224] 18 p2599 N90-24788
Finding squares and rectangles in sets of points
[RUU-CS-89-10] 18 p2601 N90-24806
Ranking intervals under visibility constraints
[RUU-CS-89-18] 18 p2602 N90-24812
Structure of linear-quadratic control
[ETN-90-96894] 18 p2602 N90-24819
More about general saddlepoint approximations
[AD-A221217] 18 p2604 N90-24832
Effective Hamiltonians and the theory of invariants
[DE90-611035] 18 p2605 N90-24836
G exchangeability and the construction of distribution-free statistics 18 p2605 N90-24837
Symposium on Applied Probability
[AD-A218760] 18 p2605 N90-24838
On the statistical analysis of growth
[ETN-90-96923] 18 p2606 N90-24841
A nonlocal free energy density functional approximation for the electrical double layer
[AD-A220664] 18 p2607 N90-24848
Sound propagation elements in evaluation of en route noise of advanced turbofan aircraft 18 p2609 N90-24861
Axions and SN 1987A: Axion trapping
[NASA-CR-186604] 18 p2612 N90-24881
Improved model for solar cosmic ray exposure in manned Earth orbital flights
[NASA-TP-2987] 18 p2639 N90-25031
A quantitative technique to estimate microburst wind shear hazard to aircraft 18 p2640 N90-25040
From where they look to what they think: Determining controller cognitive strategies from oculometer scanning data 18 p2641 N90-25041
Dynamic analysis of flexible multibody structures 18 p2642 N90-25048
Development of a finite element based delamination analysis for laminates subject to extension, bending, and torsion 18 p2642 N90-25049
Fatigue analysis of mini-mast space truss 18 p2643 N90-25052
A user-friendly, menu-driven, language-free laser characteristics curves graphing program for desk-top IBM PC compatible computers 18 p2644 N90-25056
Extension-torsion coupling behavior of advanced composite tilt-rotor blades 18 p2644 N90-25057
An investigation of a mathematical model of an optically pumped Ti(3+):Al2O3 laser system 18 p2646 N90-25063
Expansion and orthogonalization of measured modes for structure identification 18 p2647 N90-25068
Operations and support cost modeling using Markov chains 18 p2648 N90-25070
A review of instability and noise propagation in supersonic flows
[NASA-CR-186800] 19 p2655 N90-25112
Development of a microcomputer based software system for use in crewmember ejection analysis
[AD-A220398] 19 p2656 N90-25117
The effect of aircraft size on cabin floor dynamic pulses
[DOT/FAA/CT-88/15] 19 p2659 N90-25136
Ground shake test of the UH-60A helicopter airframe and comparison with NASTRAN finite element model predictions
[NASA-CR-181993] 19 p2661 N90-25143
Lecture notes on flight simulation techniques
[LR-596] 19 p2662 N90-25153
A design optimization process for Space Station Freedom
[NASA-CR-186851] 19 p2667 N90-25175
Intelligent composites containing measuring fibre optic networks for continuous self diagnosis
[ETN-90-97018] 19 p2673 N90-25200
Equivalent circuit models for ac impedance data analysis
[NASA-TM-100402] 19 p2686 N90-25277
A two layer model for the simulation of internal linear and nonlinear waves in Lake Geneva (Switzerland) 19 p2687 N90-25286
A computational efficient modelling of laminar separation bubbles
[NASA-CR-186729] 19 p2688 N90-25291
Modeling and Applications of Transport Phenomena in Porous Media, volume 1
[VKI-LS-1990-01-VOL-1] 19 p2689 N90-25296

Continuum approach and contaminant transport in ground water flows 19 p2690 N90-25301
Network modeling of fluid flow in porous media 19 p2690 N90-25306
The flow of non Newtonian fluids in porous media 19 p2691 N90-25307
Fingering in 2-D porous media: Experiments, network simulators and statistical models 19 p2691 N90-25308
Particle tracking methods and fractal statistics in groundwater modeling 19 p2691 N90-25309
Depletion mode pumping of solid state lasers [DE90-012090] 19 p2696 N90-25339
Free vibrations of thin-walled semicircular graphite-epoxy composite frames [NASA-TM-102680] 19 p2701 N90-25365
Loads analysis and testing of flight configuration solid rocket motor outer boot ring segments [NASA-TP-3028] 19 p2701 N90-25366
LEO high voltage solar array arcing response model, continuation 5 [NASA-CR-186505] 19 p2709 N90-25418
A kinematic/dynamic model for prediction of neck injury during impact acceleration 19 p2719 N90-25469
Effects of head mounted devices on head-neck dynamic response to +G(sub z) accelerations 19 p2720 N90-25471
Spacecraft external molecular contamination analysis 19 p2730 N90-25520
Some observations for the pigeon hole principle [RUU-CS-88-39] 19 p2750 N90-25624
Laboratory studies of acoustic scattering from the underside of sea ice [AD-A221333] 19 p2753 N90-25644
Analytic study of the high-frequency impedance [CEBAF-PR-89-014] 19 p2757 N90-25665
Formation of magnetic islands due to field perturbations in toroidal stellarators [DE90-012132] 19 p2759 N90-25679
Conceptual task modeling [TR-89-14] 19 p2762 N90-25693
A framework for query optimization in temporal databases [DE90-011339] 19 p2763 N90-25700
BL Lacs from the EMSS: Number-counts and implications for the luminosity function 19 p2785 N90-25849
U. radio emission from quiescent filaments [NASA-CR-186538] 19 p2797 N90-25922
Aerodynamic loads and blade vortex interaction noise prediction [ISL-PU-310/89] 20 p2802 N90-25942
The applicability of simple helicopter models for flight mechanics studies [ETN-90-96962] 20 p2808 N90-25975
Agusta methodology for pitch link loads prediction in preliminary design phase [ETN-90-97270] 20 p2808 N90-25978
Performance of a supercharged direct-injection stratified-charge rotary combustion engine [NASA-TM-103105] 20 p2809 N90-25982
Subsonic combustor flow modeling: State of the art of CFD techniques for reacting and combusting flow 20 p2810 N90-25991
Turbulent combustion modeling for turbo-jet combustion chambers 20 p2811 N90-25993
Background, current status, and prognosis of the ongoing slush hydrogen technology development program for the NASP [NASA-TM-103220] 20 p2822 N90-26055
The origin of poorly conditioned susceptibility matrix within inverse CVM algorithm in the case of Pd(sub 3)V: A comparison to the case of Ni(sub 3)V [DE90-012464] 20 p2833 N90-26110
Extension of a noninteractive reliability model for ceramic matrix composites [NASA-CR-185267] 20 p2838 N90-26142
Modelling of the processing of incompatible polymer blends [ETN-90-97211] 20 p2840 N90-26152
Simulated dynamic response of a servovalve controlled hydraulic actuator [NASA-TM-101644] 20 p2842 N90-26167
Optimal synchronization of spread spectrum sequenced by nontransferable switching operators 20 p2845 N90-26183
Radio channel measurement and modelling for future mobile radio systems 20 p2845 N90-26184
Long-range planning cost model for support of future space missions by the deep space network 20 p2854 N90-26231
Validity domain of the scalar Kirchhoff and Rayleigh-Sommerfeld diffraction theories in the near field of small phase objects: Comparison between calculation models and microwave measure [ETN-90-96963] 20 p2855 N90-26236
A model of the synchronous machine with rectifier, especially for control purposes [EUT-89-E-215] 20 p2858 N90-26256
A possibility to incorporate saturation in the simple, global model of a synchronous machine with rectifier [EUT-89-E-225] 20 p2858 N90-26258
An investigation into the numerical prediction of boundary layer transition using the K.Y. Chien turbulence model [NASA-CR-185252] 20 p2860 N90-26269
A numerical simulation of the quasi-heterodyne technique for double-pulsed holographic vibration measurements [PNR90622] 20 p2865 N90-26301
An inverse dynamic method yielding flexible manipulator state trajectories [NASA-CR-186807] 20 p2870 N90-26329
Application of symbolic computations to the constitutive modeling of structural materials [NASA-TM-103225] 20 p2876 N90-26364
Fatigue life assessment using a short crack growth model [PNR90663] 20 p2877 N90-26367
Investigation of crack-closure prediction models for fatigue in aluminium alloy sheet under flight-simulation loading [LR-619] 20 p2877 N90-26369
Modeling, simulation, and analysis of optical remote sensing systems [NASA-CR-186648] 20 p2878 N90-26376
Measuring and modeling near-surface reflected and emitted radiation fluxes at the FIFE site [NASA-CR-180953] 20 p2879 N90-26378
Nordic Symposium on Atmospheric Chemistry [CM-78] 20 p2883 N90-26403
Adjustment and validation of the mathematical prediction model for sweat rate, heart rate, and body temperature under outdoor conditions [AD-A222599] 20 p2898 N90-26486
Human performance models [FFI-90/7002] 20 p2901 N90-26502
A computer module used to calculate the horizontal control surface size of a conceptual aircraft design [NASA-CR-186872] 20 p2903 N90-26515
H-infinity control: An exploratory study [EUT-88-E-211] 20 p2915 N90-26584
On central-difference and upwind schemes [NASA-CR-182061] 20 p2917 N90-26595
Combinatorial problems using a hypercube and Hamming graphs [ETN-90-97240] 20 p2919 N90-26609
Nonlinear modeling of time series using Multivariate Adaptive Regression Splines (MARS) [AD-A222710] 20 p2921 N90-26623
Reversed residuals in autoregressive time series analysis [AD-A222711] 20 p2921 N90-26624
Evaluation of a decomposition approach for real-time scheduling using a Stochastic model [AD-A222726] 20 p2921 N90-26625
Application and extension of an analytical model of the confined acoustic beam generated by a transducer [AD-A222994] 20 p2924 N90-26639
An embedded fibre optic sensor for impact damage detection in composite materials [UTIAS-332] 20 p2926 N90-26650
Dielectric function of InGaAs in the visible [NASA-TM-103246] 20 p2932 N90-26683
A lattice gas model for thermohydrodynamics [DE90-011964] 20 p2933 N90-26690
Laboratory studies, analysis, and interpretation of the spectra of hydrocarbons present in planetary atmospheres including cyanoacetylene, acetylene, propane, and ethane 20 p2943 N90-26748
Laboratory measurements and modeling of microwave absorption by ammonia in gas mixtures applicable to giant planet atmospheres 20 p2944 N90-26750
Laboratory measurements and methane photochemistry modeling 20 p2947 N90-26770
Investigation of the Saturn dust environment from the analysis of energetic charged particle measurements [NASA-CR-186727] 20 p2950 N90-26784
Velocity measurements on a lifting rotor/airframe configuration in low speed forward flight 21 p2953 N90-26790
Aerodynamic/dynamic interaction [AD-A222263] 21 p2954 N90-26798
Obtaining consistent models of helicopter flight-data measurement errors using kinematic-compatibility and state-reconstruction methods [AD-A222533] 21 p2954 N90-26799
Finite element models of USAF aircraft structures 21 p2958 N90-26820
Damage tolerance analysis for manned hypervelocity vehicles. Volume 2: Software user's manual [AD-A222136] 21 p2959 N90-26826
A linear-eddy model of turbulent shear layer mixing 21 p2974 N90-26904
Dynamic properties of porous B4C [AD-A222850] 21 p2985 N90-26960
An interdisciplinary approach to the predictive modeling of structural adhesive bonding [AD-A221703] 21 p2988 N90-26982
Specification for HF Lowest Usable Frequency (LUF) model [AD-A222114] 21 p2996 N90-27031
Linear averaged and sampled data models for large signal control of high power factor ac-dc converters [AD-A221976] 21 p3020 N90-27170
A study of the effect of synoptic scale processes in GCM modelling [NASA-CR-184804] 21 p3021 N90-27175
The role of the topography in gravity gradiometer reductions and in the solution of the geodetic boundary value problem using analytical downward continuation [AD-A223107] 21 p3025 N90-27201
A tool for modeling concurrent real-time computation 21 p3047 N90-27321
VIP: A knowledge-based design aid for the engineering of space systems 21 p3048 N90-27327
A theoretical model of optimistic recovery in distributed systems [AD-A222055] 21 p3054 N90-27359
Robotic space simulation integration of vision algorithms into an orbital operations simulation [NASA-CR-185934] 21 p3059 N90-27395
The development of the time-delayed neural network architecture [AD-A221540] 21 p3061 N90-27403
Conjugate gradient methods for constrained least squares problems [AD-A222706] 21 p3063 N90-27411
Toeplitz matrices: Algebra and algorithms [AD-A223174] 21 p3064 N90-27416
Proceedings of Workshop on Reliability in Computational Mechanics [AD-A221694] 21 p3065 N90-27426
Model-based Gaussian and non-Gaussian clustering [AD-A222097] 21 p3066 N90-27430
Multivariate model building and model identification [AD-A221619] 21 p3067 N90-27435
Integrated structural/control design via multiobjective optimization [AD-A223088] 21 p3071 N90-27459
Air Force procedure for predicting aircraft noise around airbases: Noise Exposure Model (NOISEMAP). User's manual [AD-A223162] 21 p3072 N90-27467
The theory and simulation of plasmoid formation and propagation [AD-A222048] 21 p3079 N90-27504
Effects of organizational structure on performance: Experimental results [AD-A222871] 21 p3085 N90-27543
High resolution optical imaging through the atmosphere [AD-A221913] 21 p3097 N90-27599
United States Air Force research initiation program for 1988, volume 3 [AD-A223125] 21 p3102 N90-27615
United States Air Force research initiation program for 1988, volume 4 [AD-A223126] 21 p3102 N90-27616
Experimental identification of helicopter engine dynamics from closed loop data 22 p3104 N90-27627
Dynamics and dynamics experiments in TSS-1 22 p3129 N90-27758
Observation model and parameter partials for the JPL geodetic (GPS) modeling software 'GPSOMC' [NASA-CR-186972] 22 p3132 N90-27774
Laser surface interactions of high-T(sub c) superconductors 22 p3139 N90-27809
Calculations of chemically reacting shear flows above solid fuels 22 p3162 N90-27930
Flowfield computation of entry vehicles [NASA-CR-186946] 22 p3171 N90-27986
Calculation of surface free three dimensional flows [ONERA-RSF-5/4368-AY-002A] 22 p3176 N90-28022
The mathematical modeling of arc welding operation [DE90-013700] 22 p3183 N90-28064
Modification of the SHABERTH bearing code to incorporate RP-1 and a discussion of the traction model [NASA-TP-3017] 22 p3183 N90-28066
Acoustic emission from a growing crack 22 p3188 N90-28089
Impact of NDE-NDI methods on aircraft design, manufacture, and maintenance, from the fundamental point of view 22 p3189 N90-28093

Reliability growth modeling analysis of the space shuttle main engines based upon the Weibull process
[NASA-TM-103511] 22 p3189 N90-28098
Micromechanical model of crack growth in fiber reinforced ceramics
[NASA-CR-4321] 22 p3192 N90-28113
Numerical simulation of the middle atmosphere chemical composition and temperature under changing solar conditions 22 p3206 N90-28186
Cloud top entrainment instability and cloud top distributions 22 p3214 N90-28231
On the dynamic and thermodynamic structures of marine stratocumulus 22 p3216 N90-28244
Microphysical fundamentals governing cirrus cloud growth: Modeling studies 22 p3225 N90-28291
Instability bursts associated with Extratropical Cyclone Systems (ECSs) and a forecast index of 3 to 12 hour heavy precipitation
[NOAA-TM-NESDIS-30] 22 p3228 N90-28309
Vertically averaged spectral model for tidal circulation in estuaries. Part 1: Model formulation
[PB90-181678] 22 p3230 N90-28319
Physical characteristics of clothing materials with regard to heat transport
[IZF-1989-10] 22 p3233 N90-28336
Calculation of clothing insulation and vapour resistance
[IZF-1989-49] 22 p3234 N90-28338
Robust adaptive control: Handling the excitation problem 22 p3241 N90-28382
Polymatroids: Construction and random algorithms
[REPT-89-068] 22 p3242 N90-28388
Optical imaging of IRAS galaxies: The evolution of infrared-bright galaxies 22 p3261 N90-28465
Nonequilibrium radiation and chemistry models for aerocapture vehicle flowfields
[NASA-CR-186379] 23 p3267 N90-28490
Secondary instabilities in compressible boundary layers
[NASA-CR-182091] 23 p3269 N90-28502
The effects of structural flap-lag and pitch-lag coupling on soft inplane hingeless rotor stability in hover
[NASA-TP-3002] 23 p3269 N90-28503
Study of ground effects on flying scaled models 23 p3275 N90-28532
Cage stability analysis for SSME HPOTP bearings 23 p3292 N90-28625
Micromechanics of cyclic deformation in SSME turbopump blade materials 23 p3295 N90-28641
High temperature fatigue behavior of Haynes 188 23 p3295 N90-28642
Structural response of SSME turbine blade airfoils 23 p3297 N90-28649
Probabilistic model for fracture mechanics service life analysis 23 p3297 N90-28650
Thermal analysis of thermal barrier coatings in a high heat flux environment 23 p3297 N90-28652
Probability models for the failure of fibres and fibrous composite materials 23 p3300 N90-28665
A constitutive model for AS4/PEEK thermoplastic composites under cyclic loading
[NASA-CR-180393] 23 p3302 N90-28679
Development of comprehensive numerical schemes for predicting evaporating gas-droplets flow processes of a liquid-fueled combustor
[NASA-CR-187018] 23 p3305 N90-28693
An LQR controller design approach for a Large Gap Magnetic Suspension System (LGMSS)
[NASA-TM-101606] 23 p3316 N90-28751
New approach to HF channel modeling and simulation. Part 2: Stochastic model
[PB90-200338] 23 p3317 N90-28755
Modeling tape-wound magnetic switches
[DE90-015121] 23 p3322 N90-28782
Simulation of INPE's printed circuit laboratory production line
[INPE-4556-TDL/331] 23 p3322 N90-28784
On the use of Lagrangian variables in descriptions of unsteady boundary-layer separation
[NASA-CR-182071] 23 p3323 N90-28789
Evaluation of a hybrid kinetics/mixing-controlled combustion model for turbulent premixed and diffusion combustion using KIVA-2
[NASA-TM-103196] 23 p3323 N90-28792
An experimental investigation of a single and multiphase confined coaxial jet 23 p3324 N90-28796
Gas-jet and tangent-slot film cooling tests of a 12.5 deg cone at Mach number of 6.7
[NASA-TP-2786] 23 p3326 N90-28806
A hybrid perturbation-Galerkin technique for partial differential equations
[NASA-CR-182085] 23 p3327 N90-28814
Study of meteorological processes important in the degradation of materials through surface temperature
[PB90-222720] 23 p3336 N90-28856
Structural analysis and optimum design of geodesically stiffened composite panels
[NASA-CR-186944] 23 p3337 N90-28862
Correlation of AH-1G airframe flight vibration data with a coupled rotor-fuselage analysis
[NASA-CR-181974] 23 p3338 N90-28865
Plan, execute, and discuss vibration measurements and correlations to evaluate a NASTRAN finite element model of the AH-64 helicopter airframe
[NASA-CR-181973] 23 p3338 N90-28866
Green's functions for dislocations in bonded strips and related crack problems
[NASA-CR-185291] 23 p3340 N90-28878
A method of classification for multisource data in remote sensing based on interval-valued probabilities
[NASA-CR-187007] 23 p3343 N90-28889
Methods for multisource data analysis in remote sensing
[NASA-CR-187005] 23 p3343 N90-28890
Three functions that model empirically measured unfrozen water content data and predict relative hydraulic conductivity
[AD-A223875] 23 p3343 N90-28892
Sound propagation through atmospheric turbulence: A literature summary
[RPI-MATH-184] 23 p3350 N90-28930
Planetary-scale flow on a two-layer beta-plane channel model with topography 23 p3350 N90-28931
Gravity wave initiated convection
[NASA-CR-186868] 23 p3350 N90-28933
Automated system for meteorological analysis
[INPE-4586-TDL/332] 23 p3352 N90-28945
Vorticity balance study for a tropical region, during the Southern Hemisphere summer
[INPE-4634-TDL/336] 23 p3353 N90-28949
Methods and strategies of object localization 23 p3366 N90-29020
Planning 3-D collision-free paths using spheres 23 p3367 N90-29024
A design philosophy for multi-layer neural networks with applications to robot control 23 p3368 N90-29033
A Boltzmann machine for the organization of intelligent machines 23 p3370 N90-29040
Autoregressive-moving average models for texture classification
[INPE-4987-PRE/1549] 23 p3380 N90-29092
Second order tensor finite element
[NASA-CR-184008] 23 p3386 N90-29122
Multigrid for hypersonic inviscid flows
[NASA-CR-182082] 23 p3387 N90-29125
Criticality of the three-state chiral clock model: A renormalisation group study
[DE90-627321] 23 p3400 N90-29212
Z(6) model: Criticality and break-collape method
[DE90-627323] 23 p3401 N90-29214
An infrared sky model based on the IRAS point source data
[NASA-CR-177526] 23 p3409 N90-29265
Cepheid masses for models with enhanced opacities
[DE90-014919] 23 p3409 N90-29266
Pulsations of the white dwarf component in V471 tauri-like binaries
[DE90-014921] 23 p3409 N90-29267
Radio outbursts in extragalactic sources 23 p3414 N90-29291
Numerical simulation of hypersonic viscous flow for the design of H-2 orbiting plane (HOPE)
[NAL-TR-1028] 24 p3422 N90-29330
State estimation for systems moving through random fields 24 p3429 N90-29373
Multi-disciplinary optimization of aeroservoelastic systems
[NASA-CR-185931] 24 p3432 N90-29385
Nonlinear modeling of joint dominated structures
[NASA-CR-4324] 24 p3439 N90-29423
Cyclic voltammetry at a rotating disk, electroreduction of nitrate in acidic nickel solutions, and frequency-response analysis of porous electrodes
[DE90-015317] 24 p3447 N90-29466
Influence of convection on microstructure
[NASA-CR-186506] 24 p3448 N90-29470
Modeling and reconstruction algorithms for detection, location, and identification of subsurface anomalies
[AD-A224358] 24 p3459 N90-29539
Specification for a standard electromagnetic propagation model
[AD-A223556] 24 p3461 N90-29551
IEEE Conference on Neural Information Processing Systems, Natural and Synthetic
[AD-A223611] 24 p3461 N90-29552
Reliability analysis/assessment of advanced technologies
[AD-A223647] 24 p3465 N90-29573
Numerical simulations of the structure of supersonic shear layers
[AD-A224164] 24 p3467 N90-29587
Finite difference modeling of laser diode ignited components
[DE90-015652] 24 p3474 N90-29635
Modeling towed cable system dynamics
[AD-A223610] 24 p3476 N90-29644
Application of the complex variable solution to some problems in linear elastic materials with voids 24 p3478 N90-29658
On a generalized laminate theory with application to bending, vibration, and delamination buckling in composite laminates 24 p3478 N90-29659
Investigation of the dynamic buckling of liquid-filled tanks 24 p3478 N90-29660
Proceedings of damping '89. Volume 1: Pages AAB-1 through DCD-11
[AD-A223431] 24 p3479 N90-29664
Proceedings of Damping '89. Volume 3: Pages ICA-1 through KDC-15
[AD-A223433] 24 p3479 N90-29666
NASA radiation belt models AP-8 and AE-8
[AD-A223660] 24 p3492 N90-29737
A study of magnetic field reconnection and plasma processes in the magnetosphere
[DE90-016117] 24 p3493 N90-29741
A global model of thunderstorm electricity and the prediction of whistler duct formation 24 p3493 N90-29744
The effect of wave data assimilation on the numerical simulation of wave energy advection
[KNMI-TR-121] 24 p3496 N90-29760
Frequency and ventilation: A survey of theoretical and experimental ventilation modelling
[LR-625] 24 p3498 N90-29772
Modeling, design, and control of flexible manipulator arms: Status and trends 24 p3500 N90-29782
Dynamical modeling of serial manipulators with flexible links and joints using the method of kinematic influence 24 p3500 N90-29783
Reflections on the relationship between artificial intelligence and operations research 24 p3506 N90-29816
A discrete decentralized variable structure robotic controller 24 p3509 N90-29835
How to push a block along a wall 24 p3511 N90-29848
Linear analysis of a force reflective teleoperator 24 p3513 N90-29856
A spatial operator algebra for manipulator modeling and control 24 p3519 N90-29894
Communications Interface Driver (CID) software principles of operation
[DOT/FAA/CT-TN89/46] 24 p3526 N90-29937
An interactive optimization based, computer graphics software package. Phase 2: Users manual
[AD-A223854] 24 p3529 N90-29954
Problems in probability, statistics, and reliability
[AD-A224152] 24 p3540 N90-30016
Unification of statistical methods for continuous and discrete data
[AD-A224307] 24 p3540 N90-30017
A new diagnostics approach for repeated measures designs
[AD-A223500] 24 p3540 N90-30020
Numerical pulse propagation studies using two classical ocean waveguide models
[AD-A224118] 24 p3542 N90-30033
A model of peaked density profile and inward pinch in tokamaks
[DE90-508079] 24 p3548 N90-30072

MATHEMATICAL PROGRAMMING
NT DYNAMIC PROGRAMMING
NT LINEAR PROGRAMMING
NT NONLINEAR PROGRAMMING
NT QUADRATIC PROGRAMMING

Polymorphism and information loss in Martin-Loef's type theory
[CS-8814] 04 p0533 N90-13079
Constructing a calculus of programs
[CWI-CS-R8914] 05 p0683 N90-13979
Efficient algorithms for dilated mappings of binary trees
[NASA-CR-181980] 09 p1262 N90-17317
Nonprocedural implementation of mathematical programming algorithms
[AD-A216039] 10 p1419 N90-18179
Deterministic differential game solution: The approximate strategy method
[ESA-TT-1158] 11 p1555 N90-18956
A knowledge-based approach to improving optimization techniques in system planning 15 p2154 N90-22303
Linear programming tools for integer programming
[AD-A219013] 16 p2300 N90-23106
A vectorization algorithm for the solution of large, sparse triangular systems of equations
[AD-A219850] 17 p2446 N90-23947

Compound sets in mathematical programming modeling languages
[MEMO-834] 17 p2449 N90-23963
Inverting the flow of computation
[TR-89-10] 17 p2450 N90-23971
Bounding separable recourse functions with limited distribution information
[AD-A219504] 17 p2465 N90-24084
Solution of the optimal control problem using the software package STOMP
[MBB-FE-126/S/PUB-370] 19 p2651 N90-25087
Some studies related to a new Hexagonal Compound Parabolic Concentrator (HCPC) as a secondary in tandem with a solar tower
[DLR-FB-90-12] 24 p3465 N90-29700
The effect of wave data assimilation on the numerical simulation of wave energy advection
[KNMI-TR-121] 24 p3496 N90-29760
Formal verification of mathematical software, volume 2
[AD-A223633] 24 p3527 N90-29943

MATHEMATICS
Summary of research academic departments, 1987-1988
[AD-A213252] 05 p0716 N90-14183
Remarks on intuitionism and the philosophy of mathematics
[ITLI-LP-88-05] 17 p2440 N90-23901
The Clemson University, university research initiative program in discrete mathematics and computational analysis
[AD-A220103] 17 p2461 N90-24055
Computer animation in mathematics, science, and art
[DE90-013051] 20 p2908 N90-26538

MATRICES
On a fallacious conjecture about the stabilizability properties of solutions of the Riccati difference equation
[REPT-89-007] 16 p2305 N90-23132

MATRICES (CIRCUITS)
Memory matrix
[WO-PATENT-88/04096] 05 p0680 N90-13961
Characterization of two MMIC GaAs switch matrices at microwave frequencies
[NASA-TM-102449] 06 p0733 N90-14273
Optical shutter switching matrix
[NASA-CASE-KSC-11392-1] 15 p2167 N90-22383
High speed magneto-resistive random access memory
[NASA-CASE-NPO-17954-1-CU] 20 p2904 N90-26519

MATRICES (MATHEMATICS)
NT ADJOINTS
NT CANONICAL FORMS
NT EIGENVALUES
NT EIGENVECTORS
NT HESSIAN MATRICES
NT JORDAN FORM
NT STIFFNESS MATRIX
Studies in estimation theory, applications and implementations
[AD-A210712] 01 p0114 N90-10653
The computation and use of the asymptotic covariance matrix for measurement error models
[PB89-215321] 01 p0115 N90-10659
LINPACK routines based on the level 2 BLAS
[CWI-NM-R8811] 02 p0261 N90-11483
Realization theoretic solution of two analytic matrix equations with applications to stabilization of infinite-dimensional systems
[AD-A211118] 02 p0285 N90-11512
An improved algorithm for the determination of the system paramters of a visual binary by least squares 02 p0290 N90-11658
Microscopic approach to the generator coordinate method
[DE89-016701] 03 p0392 N90-12233
A dynamic proof of the Frobenius-Perron theorem for Metzler matrices
[AD-A211839] 03 p0392 N90-12235
Four vector-matrix primitives
[AD-A211889] 03 p0392 N90-12237
A matrix factorization and its application to large-scale linear programming
[AD-A211293] 03 p0394 N90-12244
A long time tail for random walk in random scenery
[REPT-89-08] 03 p0398 N90-12278
A well conditioned formulation for the analysis of multi-layered frequency selective surfaces using a cascaded matrix approach, revised
[RSRE-MEMO-4289-REV] 04 p0496 N90-12858
NUMVEC FORTRAN library manual chapter: Simultaneous linear equations
[CWI-NM-R8903] 04 p0541 N90-13135
The quadratic matrix inequality in singular H infinity control with state feedback
[MEMO-COSOR-89-03] 05 p0686 N90-13997
A multilevel parallel solver for block tridiagonal and banded linear systems
[AD-A213151] 05 p0688 N90-14008
The algebraic Riccati equation and singular optimal control
[MEMO-COSOR-88-31] 05 p0690 N90-14028
Fluctuations of the Lyapunov exponent in disordered systems
[PREPRINT-690] 05 p0695 N90-14063
A graph theoretic characterization for the rank of the transfer matrix of a structured system
[CWI-OS-R8819] 05 p0695 N90-14064
Some comments on the solvable Chiral Potts model
[PREPRINT-673] 05 p0696 N90-14070
Parallel eigenanalysis of finite element models in a completely connected architecture
[NASA-CR-185166] 06 p0799 N90-14652
Krylov methods preconditioned with incompletely factored matrices on the CM-2
[NASA-CR-181961] 06 p0822 N90-14779
A block QR factorization algorithm using restricted pivoting
[DE90-001921] 07 p0972 N90-15613
An improved toeplitz approximation method
[AD-A213994] 07 p0984 N90-15688
Canonical formalism for coupled beam optics
[DE90-003764] 07 p0992 N90-15734
An algorithm to compute the square root of 3x3 positive definite matrix
[DE89-635711] 08 p1109 N90-16417
Asymptotically fast triangularization of matrices over rings
[DE90-003161] 08 p1117 N90-16471
Polarization matrices of quartz
[AD-A215198] 09 p1212 N90-17027
Quantum sl(2) enveloping algebra and representations of braid group
[DE90-607044] 09 p1275 N90-17389
Factoring symmetric indefinite matrices on high-performance architectures
[NASA-CR-181982] 10 p1421 N90-18195
Ab initio R-matrix calculations of e+-molecule scattering 11 p1557 N90-18970
Comparison of artificial matrices and covariance functions
[ETN-90-95722] 12 p1679 N90-19645
Comparison of two matrix data structures for advanced CSM testbed applications
[NASA-CR-181951] 13 p1815 N90-20421
Progress in the development of high degree potential coefficient models 13 p1832 N90-20516
An improved error assessment for the GEM-T1 gravitational model 13 p1832 N90-20518
An algorithm for efficient estimation of superimposed exponential signals
[AD-A217218] 13 p1865 N90-20698
The parallel algorithm for solving the three-dimensional integral magnetostatic equations
[DE90-616529] 14 p2015 N90-21547
Parallel tridiagonalization of a general matrix using distributed-memory multiprocessors
[DE90-008902] 14 p2015 N90-21551
Fusion algebra and fusing matrices
[DE90-612798] 14 p2021 N90-21583
METCAN verification status
[NASA-TM-103119] 15 p2064 N90-21824
On the existence of a positive definite solution of the matrix equation X + A(sup tau)X(exp -1)A = I
[PB90-133976] 15 p2159 N90-22335
H2, fixed architecture, control design for large scale systems
[NASA-CR-180471] 16 p2226 N90-22698
Efficient dynamic simulation for multiple chain robotic mechanisms 16 p2280 N90-22995
A survey on the structured singular value 16 p2281 N90-22998
Parallel algorithms and architecture for computation of manipulator forward dynamics 16 p2283 N90-23010
Efficient computer algebra algorithms for polynomial matrices in control design 16 p2285 N90-23022
Extensions of output variance constrained controllers to hard constraints 16 p2292 N90-23056
Robust adaptive control: Stability and asymptotic performance
[AD-A219259] 16 p2304 N90-23127
Processes and formalisms for unbounded choice
[CS-8917] 16 p2305 N90-23135
A proof of the isoenergetic KAM: Theorem from the ordinary one
[W-8906] 16 p2305 N90-23136
A computer program to implement the Chen method of dimensional analysis
[AD-A218557] 16 p2306 N90-23142
Transfer matrices for multimode optical fiber systems
[AD-A218459] 16 p2317 N90-23210
Adaptive filtering and control
[AD-A219556] 17 p2454 N90-23998
Chebyshev polynomials are not always optimal
[NASA-CR-181465] 17 p2455 N90-24008
Numerical solution of large Lyapunov equations
[NASA-CR-180359] 17 p2456 N90-24010
Skew-symmetric matrices in classical mechanics
[MEMO-COSOR-89-23] 17 p2459 N90-24036
Sparse approximations of inverse matrices
[ETN-90-96904] 17 p2464 N90-24074
A fast, preconditioned conjugate gradient Toeplitz solver
[NASA-CR-180367] 18 p2589 N90-24731
Visual animation of parallel algorithms for matrix computations
[DE90-011076] 18 p2594 N90-24763
The HK singular value decomposition of rank deficient matrix triplets
[DE90-010114] 18 p2598 N90-24784
The application of the finite element method to an aerodynamic problem specific to propeller design
[LR-614] 19 p2656 N90-25116
Modular arithmetic and randomization for exact matroid problems: Extended abstract
[REPT-89-064] 19 p2751 N90-25628
On conditions guaranteeing two polynomial matrices possess identical zero structures
[MATHS-REPT-A-123] 19 p2751 N90-25631
On output deadbeat control of discrete-time multivariable systems
[MATHS-REPT-A-122] 20 p2915 N90-26583
The system matrix characterisation of input-output equivalence
[MATHS-REPT-A-112] 20 p2918 N90-26600
Rational cubics with G2-continuity
[MATHS-REPT-A-113] 20 p2918 N90-26601
Large sets of block designs
[ETN-90-97212] 20 p2918 N90-26602
Mobility studies in multiloop spatial linkages 20 p2922 N90-26628
An adaptive blocking strategy for matrix factorizations
[DE90-011108] 21 p3051 N90-27343
Some remarks on the generalised Bareiss and Levinson algorithms
[AD-A221957] 21 p3053 N90-27357
Improving the accuracy of inverse iteration
[AD-A221846] 21 p3056 N90-27377
The image of weighted combinatorial problems
[REPT-88-017] 21 p3057 N90-27382
The stability of differential systems with delay
[RR-377] 21 p3062 N90-27408
On finding supernodes for sparse matrix computations
[DE90-013626] 21 p3063 N90-27410
Toeplitz matrices: Algebra and algorithms
[AD-A223174] 21 p3064 N90-27416
Newton methods for large-scale linear equality-constrained minimization
[AD-A222310] 21 p3070 N90-27457
Algorithms and evaluation for regulation of linear, time-independent difference systems under position value limitation
[ETN-90-97308] 22 p3238 N90-28364
Polymatroids: Construction and random algorithms
[REPT-89-068] 22 p3242 N90-28388
Least-index resolution of degeneracy in linear complementarity problems with sufficient matrices
[DE90-014406] 23 p3390 N90-29145
Kalman filter formulations for transfer alignment of strapdown inertial units 24 p3424 N90-29342

MATRIX ANALYSIS
U MATRICES (MATHEMATICS)

MATRIX MATERIALS
Composites reinforced with thermotropic liquid crystal copolyester fibers
[AD-A211226] 02 p0191 N90-11089
Carbon fiber reinforced glass matrix composites for structural space based applications
[AD-A211682] 03 p0320 N90-11818
Proceedings of the DOD Workshop on the Manufacturing/Producibility of Organic Matrix Composites
[AD-A212577] 04 p0468 N90-12680
Magnetic resonance of polymers at surfaces
[AD-A212225] 04 p0480 N90-12753
Status of Gr/glass composites technology at UTOS 05 p0596 N90-13459
Failure processes in unidirectional composite materials 05 p0617 N90-13598
Toughening of a particulate-reinforced/ceramic-matrix composite
[AD-A213180] 05 p0618 N90-13604
Elasto-plastic analysis of unidirectional fiber-reinforced composites subjected to transverse normal loading using the finite element method 06 p0737 N90-14292

Effects of filament-matrix interfaces on the mechanical properties of SiC-reinforced Si3N4: A review
[DE90-001863] 07 p0890 N90-15144
Metal matrix composites: A promising alternative to conventional alloys 07 p0901 N90-15208
Effects of moisture on composite materials 09 p1185 N90-16866
Interfaces of organic matrices and graphite fiber composites: A review of the literature
[AD-A214504] 09 p1186 N90-16870
Review of polyarylacetylene matrices for thin-walled composites
[AD-A214921] 09 p1186 N90-16872
The processing and mechanical properties of high temperature/high performance composites. Book 4, section 3: Flow and creep strength
[AD-A216144] 10 p1349 N90-17822
Investigation of the failure modes in a metal matrix composite under thermal cycling
[AD-A216195] 10 p1349 N90-17825
Impact damage tolerance of composite cylindrical panels
[AD-A216401] 10 p1350 N90-17830
Damping loss factor determination of glass and graphite epoxy laminated composites using vertically oriented cantilever beams
[AD-A216529] 10 p1351 N90-17833
The processing and mechanical properties of high temperature/high performance composites. Book 2, section 2: Strength and fracture resistance
[AD-A216142] 11 p1478 N90-18507
The processing and mechanical properties of high temperature/high performance composites. Book 3, section 2: Strength and fracture resistance, part
[AD-A216143] 11 p1478 N90-18508
Mechanical properties and microstructure of Si3N4-whisker-reinforced Si3N4 matrix composite
[DE90-005651] 11 p1480 N90-18518
Comparison between the damage modes of thermo-hardenable and thermo-plastic composite matrices
[ONERA-RT-47/7086-M] 11 p1481 N90-18523
Identification and development of optimum SiC whiskers for silicon nitride matrix composites
[DE90-006888] 12 p1621 N90-19315
Composite laminate tailoring with probabilistic constraints and loads
[NASA-TM-102515] 13 p1766 N90-20138
Reinforcement-matrix interface effects in metal matrix composites
[MRL-TN-562] 14 p1943 N90-21120
Interfacial studies in fiber-reinforced thermoplastic-matrix composites 15 p2062 N90-21814
Matrix density effects on the mechanical properties of SiC/RBSN composites
[NASA-TM-103098] 15 p2065 N90-21826
Characterization and role of an elastomeric interphase within polyepoxy reinforced glass, both particulate and fibrous
[ISAL-89-0064] 16 p2222 N90-22676
Theory and experimental technique for nondestructive evaluation of ceramic composites
[NASA-TM-102561] 17 p2414 N90-23754
A creep model for metallic composites based on matrix testing: Application to Kanthal composites
[NASA-TM-103172] 19 p2672 N90-25193
The effect of interfacial characteristics on the mechanical performance of ceramic-ceramic composites
[AD-A223031] 20 p2829 N90-26090
The 1990 Gordon Research Conference on Composites
[AD-A222849] 21 p2971 N90-26886
A study on carbon Fiber (long fiber) reinforced copper matrix composite
[AD-A221584] 21 p2972 N90-26891
Micromechanics of interfaces in high temperature ceramics
[AD-A222027] 21 p2987 N90-26973
Development of polysilsesquioxane composites
[NASA-CR-180263] 22 p3152 N90-27872
Factors influencing the mode I interlaminar fracture resistance of toughened matrix composites 23 p3300 N90-28668
High performance brittle matrices and brittle matrix composites, book 1
[AD-A223273] 24 p3443 N90-29440
High performance brittle matrices and brittle matrix composites, book 2
[AD-A223274] 24 p3443 N90-29441
Prediction and control of processing-induced residual stresses in composites. Part 2: AS4/PEEK composite
[AD-A223696] 24 p3443 N90-29445
Development of dual fiber reinforced glass matrix composites for structural space based applications
[AD-A223801] 24 p3444 N90-29446
Non-destructive evaluation of infiltration-toughened ceramics
[DE90-629716] 24 p3453 N90-29501

MATRIX METHODS
A review of the Error of Matrix Method (EMM) for structural dynamic model comparison 02 p0177 N90-10993
Application of matrix correction methods on a plate and a truss structure
[NLR-MP-88042-U] 03 p0359 N90-12056
Rotordynamic analysis with shell elements for the transfer matrix method
[AD-A217455] 13 p1817 N90-20434
Influence of interfacial shear strength on the mechanical properties of SiC fiber reinforced reaction-bonded silicon nitride matrix composites
[NASA-TM-102462] 18 p2518 N90-24382
On conditions guaranteeing two polynomial matrices possess identical zero structures
[MATHS-REPT-A-123] 19 p2751 N90-25631
Parametrical retiming of vibrational models of structures
[ONERA-RT-9/3313-RY-080-R] 22 p3194 N90-28121

MATRIX STRESS CALCULATION
U MATRIX METHODS

MATRIX THEORY
International Conference on Operator Theory: Advances and applications
[AD-A212341] 04 p0545 N90-13170
Lattice QCD estimate of mixing parameters for heavy meson systems
[PREPRINT-687] 05 p0697 N90-14079
Vectors and matrices: Two turbo pascal units for fast program development
[AD-A218917] 16 p2300 N90-23105
On a generalization of the resolvent condition in the Kreiss matrix theorem
[TW-89-08] 18 p2603 N90-24827
Least-index resolution of degeneracy in linear complementarity problems with sufficient matrices
[DE90-014406] 23 p3390 N90-29145

MATTER (PHYSICS)
NT DARK MATTER
Interaction of radiation with matter: Atomic collision processes occurring in the presence of radiation fields
[AD-A213112] 05 p0697 N90-14078
The ultimate structure of matter: The US High Energy Physics Program from the 1950s through the 1980s
[DE90-001784] 06 p0840 N90-14887
Large scale calculations of the structure and dynamics of dense matter
[DE90-003654] 07 p0991 N90-15726
Pulsars lost and found: The second Princeton-Arecibo millisecond pulsar search 07 p1013 N90-15865
Recent progress in understanding the eruptions of classical novae
[NASA-CR-186280] 07 p1014 N90-15870
The use of hypervelocity launchers to explore previously inaccessible states of matter
[DE90-004088] 08 p1034 N90-15973
Anitproton-matter interactions in antiproton applications 11 p1560 N90-18989
The ultimate structure of matter: The high energy physics program from the 1950s through the 1980s
[DE90-005682] 12 p1713 N90-19836

MATTER-ANTIMATTER PROPULSION
Advanced propulsion concepts
[NASA-CR-185920] 21 p2969 N90-26872

MATURING
U GROWTH

MAXIMA
MINAS: An algorithm for systematic state assignment of sequential machines: Computational aspects and results
[EUT-89-E-217] 20 p2912 N90-26566

MAXIMUM ENTROPY METHOD
Power spectral estimation algorithms
[NASA-CR-186189] 06 p0828 N90-14812
Maximum entropy and equations of state for random cellular structures
[DE90-002840] 07 p1006 N90-15827
Stochastic model of the NASA/MSFC ground facility for large space structures with uncertain parameters: The maximum entropy approach, part 2
[NASA-CR-186009] 08 p1107 N90-16407
Comparison of the algebraic reconstruction technique with the maximum entropy reconstruction technique for a variety of detection tasks
[DE90-008933] 14 p2021 N90-21587

MAXIMUM LIKELIHOOD ESTIMATES
Modifying high-order aeroelastic math model of a jet transport using maximum likelihood estimation 01 p0021 N90-10106
Advances in regression: Use of models in spectroscopic data analysis
[AD-A210541] 01 p0116 N90-10665
The use of damage characterization for life prediction methodologies 02 p0185 N90-11053
Iterative network magnitude estimation and uncertainty assessment with noisy and clipped data
[AD-A210707] 02 p0265 N90-11507
A simple model for DSS-14 outage times 04 p0488 N90-12802
Multiplicative iterative algorithms for convex programming
[CWI-AM-R8808] 04 p0532 N90-13072
Estimating methods for counting process intensities: Non-parametric methods
[IMAG-RR-774-M] 06 p0834 N90-14846
Parameter estimation of linear systems in the presence of process noise using the maximum liklihood method
[ESDU-89032] 07 p0985 N90-15693
Maximum likelihood techniques in QELS 09 p1222 N90-17091
Nonparametric estimation of reliability and related functions
[AD-A215138] 09 p1234 N90-17160
Statistically based decompression tables 5: Haldane-Vann models for air diving
[AD-A214934] 09 p1251 N90-17261
Multiple symbol differential detection of uncoded and trellis coded MPSK
[NASA-CR-186288] 10 p1376 N90-17975
Estimation in a discrete tail rate family of recapture sampling models
[NASA-CR-180452] 10 p1421 N90-18197
Evaluation of two methods for acquisition of training statistics for digital analysis of areas prepared for plowing
[INPE-4901-PRE/1502] 11 p1522 N90-18763
Selection of optimal textural features for maximum likelihood image classification
[DE90-006901] 12 p1678 N90-19638
An algorithm for efficient estimation of superimposed exponential signals
[AD-A217218] 13 p1865 N90-20698
Flight path reconstruction using extended Kalman filtering techniques
[PD-FC-9001] 14 p1915 N90-20970
Evaluation of classification performance and proportion estimate of the sugar cane crop through PROCEDURE-INPE utilizing LANDSAT data
[INPE-4899-PRE/1500] 14 p1999 N90-21458
A real-time signal combining system for Ka-band feed arrays using maximum-likelihood weight estimates 15 p2076 N90-21888
Orthogonal distance regression
[PB90-151747] 15 p2160 N90-22336
Parameter estimation in linear filtering
[AD-A218566] 16 p2307 N90-23144
Ability distributions pattern probabilities and quasidensities
[AD-A218471] 16 p2308 N90-23153
More data on (possible) gamma ray (point) sources 16 p2335 N90-23309
A hybrid M-algorithm/sequential decoder for convolutional and trellis codes
[NASA-CR-186863] 20 p2906 N90-26528
Estimating the parameters of a sporadically observed queue
[DE90-012903] 20 p2917 N90-26596
Adaptive time series analysis using predictive inference and entropy
[AD-A222337] 21 p2997 N90-27033
Development and analysis of ARMA parameter estimation schemes in the presence of noise
[AD-A221794] 21 p3066 N90-27428
Model-based Gaussian and non-Gaussian clustering
[AD-A222097] 21 p3066 N90-27430
Experimental identification of helicopter engine dynamics from closed loop data 22 p3104 N90-27627
Tutorial on Reed-Solomon error correction coding
[NASA-TM-102162] 22 p3234 N90-28339
Probability models for the failure of fibres and fibrous composite materials 23 p3300 N90-28665
Fault Detection and Isolation (FDI) techniques for guidance and control systems 24 p3428 N90-29366

MAXIMUM PRINCIPLE
On the existence of a maximal weak solution for a semilinear elliptic equation
[REPT-89-06] 04 p0539 N90-13120

MAXIMUM USABLE FREQUENCY
Average diurnal and seasonal profiles of ionospheric storms 02 p0241 N90-11371
Specification for HF Maximum Usable Frequency (MUF) model
[AD-A214996] 09 p1206 N90-16990

EINMUF: An HF MUF, FOT, LUF prediction program
[AD-A221577] 21 p3055 N90-27371

MAXWELL EQUATION
Improved propagation models for discrete random media
[AD-A211085] 01 p0057 N90-10327
Gravitational nonminimally coupled electromagnetic fields: A possible solution to some idiosincrasies of Einstein-Maxwell theory
[DE89-618430] 02 p0286 N90-11635
Non-stationary computer model of the asymptotic region of an electric arc gas heater
[IPPCZ-288] 03 p0407 N90-12330
Application of a generalized Leibniz rule for calculating electromagnetic fields within continuous source regions
[AD-A212470] 04 p0492 N90-12831
Magnetically insulated electron flows in pulsed power systems
[AD-A212746] 04 p0549 N90-13196
Assessment of anomalous propagation predictions using minisonde refractivity data and the parabolic equation method 06 p0760 N90-14424
The free energy of Maxwell-Vlasov equilibria
[DE90-003318] 07 p0988 N90-15705
Production of photons in anisotropic spacetimes
[DE90-600760] 08 p1135 N90-16576
Vector fields, linear spaces and tensors in physics. Part 3: Tensor analysis and its applications
[INPE-5000-MD/41] 11 p1561 N90-18997
Characterization of thunderstorm induced Maxwell current densities in the middle atmosphere 12 p1634 N90-19391
Linearized analysis of (2+1)-dimensional Einstein-Maxwell theory
[DE90-741470] 12 p1725 N90-19913
Magnetostatic boundary-value problems in the incomplete-nonlinear formulation and methods of their solution
[DE90-615185] 13 p1877 N90-20767
Low-frequency oscillations in vlasov plasmas: The quadratic polarization approximation
[DE90-611309] 18 p2617 N90-24910
Vlasov-Maxwell equilibria of solar coronal loops
[DE90-015025] 23 p3414 N90-29289

MAXWELL-BOLTZMANN DENSITY FUNCTION
Solution of the Boltzmann equation using an energy group method
[AD-A213138] 05 p0699 N90-14096
Modification of ionic population by non-Maxwellian effects 06 p0785 N90-14565

MAXWELLIAN DISTRIBUTION (DENSITY)
U MAXWELL-BOLTZMANN DENSITY FUNCTION

MAZE LEARNING
A note on the maximum size of a rectilinear maze
[AD-A214445] 07 p0982 N90-15668

MCDONNELL AIRCRAFT
NT DC 10 AIRCRAFT
NT F-4 AIRCRAFT

MCDONNELL DOUGLAS AIRCRAFT
NT DC 10 AIRCRAFT
NT F-4 AIRCRAFT
NT F-18 AIRCRAFT

MDA
U MULTIPLE DOCKING ADAPTERS

MEADOWLANDS
U GRASSLANDS

MEAN
On finding the largest normal mean and estimating the selected mean
[AD-A211628] 03 p0394 N90-12245
Preference relations, Chisini-de Finetti means and Bayesian inference in retrieval-system modelling
[ESA-STR-230] 22 p3260 N90-28461
An investigation of the inviscid spatial instability of compressible mixing layers
[AD-A223776] 24 p3468 N90-29596

MEAN FREE PATH
Decay rate and other properties of the positronium negative ion 11 p1560 N90-18987

MEAN SQUARE VALUES
Electronic precipitator control
[NASA-CASE-LAR-13273-2] 13 p1798 N90-20320
Compensatability and optimal compensation of systems with stochastic parameters
[REPT-89-61] 17 p2457 N90-24024
Mean square error behavior for prediction in linear regression models
[AD-A219988] 17 p2466 N90-24092

MEAN TIME BETWEEN FAILURES
U MTBF

MEASURE AND INTEGRATION
NT FUNCTIONAL INTEGRATION
NT INTEGRAL CALCULUS
NT J INTEGRAL
NT LEBESGUE THEOREM
NT NUMERICAL INTEGRATION
NT RUNGE-KUTTA METHOD
NT WEIGHTING FUNCTIONS
Asynchronous integration of ordinary differential equations on multiprocessors
[DE89-014169] 02 p0263 N90-11493
Basic research on methods of calculating supersonic and hypersonic flow
[ONERA-RSF-19/1123-AY-234A] 04 p0448 N90-12565
On a new integrable Hamiltonian system with nearest neighbors interaction
[PREPRINT-667] 05 p0692 N90-14043
An objective time-integration procedure for isotropic rate-independent and rate-dependent elastic-plastic constitutive equations
[PB90-121245] 11 p1550 N90-18925
Notes on the unsteady rectilinear motion of a perfect gas. 9: The expansion to vacuum of a finite mass of uniform homentropic gas
[LR-590-9] 19 p2692 N90-25316
Weighted norm inequalities for Riemann-Liouville fractional integral
[DE90-627153] 23 p3388 N90-29132

MEASURE THEORY
U MEASURE AND INTEGRATION

MEASUREMENT
Large deviation estimates in the stochastic quantization of phi sub 2 exp 4
[PREPRINT-686] 05 p0693 N90-14050
Foundations of measurement and instrumentation
[NASA-RP-1222] 14 p1981 N90-21351
Measurement errors 17 p2359 N90-23426

MEASURING
U MEASUREMENT

MEASURING INSTRUMENTS
NT ACCELEROMETERS
NT ADVANCED VERY HIGH RESOLUTION RADIOMETER
NT ALTIMETERS
NT AMMETERS
NT ANALYZERS
NT ANEMOMETERS
NT APPROACH INDICATORS
NT ATOMIC CLOCKS
NT AUTONOMOUS SPACECRAFT CLOCKS
NT BALLOON-BORNE INSTRUMENTS
NT BAROMETERS
NT BATHYMETERS
NT BATHYTHERMOGRAPHS
NT BOLOMETERS
NT CALORIMETERS
NT CERENKOV COUNTERS
NT CLOCKS
NT CLOUD HEIGHT INDICATORS
NT COMPARATORS
NT COMPASSES
NT COULOMETERS
NT COUNTERS
NT DENSITOMETERS
NT DISTANCE MEASURING EQUIPMENT
NT DOSIMETERS
NT DRAG FORCE ANEMOMETERS
NT DYNAMOMETERS
NT ELASTOMETERS
NT ELECTRON PROBES
NT ELECTROSTATIC PROBES
NT ELLIPSOMETERS
NT ENGINE MONITORING INSTRUMENTS
NT ETALONS
NT EXTENSOMETERS
NT FABRY-PEROT INTERFEROMETERS
NT FIELD INTENSITY METERS
NT FLAME PROBES
NT FLIGHT LOAD RECORDERS
NT FLIGHT RECORDERS
NT FLIR DETECTORS
NT FLOW DIRECTION INDICATORS
NT FLOWMETERS
NT GAMMA RAY SPECTROMETERS
NT GAS METERS
NT GRAVIMETERS
NT GRAVITY GRADIOMETERS
NT HOT-FILM ANEMOMETERS
NT HOT-WIRE ANEMOMETERS
NT HOT-WIRE FLOWMETERS
NT HYDROMETERS
NT IMAGING SPECTROMETERS
NT INDICATING INSTRUMENTS
NT INFRARED DETECTORS
NT INFRARED INSTRUMENTS
NT INFRARED INTERFEROMETERS
NT INFRARED RADIOMETERS
NT INFRARED SCANNERS
NT INFRARED SPECTROMETERS
NT INTERFEROMETERS
NT ION PROBES
NT ION TRAPS (INSTRUMENTATION)
NT IONIZATION GAGES
NT IONOSONDES
NT LASER ALTIMETERS
NT LASER ANEMOMETERS
NT LASER DOPPLER VELOCIMETERS
NT LASER RANGE FINDERS
NT LASER SPECTROMETERS
NT LIGHT SCATTERING METERS
NT MACH-ZEHNDER INTERFEROMETERS
NT MAGNETIC PROBES
NT MAGNETOMETERS
NT MASS SPECTROMETERS
NT METEOROLOGICAL INSTRUMENTS
NT MICHELSON INTERFEROMETERS
NT MICROBALANCES
NT MICRODENSITOMETERS
NT MICROMETERS
NT MICROWAVE INTERFEROMETERS
NT MICROWAVE RADIOMETERS
NT MICROWAVE REFLECTOMETERS
NT MICROWAVE SENSORS
NT MOISTURE METERS
NT MONOCHROMATORS
NT NEPHELOMETERS
NT NEUTRON COUNTERS
NT NEUTRON SPECTROMETERS
NT OCULOMETERS
NT OMEGA NAVIGATION SYSTEM
NT OPTICAL MEASURING INSTRUMENTS
NT OXYGEN ANALYZERS
NT PARTICLE TELESCOPES
NT PHOTOMETERS
NT PIEZOELECTRIC GAGES
NT PLASMA PROBES
NT PNEUMATIC PROBES
NT POLARIMETERS
NT POLARISCOPES
NT POSITION INDICATORS
NT PRESSURE GAGES
NT PROFILOMETERS
NT PROPORTIONAL COUNTERS
NT PYRANOMETERS
NT PYROHELIOMETERS
NT PYROMETERS
NT QUANTUM COUNTERS
NT RADIATION COUNTERS
NT RADIATION DETECTORS
NT RADIATION MEASURING INSTRUMENTS
NT RADIATION PYROMETERS
NT RADIO ALTIMETERS
NT RADIO DIRECTION FINDERS
NT RADIO INTERFEROMETERS
NT RADIOMETERS
NT RADIOSONDES
NT RAIN GAGES
NT RANGE FINDERS
NT RAWINSONDES
NT REFLECTOMETERS
NT RHEOMETERS
NT RIOMETERS
NT SATELLITE-BORNE INSTRUMENTS
NT SCATTEROMETERS
NT SCINTILLATION COUNTERS
NT SEISMOGRAPHS
NT SHOCK MEASURING INSTRUMENTS
NT SIGNAL ANALYZERS
NT SMOKE DETECTORS
NT SOLAR SPECTROMETERS
NT SONDES
NT SONIC ANEMOMETERS
NT SPECTROMETERS
NT SPECTROPHOTOMETERS
NT SPECTRORADIOMETERS
NT SPEED INDICATORS
NT STRAIN GAGE BALANCES
NT STRAIN GAGES
NT TACHOMETERS
NT TEMPERATURE MEASURING INSTRUMENTS
NT TEMPERATURE PROBES
NT THEODOLITES
NT THERMAL CONDUCTIVITY GAGES
NT THERMOMETERS
NT TILTMETERS
NT TIME OF FLIGHT SPECTROMETERS
NT TIMING DEVICES
NT TORQUEMETERS
NT TOTAL OZONE MAPPING SPECTROMETER
NT TRANSMISSOMETERS
NT TURBULENCE METERS
NT ULTRAVIOLET DETECTORS
NT ULTRAVIOLET SPECTROMETERS
NT VARIOMETERS
NT VIBRATION METERS
NT VISCOMETERS

NT VOLTMETERS
NT WEATHER DATA RECORDERS
NT WIND VANES
Method and apparatus for determining time, direction and composition of impacting space particles
[NASA-CASE-LAR-13392-1-CU]
01 p0026 N90-10132
Three-in-one gage
[NASA-CR-183714] 01 p0072 N90-10413
Development of an automated probe for thermal conductivity measurements
[PB89-209324] 01 p0073 N90-10419
Data processing in lightning warning systems
[DE89-012495] 01 p0088 N90-10502
Flight test instrumentation and data processing at British Aerospace, Warton, U.K. 02 p0155 N90-10887
Response of standardized PVDF piezoelectric polymer gauges to direct shock pressures between 8 and 32 GPa
[DE89-016811] 02 p0224 N90-11282
The Sandia standard for PVDF (Polyvinylidene Di-Fluoride) shock sensors
[DE89-016530] 02 p0225 N90-11287
Field evaluation of the multi-depth deflectometers
[PB89-207708] 03 p0349 N90-11994
Lagrangian analysis of MIV (Magnetic Impulse-Velocity) gauge experiments on PBX 9502 using the mass-displacement moment function
[DE89-016612] 03 p0350 N90-12000
Devices and procedures for the calibration of sensors and measurement: Systems of the flight test support system ATTAS
[DFVLR-MITT-89-06] 03 p0351 N90-12007
Advanced measurement techniques, part 1
04 p0441 N90-12520
Recent tests at Langley with a University of Tennessee Space Institute (UTSI) skin friction balance
04 p0441 N90-12527
A laboratory verification sensor
05 p0599 N90-13477
The evaluation of a metered mixer for RTV silicone for RSRM nozzle backfill operations
[NASA-CR-183831] 05 p0645 N90-13763
A slow strain-rate tensile testing machine
[ARL-MAT-TM-399] 05 p0645 N90-13764
Bone mineral measurement using dual energy x ray densitometry 05 p0680 N90-13958
Measuring the thickness of austenitic weld deposits on carbon steel walls using a magnetic method
[DE89-635446] 06 p0794 N90-14628
Rocket studies of the lower ionosphere
[NASA-CR-186187] 06 p0814 N90-14735
X ray microprobe for the microcharacterization of materials
[DE89-006038] 06 p0836 N90-14863
Effective utilization of acoustic wave sensor responses: Simultaneous measurement of velocity and attenuation
[DE90-002580] 06 p0838 N90-14872
The assessment of visibility from automatic contrast Measurements 07 p0872 N90-15061
Calibration of a pulsed potential crack monitor for use in fatigue crack growth studies
[RAE-TM-M/S-1126] 08 p1089 N90-16301
Surface topography measurements over the 1 meter to 10 micrometer spatial period bandwidth
[DE90-003642] 08 p1122 N90-16501
On gauge fixing and quantization of constrained Hamiltonian systems
[DE90-600732] 08 p1135 N90-16574
Universal nondestructive MM-wave integrated circuit test fixture
[NASA-CASE-LEW-14746-1] 09 p1209 N90-17009
Changes in the volt, ohm, and temperature and long range impact of using the Josephson voltage standard
[DE90-004493] 09 p1214 N90-17039
A small, inexpensive apparatus for the determination of the density of powdered materials
[AD-A215393] 09 p1225 N90-17110
Skin friction balance
[NASA-CASE-LAR-13710-1] 09 p1226 N90-17117
The 15th Transducer Workshop --- for telemetry applications
[AD-A215515] 10 p1327 N90-17665
Piezoelectric polymer PVDF shock gauge: State of the research art
[ISL-CO-207/89] 11 p1512 N90-18705
Techniques for measurement of the optical properties of materials
[DE90-006902] 11 p1566 N90-19014
Photon statistical limitations for daytime optical tracking 12 p1643 N90-19442
Dual cathode system for electron beam instruments
[NASA-CASE-NPO-16878-1-CU]
13 p1803 N90-20351
Nine-year aging behavior of the ceramic flatpack resonator
[DE90-008044] 13 p1813 N90-20412
Foundations of measurement and instrumentation
[NASA-RP-1222] 14 p1981 N90-21351
The RAP unit: A remote autoranging picoammeter
[DE90-007711] 14 p1982 N90-21357
Error correction of the DEA (Digital Electronic Automation) coordinate measuring machines at LLNL
[DE90-008913] 14 p1983 N90-21365
Rapidly quantifying the relative distention of a human bladder
[NASA-CASE-LAR-13901-1-NP]
14 p2010 N90-21519
Circularity measuring system: A shape gauge designed especially for use on large objects
15 p2116 N90-22104
High temperature microhardness tester
[AD-A219567] 17 p2380 N90-23553
Determination of tide heights from airborne bathymetric data
[AD-A220412] 17 p2430 N90-23848
Advanced methods for the micromachining of sensors
[MBB-Z-0281/88-PUB] 19 p2650 N90-25081
Sol-gel coating on acoustic wave devices: Thin film characterization and chemical sensor development
[DE90-012224] 19 p2679 N90-25235
Electric field strength meters for the HF, VHF, and UHF bands
[BBC-RD-1990/3] 20 p2851 N90-26212
Qualification of concentrating mirror systems with the HERMES measurement system and the HELIOS simulation program
[DLR-FB-89-51] 20 p2882 N90-26394
Accuracy analysis of the space shuttle solid rocket motor profile measuring device
[NASA-TM-101131] 21 p2968 N90-26871
Using embedded microcontrollers in radar test equipment
[DE90-014997] 23 p3319 N90-28763
Operation and calibration of MRL permeameter for measurement of DC magnetic properties of materials under stress
[MRL-TN-574] 23 p3338 N90-28863
The use of automated ball indentation testing to measure flow properties and estimate fracture toughness in metallic materials
[DE90-015797] 24 p3452 N90-29493
Non-contact contour gage
[DE90-014672] 24 p3475 N90-29642
Multisensor evaluation framework
[AD-A224271] 24 p3522 N90-29913
A review of manganin gauge technology for measurements in the gigapascal range
[MRL-TR-90-5] 24 p3541 N90-30026
Diagnostic development and support of MHD test facilities
[DE90-015403] 24 p3550 N90-30083

MECHANICAL DEVICES
Comprehension processes in mechanical reasoning
[AD-A210459] 02 p0255 N90-11442
A device to extract energy from water waves
[REPT-89-34] 04 p0516 N90-12978
On the motion of compliantly-connected rigid bodies in contact. Part 2: A system for analyzing designs for assembly
[AD-A214136] 07 p0948 N90-15490
EDISON Project
[AD-A214724] 09 p1265 N90-17338
A theory of quantitative inference for artifact sets applied to a mechanical design compiler
[AD-A216535] 11 p1545 N90-18896
Modelling and computer control of a mechanical system
[W-8908] 16 p2243 N90-22794
Spatial operator algebra framework for multibody system dynamics 16 p2279 N90-22989
SKITTER/implement mechanical interface
[NASA-CR-184920] 17 p2384 N90-23578
Core sample extractor
[NASA-CR-182864] 17 p2411 N90-23740
Fourth European Space Mechanisms and Tribology Symposium
[ESA-SP-299] 18 p2535 N90-24462
Alignment positioning mechanism
[NASA-CASE-MSC-21502-1] 20 p2872 N90-26341
Motion translator
[AD-D014452] 22 p3181 N90-28053
Computer-aided engineering environment for controlled mechanical systems
[AD-A223551] 24 p3527 N90-29942

MECHANICAL DRAWINGS
U ENGINEERING DRAWINGS

MECHANICAL DRIVES
NT HELICOPTER PROPELLER DRIVE
NT MAGNETIC TAPE TRANSPORTS
NT PROPELLER DRIVE
NT TRANSMISSIONS (MACHINE ELEMENTS)
Magnetically levitated micro-robotics
02 p0270 N90-11542
Adjustable speed drive study, part 1
[DE89-017654] 03 p0342 N90-11948
Performance and modification of the MEA RF drive system 06 p0842 N90-14895
Adjustable speed drive study, June 1985 to September 1988. Part 2: Appendices
[DE90-002771] 07 p0922 N90-15332
Assessment of worm gearing for helicopter transmissions
[NASA-TM-102441] 08 p1025 N90-15923
Continuously variable gear drive transmission
[AD-D014268] 08 p1084 N90-16275
Power system modeling for a six legged walking vehicle 09 p1221 N90-17083
Film thickness in lubricated Hertzian contacts. Part 2: Point contacts
[ESDU-89045] 09 p1232 N90-17148
End point control of flexible manipulators
[AD-A217319] 14 p1986 N90-21383
The Shock and Vibration Digest, volume 21, no. 3
15 p2109 N90-22084
Development of cable drive systems for an automated assembly project 15 p2116 N90-22105
Determination of joint drives for stable end-effector motion in flexible robotic systems
16 p2288 N90-23034
Future automotive materials: Evolution or revolution
18 p2516 N90-24370
Design and use of brushless dc motor without detent torque 18 p2539 N90-24491
Adjustable speed drive applications guidebook
[DE90-014151] 23 p3321 N90-28780
Solutions to the frictional dynamics problem and the reciprocal variable feedback methodology for design and control of robot mechanisms 23 p3333 N90-28846
Preliminary results on noncollocated torque control of space robot actuators 23 p3373 N90-29057
Traction-drive force transmission for telerobotic joints
24 p3501 N90-29790
The effects of gear reduction on robot dynamics
24 p3513 N90-29861

MECHANICAL ENGINEERING
Superplastic sheet forming 06 p0743 N90-14327
A theory of quantitative inference for artifact sets applied to a mechanical design compiler
[AD-A216535] 11 p1545 N90-18896
Proceedings of the 3rd Annual Conference on Aerospace Computational Control, volume 1
[NASA-CR-186446] 16 p2279 N90-22987
Conceptual design of a Moving Belt Radiator (MBR) shuttle-attached experiment
[NASA-CR-185169] 17 p2367 N90-23474
Engineering fracture mechanics
[AD-A222699] 21 p3012 N90-27123
Preliminary study of a serial-parallel redundant manipulator 23 p3371 N90-29048

MECHANICAL FINGERS
U END EFFECTORS

MECHANICAL HANDS
U END EFFECTORS

MECHANICAL MEASUREMENT
NT DISPLACEMENT MEASUREMENT
NT DRAG MEASUREMENT
NT FLOW MEASUREMENT
NT FRICTION MEASUREMENT
NT PRESSURE MEASUREMENT
NT STRESS MEASUREMENT
NT THRUST MEASUREMENT
NT VELOCITY MEASUREMENT
NT VIBRATION MEASUREMENT
NT WIND MEASUREMENT
NT WIND VELOCITY MEASUREMENT
NT X RAY STRESS MEASUREMENT

MECHANICAL OSCILLATORS
NT PENDULUMS
The drum: Mechanical oscillators and acoustic radiators
[REPT-FB-01/88] 12 p1710 N90-19819

MECHANICAL PROPERTIES
NT ABRASION RESISTANCE
NT AEROELASTICITY
NT AEROTHERMOELASTICITY
NT ANELASTICITY
NT BRITTLENESS
NT BULK MODULUS
NT COMPRESSIBILITY
NT COMPRESSIVE STRENGTH
NT CREEP PROPERTIES
NT CREEP RUPTURE STRENGTH

NT CREEP STRENGTH
NT DIMENSIONAL STABILITY
NT DUCTILITY
NT ELASTIC PROPERTIES
NT ELASTOPLASTICITY
NT ELECTROSTRICTION
NT FATIGUE LIFE
NT FIBER STRENGTH
NT FLEXIBILITY
NT FRACTURE STRENGTH
NT HARDNESS
NT HIGH STRENGTH
NT HYDROELASTICITY
NT IMPACT STRENGTH
NT KNOOP HARDNESS
NT MAGNETOSTRICTION
NT MICROHARDNESS
NT MODULUS OF ELASTICITY
NT NOTCH STRENGTH
NT PHOTOELASTICITY
NT PHOTOPLASTICITY
NT PIEZOELECTRICITY
NT PLASTIC PROPERTIES
NT POISSON RATIO
NT PROPORTIONAL LIMIT
NT SHEAR CREEP
NT SHEAR PROPERTIES
NT SHEAR STRENGTH
NT SHELL STABILITY
NT STEADY STATE CREEP
NT STIFFNESS
NT STRESS CYCLES
NT STRESS RATIO
NT STRESS RELAXATION
NT STRUCTURAL STABILITY
NT SUPERPLASTICITY
NT TENSILE CREEP
NT TENSILE PROPERTIES
NT TENSILE STRENGTH
NT THERMAL RESISTANCE
NT THERMOELASTICITY
NT THERMOPLASTICITY
NT TOUGHNESS
NT VISCOELASTICITY
NT VISCOPLASTICITY
NT WEAR RESISTANCE
NT WELD STRENGTH
NT YIELD POINT
NT YIELD STRENGTH

Failure behavior of PEEK and its short-fiber composite systems
[AD-A210729] 01 p0035 N90-10189

Castings, from theory to practical application 01 p0042 N90-10236

Combined advanced foundry and quality control techniques to enhance reliability of castings for the aerospace industry 01 p0043 N90-10240

Thin walled cast high-strength structural parts 01 p0043 N90-10242

Advances in the technology of titanium castings 01 p0043 N90-10243

Properties of HY-100 for naval construction
[MRL-R-1149] 01 p0044 N90-10247

The quantitative analysis of fracture surfaces using fractals
[DE89-015361] 01 p0044 N90-10250

Dynamically compressed metals: Theory
[AD-A210741] 01 p0045 N90-10257

Investigation of the pyrometallurgical, physical and mechanical behavior of weld metal
[AD-A211114] 01 p0046 N90-10258

Ceramic components in machines, Cologne and Aachen, West Germany; Maastricht, The Netherlands and Brussels, Belgium
[DE89-015831] 01 p0047 N90-10264

Japanese structural ceramics research and development 01 p0048 N90-10272

Mechanical properties, solubilities, and processabilities in the design of the first super-strong liquid-crystalline polymers
[DE89-009252] 01 p0048 N90-10273

Structure-mechanical property relationships in ion implanted ceramics
[DE89-010129] 01 p0048 N90-10274

Synthesis and interfacial properties of new generation polyurethane systems
[AD-A210446] 01 p0050 N90-10286

Synthesis and physical properties of poly(perfluoroalkylether) urethanes
[AD-A210500] 01 p0050 N90-10287

A design assessment for metallic pressure vessels circumferentially reinforced with a pre-tensioned high-specific-strength anisotropic composite overwind
[AD-A209108] 01 p0079 N90-10453

Ceramic processing of bulk high-T(sub c) superconductors
[DE89-015703] 01 p0128 N90-10736

Liquid infiltrated C/SiC: An alternative material for hot space structures 02 p0182 N90-11030

Worked-in holes in three-dimensional reinforced composites 02 p0186 N90-11060

A study of the tribological and surface micromechanical properties of YBa2Cu3O7-x
[DE89-015680] 02 p0281 N90-11607

Exploratory study of niobium, titanium, zirconium and tantalum aluminides
[AD-A210658] 02 p0283 N90-11615

Coating galvanized steel
[AD-A211775] 03 p0329 N90-11869

Effect of fretting on fatigue strength of aluminium alloys
[ESDU-89004] 03 p0329 N90-11870

Material requirements for future aeroengines
[PNR90595] 04 p0456 N90-12610

Influence of the structure of epoxy network models on the volumetric, mechanical and viscoelastic properties
[ISAL-89-0024] 04 p0466 N90-12666

Composite materials for future aeroengines
[PNR90584] 04 p0466 N90-12667

The relationship between the mechanical properties of materials after press forming and their in-service properties
[CETIM-101530] 04 p0475 N90-12723

The effects of heat treatment after welding on the functional properties of assemblies of CrMo alloys. Heat treatment of a mixed assembly of A48 and 10CD9.10 alloys
[CETIM-104320] 04 p0475 N90-12724

How the common practice of heating plates of austenitic stainless steel during cooling affects their mechanical properties
[CETIM-104500] 04 p0476 N90-12725

The multivalent beta'-aluminas
[AD-A212103] 04 p0478 N90-12738

Textural and structural organization of the heat treated polymers: Mechanical properties relationships
[ETN-89-95711] 04 p0478 N90-12744

Effects of hot corrosion on the room temperature strength of structural ceramics
[AD-A212568] 04 p0481 N90-12762

A center for advanced electrical and structural polymers
[AD-A212853] 04 p0482 N90-12764

Rolling of ARALL laminates (an alternative method for post-stretching ARALL laminates)
[LR-560] 04 p0484 N90-12778

Structural vibration and shock isolator
[AD-D014202] 04 p0509 N90-12940

Proceedings of the Army Symposium on Solid Mechanics, 1989: Mechanics of Engineered Materials and Applications
[AD-A211954] 04 p0511 N90-12951

Increased fragility of deep pressed thin plates
[CETIM-13-Y-313] 04 p0513 N90-12962

Synthesis and properties of NdNiO(3) prepared by low temperature methods
[AD-A212117] 04 p0559 N90-13256

The application of cast SiC/Al to rotary engine components
[NASA-CR-179610] 05 p0581 N90-13385

Mechanical and thermal testing 05 p0605 N90-13521

Quench sensitivity in Al-Cu-Li alloys
[AD-A213055] 05 p0624 N90-13639

The effect of composition and aging treatment on the microstructure and mechanical properties of aluminum-lithium-titanium alloys
[AD-A213144] 05 p0624 N90-13640

The effects of alloying and thermal factors on the solidification and mechanical properties of gray iron
[VTT-619] 05 p0625 N90-13651

Considerations about the acceptance inspection of HS fasteners intended for controlled tightening
[CRIF-MT-175] 05 p0653 N90-13808

The Fourth Oxford International Conference on the Mechanical Properties of Materials at High Rates of Strain
[AD-A212293] 05 p0653 N90-13809

Time domain coupling of the boundary and finite element methods for elastodynamics
[AD-A213243] 05 p0654 N90-13811

Sol-gel processing science using a Sol-Gel Optics Research Facility (SGORF)
[AD-A213056] 05 p0699 N90-14095

Elastomeric impulse energy storage and transfer system
[AD-D014223] 06 p0730 N90-14255

Superplasticity: An overview 06 p0743 N90-14326

The mechanical properties of superplastically formed titanium and aluminium alloys 06 p0744 N90-14331

The 4.2 K fracture toughness of 304 stainless steel in a magnetic field
[DE90-002083] 06 p0747 N90-14347

Mechanical properties and morphology of oriented polymer blends 06 p0750 N90-14361

Bulk and shear moduli of epoxy encapsulants
[DE90-000899] 06 p0751 N90-14371

Numerical and empirical verification of the stress state in a ceramic, button-head, tensile specimen
[DE90-001645] 06 p0752 N90-14375

Practical superconductor development for electrical power applications
[DE90-001804] 06 p0771 N90-14487

Engineering approaches to the application of fracture toughness data in the nuclear industry
[DE90-001596] 06 p0800 N90-14659

Process monitoring using optical ultrasonic wave detection
[DE90-002021] 06 p0838 N90-14870

Dynamical simulation of dislocation microstructure
[DE90-003192] 06 p0857 N90-14982

Fatigue properties of SiC/Al composites 07 p0889 N90-15136

The mechanical behavior of a fiber-reinforced brittle matrix composite 07 p0889 N90-15139

Mechanical behavior of laminated composites at elevated temperatures 07 p0889 N90-15141

Effects of filament-matrix interfaces on the mechanical properties of SiC-reinforced Si3N4: A review
[DE90-001863] 07 p0890 N90-15144

New Light Alloys
[AGARD-CP-444] 07 p0897 N90-15185

Al-Li alloy developed by Pechiney 07 p0897 N90-15186

The microstructure and properties of aluminum-lithium alloys 07 p0897 N90-15187

Mechanical properties and fracture toughness of 8090-T651 plate and 2091 and 8090 sheet 07 p0897 N90-15188

Fatigue properties of Al-Li alloys 07 p0898 N90-15189

Microstructure/mechanical property relations in a mechanically alloyed aluminum 07 p0900 N90-15205

Metal matrix composites: A promising alternative to conventional alloys 07 p0901 N90-15208

Magnesium alloy technology for aerospace applications 07 p0901 N90-15209

Cryogenic mechanical properties of low density superplastic Al-Mg-Sc alloys
[DE90-002120] 07 p0904 N90-15222

Heat treatment of pulsed Nd: YAG laser welds in a Ti-14.8 wt pct Al-21.3 wt pct Nb titanium aluminide
[DE90-003484] 07 p0905 N90-15228

The effect of nitrogen and titanium on the toughness of high strength saw weld deposits
[AD-A213400] 07 p0905 N90-15230

Dispersion strengthening of high temperature niobium alloys
[AD-A213829] 07 p0906 N90-15236

Properties of aluminum-uranium alloys
[DE90-003889] 07 p0907 N90-15243

Bonding aerogels with polyurethanes
[DE90-003050] 07 p0910 N90-15258

Modifications of the Penn State Boundary Layer Research Facility for boundary layer/structure interaction experimental research
[AD-A213874] 07 p0931 N90-15391

Epoxy-resin cable terminations
[AD-A213789] 07 p0942 N90-15454

Ductile failure
[AD-A213864] 07 p0948 N90-15488

An investigation of mechanical behavior of crystalline solids
[DE90-003530] 07 p1000 N90-15787

Spray sealing: A breakthrough in integral fuel tank sealing technology 08 p1022 N90-15912

Cryogenic engineering and materials 08 p1030 N90-15949

Materials and techniques for model construction 08 p1030 N90-15954

The use of hypervelocity launchers to explore previously inaccessible states of matter
[DE90-004088] 08 p1034 N90-15973

Structure-property relationships in ion-beam surface-modified ceramics: Theory and applications
[AD-A212785] 08 p1047 N90-16054

Interdisciplinary research in viscoelasticity and rheology
[AD-A213630] 08 p1063 N90-16145

Absorption fluids data survey: 1989 update
[DE90-003985] 08 p1096 N90-16346

Nuclear weapon radiation effects on a space based interceptor weapon platform
[DE89-016258] 09 p1181 N90-16850

Effects of T-tabs and large deflections in DCB specimen tests
[NASA-TM-101677] 09 p1186 N90-16868
Extrusion of alumina-silicon carbide whisker composites
[DE90-004379] 09 p1186 N90-16869
Mechanics of iron, its stability and phase transformation
[DE89-636210] 09 p1193 N90-16913
Analysis of composite ring of compression test data
[DE90-004468] 09 p1239 N90-17194
Solar cell coverglasses with enhanced thermal and mechanical properties 10 p1343 N90-17785
Prediction of high temperature metal matrix composite ply properties
[NASA-TM-102490] 10 p1348 N90-17817
The processing and mechanical properties of high temperature/high performance composites. Book 1, section 1: Coatings and interfaces
[AD-A216141] 10 p1348 N90-17821
Non-destructive characterization of epoxy/dicyandiamide interphases using surface-enhanced Raman scattering
[AD-A215894] 10 p1353 N90-17846
Tensile mechanical properties in flat specimens of 7150-T7751
[INFORME-I-296/88] 10 p1356 N90-17860
Comparative analysis between the mechanical properties of conventional alloys and Al-Li
[INFORME-DT-317/89] 10 p1356 N90-17861
Ceramic matrix composites, new high performance materials 11 p1477 N90-18500
The processing and mechanical properties of high temperature/high performance composites. Book 2, section 2: Strength and fracture resistance
[AD-A216142] 11 p1478 N90-18507
The processing and mechanical properties of high temperature/high performance composites. Book 3, section 2: Strength and fracture resistance, part
[AD-A216143] 11 p1478 N90-18508
Preliminary evaluation of the strength of pin-joints in laminated composite materials
[DE90-006353] 11 p1481 N90-18524
A statistical evaluation of the variation in laminated composite properties resulting from ply misalignment
[DE90-006371] 11 p1481 N90-18525
Calculation of mechanical properties variations depending on matrix parameters in a composite, as a function of the test temperature
[DT-311/88] 11 p1481 N90-18526
Impact of composites in the aerospace industry
[ETN-90-96231] 11 p1481 N90-18527
Identification of a cast iron alloy containing nonstrategic elements
[NASA-CR-185174] 11 p1487 N90-18559
Model filled polymers 3. Rheological behavior of polystyrene containing crosslinked polystyrene beads
[AD-A215867] 11 p1489 N90-18567
Characterization and development report for the SA3274-1 and SA3274-2 transient voltage suppressors
[DE90-005712] 11 p1502 N90-18649
Crystal growth and mechanical properties of semiconductor alloys
[AD-A216697] 11 p1570 N90-19035
Thermo-oxidative stability studies of PMR-15 polymer matrix composites reinforced with various fibers
[NASA-TM-102439] 12 p1620 N90-19310
Modification of surface mechanical properties of high-chromium tool steel by carbon-implanted codeposited Fe-Ti films
[DE90-007502] 12 p1628 N90-19358
Liquid oxygen LOX compatibility evaluations of aluminum lithium (Al-Li) alloys: Investigation of the Alcoa 2090 and MMC weldalite 049 alloys 12 p1636 N90-19398
ROCOPT: A user friendly interactive code to optimize rocket structural components 12 p1639 N90-19415
A transient plasticity study and low cycle fatigue analysis of the Space Station Freedom photovoltaic solar array blanket
[NASA-TM-102516] 12 p1674 N90-19617
Physics and Mechanics of Cometary Materials
[ESA-SP-302] 12 p1738 N90-19989
Mechanical properties of fluffy agglomerates consisting of core-mantle-particles 12 p1743 N90-20019
Studies of the structure and properties of organic monolayers, multilayers and superlattices
[DE90-008330] 13 p1765 N90-20129
Tellurium embrittlement of type 316 steel
[AERE-R-13440] 13 p1776 N90-20192
Design and processing of strong-tough microcomposite steels
[DE90-007764] 13 p1777 N90-20197
The stress corrosion performance of diffusion bonded nickel base alloys
[DE90-008130] 13 p1777 N90-20199
An introduction to nickel aluminide alloy
[DE90-008565] 13 p1778 N90-20207
The effects of radiation on the mechanical properties of polymers used as electrical cable insulation and jacketing materials
[AERE-R-13286] 13 p1779 N90-20209
Interface science in deformation processing of ceramics
[DE90-008424] 13 p1780 N90-20219
Pyrotechnic device technology
[DE90-007683] 13 p1783 N90-20234
An electrochemical and spectroscopic study of electrode processes
[AD-A217261] 13 p1793 N90-20289
Seismic characterization of fracture properties
[DE90-007759] 13 p1841 N90-20570
Performance of Y-TZP materials between 800 C and 1200 C
[AD-A217723] 13 p1897 N90-20890
Reinforcement-matrix interface effects in metal matrix composites
[MRL-TN-562] 14 p1943 N90-21120
Resistance mechanics for laminated composite materials
[INPE-4919-RPE/594] 14 p1947 N90-21141
Compatibility of Au base thick films with solder alloys: Solid state growth of intermetallics
[DE90-009285] 14 p1952 N90-21175
Review of the state of the technology for joining ceramics for high-temperature structural applications
[DE90-009224] 14 p1956 N90-21199
Development of low thermal conductivity pan-based carbon fibers for solid rocket motor nozzle applications 15 p2063 N90-21818
Severe shock and vibration environments for electronic components
[DE90-007686] 15 p2117 N90-22113
Seal requirements in rocket propulsion
[ETN-90-96611] 16 p2205 N90-22580
A study of woven fabric-reinforced composite materials using an invariant-based orthotropic plasticity formulation 16 p2211 N90-22611
Calcium carbonate scale dissolution in water stabilized by carbon dioxide treatment
[AD-A218502] 16 p2214 N90-22633
Deformation and fracture of aluminum-lithium alloys: The effect of dissolved hydrogen 16 p2219 N90-22658
Investigation of the reaction kinetics between SiC fibers and selectively alloyed titanium matrix composites and determination of their mechanical properties 16 p2219 N90-22659
Approximate analysis for the formation of adiabatic shear bands
[AD-A218751] 16 p2221 N90-22670
Characterization and role of an elastomeric interphase within polyepoxy reinforced glass, both particulate and fibrous
[ISAL-89-0064] 16 p2222 N90-22676
Structural behavior of composites with progressive fracture
[NASA-TM-102370] 17 p2368 N90-23477
Ultrafine microstructure composites prepared by chemical vapor deposition
[AD-A219650] 17 p2369 N90-23484
Effect of surface oxygen on adhesion of carbon fiber-reinforced composites
[AD-A220777] 17 p2369 N90-23486
Demonstration centers for fiber reinforced materials
[REPT-45/89] 17 p2370 N90-23495
A study of the influence of alloying additions on the passivity of aluminium
[AD-A219630] 17 p2376 N90-23532
Acetylene terminated aspartimides and resins therefrom
[NASA-CASE-LAR-14188-1] 17 p2379 N90-23545
Soluble polysilanes: A new class of radiation sensitive O2-RIE resistant polymers for use in microlithography
[AD-A219476] 17 p2379 N90-23551
Negative electron affinity for infrared detection
[AD-A218816] 17 p2395 N90-23639
Electromagnetic machines which utilize microgeometry field structures
[AD-A219828] 17 p2398 N90-23660
Acousto-ultrasonic nondestructive evaluation of materials using laser beam generation and detection
[NASA-CR-186694] 17 p2398 N90-23664
Precision laser cutting
[DE90-009949] 17 p2407 N90-23717
Prediction of gear tooth separation in single-stage gear systems, using numerical techniques
[AD-A220442] 17 p2412 N90-23744
Dynamic mechanical analysis of polymeric materials 18 p2513 N90-24353
Ta and Nb reinforced MoSi2
[DE90-010596] 18 p2517 N90-24377
Characterization of solid state bonding between Coors AD-999 alumina and niobium
[DE90-010653] 18 p2518 N90-24379
Influence of interfacial shear strength on the mechanical properties of SiC fiber reinforced reaction-bonded silicon nitride matrix composites
[NASA-TM-102462] 18 p2518 N90-24382
Electron microscopy of interfaces in silicon carbide whisker-reinforced alumina composites
[DE90-010439] 18 p2519 N90-24386
Development and evaluation of advanced austenitic alloys
[DE90-011315] 18 p2528 N90-24425
Fatigue crack propagation in austenitic stainless steels at cryogenic temperatures
[DE90-011597] 18 p2528 N90-24426
Joining engineering ceramics
[DE90-010819] 18 p2531 N90-24445
Tribological and mechanical properties of Fe/Ti multilayered films
[DE90-011949] 18 p2565 N90-24635
Introduction to compact reinforced composite
[CBL-REPRINT-5] 19 p2673 N90-25199
The accelerated cooling in GTS plate mill
[ETN-90-97019] 19 p2682 N90-25256
Analog electronic control differential transmitter
[AD-D014508] 19 p2685 N90-25272
Performance of battery charge controllers
[DE90-011413] 19 p2686 N90-25279
Wear transition surfaces for long-term wear effects
[DE90-011314] 19 p2698 N90-25351
Flexion, extension and lateral bending responses of the cervical spine 19 p2719 N90-25468
Probabilistic approach to the certification for fatigue durability of composite structures
[DE90-505521] 20 p2828 N90-26085
The effect of interfacial characteristics on the mechanical performance of ceramic-ceramic composites
[AD-A223031] 20 p2829 N90-26090
Structures and mechanical properties of near-beta titanium alloys TiV10Fe2Al3 and TiV10Cu3Al3
[ONERA-NT-1989-3] 20 p2835 N90-26123
Mechanical properties of coatings and interfaces
[DE90-012726] 20 p2838 N90-26139
Extension of a noninteractive reliability model for ceramic matrix composites
[NASA-CR-185267] 20 p2838 N90-26142
Influence of the manufacturing conditions on the microstructure and mechanical properties of the silicon nitride
[ISAL-90-0008] 20 p2840 N90-26154
Soil experiment
[NASA-CR-184927] 20 p2842 N90-26165
Design of ceramic components with the NASA/CARES computer program
[NASA-TM-102369] 20 p2875 N90-26359
Lessons learned for composite aircraft structures qualification 21 p2956 N90-26808
An aluminum quality breakthrough for aircraft structural reliability 21 p2957 N90-26816
High temperature strength of SiC whisker-reinforced silicon nitride composites
[DE90-013822] 21 p2970 N90-26883
Applications of digital image processing in testing and evaluation of composite materials
[AD-A222939] 21 p2971 N90-26887
Manufacturing and mechanical properties of new textile fiber preforms for structural sandwich applications
[MBB-Z-0296-90-PUB] 21 p2972 N90-26895
Weldment mechanical properties of aluminum-copper-lithium alloy, 2090, at ambient and cryogenic temperatures
[DE90-014178] 21 p2981 N90-26941
Silicon containing electroconductive polymers and structures made therefrom
[NASA-CASE-NPO-17826-1-CU] 21 p2983 N90-26952
A tough performance simultaneous semi-interpenetrating polymer network
[NASA-CASE-LAR-14339-1] 21 p2984 N90-26955
Theory of ceramic/zirconia composites: Toughening, strengthening, and synergism
[AD-A222931] 21 p2985 N90-26961
Engineering fracture mechanics
[AD-A222699] 21 p3012 N90-27123
Generalization in the presence of free variables: A mechanically-checked correctness proof for one algorithm
[AD-A222681] 21 p3051 N90-27346
The effect of reinforcement stability on composition redistribution in cast aluminum metal matrix composites
[DE90-012469] 22 p3135 N90-27791
Oxygen stabilization induced enhancement in J(sub c) and T(sub c) of superconducting oxides 22 p3137 N90-27800

Kinetics and thermodynamics of ceramic/metal interface reactions related to high T(sub c) superconducting applications 22 p3141 N90-27815
Small angle generating apparatus
[AD-D014467] 22 p3246 N90-28408
Transcrystalline morphology in carbon fibre composites with thermoplastic matrix and its influence on the mechanical properties
[FOA-C-20783-2.1] 22 p3248 N90-28423
Data base for crack growth properties of materials 23 p3296 N90-28647
Mechanical behavior of thick, curved, laminated composites 23 p3299 N90-28664
Strengthening and toughening mechanisms in ceramic fiber-reinforced glass matrix composites 23 p3300 N90-28666
ARALL (ARamid ALuminum Laminate), a literature survey
[FOA-C-20782-2.5] 23 p3301 N90-28671
Electrochemical surface finishing using amino-substrates on carbon fibers in organic media. Effects of the finishing on the mechanical properties of carbon-epoxy composites
[ONERA-RT-9/3549-M] 23 p3301 N90-28672
Radiation-curable prepreg composites
[DE90-629740] 23 p3301 N90-28674
Effect of protective coatings on mechanical properties of superalloys 23 p3308 N90-28707
High temperature protective coatings: Recent trends 23 p3308 N90-28710
Mechanical testing activities related to high-performance structural ceramics
[DE90-014299] 23 p3313 N90-28734
Technical bibliography of high performance polyethylene fibers
[SNPE-NT-106/89/GTR/RP/NP] 23 p3313 N90-28736
Some studies of the vibration welding of thermoplastics 23 p3332 N90-28842
Structural testing and analytical research of turbine components
[AD-A223516] 24 p3434 N90-29396
Characterization of unnotched SCS-6/Ti-15-3 metal matrix composites at 650 C
[NASA-TM-102699] 24 p3444 N90-29450
Atomistic studies of grain boundaries in alloys and compounds
[DE90-012401] 24 p3452 N90-29492
Fundamental studies on intermetallic compounds
[ONERA-RT-4/1855-M] 24 p3453 N90-29497
Evaluation of static and fatigue properties of thin sheets of 8090-T8 aluminum-lithium alloy and observation of its fracture surfaces
[NAL-TR-1039] 24 p3453 N90-29499
Precursor structure-fiber property relationships in polyacrylonitrile-based carbon fibers
[AD-A224246] 24 p3454 N90-29503
Thermal analysis of bismaleimide matrix resins
[DE90-016283] 24 p3457 N90-29523
The investigation and production of titanium-tantalum junctions diffusion bonded at high temperature (855 C to 920 C): The influence of temperature, time pressure and roughness on the mechanical properties, and the optimisation of the bonded conditions
[BR114894] 24 p3476 N90-29646
Proceedings of damping '89. Volume 2: Pages FAA-1 through IBD-15
[AD-A223432] 24 p3479 N90-29665
Study of the reflection of surface acoustic wave from a material discontinuity boundary using a perturbation method 24 p3542 N90-30032

MECHANICAL RESONANCE
U RESONANT VIBRATION

MECHANICAL SHOCK
A critical assessment of models available for the shock initiation of heterogeneous explosives
[MRL-TR-89-17] 03 p0333 N90-11696
The Shock and Vibration Digest, volume 21, no. 9 09 p1235 N90-17168
The Shock and Vibration Digest, volume 22, no. 2 14 p2022 N90-21596
The Shock and Vibration Digest, volume 21, no. 2 15 p2109 N90-22059
The Shock and Vibration Digest, volume 21, no. 1 15 p2109 N90-22061
The Shock and Vibration Digest, volume 21, no. 3 15 p2109 N90-22064
The Shock and Vibration Digest, volume 21, no. 7 15 p2110 N90-22066
Optimum design of structures under shock and vibration environment 15 p2110 N90-22067
The Shock and Vibration Digest, volume 21, no. 8 15 p2110 N90-22068
The Shock and Vibration Digest, volume 22, no. 1 15 p2111 N90-22073
The Shock and Vibration Digest, volume 21, no. 6 15 p2163 N90-22363
Evaluation of EDR-3 vibration, shock, temperature, and humidity recording unit
[NASA-CR-184006] 22 p3177 N90-28028

MECHANICAL TWINNING
Deformation twinning in ordered intermetallic compounds
[DE89-014779] 07 p0997 N90-15767

MECHANIZATION
ESPRIT 820:QUIC. QUIC toolkit demonstrator applications
[REPT-892-440-105] 17 p2386 N90-23590
Technical evaluation report on the Guidance and Control Panel 49th Symposium on Fault Tolerant Design Concepts for Highly Integrated Flight Critical Guidance and Control Systems
[AGARD-AR-281] 20 p2813 N90-26012

MEDIA
NT ANISOTROPIC FLUIDS
NT ANISOTROPIC MEDIA
NT ELASTIC MEDIA
NT INTERGALACTIC MEDIA
NT INTERPLANETARY DUST
NT INTERPLANETARY MEDIUM
NT ZODIACAL DUST
Microscopic models for electromagnetic wave propagation in highly dispersive media
[AD-A224382] 24 p3460 N90-29540

MEDICAL ELECTRONICS
The use of lithium batteries in biomedical devices
[AD-A210789] 01 p0061 N90-10350

MEDICAL EQUIPMENT
NT ARTIFICIAL CARDIAC PACEMAKER
NT ARTIFICIAL HEART VALVES
NT PROSTHETIC DEVICES
A scheiner-principle vernier optometer
[AD-D014304] 07 p0934 N90-15405
Possibilities of Nd: YAG laser utilization in medicine
[MBB-UE-0002/88-PUB] 19 p2653 N90-25100

MEDICAL PERSONNEL
NT FLIGHT SURGEONS
Arctic cold weather medicine and accidental hypothermia
[AD-A223090] 20 p2899 N90-26487

MEDICAL SCIENCE
NT CLINICAL MEDICINE
NT ENDOCRINOLOGY
NT EPIDEMIOLOGY
NT HISTOLOGY
NT IMMUNOLOGY
NT NEUROLOGY
NT NUCLEAR MEDICINE
NT OPHTHALMOLOGY
NT ORTHOPEDICS
NT PATHOLOGY
NT RADIOBIOLOGY
NT RADIOLOGY
National Library of Medicine DOCLINE (tradename) manual
[PB89-188676] 03 p0416 N90-12390
Three-dimensional medical image analysis using local dynamic algorithm selection on a multiple-instruction, multiple-data architecture
[AD-A218024] 13 p1852 N90-20630
Micro SAINT programs for numerical methods of integration and differential equations
[AD-A218097] 13 p1878 N90-20772
Medical subject headings: Annotated alphabetic list, 1990
[PB90-100009] 14 p2036 N90-21683
Permuted medical subject headings, 1990
[PB90-100025] 14 p2036 N90-21684
Research and Technology
[NASA-TM-102161] 14 p2044 N90-21721

MEDICAL SERVICES
Activities in aerospace medicine
[ETN-90-95468] 12 p1696 N90-19739
Aeronautical decisionmaking for air ambulance program administrators
[DOT/FAA/DS-88/8] 17 p2347 N90-23368
Arctic cold weather medicine and accidental hypothermia
[AD-A223090] 20 p2899 N90-26487

MEDITERRANEAN SEA
Analysis of propagation in an inhomogeneous atmosphere in the horizontal and vertical direction using the parabolic equation method 06 p0760 N90-14421
The Mediterranean marine environment and its effects on aerosols and infrared transmission 15 p2079 N90-21909
US Navy hindcast spectral ocean wave model climatic atlas: Mediterranean Sea
[AD-A219755] 17 p2426 N90-23825
Efficient representation of the hydrographic structure of the north atlantic ocean and aspects of the circulation from objective methods
[AD-A218606] 17 p2429 N90-23841
Trace metal sources for the atlantic inflow to the Mediterranean Sea
[AD-A218607] 17 p2429 N90-23842

MEETINGS
U CONFERENCES

MEISSNER EFFECT
U DIAMAGNETISM
U SUPERCONDUCTIVITY

MELANIN
Diffraction studies of the structure of glasses and liquids
[DE90-007662] 12 p1632 N90-19381

MELT SPINNING
Establishment and initial operation of a resource facility for RSR (Rapid Solidification Rate) processed alloys in pilot quantities
[AD-A210369] 01 p0050 N90-10283
Precipitation strengthened high strength, high conductivity Cu-Cr-Nb alloys produced by chill block melt spinning
[NASA-CR-185144] 03 p0326 N90-11853
High temperature aluminum-base alloy
[AD-D014270] 08 p1043 N90-16028
The processing and mechanical properties of high temperature/high performance composites. Book 5, section 4: Processing: Matrices and composites, part 1
[AD-A216145] 10 p1349 N90-17823
The processing and mechanical properties of high temperature/high performance composites. Book 6, section 4: Processing: Matrices and composites, part 2
[AD-A216148] 10 p1349 N90-17824
The processing and mechanical properties of high temperature/high performance composites. Book 2, section 2: Strength and fracture resistance
[AD-A216142] 11 p1478 N90-18507
The processing and mechanical properties of high temperature/high performance composites. Book 3, section 2: Strength and fracture resistance, part
[AD-A216143] 11 p1478 N90-18508
Novel processing of HTS based conductors
[DE90-005956] 12 p1722 N90-19892

MELTING
NT ARC MELTING
NT FUSION (MELTING)
NT LEVITATION MELTING
NT VACUUM MELTING
Formation and modification of surface alloys by excimer laser melting and resolidification
[DE89-016968] 03 p0327 N90-11856
Noncontacting laser ultrasonic generation and detection at the surface of molten metal
[DE90-002020] 06 p0791 N90-14605
Production and processing of Cu-Cr-Nb alloys
[NASA-TM-102495] 08 p1047 N90-16053
Migration of carbon in tempered martensitic steel during excimer laser melting
[DE90-004838] 09 p1195 N90-16922
Superconducting Bi1.5Pb0.5Sr2Ca2Cu3O(x) ceramics by rapid melt quenching and glass crystallization
[NASA-CR-185184] 09 p1288 N90-17465
Pulsed laser-induced melting of intermediate Cu-Zn phases
[DE90-005404] 11 p1513 N90-18713
Elimination of platinum inclusions in phosphate laser glasses
[DE90-004479] 12 p1629 N90-19361
Techno-economic assessment of a carbothermic alumina reduction process
[DE90-007018] 13 p1772 N90-20170
High temperature chemistry of oxide superconductors
[DE90-007821] 13 p1895 N90-20875
Systematics in positron annihilation lifetime analysis of high (Tc) superconducting transitions
[DE90-008361] 13 p1896 N90-20884
Method of preparing radially homogeneous mercury cadmium telluride crystals
[NASA-CASE-MFS-25786-2] 13 p1898 N90-20896
Pressure rig for repetitive casting
[NASA-CASE-LAR-14050-1] 14 p1959 N90-21216
Control of surface melting and ablation in electromagnetic launchers via the magnetic vapor shielding mechanism
[AD-A219035] 16 p2204 N90-22578
The origin of multiple melting in polyurethane block copolymers
[AD-A220050] 17 p2381 N90-23563
A laboratory comparison of field techniques for measurement of the liquid water fraction of snow
[AD-A219587] 17 p2417 N90-23774
Damping associated with incipient melting in aluminum-indium alloys
[AD-A220241] 18 p2525 N90-24412

Cascade collapse in copper and nickel
[DE90-011115] 18 p2527 N90-24423
Improved processing of ceramic superconductors
[DE90-009721] 18 p2624 N90-24951
Feasibility of using lasers and infrared heaters as UNREP icing countermeasures
[AD-A219031] 19 p2695 N90-25333
Snow cover mapping and snowmelt runoff simulations on microcomputers 19 p2707 N90-25408
Natural melting within a spherical shell
[NASA-TM-102822] 20 p2861 N90-26274
The thermal radiative properties of metals at high temperature
[DE90-012468] 21 p2981 N90-26938
Dynamic consolidation of super hard materials
[AD-A224460] 24 p3454 N90-29505

MELTING POINTS
Composites reinforced with thermotropic liquid crystal copolyester fibers
[AD-A211226] 02 p0191 N90-11089
Thermophysical properties of isopropyl alcohol. Part 2: Thermodynamic properties at elevated pressures
[ESDU-89020-PT-2] 06 p0739 N90-14300
Summary physical data tables: Alkanes
[ESDU-PD3] 07 p0893 N90-15162
Orthobaric densities and molar volumes of liquids: Alcohols
[ESDU-89037] 07 p0897 N90-15184

MELTS (CRYSTAL GROWTH)
NT CONTAINERLESS MELTS
NT MELT SPINNING
Superconducting Bi1.5Pb0.5Sr2Ca2Cu3O(x) ceramics by rapid melt quenching and glass crystallization
[NASA-CR-185184] 09 p1288 N90-17465
Non-contact temperature measurement of a falling drop 10 p1365 N90-17912
Flux lattice melting in the high Tc superconductors 10 p1366 N90-17915
Infiltration mechanics in conventional and hybridised fibre reinforced metal matrix composites
[AERE-R-13330] 13 p1766 N90-20134
LaRC TPI 1500 series polymers
[NASA-CR-181899] 14 p1945 N90-21129
Effect of a crystal-melt interface on Taylor-vortex flow
[NASA-CR-186512] 15 p2171 N90-22408
Three-dimensional convection in cylindrical geometry 17 p2399 N90-23668
Contract crystal growth and fabrication services
[AD-A221357] 18 p2623 N90-24947
Development of a large scale Nd:YAG growth process
[DE90-010746] 18 p2624 N90-24954
Nucleation kinetics in undercooled, class-forming metallic melts
[ESA-TT-1186] 19 p2676 N90-25218
Mathematical simulation of heat exchanges and thermoelastic constraints in Czochralski crystal growth
[ETN-90-97242] 20 p2931 N90-26680
Electronic conduction in molten cryolite saturated with alumina
[DE90-015090] 23 p3400 N90-29211
Effect of a crystal-melt interface on Taylor-Vortex flow with buoyancy
[PB90-244401] 24 p3551 N90-30089

MEMBRANE ANALOGY
U MEMBRANE STRUCTURES
U STRUCTURAL ANALYSIS

MEMBRANE STRUCTURES
NT SKIN (STRUCTURAL MEMBER)
Advanced double layer capacitor
[AD-A211977] 04 p0469 N90-12688
Model system studies with a phase separated membrane bioreactor 05 p0679 N90-13954
The Shock and Vibration Digest, volume 21, no. 1 15 p2109 N90-22061
A review of approximate methods for determining the vibrational modes of membranes 15 p2109 N90-22063
An assessment of second-generation stretched-membrane mirror modules
[DE90-010243] 16 p2252 N90-22841
A preliminary design of interior structure and foundation of an inflatable lunar habitat 18 p2633 N90-24999

MEMBRANE THEORY
U STRUCTURAL ANALYSIS

MEMBRANES
NT CELL MEMBRANES (BIOLOGY)
NT ION EXCHANGE MEMBRANE ELECTROLYTES
NT MEMBRANE STRUCTURES
NT SKIN (STRUCTURAL MEMBER)
Electrical field dependence of protein conformation and channel function in lipid membranes of different compositions
[AD-A210236] 01 p0040 N90-10222
Polyheterocycle Langmuir-Blodgett films
[AD-A210625] 01 p0051 N90-10292
Preparation and evaluation of composite membranes for zinc/bromine storage batteries
[DE89-009931] 01 p0059 N90-10339
Stretched-membrane heliostats for solar central-receiver power plants
[DE89-016034] 01 p0084 N90-10476
Electroporation: Theory of basic mechanisms
[AD-A210196] 01 p0091 N90-10520
Membrane fusion: The role of polyphosphatidylinositol
[AD-A211289] 03 p0379 N90-12156
Photochemical observation of ion flows in membrane channels
[AD-A212449] 04 p0472 N90-12705
Calcium displacement caused by electromagnetic fields
[AD-A212690] 04 p0524 N90-13023
Asymptotic analysis of performance of membrane modules for gas separations
[DE90-000699] 06 p0742 N90-14316
Test and evaluation of polymeric membranes for oxygen enrichment of air
[DE90-000555] 06 p0742 N90-14321
Ordered ceramic membranes
[DE89-017426] 06 p0750 N90-14364
Comparison of structural subunits of the core light-harvesting complexes of photosynthetic bacteria
[DE90-001412] 06 p0819 N90-14765
Electrochemical investigation of electronically conductive polymers
[AD-A214019] 07 p0912 N90-15277
Membrane and durability studies for the zinc/bromine battery
[DE89-016181] 07 p0920 N90-15324
Advanced double layer capacitor
[AD-A213406] 07 p0923 N90-15341
Transport processes through monomolecular films
[AD-A213609] 07 p0923 N90-15342
Photochemical solar energy conversion utilizing semiconductors localized in membrane mimetic systems
[DE90-003450] 07 p0953 N90-15515
Using inorganic membranes to separate gases: R and D status review
[DE90-004386] 08 p1042 N90-16019
Study of silicon nitride pH response to the fabrication of microelectronic sensors
[LAAS-89229] 08 p1042 N90-16023
Silicon membrane formation
[DE90-003022] 08 p1049 N90-16064
Chemical-like behavior of electrons and holes in polymeric conductors
[AD-A214496] 09 p1196 N90-16931
A lightweight solid polymer electrolyte fuel cell with stack power density of 3kW/lb (7 kW/kg)
[AD-A216253] 10 p1401 N90-18100
Perforated monolayers
[DE90-005469] 11 p1488 N90-18566
Elastomeric electrical isolation membrane
[AD-D014365] 12 p1651 N90-19490
Advanced double layer capacitor
[AD-A217110] 12 p1656 N90-19518
Calculation of nonlinear viscoelastic processes for plastic layer textile membranes
[ETN-90-95868] 12 p1675 N90-19622
Status of stretched-membrane heliostats
[DE90-000801] 12 p1683 N90-19669
The drum: Mechanical oscillators and acoustic radiators
[REPT-FB-01/88] 12 p1710 N90-19819
CO2 diffusion and solubility in a Polystyrene/Polybutadiene block copolymer with highly oriented lamellar morphology
[AD-A217165] 13 p1779 N90-20211
The application of Dow Chemical's perfluorinated membranes in proton-exchange membrane fuel cells 13 p1823 N90-20466
Hydrogen-oxygen proton-exchange membrane fuel cells and electrolyzers 13 p1823 N90-20467
Selection and design of a stretched-membrane heliostat for today's markets
[DE90-007997] 13 p1828 N90-20495
Design and demonstration of an improved stretched-membrane heliostat
[DE90-007904] 14 p2001 N90-21470
Electrochemical synthesis of ultrathin film composite membranes
[AD-A219041] 16 p2216 N90-22643
Selective removal of organics for water reclamation
[NASA-TM-101890] 17 p2421 N90-23797
Development of membrane process for carbon dioxide separation from diving atmosphere
[AD-A222606] 20 p2901 N90-26504
Adjustable choke for fluids nozzle
[NASA-CASE-NPO-17625-1-CU] 21 p3003 N90-27070
Novel macrocyclic carriers for proton-coupled liquid membrane transport
[DE90-015529] 24 p3445 N90-29453

MEMORY
Integration of neurobiological and computational analyses of the neural network essentials for conditioned taste aversions
[AD-A210228] 01 p0094 N90-10537
Synaptic plasticity and memory formation
[AD-A211368] 03 p0379 N90-12158
Metacognition and retrieval from long-term memory at Mount Everest
[AD-A211629] 03 p0382 N90-12177
Fear-potentiated startle as a model system for analyzing learning and memory
[AD-A212131] 04 p0525 N90-13029
Effects of type of responding on memory/visual search: Responding just yes or just no can lead to inflexible performance
[AD-A212764] 04 p0526 N90-13033
Individual differences in associative learning and forgetting
[AD-A212765] 04 p0526 N90-13034
Advanced Software Development Workstation Project 06 p0827 N90-14807
Auditory pattern memory: Mechanisms of tonal sequence discrimination by human observers
[AD-A214494] 09 p1250 N90-17253
Stimulus familiarity determines recognition strategy for novel 3-D objects
[AD-A215274] 09 p1260 N90-17305
On categorizing sounds
[AD-A216417] 10 p1427 N90-18232
Organization of a large-scale cortical network
[AD-A216829] 11 p1540 N90-18863
A long-term retention advantage for spatial information learned naturally and in the laboratory
[AD-A218268] 13 p1855 N90-20644
Distortions in memory for visual displays 16 p2268 N90-22929
Analysis of neural systems involved in modulation of memory storage
[AD-A220230] 18 p2584 N90-24714
Acquiring generalizations to organize human databases
[AD-A219835] 18 p2634 N90-25004
The retrieval of information from secondary memory: A review and new findings
[AD-A222760] 20 p2899 N90-26489

MEMORY (COMPUTERS)
The MHOST finite element program: 3-D inelastic analysis methods for hot section components. Volume 3: Systems' manual
[NASA-CR-182236] 01 p0079 N90-10451
Effective resource utilization for multiprocessor join execution
[DE89-016303] 01 p0105 N90-10595
Shared memory versus message passing architectures: An application based study
[AD-A210312] 01 p0108 N90-10615
New computing systems and their impact on structural analysis and design
[NASA-CR-185831] 02 p0257 N90-11457
Ground-state coding in partially connected neural networks
[NASA-TM-102239] 03 p0391 N90-12227
Thin film magnetic memory elements
[AD-D014178] 03 p0398 N90-12281
GaAs gate dynamic memory technology
[AD-A212387] 04 p0560 N90-13266
Memory matrix
[WO-PATENT-88/04096] 05 p0680 N90-13961
Extended memory library for AFOS (Automation of Field Operations and Services) applications
[PB89-230858] 05 p0708 N90-14147
Concurrent processing adaptation of aeroplastic analysis of propfans
[NASA-TM-102455] 06 p0799 N90-14656
New devices using ferroelectric thin films
[DE90-000789] 07 p0921 N90-15328
Temporal, processor, and spatial locality in multiprocessor memory references
[AD-A213790] 07 p0969 N90-15598
The implementation of a coherent memory abstraction on a NUMA (Non-Uniform Memory Access) multiprocessor: Experiences with PLATINUM (Platform for Investigating Non-Uniform Memory)
[AD-A213909] 07 p0970 N90-15600
Memory management for large-scale NUMA (Non-Uniform Memory Access) multiprocessors
[AD-A213910] 07 p0970 N90-15601
An overview of PLATINUM: A Platform for Investiga ting Non-Uniform Memory (preliminary version)
[AD-A213911] 07 p0970 N90-15602

Evolution of an operating system for large-scale shared-memory multiprocessors
[AD-A213912] 07 p0970 N90-15603
Reconfigurable N-dimensional computer memory
[AD-D014309] 07 p0971 N90-15607
High level language memory management on parallel architectures
[DE89-015018] 07 p0971 N90-15609
Bounded polynomial randomized consensus
[AD-A213808] 07 p0984 N90-15686
Bus programmable slave module
[NASA-CASE-MSC-21387-1] 08 p1108 N90-16411
Analog hardware for delta-backpropagation neural networks
[NASA-CASE-NPO-17564-1-CU] 09 p1204 N90-16974
Solid state electrical switch employing materials with reversible phase transistors
[NASA-CASE-NPO-17621-1-CU] 09 p1209 N90-17010
Supporting shared data structures on distributed memory architectures
[NASA-CR-181981] 09 p1262 N90-17318
Merlin: A superglue for multicomputer systems
[NASA-CR-186330] 09 p1271 N90-17366
A scheme for supporting distributed data structures on multicomputers
[NASA-CR-181987] 10 p1415 N90-18152
Study on advanced information processing system
[NASA-CR-186342] 10 p1415 N90-18154
Cedar project: Original goals and progress to date
[DE90-006761] 11 p1543 N90-18880
Memory management in traceback Viterbi decoders 12 p1643 N90-19443
GeoNet 88: Calculation connection system concept for the EURAD project 12 p1687 N90-19688
The contour model architecture and assembly language
[AD-A217114] 13 p1865 N90-20697
Numerical Arc Segmentation Algorithm for a Radio Conference (NASARC), version 4.0: User's manual
[NASA-TM-101454] 14 p1964 N90-21250
CAMAC memory module: MEMO-32
[DE90-759846] 14 p2012 N90-21528
Quadratic Hadamard Memories 1
[AD-A217224] 14 p2013 N90-21534
An adaptive vector quantization scheme 15 p2077 N90-21898
Sparse distributed memory overview 15 p2141 N90-22235
The use of supercomputers for the design and analysis of constructions 16 p2277 N90-22977
CESAR LOCAL BUS
[FFI-89/7011] 17 p2440 N90-23903
Sharing memory robustly in message-passing systems
[AD-A219923] 17 p2447 N90-23950
The wakeup problem
[AD-A220534] 17 p2451 N90-23981
Implementation of an I-structure memory controller
[AD-A221397] 18 p2588 N90-24726
The one dimensional skewing problem
[RUU-CS-89-23] 18 p2596 N90-24769
A comparison of select image-compression algorithms for an electronic still camera 18 p2632 N90-24994
System for shooting of video images in realtime
[MBB-UM-0009/89-PUB] 19 p2653 N90-25097
Execution time supports for adaptive scientific algorithms on distributed memory machines
[NASA-CR-182052] 19 p2741 N90-25578
Multiprocessor architecture: Synthesis and evaluation
[NASA-CR-186618] 19 p2741 N90-25579
The basis system
[DE90-012077] 19 p2743 N90-25591
Exploiting replication in distributed systems
[NASA-CR-186410] 19 p2746 N90-25603
Computer architecture evaluation for structural dynamics computations: Project summary
[NASA-CR-186137] 20 p2903 N90-26512
Atomic snapshots of shared memory
[AD-A222765] 20 p2904 N90-26520
Capacity for patterns and sequences in Kanerva's SDM as compared to other associative memory models
[NASA-CR-180701] 20 p2905 N90-26522
Converses for write-unidirectional memories
[EUT-89-E-220] 20 p2909 N90-26546
Single-pass memory system evaluation for multiprogramming workloads
[NASA-CR-186553] 20 p2910 N90-26558
PANDA: A distributed multiprocessor operating system 20 p2911 N90-26561
Design knowledge capture for a corporate memory facility 21 p3045 N90-27304
Basic properties and limits of integrated arrays of dissipative circuit and logic elements
[AD-A224533] 24 p3464 N90-29567

MENISCI
Effects of gravity on equilibrium crystal shapes 02 p0281 N90-11602
Infiltration mechanics in conventional and hybridised fibre reinforced metal matrix composites
[AERE-R-13330] 13 p1766 N90-20134
Critical point wetting drop tower experiment
[NASA-CR-186513] 14 p1957 N90-21208

MENTAL HEALTH
Evaluation of physiological and psychological impairment of human performance in cold stressed subjects
[AD-A223635] 24 p3498 N90-29769

MENTAL PERFORMANCE
Models of mental functioning
[AD-A210456] 01 p0094 N90-10538
Toward a theory of representation design
[AD-A210885] 01 p0116 N90-10670
Comprehension processes in mechanical reasoning
[AD-A210459] 02 p0255 N90-11442
Stimulus-response compatibility in spatial precuing and symbolic identification: Effects of coding practice, retention, and transfer
[AD-A210745] 02 p0255 N90-11443
A menu of self-administered microcomputer-based neurotoxicology tests
[NASA-CR-185518] 03 p0382 N90-12175
The effect of incentives on the reliability and validity of cognitive speed tests
[AD-A211346] 03 p0383 N90-12181
Computer-based tutors for explaining and managing the process of diagnostic reasoning
[AD-A211738] 03 p0390 N90-12222
Effects of serial wet-dry-wet cold exposure: Thermal balance, physical activity, and cognitive performance
[AD-A212704] 04 p0524 N90-13025
The structural memory: A network model for human perception of serial objects
[CWI-CS-R8829] 05 p0675 N90-13930
A guide to reasoning under uncertainty
[REPT-72/87/R486U] 05 p0675 N90-13932
Where to from here. Future applications of mental models of complex performance
[DE90-002091] 07 p0967 N90-15586
Investigation of a magnetostrictive fiber optic interferometric sensor
[AD-A215666] 09 p1226 N90-17111
Reactions to emergency situations in actual and simulated flight 09 p1255 N90-17283
Expertise, stress, and pilot judgment 09 p1255 N90-17284
Performance recovery following startle: A laboratory approach to the study of behavioral response to sudden aircraft emergencies 09 p1256 N90-17286
Measuring learning ability by dynamic testing
[AD-A215273] 09 p1259 N90-17304
Alterations in the metabolic and sympathetic response to cold exposure after cold air acclimation
[AD-A216817] 10 p1412 N90-18144
Effects of dexamethasone and high terrestrial altitude on cognitive performance and affect
[AD-A217897] 13 p1851 N90-20625
Role of cognitive factors in the acquisition of cognitive skill
[AD-A218069] 13 p1854 N90-20642
Development of microcomputer-based mental acuity tests for repeated-measures studies
[NASA-CR-185607] 14 p2010 N90-21521
A study of mental models through communication between users and advisors solving software manipulation problems 15 p2176 N90-22434
Human cognitive and motor performance measures under typical cool white fluorescent illumination vs relatively high cool white illuminance/irradiance lighting
[AD-A218445] 16 p2262 N90-22892
A preliminary analysis of the SOAR architecture as a basis for general intelligence
[AD-A218913] 16 p2262 N90-22896
Cognitive efficiency considerations for good graphic design
[AD-A218976] 16 p2263 N90-22899
Cognitive architectures and rational analysis: Comment
[AD-A219199] 16 p2264 N90-22907
Information processing approaches to cognitive development
[AD-A219200] 16 p2265 N90-22908
Toward a SOAR theory of taking instructions for immediate reasoning tasks
[AD-A219201] 16 p2265 N90-22909
Laboratory replication of scientific discovery processes
[AD-A219273] 16 p2266 N90-22913
Motor and cognitive performance do not change during a ten-week submarine patrol
[AD-A218639] 16 p2276 N90-22969
Acquiring generalizations to organize human databases
[AD-A219835] 18 p2634 N90-25004
An empirically derived figure of merit for the quality of overall task performance 18 p2644 N90-25058
The role of attention in information processing implications for the design of displays
[AD-A219252] 19 p2723 N90-25486
Performance-based workload assessment: Allocation strategy and added task sensitivity 19 p2734 N90-25539
Real-time measurement of mental workload: A feasibility study 19 p2734 N90-25540
Human performance in cockpit-related systems
[NIAR-90-7] 20 p2900 N90-26495
Real-time measurement of mental workload using psychophysiological measures
[AD-A221462] 21 p3036 N90-27258
Automatic information processing and high performance skills: Acquisition, transfer, and retention
[AD-A221744] 21 p3036 N90-27260
Knowledge and distributed computation
[AD-A223100] 21 p3039 N90-27270
Attention, imagery, and memory: A neuromagnetic investigation
[AD-A224560] 24 p3499 N90-29775
Ability and metacognitive determinants of skill acquisition and transfer
[AD-A224569] 24 p3499 N90-29776
Physiological metrics of mental workload: A review of recent progress
[NASA-CR-187290] 24 p3499 N90-29777
Automatic recognition of tractability in inference relations
[AD-A223698] 24 p3538 N90-30003

MENTAL STRESS
U STRESS (PSYCHOLOGY)

MERCAPTAN
U THIOLS

MERCAPTO COMPOUNDS
U THIOLS

MERCURY (METAL)
NT MERCURY ISOTOPES
Fundamental studies of surface processes and trace analysis using solid electrodes
[AD-A216538] 11 p1483 N90-18533
A study of the influence of Hg(6(3)P2) population in a low-pressure discharge on mercury ion emission at 194.2 nm 20 p2853 N90-26223
The transfer of mercury between the atmosphere and lake or soil surfaces 20 p2886 N90-26419
The aqueous atmospheric chemistry of mercury 20 p2886 N90-26420

MERCURY (PLANET)
Small Mercury Relativity Orbiter 12 p1733 N90-19965

MERCURY ALLOYS
NT MERCURY AMALGAMS

MERCURY AMALGAMS
Solvent effects on the kinetics of electroreduction of Cu(I) at mercury
[AD-A209423] 01 p0038 N90-10211
Potential dependence of the elementary steps in the kinetics of electrode reactions involving amalgam formation
[AD-A209424] 01 p0038 N90-10212

MERCURY ARCS
UV photo-enhanced MOCVD of cadmium and cadmium telluride
[RSRE-MEMO-4208] 15 p2174 N90-22422

MERCURY CADMIUM TELLURIDES
Interstitial formation, non-equilibrium and macroscopic processes in mercury cadmium telluride
[AD-A212412] 04 p0561 N90-13267
Research on mercury cadmium telluride
[AD-A213924] 07 p0906 N90-15237
Resonance enhanced Raman studies of as-grown and laser-processed HgCdTe
[AD-A213855] 08 p1129 N90-16540
Spectroscopic techniques for the analysis of CdTe substrates used for the growth of HgCdTe
[AD-A214545] 09 p1288 N90-17466
Diffusion and defect characterization studies of mercury cadmium telluride
[AD-A214655] 09 p1289 N90-17470
Workshop on the Physics and Chemistry of Mercury Cadmium Telluride and Related II-VI compounds
[AD-A217496] 13 p1894 N90-20867
NRL hybrid reliability. Physics of failure initial study
[AD-A217986] 13 p1898 N90-20893
Method of preparing radially homogeneous mercury cadmium telluride crystals
[NASA-CASE-MFS-25786-2] 13 p1898 N90-20896
The potential for high performance HgCdTe arrays at 4 microns 14 p1976 N90-21320

High resolution imaging of the Venus night side using a Rockwell 128x128 HgCdTe array
14 p1978 N90-21330
Short wavelength HgCdTe staring focal plane for low background astronomy applications
14 p1979 N90-21336
Low noise HgCdTe 128 x 128 SWIR FPA for Hubble space telescope 14 p1979 N90-21337
Laboratory and telescope use of the NICMOS2 128 x 128 HgCdTe array 14 p1979 N90-21338
HgCdTe 256x256 NWIR FPA
14 p1981 N90-21348
Direct implantation process development and characterization in advanced Hg(1)-(x)Cd(x) Te EPI layers
[AD-A219133] 16 p2324 N90-23252
Fundamental and practical studies of metal contacts on mercury zinc telluride
[AD-A218730] 17 p2376 N90-23528
Rapid annealing of iron implanted Hg(1-x)Cd(x)Te
[AD-A222777] 21 p3082 N90-27524
Measurement of deep levels at InGaAs(P)/InP heterojunctions
[AD-A222890] 21 p3082 N90-27526
Faraday rotation mapping of mercury cadmium telluride
[AD-A224278] 23 p3311 N90-28729
Research on mercury cadmium telluride
[AD-A224250] 24 p3448 N90-29474

MERCURY COMPOUNDS
NT MERCURY TELLURIDES
Mercuric iodide room temperature gamma-ray detectors
[NASA-TM-103318] 13 p1804 N90-20357

MERCURY ION ENGINES
T4A thruster starting sequences and the design of an electromagnetic sequencer for cyclic life tests
[RAE-TR-77042] 19 p2669 N90-25179
A gas-phase high voltage electrical isolator with controlled breakdown
[RAE-TR-78030] 19 p2669 N90-25180

MERCURY ISOTOPES
An apparatus for the electrodynamic containment of charged macroparticles 04 p0486 N90-12789

MERCURY TELLURIDES
Thin film cadmium telluride, zinc telluride, and mercury zinc telluride solar cells
[DE89-009499] 06 p0804 N90-14681

MERIDIONAL FLOW
Solar cyclical trend study of the mid-latitude, quiet-time, meridional, neutral winds at winter solstice conditions
[AD-A217398] 13 p1841 N90-20568
Secondary flow calculations for axial and radial compressors 14 p1925 N90-21024

MEROMORPHIC FUNCTIONS
NT ELLIPTIC FUNCTIONS
The Painleve test for nonlinear ordinary and partial differential equations
[AD-A212894] 04 p0546 N90-13177

MERRITT ISLAND (FL)
Climate of the Kennedy Space Center and vicinity
[NASA-TM-103498] 22 p3228 N90-28307

MESFETS
U FIELD EFFECT TRANSISTORS

MESH
Method for fabricating thin film metallic meshes for use as Fabry-Perot interferometer elements, filters and other devices
[AD-D014236] 06 p0779 N90-14529
Crash-impact behavior of graphite/epoxy composite sine wave webs 23 p3300 N90-28667

MESH (MATHEMATICS)
U COMPUTATIONAL GRIDS

MESH GENERATION (MATHEMATICS)
U GRID GENERATION (MATHEMATICS)

MESOMETEOROLOGY
Coordination of mesoscale meteorological research between ASL and European groups
[AD-A210902] 01 p0089 N90-10508
Weather satellite and computer modeling approaches to assessing propagation over marine environments
06 p0764 N90-14443
A PBL-radiation model for application to regional numerical weather prediction 12 p1635 N90-19394
Synoptic-scale forcing of the low-level jet in developing baroclinic waves 12 p1692 N90-19717
Colloquium on Synoptic Meteorology
[PB90-121112] 12 p1692 N90-19720
Impact of marine boundary layer parameterization on a numerical simulation of cyclogenesis during a cold air outbreak event 16 p2256 N90-22864
Sea breeze: Induced mesoscale systems and severe weather
[NASA-CR-186367] 19 p2715 N90-25450
Coordination of mesoscale meteorological research between ASL and European groups
[AD-A223811] 24 p3495 N90-29751

MESON-NUCLEON INTERACTIONS
Exotic Higgs production at e+e- colliders
[PREPRINT-671] 05 p0698 N90-14088

MESONS
NT ETA-MESONS
NT HYPERONS
NT MUONS
NT PIONS
An experimental high energy physics program
[DE89-014695] 03 p0403 N90-12311
Minimal total cross section for e(+)e(-) yields W(+)W(-)
[NIKHEF-H/88-12] 04 p0553 N90-13222
Lattice QCD estimate of mixing parameters for heavy meson systems
[PREPRINT-687] 05 p0697 N90-14079
A lattice study of semileptonic decays of D-mesons
[PREPRINT-660] 05 p0698 N90-14086
Exotic Higgs production at e+e- colliders
[PREPRINT-671] 05 p0698 N90-14088
A covariant multiple scattering series for elastic projectile-target scattering
[NASA-TM-101942] 09 p1279 N90-17417
A beauty factory using an SRF linac and a storage ring
[CEBAF-PR-89-017] 20 p2925 N90-26644
Measurement of the masses and lifetimes of the charmed mesons D neutral, D plus and D (sub s) plus
[MPI-PAE/EXP-EL-220] 22 p3245 N90-28405
Quasistatic electron diffusion in quantum hadrodynamics
[ETN-90-97297] 22 p3255 N90-28432

MESOPAUSE
Near-mesopause temperatures at 69 N latitude in late summer 05 p0658 N90-13837
Meteor radar studies of the mesopause region and nonlinear atmospheric waves 17 p2421 N90-23799

MESOSCALE PHENOMENA
NT JET STREAMS (METEOROLOGY)
Coordination of mesoscale meteorological research between ASL and European groups
[AD-A210902] 01 p0089 N90-10508
Low level remote sensing: The Doppler Radar wind profiler 03 p0361 N90-12067
Satellite-derived rainfall estimates and propagation characteristics associated with the Mesoscale Convective Systems (MCSs)
[PB89-213417] 03 p0365 N90-12086
Analysis and modeling of summertime convective cloud and precipitation structure over the Southeastern United States
[NASA-CR-185436] 04 p0519 N90-12996
Project WIND: Experiments with the UK Meteorological Office mesoscale model
[AD-A212291] 04 p0521 N90-13006
Mesoscale acid deposition modeling studies
[NASA-CR-4262] 04 p0554 N90-13228
The identification of terrain-induced circulations using principal components
[DE90-001991] 06 p0815 N90-14739
Geosat/ERM altimeter data analysis for the determination of global oceanic mesoscale variability
07 p0949 N90-15492
Mesoscale analysis by numerical modelling coupled with satellite-based sounding 08 p1100 N90-16370
A dynamic model for forecasting new cloud development
[AD-A213939] 08 p1102 N90-16383
Some properties of so-called magnetic cloud structures in the solar wind
[IFSI-88-16] 08 p1153 N90-16678
A numerical study of the formation of mesoscale convective complexes 09 p1245 N90-17225
Numerical simulations of the rapid cyclogenesis over Canada and evolution of a cold front observed on 25-26 April 1979 (SESAME-AVE-3) 09 p1247 N90-17234
Comparison of circulation obtained through the trajectory of a drifting buoy tracked by satellite and hydrographic data in the Bransfield Strait
[INPE-4946-TDL/387] 11 p1537 N90-18850
A PBL-radiation model for application to regional numerical weather prediction 12 p1635 N90-19394
Transport of atmospheric aerosols above the Sierra Nevada slopes
[PB90-120288] 12 p1685 N90-19675
Initialization of EURAD, part 2
12 p1688 N90-19696
Boundary layer parameterization in CTM and MM4
12 p1688 N90-19697
Synoptic-scale forcing of the low-level jet in developing baroclinic waves 12 p1692 N90-19717
Colloquium on Synoptic Meteorology
[PB90-121112] 12 p1692 N90-19720
Digital simulation of a Boenline
[ISSN-0069-5882] 12 p1694 N90-19729
Evolution of finite amplitude baroclinic waves in the atmosphere and ocean
[INPE-4752-TDL/346] 12 p1695 N90-19733
Derivation of kinematic fields using wind profiler data from the 1985 pre-storm experiment
[AD-A217952] 13 p1845 N90-20592
A method for correcting and reducing the pressure data recorded at the PAM 2 stations during GALE
[AD-A218165] 13 p1846 N90-20596
An aircraft investigation of a convective boundary layer over Lake Michigan
[AD-A218175] 13 p1846 N90-20598
The influence of lateral boundary conditions, fixed surface forcings, and synoptic situations upon predictability estimates using limited area numerical models
14 p2005 N90-21492
A case study of cloud-to-ground lightning during the GALE program 15 p2132 N90-22185
Frontal structure in a mesoscale model
15 p2132 N90-22187
A study of mesoscale acid deposition in the lower Ohio River Valley 16 p2253 N90-22848
Impact of marine boundary layer parameterization on a numerical simulation of cyclogenesis during a cold air outbreak event 16 p2256 N90-22864
A study of turbulence near thunderstorm tops
[NASA-CR-186620] 16 p2258 N90-22870
PUFFY: A puff diffusion computer model
[FOA-C-40251-4.5] 17 p2421 N90-23796
Initiation and propagation of thunderstorm mesocyclones 17 p2428 N90-23838
Advanced mesoscale weather forecasting to support tactical operations on the airland battlefield
[AD-A219421] 19 p2715 N90-25449
Sea breeze: Induced mesoscale systems and severe weather
[NASA-CR-186367] 19 p2715 N90-25450
Boundary layer parameterization for use in a limited area forecast model 21 p3029 N90-27224
Lidar cloud studies for FIRE and ECLIPS
[NASA-CR-186384] 22 p3211 N90-28214
Mesoscale variability of free tropospheric humidity near San Nicolas Island during FIRE
22 p3214 N90-28234
Turbulence spectra of the FIRE stratocumulus-topped boundary layers 22 p3217 N90-28246
A cloudiness transition in a marine boundary layer
22 p3219 N90-28259
The 27-28 October 1986 FIRE cirrus case study: Meteorology and clouds 22 p3223 N90-28280
Satellite-derived cloud fields during the FIRE cirrus IFO case study 22 p3223 N90-28281
Preliminary simulations of the large-scale environment during the FIRE cirrus IFO 22 p3225 N90-28290
Instability bursts associated with Extratropical Cyclone Systems (ECSs) and a forecast index of 3 to 12 hour heavy precipitation
[NOAA-TM-NESDIS-30] 22 p3228 N90-28309
A nonhydrostatic numerical model in sigma-coordinates and simulations of mesoscale phenomena
23 p3350 N90-28932
Mesoscale Lightning Experiment (MLE): A view of lightning as seen from space during the STS-26 mission
[NASA-TM-103513] 23 p3353 N90-28951
Three-dimensional numerical study of thunderstorm downdrafts and associated outflow boundaries
24 p3494 N90-29746
Coordination of mesoscale meteorological research between ASL and European groups
[AD-A223811] 24 p3495 N90-29751

MESOSPHERE
NT MESOPAUSE
Fundamentals of middle atmospheric dynamics
[AD-A211747] 04 p0518 N90-12988
Neutral air turbulence in the middle and upper atmosphere observed during the MAC/EPSILON campaign 05 p0660 N90-13855
Polar mesosphere summer echoes and associated atmospheric gravity waves 05 p0660 N90-13856
The interaction and variation of waves and turbulence from MST radar data
[AD-A212849] 05 p0670 N90-13906
Remote sensing of atmospheric water vapour by pressure modulation radiometry
06 p0802 N90-14667
A measurement of hydroxyl in the daytime mesosphere 06 p0814 N90-14732
Millimeter-wave propagation in the mesosphere
[PB90-119868] 11 p1496 N90-18612
Investigations into the properties, conditions, and effects of the ionosphere
[AD-A217807] 14 p2005 N90-21489
The interpretation of SAGE 2 ozone measurements in the lower mesosphere 15 p2124 N90-22149

A study of gravity wave variability, saturation, and turbulence generation in the mesosphere and lower thermosphere
[AD-A220018] 17 p2424 N90-23810
Current status of SHARC, the strategic high altitude radiance code, and description of its new auroral module
[AD-A221068] 18 p2580 N90-24698
Photodissociation of O2 in the stratosphere and mesosphere: A general parametrization of the Schumman-Runge Bands 20 p2887 N90-26427
Conceptual design study for Infrared Limb Experiment (IRLE)
[NASA-CR-186950] 21 p2968 N90-26869
Solar activity influence on climatic variations of stratosphere and mesosphere in mid-latitudes 22 p3202 N90-28169
The planetary waves dynamics and interannual course of meteorological parameters of the high latitude stratosphere and mesosphere of the Northern and Southern Hemispheres during the 20th and 21st solar cycles and different phases of QBO 22 p3203 N90-28170
The mesospheric responses to short-term solar ultraviolet variability 22 p3204 N90-28174
A change of mesospheric ozone content under electron precipitation influence 22 p3207 N90-28191

MESOZOIC ERA
The patterns of fracture and the conditioning tectonics in the region of the Quadrilatero Ferrifero and part of the Migmatitic-Gnanulitic Complex in Minas Gerais (Brazil)
[INPE-4895-PRE/1496] 11 p1534 N90-18829

MESSAGE PROCESSING
Robotic vehicle message format
[AD-A210996] 01 p0110 N90-10627
The J-Machine: A fine grain concurrent computer
[AD-A211909] 03 p0384 N90-12187
On modeling resources in multiprocessor systems
[MEMO-INF-88-33] 04 p0535 N90-13095
A multilevel parallel solver for block tridiagonal and banded linear systems
[AD-A213151] 05 p0688 N90-14008
Action languages: Dimensions, effects
[NASA-CR-183368] 05 p0716 N90-14181
An overview of lynx
[AD-A213714] 07 p0975 N90-15631
A 3-D measurement system using object-oriented FORTH
[DE90-003393] 08 p1109 N90-16420
Development of a parallel link model for meteor burst communication
[AD-A215629] 09 p1208 N90-17001
Dynamic reconfiguration and link fault tolerance in a transputer network
[AD-A215105] 12 p1642 N90-19433
Queuing theory approach to modelling the dynamics of the human-computer interface
[AD-A216870] 12 p1705 N90-19788
Express cubes: Improving the performance of k-ary n-cube interconnection networks
[AD-A217117] 13 p1793 N90-20287
Fast causal multicast
[NASA-CR-186495] 14 p2013 N90-21533
CSMA/RN: A universal protocol for gigabit networks 15 p2150 N90-22280
Alternative parallel ring protocols 15 p2150 N90-22282
Modelling high data rate communication network access protocol 15 p2150 N90-22285
Fairness problems at the media access level for high-speed networks 15 p2151 N90-22287
A carrier sensed multiple access protocol for high data base rate ring networks 15 p2151 N90-22288
A knowledge-based system with learning for computer communication network design 15 p2157 N90-22319
Electronic mail systems 15 p2179 N90-22451
Message handling in the post-2000 era: Executive summary
[AD-A219983] 17 p2393 N90-23628
Sharing memory robustly in message-passing systems
[AD-A219923] 17 p2447 N90-23950
AIRNET: A real-time comunications network for aircraft
[NASA-CR-186140] 18 p2543 N90-24514
Performance analysis of local area networks
[NASA-CR-186639] 18 p2595 N90-24767
A task control architecture for autonomous robots 19 p2735 N90-25546
Reliable broadcast protocols
[NASA-CR-186411] 19 p2762 N90-25696
CORA: A direct sequence spread spectrum radio for voice and data 20 p2848 N90-26195
Synchronization of frequency shift transmission and the effect of oversampling 20 p2848 N90-26200
New approaches for rapid synchronisation frequency hoppers 20 p2849 N90-26201
MTP: An atomic multicast transport protocol
[NASA-CR-186716] 20 p2858 N90-26254
Knowledge and inhibition in asynchronous distributed systems
[TR-90-1139] 20 p2935 N90-26703
Overview of requirements and networks for voice communications and speech processing 21 p2992 N90-27007
The speech signal 21 p2992 N90-27008
Sisal on a message passing architecture
[DE90-008786] 21 p3051 N90-27342
Recovery in distributed systems using optimistic message logging and checkpointing
[AD-A222104] 21 p3054 N90-27361
The operational feature exchange language
[AD-A222497] 21 p3060 N90-27401
Potential new tactical applications of the Global Positioning System (GPS) 21 p3069 N90-27449
Hash functions: A tutorial and status report
[NPL-DITC-151/89] 22 p3238 N90-28361
Dynamic load-sharing using predicted process resource requirements
[NASA-CR-186691] 22 p3255 N90-28433
Communications Interface Driver (CID) test plan
[DOT/FAA/CT-TN89/35] 23 p3319 N90-28762
Observability of relative navigation using range-only measurements 24 p3427 N90-29360
High speed bus technology development
[AD-A224486] 24 p3463 N90-29565

MESSAGES
Electronic mail systems 15 p2179 N90-22451
The GEOSTAR location and messaging system 17 p2360 N90-23435
Taxiway sign effectiveness under reduced visibility conditions
[DOT/FAA/CT-TN90/20] 19 p2662 N90-25150
Exploiting replication in distributed systems
[NASA-CR-186410] 19 p2746 N90-25603
PANDA: A distributed multiprocessor operating system 20 p2911 N90-26561
Secure Data Network System (SDNS) network, transport, and message security protocols
[PB90-198946] 23 p3318 N90-28757

METABOLIC WASTES
NT FECES
NT HUMAN WASTES
NT URINE

METABOLISM
NT CALCIUM METABOLISM
NT CARBOHYDRATE METABOLISM
NT CATABOLISM
NT ELECTROLYTE METABOLISM
NT ENZYME ACTIVITY
NT FERMENTATION
NT HYDROGEN METABOLISM
NT OXYGEN METABOLISM
Molecular biology and physiology of methanogenic archaebacteria
[AD-A210399] 01 p0091 N90-10522
Decomposition in Arctic terrestrial environments
[DE90-001198] 06 p0809 N90-14706
Thermal remote sensing in the differentiation of soybean crops (glycine max (L.) merrill) submitted to water deficit
[INPE-4900-PRE/1501] 11 p1522 N90-18762
Study of hydrazine metabolism and toxicity
[AD-A217103] 12 p1695 N90-19736
Metabolism, seizures, and blood flow in brain following organophosphate exposure: Mechanisms of action and possible therapeutic agents
[AD-A217098] 12 p1696 N90-19740
Influence of theobromine on heat production and body temperatures in cold-exposed humans: A preliminary report
[AD-A217203] 13 p1850 N90-20618
Physical performance and carbohydrate consumption in CF commandos during a 5-day field trial
[AD-A217204] 13 p1850 N90-20619
Anaerobic metabolism of aromatic compounds by phototrophic bacteria: Biochemical aspects
[DE90-009503] 14 p2009 N90-21516
The predictability and efficiency of human walking: Metabolic, mechanical, and biophysical considerations 15 p2137 N90-22211
The physiological cost of wearing the propellant handler's ensemble at the Kennedy Space Center
[NASA-TM-102786] 16 p2275 N90-22966
An in-vitro technique to study bone metabolism in developing mouse long bone rudiments under microgravity and compression 19 p2681 N90-25248
Experiment K-6-07. Metabolic and morphologic properties of muscle fibers after spaceflight 20 p2893 N90-26461
Experiment K-6-08. Biochemical and histochemical observations of vastus medialis 20 p2893 N90-26462
Experiment K-6-21. Effect of microgravity on 1) metabolic onzymes of type 1 and type 2 muscle fibers and on 2) metabolic enzymes, neutransmitter amino acids, and neurotransmitter associated enzymes in motor and somatosensory cerebral cortex. Part 1: Metabolic enzymes of individual muscle fibers; part 2: metabolic enzymes of hippocampus and spinal cord 20 p2896 N90-26474

METABOLITES
Prediction of thermal stress casualties
[AD-A212356] 04 p0523 N90-13022

METAGALAXY
U UNIVERSE

METAL AIR BATTERIES
Cost and energy consumption estimates for the aluminum-air battery anode fuel cycle
[DE90-005810] 11 p1503 N90-18656
Exploratory battery technology development and testing report for 1988
[DE90-007996] 13 p1794 N90-20297
Investigation of a photovoltaic/battery hybrid system for powering the high arctic data communications system
[AD-A218353] 13 p1798 N90-20319
The development of a simulation program of the anode side for aluminum/air batteries
[PB90-165754] 14 p1970 N90-21286

METAL BONDING
NT METAL-METAL BONDING
Contamination removal using various solvents and methodologies
[NASA-CR-183747] 05 p0626 N90-13652
Superplastic sheet forming 06 p0743 N90-14327
Diffusion bonding of metals 06 p0744 N90-14330
Designing for superplastic alloys 06 p0744 N90-14332
Critical and subcritical crack-growth behavior along toughened ceramic/metal interfaces 07 p0889 N90-15140
Fatigue and impact strength of diffusion bonded titanium alloy joints
[RAE-TM-MAT/STR-1123] 08 p1045 N90-16043
Numerical model of bond strength measurements
[DE90-006000] 10 p1396 N90-18073
Spectroscopic evidence for carbon-carbon bonding in carbide layers on metals
[AD-A216726] 11 p1479 N90-18512
Lateral spreading of Au contacts on InP
[NASA-TM-103133] 16 p2252 N90-22843
Investigation of the techniques for the analysis of composite structures: Analysis and representation of the static and dynamic behavior of glued metal insert assemblies
[IMFL-89-44] 22 p3153 N90-27878

METAL COATINGS
NT ALUMINUM COATINGS
NT GOLD COATINGS
NT ZINC COATINGS
Multiple internal reflection Fourier transform infrared spectroscopy studies of thiocyanate adsorption on silver and gold
[AD-A210245] 01 p0041 N90-10223
Fe-Ni-Cr alloys for coatings and electroforms
[PB89-195846] 03 p0325 N90-11849
Electrolitic deposited ohmic contacts on III-V compound semiconductors: A review
[PB89-217400] 03 p0410 N90-12350
The quality of vacuum deposited surface treatments
[CETIM-107040] 04 p0476 N90-12729
Laser Raman spectroscopy in studies of corrosion and electrocatalysis
[DE90-001414] 06 p0741 N90-14311
Thermal mechanical fatigue of coated blade materials
[AD-A214258] 07 p0882 N90-15107
Metal film coatings on amorphous metallic alloys
[AD-D014308] 07 p0907 N90-15240
Arc-sprayed coatings for electromagnetic pulse protection: Assessment of physical and electrical properties
[AD-A213825] 07 p0912 N90-15275
Silver coated superconducting ceramic powder
[AD-D014300] 07 p0913 N90-15278
Experimental evaluation of new alloy coatings
[AD-A214922] 09 p1194 N90-16916
The improved adhesion of organic polymers to silica and to aluminum metal with zirconium Schiff-base block copolymer coatings
[AD-A216669] 11 p1490 N90-18575
Microstructural variations in aluminum oxide coatings deposited using a dual beam ion system
[DE90-006040] 11 p1491 N90-18583
High gloss corrosion-resistant coatings
[AD-D014403] 14 p1954 N90-21184
Corrosion control through a better understanding of the metallic substrate/organic coating interface
[AD-A220432] 17 p2377 N90-23533

Evaluation of abrasion-resistant metallized coatings for civil works applications
[AD-A221078] 18 p2530 N90-24438
Production and coating of pure boron powders
[AD-A220272] 18 p2533 N90-24452
Oxidation, sulfidation, and hot corrosion: Mechanisms and interrelationships 23 p3307 N90-28702
Synthesis and property evaluation of Y-Ba2-Cu3-O(6+x) superconductors
[AD-A223494] 24 p3552 N90-30098

METAL COMBUSTION
RAAF Orion aircraft A9-300 oxygen fire
[AD-A215496] 09 p1162 N90-16725
The fundamentals of metal combustion in composite explosives revealed by high speed microphotography
[DE90-005255] 09 p1192 N90-16910
Wick-type liquid-metal combustion
[AD-A216019] 11 p1482 N90-18530
Regression and combustion characteristics of boron containing fuels for solid fuel ramjets 22 p3161 N90-27928
Pyrolysis and combustion of solid fuels under both subsonic and supersonic conditions 22 p3161 N90-27929

METAL CORROSION
U CORROSION

METAL CRYSTALS
A rate-dependent constitutive model for Be
[DE89-017755] 03 p0327 N90-11861
Temperature dependence of positron diffusion in cubic metals
[PB89-222020] 04 p0475 N90-12722
Energy concentration induced by phase transitions in hydrogenated metals
[PREPRINT-672] 05 p0625 N90-13650
Spectral properties of one dimensional quasi-crystals
[PREPRINT-659] 06 p0850 N90-14938
Amorphization of metals by ion implantation and ion beam mixing
[DE90-620571] 16 p2221 N90-22667
Scanning tunneling microscopy of semiconductor surfaces
[AD-A223339] 24 p3552 N90-30095

METAL CUTTING
High pressure waterjet cutting industrial needs survey
[AD-A214952] 10 p1368 N90-17927
Precision laser cutting
[DE90-009949] 17 p2407 N90-23717
An effective low-profile thermite torch
[DE90-015746] 24 p3459 N90-29534

METAL DRAWING
Novel processing of HTS based conductors
[DE90-005956] 12 p1722 N90-19892

METAL FATIGUE
Fatigue crack initiation mechanics of metal aircraft structures
[AD-A210567] 01 p0045 N90-10255
Fatigue crack growth rates as a function of delta K: Variability and material property 02 p0182 N90-11031
Failure modes and mechanisms in nickel alloys: Primarily austenitic stainless steel
[DE89-016823] 02 p0198 N90-11132
A re-evaluation of fatigue threshold test procedures and the simulation and prediction of fatigue crack growth under conditions of low crack closure 02 p0231 N90-11328
The effects of temperature on fatigue crack propagation in 310 austenitic stainless steel
[DE90-000136] 03 p0328 N90-11865
Effect of fretting on fatigue strength of aluminium alloys
[ESDU-89004] 03 p0329 N90-11870
Threshold for fatigue crack propagation
[DLR-FB-89-33] 05 p0655 N90-13815
Mean stress and the exhaustion of fatigue-damage resistance
[NASA-TM-101311] 05 p0655 N90-13819
A nonlinear high temperature fracture mechanics basis for strainrange partitioning
[NASA-TM-4133] 06 p0797 N90-14642
Fatigue fracture in the presence of shot peening residual stresses: Initiation, propagation, and relaxation phenomena 06 p0797 N90-14644
Fatigue properties of Al-Li alloys 07 p0898 N90-15189
Investigation on sheet material of 8090 and 2091 aluminium-lithium alloy 07 p0898 N90-15192
Aluminum lithium alloys for Navy aircraft 07 p0898 N90-15193
Fatigue, fracture mechanics and corrosion properties of some aluminium-lithium alloys 07 p0898 N90-15194
Fatigue and fracture behaviour of a PM Al-Li alloy 07 p0899 N90-15195
Uses and properties of Al-Li on the new EH101 helicopter 07 p0900 N90-15201
The effects of Mo2C morphology and strain distribution on the fatigue properties of Fe-C-Mo dual-phase steels 07 p0901 N90-15210
Directional solidification of superalloys
[NASA-CASE-MFS-28314-1] 07 p0904 N90-15227
Guide to the selection of surface treatments for the improvement of fatigue strength of steels
[ESDU-89031] 07 p0907 N90-15245
Proceedings of the 1988 Structural Integrity Program Conference
[AD-A213545] 07 p0947 N90-15486
Fatigue behavior of vertical axis wind turbine airfoils with two weld configurations
[DE90-002628] 07 p0955 N90-15525
Method to produce titanium alloy articles with high fatigue and fracture resistance
[AD-D014278] 08 p1043 N90-16029
Method of marking titanium alloy articles having distinct microstructural regions corresponding to high creep and fatigue resistance
[AD-D014283] 08 p1043 N90-16031
Failure analysis of a missile locking hook from the F-14 jet
[AD-A214995] 09 p1194 N90-16917
Fatigue crack propagation rates for titanium alloy sheet
[ESDU-89051] 09 p1201 N90-16956
Fatigue of aluminium alloy joints with various fastener systems. Low load transfer
[ESDU-89046] 09 p1239 N90-17193
Strain induced amorphization of aluminium by manganese implantation
[DE90-607259] 10 p1356 N90-17863
Effect of a single overload upon fatigue crack growth in an aluminum-lithium alloy
[AD-A216183] 10 p1356 N90-17865
Corrosion fatigue of iron-chromium-nickel alloys: Fracture mechanics and chemistry
[DE90-006318] 11 p1487 N90-18556
Softening mechanisms and microstructural instabilities during high temperature, low cycle fatigue of Ni, Ni3Al, and their metal matrix composites
[DE90-006487] 11 p1487 N90-18557
An attempt of improving high-temperature fatigue properties of Ni-Cr-W superalloys in HTGR helium
[DE90-741482] 12 p1627 N90-19350
A compendium of sources of fracture toughness and fatigue crack growth data for metallic alloys, part 4
[NASA-TM-102646] 14 p1950 N90-21164
Structural fatigue in the 34-meter HA-Dec antennas 15 p2078 N90-21902
Environment enhanced fatigue of advanced aluminum alloys and composites 16 p2218 N90-22652
Hydrogenation of stainless steels implanted with nitrogen
[DE90-617397] 16 p2221 N90-22666
Characterisation of fatigue of aluminium alloys by acoustic emission. Part 1: Identification of source mechanism
[AERE-R-13302-PT-1] 17 p2375 N90-23522
Characterisation of fatigue of aluminium alloys by acoustic emission. Part 2: Discrimination between primary and other emissions
[AERE-R-13303-PT-2] 17 p2375 N90-23523
The effects of slip character and crack closure on the growth of small fatigue cracks in titanium-aluminium alloys
[AD-A220714] 17 p2377 N90-23534
Mechanistic modeling of corrosion fatigue crack growth of steels in aqueous solutions 18 p2524 N90-24404
Development of a design methodology for high temperature cyclic applications of materials which experience cyclic softening
[DE90-006722] 19 p2674 N90-25205
Surface condition effect on the fatigue behavior of aluminum lithium alloys
[NIAR-90-13] 19 p2674 N90-25209
A study on ultrasonic detection and characterization of partially closed fatigue cracks
[DE90-011748] 19 p2702 N90-25371
A study of the fatigue behavior in scratched samples of Al-Li alloy (2090-T3)
[IAR-89-24] 20 p2832 N90-26107
AGARD/SMP Review Damage Tolerance for Engine Structures. 3: Component Behaviour and Life Management
[AGARD-R-770] 22 p3117 N90-27704
Calculation of service life of turbomachine components 22 p3117 N90-27706
Characterization of the CP 214 T851. Dissection of a cast flat bar for a standard spar
[CEAT-PV-M4/462200] 22 p3158 N90-27905
Characterization of the 7175 T7352. Dissection of a die casting standard spar
[CEAT-PV-M5/528900] 22 p3158 N90-27906
Characterization of the 7175 T7352 101. Dissection of a die casting standard spar
[CEAT-PV-M5/5288] 22 p3158 N90-27907
Characterization of the 7010 T73651. Dissection of a sheet billet for a standard spar
[CEAT-PV-M5/521700] 22 p3158 N90-27908
Damage tolerance analysis for manned hypervelocity vehicles. Volume 1: Final technical report
[AD-A221970] 22 p3191 N90-28106
High temperature fatigue behavior of Haynes 188 23 p3295 N90-28642
Constitutive and life modeling of single crystal blade alloys for root attachment analysis 23 p3296 N90-28643
The fatigue damage behavior of a single crystal superalloy 23 p3296 N90-28644
Micromechanisms of fatigue crack growth and fracture toughness in metal matrix composites
[AD-A223863] 23 p3302 N90-28676
Fretting fatigue strength of Ti-6Al-4V at room and elevated temperatures and ways of improving it 23 p3308 N90-28709
Crack layer analysis of fatigue fracture of a beta titanium alloy 23 p3338 N90-28864
Microstructure: Property correlation --- multiaxial fatigue damage evolution in waspaloy
[NASA-CR-180406] 23 p3340 N90-28880
Multiaxial fatigue criterion for 2-1/4 Cr-1 Mo steel for use in high-temperature structural design
[DE90-016039] 24 p3452 N90-29491

METAL FIBERS
Characterization of failure processes in tungsten copper composites under fatigue loading conditions
[NASA-TM-102371] 14 p1943 N90-21123
High temperature fatigue behavior of tungsten copper composites
[NASA-TM-102404] 14 p1946 N90-21138
The assessment of metal fiber reinforced polymeric composites 18 p2514 N90-24357

METAL FILMS
Structure of amorphous silicon alloy films
[DE89-009441] 01 p0128 N90-10734
Reactive ion etching of sputtered silicon carbide and tungsten thin films for device applications
[AD-A211711] 03 p0325 N90-11847
Low temperature formation of titanium aluminide films using physical vapor deposition
[AD-A211877] 03 p0328 N90-11866
Improved performance of low-T(sub c) superconductors for detection of minimum-ionizing particles
[DE90-001985] 06 p0856 N90-14976
Critical and subcritical crack-growth behavior along toughened ceramic/metal interfaces 07 p0889 N90-15140
Correlations between surface structure and catalytic activity/selectivity
[DE90-003755] 07 p0896 N90-15181
Metal film coatings on amorphous metallic alloys
[AD-D014308] 07 p0907 N90-15240
Micron-thin Nb films recovered from Mbar shock pressures
[DE90-001509] 07 p0998 N90-15772
Two-dimensional magnetic phase transition of ultrathin iron films on Pd(100)
[DE90-003555] 07 p1000 N90-15788
Epitaxial iron films
[AD-A213551] 07 p1003 N90-15807
Adhesion of silver films to ion-bombarded alumina
[DE90-005642] 09 p1199 N90-16947
Strain induced amorphization of aluminium by manganese implantation
[DE90-607259] 10 p1356 N90-17863
Time-resolved measurements of solidification and undercooling in metals and alloys
[DE90-007074] 11 p1488 N90-18564
Polymerization of nitro compounds on silver surfaces during surface-enhanced Raman scattering
[AD-A216116] 11 p1489 N90-18569
The interaction of polycrystalline copper films with dilute aqueous solutions of cupric chloride
[AD-A216465] 11 p1569 N90-19033
Surface-plasmon enhanced nonlinear photoelectric emission from thin silver films
[DE90-007676] 13 p1884 N90-20807
Application of x ray absorption edge spectrometry to the non-destructive determination of element concentrations, coating thickness and areal densities
[AERE-R-13030] 16 p2245 N90-22802
Microstructure of thin films
[AD-A219262] 16 p2324 N90-23255
Surface and interface studies by Auger electron spectroscopy
[ETN-90-96948] 18 p2522 N90-24398
Proof of principle study of thickness measurements using characteristic x ray line ratio techniques
[AD-A221113] 18 p2535 N90-24461

Platinized tin oxide catalysts for CO2 lasers: Effects of pretreatment 18 p2559 N90-24600
Adlayer physics
[AD-A221064] 19 p2673 N90-25203
Selective metallization of carbonyl-containing polymer films
[AD-D014526] 19 p2678 N90-25230
Sequentially evaporated thin film YBa2Cu3O(7-x) superconducting microwave ring resonator
[NASA-TM-103180] 19 p2685 N90-25273
Structural and electronic studies of a:SiGe:H alloys
[DE90-000313] 19 p2710 N90-25424
Ni impurity effects on hydrogen surface chemistry and etching of Si(111)
[AD-A222083] 21 p2977 N90-26921
Photoelectron spectroscopy at limit surfaces of semiconductors with rare Earth and alkali metals
[ETN-90-97322] 22 p3249 N90-28427
Ion-beam-assisted deposition of silver films on zirconia ceramics for improved tribological behavior
[DE90-009706] 24 p3456 N90-29516
Adhesion of silver films to ion-bombarded zirconia
[DE90-010088] 24 p3456 N90-29517

METAL FINISHING
NT ELECTROPOLISHING
NT SHOT PEENING
Application of high-rate cutting tools
[AD-A214644] 09 p1203 N90-16970
Electronics design of the infrared/ultrasonic sensing for a robot gripper
[PB90-160383] 21 p3010 N90-27109

METAL FLUORIDES
NT ALUMINUM FLUORIDES
NT CALCIUM FLUORIDES
NT LANTHANUM FLUORIDES
NT LITHIUM FLUORIDES
NT SODIUM FLUORIDES
NT STRONTIUM FLUORIDES
Corrosion and corrosion inhibition of metals/alloys in methylphosphonic difluoride and decontaminating solutions
[AD-A212404] 04 p0477 N90-12734
Proceedings of the High Energy Density Matter (HEDM) Conference
[AD-A212314] 05 p0629 N90-13670
Investigation of the phase stabilizing effect of potassium fluoride on ammonium nitrate
[AD-A213042] 06 p0753 N90-14381
Ternary reciprocal system of lithium and potassium fluorides and bromides
[DE90-004938] 10 p1352 N90-17840
Investigation of the phase stabilizing effect of 4 percent potassium fluoride on ammonium nitrate
[AD-A215313] 11 p1494 N90-18599
Feasibility of a super high energy density battery of the Li/BrF3 electrochemical system
[AD-A216575] 11 p1528 N90-18799
Mechanisms of reactive etching
[AD-A217679] 13 p1770 N90-20160

METAL FOILS
Stretched-membrane heliostats for solar central-receiver power plants
[DE89-016034] 01 p0084 N90-10476
Acceleration of thin foil targets using fiber-coupled optical pulses
[DE89-016526] 02 p0275 N90-11569
Exploding metallic foil fuse modeling at Los Alamos
[DE89-016970] 03 p0350 N90-11998
Electric-gun studies of conductors in high magnetic fields and experiments in dynamic flux compression
[DE90-000815] 06 p0768 N90-14470
Experimental investigation of a fast-acting exploding metallic foil opening switch
[DE90-001051] 06 p0770 N90-14479
Arc-sprayed coatings for electromagnetic pulse protection: Assessment of physical and electrical properties
[AD-A213825] 07 p0912 N90-15275
Instrumentation of pendulum impactor using metal foil strain gauges
[PB90-122656] 10 p1387 N90-18024
High-purity beryllium foils
[DE90-006408] 12 p1626 N90-19348
High temperature insulation barrier composite
[NASA-CASE-MFS-29241-1] 17 p2368 N90-23480
Analysis of strain relaxation in Au/Ni multilayers by x ray diffraction
[IAR-89-25] 20 p2875 N90-26357
Fabrication of intermetallic compounds by solid state reaction of roll-bonded materials
[AD-A221960] 21 p2982 N90-26943

METAL FORGING
U FORGING

METAL FORMING
U FORMING TECHNIQUES
U METAL WORKING

METAL FUELS
Metallized fuel particle size study in a solid fuel ramjet
[AD-A220079] 18 p2533 N90-24451

METAL GRINDING
Crystal preparation at LBL, 1976 to 1986
[DE90-007754] 13 p1894 N90-20871

METAL HALIDES
NT ALKALI HALIDES
NT ALUMINUM CHLORIDES
NT ALUMINUM FLUORIDES
NT BARIUM FLUORIDES
NT CALCIUM CHLORIDES
NT CALCIUM FLUORIDES
NT CESIUM IODIDES
NT COPPER CHLORIDES
NT IRON CHLORIDES
NT LANTHANUM FLUORIDES
NT LITHIUM CHLORIDES
NT LITHIUM FLUORIDES
NT METAL FLUORIDES
NT SILVER HALIDES
NT SODIUM CHLORIDES
NT SODIUM FLUORIDES
NT SODIUM IODIDES
NT STRONTIUM FLUORIDES
NT TITANIUM CHLORIDES
Preparation of ultra-pure metal halides
[AD-D014529] 19 p2674 N90-25204

METAL HARDENING
U HARDENING (MATERIALS)

METAL HYDRIDES
NT BERYLLIUM HYDRIDES
NT LITHIUM HYDRIDES
Effect of adsorbed arsenic on the decomposition rate of nickel hydride
[AD-A213245] 05 p0621 N90-13624
Anomalous strain rate dependence of the serrated flow in Ni-H and Ni-C-H alloys
[AD-A213244] 05 p0624 N90-13641
Studies of the structure and properties of amorphous a-Zr76Fe24Hx
[AD-A214646] 09 p1190 N90-16897
Hydride heat pumps for upgrading spacecraft waste heat 10 p1385 N90-18013
Mass spectrometric analysis of hydrogen isotopes in metals and metal hydrides
[DE90-014118] 23 p3303 N90-28685

METAL INSULATOR SEMICONDUCTORS
U MIS (SEMICONDUCTORS)

METAL IONS
NT FERRIC IONS
X ray diffraction patterns of metal aurocyanides
[DE89-015188] 03 p0326 N90-11851
Beam dynamics of a liquid metal ion source
[DE89-015856] 03 p0401 N90-12295
An apparatus for the electrodynamic containment of charged macroparticles 04 p0486 N90-12789
Host materials for transition-metal ions
[AD-A213605] 07 p1003 N90-15808
Broad-beam multi-ampere metal ion source
[DE90-003106] 08 p1059 N90-16123
Interaction between implanted ions and intrinsic defects in silica
[DE90-006569] 13 p1892 N90-20858
The high temperature behavior of gallium and indium liquid metal ion sources
[AERE-R-13321] 16 p2217 N90-22647
Biosensors for the detection of heavy metal ions
[MBB-Z-0289-89-PUB] 17 p2433 N90-23864
Theoretical studies of electrons and electron transfer processes in fluids
[DE90-008414] 17 p2470 N90-24117
A study of the influence of Hg(6(3)P2) population in a low-pressure discharge on mercury ion emission at 194.2 nm 20 p2853 N90-26223
Synthesis, structure, and properties of a new ternary metal nitride, Ca3CrN3
[AD-A222274] 21 p2978 N90-26924
High current metal ion implantation
[AD-A223098] 21 p3083 N90-27530
Structure of metal overlayers by low energy alkali ion scattering: Cu/Ru(0001) and Sn/Pt(111)
[DE90-014453] 23 p3310 N90-28718
Proceedings of the High Energy Density Materials Contractors Conference
[AD-A223793] 24 p3484 N90-29695

METAL JOINTS
NT SOLDERED JOINTS
NT WELDED JOINTS
Influence of hole surface finish, cyclic frequency and spectrum severity on the fatigue behavior of thick section aluminum alloy pin joints
[ARL-STRUC-R-430] 06 p0745 N90-14336
Fatigue of aluminium alloy joints with various fastener systems. Low load transfer
[ESDU-89046] 09 p1239 N90-17193

METAL MATRIX COMPOSITES
NT ALUMINUM BORON COMPOSITES
NT ALUMINUM GRAPHITE COMPOSITES
NT EUTECTIC COMPOSITES
Development of graphite-magnesium composites for space applications 02 p0185 N90-11054
Accelerated aging of metal matrix composites 02 p0190 N90-11085
Inorganic composite materials in Japan: Status and trends
[PB89-230015] 03 p0319 N90-11810
Deformation behavior of SiC/2014 Al metal-matrix composite
[AD-A212095] 03 p0320 N90-11816
Low temperature formation of titanium aluminide films using physical vapor deposition
[AD-A211877] 03 p0328 N90-11866
Biaxial flexing of a fiber-reinforced aluminum composite
[AD-A212742] 04 p0468 N90-12681
Corrosion and corrosion inhibition of metals/alloys in methylphosphonic difluoride and decontaminating solutions
[AD-A212404] 04 p0477 N90-12734
Ductile failure
[AD-A212975] 05 p0618 N90-13601
Carbon fiber reinforced metal matrix composites
[AD-D014245] 06 p0737 N90-14289
Analysis of metal matrix composite structures using a microchemical constitutive theory 06 p0737 N90-14290
A generalized thermomechanical constitutive model for metal matrix composites with plastic strain and damage 06 p0737 N90-14293
Parametric studies to determine the effect of compliant layers on metal matrix composite systems
[NASA-TM-102465] 06 p0737 N90-14294
Advances and future directions in superplastic materials 06 p0744 N90-14328
Fatigue properties of SiC/Al composites 07 p0889 N90-15138
Metal matrix composites with long inorganic fibers 07 p0901 N90-15206
Short fibre and particulate reinforced metal matrix composites 07 p0901 N90-15207
Metal matrix composites: A promising alternative to conventional alloys 07 p0901 N90-15208
Ductile failure
[AD-A213864] 07 p0948 N90-15488
New materials and structural concepts for space transportation systems 09 p1179 N90-16837
Metal matrix composite: Strengthening mechanisms
[AD-A214843] 09 p1186 N90-16871
Rapid solidification processing of composites
[AD-A215175] 09 p1187 N90-16875
The mechanisms of dispersion strengthening and fracture in Al-based XD (TM) alloys
[NASA-CR-4276] 09 p1187 N90-16879
Observations of fatigue crack initiation and damage growth in notched titanium matrix composites
[NASA-TM-101688] 10 p1347 N90-17815
Prediction of high temperature metal matrix composite ply properties
[NASA-TM-102490] 10 p1348 N90-17817
The processing and mechanical properties of high temperature/high performance composites. Book 4, section 3: Flow and creep strength
[AD-A216144] 10 p1349 N90-17822
Investigation of the failure modes in a metal matrix composite under thermal cycling
[AD-A216195] 10 p1349 N90-17825
Sputter deposition of diffusion barrier coatings on SiC monofilaments for use in Ti-based composites 11 p1477 N90-18502
Laboratory for the processing and evaluation of inorganic matrix composites
[AD-A216881] 11 p1480 N90-18516
Softening mechanisms and microstructural instabilities during high temperature, low cycle fatigue of Ni, Ni3Al, and their metal matrix composites
[DE90-006487] 11 p1487 N90-18557
Demonstration of capabilities of high temperature composites analyzer code HITCAN
[NASA-TM-102560] 12 p1676 N90-19629
Infiltration mechanics in conventional and hybridised fibre reinforced metal matrix composites
[AERE-R-13330] 13 p1766 N90-20134
Evaluation of thermal and mechanical loading effects on the structural behavior of a SiC/titanium composite
[NASA-TM-102536] 13 p1767 N90-20139
Compendium of abstracts and viewgraphs.
[AD-A217189] 13 p1767 N90-20140
Summary report of the Summer Conference of the DARPA-Materials Research Council
[AD-A217380] 13 p1767 N90-20143

Summary of the DoD Metal Matrix Composites (MMC) Steering Committee Meeting, hosted by the Institute for Defense Analysis
[AD-A217611] 13 p1768 N90-20145
Fundamental aspects of and failure modes in high-temperature composites
[NASA-TM-102558] 13 p1769 N90-20151
The effect of the SiC/Al interface on matrix microstructure in 2xxx-SiCp metal matrix
[AERE-R-13591] 13 p1775 N90-20184
The ageing effect of the matrix-reinforcement interface on the ageing response of an aluminium 6061 alloy reinforced with 20vol percent SiC particulates
[AERE-R-13361] 13 p1776 N90-20193
Reinforcement-matrix interface effects in metal matrix composites
[MRL-TN-562] 14 p1943 N90-21120
Acoustic characterisation of an aluminium silicon carbide metal matrix composite
[AERE-R-13273] 14 p1943 N90-21121
High temperature fatigue behavior of tungsten copper composites
[NASA-TM-102404] 14 p1946 N90-21138
Optimal fabrication processes for unidirectional metal-matrix composites: A computational simulation
[NASA-TM-102559] 14 p1947 N90-21143
Fatigue damage growth mechanisms in continuous fiber reinforced titanium matrix composites
[NASA-TM-102594] 14 p1991 N90-21409
METCAN verification status
[NASA-TM-103119] 15 p2064 N90-21824
Fatigue crack growth in unidirectional metal matrix composite
[NASA-TM-103102] 15 p2118 N90-22117
The elastic-plastic behavior of composite materials 16 p2212 N90-22615
Fatigue crack growth in a unidirectional SCS-6/Ti-15-3 composite
[NASA-TM-103095] 16 p2217 N90-22646
NASA-UVA light aerospace alloy and structures technology program
[NASA-CR-182607] 16 p2217 N90-22651
Environment enhanced fatigue of advanced aluminum alloys and composites 16 p2218 N90-22652
Investigation of the reaction kinetics between SiC fibers and selectively alloyed titanium matrix composites and determination of their mechanical properties 16 p2219 N90-22659
Inelastic response of metal matrix composites under biaxial loading 16 p2220 N90-22661
High temperature fatigue behavior of a SiC/Ti-24Al-11Nb composite
[NASA-TM-103157] 16 p2248 N90-22822
An orthotropic theory of viscoplasticity based on overstress for thermomechanical deformation and its application to laminated metal matrix composites 17 p2415 N90-23759
High temperature oxidation of Ni3Al composites
[DE90-010145] 18 p2517 N90-24373
Development of damped metal matrix composites for advanced structural applications
[AD-A219864] 18 p2518 N90-24380
Metal matrix composites microfracture: Computational simulation
[NASA-TM-103153] 18 p2518 N90-24383
A particle-level numerical simulation of the dynamic consolidation of a metal matrix composite material
[DE90-010950] 18 p2519 N90-24387
Metal matrix composites from dynamic consolidation of powder mixtures
[DE90-010951] 18 p2519 N90-24388
Thermomechanical testing techniques for high-temparature composites: TMF behavior of SiC(SCS-6)/Ti-15-3
[NASA-TM-103171] 19 p2701 N90-25367
Towards 2000: The composite engine
[PNR90646] 20 p2811 N90-26000
The influence of microstructure on the tensile behavior of an aluminum metal matrix composite
[NASA-TM-102694] 20 p2827 N90-26082
Metal matrix composites and powder processing for aero-engine applications
[PNR90617] 20 p2828 N90-26087
Investigation of thermo-mechanical effects in silicon carbide Whisker/Al alloy composites
[AD-A222635] 20 p2828 N90-26089
Study on failure modes of SiC fiber reinforced aluminum composite materials by AE method
[DE90-505518] 21 p2971 N90-26884
Corrosion protection of metal matrix composites
[AD-A222951] 21 p2971 N90-26888
Design of helicopter components in metal matrix composites
[REPT-100-20-55] 21 p2972 N90-26894
A summary of measurements of permittivities and permeabilities of some microwave absorbing materials
[AD-A223221] 21 p2995 N90-27026
Inorganic composite materials in Japan: Status and trends
[PB90-174392] 22 p3135 N90-27789
The effect of reinforcement stability on composition redistribution in cast aluminum metal matrix composites
[DE90-012469] 22 p3135 N90-27791
Effect of shock pressure on the structure and superconducting properties of Y-Ba-Cu-O in explosively fabricated bulk metal-matrix composites 22 p3138 N90-27804
Plane strain fracture toughness test procedures for particulate metal matrix composites
[NPL-DMM(A)-3] 22 p3153 N90-27873
Study of the behavior of Al metallic matrix + SiC composite materials under fatigue tests
[ETCA-89-R-077] 22 p3154 N90-27881
Micromechanics analysis of power consolidation in manufacturing particulate-reinforced MMCs (metal matrix composites)
[DE90-014448] 23 p3299 N90-28663
Inelastic analysis of laminated composites 23 p3301 N90-28669
Micromechanisms of fatigue crack growth and fracture toughness in metal matrix composites
[AD-A223863] 23 p3302 N90-28676
A theoretical investigation into the inelastic behavior of metal-matrix composites
[AD-A223973] 23 p3302 N90-28677
Evaluation of several micromechanics models for discontinuously reinforced metal matrix composites
[NASA-TM-102719] 23 p3339 N90-28872
Evaluation of ARALL-4: An aramid fiber reinforced aluminum
[AD-A223502] 24 p3443 N90-29443
Microstructure of alpha-Al base matrix/SiC particulate composites
[DE90-014894] 24 p3444 N90-29449
Characterization of unnotched SCS-6/Ti-15-3 metal matrix composites at 650 C
[NASA-TM-102699] 24 p3444 N90-29450
Proceedings of damping '89. Volume 1: Pages AAB-1 through DCD-11
[AD-A223431] 24 p3479 N90-29664
Proceedings of damping '89. Volume 2: Pages FAA-1 through IBD-15
[AD-A223432] 24 p3479 N90-29665

METAL NITRIDES
NT ALUMINUM NITRIDES
NT GALLIUM NITRIDES
NT TITANIUM NITRIDES
Synthesis, structure, electric, and magnetic properties of CaNiN
[AD-A222273] 21 p2978 N90-26923
Synthesis, structure, and properties of a new ternary metal nitride, Ca3CrN3
[AD-A222274] 21 p2978 N90-26924

METAL OXIDE SEMICONDUCTORS
NT CMOS
NT ITO (SEMICONDUCTORS)
NT SOS (SEMICONDUCTORS)
Bias and oxide thickness dependence of trapped charge buildup in MOS devices
[AD-A210264] 01 p0131 N90-10757
The analysis of current-mirror MOSFETs for use in radiation environments
[AD-A212527] 04 p0497 N90-12866
European Solid State Device Research Conference (18th) ESSDERC 88 held in Montpellier, France on 13-16 September 1988
[AD-A210618] 04 p0558 N90-13250
An accurate timing model for fault simulation in MOS circuits
[AD-A213153] 05 p0635 N90-13702
Design of a power component with IGBT insulated grid. Static and dynamic study
[ECL-88-22] 05 p0636 N90-13710
Multisensor technologies for low cost methane detection
[PB89-235188] 05 p0645 N90-13766
Unified model of charge build up and annealing of oxide charge and interface states in SiO2 due to stress
[HMI-B-465] 05 p0704 N90-14120
Characteristics of CMOS analog integrated structures using MOSIS (Metal Oxide Semiconductor Implementation System)
[DE90-001630] 07 p0998 N90-15773
Chemical profiling of silicon nitride structures
[AD-A215643] 09 p1192 N90-16907
Evaluation of doped phthalocyanines and a chemically-sensitive field effect transistor for detecting nitrogen dioxide
[AD-A215662] 09 p1214 N90-17037
Point defects and interfaces in insulating solids
[AD-A214668] 09 p1289 N90-17471
JSEP (Joint Services Electronics Program)
[AD-A215051] 09 p1290 N90-17476
Thermal characteristics of power MOS-FETS. Results obtained with the IRF-250 10 p1330 N90-17688
An assessment of the use of resonant-mode topologies for high frequency power conversion 10 p1335 N90-17726
Techniques for high frequency power conversion 10 p1336 N90-17729
Innovations in the design and matching of magnetic components and semiconductors up performance and reliability of power converters 10 p1336 N90-17731
International Summer School on Solid State Microbatteries
[AD-A213457] 10 p1434 N90-18277
An overview of radiation-induced interface traps in MOS (Metal-Oxide Semiconductor) structures
[AD-A216101] 10 p1438 N90-18299
Charge pumping as a measurement method for the characterization of short channel MOSFETS: Review, development, and comparison of measurement process
[ETN-90-95726] 12 p1654 N90-19504
Proton responses on MOS (Metal-Oxide-Semiconductor) electronics operating at cryogenic temperatures
[AD-A217622] 13 p1894 N90-20868
Study of advanced InSb arrays for SIRTF (Space Infrared Telescope Facility) 14 p1977 N90-21325
Burnout thresholds and cross section of power MOS transistors with heavy ions
[AD-A218998] 16 p2232 N90-22736
Statistical design of MOS VLSI (Very Large Scale Integrated) circuits with designed experiments
[AD-A219654] 17 p2396 N90-23647
Timing optimization of multi-phase sequential logic
[AD-A220836] 17 p2397 N90-23656
Predicting switched-bias response from steady-state irradiations
[DE90-006770] 18 p2624 N90-24950
Fundamental studies and device development in beta silicon carbide
[AD-A219253] 19 p2676 N90-25220
Neutron and gamma irradiation effects on power semiconductor switches
[NASA-TM-103200] 19 p2686 N90-25278
Role of surface passivation in the integrated processing of MOS structures
[AD-A222630] 20 p2859 N90-26264
Subthreshold technique for fixed and interface trapped charge separation in irradiated MOSFETs
[AD-A221861] 21 p3001 N90-27061
Extended characterization of the damage by hot charge carriers in gate oxide by short channel MOS field effect transistors
[ETN-90-97313] 24 p3555 N90-30114

METAL OXIDES
NT ALKALINE EARTH OXIDES
NT ALUMINUM OXIDES
NT BARIUM OXIDES
NT BERYLLIUM OXIDES
NT BISMUTH OXIDES
NT CALCIUM OXIDES
NT CERIUM OXIDES
NT CHROMIUM OXIDES
NT COBALT OXIDES
NT COPPER OXIDES
NT GALLIUM OXIDES
NT HAFNIUM OXIDES
NT ILMENITE
NT LANTHANUM OXIDES
NT LEAD OXIDES
NT LITHIUM OXIDES
NT MAGNESIUM OXIDES
NT MANGANESE OXIDES
NT MIXED OXIDES
NT MOLYBDENUM OXIDES
NT NICKEL OXIDES
NT NIOBIUM OXIDES
NT PLATINUM OXIDES
NT PLUTONIUM OXIDES
NT POTASSIUM OXIDES
NT RUTILE
NT SAPPHIRE
NT SILVER OXIDES
NT TANTALUM OXIDES
NT TIN OXIDES
NT TITANIUM OXIDES
NT TUNGSTEN OXIDES
NT URANIUM OXIDES
NT VANADIUM OXIDES
NT YTTRIUM OXIDES
NT ZINC OXIDES
NT ZIRCONIUM OXIDES

Thermodynamic properties of some metal oxide-zirconia systems
[NASA-TM-102351] 05 p0628 N90-13666
Micro-scale simulation of dynamic compaction of oxide and metal powder mixture
[DE90-002220] 06 p0856 N90-14978
Studies of organo phosphorus-, nitrogen-, and sulfur-containing molecules
[AD-A213516] 07 p0888 N90-15135
Alloying of metals for corrosion resistance
[AD-D014313] 09 p1194 N90-16919
Pulsed laser deposition of high T(sub c) superconducting thin films
[AD-A216507] 11 p1569 N90-19034
Metal alkoxides: Models for metal oxides. Alkoxide ligands in early transition metal organometallic chemistry
[DE90-007523] 13 p1894 N90-20869
Crystal preparation at LBL, 1976 to 1986
[DE90-007754] 13 p1894 N90-20871
Electronic properties of high-temperature superconductors
[AD-A217953] 13 p1898 N90-20892
CO-oxidation catalysts: Low-temperature CO oxidation over Noble-Metal Reducible Oxide (NMRO) catalysts
18 p2556 N90-24588
Applications of low temperature CO-oxidation catalysts to breathable gases 18 p2561 N90-24615
Passive mechanisms of surfaces produced by ion beam mixing and ion implantation
[AD-A222432] 21 p2982 N90-26945
A viologen/ruthenium oxide-based microelectrochemical diode with pH-dependent current-voltage characteristics
[AD-A221961] 21 p3000 N90-27052
Scaling behaviour of relaxation dependencies in metaloxide superconductors 22 p3138 N90-27802
Experimental and kinetic modeling of acid/base redox reactions over metal oxide catalysts
[DE90-013835] 22 p3156 N90-27893

METAL PARTICLES
NT METAL POWDER
NT POWDERED ALUMINUM
NT SINTERED ALUMINUM POWDER
Subsurface hardening and flow of aluminum during the incubation period of solid particle erosion
[DE90-010141] 18 p2525 N90-24409
Non-destructive characterization of polymer/metal interfaces using Surface-Enhanced Raman Scattering (SERS)
[AD-A223105] 21 p2986 N90-26967

METAL PLATES
Surface-catalyzed air oxidation of hydrazines: Environmental chamber studies
02 p0203 N90-11159
Acceleration of metal plates
[DE89-016816] 02 p0209 N90-11197
Thin section casting program. Volume 4: Static cast product bending, straightening, and rolling
[DE89-009034] 02 p0210 N90-11202
Laser-driven miniature flyer plates for shock initiation of secondary explosives
[DE89-016587] 02 p0225 N90-11288
Interferometry and high speed photography of laser-driven flyer plates
[DE89-016990] 02 p0225 N90-11290
Axial compression buckling test on the H-2 launch vehicle satellite fairing structural element prototype (aluminum surface plate/aluminum honeycomb sandwiched curved surface plate)
[NAL-TM-563] 03 p0356 N90-12039
The relationship between the mechanical properties of materials after press forming and their in-service properties
[CETIM-101530] 04 p0475 N90-12723
Carbonitrition response of steel plates not destined for heat treatments
[CETIM-106960] 04 p0476 N90-12728
Increased fragility of deep pressed thin plates
[CETIM-13-Y-313] 04 p0513 N90-12962
Mobility power flow analysis of an L-shaped plate structure subjected to acoustic excitation
[NASA-CR-186130] 05 p0655 N90-13817
Perturbations in high-velocity gas flow
[DE90-000539] 06 p0777 N90-14520
Comparison of multidimensional calculations of long-rod impacts on oblique plates
[DE89-015275] 07 p0939 N90-15440
Advanced tribological coatings for high specific strength alloys
[AD-A214061] 09 p1196 N90-16930
Analysis of biaxial stress fields in plates cracking at elevated temperatures
[AD-A216271] 10 p1397 N90-18077
Effects of oblique impact on hypervelocity shield performance
[DE90-006936] 11 p1517 N90-18739
Experimental investigation of condensation of steam in the presence of noncondensable gases using plate heat exchangers
[DE90-002251] 12 p1682 N90-19659
Evaluation of 2090-T8E48 aluminum-lithium plates
[AD-A217262] 13 p1776 N90-20196
Superconductive microprobes for eddy current evaluation of materials
[AD-A217776] 13 p1805 N90-20361
Flat plate vibration analysis experimental and numerical fillet study
[AD-A218789] 16 p2247 N90-22818
Heat sink effects on weld bead: VPPA process
[NASA-CR-186723] 19 p2697 N90-25349
Postbuckling response of long thick plates loaded in compression including higher order transverse shearing effects
[NASA-TM-102663] 19 p2700 N90-25363
Buckling and postbuckling behavior of square compression-loaded graphite-epoxy plates with circular cutouts
[NASA-TP-3007] 20 p2826 N90-26077
A comparison of the post-buckling behavior of metallic and composite plates with centrally located cutouts
[NIAR-90-14] 20 p2875 N90-26356
The response and failure mechanisms of circular metal and composite plates subjected to underwater shock loading
[AD-A222200] 21 p3013 N90-27131
Interaction of acoustic waves generated by coupled plate
[NASA-CR-186873] 21 p3072 N90-27464
Electrodeposition of wear resistant coatings
[PB90-221839] 23 p3312 N90-28732
Buckling and postbuckling behavior of compression-loaded isotropic plates with cutouts
[NASA-TP-3024] 23 p3337 N90-28859

METAL POLISHING
NT ELECTROPOLISHING

METAL POWDER
NT POWDERED ALUMINUM
NT SINTERED ALUMINUM POWDER
Fe-Ni-Cr alloys for coatings and electroforms
[PB89-195846] 03 p0325 N90-11849
Tribological properties of PM212: A high-temperature, self-lubricating, powder metallurgy composite
[NASA-TM-102355] 04 p0465 N90-12659
Temperature effects in shock consolidation of metal powders
[DE89-016782] 04 p0474 N90-12716
Micro-scale simulation of dynamic compaction of oxide and metal powder mixture
[DE90-002220] 06 p0856 N90-14978
A small, inexpensive apparatus for the determination of the density of powdered materials
[AD-A215393] 09 p1225 N90-17110
Laboratory for the processing and evaluation of inorganic matrix composites
[AD-A216881] 11 p1480 N90-18516
Method of making a long life high current density cathode from tungsten and iridium powders using a quarternary compound as the impregnant
[AD-D014425] 14 p1958 N90-21211
Method of making a cathode from tungsten powder
[AD-D014434] 15 p2069 N90-21850
Microstructure and mechanical properties of nickel aluminide powders consolidated by extrusion and hot isostatic pressing
[DE90-009777] 15 p2070 N90-21855
Institute for Materials Science and Engineering, nondestructive evaluation: Technical activities
[PB90-132739] 15 p2108 N90-22055
Undercooling and nucleation in rapid solidification rate metal powders using solid in solid emulsification
[AD-A218527] 17 p2375 N90-23526
Development of damped metal matrix composites for advanced structural applications
[AD-A219864] 18 p2518 N90-24380
Aligned bismuth, strontium, calcium cuprate coatings on polycrystalline substrates
[AD-D014522] 19 p2678 N90-25229
Pyrolysis and combustion of solid fuels under both subsonic and supersonic conditions
22 p3161 N90-27929
Micromechanics analysis of power consolidation in manufacturing particulate-reinforced MMCs (metal matrix composites)
[DE90-014448] 23 p3299 N90-28863
An effective low-profile thermite torch
[DE90-015746] 24 p3459 N90-29534

METAL PROPELLANTS
Proceedings of the High Energy Density Matter (HEDM) Conference
[AD-A212314] 05 p0629 N90-13670
Ignition and combustion characteristics of metallized propellants
[NASA-CR-186870] 21 p2976 N90-26911
Regression and combustion characteristics of boron containing fuels for solid fuel ramjets
22 p3161 N90-27928
An experimental investigation of strand burning metallized solid propellants
[AD-A224074] 24 p3457 N90-29526

METAL SHEETS
Micromechanisms of surface friction in zinc electrogalvanized steel sheets
[DE89-011819] 01 p0077 N90-10440
Thin section casting program. Volume 1: Executive summary and overview
[DE89-009030] 02 p0209 N90-11198
Deformation of extruded titanium alloys under superplastic conditions
[RAE-TM-MAT/STR-1111] 03 p0330 N90-11876
Effect of superplastic deformation on the surface roughness of sheet
[RAE-TM-MAT/STR-1112] 03 p0359 N90-12054
Corrosion and stress corrosion of aluminium-lithium alloys 07 p0898 N90-15190
Investigation on sheet material of 8090 and 2091 aluminium-lithium alloy 07 p0898 N90-15192
Superplastic performance and properties of the Lital Alloys 07 p0899 N90-15199
Uses and properties of Al-Li on the new EH101 helicopter 07 p0900 N90-15201
Aluminum-lithium: Application of plate and sheet to fighter aircraft 07 p0900 N90-15202
Fatigue crack propagation rates for titanium alloy sheet
[ESDU-89051] 09 p1201 N90-16956
Deformation and fracture of thin sheet aluminum-lithium alloys: The effect of cryogenic temperatures
16 p2218 N90-22655
Fabricating vanadium sheet to improve symmetry of drawn parts
[DE90-011253] 19 p2682 N90-25257
Fracture toughness and failure mechanisms in commercial 2091 Al-Li sheet at cryogenic temperatures
[AD-A222803] 20 p2835 N90-26125
An expert system advisor for damage repair of composite wing skins (repairman) 21 p2956 N90-26810
Evaluation of static and fatigue properties of thin sheets of 8090-T8 aluminum-lithium alloy and observation of its fracture surfaces
[NAL-TR-1039] 24 p3453 N90-29499
Fractographic analysis of fatigue crack growth under two-blocks loading on 2024-T351 sheet specimens
[LR-628] 24 p3482 N90-29680
Effects of blocks of overloads and underloads on fatigue crack growth in 2024-T351 sheet specimens: Fractographic analysis and crack closure predictions
[LR-629] 24 p3482 N90-29681

METAL SHELLS
The microwave permeability of conducting spherical shells
[AD-A220746] 17 p2369 N90-23485

METAL SPRAYING
Preparation and characterization of alumina films prepared by a novel spray pyrolysis method
[AD-A217570] 12 p1625 N90-19339

METAL STRIPS
Method for maintaining precise suction strip porosities
[NASA-CASE-LAR-13638-1] 12 p1641 N90-19427

METAL SURFACES
Structural and surface characterization of dispersed metal catalysts
[DE89-014530] 01 p0038 N90-10208
Quantitative interpretation of auger lineshapes and electron/photon stimulated desorption
[AD-A211550] 03 p0324 N90-11842
Mechanisms of CO2 reduction metal and metal modified semiconductor electrodes
[AD-A213169] 04 p0473 N90-12712
Noncontacting laser ultrasonic generation and detection at the surface of molten metal
[DE90-002020] 06 p0791 N90-14605
A method of soldering aluminum
[AD-D014226] 06 p0792 N90-14611
Surface modification of metals by ion beams
[DE90-001285] 07 p0903 N90-15218
Laser-material interactions
[AD-A214421] 07 p0937 N90-15425
The effect of primer age on adhesion of polysulphide sealant 08 p1022 N90-15909
Selectivity of the reactions of oxygenates on transition metal surfaces
[DE90-003911] 08 p1045 N90-16040
Solid state, surface, and catalytic studies of oxides
[DE90-004850] 08 p1134 N90-16566

Ion beam modification of metals: Mechanical properties and structure
[AD-A214701] 09 p1194 N90-16915
Theory of the dissociation dynamics of small molecules on metal surfaces: Finite temperature studies
[DE90-005217] 09 p1195 N90-16923
Compound for metallic surface treatment
[DE90-004121] 09 p1196 N90-16927
Chemistry at clusters, microstructures and surfaces
[AD-A215842] 10 p1353 N90-17844
Non-destructive characterization of epoxy/dicyandiamide interphases using surface-enhanced Raman scattering
[AD-A215894] 10 p1353 N90-17846
Surface-enhanced Raman scattering
[AD-A215976] 10 p1353 N90-17849
A review of the mechanism and kinetics of electrochemical hydrogen entry and degradation of metallic systems
[AD-A216671] 10 p1355 N90-17857
Surface modification of steels and aluminum alloys to control corrosion and hydrogen embrittlement. Part 1: Chemical methods
[AD-A216272] 10 p1356 N90-17866
Chemistry-structure-property interrelationships for calcareous deposits as stand-alone coatings
[AD-A216031] 10 p1359 N90-17881
Surface-enhanced Raman scattering from model acrylic adhesive systems
[AD-A216117] 10 p1359 N90-17883
International conference on Surface Modification of Metals by Ion Beams
[AD-A215872] 12 p1626 N90-19345
Surface characterization of hydrogen charged and uncharged alpha-2 and gamma titanium aluminide alloys using AES and REELS
[NASA-CR-186561] 14 p1951 N90-21171
Inelastic electron scattering from surfaces
[DE90-009365] 14 p2025 N90-21614
Characterization of particle impact by quantitative acoustic emission
[AERE-R-13028] 16 p2246 N90-22810
Modeling and experimental studies of oxide covered metal surfaces
[DE90-009961] 17 p2375 N90-23525
An investigation of the chemistry of silane coupling agents for adhesive bonding of aluminum
[AD-A220797] 17 p2381 N90-23560
Theoretical studies of photochemical methods for semiconductor etching
[AD-A218475] 17 p2475 N90-24151
Failure mechanisms of GaAs transistors: A literature survey
[AD-A221089] 18 p2548 N90-24543
A capacitance process for contact-free microfile measurement on metallic surfaces
[ETN-90-96503] 18 p2549 N90-24549
Characterization study of polycrystalline tin oxide surfaces before and after reduction in CO
18 p2559 N90-24601
Calorimetry, activity, and micro-FTIR analysis of CO chemisorption, titration, and oxidation on supported Pt
18 p2560 N90-24606
Characterization of the surfaces of platinum/tin oxide based catalysts by Fourier Transform Infrared Spectroscopy (FTIR) 18 p2560 N90-24608
Contract crystal growth and fabrication services
[AD-A221357] 18 p2623 N90-24947
Erosion mechanisms in composite materials and ripple formation mechanism in erosion
[IAR-89-4-PT-2] 20 p2826 N90-26079
Exact results for the structured liquid-solid interface
[AD-A222762] 20 p2922 N90-26630
Structure and dynamics of water at the Pt(111) interface: Molecular dynamics study
[AD-A222628] 20 p2933 N90-26687
Ni impurity effects on hydrogen surface chemistry and etching of Si(111)
[AD-A222083] 21 p2977 N90-26921
High resolution electron energy loss spectroscopy studies of chemisorbed species on metal surfaces
[AD-A222272] 21 p2978 N90-26922
Interfacial viscosity measurements of adsorbed monolayers on metal surfaces
[AD-A221689] 21 p2979 N90-26931
Passive mechanisms of surfaces produced by ion beam mixing and ion implantation
[AD-A222432] 21 p2982 N90-26945
Characterization of polymer interphases using surface-enhanced Raman scattering
[AD-A223103] 21 p2985 N90-26965
Microscopic modeling of tribological phenomena
[AD-A222049] 21 p3011 N90-27117
The epitaxial growth of copper on the (111) surface of silicon
[DE90-013817] 21 p3082 N90-27523
High current metal ion implantation
[AD-A223098] 21 p3083 N90-27530
Surfaces and interfaces of ceramics and metals
[DE90-014381] 22 p3160 N90-27920
Electrochemistry of metal surfaces
[AD-A224551] 24 p3445 N90-29458
An electron spin resonance study of adsorbed gases in ultrahigh vacuum
[ETN-90-97323] 24 p3447 N90-29469
Scanning tunneling microscopy studies of chemisorbed layers on metal surfaces
[DE90-015623] 24 p3450 N90-29486
A viscoelastic material model for computing stresses in glass
[DE90-014851] 24 p3481 N90-29673
Light scattering from surface and sub-surface defects
[DE90-016311] 24 p3546 N90-30058
Scanning tunneling microscopy of semiconductor surfaces
[AD-A223339] 24 p3552 N90-30095

METAL VAPOR LASERS
The electrical characteristic and gain behavior as a function of the radial distance from the laser axis in a copper vapor laser
[DE90-615371] 18 p2564 N90-24630

METAL VAPORS
Heat transfer in condensation of lithium vapors
[DE90-002081] 07 p0929 N90-15375
Metal vaporisers: Bicentennial series of five historical monographs
[ISBN-0-642-13584-3] 08 p1052 N90-16081

METAL WHISKER REINFORCEMENT
U WHISKER COMPOSITES

METAL WORKING
NT AUSFORMING
NT CLADDING
NT EXPLOSIVE FORMING
NT FORGING
NT METAL DRAWING
The relationship between the mechanical properties of materials after press forming and their in-service properties
[CETIM-101530] 04 p0475 N90-12723
Rolling of ARALL laminates (an alternative method for post-stretching ARALL laminates)
[LR-560] 04 p0484 N90-12778
Cold press lubrication: Fine tuning of the CETIM Forgelub test
[CETIM-105160] 04 p0509 N90-12938
Putting alloy 2091 to work 07 p0899 N90-15197
Investigation of metal processing technology
[AD-A218835] 17 p2376 N90-23531
Determination of the heat dissipated from a specimen undergoing cyclic plasticity by a hybrid numerical/experimental method
[AD-A221575] 21 p2982 N90-26946

METAL-GAS SYSTEMS
The formation of metal-oxygen species at low temperatures
[DE90-002298] 06 p0743 N90-14323
Evaluation of a diffusion/trapping model for hydrogen ingress in high strength alloys
[AD-A215528] 09 p1194 N90-16920
The temperature variation of hydrogen diffusion coefficients in metal alloys
[NASA-TM-100397] 15 p2067 N90-21836
Hydrogen in palladium alloys: Experiments, models and simulations
[PB90-200429] 22 p3156 N90-27896

METAL-INSULATOR-METAL SEMICONDUCTORS
U MIM (SEMICONDUCTORS)

METAL-METAL BONDING
Reflection by defective diffusion bonds
[AD-A212995] 05 p0623 N90-13638

METAL-OXIDE-METAL SEMICONDUCTORS
U MOM (SEMICONDUCTORS)

METAL-WATER REACTIONS
Mitigation of stress corrosion cracking of AISI 304 stainless steel in oxygenated water at 289 C by organic species at low concentration
[DE90-005631] 12 p1628 N90-19354

METALLIC GLASSES
Establishment and initial operation of a resource facility for RSR (Rapid Solidification Rate) processed alloys in pilot quantities
[AD-A210369] 01 p0050 N90-10283
Investigations of the influence of magnetically long range ordered phases on the electronic charge transport in metallic glasses
[ETN-89-94672] 02 p0202 N90-11155
Nucleation kinetics in undercooled, glass-forming metallic melts
[DLR-FB-89-32] 05 p0624 N90-13644
Computational studies of structural and transport properties of amorphous solids
[ETN-90-96027] 05 p0628 N90-13664
Method of making carbon dioxide and chlorine free fluoride-based glass
[AD-D014260] 08 p1048 N90-16060
Studies of the structure and properties of amorphous a-Zr76Fe24Hx
[AD-A214646] 09 p1190 N90-16897
Metallaboranes as precursors to metallic glasses
[AD-A216946] 11 p1490 N90-18577
Diffraction studies of the structure of glasses and liquids
[DE90-007662] 12 p1632 N90-19381
Low temperature properties of amorphous solids
15 p2171 N90-22405
Amorphization of metals by ion implantation and ion beam mixing
[DE90-620571] 16 p2221 N90-22667
Preparation of ultra-pure metal halides
[AD-D014529] 19 p2674 N90-25204
Containerless low gravity processing of glass forming and immiscible alloys
[NASA-CR-186999] 23 p3316 N90-28747

METALLIC PLASMAS
NT CESIUM PLASMA
Dynamically compressed metals: Theory
[AD-A210741] 01 p0045 N90-10257
Theory of interacting plasmas in space
07 p0993 N90-15742
Plasmon excitation in the scattering of electromagnetic waves from good conductors
[AD-A214026] 08 p1056 N90-16107
The effect of impurity gasses on variable polarity plasma arc welded 2219 aluminum
[NASA-CR-183803] 21 p2980 N90-26935

METALLIC STARS
An observational study of disk-population globular clusters 24 p3560 N90-30145

METALLICITY
An observational study of disk-population globular clusters 24 p3560 N90-30145
The evolution of horizontal branch stars and the calibration of globular cluster ages
24 p3562 N90-30152

METALLIZING
Reactive ion etching of sputtered silicon carbide and tungsten thin films for device applications
[AD-A211711] 03 p0325 N90-11847
Niobium and niobium nitride contacts on semiconducting material
[AD-D014177] 03 p0409 N90-12347
Wear-resistant coated object
[EP-PATENT-0-289-173-A1] 05 p0624 N90-13643
Growth characteristics and electronic behavior of ultrathin epitaxial metallizations
[AD-A214794] 09 p1289 N90-17474
Infrared and X ray photoelectron spectroscopy studies of the polyimide/metal interface
[AD-A218249] 13 p1773 N90-20179
Evaluation of abrasion-resistant metallized coatings for civil works applications
[AD-A221078] 18 p2530 N90-24438
Direct writing of microstructures for solid-state electronics
[AD-A220996] 18 p2535 N90-24460
Selective metallization of carbonyl-containing polymer films
[AD-D014526] 19 p2678 N90-25230
Resistivity, adhesive strength, and residual stress measurements of thin film metallizations on single crystal quartz
[DE90-011902] 20 p2837 N90-26135

METALLOGRAPHY
Development of texture analysis and its applications to titanium aero engine components
[PNR90561] 04 p0454 N90-12602
Internal and external nitriding and nitrocarburizing of iron and iron-based alloys
[ETN-90-96012] 05 p0625 N90-13646
Performance characteristics of a three-stage railgun
[DE90-002533] 06 p0729 N90-14254
Advanced tribological coatings for high specific strength alloys
[AD-A214061] 09 p1196 N90-16930
Phase properties of the rapid cooled palladium-silicon alloy in the concentration range 40 to 58 at. percent Si
[DE90-719525] 09 p1284 N90-17444
Analytical sciences
[DE90-007965] 14 p1948 N90-21152
TEM, positron lifetime, and hardness measurements of irradiated, cold-worked, and annealed Zr-1 percent Nb
[VTT-RR-650] 19 p2676 N90-25216
Damping capacity of aluminum 6061-indium alloys
[AD-A222802] 20 p2835 N90-26124
Determination of the NDT temperature and Charpy V-notch impact properties of AAR TC128 grades B steel and A 8XX grade B steel
[PB90-207804] 23 p3309 N90-28716

METALLOIDS
NT AMORPHOUS SILICON
NT ANTIMONY
NT ANTIMONY ISOTOPES
NT ARSENIC
NT BORON
NT BORON ISOTOPES
NT GERMANIUM
NT POLONIUM ISOTOPES
NT SILICON
NT SILICON ISOTOPES
NT TELLURIUM
NT TELLURIUM ISOTOPES
The synthesis and structure of stibaindoles
[AD-A222990] 21 p2976 N90-26914
METALLORGANIC COMPOUNDS
U ORGANOMETALLIC COMPOUNDS
METALLURGY
The damage tolerance of disc materials: Metallurgical factors; relationship with processing parameters 11 p1458 N90-18398
METALS
NT ALKALI METALS
NT ALKALINE EARTH METALS
NT ALUMINUM
NT ALUMINUM ISOTOPES
NT ALUMINUM 26
NT AMERICIUM
NT ANTIMONY ISOTOPES
NT BARIUM
NT BERYLLIUM
NT BISMUTH
NT CADMIUM
NT CALCIUM
NT CALCIUM ISOTOPES
NT CERIUM
NT CESIUM
NT CESIUM VAPOR
NT CHROMIUM
NT CHROMIUM ISOTOPES
NT COBALT
NT COBALT ISOTOPES
NT COBALT 60
NT COPPER
NT COPPER ISOTOPES
NT CURIUM
NT ERBIUM
NT ERBIUM ISOTOPES
NT EUROPIUM ISOTOPES
NT GADOLINIUM ISOTOPES
NT GALLIUM
NT GALLIUM ISOTOPES
NT GOLD
NT GOLD ISOTOPES
NT HAFNIUM
NT HOLMIUM
NT INDIUM
NT IRIDIUM
NT IRON
NT IRON ISOTOPES
NT LANTHANUM
NT LANTHANUM ISOTOPES
NT LEAD (METAL)
NT LEAD ISOTOPES
NT LIQUID LITHIUM
NT LIQUID METALS
NT LIQUID SODIUM
NT LITHIUM
NT LITHIUM ISOTOPES
NT MAGNESIUM
NT MAGNESIUM ISOTOPES
NT MANGANESE
NT MANGANESE ISOTOPES
NT MERCURY (METAL)
NT MERCURY ISOTOPES
NT METAL VAPORS
NT MOLYBDENUM
NT NEODYMIUM
NT NICKEL
NT NICKEL ISOTOPES
NT NIOBIUM
NT NIOBIUM ISOTOPES
NT NOBLE METALS
NT NONFERROUS METALS
NT PALLADIUM
NT PLATINUM
NT PLUTONIUM
NT POTASSIUM
NT PRASEODYMIUM
NT RARE EARTH ELEMENTS
NT REFRACTORY METALS
NT RHODIUM
NT RUBIDIUM
NT RUTHENIUM
NT SCANDIUM
NT SILVER
NT SODIUM
NT STRONTIUM
NT TANTALUM
NT TERBIUM
NT THALLIUM
NT THULIUM
NT TIN
NT TIN ISOTOPES
NT TITANIUM
NT TRANSITION METALS
NT TUNGSTEN
NT URANIUM
NT URANIUM ISOTOPES
NT VANADIUM
NT YTTERBIUM
NT YTTRIUM
NT ZINC
NT ZIRCONIUM
The structure determination of molecular adsorbates with large unit cells or lattice-gas disorder on metal surfaces
[AD-A210926] 01 p0042 N90-10230
Investigation of the pyrometallurgical, physical and mechanical behavior of weld metal
[AD-A211114] 01 p0046 N90-10258
Electron density modulation of catalytic metal centers by substituted aryl-isocyanide ligands
[AD-A212875] 04 p0473 N90-12708
Activities report of the metallic manufacturing industry
[ISSN-0524-7705] 05 p0625 N90-13649
Stress intensity factors for cracking metal structures under rapid thermal loading. Volume 2: Theoretical background
[AD-A213297] 05 p0654 N90-13812
Interaction of hydrogen isotopes with metals: Deuterium trapped at lattice defects in palladium
[DE90-000811] 06 p0747 N90-14344
Acoustic emission during intergranular stress corrosion cracking
[DE90-002894] 06 p0749 N90-14355
Proceedings of the Latin American Conference on the Applications of the Moessbauer Effect
[DE90-600819] 07 p1002 N90-15803
Fuel resistant coatings for metal and composite fuel tanks 08 p1022 N90-15911
Metals and Ceramics Division Materials Sciences Program
[DE90-004371] 08 p1050 N90-16070
Construction of inelastic stress-strain curves from minimal materials data (computer program)
[ESDU-89052] 09 p1239 N90-17189
The Hueckel model for small metal clusters. 4: Orbital properties and cohesive energies for model clusters of up to several hundred atoms
[AD-A216161] 10 p1354 N90-17852
Materials properties numerical database system established and operational at CINDAS/Purdue University 10 p1366 N90-17919
Fast optical switch and limiter using quantum size effect in metal grain composites
[AD-D014332] 12 p1619 N90-19305
Exchange and correlation effects in the Visscher-Falicov model for metal intercalated graphite
[DE90-610553] 12 p1627 N90-19349
Numerical modelling of shocks in gases and metals
[MRL-RR-8-89] 12 p1658 N90-19525
Principles of metallic solidification 13 p1784 N90-20241
Dynamics of the solidification front 13 p1785 N90-20243
Three-dimensional fatigue crack closure behavior of metals 15 p2070 N90-21857
High Intensity Electro-Magnetic and Ultrasonic Effects on Inorganic Materials Behavior and Processing Workshop
[AD-A218884] 16 p2215 N90-22640
Archaebacterial involvement in microbial metal corrosion: Metabolism of S and Fe
[AD-A219982] 17 p2377 N90-23537
Acousto-ultrasonic nondestructive evaluation of materials using laser beam generation and detection
[NASA-CR-186694] 17 p2398 N90-23664
Numerical modelling of shocks in gases and metals
[AD-A218586] 17 p2402 N90-23684
The trace metal geochemistry of suspended oceanic particulate matter
[AD-A218604] 17 p2429 N90-23839
The biogeochemistry of metal cycling
[NASA-CR-4295] 17 p2439 N90-23897
Thermal conductivity of metals 18 p2514 N90-24356
Vibrational and optical properties of amorphous metals
[DE90-011427] 18 p2522 N90-24403
Corrosion fatigue crack propagation in metals
[NASA-CR-4301] 18 p2524 N90-24405
Electromigration in metallic microstructures
[AD-A221208] 18 p2622 N90-24942
The thermal radiative properties of metals at high temperature
[DE90-012468] 21 p2981 N90-26938
Backscatter enhancement in scattering from rough surfaces
[AD-A223110] 21 p2995 N90-27024
Metal chloride cathode for a battery
[NASA-CASE-NPO-17809-1-CU] 21 p2998 N90-27041
Load-point compliance for the arc bend-arc support fracture toughness specimen
[AD-A221618] 21 p3014 N90-27134
Mass spectrometric analysis of hydrogen isotopes in metals and metal hydrides
[DE90-014118] 23 p3303 N90-28685
High temperature surface interactions: Overview 23 p3306 N90-28699
The use of automated ball indentation testing to measure flow properties and estimate fracture toughness in metallic materials
[DE90-015797] 24 p3452 N90-29493
Proceedings of Damping '89. Volume 3: Pages ICA-1 through KDC-15
[AD-A223433] 24 p3479 N90-29666
METAMORPHISM (GEOLOGY)
Metamorphism of cosmic dust: Processing from circumstellar outflows to the cometary regolith 08 p1146 N90-16641
Quantification of structural field data in the Rio Grande do Norte basin and neighborhood
[INPE-4821-RPE/591] 11 p1533 N90-18826
The patterns of fracture and the conditioning tectonics in the region of the Quadrilatero Ferrifero and part of the Migmatitic-Gnanulitic Complex in Minas Gerais (Brazil)
[INPE-4895-PRE/1496] 11 p1534 N90-18829
Geology of Espinhaco Meridional, including the Quadrilatero Ferrifero: Integration through remote sensing data
[INPE-4904-PRE/1505] 14 p1998 N90-21450
Astronaut's guide to terrestrial impact craters
[NASA-TM-102902] 17 p2421 N90-23798
METASTABILITY
U METASTABLE STATE
METASTABLE ATOMS
CANOES 2: Dynamics of atmospheric infrared thermochemical excitation, volume 4
[AD-A213344] 05 p0667 N90-13900
METASTABLE STATE
Development of metastable processing paths for high temperature alloys
[AD-A210550] 01 p0045 N90-10254
Ordered structures and metastable alloys grown by OMVPE
[DE89-016370] 01 p0129 N90-10744
CANOES 2: Dynamics of atmospheric infrared thermochemical excitation, volume 1
[AD-A213341] 05 p0667 N90-13897
CANOES 2: Dynamics of atmospheric infrared thermochemical excitation, volume 2
[AD-A213342] 05 p0667 N90-13898
CANOES 2: Dynamics of atmospheric infrared thermochemical excitation, volume 3
[AD-A213343] 05 p0667 N90-13899
Rotational energy transfer in metastable states of heteronuclear molecules
[AD-A214425] 08 p1120 N90-16485
Joint Services Electronics Program research in electronics
[AD-A217745] 13 p1796 N90-20307
Electronically metastable molecules of high symmetry
[AD-A217768] 13 p1885 N90-20814
Theoretical studies of spin-forbidden processes within the Breit-Pauli approximation
[AD-A217778] 13 p1885 N90-20815
Controlled production and characterization of metastable intermetallics
[DE90-009384] 14 p1952 N90-21176
Rigorous analysis of low temperature stochastic Ising models: Metastability and exponential approach to equilibrium
[PREPRINT-720] 16 p2312 N90-23175
A study of the influence of Hg(6(3)P2) population in a low-pressure discharge on mercury ion emission at 194.2 nm 20 p2853 N90-26223
Molecular beam epitaxial growth, characterization, and devices of modulated semiconductor structures
[AD-A221545] 21 p3084 N90-27538
Development of metastable processing paths for high temperature alloys
[AD-A223144] 22 p3157 N90-27898
Research on the structural and electronic properties of defects in amorphous silicon
[DE90-000342] 23 p3312 N90-28730

METAZOA
U ANIMALS
METEOR BURSTS
U METEOROID SHOWERS
METEOR CRATERS
U CRATERS
METEOR HAZARDS
U METEOROID HAZARDS
METEOR TRAILS
Preliminary investigation of Faraday rotation effects and description of polarization measurements on the AFGL high latitude meteor scatter test bed
[AD-A211298] 04 p0488 N90-12806
Experimentation of a transmission system data processing by meteor bursts 20 p2850 N90-26207
METEORITE COLLISIONS
Global nonlinear optimization of spacecraft protective structures design
[NASA-TM-100387] 14 p1938 N90-21095
Design of a thermal and micrometeorite protection system for an unmanned lunar cargo lander
[NASA-CR-186682] 19 p2664 N90-25161
METEORITE COMPRESSION TESTS
U COMPRESSION TESTS
U MECHANICAL PROPERTIES
U METEORITES
METEORITE CRATERS
Radar scattering mechanisms within the meteor crater ejecta blanket: Geologic implications and relevance to Venus 03 p0424 N90-12435
Deducing the age of the dense Venus atmosphere 03 p0425 N90-12438
Astronaut's guide to terrestrial impact craters
[NASA-TM-102902] 17 p2421 N90-23798
METEORITES
NT ACHONDRITES
NT ALLENDE METEORITE
NT CARBONACEOUS CHONDRITES
NT CARBONACEOUS METEORITES
NT CHONDRITES
NT IRON METEORITES
NT MICROMETEORITES
NT MURCHISON METEORITE
Abstracts for the 52nd Annual Meeting of the Meteoritical Society
[NASA-CR-186160] 06 p0860 N90-14998
The carbon chemistry of meteorites: Relationships to comets 08 p1141 N90-16615
Evolution of carbonaceous chondrite parent bodies: Insights into cometary nuclei 08 p1145 N90-16638
Isotopic microanalysis of returned comet nucleus samples 08 p1149 N90-16655
Guide to the US collection of antarctic meteorites 1976-1988 (everything you wanted to know about the meteorite collection). Antarctic Meteorite Newsletter, Volume 13, Number 1
[NASA-TM-101939] 09 p1299 N90-17526
Proceedings of a Workshop on Antarctic Meteorite Stranding Surfaces
[NASA-CR-186575] 20 p2942 N90-26739
Proceedings of a workshop on Differences Between Antarctic and Non-Antarctic Meteorites
[NASA-CR-184918] 20 p2942 N90-26740
Carbon in comet dust 21 p3089 N90-27564
The possible presence of interstellar PAHs in meteorites and interplanetary dust particles 21 p3092 N90-27579
Raman spectroscopic studies of carbon in extra-terrestrial materials 21 p3095 N90-27589
METEORITIC COMPOSITION
Meteoritic basalts
[NASA-CR-185949] 06 p0861 N90-15004
Identification of solar nebula condensates in interplanetary dust particles and unequilibrated ordinary chondrites 08 p1144 N90-16629
Composition of dust from Comet P/Halley: The mineral fraction 08 p1144 N90-16631
The comet rendezvous asteroid flyby mission 08 p1145 N90-16639
Press abstracts of the 21st Lunar and Planetary Science Conference
[NASA-CR-186874] 20 p2941 N90-26738
Carbon in comet dust 21 p3089 N90-27564
Survival of carbon grains in shocks 21 p3090 N90-27567
Diamonds in detonation soot 21 p3094 N90-27585
METEORITIC DAMAGE
Micrometeoroid impacts on silver bus bar targets at elevated voltages 10 p1346 N90-17805
Simulation of micrometeoroid impacts by laser pulses 10 p1346 N90-17806
Technology evaluation for space station atmospheric leakage
[DE90-007844] 12 p1616 N90-19294
METEORITIC DIAMONDS
Carbon in the Galaxy: Studies from Earth and Space
[NASA-CP-3061] 21 p3089 N90-27562
Survival of carbon grains in shocks 21 p3090 N90-27567
Diamonds in detonation soot 21 p3094 N90-27585
METEORITIC DUST
U MICROMETEOROIDS
METEORITIC IONIZATION
U METEOR TRAILS
METEORITIC MICROSTRUCTURES
An atom probe study of phase decomposition in three iron meteorites
[DE89-017581] 03 p0421 N90-12420
METEOROID CONCENTRATION
Reexamination of data from the asteroid/meteoroid detector
[NASA-CR-185997] 05 p0714 N90-14175
Proceedings of a workshop on Differences Between Antarctic and Non-Antarctic Meteorites
[NASA-CR-184918] 20 p2942 N90-26740
METEOROID CRATERS
U METEORITE CRATERS
METEOROID DUST CLOUDS
NT ZODIACAL DUST
METEOROID HAZARDS
Numerical simulation of micrometeroids and debris hypervelocity impacts on Columbus pressurized modules 02 p0188 N90-11075
METEOROID PROTECTION
Key structures mechanical issues of the European Space Station and platform program Columbus 02 p0188 N90-11072
Numerical simulation of micrometeroids and debris hypervelocity impacts on Columbus pressurized modules 02 p0188 N90-11075
On protection of Freedom's solar dynamic radiator from the orbital debris environment. Part 1: Preliminary analyses and testing
[NASA-TM-102458] 06 p0736 N90-14285
Simulation of micrometeoroid impacts by laser pulses 10 p1346 N90-17806
METEOROID SHOWERS
Development of a parallel link model for meteor burst communication
[AD-A215629] 09 p1208 N90-17001
A digital Meteor-Burst Communication (MBC) propagation path simulator 20 p2847 N90-26190
Meteor burst communications systems
[AD-A221675] 21 p2997 N90-27037
METEOROIDS
NT MICROMETEOROIDS
NT ZODIACAL DUST
Reexamination of data from the asteroid/meteoroid detector
[NASA-CR-185997] 05 p0714 N90-14175
USAF/GL meteor scatter data analysis program: A user's guide
[AD-A214988] 09 p1206 N90-16989
Meteor observations using the 50 MHz MENTOR imaging Doppler interferometer
[AD-A217908] 13 p1790 N90-20276
Meteor radar studies of the mesopause region and nonlinear atmospheric waves 17 p2421 N90-23799
Meteor burst communications systems
[AD-A221675] 21 p2997 N90-27037
METEOROLOGICAL CHARTS
Meteorological support: Descriptions of application programs for accessing and displaying data
[PB89-194625] 01 p0088 N90-10500
Research highlights of the NMC (National Meteorological Center) Development Division: 1987-1988
[PB89-206478] 01 p0088 N90-10501
Diagnostic study of atmosphere-terrain interaction leading to the formation of dust clouds and poor visibilities over near east desert areas
[AD-A211243] 02 p0239 N90-11358
The development of a spatial synoptic climatological index for environmental analysis 06 p0816 N90-14744
Use of operational 0-6 and 3-9 h quantitative precipitation forecasts for predicting heavy rain events
[PB90-103946] 06 p0817 N90-14750
Precipitation distributions associated with cyclones originating over the Gulf of Mexico and surrounding coastal regions
[AD-A213644] 07 p0963 N90-15589
Global distribution of total cloud cover and cloud type amounts over the ocean
[DE90-003187] 07 p0964 N90-15574
Automated system for meteorological analysis
[INPE-4586-TDL/332] 23 p3352 N90-28945
METEOROLOGICAL FLIGHT
Meteorological atlas of the Northern Hemisphere lower stratosphere for January and February 1989 during the Airborne Arctic Stratospheric Expedition
[NASA-TM-4145] 05 p0671 N90-13908
Global stratospheric change: Requirements for a Very-High-Altitude Aircraft for Atmospheric Research
[NASA-CP-10041] 06 p0723 N90-14220
METEOROLOGICAL INSTRUMENTS
NT BAROMETERS
NT CLOUD HEIGHT INDICATORS
NT IONOSONDES
NT RADIOSONDES
NT RAIN GAGES
NT RAWINSONDES
NT WEATHER DATA RECORDERS
NT WIND VANES
Meeting Review: Workshop on Airborne Instrumentation
[PB89-174775] 01 p0007 N90-10032
A program to improve performance of AFGL (Air Force Geophysical Laboratory) automated present weather observing sensors
[AD-A207669] 01 p0087 N90-10495
The Tactical Environmental Support System (TESS(3)) 06 p0757 N90-14409
Meteorological monitoring for environmental/dose assessment and emergency response modeling: How much is enough
[DE90-002726] 06 p0818 N90-14757
Accuracy and precision of GOES data collection platforms for temperature measurements
[AD-A218798] 16 p2250 N90-22832
AFGW's upper air validator system
[AD-A219309] 16 p2258 N90-22876
Impact of a unified DMSP meteorological sensor retrieval methodology on global numerical weather prediction
[AD-A220306] 18 p2581 N90-24703
Methodology investigation calibration and quality control for new meteorological instrumentation, part 1
[AD-A221407] 18 p2582 N90-24706
Improved meteorological measurements from buoys and ships (IMET): Preliminary conventions from buoys and standards data and file formats
[PB90-241910] 22 p3229 N90-28312
Improved meteorological measurements from buoys and ships (IMET): Preliminary comparison of solar radiation air temperature shields
[PB90-241928] 22 p3229 N90-28314
METEOROLOGICAL PARAMETERS
Atmospheric transmissivity update - 1988
[AD-A209130] 01 p0085 N90-10484
Mariners Weather Log, volume 32, number 3, Summer 1988
[PB88-248075] 01 p0086 N90-10491
National Severe Storms Laboratory, fiscal year 1988
[PB89-156145] 01 p0087 N90-10493
A case study evaluation of satellite-derived rainfall estimates and their application to numerical model precipitation forecast verification
[PB89-194591] 01 p0088 N90-10499
Atmospheric environment for space shuttle (STS-29) launch
[NASA-TM-100376] 02 p0175 N90-10980
Atmospheric environment for space shuttle (STS-30) launch
[NASA-TM-100381] 02 p0175 N90-10981
Hurricane Research Division fiscal year 1988 programs, fiscal year 1989 projections
[PB89-152268] 02 p0250 N90-11418
National Center For Atmospheric Research annual report, fiscal year 1988
[PB89-208987] 02 p0252 N90-11428
Interannual variability of temperature in the upper layer of the North Pacific eastern boundary region, 1971-1987
[PB89-190227] 02 p0253 N90-11434
The sea ice margins: A summary of physical phenomena
[PB89-212328] 02 p0253 N90-11436
ASR-9 weather channel test report
[AD-A211749] 03 p0339 N90-11934
MEGALIDAR
[AD-A212074] 03 p0353 N90-12020
Radar polarimetric studies based on the MAYPOLE 1983 and 1984 field experiments
[AD-A212226] 04 p0492 N90-12830
Meteorological Satellite Center Technical Note, no. 18, 1989
[MSC-TN-18] 04 p0519 N90-12997
Project WIND: Experiments with the UK Meteorological Office mesoscale model
[AD-A212291] 04 p0521 N90-13006
Estimation of rain rate using spatial and multichannel coherence: Analysis of SSM/I data 05 p0670 N90-13905

A forecasting system using the parabolic equation: Application to surface-to-air propagation in the presence of elevated layers 06 p0760 N90-14420
Propagation prediction for the North Sea environment 06 p0760 N90-14423
The thermal behavior of natural backgrounds and its prediction by means of numerical models 06 p0762 N90-14436
Climatology of Lawrence Livermore National Laboratory [DE90-000905] 06 p0818 N90-14756
Meteorological monitoring for environmental/dose assessment and emergency response modeling: How much is enough [DE90-002726] 06 p0818 N90-14757
Winter cloud seeding potential on the Mogollon Rim [PB89-190540] 07 p0962 N90-15562
Frontal clouds and flight conditions in them [AD-A214250] 07 p0964 N90-15573
Climatic summaries and documentation for the primary meteorological Station, H. J. Andrews Experimental Forest, 1972 to 1984 [PB90-104373] 08 p1102 N90-16382
Sea surface temperature fields derived from aircraft and ship observations during FASINEX 1986 [AD-A215727] 09 p1250 N90-17250
Low elevation angle KU-band satellite measurements at Austin, Texas 10 p1373 N90-17959
Surface observation climatic summaries [AD-A215786] 10 p1406 N90-18122
On the relationship between water vapor over the oceans and sea surface temperature [NASA-CR-186199] 10 p1409 N90-18127
Sounding and surface meteorological data from the Land/Sea Breeze Experiment (LASBEX) [AD-A216269] 11 p1536 N90-18842
Proceedings of the Professional Pilots Meteorology Training Standards Conference [AD-A216618] 11 p1536 N90-18843
Transport of atmospheric aerosols above the Sierra Nevada slopes [PB90-120288] 12 p1685 N90-19675
Validation of the EURAD cloud modules 12 p1687 N90-19693
Forecasting the tornadic intensities of thunderstorms by multivariate techniques [AD-A218284] 13 p1847 N90-20602
Weather data dissemination to aircraft 14 p1907 N90-20934
Data Link Processor (DLP) project transition plan [DOT/FAA/CT-TN89/68] 14 p1965 N90-21256
Transformation and deposition of airborne gaseous and particulate pollutants during transport over the Baltic Sea [PUBL-AIR-QUALITY-5] 14 p2003 N90-21478
A survey of the maritime-aerosol data collected at South Uist and the implications for the LOWTRAN maritime aerosol model 15 p2079 N90-21908
Millimetric, infrared, and optical propagation studies over a 500 m path 15 p2080 N90-21913
Evaporation duct effects at millimeter wavelengths 15 p2080 N90-21914
Interpreting meteorological data reports for LOWTRAN Navy aerosol model extinction calculations 15 p2082 N90-21920
The naval oceanic vertical aerosol model 15 p2082 N90-21921
Lidar measurements of the optical propagation environment 15 p2084 N90-21930
Lidar measurement of concentration and turbulence in battlefield obscurants 15 p2084 N90-21931
Technique for selecting an aerosol model useful for infrared atmospheric transmittance calculations 15 p2085 N90-21934
Calculation of IR propagation statistics in the eastern Atlantic for surveillance system performance assessment 15 p2085 N90-21938
Atmospheric modelling studies: A modelling comparison between IR and millimetric atmospheric propagation 15 p2086 N90-21941
The observed three-dimensional structure of baroclinic waves in the Northern Hemisphere winter as revealed in a linear regression analysis 15 p2128 N90-22167
JARE data reports, no. 140 (meteorology 21): Meteorological data at Asuka Camp, Antarctica in 1987 [ISSN-0075-3343] 15 p2132 N90-22188
Accuracy and precision of GOES data collection platforms for temperature measurements [AD-A218798] 16 p2250 N90-22832
A study of mesoscale acid deposition in the lower Ohio River Valley 16 p2253 N90-22848
US Navy regional climatic study of southern African waters [AD-A218792] 16 p2258 N90-22874
US Navy regional climatic study of the Mozambique channel and adjacent waters [AD-A218793] 16 p2258 N90-22875
AFGW's upper air validator system [AD-A219309] 16 p2258 N90-22876
Development and use of a passive technique for measuring nitrogen dioxide in the background atmosphere 16 p2331 N90-23285
Handbook of climate of the USSR. Humidity of air, atmospheric precipitations, snow cover [AD-A220454] 17 p2427 N90-23828
Radio refractivity profiles deduced from lidar measurements [AD-A221727] 21 p3026 N90-27208
On airborne measurements of radiation from broken cloud fields [MITT-67] 21 p3027 N90-27211
The test for automatic neph-analysis chart 21 p3029 N90-27219
Evaluation of correlations between meteorological measurements and observations of lightning activity using artificial neural systems [AD-A222659] 21 p3030 N90-27229
Tactical applications of Defense Meteorological Satellite Program (DMSP) environmental data 21 p3067 N90-27439
Atmospheric environment for space shuttle (STS-33) launch [NASA-TM-100399] 22 p3200 N90-28159
A comparison of ISCCP and FIRE satellite cloud parameters 22 p3221 N90-28267
Regional conditions during the 25 October 1986 FIRE cirrus/altocumulus case study 22 p3225 N90-28287
A system for recording physical properties of clouds 22 p3227 N90-28301
Cirrus parameterization from the FIRE ER-2 observations 22 p3227 N90-28302
Atmospheric environment for Space Shuttle (STS-32) launch [NASA-TM-100400] 23 p3346 N90-28912
Atmospheric environment for Space Shuttle (STS-31) launch [NASA-TM-103508] 23 p3347 N90-28913
Atmospheric environment for space shuttle (STS-36) launch [NASA-TM-100403] 23 p3347 N90-28914
Atmospheric environment for space shuttle (STS-34) launch [NASA-TM-100396] 23 p3347 N90-28915
Estimating the spatial variability of trace gas deposition velocities [PB90-208570] 23 p3349 N90-28928
Automated system for meteorological analysis [INPE-4586-TDL/332] 23 p3352 N90-28945
Meteorological conditions over the North Atlantic Ocean during GCE/CASE/WATOX [PB90-252032] 24 p3494 N90-29747

METEOROLOGICAL PROBES
U SONDES

METEOROLOGICAL RADAR
A study of the impact of simulated satellite lidar wind observations [AD-A210430] 01 p0086 N90-10488
The effectiveness of adaptive PRF (Pulse Repetition Frequency) selection in minimizing range obscuration in the TDWR (Terminal Doppler Weather Radar) system [AD-A211267] 02 p0213 N90-11222
ASR-9 weather channel test report [AD-A211749] 03 p0339 N90-11934
Middle Atmosphere Program. Handbook for MAP, volume 28 [NASA-CR-184972] 03 p0370 N90-12117
Adaptive clutter rejection filters for airborne Doppler weather radar applied to the detection of low altitude windshear [NASA-CR-186211] 06 p0766 N90-14453
A case study of the 24 August 1986 FLOWS microburst [AD-A216939] 11 p1537 N90-18847
Rain radars for earth science geostationary platforms: Some possibilities 12 p1610 N90-19262
Cockpit display of hazardous wind shear information 14 p1905 N90-20924
Meteorologist Weather Processor (MWP) integration test plan [DOT/FAA/CT-TN89/62] 14 p2007 N90-21500
Gravity wave and turbulence studies using a high-resolution ST radar [AD-A218877] 16 p2255 N90-22860
Next generation weather radar (NEXRAD) initial operational test and evaluation. Phase 2: (IOT and E(2)) [AD-A218770] 16 p2258 N90-22873
Use of clutter residue editing maps during the Denver 1988 Terminal Doppler Weather Radar (TDWR) tests [AD-A218696] 17 p2426 N90-23822
Utilization of higher frequencies for satellite communications: Determination of atmospheric effects using experiments and models [DLR-FB-89-46] 18 p2544 N90-24518
Derivation of wind fields from Doppler measurements of a single radar and application to a cold front with narrow rainband [DLR-FB-89-61] 18 p2582 N90-24705
Analysis and improved design considerations for airborne pulse Doppler radar signal processing in the detection of hazardous windshear [NASA-CR-186792] 20 p2890 N90-26448
Ground-based weather radar compatibility with digital radio-relay microwave systems [PB90-206236] 23 p3318 N90-28756
A personal computer-based, multitasking data acquisition system [NASA-TM-4232] 23 p3382 N90-29107

METEOROLOGICAL RESEARCH AIRCRAFT
Scientific justification and development plan for a mid-sized jet research aircraft [PB89-208995] 03 p0305 N90-11731
Meeting review: The Second NCAR (National Center for Atmospheric Research) Research Aircraft Fleet Workshop [PB89-200901] 03 p0369 N90-12113
Meteorological conditions over the North Atlantic Ocean during GCE/CASE/WATOX [PB90-252032] 24 p3494 N90-29747

METEOROLOGICAL ROCKETS
U SOUNDING ROCKETS

METEOROLOGICAL SATELLITES
NT DMSP SATELLITES
NT ITOS SATELLITES
NT METEOSAT SATELLITE
NT NIMBUS 7 SATELLITE
NT NOAA SATELLITES
NT SAN MARCO SATELLITES
NT TIROS N SERIES SATELLITES
NT TIROS SATELLITES
Thermodynamic and dynamic processes in the updraft region of GALE (Genesis of Atlantic Lows Experiment) IOP (Intensive Observation Period) 9 [AD-A208139] 01 p0087 N90-10496
A case study evaluation of satellite-derived rainfall estimates and their application to numerical model precipitation forecast verification [PB89-194591] 01 p0088 N90-10499
A study of the impact of simulated 183 GHz water vapor retrievals on numerical weather prediction [AD-A210431] 01 p0088 N90-10504
Meteorological rocket observations [PB89-168769] 02 p0250 N90-11419
Composited local area forecast techniques [AD-A210802] 02 p0253 N90-11432
Meteorological Satellite Center Technical Note, no. 18, 1989 [MSC-TN-18] 04 p0519 N90-12997
A collection of papers related to heavy precipitation forecasting [PB89-230833] 05 p0671 N90-13910
Weather satellite and computer modeling approaches to assessing propagation over marine environments 06 p0764 N90-14443
Identification and quantification of synoptic structure in simulated TIROS N radiance soundings [AD-A213729] 07 p0960 N90-15553
Polar cusps latitudinal shift and its relation to the IMF-By component [IFSI-88-14] 08 p1101 N90-16377
World Weather Watch. Global observing system-satellite sub-system. Information on meteorological and other environmental satellites, second edition [WMO-411-ED-2] 08 p1103 N90-16386
Compendium of meteorological space programs, satellites, and experiments [NASA-TM-102924] 12 p1607 N90-19243
Forecasting 24 and 48 hour intensity changes, for northwestern Pacific tropical cyclones, using satellite imagery [AD-A218174] 13 p1846 N90-20597
Research programs: Meteorological prediction. Oceanic processes. Climate and global change monitoring. Satellite instrumentation and calibration 19 p2714 N90-25447
The main products and their distribution of FY-1 meteorological satellite [AD-A221582] 21 p2967 N90-26865
Dust clouds Kosa from the east Asian dust storms in 1982-1988 as observed by the GMS satellite 21 p3028 N90-27214
Reproduction of GMS IR calibration table 21 p3028 N90-27215

Distribution and movement of smokes from forest fires that occurred along the boundary of the People's Republic of China and the USSR on April-May 1987
21 p3028 N90-27216
Investigation into position accuracy of typhoon center determined on GMS imagery 21 p3028 N90-27217
Application of automatic method to estimating high-level cloud motion wind in operational system and the characteristics of the resultant wind vectors
21 p3028 N90-27218
Behavior of dust clouds from Australian dust storms in 1982-1983 as observed by the GMS
21 p3029 N90-27221
An experiment to make a new design of the Satellite Cloud Information Chart with the combination of visible and infrared data observed by the GMS
21 p3029 N90-27223
Application of Meteorological Satellite (METSAT) data to support United States forces in the North Atlantic Treaty Organization (NATO) 21 p3068 N90-27440
Tactical oceanography from space: The next decade
21 p3068 N90-27442

METEOROLOGICAL SERVICES
Forecasting convection with the AFOS (Automation of Field Operations and Services) data analysis programs. (ADAP-version 2.0) (AFOS data analysis programs-version 2.0)
[PB89-145940] 01 p0086 N90-10492
National Severe Storms Laboratory, fiscal year 1988
[PB89-156145] 01 p0087 N90-10493
A program to improve performance of AFGL (Air Force Geophysical Laboratory) automated present weather observing sensors
[AD-A207669] 01 p0087 N90-10495
Meteorological support: Descriptions of application programs for accessing and displaying data
[PB89-194625] 01 p0088 N90-10500
Meteorological rocket observations
[PB89-168769] 02 p0250 N90-11419
ASR-9 weather channel test report
[AD-A211749] 03 p0339 N90-11934
Contemporary China's meteorological enterprises (selected portions)
[AD-A210697] 03 p0373 N90-12131
World Weather Watch: Implementation
[WMO-714] 03 p0375 N90-12139
Summary of papers, studies, conference presentations: 1987-1988 (from the National Weather Service, southern region)
[PB90-103896] 06 p0817 N90-14749
Plan for the FAA air traffic operational evaluation of the Automated Surface Observing System (ASOS)
[DOT/FAA/CT-TN89/56] 14 p1914 N90-20968
Meteorologist Weather Processor (MWP) integration test plan
[DOT/FAA/CT-TN89/62] 14 p2007 N90-21500
Some results from the precipitation chemistry measurement programme in Sweden
20 p2884 N90-26410
Modernization of PRC meteorological service
[AD-A221761] 21 p3032 N90-27236
DMSP's interactive tactical terminal
21 p3068 N90-27441
Flight service automation system, model 1 full capacity, NAS operational test and evaluation integration test plan
[DOT/FAA/CT-TN90/4] 22 p3111 N90-27672
Program on development of basic understanding of severe weather phenomena
[PB90-226564] 23 p3352 N90-28943

METEOROLOGICAL STATIONS
U WEATHER STATIONS

METEOROLOGY
NT AEROLOGY
NT AGROMETEOROLOGY
NT ALPINE METEOROLOGY
NT AVIATION METEOROLOGY
NT HYDROMETEOROLOGY
NT MARINE METEOROLOGY
NT MESOMETEOROLOGY
NT MICROBURSTS (METEOROLOGY)
NT MICROMETEOROLOGY
NT NUMERICAL WEATHER FORECASTING
NT PLANETARY METEOROLOGY
NT POLAR METEOROLOGY
NT STATISTICAL WEATHER FORECASTING
NT SYNOPTIC METEOROLOGY
NT TROPICAL METEOROLOGY
NT WEATHER FORECASTING
Examples of meteorological behavior of the ionosphere 02 p0246 N90-11395
Hanford Meteorological Station computer codes. Volume 10: The ARCHIVE computer code
[DE89-016175] 02 p0252 N90-11429
Scientific justification and development plan for a mid-sized jet research aircraft
[PB89-208995] 03 p0305 N90-11731
Semi-Lagrangian, semi-implicit solutions of the shallow water equations in one dimension
[AD-A212658] 04 p0503 N90-12902
Project WIND: Experiments with the UK Meteorological Office mesoscale model
[AD-A212291] 04 p0521 N90-13006
Meteorological atlas of the Northern Hemisphere lower stratosphere for January and February 1989 during the Airborne Arctic Stratospheric Expedition
[NASA-TM-4145] 05 p0671 N90-13908
Activities report of the World Meteorological Organization
[WMO-713] 05 p0671 N90-13912
Analysis of propagation in an inhomogeneous atmosphere in the horizontal and vertical direction using the parabolic equation method 06 p0760 N90-14421
Application of surface analysis methods to studies of atmospheric deposition in forests
[DE90-000562] 06 p0810 N90-14714
Summary of papers, studies, conference presentations: 1987-1988 (from the National Weather Service, southern region)
[PB90-103896] 06 p0817 N90-14749
Antarctic surface temperature and pressure data
[DE90-000971] 07 p0963 N90-15565
Backscattering effects in DIAL due to water vapor
[SER-WISS-ABHANDL-89] 08 p1082 N90-16265
The Interactive System Meteorology and its use in meteorology and oceanography
08 p1092 N90-16320
Guide on the global observing system
[WMO-488-REV] 08 p1103 N90-16385
Rocket-triggered lightning strikes and forest fire ignition 08 p1155 N90-16690
AOIPS 3 user's guide. Volume 2: Program descriptions
[NASA-TM-100725] 09 p1247 N90-17236
Observing systems simulation experiments: Their role in meteorology
[AD-A215705] 09 p1248 N90-17243
ONR tropical cyclone motion research initiative: Data assimilation considerations for field experiment analyses
[AD-A215726] 09 p1248 N90-17244
Dose assessment during complex meteorology in the Texas Panhandle
[DE90-006026] 10 p1408 N90-18118
Report on meteorological assessment of Bald Hills incidents, phase 1
[AD-A216201] 10 p1408 N90-18123
Effect of marine atmosphere on performance of electrooptical systems
[AD-A215947] 10 p1430 N90-18252
Compendium of meteorological space programs, satellites, and experiments
[NASA-TM-102924] 12 p1607 N90-19243
Science requirements for passive microwave sensors on earth science geostationary platforms
12 p1608 N90-19251
Rain radars for earth science geostationary platforms: Some possibilities 12 p1610 N90-19262
The EURAD Model: Structure and First Results
[REPT-61] 12 p1686 N90-19680
The mesoscale meteorological model MM4 and its modifications for EURAD 12 p1686 N90-19682
An observational study of squall lines in the Amazon
[INPE-4865-TDL/376] 12 p1693 N90-19723
The Terrain-Responsive Atmospheric Code (TRAC) project plan: Development of a hazardous materials dispersion modeling capability with application to ambient air monitoring network design
[DE90-007293] 13 p1829 N90-20502
JPRS report. Science and technology. USSR: Earth sciences
[JPRS-UES-89-002] 14 p1995 N90-21432
Transformation and deposition of airborne gaseous and particulate pollutants during transport over the Baltic Sea
[PUBL-AIR-QUALITY-5] 14 p2003 N90-21478
Meteorologist Weather Processor (MWP) integration test plan
[DOT/FAA/CT-TN89/62] 14 p2007 N90-21500
Windshear case study: Denver, Colorado, July 11, 1988
[DOT/FAA/DS-89/19] 14 p2008 N90-21509
Minimizing the effects of the atmosphere in the observation of ultraviolet radiation
15 p2080 N90-21911
Evaporation duct effects at millimeter wavelengths
15 p2080 N90-21914
Report on STC/Technische Universiteit (TU) Delft Extremely High Frequency (EHF) radio relay study
15 p2081 N90-21915
Propagation environments, effects, and decision aids
15 p2081 N90-21918
On three-dimensional scaling and consistent truncation of global atmospheric models 15 p2127 N90-22164
JARE data reports, no. 140 (meteorology 21): Meteorological data at Asuka Camp, Antarctica in 1989
[ISSN-0075-3343] 15 p2132 N90-22188
An investigation of meteorological effects on currents in the shelf and continental slope seas northwest of the United Kingdom. 2: Relationships between currents at different locations and with other variables
[PB90-151911] 15 p2134 N90-22195
The HCl/aerosol problem 16 p2208 N90-22597
Monthly surface thermal forcing in the tropical Pacific from 1980 to 1983
[NASA-CR-183033] 16 p2259 N90-22877
Seasonal weather forecast verification
[DE90-009467] 17 p2425 N90-23818
Activities report in meteorological research and associated fields
[ISSN-0349-0068] 18 p2582 N90-24707
The effect of random variations of radiosonde data on the predicted FLIR performance calculated by the program UFLR
[AD-A220034] 18 p2615 N90-24896
Atmospheric environment for space shuttle (STS-28) launch
[NASA-TM-100386] 19 p2715 N90-25452
Applications of ISES for meteorology
21 p3018 N90-27160
Meteorological Satellite Center Technical Note, no. 17, 1988
[ISSN-0388-9653] 21 p3028 N90-27213
Investigation into position accuracy of typhoon center determined on GMS imagery 21 p3028 N90-27217
Case study on Pre-Typhoon Active Convective Clouds (PTACC) 21 p3029 N90-27220
Behavior of dust clouds from Australian dust storms in 1982-1983 as observed by the GMS
21 p3029 N90-27221
Dust clouds from African dust storms in 1986-1987 as observed by Meteosat 21 p3029 N90-27222
An experiment to make a new design of the Satellite Cloud Information Chart with the combination of visible and infrared data observed by the GMS
21 p3029 N90-27223
Modernization of PRC meteorological service
[AD-A221761] 21 p3032 N90-27236
Bibliography of oceanography, meteorology, and geology of Louisiana, Texas, Mississippi, Alabama, and Florida
[PB90-194663] 22 p3194 N90-28124
General overview of the solar activity effects on the lower ionosphere 22 p3206 N90-28198
Atmospheric Sciences Research in the US EPA climate program
[PB90-221870] 22 p3212 N90-28219
Improved meteorological measurements from buoys and ships (IMET): Preliminary conventions from buoys and standards data and file formats
[PB90-241910] 22 p3229 N90-28312
Study of meteorological processes important in the degradation of materials through surface temperature
[PB90-222720] 23 p3336 N90-28856
Estimating the spatial variability of trace gas deposition velocities
[PB90-208570] 23 p3349 N90-28928
An investigation of forcing mechanisms during a surprise tornadic thunderstorm
[PB90-216805] 23 p3352 N90-28940
Automated system for meteorological analysis
[INPE-4586-TDL/332] 23 p3352 N90-28945
Vorticity balance study for a tropical region, during the Southern Hemisphere summer
[INPE-4634-TDL/336] 23 p3353 N90-28949
On the dynamics of severe thunderstorms
[DE90-627922] 23 p3353 N90-28950
Meteorological conditions over the North Atlantic Ocean during GCE/CASE/WATOX
[PB90-252032] 24 p3494 N90-29747
Data catalog series for space science and applications flight missions. Volume 4B: Descriptions of data sets from meteorological and terrestrial applications spacecraft and investigations
[NASA-TM-101880] 24 p3556 N90-30123

METEORS
U METEOROIDS

METEOSAT SATELLITE
Rainfall estimation over Africa using satellite data
06 p0815 N90-14742
Proposed concept for the visible/infrared imaging radiometer for second generation Meteosat
[ETN-90-98145] 08 p1123 N90-16503
Real time environment monitoring using data from METEOSAT and NOAA imaging satellites
[NLR-MP-87070-U] 12 p1684 N90-19672
Meteorological Satellite Center Technical Note, no. 17, 1988
[ISSN-0388-9653] 21 p3028 N90-27213

Dust clouds from African dust storms in 1986-1987 as observed by Meteosat 21 p3029 N90-27222

METERS
U MEASURING INSTRUMENTS

METHACRYLATE RESINS
U ACRYLIC RESINS

METHANATION
An evaluation of the relationship between the production and use of energy and atmospheric methane emissions
[DE90-007982] 14 p2004 N90-21487

METHANE
Molecular biology and physiology of methanogenic archaebacteria
[AD-A210399] 01 p0091 N90-10522
Conversion of methane to liquid hydrocarbons
[DE89-017547] 03 p0322 N90-11831
Global data bases on distribution, characteristics and methane emission of natural wetlands: Documentation of archived data tape
[NASA-TM-4153] 03 p0365 N90-12090
Tables for the thermophysical properties of methane
[PB89-222608] 04 p0469 N90-12690
Biological and biochemical methane reactions
[PB89-232615] 04 p0516 N90-12977
Multisensor technologies for low cost methane detection
[PB89-235188] 05 p0645 N90-13766
The thermally induced gas-phase reactions of methane and oxygen: A comparison of experimental and computational results
[DE90-000785] 06 p0742 N90-14317
Greenhouse gases: Changing the global climate
[DE90-002788] 07 p0957 N90-15535
Solid-state electrolyte catalysis for methane and oxygen synthesis
[PB90-100231] 08 p1040 N90-16011
Mechanisms of the electrochemistry of small organic molecules
[PB90-100785] 08 p1040 N90-16012
High-performance LO2-CH4 engine with ceramic matrix composite materials 09 p1180 N90-16840
Full scale catalytic combustion of methane under atmospheric pressure
[DE89-772354] 10 p1351 N90-17835
Effect of propellant flowrate and purity on carbon deposition in LO2/methane gas generators
11 p1471 N90-18468
Extracting chemical information form Auger line shapes
[AD-A216729] 11 p1483 N90-18537
Synthesis and properties of a novel catalyst for the combustion of methane
[PB90-127499] 12 p1622 N90-19320
Activation of methane by transition metal-substituted aluminophosphate molecular sieves
[DE90-005663] 12 p1624 N90-19331
The extinction and structure of counterflow premixed flames
[AD-A218106] 13 p1773 N90-20178
Bis(4-(3,4-dimethylenepyrrolidyl)-phenyl) methane
[NASA-CASE-LAR-13965-1-CU]
14 p1942 N90-21118
An evaluation of the relationship between the production and use of energy and atmospheric methane emissions
[DE90-007982] 14 p2004 N90-21487
High speed commercial transport fuels considerations and research needs
[NASA-TM-102535] 15 p2072 N90-21869
Analysis of the use of a methane propellant in a biowaste resistojet
[AD-A220475] 17 p2367 N90-23473
Effects of solar ultraviolet radiation on biogeochemical dynamics in aquatic environments
[AD-A221119] 18 p2578 N90-24687
Analysis of energy spectra of the ions in the coma of Halley's comet for the evaluation of the production ratio of methane and ammonia
[ETN-90-96489] 18 p2638 N90-25026
Anthropogenic sources of NO(x), SO()x, CO, and CH4: Geographical distribution
[AERONOMICA-ACTA-A-353-1990]
19 p2713 N90-25440
Measurements of CH4, N2O, CO, H2O and O3 in the middle atmosphere by the ATMOS experiment on Spacelab 3
[NASA-TM-103476] 20 p2883 N90-26400
Laboratory studies, analysis, and interpretation of the spectra of hydrocarbons present in planetary atmospheres including cyanoacetylene, acetylene, propane, and ethane 20 p2943 N90-26748
Gaussian quadrature exponential sum modeling of near infrared methane laboratory spectra obtained at temperatures from 106 to 297 K
20 p2945 N90-26758
Measurements of the methane relaxation times for application to the infrared emission models of the upper atmospheres of outer planets and Titan
20 p2945 N90-26759
Methane overtone absorption by intracavity laser spectroscopy 20 p2946 N90-26762
Laboratory measurements and methane photochemistry modeling 20 p2947 N90-26770
Optical constants of solid methane
20 p2948 N90-26775
Four-step kinetics for methane and implications for turbulent combustion 21 p2975 N90-26906
Scalar dissipation measurements in the developing region of a jet 21 p2976 N90-26909
The computer modeling of the combustion and extinction of methane-air premixed flames by thermally stable gases
[PB90-189432] 21 p2976 N90-26910
Search for interstellar methane
21 p3094 N90-27588
Carbon in the outer solar system
21 p3096 N90-27593
Global climate change: A proposed gas industry program on global climate issues
[PB90-219296] 22 p3199 N90-28156
Oxygen/methane combustion stability investigation
23 p3293 N90-28628
Atmospheric methane data for the period 1983-1985 from the NOAA/GMCC global cooperative flask sampling network
[PB90-208588] 24 p3486 N90-29701

METHANOL
U METHYL ALCOHOL

METHOD OF CHARACTERISTICS
Method of characteristic studies for rotational flow downstream of a curved shock wave
02 p0219 N90-11252
A quasi-Lagrangian moving grid technique for investigating compressible flows
14 p1972 N90-21298

METHOD OF MOMENTS
Spectral-domain analysis of finite frequency selective surfaces
[AD-A211669] 03 p0339 N90-11932
A user's manual for the method of moments Aircraft Modeling Code (AMC)
[NASA-CR-186371] 11 p1456 N90-18390
Recent improvements to the electromagnetic surface patch code
[AD-A217479] 13 p1794 N90-20293
Is Galerkin's method really better
[DE90-008804] 14 p1967 N90-21267
Frequency analysis via the method of moment functionals
[NASA-CR-186988] 22 p3239 N90-28367
Analysis of a TM01 circular to TE10 rectangular waveguide mode converter
[AD-A224566] 24 p3464 N90-29568

METHODS
U PROCEDURES

METHYL ALCOHOL
Liquid rocket booster study. Volume 2, book 1
[NASA-CR-183600] 01 p0026 N90-10133
Results from the second year of operation of the Federal Methanol Fleet at Argonne National Laboratory
[DE89-016935] 02 p0230 N90-11319
Methanol fueled vehicles and photochemical models: An evaluation of the state of knowledge
[PB89-214225] 03 p0419 N90-12410
Assessment of costs and benefits of flexible and alternative fuel use in the US transportation sector. Technical report three: Methanol production and transportation costs
[DE90-002625] 06 p0755 N90-14396
Cold starting a neat methanol (M100) vehicle with long duration spark ignition
[PB89-230692] 06 p0792 N90-14613
Survey on synthesis technologies of methanol as an alternative fuel
[DE89-901303] 07 p0914 N90-15284
Results from the third year of operation of the Federal Methanol Fleet at Lawrence Berkeley Laboratory
[DE90-003306] 08 p1084 N90-16277
Comparison of emissions of transit buses using methanol and diesel fuel
[DE90-005552] 10 p1391 N90-18044
US Army Methanol-Fueled Administrative Vehicle Demonstration Program
[AD-A216013] 10 p1393 N90-18054
Federal methanol fleet update
[DE90-006851] 11 p1517 N90-18741
Hawaii integrated biofuels research program, phase 1
[DE90-006885] 11 p1530 N90-18811
Turbine fuel alternatives (near term)
[AD-A219405] 16 p2225 N90-22695
Results from the fourth year of operation of the Federal Methanol Fleet at Lawrence Berkeley Laboratory
[DE90-014741] 23 p3315 N90-28743

METHYL COMPOUNDS
NT ACETONITRILE
Suppression of side chain crystallization and transformation of monotropic mesophases into enantiotropic mesophases by copolymerization of the parent polymers' monomer pairs containing constitutional isomeric mesogenic side groups
[AD-A209066] 03 p0330 N90-11878
Electrochemistry in near-critical and supercritical fluids. 8: Methyl viologen, decamethylferrocene, Os(bpy)3(sup 2+) and ferrocene in acetonitrile and the effect of pressure on diffusion coefficients under supercritical conditions
[AD-A213407] 07 p0895 N90-15172
Band-to-band transitions in poly (phenyl methyl silane)
[DE90-003575] 07 p0990 N90-15720
Determination of the minimum energy conformation of alkyl substituted pyrazines
[AD-A216974] 11 p1484 N90-18539
The 1-((diorganooxyphosphonyl)-methyl)-2,4- and -2,6-diamido benzenes
[NASA-CASE-ARC-11425-4] 13 p1766 N90-20133
Single-crystal diffraction analysis of 2-(trimethylsilylethynyl) 4-nitro-N,N-dimethylaniline
[AD-A218955] 16 p2216 N90-22642
Some 1-(diorganooxyphosphonyl)methyl-2,4- and -2,6-dinitro-benzenes
[NASA-CASE-ARC-11425-3] 17 p2367 N90-23475
Mass spectrometry of poly(methyl methacrylate)s of low molecular weight 20 p2829 N90-26091
Laser induced surface chemical epitaxy
[AD-A222082] 21 p2977 N90-26920
Effect of particulate fillers on the rheology of polymer melts
[AD-A223601] 24 p3455 N90-29512

METHYL CYANIDE
U ACETONITRILE

METHYLENE
Process for crosslinking methylene-containing aromatic polymers with ionizing radiation
[NASA-CASE-LAR-13448-1] 14 p1956 N90-21198
Dynamics of micellar oligomeric and monomeric sodium 10-undecenoate
[AD-A222570] 20 p2830 N90-26099
Role of the methylene amidogen (H2CN) radical in the atmospheres of Titan and Jupiter
20 p2947 N90-26769

METHYLHYDRAZINE
Atmospheric chemistry of the fuel hydrazines
02 p0203 N90-11158
Field evaluation of a passive sampling device for hydrazines in ambient air
[NASA-TM-103456] 18 p2578 N90-24686

METRIC CONVERSION
U METRICATION

METRIC SPACE
NT HILBERT SPACE
Some remarks on the gap metric
[MEMO-COSOR-88-34] 05 p0690 N90-14029
How to cluster in parallel with neural networks
08 p1113 N90-16443
On induced Hermitian metrics for holomorphic vector bundles
[DE90-612737] 14 p2019 N90-21572
The monad construction and Hermetian-Einstein metrics
[DE90-612738] 14 p2019 N90-21573
Visualization of three dimensional data
19 p2736 N90-25553
Predissimilarities, prefilters, and ultrametrics on an arbitrary set
[IMAG-RR-970-M] 20 p2918 N90-26603
The structure of random discrete spacetime
[NASA-CR-182841] 22 p3255 N90-28429

METRIC SYSTEM
U INTERNATIONAL SYSTEM OF UNITS

METRICATION
Metric handbook for Federal officials: Recommendations of the Interagency Committee on Metric Policy
[PB89-226922] 06 p0756 N90-14400

METROLOGY
Use of the NPL linac for x ray dosimetry --- linear accelerator (linac)
[NPL-RSA(EXT)-6] 03 p0404 N90-12314
Center for Electronics and Electrical Engineering technical publication announcements covering Center programs, January-March 1989 with 1989 CEEE events calendar
[PB89-228308] 03 p0418 N90-12402
Metric handbook for Federal officials: Recommendations of the Interagency Committee on Metric Policy
[PB89-226922] 06 p0756 N90-14400

Activities report of the National Electrotechnic Institute Galileo Ferraris
[ETN-90-96178] 08 p1157 N90-16705
Earth Science Geostationary Platform Technology
[NASA-CP-3040] 12 p1608 N90-19249
Center for Atomic, Molecular, and Optical Physics: Technical activities
[PB90-133158] 14 p2022 N90-21591
Large scale metrology by computer assisted photogrammetry
[REPT-892-430-116] 16 p2239 N90-22772
A laser tracking dynamic robot metrology instrument 23 p3366 N90-29021

METROPOLITAN AREAS
U CITIES

MEXICO
Disturbances in the Arizona Monsoon 03 p0362 N90-12071
A case for archaeological reconnaissance of the Cabo Catoche-Porvenir region of the northeastern Yucatan Peninsula
[NASA-TM-102248] 16 p2249 N90-22827

MGCO
U MARS OBSERVER

MICE
Acute oral toxicity of JA-2 solid propellant in ICR mice
[AD-A217264] 13 p1848 N90-20609
Acute oral toxicity of DIGL-RP solid propellant in ICR mice
[AD-A217711] 13 p1849 N90-20613
The effects of simulated hypogravity on murine bone marrow cells 18 p2631 N90-24989

MICHELSON INTERFEROMETERS
Measurement of gas intensity at high dynamic pressures
[ISL-CO-204/89] 11 p1507 N90-18680
Velocity measurement using interferometry
[ISL-CO-221/88] 11 p1512 N90-18709
Ultra-sensitive inertial sensors via neutral-atom interferometry 12 p1735 N90-19977
Velocity Interferometer System for Any Reflector (VISAR): Displacement mode data reduction
[DE90-015027] 23 p3395 N90-29184
Velocity interferometry 24 p3420 N90-29316

MICROANALYSIS
Calibration approach to electron probe microanalysis: A study with PWA-1480, a nickel base superalloy
[NASA-TM-102393] 06 p0745 N90-14335
X ray microprobe for the microcharacterization of materials
[DE89-006038] 06 p0836 N90-14863
Practical limitations of ALCHEMI measurements on ordered intermetallic alloys
[DE90-000700] 06 p0853 N90-14957
ICP/AES (Inductively Coupled Plasma/Atomic Emission Spectroscopy): A modern analytical tool
[DE90-003822] 07 p0997 N90-15765
Mass loss during x ray microanalysis
[DE90-003954] 08 p1049 N90-16067
Workshop on Analysis of Returned Comet Nucleus Samples
[NASA-CR-184821] 08 p1140 N90-16607
Trace element abundance determinations by Synchrotron X Ray Fluorescence (SXRF) on returned comet nucleus mineral grains 08 p1142 N90-16619
Analysis of particulates of comet nucleus samples: Possible use of olivine as indicator phase 08 p1147 N90-16646
Non-destructive trace element microanalysis of as-received cometary nucleus samples using synchrotron x ray fluorescence 08 p1147 N90-16649
Isotopic microanalysis of returned comet nucleus samples 08 p1149 N90-16655
The measurement of trace elements in interplanetary dust and cometary particles by ultra-high sensitivity INAA 08 p1149 N90-16656
Oxygen concentrations on surfaces of carbon fibers
[AD-A217724] 13 p1769 N90-20152
Cosmic Dust Collection Facility: Scientific objectives and programmatic relations
[NASA-TM-102160] 14 p1939 N90-21098
Estimation of the concentration-distance profile within the electrochemical diffusion layer by Raman microprobe spectroscopy
[AD-A219521] 17 p2372 N90-23506
An analytical study of tribochemical phases with colloidal additives. Contributions made by energy filtering electron microscopy
[ECL-89-009] 17 p2374 N90-23521
Friction microprobe studies of composite surfaces
[DE90-014224] 23 p3299 N90-28662

MICROBALANCES
Quartz crystal microbalance studies of electrochemical growth of conducting polymers
[AD-A210788] 01 p0052 N90-10295
Quartz crystal microbalance analysis. 1: Evidence of anion or cation insertion into electropolymerized conducting polymers
[AD-A212304] 04 p0480 N90-12755
Quartz crystal microbalance studies: Solvent effects in conducting polymer films
[AD-A219426] 17 p2372 N90-23502

MICROBE
U MICROORGANISMS

MICROBIOLOGY
NT BACTERIOLOGY
The soil microbiology of hydrazines 02 p0205 N90-11171
JPRS report: Science and technology. USSR: Life sciences
[JPRS-ULS-90-002] 14 p1995 N90-21434
The biogeochemistry of metal cycling
[NASA-CR-4295] 17 p2439 N90-23897
Definition of a near real time microbiological monitor for space vehicles
[NASA-CR-185599] 24 p3441 N90-29430

MICROBURSTS (METEOROLOGY)
Effects of stress on judgment and decision making in dynamic tasks
[AD-A210605] 01 p0135 N90-10781
A scalar/vector potential solution for aerodynamic coefficients in wind shear 02 p0147 N90-10838
A candidate concept for display of forward-looking wind shear information
[NASA-TM-101585] 06 p0725 N90-14232
The effects of clutter-rejection filtering on estimating weather spectrum parameters
[NASA-CR-186212] 06 p0817 N90-14754
Analysis of severe atmospheric disturbances from airline flight records 07 p0869 N90-15045
Influence of windshear, downdraft and turbulence on flight safety 07 p0870 N90-15048
Relative merits of reactive and forward-look detection for wind-shear encounters during landing approach for various microburst escape strategies
[NASA-TM-4158] 07 p0882 N90-15108
Synthetic aperture radar imagery of airports and surrounding areas: Archived SAR data
[NASA-CR-4275] 11 p1453 N90-18371
Synthetic aperture radar imagery of airports and surrounding areas: Philadelphia Airport
[NASA-CR-4280] 11 p1453 N90-18372
A case study of the 24 August 1986 FLOWS microburst
[AD-A216939] 11 p1537 N90-18847
Cockpit display of hazardous weather information 14 p1906 N90-20929
Airborne Doppler radar flight experiments for the detection of microbursts 14 p1963 N90-21243
Windshear case study: Denver, Colorado, July 11, 1988
[DOT/FAA/DS-89/19] 14 p2008 N90-21509
Examination of microburst development in Colorado thunderstorm for the 5 August 1982 case
[AD-A218478] 17 p2425 N90-23820
Synthetic aperture radar imagery of airports and surrounding areas: Denver Stapleton International Airport
[NASA-CR-4305] 18 p2495 N90-24257
A quantitative technique to estimate microburst wind shear hazard to aircraft 18 p2640 N90-25040

MICROCALORIMETERS
U CALORIMETERS

MICROCHANNEL PLATES
Ion detector on the basis of microchannel plates for a high-sensitive mass spectrometer
[DE89-620335] 02 p0225 N90-11291
A microchannel plate intensified, subnanosecond, X-ray imaging camera
[DE89-017781] 03 p0350 N90-12003
Outline on the future Italian transportable laser ranging station
[CISE-4845] 05 p0649 N90-13782
Enhancement of microchannel plate gain by deposition of CsI on the channel walls
[DE90-003051] 07 p0922 N90-15334
Integration of a gated microchannel plate detector into the Nova laser system
[DE90-002981] 07 p0935 N90-15413
Development of the RAIDS (Remote Atmospheric and Ionospheric Detector System) extreme ultraviolet wedge and strip detector
[AD-A213730] 07 p0949 N90-15495
Microchannel photomultipliers in time spectrometer
[DE90-616417] 14 p1982 N90-21356
A laser-induced fluorescence technique for measurement of slot-injected fluid concentration profiles in a plate turbulent boundary layer
[AD-A221388] 18 p2553 N90-24572
Noise performance of microchannel plate imaging systems
[DE90-015037] 23 p3322 N90-28785

MICROCIRCUITS
U MICROELECTRONICS

MICROCLIMATOLOGY
Cirrus microphysics and radiative transfer: Cloud field study on October 26, 1986 22 p3224 N90-28284
Cirrus radiative characteristics and the radiative impact of small particles 22 p3224 N90-28286

MICROCOMPUTERS
NT PERSONAL COMPUTERS
Microcomputer-based tests for repeated-measures: Metric properties and predictive validities
[NASA-CR-185517] 03 p0382 N90-12174
A menu of self-administered microcomputer-based neurotoxicology tests
[NASA-CR-185518] 03 p0382 N90-12175
Basic program for raster scan display unit
[NAL-TM-560] 03 p0384 N90-12185
Utilization of a PC for finite element modeling
[AD-A214173] 07 p0971 N90-15605
Digital system for monitoring and controlling remote processes
[DE90-003935] 08 p1054 N90-16094
Super-micro computer weather prediction model
[AD-A216329] 10 p1409 N90-18124
A comparison of microcomputer training methods and sources
[AD-A216349] 10 p1413 N90-18146
A microcode compiler that runs on the IBM AT and supports cascadable microcomputers, part 2
[AD-A215889] 10 p1415 N90-18155
Microcomputer enhanced optical investigation of spreading and evaporative processes in ultra thin films
[DE90-006323] 11 p1492 N90-18585
A microcode compiler that runs on the IBM AT and supports cascadable microcomputers, part 1
[AD-A215888] 11 p1542 N90-18877
Generation of triangular form models in a microcomputer environment
[INPE-4974-PRE/1539] 14 p1997 N90-21447
Development of microcomputer-based mental acuity tests for repeated-measures studies
[NASA-CR-185607] 14 p2010 N90-21521
CAD work station for electronics designer
[DE90-616473] 14 p2015 N90-21546
Graphically-oriented nonlinear analysis of statically loaded plane frames on microcomputers
[PB90-165945] 15 p2144 N90-22248
Understanding the computing system domain of advanced computing with microcomputers
[DE90-009825] 15 p2145 N90-22251
The interactive digital video interface 16 p2271 N90-22941
Preliminary evaluation of a small wearable display
[AD-A219867] 17 p2350 N90-23385
A Kalman filter with smoothing for hurricane tracking and prediction
[AD-A220413] 17 p2426 N90-23827
Microcomputer-aided ground vibration testing
[DLR-FB-89-57] 18 p2499 N90-24279
Microcomputer for the digital regulation of permanent magnet-synchronous servomotors
[ETN-90-98507] 18 p2588 N90-24727
Iconic tracking algorithms for high energy physi cs using the TRAX-I massively parallel processor
[MPI-PAE/EXP.EL-216] 18 p2596 N90-24773
Development of a microcomputer based software system for use in crewmember ejection analysis
[AD-A220398] 19 p2656 N90-25117
Practical applications of remote sensing technology
[NASA-CR-186810] 20 p2879 N90-26377
Modernization of PRC meteorological service
[AD-A221761] 21 p3032 N90-27236
Personal computer programs for the control of subnanosecond transient digitizers with applications for device damage testing
[AD-A221458] 21 p3054 N90-27365
Graphically-oriented linear analysis of plane frames subjected to complex loadings on microcomputers
[PB90-173279] 22 p3190 N90-28102
Requirements for implementing real-time control functional modules on a hierarchical parallel pipelined system 24 p3518 N90-29891
Turbo pascal implementation of a distributed processing network of MS-DOS microcomputers connected in a master-slave configuration
[AD-A223925] 24 p3525 N90-29928
Graphic interface for attribute-based data language queries from a personal computer to the multi-lingual, multi-model, multi-backend database system over an Ethernet network
[AD-A223738] 24 p3528 N90-29948
A manual for microcomputer image analysis
[DE90-015629] 24 p3529 N90-29958

Search strategies for computer-stored information: A microcomputer tutorial 24 p3557 N90-30126

MICROCRACKS

Mechanical behavior of carbon/resin composites under delamination and cracking of transverse layers
[ONERA-RT-46/7086-M] 04 p0467 N90-12678

Mechanics of interaction of a crack with microcracks 06 p0798 N90-14650

Critical and subcritical crack-growth behavior along toughened ceramic/metal interfaces 07 p0889 N90-15140

Computed tomography of electronics
[AD-A217976] 13 p1797 N90-20314

Velocity matched optical transmitter
[AD-A217413] 13 p1887 N90-20830

Use of unbalanced laminates as a screening method for microcracking
[NASA-TM-102517] 14 p1944 N90-21124

Fracture mechanics of monolithic ceramic materials under small scale microcracking conditions 15 p2070 N90-21860

Elasto-plastic analysis for contact fatigue failure 15 p2112 N90-22078

Combining acoustic emission locations and a microcrack damage model to study development of damage in brittle materials
[DE90-005195] 15 p2117 N90-22111

The pressure dilation of a deep, jointed region of the earth
[DE90-007537] 15 p2128 N90-22170

Microcracking and toughness of ceramic-fiber/ceramic-matrix composites under high temperature
[AD-A218516] 16 p2223 N90-22680

Metal matrix composites microfracture: Computational simulation
[NASA-TM-103153] 18 p2518 N90-24383

Mechanical paint removal techniques for aircraft structures
[IAR-89-23] 19 p2682 N90-25254

A study of the fatigue behavior in scratched samples of Al-Li alloy (2090-T3)
[IAR-89-24] 20 p2832 N90-26107

Effect of boron on intergranular hot cracking in Ni-Cr-Fe superalloys containing niobium
[NASA-CR-184038] 20 p2834 N90-26115

Small crack growth and its influence in near alpha-titanium alloys
[RAE-TM-P-1171] 20 p2835 N90-26121

A tough high performance composite matrix
[NASA-CASE-LAR-14338-1] 21 p2970 N90-26881

Crack layer analysis of fatigue fracture of a beta titanium alloy 23 p3338 N90-28864

MICROCRYSTALS

Memory matrix
[WO-PATENT-88/04096] 05 p0680 N90-13961

Study of microcrystalline, silicon-carbon p-layers prepared by photo-CVD and glow discharge
[DE89-009438] 06 p0850 N90-14939

MICRODENSITOMETERS

The evolution and geometry of the outer parts of the small Magellanic cloud 14 p2040 N90-21697

MICROELECTRONICS

NT LARGE SCALE INTEGRATION
NT VERY LARGE SCALE INTEGRATION

Vacuum microelectronics for beam power and rectennas 01 p0028 N90-10146

Polyheterocycle Langmuir-Blodgett films
[AD-A210625] 01 p0051 N90-10292

Micro-cavity integrable vacuum diodes and triodes
[DE89-016649] 01 p0060 N90-10344

Performance of the CAMEX64 silicon strip readout chip
[DE89-014015] 01 p0130 N90-10747

High resolution X-ray spectroscopy using germanium microcalorimeters
[DE89-017784] 03 p0351 N90-12004

Beam assisted fabrication of 3-5/Si monolithic devices
[AD-A212046] 03 p0412 N90-12367

Microsystems techniques: Concept, significance, status of development
[MBB-UA-1110/88-PUB] 04 p0495 N90-12851

Fundamental quantum 1/f noise in ultrasmall semiconductor devices and their optimal design principles
[AD-A211947] 05 p0702 N90-14107

Integrating and enhancing tools for ASIC (Application-Specific Integrated Circuits) design using MOSIS (Metal Oxide Semiconductor Implementation Service) fabrication
[DE90-001601] 06 p0769 N90-14475

Monolithic laser diode structure for microwave generation
[AD-D014210] 06 p0782 N90-14543

Component presence-absence detection for automated visual inspection of hybrid microcircuits
[KCP-613-4050] 07 p0922 N90-15335

A study of Inter-Injection-Locked phased arrays
[AD-A214097] 07 p0925 N90-15352

Overview on radiation effects in electronics
[DE90-000841] 07 p0926 N90-15357

Solid state research
[AD-A213405] 07 p1003 N90-15806

Study of silicon nitride pH response to the fabrication of microelectronic sensors
[LAAS-89229] 08 p1042 N90-16023

Solid state microelectrochemical devices: Transistor and diode devices employing a solid polymer electrolyte
[AD-A214206] 09 p1211 N90-17019

Evaluation of doped phthalocyanines and a chemically-sensitive field effect transistor for detecting nitrogen dioxide
[AD-A215662] 09 p1214 N90-17037

Design of fiber optic probes for laser light scattering 09 p1222 N90-17090

Direct measurements of the physical diffusion of redox active species: Microelectrochemical experiments and their simulation
[AD-A215680] 09 p1280 N90-17420

Chemistry at clusters, microstructures and surfaces
[AD-A215842] 10 p1353 N90-17844

Materials processing of diamond: Etching, doping by ion implantation and contact formation
[AD-A216530] 10 p1438 N90-18301

Research project in microelectronic engineering and imaging science
[DE90-006907] 11 p1503 N90-18653

Processing, fabrication, characterization and device demonstration of high temperature superconducting ceramics
[AD-A218330] 13 p1782 N90-20231

A progress report on the Livermore Miniature Vacuum Tube Project
[DE90-008302] 13 p1794 N90-20299

Fault simulator evaluation
[AD-A217782] 13 p1796 N90-20308

In-situ differential reflectance study of the etching of SiO2 films
[AD-A217186] 13 p1893 N90-20864

Microelectronic device reliability
[AD-A218774] 17 p2394 N90-23638

Solid state research
[NASA-CR-186699] 17 p2476 N90-24160

Solid state research
[NASA-CR-186700] 17 p2477 N90-24161

Direct writing of microstructures for solid-state electronics
[AD-A220996] 18 p2535 N90-24460

Monolithic phase shifter study
[AD-A219859] 18 p2546 N90-24533

Highest integration in microelectronics: Development of digital ASICs for PARS3-LR
[MBB-UA-1151/89-PUB] 19 p2653 N90-25099

Center for Space Microelectronics Technology 1988-1989 technical report
[NASA-CR-186849] 19 p2753 N90-25642

Monolithic Optical Programmable Spectrograph (MOPS)
[AD-D014502] 19 p2757 N90-25669

Multiple target tracking in a wide-field-of-view camera system
[DE90-013488] 20 p2865 N90-26300

A viologen/ruthenium oxide-based microelectrochemical diode with pH-dependent current-voltage characteristics
[AD-A221961] 21 p3000 N90-27052

Characterization of a solid-state microelectrochemical diode employing a poly(vinyl alcohol)/phosphoric acid solid-state electrolyte: Rectification at junctions between WO3 and polyaniline
[AD-A222025] 21 p3000 N90-27054

Perspectives on high temperature superconducting electronics 22 p3139 N90-27810

Polymer research
[PB90-246638] 23 p3313 N90-28737

Adjustable speed drive applications guidebook
[DE90-014151] 23 p3321 N90-28780

Measurements of the single event upset environment in the upper atmosphere
[RAE-TM-SPACE-373] 23 p3351 N90-28934

Reliability analysis/assessment of advanced technologies
[AD-A223647] 24 p3465 N90-29573

Controlling multiple manipulators using RIPS 24 p3505 N90-29814

An advanced single event upset tester
[AD-A223613] 24 p3564 N90-30163

MICROGRAPHY

U PHOTOMICROGRAPHY

MICROGRAVITY

U REDUCED GRAVITY

MICROGRAVITY APPLICATIONS

Space Station Freedom: A foothold on the future
[NASA-NP-107/10-88] 02 p0159 N90-10907

Telescience Testbed Pilot Program
[NASA-CR-184594] 02 p0257 N90-11455

Facilities for microgravity combustion research
[NASA-TM-102014] 05 p0630 N90-13679

Proceedings of the Second Noncontact Temperature Measurement Workshop
[NASA-CR-181289] 10 p1362 N90-17894

Microgravity noncontact temperature requirements at NASA Lewis Research Center 10 p1362 N90-17897

Microgravity Science and Application Program tasks, 1989 revision
[NASA-TM-4191] 13 p1786 N90-20252

Microgravity science and applications bibliography, 1989 revision
[NASA-TM-4192] 14 p1957 N90-21207

Microgravity, the space application of the 21st century. Challenges, constraints, and strategies
[REPT-892-430-105] 16 p2226 N90-22696

Space station based Microacceleration Experiment Platform
[NASA-CR-186659] 19 p2666 N90-25167

MICROHARDNESS

Dispersion strengthening of high temperature niobium alloys
[AD-A213829] 07 p0906 N90-15236

High temperature microhardness tester
[AD-A219567] 17 p2380 N90-23553

Self-lubricating-diamond like coatings deposition
[AD-A221756] 21 p2988 N90-26983

MICROINDENTATION

U MICROHARDNESS

MICROMECHANICS

Hygrothermal effects on the complex moduli of composite laminates 01 p0033 N90-10182

Micromechanisms of surface friction in zinc electrogalvanized steel sheets
[DE89-011819] 01 p0077 N90-10440

A study of the tribological and surface micromechanical properties of YBa2Cu3O7-x
[DE89-015680] 02 p0281 N90-11607

Analysis of metal matrix composite structures using a microchemical constitutive theory 06 p0737 N90-14290

Parametric studies to determine the effect of compliant layers on metal matrix composite systems
[NASA-TM-102465] 06 p0737 N90-14294

Numerical analysis and simulation of frictional particle systems 07 p0937 N90-15430

Micromechanics of an extrusion in high-cycle fatigue with creep
[AD-A213509] 07 p0947 N90-15485

Probabilistic simulation of uncertainties in composite uniaxial strengths
[NASA-TM-102483] 08 p1040 N90-16008

Effects of high rate shear on the microstructure and deformation and fracture behavior of two high strength steels
[AD-A214107] 08 p1044 N90-16032

Prediction of high temperature metal matrix composite ply properties
[NASA-TM-102490] 10 p1348 N90-17817

A micromechanical viscoplastic stress-strain model with grain boundary sliding
[DE90-006013] 10 p1437 N90-18295

Composite laminate tailoring with probabilistic constraints and loads
[NASA-TM-102515] 13 p1766 N90-20138

Computational simulation of damping in composite structures
[NASA-TM-102567] 13 p1817 N90-20432

Multi-objective shape and material optimization of composite structures including damping
[NASA-TM-102579] 14 p1945 N90-21132

Two-dimensional damage models of fiber-reinforced composites 14 p1946 N90-21135

Micromechanics analysis of space simulated thermal deformations and stresses in continuous fiber reinforced composites
[NASA-TM-102633] 14 p1946 N90-21140

Optimal fabrication processes for unidirectional metal-matrix composites: A computational simulation
[NASA-TM-102559] 14 p1947 N90-21143

Failure mechanisms under complex loading of glass-reinforced polyester composites and their matrices: The effect of superposed hydrostatic pressures up to 300 MPa on axial tensile and compressive strengths, and in-plane shear properties of unidirtionally reinforced glass-polyester composites and the relevant polyesters 15 p2110 N90-22072

Deformation and fracture of thin sheet aluminum-lithium alloys: The effect of cryogenic temperatures
16 p2218 N90-22655
Inelastic response of metal matrix composites under biaxial loading
16 p2220 N90-22661
Non destructive testing of composite structures using embedded optical fibers: A mechanical interaction model
[ETN-90-97016] 18 p2573 N90-24661
Advanced methods for the micromachining of sensors
[MBB-Z-0281/88-PUB] 19 p2650 N90-25081
A numerical micromechanics analysis of the mechanical properties of a plain weave composite
[OUEL-1760/89] 19 p2673 N90-25201
Micromechanics of interfaces in high temperature ceramics
[AD-A222027] 21 p2987 N90-26973
Micromechanics of size effect in failure due to distributed cracking
[AD-A223211] 21 p3013 N90-27128
Micromechanical model of crack growth in fiber reinforced ceramics
[NASA-CR-4321] 22 p3192 N90-28113
Micromechanisms of fatigue crack growth and fracture toughness in metal matrix composites
[AD-A223863] 23 p3302 N90-28676
Evaluation of several micromechanics models for discontinuously reinforced metal matrix composites
[NASA-TM-102719] 23 p3339 N90-28872

MICROMETEORITES
Design of a thermal and micrometeorite protection system for an unmanned lunar cargo lander
[NASA-CR-186682] 19 p2664 N90-25161

MICROMETEOROIDS
NT ZODIACAL DUST
On protection of Freedom's solar dynamic radiator from the orbital debris environment. Part 1: Preliminary analyses and testing
[NASA-TM-102458] 06 p0736 N90-14285
Micrometeoroid impacts on silver bus bar targets at elevated voltages
10 p1346 N90-17805
Simulation of micrometeoroid impacts by laser pulses
10 p1346 N90-17806
Electric dipole antennae used as micrometeoroid detectors
[AERONOMICA-ACTA-A-351-1989]
17 p2392 N90-23623
Differentiation of three dimensional models of the zodiacal interplanetary dust cloud for experiments with micrometeoroids decay detectors on the space station
[ETN-90-96488] 18 p2637 N90-25025

MICROMETEOROLOGY
NT MICROBURSTS (METEOROLOGY)
Micrometeorological investigation of surface exchange of trace gases: A case study
[PB89-208375] 02 p0249 N90-11412
An initial look at the dynamics of the microscale flow field within a large wind farm in response to variations in the natural inflow
[DE89-009501] 06 p0804 N90-14682
Precipitation mechanisms in tropical and midlatitude convective clouds
14 p2008 N90-21507
Scintillation of millimeter-wave intensity and phase caused by turbulence and precipitation
15 p2080 N90-21912
Microphysical fundamentals governing cirrus cloud growth: Modeling studies
22 p3225 N90-28291
A comparative study of infrared radiance measurements by an ER-2 based radiometer and the LANDSAT 5 Thematic Mapper (TM-6)
22 p3226 N90-28294

MICROMETEORS
U MICROMETEOROIDS

MICROMETERS
Solid state research
[NASA-CR-186699] 17 p2476 N90-24160
Solid state research
[NASA-CR-186700] 17 p2477 N90-24161

MICROMINIATURIZATION
Miniature instrumentation for laser light scattering experiments
09 p1222 N90-17088
Development of a solar-powered infrared injection laser microminiature transmitting system
[DE90-005672] 10 p1389 N90-18034
Smart microsensors for high temperature applications, phase 1
[AD-A224151] 23 p3330 N90-28828

MICROORGANISMS
NT ARCHAEBACTERIA
NT BACTERIA
NT ESCHERICHIA
NT PSEUDOMONAS
NT SALMONELLA
The soil microbiology of hydrazines
02 p0205 N90-11171
Adaptation and resistance of ecosystems to stress
[AD-A212999] 05 p0665 N90-13889
Decomposition in Arctic terrestrial environments
[DE90-001198] 06 p0809 N90-14706
Effect of community structure on the kinetics of anaerobic degradation of aromatic compounds
[DE90-003666] 07 p0888 N90-15134
Design and operation of an outdoor microalgae test facility
[DE89-009493] 13 p1848 N90-20608
Microbially influenced corrosion of carbon steels
[DE90-012231] 21 p2980 N90-26936

MICROPARTICLES
Study of phase transformations liquid-solid-solid of ultrafine particles
[ISAL-89-0019] 08 p1042 N90-16022
From interstellar dust to comets
08 p1142 N90-16620
Submicron particle analyzer
[AD-A223558] 24 p3545 N90-30050

MICROPHONES
Voice preprocessor for digital voice applications
[AD-A214726] 09 p1205 N90-16982
Field calibration of two types of microphones in hyperbaric air
[AD-A219477] 17 p2395 N90-23642
Gradient microphone for measurement of the vectorial sound velocity
[MBB-Z-0259/89-PUB] 19 p2650 N90-25080

MICROPHOTOGRAPHS
The fundamentals of metal combustion in composite explosives revealed by high speed microphotography
[DE90-005255] 09 p1192 N90-16910

MICROPHOTOMETERS
U PHOTOMETERS

MICROPOROSITY
Carbonitrition response of steel plates not destined for heat treatments
[CETIM-106960] 04 p0476 N90-12728
Microporous structure with layered interstitial surface treatment, and method and apparatus for preparation thereof
[NASA-CASE-MSC-21487-1] 09 p1189 N90-16887
Electrochemical synthesis of ultrathin film composite membranes
[AD-A219041] 16 p2216 N90-22643

MICROPROCESSORS
A prototype silicon compiler in prolog
[AD-A210669] 02 p0257 N90-11452
Power up modification for video switcher microprocessor interface for sensor system processing system
[AD-A211543] 03 p0344 N90-11962
Specification of Viper1 in Z
[RSRE-MEMO-4195] 04 p0490 N90-12817
Specification of Viper2 in Z
[RSRE-MEMO-4217] 04 p0490 N90-12819
Automated glass fiber drawing
[DE90-000894] 06 p0751 N90-14367
Coordination of processing elements in a multiprocessor computer
[WO-PATENT-88/04075] 06 p0831 N90-14830
Autonomous automatic landing through computer vision
09 p1163 N90-16734
Transient fault behavior in a microprocessor: A case study
[NASA-CR-186240] 10 p1320 N90-17633
Technology assessment of operating systems
[AD-A216893] 10 p1421 N90-18192
Laboratory implementation of the Continuously Reconfiguring Multi-Microprocessor Flight Control System (CRMMFCS)
[AD-A217730] 13 p1758 N90-20094
X ray microimaging by diffractive techniques
[DE90-008444] 13 p1804 N90-20356
Diagnostic development and support of MHD (Magnetohydrodynamics) test facilities
[DE90-004969] 13 p1890 N90-20845
Apparatus for and a method of determining compass headings
[AD-D014436] 16 p2199 N90-22551
An experimental study of fault propagation in a jet-engine controller
[NASA-CR-181335] 17 p2354 N90-23401
High performance processing system for embedded control applications in space
18 p2507 N90-24330
SEU characterization and design dependence of the SA3300 microprocessor
[DE90-007678] 18 p2589 N90-24728
Multi-microprocessor control of a precision pan and tilt head
[RSRE-MEMO-4252] 19 p2747 N90-25613
Conception of a reconfigurable microprocessor
[ETN-90-97248] 20 p2904 N90-26517
Level-2 system: Programmers-users manual
[DE90-013324] 20 p2908 N90-26540
Advanced algorithms design and implementation in on-board microprocessor systems for engine life usage monitoring
22 p3104 N90-27628
Microprocessor chip incorporating optical signal coupling receiver
[AD-D014547] 22 p3167 N90-27964
Using embedded microcontrollers in radar test equipment
[DE90-014997] 23 p3319 N90-28763
Adjustable speed drive applications guidebook
[DE90-014151] 23 p3321 N90-28780
A microprocessor controlled strain gauge calibration module
[AR-005-579] 23 p3329 N90-28821
Engineering and the advancement of human welfare. Ten outstanding achievements 1964-1989
[ISBN-0-309-04185-6] 23 p3415 N90-29297
Reliability analysis/assessment of advanced technologies
[AD-A223647] 24 p3465 N90-29573
Approach to telerobot computing architecture
[NASA-CR-186993] 24 p3534 N90-29984
Small multipurpose stored data acquisition system
[DE90-010823] 24 p3558 N90-30134

MICROPROGRAMMING
A microcode compiler that runs on the IBM AT and supports cascadable microcomputers, part 2
[AD-A215889] 10 p1415 N90-18155
A microcode compiler that runs on the IBM AT and supports cascadable microcomputers, part 1
[AD-A215888] 11 p1542 N90-18877
CESAR sequencer
[FFI-89/7021] 19 p2744 N90-25599

MICROPULSATIONS
Analytical studies of magnetospheric pulsations
[AD-A222275] 21 p3026 N90-27205

MICROROCKET ENGINES
NT ORBIT MANEUVERING ENGINE (SPACE SHUTTLE)
Viability study of ionic microthruster tests on MECB satellite
[INPE-4973-RPE/605] 11 p1475 N90-18490

MICROSCALES
U MICROBALANCES

MICROSCOPES
NT ACOUSTIC MICROSCOPES
NT ELECTRON MICROSCOPES
NT OPTICAL MICROSCOPES
Soft x ray microscope using Fourier transform holography
[DE90-002291] 06 p0781 N90-14539
Sample holder support for microscopes
[NASA-CASE-MFS-28420-1] 21 p3010 N90-27113

MICROSCOPY
NT ELECTRON MICROSCOPY
NT SCANNING TUNNELING MICROSCOPY
Biomedical applications of synchrotron x ray microscopy
[DE90-004957] 11 p1540 N90-18867
Superconductive microprobes for eddy current evaluation of materials
[AD-A217776] 13 p1805 N90-20361
Biological soft x ray contact microscopy: Imaging living CHO-SC1 cells and other biological materials
[DE90-007560] 13 p1849 N90-20610
Isoplanatic systems in mesooptics
[DE90-009785] 17 p2406 N90-23705
In-situ topographical imaging of electrode surfaces using high resolution phase-measurement interferometric microscopy
[AD-A221021] 18 p2548 N90-24542
Microscopic modeling of tribological phenomena
[AD-A222049] 21 p3011 N90-27117

MICROSTRIP ANTENNAS
Millimeter-wave/infrared rectenna development at Georgia Tech
01 p0028 N90-10147
Dielectric covered microstrip patch antennas
[AD-A211577] 03 p0344 N90-11983
Scalar Green function method for microstrip antenna analysis based on the exact image theory
[PB89-218838] 04 p0488 N90-12805
Investigation of broadband microstrip antenna structures for application in monolithic millimeter wave arrays
[AD-A213856] 07 p0923 N90-15344
A study of loaded microstrip antennas and their applications to arrays
[AD-A214857] 09 p1205 N90-16985
Modeling antennas and scatterers of arbitrary shape embedded in layered dielectric media
[AD-A214902] 09 p1211 N90-17023
Reconfigurable antennas, monolithic microwave integrated circuits with feeding networks for microstrip antennas
[AD-A216916] 11 p1498 N90-18622
Green's functions for a theoretical model of an aperture fed stacked-patch microstrip antenna
[AD-A216280] 12 p1645 N90-19455

An L-band antenna array with integrated phase shifters
[DLR-FB-89-63] 18 p2544 N90-24519
Planar microstrip Yagi array antenna
[NASA-CASE-NPO-17873-1-CU] 21 p2994 N90-27015

MICROSTRIP DEVICES
NT MICROSTRIP ANTENNAS
NT MICROSTRIP TRANSMISSION LINES
Microwave microstrip resonator measurements of Y1Ba2Cu3O(7-x) and Bi2Sr2Ca1Cu2O(8-y) thin films
[NASA-TM-102159] 05 p0635 N90-13704
High performance millimeter-wave microstrip circulators and isolators
[NASA-CR-186276] 19 p2685 N90-25270
Double sided silicon strip detectors
[MPI-PAE/EXP-EL-217] 22 p3178 N90-28036
A double-sided silicon strip detector with capacitive read out and a new method of integrated bias coupling 22 p3178 N90-28037
Readout of double sided silicon strip detectors with high intensity integrated electronics 22 p3179 N90-28038
New developments in double sided silicon strip detectors 22 p3179 N90-28039

MICROSTRIP TRANSMISSION LINES
Calibration and de-embedding of microwave measurements using any combination of one- or two-port standards
[PB89-212674] 03 p0337 N90-11916
Characteristic impedance of microstrip lines
[NASA-TM-101581] 05 p0633 N90-13694
Stripline feed for a microstrip array of patch elements with teardrop shaped probes
[NASA-CASE-NPO-17548-1-CU] 08 p1056 N90-16104
Modeling antennas and scatterers of arbitrary shape embedded in layered dielectric media
[AD-A214902] 09 p1211 N90-17023
A study of a new time-domain method of lines and its application for the characterization of microstrip line and its discontinuities
[AD-A215441] 09 p1213 N90-17034
Planar integrated circuits for microwave transmission and reception
[AD-A217676] 12 p1656 N90-19520
Investigation of tapered multiple microstrip lines for VLSI circuits
[AD-A217855] 13 p1797 N90-20310
New ferrite-filled waveguiding structures analysed by the averaging method
[PB90-165671] 14 p1967 N90-21269
Millimeter wave filter design with suspended stripline
[AD-A219582] 17 p2395 N90-23645
Microwave conductivity of laser ablated YBaCuO superconducting films and its relation to microstrip transmission line 22 p3147 N90-27844
Analysis of microstrip lines with alternative implementation of conductors and superconductors
[NASA-TM-103182] 22 p3167 N90-27968

MICROSTRUCTURE
NT METEORITIC MICROSTRUCTURES
Microstructure morphology and quality of Al-Si castings 01 p0043 N90-10244
The quantitative analysis of fracture surfaces using fractals
[DE89-015361] 01 p0044 N90-10250
Influence of microstructure and microdamage processes on fracture at high loading rates
[AD-A210307] 01 p0045 N90-10253
Mechanisms of strength and toughness in a microalloyed, precipitation hardened steel
[AD-A210571] 01 p0045 N90-10256
Ceramic components in machines, Cologne and Aachen, West Germany; Maastricht, The Netherlands and Brussels, Belgium
[DE89-015831] 01 p0047 N90-10264
Structure-mechanical property relationships in ion implanted ceramics
[DE89-010129] 01 p0048 N90-10274
Structure of amorphous silicon alloy films
[DE89-009441] 01 p0128 N90-10734
Ceramic processing of bulk high-T(sub c) superconductors
[DE89-015703] 01 p0128 N90-10736
Fatigue crack growth rates as a function of delta K: Variability and material property 02 p0182 N90-11031
Deformation induced microstructural and microchemical changes during thermomechanical treatment
[DE89-017266] 02 p0197 N90-11127
Microstructural effects on spall fracture in 1008 steel
[DE89-016770] 02 p0198 N90-11131
Ion implantation of two titanium alloys
[DE89-016958] 02 p0198 N90-11133
Characterizations of shock-loaded aluminum-infiltrated boron carbide cermets
[DE89-016773] 02 p0201 N90-11146
Intergranular and interphase boundaries in ceramics
[DE89-016969] 02 p0202 N90-11154
Basic investigations of cutting machinability of inorganic glasses using single-point tools
[W-15/87] 02 p0210 N90-11204
A characterization of the side bonding, upset plug welding process
[DE89-015181] 02 p0229 N90-11315
A study of the tribological and surface micromechanical properties of YBa2Cu3O7-x
[DE89-015680] 02 p0281 N90-11607
Defect structures preceding amorphization by ion irradiations in YBa2Cu3O(7-delta)
[DE89-016905] 02 p0282 N90-11612
Exploratory study of niobium, titanium, zirconium and tantalum aluminides
[AD-A210658] 02 p0283 N90-11615
High-temperature ceramic superconductors
[AD-A211070] 02 p0283 N90-11618
Transport properties of thermally grown Cr2O3
[DE89-016703] 02 p0284 N90-11623
Processing and characterization of alumina platelet-reinforced mullite composites
[DE90-000057] 03 p0320 N90-11814
Mechanism of electrochemical activation of carbon electrodes: Role of graphite lattice defects
[AD-A211644] 03 p0325 N90-11845
Low temperature formation of titanium aluminide films using physical vapor deposition
[AD-A211877] 03 p0328 N90-11866
Fractographic and microstructural analysis of fatigue crack growth in a Ti-6Al-4V fan disc forging
[NLR-MP-88028-U] 03 p0330 N90-11877
Photolithography: A new tool for ceramic science
[DE90-000135] 03 p0331 N90-11885
Correlating microemulsion fuel composition, structure and combustion properties
[DE89-017779] 03 p0333 N90-11898
Development of microstructured DH diode lasers and detectors for the near and medium IR spectral domain using molecular beam epitaxy
[IPM-15/1988] 03 p0354 N90-12023
Anisotropy and microstructure of high-coercivity rare earth permanent magnets
[AD-A211905] 03 p0399 N90-12285
Characterization of the Structure and Chemistry of Defects in Materials: Proceedings, volume 138
[DE89-014796] 03 p0410 N90-12352
Effect of annealing conditions on the structural and superconducting properties of Y-Ba-Cu-O films
[AD-A211308] 03 p0413 N90-12371
Synthesis and microstructure of highly oriented PbTiO3 thin films prepared by a sol-gel method
[AD-A211735] 03 p0414 N90-12377
Laser probe vaporization/oxidation testing of high temperature composites
[AD-A211410] 04 p0465 N90-12663
Heat pipe and thermal energy storage and corrosion studies (1988)
[AD-A212655] 04 p0472 N90-12706
Temperature effects in shock consolidation of metal powders
[DE89-016782] 04 p0474 N90-12716
Rapid heating tensile tests of high-energy-rate-forged 316L stainless steel charged with hydrogen and tritium
[DE89-017869] 04 p0474 N90-12717
How the common practice of heating plates of austenitic stainless steel during cooling affects their mechanical properties
[CETIM-104500] 04 p0476 N90-12725
Carbonitrition response of steel plates not destined for heat treatments
[CETIM-106960] 04 p0476 N90-12728
Ultrastructure processing and characterization of polymers
[AD-A211460] 04 p0478 N90-12743
Textural and structural organization of the heat treated polymers: Mechanical properties relationships
[ETN-89-95711] 04 p0478 N90-12744
Microsystems techniques: Concept, significance, status of development
[MBB-UA-1110/88-PUB] 04 p0495 N90-12851
Quench sensitivity in Al-Cu-Li alloys
[AD-A213055] 05 p0624 N90-13639
The effect of composition and aging treatment on the microstructure and mechanical properties of aluminum-lithium-titanium alloys
[AD-A213144] 05 p0624 N90-13640
Correlation between microstructure and magnetic properties of porous sintered iron and porous iron containing composites
[KFK-4522] 05 p0625 N90-13647
Surfaces and interfaces of ceramic materials
[AD-A212417] 05 p0627 N90-13657
A new model for the structure of silica glass
[AD-A212972] 05 p0627 N90-13659
Computational studies of structural and transport properties of amorphous solids
[ETN-90-96027] 05 p0628 N90-13664
Superplastic sheet forming 06 p0743 N90-14327
Advances and future directions in superplastic materials 06 p0744 N90-14328
Cavitation and superplasticity 06 p0744 N90-14329
The mechanical properties of superplastically formed titanium and aluminium alloys 06 p0744 N90-14331
Phases in lanthanum-nickel-aluminum intermetallic alloys
[DE90-000651] 06 p0746 N90-14343
Embrittlement of laboratory- and reactor-aged CF-3, CF-8, and CF-8M duplex stainless steels
[DE90-002777] 06 p0748 N90-14354
Mechanical properties and morphology of oriented polymer blends 06 p0750 N90-14361
The 7th International Conference on Ceramics
[DE90-002144] 06 p0752 N90-14374
Characterization of nanophase materials by x ray diffraction and computer simulation
[DE90-002270] 06 p0752 N90-14378
Primary arm spacing in directionally solidified Pb-10 wt percent Sn alloys
[NASA-CR-185190] 06 p0756 N90-14398
Practical superconductor development for electrical power applications
[DE90-001804] 06 p0771 N90-14487
Microstructure induced by laser shock in an austenitic steel 06 p0784 N90-14558
BES welding science contractors summary report, 1988 to 1989
[DE90-001004] 06 p0793 N90-14619
The feasibility of welding of irradiated materials
[DE90-002200] 06 p0795 N90-14631
Engineering approaches to the application of fracture toughness data in the nuclear industry
[DE90-001596] 06 p0800 N90-14659
Electrode development in monolithic solid oxide fuel cells
[DE90-001910] 06 p0805 N90-14684
Process monitoring using optical ultrasonic wave detection
[DE90-002021] 06 p0838 N90-14870
Atomic matching across internal interfaces
[DE90-002266] 06 p0841 N90-14889
X ray studies of strain, interface, and impurity in semiconductors
[DE90-001525] 06 p0851 N90-14947
Flux pinning and microstructure in YBa2Cu3O7
[DE90-001562] 06 p0851 N90-14948
Superconducting and microstructural properties of shock-compacted high-T sub c oxide powders
[DE90-000823] 06 p0853 N90-14958
The effect of composition and processing on high T(sub c) superconductors containing bismuth
[DE90-002203] 06 p0854 N90-14965
Microstructure and electrical properties of bulk high-T(sub c) superconductors
[DE90-001762] 06 p0855 N90-14974
Critical and subcritical crack-growth behavior along toughened ceramic/metal interfaces 07 p0889 N90-15140
The microstructure and properties of aluminum-lithium alloys 07 p0897 N90-15187
Microstructure/mechanical property relations in a mechanically alloyed aluminum 07 p0900 N90-15205
Metal matrix composites: A promising alternative to conventional alloys 07 p0901 N90-15208
The effects of Mo2C morphology and strain distribution on the fatigue properties of Fe-C-Mo dual-phase steels 07 p0901 N90-15210
Microstructural evolution of martensitic steels during fast neutron irradiation
[DE89-016231] 07 p0902 N90-15212
Accelerated aging embrittlement of cast duplex stainless steel: Activation energy for extrapolation
[DE90-001773] 07 p0903 N90-15221
Cryogenic mechanical properties of low density superplastic Al-Mg-Sc alloys
[DE90-002120] 07 p0904 N90-15222
Heat treatment of pulsed Nd: YAG laser welds in a Ti-14.8 wt pct Al-21.3 wt pct Nb titanium aluminide
[DE90-003484] 07 p0905 N90-15228
Cast stainless steel aging: Mechanisms and predictions
[DE90-003772] 07 p0907 N90-15241
Properties of aluminum-uranium alloys
[DE90-003889] 07 p0907 N90-15243

Submerged arc welding consumables for HSLA (High Strength Low Alloy)-100 steel
[AD-A213433] 07 p0941 N90-15452
Research on amorphous silicon-germanium alloys for tandem solar cells
[DE89-009436] 07 p0950 N90-15499
Fabrication of porous ceramic electrode structures
[DE90-003548] 07 p0953 N90-15517
Micron-thin Nb films recovered from Mbar shock pressures
[DE90-001509] 07 p0998 N90-15772
Atomic scale structure of twin boundary in Y-Ba-Cu-O superconductors
[DE90-003955] 07 p1006 N90-15823
The structure of silica-polysiloxane composites and its effects on their elastomeric properties
[DE89-014768] 08 p1039 N90-16005
Method to produce titanium alloy articles with high fatigue and fracture resistance
[AD-D014278] 08 p1043 N90-16029
Method for refining microstructures on prealloyed titanium powder compacts
[AD-D014280] 08 p1043 N90-16030
Method of marking titanium alloy articles having distinct microstructural regions corresponding to high creep and fatigue resistance
[AD-D014283] 08 p1043 N90-16031
Effects of high rate shear on the microstructure and deformation and fracture behavior of two high strength steels
[AD-A214107] 08 p1044 N90-16032
Interplanar spacing for various phases in austenitic stainless steels
[DE90-602350] 08 p1045 N90-16038
Microstructural explanation for irradiation embrittlement of V-15Cr-5Ti
[DE90-004112] 08 p1045 N90-16041
Phase evolution during neutron irradiation of commercial Fe-Cr-Mn alloys
[DE90-004113] 08 p1045 N90-16042
Selection of corrosion-resistant materials for use in molten nitrate salts
[DE90-004351] 08 p1046 N90-16048
Effect of carbon on ion beam mixing of Fe-Ti bilayers
[DE90-003650] 08 p1048 N90-16056
Proposal for a study of laser acceleration of electrons using micrograting structures at ATF
[DE90-003699] 08 p1082 N90-16262
Anisotropy and microstructure of high coercivity rare earth iron permanent magnets, list of papers published
[AD-A214160] 08 p1118 N90-16476
Development of low density silica aerogel as a capture medium for hyper-velocity particles
[NASA-CR-185930] 08 p1121 N90-16489
Microstructures of Y123 films on SrTiO3, LaGaO3, and LaAlO3
[DE90-003367] 08 p1129 N90-16537
Direct determination of the morphology, structure and composition of cometary and interstellar ice analogs in the laboratory 08 p1141 N90-16612
Mechanical and SEM analysis of artificial comet nucleus samples 08 p1148 N90-16650
Effects of heat treatment on microstructure and flexural properties of unidirectional carbon-carbon composites
[AD-A214985] 09 p1186 N90-16873
Structural stability of heat treated W/B4C multilayers
[DE90-005322] 09 p1188 N90-16884
Strengthening of aluminum by oxygen implantation: Experimental results and mechanical modeling
[DE90-005960] 09 p1195 N90-16924
Theory of microemulsions in a gravitational field 09 p1224 N90-17099
Subtle porosity variation in the YBa2Cu3O(7-x) high-temperature superconductor revealed by ultrasonic imaging
[NASA-TM-102130] 09 p1235 N90-17167
Phase properties of the rapid cooled palladium-silicon alloy in the concentration range 40 to 58 at. percent Si
[DE90-719525] 09 p1284 N90-17444
Modelling directional solidification
[NASA-CR-186181] 09 p1292 N90-17487
High-temperature deformation of YBa2Cu3O(7-delta) with Ag additions
[DE90-004884] 09 p1292 N90-17491
Evolution of structure and electrical properties during crystallization of rapidly solidified Bi4Ti3O12
[DE90-005221] 09 p1292 N90-17492
High-order mixture homogenization of periodic nonlinear composites 10 p1347 N90-17814
Chemistry at clusters, microstructures and surfaces
[AD-A215842] 10 p1353 N90-17844
Characterization of the 6242 Si alloy. Centrifugal wheel in conventional forging
[REPT-NT-3967] 10 p1355 N90-17859
Fundamental studies of time-dependent response and fracture of cross-linked polymers
[AD-A216694] 10 p1360 N90-17886
Crystal and magnetic structure of Er(2)(Co(sub x)Fe(sub 1-x))(17) compounds
[DE90-004928] 10 p1436 N90-18288
Defects: Their behaviour and related design assumptions 11 p1457 N90-18397
Review of component defects, their relationship to manufacturing process, and their effect on materials behaviour (for critical rotating parts) 11 p1458 N90-18399
Future technology requirements (related to defects and quantitative material behavior to aid in implementation of damage tolerance for design of engine structures) 11 p1459 N90-18403
State of the art and future prospects for high temperature composites 11 p1477 N90-18498
Laboratory for the processing and evaluation of inorganic matrix composites
[AD-A216881] 11 p1480 N90-18516
Mechanical properties and microstructure of Si3N4-whisker-reinforced Si3N4 matrix composite
[DE90-005651] 11 p1480 N90-18518
Corrosion fatigue of iron-chromium-nickel alloys: Fracture mechanics and chemistry
[DE90-006318] 11 p1487 N90-18556
Softening mechanisms and microstructural instabilities during high temperature, low cycle fatigue of Ni, Ni3Al, and their metal matrix composites
[DE90-006487] 11 p1487 N90-18557
The mechanism, measurement, and influence of properties on the galling of metals
[DE90-006533] 11 p1487 N90-18558
Colloid and interface chemistry aspects of ceramics
[AD-A216715] 11 p1490 N90-18576
Microstructural variations in aluminum oxide coatings deposited using a dual beam ion system
[DE90-006040] 11 p1491 N90-18583
The design of advanced ceramic composites
[DE90-006613] 11 p1493 N90-18592
Microstructural characterization of silicon nitride ceramics processed by pressureless sintering, overpressure sintering, and sinter/HIP
[DE90-007126] 11 p1493 N90-18594
Creep in shear of experimental solder joints
[DE90-007062] 11 p1520 N90-18753
The interaction of polycrystalline copper films with dilute aqueous solutions of cupric chloride
[AD-A216465] 11 p1569 N90-19033
Transport effects and spectroscopy of defects in microstructures
[AD-A216718] 11 p1570 N90-19036
Dislocation behaviour in Ge(x)Si(1-x) epilayers on (001) Si
[DE90-007063] 11 p1572 N90-19051
High-purity beryllium foils
[DE90-006408] 12 p1626 N90-19348
Creep behavior of alloys based on TiAl containing TiB2 and TiN particulates
[DE90-006489] 12 p1628 N90-19355
Modification of surface mechanical properties of high-chromium tool steel by carbon-implanted codeposited Fe-Ti films
[DE90-007502] 12 p1628 N90-19358
Fabrication, phase transformation studies, and characterization of SiC-AlN-Al2OC ceramics
[DE90-006591] 12 p1631 N90-19371
Microstructural characterization of multiphase coatings produced by chemical vapor deposition
[DE90-007573] 12 p1632 N90-19379
Liquid oxygen LOX compatibility evaluations of aluminum lithium (Al-Li) alloys: Investigation of the Alcoa 2090 and MMC weldalite 049 alloys 12 p1636 N90-19398
Microstructural simulations of dynamic recrystallization
[DE90-007504] 12 p1722 N90-19895
Synthesis of alumina-coated SiC whiskers for production of SiC whisker-reinforced alumina composite materials
[DE90-007778] 13 p1768 N90-20147
Analytical electron microscopy of catalyst preparations
[DE90-008699] 13 p1773 N90-20173
The effect of the SiC/Al interface on matrix microstructure in 2xxx-SiCp metal matrix
[AERE-R-13591] 13 p1775 N90-20184
Ageing effects in welded cast CF3 stainless steel
[AERE-R-13559] 13 p1775 N90-20188
Stochastic approach to the initiation of pitting corrosion
[AERE-R-13348] 13 p1775 N90-20190
The ageing effect of the matrix-reinforcement interface on the ageing response of an aluminium 6061 alloy reinforced with 20vol percent SiC particulates
[AERE-R-13361] 13 p1776 N90-20193
Design and processing of strong-tough microcomposite steels
[DE90-007764] 13 p1777 N90-20197
The stress corrosion performance of diffusion bonded nickel base alloys
[DE90-008130] 13 p1777 N90-20199
Physical sputtering of metallic systems by charged-particle impact
[DE90-007803] 13 p1777 N90-20201
Evaluation of material homogeneity as a function of thickness of low-alloy ferritic steel
[DE90-008069] 13 p1777 N90-20202
The metallurgical mechanisms of solder fatigue
[DE90-008390] 13 p1778 N90-20206
Strength and microstructure of ceramics
[AD-A217752] 13 p1782 N90-20227
Nondestructive testing of ceramics by acoustic microscopy
[AERE-R-13350] 13 p1813 N90-20411
Time-dependent failure of silver interlayer welds
[DE90-008015] 13 p1818 N90-20440
Dielectric composite thin films
[AD-A217940] 13 p1881 N90-20791
Synthesis and properties of polycrystalline Tl2Ba2CaCu2O(x) and Tl2Ba2Ca2Cu3O(x)
[DE90-007528] 13 p1897 N90-20887
Performance of Y-TZP materials between 800 C and 1200 C
[AD-A217723] 13 p1897 N90-20890
Characterization of failure processes in tungsten copper composites under fatigue loading conditions
[NASA-TM-102371] 14 p1943 N90-21123
Strengthening mechanisms of tungsten powder reinforced uranium
[DE90-009331] 14 p1947 N90-21144
Controlled production and characterization of metastable intermetallics
[DE90-009384] 14 p1952 N90-21176
Absolute multilayer characterization at high spatial resolution via real-time soft x ray imaging
[DE90-009181] 14 p1984 N90-21371
Thermomechanical deformation testing and modeling in the presence of metallurgical instabilities
[NASA-CR-185188] 14 p1993 N90-21420
Deformation processing of YBa2Cu3O(sub x)
[DE90-007795] 14 p2030 N90-21644
Deformation and microstructure of rutile
[DE90-614113] 14 p2032 N90-21654
Anisotropy of grain growth in alumina
[DE90-009045] 14 p2032 N90-21655
Microstructure of Au/Nb multilayers
[DE90-008722] 14 p2033 N90-21662
Determination of internal strains in high-temperature superconductor composites by intense pulsed neutron source
[DE90-007799] 14 p2033 N90-21664
The effect of hydrogen and microstructure on the deformation and fracture behavior of a single crystal nickel-base superalloy
[NASA-CR-185219] 15 p2068 N90-21849
Welding behavior and welding metallurgy of ductile intermetallic alloys
[DE90-008908] 15 p2069 N90-21852
The effect of aging at 343 C on type 308 stainless steel weldments
[DE90-009232] 15 p2069 N90-21853
Microstructure and mechanical properties of nickel aluminide powders consolidated by extrusion and hot isostatic pressing
[DE90-009777] 15 p2070 N90-21855
Failure mechanisms under complex loading of glass-reinforced polyester composites and their matrices: The effect of superposed hydrostatic pressures up to 300 MPa on axial tensile and compressive strengths, and in-plane shear properties of unidirtionally reinforced glass-polyester composites and the relevant polyesters 15 p2110 N90-22072
Improved crystal bending techniques applied to the LLNL dual-arm Johann mounting x ray spectrometer
[DE90-009528] 15 p2173 N90-22415
Grain boundary intermetallic phases in alloy 718
[DE90-009812] 15 p2173 N90-22417
A comprehensive study on microstructure mechanics relationships of ceramic matrix composites
[AD-A219318] 16 p2213 N90-22627
Quantitative characterization of spatial distribution of particles in materials: Application to materials processing 16 p2219 N90-22660
Structure-property relations in aluminum-lithium alloys
[AD-A219183] 16 p2222 N90-22672
Characterization of weldments using advanced experimental techniques
[DE90-009418] 16 p2242 N90-22792
Recent advances in nondestructive evaluation made possible by novel uses of video systems
[NASA-TM-102491] 16 p2244 N90-22801
The microstructural basis of damping in high damping alloys
[AD-A219572] 16 p2248 N90-22821

High temperature superconducting thin films in Japan
16 p2311 N90-23169
A study of the relation between grain boundary type and sensitisation in a partially-sensitised AISI 304 stainless steel using electron back-scattering patterns
[AERE-R-13327] 16 p2321 N90-23234
Microstructure of thin films
[AD-A219262] 16 p2324 N90-23255
High temperature electric arc furnace and method
[NASA-CASE-MFS-28281-1] 17 p2357 N90-23415
Ultrafine microstructure composites prepared by chemical vapor deposition
[AD-A219650] 17 p2369 N90-23484
Vanadium alloys with improved resistance to helium embrittlement
[DE90-009811] 17 p2375 N90-23524
Solidification of highly undercooled liquid droplets
[AD-A218776] 17 p2376 N90-23529
Report of research activity at the Research Laboratory of Electronics 17 p2486 N90-24217
High temperature oxidation of Ni3Al composites
[DE90-010145] 18 p2517 N90-24373
State of the art and future prospects for high temperature composites
[REPT-892-430-125] 18 p2517 N90-24375
Ta and Nb reinforced MoSi2
[DE90-010596] 18 p2517 N90-24377
Influence of interfacial shear strength on the mechanical properties of SiC fiber reinforced reaction-bonded silicon nitride matrix composites
[NASA-TM-102462] 18 p2518 N90-24382
A particle-level numerical simulation of the dynamic consolidation of a metal matrix composite material
[DE90-010950] 18 p2519 N90-24387
Metal matrix composites from dynamic consolidation of powder mixtures
[DE90-010951] 18 p2519 N90-24388
Rheology and microstructure of concentrated suspensions
[DE90-009976] 18 p2520 N90-24391
Corrosion fatigue crack propagation in metals
[NASA-CR-4301] 18 p2524 N90-24405
A study of the phase decomposition of Fe-Ni-Al-Mo alloys
[DE90-010143] 18 p2524 N90-24406
Processing and properties of advanced aluminum alloys
[AD-A221292] 18 p2526 N90-24416
Morphological and structural characterization of the spinodal decomposition of Fe-Cr alloys
[DE90-010496] 18 p2526 N90-24418
Irradiation effects on impact behavior of 12Cr-1MoVW and 2 1/4Cr-1Mo steels
[DE90-011075] 18 p2527 N90-24421
Development and evaluation of advanced austenitic alloys
[DE90-011315] 18 p2528 N90-24425
Fatigue crack propagation in austenitic stainless steels at cryogenic temperatures
[DE90-011597] 18 p2528 N90-24426
The effects of cooling rate XD (trademark) TiAl weld microstructure
[DE90-011975] 18 p2528 N90-24427
Effects of microstructure and adhesion on performance of sputter-deposited MoS2 solid lubricant coatings
[AD-A220900] 18 p2530 N90-24434
Joining engineering ceramics
[DE90-010819] 18 p2531 N90-24445
Power density effects in the physical and chemical properties of sputtered diamond-like carbon thin films
[DE90-011587] 18 p2532 N90-24450
Direct writing of microstructures for solid-state electronics
[AD-A220996] 18 p2535 N90-24460
Tribological and mechanical properties of Fe/Ti multilayered films
[DE90-011949] 18 p2565 N90-24635
Irradiation assisted stress corrosion cracking
[DE90-010629] 18 p2572 N90-24656
Microstructure of sputtered superconducting films of Bi2Sr2CaCu2O(x) made by low-temperature, in situ growth
[DE90-010067] 18 p2618 N90-24916
Electromigration in metallic microstructures
[AD-A221208] 18 p2622 N90-24942
Practical superconductor development for electrical power applications
[DE90-010262] 18 p2625 N90-24957
Au-Ge-Ni-Ti ohmic contacts on gallium arsenide
[DE90-011064] 18 p2625 N90-24960
In-situ growth of superconducting films of Bi-Sr-Ca-Cu-O using magnetron sputtering
[DE90-011161] 18 p2626 N90-24962
Microstructure and stability of TiB2 and Cu multilayers
[DE90-011955] 18 p2627 N90-24968
The effect of trace amounts of antimony on the structure and properties of aluminum alloy A356.2
[DE90-010461] 19 p2674 N90-25207
Microstructures of superconducting YBa2Cu3O(7-x) thin films
[DE90-011976] 19 p2761 N90-25688
Application of high performance metals in gas turbine engines
[PNR90640] 20 p2811 N90-25999
The influence of microstructure on the tensile behavior of an aluminum metal matrix composite
[NASA-TM-102694] 20 p2827 N90-26082
Investigation of thermo-mechanical effects in silicon carbide Whisker/Al alloy composites
[AD-A222635] 20 p2828 N90-26089
Hydrogen induced fracture characteristics of single crystal nickel-based superalloys
[NASA-CR-183992] 20 p2832 N90-26108
Microstructural dependence of the cavitation damage function in FCC materials
[DE90-012898] 20 p2833 N90-26113
Microstructural design for fatigue crack growth resistance in Ni-base alloy
[PNR90632] 20 p2834 N90-26120
Structures and mechanical properties of near-beta titanium alloys TiV10Fe2Al3 and TiV10Cu3Al3
[ONERA-NT-1989-3] 20 p2835 N90-26123
Influence of the manufacturing conditions on the microstructure and mechanical properties of the silicon nitride
[ISAL-90-0008] 20 p2840 N90-26154
DoD-University research instrumentation program, FY 1986/FY 1987
[AD-A222578] 20 p2859 N90-26263
Critical current density, flux creep, and microstructure in a Bi-Sr-Ca-Cu-O system
[DE90-010457] 20 p2931 N90-26676
Composite materials with improved properties in compression: Copolymerization of 1,1-dimethyl-1-Silacyclopent-3-ene and 1,1-diphenyl-1-Silacyclopent-3-ene. Characterization of copolymer microstructures by H1, C13, and Si29 NMR spectroscopy
[AD-A221686] 21 p2972 N90-26892
Solidification processing of alloys using an applied electric field
[NASA-CASE-MFS-26083-1-CU] 21 p2981 N90-26940
Weldment mechanical properties of aluminum-copper-lithium alloy, 2090, at ambient and cryogenic temperatures
[DE90-014178] 21 p2981 N90-26941
Microstructural development in HSLA-100 steel weld metals
[AD-A222105] 21 p2982 N90-26944
Fabrication of microwave guides using high Tc superconductors
[AD-A221580] 21 p3001 N90-27059
The effect of processing, deformation and annealing on the microstructure of Y1Ba2Cu3O7-(sub delta)
[DE90-011731] 21 p3079 N90-27510
Electron-phonon interaction and transport in artificially made semiconductor microstructures
[AD-A223061] 21 p3082 N90-27529
The effect of reinforcement stability on composition redistribution in cast aluminum metal matrix composites
[DE90-012469] 22 p3135 N90-27791
Oxygen stabilization induced enhancement in J(sub c) and T(sub c) of superconducting oxides
22 p3137 N90-27800
Microstructure and magnetization of doped Y-Ba-Ca-O materials prepared by melt quench and post annealing method 22 p3138 N90-27803
Study of local structure and magnetism in high-T(sub c) copper oxide superconductors
22 p3143 N90-27824
Effects of grain size and grain boundary on critical current density of high T(sub c) superconducting oxides
22 p3146 N90-27843
Microstructures and properties of superconducting Y-Er-BaCu-O thin films obtained from disordered Y-Er-BaF2-Cu films 22 p3147 N90-27848
Grain orientation studies in superconductors
22 p3148 N90-27852
Plane strain fracture toughness test procedures for particulate metal matrix composites
[NPL-DMM(A)-3] 22 p3153 N90-27873
Elementary characterization of the pre-impregnated carbon/epoxy NCHR 914/155/34 percent-T300F from Brochier after the technical note CEAT number 1/M/87
[CEAT-PV-M7/6211] 22 p3154 N90-27884
Development of metastable processing paths for high temperature alloys
[AD-A223144] 22 p3157 N90-27898
Study of the microstructure of a titanium alloy (6246) for turbomachine compressors
[ETN-90-97450] 22 p3157 N90-27900
Methodology of the fatigue under shocks. Experimental results: 7075 T6 and 35 NCD16
[ETCA-89-R-140] 22 p3157 N90-27901
Characterization of the CP 214 T851. Dissection of a cast flat bar for a standard spar
[CEAT-PV-M4/462200] 22 p3158 N90-27905
Characterization of the 7175 T7352. Dissection of a die casting standard spar
[CEAT-PV-M5/528900] 22 p3158 N90-27906
Characterization of the 7175 T7352 101. Dissection of a die casting standard spar
[CEAT-PV-M5/5288] 22 p3158 N90-27907
Characterization of the 7010 T73651. Dissection of a sheet billet for a standard spar
[CEAT-PV-M5/521700] 22 p3158 N90-27908
High-temperature deformation of silicon
[DE90-013628] 22 p3160 N90-27919
Study of the structure of ZrO2-Al2O3 plasma sprayed coatings
[ETCA-89-R-078] 22 p3161 N90-27924
Characteristics required for thermal barriers of zirconium oxide-yttrium compounds obtained by plasma spraying. Morphological analysis by x ray diffraction
[ETCA-89-R-113] 22 p3161 N90-27925
Sintering of ceramics by laser irradiation
[ETCA-89-R-134] 22 p3161 N90-27926
The mathematical modeling of arc welding operation
[DE90-013700] 22 p3183 N90-28064
The October 27-28, 1986, FIRE cirrus case study: Cloud microstructure 22 p3224 N90-28283
Friction microprobe studies of composite surfaces
[DE90-014224] 23 p3299 N90-28662
High temperature oxidation of Al-Li alloys
23 p3307 N90-28705
Microstructure and impurity effects on tungsten heavy alloys
[AD-A224220] 23 p3311 N90-28728
High-temperature deformation and microstructural analysis for Si3N4-Sc2O3
[NASA-TM-103239] 23 p3314 N90-28740
Containerless low gravity processing of glass forming and immiscible alloys
[NASA-CR-186999] 23 p3316 N90-28747
Some studies of the vibration welding of thermoplastics 23 p3332 N90-28842
Evaluation of several micromechanics models for discontinuously reinforced metal matrix composites
[NASA-TM-102719] 23 p3339 N90-28872
Electron microscopy of transition-metal doped BiCaSrCuO
[DE90-014184] 23 p3398 N90-29202
XANES and EXAFS study of Au-substituted YBa2Cu3O(7-delta)
[NASA-TM-103291] 23 p3401 N90-29219
The overall response of composite materials undergoing large elastic deformations
[AD-A224509] 24 p3442 N90-29439
Microstructure of alpha-Al base matrix/SiC particulate composites
[DE90-014894] 24 p3444 N90-29449
Influence of convection on microstructure
[NASA-CR-186506] 24 p3448 N90-29470
Effects of low Chromium(3) concentration in electrodeposition of low contraction chromium
[AD-A223338] 24 p3449 N90-29477
A welding metallurgy study of Hastelloy Alloys B-2 and W
[DE90-011910] 24 p3449 N90-29481
The influence of solidification rate on solute redistribution and second-phase formation in stainless steel alloys
[DE90-015189] 24 p3450 N90-29482
Single-phase solidification during rapid resolidification of stainless steel alloys
[DE90-015190] 24 p3450 N90-29483
Relationship between microstructure, spinodal-like decomposition and selective electropolishing of irradiated invar-type alloys
[DE90-015293] 24 p3450 N90-29484
Tensile behavior and swelling of ternary austenitic alloys irradiated in different neutron spectra
[DE90-015295] 24 p3450 N90-29485
Investigation of the effects of microalloy constituents, surface treatment and oxidation conditions on the development and breakdown of protective oxide scales
[DE90-015710] 24 p3451 N90-29488
Wear of advanced ceramics: An overview
[DE90-012168] 24 p3456 N90-29519
Transmission electron microscopy study of ICB Al on Ge and Si(001) substrates
[DE90-015299] 24 p3553 N90-30103
Advanced materials and electrochemical processes in high-temperature solid electrolytes
[DE90-015552] 24 p3553 N90-30104

Study of hot carrier relaxation in quantum wells by subpicosecond Raman scattering
[DE90-015635] 24 p3554 N90-30107

MICROWAVE AMPLIFIERS
NT CYCLOTRON RESONANCE DEVICES
Spin-lattice relaxation and the calculation of gain, pump power, and noise temperature in ruby
04 p0486 N90-12790
A closed-cycle refrigerator for cooling maser amplifiers below 4 Kelvin
04 p0487 N90-12797
Recent developments of gigatron technology
[DE90-001067] 06 p0769 N90-14474
Gigatron: A new technology for microwave power devices
[DE90-001066] 06 p0771 N90-14483
Mechanical design of the inside launch system for electron cyclotron heating in D3-D
[DE90-003292] 07 p0995 N90-15751
Compression phenomena in hard-saturated microwave amplifiers
[AD-A214546] 09 p1204 N90-16980
Output performance of idealized microwave power amplifiers
[AD-A216797] 11 p1502 N90-18645
Numerical simulation of cross field amplifiers
[DE90-006459] 12 p1652 N90-19496
High efficiency octave bandwidth millimeter wave power amplifier
[AD-A218245] 14 p1969 N90-21280
Millimeter-wave gyroklystron amplifier experiment using a relativistic electron beam
[AD-A221209] 18 p2548 N90-24544
Microwave generation for magnetic fusion energy applications
[DE90-011042] 18 p2617 N90-24906
Design and realization of a two stage C-band low noise amplifier
[FEL-89-B265] 23 p3322 N90-28783

MICROWAVE ANTENNAS
NT HORN ANTENNAS
NT LENS ANTENNAS
NT RECTENNAS
NT SPACETENNAS
Power for the moon: Is microwave power beaming an option?
01 p0030 N90-10158
Antenna beamforming using optical processing
[NASA-CR-180844] 02 p0212 N90-11210
Scannable millimeter wave arrays, volume 1
[AD-A213895] 07 p0924 N90-15347
Scannable millimeter wave arrays, volume 2
[AD-A213896] 07 p0924 N90-15348
A study of a new time-domain method of lines and its application for the characterization of microstrip line and its discontinuities
[AD-A215441] 09 p1213 N90-17034
Millimeter wave near-field study
[NASA-CR-182014] 14 p1932 N90-21058
Optical control of an 8-element Ka-band phased array using a high-speed optoelectronic interconnect
[NASA-TM-102550] 14 p1968 N90-21275
A real-time signal combining system for Ka-band feed arrays using maximum-likelihood weight estimates
15 p2076 N90-21888
Development of an optimized compact test range
[MBB-0053/88-PUB] 19 p2651 N90-25085
High performance millimeter-wave microstrip circulators and isolators
[NASA-CR-186276] 19 p2685 N90-25270
Design of an optically controlled Ka-band GaAs MMIC phased-array antenna
[NASA-TM-103147] 20 p2857 N90-26250
Thermal-distortion analysis of an antenna strongback for geostationary high-frequency microwave applications
[NASA-TP-3016] 22 p3125 N90-27738
Design and performance of a long, over-water microwave radio link
[PB90-207994] 23 p3318 N90-28758

MICROWAVE ATTENUATION
Design of a microwave calorimeter for the microwave tokamak experiment
[DE90-004486] 10 p1387 N90-18026
Laboratory measurements and modeling of microwave absorption by ammonia in gas mixtures applicable to giant planet atmospheres
20 p2944 N90-26750
Wear metal analysis in engine oil by microwave digestion and atomic absorption spectroscopy
[AD-A223070] 21 p2985 N90-26964

MICROWAVE CIRCUITS
A general-purpose computer program for the Volterra-series analysis of nonlinear microwave circuits
[AD-A210768] 02 p0216 N90-11236
Computer aided design of monolithic microwave and millimeter wave integrated circuits and subsystems
[AD-A213656] 07 p0923 N90-15343
Universal nondestructive MM-wave integrated circuit test fixture
[NASA-CASE-LEW-14746-1] 09 p1209 N90-17009
Theoretical analysis of microwave and millimeter wave integrated circuits based on magnetic films
[AD-A214772] 09 p1211 N90-17021
Research on monolithic millimeter-wave devices
[AD-A215771] 10 p1379 N90-17996
Reconfigurable antennas, monolithic microwave integrated circuits with feeding networks for microstrip antennas
[AD-A216916] 11 p1498 N90-18622
Analysis of radiometer calibration effects with TOUCHSTONE
[NASA-CR-186476] 13 p1792 N90-20284
Performance of a 300 Mbps 1:16 serial/parallel optoelectronic receiver module
[NASA-TM-103110] 13 p1795 N90-20302
The 5th Annual Review of Progress in Applied Computational Electromagnetics
[AD-A217994] 14 p1966 N90-21258
Coplanar waveguide fed phased array antenna
[NASA-TM-102522] 14 p1968 N90-21273
Indium phosphide planar Gunn diode
[AD-A219337] 16 p2233 N90-22740
Millimeter wave filter design with suspended stripline
[AD-A219582] 17 p2395 N90-23645
Analysis and applications of the crosstie-overlay slow-wave structure
[AD-A220296] 18 p2547 N90-24537
High performance millimeter-wave microstrip circulators and isolators
[NASA-CR-186276] 19 p2685 N90-25270
High temperature superconductivity applications for electronic warfare and microwave systems
[AD-A222972] 21 p3082 N90-27528
High temperature superconducting thin film microwave circuits: Fabrication, characterization, and applications
[NASA-TM-103235] 23 p3322 N90-28786

MICROWAVE COUPLING
Topics in HPM (High-Power Microwave) generation, coupling, and interaction
[AD-A216882] 12 p1682 N90-19658

MICROWAVE EMISSION
The Owens Valley solar array
03 p0435 N90-12490
Squeezing of many-atom radiation in an optical cavity
[AD-A215736] 09 p1280 N90-17422

MICROWAVE EQUIPMENT
NT BACKWARD WAVE TUBES
NT CARCINOTRONS
NT CYCLOTRON RESONANCE DEVICES
NT HORN ANTENNAS
NT KLYSTRONS
NT LENS ANTENNAS
NT MAGNETRONS
NT MICROWAVE AMPLIFIERS
NT MICROWAVE ANTENNAS
NT MICROWAVE FILTERS
NT MICROWAVE INTERFEROMETERS
NT MICROWAVE OSCILLATORS
NT MICROWAVE RADIOMETERS
NT MICROWAVE TUBES
NT RECTENNAS
NT SPACETENNAS
NT THYRATRONS
NT TRAVELING WAVE TUBES
Microwave signal detection using modulation of polymeric optical waveguides
[DE89-017545] 03 p0337 N90-11921
A 2-MeV microwave thermionic gun
[DE89-015640] 04 p0494 N90-12844
Microwave Tokamak Experiment: An overview of the construction and checkout phase
[DE90-000834] 06 p0847 N90-14924
RF transistor thermal/electrical characterization
[DE90-001427] 07 p0920 N90-15326
A study of Inter-Injection-Locked phased arrays
[AD-A214097] 07 p0925 N90-15352
The 17.1-GHz free-electron laser as a microwave source for TeV colliders
[DE90-001506] 07 p0934 N90-15406
Life test programme of ERS-1 AMI-high power amplifier
10 p1330 N90-17684
On 140 GHz microwave FEL experiments using ELF-2
[DE90-006764] 12 p1667 N90-19576
High power, high sensitivity microwave calorimeter
[AD-D014427] 14 p1982 N90-21355
Method of making a cathode from tungsten powder
[AD-D014434] 15 p2069 N90-21850
Construction of a 345 gigahertz receiver based on superconducting tunnel junctions
[AD-A218781] 16 p2232 N90-22735
Continued development and characterization of doped layers, contacts and associated electronic devices in silicon carbide
[AD-A219234] 16 p2232 N90-22738
Optical links for microwave application
[AD-A220574] 17 p2472 N90-24134
Radars in space
21 p3015 N90-27144
High temperature superconductivity applications for electronic warfare and microwave systems
[AD-A222972] 21 p3082 N90-27528
The NASA high temperature superconductivity program
22 p3145 N90-27836
Ground-based weather radar compatibility with digital radio-relay microwave systems
[PB90-206236] 23 p3318 N90-28756

MICROWAVE FILTERS
Millimeter wave filter design with suspended stripline
[AD-A219582] 17 p2395 N90-23645
Approximation, synthesis, and development of bi-mode cavities microwave filters presenting unsymmetrical quasi-elliptic responses
[CNES-NT-124] 23 p3318 N90-28761
Microwave active filters based on coupled negative resistance method
[AD-A223269] 24 p3464 N90-29570

MICROWAVE FREQUENCIES
NT C BAND
NT EXTREMELY HIGH FREQUENCIES
NT SUPERHIGH FREQUENCIES
Design, construction and test of a frequency doubler for 183 GHz
[PB89-212591] 03 p0341 N90-11944
Helsinki University of Technology Radio Laboratory
[PB90-110677] 08 p1056 N90-16102
Development of a six port network analysis tool for the 1 to 18 GHz bandwidth range
[TELECOM-PARIS-89-D-015] 18 p2545 N90-24527
U. radio emission from quiescent filaments
[NASA-CR-186538] 19 p2797 N90-25922
A global approach to image texture analysis
[AD-A223532] 24 p3527 N90-29941
Investigation of x ray variability in highly active cool stars
[NASA-CR-183853] 24 p3560 N90-30143

MICROWAVE IMAGERY
Estimation of rain rate using spatial and multichannel coherence: Analysis of SSM/I data
05 p0670 N90-13905
Laboratory of Space Technology
[PB90-110651] 08 p1033 N90-15967
Multiparameter scatterometer for remote sensing (RADSER). Project Scatter: State-of-the-art and future applications
[INPE-4871-PRE/1482] 11 p1511 N90-18701
Coherent radar measurement of ocean currents from geostationary orbit
12 p1609 N90-19259
Applications of microwave radiometric measurements to infer tropical cyclone intensity and strength
[AD-A218273] 13 p1847 N90-20600
A correlation study of wind speed as measured by the special sensor microwave/imager and the GEOSAT altimeter
[AD-A219841] 18 p2581 N90-24701

MICROWAVE INTERFEROMETERS
Simultaneous multiple frequency interferometry: An application of homodyne phase measurement
[DE89-013975] 01 p0126 N90-10719
The space microwave interferometer and the search for cosmic background gravitational wave radiation
12 p1731 N90-19952

MICROWAVE LANDING SYSTEMS
ILS/MLS comparison tests at Miami/Tamiami, Florida Airport
[ACD-330] 01 p0005 N90-10018
The addition of Bendix MLS (Microwave Landing System) antenna patterns to MLS mathematical model
[AD-A210633] 01 p0005 N90-10020
Helicopter Visual Segment Approach Lighting System (HALS)
[ACD-330] 02 p0150 N90-10856
Simulations for computer centerline approach
[DOT/FAA/CT-TN89/41] 03 p0304 N90-11726
Independent Orbiter Assessment (IOA): FMEA/CIL assessment
[NASA-CR-185550] 03 p0314 N90-11783
Microwave Landing System (MLS) remote monitoring subsystem/remote maintenance monitoring system
[DOT/FAA/PS-89/2] 15 p2050 N90-21749
Microwave Landing System (MLS) multiple system design interoperability interface control report
[DOT/FAA/SA-89/2] 15 p2050 N90-21750
An evaluation of the accuracy of a microwave landing system area navigation system at Miami/Tamiami Florida Airport
[DOT/FAA/CT-TN89/40] 17 p2349 N90-23377

MLS mathematical model validation study using airborne MLS data from Midway Airport engineering flight tests, August 1988
[DOT/FAA/CT-TN90/2] 17 p2349 N90-23378
Position computation without elevation information for computed centerline operations
[DOT/FAA/CT-TN89/42] 17 p2349 N90-23379
Analysis of the integrity of the Microwave Landing System (MLS) data functions 24 p3428 N90-29365

MICROWAVE OSCILLATORS
NT MAGNETRONS
Low noise, high voltage supply for carcinotron backward wave oscillators 10 p1338 N90-17742
Research on monolithic millimeter-wave devices
[AD-A215771] 10 p1379 N90-17996
Hamiltonian analysis and simulation of free electron lasers
[INPE-4785-TDL/351] 11 p1567 N90-19018
Microwave oscillator with reduced phase noise by negative feedback incorporating microwave signals with suppressed carrier 12 p1643 N90-19437
Experimental demonstration of an electromagnetically pumped free-electron laser with cyclotron harmonic idlers
[AD-A218830] 17 p2408 N90-23719
Sequentially evaporated thin film YBa2Cu3O(7-x) superconducting microwave ring resonator
[NASA-TM-103180] 19 p2685 N90-25273
High temperature superconducting thin film microwave circuits: Fabrication, characterization, and applications
[NASA-TM-103235] 23 p3322 N90-28786
High power microwaves for defense and accelerator applications
[AD-A223550] 24 p3464 N90-29572
Beam and plasma physics research
[AD-A224452] 24 p3548 N90-30067

MICROWAVE POWER BEAMING
Second Beamed Space-Power Workshop
[NASA-CP-3037] 01 p0027 N90-10140
Power beaming options 01 p0027 N90-10142
History and status of beamed power technology and applications at 2.45 Gigahertz 01 p0029 N90-10150
Overview of microwave concepts
01 p0029 N90-10155
Power for the moon: Is microwave power beaming an option? 01 p0030 N90-10158
Microwave beam power 01 p0030 N90-10165
Lunar power system summary of studies for the lunar enterprise task force NASA-office of exploration
07 p1008 N90-15841
Theoretical and experimental investigation of axial power extraction from a magnetically insulated transmission line oscillator
[DE90-003486] 08 p1060 N90-16131
Millimeter-wave gyroklystron amplifier experiment using a relativistic electron beam
[AD-A221209] 18 p2548 N90-24544
Lunar orbiting microwave beam power system
[NASA-TM-103211] 19 p2667 N90-25173
Analysis of a Mars-stationary orbiting microwave power transmission system
[NASA-TM-101344] 20 p2843 N90-26172

MICROWAVE RADIATION
U MICROWAVES

MICROWAVE RADIOMETERS
Venus surface properties deduced from radar and radiometry 03 p0423 N90-12431
Radiometric observations at 20.6, 31.65, and 90.0 GHz: Continuing studies 10 p1373 N90-17958
Synthetic Aperture Interferometric Radiometer (SAIR)
12 p1610 N90-19261
Applications of microwave radiometric measurements to infer tropical cyclone intensity and strength
[AD-A218273] 13 p1847 N90-20600
Microwave brightness temperature and its relation to atmospheric general circulation features
[AD-A218312] 13 p1847 N90-20603
HgCdTe 256x256 NWIR FPA
14 p1981 N90-21348
Use of microwave satellite data to study variations in rainfall over the Indian Ocean
[NASA-CR-186408] 14 p2007 N90-21501
Characterizing microwave propagation using the AFGL microwave attenuation/transmittance/brightness temperature code
[AD-A220248] 18 p2543 N90-24513
Spatial cross-correlation of Antarctic Sea ice and seabed topography
[NASA-CR-186815] 20 p2891 N90-26451
Basic data requirements for microwave radiometer systems 21 p3015 N90-27143
Observed cloud reflectivities and liquid water paths: An update 22 p3215 N90-28237

MICROWAVE REFLECTOMETERS
Modelling and synergism: Optical and microwave remote sensing. Partial report 1: Preliminary study
[BCRS-89-23] 18 p2575 N90-24668

MICROWAVE RESONANCE
Microwave microstrip resonator measurements of Y1Ba2Cu3O(7-x) and Bi2Sr2Ca1Cu2O(8-y) thin films
[NASA-TM-102159] 05 p0635 N90-13704

MICROWAVE SCATTERING
Propagation of an elliptical laser beam through the turbulent atmosphere (vertical beams)
[PB89-208680] 03 p0352 N90-12010
Experimental and theoretical study of artificial plasma layers produced by two intersecting beams in a chamber
[NASA-CR-184598] 05 p0701 N90-14102
MODTRAN: A moderate resolution model for LOWTRAN 7
[AD-A214337] 07 p0978 N90-15650
The AGRISCATT-87 campaign: Processing of the Dutscat data
[BCRS-89-20] 15 p2122 N90-22140
Characterizing microwave propagation using the AFGL microwave attenuation/transmittance/brightness temperature code
[AD-A220248] 18 p2543 N90-24513

MICROWAVE SENSORS
Earth Science Geostationary Platform Technology
[NASA-CP-3040] 12 p1608 N90-19249
Science requirements for passive microwave sensors on earth science geostationary platforms
12 p1608 N90-19251
Characterizing microwave propagation using the AFGL microwave attenuation/transmittance/brightness temperature code
[AD-A220248] 18 p2543 N90-24513
A correlation study of wind speed as measured by the special sensor microwave/imager and the GEOSAT altimeter
[AD-A219841] 18 p2581 N90-24701
Impact of a unified DMSP meteorological sensor retrieval methodology on global numerical weather prediction
[AD-A220306] 18 p2581 N90-24703
Radars in space 21 p3015 N90-27144

MICROWAVE SOUNDING
A study of the impact of simulated 183 GHz water vapor retrievals on numerical weather prediction
[AD-A210431] 01 p0088 N90-10504
Middle Atmosphere Program. Handbook for MAP, volume 28
[NASA-CR-184972] 03 p0370 N90-12117
Estimation of rain rate using spatial and multichannel coherence: Analysis of SSM/I data
05 p0670 N90-13905
Microwave brightness temperature and its relation to atmospheric general circulation features
[AD-A218312] 13 p1847 N90-20603
Thermal-distortion analysis of an antenna strongback for geostationary high-frequency microwave applications
[NASA-TP-3016] 22 p3125 N90-27738

MICROWAVE SPECTRA
Observations of CO on Mars in the infrared and millimetre range 11 p1578 N90-19090
The microwave background in steady-state cosmology
11 p1587 N90-19150
Frequency domain techniques for analyzing picosecond optical pulses
[AD-A218856] 16 p2318 N90-23214
Laboratory measurements and modeling of microwave absorption by ammonia in gas mixtures applicable to giant planet atmospheres 20 p2944 N90-26750
Microwave spectra of van der Waals complexes of importance in planetary atmospheres
20 p2944 N90-26752

MICROWAVE SWITCHING
Channelized coplanar waveguide pin-diode switches
[NASA-TM-102289] 03 p0341 N90-11943
Characterization of two MMIC GaAs switch matrices at microwave frequencies
[NASA-TM-102449] 06 p0733 N90-14273

MICROWAVE TRANSMISSION
Power for the moon: Is microwave power beaming an option? 01 p0030 N90-10158
An experimental study of microwave transmission through a decaying plasma
[AD-A210586] 01 p0127 N90-10726
Channelized coplanar waveguide pin-diode switches
[NASA-TM-102289] 03 p0341 N90-11943
Ka-band MMIC beam steered transmitter array
04 p0488 N90-12803
Ground effects on multipath fading
[TELECOM-PARIS-88-E017] 04 p0489 N90-12812
Microwave Transport Systems for the MTX (Microwave Tokamak Experiment)
[DE90-000821] 06 p0846 N90-14921
Rectangular-to-circular waveguide transitions for high-power circular overmoded waveguides
[AD-A213925] 07 p0924 N90-15349
The Solar Power Satellite (SPS): Progress so far
07 p1008 N90-15840
Lunar power system summary of studies for the lunar enterprise task force NASA-office of exploration
07 p1008 N90-15841
Planar integrated circuits for microwave transmission and reception
[AD-A217676] 12 p1656 N90-19520
Inflatable antennas for microwave pwoer transmission
15 p2060 N90-21799
Microwave analog fiber-optic link for use in the deep space network 15 p2075 N90-21883
NASA 60 GHz intersatellite communication link definition study. Addendum A: Mixed baseband and IF signals
[NASA-CR-186337] 17 p2387 N90-23593
NASA 60 GHz intersatellite communication link definition study. Baseline document
[NASA-CR-186339] 17 p2387 N90-23594
NASA 60 GHz intersatellite links definition study. Final Review
[NASA-CR-186338] 17 p2387 N90-23595
Microwave transmission line and method of modulating the phase of a signal passed through said line
[AD-D014457] 17 p2395 N90-23640

MICROWAVE TUBES
NT BACKWARD WAVE TUBES
NT CARCINOTRONS
NT CYCLOTRON RESONANCE DEVICES
NT KLYSTRONS
NT MAGNETRONS
NT TRAVELING WAVE TUBES
Transport properties of plasmas in microwave electrothermal thrusters
[AD-A219408] 16 p2320 N90-23228

MICROWAVES
NT CENTIMETER WAVES
NT MICROWAVE EMISSION
NT MILLIMETER WAVES
Antenna technology for beamed space-power
01 p0028 N90-10149
Technical options for high average power free electron milimeter-wave and laser devices
01 p0029 N90-10151
Overview of microwave concepts
01 p0029 N90-10155
Power for the moon: Is microwave power beaming an option? 01 p0030 N90-10158
Microwave beam power 01 p0030 N90-10165
Laboratory measurements of microwave and millimeter-wave properties of planetary atmospheric constituents
[NASA-CR-185914] 01 p0141 N90-10815
HPW (High Power Microwave) testing of electronic components
[DE89-016682] 02 p0217 N90-11241
High-temperature ceramic superconductors
[AD-A211070] 02 p0283 N90-11618
Calibration and de-embedding of microwave measurements using any combination of one- or two-port standards
[PB89-212674] 03 p0337 N90-11916
Microwave signal detection using modulation of polymeric optical waveguides
[DE89-017545] 03 p0337 N90-11921
Microwave instability near transition energy
[DE90-000107] 03 p0338 N90-11922
Microwave Tokamak Experiment (MTX) ohmic heating system
[DE89-017892] 03 p0408 N90-12340
Apollo lightcraft project
[NASA-CR-186055] 04 p0464 N90-12655
DSN 70-meter antenna microwave optics design and performance improvements. Part 2: Comparison with measurements 04 p0487 N90-12800
Microwave excitation of oxygen O2 (delta 1) for an oxygen-iodine laser
[DFVLR-FB-89-23] 04 p0506 N90-12919
Microwave excited excimer laser
[ETN-90-95909] 05 p0648 N90-13781
SEM (Scanning Electron Microscope) image analysis of grain growth in microwave-annealed alumina
[DE90-001606] 06 p0746 N90-14339
Symmetric waveguide junction combiner
[AD-D014243] 06 p0768 N90-14466
Monolithic laser diode structure for microwave generation
[AD-D014210] 06 p0782 N90-14543
Microwave Tokamak Experiment (MTX) first year of operation and future plans
[DE90-000817] 06 p0846 N90-14920

MTX (Microwave Tokamak Experiment)/ELF (Electron Laser Facility) 2 microwave power measurements and calibration for the 2-GW, 140-GHz, ELF 2 Free Electron Laser (FEL)
[DE90-000825] 06 p0846 N90-14922
Microwave characterization of high-temperature superconductors
[DE90-002408] 06 p0854 N90-14968
Laboratory evaluation and application of microwave absorption properties under simulated conditions for planetary atmospheres
[NASA-CR-185916] 06 p0865 N90-15025
Intense REB (Relativistic Electron Beam) transport in a weakly magnetized plasma
[DE90-002978] 07 p0994 N90-15749
Helsinki University of Technology Radio Laboratory
[PB90-110677] 08 p1056 N90-16102
Reflection from layered media with special attention to the microwave region
[ESA-TT-1155] 08 p1057 N90-16111
Microwave screening on digital radio communication links due to multicircuit power transmission lines
[DE90-734950] 08 p1058 N90-16118
Mechanisms of microwave induced damage in biologic materials
[AD-A213480] 08 p1104 N90-16390
Two-dimensional, long-pulse simulation of microwave-induced electron layer evolution in low-pressure air
[DE90-005180] 09 p1208 N90-17004
Two-dimensional calculation of sequential electron layer formation by crossed microwave beams in air at low pressure
[DE90-005254] 09 p1286 N90-17453
On multiple edge diffraction and multiple reflections of microwaves over terrain
[AD-A216418] 10 p1377 N90-17985
Design of a microwave calorimeter for the microwave tokamak experiment
[DE90-004486] 10 p1387 N90-18026
Microwave free-electron laser applications for electron cyclotron heating of plasmas
[DE90-005203] 10 p1431 N90-18257
Microwave radiation absorption by Ho(Y)-Ba-Cu-O superconducting ceramics
[DE90-610665] 11 p1492 N90-18588
Quick, reliable estimates of high-power microwave fluences: The SNEAKY-2 program
[DE90-006347] 11 p1498 N90-18624
Instability investigation for storage mode. Microwave instability (single-bunch instability)
[NIKHEF-K/AMPS/89/05] 11 p1499 N90-18628
Determining the effects of microwave power and C-field setting on the frequency of a cesium atomic frequency standard
[AD-A216599] 11 p1501 N90-18642
Output performance of idealized microwave power amplifiers
[AD-A216797] 11 p1502 N90-18645
Signal processing device to control microwave output
[AD-A216931] 11 p1502 N90-18648
Effects of pulsed and CW (Continuous Wave) 2450 MHz radiation on transformation and chromosomes of human lymphocytes in vitro
[AD-A216500] 11 p1539 N90-18857
Processing of advanced ceramics using microwaves thermal treatments
[DE90-606349] 12 p1629 N90-19362
Sparse breakdown and statistical sneakthrough effects in low-altitude microwave propagation
[DE90-007252] 12 p1648 N90-19473
Planar integrated circuits for microwave transmission and reception
[AD-A217676] 12 p1656 N90-19520
On 140 GHz microwave FEL experiments using ELF-2
[DE90-006764] 12 p1667 N90-19576
Microwave field effect transistor
[NASA-CASE-GSC-12442-2] 13 p1792 N90-20282
Growth, characterization and device development in monocrystalline diamond films
[AD-A218211] 13 p1898 N90-20895
JPRS report: Science and technology. USSR: Electronics and electrical engineering
[JPRS-UEE-90-002] 14 p1970 N90-21284
Microwave analog fiber-optic link for use in the deep space network 15 p2075 N90-21883
Spectral measurements of the cosmic microwave background 16 p2340 N90-23334
The microwave permeability of conducting spherical shells
[AD-A220746] 17 p2369 N90-23485
Lack of behavioral effects of high-peak-power microwave pulses from an axially extracted virtual cathode oscillator
[AD-A220779] 17 p2391 N90-23618
High peak power microwave pulses at 2.37 GHz: No effects on vigilance performance in monkeys
[AD-A219570] 17 p2433 N90-23863
Periodic signatures for the detection of cosmic axions
[NASA-CR-186608] 17 p2470 N90-24122
Evolution of light domain walls interacting with dark matter, part 1
[NASA-CR-181123] 17 p2485 N90-24211
A laboratory investigation into microwave backscattering from sea ice
[NASA-CR-186621] 18 p2542 N90-24510
Near field curvature at parallel phase objects: Model examination with microwaves
[ETN-90-96499] 18 p2545 N90-24525
Research studies on extreme ultraviolet and soft x ray lasers
[AD-A220271] 18 p2562 N90-24621
Microwave generation for magnetic fusion energy applications
[DE90-011042] 18 p2617 N90-24906
RF properties of high temperature superconductors: Cavity methods
[DE90-011961] 18 p2627 N90-24969
Large scale structure and microwave background anisotropies in cosmological models and stellar photometry techniques with the wide field/planetary camera of the Hubble space telescope 18 p2637 N90-25023
A laboratory investigation into microwave backscattering from sea ice
[NASA-CR-186357] 19 p2705 N90-25390
In-band amplitude dispersion on a microwave link 20 p2846 N90-26189
Laboratory measurements of microwave and millimeter-wave properties of planetary constituents 20 p2943 N90-26745
High resolution spectroscopy in the microwave and far infrared 20 p2943 N90-26746
A summary of measurements of permittivities and permeabilities of some microwave absorbing materials
[AD-A223221] 21 p2995 N90-27026
Dependence of radar backscatter on the energetics of the air-sea interface
[AD-A221966] 21 p2996 N90-27028
Fabrication of microwave guides using high Tc superconductors
[AD-A221560] 21 p3001 N90-27059
Crossed-microwave-beam air ionization laboratory experiments
[DE90-012056] 21 p3024 N90-27195
Structure and dynamics of excited atoms
[AD-A221973] 21 p3074 N90-27474
High temperature superconductivity applications for electronic warfare and microwave systems
[AD-A222972] 21 p3082 N90-27528
Microwave conductivity of laser ablated YBaCuO superconducting films and its relation to microstrip transmission line 22 p3147 N90-27844
Optical and microwave detection using Bi-Sr-Ca-Cu-O thin films 22 p3152 N90-27870
Design and performance of a long, over-water microwave radio link
[PB90-207994] 23 p3318 N90-28758
Activities of the Division of Microwave Technology
[FOA-C-30555-3.2] 24 p3459 N90-29537
Microwave background distortions from domain walls
[NASA-CR-187272] 24 p3462 N90-29556
Characteristic microwave background distortions from collapsing domain wall bubbles
[NASA-CR-187270] 24 p3462 N90-29557
Reliability study of TWT output RF window
[AD-A223688] 24 p3465 N90-29574
An x ray source for lithography
[AD-D014596] 24 p3473 N90-29630
Production of NO, NO2 and N2O in air by breakdown with high power microwaves: A preliminary report
[AD-A223297] 24 p3495 N90-29749
Beam and plasma physics research
[AD-A224452] 24 p3548 N90-30067

MIDAIR COLLISIONS
NT BIRD-AIRCRAFT COLLISIONS
UK airmisses involving commercial air transport, May-August 1988
[ISSN-0951-6301] 03 p0303 N90-11717
UK airmisses involving commercial air transport
[CAA-2/88] 03 p0303 N90-11718
UK airmisses involving commercial air transport, January - April 1989
[ISSN-0951-6301] 16 p2197 N90-22544
Effects of monitoring under high and low taskload on detection of flashing and colored radar targets
[AD-A220313] 17 p2439 N90-23895
UK airmisses involving commercial air transport: May - August 1989
[ISSN-0951-6301] 24 p3422 N90-29335

MIDCOURSE GUIDANCE
Optimal and on-board near-optimal midcourse guidance 02 p0150 N90-10857
Engagement analysis study
[DE90-009529] 15 p2163 N90-22359

MIDCOURSE TRAJECTORIES
High resolution imaging by phase retrieval and discrimination using speckle, volume 1
[AD-A214243] 07 p0919 N90-15317
A trajectory generation and system characterization model for cislunar low-thrust spacecraft. Volume 2: Technical manual
[NASA-CR-185172] 15 p2061 N90-21807

MIDDLE ATMOSPHERE
NT MESOPAUSE
NT MESOSPHERE
NT OZONOSPHERE
NT STRATOPAUSE
NT STRATOSPHERE
Middle Atmosphere Program. Handbook for MAP, volume 28
[NASA-CR-184972] 03 p0370 N90-12117
Evidence for accurate temperatures from the inflatable falling sphere 05 p0657 N90-13835
Observation of wind corners in the middle atmosphere over Andenes (69 N) during winter 1983/84, summer 1987 and summer 1988 05 p0657 N90-13836
The DYANA campaign 1990 05 p0662 N90-13870
Characterization of thunderstorm induced Maxwell current densities in the middle atmosphere 12 p1634 N90-19391
The calculation of infrared limb emission by ozone in the terrestrial middle atmosphere 15 p2125 N90-22151
Gravity wave and turbulence studies using a high-resolution ST radar
[AD-A218877] 16 p2255 N90-22860
Measurements of CH4, N2O, CO, H2O and O3 in the middle atmosphere by the ATMOS experiment on Spacelab 3
[NASA-TM-103476] 20 p2883 N90-26400
The NASA/MSFC Global Reference Atmospheric Model, 1990 version (GRAM-90)
[NASA-CR-186717] 20 p2888 N90-26435
Middle Atmosphere Program. Handbook for MAP, volume 29. Part 1: Extended Abstracts, International Symposium on Solar Activity Forcing of the Middle Atmosphere. Part 2: MASH Workshop
[NASA-CR-186005] 22 p3201 N90-28161
Influence of solar activity on middle atmosphere associated with phases of equatorial quasi-biennial oscillation 22 p3202 N90-28168
Response of the middle atmosphere to solar UV and dynamical perturbations 22 p3204 N90-28175
Gases of the middle atmosphere and short-term solar radiation variations 22 p3204 N90-28177
Physical mechanisms of solar activity effects in the middle atmosphere 22 p3206 N90-28185
Numerical simulation of the middle atmosphere chemical composition and temperature under changing solar conditions 22 p3206 N90-28186
The effects of solar particle events on the middle atmosphere 22 p3206 N90-28189
Energy deposition of corpuscular radiation in the middle atmosphere 22 p3206 N90-28190
Solar activity influence on cosmic ray penetration in the middle atmosphere 22 p3207 N90-28192
Intensive MHD-structures penetration in the middle atmosphere initiated in the ionospheric cusp under quiet geomagnetic conditions 22 p3207 N90-28193
Effects of solar activity in the middle atmosphere dynamical regime over Eastern Siberia, USSR 22 p3207 N90-28195
A new calculation of the radiative cooling by carbon dioxide in the middle atmosphere and the lower thermosphere 22 p3210 N90-28211

MIDLATITUDE ATMOSPHERE
Numerical simulations of a midlatitude squall line 01 p0087 N90-10497
Substorm associated pulsations: A study of plasmaspheric cavity resonance, mid-latitude polarisation and geostationary orbit signatures 02 p0251 N90-11422

MIDLATITUDES
U TEMPERATE REGIONS

MIE SCATTERING
NT RAYLEIGH SCATTERING
Infrared backscattering 03 p0364 N90-12083
Infrared spectrometry of aerosols
[AD-A213303] 04 p0473 N90-12713
The effect of oblate spheroidal drops on rain attenuation at 94 GHz: Comparison between theory and experiment 06 p0763 N90-14440
An investigation of flow structure, mixing and chemical reaction in combusting turbulent flows
[AD-A216739] 11 p1483 N90-18538

The naval oceanic vertical aerosol model
15 p2082 N90-21921
Inclusion of clouds and rain in atmospheric slant path calculations
15 p2083 N90-21925
Modelling UV-visible radiation observed from space
15 p2085 N90-21937
Optical properties of cometary dust
[AD-A218790] 16 p2338 N90-23325
Premixed turbulent flame propagation
[AD-A219834] 17 p2373 N90-23515
The radiation budget of stratocumulus clouds measured by tethered balloon instrumentation: Variability of flux measurements
22 p3216 N90-28242

MIE THEORY
U MIE SCATTERING

MIGRATION
Migration of carbon in tempered martensitic steel during excimer laser melting
[DE90-004838] 09 p1195 N90-16922
A scheme for supporting distributed data structures on multicomputers
[NASA-CR-181987] 10 p1415 N90-18152
Vertical migration in operational system nucleus
[INPE-4879-RPE/593] 11 p1543 N90-18883
Microelectronic device reliability
[AD-A218774] 17 p2394 N90-23638
User's manual ROBIN: A research and notification system for bird migration
[FEL-1989-103] 23 p3270 N90-28508

MILANKOVITCH THEORY
U CLIMATOLOGY

MILITARY AIR FACILITIES
Surface Observation Climatic Summaries (SOCS) for Pease Air Force Base, New Hampshire
[AD-A215750] 10 p1408 N90-18117
The United States Air Force School of Aerospace Medicine: Special report
[AD-A217740] 13 p1851 N90-20622
A comparison of lightning network data with surface weather observations
[AD-A220003] 17 p2427 N90-23832
Source emission test of gas turbine engine test facility, Kelly AFB, TX
[AD-A223869] 23 p3282 N90-28571

MILITARY AIRCRAFT
NDI (Nondestructive Inspection) oriented corrosion control for Army aircraft. Phase 1: Inspection methods
[AD-A213368] 05 p0576 N90-13359
Design trends for Army/Air Force airplanes in the United States
[NASA-TM-4179] 16 p2342 N90-23338
Aircraft drawings index 17 p2343 N90-23340
Model designation of military aerospace vehicles
[PB90-206301] 22 p3107 N90-27646

MILITARY HELICOPTERS
NT AH-1G HELICOPTER
NT AH-64 HELICOPTER
NT CH-47 HELICOPTER
NT H-53 HELICOPTER
NT UH-1 HELICOPTER
NT UH-60A HELICOPTER
Applications of flight control system methods to an advanced combat rotorcraft
[NASA-TM-101054] 03 p0308 N90-11752
Reduced voltage and restart testing of the 1-watt integral cryogenic cooler (HD-1033B/C/D)
[AD-A215133] 09 p1203 N90-16971
Reliability testing of the Hughes temperature controlled 1/4 watt split cycle cryogenic cooler (HD-1045 (V)/UA)
[AD-A216696] 12 p1641 N90-19426
Integration of externally carried weapon systems with military helicopters
[AGARD-AR-247] 22 p3115 N90-27696
The integration of multiple avionic sensors and technologies for future military helicopters
24 p3424 N90-29344

MILITARY OPERATIONS
NT COMBAT
NT ELECTRONIC WARFARE
Communications Data Base (CDB), phase 3 (with software documentation)
[AD-A210540] 01 p0137 N90-10789
Flight testing in the Netherlands: An overview
02 p0155 N90-10884
Recommended changes in US military space policies and programs: A paper submitted to the Commission on Integrated Long-Term Strategy
[PB89-219364] 04 p0460 N90-12636
Algorithm development for SDI weapons system allocation
[AD-A212973] 04 p0534 N90-13090
Electronic warfare: Reliable equipment needed to test Air Force's electronic warfare systems
[AD-A212952] 05 p0632 N90-13687
Concerning advanced architectures for strategic defense
[DE90-001894] 06 p0836 N90-14857
Proceedings of the 17th Conference on Toxicology
[AD-A215076] 09 p1252 N90-17263
Defending against a space blockade: CADRE paper
[AD-A215881] 09 p1276 N90-17398
An investigation into the effects which aerospace industry offset trade agreements have on United States Air Force mission performance
[AD-A215093] 09 p1294 N90-17502
The global positioning system
[AD-A217266] 12 p1602 N90-19222
Limitations of the conventional role of the B-1B in the European theater
[AD-A217285] 12 p1604 N90-19230
Physical performance and carbohydrate consumption in CF commandos during a 5-day field trial
[AD-A217204] 13 p1850 N90-20619
Field assessment of wet bulb globe temperature: Present and future
[AD-A218224] 13 p1853 N90-20635
The thrust and parry of the SIOP (Single Integrated Operational Plan) and SDI
[AD-A217617] 13 p1880 N90-20784
SDI (Strategic Defense Initiative): Is its future past
[DE90-008016] 13 p1880 N90-20785
Role of free-electron lasers in strategic defense
[DE90-008028] 13 p1880 N90-20786
The Department of Defense critical technologies plan for the Committees on Armed Services United States Congress
[AD-A219300] 16 p2227 N90-22702
Environmental effects upon cross-servicing of aircraft in NATO
[AD-A218374] 17 p2343 N90-23341
Optimizing ECM techniques against monopulse acquisition and tracking radars
[AD-A220036] 17 p2393 N90-23629
Laser eye protection
[AD-A219659] 17 p2408 N90-23722
Evaluation of the head injury hazard during military parachuting
[AD-A220724] 17 p2434 N90-23870
Proceedings of the 28th Annual US Army Operations Research Symposium (AORS), volume 1
[AD-A219349] 18 p2606 N90-24842
Military space operations: Shuttle and satellite computer systems do not meet performance objectives
[GAO/IMTEC-88-7] 18 p2635 N90-25014
Advanced mesoscale weather forecasting to support tactical operations on the airland battlefield
[AD-A219421] 19 p2715 N90-25449
United States Naval Academy summary of Research, Academic Departments, 1989-1990
[AD-A221219] 19 p2800 N90-25929
ASATs vs Brilliant Pebbles
[DE90-010348] 20 p2922 N90-26626
Speech Analysis and Synthesis and Man-Machine Speech Communications for Air Operations
[AGARD-LS-170] 21 p2992 N90-27006
Tactical Applications of Space Systems
[AGARD-CP-460] 21 p3067 N90-27438
Tactical applications of Defense Meteorological Satellite Program (DMSP) environmental data
21 p3067 N90-27439
Application of Meteorological Satellite (METSAT) data to support United States forces in the North Atlantic Treaty Organization (NATO)
21 p3068 N90-27440
Hover position sensing system
21 p3069 N90-27448
Tactical applications of the UHF satellite communications system
21 p3070 N90-27451
Tactical EHF satellite communications for NATO employing non-geostationary orbits
21 p3070 N90-27454
Space-base multispectral imagery: Current and future applications and implications to the United States Army
[AD-A224048] 23 p3343 N90-28894
The potential for digital databases in flight planning and flight aiding for combat aircraft
24 p3429 N90-29371
Electro-optics engineering support for the integrated launch and recovery television surveillance system
[AD-A223450] 24 p3436 N90-29406

MILITARY SPACECRAFT
NT DMSP SATELLITES
NT RECONNAISSANCE SPACECRAFT
Rate compatible punctured codes, their use in military satellite communication systems
[AD-A216723] 11 p1497 N90-18619
NASA's Advanced Communications Technology Satellite (ACTS): Will it benefit commercial/military satellites
[AD-A217710] 14 p1939 N90-21100
Report of the Defense Science Board 1989 summer study on national space launch strategy
[AD-A222419] 21 p2963 N90-26848
Tactical Applications of Space Systems
[AGARD-CP-460] 21 p3067 N90-27438

MILITARY TECHNOLOGY
Encyclopedia of US Air Force aircraft and missile systems. Volume 2: Post-World War 2 bombers, 1945-1973
[AD-A209273] 01 p0001 N90-10001
Consumer electronics testing to fast-rise EMP (Electromagnetic Pulse) VEMPS (Vertical Electromagnetic Pulse Simulator) 2 development
[AD-A210505] 01 p0057 N90-10323
Laser techniques for ground to air applications
[FOA-C-30524-3.1] 02 p0228 N90-11309
Post crash flight analysis: Visualizing flight recorder data
[AD-A212063] 03 p0302 N90-11715
Feasibility of graphics voice telephones for the post 2000 era
[FEL-1988-26] 03 p0340 N90-11937
Twenty-five years of service, 1962-1987: Proceedings of the Air Force Studies Board Symposium on Air Force Research and Development, November 16, 1987
[PB89-198915] 03 p0415 N90-12384
FY 1990/FY 1991 biennial budget descriptive summaries for the Strategic Defense Initiative Organization
[AD-A211985] 03 p0419 N90-12409
Recommended changes in US military space policies and programs: A paper submitted to the Commission on Integrated Long-Term Strategy
[PB89-219364] 04 p0460 N90-12636
A literature study of wave propagation in the 1-60 GHz range. Application to transportable military communication systems
[FEL-1988-47] 04 p0491 N90-12825
Artificial intelligence for communication prospects
[FEL-1989-1] 04 p0537 N90-13107
Configuration development for ROMENET
[AD-A213367] 06 p0765 N90-14450
Tactical UK military satellite ground terminals: A research and development review
[RSRE-MEMO-4262] 08 p1033 N90-15972
Critical problems in very large scale computer systems
[AD-A215190] 09 p1270 N90-17365
Defense Small Business Innovation Research (SBIR) Program: Program solicitation 90.1, FY-1990
[AD-A215350] 09 p1294 N90-17503
Modern Antenna Design Using Computers and Measurement: Application to Antenna Problems of Military Interest
[AGARD-LS-165] 10 p1389 N90-17932
Suggestions for designers of navy electronic equipment, 1989 edition, revision B
[AD-A215961] 10 p1380 N90-17998
Electronic Transfer of Information and its Impact on Aerospace and Defence Research and Development
[AGARD-CP-466] 15 p2177 N90-22440
Information technology applications: A British Aerospace Military Aircraft Ltd view
15 p2180 N90-22455
A comparison of CuAlNi and other high damping alloys for the purpose of naval ship silencing applications
[AD-A218801] 16 p2221 N90-22671
The Department of Defense critical technologies plan for the Committees on Armed Services United States Congress
[AD-A219300] 16 p2227 N90-22702
The RACE (research and development in advanced technologies for Europe) program: A 1989 update
[AD-A218509] 16 p2228 N90-22713
Proceedings of the NATO Advanced Workshop on Supercomputing
[AD-A218508] 16 p2299 N90-23102
Atlas/data abstract for the United States and selected areas, fiscal year 1989
[AD-A219289] 16 p2327 N90-23270
Environmental effects upon cross-servicing of aircraft in NATO
[AD-A218374] 17 p2343 N90-23341
Auditory perception of complex sounds
[AD-A219927] 17 p2435 N90-23872
Novel numerical algorithms for sensing, discrimination, and control
[AD-A220805] 17 p2444 N90-23929
High temperature superconductivity
[AD-A219483] 17 p2476 N90-24155
Proceedings of a research workshop on Computational Condensed Matter Physics. Total Energy Methods and Physics of III-V Semiconductors
[AD-A219568] 17 p2476 N90-24156
Proceedings of the 28th Annual US Army Operations Research Symposium (AORS), volume 1
[AD-A219349] 18 p2606 N90-24842

Neck Injury in Advanced Military Aircraft Environments
[AGARD-CP-471] 19 p2717 N90-25459
Special essays for the 40th anniversary of the revolution: The chief designer discusses the F-8 2 and future fighter planes
[AD-A221587] 21 p2960 N90-26829
Tactical oceanography from space: The next decade 21 p3068 N90-27442
Index of USACERL publications, October 1984-December 1989
[AD-A221644] 21 p3088 N90-27559
Testing DoD space systems: The challenge 22 p3132 N90-27771
NDI-concept for composites in future military aircraft 22 p3184 N90-28070
Very low height drop test. Conditioning and tandem dropping of two loads conditioned in two PC6 platforms assembled by rigid structures
[REPT-89/07] 22 p3193 N90-28116
Very low height drop test. Conditioning and tandem dropping of two loads conditioned in two PC6 platforms assembled by one PD9 platform and rigid structures
[REPT-89/04] 22 p3193 N90-28117
Very low height drop test. Conditioning and tandem dropping of two loads conditionned in two PC6 platforms assembled by rigid structures
[REPT-89/08] 22 p3193 N90-28118
Air University Library index to military periodicals. Cumulative issue: January to March 1989, Volume 40, Number 1
[PB90-182296] 22 p3258 N90-28452
Enhancing PLRS with user-to-user data capability 24 p3427 N90-29359
An experimental study of voice communication over a bandlimited channel using variable bit width delta modulation
[AD-A223445] 24 p3461 N90-29548
Multi-user facility for high performance optical recording of brain activity (DURIP)
[AD-A223491] 24 p3498 N90-29768

MILKY WAY GALAXY

Infrared spectroscopy of the central few parsecs of the galaxy 11 p1585 N90-19140
On the mass to light ratios of dwarf spheroidal galaxies
[DE90-610645] 11 p1591 N90-19175
The interstellar medium of a starburst galaxy; millimeter interferometric observations of M82 16 p2329 N90-23276
Molecular clouds and the large-scale structure of the galaxy 16 p2333 N90-23295
Activities report of the Institute of Astronomical Calculations
[ETN-90-96461] 17 p2481 N90-24189
Carbon in the Galaxy: Studies from Earth and Space
[NASA-CP-3061] 21 p3089 N90-27562

MILLIMETER WAVES

Millimeter-wave/infrared rectenna development at Georgia Tech 01 p0028 N90-10147
Laboratory measurements of microwave and millimeter-wave properties of planetary atmospheric constituents
[NASA-CR-185914] 01 p0141 N90-10815
Precision materials characterization in the near millimeter and submillimeter wavelength range
[AD-A210655] 02 p0194 N90-11106
Calibration and de-embedding of microwave measurements using any combination of one- or two-port standards
[PB89-212674] 03 p0337 N90-11916
First interferometric observations with arc-sec. resolution of solar radio bursts at millimeter wavelengths 03 p0431 N90-12472
Theoretical and experimental research on a millimeter-wavelength free-electron laser
[AD-A213321] 04 p0507 N90-12925
Development of high gain three terminal devices - at millimeter wave frequencies
[AD-A213089] 05 p0635 N90-13701
Laboratory evaluation and application of microwave absorption properties under simulated conditions for planetary atmospheres
[NASA-CR-185916] 06 p0865 N90-15025
Flashlight radar: A three-dimensional imaging radar
[AD-A213439] 07 p0918 N90-15307
Focal plane antenna array for millimeter waves
[AD-D014306] 07 p0920 N90-15322
Computer aided design of monolithic microwave and millimeter wave integrated circuits and subsystems
[AD-A213656] 07 p0923 N90-15343
Scannable millimeter wave arrays, volume 1
[AD-A213895] 07 p0924 N90-15347
Scannable millimeter wave arrays, volume 2
[AD-A213896] 07 p0924 N90-15348
Helsinki University of Technology Radio Laboratory
[PB90-110677] 08 p1056 N90-16102
Low-altitude millimeter-wave propagation in the evaporation duct
[AD-A214432] 08 p1057 N90-16108
The physical foundations of radiometry and their applications in the mm-waveband
[REPT-12-88] 08 p1058 N90-16114
Outflows in high mass star-forming regions 08 p1149 N90-16657
High-efficiency Schottky-Varactor frequency multipliers at millimeter waves
[PB90-110701] 09 p1209 N90-17007
Parametric spectral estimation techniques for coherent millimeter-wave radar
[AD-A214355] 10 p1371 N90-17943
The ITALSAT experiment 10 p1374 N90-17962
Millimeter wave radar clutter program
[AD-A215772] 10 p1376 N90-17978
Research on monolithic millimeter-wave devices
[AD-A215771] 10 p1379 N90-17996
Design of a microwave calorimeter for the microwave tokamak experiment
[DE90-004486] 10 p1387 N90-18026
High performance, picosecond radiation detectors grown by molecular beam epitaxy for millimeter-wave diagnostic systems
[DE90-005547] 10 p1438 N90-18302
Millimeter-wave propagation in the mesosphere
[PB90-119868] 11 p1496 N90-18612
Performance and modeling of superconducting ring resonators at millimeter-wave frequencies
[NASA-TM-102526] 11 p1500 N90-18634
Chemistry on interstellar grains and implications for infrared spectroscopy 11 p1579 N90-19097
Detection of SN1986j in NGC891 at millimetre wavelengths 11 p1585 N90-19137
The James Clerk Maxwell telescope 11 p1589 N90-19166
Large-diameter geostationary millimeter wavelength antenna concept 12 p1609 N90-19254
Structures for remotely deployable precision antennas 12 p1609 N90-19256
Millimeter radiometer system technology 12 p1610 N90-19260
Foundations of millimeter-wave frequency acoustic microscopy 12 p1709 N90-19816
Search for far infrared radiation from optically pumped defect modes
[AD-A216976] 12 p1714 N90-19843
Conference digest: Thirteenth International Conference on Infrared and Millimeter Waves, volume 1039
[AD-A217343] 13 p1793 N90-20291
Superconductive microprobes for eddy current evaluation of materials
[AD-A217776] 13 p1805 N90-20361
Millimeter wave surface resistance of RBa2Cu3O(7-delta) (R=Y,Eu,Dy,Sm,Er) superconductors
[NASA-TM-102571] 13 p1897 N90-20886
Growth, characterization and device development in monocrystalline diamond films
[AD-A218211] 13 p1898 N90-20895
Millimeter wave near-field study
[NASA-CR-182014] 14 p1932 N90-21058
MMW SAR on RPV for battlefield surveillance 14 p1961 N90-21231
High efficiency octave bandwidth millimeter wave power amplifier
[AD-A218245] 14 p1969 N90-21280
Millimeter wavelength rectenna development 15 p2060 N90-21797
High power millimeter wave source development program 15 p2061 N90-21805
Atmospheric Propagation in the UV, Visible, IR, and mm-Wave Region and Related Systems Aspects
[AGARD-CP-454] 15 p2079 N90-21907
Scintillation of millimeter-wave intensity and phase caused by turbulence and precipitation 15 p2080 N90-21912
Evaporation duct effects at millimeter wavelengths 15 p2080 N90-21914
The mm-wave region propagation experiments by satellite 15 p2081 N90-21916
Modeling millimeter-wave propagation effects in the atmosphere 15 p2082 N90-21922
Millimetre-wave propagation in the evaporation duct 15 p2084 N90-21929
Millimeter-wave bistatic scattering by terrain 15 p2085 N90-21936
Atmospheric modelling studies: A modelling comparison between IR and millimetric atmospheric propagation 15 p2086 N90-21941
The interstellar medium of a starburst galaxy; millimeter interferometric observations of M82 16 p2329 N90-23276
Implications of the IRAS data for galactic gamma ray astronomy and EGRET 16 p2334 N90-23300
Millimeter wave filter design with suspended stripline
[AD-A219582] 17 p2395 N90-23645
Joint services electronics program: Electronics research at the University of Texas at Austin
[AD-A220834] 17 p2397 N90-23655
A laboratory comparison of field techniques for measurement of the liquid water fraction of snow
[AD-A219587] 17 p2417 N90-23774
Advanced artificial dielectric materials for millimeter wavelength applications, part A
[AD-A220221] 17 p2469 N90-24112
Precision pointing and locking capabilities combined by a linear actuator 18 p2537 N90-24475
IR and millimeter waves: Properties, models, and examples of ground target applications
[FOA-C-30541-3.3] 18 p2543 N90-24516
Millimeter-wave gyroklystron amplifier experiment using a relativistic electron beam
[AD-A221209] 18 p2548 N90-24544
Millimeter-wave acoustic transducers
[AD-A221402] 18 p2612 N90-24878
Light-millimeter wave interactions in semiconductor devices
[AD-A221214] 18 p2623 N90-24943
High performance millimeter-wave microstrip circulators and isolators
[NASA-CR-186276] 19 p2685 N90-25270
Millimeter-wave multiplexers
[AD-D014518] 19 p2685 N90-25274
Figure of merit studies of beam power concepts for advanced space exploration
[NASA-CR-186720] 20 p2854 N90-26234
Submillimeter and millimeter observations of solar system objects
[NASA-CR-186636] 20 p2940 N90-26731
Laboratory measurements of microwave and millimeter-wave properties of planetary constituents 20 p2943 N90-26745
Solid state space harmonic amplifier
[AD-D014455] 22 p3166 N90-27955
Millimeter-wave generation via plasma three-wave mixing
[AD-A222010] 22 p3247 N90-28415
Radio outbursts in extragalactic sources 23 p3414 N90-29291

MILLING

PMR graphite engine duct development
[NASA-CR-182228] 01 p0008 N90-10037
Photolithography: A new tool for ceramic science
[DE90-000135] 03 p0331 N90-11885
Application of microdesigned interfaces to studies of ceramic processing
[DE90-011633] 21 p2983 N90-26951

MILLING (MACHINING)

Machining of new materials at Aerospatiale
[REPT-892-430-104] 16 p2213 N90-22622

MILLING (MIXING)

U COMPOUNDING

MILLING MACHINES

Development, implementation and test of a computer program for the production of axisymmetric pattern moulds on a numerically controlled milling machine
[LR-593] 15 p2074 N90-21877

MIM (SEMICONDUCTORS)

Critical behavior of the thermal power near the metal-insulator transition
[PREPRINT-714] 16 p2323 N90-23244
Luminescence from electroformed metal-isolator-metal-structures
[ETN-90-97295] 22 p3249 N90-28425

MIMD (COMPUTERS)

An implementation-oriented specification of the TUMULT communication primitives
[MEMO-INF-88-34] 04 p0536 N90-13096
The 2nd Symposium on the Frontiers of Massively Parallel Computations
[NASA-TM-101918] 08 p1113 N90-16442
Dynamically allocating sets of fine-grained processors to running computations 08 p1114 N90-16447
Eigensolution of finite element problems in a completely connected parallel architecture
[NASA-TM-102450] 09 p1236 N90-17173
The design and analysis of algorithm and data structure for efficient solutions of minimum-cost network flow problems on MISD and MIMD 10 p1441 N90-18313
Three-dimensional medical image analysis using local dynamic algorithm selection on a multiple-instruction, multiple-data architecture
[AD-A218024] 13 p1852 N90-20630
Architecture independent environment for developing engineering software on MIMD computers
[NASA-CR-186562] 14 p2016 N90-21553
Concurrent computing: Numerical algorithms and some applications
[AD-A218570] 16 p2300 N90-23103

Multiprocessing on supercomputers for computational aerodynamics
[NASA-TM-102806] 17 p2347 N90-23366
The use of Lanczo's method to solve the large generalized symmetric Eigenvalue problem in parallel
[NASA-CR-182072] 20 p2907 N90-26533
Special purpose parallel computer architecture for real-time control and simulation in robotic applications
[NASA-CASE-NPO-17629-1-CU] 21 p3038 N90-27268
A programming environment for parallel vision algorithms
[AD-A221486] 21 p3055 N90-27368
Concurrent Image Processing Executive (CIPE). Volume 1: Design overview
[NASA-CR-186853] 22 p3236 N90-28348
Parallelization of a software relating to aerodynamics on MIMD type computers
[ONERA-RT-31/3479-CY] 23 p3384 N90-29114
The development and evaluation of numerical algorithms for MIMD computers
[NASA-TM-101167] 24 p3526 N90-29939
Fault tolerant design for multistage routing networks
[AD-A224267] 24 p3533 N90-29978

MINERAL DEPOSITS
Geologic interpretation of gravity anomalies
[AD-A222910] 21 p3025 N90-27199
Geologic studies in Alaska by the US geological survey, 1988
[PB90-180993] 22 p3211 N90-28213

MINERAL EXPLORATION
Summaries of the thematic conferences on remote sensing for exploration geology
[NASA-CR-185321] 05 p0664 N90-13880
Geobotanical remote sensing: A review
[INPE-5026-PRE/1565] 14 p1996 N90-21440

MINERAL OILS
Development of a high temperature FZG-Ryder gear lubricant load capacity machine
[AD-A210799] 01 p0079 N90-10449
Mutagenic responses of some petroleum-base obscurants in the Ames test
[AD-A214201] 07 p0915 N90-15295

MINERALOGY
Physiographic and geological setting of the Coastal Engineering Research Center's field research facility
[AD-A210772] 02 p0238 N90-11356
Abstracts for the 52nd Annual Meeting of the Meteoritical Society
[NASA-CR-186160] 06 p0860 N90-14998
Composition of dust from Comet P/Halley: The mineral fraction 08 p1144 N90-16631
Methods for the mineralogical and textural analysis of comet nucleus samples 08 p1147 N90-16648
Near infrared spectroscopy of Mars: Study of the surface mineralogy 11 p1579 N90-19091
Analysis of tectonic movements utilizing remote sensor products in the Southern Espinhaco (SE) region
[INPE-4830-PRE/1451] 12 p1690 N90-19708
Stored mafic/ultramafic crust and early Archean mantle depletion
[NASA-CR-186460] 12 p1691 N90-19715
Proceedings of a workshop on Differences Between Antarctic and Non-Antarctic Meteorites
[NASA-CR-184918] 20 p2942 N90-26740
Status and applications of diamond and diamond-like materials: An emerging technology
[NASA-CR-186935] 21 p2985 N90-26963
Carbon in comet dust 21 p3089 N90-27564
Survival of carbon grains in shocks 21 p3090 N90-27567
On diamond, graphitic and amorphous carbons in primitive extraterrestrial solar system materials 21 p3095 N90-27591

MINERALS
NT ASBESTOS
NT BERYL
NT CALCITE
NT CHROMITES
NT CRYOLITE
NT DOLOMITE (MINERAL)
NT GRAPHITE
NT ILMENITE
NT KAOLINITE
NT OLIVINE
NT PEROVSKITES
NT PYROLYTIC GRAPHITE
NT QUARTZ
NT SPINEL
NT YTTRIUM-ALUMINUM GARNET
NT YTTRIUM-IRON GARNET
Remote sensing applied to the monitoring of mineral extraction in the proximity of urban areas: Pros and cons
[INPE-4867-PRE/1478] 11 p1522 N90-18766
Polar prospects: A minerals treaty for Antarctica
[OTA-O-428] 17 p2480 N90-24185
Experiment K-6-01. Distribution and biochemistry of mineral and matrix in the femurs of rats 20 p2892 N90-26455

MINES (EXCAVATIONS)
Verification of the NIKE3D structural analysis code by comparison against the analytic solution for a spherical cavity under a far-field uniaxial stress
[DE90-000929] 06 p0799 N90-14653

MINES (ORDNANCE)
Fiber optic technique for surveillance and control of mine fields
[FOA-C-30526-3.1] 02 p0225 N90-11293
Limitations of the conventional role of the B-1B in the European theater
[AD-A217285] 12 p1604 N90-19230

MINIATURE ELECTRONIC EQUIPMENT
Microsystems techniques: Concept, significance, status of development
[MBB-UA-1110/88-PUB] 04 p0495 N90-12851
Electrical resistance measurements of connector-panel interfaces
[AD-A221431] 21 p3001 N90-27057
Physics and techniques for the investigation of the properties of ultra small systems
[AD-A221985] 21 p3071 N90-27461

MINIATURIZATION
NT MICROMINIATURIZATION
NT SUBMINIATURIZATION
Miniaturized triaxial laser gyro 01 p0013 N90-10061
Efficient nonlinear conversion of laser diode pumped miniature solid state laser sources
[AD-A210706] 01 p0075 N90-10433
Effects of miniature CRT (Cathode Ray Tube) location upon primary and secondary task performances
[AD-A210223] 01 p0101 N90-10573
Squirt: The prototypical mobile robot for autonomous graduate students
[AD-A212337] 04 p0510 N90-12941
A portable ionosonde in support of reliable communications 06 p0762 N90-14431
Miniature laser Doppler anemometer with a diode laser
[ISL-CO-224/88] 08 p1077 N90-16232
Miniature GPS-based guidance package 09 p1163 N90-16736
Experiments on the unsteady flow in a supersonic compressor stage 11 p1462 N90-18422
Small displacement, long life on-orbit compressor design and fabrication 11 p1475 N90-18489
Analytical and experimental investigation of miniature heat pipes, phase 2
[AD-A218945] 11 p1536 N90-18873
Low-cost small satellites for astrophysical missions
[DE90-007625] 12 p1616 N90-19293
A progress report on the Livermore Miniature Vacuum Tube Project
[DE90-008302] 13 p1794 N90-20299
An assessment of the hardness of miniature vacuum tubes to high-voltage transients
[DE90-009541] 15 p2089 N90-21956
Small strain gage applications 2
[DE90-008312] 15 p2102 N90-22026
On the design and development of a miniature ceramic gimbal bearing 15 p2115 N90-22100
Miniature traveling wave tube and method of making
[NASA-CASE-LEW-14520-1] 16 p2230 N90-22724
Radio links: Instrument technologies 17 p2358 N90-23425
Reflection oscillators employing series resonant crystals'
[NASA-CASE-GSC-13173-1] 17 p2394 N90-23635
Miniaturization of flight deflection measurement system
[NASA-CASE-LAR-13628-1] 17 p2406 N90-23707
Advanced methods for the micromachining of sensors
[MBB-Z-0281/88-PUB] 19 p2650 N90-25081
Twilight zones and cornerstones: A gnat robot double feature
[AD-A220026] 20 p2870 N90-26326
Special test and evaluation methods used for a nine-axis accelerometer
[PB90-209578] 23 p3329 N90-28822
Measurement of hand dynamics in a microsurgery environment: Preliminary data in the design of a bimanual telemicro-operation test bed 23 p3364 N90-29010
Modular digital GPS receivers 24 p3424 N90-29346

MINICOMPUTERS
CEBAF control system
[CEBAF-PR-89-013] 19 p2757 N90-25666
Graphic interface for attribute-based data language queries from a personal computer to the multi-lingual, multi-model, multi-backend database system over an Ethernet network
[AD-A223738] 24 p3528 N90-29948

MINIMA
A computational analysis of the transonic flow field of two-dimensional minimum length nozzles 06 p0718 N90-14194

MINIMAX TECHNIQUE
Periodic solutions of spatially periodic Hamiltonian systems
[AD-A210645] 01 p0113 N90-10649
Subharmonic solutions near an equilibrium point for Hamiltonian systems
[AD-A210558] 02 p0263 N90-11496
International Conference on Fixed Point Theory and Applications
[AD-A212369] 04 p0545 N90-13171
The activity selection problem: A network and game theoretic approach
[MEMO-794] 05 p0694 N90-14056
Information capacity of the matched Gaussian channel with jamming. 1: Finite-dimensional channel
[AD-A214782] 09 p1205 N90-16984
A model for comparing game theory and artificial intelligence decision making processes
[AD-A215418] 09 p1271 N90-17369
Robust control of flexible structures 15 p2058 N90-21784
Eigenvalues of dynamic max-min systems
[REPT-89-84] 17 p2465 N90-24088
Nonparametric selection, ranking and testing
[AD-A219254] 19 p2752 N90-25636
For the definition of two person zero sum games
[ETN-90-97294] 24 p3541 N90-30022

MINIMIZATION
U OPTIMIZATION

MINIMUM DRAG
Constrained spanload optimization for minimum drag of multi-lifting-surface configurations 14 p1919 N90-20992
The minimum drag profile in laminar flow: A numerical way 16 p2196 N90-22535

MINING
Report of NASA Lunar Energy Enterprise Case Study Task Force
[NASA-TM-101652] 07 p1007 N90-15836
Report of the NASA lunar energy enterprise case study task force 07 p1008 N90-15837
Analysis of the financial factors governing the profitability of lunar helium-3 07 p1008 N90-15838
Transportation and operations aspects of space energy systems 07 p1008 N90-15842
Importance of helium-3 for the future 07 p1009 N90-15843
Remote sensing applied to the monitoring of mineral extraction in the proximity of urban areas: Pros and cons
[INPE-4867-PRE/1478] 11 p1522 N90-18766
A robotically constructed production and supply base on Phobos
[NASA-CR-186234] 15 p2073 N90-21872
Human factors model concerning the man-machine interface of mining crewstations 23 p3364 N90-29011
Automation and robotics technology for intelligent mining systems 23 p3366 N90-29018
Distributed communications and control network for robotic mining 24 p3520 N90-29901

MINKOWSKI SPACE
On thick domain walls in general relativity
[NASA-CR-185926] 05 p0704 N90-14124
Stable supermembrane vacuum with a discrete spectrum
[DE89-635722] 07 p0962 N90-15561
Characteristics consequences of space-time coordinate relativization
[DE90-615201] 14 p2034 N90-21668
Introduction to gauge theories and unification
[DE90-014473] 23 p3402 N90-29225

MINOR PLANETS
U ASTEROIDS

MINORITIES
ONR (Office of Naval Research) summer scholars for the 1989 PREFACE Program
[AD-A217746] 13 p1903 N90-20919

MINORITY CARRIERS
Development of a point-contact solar cell using high-volume processing techniques
[DE90-010330] 18 p2577 N90-24683
Estimation of minority carrier diffusion lengths in InP/GaAs solar cells
[NASA-TM-103213] 20 p2824 N90-26069

MIR SPACE STATION
Examination of the background by High Energy X ray Experiment (HEXE) on the space station MIR
[ETN-90-95735] 12 p1746 N90-20041
Mir-Kvant-Hexe hard x ray light curve of SN 1987A 17 p2482 N90-24197
Observations of black hole candidates with the Mir-Kvant HEXE 17 p2483 N90-24198

The X ray spectrum of Nova Vul 1988. Mir-Kvant data
19 p2766 N90-25713
Observations of the X ray pulsars from the Kvant module 19 p2767 N90-25720
Mir-Kvant-HEXE hard X ray light curve of SN 1987A
19 p2775 N90-25776
X ray observations of the LMC field by the TTM instrument onboard the Kvant module: November 1988 to June 1989 19 p2782 N90-25825
TTM-Kvant observations of the galactic plane
19 p2783 N90-25836
Technical characteristics and functions of different types of space stations 20 p2937 N90-26712
MIR: A Soviet Space Station. Some legal aspects of international cooperation 20 p2938 N90-26715

MIRA VARIABLES
AFGL ten micron mosaic array spectrometer: Recent results 14 p1978 N90-21333

MIRROR FUSION
Spectroscopic diagnostics of high temperature plasmas
[DE90-003912] 08 p1126 N90-16522
Thermal barrier research
[DE90-009213] 16 p2319 N90-23221

MIRRORS
NT ETALONS
NT MAGNETIC MIRRORS
NT PARABOLOID MIRRORS
NT TANDEM MIRRORS
Design and operating characteristics of a CW relevant quasi-optical gyrotron with variable mirror separation
[AD-A210611] 01 p0074 N90-10425
System and performance analysis of a low density actively controlled mirror for astronomic observation
02 p0178 N90-11002
Kinematic design NC optical generator
03 p0404 N90-12316
Placing mirrors in grids
[CWI-CS-R8906] 04 p0543 N90-13154
Composite panel development at JPL
05 p0595 N90-13458
Lightweight composite reflector panels
05 p0596 N90-13462
Coherent phasing of segmented mirrors
05 p0598 N90-13474
Real-time sensing of optical alignment
05 p0599 N90-13479
The telescope mirrors 05 p0603 N90-13504
The x ray mirror and the PSPC of the supernova-rocket-project 05 p0662 N90-13867
Optical design and performance of an XUV FEL (Free-Electron Laser) oscillator
[DE90-002381] 06 p0790 N90-14599
Deferred electronic heterodyne moire deflectometry: A method for transient density fields measurement
[NASA-CR-182982] 06 p0843 N90-14907
Review of quasi-optical gyrotron development
[AD-A213491] 07 p0933 N90-15402
Material responses to incident x rays
[DE89-015366] 08 p1089 N90-16305
Surface topography measurements over the 1 meter to 10 micrometer spatial period bandwidth
[DE90-003642] 08 p1122 N90-16501
Broadband incoherent imaging using multiple aperture optics
[AD-A215708] 09 p1282 N90-17437
Placement of multiple apertures for imaging telescopes
[DE90-006991] 13 p1888 N90-20833
Design and performance analysis of adaptive optical telescopes using laser guide stars
[AD-A218025] 13 p1902 N90-20913
Absolute multilayer characterization at high spatial resolution via real-time soft x ray imaging
[DE90-009181] 14 p1984 N90-21371
Design and demonstration of an improved stretched-membrane heliostat
[DE90-007904] 14 p2001 N90-21470
The investigation of multilayer x ray reflectors as x ray optical elements
[DE90-009044] 14 p2026 N90-21621
A soft actuation system for segmented reflector articulation and isolation 15 p2113 N90-22084
Driving and latching of the Starlab pointing mirror doors 15 p2114 N90-22093
An assessment of second-generation stretched-membrane mirror modules
[DE90-010243] 16 p2252 N90-22841
Full surface interferometric testing of grazing incidence mirrors
[AD-A219394] 16 p2318 N90-23218
Design and fabrication of high damage threshold turning mirrors for the Nova laser
[DE90-012703] 19 p2696 N90-25341
Mode-medium instability and its correction with a Gaussian reflectivity mirror
[NASA-TP-3023] 19 p2758 N90-25673
Qualification of concentrating mirror systems with the HERMES measurement system and the HELIOS simulation program
[DLR-FB-89-51] 20 p2882 N90-26394
Ultra precision machining
[AD-A222422] 21 p2991 N90-27003
Adaptive optics correction in real-time for dynamic wavefront errors
[AD-A221588] 21 p3077 N90-27495
XMM space telescope: Development plan for the lightweight replicated x ray gratings
[DE90-015620] 24 p3546 N90-30055

MIS (SEMICONDUCTORS)
Properties of devices prepared with epitaxial layers on InP
[AD-A210304] 01 p0132 N90-10759
Elaboration and characterization of MISFET transistors on InP
[ECL-88-19] 05 p0636 N90-13709
Study of metal-insulator-semiconductor structures on indium phosphide, implemented by anodic oxidation
[ECL-88-10] 05 p0703 N90-14114
Manufacturing and characterization of insulator-germanium structures
[ECL-88-13] 05 p0703 N90-14115
Tritium and neutron measurements of a solid state cell
[DE90-003657] 07 p1005 N90-15820

MISALIGNMENT
Alignment positioning mechanism
[NASA-CASE-MSC-21502-1] 20 p2872 N90-26341
Kalman filter formulations for transfer alignment of strapdown inertial units 24 p3424 N90-29342

MISCIBILITY
U SOLUBILITY

MISCIBILITY GAP
Systems with a miscibility gap in the liquid state
13 p1785 N90-20245

MISFETS
U FIELD EFFECT TRANSISTORS

MISORIENTATION
U MISALIGNMENT

MISS DISTANCE
Dallas/Forth Worth simulation. Phase 2: Triple simultaneous parallel Instrument Landing System (ILS) approaches (turbojets)
[DOT/FAA/CT-90/2] 23 p3270 N90-28509

MISSILE BODIES
Study of missiles in flight
[ETN-90-97457] 22 p3109 N90-27662
Experimental study on the vortices generated by the body of a missile during flight. Part 1: Laminar boundary layer
[ONERA-RT-40/1147-AY-130A-PT-1]
22 p3110 N90-27665
Effects of flowfield turbulence on asymmetric vortices over a slender body
[AD-A224139] 23 p3328 N90-28819

MISSILE CASES
U MISSILE BODIES

MISSILE COMPONENTS
NT MISSILE BODIES
Application of Bayesian reliability concepts to cruise missile electronic components
[AD-A216208] 10 p1394 N90-18059
Simulation of the dynamic environment for missile component testing: Demonstration
[AD-A216979] 11 p1466 N90-18443
Thermal shock tests
[ETCA-89-R-163] 22 p3193 N90-28120
Proceedings of US Army Research Office Workshop on US Army Applications for Diamond and Diamondlike Materials
[AD-A224193] 23 p3314 N90-28741

MISSILE CONFIGURATIONS
Aerodynamic test and analysis of a slender generic missile configuration
[AD-A212522] 04 p0448 N90-12567
Preliminary airworthiness evaluation of the AH-64A equipped with the Air To Air Stinger (ATAS) missile system
[AD-A213030] 05 p0579 N90-13374
The role of computational fluid dynamics in missile aerodynamics 10 p1304 N90-17547
Dynamic derivatives of missiles and fighter-type configurations at high angles of attack
10 p1306 N90-17554
External flow computations for a finned 60mm ramjet in steady supersonic flight
[AD-A216998] 12 p1605 N90-19233
The role of computational fluids dynamics in missile aerodynamics
[NLR-MP-88072-U] 20 p2804 N90-25952

MISSILE CONTROL
Stability and Control of Tactical Missile Systems
[AGARD-CP-451] 01 p0011 N90-10050
The present status and the future of missile aerodynamics 01 p0012 N90-10051
Prediction of the aerodynamic stability of missiles
01 p0012 N90-10052
Missile Datcom: Enhancements for design applications
01 p0012 N90-10054
Vortex induced characteristics of missiles in unsteady maneuvers 01 p0012 N90-10057
Alternative polar homing strategies
01 p0013 N90-10059
How to control unstable missile airframes: Methodology and limitations 01 p0013 N90-10060
Miniaturized triaxial laser gyro
01 p0013 N90-10061
Remote control missile model test
01 p0013 N90-10063
Investigations of thrust vector control for high-alpha pitchover 01 p0014 N90-10067
A structured singular value approach to missile autopilot analysis 2 01 p0014 N90-10068
Analysis and testing of a high performance air-air missile 01 p0014 N90-10069
Aeroelastic analysis of missile control surfaces with structural non-linearity 01 p0015 N90-10071
Design of a Kalman filter for transfer alignment
02 p0149 N90-10848
Navigation up-date using radar mapping: Assessment and optimisation simulation tool
08 p1026 N90-15928
The implications of using integrated software support environment for design of guidance and control systems software
[AGARD-AR-229] 11 p1464 N90-18432
Optimal and near-optimal medium range air-to-air missile guidance against maneuvering targets
15 p2053 N90-21766
Engagement analysis study
[DE90-009529] 15 p2163 N90-22359
Six-degree-of-freedom missile simulation using the ADI AD 100 digital computer and ADSIM simulation language
16 p2294 N90-23068
A homing missile guidance law based on new target maneuver models
[AD-A220392] 17 p2356 N90-23410
A passive homing missile guidance law based on new target maneuver models
[AD-A220419] 17 p2356 N90-23411
Brazil, the United States, and the missile technology control regime
[AD-A220551] 17 p2362 N90-23449
Missile aerodynamics
[ISBN-0-9620629-0-1] 18 p2490 N90-24236
Synthesis and validation of feedback guidance laws for air-to-air interceptions
[LR-615] 19 p2752 N90-25639
Future applications of GPS to conventional weapons
21 p3069 N90-27447
Integrated strapdown avionics for precision guided vehicles 24 p3427 N90-29361

MISSILE DEFENSE
A review of gas-cooled reactor concepts for SDI (Strategic Defense Initiative)
[DE89-016962] 06 p0842 N90-14898
Development of advanced WTA algorithms for parallel processing
[AD-A214874] 09 p1266 N90-17341
Suboptimal period design for a maneuvering missile to evade tracking filters 12 p1650 N90-19479
Zenith Star: A structural control challenge
14 p1933 N90-21064

MISSILE DESIGN
Stability and Control of Tactical Missile Systems
[AGARD-CP-451] 01 p0011 N90-10050
The present status and the future of missile aerodynamics 01 p0012 N90-10051
Prediction of stability derivatives for missiles using the HISSS panel code 01 p0012 N90-10053
Missile Datcom: Enhancements for design applications
01 p0012 N90-10054
Prediction of dynamic derivatives
01 p0012 N90-10055
Prediction of tactical missile dynamics
01 p0012 N90-10056
Vortex induced characteristics of missiles in unsteady maneuvers 01 p0012 N90-10057
Aeroelastic tailoring procedure for controlling fin hinge moments 01 p0013 N90-10058
Alternative polar homing strategies
01 p0013 N90-10059
Remote control missile model test
01 p0013 N90-10063
Wind tunnel tests: The role of the model
01 p0013 N90-10064

Validation of missile simulation
01 p0014 N90-10066
Marginal release disturbances on advanced missiles
01 p0014 N90-10070
Experience gained in the improvement of the Aspide aerodynamic configuration for the surface to air role
01 p0015 N90-10072
Winged versus wingless airframes
01 p0015 N90-10073
Missile Aerodynamics: NEAR Conference on Missile Aerodynamics
[ISBN-0-9620629-1-X] 10 p1303 N90-17540
Historical review of missile aerodynamic developments
10 p1304 N90-17542
Missile dynamics: A critical assessment of prediction capabilities 10 p1304 N90-17543
Use of semiempirical aerodynamic methods for preliminary design 10 p1304 N90-17546
High performance missiles of the future
10 p1305 N90-17550
VLA missile development and high angle of attack behavior 10 p1305 N90-17553
Missile aerodynamics
[ISBN-0-9620629-0-1] 18 p2490 N90-24236

MISSILE DETECTION
NT RADAR DETECTION
Tracking performance evaluation
[AD-A210499] 01 p0095 N90-10540
Three-dimensional route planning for a cruise missile for minimal detection by observer
[AD-A218336] 13 p1880 N90-20787

MISSILE ENGINE CASES
U ROCKET ENGINE CASES

MISSILE GUIDANCE
U MISSILE CONTROL

MISSILE LAUNCHERS
Flowfield effects of launch on a vertically-launched missile
[AD-A214466] 09 p1160 N90-16714

MISSILE STABILIZATION
U MISSILE CONTROL
U STABILIZATION

MISSILE SYSTEMS
Encyclopedia of US Air Force aircraft and missile systems. Volume 2: Post-World War 2 bombers, 1945-1973
[AD-A209273] 01 p0001 N90-10001
Complex availability problems solved with simulation
[DE89-012610] 08 p1116 N90-16459
Historical review of missile aerodynamic developments
10 p1304 N90-17542
Appropriate aeroprediction accuracy in defining missile systems for aerodynamic flight 10 p1304 N90-17544
Computational fluid dynamics for missiles
[RAE-TM-AERO-2171] 20 p2863 N90-26288

MISSILE TESTS
Aerodynamic test and analysis of a slender generic missile configuration
[AD-A212522] 04 p0448 N90-12567
Realtime simulation at MBB today and future aspects
[MBB-UA-1134/89-PUB] 19 p2653 N90-25098

MISSILE TRACKING
Tracking performance evaluation
[AD-A210499] 01 p0095 N90-10540
Suboptimal period design for a maneuvering missile to evade tracking filters 12 p1650 N90-19479
Preliminary results of the peak experiment. ALTAIR deep-space measurements
[AD-A218622] 16 p2229 N90-22714
Using simulation to determine a strategy for positively tracking a cruise missile by CMMCA
[AD-A220526] 17 p2362 N90-23448

MISSILE TRAJECTORIES
Design of a robust controller for an unstable nonminimum phase guided missile
[AD-A216147] 10 p1323 N90-17645
Study of missiles in flight
[ETN-90-97457] 22 p3109 N90-27662

MISSILES
NT AIR TO AIR MISSILES
NT AIR TO SURFACE MISSILES
NT ANTIAIRCRAFT MISSILES
NT ANTIMISSILE MISSILES
NT ANTISHIP MISSILES
NT ANTITANK MISSILES
NT BALLISTIC MISSILES
NT CRUISE MISSILES
NT INTERCONTINENTAL BALLISTIC MISSILES
NT PRECISION GUIDED PROJECTILES
NT RAMJET MISSILES
NT SIDEWINDER MISSILES
NT SURFACE TO AIR MISSILES
NT SURFACE TO SURFACE MISSILES

Encyclopedia of US Air Force aircraft and missile systems. Volume 2: Post-World War 2 bombers, 1945-1973
[AD-A209273] 01 p0001 N90-10001
Flexible missile autopilot design studies with PC-MATLAB/386 01 p0018 N90-10088
Present and future US and Soviet chemical missiles and chemical rocket projectiles
[AD-A212199] 04 p0461 N90-12644
Weapon aerodynamics overview
[RAE-TM-AERO-2150] 08 p1018 N90-15888
Navigation of autonomous air vehicles by passive imaging sensors 08 p1026 N90-15927
Tracking flares
[ISBN-0-642-13583-5] 08 p1052 N90-16080
A survey of missile aerodynamics
10 p1303 N90-17541
Historical review of missile aerodynamic developments
10 p1304 N90-17542
Missile dynamics: A critical assessment of prediction capabilities 10 p1304 N90-17543
Appropriate aeroprediction accuracy in defining missile systems for aerodynamic flight 10 p1304 N90-17544
The use of lateral jet control at Aerospatiale
10 p1305 N90-17551
VLA missile development and high angle of attack behavior 10 p1305 N90-17553
Dynamic derivatives of missiles and fighter-type configurations at high angles of attack
10 p1306 N90-17554
Combustion instability in solid propellant rockets
[AD-A216740] 11 p1476 N90-18492
Perforation of a reinforced concrete wall by a rigid missile
[AD-A210025] 14 p1986 N90-21381
Gaithersburg Nike control and launch area preliminary assessment/site inspection, Gaithersburg, Maryland
[AD-A217791] 14 p2003 N90-21482
Material evaluation of optical fibers and payout bobbins: An overview
[AD-A220104] 17 p2473 N90-24140
Missile aerodynamics
[ISBN-0-9620629-0-1] 18 p2490 N90-24236
Ramjet and ramrocket propulsion systems for missiles
21 p2973 N90-26897
Model designation of military aerospace vehicles
[PB90-206301] 22 p3107 N90-27646

MISSION PLANNING
Space station RT and E utilization study
[NASA-CR-181707] 01 p0026 N90-10129
Task analysis of the UH-60 mission and decision rules for developing a UH-60 workload prediction model. Volume 1: Summary report
[AD-A210763] 02 p0255 N90-11446
Wave combustors for trans-atmospheric vehicles
[NASA-TM-102238] 03 p0307 N90-11742
Strategy for earth explorers in global earth sciences
[NASA-CR-185933] 03 p0364 N90-12084
Report on ESA's scientific satellites
[ESA-SP-1110] 04 p0463 N90-12649
European space technology: Celebrating twenty-five years of research and development
[ESA-BR-55] 04 p0569 N90-13322
Active rendezvous between a low-earth orbit user spacecraft and the Space Transportation System (STS) shuttle 05 p0590 N90-13436
The Hipparcos Mission. Prelaunch status. Volume 1: The Hipparcos satellite
[ESA-SP-1111-VOL-1] 05 p0603 N90-13499
Operating principle 05 p0603 N90-13500
In-orbit payload calibration 05 p0606 N90-13526
Project Argo: The design and analysis of an all-propulsive and an aeroassisted version of a manned space transportation vehicle
[NASA-CR-186047] 06 p0732 N90-14266
Communication Overview Program (COP)
06 p0762 N90-14435
Superconducting gravity gradiometer mission. Volume 1: Study team executive summary
[NASA-TM-4091-VOL-1] 07 p0959 N90-15545
Mirach 100 flight control system
08 p1025 N90-15926
An intelligence-driven RPV mission planner
08 p1027 N90-15932
Distribution of hardware and software elements in unmanned air vehicle systems 08 p1027 N90-15933
Experiment facilities for materials and fluid sciences embarked on Eureca-1
[ESA-SP-1118] 08 p1053 N90-16088
Further development and limited flight testing of the CycloCrane
[AD-A215519] 09 p1167 N90-16754
Get Away Special: The first ten years
[NASA-TM-102921] 09 p1171 N90-16775
A planning and scheduling lexicon
[NASA-CR-186061] 09 p1171 N90-16777
The European long-term space plan: A basis for autonomy and cooperation 09 p1173 N90-16784
ESA's space transportation programme
09 p1173 N90-16786
United States space transportation survey
09 p1173 N90-16787
Glavkosmos U.S.S.R. and the basic objectives of its activity 09 p1174 N90-16788
The Hermes system: Its design objectives and solutions 09 p1177 N90-16821
Toward an electrical power utility for space exploration
10 p1329 N90-17681
Solar-Terrestrial Science Strategy Workshop
[NASA-CP-3048] 10 p1444 N90-18329
Background of the workshop
10 p1444 N90-18330
Supporting tools of solar-terrestrial science
10 p1444 N90-18331
Report from upper atmospheric science
10 p1444 N90-18332
Recommendations for the future
10 p1445 N90-18338
A perspective on the use of storable propellants for future space vehicle propulsion
11 p1472 N90-18473
Mission options for an electric propulsion demonstration flight test 11 p1473 N90-18479
Physics and Mechanics of Cometary Materials
[ESA-SP-302] 12 p1738 N90-19989
Rosetta/CNSR, ESA's planetary cornerstone mission
12 p1738 N90-19990
MAX 1991. The active sun: A plan for pursuing the study of the active sun at the time of the next maximum in solar activity, January 1985
[NASA-CR-186125] 12 p1745 N90-20030
Proximity operations concept design study, task 6
[NASA-CR-181971] 13 p1761 N90-20112
Gravity field information from Gravity Probe-B
13 p1839 N90-20554
Operational computer graphics in the flight dynamics environment 13 p1859 N90-20668
Three-dimensional route planning for a cruise missile for minimal detection by observer
[AD-A218336] 13 p1880 N90-20787
A spaceborne optical interferometer: The JPL CSI mission focus 14 p1933 N90-21063
Using connected-element interferometer phase-delay data for Magellan navigation in Venus orbit
15 p2075 N90-21685
Semianalytic study of high-eccentricity orbit stability and evolution 16 p2204 N90-22574
Environmental effects upon cross-servicing of aircraft in NATO
[AD-A218374] 17 p2343 N90-23341
Project Longshot: A mission to Alpha Centauri
[NASA-CR-186052] 17 p2357 N90-23417
Archimedes mission aspects
[ETN-90-96556] 17 p2361 N90-23442
Distributed mission planning technology for Columbus
18 p2501 N90-24288
Neptune, 2000 plus: Concept of a heavy space freighter for the 21st century
[ILR-MITT-229(1989)] 18 p2509 N90-24338
MARS, an AI-based Mission Activities and Resource Scheduler
[MBB-0060/89-PUB] 19 p2650 N90-25083
Project Dawdler: A proposal in response to a low Reynolds number station keeping mission
[NASA-CR-186668] 19 p2658 N90-25128
United States planetary rover status: 1989
[NASA-CR-186843] 19 p2698 N90-25353
Operations mission planner
[NASA-CR-186846] 19 p2747 N90-25611
Signposts to the future 19 p2788 N90-25867
Mars in this decade: The great exploration
[DE90-011232] 19 p2797 N90-25920
Space exploration: Cost, schedule, and performance of NASA's Mars Observer Mission. Fact sheet for the Chairman, Subcommittee on Science, Technology, and Space, Committee on Commerce, Science, and Transportation, US Senate
[GAO/NSIAD-88-137FS] 20 p2815 N90-26021
Terrapin technologies manned Mars mission proposal
[NASA-CR-186838] 20 p2816 N90-26027
Biconic cargo return vehicle with an advanced recovery system. Volume 1: Conceptual design
[NASA-CR-186520] 20 p2821 N90-26052
Applications of different design methodologies in navigation systems and development at JPL
20 p2852 N90-26221
Launching a dream: A teachers guide to a simulated space shuttle mission
[NASA-TM-89715] 20 p2934 N90-26693
The lessons of Varsovian's reconnaissance
[NASA-TM-103207] 20 p2951 N90-26789

Spike: Artificial intelligence scheduling for Hubble space telescope 21 p3040 N90-27277
Hermes rendezvous with the space station 22 p3128 N90-27753
Life cycle cost in the conceptual design of subsonic commercial aircraft, volumes 1 and 2 23 p3275 N90-28535
Development of the electric vehicle analyzer [AD-A224201] 23 p3323 N90-28788
Coordinating the activities of a planner and an execution agent 23 p3369 N90-29035
The DELTA MONSTER: An RPV designed to investigate the aerodynamics of a delta wing platform [NASA-CR-186226] 24 p3431 N90-29381
Aircraft design for mission performance using nonlinear multiobjective optimization methods [NASA-CR-4328] 24 p3432 N90-29384

MISSISSIPPI RIVER (US)
Ice conditions along the Illinois waterway as observed on LANDSAT images, 1972 to 1985 [AD-A219745] 17 p2418 N90-23775

MITOCHONDRIA
Carbon and hydrogen metabolism of green algae in light and dark [DE90-008648] 13 p1849 N90-20612

MITOSIS
Polarity establishment, morphogenesis, and cultured plant cells in space 05 p0677 N90-13943
ELF (Extremely Low Frequency) communications system ecological monitoring program: Slime mold studies [AD-A218623] 16 p2229 N90-22715
Experiment K-6-17. Structural changes and cell turnover in the rats small intestine induced by spaceflight 20 p2895 N90-26470

MIXED CRYSTALS
Monolayer formation characteristics of novel organic molecules with nonlinear optically active moieties [AD-A210496] 01 p0121 N90-10693
Process for single crystal growth of high T(sub c) superconductors [AD-D014167] 03 p0409 N90-12346
Thermodynamic studies on the ferroelectric phase transition in neutron irradiated (Li(sub x)K(1-x))2SO4 crystals at high temperature [DE89-635786] 08 p1130 N90-16545

MIXED FLOW
U MULTIPHASE FLOW

MIXED OXIDES
Volatile divalent double metal alkoxides [AD-D014355] 10 p1438 N90-18300

MIXERS
Investigation of advanced mixer-ejector exhaust system [AD-A211943] 03 p0301 N90-11705
Cavitation-controlled ultrasonic agitator [DE90-002773] 06 p0838 N90-14871
Dual-fuel, dual-mode rocket engine [NASA-CASE-LAR-13773-1] 12 p1617 N90-19298
Energy Efficient Engine exhaust mixer model technology report addendum; phase 3 test program [NASA-CR-174799] 23 p3279 N90-28556

MIXING
NT COMPOUNDING
NT DISSOLVING
NT HOMOGENIZING
NT LAMINAR MIXING
NT PREMIXING
NT SIGNAL MIXING
NT SUSPENDING (MIXING)
NT TURBULENT MIXING
Evaluation of a metering, mixing, and dispensing system for mixing polysulfide adhesive [NASA-CR-183749] 05 p0626 N90-13654
The evaluation of a metered mixer for RTV silicone for RSRM nozzle backfill operations [NASA-CR-183831] 05 p0645 N90-13763
Development of a titanium/boron blending process [DE90-001450] 06 p0754 N90-14386
Physical models for aerosol in the marine mixed-layer 06 p0763 N90-14438
Laser mixing of titanium on silicon carbide [DE90-003216] 07 p0891 N90-15150
Swirl-stabilized flames: Fluid dynamics, mixing, and flame stability limits 08 p1040 N90-16009
Silicon-based coatings on niobium metal [DE90-003651] 08 p1048 N90-16057
Cellular thermosetting fluorodiepoxide polymers [NASA-CASE-GSC-13008-2] 09 p1199 N90-16949
Influence of ion beam mixing on the growth of high temperature oxide superconducting thin film [DE90-004837] 10 p1435 N90-18280
Numerical simulations of coherent structures in a jet flame with a noncircular cross section [AD-A216710] 11 p1483 N90-18535
Control of phase structure in polymer blends [AD-A217034] 11 p1491 N90-18580
Investigation of methods to produce a uniform cloud of fuel particles in a flame tube [NASA-TM-102376] 11 p1505 N90-18665
Effects of turbulence mixing, variable properties, and vaporization on spray droplet combustion [NASA-CR-186463] 12 p1623 N90-19326
All-fiber SFPM (Stimulated Four Photon Mixing) amplifier [AD-D014358] 12 p1713 N90-19841
Ion mixing and surface modification in metal-semiconductor systems [DE90-007557] 12 p1723 N90-19897
Secondary flows and radial mixing predictions in axial compressors 14 p1922 N90-21010
A study on secondary flow and spanwise mixing in axial flow compressors 14 p1923 N90-21012
Phase equilibrium of mixtures consisting of molecules with large size and shape differences (thermodynamic modeling of Supercritical Fluid Extraction and Retrograde Condensation, SFE/RC) [PB90-131285] 14 p1947 N90-21146
Apparatus for mixing solutions in low gravity environments [NASA-CASE-MFS-26047-1] 14 p1958 N90-21209
Microgravity acoustic mixing for particle cloud combustors [NASA-CR-185159] 14 p2023 N90-21600
Control of flow separation and mixing by aerodynamic excitation [NASA-TM-103131] 15 p2047 N90-21733
The relationship between the buoyancy of near-surface air and the potential temperature of the tropopause 15 p2128 N90-22165
Experimental study of mixing and combustion processes in a solid-propellant ducted rocket motor 17 p2367 N90-23472
Diffraction patterns and vortex rollup [AD-A219876] 17 p2461 N90-24049
Abundance differences among G and K giants 17 p2484 N90-24208
CRC low- and intermediate-temperature driveability program using gasoline-alcohol blends [AD-A221321] 18 p2533 N90-24453
Fast plasma mixing: A new excitation method for CW gas lasers [AD-A220290] 18 p2617 N90-24904
Study of seasonal variation of mixing phenomena in the hypolimnion of Lake Geneva (Switzerland) 19 p2688 N90-25287
On the fine-scale mixing in the metalimnion and the seasonal thermocline of the Leman (Lake Geneva, Switzerland) 19 p2688 N90-25288
Effect of vane twist on the performance of dome swirlers for gas turbine airblast atomizers [NASA-TM-103195] 19 p2688 N90-25289
Formation of Titanium-boron surface alloys by excimer laser mixing [DE90-013172] 20 p2834 N90-26118
Passive mechanisms of surfaces produced by ion beam mixing and ion implantation [AD-A222432] 21 p2982 N90-26945
Study of the feasibility of several mixtures [IMAG-RR-776-M] 21 p3057 N90-27379
Model of turbulent diffusion flames and nitric oxide generation [PB90-155557] 22 p3155 N90-27886
Regular and chaotic motion of uniform elliptical vortices in external linear time dependent velocity fields 23 p3268 N90-28497
An experimental investigation of a single and multiphase confined coaxial jet 23 p3324 N90-28796
Chiral Maxwell-Garnett mixing formula [PB90-189143] 23 p3391 N90-29158
Ion-beam mixing of Fe/B layers for tribological applications [DE90-010091] 24 p3456 N90-29518
An investigation of the inviscid spatial instability of compressible mixing layers [AD-A223776] 24 p3468 N90-29596
Rates of vertical mixing, gas exchange, and new productions: Estimates from seasonal gas cycles in the upper ocean near Bermuda [PB90-244781] 24 p3496 N90-29758
Tail and quantile estimation for strongly mixing stationary sequences [AD-A223472] 24 p3540 N90-30019

MIXING CIRCUITS
Cryogenic Schottky-mixer receiver front-end for 40-50 GHz [PB89-221667] 03 p0343 N90-11959
SIS (Superconductor-Insulator-Superconductor) mixer research [AD-A211607] 03 p0414 N90-12375
Advances in SIS receiver technology 05 p0597 N90-13466

MIXING LAYERS (FLUIDS)
Trailing-edge sweep and three-dimensional vortex interactions in jets and mixing layers 01 p0066 N90-10379
Numerical simulation of coherent structures in an incompressible mixing layer 01 p0067 N90-10383
Control of turbulent mixing layers [AD-A211413] 03 p0301 N90-11708
Cryogenic free jets [ESA-TT-1128] 03 p0311 N90-11767
Application of large eddy interaction model to a mixing layer [NASA-CR-185123] 05 p0572 N90-13328
A planar reacting shear layer system for the study of fluid dynamics-combustion interaction [NASA-TM-102422] 05 p0582 N90-13393
Numerical solutions of the complete Navier-Stokes equations [NASA-CR-186102] 05 p0642 N90-13747
An experimental investigation of shear layer mixing in supersonic flows 06 p0775 N90-14508
Comparative study of the vorticity field in turbulent flows: Theory, experiments, and computations [DE90-001399] 06 p0776 N90-14516
Chemical reactions in turbulent mixing flows [AD-A216273] 10 p1355 N90-17856
A numerical investigation of the compressible mixing layer [AD-A217738] 13 p1802 N90-20343
An experimental investigation of mixing in buoyant flows 15 p2090 N90-21983
Applications of remote sensing to studies of oceanic upper mixed layer dynamics 15 p2122 N90-22137
Reynolds stress closure in jet flows using instability wave modeling 16 p2196 N90-22534
The effects of compressibility on a supersonic mixing layer [AD-A219315] 16 p2197 N90-22543
Analysis of velocity and temperature fluctuations in turbulent shear flows 16 p2233 N90-22744
Three-dimensional structure of plane mixing layers 17 p2344 N90-23347
Nonlinear interactions in mixing layers and compressible heated round jets [NASA-CR-186303] 17 p2400 N90-23674
A theoretical analysis of the acoustic radiation from two-dimensional turbulent mixing layers 18 p2551 N90-24559
Supersonic combustor modeling 20 p2810 N90-25992
Modeling of supersonic reacting flow fields 21 p2973 N90-26898
A linear-eddy model of turbulent shear layer mixing 21 p2974 N90-26904
A case study of cumulus formation beneath a stratocumulus sheet: Its structure and effect on boundary layer budgets 22 p3219 N90-28256
Numerical simulation of the formation of two-dimensional and three-dimensional structures in shear layers and wakes [ESA-TT-1008] 23 p3325 N90-28802

MIXING LENGTH FLOW THEORY
Navier-Stokes analysis of airfoils with leading edge ice accretions 06 p0719 N90-14196
Boundary layer parameterization for use in a limited area forecast model 21 p3029 N90-27224

MIXTURES
NT AEROSOLS
NT AIR
NT AQUEOUS SOLUTIONS
NT BINARY MIXTURES
NT COLLOIDS
NT COMPRESSED AIR
NT DETONABLE GAS MIXTURES
NT DISPERSIONS
NT EMULSIONS
NT EUTECTICS
NT FOG
NT GAS MIXTURES
NT HIGH TEMPERATURE AIR
NT LIQUID-GAS MIXTURES
NT NUCLEAR EMULSIONS
NT POLYMER BLENDS
NT SLURRIES
NT SMOKE
NT SOLID SUSPENSIONS
NT SOLUTIONS
Effective permeability of mixtures [PB89-218952] 03 p0323 N90-11839
Airborne/spaceborne pulsed power source [AD-A211762] 04 p0495 N90-12850
The generalized van der Waals theory of pure fluids and mixtures [DE90-000504] 06 p0740 N90-14307

Simultaneous thermal analysis techniques for characterization of energetic materials
[DE90-003028] 07 p0914 N90-15289
Developmental versions of FORTRAN/77 routines for the design and analysis of mixture experiments
[DE90-003513] 07 p0974 N90-15624
Fast algorithms for estimating mixture parameters
[AD-A213869] 07 p0976 N90-15636
Alcohol and blends as motor fuels
[DE90-003517] 08 p1053 N90-16085
Control of phase structure in polymer blends
[AD-A217034] 11 p1491 N90-18580
Thermodynamic properties of supercritical mixtures
[DE90-006720] 12 p1724 N90-19909
WINCOF-I code for prediction of fan compressor unit with water ingestion
[NASA-CR-185157] 15 p2045 N90-21724
Mathematical modeling of fluid-solid mixtures
[DE90-009152] 15 p2098 N90-22007
Heat engines
[DE90-000485] 20 p2882 N90-26393
Solubility characteristics of a methacrylate copolymer
[AD-A222938] 21 p2985 N90-26962
Study of the feasibility of several mixtures
[IMAG-RR-776-M] 21 p3057 N90-27379
Dynamic consolidation of super hard materials
[AD-A224460] 24 p3454 N90-29505

MNEMONICS
Three stages and two systems of visual processing
[AD-A212670] 04 p0525 N90-13032

MOBILE COMMUNICATION SYSTEMS
NT LAND MOBILE SATELLITE SERVICE
Improving the quality of a spread-spectrum radiomobile link 06 p0761 N90-14426
Spread spectrum mobile radio communications
[AD-A213726] 07 p0918 N90-15311
Voice/data integration in mobile radio networks: Overview and future research directions
[AD-A214289] 07 p0919 N90-15319
Satellite systems integrated with the terrestrial cellular network for mobile communications
[ESA-STR-226] 08 p1057 N90-16113
Japanese propagation experiments with ETS-5 10 p1372 N90-17951
Plan of advanced satellite communication experiments using ETS-6 10 p1372 N90-17952
A CCIR aeronautical mobile satellite report 10 p1372 N90-17954
Practical applications of Loran-C for land mobile use or the possibility to use Loran-C as a vehicle-location or vehicle-navigation system
[ETN-90-96265] 11 p1455 N90-18384
Message handling in the post-2000 era: Executive summary
[AD-A219983] 17 p2393 N90-23628
Broadband analysis of ground wave propagation at a50 to 400 MHz 20 p2846 N90-26185
Measurement and simulation of widespread mobile radio channel characteristics 20 p2846 N90-26186
Packet radio network concepts for the Norwegian field army 20 p2850 N90-26206
Mobile satellite communications for civil aviation
[NLR-MP-88066-U] 20 p2855 N90-26238
An experimental study of voice communication over a bandlimited channel using variable bit width delta modulation
[AD-A223445] 24 p3461 N90-29548

MOBILITY
NT ATOMIC MOBILITIES
NT ELECTRON MOBILITY
NT HOLE MOBILITY
NT IONIC MOBILITY
Some remarks on the working principle of the rocketborne nose tip dc probes in the D-region of the ionosphere 05 p0658 N90-13839
Crosslinked, flexible, low-molecular-weight polyacrylamide gels for mobility control
[DE90-000202] 07 p0913 N90-15280
Planning systems for autonomous legged vehicles
[AD-A214242] 07 p0942 N90-15458
Nonlinear continuum mechanics and applied analysis
[AD-A213629] 12 p1709 N90-19812
Concept formation and generalization based on experimentation by an autonomous mobile robot
[DE90-001731] 13 p1810 N90-20395
Resolved motion rate and resolved acceleration servo-control of wheeled mobile robots
[DE90-002585] 13 p1811 N90-20399
Proceedings of the 4th European Conference, volume 2
[AD-A216521] 14 p1986 N90-21382
Application of novel data processing techniques to the analysis of Ion Mobility Spectrometry (IMS) data
[AD-A219976] 17 p2374 N90-23516
Design of an autonomous teleoperated cargo transporting vehicle for lunar base operations
[NASA-CR-186686] 18 p2565 N90-24633
Mobility studies in multiloop spatial linkages 20 p2922 N90-26628
Motion coordination for mobile robots in unstructured environments
[PB90-199498] 23 p3332 N90-28837
Motion coordination for a mobile manipulator system
[PB90-203076] 23 p3332 N90-28839
Remote atmospheric profiling systems for tropospheric monitoring
[PB90-216789] 23 p3349 N90-28927
HERMIES-3: A step toward autonomous mobility, manipulation, and perception 23 p3374 N90-29065
Planetary rover technology development requirements 23 p3375 N90-29067
A hardware/software environment to support R/D in intelligent machines and mobile robotic systems
[DE90-014458] 23 p3385 N90-29119

MODAL RESPONSE
Analytic signals in the damping coefficient estimation 02 p0178 N90-11003
Acoustic response analysis in the low frequency domain 02 p0179 N90-11010
Comparison of sine dwell and broadband methods for modal testing 02 p0181 N90-11025
Computation of generalized modal loads in an acoustic field define by a distribution of correlated pressures
[NASA-CR-188041] 03 p0358 N90-12047
A survey on nonproportional damping 04 p0483 N90-12773
Effect of modal truncation on derivatives of closed-loop damping ratios in structural control 07 p0882 N90-15109
Restoring force method and response estimation
[DE90-002394] 08 p1116 N90-16463
Transverse vibrations of a composite cylindrical tube of circular cross section
[AD-A219227] 16 p2248 N90-22820
Structural behavior of composites with progressive fracture
[NASA-TM-102370] 17 p2368 N90-23477
Two-dimensional modal logics for relational algebras and temporal logic of intervals
[ITLI-LP-89-03] 17 p2464 N90-24077
Modal logic as a theory of information
[ITLI-LP-89-05] 17 p2480 N90-24183
Microcomputer-aided ground vibration testing
[DLR-FB-89-57] 18 p2499 N90-24279

MODE COUPLING
U COUPLED MODES

MODE OF VIBRATION
U VIBRATION MODE

MODE SHAPES
U MODAL RESPONSE

MODEL REFERENCE ADAPTIVE CONTROL
The role of sensor directed, model based control in robotics
[DE89-014133] 01 p0077 N90-10442
Experience with model based display for advanced diagnostics and control
[DE89-015693] 01 p0082 N90-10469
Control of mechanical manipulators 07 p0938 N90-15432
Direct multivariable adaptive controller with application to wing flutter 10 p1322 N90-17642
Model-reference adaptive control applied to loadfollowing of a space-nuclear power system
[DE89-014561] 10 p1429 N90-18245
Rule-based mechanisms of learning for intelligent adaptive flight control 14 p1908 N90-20939
Experimental adaptive control of a hydraulic robot 16 p2303 N90-23121
Modelling and control of a balloon borne stabilized platform 17 p2355 N90-23408
Position control of redundant manipulators using an adaptive error-based control scheme
[NASA-CR-186812] 20 p2914 N90-26578
Manipulators with flexible links: A simple model and experiments 24 p3501 N90-29786
Model based manipulator control 24 p3509 N90-29833
Discrete-time adaptive control of robot manipulators 24 p3509 N90-29834

MODELS
NT AIRCRAFT MODELS
NT ANALOG SIMULATION
NT ASTRONOMICAL MODELS
NT ATMOSPHERIC GENERAL CIRCULATION MODELS
NT ATMOSPHERIC MODELS
NT BIOLOGICAL MODELS (MATHEMATICS)
NT BREADBOARD MODELS
NT DIGITAL SIMULATION
NT DYNAMIC MODELS
NT ENVIRONMENT MODELS
NT HYDROLOGY MODELS
NT K-EPSILON TURBULENCE MODEL
NT MATHEMATICAL MODELS
NT NUCLEAR MODELS
NT OCEAN MODELS
NT PETRI NETS
NT QUARK MODELS
NT QUARK PARTON MODEL
NT SCALE MODELS
NT SEMISPAN MODELS
NT SPACECRAFT MODELS
NT STATIC MODELS
NT STELLAR MODELS
NT THREE DIMENSIONAL MODELS
NT TURBULENCE MODELS
NT TWO DIMENSIONAL MODELS
NT WIND TUNNEL MODELS
Models of mental functioning
[AD-A210456] 01 p0094 N90-10538
Acoustic test and analysis of a counterrotating prop-fan model
[NASA-CR-179590] 01 p0119 N90-10683
A fully electromagnetic hybrid model for high density plasma simulations
[DE89-016771] 02 p0279 N90-11593
Inferring data base requirements from examples in forms 02 p0288 N90-11646
An open-loop transient thermodynamic model of the Cougar turbojet
[AD-A211774] 03 p0307 N90-11745
Proceedings of the Workshop on Compound Semiconductor Devices and Integrated Circuits (13th) held in Cabourg, France on 10-12 May 1989
[AD-A211848] 03 p0343 N90-11954
Thermal model for double-drift IMPATT diodes on diamond heat sinks
[AD-A211746] 03 p0415 N90-12380
Development of a VSAERO (Vortex Separation Aerodynamics) model of the F/A-18
[AD-A212442] 04 p0448 N90-12566
Studies of gas turbine heat transfer airfoil surfaces and end-wall cooling effects
[AD-A212451] 04 p0457 N90-12620
The comparison of the airbase simulation models airbase and sustained
[FEL-1988-66] 04 p0459 N90-12629
Laser probe vaporization/oxidation testing of high temperature composites
[AD-A211410] 04 p0465 N90-12663
Photochemical observation of ion flows in membrane channels
[AD-A212449] 04 p0472 N90-12705
An investigation of the irradiation swelling mechanisms in refractory metals at high temperatures
[AD-A211406] 04 p0474 N90-12719
Structural studies of sputter-deposited MoS2 solid lubricant films
[AD-A212407] 04 p0481 N90-12759
Height and gradient from shading
[AD-A212338] 04 p0504 N90-12908
Visualization of high-resolution digital terrain
[AD-A212149] 04 p0515 N90-12971
The GEM-T2 gravitational model
[NASA-TM-100746] 04 p0517 N90-12984
Modeling and measurement methods for high speed bipolar transistors
[REPT-11] 05 p0636 N90-13714
Steady state model to determine lake resources at risk to acid deposition in the Sierra Nevada, California
[PB89-103995] 06 p0809 N90-14705
Research on GaAs quantum-coupled structures that can be used as electron devices
[AD-A214015] 07 p0924 N90-15350
Ion-heated thermal Comptonization models and x ray spectral correlations in active galactic nuclei
[DE90-003597] 08 p1151 N90-16667
Modeling the gate I/V characteristic of a GaAs MESFET for Volterra-series analysis
[AD-A215314] 09 p1212 N90-17030
An exploratory analysis of motion sickness data: A time series approach
[AD-A215534] 09 p1253 N90-17271
Measuring learning ability by dynamic testing
[AD-A215273] 09 p1259 N90-17304
Remote sensing of evaporation ducts for Naval warfare
[AD-A214849] 10 p1374 N90-17965
Parameterization of small-scale processes
[AD-A215507] 10 p1398 N90-18082
Kalman estimation for SEDS measurements 12 p1634 N90-19393
Monostable electrovalve
[INPE-4928-RPE/595] 12 p1651 N90-19487
Recalibrating software reliability models
[NASA-CR-186407] 12 p1700 N90-19763

Modeling and realization of plane acousto-optic unilateral band modulators
[ETN-90-95824] 12 p1710 N90-19818
An equational language for specifying, querying, and updating database domains
[PB90-124694] 12 p1726 N90-19918
Petrographic working model of the Rosetta sampling and modelling subgroup for a comet nucleus 12 p1738 N90-19992
Determination of fundamental thermodynamic properties of constituent materials and performance screening of candidate systems
[AD-A218089] 13 p1769 N90-20153
MEASURE: An integrated data-analysis and model identification facility
[NASA-CR-186452] 13 p1863 N90-20686
A locally constrained parallel activation model for diagnostic reasoning
[AD-A217808] 13 p1874 N90-20747
Design of a digital model following controller of reaction wheel torques
[INPE-4753-PRE/1425] 14 p1938 N90-21093
Proceedings of the 4th European Conference, volume 2
[AD-A216521] 14 p1986 N90-21382
Generation of triangular form models in a microcomputer environment
[INPE-4974-PRE/1539] 14 p1997 N90-21447
Aeroelastic simulation of higher harmonic control 15 p2054 N90-21768
Unsteady separated flows produced by complex harmonic motions: Investigation of wing-flow interactions elicited by a mechanical model simulating dragonfly wing kinematics 15 p2100 N90-22018
The chemical basis for the origin of the genetic code and the process of protein synthesis
[NASA-CR-186590] 15 p2136 N90-22205
A study of mental models through communication between users and advisors solving software manipulation problems 15 p2176 N90-22434
An experimental study of tip shape effects on the flutter of aft-swept, flat-plate wings
[NASA-TM-4180] 16 p2199 N90-22555
Microcracking and toughness of ceramic-fiber/ceramic-matrix composites under high temperature
[AD-A218516] 16 p2223 N90-22680
A theoretical and experimental investigation of an absorption refrigeration system for application with solar energy units 16 p2226 N90-22697
An experimental investigation of support strut interference on a three-percent fighter model at high angles of attack
[AD-A219793] 17 p2345 N90-23353
Preliminary investigation into the effect of high temperature thermal anneals on the figure of merit of silicon germanium alloys
[AD-A218573] 17 p2375 N90-23527
Statistical design of MOS VLSI (Very Large Scale Integrated) circuits with designed experiments
[AD-A219654] 17 p2396 N90-23647
Evaluation methodology for software engineering
[AD-A218474] 17 p2441 N90-23913
Generation of expert systems by partial evaluation
[AD-A220427] 17 p2443 N90-23920
New transonic test sections for the NAE 5 ft x 5 ft trisonic wind tunnel
[AD-A220933] 18 p2499 N90-24278
Unique failure behavior of metal/composite aircraft structural components under crash type loads
[NASA-TM-102679] 18 p2572 N90-24660
Computer-Aided Structural Engineering (CASE) project. User's guide: A Three-Dimensional Stability Analysis/Design Program (3DSAD). Report 2: General loads module
[AD-A220331] 18 p2591 N90-24742
Acquiring generalizations to organize human databases
[AD-A219835] 18 p2634 N90-25004
Behavior of composite/metal aircraft structural elements and components under crash type loads: What are they telling us
[NASA-TM-102681] 19 p2701 N90-25368
Analysis of the biomechanic and ergonomic aspects of the cervical spine under load 19 p2719 N90-25470
Applying formal models and proofs to the verification of distributed systems
[IAR-89-7] 19 p2750 N90-25625
Theft of information in the take-grant protection model
[NASA-CR-186638] 19 p2763 N90-25702
Space plane model for visual measurement of aerodynamic heating
[DE90-505514] 20 p2803 N90-25949
H-infinity based integrated flight-propulsion control design for a STOVL aircraft in transition flight
[NASA-TM-103198] 20 p2813 N90-26011
Interfacial viscosity measurements of adsorbed monolayers on metal surfaces
[AD-A221689] 21 p2979 N90-26931
Characterization of polymer interphases using surface-enhanced Raman scattering
[AD-A223103] 21 p2985 N90-26965
Meteor burst communications systems
[AD-A221675] 21 p2997 N90-27037
Neurobehavioral effects of carbon monoxide (CO) exposure in humans: Elevated carboxyhemoglobin (COHb) and cerebrovascular responses
[AD-A222840] 21 p3034 N90-27246
Artificial intelligence techniques for modeling database user behavior 21 p3049 N90-27330
The sixth generation robot in space 21 p3049 N90-27332
Recovery in distributed systems using optimistic message logging and checkpointing
[AD-A222104] 21 p3054 N90-27361
Representing processes in the extended entity-relationship model
[DE90-013350] 21 p3086 N90-27551
Multiresolutional models of uncertainty generation and reduction 23 p3370 N90-29043
A planar rocket motor model for visualization of violent reaction due to fragment impact
[AD-A224273] 24 p3441 N90-29431
Dynamic consolidation of super hard materials
[AD-A224460] 24 p3454 N90-29505
Sounder update and field strength software modifications for Special Operations Radio Frequency Management System (SORFMS). Volume 1: Program descriptions and testing
[AD-A224510] 24 p3460 N90-29543

MODEMS
Performance of four rake modems over the non-disturbed wideband HF channel
[AD-A211589] 03 p0339 N90-11930
Trends in VLF/LF (Very Low Frequency/Low Frequency) modem performance testing
[AD-A216576] 11 p1497 N90-18614
High throughput data communication system
[AD-D014342] 12 p1642 N90-19432
High speed modem
[AD-D014319] 12 p1698 N90-19750
Evaluation of a prototype 6 tone modem
[RAE-TM-FM-28] 16 p2228 N90-22708
Binary pseudo random phase correlation in radar systems: A new approach
[RSRE-MEMO-4223] 19 p2683 N90-25263
An experimental medium speed wideband modem 20 p2847 N90-26194

MODERATION (ENERGY ABSORPTION)
NT THERMALIZATION (ENERGY ABSORPTION)

MODES
NT AXIAL MODES
NT BALLOONING MODES
NT COUPLED MODES
NT FAILURE MODES
NT LASER MODES
NT PROPAGATION MODES
NT VIBRATION MODE
NT WHISPERING GALLERY MODES

MODFETS
High energy neutron irradiation effects in GaAs modulation-Doped Field Effect Transistors (MODFETS): Threshold voltage
[AD-A210502] 01 p0132 N90-10763
Proceedings of the Joint NOSC/NRL (Naval Ocean Systems Center/Naval Research Laboratory) InP Microwave/Millimeter Wave Technology Workshop
[AD-A218216] 14 p1966 N90-21259

MODIFICATION
U REVISIONS

MODULARITY
Module algebra (revised version)
[CWI-CS-R8844-REV] 02 p0260 N90-11474
Modular specifications in process algebra with curious queues
[CWI-CS-R8821] 04 p0543 N90-13152
Manufacture and testing of a solar panel assembly comprising bifacial solar cells (AMOC-SPA) 10 p1342 N90-17773
Selection and design of a stretched-membrane heliostat for today's markets
[DE90-007997] 13 p1828 N90-20495
Real-time concurrency control and transaction scheduling
[AD-A218162] 13 p1901 N90-20909
Agile multiple aperture imager receiver development
[AD-A218956] 16 p2318 N90-23215
A Communications Antenna Pointing System (CAPS): A modular approach 18 p2537 N90-24474
Modular parser generation
[CWI-CS-R8933] 18 p2592 N90-24745
Modularity in robotic systems 23 p3365 N90-29014

MODULATION
NT AMPLITUDE MODULATION
NT DELTA MODULATION
NT DIFFERENTIAL PULSE CODE MODULATION
NT FREQUENCY MODULATION
NT FREQUENCY SHIFT KEYING
NT INTERMODULATION
NT LIGHT MODULATION
NT PHASE MODULATION
NT PHASE SHIFT KEYING
NT PULSE AMPLITUDE MODULATION
NT PULSE CODE MODULATION
NT PULSE DURATION MODULATION
NT PULSE MODULATION
NT PULSE POSITION MODULATION
NT TRAVELING WAVE MODULATION
Use of depletion edge translation for high-speed modulation and switching of lightwaves
[AD-A211186] 01 p0124 N90-10713
Wideband phase-locked angular modulator 04 p0487 N90-12798
Surface current and wave modulation measurements over bottom topography: A comparison with theory
[AD-A212469] 04 p0522 N90-13011
The modulating grid 05 p0603 N90-13505
Remote sensing of atmospheric water vapour by pressure modulation radiometry 06 p0802 N90-14667
MT's algorithm: A new algorithm to search for the optimum set of modulation indices for simultaneous range, command, and telemetry
[NASA-CR-186259] 08 p1057 N90-16110
Reflectance modulation with electrochromic Li(sub x)WO(3) films
[DE90-004571] 10 p1435 N90-18279
Thermal modulation of light beams
[AD-D014322] 12 p1713 N90-19840
Error control techniques for satellite and space communications
[NASA-CR-186221] 13 p1788 N90-20263
Advanced modulation technology development for earth station demodulator applications. Coded modulation system development
[NASA-CR-185149] 13 p1789 N90-20270
Doppler radar with multiphase modulation of transmitted and reflected signal
[NASA-CASE-MSC-18808-1] 13 p1791 N90-20280
Radar RFI at Goldstone DSS 12 and DSS 16 15 p2078 N90-21900
On decoding of multi-level MPSK modulation codes
[NASA-CR-186601] 15 p2146 N90-22261
Microwave transmission line and method of modulating the phase of a signal passed through said line
[AD-D014457] 17 p2395 N90-23640
Spectral properties of a 1.3-micrometers InGaAsP diode laser under modulation
[AD-A220066] 17 p2409 N90-23729
Analysis of neural systems involved in modulation of memory storage
[AD-A220230] 18 p2584 N90-24714
Relativistic klystron amplifiers driven by modulated intense relativistic electron beams
[AD-A221075] 18 p2607 N90-24849
A simple beam position monitor system for CEBAF
[CEBAF-PR-89-015] 19 p2757 N90-25664
Advanced Communication Processing Techniques
[AD-A223244] 21 p2996 N90-27027
A 94 GHz transmissometer
[AD-A223309] 24 p3471 N90-29618
Book of abstracts of the 1st Benelux-Japan Workshop on Information and Communication Theory
[PB90-191446] 24 p3556 N90-30124

MODULATION DOPED FETS
U MODFETS

MODULATION DOPING
Strong-inversion model of threshold voltage in modulation doped field effect transistors: The role of unintentional acceptors
[AD-A212750] 04 p0498 N90-12870

MODULATION TRANSFER FUNCTION
The relay lens systems 05 p0603 N90-13506
The detectors 05 p0604 N90-13507
Broadband incoherent imaging using multiple aperture optics
[AD-A215708] 09 p1282 N90-17437
Comparison of control structures for a bidirectional high-frequency dc-dc converter 10 p1337 N90-17737
Sensor performance analysis
[NASA-RP-1241] 17 p2418 N90-23780
Frequency analysis via the method of moment functionals
[NASA-CR-186988] 22 p3239 N90-28367

MODULATORS
NT BRAGG CELLS
NT MODEMS
Use of depletion edge translation for high-speed modulation and switching of lightwaves
[AD-A211186] 01 p0124 N90-10713
Wideband phase-locked angular modulator 04 p0487 N90-12798
Optical modulators based on polymers
[EP-PATENT-0-294-061-A1] 05 p0700 N90-14099
Modification of MEA modulator-klystron units enabling short pulse injection into a pulse-stretcher ring 06 p0841 N90-14894
Performance and modification of the MEA RF drive system 06 p0842 N90-14895
Active phase and amplitude modulator
[AD-D014318] 12 p1650 N90-19480
CdTe buffered GaAs thin-slab IR waveguide modulators and T/R filter
[AD-A215999] 12 p1651 N90-19488
Modeling and realization of plane acousto-optic unilateral band modulators
[ETN-90-95824] 12 p1710 N90-19818
Velocity matched optical transmitter
[AD-A217413] 13 p1887 N90-20830
GaAs traveling-wave optical modulators using modulated coplanar electrodes with periodic cross-tie overlays
[AD-A217731] 13 p1888 N90-20835
Double valve mechanism for an acoustic modulator
[AD-D014401] 14 p1987 N90-21386
Monolithic arrays of grating-surface-emitting diode lasers and quantum well modulators for optical communications
[NASA-CR-186772] 19 p2758 N90-25674
Optical wavefront computer for stabilizing large space structures
[AD-A221707] 21 p2967 N90-26866
Special purpose spatial light modulators
[AD-A223794] 24 p3545 N90-30052
MODULATORS-DEMODULATORS
U MODEMS
MODULES
NT AIRLOCK MODULES
NT COMMAND SERVICE MODULES
NT ELECTRONIC MODULES
NT LUNAR LANDING MODULES
NT LUNAR MODULE
NT PAYLOAD ASSIST MODULE
NT POWER MODULES (STS)
NT SERVICE MODULES
NT SPACECRAFT DOCKING MODULES
NT SPACECRAFT MODULES
Evaluation of dispersive behavior in periodic structures by discrete Fourier transform 02 p0180 N90-11014
Dynamic substructuring for modular analysis and testing 02 p0180 N90-11015
Apparatus for cooling electronic components in aircraft
[AD-D014207] 05 p0579 N90-13373
Fast serial communication module
[DE89-633753] 06 p0766 N90-14454
Performance of the 10-kV, 100-kA pulsed-power modules for the FRX-C magnetic compression experiment
[DE89-014027] 06 p0845 N90-14917
Conceptual design for the space station Freedom modular combustion facility
[NASA-TM-102037] 08 p1053 N90-16087
Bus programmable slave module
[NASA-CASE-MSC-21387-1] 08 p1108 N90-16411
Non-contact temperature measurement requirements 10 p1363 N90-17898
Amplified spontaneous emission measurements on the aurora large-aperture module
[DE90-004841] 13 p1806 N90-20369
Recent progress in photovoltaic concentrator module technology
[DE90-009007] 14 p2002 N90-21475
The Italian approach to small satellites for low cost access to space developments
[ETN-90-96552] 16 p2206 N90-22587
Concept study for UHF T/R modules
[AD-A220281] 18 p2547 N90-24536
Space station based Microacceleration Experiment Platform
[NASA-CR-186659] 19 p2666 N90-25167
Sandia's CONCEPT-90 photovoltaic concentrator module
[DE90-012243] 22 p3196 N90-28134
Modularity in robotic systems 23 p3365 N90-29014
MODULUS OF ELASTICITY
Development of elastomeric polypeptide biomaterials
[AD-A210295] 01 p0049 N90-10280
Composites reinforced with thermotropic liquid crystal copolyester fibers
[AD-A211226] 02 p0191 N90-11089
Identification of equivalent modulus of a composite beam from nonmodal vibratory tests
[ECL-89-001] 05 p0656 N90-13821
Parametric studies to determine the effect of compliant layers on metal matrix composite systems
[NASA-TM-102465] 06 p0737 N90-14294
The elastic properties of woven polymeric fabric
[DE89-015391] 07 p0909 N90-15255
Elastic moduli of copper: Electronic structure contributions from pseudopotentials and full-potential linear muffin-tin orbital band structure calculations
[DE90-004423] 08 p1044 N90-16037
Construction of inelastic stress-strain curves from minimal materials data (computer program)
[ESDU-89052] 09 p1239 N90-17189
A finite element analysis of porosity effects on materials
[AD-A216225] 10 p1359 N90-17884
Fluorinated graphite fibers as a new engineering material: Promises and challenges
[NASA-TM-102511] 12 p1618 N90-19301
Compressive strength of synthetic comet nucleus samples 12 p1741 N90-20006
Ultrastructure processing of ordered polymers
[AD-A218331] 13 p1783 N90-20232
Matrix density effects on the mechanical properties of SiC/RBSN composites
[NASA-TM-103098] 15 p2065 N90-21826
Characterization and processing of blends of polyethylene terephthalate with several liquid crystalline polymers
[AD-A219565] 17 p2380 N90-23552
Calculation of thick wall fiber binders for rotor components of modern helicopters
[MBB-UD-554/84-PUB] 19 p2660 N90-25137
MOHR CIRCLES
U FRACTURE MECHANICS
MOIRE FRINGES
A sampled-grating model of moire patterns from digital imaging
[AD-A213364] 06 p0843 N90-14902
Deferred electronic heterodyne moire deflectometry: A method for transient density fields measurement
[NASA-CR-182982] 06 p0843 N90-14907
Utilization of Moire patterns as an orbital docking aid to space shuttle/Space Station Freedom 18 p2629 N90-24980
MOIRE INTERFEROMETRY
An experimental and analytical program to develop crack tip fracture criteria
[AD-A211565] 03 p0359 N90-12051
Interferometric surface distortion detector
[AD-D014211] 06 p0842 N90-14901
Analysis of ductile fracture under biaxial loading using moire interferometry 10 p1394 N90-18060
A multipulsed dynamic diffraction moire interferometer
[DE90-009765] 16 p2230 N90-22723
A compact portable diffraction moire interferometer
[DE90-009780] 16 p2238 N90-22768
J-integral and HRR field of a stably growing crack, an experimental analysis
[AD-A220418] 17 p2416 N90-23764
MOISTURE
NT ATMOSPHERIC MOISTURE
NT SOIL MOISTURE
Crau 1987: The KNMI contribution --- KNMI (Royal Netherlands Meteorological Institute)
[KNMI-TR-110] 03 p0375 N90-12140
Description of a software library for the calculation of surface fluxes
[KNMI-TR-112] 03 p0375 N90-12141
Chemical treatment of epoxy resins to reduce moisture sensitivity and to improve the mechanical properties
[AD-A212360] 04 p0481 N90-12758
Development of a titanium/boron blending process
[DE90-001450] 06 p0754 N90-14386
Low-temperature conversion of high-moisture biomass: Continuous reactor system results
[DE90-000984] 06 p0805 N90-14683
Observational study of the macroscopic behavior of moist-convective processes 07 p0959 N90-15547
Specification for evaporation duct height calculations
[AD-A213841] 07 p0964 N90-15570
Effects of moisture on composite materials 09 p1185 N90-16866
Thiokol/Wasatch installation evaluation of the redesigned field joint protection system (concepts 1 and 3)
[NASA-CR-183860] 13 p1765 N90-20127
Moisture control in sealed electronic packages
[DE90-008136] 13 p1771 N90-20166
Structure and dynamics of the Arizona monsoon boundary
[AD-A217378] 13 p1844 N90-20586
Comparison of light duty gloves with natural and synthetic materials under wet and dry conditions
[AD-A218119] 13 p1856 N90-20649
The above-inversion moisture structure observed during FIRE 22 p3215 N90-28235
Non-destructive method for environmental breakdown of graphite fiber reinforced polymer composites
[AD-A223729] 24 p3455 N90-29515
MOISTURE CONTENT
NT ATMOSPHERIC MOISTURE
Hygrothermal effects on the complex moduli of composite laminates 01 p0033 N90-10182
Airborne gamma radiation snow water equivalent and soil moisture measurements and satellite areal extent of snow cover measuerments: A user's guide, version 3.0
[PB89-177877] 02 p0235 N90-11338
Liquid water content and droplet size calibration of the NASA Lewis Icing Research Tunnel
[NASA-TM-102447] 05 p0651 N90-13797
An evaluation of the Smith-Feddes model
[AD-A213237] 05 p0671 N90-13907
Thermodynamic analysis of chemical stability of ceramic materials in hydrogen-containing atmospheres at high temperatures
[NASA-CR-4271] 08 p1050 N90-16072
Evaluating CO, CO2 and H2O concentration by partial integration of absorption band spectra
[ISL-R-110/88] 09 p1244 N90-17219
An atlas of ECMWF analyses (1980-1987). Part 1: First moment quantities
[NASA-TM-100747-PT-1] 10 p1408 N90-18120
The effect of moisture absorption in clothing on the human heat balance
[AD-A217899] 13 p1852 N90-20626
Meteorological influences on mountain cloudwater chemistry in the eastern United States
[PB90-132432] 14 p2007 N90-21504
NASA Lewis icing research tunnel user manual
[NASA-TM-102319] 17 p2355 N90-23407
Implementation of sensor and control designs for bioregenerative systems
[NASA-CR-186655] 20 p2897 N90-26479
An eight-month climatology of marine stratocumulus cloud fraction, albedo, and integrated liquid water 22 p3214 N90-28233
Cloud optical parameters as derived from the multispectral cloud radiometer 22 p3215 N90-28239
Moisture and heat budgets of a cirrus cloud from aircraft measurements during FIRE 22 p3223 N90-28279
Cirrus clouds and climate feedback: Is the sky falling and should we go tell the king 22 p3225 N90-28288
A scheme for parameterizing cirrus cloud ice water content in general circulation models 22 p3226 N90-28292
Remote sounding through semi-transparent cirrus cloud 22 p3226 N90-28296
Three functions that model empirically measured unfrozen water content data and predict relative hydraulic conductivity
[AD-A223875] 23 p3343 N90-28892
The signals of an ice warning device in dependence on total water content and normalized icing degree
[ESA-TT-1207] 24 p3484 N90-29692
MOISTURE DETECTORS
U MOISTURE METERS
MOISTURE METERS
Crau 1987: The KNMI contribution --- KNMI (Royal Netherlands Meteorological Institute)
[KNMI-TR-110] 03 p0375 N90-12140
MOJAVE DESERT (CA)
Radar scattering from desert terrains, Pisgah/Lavic Region, California: Implications for Magellan 03 p0426 N90-12443
MOL (ORBITAL LABORATORIES)
U MANNED ORBITAL LABORATORIES
MOLDING MATERIALS
Using template/hotwire cutting to demonstrate moldless composite fabrication 18 p2515 N90-24361
Surface effect for test piece on flexural test of carbon fiber reinforced plastic laminates
[NAL-TM-601] 24 p3442 N90-29436
MOLDS
Advances in the technology of titanium castings 01 p0043 N90-10243
Development, implementation and test of a computer program for the production of axisymmetric pattern moulds on a numerically controlled milling machine
[LR-593] 15 p2074 N90-21877
Using template/hotwire cutting to demonstrate moldless composite fabrication 18 p2515 N90-24361
Compression molded polyurethane block copolymers. 1: Thermal and thermomechanical properties
[AD-A220068] 18 p2529 N90-24431

Understanding silica binders
[PNR90625] 20 p2840 N90-26150
CAD/CAM reinforces the competitive edge of European mouldmakers
[CRIF-MC-88] 20 p2908 N90-26542

MOLECULAR ABSORPTION
Study of high frequency water vapor absorption parameters
[AD-A210676] 02 p0194 N90-11108
Chemical treatment of epoxy resins to reduce moisture sensitivity and to improve the mechanical properties
[AD-A212360] 04 p0481 N90-12758
Interfacial and thin film chemistry in electron device fabrication
[AD-A214784] 09 p1289 N90-17473
Activation of methane by transition metal-substituted aluminophosphate molecular sieves
[DE90-005663] 12 p1624 N90-19331
Chemical structure and kinetics at liquid/solid interfaces
[AD-A222766] 20 p2831 N90-26105
Ultrasensitive laser spectroscopy in solids: Statistical fine structure and single-molecule detection
[AD-A222391] 21 p3074 N90-27477
High pulse energy flashlamp pumpable laser dyes
[AD-A223075] 22 p3180 N90-28042
Fifteenth International Conference on X Ray and Inner-Shell Processes
[DE90-013024] 23 p3393 N90-29170

MOLECULAR BEAM EPITAXY
Use of depletion edge translation for high-speed modulation and switching of lightwaves
[AD-A211186] 01 p0124 N90-10713
Experimental investigations of transport and optical properties of 3-5 quantum well structures grown via molecular beam epitaxy under optimal growth conditions
[AD-A210269] 01 p0132 N90-10758
The growth of gallium nitride films via the innovative technique of atomic layer epitaxy
[AD-A210380] 01 p0132 N90-10760
Trap gettering by isoelectronic doping of p-GaAs and n-GaAs grown by molecular beam epitaxy
[AD-A211162] 01 p0133 N90-10769
Development of microstructured DH diode lasers and detectors for the near and medium IR spectral domain using molecular beam epitaxy
[IPM-15/1988] 03 p0354 N90-12023
Beam assisted fabrication of 3-5/Si monolithic devices
[AD-A212046] 03 p0412 N90-12367
High speed quantum-well optoelectronic devices by MBE
[AD-A212585] 04 p0555 N90-13237
Chemical beam epitaxy of ZnSe
[AD-A213265] 05 p0621 N90-13625
Surface roughening of Ge(001) during 200 eV Xe ion bombardment and Ge molecular beam epitaxy
[DE90-000674] 07 p0998 N90-15769
Defect control and denuded trap zones in the 3-5 semiconductors
[AD-A214099] 07 p1004 N90-15814
Slow positron defect profiling of silicon epilayers
[DE90-003958] 08 p1087 N90-16288
Group 2 cubic fluorides as dielectrics for III-V compound semiconductors
[AD-A214096] 08 p1129 N90-16542
Fabrication of nanometer single crystal metallic CoSi2 structures on Si
[NASA-CASE-NPO-17736-1-CU] 09 p1286 N90-17455
Interfacial and thin film chemistry in electron device fabrication
[AD-A214784] 09 p1289 N90-17473
Growth characteristics and electronic behavior of ultrathin epitaxial metallizations
[AD-A214794] 09 p1289 N90-17474
JSEP (Joint Services Electronics Program)
[AD-A215051] 09 p1290 N90-17476
Comments on containerless bulk crystal growth and epitaxy in space and on their implications regarding non-contact temperature measurements 10 p1365 N90-17911
Temperature control and calibration issues in the growth, processing and characterization of electronic materials 10 p1365 N90-17914
High temperature superconductivity
[AD-A215491] 10 p1436 N90-18286
High performance, picosecond radiation detectors grown by molecular beam epitaxy for millimeter-wave diagnostic systems
[DE90-005547] 10 p1438 N90-18302
Digital capacity transient spectroscopy of deep structure defects in III-V-Semiconductor structures
[ETN-90-96057] 12 p1722 N90-19890
Joint Services Electronics Program research in electronics
[AD-A217745] 13 p1796 N90-20307
Investigation of the technological effects on the coupling behavior of parallel GaAlAs rib waveguide
[ETN-90-95323] 13 p1887 N90-20825
Chemical beam epitaxy of ZnSe
[AD-A217375] 13 p1893 N90-20866
CCST (Center for Compound Semiconductor Technology) research briefs
[DE90-007782] 13 p1895 N90-20874
Optical properties of zinc selenide grown using molecular beam deposition techniques
[RSRE-MEMO-4269] 15 p2174 N90-22423
Continued development and characterization of doped layers, contacts, and associated electronic devices in silicon carbide
[AD-A219211] 16 p2232 N90-22737
High temperature superconductivity
[AD-A219483] 17 p2476 N90-24155
Dielectric function of InGaAs in the visible
[NASA-TM-103246] 20 p2932 N90-26683
MBE growth technology for high quality strained III-V layers
[NASA-CASE-NPO-17723-1-CU] 20 p2932 N90-26685
Laser induced surface chemical epitaxy
[AD-A222082] 21 p2977 N90-26920
Integration of picosecond GaAs photoconductive devices with silicon circuits for optical clocking and interconnects
[DE90-012096] 21 p3080 N90-27512
Investigation on the MBE growth and properties of AlGaInAs/InP and InGaAs-InAlAs superlattices
[DE90-012248] 21 p3080 N90-27515
Growth of III-V films by control of MBE growth front stoichiometry
[NASA-CASE-NPO-17724-1-CU] 21 p3081 N90-27517
Method of forming three-dimensional semiconductor structures
[NASA-CASE-NPO-17835-1-CU] 21 p3081 N90-27518
The epitaxial growth of copper on the (111) surface of silicon
[DE90-013817] 21 p3082 N90-27523
Molecular beam epitaxial growth, characterization, and devices of modulated semiconductor structures
[AD-A221545] 21 p3084 N90-27538
High resistivity Al(x)Ga(1-x) As(y)Sb(1-y) epitaxial layers by sulfur compensation doping
[DE90-012228] 22 p3248 N90-28419
Reflection Mass Spectrometry (REMS) during 3/5 MBE
[DE90-014568] 23 p3304 N90-28690
Basic studies of 3-V high efficiency cell components
[DE90-000360] 24 p3484 N90-29696
High throughput MBE materials for MODFET's
[AD-A223452] 24 p3552 N90-30097

MOLECULAR BEAMS
Reaction of oxygen with allene
[DE89-015219] 01 p0039 N90-10216
High temperature and high resolution UV photoelectron spectroscopy using supersonic molecular beams
[DE90-000176] 03 p0323 N90-11835
Lecture notes on supersonic molecular beam sources
[MPIS-20/1988] 08 p1121 N90-16494
Interactions of molecules with surfaces
[DE90-007555] 13 p1883 N90-20806
The 18th Informal Conference on Photochemistry
[AD-A219779] 17 p2373 N90-23510
Joint services electronics program: Electronics research at the University of Texas at Austin
[AD-A220834] 17 p2397 N90-23655
Instrumentation for surface reaction dynamics
[AD-A218608] 17 p2406 N90-23708

MOLECULAR BIOLOGY
Molecular biology and physiology of methanogenic archaebacteria
[AD-A210399] 01 p0091 N90-10522
Army Science Conference Proceedings (16th) held in Fort Monroe, Virginia on 25-27 October 1988: Addenda
[AD-A210235] 01 p0143 N90-10827
DOE/CEC Workshop on Critical Evaluation of Radiobiological Data to Biophysical Modeling
[DE89-015214] 02 p0254 N90-11437
Cellular and molecular mechanisms of high pressure inotropy in cardiac muscle
[AD-A211695] 03 p0381 N90-12170
JPRS report: Science and technology. USSR: Life sciences
[JPRS-ULS-90-002] 14 p1995 N90-21434
Artificial life: The coming evolution
[DE90-008860] 14 p2009 N90-21515
Workshop on High-Field NMR and Biological Applications
[DE90-010002] 18 p2614 N90-24889
Photosynthesis in intact plants
[DE90-013699] 20 p2898 N90-26482
The 1989 Gordon Research Conference on Chronobiology
[AD-A221972] 22 p3231 N90-28322
Macromolecular calculations for the XTAL-system of crystallographic programs
[AD-A222345] 22 p3248 N90-28421
Japanese molecular biology 1990: An update
[PB90-188707] 23 p3354 N90-28958
Biomedical and environmental sciences program publications, 1989
[DE90-014785] 23 p3406 N90-29250

MOLECULAR BONDS
U CHEMICAL BONDS

MOLECULAR CHAINS
Ultrastructure processing and characterization of polymers
[AD-A211460] 04 p0478 N90-12743
The structure and properties of liquid crystal polymers 06 p0749 N90-14356
Second-generation ordered polymers
[AD-A216126] 12 p1630 N90-19365
Theory of polymer blends
[DE90-002532] 12 p1632 N90-19377
Investigation into the mechanism of polymer thread drag reduction
[AD-A217492] 13 p1800 N90-20329
A new class of lubricants derived from archaebacterial lipids
[AD-D014429] 14 p1954 N90-21185
The effect of thermal damage on the mechanical properties of polymer regrinds 18 p2515 N90-24363
Surface enrichment and evaporation in a polymer mixture of long and short chains
[DE90-010073] 18 p2529 N90-24429
The formation and structure of circumstellar and interstellar dust 21 p3091 N90-27576
Structure and dynamic properties of combined polymeric main-chain/side-chain liquid crystals
[ETN-90-97299] 22 p3160 N90-27921

MOLECULAR CLOUDS
The stability of magnetohydrodynamic shock waves in molecular clouds 02 p0292 N90-11665
Interstellar medium and infrared emission of the galactic disk 05 p0661 N90-13862
Orion B: Anatomy of a star-forming region 05 p0710 N90-14155
Very high resolution radio observations of molecular cloud cores 06 p0863 N90-15013
Shapes of star-gas waves in spiral galaxies
[NASA-CR-186289] 07 p1011 N90-15859
From interstellar dust to comets 08 p1142 N90-16620
Outflows in high mass star-forming regions 08 p1149 N90-16657
A computer program to calculate the population numbers of multi-level species
[IFSI-89-15] 08 p1151 N90-16671
Variational problems in astrophysics 09 p1298 N90-17524
Photodissociation regions: Observations and theory 11 p1579 N90-19098
IR line emission from dense photodissociation regions 11 p1580 N90-19100
IR line emission from supernovae in molecular clouds 11 p1580 N90-19102
The excitation of molecular hydrogen and its significance 11 p1582 N90-19117
Molecular hydrogen in the HII region G333.6-0.2 11 p1583 N90-19121
Hydrodynamical simulations of collisions between interstellar clouds
[DE90-006921] 11 p1590 N90-19172
The molecular cloud content of early type galaxies. 2: A molecular ring in NGC 404
[PB90-124348] 14 p2039 N90-21695
Interactions of massive stars with the interstellar medium: Bow shocks and superbubbles 15 p2186 N90-22485
The evolution of the supernova remnant IC 443 15 p2186 N90-22486
The distribution of molecular clouds in spiral galaxies 15 p2186 N90-22489
The Sagittarius B2 molecular cloud: An extreme case of a galactic center giant molecular cloud 15 p2187 N90-22493
Gamma rays, cosmic rays, and local molecular clouds 15 p2193 N90-22524
High spatial resolution isotopic CO and CS observations of M17 SW: The clumpy structure of the molecular cloud core
[MPE-PREPRINT-161] 16 p2330 N90-23283
Molecular clouds and the large-scale structure of the galaxy 16 p2333 N90-23295
Gamma rays from giant molecular clouds 16 p2334 N90-23298

Implications of the IRAS data for galactic gamma ray astronomy and EGRET
16 p2334 N90-23300
More data on (possible) gamma ray (point) sources
16 p2335 N90-23309
Spectral measurements of the cosmic microwave background
16 p2340 N90-23334
Molecular studies of dense cores
17 p2484 N90-24207
Interstellar HCN, HNC and HCO+: Stability experiments with acoustooptic spectrometers
[ETN-90-96495] 18 p2638 N90-25028
An X ray pulsar in the dark cloud Lynds 1457
19 p2767 N90-25723
Interstellar grain chemistry and organic molecules
21 p3090 N90-27569
Carbon chemistry in dense molecular clouds: Theory and observational constraints
21 p3090 N90-27571
CI, CII, and CO as tracers of gas phase carbon
21 p3091 N90-27572
Laboratory simulation of interstellar grain chemistry and the production of complex organic molecules
21 p3092 N90-27580
New observations of interstellar organic molecules
21 p3094 N90-27587
Search for interstellar methane
21 p3094 N90-27588
Implications of the IRAS data for galactic gamma-ray astronomy and EGRET
[NASA-TM-103452] 22 p3261 N90-28466
A plasma diagnostic study of two wind-blown shell nebulae: NGC 7635 and NGC 2359
23 p3410 N90-29271
Interstellar magnetic fields: An observational perspective
24 p3560 N90-30144
Carbon monoxide isotopes and clumping in giant molecular clouds
24 p3562 N90-30151

MOLECULAR COLLISIONS
Particle kinetic simulation of high altitude hypervelocity flight
[NASA-CR-186003] 02 p0147 N90-10840
New developments in the ab initio treatment of low energy electron collisions with molecules
[DE89-015294] 03 p0402 N90-12299
Spin-orbit relaxation rates of Bi(6p(3)) 2D(3/2) following photolysis of Bi(CH3)3 at lambda = 193 nm
[AD-A211792] 03 p0402 N90-12303
Fundamental molecular data to support CARS diagnostics of temperature, pressure, and species concentration
[AD-A212411] 04 p0472 N90-12704
CANOES 2: Dynamics of atmospheric infrared thermochemical excitation, volume 1
[AD-A213341] 05 p0667 N90-13897
CANOES 2: Dynamics of atmospheric infrared thermochemical excitation, volume 2
[AD-A213342] 05 p0667 N90-13898
Measurement of optical radiations in spacecraft environments
[AD-A213814] 07 p0950 N90-15497
Investigations of the interactions of radiation with matter
[AD-A213554] 07 p0991 N90-15723
Rotational energy transfer in metastable states of heteronuclear molecules
[AD-A214425] 08 p1120 N90-16485
Cluster based reaction probabilities for boron with oxygen, hydrogen, water, nitrogen, nitrous oxide, carbon dioxide, carbon monoxide, methane, tetrafluoromethane, and silane
[AD-A214554] 09 p1190 N90-16894
Singlet oxygen and iodine monofluoride collisional energy transfer mechanism
[AD-A215711] 09 p1280 N90-17421
Generation of H-, H2v(double prime), and H atoms by H2+ and H3+ ions incident upon barium surfaces
[DE90-005549] 09 p1280 N90-17423
Ab initio R-matrix calculations of e+-molecule scattering
11 p1557 N90-18970
Interactions of molecules with surfaces
[DE90-007555] 13 p1883 N90-20806
Theoretical and computer simulation study of the density fluctuations in liquid water
[PREPRINT-697] 16 p2314 N90-23191
Low frequency Raman spectra of liquid water, a molecular dynamics simulation
[PREPRINT-698] 16 p2314 N90-23192
Support for the 16th International Conference on the Physics of Electronic and Atomic Collisions
[AD-A218567] 16 p2315 N90-23200
Temperature evolution of single particle correlation functions of TIP4P water
[PREPRINT-694] 17 p2470 N90-24119
Rotational and translational effects in collisions of electronically excited diatomic hydrides
[NASA-CR-186770] 20 p2829 N90-26093
Particle simulation of hypersonic flow
[AD-A222704] 21 p2954 N90-26794
Support for the Forty-Second Annual Gaseous Electronics Conference
[AD-A222881] 21 p3073 N90-27473
State-to-state ion-molecule reaction dynamics at thermal energies
[AD-A221589] 21 p3074 N90-27479
United States Air Force research initiation program for 1988, volume 2
[AD-A223124] 21 p3102 N90-27614

MOLECULAR DIFFUSION
Photochemical observation of ion flows in membrane channels
[AD-A212449] 04 p0472 N90-12705
Non-linear optical studies of adsorbates: Spectroscopy and dynamics
[DE90-001543] 06 p0741 N90-14312
NMR measurements of solvent self-diffusion coefficients in polymer solutions
[AD-A215276] 09 p1279 N90-17419
Direct measurements of the physical diffusion of redox active species: Microelectrochemical experiments and their simulation
[AD-A215680] 09 p1280 N90-17420
Modelization of dry deposition in the Chemical Transport Model (CTM) of EURAD
12 p1688 N90-19698
Investigation into the mechanism of polymer thread drag reduction
[AD-A217492] 13 p1800 N90-20329
Molecular dynamics simulations of short-range force systems on 1024-node hypercubes
[DE90-009833] 15 p2146 N90-22259
Stratified ocean mixing
[AD-A219233] 16 p2259 N90-22881
Diffusion of penetrants in polymers
[AD-A223217] 21 p2986 N90-26969
Support for the Forty-Second Annual Gaseous Electronics Conference
[AD-A222881] 21 p3073 N90-27473

MOLECULAR DISSOCIATION
U DISSOCIATION

MOLECULAR ELECTRONICS
Approaches to orthogonally fused conducting polymers for molecular electronics
[AD-A222546] 22 p3159 N90-27915
Report on the International Workshop on Progress Towards Molecular Scale Electronics
[AD-A223758] 24 p3465 N90-29575

MOLECULAR ENERGY LEVELS
NT INTERMOLECULAR FORCES
Multiline multimode CW chemical laser performance
[AD-A210613] 01 p0075 N90-10432
Solvent effects on intervalence electron-transfer energies for biferrocene cations: Comparisons with molecular models of solvent reorganization
[AD-A210263] 01 p0120 N90-10691
Dissociation and vibrational relaxation of XeF by various collision partners
[AD-A210769] 02 p0227 N90-11300
Properties of Lennard-Jones mixtures at various temperatures and energy ratios with a size ratio of two
[PB89-235204] 04 p0471 N90-12697

MOLECULAR EXCITATION
Controlling photoinduced electron transfer rates in donor-spacer-acceptor molecules by changing the electronic properties of the spacer
[DE89-015128] 01 p0128 N90-10735
Quantum chemical investigations of the mechanism of cationic polymerization and theoretical prediction of crystal densities and decomposition pathways of energetic molecules
[AD-A210322] 02 p0200 N90-11143
Spin-orbit relaxation rates of Bi(6p(3)) 2D(3/2) following photolysis of Bi(CH3)3 at lambda = 193 nm
[AD-A211792] 03 p0402 N90-12303
Electron attachment and molecular fragmentation in laser-excited plasmas
[AD-A212098] 03 p0409 N90-12343
CANOES 2: Dynamics of atmospheric infrared thermochemical excitation, volume 4
[AD-A213344] 05 p0667 N90-13900
Excitation lifetimes and excited-state forces in chemisorbed molecules
[DE90-002578] 07 p0894 N90-15165
Rotational energy transfer in metastable states of heteronuclear molecules
[AD-A214425] 08 p1120 N90-16485
Characterization of tetrahydrogen via state-selected excitation of H2
[AD-A216239] 10 p1355 N90-17855
Determination of the minimum energy conformation of alkyl substituted pyrazines
[AD-A216974] 11 p1484 N90-18539
Studies of atmospheric molecules by multiphoton spectroscopy
[DE90-005829] 11 p1534 N90-18833
Merged beam studies into the mechanisms of hydrogen molecular ion recombination
[AD-A216469] 11 p1562 N90-19002
The excitation of molecular hydrogen and its significance
11 p1582 N90-19117
High-excitation lines of molecular hydrogen: A discriminant between shock models
11 p1582 N90-19118
Infrared heterodyne spectroscopy of polyatomic molecules in circumstellar envelopes
12 p1736 N90-19980
Reactive and anisotropic elastic scattering of highly laser-vibration-excited diatomic molecules
[MPIS-19/1988] 13 p1883 N90-20804
Dynamics of electronically excited species in gaseous and condensed phase
[AD-A217696] 13 p1884 N90-20812

MOLECULAR FLOW
NT TRANSITION FLOW
Recent leak telescope development
[DE90-004101] 09 p1225 N90-17106

MOLECULAR GASES
The molecular cloud content of early type galaxies. 2: A molecular ring in NGC 404
[PB90-124348] 14 p2039 N90-21695
Molecular evolution in astrophysical environments
16 p2332 N90-23291
Molecular gas in S106: Morphology, kinematics, and chemistry of a star forming region
17 p2484 N90-24209
Digital filtering of plume emission spectra
[NASA-TM-103135] 20 p2824 N90-26070
Absolute vacuum ultraviolet photoabsorption cross section studies of atomic and molecular species: Techniques and observational data
20 p2944 N90-26754
A laboratory investigation of the production and properties of molecular and radical species pertinent to planetary atmospheres
20 p2946 N90-26766
Optical signatures of molecular particles via mass-selected cluster spectroscopy
20 p2949 N90-26780
Impact fracture experiments simulating interstellar grain-grain collisions
21 p3093 N90-27584
Can the chirality of the ISM be measured
21 p3095 N90-27590
Interstellar magnetic fields: An observational perspective
24 p3560 N90-30144

MOLECULAR INTERACTIONS
NT MOLECULAR COLLISIONS
Monte Carlo simulations of small solute/solvent clusters: Cluster properties and phase transitions
[AD-A209559] 01 p0119 N90-10684
Properties of Lennard-Jones mixtures at various temperatures and energy ratios with a size ratio of two
[PB89-235204] 04 p0471 N90-12697
Molecular dynamics of lipid bilayers
[AD-A211492] 04 p0552 N90-13214
Transition state spectroscopy of hydrogen transfer reactions
[AD-A215041] 09 p1191 N90-16901
Hydrogen desorption from the monohydride phase on Si(100)
[AD-A215237] 09 p1191 N90-16903
Non-destructive characterization of epoxy/dicyandiamide interphases using surface-enhanced Raman scattering
[AD-A215894] 10 p1353 N90-17846
Elastic recovery and polymer-polymer interactions
[AD-A217085] 12 p1633 N90-19384
Superconductivity in Ba(1-x)BiO3
[DE90-003781] 12 p1718 N90-19869
Termolecular associations of ions in gases, recombination and electron-atom collisions
[AD-A217678] 13 p1883 N90-20805
Interactions of molecules with surfaces
[DE90-007555] 13 p1883 N90-20806
DURIP advanced polymer solid state NMR instrumentation
[AD-A221401] 18 p2531 N90-24440
Molecular interactions and properties with many-body methods
[AD-A222631] 20 p2924 N90-26642
Magnetic resonance elucidation of molecule/macromolecule interaction stereochemistry
[AD-A221444] 21 p2979 N90-26928
Supersonic jet studies of benzyl alcohols: Minimum energy conformations and torsional motion
[AD-A221815] 21 p2980 N90-26934
State-to-state ion-molecule reaction dynamics at thermal energies
[AD-A221589] 21 p3074 N90-27479

Design of organic nonlinear optical materials
[AD-A222400] 21 p3084 N90-27536
An ionic mechanism of carbon formation in flames
21 p3093 N90-27582
Solid-state N15 NMR of N15-labeled nylon 6 and nylon 11
[AD-A223271] 24 p3446 N90-29459

MOLECULAR IONS

Structural peculiarities and molecular properties of charge complexes formed on positive ion injection into dense inert gas media
[DE89-633953] 06 p0839 N90-14877
The production and spectroscopy of molecular ions isolated in solid neon
[AD-A213723] 07 p0895 N90-15174
Merged beam studies into the mechanisms of hydrogen molecular ion recombination
[AD-A216469] 11 p1562 N90-19002
Dissociative recombination of molecular ions with electrons 20 p2946 N90-26767
Spectroscopy of ions and their clusters
[AD-A223109] 21 p2977 N90-26917
State-to-state ion-molecule reaction dynamics at thermal energies
[AD-A221589] 21 p3074 N90-27479

MOLECULAR ORBITALS

Bonding in transition metal silyl dimers. Molecular orbital theory
[AD-A208269] 01 p0046 N90-10260
Computational modeling of pi-conjugated polyradicals
[AD-A210573] 01 p0113 N90-10648
A structural basis for electron transfer in bacterial photosynthesis
[DE89-015702] 01 p0120 N90-10687
A diagnostic for determining the quality of single-reference electron correlation methods
02 p0272 N90-11554
A diagnostic for determining the quality of single-reference electron correlation methods
[NASA-TM-101929] 06 p0838 N90-14874
Electronic and ionic transport in polymers
[AD-A213410] 07 p0911 N90-15270
Point defects and interfaces in insulating solids
[AD-A214668] 09 p1289 N90-17471
Preparation and properties of the system Cu(x)Pd(1-x)O (0 less than or equal to x less than or equal to 0.175)
[AD-A217567] 12 p1723 N90-19901
Investigation of optical nonlinearities, conductivity and magnetism in organometallic materials
[AD-A218548] 16 p2317 N90-23211
Electronic structure and lubrication properties of MoS2: A qualitative molecular orbital approach
[AD-A220566] 17 p2380 N90-23557
Use of ab initio theory in studying various chemical systems
[AD-A220913] 18 p2521 N90-24396
Field-induced surface chemistry of NO
[AD-A223007] 21 p2977 N90-26915
An electron spin resonance study of adsorbed gases in ultrahigh vacuum
[ETN-90-97323] 24 p3447 N90-29469
Atomistic studies of grain boundaries in alloys and compounds
[DE90-012401] 24 p3452 N90-29492

MOLECULAR OSCILLATIONS

Forty-fourth symposium on molecular spectroscopy
[AD-A210752] 02 p0195 N90-11111
Structures and energies for small borane compounds: One and two boron compounds
[AD-A212264] 04 p0471 N90-12701
Determination of stepsize parameters for intermolecular vibrational energy transfer
[DE90-003346] 07 p0990 N90-15719
Production rates for electron beams and swarms in nitrogen
[AD-A218145] 13 p1885 N90-20817
Spectroscopy of propellant-related flames
[AD-A224068] 24 p3457 N90-29525

MOLECULAR RELAXATION

Solvent relaxation in electron-transfer reactions: Comparisons between barrier-crossing dynamics in water and polar aprotic media
[AD-A210212] 01 p0040 N90-10220
Fundamental molecular data to support CARS diagnostics of temperature, pressure, and species concentration
[AD-A212411] 04 p0472 N90-12704
Determination of stepsize parameters for intermolecular vibrational energy transfer
[DE90-003346] 07 p0990 N90-15719
Chemistry at clusters, microstructures and surfaces
[AD-A215842] 10 p1353 N90-17844
A continued study of optical sound generation and amplification
[AD-A217640] 13 p1882 N90-20796
Molecular dynamics and spectroscopy at gas-solid interfaces
[AD-A217743] 13 p1885 N90-20813
Transport and relaxation properties in anisotropic superconductors 15 p2170 N90-22403
Investigation of atomistic simulation of structural and dynamic differences in glassy and liquid states of atactic poly(propylene)
[AD-A218896] 16 p2224 N90-22687
Dynamics of micellar oligomeric and monomeric sodium 10-undecenoate
[AD-A222570] 20 p2830 N90-26099
Infrared spectra of van de Waals complexes of importance in planetary atmospheres
20 p2943 N90-26749
Measurements of the methane relaxation times for application to the infrared emission models of the upper atmospheres of outer planets and Titan
20 p2945 N90-26759
Characterization of superconducting materials with muon spin rotation
[DE90-013755] 21 p3081 N90-27522
Electron-phonon interaction and transport in artificially made semiconductor microstructures
[AD-A223061] 21 p3082 N90-27529
Structure and dynamic properties of combined polymeric main-chain/side-chain liquid crystals
[ETN-90-97299] 22 p3160 N90-27921

MOLECULAR ROTATION

Multiline multimode CW chemical laser performance
[AD-A210613] 01 p0075 N90-10432
Forty-fourth symposium on molecular spectroscopy
[AD-A210752] 02 p0195 N90-11111
Production rates for electron beams and swarms in nitrogen
[AD-A218145] 13 p1885 N90-20817
Simulation of inelastic deformation in glassy polypropylene and polycarbonate
[AD-A218891] 16 p2224 N90-22686
Temperature evolution of single particle correlation functions of TIP4P water
[PREPRINT-694] 17 p2470 N90-24119

MOLECULAR SPECTRA

NT ELECTRONIC SPECTRA
NT RAMAN SPECTRA
NT ROTATIONAL SPECTRA
NT VIBRATIONAL SPECTRA
Chemiluminescent ion-molecule reactions of group-3 ions with halogens: New optical spectra and reaction dynamics
[MPIS-18/1988] 02 p0196 N90-11120
A high-resolution atlas of the infrared spectrum of the Sun and the Earth atmosphere from space: A compilation of ATMOS spectra of the region from 650 to 4800 cm (2.3 to 16 micron). Volume 1: The Sun
[NASA-RP-1224-VOL-1] 05 p0666 N90-13893
A simple model for amplified spontaneous emission in dyes
[DE90-007249] 11 p1516 N90-18730
Atomic and molecular spectra from electron-excited alkali halides
[DE90-006160] 11 p1562 N90-19004
A coal model for the carriers of the unidentified IR bands 11 p1581 N90-19110
The environment of young stellar objects studied by high-resolution infrared spectroscopy
11 p1583 N90-19120
JCMT observations of the circumstellar envelope IRC+10216 11 p1585 N90-19138
Threshold photodetachment spectroscopy of the I + HI transition state region
[AD-A218410] 16 p2260 N90-22883
Decay rate and resonance fluorescence spectrum of a molecule near a composite material surface
[AD-A219692] 19 p2671 N90-25192

MOLECULAR SPECTROSCOPY

NT RAMAN SPECTROSCOPY
Two photon absorption characterization
[AD-A210508] 01 p0121 N90-10694
Forty-fourth symposium on molecular spectroscopy
[AD-A210752] 02 p0195 N90-11111
A potential nuclear magnetic resonance imaging approach for noncontact temperature measurement
10 p1364 N90-17908
Quantum-theoretical methods and studies relating to properties of materials
[AD-A217843] 13 p1765 N90-20132
Molecular dynamics and spectroscopy at gas-solid interfaces
[AD-A217743] 13 p1885 N90-20813
Center for Atomic, Molecular, and Optical Physics: Technical activities
[PB90-133158] 14 p2022 N90-21591
Contributions to the development of SLM TEA CO2 laser sources for high resolution molecular spectroscopy
16 p2240 N90-22778
Workshop on High-Field NMR and Biological Applications
[DE90-010002] 18 p2614 N90-24889
Imaging and spectroscopy of small molecules by scanning tunneling microscopy
[AD-A222572] 20 p2924 N90-26641
Determination of molecular spectroscopic parameters and energy-transfer rates by double-resonance spectroscopy 20 p2944 N90-26755
New electronic states of NH and ND observed by resonance enhanced multiphoton ionization spectroscopy 20 p2945 N90-26760
Proceedings of the 45th Ohio State University Symposium on Molecular Spectroscopy
[AD-A224349] 24 p3445 N90-29457

MOLECULAR STRUCTURE

International Conference on Organometallic Chemistry (13th) held in Torino, Europe on 4-9 September 1988: Abstracts
[AD-A210617] 01 p0033 N90-10178
Control of synthetic peptide tertiary structure
[AD-A210339] 01 p0049 N90-10281
Hierarchical structure in polymeric solids and its influence on properties
[AD-A210918] 01 p0052 N90-10297
Monolayer formation characteristics of novel organic molecules with nonlinear optically active moieties
[AD-A210496] 01 p0121 N90-10693
Pressure induced resonance Raman effects in shocked carbon disulfide
[AD-A210665] 02 p0194 N90-11107
Molecular dynamics study of the primitive model of 1-3 electrolyte studies
[AD-A211653] 03 p0325 N90-11846
Suppression of side chain crystallization and transformation of monotropic mesophases into enantiotropic mesophases by copolymerization of the parent polymers' monomer pairs containing constitutional isomeric mesogenic side groups
[AD-A209066] 03 p0330 N90-11878
Structure/reactivity relationships of polysilazane preceramics
[AD-A212028] 03 p0332 N90-11888
The prediction of middle distillate fuel properties using liquid chromatography-proton nuclear magnetic resonance spectroscopy data
[AD-A211879] 03 p0334 N90-11899
Laser production of soft x rays by multiquantum processes and the excitation of atomic inner-shell states
[AD-A211372] 03 p0353 N90-12021
Hardening mechanisms and analysis of the structure of the TGDDM/DDS epoxy resin system (tetraglycidyl-4,4' diaminodiphenylmethane/4,4' diaminodiphenylsulfone)
[NOTE-TECHNIQUE-1988-8] 04 p0465 N90-12662
Electrically conducting organic materials: Design, synthesis and characterization
[AD-A212214] 04 p0471 N90-12700
Extended basis set calculations of atomization energies: Comparison of isogyric and direct results
[AD-A212268] 04 p0471 N90-12702
Magnetic resonance of polymers at surfaces
[AD-A212225] 04 p0480 N90-12753
Structure and properties of polymer interphases
[AD-A212796] 04 p0481 N90-12763
Laser Raman spectroscopy in studies of corrosion and electrocatalysis
[DE90-001414] 06 p0741 N90-14311
The structure and properties of liquid crystal polymers
06 p0749 N90-14356
Chemistry of large molecules
[DE90-000813] 06 p0751 N90-14366
Comparison of structural subunits of the core light-harvesting complexes of photosynthetic bacteria
[DE90-001412] 06 p0819 N90-14765
Studies of organo phosphorus-, nitrogen-, and sulfur-containing molecules
[AD-A213518] 07 p0888 N90-15135
Energetics of BCC-FCC lattice deformation in iron
[AD-A213801] 07 p0905 N90-15233
MODTRAN: A moderate resolution model for LOWTRAN 7
[AD-A214337] 07 p0978 N90-15650
Dynamics of electron transfer for a non-superexchange coherent mechanisms. 2: Numerical calculations
[AD-A213511] 07 p0990 N90-15722
Relativistic self-consistent field studies of atoms and molecules
[AD-A214101] 07 p0991 N90-15724
Large scale calculations of the structure and dynamics of dense matter
[DE90-003654] 07 p0991 N90-15726
Irradition-induced grain growth: Role of dislocations
[DE90-003565] 07 p1001 N90-15792
Carbon-13 nuclear magnetic resonance of heterocyclic salts and its precursors
[DE89-635768] 08 p1041 N90-16016

Copolymers for drag reduction in marine propulsion: New molecular structures with enhanced effectiveness
[AD-A214444] 08 p1049 N90-16062
Structure-property correlations in the design of organic metals and superconductors: An overview
[DE90-003794] 08 p1131 N90-16550
Solid state, surface, and catalytic studies of oxides
[DE90-004850] 08 p1134 N90-16566
Chemical profiling of silicon nitride structures
[AD-A215643] 09 p1192 N90-16907
Protein crystal growth in microgravity
09 p1224 N90-17102
Determination of the thermal stability of perfluoroalkylethers
[NASA-TM-102493] 10 p1358 N90-17875
Molecular dynamics simulation of sedimentation using the monotonic Lagrangian grid
[AD-A215099] 10 p1427 N90-18236
Structural study of thermo-hardenable matrices. Deformation processes of composite matrices as a function of their molecular structure
[ONERA-RT-10/3521-M] 11 p1481 N90-18522
Perforated monolayers
[DE90-005469] 11 p1488 N90-18566
Electrochemical investigations of electronically conductive polymers. Part 4: By controlling the supermolecular structure, charge transport rates can be enhanced
[AD-A216603] 11 p1490 N90-18573
Infrared cometary spectroscopy
11 p1578 N90-19086
Theory of polymer blends
[DE90-002532] 12 p1632 N90-19377
Preparation and properties of the system Cu(x)Pd(1-x)O (0 less than or equal to x less than or equal to 0.175)
[AD-A217567] 12 p1723 N90-19901
Quantum-theoretical methods and studies relating to properties of materials
[AD-A217843] 13 p1765 N90-20132
The viscoelasticity of curing thermosets
[DE90-006535] 13 p1781 N90-20221
Radiation disorder and aperiodicity in irradiated ceramics
[DE90-008253] 13 p1781 N90-20222
Positron annihilation spectroscopy: A nondestructive, submicroscopic characterization technique for structural polymers
[AD-A217748] 13 p1782 N90-20226
Development of gamma-emitting, receptor-binding radiotracers for imaging the brain and pancreas
[DE90-008314] 13 p1851 N90-20621
Dielectric composite thin films
[AD-A217940] 13 p1881 N90-20791
Electronically metastable molecules of high symmetry
[AD-A217768] 13 p1865 N90-20814
Metal alkoxides: Models for metal oxides. Alkoxide ligands in early transition metal organometallic chemistry
[DE90-007523] 13 p1894 N90-20869
Nicalon/siliconoxycarbide ceramic composites
[NASA-TM-102563] 14 p1945 N90-21133
Modelling of molecular structures and properties in physical chemistry and biophysics
[AD-A214561] 14 p1947 N90-21145
A comparison of the autoignition chemistry of n-butane and isobutane in an internal combustion engine
[DE90-009474] 15 p2067 N90-21838
Surface structure and chemistry of high surface area silica gels
[DE90-007684] 15 p2071 N90-21865
The first example of an organogallium compound containing a Ga-Te bond: Synthesis, properties, and molecular structure of ((Me3CCH2)2GaTeph)2
[AD-A219258] 16 p2210 N90-22606
Single-crystal diffraction analysis of 2-(trimethylsilylethynyl) 4-nitro-N,N-dimethylaniline
[AD-A218955] 16 p2216 N90-22642
Simulation of inelastic deformation in glassy polypropylene and polycarbonate
[AD-A218891] 16 p2224 N90-22686
The microstructural basis of damping in high damping alloys
[AD-A219572] 16 p2248 N90-22821
Threshold photodetachment spectroscopy of the I + HI transition state region
[AD-A218410] 16 p2260 N90-22883
Joint services electronics program
[AD-A220615] 17 p2397 N90-23654
The effect of thermal damage on the mechanical properties of polymer regrinds 18 p2515 N90-24363
Combustion of n-butane and isobutane in an internal combustion engine: A comparison of experimental and modeling results
[DE90-005993] 18 p2522 N90-24400
First-principles interatomic potentials for transition metals and their surfaces
[DE90-011233] 18 p2528 N90-24424
Workshop on High-Field NMR and Biological Applications
[DE90-010002] 18 p2614 N90-24889
Second order non-linear optical polyphosphazenes
[AD-A219668] 18 p2615 N90-24895
A 3D visualization system for molecular structures
18 p2641 N90-25044
Computed structures of polyimides model compounds
[NASA-TM-101674] 19 p2672 N90-25195
Advanced fuel properties, phase 1
[AD-A219788] 19 p2679 N90-25236
Chemical structure and kinetics at liquid/solid interfaces
[AD-A222766] 20 p2831 N90-26105
Molecular structure of interphases between DGEBA/BTDA adhesives and silver substances using surface-enhanced Raman scattering
[AD-A222750] 20 p2841 N90-26157
Photosynthesis in intact plants
[DE90-013699] 20 p2896 N90-26482
Computer simulation of chemical reactions in synthetic model compounds and genetically engineered active sites
[AD-A222611] 20 p2898 N90-26483
Isothermal compressibility of SPC/E water
[AD-A222723] 20 p2925 N90-26643
Resonance enhanced two-laser infrared multiple photon dissociation of gaseous ions
[AD-A221826] 21 p2970 N90-26879
Synthesis, structure, electric, and magnetic properties of CaNiN
[AD-A222273] 21 p2978 N90-26923
Magnetic resonance elucidation of molecule/macromolecule interaction stereochemistry
[AD-A221444] 21 p2979 N90-26928
Supersonic jet studies of benzyl alcohols: Minimum energy conformations and torsional motion
[AD-A221815] 21 p2980 N90-26934
Aromatic polyimides containing a dimethylsilane-linked dianhydride
[NASA-CASE-LAR-14198-1] 21 p2984 N90-26956
Molecular dynamics of physical aging processes in polymer glasses (experiment and theory)
[AD-A222848] 21 p2984 N90-26959
Characterization of polymer interphases using surface-enhanced Raman scattering
[AD-A223103] 21 p2985 N90-26965
Characterization of model polyimide/silver interphases using surface-enhanced Raman scattering
[AD-A222488] 21 p2988 N90-26979
Compressive strength of rigid-rod polymer fibers
[AD-A221886] 21 p2989 N90-26987
Microscopic modeling of tribological phenomena
[AD-A222049] 21 p3011 N90-27117
Theoretical studies of time-of-flight and atom and molecular surface collision
[AD-A221705] 21 p3075 N90-27480
Electronic and molecular structure of carbon grains
21 p3091 N90-27574
Accurate quantum chemical calculations
[NASA-TM-101932] 23 p3303 N90-28680
Surface and defect excitations in covalently bonded solids
[AD-A221995] 23 p3303 N90-28682
Fuels research, volume 1
[DE90-015393] 23 p3305 N90-28695
Proceedings of the 45th Ohio State University Symposium on Molecular Spectroscopy
[AD-A224349] 24 p3445 N90-29457
Transition metal activation and functionalization of carbon-hydrogen bonds
[DE90-015826] 24 p3451 N90-29489
High resolution transmission electron microscopy of aluminophosphates
[DE90-015632] 24 p3553 N90-30105

MOLECULAR THEORY
Molecular theory and computer simulation studies of natural and synthetic gas mixtures
[PB90-130329] 12 p1711 N90-19826
Molecular theory of fluid phase equilibria
[PB90-131277] 15 p2066 N90-21832
Molecular dynamics of physical aging processes in polymer glasses (experiment and theory)
[AD-A222848] 21 p2984 N90-26959

MOLECULAR TRAJECTORIES
Low frequency Raman spectra of liquid water, a molecular dynamics simulation
[PREPRINT-698] 16 p2314 N90-23192

MOLECULAR WEIGHT
NT LOW MOLECULAR WEIGHTS
Synthesis and interfacial properties of new generation polyurethane systems
[AD-A210446] 01 p0050 N90-10286
High-temperature gel-permeation chromatography of poly(4-methyl-1-pentene)
[DE90-002967] 07 p0893 N90-15159
Summary physical data tables: Alkanes
[ESDU-PD3] 07 p0893 N90-15162
A study of physical properties of ODPA-p-PDA polyimide films
[NASA-TM-102625] 13 p1766 N90-20137
Investigation into the mechanism of polymer thread drag reduction
[AD-A217492] 13 p1800 N90-20329
Determinations of molecular weight and molecular weight distribution of high polymers by the rheological properties
[NASA-CR-186450] 14 p1953 N90-21180
Surface enrichment and evaporation in a polymer mixture of long and short chains
[DE90-010073] 18 p2529 N90-24429
Deformation-induced structural developments of ultra-high molecular weight polyethylene
[ETN-90-96899] 18 p2529 N90-24432
Evolution of structure and viscoelasticity in diethanolamine-cured epoxy
[DE90-011256] 20 p2837 N90-26134
Polyimidazoles via aromatic nucleophilic displacement
[NASA-CASE-LAR-14145-1] 21 p2983 N90-26954
Aromatic polyimides containing a dimethylsilane-linked dianhydride
[NASA-CASE-LAR-14198-1] 21 p2984 N90-26956

MOLECULES
NT DIATOMIC MOLECULES
NT MACROMOLECULES
NT POLYATOMIC MOLECULES
Combining spontaneous molecular assembly with microfabrication to pattern surfaces: Selective binding of isonitriles to platinum microwires and characterization by electrochemistry and surface spectroscopy
[AD-A209528] 01 p0039 N90-10213
Characterization of polymeric surfaces and interfaces
[AD-A210227] 01 p0049 N90-10277
Monolayer formation characteristics of novel organic molecules with nonlinear optically active moieties
[AD-A210496] 01 p0121 N90-10693
Structure and properties of simple molecular systems at very high density
[DE89-016974] 02 p0273 N90-11557
New theoretical approaches for studying electron collisions with small molecules
[DE89-017543] 02 p0273 N90-11558
State-resolved reaction dynamics
[AD-A211613] 03 p0403 N90-12307
Standard method for measurement of nonvolatile residue on surfaces
[AD-A213324] 04 p0474 N90-12714
Molecules with enhanced electronic polarizabilities based on defect-like states in conjugated polymers
[NASA-CASE-NPO-17633-1-CU] 07 p0910 N90-15263
Studies of the adsorption/desorption behavior of explosive-like molecules
[DE90-001867] 07 p0913 N90-15283
Relativistic self-consistent field studies of atoms and molecules
[AD-A214101] 07 p0991 N90-15724
Mechanisms of the electrochemistry of small organic molecules
[PB90-100785] 08 p1040 N90-16012
Theory of the dissociation dynamics of small molecules on metal surfaces: Finite temperature studies
[DE90-005217] 09 p1195 N90-16923
Symposium on Chemical Precursors to Ceramics
[AD-A214499] 09 p1196 N90-16932
Ultrasensitive laser spectroscopy in solids: Single-molecule detection
[AD-A216085] 11 p1514 N90-18716
Determination of the mechanism of decomposition of energetic molecules
[AD-A217061] 12 p1633 N90-19388
Laser surface interactions of high-(Tc) superconductors
[DE90-006894] 12 p1669 N90-19587
The calculation of hydrogen-bonding properties
[DE90-007534] 13 p1772 N90-20168
Interactions of molecules with surfaces
[DE90-007555] 13 p1883 N90-20806
Molecular organization and electrical properties of mixed Langmuir-Blodgett multilayer thin films of polypyrrole
[DE90-007627] 13 p1894 N90-20870
Phase equilibrium of mixtures consisting of molecules with large size and shape differences (thermodynamic modeling of Supercritical Fluid Extraction and Retrograde Condensation, SFE/RC)
[PB90-131285] 14 p1947 N90-21146
Molecular theory of fluid phase equilibria
[PB90-131277] 15 p2066 N90-21832
Molecular dynamics simulations of short-range force systems on 1024-node hypercubes
[DE90-009633] 15 p2146 N90-22259

Nonlinearity parameters of polymers
15 p2164 N90-22369
Molecular evolution in astrophysical environments
16 p2332 N90-23291
Ultrafast laser investigation of a solid-state explosion
[AD-A218530] 17 p2408 N90-23718
Chemistry within molecular clusters
[AD-A219836] 18 p2520 N90-24392
Fast plasma mixing: A new excitation method for CW gas lasers
[AD-A220290] 18 p2617 N90-24904
A 3D visualization system for molecular structures
18 p2641 N90-25044
Spacecraft external molecular contamination analysis
19 p2730 N90-25520
Isothermal compressibility of SPC/E water
[AD-A222723] 20 p2925 N90-26643
Stibathiolanes: Synthesis, solid state structure, and solution behavior
[AD-A223255] 20 p2933 N90-26688
High resolution infrared spectroscopy of planetary molecules using diode lasers and Fourier transform spectrometers 20 p2943 N90-26747
Recent high resolution laboratory determinations of line broadening and intensity parameters: PH3, CH3D, and CO2 20 p2944 N90-26751
Infrared line parameters at low temperatures relevant to planetary atmospheres 20 p2944 N90-26753
Intracavity Dye-Laser Absorption Spectroscopy (IDLAS) for application to planetary molecules
20 p2945 N90-26761
UV and VUV spectroscopy and photochemistry of small molecules in a supersonic jet 20 p2947 N90-26771
Ion/molecule reactions of arsenic and phosphorus cluster ions: Ionization potentials and novel reaction pathways
[AD-A222019] 21 p2977 N90-26918
Non-destructive characterization of polymer/metal interfaces using Surface-Enhanced Raman Scattering (SERS)
[AD-A223105] 21 p2986 N90-26967
Diagnostics for hydrogen atoms and molecules in H-atom sources and beams using VUV laser light
[AD-A222340] 21 p3074 N90-27476
Interstellar grain chemistry and organic molecules
21 p3090 N90-27569
Laboratory simulation of interstellar grain chemistry and the production of complex organic molecules
21 p3092 N90-27580
Can the chirality of the ISM be measured
21 p3095 N90-27590
Hyperthermal atomic oxygen generator
[NASA-CR-186573] 22 p3155 N90-27889
Macromolecular calculations for the XTAL-system of crystallographic programs
[AD-A222345] 22 p3248 N90-28421
Infrared spectroscopic measurements on planetary atmospheric gases 23 p3412 N90-29283
Thermochemical data for silicon-containing species from ab initio electronic structure calculations
[DE90-011024] 24 p3446 N90-29463

MOLIERE FORMULA
U COSMIC RAY SHOWERS
U SECONDARY COSMIC RAYS
U SPATIAL DISTRIBUTION

MOLNIYA SATELLITES
Direct Radio Broadcasting by Satellite (DRBS): A review of the technical factors and system approaches suitable for mobile and fixed reception
[BBC-RD-1989/4] 14 p1960 N90-21221

MOLTEN SALT ELECTROLYTES
Molten carbonate fuel cell technology improvement
[DE90-001934] 07 p0950 N90-15501
An assessment and comparison of fuel cells for transportation applications
[DE90-001807] 07 p0952 N90-15508
Oxygen electrode in molten carbonate fuel cells
[DE90-002871] 07 p0952 N90-15510
Oxygen electrode in molten carbonate fuel cells
[DE90-005377] 11 p1528 N90-18796
Viscosity, density and conductivity of ImCl(HCl) sub 1.3
[AD-A218902] 16 p2216 N90-22641
Evaluation of room-temperature chloroaluminate molten salts as electrolytes for high energy density batteries
[AD-A223097] 20 p2860 N90-26267

MOLTEN SALTS
Heat capacities of 1-methyl-3-ethylimidazolium chloride-aluminum chloride molten salts
[AD-A212790] 04 p0472 N90-12707
Molten carbonate fuel cell technology improvement
[DE90-001934] 07 p0950 N90-15501
Characterization of new cathode materials for molten carbonate fuel cells
[DE90-003547] 07 p0953 N90-15516
Selection of corrosion-resistant materials for use in molten nitrate salts
[DE90-004351] 08 p1046 N90-16048
Organic cathode for a secondary battery
[NASA-CASE-NPO-17604-1-CU] 08 p1059 N90-16124
Hot filament technique for measuring the thermal conductivity of molten lithium fluoride
[NASA-TM-102506] 12 p1631 N90-19373
Direct absorption receiver
[DE90-000311] 12 p1683 N90-19667
Evaluation of thermal cycling creep-fatigue damage for a molten salt receiver
[DE90-002907] 12 p1684 N90-19670
Chemical and electrochemical studies in ionic liquids
[AD-A217742] 13 p1773 N90-20175
Mechanical properties of pure nickel alloys after long term exposures to LiOH and vacuum at 775 K
[NASA-TM-102403] 13 p1774 N90-20181
The electrochemical generation of useful chemical species from lunar materials 13 p1822 N90-20461
Ionic equilibrium between octahedral and tetrahedral complexes in liquid aluminium-sodium fluoride mixtures
[DE90-613690] 14 p1948 N90-21150
Grain orientation studies in superconductors
22 p3148 N90-27852
A high temperature molten salt thermal electrochemical cell
[AD-D014469] 22 p3195 N90-28131
Molten salt induced high temperature degradation of thermal barrier coatings 23 p3307 N90-28704
Overview on hot gas tests and molten salt corrosion experiments at the DLR 23 p3309 N90-28714

MOLYBDENUM
Secondary electron emission characteristics of molybdenum-masked, ion-textured OFHC copper
[NASA-TP-2967] 07 p0902 N90-15211
Stainless steel passivity
[AD-A214108] 08 p1044 N90-16033
An XPS and electrochemical study of the influence of molybdenum and nitrogen on the passivity of austenitic stainless steel
[AD-A214267] 08 p1044 N90-16034

MOLYBDENUM ALLOYS
Fracture toughness data base for HT9 and modified 9Cr-1Mo irradiated in several reactors up to approximately 100 dpa
[DE90-000111] 03 p0328 N90-11864
The effects of heat treatment after welding on the functional properties of assemblies of CrMo alloys. Heat treatment of a mixed assembly of A48 and 10CD9.10 alloys
[CETIM-104320] 04 p0475 N90-12724
Deformation and fracture of low alloy steels at high temperature
[DE90-001274] 07 p0902 N90-15215
A comparison of CuAlNi and other high damping alloys for the purpose of naval ship silencing applications
[AD-A218801] 16 p2221 N90-22671
A study of the phase decomposition of Fe-Ni-Al-Mo alloys
[DE90-010143] 18 p2524 N90-24406
Irradiation effects on impact behavior of 12Cr-1MoVW and 2 1/4Cr-1Mo steels
[DE90-011075] 18 p2527 N90-24421

MOLYBDENUM COMPOUNDS
NT MOLYBDENUM DISULFIDES
NT MOLYBDENUM OXIDES
Face-specific interaction of MoS4(2-1) with oriented crystals of (0001) CdX (X = Se, S)
[AD-A209519] 01 p0128 N90-10732
The effects of Mo2C morphology and strain distribution on the fatigue properties of Fe-C-Mo dual-phase steels
07 p0901 N90-15210
Ta and Nb reinforced MoSi2
[DE90-010596] 18 p2517 N90-24377

MOLYBDENUM DISULFIDES
Orientation of rf-sputter-deposited MoS2 films
[ATR-89(4752)-1] 07 p1000 N90-15784
Evaluation of a prototype lithium molybdenum disulfide secondary battery for load conditioner: Characteristics and performance of 70Wh class BC cell
[DE90-702460] 09 p1210 N90-17016
Effects of microstructure and adhesion on performance of sputter-deposited MoS2 solid lubricant coatings
[AD-A220900] 18 p2530 N90-24434
Tribological properties of PVD-applied MoS2 coatings used on space mechanisms 18 p2537 N90-24470
The advantages and limitations of sputtered molybdenum disulphide as a space lubricant
18 p2537 N90-24471
Investigation of lubrication characteristics of MoS2 films in space environment 18 p2537 N90-24472
Study of ball bearings for space use
18 p2537 N90-24477
Mechanisms add foldability to ROSAT solar panels
18 p2538 N90-24483
The performance of PTFE, lead, and MoS2 as lubricant films for ball bearings operating in vacuum at 20 K
18 p2540 N90-24495
Thick and compact MoS2 coatings
18 p2541 N90-24501
Tribology of MoS2: Effect of film thickness
18 p2541 N90-24505

MOLYBDENUM OXIDES
Molybdenum disulfide-molybdenum oxide lubricants
[AD-D014253] 08 p1048 N90-16059
Interfacial chemistry of MoS2 films on Si
[AD-A216527] 11 p1482 N90-18532
Reactive sputtering of molybdenum
[DE90-008307] 13 p1778 N90-20204
Model catalytic oxidation studies using supported monometallic and heterobimetallic oxides
[DE90-009984] 16 p2220 N90-22664

MOLYBDENUM SULFIDES
NT MOLYBDENUM DISULFIDES
Structural studies of sputter-deposited MoS2 solid lubricant films
[AD-A212407] 04 p0481 N90-12759
Photoelectron spectroscopic study of the interaction of thin Fe films with the MoS2(0001) surface
[AD-A214348] 10 p1351 N90-17836
Electronic structure and lubrication properties of MoS2: A qualitative molecular orbital approach
[AD-A220566] 17 p2380 N90-23557

MOM (SEMICONDUCTORS)
Millimeter wavelength rectenna development
15 p2060 N90-21797

MOMENT DISTRIBUTION
Force and moment measurements on delta wings in unsteady flow 08 p1068 N90-16185
A flight dynamic model of aircraft spinning
[AR-005-600] 23 p3283 N90-28576
Aerodynamic forces acting on a finite rectangular slender body
[NAL-TR-1035] 24 p3421 N90-29329

MOMENTS
NT BENDING MOMENTS
NT DIPOLE MOMENTS
NT DISTRIBUTION MOMENTS
NT LOADING MOMENTS
NT MAGNETIC MOMENTS
NT MEAN
NT MOMENTS OF INERTIA
NT ORTHOGONALITY
NT PITCHING MOMENTS
NT ROLLING MOMENTS
NT STABILITY DERIVATIVES
NT STANDARD DEVIATION
NT TORQUE
NT YAWING MOMENTS
An integrated CFD/experimental analysis of aerodynamic forces and moments
[NASA-TM-102195] 01 p0002 N90-10006
Study of forces and moments on wing-bodies at high incidence, volumes 1 and 2 05 p0575 N90-13350
Effect of unshielded and shielded horn balances on hinge moment coefficients for controls at low speeds
[ESDU-89003-A] 06 p0726 N90-14238
Hinge moment coefficient derivatives for trailing-edge controls on wings at subsonic speeds
[ESDU-89009] 06 p0726 N90-14239
Example of procedure in calculation of control hinge moments
[ESDU-89010] 06 p0727 N90-14240
In-plane forces and moments on installed inclined propellers at low forward speeds
[ESDU-89047] 09 p1161 N90-16720
Interior fluid dynamics of liquid-filled projectiles
[AD-A217630] 13 p1800 N90-20330

MOMENTS OF INERTIA
Dynamical modifications to the head, load factors from additional weight 19 p2720 N90-25472

MOMENTUM
NT ANGULAR MOMENTUM
An algorithm to calculate the beam momentum distribution from flying wire profiles
[DE89-015587] 01 p0073 N90-10418
Experimental identification of modal momentum coefficients and modal identity parameters of the FLECS structure 02 p0177 N90-10991
Estimation of the C-J pressure of explosives
[DE89-013811] 02 p0208 N90-11187
Low level remote sensing: Orographic winds
03 p0361 N90-12066
Description of a software library for the calculation of surface fluxes
[KNMI-TR-112] 03 p0375 N90-12141
Electron-positron momentum distribution measurements of high-T(sub c) superconductors and related systems
[DE89-017538] 03 p0411 N90-12358

Kinematic and kinetic analyses of drop landings
14 p2010 N90-21517
Test results and flight experience of ball bearing momentum and reaction wheels
15 p2115 N90-22099
Space station dynamics, attitude control and momentum management 16 p2287 N90-23029
The role of eddy fluxes of momentum in hurricane formation
[AD-A219417] 18 p2581 N90-24700
Quantum gravity in two dimensions and the SL(2,R) current algebra
[DE90-627215] 23 p3391 N90-29156
A new momentum management controller for the space station
[NASA-CR-187265] 24 p3440 N90-29425
The f2 dominance of the energy-momentum tensor
[DE90-508027] 24 p3460 N90-29544

MOMENTUM ENERGY
U KINETIC ENERGY

MOMENTUM THEORY
A dual potential formulation of the Navier-Stokes equations 15 p2092 N90-21972

MOMENTUM TRANSFER
Questions from the Willmarth Workshop on New Directions in Research on Turbulent Wall-Layer Structures
[AD-A211282] 02 p0221 N90-11264
Periodic-disturbance accommodating control of the space station for asymptotic momentum management 05 p0586 N90-13416
A lattice study of semileptonic decays of D-mesons
[PREPRINT-660] 05 p0698 N90-14086
A low-order model of the equatorial ocean-atmosphere system 06 p0813 N90-14730
The dynamics of dust in planetary magnetospheres 08 p1149 N90-16658
Turbulent heat and momentum transfer in recirculating and impinging flows 09 p1215 N90-17043
Research in theoretical nuclear physics
[DE90-006063] 10 p1440 N90-18309
The neoclassical transport of toroidal momentum in tokamaks
[DE90-006864] 11 p1568 N90-19023
Bose condensate in superfluid (sup 4)He and momentum distributions by deep inelastic scattering
[DE90-007541] 12 p1712 N90-19832
The electron momentum-transfer cross sections of tungsten, silicon, and silicon dioxide at energies from 0.1 to 10,000 eV
[DE90-009041] 12 p1712 N90-19833
The numerical simulation of multistage turbomachinery flows 14 p1925 N90-21025
The generally covariant representation of energy-momentum pseudotensor of gravitational field
[DE90-615203] 14 p2034 N90-21669
Incomplete fusion reactors at low and intermediate energies
[KVI-809] 16 p2316 N90-23206
Symmetry in the dynamics of a polarized fluid
[ETN-90-96896] 18 p2552 N90-24567
Fluid-loop reaction system
[NASA-CASE-NPO-17204-1-CU] 20 p2864 N90-26292
Theoretical studies of time-of-flight and atom and molecular surface collision
[AD-A221705] 21 p3075 N90-27480
Heat and momentum transfer to test samples in the high velocity plasma furnace
[AD-A222182] 21 p3079 N90-27505
Reynolds stress and the physics of turbulent momentum transport
[AD-A224172] 24 p3467 N90-29588
Effects of energy, momentum and particle transport in the near-earth solar terrestrial system
[AD-A224393] 24 p3490 N90-29726
Medium energy nuclear physics research
[DE90-015852] 24 p3544 N90-30042

MONEL (TRADEMARK)
Characterization of Monel alloys by x ray fluorescence technique
[DE90-617175] 16 p2221 N90-22665

MONITORS
An appraisal of a number of power assessment procedures being proposed for use in Chinook-Lycoming T55 engine
[AD-A210482] 01 p0009 N90-10041
The Third Conference on the Environmental Chemistry of Hydrazine Fuels
[AD-A197632] 02 p0203 N90-11157
Description of a chemiluminescence detector system specifically designed for monitoring airborne hydrazine and oxidizer propellant vapors 02 p0206 N90-11179
Progress of research on water vapor lidar
[NASA-CR-185970] 03 p0352 N90-12011
The fault monitoring and diagnosis knowledge-based system for space power systems: AMPERES, phase 1
[NASA-CR-185486] 04 p0484 N90-12654
Automated monitor and control for deep space network subsystems 04 p0486 N90-12794
The process e(-)p giving gamma e(-)p as a fast luminosity for the HERA collider
[NIKHEF-H/88-13] 04 p0553 N90-13223
Plasma separation process: Magnet move to Oak Ridge National Laboratory
[DE89-017457] 04 p0556 N90-13242
The cosmic radiation effects and activation monitor
[RAE-TM-SPACE-364] 04 p0569 N90-13318
Payload electronics and mechanisms 05 p0604 N90-13508
Pilot investigation of indoor-outdoor and personal PM10 (thoracic) and associated ionic compounds and mutagenic activity
[PB89-222723] 05 p0673 N90-13920
Optical properties monitor: Experiment definition phase
[NASA-CR-183836] 05 p0699 N90-14092
Biological effects of hyperthermia and potential risk associated with ultrasonic exposure
[PB89-100702] 06 p0820 N90-14768
Human factors survey of advanced instrumentation and controls
[DE90-002477] 06 p0821 N90-14776
Development of a real time monitor for superconductive thin film preparation
[DE89-017772] 06 p0852 N90-14952
Display interface concepts for automated fault diagnosis
[NASA-TM-101610] 07 p0881 N90-15102
HCl monitor, phase 2
[AD-A213572] 07 p0958 N90-15542
Diesel starting system monitor: Prototype development
[DE90-004425] 08 p1084 N90-16276
Keeping the pilot in the loop
[RAE-TM-FM-18] 08 p1105 N90-16396
Cosmic ray NM-64 neutron monitor data 16
[IFSI-88-21] 08 p1154 N90-16684
Nimbus 7 solar backscatter ultraviolet (SBUV) ozone products user's guide
[NASA-RP-1234] 09 p1246 N90-17227
Method and apparatus for characterizing reflected ultrasonic pulses
[NASA-CASE-LAR-13966-1] 09 p1278 N90-17408
Loran C monitor: Facilities Central Processing Unit (FCPU) port evaluation
[DOT/FAA/CT-TN89/57] 10 p1318 N90-17623
Aurora upgrade. Volume 5: Machine monitoring and control system
[AD-A215963] 10 p1393 N90-18053
A new broadband pulsed high voltage monitor
[DE90-006264] 11 p1502 N90-18651
Toroid monitor
[DIGEL-1989-8] 11 p1504 N90-18663
Accustic emission diagnostic techniques for high-field high current-density super inducting poles
[DE90-007400] 11 p1562 N90-19000
In-line wear monitor
[AD-A217799] 13 p1757 N90-20091
Airplane takeoff and landing performance monitoring system
[NASA-CASE-LAR-13734-1-CU] 13 p1758 N90-20096
The Terrain-Responsive Atmospheric Code (TRAC) project plan: Development of a hazardous materials dispersion modeling capability with application to ambient air monitoring network design
[DE90-007293] 13 p1829 N90-20502
Large screen display for the Mission Control Center 13 p1858 N90-20662
Distributed earth model/orbiter simulation 13 p1860 N90-20671
An 8.4-GHz dual-maser front-end system for Parkes reimplementation 15 p2078 N90-21905
The laminar flow element: Its use as a flow standard
[PB90-129677] 15 p2126 N90-22157
Automating security monitoring and analysis for Space Station Freedom's electric power system
[NASA-TM-103148] 15 p2158 N90-22324
HCl monitor 16 p2209 N90-22599
Nonintrusive method and apparatus for monitoring the cure of polymeric materials
[NASA-CASE-LAR-13465-1] 17 p2378 N90-23544
A PC-based imaging system for the Naval Postgraduate School Infrared Search and Target Designation (NPS-IRSTD) system
[AD-A220109] 17 p2448 N90-23955
Transient pulse monitor
[AD-A220353] 18 p2508 N90-24335
The e-beam sustained CO2 laser amplifier 18 p2561 N90-24611
Monitoring of Ritz modal generation 18 p2571 N90-24650
DURIP: Improved eye movement monitoring capabilities for studies in visual cognition
[AD-A220355] 18 p2586 N90-24722
A noncontacting motion monitoring system for an astronaut translation aid
[NASA-TM-102640] 19 p2693 N90-25325
Monitoring and control of spacecraft systems using procedural reasoning 19 p2731 N90-25524
Artificial intelligence for multi-mission planetary operations 19 p2732 N90-25532
Real-time measurement of mental workload: A feasibility study 19 p2734 N90-25540
Planning for execution monitoring on a planetary rover 19 p2735 N90-25548
Photovoltaic array space power plus diagnostics experiment 19 p2737 N90-25559
A simple beam position monitor system for CEBAF
[CEBAF-PR-89-015] 19 p2757 N90-25664
Lunar deep drill apparatus
[NASA-CR-182756] 20 p2869 N90-26322
Eye tracking device for the measurement of flight performance in simulators
[AD-A220075] 20 p2898 N90-26484
Reconfigurable integrated system architecture for future monitoring systems 22 p3106 N90-27638
Evaluation of EDR-3 vibration, shock, temperature, and humidity recording unit
[NASA-CR-184006] 22 p3177 N90-28028
Preliminary exposure study to determine the effects of acid deposition on coated steel substrates
[PB90-201799] 23 p3309 N90-28715
Simulation of INPE's printed circuit laboratory production line
[INPE-4556-TDL/331] 23 p3322 N90-28784
Remote atmospheric profiling systems for tropospheric monitoring
[PB90-216789] 23 p3349 N90-28927
Causal simulation and sensor planning in predictive monitoring 23 p3389 N90-29037
Design of a monitor and simulation terminal (master) for space station telerobotics and telescience 23 p3372 N90-29051
Independent ground monitor coverage of Global Positioning System (GPS) satellites for use by civil aviation 24 p3428 N90-29364
Definition of a near real time microbiological monitor for space vehicles
[NASA-CR-185599] 24 p3441 N90-29430
Integrated controls and health monitoring fiberoptic shaft monitor
[NASA-CR-185210] 24 p3472 N90-29622
Oxygen deficiency monitor system
[DE90-014866] 24 p3523 N90-29917
A distributed control and monitor system used in laser fusion research
[DE90-011483] 24 p3549 N90-30078
Re-analysis of data on the space radiation environment above southeast Asia
[AD-A224155] 24 p3564 N90-30162

MONKEYS
Computing with neural maps: Application to perceptual and cognitive functions
[AD-A216689] 10 p1412 N90-18143
High peak power microwave pulses at 2.37 GHz: No effects on vigilance performance in monkeys
[AD-A219570] 17 p2433 N90-23863
Program review: The lifetime effects of space radiation in rhesus monkeys
[AD-A221127] 19 p2716 N90-25454
Experiment K-6-27. Analysis of radiographs and biosamples from primate studies 20 p2897 N90-26478
Renal response to seven days of lower body positive pressure in the squirrel monkey
[NASA-CR-183355] 24 p3497 N90-29761

MONOCHROMATIC RADIATION
A scheiner-principle vernier optometer
[AD-D014304] 07 p0934 N90-15405
Scientific Colloquium in Honor of Prof. Dr. Rer. Nat. Hermann L. Jordan
[ESA-TT-1101] 23 p3391 N90-29159
Energy transmission by means of coherent quasi-mono-chromatic light beams 23 p3392 N90-29163
Information processing and perceptual characteristics of display design: The role of emergent features and objects
[AD-A223683] 24 p3558 N90-30133

MONOCHROMATORS
Design of grazing incidence monochromators involving unconventional gratings
[DE89-016341] 01 p0123 N90-10704

REFLECT: A computer program for the x ray reflectivity of bent perfect crystals
[DE90-001266] 06 p0851 N90-14946
Monochromator configurations for wavelength division multiplexing
[AD-A214833] 09 p1281 N90-17430

MONOCOQUE STRUCTURES
Monocoque structure for the SKITTER three-legged walker
[NASA-CR-184635] 18 p2534 N90-24454

MONOCRYSTALS
U SINGLE CRYSTALS

MONOCULAR VISION
Non-linear analysis of visual cortical neurons
[AD-A221543] 21 p3034 N90-27250
Dynamic monocular machine vision and applications of dynamic monocular machine vision
[LRT-WE-13-FB-88-3] 21 p3061 N90-27406

MONOLITHIC CIRCUITS
U INTEGRATED CIRCUITS

MONOMERS
Monomers, polymers and transition metal complexes based upon carboranes
[AD-A210226] 01 p0040 N90-10221
UV-curable polyurethane-methacrylate co-networks and interpenetrating networks
[AD-A210445] 01 p0050 N90-10285
Suppression of side chain crystallization and transformation of monotropic mesophases into enantiotropic mesophases by copolymerization of the parent polymers' monomer pairs containing constitutional isomeric mesogenic side groups
[AD-A209066] 03 p0330 N90-11878
New polymers made with well-characterized organometallic catalysts
[AD-A213592] 07 p0912 N90-15272
LARC-IA: A flexible backbone polyimide
[NASA-TM-102586] 09 p1196 N90-16926
New Condensation polyimides containing 1,1,1-triaryl-2,2,2-trifluoroethane structures
[NASA-CASE-LEW-14346-1] 12 p1618 N90-19300
Rigid rod molecules as liquid crystal thermosets
[AD-A217573] 13 p1770 N90-20158
Investigation of optical nonlinearities, conductivity and magnetism in organometallic materials
[AD-A218548] 16 p2317 N90-23211
Dynamics of micellar oligomeric and monomeric sodium 10-undecenoate
[AD-A222570] 20 p2830 N90-26099
Condensation polyimides
[NASA-TM-103467] 20 p2836 N90-26129
Quantitative confirmation of diffusion-limited oxidation theories
[DE90-012997] 20 p2838 N90-26143
Radical homopolymerization of a trisubstituted alkene: 1-cyclobutenecarboxylic acid and its polymer
[AD-A223188] 21 p2986 N90-26968
Progress toward synthesis of polymeric polyradicals
[AD-A223414] 24 p3455 N90-29510

MONOMOLECULAR FILMS
Transport processes through monomolecular films
[AD-A213609] 07 p0923 N90-15342

MONOPLANES
NT B-52 AIRCRAFT
NT B-58 AIRCRAFT
NT B-70 AIRCRAFT
NT BOEING 737 AIRCRAFT
NT BOEING 757 AIRCRAFT
NT C-130 AIRCRAFT
NT C-135 AIRCRAFT
NT C-140 AIRCRAFT
NT C-141 AIRCRAFT
NT DHC 2 AIRCRAFT
NT F-4 AIRCRAFT
NT F-8 AIRCRAFT
NT F-17 AIRCRAFT
NT F-86 AIRCRAFT
NT F-104 AIRCRAFT
NT P-3 AIRCRAFT
NT U-2 AIRCRAFT

MONOPOLE ANTENNAS
NT WHIP ANTENNAS

MONOPOLES
Compressibility of heavy nuclei at high temperatures
[KVI-792] 04 p0552 N90-13217
Cosmic strings and baryon decay catalysis
[NASA-CR-186074] 04 p0566 N90-13299
An extended diffusive model for calculating thermal diffusivity from single monopole tokamak heat pulse propagation
[DE90-007958] 14 p2029 N90-21637

MONOPROPELLANTS
Orbital fluid resupply assessment
11 p1475 N90-18487
A comparison between experiment and simulation for concept VIC regenerative liquid propellant guns. Part 1: 30 mm
[AD-A218556] 16 p2225 N90-22692
Structure of monopropellant spray flames at elevated pressures
[AD-A218676] 17 p2383 N90-23570

MONOPULSE ANTENNAS
Dedicated tracking of crossing targets with a phased array monopulse radar
[FEL-1988-95] 04 p0491 N90-12821
Investigations of monopulse-assisted radio location systems for the safety of surface traffic
[ETN-90-97324] 21 p2956 N90-26806

MONOPULSE RADAR
Modeling the response of a monopulse radar to impulsive jamming signals using the Block Oriented System Simulator (BOSS)
[AD-A215560] 10 p1375 N90-17969
An investigation of the transfer of monopulse tracking between two coherent point sources
[AD-A217007] 12 p1646 N90-19457
Improvement of clutter rejection by scanning motion compensation in ground-based monopulse radar
[ETN-90-96550] 16 p2228 N90-22711
Optimizing ECM techniques against monopulse acquisition and tracking radars
[AD-A220036] 17 p2393 N90-23629

MONOSACCHARIDES
NT GLUCOSE

MONOTECTIC ALLOYS
Containerless low gravity processing of glass forming and immiscible alloys
[NASA-CR-186999] 23 p3316 N90-28747

MONOTONE FUNCTIONS
A special case of second-order strictness analysis
[AD-A210829] 01 p0114 N90-10656
Sequential searching in multidimensional monotone arrays
[AD-A211938] 03 p0384 N90-12188
Monotonicity of performance measures in a processor sharing queue
[CWI-BS-R8902] 05 p0689 N90-14019
A nonparametric software reliability growth model
[NASA-CR-186438] 12 p1700 N90-19764
A monotone complementarity problem in Hilbert space
[AD-A220819] 17 p2468 N90-24105
A Markov chain identity and monotonicity of the diffusion constants for a random walk in a heterogeneous environment
[CWI-AM-R8917] 18 p2605 N90-24839
Consequences of monotonicity for Markov transition functions
[AD-A222852] 21 p3063 N90-27412

MONSOONS
Disturbances in the Arizona Monsoon
03 p0362 N90-12071
Cloud types and the tropical Earth radiation budget, revised
[NASA-CR-180475] 13 p1843 N90-20582
Structure and dynamics of the Arizona monsoon boundary
[AD-A217378] 13 p1844 N90-20586
Use of microwave satellite data to study variations in rainfall over the Indian Ocean
[NASA-CR-186408] 14 p2007 N90-21501
A linear analysis of monsoon base states associated with banded convection 15 p2130 N90-22179
Tropical squall lines of the Arizona monsoon
16 p2257 N90-22867
A numerical study of the seasonal variability of the Somali current
[AD-A220708] 17 p2427 N90-23829

MONTE CARLO METHOD
A structured singular value approach to missile autopilot analysis 2 01 p0014 N90-10068
Tracking performance evaluation
[AD-A210499] 01 p0095 N90-10540
The computation and use of the asymptotic covariance matrix for measurement error models
[PB89-215321] 01 p0115 N90-10659
Monte Carlo simulations of small solute/solvent clusters: Cluster properties and phase transitions
[AD-A209559] 01 p0119 N90-10684
Auxiliary-field transformations for repulsive potentials: A physical approach
[DE89-016677] 02 p0214 N90-11223
Development of an approximate technique for the nonlinear random vibrations analysis of hysteretic systems 02 p0233 N90-11335
On algorithms for generating computationally simple piecewise linear classifiers
[NDRE/PUBL-89/1001] 02 p0258 N90-11459
Principal components in multivariate control charts
[DE89-016828] 02 p0262 N90-11489
Microwave instability near transition energy
[DE90-000107] 03 p0338 N90-11922
A unified framework for simulating Markovian models of highly dependable systems
[AD-A212164] 03 p0396 N90-12267
Monte Carlo studies of nuclei and quantum liquid drops
[DE89-016914] 03 p0402 N90-12300
Rotational and vibrational nonequilibrium effects in rarefied, hypersonic flow
[NASA-CR-182559] 04 p0437 N90-12498
Multigrid Monte Carlo in an external U(1) gauge field
[NIKHEF-ITFA-88-52] 04 p0538 N90-13114
Stochastic process models in device physics
[AD-A212284] 04 p0547 N90-13185
Monte Carlo (importance) sampling within a Benders' decomposition algorithm for stochastic linear programs
[AD-A212854] 04 p0548 N90-13189
An autopilot design methodology for bank-to-turn missiles
[AD-A213379] 05 p0583 N90-13399
Electron heating and static sheath enhancement in front of energized RF antennas
[DE90-001334] 06 p0766 N90-14456
A new simulation method for the efficient calculation of benchmarks for detonation products equations of state
[DE90-001837] 06 p0777 N90-14522
Derivation of synthetic mission profiles from electric vehicle field data
[DE89-011125] 06 p0793 N90-14620
An observational study of intramonthly quasi-periodicities in the Northern Hemisphere, extratropical geopotential height field
06 p0813 N90-14729
Path integral simulations of liquid helium
[DE90-001171] 06 p0836 N90-14862
Theoretical methods for the study of chemical dynamics
[DE90-003122] 07 p0893 N90-15160
A simulation model for dynamic system availability analysis
[AD-A213499] 07 p0974 N90-15628
Use of the linear variate method of Monte Carlo for estimating uncertainty in thermal-hydraulic codes
[DE89-017871] 07 p0985 N90-15694
Uniform versus random sampling in physical calculations: Monte Carlo
[DE90-003247] 07 p0986 N90-15696
Variational quantum Monte Carlo calculation of electronic and structural properties of crystals
[DE90-003265] 07 p0999 N90-15781
Probabilistic simulation of uncertainties in composite uniaxial strengths
[NASA-TM-102483] 08 p1040 N90-16008
Direct Monte Carlo calculations on expansion wave structure near a wall
[ISL-CO-249/88] 08 p1064 N90-16154
The theory of hybrid stochastic algorithms
[DE90-003941] 08 p1109 N90-16421
Computer simulation of dust grain evolution
08 p1144 N90-16632
Determination of solar flare accelerated ion angular distributions from SMM gamma ray and neutron measurements and determination of the He-3/H ratio in the solar photosphere from SMM gamma ray measurements
[NASA-CR-186038] 08 p1153 N90-16676
Study of continuum higher order closure models evaluated by a statistical theory of shock structure
10 p1303 N90-17538
Plume flowfield analysis of the shuttle primary Reaction Control System (RCS) rocket engine
[NASA-CR-186315] 10 p1329 N90-17676
Contained events in Soudan 2
[DE90-005648] 10 p1449 N90-18359
Angle estimation in the presence of mainbeam interference
[AD-A216832] 11 p1498 N90-18621
Spectral functions from Quantum Monte Carlo
[DE90-004870] 11 p1572 N90-19050
Three-dimensional structural analyses of reentry vehicles
[DE90-006278] 12 p1615 N90-19291
Monte Carlo models and analysis of galactic disk gamma-ray burst distributions 12 p1636 N90-19403
Analytical optical scattering in clouds
12 p1638 N90-19413
A nonparametric software reliability growth model
[NASA-CR-186438] 12 p1700 N90-19764
Numerical solution to the problem of criticality by Monte Carlo method
[DE90-608886] 12 p1708 N90-19808
Microstructural simulations of dynamic recrystallization
[DE90-007504] 12 p1722 N90-19895

Computer simulation of recrystallization in the presence of second phase particles
[DE90-007531] 12 p1723 N90-19896
Gas diffusion in a cometary crust
12 p1742 N90-20017
Theory system reliability demonstration and burn-in design
[AD-A217775] 13 p1814 N90-20416
Ordering mechanism in substitutional Ni-Cr alloys: Theory and experiment
[DE90-006268] 14 p1949 N90-21156
A conflict analysis of 4D descent strategies in a metered, multiple-arrival route environment
[NASA-CR-182019] 15 p2055 N90-21772
Recognition and analysis of aircraft targets by radar, using structural pattern representations derived from polarimetric signatures 15 p2074 N90-21879
Diffraction-limited imaging on the 200-inch telescope
15 p2183 N90-22475
Linear and nonlinear electrical response of condensed matter: Ionic, dielectric, and mixed-conduction materials
[AD-A218771] 16 p2215 N90-22639
An examination of the full-wave method for rough surface scattering
[AD-A218664] 16 p2308 N90-23155
The sensitivity of EGRET to gamma ray polarization
16 p2335 N90-23305
A theoretical model for airborne radars
[AD-A220735] 17 p2390 N90-23615
Radar detection during scintillation
[AD-A220099] 17 p2393 N90-23630
Ultra high-speed compound semiconductors and real time signal processing
[AD-A220721] 17 p2396 N90-23651
FASTER: The Fault Tolerant Architecture Simulation Tool for Evaluating Reliability, introduction and applications
[AD-A219941] 17 p2414 N90-23755
Extreme quantile estimation in binary response models
[AD-A220150] 17 p2466 N90-24093
Applications of non-parametric density estimation
[AD-A220206] 17 p2466 N90-24094
An interactive life cycle cost forecasting tool
[AD-A220472] 17 p2480 N90-24184
Low-density flow effects for hypervelocity vehicles, phase 2
[AD-A221034] 18 p2493 N90-24249
Nonlocal free energy density functional approximations for the electrical double layer; comparison with Monte Carlo results for 2:1 salt
[AD-A220911] 18 p2521 N90-24395
The measurement of composition during the early stages of the spinodal decomposition of Fe-Cr alloys
[DE90-010471] 18 p2525 N90-24408
Radar clutter via waveguide methods
[AD-A220237] 18 p2542 N90-24512
A nonlocal free energy density functional approximation for the electrical double layer
[AD-A220664] 18 p2607 N90-24848
Ensemble Monte Carlo simulation of electron transport in AlGaAs/GaAs heterostructures
[ISBN-90-9003048-4] 18 p2622 N90-24940
X rays from the accretion column of compact objects: A Monte Carlo study 19 p2775 N90-25777
Iron lines from X ray illuminated accretion discs in AGN 19 p2790 N90-25884
X ray polarization of the reprocessed emission from accretion disk in Seyfert galaxies
19 p2792 N90-25892
Noise adaptation and correlated maneuver gating of an extended Kalman filter
[AD-A221713] 21 p3001 N90-27060
A user's manual for MCPRAM (Monte Carlo PReprocessor for AMEER) and for the fuze options in AMEER (Aero Mechanical Equation Evaluation Routines)
[DE90-013598] 21 p3051 N90-27345
Genetic algorithms: The state of the art and some research proposals
[REPT-89-058] 22 p3241 N90-28380
Theoretical thermodynamics: Equation of state and perturbation studies
[PB90-199332] 22 p3255 N90-28430
A study of the sensitivity of an imaging telescope (GRITS) for high energy gamma-ray astronomy
[NASA-CR-186921] 22 p3261 N90-28468
Surface and defect excitations in covalently bonded solids
[AD-A221995] 23 p3303 N90-28682
A study of heat and fluid flow phenomena on the gas side of circular-tube plate-fin heat exchangers
23 p3324 N90-28795
An improved method for choosing sampling points for the inspection of complex surfaces in a computer-aided manufacturing environment 23 p3380 N90-29093
The first order phase transition for six-state Potts model on two dimensional random triangle lattice
[DE90-627210] 23 p3389 N90-29140
An infrared sky model based on the IRAS point source data
[NASA-CR-177526] 23 p3409 N90-29265
Comparison of dose estimates using the buildup-factor method and a Baryon transport code (BRYNTRN) with Monte Carlo results
[NASA-TP-3021] 23 p3414 N90-29290
Techniques for autonomous GPS integrity monitoring
24 p3424 N90-29345
Extension of plasma source ion implantation to ion beam enhanced deposition
[AD-A224462] 24 p3454 N90-29506
Radar clutter via ray methods
[AD-A223796] 24 p3482 N90-29553
Tool for studying the effects of range restriction in correlation coefficient estimation
[AD-A224035] 24 p3537 N90-29996
Trapezoidal stratified Monte Carlo integration
[AD-A223565] 24 p3540 N90-30021
Monte Carlo simulation of complex spectra for opacity calculations
[DE90-015198] 24 p3561 N90-30147

MOODS
Daytime sleepiness, performance, mood, nocturnal sleep: The effect of benzodiazepine and caffeine on their relationship
[AD-A210915] 01 p0093 N90-10533
Coping strategies and mood during cold weather training
[AD-A223915] 24 p3498 N90-29773

MOON
On analytic modeling of lunar perturbations of artificial satellites of the earth
[AD-A210440] 01 p0016 N90-10078
Office of exploration overview
01 p0027 N90-10141
A lunar far-side very low frequency array
[NASA-CP-3039] 01 p0139 N90-10805
CIS-lunar space infrastructure lunar technologies: Executive summary
[NASA-CR-186220] 06 p0865 N90-15029
A quasi-economic role for lunar science
[DE90-000679] 07 p1015 N90-15876
Analysis of alternative concepts for transport systems on the Moon surface
[ETN-90-95727] 12 p1672 N90-19605
Extending terrestrial mobile robotics to a proposed lunar base
[DE89-016179] 12 p1672 N90-19606
Working on the moon: The Apollo experience
[DE90-003662] 12 p1697 N90-19744
Distributed earth model/orbiter simulation
13 p1860 N90-20671
A preliminary design of interior structure and foundation of an inflatable lunar habitat 18 p2633 N90-24999
Lunar orbiting microwave beam power system
[NASA-TM-103211] 19 p2667 N90-25173
Lunar regolith bagging system
[NASA-CR-186652] 19 p2677 N90-25224
Sunlight diffusing tent for lunar worksite
[NASA-CR-186651] 19 p2677 N90-25225
Design of a Lunar farside observatory
[NASA-CR-186671] 19 p2765 N90-25709
Lunar polar coring lander
[NASA-CR-186684] 19 p2796 N90-25917
Proceedings of a workshop on Lunar Volcanic Glasses: Scientific and Resource Potential
[NASA-CR-186631] 20 p2888 N90-26437

MOORING
Estimating the time to fatigue failure of mooring cables
[PB89-220677] 04 p0511 N90-12946

MOORINGS
U MOORING

MORALE
Aviation safety: Conditions within the air traffic control work force. Fact sheet for congressional requesters
[GAO/RCED-89-113FS] 20 p2805 N90-25958

MORL
U MANNED ORBITAL LABORATORIES

MORPHOLOGY
NT GEOMORPHOLOGY
NT ISOMORPHISM
NT POLYMORPHISM
Microstructure morphology and quality of Al-Si castings 01 p0043 N90-10244
Epitaxial GaAs on SOI wafers
[AD-A209009] 01 p0127 N90-10729
Morphological aspects of the friction of hot-filament-grown diamond thin films
[DE89-015986] 01 p0130 N90-10750
Global morphology of plasma bubbles in the low latitude ionosphere 02 p0241 N90-11369
The middle and high latitude ionosphere at approximately 550 km altitude 02 p0242 N90-11374
Modelling ionospheric density structures
02 p0242 N90-11375
Polar F layer lacuna irregularities at Dumont d'Urville
02 p0243 N90-11379
Upper ionosphere and magnetospheric-ionospheric coupling
[DE89-619727] 02 p0250 N90-11415
Ion beam annealing of Ga-implanted Si
[DE89-016857] 02 p0282 N90-11610
Temperature dependent effects during Ag deposition on Cu(110)
[DE89-016987] 03 p0327 N90-11857
On the differentiable manifold of fixed order stable linear systems
[REPT-88-89] 03 p0394 N90-12250
A morphologic study of Venus Ridge belts
03 p0423 N90-12432
The algebraic basis of mathematical morphology. Part 2: Openings and closings
[CWI-AM-R8904-PT-2] 04 p0543 N90-13150
Fundamental results from microgravity cell experiments with possible commercial applications
05 p0676 N90-13940
Polarity establishment, morphogenesis, and cultured plant cells in space 05 p0677 N90-13943
The algebraic basis of mathematical morphology. Part 1: Dilations and erosions
[CWI-AM-R8807] 05 p0695 N90-14065
Mechanical properties and morphology of oriented polymer blends 06 p0750 N90-14361
A study of the infrared emission of galactic supernova remnants 06 p0861 N90-15006
The effects of Mo2C morphology and strain distribution on the fatigue properties of Fe-C-Mo dual-phase steels
07 p0901 N90-15210
Thermally stable metal/GaAs contacts
[DE90-002122] 07 p0998 N90-15774
Ice floe identification in satellite images using mathematical morphology and clustering about principal curves
[AD-A213854] 08 p1090 N90-16311
Effects of ion dose on the morphology and crystallization of amorphous germanium
[DE90-003564] 08 p1130 N90-16547
Direct determination of the morphology, structure and composition of cometary and interstellar ice analogs in the laboratory 08 p1141 N90-16612
Morphological consequences of catalytic hydrogenation of polymers in the bulk
[DE90-007276] 11 p1494 N90-18598
Fatigue crack initiation and small crack growth in several airframe alloys
[NASA-TM-102598] 11 p1518 N90-18746
Modified dislocation structures in Ge(x)Si(1-x) double epilayers on (001) Si
[DE90-007078] 11 p1572 N90-19052
Light-scattering measurements of CVD (Chemical Vapor Deposition) silicon carbide
[DE90-007885] 12 p1632 N90-19382
Investigations of CuInSe2 thin films and contacts
[DE90-000301] 12 p1721 N90-19886
Novel processing of HTS based conductors
[DE90-005956] 12 p1722 N90-19892
Oxygen concentrations on surfaces of carbon fibers
[AD-A217724] 13 p1769 N90-20152
Design and processing of strong-tough microcomposite steels
[DE90-007764] 13 p1777 N90-20197
CO2 diffusion and solubility in a Polystyrene/Polybutadiene block copolymer with highly oriented lamellar morphology
[AD-A217165] 13 p1779 N90-20211
The effects of high intensity cycle exercise on sympatho-adrenal-medullary response patterns
[AD-A217962] 13 p1852 N90-20628
Influence of the deposition conditions on radiofrequency magnetron sputtered MoS2 films
[NASA-TP-2994] 14 p1958 N90-21210
Performance evaluation of morphological edge detectors
[INPE-4975-PRE/1540] 14 p2000 N90-21464
Interfacial studies in fiber-reinforced thermoplastic-matrix composites
15 p2062 N90-21814
Production and analysis by mass spectrometry of beams of polyglycol ions 15 p2066 N90-21835
Search for rapidly star forming galaxies at high redshift 15 p2181 N90-22465
Photoresponse of YBa2Cu3O(7-delta) granular and epitaxial superconducting thin films
[NASA-TM-103144] 16 p2231 N90-22732
Spaceborne radar observations: A guide for Magellan radar-image analysis
[NASA-CR-184998] 16 p2249 N90-22826

The effect of elevated gravity on the crystallization of the MFI zeolites, ZSM-5, and silicalite
16 p2320 N90-23231
Rheological and mechanical characteristics of poly-p-phenylene terephthalamide/nylon molecular and particulate composites
[AD-A219562] 17 p2368 N90-23482
Effect of surface oxygen on adhesion of carbon fiber-reinforced composites
[AD-A220777] 17 p2369 N90-23486
Morphology changes due to oxidative treatment of glassy carbon electrodes and its applications
[AD-A219425] 17 p2371 N90-23501
Fundamental and practical studies of metal contacts on mercury zinc telluride
[AD-A218730] 17 p2376 N90-23528
The origin of multiple melting in polyurethane block copolymers
[AD-A220050] 17 p2381 N90-23563
Compression molded polyurethane block copolymers. 3: Evaluation of microphase compositions
[AD-A220160] 17 p2382 N90-23564
CVD diamond films for tribological applications
[AD-A220265] 17 p2413 N90-23750
Erosional development of bedrock spur and gully topography in the Valles Marineris, Mars
[NASA-CR-180655] 17 p2424 N90-23813
Morphological sampling
[CWI-AM-R8913] 17 p2460 N90-24044
Molecular gas in S106: Morphology, kinematics, and chemistry of a star forming region
17 p2484 N90-24209
Morphological and structural characterization of the spinodal decomposition of Fe-Cr alloys
[DE90-010496] 18 p2526 N90-24418
The catalytic reactivity of thin film crystal surfaces
[DE90-010579] 18 p2622 N90-24937
Morphological control of inter-penetrating polymer networks 18 p2642 N90-25046
Erosion mechanisms in composite materials and ripple formation mechanism in erosion
[IAR-89-4-PT-1] 20 p2826 N90-26078
Experiment K-6-02. Biomedical, biochemical and morphological alterations of muscle and dense, fibrous connective tissues during 14 days of spaceflight
20 p2892 N90-26456
Experiment K-6-03. Gravity and skeletal growth, part 1. Part 2: Morphology and histochemistry of bone cells and vasculature of the tibia; Part 3: Nuclear volume analysis of osteoblast histogenesis in periodontal ligament cells; Part 4: Intervertebral disc swelling pressure associated with microgravity 20 p2892 N90-26457
Experiment K-6-06. Morphometric and EM analyses of tibial epiphyseal plates from Cosmos 1887 rats
20 p2893 N90-26460
Experiment K-6-08. Biochemical and histochemical observations of vastus medialis
20 p2893 N90-26462
Experiment K-6-09. Morphological and biochemical investigation of microgravity-induced nerve and muscle breakdown. Part 1: Investigation of nerve and muscle breakdown during spaceflight; Part 2: Biochemical analysis of EDL and PLT muscles 20 p2893 N90-26463
Experiment K-6-12. Morphometric studies of atrial or granules and hepatocytes. Part 1: Morphometric study of the liver; Part 2: The atrial granular accumulations
20 p2894 N90-26466
Experiment K-6-13. Morphological and biochemical examination of heart tissue. Part 1: Effects of microgravity on the myocardial fine structure of rats flown on Cosmos 1887. Ultrastructure studies. Part 2: Cellular distribution of cyclic ampdependent protein kinase regulatory subunits in heart muscle of rats flown on Cosmos 1887
20 p2894 N90-26467
Experiment K-6-16. Morphological examination of rat testes. The effect of Cosmos 1887 flight on spermatogonial population and testosterone level in rat testes
20 p2895 N90-26469
Diamonds in detonation soot
21 p3094 N90-27585
Kinetics and thermodynamics of ceramic/metal interface reactions related to high T(sub c) superconducting applications 22 p3141 N90-27815
Transcrystalline morphology in carbon fibre composites with thermoplastic matrix and its influence on the mechanical properties
[FOA-C-20783-2.1] 22 p3248 N90-28423
Structure of metal overlayers by low energy alkali ion scattering: Cu/Ru(0001) and Sn/Pt(111)
[DE90-014453] 23 p3310 N90-28718
Numerical and analytical study of nonlinear bifurcations associated with the morphological stability of two-dimensional single crystals
[PB90-209594] 23 p3398 N90-29200
A plasma diagnostic study of two wind-blown shell nebulae: NGC 7635 and NGC 2359
23 p3410 N90-29271
Precursor structure-fiber property relationships in polyacrylonitrile-based carbon fibers
[AD-A224246] 24 p3454 N90-29503
Effect of particulate fillers on the rheology of polymer melts
[AD-A223601] 24 p3455 N90-29512

MORPHOTROPISM
U ISOMORPHISM

MORTALITY
Outer continental shelf environmental assessment program. Volume 66: Principal investigators
[PB90-194747] 22 p3199 N90-28154

MOS (JAPANESE SPACECRAFT)
U JAPANESE SPACECRAFT

MOS (SEMICONDUCTORS)
U METAL OXIDE SEMICONDUCTORS

MOSAICS
Fracture analysis through photographic imagery of low spatial resolution: A contribution to the study of tectonic evoluation of the Araripe Plateau region
[INPE-4876-PRE/1487] 11 p1520 N90-18756
AFGL ten micron mosaic array spectrometer: Recent results 14 p1978 N90-21333
Digital geometric correction for MSS-LANDSAT imagery
[INPE-4627-PRE/1345] 23 p3342 N90-28886

MOSFET
U FIELD EFFECT TRANSISTORS

MOSS (SPACE STATIONS)
U SPACE STATIONS

MOSSBAUER EFFECT
Electronic structure of transition metal alloys and intermetallics: Charge transfer and its implications for Moessbauer effect measurements
[DE89-017603] 03 p0327 N90-11860
Proceedings of the Latin American Conference on the Applications of the Moessbauer Effect
[DE90-600819] 07 p1002 N90-15803
Magnetic interactions in Sn-119 substituted for Cu in antiferromagnetic and superconducting lamellar cuprates
[DE90-003661] 08 p1132 N90-16560
Studies of the structure and properties of amorphous a-Zr76Fe24Hx
[AD-A214646] 09 p1190 N90-16897
Proof of the feasibility of coherent and incoherent schemes for pumping a gamma-ray laser
[AD-A219972] 18 p2562 N90-24620
SDIO/IST ultrashort wavelength laser: Novel experimental schemes for observing the Moessbauer effect in long-lived nuclear levels and nuclear coherent states
[AD-A222607] 20 p2868 N90-26316
Studies of iron impurities in YxPr1-xBa2Cu3O7-delta
22 p3151 N90-27865
Moessbauer Effect applications using intense radioactive ion beams
[DE90-014981] 23 p3394 N90-29175

MOTILITY
U LOCOMOTION

MOTION
Effect of contrast on the perception of direction of a moving pattern
[NASA-TM-102234] 07 p0965 N90-15577
Motion detection in astronomical and ice floe images
15 p2140 N90-22231

MOTION AFTEREFFECTS
Analysis of camera movement based on a sequence of images
[TELECOM-PARIS-89-D-008] 18 p2616 N90-24901

MOTION EQUATIONS
U EQUATIONS OF MOTION

MOTION PERCEPTION
Inferences from images
[AD-A210710] 02 p0258 N90-11465
Visual motion perception
[AD-A210994] 03 p0379 N90-12160
Discriminating rigid from nonrigid motion
[AD-A211794] 03 p0383 N90-12180
Development of an integrated mobile robot system at CMU (Carnegie-Mellon University)
[AD-A212555] 04 p0510 N90-12944
An architectural model of visual motion understanding
[AD-A214327] 07 p0967 N90-15589
Development of an integrated mobile robot system at Carnegie Mellon University: June 1988
[AD-A215955] 10 p1392 N90-19049
Visual perception of structure from motion
[AD-A216416] 10 p1412 N90-18141
Human motion perception: Higher-order organization
15 p2140 N90-22226
Factors affecting the perception of transparent motion
15 p2141 N90-22233
Ames vision group research overview
15 p2143 N90-22242
Visual sensitivities and discriminations and their role in aviation
[AD-A219319] 16 p2266 N90-22917
Perceiving environmental properties from motion information: Minimal conditions
16 p2268 N90-22925
On the efficacy of cinema, or what the visual system did not evolve to do 16 p2269 N90-22934
Effects of short-term weightlessness on roll circularvection 23 p3361 N90-28992
Direct estimation of structure and motion from multiple frames
[AD-A223903] 24 p3534 N90-29985

MOTION PICTURES
Computer animation in mathematics, science, and art
[DE90-013051] 20 p2908 N90-26538
Animated computer-generated video-tape instruction using DIGLIB (Device Independent Graphics Library)
[DE90-015360] 23 p3382 N90-29105

MOTION SICKNESS
Simulator induced sickness in the CP-140 (Aurora) flight deck simulator
[AD-A213096] 05 p0673 N90-13923
Functional decor in the International Space Station: Body orientation cues and picture perception
[NASA-TM-102242] 05 p0675 N90-13931
Simulator sickness in the UH-60 (Black Hawk) flight simulator
[AD-A214434] 08 p1104 N90-16392
Simulator sickness in the AH-1S (Cobra) flight simulator
[AD-A214562] 09 p1250 N90-17254
Human factors in the naval environment: A review of motion sickness and biodynamic problems
[AD-A214733] 09 p1251 N90-17258
An exploratory analysis of motion sickness data: A time series approach
[AD-A215534] 09 p1253 N90-17271
A cepstral analysis of EEG (Electroencephalographic) signals in motion sickness studies
[AD-A215663] 09 p1253 N90-17273
Vestibular examination of motion sick student pilots
[IZF-1988-22] 12 p1696 N90-19738
Simulator sickness in the CH-47 (Chinook) flight simulator
[AD-A218214] 13 p1853 N90-20634
Space adaptation syndrome induced by a long duration +3Gx centrifuge run
[AD-A218248] 14 p2010 N90-21518
Issues in development, evaluation, and use of the NASA Preflight Adaptation Trainer (PAT)
[NASA-CR-185608] 15 p2137 N90-22212
Sensory conflict in motion sickness: An observer theory approach 16 p2273 N90-22957
Brain stem evoked responses in altered G environments
[AD-A220097] 17 p2435 N90-23874
Motion sickness, visual displays, and armored vehicle design
[AD-A222678] 20 p2902 N90-26506
Vestibular responses and motion sickness during pitch, roll, and yaw sinusoidal whole-body oscillation
[AD-A223898] 24 p3497 N90-29767

MOTION SICKNESS DRUGS
An exploratory analysis of motion sickness data: A time series approach
[AD-A215534] 09 p1253 N90-17271
A cepstral analysis of EEG (Electroencephalographic) signals in motion sickness studies
[AD-A215663] 09 p1253 N90-17273

MOTION SIMULATION
On the motion equation of an elastically supported two degree of freedon gyro
[NAL-TM-568] 02 p0223 N90-11276
Molecular dynamics study of the primitive model of 1-3 electrolyte studies
[AD-A211653] 03 p0325 N90-11846
Compensatory tracking in disturbance tasks and target following tasks. The influence of cockpit motion on performance and control behavior
[LR-511] 05 p0675 N90-13933
Classification and simulation of single and multi-degree-of-freedom motions
[AD-A214925] 09 p1231 N90-17143
Simulator sickness in the AH-1S (Cobra) flight simulator
[AD-A214562] 09 p1250 N90-17254
Homogeneous dilute turbulent particle-laden water flows 15 p2090 N90-21965
Multibody dynamics model building using graphical interfaces 16 p2297 N90-23082
Analysis of the accuracy of a proposed target motion analysis procedure
[AD-A219481] 17 p2436 N90-23880

Efficient motion planning for an L-shaped object
[RUU-CS-88-38] 17 p2463 N90-24073
Simulation of the inversion of amphibian eggs in a gravitational field using hollow glass spheres
19 p2681 N90-25251
Curvature estimation in orientation selection
[AD-A221481] 21 p3034 N90-27249
On the application of similarity laws to a scaled railway bogie model
[DLR-FB-90-06] 23 p3335 N90-28853
On the simulation of space based manipulators with contact 23 p3373 N90-29056
Vestibular responses and motion sickness during pitch, roll, and yaw sinusoidal whole-body oscillation
[AD-A223898] 24 p3497 N90-29767
The control of space manipulators subject to spacecraft attitude control saturation limits
24 p3515 N90-29871
Directing an animated scene with autonomous actors
[REPT-89-041] 24 p3531 N90-29972

MOTION SIMULATORS
User's manual for the ride motion simulator
[AD-A212855] 05 p0584 N90-13402
Kinematics and control of manipulation robots
[WTHD-187] 05 p0652 N90-13803
Simulator induced sickness in the CP-140 (Aurora) flight deck simulator
[AD-A213096] 05 p0673 N90-13923
The moving platform simulator 2: A networked real-time visual simulator with distributed processing and line-of-sight displays
[AD-A214936] 09 p1266 N90-17343
Determination of the implementation of the 3-axis attitude motion simulator digital position controller
12 p1638 N90-19409
A dynamic motion simulator for future European docking systems 15 p2113 N90-22085
Utilization of Moire patterns as an orbital docking aid to space shuttle/Space Station Freedom
18 p2629 N90-24980

MOTION STABILITY
NT AERODYNAMIC STABILITY
NT AIRCRAFT STABILITY
NT ATTITUDE STABILITY
NT BOUNDARY LAYER STABILITY
NT DIRECTIONAL STABILITY
NT FLAME STABILITY
NT FLOW STABILITY
NT GYROSCOPIC STABILITY
NT HOVERING STABILITY
NT LATERAL STABILITY
NT LONGITUDINAL STABILITY
NT LOW SPEED STABILITY
NT MAGNETOHYDRODYNAMIC STABILITY
NT ROTARY STABILITY
NT SPACECRAFT STABILITY
Analysis of a system of two weakly nonlinear coupled harmonic oscillators arising from the field of wind-induced vibrations
[REPT-89-22] 03 p0396 N90-12261
Free surface scars and striations
[AD-A212429] 04 p0503 N90-12901
Control and stability of a spinning symmetric satellite in an elliptical orbit
[AD-A216284] 10 p1326 N90-17672
Dynamics and control of tethered antennas/reflectors in orbit
[AD-A219316] 16 p2207 N90-22594

MOTIVATION
NT CONTRACT INCENTIVES
The effect of incentives on the reliability and validity of cognitive speed tests
[AD-A211346] 03 p0383 N90-12181
Human behavior
[PB90-780008] 07 p0967 N90-15584
A foundation for the design of an astronautics specification system based on dynamic motivation analysis
[ILR-MITT-220] 08 p1033 N90-15969
Ability and metacognitive determinants of skill acquisition and transfer
[AD-A224569] 24 p3499 N90-29776

MOTOR SYSTEMS (BIOLOGY)
U EFFERENT NERVOUS SYSTEMS

MOTOR VEHICLES
NT AUTOMOBILES
NT ELECTRIC AUTOMOBILES
NT ELECTRIC MOTOR VEHICLES
NT TRACKED VEHICLES
NT TRUCKS
Waveform generator signal processing software
[PB89-192660] 01 p0103 N90-10587
Distance and clearance perception using forward-looking, vehicular television systems
[DE89-014740] 03 p0405 N90-12319
Methanol fueled vehicles and photochemical models: An evaluation of the state of knowledge
[PB89-214225] 03 p0419 N90-12410
Cold starting a neat methanol (M100) vehicle with long duration spark ignition
[PB89-230692] 06 p0792 N90-14613
An approach for testing fuel-cell/battery hybrid power sources for bus applications
[DE90-002090] 08 p1083 N90-16270
Antennas on land vehicles for improved communications 10 p1370 N90-17938
Comparison of emissions of transit buses using methanol and diesel fuel
[DE90-005652] 10 p1391 N90-18044
US Army Methanol-Fueled Administrative Vehicle Demonstration Program
[AD-A216013] 10 p1393 N90-18054
Options for controlling the global warming impact from motor vehicles
[PB90-161688] 22 p3197 N90-28142

MOTORS
NT ASYNCHRONOUS MOTORS
NT ELECTRIC MOTORS
NT INDUCTION MOTORS
NT SERVOMOTORS
NT STEPPING MOTORS
NT SYNCHRONOUS MOTORS
NT TORQUE MOTORS
Extraction of recovery of plasticizers from solid propellants and munitions
[AD-D014433] 15 p2072 N90-21866
Performance measurements and energy balance of an SPS V160 Stirling motor at the German Aerospace Research Establishment
[DLR-MITT-90-03] 23 p3345 N90-28903
Utilization of a measurement process by the examination of universal motors
[ETN-90-97307] 24 p3466 N90-29581

MOUNTAINS
NT ROCKY MOUNTAINS (NORTH AMERICA)
NT SIERRA NEVADA MOUNTAINS (CA)
Ice runways near the South Pole
[AD-A211606] 03 p0335 N90-11908
Photointerpretation with instruments for evaluation of environmental impact: Mata Atlantica in Cubata
[INPE-4910-PRE/1511] 11 p1531 N90-18817
Meteorological influences on mountain cloudwater chemistry in the eastern United States
[PB90-132432] 14 p2007 N90-21504
Verification of Klett's method by comparison of lidar and transmissometer measurements
15 p2084 N90-21933
An anomalous wind between valleys: Its characteristics and a proposed explanation
[DE90-008965] 15 p2133 N90-22189
High mountain flying in ski country, USA
[PB90-160316] 22 p3107 N90-27651

MOUNTING
Progress in the design of a microgravity facility for in-orbit experiments 18 p2540 N90-24496
Vibration test procedures for orbiter sidewall-mounted payloads, phase 1
[AD-A220773] 20 p2818 N90-26037
Alignment positioning mechanism
[NASA-CASE-MSC-21502-1] 20 p2872 N90-26341
Constitutive and life modeling of single crystal blade alloys for root attachment analysis
23 p3296 N90-28643

MOUNTS
U SUPPORTS

MOVEMENT
U MOTION

MOVING TARGET INDICATORS
Modified Newton-type methods for long-range target motion analysis
[FEL-1989-82] 04 p0551 N90-13208
Efficient detection of small moving objects
[AD-A213314] 05 p0632 N90-13690
Concepts for high resolution space based SAR/ISAR systems: Preliminary design considerations
14 p1960 N90-21224
Combining zero Doppler filter calculations with MTI filter calculations to increase computational speed
[AD-A222468] 21 p2997 N90-27034

MOZAMBIQUE
US Navy regional climatic study of the Mozambique channel and adjacent waters
[AD-A218793] 16 p2258 N90-22875

MPP (COMPUTERS)
U MASSIVELY PARALLEL PROCESSORS

MRAC (SYSTEMS)
U MODEL REFERENCE ADAPTIVE CONTROL

MRCA AIRCRAFT
Development of the integrated all-weather navigation system for Tornado 02 p0149 N90-10849
Fighter escape system: The next step forward
13 p1752 N90-20059

MSAT
Vehicle antenna for the mobile satellite experiment
[NASA-CR-186109] 06 p0733 N90-14271
Field measurements in MSAT-X
10 p1371 N90-17947

MTBF
Estimating the time to fatigue failure of mooring cables
[PB89-220677] 04 p0511 N90-12946
Techniques for developing a system safety risk assessment model
[AD-A223477] 24 p3477 N90-29654

MTF
U MODULATION TRANSFER FUNCTION

MTFF (SPACE STATION)
U MAN TENDED FREE FLYERS

MTI RADAR
U MOVING TARGET INDICATORS

MUFFLERS
The Shock and Vibration Digest, volume 22, no. 2
14 p2022 N90-21596
State of the art of acoustics of active and passive mufflers 14 p2023 N90-21597

MULLITES
Processing and characterization of alumina platelet-reinforced mullite composites
[DE90-000057] 03 p0320 N90-11814

MULTI-ROLE COMBAT AIRCRAFT
U MRCA AIRCRAFT

MULTIBEAM ANTENNAS
Multibeam radar altimetry: Spaceborne feasibility and airborne experimentation
[AD-A215152] 09 p1207 N90-16995
Large antenna measurement and compensation techniques 12 p1610 N90-19263

MULTICHANNEL COMMUNICATION
Coherent multichannel techniques for integrated broadband communications subscriber lines
[AD-A209323] 01 p0055 N90-10312
Description and results of a multihop NACS simulation
[FEL-1988-48] 04 p0491 N90-12824
Frequency independent constant beamwidth directional lens antenna for very wideband and multi-channel electromagnetic communications
[AD-D014214] 06 p0765 N90-14449
Computer processing of multi-channel electromagnetic data from an airborne geophysical survey system
[PB90-138413] 14 p1965 N90-21253
A parametric detection approach using multichannel processes
[AD-A219328] 17 p2395 N90-23541

MULTICHANNEL PLATES
U MICROCHANNEL PLATES

MULTIGRID METHODS
Computational Fluid Dynamics, Volume 2
[VKI-LS-1990-03-VOL-2] 22 p3172 N90-27993
Towards a genuinely multi-dimensional upwind scheme 22 p3172 N90-27995
Tailoring explicit time-marching schemes to improve convergence characteristics 22 p3172 N90-27997
Fluctuation splitting for multidimensional convection problems: An alternative to finite volume and finite element methods 22 p3173 N90-28000
Towards a two dimensional scheme of anisotropic Godunov type. On the calculation of the velocity of the nodes in the multidimensional Lagrangian codes
[ETN-90-97458] 22 p3175 N90-28017
On the calculation of the velocity of the nodes in the multidimensional Lagrangian codes
22 p3175 N90-28019
Numerical resolution of Navier-Stokes equations using several turbulence models and applications on turbomachines
[ETN-90-97478] 23 p3326 N90-28808

MULTILAYER INSULATION
Composite multilayer insulations for thermal protection of aerospace vehicles
[NASA-TM-101071] 01 p0034 N90-10183
Fabrication of NBN based electronic devices with silicon barriers
[AD-D014230] 06 p0767 N90-14463
Preparation and characterization of alumina films prepared by a novel spray pyrolysis method
[AD-A217570] 12 p1625 N90-19339

MULTILAYER STRUCTURES
U LAMINATES

MULTIMODE RESONATORS
Theoretical and experimental investigation of coupled Ar-ion lasers
[AD-A214908] 09 p1227 N90-17122

MULTIPATH TRANSMISSION
Study of high frequency water vapor absorption parameters
[AD-A210676] 02 p0194 N90-11108

Theory and simulation of the operation of a Doppler direction finder in a multipath environment
[FEL-1988-56] 03 p0340 N90-11939
Ground effects on multipath fading
[TELECOM-PARIS-88-E017] 04 p0489 N90-12812
Improving the quality of a spread-spectrum radiomobile link 06 p0761 N90-14426
Improved reliability prediction for HF digital voice transmission 06 p0761 N90-14429
Mitigating Doppler shift effect in HF multitone data modem 06 p0764 N90-14441
TROPO: A technique for predicting propagation and modem performance of digital troposcatter systems 06 p0764 N90-14444
Modelling UHF propagation for frequency assignment in radio relay networks 06 p0764 N90-14445
The characteristics of the HF radio channel and its influence on modern HF data communication system design 06 p0765 N90-14448
Spread spectrum mobile radio communications
[AD-A213726] 07 p0918 N90-15311
Antennas on land vehicles for improved communications 10 p1370 N90-17938
Proceedings of the Thirteenth NASA Propagation Experimenters Meeting (NAPEX 13)
[NASA-CR-186062] 10 p1371 N90-17945
Field measurements in MSAT-X 10 p1371 N90-17947
LMSS drive simulator for multipath propagation 10 p1372 N90-17950
LMSS modeling status report 10 p1372 N90-17953
A CCIR aeronautical mobile satellite report 10 p1372 N90-17954
Multiple symbol differential detection of uncoded and trellis coded MPSK
[NASA-CR-186288] 10 p1376 N90-17975
Effects of amplitude distortions and IF equalization on satellite communication system bit-error rate performance
[NASA-TM-102415] 12 p1645 N90-19454
First-order intensity statistics for non-Rayleigh fading
[AD-A217572] 13 p1841 N90-20569
Direct Radio Broadcasting by Satellite (DRBS): A review of the technical factors and system approaches suitable for mobile and fixed reception
[BBC-RD-1989/4] 14 p1960 N90-21221
Model order determination methods for autoregressive radio direction finding techniques
[AD-A220707] 17 p2350 N90-23384
Innovative techniques for high-resolution imaging and precision tracking
[AD-A221380] 18 p2616 N90-24899
A global common-user system for the provision of HF propagation data 20 p2845 N90-26180
Experimental study of a digital mobile radio spread spectrum in an urban site 20 p2849 N90-26205

MULTIPHASE FLOW
NT TWO PHASE FLOW
Analysis of a model and sequential numerical method for thermal reservoir simulation
[DE89-015117] 01 p0067 N90-10384
Constitutive Relationships and Models in Continuum Theories of Multiphase Flows --- conferences
[NASA-CP-3047] 01 p0067 N90-10385
Stress in dilute suspensions 01 p0068 N90-10389
Scaling and modeling of turbulent suspension flows 01 p0069 N90-10393
Turbulence kinetic energy equation for dilute suspensions 01 p0069 N90-10394
Gas-phase flowrate effect on disintegrating cryogenic liquid-jets
[NASA-TM-102357] 02 p0223 N90-11277
Heat transfer in convective boundary layer and channel flows 06 p0774 N90-14505
The laminar to slug flow transition in Hele-Shaw flow
[DE90-000636] 06 p0777 N90-14521
Dense-spray properties: Structure and turbulence modulation
[AD-A213671] 07 p0931 N90-15387
A brief description of lattice gas models for multiphase flows and magnetohydrodynamics
[DE90-003653] 08 p1062 N90-16143
Laser velocimeter measurements of multiphase flow of solids
[DE90-007604] 14 p1974 N90-21311
Scattered-light scanner measurements of cryogenic liquid-jet breakup
[NASA-TM-102432] 15 p2101 N90-22021
Holocinematography for studies of turbulent multiphase flow
[AD-A219130] 16 p2237 N90-22765
Numerical and physical modelling of bubbly flow phenomena
[DE90-009837] 17 p2401 N90-23677
Low-gravity fluid physics: A program overview
[NASA-TM-103215] 20 p2861 N90-26273
A theoretical study of flow structure and radiation for multiphase turbulent diffusion flames
[AD-A222934] 21 p2976 N90-26913

MULTIPHOTON ABSORPTION
Shortwavelength coherent radiation: Generation and applications
[AD-A209847] 01 p0074 N90-10427

MULTIPLE ACCESS
NT CODE DIVISION MULTIPLE ACCESS
NT TIME DIVISION MULTIPLE ACCESS
Performance analysis of hybrid ARQ protocols in a slotted code division multiple-access network
[AD-A211078] 02 p0213 N90-11219
Performance of cellular frequency-hopped spread-spectrum radio networks
[AD-A214480] 09 p1204 N90-16978
Extremely high data-rate, reliable network systems research
[NASA-CR-186359] 15 p2149 N90-22278
CSMA/RN: A universal protocol for gigabit networks 15 p2150 N90-22280
A carrier sensed multiple access protocol for high data base rate ring networks 15 p2151 N90-22288
Spread-spectrum communications in non-Gaussian channels
[AD-A222886] 21 p2994 N90-27019
ATDRS payload technology research and development
[NASA-TM-103256] 23 p3287 N90-28596

MULTIPLE DOCKING ADAPTERS
Fluid connectors for operation in space 18 p2536 N90-24465

MULTIPLE FREQUENCY RADAR
U MULTISPECTRAL RADAR

MULTIPLE INSTRUCTION MULTIPLE DATA STREAM
U MIMD (COMPUTERS)

MULTIPLETS
U FINE STRUCTURE

MULTIPLEX TRANSMISSION
U MULTIPLEXING

MULTIPLEXERS
U MULTIPLEXING

MULTIPLEXING
NT FREQUENCY DIVISION MULTIPLEXING
NT TIME DIVISION MULTIPLEXING
NT WAVELENGTH DIVISION MULTIPLEXING
Some significant results from testing a Remote Multiplexing Unit (RMU) for temperature-induced errors
[DE89-009432] 01 p0073 N90-10421
Performance of the CAMEX64 silicon strip readout chip
[DE89-014015] 01 p0130 N90-10747
Independent Orbiter Assessment (IOA): Analysis of the instrumentation subsystem
[NASA-CR-185571] 02 p0164 N90-10928
Optical coherence multiplexing for interprocessor communications
[DE89-016186] 02 p0275 N90-11568
Introduction to the Mil-Std-1553B serial multiplex data bus
[RAE-TM-MM-9] 03 p0418 N90-12405
Voice Multiplex System (VMS)
[AD-A213902] 07 p0919 N90-15315
Multiplexed robotic tactile sensor fabricated from polyvinylidene fluoride film
[AD-A215354] 09 p1231 N90-17145
Automatic thresholding multichannel digital radar early warning system
[AD-D014323] 12 p1642 N90-19431
Digital video: Studio signal processing
[BBC-RD-1989/14] 12 p1648 N90-19476
A digital HDTV recorder using a cluster of four D1 DVTRs
[BBC-RD-1989/13] 12 p1649 N90-19477
A waveform capture and storage unit and its use for investigating disturbances on digital transmission links
[BBC-RD-1989/17] 12 p1649 N90-19478
Performance of a 300 Mbps 1:16 serial/parallel optoelectronic receiver module
[NASA-TM-103110] 13 p1795 N90-20302
Short wavelength HgCdTe staring focal plane for low background astronomy applications 14 p1979 N90-21336
HgCdTe 256x256 NWIR FPA 14 p1981 N90-21348
Improved Si:As BIBIB (Back-Illuminated Blocked-Impurity-Band) hybrid arrays 14 p1981 N90-21349
Fault tolerant hypercube computer system architecture
[NASA-CASE-NPO-16859-1-CU] 14 p2012 N90-21527
Automatic speech recognition in air-ground data link 18 p2640 N90-25037
Millimeter-wave multiplexers
[AD-D014518] 19 p2685 N90-25274
Design of a universal protocol subsystem architecture: Specification of functions and services
[EUT-89-E-230] 20 p2912 N90-26589
Integration of GPS and strapdown inertial subsystems into a single unit 24 p3423 N90-29340
Evaluation of dynamic range for LLNL streak cameras using high contrast pulses and pulse podiatry on the Nova laser system
[DE90-015203] 24 p3472 N90-29620

MULTIPLICATION
Non-separate arithmetic codes
[RSRE-MEMO-4215] 04 p0530 N90-13058
Studies of optical matrix multiplication and reconfigurable optical interconnect concepts
[AD-A214645] 09 p1281 N90-17427

MULTIPLIER PHOTOTUBES
U PHOTOMULTIPLIER TUBES

MULTIPLIERS
Resonant-tunneling oscillators and multipliers for submillimeter receivers 05 p0597 N90-13467
Analysis of the behaviour of a current-fed multi-stage voltage multiplier with capacitive output 10 p1338 N90-17745
Analysis and design of a HV dc/dc series resonant converter using a multi-stage voltage multiplier 10 p1338 N90-17746
An 8.4-GHz dual-maser front-end system for Parkes reimplementation 15 p2078 N90-21905
CMOS analog four-quadrant multiplier
[AD-D014507] 19 p2685 N90-25271
Formal verification of the JANUS on-line multiplier
[IMAG-RR-785-I] 20 p2909 N90-26550
VLSI architecture for a Reed-Solomon decoder
[NASA-CASE-NPO-17897-1-CU] 21 p2998 N90-27040

MULTIPOLES
General contraction of Gaussian basis sets. Part 2: Atomic natural orbitals and the calculation of atomic and molecular properties
[NASA-CR-186201] 08 p1119 N90-16482
Multipole moments in general relativity and dynamical perturbations of black-hole magnetospheres 15 p2190 N90-22509
Laboratory study of ion-neutral collisions at suprathermal energies
[AD-A222117] 21 p3074 N90-27475
Stability regimes in a helical quadrupole focusing accelerator: Theory and simulation
[AD-A221755] 21 p3079 N90-27507
Superconformal algebra and central extension of meromorphic vector fields with multipoles on super-Riemann sphere
[DE90-627211] 23 p3390 N90-29153

MULTIPROCESSING (COMPUTERS)
A multiprocessor architecture using modular arithmetic for very high precision computation
[AD-A208154] 01 p0102 N90-10579
A common distributed language approach to software integration
[NASA-CR-185499] 01 p0103 N90-10584
Effective resource utilization for multiprocessor join execution
[DE89-016303] 01 p0105 N90-10595
Exploring the benefits of multiple hardware contexts in a multiprocessor architecture: Preliminary results
[AD-A210349] 01 p0108 N90-10616
Evaluating the performance of software cache coherence
[AD-A211164] 02 p0259 N90-11468
Asynchronous integration of ordinary differential equations on multiprocessors
[DE89-014169] 02 p0263 N90-11493
Computing the two dimensional fast Fourier transform on a general purpose mesh connected multiprocessor
[DE89-016515] 02 p0266 N90-11518
Fixed point iteration on point-symmetric interference graphs
[MEMO-INF-89-23] 02 p0269 N90-11535
Sequential searching in multidimensional monotone arrays
[AD-A211938] 03 p0384 N90-12188
Processing rate sensitivities of a heterogeneous multiprocessor
[PB89-229017] 03 p0387 N90-12201
Efficient diagnosis of multiprocessor systems under probabilistic models
[NASA-CR-185965] 03 p0388 N90-12212
Parallel architectures and parallel algorithms for integrated vision systems
[NASA-CR-185990] 03 p0389 N90-12215
Fast forward dynamics algorithm for robot arms using multiprocessing
[RR-367] 03 p0391 N90-12225

On modeling resources in multiprocessor systems
[MEMO-INF-88-33] 04 p0535 N90-13095
An implementation-oriented specification of the TUMULT communication primitives
[MEMO-INF-88-34] 04 p0536 N90-13096
Path expression based operating systems
[MEMO-INF-88-68] 04 p0536 N90-13097
Real-time robot motion: The VLSI implementation via transputers
[RR-364] 04 p0537 N90-13104
LAIOS: A multiprocessor network for artificial intelligence applications
[ETN-89-95498] 04 p0537 N90-13109
Parallelism in the discrete-event simulation algorithm
[AD-A213060] 05 p0682 N90-13970
A fault-tolerant software algorithm for a network of transputers
[AD-A213092] 05 p0682 N90-13972
The Aerospace Energy Systems Laboratory: A BITBUS networking application
[NASA-TM-4149] 06 p0831 N90-14829
NETRA: A parallel architecture for integrated vision systems. 1: Architecture and organization
[NASA-CR-185955] 06 p0832 N90-14839
Temporal, processor, and spatial locality in multiprocessor memory references
[AD-A213790] 07 p0969 N90-15598
ARGOS (A Research GMMP Operating System): Overvie w and interfaces
[AD-A213871] 07 p0970 N90-15599
The implementation of a coherent memory abstraction on a NUMA (Non-Uniform Memory Access) multiprocessor: Experiences with PLATINUM (Platform for Investigating Non-Uniform Memory)
[AD-A213909] 07 p0970 N90-15600
Memory management for large-scale NUMA (Non-Uniform Memory Access) multiprocessors
[AD-A213910] 07 p0970 N90-15601
An overview of PLATINUM: A Platform for Investiga ting Non-Uniform Memory (preliminary version)
[AD-A213911] 07 p0970 N90-15602
Evolution of an operating system for large-scale shared-memory multiprocessors
[AD-A213912] 07 p0970 N90-15603
XNUSIM: Graphical interface for a multiprocessor simulator
[AD-A214176] 07 p0971 N90-15606
A signal processing language for coarse grain data flow multiprocessors
[AD-A213863] 07 p0976 N90-15635
MASC: Multiprocessor architecture for symbolic processing
[AD-A213504] 07 p0979 N90-15656
Adaptive backoff synchronization techniques
[AD-A213966] 07 p0980 N90-15658
Systolic algorithms for imaging from space
[AD-A213870] 07 p0987 N90-15701
Periodic phase adjustment distributed clock synchronization in the hard realtime environment
[AD-A213842] 07 p0988 N90-15708
Large-scale optimization via distributed systems
[AD-A215136] 09 p1270 N90-17364
CHIMERA 2: A real-time UNIX-compatible multiprocessor operating system for sensor-based control applications
[AD-A215958] 10 p1392 N90-18051
A scheme for supporting distributed data structures on multicomputers
[NASA-CR-181987] 10 p1415 N90-18152
A system for execution of JSD requirements
[INPE-4915-TDL/381] 10 p1417 N90-18170
Optical shared memory
[AD-A215090] 10 p1430 N90-18249
Parallel memory addressing using coincident optical pulses
[AD-A216302] 11 p1501 N90-18641
A scalable multiprocessor architecture using Cartesian network: Relative addressing
[AD-A216580] 11 p1542 N90-18878
Cedar project: Original goals and progress to date
[DE90-006761] 11 p1543 N90-18880
Distributed decomposition of block-angular linear programs on a hypercube computer
[AD-A216433] 11 p1545 N90-18893
Summer institute in parallel computing
[DE90-005532] 11 p1548 N90-18910
Modeling A circuit switched multiprocessor interconnect
[AD-A217122] 12 p1656 N90-19519
Generic distributed systems model
[AD-A217078] 12 p1702 N90-19773
Laboratory implementation of the Continuously Reconfiguring Multi-Microprocessor Flight Control System (CRMMFCS)
[AD-A217730] 13 p1758 N90-20094
Express cubes: Improving the performance of k-ary n-cube interconnection networks
[AD-A217117] 13 p1793 N90-20287
Three-dimensional medical image analysis using local dynamic algorithm selection on a multiple-instruction, multiple-data architecture
[AD-A218024] 13 p1852 N90-20630
NYU (New York University) ultracomputer
[AD-A217167] 13 p1863 N90-20688
(DURIP) Two-Processor Alliant FX/4 System
[AD-A217810] 13 p1864 N90-20692
RIPE: An object-oriented Robot Independent Programming Environment
[DE90-008501] 13 p1866 N90-20707
Joint Japanese-American Workshop on Future Trends in Logic Programming
[DE90-006343] 13 p1867 N90-20709
Performance tradeoffs in multithreaded processors
[AD-A217123] 13 p1871 N90-20729
A Locality-based multiprocessor cache interference model
[AD-A217126] 13 p1871 N90-20730
Parallel computer graphics algorithms for the connection machine
[AD-A217300] 13 p1872 N90-20733
Fault tolerant hypercube computer system architecture
[NASA-CASE-NPO-16859-1-CU] 14 p2012 N90-21527
Parallel tridiagonalization of a general matrix using distributed-memory multiprocessors
[DE90-008902] 14 p2015 N90-21551
NETRA: A parallel architecture for integrated vision systems 2: Algorithms and performance evaluation
[NASA-CR-186510] 14 p2017 N90-21557
A parallel multigrid method for solving elliptic partial differential equations
[DE90-007929] 14 p2021 N90-21584
SISAL 1.2: An alternative to FORTRAN for shared memory multiprocessors
[DE90-005181] 15 p2146 N90-22257
A scheme for supporting automatic data migration on multicomputers
[NASA-CR-182036] 16 p2276 N90-22973
Systematic generation of multibody equations of motion suitable for recursive and parallel manipulation 16 p2280 N90-22992
Parallel processing of real-time dynamic systems simulation on OSCAR (Optimally SCheduled Advanced multiprocessoR) 16 p2282 N90-23006
Parallel and vector computation for stochastic optimal control applications 16 p2282 N90-23007
A robot arm simulation with a shared memory multiprocessor machine 16 p2283 N90-23008
TUMULT-64: A real-time multi-processor system
[MEMO-INF-89-58] 17 p2440 N90-23904
Distributed object oriented programming
[AD-A219689] 17 p2442 N90-23918
A parallel algorithm for global routing
[NASA-CR-186152] 17 p2448 N90-23959
A network flow model for load balancing in circuit-switched multicomputers
[NASA-CR-182049] 17 p2451 N90-23977
Parallel execution of LISP programs
[AD-A219823] 17 p2451 N90-23978
Failure analysis and modeling of a multicomputer system
[NASA-CR-186697] 17 p2451 N90-23980
Sensitivity analysis of transputer workfarm topologies
[AD-A219821] 18 p2595 N90-24766
Multiprocessor architecture: Synthesis and evaluation
[NASA-CR-186618] 19 p2741 N90-25579
Modeling and synthesis of multicomputer interconnection networks
[NASA-CR-186619] 19 p2746 N90-25604
Computer architecture evaluation for structural dynamics computations: Project summary
[NASA-CR-186137] 20 p2903 N90-26512
Adaptive fault-tolerant routing in hypercube multicomputers
[NASA-CR-186781] 20 p2903 N90-26513
Applications for the scalable coherent interface
[DE90-011795] 20 p2903 N90-26514
The use of Lanczo's method to solve the large generalized symmetric Eigenvalue problem in parallel
[NASA-CR-182072] 20 p2907 N90-26533
Graphics applications utilizing parallel processing
[NASA-CR-186719] 20 p2907 N90-26534
Language support for parallel computation
[AD-A223072] 20 p2911 N90-26560
PANDA: A distributed multiprocessor operating system 20 p2911 N90-26561
Two-dimensional signal processing and storage, and theory and applications of electromagnetic measurements
[AD-A222984] 21 p2995 N90-27022
Parallel numerical simulations of axisymmetric projectile flows using zonal-overlapped grids
[AD-A221711] 21 p3005 N90-27082
A tool for modeling concurrent real-time computation 21 p3047 N90-27321
CSRD parallel service machine enhancement
[AD-A221951] 21 p3058 N90-27388
Debugging and analysis of large-scale parallel programs
[AD-A221678] 21 p3059 N90-27393
Multiprocessor realization of neural networks
[AD-A222146] 21 p3060 N90-27400
Analysis and design of algorithm-based fault-tolerant systems
[NASA-CR-186884] 22 p3236 N90-28352
Efficient mapping algorithms for scheduling robot inverse dynamics computation on a multiprocessor system 23 p3375 N90-29071
The effect of multiprocessor radius on scaling
[DE90-014772] 23 p3380 N90-29095
Piecewise linear models of processor utilization
[DE90-014774] 23 p3384 N90-29115
A discrete decentralized variable structure robotic controller 24 p3509 N90-29835
Fast algorithms for parallel architectures
[AD-A223731] 24 p3528 N90-29947
Fact system: A standardizing modelization processing for concurrent systems
[ETN-90-97286] 24 p3533 N90-29982

MULTIPROGRAMMING
Spark camera annotation and control system for the BRL (Ballistic Research Laboratory) Transonic Range Facility
[AD-A212266] 04 p0459 N90-12633
Space station dynamics, attitude control and momentum management 16 p2287 N90-23029
Single-pass memory system evaluation for multiprogramming workloads
[NASA-CR-186553] 20 p2910 N90-26558

MULTIPROPELLANTS
U ROCKET PROPELLANTS

MULTIRADAR TRACKING
U RADAR NETWORKS

MULTISENSOR APPLICATIONS
Linkoeping's A.I. Consortium (LAIC) for plan guided systems. Review of the first 18 months
[FOA-C-30528-3.4] 02 p0289 N90-11537
Multisensor technologies for low cost methane detection
[PB89-235188] 05 p0645 N90-13766
Design and implementation of two concurrent multi-sensor integration algorithms for mobile robots
[DE90-003041] 07 p0981 N90-15663
Design and implementation of a multi-sensor fusion algorithm on a hypercube computer architecture
[DE90-003682] 08 p1112 N90-16438
The AGRISCATT-87 campaign: Processing of the Dutscat data
[BCRS-89-20] 15 p2122 N90-22140
Intelligent signal processing techniques for multi-sensor surveillance systems
[AD-A218890] 16 p2262 N90-22895
Multi-sensor analysis techniques for SSME safety monitoring
[NASA-CR-185260] 22 p3124 N90-27732
A method of classification for multisource data in remote sensing based on interval-valued probabilities
[NASA-CR-187007] 23 p3343 N90-28889
Workshop on Neural Networks
[DE90-014794] 23 p3385 N90-29120
An integrated system for land navigation 24 p3430 N90-29377

MULTISPECTRAL BAND SCANNERS
NT THEMATIC MAPPERS (LANDSAT)
Investigation on analyzing computer-aided forest disease classifications
[DFVLR-FB-89-16] 03 p0369 N90-12112
Image processing of LANDSAT MSS data for buried valley detection in northern Indiana 06 p0802 N90-14668
Multispectral classification of overlapping classes with applications to forest damage areas
[DLR-FB-89-55] 18 p2574 N90-24566
CAESAR: Performance and first evaluation of application possibilities
[BCRS-89-06] 19 p2705 N90-25393
High resolution infrared measurements 22 p3221 N90-28265
Description of the MARC measuring system
[FEL-89-B170] 23 p3342 N90-28887
On-line object feature extraction for multispectral scene representation
[NASA-CR-187006] 23 p3342 N90-28888
Methods for multisource data analysis in remote sensing
[NASA-CR-187005] 23 p3343 N90-28890

Space-base multispectral imagery: Current and future applications and implications to the United States Army
[AD-A224046] 23 p3343 N90-28894

MULTISPECTRAL PHOTOGRAPHY
NT INFRARED PHOTOGRAPHY
Physically-based parameterization of spatially variable soil and vegetation using satellite multispectral data
[NASA-CR-185957] 05 p0663 N90-13879
Introduction of aerial photography in agricultural research
[BCRS-89-14] 11 p1526 N90-18784
The potential of combined use of satellite data with topographic TM information for manual/visual and digital updating of land use
[NLR-MP-88021-U] 12 p1678 N90-19639

MULTISPECTRAL RADAR
A frequency agile 94 GHz pulse-Doppler radar with dual polarisation capability 14 p1960 N90-21226
Multiband imaging systems
[AD-A223969] 23 p3343 N90-28893

MULTISTAGE COMPRESSORS
U TURBOCOMPRESSORS

MULTISTAGE ROCKET VEHICLES
NT ARIANE LAUNCH VEHICLE
NT PEGASUS AIR-LAUNCHED BOOSTER
NT SKYLARK ROCKET VEHICLE
NT TITAN LAUNCH VEHICLES
Low Earth Orbit Raider (LER) winged air launch vehicle concept
[NASA-CR-186057] 04 p0452 N90-12590

MULTISTATIC RADAR
Millimeter wave radar clutter program
[AD-A215772] 10 p1376 N90-17978
Near-field bistatic RCS (Radar Cross-Section) measurements
[AD-A217011] 12 p1646 N90-19458
Tomographic processing of synthetic aperture radar signals for enhanced resolution
[AD-A217178] 13 p1789 N90-20265
Capabilities of bistatic synthetic aperture radar for covert battlefield surveillance 14 p1961 N90-21230
Millimeter-wave bistatic scattering by terrain 15 p2085 N90-21936
Backscatter enhancement in scattering from rough surfaces
[AD-A223110] 21 p2995 N90-27024
Target signature modeling and bistatic scattering measurement studies
[NASA-CR-186611] 23 p3319 N90-28766
Activities of the Division of Microwave Technology
[FOA-C-30555-3.2] 24 p3459 N90-29537
Bistatic radar cross section of a perfectly conducting rhombus-shaped flat plate
[AD-A223418] 24 p3460 N90-29546

MULTITEMPORAL ANALYSIS
U TEMPORAL RESOLUTION

MULTIVARIATE STATISTICAL ANALYSIS
NT BIVARIATE ANALYSIS
NT COVARIANCE
NT ORTHOGONALITY
NT REGRESSION ANALYSIS
On two polynomial spaces associated with a box spline
[AD-A210559] 01 p0113 N90-10646
Evaluation of tests and design factors 02 p0176 N90-10987
Principal components in multivariate control charts
[DE89-016828] 02 p0262 N90-11489
Iterative network magnitude estimation and uncertainty assessment with noisy and clipped data
[AD-A210707] 02 p0265 N90-11507
On a classification problem: Ranking and selection approach
[AD-A211627] 03 p0397 N90-12269
Stable summability and approximation theory
[AD-A211379] 04 p0539 N90-13118
Multivariable divided difference and B-splines
[MEMO-772] 04 p0544 N90-13160
On new methods for computing with multivariate B-splines
[MEMO-783] 04 p0547 N90-13183
On the recurrence relation for multivariate B-splines with respect to dimension
[MEMO-786] 05 p0689 N90-14017
Optimal stochastic modeling and control of flexible structures
[AD-A212347] 06 p0733 N90-14269
Outlier detection in multivariate calibration
[DE90-001502] 07 p0982 N90-15672
Quasi interpolants and approximation power of multivariate splines
[AD-A213535] 07 p0983 N90-15678
Applications of modern control theory synthesis to a super-augmented aircraft
[AD-A215431] 09 p1167 N90-16753
System identification and filtering of nonlinear controlled Markov processes by canonical variate analysis
[AD-A214873] 09 p1273 N90-17381
Discrete proportional Plus Integral (PI) multivariable control laws for the Control Reconfigurable Combat Aircraft (CRCA)
[AD-A215864] 11 p1464 N90-18431
Practical methods for robust multivariable control
[AD-A216937] 11 p1550 N90-18920
Inverse scattering and tomography
[AD-A216456] 11 p1551 N90-18932
Forecasting the tornadic intensities of thunderstorms by multivariate techniques
[AD-A218284] 13 p1847 N90-20602
Multivariate analysis of launcher guidance robustness
[REPT-892-422-105] 16 p2205 N90-22581
Equipment specifications for launcher guidance using multivariable frequency methods
[REPT-892-422-106] 16 p2205 N90-22582
New multivariable capabilities of the INCA program 16 p2290 N90-23049
Transactions of the Seventh Army Conference on Applied Mathematics and Computing
[AD-A219220] 16 p2309 N90-23160
The application of kriging in the statistical analysis of anthropometric data, volume 1
[AD-A220613] 17 p2438 N90-23891
The application of kriging in the statistical analysis of anthropometric data, volume 2
[AD-A220614] 17 p2438 N90-23892
The application of kriging in the statistical analysis of anthropometric data, volume 3
[AD-A220615] 17 p2438 N90-23893
Variance reduction for quantile estimates in simulations via nonlinear controls
[AD-A222653] 20 p2916 N90-26590
Adaptive time series analysis using predictive inference and entropy
[AD-A222337] 21 p2997 N90-27033
Data analysis techniques 21 p3017 N90-27151
An outline for the RTNEPH infrared atmospheric water vapor attenuation study
[AD-A221753] 21 p3027 N90-27209
Multivariate model building and model identification
[AD-A221619] 21 p3067 N90-27435
Sensitivity of the error in multivariate statistical interpolation to parameter values
[AD-A224076] 24 p3540 N90-30015
A new diagnostics approach for repeated measures designs
[AD-A223500] 24 p3540 N90-30020

MULTIVIBRATORS
NT FLIP-FLOPS

MUON SPIN ROTATION
A (mu)SR-investigation of the mixed state of the high-Tc superconductor HoBa2Cu3O7-delta
[DE90-820802] 16 p2322 N90-23241
Characterization of superconducting materials with muon spin rotation
[DE90-013755] 21 p3081 N90-27522
Magnetic properties of high-T(sub c) superconductors: Rigid levitation, flux pinning, thermal depinning, and fluctuation 22 p3137 N90-27798

MUONS
The determination of the muon content of EAS from Cygnus X-3 05 p0715 N90-14179
Cold fusion: Alchemist's dream
[DE90-000865] 06 p0847 N90-14925
A low-threshold EAS (Extensive-Air-Shower) array for gamma-ray astronomy at Los Alamos
[DE89-016780] 08 p1139 N90-16800
Status of the expansion of the CYGNUS array at Los Alamos
[DE89-016781] 08 p1139 N90-16801
Relative muon content of UHE showers associated with Hercules X-1
[DE90-000609] 08 p1151 N90-16665
Contained events in Soudan 2
[DE90-005648] 10 p1449 N90-18359
Studies of (mu)(prime)s underground with the Soudan 2 Tracker
[DE90-005658] 10 p1449 N90-18360
Underground muon observations in the Soudan 2 detector
[DE90-005647] 11 p1594 N90-19183
Search for anisotropies in the underground cosmic ray muon flux 12 p1745 N90-20034
Cosmic ray composition and muon decoherence at the knee of the all-particle cosmic ray spectrum 12 p1745 N90-20035
Cosmic ray events in Soudan 2
[DE90-005657] 12 p1746 N90-20037
Underground muons from the direction of Cygnus X-3
[DE90-005646] 12 p1746 N90-20038
Present status of (mu)CF theory
[DE90-007547] 13 p1884 N90-20809
Studies of high energy phenomena using muons
[DE90-008272] 13 p1886 N90-20820
The behaviour of the L3 muon chambers in a magnetic field
[ETN-90-96920] 18 p2613 N90-24884
Astronomy at ultra-high energies: Results from the CYGNUS experiment
[DE90-011979] 20 p2940 N90-26732

MURCHISON METEORITE
Optical constraints of kerogen from 0.15 to 40 microns: Comparison with meteoritic organics 20 p2948 N90-26776

MUSCLES
NT CONSTRICTORS
NT MYOCARDIUM
Cellular and molecular mechanisms of high pressure inotropy in cardiac muscle
[AD-A211695] 03 p0381 N90-12170
The development of a model of the human responses to load carriage 06 p0821 N90-14775
Temperature regulation during upper body exercise: Able bodied and spinal cord injured
[AD-A215130] 09 p1252 N90-17264
Techniques for studying the effects of microgravity on model particle/cell systems 12 p1640 N90-19424
Research in human performance related to space: A compilation of three projects/proposals 16 p2629 N90-24983
Electronystagmographic findings following cervical injuries 19 p2718 N90-25486
Effects of microgravity on rat muscle 20 p2891 N90-26453
Experiment K-6-02. Biomedical, biochemical and morphological alterations of muscle and dense, fibrous connective tissues during 14 days of spaceflight 20 p2892 N90-26456
Experiment K-6-04. Trace element balance in rats during spaceflight 20 p2892 N90-26458
Experiment K-6-07. Metabolic and morphologic properties of muscle fibers after spaceflight 20 p2893 N90-26461
Experiment K-6-08. Biochemical and histochemical observations of vastus medialis 20 p2893 N90-26462
Experiment K-6-09. Morphological and biochemical investigation of microgravity-induced nerve and muscle breakdown. Part 1: Investigation of nerve and muscle breakdown during spaceflight; Part 2: Biochemical analysis of EDL and PLT muscles 20 p2893 N90-26463
Experiment K-6-10. Effects of zero gravity on myofibril protein content and isomyosin distribution in rodent skeletal muscle 20 p2894 N90-26464
Experiment K-6-11. Actin mRNA and cytochrome c mRNA concentrations in the triceps brachia muscle of rats 20 p2894 N90-26465
Experiment K-6-21. Effect of microgravity on 1) metabolic enzymes of type 1 and type 2 muscle fibers and on 2) metabolic enzymes, neutransmitter amino acids, and neurotransmitter associated enzymes in motor and somatosensory cerebral cortex. Part 1: Metabolic enzymes of individual muscle fibers; part 2: metabolic enzymes of hippocampus and spinal cord 20 p2896 N90-26474
Computer aided mechanogenesis of skeletal muscle organs from single cells in vitro
[NASA-CR-187025] 23 p3354 N90-28959

MUSCULAR FATIGUE
The effect of caffeine on endurance time to exhaustion at high altitude
[AD-A212069] 03 p0380 N90-12163
Effects of high altitude hypoxia on lung and chest wall function during exercise
[AD-A219814] 17 p2434 N90-23869

MUSCULAR FUNCTION
Control of human arm movement via optimization 15 p2159 N90-22334
Dynamical modifications to the head, load factors from additional weight 19 p2720 N90-25472
Effects of microgravity on rat muscle 20 p2891 N90-26453
Experiment K-6-07. Metabolic and morphologic properties of muscle fibers after spaceflight 20 p2893 N90-26461
Evaluation of physiological and psychological impairment of human performance in cold stressed subjects
[AD-A223635] 24 p3498 N90-29769

MUSCULAR STRENGTH
Wrist orientation effect on grip strength and endurance
[PB89-200935] 03 p0383 N90-12179
Physical performance and carbohydrate consumption in CF commandos during a 5-day field trial
[AD-A217204] 13 p1850 N90-20619
Modeling strength data for CREW CHIEF 19 p2729 N90-25516

The relationship of isometric grip strength, optimal dynamometer settings, and certain anthropometric factors
[AD-A222046] 21 p3037 N90-27264

MUSCULOSKELETAL SYSTEM
NT BONE MARROW
NT BONES
NT CARTILAGE
NT COLLAGENS
NT CONNECTIVE TISSUE
NT CONSTRICTORS
NT FEMUR
NT JOINTS (ANATOMY)
NT MUSCLES
NT SPINE
NT TIBIA
NT ULNA
NT VERTEBRAE
NT WRIST

A program for the study of skeletal muscle catabolism following physical trauma
[AD-A216569] 11 p1539 N90-18859
Techniques for studying the effects of microgravity on model particle/cell systems 12 p1640 N90-19424
The effects of high intensity cycle exercise on sympatho-adrenal-medullary response patterns
[AD-A217962] 13 p1852 N90-20628
Conservation of body calcium by increased dietary intake of potassium: A potential measure to reduce the osteoporosis process during prolonged exposure to microgravity 18 p2631 N90-24993
Neck injury prevention possibilities in a high-G-enviroment experience with high sustained + G(sub z) training of pilots in the GAF IAM human centrifuge 19 p2720 N90-25474
Experiment K-6-07. Metabolic and morphologic properties of muscle fibers after spaceflight 20 p2893 N90-26461
Insulin and insulin-like growth factor-1 induce pronounced hypertrophy of skeletal myofibers in tissue culture
[NASA-CR-187026] 23 p3354 N90-28960

MUSEUMS
Technology development: Future use of NASA's large format camera is uncertain
[GAO/NSIAD-90-142] 20 p2865 N90-26298

MUTAGENS
Pilot investigation of indoor-outdoor and personal PM10 (thoracic) and associated ionic compounds and mutagenic activity
[PB89-222723] 05 p0673 N90-13920
Mutagenic responses of some petroleum-base obscurants in the Ames test
[AD-A214201] 07 p0915 N90-15295
Chamber investigations of the fate of diesel emissions in the atmosphere, volume 1, task 3
[PB90-114422] 10 p1405 N90-18103

MUTATIONS
Computer symbiosis: Emergence of symbiotic behavior through evolution
[DE89-015247] 02 p0256 N90-11450

MYLAR (TRADEMARK)
Aging and compatibility of TNF-doped Mylar
[DE90-008508] 14 p1954 N90-21186
Selective metallization of carbonyl-containing polymer films
[AD-D014526] 19 p2678 N90-25230

MYOCARDIUM
Cellular and molecular mechanisms of high pressure inotropy in cardiac muscle
[AD-A211695] 03 p0381 N90-12170
Coronary arterial capacitance and subendocardial vascular patency throughout the cardiac cycle 11 p1538 N90-18855

N

N-BODY PROBLEM
U MANY BODY PROBLEM

N-P JUNCTIONS
U P-N JUNCTIONS

N-P-N JUNCTIONS
A GaAs p-n-p-n thyristor model
[DE90-005757] 11 p1570 N90-19039

N-TYPE SEMICONDUCTORS
Dielectric spectroscopy of semiconductors
[AD-A211989] 04 p0559 N90-13255
Defect control and denuded trap zones in the 3-5 semiconductors
[AD-A214099] 07 p1004 N90-15814
Low temperature photoluminescence study of uranium implanted into III-V semiconductors and AlGaAs
[AD-A215710] 09 p1291 N90-17484
Dopant site location in dual-implanted GaP using (111) planar channeling
[DE90-006565] 11 p1571 N90-19042
In situ growth of epitaxial superconducting YBa2Cu3O(7-x) films on insulating semiconducting and ferroelectric K(Ta, Nb)O3 by pulsed laser ablation
[DE90-006568] 11 p1571 N90-19043
Passivation and gating of GaAs and Si surfaces using pseudomorphic structures
[AD-A219351] 16 p2325 N90-23256
Improving the performance of InAs(1-x)Sb(x)/InSb infrared detectors grown by metal organic chemical vapor deposition
[DE90-009743] 18 p2625 N90-24956
Fundamental studies and device development in beta silicon carbide
[AD-A219253] 19 p2676 N90-25220
Research on mercury cadmium telluride
[AD-A224250] 24 p3448 N90-29474
Surface photovoltage spectroscopy of real n-type GaAs(110) surfaces
[DE90-627325] 24 p3551 N90-30092

NACELLES
Analysis of results from wind tunnel tests of inlets for an advanced turboprop nacelle installation
[NASA-CR-174937] 01 p0003 N90-10011
Status report on a natural laminar-flow nacelle flight experiment 04 p0445 N90-12550
Nacelle design 04 p0446 N90-12551
Nacelle aerodynamic performance 04 p0446 N90-12552
Effects of acoustic sources 04 p0446 N90-12553
A note on an acoustic response during an engine nacelle flight experiment
[NASA-TM-102585] 12 p1710 N90-19821
Measurement and prediction of propeller blade surface pressure distributions 14 p1912 N90-20961
Aerodynamic design techniques at DLR Institute for Design Aerodynamics 14 p1916 N90-20979
Interactive calculation procedures for mixed compression inlets
[NASA-CR-186581] 20 p2801 N90-25934
Energy Efficient Engine program advanced turbofan nacelle definition study
[NASA-CR-174942] 23 p3280 N90-28560

NAKED SINGULARITIES
Twistons
[RSRE-MEMO-4234] 04 p0562 N90-13275

NAMING
NT NORMS

NAP-OF-THE-EARTH NAVIGATION
Computer vision techniques for rotorcraft low altitude flight 15 p2142 N90-22237
Field-of-view assessment of low-level flight and an airdrop in the C-130 Weapon System Trainer (WST)
[AD-A218504] 16 p2200 N90-22559
Survivable penetration 24 p3428 N90-29363

NAPHTHALENE
Production of jet fuels from coal-derived liquids. Volume 11: Production of advanced endothermic fuel blends from Great Plains Gasification Plant naphtha by-product stream
[AD-A210251] 02 p0207 N90-11184
Human body regional convective heat transfer determination using sublimating naphthalene disks
[AD-A212170] 03 p0380 N90-12165

NAPPES
U FOLDS (GEOLOGY)

NARROWBAND
A new approach to HF (High Frequency) channel modeling and simulation. Part 1: Deterministic model
[PB89-203962] 03 p0336 N90-11913
Narrow band and wide angle hemispherical interference optical filter
[AD-D014238] 06 p0843 N90-14904
Broadband versus narrowband driver/power amplifier: A spectral purity comparison
[DOT/FAA/CT-TN89/73] 10 p1379 N90-17995
Narrow-bandwidth unstable laser resonator
[AD-D014362] 12 p1665 N90-19568
Long pulse narrowband XeCl laser studies
[AD-A219774] 17 p2409 N90-23724
A narrowband tactical communication system for the VHF and UHF mobile radio bands 20 p2847 N90-26192
New synchronisation techniques applicable to multi-tone transmission systems 20 p2848 N90-26199
New approach to HF channel modeling and simulation. Part 2: Stochastic model
[PB90-200338] 23 p3317 N90-28755

NASA COMMUNICATION NETWORK
U NASCOM NETWORK

NASA PROGRAMS
NT ACEE PROGRAM
NT GALILEO PROJECT
NT MAGELLAN PROJECT (NASA)
NT NASA SPACE PROGRAMS
NT NATIONAL AEROSPACE PLANE PROGRAM
NT PIONEER PROJECT
NT PROJECT SETI
NT QUIET ENGINE PROGRAM
NT SCOUT PROJECT
NT SEASAT PROGRAM
NT SUPERSONIC CRUISE AIRCRAFT RESEARCH
NT VIKING MARS PROGRAM
NT VOYAGER PROJECT
Development of pressure containment and damage tolerance technology for composite fuselage structures in large transport aircraft
[NASA-CR-3996] 01 p0034 N90-10186
The NASA experience in aeronautical R and D: Three case studies with analysis
[AD-A211486] 04 p0437 N90-12496
Issues in NASA program and project management
[NASA-SP-6101(02)] 04 p0562 N90-13277
Departments of Veterans Affairs and Housing and Urban Development, and Independent Agencies Appropriations Bill, 1990
[H-REPT-101-150] 04 p0563 N90-13281
National Aeronautics and Space Administration 04 p0563 N90-13282
Fiscal year 1990 authorization request and budget estimates for the National Aeronautics and Space Administration
[GPO-96-945] 04 p0563 N90-13283
Departments of Veterans Affairs and Housing and Urban Development, and Independent Agencies Appropriation Bill, 1990
[S-REPT-101-128] 04 p0563 N90-13284
The 1990 National Aeronautics and Space Administration Authorization
[GPO-98-466] 04 p0563 N90-13285
Department of Veterans Affairs and Housing and Urban Development, and Independent Agencies Appropriations Act, 1990
[HR-2916-PP] 04 p0564 N90-13286
National Aeronautics and Space Administration 04 p0564 N90-13287
National Aeronautics and Space Administration Authorization Act, fiscal year 1990
[S-REPT-101-157] 04 p0564 N90-13288
National Aeronautics and Space Administration Authorization Act, fiscal year 1990
[S-REPT-101-157] 04 p0564 N90-13289
NASA technology applications
[GPO-99-412] 04 p0564 N90-13290
Research and Technology annual report, 1988
[NASA-TM-101070] 04 p0569 N90-13319
Small business innovation research: Program solicitation
[NASA-TM-101869] 05 p0705 N90-14126
National Aeronautics and Space Administration Multiyear Authorization Act of 1989 05 p0709 N90-14148
National Aeronautics and Space Administration authorization
[S-HRG-101-348] 05 p0709 N90-14149
Centers for the commercial development of space
[NASA-PAM-525] 05 p0709 N90-14151
NASA commercial programs
[NASA-TM-101853] 05 p0709 N90-14152
Review of the Aerospace Safety Advisory Panel report for NASA fiscal year 1990 authorization
[GPO-24-234] 06 p0722 N90-14213
An international discussion on research in solar and space physics 06 p0859 N90-14996
Bibliography of Lewis Research Center technical publications announced in 1988
[NASA-TM-102034] 07 p1009 N90-15846
NASA Patent Abstracts Bibliography: A continuing bibliography. Section 1: Abstracts (supplement 36)
[NASA-SP-7039(36)-SECT-1] 07 p1010 N90-15851
Space operations: Listing of NASA scientific missions, 1980-2000. Fact sheet for the Chairman, Subcommittee on Space Science and Applications, Committee on Science, Space, and Technology, House of Representatives
[AD-A213493] 07 p1016 N90-15881
A comparison of European and American microgravity combustion experimental techniques 09 p1202 N90-16966
NASA Patent Abstracts Bibliography: A continuing bibliography. Section 2: Indexes (supplement 36)
[NASA-SP-7039(36)-SECT-2] 10 p1441 N90-18317
An exploration of benefits from NASA Spinoff 10 p1443 N90-18325
Solar-Terrestrial Science Strategy Workshop
[NASA-CP-3048] 10 p1444 N90-18329
Supporting tools of solar-terrestrial science 10 p1444 N90-18331
Recommendations for the future 10 p1445 N90-18338

Space station technology summary
11 p1474 N90-18482
Research Reports: 1989 NASA/ASEE Summer Faculty Fellowship Program
[NASA-CR-183837] 12 p1634 N90-19390
Development of an Ada programming support environment database SEAD (Software Engineering and Ada Database) administration manual
[NASA-CR-186064] 12 p1699 N90-19757
MAX 1991. The active sun: A plan for pursuing the study of the active sun at the time of the next maximum in solar activity, January 1985
[NASA-CR-186125] 12 p1745 N90-20030
Microgravity Science and Application Program tasks, 1989 revision
[NASA-TM-4191] 13 p1786 N90-20252
A survey of experiments and experimental facilities for active control of flexible structures
14 p1936 N90-21079
Small business innovation research. Abstracts of 1988 phase 1 awards
[NASA-TM-102991] 14 p2036 N90-21680
Small business innovation research. Abstracts of completed 1987 phase 1 projects
[NASA-TM-101797] 14 p2036 N90-21681
Vision Science and Technology at NASA: Results of a Workshop
[NASA-TM-102214-REV-1] 15 p2138 N90-22216
Index to NASA news releases and speeches, 1986
[NASA-TM-101899] 15 p2175 N90-22430
Index to NASA news releases and speeches, 1987
[NASA-TM-101900] 15 p2175 N90-22431
Index to NASA news releases and speeches, 1988
[NASA-TM-101901] 15 p2175 N90-22432
Aeronautics and space report of the President: 1987 activities 15 p2181 N90-22462
Research and Technology Objectives and Plans Summary (RTOPS)
[NASA-TM-89662] 15 p2194 N90-22528
International cooperation for Mars exploration and sample return
[NASA-CR-186511] 17 p2358 N90-23419
Advancing automation and robotics technology for the Space Station Freedom and for the US economy
[NASA-TM-102668] 17 p2439 N90-23899
Space Station Freedom Pre-Workshop Session
[NASA-TM-102913] 17 p2479 N90-24172
Small business innovation research program solicitation: Closing date July 16, 1990
[NASA-TM-101798] 17 p2479 N90-24173
The 1991 NASA authorization: National Aeronautics and Space Administration fiscal year 1991 authorization request and budget estimates
[GPO-27-291] 17 p2481 N90-24188
Research and technology 1989
[NASA-TM-100369] 17 p2486 N90-24219
National Educators' Workshop: Update 1989 Standard Experiments in Engineering Materials Science and Technology
[NASA-CP-3074] 18 p2513 N90-24350
FAA/NASA En Route Noise Symposium
[NASA-CP-3067] 18 p2608 N90-24853
En route noise: NASA propfan test aircraft (corrected data - simplified procedure)
[DOT-TSC-FA953-LR4] 18 p2608 N90-24856
En route noise: NASA propfan test aircraft (calculated source noise
[DOT-TSC-FA953-LR5] 18 p2609 N90-24857
Space exploration: NASA's deep space missions are experiencing long delays
[GAO/NSIAD-88-128BR] 18 p2635 N90-25015
Departments of Veterans Affairs and Housing and Urban Development, and Independent Agencies Appropriations for Fiscal Year 1990, part 2
[S-HRG-101-345-PT-2] 18 p2636 N90-25017
National Aeronautics and Space Administration, 2 May 1989 18 p2636 N90-25018
National Aeronautics and Space Administration, 3 May 1989 18 p2636 N90-25019
NASA/American Society for Engineering Education (ASEE) Summer Faculty Fellowship Program 1989
[NASA-CR-181894] 18 p2639 N90-25034
NASA Patent Abstracts Bibliography: A continuing bibliography. Section 1: Abstracts (supplement 37)
[NASA-SP-7039(37)-SECT-1] 19 p2763 N90-25698
NASA's experience in the international exchange of scientific and technical information in the aerospace field
[NASA-TM-103093] 19 p2764 N90-25704
Winged cargo return vehicle. Volume 1: Conceptual design
[NASA-CR-186823] 20 p2821 N90-26050
Design of sensors for control of closed loop life support systems
[NASA-CR-186656] 20 p2899 N90-26490
NASA Patent Abstracts Bibliography: A continuing bibliography. Section 2: Indexes (supplement 37)
[NASA-SP-7039(37)-SECT-2] 20 p2935 N90-26700
Brief state-of-the-art review on optical communications for the NASA ISES workshop 21 p3017 N90-27153
Departments of Veterans Affairs and Housing and Urban Development, and independent agencies appropriations for 1991. Part 4: National Aeronautics and Space Administration
[GPO-30-861] 21 p3088 N90-27561
Reports of planetary geology and geophysics program, 1989
[NASA-TM-4210] 21 p3100 N90-27606
A solar power system for an early Mars expedition
[NASA-TM-103219] 22 p3243 N90-28393
Government Information Quarterly. Volume 7, no. 2: National Aeronautics and Space Administration Scientific and Technical Information Programs. Special issue
[ISSN-0740-624X] 22 p3257 N90-28440
Introduction to National Aeronautics and Space Administration's scientific and technical information programs 22 p3257 N90-28441
Management of information in a research and development agency 22 p3257 N90-28442
The new space and Earth science information systems at NASA's archive 22 p3257 N90-28443
Scientific and technical information management
22 p3257 N90-28444
NASA scientific and technical information for the 1990s 22 p3257 N90-28445
Technology utilization: Managing the transfer of NASA aerospace technology to other industries
22 p3257 N90-28446
Communications and media services
22 p3258 N90-28449
Appendix A: NASA information services
22 p3258 N90-28451
A survey of planning and scheduling research at the NASA Ames Research Center 23 p3376 N90-29076
Preliminary analysis of NASA commercialization initiatives
[PB90-202706] 23 p3407 N90-29257

NASA SPACE PROGRAMS
NT GALILEO PROJECT
NT MAGELLAN PROJECT (NASA)
NT PIONEER PROJECT
NT PROJECT SETI
NT SCOUT PROJECT
NT SEASAT PROGRAM
NT VIKING MARS PROGRAM
NT VOYAGER PROJECT
Comparison of the space program performance of countries with space programs
[ILR-MITT-222] 05 p0709 N90-14150
An implementation plan for priorities in solar-system space physics
[NASA-CR-185375] 05 p0710 N90-14154
The Explorer program for astronomy and astrophysics
05 p0712 N90-14159
Space station attached payload program support
[NASA-CR-183838] 08 p0733 N90-14274
United States space transportation survey
09 p1173 N90-16787
US commercial launcher summary
09 p1174 N90-16793
Advanced manned launch systems
09 p1175 N90-16797
The joint DOD/NASA Advanced Launch System (ALS) programme 09 p1179 N90-16832
US Activity with the OLYMPUS satellite
10 p1374 N90-17964
The Pathfinder chemical transfer propulsion program
11 p1471 N90-18471
Aerospace Safety Advisory Panel
[NASA-TM-101748] 12 p1634 N90-19389
The partnership: Space shuttle, space science, and space station
[NASA-TM-102900] 14 p1930 N90-21050
Keeping the dream alive: Managing the Space Station Program, 1982 to 1986
[NASA-CR-4272] 18 p2633 N90-25000
Proceedings of the Second Symposium on GPS Applications in space, volume 1
[AD-A219978] 20 p2806 N90-25962
NASA authorization, 1991, volume 2
[GPO-32-196] 24 p3559 N90-30138

NASA STRUCTURAL ANALYSIS PROGRAM
U NASTRAN

NASCOM NETWORK
OMV mission simulator 13 p1860 N90-20669

NASTRAN
Aeroelastic analysis of missile control surfaces with structural non-linearity 01 p0015 N90-10071
Control/structure interaction methods for space station power systems 01 p0018 N90-10087
Composite Blade Structural Analyzer (COBSTRAN) theoretical/programmer's manual
[NASA-TM-101958] 01 p0033 N90-10181
Investigation of difficult component effects on finite element model vibration prediction for the Bell AH-1G helicopter. Volume 1: Ground vibration test results
[NASA-CR-181916-VOL-1] 03 p0360 N90-12058
A mechanical power flow capability for the finite element code NASTRAN
[AD-A212202] 04 p0513 N90-12964
Application of an efficient hybrid scheme for aeroelastic analysis of advanced propellers
[NASA-TM-102428] 05 p0576 N90-13355
Investigation of difficult component effects on finite element model vibration prediction for the Bell AG-1G helicopter. Volume 2: Correlation results
[NASA-CR-181916-VOL-2] 05 p0654 N90-13814
An iterative solution to aeroelastic effects in potential flow
[AD-A216291] 10 p1310 N90-17580
Static aeroelastic analysis of a three-dimensional generic wing
[NASA-TM-102231] 13 p1757 N90-20087
COMGEN: A computer program for generating finite element models of composite materials at the micro level
[NASA-TM-102556] 13 p1818 N90-20438
Plan, formulate, and discuss a NASTRAN finite element model of the UH-60A helicopter airframe
[NASA-CR-181975] 13 p1818 N90-20439
Subsonic flutter analysis using MSC/NASTRAN
[PB90-166786] 14 p1928 N90-21041
Experimental evaluation of active-member control of precision structures 14 p1936 N90-21084
LACE flight dynamics experiment
14 p1937 N90-21086
Eighteenth NASTRAN (R) Users' Colloquium
[NASA-CP-3069] 18 p2568 N90-24837
A NASTRAN trainer for dynamics
18 p2569 N90-24638
PCI: A PATRAN-NASTRAN model translator
18 p2569 N90-24639
A generic interface between COSMIC/NASTRAN and PATRAN (R) 18 p2569 N90-24640
Eigenvalue computations with the QUAD4 consistent-mass matrix 18 p2569 N90-24642
NASTRAN migration to UNIX
18 p2569 N90-24643
Obtaining eigensolutions for multiple frequency ranges in a single NASTRAN execution
18 p2570 N90-24644
Random vibration analysis of space flight hardware using NASTRAN 18 p2570 N90-24645
Low velocity impact analysis with NASTRAN
18 p2570 N90-24647
Transitioning of power flow in beam models with bends 18 p2570 N90-24648
Coupled BE/FE/BE approach for scattering from fluid-filled structures 18 p2570 N90-24649
Fatigue analysis of mini-mast space truss
18 p2643 N90-25052
Ground shake test of the UH-60A helicopter airframe and comparison with NASTRAN finite element model predictions
[NASA-CR-181993] 19 p2661 N90-25143
A comparison of the post-buckling behavior of metallic and composite plates with centrally located cutouts
[NIAR-90-14] 20 p2875 N90-26356
Design of ceramic components with the NASA/CARES computer program
[NASA-TM-102369] 20 p2875 N90-26359
Ceramics Analysis and Reliability Evaluation of Structures (CARES). Users and programmers manual
[NASA-TP-2916] 22 p3190 N90-28099
Liquid Rocket Booster (LRB) for the Space Transportation System (STS) systems study. Appendix E: Pressure-fed booster test bed for the liquid rocket booster study
[NASA-CR-183791-APP-E] 23 p3289 N90-28605
Plan, execute, and discuss vibration measurements and correlations to evaluate a NASTRAN finite element model of the AH-64 helicopter airframe
[NASA-CR-181973] 23 p3338 N90-28866

NATIONAL AEROSPACE PLANE PROGRAM
National Aeronautics and Space Administration
04 p0564 N90-13207
Design and demonstration of heat pipe cooling for NASP and evaluation of heating methods at high heating rates
[DE89-016995] 06 p0724 N90-14227
Slush Hydrogen (SLH2) technology development for application to the National Aerospace Plane (NASP)
[NASA-TM-102315] 06 p0732 N90-14268
National aero-spaceplane status and plans
09 p1175 N90-16801

Comparison between horizontally launched air-breathing single and two-stage to orbit space vehicles
09 p1175 N90-16802

Effects of nose bluntness and shock-shock interactions on blunt bodies in viscous hypersonic flows
[NASA-CR-186451] 14 p1910 N90-20950

Proceedings of Workshop on Atmospheric Density and Aerodynamic Drag Models for Air Force Operations, volume 1
[AD-A220381] 17 p2345 N90-23355

Background, current status, and prognosis of the ongoing slush hydrogen technology development program for the NASP
[NASA-TM-103220] 20 p2822 N90-26055

Carbon-carbon composites: Emerging materials for hypersonic flight
[NASA-TM-103472] 20 p2827 N90-26080

Prediction of the ullage gas thermal stratification in a NASP vehicle propellant tank experimental simulation using FLOW-3D
[NASA-TM-103217] 20 p2841 N90-26160

National aero-space plane: Flight mechanics
22 p3129 N90-27759

NASA Langley Research Center National Aero-Space Plane Mission simulation profile sets
[NASA-TM-102670] 23 p3276 N90-28541

NATIONAL AIRSPACE SYSTEM

Ground and Obstacle Avoidance (GOA) concept of operations
[DOT/FAA/DS-89/08] 02 p0150 N90-10855

UK airmisses involving commercial air transport, May-August 1988
[ISSN-0951-6301] 03 p0303 N90-11717

Rotorcraft low altitude CNS benefit/cost analysis: Rotorcraft operations data
[DOT/FAA/DS-89/9] 03 p0419 N90-12406

National Airspace System airspace management operational concept
[DOT/FAA/DS-89/29] 05 p0577 N90-13361

National Airspace System flight planning operational concept
[DOT/FAA/DS-89/30] 05 p0577 N90-13362

National airspace system monitoring operational concept
[NAS-SR-1330] 06 p0722 N90-14214

National airspace system: Airport movement area control operational concept
[WP-89W00161] 07 p0878 N90-15086

Control outside of independent surveillance coverage operational concept
[AD-A214163] 07 p0878 N90-15090

National airspace system plan: Facilities, equipment, associated development and other capital needs
[AD-A215882] 11 p1453 N90-18373

Weather data dissemination to aircraft
14 p1907 N90-20934

National airspace system air-ground communications operational concept
[DOT/FAA/DS-90/2] 14 p1964 N90-21249

Meteorologist Weather Processor (MWP) integration test plan
[DOT/FAA/CT-TN89/62] 14 p2007 N90-21500

National Airspace System (NAS) software life cycle management study
[AD-A221180] 19 p2657 N90-25122

Replication of NASPAC Dallas/Fort Worth study
[DOT/FAA/CT-TN90/26] 19 p2657 N90-25123

A measurement of the effectiveness of the Airway Science Program to meet Federal Aviation Administration work force needs
[NIAR-90-5] 20 p2934 N90-26694

The MODE S operational test and evaluation/integration test plan
[DOT/FAA/CT-TN89/51] 22 p3111 N90-27671

Flight service automation system, model 1 full capacity, NAS operational test and evaluation integration test plan
[DOT/FAA/CT-TN90/4] 22 p3111 N90-27672

A glossary of terms, definitions, acronyms, and abbreviations related to the National Airspace System
[DOT/FAA/CT-TN89/53] 23 p3406 N90-29249

NATIONAL AIRSPACE UTILIZATION SYSTEM

Operational trial of effect of raising minimum stack level in Heathrow stacks
[CAA-PAPER-89003] 04 p0449 N90-12573

NATIONAL PARKS

Physiognomy of vegetation cover in the PNPM identified through the TM/LANDSAT sensor: A multitemporal analysis
[INPE-4834-PRE/1464] 11 p1525 N90-18776

Transport of atmospheric aerosols above the Sierra Nevada slopes
[PB90-120288] 12 p1685 N90-19675

NATIONAL SEVERE STORMS PROJECT

Severe local storm warning verification: 1966
[PB89-226310] 03 p0374 N90-12134

NATIONS

NT ALASKA
NT ARIZONA
NT AUSTRALIA
NT BRAZIL
NT CALIFORNIA
NT CANADA
NT CHINA
NT COLORADO
NT EGYPT
NT ENGLAND
NT FINLAND
NT FLORIDA
NT FRANCE
NT HAWAII
NT ICELAND
NT ILLINOIS
NT INDONESIA
NT JAPAN
NT KENYA
NT LOUISIANA
NT MALAGASY REPUBLIC
NT MARYLAND
NT MEXICO
NT MOZAMBIQUE
NT NETHERLANDS
NT NEW HAMPSHIRE
NT NEW ZEALAND
NT NORTH CAROLINA
NT NORWAY
NT OHIO
NT OKLAHOMA
NT PORTUGAL
NT SUDAN
NT SWEDEN
NT SWITZERLAND
NT TAIWAN
NT TEXAS
NT THAILAND
NT U.S.S.R.
NT UNITED KINGDOM
NT UNITED STATES
NT UTAH
NT WEST GERMANY
NT WISCONSIN
NT ZAMBIA

The essence of spacepower: Important influences on the evolution of national spacepower
[AD-A217498] 13 p1879 N90-20781

Industrial patent activity in the US. Part 1: Time series profile by company and country of origin, 1969-1989
[PB90-214404] 22 p3259 N90-28454

NATURAL FREQUENCIES

U RESONANT FREQUENCIES

NATURAL GAS

Natural gas to liquids
[DE89-000962] 03 p0322 N90-11828

Experimental and computational study of combustion limits in natural-gas fueled internal combustion engines
[PB89-235196] 05 p0629 N90-13673

The thermally induced gas-phase reactions of methane and oxygen: A comparison of experimental and computational results
[DE90-000785] 06 p0742 N90-14317

Phase 1 supplemental development of a kinematic Stirling/Rankine commercial gas-fired heat pump system
[PB90-129974] 13 p1825 N90-20483

A comparison of the contribution of various gases to the greenhouse effect
20 p2885 N90-26414

Global climate change: A proposed gas industry program on global climate issues
[PB90-219296] 22 p3199 N90-28156

Development of advanced combustion technology for medium and high speed natural gas engines
[PB90-198565] 23 p3331 N90-28836

NATURAL LANGUAGE (COMPUTERS)

Elicitation of natural language representations of uncertainty using computer technology
[DE90-001416] 07 p0972 N90-15611

Complexity of human language comprehension
[AD-A214591] 09 p1258 N90-17299

Access to multiple underlying systems in Janus
[AD-A214585] 09 p1264 N90-17329

Research and development in natural language understanding as part of the Strategic Computing Program
[AD-A214586] 09 p1264 N90-17330

Research and development in natural language understanding as part of the Strategic Computing Program
[AD-A214587] 09 p1264 N90-17331

Parrot: The Janus paraphraser
[AD-A214588] 09 p1265 N90-17332

Research and development in natural language understanding as part of the strategic computing program
[AD-A214611] 09 p1265 N90-17333

IRUS-II user manual
[AD-A214612] 09 p1265 N90-17334

Knowledge-based extensible natural language interface technology program
[AD-A216664] 11 p1545 N90-18897

High-level connectionist models
[AD-A216581] 12 p1698 N90-19751

Human task animation from performance models and natural language input
13 p1861 N90-20678

Artificial Intelligence (AI) Center of Excellence at the University of Pennsylvania
[AD-A217393] 13 p1874 N90-20743

Connectionism and compositional semantics
[AD-A219029] 16 p2264 N90-22904

Natural language processing: A tutorial
[AD-A219096] 16 p2300 N90-23108

Syntax, semantics, and pragmatism: An integrated focus based on textual linguistic knowledge
[INPE-4992-PRE/1554] 16 p2326 N90-23262

Formal methods in knowledge representation
[TR-89-11] 17 p2450 N90-23972

Knowledge graphs and natural language
[MEMO-811] 18 p2592 N90-24746

Explanation of Bayesian conditioning for decision support systems
18 p2633 N90-25002

QATT: A natural language interface for QPE
[UIUCDCS-R-89-1535] 19 p2743 N90-25590

DEB: A Diagnostic Experience Browser using similarity networks
21 p3048 N90-27329

Encoding techniques for complex information structures in connectionist systems
[NASA-CR-186942] 22 p3238 N90-28362

The SPECIALIST: Natural language processing system
[PB90-240029] 23 p3381 N90-29098

Instruction dialogues: Teaching new skills to a robot
24 p3517 N90-29884

Interset: A natural language interface for teleoperated robotic assembly of the EASE space structure
24 p3517 N90-29885

Textual regularities applicable to full text searching: The case of family history literature
24 p3557 N90-30125

NATURAL LASERS

U LASERS

NATURAL SATELLITES

NT CHARON
NT DEIMOS
NT IAPETUS
NT IO
NT JUPITER SATELLITES
NT MOON
NT PHOBOS
NT PHOEBE
NT RHEA (ASTRONOMY)
NT SATURN SATELLITES
NT TITAN
NT TITANIA
NT TRITON

The Voyager Neptune travel guide
[NASA-CR-186108] 05 p0585 N90-13412

Minor planets and other solar system objects
05 p0608 N90-13545

The treatment of minor planets and planetary satellites
05 p0611 N90-13563

NAVIER-STOKES EQUATION

Stability and transition of three-dimensional boundary layers
01 p0062 N90-10357

Direct numerical study of leading-edge contamination
01 p0063 N90-10361

Numerical investigation of the effects of longitudinal vortices on the onset of transition in a flat plate boundary layer
01 p0063 N90-10363

Primary and secondary stability analysis applied to the DFVLR-transition swept-plate experiment
01 p0065 N90-10371

Numerical solution of three-dimensional unsteady flows: Application to instability problems
01 p0065 N90-10375

Numerical simulation of turbulent plane channel flows
01 p0067 N90-10382

A composite velocity procedure for the three-dimensional reduced Navier-Stokes equations
01 p0069 N90-10396

Two counter-rotating vortices approaching a free surface in a viscous fluid
[AD-A210495] 01 p0070 N90-10404

A high-order Lagrangian-decoupling method for the incompressible Navier-Stokes equations
[NASA-CR-181903] 01 p0111 N90-10631

A parallel numerical simulation for supersonic flows using zonal overlapped grids and local time steps for common and distributed memory multiprocessors
[DE89-015252] 02 p0147 N90-10839
An experimental study of helicity and related properties in turbulent flows
[DE89-016785] 02 p0220 N90-11259
Hopf bifurcation in the driven cavity
[NASA-TM-102334] 03 p0345 N90-11969
Viscous split algorithms for the time dependent incompressible Navier-Stokes equations
[AD-A211592] 03 p0348 N90-11985
Efficient finite element solution of Navier-Stokes equations and related topics
[AD-A211647] 03 p0348 N90-11986
Numerical computation of the viscous flow field around a prolate spheroid
[DFVLR-FB-89-22] 03 p0349 N90-11992
A multigrid algorithm for the incompressible Navier-Stokes equation
[GMD-374] 03 p0349 N90-11993
A least-squares finite element method for incompressible Navier-Stokes problems
[NASA-TM-102385] 03 p0392 N90-12231
Non-stationary computer model of the asymptotic region of an electric arc gas heater
[IPPCZ-288] 03 p0407 N90-12330
Numerical algorithms for steady and unsteady incompressible Navier-Stokes equations
[NASA-CR-186039] 04 p0437 N90-12499
Hypersonic boundary layers. Viscous effects within the shock layer
[CERT-RSF-OA-25/5005-AYD] 04 p0438 N90-12502
Interaction of Tollmien-Schlichting waves and Goertler vortices 04 p0440 N90-12515
Effect of roughness on the stability of boundary layers 04 p0440 N90-12518
Application of sound and temperature to control boundary-layer transition 04 p0443 N90-12537
Numerical study of three-dimensional spatial instability of a supersonic flat plate boundary layer
[NASA-CR-181931] 04 p0499 N90-12874
Solution of the thin-layer Navier-Stokes equations for laminar transonic flow
[PB89-221600] 04 p0500 N90-12879
A multigrid method for the Navier-Stokes and Boussinesq equations
[REPT-89-17] 04 p0501 N90-12886
An implicit Navier-Stokes solver optimised for a vector-parallel computer
[VKI-TN-169] 04 p0501 N90-12890
Upwind discretization of the steady Navier-Stokes equations
[CWI-NM-R8810] 04 p0502 N90-12891
Unsteady three-dimensional thin-layer Navier Stokes solutions on dynamic blocked grids
[AD-A212377] 04 p0503 N90-12899
Multigrid calculations of 3-D turbulent viscous flows
[NASA-CR-185154] 05 p0571 N90-13323
Computation of viscous incompressible flows
[NASA-TM-101090] 05 p0572 N90-13329
An Introduction to Hypersonic Aerodynamics
[VKI-LS-1989-01] 05 p0573 N90-13334
Gas flows in rocket motors, volume 1
[AD-A213348] 05 p0615 N90-13591
Gas flows in rocket motors. Volume 2, appendix C: Time iterative solution of viscous supersonic flow
[AD-A213349] 05 p0615 N90-13592
Gas flows in rocket motors. Volume 3, appendix D: Computer code listings
[AD-A213350] 05 p0616 N90-13593
A review of quasi-coherent structures in a numerically simulated turbulent boundary layer
[NASA-TM-102191] 05 p0638 N90-13723
Multigrid and defect correction for the steady Navier-Stokes equations: Applications to aerodynamics
[ETN-90-96011] 05 p0639 N90-13727
Numerical simulation of transition in three-dimensional boundary layers
[DLR-FB-89-12] 05 p0639 N90-13728
Numerical Methods for Flows in Turbomachinery, volume 1
[VKI-LS-1989-06-VOL-1] 05 p0640 N90-13735
Three D flows in turbine blade rows 05 p0641 N90-13739
Turbulence modeling and implementation in Navier-Stokes solvers 05 p0641 N90-13742
Numerical methods for unsteady turbomachinery flow 05 p0641 N90-13743
Navier-Stokes simulation of the crossflow instability in swept-wing flows
[NASA-CR-186122] 05 p0641 N90-13744
Numerical solutions of the complete Navier-Stokes equations
[NASA-CR-186102] 05 p0642 N90-13747
Analysis of rotary engine combustion processes based on unsteady, three-dimensional computations
[NASA-TM-102469] 05 p0642 N90-13749
Application of multi-grid methods for solving the Navier-Stokes equations
[NASA-TM-102359] 05 p0687 N90-14002
An investigation of the bursting of trailing vortices using numerical simulation 06 p0718 N90-14191
Navier-Stokes solutions of 2-D transonic flow over unconventional airfoils 06 p0719 N90-14195
Navier-Stokes analysis of airfoils with leading edge ice accretions 06 p0719 N90-14196
Efficient real gas Navier-Stokes computations of high speed flows using an LU scheme
[NASA-TM-102429] 06 p0720 N90-14203
Surface flow and heating distributions on a cylinder in near wake of Aeroassist Flight Experiment (AFE) configuration at incidence in Mach 10 Air
[NASA-TP-2954] 06 p0772 N90-14493
Numerical solution of the incompressible Navier-Stokes equations 06 p0774 N90-14501
Applications of a new exact solution of the Navier-Stokes equations to flow in pipes of varying width 06 p0774 N90-14504
The analysis and modeling of dilatational terms in compressible turbulence
[NASA-CR-181959] 06 p0776 N90-14513
Numerical simulation of the unsteady two-dimensional flow in a time-dependent doubly-connected domain 07 p0875 N90-15073
An algebraic turbulence model for flow separation caused by forward and backward facing steps
[AD-A213800] 07 p0931 N90-15389
Nonlinear viscous waves produced by an impulsively moving plate
[AD-A214014] 07 p0932 N90-15392
Numerical methods for parabolic equations and inequalities in very high dimensions
[AD-A214102] 07 p0985 N90-15690
Euler and Navier-Stokes computations for two-dimensional geometries using unstructured meshes
[NASA-CR-181977] 08 p1019 N90-15893
Numerical analysis of nonstationary fluid flow (a survey)
[PREPRINT-492] 08 p1065 N90-16159
Extrapolation techniques for finite element approximations of Stokes and Navier-Stokes flow over a backward facing step
[PREPRINT-499] 08 p1065 N90-16160
Decay estimates for the compressible Navier-Stokes equations in the half-space
[PREPRINT-46] 08 p1065 N90-16163
Visualization of 2 and 3 dimensional flows
[REPT-1] 08 p1065 N90-16164
Calculation of turbulent choppy flow mixing
[ETN-90-95929] 08 p1065 N90-16165
An improvement of convection fidelity in Euler calculations 09 p1159 N90-16709
Upper semicontinuous global attractors for viscous flow
[NASA-CR-181976] 09 p1217 N90-17056
Appendage flow computations using the INS3D computer code
[AD-A215689] 09 p1218 N90-17066
A solution method for the time-dependent Navier-Stokes equations for laminar, incompressible flow
[FFA-146] 09 p1219 N90-17075
Chaos and turbulence
[AD-A215310] 09 p1294 N90-17499
Computation of compressible viscous flows 10 p1308 N90-17567
Turbulence models for compressive flows 10 p1308 N90-17568
Shock-shock boundary layer interactions 10 p1308 N90-17569
Axial flow in corners at supersonic and hypersonic speeds 10 p1308 N90-17570
Numerical simulation of supersonic free shear layers
[AD-A216289] 10 p1310 N90-17579
Viscous three-dimensional analyses for nozzles for hypersonic propulsion
[NASA-CR-185197] 10 p1321 N90-17635
Some Navier-Stokes calculations for the CAST-10 airfoil 10 p1324 N90-17651
Comparison of two- and three-dimensional Navier-Stokes solutions with NASA experimental data for CAST-10 airfoil 10 p1325 N90-17658
Numerical studies on laminar-turbulent transition in boundary layers 10 p1383 N90-18001
Application of Jameson's type nonlinear artificial dissipation to the two-dimensional Navier-Stokes computation
[NAL-TR-1015T] 10 p1384 N90-18006
Conditions at the downstream boundary for simulations of viscous incompressible flow
[NASA-TM-102510] 10 p1422 N90-18198
Numerical simulation of three-dimensional unsteady flows in turbomachines 11 p1461 N90-18417
Measurement of velocity profiles and Reynolds stresses on an oscillating airfoil 11 p1463 N90-18427
Numerical simulations of coherent structures in a jet flame with a noncircular cross section
[AD-A216710] 11 p1483 N90-18535
Improved computational fluid dynamics for continuum hypersonic flow
[AD-A216981] 11 p1506 N90-18674
Spectral multi-domain approximation of the Navier-Stokes equations in curved complex geometries
[ONERA-NT-1987-2] 11 p1508 N90-18685
Numerical simulation of the vortex breakdown
[ONERA-RSF-4/4368-AY-004A] 11 p1509 N90-18689
Numerical solution of 3D Navier-Stokes equations with upwind implicit schemes
[NASA-TM-101656] 12 p1600 N90-19205
LAGEOS 3 and the gravitomagnetic field 12 p1733 N90-19961
Application of a three-dimensional Navier-Stokes model for a subsonic jet in a crossflow 13 p1749 N90-20045
Comparison of 3-D viscous flow computations of Mach 5 inlet with experimental data
[NASA-TM-102518] 13 p1757 N90-20090
Numerical simulation methods of incompressible flows and an application to the space shuttle main engine
[NASA-TM-100038] 13 p1800 N90-20333
Mass transfer from a sphere in an oscillating flow with zero mean velocity
[NASA-TM-102566] 13 p1801 N90-20338
A matrix-free locally-implicit scheme for Navier-Stokes equations
[AD-A218298] 13 p1803 N90-20349
On total variation diminishing schemes for transonic turbulent flow computation 14 p1909 N90-20945
Comparison of C- and O-grid generation methods using a NACA 0012 airfoil
[AD-A216375] 14 p1910 N90-20948
An evaluation of the two-dimensional Euler and Navier-Stokes calculations based on a flux-vector splitting
[PB90-166778] 14 p1912 N90-20963
An efficient airfoil design method using the Navier-Stokes equations 14 p1917 N90-20981
Optimization of aerodynamic designs using computational fluid dynamics 14 p1920 N90-20999
Parabolized calculations of turbulent three dimensional flows in a turbine duct 14 p1923 N90-21013
Centrifugal impeller geometry and its influence on secondary flows 14 p1924 N90-21020
Calculation of the secondary flow in an axial turbine 14 p1924 N90-21022
Generation and decay of secondary flows and their impact on aerodynamic performance of modern turbomachinery components 14 p1925 N90-21023
Analysis of the rotor tip leakage flow with tip cooling air ejection 14 p1926 N90-21029
Effects of secondary flow on heat transfer in rotating passages 14 p1926 N90-21031
Theoretical study of the flow in a rotating channel. Experimental study through flow visualization in a curved channel 14 p1926 N90-21032
Numerical simulation of vortex breakdown 14 p1970 N90-21288
Analysis and finite element approximation of some optimal control problems associated with the Navier-Stokes equations 14 p1972 N90-21299
Navier-Stokes analysis of turbine blade heat transfer
[NASA-TM-102496] 14 p1972 N90-21300
PROTEUS two-dimensional Navier-Stokes computer code, version 1.0. Volume 1: Analysis description
[NASA-TM-102551] 14 p1973 N90-21303
PROTEUS two-dimensional Navier-Stokes computer code, version 1.0. Volume 2: User's guide
[NASA-TM-102552] 14 p1973 N90-21306
PROTEUS two-dimensional Navier-Stokes computer code, version 1.0. Volume 3: Programmer's reference
[NASA-TM-102553] 14 p1974 N90-21307
High accuracy solutions of incompressible Navier-Stokes equations
[NASA-TM-102539] 14 p2018 N90-21567
Numerical simulation of hypersonic flow around a space plane. Part 2: Application to high angles of attack flow
[NAL-TR-1011T] 15 p2045 N90-21726
Modeling of vortex-induced oscillations based on indicial response approach
[NASA-CR-186560] 15 p2047 N90-21736
Three-dimensional simulation of vortex breakdown
[NASA-TM-102664] 15 p2049 N90-21744
A multiblock/multizone code (PAB 3D-v2) for the three-dimensional Navier-Stokes equations: Preliminary applications
[NASA-CR-182032] 15 p2049 N90-21745

Analytical study of the origin and behavior of asymmetric vortices
[NASA-TM-102796] 15 p2049 N90-21746
An upwind-differencing scheme for the incompressible Navier-Stokes equations
[NASA-TM-101051] 15 p2051 N90-21757
A dual potential formulation of the Navier-Stokes equations 15 p2092 N90-21972
Convergence acceleration of upwind relaxation methods for the Navier-Stokes equations 15 p2092 N90-21973
Mesh generation for flow computation in turbomachine 15 p2094 N90-21981
Grid patching approaches for complex three-dimensional configurations 15 p2094 N90-21985
Generation and adaptation of 3-D unstructured grids for transient problems 15 p2096 N90-21994
Computational modeling and validation for hypersonic inlets
[NASA-TM-103111] 15 p2099 N90-22011
Bifurcations in viscous flow fields. On the genesis and development of topologically complicated separated flow structures
[PB90-167156] 15 p2099 N90-22012
An unsteady time asymptotic flow in the square driven cavity
[NASA-TM-103141] 15 p2099 N90-22016
Numerical study of laminar and turbulent flows past two-dimensional and axisymmetric bodies 15 p2100 N90-22020
The minimum drag profile in laminar flow: A numerical way 16 p2196 N90-22535
The analysis and simulation of compressible turbulence
[NASA-CR-181997] 16 p2197 N90-22539
Secondary frequencies in the wake of a circular cylinder with vortex shedding
[NASA-CR-181998] 16 p2197 N90-22540
Multigrid acceleration of transonic flow computations
[ENSM-8024] 16 p2237 N90-22760
A study of supermanuever aerodynamics
[AD-A218378] 17 p2344 N90-23349
Parallel computation of supersonic flows using a three-dimensional, zonal, Navier-Stokes code
[AD-A218824] 17 p2344 N90-23350
The 3-D composite velocity solutions for subsonic/transonic flow over forebodies and afterbodies
[AD-A220370] 17 p2345 N90-23354
Multiprocessing on supercomputers for computational aerodynamics
[NASA-TM-102806] 17 p2347 N90-23366
Computational analysis of the flowfield of a two-dimensional ejector nozzle
[NASA-CR-185255] 17 p2355 N90-23406
Numerical simulation of turbulent combustion using vortex methods
[AD-A219624] 17 p2372 N90-23507
Computations of a horseshoe vortex around an endwall-mounted cylinder 17 p2400 N90-23673
Algebraic turbulence modeling for unstructured and adaptive meshes
[NASA-CR-182035] 17 p2401 N90-23676
Computational fluid dynamics
[AD-A219557] 17 p2403 N90-23686
Composite reduced Navier Stokes procedures for flow problems with strong pressure interactions
[AD-A219621] 17 p2403 N90-23687
Thin-layer Navier-Stokes solutions of the asymmetric vortical flow on a tangent ogive body
[AD-A220810] 17 p2403 N90-23690
Solution of the steady state incompressible Navier-Stokes equations at high Reynolds numbers
[VKI-TN-170] 17 p2404 N90-23692
Large eddy simulation of a fully turbulent plane channel flow
[VKI-TN-171] 17 p2404 N90-23693
Second moment models of turbulence: Complex or stratified flow
[ECL-90-02] 17 p2405 N90-23703
The effects of Reynolds number, rotor incidence angle, and surface roughness on the heat transfer distribution in a large-scale turbine rotor passage
[NASA-CR-183891] 17 p2410 N90-23731
The interaction of a supersonic streamwise vortex and a normal shock wave 18 p2491 N90-24241
Reduced order models for nonlinear aerodynamics 18 p2492 N90-24244
Low-density flow effects for hypervelocity vehicles, phase 2
[AD-A221034] 18 p2493 N90-24249
Experimental and analytical study of close-coupled ventral nozzles for ASTOVL aircraft
[NASA-TM-103170] 18 p2498 N90-24273
Computational modeling of three-dimensional compressible leading edge vortices
[AD-A221022] 18 p2553 N90-24569
NSFLEX: An implicit relaxation method for the Navier-Stokes equations for a wide range of Mach numbers
[MBB-FE-122/S/PUB-366] 19 p2651 N90-25086
Stability theory for methods to solve the Navier-Stokes equations, part 1
[FFA-TN-1988-65-PT-1] 19 p2691 N90-25312
Boundary conditions for the Navier-Stoke's equations at an artificial boundary intersecting a solid boundary
[FFA-TN-1990-11] 19 p2691 N90-25313
Three-dimensional viscous flow structures from bifurcation of a degenerate singularity with three zero eigenvalues
[LR-572] 19 p2692 N90-25314
Flow structures around non-hyperbolic singularities on the wall with one vanishing eigenvalue: A discussion of the flow structures and the unfoldings
[LR-586] 19 p2692 N90-25315
Two-dimensional Euler and Navier-Stokes Time accurate simulations of fan rotor flows
[NASA-TM-102402] 20 p2803 N90-25948
Code enhancements and validation of GASP
[NPS-PAPER-44] 20 p2861 N90-26277
The finite analytic method and its applications. Volume 1: Laminar and turbulent flows past two-dimensional and axisymmetric bodies
[AD-A222787] 20 p2864 N90-26294
On the linear and nonlinear stability of non-parallel flow 21 p3002 N90-27065
Rotating flow in radial turbomachinery
[AD-A222885] 21 p3004 N90-27073
A comparison of two central difference schemes for solving the Navier-Stokes equations
[NASA-TM-102815] 22 p3108 N90-27654
Boundary layer and shock layer in hypersonic flows
[CERT-31/5005-22-DERAT] 22 p3110 N90-27664
Calculations of chemically reacting shear flows above solid fuels 22 p3162 N90-27930
Implicit solution of three-dimensional internal turbulent flows
[NASA-TM-103099] 22 p3170 N90-27982
Numerical solution for the velocity-derivative skewness of a low-Reynolds-number decaying Navier-Stokes flow
[NASA-TM-103186] 22 p3171 N90-27985
Analytical resolution of the Oseens differential equation of inclined turning cylinder with gliding
[ETN-90-97316] 22 p3171 N90-27988
An analysis of flow models: From Navier-Stokes to potential flow equations 22 p3173 N90-28002
Discretization methods for the incompressible Navier-Stokes equations 22 p3173 N90-28003
An introduction to turbulence models 22 p3173 N90-28004
Calculation of unsteady two dimensional viscous incompressible flows by spectral methods
[ETN-90-97449] 22 p3175 N90-28015
Numerical study of turbulence in the presence of walls
[ONERA-RSF-15/3419-AY-114A] 22 p3176 N90-28024
Secondary instabilities in compressible boundary layers
[NASA-CR-182091] 23 p3269 N90-28502
Numerical resolution of Navier-Stokes equations using several turbulence models and applications on turbomachines
[ETN-90-97478] 23 p3326 N90-28808
Extrapolation procedures at outflow boundaries for the Navier-Stokes equations
[FFA-TN-1990-23] 23 p3327 N90-28811
An investigation of chaotic Kolmogorov flows
[NASA-CR-182079] 23 p3328 N90-28816
Numerical simulations of blade-vortex interactions and lifting hovering rotor flows
[AD-A224238] 24 p3417 N90-29302
Investigation of ATP blades, part 2. Validation of two-dimensional viscous flow simulation codes around thin airfoils
[NAL-TR-1046] 24 p3421 N90-29326
A boundary-layer transition model for the Navier-Stokes computation for a natural-laminar-flow airfoil
[NAL-TR-1038T] 24 p3421 N90-29328
Some topics in computational transonic aerodynamics: Revision
[NAL-TR-1018T] 24 p3422 N90-29332
Calibration of the PARC program for propulsion-type flows
[AD-A224253] 24 p3434 N90-29395
An additive turbulent decomposition of the Navier-Stokes equations implemented on highly parallel computer systems
[AD-A223678] 24 p3468 N90-29595
Secondary flow in presence of wall jets: Incorporation of compression effects in a quasi-elliptic Navier-Stokes calculation code
[ETN-90-97559] 24 p3469 N90-29602
Parallelization of a method for solving three dimensional Navier-Stokes equations on a distributed memory multiprocessor
[ONERA-RTS-1/3717-CY] 24 p3534 N90-29983
The computation and analysis of acoustic waves in transonic airfoil-vortex interactions 24 p3542 N90-30031
Effect of a crystal-melt interface on Taylor-Vortex flow with buoyancy
[PB90-244401] 24 p3551 N90-30089

NAVIGATION

NT AIR NAVIGATION
NT ALL-WEATHER AIR NAVIGATION
NT AREA NAVIGATION
NT CELESTIAL NAVIGATION
NT DEAD RECKONING
NT DIGITAL NAVIGATION
NT DOPPLER NAVIGATION
NT HYBRID NAVIGATION SYSTEMS
NT INERTIAL NAVIGATION
NT INTERPLANETARY NAVIGATION
NT LORAN
NT LORAN C
NT NAP-OF-THE-EARTH NAVIGATION
NT OMEGA NAVIGATION SYSTEM
NT RADAR NAVIGATION
NT RADIO NAVIGATION
NT SPACE NAVIGATION
NT SURFACE NAVIGATION
The role of sensor directed, model based control in robotics
[DE89-014133] 01 p0077 N90-10442
Navigation of robotic systems
[DE89-017507] 03 p0390 N90-12219
Programmable near-infrared ranging system
[AD-D014237] 06 p0843 N90-14903
Centralized and decentralized Kalman filter techniques for tracking, navigation, and control
[AD-A214245] 07 p0878 N90-15091
Sensor integration using concurrent computing on-board the ORNL mobile robot
[DE89-008740] 07 p0939 N90-15436
SIMON (SuperIntelligent Mobile Observing Navigator): A high-reliability robot for a radiation environment
[DE90-003888] 07 p0943 N90-15460
Design and implementation of two concurrent multi-sensor integration algorithms for mobile robots
[DE90-003041] 07 p0981 N90-15663
Mirach 100 flight control system 08 p1025 N90-15926
Miniature GPS-based guidance package 09 p1163 N90-16736
Advances in navigation support systems based on operational pilot's heuristics 09 p1164 N90-16737
Reusable navigation module 09 p1165 N90-16742
The development of an airborne synthetic aperture radar motion compensation system 09 p1165 N90-16745
Development of an integrated mobile robot system at Carnegie Mellon University: June 1988
[AD-A215955] 10 p1392 N90-18049
Visual navigation: Constructing and utilizing simple maps of an indoor environment
[AD-A216761] 11 p1455 N90-18382
An approach centered in production rules for a partition of environment and planning in a visual navigation system (SNV)
[INPE-4813-TDL/360] 11 p1517 N90-18737
Heli/SITAN: A terrain referenced navigation algorithm for helicopters
[DE90-005193] 12 p1602 N90-19217
Highly accurate navigation: Integration of navigation and geodesic methods
[SFB-228] 12 p1602 N90-19221
Suboptimal period design for a maneuvering missile to evade tracking filters 12 p1650 N90-19479
Extending terrestrial mobile robotics to a proposed lunar base
[DE89-016179] 12 p1672 N90-19606
A human factors testbed for ground-vehicle telerobotics research
[DE90-006618] 12 p1697 N90-19746
Parallel neural net path-planner on hypercube and transputer
[DE90-006324] 12 p1703 N90-19777
Estimation of modeled object pose from monocular images
[DE90-001678] 13 p1804 N90-20354
Robot navigation research using the HERMIES mobile robot
[DE90-001952] 13 p1810 N90-20396

Boundary equations of configuration obstacles for manipulators
[DE90-002101] 13 p1874 N90-20745
Sole means navigation and integrity through hybrid Loran-C and NAVSTAR GPS 14 p1907 N90-20933
Optimal and near-optimal medium range air-to-air missile guidance against maneuvering targets 15 p2053 N90-21766
The determination of maximum deep space station slew rates for a high Earth orbiter 15 p2075 N90-21882
A higher density VLBI catalog for navigating Magellan and Galileo 15 p2078 N90-21904
Passive navigation using image irradiance tracking 15 p2141 N90-22232
Navigation software for the MPL vertical line array
[AD-A220166] 17 p2432 N90-23860
A comparison of two neural network schemes for navigation 18 p2631 N90-24991
United States planetary rover status: 1989
[NASA-CR-186843] 19 p2698 N90-25353
A comparison of two neural network schemes for navigation 19 p2733 N90-25536
ACES: Space shuttle flight software analysis expert system 19 p2739 N90-25571
The Telecommunications and Data Acquisition Report
[NASA-CR-186852] 20 p2852 N90-26217
Goldstone intracomplex connected element interferometry 20 p2852 N90-26218
Development of an integrated mobile robot system at Carnegie-Mellon University
[AD-A222494] 21 p3011 N90-27119
Tactical Applications of Space Systems
[AGARD-CP-460] 21 p3067 N90-27438
A technology assessment of alternative communications systems for the space exploration initiative
[NASA-TM-103243] 22 p3125 N90-27736
An aeronautical mobile satellite experiment
[NASA-CR-186971] 23 p3287 N90-28593
Dynamic interaction of multiple autonomous mobile robots 23 p3333 N90-28844
Treatment of systematic errors 2: Fusion of ultrasound and visual sensor data
[DE90-014780] 23 p3334 N90-28850
Proceedings of the NASA Conference on Space Telerobotics, volume 1
[NASA-CR-186856] 23 p3362 N90-29000
Automation and robotics technology for intelligent mining systems 23 p3366 N90-29018
Map learning with indistinguishable locations 23 p3367 N90-29025
Three-dimensional motor schema based navigation 23 p3367 N90-29026
Learned navigation in unknown terrains: A retraction method 23 p3368 N90-29029
A hardware/software environment to support R/D in intelligent machines and mobile robotic systems
[DE90-014458] 23 p3385 N90-29119
Modular digital GPS receivers 24 p3424 N90-29346
An analysis of GPS as the sole means navigation system in US Navy aircraft 24 p3425 N90-29350
Distributed control architecture for CNI preprocessors 24 p3426 N90-29356
An integrated system for land navigation 24 p3430 N90-29377

NAVIGATION AIDS
NT BEACONS
NT COMPASSES
NT DISCRETE ADDRESS BEACON SYSTEM
NT NAVIGATION INSTRUMENTS
NT RADAR BEACONS
NT RADIO DIRECTION FINDERS
Guidance simulation and test support for differential GPS flight experiment
[NASA-CR-177471] 01 p0005 N90-10021
Federal Radionavigation Plan, 1988
[PB89-163075] 02 p0148 N90-10846
Modified Newton-type methods for long-range target motion analysis
[FEL-1989-82] 04 p0551 N90-13208
Control outside of independent surveillance coverage operational concept
[AD-A214163] 07 p0878 N90-15090
The automatic detection of anti-collision lights
[RSRE-MEMO-4272] 08 p1019 N90-15896
Application of multifunction inertial reference systems to fighter aircraft 09 p1164 N90-16740
Application of model based reasoning to diagnosis of faults in inertial navigation equipment
[AD-A215561] 09 p1166 N90-16750
A sample reuse method for accurate parametric empirical Bayes confidence intervals
[AD-A216198] 10 p1424 N90-18216
An error sensitivity model for Doppler positioning using transit satellites
[AD-A216724] 11 p1455 N90-18381
The Fourteenth Biennial Guidance Test Symposium, volume 1
[AD-A216925] 11 p1455 N90-18383
Sole means navigation and integrity through hybrid Loran-C and NAVSTAR GPS 14 p1907 N90-20933
ALVINN: An Autonomous Land Vehicle In a Neural Network
[AD-A218975] 16 p2243 N90-22797
Continued development and analysis of a new extended Kalman filter for the Completely Integrated Reference Instrumentation System (CIRIS)
[AD-A220106] 17 p2354 N90-23400
Location and Navigation Satellite Systems
[ISBN-2-85-428-242-6] 17 p2358 N90-23420
Navigation requirements: What they are and where they come from 17 p2358 N90-23422
Cognitive requirements for aircraft navigation
[NASA-CR-186933] 21 p2955 N90-26804
Future applications of GPS to conventional weapons 21 p3069 N90-27447
Expert system for pilot assistance: The challenge of an intensive prototyping
[ETN-90-97274] 22 p3111 N90-27674
Integrated Air Traffic Management
[DLR-MITT-89-23] 22 p3112 N90-27676
R and D aspects of the future operational concept of the BFS 22 p3112 N90-27679
On-board planning and control of 4D-trajectories in the TMA 22 p3112 N90-27680
Four-dimensional navigation and Flight Management Systems 22 p3112 N90-27681
Advanced transport operating system software upgrade: Flight management/flight controls software description
[NASA-CR-181936] 22 p3239 N90-28366
The 2-D and 3-D characterizations of GPS navigation service 24 p3425 N90-29348
Enhancing PLRS with user-to-user data capability 24 p3427 N90-29359
Observability of relative navigation using range-only measurements 24 p3427 N90-29360
The potential for digital databases in flight planning and flight aiding for combat aircraft 24 p3429 N90-29371
A land navigation demonstration vehicle with a color map display for tactical use 24 p3430 N90-29375

NAVIGATION INSTRUMENTS
NT COMPASSES
NT RADIO DIRECTION FINDERS
Development of a marine integrated navigation system 02 p0149 N90-10852
Navigation experiment NAVEX: Data storage and processing
[DFVLR-MITT-89-09] 03 p0304 N90-11727
Navigation experiment NAVEX: The equipment delay times in the Spacelab mission D1
[DFVLR-MITT-89-10] 03 p0304 N90-11728
Acquisition and recording an AMX A/C. Aeritalia experience and present trends
[ETN-89-95217] 04 p0454 N90-12598
Proceedings of the 17th Annual Gravity Gradiometer Conference
[AD-A223568] 24 p3492 N90-29735

NAVIGATION SATELLITES
NT NAVIGATION TECHNOLOGY SATELLITES
NT NAVSTAR SATELLITES
NT TRANSIT SATELLITES
Stable Kalman filters for processing clock measurement data 04 p0487 N90-12801
Inexpensive global location and tracking systems using geostationary satellites
[AD-A213025] 05 p0602 N90-13498
Expert system for Kalman filter supervision: Application to autonomous satellite navigation 09 p1164 N90-16739
Navigation experiment NAVEX data storage and processing
[ESA-TT-1175] 11 p1467 N90-18445
Navigation experiment NAVEX: The self-test delay times in the D1 Spacelab mission
[ESA-TT-1176] 11 p1467 N90-18446
Interoperability issues in the use of satellite-based navigation systems for civil aviation purposes
[AD-A217279] 12 p1602 N90-19223
Sole means navigation and integrity through hybrid Loran-C and NAVSTAR GPS 14 p1907 N90-20933
Precise estimation of tropospheric path delays with GPS techniques 15 p2074 N90-21881
Three approximate methods for estimating the best subset of GPS satellites for satellite position calculations
[AD-A220380] 17 p2350 N90-23383
Location and Navigation Satellite Systems
[ISBN-2-85-428-242-6] 17 p2358 N90-23420
General introduction to location and navigation capabilities 17 p2358 N90-23421
Proceedings of the Second Symposium on GPS Applications in Space, volume 2
[AD-A219979] 20 p2806 N90-25963
Independent ground monitor coverage of Global Positioning System (GPS) satellites for use by civil aviation 24 p3428 N90-29364

NAVIGATION TECHNOLOGY SATELLITES
Realization of a different NAVSTAR global positioning system for hydrographic surveying
[ETN-89-95720] 04 p0515 N90-12972
Back to the stars 17 p2359 N90-23429
The GPS-NAVSTAR location and navigation system 17 p2359 N90-23433

NAVIGATORS
Field-of-view assessment of low-level flight and an airdrop in the C-130 Weapon System Trainer (WST)
[AD-A218504] 16 p2200 N90-22559

NAVSTAR SATELLITES
Sentinel satellite positional precision derived from the NAVSTAR global positioning system
[AD-A211876] 03 p0303 N90-11720
Realization of a different NAVSTAR global positioning system for hydrographic surveying
[ETN-89-95720] 04 p0515 N90-12972
Dynamic analysis of the geodetic networks originating from the Navstar/Global Positioning System (GPS) satellites
[SER-C-346] 08 p1091 N90-16316
Optimization of the effective GPS data rate 14 p1907 N90-20932
Sole means navigation and integrity through hybrid Loran-C and NAVSTAR GPS 14 p1907 N90-20933
The GPS-NAVSTAR location and navigation system 17 p2359 N90-23433
Analysis, Design and Synthesis Methods for Guidance and Control Systems
[AGARD-AG-314] 24 p3423 N90-29338

NAVY
Properties of HY-100 for naval construction
[MRL-R-1149] 01 p0044 N90-10247
US Navy principal site testing concept and the F-18 02 p0151 N90-10861
Summary of research academic departments, 1987-1988
[AD-A213252] 05 p0716 N90-14183
US Navy aircraft fire protection technology 10 p1315 N90-17603
Maritime safety information in the year 2000: Listen up, Navy, the times they are a changin'
[AD-A220563] 17 p2390 N90-23611

NC-130 AIRCRAFT
U C-130 AIRCRAFT

NEAR FIELDS
New test techniques to evaluate near field effects for supersonic store carriage and separation 01 p0013 N90-10062
Near-field noise predictions of an aircraft in cruise 04 p0443 N90-12538
Calculation of the odd and even integral components of the wave resistance Green's function
[AD-A212384] 04 p0503 N90-12900
The physical optics approximation in the near-field region
[FEL-1989-100] 04 p0555 N90-13234
Aspects of Raman scattering
[AD-A213926] 07 p0992 N90-15736
A field study of solid rocket exhaust impacts on the near-field environment
[NASA-TM-4172] 10 p1405 N90-18102
Green's functions for a theoretical model of an aperture fed stacked-patch microstrip antenna
[AD-A216280] 12 p1645 N90-19455
Near-field bistatic RCS (Radar Cross-Section) measurements
[AD-A217011] 12 p1646 N90-19458
Millimeter wave near-field study
[NASA-CR-182014] 14 p1932 N90-21058
Transfer matrices for multimode optical fiber systems
[AD-A218459] 16 p2317 N90-23210
Near field curvature at parallel phase objects: Model examination with microwaves
[ETN-90-96499] 18 p2545 N90-24525
Validity domain of the scalar Kirchhoff and Rayleigh-Sommerfeld diffraction theories in the near field of small phase objects: Comparison between calculation models and microwave measure
[ETN-90-96963] 20 p2855 N90-26236
Departures from plane-wave-like coupling to a Maverick missile in the radiating near-field region of a horn antenna
[AD-A222539] 21 p2997 N90-27035
Near-field gain of pyramidal horns from 18 to 40 GHz
[PB90-155854] 22 p3164 N90-27941
Theory of planar near-field measurement
[FEL-89-B273] 22 p3244 N90-28395
Structure in the near field of the transverse jet
[AD-A224502] 24 p3467 N90-29591

NEAR INFRARED RADIATION
Study of high frequency water vapor absorption parameters
[AD-A210676] 02 p0194 N90-11108
Ionospheric total electron content, and far ultraviolet, near infrared oxygen emission 02 p0249 N90-11410
Growth and characterization of materials for tunable lasers in the near infrared spectral region
[NASA-CR-185832] 03 p0352 N90-12009
Cloud phase discrimination by near-infrared remote sensing 08 p1090 N90-16310
Short time scale variability of the BL Lac object OJ 287 in the near-infrared
[IFSI-89-3] 08 p1140 N90-16603
Near infrared spectroscopy of Mars: Study of the surface mineralogy 11 p1579 N90-19091
Near infrared spectroscopy of the supernova remnant RCW103 11 p1581 N90-19109
IRCAM observations of the Reipurth 50 IR source 11 p1583 N90-19119
Near infrared (1-4 micron) spectroscopy of SN1987A 11 p1584 N90-19133
Near-infrared spectroscopy of starburst and interacting galaxies 11 p1586 N90-19144
Infrared properties of five spiral galaxies 11 p1587 N90-19154
Fluorescent molecular hydrogen emission from star-forming galaxies 11 p1588 N90-19155
Near infrared spectroscopy and spectroscopic imaging of NGC253 11 p1588 N90-19159
Measurement system of spectral irradiance in the near infrared 11 p1588 N90-19160
Isophot-S, a low resolution 2.5 to 12 microns spectrometer for ISO 11 p1589 N90-19167
Attitude control modes for the MECB remote sensing satellites
[INPE-4755-PRE/1427] 14 p1938 N90-21094
Low noise HgCdTe 128 x 128 SWIR FPA for Hubble space telescope 14 p1979 N90-21337
Laboratory and telescope use of the NICMOS2 128 x 128 HgCdTe array 14 p1979 N90-21338
Future directions for NICMOS arrays 14 p1979 N90-21339
Fast acting optical beam deflection system
[AD-A220186] 17 p2473 N90-24141
Monolithic Optical Programmable Spectrograph (MOPS)
[AD-D014502] 19 p2757 N90-25669

NEAR ULTRAVIOLET RADIATION
Study of a 1-Hz hypocycloidal pinch (HCP) pump for production of ultraviolet lasers
[AD-A224091] 24 p3547 N90-30064

NEAR WAKES
Linear instability of supersonic plane wakes
[NASA-CR-181911] 02 p0146 N90-10833
Surface flow and heating distributions on a cylinder in near wake of Aeroassist Flight Experiment (AFE) configuration at incidence in Mach 10 Air
[NASA-TP-2954] 06 p0772 N90-14493
An experimental, analytical, and computational investigation of turbomachinery rotor flow fields 07 p0926 N90-15360
An investigation of the steady and unsteady near wake and its effect on a laminar boundary layer 23 p3324 N90-28794

NEARSHORE WATER
NT COASTAL WATER

NEBULAE
NT CRAB NEBULA
NT H I REGIONS
NT H II REGIONS
NT HERBIG-HARO OBJECTS
NT ORION NEBULA
NT PLANETARY NEBULAE
NT REFLECTION NEBULAE
Studies of elementary particles: Proposal
[DE90-001120] 06 p0839 N90-14879
Non-equilibrium chemistry in the solar nebula and early solar system: Implications for the chemistry of comets 08 p1142 N90-16618
From interstellar dust to comets 08 p1142 N90-16620
Solar nebula condensates and the composition of comets 08 p1144 N90-16634
Ice grains in the dust disk of the bipolar nebula M 1-92 11 p1584 N90-19127
Detection of SN1986j in NGC891 at millimetre wavelengths 11 p1585 N90-19137
A search for very high energy gamma rays from the Crab pulsar-nebula 14 p2043 N90-21718
A three-year study of the OH masers in Orion-KL and a study of the (3,2) transition of ammonia 15 p2183 N90-22471
Spectral signatures of X ray photoionized nebulae 19 p2778 N90-25800
A plasma diagnostic study of two wind-blown shell nebulae: NGC 7635 and NGC 2359 23 p3410 N90-29271

NECK (ANATOMY)
Factor analytic reduction of the carotid-cardiac baroreflex parameters 08 p1155 N90-16693
Guidelines for safe human exposure to impact acceleration, update A
[AD-A215287] 09 p1253 N90-17268
Neck Injury in Advanced Military Aircraft Environments
[AGARD-CP-471] 19 p2717 N90-25459
Prevalence of G-induced cervical injury in US Air Force pilots 19 p2717 N90-25460
A kinematic/dynamic model for prediction of neck injury during impact acceleration 19 p2719 N90-25469
Effects of head mounted devices on head-neck dynamic response to +G(sub z) accelerations 19 p2720 N90-25471
Neck injury prevention possibilities in a high-G-enviroment experience with high sustained +G(sub z) training of pilots in the GAF IAM human centrifuge 19 p2720 N90-25474
Risk of cervical injury in real and simulated accidents 19 p2721 N90-25475
Biofidelity of a dummy's neck during automobile collision testing 19 p2721 N90-25477
Omni-directional human head-neck response
[SAE-861893] 19 p2721 N90-25478

NEGATIVE ELECTRON AFFINITY
Negative electron affinity for infrared detection
[AD-A218816] 17 p2395 N90-23639

NEGATIVE FEEDBACK
Design of high-performance negative-feedback oscillators
[ETN-90-96698] 16 p2231 N90-22729

NEGATIVE IONS
NT ANIONS
Extraction induced emittance growth for negative ion sources
[DE89-017586] 02 p0273 N90-11559
Atomic and molecular surface and volume processes in the analysis of negative hydrogen discharges
[DE89-015705] 03 p0401 N90-12294
Investigation of boundary for the negative ion extraction in the sheet-plasma negative ion source
[DE90-719532] 09 p1286 N90-17458
Decay rate and other properties of the positronium negative ion 11 p1560 N90-18987
Positronium ions and molecules 11 p1560 N90-18990
Development of an rf-driven plasma neutralizer for negative ions
[DE90-007298] 11 p1568 N90-19027
Negative ion surface plasma source development for plasma trap injectors in Novosibirsk
[DE90-006082] 12 p1716 N90-19856
Threshold photodetachment spectroscopy of the I + HI transition state region
[AD-A218410] 16 p2260 N90-22883
Experimental investigations of low-energy (4 to 40 eV) collisions of O(-)(P2) ions and O(P3) atoms with surfaces 19 p2732 N90-25530

NEGATIVE RESISTANCE CIRCUITS
High efficiency octave bandwidth millimeter wave power amplifier
[AD-A218245] 14 p1869 N90-21280
Microwave active filters based on coupled negative resistance method
[AD-A223269] 24 p3464 N90-29570

NEODYMIUM
Depletion mode pumping of solid state lasers
[DE90-012090] 19 p2696 N90-25339

NEODYMIUM COMPOUNDS
Spectroscopy of laser properties of Nd(3+)-doped CaF2, SrF2, and BaF2
[DE90-012086] 19 p2695 N90-25337

NEODYMIUM LASERS
Overview of laser concepts 01 p0029 N90-10154
Laser-driven miniature flyer plates for shock initiation of secondary explosives
[DE89-016587] 02 p0225 N90-11288
Interferometry and high speed photography of laser-driven flyer plates
[DE89-016990] 02 p0225 N90-11290
Construction of a picosecond laser system for the investigation of semiconductors using nonlinear optical methods
[ETN-89-94664] 03 p0352 N90-12013
Laser ionization mass spectroscopy
[DE89-008039] 03 p0352 N90-12015
New laser materials
[DE89-017524] 03 p0353 N90-12017
Tunable Solid State Lasers conference edition: Tunable Solid State Lasers Topical Meeting
[AD-A212292] 04 p0506 N90-12920
Advanced source development and applications. Laser-produced plasmas: A compact soft x ray source with high peak brightness
[AD-A212677] 04 p0557 N90-13245
MM and T advanced balancing/machining
[AD-A213103] 05 p0648 N90-13775
Fast electrons in a laser generated plasma 06 p0782 N90-14545
Production of homogeneous plasmas for laser-plasma interaction experiments 06 p0782 N90-14546
Experimental study on the filamentary instability in laser-matter interactions at short wave lengths 06 p0782 N90-14547
Interaction of a low flux laser beam with a solid target 06 p0783 N90-14554
Ultrahigh-brightness lasers and their applications
[DE90-000877] 06 p0789 N90-14596
Eurolaser definition phase: A comparison of high power lasers available
[ETN-90-96061] 08 p1083 N90-16268
Spallation and dynamic fracture as an effect of laser induced shock waves in carbon based composite materials
[AD-A216540] 11 p1478 N90-18509
Performance of zig-zag slab regenerative ring amplifier laser system
[DE90-006995] 13 p1806 N90-20371
Ultra-high brightness laser research at LLNL (Lawrence Livermore National Laboratory)
[DE90-008366] 13 p1896 N90-20885
Development of an ultra-bright laser and an application to multi-photon ionization 14 p1984 N90-21372
Generation of ultrashort laser pulses from neodymium glass oscillator and regenerative amplifier 14 p1984 N90-21373
Injection-seeded Nd:YAG laser linewidth measurement using saturation spectroscopy in iodine
[DE90-009537] 15 p2103 N90-22034
MEGALIDAR proof-of-concept demonstration
[AD-A218787] 16 p2255 N90-22858
DURIP: Spontaneous Raman system for the study of enhanced combustion and non-thermal plasmas
[AD-A221410] 18 p2564 N90-24629
Development of a large scale Nd:YAG growth process
[DE90-010746] 18 p2624 N90-24954
Possibilities of Nd: YAG laser utilization in medicine
[MBB-UE-0002/88-PUB] 19 p2653 N90-25100
Frequency doubled operation of a ground state depleted laser using the Nd(3+)(4)F(sub 3/2)-(4)I(sub 9/2) transition in Y2SiO5
[DE90-012089] 19 p2695 N90-25338
Design and fabrication of high damage threshold turning mirrors for the Nova laser
[DE90-012703] 19 p2696 N90-25341
Real-time monitoring of ceramic sintering with laser ultrasonics
[DE90-012960] 20 p2838 N90-26140
Development of a multi-purpose, pulsed-laser system for solar cell processing applications
[DE90-012181] 21 p3008 N90-27096
Diode laser pumped single mode 1.3 microns Nd:YALO microlaser
[AD-A223036] 21 p3008 N90-27100
Laser surface interactions of high-T(sub c) superconductors 22 p3139 N90-27809

NEON
Hot spots Ar and Ne gas puff z-pinch
[IPPCZ-289] 05 p0701 N90-14103
The production and spectroscopy of molecular ions isolated in solid neon
[AD-A213723] 07 p0895 N90-15174
Electronic energies for Neon dimer dication radiative charge transfer
[AD-A215817] 10 p1429 N90-18244
Numerical Green's functions in optical potential calculations for positron scattering from argon and neon 11 p1557 N90-18971
Positron excitation of neon 11 p1558 N90-18973
X ray laser program report for FY 1989
[AD-A221818] 21 p3009 N90-27107
Nova LMC (Large Magellanic Cloud) 1990 no. 1: The first extragalactic neon nova
[NASA-CR-180409] 23 p3411 N90-29276
Effects of basis set contraction in relativistic calculations on neon, argon, and germanium
[AD-A223357] 24 p3446 N90-29460

NEOPLASMS
NT CANCER

NEOPRENES
U CHLOROPRENE RESINS

NEPHANALYSIS
Comparisons between the RTNEPH (Real-Time Nephanalysis) and AFGL cloud layer analysis algorithms
[AD-A216637] 11 p1536 N90-18844
Exploiting surface observations of cloudiness for globalscale nephanalyses 12 p1692 N90-19719

The test for automatic neph-analysis chart
21 p3029 N90-27219

NEPHELOMETERS
Fluorescence and elastic scattering from laser dye-filled capillaries
[AD-A217026] 11 p1484 N90-18540
An outline for the RTNEPH infrared atmospheric water vapor attenuation study
[AD-A221753] 21 p3027 N90-27209
Front range lidar, aircraft, and balloon experiment
[PB90-225301] 22 p3212 N90-28218

NEPTUNE (PLANET)
NASA Voyager 2 Neptune encounter press kit
[NASA-TM-101851] 01 p0015 N90-10076
The Voyager Neptune travel guide
[NASA-CR-186108] 05 p0585 N90-13412
Neptune's Triton: A moon rich in dry ice and carbon
[NASA-CR-186298] 08 p1152 N90-16675
Parkes radio science system design and testing for Voyager Neptune encounter 12 p1645 N90-19451
Auroral ultraviolet darkening on the outer planets
15 p2192 N90-22518
Liquid-vapor equilibrium of multicomponent cryogenic systems 20 p2948 N90-26774
Carbon in the outer solar system
21 p3096 N90-27593

NEPTUNE SATELLITES
NT TRITON

NERVA (ENGINE)
U NUCLEAR ENGINE FOR ROCKET VEHICLES

NERVES
NT GANGLIA
Perception of complex auditory patterns
[AD-A219626] 17 p2434 N90-23867
Radiological investigation of the vertebral column of candidates for military flying training the the Royal Norwegian Air Force 19 p2718 N90-25463
Experiment K-6-09. Morphological and biochemical investigation of microgravity-induced nerve and muscle breakdown. Part 1: Investigation of nerve and muscle breakdown during spaceflight; Part 2: Biochemical analysis of EDL and PLT muscles 20 p2893 N90-26463
Method and apparatus for applying a mechanical force to surface
[NASA-CASE-LAR-14009-1] 21 p3011 N90-27115

NERVOUS SYSTEM
NT AUTONOMIC NERVOUS SYSTEM
NT BRAIN
NT BRAIN STEM
NT CENTRAL NERVOUS SYSTEM
NT CEREBELLUM
NT CEREBRAL CORTEX
NT CEREBRUM
NT EFFERENT NERVOUS SYSTEMS
NT GANGLIA
NT NERVES
NT PERIPHERAL NERVOUS SYSTEM
NT PINEAL GLAND
NT SPINAL CORD
NT SYMPATHETIC NERVOUS SYSTEM
NT THALAMUS
Computational and psychophysical study of human vision using neural networks
[AD-A213290] 05 p0674 N90-13924
The acute, delayed neurotoxicity evaluation of two jet engine oil formulations
[AD-A222018] 21 p2986 N90-26972

NETHERLANDS
Flight testing in the Netherlands: An overview
02 p0155 N90-10884
Results of Agrisar-86 for the Flevopolder (Netherlands) test area
[BCRS-89-21] 11 p1527 N90-18789
Remote sensing for the classification and quantification of vegetation in Spring staging areas of Brent geese on the Frisian Islands (Netherlands)
[BCRS-89-27] 11 p1527 N90-18790
Project TTA-79: Summary project report
[ETN-90-96773] 19 p2661 N90-25146

NETS
NT NEURAL NETS
NT PETRI NETS

NETWORK ANALYSIS
NT CRITICAL PATH METHOD
NT SNEAK CIRCUIT ANALYSIS
Transaction throughput in distributed systems: A modeling study using dynamic queueing networks
[MEMO-INF-89-25] 02 p0261 N90-11479
Stochastic flows in networks
[AD-A211209] 02 p0266 N90-11515
Phoebe: A preliminary control network and rotational elements
[NASA-CR-185716] 02 p0295 N90-11680
Calibration and de-embedding of microwave measurements using any combination of one- or two-port standards
[PB89-212674] 03 p0337 N90-11916
On the precision and reliability of GPS networks computed using the double difference observable
[ETN-89-95719] 04 p0449 N90-12571
Simulation of circuits adapted to signal processing
[TELECOM-PARIS-89-E001] 04 p0489 N90-12811
Path expression based operating systems
[MEMO-INF-88-68] 04 p0536 N90-13097
The application of artificial intelligence techniques to tracing the interconnections in an integrated circuit
[TELECOM-PARIS-89-E002] 04 p0537 N90-13105
Why stochastic modeling is essential in analyzing interdicted transportation network performance
[AD-A213140] 05 p0688 N90-14007
The activity selection problem: A network and game theoretic approach
[MEMO-794] 05 p0694 N90-14056
Scaling in a non Abelian string network
[ROM1F-89-676] 05 p0695 N90-14066
Network simulator definition
[AD-A213463] 07 p0918 N90-15308
On the correctness of orphan management algorithms
[AD-A213777] 07 p0975 N90-15632
Optimistic concurrency control for nested distributed transactions
[AD-A213828] 07 p0976 N90-15634
A structural factoring approach for analyzing probabilistic networks 07 p0986 N90-15697
Integrated geodetic network analysis with stochastic prior information about the gravity field and reference ellipsoid
[SER-C-351] 08 p1091 N90-16317
Development of a parallel link model for meteor burst communication
[AD-A215629] 09 p1208 N90-17001
Sneak circuit analysis for the common man
[AD-A215275] 09 p1212 N90-17029
Network flow algorithms
[AD-A214689] 09 p1265 N90-17337
The design and analysis of algorithm and data structure for efficient solutions of minimum-cost network flow problems on MISD and MIMD 10 p1441 N90-18313
Feasibility of Mealy design for processor controlpaths
[MEMO-INF-89-53] 11 p1550 N90-18923
Modeling A circuit switched multiprocessor interconnect
[AD-A217122] 12 p1656 N90-19519
Parallel methods for solving nonlinear block bordered systems of equations
[AD-A217062] 12 p1707 N90-19806
Calibration of Hewlett-Packard network analyzers: A precision viewpoint
[NASA-CR-181989] 14 p1966 N90-21262
Networks for image acquisition, processing and display 15 p2138 N90-22218
Executive summary for the network assessment model
[AD-A218762] 16 p2229 N90-22718
The distributed bit complexity of the ring: From the anonymous to the non-anonymous case
[RUU-CS-88-33] 17 p2452 N90-23988
Short proofs on multicommodity flows and cuts
[CWI-BS-R8922] 17 p2462 N90-24061
Disjoint homotopic paths and trees in a planar graph
[CWI-BS-R8923] 17 p2462 N90-24062
Belief networks in plausible reasoning
[CWI-CS-R8927] 17 p2467 N90-24098
On ergodicity and recurrence properties of a Markov chain with an application to an open Jackson network
[TW-89-10] 17 p2467 N90-24099
Development of a six port network analysis tool for the 1 to 18 GHz bandwidth range
[TELECOM-PARIS-89-D-015] 18 p2545 N90-24527
Computing Boolean functions on anonymous networks
[CWI-CS-R8935] 18 p2602 N90-24818
Distributed computing on transitive networks: The torus
[RUU-CS-88-31] 18 p2634 N90-25007
Packet radio network concepts for the Norwegian field army 20 p2850 N90-26206
On travelling-wave-based protection of high-voltage networks
[ISBN-90-9002955-9] 20 p2858 N90-26260
Automatic line network extraction from aerial imagery of urban areas through knowledge based image analysis
[AD-A222675] 20 p2880 N90-26385
Parallel algorithm for distributed memory computers (applications to matricial algorithms)
[ETN-90-97252] 20 p2913 N90-26573
High speed all optical networks
[NASA-CR-185311] 20 p2926 N90-26649
Communications network analysis tool
[AD-A222061] 21 p2996 N90-27029
Using minimal spanning trees to compare the reliability of network topologies
[NASA-TM-4208] 24 p3539 N90-30014

NETWORK CONTROL
A contribution to the synthesis of communication switching systems with decentralized control using modular components
[ETN-89-94660] 02 p0214 N90-11226
A hybrid optimisation strategy for adaptive feed-forward layered networks
[RSRE-MEMO-4193] 03 p0391 N90-12226
Satellite range delay simulator for a matrix-switched time division multiple-access network simulator
[NASA-TM-102407] 04 p0489 N90-12813
Dynamic workload modeling of high speed token rings in a metropolitan area network
[MEMO-INF-89-21] 05 p0694 N90-14059
Configuration development for ROMENET
[AD-A213367] 06 p0765 N90-14450
JPL reuse program 06 p0825 N90-14795
Voice/data integration in mobile radio networks: Overview and future research directions
[AD-A214289] 07 p0919 N90-15319
Programs for control of an analog-signal switching network
[DE90-003645] 07 p0974 N90-15626
On the correctness of orphan management algorithms
[AD-A213777] 07 p0975 N90-15632
Optimistic concurrency control for nested distributed transactions
[AD-A213828] 07 p0976 N90-15634
Object orientated simulation on transputer arrays using time warp
[AD-A219795] 17 p2389 N90-23607
ISDN in the local environment: The CISLAN project
[MEMO-INF-89-70] 17 p2452 N90-23985
Modeling and synthesis of multicomputer interconnection networks
[NASA-CR-186619] 19 p2746 N90-25804
Analysis of random drop for gateway congestion control
[NASA-CR-186736] 20 p2935 N90-26698
Lyapunov-based control for switched power converters
[AD-A221974] 21 p3000 N90-27053
Development of probabilistic and possibilistic approaches to approximate reasoning and its applications
[AD-A221945] 21 p3039 N90-27271

NETWORK SYNTHESIS
Adaptive gigabit fiber optics local area network
[AD-A210794] 02 p0275 N90-11571
The structural memory: A network model for human perception of serial objects
[CWI-CS-R8829] 05 p0675 N90-13930
Investigation of automated task learning, decomposition and scheduling
[NASA-CR-186791] 20 p2899 N90-26488
Approaches to orthogonally fused conducting polymers for molecular electronics
[AD-A222546] 22 p3159 N90-27915

NEUMANN PROBLEM
Solution of exterior acoustic problems by the boundary element method 18 p2611 N90-24874

NEURAL NETS
Real-time support for high performance aircraft operation
[NASA-CR-185475] 01 p0015 N90-10075
Integration of neurobiological and computational analyses of the neural network essentials for conditioned taste aversions
[AD-A210228] 01 p0094 N90-10537
Parallel processing and learning in simple systems
[AD-A210225] 01 p0108 N90-10612
Regulation of nonlinear and generalized linear systems
[AD-A207725] 01 p0109 N90-10619
Optical computing based on the Hopfield model for neural networks
[AD-A211824] 03 p0389 N90-12216
Can perceptrons find Lyapunov functions: An algorithmic approach to systems stability
[RR-365] 03 p0391 N90-12224
Ground-state coding in partially connected neural networks
[NASA-TM-102239] 03 p0391 N90-12227
Self-organizing semantic maps
[PB89-212609] 04 p0529 N90-13049
A theory of networks for approximation and learning
[AD-A212359] 04 p0538 N90-13110
Gas identification system using graded temperature sensor and neural net interpretation
[AD-A213359] 05 p0622 N90-13627
Computational and psychophysical study of human vision using neural networks
[AD-A213290] 05 p0674 N90-13924

Optical neural nets for scene analysis
[AD-A213986] 07 p0976 N90-15637
Neural network models for linear programming
[DE89-015974] 07 p0979 N90-15651
A neural network for bounded linear programming
[DE89-015975] 07 p0979 N90-15652
Parallel asynchronous systems and image processing algorithms 08 p1075 N90-16218
Neural networks for data compression and invariant image recognition 08 p1075 N90-16219
Knowledge-based imaging-sensor fusion system 08 p1075 N90-16220
Connectionist model-based stereo vision for telerobotics 08 p1076 N90-16224
How to cluster in parallel with neural networks 08 p1113 N90-16443
Analog hardware for delta-backpropagation neural networks
[NASA-CASE-NPO-17564-1-CU] 09 p1204 N90-16974
Classification of acousto-optic correlation signatures of spread spectrum signals using artificial neural networks
[AD-A215045] 09 p1206 N90-16992
Payload invariant control via neural networks: Development and experimental evaluation
[AD-A215740] 09 p1260 N90-17306
Event-train restoration via backpropagation neural networks
[AD-A216308] 10 p1420 N90-18189
Neurobeamformer 2: Further exploration of adaptive beamforming via neural networks
[AD-A215118] 10 p1426 N90-18226
Binary correlators for optical computing and pattern recognition 10 p1441 N90-18318
Computation and control with neural nets
[DE90-006460] 11 p1548 N90-18911
Parallel neural net path-planner on hypercube and transputer
[DE90-006324] 12 p1703 N90-19777
Hybrid neural network and rule-based pattern recognition system capable of self-modification
[DE90-007482] 12 p1703 N90-19779
Opto-Em and devices investigation
[AD-A215033] 12 p1709 N90-19814
Joint services electronics program
[AD-A217961] 13 p1797 N90-20311
Experiments in finding neural network weights
[DE90-007696] 13 p1865 N90-20702
Robust planning and control using neural networks
[AD-A217216] 13 p1872 N90-20732
Hybrid intelligent perception system: Intelligent perception through combining artificial neural networks and an expert system
[DE90-007483] 13 p1874 N90-20746
Neural networks for aircraft control 14 p1908 N90-20937
Application of neural nets to system identification and bifurcation analysis of real world experimental data
[DE90-007539] 14 p2017 N90-21558
A real time neural net estimator of fatigue life
[NASA-TM-103117] 14 p2018 N90-21564
The classification of defects from ultrasonic measurements
[AERE-R-13306] 15 p2108 N90-22056
An approach to rescheduling activities based on determination of priority and disruptivity 15 p2153 N90-22299
Adaptive pattern recognition by mini-max neural networks as a part of an intelligent processor 15 p2156 N90-22317
Satellite image analysis using neural networks 15 p2157 N90-22321
Neural implementation of a method for solving systems of linear algebraic equations
[NPL-DITC-155/89] 15 p2162 N90-22356
Qualitative aspects of signal processing through dynamical neural networks
[PREPRINT-711] 16 p2228 N90-22709
ALVINN: An Autonomous Land Vehicle In a Neural Network
[AD-A218975] 16 p2243 N90-22797
Stochastic interactive activation and the effect of context on perception
[AD-A218929] 16 p2262 N90-22898
Connectionism and compositional semantics
[AD-A219029] 16 p2264 N90-22904
Encoding sequential structure in simple recurrent networks
[AD-A218928] 16 p2278 N90-22984
Computational chaos in massively parallel neural networks 16 p2283 N90-23012
Distributed neural control of a hexapod walking vehicle 16 p2293 N90-23061
Neural networks in support of manned space 16 p2298 N90-23088
Sentence comprehension: A parallel distributed processing approach
[AD-A218886] 16 p2300 N90-23104
Adaptive Resonance Theory 1
[AD-A219044] 16 p2304 N90-23126
Learning environment for neural networks and transient acoustics
[AD-A219000] 16 p2314 N90-23186
A neural network based speech recognition system
[AD-A219794] 17 p2389 N90-23606
DURIP-Instrumentation for recording and analyzing multiple input/output saccadic eye movement neurosensory control
[AD-A219905] 17 p2435 N90-23871
Neuromorphic optical signal processing and image understanding for automated target recognition
[AD-A219827] 17 p2437 N90-23884
Neural networks applied to signal processing
[AD-A219605] 17 p2454 N90-24000
An averaging result for random differential equations
[AD-A220364] 17 p2457 N90-24021
Optical neural nets for scene analysis
[AD-A220657] 17 p2472 N90-24135
Application of neural networks to the F/A-18 engine condition monitoring system
[AD-A219820] 18 p2497 N90-24271
A neural network for feature extraction
[AD-A220363] 18 p2597 N90-24775
Adaptive control of visually guided grasping in neural networks
[AD-A221387] 18 p2597 N90-24780
A comparison of two neural network schemes for navigation 18 p2631 N90-24991
Mars Rover imaging systems and directional filtering 18 p2648 N90-25071
Advanced mesoscale weather forecasting to support tactical operations on the airland battlefield
[AD-A219421] 19 p2715 N90-25449
A comparison of two neural network schemes for navigation 19 p2733 N90-25536
Sunspot prediction using neural networks 19 p2737 N90-25560
Neuromorphic learning of continuous-valued mappings from noise-corrupted data. Application to real-time adaptive control
[NASA-TM-4176] 19 p2747 N90-25607
Non-linear systems identification using neural networks
[RR-370] 19 p2748 N90-25616
A parallel recursive prediction error algorithm for training layered neural networks
[RR-373] 19 p2748 N90-25617
Adaptive robot control using artificial neural networks: An application in the theory of cognition
[RR-374] 19 p2748 N90-25618
A comparison of the backpropagation and recursive prediction error algorithms for training neural networks
[RR-379] 19 p2748 N90-25620
Neural networks for detecting defects in aircraft structures
[IAR-90-4] 20 p2873 N90-26345
Investigation of automated task learning, decomposition and scheduling
[NASA-CR-186791] 20 p2899 N90-26488
Assembly via disassembly: A case in machine perceptual development
[NASA-CR-186867] 20 p2900 N90-26497
Capacity for patterns and sequences in Kanerva's SDM as compared to other associative memory models
[NASA-CR-180701] 20 p2905 N90-26522
Multilayered neural networks: Learning algorithms, implementation on hypercube machines, applications
[ETN-90-97255] 20 p2913 N90-26574
Neural networks for real-time sensory data processing and sensorimotor control
[AD-A223096] 20 p2916 N90-26592
Development of probabilistic and possibilistic approaches to approximate reasoning and its applications
[AD-A221945] 21 p3039 N90-27271
Spike: Artificial intelligence scheduling for Hubble space telescope 21 p3040 N90-27277
Analog hardware for learning neural networks
[NASA-CASE-NPO-17664-1-CU] 21 p3057 N90-27384
Neural network with dynamically adaptable neurons
[NASA-CASE-NPO-17803-1-CU] 21 p3057 N90-27385
A neural network for feature extraction
[AD-A223059] 21 p3058 N90-27387
Practical issues in the complexity of neural networks
[AD-A221420] 21 p3058 N90-27389
Neural networks
[AD-A222110] 21 p3060 N90-27398
Multiprocessor realization of neural networks
[AD-A222146] 21 p3060 N90-27400
The development of the time-delayed neural network architecture
[AD-A221540] 21 p3061 N90-27403
Collective computation of neural network
[AD-A221848] 21 p3061 N90-27405
Encoding techniques for complex information structures in connectionist systems
[NASA-CR-186942] 22 p3238 N90-28362
Experimental fault characterization of a neural network
[NASA-CR-186885] 22 p3240 N90-28373
Fault-tolerance in massively parallel silicon architectures: The case of neural nets
[REPT-90-012] 22 p3240 N90-28375
Compact 4-D optical neural network architecture
[AD-A222160] 22 p3241 N90-28379
A failure diagnosis system based on a neural network classifier for the space shuttle main engine
[NASA-TM-103607] 23 p3299 N90-28659
Target detection in Gaussian noise using artificial neural systems
[AD-A223983] 23 p3320 N90-28770
Proceedings of the NASA Conference on Space Telerobotics, volume 1
[NASA-CR-186856] 23 p3362 N90-29000
Computational neural learning formalisms for manipulator inverse kinematics 23 p3368 N90-29030
Multi-layer neural networks for robot control 23 p3368 N90-29031
A hybrid architecture for the implementation of the Athena neural net model 23 p3368 N90-29032
A design philosophy for multi-layer neural networks with applications to robot control 23 p3368 N90-29033
A neural network for controlling the configuration of frame structure with elastic members 23 p3368 N90-29034
Design of a monitor and simulation terminal (master) for space station telerobotics and telescience 23 p3372 N90-29051
Learning in stochastic neural networks for constraint satisfaction problems 23 p3377 N90-29078
Recursive least-squares learning algorithms for neural networks
[DE90-014926] 23 p3380 N90-29096
Overcoming rule-based rigidity and connectionist limitations through massively-parallel case-based reasoning
[NASA-CR-186963] 23 p3384 N90-29117
Workshop on Neural Networks
[DE90-014794] 23 p3385 N90-29120
Integrating rule-based and neural-net techniques for spectral analysis
[AD-A223517] 24 p3446 N90-29462
IEEE Conference on Neural Information Processing Systems, Natural and Synthetic
[AD-A223611] 24 p3461 N90-29552
Neural networks and radar systems
[FEL-89-B65] 24 p3462 N90-29558
Macro cell placement with neural net algorithms
[REPT-90-020] 24 p3466 N90-29585
Neural nets and eddy-current testing
[DE90-016044] 24 p3478 N90-29656
A procedure concept for local reflex control of grasping 24 p3509 N90-29839

NEUROLOGY
Biomedical influences on spinal cord function
[AD-A210311] 01 p0092 N90-10527
Excitatory amino acids as transmitters in the brain
[AD-A210685] 01 p0093 N90-10532
Biological investigations of adaptive networks: Neuronal control of conditioned responses
[AD-A211043] 01 p0094 N90-10534
Parallel processing and learning in simple systems
[AD-A210225] 01 p0108 N90-10612
A theory of networks for approximation and learning
[AD-A212359] 04 p0538 N90-13110
Organization of a large-scale cortical network
[AD-A216829] 11 p1540 N90-18863
Neurotransmitter and peptide localization in human brain
[AD-A219964] 17 p2435 N90-23873
Decompression sickness affecting the temporomandibular joint
[AD-A220959] 18 p2584 N90-24715

NEUROMUSCULAR TRANSMISSION
Excitatory amino acids as transmitters in the brain
[AD-A210685] 01 p0093 N90-10532
Extrathalamic modulation of cortical function
[AD-A211044] 01 p0094 N90-10535
Synaptic plasticity and memory formation
[AD-A211368] 03 p0379 N90-12158
Neurotransmitter and peptide localization in human brain
[AD-A219964] 17 p2435 N90-23873

NEURON TRANSMISSION
U BIOELECTRICITY

NEURONS
Analog hardware for delta-backpropagation neural networks
[NASA-CASE-NPO-17564-1-CU] 09 p1204 N90-16974
Pre-treatment with tyrosine reverses hypothermia induced behavioral depression
[AD-A215211] 09 p1252 N90-17265
Acetylcholinesterase inhibition and information processing in the auditory cortex
[AD-A216092] 10 p1411 N90-18139
Organization of a large-scale cortical network
[AD-A216829] 11 p1540 N90-18863
Non-linear analysis of visual cortical neurons
[AD-A221543] 21 p3034 N90-27250
Hitting lines with two-dimensional Brownian motion
[AD-A223595] 24 p3541 N90-30027
NEUROPHYSIOLOGY
Biological investigations of adaptive networks: Neuronal control of conditioned responses
[AD-A211043] 01 p0094 N90-10534
Synaptic plasticity and memory formation
[AD-A211368] 03 p0379 N90-12158
Computational and psychophysical study of human vision using neural networks
[AD-A213290] 05 p0674 N90-13924
High compression image and image sequence coding 08 p1074 N90-16214
Neurocontrol systems and wing-fluid interactions underlying dragonfly flight 12 p1606 N90-19240
Sensory conflict in motion sickness: An observer theory approach 16 p2273 N90-22957
DURIP-Instrumentation for recording and analyzing multiple input/output saccadic eye movement neurosensory control
[AD-A219905] 17 p2435 N90-23871
Analysis of neural systems involved in modulation of memory storage
[AD-A220230] 18 p2584 N90-24714
Curvature estimation in orientation selection
[AD-A221481] 21 p3034 N90-27249
Collective computation of neural network
[AD-A221848] 21 p3061 N90-27405
Time, space and form in vision
[AD-A213889] 23 p3357 N90-28971
Neurophysiological correlates of information processing abilities during divided attention situations in air traffic controllers 23 p3360 N90-28989
Statement of research objectives and summary of research efforts
[RLE-PR-132] 23 p3415 N90-29295
NEUROSCIENCE
U NEUROLOGY
NEUROTRANSMITTERS
Peripheral nervous velocity of conduction in fighter pilots 09 p1256 N90-17287
Neurotransmitter and peptide localization in human brain
[AD-A219964] 17 p2435 N90-23873
Experiment K-6-18. Study of muscarinic and gaba (benzodiazepine) receptors in the sensory-motor cortex, hippcampus and spinal code 20 p2895 N90-26471
NEUTRAL ATMOSPHERES
Low latitude F-region dynamical processes from atomic oxygen nightglow emissions
[INPE-4999-PRE/1561] 14 p2006 N90-21494
Solar wind and high energy particle effects in the middle atmosphere 22 p3206 N90-28188
NEUTRAL ATOMS
Laser cooling of neutral atoms
[AD-A214440] 09 p1279 N90-17418
The 41st Annual Gaseous Electronics Conference
[AD-A214540] 12 p1715 N90-19851
Ultra-sensitive inertial sensors via neutral-atom interferometry 12 p1735 N90-19977
Traps for neutral atoms
[AD-A220925] 18 p2613 N90-24885
Experimental investigations of low-energy (4 to 40 eV) collisions of O(-)(P2) ions and O(P3) atoms with surfaces 19 p2732 N90-25530
Traps for neutral atoms
[AD-A221331] 19 p2754 N90-25649
NEUTRAL BEAMS
NT MOLECULAR BEAMS
NT NEUTRON BEAMS
In situ measurement of neutral beam components using the Doppler-shifted H(sub alpha) emissions in Heliotron E
[DE90-719521] 08 p1125 N90-16516
Development of an rf-driven plasma neutralizer for negative ions
[DE90-007298] 11 p1568 N90-19027
Power threshold for neutral beam current drive
[DE90-008348] 13 p1886 N90-20822
The beta limit in the DIII-D tokamak
[DE90-011896] 19 p2759 N90-25677
Proceedings of the US-Japan Fusion Cooperation Program Exchange P148 Workshop on Advanced Current Drive Concepts
[IPPJ-REV-4] 21 p3078 N90-27498
NEUTRAL BUOYANCY SIMULATION
Telerobotic application to EVA 18 p2502 N90-24298
Groundbased simulations of in-orbit operations 18 p2505 N90-24314
NEUTRAL CURRENTS
BOREX: Solar neutrino experiment via weak neutral and charged currents in boron-11
[DE90-003790] 09 p1300 N90-17530
NEUTRAL GASES
Stormtime coupling of the neutral and ionized upper atmosphere at middle latitudes 02 p0243 N90-11381
Calculation of the temperature and velocity vector of the neutral gas using EISCAT CP3-data 02 p0244 N90-11384
Laboratory simulations of the solar wind-comet interactions 07 p1015 N90-15875
Helium transport in plasma edge regions 14 p2027 N90-21625
PIC code modeling of spacecraft charging potential during electron beam injection into a background of neutral gas and plasma, part 1
[NASA-CR-186602] 15 p2059 N90-21792
Spectrum formation in active galactic nuclei and Type 2 supernovae 15 p2187 N90-22490
The ratio of neutral hydrogen to neutral helium in the local interstellar medium 15 p2189 N90-22499
Instrumentation for surface reaction dynamics
[AD-A218608] 17 p2406 N90-23708
Ion neutral gas coupling in the polar atmosphere: Use of EISCAT for the calculation of thermospheric parameters
[ETN-90-96490] 18 p2580 N90-24694
Disk mass densities in edge-on spiral galaxies 21 p3097 N90-27600
Effects of thruster firings on the shuttle environment 1: Neutral gas composition
[AD-A224404] 24 p3487 N90-29707
NEUTRAL PARTICLES
NT COLD NEUTRONS
NT FAST NEUTRONS
NT NEUTRONS
NT PHOTONEUTRONS
NT SOLAR NEUTRONS
Determination of neutral particle concentration at erosion laser plasma expansion into vacuum
[DE89-620128] 02 p0228 N90-11308
Comparison of laser and neutral particle beam discrimination
[DE89-017786] 03 p0353 N90-12018
Low energy neutral particle energy analyser by time of flight method
[DE90-719529] 08 p1125 N90-16517
Chemical interactions and light emissions from vented species
[AD-A214130] 10 p1327 N90-17668
Laboratory study of ion-neutral collisions at suprathermal energies
[AD-A222117] 21 p3074 N90-27475
NEUTRAL SHEETS
A current disruption mechanism in the neutral sheet for triggering substorm expansions
[NASA-CR-186260] 09 p1298 N90-17525
NEUTRALIZERS
The chemistry of the hypochlorite neutralization of hydrazine fuels 02 p0205 N90-11173
Development of an rf-driven plasma neutralizer for negative ions
[DE90-007298] 11 p1568 N90-19027
NEUTRINO
The number of neutrino species, confronted with the results at the recent Lepton-Photon Symposium (August 7-12, 1989)
[NOTA-INTERNA-940] 16 p2315 N90-23195
NEUTRINO BEAMS
Fermilab fixed target beams from the main injector
[DE89-014355] 01 p0122 N90-10697
NEUTRINOS
NT SOLAR NEUTRINOS
Research program in theoretical high energy physics
[DE89-013963] 01 p0121 N90-10695
Astrophysical and cosmological constraints to neutrino properties
[NASA-CR-185031] 01 p0140 N90-10809
Experimental test of PCAC hypothesis in the reactions mu neutrino-proton giving muon(-)-proton-pion(+) and mu antineutrino-proton giving muon(+)-proton-pion(-) in the delta (1232) region --- partial conserved axial current
[MPE-PAE/EXP.EL.199] 03 p0403 N90-12309
The Baksan gallium solar neutrino experiment
[DE89-016036] 03 p0429 N90-12457
Minimal total cross section for e(+)e(-) yields W(+)W(-)
[NIKHEF-H/88-12] 04 p0553 N90-13222
Unitarity limits on the mass and radius of dark matter particles
[NASA-CR-186079] 05 p0713 N90-14164
Correlation among gravitational wave and neutrino detectors data during SN1987A
[NOTA-INTERNA-932] 05 p0713 N90-14165
Nuclear physics and cosmology
[NASA-CR-186166] 05 p0713 N90-14167
A theoretical perspective on neutrino physics
[DE90-000759] 06 p0839 N90-14878
Supernovae, compact stars, and nuclear physics
[DE90-002682] 06 p0864 N90-15022
Neutrino interactions
[NOTA-INTERNA-934] 08 p1121 N90-16495
Research and development of a helium-4 based solar neutrino detector
[DE90-005416] 10 p1447 N90-18353
Search for proton decay and supernova neutrino bursts with a lunar base neutron detector
[DE90-607644] 10 p1448 N90-18358
Research in theoretical physics
[DE90-005558] 11 p1562 N90-19001
Cosmic ray events in Soudan 2
[DE90-005657] 12 p1746 N90-20037
Current drive in a supernova 15 p2187 N90-22491
Chopper for neutrinos and antineutrinos
[AD-A218402] 17 p2471 N90-24124
Axions and SN 1987A: Axion trapping
[NASA-CR-186604] 18 p2612 N90-24881
Application of solar seismology to study of the convection zone
[AD-A221975] 21 p3101 N90-27610
Biased clustering in a universe with hot dark matter and cosmic string
[FERMILAB-PUB-90/23-A] 22 p3262 N90-28473
Solar oscillation frequency and solar neutrino predictions
[DE90-014918] 23 p3413 N90-29288
Search for neutrino events in the Kamiokande-2 detector in correlation with the solar-flare activity in March 1989
[DE90-508085] 24 p3563 N90-30160
NEUTRON ACTIVATION ANALYSIS
The measurement of trace elements in interplanetary dust and cometary particles by ultra-high sensitivity INAA 08 p1149 N90-16656
Conference on Instrumental Activation Analysis: IAA 89
[DE90-615661] 19 p2694 N90-25327
NEUTRON BEAMS
Hydrogen assay foil counting system
[DE90-007415] 12 p1624 N90-19332
A requirement for Australian research: Access to big science facilities, a report by the Australian National Committee for Crystallography
[DE90-614784] 14 p1930 N90-21048
NEUTRON COUNTERS
NT NEUTRON SPECTROMETERS
Cosmic ray NM-64 neutron monitor data 16
[IFSI-88-21] 08 p1154 N90-16684
Search for proton decay and supernova neutrino bursts with a lunar base neutron detector
[DE90-607644] 10 p1448 N90-18358
The ground-level cosmic-ray event of September 29, 1989 as recorded by the Rome detectors
[NOTA-INTERNA-944] 16 p2340 N90-23336
Cosmic ray NM-64 neutron monitor data-17
[NOTA-INTERNA-945] 16 p2341 N90-23337
NEUTRON CROSS SECTIONS
Helium generation in fusion reactor materials
[DE90-013005] 23 p3393 N90-29172
Emission of quick neutrons and non-equilibrium phenomena by central shocks in the reaction 40 Ar + 40 Ca at 20 MeV/u
[ETN-90-97296] 24 p3544 N90-30043
NEUTRON DETECTORS
U NEUTRON COUNTERS
NEUTRON DIFFRACTION
Structural aspects of the phase separation in La2CuO4.032
[DE89-016183] 01 p0130 N90-10751
Neutron scattering experiments on high-temperature superconducting materials: Foreign trip report, September 13, 1988--October 4, 1988
[DE89-017451] 02 p0285 N90-11630
Report of the Specialists' Workshop on Phase Transition Studies on Hydrogen-Bonded Crystals by Neutron and X-ray Diffractometries
[DE89-906638] 02 p0285 N90-11631
Neutron scattering studies of premartensitic phenomena
[DE90-000025] 03 p0328 N90-11863

Single crystal diffraction
[DE90-000024] 03 p0412 N90-12366
Investigations of spontaneous nuclear order in copper by neutron diffraction
[ETN-90-98060] 05 p0698 N90-14090
Application of neutron diffraction NDE to high-temperature superconducting composites
[DE90-002184] 06 p0738 N90-14295
Charge transfer and bond lengths in YBa2Cu(sub 3-x)M(sub x)O(sub 6+y)
[DE90-002241] 06 p0854 N90-14966
Powder neutron diffraction study of the structural phase diagram of the Ba(sub 1-x)K(sub x)BiO3 system
[DE90-002264] 06 p0854 N90-14967
Magnetic excitations in thulium metal
[DE90-002475] 06 p0855 N90-14970
Structure and dynamics of disordered systems
[DE90-001408] 07 p0990 N90-15718
The possible occurrence of multi-phase behavior in the high T(sub c) superconductor YBa2Cu3O(sub x)
[DE90-002999] 07 p0999 N90-15777
High temperature neutron diffraction study of the formation reaction of bismuth superconductors
[DE90-004883] 08 p1134 N90-16568
Flexibility of the zeolite RHO framework: In situ x ray and neutron powder structural characterization of divalent cation-exchanged zeolite RHO
[AD-A214573] 09 p1288 N90-17467
Crystallographic and magnetic properties of (C6 D11 ND3)CuBr3 and (Zn(1-x)Mn(x))3As2: A neutron scattering study
[ECN-219] 11 p1573 N90-19055
Bose condensate in superfluid (sup 4)He and momentum distributions by deep inelastic scattering
[DE90-007541] 12 p1712 N90-19832
A requirement for Australian research: Access to big science facilities, a report by the Australian National Committee for Crystallography
[DE90-614784] 14 p1930 N90-21048
New approach to the dynamical diffraction theory in the case of three-dimensional perfect crystal
[DE90-620563] 16 p2322 N90-23240
Use of neutron diffraction in determining strains in high-temperature superconducting composites
[DE90-010404] 18 p2621 N90-24931
Texture of materials by time-of-flight neutron diffraction
[DE90-008968] 20 p2830 N90-26096

NEUTRON EMISSION
Tritium and neutron measurements of a solid state cell
[DE90-003657] 07 p1005 N90-15820
Displacement flow and deuteron drag in a metal: A path towards cold fusion
[PREPRINT-703] 16 p2320 N90-23227
Investigation of the effect of mechanical stress on cold fusion
[AD-A220123] 17 p2474 N90-24147
Emission of quick neutrons and non-equilibrium phenomena by central shocks in the reaction 40 Ar + 40 Ca at 20 MeV/u
[ETN-90-97296] 24 p3544 N90-30043

NEUTRON FLUX
U FLUX (RATE)

NEUTRON IRRADIATION
High energy neutron irradiation effects in GaAs modulation-Doped Field Effect Transistors (MODFETS): Threshold voltage
[AD-A210502] 01 p0132 N90-10763
Phase evolution during neutron irradiation of commercial Fe-Cr-Mn alloys
[DE90-004113] 08 p1045 N90-16042
Fracture toughness of ferritic alloys at very high neutron exposures
[DE90-004519] 08 p1046 N90-16046
Thermodynamic studies on the ferroelectric phase transition in neutron irradiated (Li(sub x)K(1-x))2SO4 crystals at high temperature
[DE89-635786] 08 p1130 N90-16545
Response of unirradiated and neutron-irradiated vanadium alloys to Charpy-impact loading
[DE90-004878] 11 p1486 N90-18551
An influence of fast neutron irradiation on the properties of p-i-n wide-based diodes
[DE90-611148] 18 p2550 N90-24556
An examination of the 1-MeV equivalent silicon damage methodology
[DE90-007167] 18 p2614 N90-24888
Neutron and gamma irradiation effects on power semiconductor switches
[NASA-TM-103200] 19 p2686 N90-25278
Swelling of neutron irradiated vanadium alloys
[DE90-015294] 24 p3448 N90-29472

NEUTRON PHYSICS
Proof of the feasibility of coherent and incoherent schemes for pumping a gamma-ray laser
[AD-A212315] 04 p0506 N90-12921

NEUTRON RADIOGRAPHY
Neutron autoradiography of hydrogen
[DE90-612930] 14 p1948 N90-21148
Determination of Li-Al alloy extent in tubular aluminum elements by small source neutron radiology
[DE90-009142] 14 p1952 N90-21174
Neutron radiography: Applications and systems
22 p3186 N90-28080

NEUTRON SCATTERING
Magnetic correlations in high T(sub c) oxides in the superconducting state
[DE89-016421] 01 p0130 N90-10746
Spin fluctuations and excitations in a 2D xy-ferromagnet: CoCl2 in graphite
[DE89-017600] 02 p0196 N90-11119
Neutron scattering studies of amorphous Invar alloys
[DE89-016868] 02 p0197 N90-11126
Neutron scattering experiments on high-temperature superconducting materials: Foreign trip report, September 13, 1988--October 4, 1988
[DE89-017451] 02 p0285 N90-11630
Neutron scattering studies of premartensitic phenomena
[DE90-000025] 03 p0328 N90-11863
Solid State Division
[DE90-000979] 06 p0851 N90-14945
Structure and dynamics of disordered systems
[DE90-001408] 07 p0990 N90-15718
Measurement of body fat by neutron inelastic scattering: Comments on installation, operation, and error analysis
[DE90-006765] 11 p1540 N90-18868
Neutron scattering measurements of the magnetic excitations of high-temperature superconducting materials
[DE90-006567] 12 p1721 N90-19885
Low temperature properties of amorphous solids
15 p2171 N90-22405
On the explanation of anomalies in inelastic neutron scattering by high-T(sub c) superconductors
[DE90-620561] 17 p2475 N90-24149
NMR and optical studies of piezoelectric polymers
[DE90-012459] 20 p2837 N90-26137

NEUTRON SOURCES
The Reversed-Field-Pinch (RFP) fusion neutron source: A conceptual design
[DE89-015297] 02 p0276 N90-11577
Report of the Advanced Neutron Source (ANS) Aluminum Cladding Corrosion Workshop
[DE90-001281] 07 p0903 N90-15217
Gamma-ray production cross section measurements using a white neutron source from 1 to 400 MeV
[DE90-008906] 14 p2025 N90-21610
Determination of internal strains in high-temperature superconductor composites by intense pulsed neutron source
[DE90-007799] 14 p2033 N90-21664
Neutron radiography: Applications and systems
22 p3186 N90-28080

NEUTRON SPECTRA
Crystal and magnetic structure of Er(2)(Co(sub x)Fe(sub 1-x))(17) compounds
[DE90-004926] 10 p1436 N90-18288
Hydrogen assay foil counting system
[DE90-007415] 12 p1624 N90-19332
Tensile behavior and swelling of ternary austenitic alloys irradiated in different neutron spectra
[DE90-015295] 24 p3450 N90-29485

NEUTRON SPECTROMETERS
Concept for a neutron spectrometer based on optical detection of (3)He(n, p)-3H reactions in a gas
[DE90-014776] 23 p3330 N90-28826

NEUTRON STARS
NT PULSARS
Pulsars lost and found: The second Princeton-Arecibo millisecond pulsar search 07 p1013 N90-15865
Positron annihilation in gamma-ray bursts
11 p1559 N90-18983
Sources of gravitational waves
12 p1730 N90-19942
Time-dependent two-dimensional radiation hydrodynamics of accreting matter onto highly magnetized neutron stars
[DE90-006927] 12 p1737 N90-19985
Physics of systems containing neutron stars
[NASA-CR-186002] 15 p2182 N90-22467
Does SN 1987A contain a rapidly vibrating neutron star
[CAL-371] 15 p2182 N90-22468
Does mass accretion lead to field decay in neutron stars
[CAL-394] 15 p2182 N90-22470
Gamma ray bursts: Current status of observations and theory
[NASA-TM-100398] 15 p2194 N90-22526
The dynamical evolution of dense clusters of compact stars 16 p2331 N90-23287
Gamma radiation from radio pulsars
16 p2334 N90-23302
Gamma radiation from the Crab and Vela pulsars
16 p2334 N90-23303
Gamma ray pulsars: Models and observations
16 p2335 N90-23304
What can gamma rays tell us about binary x ray sources and SNR's
16 p2336 N90-23310
Gamma ray bursts: Current status of observations and theory
16 p2336 N90-23313
What is learned from high energy bursts and flares
16 p2336 N90-23314
Noise variability in Cyg X-1 and Her X-1
17 p2483 N90-24200
EXOSAT observations of the pulse profile of Her X-1 during intermediate intensity states in a 35-day-cycle in 1985
17 p2483 N90-24201
The role of comptonisation in energy spectra of standard QPO-sources
17 p2484 N90-24205
Radiation-driven evolution of low-mass x ray binaries
18 p2637 N90-25022
Multiwavelength constraints on gamma-ray burst sources
18 p2639 N90-25032
Fast pulsars, strange stars
[DE90-011631] 19 p2765 N90-25710
Time-dependent two dimensional radiation hydrodynamics of accreting matter onto highly magnetized neutron stars
19 p2767 N90-25722
Super-critical accretion in Cir X-1
19 p2767 N90-25725
The decay of neutron star magnetic fields
19 p2769 N90-25737
Exploding neutron stars near the minimum mass: The total energy release
19 p2774 N90-25769
A theory of the rapid burster (MXB1730-335)
19 p2775 N90-25782
Accretion onto neutron stars: Radiative transfer in a strong gravitational field
19 p2776 N90-25784
EXOSAT observations of the pulse profile of Her X-1 during intermediate intensity states in a 35-day cycle in 1985
19 p2776 N90-25788
Hard X rays with a power law spectrum from a neutron star accreting through the relativistic gap
19 p2777 N90-25793
Neutron star formation in low-mass binary systems
19 p2778 N90-25797
Gamma ray bursts from magnetospheric plasma oscillations
19 p2779 N90-25805
Relativistic light bending near neutron stars
19 p2779 N90-25810
The role of comptonisation in energy spectra of standard QPO-sources
19 p2781 N90-25820
X ray burster spectra in the state of the persistent flux level. Two temperature models of the neutron star atmosphere
19 p2782 N90-25824
New results of numerical simulations of X ray binaries evolution
19 p2782 N90-25828
Optical light curves of HZ Her in the model of freely precessing neutron star
19 p2783 N90-25831
Rotating neutron stars and the equation of state of dense matter
[DE90-014185] 23 p3410 N90-29269

NEUTRON TRANSMUTATION
U NUCLEAR REACTIONS

NEUTRONS
NT COLD NEUTRONS
NT FAST NEUTRONS
NT PHOTONEUTRONS
NT SOLAR NEUTRONS
Energy dependent transport problem with generalized boundary conditions
[DE89-617843] 01 p0118 N90-10676
Tritium and neutron measurements of a solid state cell
[DE90-003657] 07 p1005 N90-15820
Isotope driven critical scattering and phase separation from mixtures of deuterated and protonated polymers
[DE90-003976] 08 p1051 N90-16076
Neutron experiments on high-temperature superconductors
[DE90-003978] 08 p1132 N90-16559
Results of an attempt to measure increased rates of the reaction D-2 + D-2 yields He-3 + n in a nonelectrochemical cold fusion experiment
[NASA-TM-102430] 09 p1280 N90-17424
On the scale of diffusion lengths observable by neutron reflection: Application to polymers
[DE90-005645] 10 p1358 N90-17878
Cold fusion research
[DE90-005611] 10 p1433 N90-18267
Fracture toughness and tensile properties of alloy HT9 in thin sections under high neutron fluences
[DE90-008386] 15 p2069 N90-21851
An analysis of the finite-differenced, even-parity discrete-ordinates equations in slab geometry
[DE90-006479] 15 p2160 N90-22337

Physics of systems containing neutron stars
[NASA-CR-186002] 15 p2182 N90-22467
Study of Sn-116 via neutron pickup and proton stripping reactions
[KVI-814] 16 p2315 N90-23199
Measurements of the single event upset environment in the upper atmosphere
[RAE-TM-SPACE-373] 23 p3351 N90-28934
Accurate calculations of neutron kerma and damage from ENDF/B-VI evaluations for silicon, chromium, iron and nickel, and comparison with ENDF/B-V results
[DE90-016020] 24 p3481 N90-29674

NEW HAMPSHIRE
Surface Observation Climatic Summaries (SOCS) for Pease Air Force Base, New Hampshire
[AD-A215750] 10 p1408 N90-18117

NEW ZEALAND
Satellite image atlas of glaciers of the world: Irian Jaya, Indonesia, and New Zealand
[PB90-230095] 24 p3483 N90-29691

NEWS
Index to NASA news releases and speeches, 1986
[NASA-TM-101899] 15 p2175 N90-22430
Index to NASA news releases and speeches, 1987
[NASA-TM-101900] 15 p2175 N90-22431
Index to NASA news releases and speeches, 1988
[NASA-TM-101901] 15 p2175 N90-22432

NEWTON METHODS
NT NEWTON-RAPHSON METHOD
An improved algorithm for the determination of the system paramters of a visual binary by least squares
02 p0290 N90-11658
A modified Newton method for unconstrained minimization
[AD-A212752] 04 p0546 N90-13174
Modified Newton-type methods for long-range target motion analysis
[FEL-1989-82] 04 p0551 N90-13208
A note on Smale's global Newton method
[AD-A215139] 09 p1267 N90-17346
On calculating analytic centers
[AD-A215635] 09 p1274 N90-17385
Computer-aided structural optimisation of aircraft structures
[BR112837] 14 p1915 N90-20973
Parallel non-linear optimization
[REPT-89-45] 15 p2151 N90-22290
A survey of search directions in interior point methods for linear programming
[REPT-89-65] 17 p2445 N90-23934
Calculation of correction terms for forces and moment measurements in radial flow field of hypersonic spheric nozzles 18 p2490 N90-24234
Direct calculation of Newton steps without accumulating Jacobians
[DE90-009702] 18 p2607 N90-24847
Efficient generalized conjugate gradient algorithms. Part 2: Implementation
[MATHS-REPT-A-118-PT-2] 20 p2908 N90-26543
Projection methods for solving nonlinear systems of equations
[NASA-TM-101878] 21 p3063 N90-27409
Newton methods for large-scale linear equality-constrained minimization
[AD-A222310] 21 p3070 N90-27457
Recursive Newton-Euler formulation of manipulator dynamics 24 p3513 N90-29862
The location of zeros using generalizations of Newton's method
[DE90-627168] 24 p3541 N90-30023

NEWTON THEORY
Optimum shape of a blunt forebody in hypersonic flow
[NASA-CR-181955] 05 p0575 N90-13351
Toward higher order tests of the gravitational interaction 12 p1731 N90-19948

NEWTON-RAPHSON METHOD
Iterative procedures for space shuttle main engine performance models 12 p1639 N90-19416
Elastic stability and nonlinear behavior of imperfect shells with initial stresses 15 p2110 N90-22070
Numerical solutions of the nonlinear theory of curved beams 15 p2110 N90-22071

NEWTONIAN FLUIDS
Rheology and microstructure of concentrated suspensions
[DE90-009976] 18 p2520 N90-24391
Theoretical studies of non-Newtonian and Newtonian fluid flow through porous media
[DE90-011610] 18 p2554 N90-24576
The flow of non Newtonian fluids in porous media
19 p2691 N90-25307
Surface dilation and fluid-dynamical behaviour of Newtonian liquids in an overflowing cylinder. 1: Pure liquids
[LR-601] 19 p2692 N90-25317

NICKEL
NT NICKEL ISOTOPES
Structural and surface characterization of dispersed metal catalysts
[DE89-014530] 01 p0038 N90-10208
An electroformed nickel-sulfur alloy for a nose cone
[DE90-000866] 06 p0745 N90-14337
Silver-nickel composite cathodes for alkaline secondary batteries
[AD-D014231] 06 p0767 N90-14464
Theoretical studies of chemisorption and surface reactions on nickel and silicon
[DE90-004849] 08 p1047 N90-16050
Spectroscopic evidence for carbon-carbon bonding in carbide layers on metals
[AD-A216726] 11 p1479 N90-18512
Time-resolved measurements of solidification and undercooling in metals and alloys
[DE90-007074] 11 p1488 N90-18564
Nanolayer reactions in aluminum-metal interfaces
[DE90-004955] 12 p1626 N90-19342
Structural comparison of nickel electrodes and precursor phases 13 p1824 N90-20472
Impedance studies of Ni/Cd and Ni/H2 cells using the cell case as a reference electrode
13 p1824 N90-20473
The application of electrochemical impedance spectroscopy for characterizing the degradation of Ni(OH)2/NiOOH electrodes 13 p1824 N90-20474
KOH concentration effect on the cycle life of nickel-hydrogen cells. Part 4: Results of failure analyses
13 p1824 N90-20475
Advances in lightweight nickel electrode technology
13 p1825 N90-20476
An investigation of the dislocation structure of the Ni/Ag phase boundary
[DE90-008428] 13 p1895 N90-20876
L shell XANES (X ray Absorption Near Edge Structure) for solid metals: Ti, V, Cr, Fe, Ni, Cu
[DE90-008043] 13 p1896 N90-20880
Microstructure and mechanical properties of nickel aluminide powders consolidated by extrusion and hot isostatic pressing
[DE90-009777] 15 p2070 N90-21855
Cascade collapse in copper and nickel
[DE90-011115] 18 p2527 N90-24423
Atomic structure of Ag/Ni interfaces
[DE90-010053] 18 p2618 N90-24914
Analysis of strain relaxation in Au/Ni multilayers by x ray diffraction
[IAR-89-25] 20 p2875 N90-26357
Ni impurity effects on hydrogen surface chemistry and etching of Si(111)
[AD-A222083] 21 p2977 N90-26921
Cyclic voltammetry at a rotating disk, electroreduction of nitrate in acidic nickel solutions, and frequency-response analysis of porous electrodes
[DE90-015317] 24 p3447 N90-29466
Relationship between microstructure, spinodal-like decomposition and selective electropolishing of irradiated invar-type alloys
[DE90-015293] 24 p3450 N90-29484
Recent progress in electronic structure calculations for defects in metals
[DE90-016323] 24 p3452 N90-29494

NICKEL ALLOYS
NT HASTELLOY (TRADEMARK)
NT INCONEL (TRADEMARK)
NT MONEL (TRADEMARK)
NT NITINOL ALLOYS
NT UDIMET ALLOYS
NT WASPALOY
Friction and wear of oxide-ceramic sliding against IN-718 nickel base alloy at 25 to 800 C in atmospheric air
[NASA-TM-102291] 01 p0046 N90-10262
Failure modes and mechanisms in nickel alloys: Primarily austenitic stainless steel
[DE89-016823] 02 p0198 N90-11132
Ignition characteristics of the nickel-based alloy UNS N07718 in pressurized oxygen
[NASA-CR-185932] 03 p0326 N90-11850
Weldability of ductile nickel aluminides
[DE89-017452] 03 p0327 N90-11859
Determination and description of the long term creep behavior of high temperature gas turbine materials
[ETN-89-94985] 03 p0329 N90-11871
Determination of the gaseous hydrogen ductile-brittle transition in copper-nickel alloys
[NASA-TM-86494] 04 p0474 N90-12715
Constitutive modeling for isotropic materials (HOST)
[NASA-CR-179522] 05 p0582 N90-13390
Constitutive modeling for isotropic materials (HOST)
[NASA-CR-174718] 05 p0582 N90-13391
Effect of adsorbed arsenic on the decomposition rate of nickel hydride
[AD-A213245] 05 p0621 N90-13624
Anomalous strain rate dependence of the serrated flow in Ni-H and Ni-C-H alloys
[AD-A213244] 05 p0624 N90-13641
Phases in lanthanum-nickel-aluminum intermetallic alloys
[DE90-000651] 06 p0746 N90-14343
Martensite transformation in NiTi alloys induced by tensile stress pulses
[DE90-001832] 06 p0747 N90-14346
Nickel beryllides and their properties
[DE90-001736] 07 p0903 N90-15220
Magnetic viscosity in Ni/Cu compositionally-modulated alloys
[DE90-002303] 07 p0904 N90-15223
The effect of dissolved ozone on the corrosion behavior of Cu-30 Ni and 304L stainless steel in 0.5 N NaCl solutions
[AD-A213804] 07 p0906 N90-15235
Hardness-damage correlations in Ta implanted single crystal Ni3Al
[DE90-005270] 09 p1293 N90-17494
Defects in monoblock cast turbine wheels
11 p1458 N90-18400
Sintering of a model nickel/alumina catalyst
[ETN-90-96270] 11 p1487 N90-18561
Mechanical properties of pure nickel alloys after long term exposures to LiOH and vacuum at 775 K
[NASA-TM-102403] 13 p1774 N90-20181
The stress corrosion performance of diffusion bonded nickel base alloys
[DE90-008130] 13 p1777 N90-20199
An introduction to nickel aluminide alloy
[DE90-008565] 13 p1778 N90-20207
Ordering mechanism in substitutional Ni-Cr alloys: Theory and experiment
[DE90-006268] 14 p1949 N90-21156
Grain boundary precipitation in Ni3Al based alloys
[AERE-R-13362] 14 p1950 N90-21161
High-temperature oxidation and sulfidation of Fe-20Cr-16Ni-4Al-1Y2O3 oxide-dispersion-strengthened alloy
[DE90-007897] 14 p1951 N90-21168
Lecture on ordered intermetallic alloys
[DE90-009011] 14 p1951 N90-21169
On the stability of amorphous silica coatings for high temperature service
[AERE-R-13425] 14 p1953 N90-21179
The temperature variation of hydrogen diffusion coefficients in metal alloys
[NASA-TM-100397] 15 p2067 N90-21836
The effect of hydrogen and microstructure on the deformation and fracture behavior of a single crystal nickel-base superalloy
[NASA-CR-185219] 15 p2068 N90-21849
A comparison of CuAlNi and other high damping alloys for the purpose of naval ship silencing applications
[AD-A218801] 16 p2221 N90-22671
A study of the phase decomposition of Fe-Ni-Al-Mo alloys
[DE90-010143] 18 p2524 N90-24406
Grain growth and phase formation in ion irradiated/annealed thin Ni-Al alloys films
[DE90-010409] 18 p2525 N90-24407
Microstructural design for fatigue crack growth resistance in Ni-base alloy
[PNR90632] 20 p2834 N90-26120
High temperature multiaxiale creep testing of Nimonic 115
[RAE-TM-P-1182] 20 p2835 N90-26122
Density changes of generation 1.5 and 2.0 copper alloys irradiated at 411 to 414 C and 529 C in FFTF-MOTA
[DE90-015291] 23 p3311 N90-28724
Oxidation of NiAl(110)
[DE90-015645] 24 p3451 N90-29487
Isotopic tailoring and other techniques used to study helium effects in austenitic alloys
[DE90-016344] 24 p3452 N90-29495
The effect of helium on microstructural evolution in austenitic steels as determined by spectral tailoring experiments
[DE90-016360] 24 p3452 N90-29496
Fundamental studies on intermetallic compounds
[ONERA-RT-4/1855-M] 24 p3453 N90-29497

NICKEL CADMIUM BATTERIES
Electrical battery model for LEO application based on absolute instantaneous state of charge
10 p1332 N90-17702
Low earth orbit nickel cadmium battery lifetime testing
10 p1334 N90-17716
Changes in impedance of Ni electrodes upon standing and cycling
[NASA-TM-102438] 10 p1401 N90-18097
The importance of batteries in unmanned missions
13 p1821 N90-20456

Laboratory testing of Energy Research Corporation ERC 160 NiCd 6 volt traction battery
[DE90-009629] 15 p2089 N90-21957
Laboratory testing of Saft SEH-5-200 6 volt traction battery
[DE90-009787] 15 p2089 N90-21958
The INEL battery data base
[DE90-010914] 18 p2550 N90-24555
NASA aerospace flight battery systems program
[NASA-TM-103237] 20 p2882 N90-26397
Hubble space telescope six-battery test bed
[NASA-TM-103506] 22 p3124 N90-27731

NICKEL COMPOUNDS
NT NICKEL OXIDES
Effect of adsorbed arsenic on the decomposition rate of nickel hydride
[AD-A213245] 05 p0621 N90-13624
New organic synthetic metals derived from BEDT-TTF, Ni(dsit)2 and BEDO-TTF
[DE90-003793] 07 p0907 N90-15242
New electrically conducting solids based on nickel(II) - bis(1,3-dithiole-2-thione-4,5-diselenolate)
[DE90-003788] 08 p1042 N90-16020
Antiferromagnetism and enhanced heat in CeM2Sn (M = Ni, Ir, Cu, Rh, Pd, and Pt
[DE90-014924] 23 p3399 N90-29206

NICKEL HYDROGEN BATTERIES
Characterization and cycle tests of lightweight nickel electrodes
[NASA-TM-102399] 04 p0470 N90-12696
Terrestrial nickel/hydrogen battery development at Johnson Controls, Inc.
[DE89-015843] 06 p0769 N90-14471
A nickel/hydrogen battery for PV systems
[DE90-001537] 07 p0926 N90-15358
Space Station Freedom energy storage system design and development 10 p1332 N90-17701
The ground testing of nickel hydrogen batteries prior to launch 10 p1333 N90-17705
Nickel hydrogen cell design for space applications 10 p1334 N90-17714
Status of the cycling tests performed with SAFT NiH2 cells dedicated to space applications 10 p1334 N90-17715
Changes in impedance of Ni electrodes upon standing and cycling
[NASA-TM-102438] 10 p1401 N90-18097
Space Electrochemical Research and Technology (SERT), 1989
[NASA-CP-3056] 13 p1821 N90-20454
Characterization testing of a 40 AHR bipolar nickel-hydrogen battery 13 p1822 N90-20463
Multi-mission Ni-H2 battery cells for the 1990's 13 p1825 N90-20477
Nickel-hydrogen capacity loss on storage 13 p1825 N90-20478
Effect of KOH concentration on LEO cycle life of IPV nickel-hydrogen flight battery cells
[NASA-TM-103127] 14 p1942 N90-21116
Effect of LEO cycling on 125 Ah advanced design IPV nickel-hydrogen battery cells
[NASA-TM-103128] 15 p2061 N90-21808
Photovoltaic power for Space Station Freedom
[NASA-TM-102569] 15 p2062 N90-21812
Electrochemical impregnation and cycle life of lightweight nickel electrodes for nickel-hydrogen cells
[NASA-TM-103140] 15 p2068 N90-21844
Analysis of thermal energy storage material with change-of-phase volumetric effects
[NASA-TM-102457] 15 p2092 N90-21974
NASA aerospace flight battery systems program
[NASA-TM-103237] 20 p2882 N90-26397

NICKEL IRON BATTERIES
The INEL battery data base
[DE90-010914] 18 p2550 N90-24555

NICKEL ISOTOPES
Cosmic ray half life of Ni-56
[DE90-000132] 08 p1153 N90-16680
Plating nickel-63 on copper coupons
[DE90-005023] 10 p1356 N90-17862

NICKEL OXIDES
Center for surface radiation damage studies
[AD-A218452] 16 p2222 N90-22678
High temperature oxidation of Ni3Al composites
[DE90-010145] 18 p2517 N90-24373

NICKEL STEELS
Contribution to the transcrystalline stress crack corrosion of austenite chromium-nickel steels
[ETN-89-94665] 02 p0199 N90-11137
Mechanical property characterization of VascoMax T-300
[AD-A212950] 05 p0623 N90-13637
Influence of sinter technical limits for the manufacturing of oscillation strained pieces made of sinter steel
[LBF-FB-184(1989)] 18 p2526 N90-24413

NICKEL ZINC BATTERIES
Cycle-life improvement of Zn/NiOOH cells by the addition of Ca(OH)2 to the zinc electrode
[DE90-004040] 08 p1062 N90-16139

NICOTINIC ACID
Niacin ingested at night causes severe hypotension
[AD-A217896] 13 p1851 N90-20624

NIGHT
Cumulative airport noise exposure metrics: An assessment of evidence for time-of-day weightings, revision
[AD-A214878] 09 p1170 N90-16773
Niacin ingested at night causes severe hypotension
[AD-A217896] 13 p1851 N90-20624
High resolution imaging of the Venus night side using a Rockwell 128x128 HgCdTe array 14 p1978 N90-21330
Optimal helicopter trajectory planning for terrain following flight
[NASA-CR-186470] 17 p2349 N90-23376
Energy storage for a lunar base by the reversible chemical reaction: CaO+H2O reversible reaction Ca(OH)2
[NASA-TM-103145] 19 p2709 N90-25419

NIGHT AIRGLOW
U NIGHTGLOW

NIGHT E LAYER
U E REGION
U NIGHT SKY

NIGHT F LAYER
U F REGION
U NIGHT SKY

NIGHT FLIGHTS (AIRCRAFT)
Human factors and safety considerations of night vision systems flight using thermal imaging systems
[AD-A223226] 21 p3037 N90-27263

NIGHT SKY
Night sky radiometric measurements during follow-on-evaluation testing of AN/PVS-7 (A, B) at Fort Benning, Georgia
[AD-A211273] 02 p0276 N90-11574
Distribution of auroral precipitation at midnight during a magnetic storm
[PB89-213136] 03 p0370 N90-12118
The optical night sky at low surface brightness: High latitude dust and faint field galaxies 15 p2185 N90-22481

NIGHT VISION
Cockpit lighting compatibility with image intensification night imaging systems: Issues and answers
[AD-A210503] 01 p0006 N90-10028
Night sky radiometric measurements during follow-on-evaluation testing of AN/PVS-7 (A, B) at Fort Benning, Georgia
[AD-A211273] 02 p0276 N90-11574
Visual acuity and stereopsis with night vision goggles
[AD-A211552] 03 p0381 N90-12167
A Scheiner-principle pocket optometer for self-evaluation and biofeedback accommodation training
[AD-A213171] 04 p0524 N90-13027
Imaging probabilities, geometry and ergonomics in limited visibility helicopter operations 07 p0872 N90-15060
The assessment of visibility from automatic contrast Measurements 07 p0872 N90-15061
Attenuating the luminous output of the AN/PVS-5A night vision goggles and its effects on visual acuity
[AD-A214895] 09 p1261 N90-17311
Reliability testing of the Hughes temperature controlled 1/4 watt split cycle cryogenic cooler (HD-1045 (V)/UA)
[AD-A216696] 12 p1641 N90-19426
Human factors engineering testing of aircraft cockpit lighting systems
[AD-A216853] 12 p1697 N90-19743
Relationship between flexibility of closure and success in pilot night vision sensor system training
[AD-A221439] 16 p2261 N90-22890
Helmet-mounted pilot night vision systems: Human factors issues 16 p2269 N90-22930
The application of kriging in the statistical analysis of anthropometric data, volume 1
[AD-A220613] 17 p2438 N90-23891
The application of kriging in the statistical analysis of anthropometric data, volume 3
[AD-A220615] 17 p2438 N90-23893
Human factors and safety considerations of night vision systems flight using thermal imaging systems
[AD-A223226] 21 p3037 N90-27263
The measurement of dark adaptation level in the presence of glare
[PB90-155987] 22 p3231 N90-28323
Human factors and safety considerations of night vision systems flight
[USAARL-89-12] 22 p3233 N90-28332

NIGHTGLOW
A self-consistent model of the most common nightglow emissions 05 p0660 N90-13853
Chemical interactions and light emissions from vented species
[AD-A214130] 10 p1327 N90-17668
Study of the atmospheric emissions of OI wavelength 557.7 nm and O2 (0,0) wavelength 761.9 nm in the equatorial region utilizing measurement of photometer on-board a rocket
[INPE-4811-TDL/358] 11 p1533 N90-18827
Low latitude F-region dynamical processes from atomic oxygen nightglow emissions
[INPE-4999-PRE/1561] 14 p2006 N90-21494
Polar BEAR UV imaging of airglow and aurora-image processing and results
[AD-A219480] 17 p2422 N90-23802

NIMBOSTRATUS CLOUDS
A case study of a quasi-stationary tropical convective line
[AD-A218325] 13 p1847 N90-20604

NIMBUS CLOUDS
U NIMBOSTRATUS CLOUDS

NIMBUS SATELLITES
NT NIMBUS 7 SATELLITE

NIMBUS 7 SATELLITE
Nimbus 7 solar backscatter ultraviolet (SBUV) ozone products user's guide
[NASA-RP-1234] 09 p1246 N90-17227
Atlas of albedo and absorbed solar radiation derived from Nimbus 7 Earth radiation budget data set, November 1978 to October 1985
[NASA-RP-1231] 09 p1247 N90-17233
Cloud types and the tropical Earth radiation budget, revised
[NASA-CR-180475] 13 p1843 N90-20582
Nimbus-7 TOMS Antarctic ozone atlas: August through November, 1989
[NASA-RP-1237] 17 p2428 N90-23837
Spatial cross-correlation of Antarctic Sea ice and seabed topography
[NASA-CR-186815] 20 p2891 N90-26451

NIOBATES
NT LITHIUM NIOBATES
Low temperature elastic and dielectric properties of incommensurate barium sodium niobate
[AD-A216969] 12 p1709 N90-19815

NIOBIUM
NT NIOBIUM ISOTOPES
Exploratory study of niobium, titanium, zirconium and tantalum aluminides
[AD-A210658] 02 p0283 N90-11615
Niobium and niobium nitride contacts on semiconducting material
[AD-D014177] 03 p0409 N90-12347
Niobium 1 percent zirconium/potassium and titanium/potassium life-test heat pipe design and testing
[DE90-002430] 07 p0954 N90-15522
Micron-thin Nb films recovered from Mbar shock pressures
[DE90-001509] 07 p0998 N90-15772
Silicon-based coatings on niobium metal
[DE90-003651] 08 p1048 N90-16057
Dynamic response for thermal control and measurement and fast radiation thermometry 10 p1367 N90-17924
Chemically prepared PZT films doped with niobium
[DE90-006811] 13 p1892 N90-20859
Microstructure of Au/Nb multilayers
[DE90-008722] 14 p2033 N90-21662
Mechanical properties of carbon-implanted niobium
[DE90-009864] 15 p2064 N90-21823
Ta and Nb reinforced MoSi2
[DE90-010596] 18 p2517 N90-24377
Characterization of solid state bonding between Coors AD-999 alumina and niobium
[DE90-010653] 18 p2518 N90-24379
Characterization of NbTi multifilamentary superconducting wires
[DE90-626245] 20 p2930 N90-26672
Crystal chemical and quantum chemical studies of Ba(Sr)-Nb oxide compounds 22 p3150 N90-27858

NIOBIUM ALLOYS
Emittance, catalysis, and dynamic oxidation of Ti-14Al-21Nb
[NASA-TP-2955] 01 p0044 N90-10248
Precipitation strengthened high strength, high conductivity Cu-Cr-Nb alloys produced by chill block melt spinning
[NASA-CR-185144] 03 p0326 N90-11853
Creep strength of niobium alloys, Nb-1%Zr and PWC-11
[NASA-TM-102390] 03 p0326 N90-11854
Dispersion strengthening of high temperature niobium alloys
[AD-A213829] 07 p0906 N90-15236

Production and processing of Cu-Cr-Nb alloys
[NASA-TM-102495] 08 p1047 N90-16053
Properties and design of multifilamentary NbTi composite superconductors
[DE90-004904] 08 p1134 N90-16569
Effect of manganese additions on the physical and superconducting properties of Nb-46.5Ti
[DE90-005393] 10 p1436 N90-18290
Low temperature specific heat and magnetic susceptibility of NbTi and NbTiMn alloys
[DE90-005390] 11 p1486 N90-18552
Ac loss measurements of two multifilamentary NbTi composite strands
[DE90-005388] 12 p1619 N90-19304
Oxidation characteristics of Ti-14Al-21Nb ingot alloy
[NASA-TP-3012] 19 p2674 N90-25206
Effect of boron on intergranular hot cracking in Ni-Cr-Fe superalloys containing niobium
[NASA-CR-184038] 20 p2834 N90-26115
Advanced processing and properties of high performance alloys
[AD-A221776] 21 p2983 N90-26948

NIOBIUM CARBIDES
Kinetics and mechanisms of primary and steady state creep in B- and Al-containing alpha silicon carbide
[AD-A210739] 02 p0283 N90-11616

NIOBIUM COMPOUNDS
NT LITHIUM NIOBATES
NT NIOBATES
NT NIOBIUM CARBIDES
NT NIOBIUM OXIDES
NT NIOBIUM STANNIDES
The characterization of Nb3Sn superconductors for use in magnets of 19 T and greater
[DE89-017758] 03 p0412 N90-12364
Fabrication of NBN based electronic devices with silicon barriers
[AD-D014230] 06 p0767 N90-14463
Edge geometry superconducting tunnel junctions utilizing an NbN/MgO/NbN thin film structure
[NASA-CASE-NPO-17812-1-CU] 09 p1286 N90-17456
Integrated optics at Lawrence Livermore National Laboratory
[DE90-003015] 10 p1431 N90-18255
TEM, positron lifetime, and hardness measurements of irradiated, cold-worked, and annealed Zr-1 percent Nb
[VTT-RR-650] 19 p2676 N90-25216

NIOBIUM ISOTOPES
Determination of hyperfine structures and Rydberg convergence limits of selected optical transitions in Nb-93 using resonance ionization spectroscopy
[PB90-110719] 08 p1122 N90-16498

NIOBIUM OXIDES
Optical waveguide fabrication by stoichiometric implantation of Ti and O into LiNbO3
[DE90-004238] 09 p1292 N90-17488
Deposition of electrooptic thin films
[DE90-010543] 18 p2619 N90-24922

NIOBIUM STANNIDES
Further studies of transverse stress effects in cable-in-conduit conductors
[DE90-001517] 06 p0771 N90-14484

NITINOL ALLOYS
Battery actuation of NITINOL at sub-zero temperatures
[AD-A211254] 02 p0216 N90-11237

NITRAMINE PROPELLANTS
Nitramine composite solid propellant modeling 02 p0207 N90-11183
Calculation of Einstein A coefficients and oscillator strengths for the A(perturbed)(2)A(1)-X(perturbed)(2)B(1) transition of NH(2)
[AD-A213837] 07 p0896 N90-15176
Determination of the mechanism of decomposition of energetic molecules
[AD-A217061] 12 p1633 N90-19388
Structure of model gas flames in nitramines
[AD-A217578] 13 p1770 N90-20159
Nitramine composite solid propellant modelling
[AD-A220198] 17 p2383 N90-23573
Temperature and OH concentrations in a solid propellant flame using absorption techniques
[AD-A222591] 20 p2830 N90-26100

NITRATES
NT AMMONIUM NITRATES
NT CELLULOSE NITRATE
NT PETN
NT SILVER NITRATES
Processing and fabrication of high temperature oxide superconductors
[AD-A210197] 01 p0131 N90-10755
Selection of corrosion-resistant materials for use in molten nitrate salts
[DE90-004351] 08 p1046 N90-16048
Heterogeneous transformation of peroxyacetylnitrate 20 p2887 N90-26430
Cyclic voltammetry at a rotating disk, electroreduction of nitrate in acidic nickel solutions, and frequency-response analysis of porous electrodes
[DE90-015317] 24 p3447 N90-29466
Tropospheric nitrogen: The influence of anthropogenic sources on distributions and deposition
[DE90-015408] 24 p3487 N90-29709

NITRATION
The 1-((diorganooxyphosphonyl)-methyl)-2,4- and -2,6-diamido benzenes
[NASA-CASE-ARC-11425-4] 13 p1766 N90-20133
Some 1-(diorganooxyphosphonyl)methyl-2,4- and -2,6-dinitro-benzenes
[NASA-CASE-ARC-11425-3] 17 p2367 N90-23475

NITRIC ACID
Profile measurements of sulfur dioxide, nitrogen oxides, and nitric acid deposition velocities in California's south coast air basin
[PB90-104001] 06 p0808 N90-14703
Measurements of tropospheric nitric acid over the Western United States and Northeastern Pacific Ocean
[NASA-TM-103470] 20 p2883 N90-26399
The global cycle of reactive nitrogen
[DE90-015041] 23 p3348 N90-28919
Tropospheric nitrogen: The influence of anthropogenic sources on distributions and deposition
[DE90-015408] 24 p3487 N90-29709

NITRIC OXIDE
The retrieval of the concentrations of nitric oxide and nitrogen dioxide from satellite solar occultation measurements at sunset and sunrise 06 p0814 N90-14733
Excitation lifetimes and excited-state forces in chemisorbed molecules
[DE90-002578] 07 p0894 N90-15165
A program of fundamental research on explosives at Los Alamos
[DE90-006509] 11 p1495 N90-18602
Estimation of the distribution of SO2 and NOX emission in Europe 12 p1688 N90-19699
Computation of hypersonic low density flows with thermochemical nonequilibrium 13 p1749 N90-20044
Model of turbulent diffusion flames and nitric oxide generation
[PB90-155557] 22 p3155 N90-27886

NITRIDES
NT ALUMINUM NITRIDES
NT BORON NITRIDES
NT GALLIUM NITRIDES
NT METAL NITRIDES
NT OXYNITRIDES
NT SILICON NITRIDES
NT TITANIUM NITRIDES
Ion implantation of two titanium alloys
[DE89-016958] 02 p0198 N90-11133
Niobium and niobium nitride contacts on semiconducting material
[AD-D014177] 03 p0409 N90-12347
Edge geometry superconducting tunnel junctions utilizing an NbN/MgO/NbN thin film structure
[NASA-CASE-NPO-17812-1-CU] 09 p1286 N90-17456
Effects of titanium on some surface properties of nitride ceramics
[AERE-R-13566] 14 p1953 N90-21178
Studies on the use of supercritical ammonia for ceramic nitride synthesis and fabrication
[NASA-TM-102570] 15 p2068 N90-21843
Synthesis, structure, and properties of Ca2ZnN2
[AD-A222012] 21 p3083 N90-27533

NITRIDING
Advances and directions of ion nitriding/carburizing
[NASA-TM-102398] 03 p0334 N90-11902
Internal and external nitriding and nitrocarburizing of iron and iron-based alloys
[ETN-90-96012] 05 p0625 N90-13646
An XPS and electrochemical study of the influence of molybdenum and nitrogen on the passivity of austenitic stainless steel
[AD-A214267] 08 p1044 N90-16034
Influence of a surface finishing on the fatigue behavior of a 32CDV13 steel
[ETCA-89-R-164] 22 p3157 N90-27902
Surface reactions of the TA6V titanium alloy under laser irradiation
[ETCA-90-R-012] 22 p3158 N90-27904

NITRILES
NT ACETONITRILE
NT ACRYLONITRILES
NT POLYACRYLONITRILE
The chemistry of hexaazatriphenylene hexanitrile, a polyfunctional heterocycle with potential utility in the formulation of thermostable polymers
[AD-A212353] 04 p0480 N90-12757
Miscibility and phase behavior of poly (enaminonitrile)/PEO blends
[AD-A222255] 21 p2987 N90-26975
Precursor structure-fiber property relationships in polyacrylonitrile-based carbon fibers
[AD-A224246] 24 p3454 N90-29503

NITRO COMPOUNDS
NT NITROBENZENES
NT NITROMETHANE
NT TRINITROTOLUENE

NITROBENZENES
NT TRINITROTOLUENE
Polymerization of nitro compounds on silver surfaces during surface-enhanced Raman scattering
[AD-A216116] 11 p1489 N90-18569

NITROCELLULOSE
U CELLULOSE NITRATE

NITROGEN
NT LIQUID NITROGEN
Evaluation of the North Atlantic seasonal nitrogen model, version 2
[DE89-016157] 01 p0090 N90-10515
Interactive computer program for the generation of enthalpy-entropy and temperature-entropy charts of nitrogen and hydrogen
[DLR-FB-89-27] 04 p0533 N90-13081
CANOES 2: Dynamics of atmospheric infrared thermochemical excitation, volume 1
[AD-A213341] 05 p0667 N90-13897
CANOES 2: Dynamics of atmospheric infrared thermochemical excitation, volume 2
[AD-A213342] 05 p0667 N90-13898
CANOES 2: Dynamics of atmospheric infrared thermochemical excitation, volume 3
[AD-A213343] 05 p0667 N90-13899
CANOES 2: Dynamics of atmospheric infrared thermochemical excitation, volume 4
[AD-A213344] 05 p0667 N90-13900
Propagation of sound in vibrationally excited nitrogen and hydrogen gas mixtures
[AD-A213002] 05 p0696 N90-14073
Phase changes in carbon and nitrogen systems: Their effects on the detonation properties of high explosives
[DE90-000829] 06 p0755 N90-14392
Nitrogen deposition to forest trees
[DE90-003285] 06 p0812 N90-14726
The dissociation energy of N2
[NASA-TM-101930] 07 p0891 N90-15153
Stainless steel passivity
[AD-A214108] 08 p1044 N90-16033
An XPS and electrochemical study of the influence of molybdenum and nitrogen on the passivity of austenitic stainless steel
[AD-A214267] 08 p1044 N90-16034
Characterization of B and N implanted fused silica
[DE90-004198] 08 p1050 N90-16069
The preparation and characterisation of oxynitride glasses and glass-ceramics
[AD-A214783] 09 p1197 N90-16935
Regulation of nitrogen uptake and assimilation: Effects of nitrogen source, root-zone pH, and aerial CO2 concentration on growth and productivity of soybeans
[NASA-CR-177546] 10 p1413 N90-18147
Evolutionary effects in B stars 14 p2041 N90-21704
Recombination lines of C I and N II in the interstellar medium 15 p2182 N90-22466
Reactions of silane in active nitrogen
[AD-A220371] 17 p2373 N90-23511
Preparation and characterization of properties of oxynitride glasses and fibers
[AD-A221334] 19 p2677 N90-25227
The global cycle of reactive nitrogen
[DE90-015041] 23 p3348 N90-28919
Electron-beam fluorescence measurements in hypersonic flows 24 p3420 N90-29318
Meteorological conditions over the North Atlantic Ocean during GCE/CASE/WATOX
[PB90-252032] 24 p3494 N90-29747

NITROGEN ATOMS
Computation of hypersonic low density flows with thermochemical nonequilibrium 13 p1749 N90-20044
Formation and deactivation of vibrationally excited atmospheric molecules
[AD-A222660] 20 p2889 N90-26442
Synthesis, structure, and properties of Ca2ZnN2
[AD-A222012] 21 p3083 N90-27533
Quenching of N(2D) by O(3P)
[AD-A221690] 23 p3303 N90-28683

NITROGEN COMPOUNDS
NT ALUMINUM NITRIDES
NT AMIDES
NT AMINO RADICAL
NT AMMONIA
NT AMMONIUM NITRATES
NT ATROPINE
NT AZIDES (INORGANIC)
NT AZIDES (ORGANIC)
NT BISMALEIMIDE
NT BORON NITRIDES
NT CAFFEINE
NT CELLULOSE NITRATE
NT CYANAMIDES
NT CYANO COMPOUNDS
NT CYANOACETYLENE
NT GALLIUM NITRIDES
NT HMX
NT HYDROCYANIC ACID
NT IMIDES
NT IMINES
NT ISOCYANATES
NT KAPTON (TRADEMARK)
NT METAL NITRIDES
NT NITRATES
NT NITRIC ACID
NT NITRIC OXIDE
NT NITRIDES
NT NITROBENZENES
NT NITROGEN DIOXIDE
NT NITROGEN FLUORIDES
NT NITROGEN OXIDES
NT NITROGEN POLYMERS
NT NITROGEN TETROXIDE
NT NITROMETHANE
NT NITROUS OXIDES
NT OXYNITRIDES
NT PETN
NT POLYIMIDES
NT RDX
NT SILICON NITRIDES
NT SILVER NITRATES
NT TITANIUM NITRIDES
NT TRINITROTOLUENE
NT TRYPTOPHAN
NT UREAS
Y-Si-Al-O-N glass fibers
[AD-A211170] 02 p0190 N90-11088
Nuclear magnetic resonance signatures of nitrogen-containing compounds
[AD-A213375] 05 p0622 N90-13628
Pentafluorothio polynitroaliphatic explosives
[AD-D014221] 06 p0753 N90-14383
Nitrogen deposition to forest trees
[DE90-003285] 06 p0812 N90-14726
Studies of organo phosphorus-, nitrogen-, and sulfur-containing molecules
[AD-A213518] 07 p0888 N90-15135
Research in energetic compounds
[AD-A214106] 10 p1360 N90-17887
A preliminary assessment of 3-Nitro-1,2,4-Triazol-5-One (NTO) as an insensitive high explosive
[AD-A215083] 10 p1360 N90-17889
Synthesis and chemistry of unsaturated metal nitrogen compounds
[AD-A216550] 12 p1622 N90-19321
Copolymer-like structures of nematic nitroimine dimers
[AD-A217574] 13 p1780 N90-20215
On the vapour phase deposition mechanism of carbon-boron-nitrogen compounds between 800 and 1000 C
[REPT-992-430-101] 16 p2214 N90-22832
Deposition to the Baltic Sea 20 p2884 N90-26404
NITROGEN DIOXIDE
Atmospheric chemistry of the fuel hydrazines
02 p0203 N90-11158
Micrometeorological investigation of surface exchange of trace gases: A case study
[PB89-208375] 02 p0249 N90-11412
Synergistic effects of nitrogen dioxide and carbon dioxide following acute inhalation exposures in rats
[PB89-214779] 03 p0377 N90-12150
The retrieval of the concentrations of nitric oxide and nitrogen dioxide from satellite solar occultation measurements at sunset and sunrise
06 p0814 N90-14733
Evaluation of doped phthalocyanines and a chemically-sensitive field effect transistor for detecting nitrogen dioxide
[AD-A215662] 09 p1214 N90-17037
Development and use of a passive technique for measuring nitrogen dioxide in the background atmosphere 16 p2331 N90-23285
Photodissociation of NO2: Influence of photolysis wavelength and temperature dependence on product formation 20 p2887 N90-26426
Laboratory and field evaluations of extrasensitive sulfur dioxide and nitrogen dioxide analyzers for acid deposition monitoring
[PB90-201062] 22 p3199 N90-28153
An electron spin resonance study of adsorbed gases in ultrahigh vacuum
[ETN-90-97323] 24 p3447 N90-29469
Production of NO, NO2 and N2O in air by breakdown with high power microwaves: A preliminary report
[AD-A223297] 24 p3495 N90-29749
NITROGEN FIXATION
U NITROGENATION
NITROGEN FLUORIDES
Synthesis of tetrafluorohydrazine
[AD-D014281] 08 p1052 N90-16083
Experimental studies on energy storage
[AD-A219032] 16 p2252 N90-22845
NITROGEN HYDRIDES
NT AMINO RADICAL
NITROGEN IONS
Ion implantation of two titanium alloys
[DE89-016958] 02 p0198 N90-11133
An explicit partition of the fusion-like cross section
[KVI-797] 04 p0553 N90-13225
Production rates for electron beams and swarms in nitrogen
[AD-A218145] 13 p1885 N90-20817
Friction and wear of tungsten carbides with nitrogen ion implants
[ECL-89-19] 17 p2371 N90-23496
NITROGEN OXIDES
NT NITRIC OXIDE
NT NITROGEN DIOXIDE
NT NITROGEN TETROXIDE
NT NITROUS OXIDES
Study of the NO3 radical decomposition reaction and the N2O5 in equilibrium with NO3 + NO2 equilibrium constant
[PB89-208961] 01 p0085 N90-10480
Electron attachment and molecular fragmentation in laser-excited plasmas
[AD-A212098] 03 p0409 N90-12343
CANOES 2: Dynamics of atmospheric infrared thermochemical excitation, volume 1
[AD-A213341] 05 p0667 N90-13897
CANOES 2: Dynamics of atmospheric infrared thermochemical excitation, volume 2
[AD-A213342] 05 p0667 N90-13898
CANOES 2: Dynamics of atmospheric infrared thermochemical excitation, volume 3
[AD-A213343] 05 p0667 N90-13899
CANOES 2: Dynamics of atmospheric infrared thermochemical excitation, volume 4
[AD-A213344] 05 p0667 N90-13900
Profile measurements of sulfur dioxide, nitrogen oxides, and nitric acid deposition velocities in California's south coast air basin
[PB90-104001] 06 p0808 N90-14703
Acid deposition
[DE90-003959] 07 p0958 N90-15544
Time and spatially dependent estimates of pollutant trace gas emissions and their effect on tropospheric ozone 09 p1243 N90-17212
Low NO(x) potential of gas turbine engines
[NASA-TM-102452] 10 p1321 N90-17636
The RADM 2 gas-phase chemical mechanism
12 p1686 N90-19684
Source attribution for tropospheric ozone in the US
[DE90-007994] 14 p2004 N90-21484
A low NOx strategy for combusting high nitrogen content fuels
[PB90-155664] 19 p2712 N90-25435
Anthropogenic sources of NO(x), SO()x, CO, and CH4: Geographical distribution
[AERONOMICA-ACTA-A-353-1990] 19 p2713 N90-25440
Aircraft exhaust emissions: An engine manufacturer's perspective
[PNR90675] 20 p2812 N90-26004
Catching our breath: Next steps for reducing urban ozone
[PB90-130451] 20 p2883 N90-26398
Measurements of CH4, N2O, CO, H2O and O3 in the middle atmosphere by the ATMOS experiment on Spacelab 3
[NASA-TM-103476] 20 p2883 N90-26400
New observations of stratospheric N2O5
[NASA-TM-103478] 20 p2883 N90-26402
Verification and improvement of the EMEP model for long-range transport and deposition of pollutants
20 p2884 N90-26405
An Eulerian transport model for NO(sub x)-compounds
20 p2884 N90-26406
Formation and deactivation of vibrationally excited atmospheric molecules
[AD-A222660] 20 p2889 N90-26442
Quenching of N(2D) by O(3P)
[AD-A221690] 23 p3303 N90-28683
The global cycle of reactive nitrogen
[DE90-015041] 23 p3348 N90-28919
Acid deposition: No such thing as a free launch
[DE90-015085] 23 p3348 N90-28920
Tropospheric nitrogen: The influence of anthropogenic sources on distributions and deposition, executive summary
[DE90-015401] 23 p3348 N90-28922
Measurements of the high altitude infrared characteristics of the atmosphere
[AD-A224401] 24 p3491 N90-29728
NITROGEN PLASMA
An experimental study of microwave transmission through a decaying plasma
[AD-A210586] 01 p0127 N90-10726
Plasma modification of poly (p-phenylenebenzobisthiazole)
[AD-A215761] 10 p1433 N90-18272
Polycrystalline diamond Junction Field Effect Transistors (JFETS)
[AD-A222238] 21 p3083 N90-27534
NITROGEN POLYMERS
Synthesis and analysis of novel polymers with potential for providing both high permselectivity and permeability in gas separation applications
[DE90-003907] 08 p1049 N90-16065
NITROGEN TETROXIDE
Thermodynamic transport properties of nitrogen tetroxide in hypercritical conditions for regenerative cooling of a rocket engine. Volume 1: Tests
[ETN-89-94975] 01 p0134 N90-10773
Thermodynamic transport properties of nitrogen tetroxide in hypercritical conditions for regenerative cooling of a rocket engine. Volume 2: Appendices
[ETN-89-94977] 01 p0134 N90-10774
Space shuttle RCS oxidizer leak repair for STS-26
11 p1474 N90-18485
NITROGENATION
Surface treatments of carbon fibers in an organic environment. Finite element analysis of pull-out tests
[ONERA-RT-7/3549-M] 04 p0471 N90-12698
NITROMETHANE
Chemistry of nitromethane at very high pressure
[DE89-008016] 01 p0039 N90-10215
In-situ study of the chemically driven flow fields in initiating homogeneous and heterogeneous nitromethane explosives
[DE89-008415] 02 p0207 N90-11186
NITROUS OXIDES
Formation kinetics of N2O in the atmosphere
20 p2886 N90-26425
Field-induced surface chemistry of NO
[AD-A223007] 21 p2977 N90-28915
Natural and anthropogenic climate change
[DE90-015528] 23 p3348 N90-28923
Production of NO, NO2 and N2O in air by breakdown with high power microwaves: A preliminary report
[AD-A223297] 24 p3495 N90-29749
NMR
U NUCLEAR MAGNETIC RESONANCE
NOAA SATELLITES
Determination of optical porperties of clouds from NOAA-AVHRR data using Apollo
08 p1092 N90-16321
Operational requirements and the geostationary platform 12 p1608 N90-19250
Real time environment monitoring using data from METEOSAT and NOAA imaging satellites
[NLR-MP-87070-U] 12 p1684 N90-19672
Overview of battery usage in NASA/GSFC LEO and GEOspacecrafts 13 p1821 N90-20455
Implementation of reflectance models in operational AVHRR radiation budget processing
[NOAA-TR-NESDIS-49] 18 p2578 N90-24688
NOBLE GASES
U RARE GASES
NOBLE METALS
NT GOLD
NT GOLD ISOTOPES
NT RUTHENIUM
NT SILVER
Surface analyses and modelling of rate multiplicity and instabilities
[DE90-005418] 10 p1352 N90-17838
Process for making a noble metal on tin oxide catalyst
[NASA-CASE-LAR-13741-1-SB] 13 p1774 N90-20180
CO-oxidation catalysts: Low-temperature CO oxidation over Noble-Metal Reducible Oxide (NMRO) catalysts
18 p2556 N90-24588
Phillips CO-oxidation catalyts for long-lived CO2 lasers: Activity and initial characterization studies
18 p2557 N90-24592

Synthesis, characterization and evaluation of CO-oxidation catalysts for high repetition rate CO2 TEA lasers
18 p2557 N90-24593
Mechanistic studies of the CO-oxidation reaction on catalysts for use in long-life CO2 lasers
18 p2558 N90-24596

NOCTILUCENCE
U LUMINESCENCE

NOE NAVIGATION
U NAP-OF-THE-EARTH NAVIGATION

NOISE (SOUND)
NT AERODYNAMIC NOISE
NT AIRCRAFT NOISE
NT BLADE SLAP NOISE
NT ENGINE NOISE
NT JET AIRCRAFT NOISE
NT PROPELLER NOISE
NT SONIC BOOMS
NT THERMAL NOISE
The effects of noise on performance
[AD-A212519] 04 p0551 N90-13209
ULF/VLF (0.001 to 50 Hz) Seismo-Acoustic Noise in the Ocean
[AD-A212942] 05 p0671 N90-13913
Control of an experiment to measure acoustic noise in the space shuttle
[NPS62-89-022] 06 p0838 N90-14869
Wind speed dependence of acoustic ambient vertical directional spectra at high frequency
[AD-A214293] 07 p0989 N90-15712
Computation of broadband mixing noise from turbomachinery
[AD-A214448] 07 p0989 N90-15713
Voice preprocessor for digital voice applications
[AD-A214726] 09 p1205 N90-16982
Recognition of environmental sounds
[AD-A214942] 09 p1259 N90-17302
Vertical directionality measurements of ambient noise in the NE Pacific
[AD-A220007] 17 p2432 N90-23856
Observations of seafloor ambient noise with an ocean bottom seismometer array
[AD-A220159] 17 p2432 N90-23858
Large aperture array measurements of the vertical ambient noise field
[AD-A220165] 17 p2432 N90-23859
Auditory perception of complex sounds
[AD-A219927] 17 p2435 N90-23872
BASEOPS default profiles for civil aircraft
[AD-A223161] 21 p2959 N90-26825
Aspects of acoustic noise generation by a laser-propelled vehicle
[DE90-012087] 21 p2964 N90-26851
Development and analysis of ARMA parameter estimation schemes in the presence of noise
[AD-A221794] 21 p3066 N90-27428
Noise from tip vortex and bubble cavitation
[AD-A221962] 21 p3072 N90-27468
Applications of ripple analysis in hydro-acoustics
[ETN-90-97015] 22 p3244 N90-28397
Methods for detecting low-frequency signals in the presence of strong winds
[AD-A223980] 23 p3320 N90-28769
Measuring the vertical directional spectra caused by sea surface sound
[AD-A223883] 23 p3354 N90-28957

NOISE ATTENUATION
U NOISE REDUCTION

NOISE ELIMINATION
U NOISE REDUCTION

NOISE GENERATORS
Development of a thermoacoustic test facility
02 p0183 N90-11041
The large European Acoustic Facility at ESTEC
02 p0187 N90-11067
Effects of acoustic sources 04 p0446 N90-12553
Influence of vane sweep on rotor-stator interaction noise
05 p0571 N90-13325
Dynamics of a class of vortex rings
07 p0926 N90-15362
Aspects of acoustic noise generation by a laser-propelled vehicle
[DE90-012087] 21 p2964 N90-26851

NOISE HAZARDS
U HAZARDS
U NOISE (SOUND)

NOISE INTENSITY
Noise data of four small propeller-driven airplanes
[PB89-216980] 03 p0400 N90-12291
The effects of noise on speech and warning signals
[AD-A212520] 04 p0551 N90-13210
Cavitation-controlled ultrasonic agitator
[DE90-002773] 06 p0838 N90-14871
Cumulative airport noise exposure metrics: An assessment of evidence for time-of-day weightings, revision
[AD-A214878] 09 p1170 N90-16773
Evaluation of two objective measures of effective auditory stimulus level
[AD-A214869] 09 p1250 N90-17255
Adaptive multiple-band CFAR (Constant-False-Alarm-Rate) detection of an optical pattern with unknown spectral distribution
[AD-A214754] 09 p1281 N90-17429
Measuring Day-Night Noise Levels (DNL) using the metrosonics db-310 sound level analyzer (Dosimeter)
[AD-A215757] 10 p1427 N90-18230
Noise levels from a VSTOL aircraft measured at ground level and at 1.2 m above the ground
[NPL-RSA(EXT)-009] 11 p1562 N90-18999
Self-tuning control techniques, implicit and explicit, with parameter estimation in Kalman filters, applied to artificial satellite attitude
[INPE-4857-TDL/368] 12 p1613 N90-19276
Noise floors of subnanosecond transient recording systems
[DE90-002339] 12 p1666 N90-19571
Lateral attenuation of military aircraft flight noise
[AD-A218041] 13 p1882 N90-20799
Airborne sound insulation of slits, joints, and sealing stripes
[PB90-128976] 14 p2023 N90-21599
Free-field propagation of high intensity noise
[NASA-CR-186577] 14 p2024 N90-21604
Prediction of length scales in a Mach reflection flowfield
15 p2069 N90-21959
Noise reduction theory acoustic barrier construction
[CRIF-MC-87] 16 p2313 N90-23183
Analyses of the predictability of noise-induced sleep disturbance
[AD-A220156] 17 p2435 N90-23876
Summary of sonic boom rise times observed during FAA community response studies over a 6-month period in the Oklahoma City area
[NASA-CR-4277] 18 p2608 N90-24852
Sound propagation elements in evaluation of en route noise of advanced turbofan aircraft
18 p2609 N90-24861
Agenda toward the development of a rational noise descriptor system relevant to human annoyance by en route aircraft noise
18 p2610 N90-24866
Additive evaluation criteria for aircraft noise
18 p2610 N90-24867
En route noise annoyance laboratory test: Preliminary results
18 p2611 N90-24870
An aircraft noise study in Norway
18 p2611 N90-24872
Aeroacoustics of advanced propellers
[NASA-TM-103137] 20 p2923 N90-26635
Aiming control: Theory and applications to dynamic control of space structures
[AD-A221532] 21 p2967 N90-26864
Post-flare effects in the lower ionosphere of middle latitudes
22 p3209 N90-28205
Structure-borne noise estimates for the PTA aircraft
[NASA-CR-4315] 22 p3244 N90-28396
Studies in automatic speech recognition and its application in aerospace
23 p3318 N90-28759
Annoyance caused by advanced turboprop aircraft flyover noise: Counter-rotating-propeller configuration
[NASA-TP-3027] 23 p3392 N90-29166
Audibility and annoyance of en route noise of unducted fan engines
[AD-A223687] 24 p3543 N90-30035

NOISE MEASUREMENT
Measurement resolution of noise directivity patterns from acoustic flight tests
[NASA-TM-4134] 01 p0118 N90-10679
The design and development of an acoustic test section for the ARA transonic wind tunnel
[PNR90574] 04 p0550 N90-13202
Acoustic recording systems for use in military aircraft
[RAE-TM-MM-11] 04 p0551 N90-13207
Recovery of particle size distribution of ultrafine aerosols from diffusional decay measurements
[AD-A213006] 05 p0621 N90-13621
Analysis of an R-SQUID noise thermometer
[VTT-PUBL-54] 05 p0645 N90-13769
A model suitable for predicting the noise associated with the ducted tail rotor of a helicopter
[ECL-88-09] 05 p0697 N90-14074
Multisqueezing of mechanical states and back-action evasion measurements
[IFSI-89-6] 08 p1123 N90-16504
Radio noise measurements in the long-wave band at Thule, Greenland
[NASA-CR-182824] 09 p1206 N90-16991
Evaluation of two objective measures of effective auditory stimulus level
[AD-A214869] 09 p1250 N90-17255
Measuring Day-Night Noise Levels (DNL) using the metrosonics db-310 sound level analyzer (Dosimeter)
[AD-A215757] 10 p1427 N90-18230
Noise levels from a VSTOL aircraft measured at ground level and at 1.2 m above the ground
[NPL-RSA(EXT)-009] 11 p1562 N90-18999
The Shock and Vibration Digest, volume 22, no. 2
14 p2022 N90-21596
State of the art of acoustics of active and passive mufflers
14 p2023 N90-21597
Airborne sound insulation of slits, joints, and sealing stripes
[PB90-128976] 14 p2023 N90-21599
Exhaust environment measurements of a turbofan engine equipped with an afterburner and 2D nozzle
[NASA-CR-4289] 15 p2052 N90-21760
Noise reduction theory acoustic barrier construction
[CRIF-MC-87] 16 p2313 N90-23183
Large aperture array measurements of the vertical ambient noise field
[AD-A220165] 17 p2432 N90-23859
Analysis of the environmental noise situation around a large Swedish prototype wind turbine
[FFA-TN-1988-16] 17 p2469 N90-24116
PTA en route noise measurements
18 p2608 N90-24855
En route noise: NASA propfan test aircraft (corrected data - simplified procedure)
[DOT-TSC-FA953-LR4] 18 p2608 N90-24856
En route noise of two turboprop aircraft
[DLR-MITT-89-18] 18 p2609 N90-24859
Noise measurements of turboprop airplanes at different overflight elevations
18 p2609 N90-24860
Preliminary thoughts on an acoustic metric for the wilderness aircraft overflight study
18 p2609 N90-24862
En route noise annoyance laboratory test: Preliminary results
18 p2611 N90-24870
Human response research update
18 p2611 N90-24873
Innovative techniques for high-resolution imaging and precision tracking
[AD-A221380] 18 p2616 N90-24899
Aero-acoustic investigations of the magnetic train Transrapid 06
[MBB-UW-0009/89-PUB] 19 p2654 N90-25104
Neuromorphic learning of continuous-valued mappings from noise-corrupted data. Application to real-time adaptive control
[NASA-TM-4176] 19 p2747 N90-25607
Data of aero acoustic measurements on ultra-light aircraft propellers
[ESA-TT-1147] 19 p2754 N90-25648
Man-made noise in a military environment
20 p2847 N90-26191
Bringing aircraft noise testing down to Earth
[PNR90642] 20 p2924 N90-26637
Aviation acoustical noise measurement
[AD-A222014] 21 p3073 N90-27469
Theoretical studies carried out in 1988 on helicopter rotor noise under subsonic conditions
[ONERA-RS-82/5094-PY] 22 p3245 N90-28402
Technique for the measurement of noise of the flow associated to the small wave numbers of the turbulence spectra
[ETN-90-97558] 24 p3469 N90-29601

NOISE POLLUTION
The effects of noise on speech and warning signals
[AD-A212520] 04 p0551 N90-13210
Cumulative airport noise exposure metrics: An assessment of evidence for time-of-day weightings, revision
[AD-A214878] 09 p1170 N90-16773
A/F32T-9 large turbo fan engine enclosed noise suppressor system (T-9 NSS), exterior far-field and interior noise, McConnell AFB, Kansas
[AD-A220535] 17 p2354 N90-23402
Updating a dosage-effect relationship for the prevalence of annoyance due to general transportation noise
[AD-A219416] 17 p2421 N90-23794
Activities report in technical-physical research
[ETN-90-96771] 17 p2487 N90-24223
Activities report in aerospace and aerodynamics
[ETN-90-96774] 17 p2487 N90-24224
FAA/NASA En Route Noise Symposium
[NASA-CP-3067] 18 p2608 N90-24853
Sound propagation elements in evaluation of en route noise of advanced turbofan aircraft
18 p2609 N90-24861
Preliminary thoughts on an acoustic metric for the wilderness aircraft overflight study
18 p2609 N90-24862

US Forest Service and National Park Service Wilderness Aircraft Overflight Study: Sociological background and study plans 18 p2609 N90-24863
Agenda toward the development of a rational noise descriptor system relevant to human annoyance by en route aircraft noise 18 p2610 N90-24866
High-speed civil transport study: Special factors [NASA-CR-181881] 23 p3276 N90-28537

NOISE PREDICTION
Acoustic design considerations: Review of rotor acoustic sources 04 p0451 N90-12585
Estimation of subsonic far-field jet-mixing noise from single-stream circular nozzles [ESDU-89041] 09 p1161 N90-16721
En route noise annoyance laboratory test: Preliminary results 18 p2611 N90-24870
High speed turboprop aeroacoustic study (counterrotation). Volume 1: Model development [NASA-CR-185241] 20 p2923 N90-26633

NOISE PREDICTION (AIRCRAFT)
Near-field noise predictions of an aircraft in cruise 04 p0443 N90-12538
A model suitable for predicting the noise associated with the ducted tail rotor of a helicopter [ECL-88-09] 05 p0697 N90-14074
Evaluation of analysis techniques for low frequency interior noise and vibration of commercial aircraft [NASA-CR-181851] 06 p0837 N90-14886
Aerodynamic loads and blade vortex interaction noise prediction [ISL-PU-310/89] 20 p2802 N90-25942
Aeroacoustics of advanced propellers [NASA-TM-103137] 20 p2923 N90-26635
The validation and application of a rotor acoustic prediction computer program [NASA-TM-101794] 21 p3072 N90-27465
Air Force procedure for predicting aircraft noise around airbases: Airbase operations program (BASEOPS) description [AD-A223069] 21 p3072 N90-27466
Air Force procedure for predicting aircraft noise around airbases: Noise Exposure Model (NOISEMAP). User's manual [AD-A223162] 21 p3072 N90-27467
Assessment System for Aircraft Noise (ASAN): Development of alpha-test prototype system software [AD-A223770] 24 p3543 N90-30036

NOISE PROPAGATION
NRL/VOA modifications to IONCAP as of 12 July 1988 [AD-A211546] 03 p0338 N90-11929
Acoustical effects of a large ridge on low-frequency sound propagation in stationary and moving atmospheres [NASA-CR-186001] 03 p0400 N90-12290
Active control of multi-dimensional random sound in ducts [NASA-TM-102653] 14 p2024 N90-21603
Free-field propagation of high intensity noise [NASA-CR-186577] 14 p2024 N90-21604
En route noise: NASA propfan test aircraft (corrected data - simplified procedure) [DOT-TSC-FA953-LR4] 18 p2608 N90-24856
En route noise: NASA propfan test aircraft (calculated source noise [DOT-TSC-FA953-LR5] 18 p2609 N90-24857
A review of instability and noise propagation in supersonic flows [NASA-CR-186800] 19 p2655 N90-25112
The validation and application of a rotor acoustic prediction computer program [NASA-TM-101794] 21 p3072 N90-27465
Theoretical studies carried out in 1988 on helicopter rotor noise under subsonic conditions [ONERA-RS-82/5094-PY] 22 p3245 N90-28402

NOISE REDUCTION
The theory and application of quadratic minimization in the active reduction of sound and vibration 01 p0119 N90-10682
Calculation of sound transmission through a cylindrical shell using ASKA acoustics 02 p0179 N90-11009
Review and analysis of the DNW/Model 360 rotor acoustic data base [NASA-TM-102253] 03 p0299 N90-11692
Multi-stage noise-reducing system [AD-D014179] 03 p0341 N90-11942
Adaptive noise cancellation for a class of nonlinear 2R filter [RR-351] 03 p0344 N90-11965
Noise data of four small propeller-driven airplanes [PB89-216980] 03 p0400 N90-12291
The NASA experience in aeronautical R and D: Three case studies with analysis [AD-A211486] 04 p0437 N90-12496
What should be done with those noisy old aircraft [PNR90562] 04 p0452 N90-12593
Re-engine with the Rolls-Royce Tay 670, the route to significant noise reduction [PNR90585] 04 p0455 N90-12606
Adaptive antenna arrays for satellite communication [NASA-CR-185989] 04 p0485 N90-12784
Removal of noise from noise-degraded speech signals [AD-A212876] 04 p0493 N90-12840
Application of active noise reduction for hearing protection and speech intelligibility improvement [IZF-1988-21] 04 p0527 N90-13042
UHB demonstrator interior noise control flight tests and analysis [NASA-CR-181897] 04 p0549 N90-13198
The commercial aircraft noise problem [PNR90577] 04 p0550 N90-13203
A frequency domain technique for improving sound field reproduction [RAE-TM-MM-10] 04 p0551 N90-13205
Estimation of rain rate using spatial and multichannel coherence: Analysis of SSM/I data 05 p0670 N90-13905
Test procedures for the evaluation of helmet and headset mounted active noise reduction systems [AD-A212991] 05 p0676 N90-13937
Fundamental quantum 1/f noise in ultrasmall semiconductor devices and their optimal design principles [AD-A211947] 05 p0702 N90-14107
A communications system with an adaptive multi-functional architecture 06 p0759 N90-14415
Sound attenuation apparatus [NASA-CASE-LAR-13968-1] 07 p0988 N90-15710
Low-noise nozzle valve [NASA-CASE-MFS-28383-1] 09 p1216 N90-17051
Study of active noise control in ducts [DE89-772353] 10 p1425 N90-18224
Fuselage design for a specified Mach-sliced area distribution [NASA-TP-2975] 11 p1455 N90-18385
Microwave oscillator with reduced phase noise by negative feedback incorporating microwave signals with suppressed carrier 12 p1643 N90-19437
The adaptive line enhancer applied to chirp detection [DE90-006772] 13 p1789 N90-20268
Common-mode rejector for pulse power diagnostics [AD-A218096] 13 p1798 N90-20316
Synopsis of early field test results from the gravity gradiometer survey system 13 p1833 N90-20525
Lateral attenuation of military aircraft flight noise [AD-A218041] 13 p1882 N90-20799
A review of gear housing dynamics and acoustics literature [NASA-CR-185148] 14 p1987 N90-21387
Transmission research activities at NASA Lewis Research Center [NASA-TM-103132] 14 p1988 N90-21394
The Shock and Vibration Digest, volume 22, no. 2 14 p2022 N90-21596
State of the art of acoustics of active and passive mufflers 14 p2023 N90-21597
Airborne sound insulation of slits, joints, and sealing stripes [PB90-128976] 14 p2023 N90-21599
Passive stabilization of a fiber optic nonlinear interferometric sensor [AD-D014438] 14 p2026 N90-21620
The Shock and Vibration Digest, volume 21, no. 8 15 p2110 N90-22068
Spline function smoothing and differentiation of noisy data on a rectangular grid [DE90-009319] 15 p2160 N90-22338
The Shock and Vibration Digest, volume 21, no. 6 15 p2163 N90-22363
Noise transmission into propeller-driven airplanes 15 p2163 N90-22364
Improvement of clutter rejection by scanning motion compensation in ground-based monopulse radar [ETN-90-96550] 16 p2228 N90-22711
Integrated control-system design via generalized LQG (GLQG) theory 16 p2286 N90-23023
Noise reduction theory acoustic barrier construction [CRIF-MC-87] 16 p2313 N90-23183
A/F32T-9 large turbo fan engine enclosed noise suppressor system (T-9 NSS), exterior far-field and interior noise, McConnell AFB, Kansas [AD-A220535] 17 p2354 N90-23402
Data quality analysis at the National Transonic Facility [NASA-CR-4303] 17 p2448 N90-23957
The effect of noise-abatement profiles on noise immissions and human annoyance underneath a subsequent climbpath 18 p2610 N90-24865
Problems of internal acoustics in two and three dimensional cavities with deformable walls using the MSC/Nastran code [DLC/STR-INT-TN-004] 18 p2612 N90-24876
Aero-acoustic investigations of the magnetic train Transrapid 06 [MBB-UW-0009/89-PUB] 19 p2654 N90-25104
Stage 2 re-engining: The only way to achieve a real stage 3 aircraft [PNR90636] 20 p2808 N90-25977
Low-speed wind tunnel investigation of the static stability and control characteristics of an advanced turboprop configuration with the propellers placed over the tail [NASA-CR-186900] 20 p2814 N90-26017
Man-made noise in a military environment 20 p2847 N90-26191
Classification regions in remote sensing imagery utilizing spatial characteristics [INPE-4913-PRE/1514] 20 p2879 N90-26381
A preliminary study of the masking of wind turbine noise by ambient sound [FFA-TN-1990-01] 20 p2923 N90-26636
Aviation acoustical noise measurement [AD-A222014] 21 p3073 N90-27469
A process for analysis, evaluation, and development of aerial servicing noise reduction measures in civil aircraft [ETN-90-97300] 22 p3244 N90-28396
Comparison of speech intelligibility in cockpit noise using SPH-4 flight helmet with and without active noise reduction [NASA-CR-177564] 23 p3271 N90-28510
Methods for detecting low-frequency signals in the presence of strong winds [AD-A223980] 23 p3320 N90-28769
Performance analysis of subspace-based parameter estimation algorithms [AD-A224523] 24 p3463 N90-29586
An assessment of the application of in situ ion-density data from DMSP to modeling of transionospheric scintillation [AD-A224392] 24 p3490 N90-29725

NOISE SPECTRA
Effects of acoustic sources 04 p0446 N90-12553
A frequency domain technique for improving sound field reproduction [RAE-TM-MM-10] 04 p0551 N90-13205
Dynamics of a class of vortex rings 07 p0926 N90-15362
The calculation of overground sound propagation in the presence of wind and temperature gradients [ESDU-89036] 07 p0989 N90-15714
Advanced Doppler tracking experiments 12 p1731 N90-19951
Free-field propagation of high intensity noise [NASA-CR-186577] 14 p2024 N90-21604
Spectral characteristics of low-angle radar ground clutter [AD-A220817] 17 p2392 N90-23622
In situ investigation of sea surface noise from a depth of one meter [AD-A220158] 17 p2432 N90-23857
Analysis of the environmental noise situation around a large Swedish prototype wind turbine [FFA-TN-1988-16] 17 p2469 N90-24116
Noise variability in Cyg X-1 and Her X-1 17 p2483 N90-24200
Innovative techniques for high-resolution imaging and precision tracking [AD-A221380] 18 p2616 N90-24899
QPOs and preferred time scales in the variability of X ray pulsars 19 p2767 N90-25721
X ray observations of GS2023+338 by the Kvant module 19 p2771 N90-25747
Noise variability in Cyg X-1 and Her X-1 19 p2771 N90-25753
A model for 1/f-type variability in active galactic nuclei 19 p2778 N90-25799
Methods for probing quasi-periodic oscillations on short time scales 19 p2780 N90-25811
Characterization of the pitting corrosion of aluminum-lithium alloys [ETCA-89-R-176] 22 p3157 N90-27903
Inertial grade fiber gyros 24 p3426 N90-29353

NOISE SUPPRESSORS
U NOISE REDUCTION

NOISE TEMPERATURE
Spin-lattice relaxation and the calculation of gain, pump power, and noise temperature in ruby 04 p0486 N90-12790
Interrelationship of spatial and radiometric resolution in the thermal infrared band [INPE-4860-TDL/371] 11 p1523 N90-18771
Ultralow noise performance of an 8.4-GHz maser-feedhorn system 15 p2076 N90-21889
Radiometric tests on wet and dry antenna reflector surface panels 15 p2076 N90-21890

NOISE THRESHOLD
Recognition of environmental sounds [AD-A214942] 09 p1259 N90-17302

Noise floors of subnanosecond transient recording systems
[DE90-002339] 12 p1666 N90-19571
Binaural masking: An analysis of models
[AD-A221668] 21 p3035 N90-27252

NOISE TOLERANCE
FAA/NASA En Route Noise Symposium
[NASA-CP-3067] 18 p2608 N90-24853
Proposed definition of the term en route in en route aircraft noise 18 p2608 N90-24854
The effect of noise-abatement profiles on noise immissions and human annoyance underneath a subsequent climbpath 18 p2610 N90-24865
Additive evaluation criteria for aircraft noise 18 p2610 N90-24867
Social survey findings on en route noise annoyance issues 18 p2610 N90-24868
Predicting the audibility and annoyance of unducted fan engines 18 p2610 N90-24869
Problems related to aircraft noise in Switzerland 18 p2611 N90-24871
Human response research update 18 p2611 N90-24873
Noise adaptation and correlated maneuver gating of an extended Kalman filter
[AD-A221713] 21 p3001 N90-27060
Annoyance caused by advanced turboprop aircraft flyover noise: Counter-rotating-propeller configuration
[NASA-TP-3027] 23 p3392 N90-29166
Workshop on Low Level Flight Training
[AGARD-AR-288] 24 p3436 N90-29404

NOMENCLATURES
Nomenclature for physical mapping of complex genomes
[DE89-015173] 06 p0859 N90-14994
Quick guide of the essential concepts used in optical digital data disk technology 17 p2479 N90-24175

NOMINAL VALUES
U APPROXIMATION

NOMOGRAMS
U NOMOGRAPHS

NOMOGRAPHS
Debris/ice/TPS assessment and photographic analysis for shuttle mission STS-31R
[NASA-TM-102790] 20 p2819 N90-26040

NONADIABATIC PROCESSES
U HEAT TRANSFER

NONAQUEOUS ELECTROLYTES
Electroactive polyaniline film deposited from non-aqueous media. 2: Effect of acid concentration in solutions
[AD-A212084] 04 p0477 N90-12737
Laser temperature-jump kinetic studies of fast reactions in nonaqueous solutions
[AD-A218819] 17 p2371 N90-23500
Electrochemical, in situ Raman spectroscopic, and conductivity studies of polypyrrole incorporating large size anions: Conducting nature of reduced form
[AD-A222739] 20 p2831 N90-26102

NONCONDENSABLE GASES
Experimental investigation of condensation of steam in the presence of noncondensable gases for open-cycle surface condensers
[DE90-003552] 08 p1097 N90-16353
Experimental investigation of condensation of steam in the presence of noncondensable gases using plate heat exchangers
[DE90-002251] 12 p1682 N90-19659

NONCONDUCTORS
U ELECTRICAL INSULATION

NONDESTRUCTIVE TESTS
NT NEUTRON RADIOGRAPHY
Generic system components of the Thiokol ultrasonic RSRM case-to-insulation bondline inspection system
[NASA-CR-183738] 01 p0031 N90-10171
Gaussmeter determination of 302 stainless steel material condition
[BDX-613-3941] 01 p0044 N90-10249
Investigation of materials and bonding using the scanning laser acoustic microscope
[KCP-613-4033] 01 p0048 N90-10270
Wave-mode coordinate analysis of L junction in LSS
[AD-A211116] 02 p0176 N90-10984
Advances in instrumentation for experimental stress and vibration analysis and its applications 02 p0187 N90-11069
Sensors for nondestructive testing and evaluation of materials
[DE89-014763] 02 p0223 N90-11279
The investigation of the fundamental limits of heterodyne holographic interferometry with the application of imaging laser generated lamb waves
[AD-A211048] 02 p0224 N90-11285
A technique to correlate fractography with NDE (Non-Destructive Evaluation) of small samples
[DE89-016904] 02 p0231 N90-11325
NDE (Non-Destructive Evaluation) publications, 1985
[PB89-229025] 03 p0356 N90-12036
An air coupled transmission mode acoustic microscope for on-line non-destructive evaluation
[AD-A211416] 04 p0511 N90-12947
Device for inspection of materials by eddy current methods
[AD-D014205] 04 p0511 N90-12948
NDI (Nondestructive Inspection) oriented corrosion control for Army aircraft. Phase 1: Inspection methods
[AD-A213368] 05 p0576 N90-13359
Nondestructive analysis of aileron fatigue and aging in a Mirage F1
[REPT-M6-594000] 05 p0580 N90-13378
Quantitative non-destructive evaluation using laser generated ultrasonic pulses 05 p0653 N90-13805
Application of neutron diffraction NDE to high-temperature superconducting composites
[DE90-002184] 06 p0738 N90-14295
Diffusion bonding of metals 06 p0744 N90-14330
Nondestructive evaluation of flaw clusters and thin layer interfaces 06 p0795 N90-14633
Assessment of the efficiency of nondestructive techniques in materials testing studies based on the information criterion
[DE89-635444] 06 p0796 N90-14634
ROBOCAL (Robotic Calorimetry): An automated NDA (Nondestructive Assay) calorimetry and gamma isotopic system
[DE90-003217] 07 p0894 N90-15168
Assessment of strength limiting flaws in ceramic heat exchanger components
[DE90-004086] 08 p1051 N90-16077
Slow positron defect profiling of silicon epilayers
[DE90-003958] 08 p1087 N90-16288
Theoretical study on creep damage detection by ultra-sonic wave measurement
[DE90-702472] 08 p1087 N90-16290
Prompt Gamma Activation Analysis (PGAA): Technique of choice for nondestructive bulk analysis of returned comet samples 08 p1144 N90-16633
Non-destructive trace element microanalysis of as-received cometary nucleus samples using synchrotron x ray fluorescence 08 p1147 N90-16649
Utilization of focused acoustic beams to inspect composite materials
[ETN-90-96084] 09 p1188 N90-16880
Nondestructive control of composite materials by holographic interferometry
[ISL-CO-244/88] 09 p1188 N90-16882
Eddy current test for bolts
[AD-A214829] 09 p1234 N90-17159
Subtle porosity variation in the YBa2Cu3O(7-x) high-temperature superconductor revealed by ultrasonic imaging
[NASA-TM-102130] 09 p1235 N90-17167
Generalized pulse equations for through-transmission evaluation of arbitrary multilayered structures
[NASA-TM-100752] 09 p1278 N90-17407
Diffusion and defect characterization studies of mercury cadmium telluride
[AD-A214655] 09 p1289 N90-17470
Non-destructive characterization of epoxy/dicyandiamide interphases using surface-enhanced Raman scattering
[AD-A215894] 10 p1353 N90-17846
Z-grid signal conditioning system user's guide and technical reference
[AD-A215122] 10 p1395 N90-18067
Boundary estimation problems arising in thermal tomography
[NASA-CR-181964] 10 p1421 N90-18193
Inspection of carbon/epoxy and aluminum honeycomb paraboloidal components by HNDT
[AD-A216796] 11 p1479 N90-18514
Hydrogen assay foil counting system
[DE90-007415] 12 p1624 N90-19332
Frequency response of electrochemical cells 12 p1639 N90-19419
Summary of the DoD Metal Matrix Composites (MMC) Steering Committee Meeting, hosted by the Institute for Defense Analysis
[AD-A217611] 13 p1768 N90-20145
Nondestructive testing of ceramics by acoustic microscopy
[AERE-R-13350] 13 p1813 N90-20411
Residual stresses: A review of their measurement and interpretation using x ray diffraction
[AERE-R-13005] 13 p1815 N90-20423
Barkhausen noise analysis and ferromagnetic materials
[AD-A217989] 13 p1881 N90-20792
Neutron autoradiography of hydrogen
[DE90-612930] 14 p1948 N90-21148
Magneto acoustic emission apparatus for testing materials for embrittlement
[NASA-CASE-LAR-13817-1] 14 p1951 N90-21170
Some recent applications of laser ultrasound to the characterisation of materials
[AERE-R-13438] 14 p1985 N90-21374
Collapsible fabric tank testing
[AD-A217861] 14 p1987 N90-21388
Ultrasonic and radiographic evaluation of advanced aerospace materials: Ceramic composites
[NASA-TM-102540] 14 p1989 N90-21401
Development of ultrasonic nondestructive methods for defect and damage characterization in composite materials 15 p2063 N90-21816
Institute for Materials Science and Engineering, nondestructive evaluation: Technical activities
[PB90-132739] 15 p2108 N90-22055
Institute for Materials Science and Engineering, Fracture and Deformation Division: Technical activities, 1989
[PB90-155359] 15 p2116 N90-22106
Impact damage in graphite/epoxy laminates: Damage characterization, acoustic emission, and finite element simulation, volumes 1 and 2 16 p2211 N90-22610
Nondestructive Testing (NDT); Ceramic Matrix Composite Materials (CMCM) — Nondestructive testing (ndc); ceramic matrix composite materials (CMMC)
[REPT-892-430-123] 16 p2222 N90-22677
Applications of laser ultrasound
[AERE-R-13106] 16 p2239 N90-22777
Two-dimensional surface strain measurement based on a variation of Yamaguchi's laser-speckle strain gauge
[NASA-TM-103162] 16 p2241 N90-22784
Recent advances in nondestructive evaluation made possible by novel uses of video systems
[NASA-TM-102491] 16 p2244 N90-22801
Application of x ray absorption edge spectrometry to the non-destructive determination of element concentrations, coating thickness and areal densities
[AERE-R-13030] 16 p2245 N90-22802
Crack detection in silicon nitride by acoustic microscopy
[AERE-R-13196] 16 p2245 N90-22803
Real-time stereo-microradiography
[AD-A218433] 16 p2245 N90-22805
On-line x ray inspection of materials and structural components using discrete element x ray detectors for digital radiographic and computed tomographic evaluation
[AD-A218911] 16 p2245 N90-22806
Acousto-ultrasonic nondestructive evaluation of materials using laser beam generation and detection
[NASA-CR-186694] 17 p2398 N90-23664
Theory and experimental technique for nondestructive evaluation of ceramic composites
[NASA-TM-102561] 17 p2414 N90-23754
Method of radiographic inspection of wooden members
[NASA-CASE-LAR-13724-1] 17 p2414 N90-23756
Nondestructive measurement of residual stresses in aircraft transparencies
[AD-A218680] 17 p2415 N90-23762
In-situ topographical imaging of electrode surfaces using high resolution phase-measurement interferometric microscopy
[AD-A221021] 18 p2548 N90-24542
The feasibility of detecting corrosion in electric fuzes using the thermal transient technique
[AD-A221385] 18 p2549 N90-24547
NDE (NonDestructive Evaluation) of ceramic heat exchangers
[DE90-010977] 18 p2554 N90-24575
Non destructive testing of composite structures using embedded optical fibers: A mechanical interaction model
[ETN-90-97016] 18 p2573 N90-24661
Low thrust rocket test facility
[NASA-TM-103206] 19 p2663 N90-25158
An approach for relating the results of quantitative nondestructive evaluation to intrinsic properties of high-performance materials
[NASA-CR-186484] 19 p2699 N90-25355
Eddy current inspection at the nuclear power plants
[VTT-RR-653] 19 p2699 N90-25357
Inspection of welds with eddy current
[TTR-RR-644] 19 p2699 N90-25358
ESA fracture control requirements
[ESA-PSS-01-401-ISSUE-1] 19 p2703 N90-25376
Acousto-optic signature analysis for inspection of the orbiter thermal protection tile bonds
[DE90-013089] 20 p2819 N90-26043
Holography and holographic interferometry
[PNR90670] 20 p2866 N90-26303
Neural networks for detecting defects in aircraft structures
[IAR-90-4] 20 p2873 N90-26345

Field experience in using laser acoustic sensing for inspection
[DE90-012954] 20 p2873 N90-26347
NDT in aerospace: The next decade (1990's)
[PNR90628] 20 p2874 N90-26348
The role of NDI in the certification of turbine engine components
[PNR90629] 20 p2874 N90-26349
Characterization of inspection performance
[NLR-MP-88068-U] 20 p2874 N90-26350
Nondestructive one- and two-dimensional doping profiling by inverse methods
[ETN-90-97264] 20 p2874 N90-26351
Development of creep-fatigue damage detection method of rotor steel by ultrasonic wave measurement
[DE90-503792] 20 p2877 N90-26365
An embedded fibre optic sensor for impact damage detection in composite materials
[UTIAS-332] 20 p2926 N90-26650
NDE (Nondestructive evaluation) of critical currents in high T(sub c) superconductors
[DE90-012953] 20 p2930 N90-26670
Characterization of impact damage in composites
21 p2957 N90-26811
Retirement for cause of the F100 engine
21 p2957 N90-26813
A general discussion of the retirement for cause inspection system 21 p2957 N90-26814
Study on failure modes of SiC fiber reinforced aluminum composite materials by AE method
[DE90-505518] 21 p2971 N90-26884
Applications of digital image processing in testing and evaluation of composite materials
[AD-A222939] 21 p2971 N90-26887
Non-destructive characterization of polymer/metal interfaces using Surface-Enhanced Raman Scattering (SERS)
[AD-A223105] 21 p2986 N90-26967
Non-destructive characterization of polymer/metal interphases using surface-enhanced Raman scattering
[AD-A222490] 21 p2988 N90-26980
Artificial intelligence in the materials processing laboratory 21 p3041 N90-27283
Physics and techniques for the investigation of the properties of ultra small systems
[AD-A221985] 21 p3071 N90-27461
Flight set 360H005 (STS-26) seals, volume 4
[NASA-CR-183904] 22 p3181 N90-28051
Impact of Emerging NDE-NDI Methods on Aircraft Design, Manufacture, and Maintenance
[AGARD-CP-462] 22 p3184 N90-28068
The role of NDI in the certification of turbine engine components 22 p3184 N90-28069
NDI-concept for composites in future military aircraft
22 p3184 N90-28070
Assessment and demonstration of the capabilities of NDI processes, equipment, and personnel
22 p3184 N90-28071
Inspection reliability 22 p3184 N90-28072
Critical inspection of high performance turbine engine components: The RFC concept
22 p3185 N90-28073
Nondestructive evaluation of adhesively-bonded joints
22 p3185 N90-28074
Ultrasonic inspection of advanced CFRP structures by computer-controlled, pulse-echo technique
22 p3185 N90-28075
An ultrasonic system for in-service non-destructive inspection of composite structures
22 p3185 N90-28076
A technique for rapid inspection of composite aircraft structure for impact damage 22 p3185 N90-28077
In-service inspection of composite components on aircraft at depot and field levels
22 p3186 N90-28078
Development of an automated ultrasonic inspection system for composite structure on in-service aircraft
22 p3186 N90-28079
Neutron radiography: Applications and systems
22 p3186 N90-28080
Progress in the detection of cracks under installed fasteners using eddy currents 22 p3186 N90-28081
Acoustic emission detection of crack presence and crack advance during flight 22 p3186 N90-28082
Development and application of Computed Tomography (CT) for inspection of aerospace components
22 p3187 N90-28083
The application of infrared thermography to the nondestructive testing of composite materials
22 p3187 N90-28084
Stenopic radiography: A non-destructive test without contact 22 p3187 N90-28086
Noncontact laser thermomechanical nondestructive evaluation for advanced coatings
22 p3187 N90-28087
Advanced NDE techniques for quantitative characterization of aircraft 22 p3188 N90-28088
Study of failure processes in fiber reinforced composites using acoustic emission techniques
22 p3188 N90-28090
Use of acoustic emission for continuous surveillance of aircraft structures 22 p3188 N90-28092
Impact of NDE-NDI methods on aircraft design, manufacture, and maintenance, from the fundamental point of view 22 p3189 N90-28093
Input-output characterization of fiber reinforced composites by P waves
[NASA-CR-185287] 22 p3189 N90-28097
Fatigue crack monitoring from initiation to through cracking in welded thick steel sections
[ARE-TM(UHS)-90203] 22 p3194 N90-28122
A comparison of single-cycle versus multi-cycle proof testing strategies 23 p3296 N90-28646
Ultrasonic verification of five wave fronts in unidirectional graphite epoxy composite
[NASA-CR-185288] 23 p3337 N90-28858
A low cost shadow moire device for the nondestructive evaluation of impact damage in composite laminates
[AD-A223451] 24 p3443 N90-29442
Non-destructive evaluation of infiltration-toughened ceramics
[DE90-629716] 24 p3453 N90-29501
Non-destructive method for environmental breakdown of graphite fiber reinforced polymer composites
[AD-A223729] 24 p3455 N90-29515
Nondestructive material characterization
[DE90-015176] 24 p3477 N90-29652

NONEQUILIBRIUM CONDITIONS
Rotational and vibrational nonequilibrium effects in rarefied, hypersonic flow
[NASA-CR-182559] 04 p0437 N90-12498
Elements of a relativistic microscopic theory of hadronic matter in equilibrium and non-equilibrium
[KVI-796] 04 p0552 N90-13218
Non-equilibrium effects of slow diffusion controlled reactions on the properties of explosives
[DE90-000822] 06 p0754 N90-14391
Non-equilibrium chemistry in the solar nebula and early solar system: Implications for the chemistry of comets
08 p1142 N90-16618
Theoretical investigation of non-equilibrium chemistry and optical radiation in hypersonic flow fields
[NASA-CR-186335] 24 p3417 N90-29300

NONEQUILIBRIUM DRAG
U FRICTION DRAG

NONEQUILIBRIUM FLOW
Particle kinetic simulation of high altitude hypervelocity flight
[NASA-CR-186003] 02 p0147 N90-10840
A study of the influence of alloying additions on the passivity of aluminium
[AD-A219630] 17 p2376 N90-23532
On upwind formulations and non equilibrium chemistry
[DLC/FLU-INT-TN-014] 17 p2403 N90-23691
A review of reaction rates and thermodynamic and transport properties for an 11-species air model for chemical and thermal nonequilibrium calculations to 30000 K
[NASA-RP-1232] 21 p3002 N90-27064

NONEQUILIBRIUM IONIZATION
Gas dynamical processes in the theory of galaxy formation 02 p0294 N90-11673
Nonequilibrium ionization in supernova remnants: The case of Tycho
[MPE-PREPRINT-153] 04 p0565 N90-13295
Improved computational fluid dynamics for continuum hypersonic flow
[AD-A216981] 11 p1506 N90-18674
Time-resolved spectroscopy of nonequilibrium ionization in laser-produced plasmas
[DE90-008663] 13 p1891 N90-20854

NONEQUILIBRIUM PLASMAS
The 10th Gordon Research Conference on Plasma Chemistry
[AD-A215161] 09 p1285 N90-17449
The 41st Annual Gaseous Electronics Conference
[AD-A214540] 12 p1715 N90-19851

NONEQUILIBRIUM RADIATION
Nonequilibrium radiation and chemistry models for aerocapture vehicle flowfields
[NASA-CR-186728] 22 p3169 N90-27973
Nonequilibrium radiation and chemistry models for aerocapture vehicle flowfields
[NASA-CR-186379] 23 p3267 N90-28490

NONEQUILIBRIUM THERMODYNAMICS
A review of reaction rates and thermodynamic and transport properties for an 11-species air model for chemical and thermal nonequilibrium calculations to 30000 K
[NASA-RP-1232] 21 p3002 N90-27064
Reduced distribution functions and nonequilibrium thermodynamics of single component fluids
[PB90-189119] 22 p3254 N90-28428

NONEUCLIDIAN GEOMETRY
U DIFFERENTIAL GEOMETRY

NONFERROUS METALS
The future of non ferrous metals in aerospace engines
[PNR90572] 04 p0475 N90-12720

NONFLAMMABLE MATERIALS
Test and evaluation: Reducing risks to military aircraft from bird collisions. Report to the Chairman, Legislation, and National Security Subcommittee, Committee on Goverment Operations, House of Représentatives
[AD-A210670] 02 p0148 N90-10845
Information compendium on nonflammable hydraulic fluid and design requirements for its adoption
[AD-A219569] 17 p2380 N90-23554

NONHOLONOMIC EQUATIONS
Redundancy of space manipulator on free-flying vehicle and its nonholonomic path planning
24 p3502 N90-29797

NONHOMOGENEITY
U INHOMOGENEITY

NONISOTROPIC PLATES
U ANISOTROPIC PLATES

NONISOTROPY
U ANISOTROPY

NONLINEAR EQUATIONS
NT NONLINEAR EVOLUTION EQUATIONS
NT QUADRATIC EQUATIONS
An iterative method for systems of nonlinear hyperbolic equations
[NASA-CR-181919] 01 p0112 N90-10638
Non-linear wave-equations for low-frequency acoustic gravity waves 02 p0240 N90-11365
Global linear representations of nonlinear systems and the adjoint map
[RR-347] 03 p0394 N90-12247
Rational expansion for nonlinear input-output maps
[RR-348] 03 p0394 N90-12248
Mapping nonlinear integro-differential equations into the frequency domain
[RR-366] 03 p0394 N90-12249
Splines and equations of nonlinear parameters
[IMAG-RR-750-M] 03 p0395 N90-12257
Self-tuning control of nonlinear Armax models --- Autoregressive Moving Average with eXogeneous (ARMAX) inputs
[RR-362] 04 p0508 N90-12930
Building a software package for solving large sparse nonlinear systems of equations
[AD-A211758] 04 p0529 N90-13055
A recursive algorithm for computing the frequency response of a class of nonlinear difference equation models
[RR-354] 04 p0539 N90-13123
The Painleve test for nonlinear ordinary and partial differential equations
[AD-A212894] 04 p0546 N90-13177
The stability of Taylor-Couette flow with radial heating
06 p0774 N90-14502
Local error estimates for discontinuous solutions of nonlinear hyperbolic equations
[NASA-CR-181960] 06 p0834 N90-14847
Interdisciplinary research in viscoelasticity and rheology
[AD-A213630] 08 p1063 N90-16145
Hidden regularity for a strongly nonlinear wave equation
[DE90-600742] 08 p1116 N90-16485
Nonlinear heat transfer and wave motion
[AD-A214911] 09 p1217 N90-17058
Approximation method for nonlinear integral equations of Hammerstein type
[DE90-600727] 09 p1272 N90-17372
Asymptotic behaviour of solutions of a degenerate quasilinear hyperbolic equation
[DE89-635713] 09 p1276 N90-17400
Nonlinear wave propagation
[AD-A215500] 10 p1375 N90-17968
Self similar solutions of the second kind of nonlinear diffusion-type equations
[DE90-606953] 10 p1422 N90-18204
On the quantum inverse problem for a new type of nonlinear Schroedinger equation for Alfven waves in plasma
[DE90-607469] 10 p1431 N90-18259
Hamiltonian analysis and simulation of free electron lasers
[INPE-4785-TDL/351] 11 p1567 N90-19018
A vectorized algorithm for 3D dynamics of a tethered satellite 12 p1640 N90-19423
A comparison between the propagators method and the decomposition method for nonlinear equations
[DE90-005783] 12 p1704 N90-19781

Iteration methods for solving nonlinear equations in Frechet spaces
[DE90-610429] 12 p1706 N90-19799
Projection-iteration methods for solving nonlinear operator equations
[DE90-610433] 12 p1707 N90-19801
Parallel methods for solving nonlinear block bordered systems of equations
[AD-A217062] 12 p1707 N90-19806
Computing mean responses in nonlinear models
[AD-A217642] 13 p1865 N90-20700
Experiments in finding neural network weights
[DE90-007696] 13 p1865 N90-20702
Parallel non-linear optimization
[REPT-89-45] 15 p2151 N90-22290
A generalized complementarity problem in Hilbert space
[DE90-009576] 15 p2163 N90-22360
Numerical investigations of nonlinear behavior in the Einstein equations 15 p2175 N90-22427
Nonlinear bifurcation study of plane Poiseuille flow
[DLR-FB-89-42] 16 p2236 N90-22756
Evidence for self-refraction in a convergence zone: NPE (Nonlinear progressive wave equation) model results
[AD-A218546] 16 p2259 N90-22879
The application of a non-linear least squares method to predicting seat transmissibility
[ISVR-TR-173] 16 p2275 N90-22967
On approximation of nonlinear boundary integral equations for the combined method
[DE90-009784] 16 p2305 N90-23130
Continuation and multi-grid methods for bifurcation problems
[AD-A218904] 16 p2307 N90-23146
Collective properties of neural systems and their relation to other physical models
[AD-A219071] 16 p2315 N90-23201
Direct calculation of Newton steps without accumulating Jacobians
[DE90-009702] 18 p2607 N90-24847
Nonlinear supersonic motions of magnetized plasma flow with mass loading
[AERONOMICA-ACTA-A-354-1990] 19 p2760 N90-25681
Parallel processors and nonlinear structural dynamics algorithms and software
[NASA-CR-186755] 20 p2907 N90-26536
Efficient implementation of minimal polynomial and reduced rank extrapolation methods
[NASA-TM-103240] 20 p2920 N90-26616
Identification techniques for nonlinear differential equations of motion
[AD-A220895] 21 p3062 N90-27407
Linear iterative solvers for implicit ODE methods
[NASA-CR-182074] 22 p3242 N90-28386
Uniform dissipative solutions for some fourth order nonlinear differential equations
[DE90-627151] 24 p3536 N90-29991
An existence theorem for periodic solutions and applications to some third order nonlinear differential equations
[DE90-627152] 24 p3536 N90-29992
Oscillatory and nonoscillatory behaviour of solutions of an equation alternately of retarded and advanced type
[DE90-627159] 24 p3536 N90-29993
A posteriori error estimates for parametrized nonlinear equations
[AD-A224067] 24 p3537 N90-29997
Symmetry and island structure of the standard map
[DE90-508076] 24 p3548 N90-30069

NONLINEAR EVOLUTION EQUATIONS

A straightforward method for finding implicit solitary wave solutions of nonlinear evolution and wave equations
[AD-A210561] 01 p0113 N90-10647
A space-time discretization procedure for wave propagation problems
[NASA-TM-102215] 08 p1105 N90-16399
Nonlinear wave propagation
[AD-A215500] 10 p1375 N90-17968
Nonlinear waves and inverse scattering
[AD-A218483] 17 p2387 N90-23597

NONLINEAR FEEDBACK

A feedback extension to the numerical solution of nonlinear boundary value problems
[AD-A219886] 17 p2461 N90-24050
On the theory of nonlinear control systems
[MEMO-813] 18 p2597 N90-24776
Transition to complicated behavior in infinite dimensional dynamical systems
[AD-A221502] 21 p3077 N90-27494

NONLINEAR FILTERS

Adaptive noise cancellation for a class of nonlinear 2R filter
[RR-351] 03 p0344 N90-11965
Nongaussian linear filtering, identification of linear systems, and the symplectic group
[CWI-PM-R8810] 04 p0547 N90-13184
Estimation and control of nonlinear and hybrid systems with applications to air-to-air guidance
[AD-A214542] 09 p1170 N90-16770
System identification and filtering of nonlinear controlled Markov processes by canonical variate analysis
[AD-A214873] 09 p1273 N90-17381
Non-linear analysis of visual cortical neurons
[AD-A221543] 21 p3034 N90-27250
Statistical methodologies for non-Gaussian noisy environments
[AD-A222137] 21 p3066 N90-27433

NONLINEAR OPTICS

Monolayer formation characteristics of novel organic molecules with nonlinear optically active moieties
[AD-A210496] 01 p0121 N90-10693
Second-order nonlinear optical devices in poled polymers
[DE89-015842] 01 p0123 N90-10703
Nonlinear optics and organic materials
[AD-A210570] 01 p0124 N90-10709
Generation of higher-order squeezing of quantum electromagnetic fields by degenerate four-wave mixing and other processes
[DE89-618392] 02 p0212 N90-11213
Nonlinear optical studies of resonant systems
[AD-A211032] 02 p0227 N90-11301
Construction of a picosecond laser system for the investigation of semiconductors using nonlinear optical methods
[ETN-89-94664] 03 p0352 N90-12013
Optics and opto-electronics systems
[AD-A212340] 05 p0699 N90-14093
Molecules with enhanced electronic polarizabilities based on defect-like states in conjugated polymers
[NASA-CASE-NPO-17633-1-CU] 07 p0910 N90-15263
Nonlinear optical material studies
[AD-A213938] 07 p0993 N90-15737
Phase equilibrium and crystal growth studies on AgGaSe2 and related nonlinear optical materials
[AD-A213650] 07 p1003 N90-15809
Studies of optical matrix multiplication and reconfigurable optical interconnect concepts
[AD-A214645] 09 p1281 N90-17427
Optically tunable gratings for optical interconnects
[AD-A216978] 12 p1714 N90-19844
Picosecond nonlinear studies of complex materials using the free electron laser
[AD-A218215] 13 p1809 N90-20387
Nonlinear optics in thin films
[AD-A217336] 13 p1887 N90-20829
Integrability and chaos in nonlinearly coupled optical beams
[DE90-007540] 13 p1888 N90-20834
A second-order nonlinear optical poly(organophosphazene)
[AD-A218408] 16 p2210 N90-22607
Single-crystal diffraction analysis of 2-(trimethylsilylethynyl) 4-nitro-N,N-dimethylaniline
[AD-A218955] 16 p2216 N90-22642
Analysis and evaluation of technical data on the photochromic and non-linear optical properties of materials
[AD-A219398] 16 p2318 N90-23219
Center for Analysis of Heterogeneous and Nonlinear Media
[AD-A219627] 17 p2403 N90-23688
Nonlinear optical responses and laser damage thresholds of films of a polarized stilbene side chain liquid crystal polymer and a phthalocyanine
[AD-A219462] 17 p2408 N90-23720
Long pulse narrowband XeCl laser studies
[AD-A219774] 17 p2409 N90-23724
Multiple beam optical processing
[AD-A219048] 17 p2471 N90-24129
Second order non-linear optical polyphosphazenes
[AD-A219868] 18 p2615 N90-24895
Transition to complicated behavior in infinite dimensional dynamical systems
[AD-A221502] 21 p3077 N90-27494
Statement of research objectives and summary of research efforts
[RLE-PR-132] 23 p3415 N90-29295
Analysis and evaluation of technical data on the photochronic and non-linear optical properties of materials
[AD-A223855] 24 p3545 N90-30053

NONLINEAR PROGRAMMING

General and numerical approach to the sphere solution in FAST 05 p0610 N90-13555
On the identification of local minimizers in inertia-controlling methods for quadratic programming
[DE89-017330] 07 p0973 N90-15616
Sequential quadratic programming algorithms for optimization
[DE90-000022] 07 p0973 N90-15617
An exact algorithm for the p-median problem
[INPE-4914-PRE/1415] 10 p1418 N90-18172
An exact algorithm for the problem of p-medians
[INPE-4924-TDL/384] 11 p1544 N90-18885
Suboptimal and hybrid numerical solution schemes for orbit transfer manoeuvres
[INPE-4991-PRE/1556] 14 p1931 N90-21054
Analysis, selection, and implementation of procedures which approve optimal artificial satellite maneuvers
[INPE-5003-TDL/397] 15 p2058 N90-21786
Multilevel decomposition approach to the preliminary sizing of a transport aircraft wing
[NASA-CR-4296] 16 p2200 N90-22557
An algorithm for the solution of dynamic linear programs 16 p2286 N90-23026
Approximate minimum-time trajectories for 2-link flexible manipulators 16 p2287 N90-23030
A design optimization process for Space Station Freedom
[NASA-CR-186851] 19 p2667 N90-25175
The Second Asilomar Workshop on Progress in Mathematical Programming
[AD-A221986] 21 p3053 N90-27358
Ascent and descent trajectory optimization of Ariane 5/Hermes 22 p3126 N90-27743
New approaches to linear and nonlinear programming
[AD-A224328] 24 p3525 N90-29932

NONLINEAR SYSTEMS

The application of TSIM software to act design and analysis on flexible aircraft 01 p0018 N90-10086
Summarizing qualitative behavior from measurements of nonlinear circuits, revision
[AD-A210919] 01 p0061 N90-10353
A new approach to control single-link flexible arms. Part I: Modelling and identification in the presence of joint friction
[AD-A210590] 01 p0078 N90-10445
Regulation of nonlinear and generalized linear systems
[AD-A207725] 01 p0109 N90-10619
Finite methods for a nonlinear allocation problem
[AD-A209719] 01 p0111 N90-10629
Stochastic control theory, nonlinear structural mechanics and applied combinatorics
[AD-A209042] 01 p0114 N90-10657
A general-purpose computer program for the Volterra-series analysis of nonlinear microwave circuits
[AD-A210768] 02 p0216 N90-11236
Nonlinear adjustment with or without constraints, applicable to geodetic models
[AD-A210820] 02 p0265 N90-11509
Mapping nonlinear integro-differential equations into the frequency domain
[RR-366] 03 p0394 N90-12249
Orthogonal least squares methods and their application to nonlinear system identification
[RR-343] 03 p0395 N90-12259
Analysis of a system of two weakly nonlinear coupled harmonic oscillators arising from the field of wind-induced vibrations
[REPT-89-22] 03 p0396 N90-12261
Fast sampling and stability of nonlinear sampled data systems. Part 2: Sampling rate estimations
[RR-341] 03 p0397 N90-12271
Modeling and analysis of nonlinear time series
[RR-355] 03 p0397 N90-12272
Fast sampling and stability of nonlinear sampled-data systems. Part 1: Existence theorems
[RR-340-PT-1] 03 p0398 N90-12276
Slow sampling and stability of nonlinear sampled-data systems
[RR-342] 03 p0398 N90-12277
Optimal observer motion for bearings-only localization and tracking 04 p0449 N90-12569
Nonlinear systems and Kolmogorov's representation theorem
[RR-363] 04 p0508 N90-12931
Fundamentals of middle atmospheric dynamics
[AD-A211747] 04 p0518 N90-12988
Building a software package for solving large sparse nonlinear systems of equations
[AD-A211758] 04 p0529 N90-13055
A functional expansion and stability for nonlinear input-output maps
[RR-359] 04 p0539 N90-13121
A new decision rule for model structure identification of a class of nonlinear dynamic systems
[RR-360] 04 p0539 N90-13122
Remarks on the control of discrete time nonlinear systems
[MEMO-770] 04 p0544 N90-13158

Transformations and representations of nonlinear systems
[MEMO-778] 04 p0544 N90-13164
Towards a complete local solution of the nonlinear model matching problem
[MEMO-781] 04 p0545 N90-13166
Nongaussian linear filtering, identification of linear systems, and the symplectic group
[CWI-PM-R8810] 04 p0547 N90-13184
Problems in nonlinear acoustics: Scattering of sound by sound, parametric receiving arrays, nonlinear effects in asymmetric sound beams and pulsed finite amplitude sound beams
[AD-A211756] 04 p0550 N90-13200
Correlation of Puma airloads: Lifting-line and wake calculation
[NASA-TM-102212] 05 p0572 N90-13327
The S.D.G., P.S.D. and the nonlinear airplane
[NLR-MP-88018-U] 05 p0578 N90-13371
Discretization and model reduction for a class of nonlinear systems 05 p0583 N90-13397
Bilinear modeling and nonlinear estimation 05 p0589 N90-13430
Using Broyden updates to approximate the Jacobian in a semi-implicit backward differentiation code
[AD-A213239] 05 p0688 N90-14010
Another approach to the local disturbance decoupling problem with stability for nonlinear systems
[MEMO-799] 05 p0691 N90-14033
A helicopter flight path controller design via a nonlinear transformation technique 06 p0727 N90-14242
Dynamics and control of flexible spacecraft during and after slewing maneuvers
[NASA-CR-186123] 06 p0733 N90-14270
Box experiments. Nonlinear effects at plasma resonance 06 p0783 N90-14555
Non-linear vibrations, stability, and dynamics of structures and mechanisms
[AD-A212152] 06 p0796 N90-14639
On strongly nonlinear vortex/wave interactions in boundary-layer transition
[NASA-CR-181963] 07 p0876 N90-15078
Nonlinear viscous waves produced by an impulsively moving plate
[AD-A214014] 07 p0932 N90-15392
Nonlinear strain-displacement relations for thin axisymmetric shells
[PB89-226013] 07 p0945 N90-15470
Continuum analogues of contragredient Lie algebras: Lie algebras with a Cartan operator and nonlinear dynamical systems
[DE89-635698] 07 p0985 N90-15691
Optimal periodic control and regulator theory based on the second variation 07 p0987 N90-15704
Element-by-element preconditioning techniques for large-scale, vectorized finite element analysis in nonlinear solid and structural mechanics 08 p1087 N90-16291
Estimation and control of nonlinear and hybrid systems with applications to air-to-air guidance
[AD-A214542] 09 p1170 N90-16770
Compression phenomena in hard-saturated microwave amplifiers
[AD-A214546] 09 p1204 N90-16980
Nonlinear modulational stability and propagation of an electromagnetic pulse in a two-component, neutral plasma
[AD-A215131] 09 p1207 N90-16994
Chaos and turbulence
[AD-A215310] 09 p1294 N90-17499
Fluid transmission line dynamics for signals of finite amplitude
[AD-A215758] 10 p1385 N90-18014
Nonlinear dynamics of domain walls and vortices in two-dimensional systems
[DE90-004840] 10 p1425 N90-18221
Experimental investigation of relationship between nonlinear field energy and emittance growth
[AD-A215813] 10 p1430 N90-18246
Control and stabilization of linear and nonlinear distributed systems
[AD-A216446] 11 p1547 N90-18908
Using special-purpose computing to examine chaotic behavior in nonlinear mappings
[AD-A216800] 11 p1549 N90-18916
Nonlinear model matching: A local solution and two worked examples
[MEMO-809] 11 p1554 N90-18948
Applications of frequency and wavenumber nonlinear digital signal processing to nonlinear hydrodynamics research
[AD-A216259] 12 p1658 N90-19530
Parallel methods for solving nonlinear block bordered systems of equations
[AD-A217062] 12 p1707 N90-19806
Nonlinear system vibration: The appearance of chaos
[DE90-007546] 12 p1708 N90-19810
Nonlinear continuum mechanics and applied analysis
[AD-A213629] 12 p1709 N90-19812
Nonlinear mechanics of unstable plasmas as related to high altitude aerodynamics
[AD-A215126] 12 p1716 N90-19852
A learning regulator for the plane longitudinal movement
[ETN-90-95381] 13 p1864 N90-20695
Computing mean responses in nonlinear models
[AD-A217642] 13 p1865 N90-20700
Robust adaptive nonlinear control under extended matching conditions
[AD-A217684] 13 p1874 N90-20744
Observer based compensators for nonlinear systems
[AD-A217426] 13 p1876 N90-20760
Nonlinear systems of partial differential equations
[AD-A217581] 13 p1877 N90-20761
Techniques for accelerating iterative methods for the solution of mathematical problems
[AD-A218272] 13 p1878 N90-20775
Observation of nonlinear reflectivity from InSb surface and optical switching application
[AD-A217184] 13 p1887 N90-20826
Nonlinear and distributed parameter models of the mini-mast truss 14 p1934 N90-21070
Elastic-plastic instability of plane frames 14 p1992 N90-21415
Determination of unknown coefficients in partical differential equations
[AD-A217169] 14 p2019 N90-21569
Quiet mode for nonlinear rotor models
[NASA-TM-102236] 15 p2051 N90-21758
Direct inversion of rigid-body rotational dynamics
[NASA-TM-102798] 15 p2055 N90-21773
Nonlinear fracture mechanics using semicircular specimens and tension-softening behavior 15 p2116 N90-22108
Approximate optimal guidance schemes for atmospheric orbital maneuvering 16 p2206 N90-22585
Bifurcational aspects of parametric resonance
[W-8904] 16 p2231 N90-22730
Optimization of a pulsed air core transformer for low impedance inductive ignition
[AD-A218748] 16 p2232 N90-22734
The (DURIP) computer simulations of plasmas, nonlinear systems, and control theory
[AD-A219070] 16 p2300 N90-23107
A computational method for general higher index nonlinear singular systems of differential equations
[AD-A219164] 16 p2307 N90-23147
Estimating short-period dynamics using an extended Kalman filter
[NASA-TM-101722] 17 p2352 N90-23392
Laser temperature-jump kinetic studies of fast reactions in nonaqueous solutions
[AD-A218819] 17 p2371 N90-23500
Nonlinear dynamics and control of flexible structures
[AD-A218372] 17 p2386 N90-23588
Nonlinear waves and inverse scattering
[AD-A218483] 17 p2387 N90-23597
Nonlinear multigrid applied to a 1D stationary semiconductor model
[CWI-NM-R8905] 17 p2398 N90-23659
Boundary conditions for nonlinear hyperbolic systems of conservation laws
[REPT-892-422-101] 17 p2404 N90-23694
Spectral properties of a 1.3-micrometers InGaAsP diode laser under modulation
[AD-A220066] 17 p2409 N90-23729
The standard map machine
[AD-A219943] 17 p2441 N90-23908
Diffraction patterns and vortex rollup
[AD-A219876] 17 p2461 N90-24049
Dynamic disturbance decoupling for nonlinear systems
[MEMO-835] 17 p2463 N90-24069
On the theory of nonlinear control systems
[MEMO-813] 18 p2597 N90-24776
More about general saddlepoint approximations
[AD-A221217] 18 p2604 N90-24832
Studies in non-linear unsteady aerodynamics
[AD-A221228] 19 p2654 N90-25108
Nonlinear optical protection against frequency agile lasers
[AD-D014535] 19 p2695 N90-25335
A control problem for Burgers' equation with bounded input/output
[NASA-CR-182062] 19 p2747 N90-25608
Minimum variance control of nonlinear systems
[RR-369] 19 p2748 N90-25615
Non-linear systems identification using neural networks
[RR-370] 19 p2748 N90-25616
Nonlinear systems, the Lie series, and the left shift operator: Application to nonlinear optimal control
[RR-376] 19 p2748 N90-25619
Non-linear systems identification using radial basis functions
[RR-378] 19 p2751 N90-25635
The interpretation of nonlinear frequency response functions
[RR-375] 19 p2753 N90-25643
Nonlinear phenomena in accretion disks: Possibility for observational verification 19 p2775 N90-25779
A contribution to the improvement of the accuracy in the parameter identification of nonlinear processes, by example of the aircraft motion
[ETN-90-96961] 20 p2808 N90-25974
Variance reduction for quantile estimates in simulations via nonlinear controls
[AD-A222653] 20 p2916 N90-26590
Non-linear axial vibrations of a cylindrical liquid column in zero-gravity
[LRT-WE-9-FB-4(1989)] 21 p2991 N90-26997
Nonlinear real-time signal processing
[AD-A222889] 21 p2994 N90-27020
Nonlinear axisymmetric free vibrations of a liquid in a cylindrical tank with an elastic bottom
[LRT-WE-9-FB-17(1989)] 21 p3006 N90-27092
The effect of nonlinearities on flexible structures
[AD-A222705] 21 p3012 N90-27124
Symmetry and global bifurcation in nonlinear solid mechanics
[AD-A221981] 21 p3013 N90-27129
Stochastic structural dynamics for aerospace applications
[AD-A221517] 21 p3013 N90-27133
Algorithms to solve nonlinear time dependent problems of engineering and physics
[AD-A221463] 21 p3055 N90-27366
Analysis and design methods for nonlinear control systems
[AD-A221621] 21 p3061 N90-27404
The stability of differential systems with delay
[RR-377] 21 p3062 N90-27408
Projection methods for solving nonlinear systems of equations
[NASA-TM-101878] 21 p3063 N90-27409
Nonlinear dynamics and control of SDI structural components
[AD-A222472] 21 p3071 N90-27458
Linear and nonlinear optical properties of quantum dots
[AD-A223050] 21 p3076 N90-27489
Observer or direct inversion 22 p3103 N90-27622
Calculation of surface free three dimensional flows
[ONERA-RSF-5/4388-AY-002A] 22 p3178 N90-28022
Optoelectronics Research Center
[AD-A221926] 22 p3246 N90-28410
Mode competition in the quasioptical gyrotron
[AD-A222181] 23 p3329 N90-28823
Parametric solution of nonlinear structure problems
[ONERA-RT-21/3542-RY-082-R] 23 p3340 N90-28874
Error detection and control for nonlinear shell analysis
[NASA-TM-102723] 23 p3340 N90-28877
Numeric fluid mechanics 23 p3392 N90-29161
Laser physics and laser spectroscopy
[AD-A224379] 24 p3473 N90-29628
Proceedings of damping '89. Volume 2: Pages FAA-1 through IBD-15
[AD-A223432] 24 p3479 N90-29665
Research in nonlinear water waves
[AD-A224065] 24 p3496 N90-29759
An improved adaptive control for repetitive motion of robots 24 p3508 N90-29831
On discrete control of nonlinear systems with applications to robotics 24 p3519 N90-29893
An efficient temporal logic for robotic task planning 24 p3521 N90-29906

NONLINEARITY

Aeroelastic analysis of missile control surfaces with structural non-linearity 01 p0015 N90-10071
On modelling nonlinear damping in distributed parameter systems 01 p0022 N90-10109
Use of the quasilinearization algorithm for the simulation of LSS slewing 01 p0022 N90-10110
Inherent bias in nonlinear least squares analysis of first-order kinetic data
[AD-A210677] 01 p0114 N90-10651
Theoretical and experimental investigation of nonlinear optoacoustics in liquids
[AD-A210427] 01 p0124 N90-10708
Passive trajectography by azimuth: Improvement of estimation quality 02 p0150 N90-10854
Development of an approximate technique for the nonlinear random vibrations analysis of hysteretic systems 02 p0233 N90-11335
Estimation on nonlinear damping in second order distributed parameter systems
[NASA-CR-181890] 02 p0263 N90-11494

Nonlinear adjustment with or without constraints, applicable to geodetic models
[AD-A210820] 02 p0265 N90-11509
Potential for parallelism in explicit linear methods
[DE89-017329] 02 p0267 N90-11523
A solution to nonlinearity problems
[DE89-016975] 02 p0270 N90-11544
Near-planar TS waves and longitudinal vortices in channel flow: Nonlinear interaction and focusing
[NASA-CR-181928] 03 p0300 N90-11698
Numerical experience with a class of algorithms for nonlinear optimization using inexact function and gradient information
[NASA-CR-181927] 03 p0392 N90-12232
Linear (passive) and non-linear guided and studies in glass
[AD-A211693] 03 p0406 N90-12325
Sensitivity of LFC techniques in the non-linear regime
04 p0442 N90-12533
Non-linear optical studies of adsorbates: Spectroscopy and dynamics
[DE90-001543] 06 p0741 N90-14312
Nonlinear quantum effects in the Maser model: A large N scaling behaviour
[DE89-631631] 06 p0787 N90-14584
Chaotic behavior in nonlinear polarization dynamics
[DE89-013453] 06 p0788 N90-14589
A study of incremental-iterative strategies for nonlinear analyses
[PB89-226005] 06 p0798 N90-14646
Hamiltonian chaos in a nonlinear polarized optical beam
[DE90-002437] 07 p0934 N90-15408
Use of the linear variate method of Monte Carlo for estimating uncertainty in thermal-hydraulic codes
[DE89-017871] 07 p0985 N90-15694
Nonlinear optical material studies
[AD-A213938] 07 p0993 N90-15737
Soft modes, freezing, and nonlinear response of a dipolar glass
[DE90-003647] 08 p1051 N90-16075
Numerical simulation of the nonlinear evolution of a perturbation in a three dimensional boundary layer
08 p1067 N90-16173
On-line estimation of mechanical nonlinearities in compliant two-link robot manipulators
08 p1085 N90-16280
Effects of T-tabs and large deflections in DCB specimen tests
[NASA-TM-101677] 09 p1186 N90-16868
An entropy-based approach to nonlinear stability
[NASA-TM-101086] 09 p1272 N90-17376
Report on the multicolor pyrometry session at the Second NASA Non-Contact Temperature-Measurement Workshop 10 p1367 N90-17926
Antennas on land vehicles for improved communications 10 p1370 N90-17938
Application of Jameson's type nonlinear artificial dissipation to the two-dimensional Navier-Stokes computation
[NAL-TR-1015T] 10 p1384 N90-18006
Proceedings of a research workshop on Nonlinear Time Series Analysis and Applications
[AD-A216541] 10 p1423 N90-18214
Analysis and evaluation of technical data on the photochromic and non-linear optical properties of materials
[AD-A216124] 10 p1431 N90-18254
Quasilinear approach to the damping of LH waves in a reactor-grade plasma
[IPPCZ-292] 10 p1432 N90-18262
Contribution to the study of stability robustness of nonlinear multivariable regulators
[INPE-4801-TDL/356] 11 p1554 N90-18950
Numerical solution of 3D Navier-Stokes equations with upwind implicit schemes
[NASA-TM-101656] 12 p1600 N90-19205
Evaluation of the heat transfer module (FAHT) of Failure Analysis Nonlinear Thermal And Structural Integrated Code (FANTASTIC) 12 p1637 N90-19407
Calculation of nonlinear viscoelastic processes for plastic layer textile membranes
[ETN-90-95868] 12 p1675 N90-19622
Status of a nonlinear water surge model in February 1988
[KNMI-WR-88-03] 12 p1695 N90-19735
Amplitude-dependent neutral modes in compressible boundary layer flows
[NASA-TM-102524] 13 p1799 N90-20326
Observation of nonlinear reflectivity from InSb surface and optical switching application
[AD-A217184] 13 p1887 N90-20826
Nonlinear plasma and beam physics in plasma wake-fields
[DE90-008812] 13 p1892 N90-20855
Nonlinear stability in fluid and plasma dynamics
[AD-A217735] 13 p1892 N90-20856
Mechanics of interface fracture
14 p1990 N90-21408
Theory and application of nonlinear normal mode initialization
[PB90-166000] 14 p2006 N90-21497
A remark on the Kelvin transform and a non-linear partial differential equation
[PB90-165622] 14 p2021 N90-21589
Passive stabilization of a fiber optic nonlinear interferometric sensor
[AD-D014438] 14 p2026 N90-21620
Nonlinear interaction of photons and phonons in electron-positron plasmas
[DE90-009341] 14 p2030 N90-21640
Accurate nonlinear control for satellites using reaction wheels
[INPE-4983-PRE/1546] 15 p2059 N90-21787
Nonlinear spline operator interpolation and sliding control of deformable maneuvering bodies
15 p2074 N90-21878
Nonlinear stability analysis and control of dynamical robotic systems 15 p2104 N90-22037
Practical nonlinear simulation of rotating machinery dynamics with application to turbine blade rubbing
15 p2104 N90-22038
On three-dimensional scaling and consistent truncation of global atmospheric models 15 p2127 N90-22164
Graphically-oriented nonlinear analysis of statically loaded plane frames on microcomputers
[PB90-165945] 15 p2144 N90-22248
Nonlinearity parameters of polymers
15 p2164 N90-22369
Semianalytic study of high-eccentricity orbit stability and evolution 16 p2204 N90-22574
A study of woven fabric-reinforced composite materials using an invariant-based orthotropic plasticity formulation
16 p2211 N90-22611
Nonlinear finite element formulation for the large displacement analysis in multibody system dynamics
16 p2284 N90-23015
Application of numerical optimization techniques to control system design for nonlinear dynamic models of aircraft 16 p2287 N90-23032
Effect on relaxation on nonlinear waves in crystals
16 p2310 N90-23165
Reconstructing primordial density fluctuations
16 p2333 N90-23293
Research on statistical techniques for signal processing
[AD-A218811] 17 p2388 N90-23599
Nonlinear interactions in mixing layers and compressible heated round jets
[NASA-CR-186303] 17 p2400 N90-23674
Non-linear dynamic analysis of geared systems, part 2
[NASA-CR-180495] 17 p2410 N90-23732
Nonlinear internal gravity wave critical layers
17 p2422 N90-23801
Behaviour in the large of numerical solutions to one-dimensional nonlinear viscoelasticity by continuous time Galerkin methods
[AD-A220197] 17 p2461 N90-24057
A time-marching method for calculating unsteady airloads on three-dimentional wings. Part 2: Full-potential formulation
[DLR-FB-89-59] 18 p2494 N90-24255
Nonlinear development of Goertler and crossflow vortices and Goertler/Tollmien-Schlichting wave interaction
[AD-A221107] 18 p2553 N90-24571
Second order non-linear optical polyphosphazenes
[AD-A219868] 18 p2615 N90-24895
Kinetic theory of low-frequency nonlinear structures in magnetized plasmas
[DE90-611306] 18 p2617 N90-24907
Renormalized microscopic theory of fluctuations in inhomogeneous magnetized plasmas
[DE90-611307] 18 p2617 N90-24908
Microscopic theory of non-linear phenomena in semiconductor superlattices
[AD-A221106] 18 p2622 N90-24941
Flexural fatigue life prediction of closed hat-section using materially nonlinear axial fatigue characteristics
18 p2645 N90-25062
Evaluation of nonlinear motion-drive algorithms for flight simulators
[UTIAS-TN-272] 19 p2662 N90-25148
Dynamic analysis of space-related linear and non-linear structures
[NASA-TM-103490] 19 p2667 N90-25174
Prediction methodologies for nonlinear aerodynamic characteristics of control surfaces
[NIAR-90-17] 20 p2801 N90-25937
Nonlinear modeling of time series using Multivariate Adaptive Regression Splines (MARS)
[AD-A222710] 20 p2921 N90-26623
On the linear and nonlinear stability of non-parallel flow 21 p3002 N90-27065
Linear and nonlinear optical properties of quantum dots
[AD-A223050] 21 p3076 N90-27489
Nonlinear multi-mode coupling of the solar gravity modes in a rotationally split multiplet 21 p3100 N90-27608
Entropy wave instability in compact ramjets
22 p3162 N90-27932
A nonlinear finite element formulation for the large displacement analysis of plates
23 p3338 N90-28867
Computerized simulation of phenomena in plasma via particles
[INPE-4595-RPE/569] 23 p3397 N90-29194
Numerical and analytical study of nonlinear bifurcations associated with the morphological stability of two-dimensional single crystals
[PB90-209594] 23 p3398 N90-29200
Control of nonlinear space-charge emittance growth
[DE90-014752] 23 p3410 N90-29270
Aerodynamic forces acting on a finite rectangular slender body
[NAL-TR-1035] 24 p3421 N90-29329
Nonlinear static and dynamic modeling of composite rotor blades including warping effects
24 p3431 N90-29382
Aircraft design for mission performance using nonlinear multiobjective optimization methods
[NASA-CR-4328] 24 p3432 N90-29384
Nonlinear modeling of joint dominated structures
[NASA-CR-4324] 24 p3439 N90-29423
On a generalized laminate theory with application to bending, vibration, and delamination buckling in composite laminates 24 p3478 N90-29659
Windshear estimation along the trajectory of an aircraft 24 p3494 N90-29745
Investigation of the application in the simulation program 'PSpice' of the Jiles-Atherton model for nonlinear magnetic materials in order to predict the degaussing of magnets
[LINO-1990-1] 24 p3541 N90-30029
The computation and analysis of acoustic waves in transonic airfoil-vortex interactions
24 p3542 N90-30031

NONNEWTONIAN FLOW

A numerical and analytical study of normal stresses and pressure differences in non-Newtonian creeping flows
16 p2234 N90-22749

NONNEWTONIAN FLUIDS

Analysis of spurt phenomena for a non-Newtonian fluid
[AD-A210560] 01 p0071 N90-10405
Stability of discontinuous shearing motions of a non-Newtonian fluid
[AD-A210643] 01 p0071 N90-10406
Stability of discontinuous steady states in shearing motion of a non-Newtonian fluid
[AD-A210644] 01 p0071 N90-10407
Quadratic dynamical systems describing shear flow of non-Newtonian fluids
[AD-A212892] 05 p0638 N90-13720
Analysis of new phenomena in shear flow of non-Newtonian fluids
[AD-A212893] 05 p0638 N90-13721
New transient algorithms for non-Newtonian flows
[AD-A213494] 07 p0930 N90-15385
Error cancellation in HPBL derivation of elastic hole-pressure error
[AD-A219854] 17 p2417 N90-23771
Modeling of free viscoelastic jets and instability mechanisms
[AD-A221672] 21 p3005 N90-27080

NONOSCILLATORY ACTION

Some aspects of Essentially Nonoscillatory (ENO) formulations for the Euler equations, part 3
[NASA-CR-4285] 14 p1910 N90-20949

NONPARAMETRIC STATISTICS

Empirical Bayes selection for the highest probability of success in negative binomial distributions
[AD-A210273] 01 p0115 N90-10660
Boundary kernel estimation of the two sample comparison density function
[AD-A210757] 02 p0268 N90-11532
Small sample theory for steady state confidence intervals
[AD-A212097] 03 p0393 N90-12242
Empirical Bayes estimation of binomial parameter with symmetric priors
[AD-A211646] 03 p0394 N90-12246
Random truncation models and Markov processes
[CWI-MS-R8817] 04 p0547 N90-13181

Nonparametric estimation of reliability and related functions
[AD-A215138] 09 p1234 N90-17160
Parametric models for A(sub n): Splitting processes and mixtures
[AD-A218421] 16 p2306 N90-23140
Bayesian nonparametric prediction and statistical inference
[AD-A218473] 16 p2308 N90-23154
Statistical inference from sampled data
[AD-A218731] 16 p2309 N90-23156
Sample size for correlation estimates
[AD-A219810] 17 p2485 N90-24085
Applications of non-parametric density estimation
[AD-A220206] 17 p2466 N90-24094
Computing environments, interactive graphics and nonparametric methods for data analysis
[DE90-016127] 24 p3530 N90-29962

NONREFLECTION
U ENERGY ABSORPTION

NONRELATIVISTIC ELECTRONS
U ELECTRONS

NONRELATIVISTIC MECHANICS
Twistons
[RSRE-MEMO-4234] 04 p0562 N90-13275

NONRIGIDITY
U FLEXIBILITY

NONTHERMAL EMISSION
U NONTHERMAL RADIATION

NONTHERMAL RADIATION
NT CYCLOTRON RADIATION
NT ION CYCLOTRON RADIATION
NT SYNCHROTRON RADIATION
Ionosphere-thermosphere coupling at high latitudes: Aspect angle dependence of non-thermal plasmas 02 p0244 N90-11382
The behavior of beams of relativistic non-thermal electrons under the influence of collisions and synchrotron losses
[NASA-CR-185983] 03 p0401 N90-12298
Non-thermal radio emission of X ray binaries 19 p2769 N90-25738

NONUNIFORM FLOW
Review and evaluation of a turbomachinery throughflow finite element code
[AD-A213058] 05 p0650 N90-13787
Flow boiling with enhancement devices for cold plate coolant channel design
[NASA-CR-186358] 15 p2089 N90-21961

NONUNIFORM MAGNETIC FIELDS
Experimental investigation of relationship between nonlinear field energy and emittance growth
[AD-A215813] 10 p1430 N90-18246
Excitation of hypersound at boundary between Type-2 superconductor and a concentrated paramagnetic compound 16 p2310 N90-23164

NONUNIFORM PLASMAS
Study of a 1-Hz hypocycloidal pinch (HCP) pump for production of ultraviolet lasers
[AD-A224091] 24 p3547 N90-30064

NONVISCOUS FLOW
U INVISCID FLOW

NORMAL DENSITY FUNCTIONS
Efficient numerical method for computation of thermohydrodynamics of laminar lubricating films
[NASA-CR-185136] 02 p0219 N90-11256
On a classification problem: Ranking and selection approach
[AD-A211627] 03 p0397 N90-12269
Analysis of distributions of Visual Meteorological Conditions (VMC) heliport data
[DOT/FAA/CT-TN89/67] 14 p2008 N90-21508
PUFFY: A puff diffusion computer model
[FOA-C-40251-4.5] 17 p2421 N90-23796
Approximate interval estimation methods for the reliability of systems using component data with exponential and Weibull distributions
[AD-A219857] 17 p2460 N90-24048
The gamma process and the Poisson distribution
[MEMO-COSOR-89-24] 17 p2466 N90-24089
Hitting lines with two-dimensional Brownian motion
[AD-A223595] 24 p3541 N90-30027

NORMAL DISTRIBUTIONS
U NORMAL DENSITY FUNCTIONS

NORMAL FORCE DISTRIBUTION
U FORCE DISTRIBUTION

NORMAL SHOCK WAVES
The stability of magnetohydrodynamic shock waves in molecular clouds 02 p0292 N90-11665
Measured and predicted aerodynamic coefficients and shock shapes for Aeroassist Flight Experiment (AFE) configuration
[NASA-TP-2956] 06 p0717 N90-14185
The interaction of a supersonic streamwise vortex and a normal shock wave 19 p2491 N90-24241

NORMALITY
A renormalization group approach to image processing: A new computational method for three-dimensional shapes in robot vision, and the computation complexity of the cooling algorithms
[AD-A214247] 07 p0977 N90-15643
Norms and perception of events
[AD-A224236] 24 p3499 N90-29774

NORMALIZING
Simple proof of renormalization group equation in the minimal subtraction scheme
[DE90-600758] 08 p1115 N90-16457

NORMALIZING (STATISTICS)
Removing stripes in GOES (Geostationary Operational Environmental Satellites) images by matching empirical distribution functions
[PB89-213359] 04 p0514 N90-12968
Some remarks on the gap metric
[MEMO-COSOR-88-34] 05 p0690 N90-14029
Some computational properties of rotation representations
[AD-A213888] 07 p0981 N90-15665
Modeling the response of a monopulse radar to impulsive jamming signals using the Block Oriented System Simulator (BOSS)
[AD-A215560] 10 p1375 N90-17969
A neural network based speech recognition system
[AD-A219794] 17 p2389 N90-23606

NORMS
Contractivity in the maximum norm for Runge-Kutta methods
[TW-89-06] 15 p2162 N90-22352

NORTH AMERICA
The effect of latent heat release on synoptic-to-planetary scale wave interactions: Observational study 03 p0362 N90-12074
The reduction correction in North America 13 p1836 N90-20540
Technology for electronic transfer of information: The present and future in North America 15 p2177 N90-22442
Evaluation of the role of ozone, acid deposition, and other airborne pollutants in the forests of eastern North America
[PB90-184896] 22 p3197 N90-28140
World weather records, 1971-1980. Volume 1: North America
[PB90-182858] 22 p3212 N90-28221
Acid deposition: No such thing as a free launch
[DE90-015085] 23 p3348 N90-28920
Catalog of strong motion stations in Eastern North America
[PB90-251984] 24 p3490 N90-29722
Meteorological conditions over the North Atlantic Ocean during GCE/CASE/WATOX
[PB90-252032] 24 p3494 N90-29747

NORTH AMERICAN AIRCRAFT
NT B-1 AIRCRAFT
NT B-70 AIRCRAFT
NT F-86 AIRCRAFT
NT X-15 AIRCRAFT

NORTH ATLANTIC TREATY ORGANIZATION (NATO)
Environmental effects upon cross-servicing of aircraft in NATO
[AD-A218374] 17 p2343 N90-23341
AGARD highlights 90/1 20 p2951 N90-26788
Potential new tactical applications of the Global Positioning System (GPS) 21 p3069 N90-27449
Tactical EHF satellite communications for NATO employing non-geostationary orbits 21 p3070 N90-27454
The NATO thesaurus project
[NASA-CR-186931] 21 p3087 N90-27552

NORTH CAROLINA
Coastal frontogenesis and associated severe weather on 13 March 1986 (GALE IOP 13)
[AD-A217708] 13 p1845 N90-20590

NORTH SEA
Climatological data for the North Sea based on observations by voluntary observing ships over the period 1961-1980
[KNMI-WR-89-02] 04 p0520 N90-13002
Propagation prediction for the North Sea environment 06 p0760 N90-14423
Phytoplankton and its contribution to the atmospheric sulfur budget of northern Europe 20 p2885 N90-26417

NORTHERN HEMISPHERE
NT ARCTIC REGIONS
Auroral and sub-auroral F-layer irregularity studies in the Northern and Southern Hemisphere during the equinox transition study September 16-26, 1984 02 p0246 N90-11393
UV ionospheric remote sensing with the polar BEAR satellite
[AD-A211359] 03 p0372 N90-12127
Coronae on Venus observations and models of origin 03 p0427 N90-12449
Current velocity and hydrographic observations in the southwestern North Atlantic Ocean: Subtropical Atlantic Climate Studies (STACS), 1988
[PB89-230825] 04 p0521 N90-13010
Meteorological atlas of the Northern Hemisphere lower stratosphere for January and February 1989 during the Airborne Arctic Stratospheric Expedition
[NASA-TM-4145] 05 p0671 N90-13908
An observational study of intramonthly quasi-periodicities in the Northern Hemisphere, extratropical geopotential height field 06 p0813 N90-14729
Multiple flow regimes in the Northern Hemisphere winter 08 p1100 N90-16372
The observed three-dimensional structure of baroclinic waves in the Northern Hemisphere winter as revealed in a linear regression analysis 15 p2128 N90-22167
VHE gamma ray emission from Northern Hemisphere X ray binaries 19 p2772 N90-25760
Total ozone time variations during the spring reversals in the high latitudinal stratosphere of the Northern Hemisphere during the 20th and 21st solar cycles 22 p3205 N90-28181

NORTHROP AIRCRAFT
NT F-18 AIRCRAFT

NORWAY
An aircraft noise study in Norway 18 p2611 N90-24872

NOSE CAPS
U NOSE CONES

NOSE CONES
NT ABLATIVE NOSE CONES
Blunt-nose inviscid airflows with coupled nonequilibrium processes 05 p0573 N90-13336
An electroformed nickel-sulfur alloy for a nose cone
[DE90-000866] 06 p0745 N90-14337

NOSE TIPS
VLA missile development and high angle of attack behavior 10 p1305 N90-17553

NOSE WHEELS
Independent Orbiter Assessment (IOA): Analysis of the nose wheel steering subsystem
[NASA-CR-185548] 02 p0163 N90-10921
Independent Orbiter Assessment (IOA): Analysis of the landing/deceleration subsystem
[NASA-CR-185569] 02 p0167 N90-10943
Independent Orbiter Assessment (IOA): Assessment of the nose wheel steering subsystem
[NASA-CR-185533] 02 p0168 N90-10947
Independent Orbiter Assessment (IOA): CIL issues resolution report, volume 2
[NASA-CR-185524-VOL-2] 02 p0170 N90-10955
Modeling and analysis of the space shuttle nose-gear tire with semianalytic finite elements
[NASA-TP-2977] 12 p1670 N90-19595

NOSES (FOREBODIES)
NT ABLATIVE NOSE CONES
NT NOSE CONES
Development of a preliminary high-angle-of-attack nose-down pitch control requirement for high-performance aircraft
[NASA-TM-101684] 12 p1600 N90-19206
Effects of nose bluntness and shock-shock interactions on blunt bodies in viscous hypersonic flows
[NASA-CR-186451] 14 p1910 N90-20950
Effective methods of controlling a junction vortex system in an incompressible, three-dimensional, turbulent flow 15 p2047 N90-21732

NOTATION
U CODING

NOTCH STRENGTH
Fatigue damage growth mechanisms in continuous fiber reinforced titanium matrix composites
[NASA-TM-102594] 14 p1991 N90-21409
The blunt notch behaviour of metal laminates: ARALL and GLARE
[LR-617] 20 p2877 N90-26368

NOTCH TESTS
NT CHARPY IMPACT TEST
Interlaminar stress concentration in fiber composites
[ETN-89-94670] 03 p0319 N90-11809
Numerical analysis of notch test damage to laminated composite plates submitted to uniaxial traction
[CETIM-107310] 04 p0467 N90-12675
Determination of the gaseous hydrogen ductile-brittle transition in copper-nickel alloys
[NASA-TM-86494] 04 p0474 N90-12715
Fatigue testing of welded steel assemblies with or without finishing treatments
[CETIM-107900] 04 p0513 N90-12961
Three-dimensional Fe analysis of the surface distribution in notched compact samples of 20 MnMoNi 55
[W-1/89] 12 p1676 N90-19625

Strength in notched and impact-damaged laminates
15 p2064 N90-21820
About the effect of loading sequence on the fatigue life of notched specimens made from steel and aluminum alloys
[LBF-FB-186(1989)] 18 p2526 N90-24414
Fracture toughness of polyimide films
[NASA-TM-103473] 20 p2836 N90-26130
Ascertaining the fracture toughness of ceramic materials by means of bending testpieces of various notch types at ambient and high temperatures
[ESA-TT-992] 23 p3312 N90-28733

NOTCHED METALS
U NOTCH TESTS

NOTCHES
Experimental observations and finite element analysis of the initiation of fiber microbuckling in notched composite laminates
[NASA-CR-186207] 19 p2699 N90-25359
Ascertaining the fracture toughness of ceramic materials by means of bending testpieces of various notch types at ambient and high temperatures
[ESA-TT-992] 23 p3312 N90-28733

NOVA LASER SYSTEM
Integration of a gated microchannel plate detector into the Nova laser system
[DE90-002981] 07 p0935 N90-15413
Improved energy and power balance at Nova targets
[DE90-007260] 13 p1807 N90-20372
Evaluation of dynamic range for LLNL streak cameras using high contrast pulses and pulse podiatry on the Nova laser system
[DE90-015203] 24 p3472 N90-29620

NOVAE
NT DWARF NOVAE
NT HERCULES NOVA
Theoretical statistics of zero-age cataclysmic variables
01 p0141 N90-10810
Recent and future x ray observations of classical novae during the outburst stage
[MPE-PREPRINT-159] 08 p1140 N90-16606
Soft x ray emission from classical novae in outburst
[DE90-006480] 11 p1595 N90-19187
Recent advances in the studies of the nova outburst
[DE90-008936] 14 p2038 N90-21691
Multi-wavelength observations of novae in outburst
[DE90-008934] 14 p2038 N90-21692
The 1989 outburst of V404 Cygni: A very unusual x ray nova
[DE90-008935] 14 p2038 N90-21693
Model atmospheres for novae during the early stages
[NASA-CR-180498] 14 p2038 N90-21694
The Al-26(rho, gamma)Si-27 reaction: Stellar origins of galactic Al-26 15 p2188 N90-22498
Infrared coronal line novae 16 p2339 N90-23328
The X ray spectrum of Nova Vul 1988. Mir-Kvant data
19 p2766 N90-25713
PW Vul: A classical nova with nearly solar abundances
[NASA-CR-185080] 23 p3411 N90-29275
The impact of IUE on studies of the nova outburst: 1986-1990
[DE90-014915] 24 p3563 N90-30156

NOXIOUS MATERIALS
U CONTAMINANTS

NOZZLE COEFFICIENT
U NOZZLE FLOW

NOZZLE DESIGN
Investigations of thrust vector control for high-alpha pitchover 01 p0014 N90-10067
Three-dimensional, two-phase, transonic, canted nozzle flows
[AD-A211528] 03 p0347 N90-11984
Flight motor set 360L001 (STS-26R). Volume 5: Nozzle component
[NASA-CR-183771] 05 p0615 N90-13588
A numerical technique for analysis of resistojet nozzle flow 06 p0775 N90-14506
Hypersonic nozzle design
[NASA-CR-186261] 07 p0876 N90-15077
Space shuttle Production Verification Motor 1 (PV-1) static fire
[NASA-CR-183784] 08 p1037 N90-15991
Parametric assessment of propulsion system mass for airbreathing launcher configurations
09 p1177 N90-16819
Low-noise nozzle valve
[NASA-CASE-MFS-28383-1] 09 p1216 N90-17051
Arcjet nozzle design impacts
11 p1473 N90-18478
Static investigation of a two-dimensional convergent-divergent exhaust nozzle with multiaxis thrust-vectoring capability
[NASA-TP-2973] 12 p1597 N90-19193
An investigation of secondary flows in nozzle guide vanes 14 p1923 N90-21016
Secondary flow predictions for a transonic nozzle guide vane 14 p1924 N90-21017
Detailed heat transfer measurements in nozzle guide vane passages in linear and annular cascades in the presence of secondary flows 14 p1926 N90-21030
Supersonic nozzle design of arbitrary cross-section
14 p1927 N90-21035
Technical Evaluation Motor no. 5 (TEM-5)
[NASA-CR-183932] 14 p1942 N90-21117
A computer program for the prediction of nozzle-propeller performance
[LR-578] 15 p2048 N90-21740
Theory and numerical analysis of single and multi-element nozzle propellers
[LR-579] 15 p2048 N90-21741
Recent improvements in the scope and accuracy of the performance prediction of nozzle propellers
[LR-598] 15 p2048 N90-21742
Analysis and design of optimized truncated scarfed nozzles subject to external flow effects
[NASA-TM-103175] 19 p2654 N90-25106
An optical study of the flow start-up process in four convergent-divergent nozzles
[AD-A222918] 21 p2963 N90-26846
TRANSTRAIN: A program to compute strain transformations in composite materials
[NASA-TM-103509] 22 p3153 N90-27877
High/variable mixture ratio O2/H2 engine
23 p3295 N90-28638
Design of an axisymmetric, contoured nozzle for the HEG
[DLR-FB-90-04] 23 p3327 N90-28812

NOZZLE EFFICIENCY
Static investigation of a two-dimensional convergent-divergent exhaust nozzle with multiaxis thrust-vectoring capability
[NASA-TP-2973] 12 p1597 N90-19193
Internal performance of two nozzles utilizing gimbal concepts for thrust vectoring
[NASA-TP-2991] 12 p1599 N90-19200
Theory and numerical analysis of single and multi-element nozzle propellers
[LR-579] 15 p2048 N90-21741
Experimental and analytical study of close-coupled ventral nozzles for ASTOVL aircraft
[NASA-TM-103170] 18 p2498 N90-24273
The affect of gravity on particle collection in inertial impactors
[DE90-013372] 23 p3393 N90-29173

NOZZLE FLOW
Investigation of advanced mixer-ejector exhaust system
[AD-A211943] 03 p0301 N90-11705
Three-dimensional, two-phase, transonic, canted nozzle flows
[AD-A211528] 03 p0347 N90-11984
Gas flows in rocket motors, volume 1
[AD-A213348] 05 p0615 N90-13591
Gas flows in rocket motors. Volume 2, appendix C: Time iterative solution of viscous supersonic flow
[AD-A213349] 05 p0615 N90-13592
Gas flows in rocket motors. Volume 3, appendix D: Computer code listings
[AD-A213350] 05 p0616 N90-13593
Coherent structures in a round jet
05 p0640 N90-13733
A computational analysis of the transonic flow field of two-dimensional minimum length nozzles
06 p0718 N90-14194
A numerical technique for analysis of resistojet nozzle flow 06 p0775 N90-14506
Engine inlet distortion in a 9.2 percent scale vectored thrust STOVL model in ground effect
[NASA-TM-102358] 10 p1307 N90-17561
Viscous three-dimensional analyses for nozzles for hypersonic propulsion
[NASA-CR-185197] 10 p1321 N90-17635
Experimental investigation of a chemical laser cavity flowfield
[AD-A216398] 10 p1390 N90-18038
Computation of hypersonic unsteady viscous flow over a cylinder 12 p1597 N90-19194
Secondary flow predictions for a transonic nozzle guide vane 14 p1924 N90-21017
Secondary flow in a turbine guide vane with low aspect ratio 14 p1924 N90-21018
The effect of secondary flow on the redistribution of the total temperature field downstream of a stationary turbine cascade 14 p1926 N90-21033
Analysis of internal flow in a ventral nozzle for STOVL aircraft
[NASA-TM-103123] 17 p2355 N90-23404
Computational analysis of the flowfield of a two-dimensional ejector nozzle
[NASA-CR-185255] 17 p2355 N90-23406
Determination of the velocity, density, maximum flux, and enthalpy profiles for a very high temperature arc jet nozzle flow
[AD-A218390] 17 p2402 N90-23682
Effect of tail size reductions on longitudinal aerodynamic characteristics of a three surface F-15 model with nonaxisymmetric nozzles
[NASA-TP-3036] 20 p2802 N90-25938
Hot gas ingestion characteristics and flow visualization of a vectored thrust STOVL concept
[NASA-TM-103212] 20 p2813 N90-26009
An optical study of the flow start-up process in four convergent-divergent nozzles
[AD-A222918] 21 p2963 N90-26846
Adjustable choke for fluids nozzle
[NASA-CASE-NPO-17625-1-CU] 21 p3003 N90-27070
Investigation of factors affecting data comparison
22 p3119 N90-27714

NOZZLE GEOMETRY
A computational analysis of the transonic flow field of two-dimensional minimum length nozzles
06 p0718 N90-14194
Internal performance of two nozzles utilizing gimbal concepts for thrust vectoring
[NASA-TP-2991] 12 p1599 N90-19200
Performance of an aero-space plane propulsion nozzle 14 p1926 N90-21034
Analysis and design of optimized truncated scarfed nozzles subject to external flow effects
[NASA-TM-103175] 19 p2654 N90-25106
Effect of tail size reductions on longitudinal aerodynamic characteristics of a three surface F-15 model with nonaxisymmetric nozzles
[NASA-TP-3036] 20 p2802 N90-25938
Low power arcjet performance
[NASA-TM-103280] 23 p3298 N90-28657
Design of an axisymmetric, contoured nozzle for the HEG
[DLR-FB-90-04] 23 p3327 N90-28812

NOZZLE THRUST COEFFICIENTS
Aerodynamics of thrust vectoring
[NASA-CR-185074] 05 p0575 N90-13354

NOZZLES
Simulation of the control characteristics of an axial piston pump and a flapper-nozzle valve combination
05 p0649 N90-13784

NTS
U NAVIGATION TECHNOLOGY SATELLITES

NUCLEAR ASTROPHYSICS
Big-bang nucleosynthesis revisited
[NASA-CR-186256] 15 p2174 N90-22426
Prospects for nuclear astrophysics with intense radioactive ion beams
[DE90-015616] 24 p3544 N90-30044

NUCLEAR AUXILIARY POWER UNITS
NT SPACE POWER REACTORS
NT SPACE POWER UNIT REACTORS
On the development of the power sources for the Ulysses and Galileo missions 10 p1331 N90-17693

NUCLEAR BINDING ENERGY
Mechanisms of CO2 reduction metal and metal modified semiconductor electrodes
[AD-A213169] 04 p0473 N90-12712
Theoretical investigations of the structures and binding energies of Be(sub n) and Mg(sub n) (n = 3-5) clusters
[NASA-TM-101931] 08 p1120 N90-16483
Positronium ions and molecules
11 p1560 N90-18990
High resolution electron energy loss spectroscopy studies of chemisorbed species on metal surfaces
[AD-A222272] 21 p2978 N90-26922

NUCLEAR BULGE (GALAXIES)
U GALACTIC BULGE

NUCLEAR CAPTURE
NT ELECTRON CAPTURE

NUCLEAR ELECTRIC POWER GENERATION
NT NUCLEAR AUXILIARY POWER UNITS
NT NUCLEAR POWER PLANTS
NT PATHFINDER NUCLEAR REACTOR
NT SPACE POWER REACTORS
NT SPACE POWER UNIT REACTORS
Activities report on KEMA R and D
[ST-REPT-VOL-6-NO-12] 03 p0367 N90-12100
Report of the NASA lunar energy enterprise case study task force 07 p1008 N90-15837
Analysis of the financial factors governing the profitability of lunar helium-3 07 p1008 N90-15838
Introduction to D-He(3) fusion reactors
07 p1008 N90-15839
Importance of helium-3 for the future
07 p1009 N90-15843
Challenges for future space power systems
10 p1331 N90-17695

Analysis of competition among kinds of energy at the era of complexed energy. (Report on overseas study)
[DE89-910213] 12 p1680 N90-19650
Nuclear technology and the space exploration missions
[NASA-TM-103156] 16 p2253 N90-22847
The nuclear battery
[DE90-630400] 24 p3462 N90-29559

NUCLEAR ELECTRIC PROPULSION
Low-earth-orbit to low-lunar-orbit laser freighter
01 p0030 N90-10160
Laser propulsion option 01 p0030 N90-10161
Laser thruster 01 p0030 N90-10164
Design study of a modular gas-cooled, closed-brayton cycle reactor for marine use
[AD-A213453] 07 p0953 N90-15518
Electric propulsion for manned Mars exploration
11 p1473 N90-18480
A radiological assessment of nuclear power and propulsion operations near Space Station Freedom
[NASA-CR-185185] 14 p1941 N90-21108
A trajectory generation and system characterization model for cislunar low-thrust spacecraft. Volume 2: Technical manual
[NASA-CR-185172] 15 p2061 N90-21807
Project Exodus
[NASA-CR-186836] 20 p2816 N90-26026

NUCLEAR EMULSIONS
Target nucleus fragmentation in O16 + (Ag,Br) interactions at 200 A GeV
[LUIP-8906] 07 p0991 N90-15727
Mesooptical Fourier transform microscope: A new device for high energy physics
[DE90-616423] 14 p2026 N90-21615

NUCLEAR ENERGY
Nuclear power in space
[GPO-23-835] 16 p2316 N90-23202

NUCLEAR ENGINE FOR ROCKET VEHICLES
A review of gas-cooled reactor concepts for SDI (Strategic Defense Initiative)
[DE89-016962] 06 p0842 N90-14898
Dynamics analyses of space power systems using the salt code
[DE90-002274] 08 p1038 N90-15995

NUCLEAR EXPLOSION EFFECT
Long wave atmospheric noise model, phase 1. Volume 2: Mode parameters
[AD-A212795] 04 p0493 N90-12837
PRPSIM: A FORTRAN code to calculate properties of radio wave propagation in a structured ionized medium. Volume 2: Theory and models
[AD-A216299] 10 p1377 N90-17983
Pulse-width dependent radiation effects on electronic components
[AD-A219517] 17 p2395 N90-23643

NUCLEAR EXPLOSIONS
NT THERMONUCLEAR EXPLOSIONS
Dynamically compressed metals: Theory
[AD-A210741] 01 p0045 N90-10257
Hydrophone investigations of earthquakes and explosion generated high-frequency seismic phases
[AD-A212055] 03 p0371 N90-12122
Seismic wave attenuation and yield determination at regional distances
[AD-A211548] 03 p0372 N90-12128
Long wave atmospheric noise model, phase 1. Volume 1: Lightning occurrence rates and propagation theory
[AD-A212794] 04 p0493 N90-12836
PRPSIM: A FORTRAN code to calculate properties of radio wave propagation in a structured ionized medium. Volume 2: Theory and models
[AD-A216299] 10 p1377 N90-17983
Computing shock waves in turbulent mixing regions
[DE90-005996] 10 p1386 N90-18021
ACIRF user's guide: Theory and examples
[AD-A216436] 11 p1496 N90-18613
A linear filtering technique for removal of low-frequency noise
[DE90-006183] 13 p1794 N90-20296
Final safety analysis report for the Ulysses mission. Volume 2 (Book 1): Accident model document
[DE90-008694] 14 p1940 N90-21103
Seismic wave propagation, attenuation and scattering over regional distances
[AD-A219358] 16 p2256 N90-22862
Pulse-width dependent radiation effects on electronic components
[AD-A219517] 17 p2395 N90-23643
Analysis of regional phases using three-component data
[AD-A219482] 17 p2422 N90-23803
Bioelectromagnetic effects of the Electromagnetic Pulse (EMP)
[AD-A221552] 21 p3033 N90-27243
The Surface Air Sampling Program
[DE90-014873] 24 p3487 N90-29711

NUCLEAR FISSION
Populations of excited states and reaction mechanisms in the emission of complex fragments
[DE90-007481] 13 p1886 N90-20819

NUCLEAR FUEL BURNUP
Modeling of combustion processes in a solid fuel particle
[DE90-009140] 16 p2214 N90-22629

NUCLEAR FUEL ELEMENTS
Scaling study for SP-100 reactor technology
[NASA-TM-897140] 08 p1122 N90-16496
TFE verification program
[DE90-008227] 18 p2614 N90-24891

NUCLEAR FUEL REPROCESSING
MHD seed recovery and regeneration
[DE89-002711] 01 p0125 N90-10715
Results of the manipulator test test stand study: Comparison of manipulators and evaluation of equipment items
[DE90-000977] 06 p0794 N90-14625

NUCLEAR FUELS
NT SPENT FUELS
Starlight: A stationary inertial-confinement-fusion reactor with nonvaporizing walls
[DE90-002315] 06 p0847 N90-14927
Particle transport in pellet fueled JET (Jet European Torus) plasmas
[DE90-008077] 13 p1891 N90-20851
Advanced space transportation technologies
18 p2645 N90-25061
Multimegawatt space nuclear power supply, phase 1. Volume 3: Annotated outline of preliminary safety assessment D180-30619-7
[DE90-012432] 20 p2926 N90-26646
Multimegawatt space nuclear power supply, phase 1. Supplement: D180-30619-8
[DE90-012433] 20 p2926 N90-26647
Overview of advanced fuel fusion
[DE90-015660] 24 p3550 N90-30085

NUCLEAR FUSION
NT CONTROLLED FUSION
Theoretical atomic physics for fusion
[DE89-017363] 02 p0274 N90-11563
The Reversed-Field-Pinch (RFP) fusion neutron source: A conceptual design
[DE89-015297] 02 p0276 N90-11577
Gordon Conference on Atomic Physics
[AD-A211946] 03 p0402 N90-12304
Highlights of papers presented at the workshop on Cold Fusion Phenomena
[DE89-016956] 03 p0407 N90-12334
An explicit partition of the fusion-like cross section
[KVI-797] 04 p0553 N90-13225
Nuclear physics and cosmology
[NASA-CR-186166] 05 p0713 N90-14167
Big Bang nucleosynthesis and the Quark-Hadron transition
[NASA-CR-186169] 05 p0713 N90-14168
Cosmology and the weak interaction
[NASA-CR-186170] 05 p0713 N90-14169
Quality assurance and quality control for the Compact Physics Research Facility (CPRF) and ZTH experiment
[DE90-002352] 06 p0796 N90-14636
Lawrence Livermore National Laboratory (LLNL) research on cold fusion
[DE90-000930] 06 p0845 N90-14915
Cold fusion: Alchemist's dream
[DE90-000865] 06 p0847 N90-14925
Stability of the Global Alfven Eigenmode in the presence of fusion alpha particles in an ignited tokamak plasma
[DE89-016618] 06 p0848 N90-14930
In-situ ion beam measurements of deuterium loading in thin foil electrochemical cells
[DE90-003162] 07 p0952 N90-15511
Upgrade plans to handle 30 to 40 Mbytes of data for D3-D
[DE90-003291] 07 p0995 N90-15750
Tunnelling effects on low energy fusion cross sections
[AD-A214010] 07 p0997 N90-15762
Tritium and neutron measurements of a solid state cell
[DE90-003657] 07 p1005 N90-15820
Analysis of the financial factors governing the profitability of lunar helium-3
07 p1008 N90-15838
Toroidal magnetic fields in terms of field-line invariants
[DE89-016610] 08 p1123 N90-16507
Near-term directions in the world stellarator program
[DE90-004361] 08 p1124 N90-16511
Theoretical study of cold nuclear fusion using barrier penetration approach
[DE90-601096] 08 p1124 N90-16513
Fracto-fusion. Mechanism of cold fusion
[DE90-719573] 08 p1125 N90-16518
Lower limit for the average angular momentum leading to fusion
[DE90-004027] 08 p1126 N90-16523
Gamma-ray observations and the distribution of interstellar aluminum-26 08 p1150 N90-16661
Nuclear reaction uncertainties in standard and non-standard cosmologies
[DE90-003594] 08 p1151 N90-16666
Determination of solar flare accelerated ion angular distributions from SMM gamma ray and neutron measurements and determination of the He-3/H ratio in the solar photosphere from SMM gamma ray measurements
[NASA-CR-186038] 08 p1153 N90-16676
Results of an attempt to measure increased rates of the reaction D-2 + D-2 yields He-3 + n in a nonelectrochemical cold fusion experiment
[NASA-TM-102430] 09 p1280 N90-17424
A preliminary investigation of cold fusion by electrolysis of heavy water
[DE90-004383] 09 p1285 N90-17447
Nuclear driving of stellar oscillations and their coupling to convection 10 p1446 N90-18345
The effects of cold dark matter on Big Bang nucleosynthesis 12 p1698 N90-19749
Measurement of cross sections: New needs and possibilities
[DE90-007248] 12 p1711 N90-19829
Record of forum on cold fusion
[DE90-749883] 12 p1717 N90-19863
Distributed bosonic states and condensed matter fusion
[AD-A217605] 12 p1718 N90-19868
Application of railgun principle to high-velocity hydrogen pellet injection for magnetic fusion reactor refueling
[DE90-008281] 13 p1761 N90-20109
Present status of (mu)CF theory
[DE90-007547] 13 p1884 N90-20809
Designing an experimenters database using the Nijssen Information Analysis Methodology (NIAM)
[DE90-008548] 13 p1900 N90-20907
West European magnetic confinement fusion research
14 p2029 N90-21634
Fusion burn dynamics in Dense Z-Pinch (DZP)
[DE90-007976] 14 p2029 N90-21638
An attempt to measure cold-fusion effects
[DE90-613248] 14 p2031 N90-21649
Operator algebra from fusion rules: The infinite number of Ising theories
[NIKHEF-H/89-7] 15 p2165 N90-22374
Japanese magnetic confinement fusion research
15 p2169 N90-22392
Big-bang nucleosynthesis revisited
[NASA-CR-186256] 15 p2174 N90-22426
Displacement flow and deuteron drag in a metal: A path towards cold fusion
[PREPRINT-703] 16 p2320 N90-23227
Investigation of the effect of mechanical stress on cold fusion
[AD-A220123] 17 p2474 N90-24147
Abundance differences among G and K giants
17 p2484 N90-24208
Probing the Big Bang with LEP
[NASA-CR-181060] 17 p2485 N90-24212
Microwave generation for magnetic fusion energy applications
[DE90-011042] 18 p2617 N90-24906
Comparative assessment of world research efforts on magnetic confinement fusion 19 p2759 N90-25680
Application of the results of carbon pellet modeling to the problem of plasma penetration
[DE90-012713] 20 p2928 N90-26658
Materials studies for magnetic fusion energy applications at low temperatures, volume 12
[PB90-157553] 22 p3248 N90-28417
Fundamental studies of fusion plasmas
[DE90-015732] 24 p3549 N90-30080

NUCLEAR GYROSCOPES
The anatomy of the gyroscope, part 3
[AGARD-AG-313] 14 p1982 N90-21359

NUCLEAR HEAT
Nuclear closed-cycle gaseous heat engine concept
[DE89-016824] 03 p0404 N90-12313

NUCLEAR INTERACTIONS
NT ELECTRON CAPTURE
NT SPIN-ORBIT INTERACTIONS
NT WEAK INTERACTIONS (FIELD THEORY)
On a new integrable Hamiltonian system with nearest neighbors interaction
[PREPRINT-667] 05 p0692 N90-14043
The effective (3)He-nucleon force in a microscopic DWBA approach to the (3)He,t charge exchange reaction --- Distorted Wave-Borne Approximation (DWBA)
[KVI-763] 05 p0697 N90-14077
A study of recoil protons in ultra-relativistic nucleus-nucleus collisions
[LUIP-8907] 06 p0838 N90-14873

The creation of high energy densities with antimatter beams
[DE90-002383] 06 p0842 N90-14899
Nuclear interactions of high energy heavy ions and applications in astrophysics
[DE90-006691] 12 p1737 N90-19984
Cosmic ray composition and muon decoherence at the knee of the all-particle cosmic ray spectrum
12 p1745 N90-20035
Strangeness enhancement in 14.6 A GeV/c Si+Au interactions?
[DE90-008826] 14 p2026 N90-21616
Fragmentation of relativistic heavy nuclei with application to cosmic ray propagation 14 p2043 N90-21716
Nucleus-nucleus collisions and the nuclear equation of state
[DE90-015427] 24 p3543 N90-30037

NUCLEAR MAGNETIC RESONANCE
NT PROTON MAGNETIC RESONANCE
NT PROTON RESONANCE
NMR evidence for a planar arene intermediate in the electron-transfer induced eta 6 to eta 4 hapticity change of a rhodium arene complex
[AD-A210211] 01 p0033 N90-10177
Applications of NMR spectroscopy to the study of zeolite synthesis
[DE89-015226] 02 p0192 N90-11095
Hardening mechanisms and analysis of the structure of the TGDDM/DDS epoxy resin system (tetraglycidyl-4,4' diaminodiphenylmethane/4,4' diaminodiphenylsulfone)
[NOTE-TECHNIQUE-1988-8] 04 p0465 N90-12662
Magnetic resonance of polymers at surfaces
[AD-A212225] 04 p0480 N90-12753
Persistent current, NMR, and ion transmission experiments in rotating He-3 superfluids --- Nuclear Magnetic Resonance (NMR)
[ISBN-952-90056-1-X] 04 p0553 N90-13221
Nuclear magnetic resonance signatures of nitrogen-containing compounds
[AD-A213375] 05 p0622 N90-13628
Perturbed angular correlations in zirconia ceramics
[DE89-017272] 06 p0751 N90-14369
Use of superconducting plates and shells to deflect magnetic noise fields: Application to MEG
[DE89-012592] 06 p0803 N90-14676
Development of NMR (Nuclear Magnetic Resonance) imaging probes for advanced ceramics
[DE90-003812] 07 p0911 N90-15269
Carbon-13 nuclear magnetic resonance of heterocyclic salts and its precursors
[DE89-635768] 08 p1041 N90-16016
NMR measurements of solvent self-diffusion coefficients in polymer solutions
[AD-A215276] 09 p1279 N90-17419
A potential nuclear magnetic resonance imaging approach for noncontact temperature measurement
10 p1364 N90-17908
NMR (Nuclear Magnetic Resonance) imaging development for the study of solids
[AD-A217073] 12 p1723 N90-19899
Copper and oxygen NMR studies on the magnetic properties of YBa2Cu3O(7-y)
[DE90-007889] 13 p1893 N90-20863
Metal alkoxides: Models for metal oxides. Alkoxide ligands in early transition metal organometallic chemistry
[DE90-007523] 13 p1894 N90-20869
Single crystal NMR of high temperature superconductors 16 p2321 N90-23236
Laser temperature-jump kinetic studies of fast reactions in nonaqueous solutions
[AD-A218819] 17 p2371 N90-23500
NMR studies of polymeric solid electrolytes
[AD-A219833] 17 p2381 N90-23562
Pulsed and modulated passage NMRON studies of cobalt-iron alloys 17 p2470 N90-24118
Density profile of terminally adsorbed polymers
[AD-A220897] 18 p2529 N90-24433
DURIP advanced polymer solid state NMR instrumentation
[AD-A221401] 18 p2531 N90-24440
Workshop on High-Field NMR and Biological Applications
[DE90-010002] 18 p2614 N90-24889
Dynamics of micellar oligomeric and monomeric sodium 10-undecenoate
[AD-A222570] 20 p2830 N90-26099
Magnetic resonance elucidation of molecule/macromolecule interaction stereochemistry
[AD-A221444] 21 p2979 N90-26928
Chemical and laser sciences division
[DE90-013532] 21 p3101 N90-27611
Magnetic properties of high-T(sub c) superconductors: Rigid levitation, flux pinning, thermal depinning, and fluctuation 22 p3137 N90-27798
Aqueous solution properties of ampholytic ionomers
[AD-A222152] 22 p3156 N90-27890
Experimental and kinetic modeling of acid/base redox reactions over metal oxide catalysts
[DE90-013835] 22 p3156 N90-27893
Solid-state N15 NMR of N15-labeled nylon 6 and nylon 11
[AD-A223271] 24 p3446 N90-29459
Investigation of YBa2Cu3O(7-sigma) by NMR and construction of an ultra low temperature cryostat
24 p3550 N90-30088

NUCLEAR MEDICINE
NT RADIOBIOLOGY
Activities report of the Kernfysisch Versneller Instituut
[ETN-89-95752] 04 p0553 N90-13219
Coded-aperture imaging in nuclear medicine
08 p1073 N90-16208
Assessment of research needs for laser technologies applied to advanced spectroscopic methods
[DE90-007402] 12 p1669 N90-19588
Software quality assurance and software safety in the biomed control system
[DE90-008072] 13 p1866 N90-20706
JPRS report: Science and technology. USSR: Life sciences
[JPRS-ULS-90-002] 14 p1995 N90-21434
Biomedical and environmental sciences program publications, 1989
[DE90-014785] 23 p3406 N90-29250

NUCLEAR MODELS
Precompound decay models for medium energy nuclear reactions
[DE90-008352] 13 p1884 N90-20808

NUCLEAR PARTICLES
NT ALPHA PARTICLES
NT ANTINEUTRINOS
NT ANTINUCLEONS
NT ANTIPARTICLES
NT ANTIPROTONS
NT BETA PARTICLES
NT BOSONS
NT ETA-MESONS
NT HYPERONS
NT MESONS
NT MUONS
NT NUCLEONS
NT PHOTOELECTRONS
NT PHOTONS
NT PIONS
NT POSITRONS

NUCLEAR PHYSICS
NT NUCLEAR ASTROPHYSICS
Gordon Conference on Atomic Physics
[AD-A211946] 03 p0402 N90-12304
Low resistivity electrodeless streamer tubes
[PREPRINT-685-89] 05 p0636 N90-13712
Nuclear physics and cosmology
[NASA-CR-186166] 05 p0713 N90-14167
Supernovae, compact stars, and nuclear physics
[DE90-002682] 06 p0864 N90-15022
NTES (Nuclear Test and Experimental Sciences) program laser facility for physics experiments Building 391 High Bay Option
[DE90-001795] 07 p0935 N90-15411
Thermal and statistical properties of nuclei and nuclear systems
[DE90-000183] 07 p0990 N90-15717
On the free carrier-negative U center interacting model for the high-T(sub c) oxide superconductor
[DE89-635908] 07 p0998 N90-15775
Elementary particle physics: Experimental
[DE90-005973] 10 p1429 N90-18242
Research in theoretical nuclear physics
[DE90-006063] 10 p1440 N90-18309
Theoretical studies in nuclear physics
[DE90-005981] 11 p1565 N90-19005
Activities report in nuclear physics
[ETN-90-95322] 13 p1883 N90-20803
JPRS report: Science and technology. USSR: Physics and mathematics
[JPRS-UPM-90-002] 14 p2022 N90-21593
Current experiments in elementary particle physics
[DE90-008062] 14 p2024 N90-21607
JPRS report: Science and technology. USSR: Physics and mathematics
[JPRS-UPM-89-001] 16 p2310 N90-23162
Biomedical and environmental sciences program publications, 1989
[DE90-014785] 23 p3406 N90-29250
Medium energy nuclear physics research
[DE90-015852] 24 p3544 N90-30042

NUCLEAR POWER GENERATION
U NUCLEAR ELECTRIC POWER GENERATION

NUCLEAR POWER PLANTS
Design study of a modular gas-cooled, closed-brayton cycle reactor for marine use
[AD-A213453] 07 p0953 N90-15518
Technical specifications requirements: Automated reasoning applications
[DE90-008799] 13 p1867 N90-20712
Eddy current inspection at the nuclear power plants
[VTT-RR-653] 19 p2699 N90-25357
The potential of renewable energy
[DE90-000322] 21 p3019 N90-27163
Neural nets and eddy-current testing
[DE90-016044] 24 p3478 N90-29656

NUCLEAR POWER REACTORS
NT PATHFINDER NUCLEAR REACTOR
NT SPACE POWER REACTORS
NT SPACE POWER UNIT REACTORS

NUCLEAR PROPULSION
NT NUCLEAR ELECTRIC PROPULSION
Heating rates in a High Energy Propulsion System (HEPS) Orbital Transfer Vehicle (OTV)
[AD-A214354] 10 p1360 N90-17888
Nuclear technology and the space exploration missions
[NASA-TM-103156] 16 p2253 N90-22847
Nuclear power systems for lunar and Mars exploration
[NASA-TM-103168] 21 p2969 N90-26873

NUCLEAR PUMPED LASERS
Beam propagation in direct nuclear pumped laser amplifiers
[DE90-009613] 15 p2104 N90-22035

NUCLEAR PUMPING
Gasdynamic phenomena in nuclear-reactor-pumped lasers
[DE90-005428] 09 p1229 N90-17131
Heat-transfer regimes in nuclear-reactor-pumped gas lasers
[DE90-002904] 15 p2103 N90-22032
Beam propagation in direct nuclear pumped laser amplifiers
[DE90-009613] 15 p2104 N90-22035

NUCLEAR QUADRUPOLE RESONANCE
Magnetic correlations in La(2-x)Sr(x)CuO4 from NQR relaxation and specific heat 22 p3143 N90-27827

NUCLEAR RADIATION
NT BETA PARTICLES
NT FAST NEUTRONS
NT GAMMA RAY BEAMS
NT GAMMA RAY BURSTS
NT GAMMA RAYS
NT NEUTRON BEAMS
NT PHOTONEUTRONS
NT SPALLATION
Proof of the feasibility of coherent and incoherent schemes for pumping a gamma-ray laser
[AD-A212315] 04 p0506 N90-12921
Final Safety Analysis Report for the Ulysses Mission. Volume 3 (Book 1): Nuclear risk analysis document
[DE90-008691] 14 p1939 N90-21101
Final safety analysis report for the Ulysses Mission. Volume 3 (Book 2): Nuclear risk analysis document-appendices
[DE90-008692] 14 p1939 N90-21102
Final safety analysis report for the Ulysses mission. Volume 2 (Book 1): Accident model document
[DE90-008694] 14 p1940 N90-21103
Space radiation studies
[NASA-CR-183991] 19 p2798 N90-25925
Environmental radioactivity measurement intercomparison exercise
[NPL-RSA(EXT)-5] 22 p3200 N90-28158

NUCLEAR REACTIONS
NT CONTROLLED FUSION
NT ELECTRON CAPTURE
NT NEUTRON EMISSION
NT NEUTRON SCATTERING
NT NUCLEAR FISSION
NT NUCLEAR FUSION
NT NUCLEAR INTERACTIONS
NT NUCLEAR SCATTERING
NT PHOTONUCLEAR REACTIONS
NT RADIOACTIVE DECAY
NT RESONANCE SCATTERING
NT SPALLATION
NT SPIN-ORBIT INTERACTIONS
NT THERMONUCLEAR REACTIONS
NT WEAK INTERACTIONS (FIELD THEORY)
Cold fusion: Alchemist's dream
[DE90-000865] 06 p0847 N90-14925
Theoretical study of cold nuclear fusion using barrier penetration approach
[DE90-601096] 08 p1124 N90-16513
Some theoretical aspects of cold fusion: A report
[DE90-601098] 08 p1125 N90-16514
Fracto-fusion. Mechanism of cold fusion
[DE90-719573] 08 p1125 N90-16518
Nuclear activity, morphology, and far infrared properties of spiral galaxies
[ETN-90-95373] 12 p1744 N90-20024

Activities report in nuclear physics
[ETN-90-95322] 13 p1883 N90-20803
Precompound decay models for medium energy nuclear reactions
[DE90-008352] 13 p1884 N90-20808
Present status of (mu)CF theory
[DE90-007547] 13 p1884 N90-20809
Populations of excited states and reaction mechanisms in the emission of complex fragments
[DE90-007481] 13 p1886 N90-20819
Gamma-ray production cross section measurements using a white neutron source from 1 to 400 MeV
[DE90-008906] 14 p2025 N90-21610
Investigation of correlations in nuclei with the (e,e'X) reaction
[ETN-90-96398] 15 p2166 N90-22377
Study of Sn-116 via neutron pickup and proton stripping reactions
[KVI-814] 16 p2315 N90-23199
Incomplete fusion reactors at low and intermediate energies
[KVI-809] 16 p2316 N90-23206
A closed form solution to HZE propagation
[NASA-TM-103482] 20 p2924 N90-26640
Accurate calculations of neutron kerma and damage from ENDF/B-VI evaluations for silicon, chromium, iron and nickel, and comparison with ENDF/B-V results
[DE90-016020] 24 p3481 N90-29674
Prospects for nuclear astrophysics with intense radioactive ion beams
[DE90-015616] 24 p3544 N90-30044

NUCLEAR REACTOR CONTROL
Model-reference adaptive control applied to loadfollowing of a space-nuclear power system
[DE89-014561] 10 p1429 N90-18245
Analysis and evaluation of ZPPR (Zero Power Physics Reactor) critical experiments for a 100 kilowatt-electric space reactor
[DE90-005634] 12 p1713 N90-19835

NUCLEAR REACTORS
NT BREEDER REACTORS
NT FUSION REACTORS
NT GAS COOLED REACTORS
NT HELIOTRONS
NT HIGH TEMPERATURE GAS COOLED REACTORS
NT LIQUID METAL FAST BREEDER REACTORS
NT PATHFINDER NUCLEAR REACTOR
NT PEBBLE BED REACTORS
NT SPACE POWER REACTORS
NT SPACE POWER UNIT REACTORS
NT SPHEROMAKS
NT STELLARATORS
NT TOKAMAK DEVICES
NT ZERO POWER REACTORS
Laser-powered lunar base 01 p0029 N90-10156
Earth orbit laser systems 01 p0030 N90-10162
Central electrical utility power for a satellite ring city in low earth orbit space 01 p0031 N90-10166
Boundary effects on the MHD dynamo in laboratory plasmas
[DE89-015207] 02 p0276 N90-11576
Wind/seismic comparisons for upgrading existing structures
[DE89-016055] 03 p0357 N90-12044
Activities report of the Joint Research Center
[ETN-89-95757] 04 p0569 N90-13321
Re-entry hazards and cosmos 1900
[FOA-C-30535-9.4] 05 p0613 N90-13583
Energy ratings for metal oxide varistors under repetitively pulsed operation
[DE90-002353] 06 p0770 N90-14480
A cost effective battery bank for I(sup 2)T testing and evaluation of electrical switchgear
[DE90-002350] 06 p0772 N90-14490
Failure probability estimate of Type 304 stainless steel piping
[DE90-000659] 06 p0796 N90-14635
Human factors survey of advanced instrumentation and controls
[DE90-002477] 06 p0821 N90-14776
Tuned-circuit Johnson noise thermometry
[DE89-016221] 07 p0925 N90-15356
The Gevaltig: An inertial fusion powered manned spacecraft design for outer solar system missions
[NASA-CR-185163] 08 p1036 N90-15985
Nuclear reaction uncertainties in standard and non-standard cosmologies
[DE90-003594] 08 p1151 N90-16666
Activities report in nuclear physics
[ETN-90-95322] 13 p1883 N90-20803
Simple light gas guns for hypervelocity studies
[DE90-008907] 14 p1931 N90-21056
West European magnetic confinement fusion research 14 p2029 N90-21634
Full wave computation of electromagnetic wave excitation, propagation, and absorption at the ion cyclotron frequency in fusion experiments
[DE90-009399] 14 p2030 N90-21642
Proceedings of the Conference on Technology-Based Confidence Building: Energy and Environment
[CNSS-PAPERS-22] 15 p2125 N90-22152
A decision support system for control and automation of dynamical processes
[AD-A219501] 17 p2454 N90-23995
Characteristics of the IAEA correlation monitor material for surveillance programmes
[VTT-RR-639] 19 p2682 N90-25258
The chemical effects of the Martian environment on power system component materials: A theoretical approach
[NASA-TM-103203] 20 p2825 N90-26074
Analysis of a Mars-stationary orbiting microwave power transmission system
[NASA-TM-101344] 20 p2843 N90-26172
The nuclear battery
[DE90-630400] 24 p3462 N90-29559
Counter-current flow limitation in thin rectangular channels
[DE90-015124] 24 p3469 N90-29599

NUCLEAR RESEARCH
QTA (QUESTIONNAIRE-TASK-ANALYSIS): An electronic tool for job/task analysis
[DE90-008944] 24 p3499 N90-29778

NUCLEAR ROCKET ENGINES
TFE verification program
[DE90-008227] 18 p2614 N90-24891

NUCLEAR SCATTERING
NT NEUTRON SCATTERING
NT RESONANCE SCATTERING
Small particle scattering and absorption
[AD-A213168] 04 p0473 N90-12711
Multiple versus single scattering of terrestrial infrared longwave radiation in an aerosol-laden planetary boundary layer
[AD-A217709] 13 p1790 N90-20272

NUCLEAR SHIELDING
U RADIATION SHIELDING

NUCLEAR SPIN
Proceedings of the Conference on High-Spin Nuclear Structure and Novel Nuclear Shapes
[DE88-013968] 06 p0839 N90-14875
Transport and relaxation properties in anisotropic superconductors 15 p2170 N90-22403
Pulsed and modulated passage NMRON studies of cobalt-iron alloys 17 p2470 N90-24118

NUCLEAR STRUCTURE
Synchrotron radiation, free electron laser, and nuclear structure
[DE89-017352] 02 p0228 N90-11306
Monte Carlo studies of nuclei and quantum liquid drops
[DE89-016914] 03 p0402 N90-12300
Investigations of spontaneous nuclear order in copper by neutron diffraction
[ETN-90-96060] 05 p0698 N90-14090
Proceedings of the Conference on High-Spin Nuclear Structure and Novel Nuclear Shapes
[DE88-013968] 06 p0839 N90-14875
Heavy ion interactions
[DE90-001410] 06 p0840 N90-14884
Heavy ion inelastic scattering with a 4(pi) gamma detector
[DE90-002709] 08 p1120 N90-16488
Theoretical aspects of electroweak and other interactions in medium energy nuclear physics
[DE90-004015] 08 p1121 N90-16493
Searching for existing nuclear data
[DE90-007535] 12 p1727 N90-19925
The basis spline method and associated techniques
[DE90-008403] 13 p1877 N90-20763

NUCLEAR WARFARE
The thrust and parry of the SIOP (Single Integrated Operational Plan) and SDI
[AD-A217617] 13 p1880 N90-20784

NUCLEAR WASTES
U RADIOACTIVE WASTES

NUCLEAR WEAPONS
Nuclear weapon radiation effects on a space based interceptor weapon platform
[DE89-016258] 09 p1181 N90-16850
Overview of defense applications of ICF (Inertial Confinement Fusion)
[DE90-005745] 10 p1433 N90-18269
Survivability and effectiveness of near-term strategic defense
[DE90-005805] 11 p1555 N90-18955
Assessing the morality of using the space environment as a platform for weapons
[AD-A217348] 13 p1879 N90-20780
SDI (Strategic Defense Initiative): Is its future past
[DE90-008016] 13 p1880 N90-20785
Brilliant pebbles
[DE90-010756] 18 p2606 N90-24845
ASATs vs Brilliant Pebbles
[DE90-010348] 20 p2922 N90-26626
Effects of ionizing radiation on the performance of selected tactical combat crews
[AD-A222880] 21 p3034 N90-27248

NUCLEATION
NT CLOUD SEEDING
Monte Carlo simulations of small solute/solvent clusters: Cluster properties and phase transitions
[AD-A209559] 01 p0119 N90-10684
Methods to decrease defect density in GaAs/Si heteroepitaxy
[DE89-016306] 01 p0131 N90-10753
Dynamics of nucleation at electrochemical interfaces via surface EXAFS and standing wave measurements
[AD-A210733] 02 p0195 N90-11109
Nucleation kinetics in undercooled, glass-forming metallic melts
[DLR-FB-89-32] 05 p0624 N90-13644
Cavitation and superplasticity 06 p0744 N90-14329
Theory of the energetics and nonclassical nucleation for martensitic transformations from partially soft lattice modes
[DE90-002182] 06 p0854 N90-14964
The influence of the substrate surface on the nucleation and growth of superconducting thin films
[DE90-003649] 06 p0857 N90-14983
Energetics of BCC-FCC lattice deformation in iron
[AD-A213801] 07 p0905 N90-15233
Study of phase transformations liquid-solid-solid of ultrafine particles
[ISAL-89-0019] 08 p1042 N90-16022
False vacuum decay in Jordan-Brans-Dicke cosmologies
[NASA-CR-186257] 09 p1293 N90-17497
Investigation of the phase stabilizing effect of 4 percent potassium fluoride on ammonium nitrate
[AD-A215313] 11 p1494 N90-18599
Investigation of the processes controlling the flame generation of refractory materials
[DE90-007564] 12 p1624 N90-19333
Nucleation of vortices in superfluid helium-4
[DE90-610675] 12 p1720 N90-19880
Ceramic oxide thin film formation utilizing biological processes
[DE90-008599] 13 p1781 N90-20225
Interfacial studies in fiber-reinforced thermoplastic-matrix composites 15 p2062 N90-21814
Martensitic transformation induced by stress pulses
[DE90-009534] 15 p2069 N90-21854
UV photo-enhanced MOCVD of cadmium and cadmium telluride
[RSRE-MEMO-4208] 15 p2174 N90-22422
The effects of zinc addition on the environmental stability of Al-Li alloys 16 p2219 N90-22657
Undercooling and nucleation in rapid solidification rate metal powders using solid in solid emulsification
[AD-A218527] 17 p2375 N90-23526
Baryogenesis in extended inflation. Part 1: Baryogenesis via production and decay of supermassive bosons
[NASA-CR-180615] 17 p2470 N90-24120
Nucleation kinetics in undercooled, class-forming metallic melts
[ESA-TT-1186] 19 p2676 N90-25218
Extended inflation from higher dimensional theories
[NASA-CR-180549] 19 p2796 N90-25916
Undercooling and solidification
[DLR-FB-90-020] 20 p2931 N90-26678
Design of organic nonlinear optical materials
[AD-A222400] 21 p3084 N90-27536
The Colorado/Missouri 1989 cirrus mini IFO 22 p3227 N90-28299
Percolation and low density materials: Theory and applications
[AD-A224237] 24 p3442 N90-29438
Mechanism of habit change for atmospheric ice crystal growth 24 p3489 N90-29717

NUCLEI
Thermal and statistical properties of nuclei and nuclear systems
[DE90-000183] 07 p0990 N90-15717
Q-2 and A dependence of delta (1232) electroexcitation in nuclei
[DE90-003470] 08 p1121 N90-16492
Heavy Nucleus Collector (HNC) project for the NASA Long Duration Exposure Facility (LDEF)
[NASA-CR-182094] 24 p3544 N90-30045

NUCLEI (NUCLEAR PHYSICS)
NT ALPHA PARTICLES
NT DEUTERONS
NT HEAVY NUCLEI
NT ODD-ODD NUCLEI
NT TRITONS
Fluctuations in transverse energy and multiplicity, energy densities, and neutral pion spectra in nucleus-nucleus collisions at 200 GeV/nucleon
[DE89-017583] 03 p0402 N90-12302
Detailed photonuclear cross-section calculations and astrophysical applications
[DE89-017531] 03 p0421 N90-12419
Activities report of the Kernfysisch Versneller Instituut
[ETN-89-95752] 04 p0553 N90-13219
Proceedings of the Conference on High-Spin Nuclear Structure and Novel Nuclear Shapes
[DE88-013968] 06 p0839 N90-14875
Rapidity densities and their fluctuations in central 200 A GeV S32 interations with Au and Ag,Br nuclei
[LUIP-8905] 07 p0989 N90-15715
Target nucleus fragmentation in O16 + (Ag,Br) interactions at 200 A GeV
[LUIP-8906] 07 p0991 N90-15727
New calculations and measurements of the Coulomb cross-section for the production of direct electron pairs by high energy nuclei
[NASA-TM-101280] 15 p2165 N90-22371
Investigation of correlations in nuclei with the (e,e'X) reaction
[ETN-90-96398] 15 p2166 N90-22377
Study of short-lived unstable nuclei by means of laser optical pumping
[AD-A222561] 21 p3009 N90-27105

NUCLEIC ACIDS
NT DEOXYRIBONUCLEIC ACID
NT RIBONUCLEIC ACIDS

NUCLEON POTENTIAL
Nucleon polarizabilities in the constituent quark model
[NOTA-INTERNA-936] 05 p0698 N90-14082

NUCLEON-NUCLEON INTERACTIONS
Fluctuations in transverse energy and multiplicity, energy densities, and neutral pion spectra in nucleus-nucleus collisions at 200 GeV/nucleon
[DE89-017583] 03 p0402 N90-12302
Experimental test of PCAC hypothesis in the reactions mu neutrino-proton giving muon(-)-proton-pion(+) and mu antineutrino-proton giving muon(+)-proton-pion(-) in the delta (1232) region --- partial conserved axial current
[MPE-PAE/EXP.EL.199] 03 p0403 N90-12309
The interacting boson approximation
[KVI-774] 04 p0552 N90-13215

NUCLEON-NUCLEON SCATTERING
The effective (3)He-nucleon force in a microscopic DWBA approach to the (3)He,t charge exchange reaction --- Distorted Wave-Borne Approximation (DWBA)
[KVI-763] 05 p0697 N90-14077
Relativistic effects in low energy nucleon-nucleon scattering
[CEBAF-PR-89-025] 21 p3075 N90-27483

NUCLEONS
Theoretical aspects of electroweak and other interactions in medium energy nuclear physics
[DE90-004015] 08 p1121 N90-16493
A covariant multiple scattering series for elastic projectile-target scattering
[NASA-TM-101942] 09 p1279 N90-17417
Contained events in Soudan 2
[DE90-005648] 10 p1449 N90-18359
Underground muon observations in the Soudan 2 detector
[DE90-005647] 11 p1594 N90-19183

NUCLEOSYNTHESIS
U NUCLEAR FUSION

NUCLEOTIDES
NT ADENOSINE TRIPHOSPHATE

NUCLIDES
NT ALUMINUM ISOTOPES
NT ALUMINUM 26
NT AMERICIUM
NT ANTIMONY ISOTOPES
NT BORON ISOTOPES
NT CALCIUM ISOTOPES
NT CARBON ISOTOPES
NT CARBON 12
NT CARBON 13
NT CARBON 14
NT CESIUM VAPOR
NT CHROMIUM ISOTOPES
NT COBALT ISOTOPES
NT COBALT 60
NT CURIUM
NT DEUTERIUM
NT ERBIUM ISOTOPES
NT EUROPIUM ISOTOPES
NT GADOLINIUM ISOTOPES
NT GALLIUM ISOTOPES
NT GOLD ISOTOPES
NT HELIUM ISOTOPES
NT HYDROGEN ISOTOPES
NT IODINE ISOTOPES
NT IRON ISOTOPES
NT ISOTOPES
NT KRYPTON ISOTOPES
NT KRYPTON 85
NT LANTHANUM ISOTOPES
NT LEAD ISOTOPES
NT LITHIUM ISOTOPES
NT MANGANESE ISOTOPES
NT MERCURY ISOTOPES
NT NICKEL ISOTOPES
NT NIOBIUM ISOTOPES
NT OXYGEN ISOTOPES
NT OXYGEN 18
NT PLUTONIUM
NT POLONIUM ISOTOPES
NT RADIOACTIVE ISOTOPES
NT RADON ISOTOPES
NT TELLURIUM
NT TELLURIUM ISOTOPES
NT TIN ISOTOPES
NT TRITIUM
NT URANIUM ISOTOPES
Cosmogenic nuclides in cometary materials: Implications for rate of mass loss and exposure history
08 p1143 N90-16623
Measurements of long-lived cosmogenic nuclides in returned comet nucleus samples
08 p1146 N90-16640

NULL HYPOTHESIS
Newton methods for large-scale linear equality-constrained minimization
[AD-A222310] 21 p3070 N90-27457

NULL ZONES
Deep null antennas and their applications to tactical VHF radio communications
[AD-A210656] 02 p0212 N90-11214
Boundary kernel estimation of the two sample comparison density function
[AD-A210757] 02 p0268 N90-11532
Null offset voltage compensator for operational amplifier
[AD-D014189] 04 p0496 N90-12859
Characterization of liquid crystal displays for optical signal processing applications
[AD-A212832] 04 p0505 N90-12910
Performance of adaptive nulling antennas in a jamming environment
[AD-A219305] 16 p2230 N90-22720
On null tratorial torsion in vacuum quadratic Poincare gauge field theory
[MATHS-REPT-A-111] 19 p2751 N90-25630
MUSE: A systolic array for adaptive nulling with 64 degrees of freedom, using Givens transformations and wafer scale integration
[AD-A223812] 24 p3529 N90-29953

NUMBER THEORY
NT ARITHMETIC
NT CONGRUENCES
NT DIOPHANTINE EQUATION
NT DIVIDING (MATHEMATICS)
NT EXPONENTS
NT FIXED POINT ARITHMETIC
NT FLOATING POINT ARITHMETIC
NT INDUCTION (MATHEMATICS)
NT INTEGERS
NT MULTIPLICATION
A modified Moebius inverse formula and its applications in physics
[DE90-612740] 14 p2022 N90-21594
On the notion of currying
[MEMO-INF-89-57] 18 p2592 N90-24749
Achromatic number is NP-complete for cographs and interval graphs
[RUU-CS-88-25] 18 p2600 N90-24803
Minimizing sums of addition chains
[RUU-CS-89-15] 18 p2635 N90-25013
A number-theoretic approach to subgroups of dihedral groups
[AD-A222857] 21 p3063 N90-27413

NUMERICAL ANALYSIS
NT APPROXIMATION
NT BORN APPROXIMATION
NT BOUNDARY INTEGRAL METHOD
NT CHEBYSHEV APPROXIMATION
NT COMPUTATIONAL CHEMISTRY
NT COMPUTATIONAL FLUID DYNAMICS
NT CONJUGATE GRADIENT METHOD
NT DIFFERENCE EQUATIONS
NT EDDINGTON APPROXIMATION
NT ERROR ANALYSIS
NT ESSENTIALLY NON-OSCILLATORY SCHEMES
NT FINITE DIFFERENCE THEORY
NT FINITE ELEMENT METHOD
NT FINITE VOLUME METHOD
NT FLUX VECTOR SPLITTING
NT HARTREE APPROXIMATION
NT INTERPOLATION
NT ITERATION
NT ITERATIVE SOLUTION
NT LEAST SQUARES METHOD
NT MEAN SQUARE VALUES
NT MONTE CARLO METHOD
NT MULTIGRID METHODS
NT NEWTON METHODS
NT NEWTON-RAPHSON METHOD
NT NOMOGRAPHS
NT NUMERICAL DIFFERENTIATION
NT NUMERICAL INTEGRATION
NT OSEEN APPROXIMATION
NT PADE APPROXIMATION
NT PARTICLE IN CELL TECHNIQUE
NT PREDICTOR-CORRECTOR METHODS
NT RAYLEIGH-RITZ METHOD
NT RELAXATION METHOD (MATHEMATICS)
NT RUNGE-KUTTA METHOD
NT TRUNCATION ERRORS
NT TVD SCHEMES
Numerical simulations of a midlatitude squall line
01 p0087 N90-10497
Numerical analysis of a class of problems in the mathematical theory of plasticity and damage
[AD-A210731] 01 p0114 N90-10855
Study for optimization of redundant vane-type flow-direction sensing systems and numerical analysis for design of the systems
[NAL-TM-571] 02 p0155 N90-10890
Numerical treatment of the thermo-structural-dynamic problems: The interpolation techniques
02 p0180 N90-11016
International conference on numerical grid generation in computational fluid dynamics
[AD-A211082] 02 p0220 N90-11262
Analytical and numerical studies in flow development
[DE89-017380] 02 p0221 N90-11269
On the numerical solution of two-point boundary value problems
[AD-A211244] 02 p0266 N90-11516
Computation of ramjet internal flowfields
[AD-A212001] 03 p0307 N90-11743
Numerical analysis, scientific computing and fundamental studies of fluid mechanics
[DE89-017554] 03 p0346 N90-11975
Numerical analysis of notch test damage to laminated composite plates submitted to uniaxial traction
[CETIM-107310] 04 p0467 N90-12675
Unsteady three-dimensional thin-layer Navier Stokes solutions on dynamic blocked grids
[AD-A212377] 04 p0503 N90-12899
Radio frequency linac driven free-electron laser configurations
[AD-A212572] 04 p0507 N90-12922
Cavity eigenmodes for the NIST/NRL (National Institute of Standards and Technology/Naval Research Laboratory) free electron laser
[AD-A212706] 04 p0507 N90-12923
A cell-centered multigrid method for three-dimensional anisotropic-diffusion and interface problems
[REPT-89-35] 04 p0540 N90-13128
Local mode smoothing analysis of various incomplete factorization iterative methods in two dimensions
[REPT-89-36] 04 p0540 N90-13129
Problems in nonlinear acoustics: Scattering of sound by sound, parametric receiving arrays, nonlinear effects in asymmetric sound beams and pulsed finite amplitude sound beams
[AD-A211756] 04 p0550 N90-13200
Ground states of a two-dimensional charged-boson system
[AD-A212363] 04 p0553 N90-13226
Study of modern instrumentation and methods for astronomic positioning in the field
[AD-A213217] 05 p0710 N90-14157
Research in mathematics and computer science at Argonne, July 1, 1986 to January 6, 1988
[DE88-010343] 06 p0822 N90-14781
Investigation of broadband microstrip antenna structures for application in monolithic millimeter wave arrays
[AD-A213856] 07 p0923 N90-15344
Stability of numerical solutions for stratified two-phase flow
[DE90-701646] 07 p0929 N90-15379
Numerical analysis and simulation of frictional particle systems 07 p0937 N90-15430
Ultra high performance, highly reliable, numeric intensive processors and systems
[AD-A214100] 07 p0980 N90-15659

Numerical optimization
[AD-A213758] 07 p0984 N90-15683
Numerical methods for parabolic equations and inequalities in very high dimensions
[AD-A214102] 07 p0985 N90-15690
Dynamics of electron transfer for a non-superexchange coherent mechanisms. 2: Numerical calculations
[AD-A213511] 07 p0990 N90-15722
Improved tangent-cone method for the Aerodynamic Preliminary Analysis System (APAS) version of the hypersonic arbitrary-body program
[NASA-TM-4165] 08 p1018 N90-15890
A physical and numerical study of the turn-off behavior of bipolar power transistors
[LAAS-89185] 08 p1061 N90-16136
A numeric analysis of incompressible, viscous flow around a symmetrical body of revolution
[ISL-CO-215/87] 08 p1064 N90-16157
Two possible configurations for the top-hat electrostatic analyzer: A numerical study
[IFSI-88-18] 08 p1077 N90-16229
The bifurcation interpreter: A step towards the automatic analysis of dynamical systems
[AD-A214618] 09 p1265 N90-17336
Compiling scientific code using partial evaluation
[AD-A215087] 09 p1270 N90-17363
Analysis and numerical solution of flow over airfoil with control flap 10 p1307 N90-17584
The Hueckel model for small metal clusters. 4: Orbital properties and cohesive energies for model clusters of up to several hundred atoms
[AD-A216161] 10 p1354 N90-17852
New type of optical bistability in polymers mediated by phonons
[AD-A216102] 10 p1359 N90-17882
Oblique impact of two cylinders in a uniform flow
[AD-A215933] 10 p1385 N90-18015
Numerical algorithms for parallel computers
[AD-A216812] 10 p1419 N90-18181
Optimization of Gaussian beam widths in acoustic propagation
[AD-A215893] 10 p1427 N90-18231
Damage in a perforated graphite-epoxy composite plate under monotonic and cyclic biaxial loading
[ESA-TT-1117] 11 p1480 N90-18521
KAM: Automatic planning and interpretation of numerical experiments using geometrical methods
[AD-A216805] 11 p1546 N90-18900
Numerical and experimental analysis of a thin liquid film on a rotating disk related to development of a spacecraft absorption cooling system
[NASA-CR-183457] 12 p1657 N90-19523
Evolution of midplate hotspot swells: Numerical solutions
[NASA-CR-186462] 12 p1691 N90-19713
Aerodynamic and kinetic processes in flames
[AD-A217796] 13 p1773 N90-20176
Modification and improvement of software for modeling multidimensional reacting fuel flows
[AD-A217789] 13 p1783 N90-20235
Micro SAINT programs for numerical methods of integration and differential equations
[AD-A216097] 13 p1878 N90-20772
MECCA program documentation
[NOAA-TR-NESDIS-46] 14 p2003 N90-21477
Theory and numerical analysis of single and multi-element nozzle propellers
[LR-579] 15 p2048 N90-21741
Experimental determination of thermal conductance in bolted joint impact in satellites
[INPE-4989-PRE/1551] 15 p2059 N90-21788
Computational methods and plasticity
[LR-583] 15 p2119 N90-22120
Stability radius of polynomials occurring in the numerical solution of initial value problems
[TW-89-04] 15 p2162 N90-22350
The synergism of analytic and numerical techniques in general relativity: Calculation of radiative spacetimes 15 p2174 N90-22425
A numerical and analytical study of normal stresses and pressure differences in non-Newtonian creeping flows 16 p2234 N90-22749
JPRS report: Science and technology. USSR: Physics and mathematics
[JPRS-UPM-89-001] 16 p2310 N90-23162
Analysis of internal flow in a ventral nozzle for STOVL aircraft
[NASA-TM-103123] 17 p2355 N90-23404
Structural behavior of composites with progressive fracture
[NASA-TM-102370] 17 p2368 N90-23477
The origin of multiple melting in polyurethane block copolymers
[AD-A220050] 17 p2381 N90-23583
Nonlinear multigrid applied to a 1D stationary semiconductor model
[CWI-NM-R8905] 17 p2398 N90-23659
Numerical study of the onset of instability in the flow past a sphere 17 p2400 N90-23672
Computations of a horseshoe vortex around an endwall-mounted cylinder 17 p2400 N90-23673
The effects of wiggler errors on free electron laser performance
[AD-A220421] 17 p2409 N90-23725
Prediction of gear tooth separation in single-stage gear systems, using numerical techniques
[AD-A220442] 17 p2412 N90-23744
J-integral and HRR field of a stably growing crack, an experimental analysis
[AD-A220418] 17 p2416 N90-23764
Interdigitated back contact silicon solar cell analysis and design recommendations for space use
[AD-A220414] 17 p2420 N90-23790
Cumulative reports and publications through December 31, 1989
[NASA-CR-182041] 17 p2439 N90-23898
The standard map machine
[AD-A219943] 17 p2441 N90-23908
Numerical solution of large Lyapunov equations
[NASA-CR-180359] 17 p2456 N90-24010
A feedback extension to the numerical solution of nonlinear boundary value problems
[AD-A219886] 17 p2461 N90-24050
The Clemson University, university research initiative program in discrete mathematics and computational analysis
[AD-A220103] 17 p2461 N90-24055
Behaviour in the large of numerical solutions to one-dimensional nonlinear viscoelasticity by continuous time Galerkin methods
[AD-A220197] 17 p2461 N90-24057
The Trickett-Welch Solution to the Behrens-Fisher problem applied to one-sided tolerance limits for random effects model
[AD-A220416] 17 p2465 N90-24086
Analysis and applications of the crosstie-overlay slow-wave structure
[AD-A220286] 18 p2547 N90-24537
Impact of a unified DMSP meteorological sensor retrieval methodology on global numerical weather prediction
[AD-A220306] 18 p2581 N90-24703
Flipper user's manual
[AD-A220788] 18 p2590 N90-24734
Development of a postprocessing and 3D graphical imaging facility
[AD-A221212] 18 p2593 N90-24755
On the use of stability regions in the numerical analysis of stability value problems
[TW-89-07] 18 p2603 N90-24826
A study of non-uniqueness and instability for convex materials
[DE90-012060] 19 p2689 N90-25294
ICASE semiannual report, April 1 - September 30, 1989
[NASA-CR-181988] 19 p2727 N90-25502
One dimensional heavy ion beam transport: Energy independent model
[NASA-CR-186722] 19 p2754 N90-25650
Research conducted at the Institute for Computer Applications in Science and Engineering in applied mathematics, numerical analysis, and computer science
[NASA-CR-182057] 20 p2903 N90-26510
Computer analysis of chromatographic data 20 p2905 N90-26521
Numerical treatment of shell crossing singularities in the spherically symmetric gravitational collapse
[ETN-90-96967] 20 p2917 N90-26598
Asymptotic analysis of dissipative waves with applications to their numerical simulation
[NASA-TM-103231] 20 p2920 N90-26615
Transient signal distortion and coupling in multilayer multiconductor MIC microstrips
[AD-A222989] 21 p3000 N90-27050
Lyapunov-based control for switched power converters
[AD-A221974] 21 p3000 N90-27053
On the theory and numerics of differential-algebraic equations
[AD-A222427] 21 p3065 N90-27422
Applications of gauge theories to enhance numerical solutions of mixed potential integral equations
[AD-A221520] 21 p3065 N90-27424
Queing networks with finite capacities
[AD-A221547] 21 p3065 N90-27425
Generalized Voronoi diagrams: Initial results
[IMAG-RR-799-M] 21 p3066 N90-27429
Novel numerical analysis method for the study of convolution equations in appearance potential spectroscopy
[ETN-90-97288] 23 p3400 N90-29210
Statistically designed study of the variables and parameters of carbon dioxide equations of state
[DE90-016196] 24 p3447 N90-29467
A numerical study of the response of the laminar unsteady separated flow about a circular cylinder to changes of boundary conditions
[DLR-FB-90-10] 24 p3471 N90-29613
A vector diagram approach to shaping inputs for vibration reduction
[AD-A223724] 24 p3480 N90-29671
Formal verification of mathematical software, volume 2
[AD-A223633] 24 p3527 N90-29943

NUMERICAL CONTROL

Combined advanced foundry and quality control techniques to enhance reliability of castings for the aerospace industry 01 p0043 N90-10240
Numerical simulation of turbulent flow downstream a sudden axisymmetric expansion
[FOA-C-20758-2.1] 02 p0222 N90-11272
Scheduling sporadic and aperiodic events in a hard real-time system
[AD-A211344] 03 p0387 N90-12205
Computer controlled MHD power consolidation and pulse-generation system
[DE89-015600] 03 p0407 N90-12333
Development of an integrated mobile robot system at CMU (Carnegie-Mellon University)
[AD-A212555] 04 p0510 N90-12944
A computer-controlled automated test system for fatigue and fracture testing
[DE90-002931] 06 p0800 N90-14661
Time bounds for real-time process control in the presence of timing uncertainty
[AD-A213791] 07 p0975 N90-15633
Computer controlled MHD power consolidation and pulse-generation system
[DE90-001224] 07 p0981 N90-15662
Computer-controlled ion beam sputter-deposition of superconducting oxide films
[AD-A213921] 07 p1004 N90-15812
D3-D cryogenic control system upgrade
[DE90-003290] 08 p1054 N90-16092
Diesel starting system monitor: Prototype development
[DE90-004425] 08 p1084 N90-16276
Bus programmable slave module
[NASA-CASE-MSC-21387-1] 08 p1108 N90-16411
Subtle porosity variation in the YBa2Cu3O(7-x) high-temperature superconductor revealed by ultrasonic imaging
[NASA-TM-102130] 09 p1235 N90-17167
Generating optimally evasive MaRV trajectories
[DE90-004496] 10 p1328 N90-17671
Effects of controlled three-dimensional perturbations on boundary layer transition
[AD-A215080] 10 p1384 N90-18011
Mechanical disturbances in high-performance superconducting dipoles
[DE90-006237] 11 p1570 N90-19040
A computer control system for the alternating gradient magnetometer 12 p1636 N90-19402
Determination of the implementation of the 3-axis attitude motion simulator digital position controller 12 p1638 N90-19409
Disturbance torque rejection properties of the NASA/JPL 70-meter antenna axis servos 12 p1644 N90-19450
A digitally controlled system for effecting and presenting a selected electrical resistance
[NASA-CASE-MFS-29149-1] 12 p1652 N90-19492
Multi-tasking computer control of video related equipment 13 p1859 N90-20665
Development, implementation and test of a computer program for the production of axisymmetric pattern moulds on a numerically controlled milling machine
[LR-593] 15 p2074 N90-21877
Computerized inspection of gear tooth surfaces
[NASA-TM-102395] 15 p2107 N90-22054
The elastic-plastic behavior of composite materials 16 p2212 N90-22615
Computer controlled cryogenic temperature controller
[AD-A218785] 16 p2227 N90-22701
Modelling and computer control of a mechanical system
[W-8908] 16 p2243 N90-22794
Application of numerical optimization techniques to control system design for nonlinear dynamic models of aircraft 16 p2287 N90-23032
A test matrix sequencer for research test facility automation
[NASA-TM-103108] 17 p2357 N90-23416
Development of a quadrupole-based Secondary-Ion Mass Spectrometry (SIMS) system at Lewis Research Center
[NASA-TM-102531] 17 p2367 N90-23476

A decision support system for control and automation of dynamical processes
[AD-A219501] 17 p2454 N90-23995
Microcomputer for the digital regulation of permanent magnet-synchronous servomotors
[ETN-90-96507] 18 p2588 N90-24727
System development and early biological tests in NASA's biomass production chamber
[NASA-TM-103494] 19 p2716 N90-25456
Computer access security code system
[NASA-CASE-NPO-17525-1-CU] 19 p2742 N90-25583
Thermionic gun control system for the CEBAF injector
[CEBAF-PR-89-028] 19 p2755 N90-25654
Ultrasonic inspection of advanced CFRP structures by computer-controlled, pulse-echo technique 22 p3185 N90-28075
Digital beam position regulation of the superconducting accelerator at Darmstadt
[ETN-90-97293] 22 p3246 N90-28406
A system architecture for a planetary rover 23 p3365 N90-29015
Reflexive obstacle avoidance for kinematically-redundant manipulators 23 p3371 N90-29047
Computer-aided engineering environment for controlled mechanical systems
[AD-A223551] 24 p3527 N90-29942

NUMERICAL DATA BASES
Defense Technical Information Center cataloging guidelines
[AD-A211000] 01 p0137 N90-10792

NUMERICAL DIFFERENTIATION
On the differentiable manifold of fixed order stable linear systems
[REPT-88-89] 03 p0394 N90-12250
Recursive linearization of multibody dynamics equations of motion 16 p2280 N90-22993

NUMERICAL FLOW VISUALIZATION
Numerical Methods for Flows in Turbomachinery, volume 2
[VKI-LS-1989-06-VOL-2] 05 p0641 N90-13741
Numerical methods for unsteady turbomachinery flow 05 p0641 N90-13743
Dynamics of a class of vortex rings 07 p0926 N90-15362
Numerical simulation of the vortex breakdown
[ONERA-RSF-4/4368-AY-004A] 11 p1509 N90-18689
Numerical investigations of heat transfer and flow rates in rotating cavities. Simulation of the movement generated by wall temperature gradients, by source-sink mass flows or by the differential rotation of the walls, under the influence or coriolis and centrifugal forces
[ETN-90-96253] 11 p1510 N90-18695
Prediction of aerodynamic performance of airfoils in low Reynolds number flows
[DLC-EST-TN-031] 17 p2346 N90-23360
Codice ETF-3D: Euler transonic flow user manual
[DLC/FLU-INT-TN-006] 17 p2346 N90-23362
Development of a system for the numerical simulation of Euler flows, with results of preliminary 3-D propeller-slipstream/exhaust-jet calculations
[NLR-TR-88008-U] 20 p2863 N90-26285
Direct numerical simulation of compressible free shear flows 21 p2974 N90-26901
Experimental study of the Taylor-Goertler instability
[ETN-90-97447] 22 p3175 N90-28014
Ultra-fast visualization of a turbulent boundary layer by a laser velocimeter
[IMFL-89-37] 22 p3181 N90-28048
An investigation of chaotic Kolmogorov flows
[NASA-CR-182079] 23 p3328 N90-28816
Calculation of flow fields by the solution of the Euler equations using an extended finite volume discretization scheme
[ESA-TT-1204] 24 p3470 N90-29605

NUMERICAL INTEGRATION
NT RUNGE-KUTTA METHOD
STS-GPS (Space Transportation System - Global Positioning System) tracking experiment for gravitation estimation: Feasibility study
[AD-A211265] 02 p0150 N90-10859
An analytical and experimental study of the elastodynamic response characteristics of planar linkage mechanism with bearing clearances 02 p0233 N90-11336
Programs for numerical integration of piece-wise smooth functions
[DE89-620449] 02 p0258 N90-11464
Spectral-domain analysis of finite frequency selective surfaces
[AD-A211669] 03 p0339 N90-11932
Increasing the real stability boundary of explicit methods
[CWI-NM-R8902] 04 p0541 N90-13134
A transient response method for linear coupled substructures
[NASA-TP-2926] 05 p0592 N90-13444
Symplectic numerical integration of Hamiltonian systems
[DE90-002380] 06 p0835 N90-14855
Numerical boundary layer calculations on the DFVLR ellipsoid of revolution 08 p1070 N90-16193
Autonomous orbit determination using GPS
[INPE-4815-TDL/361] 11 p1466 N90-18442
Micro SAINT programs for numerical methods of integration and differential equations
[AD-A218097] 13 p1878 N90-20772
Supersonic nozzle design of arbitrary cross-section 14 p1927 N90-21035
Finite element analysis of elastic contact problems with friction 15 p2105 N90-22040
Semianalytic study of high-eccentricity orbit stability and evolution 16 p2204 N90-22574
A new second-order integration algorithm for simulating mechanical dynamic systems 16 p2293 N90-23064
Effective action for induced gravity on a 2-dimensional manifold
[PREPRINT-712] 16 p2311 N90-23173
Semianalytic satellite theory
[AD-A220744] 17 p2361 N90-23444
A note on the Gaussian integration formula
[AD-A220053] 17 p2461 N90-24054
Models of intracavity frequency doubled lasers
[AD-A221182] 18 p2563 N90-24628
Natural melting within a spherical shell
[NASA-TM-102822] 20 p2861 N90-26274
Mechanics of impact energy absorption
[PB90-190836] 22 p3190 N90-28101
Calculation of turbulent air streams in driver cabs
[ETN-90-97320] 24 p3419 N90-29310
Tests of initialization procedures with the NRL limited area numerical weather prediction model
[AD-A223549] 24 p3495 N90-29750
Analytic least squares
[NPL-DES-86] 24 p3531 N90-29971
Solution of nonlinear eigenvalue problems via parallel shooting
[LR-587] 24 p3539 N90-30013

NUMERICAL STABILITY
A nonoscillatory, characteristically convected, finite volume scheme for multidimensional convection problems
[NASA-TM-102354] 02 p0263 N90-11497
Note on explicit parallel multistep Runge-Kutta methods
[CWI-NM-R8814] 02 p0268 N90-11529
On the equivalence of BS-stability and B-consistency
[CWI-NM-R8815] 02 p0268 N90-11530
Development of a VSAERO (Vortex Separation Aerodynamics) model of the F/A-18
[AD-A212442] 04 p0448 N90-12566
Vortex dynamics
[AD-A212119] 04 p0499 N90-12877
Smoothed predictor-corrector methods for solving partial differential equations
[CWI-NM-R8808] 04 p0540 N90-13131
Iterated theta method for hyperbolic equations
[CWI-NM-R8809] 04 p0540 N90-13132
Group implicit concurrent algorithms in nonlinear structural dynamics
[NASA-CR-185950] 06 p0796 N90-14638
Numerical methodologies for solving partial differential equations
[DE90-001842] 06 p0834 N90-14849
Studies in statistical signal processing
[AD-A214490] 09 p1275 N90-17393
Finite element approximations of the stokes flow problem based upon various variational principles
[DE90-608612] 12 p1659 N90-19533
Stability of a solitary wave solution to a set of coupled Boussinesq-like equations
[DE90-008927] 14 p2021 N90-21586
Dynamical approach study of spurious steady-state numerical solutions of nonlinear differential equations. Part 1: The ODE connection and its implications for algorithm development in computational fluid dynamics
[NASA-TM-102820] 15 p2160 N90-22339
The theta-methods in the numerical solution of delay differential equations
[TW-89-03] 15 p2161 N90-22349
Stability radius of polynomials occurring in the numerical solution of initial value problems
[TW-89-04] 15 p2162 N90-22350
Stability analysis of numerical methods for delay differential equations
[TW-89-09] 15 p2162 N90-22353
Kharitonov's theorem: Generalizations and algorithms 18 p2646 N90-25064
Dichotomies for certain product measures and stable processes
[AD-A222568] 20 p2921 N90-26821
Conjugate gradient methods for constrained least squares problems
[AD-A222706] 21 p3063 N90-27411

NUMERICAL WEATHER FORECASTING
A study of the impact of simulated satellite lidar wind observations
[AD-A210430] 01 p0086 N90-10488
A case study evaluation of satellite-derived rainfall estimates and their application to numerical model precipitation forecast verification
[PB89-194591] 01 p0088 N90-10499
A study of the impact of simulated 183 GHz water vapor retrievals on numerical weather prediction
[AD-A210431] 01 p0088 N90-10504
NASA/MSFC FY88 Global Scale Atmospheric Processes Research Program Review
[NASA-TM-100357] 03 p0360 N90-12059
Semi-Lagrangian, semi-implicit solutions of the shallow water equations in one dimension
[AD-A212658] 04 p0503 N90-12902
A PBL-radiation model for application to regional numerical weather prediction 12 p1635 N90-19394
Adiabatic and diabatic initialization of the AFGL (Air Force Geophysics Laboratory) global spectral model using dynamic normal mode and nonlinear normal mode methods
[AD-A218120] 13 p1846 N90-20595
The influence of lateral boundary conditions, fixed surface forcings, and synoptic situations upon predictability estimates using limited area numerical models 14 p2005 N90-21492
Theory and application of nonlinear normal mode initialization
[PB90-166000] 14 p2006 N90-21497
Impact of a unified DMSP meteorological sensor retrieval methodology on global numerical weather prediction
[AD-A220306] 18 p2581 N90-24703
A global model of thunderstorm electricity and the prediction of whistler duct formation 24 p3493 N90-29744
Tests of initialization procedures with the NRL limited area numerical weather prediction model
[AD-A223549] 24 p3495 N90-29750

NUTATION
Optical nutation in polymers irradiated by ultrashort laser pulses
[AD-A212927] 10 p1357 N90-17869
Nonlinear optical processes in one-dimensional polymers
[AD-A216103] 11 p1489 N90-18568
Laboratory simulation of the effect of rocket thrust on a precessing space vehicle
[NASA-CR-186681] 19 p2669 N90-25182
Flow induced nutation instability in spinning solid propellant rockets
[AD-A222504] 21 p2969 N90-26877
On the spatial eigenvalue approach to high Reynolds number flow in a rotating and nutating cylinder
[AD-A221710] 21 p3005 N90-27081

NUTATIONAL OSCILLATION
U NUTATION

NUTRIENTS
Continuous hydroponic wheat production using a recirculating system
[NASA-TM-102784] 11 p1538 N90-18853

NUTRITION
Utilization of non-conventional systems for conversion of biomass to food components
[NASA-CR-177545] 07 p0968 N90-15591
Physical performance and carbohydrate consumption in CF commandos during a 5-day field trial
[AD-A217204] 13 p1850 N90-20619
Proximate composition of seed and biomass from soybean plants grown at different carbon monoxide (CO_2) concentrations
[NASA-TM-103496] 20 p2897 N90-26480

NUTS (FASTENERS)
Considerations about the acceptance inspection of HS fasteners intended for controlled tightening
[CRIF-MT-175] 05 p0653 N90-13806

NYLON (TRADEMARK)
The creep behavior of an aramide fiber reinforced wound tow-strap
[LR-546] 12 p1620 N90-19312
Synthesis of poly(dimethylsiloxane) - nylon 6 diblock copolymers
[AD-A216850] 12 p1630 N90-19367
Rheological and mechanical characteristics of poly-p-phenylene terephthalamide/nylon molecular and particulate composites
[AD-A219562] 17 p2368 N90-23482

Nylon and teflon scribe effect on NBR to Chemlok 233 and NBR to NBR bond interfaces
[NASA-CR-184004] 22 p3189 N90-28095
Solid-state N15 NMR of N15-labeled nylon 6 and nylon 11
[AD-A223271] 24 p3446 N90-29459

NYLON RESINS
U POLYAMIDE RESINS

NYQUIST DIAGRAM
A robust stability result for generalised predictive control
[OUEL-1773/89] 15 p2158 N90-22330

NYQUIST FREQUENCIES
Calculating the time domain average of gear vibration data sampled at less than the Nyquist frequency
[OUEL-1768/89] 15 p2107 N90-22052

NYSTAGMUS
NT VESTIBULAR NYSTAGMUS
Vestibular responses and motion sickness during pitch, roll, and yaw sinusoidal whole-body oscillation
[AD-A223898] 24 p3497 N90-29767

O

O RING SEALS
High temperature, flexible, thermal barrier seal
[NASA-CASE-LEW-14672-1] 07 p0940 N90-15444
Space shuttle Production Verification Motor 1 (PV-1) static fire
[NASA-CR-183784] 08 p1037 N90-15991
Space shuttle solid rocket booster redesign and testing 09 p1175 N90-16804
Test data of flow field of shuttle SRM nozzle joint with bond defects, using unheated air 11 p1470 N90-18464
Flight set 360T004 (STS-30)
[NASA-CR-183927] 15 p2106 N90-22049
Flight set 360H005 (STS-28) seals, volume 4
[NASA-CR-183904] 22 p3181 N90-28051
Compatibility of elastomeric seal compounds with MIL-H-6083 and MIL-H-46170 hydraulic fluid
[AD-A224248] 24 p3454 N90-29504
Leak detection aid
[DE90-014678] 24 p3471 N90-29616

O STARS
A source of observational constraints on the structure of Wolf-Rayet winds
[DE90-001236] 06 p0864 N90-15023
The upper main sequence of OB associations. Part 2: The single-lined O stars: Spectral classification of northern stars and lines of C and N
[SER-C-PREPUBL-FASC-39] 08 p1139 N90-16602
Predictions of infrared recombinations lines in stellar winds of hot stars 11 p1585 N90-19136
O-star parameters from line profiles of wind-blanketed model atmospheres 12 p1736 N90-19982
A high galactic latitude survey of far ultraviolet excess objects 15 p2183 N90-22473
Interactions of massive stars with the interstellar medium: Bow shocks and superbubbles 15 p2186 N90-22485
An analysis of the Palomar-Green subdwarfs and white dwarfs 23 p3409 N90-29263

OBJECT PROGRAMS
ISI's (Information Sciences Institute) SDI architecture simulator: An experiment in adding new software to the system
[AD-A211314] 03 p0387 N90-12204
SIMOGEN: An object-oriented language for simulation
[AD-A213129] 05 p0682 N90-13973
Action languages: Dimensions, effects
[NASA-CR-183388] 05 p0716 N90-14181
A 3-D measurement system using object-oriented FORTH
[DE90-003393] 08 p1109 N90-16420
Object Oriented Programming Systems (OOPS) and frame representations: An investigation of programming paradigms
[NASA-CR-186084] 12 p1699 N90-19758
Implementation of a hypertext help system for GLAD (Graphics LAnguage for Database)
[AD-A217936] 13 p1868 N90-20718
STORM: A statistical object representation model
[DE90-009048] 14 p2036 N90-21686
Object-oriented databases: How are they different and what difference does it make
[REPT-89-55] 15 p2180 N90-22459
Using object-oriented analysis techniques to support system testing
[DE90-009540] 16 p2226 N90-22700
Object-oriented query languages: The notion and the issues
[REPT-89-054] 16 p2298 N90-23093
Distributed object oriented programming
[AD-A219689] 17 p2442 N90-23918
Towards elegant design of highly interactive information systems using an object-oriented approach
[REPT-89-75] 17 p2480 N90-24179
An object-oriented solution example: A flight simulator electrical system
[AD-A219190] 19 p2661 N90-25145
Object-oriented design: Deriving conceptual solutions to large-scale information processing problems
[DE90-011189] 19 p2763 N90-25699
Object oriented programming
[DE90-011797] 20 p2907 N90-26532
Resource allocation using constraint propagation 21 p3040 N90-27278
Capturing design knowledge 21 p3045 N90-27305
A diagnosis system using object-oriented fault tree models 21 p3046 N90-27313
Object oriented fault diagnosis system for space shuttle main engine redlines 21 p3046 N90-27315
An engineering approach to automatic programming 21 p3046 N90-27317
Automated extraction of knowledge for model-based diagnostics 21 p3047 N90-27318
The sixth generation robot in space 21 p3049 N90-27332
Reconfigurable integrated system architecture for future monitoring systems 22 p3106 N90-27638
Tutorial on using LISP object-oriented programming for blackboards: Solving the radar tracking problem
[AD-A224272] 24 p3525 N90-29930
A survey of object-oriented database technology
[AD-A224490] 24 p3558 N90-30130

OBLIQUE SHOCK WAVES
Convection of a pattern of vorticity through a reacting shock wave
[NASA-CR-181921] 01 p0102 N90-10576
The stability of magnetohydrodynamic shock waves in molecular clouds 02 p0292 N90-11665
Flow separation in shock wave boundary layer interactions at hypersonic speeds
[NASA-CR-4274] 08 p1017 N90-15885
Measurements of heat-transfer coefficients in the interaction regions between oblique shock waves and turbulent boundary layers with a multi-layered thin film heat transfer gauge
[DE90-004123] 09 p1216 N90-17054
Glancing shock-boundary layer interactions 10 p1309 N90-17571
Interaction of an oblique shock wave with supersonic flow over a blunt body 12 p1598 N90-19197
Interactive calculation procedures for mixed compression inlets
[NASA-CR-186581] 20 p2801 N90-25934

OBLIQUE WINGS
Static aeroelastic analysis for generic configuration aircraft
[NASA-TM-89423] 01 p0009 N90-10042
Output model-following control synthesis for an oblique-wing aircraft
[NASA-TM-100454] 12 p1606 N90-19241
Static aeroelastic analysis of a three-dimensional generic wing
[NASA-TM-102231] 13 p1757 N90-20087
Multiprocessing on supercomputers for computational aerodynamics
[NASA-TM-102606] 17 p2347 N90-23366
The aerodynamic design of the oblique flying wing supersonic transport
[NASA-CR-177552] 23 p3276 N90-28540

OBSCURATION
U OCCULTATION

OBSERVABILITY (SYSTEMS)
Optimal observer motion for bearings-only localization and tracking 04 p0449 N90-12569
Investigation of the observability of a satellite cluster in a near circular orbit
[AD-A216224] 10 p1326 N90-17662
Elements of active vibration control for rotating machinery
[NASA-TM-102368] 16 p2227 N90-22703
Observability of relative navigation using range-only measurements 24 p3427 N90-29360

OBSERVATION
NT EARTH OBSERVATIONS (FROM SPACE)
NT SATELLITE OBSERVATION
NT SKY SURVEYS (ASTRONOMY)
NT SPACE OBSERVATIONS (FROM EARTH)
NT SPOT (FRENCH SATELLITE)
NT VISUAL OBSERVATION
When and where to look to observe major solar flares 03 p0430 N90-12465
Comets: Dirty snowballs or icy dirtballs 12 p1739 N90-19994

OBSERVATION AIRCRAFT
NT U-2 AIRCRAFT
Pilotless airplanes
[AD-A211719] 03 p0305 N90-11734
Mode S data link trials, 10-11 January 1989
[RSRE-MEMO-4267] 04 p0490 N90-12815

OBSERVATORIES
NT ASTRONOMICAL OBSERVATORIES
NT ASTRONOMICAL SATELLITES
NT GAMMA RAY OBSERVATORY
NT GEOPHYSICAL OBSERVATORIES
NT HEAO
NT HEAO 1
NT HEAO 2
NT HUBBLE SPACE TELESCOPE
NT INFRARED ASTRONOMY SATELLITE
NT INFRARED SPACE OBSERVATORY (ISO)
NT IUE
NT LARGE DEPLOYABLE REFLECTOR
NT LUNAR OBSERVATORIES
NT POGO
NT ROSAT MISSION
NT SOLAR OBSERVATORIES
NT SPACE INFRARED TELESCOPE FACILITY
NT SPARTAN SATELLITES
NT X RAY ASTROPHYSICS FACILITY
Artificial intelligence approaches to astronomical observation scheduling
[NASA-CR-186277] 07 p1012 N90-15862
Major themes in the future of solar-terrestrial science 10 p1445 N90-18337
Design and performance analysis of adaptive optical telescopes using laser guide stars
[AD-A218025] 13 p1902 N90-20913
Experience with the UKIRT InSb array camera 14 p1977 N90-21327
SOFIA: Stratospheric Observatory for Infrared Astronomy 14 p1980 N90-21346
The evolution and geometry of the outer parts of the small Magellanic cloud 14 p2040 N90-21697
The determination of maximum deep space station slew rates for a high Earth orbiter 15 p2075 N90-21882
Proceedings of the International Workshop on Geomagnetic Observatory Data Acquisition and Processing
[GEOPHYSICAL-PUBL-15] 21 p3021 N90-27177

OBSIDIAN
Impact fracture experiments simulating interstellar grain-grain collisions 21 p3093 N90-27584

OBSTACLE AVOIDANCE
Kalman filter based range estimation for autonomous navigation using imaging sensors 15 p2142 N90-22238
Efficient motion planning for an L-shaped object
[RUU-CS-88-38] 17 p2463 N90-24073
Numerical approach of collision avoidance and optimal control on robotic manipulators 19 p2736 N90-25552
Method and apparatus for configuration control of redundant robots
[NASA-CASE-NPO-17801-1-CU] 21 p3010 N90-27110
Velocity filtering applied to optical flow calculations
[NASA-TM-102802] 23 p3271 N90-28512
Motion coordination for mobile robots in unstructured environments
[PB90-199498] 23 p3332 N90-28837
Cartesian control of redundant robots 23 p3363 N90-29004
Reflexive obstacle avoidance for kinematically-redundant manipulators 23 p3371 N90-29047
Guidance algorithms for a free-flying space robot 24 p3503 N90-29798

OBSTACLES
U BARRIERS

OBSTRUCTING
U BLOCKING

OCCLUSION
The 3D-POLY: A robot vision system for recognizing objects in occluded environments 02 p0229 N90-11313

OCCULTATION
NT RADIO OCCULTATION
The retrieval of the concentrations of nitric oxide and nitrogen dioxide from satellite solar occultation measurements at sunset and sunrise 06 p0814 N90-14733
The effect of windscreen bows and HUD pitch ladder format on pilot performance during simulated flight
[AD-A218139] 14 p2011 N90-21523
SAGE 3: A visible wavelength limb sounder 21 p3016 N90-27147
Zonal winds between 25 and 120 km retrieved from solar occultation spectra 24 p3489 N90-29718
Formation of hydrogen line and continuum emission in young stellar objects 24 p3562 N90-30150

OCCUPATIONAL DISEASES
Occupational safety considerations with hydrazine 02 p0207 N90-11182

Criteria for a recommended standard: Occupational exposure to hand-arm vibration
[PB90-168048] 22 p3233 N90-28331

OCCURRENCES
Additive evaluation criteria for aircraft noise
18 p2610 N90-24867

OCEAN BOTTOM
ONR/NORDA Workshop on Terrain Analysis and Quantitative Geomorphology
[AD-A210464] 01 p0086 N90-10489
The influence of a steady baroclinic deep ocean on the shelf
[PB89-198188] 01 p0089 N90-10511
A search for layering in the oceanic crust
[PB89-198220] 01 p0090 N90-10514
Surface wave ray tracing and Ms:yield determination in a laterally heterogeneous earth
[AD-A210241] 01 p0090 N90-10516
Corrosion rates of structural materials on the ocean floor
[DE89-015211] 02 p0197 N90-11123
Physiographic and geological setting of the Coastal Engineering Research Center's field research facility
[AD-A210772] 02 p0238 N90-11356
Coastal subsea permafrost and bedrock observations using dc resistivity
[AD-A210784] 02 p0253 N90-11435
Hydrophone investigations of earthquakes and explosion generated high-frequency seismic phases
[AD-A212055] 03 p0371 N90-12122
Surface current and wave modulation measurements over bottom topography: A comparison with theory
[AD-A212469] 04 p0522 N90-13011
Mid-Oceanic Ridge: A Dynamic Global System
[PB89-198691] 06 p0818 N90-14758
Dynamics of mid-ocean ridge systems
07 p0965 N90-15575
Evolution of overlapping spreading centers: A Sea Mark 2 investigation
[AD-A214278] 07 p0965 N90-15576
ZBTAB: Zenith-248 version of BLUGTAB
[AD-A214279] 08 p1108 N90-16415
The effects of abrupt topography on ocean currents as sensed by satellite remote sensing
[AD-A214123] 10 p1409 N90-18128
Segmentation of topographic profiles of the seafloor based on a self-affine model
[AD-A215938] 10 p1410 N90-18132
On the applicability of CAESAR for the remote sensing of bottom depth and bottom composition of shallow waters: A model study
[BCRS-89-13] 11 p1526 N90-18783
Stored mafic/ultramafic crust and early Archean mantle depletion
[NASA-CR-186460] 12 p1691 N90-19715
An outline for the analysis of wave induced bottom pressure fluctuations
[MRL-TN-558] 14 p2008 N90-21510
On the effectiveness of the production of antarctic bottom water in the Weddell and Ross Seas
[AD-A218873] 16 p2259 N90-22880
Modelling bottom stress in depth-averaged flows
[AD-A218605] 17 p2429 N90-23840
ULF/VLF ocean bottom seismo-acoustics
[AD-A218810] 17 p2429 N90-23843
Seismic anisotropy and large-scale porosity in the ocean floor
[AD-A220453] 17 p2431 N90-23849
Sea bottom topography with X-band SLAR
[BCRS-89-25] 17 p2431 N90-23854
Observations of seafloor ambient noise with an ocean bottom seismometer array
[AD-A220159] 17 p2432 N90-23858
Atmospheric correction of thematic mapping measurements about seabeds of the German Bay
[GKSS-89/E/47] 20 p2816 N90-26029
Evolution of overlapping spreading centers: A SeaMARC 2 investigation
[AD-A223102] 21 p3025 N90-27200
Drilling the oceanic lower crust and mantle: A global strategy for exploring the deep oceanic crust and mantle in the 1990's
[PB90-240953] 23 p3351 N90-28936
Large aperture acoustic arrays in support of reverberation studies
[AD-A224002] 23 p3393 N90-29168
Some aspects of the structure and evolution of oceanic spreading centers 24 p3496 N90-29757

OCEAN COLOR SCANNER
Ocean colour: Methods, technologies, applications
19 p2707 N90-25406

OCEAN CURRENTS
NT EL NINO
NT GULF STREAM
Observations and modelling of deep equatorial currents in the central Pacific
[PB89-198139] 03 p0377 N90-12145
Dynamics of the equatorial undercurrent and its termination
[PB89-198147] 03 p0377 N90-12146
Compendium of marine meteorological and oceanographic products of the Ocean Products Center, revision 1
[PB89-230684] 04 p0514 N90-12967
Laser wave estimation
[AD-A213867] 09 p1227 N90-17119
The effects of abrupt topography on ocean currents as sensed by satellite remote sensing
[AD-A214123] 10 p1409 N90-18128
An application of ocean wave-current refraction to the gulf stream using SEASAT SAR data
[AD-A216769] 11 p1537 N90-18851
Coherent radar measurement of ocean currents from geostationary orbit 12 p1609 N90-19259
A model of the general ocean circulation determined from a joint solution for the Earth's gravity field
13 p1838 N90-20550
Correlation of AVHRR imagery with sub-surface features in California current
[AD-A218184] 13 p1848 N90-20607
An investigation of meteorological effects on currents in the shelf and continental slope seas northwest of the United Kingdom. 2: Relationships between currents at different locations and with other variables
[PB90-151911] 15 p2134 N90-22195
Determination of the general ocean circulation using satellite altimetry from a simultaneous solution for the Earth's gravity field 16 p2203 N90-22569
On the effectiveness of the production of antarctic bottom water in the Weddell and Ross Seas
[AD-A218873] 16 p2259 N90-22880
A numerical study of the seasonal variability of the Somali current
[AD-A220708] 17 p2427 N90-23829
Modelling bottom stress in depth-averaged flows
[AD-A218605] 17 p2429 N90-23840
Efficient representation of the hydrographic structure of the north atlantic ocean and aspects of the circulation from objective methods
[AD-A218606] 17 p2429 N90-23841
Test and evaluation of surf forecasting model
[AD-A219580] 17 p2430 N90-23845
Modeling studies of the LeeUwin current using a high-resolution primitive equation model
[AD-A219595] 17 p2430 N90-23846
A numerical study of wind forcing in the eastern boundary current system off Portugal
[AD-A219596] 17 p2430 N90-23847
Ocean variability from crossover differences derived from altimeter measurements
[ETN-90-96695] 17 p2431 N90-23852
The effects of climatological and transient wind forcing on eddy generation in the California current system
[AD-A219858] 17 p2431 N90-23855
Geophysical studies related to geodetic reference frames
[AD-A220249] 18 p2574 N90-24663
A range-dependent analysis of acoustic transmission across a cold filament in the California current
[AD-A220175] 18 p2583 N90-24709
Circulation and property distributions in the Central Bering Sea, Spring, 1988
[PB90-155847] 22 p3230 N90-28317
Impact of satellite altimetric data on the numerical simulation of the general oceanic currents: Sensitivity to orbit parameters
[ETN-90-97461] 22 p3231 N90-28321
Ross Sea oceanographic data, 1983-1987: USCGC GLACIER, January-February 1983; USCGC POLAR SEA, January-February 1984; USCGC POLAR STAR, February 1984; USCGC POLAR SEA, February 1987
[PB90-243932] 23 p3354 N90-28955

OCEAN DATA ACQUISITIONS SYSTEMS
Climatological data for the North Sea based on observations by voluntary observing ships over the period 1961-1980
[KNMI-WR-89-02] 04 p0520 N90-13002
Research programs: Meteorological prediction. Oceanic processes. Climate and global change monitoring. Satellite instrumentation and calibration
19 p2714 N90-25447

OCEAN DATA PLATFORMS
U OCEAN DATA ACQUISITIONS SYSTEMS

OCEAN DATA STATIONS
U OCEAN DATA ACQUISITIONS SYSTEMS

OCEAN DYNAMICS
The influence of a steady baroclinic deep ocean on the shelf
[PB89-198188] 01 p0089 N90-10511
Observations of long Rossby waves in the northern tropical Pacific
[PB89-196331] 03 p0376 N90-12143
Observations and modelling of deep equatorial currents in the central Pacific
[PB89-198139] 03 p0377 N90-12145
Dynamics of the equatorial undercurrent and its termination
[PB89-198147] 03 p0377 N90-12146
A linearized surface condition in low speed hydrodynamics
[REPT-89-04] 04 p0501 N90-12885
A hybrid architecture for feature labelling of oceanographic satellite images
[AD-A212236] 04 p0515 N90-12975
Applications of remote sensing to studies of oceanic upper mixed layer dynamics 15 p2122 N90-22137
On the effectiveness of the production of antarctic bottom water in the Weddell and Ross Seas
[AD-A218873] 16 p2259 N90-22880
Stratified ocean mixing
[AD-A219233] 16 p2259 N90-22881
Mariners Weather Log, volume 33, number 2, Spring 1989
[PB90-146838] 20 p2889 N90-26443
Mariners Weather Log, volume 33, number 3, Summer 1989
[PB90-146846] 20 p2889 N90-26444
Study of the ocean tides by the assimilation of marigraphic and altimetric satellite data in a hydrodynamic model
[ETN-90-97460] 22 p3231 N90-28320
Impact of satellite altimetric data on the numerical simulation of the general oceanic currents: Sensitivity to orbit parameters
[ETN-90-97461] 22 p3231 N90-28321

OCEAN MODELS
The influence of a steady baroclinic deep ocean on the shelf
[PB89-198188] 01 p0089 N90-10511
IFD (Implicit Finite Difference): Interfaced with Harvard open ocean model forecasts
[AD-A210521] 01 p0090 N90-10517
A low-order model of the equatorial ocean-atmosphere system 06 p0813 N90-14730
Tuning of the OSCURS (Ocean Surface Current Simulations) numerical model to ocean surface measurements in the Gulf of Alaska
[PB89-103979] 06 p0818 N90-14759
The Polar Ice Prediction System: A sea ice forecasting system
[AD-A214600] 09 p1249 N90-17246
Evolution of finite amplitude baroclinic waves in the atmosphere and ocean
[INPE-4752-TDL/346] 12 p1695 N90-19733
A linear systems theory approach to the range-independent acoustic channel
[AD-A216551] 12 p1710 N90-19817
A model of the general ocean circulation determined from a joint solution for the Earth's gravity field
13 p1838 N90-20550
Predictability of weather and climate in a coupled ocean-atmosphere model: A dynamical systems approach
[NASA-CR-186499] 14 p2007 N90-21502
Modeling the upper ocean and its interaction with the atmosphere
[DE90-008980] 14 p2008 N90-21511
Applications of remote sensing to studies of oceanic upper mixed layer dynamics 15 p2122 N90-22137
A free surface Bryan-Cox-Semtner model
[IOS-270] 15 p2135 N90-22201
Determination of the general ocean circulation using satellite altimetry from a simultaneous solution for the Earth's gravity field 16 p2203 N90-22569
Predictability of weather and climate in a coupled ocean-atmosphere model: A dynamical systems approach 16 p2256 N90-22865
US Navy hindcast spectral ocean wave model climatic atlas: Mediterranean Sea
[AD-A219755] 17 p2426 N90-23825
A numerical study of the seasonal variability of the Somali current
[AD-A220708] 17 p2427 N90-23829
Modelling bottom stress in depth-averaged flows
[AD-A218605] 17 p2429 N90-23840
Efficient representation of the hydrographic structure of the north atlantic ocean and aspects of the circulation from objective methods
[AD-A218606] 17 p2429 N90-23841
A numerical study of wind forcing in the eastern boundary current system off Portugal
[AD-A219596] 17 p2430 N90-23847
The effects of climatological and transient wind forcing on eddy generation in the California current system
[AD-A219858] 17 p2431 N90-23855

Gulfcasting: Dynamical forecast experiments for G ulf Stream rings and meanders
[AD-A221482] 21 p3032 N90-27238
Study of the ocean tides by the assimilation of marigraphic and altimetric satellite data in a hydrodynamic model
[ETN-90-97460] 22 p3231 N90-28320
Impact of satellite altimetric data on the numerical simulation of the general oceanic currents: Sensitivity to orbit parameters
[ETN-90-97461] 22 p3231 N90-28321
Factorization of the characteristic equation for three layer ducts
[AD-A223867] 23 p3354 N90-28956
Rates of vertical mixing, gas exchange, and new productions: Estimates from seasonal gas cycles in the upper ocean near Bermuda
[PB90-244781] 24 p3496 N90-29758
Numerical pulse propagation studies using two classical ocean waveguide models
[AD-A224118] 24 p3542 N90-30033

OCEAN SURFACE
Chesapeake Bay surface salinities, 1951-88
[PB89-194583] 01 p0090 N90-10513
Laser altimeter for use over the ocean
[AD-A211252] 02 p0224 N90-11286
Interannual variability of temperature in the upper layer of the North Pacific eastern boundary region, 1971-1987
[PB89-190227] 02 p0253 N90-11434
Hydrophone investigations of earthquakes and explosion generated high-frequency seismic phases
[AD-A212055] 03 p0371 N90-12122
Equatorial oceanic response to forcing on time scales from days to months
[PB89-206775] 03 p0377 N90-12147
Feature modeling: The incorporation of a front and eddy map into optimum interpolation-based thermal analysis
[AD-A213253] 05 p0672 N90-13914
A global ocean wind stress climatology based on ECMWF (European Centre for Medium Range Weather Forecasts) analyses
[PB90-109968] 06 p0817 N90-14752
Tuning of the OSCURS (Ocean Surface Current Simulations) numerical model to ocean surface measurements in the Gulf of Alaska
[PB89-103979] 06 p0818 N90-14759
Geosat/ERM altimeter data analysis for the determination of global oceanic mesoscale variability
07 p0949 N90-15492
Specification for evaporation duct height calculations
[AD-A213841] 07 p0964 N90-15570
Further research on dynamics of marine atmospheres in tropical cyclones
[AD-A213882] 07 p0964 N90-15571
Global distribution of total cloud cover and cloud type amounts over the ocean
[DE90-003187] 07 p0964 N90-15574
Wind speed dependence of acoustic ambient vertical directional spectra at high frequency
[AD-A214293] 07 p0969 N90-15712
A statistical model of the infrared signature of a wind roughened sea
[AD-A214531] 09 p1249 N90-17245
Sea surface temperature fields derived from aircraft and ship observations during FASINEX 1986
[AD-A215727] 09 p1250 N90-17250
Remote sensing of evaporation ducts for Naval warfare
[AD-A214849] 10 p1374 N90-17965
Remote sensing: Environmental effects of surface films
[AD-A216190] 10 p1400 N90-18094
Some problems in oceanic radiative transfer
[AD-A215935] 10 p1410 N90-18131
Multiparameter scatterometer for remote sensing (RADSER). Project Scatter: State-of-the-art and future applications
[INPE-4871-PRE/1482] 11 p1511 N90-18701
Intertropical Convergence Zone (ITCZ) and its relationship with the precipitation of the north-northeast Brazilian region
[INPE-4887-TDL/378] 11 p1535 N90-18839
Earth tidal analysis based on gravimeter observations and the influence of ocean tides
[ETN-90-95721] 12 p1695 N90-19734
Zones of feasibility for retrieval of surface pressure from observations of absorption in the A band of oxygen
[DAR-TP-19] 14 p2006 N90-21495
Modeling the upper ocean and its interaction with the atmosphere
[DE90-006980] 14 p2008 N90-21511
European network of interest in the measurement and analysis of mean sea levels from tide gauge records
[PB90-151929] 15 p2134 N90-22196
Kinematics under wind waves
[AD-A219541] 17 p2430 N90-23844
Ocean variability from crossover differences derived from altimeter measurements
[ETN-90-96895] 17 p2431 N90-23852
In situ investigation of sea surface noise from a depth of one meter
[AD-A220158] 17 p2432 N90-23857
Ocean feature recognition using genetic algorithms with fuzzy fitness functions (GA/F3)
19 p2740 N90-25576
Dependence of radar backscatter on the energetics of the air-sea interface
[AD-A221966] 21 p2996 N90-27026
A preliminary analysis of threshold signal detection in ambient and signal-dependent noise environments
[AD-A222089] 21 p2996 N90-27030
Space-based wide area surveillance system studies
21 p3068 N90-27444
Remote sensing of the ocean surface with C- and Ku-band airborne scatterometers
22 p3195 N90-28129
A day-to-day comparison study of Seasat scatterometer winds with winds observed from islands in the tropical Pacific
[NASA-CR-186696] 22 p3212 N90-28223
Detection of ocean inner waves by synthetic aperture radar: Observations at Gibraltar pass
[ETN-90-97477] 23 p3353 N90-28953
Measuring the vertical directional spectra caused by sea surface sound
[AD-A223883] 23 p3354 N90-28957
Research in nonlinear water waves
[AD-A224065] 24 p3496 N90-29759

OCEAN TEMPERATURE
NT SEA SURFACE TEMPERATURE
Semi-monthly temperature and geopotential anomaly in the upper 500 meters along the Oahu-Farallon Islands great circle from November 15, 1967 through December 15, 1979
[AD-A210640] 01 p0091 N90-10518
Interannual variability of temperature in the upper layer of the North Pacific eastern boundary region, 1971-1987
[PB89-190227] 02 p0253 N90-11434
Equatorial oceanic response to forcing on time scales from days to months
[PB89-206775] 03 p0377 N90-12147
Feature modeling: The incorporation of a front and eddy map into optimum interpolation-based thermal analysis
[AD-A213253] 05 p0672 N90-13914
Specification for evaporation duct height calculations
[AD-A213841] 07 p0964 N90-15570
An investigation of meteorological effects on currents in the shelf and continental slope seas northwest of the United Kingdom. 2: Relationships between currents at different locations and with other variables
[PB90-151911] 15 p2134 N90-22195
A range-dependent analysis of acoustic transmission across a cold filament in the California current
[AD-A220175] 18 p2583 N90-24709
Circulation and property distributions in the Central Baring Sea, Spring, 1988
[PB90-155847] 22 p3230 N90-28317

OCEAN THERMAL ENERGY CONVERSION
Planning for hybrid-cycle OTEC experiments using the HMTSTA test facility at the Natural Energy Laboratory of Hawaii
[DE89-013278] 02 p0237 N90-11349
Ocean thermal energy conversion: An overview
[DE89-000838] 07 p0953 N90-15512
Conceptual design analysis for hybrid-cycle OTEC plants for co-production of electric power and desalinated water
[DE90-003551] 08 p1097 N90-16350
Experimental investigation of condensation of steam in the presence of noncondensable gases using plate heat exchangers
[DE90-002251] 12 p1682 N90-19659
Experiments on oxygen desorption from surface warm seawater under Open-Cycle Ocean Thermal Energy Conversion (OC-OTEC) conditions
[DE90-000308] 12 p1683 N90-19666
Innovative turbine concepts for open-cycle OTEC (Ocean Thermal Energy Conversion)
[DE90-000315] 13 p1827 N90-20493
Perspectives on solar energy and the environment
[DE90-007680] 13 p1828 N90-20494
Ocean energy program summary
[DE89-009481] 16 p2251 N90-22836
Ocean energy program summary. Volume 2: Research summaries
[DE89-009482] 18 p2576 N90-24677

OCEANOGRAPHIC PARAMETERS
NT OCEAN TEMPERATURE
NT SEA SURFACE TEMPERATURE
Meeting Review: Workshop on Airborne Instrumentation
[PB89-174775] 01 p0007 N90-10032
US Navy regional climatic study of the United States Atlantic Coast and associated waters
[AD-A210198] 01 p0088 N90-10503
Coastal Research Center Woods Hole Oceanographic Institution
[PB89-198238] 01 p0089 N90-10510
The sea ice margins: A summary of physical phenomena
[PB89-212328] 02 p0253 N90-11436
Statistical models for the optimal estimation of oceanic fields
[AD-A211786] 03 p0377 N90-12149
ZBTAB: Zenith-248 version of BLUGTAB
[AD-A214279] 08 p1108 N90-16415
Tidal and lunar data for Point Mugu, San Nicolas Island, and the Barking Sands Area during 1990
[AD-A214828] 09 p1249 N90-17248
Near real time VHF telemetry of near shore oceanographic data
[AD-A215756] 10 p1327 N90-17666
Parameterization of small-scale processes
[AD-A215507] 10 p1396 N90-18082
Observations of fine-scale vertical shear and strain in the upper ocean
[AD-A214476] 10 p1410 N90-18130
An improved model for the Earth's gravity field
13 p1832 N90-20515
US Navy regional climatic study of the Central East Asian coast and associated waters
[AD-A217448] 13 p1844 N90-20587
US Navy regional climatic study of southern African waters
[AD-A218792] 16 p2258 N90-22874
US Navy regional climatic study of the Mozambique channel and adjacent waters
[AD-A218793] 16 p2258 N90-22875
ULF/VLF ocean bottom seismo-acoustics
[AD-A218810] 17 p2429 N90-23843
Evolution of overlapping spreading centers: A SeaMARC 2 investigation
[AD-A223102] 21 p3025 N90-27200
Detection of ocean inner waves by synthetic aperture radar: Observations at Gibraltar pass
[ETN-90-97477] 23 p3353 N90-28953

OCEANOGRAPHY
ONR/NORDA Workshop on Terrain Analysis and Quantitative Geomorphology
[AD-A210464] 01 p0086 N90-10489
Coastal Research Center Woods Hole Oceanographic Institution
[PB89-198238] 01 p0089 N90-10510
Coastal subsea permafrost and bedrock observations using dc resistivity
[AD-A210784] 02 p0253 N90-11435
Compendium of marine meteorological and oceanographic products of the Ocean Products Center, revision 1
[PB89-230684] 04 p0514 N90-12967
A hybrid architecture for feature labelling of oceanographic satellite images
[AD-A212236] 04 p0515 N90-12975
Feature modeling: The incorporation of a front and eddy map into optimum interpolation-based thermal analysis
[AD-A213253] 05 p0672 N90-13914
Tuning of the OSCURS (Ocean Surface Current Simulations) numerical model to ocean surface measurements in the Gulf of Alaska
[PB89-103979] 06 p0818 N90-14759
The Interactive System Meteorology and its use in meteorology and oceanography
08 p1092 N90-16320
Measurement of fluctuations in the tilt of Arctic ice at the CEAREX Oceanography Camp: Experiment review, data catalog, and preliminary results
[AD-A215059] 09 p1249 N90-17249
Near real time VHF telemetry of near shore oceanographic data
[AD-A215756] 10 p1327 N90-17666
ERS-1 European remote sensing satellite: A new tool for global environmental monitoring in the 1990's
[ESA-BR-36] 11 p1526 N90-18782
Forecasters handbook for Central America and adjacent waters
[AD-A216752] 11 p1536 N90-18845
Comparison of circulation obtained through the trajectory of a drifting buoy tracked by satellite and hydrographic data in the Bransfield Strait
[INPE-4946-TDL/387] 11 p1537 N90-18850
Single antenna interferometry
[DE90-008120] 12 p1648 N90-19474
Committee on Geodesy - National Research Council
[AD-A217770] 13 p1821 N90-20452
Progress in the Determination of the Earth's Gravity Field
[NASA-CR-185721] 13 p1831 N90-20513

Continental shelf processes affecting the oceanography of the South Atlantic Bight
[DE90-008439] 13 p1848 N90-20606
JPRS report. Science and technology. USSR: Earth sciences
[JPRS-UES-88-004] 14 p1995 N90-21431
JPRS report. Science and technology. USSR: Earth sciences
[JPRS-UES-89-002] 14 p1995 N90-21432
JPRS report: Science and technology. USSR: Earth sciences
[JPRS-UES-90-005] 14 p1995 N90-21433
European network of interest in the measurement and analysis of mean sea levels from tide gauge records
[PB90-151929] 15 p2134 N90-22196
Pre-study laser bathymetry
[BCRS-89-26] 15 p2134 N90-22198
Determination of the general ocean circulation using satellite altimetry from a simultaneous solution for the Earth's gravity field 16 p2203 N90-22569
Monthly surface thermal forcing in the tropical Pacific from 1980 to 1983
[NASA-CR-183033] 16 p2259 N90-22877
Efficient representation of the hydrographic structure of the north atlantic ocean and aspects of the circulation from objective methods
[AD-A218606] 17 p2429 N90-23841
Sea bottom topography with X-band SLAR
[BCRS-89-25] 17 p2431 N90-23854
Frontogenesis in gravity currents: An example with no known applications in oceanography
[MATHS-REPT-A-117] 20 p2863 N90-26284
Applications of ISES for the oceans 21 p3017 N90-27156
Tactical applications of Defense Meteorological Satellite Program (DMSP) environmental data 21 p3067 N90-27439
Tactical oceanography from space: The next decade 21 p3068 N90-27442
Bibliography of oceanography, meteorology, and geology of Louisiana, Texas, Mississippi, Alabama, and Florida
[PB90-194663] 22 p3194 N90-28124
The influence of continental sources of aerosols on the marine stratocumulus during FIRE IFO-1 22 p3218 N90-28250
Study of the ocean tides by the assimilation of marigraphic and altimetric satellite data in a hydrodynamic model
[ETN-90-97460] 22 p3231 N90-28320
Drilling the oceanic lower crust and mantle: A global strategy for exploring the deep oceanic crust and mantle in the 1990's
[PB90-240953] 23 p3351 N90-28936
Proceedings of the 14th Annual Climate Diagnostics Workshop
[PB90-198573] 23 p3351 N90-28938
Oceanographic data exchange, 1988
[PB90-232596] 23 p3353 N90-28952
Ross Sea oceanographic data, 1983-1987: USCGC GLACIER, January-February 1983; USCGC POLAR SEA, January-February 1984; USCGC POLAR STAR, February 1984; USCGC POLAR SEA, February 1987
[PB90-243932] 23 p3354 N90-28955

OCEANS
NT ANTARCTIC OCEAN
NT ARCTIC OCEAN
NT ATLANTIC OCEAN
NT INDIAN OCEAN
NT PACIFIC OCEAN
Laser altimeter for use over the ocean
[AD-A211252] 02 p0224 N90-11286
Doppler statistics of ocean velocity variability
[AD-A211687] 03 p0377 N90-12148
ULF/VLF (0.001 to 50 Hz) Seismo-Acoustic Noise in the Ocean
[AD-A212942] 05 p0671 N90-13913
Multiple flow regimes in the Northern Hemisphere winter 08 p1100 N90-16372
Charting and Geodetic Services
[PB90-116674] 09 p1240 N90-17196
Phase space and path integral methods applied to direct and inverse ocean seismo-acoustic modeling
[AD-A214777] 09 p1249 N90-17247
Parameterization of small-scale processes
[AD-A215507] 10 p1398 N90-18082
On the relationship between water vapor over the oceans and sea surface temperature
[NASA-CR-186199] 10 p1409 N90-18127
Observations of fine-scale vertical shear and strain in the upper ocean
[AD-A214476] 10 p1410 N90-18130
Some problems in oceanic radiative transfer
[AD-A215935] 10 p1410 N90-18131
An application of ocean wave-current refraction to the gulf stream using SEASAT SAR data
[AD-A216769] 11 p1537 N90-18851
A linear systems theory approach to the range-independent acoustic channel
[AD-A216551] 12 p1710 N90-19817
Gravitational model improvement at the Goddard Space Flight Center 13 p1831 N90-20514
Numerical simulations of the cloud-capped marine boundary layer 14 p2008 N90-21506
A new stability criterion in the shallow-water system for two-dimensional coherent eddies in the atmosphere and oceans 15 p2130 N90-22176
Generalized Herglotz functions and inverse scattering problem in a finite depth ocean
[PB90-150996] 15 p2134 N90-22197
A numerical study of basic coastal upwelling processes 16 p2259 N90-22878
Ocean feature recognition using genetic algorithms with fuzzy fitness functions (GA/F3) 19 p2740 N90-25576
Radio refractivity profiles deduced from lidar measurements
[AD-A221727] 21 p3026 N90-27208
Environmental Research Laboratories programs and plans. FY-1989 and FY-1990 plans
[PB90-169988] 22 p3197 N90-28144
An injective far-field pattern operator and inverse scattering problem in a finite depth ocean
[PB90-159294] 22 p3230 N90-28318
Design and performance of a long, over-water microwave radio link
[PB90-207994] 23 p3318 N90-28758
Ross Sea oceanographic data, 1983-1987: USCGC GLACIER, January-February 1983; USCGC POLAR SEA, January-February 1984; USCGC POLAR STAR, February 1984; USCGC POLAR SEA, February 1987
[PB90-243932] 23 p3354 N90-28955
Proceedings of a Workshop on the Geoelectric and Geomagnetic Environment of Continental Margins
[AD-A223743] 24 p3493 N90-29739
Rates of vertical mixing, gas exchange, and new productions: Estimates from seasonal gas cycles in the upper ocean near Bermuda
[PB90-244781] 24 p3496 N90-29758

OCTAHEDRAL RESEARCH SATELLITES
U ENVIRONMENTAL RESEARCH SATELLITES

OCTAHEDRONS
Ionic equilibrium between octahedral and tetrahedral complexes in liquid aluminium-sodium fluoride mixtures
[DE90-613690] 14 p1948 N90-21150

OCTANE NUMBER
CRC (Coordinating Research Council) octane number requirement survey 1988
[AD-A214845] 09 p1200 N90-16954

OCTANES
Shock tube ignition of octanes
[DE90-001167] 07 p0893 N90-15164

OCULOGRAVIC ILLUSIONS
Spatial vision within egocentric and exocentric frames of reference 16 p2268 N90-22928

OCULOMETERS
Safety evaluation of infrared lamp power output for oculometer eye/head tracker system
[AD-A215809] 10 p1411 N90-18138
Comparison of oculometer and head-fixed reticle with voice or switch and touch panel for data entry on a generic tactical air combat display
[AD-A217231] 13 p1855 N90-20646
From where they look to what they think: Determining controller cognitive strategies from oculometer scanning data 18 p2641 N90-25041
Cockpit Ocular Recording System (CORS)
[NASA-CR-4281] 21 p3033 N90-27244

ODAS
U OCEAN DATA ACQUISITIONS SYSTEMS

ODD-ODD NUCLEI
The interacting boson approximation
[KVI-774] 04 p0552 N90-13215

OFFGASSING
Space station contamination modeling
[NASA-CR-183871] 23 p3286 N90-28590

OFFSHORE ENERGY SOURCES
Atlantic outer continental shelf: Description of the Mid-Atlantic environment
[PB90-100033] 11 p1537 N90-18849

OFFSHORE PLATFORMS
Development of a computer model to predict platform station keeping requirements in the Gulf of Mexico using remote sensing data
[NASA-CR-186678] 19 p2663 N90-25155

OFT
U SPACE TRANSPORTATION SYSTEM FLIGHTS

OGEE WINGS
U VARIABLE SWEEP WINGS

OGIVES
An experimental investigation of the aerodynamic characteristics of slanted base ogive cylinders using magnetic suspension technology
[NASA-CR-181708] 02 p0146 N90-10834
The determination of the aerodynamic characteristics of an ogive-cylinder body in subsonic, curved, incompressible flow, and an assessment of the effect of flow curvature
[REPT-87-13] 03 p0302 N90-11712
Three-dimensional separated flow prediction on fusiform body using Euler and boundary layer methods 16 p2234 N90-22745
Subsonic sting interference on the aerodynamic characteristics of a family of slanted-base ogive-cylinders
[NASA-CR-4299] 18 p2492 N90-24242

OGO
NT POGO

OHIO
FFT-local gravimetric geoid computation 13 p1835 N90-20536
A study of mesoscale acid deposition in the lower Ohio River Valley 16 p2253 N90-22848

OHMIC DISSIPATION
Microwave Tokamak Experiment (MTX) ohmic heating system
[DE89-017892] 03 p0408 N90-12340
Joule heating and runaway electron acceleration in a solar flare 03 p0432 N90-12478
Aerosol heating and vaporization of high-flux laser beams
[DE90-003471] 07 p0937 N90-15428
Electromagnetic fusion process and position research 13 p1785 N90-20249
Actions of magnetospheres on planetary atmospheres
[IRF-SR-203] 17 p2486 N90-24215
Dielectric determination of the glass transition temperature (T sub g) 18 p2513 N90-24352

OIL EXPLORATION
Devices and methods for in-situ combustion ignition
[DE89-000766] 06 p0740 N90-14309
Atlantic outer continental shelf: Description of the Mid-Atlantic environment
[PB90-100033] 11 p1537 N90-18849
Applications of differential GPS 24 p3425 N90-29349

OIL RECOVERY
Statistically designed study of the variables and parameters of carbon dioxide equations of state
[DE90-016196] 24 p3447 N90-29467

OILS
NT CASTOR OIL
NT CRUDE OIL
NT FUEL OILS
NT LUBRICATING OILS
NT MINERAL OILS
NT SHALE OIL
High temperature VSCF (Variable Speed Constant Frequency) generator system
[AD-A210823] 01 p0061 N90-10351
Flow visualization techniques for flight research 02 p0153 N90-10878
Thermocapillary migration of liquid droplets in a temperature gradient in a density matched system
[NASA-CR-185178] 06 p0776 N90-14512
Wear metal analysis in engine oil by microwave digestion and atomic absorption spectroscopy
[AD-A223070] 21 p2985 N90-26964

OKLAHOMA
Natural resources information system for the state of Oklahoma
[DE90-009483] 15 p2180 N90-22458
Initiation and propagation of thunderstorm mesocyclones 17 p2428 N90-23838

OLEFINS
U ALKENES

OLFACTORY PERCEPTION
Synaptic plasticity and memory formation
[AD-A211368] 03 p0379 N90-12158

OLIGOMERS
Dynamics of micellar oligomeric and monomeric sodium 10-undecenoate
[AD-A222570] 20 p2830 N90-26099
Theoretical investigations and attempted synthesis of organic magnetic polymers and oligomers
[AD-A223409] 24 p3455 N90-29509

OLIVINE
Analysis of particulates of comet nucleus samples: Possible use of olivine as indicator phase 08 p1147 N90-16646
Impact fracture experiments simulating interstellar grain-grain collisions 21 p3093 N90-27584

OME
U ORBIT MANEUVERING ENGINE (SPACE SHUTTLE)

OMEGA NAVIGATION SYSTEM
Omega system performance assessment
[AD-A210342] 01 p0056 N90-10322
South Pacific OMEGA validation analysis
[AD-A215916] 10 p1319 N90-17624
Overview of Omega signal coverage
24 p3429 N90-29368
Omega navigation signal characteristics
24 p3429 N90-29369

OMNIDIRECTIONAL ANTENNAS
NT WHIP ANTENNAS
A calibrated, omnidirectional, LF loop antenna for GWEN (Ground Wave Emergency Network)
[AD-A211264] 02 p0213 N90-11221
Very broad band VHF/UHF omnidirectional antenna design study
[AD-A215358] 09 p1207 N90-16997
Telemetry and telecommand omnidirectional antenna in the short wave band
[ETN-90-96285] 11 p1499 N90-18631
Inmarsat omni-antenna deployment mechanism
18 p2542 N90-24508
Some design considerations for small piezo-electrical ceramic transducers
[FEL-1989-68] 22 p3178 N90-28034

ON-LINE SYSTEMS
Planning an Integrated On-line Library System (IOLS)
[AD-A209406] 01 p0136 N90-10783
Online support for the intellectual activity of browsing
01 p0136 N90-10784
Defense Technical Information Center cataloging guidelines
[AD-A211000] 01 p0137 N90-10792
National Library of Medicine DOCLINE (tradename) manual
[PB89-188676] 03 p0416 N90-12390
FEDIX: An on-line information service for universities and other research organizations: User's guide, version 2.0, release 1
[DE89-016695] 03 p0417 N90-12398
An air coupled transmission mode acoustic microscope for on-line non-destructive evaluation
[AD-A211416] 04 p0511 N90-12947
A practical approach for minimum time control of the Spacecraft Control Laboratory Experiment (SCOLE), appendix A
[NASA-CR-186008] 05 p0602 N90-13495
On-line range prediction system, part 2
[NASA-CR-185889] 05 p0647 N90-13771
Efficient on-line simulations of tree machines and multidimensional turing machines by random access machines
[AD-A213152] 05 p0680 N90-13960
On the performance of on-line algorithms for partition problems
[MEMO-784] 05 p0689 N90-14015
Survey of adaptive control theory and its applications
[DE89-901270] 06 p0833 N90-14840
On-line system to measure magnetic characteristics of steel samples
[DE89-633443] 06 p0836 N90-14861
A comparative evaluation and analysis of end-user search performance in an academic environment
07 p1009 N90-15845
On-line chemical composition analyzer development
[DE90-004079] 08 p1043 N90-16026
On-line estimation of mechanical nonlinearities in compliant two-link robot manipulators
08 p1085 N90-16280
Online submicron particle sizing by dynamic light scattering using autodilution 09 p1223 N90-17095
Executive summary for designing online help systems: Report of year 1 activity
[AD-A214811] 09 p1262 N90-17320
Help design software project
[AD-A214883] 09 p1270 N90-17362
Fine tuning your search output: Word processors, desktop publishing, electronic mail, databases, and beyond
[DE90-005192] 09 p1297 N90-17517
Materials properties numerical database system established and operational at CINDAS/Purdue University 10 p1366 N90-17919
ESRIN
[ESA-BR-58] 12 p1677 N90-19831
Onboard shuttle on-line software requirements system: Prototype 13 p1858 N90-20658
SES cupola interactive display design environment
13 p1862 N90-20679
Implementation of a hypertext help system for GLAD (Graphics LAnguage for Database)
[AD-A217936] 13 p1868 N90-20718
Maintaining bridge-connected and biconnected components on-line
[AD-A215107] 13 p1875 N90-20754
Effective techniques for the identification and accommodation of disturbances
14 p1934 N90-21072
On-line assessment of weld quality using ultrasonics
[AERE-R-13401] 14 p1989 N90-21398
Nonlinear spline operator interpolation and sliding control of deformable maneuvering bodies
15 p2074 N90-21878
Automating security monitoring and analysis for Space Station Freedom's electric power system
[NASA-TM-103148] 15 p2158 N90-22324
Evaluation of optical storage technology for decision support databases 15 p2176 N90-22436
Technologies for electronic transfer of information: The present state and trends in Europe
15 p2177 N90-22441
On-line x ray inspection of materials and structural components using discrete element x ray detectors for digital radiographic and computed tomographic evaluation
[AD-A218911] 16 p2245 N90-22806
Combining high performance simulation, data acquisition, and graphics display computers
16 p2293 N90-23062
An expert system to perform on-line controller tuning
[NASA-TM-103101] 17 p2453 N90-23991
Autonomous power expert fault diagnostic system for Space Station Freedom electrical power system testbed
19 p2730 N90-25521
Continuous on-line link error rate detector
[AD-D014510] 20 p2850 N90-26209
Self-checking on-line testable static RAM
[NASA-CASE-NPO-17939-1-CU]
20 p2904 N90-26518
Formal verification of the JANUS on-line multiplier
[IMAG-RR-785-I] 20 p2909 N90-26550
On line diagnostics of rotating machinery using expert system technology 22 p3105 N90-27632
Replay and transmission of AIMS-data to mainframe computer using remote transcribers
22 p3105 N90-27634
The new space and Earth science information systems at NASA's archive 22 p3257 N90-28443
Appendix A: NASA information services
22 p3258 N90-28451
On-line object feature extraction for multispectral scene representation
[NASA-CR-187006] 23 p3342 N90-28888
Coordinating the activities of a planner and an execution agent 23 p3369 N90-29035
Grasp planning under uncertainty
23 p3370 N90-29041
An expert system to perform on-line controller restructuring for abrupt model changes
[NASA-TM-103609] 23 p3385 N90-29121
Noncontact measurement of rotating blade vibrations
[NAL-TR-1033] 24 p3483 N90-29687
Supporting large scale applications on networks of workstations
[NASA-CR-186346] 24 p3532 N90-29975
Low cost management of replicated data in fault-tolerant distributed systems
[NASA-CR-186370] 24 p3532 N90-29976
FEDIX: An on-line information service for universities and other research organizations: User's guide
[DE90-014835] 24 p3559 N90-30137

ONBOARD COMPUTERS
U AIRBORNE/SPACEBORNE COMPUTERS

ONBOARD DATA PROCESSING
On-board software 05 p0605 N90-13518
The in-orbit initialization phase
05 p0606 N90-13525
The use of digital signal processing in satellite communication 05 p0631 N90-13684
Checklist reading problems in airplanes equipped with speech recognition systems
[ILR-MITT-223(1989)] 09 p1261 N90-17314
Experimental investigations of the unsteady boundary layer on an oscillating flat plate. Optimization and validation of a code, for calculating the potential flow/boundary layer coupling of a flat plate and of an oscillating profile
[ETN-90-96254] 11 p1508 N90-18682
An approach to on-board optimization of cruise at constant altitude
[LR-581] 15 p2050 N90-21752
Onboard detection of intrinsic Ly alpha radiation from a neutral particle beam
[DE90-010341] 18 p2511 N90-24346
Information sciences experiment system
21 p3015 N90-27142
Description of SAFIRE for ISES
21 p3016 N90-27148
ERBE and CERES broadband scanning radiometers
21 p3016 N90-27149
Onboard processor technology review
21 p3017 N90-27152
Applications of ISES for geology
21 p3017 N90-27154
Applications of ISES for the oceans
21 p3017 N90-27156
Applications of ISES for coastal zone studies
21 p3018 N90-27157
Applications of ISES for instrument science
21 p3018 N90-27161
Command and control in the age of space-based surveillance 21 p3069 N90-27445
Tactical EHF satellite communications for NATO employing non-geostationary orbits
21 p3070 N90-27454
Past, present and future: Aircraft integrated monitoring systems: An ever-developing technology
22 p3103 N90-27618
Aircraft condition monitoring system for future Airbus aircraft: New concept for programming and data recording 22 p3103 N90-27619
The EFA integrated monitoring and recording system: Requirements and concept for implementation
22 p3103 N90-27620
Multichannel on-board load and fatigue monitoring
22 p3103 N90-27621
Observer or direct inversion 22 p3103 N90-27622
Advanced algorithms design and implementation in on-board microprocessor systems for engine life usage monitoring 22 p3104 N90-27628
Expert system diagnostics and parts life tracking as applied to the AV-8B aircraft for the USMC
22 p3104 N90-27629
AIMS for helicopters 22 p3106 N90-27639
The new US flight recorder regulations
22 p3106 N90-27642
Australian experience in flight recorder readout and analysis 22 p3106 N90-27644
On-board planning and control of 4D-trajectories in the TMA 22 p3112 N90-27680
On the structure of a future flight operations system
22 p3113 N90-27682
Aircraft measurements of pollution species near Bermuda and the east coast of the United States during CASE-WATOX
[PB90-159450] 22 p3197 N90-28141
Database development for the DMSP experiments
[AD-A224346] 24 p3557 N90-30129

ONBOARD EQUIPMENT
NT AIRBORNE EQUIPMENT
NT AIRBORNE LASERS
NT AIRBORNE/SPACEBORNE COMPUTERS
NT AIRCRAFT EQUIPMENT
NT EJECTION SEATS
NT SPACECRAFT ELECTRONIC EQUIPMENT
NT SPACECRAFT EQUIPMENT
Development of an automatic ground collision avoidance system using a digital terrain database
[AD-A216247] 10 p1318 N90-17621
Passive navigation using image irradiance tracking
15 p2141 N90-22232
Smart built-in test 19 p2728 N90-25512
Space operations: NASA's communications support for Earth orbiting spacecraft. Report to Chairman, Subcommittee on Space Science and Applications, Committee on Science, Space and Technology, House of Representatives
[GAO/IMTEC-89-41] 20 p2851 N90-26215
On-board planning and control of 4D-trajectories in the TMA 22 p3112 N90-27680

ONE DIMENSIONAL FLOW
Julia-Fatou-Sullivan theory for real one-dimensional dynamics
[REPT-88-100] 04 p0548 N90-13190

ONE-PHASE FLOW
U SINGLE-PHASE FLOW

ONISOTROPY
U ANISOTROPY

OOCYTES
U GAMETOCYTES

OORT CLOUD
Physical processing of cometary nuclei
08 p1148 N90-16653

OPACITY
Solar opacities constrained by solar neutrinos and solar oscillations
[DE89-016988] 02 p0297 N90-11687
Equation of state and opacity of dense plasmas
[DE90-002223] 06 p0847 N90-14926
Astophysical opacities at LLNL
[DE90-003599] 07 p1014 N90-15872
Development of low density silica aerogel as a capture medium for hyper-velocity particles
[NASA-CR-185930] 08 p1121 N90-16489
Update on the OPAL opacity code
[DE90-009946] 15 p2184 N90-22480

Monte Carlo simulation of complex spectra for opacity calculations
[DE90-015198] 24 p3561 N90-30147

OPEN CHANNEL FLOW
Activities report of the Hydraulics Research Laboratory
[ETN-90-96568] 19 p2687 N90-25281
Velocity distribution in a gravel-bed flume; for steady and unsteady flow 19 p2687 N90-25283
Spatially accelerating flow in smooth open channel 19 p2687 N90-25284

OPEN CIRCUIT VOLTAGE
Cable coupling lightning transient qualification
[NASA-CR-183826] 05 p0584 N90-13405
Definition of a design methodology and study of the driving and protection functions of a smart power switch
[LAAS-89-330] 16 p2231 N90-22727

OPEN CLUSTERS
NT PLEIADES CLUSTER
Carbon isotope ratios and lithium abundances in open cluster giants 02 p0292 N90-11664
The age of the galactic disk
[NASA-CR-186292] 07 p1013 N90-15869
The upper main sequence of OB associations. Part 2: The single-lined O stars: Spectral classification of northern stars and lines of C and N
[SER-C-PREPUBL-FASC-39] 08 p1139 N90-16602
Carbon monoxide isotopes and clumping in giant molecular clouds 24 p3562 N90-30151

OPENINGS
NT APERTURES
NT SLITS
NT SYNTHETIC APERTURES
Single fluid simulations of plasma openings switch behavior
[DE90-002643] 07 p0921 N90-15330
Cloud hole-boring with long pulse CO2 lasers
[DE90-008946] 14 p1985 N90-21377
Determination of stresses around cutouts in multilayered composite plate and shell structures 14 p1992 N90-21417
Detecting black holes in packet-radio networks (SRNTN-56)
[AD-A219636] 17 p2389 N90-23604
Buckling and postbuckling behavior of square compression-loaded graphite-epoxy plates with circular cutouts
[NASA-TP-3007] 20 p2826 N90-26077
Buckling and postbuckling behavior of compression-loaded isotropic plates with cutouts
[NASA-TP-3024] 23 p3337 N90-28859

OPERATING COSTS
Revolutionary opportunities for materials and structures study
[NASA-CR-179642] 01 p0034 N90-10184
View on recent fuel costs in airlines
[NAL-TM-569] 02 p0289 N90-11653
Designing for reliable and low maintenance cost aero engines
[PNR90570] 04 p0455 N90-12604
The Kryo-Kanal Koeln (KKK): Description of the tunnel conversion. Thermal insulation, instrumentation, operational experience, test results and operating costs 08 p1029 N90-15943
Reducing C130E Hercules operating costs in the Royal Australian Air Force and the United States Air Force by increasing cruise speeds
[AD-A215747] 10 p1319 N90-17629
Phase 1 supplemental development of a kinematic Stirling/Rankine commercial gas-fired heat pump system
[PB90-129974] 13 p1825 N90-20483
Energy Efficient Engine program advanced turbofan nacelle definition study
[NASA-CR-174942] 23 p3280 N90-28560
Energy Efficient Engine: High-pressure compressor test hardware detailed design report
[NASA-CR-180850] 23 p3281 N90-28570
Operational cost drivers 23 p3294 N90-28636
Airline productivity relating on the fuel cost. (2): Fuel consumption values and fuel efficiency
[NAL-TM-604-2] 24 p3422 N90-29333
The cost of air service fragmentation
[TT-9010] 24 p3422 N90-29334

OPERATING SYSTEMS (COMPUTERS)
NT DISK OPERATING SYSTEM (DOS)
NT UNIX (OPERATING SYSTEM)
DDN Trusted Guard Gateway: Trusted Guard Gateway (TGG) technology assessment, phase 2
[AD-A210248] 01 p0108 N90-10614
Computer availability impact on the archiving of scientific and technical reports
[AD-A210283] 01 p0136 N90-10787
A distributed debugger for Amoeba
[CWI-CS-R8828] 02 p0257 N90-11453
MSP: Modeling of concurrent processes. Version 1.00 General introduction and directions for use
[REPT-88-88] 02 p0260 N90-11477
On the Amoeba protocol
[CWI-CS-R8827] 02 p0261 N90-11480
An expert system for VM performance analysis
[REPT-89-30] 04 p0528 N90-13045
A mapping for converting Mascot designs to Ada programs
[RSRE-MEMO-4244] 04 p0531 N90-13070
Process expressions and Hoare's logic
[CWI-CS-R8905] 04 p0532 N90-13076
Path expression based operating systems
[MEMO-INF-88-68] 04 p0536 N90-13097
The role of order in distributed programs
[NASA-CR-186252] 06 p0830 N90-14826
The Aerospace Energy Systems Laboratory: A BITBUS networking application
[NASA-TM-4149] 06 p0831 N90-14829
How robust are distributed systems
[NASA-CR-186242] 06 p0832 N90-14837
Integrated approach fault tolerance-current state and future requirements
[AD-A214402] 07 p0944 N90-15465
ARGOS (A Research GMMP Operating System): Overvie w and interfaces
[AD-A213871] 07 p0970 N90-15599
The implementation of a coherent memory abstraction on a NUMA (Non-Uniform Memory Access) multiprocessor: Experiences with PLATINUM (Platform for Investigating Non-Uniform Memory)
[AD-A213909] 07 p0970 N90-15600
Memory management for large-scale NUMA (Non-Uniform Memory Access) multiprocessors
[AD-A213910] 07 p0970 N90-15601
An overview of PLATINUM: A Platform for Investiga ting Non-Uniform Memory (preliminary version)
[AD-A213911] 07 p0970 N90-15602
Evolution of an operating system for large-scale shared-memory multiprocessors
[AD-A213912] 07 p0970 N90-15603
An executive system for modeling with rational b-splines
[AD-A213460] 07 p0974 N90-15627
Methodology for developing realtime distributed systems
[AD-A214570] 09 p1296 N90-17509
The Saguaro distributed operating system
[AD-A215083] 10 p1374 N90-17966
Writing parallel, discrete-event simulations in ModSim: Insight and experience
[DE90-001833] 10 p1419 N90-18183
Technology assessment of operating systems
[AD-A216893] 10 p1421 N90-18192
The design and analysis of new techniques for transaction management in database systems 10 p1441 N90-18314
The implications of using integrated software support environment for design of guidance and control systems software
[AGARD-AR-229] 11 p1464 N90-18432
Vertical migration in operational system nucleus
[INPE-4879-RPE/593] 11 p1543 N90-18883
L: A language for solution of incremental systems in a parallel processing environment
[INPE-4816-TDL/362] 11 p1543 N90-18884
TAE Plus: Transportable Applications Environment Plus tools for building graphic-oriented applications 13 p1856 N90-20652
Applications of graphics to support a testbed for autonomous space vehicle operations 13 p1858 N90-20661
MEASURE: An integrated data-analysis and model identification facility
[NASA-CR-186452] 13 p1863 N90-20686
NYU (New York University) ultracomputer
[AD-A217167] 13 p1863 N90-20688
The HS6000/20 development system
[LINO-1989-6] 13 p1865 N90-20696
VHSIC Hardware Description Language (VHDL) benchmark suite
[AD-A217947] 13 p1868 N90-20719
Innovations in telecommunications networks 15 p2178 N90-22444
Methodology for analysis and simulation of large multidisciplinary problems 16 p2290 N90-23046
DARK (Distributed Ada Real-Time Kernel) porting and extension guide Kernel version 3.0
[AD-A219291] 16 p2301 N90-23112
BTOS database evaluation
[AD-A219304] 16 p2328 N90-23271
Multiprocessing on supercomputers for computational aerodynamics
[NASA-TM-102806] 17 p2347 N90-23366
A model of a path expression based operating system shell
[MEMO-INF-89-71] 17 p2440 N90-23906
Experiences with the Amoeba distributed operating system
[CWI-CS-R8929] 18 p2596 N90-24770
Amoeba: High performance distributed computing
[CWI-CS-R8937] 18 p2596 N90-24771
TRENDS: The aeronautical post-test database management system
[NASA-TM-101025] 19 p2662 N90-25149
Tools for distributed application management
[NASA-CR-186646] 19 p2762 N90-25692
Reliable broadcast protocols
[NASA-CR-186411] 19 p2762 N90-25696
PANDA: A distributed multiprocessor operating system 20 p2911 N90-26561
A development framework for artificial intelligence based distributed operations support systems 21 p3044 N90-27301
Linear algebra on a CRAY X-MP
[AD-A221780] 21 p3056 N90-27374
Advanced transport operating system software upgrade: Flight management/flight controls software description
[NASA-CR-181936] 22 p3239 N90-28366
Report of the Invitational Workshop on Data Integrity
[PB90-148123] 22 p3240 N90-28372
ROSES, a Robot Operating System Expert Scheduler: Methodological framework
[DE90-014782] 23 p3334 N90-28851
Concepts of concurrent programming
[AD-A223897] 23 p3382 N90-29110
System software for Soviet computers 24 p3523 N90-29921
Programming your way out of the past: ISIS and the META Project
[NASA-CR-186275] 24 p3524 N90-29922
AHTO project: Software technology for open distributed processing
[PB90-190943] 24 p3524 N90-29923
Language and system support for concurrent programming
[AD-A223760] 24 p3528 N90-29949
Low cost management of replicated data in fault-tolerant distributed systems
[NASA-CR-186370] 24 p3532 N90-29976

OPERATING TEMPERATURE
A nonintrusive method for measuring the operating temperature of a solenoid-operated valve
[DE90-007576] 13 p1804 N90-20355
Proton responses on MOS (Metal-Oxide-Semiconductor) electronics operating at cryogenic temperatures
[AD-A217622] 13 p1894 N90-20868
Turbine fuel alternatives (near term)
[AD-A219405] 16 p2225 N90-22695
Enhanced ceria solid electrolyte fuel cell development. Reduction of electronic conductivity permits use of a solid ceria electrolyte in high efficiency high power density fuel cells at temperatures compatible with metallic cell hardware
[AD-A219297] 16 p2253 N90-22846
Diode laser satellite systems for beamed power transmission
[NASA-TP-2992] 18 p2556 N90-24585

OPERATIONAL AMPLIFIERS
Null offset voltage compensator for operational amplifier
[AD-D014189] 04 p0496 N90-12859
Transient radiation hardened CMOS (Complementary Metal Oxide Semiconductor) operational amplifiers
[AD-A217972] 13 p1797 N90-20313

OPERATIONAL CALCULUS
Module algebra (revised version)
[CWI-CS-R8844-REV] 02 p0260 N90-11474
Backward analysis on higher order functions
[MEMO-INF-89-19] 02 p0268 N90-11526

OPERATIONAL PROBLEMS
Spacecraft charging effects
[RAE-TM-SPACE-375] 23 p3287 N90-28594

OPERATIONS RESEARCH
Regulation of nonlinear and generalized linear systems
[AD-A207725] 01 p0109 N90-10619
Checking the Goldbach conjecture on a vector computer
[CWI-NM-R8812] 02 p0260 N90-11475
Variable step iteration of high-order Runge-Kutta methods on parallel computers
[CWI-NM-R8817] 02 p0260 N90-11476
Transaction throughput in distributed systems: A modeling study using dynamic queueing networks
[MEMO-INF-89-25] 02 p0261 N90-11479
On the Amoeba protocol
[CWI-CS-R8827] 02 p0261 N90-11480
LINPACK routines based on the level 2 BLAS
[CWI-NM-R8811] 02 p0261 N90-11483

Fixed point iteration on point-symmetric interference graphs
[MEMO-INF-89-23] 02 p0269 N90-11535
The comparison of the airbase simulation models airbase and sustained
[FEL-1988-66] 04 p0459 N90-12629
Solving three dimensional block bidiagonal linear systems on vector computers
[REPT-89-14] 04 p0530 N90-13056
Radar and sensor array design planning for a naval missile testing center. Artificial intelligence applications
[ETCA-88-R-099] 04 p0537 N90-13108
Smoothed limit theorems for equilibrium processes
[AD-A212321] 04 p0547 N90-13186
In-orbit payload calibration 05 p0606 N90-13526
Research in optical interconnection techniques
[AD-A214028] 07 p0993 N90-15739
A planning and scheduling lexicon
[NASA-CR-186061] 09 p1171 N90-16777
Operational drivers for launcher architectures
09 p1178 N90-16828
Network flow algorithms
[AD-A214689] 09 p1265 N90-17337
Integrated silicon flip-flop sensors
[ETN-90-96271] 11 p1503 N90-18654
Parallel algorithms derivation
[AD-A216452] 11 p1545 N90-18894
Research in reliability, availability and maintainability for complex failure systems
[AD-A217744] 13 p1813 N90-20415
An integrative research review of the relationship between technology and structure: A meta-analytic synthesis
[AD-A218115] 13 p1899 N90-20903
Scheduling around a small common due date
[CWI-BS-R8914] 17 p2446 N90-23943
The existence of sensitive optimal policies in two multi-dimensional queueing models
[TW-89-11] 17 p2464 N90-24080
Note on the optimality of the generalized shortest queue policy
[TW-90-01] 17 p2464 N90-24081
Sojourn times in queueing networks
[CWI-BS-R8916] 17 p2467 N90-24102
In-orbit operations research and development program of the Toulouse Space Center 18 p2501 N90-24290
Proceedings of the 28th Annual US Army Operations Research Symposium (AORS), volume 1
[AD-A219349] 18 p2606 N90-24842
Minimizing distortion and internal forces in truss structures by simulated annealing
18 p2644 N90-25055
Operations and support cost modeling using Markov chains 18 p2648 N90-25070
Launching a dream: A teachers guide to a simulated space shuttle mission
[NASA-TM-89715] 20 p2934 N90-26693
DEVS-based intelligent control of space adapted fluid mixing 21 p3040 N90-27279
Four-dimensional navigation and Flight Management Systems 22 p3112 N90-27681
Target acquisition probability as a function of distance, calculated with PHIND
[IZF-1989-46] 22 p3244 N90-28394
ECS: Sixth year in orbit
[ESA-BR-70] 24 p3440 N90-29428
Reflections on the relationship between artificial intelligence and operations research
24 p3506 N90-29816
Preliminary hazard analysis in design application to EVA space suit
[ETN-90-97585] 24 p3523 N90-29918
New approaches to linear and nonlinear programming
[AD-A224328] 24 p3525 N90-29932

OPERATOR PERFORMANCE
SINCGARS (Single-Channel Ground/Airborne Radio System) operator performance decay
[AD-A210716] 01 p0057 N90-10326
An adaptive controller for enhancing operator performance during teleoperation
[NASA-CR-183445] 01 p0077 N90-10438
Active participation in highly automated systems: Turning the wrong stuff into the right stuff
[AD-A210218] 01 p0101 N90-10572
Human Operator Simulator (HOS) 4 user's guide
[AD-A212007] 03 p0310 N90-11763
Parallel approach separation and controller performance: A study of the impact of two separation standards
[DOT/FAA/CT-TN89/50] 04 p0449 N90-12574
Compensatory tracking in disturbance tasks and target following tasks. The influence of cockpit motion on performance and control behavior
[LR-511] 05 p0675 N90-13933
The application of queuing theory to the modelling of CP-140 aircraft communications
[AD-A213479] 07 p0918 N90-15310
Where to from here. Future applications of mental models of complex performance
[DE90-002091] 07 p0967 N90-15586
User interaction with self-learning systems
[AD-A214280] 08 p1105 N90-16395
Personality assessment in aviation selection
09 p1257 N90-17289
Brain activity during tactical decision-making. Part 3: Relationships between probe-evoked potentials, simulation performance, and on-job performance
[AD-A217207] 13 p1854 N90-20638
Mental lapses and event-related potentials
[AD-A219454] 17 p2436 N90-23878
On-board expert system for manned rendezvous operation assistance 18 p2504 N90-24309
Telepresence for space: The state of the concept
19 p2731 N90-25526
The human factors of workstation telepresence
19 p2732 N90-25528
A helmet mounted display to adapt the telerobotic environment to human vision 19 p2737 N90-25555
Aviation safety: Serious problems continue to trouble the air traffic control work force. Report to congressional requesters
[GAO/RCED-89-112] 20 p2805 N90-25959
Application of audio/speech recognition for military applications 21 p2993 N90-27014
Simulation of synthetic aperture radar 4: Summary and recommendations
[AD-A221822] 21 p2997 N90-27038
The integration of complex information from auditory and visual channels under stress
[AD-A222686] 21 p3033 N90-27245
The measurement of dark adaptation level in the presence of glare
[PB90-155987] 22 p3231 N90-28323
Situational Awareness Rating Technique (SART): The development of a tool for aircrew systems design
23 p3357 N90-28975
Tracking performance and influence of field of view
23 p3360 N90-28988
Teleoperator comfort and psychometric stability: Criteria for limiting master-controller forces of operation and feedback during telemanipulation
23 p3364 N90-29009
Performance limitations of bilateral force reflection imposed by operator dynamic characteristics
24 p3510 N90-29840
Multisensor evaluation framework
[AD-A224271] 24 p3522 N90-29913

OPERATORS (MATHEMATICS)
NT LINEAR OPERATORS
On two polynomial spaces associated with a box spline
[AD-A210559] 01 p0113 N90-10646
Parameter identification for an abstract Cauchy problem by quasilinearization
[NASA-CR-181933] 03 p0385 N90-12192
Operator product coefficients in non-diagonal conformal field theories
[PB89-216873] 03 p0399 N90-12283
Labeled trees and the efficient computation of derivations
[NASA-CR-185386] 04 p0538 N90-13113
Stable summability and approximation theory
[AD-A211379] 04 p0539 N90-13118
Modular specifications in process algebra with curious queues
[CWI-CS-R8821] 04 p0543 N90-13152
International Conference on Operator Theory: Advances and applications
[AD-A212341] 04 p0545 N90-13170
Operator product coefficients in non-diagonal conformal field theories
[NIKHEF-H/88-19] 04 p0553 N90-13224
Program transformation with abstract relation algebras
[AD-A213270] 05 p0688 N90-14011
Numerical methodologies for solving partial differential equations
[DE90-001842] 06 p0834 N90-14849
On the sum of two maximal monotone operators
[REPT-89-31] 07 p0982 N90-15669
Continuum analogues of contragredient Lie algebras: Lie algebras with a Cartan operator and nonlinear dynamical systems
[DE89-635698] 07 p0985 N90-15691
Existence, uniqueness, and approximation of a solution for a K-positive definite operator equation
[DE90-600728] 09 p1272 N90-17373
On calculating analytic centers
[AD-A215535] 09 p1274 N90-17385
On scattering by time-dependent potentials: The 2-D case
[DE89-635708] 09 p1275 N90-17390
New spacetime superalgebras and their Kac-Moody extension
[DE90-606949] 10 p1422 N90-18201
Iterative methods for nonlinear set-valued operators of the monotone type with applications to operator equations
[DE90-606950] 10 p1422 N90-18202
Recurrence conditions for average and Blackwell optimality in denumerable state Markov decision chains
[TW-89-02] 11 p1555 N90-18952
Kreim factorization of covariance operators of 2-parameter random fields and application to the likelihood ratio
[MEMO-802] 11 p1555 N90-18953
Differential operators associated with Gegenbauer polynomials. 3: The regular case
[DE90-610422] 12 p1706 N90-19795
Magnetostatic boundary-value problems in the incomplete-nonlinear formulation and methods of their solution
[DE90-615185] 13 p1877 N90-20767
On a non classical oblique derivative problem for parabolic singular integro-differential operators
[DE90-612739] 14 p2020 N90-21574
Nonlinear spline operator interpolation and sliding control of deformable maneuvering bodies
15 p2074 N90-21878
Spatial operator algebra framework for multibody system dynamics 16 p2279 N90-22989
Naturalness of polymorphism
[CS-8916] 16 p2305 N90-23134
A proof of the isoenergetic KAM: Theorem from the ordinary one
[W-8906] 16 p2305 N90-23136
The effects of caustics in acoustic inverse scattering experiments
[AD-A218454] 16 p2313 N90-23185
Improving fermion operators
[PREPRINT-710] 16 p2315 N90-23193
Mixing of DIS operators in lattice QCD
[PREPRINT-708] 16 p2323 N90-23243
Morphological sampling
[CWI-AM-R8913] 17 p2460 N90-24044
Gevrey spaces related to Lie algebras of operators
[ETN-90-96892] 17 p2468 N90-24109
Extensions of algebraic image operators: An approach to model-based vision 19 p2741 N90-25577
Nonlinear systems, the Lie series, and the left shift operator: Application to nonlinear optimal control
[RR-376] 19 p2748 N90-25619
Hopf-algebraic structure of combinatorial objects and differential operators
[NASA-CR-186360] 19 p2752 N90-25640
Galerkin finite difference Laplacian operators on isolated unstructured triangular meshes by linear combinations
[NASA-TM-103209] 20 p2861 N90-26276
Impulse response operators for structural complexes
[AD-A222374] 22 p3191 N90-28107
On the zeta-function regularization of chiral Jacobians for singular Dirac operators
[DE90-627176] 23 p3390 N90-29150
Casimir effect in a D-dimensional flat spacetime and the cut-off method
[DE90-627177] 23 p3390 N90-29151

OPERATORS (PERSONNEL)
NT AIRCRAFT PILOTS
NT PILOTS (PERSONNEL)
NT TEST PILOTS
Active participation in highly automated systems: Turning the wrong stuff into the right stuff
[AD-A210218] 01 p0101 N90-10572
Human factors survey of advanced instrumentation and controls
[DE90-002477] 06 p0821 N90-14776
An approach to elemental task learning
[DE90-006614] 12 p1697 N90-19745
The role of attention in information processing implications for the design of displays
[AD-A219252] 19 p2723 N90-25486
QTA (QUESTIONNAIRE-TASK-ANALYSIS): An electronic tool for job/task analysis
[DE90-008944] 24 p3499 N90-29778

OPHTHALMOLOGY
Prescribing spectacles for aviators
[AD-A214830] 09 p1260 N90-17310
Laser-produced plasmas in medicine
[DE90-007623] 13 p1891 N90-20849
Measurement and visualization of the shock wave caused by the impact of a pulsed YAG laser in water
[REPT-892-430-113] 16 p2240 N90-22783

OPTICAL ABSORPTION
U ELECTROMAGNETIC ABSORPTION
U LIGHT TRANSMISSION

OPTICAL AMPLIFIERS
U LIGHT AMPLIFIERS
OPTICAL BISTABILITY
New type of optical bistability in polymers mediated by phonons
[AD-A216102] 10 p1359 N90-17882
Optical Bistability, 1988
[AD-A217681] 13 p1888 N90-20832
Optical properties of zinc selenide grown using molecular beam deposition techniques
[RSRE-MEMO-4269] 15 p2174 N90-22423
Optical bistability in semiconducting material 15 p2174 N90-22424
Optical nonlinearity due to structure defects and bistability in the band discontinuity area of CdS
[ETN-90-97303] 24 p3554 N90-30112
OPTICAL COMMUNICATION
Coherent multilchannel techniques for integrated broadband communications subscriber lines
[AD-A209323] 01 p0055 N90-10312
Calculation, optimization and comparison of optical transmission systems with superheterodyne reception
[ETN-89-94651] 02 p0214 N90-11224
Laser dynamics: The system dynamics and network theory of optoelectronic integrated circuit design 02 p0226 N90-11296
Optical coherence multiplexing for interprocessor communications
[DE89-016186] 02 p0275 N90-11568
MEGALIDAR
[AD-A212074] 03 p0353 N90-12020
Design and performance of an on-satellite laser diagnostic system for a free space optical heterodyne frequency-shift-keyed communication system
[AD-A211986] 04 p0505 N90-12915
Three stages and two systems of visual processing
[AD-A212670] 04 p0525 N90-13032
Fellowships in information and stochastic systems
[AD-A212385] 04 p0563 N90-13280
Optical communication with semiconductor laser diode
[NASA-CR-185686] 05 p0647 N90-13770
Integrated optoelectronic receivers
[AD-A213376] 05 p0700 N90-14098
Shuttle Laser Technology Experiment Facility (LTEF)-to-airplane lasercom experiment: Airplane considerations
[NASA-TM-100749] 06 p0731 N90-14260
SLCSAT (Submarine Laser Communication Satellite) communication system design study
[AD-A213403] 07 p0917 N90-15304
Laser communication system with wide band magnetostrictive modulation
[AD-D014302] 07 p0937 N90-15427
OPFET (Optical Field-Effect Transistor) demodulator-downconverter for detecting microwave modulated optical signals
[AD-D014294] 08 p1060 N90-16128
Optical transmission through clouds
[AD-A214765] 09 p1248 N90-17240
Atmospheric transmission calculations for optical frequencies 10 p1373 N90-17960
Laser intersatellite transmission experiment spatial acquisition, tracking, and pointing system
[AD-A215934] 10 p1389 N90-18036
Direct detection optical intersatellite link at 220 Mbps using AlGaAs laser diode and silicon APD with 4-ary PPM signaling
[NASA-CR-186380] 12 p1646 N90-19460
Development of a receiver for a space-based laser radar system
[AD-A215079] 12 p1665 N90-19566
A space-based optical communication system utilizing fiber optics
[AD-A217333] 13 p1887 N90-20828
GaAs traveling-wave optical modulators using modulated coplanar electrodes with periodic cross-tie overlays
[AD-A217731] 13 p1888 N90-20835
Fundamental studies of photon statistics
[AD-A217825] 13 p1888 N90-20836
Optical control of an 8-element Ka-band phased array using a high-speed optoelectronic interconnect
[NASA-TM-102550] 14 p1968 N90-21275
Optical shutter switching matrix
[NASA-CASE-KSC-11392-1] 15 p2167 N90-22383
Single mode communication link
[AD-A219499] 17 p2388 N90-23601
Multiple beam optical processing
[AD-A219048] 17 p2471 N90-24129
Optical links for microwave application
[AD-A220574] 17 p2472 N90-24134
Investigations of laterally coupled all optical switches and detectors on silica fibers
[AD-A220297] 17 p2473 N90-24142
Report of research activity at the Research Laboratory of Electronics 17 p2486 N90-24217
Monolithic arrays of grating-surface-emitting diode lasers and quantum well modulators for optical communications
[NASA-CR-186772] 19 p2758 N90-25674
A two-telescope receiver design for deep space optical communications 20 p2853 N90-26226
High speed all optical networks
[NASA-CR-185311] 20 p2926 N90-26649
Diode laser pumped single mode 1.3 microns Nd:YALO microlaser
[AD-A223036] 21 p3008 N90-27100
Brief state-of-the-art review on optical communications for the NASA ISES workshop 21 p3017 N90-27153
Adaptive polarization diversity detection scheme for coherent communications and interferometric fiber sensors
[AD-D014479] 22 p3163 N90-27938
Optical communications system having a wide-core single-mode planar waveguide
[AD-D014485] 22 p3164 N90-27939
Microprocessor chip incorporating optical signal coupling receiver
[AD-D014547] 22 p3167 N90-27964
Application of integrated optical components in optical fiber communication
[FEL-89-B252] 23 p3395 N90-29183
Satellite Constellation Orbit Evaluation (SCORE) program
[AD-A223531] 24 p3438 N90-29417
OPTICAL COMPUTERS
Antenna beamforming using optical processing
[NASA-CR-180844] 02 p0212 N90-11210
Optical shared memory
[AD-A215090] 10 p1430 N90-18249
Binary correlators for optical computing and pattern recognition 10 p1441 N90-18318
Adaptive associative-processing optical computing architectures
[AD-D014317] 13 p1863 N90-20685
A hybrid architecture for the implementation of the Athena neural net model 23 p3368 N90-29032
OPTICAL CORRECTION PROCEDURE
Improvement of ultrashort pulsed laser shadowgraph photography by means of optical filters
[ISL-CO-215/88] 04 p0504 N90-12906
Geometric correction models for HRV-SPOT images
[INPE-5001-TDL/395] 11 p1521 N90-18757
Optical wavefront computer for stabilizing large space structures
[AD-A221707] 21 p2967 N90-26866
OPTICAL COUNTERMEASURES
Defense to laser light irradiation
[AD-D014286] 08 p1036 N90-15984
OPTICAL COUPLING
Theoretical and experimental investigation of coupled Ar-ion lasers
[AD-A214908] 09 p1227 N90-17122
Fiber optic transversal filter/variable delay line
[AD-D014328] 10 p1430 N90-18248
Optical amplification in 45 deg - cut BaTiO3
[AD-A216043] 11 p1566 N90-19011
Investigation of the technological effects on the coupling behavior of parallel GaAlAs rib waveguide
[ETN-90-95323] 13 p1887 N90-20825
Phase locking of two HIQ resonators
[AD-A221123] 18 p2563 N90-24627
Optical fiber to waveguide coupling technique
[AD-A221781] 21 p3077 N90-27496
Image amplification in photoreactive crystals and utilization in optical reaction systems
[ETN-90-97285] 24 p3546 N90-30059
OPTICAL DATA PROCESSING
NT SCENE ANALYSIS
Optical processing for distributed sensors in control of flexible spacecraft 01 p0021 N90-10102
Utilization of photorefractive crystals in optical image processing
[ISBN-3-923560-06-0] 02 p0225 N90-11292
Fast and objective MRTD measurement
[FEL-1988-24] 03 p0351 N90-12006
Optical computing based on the Hopfield model for neural networks
[AD-A211824] 03 p0389 N90-12216
Optical data transmission systems in radiation environment
[DE90-000174] 03 p0405 N90-12322
Characterization of liquid crystal displays for optical signal processing applications
[AD-A212832] 04 p0505 N90-12910
Optics and opto-electronics systems
[AD-A212340] 05 p0699 N90-14093
Normal points: Compression of satellite laser ranging data
[ETN-90-96008] 05 p0707 N90-14145
New devices using ferroelectric thin films
[DE90-000789] 07 p0921 N90-15328
Studies of optical matrix multiplication and reconfigurable optical interconnect concepts
[AD-A214645] 09 p1281 N90-17427
Reactive atmosphere processing of BaTiO3 and origins of its photorefractive effect
[AD-A215034] 09 p1289 N90-17475
Optical Johnson noise thermometry 10 p1363 N90-17899
Hybrid (optical/electronic) computing and digital optical computing
[AD-A214502] 10 p1416 N90-18160
Binary correlators for optical computing and pattern recognition 10 p1441 N90-18318
Application of wavefront analysis techniques to restoring of images degraded by atmospheric turbulence
[ONERA-PUBL-1989-1] 11 p1589 N90-19168
Adaptive associative-processing optical computing architectures
[AD-D014317] 13 p1863 N90-20685
Photonic processing at NASA Ames Research Center 15 p2141 N90-22234
Northeast Artificial Intelligence Consortium annual report, 1988. Volume 12: Computer architectures for very large knowledge bases
[AD-A219599] 17 p2454 N90-23999
Optical wavefront computer for stabilizing large space structures
[AD-A221707] 21 p2967 N90-26866
Optics and symbolic computing
[AD-A221443] 21 p3077 N90-27493
Solid state circuitry with optical data interfacing
[AD-D014548] 22 p3248 N90-28422
A hybrid architecture for the implementation of the Athena neural net model 23 p3368 N90-29032
Two-dimensional signal processing and storage and theory and applications of electromagnetic measurements
[AD-A224239] 24 p3459 N90-29538
Optical symbolic processor for expert system execution
[AD-A224264] 24 p3525 N90-29931
Optical signal computing
[AD-A223624] 24 p3545 N90-30051
OPTICAL DATA STORAGE MATERIALS
Optical storage technology
[AD-A224028] 23 p3407 N90-29254
OPTICAL DENSITY
Analysis of catalytically enhanced solar absorption chemical reactors. 2: Predicted characteristics of a 100 kW chemical reactor
[DE89-014743] 07 p0954 N90-15521
A high optical density measuring spectrometer
[AD-D014331] 12 p1621 N90-19318
The receiving system of a dual dye lidar to study molecular and aerosol densities at the base of the stratosphere
[AD-A218286] 13 p1843 N90-20581
OPTICAL DEPOLARIZATION
Low frequency polarized and depolarized light scattering in H-bonded liquids: CH3(CH2)n-1OH (n=1,...5)
[PREPRINT-693] 05 p0700 N90-14100
Polarization coupling in the acousto-optic interaction of surface waves 15 p2164 N90-22365
OPTICAL DEPTH
U OPTICAL THICKNESS
OPTICAL DISKS
Document preservation by electronic imaging. Volume 1: Synopsis
[PB89-226526] 06 p0858 N90-14987
Document preservation by electronic imaging. Volume 2: System and experiment description
[PB89-226534] 06 p0858 N90-14988
Document preservation by electronic imaging. Volume 3: Appendices
[PB89-226542] 06 p0858 N90-14989
Procurement of an optical disk information storage and retrieval system
[DE90-001372] 07 p1010 N90-15849
Army War College final prototype optical disk system testing and evaluation report
[DE90-008852] 14 p2036 N90-21685
Quick guide of the essential concepts used in optical digital data disk technology 17 p2479 N90-24175
Applications of PC-based digital imaging for storing microscopy images on optical disks
[DE90-011355] 19 p2763 N90-25701
Disk mass densities in edge-on spiral galaxies 21 p3097 N90-27600
Linear laser diode arrays for improvement in optical disk recording for space stations
[NASA-CR-4322] 22 p3180 N90-28047
OPTICAL EMISSION
U LIGHT EMISSION
OPTICAL EMISSION SPECTROSCOPY
NT LASER SPECTROSCOPY

Method and apparatus for determining optical absorption and emission characteristics of a crystal or non-crystalline fiber
[NASA-CASE-LAR-13963-1] 17 p2475 N90-24150

OPTICAL EQUIPMENT
NT CAMERAS
NT COLLIMATORS
NT DIFFRACTION LIMITED CAMERAS
NT ELLIPSOMETERS
NT ETALONS
NT EYEPIECES
NT FAINT OBJECT CAMERA
NT FRAMING CAMERAS
NT HIGH SPEED CAMERAS
NT IMAGE TUBES
NT INFRARED SPECTROMETERS
NT LASER DOPPLER VELOCIMETERS
NT LASER RANGE FINDERS
NT LIGHT SCATTERING METERS
NT MICRODENSITOMETERS
NT MICROWAVE REFLECTOMETERS
NT MULTISPECTRAL BAND SCANNERS
NT NEPHELOMETERS
NT OCULOMETERS
NT OPTICAL GYROSCOPES
NT OPTICAL MEASURING INSTRUMENTS
NT OPTICAL MICROSCOPES
NT OPTICAL RADAR
NT OPTICAL SCANNERS
NT PHOTOMETERS
NT POLARIMETERS
NT POLARISCOPES
NT PRISMS
NT PYROHELIOMETERS
NT REFLECTOMETERS
NT SCHMIDT CAMERAS
NT SPECTROPHOTOMETERS
NT STREAK CAMERAS
NT TELEVISION CAMERAS
NT THEMATIC MAPPERS (LANDSAT)
NT THEODOLITES
NT TOTAL OZONE MAPPING SPECTROMETER
NT TRANSMISSOMETERS
NT ULTRAVIOLET SPECTROMETERS
NT WIDE ANGLE LENSES

Polyheterocycle Langmuir-Blodgett films
[AD-A210625] 01 p0051 N90-10292
Subpicosecond optical digital computation using conjugate parametric generators
[AD-A207908] 01 p0058 N90-10330
Second-order nonlinear optical devices in poled polymers
[DE89-015842] 01 p0123 N90-10703
Applications of flight control system methods to an advanced combat rotorcraft
[NASA-TM-101054] 03 p0308 N90-11752
Kinematic design NC optical generator
03 p0404 N90-12316
Design and performance of an optical mount using cross-flexure pivots
[DE89-017551] 04 p0508 N90-12929
Control of optical systems 05 p0600 N90-13484
The modulating grid 05 p0603 N90-13505
Modeling of the Hipparcos optical system
05 p0612 N90-13572
Efficient detection of small moving objects
[AD-A213314] 05 p0632 N90-13690
Method and apparatus to enhance the sensitivity of cylindrical magnetostrictive transducer to magnetic fields
[AD-D014218] 06 p0767 N90-14459
Interferometric surface distortion detector
[AD-D014211] 06 p0842 N90-14901
Analysis and evaluation of technical data on the photochromic and non-linear optical properties of materials. Appendix: Eye/sensor protection by an optical fuse mirror at a focal plane: Feasibility assessment
[AD-A214051] 07 p0896 N90-15177
Instrumentation for cryogenic wind tunnels
08 p1030 N90-15950
Flow visualization in the cryogenic wind tunnel
08 p1030 N90-15953
Analysis and evaluation of technical data on the photochromic and non-linear optical properties of materials
[AD-A214050] 08 p1041 N90-16014
Reflectometers
[AD-D014249] 08 p1122 N90-16499
Surface topography measurements over the 1 meter to 10 micrometer spatial period bandwidth
[DE90-003642] 08 p1122 N90-16501
Micro-miniature roll rate sensor
[AD-A214778] 09 p1225 N90-17107
Comparison of drop size distributions from two droplet sizing systems
[NASA-TM-102520] 09 p1232 N90-17147
A statistical model of the infrared signature of a wind roughened sea
[AD-A214531] 09 p1249 N90-17245
The Advanced Digital-Optical Control System (ADOCS) user demonstration program
[AD-A215984] 10 p1323 N90-17644
New type of optical bistability in polymers mediated by phonons
[AD-A216102] 10 p1359 N90-17882
Highly accurate navigation: Integration of navigation and geodesic methods
[SFB-228] 12 p1602 N90-19221
Precision segmented reflector, figure verification sensor 12 p1611 N90-19272
A high optical density measuring spectrometer
[AD-D014331] 12 p1621 N90-19318
FOMA: A Fast Optical Multichannel Analyzer
[DE90-004093] 12 p1713 N90-19939
Design and test of a compact optics system for the pool boiling experiment
[NASA-TM-102530] 13 p1786 N90-20253
Simple reflection holography
[DE90-008309] 13 p1805 N90-20359
Robotic mobility system: Road following algorithms
[AD-A218107] 13 p1874 N90-20748
A space-based optical communication system utilizing fiber optics
[AD-A217333] 13 p1887 N90-20828
Velocity matched optical transmitter
[AD-A217413] 13 p1887 N90-20830
CCST (Center for Compound Semiconductor Technology) research briefs
[DE90-007782] 13 p1895 N90-20874
ASCIE: An integrated experiment to study CSI in large segmented optical systems 14 p1936 N90-21082
The anatomy of the gyroscope, part 3
[AGARD-AG-313] 14 p1982 N90-21359
An acousto-optic image correlator with a throughput rate of 1000 templates per second
[DE90-009323] 15 p2144 N90-22249
High performance holographic elements and media
[AD-A218999] 16 p2239 N90-22775
Agile multiple aperture imager receiver development
[AD-A218956] 16 p2318 N90-23215
Electromagnetic machines which utilize microgeometry field structures
[AD-A219628] 17 p2398 N90-23660
Multiple beam optical processing
[AD-A219048] 17 p2471 N90-24129
Remote optical sensing
[AD-A220780] 17 p2473 N90-24136
Wearing of cryomechanisms at 4 K
18 p2537 N90-24476
Optical signal processing
[AD-A220332] 18 p2615 N90-24897
Rome air development center cryo test facility
[AD-A220067] 19 p2662 N90-25147
Nonlinear optical protection against frequency agile lasers
[AD-D014535] 19 p2695 N90-25335
Ultra precision machining
[AD-A222422] 21 p2991 N90-27003
Optical communications system having a wide-core single-mode planar waveguide
[AD-D014485] 22 p3164 N90-27939
Improved meteorological measurements from buoys and ships (IMET): Preliminary comparison of precipitation sensors
[PB90-241902] 22 p3229 N90-28316
Effects and control of the correlation properties of light sources
[AD-A224539] 24 p3545 N90-30049
Analysis and evaluation of technical data on the photochronic and non-linear optical properties of materials
[AD-A223855] 24 p3545 N90-30053

OPTICAL FIBERS
Multimode fiber interferometry and several-mode fiber polarimetry via phase conjugation
[DE89-014226] 01 p0123 N90-10706
Fiber optic technique for surveillance and control of mine fields
[FOA-C-30526-3.1] 02 p0225 N90-11293
Fiber optics: A brief introduction
[DE89-009337] 02 p0274 N90-11567
Acceleration of thin foil targets using fiber-coupled optical pulses
[DE89-016526] 02 p0275 N90-11569
Optical fibre witnesses of fatigue damage in composite materials 04 p0465 N90-12660
Variational and asymptotic methods in open and closed waveguide analysis
[REPT-34] 04 p0554 N90-13229
Simulated Brillouin backscattering in optical fibers: A ring resonator 06 p0783 N90-14556
Interlaboratory comparison of radiation-induced attenuation in optical fibers. Part 3: Transient exposures
[DE90-000859] 07 p0992 N90-15729
Optical acoustic sensor using optical fiber
[DE89-901267] 07 p0992 N90-15730
SBS (Stimulated Brillouin Scattering) pulse distortion in multimode optical fibers: Preliminary results
[DE90-003023] 07 p0992 N90-15731
Mechanical evaluation of the differential drum concept for optical fiber pay-out
[AD-A214149] 07 p0993 N90-15740
Angle of arrival detection through analysis of optical fiber intensity patterns
[AD-A215421] 09 p1218 N90-17065
IR optical fiber-based noncontact pyrometer for drop tube instrumentation 10 p1365 N90-17909
The influence of gamma-radiation on the bandwidth of optical fibres and the reduction of the induced attenuation by bleaching and hardening the fibre
[FEL-1988-62] 12 p1714 N90-19848
Development of an ultra-bright laser and an application to multi-photon ionization 14 p1984 N90-21372
Stability studies of a pH-sensitive polymer matrix: Applications to fiber optic pH sensors
[DE90-009579] 15 p2072 N90-21867
Processing of thermotropic liquid crystalline polymers and their blends
[AD-A218804] 16 p2223 N90-22683
Transfer matrices for multimode optical fiber systems
[AD-A218459] 16 p2317 N90-23210
Single mode communication link
[AD-A219499] 17 p2388 N90-23601
Optical fiber for acoustic sensor applications
[AD-A219323] 17 p2472 N90-24130
Remote optical sensing
[AD-A220780] 17 p2473 N90-24136
Material evaluation of optical fibers and payout bobbins: An overview
[AD-A220104] 17 p2473 N90-24140
Method and apparatus for determining optical absorption and emission characteristics of a crystal or non-crystalline fiber
[NASA-CASE-LAR-13963-1] 17 p2475 N90-24150
Tests for integrating measurement of gas pressures in flight propellers
[ETN-90-96498] 18 p2494 N90-24253
Monitoring of catalyst performance in CO2 lasers using frequency modulation spectroscopy with diode lasers
18 p2561 N90-24614
Non destructive testing of composite structures using embedded optical fibers: A mechanical interaction model
[ETN-90-97016] 18 p2573 N90-24661
Intelligent composites containing measuring fibre optic networks for continuous self diagnosis
[ETN-90-97018] 19 p2673 N90-25200
Active lag angle device
[AD-D014538] 20 p2857 N90-26249
An embedded fibre optic sensor for impact damage detection in composite materials
[UTIAS-332] 20 p2926 N90-26650
Optical transmission through a polarization preserving single mode optical fiber at two Ar(+) laser wavelengths
[NASA-TM-103475] 20 p2926 N90-26651
Theory of biaxial graded-index optical fiber
[NASA-CR-186882] 20 p2927 N90-26652
A dual-wavelength passive homodyne detection unit for fiber-coupled white-light interferometers
[ETN-90-97036] 20 p2927 N90-26653
Optical fiber to waveguide coupling technique
[AD-A221781] 21 p3077 N90-27496
Solid state circuitry with optical data interfacing
[AD-D014548] 22 p3248 N90-28422
Noncontact measurement of high temperature using optical fiber sensors
[NASA-CR-186975] 23 p3329 N90-28825
Theory of biaxial graded-index optical fiber
[NASA-CR-186977] 23 p3395 N90-29180

OPTICAL FILTERS
NT INFRARED FILTERS

A remote sensor to monitor combustion products using a tunable acousto-optic filter 02 p0223 N90-11275
The Si(1-x)Nx Rugate
[AD-A211236] 02 p0275 N90-11572
A method to model fuze-performance. Part 3: Diffraction of electromagnetic radiation by an edge
[FEL-1989-22-PT-3] 03 p0340 N90-11940
Improvement of ultrashort pulsed laser shadowgraph photography by means of optical filters
[ISL-CO-215/88] 04 p0504 N90-12906
A review of laser filter materials
[AD-A213134] 05 p0648 N90-13776
Narrow band and wide angle hemispherical interference optical filter
[AD-D014238] 06 p0843 N90-14904

Design of a large angular aperture TeO2 acousto-optic tunable filter
[AD-A213999] 07 p0993 N90-15738
Fiber optic transversal filter/variable delay line
[AD-D014328] 10 p1430 N90-18248
Optical anti-aliasing filters
[AD-A215826] 10 p1430 N90-18251
Development of a receiver for a space-based laser radar system
[AD-A215079] 12 p1665 N90-19566
Visual processing in texture segregation
[AD-A216539] 12 p1696 N90-19737
Novel pulsed plasma treatment and coating process: Multilayer structures for optical computing applications
[AD-A220737] 18 p2615 N90-24894
National Aeronautics and Space Administration (NASA)/American Society for Engineering Education (ASEE) Summer Faculty Fellowship Program-1989, volume 2
[NASA-CR-185601-VOL-2] 18 p2630 N90-24985
Optical calculation of correlation filters for a robotic vision system 18 p2630 N90-24986
Velocity filtering applied to optical flow calculations
[NASA-TM-102802] 23 p3271 N90-28512

OPTICAL GENERATORS
U LASER CAVITIES

OPTICAL GYROSCOPES
Inertial grade fiber gyros 24 p3426 N90-29353

OPTICAL HETERODYNING
Design and performance of an on-satellite laser diagnostic system for a free space optical heterodyne frequency-shift-keyed communication system
[AD-A211986] 04 p0505 N90-12915
Distance measurement using laser diodes
[ETN-90-96144] 08 p1082 N90-16264
Optical interferometer in space 12 p1731 N90-19953
Heterodyne characterization of high-speed photomixers for the ultraviolet
[AD-A220914] 18 p2547 N90-24538
Optical signal processing
[AD-A220332] 18 p2615 N90-24897
A numerical simulation of the quasi-heterodyne technique for double-pulsed holographic vibration measurements
[PNR90622] 20 p2865 N90-26301
Absolute wind measurements in the lower thermosphere of Venus using infrared heterodyne spectroscopy 24 p3561 N90-30146

OPTICAL ILLUSION
Effects of short-term weightlessness on roll circularvection 23 p3361 N90-28992

OPTICAL IMAGES
U IMAGES

OPTICAL MASER MODULATION
U LIGHT MODULATION

OPTICAL MASERS
U LASERS

OPTICAL MATERIALS
Nonlinear optical material studies
[AD-A213938] 07 p0993 N90-15737
Phase equilibrium and crystal growth studies on AgGaSe2 and related nonlinear optical materials
[AD-A213650] 07 p1003 N90-15809
Analysis and evaluation of technical data on the photochromic and non-linear optical properties of materials
[AD-A219398] 16 p2318 N90-23219
Laser induced damage in optical materials: 1988
[PB90-185570] 22 p3179 N90-28041
Nonlinear optical studies of the optical and electronic properties of semiconductor heterostructures
[AD-A223408] 24 p3552 N90-30096

OPTICAL MEASUREMENT
NT ASTRONOMICAL PHOTOMETRY
NT COLORIMETRY
NT INFRARED PHOTOMETRY
NT OPTOMETRY
NT PHOTOMETRY
NT POLARIMETRY
NT SPECTROPHOTOMETRY
NT STELLAR SPECTROPHOTOMETRY
Demonstration of a dual-lidar method for measuring optical depths in the vertical
[AD-A210598] 01 p0124 N90-10711
Remote detection of boundary-layer transition by an optical system 04 p0441 N90-12524
Optical detection of space debris using a large achromatic coronagraph
[AD-A211362] 04 p0462 N90-12647
Optical properties monitor: Experiment definition phase
[NASA-CR-183836] 05 p0699 N90-14092
Reexamination of data from the asteroid/meteoroid detector
[NASA-CR-185997] 05 p0714 N90-14175
Process monitoring using optical ultrasonic wave detection
[DE90-002021] 06 p0838 N90-14870
Measurement of optical radiations in spacecraft environments
[AD-A213814] 07 p0950 N90-15497
HCl monitor, phase 2
[AD-A213572] 07 p0958 N90-15542
Advanced diagnostics for reacting flows
[AD-A214795] 09 p1285 N90-17448
Signal processing applied to photothermal techniques for materials characterization 10 p1364 N90-17902
Analysis and test of a wide angle spectrometer
[AD-A215819] 10 p1388 N90-18030
Optical measurement of precipitation
[AD-A214357] 10 p1407 N90-18116
Safety evaluation of infrared lamp power output for oculometer eye/head tracker system
[AD-A215809] 10 p1411 N90-18138
Techniques for measurement of the optical properties of materials
[DE90-006902] 11 p1566 N90-19014
Development and testing of a universally implementable recording aligning system
[SER-C-349] 12 p1691 N90-19716
Correlation of atmospheric optical turbulence and meteorological measurements
[AD-A218019] 13 p1842 N90-20576
An ellipsometric measurement of optical properties for InP surfaces
[AD-A217185] 13 p1887 N90-20827
The optical measurement of acoustic velocity fields 14 p2023 N90-21601
A video-based experimental investigation of wing rock 15 p2054 N90-21771
Evaluation and representation of two and three dimensional data fields from optical stream measurements
[MPIS-18/1989] 17 p2474 N90-24143
Feasibility study for the advanced one-dimensional high temperature optical strain measurement system, phase 3
[NASA-CR-185254] 19 p2693 N90-25324
Preliminary error budget for an optical ranging system: Range, range rate, and differenced range observables 20 p2853 N90-26227
Velocity selection to enable direct measurement of strong single atom-optical cavity coupling
[AD-A223060] 21 p3071 N90-27460
Infrared observations of the solar system in support of Large Aperture Infrared Telescope (LARITS): Calibration
[AD-A222222] 21 p3097 N90-27597
Optical and microwave detection using Bi-Sr-Ca-Cu-O thin films 22 p3152 N90-27870
Lidar cloud studies for FIRE and ECLIPS
[NASA-CR-186384] 22 p3211 N90-28214
Concept for a neutron spectrometer based on optical detection of (3)He(n, p)-3H reactions in a gas
[DE90-014776] 23 p3330 N90-28826
Real-time concentration monitoring of large aerodynamic diameter fiber aerosols using the geometric optic inversion technique
[AD-A224167] 24 p3545 N90-30048

OPTICAL MEASURING INSTRUMENTS
NT ELLIPSOMETERS
NT ETALONS
NT INFRARED SPECTROMETERS
NT LASER RANGE FINDERS
NT LIGHT SCATTERING METERS
NT MICRODENSITOMETERS
NT MICROWAVE REFLECTOMETERS
NT NEPHELOMETERS
NT OCULOMETERS
NT PHOTOMETERS
NT POLARIMETERS
NT REFLECTOMETERS
NT SPECTROPHOTOMETERS
NT THEODOLITES
NT TOTAL OZONE MAPPING SPECTROMETER
NT TRANSMISSOMETERS
NT ULTRAVIOLET SPECTROMETERS
Evaluation test of CCD area sensor for star sensor
[NAL-TM-570] 02 p0274 N90-11566
Catadioptric Optics for laser Doppler velocimeter applications
[NASA-TM-102210] 04 p0504 N90-12904
Mark-3 interferometer
[AD-A213155] 04 p0505 N90-12911
Application of a copper vapour laser to investigation of shock and blade interaction in a shock tube
[PNR90578] 04 p0506 N90-12918
Optical techniques for in-plane strain analysis in an industrial environment
[PNR90601] 04 p0512 N90-12957
Optical modulators based on polymers
[EP-PATENT-0-294-061-A1] 05 p0700 N90-14099
Spectral contents readout of birefringent sensor
[NASA-CR-179444] 06 p0843 N90-14905
Optical acoustic sensor using optical fiber
[DE89-901267] 07 p0992 N90-15730
Design and performance analysis of adaptive optical telescopes using laser guide stars
[AD-A218025] 13 p1902 N90-20913
Optical rate sensor algorithms 18 p2632 N90-24997
Acousto-optical localization of speed maneuvering flight targets
[FB-11-89] 19 p2758 N90-25676
The instrument HOSS (Hydro Optical Sensor System)
[FOA-C-30554-3.1] 22 p3248 N90-28411
Detectors and signal processing for the speed measuring system 4-01
[FEL-1989-64] 24 p3472 N90-29623

OPTICAL MEMORY (DATA STORAGE)
Optical shared memory
[AD-A215090] 10 p1430 N90-18249
Parallel memory addressing using coincident optical pulses
[AD-A216302] 11 p1501 N90-18641
Evaluation of optical storage technology for decision support databases 15 p2176 N90-22436
Technologies for electronic transfer of information: The present state and trends in Japan 15 p2177 N90-22443
Electronic transfer of information applications in the Societe Aerospatiale 15 p2179 N90-22454
Use of optical storage devices as shared resources in local area networks
[AD-A219198] 16 p2327 N90-23269
Two-dimensional signal processing and storage and theory and applications of electromagnetic measurements
[AD-A224239] 24 p3459 N90-29538

OPTICAL METHODS
U OPTICS

OPTICAL MICROSCOPES
Mesooptical Fourier transform microscope: A new device for high energy physics
[DE90-616423] 14 p2026 N90-21615
X ray optics
[AD-A221218] 18 p2616 N90-24898

OPTICAL MODULATION
U LIGHT MODULATION

OPTICAL PATHS
Subpicosecond optical digital computation using conjugate parametric generators
[AD-A207908] 01 p0058 N90-10330
Coupled multiline CW HF lasers: Experimental performance
[AD-A210844] 01 p0075 N90-10434
Study of high frequency water vapor absorption parameters
[AD-A210676] 02 p0194 N90-11108
Turbulence effects on reflected optical patterns (atmosphere and structure)
[PB89-208094] 03 p0404 N90-12315
Linear (passive) and non-linear guided and studies in glass
[AD-A211693] 03 p0406 N90-12325
Catadioptric Optics for laser Doppler velocimeter applications
[NASA-TM-102210] 04 p0504 N90-12904
Diffraction of light by ultrasonic pulses 15 p2164 N90-22366
Optical shutter switching matrix
[NASA-CASE-KSC-11392-1] 15 p2167 N90-22383
Data analysis of a two-lidar experiment
[AD-A220289] 17 p2428 N90-23834
Optical computing strategies
[AD-A219433] 17 p2472 N90-24131
Mode competition in the quasioptical gyrotron
[AD-A222181] 23 p3329 N90-28823

OPTICAL POLARIZATION
Optical phonon modes in a double heterostructure of polar crystals
[AD-A214208] 07 p1004 N90-15816
Properties and performance of the LiCaAlF6:Cr(3+) laser material
[DE90-007242] 11 p1516 N90-18728
An optical and infrared study of blazars 12 p1728 N90-19930
Polymer liquid crystals with side chain discogens
[AD-A218013] 13 p1782 N90-20228
Differential polarimetric fiber optic sensor
[AD-D014501] 19 p2757 N90-25668
Investigations of polarized light scattering from rough surfaces
[AD-A221943] 21 p3076 N90-27491
Adaptive polarization diversity detection scheme for coherent communications and interferometric fiber sensors
[AD-D014479] 22 p3163 N90-27938

OPTICAL PROPERTIES
NT ABSORPTIVITY
NT BIDIRECTIONAL REFLECTANCE
NT BIREFRINGENCE
NT BRIGHTNESS
NT BRIGHTNESS DISTRIBUTION
NT COLOR
NT DICHROISM
NT LUMINOSITY
NT OPACITY
NT OPTICAL BISTABILITY
NT OPTICAL REFLECTION
NT PHOSPHORESCENCE
NT PHOTOCONDUCTIVITY
NT RADIANCE
NT REFLECTANCE
NT REFRACTIVITY
NT SKY BRIGHTNESS
NT SPECTRAL REFLECTANCE
NT STELLAR LUMINOSITY
NT TRANSMISSIVITY
NT TRANSMITTANCE
NT TRANSPARENCE
NT WATER COLOR

Laser diode array and transmission optics
01 p0030 N90-10163
Stretched-membrane heliostats for solar central-receiver power plants
[DE89-016034] 01 p0084 N90-10476
Two photon absorption characterization
[AD-A210508] 01 p0121 N90-10694
Design of grazing incidence monochromators involving unconventional gratings
[DE89-016341] 01 p0123 N90-10704
Theoretical and experimental investigation of nonlinear optoacoustics in liquids
[AD-A210427] 01 p0124 N90-10708
Nonlinear optics and organic materials
[AD-A210570] 01 p0124 N90-10709
Study of high frequency water vapor absorption parameters
[AD-A210676] 02 p0194 N90-11108
Atmospheric aerosol size distributions and optical properties found in the marine boundary layer over the Atlantic Ocean
[AD-A210800] 02 p0252 N90-11431
Acoustic studies of new materials: Quasicrystals, low-loss glasses and high Tc superconductors
[AD-A211281] 02 p0272 N90-11551
Energy transfer and non-linear optical properties at near ultraviolet wavelengths: Rare earth 4f(yields)5d transitions in crystals and glasses
[DE90-000065] 03 p0405 N90-12321
Characterization of the Structure and Chemistry of Defects in Materials: Proceedings, volume 138
[DE89-014796] 03 p0410 N90-12352
Fundamental molecular data to support CARS diagnostics of temperature, pressure, and species concentration
[AD-A212411] 04 p0472 N90-12704
Small particle scattering and absorption
[AD-A213168] 04 p0473 N90-12711
Ultrastructure processing and characterization of polymers
[AD-A211460] 04 p0478 N90-12743
Laser initiated ignition of liquid propellant
[AD-A212342] 04 p0482 N90-12766
Cavity eigenmodes for the NIST/NRL (National Institute of Standards and Technology/Naval Research Laboratory) free electron laser
[AD-A212706] 04 p0507 N90-12923
Comments on the use of LOWTRAN in transmission calculations for sites with the ground elevated relative to sea level
[AD-A212724] 04 p0519 N90-12995
Direct computation of 3D shape invariants and the focus of expansion
[AD-A212386] 04 p0549 N90-13195
Study of the electrical and optical properties of the vanadium and nickel impurities in GaAs
[ISAL-89-0028] 04 p0559 N90-13259
Optical clock distribution to VLSI chips
[AD-A212269] 04 p0560 N90-13264
Growth and characterization of zinc sulfide films by conversion of zinc oxide films with H2S
[AD-A213345] 04 p0561 N90-13271
A figure control sensor for the Large Deployable Reflector (LDR) 05 p0594 N90-13451
Low temperature optical testing of CFRP telescope panels 05 p0596 N90-13463
Optical properties monitor: Experiment definition phase
[NASA-CR-183836] 05 p0699 N90-14092
Optical design and performance of an XUV FEL (Free-Electron Laser) oscillator
[DE90-002381] 06 p0790 N90-14599
Analysis and evaluation of technical data on the photochromic and non-linear optical properties of materials
[AD-A214212] 07 p0896 N90-15178
Laser-material interactions
[AD-A214421] 07 p0937 N90-15425
Thin films under chemical stress
[DE90-003754] 07 p0947 N90-15484
Research on high-efficiency, single-junction, monolithic, thin-film amorphous silicon solar cells, phase 2
[DE89-009496] 07 p0951 N90-15503
Nonlinear optical material studies
[AD-A213938] 07 p0993 N90-15737
Picosecond photoconductivity using a graded bandgap Al(x)Ga(1-x)As active detecting layer
[DE90-003452] 07 p1000 N90-15786
Research on materials and components for opto-electronic signal processing and computing
[AD-A213740] 07 p1003 N90-15811
Innovative optoelectronic materials and structures using OMVPE
[AD-A214192] 07 p1004 N90-15815
The middle Martian atmosphere
07 p1014 N90-15874
Design, characterization, and optical properties of phosphazene-based polymers
[DE90-004111] 08 p1050 N90-16068
Determination of optical porperties of clouds from NOAA-AVHRR data using Apollo
08 p1092 N90-16321
Eurolaser. High power excimer laser: Optical crystals
[ETN-90-95901] 08 p1132 N90-16558
Lithium cobalt oxide thin film and its electrochromism
[DE90-004570] 08 p1133 N90-16564
Electronic properties of GaAs-(Al,Ga)As quasiperiodic
[AD-A214704] 09 p1289 N90-17472
Research on high-efficiency, multi-gap, multi-junction amorphous silicon-based alloy thin-film solar cells
[DE89-009492] 10 p1402 N90-18101
Analysis and evaluation of technical data on the photochromic and non-linear optical properties of materials
[AD-A216124] 10 p1431 N90-18254
Integrated optics at Lawrence Livermore National Laboratory
[DE90-003015] 10 p1431 N90-18255
Nonlinear optical processes in one-dimensional polymers
[AD-A216103] 11 p1489 N90-18568
Evaluating a glass surface produced by ductile grinding
[DE90-006782] 11 p1496 N90-18608
Performance of a 500 watt Nd:GGG zigzag slab oscillator
[DE90-006263] 11 p1503 N90-18657
Techniques for measurement of the optical properties of materials
[DE90-006902] 11 p1566 N90-19014
A high optical density measuring spectrometer
[AD-D014331] 12 p1621 N90-19318
Analytical optical scattering in clouds
12 p1638 N90-19413
All-fiber SFPM (Stimulated Four Photon Mixing) amplifier
[AD-D014358] 12 p1713 N90-19841
The optical properties of beryllium
[DE90-006372] 12 p1715 N90-19848
Performance of zig-zag slab regenerative ring amplifier laser system
[DE90-006995] 13 p1806 N90-20371
Picosecond nonlinear studies of complex materials using the free electron laser
[AD-A218215] 13 p1809 N90-20387
Theoretical and experimental study of solid phase miscibility gaps in III/V quaternary alloys
[DE90-008430] 13 p1895 N90-20877
Laser controlled semiconductor armature for electromagnetic launchers
[AD-D014435] 14 p1931 N90-21055
Power transmission device
[AD-D014430] 14 p1969 N90-21281
Characterization and comparison of optically transparent conducting films
[DE90-000319] 14 p2033 N90-21660
Cirrus cloud optical properties measured with the University of Wisconsin high spectral resolution and volume imaging lidars 15 p2084 N90-21932
Extended optical emission in 3CR radio galaxies
15 p2193 N90-22523
A second-order nonlinear optical poly(organophosphazene)
[AD-A218408] 16 p2210 N90-22607
Single-crystal diffraction analysis of 2-(trimethylsilylethynyl) 4-nitro-N,N-dimethylaniline
[AD-A218955] 16 p2216 N90-22642
Solar Concentrator Advanced Development Program
[NASA-CR-185173] 16 p2250 N90-22834
High temperature superconducting thin films in Japan
16 p2311 N90-23169
Optical properties of novel GaAs-based semiconductors 16 p2321 N90-23235
Optical properties of cometary dust
[AD-A218790] 16 p2338 N90-23325
Negative electron affinity for infrared detection
[AD-A218816] 17 p2395 N90-23639
Nonlinear optical responses and laser damage thresholds of films of a polarized stilbene side chain liquid crystal polymer and a phthalocyanine
[AD-A219462] 17 p2408 N90-23720
A study of gravity wave variability, saturation, and turbulence generation in the mesosphere and lower thermosphere
[AD-A220018] 17 p2424 N90-23810
Data analysis of a two-lidar experiment
[AD-A220289] 17 p2428 N90-23834
Fellowship in physics/modern optics and quantum electronics
[AD-A218772] 17 p2469 N90-24111
Multiple beam optical processing
[AD-A219048] 17 p2471 N90-24129
Advanced guided wave electro-optical switches
[AD-A219784] 17 p2472 N90-24132
An assessment of the CD-FLIR as an ARGUS sensor
[AD-A220841] 17 p2473 N90-24137
Fast acting optical beam deflection system
[AD-A220186] 17 p2473 N90-24141
Optical phonons and electronic properties in double heterostructures
[AD-A219436] 17 p2475 N90-24153
Vibrational and optical properties of amorphous metals
[DE90-011427] 18 p2522 N90-24403
In-situ topographical imaging of electrode surfaces using high resolution phase-measurement interferometric microscopy
[AD-A221021] 18 p2548 N90-24542
Models of intracavity frequency doubled lasers
[AD-A221182] 18 p2563 N90-24628
Light-millimeter wave interactions in semiconductor devices
[AD-A221214] 18 p2623 N90-24943
A user-friendly, menu-driven, language-free laser characteristics curves graphing program for desk-top IBM PC compatible computers 18 p2644 N90-25056
Spectroscopy of laser properties of Nd(3+)-doped CaF2, SrF2, and BaF2
[DE90-012086] 19 p2695 N90-25337
Satellite material contaminant optical properties
19 p2732 N90-25529
Optical high-speed parallel backplane
[AD-D014504] 19 p2757 N90-25670
Optical properties and transport properties of hydrogenated amorphous silicon
[ETN-90-97215] 20 p2927 N90-26656
Ellipsometric study of YBa2Cu3O(7-x) laser ablated and co-evaporated films
[NASA-TM-103223] 20 p2932 N90-26682
An optical study of the flow start-up process in four convergent-divergent nozzles
[AD-A222918] 21 p2963 N90-26846
The thermal radiative properties of metals at high temperature
[DE90-012468] 21 p2981 N90-26938
Atmospherically induced optical contamination from orbiting thrusters
[AD-A223112] 21 p3021 N90-27174
Analysis of cirrus optical properties with data from NASA ER2 High-resolution Interferometer Sounder (HIS)
[NASA-CR-186365] 21 p3030 N90-27227
Linear and nonlinear optical properties of quantum dots
[AD-A223050] 21 p3076 N90-27489
Investigation on the MBE growth and properties of AlGaInAs/InP and InGaAs-InAlAs superlattices
[DE90-012248] 21 p3080 N90-27515
FIRE Science Results 1989
[NASA-CP-3079] 22 p3213 N90-28224
The radiation budget of stratocumulus clouds measured by tethered balloon instrumentation: Variability of flux measurements 22 p3216 N90-28242
Optical properties of marine stratocumulus clouds modified by ship track effluents
22 p3218 N90-28253
Serial interferometric fiber-optic sensor array
[AD-D014466] 22 p3246 N90-28407
Optoelectronics Research Center
[AD-A221926] 22 p3246 N90-28410
Experimental study of the optical constants of metals at high temperatures
[DE90-014732] 23 p3310 N90-28719

Semiconductor measurement technology: A software program for aiding the analysis of ellipsometric measurements, simple spectroscopic models
[PB90-216847] 23 p3398 N90-29201
Two terminal CuInSe2 based cascade cells
[DE90-000363] 24 p3485 N90-29697
Quantum well infrared detectors 1: Some calculations of their optical properties
[RSRE-MEMO-4363] 24 p3547 N90-30062

OPTICAL PUMPING
NT LASER PUMPING
A laser-driven source of polarized hydrogen and deuterium
[DE89-015130] 01 p0075 N90-10429
Precision materials characterization in the near millimeter and submillimeter wavelength range
[AD-A210655] 02 p0194 N90-11106
Photoelectron pumped phosphors
[AD-A213202] 04 p0505 N90-12912
Properties and performance of the LiCaAlF6:Cr(3+) laser material
[DE90-007242] 11 p1516 N90-18728
A simple model for amplified spontaneous emission in dyes
[DE90-007249] 11 p1516 N90-18730
Anode plasma formation as a possible mechanism for an electrical stress limit in cold cathode diodes
[DE90-007503] 12 p1655 N90-19516
Time resolved gain/loss studies under low and high power loading for the XeF C-A transition
[DE90-007506] 12 p1655 N90-19517
Blue upconversion thulium laser
[DE90-006517] 12 p1668 N90-19584
The electrical characteristic and gain behavior as a function of the radial distance from the laser axis in a copper vapor laser
[DE90-615371] 18 p2564 N90-24630
Spectroscopy of laser properties of Nd(3+)-doped CaF2, SrF2, and BaF2
[DE90-012086] 19 p2695 N90-25337
Depletion mode pumping of solid state lasers
[DE90-012090] 19 p2696 N90-25339
Gaseous optical contamination of the spacecraft environment: A review 19 p2730 N90-25519
A composition for the filling of gas-discharge tubes
[AD-A222818] 21 p2999 N90-27047
Study of short-lived unstable nuclei by means of laser optical pumping
[AD-A222561] 21 p3009 N90-27105
X ray laser program report for FY 1989
[AD-A221818] 21 p3009 N90-27107
New resonantly photo-pumped x ray laser scheme
[DE90-015044] 23 p3331 N90-28831
Model calculations for a 600 angstrom laser based on photopumping of Mo(sup 6+) by a spectral line of Mo(sup 11+)
[DE90-015202] 24 p3474 N90-29634
A distributed control and monitor system used in laser fusion research
[DE90-011483] 24 p3549 N90-30078

OPTICAL RADAR
A study of the impact of simulated satellite lidar wind observations
[AD-A210430] 01 p0086 N90-10488
Demonstration of a dual-lidar method for measuring optical depths in the vertical
[AD-A210598] 01 p0124 N90-10711
Laser altimeter for use over the ocean
[AD-A211252] 02 p0224 N90-11286
Laser techniques for ground to air applications
[FOA-C-30524-3.1] 02 p0228 N90-11309
Lidar observations of the stratospheric aerosol: Boulder, Colorado, 1985 to 1987
[PB89-203871] 02 p0251 N90-11425
Progress of research on water vapor lidar
[NASA-CR-185970] 03 p0352 N90-12011
MEGALIDAR
[AD-A212074] 03 p0353 N90-12020
Laser sounding from space: Report of the ESA Technology Working Group on Space Laser Sounding and Ranging
[ESA-SP-1108] 03 p0354 N90-12024
Measurements of aerosol properties needed to infer backscatter characteristics in support of the NASA Doppler Lidar program 03 p0364 N90-12082
Calibration of a visioceilometer, a hand held lidar system
[FEL-1988-73] 03 p0374 N90-12137
Atmospheric horizontal-inhomogeneity effects on the optical depths determined by the double-elevation-angle lidar technique
[AD-A212836] 04 p0493 N90-12839
Development of mid-infrared solid state lasers for spaceborne lidar
[NASA-CR-183290] 05 p0647 N90-13772
Near-mesopause temperatures at 69 N latitude in late summer 05 p0658 N90-13837
Diurnal variation of the sodium layer at polar latitudes in summer 05 p0662 N90-13869
Field evaluation of a Nissan laser collision avoidance system
[PB90-105602] 06 p0722 N90-14215
Remote sensing of the aerosol scattering coefficient with a multi-field-of view lidar 06 p0763 N90-14437
High resolution Doppler lidar
[NASA-CR-183288] 06 p0781 N90-14542
The lidar experiment at Andoya, Norway, during the Summer of 1988
[BONN-IR-89-16] 08 p1058 N90-16117
Backscattering effects in DIAL due to water vapor
[SER-WISS-ABHANDL-89] 08 p1082 N90-16265
Lidar technique for adjusting aerosol model number densities to existing conditions
[AD-A213846] 08 p1101 N90-16374
Ground-based deep-space LADAR for satellite detection: A parametric study
[AD-A215673] 09 p1228 N90-17126
Evaluation of a delay-Doppler imaging algorithm based on the Wigner-Ville distribution
[AD-A215827] 10 p1377 N90-17980
Effect of marine atmosphere on performance of electrooptical systems
[AD-A215947] 10 p1430 N90-18252
Doppler lidar working group report
[ESA-SP-1112] 11 p1537 N90-18848
Applications of FM-CW laser radar to antenna contour mapping 12 p1611 N90-19270
Remote Attitude Measurement Sensor (RAMS)
12 p1611 N90-19271
Development of a receiver for a space-based laser radar system
[AD-A215079] 12 p1665 N90-19566
Multi-dimensional LADAR tracking and adaptive grasping for spaceborne assembly of SDI (Strategic Defense Initiative) platforms
[AD-A218236] 13 p1791 N90-20279
The receiving system of a dual dye lidar to study molecular and aerosol densities at the base of the stratosphere
[AD-A218286] 13 p1843 N90-20581
Design and performance analysis of adaptive optical telescopes using laser guide stars
[AD-A218025] 13 p1902 N90-20913
Development of an ultra-bright laser and an application to multi-photon ionization 14 p1984 N90-21372
Atmospheric Propagation in the UV, Visible, IR, and mm-Wave Region and Related Systems Aspects
[AGARD-CP-454] 15 p2079 N90-21907
Lidar measurements of the optical propagation environment 15 p2084 N90-21930
Lidar measurement of concentration and turbulence in battlefield obscurants 15 p2084 N90-21931
Cirrus cloud optical properties measured with the University of Wisconsin high spectral resolution and volume imaging lidars 15 p2084 N90-21932
Verification of Klett's method by comparison of lidar and transmissometer measurements
15 p2084 N90-21933
Development of mid-infrared solid state lasers for spaceborne lidar
[NASA-CR-185095] 15 p2103 N90-22031
Dynamic and microphysical characteristics of cirrus clouds as revealed by aircraft, lidar, and other observations during FIRE 15 p2130 N90-22177
MEGALIDAR proof-of-concept demonstration
[AD-A218787] 16 p2255 N90-22858
Data analysis of a two-lidar experiment
[AD-A220289] 17 p2428 N90-23834
Determination of tide heights from airborne bathymetric data
[AD-A220412] 17 p2430 N90-23848
Kinetic and extraction measurements on 12C18O2
[AD-A220417] 17 p2472 N90-24133
Reports from the German Meteorological Service. No. 179: Development, realization and functioning of lidar to evaluate the atmospheric ozone profile
[ISBN-3-88148-252-0] 18 p2578 N90-24685
Atmospheric sounding with UV lidar
[FOA-C-30542-3.1] 18 p2579 N90-24692
Innovative techniques for high-resolution imaging and precision tracking
[AD-A221380] 18 p2616 N90-24899
Laser radar angular tracking
[AD-A222741] 20 p2869 N90-26319
Vertical ozone probing with lidar
20 p2885 N90-26416
The 27-28 October 1986 FIRE IFO cirrus case study: Cirrus parameter relationships derived from satellite and lidar data
[NASA-TM-103469] 20 p2890 N90-26447
Development of eye-safe lidar for aerosol measurements
[NASA-CR-186905] 20 p2901 N90-26503
Aureole lidar: Ground based measurement
[AD-A223207] 21 p3008 N90-27101
A solid-state multiple-pass amplifier for diode pumped coherent laser radar systems
[AD-A222537] 21 p3009 N90-27104
Lidar instruments proposed for Eos
21 p3016 N90-27145
Program to perform research on use of lidar for range resolved turbulence measurements
[AD-A222189] 21 p3026 N90-27204
Radio refractivity profiles deduced from lidar measurements
[AD-A221727] 21 p3026 N90-27208
Airborne CO2 Doppler lidar for wind shear detection
22 p3106 N90-27640
Lidar observations of stratospheric aerosols in 1988
[PB90-180670] 22 p3198 N90-28145
Lidar cloud studies for FIRE and ECLIPS
[NASA-CR-186384] 22 p3211 N90-28214
Front range lidar, aircraft, and balloon experiment
[PB90-225301] 22 p3212 N90-28218
Analysis of ER-2 radiometer and lidar observations from the 1987 marine stratus experiment
22 p3216 N90-28241
ETO lidar studies of cirrostratus altocumulogenitus: Another role for supercooled liquid water in cirrus cloud formation 22 p3221 N90-28269
Seasonal and interannual changes in cirrus
22 p3222 N90-28272
Interpretation of cirrus cloud properties using coincident satellite and lidar data during the FIRE cirrus IFO
22 p3223 N90-28276
Summary of results and conclusions based on analysis of volume imaging and high spectral resolution lidar data acquired during FIRE phase 1, part 1
22 p3223 N90-28278
Airborne lidar/radiometric measurements of cirrus cloud parameters and their application to LOWTRAN radiance evaluations 22 p3227 N90-28298
Summary of results and conclusions based on analysis of volume imaging and high spectral resolution lidar data acquired during FIRE phase 1, part 2
22 p3227 N90-28300
Cirrus parameterization from the FIRE ER-2 observations 22 p3227 N90-28302
The 1973-1974 lidar observations of cirrus clouds at Kwajalein 22 p3227 N90-28303
The use of an airborne lidar for mapping cirrus clouds in FIRE, phase 2 22 p3228 N90-28304
On the use of IR lidar and K(sub a)-band radar for observing cirrus clouds 22 p3228 N90-28305
Light source for dynamic testing of photo detectors
[FEL-1989-69] 22 p3247 N90-28414
Wind lidar for BEST
[CNES-NT-125] 23 p3353 N90-28947

OPTICAL RANGE FINDERS
NT LASER RANGE FINDERS

OPTICAL REFLECTION
Fiber optics: A brief introduction
[DE89-009337] 02 p0274 N90-11567
Forest mapping Nuerenberg German national forest with special emphasis on the spectral reflection behavior of pine trees 08 p1093 N90-16328
The ISO solar generator: Solar cells and OSR mixed
10 p1341 N90-17767
An ellipsometric measurement of optical properties for InP surfaces
[AD-A217185] 13 p1887 N90-20827
All-optical device and method for remapping images
[AD-D014540] 19 p2758 N90-25672

OPTICAL RELAY SYSTEMS
The relay lens systems 05 p0603 N90-13506

OPTICAL RESONATORS
Variational and asymptotic methods in open and closed waveguide analysis
[REPT-34] 04 p0554 N90-13229
Simulated Brillouin backscattering in optical fibers: A ring resonator 06 p0783 N90-14556
Narrow-bandwidth unstable laser resonator
[AD-D014362] 12 p1665 N90-19568
Sequentially evaporated thin film YBa2Cu3O(7-x) superconducting microwave ring resonator
[NASA-TM-103180] 19 p2685 N90-25273

OPTICAL SCANNERS
NT MULTISPECTRAL BAND SCANNERS
NT THEMATIC MAPPERS (LANDSAT)
Proceedings of the Conference on Application of Scanning Methodologies in Libraries
[PB89-233415] 06 p0858 N90-14990
Analysis and test of a wide angle spectrometer
[AD-A215819] 10 p1388 N90-18030
Optically tunable gratings for optical interconnects
[AD-A216978] 12 p1714 N90-19844

Induction-type metal detector with increased scanning area capability
[NASA-CASE-KSC-11386-1] 15 p2101 N90-22023
Multi-axis, 3-D, scanning LDA (Laser Doppler Anemometer) system for unsteady aerodynamics
[AD-A218571] 16 p2197 N90-22541
Research and facilities handbook 1989
[ISSN-0267-6281] 19 p2784 N90-25840
Near-angle scattering and binary optics
[AD-A224140] 23 p3396 N90-29186

OPTICAL SENSORS
U OPTICAL MEASURING INSTRUMENTS

OPTICAL SIGNALS
U OPTICAL COMMUNICATION

OPTICAL SPECTRUM
U LIGHT (VISIBLE RADIATION)
U SPECTRA

OPTICAL SWITCHING
Vanadium dioxide protective devices
[AD-A212018] 03 p0332 N90-11987
Laser glass (1989)
[DE90-002754] 07 p0909 N90-15257
Observation of nonlinear reflectivity from InSb surface and optical switching application
[AD-A217184] 13 p1887 N90-20826
Optical shutter switching matrix
[NASA-CASE-KSC-11392-1] 15 p2167 N90-22383

OPTICAL THICKNESS
Demonstration of a dual-lidar method for measuring optical depths in the vertical
[AD-A210598] 01 p0124 N90-10711
Analysis of catalytically enhanced solar absorption chemical reactors. 2: Predicted characteristics of a 100 kW chemical reactor
[DE89-014743] 07 p0954 N90-15521
Laser cooling of neutral atoms
[AD-A214440] 09 p1279 N90-17418
Structural instabilities, impurities, and defects in electronic materials
[AD-A215384] 09 p1290 N90-17481
Cirrus cloud optical properties measured with the University of Wisconsin high spectral resolution and volume imaging lidars 15 p2084 N90-21932

OPTICAL TRACKING
Ground-based deep-space LADAR for satellite detection: A parametric study
[AD-A215673] 09 p1228 N90-17126
An evaluation of an airborne laser profiling system for high precision terrain mapping
[AD-A217025] 11 p1525 N90-18780
Photon statistical limitations for daytime optical tracking 12 p1643 N90-19442
Multi-dimensional LADAR tracking and adaptive grasping for spaceborne assembly of SDI (Strategic Defense Initiative) platforms
[AD-A218236] 13 p1791 N90-20279
DURIP: Improved eye movement monitoring capabilities for studies in visual cognition
[AD-A220355] 18 p2586 N90-24722
Color image processing for navigation: Two road trackers
[AD-A222667] 20 p2916 N90-26591

OPTICAL TRANSITION
Initial optical transition radiation measurements of the electron beam for the Boeing free-electron laser experiment
[DE90-003396] 07 p0935 N90-15416
Optical emissions from bombarding atmospheric gases with heavy ions
[AD-A223544] 24 p3543 N90-30040
Establishment of a capability to measure optical transition radiation
[AD-A224094] 24 p3545 N90-30047

OPTICAL WAVEGUIDES
NT OPTICAL FIBERS
Novel physical effects in intersecting optical waveguides 02 p0274 N90-11565
Microwave signal detection using modulation of polymeric optical waveguides
[DE89-017545] 03 p0337 N90-11921
Optical guiding by plasma waves in the plasma beat wave accelerator
[AD-A214288] 07 p0997 N90-15763
Optical waveguide fabrication by stoichiometric implantation of Ti and O into LiNbO3
[DE90-004238] 09 p1292 N90-17488
CdTe buffered GaAs thin-slab IR waveguide modulators and T/R filter
[AD-A215999] 12 p1651 N90-19488
Modeling and realization of plane acousto-optic unilateral band modulators
[ETN-90-95824] 12 p1710 N90-19818
Thermal modulation of light beams
[AD-D014322] 12 p1713 N90-19840
Optically tunable gratings for optical interconnects
[AD-A216978] 12 p1714 N90-19844
Investigation of the technological effects on the coupling behavior of parallel GaAlAs rib waveguide
[ETN-90-95323] 13 p1887 N90-20825
Nonlinear optics in thin films
[AD-A217336] 13 p1887 N90-20829
Velocity matched optical transmitter
[AD-A217413] 13 p1887 N90-20830
Advanced guided wave electro-optical switches
[AD-A219784] 17 p2472 N90-24132

OPTICS
Optics of the Amsterdam pulse stretcher (AmPS)
06 p0841 N90-14893
Canonical formalism for coupled beam optics
[DE90-003764] 07 p0992 N90-15734
Gas optics applicable to free electron laser technology
[AD-A214285] 07 p0993 N90-15741

OPTIMAL CONTROL
NT LINEAR QUADRATIC GAUSSIAN CONTROL
NT LINEAR QUADRATIC REGULATOR
NT TIME OPTIMAL CONTROL
Active vibration mitigation of distributed parameter, smart-type structures using Pseudo-Feedback Optimal Control (PFOC) 01 p0024 N90-10121
Optimized resolved rate control of seven-degree-of-freedom Laboratory Telerobotic Manipulator (LTM) with application to three-dimensional graphics simulation
[NASA-TP-2938] 01 p0109 N90-10618
Stochastic control theory, nonlinear structural mechanics and applied combinatorics
[AD-A209042] 01 p0114 N90-10657
Performance analysis of hybrid ARQ protocols in a slotted code division multiple-access network
[AD-A211078] 02 p0213 N90-11219
A hybrid optimisation strategy for adaptive feed-forward layered networks
[RSRE-MEMO-4193] 03 p0391 N90-12226
Optimal observer motion for bearings-only localization and tracking 04 p0449 N90-12569
Integration of a centralized multiplexed control unit into the cockpit of an aircraft
[F6150-DT410-1-88329] 04 p0458 N90-12622
Aeroelastic control of composite lifting surfaces: Integrated aeroelastic control optimization
05 p0583 N90-13396
The dynamics and control of large flexible space structures - 12, supplement 11
[NASA-CR-185966] 05 p0602 N90-13494
Attitude and shape control of optimally designed large space structures 05 p0613 N90-13579
Simulation of the control characteristics of an axial piston pump and a flapper-nozzle valve combination
05 p0649 N90-13784
On the asymptotic convergence of the simulated annealing algorithm in the presence of a parameter dependent penalization
[MEMO-COSOR-89-16] 05 p0684 N90-13984
A priori results in linear quadratic optimal control theory
[MEMO-COSOR-89-02] 05 p0686 N90-13996
The quadratic matrix inequality in singular H infinity control with state feedback
[MEMO-COSOR-89-03] 05 p0686 N90-13997
The singular H infinity control problem with dynamic measurement feedback
[MEMO-COSOR-89-14] 05 p0687 N90-14000
The output-stabilizable subspace and linear optimal control
[MEMO-COSOR-89-15] 05 p0687 N90-14001
Optimal processes described by a parabolic differential equation with control in the coefficients, part 4
[MEMO-785-PT-4] 05 p0689 N90-14016
The regular indefinite linear quadratic problem with linear endpoint constraints
[MEMO-COSOR-88-15] 05 p0690 N90-14022
Continuity properties of one-parameter families of linear-quadratic problems without stability
[MEMO-COSOR-88-17] 05 p0690 N90-14024
Convergence properties of indefinite linear quadratic problems with receding horizon
[MEMO-COSOR-88-25] 05 p0690 N90-14026
On the output-stabilizable subspace
[MEMO-COSOR-88-27] 05 p0690 N90-14027
Optimal control of aero-assisted orbit transfer vehicles
06 p0727 N90-14241
Guidance and Control strategies for aerospace vehicles
[NASA-CR-186195] 06 p0727 N90-14243
Guidance analysis of the aeroglide plane change maneuver as a turning point problem
[NASA-TM-101639] 07 p0883 N90-15110
The application of optimal control theory for analysis of human jumping and pedaling
07 p0968 N90-15590
Optimal periodic control and regulator theory based on the second variation 07 p0987 N90-15704
The algebraic Riccati equation and singular optimal control
[MEMO-COSOR-89-11] 08 p1117 N90-16467
Stochastic adaptive control and estimation enhancement
[AD-A215486] 10 p1420 N90-18187
Optimization of sensors and actuators positioning aimed at obtaining reduced models for the synthesis of optimal control regulators of flexible structures
[INPE-4760-TDL/348] 11 p1468 N90-18450
An interactive system applied to the linear quadratic problem
[INPE-4945-TDL/386] 11 p1548 N90-18913
Output model-following control synthesis for an oblique-wing aircraft
[NASA-TM-100454] 12 p1606 N90-19241
Investigations into a new algorithm for calculating H infinity optimal controllers 12 p1637 N90-19406
Trajectory optimization in the presence of constraints
[AD-A218271] 13 p1760 N90-20104
Experimental and theoretical investigation of optimal control methods with model reduction
14 p1928 N90-21039
Suboptimal and hybrid numerical solution schemes for orbit transfer manoeuvres
[INPE-4991-PRE/1556] 14 p1931 N90-21054
Analysis and finite element approximation of some optimal control problems associated with the Navier-Stokes equations 14 p1972 N90-21299
Optimal control of an aircraft flying through a downburst 15 p2053 N90-21765
Optimal and near-optimal medium range air-to-air missile guidance against maneuvering targets
15 p2053 N90-21766
Advances in optimal active control techniques for aerospace systems; application to aircraft active landing gear 15 p2054 N90-21769
A decentralized linear quadratic control design method for flexible structures 15 p2054 N90-21770
The insertion of human dynamics models in the flight control loops of V/STOL research aircraft. Appendix 2: The optimal control model of a pilot in V/STOL aircraft control loops
[NASA-CR-186598] 15 p2055 N90-21776
Analysis, selection, and implementation of procedures which approve optimal artificial satellite maneuvers
[INPE-5003-TDL/397] 15 p2058 N90-21786
The Shock and Vibration Digest, volume 21, no. 1
15 p2109 N90-22061
Recent advances in structural control
15 p2109 N90-22062
A frame approach to the H-infinity super-optimal solution
[OUEL-1761/89] 15 p2158 N90-22327
The role of input weighting and bounding in the characteristic GPC method
[OUEL-1762/89] 15 p2158 N90-22328
Branch point placement
[OUEL-1767/89] 15 p2158 N90-22329
An intelligent interface for the design of optimal control systems
[INPE-4917-PRE/1516] 15 p2159 N90-22332
Control of human arm movement via optimization
15 p2159 N90-22334
Low order FIR and IIR filters in dynamic vision
[OUEL-1785/89] 15 p2167 N90-22384
Minimum flying qualities. Volume 3: Program CC's implementation of the human optimal control model
[AD-A218562] 16 p2201 N90-22562
Orbital maneuvers optimization for station acquisition of geostationary satellites. Deterministic and stochastic approaches
[LAAS-89-359] 16 p2206 N90-22589
Parallel and vector computation for stochastic optimal control applications 16 p2282 N90-23007
Optimum control forces for multibody systems with intermittent motion 16 p2284 N90-23016
Frequency response modeling and control of flexible structures: Computational methods
16 p2285 N90-23021
H(2)- and H(infinity)-design tools for linear time-invariant systems 16 p2286 N90-23025
A finite element based method for solution of optimal control problems 16 p2286 N90-23027
Substructural controller synthesis
16 p2292 N90-23055
A priori results in linear-quadratic optimal control theory (extended version)
[MEMO-COSOR-89-17] 16 p2304 N90-23124
Optimal helicopter trajectory planning for terrain following flight
[NASA-CR-186470] 17 p2349 N90-23376
Prediction of longitudinal pilot induced oscillations using the optimal control model
[AD-A220593] 17 p2356 N90-23412

Stochastic adaptive control and estimation enhancement
[AD-A219629] 17 p2454 N90-24001
Dynamic optimisation of thermal energy systems
[ETN-90-96900] 18 p2576 N90-24676
Progress in the polynomial solution of the standard H-infinity optimal control problem
[MEMO-817] 18 p2597 N90-24777
Solution of the optimal control problem using the software package STOMP
[MBB-FE-126/S/PUB-370] 19 p2651 N90-25087
Numerical approach of collision avoidance and optimal control on robotic manipulators
19 p2736 N90-25552
Nonlinear systems, the Lie series, and the left shift operator: Application to nonlinear optimal control
[RR-376] 19 p2748 N90-25619
Model following control system design: Preliminary ATTAS in-flight simulation test results
[PD-FC-9003] 20 p2813 N90-26010
Design of robust multivariable controllers
[AD-A222096] 21 p3060 N90-27397
Optimization of the deployment of a pair of satellites in inclined eccentric geosynchronous orbits
22 p3128 N90-27751
Stochastic dynamic programming for reservoir optimal control: Dense discretization and inflow correlation assumption made possible by parallel computing
[REPT-89-056] 22 p3238 N90-28360
Effective optimal control of a fighter aircraft engine
23 p3277 N90-28548
The dynamics and control of large flexible space structures - 13
[NASA-CR-186930] 23 p3286 N90-28591
Control and estimation for aerospace applications with system time delays 24 p3428 N90-29367
Optimal trajectories for hypervelocity flight
24 p3430 N90-29378
Proceedings of damping '89. Volume 1: Pages AAB-1 through DCD-11
[AD-A223431] 24 p3479 N90-29664
Time optimal movement of cooperating robots
24 p3505 N90-29815
Recursive multibody dynamics and discrete-time optimal control 24 p3513 N90-29860

OPTIMIZATION
NT DYNAMIC PROGRAMMING
NT FLIGHT OPTIMIZATION
NT LINEAR PROGRAMMING
NT LINEAR QUADRATIC GAUSSIAN CONTROL
NT LINEAR QUADRATIC REGULATOR
NT MATHEMATICAL PROGRAMMING
NT NONLINEAR PROGRAMMING
NT OPERATIONS RESEARCH
NT OPTIMAL CONTROL
NT QUADRATIC PROGRAMMING
NT SIMPLEX METHOD
NT TIME OPTIMAL CONTROL
NT TRAJECTORY OPTIMIZATION

CONSOLE: A CAD tandem for optimization-based design interacting with user-supplied simulators
01 p0017 N90-10085
Numerically efficient algorithm for model development of high-order systems 01 p0022 N90-10108
Control law synthesis and optimization software for large order aeroservoelastic systems
01 p0022 N90-10111
Optimal q-Markov COVER for finite precision implementation 01 p0023 N90-10117
Approximate simulation model for analysis and optimization in engineering system design
[NASA-TM-101616] 01 p0054 N90-10308
An expert system for optimal gear design
01 p0077 N90-10439
General decomposition of sequential machines: Relationships to state assignment
[AD-A208189] 01 p0102 N90-10580
Effective resource utilization for multiprocessor join execution
[DE89-016303] 01 p0105 N90-10595
Finite methods for a nonlinear allocation problem
[AD-A209719] 01 p0111 N90-10629
Numerical optimization in Hilbert space using inexact function and gradient evaluations
[NASA-CR-181926] 01 p0112 N90-10640
Monolayer formation characteristics of novel organic molecules with nonlinear optically active moieties
[AD-A210496] 01 p0121 N90-10693
A compact X-ray lithography lattice using superferric magnets
[DE89-013947] 01 p0127 N90-10728
Optimal and on-board near-optimal midcourse guidance 02 p0150 N90-10857
Integrated multidisciplinary design optimization of rotorcraft
[NASA-TM-101642] 02 p0155 N90-10889
Study for optimization of redundant vane-type flow-direction sensing systems and numerical analysis for design of the systems
[NAL-TM-571] 02 p0155 N90-10890
A review of the Error of Matrix Method (EMM) for structural dynamic model comparison
02 p0177 N90-10993
JOE: Jordan Optimized Eigensolver. A step toward a numerical Jordan form analyzer for control and interactive thermo-structural-dynamic applications
02 p0184 N90-11047
New data handling system (MDH) for mechanical tests at ESTEC 02 p0187 N90-11066
Thin section casting program. Volume 3: Vertical TSC (Thin-Section Casting) approach
[DE89-009033] 02 p0210 N90-11201
Calculation, optimization and comparison of optical transmission systems with superheterodyne reception
[ETN-89-94651] 02 p0214 N90-11224
Stochastic optimization by simulation: Some experiments with a simple steady-state queue
[AD-A210762] 02 p0265 N90-11508
Control and optimization for observations of systems governed by controlled partial differential equations
[AD-A211122] 02 p0266 N90-11513
Reduction of the Dirac equation to the Dirac-Kaehler equation
[DE89-630111] 02 p0270 N90-11541
A design procedure for the handling qualities optimization of the X-29A aircraft
[NASA-TM-4142] 03 p0308 N90-11753
Controller design for active vibration suppression of a helicopter
[DFVLR-FB-89-20] 03 p0310 N90-11760
An integrated methodology for optimizing structural composite damping
[NASA-TM-102343] 03 p0319 N90-11808
Nearly optimal algorithms and bounds for multilayer channel routing
[AD-A211913] 03 p0343 N90-11955
Airframe structural dynamic considerations in rotor design optimization
[NASA-TM-101646] 03 p0360 N90-12057
Statistical models for the optimal estimation of oceanic fields
[AD-A211786] 03 p0377 N90-12149
A hybrid optimisation strategy for adaptive feed-forward layered networks
[RSRE-MEMO-4193] 03 p0391 N90-12226
Numerical experience with a class of algorithms for nonlinear optimization using inexact function and gradient information
[NASA-CR-181927] 03 p0392 N90-12232
Optimal matching of 3-D convex polyhedra
[TELECOM-PARIS-89C003] 03 p0395 N90-12258
On the asymptotic optimality of certain empirical Bayes simultaneous testing procedures
[AD-A211649] 03 p0397 N90-12270
Integrated multidisciplinary optimization of rotorcraft: A plan for development
[NASA-TM-101617] 04 p0450 N90-12580
General approach and scope --- rotor blade design optimization 04 p0451 N90-12581
Validation of the procedures --- integrated multidisciplinary optimization of rotorcraft
04 p0451 N90-12587
Appendix: Results obtained to date --- integrated multidisciplinary optimization of rotorcraft
04 p0451 N90-12588
The computer age and traditional approximate, analytical methods 04 p0483 N90-12772
Reduction of turbulent drag: Boundary layer manipulators
[CERT-RSF-OA-74/2259-AYD]
04 p0501 N90-12889
An implicit Navier-Stokes solver optimised for a vector-parallel computer
[VKI-TN-169] 04 p0501 N90-12890
Multilevel optimization with system Optsys
[FFA-TN-1988-60] 04 p0512 N90-12953
Optimum data weighting and error calibration for estimation of gravitational parameters
[NASA-TM-100737] 04 p0517 N90-12985
On the identification of local minimizers in inertia-controlling methods for quadratic programming
[AD-A212514] 04 p0534 N90-13086
Sequential quadratic programming algorithms for optimization
[AD-A212800] 04 p0534 N90-13088
Algorithm development for SDI weapons system allocation
[AD-A212973] 04 p0534 N90-13090
On a rate of convergence of the multiknapsack value function
[CWI-MS-R8812] 04 p0542 N90-13144
On the smooth fit boundary conditions in the optimal stopping problem for semimartingales
[CWI-MS-R8819] 04 p0542 N90-13147
A modified Newton method for unconstrained minimization
[AD-A212752] 04 p0546 N90-13174
Effect of the length of the multijunction grill on its lower hybrid current drive efficiency
[IPPCZ-283] 04 p0556 N90-13240
On optimization of the multijunction grill for the lower hybrid current drive
[IPPCZ-280] 04 p0556 N90-13241
Aeroelastic control of composite lifting surfaces: Integrated aeroelastic control optimization
05 p0583 N90-13396
Discretization and model reduction for a class of nonlinear systems 05 p0583 N90-13397
Feature modeling: The incorporation of a front and eddy map into optimum interpolation-based thermal analysis
[AD-A213253] 05 p0672 N90-13914
Implementing the discrete Fourier transform on the hypercube FPS T40
[IMAG-RR-773-I] 05 p0684 N90-13983
Model reduction of weakly damped mechanical systems
[MEMO-798] 05 p0686 N90-13993
Identification of impulsive interference channels
[AD-A213154] 05 p0688 N90-14009
Global optimization and simulated annealing
[MEMO-COSOR-88-21] 05 p0690 N90-14025
Convergence properties of indefinite linear quadratic problems with receding horizon
[MEMO-COSOR-88-25] 05 p0690 N90-14026
Fundamental quantum 1/f noise in ultrasmall semiconductor devices and their optimal design principles
[AD-A211947] 05 p0702 N90-14107
Introduction to data items on flight path optimisation
[ESDU-89015] 06 p0723 N90-14221
New heating and cooling technology: Regenerative heat pump according to the Vuilleumier principle
[DE90-002701] 06 p0807 N90-14699
Parallel projected variable metric algorithms for unconstrained optimization
[NASA-CR-181930] 06 p0833 N90-14842
Application of heuristic satellite plan synthesis algorithms to requirements of the WARC-88 allotment plan
[NASA-TM-102479] 06 p0835 N90-14856
Centralized and decentralized Kalman filter techniques for tracking, navigation, and control
[AD-A214245] 07 p0878 N90-15091
Guidance analysis of the aeroglide plane change maneuver as a turning point problem
[NASA-TM-101639] 07 p0883 N90-15110
Investigation of broadband microstrip antenna structures for application in monolithic millimeter wave arrays
[AD-A213856] 07 p0923 N90-15344
Gas turbine regenerators: A method for selecting the optimum plate-finned surface pair for minimum core volume
[AD-A213430] 07 p0930 N90-15382
Comprehensive, nonintercepting electron-beam diagnostics using spontaneous emission
[DE90-003211] 07 p0935 N90-15414
NOISE: A nonlinear optimization induction free-electron laser systems engineering code
[DE90-004438] 07 p0936 N90-15420
On the analysis and optimization of a platform manipulator 07 p0938 N90-15433
New approach to the inverse problem of six-link manipulators via the optimization technique
[DE90-710044] 07 p0940 N90-15441
Base reaction optimization of redundant manipulators for space applications
[NASA-CR-186274] 07 p0941 N90-15447
Planning minimum-energy paths in an off-road environment with anisotropic traversal costs and motion constraints
[AD-A214181] 07 p0942 N90-15457
Oxygen and other atmospheric gases
[AD-A214296] 07 p0961 N90-15557
On the identification of local minimizers in inertia-controlling methods for quadratic programming
[DE89-017330] 07 p0973 N90-15616
Sequential quadratic programming algorithms for optimization
[DE90-000022] 07 p0973 N90-15617
Gradient projection techniques for large-scale optimization problems
[DE90-001986] 07 p0973 N90-15618
Optimizing and evaluating algorithms for replicated data concurrency control
[DE90-003080] 07 p0973 N90-15619

Tensor methods for unconstrained optimization using second derivatives
[AD-A213642] 07 p0983 N90-15681

Numerical optimization
[AD-A213758] 07 p0984 N90-15683

Optimization of stochastic systems via simulation
[AD-A214011] 07 p0985 N90-15689

Synthesis of control law, on a RPV, in order to minimize the number of sensors 08 p1025 N90-15925

Built in test of folded PLAs
[IMAG-RR-758-I] 08 p1061 N90-16134

Plume shape optimization of small attitude control thrusters with respect to impingement and thrust
[ISL-CO-220/88] 08 p1064 N90-16153

Mechanoelectric conversion by uniaxial constraint in piezoelectric generators: Optimization of electrical, mechanical, and physico-chemical parameters of materials
[ISAL-89-0020] 08 p1078 N90-16235

Optimization of monotonic inference algorithms in propositional and first order logic
[LAAS-89204] 08 p1111 N90-16436

Optimal step sizes in semi-stochastic approximation procedures
[ETN-90-95888] 08 p1117 N90-16469

Enhanced performance IR focal plane arrays using adaptive subtraction
[RSRE-MEMO-4286] 08 p1123 N90-16502

Near-term directions in the world stellarator program
[DE90-004381] 08 p1124 N90-16511

MHD stable high beta spheromak equilibrium
[DE90-004873] 08 p1127 N90-16529

New optimization techniques in database access and maintenance 08 p1137 N90-16586

Event-join optimization in temporal relational databases
[DE90-003117] 08 p1137 N90-16588

Optimum ascent performance of winged two-stage vehicles 09 p1177 N90-16816

The Hermes system: Its design objectives and solutions 09 p1177 N90-16821

The 1989 National Convention Record IEE Japan, part 8
[DE89-910081] 09 p1210 N90-17013

Integrated analytical evaluation and optimization of model parameters against preprocessed measurement data
[AD-A215518] 09 p1247 N90-17231

A note on Smale's global Newton method
[AD-A215139] 09 p1267 N90-17346

Large-scale optimization via distributed systems
[AD-A215136] 09 p1270 N90-17364

Image smoothing and differentiation with minimal-curvature filters
[AD-A215184] 09 p1273 N90-17382

Fabrication of ultra thin GaAs and Ge substrates for high efficiency solar cells 10 p1339 N90-17753

Reduction of 50 micron thick solar cell weight by selective back contact silver plating 10 p1342 N90-17778

Report on the multicolor pyrometry session at the Second NASA Non-Contact Temperature-Measurement Workshop 10 p1367 N90-17926

Pareto optimization design techniques for the AFIT (Air Force Institute of Technology)/AAMRL (Armstrong Aeronautical Medical Research Laboratory) anthropomorphic robotic manipulator
[AD-A216178] 10 p1414 N90-18150

Dynamic factorization in large-scale optimization
[AD-A214568] 10 p1416 N90-18161

An exact algorithm for the p-median problem
[INPE-4914-PRE/1415] 10 p1418 N90-18172

Optimization of Gaussian beam widths in acoustic propagation
[AD-A215893] 10 p1427 N90-18231

Development of free-piston Stirling engine performance and optimization codes based on Martini simulation technique
[NASA-CR-182210] 10 p1443 N90-18326

Particle detection via rotons in helium-4 superfluid
[DE90-005417] 10 p1448 N90-18354

Practical applications of Loran-C for land mobile use or the possibility to use Loran-C as a vehicle-location or vehicle-navigation system
[ETN-90-96265] 11 p1455 N90-18384

Optimization of sensors and actuators positioning aimed at obtaining reduced models for the synthesis of optimal control regulators of flexible structures
[INPE-4760-TDL/348] 11 p1468 N90-18450

Interlaminar fracture testing of carbon fibre/PEEK composites validity and applications 11 p1477 N90-18497

Optimum catalytic process for alcohol fuels from syngas
[DE90-007188] 11 p1495 N90-18604

On the range resolution of point targets with FMCW radar systems
[DLR-FB-89-47] 11 p1499 N90-18629

Optimal planning method of underground distribution system, part 2. Application to various types of system configurations
[DE89-782323] 11 p1500 N90-18636

Resonator modes in high gain free electron lasers
[DE90-006098] 11 p1514 N90-18720

Study of discharge mechanisms and the stability of transverse electric discharges in the gas mixtures
[ISL-R-114/88] 11 p1516 N90-18733

Optimization of the reference parameters in the accompanying solar panel dynamics
[INPE-4795-PRE/1449] 11 p1528 N90-18798

Optimum and heuristic algorithms for finite state machine decomposition and partitioning
[AD-A216778] 11 p1546 N90-18899

Optimum selection procedures in multi-stage screening, reliability, and time
[AD-A216811] 11 p1553 N90-18942

On the depth of combinatorial optimization problems
[MEMO-803] 11 p1554 N90-18946

Near-field bistatic RCS (Radar Cross-Section) measurements
[AD-A217011] 12 p1646 N90-19458

Development of dynamic equivalent network structures with a universal identification and optimization process
[ETN-90-95822] 12 p1654 N90-19507

CO2 laser plus optimization for harmonic generation
[AD-D014341] 12 p1665 N90-19565

Digital treatment of elastic-plastic structures by means of quadratic optimization processes from the finite element method
[ETN-90-95823] 12 p1675 N90-19621

Selection of optimal textural features for maximum likelihood image classification
[DE90-006901] 12 p1678 N90-19638

Study of the optimization of reference parameters to the dynamic constraints of solar panels
[INPE-4793-TDL/355] 12 p1681 N90-19656

An optimized algorithm for solving the nodal diffusion method on shared memory multiprocessors
[DE90-002703] 12 p1700 N90-19762

Adaptive, asynchronous stochastic global optimization algorithms for sequential and parallel computation
[AD-A217093] 12 p1702 N90-19775

Minimum cycle covering and integer flows
[AD-A216546] 12 p1705 N90-19785

Optimal layout via Boolean satisfiability
[AD-A216777] 12 p1705 N90-19787

Optimal iteration steps by stochastic approximation processes for the solution of optimization problems with twice differentiable functions
[ETN-90-95887] 12 p1708 N90-19809

Nonlinear continuum mechanics and applied analysis
[AD-A213629] 12 p1709 N90-19812

Design and performance of a multi-stage cylindrical reconnection launcher
[DE90-007820] 13 p1761 N90-20108

Composite laminate tailoring with probabilistic constraints and loads
[NASA-TM-102515] 13 p1766 N90-20138

Optimization of fracture resistance in composites
[AD-A217431] 13 p1768 N90-20144

Optimization of laminated composite plates
[AD-A217621] 13 p1768 N90-20146

On optimal distributed decision architectures in a hypothesis testing environment
[AD-A217824] 13 p1790 N90-20274

Optimization of digital filters for a short-scan interferometer
[AD-A217997] 13 p1798 N90-20315

Common-mode rejector for pulse power diagnostics
[AD-A218096] 13 p1798 N90-20316

Multi-mission Ni-H2 battery cells for the 1990's 13 p1825 N90-20477

Phase 1 supplemental development of a kinematic Stirling/Rankine commercial gas-fired heat pump system
[PB90-129974] 13 p1825 N90-20483

A unified approach to the synthesis of fully testable sequential machines
[AD-A217120] 13 p1863 N90-20687

(DURIP) Two-Processor Alliant FX/4 System
[AD-A217810] 13 p1864 N90-20692

Design decision making with multiple interacting criteria and varying relative weights
[AD-A218027] 13 p1869 N90-20721

Irredundant sequential machines via optimal logic synthesis
[AD-A217119] 13 p1873 N90-20742

Exact algorithms for output encoding, state assignment and four-level Boolean minimization
[AD-A217121] 13 p1876 N90-20756

Chemical beam epitaxy of ZnSe
[AD-A217375] 13 p1893 N90-20866

Study of possible solar heating effects on thermosonde probes: Error analysis
[AD-A218116] 13 p1903 N90-20917

Optimization of the effective GPS data rate 14 p1907 N90-20932

Computer-aided structural optimisation of aircraft structures
[BR112837] 14 p1915 N90-20973

Computational Methods for Aerodynamic Design (Inverse) and Optimization
[AGARD-CP-463] 14 p1916 N90-20976

Progress in inverse design and optimization in aerodynamics 14 p1916 N90-20977

Aerodynamic optimization by simultaneously updating flow variables and design parameters 14 p1918 N90-20991

Constrained spanload optimization for minimum drag of multi-lifting-surface configurations 14 p1919 N90-20992

Numerical optimization of target pressure distributions for subsonic and transonic airfoil design 14 p1919 N90-20993

A tool for automatic design of airfoils in different operating conditions 14 p1919 N90-20994

The use of numerical optimization for helicopter airfoil and blade design 14 p1919 N90-20995

Aerodynamic design by optimization 14 p1920 N90-20996

Numerical optimization of wings in transonic flow 14 p1920 N90-20997

Aerodynamic design via control theory 14 p1920 N90-20998

Optimization of aerodynamic designs using computational fluid dynamics 14 p1920 N90-20999

A homotopy approach to the solutions of minimum-fuel space-flight rendezvous problems 14 p1931 N90-21053

Optimization of the structural and control system for LSS with reduced-order model 14 p1935 N90-21075

Computational architecture for integrated controls and structures design 14 p1935 N90-21076

Recent experience in simultaneous control-structure optimization 14 p1936 N90-21078

Global nonlinear optimization of spacecraft protective structures design
[NASA-TM-100387] 14 p1938 N90-21095

Multi-objective shape and material optimization of composite structures including damping
[NASA-TM-102579] 14 p1945 N90-21132

Optimal fabrication processes for unidirectional metal-matrix composites: A computational simulation
[NASA-TM-102559] 14 p1947 N90-21143

Modeling the temperature dependence of the thermal conductivity of aluminum nitride
[DE90-009428] 14 p1949 N90-21154

Application of optimization in design and motion control of robot manipulators 14 p1988 N90-21393

Design and demonstration of an improved stretched-membrane heliostat
[DE90-007904] 14 p2001 N90-21470

Nonoptimal entropy generation by heat transfer in cryogenic domain
[DE90-007544] 14 p2034 N90-21667

Design and optimisation of thin foil x ray telescopes 14 p2038 N90-21690

Recent improvements in the scope and accuracy of the performance prediction of nozzle propellers
[LR-598] 15 p2048 N90-21742

Optimization and guidance of flight trajectories in the presence of windshear
[NASA-CR-186163] 15 p2049 N90-21747

A comparison of time-optimal interception trajectories for the F-8 and F-15
[NASA-CR-186300] 15 p2050 N90-21753

Conceptual design optimization study
[NASA-CR-4298] 15 p2051 N90-21755

Optimal control of an aircraft flying through a downburst 15 p2053 N90-21765

Optimal and near-optimal medium range air-to-air missile guidance against maneuvering targets 15 p2053 N90-21766

Optimal trajectories for the aeroassisted flight experiment. Part 4: Data, tables, and graphs
[NASA-CR-186164] 15 p2056 N90-21780

Electromagnetic inverse profiling of stratified media
[ETN-90-96402] 15 p2087 N90-21947

Generation, optimization, and adaptation of multidomain meshes around complex configurations 15 p2095 N90-21990

Optimum design of structures under shock and vibration environment 15 p2110 N90-22067

Optimization of power output from wind turbines 15 p2124 N90-22146

Global distribution of organo-bromine gases 15 p2124 N90-22150

Parallel non-linear optimization
[REPT-89-45] 15 p2151 N90-22290
A knowledge-based approach to improving optimization techniques in system planning 15 p2154 N90-22303
Control of human arm movement via optimization 15 p2159 N90-22334
On the existence of a positive definite solution of the matrix equation X + A(sup tau)X(exp -1)A = I
[PB90-133976] 15 p2159 N90-22335
Discrete variable structural optimization by the complex method
[LR-597] 15 p2161 N90-22341
Knowledge-based semantic query processing: An optimal transformation approach 15 p2176 N90-22437
Object-oriented databases: How are they different and what differnece does it make
[REPT-89-55] 15 p2180 N90-22459
Multilevel decomposition approach to the preliminary sizing of a transport aircraft wing
[NASA-CR-4296] 16 p2200 N90-22557
Differential equation based method for accurate approximations in optimization
[NASA-TM-102639] 16 p2200 N90-22558
Limiting performance based structural and control optimization for large vibrating structures 16 p2202 N90-22568
A comparison of CuAlNi and other high damping alloys for the purpose of naval ship silencing applications
[AD-A218801] 16 p2221 N90-22671
Nondestructive Testing (NDT); Ceramic Matrix Composite Materials (CMCM) --- Nondestructive testing (ndc); ceramic matrix composite materials (CMMC)
[REPT-892-430-123] 16 p2222 N90-22677
H2, fixed architecture, control design for large scale systems
[NASA-CR-180471] 16 p2226 N90-22698
High temperature ceramic-tubed reformer
[DE90-009617] 16 p2236 N90-22755
A free electron laser master oscillator power amplifier experiment 16 p2239 N90-22776
The use of supercomputers for the design and analysis of constructions 16 p2277 N90-22977
A survey on the structured singular value 16 p2281 N90-22998
Algorithms for computing the multivariable stability margin 16 p2281 N90-22999
Combined control-structure optimization 16 p2282 N90-23005
H(2)- and H(infinity)-design tools for linear time-invariant systems 16 p2286 N90-23025
Application of numerical optimization techniques to control system design for nonlinear dynamic models of aircraft 16 p2287 N90-23032
Implementation of generalized optimality criteria in a multidisciplinary environment 16 p2290 N90-23048
Reusing software components by specialization
[REPT-89-062] 16 p2298 N90-23094
Periodic ARMA models: Optimal prediction and minimum-phase condition
[REPT-89-006] 16 p2305 N90-23131
Towards a calculus of data refinement
[CS-8902] 16 p2326 N90-23264
Destabilization of supersonic free shear layers by parametric excitation using Mach waves generated by a wavy wall
[AD-A219655] 17 p2345 N90-23352
Overcoming the Bellman's curse of dimensionality in large optimization problems
[NASA-TM-102662] 17 p2352 N90-23391
Prospects for integration of satellite communications, navigation and monitoring functions 17 p2360 N90-23439
Geometric programming prediction of design trends for OMV protective structures
[NASA-TM-4206] 17 p2365 N90-23462
Implementation of image action plus software for image analysis of solid propellant combustion holograms
[AD-A219644] 17 p2372 N90-23508
Simulation and interdisciplinary design methodology for control-structure interaction systems 17 p2385 N90-23584
CMOS IC I(sub DDQ) testing for the 1990s
[DE90-009508] 17 p2394 N90-23634
On computing the pressure by the p version of the finite element method for Stokes problem
[AD-A219887] 17 p2404 N90-23697
Precision laser cutting
[DE90-009949] 17 p2407 N90-23717
The effects of climate change on energy planning and operations in the Pacific Northwest. Volume 1: Overview
[DE90-009464] 17 p2425 N90-23816
Neuromorphic optical signal processing and image understanding for automated target recognition
[AD-A219827] 17 p2437 N90-23884
An O(square root of n) complexity reduction for the long-step path-following algorithm for linear programming
[REPT-89-85] 17 p2445 N90-23940
Scheduling around a small common due date
[CWI-BS-R8914] 17 p2446 N90-23943
Bit-optimal election in synchronous rings
[RUU-CS-89-2] 17 p2446 N90-23945
Numerical optimization, system theoretic and software tools for the integrated design of flexible structures and their control systems
[AD-A219877] 17 p2447 N90-23949
Optimization of series expressions. Part 2: Over view of the theory and implementation
[AD-A219961] 17 p2447 N90-23952
Formal methods in knowledge representation
[TR-89-11] 17 p2450 N90-23972
A general approach to dominance in the plane
[RUU-CS-88-35] 17 p2463 N90-24072
The existence of sensitive optimal policies in two multi-dimensional queueing models
[TW-89-11] 17 p2464 N90-24080
Note on the optimality of the generalized shortest queue policy
[TW-90-01] 17 p2464 N90-24081
Universal criteria for blind deconvolution
[AD-A220853] 17 p2465 N90-24087
Probabilistic analysis of the minimum weighted flowtime scheduling problem
[CWI-BS-R8913] 17 p2466 N90-24091
ADELE: Deployment hinge using wraparound strips 18 p2538 N90-24485
New liquid cathode electrolytes in high rate cells
[AD-A219822] 18 p2546 N90-24531
Multichip packaging technology with laser-patterned interconnects
[DE90-010743] 18 p2549 N90-24552
Dynamic optimisation of thermal energy systems
[ETN-90-96900] 18 p2576 N90-24676
Summary results of an assessment of research projects in the national photovoltaics program
[DE90-008222] 18 p2577 N90-24680
Translating polygons with applications to hidden surface removal
[RUU-CS-89-31] 18 p2602 N90-24816
An improved technique for output-sensitive hidden surface removal
[RUU-CS-89-32] 18 p2602 N90-24817
A RUTCOR project in discrete applied mathematics
[AD-A221191] 18 p2604 N90-24831
Improved processing of ceramic superconductors
[DE90-009721] 18 p2624 N90-24951
On rectilinear link distance
[RUU-CS-89-13] 18 p2634 N90-25008
Minimizing sums of addition chains
[RUU-CS-89-15] 18 p2635 N90-25013
Large scale structure and microwave background anisotropies in cosmological models and stellar photometry techniques with the wide field/planetary camera of the Hubble space telescope 18 p2637 N90-25023
Kharitonov's theorem: Generalizations and algorithms 18 p2646 N90-25064
Expansion and orthogonalization of measured modes for structure identification 18 p2647 N90-25068
Development and application of an optimization procedure for space and aircraft structures
[MBB-FW-522/S/PUB-383] 19 p2650 N90-25078
An accurate numerical technique for determining flight test rate gyroscope biases prior to takeoff
[AD-A220987] 19 p2660 N90-25138
A design optimization process for Space Station Freedom
[NASA-CR-186851] 19 p2667 N90-25175
Outlook for ceramics in heat engines, 1990 - 2010: A technical and economic assessment based on a worldwide Delphi survey
[DE90-011262] 19 p2679 N90-25234
A decision-making aid for multi-layer radar absorbent coverings
[ESA-TT-1173] 19 p2684 N90-25267
The photovoltaic concentrator initiative
[DE90-011228] 19 p2710 N90-25425
The effects of different diffusion sources on silicon solar cell recombination properties
[DE90-011235] 19 p2710 N90-25426
Crystalline photovoltaic cell research, status, and future direction
[DE90-011478] 19 p2710 N90-25427
Automated control of hierarchical systems using value-driven methods 19 p2735 N90-25547
Numerical approach of collision avoidance and optimal control on robotic manipulators 19 p2736 N90-25552
Execution time supports for adaptive scientific algorithms on distributed memory machines
[NASA-CR-182052] 19 p2741 N90-25578
Analytic study of the high-frequency impedance
[CEBAF-PR-89-014] 19 p2757 N90-25665
A contribution to the economic, optimal dimensioning, and shaping of aircraft structures using a design model
[ETN-90-96966] 20 p2808 N90-25976
Plate rods and leaf springs with hybrid structure: Cross section optimization following different target criteria
[ILR-MITT-227(1989)] 20 ,p2877 N90-26366
A search routine for optimization in a wind power system with variable speed
[FOA-C-20779-2.1] 20 p2882 N90-26395
Modeling and optimization of a regenerative fuel cell system using the ASPEN process simulator
[NASA-TM-103210] 20 p2882 N90-26396
Microspacecraft and Earth observation: Electrical field (ELF) measurement project
[NASA-CR-186821] 20 p2888 N90-26436
Study of a class of non convex optimization algorithms: Implementation and applications
[ETN-90-97241] 20 p2909 N90-26552
Adaptive and comparative studies of optimization algorithms: Implementations and applications
[ETN-90-97243] 20 p2910 N90-26553
A sum rule satisfied by optimized feed-forward layered networks
[RSRE-MEMO-4341] 20 p2914 N90-26579
On networks, optimized feature extraction, and the Bayes decision
[RSRE-MEMO-4342] 20 p2914 N90-26580
Development of a method to design helicopter rotors
[REPT-100-30-03] 21 p2960 N90-26830
Communications and tracking expert systems study
[NASA-CR-185935] 21 p2992 N90-27004
Toward the optimization of a non-diffusing, two-dimensional S-shaped duct
[IAR-89-3] 21 p3003 N90-27068
Computer assisted analysis and modelling of structured problems
[AD-A222991] 21 p3052 N90-27350
EINMUF: An HF MUF, FOT, LUF prediction program
[AD-A221577] 21 p3055 N90-27371
Numerical solutions to steady-state problems with discontinuities
[AD-A222205] 21 p3064 N90-27418
Computation of efficient solutions of discretely distributed stochastic optimization problems
[ETN-90-97330] 21 p3067 N90-27436
Newton methods for large-scale linear equality-constrained minimization
[AD-A222310] 21 p3070 N90-27457
Integrated structural/control design via multiobjective optimization
[AD-A223088] 21 p3071 N90-27459
Air traffic management in Europe: Structure, tasks, potential 22 p3112 N90-27677
Four-dimensional navigation and Flight Management Systems 22 p3112 N90-27681
An introduction to space trajectories 22 p3127 N90-27749
Design optimization of short focal length photovoltaic modules
[PB90-182221] 22 p3195 N90-28133
Genetic algorithms: The state of the art and some research proposals
[REPT-89-058] 22 p3241 N90-28380
An environment to support problem solving
[ISBN-90-9003151-0] 22 p3259 N90-28458
Aerodynamic interferences of in-flight thrust reversers in ground effect 23 p3274 N90-28529
System reliability optimization of aircraft wings 23 p3275 N90-28536
Bearing optimization for SSME HPOTP application 23 p3292 N90-28622
Summary of booster propulsion/vehicle impact study results 23 p3294 N90-28635
Design optimization of gas generator hybrid propulsion boosters
[NASA-CR-181096] 23 p3299 N90-28660
High temperature oxidation of Al-Li alloys 23 p3307 N90-28705
Minimum weight design of a leaf spring tapered in thickness and width for the Hubble Space Telescope-space support equipment
[NASA-TM-4233] 23 p3340 N90-28879
A neural network for controlling the configuration of frame structure with elastic members 23 p3368 N90-29034
Efficient mapping algorithms for scheduling robot inverse dynamics computation on a multiprocessor system 23 p3375 N90-29071
Least-index resolution of degeneracy in linear complementarity problems with sufficient matrices
[DE90-014406] 23 p3390 N90-29145

An enhanced integrated aerodynamic load/dynamic optimization procedure for helicopter rotor blades
[NASA-CR-4326] 24 p3432 N90-29383
Aircraft design for mission performance using nonlinear multiobjective optimization methods
[NASA-CR-4328] 24 p3432 N90-29384
Multi-disciplinary optimization of aeroservoelastic systems
[NASA-CR-185931] 24 p3432 N90-29385
Optimization of tetrahedrical meshes for finite element calculation methods in fluids mechanics
[ETN-90-97560] 24 p3469 N90-29603
The investigation and production of titanium-tantalum junctions diffusion bonded at high temperature (855 C to 920 C): The influence of temperature, time pressure and roughness on the mechanical properties, and the optimisation of the bonded conditions
[BR114894] 24 p3476 N90-29648
Proceedings of damping '89. Volume 2: Pages FAA-1 through IBD-15
[AD-A223432] 24 p3479 N90-29665
Parallel and sparse methods for large-scale numerical optimization
[DE90-015655] 24 p3530 N90-29959
Analytic least squares
[NPL-DES-86] 24 p3531 N90-29971
Unique binary search tree representations and equality-testing of sets and sequences
[AD-A223643] 24 p3537 N90-30002
A new look at conjugate direction methods of optimization
[MATHS-REPT-A-125] 24 p3539 N90-30010

OPTIMUM CONTROL
U OPTIMAL CONTROL

OPTOELECTRONIC DEVICES
NT PHOTODIODES
NT PHOTOTRANSISTORS
Laser dynamics: The system dynamics and network theory of optoelectronic integrated circuit design
02 p0226 N90-11296
Semiconductor quantum well lasers and related optoelectronic devices on silicon, III-V
[AD-A210758] 02 p0227 N90-11299
High speed quantum-well optoelectronic devices by MBE
[AD-A212585] 04 p0555 N90-13237
Optical modulators based on polymers
[EP-PATENT-0-294-061-A1] 05 p0700 N90-14099
Characterization of B and N implanted fused silica
[DE90-004198] 08 p1050 N90-16069
First test results with a CCD camera developed by INPE
[INPE-4873-PRE/1484] 10 p1388 N90-18029
Activities report in DLR research field communication engineering and reconnaissance
[ISSN-0173-0118] 11 p1525 N90-18781
The III-V semiconductor quantum well lasers and related optoelectronic devices on silicon
[AD-A216980] 12 p1666 N90-19570
A fiber-optic current sensor for aerospace applications
[NASA-TM-103152] 16 p2239 N90-22773
Characterization by means of electrochemical impedance measurement and optoelectrochemical analysis of electrolytic, insulating, and semiconducting solution structures. Development of a cartographic analysis method for optoelectrochemical impedance
[ECL-89-15] 17 p2474 N90-24144
The III-V semiconductor quantum well lasers and related optoelectronic devices on silicon
[AD-A224120] 23 p3331 N90-28835

OPTOELECTRONIC SWITCHING
U OPTICAL SWITCHING

OPTOGALVANIC SPECTROSCOPY
Optogalvanic laser spectroscopic and interference spectroscopic experiments of isotope gap and hyperfine structure for spectrum of Europium 1 and Erbium 2
[ETN-90-95358] 12 p1623 N90-19327
Characterization by means of electrochemical impedance measurement and optoelectrochemical analysis of electrolytic, insulating, and semiconducting solution structures. Development of a cartographic analysis method for optoelectrochemical impedance
[ECL-89-15] 17 p2474 N90-24144
Examinations of hyperfine structure and isotope displacement of the elements gadolinium and europium with laser fluorescence and two photon spectroscopy
[ETN-90-97312] 24 p3447 N90-29488

OPTOMETRY
A Scheiner-principle pocket optometer for self-evaluation and biofeedback accommodation training
[AD-A213171] 04 p0524 N90-13027
A scheiner-principle vernier optometer
[AD-D014304] 07 p0934 N90-15405
Design principles of the LVT-2 model laser instrument for the measurement of visual characteristics
[AD-A214951] 09 p1228 N90-17124

OR-GATES
U GATES (CIRCUITS)

ORBIT CALCULATION
The recovery of orbital and geophysical parameters using a spaceborne laser ranging system
02 p0226 N90-11294
Sentinel satellite positional precision derived from the NAVSTAR global positioning system
[AD-A211876] 03 p0303 N90-11720
Evaluation of 15th- and 30th-order geopotential harmonic coefficients from 26 resonant satellite orbits
[RAE-TR-88045] 04 p0461 N90-12640
Orbit determination and analysis for Cosmos 236 at 15th-order resonance
[RAE-TR-88058] 04 p0461 N90-12641
An analytic development of orbit determination for a distant, planetary orbiter 04 p0485 N90-12787
The GEM-T2 gravitational model
[NASA-TM-100746] 04 p0517 N90-12984
Spacecraft Orbit Design and Analysis (SODA), version 1.0 user's guide
[NASA-CR-181932] 04 p0529 N90-13050
Orbit and attitude determination results during launch support operations for SBS-5
[PAPER-7] 05 p0587 N90-13420
GOES I/M image navigation and registration
05 p0588 N90-13422
Automation of orbit determination functions for National Aeronautics and Space Administration (NASA)-supported satellite missions 05 p0590 N90-13434
The controllability of the aeroassist flight experiment atmospheric skip trajectory 05 p0591 N90-13438
Precision of semi-geometrically determined SLR baselines vs. site occupation time
[ETN-90-96007] 05 p0665 N90-13885
Correction of ionospheric effects for the precise orbit determination of satellites 06 p0762 N90-14432
Error modeling of bias-type parameters for TOPEX orbit determination 07 p0884 N90-15117
An autonomous orbit determination system for earth satellites
[AD-A215671] 09 p1172 N90-16779
Advanced tracking systems design and analysis
[NASA-CR-183459] 10 p1376 N90-17976
An investigation of long term orbits about the planet Mars using a dynamic atmosphere model
[AD-A216111] 10 p1447 N90-18351
Orbit determination of artificial Earth satellites through estmation techniques combined with state smoothing techniques
[INPE-4959-TDL/388] 11 p1465 N90-18440
Autonomous orbit determination using GPS
[INPE-4815-TDL/361] 11 p1466 N90-18442
Using the method of matched asymptotic expansions, analytically investigate the three-dimensional, atmosphere entry problem
[AD-A216267] 11 p1468 N90-18451
Small Mercury Relativity Orbiter
12 p1733 N90-19965
Ambiguity bootstrapping to determine GPS orbits and baselines
[AD-A218206] 14 p1931 N90-21052
Using connected-element interferometer phase-delay data for Magellan navigation in Venus orbit
15 p2075 N90-21885
UD filtering and smoothing applied to orbit determination
[INPE-4966-PRE/1535] 15 p2189 N90-22501
Orbit recovery of a low Earth orbiter from GPS and ground tracking stations
[FFI-89/7012] 17 p2361 N90-23446
Theoretical principles of the FHP-GA trajectory calculation program
[FB-10-89] 19 p2663 N90-25156
Satellite orbit determination and gravity field recovery from satellite-to-satellite tracking
[LR-605] 19 p2663 N90-25157
Proceedings of the Second Symposium on GPS Applications in Space, volume 2
[AD-A219979] 20 p2806 N90-25963
A reduced-dynamic technique for precise orbit determination 20 p2852 N90-26219
Applications of different design methodologies in navigation systems and development at JPL
20 p2852 N90-26221
Galileo: Earth avoidance study report
[NASA-CR-186424] 22 p3123 N90-27730
Orbit computation 22 p3128 N90-27750
Satellite motion in an axi-symmetric gravitational field. Part 1: Perturbations due to J2 (second order) and J3
[RAE-TR-88068] 24 p3440 N90-29429
Thermal imaging assessment
[AD-A224400] 24 p3460 N90-29542

ORBIT DECAY
Impact of tether cutting on onboard navigation during the Tethered Satellite Mission-1
05 p0588 N90-13424

ORBIT EQUATIONS
U ORBITAL MECHANICS

ORBIT MANEUVERING ENGINE (SPACE SHUTTLE)
Independent Orbiter Assessment (IOA): Assessment of the orbital maneuvering system FMEA/CIL, volume 1
[NASA-CR-185544-VOL-1] 03 p0315 N90-11787
Independent Orbiter Assessment (IOA): Assessment of the orbital maneuvering subsystem, volume 2
[NASA-CR-185544-VOL-2] 03 p0315 N90-11788

ORBIT PERTURBATION
NT SATELLITE PERTURBATION
Some results on connecting orbits for a class of Hamiltonian systems
[AD-A213536] 07 p0983 N90-15679
On mean elements for satellite orbits perturbed by the zonal harmonics of the geopotential
[RAE-TM-SPACE-371] 08 p1033 N90-15971
An investigation of long term orbits about the planet Mars using a dynamic atmosphere model
[AD-A216111] 10 p1447 N90-18351
Semianalytic study of high-eccentricity orbit stability and evolution 16 p2204 N90-22574
Reference frames: Orbitography
17 p2359 N90-23427
GPS navigational performance in space rendezvous operations 18 p2504 N90-24310

ORBIT SPECTRUM UTILIZATION
Application of heuristic satellite plan synthesis algorithms to requirements of the WARC-88 allotment plan
[NASA-TM-102479] 06 p0835 N90-14856

ORBIT TRANSFER VEHICLES
Laser propulsion option 01 p0030 N90-10161
Laser thruster 01 p0030 N90-10164
Microwave beam power 01 p0030 N90-10165
Optimal trajectories for the Aeroassisted Flight Experiment. Part 1: Equations of motion in an Earth-fixed system
[NASA-CR-186134] 05 p0592 N90-13441
Optimal trajectories for the Aeroassisted Flight Experiment. Part 2: Equations of motion in an inertial system
[NASA-CR-186135] 05 p0592 N90-13442
Optimal trajectories for the aeroassisted flight experiment, 1988-89
[NASA-CR-186132] 05 p0592 N90-13443
Optimal control of aero-assisted orbit transfer vehicles
06 p0727 N90-14241
Guidance and Control strategies for aerospace vehicles
[NASA-CR-186195] 06 p0727 N90-14243
Optimal trajectories for the aeroassisted flight experiment
[NASA-CR-186133] 06 p0729 N90-14250
Singular perturbation analysis of AOTV-related trajectory optimization problems
[NASA-CR-186202] 08 p1027 N90-15936
A Mars/Phobos transportation system
[NASA-CR-186217] 09 p1230 N90-17135
Heating rates in a High Energy Propulsion System (HEPS) Orbital Transfer Vehicle (OTV)
[AD-A214354] 10 p1360 N90-17888
Flight and driving optimization of air breathing aerodynamic space vehicle
[ETN-90-95379] 12 p1607 N90-19246
Project LOCOST: Laser or Chemical Hybrid Orbital Space Transport
[NASA-CR-186822] 20 p2819 N90-26042
Project SPARC: Space-based aeroassisted reusable craft
[NASA-CR-186816] 20 p2821 N90-26051

ORBITAL ASSEMBLY
Space Station Freedom: A foothold on the future
[NASA-NP-107/10-88] 02 p0159 N90-10907
Assembly considerations for large reflectors
05 p0599 N90-13480
Onorbit electron beam welding experiment definition
[NASA-CR-183847] 07 p0938 N90-15431
Mechanized fluid connector and assembly tool system
[NASA-CASE-MSC-21434-1] 09 p1230 N90-17138
Multi-dimensional LADAR tracking and adaptive grasping for spaceborne assembly of SDI (Strategic Defense Initiative) platforms
[AD-A218236] 13 p1791 N90-20279
Definition of large components assembled on-orbit and robot compatible mechanical joints
[NASA-TM-100395] 15 p2105 N90-22043
Development of cable drive systems for an automated assembly project 15 p2116 N90-22105
On-orbit operations of the Space Station Freedom attached payloads accommodations equipment
18 p2500 N90-24283

Operations considerations in Space Station Freedom assembly 18 p2500 N90-24284
Mechanisms to assemble space structures in extravehicular environment 18 p2538 N90-24480
Control strategy for cooperating disparate manipulators
[NASA-CR-186809] 20 p2870 N90-26328
Space Station attached payloads 21 p3015 N90-27141
The challenge of assembling a space station in orbit 22 p3130 N90-27763
In-space construction and dynamics of large space structures 22 p3130 N90-27764
Utilization of space station, part 3
[NAL-TM-597-PT-3] 24 p3439 N90-29422
Interset: A natural language interface for teleoperated robotic assembly of the EASE space structure 24 p3517 N90-29885
A comparison of the Shuttle remote manipulator system and the Space Station Freedom mobile servicing center 24 p3522 N90-29910

ORBITAL ELEMENTS
On universal elements, and conversion procedures to and from position and velocity
[RAE-TM-SPACE-370] 09 p1277 N90-17406
Evaluation of influences of errors involved in orbit propagation of artificial satellites
[INPE-4962-TDL/391] 11 p1466 N90-18441
Semianalytic study of high-eccentricity orbit stability and evolution 16 p2204 N90-22574

ORBITAL FLIGHT TESTS (SHUTTLE)
U SPACE TRANSPORTATION SYSTEM FLIGHTS

ORBITAL LAUNCHING
Assembly vs. direct launch of transfer vehicles
[NASA-TM-102686] 19 p2797 N90-25921

ORBITAL MANEUVERING VEHICLES
Independent Orbiter Assessment (IOA): Analysis of the orbital maneuvering system
[NASA-CR-185554] 02 p0162 N90-10919
A Mars/Phobos transportation system
[NASA-CR-186217] 09 p1230 N90-17135
Evaluation and analysis of the orbital maneuvering vehicle video system 12 p1638 N90-19411
OMV mission simulator 13 p1860 N90-20669
The Orbital Maneuvering Vehicle Training Facility visual system concept 13 p1863 N90-20684
Autonomous integrated GPS/INS navigation experiment for OMV. Phase 1: Feasibility study
[NASA-CR-4267] 14 p1914 N90-20969
Optimal trajectories for the aeroassisted flight experiment. Part 3: Formulation, results, and analysis
[NASA-CR-186165] 14 p1930 N90-21051
Orbital Maneuvering Vehicle (OMV) three-point docking latch 15 p2114 N90-22094
Computer vision research at Marshall Space Flight Center 15 p2142 N90-22240
Geometric programming prediction of design trends for OMV protective structures
[NASA-TM-4206] 17 p2365 N90-23462
OMV (Orbital Maneuvering Vehicle) payload support concept for Pegasus boosted payloads
[AD-A218371] 17 p2365 N90-23463
A proposed change to the NASA strategy for servicing space assets 18 p2500 N90-24282
SDIO robotics in space applications 19 p2729 N90-25514
Remote operation of an orbital maneuvering vehicle in simulated docking maneuvers 19 p2736 N90-25554
Space transportation: NASA has no firm need for increasingly costly orbital maneuvering vehicle
[GAO/NSIAD-90-192] 20 p2819 N90-26041
Literature concerning control and display technology applicable to the Orbital Maneuvering Vehicle (OMV)
[NASA-CR-186790] 20 p2820 N90-26048
Biconic cargo return vehicle with an advanced recovery system. Volume 1: Conceptual design
[NASA-CR-186520] 20 p2821 N90-26052

ORBITAL MANEUVERS
Orbit and attitude determination results during launch support operations for SBS-5
[PAPER-7] 05 p0587 N90-13420
GOES-I/M ascent maneuvers from transfer orbit to station 05 p0587 N90-13421
The attitude and orbit control system 05 p0605 N90-13516
Launch and early orbit 05 p0606 N90-13524
Guidance analysis of the aeroglide plane change maneuver as a turning point problem
[NASA-TM-101639] 07 p0883 N90-15110
Overview of the Hermes in-orbit control system 09 p1178 N90-16824
Performance of large area xenon ion thrusters for orbit transfer missions 11 p1472 N90-18475
Orbital Maneuvering Vehicle (OMV) three-point docking latch 15 p2114 N90-22094
Orbit acquisition and control strategy for small satellites in inclined eccentric orbits
[ETN-90-96551] 16 p2203 N90-22573
Approximate optimal guidance schemes for atmospheric orbital maneuvering 16 p2206 N90-22585
Orbital maneuvers optimization for station acquisition of geostationary satellites. Deterministic and stochastic approaches
[LAAS-89-359] 16 p2206 N90-22589
A computer graphics system for visualizing spacecraft in orbit 16 p2272 N90-22952
Knowledge based system for Hermes orbital operations ground support
[REPT-892-440-102] 17 p2361 N90-23443
Orbit control for a regional navigation system based on tundra orbit
[AIAA-89-3619] 17 p2365 N90-23466
Robotic space simulation integration of vision algorithms into an orbital operations simulation
[NASA-CR-185934] 21 p3059 N90-27395
Noncoplanar orbit transfer optimization for an aeroassisted sortie vehicle 22 p3128 N90-27752
The dynamics of orbital maneuvering: Design and evaluation of a visual display aid for human controllers 22 p3131 N90-27767

ORBITAL MECHANICS
NT KEPLER LAWS
Adaptive structures to meet future requirements for large precision structures 02 p0178 N90-11001
An improved algorithm for the determination of the system paramters of a visual binary by least squares 02 p0290 N90-11658
An analytic development of orbit determination for a distant, planetary orbiter 04 p0485 N90-12787
Spacecraft Orbit Design and Analysis (SODA), version 1.0 user's guide
[NASA-CR-181932] 04 p0529 N90-13050
Flight Mechanics/Estimation Theory Symposium, 1989
[NASA-CP-3050] 05 p0586 N90-13413
GOES-I/M ascent maneuvers from transfer orbit to station 05 p0587 N90-13421
Shuttle relative navigation of a tethered satellite mission with current on board software 05 p0588 N90-13423
Calculation of double-lunar swingby trajectories: I. Keplerian foundation 05 p0590 N90-13435
Atmospheric drag model calibrations for spacecraft lifetime prediction 05 p0591 N90-13439
Satellite motion around an oblate planet: A perturbation solution for all orbital parameters
[AD-A216176] 10 p1326 N90-17661
Data collection and location platforms experimental network: Description of an orbit routine
[INPE-4798-NTE/287] 11 p1465 N90-18439
Using the method of matched asymptotic expansions, analytically investigate the three-dimensional, atmosphere entry problem
[AD-A216287] 11 p1468 N90-18451
Accuracy of global positioning system broadcast orbits for relative surveys
[PB90-125428] 12 p1602 N90-19218
Geographically correlated orbit error 13 p1838 N90-20551
Distributed earth model/orbiter simulation 13 p1860 N90-20671
Orbital mechanics: A learning tool on the main frame
[AD-A218799] 16 p2204 N90-22576
Low cost station keeping maneuvers for a small-satellites constellation in tundra orbits
[ETN-90-96553] 16 p2206 N90-22588
Dynamics and control of tethered antennas/reflectors in orbit
[AD-A219316] 16 p2207 N90-22594
Interactive orbital proximity operations planning system 16 p2273 N90-22953
Reference frames: Orbitography 17 p2359 N90-23427
Signal processing: Kalman filtering 17 p2359 N90-23428
Thermal and orbital analysis of Earth monitoring Sun-synchronous space experiments
[NASA-TM-101630] 19 p2666 N90-25168
The aerobraking space transfer vehicle
[NASA-CR-186819] 20 p2821 N90-26053
A reduced-dynamic technique for precise orbit determination 20 p2852 N90-26219
Lunar lander conceptual design
[NASA-CR-186233] 21 p2965 N90-26856
Orbit computation 22 p3128 N90-27750

ORBITAL MOTION
U ORBITS

ORBITAL POSITION ESTIMATION
General principles of radionavigation: Space mapping 17 p2358 N90-23423
The DORIS system 17 p2359 N90-23431
Satellite orbitography 17 p2359 N90-23432

ORBITAL RENDEZVOUS
Optimal, impulsive, time-fixed orbital rendezvous and interception with path constraints 13 p1760 N90-20102
The resupply interface mechanism RMS compatibility test 15 p2113 N90-22090
Hermes rendezvous and navigation system 18 p2504 N90-24308
Hermes rendezvous with the space station 22 p3128 N90-27753

ORBITAL RESONANCES (CELESTIAL MECHANICS)
Superhumps in accretion disks 19 p2768 N90-25728

ORBITAL SERVICING
Orbital servicing: Issue or answer
[AD-A217284] 12 p1616 N90-19295
The partnership: Space shuttle, space science, and space station
[NASA-TM-102900] 14 p1930 N90-21050
Definition of large components assembled on-orbit and robot compatible mechanical joints
[NASA-TM-100395] 15 p2105 N90-22043
The resupply interface mechanism RMS compatibility test 15 p2113 N90-22090
Orbital Maneuvering Vehicle (OMV) three-point docking latch 15 p2114 N90-22094
Second European In-Orbit Operations Technology Symposium
[ESA-SP-297] 18 p2499 N90-24280
A proposed change to the NASA strategy for servicing space assets 18 p2500 N90-24282
On-orbit operations of the Space Station Freedom attached payloads accommodations equipment 18 p2500 N90-24283
Servicing test facility: A hardware simulator for telerobotic in-orbit servicing 18 p2501 N90-24287
Advanced robotics for the on-orbit servicing 18 p2501 N90-24289
The SPIDER robotic system 18 p2501 N90-24291
Flight support system servicing aid tool 18 p2501 N90-24293
Hierarchy of on-orbit servicing interfaces 18 p2502 N90-24294
The European EVA suit: An optimized tool for Hermes/MTFF in-orbit operations 18 p2502 N90-24296
Perspective features of internal automation and robotics for supporting Columbus attached laboratory payload operations 18 p2502 N90-24297
HERA and EVA co-operation scenarios 18 p2502 N90-24299
Robot-based equipment manipulation and transportation for the Columbus free flying laboratory 18 p2503 N90-24300
Telerobotic architecture for an on-orbit servicer 18 p2503 N90-24302
A flexible teleoperation test bed for human factors experimentation 18 p2503 N90-24304
The bi-arm servicer: A multimission concept and a technological model for space robotics 18 p2504 N90-24307
Groundbased simulations of in-orbit operations 18 p2505 N90-24314
Simulation and ground-based testing of ORU-handling with a bi-arm robot 18 p2505 N90-24317
ROSED: Robotic Servicing Demonstrator 18 p2505 N90-24318
Orbital Replacement Units (ORUs) design considerations 18 p2506 N90-24320
Technology requirements for on-orbit servicing of spacecraft 18 p2506 N90-24321
Satellite servicer system flight demonstration program 18 p2506 N90-24322
Interconnecting devices conceived for in-orbit operations 18 p2506 N90-24323
Development of a fully automated fluid resupply interface system 18 p2506 N90-24324
NASREM: A functional architecture for control of the flight telerobotic servicer 18 p2506 N90-24325
EVA power tool prototype 18 p2538 N90-24482
An Earth orbiting satellite service and repair facility
[NASA-CR-186689] 19 p2665 N90-25166
Engineering test results for the Moog Single Line Disconnect
[NASA-TM-100755] 22 p3132 N90-27776
Space robotic system for proximity operations 24 p3504 N90-29806
Stability analysis of multiple-robot control systems 24 p3505 N90-29811
The flight telerobotic servicer project: A technical overview 24 p3506 N90-29821
The flight telerobotic servicer Tinman concept: System design drivers and task analysis 24 p3506 N90-29822

Research and development activities at the Goddard Space Flight Center for the flight telerobotic servicer project 24 p3507 N90-29824
The astronaut and the banana peel: An EVA retriever scenario 24 p3519 N90-29897
Next generation space robot 24 p3520 N90-29899
A comparison of the Shuttle remote manipulator system and the Space Station Freedom mobile servicing center 24 p3522 N90-29910
An intelligent, free-flying robot 24 p3522 N90-29912

ORBITAL SIMULATORS
U SPACE SIMULATORS

ORBITAL SPACE TESTS
On-orbit demonstration of GaAs solar cell and panel technologies 10 p1339 N90-17751
On-orbit results of the LIPS 3/InP homojunction solar cell experiment 10 p1344 N90-17794
SPOT 1 solar array: Three years in orbit performance evaluation 10 p1344 N90-17795
In-orbit operations research and development program of the Toulouse Space Center 18 p2501 N90-24290

ORBITAL TRANSFER
U TRANSFER ORBITS

ORBITAL VELOCITY
On universal elements, and conversion procedures to and from position and velocity
[RAE-TM-SPACE-370] 09 p1277 N90-17406
Rings of Earth detected by orbital debris radar 20 p2854 N90-26232

ORBITAL WORKERS
Mechanisms to assemble space structures in extravehicular environment 18 p2538 N90-24480
EVA power tool prototype 18 p2538 N90-24482

ORBITAL WORKSHOPS
NT SKYLAB 1

ORBITALS
NT ELECTRON ORBITALS
NT MOLECULAR ORBITALS

ORBITING LUNAR STATIONS
A lunar space station
[NASA-CR-186223] 24 p3563 N90-30158

ORBITS
NT CIRCULAR ORBITS
NT EARTH ORBITS
NT ECCENTRIC ORBITS
NT ELLIPTICAL ORBITS
NT EQUATORIAL ORBITS
NT GEOSYNCHRONOUS ORBITS
NT LUNAR ORBITS
NT PLANETARY ORBITS
NT POLAR ORBITS
NT SATELLITE ORBITS
NT SPACECRAFT ORBITS
NT STELLAR ORBITS
NT TRANSFER ORBITS
Theoretical investigations of chaotic dynamics
[AD-A207724] 01 p0134 N90-10772
Homoclinic orbits for a class of Hamiltonian systems
[AD-A210562] 03 p0391 N90-12229
Some results on connecting orbits for a class of Hamiltonian systems
[AD-A213536] 07 p0983 N90-15679
The hyperbolic Kepler's equation, and the elliptic equation revisited
[RAE-TM-SPACE-369] 09 p1274 N90-17388
Stable orbits about the Martian moons
[AD-A216400] 10 p1447 N90-18352
An error sensitivity model for Doppler positioning using transit satellites
[AD-A216724] 11 p1455 N90-18381
M51's spiral structure
[DE90-007624] 13 p1903 N90-20916
Towards a Sarkovski order for the embedding of disks maintaining their orientation
[REPT-89-43] 15 p2151 N90-22289
UD filtering and smoothing applied to orbit determination
[INPE-4966-PRE/1535] 15 p2189 N90-22501
A variational approach to heteroclinic orbits for a class of Hamiltonian systems
[AD-A219653] 17 p2460 N90-24047

ORDER-DISORDER TRANSFORMATIONS
Raman spectroscopic study of the rare earth sesquisulfides
[AD-A210610] 01 p0041 N90-10226
The structure determination of molecular adsorbates with large unit cells or lattice-gas disorder on metal surfaces
[AD-A210926] 01 p0042 N90-10230
Ordered structures and metastable alloys grown by OMVPE
[DE89-016370] 01 p0129 N90-10744
Structure and dynamics of disordered systems
[DE90-001408] 07 p0990 N90-15718
Theoretical studies on the electronic structure of high-temperature superconductors
[DE90-001301] 07 p0998 N90-15771
Contribution to the study of order effects in the Ising model framework: Ground states and phase diagrams
[ESA-TT-1118] 08 p1132 N90-16557
Statistical mechanical models for liquid and amorphous structure in covalently bonded systems
[DE90-607233] 10 p1428 N90-18240
Second-generation ordered polymers
[AD-A216126] 12 p1630 N90-19365
Optical studies of dynamical processes in disordered materials
[DE90-007080] 12 p1631 N90-19372
Ionic disorder in crystals at high temperatures with emphasis on fluorites
[AERE-R-13544] 13 p1893 N90-20862
The geometry of disorder: Report 1987 to 1990
[DE90-008250] 13 p1896 N90-20882
Ordering mechanism in substitutional Ni-Cr alloys: Theory and experiment
[DE90-006268] 14 p1949 N90-21156
Localization of vibration in disordered nearly cyclic structures 16 p2246 N90-22812
Translating polygons with applications to hidden surface removal
[RUU-CS-89-31] 18 p2602 N90-24816
The origin of poorly conditioned susceptibility matrix within inverse CVM algorithm in the case of Pd(sub 3)V: A comparison to the case of Ni(sub 3)V
[DE90-012464] 20 p2833 N90-26110
High temperature x ray diffraction and Landau theory investigations of order-disorder transition in defect NaCl-type solids
[DE90-011807] 20 p2930 N90-26673
Measurements of energy dispersion at liquid-solid interfaces: Fluorescence quenching of pyrene bound to fumed silica
[AD-A222371] 21 p2978 N90-26926
Localization effects in radiationally disordered high-temperature superconductors: Theoretical interpretation 22 p3148 N90-27853
X ray scattering studies of non-equilibrium ordering processes
[DE90-015066] 23 p3400 N90-29209
Interface formation and percusory dynamics
[AD-A224128] 23 p3402 N90-29223
Percolation and low density materials: Theory and applications
[AD-A224237] 24 p3442 N90-29438
Kinetic pathway in Stranski-Krastanov growth of Ge on Si(001)
[AD-A224324] 24 p3445 N90-29456
Microscopic aspects of the initial stages of epitaxial growth. A scanning tunneling microscopy study
[AD-A224325] 24 p3551 N90-30094
A comparative first principles study of phase stability in Ni-Ti and Ni-Al alloys around equiatomic composition
[DE90-016477] 24 p3554 N90-30111

ORES
U MINERALS

ORGANELLES
NT CHLOROPLASTS
NT MITOCHONDRIA

ORGANIC CHARGE TRANSFER SALTS
New organic synthetic metals derived from BEDT-TTF, Ni(dsit)2 and BEDO-TTF
[DE90-003793] 07 p0907 N90-15242

ORGANIC CHEMISTRY
The synthesis and structure of novel antimony thiametallacycles
[AD-A210888] 01 p0042 N90-10229
Cubane derivatives for propellant applications
[AD-A210368] 01 p0054 N90-10305
Self-assembled organic monolayer films
[AD-A212006] 03 p0323 N90-11838
Electron density modulation of catalytic metal centers by substituted aryl-isocyanide ligands
[AD-A212875] 04 p0473 N90-12708
Ion beam analysis of diffusion in polymer glasses
[AD-A212339] 04 p0480 N90-12756
Organic chemistry of cometary dust as derived from PUMA 1 data 08 p1143 N90-16628
Investigation of optical nonlinearities, conductivity and magnetism in organometallic materials
[AD-A218548] 16 p2317 N90-23211
Observation of a magic number in the ion distribution of ethene clusters
[AD-A219837] 18 p2521 N90-24393
Morphological control of inter-penetrating polymer networks 18 p2642 N90-25046
Supersonic jet studies of benzyl alcohols: Minimum energy conformations and torsional motion
[AD-A221815] 21 p2980 N90-26934
Interstellar grain chemistry and organic molecules 21 p3090 N90-27569

ORGANIC COMPOUNDS
NT ACETIC ACID
NT ACETYL COMPOUNDS
NT ACETYLENE
NT ACRYLIC ACID
NT ADENOSINE TRIPHOSPHATE
NT ALANINE
NT ALBUMINS
NT ALIPHATIC HYDROCARBONS
NT ALKANES
NT ALKENES
NT AMINO ACIDS
NT ASPARTATES
NT ATROPINE
NT AZOLES
NT AZULENE
NT BENZENE
NT BUTADIENE
NT BUTANES
NT BUTENES
NT CAFFEINE
NT CARBOHYDRATES
NT CARBOXYHEMOGLOBIN
NT CARBOXYLIC ACIDS
NT CASTOR OIL
NT CATALASE
NT CELLULOSE
NT CHOLINE
NT CHOLINESTERASE
NT CORTICOSTEROIDS
NT CUBANE
NT CYANOACETYLENE
NT CYCLIC COMPOUNDS
NT CYCLIC HYDROCARBONS
NT CYCLOBUTANE
NT CYCLOHEXANE
NT CYTOCHROMES
NT DEOXYRIBONUCLEIC ACID
NT DIENES
NT ENZYMES
NT ETHANE
NT ETHYLENE
NT ETHYLENE OXIDE
NT FATS
NT FLUOROAMINES
NT FLUOROCARBONS
NT FLUOROHYDROCARBONS
NT FLUOROPOLYMERS
NT FORMIC ACID
NT GLOBULINS
NT GLUCOSE
NT GLUCOSIDES
NT GLYCINE
NT HEMOGLOBIN
NT HETEROCYCLIC COMPOUNDS
NT HMX
NT HYDROCARBONS
NT KEROGEN
NT LIPIDS
NT MELANIN
NT METHANE
NT METHYLENE
NT NAPHTHALENE
NT NATURAL GAS
NT NICOTINIC ACID
NT OCTANES
NT ORGANIC CHARGE TRANSFER SALTS
NT ORGANIC LIQUIDS
NT ORGANIC PHOSPHORUS COMPOUNDS
NT ORGANIC SILICON COMPOUNDS
NT ORGANIC SULFUR COMPOUNDS
NT OXIDASE
NT OXYACETYLENE
NT PEPTIDES
NT PHENANTHRENE
NT PHENYLALANINE
NT PHOSPHAZENE
NT PHTHALOCYANIN
NT POLYBUTADIENE
NT POLYPEPTIDES
NT POLYTETRAFLUOROETHYLENE
NT POLYVINYL FLUORIDE
NT PROPANE
NT PROPYLENE
NT PROSTAGLANDINS
NT PROTEINS
NT PYRENES
NT PYRIDINES
NT PYRROLES
NT RDX
NT RIBONUCLEIC ACIDS
NT STARCHES
NT STILBENE
NT TEFLON (TRADEMARK)
NT TETRAHYDROFURAN
NT TOLUENE

NT TRYPTOPHAN
NT TYROSINE
NT VINYLIDENE
Organic explosives and related compounds. Environmental and health considerations
[AD-A210554] 01 p0054 N90-10306
Structure-property relationships as an aid in the rational design of (beta)-(ET)(sub 2)X organic superconductors
[DE89-016912] 03 p0410 N90-12356
Energies of organic compounds
[DE90-003174] 06 p0743 N90-14324
Analysis of ambient polar volatile organic compounds using chemical ionization-ion trap detector
[PB90-106451] 07 p0956 N90-15529
Mechanisms of the electrochemistry of small organic molecules
[PB90-100785] 08 p1040 N90-16012
Organic cathode for a secondary battery
[NASA-CASE-NPO-17604-1-CU] 08 p1059 N90-16124
Analysis of organic compounds in returned comet nucleus samples 08 p1142 N90-16617
A gas chromatograph/mass spectrometry method for determining isotopic distributions in organic compounds used in the chemical approach to stable isotope separation
[DE90-005738] 10 p1352 N90-17841
Surface-enhanced Raman scattering
[AD-A215976] 10 p1353 N90-17849
Studies of the structure and properties of organic monolayers, multilayers and superlattices
[DE90-008330] 13 p1765 N90-20129
Developments in solar photocatalysis for destruction of organics in water
[DE90-007685] 13 p1771 N90-20162
Ring expansion and equilibration in organophosphazenes, and the relationship to polymerization
[AD-A218234] 13 p1782 N90-20230
Pressure in the study of organic superconductors
[DE90-011049] 18 p2625 N90-24959
Theoretical investigations and attempted synthesis of organic magnetic polymers and oligomers
[AD-A223409] 24 p3455 N90-29509

ORGANIC LASERS
NT DYE LASERS
Eye/sensor protection against laser irradiation organic nonlinear optical materials
[AD-A210599] 01 p0093 N90-10531

ORGANIC LIQUIDS
Dimensional analysis of continuous high-capacity electrodispersion of aqueous based liquids in an organic continuous phase
[DE90-003714] 07 p0888 N90-15136
The physical-organic chemistry of surfaces, and its relevance to molecular recognition
[AD-A215987] 10 p1354 N90-17850

ORGANIC MATERIALS
NT PEAT
Computational modeling of pi-conjugated polyradicals
[AD-A210573] 01 p0113 N90-10648
Nonlinear optics and organic materials
[AD-A210570] 01 p0124 N90-10709
Interactions of hydrazines with colloidal constituents of soils 02 p0204 N90-11164
Selective removal of organics for water reclamation
[NASA-CR-185959] 02 p0255 N90-11445
Proceedings of the DOD Workshop on the Manufacturing/Producibility of Organic Matrix Composites
[AD-A212577] 04 p0468 N90-12680
Analysis and evaluation of technical data on the photochromic and non-linear optical properties of materials
[AD-A214212] 07 p0896 N90-15178
Ion bombardment experiments suggesting an origin for organic particles in pre-cometary and cometary ices 08 p1148 N90-16652
Refractory solids in chondrites and comets: How similar 08 p1148 N90-16654
Analysis and evaluation of technical data on the photochromic and non-linear optical properties of materials
[AD-A216124] 10 p1431 N90-18254
Process for crosslinking methylene-containing aromatic polymers with ionizing radiation
[NASA-CASE-LAR-13448-1] 14 p1956 N90-21198
Measurement of localized deep levels and wafer non-uniformities at 3-5 semiconductor heterojunctions
[AD-A218547] 16 p2323 N90-23248
HPLC analysis of helicopter rotor blade materials
[AD-A221121] 18 p2497 N90-24270
Anode materials for electrochemical waste destruction 18 p2514 N90-24354
Use of high-dimensional spectral data to evaluate organic matter, reflectance relationships in soils
[NASA-CR-186650] 18 p2574 N90-24865
Gaseous optical contamination of the spacecraft environment: A review 19 p2730 N90-25519
Optical constraints of kerogen from 0.15 to 40 microns: Comparison with meteoritic organics 20 p2948 N90-26776
Structure-property behavior of new organic-inorganic polymeric hybrid materials based on sol gel chemistry
[AD-A222168] 21 p2987 N90-26974
Interstellar grain chemistry and organic molecules 21 p3090 N90-27569
Carbon in the outer solar system 21 p3096 N90-27593
Organic polyradical models for organic magnetic materials
[AD-A223691] 24 p3442 N90-29435
Theoretical investigations of Pi-conjugated polyradicals as models for organic magnetic materials
[AD-A223411] 24 p3446 N90-29461

ORGANIC NITRATES
NT CELLULOSE NITRATE
NT PETN

ORGANIC PHOSPHORUS COMPOUNDS
NT PHOSPHAZENE
Studies of organo phosphorus-, nitrogen-, and sulfur-containing molecules
[AD-A213518] 07 p0888 N90-15135
Metabolism, seizures, and blood flow in brain following organophosphate exposure: Mechanisms of action and possible therapeutic agents
[AD-A217098] 12 p1696 N90-19740
A second-order nonlinear optical poly(organophosphazene)
[AD-A218408] 16 p2210 N90-22607
Retention index monitoring of volatile organic compounds using thermal desorption gas chromatography
[AD-A221117] 18 p2521 N90-24397

ORGANIC SILICON COMPOUNDS
Polymeric aluminasilazane precursors for aluminosilicon nitride
[AD-A222755] 20 p2841 N90-26158

ORGANIC SOLIDS
Self-calibrating apparatus to find dynamic compressibility of organic solids
[AD-A219780] 17 p2415 N90-23763

ORGANIC SULFUR COMPOUNDS
Novel high-rate, all solid-state, sodium and lithium/organosulfur batteries
[DE90-001014] 07 p0920 N90-15325
New electrically conducting solids based on nickel(II) - bis(1,3-dithiole-2-thione-4,5-diselenolate)
[DE90-003788] 08 p1042 N90-16020

ORGANISMS
Artificial life: The coming evolution
[DE90-008860] 14 p2009 N90-21515

ORGANIZATIONS
NT BUREAUS (ORGANIZATIONS)
NT EUROPEAN SPACE AGENCY
NT FEDERATIONS
NT NORTH ATLANTIC TREATY ORGANIZATION (NATO)
NT WORLD METEOROLOGICAL ORGANIZATION
Directory of International and Regional Organizations Conducting Standards-Related Activities, May 1989
[PB89-221147] 04 p0483 N90-12776
National Science Foundation 04 p0569 N90-13320
An investigation of application development process controls in an end-user setting: A field study 09 p1295 N90-17504
An analysis of the impacts of computer-based information systems on research and development organizations
[AD-A216283] 10 p1442 N90-18324
Calendar of selected aeronautical and space meetings
[AGARD-CAL-90/1] 11 p1574 N90-19060
An integrative research review of the relationship between technology and structure: A meta-analytic synthesis
[AD-A218115] 13 p1899 N90-20903
Cooperating intelligent systems
[NASA-CR-184982] 14 p2012 N90-21529
Facilitating knowledge sharing in organizations: Semiautonomous agents that learn to gather, classify, and distribute environmental scanning knowledge 15 p2176 N90-22435
National Aeronautics and Space Administration (NASA)/American Society for Engineering Education (ASEE) Summer Faculty Fellowship Program-1989, volume 1
[NASA-CR-185601-VOL-1] 18 p2627 N90-24972
National Aeronautics and Space Administration (NASA)/American Society for Engineering Education (ASEE) Summer Faculty Fellowship Program-1989, volume 2
[NASA-CR-185601-VOL-2] 18 p2630 N90-24985
A systematic approach to training: A training needs assessment 18 p2645 N90-25059
Effect of organizational structure on performance of decision making teams
[AD-A223160] 20 p2934 N90-26897
Industrial patent activity in the US. Part 1: Tima series profile by company and country of origin, 1969-1989
[PB90-214404] 22 p3259 N90-28454
Working implementation agreements for open systems interconnection protocols
[PB90-197948] 24 p3557 N90-30127

ORGANOMETALLIC COMPOUNDS
NT CARBOXYHEMOGLOBIN
NT CHLOROPHYLLS
NT FERROCENES
NT HEMOGLOBIN
International Conference on Organometallic Chemistry (13th) held in Torino, Europe on 4-9 September 1988: Abstracts
[AD-A210617] 01 p0033 N90-10178
The synthesis and structure of novel antimony thiametallacycles
[AD-A210888] 01 p0042 N90-10229
Bonding in transition metal silyl dimers. Molecular orbital theory
[AD-A208269] 01 p0046 N90-10260
Solvent dynamical effects in electron transfer: Evaluation of electronic matrix coupling elements for metallocene self-exchange reactions
[AD-A210306] 01 p0121 N90-10692
Synthesis of powder with gel technique
[FOA-C-20752-2.4(2.1)] 02 p0202 N90-11156
Ultra high speed compound semiconductors and real time signal processing
[AD-A211394] 03 p0413 N90-12372
Metallo-organic decomposition process for dielectric films
[AD-A211590] 04 p0495 N90-12849
New organic synthetic metals derived from BEDT-TTF, Ni(dsit)2 and BEDO-TTF
[DE90-003793] 07 p0907 N90-15242
Symposium on Chemical Precursors to Ceramics
[AD-A214499] 09 p1196 N90-16932
Perfluorinated ligands in organometallic chemistry
[AD-A216415] 11 p1476 N90-18493
Enhanced bonding of fiber reinforcements to thermoset resins 11 p1476 N90-18496
Reliability studies of ceramic capacitors
[AD-A216763] 11 p1501 N90-18643
High power semiconductor laser arrays by metalorganic chemical vapor deposition 13 p1805 N90-20363
Metal alkoxides: Models for metal oxides. Alkoxide ligands in early transition metal organometallic chemistry
[DE90-007523] 13 p1894 N90-20869
The first example of an organogallium compound containing a Ga-Te bond: Synthesis, properties, and molecular structure of ((Me3CCH2)2GaTeph)2
[AD-A219258] 16 p2210 N90-22608
Investigation of optical nonlinearities, conductivity and magnetism in organometallic materials
[AD-A218548] 16 p2317 N90-23211
Ultra high-speed compound semiconductors and real time signal processing
[AD-A220721] 17 p2396 N90-23651
Formation of high Tc superconducting films by organometallic chemical vapor deposition
[AD-D014498] 19 p2760 N90-25682
Composite materials with improved properties in compression: Synthesis and dimerization 2,3-dimethyl-5-silaspiro(4.4)nona-2,7-diene
[AD-A222552] 22 p3156 N90-27892

ORGANOMETALLIC POLYMERS
Metal-assisted syntheses of boranes and carboranes
[AD-A210728] 01 p0041 N90-10227
Transition metal catalyzed synthesis of organmetallic polymers
[AD-A212133] 04 p0478 N90-12740
New polymers made with well-characterized organometallic catalysts
[AD-A213592] 07 p0912 N90-15272
Porous ceramic bodies
[AD-D014277] 08 p1049 N90-16061
Electronic and ionic transport in polymers
[AD-A217028] 11 p1491 N90-18579
Combination primer/topcoat coating
[AD-D014445] 14 p1954 N90-21189
Modified maleic anhydride copolymers as e-beam resists
[AD-A218470] 16 p2223 N90-22679

Polymeric aluminasilazane precursors for aluminosilicon nitride
[AD-A222755] 20 p2841 N90-26158
Stibathiolanes: Synthesis, solid state structure, and solution behavior
[AD-A223255] 20 p2933 N90-26688
The synthesis and structure of stibaindoles
[AD-A222990] 21 p2976 N90-26914

ORGANS
Reliability of equivalent sphere model in blood-forming organ dose estimation
[NASA-TM-4178] 12 p1746 N90-20036
Simplified model for solar cosmic ray exposure in manned Earth orbital flights
[NASA-TM-4182] 14 p2043 N90-21715
Improved model for solar cosmic ray exposure in manned Earth orbital flights
[NASA-TP-2987] 18 p2639 N90-25031

ORIENTATION
Face-specific interaction of MoS4(2-1) with oriented crystals of (0001) CdX (X = Se, S)
[AD-A209519] 01 p0128 N90-10732
Development of a preliminary high-angle-of-attack nose-down pitch control requirement for high-performance aircraft
[NASA-TM-101684] 12 p1600 N90-19206
Determination of Earth orientation using the Global Positioning System 12 p1642 N90-19435

ORIFICE FLOW
Effect of pipe roughness on orifice flow measurement
[PB89-231484] 04 p0500 N90-12880
Measurements of coefficients of discharge for concentric flange-tapped square-edged orifice meters in water over the Reynolds number range 600 to 2,700,000
[PB89-235147] 04 p0502 N90-12892
Optimum location of flow conditioners in a 4-inch orifice meter
[PB90-111675] 09 p1216 N90-17049

ORIFICES
Two dimensional orifice array, monodisperse drop source, phase 1
[AD-A211319] 04 p0500 N90-12881
Optimum location of flow conditioners in a 4-inch orifice meter
[PB90-111675] 09 p1216 N90-17049
Turbulence scale effects on heat transfer in a linear turbine cascade
[AD-A216222] 10 p1321 N90-17637
Adjustable choke for fluids nozzle
[NASA-CASE-NPO-17625-1-CU] 21 p3003 N90-27070
In-flight investigation of shuttle tile pressure orifice installations
[NASA-TM-4219] 23 p3328 N90-28820

ORION AIRCRAFT
U P-3 AIRCRAFT

ORION NEBULA
Further observations of rotationally excited far infrared OH16 and OH18 emission in Orion-KL: Tighter constraints on the nature of the emitting region
[NASA-CR-186004] 05 p0710 N90-14156
Mapping and spectroscopy of the 3.3 microns feature in Orion 11 p1582 N90-19112

ORNITHOPTER AIRCRAFT
U RESEARCH AIRCRAFT

OROGRAPHY
Stratiform clouds and their interaction with atmospheric motions 03 p0360 N90-12060
Low level remote sensing: Orographic winds 03 p0361 N90-12066
The effect of orographic forcing on the mean flow of the stratosphere 08 p1099 N90-16367
Semigeostrophic flow over orography in a stratified rotating atmosphere 15 p2127 N90-22163
A nonhydrostatic numerical model in sigma-coordinates and simulations of mesoscale phenomena 23 p3350 N90-28932

ORR-SOMMERFELD EQUATIONS
Elimination of spurious eigenvalues in the Chebyshev tau spectral method
[PB89-209282] 03 p0345 N90-11967
Solution of the Orr-Sommerfeld equation for three dimensional incompressible flow using Galerkin method and Chebichev polynomials: The COCIP code
[CERT-46/5618-34-DERAT] 22 p3176 N90-28021

ORRERIES
U ASTRONOMICAL MODELS

ORTHO PARA CONVERSION
Development of high-activity para- to ortho-hydrogen conversion catalysts, volume 2
[AD-A218700] 16 p2215 N90-22638

ORTHOGONAL FUNCTIONS
Orthogonal least squares methods and their application to nonlinear system identification
[RR-343] 03 p0395 N90-12259
Vorticity amplification in nonorthogonal stagnation flow 08 p1064 N90-16152
Orthogonal distance regression
[PB90-151747] 15 p2160 N90-22336
Generalizations of a q-analogue of Laguerre polynomials
[REPT-89-51] 15 p2161 N90-22345
Efficient representation of the hydrographic structure of the north atlantic ocean and aspects of the circulation from objective methods
[AD-A218606] 17 p2429 N90-23841
Polynomial asymptotic estimates of Gegenbauer, Laguerre, and Jacobi polynomials
[CWI-AM-R8911] 17 p2460 N90-24043
Stability and error estimates for sinc interpolation
[CWI-AM-R8914] 18 p2599 N90-24790
Expansion and orthogonalization of measured modes for structure identification 18 p2647 N90-25068
Annual and interannual variations of Earth-emitted radiation based on a 10-year data set
[NASA-TM-103465] 20 p2887 N90-26432
Asymptotic law of the orthogonal empirical functions and applications, part 2
[IMAG-RR-792-M-PT-2] 20 p2918 N90-26605
Recurrence relations and weight functions for approximation by orthonormal polynomials
[DE90-627156] 23 p3388 N90-29134

ORTHOGONALITY
Generalizations of Laguerre polynomials
[REPT-89-25] 03 p0396 N90-12263
A generalization of Moak's q-Laguerre polynomials
[REPT-89-21] 04 p0540 N90-13126
NUMVEC FORTRAN library manual chapter: Simultaneous linear equations
[CWI-NM-R8903] 04 p0541 N90-13135
Representations of the twisted SU(2) quantum group and some q-hypergeometric orthogonal polynomials
[CWI-PM-R8809] 04 p0541 N90-13140
Symmetric waveguide junction combiner
[AD-D014243] 06 p0768 N90-14466
Two dimensional laminated shell theory including parabolic transverse shear
[AD-A213817] 07 p0948 N90-15487
Studies in statistical signal processing
[AD-A214490] 09 p1275 N90-17393
Sequentiality in orthogonal term rewriting systems
[CWI-CS-R8932] 18 p2592 N90-24744
On a class of generalized orthogonal polynomials with real zeros
[MEMO-826] 18 p2600 N90-24799
Measuring sensitivities and orthogonalities of magnetometer sensors in the Nurmijarvi coil hut 21 p3022 N90-27180
Use of the method of natural orthogonal components for derivation of S sub R-variation and digital K-indices 21 p3024 N90-27193
Parallel architectures and algorithms for image understanding
[AD-A223479] 24 p3526 N90-29940

ORTHOPEDICS
Engineering specification and system design for CAD/CAM of custom shoes: UMC project effort
[NASA-CR-186547] 15 p2145 N90-22255

ORTHOPHOTOGRAPHY
Digital production of perspective images
[SER-C-347] 12 p1701 N90-19768

ORTHOSTATIC TOLERANCE
Effect of fluid countermeasures of varying osmolarity on cardiovascular responses to orthostatic stress 18 p2626 N90-24978
Cardiovascular deconditioning of cosmonauts: Role, importance and applications of the lower body negative pressure
[ETN-90-97507] 23 p3355 N90-28964

ORTHOTROPIC PLATES
Through-thickness strain response of thick composites in compression
[AD-A217233] 13 p1767 N90-20141
Perturbation solutions in D* for buckling, vibration, and static loading of specially orthotropic plates 13 p1814 N90-20419
Postbuckling behavior of laminated specially orthotropic plates by affine transformation 13 p1814 N90-20420
Review of formulae for the buckling of simply-supported, orthotropic plates under shear load, including transverse shear effects
[PB90-167073] 14 p1994 N90-21429
The behaviour of mechanically fastened joints in composite structures 16 p2242 N90-22789
Impact response of orthotropic composite plates predicted by a one-parameter differential equation
[FFA-TN-1989-07] 17 p2369 N90-23488
Low velocity impact analysis with NASTRAN 18 p2570 N90-24647
Buckling and postbuckling behavior of square compression-loaded graphite-epoxy plates with circular cutouts
[NASA-TP-3007] 20 p2826 N90-26077

ORTHOTROPIC SHELLS
Equilibrium and stability in composite thin shell 02 p0178 N90-10998
Buckling of axially compressed imperfect orthotropic shells with elastic edge supports
[PB89-217038] 03 p0357 N90-12043
ROCOPT: A user friendly interactive code to optimize rocket structural components 12 p1639 N90-19415

OSCILLATING CYLINDERS
Response of a liquid column with respect to oscillatory rotational top- and bottom excitation
[LRT-WE-9-FB-8(1989)] 21 p3006 N90-27086
Oscillatory response of a liquid column to counter rotational excitation
[LRT-WE-9-FB-12(1989)] 21 p3006 N90-27088

OSCILLATING FLOW
An experimental investigation of transition in oscillating pipe flow 02 p0218 N90-11249
Experimental investigation to suppress flow-induced pressure oscillations in open cavities
[AD-A216285] 10 p1310 N90-17578
Mass transfer from a sphere in an oscillating flow with zero mean velocity
[NASA-TM-102566] 13 p1801 N90-20338
ULTRA-SHARP nonoscillatory convection schemes for high-speed steady multidimensional flow
[NASA-TM-102568] 14 p2019 N90-21570
Extension of a streamwise upwind algorithm to a moving grid system
[NASA-TM-102800] 15 p2048 N90-21739
Fluid oscillations in an open, flexible container
[REPT-89-69] 17 p2404 N90-23696
Heat exchanger with oscillating flow
[NASA-CASE-LAR-14033-1] 21 p3004 N90-27072
Numerical simulations of flowfields in a central-dump ramjet combustor. 3: Effects of chemistry
[AD-A224145] 23 p3282 N90-28573
Oscillatory convection
[ESA-TT-890] 23 p3325 N90-28801

OSCILLATIONS
NT AIRFOIL OSCILLATIONS
NT ELECTRON OSCILLATIONS
NT HARMONIC OSCILLATION
NT MOLECULAR OSCILLATIONS
NT NONOSCILLATORY ACTION
NT PLASMA OSCILLATIONS
NT PRESSURE OSCILLATIONS
NT SOLAR OSCILLATIONS
NT SOUTHERN OSCILLATION
NT STABLE OSCILLATIONS
NT STELLAR OSCILLATIONS
NT TRANSIENT OSCILLATIONS
NT TRANSVERSE OSCILLATION
NT WING OSCILLATIONS
Analysis of a system of two weakly nonlinear coupled harmonic oscillators arising from the field of wind-induced vibrations
[REPT-89-22] 03 p0396 N90-12261
Additions and corrections to SUPER: A program for calculating steady and oscillatory supersonic flow over a thin wing, tail plane and fin
[AD-A211771] 04 p0438 N90-12501
Unsteady aerodynamics of oscillating and rapidly pitched airfoils 07 p0875 N90-15074
Neutrino oscillations: An essay in honor of Felix Boehm
[DE90-003223] 08 p1121 N90-16491
Surface pressure distributions on a delta wing undergoing large amplitude pitching oscillations
[NASA-CR-186326] 10 p1306 N90-17558
Magnetoplasma oscillations of the wave-guided type in semiconductor superlattices
[DE90-607260] 10 p1431 N90-18258
First results from the MST (Madison Symmetric Torus) reversed field pinch
[DE90-005743] 10 p1433 N90-18268
Unsteady Aerodynamic Phenomena in Turbomachines
[AGARD-CP-468] 11 p1459 N90-18405
Numerical investigation of unsteady flow in oscillating turbine and compressor cascades 11 p1459 N90-18407
Calculation of the unsteady two-dimensional, inviscid, compressible flow around a strongly cambered oscillating single blade 11 p1460 N90-18409
Asymptotic analysis of transonic flow through oscillating cascades 11 p1462 N90-18421
Measurement of velocity profiles and Reynolds stresses on an oscillating airfoil 11 p1463 N90-18427
Injection parameters and beam oscillations during extraction
[NIKHEF-K/AMPS/89-07] 11 p1499 N90-18632

Back swing phenomenon of synchronous generator. Study on ac-dc power system simulator tests
[DE89-782321] 11 p1500 N90-18635
Experimental investigations of the unsteady boundary layer on an oscillating flat plate. Optimization and validation of a code, for calculating the potential flow/boundary layer coupling of a flat plate and of an oscillating profile
[ETN-90-96254] 11 p1508 N90-18682
Oscillation and damping behavior of fine steel test tubes, with particular consideration to destruction free proofs from hydrogen fragilization
[ETN-90-95371] 12 p1627 N90-19351
Microwave oscillator with reduced phase noise by negative feedback incorporating microwave signals with suppressed carrier 12 p1643 N90-19437
Transient and sustained resonance in very slowly varying oscillatory Hamiltonian systems with application to free-electron lasers
[DE90-005984] 12 p1666 N90-19574
An experimental study of the aeroelastic behaviour of two parallel interfering circular cylinders 12 p1673 N90-19609
Initialization of EURAD. Part 1: Utilization of ECMWF analysis data 12 p1688 N90-19695
Numerical simulations of supersonic flow through oscillating cascade sections
[NASA-TM-103100] 13 p1750 N90-20051
A video-based experimental investigation of wing rock
[AD-A218244] 13 p1755 N90-20075
Modeling of vortex-induced oscillations based on indicial response approach
[NASA-CR-186560] 15 p2047 N90-21736
A theoretical analysis of the acoustic radiation from two-dimensional turbulent mixing layers 18 p2551 N90-24559
Sustained resonance in very slowly varying oscillatory Hamiltonian systems
[DE90-010422] 18 p2598 N90-24783
Kinetic theory of low-frequency nonlinear structures in magnetized plasmas
[DE90-611306] 18 p2617 N90-24907
Low-frequency oscillations in vlasov plasmas: The quadratic polarization approximation
[DE90-611309] 18 p2617 N90-24910
Evaluation of nonlinear motion-drive algorithms for flight simulators
[UTIAS-TN-272] 19 p2662 N90-25148
Application of solar seismology to study of the convection zone
[AD-A221975] 21 p3101 N90-27610
Entropy wave instability in compact ramjets 22 p3162 N90-27932
Regular and chaotic motion of uniform elliptical vortices in external linear time dependent velocity fields 23 p3268 N90-28497
Stabilization of Taylor-Couette flow due to time-periodic outer cylinder oscillation
[PB90-219130] 23 p3323 N90-28790
Oscillatory convection
[ESA-TT-890] 23 p3325 N90-28801
Effects and tolerances of injection jitter in the SLC and future linear colliders
[DE90-014805] 23 p3394 N90-29179
Nonradial instability strips for post-AGB stars
[DE90-014922] 23 p3411 N90-29278
Oscillatory and nonoscillatory behaviour of solutions of an equation alternately of retarded and advanced type
[DE90-627159] 24 p3536 N90-29993
Adiabatic invariance and transient resonance in very slowly varying oscillatory Hamiltonian systems
[DE90-016118] 24 p3538 N90-30007
New real space correlated-basis-functions approach for the electron correlations of the semiconductor inversion layer
[DE90-627315] 24 p3551 N90-30090

OSCILLATOR STRENGTHS
Calculation of Einstein A coefficients and oscillator strengths for the A(perturbed)(2)A(1)-X(perturbed)(2)B(1) transition of NH(2)
[AD-A213837] 07 p0896 N90-15176

OSCILLATORS
NT CRYSTAL OSCILLATORS
NT HARMONIC OSCILLATORS
NT MAGNETRONS
NT MECHANICAL OSCILLATORS
NT MICROWAVE OSCILLATORS
NT PENDULUMS
NT RELAXATION OSCILLATORS
NT SYNCHRONIZED OSCILLATORS
NT VOLTAGE CONTROLLED OSCILLATORS
Master oscillator with power amplifiers: Performance of a two-element CW HF phased-laser array
[AD-A211141] 01 p0076 N90-10435
Submillimeter quantum electronics
[AD-A210439] 01 p0132 N90-10762
Resonance effect on the oscillator distribution function
[DE89-630105] 02 p0271 N90-11548
Advanced light source master oscillator
[DE90-000123] 03 p0342 N90-11953
Resonant-tunneling oscillators and multipliers for submillimeter receivers 05 p0597 N90-13467
Symmetric waveguide junction combiner
[AD-D014243] 06 p0768 N90-14486
Numerical simulations of free-electron laser oscillators
[DE89-003488] 06 p0788 N90-14588
Optical design and performance of an XUV FEL (Free-Electron Laser) oscillator
[DE90-002381] 06 p0790 N90-14599
INEX (Integrated Numerical Experiment) simulations of the Los Alamos HIBAF (High-Brightness Accelerator Free-Electron Laser) free-electron laser MOPA (Master Oscillator Power Amplifier) experiment
[DE90-002387] 06 p0790 N90-14601
A study of Inter-Injection-Locked phased arrays
[AD-A214097] 07 p0925 N90-15352
Theoretical and experimental investigation of axial power extraction from a magnetically insulated transmission line oscillator
[DE90-003486] 08 p1060 N90-16131
The bifurcation interpreter: A step towards the automatic analysis of dynamical systems
[AD-A214618] 09 p1265 N90-17336
A space-fed local oscillator for spaceborne phased arrays
[AD-A216526] 10 p1328 N90-17673
Performance of a 500 watt Nd:GGG zigzag slab oscillator
[DE90-006263] 11 p1503 N90-18657
Planar integrated circuits for microwave transmission and reception
[AD-A217676] 12 p1656 N90-19520
Development of an ultra-bright laser and an application to multi-photon ionization 14 p1984 N90-21372
Generation of ultrashort laser pulses from neodymium glass oscillator and regenerative amplifier 14 p1984 N90-21373
An 8.4-GHz dual-maser front-end system for Parkes reimplementation 15 p2078 N90-21905
Dynamics of an oscillator with three-degrees-of-freedom in a uniform windfield
[REPT-89-56] 15 p2119 N90-22121
Design of high-performance negative-feedback oscillators
[ETN-90-96698] 16 p2231 N90-22729
Bifurcational aspects of parametric resonance
[W-8904] 16 p2231 N90-22730
A free electron laser master oscillator power amplifier experiment 16 p2239 N90-22776
Quantum non-demolition stroboscopic observables and multipumping back-action evasion schemes
[PREPRINT-699] 16 p2326 N90-23260
Are quantum measurements on macroscopic bodies feasible
[PREPRINT-700] 16 p2326 N90-23261
Reflection oscillators employing series resonant crystals'
[NASA-CASE-GSC-13173-1] 17 p2394 N90-23635
Intersubband transitions in an asymmetric quantum well with a thin barrier of a delta-function potential
[AD-A220723] 17 p2477 N90-24162
Asymptotic analysis of wind-induced vibrations
[ETN-90-96903] 18 p2572 N90-24658
Stability of laser oscillator systems 18 p2641 N90-25045
Free electron laser injection oscillator
[AD-D014180] 21 p3007 N90-27095
Modified fast frequency acquisition via adaptive least squares algorithm
[NASA-CASE-NPO-17845-1-CU] 21 p3050 N90-27341
Computer simulation of micro-triode performance
[DE90-014191] 23 p3320 N90-28774
Dissipative quantum maps
[DE90-627179] 23 p3402 N90-29227
Quantum chaos and dissipation: Lyapunov exponents
[DE90-627180] 23 p3403 N90-29228
High voltage picosecond pulse generation using avalanche diodes
[DE90-015194] 24 p3465 N90-29577

OSCILLOSCOPES
Pin switch circuits instrument for microsecond velocity measurements
[AD-A210638] 01 p0074 N90-10426

OSEEN APPROXIMATION
Analytical resolution of the Oseens differential equation of inclined turning cylinder with gliding
[ETN-90-97316] 22 p3171 N90-27988

OSTEOPOROSIS
Conservation of body calcium by increased dietary intake of potassium: A potential measure to reduce the osteoporosis process during prolonged exposure to microgravity 18 p2631 N90-24993

OTOLITH ORGANS
Pre- and postflight postural control of the D1 Spacelab mission astronauts examined with a tilting room
[IZF-1988-25] 04 p0527 N90-13039
The effects of linear acceleration on perception and nystagmus 15 p2136 N90-22209

OTV
U ORBIT TRANSFER VEHICLES

OUTCROPS
Quantification of structural field data in the Rio Grande do Norte basin and neighborhood
[INPE-4821-RPE/591] 11 p1533 N90-18826

OUTER PLANET MISSIONS
U GRAND TOURS

OUTER SPACE TREATY
Manned Space Stations: Legal Issues
[ESA-SP-305] 20 p2937 N90-26711
The US/International Space Station: Legal aspects of space objects and jurisdiction and control 20 p2937 N90-26713
Damage responsibility and liability in space stations 20 p2937 N90-26714
MIR: A Soviet Space Station. Some legal aspects of international cooperation 20 p2938 N90-26715
The partnership concept and international management 20 p2938 N90-26717
The International Space Station: Conditions of access and use 20 p2938 N90-26718

OUTGASSING
Gravimetric measurements of materials outgassing applied to graphite-epoxy laminates
[NASA-TM-100753] 05 p0619 N90-13609
Improved process for HIP canning of composites
[NASA-CASE-LEW-14990-1-CU] 07 p0890 N90-15147
Coefficients of thermal expansion for a carbon-carbon composite
[DE90-004484] 09 p1188 N90-16883
Space station contamination control study: Internal combustion, phase 1
[NASA-CR-179323] 10 p1328 N90-17674
Spacecraft external molecular contamination analysis 19 p2730 N90-25520
Satellite material contaminant optical properties 19 p2732 N90-25529
Space station contamination modeling
[NASA-CR-183871] 23 p3286 N90-28590

OUTLETS
NT VENTS

OUTLETS (GEOLOGY)
U ESTUARIES

OUTLIERS (STATISTICS)
Outlier detection in multivariate calibration
[DE90-001502] 07 p0982 N90-15672

OUTPUT
NT LASER OUTPUTS
NT MASER OUTPUTS
Test generation for highly sequential circuits
[AD-A211932] 05 p0634 N90-13698
On the output-stabilizable subspace
[MEMO-COSOR-88-27] 05 p0690 N90-14027

OVENS
Signal processing device to control microwave output
[AD-A216931] 11 p1502 N90-18648
Uncertainty evaluation in an automated high temperature environmental simulation oven
[REPT-892-430-103] 16 p2203 N90-22571

OVER-THE-HORIZON RADAR
MF/HF multistatic mid-ocean radar experiments in support of SWOTHR (Surface-Wave Over-The-Horizon Radar)
[AD-A213830] 07 p0919 N90-15314
The development of over-the-horizon radar in Australia
[ISBN-0-642-13561-4] 08 p1055 N90-16099
Bermuda ionosonde tests in support of OTH-B
[NASA-TM-89359] 19 p2713 N90-25442

OVERCAST
U CLOUD COVER

OVERHAUSER EFFECT
Proton magnetometers for measurement of the Earth's magnetic field 21 p3023 N90-27188

OVERPRESSURE
Microstructural characterization of silicon nitride ceramics processed by pressureless sintering, overpressure sintering, and sinter/HIP
[DE90-007126] 11 p1493 N90-18594
Summary of sonic boom rise times observed during FAA community response studies over a 6-month period in the Oklahoma City area
[NASA-CR-4277] 18 p2608 N90-24852

Method and apparatus for assessing distillate fuel stability by oxygen overpressure
[AD-D014499] 19 p2679 N90-25237

OVERTONES
U HARMONICS

OVERVOLTAGE
Lightning and surge protection of photovoltaic installations: Two case histories, Vulcano and Kythnos
[PB89-229058] 03 p0374 N90-12135
Transient fault behavior in a microprocessor: A case study
[NASA-CR-186240] 10 p1320 N90-17633
The dielectric behavior of sulfur hexafluoride submitted to rapid transitory overvoltages
[ECL-89-16] 17 p2374 N90-23520
A linearly controlled direct-current power source for high-current inductive loads in a magnetic suspension wind tunnel
[NASA-TM-4198] 19 p2692 N90-25319
L-SWITCH: A PC-program for computing transient voltages and currents during switching off three-phase inductances
[PB90-191412] 22 p3167 N90-27961
Use of Ni63 overvoltage gap switches in the flight termination systems on boosters launched from US Army Kwajalein Atoll (USAKA)
[AD-A223866] 23 p3299 N90-28661

OXIDASE
Amperometric biosensors for glucose, lactate, and glycolate based on oxidases and redox-modified siloxane polymers
[DE90-002301] 06 p0781 N90-14541

OXIDATION
NT ELECTROCHEMICAL OXIDATION
NT PHOTOOXIDATION
Heterogeneous catalysts in water
[AD-A210742] 01 p0041 N90-10228
Emittance, catalysis, and dynamic oxidation of Ti-14Al-21Nb
[NASA-TP-2955] 01 p0044 N90-10248
Photochemically-driven biomimetic oxidation of alkanes and olefins
[DE89-011536] 02 p0193 N90-11097
Enhanced oxidation and solovolysis reactions in chemically inert microheterogeneous systems
[AD-A210748] 02 p0195 N90-11110
Hydrogen-silicon carbide interactions
[NASA-TM-102382] 02 p0200 N90-11144
Surface-catalyzed air oxidation of hydrazines: Environmental chamber studies
02 p0203 N90-11159
Trace metal catalysis of hydrazine decomposition: The role of chromium 02 p0204 N90-11163
Surface-catalyzed air oxidation reactions of hydrazines: Tubular reactor studies 02 p0204 N90-11167
The chemistry of the hypochlorite neutralization of hydrazine fuels 02 p0205 N90-11173
Fuel neutralization by ozone oxidation
02 p0206 N90-11176
Powder morphology effects in the ignition of titanium-based pyrotechnics
[DE89-017229] 02 p0208 N90-11191
Transport properties of thermally grown Cr2O3
[DE89-016703] 02 p0284 N90-11623
Conversion of methane to liquid hydrocarbons
[DE89-017547] 03 p0322 N90-11831
Computer simulation studies of the catalytic oxidation of carbon monoxide on platinum metals
[PB89-223739] 04 p0475 N90-12721
Study of metal-insulator-semiconductor structures on indium phosphide, implemented by anodic oxidation
[ECL-88-10] 05 p0703 N90-14114
Predictive aging of elastomers in air: The importance of understanding diffusion-limited oxidation effects
[DE90-001385] 06 p0751 N90-14372
Novel polyimide compositions based on 4,4': Isophthaloyldiphthalic anaydride (IDPA)
[NASA-CASE-LAR-14194-1] 07 p0890 N90-15148
A review of the effects of microalloying constituents on the formation and breakdown of protective oxide scales on high-temperature alloys at temperatures below 700 C
[DE90-001277] 07 p0902 N90-15216
Report of the Advanced Neutron Source (ANS) Aluminum Cladding Corrosion Workshop
[DE90-001281] 07 p0903 N90-15217
Products of the hypochlorite oxidation of hydrazine fuels
[AD-A213557] 07 p0915 N90-15291
Partial reduction of re-oxidation processing of Y-Ba-Cu-O sputtered thin films
[DE90-003655] 07 p0999 N90-15782
Comprehensive mechanisms for combustion chemistry: An experimental and numerical study with emphasis on applied sensitivity analysis
[DE90-003904] 08 p1041 N90-16017
Solid state, surface, and catalytic studies of oxides
[DE90-004850] 08 p1134 N90-16566
Program to study the oxidation of carbon-carbon composites and coatings on these materials
[AD-A214989] 09 p1187 N90-16874
Cluster based reaction probabilities for boron with oxygen, hydrogen, water, nitrogen, nitrous oxide, carbon dioxide, carbon monoxide, methane, tetrafluoromethane, and silane
[AD-A214554] 09 p1190 N90-16894
Study of adherent oxide scales
[AD-A215189] 09 p1198 N90-16940
Surface analyses and modelling of rate multiplicity and instabilities
[DE90-005418] 10 p1352 N90-17838
Heat treatment study of the SiC/Ti-15-3 composite system
[NASA-TP-2970] 12 p1618 N90-19302
Synthesis and properties of a novel catalyst for the combustion of methane
[PB90-127499] 12 p1622 N90-19320
Effect of temperature on the storage life of polysulfide aircraft sealants
[MRL-TR-89-31] 12 p1629 N90-19364
Control of the RADM chemistry mechanism of the gas phase 12 p1687 N90-19690
Determination of fundamental thermodynamic properties of constituent materials and performance screening of candidate systems
[AD-A218089] 13 p1769 N90-20153
Structural comparison of nickel electrodes and precursor phases 13 p1824 N90-20472
High-temperature oxidation and sulfidation of Fe-20Cr-16Ni-4Al-1Y2O3 oxide-dispersion-strengthened alloy
[DE90-007897] 14 p1951 N90-21168
Improved Thermo-Oxidative-Deposition screening tests for turbine lubricants
[AD-A217795] 14 p1954 N90-21188
Testing carbon fabric for oxidation mass loss
15 p2063 N90-21819
Detailed mechanism for oxidation of benzene
[NASA-TM-102443] 15 p2067 N90-21842
Ternary reactions among polymer substrate-organohalogen-antimony oxides under pyrolytic, oxidative and flaming conditions
[PB90-154766] 15 p2071 N90-21861
Oxidation and ignition characteristics of hydrocarbon fuels
[AD-A218666] 16 p2215 N90-22637
Improved high temperature oxidation behavior of alloys by ion implantation
[AERE-R-13309] 16 p2217 N90-22650
Model catalytic oxidation studies using supported monometallic and heterobimetallic oxides
[DE90-009984] 16 p2220 N90-22664
Experimental evaluation of chemical cleaning processes for high-lifetime silicon processing
[DE90-009332] 16 p2226 N90-22699
Catalyst for carbon monoxide oxidation
[NASA-CASE-LAR-14155-1-SB]
17 p2374 N90-23517
Fuel-rich catalytic combustion: A fuel processor for high-speed propulsion
[NASA-TM-103177] 17 p2374 N90-23518
Anode materials for electrochemical waste destruction
18 p2514 N90-24354
High temperature oxidation of Ni3Al composites
[DE90-010145] 18 p2517 N90-24373
Low-Temperature CO-Oxidation Catalysts for Long-Life CO2 Lasers
[NASA-CP-3076] 18 p2556 N90-24586
CO-oxidation catalysts: Low-temperature CO oxidation over Noble-Metal Reducible Oxide (NMRO) catalysts
18 p2556 N90-24588
Pt/SnO2-based CO-oxidation catalysts for long-life closed-cycle CO2 lasers 18 p2556 N90-24589
The oxidation of carbon monoxide using tin oxide based catalysts 18 p2557 N90-24590
LaRC-developed catalysts for CO2 lasers
18 p2557 N90-24591
Phillips CO-oxidation catalyts for long-lived CO2 lasers: Activity and initial characterization studies
18 p2557 N90-24592
Synthesis, characterization and evaluation of CO-oxidation catalysts for high repetition rate CO2 TEA lasers 18 p2557 N90-24593
Alternative catalysts for low-temperature CO-oxidation
18 p2557 N90-24594
A computer program for the design of optimum catalytic monoliths for CO2 lasers 18 p2558 N90-24595
Mechanistic studies of the CO-oxidation reaction on catalysts for use in long-life CO2 lasers
18 p2558 N90-24596
The effect of H2O and pretreatment on the activity of a Pt/SnO2 catalyst 18 p2558 N90-24597
Effect of pretreatment on a platinized tin oxide catalyst used for low-temperature CO-oxidation
18 p2558 N90-24599
In situ analysis of CO during chemisorption and oxidation on graphite: Supported Pt by FTIR-microspectrometry
18 p2559 N90-24605
Calorimetry, activity, and micro-FTIR analysis of CO chemisorption, titration, and oxidation on supported Pt
18 p2560 N90-24606
Analysis of Pt/SnO(sub x) during catalysis of CO oxidation 18 p2560 N90-24607
Characterization of the surfaces of platinum/tin oxide based catalysts by Fourier Transform Infrared Spectroscopy (FTIR) 18 p2560 N90-24608
Chemisorption studies of Pt/SnO2 catalysts
18 p2560 N90-24609
Applications of low temperature CO-oxidation catalysts to breathable gases 18 p2561 N90-24615
Potential technology transfers of research on low-temperature carbon monoxide-oxygen recombination catalysts 18 p2562 N90-24616
The catalytic reactivity of thin film crystal surfaces
[DE90-010579] 18 p2622 N90-24937
Morphological control of inter-penetrating polymer networks 18 p2642 N90-25046
Oxidation characteristics of Ti-14Al-21Nb ingot alloy
[NASA-TP-3012] 19 p2674 N90-25206
Laboratory investigations: Low Earth orbit environment chemistry with spacecraft surfaces
19 p2732 N90-25531
A resistance strain gage with repeatable and cancellable apparent strain for use to 800 C
[NASA-CR-185256] 20 p2823 N90-26083
Carbon-carbon composites: Emerging materials for hypersonic flight
[NASA-TM-103472] 20 p2827 N90-26080
Oxidation and sulfidation of Type 310S stainless steel at elevated temperatures
[DE90-010149] 20 p2832 N90-26109
Quantitative confirmation of diffusion-limited oxidation theories
[DE90-012997] 20 p2838 N90-26143
Role of surface passivation in the integrated processing of MOS structures
[AD-A222630] 20 p2859 N90-26264
The effects of pretreatment conditions on a Pt/SnO2 catalyst for the oxidation of CO in CO2 lasers
[NASA-TM-103487] 20 p2867 N90-26309
Rapid thermal processing: A study of the silicon oxidation and of the implanted boron activation
[LAAS-90051] 20 p2932 N90-26681
Diamonds in detonation soot
21 p3094 N90-27585
Modeling of carbon monoxide oxidation kinetics over NASA carbon dioxide laser catalysts
[NASA-CR-186356] 22 p3155 N90-27885
A study of catalysts and mechanisms in synthesis reactions
[DE90-015064] 23 p3304 N90-28691
Oxidation, sulfidation, and hot corrosion: Mechanisms and interrelationships 23 p3307 N90-28702
Scale adherence effects in oxidation and sulfidation
23 p3307 N90-28703
Molten salt induced high temperature degradation of thermal barrier coatings 23 p3307 N90-28704
High temperature oxidation of Al-Li alloys
23 p3307 N90-28705
Fretting wear and fretting fatigue at temperatures up to 600 C 23 p3307 N90-28706
Evaluation of high temperature protective coatings for gas turbine engines under simulated service conditions
23 p3309 N90-28712
Oxidation of NiAl(110)
[DE90-015645] 24 p3451 N90-29487
Investigation of the effects of microalloy constituents, surface treatment and oxidation conditions on the development and breakdown of protective oxide scales
[DE90-015710] 24 p3451 N90-29488
Ion-beam mixing of Fe/B layers for tribological applications
[DE90-010091] 24 p3456 N90-29518

OXIDATION RESISTANCE
Emittance, catalysis, and dynamic oxidation of Ti-14Al-21Nb
[NASA-TP-2955] 01 p0044 N90-10248
Oxidation effects on the mechanical properties of SiC fiber-reinforced reaction-bonded silicon nitride matrix composites
[NASA-TM-102360] 06 p0736 N90-14287
Nickel berylides and their properties
[DE90-001736] 07 p0903 N90-15220
Experimental evaluation of new alloy coatings
[AD-A214922] 09 p1194 N90-16916
Short wavelength laser/materials interactions
[AD-A218015] 13 p1808 N90-20386

Titanium aluminides: Processing, properties and potential
[AERE-R-13198] 14 p1949 N90-21158
High temperature insulation barrier composite
[NASA-CASE-MFS-29241-1] 17 p2368 N90-23480
Soluble polysilanes: A new class of radiation sensitive O2-RIE resistant polymers for use in microlithography
[AD-A219476] 17 p2379 N90-23551
The oxidation and corrosion of ODS alloys
[NASA-TM-102555] 19 p2675 N90-25211
NASA Langley Research Center National Aero-Space Plane Mission simulation profile sets
[NASA-TM-102670] 23 p3276 N90-28541
Thermal shock and oxidation resistance of ceramic coatings 23 p3308 N90-28711
High performance brittle matrices and brittle matrix composites, book 1
[AD-A223273] 24 p3443 N90-29440
High performance brittle matrices and brittle matrix composites, book 2
[AD-A223274] 24 p3443 N90-29441

OXIDATION-REDUCTION REACTIONS

Combining spontaneous molecular assembly with microfabrication to pattern surfaces: Selective binding of isonitriles to platinum microwires and characterization by electrochemistry and surface spectroscopy
[AD-A209528] 01 p0039 N90-10213
Solvent relaxation in electron-transfer reactions: Comparisons between barrier-crossing dynamics in water and polar aprotic media
[AD-A210212] 01 p0040 N90-10220
Heterogeneous catalysts in water
[AD-A210742] 01 p0041 N90-10228
Solvent dynamical effects in electron transfer: Evaluation of electronic matrix coupling elements for metallocene self-exchange reactions
[AD-A210306] 01 p0121 N90-10692
Dynamics of nucleation at electrochemical interfaces via surface EXAFS and standing wave measurements
[AD-A210733] 02 p0195 N90-11109
Enhanced oxidation and solovolysis reactions in chemically inert microheterogeneous systems
[AD-A210748] 02 p0195 N90-11110
Capacitive behavior in conducting polymers: The ac impedance and quartz crystal microbalance studies
[AD-A210754] 02 p0201 N90-11150
Iron (III) initiated autoxidation of 1,2,3,4-tetrahydrocarbazole: An example of electron transfer
[AD-A211857] 03 p0323 N90-11836
Effect of electrical double layer on transport limited currents at microelectrodes
[AD-A211586] 03 p0324 N90-11843
Capacitive behavior in conducting polymers
[AD-A212448] 04 p0481 N90-12760
Electrochemical parameterization of metal complex redox potentials, using the ruthenium(III)/ruthenium(II) couple to generate a ligand electrochemical series
[AD-A214439] 08 p1041 N90-16015
Kinetics of the graphite/oxygen reaction in the in-pore diffusion controlled regime. Part 3: Influence of boundary layer diffusion in kinetic experiments at temperatures 970K to 1170K
[JUEL-2284-PT-3] 08 p1042 N90-16024
Direct measurements of the physical diffusion of redox active species: Microelectrochemical experiments and their simulation
[AD-A215680] 09 p1280 N90-17420
Oxidation and reduction of Bi2Sr1.85CuO(6-y) crystals
[DE90-004246] 09 p1287 N90-17460
Linear free energy relations for multielectron transfer kinetics: A brief look at the Bronsted/Tafel analogy
[AD-A215078] 12 p1710 N90-19823
Electrochemical phase diagrams for aqueous redox systems
[AD-A217168] 13 p1770 N90-20157
Ligand-centered electron-transfer redox processes for manganese, iron, and cobalt complexes in relation to selected catalytic systems
[AD-A217957] 13 p1773 N90-20177
All-solid-state thin-film rechargeable lithium batteries using solid redox polymerization electrodes
[DE90-008665] 13 p1796 N90-20306
Quartz crystal microbalance studies: Solvent effects in conducting polymer films
[AD-A219426] 17 p2372 N90-23502
Evaluation of ion intercalation in conducting polymers
[AD-A219423] 17 p2379 N90-23549
Quartz crystal microbalance analysis: Partial cation release during oxidation of conducting polymers
[AD-A221091] 18 p2530 N90-24439
Electrochemical, in situ Raman spectroscopic, and conductivity studies of polypyrrole incorporating large size anions: Conducting nature of reduced form
[AD-A222739] 20 p2831 N90-26102
A viologen/ruthenium oxide-based microelectrochemical diode with pH-dependent current-voltage characteristics
[AD-A221961] 21 p3000 N90-27052

OXIDE FILMS

Significance of oxide skins on powder for the quality of PM Al material --- PM (press molded)
[DFVLR-FB-89-11] 03 p0329 N90-11873
Glancing angle x ray studies of oxide films
[DE89-017828] 06 p0852 N90-14953
Computer-controlled ion beam sputter-deposition of superconducting oxide films
[AD-A213921] 07 p1004 N90-15812
Lithium cobalt oxide thin film and its electrochromism
[DE90-004570] 08 p1133 N90-16564
Solid state, surface, and catalytic studies of oxides
[DE90-004850] 08 p1134 N90-16566
Investigation of low temperature multilevel dielectrics for application for radiation tolerant, submicron-scaled IC technology
[AD-A216114] 10 p1433 N90-18273
Influence of ion beam mixing on the growth of high temperature oxide superconducting thin film
[DE90-004837] 10 p1435 N90-18280
Interfacial chemistry of MoS2 films on Si
[AD-A216527] 11 p1482 N90-18532
Significance of oxide skins on powder for the quality of PM Al materials
[ESA-TT-1178] 11 p1487 N90-18560
Growth and characterization of gallium (III) oxide films
[AD-A217568] 12 p1723 N90-19902
Ceramic oxide thin film formation utilizing biological processes
[DE90-008599] 13 p1781 N90-20225
Ceramic epitaxial films and multilayers prepared by MOCVD
[DE90-011090] 18 p2532 N90-24447
Epitaxy of TiO2 thin film on sapphire by MOCVDVD
[DE90-010054] 18 p2618 N90-24915
Deposition of electrooptic thin films
[DE90-010543] 18 p2619 N90-24922
Selective electrocatalysis of anodic oxygen-transfer reactions at chemically modified, thin-film lead dioxide electrodes
[DE90-011747] 20 p2857 N90-26252
Studies on ion scattering and sputtering processes relevant to ion beam sputter deposition of multicomponent thin films
[DE90-010071] 20 p2931 N90-26675
Passive mechanisms of surfaces produced by ion beam mixing and ion implantation
[AD-A222432] 21 p2982 N90-26945

OXIDES

NT ALKALINE EARTH OXIDES
NT ALUMINUM OXIDES
NT ANHYDRIDES
NT BARIUM OXIDES
NT BERYLLIUM OXIDES
NT BISMUTH OXIDES
NT CALCIUM OXIDES
NT CARBON DIOXIDE
NT CARBON MONOXIDE
NT CERIUM OXIDES
NT CHROMIUM OXIDES
NT COBALT OXIDES
NT COPPER OXIDES
NT DIOXIDES
NT GALLIUM OXIDES
NT HAFNIUM OXIDES
NT HEAVY WATER
NT HYDROGEN PEROXIDE
NT ILMENITE
NT LANTHANUM OXIDES
NT LEAD OXIDES
NT LITHIUM OXIDES
NT MAGNESIUM OXIDES
NT MANGANESE OXIDES
NT METAL OXIDES
NT MIXED OXIDES
NT MOLYBDENUM OXIDES
NT NICKEL OXIDES
NT NIOBIUM OXIDES
NT NITRIC OXIDE
NT NITROGEN DIOXIDE
NT NITROGEN OXIDES
NT NITROGEN TETROXIDE
NT NITROUS OXIDES
NT PEROXIDES
NT PLATINUM OXIDES
NT PLUTONIUM OXIDES
NT POTASSIUM OXIDES
NT QUARTZ
NT RUTILE
NT SAPPHIRE
NT SILICON DIOXIDE
NT SILICON OXIDES
NT SILVER OXIDES
NT SULFUR DIOXIDES
NT SULFUR OXIDES
NT TANTALUM OXIDES
NT TIN OXIDES
NT TITANIUM OXIDES
NT TUNGSTEN OXIDES
NT URANIUM OXIDES
NT VANADIUM OXIDES
NT YTTRIUM OXIDES
NT ZINC OXIDES
NT ZIRCONIUM OXIDES

Materials for engine applications above 3000 deg F: An overview
[NASA-TM-100169] 01 p0034 N90-10188
Processing and fabrication of high temperature oxide superconductors
[AD-A210197] 01 p0131 N90-10755
Mechanism of electrochemical activation of carbon electrodes: Role of graphite lattice defects
[AD-A211644] 03 p0325 N90-11845
Synthesis and properties of NdNiO(3) prepared by low temperature methods
[AD-A212117] 04 p0559 N90-13256
Preparation of 110K (Bi, Pb)-Sr-Ca-Cu-O superconductor from glass precursor
[NASA-CR-185162] 05 p0702 N90-14108
A model of the isotope effect of the oxide superconductor
[DE89-635907] 06 p0855 N90-14971
A review of the effects of microalloying constituents on the formation and breakdown of protective oxide scales on high-temperature alloys at temperatures below 700 C
[DE90-001277] 07 p0902 N90-15216
Design of a large angular aperture TeO2 acousto-optic tunable filter
[AD-A213999] 07 p0993 N90-15738
Review of new energy. Superconductivity
[DE90-734947] 09 p1287 N90-17464
Performance of superconductive oxides as cathodes for lithium rechargeable batteries
[AD-A216030] 10 p1401 N90-18098
Solid oxide fuel cell cogeneration system conceptual design, program 2
[PB90-114968] 12 p1681 N90-19653
Spallation of oxide scales from 20 percent Cr/25 percent Ni/Nb stainless steel
[AERE-R-13464] 13 p1775 N90-20189
High temperature chemistry of oxide superconductors
[DE90-007821] 13 p1895 N90-20875
Development of planar geometry solid oxide fuel cell technology, phase 2
[PB90-131293] 14 p2001 N90-21467
Specific heat and critical fluctuations in anisotropic high-T(sub c) oxide superconductors
[DE90-613394] 14 p2031 N90-21651
Modeling and experimental studies of oxide covered metal surfaces
[DE90-009961] 17 p2375 N90-23525
Graft copolymers of rigid-rod poly(p-phenylenebenzobisimidazole)
[AD-A220369] 17 p2380 N90-23555
Production and coating of pure boron powders
[AD-A220272] 18 p2533 N90-24452
The oxidation and corrosion of ODS alloys
[NASA-TM-102555] 19 p2675 N90-25211
Preparation and characterization of properties of oxynitride glasses and fibers
[AD-A221334] 19 p2677 N90-25227
Oxide thermal stability on gamma titanium aluminide
[DE90-012054] 19 p2678 N90-25232
Fabrication of composite high temperature superconductor wires from Ag/YBa2Cu3O(sub x) powder produced by AgNO3 decomposition
[AD-A221936] 21 p3083 N90-27532
Ternary and quaternary oxides of Bi, Sr, and Cu 22 p3141 N90-27817
Crystal chemical and quantum chemical studies of Ba(Sr)-Nb oxide compounds 22 p3150 N90-27858
Superconductivity in the Sn-Ba-Sr-Y-Cu-O system 22 p3151 N90-27863
A YBCO RF-SQUID magnetometer and its applications 22 p3151 N90-27867
Monolithic solid oxide fuel cell technology development, phase 1A
[PB90-183237] 22 p3195 N90-28132
High temperature surface interactions: Overview 23 p3306 N90-28699
Dynamical information for Fe doped YBa2Cu3O7 superconducting oxides obtained from high temperature Moessbauer studies
[DE90-627871] 23 p3401 N90-29218
Extended characterization of the damage by hot charge carriers in gate oxide by short channel MOS field effect transistors
[ETN-90-97313] 24 p3555 N90-30114

OXIDIZERS
NT LIQUID OXYGEN
NT PHOTOCHEMICAL OXIDANTS
NT ROCKET OXIDIZERS
Inorganic halogen oxidizers
[AD-A213990] 07 p0915 N90-15294
Effect of reduced atmospheric pressure on the performance characteristics of pyrotechnic compositions containing aluminum
[AD-A214473] 09 p1200 N90-16953
Space shuttle RCS oxidizer leak repair for STS-26 11 p1474 N90-18485
A parametric heat transfer study for cryogenic ball bearings in SSME HPOTP 12 p1635 N90-19397
Airliner cabin ozone: An updated review
[AD-A219264] 16 p2276 N90-22970
Hybrid propulsion technology program
[NASA-CR-183952] 21 p2968 N90-26870
Ignition and combustion characteristics of metallized propellants
[NASA-CR-186870] 21 p2976 N90-26911
Atmospheric dispersion of solid and liquid rocket propellants
[AD-A221293] 21 p3020 N90-27173

OXYACETYLENE
An investigation of diamond film deposition in a premixed oxyacetylene flame
[AD-A212595] 04 p0561 N90-13268

OXYALKYLATION
U ALKYLATION

OXYGEN
NT LIQUID OXYGEN
NT OXYGEN ISOTOPES
NT OXYGEN 18
Reaction of oxygen with allene
[DE89-015219] 01 p0039 N90-10216
Method and apparatus for maintaining thermal control in plasma conditions
[NASA-CASE-MFS-28368-1] 01 p0125 N90-10717
A new inexpensive electrochemical meter for oxygen in sodium coolant
[DE89-630802] 02 p0194 N90-11104
Ionospheric total electron content, and far ultraviolet, near infrared oxygen emission 02 p0249 N90-11410
In-situ spectroscopic studies of transition metal macrocycles as catalysts for the electrochemical reduction of oxygen
[PB89-219273] 03 p0321 N90-11826
Ignition characteristics of the nickel-based alloy UNS N07718 in pressurized oxygen
[NASA-CR-185932] 03 p0326 N90-11850
Lifetime of singlet oxygen in aqueous hydrogen peroxide (BHP)
[AD-A211545] 03 p0403 N90-12306
Measurement and correlation of the solubility and diffusion coefficient for oxygen and chlorine in basic hydrogen peroxide
[AD-A212348] 04 p0472 N90-12703
Metallo-organic decomposition process for dielectric films
[AD-A211590] 04 p0495 N90-12849
Microwave excitation of oxygen O2 (delta 1) for an oxygen-iodine laser
[DFVLR-FB-89-23] 04 p0506 N90-12919
Semiconductor measurement technology: Database for and statistical analysis of the interlaboratory determination of the conversion coefficient for the measurement of the interstitial oxygen content of silicon by infrared absorption
[PB89-221170] 04 p0558 N90-13253
CANOES 2: Dynamics of atmospheric infrared thermochemical excitation, volume 1
[AD-A213341] 05 p0667 N90-13897
CANOES 2: Dynamics of atmospheric infrared thermochemical excitation, volume 2
[AD-A213342] 05 p0667 N90-13898
Model system studies with a phase separated membrane bioreactor 05 p0679 N90-13954
Fermentation and oxygen transfer in microgravity 05 p0679 N90-13956
The thermally induced gas-phase reactions of methane and oxygen: A comparison of experimental and computational results
[DE90-000785] 06 p0742 N90-14317
Test and evaluation of polymeric membranes for oxygen enrichment of air
[DE90-000555] 06 p0742 N90-14321
The formation of metal-oxygen species at low temperatures
[DE90-002298] 06 p0743 N90-14323
Oxygen stoichiometry, structural transitions, and thermodynamic behavior of the YBa2Cu3O(x) system
[DE89-017694] 06 p0852 N90-14951
Anisotropy of oxygen tracer diffusion in YBa2Cu3O7-delta single crystals
[DE90-001931] 06 p0856 N90-14979
Oxygen electrode in molten carbonate fuel cells
[DE90-002871] 07 p0952 N90-15510
Solid-state electrolyte catalysis for methane and oxygen synthesis
[PB90-100231] 08 p1040 N90-16011
Effects of gravity waves on the polar O2 and OH airglow 08 p1101 N90-16373
Computation of the unsteady facilitated transport of oxygen in hemoglobin
[NASA-TM-102251] 08 p1106 N90-16400
The effects of oxygen and strontium vacancies on the superconductivity of single crystals of Bi2Sr(2-x)CuO(6-y)
[DE90-004242] 08 p1133 N90-16561
Electron beam induced oxygen in YBa2Cu3O(7-x) superconductors
[DE90-004839] 08 p1133 N90-16565
Electrochemical cell for obtaining oxygen from carbon dioxide atmospheres
[NASA-CR-186225] 09 p1189 N90-16886
Strengthening of aluminum by oxygen implantation: Experimental results and mechanical modeling
[DE90-005960] 09 p1195 N90-16924
The preparation and characterisation of oxynitride glasses and glass-ceramics
[AD-A214783] 09 p1197 N90-16935
Reactions of atmospheric species with clean and H, C, and O implanted species
[AD-A214602] 09 p1244 N90-17218
Singlet oxygen and iodine monofluoride collisional energy transfer mechanism
[AD-A215711] 09 p1260 N90-17421
Optical waveguide fabrication by stoichiometric implantation of Ti and O into LiNbO3
[DE90-004238] 09 p1292 N90-17468
Effect of oxygen on the tear strength of elastomers
[AD-A215845] 10 p1359 N90-17879
Research in energetic compounds
[AD-A214106] 10 p1360 N90-17887
Simultaneous observations of the emissions OI (5577), O2A(0.1), NaD(5893) and OH(9.4) and the rotational temperatures TO2 and TOH in the upper atmosphere
[INPE-4851-TDL/366] 10 p1407 N90-18113
Lower limits on the absolute dissociative electron attachment cross section from O2 condensed on rare-gas films
[AD-A216727] 11 p1483 N90-18536
Millimeter-wave propagation in the mesosphere
[PB90-119868] 11 p1496 N90-18612
Oxygen electrode in molten carbonate fuel cells
[DE90-005377] 11 p1528 N90-18796
Design and operation of an inert gas facility for thermoelectric generator storage
[DE90-007146] 11 p1565 N90-19008
Electron stimulated O(-) desorption from O2 condensed on a rare-gas film: Evidence for an indirect Bounce trajectory
[AD-A216725] 12 p1622 N90-19322
High-purity beryllium foils
[DE90-006408] 12 p1626 N90-19348
Laser surface interactions of high-(Tc) superconductors
[DE90-006894] 12 p1669 N90-19587
Experiments on oxygen desorption from surface warm seawater under Open-Cycle Ocean Thermal Energy Conversion (OC-OTEC) conditions
[DE90-000308] 12 p1683 N90-19666
Predicting effects of global climate change on reservoir water quality and fish habitat
[DE90-003674] 12 p1689 N90-19704
Oxygen concentrations on surfaces of carbon fibers
[AD-A217724] 13 p1769 N90-20152
A technical and economic evaluation of oxygen-enriched combustion in diesel engines using water-emulsified fuels
[DE90-008095] 13 p1810 N90-20394
Oxygen electrodes for rechargeable alkaline fuel cells-II 13 p1823 N90-20469
Copper and oxygen NMR studies on the magnetic properties of YBa2Cu3O(7-y)
[DE90-007889] 13 p1893 N90-20863
O2 reduction at the IFC orbiter fuel cell O2 electrode
[NASA-TM-102580] 14 p2001 N90-21469
Zones of feasibility for retrieval of surface pressure from observations of absorption in the A band of oxygen
[DAR-TP-19] 14 p2006 N90-21495
Device for quickly sensing the amount of O2 in a combustion product gas
[NASA-CASE-LAR-13816-1] 15 p2102 N90-22025
Effect of surface oxygen on adhesion of carbon fiber-reinforced composites
[AD-A220777] 17 p2369 N90-23486
Wear of gold-plated contacts: Microscopic aspects, role of oxygen 18 p2538 N90-24479
Synthesis of ceramic superconductors under low oxygen pressure
[DE90-010415] 18 p2621 N90-24933
Contract crystal growth and fabrication services
[AD-A221357] 18 p2623 N90-24947
Thermodynamic and fluid mechanic analysis of rapid pressurization in a dead-end tube 18 p2631 N90-24990
Method and apparatus for assessing distillate fuel stability by oxygen overpressure
[AD-D014499] 19 p2679 N90-25237
Diversiform processes of ozone in the atmosphere: Introduction study
[AERONOMICA-ACTA-A-352-1990] 19 p2713 N90-25439
Mars in situ propellants: Carbon monoxide and oxygen ignition experiments
[NASA-TM-103202] 20 p2823 N90-26065
Photodissociation of O2 in the stratosphere and mesosphere: A general parametrization of the Schumman-Runge Bands 20 p2887 N90-26427
Oxygen stabilization induced enhancement in J(sub c) and T(sub c) of superconducting oxides 22 p3137 N90-27800
Effect of oxygen stoichiometry on T(sub c) of Bi-based superconductors 22 p3142 N90-27818
Study of local structure and magnetism in high-T(sub c) copper oxide superconductors 22 p3143 N90-27824
Catalytic ignition of hydrogen/oxygen 23 p3293 N90-28627
Investigation of the effects of microalloy constituents, surface treatment and oxidation conditions on the development and breakdown of protective oxide scales
[DE90-015710] 24 p3451 N90-29488
Oxygen deficiency monitor system
[DE90-014866] 24 p3523 N90-29917
Optical emissions from bombarding atmospheric gases with heavy ions
[AD-A223544] 24 p3543 N90-30040
First principles calculation of oxygen ordering in YBa2Cu3O(7-y)
[DE90-015205] 24 p3553 N90-30102
High resolution transmission electron microscopy of partial states of oxygen order in YBa2Cu3O(z)
[DE90-015637] 24 p3554 N90-30108

OXYGEN ANALYZERS
A reliable, maintenance-free oxygen sensor for aircraft using an oxygen-sensitive coating on potentiometric electrodes
[AD-A222696] 23 p3277 N90-28545

OXYGEN ATOMS
Retrieval of atomic oxygen and temperature in the thermosphere. Part 2: Feasibility of an experiment based on limb emission in the OI lines
[AD-A211807] 03 p0371 N90-12121
Retrieval of atomic oxygen and temperature in the thermosphere. Part 1: Feasibility of an experiment based on the spectrally resolved 147 micrometer limb emission
[AD-A211987] 04 p0517 N90-12986
Design development, qualification, and flight production of an ATOX resistant flexible solar array for low earth orbit mission 10 p1344 N90-17796
Simultaneous observations of the emissions OI (5577), O2A(0.1), NaD(5893) and OH(9.4) and the rotational temperatures TO2 and TOH in the upper atmosphere
[INPE-4851-TDL/366] 10 p1407 N90-18113
Absolute cross-sections for dissociative electron attachment in O2 condensed on Kr films
[AD-A216730] 11 p1570 N90-19038
Computation of hypersonic low density flows with thermochemical nonequilibrium 13 p1749 N90-20044
The effect of leveling coatings on the atomic oxygen durability of solar concentrator surfaces
[NASA-TM-102557] 14 p1941 N90-21110
Low latitude F-region dynamical processes from atomic oxygen nightglow emissions
[INPE-4999-PRE/1561] 14 p2006 N90-21494
The interpretation of SAGE 2 ozone measurements in the lower mesosphere 15 p2124 N90-22149
Synthesis and characterization of aromatic polyester and polysiloxane containing block copolymers: Multiphase transparent atomic oxygen resistant damping materials, liquid crystal films, and toughening components of sol/gel glasses
[AD-A218871] 16 p2224 N90-22685
Investigation of lubrication characteristics of MoS2 films in space environment 18 p2537 N90-24472
Laser surface interactions of high-T(sub c) superconductors 22 p3139 N90-27809
Hyperthermal atomic oxygen generator
[NASA-CR-186573] 22 p3155 N90-27889
The effects of atomic oxygen on the thermal emittance of high temperature radiator surfaces
[NASA-TM-103224] 23 p3301 N90-28670
Quenching of N(2D) by O(3P)
[AD-A221690] 23 p3303 N90-28683

OXYGEN BREATHING
Potential for reduction of decompression sickness by prebreathing with 100 percent oxygen while exercising
[AD-A213449] 07 p0966 N90-15581
The characteristics of physiological responses and tolerance evaluation of pressure breathing
[AD-A214991] 09 p1252 N90-17262
Evaluation of the Scott aviation portable protective breathing device for contaminant leakage as prescribed by FAA Action Notice A-8150.2. Phase 1: Original tests of the portable protective breathing device. Phase 2: Tests of the redesigned portable protective breathing device
[AD-A216799] 12 p1601 N90-19214
Effects of high altitude hypoxia on lung and chest wall function during exercise
[AD-A219814] 17 p2434 N90-23869

OXYGEN CONSUMPTION
The effect of caffeine on endurance time to exhaustion at high altitude
[AD-A212069] 03 p0380 N90-12163
Prediction of thermal stress casualties
[AD-A212356] 04 p0523 N90-13022
The predictability and efficiency of human walking: Metabolic, mechanical, and biophysical considerations
15 p2137 N90-22211
Work enhancement and thermal changes during intermittent work in cool water after carbohydrate loading
[AD-A222877] 21 p3034 N90-27247

OXYGEN DEFICIENCY
U HYPOXIA

OXYGEN DETECTORS
U OXYGEN ANALYZERS

OXYGEN FLUORIDES
Experimental studies on energy storage
[AD-A219032] 16 p2252 N90-22845

OXYGEN IONS
Ion implantation of two titanium alloys
[DE89-016958] 02 p0198 N90-11133
Can ion acceleration by double-cyclotron absorption produce O(+) ion conics
[IRF-PREPRINT-114] 02 p0280 N90-11600
Model of oxygen ions resonant lines emission of REB-heated plasma
[IPPCZ-294] 10 p1432 N90-18261
Thermoelectric conversion with ion conductors
[AD-A217822] 13 p1828 N90-20497
Experimental investigations of low-energy (4 to 40 eV) collisions of O(-)(P2) ions and O(P3) atoms with surfaces
19 p2732 N90-25530

OXYGEN ISOTOPES
NT OXYGEN 18
Target nucleus fragmentation in O16 + (Ag,Br) interactions at 200 A GeV
[LUIP-8906] 07 p0991 N90-15727
On the observation of a transition from fusion to multifragmentation in high multiplicity O16 induced reactions
[LUIP-8812] 08 p1119 N90-16481
Stable isotope studies of cometary analogue materials
12 p1740 N90-20001
Isotope exchange in oxide-containing catalyst
[NASA-CASE-LAR-13542-2-SB]
13 p1769 N90-20154
The 16-O photodisintegration at low energies
[NOTA-INTERNA-941] 16 p2315 N90-23196
Kinetic and extraction measurements on 12C18O2
[AD-A220417] 17 p2472 N90-24133
Rare-isotope and kinetic studies of Pt/SnO2 catalysts
18 p2558 N90-24598

OXYGEN METABOLISM
Measurement of mechanical work and energy expenditure in running and bicycling
05 p0675 N90-13935

OXYGEN PLASMA
Oxygenation and possible etching of high T(sub c) superconducting films by oxygen plasma
[DE90-004956] 12 p1719 N90-19871
Polycrystalline diamond Junction Field Effect Transistors (JFETS)
[AD-A222238] 21 p3083 N90-27534

OXYGEN PRODUCTION
New calculations of photodissociation cross-sections in the O2 Schumann-Runge system
05 p0657 N90-13834
Oxygen and other atmospheric gases
[AD-A214296] 07 p0961 N90-15557
Getting lunar ilmenite: From soils or rocks
[NASA-CR-186498] 12 p1744 N90-20029
Impact of low gravity on water electrolysis operation
[NASA-CR-185521] 15 p2072 N90-21870
Expert systems for automated maintenance of a Mars oxygen production system
[NASA-CR-186209] 15 p2138 N90-22215
Space Station Freedom environmental control and life support system phase 3 simplified integrated test detailed report
[NASA-TM-4204] 16 p2207 N90-22593

OXYGEN RECOMBINATION
CANOES 2: Dynamics of atmospheric infrared thermochemical excitation, volume 4
[AD-A213344] 05 p0667 N90-13900
Potential technology transfers of research on low-temperature carbon monoxide-oxygen recombination catalysts 18 p2562 N90-24616

OXYGEN SPECTRA
Retrieval of atomic oxygen and temperature in the thermosphere. Part 2: Feasibility of an experiment based on limb emission in the OI lines
[AD-A211807] 03 p0371 N90-12121
A self-consistent model of the most common nightglow emissions 05 p0660 N90-13853

OXYGEN SUPPLY EQUIPMENT
Comparison of protective breathing equipment performance at ground level and 8,000 feet altitude using parameters prescribed by portions of FAA action notice A-8150.2
[AD-A212852] 06 p0821 N90-14773
RAAF Orion aircraft A9-300 oxygen fire
[AD-A215496] 09 p1162 N90-16725
Hybrid propulsion technology program. Volume 1: Conceptional design package
[NASA-CR-183953] 15 p2060 N90-21793
Hybrid propulsion technology program. Volume 2: Technology definition package
[NASA-CR-183954] 15 p2060 N90-21794
Lunar base 2 (the second thousand days of a base on the Moon)
[ILR-MITT-230(1989)] 16 p2275 N90-22968

OXYGEN SYSTEMS
U OXYGEN SUPPLY EQUIPMENT

OXYGEN 18
Rare-isotope and kinetic studies of Pt/SnO2 catalysts
18 p2558 N90-24598

OXYGEN-HYDROCARBON ROCKET ENGINES
LOX/hydrocarbon combustion instability investigation
[NASA-CR-182249] 05 p0615 N90-13589
Cooling of rocket thrust chambers with liquid oxygen
[NASA-TM-103146] 16 p2210 N90-22605
Advanced Earth-to-Orbit Propulsion Technology 1988, volume 1
[NASA-CP-3012-VOL-1] 23 p3290 N90-28611
Computer code for the prediction of nozzle admittance
23 p3293 N90-28630

OXYGENATION
MOBILE4 oxygenated fuels version user's guide
[PB89-230700] 05 p0629 N90-13674
Selectivity of the reactions of oxygenates on transition metal surfaces
[DE90-003911] 08 p1045 N90-16040
Oxygenation and possible etching of high T(sub c) superconducting films by oxygen plasma
[DE90-004956] 12 p1719 N90-19871
Cation and anion tracer diffusion in YBa(sub 2)Cu(sub 3)O(sub 7-delta)
[DE90-009708] 18 p2620 N90-24927

OXYNITRIDES
Y-Si-Al-O-N glass fibers
[AD-A211170] 02 p0190 N90-11088
The preparation and characterisation of oxynitride glasses and glass-ceramics
[AD-A214783] 09 p1197 N90-16935
Preparation and characterization of properties of oxynitride glasses and fibers
[AD-A221334] 19 p2677 N90-25227

OZONE
Atmospheric chemistry of the fuel hydrazines
02 p0203 N90-11158
Ozonation of hydrazines and their associated impurities 02 p0205 N90-11174
Modeling the ozonolysis of hydrazines wastewater
02 p0205 N90-11175
Fuel neutralization by ozone oxidation
02 p0206 N90-11176
Interrelation of experimental exposure and ambient air quality data for comparison of ozone exposure indices and estimating agricultural losses
[PB89-195036] 02 p0238 N90-11353
Are ozone exceedance rates decreasing. Comment on extreme value analysis of environmental time-series: An application to trend detection in ground-level ozone
[AD-A211029] 02 p0239 N90-11357
Micrometeorological investigation of surface exchange of trace gases: A case study
[PB89-208375] 02 p0249 N90-11412
Theoretical investigation of gas-surface interactions
[NASA-CR-185492] 02 p0272 N90-11552
Studies of baroclinic instability in the presence of surface topography and stratospheric ozone
03 p0361 N90-12068
Use of satellite data and modeling to asses the influence of stratospheric processes on the troposphere
03 p0363 N90-12075
Ozone depletion, greenhouse gases, and climate change
[PB89-216097] 03 p0369 N90-12110
Sensitivity of a regional oxidant model to variations in climate parameters, volume 1 and 2
[PB89-224943] 04 p0516 N90-12981
Proceedings: US/FRG (Federal Republic of Germany) Workshop on Photochemical Ozone Problem and Its Control: US Experiences and the Situation in Europe
[PB89-233514] 05 p0666 N90-13891
CANOES 2: Dynamics of atmospheric infrared thermochemical excitation, volume 4
[AD-A213344] 05 p0667 N90-13900
Discussions of global environmental problems
[DE90-002747] 06 p0811 N90-14718
A model for the simulation of the ozone budget in the atmosphere under anthropogenic perturbation
[DE89-636294] 06 p0811 N90-14719
The retrieval of the concentrations of nitric oxide and nitrogen dioxide from satellite solar occultation measurements at sunset and sunrise
06 p0814 N90-14733
Variability of cultivar responses to ozone
[PB89-225460] 07 p0956 N90-15528
ECC (Electrochemical Concentration Cell) ozonesonde observations at Mirny, Antarctica, during 1988
[PB90-113960] 08 p1098 N90-16357
Operational ozone monitoring with the Global Ozone Monitoring Radiometer (GOMR)
[PB90-114034] 08 p1098 N90-16359
Environmental, health, and CFC substitution aspects of the ozone depletion issue
[DE90-004404] 08 p1099 N90-16363
The chemistry and dynamics of marine stratocumulus
08 p1102 N90-16381
Time and spatially dependent estimates of pollutant trace gas emissions and their effect on tropospheric ozone 09 p1243 N90-17212
Nimbus 7 solar backscatter ultraviolet (SBUV) ozone products user's guide
[NASA-RP-1234] 09 p1246 N90-17227
A 3-D dynamical/chemical GCM for simulating the anthropogenical effects on ozone
[DE90-004836] 10 p1406 N90-18108
Simulation of a weather situation with high ozone concentrations during ALPEX 12 p1686 N90-19686
The EURAD model in EUROTRAC
12 p1689 N90-19701
Air pollution-caused changes in photosynthesis: Effects on plant growth and rhizosphere functions
[DE90-007184] 13 p1829 N90-20501
The development of ultraviolet-ozone cleaning as a production process in the packaging of integrated circuits
[DE90-007960] 14 p1959 N90-21220
Effects of Air Pollution on Western Forests
[PB90-131111] 14 p2003 N90-21481
Source attribution for tropospheric ozone in the US
[DE90-007994] 14 p2004 N90-21484
The interpretation of SAGE 2 ozone measurements in the lower mesosphere 15 p2124 N90-22149
The calculation of infrared limb emission by ozone in the terrestrial middle atmosphere
15 p2125 N90-22151
Opportunities for US-USSR cooperation in the investigation of Arctic stratospheric ozone
15 p2125 N90-22154
Airliner cabin ozone: An updated review
[AD-A219264] 16 p2276 N90-22970
Feasibility study for a microwave-powered ozone sniffer aircraft
[NASA-CR-186660] 17 p2353 N90-23397
The diurnal ozone cycle in a coniferous forest: The importance of meteorology and chemistry
[CM-75] 17 p2421 N90-23795
Nimbus-7 TOMS Antarctic ozone atlas: August through November, 1989
[NASA-RP-1237] 17 p2428 N90-23837
NASA/USRA high altitude reconnaissance aircraft
[NASA-CR-186685] 18 p2496 N90-24266
High altitude ozone research balloon
[NASA-CR-186653] 19 p2654 N90-25107
Diversiform processes of ozone in the atmosphere: Introduction study
[AERONOMICA-ACTA-A-352-1990]
19 p2713 N90-25439
Catching our breath: Next steps for reducing urban ozone
[PB90-130451] 20 p2883 N90-26398
Measurements of CH4, N2O, CO, H2O and O3 in the middle atmosphere by the ATMOS experiment on Spacelab 3
[NASA-TM-103476] 20 p2883 N90-26400

The global consequences of increasing tropospheric ozone concentrations
[NASA-TM-103477] 20 p2883 N90-26401
The diurnal ozone cycle in a coniferous forest: The importance of meteorology and chemistry
20 p2886 N90-26423
Analysis of cirrus optical properties with data from NASA ER2 High-resolution Interferometer Sounder (HIS)
[NASA-CR-186365] 21 p3030 N90-27227
Evaluation of the role of ozone, acid deposition, and other airborne pollutants in the forests of eastern North America
[PB90-184896] 22 p3197 N90-28140
Response of the middle atmosphere to solar UV and dynamical perturbations 22 p3204 N90-28175
Stratospheric effects of solar ultraviolet variations on the solar rotation time scale 22 p3204 N90-28176
Gases of the middle atmosphere and short-term solar radiation variations 22 p3204 N90-28177
Atmospheric planetary waves induced by solar rotation 22 p3204 N90-28178
On the relationship between the phases of 27-day total ozone and solar activity indices in different latitudinal zones 22 p3205 N90-28180
Total ozone time variations during the spring reversals in the high latitudinal stratosphere of the Northern Hemisphere during the 20th and 21st solar cycles
22 p3205 N90-28181
The vertical ozone distribution during maximum and minimum solar activity 22 p3205 N90-28182
Diurnal and temporal variation of UV-flux and its dependence on stratospheric ozone
22 p3205 N90-28184
An influence of solar activity on latitudinal distribution of atmospheric ozone and temperature in 2-D radiative-photochemical model 22 p3206 N90-28187
Solar wind and high energy particle effects in the middle atmosphere 22 p3206 N90-28188
The effects of solar particle events on the middle atmosphere 22 p3206 N90-28189
A change of mesospheric ozone content under electron precipitation influence 22 p3207 N90-28191
Comparison of satellite derived dynamical quantities in the stratosphere of the Southern Hemisphere
22 p3210 N90-28210
Ozone for trace organic contaminant removal
[PB90-221680] 23 p3347 N90-28916
The global cycle of reactive nitrogen
[DE90-015041] 23 p3348 N90-28919
Acid deposition: No such thing as a free launch
[DE90-015085] 23 p3348 N90-28920
Tropospheric nitrogen: The influence of anthropogenic sources on distributions and deposition, executive summary
[DE90-015401] 23 p3348 N90-28922
Present state of knowledge of the upper atmosphere 1990: An assessment report
[NASA-RP-1242] 23 p3350 N90-28929
Trend analysis of total ozone data
24 p3486 N90-29703
Success of EPA's stratospheric ozone engineering research
[PB90-246265] 24 p3487 N90-29706
Tropospheric nitrogen: The influence of anthropogenic sources on distributions and deposition
[DE90-015406] 24 p3487 N90-29709
Measurements of the high altitude infrared characteristics of the atmosphere
[AD-A224401] 24 p3491 N90-29728
A study of water vapor, electrical parameters, and radio propagation
[AD-A223582] 24 p3492 N90-29736

OZONE DEPLETION
Geophysical monitoring for climatic change number 16
[PB89-159628] 01 p0087 N90-10494
Stratospheric ozone depletion
[PB89-207476] 02 p0238 N90-11354
Ozone depletion, greenhouse gases, and climate change
[NASA-CR-185323] 03 p0367 N90-12101
Ozone Research Program (German contribution to climate and atmosphere research)
[REPT-46-88] 03 p0369 N90-12111
Consumer Ozone Protection Act of 1989
[S-HRG-101-377] 06 p0809 N90-14708
International aspects of restrictions of ozone-depleting substances
[DE90-001813] 07 p0957 N90-15534
ECC (Electrochemical Concentration Cell) ozonesonde observations at South Pole, Antarctica, during 1988
[PB90-110172] 08 p1098 N90-16355
Scientific linkages in global change
[PB90-112608] 08 p1098 N90-16356
Potential impact of stratospheric ozone depletion on marine ecosystems
[PB90-112616] 08 p1098 N90-16360
Environmental, health, and CFC substitution aspects of the ozone depletion issue
[DE90-004404] 08 p1099 N90-16363
Experimental performance of ozone-safe alternative refrigerants: Experimental performance comparisons of R32, R125, R143a, R218, R134a, R152a, R124, R142b, RC318 and R143 in a refrigeration circuit
[DE90-009227] 15 p2073 N90-21876
Opportunities for US-USSR cooperation in the investigation of Arctic stratospheric ozone
15 p2125 N90-22154
On the antarctic ozone depletion during solar cycle 21
[NOTA-INTERNA-943] 16 p2253 N90-22849
Earth observation from the interstellar space
[REPT-44/89] 17 p2418 N90-23781
Nimbus-7 TOMS Antarctic ozone atlas: August through November, 1989
[NASA-RP-1237] 17 p2426 N90-23837
Reports from the German Meteorological Service. No. 179: Development, realization and functioning of lidar to evaluate the atmospheric ozone profile
[ISBN-3-88148-252-0] 18 p2578 N90-24685
Global changes in tropospheric chemistry
19 p2708 N90-25411
Results from the IVL TOR Station at Roervik, Sweden. A contribution to the EURATRAC subproject TOR
20 p2885 N90-26415
Vertical ozone probing with lidar
20 p2885 N90-26416
Stratospheric chemistry 20 p2886 N90-26424
Subjective-probability-based scenarios for uncertain input parameters: Stratospheric ozone depletion
[N-3140-EPA/JMO/RC] 22 p3199 N90-28157
The mesospheric responses to short-term solar ultraviolet variability 22 p3204 N90-28174
The effects of solar particle events on the middle atmosphere 22 p3206 N90-28189
Present state of knowledge of the upper atmosphere 1990: An assessment report
[NASA-RP-1242] 23 p3350 N90-28929

OZONE HOLE
U OZONE DEPLETION

OZONE LAYER
U OZONOSPHERE

OZONOMETRY
Operational ozone monitoring with the Global Ozone Monitoring Radiometer (GOMR)
[PB90-114034] 08 p1098 N90-16359
Nimbus 7 solar backscatter ultraviolet (SBUV) ozone products user's guide
[NASA-RP-1234] 09 p1246 N90-17227
Vertical ozone probing with lidar
20 p2885 N90-26416
The diurnal ozone cycle in a coniferous forest: The importance of meteorology and chemistry
20 p2886 N90-26423

OZONOSPHERE
Ozone Research Program (German contribution to climate and atmosphere research)
[REPT-46-88] 03 p0369 N90-12111
NASA/USRA high altitude reconnaissance aircraft
[NASA-CR-186685] 18 p2496 N90-24266
Reports from the German Meteorological Service. No. 179: Development, realization and functioning of lidar to evaluate the atmospheric ozone profile
[ISBN-3-88148-252-0] 18 p2578 N90-24685
Diversiform processes of ozone in the atmosphere: Introduction study
[AERONOMICA-ACTA-A-352-1990]
19 p2713 N90-25439

P

P WAVES
Measurements of high frequency seismic waves
[AD-A219370] 16 p2256 N90-22863
Input-output characterization of fiber reinforced composites by P waves
[NASA-CR-185287] 22 p3189 N90-28097

P-I-N DIODES
U DIODES
U P-I-N JUNCTIONS

P-I-N JUNCTIONS
Studies of high power density, pico-second rise-time light activated semiconductor switch
[AD-A210549] 01 p0061 N90-10349
Channelized coplanar waveguide pin-diode switches
[NASA-TM-102289] 03 p0341 N90-11943
Integrated optoelectronic receivers
[AD-A213376] 05 p0700 N90-14098
Preparation and properties of high deposition a-Si:H films and solar cells using disilane
[DE89-009467] 06 p0804 N90-14679
An electron-beam controlled semiconductor switch
[AD-A217181] 13 p1793 N90-20288
Coplanar waveguide discontinuities for P-I-N diode switches and filter applications
[NASA-TM-102534] 14 p1969 N90-21278
Research on amorphous silicon-based thin film photovoltaic devices. Task B: Research on stable high efficiency large area, amorphous silicon-based submodules
[DE90-000320] 14 p2002 N90-21473
An influence of fast neutron irradiation on the properties of p-i-n wide-based diodes
[DE90-611148] 18 p2550 N90-24556

P-N JUNCTIONS
Development of high performance beta-SiC field-effect transistors
[AD-A213885] 07 p0924 N90-15346
Investigations of x ray sensitive PN-CCD's
[MPE-213] 12 p1653 N90-19499

P-N-P-N JUNCTIONS
A GaAs p-n-p-n thyristor model
[DE90-005757] 11 p1570 N90-19039

P-TYPE SEMICONDUCTORS
Scanning tunneling microscopy etching of micrometer level features on p-type GaAs
[AD-A209216] 01 p0058 N90-10328
Dielectric spectroscopy of semiconductors
[AD-A211989] 04 p0559 N90-13255
Defect control and denuded trap zones in the 3-5 semiconductors
[AD-A214099] 07 p1004 N90-15814
Carbon doping of compound semiconductor epitaxial layers using carbon tetrachloride
[AD-A215053] 09 p1290 N90-17477
Workshop on Hydrogen Effects in InP and Related Compounds
[AD-A215197] 09 p1290 N90-17479
Dopant site location in dual-implanted GaP using (111) planar channeling
[DE90-006565] 11 p1571 N90-19042
Passivation and gating of GaAs and Si surfaces using pseudomorphic structures
[AD-A219351] 16 p2325 N90-23256
Improving the performance of InAs(1-x)Sb(x)/InSb infrared detectors grown by metal organic chemical vapor deposition
[DE90-009743] 18 p2625 N90-24956
Fundamental studies and device development in beta silicon carbide
[AD-A219253] 19 p2676 N90-25220
Research on mercury cadmium telluride
[AD-A224250] 24 p3448 N90-29474
Integrated technology in MCT/GaAs and MCT/Si for medium and long wavelength infrared
[AD-A223557] 24 p3552 N90-30100

P-3 AIRCRAFT
RAAF Orion aircraft A9-300 oxygen fire
[AD-A215496] 09 p1162 N90-16725
An examination of the fatigue meter records from the RAAF Orion P-3C fleet
[AD-A214000] 10 p1319 N90-17628
The reduction of smoke emissions from Allison T56 engines
[ARL-PROP-R-182] 23 p3277 N90-28547

PACIFIC ISLANDS
NT JAPAN
NT NEW ZEALAND

PACIFIC OCEAN
Mariners Weather Log, volume 32, number 3, Summer 1988
[PB88-248075] 01 p0086 N90-10491
Semi-monthly temperature and geopotential anomaly in the upper 500 meters along the Oahu-Farallon Islands great circle from November 15, 1967 through December 15, 1979
[AD-A210640] 01 p0091 N90-10518
Interannual variability of temperature in the upper layer of the North Pacific eastern boundary region, 1971-1987
[PB89-190227] 02 p0253 N90-11434
Dynamics and energetics of the South Pacific Convergence Zone during FGGE SOP-1 and South Pacific Convergence Zone and global-scale
03 p0361 N90-12065
Tropical Pacific moisture variability
03 p0362 N90-12070
Hydrophone investigations of earthquakes and explosion generated high-frequency seismic phases
[AD-A212055] 03 p0371 N90-12122
Observations of long Rossby waves in the northern tropical Pacific
[PB89-196331] 03 p0376 N90-12143
Observations and modelling of deep equatorial currents in the central Pacific
[PB89-198139] 03 p0377 N90-12145
Equatorial oceanic response to forcing on time scales from days to months
[PB89-206775] 03 p0377 N90-12147

Tuning of the OSCURS (Ocean Surface Current Simulations) numerical model to ocean surface measurements in the Gulf of Alaska
[PB89-103979] 06 p0818 N90-14759
Responding to the threat of global warming: Options for the Pacific and Asia
[DE90-003553] 07 p0957 N90-15539
Identification and quantification of synoptic structure in simulated TIROS N radiance soundings
[AD-A213729] 07 p0960 N90-15553
Segmentation of topographic profiles of the seafloor based on a self-affine model
[AD-A215938] 10 p1410 N90-18132
Forecasters handbook for Central America and adjacent waters
[AD-A216752] 11 p1536 N90-18845
Drifting buoy data from Western Tropical Pacific for the period February 1, 1986 through February 28, 1989
[PB90-113978] 12 p1695 N90-19732
A cloud climatology for the North Pacific area centered at Shemya, Alaska
[AD-A217334] 13 p1844 N90-20585
Forecasting 24 and 48 hour intensity changes, for northwestern Pacific tropical cyclones, using satellite imagery
[AD-A218174] 13 p1846 N90-20597
Monthly surface thermal forcing in the tropical Pacific from 1980 to 1983
[NASA-CR-183033] 16 p2259 N90-22877
Tropical cyclones, 1989: Central north Pacific
[PB90-182536] 17 p2428 N90-23836
The trace metal geochemistry of suspended oceanic particulate matter
[AD-A218604] 17 p2429 N90-23839
Measurements of tropospheric nitric acid over the Western United States and Northeastern Pacific Ocean
[NASA-TM-103470] 20 p2883 N90-26399
A day-to-day comparison study of Seasat scatterometer winds with winds observed from islands in the tropical Pacific
[NASA-CR-186696] 22 p3212 N90-28223
Responding to the threat of global warming: Options for the Pacific and Asia
[DE90-014756] 23 p3347 N90-28918

PACKAGES
MM and T for VHSIC multichip packages
[AD-A213259] 05 p0635 N90-13703

PACKAGING
NT ELECTRONIC PACKAGING
Multichip packaging technology with laser-patterned interconnects
[DE90-010743] 18 p2549 N90-24552

PACKET SWITCHING
Implementation issues in source coding
[NASA-CR-185327] 05 p0681 N90-13963
Multiple crossbar network: A switched high-speed local network
[DE90-001839] 06 p0831 N90-14833
Packet Radio Integrated System Module (PRISM): Design document
[AD-A214723] 09 p1205 N90-16981
Packet telemetry standard
[ESA-PSS-04-106-ISSUE-1] 11 p1467 N90-18447
An adaptive ARQ (Automatic Repeat Request) strategy for packet switching data communication networks
[AD-A216597] 11 p1497 N90-18615
Packet radio networks under dynamic jamming
[AD-A217094] 12 p1648 N90-19475
Scalable coherent interface
[DE90-008011] 15 p2149 N90-22277
An overview of Canadian radio propagation/communications technologies research
20 p2844 N90-26179
Optimal synchronization of spread spectrum sequenced by nontransferable switching operators
20 p2845 N90-26183
Interconnection networks and parallel processing
[FEL-1989-112] 22 p3240 N90-28376

PACKET TRANSMISSION
Description and results of a multihop NACS simulation
[FEL-1988-46] 04 p0491 N90-12824
Implementation issues in source coding
[NASA-CR-185327] 05 p0681 N90-13963
Analysis of a queueing model for slotted ring networks
[MEMO-796] 05 p0694 N90-14058
Broadcast file distribution on packet satellite networks
15 p2079 N90-21906
Detecting black holes in packet-radio networks (SRNTN-56)
[AD-A219636] 17 p2389 N90-23604
High-throughput, survivable protocols for CDMA packet-radio networks (SRNTN-74)
[AD-A220189] 17 p2393 N90-23631

PACKETS (COMMUNICATION)
Network analyzer for nonstatic jamming
[AD-A210759] 02 p0212 N90-11216
An approximate max-flow min-cut theorem for uniform multicommodity flow problems with applications to approximation algorithms
[AD-A211908] 03 p0386 N90-12198
Configuration development for ROMENET
[AD-A213367] 06 p0765 N90-14450
Broadcast file distribution on packet satellite networks
15 p2079 N90-21906
Performance analysis of Aloha networks with power capture and near/far effect
[AD-A218739] 16 p2229 N90-22717
Locality in parallel computation
[AD-A218733] 16 p2302 N90-23120
Unfairness caused by quadratic backoff in a packet-radio network
[AD-A219635] 17 p2388 N90-23603
Detecting black holes in packet-radio networks (SRNTN-56)
[AD-A219636] 17 p2389 N90-23604
Analysis of random drop for gateway congestion control
[NASA-CR-186736] 20 p2935 N90-26698
The need for headers: An impossibility result for communication over unreliable channels
[AD-A222823] 21 p2994 N90-27018

PACKING DENSITY
High density tape casting system
[NASA-CASE-NPO-16901-1-CU]
12 p1640 N90-19425

PACKINGS (SEALS)
Development and testing of a contactless static/dynamic shaft seal with little sealing gas requirement
[KFK-4599] 05 p0652 N90-13802
Seal requirements in rocket propulsion
[ETN-90-96611] 16 p2205 N90-22580

PADE APPROXIMATION
On the parallel solution of parabolic equations
[NASA-CR-180363] 17 p2455 N90-24009
Higher order diffusion model for a bipolar transistor
[PB90-190901] 22 p3167 N90-27960

PAIN
The reliability of clinical measurements of forward bending obtained by the use of the modified fingertip-to-floor method
[AD-A217907] 13 p1852 N90-20627
A survey of cervical pain in pilots of a Belgian F-16 Air Defence Wing 19 p2718 N90-25462

PAINTS
Electrical characteristics measurements for the TSS-1 satellite painting
[IFSI-89-7] 08 p1036 N90-15987
Ultrasonic assisted paint removal method
[AD-D014264] 08 p1119 N90-16479
The future of aircraft paint removal methods
[AD-A214946] 09 p1197 N90-16936
Principles and formulation of solar reflecting and low infrared emitting coatings for defence use
[MRL-TR-89-2] 10 p1358 N90-17874
Heat-resistant and anticorrosive paint
[DE90-006077] 12 p1630 N90-19369
Radiometric tests on wet and dry antenna reflector surface panels 15 p2076 N90-21890
Robots for aircraft coatings removal: Parameters and requirements
[DE90-009429] 15 p2106 N90-22048
Mechanical paint removal techniques for aircraft structures
[IAR-89-23] 19 p2682 N90-25254
Statistical treatment of slow strain rate data for assessment of hydrogen embrittlement in low alloy high strength steel
[ARL-MAT-R-122] 20 p2832 N90-26106
Mechanical paint removal techniques for aircraft structures
[NIAR-90-12] 20 p2842 N90-26166
UNICOAT: Development of a primer/topcoat and flexible primer for aluminum
[AD-A221803] 21 p2989 N90-26986
A summary of measurements of permittivities and permeabilities of some microwave absorbing materials
[AD-A223221] 21 p2995 N90-27026
A silver-bearing, High-Temperature, Superconducting (HTS) paint
[AD-A221616] 21 p3084 N90-27539
Evaluation of EA-934NA with 2.5 percent Cab-O-Sil
[NASA-CR-184005] 22 p3158 N90-27909
Investigation of the effects of acid deposition on materials
[PB90-158973] 22 p3197 N90-28143

PAIR PRODUCTION
Exotic Higgs production at e+e- colliders
[PREPRINT-671] 05 p0698 N90-14088
Local pairing and antiferromagnetism in high-T sub c superconductors
[AD-A213004] 05 p0703 N90-14113
Rapidity densities and their fluctuations in central 200 A GeV S32 interations with Au and Ag,Br nuclei
[LUIP-8905] 07 p0989 N90-15715
Linear electron-hole-electron pair model of high-temperature superconductivity in La(2-x)M(x)CuO4 and YBa2Cu3O(7-y): Part 2. Dependence of the superconducting transition temperatures on pressure and on hole concentration
[DE90-003012] 07 p0999 N90-15779
Production of photons in anisotropic spacetimes
[DE90-600760] 08 p1135 N90-16576
Thermal pair cloud models of MeV gamma ray emissions from Cygnus X-1 and the Galactic Center
[DE90-001168] 09 p1301 N90-17536
Antihydrogen formation in collisions of positronium with antiprotons 11 p1560 N90-18988
Positronium formation in e+ plus H- collisions
11 p1561 N90-18993
Studies of high energy phenomena using muons
[DE90-008272] 13 p1886 N90-20820
Nonlinear interaction of photons and phonons in electron-positron plasmas
[DE90-009341] 14 p2030 N90-21640
New calculations and measurements of the Coulomb cross-section for the production of direct electron pairs by high energy nuclei
[NASA-TM-101280] 15 p2165 N90-22371
Quark-antiquark pair production via gamma W fusion at high energy e(+)e(-) colliders
[PREPRINT-705] 16 p2316 N90-23205
The sensitivity of EGRET to gamma ray polarization
16 p2335 N90-23305
Quantum effects in pair cascade models of AGN spectra 19 p2789 N90-25873
Electron positron pair winds and the Eddington limit
19 p2791 N90-25888
Spherical accretion with thermal pair production as models of AGN 19 p2793 N90-25897
X ray spectral index variability in NGC 4151
19 p2795 N90-25911
Charge transfer polarisation wave and carrier pairing in the high T(sub c) copper oxides
22 p3142 N90-27820

PALEOCLIMATOLOGY
Evaluation of climatic models: Comparison of simulated and observed patterns for past climates
[DE90-001228] 06 p0817 N90-14755
Global lake-level variations from 18,000 to 0 years ago: A palaeoclimate analysis
[DE90-000998] 07 p0956 N90-15531

PALEONTOLOGY
Fluctuation history of Great Salt Lake, Utah, during the last 13,000 years, part 2
[NASA-CR-185911] 01 p0082 N90-10466
Analysis of tectonic movements utilizing remote sensor products in the Southern Espinhaco (SE) region
[INPE-4830-PRE/1451] 12 p1690 N90-19708
The 5th International symposium on palaeolimnology
[AD-A219244] 20 p2887 N90-26431

PALLADIUM
Interaction of hydrogen isotopes with metals: Deuterium trapped at lattice defects in palladium
[DE90-000811] 06 p0747 N90-14344
Characterization of nanophase materials by x ray diffraction and computer simulation
[DE90-002270] 06 p0752 N90-14378
Atomic matching across internal interfaces
[DE90-002266] 06 p0841 N90-14889
Interaction of hydrogen in palladium as prescribed by the embedded atom method
[DE90-003893] 07 p0907 N90-15244
Two-dimensional magnetic phase transition of ultrathin iron films on Pd(100)
[DE90-003555] 07 p1000 N90-15788
High resolution electron microscopy of grain boundaries in nanophase palladium
[DE90-003823] 07 p1002 N90-15800
Supercomputer applications for materials science: Ordering effects of hydrogen in palladium
[DE90-004664] 12 p1718 N90-19870
Pt/SnO2-based CO-oxidation catalysts for long-life closed-cycle CO2 lasers 18 p2556 N90-24589
Synthesis, characterization and evaluation of CO-oxidation catalysts for high repetition rate CO2 TEA lasers 18 p2557 N90-24593
Mechanistic studies of the CO-oxidation reaction on catalysts for use in long-life CO2 lasers
18 p2558 N90-24596
Review of model sensor studies on Pd/SnO2(110) surfaces 18 p2559 N90-24604

PALLADIUM ALLOYS
Effects of composition and age hardening on precious metal electrical contacts
[DE88-008791] 06 p0769 N90-14476

Hydrogen in palladium alloys: Experiments, models and simulations
[PB90-200429] 22 p3156 N90-27896

PALLADIUM COMPOUNDS
Study of palladium and chromium silicides formation in liquid phase and in solid phase
[LAAS-89040] 04 p0470 N90-12695
Preparation and properties of the system Cu(x)Pd(1-x)O (0 less than or equal to x less than or equal to 0.175)
[AD-A217567] 12 p1723 N90-19901
Antiferromagnetism and enhanced heat in CeM2Sn (M = Ni, Ir, Cu, Rh, Pd, and Pt
[DE90-014924] 23 p3399 N90-29206

PAM (MODULATION)
U PULSE AMPLITUDE MODULATION

PAN (POLYACRYLONITRILE)
U POLYACRYLONITRILE

PANEL METHOD (FLUID DYNAMICS)
Prediction of stability derivatives for missiles using the HISSS panel code 01 p0012 N90-10053
Frequency domain aerodynamic analysis of interacting rotating systems 02 p0147 N90-10837
Study of the integration of wind tunnel and computational methods for aerodynamic configurations
[NASA-TM-102196] 05 p0572 N90-13332
A technique for the prediction of aerodynamics and aeroelasticity of rotor blades 05 p0579 N90-13377
A three-dimensional potential flow analysis of dynamic fluid forces acting on a whirling centrifugal impeller bounded by a volute 05 p0637 N90-13717
Program VSAERO theory document: A computer program for calculating nonlinear aerodynamic characteristics of arbitrary configurations
[NASA-CR-4023] 06 p0720 N90-14200
On the evaluation of aerodynamic influence coefficients
[NLR-MP-87019-U] 12 p1597 N90-19191
A panel process for the calculation of the flow around a wing with front angle damping
[ETN-90-95367] 12 p1600 N90-19207
Experimental and theoretical aerodynamic characteristics of a high-lift semispan wing model
[NASA-TP-2990] 13 p1749 N90-20046
Users manual for the NASA Lewis Ice Accretion Prediction Code (LEWICE)
[NASA-CR-185129] 14 p1909 N90-20943
An intensive procedure for the design of pressure-specified three-dimensional configurations at subsonic and supersonic speeds by means of a higher-order panel method 14 p1917 N90-20982
A system for transonic wing design with geometric constraints based on an inverse method 14 p1917 N90-20983
A fast collocation method for transonic airfoil design 14 p1917 N90-20984
Probabilistic modeling for simulation of aerodynamic uncertainties in propulsion systems
[NASA-TM-102472] 14 p1927 N90-21036
Application of the TRANAIR rectangular grid approach to the aerodynamic analysis of complex configurations 15 p2096 N90-21996
The influence of the gas surface interaction on spacecraft orbital motion 17 p2365 N90-23461
A time-marching method to calculate unsteady airloads on three-dimensional wings. Part 1: Linearized formulation
[DLR-FB-89-58] 18 p2494 N90-24254
A time-marching method for calculating unsteady airloads on three-dimentional wings. Part 2: Full-potential formulation
[DLR-FB-89-59] 18 p2494 N90-24255
A lifting surface method for the calculation of steady and unsteady, incompressible propeller aerodynamics
[ESA-TT-1151] 19 p2655 N90-25113
An unsteady lifting surface method for single rotation propellers
[NASA-CR-4302] 20 p2802 N90-25940
Aerodynamic/dynamic interaction
[AD-A222263] 21 p2954 N90-26798
Study of the ground effects in the CEAT aerohydrodynamic tunnel: Using the results 23 p3274 N90-28530

PANELS
NT CURVED PANELS
NT RECTANGULAR PANELS
NT WING PANELS
Prediction of the thermal environment and thermal response of simple panels exposed to radiant heat
[NASA-TM-101660] 03 p0400 N90-12292
SiO overcoating and polishing of CFRP telescope panels 05 p0599 N90-13478
The Space Station Photovoltaic Panels Plasma Interaction Test Program: Test plan and results
[NASA-TM-102474] 05 p0613 N90-13581
Onorbit electron beam welding experiment definition
[NASA-CR-183847] 07 p0938 N90-15431
High temperature, flexible, thermal barrier seal
[NASA-CASE-LEW-14672-1] 07 p0940 N90-15444
Boundary walls, fences and hoardings: Mean and peak wind loads and overturning moments
[ESDU-89050] 09 p1239 N90-17190
Impact damage tolerance of composite cylindrical panels
[AD-A216401] 10 p1350 N90-17830
A study of the structural efficiency of fluted core graphite-epoxy panels
[NASA-TM-101681] 10 p1396 N90-18070
Investigation of collapse characteristics of cylindrical composite panels with large cutouts
[AD-A216378] 10 p1397 N90-18079
Comparison between design and installed acoustic characteristics of NASA Lewis 9- by 15-foot low-speed wind tunnel acoustic treatment
[NASA-TP-2996] 12 p1606 N90-19242
Precision segmented reflector, figure verification sensor 12 p1611 N90-19272
Interlaminar shear stress effects on the postbuckling response of graphite-epoxy panels
[NASA-TM-102626] 12 p1676 N90-19630
Study of the optimization of reference parameters to the dynamic constraints of solar panels
[INPE-4793-TDL/355] 12 p1681 N90-19656
Reusable high-temperature heat pipes and heat pipe panels
[NASA-CASE-LAR-13761-1] 13 p1799 N90-20323
Comparison of oculometer and head-fixed reticle with voice or switch and touch panel for data entry on a generic tactical air combat display
[AD-A217231] 13 p1855 N90-20646
Localization and delocalization in periodic one-dimensional dynamic systems
[AD-A217939] 13 p1882 N90-20797
Preliminary design approach for large high precision segmented reflectors
[NASA-TM-102605] 14 p1938 N90-21096
Experimental determination of thermal conductance in bolted joint impact in satellites
[INPE-4989-PRE/1551] 15 p2059 N90-21788
Radiometric tests on wet and dry antenna reflector surface panels 15 p2076 N90-21890
Experimental and computational study of the viscoplastic response of high temperature structures 16 p2220 N90-22663
Numerical studies of the active control of sound transmission through double partitions
[ISVR-TR-183] 16 p2313 N90-23181
High temperature flexible seal
[NASA-CASE-LEW-14695-1] 17 p2413 N90-23751
Diffraction about acoustically soft panels
[AD-A220850] 17 p2469 N90-24115
Future automotive materials: Evolution or revolution 18 p2516 N90-24370
Electrical resistance measurements of connector-panel interfaces
[AD-A221431] 21 p3001 N90-27057
The response and failure mechanisms of circular metal and composite plates subjected to underwater shock loading
[AD-A222200] 21 p3013 N90-27131
A method for the reduction of aerodynamic drag of road vehicles
[NASA-TM-102589] 22 p3108 N90-27656
M-52 spray booth qualification test
[NASA-CR-184003] 22 p3122 N90-27727
Transformational part-count in layered octahedral-tetrahedral truss configurations
[NASA-TM-102635] 23 p3287 N90-28598
Study of meteorological processes important in the degradation of materials through surface temperature
[PB90-222720] 23 p3336 N90-28856

PANIC
Passenger behaviour in aircraft emergencies involving smoke and fire 10 p1317 N90-17613

PANORAMIC SCANNING
Atmospheric autorotating imaging device
[NASA-CASE-NPO-17390-1-CU] 16 p2238 N90-22769

PAPER (MATERIAL)
Color printing for computer graphics. Or: How to get it off your screen and onto paper, in color
[PB89-208110] 03 p0384 N90-12184
Photochromic papers or films for noncopyable documents
[DE90-004006] 10 p1441 N90-18316
Recycling waste-paper 18 p2514 N90-24359

PARABOLAS
Two dimensional laminated shell theory including parabolic transverse shear
[AD-A213817] 07 p0948 N90-15487

PARABOLIC ANTENNAS
A closed-cycle refrigerator for cooling maser amplifiers below 4 Kelvin 04 p0487 N90-12797
Frequency independent constant beamwidth directional lens antenna for very wideband and multi-channel electromagnetic communications
[AD-D014214] 06 p0765 N90-14449
Apparatus and method for locating the axis of symmetry (center of circular cross section) of three dimensional objects
[AD-D014407] 14 p1982 N90-21354

PARABOLIC DIFFERENTIAL EQUATIONS
Parabolic equations for curves on surfaces. 2: Intersections, blow up and generalized solutions
[AD-A212890] 05 p0687 N90-14004
Optimal processes described by a parabolic differential equation with control in the coefficients, part 4
[MEMO-785-PT-4] 05 p0689 N90-14016
A forecasting system using the parabolic equation: Application to surface-to-air propagation in the presence of elevated layers 06 p0760 N90-14420
Analysis of propagation in an inhomogeneous atmosphere in the horizontal and vertical direction uaing the parabolic equation method 06 p0760 N90-14421
Propagation modeling for some horizontally varying tropospheric ducts 06 p0760 N90-14422
Assessment of anomalous propagation predictions using minisonde refractivity data and the parabolic equation method 06 p0760 N90-14424
Numerical methods for parabolic equations and inequalities in very high dimensions
[AD-A214102] 07 p0985 N90-15690
Undetermined coefficient problems for quasi-linear parabolic equations
[AD-A218462] 16 p2306 N90-23141
On the parallel solution of parabolic equations
[NASA-CR-180363] 17 p2455 N90-24009
Analytic parabolic equation solutions
[AD-A218588] 17 p2456 N90-24015
Radar clutter via waveguide methods
[AD-A220237] 18 p2542 N90-24512
The Gauss beam method for surface waves. Theory and utilization for a lateral heterogeneous spheric Earth
[ETN-90-96492] 18 p2580 N90-24695
Shock-layer bounds for a singularly perturbed equation
[NASA-CR-182080] 22 p3243 N90-28391
Study of a variable step network and comparison between the radii method and the parabolic equations, applied to the acoustic propagation in the atmosphere
[ONERA-RF-12/3641-PY] 22 p3245 N90-28401

PARABOLIC FLIGHT
Combustion Experiments During KC-135 Parabolic Flights
[ESA-SP-1113] 09 p1201 N90-16958
External flow computations for a finned 60mm ramjet in steady supersonic flight
[AD-A216998] 12 p1605 N90-19233

PARABOLIC REFLECTORS
NT PARABOLOID MIRRORS
Performance effects of tie-truss modifications for a 70-meter centerline beam waveguide antenna 04 p0486 N90-12791
Test results from a full-scale sodium reflux pool-boiler solar receiver
[DE90-003577] 12 p1684 N90-19671
An assessment of second-generation stretched-membrane mirror modules
[DE90-010243] 16 p2252 N90-22841
Beamforming devices and feed structures for a DBS flat-plate antenna
[BBC-RD-1989/12] 17 p2386 N90-23592
Feasibility study of a synthesis procedure for array feeds to improve radiation performance of large distorted reflector antennas
[NASA-CR-186641] 20 p2851 N90-26213
Wind loads and local pressure distributions on parabolic dish solar collectors
[DE90-000328] 21 p3019 N90-27166

PARABOLOID MIRRORS
Reflectometers
[AD-D014249] 08 p1122 N90-16499
An assessment of second-generation stretched-membrane mirror modules
[DE90-010243] 16 p2252 N90-22841

PARACHUTE DESCENT
Performance and quality of a wing type parachute: Parametric analysis
[REPT-88-19] 03 p0302 N90-11710
Evaluation of the head injury hazard during military parachuting
[AD-A220724] 17 p2434 N90-23870
Wind tunnel study of wake downwash behind A 6 percent scale model B1-B aircraft
[DE90-011783] 20 p2802 N90-25941

PARACHUTE FABRICS
Wind tunnel tests of a 20-gore disk-gap-band parachute
[AD-A221326] 18 p2493 N90-24251

PARACHUTES
NT DRAG CHUTES
NT RIBBON PARACHUTES
Wind tunnel tests of a 20-gore disk-gap-band parachute
[AD-A221326] 18 p2493 N90-24251
High altitude ozone research balloon
[NASA-CR-186653] 19 p2654 N90-25107
PARACHUTING
U PARACHUTE DESCENT
PARACHUTING INJURY
Parachute opening shocks during high speed ejections: Normalization 13 p1751 N90-20056
PARALLAX
NT STELLAR PARALLAX
PARALLEL COMPUTERS
NT MASSIVELY PARALLEL PROCESSORS
NT MIMD (COMPUTERS)
NT SIMD (COMPUTERS)
Shared memory versus message passing architectures: An application based study
[AD-A210312] 01 p0108 N90-10615
The rewrite rule machine project
[AD-A210528] 01 p0109 N90-10617
Variable step iteration of high-order Runge-Kutta methods on parallel computers
[CWI-NM-R8817] 02 p0260 N90-11476
An implicit Navier-Stokes solver optimised for a vector-parallel computer
[VKI-TN-169] 04 p0501 N90-12890
Performance evaluations of a parallel and expandable database computer: The multi-backend database computer
[AD-A212761] 04 p0528 N90-13046
Area-universal networks
[AD-A211863] 04 p0535 N90-13092
Block predictor (low order) corrector methods to solve ordinary differential equations on parallel computers
[IMAG-RR-757-M] 06 p0834 N90-14845
Reconfigurable N-dimensional computer memory
[AD-D014309] 07 p0971 N90-15607
High level language memory management on parallel architectures
[DE89-015018] 07 p0971 N90-15609
Investigation of the applicability of a functional programming model to fault-tolerant parallel processing for knowledge-based systems
[NASA-CR-181938] 07 p0979 N90-15654
Numerical algorithms for parallel computers
[AD-A216812] 10 p1419 N90-18181
Flosolver Mk1B: An eight processor parallel machine
[PD-CF-8941] 12 p1699 N90-19755
A time stepping algorithm for parallel computers
[DE90-008163] 13 p1873 N90-20738
Supercomputers need super arithmetic
[PB90-130253] 15 p2145 N90-22252
On the performance of algorithms for large-scale bound constrained problems
[DE90-010084] 18 p2590 N90-24736
ICASE semiannual report, April 1 - September 30, 1989
[NASA-CR-181988] 19 p2727 N90-25502
Principles of FP2: Term algebras for specification of parallel machines
[RR-789-I-IMAG-98-LIFIA] 20 p2913 N90-26571
Parallel algorithm for distributed memory computers (applications to matricial algorithms)
[ETN-90-97252] 20 p2913 N90-26573
Special purpose parallel computer architecture for real-time control and simulation in robotic applications
[NASA-CASE-NPO-17629-1-CU] 21 p3038 N90-27268
An even-parity/odd-parity formulation for deterministic transport calculations on massively parallel computers
[DE90-015036] 23 p3384 N90-29116
An additive turbulent decomposition of the Navier-Stokes equations implemented on highly parallel computer systems
[AD-A223678] 24 p3468 N90-29595
Requirements for implementing real-time control functional modules on a hierarchical parallel pipelined system 24 p3518 N90-29891
MUSE: A systolic array for adaptive nulling with 64 degrees of freedom, using Givens transformations and wafer scale integration
[AD-A223812] 24 p3529 N90-29953
Assembler for a parallel computer
[NAL-TM-586] 24 p3532 N90-29974
A high-speed KDL-RAM file system for parallel computers
[AD-A223299] 24 p3533 N90-29979
Innovative uses of parallel computers
[AD-A223578] 24 p3533 N90-29980
PARALLEL FLOW
NT PIPE FLOW
NT THREE DIMENSIONAL FLOW
Appendage flow computations using the INS3D computer code
[AD-A215689] 09 p1218 N90-17066
The evolution of linearized perturbations of parallel flows
[DE90-005978] 09 p1221 N90-17082
Goertler vortices in growing boundary layers: The leading edge receptivity problem, linear growth and the nonlinear breakdown stage
[NASA-CR-181962] 10 p1306 N90-17555
Instabilities and subharmonic resonances of subsonic heated round jets, volume 2
[NASA-CR-186058] 15 p2100 N90-22017
An experimental study of tip shape effects on the flutter of aft-swept, flat-plate wings
[NASA-TM-4180] 16 p2199 N90-22555
Parallel channel flow excursions
[DE90-009129] 16 p2235 N90-22753
Parallel computation of supersonic flows using a three-dimensional, zonal, Navier-Stokes code
[AD-A218824] 17 p2344 N90-23350
Calculation of correction terms for forces and moment measurements in radial flow field of hypersonic spheric nozzles 18 p2490 N90-24234
Parallel numerical simulations of axisymmetric projectile flows using zonal-overlapped grids
[AD-A221711] 21 p3005 N90-27082
PARALLEL PLATES
The modulating grid 05 p0603 N90-13505
Modeling of composite beams and plates for static and dynamic analysis
[NASA-CR-186459] 20 p2874 N90-26354
PARALLEL PROCESSING (COMPUTERS)
Evaluating local indirect addressing in SIMD proc essors
[NASA-CR-181845] 01 p0103 N90-10581
Proceedings of the 2nd International Conference on Vector and Parallel Computing
[AD-A209401] 01 p0103 N90-10585
A low-cost hypercube load-balance algorithm
[DE89-015739] 01 p0104 N90-10589
Effective resource utilization for multiprocessor join execution
[DE89-016303] 01 p0105 N90-10595
Applications of parallel supercomputers: Scientific results and computer science lessons
[DE89-016385] 01 p0107 N90-10611
Parallel processing and learning in simple systems
[AD-A210225] 01 p0108 N90-10612
Shared memory versus message passing architectures: An application based study
[AD-A210312] 01 p0108 N90-10615
An iterative method for systems of nonlinear hyperbolic equations
[NASA-CR-181919] 01 p0112 N90-10638
Computational and statistical issues in discrete-event simulation
[AD-A210743] 01 p0116 N90-10668
A parallel numerical simulation for supersonic flows using zonal overlapped grids and local time steps for common and distributed memory multiprocessors
[DE89-015252] 02 p0147 N90-10839
Advanced manned space flight simulation and training: An investigation of simulation host computer system concepts
[NASA-CR-185998] 02 p0160 N90-10911
Modal analysis of fluid-structure systems by parallel subspace iteration 02 p0181 N90-11024
Cellular automata and massively parallel physics
[DE89-016506] 02 p0220 N90-11257
New computing systems and their impact on structural analysis and design
[NASA-CR-185831] 02 p0257 N90-11457
Research, development, training and education using the Ada programming language
[AD-A210760] 02 p0259 N90-11466
Parallel inference based on delta processing
[CWI-CS-R8846] 02 p0261 N90-11482
A generalization of A. N. Habermann's theorem for semaphores
[REPT-88-98] 02 p0261 N90-11484
Asynchronous integration of ordinary differential equations on multiprocessors
[DE89-014169] 02 p0263 N90-11493
Computing the two dimensional fast Fourier transform on a general purpose mesh connected multiprocessor
[DE89-016515] 02 p0266 N90-11518
Potential for parallelism in explicit linear methods
[DE89-017329] 02 p0267 N90-11523
Note on explicit parallel multistep Runge-Kutta methods
[CWI-NM-R8814] 02 p0268 N90-11529
Tools to aid in the development high-performance algorithms
[DE89-012395] 03 p0386 N90-12194
Parallel graph contraction
[AD-A211916] 03 p0386 N90-12199
Parallel implementation and evaluation of motion estimation system algorithms on a distributed memory multiprocessor using knowledge based mappings
[NASA-CR-185984] 03 p0389 N90-12213
Novel techniques for data decomposition and load balancing for parallel processing of vision systems: Implementation and evaluation using a motion estimation system
[NASA-CR-185991] 03 p0389 N90-12214
Parallel architectures and parallel algorithms for integrated vision systems
[NASA-CR-185990] 03 p0389 N90-12215
Parallel processing on transputer arrays for the recognition of objects in infrared images
[RSRE-MEMO-4197] 03 p0389 N90-12217
Distributed VLSI architecture for fast Jacobian and inverse Jacobian formulations
[RR-346] 03 p0390 N90-12218
Robot inverse dynamics computation via VLSI distributed architectures
[RR-350] 03 p0390 N90-12223
Fast forward dynamics algorithm for robot arms using multiprocessing
[RR-367] 03 p0391 N90-12225
Dynamic embedding of trees in hypercubes with constant dilation and load
[AD-A211884] 03 p0392 N90-12236
Multilevel optimization with system Optsys
[FFA-TN-1988-60] 04 p0512 N90-12953
Performance evaluations of a parallel and expandable database computer: The multi-backend database computer
[AD-A212761] 04 p0528 N90-13046
A fan-in algorithm for distributed sparse numerical factorization
[AD-A211569] 04 p0529 N90-13054
Parallel and deterministic algorithms from MRF (Markov Random Fields): Surface reconstruction and integration
[AD-A212457] 04 p0533 N90-13084
NAUTILE: A physical design environment based on an object-oriented data manager
[IMAG-RR-737-I] 04 p0535 N90-13094
Formal calculations and parallesism. Solving linear systems
[ETN-89-95499] 04 p0536 N90-13098
Identification of robot dynamics: A parallel processing approach
[RR-361] 04 p0537 N90-13103
Block-structured solution of three-dimensional transonic flows using parallel processing
[AD-A212851] 05 p0572 N90-13330
Explicit modeling and concurrent processing in the simulation of multibody dynamic systems 05 p0599 N90-13481
Parallelism in the discrete-event simulation algorithm
[AD-A213060] 05 p0682 N90-13970
Implementing the discrete Fourier transform on the hypercube FPS T40
[IMAG-RR-773-I] 05 p0684 N90-13983
A multilevel parallel solver for block tridiagonal and banded linear systems
[AD-A213151] 05 p0688 N90-14008
Group implicit concurrent algorithms in nonlinear structural dynamics
[NASA-CR-185950] 06 p0796 N90-14638
Parallel eigenanalysis of finite element models in a completely connected architecture
[NASA-CR-185166] 06 p0799 N90-14652
Krylov methods preconditioned with incompletely factored matrices on the CM-2
[NASA-CR-181961] 06 p0822 N90-14779
Research in mathematics and computer science at Argonne, July 1, 1986 to January 6, 1988
[DE88-010343] 06 p0822 N90-14781
High performance parallel architectures
[DE90-001055] 06 p0823 N90-14782
Force user's manual: A portable, parallel FORTRAN
[NASA-CR-4265] 06 p0823 N90-14785
Parallel mathematical software
[DE90-002694] 06 p0829 N90-14822
Strand: A practical parallel programming language
[DE90-002861] 06 p0830 N90-14825
PCP (Parallel C Preprocessor): A parallel extension of C that is 99 percent fat free
[DE90-002813] 06 p0831 N90-14834
Generalization in backpropagation networks: An empirical study using image data
[DE89-012658] 06 p0832 N90-14835
Architectures for reasoning in parallel
[NASA-CR-186237] 06 p0832 N90-14836
NETRA: A parallel architecture for integrated vision systems. 1: Architecture and organization
[NASA-CR-185955] 06 p0832 N90-14839

Block predictor (low order) corrector methods to solve ordinary differential equations on parallel computers
[IMAG-RR-757-M] 06 p0834 N90-14845
VLSI theory and parallel supercomputing
[AD-A214035] 07 p0925 N90-15351
Research in mathematics and computer science at Argonne
[DE90-000975] 07 p0969 N90-15595
The parallel decomposition of linear programs
[DE90-003538] 07 p0974 N90-15625
Investigation of the applicability of a functional programming model to fault-tolerant parallel processing for knowledge-based systems
[NASA-CR-181938] 07 p0979 N90-15654
Adaptive backoff synchronization techniques
[AD-A213966] 07 p0980 N90-15658
PVM (Parallel Virtual Machine): A framework for parallel distributed computing
[DE90-004390] 08 p1106 N90-16403
The 2nd Symposium on the Frontiers of Massively Parallel Computations
[NASA-TM-101918] 08 p1113 N90-16442
How to cluster in parallel with neural networks
08 p1113 N90-16443
Overview and extensions of a system for routing directed graphs on SIMD architectures 08 p1113 N90-16444
Parallel algorithms for interactive manipulation of digital terrain models 08 p1113 N90-16445
Sort computation 08 p1113 N90-16446
Stochastic simulation of charged particle transport on the massively parallel processor
08 p1114 N90-16448
Estimating water flow through a hillslope using the massively parallel processor 08 p1114 N90-16449
Scan line graphics generation on the massively parallel processor 08 p1114 N90-16450
BLITZEN: A highly integrated massively parallel machine 08 p1115 N90-16453
A generic fine-grained parallel C
08 p1115 N90-16454
On the efficient exploitation of speculation under data flow paradigms of control
[AD-A214112] 08 p1115 N90-16455
Parallel processing implementation of a flight controller 09 p1165 N90-16743
Analog hardware for delta-backpropagation neural networks
[NASA-CASE-NPO-17564-1-CU]
09 p1204 N90-16974
Eigensolution of finite element problems in a completely connected parallel architecture
[NASA-TM-102450] 09 p1236 N90-17173
The EPSILON-2 hybrid dataflow architecture
[DE90-003152] 09 p1263 N90-17326
Development of advanced WTA algorithms for parallel processing
[AD-A214874] 09 p1266 N90-17341
Parallel functional computation
[AD-A214627] 09 p1269 N90-17360
Parallel logic programming and parallel systems software and hardware
[AD-A214635] 09 p1270 N90-17361
Merlin: A superglue for multicomputer systems
[NASA-CR-186330] 09 p1271 N90-17366
An analysis of scatter decomposition
[NASA-CR-181978] 09 p1276 N90-17396
Transient finite element computations on the transputer system
[NASA-CR-185199] 10 p1396 N90-18071
Hybrid (optical/electronic) computing and digital optical computing
[AD-A214502] 10 p1416 N90-18160
Writing parallel, discrete-event simulations in ModSim: insight and experience
[DE90-001833] 10 p1419 N90-18183
Efficient interconnection schemes for VLSI and parallel computation
[AD-A216405] 10 p1420 N90-18185
Theoretical and experimental analyses of parallel combinatorial algorithms
[AD-A216407] 10 p1420 N90-18186
A parallel iterative method for solving 3-dimensional elliptic partial differential equations
[DE90-005187] 10 p1422 N90-18199
Visual servoing for autonomous aircraft refueling
[AD-A216042] 11 p1455 N90-18386
Technology development and circuit design for a parallel laser programmable floating point application specific processor
[AD-A215870] 11 p1500 N90-18637
Parallel memory addressing using coincident optical pulses
[AD-A216302] 11 p1501 N90-18641
Performance characterization of the Convex C-240 computer system
[DE90-006425] 11 p1543 N90-18879
L: A language for solution of incremental systems in a parallel processing environment
[INPE-4816-TDL/362] 11 p1543 N90-18884
Parallel algorithms derivation
[AD-A216452] 11 p1545 N90-18894
Derivation of efficient parallel programs: An example from genetic sequence analysis
[DE90-005654] 11 p1547 N90-18904
Summer institute in parallel computing
[DE90-005532] 11 p1548 N90-18910
Computation and control with neural nets
[DE90-006460] 11 p1548 N90-18911
Speculative computation in multilisp
[AD-A216579] 11 p1575 N90-19067
Memory management in traceback Viterbi decoders
12 p1643 N90-19443
High-level connectionist models
[AD-A216581] 12 p1698 N90-19751
Flosolver Mk1B: An eight processor parallel machine
[PD-CF-8941] 12 p1699 N90-19755
Adaptive, asynchronous stochastic global optimization algorithms for sequential and parallel computation
[AD-A217093] 12 p1702 N90-19775
Parallel neural net path-planner on hypercube and transputer
[DE90-006324] 12 p1703 N90-19777
Parallel algorithms for boundary value problems
[NASA-TM-102498] 12 p1704 N90-19783
On the parallel efficiency of the Frederickson-McBryan multigrid
[NASA-CR-181999] 12 p1705 N90-19791
Joint services electronics program
[AD-A217961] 13 p1797 N90-20311
Parallel algorithms in the finite element approximation of flow problems
[AD-A217729] 13 p1802 N90-20341
Supercomputer environments
[AD-A217682] 13 p1863 N90-20689
A real-time parallel pipelined data-flow image-processing system
[DE90-008324] 13 p1864 N90-20691
Joint Japanese-American Workshop on Future Trends in Logic Programming
[DE90-008343] 13 p1867 N90-20709
Almost-optimum parallel speed-ups of algorithms for bipartite matching and related problems
[AD-A215111] 13 p1871 N90-20728
Advanced parallel systems
[AD-A217175] 13 p1872 N90-20731
Asynchronous design for parallel processing architectures
[AD-A217421] 13 p1872 N90-20734
Design of a simulation interface for a parellel computing environment
[DE90-008497] 13 p1873 N90-20737
A time stepping algorithm for parallel computers
[DE90-008163] 13 p1873 N90-20738
A model and implementation of multigrid for massively parallel computers
[DE90-008165] 13 p1873 N90-20739
Implementation of midcourse tracking and correlation on massively parallel computers
[DE90-008166] 13 p1873 N90-20740
A parallel architecture for real-time simulation
[AD-A218321] 13 p1873 N90-20741
Artificial Intelligence (AI) Center of Excellence at the University of Pennsylvania
[AD-A217393] 13 p1874 N90-20743
Implementation of a hypercube database system
[DE90-008440] 13 p1900 N90-20905
Cooperating intelligent systems
[NASA-CR-184982] 14 p2012 N90-21529
Parallel tridiagonalization of a general matrix using distributed-memory multiprocessors
[DE90-008902] 14 p2015 N90-21551
Hypercluster parallel processing library user's manual
[NASA-CR-185231] 14 p2016 N90-21552
Performance bounds on parallel self-initiating discrete-event
[NASA-CR-182010] 14 p2016 N90-21556
NETRA: A parallel architecture for integrated vision systems 2: Algorithms and performance evaluation
[NASA-CR-186510] 14 p2017 N90-21557
Application of neural nets to system identification and bifurcation analysis of real world experimental data
[DE90-007539] 14 p2017 N90-21558
Activities and operations of the Advanced Computing Research Facility
[DE90-007957] 14 p2017 N90-21559
A parallel multigrid method for solving elliptic partial differential equations
[DE90-007929] 14 p2021 N90-21584
Modeling high-temperature superconductors and metallic alloys on the Intel IPSC/860
[DE90-009402] 14 p2033 N90-21665
Parallel asynchronous hardware implementation of image processing algorithms 15 p2138 N90-22219
Computation and parallel implementation for early vision 15 p2139 N90-22222
Image gathering, coding, and processing: End-to-end optimization for efficient and robust acquisition of visual information 15 p2139 N90-22224
Photonic processing at NASA Ames Research Center
15 p2141 N90-22234
Sparse distributed memory overview
15 p2141 N90-22235
SISAL 1.2: An alternative to FORTRAN for shared memory multiprocessors
[DE90-005181] 15 p2146 N90-22257
Molecular dynamics simulations of short-range force systems on 1024-node hypercubes
[DE90-009833] 15 p2146 N90-22259
Scalable coherent interface
[DE90-008011] 15 p2149 N90-22277
Parallel non-linear optimization
[REPT-89-45] 15 p2151 N90-22290
The preprocessed doacross loop
[NASA-CR-182056] 16 p2276 N90-22972
A scheme for supporting automatic data migration on multicomputers
[NASA-CR-182038] 16 p2276 N90-22973
Communication overhead on the Intel iPSC-860 hypercube
[NASA-CR-182055] 16 p2278 N90-22982
Parallel processing of real-time dynamic systems simulation on OSCAR (Optimally SCheduled Advanced multiprocessoR) 16 p2282 N90-23006
A robot arm simulation with a shared memory multiprocessor machine 16 p2283 N90-23008
A unifying framework for rigid multibody dynamics and serial and parallel computational issues
16 p2283 N90-23009
Parallel algorithms and architecture for computation of manipulator forward dynamics 16 p2283 N90-23010
Computational chaos in massively parallel neural networks 16 p2283 N90-23012
Characterization of robotics parallel algorithms and mapping onto a reconfigurable SIMD machine
16 p2289 N90-23039
Proceedings of the 3rd Annual Conference on Aerospace Computational Control, volume 2
[NASA-CR-186447] 16 p2289 N90-23040
A parallel structure transient response algorithm using independent substructure response computation
16 p2290 N90-23044
Parallel conjugate gradient algorithms for manipulator dynamic simulation 16 p2290 N90-23045
A real time, FEM based optimal control algorithm and its implementation using parallel processing hardware (transistors) in a microprocessor environment
16 p2294 N90-23066
The power and efficiency of advanced software and parallel processing 16 p2296 N90-23079
On the performance of parallel algorithms
[CS-8914] 16 p2299 N90-23099
Proceedings of the NATO Advanced Workshop on Supercomputing
[AD-A218508] 16 p2299 N90-23102
Sentence comprehension: A parallel distributed processing approach
[AD-A218886] 16 p2300 N90-23104
Interconnection networks for highly parallel supercomputing architectures
[REPT-89-053] 16 p2302 N90-23118
Controlling real-time systems with parallel processes
[CS-8918] 16 p2302 N90-23119
Locality in parallel computation
[AD-A218733] 16 p2302 N90-23120
Proceedings of the 9th International Conference on Computing Methods in Applied Science and Engineering
[AD-A219307] 16 p2307 N90-23149
The cost of conservative synchronization in parallel discrete event simulations
[NASA-CR-182034] 17 p2441 N90-23912
A parallel algorithm for global routing
[NASA-CR-186152] 17 p2448 N90-23959
Concurrent Clean
[TR-89-18] 17 p2450 N90-23974
Design of finite element systems for parallel computers 17 p2450 N90-23975
Parallel execution of LISP programs
[AD-A219623] 17 p2451 N90-23978
Block Runge-Kutta methods on parallel computers
[CWI-NM-R8906] 17 p2452 N90-23982
Block Runge-Kutta methods
[CWI-NM-R8913] 17 p2452 N90-23983
Structured NC
[RUU-CS-89-6] 17 p2452 N90-23989

Northeast Artificial Intelligence Consortium annual report, 1988. Volume 12: Computer architectures for very large knowledge bases
[AD-A219599] 17 p2454 N90-23999
On the parallel solution of parabolic equations
[NASA-CR-180363] 17 p2455 N90-24009
Implementation of an I-structure memory controller
[AD-A221397] 18 p2588 N90-24726
Synchronously parallel Boltzmann machines: A mathematical model
[MEMO-COSOR-89-21] 18 p2590 N90-24732
Preconditioned time-differencing for the parallel solution of the heat equation
[DE90-010636] 18 p2590 N90-24737
Parallelizing the closure computation in automated deduction
[DE90-007792] 18 p2593 N90-24758
CERC (Center for Energy Research Computation) report: Results of the CERC Project with recommendations for ANL (Argonne National Laboratory) institutional strategies in advanced scientific computing
[DE90-008238] 18 p2594 N90-24759
Input/output algorithm for M-dimensional rectangular domain decompositions on N-dimensional hypercube multicomputers
[DE90-010494] 18 p2594 N90-24762
Visual animation of parallel algorithms for matrix computations
[DE90-011076] 18 p2594 N90-24763
Embedded diagonally implicit Runge-Kutta algorithms on parallel computers
[CWI-NM-R8912] 18 p2595 N90-24765
Sensitivity analysis of transputer workfarm topologies
[AD-A219821] 18 p2595 N90-24766
The one dimensional skewing problem
[RUU-CS-89-23] 18 p2596 N90-24769
Iconic tracking algorithms for high energy physi cs using the TRAX-I massively parallel processor
[MPI-PAE/EXP.EL-216] 18 p2596 N90-24773
Potential performance of methods for parallelism across time in ODEs
[DE90-010992] 18 p2596 N90-24774
Determination of algorithm parallelism in NP complete problems for distributed architectures
[AD-A220192] 18 p2598 N90-24786
Managing parallelism and resources in scientific dataflow programs
[AD-A221398] 18 p2635 N90-25010
Execution time supports for adaptive scientific algorithms on distributed memory machines
[NASA-CR-182052] 19 p2741 N90-25578
On the design of a concurrent image analysis system
[DE90-011388] 19 p2746 N90-25605
A parallel Newton-Euler formulation for fast dynamic simulation of robot manipulators
[RR-368] 19 p2748 N90-25614
Run-time parallelization and scheduling of loops
[NASA-CR-182039] 20 p2902 N90-26509
Research conducted at the Institute for Computer Applications in Science and Engineering in applied mathematics, numerical analysis, and computer science
[NASA-CR-182057] 20 p2903 N90-26510
Autoplan: A self-processing network model for an extended blocks world planning environment
[NASA-CR-186733] 20 p2905 N90-26526
Graphics applications utilizing parallel processing
[NASA-CR-186719] 20 p2907 N90-26534
Parallel processors and nonlinear structural dynamics algorithms and software
[NASA-CR-186755] 20 p2907 N90-26536
A parallel algorithm for surface plane intersection
[IMAG-RR-794-M] 20 p2909 N90-26549
Efficient network topologies for extensible massively parallel computers
[ETN-90-97220] 20 p2912 N90-26568
Design of a universal protocol subsystem architecture: Specification of functions and services
[EUT-89-E-230] 20 p2912 N90-26569
Parallelization of an annealing simulation applied to improving tetrahedric grids
[IMAG-RR-796-M] 20 p2913 N90-26570
Principles of FP2: Term algebras for specification of parallel machines
[RR-789-I-IMAG-98-LIFIA] 20 p2913 N90-26571
Implementation of algorithms used in calculating the tensor product of matrices on a distributed memory machine
[IMAG-RR-786-I] 20 p2913 N90-26572
Parallel algorithm for distributed memory computers (applications to matricial algorithms)
[ETN-90-97252] 20 p2913 N90-26573
Parallel/distributed direct method for solving linear systems
[NASA-TM-103229] 20 p2919 N90-26614
Two-dimensional signal processing and storage, and theory and applications of electromagnetic measurements
[AD-A222984] 21 p2995 N90-27022
Special purpose parallel computer architecture for real-time control and simulation in robotic applications
[NASA-CASE-NPO-17629-1-CU] 21 p3038 N90-27268
Sisal on a message passing architecture
[DE90-008786] 21 p3051 N90-27342
Analog hardware for learning neural networks
[NASA-CASE-NPO-17664-1-CU] 21 p3057 N90-27384
Place/transition nets with debit arcs
[NASA-CR-186932] 21 p3058 N90-27386
CSRD parallel service machine enhancement
[AD-A221951] 21 p3058 N90-27388
Debugging and analysis of large-scale parallel programs
[AD-A221678] 21 p3059 N90-27393
Parallel algorithms for computer vision
[AD-A221871] 21 p3059 N90-27394
DSIM: A distributed simulator
[NASA-CR-186880] 22 p3237 N90-28353
Stochastic dynamic programming for reservoir optimal control: Dense discretization and inflow correlation assumption made possible by parallel computing
[REPT-89-056] 22 p3238 N90-28360
Fault-tolerance in massively parallel silicon architectures: The case of neural nets
[REPT-90-012] 22 p3240 N90-28375
Interconnection networks and parallel processing
[FEL-1989-112] 22 p3240 N90-28376
Distributed transitive closure computations: The disconnection set approach
[REPT-90-014] 22 p3259 N90-28459
Educational and research activities of the Dig ital Systems Laboratory at Helsinki University of Technology
[PB90-190893] 22 p3265 N90-28486
ROSES, a Robot Operating System Expert Scheduler: Methodological framework
[DE90-014782] 23 p3334 N90-28851
The effect of multiprocessor radius on scaling
[DE90-014772] 23 p3380 N90-29095
Parallelization of a software relating to aerodynamics on MIMD type computers
[ONERA-RT-31/3479-CY] 23 p3384 N90-29114
An even-parity/odd-parity formulation for deterministic transport calculations on massively parallel computers
[DE90-015036] 23 p3384 N90-29116
Overcoming rule-based rigidity and connectionist limitations through massively-parallel case-based reasoning
[NASA-CR-186963] 23 p3384 N90-29117
Two-dimensional signal processing and storage and theory and applications of electromagnetic measurements
[AD-A224239] 24 p3459 N90-29538
Turbo pascal implementation of a distributed processing network of MS-DOS microcomputers connected in a master-slave configuration
[AD-A223925] 24 p3525 N90-29928
Parallel architectures and algorithms for image understanding
[AD-A223479] 24 p3526 N90-29940
Fast algorithms for parallel architectures
[AD-A223731] 24 p3528 N90-29947
Parallel and sparse methods for large-scale numerical optimization
[DE90-015655] 24 p3530 N90-29959
Developing tools for performance visualization of parallel algorithms
[DE90-015801] 24 p3530 N90-29960
A parallel least squares collocation conjugate gradient approach for the advection diffusion equation
[DE90-015965] 24 p3530 N90-29961
Assembler for a parallel computer
[NAL-TM-586] 24 p3532 N90-29974
Fault tolerant design for multistage routing networks
[AD-A224267] 24 p3533 N90-29978
Asynchronous design for parallel processing architectures
[AD-A223754] 24 p3533 N90-29981
Fact system: A standardizing modelization processing for concurrent systems
[ETN-90-97286] 24 p3533 N90-29982
Parallelization of a method for solving three dimensional Navier-Stokes equations on a distributed memory multiprocessor
[ONERA-RTS-1/3717-CY] 24 p3534 N90-29983

PARALLEL PROGRAMMING
The rewrite rule machine project
[AD-A210526] 01 p0109 N90-10617
Boolean functions, invariance groups and parallel complexity
[CWI-CS-R8836] 02 p0260 N90-11472
A simple definition for parallel composition of prime event structures
[CWI-CS-R8903] 04 p0532 N90-13074
Towards a parallel algorithm for the many body problem
[CS-8813] 04 p0533 N90-13078
A compilation strategy for numerical programs based on partial evaluation
[AD-A212759] 04 p0546 N90-13175
Paralation views: Abstractions for efficient scientific computing on the connection machine
[AD-A213935] 07 p0971 N90-15604
An overview of lynx
[AD-A213714] 07 p0975 N90-15631
Principles and algorithms for causal reasoning with uncertainty
[AD-A214248] 07 p0977 N90-15644
MASC: Multiprocessor architecture for symbolic processing
[AD-A213504] 07 p0979 N90-15656
Design and implementation of a multi-sensor fusion algorithm on a hypercube computer architecture
[DE90-003682] 08 p1112 N90-16438
A theory for graph-based language specification, analysis, and mapping with application to the development of parallel software
[AD-A214910] 09 p1266 N90-17342
Parallel logic programming and parallel systems software and hardware
[AD-A214635] 09 p1270 N90-17361
Writing parallel, discrete-event simulations in ModSim: Insight and experience
[DE90-001833] 10 p1419 N90-18183
Event-train restoration via backpropagation neural networks
[AD-A216308] 10 p1420 N90-18189
Technology development and circuit design for a parallel laser programmable floating point application specific processor
[AD-A215870] 11 p1500 N90-18637
Derivation of efficient parallel programs: An example from genetic sequence analysis
[DE90-005654] 11 p1547 N90-18904
Speculative computation in multilisp
[AD-A216579] 11 p1575 N90-19067
NYU (New York University) ultracomputer
[AD-A217167] 13 p1863 N90-20688
Hypercluster parallel processing library user's manual
[NASA-CR-185231] 14 p2016 N90-21552
SISAL 1.2: An alternative to FORTRAN for shared memory multiprocessors
[DE90-005181] 15 p2146 N90-22257
On the performance of parallel algorithms
[CS-8914] 16 p2299 N90-23099
Durra: A task-level description language reference manual, version 2
[AD-A219293] 16 p2301 N90-23114
Controlling real-time systems with parallel processes
[CS-8918] 16 p2302 N90-23119
Determination of algorithm parallelism in NP complete problems for distributed architectures
[AD-A220192] 18 p2598 N90-24786
Using integrity constraints to control search in knowledge base systems
[AD-A221291] 18 p2634 N90-25009
Multiprocessor architecture: Synthesis and evaluation
[NASA-CR-186618] 19 p2741 N90-25579
Language support for parallel computation
[AD-A223072] 20 p2911 N90-26560
Parallel programming with algorithmic skeletons
[DE90-010536] 20 p2911 N90-26562
Efficient network topologies for extensible massively parallel computers
[ETN-90-97220] 20 p2912 N90-26568
A programming environment for parallel vision algorithms
[AD-A221486] 21 p3055 N90-27368
Debugging and analysis of large-scale parallel programs
[AD-A221678] 21 p3059 N90-27393
AIMS test and simulation equipment 22 p3104 N90-27623
Parallelisation of a dynamic programming algorithm suitable for feature detection
[RSRE-MEMO-4349] 22 p3241 N90-28377
Concepts of concurrent programming
[AD-A223897] 23 p3382 N90-29110
Piecewise linear models of processor utilization
[DE90-014774] 23 p3384 N90-29115
Durra: A task-level description language user's manual
[AD-A223761] 24 p3528 N90-29950

PARALLEL STRIP LINES
U MICROSTRIP TRANSMISSION LINES

PARALLELEPIPEDS
FRAC-IN-THE-BOX utilization
[DE90-003648] 08 p1108 N90-16412

PARALLELOGRAMS
NT RHOMBOIDS
PARALYSIS
Temperature regulation during upper body exercise: Able bodied and spinal cord injured
[AD-A215130] 09 p1252 N90-17264
PARAMAGNETIC AMPLIFIERS
U MASERS
PARAMAGNETIC RESONANCE
NT ELECTRON PARAMAGNETIC RESONANCE
PARAMAGNETISM
Optical paramagnetic/diamagnetic gas sensor
[AD-D014368] 12 p1663 N90-19554
PARAMETER IDENTIFICATION
Numerically efficient algorithm for model development of high-order systems 01 p0022 N90-10108
On the interactive computer program IPIS for aircraft parameter identification
[NAL-TR-1000] 01 p0103 N90-10586
A unified approach to estimating tail behavior
[AD-A210961] 01 p0117 N90-10672
STS-GPS (Space Transportation System - Global Positioning System) tracking experiment for gravitation estimation: Feasibility study
[AD-A211265] 02 p0150 N90-10859
Results and practical experience using parameter identification techniques on the AM-X program at Aermacchi 02 p0153 N90-10873
Experimental identification of modal momentum coefficients and modal identity parameters of the FLECS structure 02 p0177 N90-10991
Updating of finite element model by means of normal mode parameters 02 p0177 N90-10992
Parametric identification of conservative self adjoint structures 02 p0177 N90-10994
Employment of modal survey methodologies in dynamic analysis procedures 02 p0179 N90-11006
Comparison of phase resonance, mode separation, and driven-base modal identification methods applied to the FLECS test structure 02 p0181 N90-11027
Performance and robustness of adaptive controllers for linear stochastic systems 02 p0261 N90-11485
Parameter identification for an abstract Cauchy problem by quasilinearization
[NASA-CR-181933] 03 p0385 N90-12192
Improvement of rules relating to clamp calculations
[CETIM-110610] 04 p0509 N90-12939
An error estimator for parameter choice in regulating least square problems. Application to regularized deconvolution
[IMAG-RR-744-M] 04 p0540 N90-13125
A kernel approach to estimation of the sphere radius density in Wicksell's corpuscle problem
[CWI-MS-R8809] 04 p0542 N90-13142
A semiparametric model for citation counts
[CWI-MS-R8814] 04 p0542 N90-13145
Astrometric parameter determination in FAST
05 p0610 N90-13556
The sphere solution and astrometric parameter determination in NDAC 05 p0610 N90-13557
Double star reductions in FAST
05 p0611 N90-13562
Accuracy and characteristics of the Hipparcos catalog
05 p0611 N90-13566
Parameter estimation for the Gummel-Poon transistor model
[MA-53] 05 p0635 N90-13705
Senegalese land surface change analysis and biophysical parameter estimation using NOAA AVHRR spectral data
[NASA-CR-186120] 05 p0664 N90-13883
Software development for avionics SSME control and diagnostics
[NASA-CR-184894] 05 p0681 N90-13964
The effectiveness of vane-aileron excitation in the experimental determination of flutter speed by parameter identification
[NASA-TP-2971] 07 p0880 N90-15100
Error modeling of bias-type parameters for TOPEX orbit determination 07 p0884 N90-15117
Parametric identification of discrete time series models for structural response prediction
07 p0945 N90-15472
Parameter estimation of linear systems in the presence of process noise using the maximum liklihood method
[ESDU-89032] 07 p0985 N90-15693
Maximum likelihood techniques in QELS
09 p1222 N90-17091
Boundary estimation problems arising in thermal tomography
[NASA-CR-181964] 10 p1421 N90-18193
Efficient detection and signal parameter estimation with application to high dynamic GPS receiver
[NASA-CASE-NPO-17820-1-CU]
11 p1454 N90-18379
The damage tolerance of disc materials: Metallurgical factors; relationship with processing parameters
11 p1458 N90-18398
A global approach for the identification of structural connection properties
[NASA-TM-102502] 11 p1518 N90-18745
Optimization of the reference parameters in the accompanying solar panel dynamics
[INPE-4795-PRE/1449] 11 p1528 N90-18798
Connections between the circulation in altitude and convection over South America
[INPE-4923-TDL/383] 11 p1534 N90-18828
An interactive system applied to the linear quadratic problem
[INPE-4945-TDL/386] 11 p1548 N90-18913
Satellite imagery for water quality assessment in coastal regions
[INPE-4891-PRE/1492] 12 p1678 N90-19636
Wind conditions near the ground in Federal Republic of Germany
[ISBN-3-88148-248-2] 12 p1694 N90-19727
Gravity field determination and error assessment techniques 13 p1832 N90-20517
An approximation theory for the identification of linear thermoelastic systems
[NASA-CR-182015] 13 p1877 N90-20764
CSI technology validation on an LSS ground experiment facility 14 p1937 N90-21089
Uncertainty analysis of the accident effect area of a BLEVE
[REPT-89-49] 15 p2126 N90-22160
Performance of the IMP array processing algorithm: First results
[RSRE-MEMO-4291] 15 p2148 N90-22274
Autonomous power expert system
15 p2154 N90-22306
JPL control/structure interaction test bed real-time control computer architecture 16 p2294 N90-23070
Robust adaptive control: Stability and asymptotic performance
[AD-A219259] 16 p2304 N90-23127
Estimation of Hilbert space valued parameters by the method of sieves
[AD-A218565] 16 p2306 N90-23143
Parameter estimation in linear filtering
[AD-A218566] 16 p2307 N90-23144
Spectral determinations for discrete sources with EGRET 16 p2336 N90-23312
Estimating short-period dynamics using an extended Kalman filter
[NASA-TM-101722] 17 p2352 N90-23392
Modelling and synergism: Optical and microwave remote sensing. Partial report 1: Preliminary study
[BCRS-89-23] 18 p2575 N90-24668
Active perception and exploratory robotics
[MS-CIS-89-65] 19 p2726 N90-25501
ICASE semiannual report, April 1 - September 30, 1989
[NASA-CR-181988] 19 p2727 N90-25502
Neuromorphic learning of continuous-valued mappings from noise-corrupted data. Application to real-time adaptive control
[NASA-TM-4176] 19 p2747 N90-25607
A contribution to the improvement of the accuracy in the parameter identification of nonlinear processes, by example of the aircraft motion
[ETN-90-96961] 20 p2808 N90-25974
A model of the synchronous machine with rectifier, especially for control purposes
[EUT-89-E-215] 20 p2858 N90-26256
Research conducted at the Institute for Computer Applications in Science and Engineering in applied mathematics, numerical analysis, and computer science
[NASA-CR-182057] 20 p2903 N90-26510
A new scheme for identification and control
[EUT-88-E-213] 20 p2915 N90-26586
A neural network for feature extraction
[AD-A223059] 21 p3058 N90-27387
Development and analysis of ARMA parameter estimation schemes in the presence of noise
[AD-A221794] 21 p3066 N90-27428
Identification method for estimation of electrical parameters of induction motors
[ETN-90-97306] 22 p3168 N90-27969
Determination of parameters of the Earth-Moon system: A contribution to model extension, evaluation, results
[SER-C-353] 22 p3263 N90-28479
A failure diagnosis system based on a neural network classifier for the space shuttle main engine
[NASA-TM-103607] 23 p3299 N90-28659
Estimation and representation of multidimensional mappings
[DLR-MITT-90-06] 24 p3531 N90-29967
Sensitivity of the error in multivariate statistical interpolation to parameter values
[AD-A224076] 24 p3540 N90-30015
PARAMETERIZATION
NT PARAMETER IDENTIFICATION
Quality control of castings 01 p0043 N90-10239
Subpicosecond optical digital computation using conjugate parametric generators
[AD-A207908] 01 p0058 N90-10330
An evaluation of the Chaboche and Bodner-Partom viscoplastic constitutive theories for strain rate sensitive materials 02 p0232 N90-11330
Parameter estimation in functional and partial differential equations
[AD-A211040] 02 p0265 N90-11511
Constitutive parameter measurements of lossy materials
[NASA-CR-183398] 02 p0281 N90-11603
Performance and quality of a wing type parachute: Parametric analysis
[REPT-88-19] 03 p0302 N90-11710
Structure based formal methods for software engineering
[AD-A211660] 03 p0388 N90-12207
Adaptive feedback linearization: Stability and robustness
[PB89-219497] 03 p0390 N90-12220
Numerical experience with a class of algorithms for nonlinear optimization using inexact function and gradient information
[NASA-CR-181927] 03 p0392 N90-12232
An error estimator for parameter choice in regulating least square problems. Application to regularized deconvolution
[IMAG-RR-744-M] 04 p0540 N90-13125
Physically-based parameterization of spatially variable soil and vegetation using satellite multispectral data
[NASA-CR-185957] 05 p0663 N90-13879
Some quick and efficient methods for bearing-only target motion analysis
[IMAG-RR-762-M] 05 p0693 N90-14049
Shock tube ignition of octanes
[DE90-001167] 07 p0893 N90-15164
Observational study of the macroscopic behavior of moist-convective processes 07 p0959 N90-15547
Flux parameterization techniques in the atmospheric surface layer 07 p0959 N90-15548
Calculation of source and structure parameters at regional and teleseismic distances
[AD-A214297] 07 p0961 N90-15558
Fast algorithms for estimating mixture parameters
[AD-A213869] 07 p0976 N90-15636
Some computational properties of rotation representations
[AD-A213888] 07 p0981 N90-15665
Higher order crossings from a parametric family of linear filters
[AD-A213427] 07 p0983 N90-15676
Membership-set parameter estimation via optimal bounding ellipsoids
[AD-A213807] 07 p0984 N90-15685
Parametric assessment of propulsion system mass for airbreathing launcher configurations
09 p1177 N90-16819
Efficient calculation of Ariane ascent trajectories with recursive quadratic programming
09 p1180 N90-16844
A numerical study of the formation of mesoscale convective complexes 09 p1245 N90-17225
Study on lightning parameters in the light of long gap discharge phenomena
[DE90-734987] 09 p1248 N90-17237
Infrared thermal imaging figures of merit
10 p1364 N90-17904
Parametric spectral estimation techniques for coherent millimeter-wave radar
[AD-A214355] 10 p1371 N90-17943
Parameterization of small-scale processes
[AD-A215507] 10 p1398 N90-18082
A general method of using prior information in a simultaneous equation system
[NOAA-TR-NESDIS-47] 10 p1423 N90-18209
A sample reuse method for accurate parametric empirical Bayes confidence intervals
[AD-A216198] 10 p1424 N90-18216
The Uniform Engine Test Programme
[AGARD-AR-248] 12 p1604 N90-19232
Study of the optimization of reference parameters to the dynamic constraints of solar panels
[INPE-4793-TDL/355] 12 p1681 N90-19656
Boundary layer parameterization in CTM and MM4
12 p1688 N90-19697
Reparametrization BRS cohomology in two-dimensional gravity and non-critical string theories
[DE90-741468] 12 p1725 N90-19911
Laboratory techniques for the characterisation of snow structures 12 p1741 N90-20007

Modeling the temperature dependence of the thermal conductivity of aluminum nitride
[DE90-009428] 14 p1949 N90-21154
Operation of a step tunable megawatt gyrotron
15 p2061 N90-21802
Modelling of optically and IR effective atmospheric turbulence
15 p2082 N90-21923
Nonlinearity parameters of polymers
15 p2164 N90-22369
Approximate analysis for the formation of adiabatic shear bands
[AD-A218751] 16 p2221 N90-22670
Impact of marine boundary layer parameterization on a numerical simulation of cyclogenesis during a cold air outbreak event
16 p2256 N90-22864
Robust modelling of sampled systems for time delay estimation
[REPT-89-047] 16 p2298 N90-23092
Curvature-dependent parametrization of curves and surfaces
[CS-8915] 16 p2299 N90-23100
A parametric detection approach using multichannel processes
[AD-A219328] 17 p2395 N90-23641
A solution for the variance-penalized Markov decision problem based on parametric linear programming
[TW-90-02] 17 p2467 N90-24100
A parametric study of counterflow heat exchanger transients
[IAR-89-10] 19 p2689 N90-25293
Physical parameterization of snow albedo for use in climate models
[PB90-167313] 19 p2712 N90-25433
Studies in the parameterization of cloudiness in climate models and the analysis of radiation fields in general circulation models
[NASA-CR-186378] 19 p2715 N90-25448
Non-linear systems identification using neural networks
[RR-370] 19 p2748 N90-25616
Calculation of the algebraic curves parameterization: Hamburger-Noether expansions
[IMAG-RR-798-M] 20 p2919 N90-26608
Boundary layer parameterization for use in a limited area forecast model
21 p3029 N90-27224
Design of robust multivariable controllers
[AD-A222096] 21 p3060 N90-27397
Investigation of factors affecting data comparison
22 p3119 N90-27714
Parametrical retiming of vibrational models of structures
[ONERA-RT-9/3313-RY-080-R]
22 p3194 N90-28121
July 16, 1987 revisited: Lessons for modelers
22 p3214 N90-28232
An eight-month climatology of marine stratocumulus cloud fraction, albedo, and integrated liquid water
22 p3214 N90-28233
Observed cloud reflectivities and liquid water paths: An update
22 p3215 N90-28237
Cloud optical parameters as derived from the multispectral cloud radiometer
22 p3215 N90-28239
Comparison of 30 day integrations with and without interactive clouds
22 p3222 N90-28274
Physically-based general circulation model parameterization of clouds and their radiative interaction
22 p3228 N90-28308
Robust controller design by contraction of a pole region
[ESA-TT-1042] 23 p3384 N90-29118
A posteriori error estimates for parametrized nonlinear equations
[AD-A224067] 24 p3537 N90-29997
Parametric testing for the RSRE CMOS, silicon on sapphire process
[RSRE-MEMO-4369] 24 p3555 N90-30115

PARAMETERS
U INDEPENDENT VARIABLES

PARAMETRIC AMPLIFIERS
Nonlinear acoustic interactions in superfluid helium
15 p2164 N90-22367
Millimeter-wave acoustic transducers
[AD-A221402] 18 p2612 N90-24878
Solid-state lasers for coherent communication and remote sensing
[NASA-CR-186634] 20 p2866 N90-26306

PARAMETRIC OSCILLATORS
U PARAMETRIC AMPLIFIERS

PARASITES
Computer symbiosis: Emergence of symbiotic behavior through evolution
[DE89-015247] 02 p0256 N90-11450

PARITY
Observational physics of mirror world
[NASA-CR-185923] 05 p0697 N90-14076
An even-parity/odd-parity formulation for deterministic transport calculations on massively parallel computers
[DE90-015036] 23 p3384 N90-29116
Parity violation and superconductivity in doped Mott insulators
[DE90-627493] 23 p3401 N90-29217
Fault Detection and Isolation (FDI) techniques for guidance and control systems 24 p3428 N90-29366

PARKS
NT NATIONAL PARKS

PARSING ALGORITHMS
Two VAX-PASCAL terminal interface modules for visualizing scanning and parsing
[MEMO-INF-89-17] 02 p0259 N90-11470
A table-driven approach to fast context-free parsing
[AD-A212210] 04 p0533 N90-13082
Design and implementation of the nested relational data model under the Exodus extensible database system
[AD-A215356] 09 p1296 N90-17515
Natural language processing: A tutorial
[AD-A219096] 16 p2300 N90-23108
Conceptual dependency graphs and DJ
[REPT-89-62] 17 p2445 N90-23933
Modular parser generation
[CWI-CS-R8933] 18 p2592 N90-24745
ATN design tool
[AD-A223030] 20 p2911 N90-26559

PARTIAL DIFFERENTIAL EQUATIONS
NT BIHARMONIC EQUATIONS
NT BURGER EQUATION
NT ELLIPTIC DIFFERENTIAL EQUATIONS
NT FOKKER-PLANCK EQUATION
NT GAUSS EQUATION
NT HELMHOLTZ VORTICITY EQUATION
NT LIOUVILLE EQUATIONS
NT PARABOLIC DIFFERENTIAL EQUATIONS
NT POISSON EQUATION
NT VLASOV EQUATIONS
A straightforward method for finding implicit solitary wave solutions of nonlinear evolution and wave equations
[AD-A210561] 01 p0113 N90-10647
Multiple solutions for Lagrangian systems in T superscript n
[AD-A210646] 01 p0113 N90-10650
Wavefront propagation for reaction-diffusion systems of PDE
[AD-A210862] 02 p0265 N90-11510
Control and optimization for observations of systems governed by controlled partial differential equations
[AD-A211122] 02 p0266 N90-11513
Domain decomposition for partial differential equations
[DE89-016669] 02 p0267 N90-11519
Smoothed predictor-corrector methods for solving partial differential equations
[CWI-NM-R8808] 04 p0540 N90-13131
A moving-grid interface for systems of one-dimensional time-dependent partial differential equations
[CWI-NM-R8904] 04 p0541 N90-13136
The Painleve test for nonlinear ordinary and partial differential equations
[AD-A212894] 04 p0546 N90-13177
Quadratic dynamical systems describing shear flow of non-Newtonian fluids
[AD-A212892] 05 p0638 N90-13720
Aspects of field theory related to the Zakharov problem
06 p0783 N90-14551
Research in mathematics and computer science at Argonne, July 1, 1986 to January 6, 1988
[DE88-010343] 06 p0822 N90-14781
User's guide to PMESH: A grid-generation program for single-rotation and counterrotation advanced turboprops
[NASA-CR-185156] 06 p0823 N90-14783
Numerical methodologies for solving partial differential equations
[DE90-001842] 06 p0834 N90-14849
Two-dimensional behavior of Megagauss-field-confined solid fiber Z-pinches
[DE90-000684] 06 p0845 N90-14918
Finite difference techniques and rotor blade aeroelastic partial differential equations with quasisteady aerodynamics
07 p0875 N90-15075
Knowledge representations for the automatic generation of numerical simulators for PDEs
[DE89-008036] 07 p0972 N90-15615
Physical process in MPD plasmas
[AD-A213679] 07 p0996 N90-15761
Symbol manipulation and applied mathematics
[AD-A214702] 09 p1273 N90-17378
Hybrid (optical/electronic) computing and digital optical computing
[AD-A214502] 10 p1416 N90-18160
Domain decomposition with local mesh refinement
[AD-A215806] 10 p1418 N90-18175
Self similar solutions of the second kind of nonlinear diffusion-type equations
[DE90-606953] 10 p1422 N90-18204
Convergence properties of iterative algorithms for solving the nodal diffusion equations
[DE89-016859] 12 p1707 N90-19804
A time stepping algorithm for parallel computers
[DE90-008163] 13 p1873 N90-20738
A model and implementation of multigrid for massively parallel computers
[DE90-008165] 13 p1873 N90-20739
Nonlinear systems of partial differential equations
[AD-A217581] 13 p1877 N90-20761
Application of an inverse method to the design of a radial inflow turbine
14 p1918 N90-20989
Multigrid on massively parallel computers
[DE90-008999] 14 p2017 N90-21560
High accuracy solutions of incompressible Navier-Stokes equations
[NASA-TM-102539] 14 p2018 N90-21567
Determination of unknown coefficients in partical differential equations
[AD-A217169] 14 p2019 N90-21569
On the equation: Delta u+c=Ke(sup u)
[DE90-612741] 14 p2020 N90-21575
A parallel multigrid method for solving elliptic partial differential equations
[DE90-007929] 14 p2021 N90-21584
Stability of a solitary wave solution to a set of coupled Boussinesq-like equations
[DE90-008927] 14 p2021 N90-21586
A remark on the Kelvin transform and a non-linear partial differential equation
[PB90-165622] 14 p2021 N90-21589
Numerical simulation model of hydrazine attitude control thrusters
[INPE-4965-PRE/1534] 15 p2068 N90-21848
Dual-shaped offset reflector antenna designs from solutions of the geometrical optics first-order partial differential equations
15 p2076 N90-21887
On the way to an integrated mesh generation system for industrial applications
15 p2095 N90-21989
Analytic semigroups: Applications to inverse problems for flexible structures
[NASA-CR-182047] 16 p2306 N90-23138
Undetermined coefficient problems for quasi-linear parabolic equations
[AD-A218462] 16 p2306 N90-23141
Continuation and multi-grid methods for bifurcation problems
[AD-A218904] 16 p2307 N90-23146
Adaptive mesh experiments for hyperbolic partial differential equations
[AD-A219194] 16 p2307 N90-23148
Nonlinear interactions in mixing layers and compressible heated round jets
[NASA-CR-186303] 17 p2400 N90-23674
Efficient numerical methods for evolution partial differential equations
[AD-A219790] 17 p2457 N90-24020
Convergence properties of the Runge-Kutta-Chebyshev method
[CWI-NM-R8907] 17 p2459 N90-24038
Preconditioned time-differencing for the parallel solution of the heat equation
[DE90-010636] 18 p2590 N90-24737
An investigation of a mathematical model of an optically pumped Ti(3+):Al2O3 laser system
18 p2646 N90-25063
Execution time supports for adaptive scientific algorithms on distributed memory machines
[NASA-CR-182052] 19 p2741 N90-25578
Adaptive node movement in finite-difference solutions of partial differential equations with applications to gasdynamics, part 1
[UTIAS-333-PT-1] 19 p2750 N90-25622
Adaptive node movement in finite-difference solutions of partial differential equations with applications to gasdynamics, part 2
[UTIAS-333-PT-2] 19 p2750 N90-25623
An adaptive finite element method for shock developing partial differential equation
[FFI-89/7014] 19 p2751 N90-25632
Using implicit ODE methods with iterative linear equation solvers in spectral methods
[FFI-89/7017] 19 p2751 N90-25633
Projection methods for solving nonlinear systems of equations
[NASA-TM-101878] 21 p3063 N90-27409
On domain decomposition methods for solving partial differential equations
[AD-A222975] 21 p3063 N90-27414
Separable coordinate systems for PDE
[AD-A223052] 21 p3063 N90-27415
Numerical solutions to steady-state problems with discontinuities
[AD-A222205] 21 p3064 N90-27418

Parallel performance of domain-decomposed preconditioned Krylov methods for PDEs with adaptive refinement
[AD-A222339] 21 p3064 N90-27420
A hybrid perturbation-Galerkin technique for partial differential equations
[NASA-CR-182085] 23 p3327 N90-28814
The effect of multiprocessor radius on scaling
[DE90-014772] 23 p3380 N90-29095
Asymptotic behavior of solutions of diffusion-like partial differential equations invariant to a family of affine groups
[DE90-014792] 23 p3388 N90-29130
The Cousin problems for an overdetermined system of complex partial differential equations
[DE90-627170] 23 p3389 N90-29139
Some overdetermined systems of complex partial differential equations
[DE90-627162] 24 p3536 N90-29995
Transformation group methods in plasma physics
[DE90-628755] 24 p3548 N90-30074

PARTIAL PRESSURE
Comparison of protective breathing equipment performance at ground level and 8,000 feet altitude using parameters prescribed by portions of FAA action notice A-8150.2
[AD-A212852] 06 p0821 N90-14773

PARTICLE ACCELERATION
Ionospheric irregularities due to powerful HF radio transmissions 02 p0245 N90-11389
Can ion acceleration by double-cyclotron absorption produce O(+) ion conics
[IRF-PREPRINT-114] 02 p0280 N90-11600
Heating and acceleration of coronal and chromospheric ions during solar flares 03 p0433 N90-12479
Chromospheric-coronal coupling during solar flares: Current systems and particle acceleration 03 p0433 N90-12480
Auroral particle acceleration by dc and low frequency electric fields 05 p0658 N90-13841
The auroral current - voltage relationship 05 p0658 N90-13843
Use of plasmas for the acceleration of particles to very high energy 06 p0783 N90-14553
A calculation of energetic proton spectra producedat substorm onset in the fields of the explosive reconnection model 07 p1013 N90-15866
Proposal for a study of laser acceleration of electrons using micrograting structures at ATF
[DE90-003699] 08 p1082 N90-16262
Possible measurement of the gravitational acceleration of molecules, atoms, nuclei, elementary particles, and antiparticles
[DE90-719559] 08 p1121 N90-16490
Fracto-fusion. Mechanism of cold fusion
[DE90-719573] 08 p1125 N90-16518
Determination of solar flare accelerated ion angular distributions from SMM gamma ray and neutron measurements and determination of the He-3/H ratio in the solar photosphere from SMM gamma ray measurements
[NASA-CR-186038] 08 p1153 N90-16676
Report from space plasma science 10 p1445 N90-18338
Radiation of electromagnetic waves by an accelerated charged particle in medium
[DE90-610458] 12 p1646 N90-19461
Research accomplishments and future goals in particle physics
[DE90-007296] 12 p1712 N90-19830
The inverse-square law and quantum gravity 12 p1731 N90-19949
Langmuir wave interaction with ion acoustic wave
[DE90-615407] 14 p2027 N90-21624
Current drive in a supernova 15 p2187 N90-22491
Reacceleration of pairs in compact sources 19 p2787 N90-25859
The Tempel 2 dust trail
[AD-A224395] 24 p3562 N90-30153

PARTICLE ACCELERATOR TARGETS
Fermilab fixed target beams from the main injector
[DE89-014355] 01 p0122 N90-10697
Lower limit for the average angular momentum leading to fusion
[DE90-004027] 08 p1126 N90-16523
The design of a large aperture high field dipole
[DE90-007910] 14 p1970 N90-21285

PARTICLE ACCELERATORS
NT BETATRONS
NT CYCLIC ACCELERATORS
NT CYCLOTRONS
NT ELECTRON ACCELERATORS
NT ION ACCELERATORS
NT LINEAR ACCELERATORS
NT STORAGE RINGS (PARTICLE ACCELERATORS)
NT SUPERCONDUCTING SUPER COLLIDER
NT SYNCHROTRONS
NT VAN DE GRAAFF ACCELERATORS
Lifetime testing of commercially available 3.0 (mu)f, 100 kV pulsed-power capacitors
[DE89-017230] 02 p0217 N90-11242
Investigations into the influence of the state functions on the cross sections of the direct p,gamma reactions at energies in the 100 keV range, and project of a cascade accelerator for the measurement of the p,gamma capture cross sections
[ETN-89-94662] 02 p0273 N90-11561
Measurement of the fractional momentum carried by the glutons in the low Q squared photon-gluon fusion events at the ep HERA collider
[NOTA-INTERNA-937] 05 p0698 N90-14083
Use of a krypton isotope for rapid ion changeover at the Lawrence Berkeley Laboratory 88-inch cyclotron
[NASA-CR-186107] 05 p0698 N90-14084
NIKHEF-K contributions to the 1989 Particle Accelerator Conference
[NIKHEF/AMPS/89/03] 06 p0841 N90-14891
The Amsterdam pulse stretcher project (AmPS) 06 p0841 N90-14892
Optics of the Amsterdam pulse stretcher (AmPS) 06 p0841 N90-14893
Computation and control with neural nets
[DE90-006460] 11 p1548 N90-18911
Current and future uses of accelerators in particle astrophysics
[DE90-006667] 11 p1595 N90-19186
Dynamics of plasma injection along magnetic field lines in the PBFA 2 (Particle Beam Fusion Accelerator 2) plasma opening switch
[DE90-006751] 12 p1717 N90-19862
Designing an experimenters database using the Nijssen Information Analysis Methodology (NIAM)
[DE90-008548] 13 p1900 N90-20907
Current experiments in elementary particle physics
[DE90-008062] 14 p2024 N90-21607
A measurement of the gravitational acceleration of the antiproton
[DE90-008903] 14 p2025 N90-21612
Gravitational radiation produced by high energy accelerators and high power lasers
[PREPRINT-701] 16 p2240 N90-22782
Stability regimes in a rotating quadrupole focusing accelerator
[AD-A219513] 16 p2317 N90-23209
The behaviour of the L3 muon chambers in a magnetic field
[ETN-90-96920] 18 p2613 N90-24884
RF control system development at CEBAF
[CEBAF-PR-89-026] 19 p2755 N90-25653
Thermionic gun control system for the CEBAF injector
[CEBAF-PR-89-028] 19 p2755 N90-25654
Characteristic impedances and loss data for a common stripline pickup geometry
[CEBAF-PR-89-038] 19 p2755 N90-25656
Analytic study of the high-frequency impedance
[CEBAF-PR-89-014] 19 p2757 N90-25665
Thermal management of an accelerator system in space
[DE90-013153] 20 p2922 N90-26627
Diagnostics for hydrogen atoms and molecules in H-atom sources and beams using VUV laser light
[AD-A222340] 21 p3074 N90-27476
PBFA 2 applied B ion diode beam characteristics at high voltages
[DE90-014419] 23 p3396 N90-29190
High power microwaves for defense and accelerator applications
[AD-A223550] 24 p3464 N90-29572

PARTICLE BEAMS
NT ATOMIC BEAMS
NT ELECTRON BEAMS
NT ION BEAMS
NT MOLECULAR BEAMS
NT NEUTRAL BEAMS
NT NEUTRINO BEAMS
NT NEUTRON BEAMS
NT PION BEAMS
NT PROTON BEAMS
NT RELATIVISTIC ELECTRON BEAMS
Ion sources, electron guns and beam optics
[DE89-015526] 02 p0274 N90-11562
Comparison of laser and neutral particle beam discrimination
[DE89-017786] 03 p0353 N90-12018
DART: A simulation code for charged particle beams, revision 1
[DE89-016697] 03 p0404 N90-12312
Nonpotential scattering for the density matrix and quantum gravity
[PREPRINT-688] 05 p0697 N90-14080
Experimental investigation of relationship between nonlinear field energy and emittance growth
[AD-A215813] 10 p1430 N90-18246
Optically excited states in positronium 11 p1559 N90-18985
Fifth-order aberrations in magnetic quadrupole-octupole systems
[DE90-007489] 12 p1712 N90-19831
Dynamics of plasma injection along magnetic field lines in the PBFA 2 (Particle Beam Fusion Accelerator 2) plasma opening switch
[DE90-006751] 12 p1717 N90-19862
Literature file on fast kickers and SEPTA: Components for deflection and separation of particle beams
[LINO-162] 12 p1727 N90-19924
Designing an experimenters database using the Nijssen Information Analysis Methodology (NIAM)
[DE90-008548] 13 p1900 N90-20907
Charged-particle beam research program
[DE90-007937] 14 p2026 N90-21618
Onboard detection of intrinsic Ly alpha radiation from a neutral particle beam
[DE90-010341] 18 p2511 N90-24346
Proceedings of symposium on Production and Target Interaction of Particle Beam
[IPPJ-900] 18 p2616 N90-24903
Thermal management of an accelerator system in space
[DE90-013153] 20 p2922 N90-26627
Beam diagnostics in circular machines: Review of new developments
[DE90-014986] 23 p3394 N90-29176

PARTICLE COLLISIONS
The role of particle collisions in pneumatic transport 01 p0068 N90-10392
A symplectic coherent beam-beam model
[DE89-015386] 01 p0122 N90-10701
Global ionospheric dynamics 02 p0240 N90-11366
Ion heating events observed at the EISCAT radar 02 p0244 N90-11385
Theoretical atomic physics for fusion
[DE89-017363] 02 p0274 N90-11563
Atomic and molecular surface and volume processes in the analysis of negative hydrogen discharges
[DE89-015705] 03 p0401 N90-12294
The behavior of beams of relativistic non-thermal electrons under the influence of collisions and synchrotron losses
[NASA-CR-185983] 03 p0401 N90-12298
New developments in the ab initio treatment of low energy electron collisions with molecules
[DE89-015294] 03 p0402 N90-12299
Fluctuations in transverse energy and multiplicity, energy densities, and neutral pion spectra in nucleus-nucleus collisions at 200 GeV/nucleon
[DE89-017583] 03 p0402 N90-12302
GALAX: A two-dimensional N-body code for disk galaxy dynamics
[PB89-217780] 03 p0420 N90-12415
A study of recoil protons in ultra-relativistic nucleus-nucleus collisions
[LUIP-8907] 06 p0838 N90-14873
Calculation of two-neutron multiplicity in photonuclear reactions
[NASA-TP-2968] 06 p0841 N90-14890
Progress in LTE and non-LTE transport calculations
[DE90-003394] 07 p0997 N90-15764
Electron-positron momentum distribution measurements of high-T superconductors and related systems
[DE90-002974] 07 p0999 N90-15780
LEAP: A balloon-borne search for low-energy cosmic ray antiprotons 07 p1015 N90-15878
On the observation of a transition from fusion to multifragmentation in high multiplicity O16 induced reactions
[LUIP-8812] 08 p1119 N90-16481
Interactions of molecules with surfaces
[DE90-005337] 10 p1428 N90-18237
Annihilation physics of exotic galactic dark matter particles 11 p1559 N90-18984
Antihydrogen formation in collisions of positronium with antiprotons 11 p1560 N90-18988
Positronium formation in e+ plus H- collisions 11 p1561 N90-18993
The electron momentum-transfer cross sections of tungsten, silicon, and silicon dioxide at energies from 0.1 to 10,000 eV
[DE90-009041] 12 p1712 N90-19833
Electrical resistivity of strongly coupled plasmas in intense fields
[DE90-002236] 12 p1717 N90-19861
Incoherent retrodiffusion of radiowaves in plasma with particle impulse
[ETN-90-95375] 12 p1718 N90-19864

Low velocity dust-dust collisions
12 p1741 N90-20011
Possible targeting of particle emission by mechanical stress and penetration of sublimating ice-dust-surfaces
12 p1742 N90-20016
Energy transfer between electrons and ions in collision cascades in solids
[AERE-R-13662] 13 p1883 N90-20801
Termolecular associations of ions in gases, recombination and electron-atom collisions
[AD-A217678] 13 p1883 N90-20805
Inelastic electron scattering from surfaces
[DE90-009365] 14 p2025 N90-21614
Characterization of the plasma in magnetic multidipole discharges
[DE90-613219] 14 p2028 N90-21628
Correlated electron processes in ion-atom collisions
[DE90-009477] 15 p2165 N90-22370
The number of neutrino species, confronted with the results at the recent Lepton-Photon Symposium (August 7-12, 1989)
[NOTA-INTERNA-940] 16 p2315 N90-23195
Quark-antiquark pair production via gamma W fusion at high energy e(+)e(-) colliders
[PREPRINT-705] 16 p2316 N90-23205
Baryogenesis in extended inflation. Part 1: Baryogenesis via production and decay of supermassive bosons
[NASA-CR-180615] 17 p2470 N90-24120
Hyperon production at 200 and 900 GeV cm energy
[USIP-89-02] 17 p2471 N90-24126
One dimensional heavy ion beam transport: Energy independent model
[NASA-CR-186722] 19 p2754 N90-25650
Electron-impact spectroscopy
20 p2949 N90-26779
Investigation of the Saturn dust environment from the analysis of energetic charged particle measurements
[NASA-CR-186727] 20 p2950 N90-26784
Laboratory study of ion-neutral collisions at suprathermal energies
[AD-A222117] 21 p3074 N90-27475
Theoretical studies of time-of-flight and atom and molecular surface collision
[AD-A221705] 21 p3075 N90-27480
Readout of double sided silicon strip detectors with high intensity integrated electronics 22 p3179 N90-28038
New developments in double sided silicon strip detectors 22 p3179 N90-28039
Nucleus-nucleus collisions and the nuclear equation of state
[DE90-015427] 24 p3543 N90-30037
New developments in low-energy cosmic gamma-ray detection
[UT-HE-90/07] 24 p3564 N90-30165

PARTICLE COUNTERS
U RADIATION COUNTERS

PARTICLE DECAY
U RADIOACTIVE DECAY

PARTICLE DENSITY (CONCENTRATION)
NT CARRIER DENSITY (SOLID STATE)
NT ELECTRON DENSITY (CONCENTRATION)
NT ELECTRON DENSITY PROFILES
NT ELECTRON DISTRIBUTION
NT ION DENSITY (CONCENTRATION)
NT IONOSPHERIC ELECTRON DENSITY
NT IONOSPHERIC ION DENSITY
NT MAGNETOSPHERIC ELECTRON DENSITY
NT PLASMA DENSITY
Performance of laminar-flow leading-edge test articles in cloud encounters 04 p0439 N90-12511
Dense-spray properties: Structure and turbulence modulation
[AD-A213671] 07 p0931 N90-15387
Development and utilization of new diagnostics for dense-phase pneumatic transport
[DE90-006787] 12 p1659 N90-19536
About the order of Appel's algorithm
[CS-8910] 16 p2299 N90-23097
Time-dependent density-functional theory
[AD-A220993] 18 p2604 N90-24829
The affect of gravity on particle collection in inertial impactors
[DE90-013372] 23 p3393 N90-29173

PARTICLE DETECTORS
U RADIATION COUNTERS

PARTICLE DIFFUSION
NT ELECTRON DIFFUSION
NT IONIC DIFFUSION
Plasma theory and simulation
[AD-A207952] 01 p0125 N90-10714
Some new algorithms for boundary value problems in smooth particle hydrodynamics
[AD-A211726] 03 p0348 N90-11987
Temperature dependence of positron diffusion in cubic metals
[PB89-222020] 04 p0475 N90-12722
Recovery of particle size distribution of ultrafine aerosols from diffusional decay measurements
[AD-A213006] 05 p0621 N90-13621
Numerical methods for parabolic equations and inequalities in very high dimensions
[AD-A214102] 07 p0985 N90-15690
Proposed uses of laser light scattering instruments for polymerization studies 09 p1224 N90-17100
On the scale of diffusion lengths observable by neutron reflection: Application to polymers
[DE90-005645] 10 p1358 N90-17878
Anomalous particle diffusion through a magnetic picket fence
[INPE-4841-PRE/1470] 10 p1433 N90-18270
An optimized algorithm for solving the nodal diffusion method on shared memory multiprocessors
[DE90-002703] 12 p1700 N90-19762
Improvements in macroreticular particles for ion-exchange and gel-permeation chromatography
[DE90-003717] 18 p2522 N90-24399
A study of positrons from Soviet nuclear powered satellites as tracers for magnetospheric research
[DE90-013157] 20 p2888 N90-26438
Diffusion-accommodated grain boundary sliding in a polycrystal
[DE90-012727] 20 p2930 N90-26668

PARTICLE EMISSION
NT ELECTRON EMISSION
NT FIELD EMISSION
NT ION EMISSION
NT NEUTRON EMISSION
NT PHOTOELECTRIC EMISSION
NT SECONDARY EMISSION
NT THERMIONIC EMISSION
Particle emission and charging effects induced by fracture
[AD-A210215] 01 p0080 N90-10459
ERNE: Energetic and Relativistic Nuclei and Electron experiment 04 p0568 N90-13315
Calculation of two-neutron multiplicity in photonuclear reactions
[NASA-TP-2968] 06 p0841 N90-14890
Characterization of chemicals on engine exhaust particles
[AD-A213566] 07 p0882 N90-15106
Possible targeting of particle emission by mechanical stress and penetration of sublimating ice-dust-surfaces
12 p1742 N90-20016
Advanced space transportation technologies
18 p2645 N90-25061
The Tempel 2 dust trail
[AD-A224395] 24 p3562 N90-30153

PARTICLE ENERGY
NT ELECTRON ENERGY
NT ELECTRON STATES
An experiment to search for galactic axions
05 p0710 N90-14158
A calculation of energetic proton spectra producedat substorm onset in the fields of the explosive reconnection model 07 p1013 N90-15866
LEAP: A balloon-borne search for low-energy cosmic ray antiprotons 07 p1015 N90-15878
Low energy neutral particle energy analyser by time of flight method
[DE90-719529] 08 p1125 N90-16517
A balloon measurement of the isotopic composition of galactic cosmic ray iron 14 p2043 N90-21717
Exclusive production of p, p-, pi, and pi- in photon photon collisions
[NIKHEF-H/89-9] 15 p2165 N90-22376
Quark-antiquark pair production via gamma W fusion at high energy e(+)e(-) colliders
[PREPRINT-705] 16 p2316 N90-23205
Gamma rays from pulsar wind shock acceleration
16 p2336 N90-23311
Effects of energy, momentum and particle transport in the near-earth solar terrestrial system
[AD-A224393] 24 p3490 N90-29726

PARTICLE FLUX
U FLUX (RATE)

PARTICLE FLUX DENSITY
NT PROTON FLUX DENSITY
Performance of resistive plate counters at beam flux up to 140 Hz/cm2
[NOTA-INTERNA-930] 05 p0697 N90-14081
Search for anisotropies in the underground cosmic ray muon flux 12 p1745 N90-20034

PARTICLE IN CELL TECHNIQUE
NTRFACE for MAGIC
[AD-A212858] 04 p0538 N90-13112
The inverse triax x ray diode: An alternate reduced-endpoint-energy bremsstrahlung source
[DE90-006366] 13 p1792 N90-20285

PARTICLE INTERACTIONS
NT ELECTRON CAPTURE
NT ELEMENTARY PARTICLE INTERACTIONS
NT HIGH ENERGY INTERACTIONS
NT MESON-NUCLEON INTERACTIONS
NT MOLECULAR COLLISIONS
NT MOLECULAR INTERACTIONS
NT NUCLEAR INTERACTIONS
NT NUCLEON-NUCLEON INTERACTIONS
NT PLASMA-PARTICLE INTERACTIONS
NT SPIN-ORBIT INTERACTIONS
NT STRONG INTERACTIONS (FIELD THEORY)
NT WEAK ENERGY INTERACTIONS
NT WEAK INTERACTIONS (FIELD THEORY)
Tangent map analysis of the beam-beam interaction
[DE89-015857] 01 p0120 N90-10689
Atomic effects of beta decay in astrophysics and in elementary particle physics 01 p0141 N90-10811
On the effective transport properties of composite materials 02 p0190 N90-11086
Global and local fluctuations in multiplicity and transverse energy for central ultra-relativistic heavy-ion interactions
[LUIP-8903] 02 p0272 N90-11555
Molecular dynamics study of the primitive model of 1-3 electrolyte studies
[AD-A211653] 03 p0325 N90-11846
Laser production of soft x rays by multiquantum processes and the excitation of atomic inner-shell states
[AD-A211372] 03 p0353 N90-12021
Wave particle interactions
[DE89-017527] 03 p0407 N90-12335
Observational physics of mirror world
[NASA-CR-185923] 05 p0697 N90-14076
Interaction of radiation with matter: Atomic collision processes occurring in the presence of radiation fields
[AD-A213112] 05 p0697 N90-14078
Measurement of the fractional momentum carried by the glutons in the low Q squared photon-gluon fusion events at the ep HERA collider
[NOTA-INTERNA-937] 05 p0698 N90-14083
Big Bang nucleosynthesis and the Quark-Hadron transition
[NASA-CR-186169] 05 p0713 N90-14168
Supersymmetric dark matter above the W mass
[NASA-CR-186168] 06 p0863 N90-15016
Target nucleus fragmentation in O16 + (Ag,Br) interactions at 200 A GeV
[LUIP-8906] 07 p0991 N90-15727
Neutrino interactions
[NOTA-INTERNA-934] 08 p1121 N90-16495
Proceedings of the 23rd Annual Seminar on Theoretical Physics
[DE90-601827] 08 p1135 N90-16577
BOREX: Solar neutrino experiment via weak neutral and charged currents in boron-11
[DE90-003790] 09 p1300 N90-17530
Strongly coupled one-dimensional system and the polymer
[AD-A216330] 11 p1489 N90-18571
Low-energy scattering of electrons and positrons in liquids 11 p1559 N90-18981
Once more about the sizes of fast-moving objects
[DE90-615204] 14 p2022 N90-21592
Some global problems in gauge theories (variations on a theme of Aharonov and Bohm)
[DE90-009034] 14 p2035 N90-21678
PIC code modeling of spacecraft charging potential during electron beam injection into a background of neutral gas and plasma, part 1
[NASA-CR-186602] 15 p2059 N90-21792
QCD Compton scattering at HERA energy
[NIKHEF-H/89-3] 15 p2165 N90-22372
Investigation of correlations in nuclei with the (e,e'X) reaction
[ETN-90-96398] 15 p2166 N90-22377
Replica scaling analysis of interfaces in random media
[PREPRINT-713] 16 p2312 N90-23174
Support for the 16th International Conference on the Physics of Electronic and Atomic Collisions
[AD-A218567] 16 p2315 N90-23200
One dimensional heavy ion beam transport: Energy independent model
[NASA-CR-186722] 19 p2754 N90-25650
First International Conference on Laboratory Research for Planetary Atmospheres
[NASA-CP-3077] 20 p2942 N90-26744
Ion/molecule reactions of arsenic and phosphorus cluster ions: Ionization potentials and novel reaction pathways
[AD-A222019] 21 p2977 N90-26918
Coulomb-dissociation of 156 MeV 6Li-projectiles
[KFK-4691] 21 p3075 N90-27482
Ion divergence and the stability of magnetically insulated diodes
[DE90-014565] 23 p3321 N90-28777

Sigma and pi interactions of the pyrrolic ligand sandwich-like lanthanide phthalocyanines determined from magnetic susceptibility and ligand-field theory
[AD-A223609] 24 p3443 N90-29444

PARTICLE LADEN JETS
Dense-spray properties: Structure and turbulence modulation
[AD-A213671] 07 p0931 N90-15387
The future of aircraft paint removal methods
[AD-A214946] 09 p1197 N90-16936

PARTICLE MASS
An experiment to search for galactic axions 05 p0710 N90-14158
Unitarity limits on the mass and radius of dark matter particles
[NASA-CR-186079] 05 p0713 N90-14164
An estimation of the one-loop mass shifts in open superstring theory
[DE90-719578] 08 p1136 N90-16582
Trajectory-capture cell instrumentation for measurement of dust particle mass, velocity and trajectory, and particle capture 08 p1146 N90-16644
Elementary particles and cosmology
[DE90-610648] 11 p1591 N90-19177

PARTICLE MOTION
Effect of particle velocity fluctuations on the inertia coupling in two-phase flow 01 p0066 N90-10391
The role of particle collisions in pneumatic transport 01 p0068 N90-10392
DMC (Distinct Motion Code): A rigid body motion code for determining the interaction of multiple spherical particles
[DE89-016929] 02 p0270 N90-11543
Composite vs constituent particle aspects of hole motion in the CuO2 plane
[DE89-618854] 04 p0558 N90-13251
Synchrotron-betatron parametric instability in free-electron lasers
[AD-A213373] 05 p0648 N90-13777
Ring source/force excitation of axisymmetric shell structure
[ARE-TM(UHA)-88519] 05 p0698 N90-14085
Self-field-induced chaotic electron motion in free electron lasers
[DE90-001710] 06 p0790 N90-14598
Dense-spray properties: Structure and turbulence modulation
[AD-A213671] 07 p0931 N90-15387
Canonical formalism for coupled beam optics
[DE90-003764] 07 p0992 N90-15734
Beam collector and output window for a 35 GHz 100 kW gyrotron
[INPE-4958-RPE/603] 11 p1511 N90-18699
Once more about the sizes of fast-moving objects
[DE90-615204] 14 p2022 N90-21592
Dynamics of motion charged particles in a field of two electromagnetic waves
[DE90-620690] 16 p2228 N90-22706
Bubble, Drop and Particle Unit (BDPU): A multi-user microgravity facility
[IAF-89-431] 20 p2842 N90-26164
Computerized simulation of phenomena in plasma via particles
[INPE-4595-RPE/569] 23 p3397 N90-29194
Particle dispersion in a turbulent shear flow
[AD-A224327] 24 p3467 N90-29590
Spectral structure and generation mechanism of ducted VLF whistler mode sideband waves 24 p3489 N90-29720

PARTICLE PRECIPITATION
NT ELECTRON PRECIPITATION
NT PROTON PRECIPITATION
Magnetospheric substorms as a signature of the solar terrestrial interaction 02 p0240 N90-11363
Modelling ionospheric density structures 02 p0242 N90-11375
Observations of ionosphere/magnetosphere interactions from the Dynamics Explorer satellites 02 p0242 N90-11376
Electrostatic turbulence in the high latitude ionosphere 02 p0246 N90-11392
Distribution of auroral precipitation at midnight during a magnetic storm
[PB89-213136] 03 p0370 N90-12118
Airborne measurements of the electric field and the charge precipitation particles in convective clouds: Lower positive charge centres
[ESA-TT-1157] 11 p1535 N90-18836
Electron density profiles in the background of LF absorption during Forbush-decrease and PSE 22 p3208 N90-28199

PARTICLE PRODUCTION
NT PAIR PRODUCTION
NT PHOTOPRODUCTION
Substructural dependence of the multiparticle production in relativistic heavy-ion interactions
[LUIP-8904] 07 p0989 N90-15716
Elementary particle physics: Experimental
[DE90-005973] 10 p1429 N90-18242
Research in theoretical nuclear physics
[DE90-006063] 10 p1440 N90-18309
Theoretical survey on positronium formation and ionisation in positron atom scattering 11 p1556 N90-18965
Positron scattering by atomic hydrogen using optical potentials and with positronium formation 11 p1557 N90-18966
Positronium formation in Ss state in e+-Li scattering 11 p1557 N90-18967
Angular correlation studies in noble gases 11 p1557 N90-18972
Annihilation physics of exotic galactic dark matter particles 11 p1559 N90-18984
Optically excited states in positronium 11 p1559 N90-18985
Elementary particles and cosmology
[DE90-610648] 11 p1591 N90-19177
Theoretical investigations in elementary particle physics
[DE90-007178] 13 p1883 N90-20802
The observed properties of the intermediate-degree gravity modes and their relevance to the solar neutrino paradox 15 p2193 N90-22519
Hyperon production at 200 and 900 GeV cm energy
[USIP-89-02] 17 p2471 N90-24126
Production and coating of pure boron powders
[AD-A220272] 18 p2533 N90-24452
A research program in physics of the early universe
[DE90-013319] 20 p2942 N90-26742
High energy physics at Tufts University
[DE90-014664] 23 p3394 N90-29174

PARTICLE SIZE DISTRIBUTION
The measurement of infrared spectra of dense ceramics by specular reflectance spectroscopy
[AD-A210609] 01 p0051 N90-10291
Real-time observations of aerosol composition changes
[DE89-012382] 01 p0073 N90-10422
Powder morphology effects in the ignition of titanium-based pyrotechnics
[DE89-017229] 02 p0208 N90-11191
Analysis of forest fire smoke using satellite imagery
[AD-A210657] 02 p0236 N90-11339
Atmospheric aerosol size distributions and optical properties found in the marine boundary layer over the Atlantic Ocean
[AD-A210800] 02 p0252 N90-11431
Droplet sizing instrumentation used for icing research: Operation, calibration, and accuracy
[NASA-CR-182293] 03 p0350 N90-11999
Aerosol in the Pacific troposphere 03 p0363 N90-12078
Recovery of particle size distribution of ultrafine aerosols from diffusional decay measurements
[AD-A213006] 05 p0621 N90-13621
Ordered ceramic membranes
[DE89-017426] 06 p0750 N90-14364
Particle size effects in the initiation of explosives containing reactive and nonreactive continuous phases
[DE90-000786] 06 p0754 N90-14390
Comparison of two droplet sizing systems in an icing wind tunnel
[NASA-TM-102456] 06 p0793 N90-14617
Advanced study in solid transport: Rheological behavior of dense suspension
[DE90-003369] 07 p0947 N90-15483
Beryllium dispersion near explosive firing tables: A comparison of computed and observed results
[DE90-002635] 07 p0960 N90-15550
Study of phase transformations liquid-solid-solid of ultrafine particles
[ISAL-89-0019] 08 p1042 N90-16022
Development of an elastomeric additive to improve the impact resistance of unsaturated polyester networks
[ISAL-89-0006] 08 p1050 N90-16073
Laser light scattering review 09 p1221 N90-17086
Advanced instrumentation for QELS experiments 09 p1223 N90-17093
Enhanced resolution particle size distributions by multiple angle photon correlation spectroscopy 09 p1223 N90-17094
Online submicron particle sizing by dynamic light scattering using autodilution 09 p1223 N90-17095
Light scattering instrumentation for micro gravity research 09 p1223 N90-17096
Laser light scattering as a probe of fractal colloid aggregates 09 p1223 N90-17097
Laser velocimeter seed particle sizing by the whisker particle collector and laser aerosol spectrometer methods
[PB90-111287] 09 p1224 N90-17103
Rain core structure statistics derived from radar and disdrometer measurements in the mid-Atlantic coast of the US 10 p1373 N90-17956
Fluidization mechanisms in slurry flow
[DE90-006497] 11 p1509 N90-18691
Satellites and debris in earth revolution orbits and first estimation of the collision probability
[R-8709] 12 p1615 N90-19289
Experimental and theoretical studies of light scattering by small particles
[AD-A217432] 13 p1888 N90-20831
Phase Doppler droplet sizing: Scattering angle effects
[DE90-009571] 16 p2236 N90-22754
Processing and properties of advanced aluminum alloys
[AD-A221292] 18 p2526 N90-24416
Metallized fuel particle size study in a solid fuel ramjet
[AD-A220079] 18 p2533 N90-24451
Grain-size distribution and armoring in gravel-bed rivers: A case study 19 p2687 N90-25285
Contamination of spacecraft by recontact of dumped liquids 19 p2728 N90-25508
Combustion instrumentation 20 p2811 N90-25996
Texture of materials by time-of-flight neutron diffraction
[DE90-008968] 20 p2830 N90-26096
Hypervelocity impact shield
[NASA-CASE-MSC-21420-1] 21 p2966 N90-26858
The sensitivity of several explosives to ignition in the launch environment
[AD-A221581] 21 p2990 N90-26993
Particle size distribution determined from measured scattered light
[MPIS-5/1990] 21 p3077 N90-27497
Cirrus microphysics and radiative transfer: Cloud field study on October 28, 1986 22 p3224 N90-28284
The 27-28 October 1986 FIRE IFO cirrus case study: Comparison of satellite and aircraft derived particle size 22 p3224 N90-28285
Cirrus radiative characteristics and the radiative impact of small particles 22 p3224 N90-28286
Cirrus clouds and climate feedback: Is the sky falling and should we go tell the king 22 p3225 N90-28288
Micromechanics analysis of power consolidation in manufacturing particulate-reinforced MMCs (metal matrix composites)
[DE90-014448] 23 p3299 N90-28663
Microstructure of alpha-Al base matrix/SiC particulate composites
[DE90-014894] 24 p3444 N90-29449
An experimental investigation of strand burning metallized solid propellants
[AD-A224074] 24 p3457 N90-29526
Analysis of pyrotechnic devices by laser-illuminated high speed photography
[DE90-015741] 24 p3458 N90-29530
The Tempel 2 dust trail
[AD-A224395] 24 p3562 N90-30153

PARTICLE SPIN
NT ELECTRON SPIN
NT ISOTOPIC SPIN
NT NUCLEAR SPIN
Transverse spin observables in chromodynamics
[DE90-005638] 12 p1711 N90-19824
Operator algebra from fusion rules: The infinite number of Ising theories
[NIKHEF-H/89-7] 15 p2165 N90-22374

PARTICLE TELESCOPES
First results from the MACRO (Monopole, Astrophysics, Cosmic Ray Observatory) detector at the Gran Sasso Laboratory
[DE90-003243] 07 p1011 N90-15858
PROTEL: Design, fabrication, calibration, testing, and satellite integration of a proton telescope
[AD-A214564] 09 p1183 N90-16861
A drift chamber telescope for high-Z particles
[NASA-CR-186497] 12 p1746 N90-20040

PARTICLE THEORY
Plasma theory and simulation
[AD-A207952] 01 p0125 N90-10714
Particle physics and cosmology using stellar evolution theory
[DE89-017529] 03 p0421 N90-12418
Research program in elementary particle theory
[DE90-005600] 10 p1428 N90-18241
Particle theory and cosmology
[DE90-005338] 10 p1446 N90-18346
The inverse-square law and quantum gravity 12 p1731 N90-19949
Particle transport in pellet fueled JET (Jet European Torus) plasmas
[DE90-008077] 13 p1891 N90-20851

Rings
[DE90-009035] 14 p2025 N90-21613
Time-dependent density-functional theory
[AD-A220993] 18 p2604 N90-24829
Fast pulsars, strange stars: An opportunity in radio astronomy
[DE90-015630] 24 p3563 N90-30155

PARTICLE TRACKS
USAF/GL meteor scatter data analysis program: A user's guide
[AD-A214988] 09 p1206 N90-16989
Molecular dynamics simulation of sedimentation using the monotonic Lagrangian grid
[AD-A215099] 10 p1427 N90-18236
Cold fusion research
[DE90-005611] 10 p1433 N90-18267
Studies of (mu)(prime)s underground with the Soudan 2 Tracker
[DE90-005656] 10 p1449 N90-18360
The track-etch detector for the MACRO experiment at the Gran Sasso Laboratory
[DE90-003235] 11 p1594 N90-19182
Mesooptical Fourier transform microscope: A new device for high energy physics
[DE90-616423] 14 p2026 N90-21615
Particle tracking methods and fractal statistics in groundwater modeling 19 p2691 N90-25309
Meteor burst communications systems
[AD-A221675] 21 p2997 N90-27037
New developments in low-energy cosmic gamma-ray detection
[UT-HE-90/07] 24 p3564 N90-30165

PARTICLE TRAJECTORIES
NT ELECTRON TRAJECTORIES
Experimental test of PCAC hypothesis in the reactions mu neutrino-proton giving muon(-)-proton-pion(+) and mu antineutrino-proton giving muon(+)-proton-pion(-) in the delta (1232) region --- partial conserved axial current
[MPE-PAE/EXP.EL.199] 03 p0403 N90-12309
Confinement of multiply charged ions in an ECRH mirror plasma
[DE89-016052] 03 p0406 N90-12327
Coded trajectories for the investigation of strongly unsteady flow fields 08 p1078 N90-16240
Analysis of the measuring range and the accuracy of an existing particle image velocimetry system 08 p1080 N90-16247
Trajectory-capture cell instrumentation for measurement of dust particle mass, velocity and trajectory, and particle capture 08 p1146 N90-16644
Swept wing ice accretion modeling
[NASA-TM-103114] 15 p2046 N90-21727
Rings of Earth detected by orbital debris radar 20 p2854 N90-26232
Unexpected properties of the centrifugal force
[DE90-627197] 23 p3392 N90-29164
A search for low energy cosmic ray antiprotons 24 p3564 N90-30161

PARTICLES
NT AEROSOLS
NT ALPHA PARTICLES
NT ANTINEUTRINOS
NT ANTINUCLEONS
NT ANTIPARTICLES
NT ANTIPROTONS
NT ARGON PLASMA
NT BARYONS
NT BETA PARTICLES
NT BOSONS
NT BOUNDARY LAYER PLASMAS
NT CESIUM PLASMA
NT CHARGED PARTICLES
NT COLD NEUTRONS
NT COLD PLASMAS
NT COLLISIONAL PLASMAS
NT COLLISIONLESS PLASMAS
NT CONDUCTION ELECTRONS
NT COSMIC DUST
NT COSMIC PLASMA
NT CYLINDRICAL PLASMAS
NT DENSE PLASMAS
NT DEUTERONS
NT DROPS (LIQUIDS)
NT DUST
NT ELECTRON BEAMS
NT ELECTRON PLASMA
NT ELECTRON PRECIPITATION
NT ELECTRON RADIATION
NT ELECTRON-POSITRON PAIRS
NT ELECTRON-POSITRON PLASMAS
NT ELECTRONS
NT ELEMENTARY PARTICLES
NT ENERGETIC PARTICLES
NT ETA-MESONS
NT FAST NEUTRONS
NT FERMIONS
NT FOG
NT FREE ELECTRONS
NT GLUONS
NT GRAVITONS
NT HADRONS
NT HEAVY NUCLEI
NT HELIUM PLASMA
NT HIGH ENERGY ELECTRONS
NT HIGH TEMPERATURE PLASMAS
NT HOT ELECTRONS
NT HYDROGEN PLASMA
NT HYPERONS
NT INTERPLANETARY DUST
NT IONIZED GASES
NT LASER PLASMAS
NT LEPTONS
NT LUNAR DUST
NT MAGNETIC CLOUDS
NT MESONS
NT METAL PARTICLES
NT METAL POWDER
NT METALLIC PLASMAS
NT MICROPARTICLES
NT MUONS
NT NEUTRAL PARTICLES
NT NEUTRINOS
NT NEUTRONS
NT NITROGEN PLASMA
NT NONEQUILIBRIUM PLASMAS
NT NONUNIFORM PLASMAS
NT NUCLEI (NUCLEAR PHYSICS)
NT NUCLEONS
NT ODD-ODD NUCLEI
NT OXYGEN PLASMA
NT PARTICULATES
NT PHOTOELECTRONS
NT PHOTONEUTRONS
NT PHOTONS
NT PI-ELECTRONS
NT PIONS
NT PLASMA CLOUDS
NT PLASMA FOCUS
NT PLASMA JETS
NT PLASMA LAYERS
NT PLASMA SHEATHS
NT PLASMAS (PHYSICS)
NT POLARONS
NT POSITRONS
NT POWDER (PARTICLES)
NT POWDERED ALUMINUM
NT PROTONS
NT QUARKS
NT RADIATION BELTS
NT RADIO JETS (ASTRONOMY)
NT RAINDROPS
NT RECOIL PROTONS
NT RELATIVISTIC ELECTRON BEAMS
NT RELATIVISTIC PARTICLES
NT RELATIVISTIC PLASMAS
NT ROTATING PLASMAS
NT SEMICONDUCTOR PLASMAS
NT SINTERED ALUMINUM POWDER
NT SOLAR CORPUSCULAR RADIATION
NT SOLAR COSMIC RAYS
NT SOLAR NEUTRINOS
NT SOLAR NEUTRONS
NT SOLAR PROTONS
NT SOLAR WIND
NT SOOT
NT SPACE PLASMAS
NT SPHERICAL PLASMAS
NT STELLAR WINDS
NT STRONGLY COUPLED PLASMAS
NT THERMAL PLASMAS
NT TOROIDAL PLASMAS
NT TRAPPED PARTICLES
NT TRITONS
NT ZODIACAL DUST
Heterogeneous catalysts in water
[AD-A210742] 01 p0041 N90-10228
Numerical calculations of the collapse of a cavity in the vicinity of a compliant wall
[AD-A210489] 01 p0070 N90-10403
A laser Doppler anemometry investigation of single-phase and particle-laden jet flows
[AD-A210660] 02 p0220 N90-11261
DMC (Distinct Motion Code): A rigid body motion code for determining the interaction of multiple spherical particles
[DE89-016929] 02 p0270 N90-11543
Doppler statistics of ocean velocity variability
[AD-A211687] 03 p0377 N90-12148
Experimental research in high energy physics
[DE90-000061] 03 p0408 N90-12342
Small particle scattering and absorption
[AD-A213168] 04 p0473 N90-12711
Pilot investigation of indoor-outdoor and personal PM10 (thoracic) and associated ionic compounds and mutagenic activity
[PB89-222723] 05 p0673 N90-13920
The fluid mechanics of filters 06 p0773 N90-14499
Processing and properties of nanophase oxides
[DE90-003826] 07 p0895 N90-15171
Numerical analysis and simulation of frictional particle systems 07 p0937 N90-15430
Stand-off shields for hypervelocity particles
[DE89-016182] 07 p0939 N90-15437
Development of low density silica aerogel as a capture medium for hyper-velocity particles
[NASA-CR-185930] 08 p1121 N90-16489
Chemistry on interstellar grains and implications for infrared spectroscopy 11 p1579 N90-19097
Infrared diagnostics for interstellar solid state chemistry 11 p1580 N90-19103
A review of models for the analysis of the injection of densely loaded flows into entrained flow gasifiers
[DE90-000453] 12 p1662 N90-19550
Evaluation of the response of aluminum alloys to single and multiple particle impacts
[DE90-003689] 12 p1676 N90-19626
Enhancement of mass transfer to a rotating cylinder electrode by inert particles suspended in the electrolyte
[DE90-008054] 13 p1771 N90-20165
Mathematical modeling of fluid-solid mixtures
[DE90-009152] 15 p2098 N90-22007
The effects of urban air pollution on solar radiation
[DE89-009455] 19 p2712 N90-25438
Particle simulation of hypersonic flow
[AD-A222704] 21 p2954 N90-26794
Linear and nonlinear optical properties of quantum dots
[AD-A223050] 21 p3076 N90-27489
An experimental investigation of a single and multiphase confined coaxial jet 23 p3324 N90-28796
Spatial structure of particle-orbit loss regions in l=2 helical systems
[DE90-508080] 24 p3548 N90-30073

PARTICULATE FILTERS
U FLUID FILTERS

PARTICULATE SAMPLING
Aerosol in the Pacific troposphere 03 p0363 N90-12078
Measurements of aerosol properties needed to infer backscatter characteristics in support of the NASA Doppler Lidar program 03 p0364 N90-12082
Design and calibration of an in-stack, low-pressure impactor
[AD-A213531] 07 p0882 N90-15105
Undercooling and nucleation in rapid solidification rate metal powders using solid in solid emulsification
[AD-A218527] 17 p2375 N90-23526
Sample holder support for microscopes
[NASA-CASE-MFS-28420-1] 21 p3010 N90-27113

PARTICULATES
NT SOOT
Properties of F-34 (JP-8) fuel for 1988
[AD-A210188] 01 p0053 N90-10303
Densification of particulate ceramic composites: The role of heterogeneities
[DE90-000177] 03 p0331 N90-11886
Saltation and suspension of particulate matter in air
[AD-A213618] 07 p0960 N90-15552
High temperature aluminum-base alloy
[AD-D014270] 08 p1043 N90-16028
Ambient flow studies and particulate collection measurements: A laminar flow, reduced entrainment electrostatic precipitator
[DE90-001457] 08 p1063 N90-16149
Electron beam analysis of particulate cometary material 08 p1141 N90-16613
The in-situ cometary particulate size distribution measured for one comet: P/Halley 08 p1145 N90-16637
Analysis of particulates of comet nucleus samples: Possible use of olivine as indicator phase 08 p1147 N90-16646
Ion bombardment experiments suggesting an origin for organic particles in pre-cometary and cometary ices 08 p1148 N90-16652
Underwater acoustic scattering from spherical particulates and bubbles
[AD-A214827] 09 p1279 N90-17414
Creep behavior of alloys based on TiAl containing TiB2 and TiN particulates
[DE90-006489] 12 p1628 N90-19355
Chemical composition of precipitation and wet/dry deposition of sulfur compounds around the coastal area
[DE89-782324] 12 p1685 N90-19677
Hydrodynamic interactions and transport coefficients in a suspension of spherical particles
[DE90-008301] 13 p1801 N90-20336

Overview of the methodologies used to compile large scale emissions inventories
[DE90-008518] 13 p1830 N90-20509
The trace metal geochemistry of suspended oceanic particulate matter
[AD-A218604] 17 p2429 N90-23839
Interaction of electromagnetic signals with particulate clouds
[AD-A222604] 20 p2856 N90-26244
Optical signatures of molecular particles via mass-selected cluster spectroscopy
20 p2949 N90-26780
Evaluation of several micromechanics models for discontinuously reinforced metal matrix composites
[NASA-TM-102719] 23 p3339 N90-28872
Estimating the spatial variability of trace gas deposition velocities
[PB90-208570] 23 p3349 N90-28928
Investigation of particulate formation during diesel spray combustion
[DE90-012682] 24 p3446 N90-29464
Effect of particulate fillers on the rheology of polymer melts
[AD-A223601] 24 p3455 N90-29512

PARTITIONS (MATHEMATICS)
Error control techniques for satellite and space communications
[NASA-CR-182751] 05 p0631 N90-13685
On the performance of on-line algorithms for partition problems
[MEMO-784] 05 p0689 N90-14015
Classification of modular invariant partition functions for the twisted N=2 superconformal algebra, twisted SU(2) Kac-Moody algebra and D(sub 2K) parafermions
[DE90-600767] 06 p0835 N90-14853
Intersecting line segments, ray shooting, and other applications of geometric partitioning techniques
[RUU-CS-88-26] 18 p2601 N90-24804
Storing line segments in partition trees
[RUU-CS-89-17] 18 p2601 N90-24811
Cyclic error correcting block codes for reliability increasing of VLSI networks
[ETN-90-97304] 22 p3168 N90-27968

PASCAL (PROGRAMMING LANGUAGE)
Two VAX-PASCAL terminal interface modules for visualizing scanning and parsing
[MEMO-INF-89-17] 02 p0259 N90-11470
Environment for failure region analysis: REACHER - a reachability condition derivation tool
[AD-A214183] 07 p0977 N90-15641
Parallel algorithms for interactive manipulation of digital terrain models 08 p1113 N90-16445
The development of a simulation program of the anode side for aluminum/air batteries
[PB90-165754] 14 p1970 N90-21286
Vectors and matrices: Two turbo pascal units for fast program development
[AD-A218917] 16 p2300 N90-23105
Turbo pascal implementation of a distributed processing network of MS-DOS microcomputers connected in a master-slave configuration
[AD-A223925] 24 p3525 N90-29928

PASSAGEWAYS
NT STRAITS
Apparatus for mixing solutions in low gravity environments
[NASA-CASE-MFS-26047-1] 14 p1958 N90-21209

PASSENGER AIRCRAFT
NT A-300 AIRCRAFT
NT A-310 AIRCRAFT
NT A-320 AIRCRAFT
NT BOEING 727 AIRCRAFT
NT BOEING 737 AIRCRAFT
NT BOEING 747 AIRCRAFT
NT BOEING 757 AIRCRAFT
NT CH-47 HELICOPTER
NT COMMUTER AIRCRAFT
NT DC 10 AIRCRAFT
NT EUROPEAN AIRBUS
NT H-53 HELICOPTER
NT L-1011 AIRCRAFT
International Aircraft Occupant Safety Conference and Workshop proceedings
[AD-A214452] 07 p0877 N90-15085
Heat release rate measurement for evaluating the flammability of aircraft materials
10 p1316 N90-17610
The effects of wearing passenger protective breathing equipment on evacuation times through type 3 and type 4 emergency aircraft exits in clear air and smoke. Phase 1: Evacuations in clear air. Phase 2: Evacuations in smoke
[AD-A216798] 11 p1453 N90-18374
AVION: A detailed report on the preliminary design of a 79-passenger, high-efficiency, commercial transport aircraft
[NASA-CR-186663] 17 p2353 N90-23395
A process for analysis, evaluation, and development of aerial servicing noise reduction measures in civil aircraft
[ETN-90-97300] 22 p3244 N90-28398
Aircraft evacuations: The effect of passenger motivation and cabin configuration adjacent to the exit
[CAA-PAPER-89019] 24 p3423 N90-29336

PASSENGERS
Fire safety in civil aviation 10 p1312 N90-17586
Fire hardening of an aircraft passenger cabin
10 p1315 N90-17606
Passenger behaviour in aircraft emergencies involving smoke and fire 10 p1317 N90-17613
Smokehoods donned quickly. The impact of donning smokehoods on evacuation times
10 p1317 N90-17614
The effects of wearing passenger protective breathing equipment on evacuation times through type 3 and type 4 emergency aircraft exits in clear air and smoke. Phase 1: Evacuations in clear air. Phase 2: Evacuations in smoke
[AD-A216798] 11 p1453 N90-18374
The influence of adjacent seating configurations on egress through a type 3 emergency exit
[AD-A218393] 17 p2348 N90-23371
High speed civil transport
[NASA-CR-186661] 17 p2353 N90-23396
Biodynamic simulations of an aircraft pilot/passenger in various crash environments
[NIAR-90-6] 20 p2900 N90-26494
Human factors: The human interface with aircraft interiors
[NIAR-90-18] 20 p2900 N90-26496

PASSIVATION
U PASSIVITY

PASSIVE SATELLITES
NT BEACON EXPLORER A
NT BEACON SATELLITES
NT LAGEOS (SATELLITE)

PASSIVITY
Elaboration and characterization of MISFET transistors on InP
[ECL-88-19] 05 p0636 N90-13709
Laser Raman spectroscopy in studies of corrosion and electrocatalysis
[DE90-001414] 06 p0741 N90-14311
Stainless steel passivity
[AD-A214108] 08 p1044 N90-16033
An XPS and electrochemical study of the influence of molybdenum and nitrogen on the passivity of austenitic stainless steel
[AD-A214267] 08 p1044 N90-16034
Passivation and gating of GaAs and Si surfaces using pseudomorphic structures
[AD-A219351] 16 p2325 N90-23256
A study of the influence of alloying additions on the passivity of aluminium
[AD-A219630] 17 p2376 N90-23532
New directions in InP solar cell research
[NASA-TM-103160] 17 p2398 N90-23662
Passivation of high temperature superconductors
[NASA-CASE-NPO-17949-1-CU]
20 p2932 N90-26684
PH3 surface chemistry on Si(111)-(7x7): A study by Auger spectroscopy and electron stimulated desorption methods
[AD-A221508] 21 p2979 N90-26929

PASTES
Effect of temperature on the storage life of polysulfide aircraft sealants
[MRL-TR-89-31] 12 p1629 N90-18364

PATENT APPLICATIONS
Method of producing a thin silicon-on-insulator layer
[AD-D014330] 09 p1290 N90-17478
The automation plan of the General Directorate 1 (search) of the European Patent Office
15 p2178 N90-22448
Active lag angle device
[AD-D014536] 20 p2857 N90-26249
Multicolor infrared photodetector
[AD-D014511] 20 p2865 N90-26297
Improved high power/high frequency inductor
[NASA-CASE-NPO-17830-1-CU]
21 p2998 N90-27042
Solid state circuitry with optical data interfacing
[AD-D014548] 22 p3248 N90-28422

PATENT POLICY
NASA Patent Abstracts Bibliography: A continuing bibliography. Section 1: Abstracts (supplement 36)
[NASA-SP-7039(36)-SECT-1] 07 p1010 N90-15851
NASA Patent Abstracts Bibliography: A continuing bibliography. Section 2: Indexes (supplement 36)
[NASA-SP-7039(36)-SECT-2] 10 p1441 N90-18317
NASA Patent Abstracts Bibliography: A continuing bibliography. Section 1: Abstracts (supplement 37)
[NASA-SP-7039(37)-SECT-1] 19 p2763 N90-25698
NASA Patent Abstracts Bibliography: A continuing bibliography. Section 2: Indexes (supplement 37)
[NASA-SP-7039(37)-SECT-2] 20 p2935 N90-26700
Manned Space Stations: Legal issues
[ESA-SP-305] 20 p2937 N90-26711
The astronauts' legal status: The International Space Station 20 p2938 N90-26721
Space Station intellectual property rights and US patent law 20 p2939 N90-26723
Space manufacture: Protection and valuation of innovations from a users point of view
20 p2939 N90-26724
Production activities in space: The problems of protection 20 p2939 N90-26725
Possible solutions 20 p2939 N90-26726
Legal ramifications of intellectual property
22 p3258 N90-28448

PATENTS
Continuously variable gear drive transmission
[AD-D014268] 08 p1084 N90-16275
The automation plan of the General Directorate 1 (search) of the European Patent Office
15 p2178 N90-22448
Electronic transfer of information applications in the Societe Aerospatiale 15 p2179 N90-22454
Yaw fin deployment apparatus for ejection seat
[AD-D014512] 19 p2656 N90-25118
Possible solutions 20 p2939 N90-26726
Legal ramifications of intellectual property
22 p3258 N90-28448
Industrial patent activity in the US. Part 1: Tima series profile by company and country of origin, 1969-1989
[PB90-214404] 22 p3259 N90-28454
Industrial patent activity in the US. Part 2: Alphabetical listing by company, 1969-1989
[PB90-214412] 23 p3405 N90-29246

PATH PLANNING
U TRAJECTORY PLANNING

PATHFINDER NUCLEAR REACTOR
Regenerative fuel cell systems for project pathfinder
10 p1333 N90-17708

PATHOGENESIS
Regulation of erythropoiesis in rats during space flight
[NASA-CR-177537] 23 p3378 N90-29086

PATHOGENS
Short-term bioassays may be useful in evaluating fiber/whisker hazards
[DE90-003707] 08 p1104 N90-16393

PATHOLOGICAL EFFECTS
Field management of accidental hypothermia during diving
[AD-A219560] 17 p2434 N90-23866

PATHOLOGY
Mutagenic responses of some petroleum-base obscurants in the Ames test
[AD-A214201] 07 p0915 N90-15295
The investigation of particulate matter in the lungs of smoke inhalation death victims
10 p1317 N90-17617
The importance of pathophysiological parameters in fire modelling of aircraft accidents 10 p1317 N90-17618

PATHS
Long dominating cycles and paths in graphs with large neighborhood unions
[MEMO-769] 04 p0544 N90-13157

PATIENTS
Rapidly quantifying the relative distention of a human bladder
[NASA-CASE-LAR-13901-1-NP]
14 p2010 N90-21519
Electronystagmographic findings following cervical injuries 19 p2718 N90-25466

PATTERN DISTRIBUTION
U DISTRIBUTION (PROPERTY)

PATTERN RECOGNITION
NT CHARACTER RECOGNITION
A comparison of real-time optical correlators for pattern recognition
[DE89-016416] 01 p0123 N90-10705
Microsensor and pattern recognition techniques in hydrazine detection 02 p0206 N90-11177
Simulation of synthetic aperture radar 1: Feature density and accuracy requirements
[AD-A211019] 02 p0213 N90-11218
The 3D-POLY: A robot vision system for recognizing objects in occluded environments
02 p0229 N90-11313
ANIMA: Image analyzer applied to remote sensing
[INPE-4766-PRE/1435] 02 p0256 N90-11447
On algorithms for generating computationally simple piecewise linear classifiers
[NDRE/PUBL-89/1001] 02 p0258 N90-11459

Inferences from images
[AD-A210710] 02 p0258 N90-11465
Applications of artificial intelligence to digital photogrammetry 02 p0262 N90-11486
Improved pattern recognition techniques for real time operation
[AD-A211395] 03 p0324 N90-11840
Eye movements and spatial pattern vision
[AD-A211650] 03 p0381 N90-12169
A survey of camera error sources in machine vision systems
[DE89-014072] 03 p0405 N90-12318
Automatic processing of images from the GRATE flight test tool
[DLR-FB-89-28] 04 p0454 N90-12599
Progress in the identification of airborne radar targets
[AD-A212749] 04 p0493 N90-12835
A robot which will investigate the condition of underground pipe
[PB89-230650] 04 p0508 N90-12928
A two-dimensional hybrid experimental-numerical technique for elastic-plastic stress analysis
04 p0511 N90-12949
A theory of networks for approximation and learning
[AD-A212359] 04 p0538 N90-13110
Software development for avionics SSME control and diagnostics
[NASA-CR-184894] 05 p0681 N90-13964
Weather satellite and computer modeling approaches to assessing propagation over marine environments
06 p0764 N90-14443
Pattern recognition techniques applied to the NASA-ACTS order-wire problem
06 p0764 N90-14446
NORDA's pattern analysis laboratory: Current contributions to naval mapping, charting, and geodesy
[AD-A212731] 06 p0801 N90-14665
A rough transform technique for extracting lead features from sea ice imagery
[AD-A212758] 06 p0801 N90-14666
Generalization in backpropagation networks: An empirical study using image data
[DE89-012658] 06 p0832 N90-14835
NETRA: A parallel architecture for integrated vision systems. 1: Architecture and organization
[NASA-CR-185955] 06 p0832 N90-14839
Vision in dynamic environments
[AD-A213434] 07 p0967 N90-15587
Optical neural nets for scene analysis
[AD-A213986] 07 p0976 N90-15637
Connectionist model-based stereo vision for telerobotics 08 p1076 N90-16224
Ice floe identification in satellite images using mathematical morphology and clustering about principal curves
[AD-A213854] 08 p1090 N90-16311
The development of two-dimensional object identification techniques
[NASA-CR-186203] 08 p1107 N90-16408
Pattern matching in ML: A case study in refinement
[RSRE-89004] 08 p1111 N90-16430
Interpretation of CAD (Computer Aided Design) models through IGES (Initial Graphics Exchange Specification) interface
[PB90-121294] 08 p1112 N90-16441
High speed signal extraction using electro-optic techniques
[AD-A214446] 08 p1122 N90-16500
Order filters, median recursive filter: Analysis and evaluation of performance in image processing
[ISAL-89-0017] 08 p1123 N90-16505
Measures of subjective variables in visual cognition
[AD-A215084] 09 p1259 N90-17303
Adaptive multiple-band CFAR (Constant-False-Alarm-Rate) detection of an optical pattern with unknown spectral distribution
[AD-A214754] 09 p1281 N90-17429
Electron-beam phase-only spatial light modulator for matched filtering
[AD-A215026] 09 p1282 N90-17431
Aggregate filter
[AD-A215029] 09 p1282 N90-17432
Gabor transforms for forward looking infrared image segmentation
[AD-A215046] 09 p1282 N90-17433
Hybrid optical/digital architecture for distortion invariant pattern recognition
[AD-A215628] 09 p1282 N90-17435
Computing with neural maps: Application to perceptual and cognitive functions
[AD-A216689] 10 p1412 N90-18143
Hybrid (optical/electronic) computing and digital optical computing
[AD-A214502] 10 p1416 N90-18160
Binary correlators for optical computing and pattern recognition 10 p1441 N90-18318
Recognizing three-dimensional objects without the use of models
[AD-A216766] 11 p1540 N90-18862
Derivation of an efficient rule system pattern matcher
[AD-A216801] 11 p1549 N90-18917
Visual target detection and recognition
[DE90-006903] 11 p1567 N90-19015
VLSI implementation of moment invariants for automated inspection
[DE90-005318] 12 p1652 N90-19493
Selection of optimal textural features for maximum likelihood image classification
[DE90-006901] 12 p1678 N90-19638
An approach to elemental task learning
[DE90-006614] 12 p1697 N90-19745
On the verification of hypothesized matches in model-based recognition
[AD-A214718] 12 p1699 N90-19759
Object detection and amplitude estimation based on maximum a posteriori reconstructions
[DE90-007511] 12 p1701 N90-19770
Hybrid neural network and rule-based pattern recognition system capable of self-modification
[DE90-007482] 12 p1703 N90-19779
The role of chaos in hemispheric process and attention
[AD-A217674] 13 p1854 N90-20639
The boundaries of hemispheric processing in visual pattern recognition
[AD-A217675] 13 p1854 N90-20640
Lateral asymmetry in pattern recognition: Understanding the effects of familiarity, distinction, and perspective change
[AD-A217739] 13 p1854 N90-20641
Parts of recognition
[AD-A217694] 13 p1868 N90-20714
Texture segmentation using localized spatial filtering
[AD-A218064] 13 p1869 N90-20722
Hybrid intelligent perception system: Intelligent perception through combining artificial neural networks and an expert system
[DE90-007483] 13 p1874 N90-20746
Phase-only holographic filters and their applications
[PB90-166802] 14 p1984 N90-21368
Applications of remote sensing to studies of oceanic upper mixed layer dynamics 15 p2122 N90-22137
Photonic processing at NASA Ames Research Center
15 p2141 N90-22234
Algorithms and architectures for robot vision
15 p2141 N90-22236
Instrumentation and robotic image processing using top-down model control 15 p2142 N90-22239
Computer vision research at Marshall Space Flight Center 15 p2142 N90-22240
An acousto-optic image correlator with a throughput rate of 1000 templates per second
[DE90-009323] 15 p2144 N90-22249
Symbolic pattern processing system for planar spatial structures
[DE90-001598] 15 p2146 N90-22256
Adaptive pattern recognition by mini-max neural networks as a part of an intelligent processor
15 p2156 N90-22317
Satellite image analysis using neural networks
15 p2157 N90-22321
Object detection using structural matching
[INPE-4954-PRE/1532] 15 p2159 N90-22333
Automated star pattern recognition
16 p2211 N90-22612
The analysis of polar clouds from AVHRR satellite data using pattern recognition techniques
[NASA-CR-183300] 16 p2257 N90-22868
Quantum-limited image recognition
[AD-A218425] 16 p2299 N90-23101
Adaptive Resonance Theory 1
[AD-A219044] 16 p2304 N90-23126
Auditory spectro-temporal pattern analysis
[AD-A218416] 16 p2313 N90-23184
Classification techniques for quantum-limited and classical-intensity images
[AD-A218693] 16 p2317 N90-23212
A neural network based speech recognition system
[AD-A219794] 17 p2389 N90-23606
Neuromorphic optical signal processing and image understanding for automated target recognition
[AD-A219827] 17 p2437 N90-23884
A tabular bottom up recognizer
[REPT-89-78] 17 p2445 N90-23937
Improving upon standard pattern classification algorithms by implementing them as multi-layer perceptrons
[AD-A220046] 17 p2447 N90-23954
Multiple beam optical processing
[AD-A219048] 17 p2471 N90-24129
Optical computing strategies
[AD-A219433] 17 p2472 N90-24131
Optical neural nets for scene analysis
[AD-A220657] 17 p2472 N90-24135
Iconic tracking algorithms for high energy physi cs using the TRAX-I massively parallel processor
[MPI-PAE/EXP.EL-216] 18 p2596 N90-24773
A neural network for feature extraction
[AD-A220363] 18 p2597 N90-24775
Mars Rover imaging systems and directional filtering
18 p2648 N90-25071
Advanced mesoscale weather forecasting to support tactical operations on the airland battlefield
[AD-A219421] 19 p2715 N90-25449
Extensions of algebraic image operators: An approach to model-based vision 19 p2741 N90-25577
Initial results on fault diagnosis of DSN antenna control assemblies using pattern recognition techniques
20 p2854 N90-26228
Pattern classification of textura by moment and distance autocorrelation function
[INPE-4976-PRE/1541] 20 p2879 N90-26379
A sum rule satisfied by optimized feed-forward layered networks
[RSRE-MEMO-4341] 20 p2914 N90-26579
On networks, optimized feature extraction, and the Bayes decision
[RSRE-MEMO-4342] 20 p2914 N90-26580
Speech recognition based on pattern recognition techniques 21 p2993 N90-27011
Data analysis techniques 21 p3017 N90-27151
A neural network for feature extraction
[AD-A223059] 21 p3058 N90-27387
Parallel algorithms for computer vision
[AD-A221871] 21 p3059 N90-27394
Soviet image pattern recognition research
[DE90-010912] 21 p3059 N90-27396
United States Air Force research initiation program for 1988, volume 2
[AD-A223124] 21 p3102 N90-27614
Progress in the detection of cracks under installed fasteners using eddy currents 22 p3186 N90-28081
Study of failure processes in fiber reinforced composites using acoustic emission techniques
22 p3188 N90-28090
Development of an expert system embedding pattern recognition techniques for pollution source identification
[PB90-185927] 22 p3197 N90-28139
Conference on The Perception of Structure Program and Abstracts
[AD-A222437] 22 p3232 N90-28328
Categorization and identification of simultaneous targets
[IZF-1989-22] 22 p3234 N90-28337
Parallelisation of a dynamic programming algorithm suitable for feature detection
[RSRE-MEMO-4349] 22 p3241 N90-28377
Image fusion through multi-resolution contrast decomposition
[IZF-1989-19] 22 p3247 N90-28412
Studies in automatic speech recognition and its application in aerospace 23 p3318 N90-28759
Tele-Autonomous control involving contact --- object localization
[NASA-CR-187004] 23 p3335 N90-28854
On-line object feature extraction for multispectral scene representation
[NASA-CR-187006] 23 p3342 N90-28888
A method of classification for multisource data in remote sensing based on interval-valued probabilities
[NASA-CR-187007] 23 p3343 N90-28889
Real-time edge tracking using a tactile sensor
23 p3367 N90-29023
Perceptual telerobotics 23 p3374 N90-29063
Recognition of infrared images. Part 3: The effect of image processing with a size-contrast box filter on observation performance
[IZF-1989-39] 23 p3395 N90-29182
Detection and analysis of wind fronts and current shear in digital SAR images
[FFI-89/7016] 24 p3495 N90-29755
Weighted feature selection criteria for visual servoing of a telerobot 24 p3503 N90-29801
A fast 3-D object recognition algorithm for the vision system of a special-purpose dexterous manipulator
24 p3503 N90-29803
Recognition by linear combination of models
[AD-A224268] 24 p3525 N90-29929
Machine recognition as representation and search
[AD-A223700] 24 p3528 N90-29946

PATTERN REGISTRATION

Pattern matching in ML: A case study in refinement
[RSRE-89004] 08 p1111 N90-16430
Spatial registration of TIROS-N weather satellite data
[AD-A216041] 11 p1536 N90-18841
Derivation of an efficient rule system pattern matcher
[AD-A216801] 11 p1549 N90-18917

Stereo feature matching in disparity space
[AD-A218170] 13 p1875 N90-20751
Image segmentation with detection of highlights and inter-reflections using color
[AD-A218710] 16 p2317 N90-23213
KIPSE1: A Knowledge-based Interactive Problem Solving Environment for data estimation and pattern classification 21 p3041 N90-27287
Recognition by linear combination of models
[AD-A224268] 24 p3525 N90-29929

PATTERNS
Effect of contrast on the perception of direction of a moving pattern
[NASA-TM-102234] 07 p0965 N90-15577
Radar transponder antenna pattern analysis for the space shuttle 12 p1638 N90-19414

PAVEMENTS
Definition of research needs to address airport pavement distress in cold regions
[DOT/FAA/DS-89/13] 02 p0157 N90-10896
Field evaluation of the multi-depth deflectometers
[PB89-207708] 03 p0349 N90-11994
Evaluation of a neoprene latex modified SAMI (Stress Absorbing Membrane Interlayer)
[PB89-226435] 05 p0628 N90-13665
Design temperatures for flexible airfield pavement design
[AD-A214141] 07 p0884 N90-15115
Criteria for polymer concrete on airport pavements
[DOT/FAA/DS-89/18] 14 p1929 N90-21045
Criteria for coal tar seal coats on airport pavements. Volume 2: Laboratory and field studies
[AD-A220167] 18 p2498 N90-24277
Airport pavement drainage
[DOT/FAA/RD-90/24] 22 p3122 N90-27728
Development of acceptance plans for airport pavement materials. Volume 1: Development
[DOT/FAA/RD-90/15] 23 p3284 N90-28581
Development of a thickness design procedure for stabilized layers under rigid airfield pavements
[DOT/FAA/RD-90/22] 23 p3284 N90-28582

PAYLOAD ASSIST MODULE
The development of expertise on an intelligent tutoring system 18 p2630 N90-24984

PAYLOAD CONTROL
Independent Orbiter Assessment (IOA): Analysis of the remote manipulator system
[NASA-CR-185585] 02 p0164 N90-10926
STS payload design load evolution 02 p0176 N90-10989
Reduction of dynamic response of spacecraft structures and payloads 02 p0178 N90-11000
Flight-mechanical environment on Ariane launch vehicle payloads 02 p0184 N90-11048
Modeling and control of the rapid deployment of towed airborne devices 07 p0879 N90-15092
Payload invariant control via neural networks: Development and experimental evaluation
[AD-A215740] 09 p1260 N90-17306
Astrometric Telescope Facility isolation and pointing study
[NASA-CR-177473] 10 p1328 N90-17675
Payload vibration isolation in a microgravity environment
[NASA-CR-186191] 11 p1518 N90-18744
IRIS system and future application to expandable launchers
[IAF-89-212] 20 p2818 N90-26035
Payload training methodology study
[NASA-CR-183907] 21 p2964 N90-26849
Capture of free-flying payloads with flexible space manipulators 24 p3500 N90-29784

PAYLOAD DELIVERY (STS)
Syncom 4 deploy, LDEF retrieval highlight 10-day Columbia flight
[NASA-NEWS-RELEASE-89-180] 05 p0594 N90-13448
Shuttle C: Heavy-lift vehicle of the 1990's 09 p1178 N90-16830
Advanced APS impacts on vehicle payloads 11 p1472 N90-18472
Flight control issues of the next generation space transportation launch vehicles 22 p3126 N90-27742
Concept synthesis of an equipment manipulation and transportation system EMATS 24 p3510 N90-29844
Optimal payload rate limit algorithm for zero-G manipulators 24 p3513 N90-29858

PAYLOAD DEPLOYMENT & RETRIEVAL SYSTEM
NT REMOTE MANIPULATOR SYSTEM

PAYLOAD INTEGRATION
STS payload design load evolution 02 p0176 N90-10989
Payload crew utilization for spacelab missions
[NASA-TP-2976] 06 p0730 N90-14256
Get Away Special: The first ten years
[NASA-TM-102921] 09 p1171 N90-16775
The development of a complementary expendable launch vehicle interface for an STS deployable payload 15 p2113 N90-22086
Driving and latching of the Starlab pointing mirror doors 15 p2114 N90-22093
Planning for Space Station Freedom laboratory payload integration
[NASA-CR-186751] 20 p2820 N90-26047
Integrated support structure
[NASA-CR-186835] 20 p2841 N90-26162

PAYLOAD INTEGRATION PLAN
Flight-mechanical environment on Ariane launch vehicle payloads 02 p0184 N90-11048
Shuttle C: Heavy-lift vehicle of the 1990's 09 p1178 N90-16830

PAYLOAD RETRIEVAL (STS)
Concept synthesis of an equipment manipulation and transportation system EMATS 24 p3510 N90-29844
A comparison of the Shuttle remote manipulator system and the Space Station Freedom mobile servicing center 24 p3522 N90-29910

PAYLOAD STATIONS
Space station Simulation Computer System (SCS) study for NASA/MSFC. Volume 4: Conceptual design report
[NASA-CR-183843] 13 p1762 N90-20116
Space station Simulation Computer System (SCS) study for NASA/MSFC. Volume 5: Study analysis report
[NASA-CR-183844] 13 p1763 N90-20117

PAYLOADS
NT ASTRO MISSIONS (STS)
NT EARTH RADIATION BUDGET EXPERIMENT
NT GEOPHYSICAL FLUID FLOW CELLS
NT GET AWAY SPECIALS (STS)
NT HALOGEN OCCULTATION EXPERIMENT
NT SHUTTLE IMAGING RADAR
NT SPACE SHUTTLE PAYLOADS
NT SPACE STATION PAYLOADS
NT SPACELAB
NT SPACELAB PAYLOADS
NT X RAY ASTROPHYSICS FACILITY
Simulation of shuttle flight control system structural interaction with RMS deployed payloads 01 p0020 N90-10100
Microwave beam power 01 p0030 N90-10165
Design of scientific payloads and components
[AD-A211819] 03 p0351 N90-12005
The Hipparcos Mission. Prelaunch status. Volume 1: The Hipparcos satellite
[ESA-SP-1111-VOL-1] 05 p0603 N90-13499
Overview of the Hipparcos payload 05 p0603 N90-13503
Payload electronics and mechanisms 05 p0604 N90-13508
The payload structure 05 p0604 N90-13510
Payload thermal control 05 p0604 N90-13511
In-orbit payload calibration 05 p0606 N90-13526
Observation of the solar Lyman-alpha line 05 p0662 N90-13868
The Skylark sounding rocket program and future launcher developments by British Aerospace (Space Systems) Ltd. 05 p0662 N90-13871
Unsteady aerodynamic simulation of multiple bodies in relative motion: A prototype method
[NASA-TM-102181] 06 p0717 N90-14188
Manipulation strategies for massive space payloads
[NASA-CR-186081] 06 p0728 N90-14247
Unmanned air vehicles payloads and sensors 08 p1026 N90-15930
Automated search techniques applied to optical payloads in unmanned air vehicles 08 p1026 N90-15931
Proposed concept for the visible/infrared imaging radiometer for second generation Meteosat
[ETN-90-96145] 08 p1123 N90-16503
Remote Manipulator System (RMS)-based Controls-Structures Interaction (CSI) flight experiment feasibility study
[NASA-CR-181952] 09 p1230 N90-17136
Development and use of data analysis procedures for the CRRES (Combined Release and Radiation Effects Satellite) payloads AFGL-701-2/Dosimeter and AFGL-701-4/Fluxmeter and application of the data analysis results to improve the static and dynamic models of the Earth's radiation belts
[AD-A215953] 10 p1447 N90-18348
Electric propulsion for manned Mars exploration 11 p1473 N90-18480
BEAR electrostatic analyzer: Flight results
[DE90-006511] 11 p1498 N90-18625
Payload vibration isolation in a microgravity environment
[NASA-CR-186191] 11 p1518 N90-18744
Geostationary earth science platform concepts 12 p1608 N90-19252
Space station Simulation Computer System (SCS) study for NASA/MSFC. Volume 2: Concept document
[NASA-CR-183841] 13 p1762 N90-20114
Space station Simulation Computer System (SCS) study for NASA/MSFC. Volume 3: Refined conceptual design report
[NASA-CR-183842] 13 p1762 N90-20115
Space station Simulation Computer System (SCS) study for NASA/MSFC. Volume 4: Conceptual design report
[NASA-CR-183843] 13 p1762 N90-20116
Space station Simulation Computer System (SCS) study for NASA/MSFC. Volume 5: Study analysis report
[NASA-CR-183844] 13 p1763 N90-20117
Space station Simulation Computer System (SCS) study for NASA/MSFC. Volume 6: Study issues report
[NASA-CR-183845] 13 p1763 N90-20118
Modeling and control of flexible space platforms with articulated payloads 14 p1935 N90-21073
An air-bearing weight offload system for ground test of heavy LSS structures 14 p1936 N90-21081
Controls, Astrophysics, and Structures Experiment in Space (CASES) 14 p1937 N90-21085
Feasibility study for a microwave-powered ozone sniffer aircraft
[NASA-CR-186660] 17 p2353 N90-23397
OMV (Orbital Maneuvering Vehicle) payload support concept for Pegasus boosted payloads
[AD-A218371] 17 p2365 N90-23463
Dynamic modeling and control of a flexible arm holding a non-rigid payload 18 p2507 N90-24331
Random vibration analysis of space flight hardware using NASTRAN 18 p2570 N90-24645
High altitude ozone research balloon
[NASA-CR-186653] 19 p2654 N90-25107
Advanced solar-propelled cargo spacecraft for Mars missions
[NASA-CR-186218] 19 p2665 N90-25164
Interactions between the Space Station and the environment: A preliminary assessment of EMI 19 p2737 N90-25557
Rotating-unbalanced-mass devices and methods for scanning balloon-borne-experiments, free-flying spacecraft, and space shuttle/space station attached experiments
[NASA-CASE-MFS-28425-1] 20 p2866 N90-26304
Affordable spacecraft: Design and launch alternatives. Background paper 22 p3125 N90-27737
Affordable spacecraft: Design and launch alternatives. Background paper
[PB90-203225] 22 p3126 N90-27740
Reaction-compensation technology for microgravity laboratory robots
[NASA-TM-103271] 22 p3183 N90-28082
ATDRS payload technology research and development
[NASA-TM-103256] 23 p3287 N90-28596
Development and approach to low-frequency microgravity isolation systems
[NASA-TP-2984] 23 p3317 N90-28754
Dynamic modeling and payload-adaptation control of a flexible one-link manipulator 23 p3333 N90-28843
Shuttle remote manipulator system mission preparation and operations 24 p3521 N90-29909
Database development for the DMSP experiments
[AD-A224346] 24 p3557 N90-30129

PBRE (REACTORS)
U PEBBLE BED REACTORS

PCB
U POLYCHLORINATED BIPHENYLS

PCM (MATERIALS)
U PHASE CHANGE MATERIALS

PCM (MODULATION)
U PULSE CODE MODULATION

PCM TELEMETRY
PC-based PCM telemetry data reduction system software
[DE90-000317] 13 p1761 N90-20111

PDM (MODULATION)
U PULSE DURATION MODULATION

PEACETIME
Peacetime replacement and crash damage factors for army aircraft
[AD-A218544] 17 p2348 N90-23372

PEAT
Decomposition in Arctic terrestrial environments
[DE90-001198] 06 p0809 N90-14706
Ecological study of peat landforms in Canada and Alaska
[NASA-CR-184923] 19 p2705 N90-25391

PEBBLE BED REACTORS
Design study of a modular gas-cooled, closed-brayton cycle reactor for marine use
[AD-A213453] 07 p0953 N90-15518

PECULIAR GALAXIES
Study of peculiar galaxies in the Southern Hemisphere
[INPE-4810-TDL/357] 11 p1594 N90-19184

Counterrotating cores in elliptical galaxies
16 p2332 N90-23288

PECULIAR STARS
NT SYMBIOTIC STARS

PEDOLOGY
U SOIL SCIENCE

PEEK
Failure behavior of PEEK and its short-fiber composite systems
[AD-A210729] 01 p0035 N90-10189
Orthotropic elasto-plastic behavior of AS4/APC-2 thermoplastic composite in compression
[NASA-CR-186080] 04 p0513 N90-12959
Interlaminar fracture testing of carbon fibre/PEEK composites validity and applications
11 p1477 N90-18497
Cross-sectional examination of the damage zone in impacted specimens of carbon/epoxy and carbon/PEEK composites
[NASA-TM-100391] 14 p1944 N90-21125
Characterization of the creep compliances J22 and J66 of orthotropic composites with PEEK and epoxy matrices using the nonlinear viscoelastic response of the neat resins
[MBB-Z-0258/89-PUB] 19 p2650 N90-25082
Process of three dimensional lithography in amorphous polymers
[AD-D014500] 19 p2676 N90-25221
Characterization of impact damage in composites
21 p2957 N90-26811
Dissipation of mechanical work and temperature rise in AS4/PEEK thermoplastic composite
[NASA-CR-186893] 23 p3302 N90-28678
A constitutive model for AS4/PEEK thermoplastic composites under cyclic loading
[NASA-CR-180393] 23 p3302 N90-28679

PEELING
Manual for Program PSTRESS: Peel stress computation
[NASA-CR-178408] 03 p0321 N90-11822

PEENING
NT SHOT PEENING

PEGASUS AIR-LAUNCHED BOOSTER
OMV (Orbital Maneuvering Vehicle) payload support concept for Pegasus boosted payloads
[AD-A218371] 17 p2365 N90-23463

PELLETS
Characteristics of an electron-beam rocket pellet accelerator
[DE90-001595] 06 p0729 N90-14252
Starlight: A stationary inertial-confinement-fusion reactor with nonvaporizing walls
[DE90-002315] 06 p0847 N90-14927
Microstructure and electrical properties of bulk high-T(sub c) superconductors
[DE90-001762] 06 p0855 N90-14974
Application of railgun principle to high-velocity hydrogen pellet injection for magnetic fusion reactor refueling
[DE90-008281] 13 p1761 N90-20109
Application of the results of carbon pellet modeling to the problem of plasma penetration
[DE90-012713] 20 p2928 N90-26658
Noncontact measurement of high temperature using optical fiber sensors
[NASA-CR-186975] 23 p3329 N90-28825

PENALTY FUNCTION
Convergence results for pseudospectral approximations of hyperbolic systems by a penalty type boundary treatment
[NASA-CR-181929] 03 p0391 N90-12230
Long steps with the logarithmic penalty barrier function in linear programming
[REPT-89-44] 15 p2147 N90-22265
A solution for the variance-penalized Markov decision problem based on parametric linear programming
[TW-90-02] 17 p2467 N90-24100

PENDULUMS
Equilibrium solutions of a spherical pendulum with rotating point of suspension and friction
[ESA-TT-1139] 03 p0400 N90-12288
Instrumentation of pendulum impactor using metal foil strain gauges
[PB90-122656] 10 p1387 N90-18024
Evaluation of helmet retention systems using a pendulum device
[AD-A215489] 11 p1542 N90-18874
A nearly-linear computational-cost scheme for the forward dynamics of an N-body pendulum
16 p2280 N90-22996
Computational dynamics for robotics systems using a non-strict computational approach
16 p2283 N90-23011

PENETRANTS
Diffusion of penetrants in polymers
[AD-A223217] 21 p2986 N90-26969

PENETRATION
Studies in penetration mechanics
[AD-A210713] 01 p0079 N90-10448
Evaluation of integrals related to the Debye function
[DE89-016930] 02 p0264 N90-11499
N-port theory applied to backscatter polarimetry and depolarization in foliage penetration
[AD-A213437] 07 p0917 N90-15305
MESA 3-D calculations of armor penetration by projectiles with combined obliquity and yaw
[DE89-015265] 07 p0939 N90-15438
Hydrodynamics code calculations of debris clouds produced by ball-plate impacts
[DE89-015270] 07 p0939 N90-15439
Comparison of multidimensional calculations of long-rod impacts on oblique plates
[DE89-015275] 07 p0939 N90-15440
Theoretical study of cold nuclear fusion using barrier penetration approach
[DE90-601096] 08 p1124 N90-16513
Magnetic penetration depth and intragrain critical current density in gain-aligned Tl2Ca2Ba2Cu3O10 superconductor
[DE90-004245] 08 p1133 N90-16562
Taylor impact testing
[AD-A215018] 09 p1231 N90-17144
Simulation fidelity in lightning penetration studies
[DE90-006367] 12 p1694 N90-19731
Possible targeting of particle emission by mechanical stress and penetration of sublimating ice-dust-surfaces
12 p1742 N90-20016
Focused ion beam implantation
[AD-A217987] 13 p1898 N90-20894
Boeing 727-100 test project (high energy radiated field tests)
[DOT/FAA/CT-88/33] 14 p1964 N90-21247
VAMAS project on variable weld penetration: Surface tension of the steels
[NPL-DMA(A)-188] 15 p2070 N90-21856
Role of shear instability in ballistic penetration
[AD-A219186] 16 p2244 N90-22799
Spectral methods for electromagnetic propagation and diffraction
[AD-A220291] 17 p2393 N90-23632
Dust environment modelling from encounters with comet P/Halley
17 p2485 N90-24210
X ray diffraction analysis of control and test fibers
[MTL-TR-89-58] 19 p2678 N90-25233
Measurement techniques, evaluation criteria and injury probability assessment methodologies developed for Navy ejection and crashworthy seat evaluations
19 p2721 N90-25479
Diffusion of penetrants in polymers
[AD-A223217] 21 p2986 N90-26969
A case study of cumulus formation beneath a stratocumulus sheet: Its structure and effect on boundary layer budgets
22 p3219 N90-28256
Survivable penetration
24 p3428 N90-29363
Design and evaluation of candidate pressure distribution and air data system tile penetration for the aeroassist flight experiment
[NASA-CR-4312] 24 p3471 N90-29615

PENETRATION BALLISTICS
U TERMINAL BALLISTICS

PENINSULAS
A case for archaeological reconnaissance of the Cabo Catoche-Porvenir region of the northeastern Yucatan Peninsula
[NASA-TM-102248] 16 p2249 N90-22827

PENNING DISCHARGE
Beam-plasma discharge in penetrating plasma
[DE89-630481] 02 p0280 N90-11597

PENNING EFFECT
Polarization effects in ionizing collisions with Ne*(3-P2)- and Ne**(3-D3)-atoms
[ETN-90-96891] 17 p2471 N90-24127

PENTACHLORIDES
U CHLORIDES

PENTAERYTHRITOL TETRANITRATE
U PETN

PEPTIDES
NT POLYPEPTIDES
Control of synthetic peptide tertiary structure
[AD-A210339] 01 p0049 N90-10281
Boron analogues of amino acids and derivatives
[AD-A211311] 03 p0379 N90-12157
Combined capillary electrophoresis and electrospray ionization mass spectrometry
[DE90-001903] 06 p0743 N90-14322
Arginine vasopressin lowers pulmonary artery pressure in hypoxic rats by releasing artrial natriuretic peptide
[AD-A215986] 10 p1410 N90-18134
The effects of high intensity cycle exercise on sympatho-adrenal-medullary response patterns
[AD-A217962] 13 p1852 N90-20628
The effects of graded exercise at sea level on plasma proenkephalin peptide F and catecholamine responses
[AD-A218195] 13 p1853 N90-20633

PERCENTAGE
U RATIOS

PERCEPTION
NT AUDITORY PERCEPTION
NT BINAURAL HEARING
NT CONSCIOUSNESS
NT KINESTHESIA
NT MOTION PERCEPTION
NT OLFACTORY PERCEPTION
NT PAIN
NT PROPRIOCEPTION
NT SENSORY PERCEPTION
NT SOUND LOCALIZATION
NT SPACE PERCEPTION
NT TACTILE DISCRIMINATION
NT TASTE
NT TOUCH
NT VERTICAL PERCEPTION
NT VISUAL DISCRIMINATION
NT VISUAL PERCEPTION
Effects of type of responding on memory/visual search: Responding just yes or just no can lead to inflexible performance
[AD-A212764] 04 p0526 N90-13033
The structural memory: A network model for human perception of serial objects
[CWI-CS-R8829] 05 p0675 N90-13930
Effect of contrast on the perception of direction of a moving pattern
[NASA-TM-102234] 07 p0965 N90-15577
Proximity compatibility and information display: The effects of space and color on the analysis of aircraft stall conditions
[AD-A214488] 09 p1260 N90-17309
A connectionist implementation of cognitive phonology
[AD-A219095] 16 p2264 N90-22906
Cognitive requirements for aircraft navigation
[NASA-CR-186933] 21 p2955 N90-26804
Detecting perceptual groupings in textures by continuity considerations
21 p3045 N90-27310
Content effects in mathematics problem solving
[AD-A222436] 21 p3065 N90-27423
Conference on The Perception of Structure Program and Abstracts
[AD-A222437] 22 p3232 N90-28328
Development of a methodology for icon evaluation
[NPL-DITC-159/90] 22 p3235 N90-28345
How do robots take two parts apart
23 p3374 N90-29061
Perceptual telerobotics
23 p3374 N90-29063
A tesselated probabilistic representation for spatial robot perception and navigation
23 p3376 N90-29075
Ability and metacognitive determinants of skill acquisition and transfer
[AD-A224569] 24 p3499 N90-29776
A layered abduction model of perception: Integrating bottom-up and top-down processing in a multi-sense agent
24 p3512 N90-29851
Information processing and perceptual characteristics of display design: The role of emergent features and objects
[AD-A223683] 24 p3558 N90-30133

PERCEPTRONS
U SELF ORGANIZING SYSTEMS

PERCEPTUAL ERRORS
An architectural model of visual motion understanding
[AD-A214327] 07 p0967 N90-15589
Aiding the decision maker: Perceptual and cognitive issues at the human-machine interface
[AD-A217862] 13 p1855 N90-20648
Stereoscopic distance perception
16 p2267 N90-22921
Paradoxical monocular stereopsis and perspective vergence
16 p2267 N90-22922
Distortions in memory for visual displays
16 p2268 N90-22929
Exocentric direction judgements in computer-generated displays and actual scenes
16 p2270 N90-22936
Adapting to variable prismatic displacement
16 p2271 N90-22945
Interactions of form and orientation
16 p2274 N90-22958
The effects of training on errors of perceived direction in perspective displays
[NASA-TM-102792] 22 p3232 N90-28329

PERCHLORATES
NT AMMONIUM PERCHLORATES
NT LITHIUM PERCHLORATES
NT POTASSIUM PERCHLORATES
Composite propellants with high burning rates
[FOA-C-20781-2.1] 23 p3315 N90-28744

PERCOLATION
The viscoelasticity of curing thermosets
[DE90-006535] 13 p1781 N90-20221
Mathematical modelling of intergranular attack in stainless steels: A preliminary study
[AERE-M-3698] 14 p1950 N90-21160
Clustering and uniqueness in mathematical models of percolation phenomena
[ETN-90-96400] 15 p2163 N90-22358
On the structure of Mandelbrot's percolation process and other random Cantor sets
[REPT-89-54] 15 p2163 N90-22362
Discrete approach: Percolation theory
19 p2689 N90-25297
Percolation and low density materials: Theory and applications
[AD-A224237] 24 p3442 N90-29438

PERCUSSION
Methods for improving the flowability of a percussion primer composition
[MRL-TR-89-32] 14 p1956 N90-21201
Percussive sound analysis using an autoregressive model. Application of modified covariance
[TELECOM-PARIS-89-D-016] 18 p2612 N90-24879

PERFECT GAS
U IDEAL GAS

PERFLUORO COMPOUNDS
Determination of the thermal stability of perfluoroalkylethers
[NASA-TM-102493] 10 p1358 N90-17875
Perfluorinated ligands in organometallic chemistry
[AD-A216415] 11 p1476 N90-18493
Experience with synthetic fluorinated fluid lubricants
15 p2114 N90-22095

PERFORATED PLATES
Laminar flow control perforated wing panel development
[NASA-CR-178166] 01 p0034 N90-10187
Comparison between design and installed acoustic characteristics of NASA Lewis 9- by 15-foot low-speed wind tunnel acoustic treatment
[NASA-TP-2996] 12 p1606 N90-19242
Innovative design of composite structures: The use of curvilinear fiber format to improve buckling resistance of composite plates with central circular holes
[NASA-CR-186454] 13 p1766 N90-20135
Application of the complex variable solution to some problems in linear elastic materials with voids
24 p3478 N90-29658
Parametric studies of acoustic duct attenuation ofperforated-plate-on-honeycomb absorber
[NAL-TM-603] 24 p3542 N90-30030

PERFORATED SHELLS
An investigation of hole-edge crack problem by a combined complex variable and least square method
[LR-626] 24 p3482 N90-29679

PERFORATING
Perforation of a reinforced concrete wall by a rigid missile
[AD-A210025] 14 p1986 N90-21381

PERFORATION
Simulated-airline-service flight tests of laminar-flow control with perforated-surface suction system
[NASA-TP-2966] 10 p1319 N90-17627

PERFORMANCE PREDICTION
ILS (Instrument Landing System) mathematical modeling study on the effects of proposed hangar construction west of runway 18R on localizer performance at Dallas-Fort Worth International Airport
[AD-A210631] 01 p0005 N90-10019
Large-scale Advanced Prop-fan (LAP) high speed wind tunnel test report
[NASA-CR-182125] 01 p0010 N90-10045
Stability and Control of Tactical Missile Systems
[AGARD-CP-451] 01 p0011 N90-10050
Prediction of stability derivatives for missiles using the HISSS panel code 01 p0012 N90-10053
Missile Datcom: Enhancements for design applications
01 p0012 N90-10054
Prediction of dynamic derivatives
01 p0012 N90-10055
Prediction of tactical missile dynamics
01 p0012 N90-10056
Vortex induced characteristics of missiles in unsteady maneuvers 01 p0012 N90-10057
New test techniques to evaluate near field effects for supersonic store carriage and separation
01 p0013 N90-10062
Comparison of DPCM prediction strategies for high-quality digital television bit-rate reduction
[BBC-RD-1989/8] 01 p0058 N90-10318
The third generation rigid solar array GSR3
02 p0180 N90-11017
Planning for hybrid-cycle OTEC experiments using the HMTSTA test facility at the Natural Energy Laboratory of Hawaii
[DE89-013278] 02 p0237 N90-11349
Review and analysis of the DNW/Model 360 rotor acoustic data base
[NASA-TM-102253] 03 p0299 N90-11692
Some implications of the isotropic momentarily frozen assumptions for the SPAN-MAT program
[NASA-CR-181937] 03 p0301 N90-11704
Prediction of the thermal environment and thermal response of simple panels exposed to radiant heat
[NASA-TM-101660] 03 p0400 N90-12292
Numerical simulation of unsteady rotational flow over propfan configurations
[NASA-CR-186037] 04 p0438 N90-12500
Analysis and simulation of dynamics of spacecraft power systems 04 p0463 N90-12653
Optical fibre witnesses of fatigue damage in composite materials 04 p0465 N90-12660
Multilayer theory for delamination analysis of a composite curved bar subjected to end forces and end moments
[NASA-TM-4139] 04 p0466 N90-12669
Performance of the split-symbol moments SNR estimator in the presence of inter-symbol interference
04 p0487 N90-12799
On-ground photometric calibration
05 p0605 N90-13523
In-orbit payload calibration 05 p0606 N90-13526
A three-dimensional potential flow analysis of dynamic fluid forces acting on a whirling centrifugal impeller bounded by a volute 05 p0637 N90-13717
An investigation of gear mesh failure prediction techniques
[NASA-TM-102340] 05 p0649 N90-13785
Normal force, pitching moment, and side force of forebody-cylinder combinations for angles of attack up to 90 degrees and Mach numbers up to 5
[ESDU-89014] 06 p0718 N90-14192
Effect of unshielded and shielded horn balances on hinge moment coefficients for controls at low speeds
[ESDU-89003-A] 06 p0726 N90-14238
Hinge moment coefficient derivatives for trailing-edge controls on wings at subsonic speeds
[ESDU-89009] 06 p0726 N90-14239
SRB thermal environments
[NASA-CR-183801] 06 p0734 N90-14276
Investigation of combustion instability in ramjet combustors 06 p0739 N90-14303
Numerical and empirical verification of the stress state in a ceramic, button-head, tensile specimen
[DE90-001645] 06 p0752 N90-14375
The Tactical Environmental Support System (TESS(3))
06 p0757 N90-14409
Decision-aid design factors in connection with HF communication and emitter location disciplines
06 p0758 N90-14413
RPE: A parabolic equation radio assessment model
06 p0759 N90-14419
Improved reliability prediction for HF digital voice transmission 06 p0761 N90-14429
Low level range coverage performance prediction for VHF radar 06 p0763 N90-14439
Weather satellite and computer modeling approaches to assessing propagation over marine environments
06 p0764 N90-14443
TROPO: A technique for predicting propagation and modem performance of digital troposcatter systems
06 p0764 N90-14444
Transient response of flexible rotor-bearing systems subjected to combined unbalance and ground excitations 06 p0792 N90-14616
System design and performance prediction of a free-piston Stirling engine/magnetic coupling/compressor assembly in a gas residential heat pump
[DE89-016070] 06 p0807 N90-14696
An analysis of drilling of composite materials
07 p0889 N90-15142
Predicting the performance of ceramic filters by the use of silt density index
[DE90-001316] 07 p0909 N90-15256
Parametric identification of discrete time series models for structural response prediction
07 p0945 N90-15472
Improved tangent-cone method for the Aerodynamic Preliminary Analysis System (APAS) version of the hypersonic arbitrary-body program
[NASA-TM-4165] 08 p1018 N90-15890
Multidimensional numerical simulation of large caliber ignition processes
[ISL-CO-233/88] 08 p1042 N90-16021
CIS-2 analyzer derivation of hardware parameters
[IFSI-89-13] 08 p1077 N90-16230
Performance predictions for an intermediate-sized VAWT based on performance of the 34-m VAWT test bed
[DE90-002835] 08 p1096 N90-16345
The development of a T53-L11 engine computer model
[AD-A214533] 09 p1168 N90-16760
Assessment of strength limiting flaws in ceramic heat exchanger tubes, phase 2
[DE90-004081] 09 p1220 N90-17080
Numerical predictions of local entropy generation for an impinging jet
[DE90-004671] 09 p1220 N90-17081
The use of computer programs to determine environmental compliance, predict performance, and assess impacts
[DE90-005230] 09 p1245 N90-17222
Prediction of success in flight training by single- and dual-task performance 09 p1257 N90-17293
Predicting Air Combat Maneuvering (ACM) performance 09 p1258 N90-17294
Standardized tests for research with environmental stressors: The AGARD STRES battery
09 p1258 N90-17295
The performance implications of Ada in a MASCOT 3 design
[YM-5748-M304/2] 09 p1263 N90-17324
VHSIC/VHSIC-Like reliability prediction modeling
[AD-A214601] 09 p1288 N90-17468
Computational design of low aspect ratio wing-winglet configurations for transonic wind-tunnel tests
[NASA-CR-181939] 10 p1303 N90-17539
An examination of the fatigue meter records from the RAAF Orion P-3C fleet
[AD-A214000] 10 p1319 N90-17628
A method for the prediction of supersonic compressor blade performance
[CUED/A-TURBO/TR-126] 10 p1321 N90-17634
New models and techniques for predicting radiation effects on solar array performances
10 p1344 N90-17790
Performance predictions for passive solar water heating systems. Report 1: Performance monitoring to validate site-specific estimates of passive solar water heaters. Report 2: Laboratory report. Passive solar water heater tests
[DE90-002879] 10 p1401 N90-18096
An approximate model for the performance and acoustic predictions of counterrotating propeller configurations
[NASA-CR-180667] 10 p1426 N90-18228
The effects of wind tunnel data uncertainty on aircraft point performance predictions
[AD-A216091] 11 p1456 N90-18387
Numerical prediction of axial turbine stage aerodynamics 11 p1461 N90-18416
Development of a mass averaging temperature probe
11 p1461 N90-18418
Application of variable-gain output feedback for high-alpha control
[NASA-TM-102603] 11 p1464 N90-18434
Performance parameter characterisation of various types of IR single element detectors
11 p1588 N90-19161
Three-dimensional viscous rotor flow calculations using a viscous-inviscid interaction approach
[NASA-TM-102235] 12 p1599 N90-19204
Aeroservoelasticity
[NASA-TM-102620] 12 p1603 N90-19227
Flight and driving optimization of air breathing aerodynamic space vehicle
[ETN-90-95379] 12 p1607 N90-19246
Effects of turbulence mixing, variable properties, and vaporization on spray droplet combustion
[NASA-CR-186463] 12 p1623 N90-19326
Iterative procedures for space shuttle main engine performance models 12 p1639 N90-19416
Recalibrating software reliability models
[NASA-CR-186407] 12 p1700 N90-19763
Using transonic small disturbance theory for predicting the aeroelastic stability of a flexible wind-tunnel model
[NASA-TM-102617] 13 p1749 N90-20047
Airplane takeoff and landing performance monitoring system
[NASA-CASE-LAR-13734-1-CU]
13 p1758 N90-20096
Model development in viscoplastic ratchetting
[NASA-TM-102509] 13 p1816 N90-20431
Secondary flow predictions for a transonic nozzle guide vane 14 p1924 N90-21017
Generation and decay of secondary flows and their impact on aerodynamic performance of modern turbomachinery components 14 p1925 N90-21023
Computational prediction and measurement of the flow in axial turbine cascades and stages
14 p1925 N90-21028

Development of a fracture analysis technique for use with a general-purpose finite element program
14 p1992 N90-21416
Recent improvements in the scope and accuracy of the performance prediction of nozzle propellers
[LR-598] 15 p2048 N90-21742
Validity of the two-level model for Viterbi decoder gap-cycle performance 15 p2077 N90-21896
The predictability and efficiency of human walking: Metabolic, mechanical, and biophysical considerations
15 p2137 N90-22211
Networks for image acquisition, processing and display 15 p2138 N90-22218
A modeling technique for STOVL ejector and volume dynamics
[NASA-TM-103167] 16 p2202 N90-22566
Environment enhanced fatigue of advanced aluminum alloys and composites 16 p2218 N90-22652
Deformation and fracture of thin sheet aluminum-lithium alloys: The effect of cryogenic temperatures
16 p2218 N90-22655
Integrated control-system design via generalized LQG (GLQG) theory 16 p2286 N90-23023
On the performance of parallel algorithms
[CS-8914] 16 p2299 N90-23099
Prediction of aerodynamic performance of airfoils in low Reynolds number flows
[DLC-EST-TN-031] 17 p2346 N90-23360
Correlation/validation of finite element code analyses for vibration assessment of avionic equipment
[AD-A220393] 17 p2353 N90-23398
Prediction methods of launcher aeroelastic stability. Application to the Ariane 5/Hermes vehicle. Comparison with test results
[REPT-892-422-107] 17 p2362 N90-23451
Application of neural networks to the F/A-18 engine condition monitoring system
[AD-A219820] 18 p2497 N90-24271
Predicting the audibility and annoyance of unducted fan engines 18 p2610 N90-24869
The Penguin: A low Reynolds number powered glider for station keeping missions
[NASA-CR-186667] 19 p2658 N90-25129
Evaluation of various thrust calculation techniques on an F404 engine
[NASA-TP-3001] 19 p2659 N90-25134
Ground shake test of the UH-60A helicopter airframe and comparison with NASTRAN finite element model predictions
[NASA-CR-181993] 19 p2661 N90-25143
LOX manifold tee analysis
[NASA-CR-183994] 19 p2670 N90-25188
Moving out of the galaxy: Future prospects for X Ray binaries studies 19 p2770 N90-25746
BBXRT observations of X ray binaries
19 p2778 N90-25802
Spectroscopy of AGNs with Xspect/Sodart in 1993
19 p2794 N90-25909
Enroute flight planning: The design of cooperative planning systems
[NASA-CR-186797] 20 p2806 N90-25964
Performance of a supercharged direct-injection stratified-charge rotary combustion engine
[NASA-TM-103105] 20 p2809 N90-25982
Handbook of uncertainty methodology for engine testing at Pyestock (England)
[RAE-TM-P-1179] 20 p2812 N90-26007
On controller choice for robust sliding mode performance
[MATHS-REPT-A-107] 20 p2872 N90-26337
Statistical analysis of a software reliability model
[IMAG-RR-781-M] 20 p2874 N90-26352
Modeling and optimization of a regenerative fuel cell system using the ASPEN process simulator
[NASA-TM-103210] 20 p2882 N90-26396
Retirement for cause of the F100 engine
21 p2957 N90-26813
Role of interfaces and interphases in the evolution mechanics of material systems
[AD-A222702] 21 p2971 N90-26885
Cross-validation of experimental USAF pilot training performance models
[AD-A222253] 21 p3035 N90-27257
The integration of automated knowledge acquisition with computer-aided software engineering for space shuttle expert systems 21 p3045 N90-27307
Queing networks with finite capacities
[AD-A221547] 21 p3065 N90-27425
Comparative Engine Performance Measurements
[AGARD-LS-169] 22 p3118 N90-27711
Assessment and demonstration of the capabilities of NDI processes, equipment, and personnel
22 p3184 N90-28071
Use of acoustic emission for continuous surveillance of aircraft structures 22 p3188 N90-28092
Blade tip rubbing stress prediction
23 p3290 N90-28615
Developments in test procedures for hot-salt corrosion of superalloys 23 p3306 N90-28700

PERFORMANCE TESTS
Commercial high current ignitron development
[DE89-015077] 01 p0058 N90-10331
Report on the performance and operating characteristics of the Burle C83061E QUANTACON (trademark) photomultiplier tube
[DE89-015257] 01 p0058 N90-10333
Heat transfer characteristics of igniter output plumes
[DE89-011449] 01 p0059 N90-10340
Some significant results from testing a Remote Multiplexing Unit (RMU) for temperature-induced errors
[DE89-009432] 01 p0073 N90-10421
Analysis and test of a 16-foot radial rib reflector developmental model
[NASA-TM-101648] 01 p0080 N90-10457
Tracking performance evaluation
[AD-A210499] 01 p0095 N90-10540
Director, Operational Test and Evaluation report FY-88
[AD-A206784] 01 p0135 N90-10778
Development of a marine integrated navigation system
02 p0149 N90-10852
Aircraft live fire testing 02 p0154 N90-10879
Deep null antennas and their applications to tactical VHF radio communications
[AD-A210656] 02 p0212 N90-11214
Wideband connectivity and support for Cronus cluster at USAF Electronic Systems Division
[AD-A210749] 02 p0212 N90-11215
ASIC (Application Specific Integrated Circuit) replacement for an SSI (Small Scale Integrated) component design: A case study
[DE89-013494] 02 p0215 N90-11232
Lifetime testing of commercially available 3.0 (mu)f, 100 kV pulsed-power capacitors
[DE89-017230] 02 p0217 N90-11242
Performance of four rake modems over the non-disturbed wideband HF channel
[AD-A211589] 03 p0339 N90-11930
Hybrid angular velocity reference system for the investigation of dynamic properties of strapdown gryos
[DFVLR-FB-89-25] 04 p0450 N90-12577
The role of component testing
[PNR90589] 04 p0455 N90-12608
SSME structural dynamic model development
[NASA-CR-183671] 04 p0463 N90-12650
Oxide ceramic fibers by the sol-gel methods
[AD-A211315] 04 p0478 N90-12742
Mode S data link trials, 10-11 January 1989
[RSRE-MEMO-4267] 04 p0490 N90-12815
Removal of noise from noise-degraded speech signals
[AD-A212876] 04 p0493 N90-12840
Performance analysis of large adaptive sidelobe canceller arrays with reused elements
[AD-A212888] 04 p0494 N90-12841
Design and commissioning test results for the hypervelocity launcher research complex battery power supply
[AD-A211320] 04 p0495 N90-12848
Feedback charge amplifier integrated on the detector wafer
[REPT-89-037] 04 p0496 N90-12852
The analysis of current-mirror MOSFETs for use in radiation environments
[AD-A212527] 04 p0497 N90-12866
Cold tests of quasi-optical gyrotron resonators
[AD-A212707] 04 p0498 N90-12868
Pre- and postflight postural control of the D1 Spacelab mission astronauts examined with a tilting room
[IZF-1988-25] 04 p0527 N90-13039
Expert system for test program set fault candidate selection
[AD-A213338] 04 p0535 N90-13091
Design and tests of simple, inexpensive optical beacon for use on small satellites
[AD-A213325] 04 p0555 N90-13238
A laboratory verification sensor
05 p0599 N90-13477
Electrical testing 05 p0605 N90-13520
In-orbit payload calibration 05 p0606 N90-13526
LOX/hydrocarbon combustion instability investigation
[NASA-CR-182249] 05 p0615 N90-13589
Qualification of improved joint heaters
[NASA-CR-183827] 05 p0616 N90-13594
Low resistivity electrodeless streamer tubes
[PREPRINT-685-89] 05 p0636 N90-13712
The evaluation of a metered mixer for RTV silicone for RSRM nozzle backfill operations
[NASA-CR-183831] 05 p0645 N90-13763
Performance evaluation of a six-axis generalized force-reflecting teleoperator
[NASA-CR-186106] 05 p0651 N90-13796
A counter gating circuit for acoustic emission monitoring of structures cracking under repetitive alternating loads
[ARL-MAT-TM-398] 05 p0653 N90-13808
Parallelism in the discrete-event simulation algorithm
[AD-A213060] 05 p0682 N90-13970
Performance of resistive plate counters at beam flux up to 140 Hz/cm2
[NOTA-INTERNA-930] 05 p0697 N90-14081
Effect of blade planform variation on a small-scale hovering rotor
[NASA-TM-4146] 06 p0717 N90-14186
Arcjet thruster research and technology. Phase 1: Executive summary
[NASA-CR-182106] 06 p0734 N90-14278
Flight set 360T004 (STS-30) field joint protection system, volume 7
[NASA-CR-183829] 06 p0735 N90-14280
Study of new materials for gun propellant formulations
[DE89-015285] 06 p0754 N90-14388
Zinc/bromine battery evaluation at SNL (Sandia National Laboratory)
[DE89-015847] 06 p0769 N90-14473
Laboratory testing of Sonnenschein DF6V180 6 volt traction battery
[DE90-002080] 06 p0771 N90-14486
Testing and performance of a high-gain flux-compression generator
[DE90-002808] 06 p0772 N90-14492
Field testing of a ceramic heat exchanger for heat recovery application
[DE90-002082] 06 p0778 N90-14523
A laboratory test for fuel injector deposit studies
[DE90-000802] 06 p0795 N90-14629
Performance evaluation of the Puritan-Bennett crew-member portable protective breathing device as prescribed by portions of FAA action notice A-8150.2
[AD-A211113] 06 p0821 N90-14772
Performance of the 10-kV, 100-kA pulsed-power modules for the FRX-C magnetic compression experiment
[DE89-014027] 06 p0845 N90-14917
Current launch vehicle reliability practice and data base assessment. Volume 1: Executive summary and report body
[AD-A213600] 07 p0885 N90-15121
The effect of nitrogen and titanium on the toughness of high strength saw weld deposits
[AD-A213400] 07 p0905 N90-15230
A future for LLNL (Lawrence Livermore National Laboratory) research in composite high explosives
[DE90-004442] 07 p0915 N90-15290
MF/HF multistatic mid-ocean radar experiments in support of SWOTHR (Surface-Wave Over-The-Horizon Radar)
[AD-A213830] 07 p0919 N90-15314
A nickel/hydrogen battery for PV systems
[DE90-001537] 07 p0926 N90-15358
High power density spray cooling
[AD-A213575] 07 p0930 N90-15386
SIMON (SuperIntelligent Mobile Observing Navigator): A high-reliability robot for a radiation environment
[DE90-003888] 07 p0943 N90-15460
Structural response measurements and predictions for the SANDIA 34-meter test bed
[DE90-002575] 07 p0955 N90-15524
Knowledge based text generation
[AD-A214273] 07 p0977 N90-15645
Fuel Tank Technology
[AGARD-R-771] 08 p1021 N90-15904
Aircraft fuel tank construction and testing experience
08 p1021 N90-15907
Design philosophy and construction techniques for integral fuselage fuel tanks 08 p1023 N90-15913
Performance of a highly-loaded HP compressor
[RAE-TM-P-1149] 08 p1024 N90-15919
A UK perspective on the uniform engine test programme
[RAE-TM-P-1172] 08 p1025 N90-15922
Space shuttle Production Verification Motor 1 (PV-1) static fire
[NASA-CR-183784] 08 p1037 N90-15991
Pulsed plasma mission endurance test
[AD-A213462] 08 p1037 N90-15993
Theoretical and experimental investigation of axial power extraction from a magnetically insulated transmission line oscillator
[DE90-003486] 08 p1060 N90-16131
Stand Alone Pressure Measurement Device (SAPMD) for the space shuttle Orbiter, part 1
[NASA-CR-172119-PT-1] 08 p1072 N90-16202
Stand Alone Pressure Measurement Device (SAPMD) for the space shuttle Orbiter, part 2
[NASA-CR-172119-PT-2] 08 p1072 N90-16203
Results from the third year of operation of the Federal Methanol Fleet at Lawrence Berkeley Laboratory
[DE90-003306] 08 p1084 N90-16277

Performance predictions for an intermediate-sized VAWT based on performance of the 34-m VAWT test bed
[DE90-002835] 08 p1096 N90-16345
On the selection of materials for cryogenic seals and the testing of their performance
08 p1156 N90-16696
Analysis of indirect effects of lightning on a metallic A 300 wing: Test report
[REPT-E87/645800] 09 p1162 N90-16726
Experimental evaluation of impedance control for robotic aircraft refueling
[AD-A215532] 09 p1167 N90-16755
Turbine blade data acquisition system software reference
[AD-A215134] 09 p1169 N90-16764
Turbine blade data acquisition system technical reference
[AD-A215135] 09 p1169 N90-16765
Coefficients of thermal expansion for a carbon-carbon composite
[DE90-004484] 09 p1188 N90-16883
Adhesive for composite bonding
[DE90-005683] 09 p1188 N90-16885
Evaluation of a prototype lithium molybdenum disulfide secondary battery for load conditioner: Characteristics and performance of 70Wh class BC cell
[DE90-702460] 09 p1210 N90-17016
Sealing L-alloys/FeS(x) cells for a bipolar battery
[DE90-004887] 09 p1214 N90-17040
Identification and reduction of Wakefield effects in the wiggler region of the Los Alamos free-electron laser
[DE90-004871] 09 p1228 N90-17128
Improved performance of the Boeing/LANL FEL (Free-Electron Laser) experiment: Extraction efficiency and cavity length detuning effects
[DE90-004872] 09 p1228 N90-17129
Small screw study: Fastener tensile strength and optimum thread depth
[DE90-005001] 09 p1231 N90-17141
Statistical theory of reliability
[AD-A215320] 09 p1234 N90-17161
Light-trapping concentrator cells
[DE90-004988] 09 p1242 N90-17205
Research on stable high-efficiency, large area, amorphous silicon-based solar cells, phase 2
[DE89-009491] 09 p1242 N90-17208
Physiological evaluation of men wearing three different toxicological protective systems
[AD-A215527] 09 p1261 N90-17313
Use of hypermedia as a user interface for an artificial intelligence-based problem solver
[AD-A215551] 09 p1271 N90-17370
Full surface interferometric testing of grazing incidence mirrors
[AD-A213590] 09 p1281 N90-17425
Method of producing a thin silicon-on-insulator layer
[AD-D014330] 09 p1290 N90-17478
Altitude testing of the 2D V/STOL ADEN demonstrator on an F404 engine
[NASA-CR-174824] 10 p1321 N90-17638
The design and performance of a general purpose 57 kilowatt solar array simulator for current and future large spacecraft 10 p1330 N90-17685
Assessment of in-orbit performance data of a bifacial flight experiment 10 p1344 N90-17793
Infrared thermal imaging figures of merit
10 p1364 N90-17904
Lightweight transformer demonstration
[DE90-001470] 10 p1379 N90-17991
Analysis and test of a wide angle spectrometer
[AD-A215819] 10 p1388 N90-18030
RADC reliability engineer's TOOLKIT
[AD-A215977] 10 p1394 N90-18058
Performance of superconductive oxides as cathodes for lithium rechargeable batteries
[AD-A216030] 10 p1401 N90-18098
Preliminary experimental measurement of isoplanatic angle
[AD-A215828] 10 p1407 N90-18115
Research on a two-dimensional inlet for a supersonic V/STOL propulsion system. Appendix A
[NASA-CR-174945] 11 p1451 N90-18364
The signals of an ice warning device in dependence on total water content and normalized icing degree
[DLR-FB-89-52] 11 p1454 N90-18377
Compressor performance tests in the compressor research facility 11 p1463 N90-18428
Transient pressure test article test program
11 p1470 N90-18463
Trends in VLF/LF (Very Low Frequency/Low Frequency) modem performance testing
[AD-A216576] 11 p1497 N90-18614
A new broadband pulsed high voltage monitor
[DE90-006264] 11 p1502 N90-18651
Performance of a 500 watt Nd:GGG zigzag slab oscillator
[DE90-006263] 11 p1503 N90-18657
Integrated regenerative fuel cell experimental evaluation
[NASA-CR-185183] 11 p1530 N90-18808
Anthropometry of a fit test sample used in evaluating the current and improved MCU-2/P masks
[AD-A215173] 11 p1541 N90-18873
Evaluation of helmet retention systems using a pendulum device
[AD-A215489] 11 p1542 N90-18874
Mechanical disturbances in high-performance superconducting dipoles
[DE90-006237] 11 p1570 N90-19040
A comparison of reflector antenna designs for wide-angle scanning 12 p1610 N90-19264
Radial response of the burst and transient source experiment 12 p1637 N90-19408
Reliability testing of the Hughes temperature controlled 1/4 watt split cycle cryogenic cooler (HD-1045 (V)/UA)
[AD-A216696] 12 p1641 N90-19426
Big Viterbi Decoder (BVD) results for (7,1/2) convolutional code 12 p1644 N90-19446
The 32-GHz performance of the DSS-14 70-meter antenna: 1989 configuration 12 p1645 N90-19452
Operational evaluation of initial data link air traffic control services, volume 1
[DOT/FAA/CT-90/1-VOL-1] 12 p1648 N90-19472
High power, high frequency component test facility
[NASA-TM-102500] 12 p1650 N90-19484
Progress in the CW operation of a 140 GHz gyrotron
[DE90-007382] 12 p1663 N90-19558
Solid State Photovoltaic Research Branch
[DE89-009463] 12 p1682 N90-19680
Marginal test and analysis of DRAM with masked alpha radiation
[RB-4180] 12 p1699 N90-19754
The USAF Advanced Dynamic Anthropomorphic Manikin (ADAM) 13 p1752 N90-20062
In-line wear monitor
[AD-A217799] 13 p1757 N90-20091
Flight termination system battery guidelines
[AD-A217310] 13 p1758 N90-20092
ARDEC (Armament Research, Development and Engineering Center) electric gun in-house test program
[AD-A217337] 13 p1760 N90-20105
Design and performance of a multi-stage cylindrical reconnection launcher
[DE90-007820] 13 p1761 N90-20108
Characterization testing of a 40 AHR bipolar nickel-hydrogen battery 13 p1822 N90-20463
Sodium-sulfur battery flight experiment definition study
13 p1825 N90-20479
Advanced on-site power plant development technology program
[DE90-000443] 13 p1826 N90-20484
First year's results and field experience with the latest JILA absolute gravimeter 13 p1834 N90-20529
Performance data from a wind-tunnel test of two main-rotor blade designs for a utility-class helicopter
[NASA-TM-4183] 14 p1916 N90-20974
Secondary flow predictions for a transonic nozzle guide vane 14 p1924 N90-21017
Space environment simulation of the SCD-01 satellite through heating plates
[INPE-4988-PRE/1550] 14 p1940 N90-21105
Effect of KOH concentration on LEO cycle life of IPV nickel-hydrogen flight battery cells
[NASA-TM-103127] 14 p1942 N90-21116
Selective automatic fire extinguisher for computers (SAFECOMP): Developmental test and evaluation/initial operational test and evaluation
[AD-A217790] 14 p1958 N90-21212
The development of a simulation program of the anode side for aluminum/air batteries
[PB90-165754] 14 p1970 N90-21286
Germanium Blocked Impurity Band (BIB) detectors
14 p1976 N90-21321
Ga:Ge array development 14 p1977 N90-21323
NETRA: A parallel architecture for integrated vision systems 2: Algorithms and performance evaluation
[NASA-CR-186510] 14 p2017 N90-21557
Flight motor set 360L002 (STS-27R). Volume 5: Nozzle component
[NASA-CR-183945] 15 p2062 N90-21811
Aging characteristics of Li/SO(sub 2) cells
[NASA-CR-180432] 15 p2088 N90-21954
Laboratory testing of Energy Research Corporation ERC 160 NiCd 6 volt traction battery
[DE90-009629] 15 p2089 N90-21957
Laboratory testing of Saft SEH-5-200 6 volt traction battery
[DE90-009787] 15 p2089 N90-21958
Characterization and calibration of coordinate measuring machines
[DE90-009320] 16 p2242 N90-22791
Next generation weather radar (NEXRAD) initial operational test and evaluation. Phase 2: (IOT and E(2))
[AD-A218770] 16 p2258 N90-22873
Proceedings of the 3rd Annual Conference on Aerospace Computational Control, volume 1
[NASA-CR-186446] 16 p2279 N90-22987
On randomness of random number generators
[MEMO-COSOR-89-20] 16 p2308 N90-23151
Preliminary evaluation of a small wearable display
[AD-A219867] 17 p2350 N90-23385
Performance analysis of CCSDS path service
[NASA-CR-180699] 17 p2364 N90-23457
Comparison of Goretex laminated and Dermoflex coated fabrics
[AD-A219383] 17 p2368 N90-23481
MTS high temperature testing system
[AD-A219613] 17 p2369 N90-23483
Bioluminescence for detection of trace compounds
[AD-A219435] 17 p2372 N90-23503
Unfairness caused by quadratic backoff in a packet-radio network
[AD-A219635] 17 p2388 N90-23603
Microelectronic device reliability
[AD-A218774] 17 p2394 N90-23638
UW VLSI chip tester
[AD-A220789] 17 p2397 N90-23653
Design, simulation, and testing of a field-oriented ac servo-drive using a TMS 32010 signal processor
[EMV-88-42] 17 p2397 N90-23658
Wide range stress intensity factor and crack-mouth-opening displacement expressions suitable for short crack fracture testing with arc bend-chord support samples
[AD-A218395] 17 p2415 N90-23781
Computer tomography of thermal batteries and other closed systems
[AD-A218379] 17 p2419 N90-23787
Very high frequency measurements of geometric factors in transmission line lead acid cells
[AD-A219463] 17 p2420 N90-23788
Digital terrain elevation data compact disk-read only memory prototype evaluation
[AD-A218545] 17 p2442 N90-23915
Estimation of noise field directionality: Comparison with Fourier series method
[AD-A220366] 17 p2469 N90-24114
Operational effects on crashworthy seat attenuators
[AD-A221148] 18 p2495 N90-24259
A compact joint for the ROTEX manipulator
18 p2536 N90-24467
EHF heterojunction bipolar transistors
[AD-A220984] 18 p2548 N90-24541
Performance of alumina-supported Pt catalysts in an electron-beam-sustained CO2 laser amplifier
18 p2561 N90-24613
Experimental high speed/power ratio ASIC designs using residue numbers
[AD-A220302] 18 p2591 N90-24741
Human response research update
18 p2611 N90-24873
Binary pseudo random phase correlation in radar systems: A new approach
[RSRE-MEMO-4223] 19 p2683 N90-25263
Experiments in variable frame rate analysis for speech recognition
[RSRE-MEMO-4330] 19 p2683 N90-25264
Engineering evaluation testing of the Soleq dual battery van
[DE90-012685] 19 p2698 N90-25354
CAESAR: Performance and first evaluation of application possibilities
[BCRS-89-06] 19 p2705 N90-25393
Performance testing and qualification of Sandia's third baseline photovoltaic concentrator module
[DE90-012644] 19 p2711 N90-25431
SOAR 89: Space Station. Space suit test program
19 p2727 N90-25506
Multi-microprocessor control of a precision pan and tilt head
[RSRE-MEMO-4252] 19 p2747 N90-25613
Performance evaluation of LE-7 high pressure pumps
[DE90-505523] 20 p2817 N90-26034
Heavy ion tests on programmable VLSI
[ETN-90-97254] 20 p2822 N90-26057
Development of ceramic hybrid combustor: Design and combustion test results
[DE90-503442] 20 p2839 N90-26149
Design and performance analysis of the DSS-13 beam waveguide antenna 20 p2853 N90-26225
Contribution to CMOS integrated circuit tests: Study of the stuck-on and stuck-open fault tests
[ETN-90-97256] 20 p2859 N90-26261

QM-8 final performance evaluation report: SEALS, volume 4
[NASA-CR-183958] 20 p2869 N90-26324
Interim qualification tests and procedures for terrestrial photovoltaic thin-film flat-plate modules
[DE90-000354] 20 p2881 N90-26392
The retrieval of information from secondary memory: A review and new findings
[AD-A222760] 20 p2899 N90-26489
Advanced Turbine Technology Applications Project (ATTAP)
[NASA-CR-185240] 20 p2939 N90-26728
The sensitivity of several explosives to ignition in the launch environment
[AD-A221581] 21 p2990 N90-26993
RADC/EEV diagnostic rhyme test system improvements
[AD-A223187] 21 p2995 N90-27025
Electrical resistance measurements of connector-panel interfaces
[AD-A221431] 21 p3001 N90-27057
Personal computer programs for the control of subnanosecond transient digitizers with applications for device damage testing
[AD-A221458] 21 p3054 N90-27365
AIMS test and simulation equipment
22 p3104 N90-27623
The MODE S operational test and evaluation/integration test plan
[DOT/FAA/CT-TN89/51] 22 p3111 N90-27671
Development and testing of methodology for evaluating the performance of multi-input/multi-output digital control systems
[NASA-TM-102704] 22 p3115 N90-27699
The basis for facility comparison
22 p3118 N90-27713
Investigation of factors affecting data comparison
22 p3119 N90-27714
Experience in developing an improved ground-level test capability 22 p3120 N90-27720
M-52 spray booth qualification test
[NASA-CR-184003] 22 p3122 N90-27727
Tests of an ultra-light tunnel in the anechoic wind tunnel facility CEPRA 19
[ONERA-RF-20/7294-PH] 22 p3122 N90-27729
Testing DoD space systems: The challenge
22 p3132 N90-27771
Fatigue testing apparatus
[AD-D014544] 22 p3192 N90-28108
Garment pressurizing apparatus
[AD-D014451] 22 p3232 N90-28330
Performance of the Intel iPSC/860 hypercube
[DE90-014697] 22 p3235 N90-28346
Light source for dynamic testing of photo detectors
[FEL-1989-69] 22 p3247 N90-28414
A look at tomorrow today 23 p3273 N90-28524
Validation of the F-18 high alpha research vehicle flight control and avionics systems modifications
[NASA-TM-101723] 23 p3276 N90-28542
Energy Efficient Engine exhaust mixer model technology report addendum; phase 3 test program
[NASA-CR-174799] 23 p3279 N90-28556
Energy efficient engine pin fin and ceramic composite segmented liner combustor sector rig test report
[NASA-CR-179534] 23 p3281 N90-28567
Source emission test of gas turbine engine test facility, Kelly AFB, TX
[AD-A223869] 23 p3282 N90-28571
Liquid Rocket Booster (LRB) for the Space Transportation System (STS) systems study. Appendix F: Performance and trajectory for ALS/LRB launch vehicles
[NASA-CR-183792-APP-F] 23 p3289 N90-28606
A comparison of single-cycle versus multi-cycle proof testing strategies 23 p3296 N90-28646
Mechanical testing activities related to high-performance structural ceramics
[DE90-014299] 23 p3313 N90-28734
Communications Interface Driver (CID) test plan
[DOT/FAA/CT-TN89/35] 23 p3319 N90-28762
Special test and evaluation methods used for a nine-axis accelerometer
[PB90-209578] 23 p3329 N90-28822
Performance measurements and energy balance of an SPS V160 Stirling motor at the German Aerospace Research Establishment
[DLR-MITT-90-03] 23 p3345 N90-28903
Air Force Officer Qualifying Test (AFOQT): Development of quick score composites for forms P1 and P2
[AD-A223868] 23 p3362 N90-28997
Performance evaluation of a 6 axis high fidelity generalized force reflecting teleoperator
23 p3372 N90-29052
State estimation for systems moving through random fields 24 p3429 N90-29373
Recommended practices for measurement of gas path pressures and temperatures for performance assessment of aircraft turbine engines and components
[AGARD-AR-245] 24 p3433 N90-29393
Structural testing and analytical research of turbine components
[AD-A223516] 24 p3434 N90-29396
AutoPAVER: A software package for automated pavement evaluation
[AD-A224176] 24 p3458 N90-29531
Radar receiver procedures
[AD-A224399] 24 p3460 N90-29541
Performance test plan for variable-speed ac superconducting motor
[DE90-016208] 24 p3465 N90-29579
A 94 GHz transmissometer
[AD-A223309] 24 p3471 N90-29618
Integrated controls and health monitoring fiberoptic shaft monitor
[NASA-CR-185210] 24 p3472 N90-29622
Friction, wear and electric characteristics of slip-ring brush materials for space applications. Part 1: Screening by pin-on-disk friction tests
[NAL-TR-1040] 24 p3478 N90-29657
Multisensor evaluation framework
[AD-A224271] 24 p3522 N90-29913
Survey of formal specification techniques for reactive systems
[AD-A223741] 24 p3538 N90-30005
A reduced-order extended Kalman filter for moving images
[AD-A223742] 24 p3541 N90-30028
Parametric testing for the RSRE CMOS, silicon on sapphire process
[RSRE-MEMO-4369] 24 p3555 N90-30115

PERFUSION
U DIFFUSION

PERIOD DOUBLING
On spurious steady-state solutions of explicit Runge-Kutta schemes
[NASA-TM-102819] 15 p2160 N90-22340

PERIOD EQUATIONS
U PERIODIC FUNCTIONS

PERIODIC FUNCTIONS
NT COSINE SERIES
NT SINE SERIES
NT TANGENTS
NT TRIGONOMETRIC FUNCTIONS
Periodic solutions of spatially periodic Hamiltonian systems
[AD-A210645] 01 p0113 N90-10649
On the maximum period of a permutation of N elements
[MEMO-771] 04 p0544 N90-13159
The discrete-time single-server queueing model
[MEMO-780] 04 p0544 N90-13165
Periodic solutions of Hamiltonian systems of 3-body type
[AD-A212891] 05 p0687 N90-14005
A variational approach to heteroclinic orbits for a class of Hamiltonian systems
[AD-A219853] 17 p2460 N90-24047

PERIODIC ORBITS
U ORBITS

PERIODIC PROCESSES
U CYCLES

PERIODIC VARIATIONS
NT ALTERNATIONS
NT ANNUAL VARIATIONS
NT DIURNAL VARIATIONS
Chesapeake Bay surface salinities, 1951-88
[PB89-194583] 01 p0090 N90-10513
Localized vibrations of nearly periodic structures with irregularities 06 p0798 N90-14648
An observational study of intramonthly quasi-periodicities in the Northern Hemisphere, extratropical geopotential height field
06 p0813 N90-14729
Optimal periodic control and regulator theory based on the second variation 07 p0987 N90-15704
Periodically unsteady effects on profiles, induced by separation 08 p1070 N90-16196
Identifying the circadian cycle in human information processing data using periodicity analysis: A synopsis
[AD-A214674] 09 p1251 N90-17257
Research on cascade secondary and tip-leakage flows: Periodicity and surface flow visualization
14 p1925 N90-21026
Towards a Sarkovski order for the embedding of disks maintaining their orientation
[REPT-89-43] 15 p2151 N90-22289
A 154-day periodicity in the occurrence rate of proton flares
[NASA-CR-185826] 16 p2340 N90-23333
QPOs from black-hole candidates
19 p2770 N90-25743
The impacts of Ginga results on QPO models
19 p2770 N90-25744
Variability of the X ray sources in M31
19 p2773 N90-25768
Long period variations in high mass X ray binaries and their possible relationship with SU UMa stars
19 p2777 N90-25796
The role of comptonisation in energy spectra of standard QPO-sources 19 p2781 N90-25820
Periodicity of redshift distribution in a T-3 universe
[FERMILAB-PUB-90/26-A] 22 p3262 N90-28475

PERIODICALS
Air University Library index to military periodicals. Cumulative issue: January to March 1989, Volume 40, Number 1
[PB90-182296] 22 p3258 N90-28452

PERIODICITY
U PERIODIC VARIATIONS

PERIODICITY (BIOLOGY)
U RHYTHM (BIOLOGY)

PERIPHERAL EQUIPMENT (COMPUTERS)
NT PRINTERS (DATA PROCESSING)
NT REMOTE CONSOLES

PERIPHERAL NERVOUS SYSTEM
Peripheral nervous velocity of conduction in fighter pilots 09 p1256 N90-17287

PERIPHERAL VISION
The effects of foveal load on peripheral sensitivity in the visual field
[AD-A214872] 09 p1251 N90-17260
Sensitivity of the peripheral vision to simulated aircraft ascent and descent 10 p1413 N90-18145
Detection acuity in the peripheral retina
[AD-A218183] 13 p1853 N90-20632
Maintaining spatial orientation awareness
23 p3361 N90-28993

PERIPHERIES
U BOUNDARIES

PERMAFROST
Introduction to drilling technology
12 p1740 N90-20002
Three functions that model empirically measured unfrozen water content data and predict relative hydraulic conductivity
[AD-A223875] 23 p3343 N90-28892

PERMANENT MAGNETS
Periodic permanent magnet structures
[AD-D014173] 03 p0398 N90-12280
Anisotropy and microstructure of high-coercivity rare earth permanent magnets
[AD-A211905] 03 p0399 N90-12285
Graduate fellowships in the field of hard magnetic materials
[AD-A212303] 04 p0477 N90-12733
A survey of the current state-of-the-art in high-energy-product permanent magnets
[AD-A211761] 04 p0549 N90-13193
Anisotropy and microstructure of high coercivity rare earth iron permanent magnets, list of papers published
[AD-A214160] 08 p1118 N90-16476
Permanent magnet flux-biased magnetic actuator with flux feedback
[NASA-CASE-LAR-13785-1] 09 p1277 N90-17403
Induction motor control
[NASA-TM-102533] 12 p1605 N90-19234
Theoretical and experimental studies of a brushless disk rotor motor with permanent magnetic excitation and gap windings
[ETN-90-96056] 12 p1655 N90-19512
Design of a high power density, permanent magnet, axial gap dc motor
[DE90-005449] 12 p1655 N90-19514
Magnetic hardening studies and novel techniques for preparation of high performance magnets
[AD-A217737] 13 p1881 N90-20790
Microcomputer for the digital regulation of permanent magnet-synchronous servomotors
[ETN-90-96507] 18 p2588 N90-24727
Superconducting permanent magnets
[AD-A218944] 18 p2618 N90-24912
Metallurgical processes in multi-component rare Earth-transition metal permanent magnet alloys
[AD-A222891] 21 p2982 N90-26942

PERMEABILITY
NT DIELECTRIC PERMEABILITY
Electrical field dependence of protein conformation and channel function in lipid membranes of different compositions
[AD-A210236] 01 p0040 N90-10222
Effective permeability of mixtures
[PB89-218952] 03 p0323 N90-11839
Asymptotic analysis of performance of membrane modules for gas separations
[DE90-000699] 06 p0742 N90-14316

Test and evaluation of polymeric membranes for oxygen enrichment of air
[DE90-000555] 06 p0742 N90-14321
Ordered ceramic membranes
[DE89-017426] 06 p0750 N90-14364
Improved performance polysulfide based sealant
08 p1022 N90-15910
Synthesis and analysis of novel polymers with potential for providing both high permselectivity and permeability in gas separation applications
[DE90-003907] 08 p1049 N90-16065
Some considerations on resource evaluation of The Geysers
[DE90-002119] 08 p1095 N90-16343
Basic studies on separative glass
[DE90-702436] 09 p1196 N90-16928
Chemical-like behavior of electrons and holes in polymeric conductors
[AD-A214496] 09 p1196 N90-16931
A review of the mechanism and kinetics of electrochemical hydrogen entry and degradation of metallic systems
[AD-A216671] 10 p1355 N90-17857
Helium permeability through austenitic stainless steel
[DE90-007046] 11 p1488 N90-18562
A contribution to the theory of transient conductor simulations
[ETN-90-95891] 12 p1654 N90-19511
Using image analysis to determine petrophysical properties of reservoir rocks
[DE90-000222] 12 p1680 N90-19649
Criteria for polymer concrete on airport pavements
[DOT/FAA/DS-89/18] 14 p1929 N90-21045
A casting and imaging technique for determining void geometry and relative permeability behavior of a single fracture specimen
[DE90-009192] 14 p1989 N90-21403
Quantitative confirmation of diffusion-limited oxidation theories
[DE90-012997] 20 p2838 N90-26143
Development of membrane process for carbon dioxide separation from diving atmosphere
[AD-A222606] 20 p2901 N90-26504
A summary of measurements of permittivities and permeabilities of some microwave absorbing materials
[AD-A223221] 21 p2995 N90-27026
Hyperthermal atomic oxygen generator
[NASA-CR-186573] 22 p3155 N90-27889
Chiral Maxwell-Garnett mixing formula
[PB90-189143] 23 p3391 N90-29158
Modification of polystyrene/polybutadiene block copolymer films by chemical reaction with bromine and effect on gas permeability
[AD-A223612] 24 p3455 N90-29513

PERMEATING
Modeling of hydrazine surface interactions in environmental reaction chambers
02 p0203 N90-11162

PERMITTIVITY
Capacitive energy storage at cryogenic temperatures, phase 2
[AD-A210366] 01 p0061 N90-10347
Influence of core-shell grains on the internal stress state and permittivity response of zirconia modified barium titanate
[AD-A211245] 02 p0202 N90-11153
Modeling of the dielectric behavior of composite materials
[CERT-1/1398-MO] 04 p0467 N90-12674
Porous ceramic bodies
[AD-D014277] 08 p1049 N90-16061
Plasmon excitation in the scattering of electromagnetic waves from good conductors
[AD-A214026] 08 p1056 N90-16107
The redetermination of the elastic, piezoelectric, and dielectric constants of quartz and their variation with temperature
[AD-A215025] 09 p1197 N90-16937
Electromagnetic scale models using emulsions
[AD-A214855] 09 p1211 N90-17022
Heterogeneous composite and method of making
[AD-D014337] 12 p1619 N90-19306
Alternate film dielectric materials
[DE90-007213] 12 p1632 N90-19378
Causality of plasma permittivity with loss and restoring terms
[NASA-TM-101671] 12 p1645 N90-19453
A study of physical properties of ODPA-p-PDA polyimide films
[NASA-TM-102525] 13 p1766 N90-20137
Process for lowering the dielectric constant of polyimides using diamic acid additives
[NASA-CASE-LAR-13902-1] 17 p2379 N90-23546
A summary of measurements of permittivities and permeabilities of some microwave absorbing materials
[AD-A223221] 21 p2995 N90-27026
Accurate determination of the complex permittivity of biological tissue at 90 GHz, 70 GHz, and over a broad band around 35 GHz
[AD-A222062] 21 p3033 N90-27240
Chiral Maxwell-Garnett mixing formula
[PB90-189143] 23 p3391 N90-29158

PERMUTATIONS
The organization of permutation architectures with bussed interconnections
[AD-A210832] 01 p0061 N90-10352
On the maximum period of a permutation of N elements
[MEMO-771] 04 p0544 N90-13159
Frequency agile synthetic aperture radar
[AD-D014235] 06 p0765 N90-14451

PEROVSKITES
Researches on amorphous perovskite
[DE89-900733] 08 p1128 N90-16535
Chemically prepared PZT films doped with niobium
[DE90-006811] 13 p1892 N90-20859
The effects of point defects and composition on structural phase transition
[DE90-010109] 16 p2322 N90-23238
Protons and lattice defects in perovskite-related oxides
[DE90-010957] 18 p2624 N90-24955

PEROXIDES
NT HYDROGEN PEROXIDE
The collection and analysis of atmospheric peroxides
20 p2887 N90-26428
Heterogeneous transformation of peroxyacetylnitrate
20 p2887 N90-26430

PERSONAL COMPUTERS
Personal computer process data acquisition
[DE89-017877] 06 p0828 N90-14816
Utilization of a PC for finite element modeling
[AD-A214173] 07 p0971 N90-15605
Personal computer study of finite-difference methods for the transonic small disturbance equation
[NASA-TM-102582] 08 p1019 N90-15892
RenderMan design principles
13 p1857 N90-20653
Multi-tasking computer control of video related equipment 13 p1859 N90-20665
HCI monitor 16 p2209 N90-22599
ASTEC: Controls analysis for personal computers
16 p2291 N90-23052
The Zenith Z-248 as a scientific workstation
[AD-A219991] 17 p2441 N90-23909
Shape discrimination research using an IBM PC
[AD-A219993] 17 p2447 N90-23953
A fast PC-based solver for simultaneous linear equations
[AD-A220190] 17 p2461 N90-24056
A low-cost PC-based telemetry data-reduction system
[DE90-000330] 18 p2509 N90-24339
Personal Computer (PC) thermal analyzer
[AD-A221325] 18 p2548 N90-24546
A user-friendly, menu-driven, language-free laser characteristics curves graphing program for desk-top IBM PC compatible computers 18 p2644 N90-25056
L-SWITCH: A PC program for computing transient voltages and currents during switching off three-phase inductances
[EUT-89-E-221] 20 p2858 N90-26257
PC-based closed-circuit television system
[DE90-013366] 21 p2994 N90-27017
Personal computer programs for the control of subnanosecond transient digitizers with applications for device damage testing
[AD-A221458] 21 p3054 N90-27365
Flight data replay and analysis system
22 p3105 N90-27635
Stratus: An interactive steady state mixed layer model for personal computers 22 p3219 N90-28255
The personal computer: An untapped source for the United States Army War College
[AD-A223976] 23 p3379 N90-29087
A personal computer-based, multitasking data acquisition system
[NASA-TM-4232] 23 p3382 N90-29107
Graphic interface for attribute-based data language queries from a personal computer to the multi-lingual, multi-model, multi-backend database system over an Ethernet network
[AD-A223738] 24 p3528 N90-29948
GSHELL: Multichannel analyzer/multichannel scaler emulation software for IBM-PC-compatible computers
[DE90-015396] 24 p3529 N90-29956
Automated CADAM data transfer: User's manual
[DE90-014871] 24 p3530 N90-29963
ESTEC software catalogue
[ESA-SP-1133] 24 p3531 N90-29968

PERSONALITY
Psychophysiological correlates of human adaptation in antarctica
[AD-A216679] 10 p1412 N90-18142
Effects of dexamethasone and high terrestrial altitude on cognitive performance and affect
[AD-A217897] 13 p1851 N90-20625
Personality factors in flight operations. Volume 1: Leader characteristics and crew performance in a full-mission air transport simulation
[NASA-TM-102259] 17 p2348 N90-23370

PERSONALITY TESTS
Personality characteristics of USAF pilot candidates
09 p1255 N90-17281
Leader personality and crew effectiveness: Factors influencing performance in full-mission air transport simulation 09 p1255 N90-17282
Personality assessment in aviation selection
09 p1257 N90-17289
The trials and tribulations of RAF defence mechanism testing 09 p1257 N90-17291
Study of the application of a stress reactivity test in personnel selection
[DLR-FB-89-54] 19 p2723 N90-25489

PERSONNEL
NT AIR TRAFFIC CONTROLLERS (PERSONNEL)
NT AIRCRAFT PILOTS
NT ASTRONAUTS
NT COSMONAUTS
NT CREWS
NT FLIGHT CREWS
NT FLIGHT SURGEONS
NT INSTRUCTORS
NT MEDICAL PERSONNEL
NT NAVIGATORS
NT OPERATORS (PERSONNEL)
NT ORBITAL WORKERS
NT PILOTS (PERSONNEL)
NT PROGRAMMERS
NT SCIENTISTS
NT SPACECREWS
NT TEST PILOTS
SINCGARS (Single-Channel Ground/Airborne Radio System) operator performance decay
[AD-A210716] 01 p0057 N90-10326
Hydrazine dosimetry 02 p0206 N90-11178
Rocket studies of the lower ionosphere
[NASA-CR-186187] 06 p0814 N90-14735
Physical and Electrical Standards Laboratory general operating procedures
[DE90-003515] 07 p0884 N90-15116
MANPRINT methods monograph: Aiding the development of manned system performance criteria
[AD-A213543] 07 p0968 N90-15593
MANPRINT (Manpower and Personnel Integration) evaluation: AN/TRC-170 digital troposcatter radio system
[AD-A211799] 08 p1055 N90-16100
An exploration of issues related to future space logisticians
[AD-A215374] 09 p1276 N90-17397
Psychophysiological correlates of human adaptation in antarctica
[AD-A216679] 10 p1412 N90-18142
Insulation, compressibility and absorbency of dry suit undergarments
[AD-A215944] 10 p1414 N90-18149
Source hierarchy list. Volume 1: A through D
[AD-A216050] 10 p1442 N90-18321
Source hierarchy list. Volume 2: E through N
[AD-A216051] 10 p1442 N90-18322
Airborne radar systems specialist, AFSC 118X2
[AD-A215450] 11 p1496 N90-18611
Physical performance and carbohydrate consumption in CF commandos during a 5-day field trial
[AD-A217204] 13 p1850 N90-20619
Lack of behavioral effects of high-peak-power microwave pulses from an axially extracted virtual cathode oscillator
[AD-A220779] 17 p2391 N90-23618
The integrated area measure of visual endogenous ERPs: Relation to cognitive workload and hemisphere
[AD-A223191] 21 p3035 N90-27255
Scientists, engineers, and technicians in nonmanufacturing industries: 1987. (Detailed statistical tables)
[PB90-226903] 23 p3404 N90-29235
Minimal sleep to maintain performance: Search for sleep quantum in sustained operations
[AD-A223815] 24 p3498 N90-29770
Human error classification and data collection
[DE90-631408] 24 p3522 N90-29915

PERSONNEL DEVELOPMENT
Higher education for science and technology: A background paper
[PB89-191290] 02 p0287 N90-11642

Cognitive and Neural Sciences Division 1989 programs
[AD-A212634] 06 p0820 N90-14769
Project summaries
[PB90-103987] 08 p1118 N90-16472
An exploration of issues related to future space logisticians
[AD-A215374] 09 p1276 N90-17397
Airborne radar systems specialist, AFSC 118X2
[AD-A215450] 11 p1496 N90-18611
Preparing technicians for engineering materials technology 18 p2516 N90-24369
Materials and processes for spacecraft: The ESTEC approach
[ESA-STM-244] 19 p2667 N90-25176
Automatic information processing and high performance skills: Application to training
[AD-A221709] 21 p3036 N90-27259

PERSONNEL MANAGEMENT
Middle management of research
[NASA-TM-102417] 13 p1899 N90-20901
A systematic approach to training: A training needs assessment 18 p2645 N90-25059

PERSONNEL SELECTION
NT PILOT SELECTION
Cognitive and Neural Sciences Division 1989 programs
[AD-A212634] 06 p0820 N90-14769
Human Behaviour in High Stress Situations in Aerospace Operations
[AGARD-CP-458] 09 p1254 N90-17275
Leader personality and crew effectiveness: Factors influencing performance in full-mission air transport simulation 09 p1255 N90-17282
Personality assessment in aviation selection 09 p1257 N90-17289
The incremental validity of spatial and perceptual-psychomotor tests relative to the armed services vocational aptitude battery
[AD-A220903] 18 p2585 N90-24719
Activities report of the National Aerospace Medical Center
[ETN-90-96936] 18 p2585 N90-24721
Air Force Officer Qualifying Test (AFOQT): Development of quick score composites for forms P1 and P2
[AD-A223868] 23 p3362 N90-28997

PERSPIRATION
Control of thermoregulatory sweating during exercise in the heat
[AD-A206001] 01 p0092 N90-10523
The effect of moisture absorption in clothing on the human heat balance
[AD-A217899] 13 p1852 N90-20626
Hydration effects on human physiology and exercise-heat performance
[AD-A217969] 13 p1852 N90-20629

PERTURBATION
NT ORBIT PERTURBATION
NT SATELLITE PERTURBATION
Report on the 2-D Model Intercomparison Workshop held January 11-16, 1987 in Fort Myers Beach, Florida, chapter 2 02 p0248 N90-11406
Gauge invariant cosmological perturbations with cold dark matter
[DE89-790940] 02 p0295 N90-11679
Some notes on perturbations of differential-algebraic equations
[PB89-218564] 03 p0393 N90-12243
On mean elements for satellite orbits perturbed by the zonal harmonics of the geopotential
[AD-A212322] 04 p0461 N90-12642
Magnetically insulated electron flows in pulsed power systems
[AD-A212746] 04 p0549 N90-13196
First-order Bragg SAR imagery of Kelvin wakes and moving internal wave fields
[AD-A213361] 05 p0633 N90-13691
The linear study of zonally asymmetric barotropic flows 05 p0668 N90-13902
Measurement of arithmetic error and calculation perturbations
[IMAG-RR-767-M] 05 p0692 N90-14039
On the effects of an uncertainty on evolution law in dynamical systems
[PREPRINT-689] 05 p0693 N90-14047
The stability of Taylor-Couette flow with radial heating 06 p0774 N90-14502
Atomic structure and spectral perturbations in hot dense plasmas 06 p0785 N90-14567
Perturbation methods for the calculation of gravitational waves from slightly non-spherical spacetimes with applications to stellar core collapse 06 p0863 N90-15015
Singular perturbation analysis of AOTV-related trajectory optimization problems
[NASA-CR-186202] 08 p1027 N90-15936
Planar array antenna design analysis, volume 1
[AD-A215537] 09 p1207 N90-16999
The evolution of linearized perturbations of parallel flows
[DE90-005978] 09 p1221 N90-17082
Effects of controlled three-dimensional perturbations on boundary layer transition
[AD-A215080] 10 p1384 N90-18011
Evaluation of influences of errors involved in orbit propagation of artificial satellites
[INPE-4962-TDL/391] 11 p1466 N90-18441
Tomographic investigations of weakly perturbed supersonic free jets
[MPIS-MITT-91] 12 p1600 N90-19209
Ionospheric heating with oblique waves. Volume 1: Electron density perturbations
[AD-A216260] 12 p1690 N90-19709
Evolution of finite amplitude baroclinic waves in the atmosphere and ocean
[INPE-4752-TDL/346] 12 p1695 N90-19733
Aiming control: Theory and applications to dynamic control of space structures
[AD-A217877] 13 p1764 N90-20123
The dynamics of scalar fields in the early universe 14 p2039 N90-21696
Effect of atmospheric turbulence on electro-optical systems 15 p2086 N90-21940
Normal forms for weakly non-linear perturbed wave equations
[REPT-89-41] 15 p2161 N90-22343
Multipole moments in general relativity and dynamical perturbations of black-hole magnetospheres 15 p2190 N90-22509
Recursive linearization of multibody dynamics equations of motion 16 p2280 N90-22993
A survey on the structured singular value 16 p2281 N90-22998
Algorithms for computing the multivariable stability margin 16 p2281 N90-22999
An examination of the full-wave method for rough surface scattering
[AD-A218664] 16 p2308 N90-23155
The effects of caustics in acoustic inverse scattering experiments
[AD-A218454] 16 p2313 N90-23185
Computation of low Mach number compressible flow 17 p2344 N90-23346
Examination of microburst development in Colorado thunderstorm for the 5 August 1982 case
[AD-A218478] 17 p2425 N90-23820
The problem of robust compensation for systems with unmodeled dynamics
[AD-A221246] 18 p2548 N90-24545
Finite amplitude surface waves in cooled plasmas with smeared interface
[DE90-611308] 18 p2617 N90-24909
On the receptivity problem for Goertler vortices: Vortex motions induced by wall roughness
[NASA-CR-182036] 19 p2654 N90-25109
Formation of magnetic islands due to field perturbations in toroidal stellarators
[DE90-012132] 19 p2759 N90-25679
Origin of density fluctuations in extended inflation
[NASA-CR-182652] 19 p2795 N90-25915
The effect of a three-dimensional source on the flow through a channel with square cross section
[LR-512] 20 p2863 N90-26289
Aiming control: Theory and applications to dynamic control of space structures
[AD-A221532] 21 p2967 N90-26864
Improved computational strategy for predicting the response of complex systems
[AD-A221661] 21 p3014 N90-27135
Nonlinear multi-mode coupling of the solar gravity modes in a rotationally split multiplet 21 p3100 N90-27608
Study of the origin of three dimensional structures in shear flows through external forcing
[AD-A221923] 22 p3170 N90-27980
The instability mechanism of synoptic-scale eddies 22 p3211 N90-28217
Theoretical thermodynamics: Equation of state and perturbation studies
[PB90-199332] 22 p3255 N90-28430
Aerodynamics of bodies in shear flow 23 p3268 N90-28496
Regular and chaotic motion of uniform elliptical vortices in external linear time dependent velocity fields 23 p3268 N90-28497
An investigation of the steady and unsteady near wake and its effect on a laminar boundary layer 23 p3324 N90-28794
A hybrid perturbation-Galerkin technique for partial differential equations
[NASA-CR-182085] 23 p3327 N90-28814
Geometric theory for infinite dimensional systems
[ETN-90-96922] 23 p3389 N90-29144
The formation of globular clusters 23 p3410 N90-29272

PERTURBATION THEORY
On analytic modeling of lunar perturbations of artificial satellites of the earth
[AD-A210440] 01 p0016 N90-10078
A unified view of infinitesimal perturbation analysis and likelihood ratios
[AD-A210682] 01 p0114 N90-10652
Extended basis set calculations of atomization energies: Comparison of isogyric and direct results
[AD-A212268] 04 p0471 N90-12702
Optimal control of aero-assisted orbit transfer vehicles 06 p0727 N90-14241
Localized vibrations of nearly periodic structures with irregularities 06 p0798 N90-14648
Wide-angle propagation in inhomogeneous fluids and elastic solids using perturbation methods 06 p0837 N90-14868
General many-body systems
[DE90-000685] 07 p0982 N90-15670
Relativistic self-consistent field studies of atoms and molecules
[AD-A214101] 07 p0991 N90-15724
On the domain of string perturbation theory
[DE90-800759] 08 p1135 N90-16575
The dynamics of dust in planetary magnetospheres 08 p1149 N90-16658
Numerical simulation of unstably stratified sheared flows
[DE90-005396] 10 p1384 N90-18008
Colliding natural convection boundary layer flow in a rectangular enclosure
[DE90-005397] 10 p1384 N90-18009
Thermodynamics of systems with very many components phase equilibrium
[DE90-007345] 11 p1573 N90-19059
Perturbations of test mass motion in the Schwarzschild spacetime using the method of Hamilton and Jacobi 11 p1577 N90-19083
Nonlinear system vibration: The appearance of chaos
[DE90-007546] 12 p1708 N90-19810
Drag-free satellite control 12 p1735 N90-19974
Using transonic small disturbance theory for predicting the aeroelastic stability of a flexible wind-tunnel model
[NASA-TM-102617] 13 p1749 N90-20047
Numerical simulations of supersonic flow through oscillating cascade sections
[NASA-TM-103100] 13 p1750 N90-20051
Electronic structure, alloy phase stability, and phase diagrams
[DE90-008306] 13 p1778 N90-20203
Measurement of the stimulated thermal Rayleigh scattering instability
[DE90-007849] 13 p1807 N90-20376
Perturbation solutions in D* for buckling, vibration, and static loading of specially orthotropic plates 13 p1814 N90-20419
Postbuckling behavior of laminated specially orthotropic plates by affine transformation 13 p1814 N90-20420
Discrete modeling of beds of propellant exposed to strong stimulus
[DE90-008932] 14 p1957 N90-21206
The effects of forcing on a single stream shear layer and its parent boundary layer
[NASA-CR-186529] 14 p1973 N90-21301
Chern-Simons superconductivity at finite temperature
[DE90-613393] 14 p2031 N90-21650
An experimental investigation of the physical mechanisms controlling the asymmetric flow past slender bodies at large angles of attack 15 p2053 N90-21767
Perturbation techniques in the dynamics and control of flexible manipulators
[OUEL-1772/89] 15 p2107 N90-22053
A new stability criterion in the shallow-water system for two-dimensional coherent eddies in the atmosphere and oceans 15 p2130 N90-22176
Recursive linearization of multibody dynamics equations of motion 16 p2280 N90-22993
Effect on relaxation on nonlinear waves in crystals 16 p2310 N90-23165
Prediction methods of launcher aeroelastic stability. Application to the Ariane 5/Hermes vehicle. Comparison with test results
[REPT-892-422-107] 17 p2362 N90-23451
Dynamic disturbance decoupling for nonlinear systems
[MEMO-835] 17 p2483 N90-24069
Classical theory of radiating strings
[NASA-CR-186607] 17 p2485 N90-24214
Methods of perturbation theory as a means for interactive design from bodies in a flow
[ETN-90-96502] 18 p2553 N90-24573
Sustained resonance in very slowly varying oscillatory Hamiltonian systems
[DE90-010422] 18 p2598 N90-24783

Synthesis and validation of feedback guidance laws for air-to-air interceptions
[LR-615] 19 p2752 N90-25639
An investigation of the use of singular perturbation methods and modal control theory in the derivation or aircraft control schemes
[MATHS-REPT-A-106] 20 p2814 N90-26014
Chemical structure and kinetics at liquid/solid interfaces
[AD-A222766] 20 p2831 N90-26105
Perturbation methods in the theory of waves and bifurcation phenomena 20 p2916 N90-26593
Application and extension of an analytical model of the confined acoustic beam generated by a transducer
[AD-A222994] 20 p2924 N90-26639
An introduction to space trajectories
22 p3127 N90-27749
Real time guidance and propulsion control for single-stage-to-orbit airbreathing vehicles
23 p3285 N90-28587
Formation of magnetic islands due to field perturbations in toroidal stellarator configurations
[DE90-014789] 23 p3397 N90-29191
Higher loop contributions to effective potential of gauge theory at high temperature
[DE90-627208] 23 p3403 N90-29231
Satellite motion in an axi-symmetric gravitational field. Part 1: Perturbations due to J2 (second order) and J3
[RAE-TR-88068] 24 p3440 N90-29429
Effects of basis set contraction in relativistic calculations on neon, argon, and germanium
[AD-A223357] 24 p3446 N90-29460
Unstable phenomena in mechanical systems
[AD-A223640] 24 p3537 N90-30001
Study of the reflection of surface acoustic wave from a material discontinuity boundary using a perturbation method 24 p3542 N90-30032
A comparative first principles study of phase stability in Ni-Ti and Ni-Al alloys around equiatomic composition
[DE90-016477] 24 p3554 N90-30111
On a calculation of the ground-state energy in quantum mechanics
[DE90-627182] 24 p3555 N90-30119
Introductory lectures on conformal field theory and strings
[DE90-627219] 24 p3556 N90-30120

PESTICIDES
Data Base Analyzer and Parameter Estimator (DBAPE) interactive computer program user's manual
[PB90-193053] 23 p3406 N90-29252

PETN
Free-expansion experiments and modeling in detonation: Chemistry and hydrodynamics on a laboratory scale
[DE89-007748] 01 p0053 N90-10302
Laser initiation of secondary explosives
[DE89-010229] 01 p0075 N90-10431
Crystal orientation effects in PETN explosive with 4 GPa shocks
[DE89-016996] 02 p0206 N90-11190
Fast transit gas- and condensed-phase chemistry of energetic materials
[DE90-001656] 06 p0755 N90-14395
Critical temperature analysis for a hemispherical charge of a binary explosive
[DE90-001447] 07 p0913 N90-15282

PETRI NETS
On the generation of a variable structure airport surface traffic control system
[AD-A211306] 03 p0304 N90-11724
Requirements specification with Petri nets using the cube tool methodology
[AD-A212190] 04 p0492 N90-12829
Extended performability modeling using dynamic queing networks
[MEMO-INF-89-15] 04 p0536 N90-13099
Eigenvalues of dynamic max-min systems
[REPT-89-84] 17 p2465 N90-24088
The semantics of data flow diagrams
[TR-89-16] 17 p2480 N90-24181
The proposal of a high-level stochastic Petri net
[REPT-90-005] 19 p2752 N90-25637
Place/transition nets with debit arcs
[NASA-CR-186932] 21 p3058 N90-27386

PETROGRAPHY
Using image analysis to determine petrophysical properties of reservoir rocks
[DE90-000222] 12 p1680 N90-19649
Analysis of tectonic movements utilizing remote sensor products in the Southern Espinhaco (SE) region
[INPE-4830-PRE/1451] 12 p1690 N90-19708
Geochemistry and origin of regional dolomites
[DE90-012589] 21 p3024 N90-27196

PETROLEUM
U CRUDE OIL

PETROLEUM PRODUCTS
NT ASPHALT
NT DIESEL FUELS
NT GASOLINE
NT TARS

PETROLOGY
NT PETROGRAPHY
Workshop on the Archean Mantle
[NASA-CR-186156] 06 p0814 N90-14736
Workshop on Moon in Transition: Apollo 14, KREEP, and Evolved Lunar Rocks
[NASA-CR-186153] 06 p0865 N90-15026
The Apollo 15 coarse fines (4-10 mm)
[NASA-TM-101934] 06 p0865 N90-15027
Summaries of physical research in the geosciences
[DE90-004993] 08 p1090 N90-16309
P-T condition to deformation from fluid inclusions in mylonites
[NASA-CR-186377] 12 p1690 N90-19710
Stored mafic/ultramafic crust and early Archean mantle depletion
[NASA-CR-186460] 12 p1691 N90-19715
Petrographic working model of the Rosetta sampling and modelling subgroup for a comet nucleus
12 p1738 N90-19992
Geochemistry and origin of regional dolomites
[DE90-012589] 21 p3024 N90-27196

PH
Characterization of cloud chemistry and frequency of canopy exposure to clouds in the Sierra Nevada
[PB89-104035] 06 p0817 N90-14753
Study of silicon nitride pH response to the fabrication of microelectronic sensors
[LAAS-89229] 08 p1042 N90-16023
Sticking coefficient of HCl on aerosols
16 p2208 N90-22598
Analysis of acid precipitation samples collected by state agencies: January to December 1988
[PB90-191784] 22 p3198 N90-28151
Prediction of episodic acidification in Maryland coastal plain streams
[PB90-194978] 22 p3199 N90-28152

PH FACTOR
A collaborative effort to model plant response to acidic rain
[DE90-003002] 09 p1244 N90-17215
Stability studies of a pH-sensitive polymer matrix: Applications to fiber optic pH sensors
[DE90-009579] 15 p2072 N90-21867
Shear-resistant drag reduction polymers. Part 1: Molecular investigations of polymer drag reduction and the development of laboratory screening methods
[AD-A223353] 24 p3454 N90-29508

PHANTOM AIRCRAFT
NT F-4 AIRCRAFT

PHARMACOLOGY
Parallel processing and learning in simple systems
[AD-A210225] 01 p0108 N90-10612
Preliminary study of pharmacological control of space disease
[ETN-90-95015] 05 p0674 N90-13927
Coded-aperture imaging in nuclear medicine
08 p1073 N90-16208
The United States Air Force School of Aerospace Medicine: Special report
[AD-A217740] 13 p1851 N90-20622
JPRS report: Science and technology. USSR: Life sciences
[JPRS-ULS-90-002] 14 p1995 N90-21434
Pharmacological resetting of the circadian sleep-wake cycle effects of triazolam on reentrainment of circadian rhythms in a diurnal primate
[AD-A224227] 24 p3497 N90-29764

PHASE ANGLE
U PHASE SHIFT

PHASE CHANGE MATERIALS
Potential industrial applications for composite phase-change materials as thermal energy storage media
[DE89-015170] 02 p0237 N90-11346
Phase change material for spacecraft thermal management
[AD-A211404] 04 p0462 N90-12648
Selection of phase-change and containment materials for thermal energy storage
[NASA-CR-186228] 07 p0952 N90-15508
Satellite thermal storage systems using metallic phase-change materials
[DE89-016872] 07 p0952 N90-15507
Ion beam modification of metals: Mechanical properties and structure
[AD-A214701] 09 p1194 N90-16915
Development of a high temperature storage unit for integration with solar dynamic systems
10 p1335 N90-17720
Spacecraft thermal control design data, volume 3
[ESA-PSS-03-108-ISSUE-1-VOL-3]
11 p1469 N90-18457
Failure and degradation modes in selected solar materials: A review
[DE90-009075] 14 p2002 N90-21476
Analysis of thermal energy storage material with change-of-phase volumetric effects
[NASA-TM-102457] 15 p2092 N90-21974

PHASE COHERENCE
Analysis of phase retrieval in active imaging
[AD-A221080] 18 p2563 N90-24626

PHASE CONJUGATION
Multimode fiber interferometry and several-mode fiber polarimetry via phase conjugation
[DE89-014226] 01 p0123 N90-10706
Optics and opto-electronics systems
[AD-A212340] 05 p0699 N90-14093
Beam combining by phase transition nonlinear media
[AD-A219301] 18 p2233 N90-22739

PHASE CONTROL
Dynamics and control of turbulent shear flows
[AD-A210396] 01 p0070 N90-10402
Phase control mechanism for wave energy conversion
[AD-D014354] 12 p1681 N90-19657
Fiber-optic projected-fringe digital interferometry
[NASA-TM-103252] 22 p3178 N90-28033

PHASE DETECTORS
Advanced instrumentation for aircraft icing research
[NASA-CR-185225] 14 p1921 N90-21006
Zero-G phase detector and separator
[NASA-CASE-LEW-14844-1] 15 p2101 N90-22024

PHASE DEVIATION
On linear structure and phase rotation invariant properties of block 2(sup l)-PSK modulation codes
[NASA-CR-186308] 12 p1641 N90-19429

PHASE DIAGRAMS
Interactive computer program for the generation of enthalpy-entropy and temperature-entropy charts of nitrogen and hydrogen
[DLR-FB-89-27] 04 p0533 N90-13081
Solid oxide fuel cells electrodes based on In(sub 2)O(sub 3)-PrO(sub 1.83)-ZrO(sub 2)
[DE90-002666] 06 p0806 N90-14691
Powder neutron diffraction study of the structural phase diagram of the Ba(sub 1-x)K(sub x)BiO3 system
[DE90-002264] 06 p0854 N90-14967
Gas-liquid-liquid equilibria in mixtures of water, light gases, and hydrocarbons
[DE90-003180] 07 p0894 N90-15167
Surface studies at the NSLS
[DE90-003173] 08 p1043 N90-16027
Contribution to the study of order effects in the Ising model framework: Ground states and phase diagrams
[ESA-TT-1118] 08 p1132 N90-16557
Physical properties of Bi2Sr2CuO6, the semiconducting phase, structurally distinct from the n = 1 Bi-cuprate superconductor
[DE90-004299] 08 p1133 N90-16563
Estimation of thermodynamic properties of alloys from phase diagram and other loose boundary conditions
[DE90-719511] 08 p1135 N90-16579
Phase properties of the rapid cooled palladium-silicon alloy in the concentration range 40 to 58 at. percent Si
[DE90-719525] 09 p1284 N90-17444
Pulsed laser-induced melting of intermediate Cu-Zn phases
[DE90-005404] 11 p1513 N90-18713
What influences order parameters across the superconducting phase boundary
[DE90-610663] 11 p1572 N90-19047
Thermodynamics of systems with very many components phase equilibrium
[DE90-007345] 11 p1573 N90-19059
Fabrication, phase transformation studies, and characterization of SiC-AlN-Al2OC ceramics
[DE90-006591] 12 p1631 N90-19371
Molecular theory and computer simulation studies of natural and synthetic gas mixtures
[PB90-130329] 12 p1711 N90-19826
Electrochemical phase diagrams for aqueous redox systems
[AD-A217168] 13 p1770 N90-20157
Electronic structure, alloy phase stability, and phase diagrams
[DE90-008306] 13 p1778 N90-20203
Phase equilibria and solution thermodynamics of bismuth-lead alloys
[PB90-138421] 14 p1950 N90-21163
Controlled production and characterization of metastable intermetallics
[DE90-009384] 14 p1952 N90-21176
Molecular theory of fluid phase equilibria
[PB90-131277] 15 p2066 N90-21832

Improvement study of iron disilicide thermoelectric materials
[AD-A218946] 16 p2252 N90-22844
NMR studies of polymeric solid electrolytes
[AD-A219833] 17 p2381 N90-23562
Electronic structure and phase stability properties of Al-Li alloys
[DE90-010632] 18 p2525 N90-24410
A first principles examination of phase stability in FCC-based ordered Ni-V alloys
[DE90-010635] 18 p2525 N90-24411
Chemical and crystallographic phase behavior in the Ba(1-x)K(x)BiO3 system
[DE90-010072] 18 p2618 N90-24917
The origin of poorly conditioned susceptibility matrix within inverse CVM algorithm in the case of Pd(sub 3)V: A comparison to the case of Ni(sub 3)V
[DE90-012464] 20 p2833 N90-26110
Phase compatibilities of YBa2Cu3O(9-delta) type structure in quintenary systems Y-Ba-Cu-O-X (impurity)
22 p3145 N90-27834
Development of metastable processing paths for high temperature alloys
[AD-A223144] 22 p3157 N90-27898
Phase diagram and thermodynamic data for the Am-Pu system
[NPL-DMM(A)-5] 22 p3255 N90-28431
Trajectories of renormalization group flows on the phase diagram of N=2 superconformal field theories
[DE90-627212] 23 p3391 N90-29154
Topology of singularities and phase diagram of N=2 superconformal field theories
[DE90-627213] 23 p3391 N90-29155
First principles calculation of oxygen ordering in YBa2Cu3O(7-y)
[DE90-015205] 24 p3553 N90-30102

PHASE ERROR
An Energy Spectrum Compressor system (ESC) for the Amsterdam pulse stretcher (AmPS)
06 p0842 N90-14896
On linear structure and phase rotation invariant properties of block 2(sup I)-PSK modulation codes
[NASA-CR-186308] 12 p1641 N90-19429
Measurement errors 17 p2359 N90-23426
Combined effects of fast and selective fading on performance of PSK and MSK with coherent detection
20 p2849 N90-26204
Modified fast frequency acquisition via adaptive least squares algorithm
[NASA-CASE-NPO-17845-1-CU]
21 p3050 N90-27341

PHASE LOCK DEMODULATORS
Phase ambiguity resolution for offset QPSK modulation systems
[NASA-CASE-NPO-17853-1-CU]
09 p1204 N90-16975

PHASE LOCKED SYSTEMS
Coupled multiline CW HF lasers: Experimental performance
[AD-A210844] 01 p0075 N90-10434
Wideband phase-locked angular modulator
04 p0487 N90-12798
The 22 GHz Radioastron receiver: Development of prototype components during the year 1988
[PB89-212583] 07 p0920 N90-15323
Theoretical and experimental investigation of coupled Ar-ion lasers
[AD-A214908] 09 p1227 N90-17122
Experimental and theoretical study of CO2 staggered hollow-bore array lasers
[AD-A212921] 10 p1389 N90-18032
The effects of sinusoidal interference on the second-order carrier tracking loop preceded by a bandpass limiter in the Block 4 receiver 12 p1644 N90-19449
Experimental investigation of the mechanisms underlying vortex kinematics in unsteady separated flows
[AD-A217889] 13 p1802 N90-20346
Strain and dynamic measurements using fiber optic sensors embedded into graphite/epoxy tubes
14 p1937 N90-21090
Radio links: Instrument technologies
17 p2358 N90-23425
Phase locking of two HIQ resonators
[AD-A221123] 18 p2563 N90-24627
Sustained resonance in very slowly varying oscillatory Hamiltonian systems
[DE90-010422] 18 p2598 N90-24783
An approach to systematic phase-lock loop design
[ETN-90-96905] 19 p2686 N90-25280
New approaches for rapid synchronisation frequency hoppers 20 p2849 N90-26201
Direct drive robotic hand
[NASA-CASE-NPO-17917-1-CU]
20 p2872 N90-26339
Integration of GPS/INS with partitioned filters
24 p3425 N90-29347

PHASE MATCHING
Aspects of Raman scattering
[AD-A213926] 07 p0992 N90-15736
The super-gratings: How to improve the limiting resolution of grating spectrometers
[PREPRINT-695] 16 p2204 N90-22577
Nonlinear spectroscopy of multicomponent droplets and 2- and 3-dimensional measurements in flames
[AD-A218569] 16 p2215 N90-22636
Laser physics and laser spectroscopy
[AD-A224379] 24 p3473 N90-29628

PHASE MODULATION
NT PHASE SHIFT KEYING
Error control techniques for satellite and space communications
[NASA-CR-182751] 05 p0631 N90-13685
Active phase and amplitude modulator
[AD-D014318] 12 p1650 N90-19480
Thermal modulation of light beams
[AD-D014322] 12 p1713 N90-19840
Weather data dissemination to aircraft
14 p1907 N90-20934
Multiwave diffraction analysis of transmission phase gratings
[RSRE-MEMO-4325] 15 p2087 N90-21948
High performance holographic elements and media
[AD-A218999] 16 p2239 N90-22775
Binary pseudo random phase correlation in radar systems: A new approach
[RSRE-MEMO-4223] 19 p2683 N90-25263
Optical wavefront computer for stabilizing large space structures
[AD-A221707] 21 p2967 N90-26866

PHASE RESPONSE
U FREQUENCY RESPONSE
U PHASE SHIFT

PHASE RULE
SGTE data for pure elements
[NPL-DMA(A)-195] 15 p2181 N90-22460

PHASE SEPARATION (MATERIALS)
La(sub 2)MO(sub 4 + delta) (M = Cu, Ni, Co): Phase separation and superconductivity resulting from excess oxygen defects
[DE90-001988] 08 p1128 N90-16534
Polymer solution phase separation: Microgravity simulation 09 p1224 N90-17101
Mechano-caloric cooling device
[NASA-CR-186316] 12 p1662 N90-19552
Grain boundary intermetallic phases in alloy 718
[DE90-009812] 15 p2173 N90-22417
Rheological and mechanical characteristics of poly-p-phenylene terephthalamide/nylon molecular and particulate composites
[AD-A219562] 17 p2368 N90-23482
Discrete approach: Percolation theory
19 p2689 N90-25297
Heterogeneity description using fractal concepts
19 p2690 N90-25299

PHASE SHIFT
NT SAGNAC EFFECT
Simultaneous multiple frequency interferometry: An application of homodyne phase measurement
[DE89-013975] 01 p0126 N90-10719
Effect of the length of the multijunction grill on its lower hybrid current drive efficiency
[IPPCZ-283] 04 p0556 N90-13240
On optimization of the multijunction grill for the lower hybrid current drive
[IPPCZ-280] 04 p0556 N90-13241
Energy exchange of interacting solitons in multidimensions
[PREPRINT-662] 05 p0696 N90-14071
The phase gradient autofocus algorithm: An optimal estimator of the phase derivative
[DE90-000895] 06 p0828 N90-14814
Aspects of Raman scattering
[AD-A213926] 07 p0992 N90-15736
Multilayer optical elements for generation and analysis of circularly polarized x rays
[DE90-006103] 10 p1430 N90-18250
On linear structure and phase rotation invariant properties of block 2(sup I)-PSK modulation codes
[NASA-CR-186308] 12 p1641 N90-19429
Dual-mode latching reciprocal ferrite phase shifter
[FEL-1988-55] 12 p1652 N90-19497
Doppler radar with multiphase modulation of transmitted and reflected signal
[NASA-CASE-MSC-18808-1] 13 p1791 N90-20280
Transport and relaxation properties in anisotropic superconductors 15 p2170 N90-22403
Transport properties of anisotropic superconductors
15 p2170 N90-22404
Simulation and analysis of a MFQPSK signal transmitted through an acoustic medium
[AD-A220345] 17 p2393 N90-23633
An L-band antenna array with integrated phase shifters
[DLR-FB-89-63] 18 p2544 N90-24519
Novel approaches to sensitivity enhancement of ring laser gyros
[AD-A224335] 24 p3471 N90-29617

PHASE SHIFT CIRCUITS
NT CIRCULATORS (PHASE SHIFT CIRCUITS)
Finite element analysis of propagation in waveguide components with application to ferrite phase shifters
[FOA-C-30529-3.2] 09 p1204 N90-16977
Beamforming devices and feed structures for a DBS flat-plate antenna
[BBC-RD-1989/12] 17 p2386 N90-23592
Serrodyning by means of a digital phase shifter
[AD-A219593] 17 p2396 N90-23646
Monolithic phase shifter study
[AD-A219859] 18 p2546 N90-24533

PHASE SHIFT KEYING
Mitigating Doppler shift effect in HF multitone data modem 06 p0764 N90-14441
Phase ambiguity resolution for offset QPSK modulation systems
[NASA-CASE-NPO-17853-1-CU]
09 p1204 N90-16975
Error detection and correction for a multiple frequency quaternary phase shift keyed signal
[AD-A215706] 09 p1208 N90-17003
On linear structure and phase rotation invariant properties of block 2(sup I)-PSK modulation codes
[NASA-CR-186308] 12 p1641 N90-19429
Costas loop lock detection in the advanced receiver
12 p1643 N90-19441
Advanced modulation technology development for earth station demodulator applications. Coded modulation system development
[NASA-CR-185149] 13 p1789 N90-20270
QPSK carrier-acquisition performance in the advanced receiver 2 15 p2076 N90-21892
On decoding of multi-level MPSK modulation codes
[NASA-CR-186601] 15 p2146 N90-22261
Multi-level trellis coded modulation and multi-stage decoding
[NASA-CR-186861] 19 p2743 N90-25593
Combined effects of fast and selective fading on performance of PSK and MSK with coherent detection
20 p2849 N90-26204
QPSK loop lock detection in the advanced receiver
20 p2854 N90-26230
Studies of ECCM improvements for frequency-hopping CPFSK systems
[AD-A222995] 21 p2995 N90-27023

PHASE TRANSFORMATIONS
NT ARC MELTING
NT BOILING
NT COAL LIQUEFACTION
NT EVAPORATION
NT EVAPOTRANSPIRATION
NT FILM BOILING
NT FREEZING
NT FUSION (MELTING)
NT LEVITATION MELTING
NT LIQUEFACTION
NT MARTENSITIC TRANSFORMATION
NT MELTING
NT SUBLIMATION
NT TRANSPIRATION
NT VACUUM MELTING
NT VAPORIZING
NT ZONE MELTING
Computer simulations of polymer dynamics in the solid state
[DE89-010337] 01 p0048 N90-10275
Monte Carlo simulations of small solute/solvent clusters: Cluster properties and phase transitions
[AD-A209559] 01 p0119 N90-10684
Mott transition: Low-energy excitations and superconductivity
[DE89-617778] 01 p0129 N90-10741
Progress report on grain boundaries
[DE89-015541] 01 p0130 N90-10749
Time-resolved mass spectrometry technique for studying fast transient CHNO explosive decomposition kinetics
[DE89-016540] 02 p0193 N90-11101
Solidification front/viscous phase transitions, forward-backward heat equations
[AD-A211068] 02 p0195 N90-11114
X-ray and gamma-ray spectroscopy of solids under pressure
[DE89-017271] 02 p0196 N90-11118

Thermal expansion and phase transformation studies on some materials by high temperature X-ray powder diffractometry
[DE89-631032] 02 p0198 N90-11130
Precipitation and transformation toughening of Al-Mg signals
[ETN-89-94675] 02 p0199 N90-11138
Shock induced dissociation of polyethylene
[DE89-016983] 02 p0221 N90-11267
Structure and properties of simple molecular systems at very high density
[DE89-016974] 02 p0273 N90-11557
Chevron layer structures in Surface Stabilized Ferroelectric Liquid Crystal (SSFLC) cells filled with a material which exhibits the chiral nematic to smectic C* phase transition
[DE89-016985] 02 p0285 N90-11628
Neutron scattering experiments on high-temperature superconducting materials: Foreign trip report, September 13, 1988--October 4, 1988
[DE89-017451] 02 p0285 N90-11630
Report of the Specialists' Workshop on Phase Transition Studies on Hydrogen-Bonded Crystals by Neutron and X-ray Diffractometries
[DE89-906638] 02 p0285 N90-11631
Shock dissociation of molecular fluids: A possibility of first-order phase change
[DE89-016647] 03 p0322 N90-11829
New mechanism for toughening ceramic materials
[AD-A211651] 03 p0332 N90-11892
Properties of strongly coupled multi-ionic plasmas
[DE89-017782] 03 p0408 N90-12339
Flare-in texture in rotating superfluid (3)He-B
[PB89-218994] 03 p0412 N90-12368
A critical assessment of thermodynamic and phase diagram data for the Ga-In system
[NPL-DMA(A)-174] 03 p0415 N90-12382
Analysis of the performance of heat pipes and phase-change materials with multiple localized heat sources for space applications
[AD-A212232] 04 p0503 N90-12898
Synthesis and properties of NdNiO(3) prepared by low temperature methods
[AD-A212117] 04 p0559 N90-13256
Statistical mechanics of strings and topology
[ROM1F-89-683] 05 p0696 N90-14068
Big Bang nucleosynthesis and the Quark-Hadron transition
[NASA-CR-186169] 05 p0713 N90-14168
Shock-induced solid state reactions and phase transitions: X ray profile studies on shock-modified Fe3O4 and ZrO2 powders
[DE90-000669] 06 p0741 N90-14315
The metallurgical determinants of toughness as cryogenic temperature
[DE90-002331] 06 p0748 N90-14351
First-principles interatomic potentials in transition metals: Multi-ion interactions and their analytic representation
[DE90-001990] 06 p0748 N90-14353
Investigation of the phase stabilizing effect of potassium fluoride on ammonium nitrate
[AD-A213042] 06 p0753 N90-14381
Phase changes in carbon and nitrogen systems: Their effects on the detonation properties of high explosives
[DE90-000829] 06 p0755 N90-14392
Oxygen stoichiometry, structural transitions, and thermodynamic behavior of the YBa2Cu3O(x) system
[DE89-017694] 06 p0852 N90-14951
Muon SR investigation of magnetism and superconductivity in (Y(1-x)Pr(x))Ba2Cu3O7
[DE90-000689] 06 p0852 N90-14956
Theory of the energetics and nonclassical nucleation for martensitic transformations from partially soft lattice modes
[DE90-002182] 06 p0854 N90-14964
Crack tip toughening by inclusions with pairs of shear transformations
[DE89-007845] 07 p0909 N90-15254
Phase transition in polymer blends and structure of ionomers
[DE90-003525] 07 p0911 N90-15266
The possible occurrence of multi-phase behavior in the high T(sub c) superconductor YBa2Cu3O(sub x)
[DE90-002999] 07 p0999 N90-15777
Bulk wave characterization of high T(sub c) superconductors
[AD-A214030] 07 p1004 N90-15813
Study of phase transformations liquid-solid-solid of ultrafine particles
[ISAL-89-0019] 08 p1042 N90-16022
Fundamental studies of beta phase decomposition modes in titanium alloys
[AD-A214424] 08 p1044 N90-16035
Phase evolution during neutron irradiation of commercial Fe-Cr-Mn alloys
[DE90-004113] 08 p1045 N90-16042
Soft modes, freezing, and nonlinear response of a dipolar glass
[DE90-003647] 08 p1051 N90-16075
On the observation of a transition from fusion to multifragmentation in high multiplicity O16 induced reactions
[LUIP-8812] 08 p1119 N90-16481
Superflow induced phase transition in the axial vortex-free texture of rotating superfluid He-3-B
[PB90-110388] 08 p1127 N90-16531
Thermodynamic studies on the ferroelectric phase transition in neutron irradiated (Li(sub x)K(1-x))2SO4 crystals at high temperature
[DE89-635786] 08 p1130 N90-16545
Physical properties of Bi2Sr2CuO6, the semiconducting phase, structurally distinct from the n = 1 Bi-cuprate superconductor
[DE90-004299] 08 p1133 N90-16563
Kosterlitz-Thouless phase transition in two-dimensional hierarchical Coulomb gases
[DE89-618399] 09 p1189 N90-16890
Mechanics of iron, its stability and phase transformation
[DE89-636210] 09 p1193 N90-16913
Phase stability of a manganese-stabilized low-activation martensitic steel
[DE90-004114] 09 p1193 N90-16914
Zirconia based ceramics
[DE90-606358] 09 p1199 N90-16946
Coherent phase transformation under nonhydrostatic stress-wave loading
[DE90-005719] 10 p1396 N90-18072
Nonlinear dynamics of domain walls and vortices in two-dimensional systems
[DE90-004840] 10 p1425 N90-18221
Investigation of the phase stabilizing effect of 4 percent potassium fluoride on ammonium nitrate
[AD-A215313] 11 p1494 N90-18599
Modeling convective Marangoni flows with void movement in the presence of solid-liquid phase change
[DE90-006474] 11 p1509 N90-18690
Kinetic relations and the propagation of phase boundaries in solids
[AD-A215881] 11 p1519 N90-18747
Particle physics and cosmology
[DE90-006547] 11 p1590 N90-19171
Advanced ceramics
[DE90-608004] 12 p1630 N90-19370
Fabrication, phase transformation studies, and characterization of SiC-AlN-Al2OC ceramics
[DE90-006591] 12 p1631 N90-19371
Computation at the edge of chaos: Phase transition and emergent computation
[DE90-007488] 12 p1708 N90-19811
Low temperature elastic and dielectric properties of incommensurate barium sodium niobate
[AD-A216969] 12 p1709 N90-19815
The effects of gradients on boundary stability
[DE90-007428] 12 p1722 N90-19894
Studies of the structure and properties of organic monolayers, multilayers and superlattices
[DE90-008330] 13 p1765 N90-20129
Copolymer-like structures of nematic nitroimine dimers
[AD-A217574] 13 p1780 N90-20215
Welding behavior and welding metallurgy of ductile intermetallic alloys
[DE90-008908] 15 p2069 N90-21852
Extraction of recovery of plasticizers from solid propellants and munitions
[AD-D014433] 15 p2072 N90-21868
A weak formulation for phase-change problems with bulk movement due to unequal densities
[DE90-009398] 15 p2163 N90-22361
Preparation and characterization of Cu2ZnGeS(4-y)Se(y)
[AD-A217469] 15 p2171 N90-22407
Topological defects in extended inflation
[NASA-CR-186594] 15 p2190 N90-22505
Center for surface radiation damage studies
[AD-A218452] 16 p2222 N90-22678
Investigation of atomistic simulation of structural and dynamic differences in glassy and liquid states of atactic poly(propylene)
[AD-A218896] 16 p2224 N90-22687
Beam combining by phase transition nonlinear media
[AD-A219301] 16 p2233 N90-22739
Characterization of weldments using advanced experimental techniques
[DE90-009418] 16 p2242 N90-22792
The effects of point defects and composition on structural phase transition
[DE90-010109] 16 p2322 N90-23238
Undercooling and nucleation in rapid solidification rate metal powders using solid in solid emulsification
[AD-A218527] 17 p2375 N90-23526
US Army Research Office Workshop on Smart Materials, Structures and Mathematical Issues proceedings
[AD-A218528] 17 p2468 N90-24110
Baryogenesis in extended inflation. Part 1: Baryogenesis via production and decay of supermassive bosons
[NASA-CR-180615] 17 p2470 N90-24120
A study of the phase decomposition of Fe-Ni-Al-Mo alloys
[DE90-010143] 18 p2524 N90-24406
Shape memory alloys for robot grippers and mechanical hands 18 p2536 N90-24466
Phase stability in the Al(6-x)Cu(x)Zr2 system for 0 less than x less than 1.0
[DE90-010620] 18 p2620 N90-24925
Nucleation kinetics in undercooled, class-forming metallic melts
[ESA-TT-1186] 19 p2676 N90-25218
Aligned bismuth, strontium, calcium cuprate coatings on polycrystalline substrates
[AD-D014522] 19 p2678 N90-25229
Extended inflation from higher dimensional theories
[NASA-CR-180549] 19 p2796 N90-25916
Dynamical solvent effects on electron-transfer processes: Recent progress and perspectives
[AD-A222603] 20 p2830 N90-26101
Twin boundaries, interfaces and modulated structures in martensites
[DE90-012899] 20 p2833 N90-26111
Fractal structure and fractal time in silica sol-gels
[DE90-013197] 20 p2838 N90-26144
Low-gravity fluid physics: A program overview
[NASA-TM-103215] 20 p2861 N90-26273
Natural melting within a spherical shell
[NASA-TM-102822] 20 p2861 N90-26274
Molecular beam epitaxial growth, characterization, and devices of modulated semiconductor structures
[AD-A221545] 21 p3084 N90-27538
A continuum model for phase transformation in thermoelastic solids
[AD-A222353] 21 p3085 N90-27542
Stabilization of high T(sub c) phase in bismuth cuprate superconductor by lead doping 22 p3144 N90-27832
Evaluation of advanced austenitic alloys relative to alloy design criteria for steam service. Part 1: Lean stainless steel
[DE90-014765] 23 p3310 N90-28720
The first order phase transition for six-state Potts model on two dimensional random triangle lattice
[DE90-627210] 23 p3389 N90-29140
Microwave background distortions from domain walls
[NASA-CR-187272] 24 p3462 N90-29556
Characteristic microwave background distortions from collapsing domain wall bubbles
[NASA-CR-187270] 24 p3462 N90-29557
First principles calculation of oxygen ordering in YBa2Cu3O(7-y)
[DE90-015205] 24 p3553 N90-30102

PHASE VELOCITY

Investigations of Eurasian seismic sources and upper mantle structure
[AD-A211806] 03 p0371 N90-12120
Long wave atmospheric noise model, phase 1. Volume 1: Lightning occurrence rates and propagation theory
[AD-A212794] 04 p0493 N90-12836
Optical guiding by plasma waves in the plasma beat wave accelerator
[AD-A214288] 07 p0997 N90-15763
An experimental study of the effect of streamwise vortices on unsteady turbulent boundary-layer separation 09 p1215 N90-17045
Instabilities and subharmonic resonances of subsonic heated round jets, volume 2
[NASA-CR-186058] 15 p2100 N90-22017
A theoretical investigation of gravity-wave-generated stress and vorticity in the planetary boundary layer 15 p2191 N90-22512
Nonlinear spectroscopy of multicomponent droplets and 2- and 3-dimensional measurements in flames
[AD-A218569] 16 p2215 N90-22636
Nonlinear internal gravity wave critical layers 17 p2422 N90-23801
Normal-mode and phase-integral methods for determining phase and group velocities in simple underwater acoustic ducts
[AD-A221393] 18 p2612 N90-24877

PHASE-SPACE INTEGRAL

Lie-algebraic aspects of the classical nonrelativistic Calogero-Moser models
[CWI-AM-R8901] 04 p0542 N90-13148

PHASED ARRAYS

Gyrotron development for space power beaming 01 p0028 N90-10148

Coupled multiline CW HF lasers: Experimental performance
[AD-A210844] 01 p0075 N90-10434
Master oscillator with power amplifiers: Performance of a two-element CW HF phased-laser array
[AD-A211141] 01 p0076 N90-10435
Antenna beamforming using optical processing
[NASA-CR-180844] 02 p0212 N90-11210
Proceedings of the 1988 Antenna Applications Symposium, volume 1
[AD-A211396] 03 p0338 N90-11928
Dedicated tracking of crossing targets with a phased array monopulse radar
[FEL-1988-95] 04 p0491 N90-12821
Vehicle antenna for the mobile satellite experiment
[NASA-CR-186109] 06 p0733 N90-14271
Proceedings of the Antenna Applications Symposium, volume 2
[AD-A213815] 07 p0919 N90-15313
A study of Inter-Injection-Locked phased arrays
[AD-A214097] 07 p0925 N90-15352
A multichannel processing approach to real time network detection, phase association, and threshold monitoring
[AD-A213940] 07 p0980 N90-15657
Large angle off-axis beam steering of a phased telescope array
[AD-D014269] 08 p1060 N90-16127
A space-fed local oscillator for spaceborne phased arrays
[AD-A216526] 10 p1328 N90-17673
Lower bounds on multiple-source direction finding in the presence of direction-dependent antenna-array-calibration errors
[AD-A215825] 10 p1376 N90-17979
Experimental and theoretical study of CO2 staggered hollow-bore array lasers
[AD-A212921] 10 p1389 N90-18032
Science requirements for passive microwave sensors on earth science geostationary platforms
12 p1608 N90-19251
Performance of a 300 Mbps 1:16 serial/parallel optoelectronic receiver module
[NASA-TM-103110] 13 p1795 N90-20302
The PHARUS project: Design of a polarimetric C-band SAR in the Netherlands 14 p1961 N90-21228
Concept for a spaceborne Synthetic Aperture Radar (SAR) sensor based on active phased array technology
14 p1962 N90-21234
A motion compensation study for the PHARUS project
14 p1962 N90-21235
Bit-error-rate testing of fiber optic data links for MMIC-based phased array antennas
[NASA-TM-102523] 14 p1966 N90-21261
Coplanar waveguide fed phased array antenna
[NASA-TM-102522] 14 p1968 N90-21273
Optical control of an 8-element Ka-band phased array using a high-speed optoelectronic interconnect
[NASA-TM-102550] 14 p1968 N90-21275
The effect of mechanical deformation on the radiation patterns of large space-based arrays
[AD-A219288] 16 p2230 N90-22719
Low-sidelobe phased array antenna characteristics using the planar near-field Scanning technique: Theory and experiment
[AD-A220611] 17 p2390 N90-23613
High performance millimeter-wave microstrip circulators and isolators
[NASA-CR-186276] 19 p2685 N90-25270
Design of an optically controlled Ka-band GaAs MMIC phased-array antenna
[NASA-TM-103147] 20 p2857 N90-26250
ATDRS payload technology research and development
[NASA-TM-103256] 23 p3287 N90-28596

PHENANTHRENE
Synthesis and chemistry of unsaturated metal nitrogen compounds
[AD-A216550] 12 p1622 N90-19321

PHENOL FORMALDEHYDE
Structure and properties of resorcinol-formaldehyde gels
[DE90-005201] 10 p1358 N90-17876

PHENOLIC EPOXY RESINS
The interface chemistry of phenolic and epoxy adhesives with a model aluminium surface
[MBB-Z-0288-89-PUB] 18 p2531 N90-24441

PHENOLIC RESINS
NT PHENOLIC EPOXY RESINS
Structure and properties of resorcinol-formaldehyde gels
[DE90-005201] 10 p1358 N90-17876
Proceedings of the Advisory Committee on Standardization of Carbon-Phenolic Test Methods and Specifications
[NASA-CR-186478] 15 p2063 N90-21817
Tribomaterial factors in space mechanism brake performance 15 p2114 N90-22096
An examination of impact damage in glass-phenolic and aluminum honeycomb core composite panels
[NASA-TP-3042] 22 p3153 N90-27876

PHENOLS
Organic polyradical models for organic magnetic materials
[AD-A223691] 24 p3442 N90-29435
Progress toward synthesis of polymeric polyradicals
[AD-A223414] 24 p3455 N90-29510

PHENOMENOLOGY
Performance and modeling of superconducting ring resonators at millimeter-wave frequencies
[NASA-TM-102526] 11 p1500 N90-18634
Flux creep in Bi2Sr2CaCu2O8(sub +x) single crystals
22 p3136 N90-27794

PHENYLALANINE
Advanced biosensors for amino acid detection
[AD-A214029] 08 p1076 N90-16225

PHENYLS
NT POLYCHLORINATED BIPHENYLS
NT POLYPHENYLS
High temperature insulators
[AD-D014193] 04 p0479 N90-12751
Bis(4-(3,4-dimethylenepyrrolidyl)-phenyl) methane
[NASA-CASE-LAR-13965-1-CU] 14 p1942 N90-21118
Boron-containing organosilane polymers and ceramic materials thereof
[NASA-CASE-ARC-11649-2-SB] 14 p1952 N90-21177
Acetylene terminated aspartimides and resins therefrom
[NASA-CASE-LAR-14188-1] 17 p2379 N90-23545

PHILOSOPHY
Understanding developments in computer technology: A pragmatic and synthetic interpretation
07 p0971 N90-15608
Remarks on intuitionism and the philosophy of mathematics
[ITLI-LP-88-05] 17 p2440 N90-23901

PHOBIAS
NT FEAR

PHOBOS
Soviet Mars program 02 p0158 N90-10903
Stable orbits about the Martian moons
[AD-A216400] 10 p1447 N90-18352
A robotically constructed production and supply base on Phobos
[NASA-CR-186234] 15 p2073 N90-21872

PHOEBE
Phoebe: A preliminary control network and rotational elements
[NASA-CR-185716] 02 p0295 N90-11680

PHONEMES
Attention and vigilance in speech perception
[AD-A210493] 01 p0095 N90-10539
Triphone clustering in the ARM system
[RSRE-MEMO-4357] 22 p3166 N90-27952
Experiments with grand variance in the ARM continuous speech recognition system
[RSRE-MEMO-4359] 22 p3166 N90-27954

PHONETICS
Attention and vigilance in speech perception
[AD-A210493] 01 p0095 N90-10539
Speech synthesis: From segmental synthesis to acoustic rules, using temporal decomposition
[TELECOM-88-E-019] 10 p1375 N90-17972
A connectionist implementation of cognitive phonology
[AD-A219095] 16 p2264 N90-22906
Speech recognition based on pattern recognition techniques 21 p2993 N90-27011

PHONONS
Quasi-diffusion between phonon and roton gases in two- and three-dimensional liquid helium
[AD-A210565] 02 p0192 N90-11096
Study of disorder and strain in semiconductor heterostructures and superlattices by Raman scattering
02 p0280 N90-11601
On the choice of trial function in theoretical calculations of the thermal conductivity
[DE90-001733] 07 p0897 N90-15182
General many-body systems
[DE90-000685] 07 p0982 N90-15670
Phonons and charge-transfer excitations in HTS superconductors
[DE89-016616] 07 p0997 N90-15768
Cu-O chains in YBa2Cu3O(7-delta) and the phonon mechanism of high-Tc superconductivity
[DE90-603502] 07 p1003 N90-15805
Interface phonons in semiconductor double heterostructures
[AD-A213732] 07 p1003 N90-15810
Phonon anomaly at T(sub c) in (Y/ER)Ba2Cu3O(7-delta)
[DE90-003562] 08 p1129 N90-16539
Electronic properties of GaAs-(Al,Ga)As quasiperiodic
[AD-A214704] 09 p1289 N90-17472
New type of optical bistability in polymers mediated by phonons
[AD-A216102] 10 p1359 N90-17882
Phonon dispersion and Kohn anomalies in the alloy Cu(0.84)Al(0.16)
[DE90-005578] 10 p1428 N90-18239
A modified Moebius inverse formula and its applications in physics
[DE90-612740] 14 p2022 N90-21594
Nonlinear interaction of photons and phonons in electron-positron plasmas
[DE90-009341] 14 p2030 N90-21640
Coupled magnetoplasmon-phonon modes at the surface of a semi-infinite semiconductor superlattice
[DE90-612904] 14 p2031 N90-21647
Millimeter-wave acoustic transducers
[AD-A221402] 18 p2612 N90-24878
Phase-sensitive optical detection of ballistic phonon pulses using frequency-modulation spectroscopy and persistent spectral holes
[AD-A221521] 21 p2979 N90-26930
Coupled bipolarons and optical phonons as a model for high-T(sub c) superconductors
22 p3149 N90-27854
Subpicosecond Raman study of hot electrons and hot phonons in GaAs
[DE90-015634] 24 p3553 N90-30106

PHOSPHATES
NT ADENOSINE TRIPHOSPHATE
NT CALCIUM PHOSPHATES
Polyelectrolyte-diffused zinc phosphate conversion coatings and polyacid coupling primers for corrosion protection of steel and aluminum, and alkali-catalyzed hydrolysis of polyimide-based materials
[AD-A212240] 04 p0480 N90-12754
Activation of methane by transition metal-substituted aluminophosphate molecular sieves
[DE90-005663] 12 p1624 N90-19331
Elimination of platinum inclusions in phosphate laser glasses
[DE90-004479] 12 p1629 N90-19361
Short-range structure of fluorine-modified phosphate glass
[DE90-013494] 20 p2839 N90-26145
High resolution transmission electron microscopy of aluminophosphates
[DE90-015632] 24 p3553 N90-30105

PHOSPHAZENE
Design, characterization, and optical properties of phosphazene-based polymers
[DE90-004111] 08 p1050 N90-16068
A preliminary assessment of 3-Nitro-1,2,4-Triazol-5-One (NTO) as an insensitive high explosive
[AD-A215063] 10 p1360 N90-17889
Synthesis of new polyphosphazene elastomers
[AD-A217585] 13 p1780 N90-20216
Ring expansion and equilibration in organophosphazenes, and the relationship to polymerization
[AD-A218234] 13 p1782 N90-20230
A second-order nonlinear optical poly(organophosphazene)
[AD-A218408] 16 p2210 N90-22607
Second order non-linear optical polyphosphazenes
[AD-A219868] 18 p2615 N90-24895
Fluorescent probe investigation of a water-soluble polyphosphazene
[AD-A222317] 21 p2978 N90-26925

PHOSPHIDES
NT BORON PHOSPHIDES
NT GALLIUM PHOSPHIDES
NT INDIUM PHOSPHIDES

PHOSPHINES
The adsorption and thermal decomposition of PH3 on Si(111)-(7x7)
[AD-A222417] 21 p2978 N90-26927
PH3 surface chemistry on Si(111)-(7x7): A study by Auger spectroscopy and electron stimulated desorption methods
[AD-A221508] 21 p2979 N90-26929

PHOSPHORESCENCE
Mapping of upper electronic reaction surfaces by tuned laser photolysis and by absorption and emission spectroscopies
[DE90-000125] 06 p0741 N90-14314

PHOSPHORIC ACID
Membrane fusion: The role of polyphosphatidylinositol
[AD-A211289] 03 p0379 N90-12156
Electrochemical characteristics of acid electrolytes for fuel cells
[PB90-244385] 24 p3484 N90-29693

PHOSPHORIC ACID FUEL CELLS
Impact of fundamental technical improvements
[PB89-218010] 01 p0083 N90-10472
Improved anode catalysts for coal gas-fueled phosphoric acid fuel cells
[DE90-004016] 08 p1096 N90-16347
Gas cooled fuel cell systems technology development program
[DE90-000446] 12 p1683 N90-19668
Fuel cell systems program plan, FY 1990
[DE90-008178] 14 p2002 N90-21471

PHOSPHORS
Photoelectron pumped phosphors
[AD-A213202] 04 p0505 N90-12912
Solid-state fluorescence above 1000 C: Application to high-temperature laser thermography
[DE90-006422] 11 p1514 N90-18721
Evaluating thermographic phosphors in an operating turbine engine
[DE90-004874] 15 p2105 N90-22044
Engine testing of thermographic phosphors
[DE90-013269] 22 p3182 N90-28059

PHOSPHORUS
The 1-((diorganooxyphosphonyl)-methyl)-2,4- and -2,6-diamido benzenes
[NASA-CASE-ARC-11425-4] 13 p1766 N90-20133
Electron beam induced damage in PECVD Si3N4 and SiO2 films on InP
[NASA-TM-102544] 13 p1810 N90-20393
Some 1-(diorganooxyphosphonyl)methyl-2,4- and -2,6-dinitro-benzenes
[NASA-CASE-ARC-11425-3] 17 p2367 N90-23475
Studies on phosphorus segregation in austenite
[ISBN-952-90-1488-0] 18 p2526 N90-24417
Ion/molecule reactions of arsenic and phosphorus cluster ions: Ionization potentials and novel reaction pathways
[AD-A222019] 21 p2977 N90-26918
Thermographic phosphor technique
24 p3421 N90-29324

PHOSPHORUS COMPOUNDS
NT ADENOSINE TRIPHOSPHATE
NT BORON PHOSPHIDES
NT CALCIUM PHOSPHATES
NT GALLIUM PHOSPHIDES
NT INDIUM PHOSPHIDES
NT ORGANIC PHOSPHORUS COMPOUNDS
NT PHOSPHATES
NT PHOSPHAZENE
NT PHOSPHINES
NT PHOSPHORIC ACID
NT PHOSPHORUS POLYMERS

PHOSPHORUS POLYMERS
A second-order nonlinear optical poly(organophosphazene)
[AD-A218408] 16 p2210 N90-22607

PHOSPHORYLATION
Membrane fusion: The role of polyphosphatidylinositol
[AD-A211289] 03 p0379 N90-12156

PHOTOABSORPTION
Investigations of the interactions of radiation with matter
[AD-A213554] 07 p0991 N90-15723
Fluorescence from photoexcitation of Cl2 at 50 to 105 nm
[NASA-CR-186206] 09 p1189 N90-16888
Absolute vacuum ultraviolet photoabsorption cross section studies of atomic and molecular species: Techniques and observational data
20 p2944 N90-26754
High resolution, low temperature photoabsorption cross-section of C2H2 with application to Saturn's atmosphere 20 p2945 N90-26757

PHOTOACOUSTIC SPECTROSCOPY
A feasibility study for using CARS in temperature and volumetric measurement as a function of time
[ISL-CO-223/88] 09 p1226 N90-17116

PHOTOCATHODES
Enhancement of microchannel plate gain by deposition of CsI on the channel walls
[DE90-003051] 07 p0922 N90-15334
Center for X Ray Optics, 1988
[DE90-003300] 07 p0992 N90-15732
Quantum yield of photocathodes in far and extreme ultraviolet wavelength area
[ETN-90-95731] 12 p1654 N90-19505
Long-term flat-field behavior in LLNL streak cameras: Preliminary results
[DE90-015615] 24 p3472 N90-29621

PHOTOCHEMICAL OXIDANTS
Stratospheric ozone depletion
[PB89-207476] 02 p0238 N90-11354
Proceedings: US/FRG (Federal Republic of Germany) Workshop on Photochemical Ozone Problem and Its Control: US Experiences and the Situation in Europe
[PB89-233514] 05 p0686 N90-13891

PHOTOCHEMICAL REACTIONS
NT PHOTOCHROMISM
NT PHOTODECOMPOSITION
NT PHOTOLYSIS
NT PHOTOSYNTHESIS
Silicon dioxide deposition at 100 deg C using vacuum ultraviolet light
[TR-0088(3945-07)-6] 01 p0047 N90-10269
Paper 1. Impact of volcanic aerosols on stratospheric chemistry. Paper 2. O2 (1 sigma g +) and O2 (1 delta g) in the H + O2 reaction system. Paper 3. Barotropic instability of zonal jets on Mars, Earth and Venus
01 p0084 N90-10477
Photochemically-driven biomimetic oxidation of alkanes and olefins
[DE89-011536] 02 p0193 N90-11097
Two-Dimensional Intercomparison of Stratospheric Models
[NASA-CP-3042] 02 p0248 N90-11405
Report on the 2-D Model Intercomparison Workshop held January 11-16, 1987 in Fort Myers Beach, Florida, chapter 2 02 p0248 N90-11406
Report of the 1988 2-D Intercomparison Workshop, chapter 3 02 p0248 N90-11407
Model documentation, chapter 4
02 p0249 N90-11408
Introduction and data summary, chapter 5
02 p0249 N90-11409
Electron transfer reactions
[AD-A210711] 02 p0271 N90-11545
Methanol fueled vehicles and photochemical models: An evaluation of the state of knowledge
[PB89-214225] 03 p0419 N90-12410
Venus volcanism: Rate estimates from laboratory studies of sulfur gas-solid reactions 03 p0422 N90-12428
Chemical and photochemical reactivity in microemulsions and waterless microemulsions
[AD-A211776] 04 p0470 N90-12692
Photochemical observation of ion flows in membrane channels
[AD-A212449] 04 p0472 N90-12705
Small particle scattering and absorption
[AD-A213168] 04 p0473 N90-12711
The retrieval of the concentrations of nitric oxide and nitrogen dioxide from satellite solar occultation measurements at sunset and sunrise
06 p0814 N90-14733
Characterization of chemicals on engine exhaust particles
[AD-A213566] 07 p0882 N90-15106
Excimer emission from alkali diatomic and alkaline-earth-noble-gas molecules
[AD-A214246] 07 p0896 N90-15179
Interfacial systems for photochemical energy conversion
[DE90-003181] 07 p0953 N90-15514
Photochemical solar energy conversion utilizing semiconductors localized in membrane mimetic systems
[DE90-003450] 07 p0953 N90-15515
NO2 photodissociation dynamics
[AD-A214422] 07 p0962 N90-15560
The chemistry and dynamics of marine stratocumulus
08 p1102 N90-16381
Development of flow visualization and nonintrusive velocity measurement in turbulent flow
[ETN-90-96077] 09 p1161 N90-16717
Initiation precursors and initiators in laser-induced copolymerization of styrene and maleic anhydride in acetone
[NASA-TM-4166] 10 p1346 N90-17810
Photoinduced electron transfer processes in homogeneous and microheterogeneous solutions
[DE90-006048] 10 p1352 N90-17842
Chemistry at clusters, microstructures and surfaces
[AD-A215842] 10 p1353 N90-17844
A 3-D dynamical/chemical GCM for simulating the anthropogenical effects on ozone
[DE90-004836] 10 p1406 N90-18108
Simultaneous observations of the emissions OI (5577), O2A(0.1), NaD(5893) and OH(9.4) and the rotational temperatures TO2 and TOH in the upper atmosphere
[INPE-4851-TDL/368] 10 p1407 N90-18113
Report from upper atmospheric science
10 p1444 N90-18332
Temperature dependence of photon-gated persistent spectral hole-burning for the meso-tetra-p-tolyl Zn-tetrabenzoporphyrin/chloroform system in poly(methylmethacrylate)
[AD-A216086] 11 p1482 N90-18531
Ultrafast chemical dynamics of reactions in beams
[AD-A216319] 11 p1514 N90-18717
Chemical vapor deposition and photochemical vapor deposition of amorphous silicon photovoltaic devices
[DE89-009510] 11 p1529 N90-18803
Study of the atmospheric emissions of OI wavelength 557.7 nm and O2 (0,0) wavelength 761.9 nm in the equatorial region utilizing measurement of photometer on-board a rocket
[INPE-4811-TDL/358] 11 p1533 N90-18827
The role of clouds in the photochemistry of the background troposphere 12 p1688 N90-19694
Biological applications and effects of optical masers
[AD-A217910] 13 p1808 N90-20385
Use of environmental monitoring data in evaluation of atmospheric modeling results
[DE90-008607] 13 p1831 N90-20510
Molecular dynamics and spectroscopy at gas-solid interfaces
[AD-A217743] 13 p1885 N90-20813
Determination of rates of reaction in the gas-phase in the troposphere: Theory and practice. 2: Rate of direct photoreaction: Screening-level test guideline-spectroscopic determination of the cross section and the maximum rate of direct photoreaction in sunlight
[PB90-146291] 15 p2125 N90-22156
Auroral ultraviolet darkening on the outer planets
15 p2192 N90-22518
Interaction of atomic hydrogen with pico- and femtosecond laser pulses
[AD-A218426] 16 p2241 N90-22785
Development and use of a passive technique for measuring nitrogen dioxide in the background atmosphere 16 p2331 N90-23285
The 18th Informal Conference on Photochemistry
[AD-A219779] 17 p2373 N90-23510
Informal conference on the Chemistry of Energetic Azides, Isocyanates, and Related Species
[AD-A219825] 17 p2373 N90-23514
Soluble polysilanes: A new class of radiation sensitive O2-RIE resistant polymers for use in microlithography
[AD-A219476] 17 p2379 N90-23551
Theoretical studies of photochemical methods for semiconductor etching
[AD-A218475] 17 p2475 N90-24151
Electronic and ionic transport in processable conducting polymers
[AD-A221045] 18 p2530 N90-24436
In vitro photoreactivation of transforming DNA of bacillus subtilis spores after irradiation with UV light
[DLR-FB-89-45] 18 p2583 N90-24710
New observations of stratospheric N2O5
[NASA-TM-103478] 20 p2883 N90-26402
A comparison of the contribution of various gases to the greenhouse effect 20 p2885 N90-26414
Measurements of monoterpenes in a coniferous forest
20 p2886 N90-26421
Stratospheric chemistry 20 p2886 N90-26424
Heterogeneous transformation of peroxyacetylnitrate
20 p2887 N90-26430
Soft x ray resist characterization: Studies with a laser plasma x ray source
[DE90-013493] 20 p2928 N90-26661
Laboratory studies, analysis, and interpretation of the spectra of hydrocarbons present in planetary atmospheres including cyanoacetylene, acetylene, propane, and ethane 20 p2943 N90-26748
Absolute vacuum ultraviolet photoabsorption cross section studies of atomic and molecular species: Techniques and observational data
20 p2944 N90-26754
Novel laser gain and time-resolved FTIR studies of photochemistry 20 p2945 N90-26758
Chemical kinetics and modeling of planetary atmospheres 20 p2946 N90-26763
Laboratory measurements and methane photochemistry modeling 20 p2947 N90-26770
UV and VUV spectroscopy and photochemistry of small molecules in a supersonic jet 20 p2947 N90-26771
Laboratory studies of photodissociation processes relevant to the formation of cometary radicals
20 p2947 N90-26772
United States Air Force research initiation program for 1988, volume 1
[AD-A223123] 21 p3101 N90-27613
Photo-sensitized ignition of hydrogen/oxygen mixtures for hypersonic flight vehicles 22 p3163 N90-27935
Tropospheric nitrogen: The influence of anthropogenic sources on distributions and deposition, executive summary
[DE90-015401] 23 p3348 N90-28922
Organic polyradical models for organic magnetic materials
[AD-A223691] 24 p3442 N90-29435
Theoretical investigations and attempted synthesis of organic magnetic polymers and oligomers
[AD-A223409] 24 p3455 N90-29509
Chemical stabilization of laser dyes
[AD-A224219] 24 p3473 N90-29627
Trend analysis of total ozone data
24 p3486 N90-29703

Tropospheric nitrogen: The influence of anthropogenic sources on distributions and deposition
[DE90-015408] 24 p3487 N90-29709

PHOTOCHEMISTRY
U PHOTOCHEMICAL REACTIONS

PHOTOCHROMISM
Analysis and evaluation of technical data on the photochromic and non-linear optical properties of materials
[AD-A214212] 07 p0896 N90-15178
Photochromic papers or films for noncopyable documents
[DE90-004006] 10 p1441 N90-18316
Analysis and evaluation of technical data on the photochromic and non-linear optical properties of materials
[AD-A219398] 16 p2318 N90-23219
All-optical photochromic spatial light modulators based on photoinduced electron transfer in rigid matrices
[NASA-CASE-NPO-17612-1-CU] 21 p3076 N90-27487
Analysis and evaluation of technical data on the photochronic and non-linear optical properties of materials
[AD-A223855] 24 p3545 N90-30053

PHOTOCLINOMETRY
U PHOTOGRAMMETRY

PHOTOCONDUCTIVITY
Physics of high energy photoconductive switches
[AD-A210341] 01 p0060 N90-10345
High power, solid state RF pulse generators
[AD-D014172] 03 p0341 N90-11941
Energy transfer and non-linear optical properties at near ultraviolet wavelengths: Rare earth 4f(yields)5d transitions in crystals and glasses
[DE90-000065] 03 p0405 N90-12321
Subnanosecond linear GaAs photoconductive switching, revision 1
[DE89-017739] 03 p0412 N90-12363
Multiband photoconductive detector based on layered semiconductor quantum wells
[AD-D014232] 06 p0849 N90-14936
Picosecond photoconductivity using a graded bandgap Al(x)Ga(1-x)As active detecting layer
[DE90-003452] 07 p1000 N90-15786
Research on stable high-efficiency, large area, amorphous silicon-based solar cells, phase 2
[DE89-009491] 09 p1242 N90-17208
Transient photoconduction in doped polymers: Spatial and energetic disorder
[ETN-90-95917] 12 p1631 N90-19376
Hot carrier in subpicosecond photoconductive experiments
[AD-A219874] 17 p2477 N90-24166
Research on stable, large-area, amorphous silicon based submodules, phase 3
[DE90-000339] 23 p3399 N90-29204

PHOTOCONDUCTORS
Analysis of the performance of gallium arsenide photoavalanche switches
[DE89-015774] 01 p0129 N90-10739
Development of FIR arrays with integrating amplifiers 05 p0598 N90-13473
Avalanche photoconductive switching
[DE90-002980] 07 p0922 N90-15337
Interfacial and thin film chemistry in electron device fabrication
[AD-A214784] 09 p1289 N90-17473
High performance, picosecond radiation detectors grown by molecular beam epitaxy for millimeter-wave diagnostic systems
[DE90-005547] 10 p1438 N90-18302
Stressed Ge:Ga photoconductors for space-based astronomy. (Is there life beyond 120 micron) 14 p1975 N90-21315
Near contact phenomena and transient effects in far infrared photoconductors 14 p1976 N90-21316
Germanium Blocked Impurity Band (BIB) detectors 14 p1976 N90-21321
Ga:Ge array development 14 p1977 N90-21323
Stressed detector arrays for airborne astronomy 14 p1978 N90-21332
Initial astronomical results with a new 5-14 micron Si:Ga 58x62 DRO array camera 14 p1978 N90-21334
Status of the isophot detector development 14 p1980 N90-21342
ISO/LWS: Detector status 14 p1980 N90-21343
Fast acting optical beam deflection system
[AD-A220186] 17 p2473 N90-24141
Integration of picosecond GaAs photoconductive devices with silicon circuits for optical clocking and interconnects
[DE90-012096] 21 p3080 N90-27512

PHOTOCURRENTS
U ELECTRIC CURRENT
U PHOTOELECTRIC EMISSION

PHOTODECOMPOSITION
An investigation of the degradation and stabilization of polymer systems
[AD-A210362] 01 p0049 N90-10282
Plasma modification of poly (p-phenylenebenzobisthiazole)
[AD-A215761] 10 p1433 N90-18272
The 16-O photodisintegration at low energies
[NOTA-INTERNA-941] 16 p2315 N90-23196
Relativistic corrections to He-3 photodisintegration sum rules
[NOTA-INTERNA-942] 16 p2315 N90-23197

PHOTODETACHMENT
Transition state spectroscopy of hydrogen transfer reactions
[AD-A215041] 09 p1191 N90-16901
Electron production, electron attachment, and charge recombination process in high pressure gas discharges
[AD-A216301] 10 p1434 N90-18274
Femtosecond studies of electron photodetachment of simple ions in liquid water: Solvation and geminate recombination dynamics
[AD-A218520] 16 p2215 N90-22634
Threshold photodetachment spectroscopy of the I + HI transition state region
[AD-A218410] 16 p2260 N90-22883
Experimental investigations of low-energy (4 to 40 eV) collisions of O(-)(P2) ions and O(P3) atoms with surfaces 19 p2732 N90-25530

PHOTODETECTORS
U PHOTOMETERS

PHOTODIODES
Switched power workshop: Introduction and summary
[DE90-000036] 03 p0342 N90-11952
Optical communication with semiconductor laser diode
[NASA-CR-185886] 05 p0647 N90-13770
High-efficiency large-area CdTe modules
[DE89-009498] 06 p0806 N90-14689
Method of sensitizing PB-Salt epitaxial films for Schottky diodes
[AD-D014244] 06 p0850 N90-14937
Research on materials and components for opto-electronic signal processing and computing
[AD-A213740] 07 p1003 N90-15811
Bioluminescence for detection of trace compounds
[AD-A213458] 09 p1189 N90-16889
NASA Laser Light Scattering Advanced Technology Development Workshop, 1988
[NASA-CP-10033] 09 p1221 N90-17085
Photon counting modules using RCA silicon avalanche photodiodes 09 p1222 N90-17089
Study and implementation of a monolithic photoreceiver integrating a photodiode and a junction field effect transistor in GaInAs with polarization resistance
[IDI-18902] 10 p1379 N90-17990
Current status of InAsSb strained layer superlattice infrared detectors: Demonstration of a high detectivity, 10 micron photodiode
[DE90-000800] 10 p1434 N90-18276
State of the art in semiconductor detectors
[DE90-005567] 11 p1512 N90-18706
Contact formation on (Hg,Cd) Te
[AD-A217088] 12 p1723 N90-19900
NRL hybrid reliability. Physics of failure initial study
[AD-A217986] 13 p1898 N90-20893
Bioluminescence for detection of trace compounds
[AD-A219435] 17 p2372 N90-23503
Investigations of laterally coupled all optical switches and detectors on silica fibers
[AD-A220297] 17 p2473 N90-24142
Heterodyne characterization of high-speed photomixers for the ultraviolet
[AD-A220914] 18 p2547 N90-24538
Tin doping of InSb grown by MOCVD using tetraethyltin
[DE90-009727] 18 p2620 N90-24929
Improving the performance of InAs(1-x)Sb(x)/InSb infrared detectors grown by metal organic chemical vapor deposition
[DE90-009743] 18 p2625 N90-24956
Optical techniques for determination of normal shock position in supersonic flows for aerospace applications
[NASA-TM-103201] 19 p2693 N90-25323
Tracking a head-mounted display in a room-sized environment with head-mounted cameras
[AD-A222545] 21 p3037 N90-27266
Radiation effects in InAsSb strained-layer superlattice photodiodes induced by dose-rate and transient x ray environments
[DE90-015000] 23 p3400 N90-29208

PHOTODISSOCIATION
Photodissociation of XeF2 (xenon difluoride) at 193 nm
[AD-A211663] 04 p0506 N90-12916
New calculations of photodissociation cross-sections in the O2 Schumann-Runge system 05 p0657 N90-13834
NO2 photodissociation dynamics
[AD-A214422] 07 p0962 N90-15560
Photodissociation regions: Observations and theory 11 p1579 N90-19098
IR line emission from dense photodissociation regions 11 p1580 N90-19100
DURIP FTIR studies of solid state reaction dynamics
[AD-A217713] 13 p1773 N90-20174
DURIP theoretical/experimental investigations of highly energetic dication species
[AD-A217771] 13 p1808 N90-20383
Electronically metastable molecules of high symmetry
[AD-A217768] 13 p1885 N90-20814
The 18th Informal Conference on Photochemistry
[AD-A219779] 17 p2373 N90-23510
Photodissociation of O2 in the stratosphere and mesosphere: A general parametrization of the Schumman-Runge Bands 20 p2887 N90-26427
Absolute vacuum ultraviolet photoabsorption cross section studies of atomic and molecular species: Techniques and observational data 20 p2944 N90-26754
Laboratory studies of photodissociation processes relevant to the formation of cometary radicals 20 p2947 N90-26772
Optical signatures of molecular particles via mass-selected cluster spectroscopy 20 p2949 N90-26780
Resonance enhanced two-laser infrared multiple photon dissociation of gaseous ions
[AD-A221826] 21 p2970 N90-26879
Photo-sensitized ignition of hydrogen/oxygen mixtures for hypersonic flight vehicles 22 p3163 N90-27935
The mesospheric responses to short-term solar ultraviolet variability 22 p3204 N90-28174

PHOTOELASTIC ANALYSIS
The stress analysis of thin-walled screwed tubular joints 06 p0796 N90-14637
A photoelastic analysis of the strain field around impact damage in a graphite fibre reinforced panel subjected to compression loads
[FFA-TN-1989-48] 19 p2703 N90-25379

PHOTOELASTIC STRESS MEASUREMENT
U PHOTOELASTIC ANALYSIS

PHOTOELASTICITY
Micro-miniature roll rate sensor
[AD-A214778] 09 p1225 N90-17107
Stress field near crack tip: An experimental evaluation of the three dimensional variation
[AD-A217878] 13 p1818 N90-20441
A spectral analysis approach to wave propagation in layered solids 15 p2120 N90-22131
Nondestructive measurement of residual stresses in aircraft transparencies
[AD-A218680] 17 p2415 N90-23782
Photoelasticity: A cost effective design tool 21 p2958 N90-26819

PHOTOELECTRIC CATHODES
U PHOTOCATHODES

PHOTOELECTRIC CELLS
NT PHOTOVOLTAIC CELLS
NT SOLAR CELLS

PHOTOELECTRIC EFFECT
NT PHOTOCONDUCTIVITY
NT PHOTOELECTRIC EMISSION
NT PHOTOIONIZATION
NT PHOTOVOLTAIC EFFECT
Technology of fast spark gaps
[AD-A214199] 07 p0925 N90-15353
Metal coordination polymers as potential high-energy lithographic resists
[AD-A216668] 11 p1490 N90-18574

PHOTOELECTRIC EMISSION
Superconductivity from valence fluctuations with finite U
[DE89-015302] 01 p0129 N90-10742
On the photoemission spectrum and optical gap in La2CuO4
[DE89-015281] 02 p0281 N90-11605
A fermi liquid electric structure and the nature of the carriers in high-T(sub c) cuprates: A photoemission study
[DE89-016774] 02 p0284 N90-11624
State-resolved reaction dynamics
[AD-A211613] 03 p0403 N90-12307
Surface, interface, and bulk properties of high T(sub c) superconductors
[AD-A211490] 03 p0413 N90-12373
High resolution-angle resolved photoemission studies of high temperature superconductors
[DE89-017691] 06 p0852 N90-14950

International Conference on Materials and Mechanisms of Superconductivity: High Temperature Superconductors
[AD-A215343] 09 p1290 N90-17480
Normal state electronic structure and the superconducting energy gap in HTSC's as determined from photoemission spectroscopy
[DE90-004857] 09 p1292 N90-17489
Research investigation directed toward extending the useful range of the electromagnetic spectrum
[AD-A217460] 13 p1789 N90-20267
Surface-plasmon enhanced nonlinear photoelectric emission from thin silver films
[DE90-007676] 13 p1884 N90-20807

PHOTOELECTRIC GENERATORS
NT PHOTOVOLTAIC CELLS
NT SOLAR CELLS

PHOTOELECTRIC MATERIALS
Photoelectrochemical behavior of type n of GaAs in concentrated iodide media and realization of an experimental device
[ECL-88-18] 05 p0703 N90-14117

PHOTOELECTRICITY
NT PHOTOCONDUCTIVITY
NT PHOTOELECTRIC EFFECT
NT PHOTOELECTRIC EMISSION
NT PHOTOIONIZATION
NT PHOTOVOLTAIC EFFECT
QCD Compton scattering at HERA energy
[NIKHEF-H/89-3] 15 p2165 N90-22372
Structural and electronic studies of a:SiGe:H alloys
[DE90-000313] 19 p2710 N90-25424
A fast lightstripe rangefinding system with smart VLSI sensor 23 p3366 N90-29019

PHOTOELECTROCHEMICAL DEVICES
Photoelectrochemical behavior of type n of GaAs in concentrated iodide media and realization of an experimental device
[ECL-88-18] 05 p0703 N90-14117

PHOTOELECTROCHEMISTRY
Perfluorinated ligands in organometallic chemistry
[AD-A216415] 11 p1476 N90-18493
Studies of photochemically and electrochemically driven electron transport in zeolites
[DE90-007659] 12 p1624 N90-19335
Scanning laser photocurrent spectroscopy of electrochemically grown bismuth sulphide films
[AERE-M-3709] 16 p2217 N90-22649
Characterization by means of electrochemical impedance measurement and optoelectrochemical analysis of electrolytic, insulating, and semiconducting solution structures. Development of a cartographic analysis method for optoelectrochemical impedance
[ECL-89-15] 17 p2474 N90-24144

PHOTOELECTROMAGNETIC DETECTORS
U RADIATION MEASURING INSTRUMENTS

PHOTOELECTRON SPECTROSCOPY
High temperature and high resolution UV photoelectron spectroscopy using supersonic molecular beams
[DE90-000176] 03 p0323 N90-11835
Synthesis conductivity, and x ray photoelectron spectrum of Bi2Sr2Cu(sub 7+x). A new ternary bismuth-oxide system exhibiting metallic conductivity
[DE90-003010] 07 p0999 N90-15778
Transition state spectroscopy of hydrogen transfer reactions
[AD-A215041] 09 p1191 N90-16901
Photoelectron spectroscopic study of the interaction of thin Fe films with the MoS2(0001) surface
[AD-A214348] 10 p1351 N90-17836
Understanding electronegative effects in core-level electron spectroscopies; application to the high temperature superconductors
[AD-A216728] 11 p1570 N90-19037
Infrared and X ray photoelectron spectroscopy studies of the polyimide/metal interface
[AD-A218249] 13 p1773 N90-20179
Surface physics instrumentation
[AD-A220460] 17 p2373 N90-23512
Photoelectron spectroscopy at limit surfaces of semiconductors with rare Earth and alkali metals
[ETN-90-97322] 22 p3249 N90-28427
Preliminary exposure study to determine the effects of acid deposition on coated steel substrates
[PB90-201799] 23 p3309 N90-28715

PHOTOELECTRONICS
U PHOTOELECTRICITY

PHOTOELECTRONS
Photoelectron pumped phosphors
[AD-A213202] 04 p0505 N90-12912
A Scanning Photoelectron Microscope (SPEM) at the National Synchrotron Light Source (NSLS)
[DE90-001551] 06 p0780 N90-14537

PHOTOEMISSION
U PHOTOELECTRIC EMISSION

PHOTOEMISSIVITY
U EMISSIVITY
U PHOTOELECTRIC EMISSION

PHOTOEMITTERS
U PHOTOELECTRIC MATERIALS

PHOTOGEOLOGY
An attempt to draw conclusions from the vegetation to the geological underground in the area of Amberg (Germany, F.R.) by means of digital image processing of TM data
[DFVLR-FB-89-24] 04 p0515 N90-12974
Analysis of photogeologic lineaments in the Ithacare (BA) region: A proposed methodology
[INPE-4855-PRE/1478] 12 p1677 N90-19635

PHOTOGRAMMETRY
Applications of artificial intelligence to digital photogrammetry 02 p0262 N90-11486
Focal research effort points of the Institute of Applied Geodesy in the field of digital image processing 08 p1094 N90-16333
Applications of the GPS in photogrammetry
[ETN-90-96004] 12 p1680 N90-19648
Committee on Geodesy - National Research Council
[AD-A217770] 13 p1821 N90-20452
Space environment robot vision system 15 p2143 N90-22245
Large scale metrology by computer assisted photogrammetry
[REPT-892-430-116] 16 p2239 N90-22772
The use of additional Global Positioning System (GPS) observations in large scale photogrammetry
[ETN-90-96693] 17 p2418 N90-23778

PHOTOGRAPH INTERPRETATION
U PHOTOINTERPRETATION

PHOTOGRAPHIC EMULSIONS
NT NUCLEAR EMULSIONS

PHOTOGRAPHIC EQUIPMENT
NT CAMERAS
NT DIFFRACTION LIMITED CAMERAS
NT FAINT OBJECT CAMERA
NT FRAMING CAMERAS
NT HIGH SPEED CAMERAS
NT SCHMIDT CAMERAS
NT STREAK CAMERAS
NT TELEVISION CAMERAS

PHOTOGRAPHIC FILM
Development of X diagnostics around the pulse 1 laser 06 p0787 N90-14580

PHOTOGRAPHIC MEASUREMENT
NT PHOTOGRAMMETRY

PHOTOGRAPHS
NT MARS PHOTOGRAPHS
NT MICROPHOTOGRAPHS
NT MOTION PICTURES
Debris/ice/TPS assessment and photographic analysis for Shuttle Mission STS-33R
[NASA-TM-102785] 09 p1180 N90-16846
Fracture analysis through photographic imagery of low spatial resolution: A contribution to the study of tectonic evoluation of the Araripe Plateau region
[INPE-4876-PRE/1487] 11 p1520 N90-18756
Recognizing three-dimensional objects without the use of models
[AD-A216766] 11 p1540 N90-18862
Characterization of linear structures from remote sensing data; Espinhaco Meridional (MG) sierra
[INPE-4905-PRE/1506] 14 p1997 N90-21449
Geology of Espinhaco Meridional, including the Quadrilatero Ferrifero: integration through remote sensing data
[INPE-4904-PRE/1505] 14 p1998 N90-21450
Debris/ice/TPS assessment and photographic analysis for Shuttle Mission STS-36
[NASA-TM-102789] 16 p2205 N90-22583
Periphery camera system
[AD-A221281] 18 p2555 N90-24583
Video photographic considerations for measuring the proximity of a probe aircraft with a smoke seeded trailing vortex
[NASA-TM-102691] 19 p2657 N90-25120
Debris/ice/TPS assessment and photographic analysis for shuttle mission STS-31R
[NASA-TM-102790] 20 p2819 N90-26040
Stenopic radiography: A non-destructive test without contact 22 p3187 N90-28086
Multiband imaging systems
[AD-A223969] 23 p3343 N90-28893
National Archives preservation research priorities: Past and present
[PB90-206210] 23 p3405 N90-29242

PHOTOGRAPHY
NT ACOUSTICAL HOLOGRAPHY
NT AERIAL PHOTOGRAPHY
NT ALL SKY PHOTOGRAPHY
NT ASTRONOMICAL PHOTOGRAPHY
NT AUTORADIOGRAPHY
NT CINEMATOGRAPHY
NT COLOR PHOTOGRAPHY
NT FRACTOGRAPHY
NT FRAME PHOTOGRAPHY
NT HIGH SPEED PHOTOGRAPHY
NT HOLOGRAPHY
NT INFRARED IMAGERY
NT INFRARED PHOTOGRAPHY
NT MULTISPECTRAL PHOTOGRAPHY
NT ORTHOPHOTOGRAPHY
NT PHOTOMICROGRAPHY
NT SATELLITE-BORNE PHOTOGRAPHY
NT SCHLIEREN PHOTOGRAPHY
NT SHADOWGRAPH PHOTOGRAPHY
NT SPACEBORNE PHOTOGRAPHY
NT STEREOPHOTOGRAPHY
NT STEREOSCOPY
NT STREAK PHOTOGRAPHY
NT ULTRAVIOLET PHOTOGRAPHY
NT UNDERWATER PHOTOGRAPHY
NT WHITE LIGHT HOLOGRAPHY
Orbital remote sensing in the decade of the nineties: New approaches and challenges in geology
[INPE-4838-PRE/1467] 11 p1521 N90-18758
Spacecraft optical contamination environment
[AD-A218088] 13 p1889 N90-20838
A manual for analysis of hemispherical canopy photography
[DE90-014718] 23 p3342 N90-28885

PHOTOINTERPRETATION
Computer-aided boundary delineation of agricultural lands
[NASA-TM-102243] 08 p1091 N90-16313
Study of alteration covers of part of the Sao Paulo State through remote sensing data
[INPE-4849-TDL/364] 10 p1399 N90-18086
Remote sensing in agriculture: Basic concepts, methodology and applications
[INPE-4806-MD/39] 10 p1399 N90-18088
Photointerpretation with instruments for evaluation of environmental impact: Mata Atlantica in Cubata
[INPE-4910-PRE/1511] 11 p1531 N90-18817
LANDSAT-5 data in the study of wheat and bean crops
[INPE-4746-RPE/580] 13 p1819 N90-20444
A system for analysis and interpretation of lineaments in remote sensing images
[INPE-4893-PRE/1494] 13 p1840 N90-20565
Monitoring of agrocattle-raising projects through visual/digital analysis of LANDSAT-TM imagery south of Para state
[INPE-4982-PRE/1542] 14 p1996 N90-21442
Survey of land use through remote sensing
[INPE-5032-MD/042] 14 p1996 N90-21443
Comparison of methods of space color transformations for enhancement of colored images
[INPE-4977-PRE/1542] 23 p3341 N90-28881

PHOTOIONIZATION
Synchrotron-radiation experiments with recoil ions
[DE89-017579] 03 p0402 N90-12301
Energy transfer and non-linear optical properties at near ultraviolet wavelengths: Rare earth 4f(yields)5d transitions in crystals and glasses
[DE90-000065] 03 p0405 N90-12321
Electron attachment and molecular fragmentation in laser-excited plasmas
[AD-A212098] 03 p0409 N90-12343
Oxygen and other atmospheric gases
[AD-A214296] 07 p0961 N90-15557
Investigations of the interactions of radiation with matter
[AD-A213554] 07 p0991 N90-15723
New approach to omega PPCs (Propagation Corrections)
[AD-A215610] 09 p1207 N90-17000
Studies of atmospheric molecules by multiphoton spectroscopy
[DE90-005829] 11 p1534 N90-18833
An implication of the IR identification of PAHs: The heating of the diffuse is gas 11 p1582 N90-19113
DURIP FTIR studies of solid state reaction dynamics
[AD-A217713] 13 p1773 N90-20174
Atmospheric chemiluminescence: COCHISE and FACELIF experiments
[AD-A218121] 13 p1843 N90-20578
Electronically metastable molecules of high symmetry
[AD-A217768] 13 p1885 N90-20814
Spectrum formation in active galactic nuclei and Type 2 supernovae 15 p2187 N90-22490
Measurements and simulation of controlled beamfront motion in the Laser Controlled Collective Accelerator
[DE90-009992] 16 p2240 N90-22780
Infrared coronal line novae 16 p2339 N90-23328
The 18th Informal Conference on Photochemistry
[AD-A219779] 17 p2373 N90-23510

Prediction of high-voltage, broadband RF pulse generation from an air gas avalanche switch
[DE90-010183] 18 p2549 N90-24551
Spectral signatures of X ray photoionized nebulae 19 p2778 N90-25800
Formation and deactivation of vibrationally excited atmospheric molecules
[AD-A222660] 20 p2889 N90-26442
Role of the methylene amidogen (H2CN) radical in the atmospheres of Titan and Jupiter 20 p2947 N90-26769
Diagnostics for hydrogen atoms and molecules in H-atom sources and beams using VUV laser light
[AD-A222340] 21 p3074 N90-27476
Detection of vibrationally excited H2(v double prime) for H(-) production
[AD-A222560] 22 p3180 N90-28044
Fifteenth International Conference on X Ray and Inner-Shell Processes
[DE90-013024] 23 p3393 N90-29170
A plasma diagnostic study of two wind-blown shell nebulae: NGC 7635 and NGC 2359 23 p3410 N90-29271
Formation of hydrogen line and continuum emission in young stellar objects 24 p3562 N90-30150

PHOTOLITHOGRAPHY
Characterization of 4/3 technology large-scale integrated circuit on polysilicon processes
[BDX-613-3971] 01 p0059 N90-10335
Negative-working electron beam resist based on poly(methyl methacrylate)
[AD-A207834] 01 p0128 N90-10733
Photolithography: A new tool for ceramic science
[DE90-000135] 03 p0331 N90-11885
Critical and subcritical crack-growth behavior along toughened ceramic/metal interfaces 07 p0889 N90-15140
Research on GaAs quantum-coupled structures that can be used as electron devices
[AD-A214015] 07 p0924 N90-15350
Photoresponse of YBa2Cu3O(7-delta) granular and epitaxial superconducting thin films
[NASA-TM-103144] 16 p2231 N90-22732
Soluble polysilanes: A new class of radiation sensitive O2-RIE resistant polymers for use in microlithography
[AD-A219476] 17 p2379 N90-23551
Application of microdesigned interfaces to studies of ceramic processing
[DE90-011633] 21 p2983 N90-26951
Flux motion effects in Tl-Ca-Ba-Cu-O thin films
[DE90-012176] 21 p3080 N90-27514
Dynamical properties of two-dimensional Josephson junction arrays
[AD-A223965] 23 p3402 N90-29221

PHOTOLUMINESCENCE
NT X RAY FLUORESCENCE
Radiationless transitions and excited-state absorption of low-field chromium complexes in solids
[AD-A210653] 02 p0194 N90-11105
Luminescence in applied magnetic fields
[AD-A211551] 03 p0399 N90-12287
Elaboration and characterization of MISFET transistors on InP
[ECL-88-19] 05 p0636 N90-13709
Study of surface uniformity of semiconductors 3 to 5 by photoluminescence imagery
[EGL-88-15] 05 p0703 N90-14116
GaAs and GaAs:In: Influence of surface treatments and characterization of homogeneity by photoluminescent imagery
[ECL-88-24] 05 p0704 N90-14118
Spectroscopic techniques for the analysis of CdTe substrates used for the growth of HgCdTe
[AD-A214545] 09 p1288 N90-17466
Excited state lifetime measurements of ytterbium in indium phosphide
[AD-A215709] 09 p1291 N90-17483
Low temperature photoluminescence study of uranium implanted into III-V semiconductors and AlGaAs
[AD-A215710] 09 p1291 N90-17484
Selective excitation luminescence and photoluminescence investigations of ytterbium doped InP, GaAs and AlGaAs
[AD-A215713] 09 p1291 N90-17485
Luminescence of lanthanides and actinides implanted into binary III-V semiconductors and AlGaAs
[AD-A215759] 11 p1569 N90-19031
The possible presence of interstellar PAHs in meteorites and interplanetary dust particles 21 p3092 N90-27579
Subpicosecond Raman study of hot electrons and hot phonons in GaAs
[DE90-015634] 24 p3553 N90-30106

PHOTOLYSIS
An investigation of the degradation and stabilization of polymer systems
[AD-A210362] 01 p0049 N90-10282
Photolysis of spacecraft contaminants
[AD-A211715] 03 p0317 N90-11801
Spin-orbit relaxation rates of Bi(6p(3)) 2D(3/2) following photolysis of Bi(CH3)3 at lambda = 193 nm
[AD-A211792] 03 p0402 N90-12303
Photodissociation of XeF2 (xenon difluoride) at 193 nm
[AD-A211663] 04 p0506 N90-12916
Corrections for non-ideal effects in reflected shock waves at low Mach numbers
[DE90-002192] 06 p0721 N90-14208
Mapping of upper electronic reaction surfaces by tuned laser photolysis and by absorption and emission spectroscopies
[DE90-000125] 06 p0741 N90-14314
Studies of photochemically and electrochemically driven electron transport in zeolites
[DE90-007659] 12 p1824 N90-19335
Infrared absorption spectroscopy and chemical kinetics of free radicals
[DE90-009469] 15 p2067 N90-21837
UV photo-enhanced MOCVD of cadmium and cadmium telluride
[RSRE-MEMO-4208] 15 p2174 N90-22422
IR transition moments and collisional dynamics of vibrationally excited OH radicals via time-resolved laser absorption spectroscopy
[AD-A221005] 18 p2580 N90-24696
Photodissociation of NO2: Influence of photolysis wavelength and temperature dependence on product formation 20 p2887 N90-26426
Rate constant for reaction of atomic hydrogen with germane 20 p2947 N90-26768
Laboratory simulation of interstellar grain chemistry and the production of complex organic molecules 21 p3092 N90-27580

PHOTOMAPPING
Introduction of aerial photography in agricultural research
[BCRS-89-14] 11 p1526 N90-18784
Digital processing of TM/LANDSAT data in monitoring interior water
[INPE-4956-PRE/1533] 14 p1997 N90-21448
Topographic mapping from SPOT satellite imagery
[ETN-90-96689] 17 p2418 N90-23777
Method to image high speed events using a standard video camera
[AD-D014556] 22 p3177 N90-28030

PHOTOMAPS
Height and gradient from shading
[AD-A212338] 04 p0504 N90-12908

PHOTOMETERS
NT TOTAL OZONE MAPPING SPECTROMETER
NT ULTRAVIOLET SPECTROMETERS
Adaptive machine vision
[AD-A208130] 01 p0076 N90-10436
Characterization of GaAs/Si/GaAs heterointerfaces
[DE89-016302] 01 p0131 N90-10752
Laser physics and laser techniques
[AD-A211117] 02 p0227 N90-11302
SWAN: A study of solar wind anisotropies 04 p0568 N90-13312
Optical communication with semiconductor laser diode
[NASA-CR-185886] 05 p0647 N90-13770
Multiband photoconductive detector based on layered semiconductor quantum wells
[AD-D014232] 06 p0849 N90-14936
Optical paramagnetic/diamagnetic gas sensor
[AD-D014368] 12 p1663 N90-19554
Mercuric iodide room temperature gamma-ray detectors
[NASA-TM-103318] 13 p1804 N90-20357
Ga:Ge array development 14 p1977 N90-21323
Initial astronomical results with a new 5-14 micron Si:Ga 58x62 DRO array camera 14 p1978 N90-21334
Alternating gradient photodetector
[NASA-CASE-NPO-17235-1-CU] 14 p1982 N90-21358
Innovative techniques for high-resolution imaging and precision tracking
[AD-A221380] 18 p2616 N90-24899
Multicolor infrared photodetector
[AD-D014511] 20 p2865 N90-26297
Light source for dynamic testing of photo detectors
[FEL-1989-69] 22 p3247 N90-28414

PHOTOMETRY
NT ASTRONOMICAL PHOTOMETRY
NT INFRARED PHOTOMETRY
NT SPECTROPHOTOMETRY
NT STELLAR SPECTROPHOTOMETRY
Spatial characteristics of airglow and solar scatter radiance from the earth's atmosphere
[AD-A211358] 03 p0372 N90-12126
On-ground photometric calibration 05 p0605 N90-13523
Minor planets and other solar system objects 05 p0608 N90-13545
Overview of the Tycho data analysis 05 p0610 N90-13558
Photometry: Main mission and Tycho 05 p0610 N90-13560
Double star reductions in NDAC 05 p0610 N90-13561
Photometric analyses of abundances in dwarf spheroidal galaxies and globular clusters 12 p1736 N90-19978
InSb DRO array characteristics 14 p1977 N90-21326
AFGL ten micron mosaic array spectrometer: Recent results 14 p1978 N90-21333
Introduction to the Infrared Space Observatory (ISO) 14 p1979 N90-21340
Analysis of gamma squared Velorum photometry from the South Pole 15 p2183 N90-22472
Retention index monitoring of volatile organic compounds using thermal desorption gas chromatography
[AD-A221117] 18 p2521 N90-24397
Large scale structure and microwave background anisotropies in cosmological models and stellar photometry techniques with the wide field/planetary camera of the Hubble space telescope 18 p2637 N90-25023
Dynamic and photometric evolutionary models of tidal tails and ripples 18 p2637 N90-25024
UBVRI-photopolarimetry and the X ray dips of V471 Tau 19 p2775 N90-25781
The long-term optical behaviour of X Per = 3U 0352+30 19 p2776 N90-25783
SIRTF: Probing the dark corners of the galaxy 21 p3091 N90-27577
Infrared observations of the solar system in support of Large Aperture Infrared Telescope (LARITS): Calibration
[AD-A222222] 21 p3097 N90-27597

PHOTOMICROGRAPHY
Research project in microelectronic engineering and imaging science
[DE90-006907] 11 p1503 N90-18653

PHOTOMULTIPLIER TUBES
Report on the performance and operating characteristics of the Burle C83061E QUANTACON (trademark) photomultiplier tube
[DE89-015257] 01 p0058 N90-10333
Photoelectron pumped phosphors
[AD-A213202] 04 p0505 N90-12912
The solid state photomultiplier: Status of photon counting beyond the near-infrared 14 p1976 N90-21319
Microchannel photomultipliers in time spectrometer
[DE90-616417] 14 p1982 N90-21356
CMOS analog four-quadrant multiplier
[AD-D014507] 19 p2685 N90-25271

PHOTON BEAMS
B factory via conversion of 1 TeV electron beams into 1 TeV photon beams
[DE89-017692] 04 p0505 N90-12914
Multilayer optical elements for generation and analysis of circularly polarized x rays
[DE90-006103] 10 p1430 N90-18250
A study of the interaction of light with surfaces of sub-micron dimensions
[DE90-006646] 11 p1571 N90-19048
Transient annealing characterization of irradiated MOSFETS
[AD-A223877] 23 p3401 N90-29220

PHOTON DENSITY
Production of photons in anisotropic spacetimes
[DE90-600760] 08 p1135 N90-16576
Hard X ray observations of AGN 19 p2791 N90-25889

PHOTON-ELECTRON INTERACTION
International workshop on Beam Injection Assessment of Defects in Semiconductors
[AD-A210842] 02 p0283 N90-11617
B factory via conversion of 1 TeV electron beams into 1 TeV photon beams
[DE89-017692] 04 p0505 N90-12914

PHOTONEUTRONS
The 16-O photodisintegration at low energies
[NOTA-INTERNA-941] 16 p2315 N90-23196

PHOTONIC PROPULSION
NT LASER PROPULSION

PHOTONIC SWITCHING
U OPTICAL SWITCHING

PHOTONICS
Optical Bistability, 1988
[AD-A217681] 13 p1888 N90-20832

Electronic and photonic power applications
[DE90-015567] 24 p3485 N90-29698

PHOTONS
Two photon absorption characterization
[AD-A210508] 01 p0121 N90-10694
Dielectronic excitation and recombination in crystal channels
[DE89-016864] 02 p0284 N90-11625
Solar opacities constrained by solar neutrinos and solar oscillations
[DE89-016988] 02 p0297 N90-11687
Quantitative interpretation of auger lineshapes and electron/photon stimulated desorption
[AD-A211550] 03 p0324 N90-11842
Laser production of soft x rays by multiquantum processes and the excitation of atomic inner-shell states
[AD-A211372] 03 p0353 N90-12021
Measurement of the light flux density patterns from luminaires proposed as photon sources for photosynthesis during space travel
[NASA-CR-186124] 05 p0672 N90-13916
Measurement of the fractional momentum carried by the glutons in the low Q squared photon-gluon fusion events at the ep HERA collider
[NOTA-INTERNA-937] 05 p0698 N90-14083
Nonresonant and resonant multiphoton ionization of (NO)(sub n) and Ar(sub n)NO clusters with picosecond laser pulses
[DE89-016853] 06 p0791 N90-14607
Is the number of photons conserved in an expanding universe
[DE89-618836] 06 p0864 N90-15018
NO2 photodissociation dynamics
[AD-A214422] 07 p0952 N90-15560
Photon counting modules using RCA silicon avalanche photodiodes 09 p1222 N90-17089
Persistant spectral hole-burning: Photon-gating and fundamental statistical limits
[AD-A216084] 11 p1501 N90-18640
Angular correlation studies in noble gases 11 p1557 N90-18972
Research in theoretical physics
[DE90-005558] 11 p1562 N90-19001
Photon statistical limitations for daytime optical tracking 12 p1643 N90-19442
The EGS4 Code System: Solution of gamma-ray and electron transport problems
[DE90-008100] 12 p1713 N90-19838
All-fiber SFPM (Stimulated Four Photon Mixing) amplifier
[AD-D014358] 12 p1713 N90-19841
Toward higher order tests of the gravitational interaction 12 p1731 N90-19948
Research investigation directed toward extending the useful range of the electromagnetic spectrum
[AD-A217460] 13 p1789 N90-20267
Determinations of photon spectra
[AD-A218003] 13 p1885 N90-20816
Fundamental studies of photon statistics
[AD-A217825] 13 p1888 N90-20836
On the creation of gravitational wave by photon in external electromagnetic field
[DE90-613366] 14 p1967 N90-21265
The solid state photomultiplier: Status of photon counting beyond the near-infrared 14 p1976 N90-21319
Gamma-ray production cross section measurements using a white neutron source from 1 to 400 MeV
[DE90-008906] 14 p2025 N90-21610
Nonlinear interaction of photons and phonons in electron-positron plasmas
[DE90-009341] 14 p2030 N90-21640
Problems in radiative transfer in astrophysics: An escape probability treatment of line overlap and a model of the masers around VX Sgr 14 p2041 N90-21705
Horizon problem in cosmological models with non zero
[DE90-613367] 14 p2042 N90-21708
Exclusive production of p, p-, pi, and pi- in photon photon collisions
[NIKHEF-H/89-9] 15 p2165 N90-22376
The illusive Geminga: What is it 16 p2335 N90-23307
Dose analysis of the model 112A Pulserad pulsed x ray generator by its CYLTRAN
[AD-A220372] 17 p2471 N90-24125
Astronomy at ultra-high energies: Results from the CYGNUS experiment
[DE90-011979] 20 p2940 N90-26732
First International Conference on Laboratory Research for Planetary Atmospheres
[NASA-CP-3077] 20 p2942 N90-26744
Photon sputtering of H2O ices: A preliminary report 20 p2949 N90-26783
Unexpected properties of the centrifugal force
[DE90-627197] 23 p3392 N90-29164

PHOTONUCLEAR REACTIONS
Detailed photonuclear cross-section calculations and astrophysical applications
[DE89-017531] 03 p0421 N90-12419
Calculation of two-neutron multiplicity in photonuclear reactions
[NASA-TP-2968] 06 p0841 N90-14890
Proceedings of the specialists' meeting on physics and engineering of fission and spallation
[DE90-719706] 08 p1125 N90-16519
Proof of the feasibility of coherent and incoherent schemes for pumping a gamma-ray laser
[AD-A219972] 18 p2562 N90-24620
A site for the astrophysical gamma ray process
[DE90-013473] 20 p2950 N90-26787

PHOTOOXIDATION
An investigation of the degradation and stabilization of polymer systems
[AD-A210362] 01 p0049 N90-10282
Interfacial and thin film chemistry in electron device fabrication
[AD-A214784] 09 p1289 N90-17473
The RADM 2 gas-phase chemical mechanism 12 p1686 N90-19684
Source attribution for tropospheric ozone in the US
[DE90-007994] 14 p2004 N90-21484
Pyrotechnic materials ignited using lasers. High energy photopyrotechnic chains
[REPT-892-430-121] 16 p2225 N90-22691

PHOTOPLASTICITY
Structural and optical properties of DMP-128 holograms during environmental testing
[AD-A221691] 21 p3007 N90-27094

PHOTOPRODUCTION
B factory via conversion of 1 TeV electron beams into 1 TeV photon beams
[DE89-017692] 04 p0505 N90-12914
Measurement of the fractional momentum carried by the glutons in the low Q squared photon-gluon fusion events at the ep HERA collider
[NOTA-INTERNA-937] 05 p0698 N90-14083
Theoretical aspects of electroweak and other interactions in medium energy nuclear physics
[DE90-004015] 08 p1121 N90-16493

PHOTORECEPTORS
Filling in the retinal image 15 p2140 N90-22229
Polarization contrast vision
[AD-A221423] 21 p3076 N90-27492

PHOTOREDUCTION
U PHOTOCHEMICAL REACTIONS

PHOTORESISTIVITY
U PHOTOCONDUCTIVITY

PHOTORESISTORS
U PHOTOCONDUCTORS

PHOTOSENSITIVITY
NT LIGHT ADAPTATION
NT PHOTOTROPISM
Graded bandgap solar cells
[AD-A211537] 03 p0367 N90-12097
New devices using ferroelectric thin films
[DE90-000789] 07 p0921 N90-15328
Center for X Ray Optics, 1988
[DE90-003300] 07 p0992 N90-15732
Develop techniques for ion implantation of PLZT for adaptive optics
[AD-A216005] 10 p1431 N90-18253
Photochromic papers or films for noncopyable documents
[DE90-004006] 10 p1441 N90-18316
Stability studies of a pH-sensitive polymer matrix: Applications to fiber optic pH sensors
[DE90-009579] 15 p2072 N90-21867

PHOTOSENSORS
U PHOTOELECTRICITY
U RADIATION MEASURING INSTRUMENTS

PHOTOSPHERE
MHD (magnetohydrodynamic) modeling of solar and interplanetary processes
[PB89-215461] 03 p0420 N90-12416
Rotation of the photospheric magnetic fields: A north-south asymmetry
[NASA-CR-186159] 05 p0715 N90-14177
Determination of solar flare accelerated ion angular distributions from SMM gamma ray and neutron measurements and determination of the He-3/H ratio in the solar photosphere from SMM gamma ray measurements
[NASA-CR-186038] 08 p1153 N90-16676
A comparison of photospheric and circumstellar (HCN)/(CO)-ratios for bright carbon stars
[PB90-151101] 15 p2184 N90-22477
Super-critical accretion in Cir X-1 19 p2767 N90-25725
Nonpotential magnetic fields at sites of gamma ray flares
[NASA-TM-103493] 20 p2950 N90-26785

PHOTOSYNTHESIS
Biochemical cycling and fluxes between the deep euphotic zone and other oceanic realms
[PB89-152458] 01 p0089 N90-10509
A structural basis for electron transfer in bacterial photosynthesis
[DE89-015702] 01 p0120 N90-10687
Controlling photoinduced electron transfer rates in donor-spacer-acceptor molecules by changing the electronic properties of the spacer
[DE89-015128] 01 p0128 N90-10735
Photochemically-driven biomimetic oxidation of alkanes and olefins
[DE89-011536] 02 p0193 N90-11097
Measurement of the light flux density patterns from luminaires proposed as photon sources for photosynthesis during space travel
[NASA-CR-186124] 05 p0672 N90-13916
Factors affecting electron spin polarization in photosynthetic systems
[DE90-000196] 06 p0819 N90-14764
Comparison of structural subunits of the core light-harvesting complexes of photosynthetic bacteria
[DE90-001412] 06 p0819 N90-14765
Dynamics of carbon dioxide exchange of a wheat community grown in a semi-closed environment 08 p1155 N90-16689
Energy transfer and photochemistry in biomimetic solar conversion
[PB90-114562] 12 p1681 N90-19652
Air pollution-caused changes in photosynthesis: Effects on plant growth and rhizosphere functions
[DE90-007184] 13 p1829 N90-20501
Carbon and hydrogen metabolism of green algae in light and dark
[DE90-008648] 13 p1849 N90-20612
Photosynthetic water splitting, phase 2
[PB90-132671] 15 p2066 N90-21833
Effects of air temperature on atmospheric CO2-plant growth relationships
[DE90-010159] 17 p2420 N90-23793
Carbon dioxide and water exchange rates by a wheat crop in NASA's biomass production chamber: Results from an 86-day study (January to April 1989)
[NASA-TM-102788] 19 p2716 N90-25453
System development and early biological tests in NASA's biomass production chamber
[NASA-TM-103494] 19 p2716 N90-25456
Gas exchange characteristics as indicators of the basic limiting factors in photosynthesis
[DE90-012399] 20 p2898 N90-26481
Photosynthesis in intact plants
[DE90-013699] 20 p2898 N90-26482
Greenhouse design for a Martian colony: Structural, solar collection and light distribution systems
[NASA-CR-186818] 20 p2901 N90-26501
Grassland/atmosphere response to changing climate: Coupling regional and local scales
[DE90-015814] 24 p3487 N90-29710

PHOTOTHERMAL CONVERSION
Predictive aging of polymers
[NASA-CASE-NPO-17524-1-CU] 01 p0046 N90-10261

PHOTOTHERMOTROPISM
U ANISOTROPY
U PHOTOTROPISM
U TEMPERATURE EFFECTS

PHOTOTRANSISTORS
Investigations of laterally coupled all optical switches and detectors on silica fibers
[AD-A220297] 17 p2473 N90-24142

PHOTOTROPISM
Anaerobic metabolism of aromatic compounds by phototrophic bacteria: Biochemical aspects
[DE90-009503] 14 p2009 N90-21516

PHOTOTUBES
NT PHOTOMULTIPLIER TUBES

PHOTOVOLTAGES
Transient pulse monitor
[AD-A220353] 18 p2508 N90-24335
Scanning electron microscopy by photovoltage contrast imaging
[AD-D014517] 19 p2760 N90-25684
Surface photovoltage spectroscopy of real n-type GaAs(110) surfaces
[DE90-627325] 24 p3551 N90-30092

PHOTOVOLTAIC CELLS
NT SOLAR CELLS
United States photovoltaic concentrator technology process and new program initiative
[DE89-013812] 01 p0083 N90-10475
Lightning and surge protection of photovoltaic installations: Two case histories, Vulcano and Kythnos
[PB89-229058] 03 p0374 N90-12135
A nickel/hydrogen battery for PV systems
[DE90-001537] 07 p0926 N90-15358

Sizing and selection of batteries for stand-alone photovoltaic systems
[DE90-002990] 08 p1060 N90-16129
Ga0.47In0.53As cells for GaAs-stacked photovoltaic tandems 10 p1338 N90-17749
GaAs cells on Si substrates: A new challenge for space photovoltaic applications 10 p1339 N90-17750
Aeolian removal of dust from photovoltaic surfaces on Mars
[NASA-TM-102507] 12 p1617 N90-19299
A transient plasticity study and low cycle fatigue analysis of the Space Station Freedom photovoltaic solar array blanket
[NASA-TM-102516] 12 p1674 N90-19617
Solid State Photovoltaic Research Branch
[DE89-009463] 12 p1682 N90-19660
Investigation of a photovoltaic/battery hybrid system for powering the high arctic data communications system
[AD-A218353] 13 p1798 N90-20319
Infrared ground-based astronomy with the Hughes 256 X 256 PtSi array 14 p1978 N90-21331
Research on amorphous silicon-based thin film photovoltaic devices. Task B: Research on stable high efficiency large area, amorphous silicon-based submodules
[DE90-000320] 14 p2002 N90-21473
Recent progress in photovoltaic concentrator module technology
[DE90-009007] 14 p2002 N90-21475
Analysis of thermal energy storage material with change-of-phase volumetric effects
[NASA-TM-102457] 15 p2092 N90-21974
Photovoltaic advanced research and development project: Solar radiation research
[DE90-000302] 16 p2251 N90-22839
Photovoltaic measurements and performance branch
[DE90-000324] 18 p2577 N90-24681
Photovoltaic concentrator technology development
[DE90-011479] 18 p2577 N90-24684
The photovoltaic concentrator initiative
[DE90-011228] 19 p2710 N90-25425
Crystalline photovoltaic cell research, status, and future direction
[DE90-011478] 19 p2710 N90-25427
Performance testing and qualification of Sandia's third baseline photovoltaic concentrator module
[DE90-012644] 19 p2711 N90-25431
Photovoltaic array space power plus diagnostics experiment 19 p2737 N90-25559
Interim qualification tests and procedures for terrestrial photovoltaic thin-film flat-plate modules
[DE90-000354] 20 p2881 N90-26392
Design optimization of short focal length photovoltaic modules
[PB90-182221] 22 p3195 N90-28133
Sandia's CONCEPT-90 photovoltaic concentrator module
[DE90-012243] 22 p3196 N90-28134

PHOTOVOLTAIC CONVERSION
Photovoltaic system research status
[DE89-016764] 03 p0366 N90-12094
Photovoltaic Measurements and Performance Branch
[DE89-009500] 06 p0807 N90-14695
High-efficiency copper ternary thin film solar cells
[DE89-009470] 09 p1242 N90-17207
Research on amorphous silicon based thin film photovoltaic devices. Phase 2: Research on stable high-efficiency, large area amorphous silicon based submodules
[DE89-009515] 09 p1243 N90-17209
European Space Power, volume 2
[ESA-SP-294-VOL-2] 10 p1338 N90-17748
Ga0.47In0.53As cells for GaAs-stacked photovoltaic tandems 10 p1338 N90-17749
GaAs cells on Si substrates: A new challenge for space photovoltaic applications 10 p1339 N90-17750
On-orbit demonstration of GaAs solar cell and panel technologies 10 p1339 N90-17751
AlGaAs/GaAs solar cells with efficiencies greater than 22 percent 10 p1339 N90-17755
Manufacture and testing of a solar panel assembly comprising bifacial solar cells (AMOC-SPA) 10 p1342 N90-17773
NASA advanced space photovoltaic technology: Status, potential and future mission applications 10 p1342 N90-17775
High-efficient solar cells for space application 10 p1342 N90-17777
GaAs back point contact solar cell simulation 10 p1343 N90-17781
The INMARSAT-2 solar generator panels 10 p1343 N90-17782
Solar cell electrodynamic characteristics test equipment 10 p1344 N90-17791
Assessment of in-orbit performance data of a bifacial flight experiment 10 p1344 N90-17793
SPOT 1 solar array: Three years in orbit performance evaluation 10 p1344 N90-17795
The advanced photovoltaic solar array program 10 p1345 N90-17797
In-orbit performance of CS-3a spacecraft GaAs solar array 10 p1346 N90-17804
Improved solar cells testing fixtures 10 p1346 N90-17807
Study on the measures to promote the use of photovoltaic power generating system overseas
[DE90-742056] 11 p1530 N90-18807
Photovoltaic energy
[DE89-009473] 13 p1826 N90-20486
Recent results from advanced research on space solar cells at NASA
[NASA-TM-102485] 14 p1968 N90-21274
Improvement of small-area, amorphous-silicon thin-film photovoltaics on polymer substrate
[DE90-000314] 14 p2002 N90-21472
Space Station Freedom solar array panels plasma interaction test facility
[NASA-TM-102475] 15 p2186 N90-22488
Photovoltaic advanced research and development project: Solar radiation research
[DE90-000302] 16 p2251 N90-22839
Summary results of an assessment of research projects in the national photovoltaics program
[DE90-008222] 18 p2577 N90-24680
Photovoltaic measurements and performance branch
[DE90-000324] 18 p2577 N90-24681
The chemical effects of the Martian environment on power system component materials: A theoretical approach
[NASA-TM-103203] 20 p2825 N90-26074
Storage battery operation technique of photovoltaic system to prevent the imbalance of state of charge
[DE90-503032] 20 p2858 N90-26255
Megawatt solar power systems for lunar surface operations
[NASA-CR-186509] 20 p2881 N90-26391
Electronic and photonic power applications
[DE90-015567] 24 p3485 N90-29698

PHOTOVOLTAIC EFFECT
CuInSe2 and CdTe: Scale-up for manufacturing
[DE89-009503] 13 p1827 N90-20489
Power transmission device
[AD-D014430] 14 p1969 N90-21281
Short wavelength HgCdTe staring focal plane for low background astronomy applications 14 p1979 N90-21336
Photovoltaic Program Branch
[DE90-000318] 15 p2123 N90-22142
Direct conversion technology
[NASA-CR-186795] 18 p2576 N90-24675
Summary results of an assessment of research projects in the national photovoltaics program
[DE90-008222] 18 p2577 N90-24680
Photovoltaic Energy Program summary. Volume 2: Research summaries
[DE89-009474] 19 p2710 N90-25422
Scanning electron microscopy by photovoltage contrast imaging
[AD-D014517] 19 p2760 N90-25684
Effects of energy, momentum and particle transport in the near-earth solar terrestrial system
[AD-A224393] 24 p3490 N90-29726
Photoinduced and holographically reinforced light diffusion in electrooptic crystals
[ETN-90-97321] 24 p3547 N90-30060
Integrated technology in MCT/GaAs and MCT/Si for medium and long wavelength infrared
[AD-A223557] 24 p3552 N90-30100

PHTHALATES
Rheological and mechanical characteristics of poly-p-phenylene terephthalamide/nylon molecular and particulate composites
[AD-A219562] 17 p2368 N90-23482

PHTHALOCYANIN
Femtosecond dynamics of fluoro-aluminum phthal ocyanine and linear alkane molecules
[AD-A210939] 01 p0133 N90-10766
Multicolor electrochromic displays exploratory development
[AD-A212004] 03 p0303 N90-11721
Evaluation of doped phthalocyanines and a chemically-sensitive field effect transistor for detecting nitrogen dioxide
[AD-A215662] 09 p1214 N90-17037
Nonlinear optical responses and laser damage thresholds of films of a polarized stilbene side chain liquid crystal polymer and a phthalocyanine
[AD-A219462] 17 p2408 N90-23720
Sigma and pi interactions of the pyrrolic ligand sandwich-like lanthanide phthalocyanines determined from magnetic susceptibility and ligand-field theory
[AD-A223609] 24 p3443 N90-29444

PHUGOID OSCILLATIONS
U OSCILLATIONS
U OSCILLATORS
U PITCH (INCLINATION)

PHYSICAL CHEMISTRY
NT QUANTUM CHEMISTRY
Physical processing of cometary nuclei 08 p1148 N90-16653
Laboratory studies of cometary ice analogues 12 p1739 N90-19997
Physico-chemical properties of formaldehyde-ice-dust mixtures 12 p1740 N90-20000
Crustal strength of different model comet materials 12 p1740 N90-20003
Modelling of molecular structures and properties in physical chemistry and biophysics
[AD-A214561] 14 p1947 N90-21145
QATT: A natural language interface for QPE
[UIUCDCS-R-89-1535] 19 p2743 N90-25590
A lightweight solid polymer electrolyte fuel cell with stack power density of 3 kW/lb (7kW/kg)
[AD-A223068] 21 p3020 N90-27189
Energetics and crystal chemistry of Ruddlesden-Popper type structures in high T(sub c) ceramic superconductors 22 p3141 N90-27814

PHYSICAL ENDURANCE
U PHYSICAL FITNESS

PHYSICAL EXAMINATIONS
Activities in aerospace medicine
[ETN-90-95468] 12 p1696 N90-19739
Decompression sickness affecting the temporomandibular joint
[AD-A220959] 18 p2584 N90-24715
Activities report of the National Aerospace Medical Center
[ETN-90-96936] 18 p2585 N90-24721

PHYSICAL EXERCISE
Control of thermoregulatory sweating during exercise in the heat
[AD-A206001] 01 p0092 N90-10523
Exertional heatstroke: An international perspective. An introduction: The role of exercise in the etiology of exertional heatstroke
[AD-A212242] 04 p0523 N90-13020
Exercise countermeasures for bed rest deconditioning
[NASA-TM-101045] 05 p0674 N90-13926
Measurement of mechanical work and energy expenditure in running and bicycling 05 p0675 N90-13935
Potential for reduction of decompression sickness by prebreathing with 100 percent oxygen while exercising
[AD-A213449] 07 p0966 N90-15581
The application of optimal control theory for analysis of human jumping and pedaling 07 p0968 N90-15590
Effectiveness of progressive resistance training for increasing maximal repetitive lifting capacity
[AD-A215286] 09 p1252 N90-17267
The role of blood volume in determining the cardiovascular adjustments to exercise 11 p1538 N90-18854
The reliability of clinical measurements of forward bending obtained by the use of the modified fingertip-to-floor method
[AD-A217907] 13 p1852 N90-20627
The effects of high intensity cycle exercise on sympatho-adrenal-medullary response patterns
[AD-A217962] 13 p1852 N90-20628
Hydration effects on human physiology and exercise-heat performance
[AD-A217969] 13 p1852 N90-20629
The effects of graded exercise at sea level on plasma proenkephalin peptide F and catecholamine responses
[AD-A218195] 13 p1853 N90-20633
Kinematic and kinetic analyses of drop landings 14 p2010 N90-21517
Effects of cholinergic drugs on exercise performance and simple reaction time of rhesus monkeys
[AD-A219455] 17 p2433 N90-23862
Effect of low air velocities on thermal homeostasis and comfort during exercise at space station operational temperature and humidity 18 p2628 N90-24975
Overtraining and exercise motivation: A research prospectus 18 p2629 N90-24982
The use of underwater dynamometry to evaluate two space suits 18 p2632 N90-24995
Effects of microgravity on rat muscle 20 p2891 N90-26453
Experiment K-6-09. Morphological and biochemical investigation of microgravity-induced nerve and muscle breakdown. Part 1: Investigation of nerve and muscle breakdown during spaceflight; Part 2: Biochemical analysis of EDL and PLT muscles 20 p2893 N90-26463
Joint US/USSR study: Comparison of effects of horizontal and head-down bed rest
[NASA-TP-3037] 23 p3355 N90-28965

PHYSICAL FITNESS
Demonstration of replicable dimensions of health behaviors
[AD-A211920] 03 p0380 N90-12161
The effect of concurrent strength and endurance training on electromechanical delay, maximum voluntary contraction, and rate of force development
[AD-A213316] 04 p0525 N90-13028
Effectiveness of progressive resistance training for increasing maximal repetitive lifting capacity
[AD-A215286] 09 p1252 N90-17267
Physiological and perceptual responses to prolonged treadmill load carriage
[AD-A218910] 16 p2260 N90-22886
Effects of high altitude hypoxia on lung and chest wall function during exercise
[AD-A219814] 17 p2434 N90-23869
The relationship of isometric grip strength, optimal dynamometer settings, and certain anthropometric factors
[AD-A222046] 21 p3037 N90-27264
Physiological reactions to heat stress; quantifying the effects of individual parameters
[IZF-1989-30] 22 p3232 N90-28326
PHYSICAL OPTICS
Surface reflection: Physical and geometrical perspectives
[AD-A210592] 01 p0124 N90-10710
Nonprincipal-plane scattering from flat plates: Second-order and corner diffraction and pattern control of horn antennas
[NASA-CR-185485] 02 p0211 N90-11205
Part A: Nonprincipal-plane scattering from flat plates: Second-order and corner diffractions
02 p0211 N90-11206
Constitutive parameter measurements of lossy materials
[NASA-CR-183398] 02 p0281 N90-11603
A method to model fuze-performance. Part 3: Diffraction of electromagnetic radiation by an edge
[FEL-1989-22-PT-3] 03 p0340 N90-11940
A method to model fuze performance. Part 2: Calculation of target reflections with physical optics
[FEL-1989-21-PT-2] 04 p0491 N90-12822
The physical optics approximation in the near-field region
[FEL-1989-100] 04 p0555 N90-13234
Analytical optical scattering in clouds
12 p1638 N90-19413
PHYSICAL PROPERTIES
The prediction of middle distillate fuel properties using liquid chromatography-proton nuclear magnetic resonance spectroscopy data
[AD-A211879] 03 p0334 N90-11899
PHYSICAL WORK
Investigation of the effects of external supports on manual lifting
[PB90-103367] 09 p1260 N90-17307
Space station based Microacceleration Experiment Platform
[NASA-CR-186659] 19 p2666 N90-25167
Teleoperator comfort and psychometric stability: Criteria for limiting master-controller forces of operation and feedback during telemanipulation
23 p3364 N90-29009
PHYSICS
Elementary and middle school science improvement project
[NASA-CR-183768] 05 p0705 N90-14125
PHYSIOGRAPHY
U GEOMORPHOLOGY
PHYSIOLOGICAL DEFENSES
NT IMMUNE SYSTEMS
Effects of pyridostigmine bromide on A-10 pilots during execution of a simulated mission: Physiology
[AD-A221222] 18 p2584 N90-24717
PHYSIOLOGICAL EFFECTS
NT HEMODYNAMIC RESPONSES
NT PHYSIOLOGICAL RESPONSES
Biological effects of power frequency electric and magnetic fields: Background paper
[PB89-209985] 02 p0254 N90-11439
Synergistic effects of nitrogen dioxide and carbon dioxide following acute inhalation exposures in rats
[PB89-214779] 03 p0377 N90-12150
Effects of atmospheric mix and toxic fumes on military performance
[PB89-223630] 04 p0522 N90-13015
Biochemical and physiological changes in glider pilots during multihour flights
[DLR-FB-89-29] 04 p0523 N90-13018
The effects of noise on performance
[AD-A212519] 04 p0551 N90-13209
Exploring the living universe: A strategy for space life sciences
[NASA-TM-101891] 06 p0822 N90-14778
Use of lower body negative pressure as a countermeasure to negative Gz acceleration
[AD-A213927] 07 p0967 N90-15583
The 1988-1989 NASA space/gravitational biology accomplishments
[NASA-TM-4160] 09 p1250 N90-17251
Investigation of the effects of external supports on manual lifting
[PB90-103367] 09 p1260 N90-17307
The role of blood volume in determining the cardiovascular adjustments to exercise
11 p1538 N90-18854
Effects of pulsed and CW (Continuous Wave) 2450 MHz radiation on transformation and chromosomes of human lymphocytes in vitro
[AD-A216500] 11 p1539 N90-18857
Fourth International Conference on Fusion Reactor Materials
[DE90-006142] 11 p1568 N90-19025
Windblast protection for advanced ejection seats
13 p1752 N90-20063
Heat exhaustion in a rat model: Lithium as a biochemical probe
[AD-A219361] 16 p2260 N90-22884
Assessment System for Aircraft Noise (ASAN) citation database. Volume 1: User's manual
[AD-A219175] 16 p2314 N90-23188
Assessment System for Aircraft Noise (ASAN) citation database. Volume 2: Database update manual
[AD-A219176] 16 p2314 N90-23189
Assessment System for Aircraft Noise (ASAN) citation database. Volume 3: New citation review procedures
[AD-A219177] 16 p2314 N90-23190
Physiological and perceptual responses to prolonged treadmill load carriage
[AD-A218809] 17 p2433 N90-23865
Strategies to sustain and enhance performance in stressful environments
[AD-A221224] 18 p2583 N90-24711
Research in human performance related to space: A compilation of three projects/proposals
18 p2629 N90-24983
Biochemical and physiological changes in glider pilots during multi-hour flights
[ESA-TT-1183] 19 p2722 N90-25484
Damage measurements on optical materials for use in high-peak-power lasers
[DE90-013489] 20 p2868 N90-26314
Laser damage database at 1064 nm
[DE90-013490] 20 p2868 N90-26315
Further studies of 60 Hz exposure effects on human function
[DE90-014377] 23 p3355 N90-28962
PHYSIOLOGICAL FACTORS
Wrist orientation effect on grip strength and endurance
[PB89-200935] 03 p0383 N90-12179
Pre- and postflight postural control of the D1 Spacelab mission astronauts examined with a tilting room
[IZF-1988-25] 04 p0527 N90-13039
PHYSIOLOGICAL RESPONSES
NT HEMODYNAMIC RESPONSES
Daytime sleepiness, performance, mood, nocturnal sleep: The effect of benzodiazepine and caffeine on their relationship
[AD-A210915] 01 p0093 N90-10533
Biological investigations of adaptive networks: Neuronal control of conditioned responses
[AD-A211043] 01 p0094 N90-10534
Thermoregulatory responses to intermittent exercise are influenced by knit structure of underwear
[AD-A209087] 01 p0095 N90-10541
Cardiovascular, renal, electrolyte, and hormonal changes in man during gravitational stress, weightlessness, and simulated weightlessness: Lower body positive pressure applied by the antigravity suit
[NASA-TM-102232] 04 p0522 N90-13013
The relationship between subjective and objective measures of simulator-induced ataxia
[AD-A213095] 05 p0673 N90-13922
Gravity receptors and responses
05 p0678 N90-13948
The development of a model of the human responses to load carriage 06 p0821 N90-14775
Cryogenic engineering and materials
08 p1030 N90-15949
Factor analytic reduction of the carotid-cardiac baroreflex parameters 08 p1155 N90-16693
The characteristics of physiological responses and tolerance evaluation of pressure breathing
[AD-A214991] 09 p1252 N90-17262
Pre-treatment with tyrosine reverses hypothermia induced behavioral depression
[AD-A215211] 09 p1252 N90-17265
Sensations of temperature and humidity during intermittent exercise and the influence of underwear knit structure
[AD-A215285] 09 p1252 N90-17266
Psychological and physiological responses of blacks and caucasians to hand cooling
[AD-A215646] 09 p1253 N90-17272
Stress and performance during a simulated flight in a F-16 simulator 09 p1256 N90-17285
Performance recovery following startle: A laboratory approach to the study of behavioral response to sudden aircraft emergencies 09 p1256 N90-17286
Physiological evaluation of men wearing three different toxicological protective systems
[AD-A215527] 09 p1261 N90-17313
The importance of pathophysiological parameters in fire modelling of aircraft accidents 10 p1317 N90-17618
Influence of theobromine on heat production and body temperatures in cold-exposed humans: A preliminary report
[AD-A217203] 13 p1850 N90-20618
A comparison of the mechanisms of cold- and microgravity-induced fluid loss
[AD-A218098] 13 p1852 N90-20631
Effective calibration of heat flux transducers for experimental use
[AD-A218262] 13 p1853 N90-20636
Physiological and perceptual responses to prolonged treadmill load carriage
[AD-A218910] 16 p2260 N90-22886
The physiological cost of wearing the propellant handler's ensemble at the Kennedy Space Center
[NASA-TM-102786] 16 p2275 N90-22966
Physiological and perceptual responses to prolonged treadmill load carriage
[AD-A218809] 17 p2433 N90-23865
Effect of laser glare and aircraft windscreen on visual search performance under low ambient lighting
[AD-A219456] 17 p2437 N90-23888
Effect of fluid countermeasures of varying osmolarity on cardiovascular responses to orthostatic stress
18 p2628 N90-24978
The retrieval of information from secondary memory: A review and new findings
[AD-A222760] 20 p2899 N90-26489
Physiological reactions to heat stress; quantifying the effects of individual parameters
[IZF-1989-30] 22 p3232 N90-28326
Fluid and electrolyte homeostasis during spaceflight: Elucidation of mechanisms in a primate
[NASA-CR-177548] 23 p3378 N90-29085
Renal response to seven days of lower body positive pressure in the squirrel monkey
[NASA-CR-183355] 24 p3497 N90-29761
Vestibular responses and motion sickness during pitch, roll, and yaw sinusoidal whole-body oscillation
[AD-A223898] 24 p3497 N90-29767
PHYSIOLOGICAL TESTS
NT VESTIBULAR TESTS
Wrist orientation effect on grip strength and endurance
[PB89-200935] 03 p0383 N90-12179
Physiological and perceptual responses to prolonged treadmill load carriage
[AD-A218910] 16 p2260 N90-22886
Electrocardiogram of military aircraft pilots measured during real flight missions: Study of the variability of the cardiac rhythm in correlation with working stress
[ETN-90-97453] 22 p3231 N90-28324
Predicting F/A-18 fleet replacement squadron performance using an automated battery of performance-based tests
[AD-A223899] 23 p3277 N90-28543
PHYSIOLOGY
NT ELECTROPHYSIOLOGY
NT EXERCISE PHYSIOLOGY
NT GRAVITATIONAL PHYSIOLOGY
NT HEMATOPOIETIC SYSTEM
NT NEUROPHYSIOLOGY
NT PSYCHOPHYSIOLOGY
NT WORKLOADS (PSYCHOPHYSIOLOGY)
Continuous gas exchange measurements using individual fascicle cuvettes: The tubule system
[DE90-004932] 10 p1405 N90-18105
Regulation of nitrogen uptake and assimilation: Effects of nitrogen source, root-zone pH, and aerial CO2 concentration on growth and productivity of soybeans
[NASA-CR-177546] 10 p1413 N90-18147
Studies of 60-Hz exposure effects on human function
[DE90-009473] 15 p2137 N90-22210
The physiological cost of wearing the propellant handler's ensemble at the Kennedy Space Center
[NASA-TM-102786] 16 p2275 N90-22966
Research in human performance related to space: A compilation of three projects/proposals
18 p2629 N90-24983

Effects of microgravity on rat bone, cartilage and connective tissues 20 p2891 N90-26454
Joint US/USSR study: Comparison of effects of horizontal and head-down bed rest
[NASA-TP-3037] 23 p3355 N90-28965
Physiological metrics of mental workload: A review of recent progress
[NASA-CR-187290] 24 p3499 N90-29777

PHYTOPLANKTON
Some problems in oceanic radiative transfer
[AD-A215935] 10 p1410 N90-18131
Phytoplankton and its contribution to the atmospheric sulfur budget of northern Europe 20 p2885 N90-26417
Cloud reflectance characteristics in the presence of variable Dimethylsulfide (DMS) sources
[AD-A222806] 21 p3024 N90-27197

PI-ELECTRONS
Algorithms for calorimeter simulation with parameterized showers by example of H1 detectors
[MPI-PAE/EXP.EL-200] 12 p1711 N90-19828

PICKOFFS
U SENSORS

PICKUPS
U SENSORS

PICOSECOND PULSES
Air breakdown photography in the picosecond domain
[DE89-016775] 03 p0322 N90-11830
Nonresonant and resonant multiphoton ionization of (NO)(sub n) and Ar(sub n)NO clusters with picosecond laser pulses
[DE89-016853] 06 p0791 N90-14607
Picosecond Laser Facility
[AD-A217784] 13 p1808 N90-20384
Picosecond nonlinear studies of complex materials using the free electron laser
[AD-A218215] 13 p1809 N90-20387
Generation of ultrashort laser pulses from neodymium glass oscillator and regenerative amplifier 14 p1984 N90-21373
Frequency domain techniques for analyzing picosecond optical pulses
[AD-A218856] 16 p2318 N90-23214
Picosecond laser pulse interactions with metallic and semiconducting surfaces
[AD-A219680] 17 p2408 N90-23723
High voltage picosecond pulse generation using avalanche diodes
[DE90-015194] 24 p3465 N90-29577

PICTURE ELEMENTS
U PIXELS

PIERCING
The nature of cometary materials 08 p1147 N90-16647
Bird impact tests on asymmetric sandwich structures made in Kevlar 49
[CEAT-NT-10/S/83-5] 09 p1162 N90-16727
Bird impact tests on curved structures of the type Sandwich-Kevlar-Nida for normal and angular shooting
[CEAT-NT-10/S/83-4] 09 p1162 N90-16728
Hypervelocity impact shield
[NASA-CASE-MSC-21420-1] 21 p2966 N90-26858

PIEZOELECTRIC CERAMICS
NT LEAD ZIRCONATE TITANATES
Piezoelectric ceramic modeling and characterization at high levels of mechanical activity
[ISAL-89-0030] 08 p1051 N90-16074
Ultrasonic inspection of advanced CFRP structures by computer-controlled, pulse-echo technique 22 p3185 N90-28075
Piezoelectric and electrostrictive materials for transducer applications, volume 2
[AD-A223561] 24 p3480 N90-29669

PIEZOELECTRIC GAGES
Mechanoelectric conversion by uniaxial constraint in piezoelectric generators: Optimization of electrical, mechanical, and physico-chemical parameters of materials
[ISAL-89-0020] 08 p1078 N90-16235
The study of VF2/VF3 piezoelectric copolymeteres submitted to shocks
[ISL-CO-210/9] 20 p2931 N90-26679

PIEZOELECTRIC TRANSDUCERS
NT PIEZOELECTRIC GAGES
Polarization matrices of lithium tetraborate
[AD-A210774] 02 p0195 N90-11112
Detection of flow instabilities at airfoil profiles using piezoelectric arrays 08 p1067 N90-16175
Colinear fluctuating wall shear stress and fluctuating pressure transducer
[AD-D014296] 08 p1076 N90-16226
Determination of dynamic surface forces using piezoelectric arrays 08 p1080 N90-16249
The use of piezofoil sensors for the determination of the unsteady pressure distribution at the surface of a gas turbine blade 08 p1080 N90-16250
Temperature and coupling behavior of resonators and transducers of lithium tetraborate driven by lateral and thickness fields
[AD-A219548] 17 p2395 N90-23644
Terbium-dysprosium magnetostrictive high power transducers
[AD-D014509] 19 p2753 N90-25641
Some design considerations for small piezo-electrical ceramic transducers
[FEL-1989-68] 22 p3178 N90-28034
Nondestructive material characterization
[DE90-015176] 24 p3477 N90-29652
Piezoelectric and electrostrictive materials for transducer applications, volume 1
[AD-A223560] 24 p3480 N90-29668
Piezoelectric and electrostrictive materials for transducer applications, volume 2
[AD-A223561] 24 p3480 N90-29669

PIEZOELECTRICITY
Behaviour of VF(sub 2)/VF(sub 3) piezoelectric copolymers under shock loading
[DE89-016538] 02 p0201 N90-11145
Response of standardized PVDF piezoelectric polymer gauges to direct shock pressures between 8 and 32 GPa
[DE89-016811] 02 p0224 N90-11282
The Sandia standard for PVDF (Polyvinylidene Di-Fluoride) shock sensors
[DE89-016530] 02 p0225 N90-11287
SAW (Surface Acoustic Wave) transducer with improved bus-bar design
[AD-D014250] 08 p1060 N90-16125
Mechanoelectric conversion by uniaxial constraint in piezoelectric generators: Optimization of electrical, mechanical, and physico-chemical parameters of materials
[ISAL-89-0020] 08 p1078 N90-16235
The redetermination of the elastic, piezoelectric, and dielectric constants of quartz and their variation with temperature
[AD-A215025] 09 p1197 N90-16937
Surface acoustic wave sensors and piezoelectric actuators for investigations of transitional and turbulent flows
[AD-A214889] 09 p1279 N90-17415
Development and test of power amplifiers for the driving of low-voltage piezo-actuators in multistable interferometers
[DLR-MITT-89-19] 11 p1504 N90-18662
Piezoelectric polymer PVDF shock gauge: State of the research art
[ISL-CO-207/89] 11 p1512 N90-18705
Temperature compensated crystal oscillator (TCXO) with improved temperature compensation
[AD-D014334] 12 p1650 N90-19482
Field effect transistor structures based on strain induced polarization charges
[DE90-007247] 12 p1655 N90-19515
Experimental evaluation of active-member control of precision structures 14 p1936 N90-21084
Active control of bearing preload using piezoelectric translators 15 p2115 N90-22098
Shaping radiation pattern of excimer laser by means of controllable intracavity mirror 16 p2310 N90-23166
Piezoelectric and pyroelectric effects of a crystalline polymer 18 p2515 N90-24360
NMR and optical studies of piezoelectric polymers
[DE90-012459] 20 p2837 N90-26137
The study of VF2/VF3 piezoelectric copolymeteres submitted to shocks
[ISL-CO-210/9] 20 p2931 N90-26679
Piezoelectric and electrostrictive materials for transducer applications, volume 1
[AD-A223560] 24 p3480 N90-29668

PIEZORESISTIVE TRANSDUCERS
NT PIEZOELECTRIC GAGES
Fluctuating pressures measured beneath a high-temperature, turbulent boundary layer on a flat plate at Mach number of 5
[NASA-TP-2947] 01 p0118 N90-10680
Evaluation of shock isolation techniques for a piezoresistive accelerometer
[DE89-014496] 06 p0780 N90-14535

PIGMENTS
NT CHLOROPHYLLS
NT CYTOCHROMES
NT MELANIN

PILE FOUNDATIONS
Geotechnical instrumentation
[PB89-198675] 07 p0933 N90-15398

PILOT ERROR
Classification and reduction of pilot error
[NASA-CR-181867] 01 p0004 N90-10014
Fatigue, pilot deviations and time of day
[NASA-CR-185369] 04 p0526 N90-13035
Review of serious aircraft accidents in the Belgian Air Force: Causes and comparison with selection data 09 p1254 N90-17277
Accidents in fighter aircraft caused by human factors. Why do they occur 09 p1254 N90-17278
Spatial displays as a means to increase pilot situational awareness 16 p2272 N90-22951
Spatial disorientation incidents in the RNLAF F16 and F5 aircraft and suggestions for prevention 23 p3357 N90-28973
Loss of alertness and consciousness from pilot position during long range flight 23 p3360 N90-28990

PILOT INDUCED OSCILLATION
Prediction of longitudinal pilot induced oscillations using the optimal control model
[AD-A220593] 17 p2356 N90-23412

PILOT PERFORMANCE
The effect of higher education variables on cadet performance during 1987 light aircraft training
[AD-A210199] 01 p0094 N90-10536
Helicopter Visual Segment Approach Lighting System (HALS)
[ACD-330] 02 p0150 N90-10856
Heliport surface maneuvering test results
[ACD-330] 02 p0157 N90-10897
Field-of-View variations and stripe-texturing effects on assault landing performance in the C-130 weapon system trainer
[AD-A212763] 04 p0459 N90-12634
Fatigue, pilot deviations and time of day
[NASA-CR-185369] 04 p0526 N90-13035
Spatial tests for aviators
[IZF-1988-15] 04 p0527 N90-13041
Human factors research in aircrew performance and training
[AD-A213285] 05 p0676 N90-13938
A candidate concept for display of forward-looking wind shear information
[NASA-TM-101585] 06 p0725 N90-14232
Workload induced spatio-temporal distortions and safety of flight
[DE89-016613] 06 p0820 N90-14771
The human element: The key to safe, civil operations in adverse weather 07 p0869 N90-15042
Classification of windshear severity 07 p0870 N90-15049
Canard versus aft-tail ride qualities performance and pilot command response 07 p0871 N90-15053
Aircraft response and pilot behaviour during a wake vortex encounter perpendicular to the vortex axis 07 p0871 N90-15057
Imaging probabilities, geometry and ergonomics in limited visibility helicopter operations 07 p0872 N90-15060
Model for measuring complex performance in an aviation environment
[DE90-002055] 07 p0967 N90-15585
Piloted simulation of a ground-based time-control concept for air traffic control
[NASA-TM-101085] 08 p1020 N90-15898
Keeping the pilot in the loop
[RAE-TM-FM-18] 08 p1105 N90-16396
Accidents in fighter aircraft caused by human factors. Why do they occur 09 p1254 N90-17278
Psychological reactions of pilots involved in accidents in the Swedish Air Force 09 p1254 N90-17279
Personality characteristics of USAF pilot candidates 09 p1255 N90-17281
Expertise, stress, and pilot judgment 09 p1255 N90-17284
Stress and performance during a simulated flight in a F-16 simulator 09 p1256 N90-17285
Peripheral nervous velocity of conduction in fighter pilots 09 p1256 N90-17287
The trials and tribulations of RAF defence mechanism testing 09 p1257 N90-17291
Predicting Air Combat Maneuvering (ACM) performance 09 p1258 N90-17294
Development of a performance-based test of gaze capability: A threshold approach
[AD-A214675] 09 p1259 N90-17301
Proximity compatibility and information display: The effects of space and color on the analysis of aircraft stall conditions
[AD-A214488] 09 p1260 N90-17309
Checklist reading problems in airplanes equipped with speech recognition systems
[ILR-MITT-223(1989)] 09 p1261 N90-17314
Delivery performance of conventional aircraft by terminal-area, time-based air traffic control: A real-time simulation evaluation
[NASA-TP-2978] 11 p1454 N90-18378
Three input concepts for flight crew interaction with information presented on a large-screen electronic cockpit display
[NASA-TM-4173] 11 p1457 N90-18394

A learning regulator for the plane longitudinal movement
[ETN-90-95381] 13 p1864 N90-20695
An early overview of tiltrotor aircraft characteristics and pilot procedures in civil transport applications
[DOT/FAA/DS-89/37] 14 p1921 N90-21003
Stereopsis cueing effects on hover-in-turbulence performance in a simulated rotorcraft
[NASA-TP-2980] 14 p1921 N90-21004
Field-of-view assessment of low-level flight and an airdrop in the C-130 Weapon System Trainer (WST)
[AD-A218504] 16 p2200 N90-22559
Model-based method for terrain-following display design
[AD-A219302] 16 p2201 N90-22563
Visual behavior in the F-15 simulator for air-to-air combat
[AD-A218648] 16 p2262 N90-22893
Spatial displays as a means to increase pilot situational awareness 16 p2272 N90-22951
Synthetic perspective optical flow: Influence on pilot control tasks 16 p2273 N90-22956
Fighter agility metrics, research, and test
[NASA-CR-186118] 17 p2351 N90-23386
Target selection in anti-tank helicopter operations: Relative weight of cues in target evaluation judgements
[FOA-C-50072-5.2] 17 p2436 N90-23881
Target selection in anti-tank operations: Effects of experience
[FOA-C-50073-5.2] 17 p2436 N90-23882
Mode of presentation of cues in policy capturing: A comparison between verbal and pictorial presentation of targets in judgement of probability to fire
[FOA-C-50074-5.2] 17 p2436 N90-23883
Helicopter controllability
[AD-A220078] 18 p2498 N90-24275
Effects of pyridostigmine bromide on A-10 pilots during execution of a simulated mission: Physiology
[AD-A221222] 18 p2584 N90-24717
Activities report of the National Aerospace Medical Center
[ETN-90-96936] 18 p2585 N90-24721
An empirically derived figure of merit for the quality of overall task performance 18 p2644 N90-25058
Mobility of the head and load effects: Experimental approach in a centrifuge 19 p2720 N90-25473
The prediction of professional success of licenced pilots: The validity of flight experience in comparison with standardized psychological aptitude tests
[DLR-FB-89-53] 19 p2723 N90-25488
Eye tracking device for the measurement of flight performance in simulators
[AD-A220075] 20 p2898 N90-26484
Pilot interaction with automated airborne decision making systems
[NASA-CR-186730] 20 p2899 N90-26492
Psychophysiological assessment of pilot workload in an applied setting
[AD-A222707] 20 p2902 N90-26507
Dallas/Fort Worth simulation, volume 1
[DOT/FAA/CT-TN89/28-VOL-1] 21 p2955 N90-26802
Cockpit Ocular Recording System (CORS)
[NASA-CR-4281] 21 p3033 N90-27244
Cross-validation of experimental USAF pilot training performance models
[AD-A222253] 21 p3035 N90-27257
Tips on desert flying
[PB90-233222] 22 p3110 N90-27670
Situational Awareness in Aerospace Operations
[AGARD-CP-478] 23 p3357 N90-28972
Spatial disorientation incidents in the RNLAF F16 and F5 aircraft and suggestions for prevention 23 p3357 N90-28973
A methodology for the objective measurement of pilot situation awareness 23 p3357 N90-28974
Performance-based measures of merit for tactical situation awareness 23 p3358 N90-28976
Evaluation of the Situational Awareness Rating Technique (SART) as a tool for aircrew systems design 23 p3358 N90-28977
Attention gradients in situation awareness 23 p3358 N90-28978
Towards a future cockpit: The prototyping and pilot integration of the Mission Management Aid (MMA) 23 p3358 N90-28979
The three-dimensional structure of visual attention and its implications for display design 23 p3359 N90-28980
Counterair situation awareness display for Army aviation 23 p3359 N90-28982
The simulation of localized sounds for improved situational awareness 23 p3359 N90-28984
The effects of acoustic orientation cues on instrument flight performance in a flight simulator 23 p3359 N90-28985
Experimental tests on the minimal visual acuity required for safe air crew and air control personnel performance 23 p3360 N90-28987
Loss of alertness and consciousness from pilot position during long range flight 23 p3360 N90-28990
Evaluation of the performance capability of the aviator under hypoxic conditions operational expenence 23 p3361 N90-28991
Effects of short-term weightlessness on roll circularvection 23 p3361 N90-28992
Maintaining spatial orientation awareness 23 p3361 N90-28993
Proprioception in aircraft control
[IZF-1989-43] 23 p3377 N90-29082
Workshop on Low Level Flight Training
[AGARD-AR-288] 24 p3436 N90-29404
Visual processing: Implications for helmet mounted displays
[AD-A223488] 24 p3522 N90-29916

PILOT PLANTS
Thin section casting program. Volume 2-A: Appendix to volume 2
[DE89-009032] 02 p0210 N90-11200

PILOT SELECTION
The effect of higher education variables on cadet performance during 1987 light aircraft training
[AD-A210199] 01 p0094 N90-10536
Human factors research in aircrew performance and training
[AD-A213285] 05 p0676 N90-13938
Review of serious aircraft accidents in the Belgian Air Force: Causes and comparison with selection data 09 p1254 N90-17277
Accidents in fighter aircraft caused by human factors. Why do they occur 09 p1254 N90-17278
Personality characteristics of USAF pilot candidates 09 p1255 N90-17281
Training and selecting individuals for high levels of information processing load 09 p1256 N90-17288
Principle guidelines for the psychological screening of candidate pilots for the Belgian Air Force 09 p1257 N90-17292
Pilot candidate selection
[AD-A217296] 12 p1696 N90-19742
Aeronautical decisionmaking for air ambulance program administrators
[DOT/FAA/DS-88/8] 17 p2347 N90-23368
The prediction of professional success of licenced pilots: The validity of flight experience in comparison with standardized psychological aptitude tests
[DLR-FB-89-53] 19 p2723 N90-25488
Study of the application of a stress reactivity test in personnel selection
[DLR-FB-89-54] 19 p2723 N90-25489
TOM: Test of multiple task performance, user manual
[DLR-FB-89-60] 19 p2723 N90-25490
International application of the DLR test-system: First year of cooperation with IBERIA in pilot selection
[DLR-FB-90-05] 19 p2723 N90-25491
Cross-validation of experimental USAF pilot training performance models
[AD-A222253] 21 p3035 N90-27257
Predicting F/A-18 fleet replacement squadron performance using an automated battery of performance-based tests
[AD-A223899] 23 p3277 N90-28543

PILOT TRAINING
The effect of higher education variables on cadet performance during 1987 light aircraft training
[AD-A210199] 01 p0094 N90-10536
Field-of-View variations and stripe-texturing effects on assault landing performance in the C-130 weapon system trainer
[AD-A212763] 04 p0459 N90-12634
A Scheiner-principle pocket optometer for self-evaluation and biofeedback accommodation training
[AD-A213171] 04 p0524 N90-13027
A comparison of two subject-controlled attitude measures during somatogravic illusion exposure
[AD-A212528] 04 p0525 N90-13031
Human factors research in aircrew performance and training
[AD-A213285] 05 p0676 N90-13938
Development of the AH-64 display symbology training module
[AD-A213456] 07 p0968 N90-15592
Backward transfer and skill acquisition in the AH-1 flight and weapons simulator
[AD-A213432] 09 p1170 N90-16772
Hermes training aircraft 09 p1178 N90-16827
Personality characteristics of USAF pilot candidates 09 p1255 N90-17281
Training and selecting individuals for high levels of information processing load 09 p1256 N90-17288
The trials and tribulations of RAF defence mechanism testing 09 p1257 N90-17291
Proceedings of the Professional Pilots Meteorology Training Standards Conference
[AD-A216618] 11 p1536 N90-18843
Pilot candidate selection
[AD-A217296] 12 p1696 N90-19742
Minimum flying qualities. Volume 1: Piloted simulation evaluation of multiple axis flying qualities
[AD-A218560] 16 p2200 N90-22560
Visual behavior in the F-15 simulator for air-to-air combat
[AD-A218648] 16 p2262 N90-22893
Aeronautical decisionmaking for air ambulance program administrators
[DOT/FAA/DS-88/8] 17 p2347 N90-23368
Pilot decision-making training
[AD-A221349] 18 p2585 N90-24720
Neck injury prevention possibilities in a high-G-enviroment experience with high sustained +G(sub z) training of pilots in the GAF IAM human centrifuge 19 p2720 N90-25474
Cross-validation of experimental USAF pilot training performance models
[AD-A222253] 21 p3035 N90-27257
Predicting F/A-18 fleet replacement squadron performance using an automated battery of performance-based tests
[AD-A223899] 23 p3277 N90-28543
Maintaining spatial orientation awareness 23 p3361 N90-28993

PILOTED CENTRIFUGES
U HUMAN CENTRIFUGES

PILOTLESS AIRCRAFT
NT TARGET DRONE AIRCRAFT
Guidance and Control of Unmanned Air Vehicles
[AGARD-CP-436] 08 p1025 N90-15924
Unmanned air vehicles payloads and sensors 08 p1026 N90-15930
Distribution of hardware and software elements in unmanned air vehicle systems 08 p1027 N90-15933
Technology and evaluation of unmanned air vehicles 08 p1027 N90-15934
Design of a natural laminar flow airfoil for an unmanned aircraft
[PD-CF-9004] 14 p1916 N90-20975
Initial flight test of half-scale unmanned air vehicle
[AD-A219584] 17 p2351 N90-23388

PILOTS
Vestibular examination of motion sick student pilots
[IZF-1988-22] 12 p1696 N90-19738

PILOTS (PERSONNEL)
NT AIRCRAFT PILOTS
NT TEST PILOTS
Human performance in continuous/sustained operations and the demands of extended work/rest schedules: An annotated bibliography, volume 2
[AD-A210504] 01 p0093 N90-10530
Biochemical and physiological changes in glider pilots during multihour flights
[DLR-FB-89-29] 04 p0523 N90-13018
Human factors research in aircrew performance and training
[AD-A213285] 05 p0676 N90-13938

PINCH EFFECT
NT PLASMA PINCH
NT REVERSE FIELD PINCH
NT THETA PINCH
NT ZETA PINCH
A solvable self-similar model of the sausage instability in a resistive Z-pinch
[AD-A213137] 05 p0688 N90-14006
Hot spots Ar and Ne gas puff z-pinch
[IPPCZ-289] 05 p0701 N90-14103
Laser probing non-cylindrical Z-pinch in near-isolator region of a discharged chamber
[DE89-632018] 06 p0844 N90-14912
Enhanced pinch effect due to electrostatic potential
[DE90-007088] 13 p1890 N90-20844
New methods in plasma simulation
[DE90-007507] 13 p1890 N90-20847
A model of peaked density profile and inward pinch in tokamaks
[DE90-508079] 24 p3548 N90-30072

PINEAL GLAND
Experiment K-6-19. Pineal physiology in microgravity: Relation to rat gonadal function 20 p2895 N90-26472
Melatonin, light and, circadian cycles
[AD-A223196] 21 p3035 N90-27256

PINHOLES
Comparison of currents predicted by NASCAP/LEO model simulations with elementary Langmuir-type bare probe models for an insulated cable containing a single pinhole
[NASA-TM-102486] 20 p2821 N90-26054

PINNING
NT FLUX PINNING

Effects of non-linearity in the variation of pinning potential with current-density on magnetic flux creep in high and low T(sub c) superconductors
[DE90-003952] 07 p1005 N90-15822
Pinning, flow and plastic deformation of flux vortices in high T(sub c) superconductors 22 p3136 N90-27796
Measurement of H(sub c1) in a single crystal of YBa2Cu3O7 with low pinning 22 p3151 N90-27864

PINS
Worked-in holes in three-dimensional reinforced composites 02 p0186 N90-11060
Influence of hole surface finish, cyclic frequency and spectrum severity on the fatigue behavior of thick section aluminum alloy pin joints
[ARL-STRUC-R-430] 06 p0745 N90-14336
Preliminary evaluation of the strength of pin-joints in laminated composite materials
[DE90-006353] 11 p1481 N90-18524
The behaviour of mechanically fastened joints in composite structures 16 p2242 N90-22789
Controlled crack growth specimen for brittle systems
[NASA-TM-103126] 17 p2378 N90-23543
Friction, wear and electric characteristics of slip-ring brush materials for space applications. Part 1: Screening by pin-on-disk friction tests
[NAL-TR-1040] 24 p3478 N90-29657

PION BEAMS
Low resistivity electrodeless streamer tubes
[PREPRINT-685-89] 05 p0636 N90-13712
Performance of resistive plate counters at beam flux up to 140 Hz/cm2
[NOTA-INTERNA-930] 05 p0697 N90-14081

PIONEER F SPACE PROBE
U PIONEER 10 SPACE PROBE

PIONEER G SPACE PROBE
U PIONEER 11 SPACE PROBE

PIONEER PROJECT
The Pioneer Venus Orbiter: 11 years of data. A laboratory for atmospheres seminar talk
[NASA-TM-100761] 16 p2328 N90-23273

PIONEER SATURN SPACECRAFT
U PIONEER 11 SPACE PROBE

PIONEER SPACE PROBES
NT PIONEER 10 SPACE PROBE
NT PIONEER 11 SPACE PROBE

PIONEER VENUS ORBITER
U PIONEER VENUS 1 SPACECRAFT

PIONEER VENUS SPACECRAFT
NT PIONEER VENUS 1 SPACECRAFT
A survey of planning and scheduling research at the NASA Ames Research Center 23 p3376 N90-29076

PIONEER VENUS 1 SPACECRAFT
The Pioneer Venus Orbiter: 11 years of data. A laboratory for atmospheres seminar talk
[NASA-TM-100761] 16 p2328 N90-23273
Investigation of plasma density bulge in front of Venus bow shock
[NASA-CR-186937] 22 p3262 N90-28476

PIONEER 12 SPACE PROBE
U PIONEER VENUS SPACECRAFT

PIONEER 10 SPACE PROBE
Pioneers 10 and 11 deep space missions
[NASA-TM-102269] 10 p1448 N90-18355
Digital Doppler extraction demonstration with the advanced receiver 15 p2076 N90-21893

PIONEER 11 SPACE PROBE
Pioneers 10 and 11 deep space missions
[NASA-TM-102269] 10 p1448 N90-18355

PIONS
Fluctuations in transverse energy and multiplicity, energy densities, and neutral pion spectra in nucleus-nucleus collisions at 200 GeV/nucleon
[DE89-017583] 03 p0402 N90-12302
Heavy ion interactions
[DE90-001410] 06 p0840 N90-14884

PIPE FLOW
The structure of Reynolds stress in the near wall region of a turbulent pipe flow 02 p0218 N90-11247
An experimental investigation of transition in oscillating pipe flow 02 p0218 N90-11249
Effect of pipe roughness on orifice flow measurement
[PB89-231484] 04 p0500 N90-12880
Two-phase flow pressure losses in pipeline fittings
[ESDU-89012] 04 p0500 N90-12883
An improved algorithm for the modeling of vapor flow in heat pipes
[NASA-CR-185179] 05 p0642 N90-13748
An investigation of the bursting of trailing vortices using numerical simulation 06 p0718 N90-14191
Selection of the energy-efficient enhancement geometry for single-phase turbulent flow inside tubes
[DE89-017690] 06 p0777 N90-14519
Pipe and bend erosion by pneumatic transport of solids at high temperature
[DE89-015741] 06 p0778 N90-14524
Reduction of erosion in elbows due to flow modifications, phase 2
[DE89-011702] 07 p0932 N90-15394
Pressure losses in flow through a sudden contraction of duct area
[ESDU-89040] 09 p1220 N90-17077
Boiling inside tubes: Pressure drop in straitht tubes with upward or horizontal flow
[ESDU-89039] 09 p1220 N90-17078
Incompressible flow friction factors in a simulated heat pipe
[AD-A216288] 10 p1386 N90-18018
Separation bubbles at high Reynolds number: Measurement and computation
[CUED/A-AERO/15] 12 p1657 N90-19525
Experimental and analytical investigation of adiabatic critical water air two phase flow in small diameter tubes
[TB-88/1] 12 p1660 N90-19540
On the way to an integrated mesh generation system for industrial applications 15 p2095 N90-21989
Turbulence in slurry pipe flow
[DE90-008940] 15 p2098 N90-22006
Mathematical modeling of fluid-solid mixtures
[DE90-009152] 15 p2098 N90-22007
Some observations on liquid flow through filters
[AERE-R-13300] 16 p2234 N90-22748

PIPE NOZZLES
Fatigue resistance of pressure vessels in high strength steels effect of some improvement techniques
[CRIF-MT-176] 05 p0652 N90-13799

PIPELINES
Two-phase flow pressure losses in pipeline fittings
[ESDU-89012] 04 p0500 N90-12883
Pipeline vibrations. Fluid transients in non-rigid, unbranched planar piping systems
[ESDU-89030] 07 p0948 N90-15491
Microbially influenced corrosion of carbon steels
[DE90-012231] 21 p2980 N90-26936

PIPELINING (COMPUTERS)
A distributed pipelined architecture of the recursive Lagrangian equations of motion for robot manipulators with VLSI implementation --- VLSI (very large scale integration)
[RR-353] 03 p0344 N90-11966
Efficient algorithms for dilated mappings of binary trees
[NASA-CR-181980] 09 p1262 N90-17317
A real-time parallel pipelined data-flow image-processing system
[DE90-008324] 13 p1864 N90-20691
Intensity dependent spread processor and workstation 15 p2143 N90-22244
The one dimensional skewing problem
[RUU-CS-89-23] 18 p2596 N90-24769
Design of a universal protocol subsystem architecture: Specification of functions and services
[EUT-89-E-230] 20 p2912 N90-26569
Efficient instruction sequencing with inline target insertion
[NASA-CR-185341] 21 p3052 N90-27348
Implementation and design of a teleoperation system based on a VMEBUS/68020 pipelined architecture 23 p3372 N90-29053
Basic properties and limits of integrated arrays of dissipative circuit and logic elements
[AD-A224533] 24 p3464 N90-29567

PIPES (TUBES)
NT GAS PIPES
Surface-catalyzed air oxidation reactions of hydrazines: Tubular reactor studies 02 p0204 N90-11167
Analysis of coaxial wire measurement of longitudinal coupling impedance
[DE89-015748] 02 p0215 N90-11230
Doubly-fluted tubes and enhanced tubes in confined crossflow
[PB89-217921] 03 p0345 N90-11971
Autofrettage-stress distribution under load and retained stresses after depressurization
[AD-A212090] 03 p0358 N90-12048
Theoretical evaluation of defects in pressure vessels and pipings
[CRIF-MT-174] 05 p0651 N90-13798
Applications of a new exact solution of the Navier-Stokes equations to flow in pipes of varying width 06 p0774 N90-14504
Failure probability estimate of Type 304 stainless steel piping
[DE90-000659] 06 p0796 N90-14635
Heat transfer of buried pipe for heat pump application
[DE90-000580] 06 p0807 N90-14697
Laminar forced convection inside externally finned tubes
[DE89-636431] 07 p0928 N90-15373
Investigation of loads generated by temperature transients in pipes
[DE89-636433] 07 p0932 N90-15395
Eddy-current inspection of shuttle heat exchanger tube welds
[NASA-CR-186302] 07 p0943 N90-15462
Using the singularity-separating method to study how to decrease the pressure at the end of a tube
[PREPRINT-490] 08 p1065 N90-16158
Estimation of subsonic far-field jet-mixing noise from single-stream circular nozzles
[ESDU-89041] 09 p1161 N90-16721
Turbulent heat and momentum transfer in recirculating and impinging flows 09 p1215 N90-17043
Elastic-plastic analysis of a thick-walled composite tube subjected to internal pressure
[AD-A215258] 09 p1238 N90-17187
Elastic stress concentration factors. Geometric discontinuities in rods and tubes of isotropic materials
[ESDU-89048] 09 p1239 N90-17192
FLUSH: A tool for the design of slush hydrogen flow systems
[NASA-TM-102467] 10 p1361 N90-17890
Space shuttle RCS oxidizer leak repair for STS-26 11 p1474 N90-18485
Failure probability estimate of Type 304 stainless steel piping
[DE90-003896] 11 p1486 N90-18550
Oscillation and damping behavior of fine steel test tubes, with particular consideration to destruction free proofs from hydrogen fragilization
[ETN-90-95371] 12 p1627 N90-19351
Determination of flow-regime boundaries for cohesive particles
[DE90-007425] 13 p1800 N90-20332
Determination of Li-Al alloy extent in tubular aluminum elements by small source neutron radiology
[DE90-009142] 14 p1952 N90-21174
A numerical model for the determination of periodic solutions of pipes subjected to non-conservative loads
[DE90-614756] 14 p1993 N90-21423
Program CICC: Flow and heat transfer in Cable In Conduit Conductors, user's manual
[DE90-007924] 14 p2033 N90-21661
Turbulence in slurry pipe flow
[DE90-008940] 15 p2098 N90-22006
Mathematical modeling of fluid-solid mixtures
[DE90-009152] 15 p2098 N90-22007
Design of a telescoping tube system for access and handling equipment 15 p2116 N90-22102
An investigation of the generation and radiation of aerodynamic noise in real piping systems 15 p2164 N90-22368
The elastic-plastic behavior of composite materials 16 p2212 N90-22615
Calcium carbonate scale dissolution in water stabilized by carbon dioxide treatment
[AD-A218502] 16 p2214 N90-22633
Tubular space truss structure for SKITTER 2 robot
[NASA-CR-184922] 17 p2384 N90-23580
Periphery camera system
[AD-A221281] 18 p2555 N90-24583
Experimental characterization of the effects of pneumatic tubing on unsteady pressure measurements
[NASA-TM-4171] 22 p3116 N90-27703
Behavior of aramid/epoxy wounded tubes under uniaxial and biaxial loading
[ETCA-89-R-150] 23 p3339 N90-28873

PISTON ENGINES
NT DIESEL ENGINES
NT FREE-PISTON ENGINES
NT STIRLING ENGINES
System design and performance prediction of a free-piston Stirling engine/magnetic coupling/compressor assembly in a gas residential heat pump
[DE89-016070] 06 p0807 N90-14696
Development of free-piston Stirling engine performance and optimization codes based on Martini simulation technique
[NASA-CR-182210] 10 p1443 N90-18326

PISTONS
Sliding seal materials for low heat rejection engines
[NASA-CR-182262] 03 p0331 N90-11882
Simulation of the control characteristics of an axial piston pump and a flapper-nozzle valve combination 05 p0649 N90-13784
Lightweight piston architecture
[NASA-CASE-LAR-13926-1] 15 p2105 N90-22042
Elastomeric mount for thrust bearing shoe
[AD-D014465] 22 p3181 N90-28054

PITCH (INCLINATION)
The dynamics of circular plates with patch damping: A numerical and experimental study 02 p0232 N90-11329
Unsteady aerodynamics with applications to flight mechanics
[AD-A211944] 03 p0301 N90-11706
Development of a three-axis trim program
[AD-A212883] 06 p0726 N90-14237

A pitch control law for compensation of the phugoid mode induced by windshears 07 p0870 N90-15051
Design of integrated pitch axis for autopilot/autothrottle and integrated lateral axis for autopilot/yaw damper for NASA TSRV airplane using integral LQG methodology [NASA-CR-4268] 09 p1169 N90-16768

PITCH (MATERIAL)
Carbon fiber reinforced glass matrix composites for structural space based applications [AD-A211682] 03 p0320 N90-11818

PITCH ANGLES
U PITCH (INCLINATION)

PITCH ATTITUDE CONTROL
U LONGITUDINAL CONTROL

PITCHING MOMENTS
Normal-force-curve and pitching-moment-curve slopes of forebody-cylinder combinations at zero angle of attack for Mach numbers up to 5 [ESDU-89008] 03 p0301 N90-11709
Normal force, pitching moment, and side force of forebody-cylinder combinations for angles of attack up to 90 degrees and Mach numbers up to 5 [ESDU-89014] 06 p0718 N90-14192
Flow visualization of the effect of pitch rate on the vortex development on the scale model of a F-18 fighter aircraft [AD-A214244] 07 p0876 N90-15080
The response of helicopter rotors to vibratory airload [AD-A215678] 09 p1167 N90-16756
Body effect on wing angle of attack and pitching moment at zero lift at low speeds [ESDU-89042] 09 p1167 N90-16757
Study of the ground effects in the CEAT aerohydrodynamic tunnel: Using the results 23 p3274 N90-28530

PITOT TUBES
Evaluation of water cooled supersonic temperature and pressure probes for application to 2000 F flows [NASA-TM-102612] 19 p2753 N90-25645

PITTING
Coatings for gas turbine compressors [NLR-MP-88045-U] 03 p0308 N90-11750
Unsteady diffusion from a hemispherical pit [NPL-DMA(A)-190] 04 p0553 N90-13220
The effect of dissolved chlorine on the pitting behavior of 304L stainless steel in a 0.5 N NaCl solution [AD-A213803] 07 p0905 N90-15234
The effect of dissolved ozone on the corrosion behavior of Cu-30 Ni and 304L stainless steel in 0.5 N NaCl solutions [AD-A213804] 07 p0906 N90-15235
Stochastic approach to the initiation of pitting corrosion [AERE-R-13348] 13 p1775 N90-20190
Current fluctuations associated with localised corrosion: Mechanistic studies of the early stages of pitting and stress corrosion cracking of stainless steel [AERE-R-13531] 14 p1950 N90-21159
Corrosion behavior of mild steel in high pH aqueous media [PB90-131152] 14 p1950 N90-21162
Surface pitting fatigue life of noninvolute, low-contact-ratio gears [NASA-TM-103116] 16 p2242 N90-22790
A study of the influence of alloying additions on the passivity of aluminium [AD-A219630] 17 p2376 N90-23532
Characterization of the pitting corrosion of aluminum-lithium alloys [ETCA-89-R-176] 22 p3157 N90-27903

PITUITARY GLAND
Experiment K-6-20. The effect of spaceflight on pituitary oxytocin and vasopressin content of rats 20 p2896 N90-26473
Experiment K-6-22. Growth hormone regulation, synthesis and secretion in microgravity. Part 1: Somatotroph physiology. Part 2: Immunohistochemical analysis of hypothalamic hormones. Part 3: Plasma analysis 20 p2896 N90-26475

PITUITARY HORMONES
The pituitary growth hormone cell in space 05 p0676 N90-13941
Experiment K-6-22. Growth hormone regulation, synthesis and secretion in microgravity. Part 1: Somatotroph physiology. Part 2: Immunohistochemical analysis of hypothalamic hormones. Part 3: Plasma analysis 20 p2896 N90-26475

PIVOTS
Pivotal mono wing cruise missile with wing deployment and fastener mechanism [AD-D014191] 04 p0452 N90-12594
Design and performance of an optical mount using cross-flexure pivots [DE89-017551] 04 p0508 N90-12929
Constructibility limits of multiflow wind turbines with pivots [ILR-MITT-215] 12 p1682 N90-19662
Hitching mechanism for lunar dump train [NASA-CR-183034] 19 p2697 N90-25344

PIXELS
Estimated UV clutter levels at 10-100 meter sensor pixel resolution extrapolated from recent polar bear measurements [AD-A211357] 03 p0372 N90-12125
Image preprocessing by modified median filter [AD-D014199] 04 p0492 N90-12828
Video line processor [AD-D014198] 04 p0497 N90-12861
SAS graphics in DCF [PNR90563] 06 p0756 N90-14399
A logic for the pixel assignment step of imagery classification predicated on class structure 07 p0949 N90-15493
Detection of edges using local geometry 08 p1074 N90-16213
Simulation of shading in synthetic surfaces [INPE-4869-PRE/1480] 10 p1326 N90-17660
Project Floval: Correction of relief effects in eucalyptus reforestration [INPE-4814-RPE/590] 11 p1525 N90-18777
A method for determination of control pixels for LANSAT using a reflector [INPE-4884-PRE/1491] 12 p1677 N90-19632
Shade images of forested areas obtained from LANDSAT MSS data [NASA-TM-102939] 14 p1995 N90-21436
Subsystem TM Precision: Progress and perspective [INPE-5006-PRE/1563] 14 p2000 N90-21461

PLAINS
NT COASTAL PLAINS
NT FLOOD PLAINS
Use of ground penetrating radar to define recharge areas in the Central Sand Plain [PB89-224885] 04 p0490 N90-12814

PLANAR STRUCTURES
On the 2-extendability of planar graphs [AD-A210289] 01 p0112 N90-10642
Robust spatial calibration of a planar positron camera [AD-A210773] 02 p0224 N90-11284
Planar sliding of a rigid body with dry friction: Limit surfaces and dynamics of motion 02 p0229 N90-11314
An analytical and experimental study of the elastodynamic response characteristics of planar linkage mechanism with bearing clearances 02 p0233 N90-11336
Inferences from images [AD-A210710] 02 p0258 N90-11465
Acceleration sets of planar manipulators. Part 1: Theory [AD-A213162] 04 p0510 N90-12945
Analysis of the non-planar response of a cantilever, with the aid of computerized symbolic manipulation [AD-A212421] 04 p0545 N90-13172
Acceleration sets of planar manipulators. Part 2: Applications and experiments [AD-A213336] 05 p0650 N90-13791
High temperature aluminum-base alloy [AD-D014270] 08 p1043 N90-16028
Development of planar geometry solid oxide fuel cells [PB90-100769] 08 p1095 N90-16341
Planar array antenna design analysis, volume 1 [AD-A215537] 09 p1207 N90-16999
A statistical study of the surface accuracy of a planar truss beam [NASA-TM-4161] 09 p1235 N90-17171
Internal transmission line filter element [AD-D014353] 12 p1651 N90-19489
Experimental investigations on channelized coplanar waveguide [NASA-TM-102494] 13 p1792 N90-20286
Dual cathode system for electron beam instruments [NASA-CASE-NPO-16878-1-CU] 13 p1803 N90-20351
A homotopy approach to the solutions of minimum-fuel space-flight rendezvous problems 14 p1931 N90-21053
A new rectangular waveguide to coplanar waveguide transition [NASA-TM-102477] 14 p1966 N90-21263
Coplanar waveguide fed phased array antenna [NASA-TM-102522] 14 p1968 N90-21273
Coplanar waveguide discontinuities for P-I-N diode switches and filter applications [NASA-TM-102534] 14 p1969 N90-21278
Elastic-plastic instability of plane frames 14 p1992 N90-21415
Graphically-oriented nonlinear analysis of statically loaded plane frames on microcomputers [PB90-165945] 15 p2144 N90-22248
Symbolic pattern processing system for planar spatial structures [DE90-001598] 15 p2146 N90-22256
Polarization coupling in the acousto-optic interaction of surface waves 15 p2164 N90-22365
Control of a flexible planar truss using proof mass actuators 16 p2288 N90-23035
Low-sidelobe phased array antenna characteristics using the planar near-field Scanning technique: Theory and experiment [AD-A220611] 17 p2390 N90-23613
On the planar translation of two bodies in a uniform flow [AD-A220143] 17 p2404 N90-23698
Millimeter-wave multiplexers [AD-D014518] 19 p2685 N90-25274
Forbidden tangential orbit transfers between intersecting Keplerian orbits [NASA-TP-3031] 20 p2816 N90-26028
Planar microstrip Yagi array antenna [NASA-CASE-NPO-17873-1-CU] 21 p2994 N90-27015
Maintenance of a minimum spanning forest in a dynamic planar graph [AD-A221425] 21 p3054 N90-27362
Optical communications system having a wide-core single-mode planar waveguide [AD-D014485] 22 p3164 N90-27939
Graphically-oriented linear analysis of plane frames subjected to complex loadings on microcomputers [PB90-173279] 22 p3190 N90-28102
Optimal trajectories for hypervelocity flight 24 p3430 N90-29378
A planar rocket motor model for visualization of violent reaction due to fragment impact [AD-A224273] 24 p3441 N90-29431

PLANE STRAIN
Plane strain fracture toughness test procedures for particulate metal matrix composites [NPL-DMM(A)-3] 22 p3153 N90-27873
Comparison of crack closure result obtained by 3D elastic-plastic FEM and modified Dugdale model [FFA-TN-1990-18] 24 p3481 N90-29675

PLANE STRESS
An investigation into the foundations of elastic-plastic fracture mechanics 15 p2120 N90-22130
Axisymmetric and cylindrically orthotropic analysis of filament winding 16 p2246 N90-22811
Weak-beam electron microscopy of dislocation splitting in TiAl: Relationship to plasticity [ESA-TT-1159] 19 p2676 N90-25217

PLANE WAVES
Computations of the refraction of a plane shock wave at a slow-fast gas interface [DE89-016508] 02 p0220 N90-11258
Experimental investigation of a planar shock wave over a double wedge [AD-A211366] 03 p0347 N90-11981
Mobility power flow analysis of an L-shaped plate structure subjected to acoustic excitation [NASA-CR-186130] 05 p0655 N90-13817
A new technique for simulating composite material. Task 2: Analytical solutions with Generalized Impedance Boundary Conditions (GIBCs) [NASA-CR-186249] 07 p0890 N90-15146
Focal plane antenna array for millimeter waves [AD-D014306] 07 p0920 N90-15322
Observation of atomic relaxation near an interface through detection of emitted fluorescence [AD-A214308] 07 p0991 N90-15725
A space-time discretization procedure for wave propagation problems [NASA-TM-102215] 08 p1105 N90-16399
Angle of arrival detection through analysis of optical fiber intensity patterns [AD-A215421] 09 p1218 N90-17065
A numerical and theoretical study of seismic wave diffraction in complex geologic structure [AD-A218209] 14 p2005 N90-21490
Active control of multi-dimensional random sound in ducts [NASA-TM-102653] 14 p2024 N90-21603
The interaction between a plane shock wave and a cylindrical afterbody 15 p2046 N90-21728
Scattering of a plane electromagnetic wave from a semicircular crack in a perfectly conducting ground plane [AD-A219310] 16 p2230 N90-22721
Effect on relaxation on nonlinear waves in crystals 16 p2310 N90-23165
Spectral methods for electromagnetic propagation and diffraction [AD-A220291] 17 p2393 N90-23632
Analysis of regional phases using three-component data [AD-A219482] 17 p2422 N90-23803

Development of an optimized compact test range
[MBB-0053/88-PUB] 19 p2651 N90-25085
Transient electromagnetic scattering on anisotropic media
[DE90-011802] 19 p2683 N90-25262
A study of non-uniqueness and instability for convex materials
[DE90-012060] 19 p2689 N90-25294
Departures from plane-wave-like coupling to a Maverick missile in the radiating near-field region of a horn antenna
[AD-A222539] 21 p2997 N90-27035
Integrated optics interdigitated-electrode switches
[AD-A223245] 21 p3076 N90-27490
Electromagnetic scattering from two-dimensional thick material junctions
[NASA-CR-186468] 23 p3319 N90-28767
Elastic interfaces
[REPT-90-003] 24 p3493 N90-29742

PLANET EPHEMERIDES
Minor planets and other solar system objects
05 p0608 N90-13545
The treatment of minor planets and planetary satellites 05 p0611 N90-13563

PLANET ORIGINS
U PLANETARY EVOLUTION

PLANETARY ATMOSPHERES
NT JUPITER ATMOSPHERE
NT MARS ATMOSPHERE
NT PLANETARY IONOSPHERES
NT SATURN ATMOSPHERE
NT VENUS ATMOSPHERE
NT VENUS CLOUDS
Paper 1. Impact of volcanic aerosols on stratospheric chemistry. Paper 2. O2 (1 sigma g +) and O2 (1 delta g) in the H + O2 reaction system. Paper 3. Barotropic instability of zonal jets on Mars, Earth and Venus
01 p0084 N90-10477
Laboratory measurements of microwave and millimeter-wave properties of planetary atmospheric constituents
[NASA-CR-185914] 01 p0141 N90-10815
The Voyager Neptune travel guide
[NASA-CR-186108] 05 p0585 N90-13412
Laboratory evaluation and application of microwave absorption properties under simulated conditions for planetary atmospheres
[NASA-CR-185916] 06 p0865 N90-15025
Science exploration opportunities for manned missions to the Moon, Mars, Phobos, and an asteroid
[NASA-CR-186295] 09 p1171 N90-16776
IR spectroscopy of planets and satellites; Venus, Mars, giant planets, and Titan 11 p1578 N90-19085
Measurements of the D/H ratio in planetary atmospheres by ground based infrared spectroscopy
11 p1578 N90-19088
Jupiter's drifting decametric bursts with the changing time scale
[DE90-618870] 15 p2192 N90-22517
Auroral ultraviolet darkening on the outer planets
15 p2192 N90-22518
Actions of magnetospheres on planetary atmospheres
[IRF-SR-203] 17 p2486 N90-24215
Submillimeter and millimeter observations of solar system objects
[NASA-CR-186636] 20 p2940 N90-26731
First International Conference on Laboratory Research for Planetary Atmospheres
[NASA-CP-3077] 20 p2942 N90-26744
Laboratory measurements of microwave and millimeter-wave properties of planetary constituents
20 p2943 N90-26745
Laboratory studies, analysis, and interpretation of the spectra of hydrocarbons present in planetary atmospheres including cyanoacetylene, acetylene, propane, and ethane 20 p2943 N90-26748
Infrared spectra of van de Waals complexes of importance in planetary atmospheres
20 p2943 N90-26749
Recent high resolution laboratory determinations of line broadening and intensity parameters: PH3, CH3D, and CO2 20 p2944 N90-26751
Microwave spectra of van der Waals complexes of importance in planetary atmospheres
20 p2944 N90-26752
Infrared line parameters at low temperatures relevant to planetary atmospheres 20 p2944 N90-26753
Determination of molecular spectroscopic parameters and energy-transfer rates by double-resonance spectroscopy 20 p2944 N90-26755
Novel laser gain and time-resolved FTIR studies of photochemistry 20 p2945 N90-26756
High resolution, low temperature photoabsorption cross-section of C2H2 with application to Saturn's atmosphere 20 p2945 N90-26757
Measurements of the methane relaxation times for application to the infrared emission models of the upper atmospheres of outer planets and Titan
20 p2945 N90-26759
Intracavity Dye-Laser Absorption Spectroscopy (IDLAS) for application to planetary molecules
20 p2945 N90-26761
Methane overtone absorption by intracavity laser spectroscopy 20 p2946 N90-26762
Chemical kinetics and modeling of planetary atmospheres 20 p2946 N90-26763
A laboratory investigation of the production and properties of molecular and radical species pertinent to planetary atmospheres 20 p2946 N90-26766
The applications of chemical thermodynamics and chemical kinetics to planetary atmospheres research
20 p2948 N90-26773
Optical constants of solid methane
20 p2948 N90-26775
Optical signatures of molecular particles via mass-selected cluster spectroscopy
20 p2949 N90-26780
Proton irradiation of simple gas mixtures: Influence of irradiation parameters 20 p2949 N90-26782
Infrared spectroscopic measurements on planetary atmospheric gases 23 p3412 N90-29283

PLANETARY BASES
Figure of merit studies of beam power concepts for advanced space exploration
[NASA-CR-186720] 20 p2854 N90-26234
Press abstracts of the 21st Lunar and Planetary Science Conference
[NASA-CR-186874] 20 p2941 N90-26738

PLANETARY BOUNDARY LAYER
Thermodynamic and dynamic processes in the updraft region of GALE (Genesis of Atlantic Lows Experiment) IOP (Intensive Observation Period) 9
[AD-A208139] 01 p0087 N90-10496
A one-dimensional shipboard model for forecasting refractive effects in the planetary boundary layer
06 p0764 N90-14442
A PBL-radiation model for application to regional numerical weather prediction 12 p1635 N90-19394
Multiple versus single scattering of terrestrial infrared longwave radiation in an aerosol-laden planetary boundary layer
[AD-A217709] 13 p1790 N90-20272
A theoretical investigation of gravity-wave-generated stress and vorticity in the planetary boundary layer
15 p2191 N90-22512
A new stochastic model of turbulent dispersion in the convective planetary boundary layer and the results of the Atterbury-87 field study 16 p2254 N90-22853
Boundary layer parameterization for use in a limited area forecast model 21 p3029 N90-27224
A unified view of convective transports by stratocumulus clouds, shallow cumulus clouds, and deep convection
22 p3219 N90-28254
Diffusion in the surface layer of the convective boundary layer
[AD-A224125] 23 p3349 N90-28924

PLANETARY COMPOSITION
Topical Conference on the Origin of the Earth
[NASA-CR-185061] 15 p2128 N90-22166
High resolution infrared spectroscopy of planetary molecules using diode lasers and Fourier transform spectrometers 20 p2943 N90-26747

PLANETARY CORES
NT EARTH CORE
High pressure studies of planetary matter
[DE89-017738] 03 p0428 N90-12455

PLANETARY CRATERS
Potential for observing and discriminating impact craters and comparable volcanic landforms on Magellan radar images 03 p0423 N90-12429
Deducing the age of the dense Venus atmosphere
03 p0425 N90-12438
Impact cratering and the surface age of Venus: The Pre-Magellan controversy 03 p0426 N90-12446

PLANETARY CRUSTS
NT EARTH CRUST
Divergent plate boundaries and crustal spreading on Venus: Evidence from Aphrodite Terra
03 p0422 N90-12427
Tectonism on Venus: A review
03 p0425 N90-12440
Crustal deformation: Earth vs Venus
03 p0427 N90-12450
MEVTV Workshop on Early Tectonic and Volcanic Evolution of Mars
[NASA-CR-186098] 21 p3021 N90-27176

PLANETARY ENTRY
U ATMOSPHERIC ENTRY

PLANETARY ENVIRONMENTS
NT JUPITER ATMOSPHERE
NT MARS ATMOSPHERE
NT MARS ENVIRONMENT
NT PLANETARY ATMOSPHERES
NT PLANETARY IONOSPHERES
NT PLANETARY MAGNETOSPHERES
NT SATURN ATMOSPHERE
NT VENUS ATMOSPHERE
NT VENUS CLOUDS

PLANETARY EVOLUTION
Office of exploration overview
01 p0027 N90-10141
Deducing the age of the dense Venus atmosphere
03 p0425 N90-12438
Clotho Tessera, Venus: A fragment of Fortuna Tessera 03 p0425 N90-12439
Eastern Ishtar Terra: Tectonic evolution derived from recognized features 03 p0428 N90-12451
Reports of planetary geology and geophysics program, 1988
[NASA-TM-4130] 03 p0428 N90-12454
Workshop on the Archean Mantle
[NASA-CR-186156] 06 p0814 N90-14736
The volatile composition of comets
[NASA-CR-186281] 07 p1014 N90-15871
Mission to Mars. Report of the Mars exploration study team
[ESA-SP-1117] 08 p1033 N90-15968
Science exploration opportunities for manned missions to the Moon, Mars, Phobos, and an asteroid
[NASA-CR-186295] 09 p1171 N90-16776
Tectonic history of the terrestrial planets
[NASA-CR-186309] 09 p1246 N90-17229
Topical Conference on the Origin of the Earth
[NASA-CR-185061] 15 p2128 N90-22166
Reports of planetary astronomy, 1990
[NASA-TM-4205] 20 p2940 N90-26730
Carbon chemistry in dense molecular clouds: Theory and observational constraints 21 p3090 N90-27571
Near-infrared speckle observations of T Tauri stars and a multi-wavelength study of the prototype star T Tauri
23 p3409 N90-29264

PLANETARY EXPLORATION
U SPACE EXPLORATION

PLANETARY GEOLOGY
NT MARS VOLCANOES
Abstracts for the Venus Geoscience Tutorial and Venus Geologic Mapping Workshop
[NASA-CR-185432] 03 p0422 N90-12423
Geology of Southern Guinevere Planitia, Venus, based on analyses of Goldstone radar data
03 p0422 N90-12424
Characteristics, distribution and geologic/terrain associations of small dome-like hills on Venus
03 p0422 N90-12425
Tessera terrain: Characteristics and models of origin
03 p0422 N90-12426
Contrasting landform perception with varied radar illumination geometries and at simulated resolutions of Venera and Magellan 03 p0423 N90-12430
Venus surface properties deduced from radar and radiometry 03 p0423 N90-12431
A morphologic study of Venus Ridge belts
03 p0423 N90-12432
Evidence for volcanism in NW Ishtar Terra, Venus
03 p0424 N90-12433
Radar scattering mechanisms within the meteor crater ejecta blanket: Geologic implications and relevance to Venus 03 p0424 N90-12435
Aeolian processes on Venus
03 p0425 N90-12436
Architecture of orogenic belts and convergent zones in Western Ishtar Terra, Venus
03 p0425 N90-12437
Clotho Tessera, Venus: A fragment of Fortuna Tessera 03 p0425 N90-12439
Crater identification and resolution of lunar radar images 03 p0426 N90-12441
Venus: Mantle convection, hotspots, and tectonics
03 p0426 N90-12442
Radar scattering from desert terrains, Pisgah/Lavic Region, California: Implications for Magellan
03 p0426 N90-12443
Lakshmi Planum: A distinctive highland volcanic province 03 p0426 N90-12444
Volcanism on Venus: Large shields and major accumulations of small domes 03 p0426 N90-12445
Impact cratering and the surface age of Venus: The Pre-Magellan controversy 03 p0426 N90-12446
Geology of the Venus equatorial region from Pioneer Venus radar imaging 03 p0427 N90-12447
Venus and the Archean Earth: Thermal considerations
03 p0427 N90-12448
Crustal deformation: Earth vs Venus
03 p0427 N90-12450

Eastern Ishtar Terra: Tectonic evolution derived from recognized features 03 p0428 N90-12451
Three ages of Venus 03 p0428 N90-12453
Reports of planetary geology and geophysics program, 1988
[NASA-TM-4130] 03 p0428 N90-12454
Near infrared spectroscopy of Mars: Study of the surface mineralogy 11 p1579 N90-19091
Aeolian removal of dust from photovoltaic surfaces on Mars
[NASA-TM-102507] 12 p1617 N90-19299
Topical Conference on the Origin of the Earth
[NASA-CR-185061] 15 p2128 N90-22166
Quantitative studies of the Martian south polar region using spacecraft images 15 p2191 N90-22514
The Pioneer Venus Orbiter: 11 years of data. A laboratory for atmospheres seminar talk
[NASA-TM-100761] 16 p2328 N90-23273
Remote Sensing and the Earth's Environment
[ESA-SP-301] 19 p2706 N90-25398
Scientific guidelines for preservation of samples collected from Mars
[NASA-TM-4184] 19 p2796 N90-25918
Directory of research projects: Planetary geology and geophysics program
[NASA-TM-4211] 20 p2942 N90-26743
MEVTV Workshop on Early Tectonic and Volcanic Evolution of Mars
[NASA-CR-186098] 21 p3021 N90-27176
Reports of planetary geology and geophysics program, 1989
[NASA-TM-4210] 21 p3100 N90-27606

PLANETARY IONOSPHERES
Global ionospheric dynamics 02 p0240 N90-11366
The Pioneer Venus Orbiter: 11 years of data. A laboratory for atmospheres seminar talk
[NASA-TM-100761] 16 p2328 N90-23273

PLANETARY MAGNETIC FIELDS
Spacecraft attitude determination using the earth's magnetic field 05 p0589 N90-13429
Equilibrium and stability analysis of magnetospheric plasmas 15 p2057 N90-21782

PLANETARY MAGNETOSPHERES
Research in cosmic and gamma ray astrophysics
[NASA-CR-185451] 04 p0569 N90-13316
The Voyager Neptune travel guide
[NASA-CR-185108] 05 p0585 N90-13412
Particle simulations in magnetospheric plasmas
[NASA-CR-186238] 06 p0848 N90-14934
The dynamics of dust in planetary magnetospheres 08 p1149 N90-16658
Actions of magnetospheres on planetary atmospheres
[IRF-SR-203] 17 p2486 N90-24215

PLANETARY MANTLES
NT EARTH MANTLE
Divergent plate boundaries and crustal spreading on Venus: Evidence from Aphrodite Terra 03 p0422 N90-12427
Venus: Mantle convection, hotspots, and tectonics 03 p0426 N90-12442
Venus and the Archean Earth: Thermal considerations 03 p0427 N90-12448

PLANETARY MAPPING
Phoebe: A preliminary control network and rotational elements
[NASA-CR-185716] 02 p0295 N90-11680
Abstracts for the Venus Geoscience Tutorial and Venus Geologic Mapping Workshop
[NASA-CR-185432] 03 p0422 N90-12423
Characteristics, distribution and geologic/terrain associations of small dome-like hills on Venus 03 p0422 N90-12425
Tessera terrain: Characteristics and models of origin 03 p0422 N90-12426
Divergent plate boundaries and crustal spreading on Venus: Evidence from Aphrodite Terra 03 p0422 N90-12427
Potential for observing and discriminating impact craters and comparable volcanic landforms on Magellan radar images 03 p0423 N90-12429
Architecture of orogenic belts and convergent zones in Western Ishtar Terra, Venus 03 p0425 N90-12437
Clotho Tessera, Venus: A fragment of Fortuna Tessera 03 p0425 N90-12439
Venus: Mantle convection, hotspots, and tectonics 03 p0426 N90-12442
Lakshmi Planum: A distinctive highland volcanic province 03 p0426 N90-12444
Volcanism on Venus: Large shields and major accumulations of small domes 03 p0426 N90-12445
Impact cratering and the surface age of Venus: The Pre-Magellan controversy 03 p0426 N90-12446
Eastern Ishtar Terra: Tectonic evolution derived from recognized features 03 p0428 N90-12451
Three ages of Venus 03 p0428 N90-12453
The Magellan Venus explorer's guide
[NASA-CR-186968] 23 p3286 N90-28592
First results in terrain mapping for a roving planetary explorer 23 p3375 N90-29066

PLANETARY METEOROLOGY
Synoptic/planetary-scale interactions and blocking over the North Atlantic Ocean 03 p0360 N90-12061
Application of dynamical systems theory to global weather phenomena revealed by satellite imagery 03 p0361 N90-12063

PLANETARY NEBULAE
Identification of solar nebula condensates in interplanetary dust particles and unequilibrated ordinary chondrites 08 p1144 N90-16629
Airborne observations of the infrared emission bands 11 p1580 N90-19101
Planetary nebulae 11 p1583 N90-19122
A survey of PAH emission in HII regions, planetary and proto-planetary nebulae 11 p1584 N90-19129
Unidentified infrared features in proto-planetary nebulae 11 p1584 N90-19130
Dust in planetary nebulae: IRSPEC observations in the 3.0 micron-3.8 micron range 11 p1584 N90-19132
The microchannel plate camera as a detector at high resolution spectrographs: Experiments for velocity distribution in planetary nebulae
[ETN-90-95733] 12 p1664 N90-19560
Signature objects: Preliminaries for the satellite project HIPPARCOS/TYCHO
[ETN-90-95730] 12 p1729 N90-19934
Model calculations for dynamic development of planetary nebulae
[ETN-90-95734] 12 p1744 N90-20025
Structural experiments of planetary nebulae: Charge-coupled devices, image reduction under MIDAS, information representation, and development of an evolution classification for PN's
[ETN-90-95736] 12 p1744 N90-20026
Recombination lines of C I and N II in the interstellar medium 15 p2182 N90-22466
Investigation of the late stages of stellar evolution: Mass loss from evolved stars 15 p2187 N90-22492
The dynamic instability of adiabatic blastwaves
[NASA-CR-182498] 17 p2401 N90-23679
On planetary nebulae as sources of carbon dust: Infrared emission from planetary nebulae of the galactic halo 21 p3093 N90-27583
The ionization structure of planetary nebulae 10: NGC 2392
[NASA-CR-186960] 23 p3411 N90-29274

PLANETARY ORBITS
An analytic development of orbit determination for a distant, planetary orbiter 04 p0485 N90-12787
Manned spacecraft
[AD-A214218] 07 p0887 N90-15129
Vector fields, linear spaces and tensors in physics. Part 3: Tensor analysis and its applications
[INPE-5000-MD/41] 11 p1561 N90-18997
Use of random Martian atmosphere to evaluate potential entry guidance schemes
[NASA-TM-102606] 13 p1764 N90-20122
Reports of planetary astronomy, 1990
[NASA-TM-4205] 20 p2940 N90-26730

PLANETARY RADIATION
High resolution imaging of the Venus night side using a Rockwell 128x128 HgCdTe array 14 p1978 N90-21330

PLANETARY RINGS
NT SATURN RINGS
The Voyager Neptune travel guide
[NASA-CR-186108] 05 p0585 N90-13412

PLANETARY SATELLITES
U NATURAL SATELLITES

PLANETARY SPACE FLIGHT
U INTERPLANETARY FLIGHT

PLANETARY SPACECRAFT
U INTERPLANETARY SPACECRAFT

PLANETARY SURFACES
NT MARS SURFACE
NT VENUS SURFACE
A dynamical study of Jupiter's Great Red Spot 02 p0295 N90-11681
The nature of cometary materials 08 p1147 N90-16647
United States planetary rover status: 1989
[NASA-CR-186843] 19 p2698 N90-25353
Planning for execution monitoring on a planetary rover 19 p2735 N90-25548
Analysis of a Mars-stationary orbiting microwave power transmission system
[NASA-TM-101344] 20 p2843 N90-26172
A system architecture for a planetary rover 23 p3365 N90-29015
Planetary rover technology development requirements 23 p3375 N90-29067

PLANETARY SYSTEMS
NT SOLAR SYSTEM

PLANETARY TEMPERATURE
Large impact events and atmospheric evolution on the terrestrial planets 12 p1744 N90-20028

PLANETARY WAVES
Application of dynamical systems theory to global weather phenomena revealed by satellite imagery 03 p0361 N90-12063
The effect of latent heat release on synoptic-to-planetary wave interactions and its implication for satellite observations: Theoretical modeling 03 p0362 N90-12073
The effect of latent heat release on synoptic-to-planetary scale wave interactions: Observational study 03 p0362 N90-12074
Laboratory and theoretical models of planetary-scale instabilities and waves 03 p0363 N90-12076
Observations of long Rossby waves in the northern tropical Pacific
[PB89-196331] 03 p0376 N90-12143
Long wave propagation assessment 06 p0758 N90-14414
The effect of orographic forcing on the mean flow of the stratosphere 08 p1099 N90-16367
Evolution of atmospheric baroclinic waves 16 p2254 N90-22855
Meteor radar studies of the mesopause region and nonlinear atmospheric waves 17 p2421 N90-23799
Annual and interannual variations of Earth-emitted radiation based on a 10-year data set
[NASA-TM-103465] 20 p2887 N90-26432
The planetary waves dynamics and interannual course of meteorological parameters of the high latitude stratosphere and mesosphere of the Northern and Southern Hemispheres during the 20th and 21st solar cycles and different phases of QBO 22 p3203 N90-28170
Atmospheric planetary waves induced by solar rotation 22 p3204 N90-28178
Resonant Rossby waves and solar activity 22 p3205 N90-28179
Total ozone time variations during the spring reversals in the high latitudinal stratosphere of the Northern Hemisphere during the 20th and 21st solar cycles 22 p3205 N90-28181

PLANETESIMALS
U PROTOPLANETS

PLANETOLOGY
Data catalog series for space science and applications flight missions. Volume 5A: Descriptions of astronomy, astrophysics, and solar physics spacecraft and investigations. Volume 5B: Descriptions of data sets from astronomy, astrophysics, and solar physics spacecraft and investigations
[NASA-TM-101908] 24 p3437 N90-29413
Data catalog series for space science and applications flight flight missions. Volume 2B: Descriptions of data sets from geostationary and high-altitude scientific spacecraft and investigations
[NASA-TM-101909] 24 p3437 N90-29414
Data catalog series for space science and applications flight missions. Volume 1A: Descriptions of planetary and heliocentric spacecraft and investigations, second edition
[NASA-TM-101910] 24 p3438 N90-29415
Data catalog series for space science and applications flight missions. Volume 6: Master index volume
[NASA-TM-101913] 24 p3438 N90-29416
Data catalog series for space science and applications flight missions. Volume 3B: Descriptions of data sets from low- and medium-altitude scientific spacecraft and investigations
[NASA-TM-89680] 24 p3560 N90-30140
Data catalog series for space science and applications flight missions. Volume 1B: Descriptions of data sets from planetary and heliocentric spacecraft and investigations
[NASA-TM-89695] 24 p3561 N90-30148

PLANETS
NT EARTH (PLANET)
NT GAS GIANT PLANETS
NT JUPITER (PLANET)
NT MARS (PLANET)
NT MERCURY (PLANET)
NT NEPTUNE (PLANET)
NT PLUTO (PLANET)
NT SATURN (PLANET)
NT TERRESTRIAL PLANETS
NT URANUS (PLANET)
NT VENUS (PLANET)
Satellite motion around an oblate planet: A perturbation solution for all orbital parameters
[AD-A216176] 10 p1326 N90-17661
Large impact events and atmospheric evolution on the terrestrial planets 12 p1744 N90-20028

Extraterrestrial life in the universe
[NASA-TM-102363] 15 p2181 N90-22464

PLANFORMS
NT DELTA WINGS
NT RECTANGULAR PANELS
NT RECTANGULAR PLANFORMS
NT RECTANGULAR PLATES
NT RECTANGULAR WINGS
NT SWEPT FORWARD WINGS
NT SWEPTBACK WINGS
NT VARIABLE SWEEP WINGS
NT WING PLANFORMS
Prediction of forces and moments for flight vehicle control effectors. Part 2: An analysis of delta wing aerodynamic control effectiveness in ground effect
[NASA-CR-186572] 15 p2047 N90-21735

PLANIGRAPHY
U TOMOGRAPHY

PLANKTON
NT PHYTOPLANKTON
Observations of fine-scale vertical shear and strain in the upper ocean
[AD-A214476] 10 p1410 N90-18130

PLANKTON BLOOM
U PLANKTON

PLANNING
NT AIRPORT PLANNING
NT MANAGEMENT PLANNING
NT MISSION PLANNING
NT PRODUCTION PLANNING
NT PROJECT PLANNING
NT REGIONAL PLANNING
NT TASK PLANNING (ROBOTICS)
NT TRAJECTORY PLANNING
NT URBAN PLANNING
Differences in writers initial task representations
[AD-A210433] 01 p0136 N90-10788
The Air Force Flight Test Center Flight Test Safety Program 02 p0153 N90-10872
Advanced Turbine Technology Applications Program, (ATTAP): A plan for improving the prototype production of ceramic components for the gas turbine engine, 1988--1992
[DE89-015566] 02 p0230 N90-11320
Linkoeping's A.I. Consortium (LAIC) for plan guided systems. Review of the first 18 months
[FOA-C-30528-3.4] 02 p0269 N90-11537
Planning in writing: The cognition of a constructive process
[AD-A210434] 02 p0288 N90-11648
Coupling rule-based and object-oriented programming for the classification of machined features
[DE89-017705] 03 p0334 N90-11903
An optimum trajectory planner for robot manipulators in joint-space and under physical constraints
[RR-349] 03 p0355 N90-12029
Reasoning about change and exceptions in automated process planning
[DE89-017706] 03 p0386 N90-12195
Problem-dependent transformations of 3D terrain elevation maps into cost precursor maps
[PB89-218127] 04 p0514 N90-12969
Battery technology assessment and R and D plan
[DE90-002007] 06 p0772 N90-14489
An expert system for quality assurance (a.k.a.) QA Express
[DE90-003887] 07 p0944 N90-15467
Annual operating plan for fiscal year 1990 for chemical/hydrogen energy systems program
[DE90-003964] 07 p0955 N90-15527
The first 1000 days of a future lunar base
[ILR-MITT-224] 08 p1033 N90-15970
Federal roles to realize national energy-efficiency opportunities in the 1990s
[DE90-004410] 08 p1096 N90-16348
Invention and innovation: Alternative mechanisms for enhancing organizational competitiveness
[DE89-015858] 08 p1136 N90-16584
Optimal planning method of underground distribution system, part 2. Application to various types of system configurations
[DE89-782323] 11 p1500 N90-18636
Approaches to the planning of coherent text
[AD-A216463] 11 p1545 N90-18895
Working on the moon: The Apollo experience
[DE90-003662] 12 p1697 N90-19744
Experimental validation of extended image reconstruction using bispectral speckle interferometry
[DE90-008545] 13 p1772 N90-20171
Swing-free movement of simply suspended objects employing parameter estimation
[DE90-002238] 13 p1811 N90-20398
Controlling Summer Heat Islands: Proceedings
[DE90-008075] 13 p1830 N90-20508
Robust planning and control using neural networks
[AD-A217216] 13 p1872 N90-20732
Principles of Very Large Scale Integrated (VLSI) system planning 15 p2088 N90-21950
The 1990 Goddard Conference on Space Applications of Artificial Intelligence
[NASA-CP-3068] 15 p2152 N90-22294
The application of connectionism to query planning/scheduling in intelligent user interfaces 15 p2152 N90-22295
SURE (Science User Resource Expert): A science planning and scheduling assistant for a resource based environment 15 p2153 N90-22302
A knowledge-based approach to improving optimization techniques in system planning 15 p2154 N90-22303
US access to space: Launch vehicle choices for 1990 to 2010 16 p2205 N90-22579
Environmental effects upon cross-servicing of aircraft in NATO
[AD-A218374] 17 p2343 N90-23341
CMOS IC I(sub DDQ) testing for the 1990s
[DE90-009508] 17 p2394 N90-23634
The effects of climate change on energy planning and operations in the Pacific Northwest. Volume 1: Overview
[DE90-009464] 17 p2425 N90-23816
Sequencing and scheduling: Algorithms and complexity
[CWI-BS-R8909] 17 p2446 N90-23942
Summary results of an assessment of research projects in the national photovoltaics program
[DE90-008222] 18 p2577 N90-24680
Understanding our genetic inheritance. The US Human Genome project: The first five years, FY 1991-1995
[DE90-008240] 18 p2584 N90-24718
Mobile transporter path planning 19 p2727 N90-25505
Enroute flight planning: The design of cooperative planning systems
[NASA-CR-186797] 20 p2806 N90-25964
Structural Mechanics Division research and technology plans for FY 1990 and accomplishments for FY 1989
[NASA-TM-102654] 20 p2876 N90-26361
Investigation of automated task learning, decomposition and scheduling
[NASA-CR-186791] 20 p2899 N90-26488
Autoplan: A self-processing network model for an extended blocks world planning environment
[NASA-CR-186733] 20 p2905 N90-26526
Integrating planning and reactive control 23 p3377 N90-29077
Integrating planning, execution, and learning 23 p3377 N90-29079
Vehicle path-planning in three dimensions using optics analogs for optimizing visibility and energy cost 24 p3512 N90-29853
Precedence relationship representations of mechanical assembly sequences 24 p3514 N90-29866
The indexed time table approach for planning and acting 24 p3521 N90-29907

PLANT DISEASES
Investigation of the usefulness of LANDSAT 5 thematic mapper data for mapping forest disease
[DFVLR-FB-89-06] 03 p0365 N90-12088
Signature analysis and classification of pine of different vitality classes using airborne thematic mapper data
[DFVLR-FB-89-07] 03 p0365 N90-12089

PLANT STRESS
Air pollution-caused changes in photosynthesis: Effects on plant growth and rhizosphere functions
[DE90-007184] 13 p1829 N90-20501
Vegetation stress monitoring by fluorescence 19 p2708 N90-25414

PLANTING
Dynamics of carbon dioxide exchange of a wheat community grown in a semi-closed environment 08 p1155 N90-16689
Relationship of radiometric field measurements of wheat in the Assis-Safra region, 1988
[INPE-4949-RPE/598] 13 p1819 N90-20443
Wheat productivity estimate through field radiometry
[INPE-4994-PRE/1556] 14 p2000 N90-21460
Spectral response of wheat and its relationship with agronomic variables in the tropical region
[INPE-5018-RPE/612] 15 p2122 N90-22138
A proposal to demonstrate production of salad crops in the space station mockup facility with particular attention to space, energy, and labor constraints
[NASA-CR-186811] 19 p2725 N90-25500

PLANTS (BOTANY)
NT ALGAE
NT AQUATIC PLANTS
NT CONIFERS
NT COTTON
NT FUNGI
NT GRASSES
NT LEGUMINOUS PLANTS
NT PHYTOPLANKTON
NT SOYBEANS
NT SUGAR CANE
NT TREES (PLANTS)
Global data bases on distribution, characteristics and methane emission of natural wetlands: Documentation of archived data tape
[NASA-TM-4153] 03 p0365 N90-12090
How to detect when cells in space perceive gravity 05 p0678 N90-13946
Effects of microgravity on growth hormone concentration and distribution in plants 05 p0678 N90-13947
Gravity receptors and responses 05 p0678 N90-13948
Gravitropism in plants: Hydraulics and wall growth properties of responding cells 05 p0678 N90-13950
A collaborative effort to model plant response to acidic rain
[DE90-003002] 09 p1244 N90-17215
ELF (Extremely Low Frequency) communications system ecological monitoring program: Summary of 1988 progress
[AD-A216153] 10 p1377 N90-17981
ELF (Extremely Low Frequency) communications systems ecological monitoring program: Wetland studies
[AD-A218632] 16 p2229 N90-22716
Design and implementation of sensor systems for control of a closed-loop life support system
[NASA-CR-186675] 19 p2725 N90-25497
Flora and threatened and endangered plants of John F. Kennedy Space Center, Florida
[NASA-TM-102791] 23 p3349 N90-28925

PLANTS (INDUSTRIES)
U INDUSTRIAL PLANTS

PLASMA ACCELERATION
Experimental studies of plasma wake-field acceleration and focusing
[DE89-016718] 02 p0279 N90-11591

PLASMA ACCELERATORS
NT COAXIAL PLASMA ACCELERATORS
Theoretical and computational studies of magnetic insulation and other plasma-opening-switch phenomena
[DE90-004421] 07 p0996 N90-15757
Optical guiding by plasma waves in the plasma beat wave accelerator
[AD-A214288] 07 p0997 N90-15763

PLASMA ARC SPRAYING
U ARC SPRAYING

PLASMA ARC WELDING
Material properties of 2219-T851 aluminum alloy plasma welded compared to TIG welding 02 p0182 N90-11032
Heat sink effects on weld bead: VPPA process 12 p1639 N90-19418
Heat sink effects on weld bead: VPPA process
[NASA-CR-186723] 19 p2697 N90-25349
The effect of impurity gasses on variable polarity plasma arc welded 2219 aluminum
[NASA-CR-183803] 21 p2980 N90-26935
Power beam technology at Los Alamos: A review of research and development activities
[DE90-009002] 22 p3182 N90-28057
Robotic and automatic welding development at the Marshall Space Flight Center 23 p3298 N90-28656

PLASMA ARCS
U PLASMA JETS

PLASMA BUBBLES
Low latitude F-region dynamical processes from atomic oxygen nightglow emissions
[INPE-4999-PRE/1561] 14 p2006 N90-21494

PLASMA CHEMISTRY
The 10th Gordon Research Conference on Plasma Chemistry
[AD-A215161] 09 p1285 N90-17449
Pulsed-discharge carbon dioxide lasers 18 p2556 N90-24587
Production of NO, NO2 and N2O in air by breakdown with high power microwaves: A preliminary report
[AD-A223297] 24 p3495 N90-29749

PLASMA CLOUDS
NT MAGNETIC CLOUDS
Short wavelength striations on expanding plasma clouds
[DE89-016585] 02 p0250 N90-11416
A beam induced upset during the flight of the ECHO-7 rocket
[NASA-CR-186089] 03 p0309 N90-11755
Two-meter laser material response impulse measurements
[AD-A215834] 12 p1665 N90-19567

PLASMA COMPOSITION
Vacuum deposition by pulsed laser radiation: Plasma composition, deposition techniques, and thin film properties
[ETN-90-97263] 20 p2931 N90-26677

PLASMA COMPRESSION
Initial results from FRC (Field-Reversed Configuration) compression experiments on FRX-C/LSM
[DE90-003390] 07 p0995 N90-15754
Design of a spheromak compressor driven by high explosives
[DE90-003652] 08 p1086 N90-16283
High growth rate diamond synthesis in a large area atmospheric pressure inductively coupled plasma
[AD-A216090] 11 p1567 N90-19019
PLASMA CONDUCTIVITY
Workshop on Hydrogen Effects in InP and Related Compounds
[AD-A215197] 09 p1290 N90-17479
PLASMA CONFINEMENT
U PLASMA CONTROL
PLASMA CONTROL
Observations of azimuthal asymmetry for certain FRC operating regimes
[DE89-015300] 01 p0126 N90-10721
Massachusetts Institute of Technology Plasma Fusion Center
[DE89-016050] 01 p0126 N90-10723
Hybrid particle-fluid approach to low-frequency turbulence in magnetically confined plasmas
[DE89-015904] 02 p0277 N90-11579
A study of runaway electron confinement and theory of neoclassical MHD turbulence
[DE89-016728] 02 p0277 N90-11584
Launched electrons in plasma opening switches
[DE89-016886] 02 p0279 N90-11596
Compact torus configurations with high frequency driven currents
[ETN-89-94674] 02 p0280 N90-11598
Confinement of multiply charged ions in an ECRH mirror plasma
[DE89-016052] 03 p0406 N90-12327
Control of plasma position in the CASTOR tokamak
[IPPCZ-284] 03 p0407 N90-12332
Computation of electromagnetic effects in a tokamak due to a plasma disruption
[DE90-001764] 06 p0848 N90-14931
Studies of plasma performance and transport in the Advanced Toroidal Facility (ATF)
[DE90-001737] 07 p0994 N90-15746
Design of DIII-D advanced divertor
[DE90-003343] 07 p0995 N90-15752
Magnetic mirror confinement concepts system studies
[DE90-003667] 07 p0995 N90-15753
Theoretical and computational studies of magnetic insulation and other plasma-opening-switch phenomena
[DE90-004421] 07 p0996 N90-15757
Hollow-cathode experiments to support electrodynamic tether applications
[IFSI-89-5] 08 p1036 N90-15986
Initial deuterium confinement studies in DIII-D tokamak: DIII-D milestone report number 58
[DE90-003942] 08 p1124 N90-16509
Recent progress on the HESS (High Explosive Spheromak Source) experiment
[DE90-003218] 08 p1125 N90-16520
Plasma assisted chemical vapor deposition of diamond films
[AD-A214641] 09 p1197 N90-16934
Density clamping phenomena in electron cyclotron resonance heated plasmas on Heliotron E
[DE90-719523] 09 p1284 N90-17442
Dissipative trapped electron modes in ell equals 2 torsatrons
[DE90-004919] 10 p1431 N90-18256
Results of the H-mode experiments with JT-60 outer and lower divertors
[DE90-733146] 10 p1432 N90-18265
First pump limiter experiments in TORE SUPRA
[DE90-004968] 10 p1432 N90-18266
Anomalous particle diffusion through a magnetic picket fence
[INPE-4841-PRE/1470] 10 p1433 N90-18270
Overview of recent results from the Advanced Toroidal Facility
[DE90-005673] 12 p1716 N90-19853
Anomalous transport in toroidal plasmas
[DE90-006549] 12 p1717 N90-19859
Theory of field reversed configurations
[DE90-006702] 12 p1717 N90-19860
Improved energy and power balance at Nova targets
[DE90-007260] 13 p1807 N90-20372
Power threshold for neutral beam current drive
[DE90-008348] 13 p1886 N90-20822
The impedance of energy efficiency of a coaxial magnetized plasma source used for spheromak formation and sustainment
[DE90-003220] 13 p1889 N90-20841
The ANU (Australian National University) Heliac Program
[DE90-006620] 13 p1890 N90-20843
Difference in electron thermal diffusivity and profile between interior and exterior of TFTR L-mode plasmas
[DE90-007479] 13 p1890 N90-20846
High elongation plasmas
[DE90-007575] 13 p1891 N90-20848
West European magnetic confinement fusion research 14 p2029 N90-21634
Applied plasma physics
[DE90-007932] 14 p2029 N90-21635
Magnetic turbulence versus safety factor in the Tokapole 2 tokamak 15 p2168 N90-22391
Japanese magnetic confinement fusion research 15 p2169 N90-22392
Impurity control in toroidal devices
[DE90-618585] 15 p2170 N90-22399
Advances in spheromak understanding and parameters
[DE90-012052] 19 p2759 N90-25678
Comparative assessment of world research efforts on magnetic confinement fusion 19 p2759 N90-25680
Confinement of nonneutral plasma in unconventional geometries
[DE90-013048] 20 p2928 N90-26659
The effects of carbonization on the confinement properties of the DIII-D H-mode
[DE90-013297] 20 p2928 N90-26660
Physics of the L to H transition in DIII-D
[DE90-014120] 23 p3396 N90-29187
Temperature-gradient instability induced by conducting end walls
[DE90-014334] 23 p3396 N90-29188
Stellarator status, 1989
[DE90-014791] 23 p3397 N90-29192
Spatial structure of particle-orbit loss regions in l=2 helical systems
[DE90-508080] 24 p3548 N90-30073
Structure of magnetic field in tokamaks
[DE90-628904] 24 p3549 N90-30075
Magnetic surfaces in tokamaks
[DE90-628905] 24 p3549 N90-30076
PLASMA COOLING
Liquid and solid ion plasmas
[AD-A212415] 04 p0557 N90-13244
Experimental study of population inversion and spectral line broadening in a plasma containing a mixture of high Z and low Z ions
[DE90-007552] 14 p2027 N90-21622
PLASMA CURRENTS
Compact torus configurations with high frequency driven currents
[ETN-89-94674] 02 p0280 N90-11598
Plasma-anode electron gun research
[AD-A211547] 03 p0312 N90-11773
Effect of the length of the multijunction grill on its lower hybrid current drive efficiency
[IPPCZ-283] 04 p0556 N90-13240
On optimization of the multijunction grill for the lower hybrid current drive
[IPPCZ-280] 04 p0556 N90-13241
The Space Station Photovoltaic Panels Plasma Interaction Test Program: Test plan and results
[NASA-TM-102474] 05 p0613 N90-13581
Effects of ionospheric modification on system performance 20 p2849 N90-26202
Application of the results of carbon pellet modeling to the problem of plasma penetration
[DE90-012713] 20 p2928 N90-26658
The effects of carbonization on the confinement properties of the DIII-D H-mode
[DE90-013297] 20 p2928 N90-26660
Combined electron cyclotron ray tracing and transport code studies in the compact ignition tokamak
[DE90-014097] 23 p3396 N90-29189
PLASMA CYLINDERS
NT CYLINDRICAL PLASMAS
On the thermal stability of flow of a radiating two-component plasma in a porous medium between two rotating cylinders
[DE89-636426] 06 p0847 N90-14928
PLASMA DECAY
An experimental study of microwave transmission through a decaying plasma
[AD-A210586] 01 p0127 N90-10726
Experimental and theoretical study of artificial plasma layers produced by two intersecting beams in a chamber
[NASA-CR-184598] 05 p0701 N90-14102
Limitations in the growing of a plasma wave produced by heterodyning two lasers due to modulations and decay instabilities 06 p0783 N90-14552
Model of oxygen ions resonant lines emission of REB-heated plasma
[IPPCZ-294] 10 p1432 N90-18261
Anomalous decay of Langmuir turbulence. High power, high frequency radiation from beam-plasma interaactions
[AD-A224282] 24 p3547 N90-30065
PLASMA DENSITY
Simultaneous multiple frequency interferometry: An application of homodyne phase measurement
[DE89-013975] 01 p0126 N90-10719
Scattering of an ICRF magnetosonic wave by plasma density turbulence
[DE89-015223] 01 p0126 N90-10720
Numerical simulation of the compressible Orszag-Tang vortex
[AD-A210465] 01 p0127 N90-10725
ANTHEM simulation of plasma opening switches
[DE89-016617] 02 p0217 N90-11239
Studies of a strongly coupled plasma produced in a capillary discharge
[DE89-016611] 02 p0277 N90-11581
ANTHEM simulation of the early time magnetic field penetration of the plasma surrounding a high density Z-pinch
[DE89-016980] 02 p0277 N90-11585
Producing of an ECR plasma using 2450MHz Whistler wave and the investigating of its parameters
[DE89-618689] 02 p0278 N90-11586
Experimental studies of plasma wake-field acceleration and focusing
[DE89-016718] 02 p0279 N90-11591
Beam-plasma discharge in penetrating plasma
[DE89-630481] 02 p0280 N90-11597
Magnetically insulated electron flows in pulsed power systems
[AD-A212746] 04 p0549 N90-13196
Resonance cone diagnostics in the mid-latitude ionosphere 05 p0658 N90-13840
Experimental and theoretical study of artificial plasma layers produced by two intersecting beams in a chamber
[NASA-CR-184598] 05 p0701 N90-14102
Strategic characteristics of Dynamics Explorer 1 retarding ion mass spectrometer and the consequences for core plasma measurements
[AD-A214013] 07 p0886 N90-15125
Frequency shift induced in laser pulses by plasma density variations
[AD-A214195] 07 p0936 N90-15424
Microfluctuations of plasma density in a theta-pinch and spatial coherency of a probing laser beam
[DE90-603347] 07 p0996 N90-15760
Langmuir wave interaction with ion-sound one. Part 1: Stochastic effects
[DE90-603368] 08 p1118 N90-16474
The lower hybrid drift instability and the evolution of plasma gradients
[DE90-006521] 11 p1568 N90-19021
Study on rotating plasma with submillimeter laser interferometer
[DE90-615387] 14 p2027 N90-21623
Helium transport in plasma edge regions 14 p2027 N90-21625
A simplified theoretical model for the laser-induced optogalvanic effect
[DE90-613121] 14 p2028 N90-21626
Characterization of the plasma in magnetic multidipole discharges
[DE90-613219] 14 p2028 N90-21628
Analytical theory of the Bunemann instability for electron runaway
[IPF-88-3] 16 p2319 N90-23224
An analytic/empirical model of the middle and low latitude ionosphere
[AD-A220004] 17 p2423 N90-23809
Plasma cloaking: Air chemistry, broadband absorption, and plasma generation
[AD-A222044] 21 p3078 N90-27503
Investigation of plasma density bulge in front of Venus bow shock
[NASA-CR-186937] 22 p3262 N90-28476
A model of peaked density profile and inward pinch in tokamaks
[DE90-508079] 24 p3548 N90-30072
UCD-LLNL collaboration on basic plasma physics research in inertial confinement fusion
[DE90-015771] 24 p3549 N90-30081
PLASMA DIAGNOSTICS
Observations of azimuthal asymmetry for certain FRC operating regimes
[DE89-015300] 01 p0126 N90-10721
Generation of 3/2 omega sub o radiation in inhomogeneous plasmas under the irradiation of intense electromagnetic waves
[DE89-015723] 01 p0126 N90-10722
Massachusetts Institute of Technology Plasma Fusion Center
[DE89-016050] 01 p0126 N90-10723
PISCES program plasma-surface interactions research
[DE89-015622] 02 p0276 N90-11578
Confinement of multiply charged ions in an ECRH mirror plasma
[DE89-016052] 03 p0406 N90-12327

The soft x ray telescope for Solar-A
03 p0432 N90-12475
Research on heating, instabilities, turbulence and RF emission from electric field dominated plasmas
[AD-A212122] 04 p0557 N90-13243
Resonance cone diagnostics in the mid-latitude ionosphere 05 p0658 N90-13840
Laser probing non-cylindrical Z-pinch in near-isolator region of a discharged chamber
[DE89-632018] 06 p0844 N90-14912
Ion collection by probing objects in flowing magnetized plasmas
[DE90-001711] 06 p0845 N90-14916
Microwave Tokamak Experiment (MTX) first year of operation and future plans
[DE90-000817] 06 p0846 N90-14920
Precision timing and interlocks systems for FEL (Free-Electron Laser) heating experiments on MTX (Microwave Tokamak Experiment)
[DE90-000833] 06 p0847 N90-14923
Microwave Tokamak Experiment: An overview of the construction and checkout phase
[DE90-000834] 06 p0847 N90-14924
Microfluctuations of plasma density in a theta-pinch and spatial coherency of a probing laser beam
[DE90-603347] 07 p0996 N90-15760
In situ measurement of neutral beam components using the Doppler-shifted H(sub alpha) emissions in Heliotron E
[DE90-719521] 08 p1125 N90-16516
Low energy neutral particle energy analyser by time of flight method
[DE90-719529] 08 p1125 N90-16517
Spectroscopic diagnostics of high temperature plasmas
[DE90-003912] 08 p1126 N90-16522
Advanced diagnostics for reacting flows
[AD-A215050] 09 p1217 N90-17060
Advanced diagnostics for reacting flows
[AD-A214795] 09 p1285 N90-17448
The 10th Gordon Research Conference on Plasma Chemistry
[AD-A215161] 09 p1285 N90-17449
Spectral characteristics of arc-heated low density plasma flows (IV) air and N2-CO2 mixture plasmas
[NAL-TR-1012] 09 p1285 N90-17451
A 13-point Thomson scattering system for JFT-2M plasma
[DE90-733140] 10 p1432 N90-18263
Plasma diagnostics generated in the Compact Torus of UNICAMP
[INPE-4862-RPE/593] 10 p1433 N90-18271
Measurement of the space potential of a high-temperature plasma by fast atomic beam scattering on an ion probe beam
[DE90-006118] 11 p1567 N90-19020
Computerized analysis of hydrogen plasma in a compact H(sup -) cusp source
[DE90-006881] 11 p1569 N90-19029
FOMA: A Fast Optical Multichannel Analyzer
[DE90-004093] 12 p1713 N90-19839
Particle transport in pellet fueled JET (Jet European Torus) plasmas
[DE90-008077] 13 p1891 N90-20851
Time-resolved spectroscopy of nonequilibrium ionization in laser-produced plasmas
[DE90-008663] 13 p1891 N90-20854
The investigation of multilayer x ray reflectors as x ray optical elements
[DE90-009044] 14 p2026 N90-21621
Study on rotating plasma with submillimeter laser interferometer
[DE90-615387] 14 p2027 N90-21623
Characterization of the plasma in magnetic multidipole discharges
[DE90-613219] 14 p2028 N90-21628
Applied plasma physics
[DE90-007932] 14 p2029 N90-21635
Thermal barrier research
[DE90-009213] 16 p2319 N90-23221
Activities report of the Institute for Plasma Research
[ETN-90-96467] 16 p2319 N90-23225
The effects of carbonization on the confinement properties of the DIII-D H-mode
[DE90-013297] 20 p2928 N90-26660
A study on the heating and diagnostic of a tokamak plasma by electromagnetic waves of the electron cyclotron range of frequencies
[DE90-791312] 21 p3078 N90-27499
Laser spectroscopy of plasmas
[AD-A221978] 21 p3078 N90-27502
Laser diagnostics of plasma thrusters
[AD-A221682] 21 p3079 N90-27506
High power arcjet
[NASA-CR-183086] 23 p3298 N90-28658
PBFA 2 applied B ion diode beam characteristics at high voltages
[DE90-014419] 23 p3396 N90-29190
Computerized simulation of phenomena in plasma via particles
[INPE-4595-RPE/569] 23 p3397 N90-29194
Investigation of laser diagnostics of PACVO (Plasma Assisted Chemical Vapor Deposition) processes for depositing hard face coatings
[DE90-016209] 24 p3457 N90-29522
Lectures in plasma diagnostics
[DE90-015825] 24 p3550 N90-30086
Compact toroid research
[DE90-016123] 24 p3550 N90-30087

PLASMA DIFFUSION
Proceedings of the Workshop on Compound Semiconductor Devices and Integrated Circuits (13th) held in Cabourg, France on 10-12 May 1989
[AD-A211848] 03 p0343 N90-11954
Incoherent retrodiffusion of radiowaves in plasma with particle impulse
[ETN-90-95375] 12 p1718 N90-19864
Study on rotating plasma with submillimeter laser interferometer
[DE90-615387] 14 p2027 N90-21623

PLASMA DIODES
Generation and focusing of pulsed intense ion beams
[DE89-017558] 03 p0408 N90-12338
Anode plasma formation as a possible mechanism for an electrical stress limit in cold cathode diodes
[DE90-007503] 12 p1655 N90-19516
Polycrystalline diamond Junction Field Effect Transistors (JFETS)
[AD-A222238] 21 p3083 N90-27534
Unipolar arcing on the cathode surface of a high voltage diode
[AD-A224122] 23 p3322 N90-28787

PLASMA DISCHARGES
U PLASMA JETS

PLASMA DISPERSION
U PLASMA DIFFUSION

PLASMA DRIFT
Plasma theory and simulation
[AD-A207952] 01 p0125 N90-10714
Particle simulation in curvilinear coordinate systems
[DE89-016727] 02 p0277 N90-11583
Ion collection by probing objects in flowing magnetized plasmas
[DE90-001711] 06 p0845 N90-14916
Nonlinear wave coupling and clumps in drift wave turbulence theory
[DE90-004103] 08 p1063 N90-16150
Solar flares and dynamics of Langmuir waves in current-carrying plasmas
[IPPCZ-291] 14 p2042 N90-21710
Three-dimensional simulations of simple electron drift wave turbulence in tokamak geometry
[DE90-009581] 15 p2169 N90-22398

PLASMA DYNAMICS
Development of computer codes to model dynamics of the earth's magnetosphere
[AD-A211532] 04 p0517 N90-12987
Research on heating, instabilities, turbulence and RF emission from electric field dominated plasmas
[AD-A212122] 04 p0557 N90-13243
Strategic characteristics of Dynamics Explorer 1 retarding ion mass spectrometer and the consequences for core plasma measurements
[AD-A214013] 07 p0886 N90-15125
Active probing of space plasmas
[AD-A216867] 12 p1716 N90-19855
Nonlinear stability in fluid and plasma dynamics
[AD-A217735] 13 p1892 N90-20856
Hybrid modeling of plasmas and applications to fusion and space physics 15 p2168 N90-22387
Statement of research objectives and summary of research efforts
[RLE-PR-132] 23 p3415 N90-29295

PLASMA ELECTRODES
Plasma-anode electron gun research
[AD-A211547] 03 p0312 N90-11773
True asymptotic plasma-sheath matching with an asymptotically correct collisional presheath
[AD-A212857] 05 p0701 N90-14104

PLASMA ENGINES
NASA/USRA advanced space design program: The laser powered interorbital vehicle
[NASA-CR-186044] 04 p0462 N90-12646
Energy deposition in low power coaxial plasma thrusters 06 p0844 N90-14911
Physical process in MPD plasmas
[AD-A213679] 07 p0996 N90-15761
Pulsed plasma mission endurance test
[AD-A213462] 08 p1037 N90-15993
The effects of magnetic nozzle configurations on plasma thrusters
[NASA-CR-186465] 14 p1941 N90-21109
Transport properties of plasmas in microwave electrothermal thrusters
[AD-A219408] 16 p2320 N90-23228
Laser diagnostics of plasma thrusters
[AD-A221682] 21 p3079 N90-27506

PLASMA EQUILIBRIUM
The dense Z-pinch as a plasma radiation source. 1: Quasi-static Bennett model
[AD-A210600] 01 p0127 N90-10727
Electromagnetic jets in pulsar magnetospheres and near magnetized accretion disks 02 p0294 N90-11675
Three-dimensional equilibria and Mercier stability calculations
[DE89-015907] 04 p0556 N90-13239
Stability of the Global Alfven Eigenmode in the presence of fusion alpha particles in an ignited tokamak plasma
[DE89-016618] 06 p0848 N90-14930
The free energy principle, negative energy modes, and stability
[DE90-005368] 11 p1573 N90-19056
Resonant MHD modes with toroidal coupling
[DE90-010077] 16 p2319 N90-23222
Numerical methods for the problem of the free-boundary plasma equilibrium in a stellarator (torsatron)
[DE90-620580] 16 p2319 N90-23223
Experiments at high elongations in DIII-D
[DE90-013217] 21 p3078 N90-27500

PLASMA ETCHING
Reactive ion etching of SiC thin films by mixtures of fluorinated gases and oxygen
[AD-A211046] 02 p0195 N90-11113
Reactive ion etching of sputtered silicon carbide and tungsten thin films for device applications
[AD-A211711] 03 p0325 N90-11847
Mechanisms in reactive ion etching of silicon carbide thin films
[AD-A213018] 05 p0634 N90-13700
The 10th Gordon Research Conference on Plasma Chemistry
[AD-A215161] 09 p1285 N90-17449
Proceedings of the Joint NOSC/NRL (Naval Ocean Systems Center/Naval Research Laboratory) InP Microwave/Millimeter Wave Technology Workshop
[AD-A218216] 14 p1966 N90-21259

PLASMA FLOW
U MAGNETOHYDRODYNAMIC FLOW

PLASMA FOCUS
Experimental studies of plasma wake-field acceleration and focusing
[DE89-016718] 02 p0279 N90-11591
Oblique ionospheric heating and effects on radio propagation
[AD-A214756] 09 p1205 N90-16983
A continuous plasma final focus
[DE90-006096] 11 p1568 N90-19024
Activities report of the Institute for Plasma Research
[ETN-90-96467] 16 p2319 N90-23225

PLASMA FREQUENCIES
Simultaneous multiple frequency interferometry: An application of homodyne phase measurement
[DE89-013975] 01 p0126 N90-10719
Study of a 1-Hz hypocycloidal pinch (HCP) pump for production of ultraviolet lasers
[AD-A224091] 24 p3547 N90-30064

PLASMA GENERATION
U PLASMA GENERATORS

PLASMA GENERATORS
NT PLASMA GUNS
NT TOKAMAK DEVICES
Hermes plasma wind tunnel. Preliminary study, phase A1: Text
[DVG-HER-TN-002-PT-1] 04 p0459 N90-12631
Hermes plasma wind tunnel. Preliminary study, phase A1: Annexes, tables, figures
[DVG-HER-TN-002-PT-2] 04 p0459 N90-12632
Activities report in laser matter interactions
[ETN-90-95515] 06 p0782 N90-14544
Plasma cloaking: Air chemistry, broadband absorption, and plasma generation
[AD-A222044] 21 p3078 N90-27503

PLASMA GUNS
Plasma gun with coaxial powder feed and adjustable cathode
[NASA-CASE-LEW-14901-1] 01 p0126 N90-10718
Progress with small, high-magnetic-field spheromaks in CTX
[DE90-003395] 08 p1127 N90-16527

PLASMA HEATING
NT ELECTRON CYCLOTRON HEATING
Scattering of an ICRF magnetosonic wave by plasma density turbulence
[DE89-015223] 01 p0126 N90-10720

Kinetic effects in Alfven wave heating. Part 2: Propagation and absorption with a single minority species
[DE89-016619] 01 p0126 N90-10724
Projections for a steady-state tokamak reactor based on ITER
[DE89-016678] 02 p0278 N90-11589
Hermes plasma wind tunnel. Preliminary study, phase A1: Text
[DVG-HER-TN-002-PT-1] 04 p0459 N90-12631
Hermes plasma wind tunnel. Preliminary study, phase A1: Annexes, tables, figures
[DVG-HER-TN-002-PT-2] 04 p0459 N90-12632
Effect of the length of the multijunction grill on its lower hybrid current drive efficiency
[IPPCZ-283] 04 p0556 N90-13240
Research on heating, instabilities, turbulence and RF emission from electric field dominated plasmas
[AD-A212122] 04 p0557 N90-13243
Electron heating and static sheath enhancement in front of energized RF antennas
[DE90-001334] 06 p0766 N90-14456
Propulsion research on the hybrid plume rocket
[AD-A214420] 07 p0887 N90-15132
Density clamping phenomena in electron cyclotron resonance heated plasmas on Heliotron E
[DE90-719523] 09 p1284 N90-17442
Investigation of boundary for the negative ion extraction in the sheet-plasma negative ion source
[DE90-719532] 09 p1286 N90-17458
Microwave free-electron laser applications for electron cyclotron heating of plasmas
[DE90-005203] 10 p1431 N90-18257
Model of oxygen ions resonant lines emission of REB-heated plasma
[IPPCZ-294] 10 p1432 N90-18261
Nonlinear mechanics of unstable plasmas as related to high altitude aerodynamics
[AD-A215126] 12 p1716 N90-19852
Overview of recent results from the Advanced Toroidal Facility
[DE90-005673] 12 p1716 N90-19853
Negative ion surface plasma source development for plasma trap injectors in Novosibirsk
[DE90-006082] 12 p1716 N90-19856
Computation of coupling elements between waveguides and modes for large launching structures
[IPPCZ-290] 13 p1890 N90-20842
Fusion burn dynamics in Dense Z-Pinch (DZP)
[DE90-007976] 14 p2029 N90-21638
Full wave computation of electromagnetic wave excitation, propagation, and absorption at the ion cyclotron frequency in fusion experiments
[DE90-009399] 14 p2030 N90-21642
Solar flares and dynamics of Langmuir waves in current-carrying plasmas
[IPPCZ-291] 14 p2042 N90-21710
Parasitic coupling of the fringing fields of an Ion-Bernstein wave antenna
[DE90-009918] 17 p2387 N90-23596
Effects of ionospheric modification on system performance 20 p2849 N90-26202
The effects of carbonization on the confinement properties of the DIII-D H-mode
[DE90-013297] 20 p2928 N90-26660
A study on the heating and diagnostic of a tokamak plasma by electromagnetic waves of the electron cyclotron range of frequencies
[DE90-791312] 21 p3078 N90-27499
Lower thermosphere (80-100 km) dynamics response to solar and geomagnetic activity: Overview
22 p3207 N90-28194
High average power CW FELS (Free Electron Laser) for application to plasma heating: Designs and experiments
[DE90-011085] 24 p3474 N90-29633
Stochastic properties of the plasma wave heating map
[DE90-508077] 24 p3548 N90-30070
A model of peaked density profile and inward pinch in tokamaks
[DE90-508079] 24 p3548 N90-30072
Fundamental studies of fusion plasmas
[DE90-015732] 24 p3549 N90-30080

PLASMA INSTABILITY
U MAGNETOHYDRODYNAMIC STABILITY

PLASMA INTERACTIONS
NT LASER PLASMA INTERACTIONS
NT PLASMA-ELECTROMAGNETIC INTERACTION
NT PLASMA-PARTICLE INTERACTIONS
Dynamically compressed metals: Theory
[AD-A210741] 01 p0045 N90-10257
Plasma-anode electron gun research
[AD-A211547] 03 p0312 N90-11773
Calcium displacement caused by electromagnetic fields
[AD-A212690] 04 p0524 N90-13023
Proceedings of the 10 May 1989 Antiproton Technology Workshop: Addendum
[AD-A212804] 04 p0554 N90-13227
The Space Station Photovoltaic Panels Plasma Interaction Test Program: Test plan and results
[NASA-TM-102474] 05 p0613 N90-13581
Frequency shift induced in laser pulses by plasma density variations
[AD-A214195] 07 p0936 N90-15424
Theory of interacting plasmas in space
07 p0993 N90-15742
Laboratory simulations of the solar wind-comet interactions 07 p1015 N90-15875
Environmental constraints for polar platform design
[RAE-TR-89014] 09 p1181 N90-16849
Chemical interactions and light emissions from vented species
[AD-A214130] 10 p1327 N90-17668
Solar arrays in the LEO-plasma environment: A model for leakage current phenomena deduced from experimental and theoretical studies
10 p1345 N90-17802
Report from space plasma science
10 p1445 N90-18336
Active probing of space plasmas
[AD-A216867] 12 p1716 N90-19855
The nonlinear interaction of intense laser pulses in plasmas
[AD-A217604] 12 p1718 N90-19867
USU center of excellence in theory and analysis of the geo-plasma environment
[AD-A217736] 13 p1759 N90-20101
Space Station Freedom solar array panels plasma interaction test facility
[NASA-TM-102475] 15 p2186 N90-22488
Characterization of plasma flow through magnetic nozzles
[AD-A221044] 18 p2617 N90-24905
Space environments and their effects on space automation and robotics 19 p2735 N90-25543
Effects of energy, momentum and particle transport in the near-earth solar terrestrial system
[AD-A224393] 24 p3490 N90-29726
Anomalous decay of Langmuir turbulence. High power, high frequency radiation from beam-plasma interactions
[AD-A224282] 24 p3547 N90-30065

PLASMA JET WIND TUNNELS
Hermes plasma wind tunnel. Preliminary study, phase A1: Text
[DVG-HER-TN-002-PT-1] 04 p0459 N90-12631
Hermes plasma wind tunnel. Preliminary study, phase A1: Annexes, tables, figures
[DVG-HER-TN-002-PT-2] 04 p0459 N90-12632
Aerodynamic simulation conditions in arc heated wind tunnels 09 p1180 N90-16843
SIMOUN: An optimized supersonic high temperature wind tunnel for testing construction materials to be used on the spaceplane
[REPT-892-430-111] 16 p2203 N90-22572

PLASMA JETS
NT RADIO JETS (ASTRONOMY)
Diamondlike carbon coatings for optical systems
[AD-A211255] 02 p0276 N90-11573
Studies of a strongly coupled plasma produced in a capillary discharge
[DE89-016611] 02 p0277 N90-11581
Electromagnetic jets in pulsar magnetospheres and near magnetized accretion disks 02 p0294 N90-11675
Plasma-anode electron gun research
[AD-A211547] 03 p0312 N90-11773
Microwave Tokamak Experiment (MTX) first year of operation and future plans
[DE90-000817] 06 p0846 N90-14920
Evaluation of space plasma data: Effects upon spacecraft materials and predictions of hazardous conditions; polar ARCS
[AD-A219509] 17 p2474 N90-24145
Quantitative spectroscopy of x ray laser plasmas in pulsed power devices
[AD-A221964] 21 p3078 N90-27501

PLASMA LAYERS
NT PLASMA SHEATHS
Computer simulations of electromagnetic ion instabilities in the plasma sheet boundary layer
[DE89-016596] 02 p0278 N90-11588
Numerical study of the current sheet and PSBL in a magnetotail model
[NASA-CR-183289] 02 p0293 N90-11669
The physics of double layers and their role in astrophysics
[TRITA-EPP-89-03] 03 p0421 N90-12421
Experimental and theoretical study of artificial plasma layers produced by two intersecting beams in a chamber
[NASA-CR-184598] 05 p0701 N90-14102
Novel pulsed plasma treatment and coating process: Multilayer structures for optical computing applications
[AD-A220737] 18 p2615 N90-24894
On the nature of the plasma sheet boundary layer
[DE90-013158] 20 p2889 N90-26439

PLASMA LIFETIME
Plasma cloaking: Air chemistry, broadband absorption, and plasma generation
[AD-A222044] 21 p3078 N90-27503

PLASMA LOSS
Characterization of the plasma in magnetic multidipole discharges
[DE90-613219] 14 p2028 N90-21628

PLASMA OSCILLATIONS
GOLF: Global Oscillations at Low Frequencies for the SOHO mission 04 p0566 N90-13304
High-frequency instability of the sheath-plasma resonance
[NASA-CR-186127] 06 p0844 N90-14910
CW ultraviolet laser excited with an electron beam
[AD-A214928] 09 p1227 N90-17123
Gamma ray bursts from magnetospheric plasma oscillations 19 p2779 N90-25805
Computerized simulation of phenomena in plasma via particles
[INPE-4595-RPE/569] 23 p3397 N90-29194
Control of helium accumulation
[DE90-015658] 24 p3550 N90-30084

PLASMA PERTURBATION
U PLASMA OSCILLATIONS

PLASMA PHYSICS
Plasma waves in the earth's foreshock, bow shock, and magnetosheath 01 p0086 N90-10486
Plasma theory and simulation
[AD-A207952] 01 p0125 N90-10714
Theoretical plasma physics
[DE90-000009] 03 p0408 N90-12341
MHD (magnetohydrodynamic) modeling of solar and interplanetary processes
[PB89-215461] 03 p0420 N90-12416
Plasma separation process: Magnet move to Oak Ridge National Laboratory
[DE89-017457] 04 p0556 N90-13242
Time evolution of the electron swarm energy distribution function
[AD-A212967] 04 p0557 N90-13247
An implementation plan for priorities in solar-system space physics
[NASA-CR-185375] 05 p0710 N90-14154
Fundamental studies of fusion plasmas
[DE90-002343] 06 p0848 N90-14933
Particle simulations in magnetospheric plasmas
[NASA-CR-186238] 06 p0848 N90-14934
Upgrade plans to handle 30 to 40 Mbytes of data for D3-D
[DE90-003291] 07 p0995 N90-15750
Data file management in the D3-D data acquisition and analysis computer systems
[DE90-003289] 07 p1010 N90-15850
Stress analysis of the Princeton Plasma Physics Laboratory 1/2- x 1/2-inch shear/compression test fixture
[DE90-004401] 08 p1124 N90-16512
Study on edge plasma physics and particle control in the Heliotron E device
[DE90-719524] 09 p1284 N90-17443
Report from ionospheric science
10 p1444 N90-18333
Report from magnetospheric science
10 p1444 N90-18334
Scientific activity programs for 1988-1990
[IFSI-88-23] 10 p1445 N90-18340
JPRS report: Science and technology. USSR: Physics and mathematics
[JPRS-UPM-90-002] 14 p2022 N90-21593
Numerical code AEOLUS-E1 for analysing free-boundary resistive MHD mode
[DE90-759903] 14 p2028 N90-21630
Hybrid modeling of plasmas and applications to fusion and space physics 15 p2168 N90-22387
Plasma contactor research, 1989
[NASA-CR-185212] 15 p2168 N90-22389
NSSDC data listing
[NASA-TM-102989] 15 p2180 N90-22456
JPRS report: Science and technology. USSR: Physics and mathematics
[JPRS-UPM-89-001] 16 p2310 N90-23162
Report of research activity at the Research Laboratory of Electronics 17 p2486 N90-24217
Sensitivity analysis with a simple charging code
[RAE-TM-SPACE-374] 20 p2929 N90-26662
The theory and simulation of plasmoid formation and propagation
[AD-A222048] 21 p3079 N90-27504
Physics of the L to H transition in DIII-D
[DE90-014120] 23 p3396 N90-29187

CARS spectroscopy and applications
24 p3420 N90-29321
The worldwide ionospheric data base
[NASA-TM-101823] 24 p3488 N90-29714
Beam and plasma physics research
[AD-A224452] 24 p3548 N90-30067
Transformation group methods in plasma physics
[DE90-628755] 24 p3548 N90-30074
Transport of nonneutral plasmas
[AD-A223457] 24 p3549 N90-30077
UCD-LLNL collaboration on basic plasma physics research in inertial confinement fusion
[DE90-015771] 24 p3549 N90-30081

PLASMA PINCH
NT THETA PINCH
NT ZETA PINCH
The dense Z-pinch as a plasma radiation source. 1: Quasi-static Bennett model
[AD-A210600] 01 p0127 N90-10727
Advanced concepts theory
[AD-A211665] 03 p0409 N90-12344
Nonlinear plasma and beam physics in plasma wake-fields
[DE90-008812] 13 p1892 N90-20855
Advanced concepts theory annual report, 1989
[AD-A220768] 17 p2474 N90-24146
Millimeter-wave generation via plasma three-wave mixing
[AD-A222010] 22 p3247 N90-28415

PLASMA POTENTIALS
An iterative method to solve the nonlinear Poisson's equation in the case of plasma tangential discontinuities
[AERONOMICA-ACTA-A-346-1989]
05 p0692 N90-14045
Electron heating and static sheath enhancement in front of energized RF antennas
[DE90-001334] 06 p0766 N90-14456
Investigation of boundary for the negative ion extraction in the sheet-plasma negative ion source
[DE90-719532] 09 p1286 N90-17458
Plasma contactor research, 1989
[NASA-CR-185212] 15 p2168 N90-22389
Solar array arcing in plasmas
19 p2737 N90-25558

PLASMA POWER SOURCES
NT PLASMA ENGINES
Magnetically insulated electron flows in pulsed power systems
[AD-A212746] 04 p0549 N90-13196
Review of quasi-optical gyrotron development
[AD-A213491] 07 p0933 N90-15402

PLASMA PROBES
NT ELECTROSTATIC PROBES
Laser spectroscopy of plasmas
[AD-A221978] 21 p3078 N90-27502

PLASMA PROPULSION
NASA/USRA advanced space design program: The laser powered interorbital vehicle
[NASA-CR-186044] 04 p0462 N90-12646
Test facility and preliminary performance of a 100 kW class MPD thruster 11 p1472 N90-18476
Transport properties of plasmas in microwave electrothermal thrusters
[AD-A219408] 16 p2320 N90-23228
Geometric effects in applied-field MPD thrusters
[NASA-TM-103259] 22 p3134 N90-27782

PLASMA PUMPING
Study of a 1-Hz hypocycloidal pinch (HCP) pump for production of ultraviolet lasers
[AD-A224091] 24 p3547 N90-30064

PLASMA RADIATION
The dense Z-pinch as a plasma radiation source. 1: Quasi-static Bennett model
[AD-A210600] 01 p0127 N90-10727
Advanced concepts theory
[AD-A211665] 03 p0409 N90-12344
Proceedings of the 10 May 1989 Antiproton Technology Workshop: Addendum
[AD-A212804] 04 p0554 N90-13227
Study of lithium-like ions for amplifying radiation below 100 angstroms. Experiment at the Rutherford Appleton Laboratory 06 p0786 N90-14572
Radiation of plasma waves from large space structures in low earth orbit
[AD-A215062] 09 p1182 N90-16856
Scaling Z-pinch plasmas with atomic number for a given K-shell emission
[AD-A215703] 09 p1285 N90-17450
X ray spectra produced by NaF implosions
[AD-A215803] 10 p1429 N90-18243
The nonlinear interaction of intense laser pulses in plasmas
[AD-A217604] 12 p1718 N90-19867
An electron-beam controlled semiconductor switch
[AD-A217181] 13 p1793 N90-20288
Nonlinear spectroscopy of multicomponent droplets and 2- and 3-dimensional measurements in flames
[AD-A218569] 16 p2215 N90-22636
Advanced concepts theory annual report, 1989
[AD-A220768] 17 p2474 N90-24146
X ray laser program report for FY 1989
[AD-A221818] 21 p3009 N90-27107
Solar-geophysical data number 544, December 1989. Part 2 (Comprehensive reports). Data for June 1989 and miscellaneous
[PB90-171679] 22 p3264 N90-28482

PLASMA RESONANCE
Resonance cone diagnostics in the mid-latitude ionosphere 05 p0658 N90-13840
Box experiments. Nonlinear effects at plasma resonance 06 p0783 N90-14555
Simulated Brillouin backscattering in optical fibers: A ring resonator 06 p0783 N90-14556
High-frequency instability of the sheath-plasma resonance
[NASA-CR-186127] 06 p0844 N90-14910
Plasmon excitation in the scattering of electromagnetic waves from good conductors
[AD-A214026] 08 p1056 N90-16107
Finite amplitude surface waves in cooled plasmas with smeared interface
[DE90-611308] 18 p2617 N90-24909

PLASMA RINGS
U TOROIDAL PLASMAS

PLASMA SHEATHS
Plasma theory and simulation
[AD-A207952] 01 p0125 N90-10714
True asymptotic plasma-sheath matching with an asymptotically correct collisional presheath
[AD-A212857] 05 p0701 N90-14104
High-frequency instability of the sheath-plasma resonance
[NASA-CR-186127] 06 p0844 N90-14910
Near-surface sputtered particle transport for an oblique incidence magnetic field plasma
[DE90-004422] 07 p0996 N90-15758
Electron populations above the nightside auroral oval during magnetic quiet times
[IRF-PREPRINT-116] 19 p2714 N90-25445
Comparison of currents predicted by NASCAP/LEO model simulations with elementary Langmuir-type bare probe models for an insulated cable containing a single pinhole
[NASA-TM-102486] 20 p2821 N90-26054
The near-Earth orbital environment coupling to its energy sources
[AD-A222435] 21 p3026 N90-27206
Lectures in plasma diagnostics
[DE90-015825] 24 p3550 N90-30086

PLASMA SOUND WAVES
U MAGNETOHYDRODYNAMIC WAVES
U PLASMA WAVES

PLASMA SPECTRA
Numerical simulation of the compressible Orszag-Tang vortex
[AD-A210465] 01 p0127 N90-10725
Calculations of soft x ray emission of REB-heated plasma
[IPPCZ-287] 03 p0407 N90-12329
Transversal inhomogeneity and radiative transfer in plasmas obtained by laser impact
06 p0785 N90-14568
ICP/AES (Inductively Coupled Plasma/Atomic Emission Spectroscopy): A modern analytical tool
[DE90-003822] 07 p0997 N90-15765
Spectroscopy of ions and their clusters
[AD-A223109] 21 p2977 N90-26917
The near-Earth orbital environment coupling to its energy sources
[AD-A222435] 21 p3026 N90-27206
Soft x ray emission spectra from laser-irradiated high-Z targets
[AD-A223552] 24 p3552 N90-30099

PLASMA SPRAYING
Plasma gun with coaxial powder feed and adjustable cathode
[NASA-CASE-LEW-14901-1] 01 p0126 N90-10718
Surfaces and interfaces of ceramic materials
[AD-A212417] 05 p0627 N90-13657
Improved process for HIP canning of composites
[NASA-CASE-LEW-14990-1-CU]
07 p0890 N90-15147
Structural analysis of zirconium-aluminum plasma deposits
[ETCA-89-R-073] 08 p1046 N90-16045
Study of the structure of ZrO2-Al2O3 plasma sprayed coatings
[ETCA-89-R-078] 22 p3161 N90-27924
Characteristics required for thermal barriers of zirconium oxide-yttrium compounds obtained by plasma spraying. Morphological analysis by x ray diffraction
[ETCA-89-R-113] 22 p3161 N90-27925
Vacuum application of thermal barrier plasma coatings
23 p3298 N90-28653

PLASMA STABILITY
U MAGNETOHYDRODYNAMIC STABILITY

PLASMA TEMPERATURE
Studies of a strongly coupled plasma produced in a capillary discharge
[DE89-016611] 02 p0277 N90-11581
The soft x ray telescope for Solar-A
03 p0432 N90-12475
Experimental and theoretical study of artificial plasma layers produced by two intersecting beams in a chamber
[NASA-CR-184598] 05 p0701 N90-14102
Advanced diagnostics for reacting flows
[AD-A215050] 09 p1217 N90-17060
Spectral characteristics of arc-heated low density plasma flows (IV) air and N2-CO2 mixture plasmas
[NAL-TR-1012] 09 p1285 N90-17451

PLASMA THEORY
U PLASMA PHYSICS

PLASMA TURBULENCE
Scattering of an ICRF magnetosonic wave by plasma density turbulence
[DE89-015223] 01 p0126 N90-10720
Research on heating, instabilities, turbulence and RF emission from electric field dominated plasmas
[AD-A212122] 04 p0557 N90-13243
Strong Langmuir turbulence and second harmonics in laser-matter interactions 06 p0782 N90-14548
Nonlinear wave coupling and clumps in drift wave turbulence theory
[DE90-004103] 08 p1063 N90-16150
Proceedings of a contractors meeting on Combustion Rocket Propulsion Diagnostics of Reacting Flow
[AD-A216445] 12 p1617 N90-19297
Nonlinear mechanics of unstable plasmas as related to high altitude aerodynamics
[AD-A215126] 12 p1716 N90-19852
Spontaneous magnetic reconnection in a turbulent plasma 13 p1889 N90-20840
Center of excellence in theoretical geoplasma research
[AD-A215035] 14 p2005 N90-21488

PLASMA WAVES
NT ELECTROSTATIC WAVES
Plasma waves in the earth's foreshock, bow shock, and magnetosheath 01 p0086 N90-10486
Hybrid particle-fluid approach to low-frequency turbulence in magnetically confined plasmas
[DE89-015904] 02 p0277 N90-11579
Producing of an ECR plasma using 2450MHz Whistler wave and the investigating of its parameters
[DE89-618689] 02 p0278 N90-11586
CRRES (Combined Release and Radiation Effects Satellite) SPACERAD plasma wave experiment
[AD-A210791] 02 p0278 N90-11587
Experimental studies of plasma wake-field acceleration and focusing
[DE89-016718] 02 p0279 N90-11591
Beam-plasma discharge in penetrating plasma
[DE89-630481] 02 p0280 N90-11597
Quantitative methods for waves in space plasmas
[PB89-210256] 02 p0280 N90-11599
Coherency properties of strong Langmuir turbulence
[DE89-009290] 03 p0371 N90-12119
Wave particle interactions
[DE89-017527] 03 p0407 N90-12335
The supersonic anisotropic collapse of Langmuir waves 06 p0783 N90-14550
Limitations in the growing of a plasma wave produced by heterodyning two lasers due to modulations and decay instabilities 06 p0783 N90-14552
Use of plasmas for the acceleration of particles to very high energy 06 p0783 N90-14553
Box experiments. Nonlinear effects at plasma resonance 06 p0783 N90-14555
Toroidal rotation retardation and ion anomalous transport by drift waves in a tokamak
[DE89-634427] 06 p0844 N90-14913
Particle simulations in magnetospheric plasmas
[NASA-CR-186238] 06 p0848 N90-14934
Optical guiding by plasma waves in the plasma beat wave accelerator
[AD-A214288] 07 p0997 N90-15763
On averaged force acting on a particle in HF electromagnetic field
[DE90-600984] 08 p1057 N90-16109
Nonlinear wave coupling and clumps in drift wave turbulence theory
[DE90-004103] 08 p1063 N90-16150

Design of a spheromak compressor driven by high explosives
[DE90-003652] 08 p1086 N90-16283
Radiation of plasma waves from large space structures in low earth orbit
[AD-A215062] 09 p1182 N90-16856
Particle simulations in magnetospheric plasmas
[AD-A216256] 11 p1534 N90-18831
Magnetic field generation by acoustic oscillations in solar atmosphere
[DE90-606054] 11 p1594 N90-19180
Nonlinear interaction of electrostatic waves at a narrow inhomogeneous layer of a warm magnetoactive plasma
[DE90-610624] 12 p1717 N90-19857
Nonlinear plasma and beam physics in plasma wake-fields
[DE90-008812] 13 p1892 N90-20855
On the relativistic Vlasov equation in guiding-center coordinates
[DE90-613241] 14 p2028 N90-21629
Dynamics of cavitons in strong Langmuir turbulence
[DE90-008918] 14 p2029 N90-21633
Cyclotron maser and plasma wave growth in magnetic loops
[NASA-CR-179862] 15 p2170 N90-22402
Sound waves in weakly ionized gas
[DE90-620704] 16 p2313 N90-23180
Parasitic coupling of the fringing fields of an Ion-Bernstein wave antenna
[DE90-009918] 17 p2387 N90-23596
Self-similar Langmuir collapse
[DE90-611310] 18 p2617 N90-24911
Analytical studies of magnetospheric pulsations
[AD-A222275] 21 p3026 N90-27205
Proceedings of the US-Japan Fusion Cooperation Program Exchange P148 Workshop on Advanced Current Drive Concepts
[IPPJ-REV-4] 21 p3078 N90-27498
A study on the heating and diagnostic of a tokamak plasma by electromagnetic waves of the electron cyclotron range of frequencies
[DE90-791312] 21 p3078 N90-27499
The plasma wave signature of a 'magnetic hole' in the vicinity of the magnetopause
[NASA-CR-187027] 22 p3212 N90-28220
Electron acoustic and magnetoacoustic modes in a magnetized beam plasma system
[DE90-627473] 23 p3398 N90-29199
Stochastic properties of the plasma wave heating map
[DE90-508077] 24 p3548 N90-30070
Structure of magnetic field in tokamaks
[DE90-626904] 24 p3549 N90-30075

PLASMA-ELECTROMAGNETIC INTERACTION
NT LASER PLASMA INTERACTIONS
A beam induced upset during the flight of the ECHO-7 rocket
[NASA-CR-186089] 03 p0309 N90-11755
Computation of coupling elements between waveguides and modes for large launching structures
[IPPCZ-290] 13 p1890 N90-20842
Forced scattering of electromagnetic waves on electron beam in periodically inhomogeneous plasma
[DE90-620705] 16 p2228 N90-22707
Effects of ionospheric modification on system performance 20 p2849 N90-26202
Millimeter-wave generation via plasma three-wave mixing
[AD-A222010] 22 p3247 N90-28415

PLASMA-PARTICLE INTERACTIONS
Beam-plasma discharge in penetrating plasma
[DE89-630481] 02 p0280 N90-11597
The interaction of supernovae and pulsars with the circumstellar environment 02 p0293 N90-11671

PLASMAGUIDES
Forced scattering of electromagnetic waves on electron beam in periodically inhomogeneous plasma
[DE90-620705] 16 p2228 N90-22707

PLASMAS (PHYSICS)
NT ARGON PLASMA
NT BETA PARTICLES
NT BOUNDARY LAYER PLASMAS
NT CESIUM PLASMA
NT COLD PLASMAS
NT COLLISIONAL PLASMAS
NT COLLISIONLESS PLASMAS
NT COSMIC PLASMA
NT CYLINDRICAL PLASMAS
NT DENSE PLASMAS
NT ELECTRON PLASMA
NT ELECTRON-POSITRON PLASMAS
NT HELIUM PLASMA
NT HIGH TEMPERATURE PLASMAS
NT HYDROGEN PLASMA
NT LASER PLASMAS
NT METALLIC PLASMAS
NT NITROGEN PLASMA
NT NONEQUILIBRIUM PLASMAS
NT NONUNIFORM PLASMAS
NT OXYGEN PLASMA
NT PLASMA FOCUS
NT RELATIVISTIC PLASMAS
NT ROTATING PLASMAS
NT SEMICONDUCTOR PLASMAS
NT SOLAR WIND
NT SPACE PLASMAS
NT SPHERICAL PLASMAS
NT STELLAR WINDS
NT STRONGLY COUPLED PLASMAS
NT THERMAL PLASMAS
NT TOROIDAL PLASMAS
Method and apparatus for maintaining thermal control in plasma conditions
[NASA-CASE-MFS-28368-1] 01 p0125 N90-10717
Scattering of an ICRF magnetosonic wave by plasma density turbulence
[DE89-015223] 01 p0126 N90-10720
ANTHEM simulation of plasma opening switches
[DE89-016617] 02 p0217 N90-11239
Ionospheric Structure and Variability on a Global Scale and Interactions with Atmosphere and Magnetosphere
[AGARD-CP-441] 02 p0239 N90-11361
Balance equations for ionospheric plasmas with different partial temperatures 02 p0240 N90-11364
Global morphology of plasma bubbles in the low latitude ionosphere 02 p0241 N90-11369
Ionosphere-thermosphere coupling at high latitudes: Aspect angle dependence of non-thermal plasmas 02 p0244 N90-11382
Small-scale irregularities and global plasma dynamics in the high-latitude ionosphere 02 p0246 N90-11394
Boundary effects on the MHD dynamo in laboratory plasmas
[DE89-015207] 02 p0276 N90-11576
ANTHEM simulation of the early time magnetic field penetration of the plasma surrounding a high density Z-pinch
[DE89-016980] 02 p0277 N90-11585
CRRES (Combined Release and Radiation Effects Satellite) SPACERAD plasma wave experiment
[AD-A210791] 02 p0278 N90-11587
Solid fiber Z-pinches: Cold-start computations
[DE89-016768] 02 p0279 N90-11592
A fully electromagnetic hybrid model for high density plasma simulations
[DE89-016771] 02 p0279 N90-11593
Beam-plasma discharge in penetrating plasma
[DE89-630481] 02 p0280 N90-11597
Ion bombardment of Io and Mercury 02 p0296 N90-11682
Plasma-deposited amorphous hydrogenated carbon films and their tribological properties
[NASA-TM-102379] 03 p0331 N90-11880
Advances and directions of ion nitriding/carburizing
[NASA-TM-102398] 03 p0334 N90-11902
Electron cyclotron emission and absorption experiment on the CASTOR tokamak
[IPPCZ-285] 03 p0407 N90-12331
Control of plasma position in the CASTOR tokamak
[IPPCZ-284] 03 p0407 N90-12332
Joule heating and runaway electron acceleration in a solar flare 03 p0432 N90-12478
Development of a numerical solution to the time dependent kinetic equation 03 p0433 N90-12481
Advanced source development and applications. Laser-produced plasmas: A compact soft x ray source with high peak brightness
[AD-A212677] 04 p0557 N90-13245
Mechanisms in reactive ion etching of silicon carbide thin films
[AD-A213018] 05 p0634 N90-13700
Hot spots Ar and Ne gas puff z-pinch
[IPPCZ-289] 05 p0701 N90-14103
Energy deposition in low power coaxial plasma thrusters 06 p0844 N90-14911
Two-dimensional behavior of Megagauss-field-confined solid fiber Z-pinches
[DE90-000684] 06 p0845 N90-14918
Fundamental studies of fusion plasmas
[DE90-002343] 06 p0848 N90-14933
SCATHA (Spacecraft Charging At High Altitudes) atlas data base, volume 2
[AD-A214205] 07 p0887 N90-15128
Intense REB (Relativistic Electron Beam) transport in a weakly magnetized plasma
[DE90-002978] 07 p0994 N90-15749
The 17th AINSE Plasma Physics Conference: Conference handbook
[DE90-600936] 07 p0996 N90-15759
Physical process in MPD plasmas
[AD-A213679] 07 p0996 N90-15761
Second harmonic electron cyclotron heating in low and over density plasmas in Heliotron DR
[DE90-719519] 08 p1125 N90-16515
Ion bombardment experiments suggesting an origin for organic particles in pre-cometary and cometary ices 08 p1148 N90-16652
Dissipative effects in Friedmann universes
[DE89-618838] 08 p1150 N90-16663
Nonlinear modulational stability and propagation of an electromagnetic pulse in a two-component, neutral plasma
[AD-A215131] 09 p1207 N90-16994
Study on edge plasma physics and particle control in the Heliotron E device
[DE90-719524] 09 p1284 N90-17443
A design procedure for a slotted waveguide with probe-fed slots radiating into plasma
[DE90-004168] 09 p1284 N90-17446
Investigation of boundary for the negative ion extraction in the sheet-plasma negative ion source
[DE90-719532] 09 p1286 N90-17458
Plasma and ion fluorination for chemical hardening of synthetic rubbers
[AD-A216388] 10 p1360 N90-17885
Electron-beam induced damage in thin insulating films on compound semiconductors
[NASA-CR-185177] 10 p1378 N90-17987
Magnetoplasma oscillations of the wave-guided type in semiconductor superlattices
[DE90-607260] 10 p1431 N90-18258
On the quantum inverse problem for a new type of nonlinear Schroedinger equation for Alfven waves in plasma
[DE90-607469] 10 p1431 N90-18259
Model of oxygen ions resonant lines emission of REB-heated plasma
[IPPCZ-294] 10 p1432 N90-18261
Quasilinear approach to the damping of LH waves in a reactor-grade plasma
[IPPCZ-292] 10 p1432 N90-18262
A 13-point Thomson scattering system for JFT-2M plasma
[DE90-733140] 10 p1432 N90-18263
Numerical simulation of non-inductive current drive for tokamak plasmas with time-varying electron temperatures
[DE90-733144] 10 p1432 N90-18264
First pump limiter experiments in TORE SUPRA
[DE90-004968] 10 p1432 N90-18266
First results from the MST (Madison Symmetric Torus) reversed field pinch
[DE90-005743] 10 p1433 N90-18268
Anomalous particle diffusion through a magnetic picket fence
[INPE-4841-PRE/1470] 10 p1433 N90-18270
Plasma modification of poly (p-phenylenebenzobisthiazole)
[AD-A215761] 10 p1433 N90-18272
Streaming gravity mode instability
[DE90-610619] 11 p1535 N90-18835
Hamiltonian analysis and simulation of free electron lasers
[INPE-4785-TDL/351] 11 p1567 N90-19018
Development of an rf-driven plasma neutralizer for negative ions
[DE90-007298] 11 p1568 N90-19027
Magnetohydrodynamic modeling of plasma opening switches and gas puff plasmas
[DE90-005825] 11 p1569 N90-19028
Investigation of a simulated tritium plasma using Coherent Anti-Stokes Raman Spectroscopy (CARS)
[DE90-005696] 12 p1622 N90-19319
Causality of plasma permittivity with loss and restoring terms
[NASA-TM-101671] 12 p1645 N90-19453
Longitudinal traveling waves bifurcating from Vlasov plasma equilibria 12 p1715 N90-19850
Nonlinear mechanics of unstable plasmas as related to high altitude aerodynamics
[AD-A215126] 12 p1716 N90-19852
Negative ion surface plasma source development for plasma trap injectors in Novosibirsk
[DE90-006082] 12 p1716 N90-19856
Plasma simulation on magnetohydrodynamic time scales
[DE90-007490] 12 p1718 N90-19865
An electrical model for plasma armature voltage
[DE90-007530] 12 p1718 N90-19866
Electron beam induced damage in PECVD Si3N4 and SiO2 films on InP
[NASA-TM-102544] 13 p1810 N90-20393
Solar cyclical trend study of the mid-latitude, quiet-time, meridional, neutral winds at winter solstice conditions
[AD-A217398] 13 p1841 N90-20568

The impedance of energy efficiency of a coaxial magnetized plasma source used for spheromak formation and sustainment
[DE90-003220] 13 p1889 N90-20841
New methods in plasma simulation
[DE90-007507] 13 p1890 N90-20847
High elongation plasmas
[DE90-007575] 13 p1891 N90-20848
Instabilities and vortex dynamics in shear flow of magnetized plasmas
[DE90-009448] 14 p2030 N90-21643
Solar flares and dynamics of Langmuir waves in current-carrying plasmas
[IPPCZ-291] 14 p2042 N90-21710
Equilibrium and stability analysis of magnetospheric plasmas 15 p2057 N90-21782
Gas-puff z-pinch experiment
[IPPCZ-286] 15 p2167 N90-22385
Hybrid modeling of plasmas and applications to fusion and space physics 15 p2168 N90-22387
The MHD structure of an open magnetotail boundary 15 p2168 N90-22388
Plasma contactor research, 1989
[NASA-CR-185212] 15 p2168 N90-22389
The (DURIP) computer simulations of plasmas, nonlinear systems, and control theory
[AD-A219070] 16 p2300 N90-23107
Measurement of plasma-neutralized super-vacuum currents in a gyrotron configuration
[AD-A218505] 16 p2316 N90-23207
Gas dynamic theory of flight of fast electron flux in plasma
[DE90-618767] 16 p2319 N90-23220
Molecular evolution in astrophysical environments 16 p2332 N90-23291
Electric dipole antennae used as micrometeoroid detectors
[AERONOMICA-ACTA-A-351-1989] 17 p2392 N90-23623
Technical accomplishments of the NASA Lewis Research Center, 1989
[NASA-TM-102296] 17 p2486 N90-24220
Flight model discharge system
[AD-A220261] 18 p2510 N90-24342
Pulsed-discharge carbon dioxide lasers 18 p2556 N90-24587
Dissociation phenomena in electron-beam sustained carbon dioxide lasers 18 p2560 N90-24610
MIT (Massachusetts Institute of Technology) short-wavelength laser project
[DE90-008975] 18 p2562 N90-24619
Novel pulsed plasma treatment and coating process: Multilayer structures for optical computing applications
[AD-A220737] 18 p2615 N90-24894
Fast plasma mixing: A new excitation method for CW gas lasers
[AD-A220290] 18 p2617 N90-24904
Kinetic theory of low-frequency nonlinear structures in magnetized plasmas
[DE90-611306] 18 p2617 N90-24907
Renormalized microscopic theory of fluctuations in inhomogeneous magnetized plasmas
[DE90-611307] 18 p2617 N90-24908
AFE dynamic effects in inhomogeneous plasmas 18 p2643 N90-25053
Technology for low pressure plasma processes, a new approach: The plasma box concept
[MBB-UE-0003/89-PUB] 19 p2653 N90-25101
Discharge transient coupling in large space power systems 19 p2735 N90-25544
Interactions between the Space Station and the environment: A preliminary assessment of EMI 19 p2737 N90-25557
The beta limit in the DIII-D tokamak
[DE90-011896] 19 p2759 N90-25677
Accretion onto neutron stars: Radiative transfer in a strong gravitational field 19 p2776 N90-25784
Sensitivity analysis with a simple charging code
[RAE-TM-SPACE-374] 20 p2929 N90-26662
Advanced propulsion concepts
[NASA-CR-185920] 21 p2969 N90-26872
Electrodynamics of the high latitude ionosphere
[AD-A223229] 21 p3026 N90-27203
Proceedings of the US-Japan Fusion Cooperation Program Exchange P148 Workshop on Advanced Current Drive Concepts
[IPPJ-REV-4] 21 p3078 N90-27498
Experiments at high elongations in DIII-D
[DE90-013217] 21 p3078 N90-27500
Laser spectroscopy of plasmas
[AD-A221978] 21 p3078 N90-27502
The theory and simulation of plasmoid formation and propagation
[AD-A222048] 21 p3079 N90-27504
Heat and momentum transfer to test samples in the high velocity plasma furnace
[AD-A222182] 21 p3079 N90-27505
The influence of IMF on the lower ionosphere plasma in high and middle latitudes 22 p3208 N90-28200
Computerized simulation of phenomena in plasma via particles
[INPE-4595-RPE/569] 23 p3397 N90-29194
Ignition and burn control characteristics of thermonuclear plasmas
[DE90-015385] 23 p3398 N90-29197
Measurement of gravitational acceleration of antimatter
[DE90-627464] 23 p3403 N90-29233
A plasma diagnostic study of two wind-blown shell nebulae: NGC 7635 and NGC 2359 23 p3410 N90-29271
Theoretical studies of proton beams in solar flare loops 23 p3413 N90-29286
Extension of plasma source ion implantation to ion beam enhanced deposition
[AD-A224462] 24 p3454 N90-29506
Investigation of laser diagnostics of PACVO (Plasma Assisted Chemical Vapor Deposition) processes for depositing hard face coatings
[DE90-016209] 24 p3457 N90-29522
Ionospheric irregularities: Source, structure, plasma processes and effects on sensor systems
[AD-A223908] 24 p3490 N90-29723
Investigation of structure and transport processes in the high latitude ionospheric plasma using ground based and airborne digisondes
[AD-A224397] 24 p3491 N90-29727
A study of magnetic field reconnection and plasma processes in the magnetosphere
[DE90-016117] 24 p3493 N90-29741
A review of self generated B-field in ICF corona
[DE90-627479] 24 p3547 N90-30063
Tokamak plasma shape identification with a Legendre-Fourier expansion of the vacuum poloidal flux function in the toroidal coordinates
[DE90-508031] 24 p3548 N90-30068
Fundamental studies of fusion plasmas
[DE90-015732] 24 p3549 N90-30080

PLASMASPHERE
Short wavelength striations on expanding plasma clouds
[DE89-016585] 02 p0250 N90-11416
Development of computer codes to model dynamics of the earth's magnetosphere
[AD-A211532] 04 p0517 N90-12987
Optical observations of interplanetary pick-up ions: The experiment Helly 05 p0661 N90-13863
USU center of excellence in theory and analysis of the geo-plasma environment
[AD-A217736] 13 p1759 N90-20101
Solar flares and magnetospheric particles: Investigations based upon the ONR-602 and ONR-604 experiments
[AD-A218844] 16 p2340 N90-23332
The near-Earth orbital environment coupling to its energy sources
[AD-A222435] 21 p3026 N90-27206
New Voyager radio spectrograms of Uranus
[NASA-CR-180381] 23 p3412 N90-29284

PLASMOIDS
U PLASMAS (PHYSICS)

PLASMONS
Plasmon excitation in the scattering of electromagnetic waves from good conductors
[AD-A214026] 08 p1056 N90-16107
Surface-plasmon enhanced nonlinear photoelectric emission from thin silver films
[DE90-007676] 13 p1884 N90-20807
US-Japan Workshop on Atomic Collisions in Solids: Abstracts of lectures
[DE90-008979] 14 p2025 N90-21611
Coupled magnetoplasmon-phonon modes at the surface of a semi-infinite semiconductor superlattice
[DE90-612904] 14 p2031 N90-21647
Nonreciprocal components in the 140 and 220 GHz bands utilizing magnetoplasmons on semiconducting substrates
[AD-A219136] 16 p2324 N90-23253

PLASTIC ANISOTROPY
NT ELASTIC ANISOTROPY
Analysis of biaxial stress fields in plates cracking at elevated temperatures
[AD-A216271] 10 p1397 N90-18077

PLASTIC COATINGS
Polyelectrolyte-diffused zinc phosphate conversion coatings and polyacid coupling primers for corrosion protection of steel and aluminum, and alkali-catalyzed hydrolysis of polyimide-based materials
[AD-A212240] 04 p0480 N90-12754
Abrasion resistant coatings on plastics 18 p2529 N90-24428

PLASTIC DEFORMATION
Fatigue crack initiation mechanics of metal aircraft structures
[AD-A210567] 01 p0045 N90-10255
Studies in penetration mechanics
[AD-A210713] 01 p0079 N90-10448
Microstructural effects on spall fracture in 1008 steel
[DE89-016770] 02 p0198 N90-11131
Deformation of Ti-6Al-4V bar and extrusion under superplastic forming conditions
[RAE-TM-MAT/STR-1110] 03 p0330 N90-11875
Deformation of extruded titanium alloys under superplastic conditions
[RAE-TM-MAT/STR-1111] 03 p0330 N90-11876
A model for long-term creep and the effects of physical ageing in poly (butylene terephthalate)
[NPL-DMA(A)-182] 03 p0333 N90-11895
An application of the J-integral to an incremental analysis of blunting crack behavior
[DE89-016844] 03 p0358 N90-12046
Autofrettage-stress distribution under load and retained stresses after depressurization
[AD-A212090] 03 p0358 N90-12048
An experimental and analytical program to develop crack tip fracture criteria
[AD-A211565] 03 p0359 N90-12051
Deformation of electron beam welded Ti-6Al-4V alloy sheet under superplastic conditions
[RAE-TM-MAT/STR-1109] 03 p0359 N90-12053
Effect of superplastic deformation on the surface roughness of sheet
[RAE-TM-MAT/STR-1112] 03 p0359 N90-12054
A two-parameter representation of dynamic dislocation distributions
[AD-A212249] 04 p0560 N90-13263
Field-effect spectroscopy of interface states
[AD-A212998] 05 p0703 N90-14112
Approximate methods for dynamic plastic deformation of structures
[DE90-002214] 06 p0800 N90-14660
Isothermal fatigue behavior of Sn-Pb solar joints
[DE90-003280] 07 p0943 N90-15464
Deformation and fracture of ordered intermetallic compounds
[DE90-007422] 11 p1488 N90-18563
An objective time-integration procedure for isotropic rate-independent and rate-dependent elastic-plastic constitutive equations
[PB90-121245] 11 p1550 N90-18925
Three-dimensional Fe analysis of the surface distribution in notched compact samples of 20 MnMoNi 55
[W-1/89] 12 p1676 N90-19625
Elasto-plastic large deformation analysis of thin-walled structures
[PB90-164757] 14 p1994 N90-21426
Contact mechanics for three-dimensional geometries 15 p2111 N90-22076
The mechanics of shear band formation in thermal viscoplastic materials at high rates of loading 15 p2120 N90-22128
Simulation of inelastic deformation in glassy polypropylene and polycarbonate
[AD-A218891] 16 p2224 N90-22686
Strain softening in viscoelasticity of the rate type
[AD-A219915] 17 p2417 N90-23772
The effect of local thinning on the remaining life of superheater tubes
[VTT-RR-631] 19 p2703 N90-25377
Microscopic modeling of tribological phenomena
[AD-A222049] 21 p3011 N90-27117
Pinning, flow and plastic deformation of flux vortices in high T(sub c) superconductors 22 p3136 N90-27796
Influence of microslidings on the macroscopic behavior of composite textiles
[ETN-90-97459] 22 p3154 N90-27880
Micromechanics of cyclic deformation in SSME turbopump blade materials 23 p3295 N90-28641
Microstructure: Property correlation --- multiaxial fatigue damage evolution in waspaloy
[NASA-CR-180406] 23 p3340 N90-28880
Comparison of crack closure result obtained by 3D elastic-plastic FEM and modified Dugdale model
[FFA-TN-1990-18] 24 p3481 N90-29675
A method for modeling kinematic hardening and cyclic strain effects
[ONERA-RT-77/1765-RY-089-R] 24 p3481 N90-29677

PLASTIC FILMS
U POLYMERIC FILMS

PLASTIC FLOW
Studies in penetration mechanics
[AD-A210713] 01 p0079 N90-10448
Autofrettage-stress distribution under load and retained stresses after depressurization
[AD-A212090] 03 p0358 N90-12048

Anomalous strain rate dependence of the serrated flow in Ni-H and Ni-C-H alloys
[AD-A213244] 05 p0624 N90-13641
Analysis of new phenomena in shear flow of non-Newtonian fluids
[AD-A212893] 05 p0638 N90-13721
An implicit time-integration procedure for a set of internal variable constitutive equations for isotropic elasto-viscoplasticity
[PB90-121302] 08 p1117 N90-16470
The mechanics of shear band formation in thermal viscoplastic materials at high rates of loading 15 p2120 N90-22128
Pinning, flow and plastic deformation of flux vortices in high T(sub c) superconductors 22 p3136 N90-27796

PLASTIC MEMORY
Shape memory alloys for robot grippers and mechanical hands 18 p2536 N90-24466

PLASTIC PROPELLANTS
The sensitivity of several explosives to ignition in the launch environment
[AD-A221581] 21 p2990 N90-26993

PLASTIC PROPERTIES
NT ELASTOPLASTICITY
NT PHOTOPLASTICITY
NT SUPERPLASTICITY
NT THERMOPLASTICITY
NT VISCOPLASTICITY
NT YIELD POINT
Numerical analysis of a class of problems in the mathematical theory of plasticity and damage
[AD-A210731] 01 p0114 N90-10655
Modeling the temperature rise at the tip of a fast crack
[AD-A212418] 04 p0514 N90-12966
A theory of damage in brittle and cementitious materials, part 1
[AD-A212940] 05 p0627 N90-13658
A generalized thermomechanical constitutive model for metal matrix composites with plastic strain and damage 06 p0737 N90-14293
Superplasticity
[AGARD-LS-168] 06 p0743 N90-14325
A theoretical investigation of the column behavior of cold-formed square hollow sections
[PB89-225981] 06 p0797 N90-14645
Development of a rate independent plasticity theory for general cyclic loading 07 p0945 N90-15471
Burst pressure prediction of metallic/fibre reinforced rocket motor cases using an elasto-plastic instability analysis
[RARDE-1/89] 08 p1038 N90-15997
BAM: German Federal Institute for Materials Research and Testing, Berlin
[DE90-004293] 08 p1090 N90-16307
An implicit time-integration procedure for a set of internal variable constitutive equations for isotropic elasto-viscoplasticity
[PB90-121302] 08 p1117 N90-16470
A summary of the Bodner-Stouffer constitutive model
[AD-A214532] 09 p1237 N90-17182
An objective time-integration procedure for isotropic rate-independent and rate-dependent elastic-plastic constitutive equations
[PB90-121245] 11 p1550 N90-18925
A transient plasticity study and low cycle fatigue analysis of the Space Station Freedom photovoltaic solar array blanket
[NASA-TM-102516] 12 p1674 N90-19617
Three-dimensional elastic-plastic analysis of shallow cracks in single-edge-crack-tension specimens
[NASA-TM-102636] 14 p1945 N90-21130
Deformation processing of YBa2Cu3O(sub x)
[DE90-007795] 14 p2030 N90-21644
Three-dimensional fatigue crack closure behavior of metals 15 p2070 N90-21857
The Shock and Vibration Digest, volume 21, no. 8 15 p2110 N90-22068
Recent progress in the dynamic plastic behavior of structures, part 5 15 p2110 N90-22069
A study of creep damage using microradiography and continuum damage mechanics 15 p2117 N90-22109
A study of woven fabric-reinforced composite materials using an invariant-based orthotropic plasticity formulation 16 p2211 N90-22611
Approximate analysis for the formation of adiabatic shear bands
[AD-A218751] 16 p2221 N90-22670
Role of shear instability in ballistic penetration
[AD-A219186] 16 p2244 N90-22799
Development of a device for surface tension measurement and phenomenological rheology
[ECL-89-12] 17 p2382 N90-23568
A feedback extension to the numerical solution of nonlinear boundary value problems
[AD-A219886] 17 p2461 N90-24050
Processing and properties of advanced aluminum alloys
[AD-A221292] 18 p2526 N90-24416
Computational methods and plasticity
[PB90-167917] 18 p2571 N90-24652
A numerical study of plasticity induced closure in short cracks by the finite element method
[AD-A220471] 18 p2571 N90-24654
Determination of the heat dissipated from a specimen undergoing cyclic plasticity by a hybrid numerical/experimental method
[AD-A221575] 21 p2982 N90-26946
Processing and characterization of high strength, high ductility Hadfield steel
[AD-A221769] 21 p2982 N90-26947
Plastic superconductor bearings any size, any shape, 77 k and up 22 p3145 N90-27838
Studies on crack mechanics
[AD-A223634] 24 p3480 N90-29670
A method for modeling kinematic hardening and cyclic strain effects
[ONERA-RT-77/1765-RY-089-R] 24 p3481 N90-29677

PLASTIC YIELDING
U PLASTIC DEFORMATION

PLASTICITY
U PLASTIC PROPERTIES

PLASTICIZERS
NMR measurements of solvent self-diffusion coefficients in polymer solutions
[AD-A215276] 09 p1279 N90-17419
Preparation, characterisation and cookoff behaviour of booster compositions prepared from RDX and acrylic or ethylene-vinyl acetate dispersions
[MRL-TR-89-44] 14 p1957 N90-21203
Extraction of recovery of plasticizers from solid propellants and munitions
[AD-D014433] 15 p2072 N90-21868

PLASTICS
NT ACRYLIC RESINS
NT ADDITION RESINS
NT CARBON FIBER REINFORCED PLASTICS
NT EPOXY RESINS
NT GLASS FIBER REINFORCED PLASTICS
NT KEVLAR (TRADEMARK)
NT NYLON (TRADEMARK)
NT PEEK
NT PHENOLIC EPOXY RESINS
NT PHENOLIC RESINS
NT POLYAMIDE RESINS
NT POLYBUTADIENE
NT POLYESTER RESINS
NT POLYETHYLENE TEREPHTHALATE
NT POLYETHYLENES
NT POLYMETHYL METHACRYLATE
NT POLYPROPYLENE
NT POLYSTYRENE
NT POLYTETRAFLUOROETHYLENE
NT POLYVINYL ALCOHOL
NT POLYVINYL FLUORIDE
NT REINFORCED PLASTICS
NT SYNTHETIC RESINS
NT TEFLON (TRADEMARK)
NT THERMOPLASTIC FILMS
NT THERMOPLASTIC RESINS
NT THERMOSETTING RESINS
NT VINYL COPOLYMERS
Modeling the temperature rise at the tip of a fast crack
[AD-A212418] 04 p0514 N90-12966
Ductile failure
[AD-A212975] 05 p0618 N90-13601
Studies on deformation and fracture of viscoelastic composite materials
[AD-A216095] 10 p1348 N90-17819
Assessment of biobased materials
[DE90-000300] 13 p1780 N90-20220
Mechanical testing of selected engineering plastics
[DE90-008186] 16 p2222 N90-22673
Durable heat diaphragm from ordered polymer films
[AD-A220794] 17 p2381 N90-23559
National Educators' Workshop: Update 1989 Standard Experiments in Engineering Materials Science and Technology
[NASA-CP-3074] 18 p2513 N90-24350
PVDF contact probes
[VTT-RR-623] 20 p2857 N90-26253
Method of obtaining current-conducting polymer materials
[AD-A222129] 22 p3159 N90-27914
Aircraft battle damage repair of transparencies
[AD-A224168] 24 p3432 N90-29387

PLASTISOLS
NT SMOKE

PLATE (METAL)
U METAL PLATES

PLATE THEORY
Analysis of metal matrix composite structures using a microchemical constitutive theory 06 p0737 N90-14290
Two new techniques for predicting delamination growth in laminated plates 09 p1185 N90-16865
A higher-order plate theory with ideal finite element suitability
[AD-A216163] 10 p1397 N90-18075
Direct formulation of a 4-node hybrid shell element with rotational degrees of freedom
[NASA-CR-4282] 14 p1991 N90-21411
Accuracy of the QUAD4 thick shell element 18 p2569 N90-24641
Variational formulation and finite element implementation of Pagano's theory of laminated plates 24 p3442 N90-29437
Application of the complex variable solution to some problems in linear elastic materials with voids 24 p3478 N90-29658

PLATEAUS
NT GREAT BASIN (US)

PLATES
Mechanical properties and fracture toughness of 8090-T651 plate and 2091 and 8090 sheet 07 p0897 N90-15188
Uses and properties of Al-Li on the new EH101 helicopter 07 p0900 N90-15201
Aluminum-lithium: Application of plate and sheet to fighter aircraft 07 p0900 N90-15202
Fully articulated four-point-bend loading fixture
[NASA-CASE-LEW-14776-1] 07 p0940 N90-15445
Computer simulations and experiments to study the fracture of rods by flying plates
[DE90-008308] 13 p1817 N90-20437
Wave receptance analysis of vibrating beams and stiffened plates 14 p1993 N90-21419
A modification of a low-order Reissner-Mindlin plate bending element
[PB90-165630] 14 p1994 N90-21428
Pressurized bellows flat contact heat exchanger interface
[NASA-CASE-MSC-21271-1] 15 p2097 N90-21999

PLATES (STRUCTURAL MEMBERS)
NT ANISOTROPIC PLATES
NT CIRCULAR PLATES
NT CORRUGATED PLATES
NT ELASTIC PLATES
NT END PLATES
NT METAL PLATES
NT ORTHOTROPIC PLATES
NT PERFORATED PLATES
NT RECTANGULAR PLATES
NT REINFORCED PLATES
Design guide for predicting nonlinear random response (including snap-through) of buckled plates
[NASA-CR-181877] 01 p0118 N90-10681
Application of matrix correction methods on a plate and a truss structure
[NLR-MP-88042-U] 03 p0359 N90-12056
A study of the impact of a ball bearing on a long fiber composite plate with a carbon matrix, part 2
[ETCA-88-R-088-PT-2] 04 p0467 N90-12673
Transverse (through-the-thickness) shear stiffnesses of fibre reinforced composite laminated plates (computer program)
[ESDU-89013] 07 p0891 N90-15152
Two new techniques for predicting delamination growth in laminated plates 09 p1185 N90-16865
Damage in a perforated graphite-epoxy composite plate under monotonic and cyclic biaxial loading
[ESA-TT-1117] 11 p1480 N90-18521
A study of the vibrational transmission through flanged joints
[ISVR-TR-181] 11 p1520 N90-18755
Test component attachment effects on resonant plate pyrotechnic shock simulation
[DE90-006478] 12 p1662 N90-19551
Development of finite beam and shell elements for structures under great inelastic deformations
[ETN-90-95869] 12 p1675 N90-19623
Interlaminar shear stress effects on the postbuckling response of graphite-epoxy panels
[NASA-TM-102626] 12 p1676 N90-19630
Postbuckling behavior of laminated specially orthotropic plates by affine transformation 13 p1814 N90-20420
Micromechanics analysis of space simulated thermal deformations and stresses in continuous fiber reinforced composites
[NASA-TM-102633] 14 p1946 N90-21140
Determination of stresses around cutouts in multilayered composite plate and shell structures 14 p1992 N90-21417
Progression of damage and fracture in composites under dynamic loading
[NASA-TM-103118] 15 p2065 N90-21825

The Shock and Vibration Digest, volume 21, no. 8
15 p2110 N90-22068
Recent progress in the dynamic plastic behavior of structures, part 5
15 p2110 N90-22069
Explicit modeling of composite plates and beams in the dynamics of multibody systems
16 p2285 N90-23019
The accelerated cooling in GTS plate mill
[ETN-90-97019] 19 p2682 N90-25256
The stress intensity factor and stress concentration for a finite plate with a single crack emanating from a hole
[LR-607] 19 p2704 N90-25385
Reliability analysis of continuous fiber composite laminates
[NASA-CR-185265] 20 p2878 N90-26372
Modal interaction in postbuckled plates. Theory
[NASA-TP-2943] 21 p3012 N90-27121
A nonlinear finite element formulation for the large displacement analysis of plates
23 p3338 N90-28867
On a generalized laminate theory with application to bending, vibration, and delamination buckling in composite laminates
24 p3478 N90-29659

PLATES (TECTONICS)
The recovery of orbital and geophysical parameters using a spaceborne laser ranging system
02 p0226 N90-11294
Divergent plate boundaries and crustal spreading on Venus: Evidence from Aphrodite Terra
03 p0422 N90-12427
Strain accumulation and surface deformation along the San Andreas, California
[NASA-CR-185893] 05 p0666 N90-13894
Dynamics of mid-ocean ridge systems
07 p0965 N90-15575
Mid-term report on the study and development results of the Sunshine Project in fiscal 1987. Study on the evaluation technology of geothermal sources in Japan
[DE90-710708] 10 p1400 N90-18095
The interpretation of crustal dynamics data in terms of plate interactions and active tectonics of the Anatolian plate and surrounding regions in the Middle East
[NASA-CR-186200] 11 p1533 N90-18824

PLATFORMS
Improved solar cells testing fixtures
10 p1346 N90-17807

PLATING
NT ELECTROPLATING
NT ION PLATING
Determination of iron in chromium plating and polishing solutions by atomic absorption spectrometry
[AD-A214467] 09 p1189 N90-16892
Determination of trivalent chromium ions in chromium plating solutions by ultraviolet-visible spectrophotometry
[AD-A215688] 10 p1351 N90-17837
Electrodeposition of wear resistant coatings
[PB90-221839] 23 p3312 N90-28732

PLATINUM
Structural and surface characterization of dispersed metal catalysts
[DE89-014530] 01 p0038 N90-10208
Computer simulation studies of the catalytic oxidation of carbon monoxide on platinum metals
[PB89-223739] 04 p0475 N90-12721
Correlations between surface structure and catalytic activity/selectivity
[DE90-003755] 07 p0896 N90-15181
Evaluation of platinum silicide and indium antimonide as detector materials for space-based remote sensing in the 3.0-to-5.0 micrometer wavelength band
[AD-A216182] 10 p1354 N90-17853
Fundamental studies of surface processes and trace analysis using solid electrodes
[AD-A216538] 11 p1483 N90-18533
Structure and reactivity of model thin film catalysts
[DE90-007365] 11 p1485 N90-18546
Multicomponent glass surfaces structure and adsorption
[DE90-007179] 11 p1493 N90-18596
Elimination of platinum inclusions in phosphate laser glasses
[DE90-004479] 12 p1629 N90-19361
Recent advances in solid polymer electrolyte fuel cell technology with low platinum loading electrodes
13 p1823 N90-20465
Pt/SnO2-based CO-oxidation catalysts for long-life closed-cycle CO2 lasers
18 p2556 N90-24589
Synthesis, characterization and evaluation of CO-oxidation catalysts for high repetition rate CO2 TEA lasers
18 p2557 N90-24593
The effect of H2O and pretreatment on the activity of a Pt/SnO2 catalyst
18 p2558 N90-24597
Platinized tin oxide catalysts for CO2 lasers: Effects of pretreatment
18 p2559 N90-24600
ISS and TPD study of the adsorption and interaction of CO and H2 on polycrystalline Pt
18 p2559 N90-24602
In situ analysis of CO during chemisorption and oxidation on graphite: Supported Pt by FTIR-microspectrometry
18 p2559 N90-24605
Calorimetry, activity, and micro-FTIR analysis of CO chemisorption, titration, and oxidation on supported Pt
18 p2560 N90-24606
Analysis of Pt/SnO(sub x) during catalysis of CO oxidation
18 p2560 N90-24607
Characterization of the surfaces of platinum/tin oxide based catalysts by Fourier Transform Infrared Spectroscopy (FTIR)
18 p2560 N90-24608
Chemisorption studies of Pt/SnO2 catalysts
18 p2560 N90-24609
Performance of alumina-supported Pt catalysts in an electron-beam-sustained CO2 laser amplifier
18 p2561 N90-24613
A resistance strain gage with repeatable and cancellable apparent strain for use to 800 C
[NASA-CR-185256] 20 p2823 N90-26063
The application of HREELS to model catalysts: CO and C2H4 adsorption on Pt/Al2O3
[AD-A222744] 20 p2831 N90-26103
Field-induced surface chemistry of NO
[AD-A223007] 21 p2977 N90-26915
Structure of metal overlayers by low energy alkali ion scattering: Cu/Ru(0001) and Sn/Pt(111)
[DE90-014453] 23 p3310 N90-28718
Scanning tunneling microscopy studies of chemisorbed layers on metal surfaces
[DE90-015623] 24 p3450 N90-29486

PLATINUM COMPOUNDS
NT PLATINUM OXIDES
Evaluation of platinum silicide and indium antimonide as detector materials for space-based remote sensing in the 3.0-to-5.0 micrometer wavelength band
[AD-A216182] 10 p1354 N90-17853
Antiferromagnetism and enhanced heat in CeM2Sn (M = Ni, Ir, Cu, Rh, Pd, and Pt
[DE90-014924] 23 p3399 N90-29206
Evidence for a coherence gap in Ce3Bi4Pt3
[DE90-014925] 23 p3399 N90-29207

PLATINUM OXIDES
Effect of pretreatment on a platinized tin oxide catalyst used for low-temperature CO-oxidation
18 p2558 N90-24599
Characterization of the surfaces of platinum/tin oxide based catalysts by Fourier transform spectroscopy (FTIR)
18 p2643 N90-25054

PLEIADES CLUSTER
The Moon has set
[REPT-89-07] 12 p1728 N90-19933

PLEXIGLASS (TRADEMARK)
U POLYMETHYL METHACRYLATE

PLOTTERS
NT X-Y PLOTTERS
EZVIDEO, FORTRAN graphics routines for the IBM AT
[DE90-004409] 08 p1109 N90-16422
A computer graphics package
[ARE-TM(UDT)-89111] 23 p3380 N90-29094

PLOTTING
Model filled polymers 3. Rheological behavior of polystyrene containing crosslinked polystyrene beads
[AD-A215867] 11 p1489 N90-18567
A numerical solution to the Boltzmann equation for use in calculating pumping rates in a CO2 discharge laser
[AD-A216376] 11 p1514 N90-18718
Basic graphics routine technical manual
[AD-A219409] 16 p2302 N90-23117
Documentation of program Tankplot
[FFI-89/7019] 20 p2908 N90-26541
A computer graphics package
[ARE-TM(UDT)-89111] 23 p3380 N90-29094
Realtime multi-plot graphics system
[NASA-CR-4304] 24 p3523 N90-29919

PLOTTING INSTRUMENTS
U PLOTTERS

PLOWED FIELDS
U FARMLANDS

PLOWING
Evaluation of two methods for acquisition of training statistics for digital analysis of areas prepared for plowing
[INPE-4901-PRE/1502] 11 p1522 N90-18763

PLUGGING
A characterization of the side bonding, upset plug welding process
[DE89-015181] 02 p0229 N90-11315

PLUGS
The effects of hearing protectors on speech communication and the perception of warning signals
[AD-A212521] 04 p0492 N90-12832
Shape instabilities of plate-like structures. 1: Experimental observations in heavily cold worked in situ composites
[AD-A212251] 04 p0523 N90-13021
Comparative evaluation of Allison T56 engine chip detectors
[AD-A221864] 21 p2960 N90-26832
Underwater connect and disconnect plug and receptacle
[AD-D014175] 21 p2998 N90-27039

PLUMBANE
U LEAD COMPOUNDS
U METAL HYDRIDES

PLUMES
NT ROCKET EXHAUST
Boost-phase discrimination research activities
[NASA-TM-101889] 01 p0032 N90-10176
Heat transfer characteristics of igniter output plumes
[DE89-011449] 01 p0059 N90-10340
Investigation of advanced mixer-ejector exhaust system
[AD-A211943] 03 p0301 N90-11705
The shape of the probability density function of short-term concentration fluctuations of plumes in the atmospheric boundary layer
[AD-A212632] 04 p0548 N90-13188
Development of a shuttle plume radiation heating indicator
[NASA-CR-183679] 05 p0614 N90-13584
Air quality simulation model performance for one-hour averages
[PB89-233506] 05 p0665 N90-13890
Convective boundary layer and modeling of dispersion
06 p0813 N90-14731
Propulsion research on the hybrid plume rocket
[AD-A214420] 07 p0887 N90-15132
Plume shape optimization of small attitude control thrusters with respect to impingement and thrust
[ISL-CO-220/88] 08 p1064 N90-16153
Simulation of pollutant transport using a mesoscale grid circulation model
[GKSS-89/E/24] 08 p1099 N90-16365
Plume flowfield analysis of the shuttle primary Reaction Control System (RCS) rocket engine
[NASA-CR-186315] 10 p1329 N90-17676
Evolution of midplate hotspot swells: Numerical solutions
[NASA-CR-186462] 12 p1691 N90-19713
An analytic model of axisymmetric mantle plume due to thermal and chemical diffusion
[NASA-CR-186461] 12 p1691 N90-19714
Y1Ba2Cu3O(7-x) laser-ablation plume dynamics measurement by nanosecond response ion probe: Comparison with optical measurements
[DE90-007658] 13 p1807 N90-20375
Sulphur silicate interactions on the Jovian satellite Io
15 p2192 N90-22515
PUFFY: A puff diffusion computer model
[FOA-C-40251-4.5] 17 p2421 N90-23796
Spacecraft contamination programs within the Air Force Systems Command Laboratories
19 p2727 N90-25507
Evaluation of water cooled supersonic temperature and pressure probes for application to 2000 F flows
[NASA-TM-102612] 19 p2753 N90-25645
Digital filtering of plume emission spectra
[NASA-TM-103135] 20 p2824 N90-26070
Preliminary plume characteristics of an arcjet thruster
[NASA-TM-103241] 20 p2825 N90-26071
Hypervelocity impact shield
[NASA-CASE-MSC-21420-1] 21 p2966 N90-26858
Evaluation of the wake effects on plume dispersion using video image analysis
[PB90-186354] 22 p3169 N90-27972
Barotropic mechanisms associated with tropical plume formation
24 p3489 N90-29719
Wind tunnel, field, and numerical investigations of plume downwash and dispersion at an arctic industrial site
24 p3489 N90-29721

PLUTO (PLANET)
Carbon in the outer solar system
21 p3096 N90-27593

PLUTONIUM
Multiple martensitic transformations, incommensurate/commensurate phases, and charge-density-wave states in plutonium metal: Their consequences
[DE90-001235] 06 p0748 N90-14350

PLUTONIUM CARBIDES
U PLUTONIUM COMPOUNDS

PLUTONIUM COMPOUNDS
NT PLUTONIUM OXIDES
Phase diagram and thermodynamic data for the Am-Pu system
[NPL-DMM(A)-5] 22 p3255 N90-28431

PLUTONIUM OXIDES
Draft Environmental Impact Statement for the Ulysses Mission (Tier 2)
[NASA-TM-102903] 06 p0812 N90-14727
Final Environmental Impact Statement for the Ulysses Mission (Tier 2)
[NASA-TM-101104] 15 p2126 N90-22162

PLUVIOGRAPHS
U RAIN GAGES
U RECORDING INSTRUMENTS

PLY ORIENTATION
Mechanical behavior of carbon/resin composites under delamination and cracking of transverse layers
[ONERA-RT-46/7086-M] 04 p0467 N90-12678
Localization of ultrasound in thick composites
[AD-A212994] 05 p0618 N90-13602
Three-dimensional stress analysis of plain weave composites
[NASA-TM-101672] 10 p1347 N90-17813
A statistical evaluation of the variation in laminated composite properties resulting from ply misalignment
[DE90-006371] 11 p1481 N90-18525
Residual stresses in laminated thermoplastic matrix composites 15 p2063 N90-21815

PNEUMATIC CONTROL
Analysis of high speed pneumatic actuation systems under rotary directional on-off flow control 04 p0507 N90-12926
Bi-directional thruster development and test report
[NASA-CR-182013] 15 p2058 N90-21785

PNEUMATIC EQUIPMENT
NT GAS VALVES
Flight evaluation of a pneumatic system for unsteady pressure measurements using conventional sensors
[NASA-TM-4131] 06 p0724 N90-14225
Bi-directional thruster development and test report
[NASA-CR-182013] 15 p2058 N90-21785

PNEUMATIC PROBES
Compensating for pneumatic distortion in pressure sensing devices
[NASA-TM-101716] 12 p1603 N90-19224
The calibration and measuring procedure of a five-hole hemispherical head probe in compressible flow
[LR-585] 15 p2099 N90-22013
Off-design loss measurements in a compressor cascade
[AD-A220094] 18 p2552 N90-24564
Experimental characterization of the effects of pneumatic tubing on unsteady pressure measurements
[NASA-TM-4171] 22 p3116 N90-27703

PNEUMATIC RESET
U PNEUMATIC CONTROL

PNEUMATICS
The role of particle collisions in pneumatic transport 01 p0068 N90-10392
Pipe and bend erosion by pneumatic transport of solids at high temperature
[DE89-015741] 06 p0778 N90-14524
Formulation and verification of a technique for compensation of pneumatic attenuation errors in airborne pressure sensing devices 09 p1221 N90-17084
Development and utilization of new diagnostics for dense-phase pneumatic transport
[DE90-006787] 12 p1659 N90-19536

POCKELS EFFECT
U BIREFRINGENCE

PODS (EXTERNAL STORES)
Independent Orbiter Assessment (IOA): Analysis of the orbital maneuvering system
[NASA-CR-185554] 02 p0162 N90-10919
Independent Orbiter Assessment (IOA): Analysis of the reaction control system, volume 3
[NASA-CR-185532-VOL-3] 02 p0167 N90-10940

POGO
Relationship between the current and the width of the POGO electrojet during the solstices
[DE89-619725] 04 p0565 N90-13294

POINCARE PROBLEM
The behavior of matter under nonequilibrium conditions: Fundamental aspects and applications
[DE90-002522] 07 p0892 N90-15157
A new class of exact solutions of the vacuum quadratic Poincare gauge field theory
[MATHS-REPT-A-119] 20 p2933 N90-26691
On trivector torsion in vacuum quadratic Poincare gauge field theory
[MATHS-REPT-A-121] 20 p2933 N90-26692

POINT DEFECTS
NT VACANCIES (CRYSTAL DEFECTS)
Characterization of the Structure and Chemistry of Defects in Materials: Proceedings, volume 138
[DE89-014796] 03 p0410 N90-12352
Molecular-dynamics study of the amorphization of CuTi
[DE90-003563] 07 p1001 N90-15791
Point defects and interfaces in insulating solids
[AD-A214668] 09 p1289 N90-17471
Ion implantation-induced amorphization of ceramic oxides
[DE90-006564] 11 p1571 N90-19041
Self-consistant calculation of point and pair structure defects in silicium
[ETN-90-96059] 12 p1722 N90-19891
The stress-driven redistribution of point defects in the vicinity of crack-like singularities
[AERE-R-12898] 13 p1815 N90-20424
Ionic disorder in crystals at high temperatures with emphasis on fluorites
[AERE-R-13544] 13 p1893 N90-20862
The effects of point defects and composition on structural phase transition
[DE90-010109] 16 p2322 N90-23238
Photorefractive damage mechanisms in electro-optic materials
[AD-A219786] 17 p2476 N90-24157

POINT MATCHING METHOD (MATHEMATICS)
U BOUNDARY VALUE PROBLEMS

POINT SOURCES
Use of the Egret instrument in studies of the origin of the cosmic radiation. 2: Spectral signatures of discrete cosmic-ray sources
[DE90-003595] 08 p1154 N90-16682
Research in theoretical physics
[DE90-005558] 11 p1562 N90-19001
IRCAM observations of the Reipurth 50 IR source 11 p1583 N90-19119
An investigation of the transfer of monopulse tracking between two coherent point sources
[AD-A217007] 12 p1646 N90-19457
Emission data for the EURAD project 12 p1688 N90-19700
An analytic model of axisymmetric mantle plume due to thermal and chemical diffusion
[NASA-CR-186461] 12 p1691 N90-19714
Research accomplishments and future goals in particle physics
[DE90-007296] 12 p1712 N90-19830
Search for anisotropies in the underground cosmic ray muon flux 12 p1745 N90-20034
New water vapor masers in the Southern Hemisphere
[INPE-4844-PRE/1473] 14 p2037 N90-21689
A search for very high energy gamma rays from the Crab pulsar-nebula 14 p2043 N90-21718
Photometric monitoring of early type emission line stars 15 p2184 N90-22478
More data on (possible) gamma ray (point) sources 16 p2335 N90-23309
Spectral determinations for discrete sources with EGRET 16 p2336 N90-23312
Self-consistent Comptonised models for the spectra of low mass X ray binaries 19 p2780 N90-25817
An infrared sky model based on the IRAS point source data
[NASA-CR-177526] 23 p3409 N90-29265

POINT SPREAD FUNCTIONS
Effect of central obscuration on the LDR point spread function 05 p0598 N90-13475

POINT TO POINT COMMUNICATION
NT NASCOM NETWORK

POINTING CONTROL SYSTEMS
The Spartan 1 mission
[NASA-TM-101887] 01 p0015 N90-10077
Analysis of the flight dynamics of the Solar Maximum Mission (SMM) off-sun scientific pointing 05 p0590 N90-13432
Report of the Asilomar 3 LDR Workshop
[NASA-CR-184656] 05 p0594 N90-13449
Pointing control for LDR 05 p0595 N90-13453
Space telescope pointing control 05 p0595 N90-13454
Astrometric Telescope Facility isolation and pointing study
[NASA-CR-177473] 10 p1328 N90-17675
Laser intersatellite transmission experiment spatial acquisition, tracking, and pointing system
[AD-A215934] 10 p1389 N90-18036
Preliminary design of a pointer for movement of a solar simulator
[INPE-4864-TDL/375] 11 p1517 N90-18736
Disturbance torque rejection properties of the NASA/JPL 70-meter antenna axis servos 12 p1644 N90-19450
Aiming control: Theory and applications to dynamic control of space structures
[AD-A217877] 13 p1764 N90-20123
A general-purpose balloon-borne pointing system for solar scientific instruments
[NASA-TP-3013] 14 p1959 N90-21219
Nonlinear spline operator interpolation and sliding control of deformable maneuvering bodies 15 p2074 N90-21878
Balanced bridge feedback control system
[NASA-CASE-NPO-17430-1-CU] 15 p2088 N90-21951
Driving and latching of the Starlab pointing mirror doors 15 p2114 N90-22093
Active control of bearing preload using piezoelectric translators 15 p2115 N90-22098
Sliding control of pointing and tracking with operator spline estimation 16 p2281 N90-22997
Nonlinear dynamics and control of flexible structures
[AD-A218372] 17 p2386 N90-23588
Fourth European Space Mechanisms and Tribology Symposium
[ESA-SP-299] 18 p2535 N90-24462
A Communications Antenna Pointing System (CAPS): A modular approach 18 p2537 N90-24474
Precision pointing and locking capabilities combined by a linear actuator 18 p2537 N90-24475
Hemispherical pointing mechanism 18 p2541 N90-24502
Rotating-unbalanced-mass devices for scanning balloon-borne experiments, free-flying spacecraft, and space shuttle/space station experiments
[NASA-TP-3030] 19 p2682 N90-25255
Application of inertial instruments for DSN antenna pointing and tracking 20 p2853 N90-26224
Aiming control: Theory and applications to dynamic control of space structures
[AD-A221532] 21 p2967 N90-26864
The instrument pointing system: Precision attitude control in space 22 p3129 N90-27756
Pointing control system for the Teal Ruby experiment 24 p3429 N90-29370

POINTS (MATHEMATICS)
NT FIXED POINTS (MATHEMATICS)
A point in betaZ/Z not contained in a maximal orbit closure
[REPT-89-26] 04 p0540 N90-13127
A statistical analysis of spatial point patterns, a case study
[CWI-MS-R8813] 04 p0547 N90-13180
Branch point placement
[OUEL-1767/89] 15 p2158 N90-22329
A survey of search directions in interior point methods for linear programming
[REPT-89-65] 17 p2445 N90-23934
Finding squares and rectangles in sets of points
[RUU-CS-89-10] 18 p2601 N90-24806

POISEUILLE FLOW
U LAMINAR FLOW

POISONS
NT CARBAMATES (TRADENAME)
NT PESTICIDES
NT URETHANES

POISSON DENSITY FUNCTIONS
Lie-algebraic aspects of the classical nonrelativistic Calogero-Moser models
[CWI-AM-R8901] 04 p0542 N90-13148
Fellowships in information and stochastic systems
[AD-A212385] 04 p0563 N90-13280
R-matrices and higher Poisson brackets for integrable systems
[PREPRINT-669] 05 p0696 N90-14069
Note on the optimality of the generalized shortest queue policy
[TW-90-01] 17 p2464 N90-24081
The gamma process and the Poisson distribution
[MEMO-COSOR-89-24] 17 p2466 N90-24089
The M/G/1 queue with permanent customers
[CWI-BS-R8919] 17 p2467 N90-24096

POISSON EQUATION
Particle simulation in curvilinear coordinate systems
[DE89-016727] 02 p0277 N90-11583
A multigrid algorithm for the incompressible Navier-Stokes equation
[GMD-374] 03 p0349 N90-11993
Thermionic emission including both space charge and image forces
[AD-A212732] 04 p0498 N90-12869
An iterative method to solve the nonlinear Poisson's equation in the case of plasma tangential discontinuities
[AERONOMICA-ACTA-A-346-1989] 05 p0692 N90-14045
R-matrices and higher Poisson brackets for integrable systems
[PREPRINT-669] 05 p0696 N90-14069
Multigrid methods for two- and three-dimensional Poisson-type equations on the sphere
[GMD-391] 08 p1117 N90-16468
Experimental validation of extended image reconstruction using bispectral speckle interferometry
[DE90-008545] 13 p1772 N90-20171
The reduction correction in North America 13 p1836 N90-20540

Compact scheme for systems of equations applied to fundamental problems of mechanics of continua
[NASA-CR-186494] 14 p1971 N90-21292
On the way to an integrated mesh generation system for industrial applications 15 p2095 N90-21989
The gamma process and the Poisson distribution
[MEMO-COSOR-89-24] 17 p2466 N90-24089
A Lyapunov bound for solutions of Poisson's equation
[AD-A220223] 18 p2599 N90-24787
Nondestructive one- and two-dimensional doping profiling by inverse methods
[ETN-90-97264] 20 p2874 N90-26351

POISSON PROCESS
U POISSON DENSITY FUNCTIONS
U STOCHASTIC PROCESSES

POISSON RATIO
Design and evaluation of a new biaxial testing method for sheet material (SUPERBAT)
[LR-548] 05 p0656 N90-13824
Construction of inelastic stress-strain curves from minimal materials data (computer program)
[ESDU-89052] 09 p1239 N90-17189
Postbuckling behavior of laminated specially orthotropic plates by affine transformation 13 p1814 N90-20420
Failure analysis of woven hybrid composite using a finite element method
[OUEL-1791/89] 15 p2065 N90-21828

POLAR AURORAS
U AURORAS

POLAR CAP ABSORPTION
Solar cosmic ray effects in the lower ionosphere 22 p3208 N90-28201
Post-flare effects in the lower ionosphere of middle latitudes 22 p3209 N90-28205

POLAR CAPS
Studies of time-dependent polar cap convection patterns 02 p0251 N90-11421
Airfields on antarctic glacier ice
[AD-A217638] 13 p1759 N90-20097
Quantitative studies of the Martian south polar region using spacecraft images 15 p2191 N90-22514
A study of auroral activity in the nightside polar cap 16 p2254 N90-22852
Evaluation of space plasma data: Effects upon spacecraft materials and predictions of hazardous conditions; polar ARCS
[AD-A219509] 17 p2474 N90-24145

POLAR COORDINATES
Polar coordinate laser writer for binary optics fabrication
[AD-A222827] 21 p3008 N90-27097

POLAR CUSPS
Polar cusps latitudinal shift and its relation to the IMF-By component
[IFSI-88-14] 08 p1101 N90-16377

POLAR IONOSPHERE BEACON
U BEACON SATELLITES

POLAR METEOROLOGY
Investigations of polar air stream cyclogenesis based on numerical simulations with a mesoscale model
[PB89-214563] 03 p0373 N90-12132
Applications of ISES for meteorology 21 p3018 N90-27160

POLAR ORBIT GEOPHYSICAL OBSERVATORY
U POGO

POLAR ORBITS
Attitude control modes for the MECB remote sensing satellites
[INPE-4755-PRE/1427] 14 p1938 N90-21094
Database development for the DMSP experiments
[AD-A224346] 24 p3557 N90-30129

POLAR PLATFORMS (SPACE STATIONS)
U SPACE STATION POLAR PLATFORMS

POLAR REGIONS
NT ANTARCTIC REGIONS
NT ARCTIC REGIONS
NT ROSS ICE SHELF
Kiruna geophysical data: Data Summary 88/7-9, July - September 1988
[PB89-210249] 01 p0086 N90-10487
Simulation of the polar cap F region ionization using an experimental convection electric field 02 p0241 N90-11370
VLF/LF radio wave studies of the structure and variability of the equatorial, mid-latitude and polar ionosphere below 100 km 02 p0242 N90-11373
Observations of ionosphere/magnetosphere interactions from the Dynamics Explorer satellites 02 p0242 N90-11376
Empirical models of convection electric fields and electrostatic potential at high latitude from EISCAT observations: Preliminary results 02 p0243 N90-11377
Polar F layer lacuna irregularities at Dumont d'Urville 02 p0243 N90-11379
On the possibility of producing artificial ionization and polar aurora in the ionosphere by radio-waves emitted from the ground 02 p0245 N90-11388
Role of chemical effects in daytime high latitude trough formation
[AD-A211772] 04 p0518 N90-12989
Cloud cover determination in polar regions from satellite imagery *
[NASA-CR-186096] 04 p0520 N90-13003
Enhanced electron density layers in the high-latitude lower ionosphere 05 p0657 N90-13832
The electrodynamics of the polar ionosphere with special emphasis on the dayside cleft region 05 p0658 N90-13838
Polar mesosphere summer echoes and associated atmospheric gravity waves 05 p0660 N90-13856
Diurnal variation of the sodium layer at polar latitudes in summer 05 p0662 N90-13869
Auroral and sub-auroral interaction at the F region ionosphere
[AD-A213284] 05 p0666 N90-13896
Three dimensional analysis of the structure of the atmosphere in polar environments by vertical satellite sounding. Interest for the meteorological forecasts at high latitudes
[ETN-90-95506] 05 p0671 N90-13911
The effect of orographic forcing on the mean flow of the stratosphere 08 p1099 N90-16367
Polar cusps latitudinal shift and its relation to the IMF-By component
[IFSI-88-14] 08 p1101 N90-16377
New approach to omega PPCs (Propagation Corrections)
[AD-A215610] 09 p1207 N90-17000
The Polar Ice Prediction System: A sea ice forecasting system
[AD-A214600] 09 p1249 N90-17246
Alterations in the metabolic and sympathetic response to cold exposure after cold air acclimation
[AD-A216817] 10 p1412 N90-18144
Center of excellence in theoretical geoplasma research
[AD-A215035] 14 p2005 N90-21488
A high galactic latitude survey of far ultraviolet excess objects 15 p2183 N90-22473
The optical night sky at low surface brightness: High latitude dust and faint field galaxies 15 p2185 N90-22481
SeaRISE: A Multidisciplinary Research Initiative to Predict Rapid Changes in Global Sea Level Caused by Collapse of Marine Ice Sheets
[NASA-CP-3075] 16 p2249 N90-22824
Electrodynamics of the high latitude ionosphere
[AD-A223229] 21 p3026 N90-27203
Report from GPS MANPACK tests in Spitsbergen area (Norway)
[FFI-90/7007] 22 p3114 N90-27692
The influence of IMF on the lower ionosphere plasma in high and middle latitudes 22 p3208 N90-28200
Effects of energy, momentum and particle transport in the near-earth solar terrestrial system
[AD-A224393] 24 p3490 N90-29726
Investigation of structure and transport processes in the high latitude ionospheric plasma using ground based and airborne digisondes
[AD-A224397] 24 p3491 N90-29727
Studies of ionospheric dynamics utilizing data from DMSP
[AD-A223370] 24 p3492 N90-29733

POLAR SUBSTORMS
The auroral energy deposition over the polar ionosphere during substorms
[AD-A210522] 01 p0086 N90-10490

POLARIMETERS
Bragg crystal polarimeters
[NASA-CR-181331] 01 p0073 N90-10423
Spectropolarimetry, variability, and the taxonomy of active galactic nuclei 02 p0292 N90-11667
The SMM UV observations of Active Region 5395 03 p0434 N90-12485
Spectropolarimetry as a diagnostic of the interstellar medium 11 p1579 N90-19096
The PHARUS project: Design of a polarimetric C-band SAR in the Netherlands 14 p1961 N90-21228
Radar scatterometry and polarimetry at 220 GHz 15 p2085 N90-21935
LEP and CEBAF polarimeters
[CEBAF-PR-89-010] 19 p2757 N90-25667
Eos visible imagers 21 p3016 N90-27146

POLARIMETRY
Multimode fiber interferometry and several-mode fiber polarimetry via phase conjugation
[DE89-014226] 01 p0123 N90-10706
Radar polarimetric studies based on the MAYPOLE 1983 and 1984 field experiments
[AD-A212226] 04 p0492 N90-12830
Investigation of the properties of radar backscatter from sea ice
[AD-A212808] 04 p0493 N90-12838
N-port theory applied to backscatter polarimetry and depolarization in foliage penetration
[AD-A213437] 07 p0917 N90-15305
Polarimetric SAR antenna characterization
[AD-A213438] 07 p0917 N90-15306
Flashlight radar: A three-dimensional imaging radar
[AD-A213439] 07 p0918 N90-15307
Near-infrared polarimetry and spectroscopy of comets 07 p1011 N90-15857
Algorithms for optimal processing of polarimetric radar data
[AD-A217330] 13 p1876 N90-20758
A motion compensation study for the PHARUS project 14 p1962 N90-21235
Introduction to the Infrared Space Observatory (ISO) 14 p1979 N90-21340
Status of the isophot detector development 14 p1980 N90-21342
A laboratory investigation into microwave backscattering from sea ice
[NASA-CR-186357] 19 p2705 N90-25390
Differential polarimetric fiber optic sensor
[AD-D014501] 19 p2757 N90-25668
UBVRI-photopolarimetry and the X ray dips of V471 Tau 19 p2775 N90-25781

POLARISCOPES
Stress field near crack tip: An experimental evaluation of the three dimensional variation
[AD-A217878] 13 p1818 N90-20441

POLARITONS
NT PLASMONS

POLARITY
Heat sink effects on weld bead: VPPA process 12 p1639 N90-19418
The role of polarity on the stability of graphitic compounds
[DE90-006528] 13 p1780 N90-20218
The dynamic electric microfield in ionic and polar media
[AD-A222534] 22 p3156 N90-27891

POLARIZATION (CHARGE SEPARATION)
NT DIELECTRIC POLARIZATION
IBM PC analysis of polarization resistance data
[AD-A212294] 04 p0477 N90-12732
Polarization of Li/SOCl2 cells
[DE90-000883] 06 p0804 N90-14680
A search for the electric dipole of the electron
[DE90-001572] 08 p1120 N90-16484
Polarization matrices of quartz
[AD-A215198] 09 p1212 N90-17027
Field effect transistor structures based on strain induced polarization charges
[DE90-007247] 12 p1655 N90-19515
Polarization observables in deuteron photo- and electro-disintegration
[CEBAF-PR-89-022] 19 p2756 N90-25659
Subthreshold technique for fixed and interface trapped charge separation in irradiated MOSFETs
[AD-A221861] 21 p3001 N90-27061

POLARIZATION (SPIN ALIGNMENT)
A laser-driven source of polarized hydrogen and deuterium
[DE89-015130] 01 p0075 N90-10429
Factors affecting electron spin polarization in photosynthetic systems
[DE90-000196] 06 p0819 N90-14764

POLARIZATION (WAVES)
NT CIRCULAR POLARIZATION
NT CROSS POLARIZATION
NT ELLIPTICAL POLARIZATION
NT LINEAR POLARIZATION
Preliminary investigation of Faraday rotation effects and description of polarization measurements on the AFGL high latitude meteor scatter test bed
[AD-A211298] 04 p0488 N90-12806
Anisotropy of electron distributions related to the anisotropy and polarization of the continuous emitted x rays 06 p0785 N90-14566
Chaotic behavior in nonlinear polarization dynamics
[DE89-013453] 06 p0788 N90-14589
Hamiltonian chaos in a nonlinear polarized optical beam
[DE90-002437] 07 p0934 N90-15408
Polarization radar processing technology
[AD-A215242] 10 p1374 N90-17967
Millimeter-wave propagation in the mesosphere
[PB90-119868] 11 p1496 N90-18612
New parameter-free polarization potentials in low-energy positron collisions 11 p1557 N90-18968
Vector circuit theory for multilayered isotropic and chiral structures: Reflection and transmission
[PB90-122474] 12 p1652 N90-19495

Earth-orbiting resonant-mass gravitational wave detectors 12 p1731 N90-19954
Pulsar timing and gravitational waves 12 p1732 N90-19955
General relativistic x ray (UV) polarization rotations as a quantitative test for black holes 12 p1732 N90-19957
A frequency agile 94 GHz pulse-Doppler radar with dual polarisation capability 14 p1960 N90-21226
A numerical and theoretical study of seismic wave diffraction in complex geologic structure
[AD-A218209] 14 p2005 N90-21490
Charge transfer polarisation wave and carrier pairing in the high T(sub c) copper oxides 22 p3142 N90-27820
The color of polarization in cuprate superconductors 22 p3144 N90-27830
Apparatus and method for minimizing polarization-induced signal fading in an interferometric fiber-optic sensor using input-polarization control
[AD-D014492] 22 p3164 N90-27940
Regional conditions during the 25 October 1986 FIRE cirrus/altocumulus case study 22 p3225 N90-28287
Asymmetric depolarization in powerful extragalactic radio sources 22 p3264 N90-28484

POLARIZATION CHARACTERISTICS
Nucleon polarizabilities in the constituent quark model
[NOTA-INTERNA-936] 05 p0698 N90-14082
Development and polarization of ferroelectric polymer gauges, for dynamical acceleration experiments, as those in ballistics shocks
[ISL-R-119/88] 11 p1511 N90-18703
Recognition and analysis of aircraft targets by radar, using structural pattern representations derived from polarimetric signatures 15 p2074 N90-21879
Remote sensing of Earth terrain
[NASA-CR-186868] 20 p2880 N90-26382

POLARIZATION CHARTS
U GRAPHS (CHARTS)
U POLARIZATION (WAVES)

POLARIZED ELASTIC WAVES
Effect of constitutive modeling on the dynamic development of shear bands in viscoplastic materials
[AD-A220443] 17 p2416 N90-23765

POLARIZED ELECTROMAGNETIC RADIATION
NT POLARIZED LIGHT
NT SYNCHROTRON RADIATION
The extended equivalent source technique with underdetermined sources
[DE90-006989] 11 p1499 N90-18627
Scattering of a plane electromagnetic wave from a semicircular crack in a perfectly conducting ground plane
[AD-A219310] 16 p2230 N90-22721
Stability regimes in a rotating quadrupole focusing accelerator
[AD-A219513] 16 p2317 N90-23209
Symmetry in the dynamics of a polarized fluid
[ETN-90-96896] 18 p2552 N90-24567

POLARIZED LIGHT
Low frequency polarized and depolarized light scattering in H-bonded liquids: CH3(CH2)n-1OH (n=1,...5)
[PREPRINT-693] 05 p0700 N90-14100
Porosity and ice-dust mixtures in cometary particles 12 p1743 N90-20018
Polarization: Effects on second harmonic power in light scattering by free electrons
[DE90-612842] 14 p2025 N90-21608
Investigations of polarized light scattering from rough surfaces
[AD-A221943] 21 p3076 N90-27491
Polarization contrast vision
[AD-A221423] 21 p3076 N90-27492
Apparatus and method for minimizing polarization-induced signal fading in an interferometric fiber-optic sensor using input-polarization control
[AD-D014492] 22 p3164 N90-27940
Near-infrared speckle observations of T Tauri stars and a multi-wavelength study of the prototype star T Tauri 23 p3409 N90-29264

POLARIZED RADIATION
NT POLARIZED ELASTIC WAVES
NT POLARIZED ELECTROMAGNETIC RADIATION
NT POLARIZED LIGHT
NT SYNCHROTRON RADIATION
X ray polarization of the reprocessed emission from accretion disk in Seyfert galaxies 19 p2792 N90-25892

POLARIZERS
Analysis and realization of integrated optical polarizers and absorbers on LiNbO3
[ETN-90-96504] 18 p2623 N90-24949

POLARONS
Coupled bipolarons and optical phonons as a model for high-T(sub c) superconductors 22 p3149 N90-27854
Spin bipolaron in the framework of emery model for high-T(sub c) copper oxide superconductors 22 p3149 N90-27856

POLICIES
NT ENERGY POLICY
NT PATENT POLICY
NT PROCUREMENT POLICY
Sagdeyev discusses space missions, policy, Mars plans 02 p0159 N90-10906
The transfer and diffusion of new technologies: A review of the economics literature
[DE89-015671] 02 p0290 N90-11655
Policies to encourage private sector responses to potential climate change
[DE89-017244] 03 p0368 N90-12107
Electronic warfare: Reliable equipment needed to test Air Force's electronic warfare systems
[AD-A212952] 05 p0632 N90-13687
Total quality management: Directorate of Contract Management master plan
[AD-A212867] 05 p0705 N90-14131
Metric handbook for Federal officials: Recommendations of the Interagency Committee on Metric Policy
[PB89-226922] 06 p0756 N90-14400
A dynamic systems engineering methodology research study. Phase 2: Evaluating methodologies, tools, and techniques for applicability to NASA's systems projects
[NASA-CR-181319] 06 p0857 N90-14985
DOD (Department of Defense) Freedom of Information Act Program (incorporating changes 1 and 2)
[PB90-104753] 06 p0859 N90-14993
Global climate change and NEPA (National Environmental Policy Act) analyses
[DE90-003704] 07 p0958 N90-15540
Safety and cryogenic wind tunnels 08 p1032 N90-15960
Round trip to orbit. Human spaceflight alternatives: Special report
[OTA-ISC-419] 08 p1033 N90-15966
The SMITE approach to security
[RSRE-89014] 08 p1106 N90-16404
Dispelling the North American acid rain clouds: Developing a framework for political consensus through the identification of elite viewpoints, volumes 1 and 2 09 p1243 N90-17213
An investigation into the effects which aerospace industry offset trade agreements have on United States Air Force mission performance
[AD-A215093] 09 p1294 N90-17502
Survey on the social and economic influences of wide-spreading heat-pump technology
[DE89-782294] 12 p1658 N90-19526
Regional remote sensing laboratory
[INPE-4922-PRE/1519] 14 p2001 N90-21465
International science and technology policies: Testimony before the Subcommittee on International Scientific Cooperation, Committee on Science, Space, and Technology, United States House of Representatives
[DE90-009416] 15 p2181 N90-22463
The environmental liabilities of government contractors and agencies 17 p2481 N90-24186
Social survey findings on en route noise annoyance issues 18 p2610 N90-24868
Theft of information in the take-grant protection model
[NASA-CR-186638] 19 p2763 N90-25702
AGARD highlights 90/1 20 p2951 N90-26788
Strategic defense initiative: Three reasons to stay the course
[AD-A222246] 21 p3070 N90-27456
Helping America compete: The role of Federal scientific and technical information
[OTA-CIT-454] 21 p3086 N90-27549
Policy options for stabilizing global climate. Volume 1: Chapters 1-6
[PB90-182304] 22 p3198 N90-28146
Policy options for stabilizing global climate. Volume 2: Chapters 7-9
[PB90-182312] 22 p3198 N90-28147
Role of grid-based, reactive air quality modeling in policy analysis: Perspectives and implications, as drawn from a case study
[PB90-187204] 22 p3198 N90-28150
Report of the Invitational Workshop on Data Integrity
[PB90-148123] 22 p3240 N90-28372
Legal ramifications of intellectual property 22 p3258 N90-28448
State science and technology indicators: An exploratory profile and analysis
[PB90-246711] 23 p3408 N90-29259
Global Climate Change: Seeking a Global Consensus
[S-HRG-101-842] 24 p3486 N90-29704

POLISHING
NT ELECTROPOLISHING
Determination of iron in chromium plating and polishing solutions by atomic absorption spectrometry
[AD-A214467] 09 p1189 N90-16892
Stochastic approach to the initiation of pitting corrosion
[AERE-R-13348] 13 p1775 N90-20190
Crystal preparation at LBL, 1976 to 1986
[DE90-007754] 13 p1894 N90-20871
Lapping: Polishing and shear mode grinding
[DE90-015188] 24 p3458 N90-29533

POLITICS
Dispelling the North American acid rain clouds: Developing a framework for political consensus through the identification of elite viewpoints, volumes 1 and 2 09 p1243 N90-17213
Remote sensing applied to vegetation as subsidized in municipal planning
[INPE-4908-PRE/1509] 11 p1523 N90-18770
The essence of spacepower: Important influences on the evolution of national spacepower
[AD-A217498] 13 p1879 N90-20781

POLLUTANTS
U CONTAMINANTS

POLLUTION
NT AIR POLLUTION
NT ENVIRONMENT POLLUTION
NT GLOBAL AIR POLLUTION
NT INDOOR AIR POLLUTION
NT NOISE POLLUTION
NT WATER POLLUTION
Application of high performance liquid chromatography/mass spectrometry to environmental analysis
[PB90-116963] 11 p1531 N90-18814
Wearing of cryomechanisms at 4 K 18 p2537 N90-24476
Pollutants: Production and methods of reduction
[CIT/SME/VKI/RS/6] 20 p2810 N90-25990
Cloud reflectance characteristics in the presence of variable Dimethylsulfide (DMS) sources
[AD-A222806] 21 p3024 N90-27197

POLLUTION CONTROL
Potential technologies for collection and destruction of CFCs (Chlorofluorocarbons), halons, and related compounds
[PB89-219968] 03 p0368 N90-12105
Effects of tacky mat contamination on bond degradation for Chemlok/liner and NBR/liner bonds
[NASA-CR-183742] 05 p0626 N90-13653
Proceedings: US/FRG (Federal Republic of Germany) Workshop on Photochemical Ozone Problem and Its Control: US Experiences and the Situation in Europe
[PB89-233514] 05 p0666 N90-13891
Consumer Ozone Protection Act of 1989
[S-HRG-101-377] 06 p0809 N90-14708
A preliminary analysis of US CO2 emissions reduction potential from energy conservation and the substitution of natural gas for coal in the period to 2010
[DOE/NBB-0085] 12 p1684 N90-19673
Catching our breath: Next steps for reducing urban ozone
[PB90-130451] 20 p2883 N90-26398
Options for controlling the global warming impact from motor vehicles
[PB90-161688] 22 p3197 N90-28142
National air quality and emissions trends report, 1988
[PB90-200114] 23 p3346 N90-28909
Environmental quality, 1970 - 1990
[PB90-214610] 24 p3487 N90-29705
SamTrack: A sample tracking system for environmental monitoring
[DE90-016026] 24 p3488 N90-29712

POLLUTION MONITORING
Interrelation of experimental exposure and ambient air quality data for comparison of ozone exposure indices and estimating agricultural losses
[PB89-195036] 02 p0238 N90-11353
Air quality simulation model performance for one-hour averages
[PB89-233506] 05 p0665 N90-13890
Nitrogen deposition to forest trees
[DE90-003285] 06 p0812 N90-14726
Environmental surveillance data
[DE90-001275] 07 p0956 N90-15532
Chamber investigations of the fate of diesel emissions in the atmosphere, volume 1, task 3
[PB90-114422] 10 p1405 N90-18103
Application of high performance liquid chromatography/mass spectrometry to environmental analysis
[PB90-116963] 11 p1531 N90-18814
Development of a laser fluorosensor for the aircraft supported analysis of maritime toxic agents loads: Definition phase
[ETN-90-95320] 13 p1829 N90-20499

The laminar flow element: Its use as a flow standard
[PB90-129677] 15 p2126 N90-22157
The distribution of middle tropospheric carbon monoxide during early October 1984
[NASA-TM-103485] 23 p3346 N90-28906

POLLUTION TRANSPORT
The suitability of diffusion and wind-field techniques for an emergency-response dispersion model
[PB89-190219] 01 p0085 N90-10481
Meteorological monitoring for environmental/dose assessment and emergency response modeling: How much is enough
[DE90-002726] 06 p0818 N90-14757
Vertical distribution of pollutants in the presence of convective storms
[DE90-002590] 07 p0960 N90-15549
Simulation of pollutant transport using a mesoscale grid circulation model
[GKSS-89/E/24] 08 p1099 N90-16365
Transport of atmospheric aerosols above the Sierra Nevada slopes
[PB90-120288] 12 p1685 N90-19675
On the question of spray effects
12 p1687 N90-19691
Boundary layer parameterization in CTM and MM4
12 p1688 N90-19697
Modelization of dry deposition in the Chemical Transport Model (CTM) of EURAD 12 p1688 N90-19698
Sensitivity studies in a two-dimensional atmospheric transport model
[DAR-TP-18] 14 p2006 N90-21496
Global distribution of organo-bromine gases
15 p2124 N90-22150
The ASCOT 1988 valley/tributary interaction study
[DE90-009043] 15 p2133 N90-22191
Nordic Symposium on Atmospheric Chemistry
[CM-78] 20 p2883 N90-26403
Deposition to the Baltic Sea 20 p2884 N90-26404
Verification and improvement of the EMEP model for long-range transport and deposition of pollutants
20 p2884 N90-26405
An Eulerian transport model for NO(sub x)-compounds
20 p2884 N90-26406
The long-term variation of lead-210 in relation to particle-bound sulphur in surface air in Finland
20 p2884 N90-26407
Further development and application of an atmospheric chemistry trajectory model 20 p2884 N90-26408
The transfer of mercury between the atmosphere and lake or soil surfaces 20 p2886 N90-26419
The aqueous atmospheric chemistry of mercury
20 p2886 N90-26420
Atmospheric dispersion of solid and liquid rocket propellants
[AD-A221293] 21 p3020 N90-27173
Acid deposition in Maryland: Summary of results through 1989
[PB90-229782] 22 p3200 N90-28160
Meteorological conditions over the North Atlantic Ocean during GCE/CASE/WATOX
[PB90-252032] 24 p3494 N90-29747

POLOIDAL FLUX
Tokamak plasma shape identification with a Legendre-Fourier expansion of the vacuum poloidal flux function in the toroidal coordinates
[DE90-508031] 24 p3548 N90-30068

POLONIUM
NT POLONIUM ISOTOPES

POLONIUM ISOTOPES
Radon concentration over the Brazilian Amazon Basin during the wet season (Belem-Manaus GTE-ABLE-2B flight of April 24, 1987)
[INPE-4892-PRE/1493] 14 p2004 N90-21486

POLYACETYLENE
A literature survey of inherently conducting polymers
[FOA-C-20763-2.4] 05 p0628 N90-13668

POLYACRYLATES
U ACRYLIC RESINS

POLYACRYLONITRILE
Method for stabilization of pan-based carbon fibers
[AD-D014228] 06 p0736 N90-14288
Effects of heat treatment on microstructure and flexural properties of unidirectional carbon-carbon composites
[AD-A214985] 09 p1186 N90-16873
Development of low thermal conductivity pan-based carbon fibers for solid rocket motor nozzle applications
15 p2063 N90-21818

POLYAMIDE RESINS
NT KEVLAR (TRADEMARK)
NT NYLON (TRADEMARK)
Wet spinning of solid polyamic acid fibers
[NASA-CASE-LAR-14162-1] 07 p0910 N90-15259
Crosslinked, flexible, low-molecular-weight polyacrylamide gels for mobility control
[DE90-000202] 07 p0913 N90-15280
Rheological and mechanical characteristics of poly-p-phenylene terephthalamide/nylon molecular and particulate composites
[AD-A219562] 17 p2368 N90-23482
Solid-state N15 NMR of N15-labeled nylon 6 and nylon 11
[AD-A223271] 24 p3446 N90-29459

POLYATOMIC MOLECULES
NT DIATOMIC MOLECULES
A diagnostic for determining the quality of single-reference electron correlation methods
02 p0272 N90-11554
New developments in the ab initio treatment of low energy electron collisions with molecules
[DE89-015294] 03 p0402 N90-12299
Molecular dynamics of lipid bilayers
[AD-A211492] 04 p0552 N90-13214
Determination of stepsize parameters for intermolecular vibrational energy transfer
[DE90-003346] 07 p0990 N90-15719
Cluster based reaction probabilities for boron with oxygen, hydrogen, water, nitrogen, nitrous oxide, carbon dioxide, carbon monoxide, methane, tetrafluoromethane, and silane
[AD-A214554] 09 p1190 N90-16894
IR spectrophotometry of bright carbon stars
11 p1584 N90-19131
Infrared heterodyne spectroscopy of polyatomic molecules in circumstellar envelopes
12 p1736 N90-19980
DURIP FTIR studies of solid state reaction dynamics
[AD-A217713] 13 p1773 N90-20174
Laser enhanced chemical reactions
[DE90-008273] 13 p1807 N90-20377
Picosecond laser study of polyatomic molecules
[DE90-008647] 13 p1808 N90-20381
Polyatomic reaction dynamics
[DE90-008668] 13 p1884 N90-20811
Electronically metastable molecules of high symmetry
[AD-A217768] 13 p1885 N90-20814
Determination of molecular spectroscopic parameters and energy-transfer rates by double-resonance spectroscopy 20 p2944 N90-26755
Kinetics and thermochemistry of polyatomic free radicals: New results and new understandings
20 p2946 N90-26764
Spectroscopy of ions and their clusters
[AD-A223109] 21 p2977 N90-26917
Theoretical investigation of gas-surface interactions
[NASA-CR-186881] 22 p3245 N90-28403
Experimental studies leading to energy storage. Spectroscopy and dynamics of polyatomic hydrogen in liquid, solid and gaseous hydrogen plasmas
[AD-A224343] 24 p3547 N90-30066

POLYBLENDS
U POLYMER BLENDS

POLYBUTADIENE
Blow-out of rubber blocks due to internal heating
[AD-A215730] 09 p1198 N90-16943
Morphological consequences of catalytic hydrogenation of polymers in the bulk
[DE90-007276] 11 p1494 N90-18598
CO2 diffusion and solubility in a Polystyrene/Polybutadiene block copolymer with highly oriented lamellar morphology
[AD-A217165] 13 p1779 N90-20211
RSRM-9 (360L009): Ballistics mass properties
[NASA-CR-183944] 20 p2823 N90-26064
Modification of polystyrene/polybutadiene block copolymer films by chemical reaction with bromine and effect on gas permeability
[AD-A223612] 24 p3455 N90-29513

POLYCARBONATES
NT LEXAN (TRADEMARK)
Conference on Aerospace Transparent Materials and Enclosures (15th) 16-20 January 1989. Volume 2: Sessions 6-9
[AD-A210201] 01 p0006 N90-10024
An investigation of the degradation and stabilization of polymer systems
[AD-A210362] 01 p0049 N90-10282
Interfacial adsorption and crystallization of polycarbonate in carbon fiber composites
[AD-A211230] 02 p0191 N90-11090
Physical ageing and short term creep in amorphous and semicrystalline polymers
[NPL-DMA(A)-185] 04 p0479 N90-12745
Synthesis and analysis of novel polymers with potential for providing both high permselectivity and permeability in gas separation applications
[DE90-003907] 08 p1049 N90-16065
Polycarbonate article with chemical resistant coating
[NASA-CASE-MSC-21503-1] 09 p1195 N90-16925
The structural basis for fatigue initiation in glassy polymers
[DE90-009342] 14 p1956 N90-21200
Thermomechanical properties of polymeric materials and related stresses
[NASA-TM-100758] 15 p2071 N90-21864
Simulation of inelastic deformation in glassy polypropylene and polycarbonate
[AD-A218891] 16 p2224 N90-22686
The effect of thermal damage on the mechanical properties of polymer regrinds 18 p2515 N90-24363
Some studies of the vibration welding of thermoplastics 23 p3332 N90-28842

POLYCHLORINATED BIPHENYLS
The 25-KVA amorphous metal-core transformer developmental test report
[AD-A215444] 09 p1213 N90-17035

POLYCRYSTALS
Alternative fabrication techniques for high-efficiency CuInSe2 and CuInSe2-alloy films and cells
[DE89-009451] 01 p0083 N90-10474
Femtosecond dynamics of fluoro-aluminum phthalocyanine and linear alkane molecules
[AD-A210939] 01 p0133 N90-10766
Laser grooved and polycrystalline silicon solar cell research
[DE89-015196] 02 p0237 N90-11347
Proceedings of the Polycrystalline Thin Film Program Meeting
[DE89-009457] 02 p0237 N90-11348
Analysis of loss mechanisms in polycrystalline thin-film solar cells
[DE89-009454] 03 p0366 N90-12093
RF performance of polycrystalline high-T(sub c) superconductors
[DE89-017671] 03 p0411 N90-12359
Surface, interface, and bulk properties of high T(sub c) superconductors
[AD-A211490] 03 p0413 N90-12373
Spectroscopic ellipsometry characterization of CVD deposition and doping of polysilicon multilayer structures
[RSRE-MEMO-4258] 04 p0466 N90-12671
Synthesis and properties of NdNiO(3) prepared by low temperature methods
[AD-A212117] 04 p0559 N90-13256
A two-parameter representation of dynamic dislocation distributions
[AD-A212249] 04 p0560 N90-13263
Surfaces and interfaces of ceramic materials
[AD-A212417] 05 p0627 N90-13657
US Polycrystalline Thin Film Solar Cells Program
[DE89-009506] 07 p0951 N90-15504
Structural, magnetic and electrical properties of La(sub 2-x) Ba(sub x) NiO4
[AD-A214347] 10 p1434 N90-18278
Fundamental studies of surface processes and trace analysis using solid electrodes
[AD-A216538] 11 p1483 N90-18533
Research relating to crystalline silicon-film on a foreign substrate
[DE90-005720] 11 p1491 N90-18582
High growth rate diamond synthesis in a large area atmospheric pressure inductively coupled plasma
[AD-A216090] 11 p1567 N90-19019
The interaction of polycrystalline copper films with dilute aqueous solutions of cupric chloride
[AD-A216465] 11 p1569 N90-19033
Electron beam generation by electron bombardment induced cathode emission
[AD-A218203] 13 p1798 N90-20318
Chemically prepared PZT films doped with niobium
[DE90-006811] 13 p1892 N90-20859
Synthesis and properties of polycrystalline Tl2Ba2CaCu2O(x) and Tl2Ba2Ca2Cu3O(x)
[DE90-007528] 13 p1897 N90-20887
Formation of subsurface aluminum layers in beryllium by ion implantation and post-implant annealing
[DE90-007975] 14 p1951 N90-21172
Review and statistical analysis of the ultrasonic velocity method for estimating the porosity fraction in polycrystalline materials
[NASA-TM-102501-REV] 14 p1989 N90-21402
Mechanical properties of carbon-implanted niobium
[DE90-009864] 15 p2064 N90-21823
Photovoltaic Program Branch
[DE90-000318] 15 p2123 N90-22142
Characterization and processing of blends of polyethylene terephthalate with several liquid crystalline polymers
[AD-A219565] 17 p2380 N90-23552
Characterization study of polycrystalline tin oxide surfaces before and after reduction in CO
18 p2559 N90-24601
ISS and TPD study of the adsorption and interaction of CO and H2 on polycrystalline Pt
18 p2559 N90-24602
Highly-textured thallium-barium-calcium-copper-oxide polycrystalline superconducting films on silver substrates
[DE90-011972] 18 p2627 N90-24970

Aligned bismuth, strontium, calcium cuprate coatings on polycrystalline substrates
[AD-D014522] 19 p2678 N90-25229
Diffusion-accommodated grain boundary sliding in a polycrystal
[DE90-012727] 20 p2930 N90-26668
Application of microdesigned interfaces to studies of ceramic processing
[DE90-011633] 21 p2983 N90-26951
Nonlinear material response to very rapid energy deposition
[AD-A221932] 21 p2989 N90-26988
Composite ceramic superconducting wires for electric motor applications
[AD-A222085] 21 p3001 N90-27055
Polycrystalline thin film cadmium telluride n-i-p solar cells
[DE90-000351] 21 p3019 N90-27167
Flux motion effects in Tl-Ca-Ba-Cu-O thin films
[DE90-012176] 21 p3080 N90-27514
Fracture-EXAFS: A new method for the study of interfaces in thin films and polycrystalline materials
[DE90-013736] 21 p3081 N90-27521
Polycrystalline diamond Junction Field Effect Transistors (JFETS)
[AD-A222238] 21 p3083 N90-27534
Elliptical flux vortices in polycrystalline YBa2Cu3O7
22 p3136 N90-27795
Low frequency electrical noise across contacts between a normal conductor and superconducting bulk YBa2Cu3O7 22 p3146 N90-27841
Hyperthermal atomic oxygen generator
[NASA-CR-186573] 22 p3155 N90-27889
Mechanical property measurement of polycrystalline diamond films
[AD-A224037] 23 p3402 N90-29222
Polycrystalline diamond Junction Field Effect Transistors (JFETS)
[AD-A223784] 24 p3465 N90-29576

POLYESTER RESINS
New Fabric Development Program
[AD-A211549] 03 p0332 N90-11891
Instrumented impact testing of fabric-reinforced composite materials
[AD-A216764] 11 p1479 N90-18513
Processing of thermotropic liquid crystalline polymers and their blends
[AD-A218804] 16 p2223 N90-22683
The assessment of metal fiber reinforced polymeric composites 18 p2514 N90-24357

POLYESTERS
Synthesis and analysis of novel polymers with potential for providing both high permselectivity and permeability in gas separation applications
[DE90-003907] 08 p1049 N90-16065
Development of an elastomeric additive to improve the impact resistance of unsaturated polyester networks
[ISAL-89-0006] 08 p1050 N90-16073
Criteria for polymer concrete on airport pavements
[DOT/FAA/DS-89/18] 14 p1929 N90-21045
Low energy ion generator
[DE90-759905] 14 p1955 N90-21195
Failure mechanisms under complex loading of glass-reinforced polyester composites and their matrices: The effect of superposed hydrostatic pressures up to 300 MPa on axial tensile and compressive strengths, and in-plane shear properties of unidirtionally reinforced glass-polyester composites and the relevant polyesters
15 p2110 N90-22072
Synthesis and properties of a thermotropic copolyester based on 4,4 prime-dihydroxy-a,a prime-dimethylbenzalazine
[AD-A218803] 16 p2223 N90-22682
Characterization and processing of blends of polyethylene terephthalate with several liquid crystalline polymers
[AD-A219565] 17 p2380 N90-23552
Laboratory evaluation of two new high-performance polyester batting insulation materials
[AD-A222291] 21 p2987 N90-26976
The response and failure mechanisms of circular metal and composite plates subjected to underwater shock loading
[AD-A222200] 21 p3013 N90-27131

POLYETHER RESINS
NT PEEK
NT POLYMETHYL METHACRYLATE

POLYETHERETHERKETONES
U PEEK

POLYETHYLENE TEREPHTHALATE
Physical ageing and short term creep in amorphous and semicrystalline polymers
[NPL-DMA(A)-185] 04 p0479 N90-12745
Electronic and ionic transport in polymers
[AD-A213410] 07 p0911 N90-15270
Characterization and processing of blends of polyethylene terephthalate with several liquid crystalline polymers
[AD-A219565] 17 p2380 N90-23552
Process of three dimensional lithography in amorphous polymers
[AD-D014500] 19 p2678 N90-25221
Electric properties of highly oriented rigid chain, polymeric liquid crystals
[ETN-90-97287] 22 p3248 N90-28424

POLYETHYLENES
NT POLYETHYLENE TEREPHTHALATE
Shock induced dissociation of polyethylene
[DE89-016983] 02 p0221 N90-11267
Assessment of thin film batteries based on polymer electrolytes. Part 1: Energy density
[AD-A212111] 03 p0343 N90-11958
Solid state microelectrochemical devices: Transistor and diode devices employing a solid polymer electrolyte
[AD-A214206] 09 p1211 N90-17019
The size of the alkyl group R is the principal factor determining the wettability of surface-functionalized polyethylenes (PE-CONHR and PE-CO2R) by water
[AD-A216007] 10 p1354 N90-17851
Extracting chemical information form Auger line shapes
[AD-A216729] 11 p1483 N90-18537
Carbon black/polyethylene composites for PTC (Positive Temperature Coefficient) thermistor applications
[AD-A215988] 12 p1619 N90-19307
Research and development on enhanced degradable plastics
[AD-A217180] 13 p1779 N90-20212
Mechanics of necking, crazing, and crack growth in polymers 17 p2378 N90-23540
Deformation-induced structural developments of ultra-high molecular weight polyethylene
[ETN-90-96899] 18 p2529 N90-24432
The yield and post-yield behavior of high-density polyethylene
[NASA-CR-186574] 19 p2676 N90-25219
X ray diffraction analysis of control and test fibers
[MTL-TR-89-58] 19 p2678 N90-25233
Investigation of the effects of acid deposition on materials
[PB90-158973] 22 p3197 N90-28143
Technical bibliography of high performance polyethylene fibers
[SNPE-NT-106/89/GTR/RP/NP] 23 p3313 N90-28736

POLYGONS
NT RECTANGLES
NT RHOMBOIDS
NT SQUARES (MATHEMATICS)
NT TRAPEZOIDS
NT TRIANGLES
Description and manipulation of convex polygons using polarity
[IMAG-RR-771-M] 05 p0692 N90-14041
Formation of turbulent layers in the separated region around a body with polygonal cross section at large incidence and rolling
[ISL-R-101/88] 09 p1219 N90-17071
Solving computer graphics problems through boolean combinations of polygons
[AD-A214788] 09 p1273 N90-17380
The h-p version of the boundary element method with geometric mesh on polygonal domains
[AD-A215815] 10 p1423 N90-18211
Grouping for recognition
[AD-A216716] 11 p1549 N90-18915
Binary space partitioning trees and their uses
13 p1857 N90-20657
Simplified linear-time Jordan sorting and polygon clipping
[AD-A215110] 13 p1864 N90-20693
Finding minimum area k-gons
[RUU-CS-89-7] 17 p2449 N90-23967
Computational geometry and its application to computer graphics
[RUU-CS-89-8] 17 p2449 N90-23968
Translating polygons with applications to hidden surface removal
[RUU-CS-89-31] 18 p2602 N90-24816
Hierarchical structure of polygonal data for spatial analysis and representation of cartographical data
[INPE-4986-PRE/1548] 20 p2879 N90-26380
Generalized Voronoi diagrams: Initial results
[IMAG-RR-799-M] 21 p3066 N90-27429

POLYHEDRONS
NT OCTAHEDRONS
NT PARALLELEPIPEDS
NT TETRAHEDRONS
Optimal matching of 3-D convex polyhedra
[TELECOM-PARIS-89C003] 03 p0395 N90-12258
Data structures for the representation and manipulation of polyhedrons
[IMAG-RR-772-M] 05 p0692 N90-14042
Applications of polyhedral combinatorics to multicommodity flows and compact surfaces
[CWI-BS-R8921] 17 p2462 N90-24060
Kharitonov's theorem: Generalizations and algorithms
18 p2648 N90-25064
Investigation of maximum achievable body torque for a walking machine with friction cone constraints
[PB90-203175] 23 p3332 N90-28838

POLYIMIDE RESINS
The chemistry of hexaazatriphenylene hexanitrile, a polyfunctional heterocycle with potential utility in the formulation of thermostable polymers
[AD-A212353] 04 p0480 N90-12757
A novel heat resistant blend produced by compositional quenching: A thermoplastic polyimide impact modified with a fluoroelastomer
[AD-A213724] 07 p0912 N90-15273
Infrared and X ray photoelectron spectroscopy studies of the polyimide/metal interface
[AD-A218249] 13 p1773 N90-20179
Condensation polyimides
[NASA-TM-103467] 20 p2836 N90-26129
Characterization of polymer interphases using surface-enhanced Raman scattering
[AD-A223103] 21 p2985 N90-26965
Characterization of PMDI/HOPG interfaces by SERS using a silver overlayer configuration
[AD-A223104] 21 p2985 N90-26966
Characterization of model polyimide/silver interphases using surface-enhanced Raman scattering
[AD-A222488] 21 p2988 N90-26979
Autoclavable addition polyimides for 371 C composite applications
[NASA-TM-103233] 22 p3153 N90-27874

POLYIMIDES
NT BISMALEIMIDE
NT KAPTON (TRADEMARK)
The 3F condensation polyimides: Review and update
[NASA-TM-102353] 06 p0750 N90-14363
Novel polyimide compositions based on 4,4': Isophthaloyldiphthalic anaydride (IDPA)
[NASA-CASE-LAR-14194-1] 07 p0890 N90-15148
Wet spinning of solid polyamic acid fibers
[NASA-CASE-LAR-14162-1] 07 p0910 N90-15259
Polyimides with carbonyl and ether connecting groups between the aromatic rings
[NASA-CASE-LAR-14001-1] 07 p0910 N90-15260
LARC-IA: A flexible backbone polyimide
[NASA-TM-102586] 09 p1196 N90-16826
New Condensation polyimides containing 1,1,1-triaryl-2,2,2-trifluoroethane structures
[NASA-CASE-LEW-14346-1] 12 p1618 N90-19300
A study of physical properties of ODPA-p-PDA polyimide films
[NASA-TM-102625] 13 p1766 N90-20137
Bis(4-(3,4-dimethylenepyrrolidyl)-phenyl) methane
[NASA-CASE-LAR-13965-1-CU] 14 p1942 N90-21118
Process for lowering the dielectric constant of polyimides using diamic acid additives
[NASA-CASE-LAR-13902-1] 17 p2379 N90-23546
Computed structures of polyimides model compounds
[NASA-TM-101674] 19 p2672 N90-25195
Condensation polyimides
[NASA-TM-103467] 20 p2836 N90-26129
Fracture toughness of polyimide films
[NASA-TM-103473] 20 p2836 N90-26130
Characterization of a thermally imidized soluble polyimide film
[NASA-TM-103484] 20 p2836 N90-26131
A tough high performance composite matrix
[NASA-CASE-LAR-14338-1] 21 p2970 N90-26881
Polyimidazoles via aromatic nucleophilic displacement
[NASA-CASE-LAR-14145-1] 21 p2983 N90-26954
A tough performance simultaneous semi-interpenetrating polymer network
[NASA-CASE-LAR-14339-1] 21 p2984 N90-26955
Aromatic polyimides containing a dimethylsilane-linked dianhydride
[NASA-CASE-LAR-14198-1] 21 p2984 N90-26956
Evaluations of new polyimide films for flexible circuit applications at EG and G Mound Applied Technologies
[DE90-014117] 23 p3312 N90-28731

POLYISOPRENES
Analysis of spurt phenomena for a non-Newtonian fluid
[AD-A210560] 01 p0071 N90-10405

POLYMER BLENDS
A center for advanced electrical and structural polymers
[AD-A212853] 04 p0482 N90-12764
Mechanical properties and morphology of oriented polymer blends 06 p0750 N90-14361

Phase transition in polymer blends and structure of ionomers
[DE90-003525] 07 p0911 N90-15266
Control of phase structure in polymer blends
[AD-A217034] 11 p1491 N90-18580
Theory of polymer blends
[DE90-002532] 12 p1632 N90-19377
On the dynamics of polymer mixtures in solution using the RPA
[DE90-613689] 14 p1948 N90-21149
Processing of thermotropic liquid crystalline polymers and their blends
[AD-A218804] 16 p2223 N90-22683
Characterization and processing of blends of polyethylene terephthalate with several liquid crystalline polymers
[AD-A219565] 17 p2380 N90-23552
DURIP advanced polymer solid state NMR instrumentation
[AD-A221401] 18 p2531 N90-24440
Modelling of the processing of incompatible polymer blends
[ETN-90-97211] 20 p2840 N90-26152
Liquid crystalline polymers
[NASA-CR-186949] 21 p2986 N90-26971
Miscibility and phase behavior of poly (enaminonitrile)/PEO blends
[AD-A222255] 21 p2987 N90-26975

POLYMER CHEMISTRY
New polymer precursors to boron and silicon nitrides
[AD-A210287] 01 p0049 N90-10279
Development of elastomeric polypeptide biomaterials
[AD-A210295] 01 p0049 N90-10280
Transport studies of conducting polymers
02 p0200 N90-11140
Thermodynamic principles of the process of the effect of electromagnetic fields on a polymer melt
[AD-A210698] 02 p0201 N90-11149
Ultrastructure processing and characterization of polymers
[AD-A211460] 04 p0478 N90-12743
The chemistry of hexaazatriphenylene hexanitrile, a polyfunctional heterocycle with potential utility in the formulation of thermostable polymers
[AD-A212353] 04 p0480 N90-12757
Synthesis of inorganic polymers as glass precursors and for other uses. Preceramic block or graft copolymers as potential precursors to nanocomposite materials
[AD-A211978] 05 p0626 N90-13655
The 3F condensation polyimides: Review and update
[NASA-TM-102353] 06 p0750 N90-14363
Synthesis and properties of new preceramic materials
[DE90-002562] 06 p0752 N90-14373
Interfacial systems for photochemical energy conversion
[DE90-003181] 07 p0953 N90-15514
Design, characterization, and optical properties of phosphazene-based polymers
[DE90-004111] 08 p1050 N90-16068
NMR measurements of solvent self-diffusion coefficients in polymer solutions
[AD-A215276] 09 p1279 N90-17419
Chemistry at clusters, microstructures and surfaces
[AD-A215842] 10 p1353 N90-17844
Polymeric materials science in the microgravity environment 10 p1365 N90-17913
Laboratory for the processing and evaluation of inorganic matrix composites
[AD-A216881] 11 p1480 N90-18516
Dynamics and stabilization of materials possessing high energy content
[AD-A216320] 11 p1489 N90-18570
New Condensation polyimides containing 1,1,1-triaryl-2,2,2-trifluoroethane structures
[NASA-CASE-LEW-14346-1] 12 p1618 N90-19300
Materials Science Programs, fiscal year 1989
[DE90-008169] 13 p1765 N90-20131
Synthesis of new polyphosphazene elastomers
[AD-A217585] 13 p1780 N90-20216
Determinations of molecular weight and molecular weight distribution of high polymers by the rheological properties
[NASA-CR-186450] 14 p1953 N90-21180
Polysiloxanes derived from the controlled hydrolysis of tetraethoxysilane as precursors to silica for use in ceramic processing
[NASA-TM-102489] 15 p2070 N90-21858
Graft copolymers of rigid-rod poly(p-phenylenebenzobisimidazole)
[AD-A220369] 17 p2380 N90-23555
Thermal analysis of Acetylene Terminated Sulfone (ATS) resin
[AD-A220775] 17 p2381 N90-23558
Morphological control of inter-penetrating polymer networks 18 p2642 N90-25046
Quantitative confirmation of diffusion-limited oxidation theories
[DE90-012997] 20 p2838 N90-26143
Fractal structure and fractal time in silica sol-gels
[DE90-013197] 20 p2838 N90-26144
One-dimensional sigma-conjugated polysilylenes: Science and technology
[DE90-012902] 20 p2839 N90-26146
Development of microencapsulation techniques
[AD-A223032] 20 p2841 N90-26159
Composite materials with improved properties in compression. Appendix 1: Cyclopropanation of poly(1-methyl 1-phenyl 1-sila-cis-pent-3-ene). Synthesis and characterization of poly(1-methyl 3,4-methylene-1-phenyl 1-sila-cis-pent-3-ene)
[AD-A221494] 21 p2971 N90-26889
Polyarylacetylene resin composites
[AD-A221507] 21 p2972 N90-26890
Fluorescent probe investigation of a water-soluble polyphosphazene
[AD-A222317] 21 p2978 N90-26925
Elastomers and other organic composites
[AD-A222772] 21 p2984 N90-26958
Diffusion of penetrants in polymers
[AD-A223217] 21 p2986 N90-26969
Liquid crystalline polymers
[NASA-CR-186949] 21 p2986 N90-26971
Structure-property behavior of new organic-inorganic polymeric hybrid materials based on sol gel chemistry
[AD-A222168] 21 p2987 N90-26974
Miscibility and phase behavior of poly (enaminonitrile)/PEO blends
[AD-A222255] 21 p2987 N90-26975
United States Air Force research initiation program for 1988, volume 2
[AD-A223124] 21 p3102 N90-27614
Development of polysilsesquioxane composites
[NASA-CR-180263] 22 p3152 N90-27872
Method of obtaining current-conducting polymer materials
[AD-A222129] 22 p3159 N90-27914
Organic polyradical models for organic magnetic materials
[AD-A223691] 24 p3442 N90-29435
Processing of polymers using supercritical fluids
[AD-A223681] 24 p3455 N90-29514

POLYMER MATRIX COMPOSITES
NT CARBON FIBER REINFORCED PLASTICS
NT EPOXY MATRIX COMPOSITES
NT GLASS FIBER REINFORCED PLASTICS
NT REINFORCED PLASTICS
Inorganic composite materials in Japan: Status and trends
[PB89-230015] 03 p0319 N90-11810
Ballistic properties of composite materials for personnel protection
[MRL-TR-89-6] 04 p0465 N90-12661
Magnetic resonance of polymers at surfaces
[AD-A212225] 04 p0480 N90-12753
Orthotropic elasto-plastic behavior of AS4/APC-2 thermoplastic composite in compression
[NASA-CR-186080] 04 p0513 N90-12959
SESAME equation of state for a polymer composite: Phenolic refrasil
[LA-11512-MS] 07 p0910 N90-15264
New materials and structural concepts for space transportation systems 09 p1179 N90-16837
Thermo-oxidative stability studies of PMR-15 polymer matrix composites reinforced with various fibers
[NASA-TM-102439] 12 p1620 N90-19310
Transient photoconduction in doped polymers: Spatial and energetic disorder
[ETN-90-95917] 12 p1631 N90-19376
Use of unbalanced laminates as a screening method for microcracking
[NASA-TM-102517] 14 p1944 N90-21124
Self-lubricating polymer composites and polymer transfer film lubrication for space applications
[NASA-TM-102492] 15 p2071 N90-21862
Structural behavior of composites with progressive fracture
[NASA-TM-102370] 17 p2368 N90-23477
Rheological and mechanical characteristics of poly-p-phenylene terephthalamide/nylon molecular and particulate composites
[AD-A219562] 17 p2368 N90-23482
Rate dependent constitutive models for fiber reinforced polymer composites
[NASA-TM-102665] 17 p2370 N90-23492
Development of testing and analysis methodology to assess the long term durability of polymeric composites at high temperatures
[NASA-TM-102714] 23 p3339 N90-28871

POLYMER PHYSICS
Lithium polymer electrolyte battery, electrochemical behavior of cathode materials
[AD-A210755] 02 p0216 N90-11235
Configurational statistics of strings, fractals and polymer physics. Part 2: Non Abelian strings
[ROM1F-89-680-PT-2] 05 p0696 N90-14067
String correlations and galaxies formation
[ROM1F-89-677] 05 p0713 N90-14170
Non Abelian string correlations and galaxies formation
[ROM1F-89-678] 05 p0714 N90-14171
Des Cloizeaux's law for strings and galaxies formation. Part 1: Abelian configurations
[ROM1F-89-681-PT-1] 05 p0714 N90-14172
Determinations of molecular weight and molecular weight distribution of high polymers by the rheological properties
[NASA-CR-186450] 14 p1953 N90-21180
Modelling of the processing of incompatible polymer blends
[ETN-90-97211] 20 p2840 N90-26152
Approaches to orthogonally fused conducting polymers for molecular electronics
[AD-A222546] 22 p3159 N90-27915
Structure and dynamic properties of combined polymeric main-chain/side-chain liquid crystals
[ETN-90-97299] 22 p3160 N90-27921

POLYMERIC FILMS
NT KAPTON (TRADEMARK)
NT MYLAR (TRADEMARK)
Polyheterocycle Langmuir-Blodgett films
[AD-A210625] 01 p0051 N90-10292
Quartz crystal microbalance studies of electrochemical growth of conducting polymers
[AD-A210788] 01 p0052 N90-10295
Impedance analysis of ionic transport in polypyrrole-polyazulene copolymer and its charge-discharge characteristics
[AD-A210979] 01 p0052 N90-10299
Rechargeable lithium/polymer cathode batteries
[AD-A210978] 01 p0062 N90-10354
Second-order nonlinear optical devices in poled polymers
[DE89-015842] 01 p0123 N90-10703
Method and apparatus for maintaining thermal control in plasma conditions
[NASA-CASE-MFS-28368-1] 01 p0125 N90-10717
Negative-working electron beam resist based on poly(methyl methacrylate)
[AD-A207834] 01 p0128 N90-10733
Femtosecond dynamics of fluoro-aluminum phthalocyanine and linear alkane molecules
[AD-A210939] 01 p0133 N90-10766
Dynamics of nucleation at electrochemical interfaces via surface EXAFS and standing wave measurements
[AD-A210733] 02 p0195 N90-11109
Capacitive behavior in conducting polymers: The ac impedance and quartz crystal microbalance studies
[AD-A210754] 02 p0201 N90-11150
Cell performance of ultra-thin polymer cathode system: Theoretical energy and power density projections
[AD-A210786] 02 p0202 N90-11151
Electrolyte dependence of charge injection processes for electroactive polymer films
[AD-A210787] 02 p0202 N90-11152
New secondary batteries utilizing electronically conductive polymer cathodes
[NASA-CR-185885] 02 p0215 N90-11227
Method of modifying the dielectric properties of an organic polymer film
[AD-D014171] 03 p0330 N90-11879
Electroactive polyaniline film deposited from non-aqueous media. 2: Effect of acid concentration in solutions
[AD-A212084] 04 p0477 N90-12737
Optical modulators based on polymers
[EP-PATENT-0-294-061-A1] 05 p0700 N90-14099
The 3F condensation polyimides: Review and update
[NASA-TM-102353] 06 p0750 N90-14363
Heat and mass transfer design issues in PEM fuel cell hardware
[DE89-016779] 06 p0804 N90-14677
Electronic materials high-T(sub c) superconductivity polymers and composites structural materials surface science and catalysts industry participation
[NASA-CR-186063] 07 p0890 N90-15145
Optical properties and laser damage measurements of inorganic polymer films
[DE90-003633] 07 p0911 N90-15267
Thin films under chemical stress
[DE90-003754] 07 p0947 N90-15484
Mass loss during x ray microanalysis
[DE90-003954] 08 p1049 N90-16067
Chemical-like behavior of electrons and holes in polymeric conductors
[AD-A214496] 09 p1196 N90-16931

Surface-enhanced Raman scattering
[AD-A215976] 10 p1353 N90-17849
The size of the alkyl group R is the principal factor determining the wettability of surface-functionalized polyethylenes (PE-CONHR and PE-CO2R) by water
[AD-A216007] 10 p1354 N90-17851
Surface-enhanced Raman scattering from model acrylic adhesive systems
[AD-A216117] 10 p1359 N90-17883
Plasma modification of poly (p-phenylenebenzobisthiazole)
[AD-A215761] 10 p1433 N90-18272
Electronic and ionic transport in polymers
[AD-A217028] 11 p1491 N90-18579
Cell performance of ultra-thin polymer cathode systems. Part 1: Anion intercalating polymer cathode
[AD-A216037] 11 p1501 N90-18639
Heterogeneous composite and method of making
[AD-D014337] 12 p1619 N90-19306
Alternate film dielectric materials
[DE90-007213] 12 p1632 N90-19378
Infrared and X ray photoelectron spectroscopy studies of the polyimide/metal interface
[AD-A218249] 13 p1773 N90-20179
Sol-gel derived polytitanosiloxane coatings
[DE90-004186] 13 p1779 N90-20210
CO2 diffusion and solubility in a Polystyrene/Polybutadiene block copolymer with highly oriented lamellar morphology
[AD-A217165] 13 p1779 N90-20211
Research and development on enhanced degradable plastics
[AD-A217180] 13 p1779 N90-20212
Tensile film clamps and mounting block for the rheovibron and autovibron viscoelastometer
[NASA-CASE-LAR-13696-1] 13 p1812 N90-20409
Molecular organization and electrical properties of mixed Langmuir-Blodgett multilayer thin films of polypyrrole
[DE90-007627] 13 p1894 N90-20870
Low energy ion generator
[DE90-759905] 14 p1955 N90-21195
Improvement of small-area, amorphous-silicon thin-film photovoltaics on polymer substrate
[DE90-000314] 14 p2002 N90-21472
Electrochemical synthesis of ultrathin film composite membranes
[AD-A219041] 16 p2216 N90-22643
High performance holographic elements and media
[AD-A218999] 16 p2239 N90-22775
Morphology changes due to oxidative treatment of glassy carbon electrodes and its applications
[AD-A219425] 17 p2371 N90-23501
Quartz crystal microbalance studies: Solvent effects in conducting polymer films
[AD-A219426] 17 p2372 N90-23502
Evaluation of ion intercalation in conducting polymers
[AD-A219423] 17 p2379 N90-23549
XPS studies of doped polypyrrole films
[AD-A219424] 17 p2379 N90-23550
Durable heat diaphragm from ordered polymer films
[AD-A220794] 17 p2381 N90-23559
NMR studies of polymeric solid electrolytes
[AD-A219833] 17 p2381 N90-23562
Nonlinear optical responses and laser damage thresholds of films of a polarized stilbene side chain liquid crystal polymer and a phthalocyanine
[AD-A219462] 17 p2408 N90-23720
Quartz crystal microbalance analysis: Partial cation release during oxidation of conducting polymers
[AD-A221091] 18 p2530 N90-24439
Second order non-linear optical polyphosphazenes
[AD-A219868] 18 p2615 N90-24895
Selective metallization of carbonyl-containing polymer films
[AD-D014526] 19 p2678 N90-25230
Characterization of a thermally imidized soluble polyimide film
[NASA-TM-103484] 20 p2836 N90-26131
Development of membrane process for carbon dioxide separation from diving atmosphere
[AD-A222606] 20 p2901 N90-26504
The role of heat transfer during reactive-ion etching of polymer films
[AD-A222072] 21 p2977 N90-26919
Characterization of PMDI/HOPG interfaces by SERS using a silver overlayer configuration
[AD-A223104] 21 p2985 N90-26966
Non-destructive characterization of polymer/metal interfaces using Surface-Enhanced Raman Scattering (SERS)
[AD-A223105] 21 p2986 N90-26967
Environmental integrity of coating/metal interface
[AD-A222426] 21 p2987 N90-26978
Non-destructive characterization of polymer/metal interphases using surface-enhanced Raman scattering
[AD-A222490] 21 p2988 N90-26980
Cell performance of ultra-thin polymer cathode cell systems. Part 2: Cation intercalating composite polymer cathode
[AD-A221919] 21 p3020 N90-27172
A reliable, maintenance-free oxygen sensor for aircraft using an oxygen-sensitive coating on potentiometric electrodes
[AD-A222696] 23 p3277 N90-28545
Modification of polystyrene/polybutadiene block copolymer films by chemical reaction with bromine and effect on gas permeability
[AD-A223612] 24 p3455 N90-29513

POLYMERIZATION
NT COPOLYMERIZATION
NT DIMERIZATION
Predictive aging of polymers
[NASA-CASE-NPO-17524-1-CU] 01 p0046 N90-10261
Mechanical properties, solubilities, and processabilities in the design of the first super-strong liquid-crystalline polymers
[DE89-009252] 01 p0048 N90-10273
Computer simulations of polymer dynamics in the solid state
[DE89-010337] 01 p0048 N90-10275
Quantum chemical investigations of the mechanism of cationic polymerization and theoretical prediction of crystal densities and decomposition pathways of energetic molecules
[AD-A210322] 02 p0200 N90-11143
Electronic and ionic transport in polymers
[AD-A210654] 02 p0201 N90-11148
Method of modifying the dielectric properties of an organic polymer film
[AD-D014171] 03 p0330 N90-11879
Synthesis and high temperature chemistry of methylsilsesquioxane polymers produced by titanium catalyzed redistribution of methylhydridooligo- and polysiloxanes
[AD-A212000] 04 p0477 N90-12736
Polymer characterization by electrohydrodynamic ionization mass spectrometry
[AD-A212130] 04 p0478 N90-12739
Quartz crystal microbalance analysis. 1: Evidence of anion or cation insertion into electropolymerized conducting polymers
[AD-A212304] 04 p0480 N90-12755
Synthesis of energetic single phase and multi-phase polymers
[AD-A212539] 04 p0481 N90-12761
Synthesis of inorganic polymers as glass precursors and for other uses. Preceramic block or graft copolymers as potential precursors to nanocomposite materials
[AD-A211978] 05 p0626 N90-13655
Method for stabilization of pan-based carbon fibers
[AD-D014228] 06 p0736 N90-14288
The 3F condensation polyimides: Review and update
[NASA-TM-102353] 06 p0750 N90-14363
Challenges in processing for polymer composites
[DE90-002224] 06 p0752 N90-14376
Superconducting film fabrication by the sol-gel process
[DE90-002069] 07 p0909 N90-15252
Molecules with enhanced electronic polarizabilities based on defect-like states in conjugated polymers
[NASA-CASE-NPO-17633-1-CU] 07 p0910 N90-15263
New polymers made with well-characterized organometallic catalysts
[AD-A213592] 07 p0912 N90-15272
Electrochemical investigation of electronically conductive polymers
[AD-A214019] 07 p0912 N90-15277
The structure of silica-polysiloxane composites and its effects on their elastomeric properties
[DE89-014768] 08 p1039 N90-16005
The physical properties of microcellular composite foams
[DE90-003658] 08 p1048 N90-16058
Synthesis and analysis of novel polymers with potential for providing both high permselectivity and permeability in gas separation applications
[DE90-003907] 08 p1049 N90-16065
Design, characterization, and optical properties of phosphazene-based polymers
[DE90-004111] 08 p1050 N90-16068
Effects of heat treatment on microstructure and flexural properties of unidirectional carbon-carbon composites
[AD-A214985] 09 p1186 N90-16873
Cellular thermosetting fluorodiepoxide polymers
[NASA-CASE-GSC-13008-2] 09 p1199 N90-16949
Copolyimide with a combination of flexibilizing groups
[NASA-CASE-LAR-13821-1] 09 p1199 N90-16950
Influence of wall strain rate, polymer concentration, and channel height upon drag reduction and turbulent structure
[AD-A215378] 09 p1218 N90-17064
Proposed uses of laser light scattering instruments for polymerization studies 09 p1224 N90-17100
Structure and properties of resorcinol-formaldehyde gels
[DE90-005201] 10 p1358 N90-17876
New type of optical bistability in polymers mediated by phonons
[AD-A216102] 10 p1359 N90-17882
Polymeric materials science in the microgravity environment 10 p1365 N90-17913
Materials properties numerical database system established and operational at CINDAS/Purdue University 10 p1366 N90-17919
Perforated monolayers
[DE90-005469] 11 p1488 N90-18566
Polymerization of nitro compounds on silver surfaces during surface-enhanced Raman scattering
[AD-A216116] 11 p1489 N90-18569
Electrochemical investigations of novel solid redox polymerization electrodes
[DE90-006087] 11 p1492 N90-18584
Morphological consequences of catalytic hydrogenation of polymers in the bulk
[DE90-007276] 11 p1494 N90-18598
New Condensation polyimides containing 1,1,1-triaryl-2,2,2-trifluoroethane structures
[NASA-CASE-LEW-14346-1] 12 p1618 N90-19300
Second-generation ordered polymers
[AD-A216126] 12 p1630 N90-19365
Synthesis of poly(dimethylsiloxane) - nylon 6 diblock copolymers
[AD-A216850] 12 p1630 N90-19367
The 1-((diorganooxyphosphonyl)-methyl)-2,4- and -2,6-diamido benzenes
[NASA-CASE-ARC-11425-4] 13 p1766 N90-20133
Rigid rod molecules as liquid crystal thermosets
[AD-A217573] 13 p1770 N90-20158
Synthesis of new polyphosphazene elastomers
[AD-A217585] 13 p1780 N90-20216
The viscoelasticity of curing thermosets
[DE90-006535] 13 p1781 N90-20221
Ring expansion and equilibration in organophosphazenes, and the relationship to polymerization
[AD-A218234] 13 p1782 N90-20230
Novel electrodes for advanced energy storage systems
[DE90-008667] 13 p1828 N90-20496
Process for crosslinking methylene-containing aromatic polymers with ionizing radiation
[NASA-CASE-LAR-13448-1] 14 p1956 N90-21198
The structural basis for fatigue initiation in glassy polymers
[DE90-009342] 14 p1956 N90-21200
Polysiloxanes derived from the controlled hydrolysis of tetraethoxysilane as precursors to silica for use in ceramic processing
[NASA-TM-102489] 15 p2070 N90-21858
Nonlinearity parameters of polymers 15 p2164 N90-22369
Polymerization of composites
[REPT-892-430-102] 16 p2213 N90-22621
Polymerization of composite materials: A technique developed by Aerospatiale
[REPT-892-430-107] 16 p2213 N90-22623
Dehydrogenative polymerization of silanes to polysilanes: A monomeric copper(2) siloxide
[AD-A218550] 16 p2223 N90-22681
Theoretical studies of silicon chemistry
[AD-A219232] 16 p2225 N90-22690
Some 1-(diorganooxyphosphonyl)methyl-2,4- and -2,6-dinitro-benzenes
[NASA-CASE-ARC-11425-3] 17 p2367 N90-23475
Nonintrusive method and apparatus for monitoring the cure of polymeric materials
[NASA-CASE-LAR-13465-1] 17 p2378 N90-23544
Soluble polysilanes: A new class of radiation sensitive O2-RIE resistant polymers for use in microlithography
[AD-A219476] 17 p2379 N90-23551
Abrasion resistant coatings on plastics 18 p2529 N90-24428
Density profile of terminally adsorbed polymers
[AD-A220897] 18 p2529 N90-24433
Processing polymeric powders 18 p2647 N90-25069
Condensation polyimides
[NASA-TM-103467] 20 p2836 N90-26129
Characterization of a thermally imidized soluble polyimide film
[NASA-TM-103484] 20 p2836 N90-26131

Radical homopolymerization of a trisubstituted alkene: 1-cyclobutenecarboxylic acid and its polymer
[AD-A223188] 21 p2986 N90-26968
Aqueous solution properties of ampholytic ionomers
[AD-A222152] 22 p3156 N90-27890
Potential dependence of the conductivity of highly oxidized polythiophenes, polypyrroles, and polyaniline: Finite windows of high conductivity
[AD-A222024] 22 p3159 N90-27912
Approaches to orthogonally fused conducting polymers for molecular electronics
[AD-A222546] 22 p3159 N90-27915
Polymer research
[PB90-246638] 23 p3313 N90-28737
Theoretical investigations and attempted synthesis of organic magnetic polymers and oligomers
[AD-A223409] 24 p3455 N90-29509
Progress toward synthesis of polymeric polyradicals
[AD-A223414] 24 p3455 N90-29510
Chemical stabilization of laser dyes
[AD-A224219] 24 p3473 N90-29627

POLYMERS
Monomers, polymers and transition metal complexes based upon carboranes
[AD-A210226] 01 p0040 N90-10221
Characterization of polymeric surfaces and interfaces
[AD-A210227] 01 p0049 N90-10277
Magnetic resonance of polymers at surfaces
[AD-A212225] 04 p0480 N90-12753
Analysis of new phenomena in shear flow of non-Newtonian fluids
[AD-A212893] 05 p0638 N90-13721
The structure and properties of liquid crystal polymers
06 p0749 N90-14356
The elastic properties of woven polymeric fabric
[DE89-015391] 07 p0909 N90-15255
Heat capacities of solid polymers (The Advanced THermal Analysis System, ATHAS)
[DE90-007130] 11 p1493 N90-18595
A study on deformation and break-up of dispersed particles in elongational flow
[ETN-90-96268] 11 p1508 N90-18684
Material instabilities in solids
[AD-A218451] 16 p2247 N90-22817
Structure-property behavior of new organic-inorganic polymeric hybrid materials based on sol gel chemistry
[AD-A222168] 21 p2987 N90-26974

POLYMETHYL METHACRYLATE
Negative-working electron beam resist based on poly(methyl methacrylate)
[AD-A207834] 01 p0128 N90-10733
Heterogeneous combustion processes under microgravity conditions 09 p1202 N90-16965
Fire propagation in concurrent flows
[PB90-151754] 15 p2066 N90-21834
The pyrolysis of polymethylmethacrylate during combustion in a solid fuel combustion chamber
[LR-531] 15 p2068 N90-21845
Process of three dimensional lithography in amorphous polymers
[AD-D014500] 19 p2676 N90-25221
Organic polyradical models for organic magnetic materials
[AD-A223691] 24 p3442 N90-29435

POLYMORPHISM
Type reconstruction with first-class polymorphic values
[AD-A210833] 01 p0106 N90-10605
Polymorphism and information loss in Martin-Loef's type theory
[CS-8814] 04 p0533 N90-13079
Energetics of BCC-FCC lattice deformation in iron
[AD-A213801] 07 p0905 N90-15233
Investigation of the phase stabilizing effect of 4 percent potassium fluoride on ammonium nitrate
[AD-A215313] 11 p1494 N90-18599
Object Oriented Programming Systems (OOPS) and frame representations: An investigation of programming paradigms
[NASA-CR-186084] 12 p1699 N90-19758
Naturalness of polymorphism
[CS-8916] 16 p2305 N90-23134

POLYNOMIALS
NT BINOMIALS
NT DYADICS
NT HERMITIAN POLYNOMIAL
Finding isolated zero points of complex polynomial mappings
[DE89-617523] 01 p0111 N90-10633
On the coefficients of differentiated expansions of ultraspherical polynomials
[NASA-CR-181913] 01 p0112 N90-10637
On two polynomial spaces associated with a box spline
[AD-A210559] 01 p0113 N90-10646
Studies in estimation theory, applications and implementations
[AD-A210712] 01 p0114 N90-10653
Sequential design of experiments with physically based models 23
[AD-A211918] 03 p0393 N90-12239
On the communication complexity of solving a polynomial equation
[AD-A211945] 03 p0393 N90-12240
A simple proof of a differential equation for generalizations of Laguerre polynomials
[REPT-89-15] 03 p0395 N90-12253
Generalizations of Laguerre polynomials
[REPT-89-25] 03 p0396 N90-12263
Modeling and analysis of nonlinear time series
[RR-355] 03 p0397 N90-12272
A generalization of Moak's q-Laguerre polynomials
[REPT-89-21] 04 p0540 N90-13126
On some integral relations involving a generalized hypergeometric polynomial
[DE90-600729] 06 p0835 N90-14852
Bounded polynomial randomized consensus
[AD-A213808] 07 p0984 N90-15686
On calculating analytic centers
[AD-A215635] 09 p1274 N90-17385
Studies in statistical signal processing
[AD-A214490] 09 p1275 N90-17393
Efficient preconditioning for the p-version finite element method in two dimensions
[AD-A216210] 11 p1551 N90-18928
Finding critical independent sets and critical vertex subsets are polynomial problems
[AD-A216547] 11 p1552 N90-18938
Some easily analyzable convolutional codes
12 p1644 N90-19444
Differential operators associated with Gegenbauer polynomials. 3: The regular case
[DE90-610422] 12 p1706 N90-19795
Component count and preliminary assembly considerations for large space truss structures
[NASA-TM-102604] 13 p1763 N90-20121
Cell averaging Chebyshev methods for hyperbolic problems
[NASA-CR-182028] 13 p1877 N90-20768
Euler's theorem for polynomials
[AD-A218148] 13 p1878 N90-20774
Techniques for accelerating iterative methods for the solution of mathematical problems
[AD-A218272] 13 p1878 N90-20775
Elastic-plastic instability of plane frames
14 p1992 N90-21415
Generalizations of a q-analogue of Laguerre polynomials
[REPT-89-51] 15 p2161 N90-22345
Stability radius of polynomials occurring in the numerical solution of initial value problems
[TW-89-04] 15 p2162 N90-22350
Efficient computer algebra algorithms for polynomial matrices in control design 16 p2285 N90-23022
Ply cracking in composite laminates
17 p2368 N90-23478
Explicitly solvable complex Chebyshev approximation problems related to sine polynomials
[NASA-CR-181575] 17 p2455 N90-24007
Chebyshev polynomials are not always optimal
[NASA-CR-181465] 17 p2455 N90-24008
On Bernstein type inequalities and a weighted Chebyshev approximation problem on ellipses
[NASA-CR-180368] 17 p2456 N90-24011
M-estimators in linear models with long range dependent errors
[AD-A219921] 17 p2461 N90-24053
Computational tools for multi-linked flexible structures
[NASA-CR-186139] 17 p2462 N90-24058
Optimization and optimality test for the max-cut problem
[MEMO-830] 17 p2463 N90-24066
Progress in the polynomial solution of the standard H-infinity optimal control problem
[MEMO-817] 18 p2597 N90-24777
On a class of generalized orthogonal polynomials with real zeros
[MEMO-826] 18 p2600 N90-24799
Kharitonov's theorem: Generalizations and algorithms
18 p2646 N90-25064
Time-optimal aircraft pursuit-evasion with a weapon envelope constraint
[NASA-CR-186640] 19 p2658 N90-25126
Extensions of algebraic image operators: An approach to model-based vision 19 p2741 N90-25577
Random pseudo-polynomial algorithms in combinatorial programming
[REPT-89-067] 19 p2744 N90-25597
On two transformations in the generalized theory of linear systems
[MATHS-REPT-A-109] 19 p2751 N90-25629
On conditions guaranteeing two polynomial matrices possess identical zero structures
[MATHS-REPT-A-123] 19 p2751 N90-25631
Search of primitive polynomials over finite fields
[IMAG-RR-797-M] 20 p2918 N90-26607
Calculation of the algebraic curves parameterization: Hamburger-Noether expansions
[IMAG-RR-798-M] 20 p2919 N90-26608
Efficient implementation of minimal polynomial and reduced rank extrapolation methods
[NASA-TM-103240] 20 p2920 N90-26616
An outline for the RTNEPH infrared atmospheric water vapor attenuation study
[AD-A221753] 21 p3027 N90-27209
Learning binary relations and total orders
[AD-A221643] 21 p3059 N90-27392
Real-time adaptive aircraft scheduling
[NASA-CR-177558] 22 p3110 N90-27669
Tutorial on Reed-Solomon error correction coding
[NASA-TM-102162] 22 p3234 N90-28339
Efficient algorithms for a class of partitioning problems
[NASA-CR-182073] 22 p3237 N90-28357
Polymatroids: Construction and random algorithms
[REPT-89-068] 22 p3242 N90-28388
Product integration rules at Clenshaw-Curtis and related points: A robust implementation
[DE90-627158] 23 p3382 N90-29106
The center of the enveloping algebra of the semidirect product of the Heisenberg lie algebra h(sub n) and a reductive Lie algebra S the rank of which is equal to 1 or 2
[DE90-627155] 23 p3388 N90-29133
Recurrence relations and weight functions for approximation by orthonormal polynomials
[DE90-627156] 23 p3388 N90-29134
Automatic recognition of tractability in inference relations
[AD-A223698] 24 p3538 N90-30003

POLYPEPTIDES
Electrical field dependence of protein conformation and channel function in lipid membranes of different compositions
[AD-A210236] 01 p0040 N90-10222
Polypeptide inhibitors of mineral scaling and corrosion
[AD-A210507] 01 p0041 N90-10225
Development of elastomeric polypeptide biomaterials
[AD-A210295] 01 p0049 N90-10280
Synthetic polypeptide composites for sensor applications
[AD-A210797] 01 p0052 N90-10296
Comparison of structural subunits of the core light-harvesting complexes of photosynthetic bacteria
[DE90-001412] 06 p0819 N90-14765

POLYPHENYLS
Band-to-band transitions in poly (phenyl methyl silane)
[DE90-003575] 07 p0990 N90-15720
Rheological and mechanical characteristics of poly-p-phenylene terephthalamide/nylon molecular and particulate composites
[AD-A219562] 17 p2368 N90-23482

POLYPROPYLENE
High-temperature gel-permeation chromatography of poly(4-methyl-1-pentene)
[DE90-002967] 07 p0893 N90-15159
Simulation of inelastic deformation in glassy polypropylene and polycarbonate
[AD-A218891] 16 p2224 N90-22686
Investigation of atomistic simulation of structural and dynamic differences in glassy and liquid states of atactic poly(propylene)
[AD-A218896] 16 p2224 N90-22687
Graft copolymers of rigid-rod poly(p-phenylenebenzobisimidazole)
[AD-A220369] 17 p2380 N90-23555
Compression molded polyurethane block copolymers. 3: Evaluation of microphase compositions
[AD-A220160] 17 p2382 N90-23564
Some studies of the vibration welding of thermoplastics 23 p3332 N90-28842

POLYSACCHARIDES
NT CELLULOSE
NT STARCHES

POLYSTATION DOPPLER TRACKING SYSTEM
Innovative techniques for high-resolution imaging and precision tracking
[AD-A221380] 18 p2616 N90-24899

POLYSTYRENE
Positron annihilation studies of interpenetrating polymer networks
[AD-A212162] 03 p0332 N90-11890
Model filled polymers I. Synthesis of crosslinked monodisperse polystyrene beads
[AD-A213228] 05 p0627 N90-13660
The physical properties of microcellular composite foams
[DE90-003658] 08 p1048 N90-16058

Diblock copolymers at surfaces
[DE90-005406] 08 p1051 N90-16079
On the scale of diffusion lengths observable by neutron reflection: Application to polymers
[DE90-005645] 10 p1358 N90-17878
Investigation of multiple scattering in aqueous suspensions of non-absorbing polystrene microspheres using spectrophotometry
[BCRS-89-09] 11 p1485 N90-18549
Model filled polymers 3. Rheological behavior of polystyrene containing crosslinked polystyrene beads
[AD-A215867] 11 p1489 N90-18567
CO2 diffusion and solubility in a Polystyrene/Polybutadiene block copolymer with highly oriented lamellar morphology
[AD-A217165] 13 p1779 N90-20211
Development of intrinsic IPT scintillator
[DE90-007906] 14 p1984 N90-21367
Nonlinear optical responses and laser damage thresholds of films of a polarized stilbene side chain liquid crystal polymer and a phthalocyanine
[AD-A219462] 17 p2408 N90-23720
Diffusion of penetrants in polymers
[AD-A223217] 21 p2986 N90-26969
Progress toward synthesis of polymeric polyradicals
[AD-A223414] 24 p3455 N90-29510
Modification of polystyrene/polybutadiene block copolymer films by chemical reaction with bromine and effect on gas permeability
[AD-A223612] 24 p3455 N90-29513

POLYSULFIDES
Evaluation of a metering, mixing, and dispensing system for mixing polysulfide adhesive
[NASA-CR-183749] 05 p0626 N90-13654
Integral fuel tank sealing practice at British Aerospace (Kingston) 08 p1021 N90-15905
The effect of primer age on adhesion of polysulphide sealant 08 p1022 N90-15909
Improved performance polysulfide based sealant 08 p1022 N90-15910
Effect of temperature on the storage life of polysulfide aircraft sealants
[MRL-TR-89-31] 12 p1629 N90-19364
Synthesis and characterization of aromatic polyester and polysiloxane containing block copolymers: Multiphase transparent atomic oxygen resistant damping materials, liquid crystal films, and toughening components of sol/gel glasses
[AD-A218871] 16 p2224 N90-22685

POLYTETRAFLUOROETHYLENE
NT TEFLON (TRADEMARK)
The performance of PTFE, lead, and MoS2 as lubricant films for ball bearings operating in vacuum at 20 K 18 p2540 N90-24495

POLYTOPES
On calculating analytic centers
[AD-A215635] 09 p1274 N90-17385
Kharitonov's theorem: Generalizations and algorithms 18 p2646 N90-25064

POLYURETHANE FOAM
Electronic encapsulation using foam with bonded metal covers for a filter pack
[DE89-014010] 01 p0048 N90-10276
The optimum polymer binder for pressable high performance explosives: A preliminary evaluation
[ETN-90-97612] 24 p3457 N90-29524

POLYURETHANE RESINS
An investigation of the degradation and stabilization of polymer systems
[AD-A210362] 01 p0049 N90-10282
Comparison of carboxylated and sulfonated model polyurethane ionomers
[AD-A210438] 01 p0050 N90-10284
UV-curable polyurethane-methacrylate co-networks and interpenetrating networks
[AD-A210445] 01 p0050 N90-10285
Synthesis and interfacial properties of new generation polyurethane systems
[AD-A210446] 01 p0050 N90-10286
Synthesis and physical properties of poly(perfluoroalkylether) urethanes
[AD-A210500] 01 p0050 N90-10287
Polyelectrolyte-diffused zinc phosphate conversion coatings and polyacid coupling primers for corrosion protection of steel and aluminum, and alkali-catalyzed hydrolysis of polyimide-based materials
[AD-A212240] 04 p0480 N90-12754
The corrosion protection of 6061-T6 aluminum by a polyurethane-sealed anodized coat
[NASA-TM-100394] 14 p1955 N90-21191
Thermomechanical properties of polymeric materials and related stresses
[NASA-TM-100758] 15 p2071 N90-21864
Durable heat diaphragm from ordered polymer films
[AD-A220794] 17 p2381 N90-23559
Compression molded polyurethane block copolymers. 3: Evaluation of microphase compositions
[AD-A220160] 17 p2382 N90-23564
Compression molded polyurethane block copolymers. 1: Thermal and thermomechanical properties
[AD-A220068] 18 p2529 N90-24431

POLYVINYL ALCOHOL
Characterization of a solid-state microelectrochemical diode employing a poly(vinyl alcohol)/phosphoric acid solid-state electrolyte: Rectification at junctions between WO3 and polyaniline
[AD-A222025] 21 p3000 N90-27054

POLYVINYL FLUORIDE
Piezoelectric polymer PVDF shock gauge: State of the research art
[ISL-CO-207/89] 11 p1512 N90-18705
Piezoelectric and pyroelectric effects of a crystalline polymer 18 p2515 N90-24360

PONDEROMOTIVE FORCES
Simple analytic potentials for linear ion traps 12 p1642 N90-19436

PONDS
Environmental Projects. Volume 8: Modifications of wastewater evaporation ponds
[NASA-CR-186099] 06 p0808 N90-14700
Design and operation of an outdoor microalgae test facility
[DE89-009493] 13 p1848 N90-20808

PONTRYAGIN PRINCIPLE
Minimum-variance reduced-order estimation algorithms from Pontrygin's minimum principle 01 p0021 N90-10105
Modeling, simulation, and analyses of attitude control for the Crew/Equipment Retriever (CER) proposed for space station
[AD-A208140] 01 p0025 N90-10125
Numerical approach of collision avoidance and optimal control on robotic manipulators 19 p2736 N90-25552

POPULATION INVERSION
Spin-lattice relaxation and the calculation of gain, pump power, and noise temperature in ruby 04 p0486 N90-12790
Activities report in laser matter interactions
[ETN-90-95515] 06 p0782 N90-14544
Population inversions calculated for lithium-like ions in a plasma 06 p0786 N90-14571
X ray laser with enhanced x ray gain through photodepopulation
[AD-D014448] 14 p1985 N90-21375
Experimental study of population inversion and spectral line broadening in a plasma containing a mixture of high Z and low Z ions
[DE90-007552] 14 p2027 N90-21622
Fast plasma mixing: A new excitation method for CW gas lasers
[AD-A220290] 18 p2617 N90-24904

POPULATION THEORY
Selecting multinomial populations
[AD-A219256] 16 p2309 N90-23159
Proof of the feasibility of coherent and incoherent schemes for pumping a gamma-ray laser
[AD-A219972] 18 p2562 N90-24620
Tool for studying the effects of range restriction in correlation coefficient estimation
[AD-A224035] 24 p3537 N90-29996

POPULATIONS
Summary of 1987 and 1988 manatee aerial surveys at Kennedy Space Center
[NASA-TM-102783] 06 p0802 N90-14669
Destabilization of tokamak pressure-gradient driven instabilities by energetic alpha populations
[DE90-003716] 07 p0996 N90-15756
The use of photographs for identification and analysis of urban residential sectors, with planning views
[INPE-4788-PRE/1448] 10 p1399 N90-18087
Electron energy distributions and vibrational population distributions
[DE90-005550] 12 p1711 N90-19825
Populations of excited states and reaction mechanisms in the emission of complex fragments
[DE90-007481] 13 p1886 N90-20819
Selecting multinomial populations
[AD-A219256] 16 p2309 N90-23159
The effects of simulated hypogravity on murine bone marrow cells 18 p2631 N90-24989
Nonparametric selection, ranking and testing
[AD-A219254] 19 p2752 N90-25636
A study of the influence of Hg(6(3)P2) population in a low-pressure discharge on mercury ion emission at 194.2 nm 20 p2853 N90-26223
Proceedings of a workshop on Differences Between Antarctic and Non-Antarctic Meteorites
[NASA-CR-184918] 20 p2942 N90-26740

PORES
U POROSITY

POROSITY
NT MICROPOROSITY
Porosity and crack initiation during low cycle fatigue
[AD-A210989] 01 p0081 N90-10464
Thermochemical model for shock-induced chemical reactions in porous thermite: The heat detonation model
[DE89-016528] 02 p0193 N90-11100
Ultrasonic evaluation of porosity in aluminum cast materials
[AD-A213548] 07 p0905 N90-15232
Characterization of new cathode materials for molten carbonate fuel cells
[DE90-003547] 07 p0953 N90-15516
Fabrication of porous ceramic electrode structures
[DE90-003548] 07 p0953 N90-15517
Porous ceramic bodies
[AD-D014277] 08 p1049 N90-16061
Basic studies on separative glass
[DE90-702436] 09 p1196 N90-16928
Subtle porosity variation in the YBa2Cu3O(7-x) high-temperature superconductor revealed by ultrasonic imaging
[NASA-TM-102130] 09 p1235 N90-17167
A finite element analysis of porosity effects on materials
[AD-A216225] 10 p1359 N90-17884
Perforated monolayers
[DE90-005469] 11 p1488 N90-18566
Characterization of reaction kinetics in a porous electrode
[NASA-CR-186504] 12 p1625 N90-19340
Method for maintaining precise suction strip porosities
[NASA-CASE-LAR-13638-1] 12 p1641 N90-19427
Origin and effect of pores in aluminum welded joints
[REPT-87M/43/05720/SCP/GRF] 12 p1675 N90-19620
Using image analysis to determine petrophysical properties of reservoir rocks
[DE90-000222] 12 p1680 N90-19649
A test of the interstellar dust model of comets 12 p1739 N90-19995
Porosity and ice-dust mixtures in cometary particles 12 p1743 N90-20018
Review and statistical analysis of the ultrasonic velocity method for estimating the porosity fraction in polycrystalline materials
[NASA-TM-102501-REV] 14 p1989 N90-21402
Modeling and Applications of Transport Phenomena in Porous Media, volume 1
[VKI-LS-1990-01-VOL-1] 19 p2689 N90-25296
Characterization of porous media: Pore level 19 p2690 N90-25303
Characterization of porous media: Field level 19 p2690 N90-25304
Characterization of fluids in porous media 19 p2690 N90-25305
Network modeling of fluid flow in porous media 19 p2690 N90-25306
Nondestructive x ray methods for characterization of advanced aerospace materials
[DE90-011751] 19 p2699 N90-25356
Regenerative Cu La zeolite supported desulfurizing sorbents
[NASA-CASE-NPO-17480-1-CU] 20 p2830 N90-26098
The interaction of polymeric materials with ceramic surfaces with special reference to the behaviour of bioceramics 20 p2836 N90-26127
Dynamic properties of porous B4C
[AD-A222850] 21 p2985 N90-26960
On modeling the effect of pore shapes on ductile fracture
[AD-A221774] 21 p3014 N90-27136
The fatigue damage behavior of a single crystal superalloy 23 p3296 N90-28644
A new low density, high porosity lithium hydride-beryllium hydride foam
[DE90-015150] 23 p3313 N90-28739
Cyclic voltammetry at a rotating disk, electroreduction of nitrate in acidic nickel solutions, and frequency-response analysis of porous electrodes
[DE90-015317] 24 p3447 N90-29466
Apparatus to determine the complex mass of a viscous fluid contained in a rigid porous solid from acoustic pressure measurements
[AD-A223709] 24 p3472 N90-29619
High resolution transmission electron microscopy of aluminophosphates
[DE90-015632] 24 p3553 N90-30105

POROUS AIRFOILS
U POROUS BOUNDARY LAYER CONTROL

POROUS BOUNDARY LAYER CONTROL
An experimental evaluation of slots versus porous strips for laminar-flow applications 04 p0442 N90-12530

Results of LFC experiment on slotted swept supercritical airfoil in Langley's 8-foot transonic pressure tunnel
04 p0442 N90-12531
Kinetics of the graphite/oxygen reaction in the in-pore diffusion controlled regime. Part 3: Influence of boundary layer diffusion in kinetic experiments at temperatures 970K to 1170K
[JUEL-2284-PT-3] 08 p1042 N90-16024
Propagation of transient acoustic waves in porous media
[ETN-90-96401] 15 p2099 N90-22015

POROUS MATERIALS
Fracture mechanics of porous materials
[DE90-000023] 06 p0800 N90-14657
On the thermal stability of flow of a radiating two-component plasma in a porous medium between two rotating cylinders
[DE89-636426] 06 p0847 N90-14928
A finite element analysis of porosity effects on materials
[AD-A216225] 10 p1359 N90-17884
An experimental investigation of the thermal conductivity of porous adsorbents
[AD-A217854] 13 p1899 N90-20899
Method of making a long life high current density cathode from tungsten and iridium powders using a quarternary compound as the impregnant
[AD-D014425] 14 p1958 N90-21211
Ablative cooling of aerodynamically heated radomes
[AD-D014426] 14 p1971 N90-21293
Electrochemical synthesis of ultrathin film composite membranes
[AD-A219041] 16 p2216 N90-22643
Theoretical studies of non-Newtonian and Newtonian fluid flow through porous media
[DE90-011610] 18 p2554 N90-24576
Modeling and Applications of Transport Phenomena in Porous Media, volume 1
[VKI-LS-1990-01-VOL-1] 19 p2689 N90-25296
Discrete approach: Percolation theory
19 p2689 N90-25297
Instabilities: Miscible and immiscible flows
19 p2689 N90-25298
Heterogeneity description using fractal concepts
19 p2690 N90-25299
Reaction and transport in porous media
19 p2690 N90-25300
Continuum approach and contaminant transport in ground water flows
19 p2690 N90-25301
Modeling and Applications of Transport Phenomena in Porous Media, volume 2
[VKI-LS-1990-01-VOL-2] 19 p2690 N90-25302
Characterization of porous media: Pore level
19 p2690 N90-25303
Characterization of porous media: Field level
19 p2690 N90-25304
Characterization of fluids in porous media
19 p2690 N90-25305
Network modeling of fluid flow in porous media
19 p2690 N90-25306
The flow of non Newtonian fluids in porous media
19 p2691 N90-25307
Fingering in 2-D porous media: Experiments, network simulators and statistical models
19 p2691 N90-25308
Particle tracking methods and fractal statistics in groundwater modeling
19 p2691 N90-25309
Viscous fingering in porous media: A discussion of the small length scale cut-off
19 p2691 N90-25311
On modeling the effect of pore shapes on ductile fracture
[AD-A221774] 21 p3014 N90-27136
Asymptotic behavior of solutions of diffusion-like partial differential equations invariant to a family of affine groups
[DE90-014792] 23 p3388 N90-29130
Apparatus to determine the complex mass of a viscous fluid contained in a rigid porous solid from acoustic pressure measurements
[AD-A223709] 24 p3472 N90-29619

POROUS WALLS
Comparison of NAE porous wall and NASA adaptive wall test results using the NAE CAST-10 airfoil model
10 p1325 N90-17656

PORPHYRINS
NT CHLOROPHYLLS
Photochemically-driven biomimetic oxidation of alkanes and olefins
[DE89-011536] 02 p0193 N90-11097
Electrochemical, in situ Raman spectroscopic, and conductivity studies of polypyrrole incorporating large size anions: Conducting nature of reduced form
[AD-A222739] 20 p2831 N90-26102

PORTABLE EQUIPMENT
Test-retest reliability of oxford Medilog 9000 sleep recording and SS-90-3 sleep stage scoring
[AD-A211165] 02 p0254 N90-11440
Intrinsically safe 5-V, 4-A rechargeable power supply
[PB90-103235] 09 p1209 N90-17006
Hot air heat gun
[AD-D014312] 09 p1217 N90-17061
Evaluation of the Scott aviation portable protective breathing device for contaminant leakage as prescribed by FAA Action Notice A-8150.2. Phase 1: Original tests of the portable protective breathing device. Phase 2: Tests of the redesigned portable protective breathing device
[AD-A216799] 12 p1601 N90-19214
A compact portable diffraction moire interferometer
[DE90-009780] 16 p2238 N90-22768
Preliminary evaluation of a small wearable display
[AD-A219867] 17 p2350 N90-23385

PORTUGAL
A numerical study of wind forcing in the eastern boundary current system off Portugal
[AD-A219596] 17 p2430 N90-23847

POSITION (LOCATION)
NT SOLAR POSITION
Dependency-directed localization of software bugs
[AD-A210837] 01 p0106 N90-10606
Ionospheric limitations to the accuracy of SSL estimates of HF transmitter locations
02 p0248 N90-11403
Markov processes in Hilbert space and continuous spontaneous localization of systems of identical particles
[DE89-618396] 02 p0270 N90-11540
Evaluation test of CCD area sensor for star sensor
[NAL-TM-570] 02 p0274 N90-11566
Doppler statistics of ocean velocity variability
[AD-A211687] 03 p0377 N90-12148
Acoustic controlled rotation and orientation
[NASA-CASE-NPO-16995-1-CU]
03 p0400 N90-12289
Optimal observer motion for bearings-only localization and tracking
04 p0449 N90-12569
Sound Localization by Human Observers symposium proceedings
[AD-A212877] 04 p0524 N90-13026
Inexpensive global location and tracking systems using geostationary satellites
[AD-A213025] 05 p0602 N90-13498
Spatiotemporal characteristics of visual localization, phase 2
[AD-A212934] 05 p0674 N90-13929
Where is an object before you look at it
[NOTA-INTERNA-935] 05 p0704 N90-14123
Study of modern instrumentation and methods for astronomic positioning in the field
[AD-A213217] 05 p0710 N90-14157
Decision-aid design factors in connection with HF communication and emitter location disciplines
06 p0758 N90-14413
Adaptive clutter rejection filters for airborne Doppler weather radar applied to the detection of low altitude windshear
[NASA-CR-186211] 06 p0766 N90-14453
Robotic vision system
[AD-D014246] 06 p0832 N90-14838
National airspace system: Airport movement area control operational concept
[WP-89W00181] 07 p0878 N90-15086
Feasibility study of using industrial robot for ultrasound testing
[DE90-002977] 07 p0943 N90-15461
Location of interior impact source in randomly excited structures
[DE90-001092] 07 p0945 N90-15474
Analytical techniques for tracking filter implementation
08 p1021 N90-15903
Parallel algorithm for determining motion vectors in ice floe images by matching edge features
08 p1114 N90-16451
Position fixing by detection of roads and rivers
09 p1163 N90-16733
Modeling the effects of the use of GPS (Global Positioning System) derived altitude indication in the C-17A airdrop system
[AD-A215366] 09 p1166 N90-16748
Screening actuator locations for static shape control
[NASA-CR-181970] 09 p1182 N90-16851
Optimum location of flow conditioners in a 4-inch orifice meter
[PB90-111675] 09 p1216 N90-17049
Three position estimation procedures
[AD-A214992] 09 p1276 N90-17395
On universal elements, and conversion procedures to and from position and velocity
[RAE-TM-SPACE-370] 09 p1277 N90-17406
Practical applications of Loran-C for land mobile use or the possibility to use Loran-C as a vehicle-location or vehicle-navigation system
[ETN-90-96265] 11 p1455 N90-18384
Data collection and location platforms experimental network: Description of an orbit routine
[INPE-4798-NTE/287] 11 p1465 N90-18439
Thermal coefficient of delay for various coaxial and fiber-optic cables
12 p1643 N90-19439
Drifting buoy data from Western Tropical Pacific for the period February 1, 1986 through February 28, 1989
[PB90-113978] 12 p1695 N90-19732
Estimation of modeled object pose from monocular images
[DE90-001678] 13 p1804 N90-20354
Localization and delocalization in periodic one-dimensional dynamic systems
[AD-A217939] 13 p1882 N90-20797
Apparatus and method for locating the axis of symmetry (center of circular cross section) of three dimensional objects
[AD-D014407] 14 p1982 N90-21354
Localization of vibration in disordered nearly cyclic structures
16 p2246 N90-22812
Position computation without elevation information for computed centerline operations
[DOT/FAA/CT-TN89/42] 17 p2349 N90-23379
Three approximate methods for estimating the best subset of GPS satellites for satellite position calculations
[AD-A220380] 17 p2350 N90-23383
LOCSTAR: A satellite radiodetermination system for Europe
17 p2360 N90-23436
Comparison of navigation systems
17 p2360 N90-23438
Astronaut's guide to terrestrial impact craters
[NASA-TM-102902] 17 p2421 N90-23798
Diagnosis of auroral dynamics using global auroral imaging with emphasis on large-scale evolutions
[NASA-CR-186623] 17 p2422 N90-23804
Down-range imaging of radar targets
[AD-A221084] 18 p2544 N90-24521
The use of remote sensing for the localization of seepage near the Twenthe canal, Netherlands
[BCRS-89-30] 18 p2575 N90-24669
Ray shooting, implicit point location, and related queries in arrangements of segments
[RUU-CS-89-11] 18 p2601 N90-24807
AFE dynamic effects in inhomogeneous plasmas
18 p2643 N90-25053
Yaw fin deployment apparatus for ejection seat
[AD-D014512] 19 p2656 N90-25118
Optical techniques for determination of normal shock position in supersonic flows for aerospace applications
[NASA-TM-103201] 19 p2693 N90-25323
The use of PLAID in the Space Station Freedom viewing analysis
19 p2729 N90-25517
Visualization of three dimensional data
19 p2736 N90-25553
Adaptive node movement in finite-difference solutions of partial differential equations with applications to gasdynamics, part 1
[UTIAS-333-PT-1] 19 p2750 N90-25622
Qualitative evaluation of a conformal velocity vector display for use at high angles-of-attack in fighter aircraft
[NASA-TM-102629] 20 p2809 N90-25981
A reduced-dynamic technique for precise orbit determination
20 p2852 N90-26219
Electromagnetic inverse scattering of buried objects
[ETN-90-97216] 20 p2856 N90-26242
Video camera system for locating bullet holes in targets at a ballistics tunnel
[NASA-TM-4197] 20 p2865 N90-26296
Position control of redundant manipulators using an adaptive error-based control scheme
[NASA-CR-186812] 20 p2914 N90-26578
Molecular dynamics of physical aging processes in polymer glasses (experiment and theory)
[AD-A222848] 21 p2984 N90-26959
Applications of ISES for instrument science
21 p3018 N90-27161
Investigation into position accuracy of typhoon center determined on GMS imagery
21 p3028 N90-27217
Curvature estimation in orientation selection
[AD-A221481] 21 p3034 N90-27249
Further research on heading in text
[AD-A221511] 21 p3087 N90-27557
Position finding and ground target direction finding by an aircraft with a gimballed video camera
[DLR-FB-89-62] 22 p3111 N90-27673
Motion translator
[AD-D014452] 22 p3181 N90-28053
Using the x ray region of the electromagnetic spectrum for alignment: Overview, geometric optics, and design considerations
[DE90-014798] 23 p3317 N90-28752

Study of the relationships between radar structure and the electrical activity of clouds
[ETN-90-97488] 23 p3352 N90-28946
Kinematics, controls, and path planning results for a redundant manipulator 23 p3363 N90-29005
Methods and strategies of object localization 23 p3366 N90-29020
Robot Acting on Moving Bodies (RAMBO): Interaction with tumbling objects 23 p3366 N90-29022
Real-time edge tracking using a tactile sensor 23 p3367 N90-29023
Map learning with indistinguishable locations 23 p3367 N90-29025
Satellite-map position estimation for the Mars rover 23 p3375 N90-29069
An improved method for choosing sampling points for the inspection of complex surfaces in a computer-aided manufacturing environment 23 p3380 N90-29093
PLRS: A new spread spectrum position location reporting system 24 p3427 N90-29358
Enhancing PLRS with user-to-user data capability 24 p3427 N90-29359
Guidance and control techniques for airborne transfer alignment and SAR motion compensation 24 p3429 N90-29372
A method of determining a laser-velocimeter focal point and measuring its beam properties using a hot-wire anemometer
[NAL-TR-1043] 24 p3473 N90-29626
Use of 3D vision for fine robot motion 24 p3503 N90-29804
Controlling multiple manipulators using RIPS 24 p3505 N90-29814

POSITION ERRORS
Robust spatial calibration of a planar positron camera
[AD-A210773] 02 p0224 N90-11284
RTSIN1: A model of a strapdown INS on a two-axis rate table
[AD-A212406] 04 p0450 N90-12579
Wavefront error sensing for LDR 05 p0595 N90-13455
Analytical techniques for tracking filter implementation 08 p1021 N90-15903
An error sensitivity model for Doppler positioning using transit satellites
[AD-A216724] 11 p1455 N90-18381
Location recognition using stereo vision
[AD-A218218] 13 p1875 N90-20752
Mark 3 interferometer
[AD-A217188] 13 p1902 N90-20912
The role of orbit errors in processing of satellite altimeter data
[ETN-90-96699] 16 p2204 N90-22575
Three approximate methods for estimating the best subset of GPS satellites for satellite position calculations
[AD-A220380] 17 p2350 N90-23383
Helicopter Airborne Laser Positioning System (HALPS)
[NASA-TM-102814] 17 p2354 N90-23399
On the calibration of an autocollimator-comparator guide of a vertical target levelling rod differing from the ABBE's principle
[ISBN-951-754-887-7] 19 p2694 N90-25331
Continuous on-line link error rate detector
[AD-D014510] 20 p2850 N90-26209
Applications of differential GPS 24 p3425 N90-29349
The determination of PDOP (Position Dilution of Precision) in GPS 24 p3425 N90-29351
Analysis of the integrity of the Microwave Landing System (MLS) data functions 24 p3428 N90-29365
Omega navigation signal characteristics 24 p3429 N90-29369
State estimation for systems moving through random fields 24 p3429 N90-29373
An integrated system for land navigation 24 p3430 N90-29377

POSITION INDICATORS
NT RADIO DIRECTION FINDERS
Automatic processing of images from the GRATE flight test tool
[DLR-FB-89-28] 04 p0454 N90-12599
GPS network analysis: The influence of stochastic prior information of orbital elements on ground station position measures
[TR-4-1988] 08 p1020 N90-15901
Enhancing PLRS with user-to-user data capability 24 p3427 N90-29359

POSITION SENSING
The 1988 year end report for road following at Carnegie-Mellon
[NASA-CR-185967] 01 p0078 N90-10446
A figure control sensor for the Large Deployable Reflector (LDR) 05 p0594 N90-13451
Techniques for extreme attitude suspension of a wind tunnel model in a magnetic suspension and balance system
[NASA-CR-181895] 06 p0728 N90-14245
Heli/SITAN: A terrain referenced navigation algorithm for helicopters
[DE90-005193] 12 p1602 N90-19217
Development and testing of a universally implementable recording aligning system
[SER-C-349] 12 p1691 N90-19716
An electronic spirit level tilt sensor
[ETN-90-96697] 17 p2406 N90-23710
Optical techniques for determination of normal shock position in supersonic flows for aerospace applications
[NASA-TM-103201] 19 p2693 N90-25323
Assembly via disassembly: A case in machine perceptual development
[NASA-CR-186867] 20 p2900 N90-26497
Hover position sensing system 21 p3069 N90-27448
Position finding and ground target direction finding by an aircraft with a gimballed video camera
[DLR-FB-89-62] 22 p3111 N90-27673
Tele-Autonomous control invol.ing contact --- object localization
[NASA-CR-187004] 23 p3335 N90-28854

POSITIONING
Geodetic point positioning with GPS (Global Positioning System) carrier beat phase data from the CASA UNO experiment
[AD-A211955] 04 p0514 N90-12970
Placing mirrors in grids
[CWI-CS-R8906] 04 p0543 N90-13154
Correction of ionospheric effects for the precise orbit determination of satellites 06 p0762 N90-14432
Enhanced satellite geodesy through the addition of a pseudorange observable
[AD-A214987] 09 p1241 N90-17200
Optimization of sensors and actuators positioning aimed at obtaining reduced models for the synthesis of optimal control regulators of flexible structures
[INPE-4760-TDL/348] 11 p1468 N90-18450
Robot crane technology program
[PB90-111667] 11 p1516 N90-18734
Positioning control of highest accuracy for very dynamic coupled system
[ETN-90-95893] 12 p1701 N90-19769
The development of a real-time decimeter-level positioning system using Global Positioning System (GPS) technology
[AD-A218695] 16 p2199 N90-22552
Guidelines, operational procedures, and quality control for the estimation of geodetic point positions from GPS data collected with the TI4100 receiver
[AD-A218460] 16 p2250 N90-22829
Direction of movement effects under transformed visual/motor mappings 16 p2272 N90-22947
Perception-action relationships reconsidered in light of spatial display instruments 16 p2272 N90-22949
Helicopter Airborne Laser Positioning System (HALPS)
[NASA-TM-102814] 17 p2354 N90-23399
Alignment positioning mechanism
[NASA-CASE-MSC-21502-1] 20 p2872 N90-26341
Eye tracking device for the measurement of flight performance in simulators
[AD-A220075] 20 p2898 N90-26484
Beam rider for an Articulated Robot Manipulator (ARM) accurate positioning of long flexible manipulators
[NASA-CR-185151] 20 p2914 N90-26581
Method and apparatus for applying a mechanical force to surface
[NASA-CASE-LAR-14009-1] 21 p3011 N90-27115
Towards an understanding of camera fixation
[PB90-160342] 22 p3177 N90-28027
Video-rate visual servoing for robots
[AD-A218711] 22 p3181 N90-28052
Measurement of hand dynamics in a microsurgery environment: Preliminary data in the design of a bimanual telemicro-operation test bed 23 p3364 N90-29010
Modular digital GPS receivers 24 p3424 N90-29346
Applications of differential GPS 24 p3425 N90-29349
The determination of PDOP (Position Dilution of Precision) in GPS 24 p3425 N90-29351
Enhancing PLRS with user-to-user data capability 24 p3427 N90-29359
Analysis of the integrity of the Microwave Landing System (MLS) data functions 24 p3428 N90-29365
The potential for digital databases in flight planning and flight aiding for combat aircraft 24 p3429 N90-29371
Modeling and reconstruction algorithms for detection, location, and identification of subsurface anomalies
[AD-A224358] 24 p3459 N90-29539
Active vibration damping of flexible structures
[DLR-FB-90-03] 24 p3481 N90-29676
Traction-drive force transmission for telerobotic joints 24 p3501 N90-29790
Modeling and sensory feedback control for space manipulators 24 p3504 N90-29807

POSITIONING DEVICES (MACHINERY)
NT BOOMS (EQUIPMENT)
NT CAMS
New tool-holding concept
[DE90-000880] 06 p0794 N90-14624
Gripping device
[NASA-CASE-MSC-21365-1] 13 p1812 N90-20408
Digital beam position regulation of the superconducting accelerator at Darmstadt
[ETN-90-97293] 22 p3246 N90-28406

POSITIVE FEEDBACK
Active control of a flexible structure using a modal positive position feedback controller
[NASA-CR-186338] 09 p1272 N90-17371

POSITIVE IONS
NT CATIONS
Instability of the behavior of high resistivity silicon detectors due to the presence of oxide charges
[REPT-89-038] 04 p0559 N90-13260
Structural peculiarities and molecular properties of charge complexes formed on positive ion injection into dense inert gas media
[DE89-633953] 06 p0839 N90-14877
A double focussing mass-spectrometer for simultaneous ion measurements in the stratosphere
[AERONOMICA-ACTA-A-350-1989] 08 p1102 N90-16379

POSITRON ANNIHILATION
Positron annihilation studies of interpenetrating polymer networks
[AD-A212162] 03 p0332 N90-11890
Electron-positron momentum distribution measurements of high-T(sub c) superconductors and related systems
[DE89-017538] 03 p0411 N90-12358
The AMY Experiment
[DE90-001153] 06 p0839 N90-14880
Electron-positron momentum distribution measurements of high-T superconductors and related systems
[DE90-002974] 07 p0999 N90-15780
Inelastic scattering of positrons with sodium 11 p1556 N90-18961
GRIS observations of the Galactic Center 11 p1559 N90-18982
Positron annihilation in gamma-ray bursts 11 p1559 N90-18983
Positronium ions and molecules 11 p1560 N90-18990
Positron annihilation induced Auger electron spectroscopy 11 p1561 N90-18996
Positron annihilation spectroscopy: A nondestructive, submicroscopic characterization technique for structural polymers
[AD-A217748] 13 p1782 N90-20226
The electronic properties of high (Tc) superconductors probed by positron annihilation
[DE90-008354] 13 p1896 N90-20883
Systematics in positron annihilation lifetime analysis of high (Tc) superconducting transitions
[DE90-008361] 13 p1896 N90-20884

POSITRONIUM
Annihilation in Gases and Galaxies
[NASA-CP-3058] 11 p1555 N90-18957
Inelastic collisions of positrons with one-valence-electron targets 11 p1556 N90-18963
Theoretical survey on positronium formation and ionisation in positron atom scattering 11 p1556 N90-18965
Positronium formation in Ss state in e+-Li scattering 11 p1557 N90-18967
Positronium reflection and positronium beams 11 p1559 N90-18980
Optically excited states in positronium 11 p1559 N90-18985
Stark and Zeeman effects on laser cooling of positronium 11 p1560 N90-18986
Decay rate and other properties of the positronium negative ion 11 p1560 N90-18987
Antihydrogen formation in collisions of positronium with antiprotons 11 p1560 N90-18988
Positronium ions and molecules 11 p1560 N90-18990
Positronium formation in e+ plus H- collisions 11 p1561 N90-18993

POSITRONS
Electron-positron momentum distribution measurements of high-T(sub c) superconductors and related systems
[DE89-017538] 03 p0411 N90-12358
Temperature dependence of positron diffusion in cubic metals
[PB89-222020] 04 p0475 N90-12722

Interaction of low-energy electrons and positrons with condensed matter: Stopping powers and inelastic mean free paths from optical data
[DE90-001001] 06 p0840 N90-14882
Slow positron defect profiling of silicon epilayers
[DE90-003958] 08 p1087 N90-16288
Annihilation in Gases and Galaxies
[NASA-CP-3058] 11 p1555 N90-18957
Positron-alkali atom scattering
11 p1556 N90-18958
Scattering of positrons and electrons by alkali atoms
11 p1556 N90-18959
Elastic scattering of e- and e+ from Rb and Cd
11 p1556 N90-18960
Positron collisions with alkali-metal atoms
11 p1556 N90-18962
Inelastic collisions of positrons with one-valence-electron targets 11 p1556 N90-18963
Positron-rubidium scattering 11 p1556 N90-18964
Positron scattering by atomic hydrogen using optical potentials and with positronium formation
11 p1557 N90-18966
New parameter-free polarization potentials in low-energy positron collisions 11 p1557 N90-18968
The calculation of the contributions to low energy e+H2 scattering from sigma u+ and Pion u symmetries using the Kohn variational method 11 p1557 N90-18969
Ab initio R-matrix calculations of e+-molecule scattering 11 p1557 N90-18970
Numerical Green's functions in optical potential calculations for positron scattering from argon and neon
11 p1557 N90-18971
Positron excitation of neon 11 p1558 N90-18973
Positron-inert gas differential elastic scattering
11 p1558 N90-18974
Differential elastic scattering cross sections for 54.9eV positrons incident on helium 11 p1558 N90-18975
Total cross sections for positrons scattered elastically from helium based on new measurements of total ionization cross sections 11 p1558 N90-18976
Ionisation of atomic hydrogen by positron impact
11 p1558 N90-18977
Multiple-ionization of xenon atoms by positron impact
11 p1558 N90-18978
Double ionization of helium by particle impact
11 p1558 N90-18979
Low-energy scattering of electrons and positrons in liquids 11 p1559 N90-18981
Search for resonances in positron-atom systems
11 p1560 N90-18991
Resonances in low-energy positron-alkali scattering
11 p1560 N90-18992
Positron-molecule bound states and positive ion production 11 p1561 N90-18994
Initial results of positron ionization mass spectrometry
11 p1561 N90-18995
Positron trapping in semiconductors
[PB90-165606] 15 p2172 N90-22410
Monoenergetic positron beam studies of near-surface phenomena
[ETN-90-96947] 18 p2613 N90-24887
A study of positrons from Soviet nuclear powered satellites as tracers for magnetospheric research
[DE90-013157] 20 p2888 N90-26438
Slow positron beam generator for lifetime studies
[NASA-CASE-LAR-14250-1-SB]
21 p3073 N90-27472
A double-sided silicon strip detector with capacitive read out and a new method of integrated bias coupling
22 p3178 N90-28037
New developments in double sided silicon strip detectors 22 p3179 N90-28039

POST BOOST PROPULSION SYSTEM
Optimum ascent performance of winged two-stage vehicles 09 p1177 N90-16816

POSTFLIGHT ANALYSIS
Flight Motor Set 360L003 (STS-29R)
[NASA-CR-183739-VOL-1] 01 p0031 N90-10170
Independent Orbiter Assessment (IOA): Analysis of the instrumentation subsystem
[NASA-CR-185571] 02 p0164 N90-10928
Post crash flight analysis: Visualizing flight recorder data
[AD-A212063] 03 p0302 N90-11715
Kalman estimation for SEDS measurements
12 p1634 N90-19393
Flight motor set 360L002 (STS-27R). Volume 5: Nozzle component
[NASA-CR-183945] 15 p2062 N90-21811
UD filtering and smoothing applied to orbit determination
[INPE-4966-PRE/1535] 15 p2189 N90-22501
Space radiation studies
[NASA-CR-183991] 19 p2798 N90-25925
An automated calibration laboratory for flight research instrumentation: Requirements and a proposed design approach
[NASA-TM-101719] 20 p2912 N90-26564
Flight set 360H005 (STS-28) seals, volume 4
[NASA-CR-183904] 22 p3181 N90-28051

POSTLAUNCH REPORTS
Flight Motor Set 360L003 (STS-29R)
[NASA-CR-183739-VOL-1] 01 p0031 N90-10170
Debris/ice/TPS assessment and photographic analysis for Shuttle Mission STS-34
[NASA-TM-102153] 05 p0594 N90-13447
Mission report on the Orbiter Camera Payload System (OCPS) Large Format Camera (LFC) and Attitude Reference System (ARS)
[NASA-CR-186273] 09 p1240 N90-17197

POSTMISSION ANALYSIS (SPACECRAFT)
Flight motor set 360L002 (STS-27R). Volume 5: Nozzle component
[NASA-CR-183945] 15 p2062 N90-21811

POSTULATES
U AXIOMS

POSTURE
Age-related changes in human posture control: Motor coordination tests
[NASA-CR-185855] 03 p0383 N90-12178
Cardiovascular, renal, electrolyte, and hormonal changes in man during gravitational stress, weightlessness, and simulated weightlessness: Lower body positive pressure applied by the antigravity suit
[NASA-TM-102232] 04 p0522 N90-13013
Pre- and postflight postural control of the D1 Spacelab mission astronauts examined with a tilting room
[IZF-1988-25] 04 p0527 N90-13039
The effects of linear acceleration on perception and nystagmus 15 p2136 N90-22209
Motion coordination for mobile robots in unstructured environments
[PB90-199498] 23 p3332 N90-28837

POTABLE LIQUIDS
NT POTABLE WATER

POTABLE WATER
Selective removal of organics for water reclamation
[NASA-CR-185959] 02 p0255 N90-11445
Calcium carbonate scale dissolution in water stabilized by carbon dioxide treatment
[AD-A218502] 16 p2214 N90-22633
Electrochemical control of iodine disinfectant for space transportation system and space station potable water
18 p2629 N90-24981
Ozone for trace organic contaminant removal
[PB90-221680] 23 p3347 N90-28916

POTASSIUM
Radial heat flux limits in potassium heat pipes: An experimental and analytical investigation
[DE90-002655] 07 p0932 N90-15396
Niobium 1 percent zirconium/potassium and titanium/potassium life-test heat pipe design and testing
[DE90-002430] 07 p0954 N90-15522
An evaluation of metal salts of 3-nitro-1,2,4-triazol-5-one (NTO) as potential primary explosives
[MRL-TN-563] 14 p1956 N90-21202
Conservation of body calcium by increased dietary intake of potassium: A potential measure to reduce the osteoporosis process during prolonged exposure to microgravity 18 p2631 N90-24993

POTASSIUM COMPOUNDS
NT POTASSIUM HYDROXIDES
NT POTASSIUM OXIDES
NT POTASSIUM PERCHLORATES
Investigation of the phase stabilizing effect of potassium fluoride on ammonium nitrate
[AD-A213042] 06 p0753 N90-14381
Thermodynamic studies on the ferroelectric phase transition in neutron irradiated (Li(sub x)K(1-x))2SO4 crystals at high temperature
[DE89-635786] 08 p1130 N90-16545
Ternary reciprocal system of lithium and potassium fluorides and bromides
[DE90-004938] 10 p1352 N90-17840
Investigation of the phase stabilizing effect of 4 percent potassium fluoride on ammonium nitrate
[AD-A215313] 11 p1494 N90-18599

POTASSIUM HYDROXIDES
The application of electrochemical impedance spectroscopy for characterizing the degradation of Ni(OH)2/NiOOH electrodes 13 p1824 N90-20474
KOH concentration effect on the cycle life of nickel-hydrogen cells. Part 4: Results of failure analyses
13 p1824 N90-20475
Effect of KOH concentration on LEO cycle life of IPV nickel-hydrogen flight battery cells
[NASA-TM-103127] 14 p1942 N90-21116
Effect of LEO cycling on 125 Ah advanced design IPV nickel-hydrogen battery cells
[NASA-TM-103128] 15 p2061 N90-21808

POTASSIUM OXIDES
In situ growth of epitaxial superconducting YBa2Cu3O(7-x) films on insulating semiconducting and ferroelectric K(Ta, Nb)O3 by pulsed laser ablation
[DE90-006568] 11 p1571 N90-19043
Deposition of electrooptic thin films
[DE90-010543] 18 p2619 N90-24922

POTASSIUM PERCHLORATES
Pyrotechnic ignition studies using a gun tunnel
[DE89-012496] 01 p0060 N90-10341
Consequence of condensed-phase formation in transient burning of TiHx/KClO in a closed system
[DE89-013922] 02 p0208 N90-11188

POTENTIAL
Precise solution for a finite set of spherical coefficients from equiangular gridded data 13 p1833 N90-20522
Very accurate upward continuation to low heights in a test of non-Newtonian theory 13 p1837 N90-20548

POTENTIAL ENERGY
NT BIOELECTRIC POTENTIAL
NT COULOMB POTENTIAL
NT ELECTRIC POTENTIAL
NT GEOPOTENTIAL HEIGHT
NT IONIZATION POTENTIALS
NT LOW VOLTAGE
NT OPEN CIRCUIT VOLTAGE
NT PHOTOVOLTAGES
NT PLASMA POTENTIALS
NT QUANTUM WELLS
NT THRESHOLD VOLTAGE
Multiple solutions for Lagrangian systems in T superscript n
[AD-A210646] 01 p0113 N90-10650
Monte Carlo simulations of small solute/solvent clusters: Cluster properties and phase transitions
[AD-A209559] 01 p0119 N90-10684
Phase behavior of pure and mixed systems at high pressure
[DE89-017734] 03 p0322 N90-11832
On the spectrum of the staggered Dirac operator at finite chemical potential
[ITFA-88-53] 04 p0561 N90-13272
The auroral current - voltage relationship
05 p0658 N90-13843
Elastomeric impulse energy storage and transfer system
[AD-D014223] 06 p0730 N90-14255
A guide for estimating potential energy savings from increased solar reflectance of a low-sloped roof
[DE90-003720] 07 p0955 N90-15526
Electronic energies for Neon dimer dication radiative charge transfer
[AD-A215817] 10 p1429 N90-18244
Experimental investigation of relationship between nonlinear field energy and emittance growth
[AD-A215813] 10 p1430 N90-18246
Numerical Green's functions in optical potential calculations for positron scattering from argon and neon
11 p1557 N90-18971
Polyatomic reaction dynamics
[DE90-008668] 13 p1884 N90-20811
Theoretical studies of spin-forbidden processes within the Breit-Pauli approximation
[AD-A217778] 13 p1885 N90-20815
First-principles interatomic potentials for transition metals and their surfaces
[DE90-011233] 18 p2528 N90-24424
The potential of renewable energy
[DE90-000322] 21 p3019 N90-27163
Laboratory experiments on stability and entrainment of oceanic stratocumulus. Part 1: Instability experiment
22 p3220 N90-28263

POTENTIAL FIELDS
Potential theory of radiation 12 p1635 N90-19395
Nonpotential magnetic fields at sites of gamma ray flares
[NASA-TM-103493] 20 p2950 N90-26785

POTENTIAL FLOW
NT EQUIPOTENTIALS
Two-phase potential flow 01 p0067 N90-10387
Numerical calculations of the collapse of a cavity in the vicinity of a compliant wall
[AD-A210489] 01 p0070 N90-10403
Steady and unsteady potential flow around thin annular wings and engines with simulation of jet engine flow
[DFVLR-FB-89-18] 03 p0302 N90-11711
Program VSAERO theory document: A computer program for calculating nonlinear aerodynamic characteristics of arbitrary configurations
[NASA-CR-4023] 06 p0720 N90-14200
Solution of potential flow past an elastic body using the boundary element technique
[AD-A213843] 07 p0931 N90-15390

Formation of a pair of turbulent layers in the region of a flow around an axisymmetric body with an incidence angle
[ISL-R-130/87] 09 p1219 N90-17070
Formation of turbulent layers in the separated region around a body with polygonal cross section at large incidence and rolling
[ISL-R-101/88] 09 p1219 N90-17071
An iterative solution to aeroelastic effects in potential flow
[AD-A216291] 10 p1310 N90-17580
Modeling the wake as a continuous vortex sheet in a potential-flow solution using vortex panels
[AD-A216220] 10 p1385 N90-18016
Aerodynamics of unsteady systems. Numerical study of potential flow/boundary layer coupling
[ETN-90-96257] 11 p1452 N90-18367
Experimental investigations of the unsteady boundary layer on an oscillating flat plate. Optimization and validation of a code, for calculating the potential flow/boundary layer coupling of a flat plate and of an oscillating profile
[ETN-90-96254] 11 p1508 N90-18682
Users manual for the NASA Lewis Ice Accretion Prediction Code (LEWICE)
[NASA-CR-185129] 14 p1909 N90-20943
Discrete-vortex model for the symmetric-vortex flow on cones
[NASA-TP-2989] 14 p1909 N90-20946
Multigrid accelerated relaxation solution of transonic full potential flow equation
[PD-CF-8942] 14 p1910 N90-20951
A dual potential formulation of the Navier-Stokes equations 15 p2092 N90-21972
Unsteady potential flow past a propeller blade section
[NASA-CR-4307] 18 p2493 N90-24246
Sideslip-induced static pressure errors in flight-test measurements
[NASA-TM-102848] 22 p3116 N90-27702
An analysis of flow models: From Navier-Stokes to potential flow equations 22 p3173 N90-28002
Experimental study of an unsteady boundary layer on an oscillating plane plate. Optimization and validation of calculation code for the analysis of the potential flow/boundary layer coupling in the neighborhood of a plane plate and an oscillating profile
[ETN-90-97436] 22 p3175 N90-28013
Flow coupling between a rotor and a stator in turbomachinery
[AD-A223882] 23 p3282 N90-28572

POTENTIAL GRADIENTS
Observations of atmospheric electricity, 1988
[GEOPHYSICAL-PUBL-10] 14 p2006 N90-21499

POTENTIAL THEORY
Application of a generalized Leibniz rule for calculating electromagnetic fields within continuous source regions
[AD-A212470] 04 p0492 N90-12831
A fast algorithm for the evaluation of heat potentials
[AD-A211316] 04 p0529 N90-13052
An experimental investigation of viscous aspects of propeller blade flow 09 p1159 N90-16711
Potential theory of radiation 12 p1635 N90-19395
On the planar translation of two bodies in a uniform flow
[AD-A220143] 17 p2404 N90-23698
Intersubband transitions in an asymmetric quantum well with a thin barrier of a delta-function potential
[AD-A220723] 17 p2477 N90-24162
The integrated area measure of visual endogenous ERPs: Relation to cognitive workload and hemisphere
[AD-A223191] 21 p3035 N90-27255
Higher loop contributions to effective potential of gauge theory at high temperature
[DE90-627208] 23 p3403 N90-29231

POTENTIOMETRIC ANALYSIS
A reliable, maintenance-free oxygen sensor for aircraft using an oxygen-sensitive coating on potentiometric electrodes
[AD-A222696] 23 p3277 N90-28545

POTENTIOMETRY
U POTENTIOMETRIC ANALYSIS

POWDER (PARTICLES)
NT METAL POWDER
NT POWDERED ALUMINUM
NT SINTERED ALUMINUM POWDER
Japanese structural ceramics research and development 01 p0048 N90-10272
Preparation, purification and densification of zinc sulfide powder from organometallics
[AD-A210943] 01 p0052 N90-10298
Processing and fabrication of high temperature oxide superconductors
[AD-A210197] 01 p0131 N90-10755
Low temperature processing of reaction sintered silicon nitride
[DE89-017455] 02 p0191 N90-11092
Freeze-dried processing of tungsten heavy alloys
[DE89-015171] 02 p0197 N90-11122
Basic research on processing of ceramics for space structures
[AD-A205954] 02 p0199 N90-11139
Synthesis of powder with gel technique
[FOA-C-20752-2.4(2.1)] 02 p0202 N90-11156
Powder morphology effects in the ignition of titanium-based pyrotechnics
[DE89-017229] 02 p0208 N90-11191
Effects of shock-modification on superconductivity in Tl2Ca2Ba2Cu3Oy and Bi2CaSr2Cu2Ox
[DE89-017231] 02 p0285 N90-11629
Significance of oxide skins on powder for the quality of PM Al material --- PM (press molded)
[DFVLR-FB-89-11] 03 p0329 N90-11873
Densification of particulate ceramic composites: The role of heterogeneities
[DE90-000177] 03 p0331 N90-11886
Temperature effects in shock consolidation of metal powders
[DE89-016782] 04 p0474 N90-12716
Shock-induced solid state reactions and phase transitions: X ray profile studies on shock-modified Fe3O4 and ZrO2 powders
[DE90-000669] 06 p0741 N90-14315
Superconducting and microstructural properties of shock-compacted high-T sub c oxide powders
[DE90-000823] 06 p0853 N90-14958
Powder neutron diffraction study of the structural phase diagram of the Ba(sub 1-x)K(sub x)BiO3 system
[DE90-002264] 06 p0854 N90-14967
Ceramic powder characterization
[DE90-001282] 07 p0908 N90-15249
IEA/Annex 2 powder characterization cooperative program
[AD-A213540] 07 p0911 N90-15271
Processing and fabrication of YBa2Cu4O8 and YBa2Cu4O8/YBa2Cu3O(x) composites
[DE90-003559] 07 p1001 N90-15789
Synthesis of air-sinterable lanthanum chromite powders
[DE90-004681] 08 p1046 N90-16049
Fractographic analysis of long rod penetrator-armor ceramic interactions
[AD-A215172] 09 p1197 N90-16938
Agglomeration of ceramic powders
09 p1223 N90-17098
Flexibility of the zeolite RHO framework: In situ x ray and neutron powder structural characterization of divalent cation-exchanged zeolite RHO
[AD-A214573] 09 p1288 N90-17467
Synthesis of high-purity sinterable silicon nitride powder
[DE90-007050] 11 p1493 N90-18593
Analysis of propulsive powder combustion products and their corrosive effects
[ISL-CO-248/88] 11 p1495 N90-18605
Investigation of the processes controlling the flame generation of refractory materials
[DE90-007564] 12 p1624 N90-19333
An investigation of the mechanisms of solid state powder reaction in the combustion synthesis and sintering of high temperature materials
[DE90-007880] 13 p1777 N90-20198
Determination of flow-regime boundaries for cohesive particles
[DE90-007425] 13 p1800 N90-20332
Magnetic hardening studies and novel techniques for preparation of high performance magnets
[AD-A217737] 13 p1881 N90-20790
Millimeter wave surface resistance of RBa2Cu3O(7-delta) (R = Y,Eu,Dy,Sm,Er) superconductors
[NASA-TM-102571] 13 p1897 N90-20886
ZELED analysis of aperiodicity and bond lengths in ceramic powders
[DE90-612932] 14 p1955 N90-21193
Method of making a long life high current density cathode from tungsten and iridium powders using a quarternary compound as the impregnant
[AD-D014425] 14 p1958 N90-21211
Alternative materials for solid oxide fuel cells
[DE90-008615] 14 p2001 N90-21468
Shock compression of solids: A tutorial
[DE90-009185] 14 p2032 N90-21659
Test method for fire extinguishing powder, Nordtest project 675-87
[PB90-166984] 15 p2073 N90-21874
A low temperature calorimetric study of several high-T(sub c) superconductors 16 p2322 N90-23237
Production and coating of pure boron powders
[AD-A220272] 18 p2533 N90-24452
Synthesis of ceramic superconductors under low oxygen pressure
[DE90-010415] 18 p2621 N90-24933
Real space method of powder diffraction for non-periodic and nearly periodic materials
[DE90-010537] 18 p2621 N90-24935
Processing polymeric powders
18 p2647 N90-25069
Synthesis of high purity sinterable silicon carbide powder
[DE90-012029] 20 p2828 N90-26084
The EISI (Elemental and Interplanar Spacing Index) index: A search/match tool for electron diffraction phase analysis
[DE90-010832] 20 p2830 N90-26097
Development of a sealed bipolar Li-alloy/FeS2 battery for electric vehicles
[DE90-013650] 21 p2999 N90-27045
Fabrication of composite high temperature superconductor wires from Ag/YBa2Cu3O(sub x) powder produced by AgNO3 decomposition
[AD-A221936] 21 p3083 N90-27532
Nature and origin of interstellar diamond from the Allende CV3 meteorite 21 p3092 N90-27581
Synthesis of Y1Ba2Cu3O(sub x) superconducting powders by intermediate phase reaction
22 p3149 N90-27855
A high temperature molten salt thermal electrochemical cell
[AD-D014469] 22 p3195 N90-28131
Powder processing of aluminides
[DE90-015314] 24 p3444 N90-29447
Processing of nanocrystalline ceramics
[DE90-015700] 24 p3456 N90-29520

POWDER METALLURGY
Establishment and initial operation of a resource facility for RSR (Rapid Solidification Rate) processed alloys in pilot quantities
[AD-A210369] 01 p0050 N90-10283
Exploratory study of niobium, titanium, zirconium and tantalum aluminides
[AD-A210658] 02 p0283 N90-11615
Elevated temperature aluminum-titanium alloy by powder metallurgy process
[AD-D014165] 03 p0326 N90-11852
Current research in advanced materials
[DE89-017466] 03 p0331 N90-11884
Tribological properties of PM212: A high-temperature, self-lubricating, powder metallurgy composite
[NASA-TM-102355] 04 p0465 N90-12659
Dynamic sintering of metallic powders by laser shock
06 p0784 N90-14559
Micro-scale simulation of dynamic compaction of oxide and metal powder mixture
[DE90-002220] 06 p0856 N90-14978
New Light Alloys
[AGARD-CP-444] 07 p0897 N90-15185
Fatigue and fracture behaviour of a PM Al-Li alloy
07 p0899 N90-15195
High performance powder metallurgy aluminum alloys: An overview 07 p0900 N90-15204
Method for refining microstructures on prealloyed titanium powder compacts
[AD-D014280] 08 p1043 N90-16030
Structural analysis of zirconium-aluminum plasma deposits
[ETCA-89-R-073] 08 p1046 N90-16045
Shock-induced reaction synthesis of aluminides and silicides
[DE90-003948] 08 p1049 N90-16066
Significance of oxide skins on powder for the quality of PM Al materials
[ESA-TT-1178] 11 p1487 N90-18560
Constitutive data acquisition and modelling in aluminium 2014 alloy
[AERE-R-13651] 13 p1775 N90-20186
Improved toughness alloys based on titanium aluminides
[AD-A218149] 13 p1778 N90-20208
Ductile alloy encapsulated ceramic armor development
[AD-A217632] 14 p1954 N90-21183
Microstructure and mechanical properties of nickel aluminide powders consolidated by extrusion and hot isostatic pressing
[DE90-009777] 15 p2070 N90-21855
Elevated temperature crack growth in advanced powder metallurgy aluminum alloys 16 p2218 N90-22653
Elevated temperature crack growth in aluminum alloys: Tensile deformation of 2618 and FVS0812 aluminum alloys 16 p2218 N90-22654
One step HIP canning of powder metallurgy composites
[NASA-CASE-LEW-14719-1] 17 p2370 N90-23493
Undercooling and nucleation in rapid solidification rate metal powders using solid in solid emulsification
[AD-A218527] 17 p2375 N90-23526
Consortium for materials development in space
[NASA-CR-186534] 17 p2383 N90-23575

Advanced artificial dielectric materials for millimeter wavelength applications, part A
[AD-A220221] 17 p2469 N90-24112
The influence of microstructure on the tensile behavior of an aluminum metal matrix composite
[NASA-TM-102694] 20 p2827 N90-26082
Metal matrix composites and powder processing for aero-engine applications
[PNR90617] 20 p2828 N90-26087
Strengthening in heavily cold worked Cu-20 vol. percent Fe in situ composites
[DE90-011741] 22 p3135 N90-27790
Micromechanics analysis of power consolidation in manufacturing particulate-reinforced MMCs (metal matrix composites)
[DE90-014448] 23 p3299 N90-28663
Micromechanisms of fatigue crack growth and fracture toughness in metal matrix composites
[AD-A223863] 23 p3302 N90-28676
Powder processing of aluminides
[DE90-015314] 24 p3444 N90-29447

POWDERED ALUMINUM
NT SINTERED ALUMINUM POWDER
Structural analysis of zirconium-aluminum plasma deposits
[ETCA-89-R-073] 08 p1046 N90-16045
Significance of oxide skins on powder for the quality of PM Al materials
[ESA-TT-1178] 11 p1487 N90-18560
Ductile alloy encapsulated ceramic armor development
[AD-A217632] 14 p1954 N90-21183
High energy-density liquid rocket fuel performance
[NASA-CR-185279] 23 p3315 N90-28742

POWDERED METALS
U METAL POWDER

POWER AMPLIFIERS
Master oscillator with power amplifiers: Performance of a two-element CW HF phased-laser array
[AD-A211141] 01 p0076 N90-10435
Control of plasma position in the CASTOR tokamak
[IPPCZ-284] 03 p0407 N90-12332
Proof-of-principle experiment for a hot electron pumped XUV amplifier
[DE90-000820] 06 p0787 N90-14586
Life test programme of ERS-1 AMI-high power amplifier 10 p1330 N90-17684
Broadband versus narrowband driver/power amplifier: A spectral purity comparison
[DOT/FAA/CT-TN89/73] 10 p1379 N90-17995
Output performance of idealized microwave power amplifiers
[AD-A216797] 11 p1502 N90-18645
Development and test of power amplifiers for the driving of low-voltage piezo-actuators in multistable interferometers
[DLR-MITT-89-19] 11 p1504 N90-18662
High efficiency octave bandwidth millimeter wave power amplifier
[AD-A218245] 14 p1969 N90-21280
A free electron laser master oscillator power amplifier experiment 16 p2239 N90-22776
MIT (Massachusetts Institute of Technology) short-wavelength laser project
[DE90-008975] 18 p2562 N90-24619

POWER BEAMING
NT LASER POWER BEAMING
NT MICROWAVE POWER BEAMING
NT SATELLITE POWER TRANSMISSION
Power beaming options 01 p0027 N90-10142
Gyrotron development for space power beaming 01 p0028 N90-10148
Antenna technology for beamed space-power 01 p0028 N90-10149
Technical options for high average power free electron milimeter-wave and laser devices 01 p0029 N90-10151
Applicability of the beamed power concept to lunar rovers, construction, mining, explorers and other mobile equipment 01 p0030 N90-10159
Central electrical utility power for a satellite ring city in low earth orbit space 01 p0031 N90-10166
Transportation and operations aspects of space energy systems 07 p1008 N90-15842
A new method for power generation and distribution in outer space
[DE90-005571] 09 p1243 N90-17211
Space power generation and distribution
[DE90-008676] 14 p2002 N90-21474
Figure of merit studies of beam power concepts for advanced space exploration
[NASA-CR-186720] 20 p2854 N90-26234
Analysis of vibrational power transmission through a beam system including a flexible section
[ISVR-TR-176] 23 p3340 N90-28875

POWER CONDITIONING
A battery-powered, solid state magnetic compressor with applications for high PRF accelerators and lasers
[DE89-015770] 01 p0058 N90-10332
Assessment of space power related measurement requirements of the Strategic Defense Initiative
[PB89-209357] 02 p0236 N90-11343
Photovoltaic system research status
[DE89-016764] 03 p0366 N90-12094
Analysis and simulation of dynamics of spacecraft power systems 04 p0463 N90-12653
The US space station and its electric power system
[NASA-TM-101974] 05 p0616 N90-13596
Research on GaAs quantum-coupled structures that can be used as electron devices
[AD-A214015] 07 p0924 N90-15350
Electron assisted glow discharges for conditioning fusion tokamak devices
[DE90-004104] 09 p1284 N90-17445
New power system modelling approaches on the basis of equivalent state variables 10 p1330 N90-17687
The spacebus power conditioning application to the Eutelsat 2 spacecraft 10 p1330 N90-17689
The subsystem regulator, the next generation in satellite regulated power conditioning 10 p1331 N90-17690
Analysis of power bus topologies used in telecommunications satellites 10 p1331 N90-17691
The MECB data collecting satellite power supply subsystem 10 p1332 N90-17699
The modular power subsystem 10 p1332 N90-17700
Power processing unit for 20mN-class ion engine system 10 p1336 N90-17732
Variable structure control system applied to multilevel power conditioning converters 10 p1336 N90-17734
State variable modelling for the audiosusceptibility evaluations of current controlled zero ripple structures 10 p1337 N90-17735
Comparison of control structures for a bidirectional high-frequency dc-dc converter 10 p1337 N90-17737
Analysis of the CUK converter in delta V mode by charge and flux balances 10 p1337 N90-17738
A complete EPC simulation 10 p1337 N90-17741
Power conditioning for active array SAR antennas 10 p1338 N90-17744
Analysis and design of a HV dc/dc series resonant converter using a multi-stage voltage multiplier 10 p1338 N90-17745
Design development and qualification of a solar array with OSRs (SSM) bonded to the ISO spacecraft rigid sunshield 10 p1341 N90-17768
Power conditioning techniques
[NASA-TM-102577] 13 p1795 N90-20301
Electric power scheduling: A distributed problem-solving approach
[NASA-TM-103149] 15 p2157 N90-22323
Experimental demonstration of an electromagnetically pumped free-electron laser with cyclotron harmonic idlers
[AD-A218830] 17 p2408 N90-23719
Research studies on extreme ultraviolet and soft x ray lasers
[AD-A220271] 18 p2562 N90-24621
Conceptual definition of a high voltage power supply test facility
[NASA-CR-185216] 19 p2666 N90-25172
An analysis of space power system masses
[NASA-TM-103199] 19 p2669 N90-25184
Linear averaged and sampled data models for large signal control of high power factor ac-dc converters
[AD-A221976] 21 p3020 N90-27170
Hubble space telescope six-battery test bed
[NASA-TM-103506] 22 p3124 N90-27731

POWER CONVERTERS
An assessment of the use of resonant-mode topologies for high frequency power conversion 10 p1335 N90-17726
A new vision to model the parallel resonant converter 10 p1336 N90-17727
Techniques for high frequency power conversion 10 p1336 N90-17729
Dynamical model of series-resonant converter with peak capacitor voltage predictor and switching frequency control 10 p1336 N90-17730
Innovations in the design and matching of magnetic components and semiconductors up performance and reliability of power converters 10 p1336 N90-17731
Power processing unit for 20mN-class ion engine system 10 p1336 N90-17732
Linear and non-linear control of high-order converters after reducing the order by appropriate techniques 10 p1336 N90-17733
Comparison of control structures for a bidirectional high-frequency dc-dc converter 10 p1337 N90-17737
Programmatic status of NASA's CSTI high capacity power Stirling space power converter program
[NASA-TM-103142] 16 p2210 N90-22606
Lyapunov-based control for switched power converters
[AD-A221974] 21 p3000 N90-27053
Linear averaged and sampled data models for large signal control of high power factor ac-dc converters
[AD-A221976] 21 p3020 N90-27170
Generalized averaging method for power conversion circuits
[AD-A221977] 21 p3020 N90-27171
Electrical characterization of a Mapham inverter using pulse testing techniques
[NASA-TM-103254] 22 p3134 N90-27784

POWER DENSITY (ELECTROMAGNETIC)
U RADIANT FLUX DENSITY

POWER EFFICIENCY
The effect of electrode configuration on arcjet performance
[NASA-TM-102346] 02 p0189 N90-11081
X.2 limited flight test plan
[AD-A214412] 07 p0880 N90-15099
Piezoelectric ceramic modeling and characterization at high levels of mechanical activity
[ISAL-89-0030] 08 p1051 N90-16074
Permanent magnet flux-biased magnetic actuator with flux feedback
[NASA-CASE-LAR-13785-1] 09 p1277 N90-17403
Energy Efficient Engine exhaust mixer model technology report addendum; phase 3 test program
[NASA-CR-174799] 23 p3279 N90-28556

POWER FACTOR CONTROLLERS
Power factor controller study
[DE89-017655] 06 p0767 N90-14458
Adjustable speed drive study, June 1985 to September 1988. Part 2: Appendices
[DE90-002771] 07 p0922 N90-15332
The subsystem regulator, the next generation in satellite regulated power conditioning 10 p1331 N90-17690
Linear averaged and sampled data models for large signal control of high power factor ac-dc converters
[AD-A221976] 21 p3020 N90-27170

POWER GENERATORS
U ELECTRIC GENERATORS

POWER LIMITED SPACECRAFT
A space-based optical communication system utilizing fiber optics
[AD-A217333] 13 p1887 N90-20828

POWER LIMITERS
A review of laser filter materials
[AD-A213134] 05 p0648 N90-13776

POWER LINES
Microwave screening on digital radio communication links due to multicircuit power transmission lines
[DE90-734950] 08 p1058 N90-16118
The 1989 National Convention Record IEE Japan, part 11
[DE89-910083] 09 p1210 N90-17014
Conceptual design of high Tc superconducting power cable and its economic evaluation
[DE90-734940] 09 p1287 N90-17462
Characterization of electron flow in positive-polarity linear-induction accelerators
[DE90-014998] 23 p3394 N90-29177

POWER MODULES (STS)
Independent Orbiter Assessment (IOA): Assessment of the electrical power distribution and control subsystem, volume 1
[NASA-CR-185557-VOL-1] 03 p0313 N90-11779
Independent Orbiter Assessment (IOA): Assessment of the electrical power distribution and control subsystem, volume 2
[NASA-CR-185557-VOL-2] 03 p0313 N90-11780
Independent Orbiter Assessment (IOA): Assessment of the electrical power distribution and control subsystem, volume 3
[NASA-CR-185557-VOL-3] 03 p0313 N90-11781

POWER PROCESSING SYSTEMS
U POWER CONDITIONING

POWER SERIES
NT TAYLOR SERIES
Series reversion/inversion of Lambert's time function
[AD-A216243] 12 p1607 N90-19245

POWER SPECTRA
A mechanical power flow capability for the finite element code NASTRAN
[AD-A212202] 04 p0513 N90-12964
The S.D.G., P.S.D. and the nonlinear airplane
[NLR-MP-88018-U] 05 p0578 N90-13371
Power spectral estimation algorithms
[NASA-CR-186189] 06 p0828 N90-14812
A two dimensional power spectral estimate for some nonstationary processes
[NASA-CR-186100] 06 p0833 N90-14843

Array signal processing: New techniques for direction finding and spectrum estimation
[AD-A213883] 07 p0924 N90-15345
Finite word length considerations in high resolution spectral estimation
[AD-A214684] 09 p1273 N90-17377
Optical measurement of precipitation
[AD-A214357] 10 p1407 N90-18116
Power spectral densities for selected digital phase-continuous MFSK (M-ary Frequency Shift Keying) emissions
[PB90-129990] 12 p1647 N90-19463
Theory and experimental technique for nondestructive evaluation of ceramic composites
[NASA-TM-102561] 17 p2414 N90-23754
Construction of a hybrid angular velocity reference system for investigation of the dynamic characteristics of strapdown gyros
[ESA-TT-1181] 19 p2694 N90-25332
The Z/atoll classification 19 p2769 N90-25740
X ray observations of GS2023+338 by the Kvant module 19 p2771 N90-25747
Noise variability in Cyg X-1 and Her X-1 19 p2771 N90-25753
A model for 1/f-type variability in active galactic nuclei 19 p2778 N90-25799
Timing analysis of binary X ray pulsars observed by HEAO 1 19 p2781 N90-25822
Long timescale X ray variability in AGN 19 p2788 N90-25868
X ray AGN variability with hour to month timescales 19 p2788 N90-25869
The X ray time variability of NGC 6814 revisited 19 p2790 N90-25882
Formation of design envelope criterion in terms of deterministic spectral procedure
[RAE-TM-SS-9] 20 p2804 N90-25953
Observations of plasma structure freezing scale at equatorial latitudes
[AD-A222529] 21 p3026 N90-27207
Spatial scales of cirrus cloud properties 22 p3222 N90-28275
Estimation of power spectral density of runway roughness
[NAL-TR-1037] 24 p3437 N90-29411

POWER SUPPLY CIRCUITS
European Space Power, volume 1
[ESA-SP-294-VOL-1] 10 p1329 N90-17678
The 120 VDC test bed for Columbus power system 10 p1329 N90-17679
Japanese experiment module electrical power system 10 p1329 N90-17680
New power system modelling approaches on the basis of equivalent state variables 10 p1330 N90-17687
Design considerations and lessons learned on the European retrievable carrier 10 p1332 N90-17698
The MECB data collecting satellite power supply subsystem 10 p1332 N90-17699
The 120V 20A PWM switch for applications in high power distribution 10 p1335 N90-17724
A complete EPC simulation 10 p1337 N90-17741
High power medium voltage electronic load 10 p1338 N90-17747

POWER TRANSMISSION
Microwave screening on digital radio communication links due to multicircuit power transmission lines
[DE90-734950] 08 p1058 N90-16118
Power transmission device
[AD-D014430] 14 p1969 N90-21281
Free-Space Power Transmission
[NASA-CP-10016] 15 p2060 N90-21795

POWER TRANSMISSION (LASERS)
U LASER POWER BEAMING

POWER TRANSMISSION (MICROWAVE)
U MICROWAVE POWER BEAMING

POWERED LIFT AIRCRAFT
The NASA experience in aeronautical R and D: Three case studies with analysis
[AD-A211486] 04 p0437 N90-12496
Powered-lift aircraft technology
[NASA-SP-501] 04 p0452 N90-12589
FAA Rotorcraft Research, Engineering, and Development Bibliography 1962-1989
[AD-A224256] 24 p3417 N90-29299

POYNTING THEOREM
Satellite measurements of magnetospheric Poynting flux
[AD-A224391] 24 p3490 N90-29724

PPM (MODULATION)
U PULSE POSITION MODULATION

PRACTICES
U PROCEDURES

PRAIRIES
U GRASSLANDS

PRANDTL NUMBER
Time-dependent free convection in low Prandtl number fluids
[DE90-003053] 07 p0929 N90-15377
Multicellular natural convection in a narrow vertical slot
[AD-A216411] 11 p1505 N90-18668
Effect of a crystal-melt interface on Taylor-vortex flow
[NASA-CR-186512] 15 p2171 N90-22408
Low Prandtl number convection in a rectangular cavity with longitudinal thermal gradient and transverse g-jitters
[REPT-892-430-109] 17 p2404 N90-23695

PRASEODYMIUM
Muon SR investigation of magnetism and superconductivity in (Y(1-x)Pr(x))Ba2Cu3O7
[DE90-000689] 06 p0852 N90-14956
An experimental investigation of the thermal conductivity of porous adsorbents
[AD-A217854] 13 p1899 N90-20899
Studies of iron impurities in YxPr1-xBa2Cu3O7-delta 22 p3151 N90-27865

PRE-MAIN SEQUENCE STARS
NT T TAURI STARS
Outflows in high mass star-forming regions 08 p1149 N90-16657
Photometric monitoring of early type emission line stars 15 p2184 N90-22478
Evolutionary models of the rotating sun and implications for other low mass stars 16 p2339 N90-23329
Near-infrared speckle observations of T Tauri stars and a multi-wavelength study of the prototype star T Tauri 23 p3409 N90-29264

PREAMPLIFIERS
Feedback charge amplifier integrated on the detector wafer
[REPT-89-037] 04 p0496 N90-12652
Direct detection optical intersatellite link at 220 Mbps using AlGaAs laser diode and silicon APD with 4-ary PPM signaling
[NASA-CR-186380] 12 p1646 N90-19460
Short wavelength HgCdTe staring focal plane for low background astronomy applications 14 p1979 N90-21336
Status of the isophot detector development 14 p1980 N90-21342
Apparatus for and a method of determining compass headings
[AD-D014436] 16 p2199 N90-22551

PREBURNERS
Combustion characteristics of oxygen/hydrogen high pressure preburners for staged combustion cycle rocket engine
[NAL-TR-1044] 24 p3441 N90-29434

PRECAMBRIAN PERIOD
The patterns of fracture and the conditioning tectonics in the region of the Quadrilatero Ferrifero and part of the Migmatitic-Gnanulitic Complex in Minas Gerais (Brazil)
[INPE-4895-PRE/1496] 11 p1534 N90-18829
Geology of Espinhaco Meridional, including the Quadrilatero Ferrifero: Integration through remote sensing data
[INPE-4904-PRE/1505] 14 p1998 N90-21450
Contribution for the study of the evolution of part of the Espinhaco supergroup and its foundation through fracture analysis
[INPE-4907-PRE/1508] 14 p1999 N90-21459

PRECAUTIONS
U ACCIDENT PREVENTION

PRECESSION
NT PROTON PRECESSION
NT QUENCHING (ATOMIC PHYSICS)
Optical light curves of HZ Her in the model of freely precessing neutron star 19 p2783 N90-25831

PRECIOUS METALS
U NOBLE METALS

PRECIPITATES
Effects of precipitate distribution on 293 K and 77 K properties of 2090-T81 weldments
[DE90-002332] 06 p0747 N90-14349

PRECIPITATION (CHEMISTRY)
Characterization and evaluation of acid rain in East Central Florida from 1978 to 1987: Ten year summary report
[NASA-TM-102149] 01 p0084 N90-10478
The influence of carbide precipitation on the creep rupture behavior of high temperature alloys
[JUEL-2211] 08 p1046 N90-16044
Human serum albumin crystals and method of preparation
[NASA-CASE-MFS-28234-1] 13 p1850 N90-20616
SiO(x) precipitation: Defect density correlation with the n+ substrate resistivity
[DE90-005593] 13 p1895 N90-20878
A study of mesoscale acid deposition in the lower Ohio River Valley 16 p2253 N90-22848
Precipitation on dislocations in Al-Li-Cc-Mg-Zr
[AD-A221124] 18 p2526 N90-24415
Problems of enclosed crystal interfaces
[DE90-011594] 21 p3079 N90-27509
Synthesis and property evaluation of Y-Ba2-Cu3-O(6+x) superconductors
[AD-A223494] 24 p3552 N90-30098

PRECIPITATION (METEOROLOGY)
NT ACID RAIN
NT HAIL
NT RAIN
NT SNOW
NT SNOW COVER
A program to improve performance of AFGL (Air Force Geophysical Laboratory) automated present weather observing sensors
[AD-A207669] 01 p0087 N90-10495
US Navy regional climatic study of the United States Atlantic Coast and associated waters
[AD-A210198] 01 p0088 N90-10503
Global distribution of moisture, evaporation-precipitation, and diabatic heating rates 03 p0362 N90-12069
A statistical intercomparison of temperature and precipitation predicted by four general circulation models with historical data
[DE89-017785] 03 p0369 N90-12108
Analysis and modeling of summertime convective cloud and precipitation structure over the Southeastern United States
[NASA-CR-185436] 04 p0519 N90-12996
A collection of papers related to heavy precipitation forecasting
[PB89-230833] 05 p0671 N90-13910
Climate system research studies of global and regional instrumental data
[DE90-001205] 06 p0809 N90-14707
Adverse weather operations during the Canadian Atlantic storms program 07 p0871 N90-15052
The collection of non-conus aircraft icing data along with an identification of the geographical areas of potential severe icing and a study of a method of remote determining atmospheric icing data
[AD-A215055] 09 p1162 N90-16724
Surface observation climatic summaries
[AD-A215786] 10 p1408 N90-18122
On the relationship between water vapor over the oceans and sea surface temperature
[NASA-CR-186199] 10 p1409 N90-18127
Intertropical Convergence Zone (ITCZ) and its relationship with the precipitation of the north-northeast Brazilian region
[INPE-4887-TDL/378] 11 p1535 N90-18839
Validation of the EURAD cloud modules 12 p1687 N90-19693
United States Historical Climatology Network (HCN) serial temperature and precipitation data
[DE90-008029] 13 p1830 N90-20506
An intercomparison of general circulation model predictions of regional climate change
[DE90-008325] 13 p1845 N90-20589
Precipitation mechanisms in tropical and midlatitude convective clouds 14 p2008 N90-21507
Scintillation of millimeter-wave intensity and phase caused by turbulence and precipitation 15 p2080 N90-21912
Models of aerosols, clouds, and precipitation for atmospheric propagation studies 15 p2081 N90-21919
Handbook of climate of the USSR. Humidity of air, atmospheric precipitations, snow cover
[AD-A220454] 17 p2427 N90-23828
A correlation study of wind speed as measured by the special sensor microwave/imager and the GEOSAT altimeter
[AD-A219841] 18 p2581 N90-24701
Some results from the precipitation chemistry measurement programme in Sweden 20 p2884 N90-26410
The aqueous atmospheric chemistry of mercury 20 p2886 N90-26420
A LOWTRAN7 sensitivity study in the 8-12 and 3-5 micron bands: Includes comparison with LOWTRAN6 results
[AD-A222094] 21 p3031 N90-27231
Daily temperature, solar radiation, wind speed, cloud cover, and precipitation data recorded at the meteorological station for calendar years 1957--1988
[DE90-014399] 23 p3352 N90-28941

PRECIPITATION HARDENING
Mechanisms of strength and toughness in a microalloyed, precipitation hardened steel
[AD-A210571] 01 p0045 N90-10256
Strain aging in tungsten-heavy alloys
[AD-A211166] 01 p0046 N90-10259

Accelerated aging of metal matrix composites
02 p0190 N90-11085
Precipitation and transformation toughening of Al-Mg signals
[ETN-89-94675] 02 p0199 N90-11138
Precipitation strengthened high strength, high conductivity Cu-Cr-Nb alloys produced by chill block melt spinning
[NASA-CR-185144] 03 p0326 N90-11853
Effects of composition and age hardening on precious metal electrical contacts
[DE88-008791] 06 p0769 N90-14476
Evaluation of a diffusion/trapping model for hydrogen ingress in high strength alloys
[AD-A215528] 09 p1194 N90-16920
Thermomechanical deformation testing and modeling in the presence of metallurgical instabilities
[NASA-CR-185188] 14 p1993 N90-21420
Fracture-tough, corrosion-resistant bearing steels
[NASA-CR-186796] 19 p2675 N90-25213
Density changes of generation 1.5 and 2.0 copper alloys irradiated at 411 to 414 C and 529 C in FFTF-MOTA
[DE90-015291] 23 p3311 N90-28724

PRECIPITATION PARTICLE MEASUREMENT
Comparison of two droplet sizing systems in an icing wind tunnel
[NASA-TM-102456] 06 p0793 N90-14617
Airborne measurements of the electric field and the charge precipitation particles in convective clouds: Lower positive charge centres
[ESA-TT-1157] 11 p1535 N90-18836

PRECIPITATORS
NT ELECTROSTATIC PRECIPITATORS
Electronic precipitator control
[NASA-CASE-LAR-13273-2] 13 p1798 N90-20320

PRECISION
Contribution of the precision determination of noise powers in the MHz and lower GHz frequency range
[PTB-E-33] 03 p0340 N90-11935
COBE nonspinning attitude propagation
05 p0587 N90-13418
Comparison of artificial matrices and covariance functions
[ETN-90-95722] 12 p1679 N90-19645
Foundations of measurement and instrumentation
[NASA-RP-1222] 14 p1981 N90-21351
Design considerations for precision and reliability in space mechanisms 18 p2536 N90-24463
Ultra precision machining
[AD-A222422] 21 p2991 N90-27003

PRECISION GUIDED PROJECTILES
Identification of stability and control parameters of a brilliant ammunition 01 p0014 N90-10065
Integrated strapdown avionics for precision guided vehicles 24 p3427 N90-29361

PRECONDITIONING
Element-by-element preconditioning techniques for large-scale, vectorized finite element analysis in nonlinear solid and structural mechanics 08 p1087 N90-16291
Efficient preconditioning for the p-version finite element method in two dimensions
[AD-A216210] 11 p1551 N90-18928
Computation of low Mach number compressible flow
17 p2344 N90-23346
Using implicit ODE methods with iterative linear equation solvers in spectral methods
[FFI-89/7017] 19 p2751 N90-25633

PREDICTION ANALYSIS TECHNIQUES
Prediction of the aerodynamic stability of missiles
01 p0012 N90-10052
Leading edge transition by contamination in hypersonic flow 01 p0063 N90-10360
Goertler instability on an airfoil: Comparison of marching solution with experimental observations
01 p0063 N90-10364
IFD (Implicit Finite Difference): Interfaced with Harvard open ocean model forecasts
[AD-A210521] 01 p0090 N90-10517
Tracking performance evaluation
[AD-A210499] 01 p0095 N90-10540
A review of the Error of Matrix Method (EMM) for structural dynamic model comparison
02 p0177 N90-10993
Mathematical model and predictions for static and dynamic behavior of solar array structure
02 p0184 N90-11049
The use of damage characterization for life prediction methodologies 02 p0185 N90-11053
Intrinsic damage and strength criteria for advanced composite laminates in space applications
02 p0187 N90-11071
Numerical simulation of turbulent flow downstream a sudden axisymmetric expansion
[FOA-C-20758-2.1] 02 p0222 N90-11272
Coordinated multi-parameter measurements and predictions of the global-scale ionosphere
02 p0247 N90-11397
Computational methods for complex flowfields
[AD-A211485] 03 p0347 N90-11983
Stability theory applications to laminar-flow control
04 p0439 N90-12513
CFD methods for drag prediction and analysis currently in use in UK
[RAE-TM-AERO-2146] 04 p0448 N90-12563
Exponential modeling using combined forward and backward prediction
[AD-A212317] 04 p0545 N90-13169
A technique for the prediction of aerodynamics and aeroelasticity of rotor blades 05 p0579 N90-13377
Atmospheric drag model calibrations for spacecraft lifetime prediction 05 p0591 N90-13439
Lifetime predictions for the Solar Maximum Mission (SMM) and San Marco spacecraft
05 p0591 N90-13440
Effects of joints in truss structures
05 p0600 N90-13486
Sufficiency and necessity in reliability modeling
[NASA-CR-186119] 05 p0635 N90-13706
Mean stress and the exhaustion of fatigue-damage resistance
[NASA-TM-101311] 05 p0655 N90-13819
An evaluation of a fatigue crack growth prediction model for variable-amplitude loading (PREFFAS)
[LR-537] 05 p0656 N90-13822
Prediction of the 10 cm solar flux index
05 p0662 N90-13872
Orthobaric densities and molar volumes of liquids. Introduction to data items issued after July 1989
[ESDU-89018] 06 p0738 N90-14298
Propagation-based decision aids in the U.S. Navy
06 p0757 N90-14410
Engineer's Refractive Effects Prediction System (EREPS) 06 p0758 N90-14411
The FTZ HF propagation model for use on small computers and its accuracy 06 p0765 N90-14447
Parametric identification of discrete time series models for structural response prediction
07 p0945 N90-15472
On the motion of compliantly-connected rigid bodies in contact. Part 1: The motion prediction problem
[AD-A214135] 07 p0948 N90-15489
Identification and quantification of synoptic structure in simulated Tiros N radiance soundings
07 p0959 N90-15546
On the observation of a transition from fusion to multifragmentation in high multiplicity O16 induced reactions
[LUIP-8812] 08 p1119 N90-16481
Formulation and verification of a technique for compensation of pneumatic attenuation errors in airborne pressure sensing devices 09 p1221 N90-17084
The Polar Ice Prediction System: A sea ice forecasting system
[AD-A214600] 09 p1249 N90-17246
An analysis of scatter decomposition
[NASA-CR-181978] 09 p1276 N90-17396
Predicted and measured boundary layer refraction for advanced turboprop propeller noise
[NASA-TM-102365] 09 p1279 N90-17413
Chaos and turbulence
[AD-A215310] 09 p1294 N90-17499
Prediction methods for store separation
10 p1305 N90-17549
Dynamic derivatives of missiles and fighter-type configurations at high angles of attack
10 p1306 N90-17554
A study of the structural efficiency of fluted core graphite-epoxy panels
[NASA-TM-101681] 10 p1396 N90-18070
Baseline experiment for active control of structural vibrations
[AD-A216194] 10 p1397 N90-18076
The effects of wind tunnel data uncertainty on aircraft point performance predictions
[AD-A216091] 11 p1456 N90-18387
Numerical investigation of unsteady flow in oscillating turbine and compressor cascades
11 p1459 N90-18407
Development of an experimental space station model for structural dynamics research
[NASA-TM-102601] 11 p1519 N90-18751
A PBL-radiation model for application to regional numerical weather prediction 12 p1635 N90-19394
Potential theory of radiation 12 p1635 N90-19395
The influence of a wall function on turbine blade heat transfer prediction 12 p1640 N90-19421
Simple analytic potentials for linear ion traps
12 p1642 N90-19436
The effects of sinusoidal interference on the second-order carrier tracking loop preceded by a bandpass limiter in the Block 4 receiver 12 p1644 N90-19449
Synoptic-scale forcing of the low-level jet in developing baroclinic waves 12 p1692 N90-19717
Escape systems research at RAE
13 p1751 N90-20058
Relationship of radiometric field measurements of wheat in the Assis-Safra region, 1988
[INPE-4949-RPE/598] 13 p1819 N90-20443
Progress in the Determination of the Earth's Gravity Field
[NASA-CR-185721] 13 p1831 N90-20513
Gravity field determination and error assessment techniques 13 p1832 N90-20517
The use of high-resolution terrain data in gravity field prediction 13 p1835 N90-20533
The role of topography in geodetic gravity field modelling 13 p1835 N90-20534
Fourier transform methods in local gravity modeling
13 p1836 N90-20538
Determination of mean gravity anomalies in the Taiwan Island 13 p1837 N90-20547
Adiabatic and diabatic initialization of the AFGL (Air Force Geophysics Laboratory) global spectral model using dynamic normal mode and nonlinear normal mode methods
[AD-A218120] 13 p1846 N90-20595
An algorithm for efficient estimation of superimposed exponential signals
[AD-A217218] 13 p1865 N90-20698
VAPEPS user's reference manual, version 5.0
[NASA-CR-180781] 13 p1868 N90-20713
Precompound decay models for medium energy nuclear reactions
[DE90-008352] 13 p1884 N90-20808
The electronic properties of high (Tc) superconductors probed by positron annihilation
[DE90-008354] 13 p1896 N90-20883
Measurement and prediction of propeller blade surface pressure distributions 14 p1912 N90-20961
Aerodynamic design via control theory
14 p1920 N90-20998
Secondary Flows in Turbomachines
[AGARD-CP-469] 14 p1922 N90-21009
Secondary flows and radial mixing predictions in axial compressors 14 p1922 N90-21010
The effects of compressor endwall flow on airfoil incidence and deviation 14 p1922 N90-21011
Secondary flow in a turbine guide vane with low aspect ratio 14 p1924 N90-21018
Calculation of the secondary flow in an axial turbine
14 p1924 N90-21022
Losses in the tip-leakage flow of a planar cascade of turbine blades 14 p1925 N90-21027
Computer codes for the evaluation of thermodynamic properties, transport properties, and equilibrium constants of an 11-species air model
[NASA-TM-102602] 14 p1972 N90-21297
Improved analytical capabilities for foil air bearings, phase 1
[AD-A218071] 14 p1987 N90-21389
NASA airframe structural integrity program
[NASA-TM-102637] 14 p1993 N90-21422
Recent improvements in the scope and accuracy of the performance prediction of nozzle propellers
[LR-598] 15 p2048 N90-21742
Millimetric, infrared, and optical propagation studies over a 500 m path 15 p2080 N90-21913
Modelling of optically and IR effective atmospheric turbulence 15 p2082 N90-21923
UV spectral simulations using LOWTRAN 7
15 p2083 N90-21928
Multiblock topology specification and grid generation for complete aircraft configurations
15 p2094 N90-21986
Review of analysis methods for mechanically fastened joints in composites
[LR-599] 15 p2107 N90-22050
Fatigue crack growth predictions for variable-amplitude and spectrum loading
[LR-526] 15 p2118 N90-22118
Uncertainty analysis of the accident effect area of a BLEVE
[REPT-89-49] 15 p2126 N90-22160
On three-dimensional scaling and consistent truncation of global atmospheric models 15 p2127 N90-22164
Satellite versus GCM-simulated radiation balance: Comparisons and implications for climate modeling
15 p2131 N90-22180
The Shock and Vibration Digest, volume 21, no. 6
15 p2163 N90-22363
Noise transmission into propeller-driven airplanes
15 p2163 N90-22364

A life prediction model for laminated composite structural components
[NASA-CR-186587] 16 p2212 N90-22614
Inelastic response of metal matrix composites under biaxial loading 16 p2220 N90-22661
Impact of marine boundary layer parameterization on a numerical simulation of cyclogenesis during a cold air outbreak event 16 p2256 N90-22864
An innovations approach to decoupling of multibody dynamics and control 16 p2280 N90-22994
Bayesian nonparametric prediction and statistical inference
[AD-A218473] 16 p2308 N90-23154
An examination of the full-wave method for rough surface scattering
[AD-A218664] 16 p2308 N90-23155
A computer code for the prediction of aerodynamic characteristics of lifting airfoils at transonic speed
[DLC-EST-TN-030] 17 p2346 N90-23359
Rate dependent constitutive models for fiber reinforced polymer composites
[NASA-TM-102665] 17 p2370 N90-23492
Engineer's Refractive Effects Prediction System (EREPS), revision 2.0
[AD-A220742] 17 p2391 N90-23616
Prediction of gear tooth separation in single-stage gear systems, using numerical techniques
[AD-A220442] 17 p2412 N90-23744
Adding a dimension: Time as a factor in the generalizability of predictive relationships
[AD-A219679] 17 p2438 N90-23890
Mean square error behavior for prediction in linear regression models
[AD-A219988] 17 p2466 N90-24092
Low-density flow effects for hypervelocity vehicles, phase 2
[AD-A221034] 18 p2493 N90-24249
Self-similar Langmuir collapse
[DE90-611310] 18 p2617 N90-24911
Flexural fatigue life prediction of closed hat-section using materially nonlinear axial fatigue characteristics
18 p2645 N90-25062
A computational efficient modelling of laminar separation bubbles
[NASA-CR-186729] 19 p2688 N90-25291
Remote sensing for better understanding of the system Earth 19 p2706 N90-25399
A comparison of the backpropagation and recursive prediction error algorithms for training neural networks
[RR-379] 19 p2748 N90-25620
BL Lacs from the EMSS: Number-counts and implications for the luminosity function
19 p2785 N90-25849
Efficiency study comparing two helicopter planetary reduction stages
[NASA-TM-103106] 20 p2871 N90-26334
Investigation of crack-closure prediction models for fatigue in aluminium alloy sheet under flight-simulation loading
[LR-619] 20 p2877 N90-26369
Modeling and optimization of a regenerative fuel cell system using the ASPEN process simulator
[NASA-TM-103210] 20 p2882 N90-26396
Aeroacoustics of advanced propellers
[NASA-TM-103137] 20 p2923 N90-26635
Rotorcraft aeromechanical stability-methodology assessment. Phase 2: Workshop
[NASA-TM-102272] 21 p2955 N90-26800
Proceedings of the 1987 Aircraft/Engine Structural Integrity Program (ASIP/ENSIP) Conference
[AD-A198037] 21 p2956 N90-26807
Computerized corrosion forecasting model for C-5 aircraft 21 p2957 N90-26815
An interdisciplinary approach to the predictive modeling of structural adhesive bonding
[AD-A221703] 21 p2988 N90-26982
Specification for HF Lowest Usable Frequency (LUF) model
[AD-A222114] 21 p2996 N90-27031
The existence of smooth densities for the prediction filtering and smoothing problems
[AD-A222108] 21 p3066 N90-27432
The validation and application of a rotor acoustic prediction computer program
[NASA-TM-101794] 21 p3072 N90-27465
Air Force procedure for predicting aircraft noise around airbases: Noise Exposure Model (NOISEMAP). User's manual
[AD-A223162] 21 p3072 N90-27467
Inspection reliability 22 p3184 N90-28072
Role of grid-based, reactive air quality modeling in policy analysis: Perspectives and implications, as drawn from a case study
[PB90-187204] 22 p3198 N90-28150
Dynamic load-sharing using predicted process resource requirements
[NASA-CR-186891] 22 p3255 N90-28433
Prediction of subsonic vortex shedding from forebodies with chines
[NASA-CR-4323] 23 p3268 N90-28494
Control research in the NASA high-alpha technology program 23 p3272 N90-28516
Unsteady aerodynamics of controls
23 p3273 N90-28525
Flow coupling between a rotor and a stator in turbomachinery
[AD-A223882] 23 p3282 N90-28572
High temperature fatigue behavior of Haynes 188
23 p3295 N90-28642
Constitutive and life modeling of single crystal blade alloys for root attachment analysis
23 p3296 N90-28643
The fatigue damage behavior of a single crystal superalloy 23 p3296 N90-28644
Probabilistic model for fracture mechanics service life analysis 23 p3297 N90-28650
Thermal analysis of thermal barrier coatings in a high heat flux environment 23 p3297 N90-28652
Characterization of unnotched SCS-6/Ti-15-3 metal matrix composites at 650 C
[NASA-TM-102699] 24 p3444 N90-29450
Chemical kinetic and aerodynamic structures of flames
[AD-A224281] 24 p3445 N90-29455
Theoretical investigations of Pi-conjugated polyradicals as models for organic magnetic materials
[AD-A223411] 24 p3446 N90-29461
Proceedings of damping '89. Volume 1: Pages AAB-1 through DCD-11
[AD-A223431] 24 p3479 N90-29664
Simulation and measurement of the heat exchange between the urban canopy and boundary layers
24 p3486 N90-29702
Global Climate Change: Seeking a Global Consensus
[S-HRG-101-842] 24 p3486 N90-29704

PREDICTIONS

NT FLOOD PREDICTIONS
NT IMPACT PREDICTION
NT LINEAR PREDICTION
NT NOISE PREDICTION
NT NOISE PREDICTION (AIRCRAFT)
NT PERFORMANCE PREDICTION

Predictive aging of polymers
[NASA-CASE-NPO-17524-1-CU] 01 p0046 N90-10261
Turbulence modelling of three-dimensional shear flows
01 p0066 N90-10381
Applications of the hybrid automated reliability predictor: Revised edition
[NASA-TP-2760-REV] 02 p0257 N90-11454
Studies on predicting the resynchronization of the circadian system after transmedian flights
[DFVLR-FB-89-10] 03 p0382 N90-12172
The onset of the solar active cycle 22
03 p0434 N90-12488
Aerodynamic test and analysis of a slender generic missile configuration
[AD-A212522] 04 p0448 N90-12567
Shear fatigue testing and life prediction of fibre composites
[REPT-8519] 04 p0466 N90-12668
Asymptotic analyses of the structures and characteristics of flames 04 p0468 N90-12683
An investigation on combined extension and bending of thin sheets with a central crack
[LR-561] 04 p0512 N90-12958
Thermal barrier coating life prediction model development, phase 1
[NASA-CR-182230] 05 p0581 N90-13388
Hybrid deployable support truss designs for LDR
05 p0600 N90-13485
On-line range prediction system, part 2
[NASA-CR-185889] 05 p0647 N90-13771
Climate predictability: A dynamical view
[AERONOMICA-ACTA-A-347-1989] 05 p0671 N90-13909
Expected supernovae rates and gravitational waves detection
[NOTA-INTERNA-933] 05 p0713 N90-14166
Detectable gravitational waves by supernova SN 1987 A pulsar relic
[PREPRINT-658] 05 p0714 N90-14174
Orthobaric densities and molar volumes of liquids. Aromatic hydrocarbons
[ESDU-89019] 06 p0738 N90-14299
Predictive aging of elastomers in air: The importance of understanding diffusion-limited oxidation effects
[DE90-001385] 06 p0751 N90-14372
The parabolic equation approach to predicting tropospheric propagation effects in operational environments 06 p0759 N90-14418
Assessment of anomalous propagation predictions using minisonde refractivity data and the parabolic equation method 06 p0760 N90-14424
Boundary element analysis of single and multidomain problems in acoustics 06 p0837 N90-14867
Gamma ray lines from dark matter annihilation
[DE90-000779] 06 p0864 N90-15021
The radar-based short term prediction of the time-space evolution of rain fields
[AD-A213802] 07 p0918 N90-15312
Comparison of engine knock predictions using a fully-detailed and a reduced chemical kinetic mechanism
[DE90-002805] 07 p0941 N90-15448
Pipeline vibrations. Fluid transients in non-rigid, unbranched planar piping systems
[ESDU-89030] 07 p0948 N90-15491
Elicitation of natural language representations of uncertainty using computer technology
[DE90-001416] 07 p0972 N90-15611
Gradient projection techniques for large-scale optimization problems
[DE90-001986] 07 p0973 N90-15618
Two new techniques for predicting delamination growth in laminated plates 09 p1185 N90-16865
Missile dynamics: A critical assessment of prediction capabilities 10 p1304 N90-17543
Appropriate aeroprediction accuracy in defining missile systems for aerodynamic flight 10 p1304 N90-17544
Observations of fatigue crack initiation and damage growth in notched titanium matrix composites
[NASA-TM-101688] 10 p1347 N90-17815
F-15B high angle-of-attack phenomena and spin prediction using bifurcation analysis
[AD-A217366] 13 p1754 N90-20073
The influence of lateral boundary conditions, fixed surface forcings, and synoptic situations upon predictability estimates using limited area numerical models
14 p2005 N90-21492
Predictability of weather and climate in a coupled ocean-atmosphere model: A dynamical systems approach
[NASA-CR-186499] 14 p2007 N90-21502
Tropical cyclone track predictability and the adjoint method of data assimilation
[AD-A218324] 14 p2007 N90-21505
Prediction of forces and moments for flight vehicle control effectors. Part 1: Validation of methods for predicting hypersonic vehicle controls forces and moments
[NASA-CR-186571] 15 p2047 N90-21734
The solution of scattering and radiation problems for complex configurations based on 3-D grid and patch models 15 p2096 N90-21997
The role of input weighting and bounding in the characteristic GPC method
[OUEL-1762/89] 15 p2158 N90-22328
A robust stability result for generalised predictive control
[OUEL-1773/89] 15 p2158 N90-22330
Bicausal representations and multivariable generalized predictive control
[OUEL-1781/89] 15 p2159 N90-22331
A numerical and analytical study of normal stresses and pressure differences in non-Newtonian creeping flows
16 p2234 N90-22749
An investigation of the three-dimensional flow field in a centrifugal compressor 16 p2235 N90-22751
Predictability of weather and climate in a coupled ocean-atmosphere model: A dynamical systems approach 16 p2256 N90-22865
Relationship between flexibility of closure and success in pilot night vision sensor system training
[AD-A221439] 16 p2261 N90-22890
Periodic ARMA models: Optimal prediction and minimum-phase condition
[REPT-89-006] 16 p2305 N90-23131
Tropical-extratropical interaction in a model atmosphere 17 p2422 N90-23800
Analyses of the predictability of noise-induced sleep disturbance
[AD-A220156] 17 p2435 N90-23876
The interaction of a supersonic streamwise vortex and a normal shock wave 18 p2491 N90-24241
Incorporation of a progressive failure analysis method in the CSM testbed software system
18 p2640 N90-25036
A review of instability and noise propagation in supersonic flows
[NASA-CR-186800] 19 p2655 N90-25112
Development of a computer model to predict platform station keeping requirements in the Gulf of Mexico using remote sensing data
[NASA-CR-186678] 19 p2663 N90-25155

Seasonal LAI in slash pine estimated with LANDSAT TM
[NASA-TM-102278] 19 p2706 N90-25397
A kinematic/dynamic model for prediction of neck injury during impact acceleration 19 p2719 N90-25469
The prediction of professional success of licenced pilots: The validity of flight experience in comparison with standardized psychological aptitude tests
[DLR-FB-89-53] 19 p2723 N90-25488
An investigation into the numerical prediction of boundary layer transition using the K.Y. Chien turbulence model
[NASA-CR-185252] 20 p2860 N90-26269
Elevated temperature crack growth
[NASA-CR-182247] 20 p2875 N90-26355
An expert system based software sizing tool, phase 2
[NASA-CR-186706] 20 p2905 N90-26525
Laboratory measurements and methane photochemistry modeling 20 p2947 N90-26770
High productivity testing 21 p2962 N90-26843
EINMUF: An HF MUF, FOT, LUF prediction program
[AD-A221577] 21 p3055 N90-27371
Development of a linearized unsteady aerodynamic analysis for cascade gust response predictions
[NASA-CR-4308] 22 p3108 N90-27655
Study of the ocean tides by the assimilation of marigraphic and altimetric satellite data in a hydrodynamic model
[ETN-90-97460] 22 p3231 N90-28320
An investigation of crack-tip stress field criteria for predicting cleavage-crack initiation
[DE90-015597] 24 p3480 N90-29672
Effects of blocks of overloads and underloads on fatigue crack growth in 2024-T351 sheet specimens: Fractographic analysis and crack closure predictions
[LR-629] 24 p3482 N90-29681

PREDICTOR-CORRECTOR METHODS
Smoothed predictor-corrector methods for solving partial differential equations
[CWI-NM-R8808] 04 p0540 N90-13131
Block predictor (low order) corrector methods to solve ordinary differential equations on parallel computers
[IMAG-RR-757-M] 06 p0834 N90-14845
Computation of hypersonic unsteady viscous flow over a cylinder 12 p1597 N90-19194
Fundamental limitations of qualitative simulation
[MEMO-INF-89-56] 18 p2600 N90-24802
Numerical analysis of three-dimensional particle-laden flow equations
[IAR-90-2] 20 p2860 N90-26268

PREDICTORS
U PREDICTIONS

PREFLIGHT ANALYSIS
Mathematical model and predictions for static and dynamic behavior of solar array structure
02 p0184 N90-11049
The EFA integrated monitoring and recording system: Requirements and concept for implementation
22 p3103 N90-27620
Start-up built-in test for the DISCUS fault tolerant, fly-by-wire computer system 22 p3104 N90-27625
Shuttle remote manipulator system mission preparation and operations 24 p3521 N90-29909

PREFORMS
Computer synthesis of ceramic preforms for molten-metal infiltration
[DE90-000826] 06 p0751 N90-14370
Lightweight piston architecture
[NASA-CASE-LAR-13926-1] 15 p2105 N90-22042
Braided composite fasteners and method for producing same
[NASA-CASE-LAR-14062-1] 21 p3010 N90-27114

PREHEATERS
U HEATING EQUIPMENT

PREHEATING
U HEATING

PREIMPREGNATION
Preliminary experiments on filament winding nylon impregnated glass fibers (FIT)
[LR-545] 05 p0628 N90-13669

PRELAUNCH SUMMARIES
Atmospheric environment for space shuttle (STS-29) launch
[NASA-TM-100376] 02 p0175 N90-10980
Atmospheric environment for space shuttle (STS-30) launch
[NASA-TM-100381] 02 p0175 N90-10981
Debris/ice/TPS assessment and photographic analysis for Shuttle Mission STS-34
[NASA-TM-102153] 05 p0594 N90-13447
Assembly, integration, and verification
05 p0605 N90-13519
Cosmic Background Explorer (COBE) press kit
[P89-10172] 17 p2364 N90-23459

PRELAUNCH TESTS
A high precision gravity compensation system for the deployment test of the ERS-1 SAR antenna
02 p0183 N90-11038
The Hipparcos Mission. Prelaunch status. Volume 1: The Hipparcos satellite
[ESA-SP-1111-VOL-1] 05 p0603 N90-13499
Electrical testing 05 p0605 N90-13520
On-ground photometric calibration
05 p0605 N90-13523
The Hipparcos Mission. Prelaunch status. Volume 3: The data reductions
[ESA-SP-1111-VOL-3] 05 p0609 N90-13548
QM-8 field joint protection system, volume 7
[NASA-CR-183748] 05 p0614 N90-13586
The Ariane-5 Programme 09 p1176 N90-16808
The ground testing of nickel hydrogen batteries prior to launch 10 p1333 N90-17705
First Vulcain engine test results
[MBB-UK-0054/88-PUB] 19 p2652 N90-25093

PRELOADING
U PRESTRESSING

PREMIXED FLAMES
Premixed turbulent flame propagation
[AD-A211489] 03 p0324 N90-11841
Asymptotic analyses of the structures and characteristics of flames 04 p0468 N90-12683
Investigation of fuel additive effects on sooting flames
[AD-A212925] 04 p0473 N90-12709
An investigation of diamond film deposition in a premixed oxyacetylene flame
[AD-A212595] 04 p0561 N90-13268
Kinetics and mechanism of soot formation in hydrocarbon combustion
[NASA-CR-186162] 06 p0740 N90-14305
A tomographic study of premixed turbulent stagnation point flames
[DE90-002462] 07 p0892 N90-15156
Combustion Experiments During KC-135 Parabolic Flights
[ESA-SP-1113] 09 p1201 N90-16958
Premixed flames in microgravity
09 p1201 N90-16959
The extinction and structure of counterflow premixed flames
[AD-A218106] 13 p1773 N90-20178
Studies on reactive flows 15 p2066 N90-21831
Numerical investigation of turbulent flame sheets
[AD-A218553] 16 p2215 N90-22635
Two-dimensional velocimetry instrumentation
[AD-A218450] 16 p2239 N90-22774
Premixed turbulent flame propagation
[AD-A219834] 17 p2373 N90-23515
The computer modeling of the combustion and extinction of methane-air premixed flames by thermally stable gases
[PB90-189432] 21 p2976 N90-26910
The spatial scalar structure of premixed turbulent stagnation point flames
[DE90-014189] 23 p3303 N90-28686

PREMIXING
Low NO(x) potential of gas turbine engines
[NASA-TM-102452] 10 p1321 N90-17636
Turbulent combustion modeling for turbo-jet combustion chambers 20 p2811 N90-25993

PREPARATION
NT PRECONDITIONING
NT PRESTRESSING
NT PRETREATMENT
Electrochemical preparation of silver oxide electrodes having high thermal stability
[AD-D014224] 06 p0767 N90-14460
Ultrasonic assisted paint removal method
[AD-D014264] 08 p1119 N90-16479
Authors guide to the publishing procedures at Defence Research Establishment Suffield
[AD-A223101] 21 p3087 N90-27554

PREPOLYMERS
NT DIMERS
NT TRIMERS
UV-curable polyurethane-methacrylate co-networks and interpenetrating networks
[AD-A210445] 01 p0050 N90-10285
Design, characterization, and optical properties of phosphazene-based polymers
[DE90-004111] 08 p1050 N90-16068
Morphological control of inter-penetrating polymer networks 18 p2642 N90-25046
Autoclavable addition polyimides for 371 C composite applications
[NASA-TM-103233] 22 p3153 N90-27874

PREPREGS
A capacitive technique for real-time monitoring polymer coating thickness on carbon filaments during prepregging process
[NASA-TM-101682] 06 p0780 N90-14533
Evaluation and choice algorithms of cost optimal prepreg-application processes: Production of strongly charged plane parts made of fiber reinforced plastics
[ETN-90-95895] 12 p1620 N90-19313
Morphological control of inter-penetrating polymer networks 18 p2642 N90-25046
A characterization of V-391/H46-8B, A toughened BMI prepreg system produced by US Polymeric
[AD-A221772] 21 p2989 N90-26985
Elementary characterization of the pre-impregnated carbon/epoxy NCHR 914/155/34 percent-T300F from Brochier after the technical note CEAT number 1/M/87
[CEAT-PV-M7/6211] 22 p3154 N90-27884
Radiation-curable prepreg composites
[DE90-629740] 23 p3301 N90-28674

PREPROCESSING
Automatic classification of spectra from the Infrared Astronomical Satellite (IRAS)
[NASA-RP-1217] 01 p0140 N90-10807
Image preprocessing by modified median filter
[AD-D014199] 04 p0492 N90-12828
Interface between MEDUSA and GIFTS for shell structures
[LR-553] 05 p0684 N90-13985
PCP (Parallel C Preprocessor): A parallel extension of C that is 99 percent fat free
[DE90-002813] 06 p0831 N90-14834
Geometric correction models for HRV-SPOT images
[INPE-5001-TDL/395] 11 p1521 N90-18757
The preprocessed doacross loop
[NASA-CR-182056] 16 p2276 N90-22972
Translating polygons with applications to hidden surface removal
[RUU-CS-89-31] 18 p2602 N90-24816
Maintaining multiple representations of dynamic data structures
[RUU-CS-88-27] 18 p2634 N90-25005
OMS FDIR: Initial prototyping
19 p2738 N90-25562
Run-time parallelization and scheduling of loops
[NASA-CR-182039] 20 p2902 N90-26509
A user's manual for MCPRAM (Monte Carlo PReprocessor for AMEER) and for the fuze options in AMEER (Aero Mechanical Equation Evaluation Routines)
[DE90-013598] 21 p3051 N90-27345
Efficient algorithms for a class of partitioning problems
[NASA-CR-182073] 22 p3237 N90-28357

PRESELECTORS
U PREAMPLIFIERS

PRESENTATION
Mode of presentation of cues in policy capturing: A comparison between verbal and pictorial presentation of targets in judgement of probability to fire
[FOA-C-50074-5.2] 17 p2436 N90-23883

PRESERVING
Scientific guidelines for preservation of samples collected from Mars
[NASA-TM-4184] 19 p2796 N90-25918
National Archives preservation research priorities: Past and present
[PB90-206210] 23 p3405 N90-29242

PRESIDENTIAL REPORTS
Federal support to universities, colleges, and selected nonprofit institutions: Fiscal year 1988 (detailed statistical tables)
[PB90-226887] 23 p3404 N90-29236

PRESINTERING
U SINTERING

PRESSING (FORMING)
The relationship between the mechanical properties of materials after press forming and their in-service properties
[CETIM-101530] 04 p0475 N90-12723
Cold press lubrication: Fine tuning of the CETIM Forgelub test
[CETIM-105160] 04 p0509 N90-12938
Investigation of metal processing technology
[AD-A218835] 17 p2376 N90-23531

PRESSURE
NT ATMOSPHERIC PRESSURE
NT BLOOD PRESSURE
NT CRITICAL PRESSURE
NT DENSIFICATION
NT DIFFERENTIAL PRESSURE
NT DYNAMIC PRESSURE
NT FLUID PRESSURE
NT GAS PRESSURE
NT HIGH ALTITUDE PRESSURE
NT HIGH PRESSURE
NT HIGH VACUUM
NT HYDROSTATIC PRESSURE
NT HYPERTENSION
NT HYPOTENSION
NT ILLUMINANCE
NT INTERNAL PRESSURE
NT LOW PRESSURE

NT LOWER BODY NEGATIVE PRESSURE
NT LUMINANCE
NT LUMINOUS INTENSITY
NT OVERPRESSURE
NT PARTIAL PRESSURE
NT SOUND PRESSURE
NT STAGNATION PRESSURE
NT STATIC PRESSURE
NT SUPERCRITICAL PRESSURES
NT THRUST CHAMBER PRESSURE
NT TRANSIENT PRESSURES
NT TRANSITION PRESSURE
NT ULTRAHIGH VACUUM
NT VACUUM
NT VAPOR PRESSURE
NT WALL PRESSURE
NT WATER PRESSURE
NT WIND PRESSURE

Pressure correction splitting methods for the computation of oscillatory free convection in low Pr fluids
[CWI-NM-R8816] 02 p0222 N90-11271

Pressure sensitive release device
[AD-D014220] 06 p0792 N90-14610

Measurements of surface pressures on an operating vertical-axis wind turbine
[DE90-005722] 11 p1529 N90-18805

Difference in electron thermal diffusivity and profile between interior and exterior of TFTR L-mode plasmas
[DE90-007479] 13 p1890 N90-20846

Fabrication of intermetallic compounds by solid state reaction of roll-bonded materials
[AD-A221960] 21 p2982 N90-26943

Dynamic consolidation of super hard materials
[AD-A224460] 24 p3454 N90-29505

PRESSURE BREATHING

The characteristics of physiological responses and tolerance evaluation of pressure breathing
[AD-A214991] 09 p1252 N90-17262

The +Gz protection in the future: Review of scientific literature
[AD-A217887] 13 p1851 N90-20623

PRESSURE BROADENING

Determination of molecular spectroscopic parameters and energy-transfer rates by double-resonance spectroscopy 20 p2944 N90-26755

PRESSURE CABINS

U PRESSURIZED CABINS

PRESSURE CHAMBERS

NT HYPERBARIC CHAMBERS
NT VACUUM CHAMBERS

Aeritalia Space Systems Group, Turin, Italy
[EOARD-LR-89-041] 02 p0159 N90-10908

PRESSURE DEPENDENCE

Structure and properties of simple molecular systems at very high density
[DE89-016974] 02 p0273 N90-11557

Absolute pressure dependence of the second ionization level of EL2 in GaAs
[DE90-007761] 13 p1894 N90-20872

Pressure dependence of thermoelectric power of high T(sub c) 123 compound
[PD-MT-9001] 20 p2829 N90-26092

Toxicological aspects of fire onboard aircrafts: Role of the pressurization and ventilation in the cockpit
[ETN-90-97452] 22 p3233 N90-28335

PRESSURE DISTRIBUTION

Computation of generalized modal loads in an acoustic field define by a distribution of correlated pressures
[NASA-CR-186041] 03 p0358 N90-12047

Status report on a natural laminar-flow nacelle flight experiment 04 p0445 N90-12550

Nacelle design 04 p0446 N90-12551

Nacelle aerodynamic performance 04 p0446 N90-12552

Effects of acoustic sources 04 p0446 N90-12553

Supersonic boundary-layer transition on the LaRC F-106 and the DFRF F-15 aircraft. Part 2: Aerodynamic predictions 04 p0447 N90-12559

Prediction of unsteady blade surface pressures on an advanced propeller at an angle of attack
[NASA-TM-102374] 04 p0447 N90-12560

Development of a VSAERO (Vortex Separation Aerodynamics) model of the F/A-18
[AD-A212442] 04 p0448 N90-12566

A computationally efficient modelling of laminar separation bubbles
[NASA-CR-185854] 04 p0490 N90-12872

Transonic Euler solutions on mutually interfering finned bodies
[AD-A213395] 05 p0572 N90-13331

Pressure correction calculation procedures for 3D viscous flow 05 p0641 N90-13738

Ring source/force excitation of axisymmetric shell structure
[ARE-TM(UHA)-88519] 05 p0698 N90-14085

Static pressure distribution in an angular channel with helicoidal wire
[DE89-636474] 07 p0928 N90-15374

Modifications of the Penn State Boundary Layer Research Facility for boundary layer/structure interaction experimental research
[AD-A213874] 07 p0931 N90-15391

Nonlinear viscous waves produced by an impulsively moving plate
[AD-A214014] 07 p0932 N90-15392

Optical acoustic sensor using optical fiber
[DE89-901267] 07 p0992 N90-15730

Pressure measurement technique in the wind tunnel division of DFVLR
[ESA-TT-1145] 08 p1032 N90-15963

An electronic pressure profile display system for aeronautic test facilities
[NASA-TM-102478] 08 p1032 N90-15964

Laboratory studies of isolated eddies in a rotating fluid
[AD-A213903] 08 p1063 N90-16146

Determination of the N-factor in the Brunswick (Federal Rep. of Germany) transonic wind tunnel using measurements of pressure distributions and transition points, and the Sally method 08 p1067 N90-16177

Two-Dimensional Measuring Techniques
[DGLR-PAPERS-88-04] 08 p1078 N90-16236

The use of piezofoil sensors for the determination of the unsteady pressure distribution at the surface of a gas turbine blade 08 p1080 N90-16250

Use of the film-of-oil technique for profile measurements in the Transonic Wind tunnel Brunswick (TWB)
08 p1080 N90-16252

Surface pressure distributions on a delta wing undergoing large amplitude pitching oscillations
[NASA-CR-186326] 10 p1306 N90-17558

Effect of riblets on flow separation from a cylinder and an airfoil in subsonic flow
[AD-A216197] 10 p1309 N90-17574

Experimental investigation to suppress flow-induced pressure oscillations in open cavities
[AD-A216285] 10 p1310 N90-17578

Some Navier-Stokes calculations for the CAST-10 airfoil 10 p1324 N90-17651

Turbulent boundary layer pressure field-induced vibrations in a thin flexible plate under water
10 p1383 N90-18002

Modeling the pressure-strain correlation of turbulence: An invariant dynamical systems approach
[NASA-CR-181979] 10 p1383 N90-18003

Incompressible flow friction factors in a simulated heat pipe
[AD-A216288] 10 p1386 N90-18018

Supersonic wind tunnel investigation of a tubular projectile
[ISL-CO-306/89] 11 p1452 N90-18366

Calculation of excrescence drag magnification due to pressure gradient at high subsonic speeds
[ESDU-87004] 12 p1598 N90-19195

A panel process for the calculation of the flow around a wing with front angle damping
[ETN-90-95367] 12 p1600 N90-19207

Measurement and prediction of propeller blade surface pressure distributions 14 p1912 N90-20961

An intensive procedure for the design of pressure-specified three-dimensional configurations at subsonic and supersonic speeds by means of a higher-order panel method 14 p1917 N90-20982

A system for transonic wing design with geometric constraints based on an inverse method
14 p1917 N90-20983

Numerical optimization of target pressure distributions for subsonic and transonic airfoil design
14 p1919 N90-20993

Numerical optimization of wings in transonic flow
14 p1920 N90-20997

Secondary Flows in Turbomachines
[AGARD-CP-469] 14 p1922 N90-21009

Double valve mechanism for an acoustic modulator
[AD-D014401] 14 p1987 N90-21386

An experimental investigation of the physical mechanisms controlling the asymmetric flow past slender bodies at large angles of attack
15 p2053 N90-21767

Reynolds stress closure in jet flows using instability wave modeling 16 p2196 N90-22534

Large-scale advanced propeller blade pressure distributions: Prediction and data
[NASA-TM-102316] 16 p2201 N90-22564

Pressure and shear stress measurement uncertainty for DARPA SUBOFF experiment
[AD-A219109] 16 p2243 N90-22798

Pressure measurements on a 5.35 m HAWT in CARDC 12 x 16 m wind tunnel compared to theoretical pressure distributions
[FFA-TN-1989-46] 17 p2347 N90-23365

Theoretical analysis and pressure distribution of thin-walled metal inverbuckle energy absorbing tubes
17 p2414 N90-23758

Unsteady potential flow past a propeller blade section
[NASA-CR-4307] 18 p2493 N90-24246

New transonic test sections for the NAE 5 ft x 5 ft trisonic wind tunnel
[AD-A220933] 18 p2499 N90-24278

Fluid dynamic and acoustic experiments on turbomachine rotors subject to variable flow conditions
[AD-A220298] 18 p2552 N90-24565

Coupled BE/FE/BE approach for scattering from fluid-filled structures 18 p2570 N90-24649

Aerodynamic loads and blade vortex interaction noise prediction
[ISL-PU-310/89] 20 p2802 N90-25942

Application of laminar flow control to supersonic transport configurations
[NASA-CR-181917] 20 p2803 N90-25944

Installation and pretest analysis of DARPA suboff model in the DTRC anechoic wind tunnel
[AD-A221497] 21 p2955 N90-26801

The SKY SHARK: An RPV designed to investigate the pressure distribution on a lifting surface
[NASA-CR-186222] 21 p2959 N90-26824

Model tilt-rotor hover performance and surface pressure measurement
[AD-A222535] 21 p2959 N90-26827

Toward the optimization of a non-diffusing, two-dimensional S-shaped duct
[IAR-89-3] 21 p3003 N90-27068

Wind loads and local pressure distributions on parabolic dish solar collectors
[DE90-000328] 21 p3019 N90-27166

The dynamics and control of fluctuating pressure loads in the reattachment region of a supersonic free shear layer
[NASA-CR-184943] 22 p3108 N90-27652

Study of the ground effects in the CEAT aerohydrodynamic tunnel: Using the results
23 p3274 N90-28530

Measurement of the steady surface pressure distribution on a single rotation large scale advanced prop-fan blade at Mach numbers from 0.03 to 0.78
[NASA-CR-182124] 23 p3278 N90-28552

Military aircrew seating: A human factors engineering approach
[AD-A218049] 23 p3362 N90-28999

Numerical pulse propagation studies using two classical ocean waveguide models
[AD-A224118] 24 p3542 N90-30033

PRESSURE DRAG

NT INTERFERENCE DRAG
NT SUPERSONIC DRAG
NT WAVE DRAG

Sting-support interference on afterbody drag at transonic speeds
[NAL-TM-EA-8902] 23 p3267 N90-28492

PRESSURE DROP

Pressure losses in flow through a sudden contraction of duct area
[ESDU-89040] 09 p1220 N90-17077

Boiling inside tubes: Pressure drop in straitht tubes with upward or horizontal flow
[ESDU-89039] 09 p1220 N90-17078

PRESSURE EFFECTS

A study of high-lift airfoils at high Reynolds numbers in the Langley low-turbulence pressure tunnel
[NASA-TM-89125] 01 p0001 N90-10002

Pressure induced resonance Raman effects in shocked carbon disulfide
[AD-A210665] 02 p0194 N90-11107

Balance equations for ionospheric plasmas with different partial temperatures 02 p0240 N90-11364

Phase behavior of pure and mixed systems at high pressure
[DE89-017734] 03 p0322 N90-11832

Ignition characteristics of the nickel-based alloy UNS N07718 in pressurized oxygen
[NASA-CR-185932] 03 p0326 N90-11850

VISAR wave profile measurements in supra-compressed HE
[DE89-017736] 03 p0346 N90-11976

Characteristics of flyer impact for one-dimensional shock-wave st..ly applications
[DE89-017887] 03 p0346 N90-11977

Shock pressure determination in detonator wires
[DE89-017756] 03 p0350 N90-12002

High pressure studies of planetary matter
[DE89-017738] 03 p0428 N90-12455

Stage effects on stalling and recovery of a high-speed 10-stage axial-flow compressor
04 p0454 N90-12600

Projectile impact Hugoniot parameters for selected materials
[DE90-000891] 06 p0793 N90-14618

Shock-wave characterization of energetic booster-rocket propellant WAK-2 and its simulant UGS
[DE90-002633] 07 p0914 N90-15285
Burning rates of two cast nitramine explosives using a hybrid closed bomb-strand burner
[DE90-002785] 07 p0914 N90-15286
Oxygen electrode in molten carbonate fuel cells
[DE90-002871] 07 p0952 N90-15510
Micron-thin Nb films recovered from Mbar shock pressures
[DE90-001509] 07 p0998 N90-15772
The use of hypervelocity launchers to explore previously inaccessible states of matter
[DE90-004088] 08 p1034 N90-15973
Space shuttle Production Verification Motor 1 (PV-1) static fire
[NASA-CR-183784] 08 p1037 N90-15991
Thermodynamic analysis of chemical stability of ceramic materials in hydrogen-containing atmospheres at high temperatures
[NASA-CR-4271] 08 p1050 N90-16072
Summary of a decade of railgun development for high-pressure research
[DE90-005247] 09 p1172 N90-16780
Raman spectroscopic analysis of impregnated cathodes
[AD-A214559] 09 p1190 N90-16895
Ballast system for maintaining constant pressure in a glove box
[NASA-CASE-NPO-17786-1-CU] 09 p1224 N90-17104
Transient pressure test article test program 11 p1470 N90-18463
Study of the dynamical behavior of copper in a shock wave
[ISL-R-123/88] 11 p1507 N90-18679
Possible targeting of particle emission by mechanical stress and penetration of sublimating ice-dust-surfaces 12 p1742 N90-20016
An investigation of the mechanisms of solid state powder reaction in the combustion synthesis and sintering of high temperature materials
[DE90-007880] 13 p1777 N90-20198
The effect of adverse pressure gradient on turbulent burst structure in low-Reynolds number equilibrium boundary layers
[AD-A217308] 13 p1799 N90-20327
Laser-induced shock waves effects in materials
[DE90-007626] 13 p1807 N90-20379
Shock initiation sensitivity of damaged TP-H1207C composite propellant
[DE90-008509] 14 p1957 N90-21205
An internal/external pressure, tension/compression multiaxial fatigue system
[DE90-009510] 14 p1994 N90-21430
The pressure dilation of a deep, jointed region of the earth
[DE90-007537] 15 p2128 N90-22170
Design and construction of a packed column simulator operating under atmospheric and reduced pressure
[ISAL-89-60] 16 p2236 N90-22757
The pressure loaded volumetric ceramic receiver
[DLR-MITT-89-17] 16 p2252 N90-22842
Superconducting and normal compounds: Some high field/high pressure effects 16 p2320 N90-23229
Structure of monopropellant spray flames at elevated pressures
[AD-A218676] 17 p2383 N90-23570
AECM3: Acoustic Emission Conditions for failure prediction of winding carbon structures
[REPT-892-430-115] 18 p2517 N90-24374
Pressure in the study of organic superconductors
[DE90-011049] 18 p2625 N90-24959
Advanced launch vehicle configurations and performance trades 22 p3126 N90-27744
Effect of shock pressure on the structure and superconducting properties of Y-Ba-Cu-O in explosively fabricated bulk metal-matrix composites 22 p3138 N90-27804
Liquid Rocket Booster (LRB) for the Space Transportation System (STS) systems study. Appendix A: Stress analysis report for the pump-fed and pressure-fed liquid rocket booster
[NASA-CR-183787-APP-A] 23 p3288 N90-28601
Cavity aeroacoustics
[AD-A223853] 24 p3418 N90-29307

PRESSURE FIELDS
U PRESSURE DISTRIBUTION

PRESSURE GAGES
NT BAROMETERS
NT IONIZATION GAGES
NT PIEZOELECTRIC GAGES
Portable digital pressure indicator for calibrating magnetic tape recorders
[NASA-TM-101650] 07 p0933 N90-15401

PRESSURE GRADIENTS
Stability of discontinuous shearing motions of a non-Newtonian fluid
[AD-A210643] 01 p0071 N90-10406
Stability of discontinuous steady states in shearing motion of a non-Newtonian fluid
[AD-A210644] 01 p0071 N90-10407
Three-dimensional shear flows: Analysis of the track and angle of incidence
[CERT-RTS-OA-31/5025-AYD] 04 p0501 N90-12888
An experimental study of the time-dependent behavior of the appendage-body junction vortex
[AD-A213465] 07 p0930 N90-15384
Destabilization of tokamak pressure-gradient driven instabilities by energetic alpha populations
[DE90-003716] 07 p0996 N90-15756
Depressurization test on hot gas duct
[DE90-710058] 09 p1236 N90-17176
Numerical simulation of the incompressible inhomogeneous turbulence in a plane channel flow
[ONERA-NT-1988-5] 11 p1508 N90-18686
Calculation of excrescence drag magnification due to pressure gradient at high subsonic speeds
[ESDU-87004] 12 p1598 N90-19195
The effect of adverse pressure gradient on turbulent burst structure in low-Reynolds number equilibrium boundary layers
[AD-A217308] 13 p1799 N90-20327
Experimental feasibility of investigating acoustic waves in Couette flow with entropy and pressure gradients
[NASA-TM-102621] 13 p1882 N90-20795
Experimental study of a three-dimensional shear-driven turbulent boundary layer with streamwise adverse pressure gradient 17 p2399 N90-23669
Flow structures around non-hyperbolic singularities on the wall with one vanishing eigenvalue: A discussion of the flow structures and the unfoldings
[LR-586] 19 p2692 N90-25315
Experimental investigation of Tollmien-Schlichting instability and transition in similar boundary layer flow in an adverse pressure gradient (Hartree beta = -0.14)
[LR-604] 19 p2692 N90-25318
Vortex-induced boundary layer separation
[AD-A221564] 21 p3005 N90-27078
Structure in the near field of the transverse jet
[AD-A224502] 24 p3467 N90-29591

PRESSURE MEASUREMENT
Introduction to total- and partial-pressure measurements in vacuum systems
[NASA-RP-1219] 01 p0072 N90-10412
Three-in-one gage
[NASA-CR-183714] 01 p0072 N90-10413
Fluctuating pressures measured beneath a high-temperature, turbulent boundary layer on a flat plate at Mach number of 5
[NASA-TP-2947] 01 p0118 N90-10680
Measurements of pressures on the tail and aft fuselage of an airplane model during rotary motions at spin attitudes
[NASA-TP-2939] 02 p0145 N90-10829
The near-wake flow structure of wake-cylinder interaction and surface loading of cylinder 02 p0218 N90-11248
Jet-flow from shock tubes
[AD-A210651] 02 p0220 N90-11260
A remote sensor to monitor combustion products using a tunable acousto-optic filter 02 p0223 N90-11275
Measurement of pressure fluctuations in a resonant chamber with laser-induced iodine fluorescence
[ESA-TT-1123] 03 p0406 N90-12326
Preliminary experience with high response pressure measurements in a multistage, high speed compressor
[RAE-TM-P-1141] 04 p0457 N90-12619
Pressure measurement techniques in use at the Royal Aerospace Establishment 05 p0574 N90-13347
A wall interference assessment/correction interface measurement system for the NASA/ARC 12-ft PWT
[NASA-CR-185474] 05 p0584 N90-13401
Flight evaluation of a pneumatic system for unsteady pressure measurements using conventional sensors
[NASA-TM-4131] 06 p0724 N90-14225
Laser velocimeter and total pressure measurements in circular-to-rectangular transition ducts
[NASA-CR-182286] 06 p0772 N90-14494
Portable digital pressure indicator for calibrating magnetic tape recorders
[NASA-TM-101650] 07 p0933 N90-15401
Antarctic surface temperature and pressure data
[DE90-000971] 07 p0963 N90-15565
Pressure measurement technique in the wind tunnel division of DFVLR
[ESA-TT-1145] 08 p1032 N90-15963
Stand Alone Pressure Measurement Device (SAPMD) for the space shuttle Orbiter, part 1
[NASA-CR-172119-PT-1] 08 p1072 N90-16202
Stand Alone Pressure Measurement Device (SAPMD) for the space shuttle Orbiter, part 2
[NASA-CR-172119-PT-2] 08 p1072 N90-16203
Study of pressure sensors in hydrodynamic turbulent boundary layer
[ONERA-RF-17/7218-PY] 09 p1218 N90-17067
Fluid transmission line dynamics for signals of finite amplitude
[AD-A215758] 10 p1385 N90-18014
An atlas of ECMWF analyses (1980-1987). Part 1: First moment quantities
[NASA-TM-100747-PT-1] 10 p1408 N90-18120
Aerodynamic testing of a rotating wind turbine blade
[DE90-000312] 11 p1451 N90-18362
Methods for making unsteady aerodynamic pressure measurements in a rotating turbine stage 11 p1463 N90-18426
Piezoelectric polymer PVDF shock gauge: State of the research art
[ISL-CO-207/89] 11 p1512 N90-18705
Measurements of surface pressures on an operating vertical-axis wind turbine
[DE90-005722] 11 p1529 N90-18805
Study of the turbulent boundary layer on an afterbody
[TM-EA-8901] 12 p1601 N90-19212
Compensating for pneumatic distortion in pressure sensing devices
[NASA-TM-101716] 12 p1603 N90-19224
Exhaust environment measurements of a turbofan engine equipped with an afterburner and 2D nozzle
[NASA-CR-4289] 15 p2052 N90-21760
The calibration and measuring procedure of a five-hole hemispherical head probe in compressible flow
[LR-585] 15 p2099 N90-22013
Pressure and shear stress measurement uncertainty for DARPA SUBOFF experiment
[AD-A219109] 16 p2243 N90-22798
Pressure measurements on a 5.35 m HAWT in CARDC 12 x 16 m wind tunnel compared to theoretical pressure distributions
[FFA-TN-1989-46] 17 p2347 N90-23365
Heat transfer and pressure measurements for the SSME fuel-side turbopump
[NASA-CR-184928] 17 p2355 N90-23405
Aerodynamic pressure measurements on a rotating wind turbine blade
[DE90-000327] 18 p2494 N90-24256
Investigation of the vortex flow over a sharp-edged delta wing in the transonic speed regime
[LR-594] 19 p2656 N90-25115
Evaluation of water cooled supersonic temperature and pressure probes for application to 2000 F flows
[NASA-TM-102612] 19 p2753 N90-25645
Installation and pretest analysis of DARPA suboff model in the DTRC anechoic wind tunnel
[AD-A221497] 21 p2955 N90-26801
Experimental characterization of the effects of pneumatic tubing on unsteady pressure measurements
[NASA-TM-4171] 22 p3116 N90-27703
In-flight flow visualization with pressure measurements at low speeds on the NASA F-18 high alpha research vehicle
[NASA-TM-101726] 23 p3270 N90-28505
Determination of the ground effect on the characteristics of the A320 aircraft 23 p3275 N90-28534
Gas-jet and tangent-slot film cooling tests of a 12.5 deg cone at Mach number of 6.7
[NASA-TP-2786] 23 p3326 N90-28806
Recommended practices for measurement of gas path pressures and temperatures for performance assessment of aircraft turbine engines and components
[AGARD-AR-245] 24 p3433 N90-29393
Proceedings of a discussion meeting on Thermodynamics of Alloys
[AD-A224336] 24 p3449 N90-29476
Design and evaluation of candidate pressure distribution and air data system tile penetration for the aeroassist flight experiment
[NASA-CR-4312] 24 p3471 N90-29615
Apparatus to determine the complex mass of a viscous fluid contained in a rigid porous solid from acoustic pressure measurements
[AD-A223709] 24 p3472 N90-29619
Non-contact contour gage
[DE90-014672] 24 p3475 N90-29642

PRESSURE OSCILLATIONS
Combustion instabilities in liquid-fueled propulsion systems: An overview 01 p0035 N90-10192
Characteristics of combustion driven pressure oscillations in advanced turbo-fan engines with afterburner 01 p0035 N90-10194
Low frequency and high frequency combustion oscillation phenomena inside a rocket combustion chamber fed by liquid or gaseous propellants 01 p0036 N90-10197

Effects of low-frequency instabilities on the operation of Ramjet air inlets 01 p0036 N90-10198
Recent developments in Ramjet pressure oscillation technology 01 p0036 N90-10199
Attenuation of reheat buzz by active control 01 p0036 N90-10201
Numerical simulation of pressure oscillations in a ramjet combustor 01 p0037 N90-10202
Very-low-frequency oscillations in liquid-fueled ramjets 01 p0037 N90-10204
Oscillations in non-axisymmetric dump combustors 01 p0037 N90-10205
Combustion-driven oscillation in large combustion systems for power generation 01 p0038 N90-10207
Development of a thermoacoustic test facility 02 p0183 N90-11041
Observational studies of low-frequency oscillations in the Southern Hemisphere 02 p0250 N90-11420
Measurement of pressure fluctuations in a resonant chamber with laser-induced iodine fluorescence [ESA-TT-1123] 03 p0406 N90-12326
Fundamental studies of turbulent wall pressure fluctuations with applications to advanced acoustic sensor systems [AD-A213041] 04 p0552 N90-13212
Small amplitude liquid oscillations in a rectangular container under zero-gravity [LRT-WE-9-FB-2(1989)] 08 p1066 N90-16167
Experimental investigation to suppress flow-induced pressure oscillations in open cavities [AD-A216285] 10 p1310 N90-17578
Wick-type liquid-metal combustion [AD-A216019] 11 p1482 N90-18530
Investigation of SSME alternate high pressure fuel turbopump lift-off seal fluid and structural dynamic interaction 12 p1636 N90-19400
An outline for the analysis of wave induced bottom pressure fluctuations [MRL-TN-558] 14 p2008 N90-21510
An intercomparison of intraseasonal variability in general circulation models and observations [NASA-TM-100764] 21 p3030 N90-27228
The dynamics and control of fluctuating pressure loads in the reattachment region of a supersonic free shear layer [NASA-CR-184943] 22 p3108 N90-27652
Low-frequency cloud-radiation interactions 22 p3225 N90-28289
Tests of initialization procedures with the NRL limited area numerical weather prediction model [AD-A223549] 24 p3495 N90-29750

PRESSURE PROBES
U PRESSURE SENSORS

PRESSURE RATIO
Experiments on the unsteady flow in a supersonic compressor stage 11 p1462 N90-18422

PRESSURE RECOVERY
Some observations on transitory stall in conical diffusers [NASA-TM-102387] 04 p0447 N90-12561

PRESSURE REDUCTION
Two-phase flow pressure losses in pipeline fittings [ESDU-89012] 04 p0500 N90-12883
Potential for reduction of decompression sickness by prebreathing with 100 percent oxygen while exercising [AD-A213449] 07 p0966 N90-15581
Using the singularity-separating method to study how to decrease the pressure at the end of a tube [PREPRINT-490] 08 p1065 N90-16158
Depressurization test on hot gas duct [DE90-710058] 09 p1236 N90-17176
System for venting gas from a liquid storage tank [NASA-CASE-MSC-21253-1] 13 p1787 N90-20254
Secondary flow predictions for a transonic nozzle guide vane 14 p1924 N90-21017
Pseudo-steady diffusional growth or collapse of bubbles rising in time dependent pressure fields [AD-A218825] 16 p2237 N90-22764

PRESSURE REGULATORS
Tank pressure control experiment on the space shuttle [NASA-TM-102313] 05 p0615 N90-13590
Bio-reactor chamber [NASA-CASE-MSC-20929-1] 09 p1250 N90-17252
Electronically Variable Pressure Regulator (EVPR) 11 p1474 N90-18484

PRESSURE SENSORS
Analysis and construction of contact and tactile sensors [DE89-013992] 01 p0072 N90-10416
Advanced measurement techniques, part 1 04 p0441 N90-12520
Flight evaluation of a pneumatic system for unsteady pressure measurements using conventional sensors [NASA-TM-4131] 06 p0724 N90-14225
Calibration of seven-hole pressure probes for use in fluid flows with large angularity [NASA-TM-102200] 07 p0933 N90-15399
Pressure measurement technique in the wind tunnel division of DFVLR [ESA-TT-1145] 08 p1032 N90-15963
Stand Alone Pressure Measurement Device (SAPMD) for the space shuttle Orbiter, part 1 [NASA-CR-172119-PT-1] 08 p1072 N90-16202
Stand Alone Pressure Measurement Device (SAPMD) for the space shuttle Orbiter, part 2 [NASA-CR-172119-PT-2] 08 p1072 N90-16203
Colinear fluctuating wall shear stress and fluctuating pressure transducer [AD-D014296] 08 p1076 N90-16226
Formulation and verification of a technique for compensation of pneumatic attenuation errors in airborne pressure sensing devices 09 p1221 N90-17084
A small, inexpensive apparatus for the determination of the density of powdered materials [AD-A215393] 09 p1225 N90-17110
Zero-gravity vortex vent and PVT gaging system 11 p1475 N90-18486
Compensating for pneumatic distortion in pressure sensing devices [NASA-TM-101716] 12 p1603 N90-19224
Circumferential pressure probe [NASA-CASE-LAR-13775-1] 17 p2406 N90-23706
Tests for integrating measurement of gas pressures in flight propellers [ETN-90-96498] 18 p2494 N90-24253
A reliable, maintenance-free oxygen sensor for aircraft using an oxygen-sensitive coating on potentiometric electrodes [AD-A222696] 23 p3277 N90-28545
Improved meteorological measurements from buoys and ships (IMET): Preliminary report on barometric pressure sensors [PB90-242116] 24 p3494 N90-29748

PRESSURE SUITS
NT EXTRAVEHICULAR MOBILITY UNITS
NT SPACE SUITS
Integrated G-suit/immersion suit [AD-A212989] 06 p0821 N90-14774
Manned spacecraft [AD-A214218] 07 p0887 N90-15129
Use of lower body negative pressure as a countermeasure to negative Gz acceleration [AD-A213927] 07 p0967 N90-15583
TALON and CRADLE: Systems for the rescue of tumbling spacecraft and astronauts, a preliminary design 09 p1181 N90-16847
Requirements for protective pressure suits for the Hermes spacecrew 13 p1753 N90-20065
The +Gz protection in the future: Review of scientific literature [AD-A217887] 13 p1851 N90-20623
Aircrew life support systems enhancement [AD-A222626] 20 p2902 N90-26505

PRESSURE TRANSDUCERS
U PRESSURE SENSORS

PRESSURE VESSELS
NT PREBURNERS
A design assessment for metallic pressure vessels circumferentially reinforced with a pre-tensioned high-specific-strength anisotropic composite overwind [AD-A209108] 01 p0079 N90-10453
Autofrettage-stress distribution under load and retained stresses after depressurization [AD-A212090] 03 p0358 N90-12048
Theoretical evaluation of defects in pressure vessels and pipings [CRIF-MT-174] 05 p0651 N90-13798
Fatigue resistance of pressure vessels in high strength steels effect of some improvement techniques [CRIF-MT-176] 05 p0652 N90-13799
Measuring the thickness of austenitic weld deposits on carbon steel walls using a magnetic method [DE89-635446] 06 p0794 N90-14628
BAM: German Federal Institute for Materials Research and Testing, Berlin [DE90-004293] 08 p1090 N90-16307
Stress analysis in pressure vessels by mixed finite element methods taking into account shear deformation [DE90-606755] 09 p1233 N90-17152
Methodology used for gas analysis and control of trace chemical contaminants at a hyperbaric facility. 1: Gas sampling [AD-A216155] 10 p1325 N90-17659
Nickel hydrogen cell design for space applications 10 p1334 N90-17714
High elongation plasmas [DE90-007575] 13 p1891 N90-20848
An internal/external pressure, tension/compression multiaxial fatigue system [DE90-009510] 14 p1994 N90-21430
Effect of LEO cycling on 125 Ah advanced design IPV nickel-hydrogen battery cells [NASA-TM-103128] 15 p2061 N90-21808
Continued research on the strain to failure of thick-walled cylinders subjected to internal pressure [DE90-008952] 15 p2118 N90-22115
Characteristics of the IAEA correlation monitor material for surveillance programmes [VTT-RR-639] 19 p2682 N90-25258
Creep and creep rupture of strongly reinforced metallic composites [NASA-CR-185286] 22 p3192 N90-28110
Fabrication of spherical pressure vessels from composite materials [INPE-4598-RPE/570] 23 p3302 N90-28675
Guidelines for pressure vessel safety assessment [PB90-219619] 23 p3316 N90-28749
An investigation of crack-tip stress field criteria for predicting cleavage-crack initiation [DE90-015597] 24 p3480 N90-29672

PRESSURE WAVES
U ELASTIC WAVES

PRESSURE WELDING
NT DIFFUSION WELDING
NT ULTRASONIC WELDING

PRESSURIZED CABINS
Development of pressure containment and damage tolerance technology for composite fuselage structures in large transport aircraft [NASA-CR-3996] 01 p0034 N90-10186
Independent Orbiter Assessment (IOA): Analysis of the atmospheric revitalization pressure control subsystem [NASA-CR-185593] 02 p0163 N90-10925
Independent Orbiter Assessment (IOA): Assessment of the atmospheric revitalization pressure control subsystem FMEA/CIL [NASA-CR-185594] 02 p0170 N90-10957
Numerical simulation of micrometeroids and debris hypervelocity impacts on Columbus pressurized modules 02 p0188 N90-11075
Long cycle pressurized logistics module: An Italian contribution to the Space Station Freedom logistics scenario [IAF-89-083] 20 p2822 N90-26058

PRESSURIZING
Independent Orbiter Assessment (IOA): Analysis of the reaction control system, volume 2 [NASA-CR-185532-VOL-2] 02 p0167 N90-10939
Independent Orbiter Assessment (IOA): Analysis of the reaction control system, volume 3 [NASA-CR-185532-VOL-3] 02 p0167 N90-10940
Independent Orbiter Assessment (IOA): Assessment of the reaction control system, volume 1 [NASA-CR-185543-VOL-1] 03 p0316 N90-11793
Independent Orbiter Assessment (IOA): Assessment of the reaction control system, volume 2 [NASA-CR-185543-VOL-2] 03 p0316 N90-11794
Independent Orbiter Assessment (IOA): Assessment of the reaction control system, volume 3 [NASA-CR-185543-VOL-3] 03 p0316 N90-11795
Independent Orbiter Assessment (IOA): Assessment of the reaction control system, volume 4 [NASA-CR-185543-VOL-4] 03 p0316 N90-11796
Independent Orbiter Assessment (IOA): Assessment of the reaction control system, volume 5 [NASA-CR-185543-VOL-5] 03 p0316 N90-11797
Apparatus and method for monitoring pressure leaks from a sealed system [AD-D014168] 03 p0349 N90-11995
Autofrettage-stress distribution under load and retained stresses after depressurization [AD-A212090] 03 p0358 N90-12048
Tensile behavior of cylindrical pressure tanks in fiber assembling + metal hybrid structure [ILR-MITT-213] 12 p1675 N90-19618
Thermodynamic and fluid mechanic analysis of rapid pressurization in a dead-end tube 18 p2631 N90-24990
Garment pressurizing apparatus [AD-D014451] 22 p3232 N90-28330

PRESTON TUBES
U PITOT TUBES
U SPEED INDICATORS

PRESTRAINING
U PRESTRESSING

PRESTRESSING
Theoretical models of earthquake phenomena and the physical significance of seismic moment tensor expansions [AD-A213813] 07 p0961 N90-15556
Active control of bearing preload using piezoelectric translators 15 p2115 N90-22098
A cable-rigidized 3D pantograph 18 p2538 N90-24484

PRETREATMENT
NT PRESTRESSING

Stochastic approach to the initiation of pitting corrosion
[AERE-R-13348] 13 p1775 N90-20190
The effect of H2O and pretreatment on the activity of a Pt/SnO2 catalyst 18 p2558 N90-24597
Effect of pretreatment on a platinized tin oxide catalyst used for low-temperature CO-oxidation 18 p2558 N90-24599
Platinized tin oxide catalysts for CO2 lasers: Effects of pretreatment 18 p2559 N90-24600
The effects of pretreatment conditions on a Pt/SnO2 catalyst for the oxidation of CO in CO2 lasers
[NASA-TM-103487] 20 p2867 N90-26309

PRETWISTING
U PRESTRESSING
U TWISTING

PREVENTION
NT ACCIDENT PREVENTION
NT CORROSION PREVENTION
NT FIRE PREVENTION
NT ICE PREVENTION
Novel carbamates, their production and their use as fuels additives
[EP-PATENT-0-298-636-A-1] 05 p0629 N90-13676
Non-ejection neck injuries in high performance aircraft 19 p2717 N90-25461
Neck injury prevention possibilities in a high-G-enviroment experience with high sustained +G(sub z) training of pilots in the GAF IAM human centrifuge 19 p2720 N90-25474
A computer simulation model for studying cervical spine injury prevention 19 p2721 N90-25476
Final design for a comprehensive orbital debris management program
[NASA-CR-186674] 22 p3126 N90-27739

PRIMARY BATTERIES
NT ALKALINE BATTERIES
NT METAL AIR BATTERIES
NT NICKEL ZINC BATTERIES
NT SODIUM SULFUR BATTERIES
NT THERMAL BATTERIES
The use of lithium batteries in biomedical devices
[AD-A212187] 04 p0497 N90-12863
NASA aerospace flight battery systems program
[NASA-TM-103237] 20 p2882 N90-26397

PRIMARY COSMIC RAYS
NT SOLAR COSMIC RAYS

PRIMATES
NT HUMAN BEINGS
NT MONKEYS
Time, space and form in vision
[AD-A213889] 23 p3357 N90-28971

PRIMERS
The effect of primer age on adhesion of polysulphide sealant 08 p1022 N90-15909
Methods for improving the flowability of a percussion primer composition
[MRL-TR-89-32] 14 p1956 N90-21201

PRIMERS (COATINGS)
Coating galvanized steel
[AD-A211775] 03 p0329 N90-11869
Structure and properties of polymer interphases
[AD-A212796] 04 p0481 N90-12763
Combination primer/topcoat coating
[AD-D014445] 14 p1954 N90-21189
UNICOAT: Development of a primer/topcoat and flexible primer for aluminum
[AD-A221803] 21 p2989 N90-26986

PRIMITIVE EQUATIONS
Four vector-matrix primitives
[AD-A211889] 03 p0392 N90-12237
Diagnostic and kinematic fields associated with curved and straight jet streaks using a two-layer primitive equation model 08 p1100 N90-16371
Modeling studies of the LeeUwin current using a high-resolution primitive equation model
[AD-A219595] 17 p2430 N90-23846

PRINCIPAL COMPONENTS ANALYSIS
Model reduction of weakly damped mechanical systems
[MEMO-798] 05 p0686 N90-13993
Observational study of the macroscopic behavior of moist-convective processes 07 p0959 N90-15547
A comparison of variance-controlled and non-controlled principal components
[AD-A220530] 18 p2598 N90-24782
Data analysis techniques 21 p3017 N90-27151

PRINTED CIRCUITS
Cleaning of printed circuit assemblies with surface-mounted components
[DE89-013609] 03 p0341 N90-11945
Vehicle antenna for the mobile satellite experiment
[NASA-CR-186109] 06 p0733 N90-14271
Computer-Aided Design for Built-In-Test (CADBIT). Volume 1: Technical issues
[AD-A215737] 09 p1268 N90-17353
Computer-Aided Design for Built-In-Test (CADBIT). Volume 2: BIT Library
[AD-A215738] 09 p1268 N90-17354
Computer-Aided Design for Built-In-Test (CADBIT). Volume 3: Software specification
[AD-A215739] 09 p1268 N90-17355
Ion chromatography in the manufacture of multilayer circuit boards
[DE90-005560] 11 p1503 N90-18652
Computed tomography of electronics
[AD-A217976] 13 p1797 N90-20314
Report on the fifth workshop on synchrotron x ray lithography
[DE90-007903] 15 p2172 N90-22411
Correlation/validation of finite element code analyses for vibration assessment of avionic equipment
[AD-A220393] 17 p2353 N90-23398
Personal Computer (PC) thermal analyzer
[AD-A221325] 18 p2548 N90-24546
Selective metallization of carbonyl-containing polymer films
[AD-D014526] 19 p2678 N90-25230
Non-contacting printed circuit waveguide elements
[AD-D014489] 22 p3166 N90-27957
Simulation of INPE's printed circuit laboratory production line
[INPE-4556-TDL/331] 23 p3322 N90-28784
CAD models for inductive strips in homogeneous finline: The methodology
[AD-A224446] 24 p3463 N90-29564
Using multiple sensors for printed circuit board insertion 24 p3514 N90-29867

PRINTERS
NT PRINTERS (DATA PROCESSING)
Faster simulation plots 16 p2295 N90-23071
Polar coordinate laser writer for binary optics fabrication
[AD-A222827] 21 p3008 N90-27097

PRINTERS (DATA PROCESSING)
Electronic publishing: Guide to selection
[PB89-214753] 02 p0256 N90-11448
SAS graphics in DCF
[PNR90563] 06 p0756 N90-14399

PRINTING
NT LITHOGRAPHY
NT PHOTOLITHOGRAPHY
Color printing for computer graphics. Or: How to get it off your screen and onto paper, in color
[PB89-208110] 03 p0384 N90-12184
Desk top publishing: What you need to know 15 p2178 N90-22449
Electronic publishing with Standard Generalized Markup Language (SGML) 15 p2179 N90-22450
Post script code for grey-scaled displays
[AD-A223099] 21 p3053 N90-27354
Authors guide to the publishing procedures at Defence Research Establishment Suffield
[AD-A223101] 21 p3087 N90-27554
Further research on heading in text
[AD-A221511] 21 p3087 N90-27557
A computer graphics package
[ARE-TM(UDT)-89111] 23 p3380 N90-29094

PRIORITIES
Toward an understanding of global change: Initial priorities for US contributions to the International Geosphere-Biosphere Program
[NASA-CR-185873] 04 p0516 N90-12980
Concurrence control for transactions with priorities
[NASA-CR-186241] 07 p0986 N90-15699
Concurrency control for transactions with priorities
[NASA-CR-186268] 09 p1263 N90-17323
Priority arbitration with busses
[AD-A216392] 12 p1704 N90-19784
Priority inversion and its prevention
[AD-A218613] 17 p2467 N90-24101
Social survey findings on en route noise annoyance issues 18 p2610 N90-24868
National Archives preservation research priorities: Past and present
[PB90-206210] 23 p3405 N90-29242

PRISMS
AFGL ten micron mosaic array spectrometer: Recent results 14 p1978 N90-21333

PRIVACY
On the privacy problems involved in allowing access to computers via the public telephone system
[RSRE-88006] 07 p0917 N90-15303
Privacy-enhanced electronic mail
[PCS-TR90-150-REV-1] 19 p2683 N90-25261

PRIVATE AIRCRAFT
U GENERAL AVIATION AIRCRAFT

PROBABILITY
U PROBABILITY THEORY

PROBABILITY DENSITY FUNCTIONS
NT NORMAL DENSITY FUNCTIONS
NT RAYLEIGH DISTRIBUTION
NT WEIBULL DENSITY FUNCTIONS
Analytical study of mistuning/friction/aerodynamics interaction in a bladed disk assembly
[AD-A211139] 02 p0156 N90-10893
Boundary kernel estimation of the two sample comparison density function
[AD-A210757] 02 p0268 N90-11532
Estimating functionals related to a density by a class of statistics based on spacings
[REPT-89-11] 03 p0398 N90-12275
Likelihood cross-validation bandwidth selection for nonparametric kernel density estimators
[REPT-89-10] 03 p0398 N90-12279
A kernel approach to estimation of the sphere radius density in Wicksell's corpuscle problem
[CWI-MS-R8809] 04 p0542 N90-13142
Nongaussian linear filtering, identification of linear systems, and the symplectic group
[CWI-PM-R8810] 04 p0547 N90-13184
The shape of the probability density function of short-term concentration fluctuations of plumes in the atmospheric boundary layer
[AD-A212632] 04 p0548 N90-13188
Counterexamples to Robertson's conjecture
[MEMO-COSOR-88-32] 05 p0693 N90-14048
Probability density function of optical scintillations (scintillation distribution)
[PB89-103912] 06 p0843 N90-14906
Multiple flow regimes in the Northern Hemisphere winter 08 p1100 N90-16372
Bayesian characterization and detection of rare binary signature events
[AD-A221116] 18 p2606 N90-24844
PDF modeling of chemical nonequilibrium effects in turbulent nonpremixed jet flames 21 p2975 N90-26908
Triphone clustering in the ARM system
[RSRE-MEMO-4357] 22 p3166 N90-27952
Experiments with grand variance in the ARM continuous speech recognition system
[RSRE-MEMO-4359] 22 p3166 N90-27954
Subjective-probability-based scenarios for uncertain input parameters: Stratospheric ozone depletion
[N-3140-EPA/JMO/RC] 22 p3199 N90-28157
Effects of parameter uncertainties on software development effort estimates
[AD-A223304] 24 p3526 N90-29938
Angle sample variance of azimuthally spread scattering processes, using a two-element array
[AD-A223572] 24 p3542 N90-30034

PROBABILITY DISTRIBUTION FUNCTIONS
Discrete-time conversion for simulating finite-horizon Markov processes
[AD-A210683] 01 p0116 N90-10666
Multi-sample functional statistical data analysis
[AD-A210992] 01 p0117 N90-10673
Stochastic flows in networks
[AD-A211209] 02 p0266 N90-11515
Alias-free Wigner distribution function and complex ambiguity function for discrete-time samples
[AD-A211050] 02 p0269 N90-11533
Fixed point iteration on point-symmetric interference graphs
[MEMO-INF-89-23] 02 p0269 N90-11535
Dynamics of an M-level atom interacting with cavity fields: Properties of photon statistics
[AD-A211321] 04 p0552 N90-13213
Theory of goodness of fit tests and scanning innovation martingales
[CWI-BS-R8904] 05 p0693 N90-14046
On the effects of an uncertainty on evolution law in dynamical systems
[PREPRINT-689] 05 p0693 N90-14047
Uniform versus random sampling in physical calculations: Monte Carlo
[DE90-003247] 07 p0986 N90-15696
Strong large deviation and local limit theorems
[AD-A213610] 07 p0986 N90-15698
Strong moderate deviation theorems
[MEMO-804] 11 p1555 N90-18954
Determinations of photon spectra
[AD-A218003] 13 p1885 N90-20816
Ability distributions pattern probabilities and quasidensities
[AD-A218471] 16 p2308 N90-23153
Universal criteria for blind deconvolution
[AD-A220853] 17 p2465 N90-24087
Probabilistic analysis of the minimum weighted flowtime scheduling problem
[CWI-BS-R8913] 17 p2466 N90-24091
Evaluation of a decomposition approach for real-time scheduling using a Stochastic model
[AD-A222726] 20 p2921 N90-26625

Learning binary relations and total orders
[AD-A221643] 21 p3059 N90-27392
Statistical methodologies for non-Gaussian noisy environments
[AD-A222137] 21 p3066 N90-27433
The structure of random discrete spacetime
[NASA-CR-182841] 22 p3255 N90-28429
Computer-Aided Structural Engineering (CASE) project: Investigation and design of U-frame structures using program CUFRBC. Volume A: Program criteria and documentation
[AD-A224387] 24 p3525 N90-29934

PROBABILITY THEORY

Empirical Bayes selection for the highest probability of success in negative binomial distributions
[AD-A210273] 01 p0115 N90-10660
On lower confidence for PCS in truncated location parameter models
[AD-A210274] 01 p0115 N90-10661
Selection of the best with a preliminary test for two-parameter exponential distributions
[AD-A210275] 01 p0115 N90-10662
Research in mathematics and computer science: Calculation of the probability of undetected error for certain error detection codes, phase 1
[AD-A210302] 01 p0115 N90-10664
A unified approach to estimating tail behavior
[AD-A210961] 01 p0117 N90-10672
Radon transform analysis of a probabilistic method for image generation
[AD-A207814] 01 p0123 N90-10702
Development of an approximate technique for the nonlinear random vibrations analysis of hysteretic systems 02 p0233 N90-11335
Partially specified probability measures in expert systems
[CWI-CS-R8842] 02 p0269 N90-11536
Statistical models for the optimal estimation of oceanic fields
[AD-A211786] 03 p0377 N90-12149
Efficient diagnosis of multiprocessor systems under probabilistic models
[NASA-CR-185965] 03 p0388 N90-12212
On a classification problem: Ranking and selection approach
[AD-A211627] 03 p0397 N90-12269
Some 1(sub p) invariant probability measures
[REPT-88-91] 03 p0397 N90-12273
Fuzzy logic and the generalized modus ponens
[REPT-88-92] 03 p0397 N90-12274
Optical detection of space debris using a large achromatic coronagraph
[AD-A211362] 04 p0462 N90-12647
On the decoder error probability of linear codes 04 p0486 N90-12793
A simple model for DSS-14 outage times 04 p0488 N90-12802
On a rate of convergence of the multiknapsack value function
[CWI-MS-R8812] 04 p0542 N90-13144
Different notions of uncertainty in quasi-probabilistic models
[CWI-CS-R8847] 04 p0547 N90-13182
Stochastic process models in device physics
[AD-A212284] 04 p0547 N90-13185
Smoothed limit theorems for equilibrium processes
[AD-A212321] 04 p0547 N90-13186
The shape of the probability density function of short-term concentration fluctuations of plumes in the atmospheric boundary layer
[AD-A212632] 04 p0548 N90-13188
Probabilistic finite element analysis of dynamic structural response
[AD-A213249] 05 p0650 N90-13789
Why stochastic modeling is essential in analyzing interdicted transportation network performance
[AD-A213140] 05 p0688 N90-14007
Counterexamples to Robertson's conjecture
[MEMO-COSOR-88-32] 05 p0693 N90-14048
Estimation of convolution tail behavior
[MEMO-COSOR-89-04] 05 p0693 N90-14051
Failure probability estimate of Type 304 stainless steel piping
[DE90-000659] 06 p0796 N90-14635
Centralized and decentralized Kalman filter techniques for tracking, navigation, and control
[AD-A214245] 07 p0878 N90-15091
Two basic partial orderings for distributions derived from Schur functions and majorization
[AD-A213703] 07 p0984 N90-15682
Cluster based reaction probabilities for boron with oxygen, hydrogen, water, nitrogen, nitrous oxide, carbon dioxide, carbon monoxide, methane, tetrafluoromethane, and silane
[AD-A214554] 09 p1190 N90-16894
Heavy-section steel technology program fracture issues
[DE90-005264] 09 p1240 N90-17195
An algorithm for finding characteristic roots of quasi-triangular Markov chains
[AD-A215490] 10 p1421 N90-18196
Proceedings of a research workshop on Nonlinear Time Series Analysis and Applications
[AD-A216541] 10 p1423 N90-18214
Probability of failure and risk assessment of propulsion structural components 11 p1471 N90-18470
Failure probability estimate of Type 304 stainless steel piping
[DE90-003896] 11 p1486 N90-18550
Multistage forest volume estimation using a sampling system with probability variables
[INPE-4897-PRE/1498] 11 p1523 N90-18769
A comparison of void distributions in Abell cluster catalogue with numerical simulations
[DE90-610640] 11 p1590 N90-19173
Security calculations of rip reached construction elements by means of probabilistic breaking mechanics and a Markov process
[ETN-90-95890] 12 p1676 N90-19624
Theory and applications of belief functions
[AD-A217092] 12 p1702 N90-19774
Use of Coxian-type distributions in a general model of the maximum of bivariate random variables
[PB90-121229] 12 p1704 N90-19780
Distributed detection by a large team of sensors in tandem
[AD-A216607] 12 p1708 N90-19807
Development of acceleration exposure limits for advanced escape systems 13 p1751 N90-20055
Determination of fundamental thermodynamic properties of constituent materials and performance screening of candidate systems
[AD-A218089] 13 p1769 N90-20153
Error control techniques for satellite and space communications
[NASA-CR-186221] 13 p1788 N90-20263
On optimal distributed decision architectures in a hypothesis testing environment
[AD-A217824] 13 p1790 N90-20274
Research in reliability, availability and maintainability for complex failure systems
[AD-A217744] 13 p1813 N90-20415
A paradoxical result in unconditionally secure authentication codes, and an explanation
[DE90-008529] 13 p1867 N90-20710
Probabilistic analysis of algorithms for NP-complete problems
[AD-A217880] 13 p1868 N90-20716
A Locality-based multiprocessor cache interference model
[AD-A217126] 13 p1871 N90-20730
Stochastic robustness of linear control systems 14 p1908 N90-20941
Probabilistic modeling for simulation of aerodynamic uncertainties in propulsion systems
[NASA-TM-102472] 14 p1927 N90-21036
Final safety analysis report for the Ulysses Mission. Volume 2: Accident model document-appendices
[DE90-008695] 14 p1940 N90-21104
Problems in radiative transfer in astrophysics: An escape probability treatment of line overlap and a model of the masers around VX Sgr 14 p2041 N90-21705
A stress-strength interference approach to fast and delayed fracture reliability analysis for ceramic components 15 p2070 N90-21859
Calculation of IR propagation statistics in the eastern Atlantic for surveillance system performance assessment 15 p2085 N90-21938
Probabilistic finite elements: Applications to fracture and fatigue 15 p2121 N90-22134
General purpose heat source radioisotope thermoelectric generator program. Book 1: Accident analysis
[REPT-90SDS4202-BK-1] 15 p2166 N90-22379
General purpose heat source radioisotope thermoelectric generator. Book 2: Accident analysis, appendices
[REPT-90SDS4202-BK-2] 15 p2166 N90-22380
The association of supernovae with regions of recent star formation in late-type galaxies 15 p2188 N90-22497
Probabilistic structural analysis of aerospace components using NESSUS
[NASA-TM-102324] 16 p2248 N90-22823
A theory of Bayesian data analysis
[AD-A218420] 16 p2308 N90-23152
Ability distributions pattern probabilities and quasidensities
[AD-A218471] 16 p2308 N90-23153
A scattering center based numerical simulation of small scale atmospheric turbulence 16 p2312 N90-23179
A theory of control for infinite dimensional systems with application to large scale space structures
[AD-A219937] 17 p2366 N90-23469
Computer-aided mathematical analysis of probability of intercept for ground-based communication intercept system
[AD-A219856] 17 p2392 N90-23627
An asymmetric shortest queue problem
[MEMO-COSOR-89-22] 17 p2459 N90-24035
Bayesian learning
[NASA-CR-181528] 17 p2465 N90-24082
Probabilistic analysis of the minimum weighted flowtime scheduling problem
[CWI-BS-R8913] 17 p2466 N90-24091
Belief networks in plausible reasoning
[CWI-CS-R8927] 17 p2467 N90-24098
Effects of internal hydrogen on the vacancy loop formation probability in Al
[DE90-011114] 18 p2527 N90-24422
Review of probabilistic analysis of dynamic response of systems with random parameters
[NASA-CR-186171] 18 p2568 N90-24636
Evaluation of Stochastic models for estimating the persistence probability of cloud-free lines-of-sight
[AD-A220283] 18 p2581 N90-24702
A general method for approximating improper integrals
[AD-A221153] 18 p2604 N90-24830
Symposium on Applied Probability
[AD-A218760] 18 p2605 N90-24838
Predicting the audibility and annoyance of unducted fan engines 18 p2610 N90-24869
A Bayesian approach to reliability and confidence 18 p2628 N90-24974
Explanation of Bayesian conditioning for decision support systems 18 p2633 N90-25002
Operations and support cost modeling using Markov chains 18 p2648 N90-25070
Measurement techniques, evaluation criteria and injury probability assessment methodologies developed for Navy ejection and crashworthy seat evaluations 19 p2721 N90-25479
On the relation between various levels of target acquisition
[IZF-1989-38] 19 p2724 N90-25492
Hardware and software reliability estimation using simulations
[NASA-CR-186637] 19 p2741 N90-25580
Neuromorphic learning of continuous-valued mappings from noise-corrupted data. Application to real-time adaptive control
[NASA-TM-4176] 19 p2747 N90-25607
Some observations for the pigeon hole principle
[RUU-CS-88-39] 19 p2750 N90-25624
Statistical treatment of slow strain rate data for assessment of hydrogen embrittlement in low alloy high strength steel
[ARL-MAT-R-122] 20 p2832 N90-26106
A new technique in the global reliability of cyclic communications network
[NASA-TM-103479] 20 p2851 N90-26214
The variably trimmed mean CFAR detector for nonhomogeneous background
[AD-A222801] 20 p2856 N90-26243
Design of ceramic components with the NASA/CARES computer program
[NASA-TM-102369] 20 p2875 N90-26359
Software requirements: Guidance and control software development specification
[NASA-CR-182058] 20 p2906 N90-26527
Closed-form solution of decomposable stochastic models
[NASA-TM-103466] 20 p2920 N90-26619
A linear-eddy model of turbulent shear layer mixing 21 p2974 N90-26904
Multistage estimation of received carrier signal parameters under very high dynamic conditions of the receiver
[NASA-CASE-NPO-17911-1-CU] 21 p2994 N90-27016
A preliminary analysis of threshold signal detection in ambient and signal-dependent noise environments
[AD-A222089] 21 p2996 N90-27030
Development of probabilistic and possibilistic approaches to approximate reasoning and its applications
[AD-A221945] 21 p3039 N90-27271
Dynamic test input generation for multiple-fault isolation 21 p3040 N90-27280
STATLIB: NSWC library of statistical programs and subroutines
[AD-A221538] 21 p3055 N90-27370
Multi-Hilbertian spaces and their duals
[AD-A222344] 21 p3064 N90-27421
Real-time adaptive aircraft scheduling
[NASA-CR-177558] 22 p3110 N90-27669

Possible trajectory profiles to achieve the geostationary orbit without any drift phase 22 p3127 N90-27745
Ceramics Analysis and Reliability Evaluation of Structures (CARES). Users and programmers manual [NASA-TP-2916] 22 p3190 N90-28099
A solar power system for an early Mars expedition [NASA-TM-103219] 22 p3243 N90-28393
Target acquisition probability as a function of distance, calculated with PHIND [IZF-1989-46] 22 p3244 N90-28394
Probabilistic structural analysis methods development for SSME 23 p3291 N90-28616
Probability models for the failure of fibres and fibrous composite materials 23 p3300 N90-28665
A method of classification for multisource data in remote sensing based on interval-valued probabilities [NASA-CR-187007] 23 p3343 N90-28889
Multiresolutional models of uncertainty generation and reduction 23 p3370 N90-29043
An experimental study of voice communication over a bandlimited channel using variable bit width delta modulation [AD-A223445] 24 p3461 N90-29548
Problems in probability, statistics, and reliability [AD-A224152] 24 p3540 N90-30016
For the definition of two person zero sum games [ETN-90-97294] 24 p3541 N90-30022
Audibility and annoyance of en route noise of unducted fan engines [AD-A223687] 24 p3543 N90-30035

PROBLEM SOLVING
NT ALTERNATING DIRECTION IMPLICIT METHODS
NT ASYMPTOTIC METHODS
NT ITERATIVE SOLUTION
NT THEOREM PROVING
Iterative performance and an adaptive procedure for viscous flow problems 01 p0069 N90-10397
A decision support approach to the file allocation problem in a distributed computing system 01 p0107 N90-10609
Northeast Artificial Intelligence Consortium annual report for 1987. Volume 7, part A: Time oriented problem solving [AD-A210331] 01 p0110 N90-10622
Finite methods for a nonlinear allocation problem [AD-A209719] 01 p0111 N90-10629
Numerical optimization in Hilbert space using inexact function and gradient evaluations [NASA-CR-181926] 01 p0112 N90-10640
Application of a hybrid generation/utility assessment heuristic to a class of scheduling problems [NASA-TM-102367] 01 p0117 N90-10674
Motivating the notion of generic design within information processing theory: The design problem space [AD-A210266] 01 p0136 N90-10786
On the effective transport properties of composite materials 02 p0190 N90-11086
A survey of research methods to study design [AD-A211213] 02 p0262 N90-11491
Domain decomposition for partial differential equations [DE89-016669] 02 p0267 N90-11519
Eigensolutions for the reflection problem involving the interface of two chiral half spaces [PB89-221592] 03 p0338 N90-11926
Viscous split algorithms for the time dependent incompressible Navier-Stokes equations [AD-A211592] 03 p0348 N90-11985
The nonconvex multi-dimensional Riemann problem for Hamilton-Jacobi equations [NASA-CR-181887] 03 p0384 N90-12182
The use of Lanczos's method to solve the large generalized symmetric definite eigenvalue problem [NASA-CR-181914] 03 p0385 N90-12193
Taxonomic syntax for first order inference [AD-A211618] 03 p0390 N90-12221
Computer-based tutors for explaining and managing the process of diagnostic reasoning [AD-A211738] 03 p0390 N90-12222
Microscopic approach to the generator coordinate method [DE89-016701] 03 p0392 N90-12233
On the communication complexity of solving a polynomial equation [AD-A211945] 03 p0393 N90-12240
A multigrid method combined with defect correction for free convection problems at high Rayleigh numbers [REPT-89-27] 03 p0396 N90-12264
Distributed knowledge-based systems [AD-A211984] 03 p0418 N90-12401
Solving 3D block bidiagonal linear systems on vector computers [CWI-NM-R8819] 04 p0530 N90-13061
On the identification of local minimizers in inertia-controlling methods for quadratic programming [AD-A212514] 04 p0534 N90-13086
NTRFACE for MAGIC [AD-A212858] 04 p0538 N90-13112
Stable and unstable subspaces of a critical functional differential equation [PB89-220651] 04 p0538 N90-13115
On the existence of a maximal weak solution for a semilinear elliptic equation [REPT-89-06] 04 p0539 N90-13120
Remarks on the control of discrete time nonlinear systems [MEMO-770] 04 p0544 N90-13158
Towards a complete local solution of the nonlinear model matching problem [MEMO-781] 04 p0545 N90-13166
A modified Newton method for unconstrained minimization [AD-A212752] 04 p0546 N90-13174
The relationship between subjective and objective measures of simulator-induced ataxia [AD-A213095] 05 p0673 N90-13922
A priori results in linear quadratic optimal control theory [MEMO-COSOR-89-02] 05 p0686 N90-13996
The totally singular linear quadratic problem with indefinite cost [MEMO-COSOR-89-05] 05 p0687 N90-13998
The output-stabilizable subspace and linear optimal control [MEMO-COSOR-89-15] 05 p0687 N90-14001
Application of multi-grid methods for solving the Navier-Stokes equations [NASA-TM-102359] 05 p0687 N90-14002
Parabolic equations for curves on surfaces. 2: Intersections, blow up and generalized solutions [AD-A212890] 05 p0687 N90-14004
Periodic solutions of Hamiltonian systems of 3-body type [AD-A212891] 05 p0687 N90-14005
Using Broyden updates to approximate the Jacobian in a semi-implicit backward differentiation code [AD-A213239] 05 p0688 N90-14010
On the performance of on-line algorithms for partition problems [MEMO-784] 05 p0689 N90-14015
On the nonexistence of a strong solution in the boundary problem for a sticky Brownian motion [CWI-BS-R8901] 05 p0689 N90-14018
The regular indefinite linear quadratic problem with linear endpoint constraints [MEMO-COSOR-88-15] 05 p0690 N90-14022
Continuity properties of one-parameter families of linear-quadratic problems without stability [MEMO-COSOR-88-17] 05 p0690 N90-14024
Solving a specific Thue-Mahler equation [MEMO-793] 05 p0691 N90-14032
Another approach to the local disturbance decoupling problem with stability for nonlinear systems [MEMO-799] 05 p0691 N90-14033
Practice of bivariate quadratic simplicial splines [MEMO-800] 05 p0691 N90-14034
Theory of goodness of fit tests and scanning innovation martingales [CWI-BS-R8904] 05 p0693 N90-14046
Note on Urbanik's class L(sub n) --- self-decomposability of functions [MEMO-COSOR-89-07] 05 p0694 N90-14053
Reverse self-decomposability --- for characteristic functions [MEMO-COSOR-89-08] 05 p0694 N90-14054
The activity selection problem: A network and game theoretic approach [MEMO-794] 05 p0694 N90-14056
Introduction to data items on flight path optimisation [ESDU-89015] 06 p0723 N90-14221
Human factors aspects of decision support systems 06 p0757 N90-14408
Numerical methodologies for solving partial differential equations [DE90-001842] 06 p0834 N90-14849
On the identification of local minimizers in inertia-controlling methods for quadratic programming [DE89-017330] 07 p0973 N90-15616
A note on the maximum size of a rectilinear maze [AD-A214445] 07 p0982 N90-15668
Recent progress in relativistic klystron research [DE90-000942] 08 p1059 N90-16121
An algorithm to compute the square root of 3x3 positive definite matrix [DE89-635711] 08 p1109 N90-16417
Complex availability problems solved with simulation [DE89-012610] 08 p1116 N90-16459
Hidden regularity for a strongly nonlinear wave equation [DE90-600742] 08 p1116 N90-16465
America's shuttle returns to space 09 p1174 N90-16792
EDISON Project [AD-A214724] 09 p1265 N90-17338
Compiling scientific code using partial evaluation [AD-A215087] 09 p1270 N90-17363
Use of hypermedia as a user interface for an artificial intelligence-based problem solver [AD-A215551] 09 p1271 N90-17370
Structural understanding in problem solving [AD-A214776] 09 p1273 N90-17379
Asymptotic behaviour of solutions of a degenerate quasilinear hyperbolic equation [DE89-635713] 09 p1276 N90-17400
Faster scaling algorithms for general graph matching problems [AD-A215112] 10 p1417 N90-18163
An exact algorithm for the p-median problem [INPE-4914-PRE/1415] 10 p1418 N90-18172
Decomposition for optimal synthesis in a parallel computing environment 10 p1419 N90-18184
Self similar solutions of the second kind of nonlinear diffusion-type equations [DE90-606953] 10 p1422 N90-18204
An approach centered in production rules for a partition of environment and planning in a visual navigation system (SNV) [INPE-4813-TDL/360] 11 p1517 N90-18737
An integrated vision on methodologies and environments for modeling and simulation assisted by computer [INPE-4861-TDL/372] 11 p1544 N90-18886
Differential-geometric techniques for solving differential algebraic equations [AD-A216503] 11 p1552 N90-18934
The formation and use of knowledge structures in problem solving domains [AD-A216512] 11 p1552 N90-18936
Finding critical independent sets and critical vertex subsets are polynomial problems [AD-A216547] 11 p1552 N90-18938
Schema-based theories of problem solving [AD-A216717] 11 p1552 N90-18939
Elastic solutions in a semi-infinite solid with an ellipsoidal inclusion [AD-A217063] 12 p1625 N90-19338
The 0-1 multiknapsack problem: Heuristic and reduction methods [INPE-4894-PRE/1495] 12 p1704 N90-19782
A matrix-free locally-implicit scheme for Navier-Stokes equations [AD-A218298] 13 p1803 N90-20349
The inverse gravimetric problem in gravity modelling 13 p1835 N90-20535
Experiments in finding neural network weights [DE90-007696] 13 p1865 N90-20702
Institute for Computational Mechanics in Propulsion (ICOMP) fourth annual review, 1989 [NASA-TM-102519] 13 p1878 N90-20769
Techniques for accelerating iterative methods for the solution of mathematical problems [AD-A218272] 13 p1878 N90-20775
Subsonic and transonic blade design by means of analysis codes 14 p1917 N90-20985
Mechanics of interface fracture 14 p1990 N90-21408
Cooperating intelligent systems [NASA-CR-184982] 14 p2012 N90-21529
Multigrid on massively parallel computers [DE90-008999] 14 p2017 N90-21560
High accuracy solutions of incompressible Navier-Stokes equations [NASA-TM-102539] 14 p2018 N90-21567
Numerical code AEOLUS-E1 for analysing free-boundary resistive MHD mode [DE90-759903] 14 p2028 N90-21630
STORM: A statistical object representation model [DE90-009048] 14 p2036 N90-21686
Neural implementation of a method for solving systems of linear algebraic equations [NPL-DITC-155/89] 15 p2162 N90-22356
A generalized complementarity problem in Hilbert space [DE90-009576] 15 p2163 N90-22360
A study of mental models through communication between users and advisors solving software manipulation problems 15 p2176 N90-22434
Nonstrictly hyperbolic conservation laws [AD-A218525] 16 p2237 N90-22762
Towards the knowledge level in SOAR: The role of the architecture in the use of knowledge [NASA-CR-186615] 16 p2262 N90-22897
What makes some problems hard: Explorations in the problem space of difficulty [AD-A219002] 16 p2263 N90-22901
Discovering problem solving strategies: What humans do and machines don't (yet) [AD-A219008] 16 p2263 N90-22902

Laboratory replication of scientific discovery processes
[AD-A219273] 16 p2266 N90-22913
Hatching a theory of incubation effects
[AD-A219275] 16 p2266 N90-22915
Non-LIFO (Last-In-First-Out) execution of cognitive procedures
[AD-A219277] 16 p2266 N90-22916
Using deflation in the pole assignment problem with output feedback 16 p2282 N90-23004
Linear programming tools for integer programming
[AD-A219013] 16 p2300 N90-23106
Automated electric power management and control for Space Station Freedom
[NASA-TM-103151] 16 p2304 N90-23125
Scientific discovery as problem solving
[AD-A218887] 16 p2307 N90-23145
Explanation generation in expert systems (a literature review and implementation)
[AD-A218741] 16 p2327 N90-23268
Explanation and the theory of expert problem solving
[AD-A220861] 17 p2444 N90-23930
Intelligent, real-time problem solving
[AD-A219929] 17 p2455 N90-24006
Dynamic constraints networks
[AD-A219778] 17 p2457 N90-24018
Convergence of one-leg multistep methods for stiff nonlinear initial value problems
[CWI-NM-R8911] 17 p2459 N90-24040
An H(m)sub 0 interpolation result
[AD-A219888] 17 p2461 N90-24051
A fast PC-based solver for simultaneous linear equations
[AD-A220190] 17 p2461 N90-24056
Optimization and optimality test for the max-cut problem
[MEMO-830] 17 p2463 N90-24066
On a problem of F. Ruskey
[MEMO-832] 17 p2463 N90-24068
Contractivity of Runge-Kutta methods
[TW-89-12] 17 p2464 N90-24079
A simple output-sensitive algorithm for hidden surface removal
[RUU-CS-89-26] 18 p2592 N90-24751
Intelligent real-time problem-solving: Issues, concepts and research methodology
[AD-A218868] 18 p2598 N90-24781
Solving problems by interrogating sets of knowledge systems: Toward a theory of multiple knowledge systems 18 p2629 N90-24979
Autonomous power expert system
[NASA-CR-185263] 19 p2670 N90-25187
ICASE semiannual report, April 1 - September 30, 1989
[NASA-CR-181988] 19 p2727 N90-25502
A comparison of two neural network schemes for navigation 19 p2733 N90-25536
Ocean feature recognition using genetic algorithms with fuzzy fitness functions (GA/F3)
19 p2740 N90-25576
Intelligent Real-Time Problem Solving
[AD-A220357] 19 p2750 N90-25621
Modular arithmetic and randomization for exact matroid problems: Extended abstract
[REPT-89-064] 19 p2751 N90-25628
Enroute flight planning: The design of cooperative planning systems
[NASA-CR-186797] 20 p2806 N90-25964
Informatics aspects of large flow calculations on the SX-2 supercomputer
[NLR-MP-88037-U] 20 p2864 N90-26290
Reusable rocket engine turbopump health monitoring system, part 3
[NASA-CR-182294] 20 p2869 N90-26320
Pilot interaction with automated airborne decision making systems
[NASA-CR-186730] 20 p2899 N90-26492
Innovative design systems: Where are we, and where do we go from here
[AD-A222586] 20 p2910 N90-26556
Mathematical problem-solving transfer: The effects of cognitive load and attention a schema acquisition and rule automation 20 p2917 N90-26594
Unification and disunification: Theory and applications
[ETN-90-97247] 20 p2919 N90-26610
Efficient implementation of minimal polynomial and reduced rank extrapolation methods
[NASA-TM-103240] 20 p2920 N90-26616
Qualitative and quantitative reasoning about thermodynamics
[NASA-CR-186788] 20 p2933 N90-26689
A new class of exact solutions of the vacuum quadratic Poincare gauge field theory
[MATHS-REPT-A-119] 20 p2933 N90-26691
On trivector torsion in vacuum quadratic Poincare gauge field theory
[MATHS-REPT-A-121] 20 p2933 N90-26692
Rule acquisition events in the discovery of problem solving strategies
[AD-A222426] 21 p3037 N90-27265
KIPSE1: A Knowledge-based Interactive Problem Solving Environment for data estimation and pattern classification 21 p3041 N90-27287
Establishing a communications-intensive network to resolve artificial intelligence issues within NASA's Space Station Freedom research centers community
21 p3042 N90-27291
Case-based reasoning in design: An apologia
21 p3045 N90-27308
Derivation of sorting programs
21 p3047 N90-27319
A tool for modeling concurrent real-time computation
21 p3047 N90-27321
DEB: A Diagnostic Experience Browser using similarity networks 21 p3048 N90-27329
The sixth generation robot in space
21 p3049 N90-27332
Computer assisted analysis and modelling of structured problems
[AD-A222991] 21 p3052 N90-27350
Algorithms to solve nonlinear time dependent problems of engineering and physics
[AD-A221463] 21 p3055 N90-27366
Context propagation truth maintenance system
[RR-779-I] 21 p3057 N90-27380
On domain decomposition methods for solving partial differential equations
[AD-A222975] 21 p3063 N90-27414
Investigations on improved iterative methods for solving sparse systems of linear equations
[AD-A221980] 21 p3064 N90-27417
Content effects in mathematics problem solving
[AD-A222436] 21 p3065 N90-27423
Computation of efficient solutions of discretely distributed stochastic optimization problems
[ETN-90-97330] 21 p3067 N90-27436
Newton methods for large-scale linear equality-constrained minimization
[AD-A222310] 21 p3070 N90-27457
On line diagnostics of rotating machinery using expert system technology 22 p3105 N90-27632
Stochastic dynamic programming for reservoir optimal control: Dense discretization and inflow correlation assumption made possible by parallel computing
[REPT-89-056] 22 p3238 N90-28360
Linear iterative solvers for implicit ODE methods
[NASA-CR-182074] 22 p3242 N90-28386
Polymatroids: Construction and random algorithms
[REPT-89-068] 22 p3242 N90-28388
An environment to support problem solving
[ISBN-90-9003151-0] 22 p3259 N90-28458
Parametric solution of nonlinear structure problems
[ONERA-RT-21/3542-RY-082-R] 23 p3340 N90-28874
Learned navigation in unknown terrains: A retraction method 23 p3368 N90-29029
State-based scheduling: An architecture for telescope observation scheduling 23 p3369 N90-29038
Approximation algorithms for planning and control
23 p3370 N90-29042
A tesselated probabilistic representation for spatial robot perception and navigation 23 p3376 N90-29075
A user modelling approach for computer-based critiquing
[AD-A224042] 23 p3379 N90-29088
Documenting the decision structure in software development
[NASA-CR-186865] 23 p3382 N90-29108
Technical writing for software engineers
[AD-A223872] 23 p3382 N90-29109
Asymptotics of Laplace-Dirichlet integrals
[DE90-627165] 23 p3388 N90-29137
The Cousin problems for an overdetermined system of complex partial differential equations
[DE90-627170] 23 p3389 N90-29139
Generic task problem solvers in Soar
24 p3521 N90-29904
An efficient temporal logic for robotic task planning
24 p3521 N90-29906
Tutorial on using LISP object-oriented programming for blackboards: Solving the radar tracking problem
[AD-A224272] 24 p3525 N90-29930
An instability theorem for a certain sixth order differential equation
[DE90-627150] 24 p3536 N90-29990
Periodic solutions of certain fifth order differential equations
[DE90-627160] 24 p3536 N90-29994
An algebraic hierarchical basis preconditioner
[DE90-015875] 24 p3538 N90-30008
Problems in probability, statistics, and reliability
[AD-A224152] 24 p3540 N90-30016

PROCEDURES
NT BOUNDARY INTEGRAL METHOD
NT CREW PROCEDURES (INFLIGHT)
NT FINITE ELEMENT METHOD
NT FINITE VOLUME METHOD
NT OPTICAL CORRECTION PROCEDURE
NT PANEL METHOD (FLUID DYNAMICS)
Coupling rule-based and object-oriented programming for the classification of machined features
[DE89-017705] 03 p0334 N90-11903
An algebra for process creation
[CWI-CS-R8907] 04 p0543 N90-13155
A design procedure for a slotted waveguide with probe-fed slots radiating into plasma
[DE90-004168] 09 p1284 N90-17446
Space station contamination control study: Internal combustion, phase 1
[NASA-CR-179323] 10 p1328 N90-17674
En route noise: NASA propfan test aircraft (corrected data - simplified procedure)
[DOT-TSC-FA953-LR4] 18 p2608 N90-24856
Experience in developing an improved altitude test capability 22 p3120 N90-27719
Experience in developing an improved ground-level test capability 22 p3120 N90-27720
General test plan 22 p3120 N90-27721
Development of standards for superconductors
[PB90-196536] 22 p3248 N90-28418
Recommended practices for measurement of gas path pressures and temperatures for performance assessment of aircraft turbine engines and components
[AGARD-AR-245] 24 p3433 N90-29393
SamTrack: A sample tracking system for environmental monitoring
[DE90-016026] 24 p3488 N90-29712

PROCEEDINGS
U CONFERENCES
U CONGRESSIONAL REPORTS

PROCESS CONTROL (INDUSTRY)
Establishment and initial operation of a resource facility for RSR (Rapid Solidification Rate) processed alloys in pilot quantities
[AD-A210369] 01 p0050 N90-10283
Advanced GaAs process modeling, volume 1
[AD-A210385] 01 p0132 N90-10761
Thin section casting program. Volume 3: Vertical TSC (Thin-Section Casting) approach
[DE89-009033] 02 p0210 N90-11201
Sensors for nondestructive testing and evaluation of materials
[DE89-014763] 02 p0223 N90-11279
An extension of Cochran's test for homogeneity of variances
[AD-A211054] 02 p0269 N90-11534
Current research in advanced materials
[DE89-017466] 03 p0331 N90-11884
Optimal processes described by a parabolic differential equation with control in the coefficients, part 4
[MEMO-785-PT-4] 05 p0689 N90-14016
Automated glass fiber drawing
[DE90-000894] 06 p0751 N90-14367
Ion beam analysis and modification of thin-film, high-temperature superconductors
[DE90-000918] 06 p0850 N90-14941
The effect of composition and processing on high T(sub c) superconductors containing bismuth
[DE90-002203] 06 p0854 N90-14965
Processing and properties of nanophase oxides
[DE90-003826] 07 p0895 N90-15171
Mechanistic modeling of epoxy resins
[DE89-015119] 07 p0908 N90-15247
Automated convection soldering
[KCP-613-4005] 07 p0916 N90-15300
Back to basics
[DE90-002734] 07 p0943 N90-15463
Integrated approach fault tolerance-current state and future requirements
[AD-A214402] 07 p0944 N90-15465
Time bounds for real-time process control in the presence of timing uncertainty
[AD-A213791] 07 p0975 N90-15633
Processing and fabrication of YBa2Cu4O8 and YBa2Cu4O8/YBa2Cu3O(x) composites
[DE90-003559] 07 p1001 N90-15789
On-line chemical composition analyzer development
[DE90-004079] 08 p1043 N90-16026
Silicon membrane formation
[DE90-003022] 08 p1049 N90-16064
Development and evaluation of a process to produce hydrogen from coal
[DE90-003937] 08 p1052 N90-16084
Digital system for monitoring and controlling remote processes
[DE90-003935] 08 p1054 N90-16094

Application of artificial intelligence control to the vapor-liquid-solid silicon carbide whisker process
[DE90-007835] 11 p1480 N90-18519
Control of phase structure in polymer blends
[AD-A217034] 11 p1491 N90-18580
Optimum catalytic process for alcohol fuels from syngas
[DE90-007188] 11 p1495 N90-18604
Ion chromatography in the manufacture of multilayer circuit boards
[DE90-005560] 11 p1503 N90-18652
Techno-economic assessment of a carbothermic alumina reduction process
[DE90-007018] 13 p1772 N90-20170
Deformation processing of YBa2Cu3O(sub x)
[DE90-007795] 14 p2030 N90-21644
Toughened YBa2Cu3O(sub x)/ZrO2 composites
[DE90-007796] 14 p2031 N90-21645
Overview of current bulk and thick film high temperature superconductor processing strategies
[DE90-008949] 15 p2172 N90-22414
ESPRIT 820:QUIC. QUIC toolkit demonstrator applications
[REPT-892-440-105] 17 p2386 N90-23590
National Educators' Workshop: Update 1989 Standard Experiments in Engineering Materials Science and Technology
[NASA-CP-3074] 18 p2513 N90-24350
Experiments and other methods for developing expertise with design of experiments in a classroom setting 18 p2516 N90-24367
Manual and computer-aided materials selection for industrial production: An exercise in decision making 18 p2516 N90-24368
Processing and properties of advanced aluminum alloys
[AD-A221292] 18 p2526 N90-24416
Conceptual task modeling
[TR-89-14] 19 p2762 N90-25693
Integrating expert systems with solid modeling through interprocess communications and the applications interface specification
[DE90-012996] 20 p2907 N90-26537
On the robust stability of MIMO linear feedback systems
[EUT-88-E-212] 20 p2915 N90-26585
A new scheme for identification and control
[EUT-88-E-213] 20 p2915 N90-26586
Filler metal development for Hastelloy alloy XR
[DE90-791084] 21 p2981 N90-26939
Advanced processing and properties of high performance alloys
[AD-A221776] 21 p2983 N90-26948
Application of microdesigned interfaces to studies of ceramic processing
[DE90-011633] 21 p2983 N90-26951
Development of a multi-purpose, pulsed-laser system for solar cell processing applications
[DE90-012181] 21 p3008 N90-27096
Microstructures and properties of superconducting Y-Er-BaCu-O thin films obtained from disordered Y-Er-BaF2-Cu films 22 p3147 N90-27848
Tolerating failures of continuous-valued sensors
[NASA-CR-187028] 22 p3178 N90-28035
Algorithmic components in evaluating systems dependability
[REPT-88-044] 22 p3237 N90-28358
Adjustable speed drive applications guidebook
[DE90-014151] 23 p3321 N90-28780
Processing of polymers using supercritical fluids
[AD-A223681] 24 p3455 N90-29514
Planar waveguide spectrometer
[DE90-016308] 24 p3546 N90-30057

PROCESSORS (COMPUTERS)
U CENTRAL PROCESSING UNITS

PROCUREMENT
NT GOVERNMENT PROCUREMENT
Acquisition of an analytical x ray and image analysis system
[AD-A221376] 18 p2593 N90-24756
Technical guide on documentation requirements for open market contract acquisitions of information resources
[NASA-TM-102650] 19 p2762 N90-25695
Preparing software conversion studies
[PB90-235623] 23 p3381 N90-29099

PROCUREMENT MANAGEMENT
Project ORION microcomputer management system
[AD-A212945] 05 p0680 N90-13959
Program manager's handbook
[AD-A214338] 07 p1009 N90-15844

PROCUREMENT POLICY
Defense Small Business Innovation Research (SBIR) Program: Program solicitation 90.1, FY-1990
[AD-A215350] 09 p1294 N90-17503
Component selection, procurement and control for ESA space systems
[ESA-PSS-01-60-ISSUE-2] 11 p1574 N90-19062
Small business innovation research program solicitation: Closing date July 16, 1990
[NASA-TM-101798] 17 p2479 N90-24173

PRODUCT DEVELOPMENT
NT WEAPONS DEVELOPMENT
Japanese structural ceramics research and development 01 p0048 N90-10272
The service module structure of the IOS spacecraft development and qualification program 02 p0181 N90-11021
Product assurance 05 p0605 N90-13522
Process for producing a shaped, extruded product from a crosslinkable polymeric composition
[GB-PATENT-2-201-677-A] 05 p0627 N90-13662
Crosslinkable polymer
[GB-PATENT-2-205-846-A] 05 p0628 N90-13663
Kinematics and control of manipulation robots
[WTHD-187] 05 p0652 N90-13803
Further development of the PIV method for use in the large wind tunnel 08 p1080 N90-16248
French approach to space technology transfer 11 p1576 N90-19074
Identification of and response to market demand 11 p1577 N90-19078
An example of technology transfer by Aerospatiale: Fire protection materials 11 p1577 N90-19082
Compton amplifier
[DIGEL-1985-5] 12 p1654 N90-19506
Design of a pyrometer for temperature measurements on the solid fuel combustion chamber
[LR-530] 12 p1664 N90-19561
Development and construction of external laser components for hardening and coating
[MT-15/87] 13 p1806 N90-20364
A review of the suitability of available Computer Aided Software Engineering (CASE) tools for the small software development environment
[AD-A218276] 13 p1870 N90-20726
Strategy of supercomputer development 16 p2278 N90-22981
Lessons learned from the T-46A durability and damage tolerance program 21 p2957 N90-26812
Cost effective technology
[PNR90664] 21 p2991 N90-27002
Scope and conception of the pilot support system ASPIO
[LRT-WE-13-FB-88-1] 22 p3233 N90-28334
Application of integrated optical components in optical fiber communication
[FEL-89-B252] 23 p3395 N90-29183
Realization of equipment for manufacturing titanium alloy electrodes for first step melting
[ONERA-RT-15/3578-M] 24 p3453 N90-29498

PRODUCTION
Long-range plan for a research project on carbon monoxide production and prediction
[PB90-209602] 23 p3346 N90-28910

PRODUCTION COSTS
NT AIRCRAFT PRODUCTION COSTS
ERIS: Engineering Resource Information System
[AD-A213357] 05 p0707 N90-14144
The extension of technology and the control of production costs in advanced satellite systems
[AD-A215104] 09 p1183 N90-16857
Advanced development environments, continuation
[AD-A220510] 17 p2443 N90-23923
Innovative techniques for the production of low cost 2D laser diode arrays
[AD-A223575] 24 p3474 N90-29632
High throughput MBE materials for MODFET's
[AD-A223452] 24 p3552 N90-30097

PRODUCTION ENGINEERING
NT PRODUCTION PLANNING
Aerospace system unified life cycle engineering producibility measurement issues
[AD-A210937] 01 p0106 N90-10607
Estimating the relationships between the state of the art of technology and production cost for the US aircraft
[AD-A212127] 04 p0437 N90-12495
Process for producing a shaped, extruded product from a crosslinkable polymeric composition
[GB-PATENT-2-201-677-A] 05 p0627 N90-13662
ERIS: Engineering Resource Information System
[AD-A213357] 05 p0707 N90-14144
Challenges in processing for polymer composites
[DE90-002224] 06 p0752 N90-14376
Current launch vehicle reliability practice and data base assessment. Volume 1: Executive summary and report body
[AD-A213600] 07 p0885 N90-15121
Sequential rapid communication visual displays
[AD-D014282] 08 p1056 N90-16106
Industrial Modernization Incentives Program: Computer-aided log book
[AD-A214614] 09 p1265 N90-17335
The use of technology transfer centers by department of defense industrial facilities
[AD-A216863] 10 p1443 N90-18328
The Executive Workshop on Cost/Performance Measurement. Volume 1: Executive summary
[AD-A216745] 11 p1546 N90-18898
A locally constrained parallel activation model for diagnostic reasoning
[AD-A217808] 13 p1874 N90-20747
Radiation-hard-high-efficiency InP space solar cell development
[AD-A220500] 17 p2420 N90-23791
The Army/Air Force RAMCAD (Reliability And Maintainability Computer-Aided Design) program
[AD-A220923] 18 p2593 N90-24753

PRODUCTION MANAGEMENT
Current launch vehicle reliability practice and data base assessment. Volume 1: Executive summary and report body
[AD-A213600] 07 p0885 N90-15121
The influence of contract type in program execution/V-22 Osprey: A case study
[AD-A220011] 17 p2484 N90-24206
Quality function deployment as a mechanism for process characterization and control
[DE90-014755] 23 p3337 N90-28857

PRODUCTION METHODS
U PRODUCTION ENGINEERING

PRODUCTION PLANNING
The influence of contract type in program execution/V-22 Osprey: A case study
[AD-A220011] 17 p2484 N90-24206
Aircraft modifications cost analysis. Volume 1: Overview of the study
[AD-A220764] 19 p2649 N90-25074
Crystalline photovoltaic cell research, status, and future direction
[DE90-011478] 19 p2710 N90-25427

PRODUCTIVITY
Using computer design and simulation to improve manufacturing productivity
[AD-A210338] 01 p0105 N90-10598
Using computer design and simulation to improve manufacturing productivity, report period 1, 2 and 3
[AD-A210255] 02 p0258 N90-11462
Working with people to improve productivity and quality: A bibliography with indexes, 1984-1988
[NASA-SP-7078] 03 p0415 N90-12385
The Materials Division: A case study
[NASA-TM-102380] 05 p0617 N90-13597
Submerged arc welding consumables for HSLA (High Strength Low Alloy)-100 steel
[AD-A213433] 07 p0941 N90-15452
Productivity and cryogenic wind tunnels 08 p1032 N90-15961
The application of a computer data acquisition system for a new high temperature tribometer
[NASA-TM-102508] 10 p1347 N90-17811
Regulation of nitrogen uptake and assimilation: Effects of nitrogen source, root-zone pH, and aerial CO2 concentration on growth and productivity of soybeans
[NASA-CR-177546] 10 p1413 N90-18147
National airspace system plan: Facilities, equipment, associated development and other capital needs
[AD-A215882] 11 p1453 N90-18373
A perspective of software reuse
[AD-A216911] 11 p1546 N90-18901
Wheat productivity estimate through field radiometry
[INPE-4994-PRE/1556] 14 p2000 N90-21460
Advanced manufacturing technology: A Department of Energy technology transfer initiative
[DE90-008601] 14 p2037 N90-21688
Impact of meteorology on the agricultural sector: Compilation and analysis of projects
[INPE-4846-PRE/1475] 16 p2257 N90-22866
A proposal to demonstrate production of salad crops in the space station mockup facility with particular attention to space, energy, and labor constraints
[NASA-CR-186811] 19 p2725 N90-25500
High productivity testing 21 p2962 N90-26843
Applications of ISES for the atmospheric sciences 21 p3017 N90-27155
Enhancing US competitiveness through Federal scientific and technical information: Issues and opportunities 22 p3258 N90-28450
Total quality management: A recipe for success
[AD-A223287] 24 p3556 N90-30122

PRODUCTS
NT ASPHALT
NT DIESEL FUELS
NT GASOLINE

NT GREASES
NT REACTION PRODUCTS
NT TARS

PROFICIENCY
U ABILITIES

PROFILE METHOD (FORECASTING)
A methodology for the concept definition of advanced space transportation systems 09 p1176 N90-16813

PROFILOMETERS
Full surface interferometric testing of grazing incidence mirrors
[AD-A219394] 16 p2318 N90-23218

PROGRAM MANAGEMENT
U PROJECT MANAGEMENT

PROGRAM VERIFICATION (COMPUTERS)
Initial flight qualification and operational maintenance of X-29A flight software
[NASA-TM-101703] 01 p0005 N90-10023
Validation of missile simulation 01 p0014 N90-10066
High accuracy coordinate determination using the global positioning system 02 p0150 N90-10858
ATTAS flight testing experiences 02 p0151 N90-10862
Validation of NEC (Numerical Electromagnetics Code) for antennas near ground
[DE89-016502] 02 p0212 N90-11212
A distributed debugger for Amoeba
[CWI-CS-R8828] 02 p0257 N90-11453
A verification exercise relating to specification styles in LOTOS
[MEMO-INF-89-18] 02 p0259 N90-11471
Truth maintenance systems and their implementation in PROLOG
[MEMO-INF-89-13] 04 p0531 N90-13064
Expert system for test program set fault candidate selection
[AD-A213338] 04 p0535 N90-13091
Validation of the Hipparcos catalog 05 p0611 N90-13564
Data simulations in the NDAC consortium 05 p0612 N90-13574
The development of a program analysis environment for Ada
[NASA-CR-185860] 05 p0681 N90-13962
Multi-level specification and verification of real-time software
[AD-A213227] 05 p0683 N90-13975
Validation of a computer code for analysis of subsonic aerodynamic performance of wings with flaps in combination with a canard or horizontal tail and an application to optimization
[NASA-TP-2961] 06 p0717 N90-14187
Development of a three-axis trim program
[AD-A212883] 06 p0726 N90-14237
Verification of the NIKE3D structural analysis code by comparison against the analytic solution for a spherical cavity under a far-field uniaxial stress
[DE90-000929] 06 p0799 N90-14653
QUEST/Ada: Query utility environment for software testing of Ada
[NASA-CR-186121] 06 p0823 N90-14787
Initial Ada components evaluation 06 p0826 N90-14803
Environment for failure region analysis: REACHER - a reachability condition derivation tool
[AD-A214183] 07 p0977 N90-15641
The StarLite project
[AD-A214193] 07 p0977 N90-15642
Stochastic model of the NASA/MSFC ground facility for large space structures with uncertain parameters: The maximum entropy approach, part 2
[NASA-CR-186009] 08 p1107 N90-16407
Pattern matching in ML: A case study in refinement
[RSRE-89004] 08 p1111 N90-16430
Validation of an exponentially decreasing failure rate software reliability model
[AD-A215546] 09 p1235 N90-17165
A knowledge based approach to program debugging
[AD-A214941] 09 p1266 N90-17344
CHIMERA 2: A real-time UNIX-compatible multiprocessor operating system for sensor-based control applications
[AD-A215958] 10 p1392 N90-18051
Software verification plan for GCS --- guidance and control software
[NASA-TM-101668] 10 p1394 N90-18057
Research at New York University's Ultracomputer Research Laboratory
[DE90-005471] 10 p1417 N90-18167
Estimation in a discrete tail rate family of recapture sampling models
[NASA-CR-180452] 10 p1421 N90-18197
Software verification and validation: Its role in computer assurance and its relationship with software project management standards
[PB90-111691] 14 p2012 N90-21530
METCAN verification status
[NASA-TM-103119] 15 p2064 N90-21824
Spacecraft command verification: The AI solution 15 p2154 N90-22307
A verification library for multibody simulation software 16 p2298 N90-23089
Autonomous low earth orbit navigation
[REPT-892-440-101] 17 p2364 N90-23458
Automatic runtime consistency checking and debugging of formally specified programs
[AD-A218855] 17 p2442 N90-23916
The semantics of TRIDL
[TR-89-17] 17 p2450 N90-23973
Failure analysis and modeling of a multicomputer system
[NASA-CR-186697] 17 p2451 N90-23980
MARS, an AI-based Mission Activities and Resource Scheduler
[MBB-0060/89-PUB] 19 p2650 N90-25083
Making real-time reactive systems reliable
[NASA-CR-186642] 20 p2873 N90-26344
Verification-correction of a program for including uncertainties in the robot automatic programming
[ETN-90-97246] 20 p2915 N90-26588
Payload training methodology study
[NASA-CR-183907] 21 p2964 N90-26849
The identification of software failure regions
[AD-A223058] 21 p3052 N90-27352
Conceptual design of an integrated system for software systems design implementation and testing
[ETN-90-97318] 21 p3057 N90-27381
Rapid prototyping of formal specifications using Miranda
[NPL-DITC-150/89] 21 p3057 N90-27383
Debugging and analysis of large-scale parallel programs
[AD-A221678] 21 p3059 N90-27393
Development, implementation, and validation of control algorithms for the dual-arm robotic manipulation of a single object
[AD-A222502] 21 p3060 N90-27402
Experimental study on the vortices generated by the body of a missile during flight. Part 1: Laminar boundary layer
[ONERA-RT-40/1147-AY-130A-PT-1] 22 p3110 N90-27665
Verification of the naval oceanic vertical aerosol model during FIRE 22 p3219 N90-28257
An Ada evaluation report for the Verdix Corp. VADS version 5.5 release h compiler
[NPL-DITC-145/89] 22 p3235 N90-28342
Strategies for tutoring multiple bugs
[AD-A223921] 24 p3524 N90-29927
Formal verification of mathematical software, volume 2
[AD-A223633] 24 p3527 N90-29943
Formal design and verification of a reliable computing platform for real-time control. Phase 1: Results
[NASA-TM-102716] 24 p3530 N90-29965
Assembler for a parallel computer
[NAL-TM-586] 24 p3532 N90-29974
Survey of formal specification techniques for reactive systems
[AD-A223741] 24 p3538 N90-30005

PROGRAMMED INSTRUCTION
NT COMPUTER ASSISTED INSTRUCTION
Conceptual dependency theory and robot programming
[REPT-89-20] 04 p0537 N90-13106
The employment of SITIM-150 as an instructional objective for training in remote sensing
[INPE-4833-PRE/1463] 10 p1440 N90-18310
TOPAS preparation study: Summary representation of the study results
[OHB-TN-TOP-011/87] 12 p1607 N90-19244

PROGRAMMERS
Concurrent Image Processing Executive (CIPE). Volume 2: Programmer's guide
[NASA-CR-186854] 22 p3236 N90-28349

PROGRAMMING (SCHEDULING)
Software Engineering Exercise (SEE) guidelines
[AD-A212510] 04 p0534 N90-13085
Ada-Linda preliminary report: Motivation, informal description, and examples
[AD-A216004] 11 p1545 N90-18892

PROGRAMMING LANGUAGES
NT ADA (PROGRAMMING LANGUAGE)
NT ALGOL
NT APL (PROGRAMMING LANGUAGE)
NT ASSEMBLY LANGUAGE
NT BASIC (PROGRAMMING LANGUAGE)
NT C (PROGRAMMING LANGUAGE)
NT CONTEXT FREE LANGUAGES
NT FORTRAN
NT HIGH LEVEL LANGUAGES
NT LISP (PROGRAMMING LANGUAGE)
NT NATURAL LANGUAGE (COMPUTERS)
NT PASCAL (PROGRAMMING LANGUAGE)
NT PROLOG (PROGRAMMING LANGUAGE)
A common distributed language approach to software integration
[NASA-CR-185499] 01 p0103 N90-10584
A special case of second-order strictness analysis
[AD-A210829] 01 p0114 N90-10656
A verification exercise relating to specification styles in LOTOS
[MEMO-INF-89-18] 02 p0259 N90-11471
Boolean functions, invariance groups and parallel complexity
[CWI-CS-R8836] 02 p0260 N90-11472
Experience with CST: Programming and implementation
[AD-A211882] 03 p0386 N90-12197
Adoption of software engineering innovations in organizations
[AD-A211573] 03 p0387 N90-12206
Structure based formal methods for software engineering
[AD-A211660] 03 p0388 N90-12207
A language for assembly instructions
[REPT-88-90] 03 p0388 N90-12209
LOTOS tools based on the Cornell synthesizer generator
[MEMO-INF-89-5] 04 p0530 N90-13062
Abstract grammars based on transductions
[MEMO-INF-89-7-REV] 04 p0531 N90-13063
A simple definition for parallel composition of prime event structures
[CWI-CS-R8903] 04 p0532 N90-13074
SIMOGEN: An object-oriented language for simulation
[AD-A213129] 05 p0682 N90-13973
Action languages: Dimensions, effects
[NASA-CR-183388] 05 p0716 N90-14181
Research in mathematics and computer science at Argonne, July 1, 1986 to January 6, 1988
[DE88-010343] 06 p0822 N90-14781
Continuation of research in software for space operations support
[NASA-CR-186092] 06 p0827 N90-14808
Using object-oriented development to support prototyping
[DE90-000547] 06 p0829 N90-14821
Strand: A practical parallel programming language
[DE90-002861] 06 p0830 N90-14825
Paralation views: Abstractions for efficient scientific computing on the connection machine
[AD-A213935] 07 p0971 N90-15604
A signal processing language for coarse grain data flow multiprocessors
[AD-A213863] 07 p0976 N90-15635
The application of Z to the specification of air traffic control systems. 1: An initial specification of the radar processing activity
[RSRE-MEMO-4280] 08 p1020 N90-15900
Pattern matching in ML: A case study in refinement
[RSRE-89004] 08 p1111 N90-16430
The NODEN hardware description language
[RSRE-89011] 08 p1111 N90-16431
A guide to IRUS-2 application development
[AD-A214758] 09 p1266 N90-17340
A theory for graph-based language specification, analysis, and mapping with application to the development of parallel software
[AD-A214910] 09 p1266 N90-17342
The Cronus distributed DBMS (Database Management System) project
[AD-A214478] 09 p1295 N90-17508
The Saguaro distributed operating system
[AD-A215083] 10 p1374 N90-17966
Research at New York University's Ultracomputer Research Laboratory
[DE90-005471] 10 p1417 N90-18167
Technology assessment of computer languages
[AD-A216940] 10 p1419 N90-18182
Derivation of efficient parallel programs: An example from genetic sequence analysis
[DE90-005654] 11 p1547 N90-18904
RALPH: An automatic Robot Assembly Language Programmer: An overview
[PB90-120973] 11 p1548 N90-18912
Speculative computation in multilisp
[AD-A216579] 11 p1575 N90-19067
Design and architecture of fourth and fifth generation software engineering environments
[ETN-90-95365] 12 p1698 N90-19752
Using Rexx to coordinate relational commands
[DE90-007569] 12 p1702 N90-19772

An equational language for specifying, querying, and updating database domains
[PB90-124694] 12 p1726 N90-19918
Massively-parallel computational fluid dynamics
[AD-A217732] 13 p1802 N90-20342
TAE Plus: Transportable Applications Environment Plus tools for building graphic-oriented applications
13 p1856 N90-20652
Research in programming languages and software engineering
[AD-A217765] 13 p1868 N90-20715
Implementation of a hypertext help system for GLAD (Graphics LAnguage for Database)
[AD-A217936] 13 p1868 N90-20718
VHSIC Hardware Description Language (VHDL) benchmark suite
[AD-A217947] 13 p1868 N90-20719
Implementation of a hypercube database system
[DE90-008440] 13 p1900 N90-20905
SISAL 1.2: An alternative to FORTRAN for shared memory multiprocessors
[DE90-005181] 15 p2146 N90-22257
Electronic publishing with Standard Generalized Markup Language (SGML) 15 p2179 N90-22450
Six-degree-of-freedom aircraft simulation with mixed-data structure using the applied dynamics simulation language, ADSIM 16 p2294 N90-23067
Six-degree-of-freedom missile simulation using the ADI AD 100 digital computer and ADSIM simulation language
16 p2294 N90-23068
The Durra application debugger/monitor
[AD-A219290] 16 p2301 N90-23111
Durra: A task-level description language reference manual, version 2
[AD-A219293] 16 p2301 N90-23114
Implementation of image action plus software for image analysis of solid propellant combustion holograms
[AD-A219644] 17 p2372 N90-23508
Proceeding of the Embedded AI Languages Workshop
[AD-A218531] 17 p2442 N90-23914
Advanced development environments, continuation
[AD-A220510] 17 p2443 N90-23923
WireLisp: Combining graphics and procedures in a circuit specification language
[AD-A220740] 17 p2444 N90-23927
Conceptual dependency graphs and DJ
[REPT-89-62] 17 p2445 N90-23933
An abstract data model for the IDEF sub 0 graphical analysis language
[AD-A219855] 17 p2446 N90-23948
A process specification formalism based on static COLD
[CWI-CS-R8930] 17 p2448 N90-23960
Specification modules in LOTOS
[MEMO-INF-89-46] 17 p2449 N90-23965
The semantics of TRIDL
[TR-89-17] 17 p2450 N90-23973
Concurrent Clean
[TR-89-18] 17 p2450 N90-23974
Higher order attribute grammars
[RUU-CS-89-4] 18 p2590 N90-24735
Performance analysis of local area networks
[NASA-CR-186639] 18 p2595 N90-24767
Design of a specification language by abstract syntax engineering
[CWI-CS-R8934] 18 p2599 N90-24789
Functional description of a command and control language tutor 19 p2739 N90-25567
The basis system
[DE90-012077] 19 p2743 N90-25591
Outline and realization of a polymorphic language extension for ELAN
[TR-89-23] 19 p2743 N90-25592
The Knuth-Bendix completion algorithm and its specification in Z
[RSRE-MEMO-4323] 19 p2745 N90-25601
Object oriented programming
[DE90-011797] 20 p2907 N90-26532
Principles of FP2: Term algebras for specification of parallel machines
[RR-789-I-IMAG-98-LIFIA] 20 p2913 N90-26571
Establishing a communications-intensive network to resolve artificial intelligence issues within NASA's Space Station Freedom research centers community
21 p3042 N90-27291
Ada as an implementation language for knowledge based systems 21 p3050 N90-27337
Sisal on a message passing architecture
[DE90-008786] 21 p3051 N90-27342
Post script code for grey-scaled displays
[AD-A223099] 21 p3053 N90-27354
An algorithm for automated surface modelling in unigraphics
[AD-A223219] 21 p3053 N90-27355
Knowledge representation in PARKA
[AD-A221471] 21 p3055 N90-27367
Rapid prototyping of formal specifications using Miranda
[NPL-DITC-150/89] 21 p3057 N90-27383
The operational feature exchange language
[AD-A222497] 21 p3060 N90-27401
Proving Boolean equivalence with Prolog
[AD-A221766] 21 p3065 N90-27427
Study of an environment using formal reasoning. DILOG: State of the art and prototype
[CERT-1/334300-DERI] 22 p3239 N90-28368
Updates and consistency in the LOGRES language
[REPT-90-017] 22 p3239 N90-28369
Integrating mono-valued functions in deductive databases: A recursive extension of MILANT
[REPT-90-018] 22 p3239 N90-28370
A model parametric real-time logic
[REPT-90-010] 22 p3241 N90-28381
THREAD: A programming environment for interactive planning-level robotics applications
24 p3505 N90-29810
A VHDL interface for Altera design files
[AD-A224476] 24 p3523 N90-29920
System software for Soviet computers
24 p3523 N90-29921
Graphic interface for attribute-based data language queries from a personal computer to the multi-lingual, multi-model, multi-backend database system over an Ethernet network
[AD-A223738] 24 p3528 N90-29948
Language and system support for concurrent programming
[AD-A223760] 24 p3528 N90-29949
Durra: A task-level description language user's manual
[AD-A223761] 24 p3528 N90-29950
MacRootLocus: A CAD design tool for feedback control systems
[AD-A223772] 24 p3528 N90-29951
Software design for high integrity systems
[ETN-90-97517] 24 p3530 N90-29966

PROGRAMS

NT ACEE PROGRAM
NT AGRISTARS PROJECT
NT APOLLO SOYUZ TEST PROJECT
NT BRAZILIAN SPACE PROGRAM
NT CHINESE SPACE PROGRAM
NT DEFENSE PROGRAM
NT EUROPEAN SPACE PROGRAMS
NT FRENCH SPACE PROGRAM
NT GALILEO PROJECT
NT GEOGRAPHIC APPLICATIONS PROGRAM
NT GLOBAL ATMOSPHERIC RESEARCH PROGRAM
NT INDIAN SPACE PROGRAM
NT ITALIAN SPACE PROGRAM
NT JAPANESE SPACE PROGRAM
NT LUNAR PROGRAMS
NT MAGELLAN PROJECT (NASA)
NT NASA PROGRAMS
NT NASA SPACE PROGRAMS
NT NATIONAL AEROSPACE PLANE PROGRAM
NT PIONEER PROJECT
NT PROJECT SETI
NT PROJECTS
NT QUIET ENGINE PROGRAM
NT SCANNER PROJECT
NT SCOUT PROJECT
NT SEASAT PROGRAM
NT SOURCE PROGRAMS
NT SPACE PROGRAMS
NT SUPERSONIC CRUISE AIRCRAFT RESEARCH
NT SWEDISH SPACE PROGRAM
NT U.S.S.R. SPACE PROGRAM
NT UNIVERSITY PROGRAM
NT VIKING MARS PROGRAM
NT VOYAGER PROJECT

PROGRESS

Solid fuel combustion chamber
[LR-562] 15 p2068 N90-21846

PROJECT MANAGEMENT

Evaluation of mid-to-long term basic research for environmental restoration
[DE89-015621] 02 p0238 N90-11355
Preference propagation in temporal/capacity constraint graphs
[AD-A210668] 02 p0264 N90-11506
Twenty-five years of service, 1962-1987: Proceedings of the Air Force Studies Board Symposium on Air Force Research and Development, November 16, 1987
[PB89-198915] 03 p0415 N90-12384
Issues in NASA program and project management
[NASA-SP-6101(02)] 04 p0562 N90-13277
SOI: The Solar Oscillations Imager on SOHO
04 p0567 N90-13306
Assembly, integration, and verification
05 p0605 N90-13519
Project ORION microcomputer management system
[AD-A212945] 05 p0680 N90-13959
The Explorer program for astronomy and astrophysics
05 p0712 N90-14159
Sandia Satellite Program summary of operational procedures
[DE90-000892] 06 p0728 N90-14249
Space station attached payload program support
[NASA-CR-183838] 06 p0733 N90-14274
Exploring the living universe: A strategy for space life sciences
[NASA-TM-101891] 06 p0822 N90-14778
A dynamic systems engineering methodology research study. Phase 2: Evaluating methodologies, tools, and techniques for applicability to NASA's systems projects
[NASA-CR-181319] 06 p0857 N90-14985
Developing integrated parametric planning models for budgeting and managing complex projects
[NASA-CR-186006] 06 p0857 N90-14986
Physical and Electrical Standards Laboratory general operating procedures
[DE90-003515] 07 p0884 N90-15116
Back to basics
[DE90-002734] 07 p0943 N90-15463
Solid fuel combustion chamber, phase 10
[LR-536] 08 p1038 N90-16000
Establishment of the Innovative Technology Utilization Center at West Virginia University
[PB90-114711] 08 p1138 N90-16594
The joint DOD/NASA Advanced Launch System (ALS) programme 09 p1179 N90-16832
Project management in successful reliability and maintainability improvement programs
[AD-A215424] 09 p1234 N90-17162
An investigation of application development process controls in an end-user setting: A field study
09 p1295 N90-17504
NASA Propagation Information Center
10 p1371 N90-17946
Broadband versus narrowband driver/power amplifier: A spectral purity comparison
[DOT/FAA/CT-TN89/73] 10 p1379 N90-17995
Long term planning for space flight activities within the DFVLR
[DFVLR-IB-303-88/2] 11 p1465 N90-18438
Refurbishment and modification of the Metric Camera (RMK) for reflight on EOM-1 Spacelab mission
[ETN-90-96284] 11 p1512 N90-18710
Activities report in German aerospace
[ISSN-0070-3966] 11 p1595 N90-19189
Operational evaluation of initial data link air traffic control services, volume 1
[DOT/FAA/CT-90/1-VOL-1] 12 p1648 N90-19472
Development of an Ada programming support environment database SEAD (Software Engineering and Ada Database) administration manual
[NASA-CR-186064] 12 p1699 N90-19757
Spacecraft escape 13 p1753 N90-20066
Reorganization of the German space administration. Foundation of DARA
[REPT-16/89] 13 p1899 N90-20902
Fuel cell systems program plan, FY 1990
[DE90-008178] 14 p2002 N90-21471
Software verification and validation: Its role in computer assurance and its relationship with software project management standards
[PB90-111691] 14 p2012 N90-21530
Solid fuel combustion chamber
[LR-562] 15 p2068 N90-21846
Solid fuel combustion chamber
[LR-591] 15 p2068 N90-21847
Information technology applications: A British Aerospace Military Aircraft Ltd view 15 p2180 N90-22455
The automation management to support research and development 16 p2277 N90-22978
Methodology for analysis and simulation of large multidisciplinary problems 16 p2290 N90-23046
ADELE: Deployment hinge using wraparound strips
18 p2538 N90-24485
Keeping the dream alive: Managing the Space Station Program, 1982 to 1986
[NASA-CR-4272] 18 p2633 N90-25000
Space shuttle: Changes to the solid rocket motor contract
[GAO/NSIAD-88-203] 18 p2636 N90-25016
OMS FDIR: Initial prototyping
19 p2738 N90-25562
The conceptual task model: A specification technique between requirements engineering and program development
[TR-89-15] 19 p2762 N90-25694
Program plan: International aircraft operator data base
[IAR-90-1] 19 p2763 N90-25697
A long look back: ESA's faint object camera. The story of the faint object camera, one of ESA's contributions to the Hubble space telescope
[ESA-BR-67] 19 p2784 N90-25839

The Telecommunications and Data Acquisition Report
[NASA-CR-186852] 20 p2852 N90-26217
Making it happen: Project management
[PNR90618] 20 p2934 N90-26695
Electric vehicle battery R/D in the context of a propulsion system
[DE90-013667] 21 p2999 N90-27046
R and D aspects of the future operational concept of the BFS 22 p3112 N90-27679
Space program safety: Funding for NASA's safety organizations should be centralized
[GAO/NSIAD-90-187] 22 p3255 N90-28434
Procedures for DOE-Navy exchange and approval of engineering information and material management required for production of W88-0/Mk5 RBA (reentry body assembly)
[DE90-014763] 23 p3287 N90-28595
A FAA Technical Center project transition plan: Mode S
[DOT/FAA/CT-TN90/17] 23 p3319 N90-28765
Long-range plan for a research project on carbon monoxide production and prediction
[PB90-209602] 23 p3346 N90-28910
Planetary rover technology development requirements 23 p3375 N90-29067
GPS integrity requirements for use by civil aviation 24 p3423 N90-29339
Activities report of the European Space Agency
[ISSN-0258-025X] 24 p3565 N90-30169

PROJECT PLANNING
Liquid rocket booster study. Volume 2, book 3, appendices 2-5: PPIP, transition plan, AMOS plan, and environmental analysis
[NASA-CR-183602] 01 p0027 N90-10139
Studies of the European transonic wind tunnel
[ONERA-RSF-12/0694-GY] 04 p0562 N90-13278
Developing integrated parametric planning models for budgeting and managing complex projects
[NASA-CR-186006] 06 p0857 N90-14986
National program plan for electric vehicle battery research and development: Technical plan
[DE90-002023] 08 p1083 N90-16269
Technology maturity assessment methodology SDIO systems SETA
[AD-A214571] 09 p1294 N90-17501
The GSR3: A new approach for solar array deployments 10 p1340 N90-17762
Atmospheric Radiation Measurement Program plan
[DE90-006349] 12 p1689 N90-19705
National Action Plan on Superconductivity Research and Development
[PB89-138512] 12 p1720 N90-19883
Research and development quality assurance planning
[DE90-003687] 13 p1813 N90-20413
Atmospheric Radiation Measurement Program Plan
[DE90-008108] 13 p1829 N90-20504
Middle management of research
[NASA-TM-102417] 13 p1899 N90-20901
Fuel cell systems program plan, FY 1990
[DE90-008178] 14 p2002 N90-21471
Large space systems antenna technology 15 p2060 N90-21798
Solid fuel combustion chamber
[LR-591] 15 p2068 N90-21847
SeaRISE: A Multidisciplinary Research Initiative to Predict Rapid Changes in Global Sea Level Caused by Collapse of Marine Ice Sheets
[NASA-CP-3075] 16 p2249 N90-22824
Lunar base 2 (the second thousand days of a base on the Moon)
[ILR-MITT-230(1989)] 16 p2275 N90-22968
Human exploration of space: A review of NASA's 90-day study and alternatives
[NASA-CR-186394] 17 p2357 N90-23418
Satellite navigation system projects: European complement to GPS (CE-GPS), NAVSAT 17 p2360 N90-23434
Implementation of location programmes 17 p2360 N90-23440
Conceptual design of a Moving Belt Radiator (MBR) shuttle-attached experiment
[NASA-CR-185189] 17 p2367 N90-23474
Materials and processes for spacecraft: The ESTEC approach
[ESA-STM-244] 19 p2667 N90-25176
Program plan: International aircraft operator data base
[IAR-90-1] 19 p2763 N90-25697
The Federal Aviation Administration plan for research, engineering and development. Volume 1: Program plan
[AD-A221263] 19 p2800 N90-25930
The Federal Aviation Administration plan for research, engineering and development. Volume 2: Project descriptions
[AD-A221264] 19 p2800 N90-25931
Background, current status, and prognosis of the ongoing slush hydrogen technology development program for the NASP
[NASA-TM-103220] 20 p2822 N90-26055
The MODE S operational test and evaluation/integration test plan
[DOT/FAA/CT-TN89/51] 22 p3111 N90-27671
Flight service automation system, model 1 full capacity, NAS operational test and evaluation integration test plan
[DOT/FAA/CT-TN90/4] 22 p3111 N90-27672
A FAA Technical Center project transition plan: Mode S
[DOT/FAA/CT-TN90/17] 23 p3319 N90-28765
Long-range plan for a research project on carbon monoxide production and prediction
[PB90-209602] 23 p3346 N90-28910
A survey of planning and scheduling research at the NASA Ames Research Center 23 p3376 N90-29076

PROJECT SETI
The NASA SETI sky survey: Recent developments 04 p0488 N90-12804

PROJECTILE CRATERING
Role of shear instability in ballistic penetration
[AD-A219186] 16 p2244 N90-22799

PROJECTILE PENETRATION
U TERMINAL BALLISTICS

PROJECTILES
NT HYPERVELOCITY PROJECTILES
NT PRECISION GUIDED PROJECTILES
NT SABOT PROJECTILES
Remarks on certain aspects of solid explosive detonation via small projectile impact
[AD-A210648] 01 p0054 N90-10307
Studies in penetration mechanics
[AD-A210713] 01 p0079 N90-10448
EPIC-2 calculated impact loading histories of thin plates
[AD-A210557] 01 p0081 N90-10461
Fracture and three dimensional stress analyses of 7075 aluminum projectile components under spin and inertia load
[AD-A210986] 01 p0081 N90-10463
The temporal development of collision cascades in the binary collision approximation
[DE89-015860] 01 p0122 N90-10699
Gas-accelerated plate stability study
[DE89-016880] 02 p0225 N90-11289
Evaluation of integrals related to the Debye function
[DE89-016930] 02 p0264 N90-11499
Present and future US and Soviet chemical missiles and chemical rocket projectiles
[AD-A212199] 04 p0461 N90-12644
Stress waves through projectile joints and interfaces
[AD-A212201] 04 p0513 N90-12963
Current management for improved railgun performance
[AD-A212887] 05 p0593 N90-13445
Solving the blow-by problem in a two-stage gun
[DE90-000842] 06 p0728 N90-14246
Acceleration of small, light projectiles (including hydrogen isotopes) to high speeds using a two-stage light gas gun
[DE90-002479] 06 p0729 N90-14253
Performance characteristics of a three-stage railgun
[DE90-002533] 06 p0729 N90-14254
Elastomeric impulse energy storage and transfer system
[AD-D014223] 06 p0730 N90-14255
An electroformed nickel-sulfur alloy for a nose cone
[DE90-000866] 06 p0745 N90-14337
Electric-gun studies of conductors in high magnetic fields and experiments in dynamic flux compression
[DE90-000815] 06 p0768 N90-14470
Projectile impact Hugoniot parameters for selected materials
[DE90-000891] 06 p0793 N90-14618
MESA 3-D calculations of armor penetration by projectiles with combined obliquity and yaw
[DE89-015265] 07 p0939 N90-15438
The use of hypervelocity launchers to explore previously inaccessible states of matter
[DE90-004088] 08 p1034 N90-15973
Stability and fragmentation of ejecta in hypervelocity impact
[DE90-004087] 08 p1085 N90-16278
Summary of a decade of railgun development for high-pressure research
[DE90-005247] 09 p1172 N90-16780
A covariant multiple scattering series for elastic projectile-target scattering
[NASA-TM-101942] 09 p1279 N90-17417
Hypervelocity acceleration and impact experiments with the LLNL electric gun
[DE90-006924] 10 p1326 N90-17664
Supersonic wind tunnel investigation of a tubular projectile
[ISL-CO-306/89] 11 p1452 N90-18366
Measurement of gas leaks between a projectile and the walls of a tube in a ballistic compressor
[ISL-CO-250/88] 11 p1510 N90-18694
Effects of oblique impact on hypervelocity shield performance
[DE90-006936] 11 p1517 N90-18739
External flow computations for a finned 60mm ramjet in steady supersonic flight
[AD-A216998] 12 p1605 N90-19233
Computational fluid dynamics method for low Reynolds number flow in a precessing/spinning, liquid filled cylinder with rounded endcaps
[AD-A216997] 12 p1659 N90-19531
ARDEC (Armament Research, Development and Engineering Center) electric gun in-house test program
[AD-A217337] 13 p1760 N90-20105
A 10-stage reconnection demonstration launcher
[DE90-007653] 13 p1760 N90-20106
Diagnostics and firing control for the cylindrical reconnection launcher
[DE90-007677] 13 p1761 N90-20107
Design and performance of a multi-stage cylindrical reconnection launcher
[DE90-007820] 13 p1761 N90-20108
Evaluation of 2090-T8E48 aluminum-lithium plates
[AD-A217262] 13 p1776 N90-20196
Interior fluid dynamics of liquid-filled projectiles
[AD-A217630] 13 p1800 N90-20330
Simple light gas guns for hypervelocity studies
[DE90-008907] 14 p1931 N90-21056
Railgun performance with a two-stage light-gas gun injector
[DE90-009183] 14 p1932 N90-21057
Ablative cooling of aerodynamically heated radomes
[AD-D014426] 14 p1971 N90-21293
Perforation of a reinforced concrete wall by a rigid missile
[AD-A210025] 14 p1986 N90-21381
Current management for improved railgun performance 15 p2057 N90-21781
Active primary lithium thionyl chloride battery for artillery applications
[DE90-009511] 15 p2089 N90-21955
Large-scale simulations of monolithic and segmented projectiles impacting spaced armor
[AD-A219374] 16 p2244 N90-22800
Effects of X radiation on the LAMPSHADE orbital debris satellite shield, 2
[DE90-008214] 18 p2510 N90-24341
X ray diffraction analysis of control and test fibers
[MTL-TR-89-58] 19 p2678 N90-25233
A computational study of the effectiveness of coating materials for KE projectile fins subjected to the combined effects of inbore and aerodynamic heating
[AD-A222595] 20 p2840 N90-26155
Magnetic flux leakage versus ultrasonic correlation
[AD-A222112] 21 p3071 N90-27462
Collision forces for compliant projectiles
[NASA-TM-4203] 22 p3192 N90-28111
Projectile supersonic drag characteristics
[AD-A224217] 23 p3270 N90-28506
Supersonic/hypersonic aerodynamics and heat transfer for projectile design using viscous-inviscid interaction
[AD-A224354] 24 p3418 N90-29303
SONA: A measurement system for the determination of the end-of-flight burst behaviour of projectiles equipped with proximity fuses
[FEL-89-A293] 24 p3459 N90-29536
Detectors and signal processing for the speed measuring system 4-01
[FEL-1989-64] 24 p3472 N90-29623

PROJECTIVE GEOMETRY
Formal groups and differential equations
[ETN-90-96924] 18 p2603 N90-24825

PROJECTORS
Large screen display for the Mission Control Center 13 p1858 N90-20662
Some design considerations for small piezo-electrical ceramic transducers
[FEL-1989-68] 22 p3178 N90-28034

PROJECTS
NT AGRISTARS PROJECT
NT APOLLO SOYUZ TEST PROJECT
NT GALILEO PROJECT
NT MAGELLAN PROJECT (NASA)
NT PIONEER PROJECT
NT PROJECT SETI
NT SCANNER PROJECT
NT SCOUT PROJECT
NT VOYAGER PROJECT
Activities report of the National Electrotechnic Institute Galileo Ferraris
[ETN-90-96178] 08 p1157 N90-16705

The AGRISCATT-87 campaign: Processing of the Dutscat data
[BCRS-89-20] 15 p2122 N90-22140
Pre-study laser bathymetry
[BCRS-89-26] 15 p2134 N90-22198
Archimedes mission aspects
[ETN-90-96556] 17 p2361 N90-23442
Project TTA-79: Summary project report
[ETN-90-96773] 19 p2661 N90-25146
Activities report of the Institute of Sound and Vibration Research
[ETN-90-97604] 24 p3565 N90-30170

PROLATE SPHEROIDS
Numerical computation of the viscous flow field around a prolate spheroid
[DFVLR-FB-89-22] 03 p0349 N90-11992

PROLOG (PROGRAMMING LANGUAGE)
A formatting style for typesetting and distributing draft international standards
[NPL-DITC-143/89] 04 p0530 N90-13059
Truth maintenance systems and their implementation in PROLOG
[MEMO-INF-89-13] 04 p0531 N90-13064
LAIOS: A multiprocessor network for artificial intelligence applications
[ETN-89-95498] 04 p0537 N90-13109
On the safe approximation of PROLOG programs
[CWI-CS-R8913] 05 p0683 N90-13978
Conceptual modeling via logic programming
[AD-A219785] 17 p2442 N90-23919
Intelligent tutoring systems: An exploratory study of ITS and their implementation in Prolog
[RUU-CS-88-37] 18 p2597 N90-24779

PROMINENCES
NT SOLAR PROMINENCES

PROOFS
U PROVING

PROP-FAN TECHNOLOGY
Large scale prop-fan structural design study. Volume 1: Initial concepts
[NASA-CR-174992] 01 p0010 N90-10043
Large scale prop-fan structural design study. Volume 2: Preliminary design of SR-7
[NASA-CR-174993] 01 p0010 N90-10044
Large-scale Advanced Prop-fan (LAP) high speed wind tunnel test report
[NASA-CR-182125] 01 p0010 N90-10045
Large-scale Advanced Prop-fan (LAP) technology assessment report
[NASA-CR-182142] 01 p0010 N90-10046
Full scale technology demonstration of a modern counterrotating unducted fan engine concept: Component test
[NASA-CR-180868] 01 p0010 N90-10047
Full scale technology demonstration of a modern counterrotating unducted fan engine concept. Design report
[NASA-CR-180867] 01 p0010 N90-10048
Full scale technology demonstration of a modern counterrotating unducted fan engine concept. Engine test
[NASA-CR-180869] 01 p0011 N90-10049
Acoustic test and analysis of a counterrotating prop-fan model
[NASA-CR-179590] 01 p0119 N90-10683
Propfan Test Assessment (PTA): Flight test report
[NASA-CR-182278] 03 p0306 N90-11738
Propfan Test Assessment (PTA)
[NASA-CR-185138] 03 p0306 N90-11739
Numerical simulation of unsteady rotational flow over propfan configurations
[NASA-CR-186037] 04 p0438 N90-12500
Large-scale Advanced Prop-fan (LAP) static rotor test report
[NASA-CR-180848] 04 p0457 N90-12617
The design and development of an acoustic test section for the ARA transonic wind tunnel
[PNR90574] 04 p0550 N90-13202
Unsteady Euler analysis of the flow field of a propfan at an angle of attack
[NASA-TM-102426] 10 p1426 N90-18229
Structural tailoring of select fiber composite structures
[NASA-TM-102484] 14 p1946 N90-21137
Unsteady Euler solutions on dynamic blocked grids for complex configurations 15 p2094 N90-21982
Investigation of advanced counterrotation blade configuration concepts for high speed turboprop systems, task 1: Ducted propfan analysis
[NASA-CR-185217] 16 p2202 N90-22567
Experimental performance and acoustic investigation of modern, counterrotating blade concepts
[NASA-CR-185158] 17 p2352 N90-23393
Advanced gearbox technology
[NASA-CR-179625] 18 p2498 N90-24274
En route noise: NASA propfan test aircraft (corrected data - simplified procedure)
[DOT-TSC-FA953-LR4] 18 p2608 N90-24856
En route noise: NASA propfan test aircraft (calculated source noise
[DOT-TSC-FA953-LR5] 18 p2609 N90-24857
En route noise of turboprop aircraft and their acceptability: Report of tests 18 p2609 N90-24858
En route noise of two turboprop aircraft
[DLR-MITT-89-18] 18 p2609 N90-24859
Noise measurements of turboprop airplanes at different overflight elevations 18 p2609 N90-24860
When propfans cruise, will LDN 65 fly 18 p2610 N90-24864
En route noise annoyance laboratory test: Preliminary results 18 p2611 N90-24870
Euler analysis comparison with LDV data for an advanced counter-rotation propfan at cruise
[NASA-TM-103249] 20 p2803 N90-25946
Structural analysis and optimization of a propfan blade using a finite element method
[DLR-FB-90-01] 20 p2812 N90-26006
Aeroacoustics of advanced propellers
[NASA-TM-103137] 20 p2923 N90-26635
Measurement of the steady surface pressure distribution on a single rotation large scale advanced prop-fan blade at Mach numbers from 0.03 to 0.78
[NASA-CR-182124] 23 p3278 N90-28552

PROPAGATION (EXTENSION)
NT CRACK PROPAGATION
NT FLAME PROPAGATION

PROPAGATION MODES
NT WHISPERING GALLERY MODES
Wave-mode coordinate analysis of L junction in LSS
[AD-A211116] 02 p0176 N90-10984
Wide-angle propagation in inhomogeneous fluids and elastic solids using perturbation methods 06 p0837 N90-14868
Computation of coupling elements between waveguides and modes for large launching structures
[IPPCZ-290] 13 p1890 N90-20842
Analysis of a TM01 circular to TE10 rectangular waveguide mode converter
[AD-A224566] 24 p3464 N90-29568

PROPAGATION VELOCITY
A compilation of digitized satellite imagery of the Gulf Stream (1982, 1983, and 1985)
[AD-A210243] 01 p0082 N90-10467
Shock pressure determination in detonator wires
[DE89-017756] 03 p0350 N90-12002
A numerical study of thin flame representations
[DE89-017889] 06 p0741 N90-14313
New approach to omega PPCs (Propagation Corrections)
[AD-A215610] 09 p1207 N90-17000
A neural network based speech recognition system
[AD-A219794] 17 p2389 N90-23606

PROPANE
Test method for fire extinguishing powder, Nordtest project 675-87
[PB90-166984] 15 p2073 N90-21874
Critical evaluation of Jet-A spray combustion using propane chemical kinetics in gas turbine combustion simulated by KIVA-2
[NASA-TM-103173] 20 p2843 N90-26170
Laboratory studies, analysis, and interpretation of the spectra of hydrocarbons present in planetary atmospheres including cyanoacetylene, acetylene, propane, and ethane 20 p2943 N90-26748
Structure and radiation properties of turbulent diffusion flames
[PB90-218777] 22 p3155 N90-27887

PROPELLANT ADDITIVES
NT PROPELLANT BINDERS
Homogeneous catalysts in hypersonic combustion
[DE89-015258] 02 p0193 N90-11098
N-Hexyl Carborane (NHC) as combustion catalyst in composite propellants
[FOA-C-20755-2.1] 02 p0209 N90-11193
Calculation of Einstein A coefficients and oscillator strengths for the A(perturbed)(2)A(1)-X(perturbed)(2)B(1) transition of NH(2)
[AD-A213837] 07 p0896 N90-15176
Investigation of the phase stabilizing effect of 4 percent potassium fluoride on ammonium nitrate
[AD-A215313] 11 p1494 N90-18599
Ignition and combustion characteristics of metallized propellants
[NASA-CR-186870] 21 p2976 N90-26911
High energy-density liquid rocket fuel performance
[NASA-CR-185279] 23 p3315 N90-28742
An experimental investigation of strand burning metallized solid propellants
[AD-A224074] 24 p3457 N90-29526

PROPELLANT BINDERS
A surface coupled flamelet approach to dynamic response in heterogeneous propellant combustion 06 p0739 N90-14302
Using small scale tests to estimate the failure diameter of a propellant
[DE90-001166] 07 p0913 N90-15281
A study of near tip phenomena for cracks in a particulate composite 10 p1395 N90-18062

PROPELLANT CHEMISTRY
Cubane derivatives for propellant applications
[AD-A210368] 01 p0054 N90-10305
The mobile combustion diagnostic fixture and its application to the study of propellant combustion. Part 1: Investigation of the low pressure combustion of LOVA XM39 propellant
[AD-A213272] 05 p0621 N90-13626
Calculation of Einstein A coefficients and oscillator strengths for the A(perturbed)(2)A(1)-X(perturbed)(2)B(1) transition of NH(2)
[AD-A213837] 07 p0896 N90-15176

PROPELLANT COMBUSTION
NT SOLID PROPELLANT COMBUSTION
NT SOLID PROPELLANT IGNITION
Combustion Instabilities in Liquid-Fuelled Propulsion Systems
[AGARD-CP-450] 01 p0035 N90-10191
Low frequency and high frequency combustion oscillation phenomena inside a rocket combustion chamber fed by liquid or gaseous propellants 01 p0036 N90-10197
Nitramine composite solid propellant modeling 02 p0207 N90-11183
Laser initiated ignition of liquid propellant
[AD-A212342] 04 p0482 N90-12766
The mobile combustion diagnostic fixture and its application to the study of propellant combustion. Part 1: Investigation of the low pressure combustion of LOVA XM39 propellant
[AD-A213272] 05 p0621 N90-13626
A surface coupled flamelet approach to dynamic response in heterogeneous propellant combustion 06 p0739 N90-14302
Spectral studies of solid propellant combustion. 2: Emission and absorption results for M-30 and HMX1 propellants
[AD-A213857] 07 p0915 N90-15292
Research in energetic compounds
[AD-A214106] 10 p1360 N90-17887
Test data of flow field of shuttle SRM nozzle joint with bond defects, using unheated air 11 p1470 N90-18464
Extraction of recovery of plasticizers from solid propellants and munitions
[AD-D014433] 15 p2072 N90-21868
Structure of monopropellant spray flames at elevated pressures
[AD-A218676] 17 p2383 N90-23570
Nitramine composite solid propellant modelling
[AD-A220198] 17 p2383 N90-23573
An evaluation of imbedded thermocouples as a solid-propellant combustion diagnostic
[AD-A219947] 17 p2406 N90-23711
Combustor design and analysis using the Rocket Combustor Interactive Design (ROCCID) methodology
[NASA-TM-103165] 18 p2513 N90-24349
Mars in situ propellants: Carbon monoxide and oxygen ignition experiments
[NASA-TM-103202] 20 p2823 N90-26065
Temperature and OH concentrations in a solid propellant flame using absorption techniques
[AD-A222591] 20 p2830 N90-26100
Energy Efficient Engine (E3) combustion system component technology performance report
[NASA-CR-168274] 23 p3279 N90-28555
Oxygen/methane combustion stability investigation 23 p3293 N90-28628
Combustion instability coupling with feed system acoustics 23 p3293 N90-28629
Tripropellant combustion process 23 p3293 N90-28631
High/variable mixture ratio oxygen/hydrogen engines 23 p3295 N90-28637
High energy-density liquid rocket fuel performance
[NASA-CR-185279] 23 p3315 N90-28742
Evaluation of the STM4-120 kinematic Stirling engine
[DE90-013836] 23 p3344 N90-28897
AFOSR/ONR Contractors' Meeting on Combustion Rocket Propulsion Diagnostics of Reacting Flow
[AD-A224411] 24 p3441 N90-29432
Investigation of fluid dynamic performance of LE-7 liquid oxygen pump
[NAL-TR-1020] 24 p3476 N90-29650

PROPELLANT DECOMPOSITION
Laser initiated ignition of liquid propellant
[AD-A212342] 04 p0482 N90-12766

Calculation of Einstein A coefficients and oscillator strengths for the A(perturbed)(2)A(1)-X(perturbed)(2)B(1) transition of NH(2)
[AD-A213837] 07 p0896 N90-15176
Analysis of the use of a methane propellant in a biowaste resistojet
[AD-A220475] 17 p2367 N90-23473

PROPELLANT EXPLOSIONS
Discrete modeling of beds of propellant exposed to strong stimulus
[DE90-008932] 14 p1957 N90-21206
Solid rocket propellant initiation via particle beam heating
[AD-A221900] 21 p2969 N90-26878

PROPELLANT GRAINS
A study of near tip phenomena for cracks in a particulate composite 10 p1395 N90-18062
Concentric layer ramjet fuel
[AD-D014443] 14 p1941 N90-21111
Metallized fuel particle size study in a solid fuel ramjet
[AD-A220079] 18 p2533 N90-24451
RSRM-9 (360L009): Ballistics mass properties
[NASA-CR-183944] 20 p2823 N90-26064
An experimental investigation of strand burning metallized solid propellants
[AD-A224074] 24 p3457 N90-29526

PROPELLANT OXIDIZERS
U ROCKET OXIDIZERS

PROPELLANT PROPERTIES
NT PROPELLANT SENSITIVITY

PROPELLANT SENSITIVITY
Shock-wave characterization of energetic booster-rocket propellant WAK-2 and its simulant UGS
[DE90-002633] 07 p0914 N90-15285
Research in energetic compounds
[AD-A214106] 10 p1360 N90-17887
Shock initiation sensitivity of damaged TP-H1207C composite propellant
[DE90-008509] 14 p1957 N90-21205
Workshop on ESD (Electrostatic Discharge) Ignition of Composite Solid Propellants
[AD-A218599] 17 p2382 N90-23569

PROPELLANT STORAGE
Evaluation of supercritical cryogen storage and transfer systems for future NASA missions
[NASA-TM-102394] 02 p0160 N90-10912
Independent Orbiter Assessment (IOA): Analysis of the reaction control system, volume 2
[NASA-CR-185532-VOL-2] 02 p0167 N90-10939
Independent Orbiter Assessment (IOA): Analysis of the reaction control system, volume 3
[NASA-CR-185532-VOL-3] 02 p0167 N90-10940
Evolutionary space station fluids management strategies
[NASA-CR-185137] 02 p0175 N90-10983
Independent Orbiter Assessment (IOA): Assessment of the orbital maneuvering system FMEA/CIL, volume 1
[NASA-CR-185544-VOL-1] 03 p0315 N90-11787
Independent Orbiter Assessment (IOA): Assessment of the reaction control system, volume 1
[NASA-CR-185543-VOL-1] 03 p0316 N90-11793
Independent Orbiter Assessment (IOA): Assessment of the reaction control system, volume 2
[NASA-CR-185543-VOL-2] 03 p0316 N90-11794
Independent Orbiter Assessment (IOA): Assessment of the reaction control system, volume 3
[NASA-CR-185543-VOL-3] 03 p0316 N90-11795
Independent Orbiter Assessment (IOA): Assessment of the reaction control system, volume 4
[NASA-CR-185543-VOL-4] 03 p0316 N90-11796
Independent Orbiter Assessment (IOA): Assessment of the reaction control system, volume 5
[NASA-CR-185543-VOL-5] 03 p0316 N90-11797
Atomic hydrogen as a launch vehicle propellant
[NASA-TM-102459] 06 p0735 N90-14284
Investigation of the phase stabilizing effect of potassium fluoride on ammonium nitrate
[AD-A213042] 06 p0753 N90-14381
Investigation of the phase stabilizing effect of 4 percent potassium fluoride on ammonium nitrate
[AD-A215313] 11 p1494 N90-18599
Laboratory tests to determine the chemical and physical characteristics of propellant-solvent-fuel oil mixtures
[AD-A222270] 21 p2990 N90-26991

PROPELLANT TANKS
Independent Orbiter Assessment (IOA): Assessment of the electrical power generation/power reactant storage and distribution subsystem FMEA/CIL
[NASA-CR-185545] 02 p0163 N90-10923
Tank pressure control experiment on the space shuttle
[NASA-TM-102313] 05 p0615 N90-13500
Large scale metrology by computer assisted photogrammetry
[REPT-892-430-116] 16 p2239 N90-22772
Prediction of the ullage gas thermal stratification in a NASP vehicle propellant tank experimental simulation using FLOW-3D
[NASA-TM-103217] 20 p2841 N90-26160

PROPELLANT TESTS
The measurement, modeling, and prediction of traction for rocket propellant 1
[NASA-CR-185186] 12 p1633 N90-19386

PROPELLANT TRANSFER
Evaluation of supercritical cryogen storage and transfer systems for future NASA missions
[NASA-TM-102394] 02 p0160 N90-10912
Independent Orbiter Assessment (IOA): Analysis of the orbiter main propulsion system
[NASA-CR-185584] 02 p0164 N90-10927
Independent Orbiter Assessment (IOA): Assessment of the orbiter main propulsion system FMEA/CIL, volume 1
[NASA-CR-185559-VOL-1] 03 p0312 N90-11775
Independent Orbiter Assessment (IOA): Assessment of the main propulsion subsystem FMEA/CIL, volume 2
[NASA-CR-185559-VOL-2] 03 p0313 N90-11776
Independent Orbiter Assessment (IOA): Assessment of the main propulsion subsystem FMEA/CIL, volume 3
[NASA-CR-185559-VOL-3] 03 p0313 N90-11777
Independent Orbiter Assessment (IOA): Assessment of the main propulsion subsystem FMEA/CIL, volume 4
[NASA-CR-185559-VOL-4] 03 p0313 N90-11778
Orbital fluid resupply assessment
11 p1475 N90-18487
Initial experimentation on the nonvented fill of a 0.14m3 (5 ft. 3) dewar with nitrogen and hydrogen
[NASA-TM-103155] 20 p2862 N90-26278
Engineering test results for the Moog Single Line Disconnect
[NASA-TM-100755] 22 p3132 N90-27776

PROPELLANTS
NT COMPOSITE PROPELLANTS
NT CRYOGENIC ROCKET PROPELLANTS
NT DOUBLE BASE PROPELLANTS
NT DOUBLE BASE ROCKET PROPELLANTS
NT GASEOUS ROCKET PROPELLANTS
NT GELLED ROCKET PROPELLANTS
NT GUN PROPELLANTS
NT HIGH ENERGY PROPELLANTS
NT HIGH TEMPERATURE PROPELLANTS
NT HMX
NT HTPB PROPELLANTS
NT HYBRID PROPELLANTS
NT HYPERGOLIC ROCKET PROPELLANTS
NT LIQUID ROCKET PROPELLANTS
NT METAL PROPELLANTS
NT MONOPROPELLANTS
NT NITRAMINE PROPELLANTS
NT PLASTIC PROPELLANTS
NT RDX
NT ROCKET PROPELLANTS
NT RP-1 ROCKET PROPELLANTS
NT SLURRY PROPELLANTS
NT SLUSH HYDROGEN
NT SOLID PROPELLANTS
NT SOLID ROCKET PROPELLANTS
NT STORABLE PROPELLANTS
NT TATB
Cubane derivatives for propellant applications
[AD-A210368] 01 p0054 N90-10305
Organic explosives and related compounds. Environmental and health considerations
[AD-A210554] 01 p0054 N90-10306
The mobile combustion diagnostic fixture and its application to the study of propellant combustion. Part 1: Investigation of the low pressure combustion of LOVA XM39 propellant
[AD-A213272] 05 p0621 N90-13626
Evaluation of selected computer models for modeling pyrotechnic and propellant devices
[AD-A213003] 05 p0629 N90-13671
Thermochemical calculations with inert compounds
[FOA-C-20759-2.1] 05 p0630 N90-13677
Stick propellant x ray inspection
[AD-A212601] 06 p0753 N90-14380
Ignitability test method and apparatus
[NASA-CASE-LAR-13996-1-SB] 07 p0893 N90-15161
Acquisition of analytical instruments for combustion research
[AD-A214495] 09 p1190 N90-16893
Measurement of the speed and temperature of ignition gases
[ISL-CO-246/88] 09 p1192 N90-16908
Analysis of liquid propellant exposed to elastomeric materials
[AD-A214465] 09 p1200 N90-16952
Effect of propellant flowrate and purity on carbon deposition in LO2/methane gas generators
11 p1471 N90-18468
Stress analysis of rocket motors with viscoelastic propellant by a mixed finite element model
14 p1941 N90-21112
Discrete modeling of beds of propellant exposed to strong stimulus
[DE90-008932] 14 p1957 N90-21206
The physiological cost of wearing the propellant handler's ensemble at the Kennedy Space Center
[NASA-TM-102786] 16 p2275 N90-22966
Laboratory simulation of the effect of rocket thrust on a precessing space vehicle
[NASA-CR-186681] 19 p2669 N90-25182
Mars in situ propellants: Carbon monoxide and oxygen ignition experiments
[NASA-TM-103202] 20 p2823 N90-26065
Analysis of scramjet engine characteristics
[NAL-TR-1041] 24 p3434 N90-29398

PROPELLER BLADES
User's manual for PEPSIG NASA tip vortex version
[NASA-CR-182178] 02 p0146 N90-10835
Computation of the tip vortex flowfield for advanced aircraft propellers
[NASA-CR-182179] 02 p0146 N90-10836
Prediction of unsteady blade surface pressures on an advanced propeller at an angle of attack
[NASA-TM-102374] 04 p0447 N90-12560
Large-scale Advanced Prop-fan (LAP) static rotor test report
[NASA-CR-180848] 04 p0457 N90-12617
Effect of reduced aft diameter and increased blade number on high-speed counterrotation propeller performance
[NASA-TM-102077] 05 p0575 N90-13352
Application of an efficient hybrid scheme for aeroelastic analysis of advanced propellers
[NASA-TM-102428] 05 p0576 N90-13355
An experimental investigation of viscous aspects of propelier blade flow 09 p1159 N90-16711
Relating flow between counter-rotating propellers to aerodynamic interaction noise 14 p1909 N90-20944
Measurement and prediction of propeller blade surface pressure distributions 14 p1912 N90-20961
Aerofoil design techniques 14 p1916 N90-20978
Large-scale advanced propeller blade pressure distributions: Prediction and data
[NASA-TM-102316] 16 p2201 N90-22564
Unsteady potential flow past a propeller blade section
[NASA-CR-4307] 18 p2493 N90-24246
Agusta methodology for pitch link loads prediction in preliminary design phase
[ETN-90-97270] 20 p2808 N90-25978
Low-speed wind tunnel investigation of the static stability and control characteristics of an advanced turboprop configuration with the propellers placed over the tail
[NASA-CR-186900] 20 p2814 N90-26017
Investigation of the techniques for the analysis of composite structures: Analysis and representation of the static and dynamic behavior of glued metal insert assemblies
[IMFL-89-44] 22 p3153 N90-27878
Vortice-propeller interaction
[LIMSI-89-9] 23 p3326 N90-28809
Investigation of ATP blades, part 2. Validation of two-dimensional viscous flow simulation codes around thin airfoils
[NAL-TR-1046] 24 p3421 N90-29326

PROPELLER DRIVE
NT HELICOPTER PROPELLER DRIVE
X.2 limited flight test plan
[AD-A214412] 07 p0880 N90-15099
Computation of viscous flow around a propeller-shaft configuration with infinite-pitch rectangular blades
14 p1912 N90-20958

PROPELLER EFFICIENCY
The design and development of an acoustic test section for the ARA transonic wind tunnel
[PNR90574] 04 p0550 N90-13202
Application of an efficient hybrid scheme for aeroelastic analysis of advanced propellers
[NASA-TM-102428] 05 p0576 N90-13355
Computation of viscous flow around a propeller-shaft configuration with infinite-pitch rectangular blades
14 p1912 N90-20958
A computer program for the prediction of nozzle-propeller performance
[LR-578] 15 p2048 N90-21740
Theory and numerical analysis of single and multi-element nozzle propellers
[LR-579] 15 p2048 N90-21741
Experimental performance and acoustic investigation of modern, counterrotating blade concepts
[NASA-CR-185158] 17 p2352 N90-23393

PROPELLER FANS
Concurrent processing adaptation of aeroplastic analysis of propfans
[NASA-TM-102455] 06 p0799 N90-14656

Unsteady Euler analysis of the flow field of a propfan at an angle of attack
[NASA-TM-102426] 10 p1426 N90-18229
Unsteady Euler solutions on dynamic blocked grids for complex configurations 15 p2094 N90-21982
Investigation of advanced counterrotation blade configuration concepts for high speed turboprop systems, task 1: Ducted propfan analysis
[NASA-CR-185217] 16 p2202 N90-22567
En route noise: NASA propfan test aircraft (corrected data - simplified procedure)
[DOT-TSC-FA953-LR4] 18 p2608 N90-24856
En route noise: NASA propfan test aircraft (calculated source noise
[DOT-TSC-FA953-LR5] 18 p2609 N90-24857
En route noise of two turboprop aircraft
[DLR-MITT-89-18] 18 p2609 N90-24859
Noise measurements of turboprop airplanes at different overflight elevations 18 p2609 N90-24860
When propfans cruise, will LDN 65 fly 18 p2610 N90-24864
Euler analysis comparison with LDV data for an advanced counter-rotation propfan at cruise
[NASA-TM-103249] 20 p2803 N90-25946
Aeroacoustics of advanced propellers
[NASA-TM-103137] 20 p2923 N90-26635
Structure-borne noise estimates for the PTA aircraft
[NASA-CR-4315] 22 p3244 N90-28396

PROPELLER NOISE
An investigation of counterrotating tip vortex interaction
[NASA-CR-185135] 02 p0271 N90-11549
Noise data of four small propeller-driven airplanes
[PB89-216980] 03 p0400 N90-12291
Evaluation of analysis techniques for low frequency interior noise and vibration of commercial aircraft
[NASA-CR-181851] 06 p0837 N90-14866
Predicted and measured boundary layer refraction for advanced turboprop propeller noise
[NASA-TM-102365] 09 p1279 N90-17413
The radiation of sound from a propeller at angle of attack
[NASA-CR-4264] 14 p2023 N90-21602
En route noise of turboprop aircraft and their acceptability: Report of tests 18 p2609 N90-24858
En route noise of two turboprop aircraft
[DLR-MITT-89-18] 18 p2609 N90-24859
When propfans cruise, will LDN 65 fly 18 p2610 N90-24864
Annoyance caused by advanced turboprop aircraft flyover noise: Counter-rotating-propeller configuration
[NASA-TP-3027] 23 p3392 N90-29166

PROPELLER SLIPSTREAMS
Recent improvements in the scope and accuracy of the performance prediction of nozzle propellers
[LR-598] 15 p2048 N90-21742
Development of a system for the numerical simulation of Euler flows, with results of preliminary 3-D propeller-slipstream/exhaust-jet calculations
[NLR-TR-88008-U] 20 p2863 N90-26285

PROPELLERS
NT CONTRAROTATING PROPELLERS
NT PROPELLER FANS
NT SHROUDED PROPELLERS
NT VARIABLE PITCH PROPELLERS
Large scale prop-fan structural design study. Volume 2: Preliminary design of SR-7
[NASA-CR-174993] 01 p0010 N90-10044
Evaluation of the improved OV-10 anti-icing system, phase 2
[AD-A213928] 07 p0877 N90-15083
An experimental investigation of viscous aspects of propeller blade flow 09 p1159 N90-16711
In-plane forces and moments on installed inclined propellers at low forward speeds
[ESDU-89047] 09 p1161 N90-16720
Noise of a simulated installed model counterrotation propeller at angle-of-attack and takeoff/approach conditions
[NASA-TM-102440] 13 p1881 N90-20794
Laser-velocimeter-measured flow field around an advanced, swept, eight-blade propeller at Mach 0.8
[NASA-TP-2462] 14 p1909 N90-20942
Relating flow between counter-rotating propellers to aerodynamic interaction noise 14 p1909 N90-20944
Aerodynamic optimization by simultaneously updating flow variables and design parameters 14 p1918 N90-20991
Theory and numerical analysis of single and multi-element nozzle propellers
[LR-579] 15 p2048 N90-21741
Tests for integrating measurement of gas pressures in flight propellers
[ETN-90-96498] 18 p2494 N90-24253
Fluid dynamic and acoustic experiments on turbomachine rotors subject to variable flow conditions
[AD-A220298] 18 p2552 N90-24565
FAA/NASA En Route Noise Symposium
[NASA-CP-3067] 18 p2608 N90-24853
En route noise of turboprop aircraft and their acceptability: Report of tests 18 p2609 N90-24858
A lifting surface method for the calculation of steady and unsteady, incompressible propeller aerodynamics
[ESA-TT-1151] 19 p2655 N90-25113
The application of the finite element method to an aerodynamic problem specific to propeller design
[LR-614] 19 p2656 N90-25116
An unsteady lifting surface method for single rotation propellers
[NASA-CR-4302] 20 p2802 N90-25940
Aeroacoustics of advanced propellers
[NASA-TM-103137] 20 p2923 N90-26635
Noise from tip vortex and bubble cavitation
[AD-A221962] 21 p3072 N90-27468
Structure-borne noise estimates for the PTA aircraft
[NASA-CR-4315] 22 p3244 N90-28396
Investigation of ATP blades, part 2. Validation of two-dimensional viscous flow simulation codes around thin airfoils
[NAL-TR-1046] 24 p3421 N90-29326
Generalized Advanced Propeller Analysis System (GAPAS). Volume 2: Computer program user manual
[NASA-CR-185277] 24 p3434 N90-29394

PROPORTIONAL CONTROL
Discrete proportional Plus Integral (PI) multivariable control laws for the Control Reconfigurable Combat Aircraft (CRCA)
[AD-A215664] 11 p1464 N90-18431
Modelling and control of a balloon borne stabilized platform 17 p2355 N90-23408

PROPORTIONAL COUNTERS
The x ray mirror and the PSPC of the supernova-rocket-project 05 p0662 N90-13867
The softest Einstein AGN (Active Galactic Nuclei)
[DE89-009389] 06 p0864 N90-15020
In-line wear monitor
[AD-A217799] 13 p1757 N90-20091
The Einstein All-Sky IPC slew survey 19 p2787 N90-25865
The dependence of the soft X ray spectral slope with radio property, luminosity, and redshift, for a large sample of AGN from the Einstein IPC data base 19 p2789 N90-25876
Spatial and spectral features of soft diffuse X ray background seen by the Einstein observatory 19 p2792 N90-25895
Einstein SSS + MPC observations of Seyfert type galaxies 19 p2795 N90-25913
X ray spectra of cataclysmic variables
[NASA-CR-187002] 23 p3412 N90-29280

PROPORTIONAL LIMIT
Strength under various modes of deformation
[AD-A222412] 21 p3013 N90-27132

PROPRIOCEPTION
Proprioception in aircraft control
[IZF-1989-43] 23 p3377 N90-29082

PROPULSION
NT ASCENT PROPULSION SYSTEMS
NT AUXILIARY PROPULSION
NT CHEMICAL PROPULSION
NT ELECTRIC PROPULSION
NT ELECTROMAGNETIC PROPULSION
NT HYBRID PROPULSION
NT ION PROPULSION
NT JET PROPULSION
NT LASER PROPULSION
NT LOW THRUST PROPULSION
NT MARINE PROPULSION
NT MATTER-ANTIMATTER PROPULSION
NT NUCLEAR ELECTRIC PROPULSION
NT NUCLEAR PROPULSION
NT PLASMA PROPULSION
NT SPACE STATION PROPULSION
NT SPACECRAFT PROPULSION
Fuel cells for vehicle propulsion applications: A thermodynamic systems analysis
[DE89-017689] 03 p0342 N90-11950
AGARD Highlights 89/2 06 p0717 N90-14184
CIS-lunar space infrastructure lunar technologies: Executive summary
[NASA-CR-186220] 06 p0865 N90-15029
Appropriate aeroprediction accuracy in defining missile systems for aerodynamic flight 10 p1304 N90-17544
AFOSR/ONR (Air Force Office of Scientific Research/Office of Naval Research) Contractors' Meeting on Combustion Rocket Propulsion Diagnostics of Reacting Flow
[AD-A216094] 11 p1476 N90-18491
Proceedings of a contractors meeting on Combustion Rocket Propulsion Diagnostics of Reacting Flow
[AD-A216445] 12 p1617 N90-19297
Fuel-rich catalytic combustion: A fuel processor for high-speed propulsion
[NASA-TM-103177] 17 p2374 N90-23518
Technical accomplishments of the NASA Lewis Research Center, 1989
[NASA-TM-102296] 17 p2486 N90-24220
Conceptual design and analysis of roads and road construction machinery for initial lunar base operations
[NASA-CR-186673] 18 p2535 N90-24459
H-infinity based integrated flight-propulsion control design for a STOVL aircraft in transition flight
[NASA-TM-103198] 20 p2813 N90-26011
RSRM-9 (360L009): Ballistics mass properties
[NASA-CR-183944] 20 p2823 N90-26064
Supersonic reacting internal flow fields
[NASA-TM-103480] 20 p2829 N90-26094
Advanced launch vehicle configurations and performance trades 22 p3126 N90-27744
Autonomous propulsion system requirements for placement of an STS (Space Transportation System) external tank in low Earth orbit
[PB90-183302] 22 p3133 N90-27777
Flight motor set 360L006 (STS-34). Volume 1: System overview
[NASA-CR-184007] 22 p3133 N90-27781
An investigation of solid-fuel, dual-mode combustion ramjets 22 p3162 N90-27933
STOVL fighter propulsion reliability, maintainability, and supportability characterization
[AD-A224221] 23 p3282 N90-28574
Real time guidance and propulsion control for single-stage-to-orbit airbreathing vehicles 23 p3285 N90-28587
Operational cost drivers 23 p3294 N90-28636
Solid fuel combustion chamber
[LR-634] 24 p3441 N90-29433

PROPULSION SYSTEM CONFIGURATIONS
NT ASCENT PROPULSION SYSTEMS
Cycle analysis of scramjet engines
[NAL-TR-1002] 01 p0008 N90-10035
Liquid rocket booster study. Volume 2, book 4, appendices 6-8: Reports of Rocketdyne, Pratt and Whitney, and TRW
[NASA-CR-183603] 01 p0027 N90-10135
Liquid rocket booster study. Volume 2, book 2, appendix 1: Trades studies
[NASA-CR-183601] 01 p0027 N90-10136
Liquid rocket booster study. Volume 1: Executive summary
[NASA-CR-183599] 01 p0027 N90-10137
History and status of beamed power technology and applications at 2.45 Gigahertz 01 p0029 N90-10150
Materials for engine applications above 3000 deg F: An overview
[NASA-TM-100169] 01 p0034 N90-10188
Combustion Instabilities in Liquid-Fuelled Propulsion Systems
[AGARD-CP-450] 01 p0035 N90-10191
Combustion instabilities in liquid-fueled propulsion systems: An overview 01 p0035 N90-10192
Independent Orbiter Assessment (IOA): Assessment of the manned maneuvering unit
[NASA-CR-185564] 02 p0173 N90-10974
STOVL propulsion system volume dynamics approximations
[NASA-TM-102397] 03 p0306 N90-11740
Independent Orbiter Assessment (IOA): Assessment of the orbiter main propulsion system FMEA/CIL, volume 1
[NASA-CR-185559-VOL-1] 03 p0312 N90-11775
Independent Orbiter Assessment (IOA): Assessment of the main propulsion subsystem FMEA/CIL, volume 2
[NASA-CR-185559-VOL-2] 03 p0313 N90-11776
Independent Orbiter Assessment (IOA): Assessment of the main propulsion subsystem FMEA/CIL, volume 3
[NASA-CR-185559-VOL-3] 03 p0313 N90-11777
Independent Orbiter Assessment (IOA): Assessment of the main propulsion subsystem FMEA/CIL, volume 4
[NASA-CR-185559-VOL-4] 03 p0313 N90-11778
Large-scale Advanced Prop-fan (LAP) static rotor test report
[NASA-CR-180848] 04 p0457 N90-12617
SSME LOX post flow analysis/fluid structure interaction. Volume 2: Fluid structure interaction
[NASA-CR-183678] 05 p0637 N90-13716
Qualification of the 4th stage propulsor of the Brazilian launcher. SLV: A new sounding rocket 05 p0661 N90-13860
Main propulsion system test requirements for the two-engine Shuttle-C
[NASA-TM-100382] 06 p0735 N90-14282
Comparison between horizontally launched air-breathing single and two-stage to orbit space vehicles 09 p1175 N90-16802

Transportation systems for manned space missions
09 p1176 N90-16805
Space transportation booster engine configuration study. Addendum: Design definition document
[NASA-CR-183854] 09 p1184 N90-16862
Effects of scaling on the performance of magnetoplasmadynamic thrusters
[AD-A215690] 09 p1184 N90-16863
Booster propulsion/vehicle impact study, 2
[NASA-CR-179313] 10 p1346 N90-17809
The 1989 JANNAF Propulsion Meeting, volume 1
[CPIA-PUBL-515-VOL-1] 11 p1470 N90-18462
A perspective on the use of storable propellants for future space vehicle propulsion
11 p1472 N90-18473
Electric propulsion options for 10 kW class earth-space missions 11 p1472 N90-18474
Performance of large area xenon ion thrusters for orbit transfer missions 11 p1472 N90-18475
Mission options for an electric propulsion demonstration flight test 11 p1473 N90-18479
Electric propulsion for manned Mars exploration
11 p1473 N90-18480
Controllable propulsion for escape systems control
13 p1753 N90-20064
Advanced launch vehicle propulsion at the NASA Lewis Research Center
[NASA-TM-103096] 13 p1761 N90-20110
Performance of an aero-space plane propulsion nozzle 14 p1926 N90-21034
Probabilistic modeling for simulation of aerodynamic uncertainties in propulsion systems
[NASA-TM-102472] 14 p1927 N90-21036
Exhaust nozzles for propulsion systems with emphasis on supersonic cruise aircraft
[NASA-RP-1235] 14 p1927 N90-21037
A candidate architecture for monitoring and control in chemical transfer propulsion systems
[NASA-TM-103161] 16 p2208 N90-22595
AVION: A detailed report on the preliminary design of a 79-passenger, high-efficiency, commercial transport aircraft
[NASA-CR-186663] 17 p2353 N90-23395
Analysis of internal flow in a ventral nozzle for STOVL aircraft
[NASA-TM-103123] 17 p2355 N90-23404
Advanced gearbox technology
[NASA-CR-179625] 18 p2498 N90-24274
Advanced space transportation technologies
18 p2645 N90-25061
Nuclear power systems for lunar and Mars exploration
[NASA-TM-103168] 21 p2969 N90-26873
Ramjet and ramrocket propulsion systems for missiles
21 p2973 N90-26897
Advanced propulsion for LEO and GEO platforms
[NASA-TM-103228] 22 p3134 N90-27785
Liquid Rocket Booster (LRB) for the Space Transportation System (STS) systems study. Appendix B: Liquid rocket booster acoustic and thermal environments
[NASA-CR-183788-APP-B] 23 p3288 N90-28602
High/variable mixture ratio O2/H2 engine
23 p3295 N90-28638

PROPULSION SYSTEM PERFORMANCE

Performance potential of an advanced technology Mach 3 turbojet engine installed on a conceptual high-speed civil transport
[NASA-TM-4144] 01 p0008 N90-10034
Report on an overseas visit, June 1988
[AD-A210374] 01 p0009 N90-10040
Flight Motor Set 360L003 (STS-29R)
[NASA-CR-183739-VOL-1] 01 p0031 N90-10170
A rocket engine design expert system
[NASA-TM-102373] 01 p0032 N90-10172
Experimental study on the stability of small rocket engines with storable liquid propellants
01 p0036 N90-10196
Gas turbine performance analysis
[PNR90599] 04 p0456 N90-12614
RSRM-3 (360L003) ballistics/mass properties report
[NASA-CR-183716] 04 p0463 N90-12651
Ballistics/mass properties
[NASA-CR-183723] 04 p0463 N90-12652
SSME LOX post flow analysis/fluid structure interaction. Volume 2: Fluid structure interaction
[NASA-CR-183678] 05 p0637 N90-13716
Main propulsion system test requirements for the two-engine Shuttle-C
[NASA-TM-100382] 06 p0735 N90-14282
Vulcain engine development status
09 p1176 N90-16810
Performance integration of a reusable launch vehicle with hybrid airbreathing rocket propulsion
09 p1177 N90-16820
Advanced APS impacts on vehicle payloads
11 p1472 N90-18472
Electric propulsion options for 10 kW class earth-space missions 11 p1472 N90-18474
Performance of large area xenon ion thrusters for orbit transfer missions 11 p1472 N90-18475
Test facility and preliminary performance of a 100 kW class MPD thruster 11 p1472 N90-18476
Mission options for an electric propulsion demonstration flight test 11 p1473 N90-18479
Electric propulsion for manned Mars exploration
11 p1473 N90-18480
Rapid near-optimal trajectory generation and guidance law development for single-stage-to-orbit airbreathing vehicles
[NASA-CR-186299] 12 p1612 N90-19275
Controllable propulsion for escape systems control
13 p1753 N90-20064
Advanced launch vehicle propulsion at the NASA Lewis Research Center
[NASA-TM-103096] 13 p1761 N90-20110
Performance of an aero-space plane propulsion nozzle 14 p1926 N90-21034
Probabilistic modeling for simulation of aerodynamic uncertainties in propulsion systems
[NASA-TM-102472] 14 p1927 N90-21036
Exhaust nozzles for propulsion systems with emphasis on supersonic cruise aircraft
[NASA-RP-1235] 14 p1927 N90-21037
Technical Evaluation Motor no. 5 (TEM-5)
[NASA-CR-183932] 14 p1942 N90-21117
Assessment of High Temperature Superconducting (HTS) electric motors for rotorcraft propulsion
[NASA-CR-185222] 15 p2052 N90-21761
Preliminary design of a long-endurance Mars aircraft
[NASA-CR-185243] 15 p2052 N90-21763
A candidate architecture for monitoring and control in chemical transfer propulsion systems
[NASA-TM-103161] 16 p2208 N90-22595
Application of ultracapacitors in electric vehicle propulsion systems
[DE90-010884] 18 p2550 N90-24554
From 1959-1989: 30 years of service experience with ramjets
[PNR90677] 19 p2660 N90-25139
Spacecraft external molecular contamination analysis
19 p2730 N90-25520
The Screem-J4D: A proposal in response to a low Reynolds number station keeping mission
[NASA-CR-186664] 20 p2807 N90-25968
The effect of interplanetary trajectory options on a manned Mars aerobrake configuration
[NASA-TP-3019] 20 p2818 N90-26036
Supersonic reacting internal flow fields
[NASA-TM-103480] 20 p2829 N90-26094
Space Propulsion Hazards Analysis Manual (SPHAM), volume 1
[AD-A219607] 21 p2969 N90-26874
Space Propulsion Hazards Analysis Manual (SPHAM), volume 2
[AD-A219608] 21 p2969 N90-26875
Ramjet and ramrocket propulsion systems for missiles
21 p2973 N90-26897
Advanced propulsion for LEO and GEO platforms
[NASA-TM-103228] 22 p3134 N90-27785
Propulsion system-flight control integration and optimization: Flight evaluation and technology transition
[NASA-TM-4207] 23 p3278 N90-28551
Liquid Rocket Booster (LRB) for the Space Transportation System (STS) systems study. Appendix B: Liquid rocket booster acoustic and thermal environments
[NASA-CR-183788-APP-B] 23 p3288 N90-28602
Effects of friction and end losses on MHD thruster efficiency
[DE90-013673] 23 p3289 N90-28608
Advanced Earth-to-Orbit Propulsion Technology 1988, volume 1
[NASA-CP-3012-VOL-1] 23 p3290 N90-28611
Low power arcjet performance
[NASA-TM-103280] 23 p3298 N90-28657
Solid fuel combustion chamber
[LR-634] 24 p3441 N90-29433

PROPULSIVE EFFICIENCY

NT PROPELLER EFFICIENCY
Independent Orbiter Assessment (IOA): Analysis of the manned maneuvering unit
[NASA-CR-185565] 02 p0161 N90-10913
Fuel cells for vehicle propulsion applications: A thermodynamic systems analysis
[DE89-017689] 03 p0342 N90-11950
RSRM-3 (360L003) ballistics/mass properties report
[NASA-CR-183716] 04 p0463 N90-12651
Ballistics/mass properties
[NASA-CR-183723] 04 p0463 N90-12652
Aircraft propulsion: Leading the way in aviation
[LR-532] 05 p0583 N90-13395
Energy deposition in low power coaxial plasma thrusters 06 p0844 N90-14911
Mission-dependent selection of propulsion systems for reusable launch vehicles 09 p1177 N90-16815
Parametric assessment of propulsion system mass for airbreathing launcher configurations
09 p1177 N90-16819
Advanced APS impacts on vehicle payloads
11 p1472 N90-18472
AVION: A detailed report on the preliminary design of a 79-passenger, high-efficiency, commercial transport aircraft
[NASA-CR-186663] 17 p2353 N90-23395
Energy Efficient Engine (E3) combustion system component technology performance report
[NASA-CR-168274] 23 p3279 N90-28555
Energy Efficient Engine core design and performance report
[NASA-CR-168069] 23 p3279 N90-28559
Energy Efficient Engine integrated core/low spool test hardware design report
[NASA-CR-168137] 23 p3281 N90-28566
Energy Efficient Engine: High-pressure compressor test hardware detailed design report
[NASA-CR-180850] 23 p3281 N90-28570
Effects of friction and end losses on MHD thruster efficiency
[DE90-013673] 23 p3289 N90-28608

PROPYL COMPOUNDS

Determination of the minimum energy conformation of alkyl substituted pyrazines
[AD-A216974] 11 p1484 N90-18539

PROPYLENE

Rechargeable lithium/polymer cathode batteries
[AD-A210978] 01 p0062 N90-10354
Quantitative confirmation of diffusion-limited oxidation theories
[DE90-012997] 20 p2838 N90-26143
Structure and radiation properties of turbulent diffusion flames
[PB90-218777] 22 p3155 N90-27887

PROPYLENE OXIDE

Graft copolymers of rigid-rod poly(p-phenylenebenzobisimidazole)
[AD-A220369] 17 p2380 N90-23555

PROSTAGLANDINS

A program for the study of skeletal muscle catabolism following physical trauma
[AD-A216569] 11 p1539 N90-18859

PROSTHETIC DEVICES

Electromagnetic machines which utilize microgeometry field structures
[AD-A219828] 17 p2398 N90-23660
The interaction of polymeric materials with ceramic surfaces with special reference to the behaviour of bioceramics 20 p2836 N90-26127
Rotationally actuated prosthetic helping hand
[NASA-CASE-MFS-28426-1] 21 p3036 N90-27261

PROTECTION

NT CIRCUIT PROTECTION
NT CORROSION PREVENTION
NT ENVIRONMENT PROTECTION
NT EYE PROTECTION
NT METEOROID PROTECTION
NT RADIATION PROTECTION
NT RADIATION SHIELDING
NT SOLAR RADIATION SHIELDING
NT THERMAL PROTECTION
Flight set 360T004 (STS-30) field joint protection system, volume 7
[NASA-CR-183829] 06 p0735 N90-14280
Means for protecting electroexplosive devices which are subject to a wide variety of radio frequency
[AD-D014219] 06 p0753 N90-14382
Performance evaluation of the Puritan-Bennett crew-member portable protective breathing device as prescribed by portions of FAA action notice A-8150.2
[AD-A211113] 06 p0821 N90-14772
Effects of lightning on operations of aerospace vehicles 07 p0873 N90-15065
Fuel tank explosion protection
08 p1023 N90-15914
Aircraft Fire Safety
[AGARD-CP-467] 10 p1311 N90-17581
A review of UK civil aviation fire and cabin safety research 10 p1312 N90-17587
The research program at the Civil Aeromedical Institute concerning protective breathing equipment for use by crew and passengers in an aviation smoke/fume environment
10 p1317 N90-17616
Lightning protection apparatus for RF equipment and the like
[AD-D014336] 12 p1650 N90-19483
The USAF Advanced Dynamic Anthropomorphic Manikin (ADAM) 13 p1752 N90-20062
Windblast protection for advanced ejection seats
13 p1752 N90-20063
Spacecraft escape 13 p1753 N90-20066

Pressure rig for repetitive casting
[NASA-CASE-LAR-14050-1] 14 p1959 N90-21216
The internet worm
[NASA-CR-181576] 17 p2441 N90-23910
Forward canopy feasibility and Thru-The-Canopy (TTC) ejection system study
[AD-A220360] 18 p2495 N90-24258
Some comments on techniques for resisting computer viruses
[AD-A221097] 18 p2593 N90-24754
Design of a thermal and micrometeorite protection system for an unmanned lunar cargo lander
[NASA-CR-186682] 19 p2664 N90-25161
Non-ejection neck injuries in high performance aircraft 19 p2717 N90-25461
Radiological investigation of the vertebral column of candidates for military flying training the the Royal Norwegian Air Force 19 p2718 N90-25463
Theft of information in the take-grant protection model
[NASA-CR-186638] 19 p2763 N90-25702
Carbon-carbon composites: Emerging materials for hypersonic flight
[NASA-TM-103472] 20 p2827 N90-26080
On travelling-wave-based protection of high-voltage networks
[ISBN-90-9002955-9] 20 p2858 N90-26260
A Protection And Detection Surface (PADS) for damage tolerance
[NASA-TP-3011] 22 p3135 N90-27788
Basic mechanisms for computer security
[RSRE-89024] 22 p3235 N90-28347

PROTECTIVE CLOTHING
NT EXTRAVEHICULAR MOBILITY UNITS
NT HELMETS
NT PRESSURE SUITS
NT SPACE SUITS
Concepts for microgravity experiments utilizing gloveboxes
[NASA-TM-100378] 02 p0209 N90-11195
Prediction of thermal stress casualties
[AD-A212356] 04 p0523 N90-13022
Integrated G-suit/immersion suit
[AD-A212989] 06 p0821 N90-14774
Physiological evaluation of men wearing three different toxicological protective systems
[AD-A215527] 09 p1261 N90-17313
Smokehoods donned quickly. The impact of donning smokehoods on evacuation times 10 p1317 N90-17614
Some practical advice on cold weather clothing
[AD-A215936] 10 p1414 N90-18148
Insulation, compressibility and absorbency of dry suit undergarments
[AD-A215944] 10 p1414 N90-18149
Anthropometry of a fit test sample used in evaluating the current and improved MCU-2/P masks
[AD-A215173] 11 p1541 N90-18873
Minutes of the 23rd Eplosives Safety Seminar, volume 2
[AD-A218265] 14 p1959 N90-21214
The physiological cost of wearing the propellant handler's ensemble at the Kennedy Space Center
[NASA-TM-102786] 16 p2275 N90-22966
Laboratory evaluation of two new high-performance polyester batting insulation materials
[AD-A222291] 21 p2987 N90-26976
Physical characteristics of clothing materials with regard to heat transport
[IZF-1989-10] 22 p3233 N90-28336

PROTECTIVE COATINGS
NT ANODIC COATINGS
NT CERAMIC COATINGS
NT PRIMERS (COATINGS)
NT REFRACTORY COATINGS
Diamondlike carbon coatings for optical systems
[AD-A211255] 02 p0276 N90-11573
Vanadium dioxide protective devices
[AD-A212018] 03 p0332 N90-11887
Surface treatments of carbon fibers in an organic environment. Finite element analysis of pull-out tests
[ONERA-RT-7/3549-M] 04 p0471 N90-12698
The quality of vacuum deposited surface treatments
[CETIM-107040] 04 p0476 N90-12729
Polyelectrolyte-diffused zinc phosphate conversion coatings and polyacid coupling primers for corrosion protection of steel and aluminum, and alkali-catalyzed hydrolysis of polyimide-based materials
[AD-A212240] 04 p0480 N90-12754
SiO overcoating and polishing of CFRP telescope panels 05 p0599 N90-13478
Wear-resistant coated object
[EP-PATENT-0-289-173-A1] 05 p0624 N90-13643
A review of the effects of microalloying constituents on the formation and breakdown of protective oxide scales on high-temperature alloys at temperatures below 700 C
[DE90-001277] 07 p0902 N90-15216
Fuel resistant coatings for metal and composite fuel tanks 08 p1022 N90-15911
Ultrasonic assisted paint removal method
[AD-D014264] 08 p1119 N90-16479
Polycarbonate article with chemical resistant coating
[NASA-CASE-MSC-21503-1] 09 p1195 N90-16925
Advanced tribological coatings for high specific strength alloys
[AD-A214061] 09 p1196 N90-16930
Study of adherent oxide scales
[AD-A215189] 09 p1198 N90-16940
Solar cell coverglasses with enhanced thermal and mechanical properties 10 p1343 N90-17785
Surface modification of steels and aluminum alloys to control corrosion and hydrogen embrittlement. Part 1: Chemical methods
[AD-A216272] 10 p1356 N90-17866
Chemistry-structure-property interrelationships for calcareous deposits as stand-alone coatings
[AD-A216031] 10 p1359 N90-17881
Sputter deposition of diffusion barrier coatings on SiC monofilaments for use in Ti-based composites 11 p1477 N90-18502
Aeolian removal of dust from photovoltaic surfaces on Mars
[NASA-TM-102507] 12 p1617 N90-19299
Effect of barrier layers in burn-through experiments with 351-nm laser illumination
[DE90-006806] 12 p1667 N90-19577
Molding solidification 13 p1785 N90-20246
The effect of leveling coatings on the atomic oxygen durability of solar concentrator surfaces
[NASA-TM-102557] 14 p1941 N90-21110
High gloss corrosion-resistant coatings
[AD-D014403] 14 p1954 N90-21184
Combination primer/topcoat coating
[AD-D014445] 14 p1954 N90-21189
Energy beam treatment for improved adhesion of coatings to surfaces
[AD-D014449] 14 p1954 N90-21190
Comparison of Goretex laminated and Dermoflex coated fabrics
[AD-A219383] 17 p2368 N90-23481
Corrosion control through a better understanding of the metallic substrate/organic coating interface
[AD-A220432] 17 p2377 N90-23533
Archaebacterial involvement in microbial metal corrosion: Metabolism of S and Fe
[AD-A219982] 17 p2377 N90-23537
Quality evaluation of coatings by automatic scratch testing
[AD-A219331] 17 p2379 N90-23548
Criteria for coal tar seal coats on airport pavements. Volume 2: Laboratory and field studies
[AD-A220167] 18 p2498 N90-24277
Abrasion resistant coatings on plastics 18 p2529 N90-24428
Failure mechanism of urethane elastomer coated fabric collapsible fuel tanks
[AD-A221033] 18 p2530 N90-24435
Hazards protection for space suits and spacecraft
[NASA-CASE-MSC-21366-1] 19 p2725 N90-25498
Laboratory investigations: Low Earth orbit environment chemistry with spacecraft surfaces 19 p2732 N90-25531
Passive mechanisms of surfaces produced by ion beam mixing and ion implantation
[AD-A222432] 21 p2982 N90-26945
Environmental integrity of coating/metal interface
[AD-A222426] 21 p2987 N90-26978
Corrosion-inhibiting coating composition
[AD-D014546] 22 p3159 N90-27916
High-temperature, corrosion-preventive coating
[AD-D014557] 22 p3160 N90-27918
Noncontact laser thermomechanical nondestructive evaluation for advanced coatings 22 p3187 N90-28087
Molten salt induced high temperature degradation of thermal barrier coatings 23 p3307 N90-28704
Effect of protective coatings on mechanical properties of superalloys 23 p3308 N90-28707
High temperature protective coatings: Recent trends 23 p3308 N90-28710
Evaluation of high temperature protective coatings for gas turbine engines under simulated service conditions 23 p3309 N90-28712
Overview on hot gas tests and molten salt corrosion experiments at the DLR 23 p3309 N90-28714
Preliminary exposure study to determine the effects of acid deposition on coated steel substrates
[PB90-201799] 23 p3309 N90-28715
Electrodeposition of wear resistant coatings
[PB90-221839] 23 p3312 N90-28732
Use of electron spectroscopies in the tribological evaluation of diamond films
[DE90-014421] 23 p3334 N90-28848
Investigation of laser diagnostics of PACVD (Plasma Assisted Chemical Vapor Deposition) processes for depositing hard face coatings
[DE90-016209] 24 p3457 N90-29522

PROTECTORS
NT EAR PROTECTORS
Independent Orbiter Assessment (IOA): Analysis of the backup flight system
[NASA-CR-185567] 02 p0165 N90-10932

PROTEIN CRYSTAL GROWTH
Protein crystal growth in low gravity
[NASA-CR-186082] 04 p0483 N90-12770
Protein crystal growth in microgravity 09 p1224 N90-17102
Protein crystal growth in low gravity
[NASA-CR-186243] 20 p2929 N90-26663

PROTEIN SYNTHESIS
Control of synthetic peptide tertiary structure
[AD-A210339] 01 p0049 N90-10281
Protein crystal growth in low gravity
[NASA-CR-186082] 04 p0483 N90-12770
The chemical basis for the origin of the genetic code and the process of protein synthesis
[NASA-CR-186590] 15 p2136 N90-22205
Experiment K-6-11. Actin mRNA and cytochrome c mRNA concentrations in the tricepts brachia muscle of rats 20 p2894 N90-26465
Insulin and insulin-like growth factor-1 induce pronounced hypertrophy of skeletal myofibers in tissue culture
[NASA-CR-187026] 23 p3354 N90-28960

PROTEINS
NT ALBUMINS
NT ASPARTATES
NT CARBOXYHEMOGLOBIN
NT CATALASE
NT CHOLINESTERASE
NT CYTOCHROMES
NT ENZYMES
NT GLOBULINS
NT HEMOGLOBIN
NT MELANIN
NT OXIDASE
Electrical field dependence of protein conformation and channel function in lipid membranes of different compositions
[AD-A210236] 01 p0040 N90-10222
Electron transfer reactions
[AD-A210711] 02 p0271 N90-11545
Protein crystal growth in low gravity
[NASA-CR-186082] 04 p0483 N90-12770
Combined capillary electrophoresis and electrospray ionization mass spectrometry
[DE90-001903] 06 p0743 N90-14322
Characterization of biopolymer surfaces using scanning microscopies
[AD-A216572] 11 p1490 N90-18572
A program for the study of skeletal muscle catabolism following physical trauma
[AD-A216569] 11 p1539 N90-18859
Study of rifampicin fixation on plasma proteins by derivative spectrophotometry
[CERMA-89-25] 11 p1540 N90-18866
Hanging drop crystal growth apparatus and method
[NASA-CASE-MFS-28206-1-SB] 16 p2322 N90-23242
Crystal growth apparatus
[NASA-CASE-MFS-28182-1] 17 p2478 N90-24169
Experiment K-6-10. Effects of zero gravity on myofibril protein content and isomyosin distribution in rodent skeletal muscle 20 p2894 N90-26464
Experiment K-6-11. Actin mRNA and cytochrome c mRNA concentrations in the tricepts brachia muscle of rats 20 p2894 N90-26465
Experiment K-6-14. Hepatic function in rats after spaceflight 20 p2895 N90-26468
Experiment K-6-20. The effect of spaceflight on pituitary oxytocin and vasopressin content of rats 20 p2896 N90-26473
Proximate composition of seed and biomass from soybean plants grown at different carbon monoxide (CO2) concentrations
[NASA-TM-103496] 20 p2897 N90-26480
Pseudomonas diagnostic assay
[NASA-CASE-NPO-17653-1-CU] 21 p3032 N90-27239

PROTOCOL (COMPUTERS)
Robotic vehicle message format
[AD-A210996] 01 p0110 N90-10627
Performance analysis of hybrid ARQ protocols in a slotted code division multiple-access network
[AD-A211078] 02 p0213 N90-11219
On the Amoeba protocol
[CWI-CS-R8827] 02 p0261 N90-11480
A survey of research methods to study design
[AD-A211213] 02 p0262 N90-11491

Adaptive gigabit fiber optics local area network
[AD-A210794] 02 p0275 N90-11571
A real-time locking protocol
[AD-A211514] 03 p0418 N90-12403
Analysis and modeling of summertime convective cloud and precipitation structure over the Southeastern United States
[NASA-CR-185436] 04 p0519 N90-12996
Spacelab system analysis: The modified free access protocol: An access protocol for communication systems with periodic and Poisson traffic
[NASA-CR-183805] 05 p0602 N90-13497
On stability of queueing models of local area networks with slotted ring protocols
[MEMO-795] 05 p0694 N90-14057
The characteristics of the HF radio channel and its influence on modern HF data communication system design 06 p0765 N90-14448
The Delta-t transport protocol: Features and experience useful for high performance networks
[DE89-016542] 06 p0831 N90-14832
Multiple crossbar network: A switched high-speed local network
[DE90-001839] 06 p0831 N90-14833
Satellite systems integrated with the terrestrial cellular network for mobile communications
[ESA-STR-228] 08 p1057 N90-16113
The DAB model of drawing processes 08 p1155 N90-16691
Method and apparatus for positioning a robotic end effector
[NASA-CASE-MSC-21476-1] 09 p1230 N90-17137
The use of efficient broadcast protocols in asynchronous distributed systems
[NASA-CR-186272] 09 p1269 N90-17358
A specification and analysis of the IEEE (Institute of Electrical and Electronic Engineers) token ring protocol
[AD-A214567] 09 p1269 N90-17359
Internet protocol handbook. Volume 4: The Domain Name System (DNS) handbook
[AD-A214698] 09 p1296 N90-17512
On board cross support scenarios
[INPE-5005-PRE/1562] 14 p1967 N90-21268
Cooperating intelligent systems
[NASA-CR-184982] 14 p2012 N90-21529
Fast causal multicast
[NASA-CR-186495] 14 p2013 N90-21533
Broadcast file distribution on packet satellite networks 15 p2079 N90-21906
Scalable coherent interface
[DE90-008011] 15 p2149 N90-22277
Extremely high data-rate, reliable network systems research
[NASA-CR-186359] 15 p2149 N90-22278
Traffic placement policies for a multi-band network 15 p2149 N90-22279
CSMA/RN: A universal protocol for gigabit networks 15 p2150 N90-22280
Alternative parallel ring protocols 15 p2150 N90-22282
Performance of gigabit FDDI 15 p2150 N90-22283
Distributed simulation of network protocols 15 p2150 N90-22284
Modelling high data rate communication network access protocol 15 p2150 N90-22285
Extensibility and limitations of FDDI 15 p2151 N90-22286
Fairness problems at the media access level for high-speed networks 15 p2151 N90-22287
A carrier sensed multiple access protocol for high data base rate ring networks 15 p2151 N90-22288
High-throughput, survivable protocols for CDMA packet-radio networks (SRNTN-74)
[AD-A220189] 17 p2393 N90-23631
The cost of conservative synchronization in parallel discrete event simulations
[NASA-CR-182034] 17 p2441 N90-23912
Fast casual multicast
[NASA-CR-186643] 17 p2462 N90-24059
On the use of equational type logic for software engineering and protocol design
[MEMO-INF-89-52] 18 p2592 N90-24748
Performance analysis of local area networks
[NASA-CR-186639] 18 p2595 N90-24767
How to construct an atomic variable
[CWI-CS-R8939] 18 p2596 N90-24772
Analysis of a queueing model of the Orwell slotted ring
[MEMO-812] 18 p2606 N90-24843
Some issues related to simulation of the tracking and communications computer network 18 p2630 N90-24988
An expert system to advise astronauts during experiments: The protocol manager module 19 p2730 N90-25522
SHAPA: An interactive software tool for protocol analysis applied to aircrew communications and workload 19 p2734 N90-25541
Exploiting replication in distributed systems
[NASA-CR-186410] 19 p2746 N90-25603
Reliable broadcast protocols
[NASA-CR-186411] 19 p2762 N90-25696
Extension of a noninteractive reliability model for ceramic matrix composites
[NASA-CR-185267] 20 p2838 N90-26142
A versatile integrated block codes encoder-decoder 20 p2848 N90-26197
MTP: An atomic multicast transport protocol
[NASA-CR-186716] 20 p2858 N90-26254
Formal verification of distributed computing systems: Logic characterization of behaviour equivalence
[LAAS-89386] 20 p2910 N90-26555
Design of a universal protocol subsystem architecture: Specification of functions and services
[EUT-89-E-230] 20 p2912 N90-26569
Analysis of random drop for gateway congestion control
[NASA-CR-186736] 20 p2935 N90-26698
Knowledge and inhibition in asynchronous distributed systems
[TR-90-1139] 20 p2935 N90-26703
The need for headers: An impossibility result for communication over unreliable channels
[AD-A222823] 21 p2994 N90-27018
Secure Data Network System (SDNS) network, transport, and message security protocols
[PB90-198946] 23 p3318 N90-28757
Coordinating the activities of a planner and an execution agent 23 p3369 N90-29035
High speed bus technology development
[AD-A224486] 24 p3463 N90-29565
Working implementation agreements for open systems interconnection protocols
[PB90-197948] 24 p3557 N90-30127

PROTON BEAMS
Thermal initiation of confined primary explosives with a proton beam
[AD-A212954] 04 p0482 N90-12767
Direction-dependent stopping power and beam deflection in anisotropic solids
[DE90-001076] 06 p0840 N90-14883

PROTON DAMAGE
Radiation effects in ITO/InP solar cells 10 p1340 N90-17757

PROTON FLUX DENSITY
Cosmic strings and ultra-high energy cosmic rays
[NASA-CR-185924] 03 p0435 N90-12492

PROTON IMPACT
Double ionization of helium by particle impact 11 p1558 N90-18979

PROTON IRRADIATION
Assessment of bifacial silicon solar cells for space applications 10 p1342 N90-17779
Influence of high energy radiation on critical parameters of superconducting ceramics YBa2Cu3O7
[DE90-620562] 16 p2322 N90-23239
Proton irradiation of simple gas mixtures: Influence of irradiation parameters 20 p2949 N90-26782

PROTON MAGNETIC RESONANCE
The prediction of middle distillate fuel properties using liquid chromatography-proton nuclear magnetic resonance spectroscopy data
[AD-A211879] 03 p0334 N90-11899

PROTON PRECESSION
Proton magnetometers for measurement of the Earth's magnetic field 21 p3023 N90-27188

PROTON PRECIPITATION
A change of mesospheric ozone content under electron precipitation influence 22 p3207 N90-28191
Solar cosmic ray effects in the lower ionosphere 22 p3208 N90-28201
Ionospheric effects of the extreme solar activity of February 1986 22 p3210 N90-28207

PROTON RESONANCE
The Al-26(rho, gamma)Si-27 reaction: Stellar origins of galactic Al-26 15 p2188 N90-22498

PROTON TELESCOPES
U PARTICLE TELESCOPES

PROTONS
NT RECOIL PROTONS
NT SOLAR PROTONS
The grand unified photon spectrum: A coherent view of the diffuse extragalactic background radiation
[NASA-CR-186077] 05 p0715 N90-14180
Narrow one-channel resonances and their manifestation in the pure elastic scattering of unpolarized particles
[DE89-632177] 06 p0839 N90-14876
A calculation of energetic proton spectra producedat substorm onset in the fields of the explosive reconnection model 07 p1013 N90-15866
Workshop on Hydrogen Effects in InP and Related Compounds
[AD-A215197] 09 p1290 N90-17479
Advanced space power PEM fuel cell systems 10 p1333 N90-17707
Search for proton decay and supernova neutrino bursts with a lunar base neutron detector
[DE90-607644] 10 p1448 N90-18358
Contained events in Soudan 2
[DE90-005648] 10 p1449 N90-18359
Solid-state proton conductors
[DE90-007595] 11 p1531 N90-18812
Defect structures in copper and gold irradiated with fast neutrons, 14 MeV neutrons and 600 to 800 MeV protons
[DE90-007529] 12 p1629 N90-19359
The application of Dow Chemical's perfluorinated membranes in proton-exchange membrane fuel cells 13 p1823 N90-20466
Stopping power for protons in Al for the whole range of velocities
[DE90-008558] 13 p1884 N90-20810
Proton responses on MOS (Metal-Oxide-Semiconductor) electronics operating at cryogenic temperatures
[AD-A217622] 13 p1894 N90-20868
Ultrahigh-energy particle flux from cosmic strings
[NASA-CR-186592] 15 p2194 N90-22525
Study of Sn-116 via neutron pickup and proton stripping reactions
[KVI-814] 16 p2315 N90-23199
Protons and lattice defects in perovskite-related oxides
[DE90-010957] 18 p2624 N90-24955
The charged particle radiation environment for AXAF
[NASA-TM-100405] 20 p2942 N90-26741
Investigation of the Saturn dust environment from the analysis of energetic charged particle measurements
[NASA-CR-186727] 20 p2950 N90-26784
A site for the astrophysical gamma ray process
[DE90-013473] 20 p2950 N90-26787
A study of the sensitivity of an imaging telescope (GRITS) for high energy gamma-ray astronomy
[NASA-CR-186921] 22 p3261 N90-28468
Theoretical studies of proton beams in solar flare loops 23 p3413 N90-29286
A search for low energy cosmic ray antiprotons 24 p3564 N90-30161

PROTOPLANETS
Neptune's Triton: A moon rich in dry ice and carbon
[NASA-CR-186298] 08 p1152 N90-16675
A survey of PAH emission in HII regions, planetary and proto-planetary nebulae 11 p1584 N90-19129
Unidentified infrared features in proto-planetary nebulae 11 p1584 N90-19130
Low velocity dust-dust collisions 12 p1741 N90-20011
Mechanical properties of fluffy agglomerates consisting of core-mantle-particles 12 p1743 N90-20019

PROTOPLASTS
The effect of clinostat rotation on plant protoplasts 19 p2681 N90-25247

PROTOSTARS
NT PRE-MAIN SEQUENCE STARS
NT T TAURI STARS
The stability of magnetohydrodynamic shock waves in molecular clouds 02 p0292 N90-11665
Mathematical method for the study and teaching of stellar and protostellar structure 02 p0292 N90-11666
Variational problems in astrophysics 09 p1298 N90-17524
The infrared spectral signature of star formation 11 p1582 N90-19114

PROTOTYPES
A decision support approach to the file allocation problem in a distributed computing system 01 p0107 N90-10609
The Experimental Aircraft Flight Test Programme 02 p0152 N90-10865
Flight testing a newly-designed stand-off weapon dispenser 02 p0154 N90-10880
Realtime processing and display 02 p0155 N90-10886
Thin section casting program. Volume 3: Vertical TSC (Thin-Section Casting) approach
[DE89-009033] 02 p0210 N90-11201
A prototype silicon compiler in prolog
[AD-A210669] 02 p0257 N90-11452
Case study on rapid software prototyping and automated software generation: An inertial navigation system
[AD-A212272] 04 p0450 N90-12578
ISI's (Information Sciences Institute) SDI architecture simulator: Initial prototype user interface
[AD-A211325] 04 p0529 N90-13053

The development of a program analysis environment for Ada
[NASA-CR-185860] 05 p0681 N90-13962
Manipulation strategies for massive space payloads
[NASA-CR-186081] 06 p0728 N90-14247
Integrated G-suit/immersion suit
[AD-A212989] 06 p0821 N90-14774
QUEST/Ada: Query utility environment for software testing of Ada
[NASA-CR-186121] 06 p0823 N90-14787
Using object-oriented development to support prototyping
[DE90-000547] 06 p0829 N90-14821
The use of prototypes in selected foreign fighter aircraft development programs: Rafale, EAP, Lavi, and Gripen
[AD-A214500] 09 p1159 N90-16707
Guidance and control considerations for a maneuvering aerial target system 09 p1165 N90-16746
Noise and sonic boom impact technology. Initial development of an Assessment System for Aircraft Noise (ASAN). Volume 2: System design strategy
[AD-A214454] 09 p1278 N90-17411
Rapid prototyping of tools
[AD-A215956] 10 p1392 N90-18050
Space station technology summary 11 p1474 N90-18482
Electronically Variable Pressure Regulator (EVPR) 11 p1474 N90-18484
Zero-gravity vortex vent and PVT gaging system 11 p1475 N90-18486
Small displacement, long life on-orbit compressor design and fabrication 11 p1475 N90-18489
Digital integrator
[DIGEL-1989-2] 12 p1654 N90-19508
Deceit: A flexible distributed file system
[NASA-CR-186412] 12 p1726 N90-19923
Phase 1 supplemental development of a kinematic Stirling/Rankine commercial gas-fired heat pump system
[PB90-129974] 13 p1825 N90-20483
Measurement of the reflectance ratio of natural light in the sea
[IOS-265] 15 p2135 N90-22199
Facilitating knowledge sharing in organizations: Semiautonomous agents that learn to gather, classify, and distribute environmental scanning knowledge 15 p2176 N90-22435
Evaluation of a prototype 6 tone modem
[RAE-TM-FM-28] 16 p2228 N90-22708
An evaluation of the accuracy of a microwave landing system area navigation system at Miami/Tamiami Florida Airport
[DOT/FAA/CT-TN89/40] 17 p2349 N90-23377
Ultrahigh carbon steels and their laminates
[AD-A218780] 17 p2376 N90-23530
Qualitative models for space system engineering
[NASA-CR-180682] 17 p2385 N90-23585
Unfairness caused by quadratic backoff in a packet-radio network
[AD-A219635] 17 p2388 N90-23603
Digital terrain elevation data compact disk-read only memory prototype evaluation
[AD-A218545] 17 p2442 N90-23915
Measurement techniques, evaluation criteria and injury probability assessment methodologies developed for Navy ejection and crashworthy seat evaluations 19 p2721 N90-25479
Operations mission planner
[NASA-CR-186846] 19 p2747 N90-25611
IRDS prototyping with applications to the representation of EA/RA models
[NASA-CR-186066] 21 p3039 N90-27273
Expert system for pilot assistance: The challenge of an intensive prototyping
[ETN-90-97274] 22 p3111 N90-27674
Extended range tankless water heater
[DE90-014474] 23 p3316 N90-28750
A laser spectrometer and wavemeter for pulsed lasers
[NASA-CR-181731] 23 p3331 N90-28832
Issues in expanding the software base management system supporting the Computer Aided Prototyping System (CAPS)
[AD-A224344] 24 p3525 N90-29933

PROVING
NT THEOREM PROVING
Checking the Goldbach conjecture on a vector computer
[CWI-NM-R8812] 02 p0260 N90-11475
Validation of the procedures --- integrated multidisciplinary optimization of rotorcraft 04 p0451 N90-12587
Proving total correctness of recursive procedures
[CWI-CS-R8904] 04 p0532 N90-13075
Process expressions and Hoare's logic
[CWI-CS-R8905] 04 p0532 N90-13076
Meixner-Pollaczek polynomials and the Heisenberg algebra
[CWI-PM-R8806] 04 p0541 N90-13138
A validation of the proposed NATO standard method to determine target acquisition distances with image intensifiers
[IZF-1988-8] 04 p0554 N90-13230
More on the super WZW theory
[NIKHEF-H/88-11] 04 p0562 N90-13273
Assembly, integration, and verification 05 p0605 N90-13519
On the safe approximation of PROLOG programs
[CWI-CS-R8913] 05 p0683 N90-13978
Counterexamples to Robertson's conjecture
[MEMO-COSOR-88-32] 05 p0693 N90-14048
A hundred impossibility proofs for distributed computing
[AD-A216391] 10 p1419 N90-18180
Comparison of 3-D viscous flow computations of Mach 5 inlet with experimental data
[NASA-TM-102518] 13 p1757 N90-20090
Code ETF-3D. Euler transonic flow: Validation manual
[DLC/FLU-INT-TN-007] 18 p2493 N90-24248
Applying formal models and proofs to the verification of distributed systems
[IAR-89-7] 19 p2750 N90-25625
Earth Radiation Budget Experiment (ERBE) validation
[NASA-TM-103481] 20 p2888 N90-26433
Formal verification of the JANUS on-line multiplier
[IMAG-RR-785-I] 20 p2909 N90-26550
Formal verification of distributed computing systems: Logic characterization of behaviour equivalence
[LAAS-89386] 20 p2910 N90-26555
Severe local storm warning verification: 1989
[PB90-248592] 22 p3229 N90-28313

PROVISIONING
Air Force flight feeding. Volume 1: Evaluation of current system and alternative concepts
[AD-A212789] 04 p0527 N90-13043

PROXIMITY
Optimal matching of 3-D convex polyhedra
[TELECOM-PARIS-89C003] 03 p0395 N90-12258
Proximity compatibility and information display: The effects of space and color on the analysis of aircraft stall conditions
[AD-A214488] 09 p1260 N90-17309
Proximity operations concept design study, task 6
[NASA-CR-181971] 13 p1761 N90-20112
Igniter adapter-to-igniter chamber deflection test
[NASA-CR-184002] 22 p3133 N90-27780
Space robotic system for proximity operations 24 p3504 N90-29806

PRUSSIC ACID
U HYDROCYANIC ACID

PSEUDOMONAS
Pseudomonas diagnostic assay
[NASA-CASE-NPO-17653-1-CU] 21 p3032 N90-27239

PSEUDOPOTENTIALS
First-principles interatomic potentials in transition metals: Multi-ion interactions and their analytic representation
[DE90-001990] 06 p0748 N90-14353
Theoretical studies of electrons and electron transfer processes in fluids
[DE90-008414] 17 p2470 N90-24117

PSEUDORANDOM SEQUENCES
Measurement of the impulse response of the human visual system using correlation techniques
[AD-A215667] 09 p1254 N90-17274
Discrete mathematics for communication systems
[AD-A220430] 17 p2457 N90-24022
Binary pseudo random phase correlation in radar systems: A new approach
[RSRE-MEMO-4223] 19 p2683 N90-25263
Matrix generators for production of equally distributed pseudorandom vectors
[ETN-90-97291] 22 p3243 N90-28390

PSYCHOACOUSTICS
Test procedures for the evaluation of helmet and headset mounted active noise reduction systems
[AD-A212991] 05 p0676 N90-13937
On categorizing sounds
[AD-A216417] 10 p1427 N90-18232
Updating a dosage-effect relationship for the prevalence of annoyance due to general transportation noise
[AD-A219416] 17 p2421 N90-23794
Complex auditory signals
[AD-A224127] 23 p3356 N90-28969
Annoyance caused by advanced turboprop aircraft flyover noise: Counter-rotating-propeller configuration
[NASA-TP-3027] 23 p3392 N90-29166

PSYCHOLOGICAL EFFECTS
NT DESYNCHRONIZATION (BIOLOGY)
NT ILLUSIONS
NT JET LAG
NT OCULOGRAVIC ILLUSIONS
NT OPTICAL ILLUSION
Psychological mechanisms involved in the disorientation of pilots due to flight conditions
[ETN-89-95014] 04 p0527 N90-13040
Psychological reactions of pilots involved in accidents in the Swedish Air Force 09 p1254 N90-17279
Strategies to sustain and enhance performance in stressful environments
[AD-A221224] 18 p2583 N90-24711

PSYCHOLOGICAL FACTORS
Simulator sickness in the UH-60 (Black Hawk) flight simulator
[AD-A214434] 08 p1104 N90-16392
Review of serious aircraft accidents in the Belgian Air Force: Causes and comparison with selection data 09 p1254 N90-17277
The descent from the Olimpus: The effect of accidents on aircrew survivors 09 p1255 N90-17280
Systematicity as a selection constraint in analogical mapping
[AD-A216029] 11 p1541 N90-18869
Aiding the decision maker: Perceptual and cognitive issues at the human-machine interface
[AD-A217862] 13 p1855 N90-20648
The perceptual interaction of graphical attributes in thirteen bivariate displays
[AD-A217980] 13 p1868 N90-20720
The psychology of computer displays in the modern mission control center
[NASA-TM-100451] 15 p2137 N90-22213
Learning artificial grammars with competitive chunking
[AD-A219270] 16 p2265 N90-22911
Personality factors in flight operations. Volume 1: Leader characteristics and crew performance in a full-mission air transport simulation
[NASA-TM-102259] 17 p2348 N90-23370
Hand shaping: A paradigm for cognitive/motoric interaction
[AD-A219908] 17 p2437 N90-23885
Optimism and cardiovascular reactivity to psychological and cold pressor stress
[AD-A223818] 24 p3498 N90-29771
Norms and perception of events
[AD-A224236] 24 p3499 N90-29774
Information processing and perceptual characteristics of display design: The role of emergent features and objects
[AD-A223683] 24 p3558 N90-30133

PSYCHOLOGICAL INDEXES
U PSYCHOLOGICAL TESTS

PSYCHOLOGICAL TESTS
Microcomputer-based tests for repeated-measures: Metric properties and predictive validities
[NASA-CR-185517] 03 p0382 N90-12174
A menu of self-administered microcomputer-based neurotoxicology tests
[NASA-CR-185518] 03 p0382 N90-12175
The effect of incentives on the reliability and validity of cognitive speed tests
[AD-A211346] 03 p0383 N90-12181
Principle guidelines for the psychological screening of candidate pilots for the Belgian Air Force 09 p1257 N90-17292
Systematicity as a selection constraint in analogical mapping
[AD-A216029] 11 p1541 N90-18869
Appropriateness measurement for computerized adaptive tests
[AD-A216121] 11 p1541 N90-18870
Development of microcomputer-based mental acuity tests for repeated-measures studies
[NASA-CR-185607] 14 p2010 N90-21521
The incremental validity of spatial and perceptual-psychomotor tests relative to the armed services vocational aptitude battery
[AD-A220903] 18 p2585 N90-24719
Activities report of the National Aerospace Medical Center
[ETN-90-96936] 18 p2585 N90-24721
The prediction of professional success of licenced pilots: The validity of flight experience in comparison with standardized psychological aptitude tests
[DLR-FB-89-53] 19 p2723 N90-25488
Study of the application of a stress reactivity test in personnel selection
[DLR-FB-89-54] 19 p2723 N90-25489
TOM: Test of multiple task performance, user manual
[DLR-FB-89-60] 19 p2723 N90-25490
International application of the DLR test-system: First year of cooperation with IBERIA in pilot selection
[DLR-FB-90-05] 19 p2723 N90-25491

Differential psychological analysis of a computer-based audio-visual test of vigilance
[ESA-TT-1136] 19 p2724 N90-25494
Human performance in cockpit-related systems
[NIAR-90-7] 20 p2900 N90-26495
Cross-validation of experimental USAF pilot training performance models
[AD-A222253] 21 p3035 N90-27257

PSYCHOLOGY
NT AVIATION PSYCHOLOGY
NT COGNITIVE PSYCHOLOGY
NT PSYCHOACOUSTICS
NT PSYCHOPHYSICS
Human performance in continuous/sustained operations and the demands of extended work/rest schedules: An annotated bibliography, volume 2
[AD-A210504] 01 p0093 N90-10530
Comprehension processes in mechanical reasoning
[AD-A210459] 02 p0255 N90-11442
Human behavior
[PB90-780008] 07 p0967 N90-15584
Joint University Program for Air Transportation Research, 1988-1989
[NASA-CP-3063] 14 p1905 N90-20921
A connectionist implementation of cognitive phonology
[AD-A219095] 16 p2264 N90-22906
Hatching a theory of incubation effects
[AD-A219275] 16 p2266 N90-22915
The integrated area measure of visual endogenous ERPs: Relation to cognitive workload and hemisphere
[AD-A223191] 21 p3035 N90-27255
Human factors evaluation and validation criteria for quality training programs: Development, presentation, and assessment
[DE90-014724] 23 p3377 N90-29081
Norms and perception of events
[AD-A224236] 24 p3499 N90-29774

PSYCHOMETRICS
Watchfulness and attention during weightlessness simulations: Use of computerized psychometric tests
[REPT-89-TOU-3-1045] 05 p0674 N90-13928
Measuring learning ability by dynamic testing
[AD-A215273] 09 p1259 N90-17304
Subjective Workload Assessment Technique (SWAT): A user's guide
[AD-A215405] 09 p1261 N90-17312
Tool for studying the effects of range restriction in correlation coefficient estimation
[AD-A224035] 24 p3537 N90-29996

PSYCHOMOTOR PERFORMANCE
Microcomputer-based tests for repeated-measures: Metric properties and predictive validities
[NASA-CR-185517] 03 p0382 N90-12174
A menu of self-administered microcomputer-based neurotoxicology tests
[NASA-CR-185518] 03 p0382 N90-12175
Personality characteristics of USAF pilot candidates 09 p1255 N90-17281
Human cognitive and motor performance measures under typical cool white fluorescent illumination vs relatively high cool white illuminance/irradiance lighting
[AD-A218445] 16 p2262 N90-22892
Visual selective attention
[AD-A219204] 16 p2265 N90-22910
Separate visual representations for perception and for visually guided behavior 16 p2269 N90-22931
Direction of movement effects under transformed visual/motor mappings 16 p2272 N90-22947
Motor and cognitive performance do not change during a ten-week submarine patrol
[AD-A218639] 16 p2276 N90-22969
High peak power microwave pulses at 2.37 GHz: No effects on vigilance performance in monkeys
[AD-A219570] 17 p2433 N90-23863
The incremental validity of spatial and perceptual-psychomotor tests relative to the armed services vocational aptitude battery
[AD-A220903] 18 p2585 N90-24719
Predicting F/A-18 fleet replacement squadron performance using an automated battery of performance-based tests
[AD-A223899] 23 p3277 N90-28543
Evaluation of the performance capability of the aviator under hypoxic conditions operational experience 23 p3361 N90-28991

PSYCHOPHYSICS
NT PSYCHOACOUSTICS
Inferences from images
[AD-A210710] 02 p0258 N90-11465
Computational and psychophysical study of human vision using neural networks
[AD-A213290] 05 p0674 N90-13924
Spatiotemporal characteristics of visual localization, phase 2
[AD-A212934] 05 p0674 N90-13929
High compression image and image sequence coding 08 p1074 N90-16214
The perceptual buildup of three-dimensional structure from motion
[AD-A214640] 09 p1259 N90-17300
Visual perception of structure from motion
[AD-A216416] 10 p1412 N90-18141
A self-organizing multiple-view representation of three-dimensional objects
[AD-A216711] 11 p1541 N90-18871
Psychological studies of visual cortical function
[AD-A217029] 11 p1541 N90-18872
Detection acuity in the peripheral retina
[AD-A218183] 13 p1853 N90-20632
Parts of recognition
[AD-A217694] 13 p1868 N90-20714
Curvature estimation in orientation selection
[AD-A221481] 21 p3034 N90-27249
Complex auditory signals
[AD-A224127] 23 p3356 N90-28969
Auditory processing of complex sounds across frequency channels
[AD-A224147] 23 p3356 N90-28970
Time, space and form in vision
[AD-A213889] 23 p3357 N90-28971
Statement of research objectives and summary of research efforts
[RLE-PR-132] 23 p3415 N90-29295

PSYCHOPHYSIOLOGY
NT WORKLOADS (PSYCHOPHYSIOLOGY)
Psychophysiological correlates of human adaptation in antarctica
[AD-A216679] 10 p1412 N90-18142
Computing with neural maps: Application to perceptual and cognitive functions
[AD-A216689] 10 p1412 N90-18143
Seeing by exploring 16 p2268 N90-22923
Mental lapses and event-related potentials
[AD-A219454] 17 p2436 N90-23878
Psychophysiological assessment of pilot workload in an applied setting
[AD-A222707] 20 p2902 N90-26507
The effects of luminance boundaries on color perception
[AD-A221544] 21 p3034 N90-27251
Real-time measurement of mental workload using psychophysiological measures
[AD-A221462] 21 p3036 N90-27258

PUBLIC HEALTH
Human health studies of carbon monoxide (CO) under conditions of military weapons systems crewman exposures. Protocol 1: Formation of COHb
[AD-A210344] 01 p0092 N90-10528
Demonstration of replicable dimensions of health behaviors
[AD-A211920] 03 p0380 N90-12161
Measuring the demand for environmental studies
[PB90-100207] 09 p1244 N90-17214
Safety Status Report for the Ulysses mission. Book 1: Risk analysis. General purpose heat source radiosotope thermoelectric generator program
[DE90-006826] 12 p1614 N90-19282
Safety status report for the Ulysses mission. Book 2: Risk analysis. General purpose heat source radiosotope thermoelectric generator program
[DE90-006827] 12 p1614 N90-19283
The pollution hazard assessment system: Documentation and users manual
[AD-A217108] 12 p1689 N90-19706
Final Safety Analysis Report for the Ulysses Mission. Volume 3 (Book 1): Nuclear risk analysis document
[DE90-008691] 14 p1939 N90-21101
Studies of 60-Hz exposure effects on human function
[DE90-009473] 15 p2137 N90-22210
Further studies of 60 Hz exposure effects on human function
[DE90-014377] 23 p3355 N90-28962

PUBLIC LAW
NT LEGAL LIABILITY

PUBLIC RELATIONS
Index to NASA news releases and speeches, 1986
[NASA-TM-101899] 15 p2175 N90-22430
Index to NASA news releases and speeches, 1987
[NASA-TM-101900] 15 p2175 N90-22431
Index to NASA news releases and speeches, 1988
[NASA-TM-101901] 15 p2175 N90-22432

PUBLICATIONS
U DOCUMENTS

PULMONARY CIRCULATION
The characteristics of physiological responses and tolerance evaluation of pressure breathing
[AD-A214991] 09 p1252 N90-17262
Arginine vasopressin lowers pulmonary artery pressure in hypoxic rats by releasing artrial natruretic peptide
[AD-A215986] 10 p1410 N90-18134

PULSAR MAGNETOSPHERES
Electromagnetic jets in pulsar magnetospheres and near magnetized accretion disks 02 p0294 N90-11675
Ultrarelativistic envelope solitons in electron-positron plasma of the pulsar magnetosphere
[DE90-613289] 14 p1967 N90-21264
Gamma ray pulsars: Models and observations 16 p2335 N90-23304
The high-energy properties of X ray pulsars 19 p2767 N90-25719

PULSARS
The interaction of supernovae and pulsars with the circumstellar environment 02 p0293 N90-11671
Detectable gravitational waves by supernova SN 1987 A pulsar relic
[PREPRINT-658] 05 p0714 N90-14174
Supernovae, compact stars, and nuclear physics
[DE90-002682] 06 p0864 N90-15022
Pulsars lost and found: The second Princeton-Arecibo millisecond pulsar search 07 p1013 N90-15865
Pulsations of delta Scuti stars
[DE90-003213] 08 p1139 N90-16598
On the interaction of a pulsar with the ambient medium utilizing x ray images of the Crab nebula
[MPE-215] 08 p1140 N90-16604
An atlas of aperiodic variability in HMXB
[MPE-PREPRINT-158] 08 p1140 N90-16605
Relative muon content of UHE showers associated with Hercules X-1
[DE90-000609] 08 p1151 N90-16865
Strange-quark-matter stars
[DE90-006102] 10 p1446 N90-18347
Pulsar timing and gravitational waves 12 p1732 N90-19955
Time-dependent two-dimensional radiation hydrodynamics of accreting matter onto highly magnetized neutron stars
[DE90-006927] 12 p1737 N90-19985
Ultrarelativistic envelope solitons in electron-positron plasma of the pulsar magnetosphere
[DE90-613289] 14 p1967 N90-21264
A search for very high energy gamma rays from the Crab pulsar-nebula 14 p2043 N90-21718
Does mass accretion lead to field decay in neutron stars
[CAL-394] 15 p2182 N90-22470
Very high energy gamma rays from the Crab nebula and pulsar 15 p2194 N90-22527
Radio pulsar timing observations for GRO 16 p2334 N90-23301
Gamma radiation from radio pulsars 16 p2334 N90-23302
Gamma radiation from the Crab and Vela pulsars 16 p2334 N90-23303
Gamma ray pulsars: Models and observations 16 p2335 N90-23304
The illusive Geminga: What is it 16 p2335 N90-23307
More data on (possible) gamma ray (point) sources 16 p2335 N90-23309
Gamma rays from pulsar wind shock acceleration 16 p2336 N90-23311
Fast pulsars, strange stars
[DE90-011631] 19 p2765 N90-25710
Ginga observations of X ray pulsars 19 p2766 N90-25718
The high-energy properties of X ray pulsars 19 p2767 N90-25719
Observations of the X ray pulsars from the Kvant module 19 p2767 N90-25720
QPOs and preferred time scales in the variability of X ray pulsars 19 p2767 N90-25721
An X ray pulsar in the dark cloud Lynds 1457 19 p2767 N90-25723
Radiation-driven evolution and statistics of low-mass X ray binaries 19 p2770 N90-25745
A search for radio pulsars in globular clusters and transient X ray sources 19 p2772 N90-25755
VHE gamma ray emission from Southern Hemisphere X ray binaries 19 p2772 N90-25758
Evidence of a 12 ms pulsar in Cygnus X-3 19 p2772 N90-25759
Correlations between X ray luminosity and pulse shape as well as spectral shape in binary X ray pulsars 19 p2773 N90-25767
X ray timing and spectral measurements of the X ray pulsar 4U 1538-52 19 p2774 N90-25770
HEAO-1 and IR observations of the X ray pulsar 1E2259+586 19 p2774 N90-25773
Hard X ray pulses from Vela X-1 19 p2777 N90-25791
New X ray pulsars discovered with the Ginga satellite 19 p2777 N90-25795
Properties of circumstellar matter in GX301-2 observed by Tenma 19 p2778 N90-25798

Timing analysis of binary X ray pulsars observed by HEAO 1 19 p2781 N90-25822
EXOSAT observation of the pulsar PSR 1509-58 19 p2782 N90-25829
Accretion induced collapse and field decay 19 p2783 N90-25833
A multi-wavelength campaign to observe Scorpius X-1: Preliminary results from the X ray data 19 p2783 N90-25835
EXOSAT medium energy observations of binary X ray pulsar 4U1538-52 19 p2783 N90-25837
Kappa effect pulsational instability for hot extreme helium stars [DE90-014920] 23 p3411 N90-29277
Pulsations of B star models by an opacity mechanism [DE90-014923] 23 p3412 N90-29279
Gamma ray evidence for cosmic ray sources 23 p3414 N90-29292
Fast pulsars, strange stars: An opportunity in radio astronomy [DE90-015630] 24 p3563 N90-30155

PULSATING FLOW
U UNSTEADY FLOW

PULSE (CARDIOVASCULAR)
U HEART RATE

PULSE AMPLITUDE
Calibration of a pulsed potential crack monitor for use in fatigue crack growth studies [RAE-TM-M/S-1126] 08 p1089 N90-16301
Generalized pulse equations for through-transmission evaluation of arbitrary multilayered structures [NASA-TM-100752] 09 p1278 N90-17407
Experimental investigations concerning the propagation of second-sound pulses at critical heat flux [MPIS-12/1989] 16 p2313 N90-23182
Correlations between X ray luminosity and pulse shape as well as spectral shape in binary X ray pulsars 19 p2773 N90-25767
EXOSAT observations of the pulse profile of Her X-1 during intermediate intensity states in a 35-day cycle in 1985 19 p2776 N90-25788
New X ray pulsars discovered with the Ginga satellite 19 p2777 N90-25795
In-band amplitude dispersion on a microwave link 20 p2846 N90-26189

PULSE AMPLITUDE MODULATION
Means for protecting electroexplosive devices which are subject to a wide variety of radio frequency [AD-D014219] 06 p0753 N90-14382

PULSE CODE MODULATION
NT DELTA MODULATION
NT DIFFERENTIAL PULSE CODE MODULATION
Multi-level bandwidth efficient block modulation codes [NASA-CR-185484] 01 p0056 N90-10317
Independent Orbiter Assessment (IOA): Analysis of the instrumentation subsystem [NASA-CR-185571] 02 p0164 N90-10928
Type-specific dynamic measurements on wind turbines at the test site Schnittlingen (Germany, F.R.) [DFVLR-MITT-88-31] 03 p0367 N90-12099
Acquisition and recording an AMX A/C. Aeritalia experience and present trends [ETN-89-95217] 04 p0454 N90-12598
Enhanced satellite geodesy through the addition of a pseudorange observable [AD-A214987] 09 p1241 N90-17200
PC-based PCM (Pulse Code Modulation) telemetry data reduction system hardware [DE90-000316] 12 p1612 N90-19273
A waveform capture and storage unit and its use for investigating disturbances on digital transmission links [BBC-RD-1989/17] 12 p1649 N90-19478
General forms and properties of zero cross-correlation radar waveforms [AD-A217779] 13 p1790 N90-20273

PULSE COMMUNICATION
Assessment of voice coders for ATC/pilot voice communications via satellite digital communication channels [CAA-PAPER-89004] 04 p0489 N90-12807
Mitigating Doppler shift effect in HF multitone data modem 06 p0764 N90-14441
Network simulator definition [AD-A213463] 07 p0918 N90-15308
Microwave screening on digital radio communication links due to multicircuit power transmission lines [DE90-734950] 08 p1058 N90-16118
An approach to the development of software for computer-aided design of satellite communications receivers for operation in scintillating channels [AD-A215299] 09 p1267 N90-17349
Performance measurements for a laboratory-simulated 30/20 GHz communication satellite transponder [NASA-TM-102424] 10 p1376 N90-17977
A digital Meteor-Burst Communication (MBC) propagation path simulator 20 p2847 N90-26190
RADC/EEV diagnostic rhyme test system improvements [AD-A223187] 21 p2995 N90-27025

PULSE COMPRESSION
Improved amorphous metal materials for magnetic pulse compression [DE90-005723] 11 p1486 N90-18555
Coating possibilities for magnetic switches [DE90-006536] 11 p1504 N90-18659
General forms and properties of zero cross-correlation radar waveforms [AD-A217779] 13 p1790 N90-20273
Core cooling studies at LLNL (Lawrence Livermore National Laboratory) and Sandia [DE90-008303] 13 p1795 N90-20300
Development of an ultra-bright laser and an application to multi-photon ionization 14 p1984 N90-21372
Alternative solutions for Hilbert filtering in a pulse compression radar [FEL-89-C226] 22 p3165 N90-27950
Development of an all solid state 6 kHz pulse generator for driving free electron laser amplifiers [AD-A224105] 24 p3463 N90-29561

PULSE DIFFRACTION
Diffraction of light by ultrasonic pulses 15 p2164 N90-22366

PULSE DOPPLER RADAR
NT MONOPULSE RADAR
A frequency agile 94 GHz pulse-Doppler radar with dual polarisation capability 14 p1960 N90-21226
Users guide for an Airborne Windshear Doppler Radar Simulation (AWDRS) program [NASA-CR-182025] 19 p2657 N90-25121
Analysis and improved design considerations for airborne pulse Doppler radar signal processing in the detection of hazardous windshear [NASA-CR-186792] 20 p2890 N90-26448

PULSE DURATION
Pre-pulses: Signature of a trigger process in short (less than 60 secs) solar hard x ray flares 03 p0432 N90-12476
Pulsed plasma mission endurance test [AD-A213462] 08 p1037 N90-15993
EXOSAT measurements of the pulse period of Vela X-1 [MPE-PREPRINT-157] 08 p1152 N90-16673
Optical nutation in polymers irradiated by ultrashort laser pulses [AD-A212927] 10 p1357 N90-17869
Experimental and theoretical studies of light scattering by small particles [AD-A217432] 13 p1888 N90-20831
Intensity to frequency conversion technique in intensity modulated fiber optic sensing systems [NASA-TM-102562] 14 p1969 N90-21277
Diffraction of light by ultrasonic pulses 15 p2164 N90-22366
A multipulsed dynamic diffraction moire interferometer [DE90-009765] 16 p2230 N90-22723
EXOSAT observations of the pulse profile of Her X-1 during intermediate intensity states in a 35-day-cycle in 1985 17 p2483 N90-24201
The pulsed light curve of Vela X-1 17 p2483 N90-24202
Spectral variability of LMC X-4 17 p2483 N90-24204
X ray timing and spectral measurements of the X ray pulsar 4U 1538-52 19 p2774 N90-25770
EXOSAT observations of the pulse profile of Her X-1 during intermediate intensity states in a 35-day cycle in 1985 19 p2776 N90-25788
Timing analysis of binary X ray pulsars observed by HEAO 1 19 p2781 N90-25822
EXOSAT medium energy observations of binary X ray pulsar 4U1538-52 19 p2783 N90-25837
Free electron laser injection oscillator [AD-D014180] 21 p3007 N90-27095
Generalized averaging method for power conversion circuits [AD-A221977] 21 p3020 N90-27171

PULSE DURATION MODULATION
PWM converter topologies 10 p1335 N90-17721
The 120V 20A PWM switch for applications in high power distribution 10 p1335 N90-17724
An assessment of the use of resonant-mode topologies for high frequency power conversion 10 p1335 N90-17726
High speed digital control of high frequency PWM converters 10 p1337 N90-17736
Simple pole/zero modelling of conductance controllers 10 p1337 N90-17739
High power medium voltage electronic load 10 p1338 N90-17747
Instability investigation for storage mode. Microwave instability (single-bunch instability) [NIKHEF-K/AMPS/89/05] 11 p1499 N90-18628
Generalized averaging method for power conversion circuits [AD-A221977] 21 p3020 N90-27171

PULSE GENERATORS
Magnetic flux compression [DE89-016991] 02 p0271 N90-11546
Simulation of the EMP (Electromagnetic Pulse) from ESD (Electrostatic Discharge) [DE89-014484] 03 p0337 N90-11918
High power, solid state RF pulse generators [AD-D014172] 03 p0341 N90-11941
High gain flux compression generator fabrication issues [DE89-017888] 03 p0342 N90-11951
Computer controlled MHD power consolidation and pulse-generation system [DE89-015600] 03 p0407 N90-12333
Subnanosecond linear GaAs photoconductive switching, revision 1 [DE89-017739] 03 p0412 N90-12363
The design, construction, performance and calibration of pulse generators to fulfil the requirements of specifications defence standard 59-41, FS(F) 510 and FS(S) 457 [RAE-TM-FS(F)-550] 04 p0496 N90-12857
A software-based controller for generation of synchronized pulses for use with rotating machinery [DE89-016672] 06 p0770 N90-14477
Laser activities 06 p0786 N90-14576
Performance of the 10-kV, 100-kA pulsed-power modules for the FRX-C magnetic compression experiment [DE89-014027] 06 p0845 N90-14917
Design of a bounded wave EMP (Electromagnetic Pulse) simulator [AD-A214137] 07 p0919 N90-15316
Avalanche photoconductive switching [DE90-002980] 07 p0922 N90-15337
Computer controlled MHD power consolidation and pulse-generation system [DE90-001224] 07 p0981 N90-15662
Electrical safety in the high voltage laboratory [DE90-003026] 08 p1060 N90-16130
Diode pumped monolithic Nd:YLF 1.053 micron mini-laser and its application to injection seeding [DE90-005323] 10 p1390 N90-18040
Aurora upgrade. Volume 5: Machine monitoring and control system [AD-A215963] 10 p1393 N90-18053
Blue upconversion thulium laser [DE90-006517] 12 p1668 N90-19584
Programmable generation of linear frequency modulated pulses 14 p1961 N90-21232
Gas-puff z-pinch experiment [IPPCZ-286] 15 p2167 N90-22385
Dose analysis of the model 112A Pulserad pulsed x ray generator by its CYLTRAN [AD-A220372] 17 p2471 N90-24125
A 6.4 kV pulse generator with transformers [DIGEL-1989-1] 21 p3002 N90-27063
Light source for dynamic testing of photo detectors [FEL-1989-69] 22 p3247 N90-28414
Development of an all solid state 6 kHz pulse generator for driving free electron laser amplifiers [AD-A224105] 24 p3463 N90-29561
High voltage picosecond pulse generation using avalanche diodes [DE90-015194] 24 p3465 N90-29577

PULSE HEIGHT
U PULSE AMPLITUDE

PULSE MODULATION
NT DELTA MODULATION
NT DIFFERENTIAL PULSE CODE MODULATION
NT PULSE AMPLITUDE MODULATION
NT PULSE CODE MODULATION
NT PULSE DURATION MODULATION
NT PULSE POSITION MODULATION
High speed signal extraction using electro-optic techniques [AD-A214446] 08 p1122 N90-16500

PULSE POSITION MODULATION
Direct detection optical intersatellite link at 220 Mbps using AlGaAs laser diode and silicon APD with 4-ary PPM signaling [NASA-CR-186380] 12 p1646 N90-19460

PULSE RADAR
NT MONOPULSE RADAR
NT PULSE DOPPLER RADAR
The effectiveness of adaptive PRF (Pulse Repetition Frequency) selection in minimizing range obscuration in the TDWR (Terminal Doppler Weather Radar) system [AD-A211267] 02 p0213 N90-11222
Specification for radar free-space detection range and free-space intercept range calculations [AD-A213158] 04 p0494 N90-12843

Adaptive processor emulation development
[AD-A214392] 10 p1371 N90-17944

PULSE RATE

The effectiveness of adaptive PRF (Pulse Repetition Frequency) selection in minimizing range obscuration in the TDWR (Terminal Doppler Weather Radar) system
[AD-A211267] 02 p0213 N90-11222

An analysis of the anomalous high-current cathode emission in pseudospark and back-of-the-cathode lighted thyratron switches
[AD-A215328] 10 p1378 N90-17988

Experimental investigations concerning the propagation of second-sound pulses at critical heat flux
[MPIS-12/1989] 16 p2313 N90-23182

Detection of 2.93 ms pulsations in Sco X-1
19 p2774 N90-25772

EXOSAT observations of the pulse profile of Her X-1 during intermediate intensity states in a 35-day cycle in 1985 19 p2776 N90-25788

Einstein SSS and MPC observations of Aql X-1 and 4U1820-30 19 p2777 N90-25790

PULSE RECORDERS

U COUNTERS

PULSE TIME MODULATION

NT PULSE DURATION MODULATION
NT PULSE POSITION MODULATION

PULSE WIDTH

U PULSE DURATION

PULSE WIDTH MODULATION

U PULSE DURATION MODULATION

PULSED LASERS

NT Q SWITCHED LASERS
NT ULTRASHORT PULSED LASERS
NT ULTRAVIOLET LASERS

Elements of a 200 watt pulsed excimer laser
02 p0226 N90-11295

Research in X-ray optics with the ultimate aim of constructing a synchrotron radiation pumped soft X-ray lithium laser
[DE89-016788] 02 p0227 N90-11304

Advanced source development and applications. Laser-produced plasmas: A compact soft x ray source with high peak brightness
[AD-A212677] 04 p0557 N90-13245

Optical communication with semiconductor laser diode
[NASA-CR-185886] 05 p0647 N90-13770

MM and T advanced balancing/machining
[AD-A213103] 05 p0648 N90-13775

Experimental study of the shock waves generated by high energy laser pulses 06 p0784 N90-14557

Development of X diagnostics with 1 Gw laser pulses
06 p0786 N90-14578

Development of X diagnostics around the pulse 1 laser 06 p0787 N90-14580

Ultrahigh-brightness lasers and their applications
[DE90-000877] 06 p0789 N90-14596

Nonresonant and resonant multiphoton ionization of (NO)(sub n) and Ar(sub n)NO clusters with picosecond laser pulses
[DE89-016853] 06 p0791 N90-14607

Laser-supported detonation waves and pulsed laser propulsion
[DE90-002753] 07 p0935 N90-15412

Frequency shift induced in laser pulses by plasma density variations
[AD-A214195] 07 p0936 N90-15424

Optical flow measuring method using diode lasers, phase coupled arrays, and high frequency pulsed diode lasers
08 p1067 N90-16176

High frequency pulsed diode lasers and phase-coupled diode arrays for aerodynamics 08 p1078 N90-16238

Eurolaser definition phase: A comparison of high power lasers available
[ETN-90-96061] 08 p1083 N90-16268

Resonance enhanced Raman studies of as-grown and laser-processed HgCdTe
[AD-A213855] 08 p1129 N90-16540

Nondestructive control of composite materials by holographic interferometry
[ISL-CO-244/88] 09 p1188 N90-16882

Optical nutation in polymers irradiated by ultrashort laser pulses
[AD-A212927] 10 p1357 N90-17869

New type of optical bistability in polymers mediated by phonons
[AD-A216102] 10 p1359 N90-17882

Cinenholography: A relation between the coherence length of the laser and the object velocity
[ISL-CO-234/88] 11 p1515 N90-18724

Effects produced by pulsed CO2 lasers
[ISL-R-112/88] 11 p1516 N90-18731

Pulsed laser deposition of high T(sub c) superconducting thin films
[AD-A216507] 11 p1569 N90-19034

In situ growth of epitaxial superconducting YBa2Cu3O(7-x) films on insulating semiconducting and ferroelectric K(Ta, Nb)O3 by pulsed laser ablation
[DE90-006568] 11 p1571 N90-19043

In situ growth of high quality epitaxial YBa2Cu3O(7-x) thin films at moderate temperatures by pulsed laser ablation
[DE90-006629] 11 p1571 N90-19045

The nonlinear interaction of intense laser pulses in plasmas
[AD-A217604] 12 p1718 N90-19867

Pulsed laser photothermal spectroscopy of liquids and solids
[DE90-008642] 13 p1808 N90-20380

Picosecond Laser Facility
[AD-A217784] 13 p1808 N90-20384

Ultra-high brightness laser research at LLNL (Lawrence Livermore National Laboratory)
[DE90-008366] 13 p1896 N90-20885

Generation of ultrashort laser pulses from neodymium glass oscillator and regenerative amplifier
14 p1984 N90-21373

Pulsed laser processing of high temperature superconducting thin films
[DE90-008928] 15 p2172 N90-22413

In-situ pulsed laser deposition of high-T(sub c) YBa(sub 2)Cu(sub 3)O(sub 7) superconducting thin films on (100) LaAlO3 substrates
[DE90-009861] 15 p2173 N90-22418

Interaction of atomic hydrogen with pico- and femtosecond laser pulses
[AD-A218426] 16 p2241 N90-22785

Frequency domain techniques for analyzing picosecond optical pulses
[AD-A218856] 16 p2318 N90-23214

Picosecond laser pulse interactions with metallic and semiconducting surfaces
[AD-A219680] 17 p2408 N90-23723

In-situ processing of epitaxial and textured high (Tc) superconducting HoBa2Cu3O(7-x) thin films by pulsed laser evaporation technique
[DE90-009828] 17 p2474 N90-24148

Use of the Xybion ISG-camera in the RETRA-1000 TV-Holography unit
[AD-A219842] 18 p2554 N90-24577

Pulsed-discharge carbon dioxide lasers
18 p2556 N90-24587

LaRC-developed catalysts for CO2 lasers
18 p2557 N90-24591

Synthesis, characterization and evaluation of CO-oxidation catalysts for high repetition rate CO2 TEA lasers 18 p2557 N90-24593

A computer program for the design of optimum catalytic monoliths for CO2 lasers 18 p2558 N90-24595

The effect of H2O and pretreatment on the activity of a Pt/SnO2 catalyst 18 p2558 N90-24597

Rare-isotope and kinetic studies of Pt/SnO2 catalysts
18 p2558 N90-24598

Dissociation phenomena in electron-beam sustained carbon dioxide lasers 18 p2560 N90-24610

DURIP: Spontaneous Raman system for the study of enhanced combustion and non-thermal plasmas
[AD-A221410] 18 p2564 N90-24629

SiC film deposited by pulsed excimer laser ablation
[DE90-010634] 18 p2622 N90-24938

Diode laser-pumped solid-state lasers: A breakthrough in modern laser technology
[MBB-Z-0276/89-PUB] 19 p2649 N90-25077

A room-temperature, laser diode-pumped, Q-switched, 2 micron, thulium-doped, solid state laser
[AD-D014527] 19 p2695 N90-25334

Superconductivity in nonsymmetric epitaxial YBa2Cu3O(sub 7-delta)-PrBa2Cu3O(sub 7-delta) superlattices grown by pulsed laser ablation
[DE90-011637] 19 p2761 N90-25687

A numerical simulation of the quasi-heterodyne technique for double-pulsed holographic vibration measurements
[PNR90622] 20 p2865 N90-26301

Holography and holographic interferometry
[PNR90670] 20 p2866 N90-26303

New discharge pumping method for CO2 lasers
[AD-A220898] 20 p2866 N90-26307

Vacuum deposition by pulsed laser radiation: Plasma composition, deposition techniques, and thin film properties
[ETN-90-97263] 20 p2931 N90-26677

Phase-sensitive optical detection of ballistic phonon pulses using frequency-modulation spectroscopy and persistent spectral holes
[AD-A221521] 21 p2979 N90-26930

Development of a multi-purpose, pulsed-laser system for solar cell processing applications
[DE90-012181] 21 p3008 N90-27096

Pulsed laser deposition of high (Tc) superconducting thin films: Present and future
[DE90-011950] 21 p3080 N90-27511

High pulse energy flashlamp pumpable laser dyes
[AD-A223075] 22 p3180 N90-28042

A laser spectrometer and wavemeter for pulsed lasers
[NASA-CR-181731] 23 p3331 N90-28832

Tunable CW single-frequency source for injection seeding 2-micrometer lasers
[AD-A223979] 23 p3331 N90-28834

Nondestructive material characterization
[DE90-015176] 24 p3477 N90-29652

PULSED RADIATION

NT ELECTROMAGNETIC PULSES
NT SYSTEM GENERATED ELECTROMAGNETIC PULSES

Generation and focusing of pulsed intense ion beams
[DE89-017558] 03 p0408 N90-12338

Interlaboratory comparison of radiation-induced attenuation in optical fibers. Part 3: Transient exposures
[DE90-000859] 07 p0992 N90-15729

Effects of pulsed and CW (Continuous Wave) 2450 MHz radiation on transformation and chromosomes of human lymphocytes in vitro
[AD-A216500] 11 p1539 N90-18857

Topics in HPM (High-Power Microwave) generation, coupling, and interaction
[AD-A216882] 12 p1682 N90-19658

Core cooling studies at LLNL (Lawrence Livermore National Laboratory) and Sandia
[DE90-008303] 13 p1795 N90-20300

Lack of behavioral effects of high-peak-power microwave pulses from an axially extracted virtual cathode oscillator
[AD-A220779] 17 p2391 N90-23618

Dose analysis of the model 112A Pulserad pulsed x ray generator by its CYLTRAN
[AD-A220372] 17 p2471 N90-24125

X ray timing and spectral measurements of the X ray pulsar 4U 1538-52 19 p2774 N90-25770

Detection of 2.93 ms pulsations in Sco X-1
19 p2774 N90-25772

Properties of circumstellar matter in GX301-2 observed by Tenma 19 p2778 N90-25798

Orbitally modulated VHE gamma rays from Cen X-3
19 p2780 N90-25812

The pulsed light curve of Vela X-1
19 p2781 N90-25819

EXOSAT medium energy observations of binary X ray pulsar 4U1538-52 19 p2783 N90-25837

PULSES

NT ELECTRIC PULSES
NT ELECTROMAGNETIC PULSES
NT GEOMAGNETIC PULSATIONS
NT MICROPULSATIONS
NT PICOSECOND PULSES
NT SYSTEM GENERATED ELECTROMAGNETIC PULSES

High power, solid state RF pulse generators
[AD-D014172] 03 p0341 N90-11941

Airborne/spaceborne pulsed power source
[AD-A211762] 04 p0495 N90-12850

Magnetically insulated electron flows in pulsed power systems
[AD-A212746] 04 p0549 N90-13196

Quantitative non-destructive evaluation using laser generated ultrasonic pulses 05 p0653 N90-13805

Countermeasures to microgravity
05 p0680 N90-13957

Influence of RF-parameters on beam lifetime
[NIKHEF-K/AMPS/89-06] 05 p0699 N90-14091

Martensite transformation in NiTi alloys induced by tensile stress pulses
[DE90-001832] 06 p0747 N90-14346

Frequency agile synthetic aperture radar
[AD-D014235] 06 p0765 N90-14451

NIKHEF-K contributions to the 1989 Particle Accelerator Conference
[NIKHEF/AMPS/89/03] 06 p0841 N90-14891

The Amsterdam pulse stretcher project (AmPS)
06 p0841 N90-14892

Optics of the Amsterdam pulse stretcher (AmPS)
06 p0841 N90-14893

Modification of MEA modulator-klystron units enabling short pulse injection into a pulse-stretcher ring
06 p0841 N90-14894

An Energy Spectrum Compressor system (ESC) for the Amsterdam pulse stretcher (AmPS)
06 p0842 N90-14896

SBS (Stimulated Brillouin Scattering) pulse distortion in multimode optical fibers: Preliminary results
[DE90-003023] 07 p0992 N90-15731

Method and apparatus for characterizing reflected ultrasonic pulses
[NASA-CASE-LAR-13966-1] 09 p1278 N90-17408

Laser-matter interaction at intensities of 10(sup 12) W/cm(sup 2) and below
[DE90-007536] 12 p1669 N90-19590
Common-mode rejector for pulse power diagnostics
[AD-A218096] 13 p1798 N90-20316
Determinations of photon spectra
[AD-A218003] 13 p1885 N90-20816
Martensitic transformation induced by stress pulses
[DE90-009534] 15 p2069 N90-21854
Novel pulsed plasma treatment and coating process: Multilayer structures for optical computing applications
[AD-A220737] 18 p2615 N90-24894
Phase-sensitive optical detection of ballistic phonon pulses using frequency-modulation spectroscopy and persistent spectral holes
[AD-A221521] 21 p2979 N90-26930
Nonlinear material response to very rapid energy deposition
[AD-A221932] 21 p2989 N90-26988
Long pulse diode experiments
[DE90-016218] 24 p3465 N90-29578
Evaluation of dynamic range for LLNL streak cameras using high contrast pulses and pulse podiatry on the Nova laser system
[DE90-015203] 24 p3472 N90-29620
Subpicosecond Raman study of hot electrons and hot phonons in GaAs
[DE90-015634] 24 p3553 N90-30106

PULTRUSION
Pultrusion process development for long space boom model
[NASA-TM-4017] 16 p2214 N90-22628

PUMP IMPELLERS
Experimental investigation of the effect of cavitation on the rotordynamic forces on a whirling centrifugal pump impeller 15 p2105 N90-22039
Experimental investigation of the hydrodynamic forces on the shroud of a centrifugal pump impeller
[NASA-CR-186952] 21 p3009 N90-27108

PUMPS
NT AXIAL FLOW PUMPS
NT CENTRIFUGAL PUMPS
NT ELECTROMAGNETIC PUMPS
NT FUEL PUMPS
NT JET PUMPS
NT TURBINE PUMPS
Simulation of the control characteristics of an axial piston pump and a flapper-nozzle valve combination 05 p0649 N90-13784
Eurolaser CO2 laser
[ETN-90-95907] 06 p0787 N90-14582
Efficiency measurement of high pressure cryogenic rocket pumps
[NAL-TR-1022] 10 p1391 N90-18042
First pump limiter experiments in TORE SUPRA
[DE90-004968] 10 p1432 N90-18266
Study on the thermodynamical and mechanical conditions for the generation of high operating pressures with liquefied gases for low and very low flow rates
[ESA-TT-1148] 11 p1510 N90-18696
BASG thermomechanical pump helium 2 transfer tests
[NASA-CR-177541] 14 p1939 N90-21097
Performance evaluation of LE-7 high pressure pumps
[DE90-505523] 20 p2817 N90-26034

PUNCTURING
U PIERCING

PUPIL SIZE
Effects of miniature CRT (Cathode Ray Tube) location upon primary and secondary task performances
[AD-A210223] 01 p0101 N90-10573

PURGING
Independent Orbiter Assessment (IOA): Analysis of the purge, vent and drain subsystem
[NASA-CR-185547] 02 p0172 N90-10969

PURIFICATION
NT AIR PURIFICATION
Preparation, purification and densification of zinc sulfide powder from organometallics
[AD-A210943] 01 p0052 N90-10298
Results of an attempt to measure increased rates of the reaction D-2 + D-2 yields He-3 + n in a nonelectrochemical cold fusion experiment
[NASA-TM-102430] 09 p1280 N90-17424
The chemical basis for the origin of the genetic code and the process of protein synthesis
[NASA-CR-186590] 15 p2136 N90-22205
Preparation of ultra-pure metal halides
[AD-D014529] 19 p2674 N90-25204

PURIFIERS
U PURIFICATION

PURINES
NT CAFFEINE

PURITY
The improved corrosion resistance of ultra high purity magnesium alloy castings 01 p0044 N90-10245
Broadband versus narrowband driver/power amplifier: A spectral purity comparison
[DOT/FAA/CT-TN89/73] 10 p1379 N90-17995
Effect of propellant flowrate and purity on carbon deposition in LO2/methane gas generators 11 p1471 N90-18468
High-purity beryllium foils
[DE90-006408] 12 p1626 N90-19348
Improvement study of iron disilicide thermoelectric materials
[AD-A218946] 16 p2252 N90-22844
Pre-concentration method for inductively coupled plasma-mass spectrometry
[PB90-181348] 19 p2673 N90-25202
Synthesis of high purity sinterable silicon carbide powder
[DE90-012029] 20 p2828 N90-26084

PURSUIT TRACKING
DURIP: Improved eye movement monitoring capabilities for studies in visual cognition
[AD-A220355] 18 p2586 N90-24722

PWM (MODULATION)
U PULSE DURATION MODULATION

PYLONS
Application of fracture mechanics and half-cycle method to the prediction of fatigue life of B-52 aircraft pylon components
[NASA-TM-88277] 05 p0655 N90-13820
Effect of pylon wake with and without pylon blowing on propeller thrust
[NASA-TM-4162] 06 p0718 N90-14190
Compression pylon
[NASA-CASE-LAR-13777-1] 13 p1755 N90-20078

PYRANOMETERS
Pyranometry
[DWD-14] 12 p1682 N90-19661
Improved meteorological measurements from buoys and ships (IMET): Preliminary comparison of pyranometers
[PB90-241936] 22 p3229 N90-28315

PYRAZINES
Determination of the minimum energy conformation of alkyl substituted pyrazines
[AD-A216974] 11 p1484 N90-18539

PYRENES
Measurements of energy dispersion at liquid-solid interfaces: Fluorescence quenching of pyrene bound to fumed silica
[AD-A222371] 21 p2978 N90-26926

PYREX (TRADEMARK)
U BOROSILICATE GLASS

PYRIDINES
Electrochemistry in near-critical and supercritical fluids. Part 7: SO2
[AD-A208207] 01 p0039 N90-10214
Carbon-13 nuclear magnetic resonance of heterocyclic salts and its precursors
[DE89-635768] 08 p1041 N90-16016
Luminescence probe studies of ionomers. Part 3: Distribution of decay rate constants for tris bipyridyl Ruthenium(II) in Nafion membranes
[AD-A215885] 10 p1359 N90-17880
Modes of attachment of pyridine to gold surfaces
[AD-A219519] 17 p2372 N90-23504
An examination of the relationship between SERS intensities and surface concentration for pyridine adsorbed at the gold/aqueous solution interface
[AD-A219520] 17 p2372 N90-23505
Density profile of terminally adsorbed polymers
[AD-A220897] 18 p2529 N90-24433
Effects of pyridostigmine bromide on A-10 pilots during execution of a simulated mission: Physiology
[AD-A221222] 18 p2584 N90-24717

PYROELECTRICITY
Synthetic polypeptide composites for sensor applications
[AD-A210797] 01 p0052 N90-10296
Readout and signal conditioning for a linear pyroelectric array
[RSRE-MEMO-4102] 04 p0504 N90-12905
Piezoelectric and pyroelectric effects of a crystalline polymer 18 p2515 N90-24360

PYROGRAPHALLOY
U COMPOSITE MATERIALS
U PYROLYTIC GRAPHITE
U REFRACTORY MATERIALS

PYROHELIOMETERS
Pyranometry
[DWD-14] 12 p1682 N90-19661

PYROLYSIS
Structure/reactivity relationships of polysilazane preceramics
[AD-A212028] 03 p0332 N90-11888
Pyrolytic production of ceramic composites from silicates
[ETCA-89-R-012] 04 p0479 N90-12746
Continuing studies of liquid propellant drops in hot, high-pressure environments
[AD-A212265] 04 p0482 N90-12765
The conversion of carbonaceous materials to clean carbon and co-product gaseous fuel
[DE90-001561] 06 p0754 N90-14387
New polymers made with well-characterized organometallic catalysts
[AD-A213592] 07 p0912 N90-15272
Characterization of the thermal degradation of selected energetic materials and mixtures by Rapid-Scan Fourier Transform Infrared (RSFTIR) spectroscopy
[AD-A214411] 07 p0916 N90-15296
Comprehensive mechanisms for combustion chemistry: An experimental and numerical study with emphasis on applied sensitivity analysis
[DE90-003904] 08 p1041 N90-16017
Method of making carbon dioxide and chlorine free fluoride-based glass
[AD-D014260] 08 p1048 N90-16060
Silicon carbo-nitride ceramic matrix composites by polymer pyrolysis 11 p1477 N90-18499
Hawaii integrated biofuels research program, phase 1
[DE90-006885] 11 p1530 N90-18811
Preparation and characterization of alumina films prepared by a novel spray pyrolysis method
[AD-A217570] 12 p1625 N90-19339
Determination of the mechanism of decomposition of energetic molecules
[AD-A217061] 12 p1633 N90-19388
Growth and characterization of gallium (III) oxide films
[AD-A217568] 12 p1723 N90-19902
Non-noble electrocatalysts for alkaline fuel cells 13 p1824 N90-20470
Fire propagation in concurrent flows
[PB90-151754] 15 p2066 N90-21834
The pyrolysis of polymethylmethacrylate during combustion in a solid fuel combustion chamber
[LR-531] 15 p2068 N90-21845
Ternary reactions among polymer substrate-organohalogen-antimony oxides under pyrolytic, oxidative and flaming conditions
[PB90-154766] 15 p2071 N90-21861
Fuel-rich catalytic combustion: A fuel processor for high-speed propulsion
[NASA-TM-103177] 17 p2374 N90-23518
Diagnostics of glow discharges used to produce hydrogenated amorphous silicon films
[DE90-000329] 18 p2522 N90-24402
The preparation of ACEL thin films
[AD-A222919] 21 p2999 N90-27048
Development of polysilsesquioxane composites
[NASA-CR-180263] 22 p3152 N90-27872
Regression and combustion characteristics of boron containing fuels for solid fuel ramjets 22 p3161 N90-27928
Pyrolysis and combustion of solid fuels under both subsonic and supersonic conditions 22 p3161 N90-27929
Investigation of particulate formation during diesel spray combustion
[DE90-012682] 24 p3446 N90-29464

PYROLYTIC GRAPHITE
Feasibility of intercalated graphite railgun armatures
[NASA-TM-102546] 14 p1953 N90-21181
In situ analysis of CO during chemisorption and oxidation on graphite: Supported Pt by FTIR-microspectrometry 18 p2559 N90-24605
Characterization of PMDI/HOPG interfaces by SERS using a silver overlayer configuration
[AD-A223104] 21 p2985 N90-26966
Characterization of model polyimide/silver interphases using surface-enhanced Raman scattering
[AD-A222488] 21 p2988 N90-26979

PYROLYTIC MATERIALS
NT PYROLYTIC GRAPHITE
Pyrolytic production of ceramic composites from silicates
[ETCA-89-R-012] 04 p0479 N90-12746
Growth and characterization of zinc sulfide films by conversion of zinc oxide films with H2S
[AD-A213345] 04 p0561 N90-13271
Polymeric aluminasilazane precursors for aluminosilicon nitride
[AD-A222755] 20 p2841 N90-26158
United States Air Force research initiation program for 1988, volume 2
[AD-A223124] 21 p3102 N90-27614

PYROMETALLURGY
Investigation of the pyrometallurgical, physical and mechanical behavior of weld metal
[AD-A211114] 01 p0046 N90-10258
Containerless Processing of Metals: Undercooling and Solidification
[DLR-MITT-89-15] 05 p0625 N90-13645

Correlation between microstructure and magnetic properties of porous sintered iron and porous iron containing composites
[KFK-4522] 05 p0625 N90-13647

PYROMETERS
NT RADIATION PYROMETERS
Noncontact temperature pattern measuring device
[NASA-CASE-NPO-17824-1-CU] 09 p1229 N90-17132
IR optical fiber-based noncontact pyrometer for drop tube instrumentation 10 p1365 N90-17909
Non-contact temperature measurement of a falling drop 10 p1365 N90-17912
Dynamic response for thermal control and measurement and fast radiation thermometry 10 p1367 N90-17924
Report on the multicolor pyrometry session at the Second NASA Non-Contact Temperature-Measurement Workshop 10 p1367 N90-17926
Development of the blackbody probe type pyrometer, part 1. Experimental study on the fundamental characteristics
[DE89-782288] 12 p1663 N90-19553
Design of a pyrometer for temperature measurements on the solid fuel combustion chamber
[LR-530] 12 p1664 N90-19561
Multiwavelength pyrometry to correct for reflected radiation
[NASA-TM-102578] 17 p2407 N90-23714
Noncontact measurement of high temperature using optical fiber sensors
[NASA-CR-186975] 23 p3329 N90-28825

PYROMETRY
U TEMPERATURE MEASUREMENT

PYROTECHNICS
NT HMX
Heat transfer characteristics of igniter output plumes
[DE89-011449] 01 p0059 N90-10340
Pyrotechnic ignition studies using a gun tunnel
[DE89-012496] 01 p0060 N90-10341
Independent Orbiter Assessment (IOA): Analysis of the pyrotechnics subsystem
[NASA-CR-185530] 02 p0168 N90-10945
Independent Orbiter Assessment (IOA): Assessment of the pyrotechnics subsystem
[NASA-CR-185531] 02 p0168 N90-10946
Powder morphology effects in the ignition of titanium-based pyrotechnics
[DE89-017229] 02 p0208 N90-11191
The Shock and Vibration Digest, volume 21, no. 10 04 p0483 N90-12771
Pyrotechnic shock structural response 04 p0483 N90-12774
Evaluation of selected computer models for modeling pyrotechnic and propellant devices
[AD-A213003] 05 p0629 N90-13671
Development of a titanium/boron blending process
[DE90-001450] 06 p0754 N90-14386
Very low energy ignition of pyrotechnics using a Semiconductor Bridge (SCB)
[DE90-002645] 08 p1052 N90-16082
Effect of reduced atmospheric pressure on the performance characteristics of pyrotechnic compositions containing aluminum
[AD-A214473] 09 p1200 N90-16953
Analysis of propulsive powder combustion products and their corrosive effects
[ISL-CO-248/88] 11 p1495 N90-18605
Test component attachment effects on resonant plate pyrotechnic shock simulation
[DE90-006478] 12 p1662 N90-19551
Pyrotechnic device technology
[DE90-007683] 13 p1783 N90-20234
Double swivel toggle release
[NASA-CASE-MSC-21436-1] 14 p1987 N90-21390
Extraction of recovery of plasticizers from solid propellants and munitions
[AD-D014433] 15 p2072 N90-21868
Qualification test rationale for measuring the resistance of equipment to pyrotechnic shock
[REPT-892-430-117] 16 p2207 N90-22590
Ignition testing of low-energy laser diode ignited components
[DE90-009968] 16 p2214 N90-22630
Pyrotechnic materials ignited using lasers. High energy photopyrotechnic chains
[REPT-892-430-121] 16 p2225 N90-22691
Titanium-boron mixtures as variable heat sources
[DE90-009729] 18 p2522 N90-24401
A high temperature molten salt thermal electrochemical cell
[AD-D014469] 22 p3195 N90-28131
Development and evaluation of hermetic laser diode ignited pyrotechnic components
[DE90-015745] 24 p3458 N90-29529
Analysis of pyrotechnic devices by laser-illuminated high speed photography
[DE90-015741] 24 p3458 N90-29530
An effective low-profile thermite torch
[DE90-015746] 24 p3459 N90-29534
Finite difference modeling of laser diode ignited components
[DE90-015652] 24 p3474 N90-29635

PYROXYLIN
U CELLULOSE NITRATE

PYRROLES
NT TRYPTOPHAN
Quartz crystal microbalance studies of electrochemical growth of conducting polymers
[AD-A210788] 01 p0052 N90-10295
Impedance analysis of ionic transport in polypyrrole-polyazulene copolymer and its charge-discharge characteristics
[AD-A210979] 01 p0052 N90-10299
Rechargeable lithium/polymer cathode batteries
[AD-A210978] 01 p0062 N90-10354
Cell performance of ultra-thin polymer cathode system: Theoretical energy and power density projections
[AD-A210786] 02 p0202 N90-11151
Quartz crystal microbalance analysis. 1: Evidence of anion or cation insertion into electropolymerized conducting polymers
[AD-A212304] 04 p0480 N90-12755
Electrochemical investigation of electronically conductive polymers
[AD-A214019] 07 p0912 N90-15277
Electronic and ionic transport in polymers
[AD-A217028] 11 p1491 N90-18579
Chemical and electrochemical studies in ionic liquids
[AD-A217742] 13 p1773 N90-20175
Molecular organization and electrical properties of mixed Langmuir-Blodgett multilayer thin films of polypyrrole
[DE90-007627] 13 p1894 N90-20870
Morphology changes due to oxidative treatment of glassy carbon electrodes and its applications
[AD-A219425] 17 p2371 N90-23501
XPS studies of doped polypyrrole films
[AD-A219424] 17 p2379 N90-23550
Quartz crystal microbalance analysis: Partial cation release during oxidation of conducting polymers
[AD-A221091] 18 p2530 N90-24439
Electrochemical, in situ Raman spectroscopic, and conductivity studies of polypyrrole incorporating large size anions: Conducting nature of reduced form
[AD-A222739] 20 p2831 N90-26102
Pyrromethene-BF2 complexes as laser dyes
[AD-A223562] 24 p3473 N90-29631

P3V AIRCRAFT
U P-3 AIRCRAFT

P78-2 SATELLITE
U SCATHA SATELLITE

Q

Q FACTORS
Bulk acoustic wave resonators made of amorphous materials
[ONERA-NT-1989-4] 09 p1279 N90-17416
Design of sharp cutoff filters with low quality factors
[AD-A223130] 21 p3000 N90-27051

Q SWITCHED LASERS
Efficient nonlinear conversion of laser diode pumped miniature solid state laser sources
[AD-A210708] 01 p0075 N90-10433
Development of mid-infrared solid state lasers for spaceborne lidar
[NASA-CR-185095] 15 p2103 N90-22031
A room-temperature, laser diode-pumped, Q-switched, 2 micron, thulium-doped, solid state laser
[AD-D014527] 19 p2695 N90-25334

Q VALUES
A simple method using MAFIA to calculate external Q values of waveguide-loaded cavities
[DE90-741487] 12 p1647 N90-19465
Generalizations of a q-analogue of Laguerre polynomials
[REPT-89-51] 15 p2161 N90-22345

QCD
U QUANTUM CHROMODYNAMICS

QSO (RADIO SOURCES)
U QUASARS

QUADRATIC EQUATIONS
Calculation of transient response from time-harmonic spectrum
[AD-A211972] 03 p0393 N90-12241
Quadratic dynamical systems describing shear flow of non-Newtonian fluids
[AD-A212892] 05 p0638 N90-13720
Definition, determination and characterization of acceleration sets for spatial manipulators
[AD-A213366] 05 p0651 N90-13793
Approximations to joint distributions of definite quadratic forms
[AD-A216434] 11 p1551 N90-18930
Theoretical modeling studies of the marine planetary
[AD-A217200] 13 p1841 N90-20567
A Chinese bibliography on quadratic systems of differential equations
[REPT-89-39] 15 p2161 N90-22342
Topological classification of structurally stable quadratic systems without limit cycles
[REPT-89-66] 17 p2457 N90-24025
A bibliography of the qualitative theory of quadratic systems of differential equations in the plane
[REPT-89-71] 17 p2458 N90-24029
Quadratic systems with three saddles and one antisaddle
[REPT-89-80] 17 p2458 N90-24033
Infinite separatrix cycles in the critical case, divergence and uniqueness of limit cycles of a quadratic differential system
[REPT-89-87] 17 p2458 N90-24034
Progress in the polynomial solution of the standard H-infinity optimal control problem
[MEMO-817] 18 p2597 N90-24777
On null tratorial torsion in vacuum quadratic Poincare gauge field theory
[MATHS-REPT-A-111] 19 p2751 N90-25630

QUADRATIC PROGRAMMING
On the identification of local minimizers in inertia-controlling methods for quadratic programming
[AD-A212514] 04 p0534 N90-13086
Sequential quadratic programming algorithms for optimization
[AD-A212800] 04 p0534 N90-13088
On the identification of local minimizers in inertia-controlling methods for quadratic programming
[DE89-017330] 07 p0973 N90-15616
Sequential quadratic programming algorithms for optimization
[DE90-000022] 07 p0973 N90-15617
Gradient projection techniques for large-scale optimization problems
[DE90-001986] 07 p0973 N90-15618
Piecewise linear-quadratic programming and its applications
[AD-A214489] 09 p1264 N90-17328
Digital treatment of elastic-plastic structures by means of quadratic optimization processes from the finite element method
[ETN-90-95823] 12 p1675 N90-19621
Fractional state feedback control of undamped and viscoelastically-damped structures
[AD-A220477] 17 p2412 N90-23746
On the performance of algorithms for large-scale bound constrained problems
[DE90-010084] 18 p2590 N90-24736
The Second Asilomar Workshop on Progress in Mathematical Programming
[AD-A221986] 21 p3053 N90-27358
Ascent and descent trajectory optimization of Ariane 5/Hermes 22 p3126 N90-27743

QUADRATURE APPROXIMATION
U QUADRATURES

QUADRATURES
Faster Phong shading via angular interpolation
[CWI-CS-R8909] 04 p0543 N90-13156
Mitigating Doppler shift effect in HF multitone data modem 06 p0764 N90-14441
Thin-plate spline quadrature of geodetic integrals 13 p1836 N90-20539
QPSK carrier-acquisition performance in the advanced receiver 2 15 p2076 N90-21892
Simulation and analysis of a MFQPSK signal transmitted through an acoustic medium
[AD-A220345] 17 p2393 N90-23633
Numerical solution of large Lyapunov equations
[NASA-CR-180359] 17 p2456 N90-24010
Multi-level trellis coded modulation and multi-stage decoding
[NASA-CR-186861] 19 p2743 N90-25593
QPSK loop lock detection in the advanced receiver 20 p2854 N90-26230
Gaussian quadrature exponential sum modeling of near infrared methane laboratory spectra obtained at temperatures from 106 to 297 K 20 p2945 N90-26758
Modified fast frequency acquisition via adaptive least squares algorithm
[NASA-CASE-NPO-17845-1-CU] 21 p3050 N90-27341

QUADRUPOLE LENSES
U MAGNETIC LENSES

QUADRUPOLE NETWORKS
Preliminary results from the quadrupole probe on NEED-1
[FFI-89/7015] 19 p2714 N90-25446
QUADRUPOLES
A solution to nonlinearity problems
[DE89-016975] 02 p0270 N90-11544
B-Factory Final Focus System using superconducting quadrupoles
[DE90-004432] 08 p1131 N90-16552
Fifth-order aberrations in magnetic quadrupole-octupole systems
[DE90-007489] 12 p1712 N90-19831
Icarus lander 12 p1733 N90-19964
Development of a quadrupole-based Secondary-Ion Mass Spectrometry (SIMS) system at Lewis Research Center
[NASA-TM-102531] 17 p2367 N90-23476
Inhomogeneous electric field effects in a linear RF quadruple trap 20 p2853 N90-26222
Stability regimes in a helical quadrupole focusing accelerator: Theory and simulation
[AD-A221755] 21 p3079 N90-27507
QUALIFICATIONS
Qualification of diode foil materials for excimer lasers
[DE90-000602] 06 p0789 N90-14593
An exploration of issues related to future space logisticians
[AD-A215374] 09 p1276 N90-17397
Monostable electrovalve
[INPE-4928-RPE/595] 12 p1651 N90-19487
Spacecraft escape 13 p1753 N90-20066
Spacelab qualified infrared imager for microgravity science experiments
[NASA-TM-102503] 13 p1804 N90-20352
Sole means navigation and integrity through hybrid Loran-C and NAVSTAR GPS 14 p1907 N90-20932
QM-8 final performance evaluation report: SEALS, volume 4
[NASA-CR-183958] 20 p2869 N90-26324
Qualification of concentrating mirror systems with the HERMES measurement system and the HELIOS simulation program
[DLR-FB-89-51] 20 p2882 N90-26394
M-52 spray booth qualification test
[NASA-CR-184003] 22 p3122 N90-27727
Flexible space-based robot modelling and real-time simulation 22 p3131 N90-27769
QM-6 final performance evaluation report igniter, volume 6
[NASA-CR-184001] 22 p3133 N90-27779
Nondestructive evaluation of adhesively-bonded joints 22 p3185 N90-28074
QUALITATIVE ANALYSIS
A new inexpensive electrochemical meter for oxygen in sodium coolant
[DE89-630802] 02 p0194 N90-11104
Enhanced oxidation and solovolysis reactions in chemically inert microheterogeneous systems
[AD-A210748] 02 p0195 N90-11110
Compositional analysis of steels by X-ray fluorescence spectrometry
[DE89-630803] 02 p0198 N90-11129
Discrete event simulation tool for analysis of qualitative models of continuous processing systems
[NASA-CASE-MSC-21465-1] 08 p1107 N90-16410
Descriptive simulation: Combining symbolic and numerical methods in the analysis of chemical reaction mechanisms
[AD-A214678] 09 p1190 N90-16898
Absolute wind measurements in the lower thermosphere of Venus using infrared heterodyne spectroscopy
[NASA-CR-4290] 21 p3100 N90-27605
QUALITY
NT AIR QUALITY
NT ENVIRONMENTAL QUALITY
NT RIDING QUALITY
NT WATER QUALITY
Differences in writers initial task representations
[AD-A210433] 01 p0136 N90-10788
Proceedings of the 4th European Conference, volume 2
[AD-A216521] 14 p1986 N90-21382
QUALITY CONTROL
Generic system components of the Thiokol ultrasonic RSRM case-to-insulation bondline inspection system
[NASA-CR-183738] 01 p0031 N90-10171
Castings Airworthiness
[AGARD-R-762] 01 p0042 N90-10231
US Air Force certification of castings 01 p0042 N90-10232
Casting factors imposed by the French regulation for foundry castings used in military aircraft 01 p0042 N90-10233
The question of the casting factor 01 p0043 N90-10238
Quality control of castings 01 p0043 N90-10239
Combined advanced foundry and quality control techniques to enhance reliability of castings for the aerospace industry 01 p0043 N90-10240
The creation of quality: New directions in the production of aeronautics castings 01 p0043 N90-10241
Thin walled cast high-strength structural parts 01 p0043 N90-10242
Microstructure morphology and quality of Al-Si castings 01 p0043 N90-10244
Development of Information Quality Engineering (IQE) methodology for information resource management
[AD-A210615] 01 p0137 N90-10791
Lifetime testing of commercially available 3.0 (mu)f, 100 kV pulsed-power capacitors
[DE89-017230] 02 p0217 N90-11242
Principal components in multivariate control charts
[DE89-016828] 02 p0262 N90-11489
An extension of Cochran's test for homogeneity of variances
[AD-A211054] 02 p0269 N90-11534
Working with people to improve productivity and quality: A bibliography with indexes, 1984-1988
[NASA-SP-7078] 03 p0415 N90-12385
The application of quality assurance to engineering management
[DE89-009955] 03 p0416 N90-12386
The role of component testing
[PNR90589] 04 p0455 N90-12608
NDI (Nondestructive Inspection) oriented corrosion control for Army aircraft. Phase 1: Inspection methods
[AD-A213368] 05 p0576 N90-13359
Electrical testing 05 p0605 N90-13520
Product assurance 05 p0605 N90-13522
The Materials Division: A case study
[NASA-TM-102380] 05 p0617 N90-13597
Arc current control of a robotic welding system: Modeling and control system design
[AD-A213150] 05 p0650 N90-13788
Total quality management implementation strategy: Directorate of Quality Assurance
[AD-A212863] 05 p0705 N90-14127
Total quality management plan: Technical and logistics services
[AD-A212864] 05 p0705 N90-14128
Total quality management implementing plan: Office of small and disadvantaged business utilization
[AD-A212865] 05 p0705 N90-14129
Total quality management plan: Office of Congressional Affairs
[AD-A212866] 05 p0705 N90-14130
Total quality management: Directorate of Contract Management master plan
[AD-A212867] 05 p0705 N90-14131
Total quality management plan: Office of Public Affairs
[AD-A212868] 05 p0705 N90-14132
Executive overview and introduction to the SMAP information system life-cycle and documentation standards
[NASA-TM-101765] 05 p0706 N90-14134
Information system life-cycle and documentation standards, volume 1
[NASA-TM-101856] 05 p0706 N90-14135
Management plan documentation standard and Data Item Descriptions (DID). Volume of the information system life-cycle and documentation standards, volume 2
[NASA-TM-101857] 05 p0706 N90-14136
Product specification documentation standard and Data Item Descriptions (DID). Volume of the information system life-cycle and documentation standards, volume 3
[NASA-TM-101858] 05 p0706 N90-14137
Assurance specification documentation standard and Data Item Descriptions (DID). Volume of the information system life-cycle and documentation standards, volume 4
[NASA-TM-101859] 05 p0706 N90-14138
Management control and status reports documentation standard and Data Item Descriptions (DID). Volume of the information system life-cycle and documentation standards, volume 5
[NASA-TM-101860] 05 p0706 N90-14139
Review of the Aerospace Safety Advisory Panel report for NASA fiscal year 1990 authorization
[GPO-24-234] 06 p0722 N90-14213
Electrothermal response testing more than a quality assurance tool
[DE90-001449] 06 p0780 N90-14536
Quality assurance and quality control for the Compact Physics Research Facility (CPRF) and ZTH experiment
[DE90-002352] 06 p0796 N90-14636
Physical and Electrical Standards Laboratory general operating procedures
[DE90-003515] 07 p0884 N90-15116
Back to basics
[DE90-002734] 07 p0943 N90-15463
An expert system for quality assurance (a.k.a.) QA Express
[DE90-003887] 07 p0944 N90-15467
Project management in successful reliability and maintainability improvement programs
[AD-A215424] 09 p1234 N90-17162
A guide to quality assurance indicators for the defense electronics industry
[AD-A215630] 09 p1235 N90-17166
Assessment of solar cell quality criteria 10 p1342 N90-17776
Study of defect distribution in manufacturing test E8 No. 2 (program A-330/340)
[INFORME-I-366/89] 10 p1358 N90-17872
KAPSE Interface Team (KIT) public report, volume 8, part 2
[AD-A215840] 10 p1419 N90-18178
Total quality management: An application in a research and development laboratory
[AD-A215808] 10 p1440 N90-18312
Methods for trend analysis: Examples with problem/failure data 12 p1635 N90-19396
A guide to performing and documenting safety analyses
[DE90-008688] 13 p1788 N90-20261
Product assurance technology for procuring reliable, radiation-hard, custom LSI/VLSI electronics
[NASA-CR-185954] 13 p1791 N90-20281
Research and development quality assurance planning
[DE90-003687] 13 p1813 N90-20413
Transaction processing in a quality control laboratory
[DE90-004655] 13 p1813 N90-20414
Overview of the methodologies used to compile large scale emissions inventories
[DE90-008518] 13 p1830 N90-20509
Software quality assurance and software safety in the biomed control system
[DE90-008072] 13 p1866 N90-20706
Quality at a glance
[AD-A217297] 14 p1989 N90-21400
Software verification and validation: Its role in computer assurance and its relationship with software project management standards
[PB90-111691] 14 p2012 N90-21530
Advanced manufacturing technology: A Department of Energy technology transfer initiative
[DE90-008601] 14 p2037 N90-21688
Testing of an advanced thermochemical conversion reactor system
[DE90-007989] 15 p2123 N90-22141
Software quality assurance: Towards a measurable quality improvement
[REPT-89-42] 15 p2147 N90-22264
Natural resources information system for the state of Oklahoma
[DE90-009483] 15 p2180 N90-22458
Guidelines, operational procedures, and quality control for the estimation of geodetic point positions from GPS data collected with the TI4100 receiver
[AD-A218460] 16 p2250 N90-22829
Full surface interferometric testing of grazing incidence mirrors
[AD-A219394] 16 p2318 N90-23218
Some elementary questions on software quality control
[REPT-89-83] 17 p2445 N90-23939
Data quality analysis at the National Transonic Facility
[NASA-CR-4303] 17 p2448 N90-23957
HPLC analysis of helicopter rotor blade materials
[AD-A221121] 18 p2497 N90-24270
Design considerations for precision and reliability in space mechanisms 18 p2536 N90-24463
Methodology investigation calibration and quality control for new meteorological instrumentation, part 1
[AD-A221407] 18 p2582 N90-24706
A Bayesian approach to reliability and confidence 18 p2628 N90-24974
Evaluating Statistical Process Control (SPC) techniques and computing the uncertainty of force calibrations 18 p2631 N90-24992
Performance of battery charge controllers
[DE90-011413] 19 p2686 N90-25279
Software quality assurance plan for GCS
[NASA-CR-182045] 19 p2743 N90-25588
Space shuttle: Follow-up evaluation of NASA's solid rocket motor procurement. Report to the Chairman, Committee on Government Operations, House of Representatives
[GAO/NSIAD-89-89] 20 p2824 N90-26066
Characterization of inspection performance
[NLR-MP-88068-U] 20 p2874 N90-26350
Dendritic web silicon photovoltaic cell research
[DE90-011786] 20 p2880 N90-26387

Proceedings of the 1987 Aircraft/Engine Structural Integrity Program (ASIP/ENSIP) Conference
[AD-A198037] 21 p2956 N90-26807
An aluminum quality breakthrough for aircraft structural reliability 21 p2957 N90-26816
Quality evaluation of speech processing systems 21 p2993 N90-27012
Knowledge based quality assurance tools
[AD-A223064] 21 p3053 N90-27353
DMSP's interactive tactical terminal 21 p3068 N90-27441
Multichannel on-board load and fatigue monitoring 22 p3103 N90-27621
Computer modeling and data processing methods: An essential part of jet engine condition monitoring and fault diagnosis 22 p3104 N90-27626
Evaluation of composite components on the Bell 206L and Sikorsky S-76 helicopters
[NASA-TM-4195] 22 p3135 N90-27787
Power beam technology at Los Alamos: A review of research and development activities
[DE90-009002] 22 p3182 N90-28057
Neutron radiography: Applications and systems 22 p3186 N90-28080
Quality assurance support for the National Atmospheric Deposition Program and national trends network monitoring activities: 1987-1990
[PB90-187162] 22 p3198 N90-28149
Environmental radioactivity measurement intercomparison exercise
[NPL-RSA(EXT)-5] 22 p3200 N90-28158
Computer support for conducting supportability trade-offs in a team setting
[AD-A222002] 22 p3237 N90-28355
Proceedings of the Conference on Artificial Intelligence in the Department of Energy Complex
[DE90-011634] 22 p3241 N90-28378
Space program safety: Funding for NASA's safety organizations should be centralized
[GAO/NSIAD-90-187] 22 p3255 N90-28434
Assuring both quality and creativity in basic research
[DE90-011489] 22 p3256 N90-28435
Development of acceptance plans for airport pavement materials. Volume 1: Development
[DOT/FAA/RD-90/15] 23 p3284 N90-28581
Adjustable speed drive applications guidebook
[DE90-014151] 23 p3321 N90-28780
Automated system for meteorological analysis
[INPE-4586-TDL/332] 23 p3352 N90-28945
Human factors evaluation and validation criteria for quality training programs: Development, presentation, and assessment
[DE90-014724] 23 p3377 N90-29081
Utilization of a measurement process by the examination of universal motors
[ETN-90-97307] 24 p3466 N90-29581
Total quality management: A recipe for success
[AD-A223287] 24 p3556 N90-30122

QUALITY FACTORS
U Q FACTORS

QUANTILES
Variance reduction for quantile estimates in simulations via nonlinear controls
[AD-A222653] 20 p2916 N90-26590

QUANTITATIVE ANALYSIS
The quantitative analysis of fracture surfaces using fractals
[DE89-015361] 01 p0044 N90-10250
Enhanced oxidation and solvolysis reactions in chemically inert microheterogeneous systems
[AD-A210748] 02 p0195 N90-11110
Improved method for determination of helium-4 in helium-3 by mass spectrometry
[PB89-201404] 04 p0469 N90-12686
Analysis of biaxial stress fields in plates cracking at elevated temperatures
[AD-A216271] 10 p1397 N90-18077
Extracting chemical information form Auger line shapes
[AD-A216729] 11 p1483 N90-18537
Evaluation of a commercial gas chromatography/matrix isolation-infrared spectrometer for quantitative analysis of priority pollutants
[DE90-006033] 11 p1484 N90-18542
Erosion monitoring using remote sensing, part 2
[BCRS-89-15] 11 p1526 N90-18785
Variations in volatiles in magma bodies based on studies of melt inclusions
[DE90-006272] 11 p1532 N90-18821
A method of estimating temperature profiles and chemical differentiation in the near surface layers of porous comet nuclei: First results for comet P/Churyumov-Gerasimenko 12 p1742 N90-20013
Characterization of Monel alloys by x ray fluorescence technique
[DE90-617175] 16 p2221 N90-22665
Quantitative determination of 1, 2-ethanediol contamination in used diesel lubricating oils by gas chromatography/mass spectrometry
[AD-A218592] 17 p2371 N90-23498
Neural networks for real-time sensory data processing and sensorimotor control
[AD-A223096] 20 p2916 N90-26592
Qualitative and quantitative reasoning about thermodynamics
[NASA-CR-186788] 20 p2933 N90-26689

QUANTITY
U AMOUNT

QUANTIZATION
U MEASUREMENT

QUANTIZER
U COUNTERS

QUANTUM CHEMISTRY
Descriptive simulation: Combining symbolic and numerical methods in the analysis of chemical reaction mechanisms
[AD-A214678] 09 p1190 N90-16898
Molecular interactions and properties with many-body methods
[AD-A222631] 20 p2924 N90-26642
Theoretical investigation of gas-surface interactions
[NASA-CR-186881] 22 p3245 N90-28403
Accurate quantum chemical calculations
[NASA-TM-101932] 23 p3303 N90-28680

QUANTUM CHROMODYNAMICS
On the spectrum of the staggered Dirac operator at finite chemical potential
[ITFA-88-53] 04 p0561 N90-13272
Lattice QCD estimate of mixing parameters for heavy meson systems
[PREPRINT-687] 05 p0697 N90-14079
Neutrino interactions
[NOTA-INTERNA-934] 08 p1121 N90-16495
Proceedings of the 23rd Annual Seminar on Theoretical Physics
[DE90-601827] 08 p1135 N90-16577
Transverse spin observables in chromodynamics
[DE90-005638] 12 p1711 N90-19824
The renormalization group and lattice QCD
[DE90-004860] 12 p1724 N90-19905
QCD Compton scattering at HERA energy
[NIKHEF-H/89-3] 15 p2165 N90-22372
Mixing of DIS operators in lattice QCD
[PREPRINT-708] 16 p2323 N90-23243
Lattice field theory
[PREPRINT-719] 16 p2323 N90-23245
Chiral interface at the finite temperature transition point of QCD
[NASA-CR-186605] 17 p2470 N90-24121
Axions and SN 1987A: Axion trapping
[NASA-CR-186604] 18 p2612 N90-24881

QUANTUM COUNTERS
Quantum non-demolition stroboscopic observables and multipumping back-action evasion schemes
[PREPRINT-699] 16 p2326 N90-23260
Are quantum measurements on macroscopic bodies feasible
[PREPRINT-700] 16 p2326 N90-23261

QUANTUM EFFICIENCY
Research on high-efficiency, single-junction, monolithic, thin-film amorphous silicon solar cells, phase 2
[DE89-009496] 07 p0951 N90-15503
Limits of efficiency of solar cells under AMO-spectrum illumination: Comparison between Si and GaAs cells 10 p1343 N90-17784
Evaluation of platinum silicide and indium antimonide as detector materials for space-based remote sensing in the 3.0-to-5.0 micrometer wavelength band
[AD-A216182] 10 p1354 N90-17853
Radiation-hard high-efficiency InP space solar cell development
[AD-A216857] 11 p1528 N90-18800
Quantum yield of photocathodes in far and extreme ultraviolet wavelength area
[ETN-90-95731] 12 p1654 N90-19505
A new thermal sensor for x ray microcalorimetry
[DE90-008547] 13 p1805 N90-20360
InSb DRO array characteristics 14 p1977 N90-21326
Infrared ground-based astronomy with the Hughes 256 X 256 PtSi array 14 p1978 N90-21331
Short wavelength HgCdTe staring focal plane for low background astronomy applications 14 p1979 N90-21336
Improved Si:As BIBIB (Back-Illuminated Blocked-Impurity-Band) hybrid arrays 14 p1981 N90-21349
Development of a unique laboratory standard indium gallium arsenide detector for the 500 to 1700 micron spectral region, phase 2
[NASA-CR-180482] 16 p2238 N90-22767
IR transition moments and collisional dynamics of vibrationally excited OH radicals via time-resolved laser absorption spectroscopy
[AD-A221005] 18 p2580 N90-24696
Research on high-efficiency, multiple-gap, multi-junction amorphous silicon-based alloy thin-film solar cells
[DE90-000338] 23 p3344 N90-28896
Two terminal CuInSe2 based cascade cells
[DE90-000363] 24 p3485 N90-29697

QUANTUM ELECTRODYNAMICS
A theoretical high energy physics program
[DE89-012685] 01 p0121 N90-10696
Critical magnetic fields (H(sub c2), H(sub c1)) and kappa in YBa2(Cu0.98M0.02)3O(7+delta), M=Ni, Al, and Cu
[DE89-016412] 01 p0130 N90-10745
Free-electron laser theory
[DE89-620145] 02 p0226 N90-11298
On the role of Coulomb forces in atomic radiative emission
[IRF-PREPRINT-106] 03 p0403 N90-12308
On the spectrum of the staggered Dirac operator at finite chemical potential
[ITFA-88-53] 04 p0561 N90-13272
Quantum non-demolition stroboscopic observables and multipumping back-action evasion schemes
[PREPRINT-699] 16 p2326 N90-23260
Quantum ballistic and adiabatic electron transport, studied with quantum point contacts
[ETN-90-97262] 20 p2889 N90-26440
Introduction to gauge theories and unification
[DE90-014473] 23 p3402 N90-29225

QUANTUM ELECTRONICS
Quantum 1/F noise in solid state devices in particular Hg1-(sub x)Cd(sub x)Te N(+)-P diodes
[AD-A209365] 01 p0128 N90-10730
Submillimeter quantum electronics
[AD-A210439] 01 p0132 N90-10762
Nonlinear optical studies of resonant systems
[AD-A211032] 02 p0227 N90-11301
SIS (Superconductor-Insulator-Superconductor) mixer research
[AD-A211607] 03 p0414 N90-12375
Joint Services Electronics Program
[AD-A212309] 04 p0497 N90-12864
Multiband photoconductive detector based on layered semiconductor quantum wells
[AD-D014232] 06 p0849 N90-14936
Chemisorption under stress
[AD-A213785] 07 p0895 N90-15175
Research on GaAs quantum-coupled structures that can be used as electron devices
[AD-A214015] 07 p0924 N90-15350
Solid state research
[AD-A213405] 07 p1003 N90-15806
Rotational energy transfer in metastable states of heteronuclear molecules
[AD-A214425] 08 p1120 N90-16485
Proceedings of the conference on Hot Carriers in Semiconductors
[AD-A215544] 09 p1291 N90-17482
Fast optical switch and limiter using quantum size effect in metal grain composites
[AD-D014332] 12 p1619 N90-19305
Joint Services Electronics Program research in electronics
[AD-A217745] 13 p1796 N90-20307
Superconductive microprobes for eddy current evaluation of materials
[AD-A217776] 13 p1805 N90-20361
JPRS report: Science and technology. USSR: Electronics and electrical engineering
[JPRS-UEE-90-002] 14 p1970 N90-21284
Fellowship in physics/modern optics and quantum electronics
[AD-A218772] 17 p2469 N90-24111
Multiple beam optical processing
[AD-A219048] 17 p2471 N90-24129
Investigations of laterally coupled all optical switches and detectors on silica fibers
[AD-A220297] 17 p2473 N90-24142
Molecular beam epitaxial growth of heterostructures to study quantum interference phenomena
[AD-A219442] 17 p2475 N90-24154
Solid state research
[NASA-CR-186699] 17 p2476 N90-24160
Solid state research
[NASA-CR-186700] 17 p2477 N90-24161
Intersubband transitions in an asymmetric quantum well with a thin barrier of a delta-function potential
[AD-A220723] 17 p2477 N90-24162
Report of research activity at the Research Laboratory of Electronics 17 p2486 N90-24217
Towards a quantum pump of electric charges and currents
[AD-A221257] 18 p2607 N90-24851

Quantum ballistic and adiabatic electron transport, studied with quantum point contacts
[ETN-90-97262] 20 p2889 N90-26440
Laser induced surface chemical epitaxy
[AD-A222082] 21 p2977 N90-26920
Quasistatic electron diffusion in quantum hadrodynamics
[ETN-90-97297] 22 p3255 N90-28432
The III-V semiconductor quantum well lasers and related optoelectronic devices on silicon
[AD-A224120] 23 p3331 N90-28835
Statement of research objectives and summary of research efforts
[RLE-PR-132] 23 p3415 N90-29295
Report on the International Workshop on Progress Towards Molecular Scale Electronics
[AD-A223758] 24 p3465 N90-29575
Novel approaches to sensitivity enhancement of ring laser gyros
[AD-A224335] 24 p3471 N90-29617

QUANTUM MECHANICS
NT QUANTUM ELECTRODYNAMICS
Lattice fields and strong interactions
[DE89-015099] 01 p0135 N90-10777
Generation of higher-order squeezing of quantum electromagnetic fields by degenerate four-wave mixing and other processes
[DE89-618392] 02 p0212 N90-11213
Alias-free Wigner distribution function and complex ambiguity function for discrete-time samples
[AD-A211050] 02 p0269 N90-11533
Markov processes in Hilbert space and continuous spontaneous localization of systems of identical particles
[DE89-618396] 02 p0270 N90-11540
A high level Ab initio study of the anionic hydrogen-bonded complexes FH-CN-, FH-NC-, H2O-CN- and H2O-NC- 02 p0272 N90-11553
Origins of high-temperature superconductivity in the new copper oxide based ceramic superconductors
[DE89-016543] 02 p0284 N90-11622
Quantum-mechanical derivation of the Davydov equations for multi-quanta states
[DE89-015250] 03 p0401 N90-12297
Resonant quasiparticle-ion scattering in anisotropic superfluid (3)He
[PB89-221618] 03 p0413 N90-12369
Nonpotential scattering for the density matrix and quantum gravity
[PREPRINT-688] 05 p0697 N90-14080
Where is an object before you look at it
[NOTA-INTERNA-935] 05 p0704 N90-14123
Nonlinear quantum effects in the Maser model: A large N scaling behaviour
[DE89-631631] 06 p0787 N90-14584
Theoretical methods for the study of chemical dynamics
[DE90-003122] 07 p0893 N90-15160
Lefschetz trace formula and BRST
[DE89-635705] 07 p1007 N90-15835
Continuous spontaneous reduction model involving gravity
[DE90-600730] 08 p1135 N90-16573
The (2+1)-dimensional quantum gravity
[DE90-719556] 08 p1136 N90-16580
Double-periodic wormholes in theories with global symmetries
[DE90-719575] 08 p1136 N90-16581
Theory of the dissociation dynamics of small molecules on metal surfaces: Finite temperature studies
[DE90-005217] 09 p1195 N90-16923
Quantum sl(2) enveloping algebra and representations of braid group
[DE90-607044] 09 p1275 N90-17389
Research program in elementary particle theory
[DE90-005600] 10 p1428 N90-18241
On the quantum inverse problem for a new type of nonlinear Schroedinger equation for Alfven waves in plasma
[DE90-607469] 10 p1431 N90-18259
Scale transformations, the energy-momentum tensor, and the equation of state
[DE90-005372] 10 p1440 N90-18308
Systematics in positron annihilation lifetime analysis of high (Tc) superconducting transitions
[DE90-008361] 13 p1896 N90-20884
Center for Atomic, Molecular, and Optical Physics: Technical activities
[PB90-133158] 14 p2022 N90-21591
Local supersymmetry in non-relativistic systems
[DE90-612751] 14 p2034 N90-21670
Quantum mechanics in Riemannian space-time
[DE90-620448] 16 p2325 N90-23257
Baryogenesis in extended inflation. Part 1: Baryogenesis via production and decay of supermassive bosons
[NASA-CR-180615] 17 p2470 N90-24120
Fields, particles, groups: Bertel Laurents 60th Anniversary Symposium
[ETN-90-96596] 17 p2478 N90-24170
Identifying decohering paths in closed quantum systems
[NASA-CR-182853] 19 p2761 N90-25690
Important experiments to test for longer-ranged new gravitational forces
[DE90-012102] 20 p2888 N90-26434
A research program in theoretical high energy physics
[DE90-013322] 20 p2926 N90-26648
High intensity effects in Raman scattering
[DE90-012093] 21 p3076 N90-27486
Dissipative quantum maps
[DE90-627179] 23 p3402 N90-29227
Quantum chaos and dissipation: Lyapunov exponents
[DE90-627180] 23 p3403 N90-29228
Old and new ideas in the theory of quantum measurement
[DE90-627181] 23 p3403 N90-29229
Report on the International Workshop on Progress Towards Molecular Scale Electronics
[AD-A223758] 24 p3465 N90-29575
On a calculation of the ground-state energy in quantum mechanics
[DE90-627182] 24 p3555 N90-30119

QUANTUM OPTICS
Multisqueezing of mechanical states and back-action evasion measurements
[IFSI-89-6] 08 p1123 N90-16504
Classification techniques for quantum-limited and classical-intensity images
[AD-A218693] 16 p2317 N90-23212

QUANTUM STATISTICS
More on the super WZW theory
[NIKHEF-H/88-11] 04 p0562 N90-13273
Where is an object before you look at it
[NOTA-INTERNA-935] 05 p0704 N90-14123
Existence of Bose-Einstein condensation in one and two dimensions
[DE89-635910] 09 p1294 N90-17498
Few-body collisions in a weakly interacting Bose gas
[ETN-90-96893] 18 p2613 N90-24886

QUANTUM THEORY
Quantum 1/F noise in solid state devices in particular Hg1-(sub x)Cd(sub x)Te N(+)-P diodes
[AD-A209365] 01 p0128 N90-10730
The origin of the universe from quantum chaos: An introduction to current ideas
[AD-A210441] 01 p0141 N90-10813
Semiconductor quantum well lasers and related optoelectronic devices on silicon, III-V
[AD-A210758] 02 p0227 N90-11299
A diagnostic for determining the quality of single-reference electron correlation methods 02 p0272 N90-11554
Superfiled formulation of Chern-Simons supersymmetry
[DE89-618459] 02 p0286 N90-11636
General action for topological quantum field theories
[DE89-618460] 02 p0286 N90-11637
Moduli spaces and topological quantum field theories
[DE89-016943] 02 p0287 N90-11639
Monte Carlo studies of nuclei and quantum liquid drops
[DE89-016914] 03 p0402 N90-12300
Gordon Conference on Atomic Physics
[AD-A211946] 03 p0402 N90-12304
Representations of the twisted SU(2) quantum group and some q-hypergeometric orthogonal polynomials
[CWI-PM-R8809] 04 p0541 N90-13140
The addition formula for little q-Legendre polynomials and the SU(2) quantum group
[CWI-AM-R8906] 04 p0543 N90-13151
Strings, p-branes and Skyrmions in curved space 04 p0565 N90-13293
Fundamental quantum 1/f noise in ultrasmall semiconductor devices and their optimal design principles
[AD-A211947] 05 p0702 N90-14107
Chemisorption under stress
[AD-A213785] 07 p0895 N90-15175
Research on GaAs quantum-coupled structures that can be used as electron devices
[AD-A214015] 07 p0924 N90-15350
Relativistic self-consistent field studies of atoms and molecules
[AD-A214101] 07 p0991 N90-15724
Tunnelling effects on low energy fusion cross sections
[AD-A214010] 07 p0997 N90-15762
Interface phonons in semiconductor double heterostructures
[AD-A213732] 07 p1003 N90-15810
The theory of hybrid stochastic algorithms
[DE90-003941] 08 p1109 N90-16421
Multiplet classification of highest weight modules over quantum universal enveloping algebras: The U(sub q)(sl(3,C)) example
[DE90-600720] 08 p1116 N90-16464
The off-shell closed strings as the topological open membranes: Dynamical transmutation of world sheet dimension
[DE89-635721] 08 p1134 N90-16571
Double-periodic wormholes in theories with global symmetries
[DE90-719575] 08 p1136 N90-16581
Quantum fields in cosmological space-times: A soluble example
[DE89-618837] 08 p1150 N90-16662
Proceedings of the conference on Hot Carriers in Semiconductors
[AD-A215544] 09 p1291 N90-17482
Simplicial lattices in classical and quantum gravity: Mathematical structure and application 10 p1439 N90-18304
Solution of a class of conformal quantum field theory models in D-dimensional space
[DE90-607094] 10 p1439 N90-18306
Theoretical and experimental high energy physics
[DE90-006168] 11 p1565 N90-19006
Transport effects and spectroscopy of defects in microstructures
[AD-A216718] 11 p1570 N90-19036
Spectral functions from Quantum Monte Carlo
[DE90-004870] 11 p1572 N90-19050
Geometric continuum regularization of quantum field theory
[DE90-006099] 11 p1573 N90-19058
Quantum cosmological origin of large scale structures of the universe
[DE90-610647] 11 p1591 N90-19176
Goldstone excitation and symmetry breaking mechanism in superfluid He-4
[DE90-610676] 12 p1720 N90-19881
Quantum field theory on higher-genus Riemann surfaces
[DE90-741469] 12 p1725 N90-19912
Gravitational consequences of modern field theories 12 p1730 N90-19947
The inverse-square law and quantum gravity 12 p1731 N90-19949
Quantum-theoretical methods and studies relating to properties of materials
[AD-A217843] 13 p1765 N90-20132
Optical Bistability, 1988
[AD-A217681] 13 p1888 N90-20832
Linking numbers and variational method
[DE90-612793] 14 p2020 N90-21582
Fusion algebra and fusing matrices
[DE90-612798] 14 p2021 N90-21583
Studies in quantum field theory
[DE90-008731] 14 p2035 N90-21677
The 2 + 1 dimensional quantum gravity and the Braid group
[DE90-009036] 14 p2035 N90-21679
Toward quantum corrections in black hole thermodynamics 14 p2040 N90-21702
Optical phonons and electronic properties in double heterostructures
[AD-A219436] 17 p2475 N90-24153
Molecular beam epitaxial growth of heterostructures to study quantum interference phenomena
[AD-A219442] 17 p2475 N90-24154
Proceedings of a research workshop on Computational Condensed Matter Physics. Total Energy Methods and Physics of III-V Semiconductors
[AD-A219568] 17 p2476 N90-24156
Electromigration in metallic microstructures
[AD-A221208] 18 p2622 N90-24942
Quantum-confined hole states in double-barrier resonant tunneling structures
[AD-A221342] 18 p2623 N90-24946
Quantum effects in pair cascade models of AGN spectra 19 p2789 N90-25873
Excimer laser fragmentation studies of selected oximes: Nascent OH internal energy distributions and the search of H2CN fluorescence
[AD-A222622] 20 p2868 N90-26317
A composition for the filling of gas-discharge tubes
[AD-A222818] 21 p2999 N90-27047
Activities report of the Werner-Heisenberg Institute for Physics, Munich, Federal Republic of Germany
[ISSN-0173-6256] 21 p3075 N90-27481
High pulse energy flashlamp pumpable laser dyes
[AD-A223075] 22 p3180 N90-28042
Wigner symbols, quantum dynamics, and the kicked rotator
[AD-A224024] 23 p3403 N90-29234
Higher order equations of motion
[DE90-627522] 24 p3543 N90-30038

On Dirac's conjecture for Hamiltonian systems with first and second class constraints
[DE90-627206] 24 p3555 N90-30116
Workshop on Low-Dimensional Quantum Field Theory and its Applications
[DE90-508071] 24 p3555 N90-30118

QUANTUM WELLS
Use of depletion edge translation for high-speed modulation and switching of lightwaves
[AD-A211186] 01 p0124 N90-10713
Experimental investigations of transport and optical properties of 3-5 quantum well structures grown via molecular beam epitaxy under optimal growth conditions
[AD-A210269] 01 p0132 N90-10758
Submillimeter quantum electronics
[AD-A210439] 01 p0132 N90-10762
Semiconductor quantum well lasers and related optoelectronic devices on silicon, III-V
[AD-A210758] 02 p0227 N90-11299
Nonlinear optical studies of resonant systems
[AD-A211032] 02 p0227 N90-11301
Energy relaxation of light holes in InAs(.15)Sb(.85)/InSb multiple quantum wells
[DE89-016035] 03 p0409 N90-12349
High speed quantum-well optoelectronic devices by MBE
[AD-A212585] 04 p0555 N90-13237
Elastic impurity scattering in double-barrier resonant tunneling structures
[AD-A212850] 05 p0702 N90-14110
Multiband photoconductive detector based on layered semiconductor quantum wells
[AD-D014232] 06 p0849 N90-14936
Research on materials and components for opto-electronic signal processing and computing
[AD-A213740] 07 p1003 N90-15811
Theory of the electronic and optical properties of semiconductor heterostructures
[AD-A214132] 08 p1130 N90-16544
Structural instabilities, impurities, and defects in electronic materials
[AD-A215384] 09 p1290 N90-17481
Density of electronic states in a biased resonant tunneling structure
[AD-A215735] 09 p1291 N90-17486
The III-V semiconductor quantum well lasers and related optoelectronic devices on silicon
[AD-A216980] 12 p1666 N90-19570
Optical bistability in semiconducting material
15 p2174 N90-22424
Optical properties of novel GaAs-based semiconductors
16 p2321 N90-23235
Vertical emitting, ring geometry, ultra-low threshold, and ultra-high speed quantum well lasers for optical interconnect
[AD-A219946] 17 p2409 N90-23727
Intersubband transitions in an asymmetric quantum well with a thin barrier of a delta-function potential
[AD-A220723] 17 p2477 N90-24162
Novel pulsed plasma treatment and coating process: Multilayer structures for optical computing applications
[AD-A220737] 18 p2615 N90-24894
Monolithic arrays of grating-surface-emitting diode lasers and quantum well modulators for optical communications
[NASA-CR-186772] 19 p2758 N90-25674
Multicolor infrared photodetector
[AD-D014511] 20 p2865 N90-26297
Laser induced surface chemical epitaxy
[AD-A222082] 21 p2977 N90-26920
Vertical emitting, ring geometry, ultra-low threshold, and ultra-high speed quantum well lasers for optical interconnect
[AD-A222932] 21 p3008 N90-27098
Growth of III-V films by control of MBE growth front stoichiometry
[NASA-CASE-NPO-17724-1-CU]
21 p3081 N90-27517
Electron-phonon interaction and transport in artificially made semiconductor microstructures
[AD-A223061] 21 p3082 N90-27529
The III-V semiconductor quantum well lasers and related optoelectronic devices on silicon
[AD-A224120] 23 p3331 N90-28835
Quantum well infrared detectors 1: Some calculations of their optical properties
[RSRE-MEMO-4363] 24 p3547 N90-30062
Nonlinear optical studies of the optical and electronic properties of semiconductor heterostructures
[AD-A223408] 24 p3552 N90-30096
Study of hot carrier relaxation in quantum wells by subpicosecond Raman scattering
[DE90-015635] 24 p3554 N90-30107
Manufacturing and characterization of liquid-phase epitaxy layers with atomic levels at the crystal surface and at the hetero limit surfaces in the system GaAs-AlGaAs
[ETN-90-97310] 24 p3554 N90-30113

QUARK MODELS
NT QUARK PARTON MODEL
Nucleon polarizabilities in the constituent quark model
[NOTA-INTERNA-936] 05 p0698 N90-14082
The number of neutrino species, confronted with the results at the recent Lepton-Photon Symposium (August 7-12, 1989)
[NOTA-INTERNA-940] 16 p2315 N90-23195

QUARK PARTON MODEL
Neutrino interactions
[NOTA-INTERNA-934] 08 p1121 N90-16495

QUARKS
Cosmic strings and baryon decay catalysis
[NASA-CR-186074] 04 p0566 N90-13299
Big Bang nucleosynthesis and the Quark-Hadron transition
[NASA-CR-186169] 05 p0713 N90-14168
Transverse spin observables in chromodynamics
[DE90-005638] 12 p1711 N90-19824
Quark-antiquark pair production via gamma W fusion at high energy e(+)e(-) colliders
[PREPRINT-705] 16 p2316 N90-23205
Fast pulsars, strange stars: An opportunity in radio astronomy
[DE90-015630] 24 p3563 N90-30155

QUARRIES
U MINES (EXCAVATIONS)

QUARTZ
Field-assisted bonding of single crystal quartz
[DE89-015407] 03 p0410 N90-12353
The redetermination of the elastic, piezoelectric, and dielectric constants of quartz and their variation with temperature
[AD-A215025] 09 p1197 N90-16937
Finite element analysis of a quartz rotation sensor
[DE90-006959] 12 p1664 N90-19562
Resistivity, adhesive strength, and residual stress measurements of thin film metallizations on single crystal quartz
[DE90-011902] 20 p2837 N90-26135

QUARTZ CRYSTALS
Quartz crystal microbalance studies of electrochemical growth of conducting polymers
[AD-A210788] 01 p0052 N90-10295
Capacitive behavior in conducting polymers: The ac impedance and quartz crystal microbalance studies
[AD-A210754] 02 p0201 N90-11150
Field-assisted bonding of single crystal quartz
[DE89-015407] 03 p0410 N90-12353
Quartz crystal microbalance analysis. 1: Evidence of anion or cation insertion into electropolymerized conducting polymers
[AD-A212304] 04 p0480 N90-12755
Quartz crystal resonator mass loading
[AD-A215199] 09 p1212 N90-17028
Quartz crystal microbalance studies: Solvent effects in conducting polymer films
[AD-A219426] 17 p2372 N90-23502
Quartz crystal microbalance analysis: Partial cation release during oxidation of conducting polymers
[AD-A221091] 18 p2530 N90-24439

QUARTZ TRANSDUCERS
Polarization matrices of quartz
[AD-A215198] 09 p1212 N90-17027

QUASARS
The ratio to X-ray spectral shape and variability of blazars
02 p0297 N90-11688
The low-ion QSO absorption-line systems
05 p0712 N90-14162
VLA and VLBI observations of core dominated quasars
06 p0860 N90-15002
The softest Einstein AGN (Active Galactic Nuclei)
[DE89-009389] 06 p0864 N90-15020
The disk-halo connection and the nature of the interstellar medium
[NASA-CR-186286] 07 p1012 N90-15860
Scientific investigations of the Space Research Group
[ISBN-0-642-13252-6] 08 p1138 N90-16595
H-alpha emission lines in high redshift quasars
11 p1587 N90-19149
Nearly simultaneous optical, ultraviolet, and x ray observations of three PG quasars
[NASA-CR-186355] 12 p1728 N90-19932
Spectrum formation in active galactic nuclei and Type 2 supernovae
15 p2187 N90-22490
Spectral plane quasars, spectral turn-over, and frequency atlas
[INPE-5011-TDL/399] 16 p2329 N90-23277
Skewering the universe with QSO lines of sight: Lyman alpha clouds as probes of large scale structure
16 p2329 N90-23278
Spectroscopic observations of high redshift QSOs: Galaxies and the intergalactic medium at early epochs
16 p2330 N90-23280
The dynamical evolution of dense clusters of compact stars
16 p2331 N90-23287
Studies in gravitational lensing and numerical hydrodynamics
16 p2332 N90-23290
Gamma rays from active galactic nuclei
16 p2337 N90-23316
The high energy source 3C 273
16 p2337 N90-23318
Institute of Astronomy
17 p2481 N90-24190
Sco X-1 the microquasar: New VLA and VLBI results
19 p2775 N90-25780
The spectra (2 to 10 keV) of high luminosity quasars
19 p2786 N90-25852
Multifrequency observation of blazars
19 p2786 N90-25857
X ray spectra of OVV QSOs
19 p2787 N90-25863
QSO optical counts and constraints on the X ray background
19 p2789 N90-25877
The EUV spectral shape of the big-bump in HS1700+6416 and F9: A genuine difference between Seyfert's and QSO's
19 p2789 N90-25878
Long term multi-frequency study of 3C 273
19 p2790 N90-25879
Optical FeII emission and the BLR structure in QSOs
19 p2793 N90-25899
Comparing measurements of AGN X ray spectra with the shape of the diffuse X ray background spectrum
19 p2793 N90-25902
Variability of the continuum emission of GQ Comae
19 p2793 N90-25903
The soft X ray excess in Einstein quasar spectra
19 p2794 N90-25910
Strong associated C 4 absorption in low redshift quasars
[NASA-CR-186936] 22 p3262 N90-28469
Quasar pairs and quasar's peculiar velocity
[FERMILAB-PUB-90/25-A] 22 p3262 N90-28474
Periodicity of redshift distribution in a T-3 universe
[FERMILAB-PUB-90/26-A] 22 p3262 N90-28475
Quasars in galaxy cluster environments
22 p3263 N90-28477
Asymmetric depolarization in powerful extragalactic radio sources
22 p3264 N90-28484

QUASI-PARTICLES
U ELEMENTARY EXCITATIONS

QUASI-STEADY STATES
Discrete approach: Percolation theory
19 p2689 N90-25297
Numerical and analytical study of nonlinear bifurcations associated with the morphological stability of two-dimensional single crystals
[PB90-209594] 23 p3398 N90-29200

QUASI-STELLAR RADIO SOURCES
U QUASARS

QUASILINEARITY
U NONLINEARITY

QUATERNARY ALLOYS
High-efficiency CuInSe2 and CuInGaSe2 based cells and materials research
[DE89-009449] 01 p0083 N90-10471
Theoretical and experimental study of solid phase miscibility gaps in III/V quaternary alloys
[DE90-008430] 13 p1895 N90-20877
Ternary and quaternary oxides of Bi, Sr, and Cu
22 p3141 N90-27817

QUATERNIONS
An algorithm for the systematic disturbance of optimal rotational solutions
[NASA-TM-101089] 01 p0102 N90-10575
Simultaneous quaternion estimation (QUEST) and bias determination
05 p0587 N90-13417
Direct inversion of rigid-body rotational dynamics
[NASA-TM-102798] 15 p2055 N90-21773
Geometrical properties of an internal local octonionic space in a non-Riemannian manifold
[DE90-627175] 23 p3390 N90-29149

QUENCHING
Development of metastable processing paths for high temperature alloys
[AD-A210550] 01 p0045 N90-10254

QUENCHING (ATOMIC PHYSICS)
CANOES 2: Dynamics of atmospheric infrared thermochemical excitation, volume 1
[AD-A213341] 05 p0667 N90-13897
CANOES 2: Dynamics of atmospheric infrared thermochemical excitation, volume 2
[AD-A213342] 05 p0667 N90-13898
CANOES 2: Dynamics of atmospheric infrared thermochemical excitation, volume 3
[AD-A213343] 05 p0667 N90-13899
CANOES 2: Dynamics of atmospheric infrared thermochemical excitation, volume 4
[AD-A213344] 05 p0667 N90-13900

Lattice QCD estimate of mixing parameters for heavy meson systems
[PREPRINT-687] 05 p0697 N90-14079
State to state kinetics of XeCl*
[AD-A215895] 10 p1353 N90-17847
Stark and Zeeman effects on laser cooling of positronium 11 p1560 N90-18986
Reactions of N2A3 sigma u + and candidates for short wavelengths lasers
[DE90-009514] 15 p2103 N90-22033
Rotational and translational effects in collisions of electronically excited diatomic hydrides
[NASA-CR-186770] 20 p2829 N90-26093
Fluorescent probe investigation of a water-soluble polyphosphazene
[AD-A222317] 21 p2978 N90-26925
Quenching of N(2D) by O(3P)
[AD-A221690] 23 p3303 N90-28683

QUENCHING (COOLING)
Calculation of surface heat transfer parameters during quenching from surface thermocouple signals
[DE89-011620] 07 p0904 N90-15224
Undercooling and solidification
[DLR-FB-90-020] 20 p2931 N90-26678
Microstructural development in HSLA-100 steel weld metals
[AD-A222105] 21 p2982 N90-26944

QUERY LANGUAGES
Abbreviated query interpretation in extended entity-relationship oriented databases
[DE90-003114] 08 p1137 N90-16587
Parrot: The Janus paraphraser
[AD-A214588] 09 p1265 N90-17332
IRUS-II user manual
[AD-A214612] 09 p1265 N90-17334
Guidelines for the use of the SAME
[AD-A215846] 11 p1544 N90-18888
A human factors experimental comparison of two database query languages 11 p1574 N90-19064
Knowledge-based semantic query processing: An optimal transformation approach 15 p2176 N90-22437
Object-oriented query languages: The notion and the issues
[REPT-89-054] 16 p2298 N90-23093
A framework for query optimization in temporal databases
[DE90-011339] 19 p2763 N90-25700
Evaluating recursive queries in distributed databases
[REPT-90-015] 22 p3260 N90-28460
Preference relations, Chisini-de Finetti means and Bayesian inference in retrieval-system modelling
[ESA-STR-230] 22 p3260 N90-28461
Formal semantics of SQL queries
[REPT-89-069] 24 p3531 N90-29973
Accessing network databases via SQL transactions in a multi-model database system
[AD-A223946] 24 p3557 N90-30128

QUEUEING THEORY
Network analyzer for nonstatic jamming
[AD-A210759] 02 p0212 N90-11216
Transaction throughput in distributed systems: A modeling study using dynamic queueing networks
[MEMO-INF-89-25] 02 p0261 N90-11479
Stochastic optimization by simulation: Some experiments with a simple steady-state queue
[AD-A210762] 02 p0265 N90-11508
A simulation study of landing time allocation procedures for use in computer-assisted air traffic management systems
[AD-A212159] 03 p0303 N90-11722
The conditional-event approach to distributed simulation
[NASA-CR-185890] 03 p0387 N90-12200
The M/G/1 processor sharing queue as the almost sure limit of feedback queues
[REPT-89-32] 04 p0528 N90-13044
Extended performability modeling using dynamic queing networks
[MEMO-INF-89-15] 04 p0536 N90-13099
Modular specifications in process algebra with curious queues
[CWI-CS-R8821] 04 p0543 N90-13152
The discrete-time single-server queueing model
[MEMO-780] 04 p0544 N90-13165
Waiting times in polling systems with Markovian server routing
[CWI-BS-R8905] 05 p0685 N90-13989
Monotonicity of performance measures in a processor sharing queue
[CWI-BS-R8902] 05 p0689 N90-14019
Workloads and waiting times in single-server systems with multiple customer classes
[CWI-BS-R8906] 05 p0689 N90-14020
Simple appoximations for second moment characteristics of the sojurn time in the M/G/1 processor sharing queue
[CWI-BS-R8907] 05 p0694 N90-14055
On stability of queueing models of local area networks with slotted ring protocols
[MEMO-795] 05 p0694 N90-14057
Analysis of a queueing model for slotted ring networks
[MEMO-796] 05 p0694 N90-14058
Dynamic workload modeling of high speed token rings in a metropolitan area network
[MEMO-INF-89-21] 05 p0694 N90-14059
The application of queuing theory to the modelling of CP-140 aircraft communications
[AD-A213479] 07 p0918 N90-15310
Queues with negative arrivals
[AD-A213860] 07 p0984 N90-15687
Development of a parallel link model for meteor burst communication
[AD-A215629] 09 p1208 N90-17001
An algorithm for finding characteristic roots of quasi-triangular Markov chains
[AD-A215490] 10 p1421 N90-18196
A survey of performability modelling tools
[MEMO-INF-89-50] 11 p1547 N90-18907
Using dynamic queueing networks as a tool for specifying performability models
[MEMO-INF-89-51] 11 p1554 N90-18949
Recurrence conditions for average and Blackwell optimality in denumerable state Markov decision chains
[TW-89-02] 11 p1555 N90-18952
Queuing theory approach to modelling the dynamics of the human-computer interface
[AD-A216870] 12 p1705 N90-19788
An approximation for the response time of an open CP-disk system
[MEMO-COSOR-89-19] 16 p2327 N90-23266
Rate-based congestion control in networks with smart links, revision
[NASA-CR-186698] 17 p2452 N90-23987
An asymmetric shortest queue problem
[MEMO-COSOR-89-22] 17 p2459 N90-24035
The existence of sensitive optimal policies in two multi-dimensional queueing models
[TW-89-11] 17 p2464 N90-24080
Note on the optimality of the generalized shortest queue policy
[TW-90-01] 17 p2464 N90-24081
The M/G/1 queue with permanent customers
[CWI-BS-R8919] 17 p2467 N90-24096
Sojourn times in queueing networks
[CWI-BS-R8916] 17 p2467 N90-24102
Uniform limit theorems for synchronous processes with applications to queues
[AD-A220224] 18 p2599 N90-24788
Analysis of a queueing model of the Orwell slotted ring
[MEMO-812] 18 p2606 N90-24843
Computer architecture evaluation for structural dynamics computations: Project summary
[NASA-CR-186137] 20 p2903 N90-26512
Estimating the parameters of a sporadically observed queue
[DE90-012903] 20 p2917 N90-26596
Queing networks with finite capacities
[AD-A221547] 21 p3065 N90-27425

QUIET ENGINE PROGRAM
What should be done with those noisy old aircraft
[PNR90562] 04 p0452 N90-12593
Re-engine with the Rolls-Royce Tay 670, the route to significant noise reduction
[PNR90585] 04 p0455 N90-12606
The commercial aircraft noise problem
[PNR90577] 04 p0550 N90-13203

R

RACAH COEFFICIENT
Automated angular momentum recoupling algebra
[DE90-011988] 19 p2750 N90-25626

RACE FACTORS
Psychological and physiological responses of blacks and caucasians to hand cooling
[AD-A215646] 09 p1253 N90-17272

RACKS (FRAMES)
Pivotal mono wing cruise missile with wing deployment and fastener mechanism
[AD-D014191] 04 p0452 N90-12594
A robot end effector exchange mechanism for space applications 15 p2113 N90-22088
Rod gripper, changer, and storage system
[NASA-CR-183154] 17 p2411 N90-23739
Graphical explanation in an expert system for Space Station Freedom rack integration 21 p3044 N90-27299

RACON BEACONS
U RADAR BEACONS

RADAR
NT AIRBORNE SURVEILLANCE RADAR
NT COHERENT RADAR
NT DOPPLER RADAR
NT EISCAT RADAR SYSTEM (EUROPE)
NT IMAGING RADAR
NT INCOHERENT SCATTER RADAR
NT INFRARED RADAR
NT METEOROLOGICAL RADAR
NT MONOPULSE RADAR
NT MOVING TARGET INDICATORS
NT MULTISPECTRAL RADAR
NT MULTISTATIC RADAR
NT OPTICAL RADAR
NT OVER-THE-HORIZON RADAR
NT PULSE DOPPLER RADAR
NT PULSE RADAR
NT RADAR MEASUREMENT
NT RANGE AND RANGE RATE TRACKING
NT SATELLITE-BORNE RADAR
NT SEARCH RADAR
NT SECONDARY RADAR
NT SIDE-LOOKING RADAR
NT SPACE BASED RADAR
NT SURVEILLANCE RADAR
NT SYNTHETIC APERTURE RADAR
NT TRACKING RADAR
The Swedish defense research needs: For surveillance and seeker applications
[FOA-C-30520-3.3] 02 p0298 N90-11691
A radar simulation program for a 1024-processor hypercube
[DE89-014494] 06 p0766 N90-14455
High resolution, wide band Chirp-Z signal analyzer
[AD-D014240] 06 p0768 N90-14465
The radar-based short term prediction of the time-space evolution of rain fields
[AD-A213802] 07 p0918 N90-15312
Adaptive canceller limitations caused by I,Q mismatch errors
[AD-A214287] 07 p0919 N90-15318
Interference rejection and detection performance of the smallest of circuit
[AD-A215153] 09 p1212 N90-17025
Polarization radar processing technology
[AD-A215242] 10 p1374 N90-17967
Navigation experiment NAVEX data storage and processing
[ESA-TT-1175] 11 p1467 N90-18445
Automatic thresholding multichannel digital radar early warning system
[AD-D014323] 12 p1642 N90-19431
Algorithms for optimal processing of polarimetric radar data
[AD-A217330] 13 p1876 N90-20758
Research on statistical techniques for signal processing
[AD-A218811] 17 p2388 N90-23599
A theoretical model for airborne radars
[AD-A220735] 17 p2390 N90-23615
Engineer's Refractive Effects Prediction System (EREPS), revision 2.0
[AD-A220742] 17 p2391 N90-23616
Fields, particles, groups: Bertel Laurents 60th Anniversary Symposium
[ETN-90-96596] 17 p2478 N90-24170
Bayesian characterization and detection of rare binary signature events
[AD-A221116] 18 p2606 N90-24844
The variably trimmed mean CFAR detector for nonhomogeneous background
[AD-A222801] 20 p2856 N90-26243
Simulation of synthetic aperture radar 4: Summary and recommendations
[AD-A221822] 21 p2997 N90-27038
Alternative solutions for Hilbert filtering in a pulse compression radar
[FEL-89-C226] 22 p3165 N90-27950
Using embedded microcontrollers in radar test equipment
[DE90-014997] 23 p3319 N90-28763
Target detection in Gaussian noise using artificial neural systems
[AD-A223983] 23 p3320 N90-28770
Radar clutter via ray methods
[AD-A223796] 24 p3462 N90-29553

RADAR ABSORBERS
A decision-making aid for multi-layer radar absorbent coverings
[ESA-TT-1173] 19 p2684 N90-25267

RADAR ALTIMETERS
U RADIO ALTIMETERS

RADAR ANTENNAS
Power conditioning for active array SAR antennas
10 p1338 N90-17744
Applications of FM-CW laser radar to antenna contour mapping
12 p1611 N90-19270
Radar transponder antenna pattern analysis for the space shuttle
12 p1638 N90-19414
An investigation of the transfer of monopulse tracking between two coherent point sources
[AD-A217007] 12 p1646 N90-19457
ROSAR (Helicopter-Rotor based Synthetic Aperture Radar)
14 p1961 N90-21229
Concept for a spaceborne Synthetic Aperture Radar (SAR) sensor based on active phased array technology
14 p1962 N90-21234
Feasibility of a synthetic aperture Radar with Rotative Antennas (ROSAR)
[MBB-S/PUB-0385] 19 p2651 N90-25088
Concepts for high resolution space based SAR/ISAR systems
[MBB-UK-0057/89-PUB] 19 p2652 N90-25096
Target signature modeling and bistatic scattering measurement studies
[NASA-CR-186611] 23 p3319 N90-28766
Analysis and design of modifications for improved performance of the AFIT radar cross section measurement chamber
[AD-A223352] 24 p3460 N90-29545

RADAR APPROACH CONTROL
Design of a final approach spacing tool for TRACON air traffic control
[NASA-TM-102229] 02 p0147 N90-10841
The application of Z to the specification of air traffic control systems. 1: An initial specification of the radar processing activity
[RSRE-MEMO-4280] 08 p1020 N90-15900
Tracking performance of the AN/GPN-22 precision approach radar
[FEL-1988-34] 12 p1647 N90-19467
Study improvement training facilities ground control air traffic controllers. Part 1: Alternative solutions and their consequences
[FEL-89-A257-PT-1] 24 p3431 N90-29380
Study improvement training facilities ground control air traffic controllers. Part 2: Functional analysis approach control trainer
[FEL-89-A280-PT-2] 24 p3436 N90-29409

RADAR ASTRONOMY
Geology of Southern Guinevere Planitia, Venus, based on analyses of Goldstone radar data
03 p0422 N90-12424
The Telecommunications and Data Acquisition Report
[NASA-CR-186479] 15 p2074 N90-21880
Laboratory measurements and modeling of microwave absorption by ammonia in gas mixtures applicable to giant planet atmospheres
20 p2944 N90-26750

RADAR BEACONS
NT DISCRETE ADDRESS BEACON SYSTEM
Data link test and analysis system/ATCRBS transponder test system technical reference
[DOT/FAA/CT-TN90/7] 21 p2955 N90-26803
The MODE S operational test and evaluation/integration test plan
[DOT/FAA/CT-TN89/51] 22 p3111 N90-27671

RADAR BEAMS
Concepts for high resolution space based SAR/ISAR systems: Preliminary design considerations
14 p1960 N90-21224
Trade-offs in a space based surveillance radar
14 p1960 N90-21225

RADAR CLUTTER MAPS
Use of clutter residue editing maps during the Denver 1988 Terminal Doppler Weather Radar (TDWR) tests
[AD-A218696] 17 p2426 N90-23822

RADAR CORNER REFLECTORS
Scattering from coated structures and antenna pattern control using impedance surfaces, part A/B
[NASA-CR-186671] 20 p2854 N90-26233

RADAR CROSS SECTIONS
Efficient algorithm for calculation of radar cross section
[AD-A210785] 02 p0213 N90-11217
Specification for radar free-space detection range and free-space intercept range calculations
[AD-A213158] 04 p0494 N90-12843
The physical optics approximation in the near-field region
[FEL-1989-100] 04 p0555 N90-13234
Flashlight radar: A three-dimensional imaging radar
[AD-A213439] 07 p0918 N90-15307
Plasmon excitation in the scattering of electromagnetic waves from good conductors
[AD-A214026] 08 p1056 N90-16107
Compact ranges in antenna and RCS measurements
10 p1371 N90-17940
Automation of an RCS (Radar Cross Section) measurement system and its application to investigate the electromagnetic scattering from scale model aircraft canopies
[AD-A215741] 10 p1375 N90-17970
Near-field bistatic RCS (Radar Cross-Section) measurements
[AD-A217011] 12 p1646 N90-19458
Electromagnetic properties of material coated surfaces
[NASA-CR-186466] 12 p1647 N90-19466
Simulation of radar scattering from rough surfaces
[AD-A217841] 13 p1790 N90-20275
The 5th Annual Review of Progress in Applied Computational Electromagnetics
[AD-A217994] 14 p1966 N90-21258
Measurement and analysis of the electromagnetic scattering of a geodesic array of triangular trihedral corner reflectors
[AD-A220457] 17 p2389 N90-23608
Backscatter enhancement in scattering from rough surfaces
[AD-A223110] 21 p2995 N90-27024
Dependence of radar backscatter on the energetics of the air-sea interface
[AD-A221966] 21 p2996 N90-27028
Analysis and design of modifications for improved performance of the AFIT radar cross section measurement chamber
[AD-A223352] 24 p3460 N90-29545
Bistatic radar cross section of a perfectly conducting rhombus-shaped flat plate
[AD-A223418] 24 p3460 N90-29546
High range resolution radar cross-section profiles: A preliminary analysis
[AD-A223448] 24 p3461 N90-29550

RADAR DATA
Specification of Viper1 in Z
[RSRE-MEMO-4195] 04 p0490 N90-12817
Specification of Viper2 in Z
[RSRE-MEMO-4217] 04 p0490 N90-12819
The interaction and variation of waves and turbulence from MST radar data
[AD-A212849] 05 p0670 N90-13906
Applications of acousto-optical correlation devices in radar signal processing
[AD-A216624] 11 p1497 N90-18616
Simulation of synthetic aperture radar 3: Evaluation of prototype digital feature analysis data
[AD-A216750] 11 p1498 N90-18620
Algorithms for optimal processing of polarimetric radar data
[AD-A217330] 13 p1876 N90-20758
Windshear case study: Denver, Colorado, July 11, 1988
[DOT/FAA/DS-89/19] 14 p2008 N90-21509
Improving a data-acquisition software system with abstract data type components
15 p2078 N90-21901
Meteor radar studies of the mesopause region and nonlinear atmospheric waves
17 p2421 N90-23799
Sea bottom topography with X-band SLAR
[BCRS-89-25] 17 p2431 N90-23854
Conception and results of the DLR realtime azimuth processor for the E-SAR system
[ESA-TT-1184] 19 p2684 N90-25268
Study of the relationships between radar structure and the electrical activity of clouds
[ETN-90-97488] 23 p3352 N90-28946
A personal computer-based, multitasking data acquisition system
[NASA-TM-4232] 23 p3382 N90-29107

RADAR DETECTION
Specification for radar free-space detection range and free-space intercept range calculations
[AD-A213158] 04 p0494 N90-12843
Adaptive clutter rejection filters for airborne Doppler weather radar applied to the detection of low altitude windshear
[NASA-CR-186211] 06 p0766 N90-14453
The lidar experiment at Andoya, Norway, during the Summer of 1988
[BONN-IR-89-16] 08 p1058 N90-16117
Long term integration for radar detection of small targets in clutter
09 p1203 N90-16972
Aspects of VHF radars illustrated by the example of an experimental system
[REPT-1-89] 12 p1647 N90-19468
Radar detection of lightning and electric fields
[AD-A217894] 13 p1842 N90-20574
Concept for a spaceborne Synthetic Aperture Radar (SAR) sensor based on active phased array technology
14 p1962 N90-21234
Airborne Doppler radar flight experiments for the detection of microbursts
14 p1963 N90-21243
Concept and results of the DLR realtime SAR processor
14 p1963 N90-21244
Intelligent signal processing techniques for multi-sensor surveillance systems
[AD-A216890] 16 p2262 N90-22895
Radar detection during scintillation
[AD-A220099] 17 p2393 N90-23630
Effects of monitoring under high and low taskload on detection of flashing and colored radar targets
[AD-A220313] 17 p2439 N90-23895

RADAR DIRECTION FINDERS
U RADIO DIRECTION FINDERS

RADAR ECHOES
NT CLUTTER
Small-scale irregularities and global plasma dynamics in the high-latitude ionosphere
02 p0246 N90-11394
Pacific marine radar sea scatter experimental results
[AD-A211593] 03 p0339 N90-11931
Investigation of the properties of radar backscatter from sea ice
[AD-A212808] 04 p0493 N90-12838
Multiparameter radar estimation of raindrop size distribution
[AD-A212410] 04 p0521 N90-13007
First-order Bragg SAR imagery of Kelvin wakes and moving internal wave fields
[AD-A213361] 05 p0633 N90-13691
Propagation-based decision aids in the U.S. Navy
06 p0757 N90-14410
Radar detection of lightning and electric fields
[AD-A217894] 13 p1842 N90-20574
A fast ISAR-imaging process and its inherent degrading effects on image quality
14 p1963 N90-21239
Radar target image by ISAR case study
14 p1963 N90-21242
Measurement and analysis of the electromagnetic scattering of a geodesic array of triangular trihedral corner reflectors
[AD-A220457] 17 p2389 N90-23608
Millimeter - wave radar scattering from terrain: Data handbook
[AD-A220770] 17 p2391 N90-23617
High-resolution radar imaging
[AD-A220809] 17 p2391 N90-23620
Dependence of radar backscatter on the energetics of the air-sea interface
[AD-A221966] 21 p2996 N90-27028

RADAR EQUIPMENT
NT DISCRETE ADDRESS BEACON SYSTEM
NT RADAR ANTENNAS
NT RADAR BEACONS
NT RADAR CORNER REFLECTORS
NT RADAR RECEIVERS
NT RADAR TRANSMITTERS
NT RETROREFLECTORS
Tropospheric influences on satellite-Earth paths and their determination by means of radar measurements
[ESA-TT-1143] 04 p0480 N90-12639
Method for eliminating self-screening noise jamming in radar systems
[AD-D014271] 08 p1056 N90-16105
A technique for the generation of range-height-angle charts
[AD-A214534] 09 p1204 N90-16979
PRPSIM: A FORTRAN code to calculate properties of radio wave propagation in a structured ionized medium. Volume 2: Theory and models
[AD-A216299] 10 p1377 N90-17983
Finite element modeling and thermal simulations of transistor integrated circuits
[AD-A215928] 10 p1380 N90-17997
Heli/SITAN: A terrain referenced navigation algorithm for helicopters
[DE90-005193] 12 p1602 N90-19217
Development of a receiver for a space-based laser radar system
[AD-A215079] 12 p1665 N90-19566
Design options for space-based radar systems
[ETN-90-96548] 16 p2228 N90-22710
Optimizing ECM techniques against monopulse acquisition and tracking radars
[AD-A220036] 17 p2393 N90-23629
Concept study for UHF T/R modules
[AD-A220281] 18 p2547 N90-24536
Lightweight, broadband, pulsed, frequency agile, self-screening jammer for airborne deployment
[AD-D014468] 22 p3163 N90-27937

RADAR GEOLOGY
Abstracts for the Venus Geoscience Tutorial and Venus Geologic Mapping Workshop
[NASA-CR-185432] 03 p0422 N90-12423
Geology of Southern Guinevere Planitia, Venus, based on analyses of Goldstone radar data
03 p0422 N90-12424
Tessera terrain: Characteristics and models of origin
03 p0422 N90-12426

Geocoded spaceborne SAR products for geological applications 19 p2708 N90-25410

RADAR IMAGERY

Ionosphere-thermosphere coupling at high latitudes: Aspect angle dependence of non-thermal plasmas 02 p0244 N90-11382

An ionospheric model for HF sky-wave backscatter radar 02 p0247 N90-11401

Potential for observing and discriminating impact craters and comparable volcanic landforms on Magellan radar images 03 p0423 N90-12429

Contrasting landform perception with varied radar illumination geometries and at simulated resolutions of Venera and Magellan 03 p0423 N90-12430

Venus surface properties deduced from radar and radiometry 03 p0423 N90-12431

A morphologic study of Venus Ridge belts 03 p0423 N90-12432

Evidence for volcanism in NW Ishtar Terra, Venus 03 p0424 N90-12433

Analysis of radar images of the active volcanic zone at Krafla, Iceland: The effects of look azimuth biasing 03 p0424 N90-12434

Crater identification and resolution of lunar radar images 03 p0426 N90-12441

Radar scattering from desert terrains, Pisgah/Lavic Region, California: Implications for Magellan 03 p0426 N90-12443

Geology of the Venus equatorial region from Pioneer Venus radar imaging 03 p0427 N90-12447

Stress distribution and topography of Tellus Regio, Venus 03 p0428 N90-12452

On a fast two-dimensional radar imaging process for rotating targets, and an analysis of its image quality [ESA-TT-1142] 04 p0489 N90-12808

Conception and results of the DLR realtime azimuth processor for the E-SAR system [DLR-FB-89-30] 04 p0492 N90-12827

Progress in the identification of airborne radar targets [AD-A212749] 04 p0493 N90-12835

First-order Bragg SAR imagery of Kelvin wakes and moving internal wave fields [AD-A213361] 05 p0633 N90-13691

Analysis of propagation in an inhomogeneous atmosphere in the horizontal and vertical direction using the parabolic equation method 06 p0760 N90-14421

Flashlight radar: A three-dimensional imaging radar [AD-A213439] 07 p0918 N90-15307

Investigation of the topographic components of the image content of radar pictures 08 p1094 N90-16332

The development of an airborne synthetic aperture radar motion compensation system 09 p1165 N90-16745

Fractal geometry segmentation of polarimetric synthetic aperture radar images [AD-A216278] 10 p1377 N90-17982

Synthetic aperture radar imagery of airports and surrounding areas: Archived SAR data [NASA-CR-4275] 11 p1453 N90-18371

Synthetic aperture radar imagery of airports and surrounding areas: Philadelphia Airport [NASA-CR-4280] 11 p1453 N90-18372

Simulation of synthetic aperture radar 3: Evaluation of prototype digital feature analysis data [AD-A216750] 11 p1498 N90-18620

Orbital remote sensing in the decade of the nineties: New approaches and challenges in geology [INPE-4836-PRE/1467] 11 p1521 N90-18758

Analysis of photogeologic lineaments in the Ithacare (BA) region: A proposed methodology [INPE-4855-PRE/1478] 12 p1677 N90-19635

Analysis of tectonic movements utilizing remote sensor products in the Southern Espinhaco (SE) region [INPE-4830-PRE/1451] 12 p1690 N90-19708

Atmospheric wind measurements using a 50 MHz imaging Doppler Interferometer radar [AD-A218277] 13 p1847 N90-20601

SAR and ISAR imagery of marine targets 14 p1962 N90-21237

Radar observations of a formation of two fighters: A case study for ISAR imaging 14 p1963 N90-21240

The 1D-ISAR imaging of manoeuvering aircraft 14 p1963 N90-21241

Radar target image by ISAR case study 14 p1963 N90-21242

Image simulation of geometric targets for synthetic aperture radar 14 p1964 N90-21245

SAR image coding 14 p1964 N90-21246

Automatic classification of images [AD-D014437] 14 p1966 N90-21260

Results of the Gondwana Project: An example of intercontinental geologic correlation utilizing LANDSAT imagery [INPE-4870-PRE/1481] 14 p1995 N90-21437

Characterization of linear structures from remote sensing data; Espinhaco Meridional (MG) sierra [INPE-4905-PRE/1506] 14 p1997 N90-21449

Spaceborne radar observations: A guide for Magellan radar-image analysis [NASA-CR-184998] 16 p2249 N90-22826

A theoretical model for airborne radars [AD-A220735] 17 p2390 N90-23615

High-resolution radar imaging [AD-A220809] 17 p2391 N90-23620

Synthetic aperture radar imagery of airports and surrounding areas: Denver Stapleton International Airport [NASA-CR-4305] 18 p2495 N90-24257

Automated segmentation and extraction of area terrain features from radar imagery [AD-A221096] 18 p2544 N90-24522

Sweep width determination for HU-25B airborne radars: Life raft and recreational boat targets [AD-A221362] 18 p2545 N90-24524

Conception and results of the DLR realtime azimuth processor for the E-SAR system [ESA-TT-1184] 19 p2684 N90-25268

The browse file of NASA/JPL quick-look radar images from the Loch Linnhe 1989 experiment [NASA-CR-186855] 20 p2935 N90-26701

RADAR MAPS

Simulation of synthetic aperture radar 1: Feature density and accuracy requirements [AD-A211019] 02 p0213 N90-11218

Navigation up-date using radar mapping: Assessment and optimisation simulation tool 08 p1026 N90-15928

Simulation of synthetic aperture radar 3: Evaluation of prototype digital feature analysis data [AD-A216750] 11 p1498 N90-18620

The Magellan Venus explorer's guide [NASA-CR-186968] 23 p3286 N90-28592

RADAR MEASUREMENT

Middle Atmosphere Program. Handbook for MAP, volume 28 [NASA-CR-184972] 03 p0370 N90-12117

Use of ground penetrating radar to define recharge areas in the Central Sand Plain [PB89-224885] 04 p0490 N90-12814

Radar polarimetric studies based on the MAYPOLE 1983 and 1984 field experiments [AD-A212226] 04 p0492 N90-12830

The effects of clutter-rejection filtering on estimating weather spectrum parameters [NASA-CR-186212] 06 p0817 N90-14754

Flashlight radar: A three-dimensional imaging radar [AD-A213439] 07 p0918 N90-15307

Analytical techniques for tracking filter implementation 08 p1021 N90-15903

Modern Antenna Design Using Computers and Measurement: Application to Antenna Problems of Military Interest [AGARD-LS-165] 10 p1369 N90-17932

Millimeter wave radar clutter program [AD-A215772] 10 p1376 N90-17978

Coherent radar measurement of ocean currents from geostationary orbit 12 p1609 N90-19259

Near-field bistatic RCS (Radar Cross-Section) measurements [AD-A217011] 12 p1646 N90-19458

Simulation of radar and radiometer signals remote sensing cometary surface and subsurface structures 12 p1740 N90-20005

Atmospheric wind measurements using a 50 MHz imaging Doppler Interferometer radar [AD-A218277] 13 p1847 N90-20601

Problems in ISAR processing with range resolution by stepped frequency bursts 14 p1962 N90-21238

Investigations into the properties, conditions, and effects of the ionosphere [AD-A217807] 14 p2005 N90-21489

Lidar measurements of the optical propagation environment 15 p2084 N90-21930

Lidar measurement of concentration and turbulence in battlefield obscurants 15 p2084 N90-21931

Verification of Klett's method by comparison of lidar and transmissometer measurements 15 p2084 N90-21933

Initiation and propagation of thunderstorm mesocyclones 17 p2428 N90-23838

A laboratory investigation into microwave backscattering from sea ice [NASA-CR-186621] 18 p2542 N90-24510

Cloud dynamics and cloud microphysics by radar measurements 19 p2707 N90-25402

Estimation of convective rain volumes utilizing the are-time-integral technique [NASA-CR-186814] 20 p2890 N90-26449

Development of eye-safe lidar for aerosol measurements [NASA-CR-186905] 20 p2901 N90-26503

Dependence of radar backscatter on the energetics of the air-sea interface [AD-A221966] 21 p2996 N90-27028

High resolution exponential modeling of fully polarized radar returns [AD-A221432] 21 p2997 N90-27036

Aureole lidar: Ground based measurement [AD-A223207] 21 p3008 N90-27101

Program to perform research on use of lidar for range resolved turbulence measurements [AD-A222189] 21 p3026 N90-27204

Radio refractivity profiles deduced from lidar measurements [AD-A221727] 21 p3026 N90-27208

RADAR NAVIGATION

Navigation up-date using radar mapping: Assessment and optimisation simulation tool 08 p1026 N90-15928

Survivable penetration 24 p3428 N90-29363

An Ada-based marine radar simulator for collision avoidance training [ETN-90-97611] 24 p3531 N90-29970

RADAR NETWORKS

Multitarget tracking by single sensor: Analysis of the main approaches developed in this area [ESA-TT-1171] 11 p1500 N90-18633

RADAR OBSERVATION

U RADAR TRACKING

RADAR RANGE

Base level management of radio frequency radiation protection program [AD-A211787] 03 p0381 N90-12171

Low level range coverage performance prediction for VHF radar 06 p0783 N90-14439

A technique for the generation of range-height-angle charts [AD-A214534] 09 p1204 N90-16979

Compact ranges in antenna and RCS measurements 10 p1371 N90-17940

Automation of an RCS (Radar Cross Section) measurement system and its application to investigate the electromagnetic scattering from scale model aircraft canopies [AD-A215741] 10 p1375 N90-17970

An investigation of the transfer of monopulse tracking between two coherent point sources [AD-A217007] 12 p1646 N90-19457

RADAR RECEIVERS

Specification for environmental measurements to assess radar sensors [AD-A219127] 16 p2250 N90-22833

Radar receiver procedures [AD-A224399] 24 p3460 N90-29541

RADAR REFLECTIONS

U RADAR ECHOES

RADAR REFLECTORS

NT RADAR CORNER REFLECTORS

RADAR RESOLUTION

On the range resolution of point targets with FMCW radar systems [DLR-FB-89-47] 11 p1499 N90-18629

Tomographic processing of synthetic aperture radar signals for enhanced resolution [AD-A217178] 13 p1789 N90-20265

High Resolution Air- and Spaceborne Radar [AGARD-CP-459] 14 p1960 N90-21223

Down-range imaging of radar targets [AD-A221084] 18 p2544 N90-24521

RADAR SCANNING

MMW SAR on RPV for battlefield surveillance 14 p1961 N90-21231

RADAR SCATTERING

Pacific marine radar sea scatter experimental results [AD-A211593] 03 p0339 N90-11931

Spectral-domain analysis of finite frequency selective surfaces [AD-A211669] 03 p0339 N90-11932

Radar scattering mechanisms within the meteor crater ejecta blanket: Geologic implications and relevance to Venus 03 p0424 N90-12435

Radar scattering from desert terrains, Pisgah/Lavic Region, California: Implications for Magellan 03 p0426 N90-12443

Improvement and extension of a radar forest backscattering model [NASA-CR-186083] 04 p0515 N90-12973

Stochastic modelling of EM scattering from foliage [AD-A213118] 05 p0632 N90-13689

Measurement and computer simulation of antennas on ships and aircraft for results of operational reliability 10 p1369 N90-17936

Synthetic aperture radar imagery of airports and surrounding areas: Archived SAR data
[NASA-CR-4275] 11 p1453 N90-18371
Electromagnetic properties of material coated surfaces
[NASA-CR-186466] 12 p1647 N90-19466
Simulation of radar scattering from rough surfaces
[AD-A217841] 13 p1790 N90-20275
The PHARUS project: Design of a polarimetric C-band SAR in the Netherlands 14 p1961 N90-21228
A solution for real time motion compensation for SAR without using inertial navigation systems
14 p1962 N90-21236
Millimeter - wave radar scattering from terrain: Data handbook
[AD-A220770] 17 p2391 N90-23617
Target signature modeling and bistatic scattering measurement studies
[NASA-CR-186611] 23 p3319 N90-28766

RADAR SIGNATURES
Progress in the identification of airborne radar targets
[AD-A212749] 04 p0493 N90-12835
Active and passive remote sensing of ice
[AD-A214863] 09 p1241 N90-17199
Temporal statistics of low-angle ground clutter
[AD-A220816] 17 p2391 N90-23621
A comparison of the K-pulse and E-pulse techniques for aspect independent radar target identification
[AD-A220172] 18 p2542 N90-24511
High resolution exponential modeling of fully polarized radar returns
[AD-A221432] 21 p2997 N90-27036
Target signature modeling and bistatic scattering measurement studies
[NASA-CR-186611] 23 p3319 N90-28766

RADAR TARGETS
Dedicated tracking of crossing targets with a phased array monopulse radar
[FEL-1988-95] 04 p0491 N90-12821
Progress in the identification of airborne radar targets
[AD-A212749] 04 p0493 N90-12835
Studies of quantitative methods for imaging from scattered fields
[AD-A214047] 07 p0976 N90-15638
Long term integration for radar detection of small targets in clutter 09 p1203 N90-16972
A technique for the generation of range-height-angle charts
[AD-A214534] 09 p1204 N90-16979
High resolution radar target modeling using ARMA (Autoregressive Moving Average) models
[AD-A218212] 13 p1791 N90-20278
Algorithms for optimal processing of polarimetric radar data
[AD-A217330] 13 p1876 N90-20758
Radar target image by ISAR case study
14 p1963 N90-21242
Recognition and analysis of aircraft targets by radar, using structural pattern representations derived from polarimetric signatures 15 p2074 N90-21879
High-resolution radar imaging
[AD-A220809] 17 p2391 N90-23620
Neuromorphic optical signal processing and image understanding for automated target recognition
[AD-A219827] 17 p2437 N90-23884
Effects of monitoring under high and low taskload on detection of flashing and colored radar targets
[AD-A220313] 17 p2439 N90-23895
A comparison of the K-pulse and E-pulse techniques for aspect independent radar target identification
[AD-A220172] 18 p2542 N90-24511
Down-range imaging of radar targets
[AD-A221084] 18 p2544 N90-24521
Sweep width determination for HU-25B airborne radars: Life raft and recreational boat targets
[AD-A221362] 18 p2545 N90-24524
Backscatter enhancement in scattering from rough surfaces
[AD-A223110] 21 p2995 N90-27024
Target detection in Gaussian noise using artificial neural systems
[AD-A223983] 23 p3320 N90-28770

RADAR TRACKING
Relation of wind field and buoyancy to rainfall inferred from radar
[PB89-208326] 02 p0251 N90-11424
Multiparameter radar estimation of raindrop size distribution
[AD-A212410] 04 p0521 N90-13007
Turbulence spectral widths view angle independence as observed by Doppler radar
[DOT/FAA/SA-89/2] 07 p0963 N90-15566
Modeling the response of a monopulse radar to impulsive jamming signals using the Block Oriented System Simulator (BOSS)
[AD-A215560] 10 p1375 N90-17969
Tracking performance of the AN/GPN-22 precision approach radar
[FEL-1988-34] 12 p1647 N90-19467
Advanced Doppler tracking experiments
12 p1731 N90-19951
High resolution radar target modeling using ARMA (Autoregressive Moving Average) models
[AD-A218212] 13 p1791 N90-20278
Wideband S band transmitter
[AD-A217620] 13 p1794 N90-20295
Trade-offs in a space based surveillance radar
14 p1960 N90-21225
Capabilities of bistatic synthetic aperture radar for covert battlefield surveillance 14 p1961 N90-21230
Radar observations of a formation of two fighters: A case study for ISAR imaging 14 p1963 N90-21240
Radar target image by ISAR case study
14 p1963 N90-21242
Determination of the general ocean circulation using satellite altimetry from a simultaneous solution for the Earth's gravity field 16 p2203 N90-22569
Intelligent signal processing techniques for multi-sensor surveillance systems
[AD-A218890] 16 p2262 N90-22895
Using simulation to determine a strategy for positively tracking a cruise missile by CMMCA
[AD-A220526] 17 p2362 N90-23448
Sweep width determination for HU-25B airborne radars: Life raft and recreational boat targets
[AD-A221362] 18 p2545 N90-24524
Laser radar angular tracking
[AD-A222741] 20 p2869 N90-26319
User's manual ROBIN: A research and notification system for bird migration
[FEL-1989-103] 23 p3270 N90-28508
Tutorial on using LISP object-oriented programming for blackboards: Solving the radar tracking problem
[AD-A224272] 24 p3525 N90-29930

RADAR TRANSMISSION
Radar polarimetric studies based on the MAYPOLE 1983 and 1984 field experiments
[AD-A212226] 04 p0492 N90-12830
Innovative techniques for high-resolution imaging and precision tracking
[AD-A221380] 18 p2616 N90-24899
Software set-up for data processing of depolarization due to rain and ice crystals in the Olympus project
[EUT-89-E-218] 20 p2855 N90-26240
Neural networks and radar systems
[FEL-89-B65] 24 p3462 N90-29558

RADAR TRANSMITTERS
Frequency agile synthetic aperture radar
[AD-D014235] 06 p0765 N90-14451
Wideband S band transmitter
[AD-A217620] 13 p1794 N90-20295
Ground-based weather radar compatibility with digital radio-relay microwave systems
[PB90-206236] 23 p3318 N90-28756

RADIAL FLOW
A theoretical study of ingress for shrouded rotating disk systems with radial outflow
[PNR90586] 04 p0455 N90-12607
An interactive grid generation procedure for axial and radial flow turbomachinery
[NASA-CR-185167] 05 p0682 N90-13968
An experimental investigation of viscous aspects of propeller blade flow 09 p1159 N90-16711
Activation uniformity dependence of undoped semi-insulating GaAs on post-implant annealing conditions
[ETN-90-96549] 16 p2323 N90-23246
Calculation of correction terms for forces and moment measurements in radial flow field of hypersonic spheric nozzles 18 p2490 N90-24234

RADIAL VELOCITY
Kilometric type III radio bursts and interplanetary transients 06 p0867 N90-15038
The possible X ray triple 4U2129+47 (=V1727 Cygni)
19 p2768 N90-25732

RADIANCE
Offaxis radiance studies for infrared sensors
[AD-A210790] 02 p0275 N90-11570
Retrieval of atomic oxygen and temperature in the thermosphere. Part 2: Feasibility of an experiment based on limb emission in the OI lines
[AD-A211807] 03 p0371 N90-12121
Comparison of the LOWTRAN 7 code and S3-4 satellite measurements of UV radiance
[AD-A211356] 03 p0372 N90-12124
Spatial characteristics of airglow and solar scatter radiance from the earth's atmosphere
[AD-A211358] 03 p0372 N90-12126
The effects of seasonal and latitudinal earth infrared radiance variations on ERBS attitude control
05 p0586 N90-13414
Synoptic scale tropical waves in multichannel satellite radiance data 06 p0816 N90-14745
Identification and quantification of synoptic structure in simulated Tiros N radiance soundings
07 p0959 N90-15546
Identification and quantification of synoptic structure in simulated TIROS N radiance soundings
[AD-A213729] 07 p0960 N90-15553
Description of SHARC: The Strategic High-Altitude Radiance Code
[AD-A213806] 07 p0961 N90-15555
Atmospheric transmittance determination from a two-angle measurement of radiance change
[AD-A213847] 08 p1101 N90-16375
Two adaptive techniques let progressive refinement outperform the traditional radiosity algorithm
[AD-A215174] 09 p1267 N90-17347
Non-contact true temperature measurements in the microgravity environment 10 p1364 N90-17906
Project Floval: Correction of relief effects in eucalyptus reforestration
[INPE-4814-RPE/590] 11 p1525 N90-18777
LOWTRAN 7: Status, review, and impact for short-to-long-wavelength infrared applications
15 p2081 N90-21917
Models of aerosols, clouds, and precipitation for atmospheric propagation studies
15 p2081 N90-21919
UV spectral simulations using LOWTRAN 7
15 p2083 N90-21928
Long term intensity stability of Auger electron spectrometers: Instructions for the interlaboratory comparison
[NPL-DMM(A)-1] 15 p2102 N90-22027
An intensity expression organising spectral line intensity data
[IRF-SR-202] 17 p2373 N90-23513
Sensor performance analysis
[NASA-RP-1241] 17 p2418 N90-23780
Current status of SHARC, the strategic high altitude radiance code, and description of its new auroral module
[AD-A221068] 18 p2580 N90-24698
The 27-28 October 1986 FIRE IFO Cirrus case study: Comparison of radiative transfer theory with observations by satellite and aircraft
[NASA-TM-103468] 20 p2890 N90-26446
On estimating scale invariance in stratocumulus cloud fields 22 p3213 N90-28227
Intercomparisons of GOES-derived cloud parameters and surface observations over San Nicolas Island
22 p3214 N90-28229
High resolution infrared measurements
22 p3221 N90-28265
Comparison of 30 day integrations with and without interactive clouds 22 p3222 N90-28274
Interpretation of cirrus cloud properties using coincident satellite and lidar data during the FIRE cirrus IFO
22 p3223 N90-28276
Properties of cirrus from multispectral AVHRR imagery data 22 p3223 N90-28277
Cirrus radiative characteristics and the radiative impact of small particles 22 p3224 N90-28286
A comparative study of infrared radiance measurements by an ER-2 based radiometer and the LANDSAT 5 Thematic Mapper (TM-6) 22 p3226 N90-28294
Airborne lidar/radiometric measurements of cirrus cloud parameters and their application to LOWTRAN radiance evaluations 22 p3227 N90-28298
Cirrus parameterization from the FIRE ER-2 observations 22 p3227 N90-28302
Simulation of long range atmosphere effects in short range thermal infrared and CCD images
[IZF-1989-27] 22 p3247 N90-28413

RADIANT COOLING
Upcoming planetary missions and the applicability of high temperature superconductor bolometers
22 p3140 N90-27811

RADIANT ENERGY
U RADIATION

RADIANT FLUX DENSITY
NT ILLUMINANCE
NT IRRADIANCE
NT LUMINANCE
NT LUMINOUS INTENSITY
NT PARTICLE FLUX DENSITY
NT PROTON FLUX DENSITY
NT RADIANCE
NT SOLAR CONSTANT
NT SOLAR FLUX DENSITY
Squeezing of many-atom radiation in an optical cavity
[AD-A215736] 09 p1280 N90-17422
Earth radiation budget and climate
19 p2707 N90-25403
The behaviour of SS433 and Cygnus X-3 at low frequency 19 p2772 N90-25756

Sco X-1 the microquasar: New VLA and VLBI results
19 p2775 N90-25780
A new transient X ray burst source near GX 1+4
19 p2782 N90-25826
EXOSAT observation of the pulsar PSR 1509-58
19 p2782 N90-25829
Qualification of concentrating mirror systems with the HERMES measurement system and the HELIOS simulation program
[DLR-FB-89-51] 20 p2882 N90-26394
Computer modeling wave propagation with a variation of the Helmholtz-Kirchhoff relation
[AD-A222746] 20 p2927 N90-26657
ERBE and CERES broadband scanning radiometers
21 p3016 N90-27149
Energy transmission by means of coherent quasi-mono-chromatic light beams
23 p3392 N90-29163
Some studies related to a new Hexagonal Compound Parabolic Concentrator (HCPC) as a secondary in tandem with a solar tower
[DLR-FB-90-12] 24 p3485 N90-29700

RADIANT HEATING
Prediction of the thermal environment and thermal response of simple panels exposed to radiant heat
[NASA-TM-101660] 03 p0400 N90-12292
Development of a shuttle plume radiation heating indicator
[NASA-CR-183679] 05 p0614 N90-13584
Measurement of radiation property of long infrared emitter and examination of infrared radiation heating process
[DE90-741971] 10 p1425 N90-18222
Heat transfer definitions and equations
[ESDU-89022] 12 p1657 N90-19522

RADIANT INTENSITY
U RADIANT FLUX DENSITY

RADIATION
An analysis of the finite-differenced, even-parity discrete-ordinates equations in slab geometry
[DE90-006479] 15 p2160 N90-22337
Shaping radiation pattern of excimer laser by means of controllable intracavity mirror
16 p2310 N90-23166

RADIATION ABSORPTION
NT ELECTROMAGNETIC ABSORPTION
NT GAMMA RAY ABSORPTION
NT INFRARED ABSORPTION
NT MOLECULAR ABSORPTION
NT MULTIPHOTON ABSORPTION
NT PHOTOABSORPTION
NT POLAR CAP ABSORPTION
NT ULTRAVIOLET ABSORPTION
NT X RAY ABSORPTION
Acoustic studies of new materials: Quasicrystals, low-loss glasses and high Tc superconductors
[AD-A211281] 02 p0272 N90-11551
Parametric study of power absorption from electromagnetic waves by small ferrite spheres
[NASA-TP-2949] 03 p0399 N90-12282
Small particle scattering and absorption
[AD-A213168] 04 p0473 N90-12711
Stochastic modelling of EM scattering from foliage
[AD-A213118] 05 p0632 N90-13689
Atlas of albedo and absorbed solar radiation derived from Nimbus 6 earth radiation budget data set, July 1975 to May 1978
[NASA-RP-1230] 06 p0815 N90-14741
Analysis of catalytically enhanced solar absorption chemical reactors: 1 - numerical model description
[DE89-014742] 07 p0951 N90-15505
Cloud phase discrimination by near-infrared remote sensing 08 p1090 N90-16310
Atmospheric transmittance determination from a two-angle measurement of radiance change
[AD-A213847] 08 p1101 N90-16375
Mechanisms of microwave induced damage in biologic materials
[AD-A213480] 08 p1104 N90-16390
PRPSIM: A FORTRAN code to calculate properties of radio wave propagation in a structured ionized medium. Volume 2: Theory and models
[AD-A216299] 10 p1377 N90-17983
Some problems in oceanic radiative transfer
[AD-A215935] 10 p1410 N90-18131
Microwave radiation absorption by Ho(Y)-Ba-Cu-O superconducting ceramics
[DE90-610665] 11 p1492 N90-18588
Research in theoretical physics
[DE90-005558] 11 p1562 N90-19001
CO2 laser plus optimization for harmonic generation
[AD-D014341] 12 p1665 N90-19565
The pressure loaded volumetric ceramic receiver
[DLR-MITT-89-17] 16 p2252 N90-22842
Earth radiation budget and climate
19 p2707 N90-25403
Is KO Vel (E1013-477) an intermediate polar
19 p2773 N90-25766
An outline for the RTNEPH infrared atmospheric water vapor attenuation study
[AD-A221753] 21 p3027 N90-27209
On airborne measurements of radiation from broken cloud fields
[MITT-67] 21 p3027 N90-27211
NPL absorbed dose graphite calorimeter correction for the effect of the gaps around the core
[NPL-RSA(EXT)-12] 22 p3178 N90-28032
Laser beam stop
[AD-D014595] 24 p3473 N90-29629
A study of water vapor, electrical parameters, and radio propagation
[AD-A223582] 24 p3492 N90-29736

RADIATION BELTS
CRRES (Combined Release and Radiation Effects Satellite) SPACERAD plasma wave experiment
[AD-A210791] 02 p0278 N90-11587
JPRS Report: Science and technology. USSR: Space. Soviet space program to the year 2000
[JPRS-USP-89-008] 06 p0728 N90-14248
The effects of natural and enhanced Van Allen Belt radiation on a space based weapon platform
[DE89-016219] 08 p1154 N90-16685
PROTEL: Design, fabrication, calibration, testing, and satellite integration of a proton telescope
[AD-A214564] 09 p1183 N90-16861
Development and use of data analysis procedures for the CRRES (Combined Release and Radiation Effects Satellite) payloads AFGL-701-2/Dosimeter and AFGL-701-4/Fluxmeter and application of the data analysis results to improve the static and dynamic models of the Earth's radiation belts
[AD-A215953] 10 p1447 N90-18348
NASA radiation belt models AP-8 and AE-8
[AD-A223660] 24 p3492 N90-29737
Re-analysis of data on the space radiation environment above south-east Asia
[RAE-TR-89048] 24 p3565 N90-30166

RADIATION CHEMISTRY
NT PHOTODECOMPOSITION
NT PHOTODISSOCIATION
NT PHOTOLYSIS

RADIATION COUNTERS
NT CERENKOV COUNTERS
NT NEUTRON COUNTERS
NT NEUTRON SPECTROMETERS
NT PARTICLE TELESCOPES
NT PROPORTIONAL COUNTERS
NT QUANTUM COUNTERS
NT SCINTILLATION COUNTERS
Report on the performance and operating characteristics of the Burle C83061E QUANTACON (trademark) photomultiplier tube
[DE89-015257] 01 p0058 N90-10333
Ion detector on the basis of microchannel plates for a high-sensitive mass spectrometer
[DE89-620335] 02 p0225 N90-11291
Survey of the response of standard limited streamer tubes over the complete range of three-component gas mixtures of isobutane, CO(sub 2), argon
[DE89-016692] 04 p0499 N90-12875
Performance of resistive plate counters at beam flux up to 140 Hz/cm2
[NOTA-INTERNA-930] 05 p0697 N90-14081
Superconducting magnets in space
[DE90-002671] 06 p0837 N90-14865
Photon counting modules using RCA silicon avalanche photodiodes 09 p1222 N90-17089
Elementary particle physics: Experimental
[DE90-005973] 10 p1429 N90-18242
Particle detection via rotons in helium-4 superfluid
[DE90-005417] 10 p1448 N90-18354
The track-etch detector for the MACRO experiment at the Gran Sasso Laboratory
[DE90-003235] 11 p1594 N90-19182
Radial response of the burst and transient source experiment 12 p1637 N90-19408
Detector to study low-flex hard x ray/gamma ray sources
[UT-HE-90/08] 24 p3564 N90-30164

RADIATION DAMAGE
NT LASER DAMAGE
Particle emission and charging effects induced by fracture
[AD-A210215] 01 p0080 N90-10459
Photolysis of spacecraft contaminants
[AD-A211715] 03 p0317 N90-11801
Growth and characterization of materials for tunable lasers in the near infrared spectral region
[NASA-CR-185832] 03 p0352 N90-12009
Radiation damage and its influence on source requirements for high resolution x ray holography
[DE90-002508] 06 p0781 N90-14540
Microstructural evolution of martensitic steels during fast neutron irradiation
[DE89-016231] 07 p0902 N90-15212
Fusion reactor materials
[DE90-000976] 07 p0994 N90-15744
Material responses to incident x rays
[DE89-015366] 08 p1089 N90-16305
Mechanisms of microwave induced damage in biologic materials
[AD-A213480] 08 p1104 N90-16390
New models and techniques for predicting radiation effects on solar array performances
10 p1344 N90-17790
Review of synergistic environmental interactions: Guidelines for new testing approaches on future solar arrays 10 p1345 N90-17803
Electron-beam induced damage in thin insulating films on compound semiconductors
[NASA-CR-185177] 10 p1378 N90-17987
Identification and solution of a charging problem in a high-altitude detector
[DE90-008637] 12 p1616 N90-19296
Irradiation-induced amorphization and elastic shear instability in intermetallic compounds
[DE90-004845] 12 p1625 N90-19341
Effect of electron-excitation on radiation damage in ion-irradiated FCC metals
[DE90-719537] 12 p1626 N90-19344
Evaluation of radiation-induced sensitization using electrochemical potentiokinetic reactivation technique for austenitic stainless steels
[DE90-002708] 12 p1627 N90-19352
X ray specular reflection studies of silicon coated by organic monolayers (alkylsiloxanes)
[AD-A217418] 13 p1779 N90-20213
Measurement of proton induced radiation damage to CMOS transistors and pin diodes
[DE90-007836] 13 p1792 N90-20283
Electron beam induced damage in PECVD Si3N4 and SiO2 films on InP
[NASA-TM-102544] 13 p1810 N90-20393
Proton responses on MOS (Metal-Oxide-Semiconductor) electronics operating at cryogenic temperatures
[AD-A217622] 13 p1894 N90-20868
Stressed Ge:Ga photoconductors for space-based astronomy. (Is there life beyond 120 micron)
14 p1975 N90-21315
Development of intrinsic IPT scintillator
[DE90-007906] 14 p1984 N90-21367
Center for surface radiation damage studies
[AD-A218452] 16 p2222 N90-22678
A study of low level laser retinal damage
[AD-A218919] 16 p2261 N90-22887
Investigation of lubrication characteristics of MoS2 films in space environment 18 p2537 N90-24472
Monoenergetic positron beam studies of near-surface phenomena
[ETN-90-96947] 18 p2613 N90-24887
An examination of the 1-MeV equivalent silicon damage methodology
[DE90-007167] 18 p2614 N90-24888
Optical properties monitor: Experiment definition phase
[NASA-CR-4293] 19 p2666 N90-25170
The effect of crystal orientation on damage accumulation in chromium-implanted Al2O3
[DE90-012294] 20 p2931 N90-26674
Mechanisms of microwave induced damage in biologic materials
[AD-A222454] 21 p3033 N90-27242
The effects of space radiation on thin films of YBa2Cu3O(sub 7-x) 22 p3147 N90-27845
Use of Ni63 overvoltage gap switches in the flight termination systems on boosters launched from US Army Kwajalein Atoll (USAKA)
[AD-A223866] 23 p3299 N90-28661
Accurate calculations of neutron kerma and damage from ENDF/B-VI evaluations for silicon, chromium, iron and nickel, and comparison with ENDF/B-V results
[DE90-016020] 24 p3481 N90-29674
An advanced single event upset tester
[AD-A223613] 24 p3564 N90-30163

RADIATION DETECTORS
NT DOSIMETERS
Studies of elementary particles
[DE89-014859] 01 p0119 N90-10685
The detection of soft X-rays with charged coupled detectors 01 p0138 N90-10798
A liquid xenon imaging telescope for 1-30 MeV gamma-ray astrophysics
[NASA-CR-185999] 02 p0291 N90-11662
A microchannel plate intensified, subnanosecond, X-ray imaging camera
[DE89-017781] 03 p0350 N90-12003

Electron cyclotron emission and absorption experiment on the CASTOR tokamak
[IPPCZ-285] 03 p0407 N90-12331
Observation of the solar Lyman-alpha line
05 p0662 N90-13868
Correlation among gravitational wave and neutrino detectors data during SN1987A
[NOTA-INTERNA-932] 05 p0713 N90-14165
A fiber-fed imaging spectrometer
[DE90-001008] 06 p0781 N90-14538
Reflectometers
[AD-D014249] 08 p1122 N90-16499
The GALLEX Project
[DE90-005573] 09 p1300 N90-17534
L x ray spectrometry in vivo with a Si(Li)-NaI(Tl)
[DE90-005649] 10 p1387 N90-18028
High performance, picosecond radiation detectors grown by molecular beam epitaxy for millimeter-wave diagnostic systems
[DE90-005547] 10 p1438 N90-18302
Studies of (mu)(prime)s underground with the Soudan 2 Tracker
[DE90-005656] 10 p1449 N90-18360
Underground muon observations in the Soudan 2 detector
[DE90-005647] 11 p1504 N90-19183
Background studies in gas ionizing x ray detectors
12 p1636 N90-19399
Digital integrator
[DIGEL-1989-2] 12 p1654 N90-19508
The space microwave interferometer and the search for cosmic background gravitational wave radiation
12 p1731 N90-19952
Earth-orbiting resonant-mass gravitational wave detectors 12 p1731 N90-19954
Space telescope searches for black holes in galactic nuclei 12 p1732 N90-19958
Frequency stable high power lasers in space
12 p1734 N90-19969
Cosmic ray events in Soudan 2
[DE90-005657] 12 p1746 N90-20037
Stressed Ge:Ga photoconductors for space-based astronomy. (Is there life beyond 120 micron)
14 p1975 N90-21315
Germanium Blocked Impurity Band (BIB) detectors
14 p1976 N90-21321
Short wavelength HgCdTe staring focal plane for low background astronomy applications
14 p1979 N90-21336
Status of the isophot detector development
14 p1980 N90-21342
ISO/LWS: Detector status 14 p1980 N90-21343
Tests of the Rockwell Si:As Back-Illuminated Blocked-Impurity Band (BIBIB) detectors
14 p1981 N90-21350
Double sided silicon strip detectors
[MPI-PAE/EXP-EL-217] 22 p3178 N90-28036
A double-sided silicon strip detector with capacitive read out and a new method of integrated bias coupling
22 p3178 N90-28037
Readout of double sided silicon strip detectors with high intensity integrated electronics 22 p3179 N90-28038
Enrichment services for chromium isotopes for the GALLEX (gallium experiment) international collaboration experiment on solar neutrino flux
[DE90-014300] 23 p3413 N90-29285

RADIATION DISTRIBUTION
NT ANTENNA RADIATION PATTERNS
NT DIFFRACTION PATTERNS
NT SIDELOBES
On the role of Coulomb forces in atomic radiative emission
[IRF-PREPRINT-106] 03 p0403 N90-12308
Wire grid modeling of the linear tapered slot antenna
[AD-A212977] 04 p0494 N90-12842
Interaction of radiation with matter: Atomic collision processes occurring in the presence of radiation fields
[AD-A213112] 05 p0697 N90-14078
Potential theory of radiation 12 p1635 N90-19395
Analysis of a high harmonic rectangular gyrotron using ribbon beams 15 p2061 N90-21801
Modelling UV-visible radiation observed from space
15 p2085 N90-21937
Satellite versus GCM-simulated radiation balance: Comparisons and implications for climate modeling
15 p2131 N90-22180
Spectrum formation in active galactic nuclei and Type 2 supernovae 15 p2187 N90-22490
The diffuse galactic gamma ray emission
16 p2333 N90-23296
Equilibrium radiative heating tables for Earth entry
[NASA-TM-102652] 17 p2401 N90-23675
Development of a hybrid adaptive beamformer
[AD-A219652] 17 p2471 N90-24128
Studies in the parameterization of cloudiness in climate models and the analysis of radiation fields in general circulation models
[NASA-CR-186378] 19 p2715 N90-25448
Application and extension of an analytical model of the confined acoustic beam generated by a transducer
[AD-A222994] 20 p2924 N90-26639
A preliminary analysis of threshold signal detection in ambient and signal-dependent noise environments
[AD-A222089] 21 p2996 N90-27030
Solar UV variability 22 p3201 N90-28162
Satellite-derived cloud and radiation fields over the marine stratocumulus IFO 22 p3216 N90-28240
The effects of clouds on CO2 forcing
22 p3222 N90-28271
Radiative properties of cirrus clouds inferred from broadband measurements during FIRE
22 p3226 N90-28295
IR spectral characteristics of cirrus clouds
22 p3226 N90-28297
Propagation of electromagnetic radiation in a random field of gravitational waves and space radio interferometry
[DE90-627196] 23 p3319 N90-28764
Fluctuations in cosmic background radiation
[INPE-4579-PRE/1313] 23 p3415 N90-29294

RADIATION DOSAGE
Ozonation of hydrazines and their associated impurities 02 p0205 N90-11174
The analysis of current-mirror MOSFETs for use in radiation environments
[AD-A212527] 04 p0497 N90-12866
Radiation damage and its influence on source requirements for high resolution x ray holography
[DE90-002508] 06 p0781 N90-14540
Analysis and evaluation of technical data on the photochromic and non-linear optical properties of materials
[AD-A214050] 08 p1041 N90-16014
Estimates of galactic cosmic ray shielding requirements during solar minimum
[NASA-TM-4167] 09 p1300 N90-17535
L x ray spectrometry in vivo with a Si(Li)-NaI(Tl)
[DE90-005649] 10 p1387 N90-18028
Dose assessment during complex meteorology in the Texas Panhandle
[DE90-006026] 10 p1408 N90-18118
Radiation exposure for manned Mars surface missions
[NASA-TP-2979] 10 p1448 N90-18357
Effects of pulsed and CW (Continuous Wave) 2450 MHz radiation on transformation and chromosomes of human lymphocytes in vitro
[AD-A216500] 11 p1539 N90-18857
Performance of a coincidence based blood activity monitor
[DE90-006105] 11 p1540 N90-18865
Reliability of equivalent sphere model in blood-forming organ dose estimation
[NASA-TM-4178] 12 p1746 N90-20036
A radiological assessment of nuclear power and propulsion operations near Space Station Freedom
[NASA-CR-185185] 14 p1941 N90-21108
Simplified model for solar cosmic ray exposure in manned Earth orbital flights
[NASA-TM-4182] 14 p2043 N90-21715
Lack of behavioral effects of high-peak-power microwave pulses from an axially extracted virtual cathode oscillator
[AD-A220779] 17 p2391 N90-23618
Pulse-width dependent radiation effects on electronic components
[AD-A219517] 17 p2395 N90-23643
Effects of large doses of high energy electrons on a YBa2Cu3O6(+)delta high temperature superconductor
[AD-A220423] 17 p2476 N90-24158
Shutter mechanism for controlling the exposure of samples to solar radiation 18 p2540 N90-24498
Improved model for solar cosmic ray exposure in manned Earth orbital flights
[NASA-TP-2987] 18 p2639 N90-25031
Neutron and gamma irradiation effects on power semiconductor switches
[NASA-TM-103200] 19 p2686 N90-25278
The US Experiments Flown on the Soviet Biosatellite Cosmos 1887
[NASA-TM-102254] 20 p2891 N90-26452
Experiment K-6-24, K-6-25, K-6-26. Radiation dosimetry and spectrometry 20 p2897 N90-26477
Effects of protracted ionizing radiation dosage on humans and animals: A brief review of selected investigations
[AD-A222240] 21 p3033 N90-27241
Mechanisms of microwave induced damage in biologic materials
[AD-A222454] 21 p3033 N90-27242
NPL absorbed dose graphite calorimeter correction for the effect of the gaps around the core
[NPL-RSA(EXT)-12] 22 p3178 N90-28032
Further studies of 60 Hz exposure effects on human function
[DE90-014377] 23 p3355 N90-28962
Comparison of dose estimates using the buildup-factor method and a Baryon transport code (BRYNTRN) with Monte Carlo results
[NASA-TP-3021] 23 p3414 N90-29290
A tandem system of ionization chambers for effective energy determination of unknown X-radiation fields
[DE90-630463] 24 p3436 N90-29405

RADIATION EFFECTS
NT LASER DAMAGE
NT RADIATION DAMAGE
NT RADIATION INJURIES
NT SINGLE EVENT UPSETS
Biomedical studies with the free electron laser
[AD-A208927] 01 p0091 N90-10519
Eye/sensor protection against laser irradiation organic nonlinear optical materials
[AD-A210599] 01 p0093 N90-10531
Grain boundary chemistry in irradiated stainless steel and its influence on environmental degradation
[DE89-016827] 02 p0197 N90-11125
Report of the 1988 2-D Intercomparison Workshop, chapter 3 02 p0248 N90-11407
Introduction and data summary, chapter 5
02 p0249 N90-11409
PISCES program plasma-surface interactions research
[DE89-015622] 02 p0276 N90-11578
CRRES (Combined Release and Radiation Effects Satellite) SPACERAD plasma wave experiment
[AD-A210791] 02 p0278 N90-11587
Computer simulations of radiation damage in amorphous solids
[PB89-212682] 03 p0322 N90-11827
Fracture toughness data base for HT9 and modified 9Cr-1Mo irradiated in several reactors up to approximately 100 dpa
[DE90-000111] 03 p0328 N90-11864
Use of satellite data and modeling to asses the influence of stratospheric processes on the troposphere
03 p0363 N90-12075
Investigation of resonant ac-dc magnetic field effects
[AD-A211612] 03 p0379 N90-12159
Optical data transmission systems in radiation environment
[DE90-000174] 03 p0405 N90-12322
Calcium displacement caused by electromagnetic fields
[AD-A212690] 04 p0524 N90-13023
The cosmic radiation effects and activation monitor
[RAE-TM-SPACE-364] 04 p0569 N90-13318
Life science research in space
[ESA-SP-1105] 05 p0672 N90-13917
NRL (Naval Research Laboratory) Review
[AD-A212888] 05 p0716 N90-14182
Operational Decision Aids for Exploiting or Mitigating Electromagnetic Propagation Effects
[AGARD-CP-453] 06 p0757 N90-14405
The effects of heavy particle radiation on semiconductor devices
[DE90-001679] 06 p0854 N90-14962
Aircraft testing in the electromagnetic environment
07 p0873 N90-15066
Helium-induced weld cracking in irradiated 304 stainless steel
[DE90-001312] 07 p0903 N90-15219
Cast stainless steel aging: Mechanisms and predictions
[DE90-003772] 07 p0907 N90-15241
Overview on radiation effects in electronics
[DE90-000841] 07 p0926 N90-15357
Interlaboratory comparison of radiation-induced attenuation in optical fibers. Part 3: Transient exposures
[DE90-000859] 07 p0992 N90-15729
Fusion reactor materials
[DE90-000976] 07 p0994 N90-15744
Progress in LTE and non-LTE transport calculations
[DE90-003394] 07 p0997 N90-15764
Irradition-induced grain growth: Role of dislocations
[DE90-003565] 07 p1001 N90-15792
Ion-irradiation effects in Tl2Ca2Ba2Cu3O10 superconductors
[DE90-003840] 07 p1002 N90-15802
Power semiconductor devices for space nuclear power systems
[DE90-001178] 07 p1005 N90-15819
Interplanar spacing for various phases in austenitic stainless steels
[DE90-602350] 08 p1045 N90-16038
Phase evolution during neutron irradiation of commercial Fe-Cr-Mn alloys
[DE90-004113] 08 p1045 N90-16042

Modeling dislocation evolution in irradiated alloys
[DE90-004921] 08 p1047 N90-16051
Development of a diamond insulator for thermionic applications
[DE90-002849] 08 p1048 N90-16055
On the HEMP (High-Altitude Electromagnetic Pulse) response of protective relays
[DE90-003718] 08 p1061 N90-16138
Mechanisms of microwave induced damage in biologic materials
[AD-A213480] 08 p1104 N90-16390
The 1MeV-electron irradiation induced defects in epitaxially grown 3C-SiC
[DE90-719574] 08 p1131 N90-16554
Electron beam induced oxygen in YBa2Cu3O(7-x) superconductors
[DE90-004839] 08 p1133 N90-16565
Radiation modification of cometary materials: Laboratory simulations 08 p1143 N90-16626
The effects of natural and enhanced Van Allen Belt radiation on a space based weapon platform
[DE89-016219] 08 p1154 N90-16685
Environmental constraints for polar platform design
[RAE-TR-89014] 09 p1181 N90-16849
Nuclear weapon radiation effects on a space based interceptor weapon platform
[DE89-016258] 09 p1181 N90-16850
Heavy-section steel technology program fracture issues
[DE90-005264] 09 p1240 N90-17195
Integrated analytical evaluation and optimization of model parameters against preprocessed measurement data
[AD-A215518] 09 p1247 N90-17231
Proceedings of the 17th Conference on Toxicology
[AD-A215076] 09 p1252 N90-17263
Structural alterations in the cornea from exposure to infrared radiation
[AD-A215340] 09 p1253 N90-17269
Effects of O2 ion bombardment of Y-BaCu-oxide during thin film growth
[DE90-005315] 09 p1293 N90-17495
New models and techniques for predicting radiation effects on solar array performances 10 p1344 N90-17790
International Summer School on Solid State Microbatteries
[AD-A213457] 10 p1434 N90-18277
An overview of radiation-induced interface traps in MOS (Metal-Oxide Semiconductor) structures
[AD-A216101] 10 p1438 N90-18299
Development and use of data analysis procedures for the CRRES (Combined Release and Radiation Effects Satellite) payloads AFGL-701-2/Dosimeter and AFGL-701-4/Fluxmeter and application of the data analysis results to improve the static and dynamic models of the Earth's radiation belts
[AD-A215953] 10 p1447 N90-18348
Response of unirradiated and neutron-irradiated vanadium alloys to Charpy-impact loading
[DE90-004878] 11 p1486 N90-18551
Effects of pulsed and CW (Continuous Wave) 2450 MHz radiation on transformation and chromosomes of human lymphocytes in vitro
[AD-A216500] 11 p1539 N90-18857
Fourth International Conference on Fusion Reactor Materials
[DE90-006142] 11 p1568 N90-19025
Radiation-induced density changes and creep in surface layers of glass
[DE90-008112] 12 p1633 N90-19383
Transmission and reflection studies of thin films in the vacuum ultraviolet 12 p1638 N90-19412
The influence of gamma-radiation on the bandwidth of optical fibres and the reduction of the induced attenuation by bleaching and hardening the fibre
[FEL-1988-62] 12 p1714 N90-19846
Physical sputtering of metallic systems by charged-particle impact
[DE90-007803] 13 p1777 N90-20201
The effects of radiation on the mechanical properties of polymers used as electrical cable insulation and jacketing materials
[AERE-R-13286] 13 p1779 N90-20209
Radiation disorder and aperiodicity in irradiated ceramics
[DE90-008253] 13 p1781 N90-20222
Measurement of proton induced radiation damage to CMOS transistors and pin diodes
[DE90-007836] 13 p1792 N90-20283
A progress report on the Livermore Miniature Vacuum Tube Project
[DE90-008302] 13 p1794 N90-20299
Short wavelength laser/materials interactions
[AD-A218015] 13 p1808 N90-20386
Software quality assurance and software safety in the biomed control system
[DE90-008072] 13 p1866 N90-20706
Interaction between implanted ions and intrinsic defects in silica
[DE90-006569] 13 p1892 N90-20858
Final Safety Analysis Report for the Ulysses Mission. Volume 3 (Book 1): Nuclear risk analysis document
[DE90-008691] 14 p1939 N90-21101
Final safety analysis report for the Ulysses Mission. Volume 3 (Book 2): Nuclear risk analysis document-appendices
[DE90-008692] 14 p1939 N90-21102
Final safety analysis report for the Ulysses mission. Volume 2 (Book 1): Accident model document
[DE90-008694] 14 p1940 N90-21103
Grain boundary chemistry effects on irradiation-assisted stress corrosion cracking
[DE90-008623] 14 p1951 N90-21167
Aging and compatibility of TNF-doped Mylar
[DE90-008508] 14 p1954 N90-21186
Study of advanced InSb arrays for SIRTF (Space Infrared Telescope Facility) 14 p1977 N90-21325
ISO camera array development status 14 p1980 N90-21344
Laboratory characterization of direct readout Si:Sb and Si:Ga infrared detector arrays 14 p1980 N90-21347
JPRS report: Science and technology. USSR: Life sciences
[JPRS-ULS-90-002] 14 p1995 N90-21434
Biological effects of ELF (Extremely-Low-Frequency) electric and magnetic fields
[DE90-008634] 14 p2009 N90-21514
Proceedings of the 6th Regional Symposium on Biophysics
[DE90-619618] 15 p2136 N90-22206
Experiments with a laser interferometric gravitational wave antenna 15 p2184 N90-22476
High Intensity Electro-Magnetic and Ultrasonic Effects on Inorganic Materials Behavior and Processing Workshop
[AD-A218884] 16 p2215 N90-22640
Laser retinal effects: Electrophysiological determination in visual cortical cells of monkeys and cats
[AD-A218937] 16 p2261 N90-22888
Exposure of human cells to electromagnetic fields
[AD-A219377] 16 p2261 N90-22889
Influence of high energy radiation on critical parameters of superconducting ceramics YBa2Cu3O7
[DE90-620562] 16 p2322 N90-23239
Vanadium alloys with improved resistance to helium embrittlement
[DE90-009811] 17 p2375 N90-23524
Lack of behavioral effects of high-peak-power microwave pulses from an axially extracted virtual cathode oscillator
[AD-A220779] 17 p2391 N90-23618
Pulse-width dependent radiation effects on electronic components
[AD-A219517] 17 p2395 N90-23643
Test diagnostics of RF effects in integrated circuits
[AD-A219737] 17 p2396 N90-23648
High peak power microwave pulses at 2.37 GHz: No effects on vigilance performance in monkeys
[AD-A219570] 17 p2433 N90-23863
Effects of large doses of high energy electrons on a YBa2Cu3O6(+)delta high temperature superconductor
[AD-A220423] 17 p2476 N90-24158
Irradiation effects on impact behavior of 12Cr-1MoVW and 2 1/4Cr-1Mo steels
[DE90-011075] 18 p2527 N90-24421
Effects of internal hydrogen on the vacancy loop formation probability in Al
[DE90-011114] 18 p2527 N90-24422
Mechanism for deployment and retraction of biological samples 18 p2540 N90-24499
A new technique for hardening optically-triggered thyristors
[DE90-006769] 18 p2549 N90-24550
Irradiation assisted stress corrosion cracking
[DE90-010629] 18 p2572 N90-24656
Effects of solar ultraviolet radiation on biogeochemical dynamics in aquatic environments
[AD-A221119] 18 p2578 N90-24687
SEU characterization and design dependence of the SA3300 microprocessor
[DE90-007678] 18 p2589 N90-24728
Microstructure and stability of TiB2 and Cu multilayers
[DE90-011955] 18 p2627 N90-24968
TEM, positron lifetime, and hardness measurements of irradiated, cold-worked, and annealed Zr-1 percent Nb
[VTT-RR-650] 19 p2676 N90-25216
The effects of urban air pollution on solar radiation
[DE89-009455] 19 p2712 N90-25438
Program review: The lifetime effects of space radiation in rhesus monkeys
[AD-A221127] 19 p2716 N90-25454
Experiment K-6-16. Morphological examination of rat testes. The effect of Cosmos 1887 flight on spermatogonial population and testosterone level in rat testes 20 p2895 N90-26469
Experiment K-6-24, K-6-25, K-6-26. Radiation dosimetry and spectrometry 20 p2897 N90-26477
The charged particle radiation environment for AXAF
[NASA-TM-100405] 20 p2942 N90-26741
Accurate determination of the complex permittivity of biological tissue at 90 GHz, 70 GHz, and over a broad band around 35 GHz
[AD-A222062] 21 p3033 N90-27240
Effects of ionizing radiation on the performance of selected tactical combat crews
[AD-A222880] 21 p3034 N90-27248
Density changes of generation 1.5 and 2.0 copper alloys irradiated at 411 to 414 C and 529 C in FFTF-MOTA
[DE90-015291] 23 p3311 N90-28724
Bandwidth and signal-to-noise ratio enhancement of the NPS transient electromagnetic scattering laboratory
[AD-A224144] 23 p3320 N90-28771
Natural and anthropogenic climate change
[DE90-015528] 23 p3348 N90-28923
Radiation effects in InAsSb strained-layer superlattice photodiodes induced by dose-rate and transient x ray environments
[DE90-015000] 23 p3400 N90-29208
Transient annealing characterization of irradiated MOSFETS
[AD-A223877] 23 p3401 N90-29220
Swelling of neutron irradiated vanadium alloys
[DE90-015294] 24 p3448 N90-29472
Tensile behavior and swelling of ternary austenitic alloys irradiated in different neutron spectra
[DE90-015295] 24 p3450 N90-29485
The effect of helium on microstructural evolution in austenitic steels as determined by spectral tailoring experiments
[DE90-016360] 24 p3452 N90-29496
Effects of energy, momentum and particle transport in the near-earth solar terrestrial system
[AD-A224393] 24 p3490 N90-29726
High resolution transmission electron microscopy of partial states of oxygen order in YBa2Cu3O(z)
[DE90-015637] 24 p3554 N90-30108

RADIATION EMISSION
U RADIATION

RADIATION EXPOSURE
U RADIATION DOSAGE

RADIATION FIELDS
U RADIATION DISTRIBUTION

RADIATION HARDENING
Vacuum microelectronics for beam power and rectennas 01 p0028 N90-10148
Micro-cavity integrable vacuum diodes and triodes
[DE89-016649] 01 p0060 N90-10344
Design of a bounded wave EMP (Electromagnetic Pulse) simulator
[AD-A214137] 07 p0919 N90-15316
Proposed activities to prepare for testing advanced/stealth weapons systems
[AD-A214453] 07 p0920 N90-15321
Power semiconductor devices for space nuclear power systems
[DE90-001178] 07 p1005 N90-15819
Analysis and evaluation of technical data on the photochromic and non-linear optical properties of materials
[AD-A214050] 08 p1041 N90-16014
Spacecraft environmental anomalies handbook
[NASA-CR-186331] 09 p1182 N90-16852
Chemical profiling of silicon nitride structures
[AD-A215643] 09 p1192 N90-16907
Space radiation effects on electronics
[DE90-602874] 10 p1378 N90-17986
Radiation-hard high-efficiency InP space solar cell development
[AD-A216857] 11 p1528 N90-18800
A GaAs p-n-p-n thyristor model
[DE90-005757] 11 p1570 N90-19039
Product assurance technology for procuring reliable, radiation-hard, custom LSI/VLSI electronics
[NASA-CR-185954] 13 p1791 N90-20281
Measurement of proton induced radiation damage to CMOS transistors and pin diodes
[DE90-007836] 13 p1792 N90-20283
Radiation-hardened wafer scale integration
[AD-A217332] 13 p1793 N90-20290
Transient radiation hardened CMOS (Complementary Metal Oxide Semiconductor) operational amplifiers
[AD-A217972] 13 p1797 N90-20313

An assessment of the hardness of miniature vacuum tubes to high-voltage transients
[DE90-009541] 15 p2089 N90-21956
Burnout thresholds and cross section of power MOS transistors with heavy ions
[AD-A218998] 16 p2232 N90-22736
Vanadium alloys with improved resistance to helium embrittlement
[DE90-009811] 17 p2375 N90-23524
The mechanical properties of Cu/TiB2 multilayer structures
[DE90-010608] 18 p2517 N90-24378
A new technique for hardening optically-triggered thyristors
[DE90-006769] 18 p2549 N90-24550
SEU characterization and design dependence of the SA3300 microprocessor
[DE90-007678] 18 p2589 N90-24728
An examination of the 1-MeV equivalent silicon damage methodology
[DE90-007167] 18 p2614 N90-24888
Predicting switched-bias response from steady-state irradiations
[DE90-006770] 18 p2624 N90-24950
The scalability of OTR (Out-of-core Thermionic Reactor) space nuclear power systems
[DE90-013553] 21 p3075 N90-27485

RADIATION HAZARDS
Draft Environmental Impact Statement for the Ulysses Mission (Tier 2)
[NASA-TM-102903] 06 p0812 N90-14727
Safety evaluation report for Galileo: Volume 1
[DE90-003086] 07 p0886 N90-15122
Safety evaluation report for Galileo, volume 2
[DE90-003087] 07 p0886 N90-15123
Dose assessment during complex meteorology in the Texas Panhandle
[DE90-006026] 10 p1408 N90-18118
Safety evaluation of infrared lamp power output for oculometer eye/head tracker system
[AD-A215809] 10 p1411 N90-18138
Development and use of data analysis procedures for the CRRES (Combined Release and Radiation Effects Satellite) payloads AFGL-701-2/Dosimeter and AFGL-701-4/Fluxmeter and application of the data analysis results to improve the static and dynamic models of the Earth's radiation belts
[AD-A215953] 10 p1447 N90-18348
Safety analysis for the Galileo light-weight radioisotope heater unit
[DE90-007147] 11 p1566 N90-19009
Safety Status Report for the Ulysses mission. Book 1: Risk analysis. General purpose heat source radioisotope thermoelectric generator program
[DE90-006826] 12 p1614 N90-19282
Safety Status Report for the Ulysses mission: Summary. General purpose heat source radioisotope thermoelectric generator program
[DE90-006828] 12 p1614 N90-19284
Safety Status Report for the Ulysses mission. Book 2: Accident analysis-appendices. General purpose heat source radioisotope thermoelectric generator program
[DE90-006830] 12 p1614 N90-19286
Final Safety Analysis Report for the Ulysses Mission. Volume 3 (Book 1): Nuclear risk analysis document
[DE90-008691] 14 p1939 N90-21101
Final safety analysis report for the Ulysses Mission. Volume 3 (Book 2): Nuclear risk analysis document-appendices
[DE90-008692] 14 p1939 N90-21102
Final safety analysis report for the Ulysses mission. Volume 2 (Book 1): Accident model document
[DE90-008694] 14 p1940 N90-21103
Final safety analysis report for the Ulysses mission. Volume 1: Reference design document
[DE90-008693] 14 p1940 N90-21107
Boeing 727-100 test project (high energy radiated field tests)
[DOT/FAA/CT-88/33] 14 p1964 N90-21247
Final environmental impact statement for the Galileo Mission (Tier 2)
[NASA-TM-102925] 15 p2124 N90-22147
Draft environmental impact statement for the Galileo Mission (Tier 2)
[NASA-TM-102926] 15 p2124 N90-22148
Final Environmental Impact Statement for the Ulysses Mission (Tier 2)
[NASA-TM-101104] 15 p2126 N90-22162
General purpose heat source radioisotope thermoelectric generator program. Book 1: Accident analysis
[REPT-90SDS4202-BK-1] 15 p2166 N90-22379
High peak power microwave pulses at 2.37 GHz: No effects on vigilance performance in monkeys
[AD-A219570] 17 p2433 N90-23863

RADIATION HEATING
U RADIANT HEATING

RADIATION INJURIES
Treatment of laser-induced retinal injuries
[AD-A210284] 01 p0092 N90-10526
Effects of protracted ionizing radiation dosage on humans and animals: A brief review of selected investigations
[AD-A222240] 21 p3033 N90-27241

RADIATION INTENSITY
U RADIANT FLUX DENSITY

RADIATION LAWS
NT KIRCHHOFF LAW OF RADIATION
A theory of the rapid burster (MXB1730-335) 19 p2775 N90-25782
Multiwavelength observations of BL Lacertae 19 p2791 N90-25886

RADIATION MEASUREMENT
Calculations of soft x ray emission of REB-heated plasma
[IPPCZ-287] 03 p0407 N90-12329
Electron cyclotron emission and absorption experiment on the CASTOR tokamak
[IPPCZ-285] 03 p0407 N90-12331
Initial optical transition radiation measurements of the electron beam for the Boeing free-electron laser experiment
[DE90-003396] 07 p0935 N90-15416
Environmental surveillance data
[DE90-001275] 07 p0956 N90-15532
Measurement of radiation property of long infrared emitter and examination of infrared radiation heating process
[DE90-741971] 10 p1425 N90-18222
Atmospheric Radiation Measurement Program plan
[DE90-006349] 12 p1689 N90-19705
Detecting gravity waves from binary black holes 12 p1730 N90-19943
Atmospheric Radiation Measurement Program Plan
[DE90-008108] 13 p1829 N90-20504
Non-random uncertainties in the calibration of protection-level secondary standards
[NPL-RS(EXT)-110] 15 p2166 N90-22378
Derivation of radiation beam non-uniformity corrections for the calibration of large volume ionisation chambers
[NPL-RSA(EXT)-11] 15 p2167 N90-22382
Onboard detection of intrinsic Ly alpha radiation from a neutral particle beam
[DE90-010341] 18 p2511 N90-24346
Implementation of reflectance models in operational AVHRR radiation budget processing
[NOAA-TR-NESDIS-49] 18 p2578 N90-24688
Reports of workshops on Probe Measurements of Particles and Radiation in the Atmosphere of Titan
[NASA-TM-102218] 19 p2797 N90-25919
Two-dimensional signal processing and storage, and theory and applications of electromagnetic measurements
[AD-A222984] 21 p2995 N90-27022
A comparative study of infrared radiance measurements by an ER-2 based radiometer and the LANDSAT 5 Thematic Mapper (TM-6) 22 p3226 N90-28294
Improved meteorological measurements from buoys and ships (IMET): Preliminary comparison of pyranometers
[PB90-241936] 22 p3229 N90-28315
Ground level atmospheric gamma ray flux measurements in the 1 to 6 MeV range 22 p3264 N90-28483
Establishment of a capability to measure optical transition radiation
[AD-A224094] 24 p3545 N90-30047
An advanced single event upset tester
[AD-A223613] 24 p3564 N90-30163
Re-analysis of data on the space radiation environment above south-east Asia
[RAE-TR-89048] 24 p3565 N90-30166

RADIATION MEASURING INSTRUMENTS
NT ADVANCED VERY HIGH RESOLUTION RADIOMETER
NT BOLOMETERS
NT CERENKOV COUNTERS
NT DOSIMETERS
NT ELECTROSTATIC PROBES
NT FLIR DETECTORS
NT INFRARED DETECTORS
NT INFRARED INSTRUMENTS
NT INFRARED RADIOMETERS
NT INFRARED SCANNERS
NT INFRARED SPECTROMETERS
NT MICROWAVE RADIOMETERS
NT NEUTRON COUNTERS
NT NEUTRON SPECTROMETERS
NT PARTICLE TELESCOPES
NT PHOTOMETERS
NT PROPORTIONAL COUNTERS
NT PYRANOMETERS
NT QUANTUM COUNTERS
NT RADIATION COUNTERS
NT RADIATION DETECTORS
NT RADIOMETERS
NT RIOMETERS
NT SCINTILLATION COUNTERS
NT SOLAR SPECTROMETERS
NT SPECTROPHOTOMETERS
NT SPECTRORADIOMETERS
NT TOTAL OZONE MAPPING SPECTROMETER
NT ULTRAVIOLET DETECTORS
NT ULTRAVIOLET SPECTROMETERS
Center for Electronics and Electrical Engineering technical publication announcements covering Center programs, January-March 1989 with 1989 CEEE events calendar
[PB89-228308] 03 p0418 N90-12402
Beyond the IDMY (International Daylighting Measurements Year): A network instrument for low-cost data acquisition
[DE90-002722] 06 p0815 N90-14740
Characteristics of the IAEA correlation monitor material for surveillance programmes
[VTT-RR-639] 19 p2682 N90-25258
Re-analysis of data on the space radiation environment above southeast Asia
[AD-A224155] 24 p3564 N90-30162

RADIATION MEDICINE
U NUCLEAR MEDICINE

RADIATION METERS
U RADIATION MEASURING INSTRUMENTS

RADIATION NOISE
U ELECTROMAGNETIC NOISE

RADIATION PRESSURE
NT ILLUMINANCE
NT LUMINANCE
NT LUMINOUS INTENSITY
NT SOUND PRESSURE

RADIATION PROTECTION
NT RADIATION SHIELDING
NT SOLAR RADIATION SHIELDING
DOE/CEC Workshop on Critical Evaluation of Radiobiological Data to Biophysical Modeling
[DE89-015214] 02 p0254 N90-11437
Base level management of radio frequency radiation protection program
[AD-A211787] 03 p0381 N90-12171
Base level management of radio frequency radiation protection program
[AD-A211759] 04 p0523 N90-13017
Safety evaluation report for Galileo: Volume 1
[DE90-003086] 07 p0886 N90-15122
Safety evaluation report for Galileo, volume 2
[DE90-003087] 07 p0886 N90-15123
Interlaboratory comparison of radiation-induced attenuation in optical fibers. Part 3: Transient exposures
[DE90-000859] 07 p0992 N90-15729
On the HEMP (High-Altitude Electromagnetic Pulse) response of protective relays
[DE90-003718] 08 p1061 N90-16138
Space nuclear safety program
[DE90-006436] 11 p1565 N90-19007
Safety Status Report for the Ulysses mission. Book 1: Risk analysis. General purpose heat source radioisotope thermoelectric generator program
[DE90-006826] 12 p1614 N90-19282
Safety status report for the Ulysses mission. Book 2: Risk analysis. General purpose heat source radioisotope thermoelectric generator program
[DE90-006827] 12 p1614 N90-19283
Safety Status Report for the Ulysses mission: Summary. General purpose heat source radioisotope thermoelectric generator program
[DE90-006828] 12 p1614 N90-19284
A guide to performing and documenting safety analyses
[DE90-008687] 13 p1788 N90-20260
Final safety analysis report for the Ulysses Mission. Volume 3 (Book 2): Nuclear risk analysis document-appendices
[DE90-008692] 14 p1939 N90-21102
Final safety analysis report for the Ulysses Mission. Volume 2: Accident model document-appendices
[DE90-008695] 14 p1940 N90-21104
General purpose heat source radioisotope thermoelectric generator program. Book 1: Accident analysis
[REPT-90SDS4202-BK-1] 15 p2166 N90-22379
Prevention of significant deterioration application for approval to construct SP-100 Ground Engineering System Test Site
[DE90-007986] 15 p2166 N90-22381
Program review: The lifetime effects of space radiation in rhesus monkeys
[AD-A221127] 19 p2716 N90-25454

Hazards protection for space suits and spacecraft
[NASA-CASE-MSC-21366-1] 19 p2725 N90-25498

RADIATION PYROMETERS
Infrared temperature measurement with automatic consideration of emissivity
[ESA-TT-1131] 03 p0351 N90-12008
A multicolor imaging pyrometer
10 p1364 N90-17905

RADIATION RESISTANCE
U RADIATION TOLERANCE

RADIATION SHIELDING
NT SOLAR RADIATION SHIELDING
Starlight: A stationary inertial-confinement-fusion reactor with nonvaporizing walls
[DE90-002315] 06 p0847 N90-14927
Arc-sprayed coatings for electromagnetic pulse protection: Assessment of physical and electrical properties
[AD-A213825] 07 p0912 N90-15275
Interlaboratory comparison of radiation-induced attenuation in optical fibers. Part 3: Transient exposures
[DE90-000859] 07 p0992 N90-15729
Evaluation of potential cold x ray shield materials tested on Proto II
[DE90-004348] 08 p1039 N90-16003
Scaling study for SP-100 reactor technology
[NASA-TM-897140] 08 p1122 N90-16496
Estimates of galactic cosmic ray shielding requirements during solar minimum
[NASA-TM-4167] 09 p1300 N90-17535
Space radiation effects on electronics
[DE90-602874] 10 p1378 N90-17986
Simplified model for solar cosmic ray exposure in manned Earth orbital flights
[NASA-TM-4182] 14 p2043 N90-21715
Prevention of significant deterioration application for approval to construct SP-100 Ground Engineering System Test Site
[DE90-007986] 15 p2166 N90-22381
Improved model for solar cosmic ray exposure in manned Earth orbital flights
[NASA-TP-2987] 18 p2639 N90-25031
Neutron and gamma irradiation effects on power semiconductor switches
[NASA-TM-103200] 19 p2686 N90-25278
Experiment K-6-24, K-6-25, K-6-26. Radiation dosimetry and spectrometry 20 p2897 N90-26477
Lunar lander conceptual design
[NASA-CR-186233] 21 p2965 N90-26856
Comparison of dose estimates using the buildup-factor method and a Baryon transport code (BRYNTRN) with Monte Carlo results
[NASA-TP-3021] 23 p3414 N90-29290

RADIATION SICKNESS
Effects of ionizing radiation on the performance of selected tactical combat crews
[AD-A222880] 21 p3034 N90-27248

RADIATION SOURCES
NT MONOCHROMATORS
NT NEUTRON SOURCES
NT POINT SOURCES
The dense Z-pinch as a plasma radiation source. 1: Quasi-static Bennett model
[AD-A210600] 01 p0127 N90-10727
An experimental high energy physics program
[DE89-014695] 03 p0403 N90-12311
Use of a krypton isotope for rapid ion changeover at the Lawrence Berkeley Laboratory 88-inch cyclotron
[NASA-CR-186107] 05 p0698 N90-14084
Intense REB (Relativistic Electron Beam) transport in a weakly magnetized plasma
[DE90-002978] 07 p0994 N90-15749
Radiation of plasma waves from large space structures in low earth orbit
[AD-A215062] 09 p1182 N90-16856
Solid state lasers for use in non-contact temperature measurements 10 p1363 N90-17901
An investigation of the transfer of monopulse tracking between two coherent point sources
[AD-A217007] 12 p1646 N90-19457
Sources of gravitational waves
12 p1730 N90-19942
Detecting gravity waves from binary black holes
12 p1730 N90-19943
The pregalactic cosmic gravitational wave background
12 p1730 N90-19945
The space microwave interferometer and the search for cosmic background gravitational wave radiation
12 p1731 N90-19952
X ray timing observations and gravitational physics
12 p1732 N90-19956
A drift chamber telescope for high-Z particles
[NASA-CR-186497] 12 p1746 N90-20040
Free electron lasers driven by linear induction accelerators: High power radiation sources
15 p2060 N90-21800
Minimizing the effects of the atmosphere in the observation of ultraviolet radiation
15 p2080 N90-21911
The synergism of analytic and numerical techniques in general relativity: Calculation of radiative spacetimes
15 p2174 N90-22425
COS-B gamma ray sources beyond the predicted diffuse emission 16 p2335 N90-23308
Multiwavelength pyrometry to correct for reflected radiation
[NASA-TM-102578] 17 p2407 N90-23714
High resolution spectroscopy in the microwave and far infrared 20 p2943 N90-26746
Variable magnification variable dispersion glancing incidence imaging x ray spectroscopic telescope
[NASA-CASE-MFS-28013-3] 21 p3096 N90-27594
Multispectral variable magnification glancing incidence x ray telescope
[NASA-CASE-MFS-28013-4] 21 p3096 N90-27595
Gamma ray evidence for cosmic ray sources
23 p3414 N90-29292

RADIATION SPECTRA
NT ABSORPTION SPECTRA
NT BALMER SERIES
NT ELECTROMAGNETIC SPECTRA
NT ELECTRONIC SPECTRA
NT EMISSION SPECTRA
NT FRAUNHOFER LINES
NT GAMMA RAY SPECTRA
NT H ALPHA LINE
NT H BETA LINE
NT H LINES
NT INFRARED SPECTRA
NT K LINES
NT LINE SPECTRA
NT LYMAN SPECTRA
NT MICROWAVE SPECTRA
NT RADIO SPECTRA
NT RAMAN SPECTRA
NT RYDBERG SERIES
NT SOLAR SPECTRA
NT STELLAR SPECTRA
NT UBV SPECTRA
NT ULTRAVIOLET SPECTRA
NT VIBRATIONAL SPECTRA
NT VISIBLE SPECTRUM
NT X RAY SPECTRA
X ray spectra produced by NaF implosions
[AD-A215803] 10 p1429 N90-18243
JACEE long duration balloon flights
[DE90-006008] 12 p1746 N90-20039

RADIATION THERAPY
Life sciences: Lawrence Berkeley Laboratory, 1988
[DE90-008061] 13 p1849 N90-20611
Effects of protracted ionizing radiation dosage on humans and animals: A brief review of selected investigations
[AD-A222240] 21 p3033 N90-27241

RADIATION TOLERANCE
TWIRE: A test program for VLF airborne transmissions
[AD-A210516] 01 p0057 N90-10324
Improved performance polysulfide based sealant
08 p1022 N90-15910
Radiation resistance of solar cells for space application. 1: Study on the irradiation procedure of electron beams
[DE90-719546] 08 p1096 N90-16349
Structural alterations in the cornea from exposure to infrared radiation
[AD-A215340] 09 p1253 N90-17269
Radiation effects in ITO/InP solar cells
10 p1340 N90-17757
Indium phosphide solar cell research in the United States: Comparison with non-photovoltaic sources
10 p1340 N90-17758
High-efficient solar cells for space application
10 p1342 N90-17777
Assessment of bifacial silicon solar cells for space applications 10 p1342 N90-17779
Design development, qualification, and flight production of an ATOX resistant flexible solar array for low earth orbit mission 10 p1344 N90-17796
The solar array design of the Vesta small bodies spacecraft 10 p1345 N90-17799
Soluble polysilanes: A new class of radiation sensitive O2-RIE resistant polymers for use in microlithography
[AD-A219476] 17 p2379 N90-23551
Neutron and gamma irradiation effects on power semiconductor switches
[NASA-TM-103200] 19 p2686 N90-25278
Program review: The lifetime effects of space radiation in rhesus monkeys
[AD-A221127] 19 p2716 N90-25454

RADIATION TRANSPORT
Particle transport simulation for spaceborne, NaI gamma-ray spectrometers
[AD-A205150] 04 p0564 N90-13292
Environmental constraints for polar platform design
[RAE-TR-89014] 09 p1181 N90-16849
Report from space plasma science
10 p1445 N90-18336
Computer simulation of time-dependent spherically symmetric spacetimes containing radiating fluids: Formalism and code tests 15 p2185 N90-22483
An even-parity/odd-parity formulation for deterministic transport calculations on massively parallel computers
[DE90-015036] 23 p3384 N90-29116
Comparison of dose estimates using the buildup-factor method and a Baryon transport code (BRYNTRN) with Monte Carlo results
[NASA-TP-3021] 23 p3414 N90-29290
Predictions of radiation backgrounds for GRO/OSSE
[RAE-TM-SPACE-372] 23 p3414 N90-29293

RADIATIVE HEAT TRANSFER
On the thermal stability of flow of a radiating two-component plasma in a porous medium between two rotating cylinders
[DE89-636426] 06 p0847 N90-14928
Multi-dimensional discrete ordinates solutions to combined mode radiation heat transfer problems and their application to a free-falling particle, direct absorption solar receiver
[DE90-004987] 09 p1300 N90-17531
Spacecraft thermal control design data, volume 1
[ESA-PSS-03-108-ISSUE-1-VOL-1]
11 p1468 N90-18455
Condensation fluid dynamics and heat transfer on rotating spherical surfaces in a microgravitational field
[DE90-005540] 11 p1495 N90-18607
Apparatus for measuring high-flux heat transfer in radiatively heated compact exchangers
[NASA-CR-186333] 22 p3122 N90-27726
Radiative heat transfer
[PB90-247602] 23 p3327 N90-28813
Theoretical investigation of non-equilibrium chemistry and optical radiation in hypersonic flow fields
[NASA-CR-186335] 24 p3417 N90-29300

RADIATIVE LIFETIME
Lifetime of singlet oxygen in aqueous hydrogen peroxide (BHP)
[AD-A211545] 03 p0403 N90-12306
Excited state lifetime measurements of ytterbium in indium phosphide
[AD-A215709] 09 p1291 N90-17483
Measurements of the methane relaxation times for application to the infrared emission models of the upper atmospheres of outer planets and Titan
20 p2945 N90-26759
The heat of formation of CN radicals and radiative lifetimes of the A 1 Sigma - state of C2N2
20 p2946 N90-26765
Measurement of the masses and lifetimes of the charmed mesons D neutral, D plus and D (sub s) plus
[MPI-PAE/EXP-EL-220] 22 p3245 N90-28405
UV-induced degradation of the Si-SiO2 interface: Applications to the point contact solar cell
[DE90-013843] 23 p3344 N90-28898

RADIATIVE RECOMBINATION
Recombination lines of C I and N II in the interstellar medium 15 p2182 N90-22466
X ray laser program report for FY 1989
[AD-A221818] 21 p3009 N90-27107

RADIATIVE TRANSFER
NT RADIATIVE HEAT TRANSFER
Two-Dimensional Intercomparison of Stratospheric Models
[NASA-CP-3042] 02 p0248 N90-11405
Introduction and data summary, chapter 5
02 p0249 N90-11409
Gas dynamical processes in the theory of galaxy formation 02 p0294 N90-11673
Stratiform clouds and their interaction with atmospheric motions 03 p0360 N90-12060
The effect of latent heat release on synoptic-to-planetary wave interactions and its implication for satellite observations: Theoretical modeling
03 p0362 N90-12073
Activities report in laser matter interactions
[ETN-90-95515] 06 p0782 N90-14544
Atomic structure and spectral perturbations in hot dense plasmas 06 p0785 N90-14567
Transversal inhomogeneity and radiative transfer in plasmas obtained by laser impact
06 p0785 N90-14568
XRAD: A one dimensional Lagrangian code with radiative transport 06 p0785 N90-14570
Identification and quantification of synoptic structure in simulated TIROS N radiance soundings
[AD-A213729] 07 p0960 N90-15553
Optical transmission through clouds
[AD-A214765] 09 p1248 N90-17240

Two adaptive techniques let progressive refinement outperform the traditional radiosity algorithm
[AD-A215174] 09 p1267 N90-17347
Some problems in oceanic radiative transfer
[AD-A215935] 10 p1410 N90-18131
Electronic energies for Neon dimer dication radiative charge transfer
[AD-A215817] 10 p1429 N90-18244
Numerical simulations of the cloud-capped marine boundary layer 14 p2008 N90-21506
Thomson scattering in a magnetic field
14 p2040 N90-21699
A theoretical study of circumstellar dust around Ae/Be stars 14 p2040 N90-21700
Problems in radiative transfer in astrophysics: An escape probability treatment of line overlap and a model of the masers around VX Sgr 14 p2041 N90-21705
Propagation environments, effects, and decision aids
15 p2081 N90-21918
The emission lines in the ultra-violet spectrum of Beta Lyrae 15 p2183 N90-22474
Modelling late-time atmospheres of supernovae
15 p2189 N90-22500
Spectral measurements of the cosmic microwave background 16 p2340 N90-23334
Molecular studies of dense cores
17 p2484 N90-24207
Studies in the parameterization of cloudiness in climate models and the analysis of radiation fields in general circulation models
[NASA-CR-186378] 19 p2715 N90-25448
Accretion onto neutron stars: Radiative transfer in a strong gravitational field 19 p2776 N90-25784
Detailed non-LTE calculations of the iron emission from NGC 1068 19 p2788 N90-25872
The 27-28 October 1986 FIRE IFO Cirrus case study: Comparison of radiative transfer theory with observations by satellite and aircraft
[NASA-TM-103468] 20 p2890 N90-26446
Sources of cloud nuclei and development of remote sensing techniques for cloud parameters
[AD-A222464] 21 p3031 N90-27233
A new calculation of the radiative cooling by carbon dioxide in the middle atmosphere and the lower thermosphere 22 p3210 N90-28211
Reflectivities of uniform and broken stratiform clouds: An update 22 p3215 N90-28236
Relationship between the longwave cloud radiative forcing at the surface and the top of the atmosphere
22 p3222 N90-28273
Cirrus microphysics and radiative transfer: Cloud field study on October 28, 1986 22 p3224 N90-28284
Radiative diffusivity factors in cirrus and stratocumulus clouds: Application to two-stream models
22 p3226 N90-28293
A comparative study of infrared radiance measurements by an ER-2 based radiometer and the LANDSAT 5 Thematic Mapper (TM-6) 22 p3226 N90-28294
Radiative properties of cirrus clouds inferred from broadband measurements during FIRE
22 p3226 N90-28295
Remote sounding through semi-transparent cirrus cloud 22 p3226 N90-28296
IR spectral characteristics of cirrus clouds
22 p3226 N90-28297
Measurements of the high altitude infrared characteristics of the atmosphere
[AD-A224401] 24 p3491 N90-29728

RADICALS
NT AMINO RADICAL
NT FREE RADICALS
NT HYDROXYL RADICALS
Computational modeling of pi-conjugated polyradicals
[AD-A210573] 01 p0113 N90-10648
Electrically conducting organic materials: Design, synthesis and characterization
[AD-A212214] 04 p0471 N90-12700
Pentafluorothio polynitroaliphatic explosives
[AD-D014221] 06 p0753 N90-14383
Hydrogen radical enhanced growth of solar cells
[DE89-009497] 06 p0806 N90-14694
On pure radical in semigroups with zero
[DE90-606954] 10 p1422 N90-18205
Ring expansion and equilibration in organophosphazenes, and the relationship to polymerization
[AD-A218234] 13 p1782 N90-20230
Electron-impact ionization and electron attachment cross sections of radicals important in transient gaseous discharges
[AD-A217510] 13 p1806 N90-20366
Combined effect of isotopic substitution, temperature, and magnetic field on the lifetimes of triplet biradicals
[AD-A219711] 17 p2372 N90-23509
Nonlinear optical responses and laser damage thresholds of films of a polarized stilbene side chain liquid crystal polymer and a phthalocyanine
[AD-A219462] 17 p2408 N90-23720
The heat of formation of CN radicals and radiative lifetimes of the A 1 Sigma - state of C2N2
20 p2946 N90-26765
A laboratory investigation of the production and properties of molecular and radical species pertinent to planetary atmospheres 20 p2946 N90-26766
Role of the methylene amidogen (H2CN) radical in the atmospheres of Titan and Jupiter
20 p2947 N90-26769
Laboratory studies of photodissociation processes relevant to the formation of cometary radicals
20 p2947 N90-26772
Organic polyradical models for organic magnetic materials
[AD-A223691] 24 p3442 N90-29435
Theoretical investigations and attempted synthesis of organic magnetic polymers and oligomers
[AD-A223409] 24 p3455 N90-29509

RADII
Small-radius bending loss in single-mode fibers
[AD-A211822] 03 p0405 N90-12323
A kernel approach to estimation of the sphere radius density in Wicksell's corpuscle problem
[CWI-MS-R8809] 04 p0542 N90-13142
Measurements of bubble properties using a multi-frequency sound field
[AD-A212591] 04 p0551 N90-13211
A two-parameter representation of dynamic dislocation distributions
[AD-A212249] 04 p0560 N90-13263

RADIO ALTIMETERS
Laser altimeter for use over the ocean
[AD-A211252] 02 p0224 N90-11286
Multibeam radar altimetry: Spaceborne feasibility and airborne experimentation
[AD-A215152] 09 p1207 N90-16995
An evaluation of an airborne laser profiling system for high precision terrain mapping
[AD-A217025] 11 p1525 N90-18780
Heli/SITAN: A terrain referenced navigation algorithm for helicopters
[DE90-005193] 12 p1602 N90-19217
Rosetta/CNSR altimeter and sounding radar
12 p1741 N90-20009
Satellite radar altimetry over ice. Volume 1: Processing and corrections of Seasat data over Greenland
[NASA-RP-1233-VOL-1] 13 p1840 N90-20562
Satellite radar altimetry over ice. Volume 2: Users' guide for Greenland elevation data from Seasat
[NASA-RP-1233-VOL-2] 13 p1840 N90-20563
Satellite radar altimetry over ice. Volume 4: Users' guide for Antarctica elevation data from Seasat
[NASA-RP-1233-VOL-4] 13 p1840 N90-20564
A correlation study of wind speed as measured by the special sensor microwave/imager and the GEOSAT altimeter
[AD-A219841] 18 p2581 N90-24701

RADIO ANTENNAS
NT HORN ANTENNAS
NT LENS ANTENNAS
NT MICROWAVE ANTENNAS
NT SPACETENNAS
Deep null antennas and their applications to tactical VHF radio communications
[AD-A210656] 02 p0212 N90-11214
Performance effects of tie-truss modifications for a 70-meter centerline beam waveguide antenna
04 p0486 N90-12791
Electron heating and static sheath enhancement in front of energized RF antennas
[DE90-001334] 06 p0766 N90-14456
Large antenna measurement and compensation techniques 12 p1610 N90-19263
Environmental projects, volume 10. Environmental assessment: New 34-meter antenna at Apollo site
[NASA-CR-186448] 14 p2003 N90-21480

RADIO ASSISTED DETECTION AND RANGING
U RADAR

RADIO ASTRONOMY
A lunar far-side very low frequency array
[NASA-CP-3039] 01 p0139 N90-10805
Analysis of nearly simultaneous X-ray and optical observations of active galactic nuclei
01 p0139 N90-10806
Project Radioastron 02 p0158 N90-10901
Integrating detectors and their application to infrared astronomy 02 p0290 N90-11659
The Telecommunications and Data Acquisition Report
[NASA-CR-185093] 04 p0485 N90-12786
A statistical study of radio-source structure effects on astrometric very long baseline interferometry observations 04 p0485 N90-12788
Performance of the image statistics decoder in conjunction with the Goldstone-VLA array
04 p0487 N90-12796
A search for the effects of active magnetic fields in extra-galactic radio sources 05 p0712 N90-14161
Laboratory evaluation and application of microwave absorption properties under simulated conditions for planetary atmospheres
[NASA-CR-185916] 06 p0865 N90-15025
The 22 GHz Radioastron receiver: Development of prototype components during the year 1988
[PB89-212583] 07 p0920 N90-15323
Scientific investigations of the Space Research Group
[ISBN-0-642-13252-6] 08 p1138 N90-16595
Study of peculiar galaxies in the Southern Hemisphere
[INPE-4810-TDL/357] 11 p1594 N90-19184
The Telecommunications and Data Acquisition Report
[NASA-CR-185033] 12 p1642 N90-19434
Parkes radio science system design and testing for Voyager Neptune encounter 12 p1645 N90-19451
The Telecommunications and Data Acquisition Report
[NASA-CR-186479] 15 p2074 N90-21880
Jupiter's drifting decametric bursts with the changing time scale
[DE90-618870] 15 p2192 N90-22517
Molecular clouds and the large-scale structure of the galaxy 16 p2333 N90-23295
Report of research activity at the Research Laboratory of Electronics 17 p2486 N90-24217
New Voyager radio spectrograms of Uranus
[NASA-CR-180381] 23 p3412 N90-29284
Radio outbursts in extragalactic sources
23 p3414 N90-29291
Statement of research objectives and summary of research efforts
[RLE-PR-132] 23 p3415 N90-29295
Fast pulsars, strange stars: An opportunity in radio astronomy
[DE90-015630] 24 p3563 N90-30155

RADIO ATTENUATION
Ground effects on multipath fading
[TELECOM-PARIS-88-E017] 04 p0489 N90-12812
Rain-fade simulation and power augmentation for satellite communication systems
[NASA-TM-103134] 23 p3319 N90-28768

RADIO BROADCASTING
U BROADCASTING

RADIO BURSTS
NT SOLAR RADIO BURSTS
NT TYPE 3 BURSTS
Radar detection during scintillation
[AD-A220099] 17 p2393 N90-23630
Observations of the X ray pulsars from the Kvant module 19 p2767 N90-25720
Long period variations in high mass X ray binaries and their possible relationship with SU UMa stars
19 p2777 N90-25796
Identification of galactic bulge X ray bursts with persistent X ray counterparts 19 p2780 N90-25813
X ray burster spectra in the state of the persistent flux level. Two temperature models of the neutron star atmosphere 19 p2782 N90-25824
A new transient X ray burst source near GX 1+4
19 p2782 N90-25826
Post-flare effects in the lower ionosphere of middle latitudes 22 p3209 N90-28205
Radio outbursts in extragalactic sources
23 p3414 N90-29291

RADIO COMMUNICATION
NT CODE DIVISION MULTIPLE ACCESS
NT RADIO RELAY SYSTEMS
NT RADIO TELEMETRY
NT TELEPHONY
NT TIME DIVISION MULTIPLE ACCESS
Deep null antennas and their applications to tactical VHF radio communications
[AD-A210656] 02 p0212 N90-11214
Network analyzer for nonstatic jamming
[AD-A210759] 02 p0212 N90-11216
Independent Orbiter Assessment (IOA): Assessment of the communication and tracking subsystem, volume 1
[NASA-CR-185528-VOL-1] 03 p0315 N90-11789
Independent Orbiter Assessment (IOA): Assessment of the communication and tracking subsystem, volume 2
[NASA-CR-185528-VOL-2] 03 p0315 N90-11790
Independent Orbiter Assessment (IOA): Assessment of the communication and tracking subsystem, volume 3
[NASA-CR-185528-VOL-3] 03 p0315 N90-11791
A new approach to HF (High Frequency) channel modeling and simulation. Part 1: Deterministic model
[PB89-203962] 03 p0336 N90-11913
Preliminary investigation of Faraday rotation effects and description of polarization measurements on the AFGL high latitude meteor scatter test bed
[AD-A211298] 04 p0488 N90-12806

A literature study of wave propagation in the 1-60 GHz range. Application to transportable military communication systems
[FEL-1988-47] 04 p0491 N90-12825
Inexpensive global location and tracking systems using geostationary satellites
[AD-A213025] 05 p0602 N90-13498
Long-range plan for management and use of the radio spectrum by agencies and establishments of the Federal Government
[PB89-232367] 05 p0633 N90-13693
PROPHET and future signal warfare decision aids 06 p0758 N90-14412
A communications system with an adaptive multi-functional architecture 06 p0759 N90-14415
Spread spectrum mobile radio communications
[AD-A213726] 07 p0918 N90-15311
Voice/data integration in mobile radio networks: Overview and future research directions
[AD-A214289] 07 p0919 N90-15319
Helsinki University of Technology Radio Laboratory
[PB90-110677] 08 p1056 N90-16102
Satellite systems integrated with the terrestrial cellular network for mobile communications
[ESA-STR-228] 08 p1057 N90-16113
Microwave screening on digital radio communication links due to multicircuit power transmission lines
[DE90-734950] 08 p1058 N90-16118
Development of a parallel link model for meteor burst communication
[AD-A215629] 09 p1208 N90-17001
Antenna design methods adapted to radio communication
[TELECOM-88-E-018] 10 p1375 N90-17971
An introduction to high frequency radioteletype systems
[PB90-145533] 14 p1965 N90-21252
Prediction of VHF/UHF mobile reception in urban areas: Comparison with measurements in London
[BBC-RD-1989/11] 14 p1965 N90-21255
Automatic speech recognition in air-ground data link 18 p2640 N90-25037
Conceptual definition of a high voltage power supply test facility
[NASA-CR-185216] 19 p2666 N90-25172
Propagation Effects and Circuit Performance of Modern Military Radio Systems with Particular Emphasis on Those Employing Bandspreading
[AGARD-CP-442] 20 p2844 N90-26178
An overview of Canadian radio propagation/communications technologies research 20 p2844 N90-26179
Progress and remaining issues in the development of a wideband HF channel model and simulation 20 p2845 N90-26182
Broadband analysis of ground wave propagation at a50 to 400 MHz 20 p2846 N90-26185
CORA: A direct sequence spread spectrum radio for voice and data 20 p2848 N90-26195
Experimentation of a transmission system data processing by meteor bursts 20 p2850 N90-26207
Continuous on-line link error rate detector
[AD-D014510] 20 p2850 N90-26209
Design and performance of a long, over-water microwave radio link
[PB90-207994] 23 p3318 N90-28758
Rain-fade simulation and power augmentation for satellite communication systems
[NASA-TM-103134] 23 p3319 N90-28768
An assessment of the application of in situ ion-density data from DMSP to modeling of transionospheric scintillation
[AD-A222695] 24 p3491 N90-29730

RADIO DIRECTION FINDERS
Theory and simulation of the operation of a Doppler direction finder in a multipath environment
[FEL-1988-56] 03 p0340 N90-11939
Model order determination methods for autoregressive radio direction finding techniques
[AD-A220707] 17 p2350 N90-23384

RADIO EMISSION
NT HYDROXYL EMISSION
NT RADIO BURSTS
NT SOLAR RADIO BURSTS
NT SOLAR RADIO EMISSION
NT TYPE 3 BURSTS
Study of peculiar galaxies in the Southern Hemisphere
[INPE-4810-TDL/357] 11 p1594 N90-19184
Radar detection of lightning and electric fields
[AD-A217894] 13 p1842 N90-20574
New water vapor masers in the Southern Hemisphere
[INPE-4844-PRE/1473] 14 p2037 N90-21689
Flare stars at radio wavelengths
[NASA-CR-186539] 14 p2044 N90-21719
Non-thermal radio emission of X ray binaries 19 p2769 N90-25738
U. radio emission from quiescent filaments
[NASA-CR-186538] 19 p2797 N90-25922
The natural VLF emission as diagnostics and estimation means of the fluxes of solar x ray bursts 22 p3209 N90-28206

RADIO EQUIPMENT
NT HORN ANTENNAS
NT IONOSONDES
NT LENS ANTENNAS
NT MICROWAVE ANTENNAS
NT RADIO ANTENNAS
NT RADIO FILTERS
NT RADIO RECEIVERS
NT RADIO TELESCOPES
NT RADIO TRANSMITTERS
NT RADIOSONDES
NT RAWINSONDES
NT RECEPTION DIVERSITY
NT RECTENNAS
NT SPACECRAFT ANTENNAS
NT SPACETENNAS
NT SUPERHETERODYNE RECEIVERS
NT TRANSMITTER RECEIVERS
NT TRANSPONDERS
NT VERY HIGH FREQUENCY RADIO EQUIPMENT
NT VERY LARGE ARRAY (VLA)
SINCGARS (Single-Channel Ground/Airborne Radio System) operator performance decay
[AD-A210716] 01 p0057 N90-10326
A literature study of wave propagation in the 1-60 GHz range. Application to transportable military communication systems
[FEL-1988-47] 04 p0491 N90-12825
MANPRINT (Manpower and Personnel Integration) evaluation: AN/TRC-170 digital troposcatter radio system
[AD-A211799] 08 p1055 N90-16100
Parkes radio science system design and testing for Voyager Neptune encounter 12 p1645 N90-19451
Packet radio networks under dynamic jamming
[AD-A217094] 12 p1648 N90-19475
Executive summary for the network assessment model
[AD-A218762] 16 p2229 N90-22718
Radio links: Instrument technologies 17 p2358 N90-23425
Unfairness caused by quadratic backoff in a packet-radio network
[AD-A219635] 17 p2388 N90-23603
Detecting black holes in packet-radio networks (SRNTN-56)
[AD-A219636] 17 p2389 N90-23604
High-throughput, survivable protocols for CDMA packet-radio networks (SRNTN-74)
[AD-A220189] 17 p2393 N90-23631
Design of a Lunar farside observatory
[NASA-CR-186671] 19 p2765 N90-25709
A novel communication network simulator
[AD-A223045] 20 p2857 N90-26248
Design of sharp cutoff filters with low quality factors
[AD-A223130] 21 p3000 N90-27051

RADIO FILTERS
Adaptive noise cancellation for a class of nonlinear 2R filter
[RR-351] 03 p0344 N90-11965
Lightning protection apparatus for RF equipment and the like
[AD-D014336] 12 p1650 N90-19483
Surface acoustic wave filters in ZnO-SiO2-Si layered structures: Design, technology, and monolithic integration with electronic circuitry
[ETN-90-97218] 20 p2924 N90-26638

RADIO FREQUENCIES
NT C BAND
NT EXTREMELY HIGH FREQUENCIES
NT EXTREMELY LOW RADIO FREQUENCIES
NT HIGH FREQUENCIES
NT LOW FREQUENCIES
NT MICROWAVE FREQUENCIES
NT SUPERHIGH FREQUENCIES
NT ULTRAHIGH FREQUENCIES
NT VERY HIGH FREQUENCIES
NT VERY LOW FREQUENCIES
Manual of regulations and procedures for federal radio frequency management, May 1986 edition: Revisions for January 1989
[PB89-193791] 01 p0056 N90-10320
An experimental study of microwave transmission through a decaying plasma
[AD-A210586] 01 p0127 N90-10726
High power, solid state RF pulse generators
[AD-D014172] 03 p0341 N90-11941
Base level management of radio frequency radiation protection program
[AD-A211787] 03 p0381 N90-12171
RF performance of polycrystalline high-T(sub c) superconductors
[DE89-017671] 03 p0411 N90-12359
Preliminary report on the feasibility of high power Electronic Warfare (EW) using explosive energy sources
[MRL-TR-89-3] 04 p0483 N90-12775
RF and dc desensitized electroexplosive device
[AD-D014206] 04 p0497 N90-12862
Radio frequency linac driven free-electron laser configurations
[AD-A212572] 04 p0507 N90-12922
Synthesis and study of materials for superconducting electronics
[AD-A212966] 04 p0561 N90-13270
Microwave microstrip resonator measurements of Y1Ba2Cu3O(7-x) and Bi2Sr2Ca1Cu2O(8-y) thin films
[NASA-TM-102159] 05 p0635 N90-13704
Influence of RF-parameters on beam lifetime
[NIKHEF-K/AMPS/89-06] 05 p0699 N90-14091
Means for protecting electroexplosive devices which are subject to a wide variety of radio frequency
[AD-D014219] 06 p0753 N90-14382
The characteristics of the HF radio channel and its influence on modern HF data communication system design 06 p0765 N90-14448
High-frequency instability of the sheath-plasma resonance
[NASA-CR-186127] 06 p0844 N90-14910
Fundamental studies of fusion plasmas
[DE90-002343] 06 p0848 N90-14933
RF superconductivity research and development at Los Alamos National Laboratory
[DE90-002440] 06 p0855 N90-14969
Fiber optic sensing system
[NASA-CASE-LEW-14795-1] 07 p0992 N90-15733
Packet Radio Integrated System Module (PRISM): Design document
[AD-A214723] 09 p1205 N90-16981
Bulk acoustic wave resonators made of amorphous materials
[ONERA-NT-1989-4] 09 p1279 N90-17416
Radio continuum maps at 22 GHz of the H II regions RCW57 and W49
[INPE-4787-TDL/353] 10 p1446 N90-18343
RF modal quantity gaging 11 p1474 N90-18483
ACIRF user's guide: Theory and examples
[AD-A216436] 11 p1496 N90-18613
Lightning protection apparatus for RF equipment and the like
[AD-D014336] 12 p1650 N90-19483
Influence of the déposition conditions on radiofrequency magnetron sputtered MoS2 films
[NASA-TP-2994] 14 p1958 N90-21210
Boeing 727-100 test project (high energy radiated field tests)
[DOT/FAA/CT-88/33] 14 p1964 N90-21247
The mm-wave region propagation experiments by satellite 15 p2081 N90-21916
HF propagation through actively modified ionospheres
[DE90-008931] 16 p2227 N90-22705
The 30-GHz monolithic receive module
[NASA-CR-180849] 18 p2545 N90-24528
RF properties of high temperature superconductors: Cavity methods
[DE90-011961] 18 p2627 N90-24969
Digital radio link: Controlled simulator for frequency selective fading
[FOA-C-30527-3.5] 19 p2683 N90-25259
RF control system development at CEBAF
[CEBAF-PR-89-026] 19 p2755 N90-25653
Design of CEBAF's RF separator and results of cold tests
[CEBAF-PR-89-021] 19 p2756 N90-25658
On using a superconducting linac to drive a short wavelength FEL
[CEBAF-PR-89-019] 19 p2756 N90-25660
Analysis of a Mars-stationary orbiting microwave power transmission system
[NASA-TM-101344] 20 p2843 N90-26172
Radio channel measurement and modelling for future mobile radio systems 20 p2845 N90-26184
Measurement and simulation of widespread mobile radio channel characteristics 20 p2846 N90-26186
Estimation of the impulse response of a broadband mobile radio channel in suburbia at 910 MHz 20 p2846 N90-26187
A narrowband tactical communication system for the VHF and UHF mobile radio bands 20 p2847 N90-26192
Multiple-access techniques for communication over dispersive radio channels 20 p2848 N90-26196
Experimental study of a digital mobile radio spread spectrum in an urban site 20 p2849 N90-26205
Inhomogeneous electric field effects in a linear RF quadruple trap 20 p2853 N90-26222

DSS 15, 45, and 65 34-meter high efficiency antenna radio frequency performance enhancement by tilt added to the subreflector during elevation angle changes
20 p2854 N90-26229
Spread-spectrum communications in non-Gaussian channels
[AD-A222886] 21 p2994 N90-27019
Brief state-of-the-art review on optical communications for the NASA ISES workshop 21 p3017 N90-27153
Crossed-microwave-beam air ionization laboratory experiments
[DE90-012056] 21 p3024 N90-27195
Lightweight, broadband, pulsed, frequency agile, self-screening jammer for airborne deployment
[AD-D014468] 22 p3163 N90-27937
Solid state space harmonic amplifier
[AD-D014455] 22 p3186 N90-27955
Improved compact optical RF spectrum analyzer
[AD-D014481] 22 p3177 N90-28026
A radio frequency user's guide to the space environment services center geophysical alert broadcasts
[PB90-240631] 23 p3351 N90-28935
RF power generation for future linear colliders
[DE90-014804] 23 p3394 N90-29178
Modular digital GPS receivers
24 p3424 N90-29346

RADIO FREQUENCY DISCHARGE
Hydrogenated amorphous and microcrystalline silicon deposited from silane-hydrogen mixtures
[ETN-90-96267] 11 p1493 N90-18590

RADIO FREQUENCY HEATING
Radio frequency (13.56 MHz) energy enhances rewarming from mild hypothermia
[AD-A212703] 04 p0524 N90-13024
Experiments on linear high beta helical axis stellarators to study simulated toroidal effects and Alfven-wave heating
[DE90-001704] 07 p0994 N90-15745
Computation of coupling elements between waveguides and modes for large launching structures
[IPPCZ-290] 13 p1890 N90-20842
Computer simulation of ionospheric radio frequency heating
[DE90-009478] 15 p2087 N90-21944

RADIO FREQUENCY INTERFERENCE
NT ATMOSPHERICS
NT CHIRP
NT CHIRP SIGNALS
NT COSMIC NOISE
NT ELECTROMAGNETIC NOISE
NT HISS
NT IONOSPHERIC NOISE
NT SHOT NOISE
NT THERMAL NOISE
NT WHISTLERS
NT WHITE NOISE
Coupled multiline CW HF lasers: Experimental performance
[AD-A210844] 01 p0075 N90-10434
An experimental SMI adaptive antenna array for weak interfering signals
[NASA-CR-185976] 02 p0212 N90-11211
Offaxis radiance studies for infrared sensors
[AD-A210790] 02 p0275 N90-11570
Adaptive antenna arrays for satellite communication
[NASA-CR-185989] 04 p0485 N90-12784
Digital radio link: Wave propagation investigations on a 13 GHz line-of-sight path
[PB89-213128] 04 p0485 N90-12785
Automatic communications channel interference monitoring
[RSRE-MEMO-4243] 04 p0491 N90-12820
Long wave atmospheric noise model, phase 1. Volume 1: Lightning occurrence rates and propagation theory
[AD-A212794] 04 p0493 N90-12836
Long wave atmospheric noise model, phase 1. Volume 2: Mode parameters
[AD-A212795] 04 p0493 N90-12837
Performance of cellular frequency-hopped spread-spectrum radio networks
[AD-A214480] 09 p1204 N90-16978
Radio noise measurements in the long-wave band at Thule, Greenland
[NASA-CR-182824] 09 p1206 N90-16991
Near real time VHF telemetry of near shore oceanographic data
[AD-A215756] 10 p1327 N90-17666
Antenna design methods adapted to radio communication
[TELECOM-88-E-018] 10 p1375 N90-17971
Radio interference in the near-earth environment
[NASA-CR-180479] 11 p1498 N90-18623
The effects of sinusoidal interference on the second-order carrier tracking loop preceded by a bandpass limiter in the Block 4 receiver 12 p1644 N90-19449
Radar RFI at Goldstone DSS 12 and DSS 16
15 p2078 N90-21900
Test diagnostics of RF effects in integrated circuits
[AD-A219737] 17 p2396 N90-23648
Bermuda ionosonde tests in support of OTH-B
[NASA-TM-89359] 19 p2713 N90-25442
Solar array arcing in plasmas
19 p2737 N90-25558
Propagation Effects and Circuit Performance of Modern Military Radio Systems with Particular Emphasis on Those Employing Bandspreading
[AGARD-CP-442] 20 p2844 N90-26178
A global common-user system for the provision of HF propagation data 20 p2845 N90-26180
Experimental analysis of the HF linkage
20 p2845 N90-26181
Progress and remaining issues in the development of a wideband HF channel model and simulation
20 p2845 N90-26182
Performance analysis of subspace-based parameter estimation algorithms
[AD-A224523] 24 p3463 N90-29566
An assessment of the application of in situ ion-density data from DMSP to modeling of transionospheric scintillation
[AD-A224392] 24 p3490 N90-29725

RADIO FREQUENCY NOISE
U ELECTROMAGNETIC NOISE

RADIO FREQUENCY RADIATION
U RADIO WAVES

RADIO GALAXIES
Radio and optical observations of nearby active galaxies 06 p0860 N90-15000
MERLIN and VLBI observations of the radio galaxy Virgo A 06 p0860 N90-15001
Search for rapidly star forming galaxies at high redshift 15 p2181 N90-22465
Extended optical emission in 3CR radio galaxies
15 p2193 N90-22523
Extended line emission in AGN: Looking at the central engine 19 p2788 N90-25870
X ray constraints on the beaming hypothesis for BL Lacertae objects 19 p2793 N90-25900
Radio loud far-infrared galaxies
[DE90-012993] 20 p2950 N90-26786
Asymmetric depolarization in powerful extragalactic radio sources 22 p3264 N90-28484

RADIO INTERFERENCE
U RADIO FREQUENCY INTERFERENCE

RADIO INTERFEROMETERS
First interferometric observations with arc-sec. resolution of solar radio bursts at millimeter wavelengths
03 p0431 N90-12472
MERLIN and VLBI observations of the radio galaxy Virgo A 06 p0860 N90-15001
Feasibility of millimeter-accuracy geodetic positioning and vehicle tracking with repeater satellites
[AD-A214755] 09 p1182 N90-16854

RADIO JETS (ASTRONOMY)
Asymmetric depolarization in powerful extragalactic radio sources 22 p3264 N90-28484

RADIO NAVIGATION
NT LORAN
NT LORAN C
Federal Radionavigation Plan, 1988
[PB89-163075] 02 p0148 N90-10846
South Pacific OMEGA validation analysis
[AD-A215916] 10 p1319 N90-17624
The Telecommunications and Data Acquisition Report
[NASA-CR-186479] 15 p2074 N90-21880
US Coast guard radionavigation system user survey
[AD-A218480] 17 p2349 N90-23380
General principles of radionavigation: Space mapping
17 p2358 N90-23423
Location and navigation technology: Putting theory into practice 17 p2358 N90-23424
Comparison of navigation systems
17 p2360 N90-23438
Investigations of monopulse-assisted radio location systems for the safety of surface traffic
[ETN-90-97324] 21 p2956 N90-26806
Global positioning system overview/status
21 p3069 N90-27446

RADIO OBSERVATION
Radio and optical observations of nearby active galaxies 06 p0860 N90-15000
Very high resolution radio observations of molecular cloud cores 06 p0863 N90-15013
Radio pulsar timing observations for GRO
16 p2334 N90-23301
Multiwavelength constraints on gamma-ray burst sources 18 p2639 N90-25032
New Voyager radio spectrograms of Uranus
[NASA-CR-180381] 23 p3412 N90-29284

RADIO OCCULTATION
Laboratory evaluation and application of microwave absorption properties under simulated conditions for planetary atmospheres
[NASA-CR-185916] 06 p0855 N90-15025
Waves in Saturn's rings probed by radio occultation
15 p2191 N90-22511
Laboratory measurements of microwave and millimeter-wave properties of planetary constituents
20 p2943 N90-26745
Laboratory measurements and modeling of microwave absorption by ammonia in gas mixtures applicable to giant planet atmospheres 20 p2944 N90-26750

RADIO PHYSICS
Extended optical emission in 3CR radio galaxies
15 p2193 N90-22523

RADIO PROBING
Preliminary comparison of temperature soundings obtained from simultaneous radiometric, radio-acoustic, and rawinsonde measurements
[PB90-119835] 11 p1535 N90-18838

RADIO PROPAGATION
U RADIO TRANSMISSION

RADIO RECEIVERS
NT SUPERHETERODYNE RECEIVERS
NT TRANSMITTER RECEIVERS
The 22 GHz Radioastron receiver: Development of prototype components during the year 1988
[PB89-212583] 07 p0920 N90-15323
Construction of a 345 gigahertz receiver based on superconducting tunnel junctions
[AD-A218781] 16 p2232 N90-22735
A survey of equatorial magnetospheric wave activity between 5 and 8 R(sub E)
[AD-A220137] 17 p2424 N90-23812
Establishing a GPS-baseline between Seattle, Washington and Monterey, California
[AD-A220069] 18 p2495 N90-24262
A global common-user system for the provision of HF propagation data 20 p2845 N90-26180

RADIO RECEPTION
Influence of ionospheric variations on high-reliability HF systems utilizing large bases 02 p0248 N90-11404
Radio links: Instrument technologies
17 p2358 N90-23425

RADIO RELAY SYSTEMS
NT CODE DIVISION MULTIPLE ACCESS
NT TIME DIVISION MULTIPLE ACCESS
Modelling UHF propagation for frequency assignment in radio relay networks 06 p0764 N90-14445
User-friendly software for the design of digital line-of-sight radio links
[PB90-118472] 12 p1700 N90-19760
Random access transmission algorithms for data local area networks
[AD-A216443] 12 p1700 N90-19761
High stability radio links 12 p1734 N90-19970
Report on STC/Technische Universiteit (TU) Delft Extremely High Frequency (EHF) radio relay study
15 p2081 N90-21915
NASA 60 GHz intersatellite communication link definition study. Addendum A: Mixed baseband and IF signals
[NASA-CR-186337] 17 p2387 N90-23593
NASA 60 GHz intersatellite communication link definition study. Baseline document
[NASA-CR-186339] 17 p2387 N90-23594
NASA 60 GHz intersatellite links definition study. Final Review
[NASA-CR-186338] 17 p2387 N90-23595
Ground-based weather radar compatibility with digital radio-relay microwave systems
[PB90-206236] 23 p3318 N90-28756

RADIO SIGNAL ATTENUATION
U RADIO ATTENUATION

RADIO SIGNAL PROPAGATION
U RADIO TRANSMISSION

RADIO SIGNALS
A modern trans-ionospheric propagation sensing system 06 p0761 N90-14430
Performance of cellular frequency-hopped spread-spectrum radio networks
[AD-A214480] 09 p1204 N90-16978
Observations of fine-scale vertical shear and strain in the upper ocean
[AD-A214476] 10 p1410 N90-18130
Navigation experiment NAVEX: The self-test delay times in the D1 Spacelab mission
[ESA-TT-1176] 11 p1467 N90-18446
Optical excisor modeling
[AD-A219338] 16 p2230 N90-22722
Optical signal processing
[AD-A220332] 18 p2615 N90-24897
Radio refractivity profiles deduced from lidar measurements
[AD-A221727] 21 p3026 N90-27208

RADIO SOURCES (ASTRONOMY)
NT EXTRAGALACTIC RADIO SOURCES
NT PULSARS
NT QUASARS
NT RADIO GALAXIES
NT RADIO JETS (ASTRONOMY)
NT RADIO STARS
A statistical study of radio-source structure effects on astrometric very long baseline interferometry observations 04 p0485 N90-12788
The correlation between radio and far-infrared emission for disk galaxies 11 p1588 N90-19158
The 32-GHz performance of the DSS-14 70-meter antenna: 1989 configuration 12 p1645 N90-19452
Observations of Cygnus X-2 at x ray, UV, optical and radio frequencies
[MPE-PREPRINT-163] 17 p2481 N90-24191
Radio observations of the x ray binary Cygnus X-2 17 p2482 N90-24195
Multiwavelength observations of BL Lacertae 19 p2791 N90-25886
High resolution optical imaging through the atmosphere
[AD-A221913] 21 p3097 N90-27599
RADIO SPECTRA
NT MICROWAVE SPECTRA
Long-range plan for management and use of the radio spectrum by agencies and establishments of the Federal Government
[PB89-232367] 05 p0633 N90-13693
Experimental study of a digital mobile radio spread spectrum in an urban site 20 p2849 N90-26205
RADIO STARS
NT PULSARS
The behaviour of SS433 and Cygnus X-3 at low frequency 19 p2772 N90-25756
RADIO TELEMETRY
Multimedia system control
[AD-A219392] 16 p2276 N90-22971
RADIO TELESCOPES
NT VERY LARGE ARRAY (VLA)
Project Radioastron 02 p0158 N90-10901
Cryogenic Schottky-mixer receiver front-end for 40-50 GHz
[PB89-221667] 03 p0343 N90-11959
RADIO TRACKING
Feasibility of millimeter-accuracy geodetic positioning and vehicle tracking with repeater satellites
[AD-A214755] 09 p1182 N90-16854
RADIO TRANSMISSION
NT IONOSPHERIC F-SCATTER PROPAGATION
NT IONOSPHERIC PROPAGATION
NT MICROWAVE ATTENUATION
NT MICROWAVE TRANSMISSION
NT MULTIPATH TRANSMISSION
NT SHORT WAVE RADIO TRANSMISSION
NT SPREAD SPECTRUM TRANSMISSION
Ionospheric irregularities due to powerful HF radio transmissions 02 p0245 N90-11389
TEC (Total Electron Content) models
[AD-A211553] 03 p0372 N90-12129
Long wave propagation assessment 06 p0758 N90-14414
RPE: A parabolic equation radio assessment model 06 p0759 N90-14419
New perspectives for the inversion of backscatter ionograms 06 p0761 N90-14427
Packet Radio Integrated System Module (PRISM): Design document
[AD-A214723] 09 p1205 N90-16981
PRPSIM: A FORTRAN code to calculate properties of radio wave propagation in a structured ionized medium. Volume 2: Theory and models
[AD-A216299] 10 p1377 N90-17983
Experimental measurements in secondary radar field: Conception and first results
[ETN-90-96074] 12 p1648 N90-19471
JPRS report: Science and technology. USSR: Electronics and electrical engineering
[JPRS-UEE-90-002] 14 p1970 N90-21284
Preliminary results of the peak experiment. ALTAIR deep-space measurements
[AD-A218622] 16 p2229 N90-22714
Radio links: Instrument technologies 17 p2358 N90-23425
An analysis of propagation in a surface duct over a periodically rough Earth
[AD-A220565] 17 p2390 N90-23612
An overview of Canadian radio propagation/communications technologies research 20 p2844 N90-26179
Optimal synchronization of spread spectrum sequenced by nontransferable switching operators 20 p2845 N90-26183
Radio channel measurement and modelling for future mobile radio systems 20 p2845 N90-26184
Measurement and simulation of widespread mobile radio channel characteristics 20 p2846 N90-26186
Wideband characterization of forest propagation channels 20 p2846 N90-26188
Man-made noise in a military environment 20 p2847 N90-26191
Multiple-access techniques for communication over dispersive radio channels 20 p2848 N90-26196
Minimization of the cost of information transfer in HF spread spectrum transmission 20 p2848 N90-26198
New synchronisation techniques applicable to multi-tone transmission systems 20 p2848 N90-26199
Effects of ionospheric modification on system performance 20 p2849 N90-26202
Combined effects of fast and selective fading on performance of PSK and MSK with coherent detection 20 p2849 N90-26204
Packet radio network concepts for the Norwegian field army 20 p2850 N90-26206
The effects on antenna-filtered scintillation parameters of non-zero antenna pointing angles
[AD-A223840] 24 p3462 N90-29554
A study of water vapor, electrical parameters, and radio propagation
[AD-A223582] 24 p3492 N90-29736
RADIO TRANSMITTERS
NT IONOSONDES
NT RADIOSONDES
NT RAWINSONDES
NT TRANSMITTER RECEIVERS
Description and results of a multihop NACS simulation
[FEL-1988-46] 04 p0491 N90-12824
Wideband S band transmitter
[AD-A217620] 13 p1794 N90-20295
A global common-user system for the provision of HF propagation data 20 p2845 N90-26180
Preliminary error budget for an optical ranging system: Range, range rate, and differenced range observables 20 p2853 N90-26227
RADIO WAVES
NT CENTIMETER WAVES
NT DECAMETRIC WAVES
NT EXTRATERRESTRIAL RADIO WAVES
NT HYDROXYL EMISSION
NT LONG WAVE RADIATION
NT MICROWAVE EMISSION
NT MICROWAVES
NT MILLIMETER WAVES
NT RADIO BURSTS
NT RADIO EMISSION
NT SHORT WAVE RADIATION
NT SKY WAVES
NT SOLAR RADIO BURSTS
NT SOLAR RADIO EMISSION
NT SUBMILLIMETER WAVES
NT TYPE 3 BURSTS
NT WHISTLERS
VLF/LF radio wave studies of the structure and variability of the equatorial, mid-latitude and polar ionosphere below 100 km 02 p0242 N90-11373
On the possibility of producing artificial ionization and polar aurora in the ionosphere by radio-waves emitted from the ground 02 p0245 N90-11388
Radio propagation conditions forecast above a low latitude region 02 p0247 N90-11400
Handbook of radio wave propagation loss (100-20,000 MHz), part 2
[PB89-195473] 03 p0336 N90-11912
Modeling of diffraction reflection and clutter loss in UHF radio wave propagation
[FEL-1988-28] 03 p0340 N90-11938
Base level management of radio frequency radiation protection program
[AD-A211787] 03 p0381 N90-12171
Physics of the tropospheric radiopropagation
[DE89-619726] 04 p0485 N90-12783
Preliminary investigation of Faraday rotation effects and description of polarization measurements on the AFGL high latitude meteor scatter test bed
[AD-A211298] 04 p0488 N90-12806
Base level management of radio frequency radiation protection program
[AD-A211759] 04 p0523 N90-13017
Far infrared, submm and mm spectroscopy of the galactic center: Radio arc and +20/+50 km s (exp -1) clouds
[NASA-CR-185497] 04 p0565 N90-13296
The importance of environmental data 06 p0757 N90-14406
South Pacific OMEGA validation analysis
[AD-A215916] 10 p1319 N90-17624
PRPSIM: A FORTRAN code to calculate properties of radio wave propagation in a structured ionized medium. Volume 2: Theory and models
[AD-A216299] 10 p1377 N90-17983
Incoherent retrodiffusion of radiowaves in plasma with particle impulse
[ETN-90-95375] 12 p1718 N90-19664
Flare stars at radio wavelengths
[NASA-CR-186539] 14 p2044 N90-21719
Modeling millimeter-wave propagation effects in the atmosphere 15 p2082 N90-21922
Astronomy at ultra-high energies: Results from the CYGNUS experiment
[DE90-011979] 20 p2940 N90-26732
Amplitude and phase scintillation and ionospheric irregularities at sub-auroral latitudes
[AD-A222861] 21 p3025 N90-27198
The 27-day versus 13.5-day variations in the solar Lyman-alpha radiation and the radio wave absorption in the lower ionosphere over Europe 22 p3209 N90-28203
RF power generation for future linear colliders
[DE90-014804] 23 p3394 N90-29178
An assessment of the application of in situ ion-density data from DMSP to modeling of transionospheric scintillation
[AD-A222695] 24 p3491 N90-29730
A feasibility study for D-region equatorial ionosphere research using VLF radiowaves
[AD-A223685] 24 p3492 N90-29738
RADIOACTIVE CONTAMINANTS
Draft Environmental Impact Statement for the Ulysses Mission (Tier 2)
[NASA-TM-102903] 06 p0812 N90-14727
Simulation of the propagation of radiactive substances from the example of Chernobyl (USSR) 12 p1686 N90-19685
Boundary layer parameterization in CTM and MM4 12 p1688 N90-19697
Final Environmental Impact Statement for the Ulysses Mission (Tier 2)
[NASA-TM-101104] 15 p2126 N90-22162
Environmental radioactivity measurement intercomparison exercise
[NPL-RSA(EXT)-5] 22 p3200 N90-28158
RADIOACTIVE DECAY
NT NEUTRON EMISSION
Gamma radiation background measurements from Spacelab 2
[NASA-CR-183782] 02 p0297 N90-11689
Recovery of particle size distribution of ultrafine aerosols from diffusional decay measurements
[AD-A213006] 05 p0621 N90-13621
Mapping of upper electronic reaction surfaces by tuned laser photolysis and by absorption and emission spectroscopies
[DE90-000125] 06 p0741 N90-14314
Excitation lifetimes and excited-state forces in chemisorbed molecules
[DE90-002578] 07 p0894 N90-15165
Cosmic ray half life of (54)Mn
[DE90-000134] 07 p1016 N90-15880
Cosmic ray half life of Ni-56
[DE90-000132] 08 p1153 N90-16680
Search for proton decay and supernova neutrino bursts with a lunar base neutron detector
[DE90-607644] 10 p1448 N90-18358
Contained events in Soudan 2
[DE90-005648] 10 p1449 N90-18359
Helium permeability through austenitic stainless steel
[DE90-007046] 11 p1488 N90-18562
Underground muon observations in the Soudan 2 detector
[DE90-005647] 11 p1594 N90-19183
Precompound decay models for medium energy nuclear reactions
[DE90-008352] 13 p1884 N90-20808
Theoretical studies of spin-forbidden processes within the Breit-Pauli approximation
[AD-A217778] 13 p1885 N90-20815
Populations of excited states and reaction mechanisms in the emission of complex fragments
[DE90-007481] 13 p1886 N90-20819
Characteristics consequences of space-time coordinate relativization
[DE90-615201] 14 p2034 N90-21668
Does mass accretion lead to field decay in neutron stars
[CAL-394] 15 p2182 N90-22470
Cosmic strings and baryon decay
[NASA-CR-182842] 19 p2754 N90-25651
The long-term variation of lead-210 in relation to particle-bound sulphur in surface air in Finland 20 p2884 N90-26407
Measurements of energy dispersion at liquid-solid interfaces: Fluorescence quenching of pyrene bound to fumed silica
[AD-A222371] 21 p2978 N90-26926

Study of short-lived unstable nuclei by means of laser optical pumping
[AD-A222561] 21 p3009 N90-27105
Crossed-microwave-beam air ionization laboratory experiments
[DE90-012056] 21 p3024 N90-27195
A double-sided silicon strip detector with capacitive read out and a new method of integrated bias coupling
22 p3178 N90-28037
Electronic and photonic power applications
[DE90-015567] 24 p3485 N90-29698

RADIOACTIVE ELEMENTS
U RADIOACTIVE ISOTOPES

RADIOACTIVE ISOTOPES
NT AMERICIUM
NT CARBON 14
NT COBALT 60
NT COPPER ISOTOPES
NT CURIUM
NT GOLD ISOTOPES
NT KRYPTON 85
NT PLUTONIUM
NT TRITIUM
Automatic analysis and exploitation of the flow visualization images
[ETN-89-95712] 04 p0501 N90-12887
Safety evaluation report for Galileo: Volume 1
[DE90-003086] 07 p0886 N90-15122
ROBOCAL (Robotic Calorimetry): An automated NDA (Nondestructive Assay) calorimetry and gamma isotopic system
[DE90-003217] 07 p0894 N90-15168
Measurements of long-lived cosmogenic nuclides in returned comet nucleus samples
08 p1146 N90-16640
Performance of a coincidence based blood activity monitor
[DE90-006105] 11 p1540 N90-18865
The TISOL facility at TRIUMF
[DE90-006882] 12 p1713 N90-19837
The long-term variation of lead-210 in relation to particle-bound sulphur in surface air in Finland
20 p2884 N90-26407
Use of Ni63 overvoltage gap switches in the flight termination systems on boosters launched from US Army Kwajalein Atoll (USAKA)
[AD-A223866] 23 p3299 N90-28661
Moessbauer Effect applications using intense radioactive ion beams
[DE90-014981] 23 p3394 N90-29175

RADIOACTIVE MATERIALS
Spoken commands control robot that handles radioactive materials
[DE89-012632] 02 p0262 N90-11488
ROBOCAL (Robotic Calorimetry): An automated NDA (Nondestructive Assay) calorimetry and gamma isotopic system
[DE90-003217] 07 p0894 N90-15168
Technology of fast spark gaps
[AD-A214199] 07 p0925 N90-15353
Examples of robots and teleoperators at the Savannah River Site
[DE90-004659] 08 p1086 N90-16284
A new type of radioluminescent light source
[DE90-004294] 09 p1210 N90-17015
National emissions standards for hazardous air pollutants application for approval of construction SP-100 ground engineering system test site
[DE90-007985] 16 p2316 N90-23203

RADIOACTIVE NUCLIDES
U RADIOACTIVE ISOTOPES

RADIOACTIVE WASTES
Evapotranspiration studies for protective barriers: Experimental plans
[DE90-005206] 10 p1405 N90-18106
RIPE: An object-oriented Robot Independent Programming Environment
[DE90-008501] 13 p1866 N90-20707
In-situ fracture stiffness determination
[DE90-009202] 15 p2129 N90-22173
Transport of gases through concrete
[AERE-G-4977] 16 p2234 N90-22747
Object-oriented design: Deriving conceptual solutions to large-scale information processing problems
[DE90-011189] 19 p2763 N90-25699
Environmental radioactivity measurement intercomparison exercise
[NPL-RSA(EXT)-5] 22 p3200 N90-28158

RADIOACTIVITY
Radioactivity induced in gamma-ray spectrometers
[RAE-TM-SPACE-363] 04 p0569 N90-13317
The cosmic radiation effects and activation monitor
[RAE-TM-SPACE-364] 04 p0569 N90-13318
Coded-aperture imaging in nuclear medicine
08 p1073 N90-16208
Performance of a coincidence based blood activity monitor
[DE90-006105] 11 p1540 N90-18865
Application of natural isotopes in groundwater for solving environmental problems
[DE90-000223] 12 p1689 N90-19703
Predictions of radiation backgrounds for GRO/OSSE
[RAE-TM-SPACE-372] 23 p3414 N90-29293

RADIOBIOLOGY
DOE/CEC Workshop on Critical Evaluation of Radiobiological Data to Biophysical Modeling
[DE89-015214] 02 p0254 N90-11437
USSR Space Life Sciences Digest, issue 23
[NASA-CR-3922(27)] 03 p0378 N90-12154
Proceedings of the 6th Regional Symposium on Biophysics
[DE90-619618] 15 p2136 N90-22206
Field evaluation of a passive sampling device for hydrazines in ambient air
[NASA-TM-103456] 18 p2578 N90-24686
Program review: The lifetime effects of space radiation in rhesus monkeys
[AD-A221127] 19 p2716 N90-25454
Experiment K-6-24, K-6-25, K-6-26. Radiation dosimetry and spectrometry 20 p2897 N90-26477
Effects of ionizing radiation on the performance of selected tactical combat crews
[AD-A222880] 21 p3034 N90-27248
Biomedical and environmental sciences program publications, 1989
[DE90-014785] 23 p3406 N90-29250

RADIOCHEMISTRY
The Baksan gallium solar neutrino experiment
[DE89-016036] 03 p0429 N90-12457

RADIOGRAPHY
NT AUTORADIOGRAPHY
NT COMPUTER AIDED TOMOGRAPHY
NT NEUTRON RADIOGRAPHY
NT TOMOGRAPHY
NDE (Non-Destructive Evaluation) publications, 1985
[PB89-229025] 03 p0356 N90-12036
Damage in a perforated graphite-epoxy composite plate under monotonic and cyclic biaxial loading
[ESA-TT-1117] 11 p1480 N90-18521
Real-time stereo-microradiography
[AD-A218433] 16 p2245 N90-22805
Method of radiographic inspection of wooden members
[NASA-CASE-LAR-13724-1] 17 p2414 N90-23756
Experiment K-6-27. Analysis of radiographs and biosamples from primate studies
20 p2897 N90-26478
Soft x ray resist characterization: Studies with a laser plasma x ray source
[DE90-013493] 20 p2928 N90-26661
Stenopic radiography: A non-destructive test without contact 22 p3187 N90-28086
Improvement of the detail reconnaissance in radiographic irradiation images by digital image restoration
[ETN-90-97311] 22 p3189 N90-28096

RADIOISOTOPE BATTERIES
Draft Environmental Impact Statement for the Ulysses Mission (Tier 2)
[NASA-TM-102903] 06 p0812 N90-14727
Safety Status Report for the Ulysses mission. Book 1: Accident analysis. General purpose heat source radioisotope thermoelectric generator program
[DE90-006829] 12 p1614 N90-19285
Final Safety Analysis Report for the Ulysses Mission. Volume 3 (Book 1): Nuclear risk analysis document
[DE90-008691] 14 p1939 N90-21101
Final safety analysis report for the Ulysses mission. Volume 2 (Book 1): Accident model document
[DE90-008694] 14 p1940 N90-21103
Preliminary design of a long-endurance Mars aircraft
[NASA-CR-185243] 15 p2052 N90-21763
Draft environmental impact statement for the Galileo Mission (Tier 2)
[NASA-TM-102926] 15 p2124 N90-22148
Final Environmental Impact Statement for the Ulysses Mission (Tier 2)
[NASA-TM-101104] 15 p2126 N90-22162
General purpose heat source radioisotope thermoelectric generator program. Book 1: Accident analysis
[REPT-90SDS4202-BK-1] 15 p2166 N90-22379
General purpose heat source radioisotope thermoelectric generator. Book 2: Accident analysis, appendices
[REPT-90SDS4202-BK-2] 15 p2166 N90-22380
GPHS-RTG response to Challenger type accident
19 p2665 N90-25163

RADIOLOGY
Final safety analysis report for the Ulysses Mission. Volume 3 (Book 2): Nuclear risk analysis document-appendices
[DE90-008692] 14 p1939 N90-21102
A radiological assessment of nuclear power and propulsion operations near Space Station Freedom
[NASA-CR-185185] 14 p1941 N90-21108
Conference on Instrumental Activation Analysis: IAA 89
[DE90-615661] 19 p2694 N90-25327
Radiological investigation of the vertebral column of candidates for military flying training the the Royal Norwegian Air Force 19 p2718 N90-25463

RADIOMETERS
NT ADVANCED VERY HIGH RESOLUTION RADIOMETER
NT INFRARED DETECTORS
NT INFRARED RADIOMETERS
NT INFRARED SCANNERS
NT MICROWAVE RADIOMETERS
NT SPECTRORADIOMETERS
Spectrometer technology recommendations
05 p0597 N90-13468
A four channel He-3 cooled balloon-borne bolometer radiometer 05 p0597 N90-13469
Reflection indicatrices of natural surfaces for AVHRR channels 1 and 2
[DLR-MITT-89-16] 05 p0664 N90-13882
Remote sensing of atmospheric water vapour by pressure modulation radiometry
06 p0802 N90-14667
The physical foundations of radiometry and their applications in the mm-waveband
[REPT-12-88] 08 p1058 N90-16114
Model-based quantification of image quality
08 p1072 N90-16206
Operational ozone monitoring with the Global Ozone Monitoring Radiometer (GOMR)
[PB90-114034] 08 p1098 N90-16359
Radiometric study of wheat and bean crops in three types of latossolo
[INPE-4843-PRE/1472] 11 p1523 N90-18767
Spectral response of wheat and its relationship with agronomical prameters
[INPE-4950-RPE/599] 11 p1524 N90-18774
Design of a low-frequency (5-20 GHz), 15-meter-diameter passive radiometer for geostationary earth science platforms 12 p1609 N90-19255
Millimeter radiometer system technology
12 p1610 N90-19260
Synthetic Aperture Interferometric Radiometer (SAIR)
12 p1610 N90-19261
Analysis of radiometer calibration effects with TOUCHSTONE
[NASA-CR-186476] 13 p1792 N90-20284
Relationship of radiometric field measurements of wheat in the Assis-Safra region, 1988
[INPE-4949-RPE/598] 13 p1819 N90-20443
Wheat productivity estimate through field radiometry
[INPE-4994-PRE/1556] 14 p2000 N90-21460
Radiometric tests on wet and dry antenna reflector surface panels 15 p2076 N90-21890
Spectral response of wheat and its relationship with agronomic variables in the tropical region
[INPE-5018-RPE/612] 15 p2122 N90-22138
Field reports on radiometric campaigns of soybeans in the Federal district: Safra 88/89
[INPE-5021-RPE/615] 15 p2122 N90-22139
Calibration technique for heat flux sensors used in fire experiments and standard fire tests
[DOT/FAA/CT-89/26] 19 p2694 N90-25329
Annual and interannual variations of Earth-emitted radiation based on a 10-year data set
[NASA-TM-103465] 20 p2887 N90-26432
Experiments with unsteady, free surface, three-dimensional vortices in a thermally stable, stratified fluid
[AD-A222088] 21 p2954 N90-26796
Conceptual design study for Infrared Limb Experiment (IRLE)
[NASA-CR-186950] 21 p2968 N90-26869
Description of SAFIRE for ISES
21 p3016 N90-27148
ERBE and CERES broadband scanning radiometers
21 p3016 N90-27149
Cloud reflectance characteristics in the presence of variable Dimethylsulfide (DMS) sources
[AD-A222806] 21 p3024 N90-27197
Analysis of cirrus optical properties with data from NASA ER2 High-resolution Interferometer Sounder (HIS)
[NASA-CR-186365] 21 p3030 N90-27227
Integrated radiometric profiler for atmospheric humidity and temperature measurements
[AD-A221931] 21 p3032 N90-27237

Spectral absorption of marine stratocumulus clouds derived from in situ cloud radiation measurements
22 p3215 N90-28238
Cloud optical parameters as derived from the multispectral cloud radiometer 22 p3215 N90-28239
Analysis of ER-2 radiometer and lidar observations from the 1987 marine stratus experiment
22 p3216 N90-28241
Cirrus parameterization from the FIRE ER-2 observations 22 p3227 N90-28302
Technical activities 1989, Electron and Optical Physics Division
[PB90-207267] 23 p3415 N90-29296
Characteristics of pushbroom scanning type radiometer utilizing linear sensors
[NAL-TR-1024] 24 p3472 N90-29625

RADIOMETRIC CORRECTION
Real-time adaptive radiometric correction for imaging radars systems 14 p1962 N90-21233
Applications of remote sensing to studies of oceanic upper mixed layer dynamics 15 p2122 N90-22137
Multispectral classification of overlapping classes with applications to forest damage areas
[DLR-FB-89-55] 18 p2574 N90-24666
Atmospheric correction of thematic mapping measurements about seabeds of the German Bay
[GKSS-89/E/47] 20 p2816 N90-26029
Data analysis techniques 21 p3017 N90-27151

RADIOMETRIC RECTIFICATION
U RADIOMETRIC CORRECTION

RADIOMETRIC RESOLUTION
Removing stripes in GOES (Geostationary Operational Environmental Satellites) images by matching empirical distribution functions
[PB89-213359] 04 p0514 N90-12968
The physical foundations of radiometry and their applications in the mm-waveband
[REPT-12-88] 08 p1058 N90-16114
Observations of attenuation at 20.6, 31.65 and 90.0 GHz: Preliminary results from Wallops Island, VA
10 p1373 N90-17957
Interrelationship of spatial and radiometric resolution in the thermal infrared band
[INPE-4860-TDL/371] 11 p1523 N90-18771
Real-time adaptive radiometric correction for imaging radars systems 14 p1962 N90-21233
Multiresolution and time-frequency representations of signals
[REPT-89-47] 15 p2087 N90-21946
Integrated radiometric profiler for atmospheric humidity and temperature measurements
[AD-A221931] 21 p3032 N90-27237

RADIONUCLIDES
U RADIOACTIVE ISOTOPES

RADIOSENSITIVITY
U RADIATION TOLERANCE

RADIOSONDES
NT IONOSONDES
NT RAWINSONDES
The effect of random variations of radiosonde data on the predicted FLIR performance calculated by the program UFLR
[AD-A220034] 18 p2615 N90-24896

RADIOTHERAPY
U RADIATION THERAPY

RADIUS
U RADII

RADOMES
Ablative cooling of aerodynamically heated radomes
[AD-D014426] 14 p1971 N90-21293

RADON
NT RADON ISOTOPES
Radon transform analysis of a probabilistic method for image generation
[AD-A207814] 01 p0123 N90-10702

RADON ISOTOPES
Radon concentration over the Brazilian Amazon Basin during the wet season (Belem-Manaus GTE-ABLE-2B flight of April 24, 1987)
[INPE-4892-PRE/1493] 14 p2004 N90-21486

RAFTS
NT LIFE RAFTS

RAIL TRANSPORTATION
Evaluation of EDR-3 vibration, shock, temperature, and humidity recording unit
[NASA-CR-184006] 22 p3177 N90-28028
On the application of similarity laws to a scaled railway bogie model
[DLR-FB-90-06] 23 p3335 N90-28853

RAILGUN ACCELERATORS
Current management for improved railgun performance
[AD-A212887] 05 p0593 N90-13445
Performance characteristics of a three-stage railgun
[DE90-002533] 06 p0729 N90-14254
Summary of a decade of railgun development for high-pressure research
[DE90-005247] 09 p1172 N90-16780
Computational and experimental of railgun structural performance
[DE90-006418] 12 p1607 N90-19247
Muzzle shunt augmentation of conventional railguns
[DE90-007505] 12 p1607 N90-19248
An electrical model for plasma armature voltage
[DE90-007530] 12 p1718 N90-19868
A 10-stage reconnection demonstration launcher
[DE90-007653] 13 p1760 N90-20106
Diagnostics and firing control for the cylindrical reconnection launcher
[DE90-007677] 13 p1761 N90-20107
Application of railgun principle to high-velocity hydrogen pellet injection for magnetic fusion reactor refueling
[DE90-008281] 13 p1761 N90-20109
Laser controlled semiconductor armature for electromagnetic launchers
[AD-D014435] 14 p1931 N90-21055
Railgun performance with a two-stage light-gas gun injector
[DE90-009183] 14 p1932 N90-21057
Feasibility of intercalated graphite railgun armatures
[NASA-TM-102546] 14 p1953 N90-21181
Current management for improved railgun performance 15 p2057 N90-21781
Application of a rechargeable, small caliber railgun power supply
[AD-A224207] 24 p3438 N90-29418

RAILROADS
U RAIL TRANSPORTATION

RAIN
NT ACID RAIN
Effects of rain attenuation on satellite EHF (Extremely High Frequency) communications in the US
[AD-A210517] 01 p0057 N90-10325
A case study evaluation of satellite-derived rainfall estimates and their application to numerical model precipitation forecast verification
[PB89-194591] 01 p0088 N90-10499
Relation of wind field and buoyancy to rainfall inferred from radar
[PB89-208326] 02 p0251 N90-11424
Global atmospheric moisture variability
03 p0361 N90-12062
Satellite-derived rainfall estimates and propagation characteristics associated with the Mesoscale Convective Systems (MCSs)
[PB89-213417] 03 p0365 N90-12086
Radar polarimetric studies based on the MAYPOLE 1983 and 1984 field experiments
[AD-A212226] 04 p0492 N90-12830
A numerical study of rain-induced surface gravity wave attenuation
[AD-A212762] 04 p0549 N90-13197
Applied atmospheric resources research program in Thailand
[PB89-235402] 05 p0668 N90-13903
Estimation of rain rate using spatial and multichannel coherence: Analysis of SSM/I data
05 p0670 N90-13905
Rainfall estimation over Africa using satellite data
06 p0815 N90-14742
Frequency distributions of heavy rainstorms in Illinois
[PB90-100215] 06 p0816 N90-14748
Use of operational 0-6 and 3-9 h quantitative precipitation forecasts for predicting heavy rain events
[PB90-103946] 06 p0817 N90-14750
The radar-based short term prediction of the time-space evolution of rain fields
[AD-A213802] 07 p0918 N90-15312
Estimating water flow through a hillslope using the massively parallel processor 08 p1114 N90-16449
Case studies in data analysis
[AD-A215342] 09 p1248 N90-17241
Rain attenuation measurements: Variability and data quality assessment 10 p1373 N90-17955
Remote sensing and run-off modelling in the Lake Victoria Basin, Kenya
[BCRS-89-19] 11 p1526 N90-18788
Rain radars for earth science geostationary platforms: Some possibilities 12 p1610 N90-19262
An estimation of rainfall amounts using radar-derived Z-R relationships
[AD-A217950] 13 p1845 N90-20591
Use of microwave satellite data to study variations in rainfall over the Indian Ocean
[NASA-CR-186408] 14 p2007 N90-21501
Inclusion of clouds and rain in atmospheric slant path calculations 15 p2083 N90-21925
An analytic study of nonsteady two-phase laminar boundary layer around an airfoil
18 p2643 N90-25051
Natural and anthropogenic components in bulk precipitation at Blidoe (archipelago of Stockholm, Sweden) 20 p2884 N90-26409
Estimation of convective rain volumes utilizing the are-time-integral technique
[NASA-CR-186814] 20 p2890 N90-26449
Prediction of episodic acidification in Maryland coastal plain streams
[PB90-194978] 22 p3199 N90-28152
A nonhydrostatic numerical model in sigma-coordinates and simulations of mesoscale phenomena
23 p3350 N90-28932
Annual course of precipitation over much of the US: Observed versus GCM simulation
[PB90-221656] 23 p3352 N90-28942

RAIN FORESTS
Mapping and monitoring land use and land degradation in part of East Kalimantan, Indonesia, using aerospace remote sensing techniques: A SPOT case study
[BCRS-88-16B] 19 p2705 N90-25394
Study of anomalies in transition vegetation in Alto Xingo-NT, through remote sensing techniques
[INPE-4601-TDL/334] 23 p3343 N90-28891

RAIN GAGES
A case study evaluation of satellite-derived rainfall estimates and their application to numerical model precipitation forecast verification
[PB89-194591] 01 p0088 N90-10499
Optical measurement of precipitation
[AD-A214357] 10 p1407 N90-18116
An estimation of rainfall amounts using radar-derived Z-R relationships
[AD-A217950] 13 p1845 N90-20591
Quality assurance support for the National Atmospheric Deposition Program and national trends network monitoring activities: 1987-1990
[PB90-187162] 22 p3198 N90-28149
Improved meteorological measurements from buoys and ships (IMET): Preliminary comparison of precipitation sensors
[PB90-241902] 22 p3229 N90-28316

RAINDROPS
Multiparameter radar estimation of raindrop size distribution
[AD-A212410] 04 p0521 N90-13007
The effect of oblate spheroidal drops on rain attenuation at 94 GHz: Comparison between theory and experiment
06 p0763 N90-14440
A numerical model for the axisymmetric equilibrium shape of drops in uniform motion: Effects of external flow, electric field and surface charge
07 p0874 N90-15071
Rain core structure statistics derived from radar and disdrometer measurements in the mid-Atlantic coast of the US 10 p1373 N90-17956

RAINSTORMS
NT THUNDERSTORMS
Frequency distributions and hydroclimatic characteristics of heavy rainstorms in Illinois
[PB89-203988] 02 p0252 N90-11427
Frequency distributions of heavy rainstorms in Illinois
[PB90-100215] 06 p0816 N90-14748

RAMAN EFFECT
U RAMAN SPECTRA

RAMAN LASERS
Volumetric analysis by spontaneous Raman diffusion in a supersonic wind tunnel
[ISL-R-109/88] 04 p0448 N90-12564
Development of an anti-Stokes coherent Raman diffusion system for measuring hypersonic flow
[ONERA-RSF-1/7301-PY] 04 p0459 N90-12630
Energy conversion efficiency in high current Raman regime Free Electron Laser (FEL). 1: Single mode analysis
[DE90-719527] 09 p1227 N90-17120
Analysis of turbulent density fluctuations by means of spontaneous Raman diffusion
[ISL-R-103/89] 20 p2863 N90-26287
Laser techniques for studying chemical vapor deposition
[DE90-012921] 20 p2867 N90-26311
Diagnostics for hydrogen atoms and molecules in H-atom sources and beams using VUV laser light
[AD-A222340] 21 p3074 N90-27476

RAMAN SCATTERING
U RAMAN SPECTRA

RAMAN SPECTRA
Stimulated rotational Raman scattering
[DE89-016427] 01 p0075 N90-10430
Vibrational spectroscopic study of the kaolinite-hydrazine intercalation complex
02 p0204 N90-11166
Study of disorder and strain in semiconductor heterostructures and superlattices by Raman scattering
02 p0280 N90-11601

Progress of research on water vapor lidar
[NASA-CR-185970] 03 p0352 N90-12011
Pulsed-laser-excited Raman spectra of shock compressed triaminotrinitrobenzene
[DE90-000668] 03 p0353 N90-12019
MEGALIDAR
[AD-A212074] 03 p0353 N90-12020
Aspects of Raman scattering
[AD-A213926] 07 p0992 N90-15736
Characterization of MOCVD (Metal Organic Chemical Vapor Deposition) grown epitaxial ceramic oxide thin films
[DE90-003561] 07 p1001 N90-15790
Optical phonon modes in a double heterostructure of polar crystals
[AD-A214208] 07 p1004 N90-15816
Electronic properties of GaAs-(Al,Ga)As quasiperiodic
[AD-A214704] 09 p1289 N90-17472
Non-destructive characterization of epoxy/dicyandiamide interphases using surface-enhanced Raman scattering
[AD-A215894] 10 p1353 N90-17846
Surface-enhanced Raman scattering
[AD-A215976] 10 p1353 N90-17849
Surface-enhanced Raman scattering from model acrylic adhesive systems
[AD-A216117] 10 p1359 N90-17883
Polymerization of nitro compounds on silver surfaces during surface-enhanced Raman scattering
[AD-A216116] 11 p1489 N90-18569
Modelling Doppler broadening in Raman propagation
[DE90-008042] 13 p1789 N90-20269
Structural comparison of nickel electrodes and precursor phases 13 p1824 N90-20472
Relativistic stimulated Brillouin and Raman scattering in a laser-produced plasma
[DE90-613123] 14 p2028 N90-21627
High resolution stimulated Raman-Brillouin spectroscopy in gases and solids
[DE90-009535] 15 p2067 N90-21840
Brillouin gain spectroscopy in glasses and crystals
[DE90-009536] 15 p2067 N90-21841
Nonlinear spectroscopy of multicomponent droplets and 2- and 3-dimensional measurements in flames
[AD-A218569] 16 p2215 N90-22636
Low frequency Raman spectra of liquid water, a molecular dynamics simulation
[PREPRINT-698] 16 p2314 N90-23192
An examination of the relationship between SERS intensities and surface concentration for pyridine adsorbed at the gold/aqueous solution interface
[AD-A219520] 17 p2372 N90-23505
Estimation of the concentration-distance profile within the electrochemical diffusion layer by Raman microprobe spectroscopy
[AD-A219521] 17 p2372 N90-23506
DURIP: Spontaneous Raman system for the study of enhanced combustion and non-thermal plasmas
[AD-A221410] 18 p2564 N90-24629
Molecular structure of interphases between DGEBA/BTDA adhesives and silver substances using surface-enhanced Raman scattering
[AD-A222750] 20 p2841 N90-26157
Analysis of turbulent density fluctuations by means of spontaneous Raman diffusion
[ISL-R-103/89] 20 p2863 N90-26287
Development of eye-safe lidar for aerosol measurements
[NASA-CR-186905] 20 p2901 N90-26503
Raman scattering measurements using UV excimer lasers 21 p2974 N90-26902
Concentration, temperature, and density in a hydrogen-air flame by excimer-induced Raman scattering 21 p2974 N90-26903
Characterization of polymer interphases using surface-enhanced Raman scattering
[AD-A223103] 21 p2985 N90-26965
Characterization of PMDI/HOPG interfaces by SERS using a silver overlayer configuration
[AD-A223104] 21 p2985 N90-26966
Non-destructive characterization of polymer/metal interfaces using Surface-Enhanced Raman Scattering (SERS)
[AD-A223105] 21 p2986 N90-26967
Characterization of model polyimide/silver interphases using surface-enhanced Raman scattering
[AD-A222488] 21 p2988 N90-26979
Non-destructive characterization of polymer/metal interphases using surface-enhanced Raman scattering
[AD-A222490] 21 p2988 N90-26980
Beam combining of excimer lasers by stimulated Raman scattering
[AD-A222973] 21 p3008 N90-27099
High intensity effects in Raman scattering
[DE90-012093] 21 p3076 N90-27486
The possible presence of interstellar PAHs in meteorites and interplanetary dust particles 21 p3092 N90-27579
Raman spectroscopic studies of carbon in extra-terrestrial materials 21 p3095 N90-27589
Feasibility of the temperature measurements in hypersonic flow by multibeam coherent Raman anti-Stokes scattering
[ONERA-RF-56/7131-PY] 24 p3419 N90-29312
CARS spectroscopy and applications 24 p3420 N90-29321
Study of hot carrier relaxation in quantum wells by subpicosecond Raman scattering
[DE90-015635] 24 p3554 N90-30107

RAMAN SPECTROSCOPY
Raman characterization of high temperature materials using an imaging detector
[DE89-016308] 01 p0040 N90-10219
Raman spectroscopic study of the rare earth sesquisulfides
[AD-A210610] 01 p0041 N90-10226
Pressure induced resonance Raman effects in shocked carbon disulfide
[AD-A210665] 02 p0194 N90-11107
Laser Raman spectroscopy: A literature review
[FOA-C-20753-2.3] 02 p0196 N90-11121
Volumetric analysis by spontaneous Raman diffusion in a supersonic wind tunnel
[ISL-R-109/88] 04 p0448 N90-12564
Fundamental molecular data to support CARS diagnostics of temperature, pressure, and species concentration
[AD-A212411] 04 p0472 N90-12704
Ion beam analysis of diffusion in polymer glasses
[AD-A212339] 04 p0480 N90-12756
Study of the hydroxyl radical by DRASC resonance in a high pressure flame --- Diffusion Raman Anti-Stokes Coherence (DRASC)
[ONERA-RS-53/7131-PY] 05 p0622 N90-13632
Laser Raman spectroscopy in studies of corrosion and electrocatalysis
[DE90-001414] 06 p0741 N90-14311
Raman spectroscopic analysis of impregnated cathodes
[AD-A214559] 09 p1190 N90-16895
A feasibility study for using CARS in temperature and volumetric measurement as a function of time
[ISL-CO-223/88] 09 p1226 N90-17116
Surface-enhanced Raman scattering
[AD-A215976] 10 p1353 N90-17849
Investigation of a simulated tritium plasma using Coherent Anti-Stokes Raman Spectroscopy (CARS)
[DE90-005696] 12 p1622 N90-19319
Spatially high-resolution flame diagnosis by means of spontaneous Raman spectroscopy
[ETN-90-95870] 12 p1623 N90-19328
Research investigation directed toward extending the useful range of the electromagnetic spectrum
[AD-A217450] 13 p1789 N90-20267
Electrochemical, in situ Raman spectroscopic, and conductivity studies of polypyrrole incorporating large size anions: Conducting nature of reduced form
[AD-A222739] 20 p2831 N90-26102
Short-range structure of fluorine-modified phosphate glass
[DE90-013494] 20 p2839 N90-26145
Study of the radical OH in a high pressure flame by resonant DRASC
[ONERA-RF-57/7131-PY] 23 p3305 N90-28692
Investigation of particulate formation during diesel spray combustion
[DE90-012682] 24 p3446 N90-29464

RAMJET ENGINES
NT SUPERSONIC COMBUSTION RAMJET ENGINES
NT TURBORAMJET ENGINES
Recent developments in Ramjet pressure oscillation technology 01 p0036 N90-10199
Numerical simulation of pressure oscillations in a ramjet combustor 01 p0037 N90-10202
Very-low-frequency oscillations in liquid-fueled ramjets 01 p0037 N90-10204
Acoustic-vortex-chemical interactions in an idealized ramjet 01 p0037 N90-10206
A simulator for a hydrocarbon ramrocket fuel gas generator: First phase development
[AR-005-621] 02 p0189 N90-11080
Computation of ramjet internal flowfields
[AD-A212001] 03 p0307 N90-11743
Analytical studies of three-dimensional combustion processes
[AD-A211903] 03 p0323 N90-11837
Apparatus for cooling electronic components in aircraft
[AD-D014207] 05 p0579 N90-13373
Acoustic-vortical-combustion interaction in a solid fuel ramjet simulator 06 p0726 N90-14234
Investigation of combustion instability in ramjet combustors 06 p0739 N90-14303
External flow computations for a finned 60mm ramjet in steady supersonic flight
[AD-A216998] 12 p1605 N90-19233
Modification and improvement of software for modeling multidimensional reacting fuel flows
[AD-A217789] 13 p1783 N90-20235
Concentric layer ramjet fuel
[AD-D014443] 14 p1941 N90-21111
Metallized fuel particle size study in a solid fuel ramjet
[AD-A220079] 18 p2533 N90-24451
From 1959-1989: 30 years of service experience with ramjets
[PNR90677] 19 p2660 N90-25139
Gas Turbine Combustion, volume 1
[VKI-LS-1990-02-VOL-1] 20 p2810 N90-25985
Liquid fueled ramjet combustion instability: Acoustical and vortical interactions with burning sprays
[AD-A222752] 20 p2831 N90-26104
Ramjet and ramrocket propulsion systems for missiles 21 p2973 N90-26897
The 26th JANNAF Combustion Meeting, volume 1
[CPIA-PUBL-529-VOL-1] 22 p3161 N90-27927
Regression and combustion characteristics of boron containing fuels for solid fuel ramjets 22 p3161 N90-27928
Calculation of the combustion distribution in a liquid-fuel ramjet 22 p3162 N90-27931
Entropy wave instability in compact ramjets 22 p3162 N90-27932
An investigation of solid-fuel, dual-mode combustion ramjets 22 p3162 N90-27933
Numerical simulations of flowfields in a central-dump ramjet combustor. 3: Effects of chemistry
[AD-A224145] 23 p3282 N90-28573
Solid fuel combustion chamber
[LR-634] 24 p3441 N90-29433

RAMJET MISSILES
Steady flow combustion model for solid-fuel ramjet projectiles
[BRL-TR-2987] 07 p0893 N90-15163

RANDOM ACCESS
Computational complexity of random access models
[AD-A217685] 13 p1865 N90-20701
CSMA/RN: A universal protocol for gigabit networks 15 p2150 N90-22280
Fairness problems at the media access level for high-speed networks 15 p2151 N90-22287
Locality in parallel computation
[AD-A218733] 16 p2302 N90-23120

RANDOM ACCESS MEMORY
Performance analysis of hybrid ARQ protocols in a slotted code division multiple-access network
[AD-A211078] 02 p0213 N90-11219
Efficient on-line simulations of tree machines and multidimensional turing machines by random access machines
[AD-A213152] 05 p0680 N90-13960
Marginal test and analysis of DRAM with masked alpha radiation
[RB-4180] 12 p1699 N90-19754
Random access transmission algorithms for data local area networks
[AD-A216443] 12 p1700 N90-19761
Computational complexity of random access models
[AD-A217685] 13 p1865 N90-20701
A study of caching in capability computers
[RSRE-89015] 15 p2149 N90-22276
Self-checking on-line testable static RAM
[NASA-CASE-NPO-17939-1-CU] 20 p2904 N90-26518
High speed magneto-resistive random access memory
[NASA-CASE-NPO-17954-1-CU] 20 p2904 N90-26519
Bloch-line memory element and RAM memory
[AD-D014488] 22 p3234 N90-28340

RANDOM DISTRIBUTIONS
U STATISTICAL DISTRIBUTIONS

RANDOM ERRORS
On the decoder error probability of linear codes 04 p0486 N90-12793
Electron beam propagation through a magnetic wiggler with random field errors
[AD-A212705] 04 p0498 N90-12867
The use of local polynomial approximations in a knot-placement strategy for least squares spline fitting
[NPL-DITC-148/89] 15 p2162 N90-22355

RANDOM LOADS
NT GUST LOADS

RANDOM NOISE
NT RANDOM SIGNALS
Performance of the split-symbol moments SNR estimator in the presence of inter-symbol interference 04 p0487 N90-12799

Information capacity of the matched Gaussian channel with jamming. 1: Finite-dimensional channel
[AD-A214782] 09 p1205 N90-16984
Results on the detection of signals in spherically invariant random noise
[AD-A214933] 09 p1206 N90-16988
Coding capacity for a class of additive channels
[AD-A215054] 09 p1206 N90-16993
Information capacity of the stationary Gaussian channel
[AD-A215408] 09 p1207 N90-16998
Absolute continuity and mutual information for Gaussian mixtures
[AD-A215185] 09 p1274 N90-17383
Two dimensional modifications of Gaussian laser light bundles
[AD-A215207] 10 p1389 N90-18033
Adaptive state estimation and sampling rate analysis for invariant linear dynamic systems in time
[INPE-4960-TDL/389] 11 p1554 N90-18951
Effective techniques for the identification and accommodation of disturbances
14 p1934 N90-21072
Active control of multi-dimensional random sound in ducts
[NASA-TM-102653] 14 p2024 N90-21603
Parallel and vector computation for stochastic optimal control applications 16 p2282 N90-23007
Universal criteria for blind deconvolution
[AD-A220853] 17 p2465 N90-24087
Multiple-access techniques for communication over dispersive radio channels 20 p2848 N90-26196
Control of orbiting large space structural systems with discrete time observational data and random measurement noise
[AD-A222476] 21 p2967 N90-26863
Statistical methodologies for non-Gaussian noisy environments
[AD-A222137] 21 p3066 N90-27433

RANDOM NUMBERS
On the structure of Mandelbrot's percolation process and other random Cantor sets
[REPT-89-54] 15 p2163 N90-22362
On randomness of random number generators
[MEMO-COSOR-89-20] 16 p2308 N90-23151
Long period pseudo random number sequence generator
[NASA-CASE-NPO-17241-1-CU]
17 p2394 N90-23636
STATLIB: NSWC library of statistical programs and subroutines
[AD-A221538] 21 p3055 N90-27370

RANDOM PROCESSES
NT RANDOM WALK
Stopping rules for a class of random methods for detecting necessary linear inequality constraints
[MEMO-777] 05 p0683 N90-13977
Random Markov processes and uniform martingales
[CWI-BS-R8908] 05 p0690 N90-14021
Algorithmic randomness, physical entropy, measurements, and the second law
[DE90-002413] 06 p0830 N90-14823
Location of interior impact source in randomly excited structures
[DE90-001092] 07 p0945 N90-15474
Numerical solution to the problem of criticality by Monte Carlo method
[DE90-608886] 12 p1708 N90-19808
On randomness of random number generators
[MEMO-COSOR-89-20] 16 p2308 N90-23151
Control of randomly sampled robotic systems
[AD-A218948] 16 p2309 N90-23157
A white noise theory of infinite dimensional calculus
[AD-A221253] 18 p2607 N90-24850

RANDOM SAMPLING
Multi-sample functional statistical data analysis
[AD-A210992] 01 p0117 N90-10673
Slow sampling and stability of nonlinear sampled-data systems
[RR-342] 03 p0398 N90-12277
A logic for the pixel assignment step of imagery classification predicated on class structure
07 p0949 N90-15493
Uniform versus random sampling in physical calculations: Monte Carlo
[DE90-003247] 07 p0986 N90-15696
Laboratory techniques for the characterisation of snow structures 12 p1741 N90-20007
Counting and reporting intersections in arrangements of line segments
[RUU-CS-89-12] 18 p2601 N90-24808
On the stability of robotic systems with random communication rates 24 p3514 N90-29865

RANDOM SIGNALS
Kreim factorization of covariance operators of 2-parameter random fields and application to the likelihood ratio
[MEMO-802] 11 p1555 N90-18953
Time-varying filter modelling and time-frequency characterisation of nonstationary sound fields due to a moving source 16 p2312 N90-23178

RANDOM VARIABLES
Asymptotic robustness in regression and autoregression based on Lindeberg conditions
[AD-A210725] 01 p0114 N90-10654
Markov chain moment formulas for regenerative simulation
[AD-A210684] 01 p0116 N90-10667
Fast computation using faulty hypercubes
[AD-A211910] 03 p0393 N90-12238
Domain of attraction of an operator between supremum and sum
[REPT-89-05] 04 p0539 N90-13119
Tail triviality for sums of stationary random variables
[CWI-MS-R8810] 04 p0542 N90-13143
Strong moderate deviation theorems for m-dependent random variables
[AD-A212618] 04 p0546 N90-13173
Random truncation models and Markov processes
[CWI-MS-R8817] 04 p0547 N90-13181
Distribution of a sum of n random variables and a central limit theorem based on moments or on coefficients of polynomial dependence
[IMAG-RR-768-M] 05 p0692 N90-14040
Self-decomposable distributions and branching processes
[MEMO-COSOR-89-06] 05 p0693 N90-14052
Note on Urbanik's class L(sub n) --- self-decomposability of functions
[MEMO-COSOR-89-07] 05 p0694 N90-14053
Reverse self-decomposability --- for characteristic functions
[MEMO-COSOR-89-08] 05 p0694 N90-14054
Strong large deviation and local limit theorems
[AD-A213610] 07 p0986 N90-15698
Statistics of a chi-square random variable obtained from independent Gaussian samples with a non-zero mean and arbitrary variance
[AD-A214477] 09 p1275 N90-17392
Use of Coxian-type distributions in a general model of the maximum of bivariate random variables
[PB90-121229] 12 p1704 N90-19780
Dynamic response of structures with uncertain parameters 15 p2119 N90-22125
On rates of convergence and asymptotic normality in the multiknapsack problem
[CWI-BS-R8912] 17 p2460 N90-24045
The Trickett-Welch Solution to the Behrens-Fisher problem applied to one-sided tolerance limits for random effects model
[AD-A220416] 17 p2465 N90-24086
Review of probabilistic analysis of dynamic response of systems with random parameters
[NASA-CR-186171] 18 p2568 N90-24636
The effect of random variations of radiosonde data on the predicted FLIR performance calculated by the program UFLR
[AD-A220034] 18 p2615 N90-24896
Dichotomies for certain product measures and stable processes
[AD-A222568] 20 p2921 N90-26621
Effects of parameter uncertainties on software development effort estimates
[AD-A223304] 24 p3526 N90-29938

RANDOM VIBRATION
The 59th Shock and Vibration Symposium, volume 1
[AD-A214578] 09 p1238 N90-17183
Use of chaotic and random vibrations to generate high frequency test inputs. Part 2: Chaotic vibrations
[DE90-007153] 12 p1676 N90-19627
Use of chaotic and random vibrations to generate high frequency test inputs
[DE90-007412] 12 p1678 N90-19628
Probabilistic analysis of bladed turbine disks and the effect of mistuning
[NASA-TM-102564] 15 p2072 N90-21871
Random vibration analysis of space flight hardware using NASTRAN 18 p2570 N90-24645
Stochastic structural dynamics for aerospace applications
[AD-A221517] 21 p3013 N90-27133

RANDOM WALK
A long time tail for random walk in random scenery
[REPT-89-08] 03 p0398 N90-12278
Electron beam propagation through a magnetic wiggler with random field errors
[AD-A212705] 04 p0498 N90-12867
A diffusion on a fractal state space
[AD-A213555] 07 p0988 N90-15707
The effects of wiggler errors on free electron laser performance
[AD-A220421] 17 p2409 N90-23725
On a class of N-dimensional associated random walks and the hitting point identity
[CWI-BS-R8911] 17 p2466 N90-24090
Associated distributions in the analysis of two-dimensional random walks
[CWI-BS-R8917] 17 p2466 N90-24095
Diffusion in lattices with anisotropic scatterers
[CWI-AM-R8921] 18 p2599 N90-24792
A Markov chain identity and monotonicity of the diffusion constants for a random walk in a heterogeneous environment
[CWI-AM-R8917] 18 p2605 N90-24839
Particle tracking methods and fractal statistics in groundwater modeling 19 p2691 N90-25309

RANGE (EXTREMES)
NT FREQUENCY RANGES
NT PROPORTIONAL LIMIT
Are ozone exceedance rates decreasing. Comment on extreme value analysis of environmental time-series: An application to trend detection in ground-level ozone
[AD-A211029] 02 p0239 N90-11357
A closer look at the visioceilometer
[FEL-1989-80] 03 p0374 N90-12138
The regular indefinite linear quadratic problem with linear endpoint constraints
[MEMO-COSOR-88-15] 05 p0690 N90-14022
Convergence properties of indefinite linear quadratic problems with receding horizon
[MEMO-COSOR-88-25] 05 p0690 N90-14026

RANGE AND RANGE RATE TRACKING
Precision of semi-geometrically determined SLR baselines vs. site occupation time
[ETN-90-96007] 05 p0665 N90-13885
Normal points: Compression of satellite laser ranging data
[ETN-90-96008] 05 p0707 N90-14145
An improved model for the Earth's gravity field
13 p1832 N90-20515
Preliminary error budget for an optical ranging system: Range, range rate, and differenced range observables
20 p2853 N90-26227

RANGE CONTROL
U TRAJECTORY CONTROL

RANGE ERRORS
M-estimators in linear models with long range dependent errors
[AD-A219921] 17 p2461 N90-24053

RANGE FINDERS
NT LASER RANGE FINDERS
On-line range prediction system, part 2
[NASA-CR-185889] 05 p0647 N90-13771
Outline on the future Italian transportable laser ranging station
[CISE-4845] 05 p0649 N90-13782
Vision science and technology for supervised intelligent space robots 15 p2139 N90-22221
Observability of relative navigation using range-only measurements 24 p3427 N90-29360

RANGE INDICATORS
U RANGE FINDERS

RANGE MEASUREMENT
U RANGEFINDING

RANGEFINDING
NT LUNAR RANGEFINDING
NT SOUND RANGING
Laser techniques for ground to air applications
[FOA-C-30524-3.1] 02 p0228 N90-11309
Discrete filtering techniques applied to sequential GPS range measurements
[NASA-CR-177472] 03 p0305 N90-11730
A modern trans-ionospheric propagation sensing system 06 p0761 N90-14430
Programmable near-infrared ranging system
[AD-D014237] 06 p0843 N90-14903
China-built airborne synchronous laser ranger the new L-8 jet trainer aircraft
[AD-A213835] 07 p0936 N90-15422
MT's algorithm: A new algorithm to search for the optimum set of modulation indices for simultaneous range, command, and telemetry
[NASA-CR-186259] 08 p1057 N90-16110
Parallel algorithm for determining motion vectors in ice floe images by matching edge features
08 p1114 N90-16451
On the range resolution of point targets with FMCW radar systems
[DLR-FB-89-47] 11 p1499 N90-18629
Improved ranging systems 12 p1735 N90-19973
Multi-dimensional LADAR tracking and adaptive grasping for spaceborne assembly of SDI (Strategic Defense Initiative) platforms
[AD-A218236] 13 p1791 N90-20279

An assessment of the potential of continuous-wave ranging for measuring the distance to a highly reflective, infinite sheet
[NASA-TM-101680] 14 p1969 N90-21279
Development of a dynamic modeling technique and its application to the analysis and control of a high-precision robotic manipulator 14 p1987 N90-21391
Minimizing the effects of the atmosphere in the observation of ultraviolet radiation 15 p2080 N90-21911
The optical night sky at low surface brightness: High latitude dust and faint field galaxies 15 p2185 N90-22481
Remote operation of an orbital maneuvering vehicle in simulated docking maneuvers 19 p2736 N90-25554
Preliminary error budget for an optical ranging system: Range, range rate, and differenced range observables 20 p2853 N90-26227
The application of SAW devices in expanded frequency spectrum communications
[AD-A222958] 21 p2994 N90-27021
Program to perform research on use of lidar for range resolved turbulence measurements
[AD-A222189] 21 p3026 N90-27204
Velocity filtering applied to optical flow calculations
[NASA-TM-102802] 23 p3271 N90-28512
A fast lightstripe rangefinding system with smart VLSI sensor 23 p3366 N90-29019
A laser tracking dynamic robot metrology instrument 23 p3366 N90-29021
Techniques for autonomous GPS integrity monitoring 24 p3424 N90-29345
The determination of PDOP (Position Dilution of Precision) in GPS 24 p3425 N90-29351
JTIDS relative navigation: Principles, architecture, and inertial mixing 24 p3426 N90-29357

RANGES (FACILITIES)
NT BALLISTIC RANGES
NT TEST RANGES
Research and test facilities for development of technologies and experiments with commercial applications
[NASA-TM-101789] 02 p0159 N90-10909

RANGING
U RANGEFINDING

RANK TESTS
Asymptotic expansions for two-stage rank tests
[MEMO-773] 04 p0544 N90-13161
A graph theoretic characterization for the rank of the transfer matrix of a structured system
[CWI-OS-R8819] 05 p0695 N90-14064

RANKINE CYCLE
Shock induced disasociation of polyethylene
[DE89-016983] 02 p0221 N90-11267
The nuclear battery
[DE90-630400] 24 p3462 N90-29559

RANKINE-HUGONIOT RELATION
Theoretical Hugoniot of liquid hydrogen fluoride
[DE89-016504] 02 p0193 N90-11099
Estimation of the C-J pressure of explosives
[DE89-013811] 02 p0208 N90-11187
Projectile impact Hugoniot parameters for selected materials
[DE90-000891] 06 p0793 N90-14618
Interaction of minor ions with fast and slow shocks
[NASA-CR-186372] 11 p1594 N90-19181
Laser-induced shock waves effects in materials
[DE90-007626] 13 p1807 N90-20379

RANKING
Studies in estimation theory, applications and implementations
[AD-A210712] 01 p0114 N90-10653
On a classification problem: Ranking and selection approach
[AD-A211627] 03 p0397 N90-12269
Case tool evaluation system
[DE90-003696] 08 p1108 N90-16413
Ranking intervals under visibility constraints
[RUU-CS-89-18] 18 p2602 N90-24812
Nonparametric selection, ranking and testing
[AD-A219254] 19 p2752 N90-25636
Establishing viable task domains for telerobot demonstrations 24 p3518 N90-29886

RAPCON (CONTROL)
U RADAR APPROACH CONTROL

RAPID EYE MOVEMENT STATE
Test-retest reliability of oxford Medilog 9000 sleep recording and SS-90-3 sleep stage scoring
[AD-A211165] 02 p0254 N90-11440

RAPID QUENCHING (METALLURGY)
Establishment and initial operation of a resource facility for RSR (Rapid Solidification Rate) processed alloys in pilot quantities
[AD-A210389] 01 p0050 N90-10283
Kinetic processes in advanced alloys
[AD-A212049] 03 p0329 N90-11867
Production and processing of Cu-Cr-Nb alloys
[NASA-TM-102495] 08 p1047 N90-16053
Rapid solidification processing of composites
[AD-A215175] 09 p1187 N90-16875
Superconducting Bi1.5Pb0.5Sr2Ca2Cu3O(x) ceramics by rapid melt quenching and glass crystallization
[NASA-CR-185184] 09 p1288 N90-17465
Evolution of structure and electrical properties during crystallization of rapidly solidified Bi4Ti3O12
[DE90-005221] 09 p1292 N90-17492
Undercooling and nucleation in rapid solidification rate metal powders using solid in solid emulsification
[AD-A218527] 17 p2375 N90-23526

RAPID SOLIDIFICATION
U RAPID QUENCHING (METALLURGY)
U SOLIDIFICATION

RAPID TRANSIT SYSTEMS
California air transportation study: A transportation system for the California Corridor of the year 2010
[NASA-CR-186219] 06 p0722 N90-14212
Markets for high-speed intercity Maglev technology: A systems analysis approach
[DE89-017683] 06 p0794 N90-14623

RARE EARTH ALLOYS
NT ERBIUM ALLOYS
NT LANTHANUM ALLOYS
Anisotropy and microstructure of high-coercivity rare earth permanent magnets
[AD-A211905] 03 p0399 N90-12285
High power transducers
[AD-D014225] 06 p0767 N90-14461
Anisotropy and microstructure of high coercivity rare earth iron permanent magnets, list of papers published
[AD-A214160] 08 p1118 N90-16476
Fundamental studies of new magnetic heterostructures: Their growth, crystallographic structure, magnetic, and electronic properties
[DE90-007381] 11 p1572 N90-19053
Fifth-order aberrations in magnetic quadrupole-octupole systems
[DE90-007489] 12 p1712 N90-19831

RARE EARTH COMPOUNDS
NT CERIUM COMPOUNDS
NT CERIUM OXIDES
NT DYSPROSIUM COMPOUNDS
NT NEODYMIUM COMPOUNDS
NT TERBIUM COMPOUNDS
NT YTTERBIUM COMPOUNDS
Graduate fellowships in the field of hard magnetic materials
[AD-A212303] 04 p0477 N90-12733
Thermodynamic properties of some metal oxide-zirconia systems
[NASA-TM-102351] 05 p0628 N90-13666
A new approach for the utilization of electron paramagnetic resonance and an investigation of copper oxide superconductors
[AD-A213833] 09 p1277 N90-17404
Luminescence of lanthanides and actinides implanted into binary III-V semiconductors and AlGaAs
[AD-A215759] 11 p1569 N90-19031
Magnetic hardening studies and novel techniques for preparation of high performance magnets
[AD-A217737] 13 p1881 N90-20790
Fundamental studies of strongly magnetic rare earth-transition metal alloys
[DE90-012458] 21 p2960 N90-26937
Metallurgical processes in multi-component rare Earth-transition metal permanent magnet alloys
[AD-A222891] 21 p2982 N90-26942

RARE EARTH ELEMENTS
NT CERIUM
NT ERBIUM
NT ERBIUM ISOTOPES
NT EUROPIUM ISOTOPES
NT GADOLINIUM ISOTOPES
NT HOLMIUM
NT LANTHANUM
NT LANTHANUM ISOTOPES
NT NEODYMIUM
NT PRASEODYMIUM
NT SCANDIUM
NT TERBIUM
NT THULIUM
NT YTTERBIUM
NT YTTRIUM
A review of the literature on the toxicity of rare-earth metals as it pertains to the engineering demonstration system surrogate testing
[DE90-008049] 13 p1851 N90-20620
Excitation of hypersound at boundary between Type-2 superconductor and a concentrated paramagnetic compound 16 p2310 N90-23164
Formation of high Tc superconducting films by organometallic chemical vapor deposition
[AD-D014498] 19 p2760 N90-25682
Photoelectron spectroscopy at limit surfaces of semiconductors with rare Earth and alkali metals
[ETN-90-97322] 22 p3249 N90-28427

RARE GAS-HALIDE LASERS
NT KRYPTON FLUORIDE LASERS
NT XENON CHLORIDE LASERS
NT XENON FLUORIDE LASERS
Elements of a 200 watt pulsed excimer laser 02 p0226 N90-11295

RARE GASES
NT ARGON
NT HELIUM
NT HELIUM ISOTOPES
NT KRYPTON
NT KRYPTON ISOTOPES
NT KRYPTON 85
NT LIQUID HELIUM
NT LIQUID HELIUM 2
NT NEON
NT RADON
NT RADON ISOTOPES
NT XENON
Dissociation and vibrational relaxation of XeF by various collision partners
[AD-A210769] 02 p0227 N90-11300
A nonlinear-optical method for combining high power laser beams
[AD-A211730] 03 p0354 N90-12022
Structural peculiarities and molecular properties of charge complexes formed on positive ion injection into dense inert gas media
[DE89-633953] 06 p0839 N90-14877
Excimer emission from alkali diatomic and alkaline-earth-noble-gas molecules
[AD-A214246] 07 p0896 N90-15179
Absorption experiments on electron-beam pumped rare gases
[DE90-006504] 11 p1515 N90-18722
Angular correlation studies in noble gases 11 p1557 N90-18972
Positron-inert gas differential elastic scattering 11 p1558 N90-18974
Absolute cross-sections for dissociative electron attachment in O2 condensed on Kr films
[AD-A216730] 11 p1570 N90-19038
Electron stimulated O(-) desorption from O2 condensed on a rare-gas film: Evidence for an indirect Bounce trajectory
[AD-A216725] 12 p1622 N90-19322
LLE review
[DE90-008958] 14 p1985 N90-21378
Requirements for long-life operation of inert gas hollow cathodes: Preliminary report
[NASA-TM-103242] 22 p3134 N90-27783
An electron spin resonance study of adsorbed gases in ultrahigh vacuum
[ETN-90-97323] 24 p3447 N90-29469

RAREFACTION
Experimental techniques in the field of low density aerodynamics
[AGARD-AG-318(FR)] 21 p2953 N90-26792

RAREFACTION WAVES
U ELASTIC WAVES

RAREFIED GAS DYNAMICS
Computational fluid dynamics
[NASA-TM-102922] 09 p1216 N90-17052
Experimental techniques in the field of low density aerodynamics
[AGARD-AG-318(FR)] 21 p2953 N90-26792
Electron beam for velocity determination 24 p3420 N90-29319

RAREFIED GASES
NT COSMIC GASES
NT INTERSTELLAR GAS
The aerodynamic characteristics of power-law bodies in continuum and transitional hypersonic flow
[RAE-TM-AERO-2164] 16 p2196 N90-22537

RASERS
U MASERS

RASTER SCANNING
Basic program for raster scan display unit
[NAL-TM-560] 03 p0384 N90-12185
Rotating-unbalanced-mass devices and methods for scanning balloon-borne-experiments, free-flying spacecraft, and space shuttle/space station attached experiments
[NASA-CASE-MFS-28425-1] 20 p2865 N90-26304
Fast interactive image generation of line and surface oriented objects in raster systems
[ETN-90-97290] 23 p3381 N90-29102

RATE METERS
U MEASURING INSTRUMENTS

RATES (PER TIME)
NT ACCELERATION (PHYSICS)
NT ACOUSTIC VELOCITY
NT AIRSPEED

NT ANGULAR ACCELERATION
NT ANGULAR VELOCITY
NT BIT ERROR RATE
NT BURNING RATE
NT COLLISION PARAMETERS
NT COLLISION RATES
NT CRITICAL VELOCITY
NT CURRENT DENSITY
NT DECAY RATES
NT DECELERATION
NT DRIFT RATE
NT ELECTRON ACCELERATION
NT EVAPORATION RATE
NT EXHAUST VELOCITY
NT FLOW VELOCITY
NT FLUX (RATE)
NT FLUX DENSITY
NT GROUND SPEED
NT GROUP VELOCITY
NT HEART RATE
NT HEAT FLUX
NT HIGH ACCELERATION
NT HIGH SPEED
NT HYPERSONIC SPEED
NT ILLUMINANCE
NT IMPACT ACCELERATION
NT ION PRODUCTION RATES
NT IRRADIANCE
NT LOADING RATE
NT LOW SPEED
NT LUMINANCE
NT LUMINOUS INTENSITY
NT MAGNETIC FLUX
NT MASS FLOW RATE
NT ORBITAL VELOCITY
NT PARTICLE ACCELERATION
NT PARTICLE FLUX DENSITY
NT PHASE VELOCITY
NT PHOTON DENSITY
NT PLASMA ACCELERATION
NT PROPAGATION VELOCITY
NT PROTON FLUX DENSITY
NT PULSE RATE
NT RADIAL VELOCITY
NT RADIANCE
NT RADIANT FLUX DENSITY
NT RECOMBINATION COEFFICIENT
NT RESPIRATORY RATE
NT ROTOR SPEED
NT SOLAR CONSTANT
NT SOLAR FLUX
NT SOLAR FLUX DENSITY
NT SOLAR WIND VELOCITY
NT SOUND INTENSITY
NT STRAIN ENERGY RELEASE RATE
NT STRAIN RATE
NT SUBSONIC SPEED
NT SUPERSONIC SPEED
NT TIP SPEED
NT TRANSONIC SPEED
NT TRANSVERSE ACCELERATION
NT WIND VELOCITY
NT ZERO SOUND

Spin-orbit relaxation rates of Bi(6p(3)) 2D(3/2) following photolysis of Bi(CH3)3 at lambda = 193 nm
[AD-A211792] 03 p0402 N90-12303

Micro-miniature roll rate sensor
[AD-A214778] 09 p1225 N90-17107

The strength of weak learnability
[AD-A216389] 10 p1420 N90-18190

Rate compatible punctured codes, their use in military satellite communication systems
[AD-A216723] 11 p1497 N90-18619

Research and development on enhanced degradable plastics
[AD-A217180] 13 p1779 N90-20212

Navigation experiment NAVEX: Measurements and performance of the spaceborne clocks
[DLR-FB-89-43] 18 p2555 N90-24580

Optical rate sensor algorithms
18 p2632 N90-24997

Estimation of defective rate of mechanic-hydraulic components
[ETN-90-97275] 21 p3011 N90-27120

Further experiments in variable frame rate analysis for speech recognition
[RSRE-MEMO-4336] 22 p3165 N90-27951

The influence of solidification rate on solute redistribution and second-phase formation in stainless steel alloys
[DE90-015189] 24 p3450 N90-29482

RATINGS

Insulation, compressibility and absorbency of dry suit undergarments
[AD-A215944] 10 p1414 N90-18149

Proceedings of a workshop on Future Airport Passenger Terminals
[PB90-213620] 23 p3284 N90-28580

RATIONS

Air Force flight feeding. Volume 1: Evaluation of current system and alternative concepts
[AD-A212789] 04 p0527 N90-13043

Physical performance and carbohydrate consumption in CF commandos during a 5-day field trial
[AD-A217204] 13 p1850 N90-20619

RATIOS

NT ASPECT RATIO
NT COMPRESSION RATIO
NT DIMENSIONLESS NUMBERS
NT FUEL-AIR RATIO
NT HIGH ASPECT RATIO
NT HIGH REYNOLDS NUMBER
NT INDEXES (RATIOS)
NT KP INDEX
NT LIFT DRAG RATIO
NT LOW ASPECT RATIO
NT LOW REYNOLDS NUMBER
NT MACH NUMBER
NT MASS RATIOS
NT MASS TO LIGHT RATIOS
NT POISSON RATIO
NT PRANDTL NUMBER
NT PRESSURE RATIO
NT RAYLEIGH NUMBER
NT REYNOLDS NUMBER
NT SCHMIDT NUMBER
NT SIGNAL TO NOISE RATIOS
NT SIMILARITY NUMBERS
NT STRESS RATIO
NT STROUHAL NUMBER
NT THICKNESS RATIO

Synthesis and physical properties of poly(perfluoroalkylether) urethanes
[AD-A210500] 01 p0050 N90-10287

Comets: Dirty snowballs or icy dirtballs
12 p1739 N90-19994

RATS

Acute oral toxicity of DIGL-RP solid propellant in Sprague-Dawley rats
[AD-A217712] 13 p1849 N90-20614

Biological effects of ELF (Extremely-Low-Frequency) electric and magnetic fields
[DE90-008634] 14 p2009 N90-21514

Excitatory and inhibitory backward conditioning in the rat 15 p2135 N90-22204

Heat exhaustion in a rat model: Lithium as a biochemical probe
[AD-A219361] 16 p2260 N90-22884

Effects of microgravity on rat muscle
20 p2891 N90-26453

Effects of microgravity on rat bone, cartilage and connective tissues 20 p2891 N90-26454

Experiment K-6-01. Distribution and biochemistry of mineral and matrix in the femurs of rats
20 p2892 N90-26455

Experiment K-6-03. Gravity and skeletal growth, part 1. Part 2: Morphology and histochemistry of bone cells and vasculature of the tibia; Part 3: Nuclear volume analysis of osteoblast histogenesis in periodontal ligament cells; Part 4: Intervertebral disc swelling pressure associated with microgravity 20 p2892 N90-26457

Experiment K-6-04. Trace element balance in rats during spaceflight 20 p2892 N90-26458

Experiment K-6-05. The maturaton of bone and dentin matrices in rats flown on Cosmos 1887
20 p2893 N90-26459

Experiment K-6-06. Morphometric and EM analyses of tibial epiphyseal plates from Cosmos 1887 rats
20 p2893 N90-26460

Experiment K-6-08. Biochemical and histochemical observations of vastus medialis
20 p2893 N90-26462

Experiment K-6-09. Morphological and biochemical investigation of microgravity-induced nerve and muscle breakdown. Part 1: Investigation of nerve and muscle breakdown during spaceflight; Part 2: Biochemical analysis of EDL and PLT muscles 20 p2893 N90-26463

Experiment K-6-10. Effects of zero gravity on myofibril protein content and isomyosin distribution in rodent skeletal muscle 20 p2894 N90-26464

Experiment K-6-11. Actin mRNA and cytochrome c mRNA concentrations in the tricepts brachia muscle of rats 20 p2894 N90-26465

Experiment K-6-12. Morphometric studies of atrial or granules and hepatocytes. Part 1: Morphometric study of the liver; Part 2: The atrial granular accumulations
20 p2894 N90-26466

Experiment K-6-13. Morphological and biochemical examination of heart tissue. Part 1: Effects of microgravity on the myocardial fine structure of rats flown on Cosmos 1887. Ultrastructure studies. Part 2: Cellular distribution of cyclic ampdependent protein kinase regulatory subunits in heart muscle of rats flown on Cosmos 1887
20 p2894 N90-26467

Experiment K-6-14. Hepatic function in rats after spaceflight 20 p2895 N90-26468

Experiment K-6-16. Morphological examination of rat testes. The effect of Cosmos 1887 flight on spermatogonial population and testosterone level in rat testes
20 p2895 N90-26469

Experiment K-6-17. Structural changes and cell turnover in the rats small intestine induced by spaceflight
20 p2895 N90-26470

Experiment K-6-18. Study of muscarinic and gaba (benzodiazepine) receptors in the sensory-motor cortex, hippcampus and spinal code 20 p2895 N90-26471

Experiment K-6-19. Pineal physiology in microgravity: Relation to rat gonadal function
20 p2895 N90-26472

Experiment K-6-20. The effect of spaceflight on pituitary oxytocin and vasopressin content of rats
20 p2896 N90-26473

Experiment K-6-22. Growth hormone regulation, synthesis and secretion in microgravity. Part 1: Somatotroph physiology. Part 2: Immunohistochemical analysis of hypothalamic hormones. Part 3: Plasma analysis 20 p2896 N90-26475

Experiment K-6-23. Effect of spaceflight on levels and function of immune cells 20 p2897 N90-26476

RAWINSONDES

Preliminary comparison of temperature soundings obtained from simultaneous radiometric, radio-acoustic, and rawinsonde measurements
[PB90-119835] 11 p1535 N90-18838

RAY ACOUSTICS

U GEOMETRICAL ACOUSTICS

RAY OPTICS

U GEOMETRICAL OPTICS

RAY TRACING

Surface wave ray tracing and Ms:yield determination in a laterally heterogeneous earth
[AD-A210241] 01 p0090 N90-10516

A technique for the generation of range-height-angle charts
[AD-A214534] 09 p1204 N90-16979

Design of fiber optic probes for laser light scattering
09 p1222 N90-17090

Optimization of Gaussian beam widths in acoustic propagation
[AD-A215893] 10 p1427 N90-18231

Thermal radiation characteristics of nonisothermal cylindrical enclosures using a numerical ray tracing technique
[NASA-TM-102527] 14 p1972 N90-21296

Design and optimisation of thin foil x ray telescopes
14 p2038 N90-21690

The effects of caustics in acoustic inverse scattering experiments
[AD-A218454] 16 p2313 N90-23185

Some ray tracing problems related to circles and ellipses
[AD-A219306] 16 p2318 N90-23217

The Gauss beam method for surface waves. Theory and utilization for a lateral heterogeneous spheric Earth
[ETN-90-96492] 18 p2580 N90-24695

Intersecting line segments, ray shooting, and other applications of geometric partitioning techniques
[RUU-CS-88-26] 18 p2601 N90-24804

PTA en route noise measurements
18 p2608 N90-24855

A few modeling and rendering techniques for computer graphics and their implementation on ultra hardware
18 p2640 N90-25038

Combined electron cyclotron ray tracing and transport code studies in the compact ignition tokamak
[DE90-014097] 23 p3396 N90-29189

High power oblique incidence HF ionospheric modification
[AD-A224402] 24 p3491 N90-29729

Regional phase propagation in three dimensionally heterogeneous media
[AD-A223279] 24 p3491 N90-29731

Ray traced scalar fields with shaded polygonal output
[DE90-011023] 24 p3529 N90-29955

RAYLEIGH DISTRIBUTION

First-order intensity statistics for non-Rayleigh fading
[AD-A217572] 13 p1841 N90-20569

Diffusion in lattices with anisotropic scatterers
[CWI-AM-R8921] 18 p2599 N90-24792

RAYLEIGH EQUATIONS

Normal forms for weakly non-linear perturbed wave equations
[REPT-89-41] 15 p2161 N90-22343

RAYLEIGH NUMBER
A multigrid method combined with defect correction for free convection problems at high Rayleigh numbers
[REPT-89-27] 03 p0396 N90-12264
Experiments of thermoconvection in a cubic cell
[MPIS-6/1989] 12 p1661 N90-19544

RAYLEIGH SCATTERING
MEGALIDAR
[AD-A212074] 03 p0353 N90-12020
Spatial characteristics of airglow and solar scatter radiance from the earth's atmosphere
[AD-A211358] 03 p0372 N90-12126
Backscattering effects in DIAL due to water vapor
[SER-WISS-ABHANDL-89] 08 p1082 N90-16265
Advanced diagnostics for reacting flows
[AD-A214795] 09 p1285 N90-17448
Measurement of the stimulated thermal Rayleigh scattering instability
[DE90-007849] 13 p1807 N90-20376
Modelling UV-visible radiation observed from space 15 p2085 N90-21937
Quasi-static analysis of scattering from a chiral sphere
[PB90-189135] 22 p3164 N90-27943

RAYLEIGH WAVES
Surface wave ray tracing and Ms:yield determination in a laterally heterogeneous earth
[AD-A210241] 01 p0090 N90-10516
Investigations of Eurasian seismic sources and upper mantle structure
[AD-A211806] 03 p0371 N90-12120
Theoretical and experimental approach of wave phenomena in free jets
[ISL-CO-247/88] 09 p1219 N90-17069
The propagation of time harmonic Rayleigh-Lamb waves in a bimaterial plate
[AD-A216834] 11 p1519 N90-18749
Laser-induced shock waves effects in materials
[DE90-007626] 13 p1807 N90-20379
Normal forms for weakly non-linear perturbed wave equations
[REPT-89-41] 15 p2161 N90-22343
Study of a method for measuring the dimensions of cracks on the surface of ceramics by Rayleigh waves
[ETCA-89-R-024] 22 p3160 N90-27922
Characterization by ultrasonic tests of ceramics submitted to thermal shocks: influence of several parameters on the crack dimensioning
[ETCA-89-R-060] 22 p3160 N90-27923

RAYLEIGH-BENARD CONVECTION
Structures instabilities in filament liquid crystals
[ETN-90-95916] 12 p1721 N90-19888
Mass transfer induced convection near gas-liquid interfaces
[ETN-90-96925] 18 p2552 N90-24568

RAYLEIGH-RITZ METHOD
The Shock and Vibration Digest, volume 21, no. 10 04 p0483 N90-12771
The computer age and traditional approximate, analytical methods 04 p0483 N90-12772
The coupling effects of kinematics and flexibility on the Lagrangian dynamic formulation of open chain deformable links 16 p2284 N90-23018

RAYON
New Fabric Development Program
[AD-A211549] 03 p0332 N90-11891

RAYS
Ray shooting, implicit point location, and related queries in arrangements of segments
[RUU-CS-89-11] 18 p2601 N90-24807

RDX
An evaluation of ethylene-vinyl acetate copolymers as desensitizers for RDX in insensitive booster compositions prepared by slurry coating technology
[MRL-TR-89-33] 12 p1633 N90-19385
Condensed phase kinetic deuterium isotope effects in high energy phenomena: Mechanistic investigations and relationships
[AD-A217161] 13 p1770 N90-20156
Preparation, characterisation and cookoff behaviour of booster compositions prepared from RDX and acrylic or ethylene-vinyl acetate dispersions
[MRL-TR-89-44] 14 p1957 N90-21203
Study of the induction time in isothermal decomposition of explosives
[DE90-014906] 23 p3315 N90-28745

REACTANCE
A high frequency (20 kHz) power electronics reactive-current compensator with insulated gate bipolar transistors as semiconductor switches
[EMV-88-54] 17 p2399 N90-23665

REACTANCE AMPLIFIERS
U PARAMETRIC AMPLIFIERS

REACTION BONDING
Oxidation effects on the mechanical properties of SiC fiber-reinforced reaction-bonded silicon nitride matrix composites
[NASA-TM-102360] 06 p0736 N90-14287
Development of a reliable fabrication technique to produce intermetallic compounds
[AD-A215004] 09 p1194 N90-16918

REACTION JETS
U JET FLOW
U JET THRUST

REACTION KINETICS
Solvent effects on the kinetics of electroreduction of Cu(I) at mercury
[AD-A209423] 01 p0038 N90-10211
Potential dependence of the elementary steps in the kinetics of electrode reactions involving amalgam formation
[AD-A209424] 01 p0038 N90-10212
Reaction of oxygen with allene
[DE89-015219] 01 p0039 N90-10216
Direct numerical simulation of turbulent free shear flows
[AD-A210161] 01 p0040 N90-10218
Attenuated total reflection FTIR spectroscopy for measuring interfacial reaction kinetics at silica surfaces
[AD-A210314] 01 p0041 N90-10224
Free-expansion experiments and modeling in detonation: Chemistry and hydrodynamics on a laboratory scale
[DE89-007748] 01 p0053 N90-10302
Critical reaction rates in hypersonic combustion chemistry
[DE89-014278] 02 p0156 N90-10892
Simplified rate-law integration for reactions which are first order in each of two reactants
[NASA-CR-185408] 02 p0192 N90-11093
Time-resolved mass spectrometry technique for studying fast transient CHNO explosive decomposition kinetics
[DE89-016540] 02 p0193 N90-11101
Chemiluminescent ion-molecule reactions of group-3 ions with halogens: New optical spectra and reaction dynamics
[MPIS-18/1988] 02 p0196 N90-11120
Hydrogen-silicon carbide interactions
[NASA-TM-102382] 02 p0200 N90-11144
A shock initiation model for fine-grained hexanitrostilbene
[DE89-007641] 02 p0207 N90-11185
Shock initiation of LX-17 as a function of its initial temperature
[DE89-017730] 02 p0208 N90-11192
NCAR (National Center for Atmospheric Research) master mechanism of the gas phase chemistry, version 2.0
[PB89-208979] 02 p0249 N90-11413
Theoretical investigation of gas-surface interactions
[NASA-CR-185492] 02 p0272 N90-11552
Thermodynamics, kinetics, and interface morphologies of phase formation reactions between metals and Gallium Arsenide: Bulk vs thin-film studies
[DE89-016469] 02 p0284 N90-11621
Transport properties of thermally grown Cr2O3
[DE89-016703] 02 p0284 N90-11623
Natural gas to liquids
[DE89-000982] 03 p0322 N90-11828
Conversion of methane to liquid hydrocarbons
[DE89-017547] 03 p0322 N90-11831
Synthesis and chemistry of strained and conjugated fluorocarbons
[AD-A211633] 03 p0324 N90-11844
Mechanism of electrochemical activation of carbon electrodes: Role of graphite lattice defects
[AD-A211644] 03 p0325 N90-11845
Kinetic processes in advanced alloys
[AD-A212049] 03 p0329 N90-11867
Shock-induced reaction in several liquids
[DE89-016594] 03 p0346 N90-11973
VISAR wave profile measurements in supra-compressed HE
[DE89-017736] 03 p0346 N90-11976
Kinetics of diffusion-controlled reactions
[AD-A212161] 03 p0399 N90-12286
Spin-orbit relaxation rates of Bi(6p(3)) 2D(3/2) following photolysis of Bi(CH3)3 at lambda = 193 nm
[AD-A211792] 03 p0402 N90-12303
Measurement and correlation of the solubility and diffusion coefficient for oxygen and chlorine in basic hydrogen peroxide
[AD-A212348] 04 p0472 N90-12703
FLIC (FLame with Implicit Convection): A detailed, two-dimensional flame model
[AD-A212953] 04 p0473 N90-12710
Mechanisms of CO2 reduction metal and metal modified semiconductor electrodes
[AD-A213169] 04 p0473 N90-12712
An investigation of the irradiation swelling mechanisms in refractory metals at high temperatures
[AD-A211406] 04 p0474 N90-12719
Computer simulation studies of the catalytic oxidation of carbon monoxide on platinum metals
[PB89-223739] 04 p0475 N90-12721
Role of chemical effects in daytime high latitude trough formation
[AD-A211772] 04 p0518 N90-12989
Transport phenomena and interfacial kinetics in multiphase combustion systems
[AD-A212932] 05 p0621 N90-13620
Nucleation kinetics in undercooled, glass-forming metallic melts
[DLR-FB-89-32] 05 p0624 N90-13644
Physical phenomena and the microgravity response 05 p0677 N90-13945
Numerical modeling of supersonic turbulent reacting free shear layers 06 p0719 N90-14197
The thermally induced gas-phase reactions of methane and oxygen: A comparison of experimental and computational results
[DE90-000785] 06 p0742 N90-14317
Reactive flow measurements and calculations for ZrH2-based composite explosives
[DE90-000831] 06 p0755 N90-14393
Fast transit gas- and condensed-phase chemistry of energetic materials
[DE90-001656] 06 p0755 N90-14395
Effect of community structure on the kinetics of anaerobic degradation of aromatic compounds
[DE90-003666] 07 p0888 N90-15134
Theoretical methods for the study of chemical dynamics
[DE90-003122] 07 p0893 N90-15160
Shock tube ignition of octanes
[DE90-001167] 07 p0893 N90-15164
Mechanistic modeling of epoxy resins
[DE89-015119] 07 p0908 N90-15247
Burning rates of two cast nitramine explosives using a hybrid closed bomb-strand burner
[DE90-002785] 07 p0914 N90-15286
Comparison of engine knock predictions using a fully-detailed and a reduced chemical kinetic mechanism
[DE90-002805] 07 p0941 N90-15448
Dynamics of electron transfer for a nonsuperexchange coherent mechanism, 1
[AD-A213450] 07 p0990 N90-15721
Dynamics analyses of space power systems using the salt code
[DE90-002274] 08 p1038 N90-15995
Kinetics of the graphite/oxygen reaction in the in-pore diffusion controlled regime. Part 3: Influence of boundary layer diffusion in kinetic experiments at temperatures 970K to 1170K
[JUEL-2284-PT-3] 08 p1042 N90-16024
Solid state, surface, and catalytic studies of oxides
[DE90-004850] 08 p1134 N90-16566
Nuclear reaction uncertainties in standard and non-standard cosmologies
[DE90-003594] 08 p1151 N90-16666
Investigation into the feasibility of using solid fuel ramjets for high supersonic/low hypersonic tactical missiles
[AD-A214737] 09 p1168 N90-16761
Cluster based reaction probabilities for boron with oxygen, hydrogen, water, nitrogen, nitrous oxide, carbon dioxide, carbon monoxide, methane, tetrafluoromethane, and silane
[AD-A214554] 09 p1190 N90-16894
Descriptive simulation: Combining symbolic and numerical methods in the analysis of chemical reaction mechanisms
[AD-A214678] 09 p1190 N90-16898
Hydrogen desorption from the monohydride phase on Si(100)
[AD-A215237] 09 p1191 N90-16903
Kinetics of boron hydride interconversion reactions
[AD-A215386] 09 p1192 N90-16906
Development of a reliable fabrication technique to produce intermetallic compounds
[AD-A215004] 09 p1194 N90-16918
Advanced diagnostics for reacting flows
[AD-A215050] 09 p1217 N90-17060
Proposed uses of laser light scattering instruments for polymerization studies 09 p1224 N90-17100
Statistically based decompression tables 5: Haldane-Vann models for air diving
[AD-A214934] 09 p1251 N90-17261
NMR measurements of solvent self-diffusion coefficients in polymer solutions
[AD-A215276] 09 p1279 N90-17419
Results of an attempt to measure increased rates of the reaction D-2 + D-2 yields He-3 + n in a nonelectrochemical cold fusion experiment
[NASA-TM-102430] 09 p1280 N90-17424

Oxidation and reduction of Bi2Sr1.85CuO(6-y) crystals
[DE90-004246] 09 p1287 N90-17460
Superconducting Bi1.5Pb0.5Sr2Ca2Cu3O(x) ceramics by rapid melt quenching and glass crystallization
[NASA-CR-185184] 09 p1288 N90-17465
Flammability testing of aircraft cabin materials
10 p1316 N90-17611
Low NO(x) potential of gas turbine engines
[NASA-TM-102452] 10 p1321 N90-17636
Surface analyses and modelling of rate multiplicity and instabilities
[DE90-005418] 10 p1352 N90-17838
State to state kinetics of XeCl*
[AD-A215895] 10 p1353 N90-17847
Hydrogen sulfide effect on hydrogen entry into iron: A mechanistic study
[AD-A216214] 10 p1354 N90-17854
A review of the mechanism and kinetics of electrochemical hydrogen entry and degradation of metallic systems
[AD-A216671] 10 p1355 N90-17857
Control of titanium diboride SHS reactions by inert dilutions and mechanical constraint
[AD-A214378] 10 p1357 N90-17870
Luminescence probe studies of ionomers. Part 3: Distribution of decay rate constants for tris bipyridyl Ruthenium(II) in Nafion membranes
[AD-A215885] 10 p1359 N90-17880
Fundamental studies of time-dependent response and fracture of cross-linked polymers
[AD-A216694] 10 p1360 N90-17886
Combustion process science and technology
10 p1366 N90-17916
High temperature interaction of SO2 with oxide sorbents
[DE90-000435] 11 p1485 N90-18545
Pulsed laser-induced melting of intermediate Cu-Zn phases
[DE90-005404] 11 p1513 N90-18713
Ultrafast chemical dynamics of reactions in beams
[AD-A216319] 11 p1514 N90-18717
Kinetic relations and the propagation of phase boundaries in solids
[AD-A215881] 11 p1519 N90-18747
The interaction of polycrystalline copper films with dilute aqueous solutions of cupric chloride
[AD-A216465] 11 p1569 N90-19033
Proceedings of a contractors meeting on Combustion Rocket Propulsion Diagnostics of Reacting Flow
[AD-A216445] 12 p1617 N90-19297
Characterization of reaction kinetics in a porous electrode
[NASA-CR-186504] 12 p1625 N90-19340
Second-generation ordered polymers
[AD-A216126] 12 p1630 N90-19365
Determination of the mechanism of decomposition of energetic molecules
[AD-A217061] 12 p1633 N90-19388
Laboratory studies of free radical reactions in cloudwater
[DE90-003961] 12 p1694 N90-19730
Summary report of the Summer Conference of the DARPA-Materials Research Council
[AD-A217380] 13 p1767 N90-20143
Structure of model gas flames in nitramines
[AD-A217578] 13 p1770 N90-20159
Corrosion properties of Fe3Al in H2S-H2-H2O mixtures
[DE90-004936] 13 p1772 N90-20167
DURIP FTIR studies of solid state reaction dynamics
[AD-A217713] 13 p1773 N90-20174
Aerodynamic and kinetic processes in flames
[AD-A217796] 13 p1773 N90-20176
The extinction and structure of counterflow premixed flames
[AD-A218106] 13 p1773 N90-20178
Polyatomic reaction dynamics
[DE90-008668] 13 p1884 N90-20811
Populations of excited states and reaction mechanisms in the emission of complex fragments
[DE90-007481] 13 p1886 N90-20819
Computer codes for the evaluation of thermodynamic properties, transport properties, and equilibrium constants of an 11-species air model
[NASA-TM-102602] 14 p1972 N90-21297
Laser studies of chemical dynamics at the gas-solid interface
[DE90-008698] 14 p1986 N90-21380
The Chemkin Thermodynamic Data Base
[DE90-007953] 14 p2035 N90-21676
On the use of external burning to reduce aerospace vehicle transonic drag
[NASA-TM-103107] 15 p2052 N90-21762
Testing carbon fabric for oxidation mass loss
15 p2063 N90-21819
Studies on reactive flows 15 p2066 N90-21831
Infrared absorption spectroscopy and chemical kinetics of free radicals
[DE90-009469] 15 p2067 N90-21837
A comparison of the autoignition chemistry of n-butane and isobutane in an internal combustion engine
[DE90-009474] 15 p2067 N90-21838
Detailed mechanism for oxidation of benzene
[NASA-TM-102443] 15 p2067 N90-21842
Determination of rates of reaction in the gas-phase in the troposphere: Theory and practice. 2: Rate of direct photoreaction: Screening-level test guideline-spectroscopic determination of the cross section and the maximum rate of direct photoreaction in sunlight
[PB90-146291] 15 p2125 N90-22156
The Al-26(rho, gamma)Si-27 reaction: Stellar origins of galactic Al-26 15 p2188 N90-22498
Modeling of combustion processes in a solid fuel particle
[DE90-009140] 16 p2214 N90-22629
Investigation of the reaction kinetics between SiC fibers and selectively alloyed titanium matrix composites and determination of their mechanical properties
16 p2219 N90-22659
An effective He-3 nucleon force for the He-3, t) charge exchange reaction
[KVI-813] 16 p2315 N90-23198
Incomplete fusion reactors at low and intermediate energies
[KVI-809] 16 p2316 N90-23206
Analysis of the use of a methane propellant in a biowaste resistojet
[AD-A220475] 17 p2367 N90-23473
Diffusion in the thermal degradation of NC base propellants
[AD-A219831] 17 p2383 N90-23572
Selective removal of organics for water reclamation
[NASA-TM-101890] 17 p2421 N90-23797
Use of ab initio theory in studying various chemical systems
[AD-A220913] 18 p2521 N90-24396
Combustion of n-butane and isobutane in an internal combustion engine: A comparison of experimental and modeling results
[DE90-005993] 18 p2522 N90-24400
Mechanistic modeling of corrosion fatigue crack growth of steels in aqueous solutions 18 p2524 N90-24404
Studies of chemistry and diffusion on silicon and gallium arsenide surfaces using laser-induced thermal desorption
[AD-A220946] 18 p2547 N90-24539
Pt/SnO2-based CO-oxidation catalysts for long-life closed-cycle CO2 lasers 18 p2556 N90-24589
In situ analysis of CO during chemisorption and oxidation on graphite: Supported Pt by FTIR-microspectromeiry
18 p2559 N90-24605
Calorimetry, activity, and micro-FTIR analysis of CO chemisorption, titration, and oxidation on supported Pt
18 p2560 N90-24606
Chemisorption studies of Pt/SnO2 catalysts
18 p2560 N90-24609
IR transition moments and collisional dynamics of vibrationally excited OH radicals via time-resolved laser absorption spectroscopy
[AD-A221005] 18 p2580 N90-24696
The catalytic reactivity of thin film crystal surfaces
[DE90-010579] 18 p2622 N90-24937
Low thrust rocket test facility
[NASA-TM-103206] 19 p2663 N90-25158
Oxidation characteristics of Ti-14Al-21Nb ingot alloy
[NASA-TP-3012] 19 p2674 N90-25206
Reaction and transport in porous media
19 p2690 N90-25300
An analysis of the contact sintering process in III-V solar cells
[NASA-TM-103179] 19 p2709 N90-25420
Diversiform processes of ozone in the atmosphere: Introduction study
[AERONOMICA-ACTA-A-352-1990]
19 p2713 N90-25439
Synthesis of high purity sinterable silicon carbide powder
[DE90-012029] 20 p2828 N90-26084
Carbon deposition model for oxygen-hydrocarbon combustion. Task 6: Data analysis and formulation of an empirical model
[NASA-CR-183986] 20 p2829 N90-26095
Liquid fueled ramjet combustion instability: Acoustical and vortical interactions with burning sprays
[AD-A222752] 20 p2831 N90-26104
Chemical structure and kinetics at liquid/solid interfaces
[AD-A222766] 20 p2831 N90-26105
Critical evaluation of Jet-A spray combustion using propane chemical kinetics in gas turbine combustion simulated by KIVA-2
[NASA-TM-103173] 20 p2843 N90-26170
Formation kinetics of N2O in the atmosphere
20 p2886 N90-26425
First International Conference on Laboratory Research for Planetary Atmospheres
[NASA-CP-3077] 20 p2942 N90-26744
Novel laser gain and time-resolved FTIR studies of photochemistry 20 p2945 N90-26756
Chemical kinetics and modeling of planetary atmospheres 20 p2946 N90-26763
Kinetics and thermochemistry of polyatomic free radicals: New results and new understandings
20 p2946 N90-26764
The heat of formation of CN radicals and radiative lifetimes of the A 1 Sigma - state of C2N2
20 p2946 N90-26765
A laboratory investigation of the production and properties of molecular and radical species pertinent to planetary atmospheres 20 p2946 N90-26766
Rate constant for reaction of atomic hydrogen with germane 20 p2947 N90-26768
Role of the methylene amidogen (H2CN) radical in the atmospheres of Titan and Jupiter
20 p2947 N90-26769
Laboratory measurements and methane photochemistry modeling 20 p2947 N90-26770
The applications of chemical thermodynamics and chemical kinetics to planetary atmospheres research
20 p2948 N90-26773
Ramjet and ramrocket propulsion systems for missiles
21 p2973 N90-26897
Flame extinction in compressible flow
21 p2973 N90-26899
Non-premixed turbulent CO/H2 flames at local extinction conditions 21 p2975 N90-26907
PDF modeling of chemical nonequilibrium effects in turbulent nonpremixed jet flames
21 p2975 N90-26908
Measurements of energy dispersion at liquid-solid interfaces: Fluorescence quenching of pyrene bound to fumed silica
[AD-A222371] 21 p2978 N90-26926
Turbulent reacting flows and supersonic combustion
[AD-A221793] 21 p2979 N90-26933
Fabrication of intermetallic compounds by solid state reaction of roll-bonded materials
[AD-A221960] 21 p2982 N90-26943
A review of reaction rates and thermodynamic and transport properties for an 11-species air model for chemical and thermal nonequilibrium calculations to 30000 K
[NASA-RP-1232] 21 p3002 N90-27064
A unifying picture of gas-phase formation and growth of PAH (Polycyclic Aromatic Hydrocarbons), soot, diamond and graphite 21 p3091 N90-27575
An ionic mechanism of carbon formation in flames
21 p3093 N90-27582
AMSAHTS 1990: Advances in Materials Science and Applications of High Temperature Superconductors
[NASA-CP-10043] 22 p3136 N90-27792
Kinetics and thermodynamics of ceramic/metal interface reactions related to high T(sub c) superconducting applications 22 p3141 N90-27815
Synthesis of Y1Ba2Cu3O(sub x) superconducting powders by intermediate phase reaction
22 p3149 N90-27855
Modeling of carbon monoxide oxidation kinetics over NASA carbon dioxide laser catalysts
[NASA-CR-186356] 22 p3155 N90-27885
Model of turbulent diffusion flames and nitric oxide generation
[PB90-155557] 22 p3155 N90-27886
Experimental and kinetic modeling of acid/base redox reactions over metal oxide catalysts
[DE90-013835] 22 p3156 N90-27893
Calculations of chemically reacting shear flows above solid fuels 22 p3162 N90-27930
An investigation of solid-fuel, dual-mode combustion ramjets 22 p3162 N90-27933
Photo-sensitized ignition of hydrogen/oxygen mixtures for hypersonic flight vehicles 22 p3163 N90-27935
Modeling of knock in spark-ignition engines
[DE90-010875] 22 p3182 N90-28058
Numerical simulations of flowfields in a central-dump ramjet combustor. 3: Effects of chemistry
[AD-A224145] 23 p3282 N90-28573
Quenching of N(2D) by O(3P)
[AD-A221690] 23 p3303 N90-28683
The spatial scalar structure of premixed turbulent stagnation point flames
[DE90-014189] 23 p3303 N90-28686
Analyses of spray and droplet ignition for pure and multicomponent fuels 23 p3304 N90-28688
Evaluation of a hybrid kinetics/mixing-controlled combustion model for turbulent premixed and diffusion combustion using KIVA-2
[NASA-TM-103196] 23 p3323 N90-28792

Numerical simulation of reactive turbulent flows
[ETN-90-97476] 23 p3326 N90-28807
Chemical kinetic and aerodynamic structures of flames
[AD-A224281] 24 p3445 N90-29455
Transition metal activation and functionalization of carbon-hydrogen bonds
[DE90-015826] 24 p3451 N90-29489
Kinetics and structure of silicate sol-gels
[DE90-015702] 24 p3458 N90-29521
Proceedings of the High Energy Density Materials Contractors Conference
[AD-A223793] 24 p3484 N90-29695
Synthesis and property evaluation of Y-Ba2-Cu3-O(6+x) superconductors
[AD-A223494] 24 p3552 N90-30098

REACTION PRODUCTS
Surface-catalyzed air oxidation reactions of hydrazines: Tubular reactor studies 02 p0204 N90-11167
The chemistry of the hypochlorite neutralization of hydrazine fuels 02 p0205 N90-11173
Gaseous optical contamination of the spacecraft environment: A review 19 p2730 N90-25519

REACTION RATE
U REACTION KINETICS

REACTION TIME
Monolayer formation characteristics of novel organic molecules with nonlinear optically active moieties
[AD-A210496] 01 p0121 N90-10693
Performance recovery following startle: A laboratory approach to the study of behavioral response to sudden aircraft emergencies 09 p1256 N90-17286
Feedback effects in computer-based skill learning
[AD-A214560] 09 p1258 N90-17298
Spectral properties of a 1.3-micrometers InGaAsP diode laser under modulation
[AD-A220066] 17 p2409 N90-23729
Effects of cholinergic drugs on exercise performance and simple reaction time of rhesus monkeys
[AD-A219455] 17 p2433 N90-23862
The retrieval of information from secondary memory: A review and new findings
[AD-A222760] 20 p2899 N90-26489
Transient signal distortion and coupling in multilayer multiconductor MIC microstrips
[AD-A222989] 21 p3000 N90-27050
Categorization and identification of simultaneous targets
[IZF-1989-22] 22 p3234 N90-28337

REACTION WHEELS
Analytical derivation and verification of zero-gyro control for the IUE satellite
[NASA-TM-100748] 05 p0645 N90-13767
Feasibility of using Extreme Ultraviolet Explorer (EUVE) reaction wheels to satisfy Space Infrared Telescope Facility (SIRTF) maneuver requirements
[NASA-TM-100389] 12 p1663 N90-19556
Design of a digital model following controller of reaction wheel torques
[INPE-4753-PRE/1425] 14 p1938 N90-21093
Accurate nonlinear control for satellites using reaction wheels
[INPE-4983-PRE/1546] 15 p2059 N90-21787
Test results and flight experience of ball bearing momentum and reaction wheels
15 p2115 N90-22099
The large wheel actuator LDR 100-0: Development status and test results 18 p2539 N90-24487

REACTIVITY
Preparation, purification and densification of zinc sulfide powder from organometallics
[AD-A210943] 01 p0052 N90-10298
KIVA reactive hydrodynamics code applied to detonations in high vacuum
[DE89-016979] 03 p0346 N90-11974
Chemical and photochemical reactivity in microemulsions and waterless microemulsions
[AD-A211776] 04 p0470 N90-12692
Mechanisms in reactive ion etching of silicon carbide thin films
[AD-A213018] 05 p0634 N90-13700
Chemistry of large molecules
[DE90-000813] 06 p0751 N90-14366
Particle size effects in the initiation of explosives containing reactive and nonreactive continuous phases
[DE90-000786] 06 p0754 N90-14390
Reactive flow measurements and calculations for ZrH2-based composite explosives
[DE90-000831] 06 p0755 N90-14393
A measurement of hydroxyl in the daytime mesosphere 06 p0814 N90-14732
Cluster based reaction probabilities for boron with oxygen, hydrogen, water, nitrogen, nitrous oxide, carbon dioxide, carbon monoxide, methane, tetrafluoromethane, and silane
[AD-A214554] 09 p1190 N90-16894
Reactive atmosphere processing of BaTiO3 and origins of its photorefractive effect
[AD-A215034] 09 p1289 N90-17475
Survey on energy conversion of CO2 gas. Approach to solution of CO2 gas problems
[DE90-742055] 10 p1352 N90-17843
Structure and reactivity of model thin film catalysts
[DE90-007365] 11 p1485 N90-18546
Synthesis and chemistry of unsaturated metal nitrogen compounds
[AD-A216550] 12 p1622 N90-19321
Mechanisms of reactive etching
[AD-A217679] 13 p1770 N90-20160
Reactive sputtering of molybdenum
[DE90-008307] 13 p1778 N90-20204
An electrochemical and spectroscopic study of electrode processes
[AD-A217261] 13 p1793 N90-20289
Advanced calcium thionyl chloride high power battery
[AD-A216685] 13 p1825 N90-20482
Hydrocarbon-fuel/combustion-chamber-liner materials compatibility
[NASA-CR-185203] 14 p1950 N90-21165
Testing carbon fabric for oxidation mass loss
15 p2063 N90-21819
Studies on reactive flows 15 p2066 N90-21831
Experience with synthetic fluorinated fluid lubricants
15 p2114 N90-22095
Investigation of optical nonlinearities, conductivity and magnetism in organometallic materials
[AD-A218548] 16 p2317 N90-23211
Development of high performance beta-SiC field-effect transistors
[AD-A218392] 17 p2394 N90-23637
In situ analysis of CO during chemisorption and oxidation on graphite: Supported Pt by FTIR-microspectrometry
18 p2559 N90-24605
The catalytic reactivity of thin film crystal surfaces
[DE90-010579] 18 p2622 N90-24937
Making real-time reactive systems reliable
[NASA-CR-186642] 20 p2873 N90-26344
Production of superconductor/carbon bicomponent fibers 22 p3138 N90-27805
Reflection Mass Spectrometry (REMS) during 3/5 MBE
[DE90-014568] 23 p3304 N90-28690
The global cycle of reactive nitrogen
[DE90-015041] 23 p3348 N90-28919

REACTOR CHEMISTRY
U RADIOCHEMISTRY

REACTOR CORES
Prevention of significant deterioration application for approval to construct SP-100 Ground Engineering System Test Site
[DE90-007986] 15 p2166 N90-22381
Gas production and behavior in the coolant of the SP-100 space nuclear power system
[DE90-010674] 18 p2614 N90-24890

REACTOR DESIGN
The Reversed-Field-Pinch (RFP) fusion neutron source: A conceptual design
[DE89-015297] 02 p0276 N90-11577
Introductory testimony: Hearing on nuclear power in space
[DE90-001137] 06 p0842 N90-14897
Starlight: A stationary inertial-confinement-fusion reactor with nonvaporizing walls
[DE90-002315] 06 p0847 N90-14927
Design of DIII-D advanced divertor
[DE90-003343] 07 p0995 N90-15752
Analysis and evaluation of ZPPR (Zero Power Physics Reactor) critical experiments for a 100 kilowatt-electric space reactor
[DE90-005634] 12 p1713 N90-19835
Fusion technology development
[DE90-007933] 14 p2029 N90-21636
Photosynthetic water splitting, phase 2
[PB90-132671] 15 p2066 N90-21833
Energy storage for a lunar base by the reversible chemical reaction: CaO+H2O reversible reaction Ca(OH)2
[NASA-TM-103145] 19 p2709 N90-25419

REACTOR FUELS
U NUCLEAR FUELS

REACTOR MATERIALS
Microstructural evolution of martensitic steels during fast neutron irradiation
[DE89-016231] 07 p0902 N90-15212
Report of the Advanced Neutron Source (ANS) Aluminum Cladding Corrosion Workshop
[DE90-001281] 07 p0903 N90-15217
Fusion reactor materials
[DE90-000976] 07 p0994 N90-15744
Interplanar spacing for various phases in austenitic stainless steels
[DE90-602350] 08 p1045 N90-16038
Fracture toughness of ferritic alloys at very high neutron exposures
[DE90-004519] 08 p1046 N90-16046
Phase stability of a manganese-stabilized low-activation martensitic steel
[DE90-004114] 09 p1193 N90-16914
Fourth International Conference on Fusion Reactor Materials
[DE90-006142] 11 p1568 N90-19025
Fusion technology development
[DE90-007933] 14 p2029 N90-21636
Monoenergetic positron beam studies of near-surface phenomena
[ETN-90-96947] 18 p2613 N90-24887
Study on application of ultrasonic wave measurement to creep-fatigue damage detection
[DE89-782317] 19 p2700 N90-25361
Multimegawatt space nuclear power supply, phase 1. Supplement: D180-30619-8
[DE90-012433] 20 p2926 N90-26647
Filler metal development for Hastelloy alloy XR
[DE90-791084] 21 p2981 N90-26939
Density changes of generation 1.5 and 2.0 copper alloys irradiated at 411 to 414 C and 529 C in FFTF-MOTA
[DE90-015291] 23 p3311 N90-28724
Helium generation in fusion reactor materials
[DE90-013005] 23 p3393 N90-29172
Accurate calculations of neutron kerma and damage from ENDF/B-VI evaluations for silicon, chromium, iron and nickel, and comparison with ENDF/B-V results
[DE90-016020] 24 p3481 N90-29674

REACTOR SAFETY
Course A: Numerical modeling of two-phase flows for presentation at Ecole d'Ete d'Analyse Numerique
[DE90-002074] 06 p0778 N90-14526
Results of the manipulator test test stand study: Comparison of manipulators and evaluation of equipment items
[DE90-000977] 06 p0794 N90-14625
Critical time step estimation for three-dimensional explicit impact analysis
[DE90-002187] 06 p0801 N90-14662
Niobium 1 percent zirconium/potassium and titanium/potassium life-test heat pipe design and testing
[DE90-002430] 07 p0954 N90-15522
Dynamics analyses of space power systems using the salt code
[DE90-002274] 08 p1038 N90-15995
Depressurization test on hot gas duct
[DE90-710058] 09 p1236 N90-17176
Heavy-section steel technology program fracture issues
[DE90-005264] 09 p1240 N90-17195
Space nuclear safety program
[DE90-006436] 11 p1565 N90-19007
A nonintrusive method for measuring the operating temperature of a solenoid-operated valve
[DE90-007576] 13 p1804 N90-20355
Proceedings of the Conference on Technology-Based Confidence Building: Energy and Environment
[CNSS-PAPERS-22] 15 p2125 N90-22152
Prevention of significant deterioration application for approval to construct SP-100 Ground Engineering System Test Site
[DE90-007986] 15 p2166 N90-22381
Magnetic turbulence versus safety factor in the Tokapole 2 tokamak 15 p2168 N90-22391
National emissions standards for hazardous air pollutants application for approval of construction SP-100 ground engineering system test site
[DE90-007985] 16 p2316 N90-23203
A decision support system for control and automation of dynamical processes
[AD-A219501] 17 p2454 N90-23995
Multimegawatt space nuclear power supply, phase 1. Volume 2: Phase 2 plan D180-30619-6
[DE90-012431] 20 p2925 N90-26645
Multimegawatt space nuclear power supply, phase 1. Volume 3: Annotated outline of preliminary safety assessment D180-30619-7
[DE90-012432] 20 p2926 N90-26646

REACTOR TECHNOLOGY
Experience with model based display for advanced diagnostics and control
[DE89-015693] 01 p0082 N90-10469
The Reversed-Field-Pinch (RFP) fusion neutron source: A conceptual design
[DE89-015297] 02 p0276 N90-11577
Activities report of the Joint Research Center
[ETN-89-95757] 04 p0569 N90-13321
Human factors survey of advanced instrumentation and controls
[DE90-002477] 06 p0821 N90-14776
Starlight: A stationary inertial-confinement-fusion reactor with nonvaporizing walls
[DE90-002315] 06 p0847 N90-14927

Fundamental studies of fusion plasmas
[DE90-002343] 06 p0848 N90-14933
Static pressure distribution in an angular channel with helicoidal wire
[DE89-636474] 07 p0928 N90-15374
The search for solid state fusion lasers
[DE89-012301] 07 p0934 N90-15410
Design of DIII-D advanced divertor
[DE90-003343] 07 p0995 N90-15752
Introduction to D-He(3) fusion reactors
07 p1008 N90-15839
Scaling study for SP-100 reactor technology
[NASA-TM-897140] 08 p1122 N90-16496
Failure probability estimate of Type 304 stainless steel piping
[DE90-003896] 11 p1486 N90-18550
Theory of field reversed configurations
[DE90-006702] 12 p1717 N90-19860
Using formal methods to develop a paradigm for software design
[DE90-005633] 13 p1866 N90-20703
West European magnetic confinement fusion research
14 p2029 N90-21634
Fusion technology development
[DE90-007933] 14 p2029 N90-21636
TOODEE: A two-dimensional, time-dependent heat conduction program
[DE90-009631] 15 p2099 N90-22010
Proceedings of the Conference on Technology-Based Confidence Building: Energy and Environment
[CNSS-PAPERS-22] 15 p2125 N90-22152
Incomplete fusion reactors at low and intermediate energies
[KVI-809] 16 p2316 N90-23206
Advances in spheromak understanding and parameters
[DE90-012052] 19 p2759 N90-25678
Multimegawatt space nuclear power supply, phase 1. Volume 3: Annotated outline of preliminary safety assessment D180-30619-7
[DE90-012432] 20 p2926 N90-26646

READ-ONLY MEMORY DEVICES
Technology development and circuit design for a parallel laser programmable floating point application specific processor
[AD-A215870] 11 p1500 N90-18637
National Technical Information Service 1989 Users Conference proceedings
[PB90-142563] 12 p1726 N90-19921
Technologies for electronic transfer of information: The present state and trends in Japan
15 p2177 N90-22443
Electronic transfer of information applications in the Societe Aerospatiale 15 p2179 N90-22454
Digital terrain elevation data compact disk-read only memory prototype evaluation
[AD-A218545] 17 p2442 N90-23915
Failure of the ERBE scanner instrument aboard NOAA 10 spacecraft and results of failure analysis
[NASA-TM-102661] 19 p2694 N90-25328
Optical storage technology
[AD-A224028] 23 p3407 N90-29254

READING
Topographic map reading
[AD-A211269] 02 p0236 N90-11340
A survey of concurrent readers and writers
[CWI-CS-R8936] 19 p2741 N90-25581

READJUSTMENT
U ADJUSTING

READOUT
Performance of the CAMEX64 silicon strip readout chip
[DE89-014015] 01 p0130 N90-10747
Spectral contents readout of birefringent sensor
[NASA-CR-179444] 06 p0843 N90-14905
Liquid level measurement system for analog and digital readout
[AD-D014297] 08 p1076 N90-16227
Laboratory characterization of direct readout Si:Sb and Si:Ga infrared detector arrays 14 p1980 N90-21347
Australian experience in flight recorder readout and analysis 22 p3106 N90-27644
Automation of the readout, transcription and evaluation of digital flight data at DLR 22 p3106 N90-27645
Double sided silicon strip detectors
[MPI-PAE/EXP-EL-217] 22 p3178 N90-28036
A double-sided silicon strip detector with capacitive read out and a new method of integrated bias coupling
22 p3178 N90-28037

REAL GASES
Efficient real gas Navier-Stokes computations of high speed flows using an LU scheme
[NASA-TM-102429] 06 p0720 N90-14203
High enthalpy hypersonic wind tunnel F4: General description and associated instrumentation
18 p2489 N90-24228
Mission of LARVE 18 p2489 N90-24229

REAL NUMBERS
NT INTEGERS

REAL TIME OPERATION
Analysis and testing of a high performance air-air missile 01 p0014 N90-10069
Real-time support for high performance aircraft operation
[NASA-CR-185475] 01 p0015 N90-10075
Real-time observations of aerosol composition changes
[DE89-012382] 01 p0073 N90-10422
Optimized resolved rate control of seven-degree-of-freedom Laboratory Telerobotic Manipulator (LTM) with application to three-dimensional graphics simulation
[NASA-TP-2938] 01 p0109 N90-10618
A comparison of real-time optical correlators for pattern recognition
[DE89-016416] 01 p0123 N90-10705
Real-time flight test analysis and display techniques for the X-29A aircraft 02 p0152 N90-10866
Identification Friend, Foe or Neutral Joint Test
02 p0154 N90-10881
Realtime processing and display
02 p0155 N90-10886
Flight test instrumentation and data processing at British Aerospace, Warton, U.K. 02 p0155 N90-10887
Improved pattern recognition techniques for real time operation
[AD-A211395] 03 p0324 N90-11840
Scheduling sporadic and aperiodic events in a hard real-time system
[AD-A211344] 03 p0387 N90-12205
Ultra high speed compound semiconductors and real time signal processing
[AD-A211394] 03 p0413 N90-12372
A real-time locking protocol
[AD-A211514] 03 p0418 N90-12403
Real-time simulation of an F110/STOVL turbofan engine
[NASA-TM-102409] 04 p0457 N90-12618
Preliminary experience with high response pressure measurements in a multistage, high speed compressor
[RAE-TM-P-1141] 04 p0457 N90-12619
On a fast two-dimensional radar imaging process for rotating targets, and an analysis of its image quality
[ESA-TT-1142] 04 p0489 N90-12808
A real-time wind model using digital data from aircraft
[RSRE-MEMO-4309] 04 p0521 N90-13005
A transformational method for verifying safety properties in real time systems
[AD-A211925] 04 p0529 N90-13051
A mapping for converting Mascot designs to Ada programs
[RSRE-MEMO-4244] 04 p0531 N90-13070
Visual perception processing in a hierarchical control system: Level 1
[PB89-221188] 04 p0536 N90-13101
Computer-based tools for assisting air traffic controllers with arrivals flow management
[RSRE-88001] 05 p0577 N90-13366
The role of the host in a cooperating mainframe and workstation environment, volumes 1 and 2
[NASA-CR-185463-VOL-1/2] 05 p0602 N90-13496
Launch and early orbit 05 p0606 N90-13524
The in-orbit initialization phase
05 p0606 N90-13525
Novel in situ spectroscopic ellipsometer for real time analysis of CVD diamond films
[AD-A213218] 05 p0644 N90-13762
Kinematics and control of manipulation robots
[WTHD-187] 05 p0652 N90-13803
ALIS: An Auroral Large Imaging System in northern Scandinavia 05 p0663 N90-13877
Ada task scheduling: A focused Ada investigation
[NASA-CR-186072] 05 p0682 N90-13967
Multi-level specification and verification of real-time software
[AD-A213227] 05 p0683 N90-13975
Flight software development for the isothermal dendritic growth experiment
[NASA-TM-102412] 05 p0685 N90-13988
A knowledge-based flight status monitor for real-time application in digital avionics systems
[NASA-TM-101710] 05 p0686 N90-13995
Real time image enhancement during underwater recovery operations
[AD-A213139] 05 p0700 N90-14097
The biocorrosion of copper by biopolymers as examined in situ, in real time FT-IR/CIR/ATR in conjunction with pre and post XPS/AES
[DE90-002086] 06 p0747 N90-14348
Propagation assessment and tactical decision aids
06 p0757 N90-14407
PROPHET and future signal warfare decision aids
06 p0758 N90-14412
A communications system with an adaptive multi-functional architecture 06 p0759 N90-14415
Assessment of anomalous propagation predictions using minisonde refractivity data and the parabolic equation method 06 p0760 N90-14424
New perspectives for the inversion of backscatter ionograms 06 p0761 N90-14427
A modern trans-ionospheric propagation sensing system 06 p0761 N90-14430
A portable ionosonde in support of reliable communications 06 p0762 N90-14431
The use of broadcast signals for passive sensing in automated HF communication systems
06 p0762 N90-14433
An image compression algorithm for a high-resolution digital still camera
[NASA-CR-185079] 06 p0780 N90-14532
Application of reusable software components at the SEI 06 p0826 N90-14804
Continuation of research in software for space operations support
[NASA-CR-186092] 06 p0827 N90-14808
Robotic vision system
[AD-D014246] 06 p0832 N90-14838
Realtime tracking system for wide-field-of-view telescope
[DE90-001147] 06 p0843 N90-14908
Development of a real time monitor for superconductive thin film preparation
[DE89-017772] 06 p0852 N90-14952
Implementing fault-tolerant sensors
[NASA-CR-186251] 07 p0933 N90-15400
Time bounds for real-time process control in the presence of timing uncertainty
[AD-A213791] 07 p0975 N90-15633
A multichannel processing approach to real time network detection, phase association, and threshold monitoring
[AD-A213940] 07 p0980 N90-15657
Ultra high performance, highly reliable, numeric intensive processors and systems
[AD-A214100] 07 p0980 N90-15659
Concurrence control for transactions with priorities
[NASA-CR-186241] 07 p0986 N90-15699
Periodic phase adjustment distributed clock synchronization in the hard realtime environment
[AD-A213842] 07 p0988 N90-15708
Electro-optic sensors for surveillance and target acquisition 08 p1026 N90-15929
An intelligence-driven RPV mission planner
08 p1027 N90-15932
An electronic pressure profile display system for aeronautic test facilities
[NASA-TM-102478] 08 p1032 N90-15964
RETE experiment activity at the TSS-1 POCC
[IFSI-89-12] 08 p1036 N90-15988
Digital system for monitoring and controlling remote processes
[DE90-003935] 08 p1054 N90-16094
Sequential rapid communication visual displays
[AD-D014282] 08 p1056 N90-16106
Keeping the pilot in the loop
[RAE-TM-FM-18] 08 p1105 N90-16396
Dynamic architecture computer
[AD-A214262] 08 p1106 N90-16402
Autonomous automatic landing through computer vision 09 p1163 N90-16734
Advances in navigation support systems based on operational pilot's heuristics 09 p1164 N90-16737
NASA/RAE cooperation on a knowlede based flight status monitor 09 p1164 N90-16738
Expert system for Kalman filter supervision: Application to autonomous satellite navigation
09 p1164 N90-16739
Intelligent landmarks recognition in satellites images
09 p1165 N90-16741
Delta 181 sensor module command center
[AD-A214868] 09 p1182 N90-16855
AOIPS 3 user's guide. Volume 2: Program descriptions
[NASA-TM-100725] 09 p1247 N90-17236
The performance implications of Ada in a MASCOT 3 design
[YM-5748-M304/2] 09 p1263 N90-17324
Industrial Modernization Incentives Program: Computer-aided log book
[AD-A214614] 09 p1265 N90-17335
The moving platform simulator 2: A networked real-time visual simulator with distributed processing and line-of-sight displays
[AD-A214936] 09 p1266 N90-17343
Active control of a flexible structure using a modal positive position feedback controller
[NASA-CR-186336] 09 p1272 N90-17371

Studies of optical matrix multiplication and reconfigurable optical interconnect concepts
[AD-A214645] 09 p1281 N90-17427
The real-time roll-back and recovery of transactions in database systems
[AD-A214471] 09 p1295 N90-17506
Methodology for developing realtime distributed systems
[AD-A214570] 09 p1296 N90-17509
Use of anomolous thermal imaging effects for multi-mode systems control during crystal growth
10 p1365 N90-17910
Compact ranges in antenna and RCS measurements
10 p1371 N90-17940
CHIMERA 2: A real-time UNIX-compatible multiprocessor operating system for sensor-based control applications
[AD-A215958] 10 p1392 N90-18051
Proposition for an airborne remote sensing system
[INPE-4872-PRE/1483] 10 p1399 N90-18090
Hypercube expert system shell-applying production parallelism
[AD-A215762] 10 p1418 N90-18173
Delivery performance of conventional aircraft by terminal-area, time-based air traffic control: A real-time simulation evaluation
[NASA-TP-2978] 11 p1454 N90-18378
SHARP: A multi-mission artificial intelligence system for spacecraft telemetry monitoring and diagnosis
[NASA-CR-186285] 11 p1467 N90-18444
Ultrafast chemical dynamics of reactions in beams
[AD-A216319] 11 p1514 N90-18717
Comparisons between the RTNEPH (Real-Time Nephanalysis) and AFGL cloud layer analysis algorithms
[AD-A216637] 11 p1536 N90-18844
A rule-based paradigm for intelligent adaptive flight control 12 p1605 N90-19238
A computer control system for the alternating gradient magnetometer 12 p1636 N90-19402
Advanced control schemes and kinematic analysis for a kinematically redundant 7 DOF manipulator
[NASA-CR-186175] 12 p1671 N90-19599
Potential role of avionics in escape systems
13 p1752 N90-20060
Airplane takeoff and landing performance monitoring system
[NASA-CASE-LAR-13734-1-CU] 13 p1758 N90-20096
A data acquisition parallel bus for wind tunnels at ARL (Aeronautical Research Laboratory)
[AD-A218052] 13 p1759 N90-20098
The Real Time Display Builder (RTDB)
13 p1857 N90-20656
Design considerations for a space database
13 p1858 N90-20659
Operational computer graphics in the flight dynamics environment 13 p1859 N90-20668
Real-time graphics for the Space Station Freedom cupola, developed in the Systems Engineering Simulator
13 p1862 N90-20683
MEASURE: An integrated data-analysis and model identification facility
[NASA-CR-186452] 13 p1863 N90-20686
A real-time parallel pipelined data-flow image-processing system
[DE90-008324] 13 p1864 N90-20691
A parallel architecture for real-time simulation
[AD-A218321] 13 p1873 N90-20741
Real-time concurrency control and transaction scheduling
[AD-A218162] 13 p1901 N90-20909
Rule-based mechanisms of learning for intelligent adaptive flight control 14 p1908 N90-20939
Perspectives on the use of rule-based control
14 p1908 N90-20940
Effective techniques for the identification and accommodation of disturbances
14 p1934 N90-21072
Effect of KOH concentration on LEO cycle life of IPV nickel-hydrogen flight battery cells
[NASA-TM-103127] 14 p1942 N90-21116
Real-time adaptive radiometric correction for imaging radars systems 14 p1962 N90-21233
A solution for real time motion compensation for SAR without using inertial navigation systems
14 p1962 N90-21236
Concept and results of the DLR realtime SAR processor 14 p1963 N90-21244
A real-time rejection circuit to automatically reject multiple interfering hopping signals while passing a lower level desired signal
[AD-D014424] 14 p1965 N90-21251
Strategies for concurrent processing of complex algorithms in data driven architectures
[NASA-CR-186515] 14 p2013 N90-21535
A real time neural net estimator of fatigue life
[NASA-TM-103117] 14 p2018 N90-21564
A real-time signal combining system for Ka-band feed arrays using maximum-likelihood weight estimates
15 p2076 N90-21888
The application of connectionism to query planning/scheduling in intelligent user interfaces
15 p2152 N90-22295
Computer conferencing: Minds meeting anywhere anytime 15 p2179 N90-22452
The development of a real-time decimeter-level positioning system using Global Positioning System (GPS) technology
[AD-A218695] 16 p2199 N90-22552
Inertial navigation system simulator: Behavioral specification, revision
[AD-A219294] 16 p2199 N90-22554
Model-based method for terrain-following display design
[AD-A219302] 16 p2201 N90-22563
Automated star pattern recognition
16 p2211 N90-22612
Using object-oriented analysis techniques to support system testing
[DE90-009540] 16 p2226 N90-22700
Real-time stereo-microradiography
[AD-A218433] 16 p2245 N90-22805
The perception of geometrical structure from congruence 16 p2270 N90-22935
Interactive displays in medical art
16 p2271 N90-22940
Parallel processing of real-time dynamic systems simulation on OSCAR (Optimally SCheduled Advanced multiprocessoR) 16 p2282 N90-23006
Computational dynamics for robotics systems using a non-strict computational approach
16 p2283 N90-23011
An algorithm for the solution of dynamic linear programs 16 p2286 N90-23026
A finite element based method for solution of optimal control problems 16 p2286 N90-23027
Space station dynamics, attitude control and momentum management 16 p2287 N90-23029
Proceedings of the 3rd Annual Conference on Aerospace Computational Control, volume 2
[NASA-CR-186447] 16 p2289 N90-23040
A real time, FEM based optimal control algorithm and its implementation using parallel processing hardware (transistors) in a microprocessor environment
16 p2294 N90-23066
Six-degree-of-freedom aircraft simulation with mixed-data structure using the applied dynamics simulation language, ADSIM 16 p2294 N90-23067
Real-time closed-loop simulation and upset evaluation of control systems in harsh electromagnetic environments 16 p2294 N90-23069
JPL control/structure interaction test bed real-time control computer architecture 16 p2294 N90-23070
Comparative evaluations of four specification methods for real-time systems
[AD-A219187] 16 p2300 N90-23109
DARK (Distributed Ada Real-Time Kernel) porting and extension guide Kernel version 3.0
[AD-A219291] 16 p2301 N90-23112
Version description and installation guide Kernel version 3.0
[AD-A219292] 16 p2301 N90-23113
Durra: A task-level description language reference manual, version 2
[AD-A219293] 16 p2301 N90-23114
Controlling real-time systems with parallel processes
[CS-8918] 16 p2302 N90-23119
Experimental adaptive control of a hydraulic robot
16 p2303 N90-23121
Photoreflectance for in-situ characterization of MOCVD growth of semiconductors under micro-gravity conditions
[NASA-CR-186600] 17 p2383 N90-23576
Polar BEAR UV imaging of airglow and aurora-image processing and results
[AD-A219480] 17 p2422 N90-23802
A comparison of lightning network data with surface weather observations
[AD-A220003] 17 p2427 N90-23832
TUMULT-64: A real-time multi-processor system
[MEMO-INF-89-58] 17 p2440 N90-23904
Proceeding of the Embedded AI Languages Workshop
[AD-A218531] 17 p2442 N90-23914
Hartstone: Synthetic benchmark requirements for hard real-time applications
[AD-A219326] 17 p2442 N90-23917
Real time adaptive control of an Autonomous Underwater Vehicle (AUV)
[AD-A219544] 17 p2454 N90-23996
Northeast Artificial Intelligence Consortium annual report, 1988. Volume 12: Computer architectures for very large knowledge bases
[AD-A219599] 17 p2454 N90-23999
Intelligent, real-time problem solving
[AD-A219929] 17 p2455 N90-24006
DDTF improvements for more accurate space docking simulation 18 p2504 N90-24311
The real-time Hermes robot arm simulator: HSF-P
18 p2506 N90-24319
AIRNET: A real-time comunications network for aircraft
[NASA-CR-186140] 18 p2543 N90-24514
Real time inverse kinematics with joint limits and spatial constraints
[AD-A220462] 18 p2586 N90-24723
ISIS and META projects
[NASA-CR-186624] 18 p2590 N90-24733
Real time automatic programming
[AD-A220162] 18 p2591 N90-24740
Results of the REALAN project: Replacing the Ethernet access mechanism by the real-time access mechanism of Twentenet
[MEMO-INF-89-55] 18 p2596 N90-24768
Intelligent real-time problem-solving: Issues, concepts and research methodology
[AD-A218868] 18 p2598 N90-24781
System for shooting of video images in realtime
[MBB-UM-0009/89-PUB] 19 p2653 N90-25097
Evaluation of various thrust calculation techniques on an F404 engine
[NASA-TP-3001] 19 p2659 N90-25134
Autonomous power expert system
[NASA-CR-185263] 19 p2670 N90-25187
Conception and results of the DLR realtime azimuth processor for the E-SAR system
[ESA-TT-1184] 19 p2684 N90-25268
Bermuda ionosonde tests in support of OTH-B
[NASA-TM-89359] 19 p2713 N90-25442
NASA systems autonomy demonstration project: Advanced automation demonstration of Space Station Freedom thermal control system
19 p2728 N90-25510
An approach to a real-time distribution system
19 p2733 N90-25535
Real-time measurement of mental workload: A feasibility study 19 p2734 N90-25540
Evaluation of off-road terrain with static stereo and monoscopic displays 19 p2740 N90-25575
Neuromorphic learning of continuous-valued mappings from noise-corrupted data. Application to real-time adaptive control
[NASA-TM-4176] 19 p2747 N90-25807
Intelligent Real-Time Problem Solving
[AD-A220357] 19 p2750 N90-25621
Methods and apparatus for providing real-time control of a gaseous propellant rocket propulsion system
[NASA-CASE-MSC-21542-1] 20 p2825 N90-26073
Real-time monitoring of ceramic sintering with laser ultrasonics
[DE90-012960] 20 p2838 N90-26140
Guidance and control system for an autonomous underwater vehicle
[AD-A222709] 20 p2873 N90-26343
Making real-time reactive systems reliable
[NASA-CR-186642] 20 p2873 N90-26344
A real-time optical 3D tracker for head-mounted display systems
[AD-A222747] 20 p2902 N90-26508
ISIS and META projects
[NASA-CR-186645] 20 p2905 N90-26524
Software requirements: Guidance and control software development specification
[NASA-CR-182058] 20 p2906 N90-26527
A real-time robot arm collision detection system
[NASA-CR-185878] 20 p2915 N90-26582
Neural networks for real-time sensory data processing and sensorimotor control
[AD-A223096] 20 p2916 N90-26592
The browse file of NASA/JPL quick-look radar images from the Loch Linnhe 1989 experiment
[NASA-CR-186855] 20 p2935 N90-26701
Nonlinear real-time signal processing
[AD-A222889] 21 p2994 N90-27020
Earth Sciences Requirements for the Information Sciences Experiment System
[NASA-CP-3072] 21 p3015 N90-27140
Information sciences experiment system
21 p3015 N90-27142
Description of SAFIRE for ISES
21 p3016 N90-27148
ERBE and CERES broadband scanning radiometers
21 p3016 N90-27149
Applications of ISES for geology
21 p3017 N90-27154

Applications of ISES for the atmospheric sciences
21 p3017 N90-27155
Applications of ISES for the oceans
21 p3017 N90-27156
Applications of ISES for coastal zone studies
21 p3018 N90-27157
Applications of ISES for vegetation and land use
21 p3018 N90-27158
Applications of ISES for snow, ice, and sea state
21 p3018 N90-27159
Applications of ISES for meteorology
21 p3018 N90-27160
Applications of ISES for instrument science
21 p3018 N90-27161
INTERMAGNET 21 p3023 N90-27190
Gulfcasting: Dynamical forecast experiments for G ulf Stream rings and meanders
[AD-A221482] 21 p3032 N90-27238
Real-time measurement of mental workload using psychophysiological measures
[AD-A221462] 21 p3036 N90-27258
A real-time optical 6D tracker for head-mounted display systems
[AD-A222884] 21 p3036 N90-27262
Special purpose parallel computer architecture for real-time control and simulation in robotic applications
[NASA-CASE-NPO-17629-1-CU]
21 p3038 N90-27268
A computer for low contest-switch time
[AD-A222883] 21 p3038 N90-27269
An architecture for intelligent task interruption
21 p3041 N90-27284
Attitude Determination and Control System (ADCS) and Maintenance and Diagnostic System (MDS): A maintenance and diagnostic system for Space Station Freedom 21 p3043 N90-27295
The real-time learning mechanism of the Scientific Research Associates Advanced Robotic System (SRAARS) 21 p3046 N90-27312
An application generator for rapid prototyping of Ada real-time control software 21 p3046 N90-27316
A structure for maturing intelligent tutoring system student models 21 p3047 N90-27320
A tool for modeling concurrent real-time computation
21 p3047 N90-27321
Modified fast frequency acquisition via adaptive least squares algorithm
[NASA-CASE-NPO-17845-1-CU]
21 p3050 N90-27341
A programming environment for parallel vision algorithms
[AD-A221486] 21 p3055 N90-27368
ARMTRAK: A domain for the unified study of natural language, planning, and active vision
[AD-A221701] 21 p3056 N90-27373
Neural network with dynamically adaptable neurons
[NASA-CASE-NPO-17803-1-CU]
21 p3057 N90-27385
Dynamic monocular machine vision and applications of dynamic monocular machine vision
[LRT-WE-13-FB-88-3] 21 p3061 N90-27406
Tactical applications of Defense Meteorological Satellite Program (DMSP) environmental data
21 p3067 N90-27439
Command and control in the age of space-based surveillance 21 p3069 N90-27445
Real-time adaptive aircraft scheduling
[NASA-CR-177558] 22 p3110 N90-27669
Expert system for pilot assistance: The challenge of an intensive prototyping
[ETN-90-97274] 22 p3111 N90-27674
Flexible space-based robot modelling and real-time simulation 22 p3131 N90-27769
An ultrasonic system for in-service non-destructive inspection of composite structures
22 p3185 N90-28076
In-service inspection of composite components on aircraft at depot and field levels
22 p3186 N90-28078
Inspection system for in-situ inspection of aircraft composite structures 22 p3188 N90-28091
Applications of X windows in astronautics: Status and prospects
[MBB-UO-0082-90-PUB] 22 p3238 N90-28365
A model parametric real-time logic
[REPT-90-010] 22 p3241 N90-28381
Real time guidance and propulsion control for single-stage-to-orbit airbreathing vehicles
23 p3285 N90-28587
Using the x ray region of the electromagnetic spectrum for alignment: Overview, geometric optics, and design considerations
[DE90-014798] 23 p3317 N90-28752
Real-time aerodynamic heating and surface temperature calculations for hypersonic flight simulation
[NASA-TM-4222] 23 p3327 N90-28815
A laser spectrometer and wavemeter for pulsed lasers
[NASA-CR-181731] 23 p3331 N90-28832
Experiments in the dynamic and strategic control of cooperating manipulators 23 p3333 N90-28845
Solutions to the frictional dynamics problem and the reciprocal variable feedback methodology for design and control of robot mechanisms 23 p3333 N90-28846
A real time evaluation of the use of a perspective format to promote situational awareness in users of air to air tactical displays 23 p3359 N90-28981
A 17 degree of freedom anthropomorphic manipulator
23 p3362 N90-29001
Real-time edge tracking using a tactile sensor
23 p3367 N90-29023
Coordinating the activities of a planner and an execution agent 23 p3369 N90-29035
Perceptual telerobotics 23 p3374 N90-29063
Parallel algorithms for computation of the manipulator inertia matrix 23 p3376 N90-29072
An expert system to perform on-line controller restructuring for abrupt model changes
[NASA-TM-103609] 23 p3385 N90-29121
Distributed control architecture for CNI preprocessors
24 p3426 N90-29356
JTIDS relative navigation: Principles, architecture, and inertial mixing 24 p3426 N90-29357
A land navigation demonstration vehicle with a color map display for tactical use 24 p3430 N90-29375
Inertial navigation system simulator program: Top-level design
[AD-A223762] 24 p3431 N90-29379
The function of the Interactive Model Assembly Program (IMAP) for a flight simulator
[NAL-TR-1034] 24 p3437 N90-29412
Definition of a near real time microbiological monitor for space vehicles
[NASA-CR-185599] 24 p3441 N90-29430
Integrated controls and health monitoring fiberoptic shaft monitor
[NASA-CR-185210] 24 p3472 N90-29622
Concept for a reference model Architecture for Real-Time Intelligent Control Systems (ARTICS)
[PB90-220286] 24 p3475 N90-29638
Weighted feature selection criteria for visual servoing of a telerobot 24 p3503 N90-29801
Experiments in cooperative manipulation: A system perspective 24 p3505 N90-29812
Controlling multiple manipulators using RIPS
24 p3505 N90-29814
Real-time cartesian force feedback control of a teleoperated robot 24 p3513 N90-29857
Performance constraints and compensation for teleoperation with delay 24 p3517 N90-29881
The JPL telerobotic Manipulator Control and Mechanization (MCM) subsystem
24 p3519 N90-29892
The indexed time table approach for planning and acting 24 p3521 N90-29907
Realtime multi-plot graphics system
[NASA-CR-4304] 24 p3523 N90-29919
Formal design and verification of a reliable computing platform for real-time control. Phase 1: Results
[NASA-TM-102716] 24 p3530 N90-29965
Real-time concentration monitoring of large aerodynamic diameter fiber aerosols using the geometric optic inversion technique
[AD-A224167] 24 p3545 N90-30048
Submicron particle analyzer
[AD-A223558] 24 p3545 N90-30050
A compact real-time acousto-optic image correlator
[DE90-015564] 24 p3546 N90-30054

REAL VARIABLES
NT ABEL FUNCTION
NT ASYMPTOTES
NT ASYMPTOTIC SERIES
NT BESSEL FUNCTIONS
NT BIHARMONIC EQUATIONS
NT BURGER EQUATION
NT CALCULUS OF VARIATIONS
NT CAMPBELL-HAUSDORFF SERIES
NT COSINE SERIES
NT CURL (VECTORS)
NT DIFFERENTIAL EQUATIONS
NT EINSTEIN EQUATIONS
NT ELLIPTIC DIFFERENTIAL EQUATIONS
NT EXISTENCE THEOREMS
NT EXTREMUM VALUES
NT FOKKER-PLANCK EQUATION
NT FOURIER SERIES
NT FUNCTIONAL INTEGRATION
NT GAUSS EQUATION
NT GREEN'S FUNCTIONS
NT HANKEL FUNCTIONS
NT HELMHOLTZ VORTICITY EQUATION
NT HYPERBOLIC DIFFERENTIAL EQUATIONS
NT HYPERBOLIC FUNCTIONS
NT HYPERPLANES
NT INTEGRAL CALCULUS
NT J INTEGRAL
NT JACOBI INTEGRAL
NT JACOBI MATRIX METHOD
NT KERNEL FUNCTIONS
NT LEBESGUE THEOREM
NT LIAPUNOV FUNCTIONS
NT LIMITS (MATHEMATICS)
NT LINEAR EQUATIONS
NT LINEAR EVOLUTION EQUATIONS
NT LIOUVILLE EQUATIONS
NT MAXIMA
NT MEASURE AND INTEGRATION
NT MINIMA
NT NEUMANN PROBLEM
NT NONLINEAR EQUATIONS
NT NONLINEAR EVOLUTION EQUATIONS
NT NUMERICAL DIFFERENTIATION
NT NUMERICAL INTEGRATION
NT PADE APPROXIMATION
NT PARABOLIC DIFFERENTIAL EQUATIONS
NT PARTIAL DIFFERENTIAL EQUATIONS
NT PERIODIC FUNCTIONS
NT POISSON EQUATION
NT POWER SERIES
NT QUADRATIC EQUATIONS
NT RICCATI EQUATION
NT RUNGE-KUTTA METHOD
NT SERIES (MATHEMATICS)
NT SINE SERIES
NT TANGENTS
NT TAYLOR SERIES
NT TRIGONOMETRIC FUNCTIONS
NT VECTOR ANALYSIS
NT VLASOV EQUATIONS
NT VORTICITY
NT VORTICITY EQUATIONS
NT WEIERSTRASS FUNCTIONS
NT WEIGHTING FUNCTIONS

REARWARD FACING STEPS
U BACKWARD FACING STEPS

REATTACHED FLOW
Simultaneous detection of separation and transition in surface shear layers 01 p0064 N90-10368
Separation bubbles at high Reynolds number: Measurement and computation
[CUED/A-AERO/15] 12 p1657 N90-19525
Method and apparatus for detecting laminar flow separation and reattachment
[NASA-CASE-LAR-13952-1-SB]
12 p1659 N90-19534

REB
U RELATIVISTIC ELECTRON BEAMS

RECEIVERS
NT RADAR RECEIVERS
NT RADIO RECEIVERS
NT SUPERHETERODYNE RECEIVERS
NT TRANSMITTER RECEIVERS
Vacuum microelectronics for beam power and rectennas 01 p0028 N90-10146
Antenna technology for beamed space-power
01 p0028 N90-10149
Performance of a broadbanded ultrasonic transducer with coaxially mounted, nondirectional receiver
[DE89-015838] 01 p0060 N90-10343
Sensitivity of optoelectronic receivers
[AD-A211823] 03 p0338 N90-11923
Integrated optoelectronic receivers
[AD-A213376] 05 p0700 N90-14098
A heat receiver design for solar dynamic space power systems
[NASA-TM-102473] 06 p0735 N90-14283
SLCSAT (Submarine Laser Communication Satellite) communication system design study
[AD-A213403] 07 p0917 N90-15304
Satellite broadcasting: Requirements for the receiving antenna
[BBC-RD-1989/5] 08 p1055 N90-16098
Helsinki University of Technology Radio Laboratory
[PB90-110677] 08 p1056 N90-16102
Improved optics for laser light scattering
09 p1222 N90-17092
Polarization radar processing technology
[AD-A215242] 10 p1374 N90-17967
Efficient detection and signal parameter estimation with application to high dynamic GPS receiver
[NASA-CASE-NPO-17820-1-CU]
11 p1454 N90-18379
Development of a receiver for a space-based laser radar system
[AD-A215079] 12 p1665 N90-19566
Solar and thermic utilization in high temperature area: Research and development
[ETN-90-96062] 12 p1682 N90-19663

Direct absorption receiver
[DE90-000311] 12 p1683 N90-19667
Performance of a 300 Mbps 1:16 serial/parallel optoelectronic receiver module
[NASA-TM-103110] 13 p1795 N90-20302
Ridge regression processing
14 p1907 N90-20931
Direct Radio Broadcasting by Satellite (DRBS): A review of the technical factors and system approaches suitable for mobile and fixed reception
[BBC-RD-1989/4] 14 p1960 N90-21221
Feasibility of using frequency offset on very high frequency air/ground voice channels
[DOT/FAA/CT-TN89/71] 14 p1964 N90-21248
A functional description of the advanced receiver
15 p2076 N90-21891
QPSK carrier-acquisition performance in the advanced receiver 2
15 p2076 N90-21892
Digital Doppler extraction demonstration with the advanced receiver
15 p2076 N90-21893
Broadcast file distribution on packet satellite networks
15 p2079 N90-21906
Agile multiple aperture imager receiver development
[AD-A218956] 16 p2318 N90-23215
Frequency assignments for HFDF receivers in a search and rescue network
[AD-A220529] 17 p2390 N90-23610
Miniaturization of flight deflection measurement system
[NASA-CASE-LAR-13628-1] 17 p2406 N90-23707
The 30-GHz monolithic receive module
[NASA-CR-180849] 18 p2545 N90-24528
Antennas for portable VHF-FM receivers
[BBC-RD-1990/1] 20 p2850 N90-26211
A novel multireceiver communications system configuration based on optimal estimation theory
[NASA-CR-186847] 20 p2851 N90-26216
A two-telescope receiver design for deep space optical communications
20 p2853 N90-26226
QPSK loop lock detection in the advanced receiver
20 p2854 N90-26230
A preliminary analysis of threshold signal detection in ambient and signal-dependent noise environments
[AD-A222089] 21 p2996 N90-27030
Measured effects of repeater jamming on direct-sequence spread spectrum receivers that use envelope detectors
[AD-A222231] 21 p2996 N90-27032
Aureole lidar: Ground based measurement
[AD-A223207] 21 p3008 N90-27101
Report from GPS MANPACK tests in Spitsbergen area (Norway)
[FFI-90/7007] 22 p3114 N90-27692
Modular digital GPS receivers
24 p3424 N90-29346

RECEIVING SYSTEMS
U RECEIVERS

RECEPTION DIVERSITY
The Australian experiment with ETS-V
10 p1372 N90-17949
Radar detection of lightning and electric fields
[AD-A217894] 13 p1842 N90-20574
Understanding tropscatter propagation
[AD-A220969] 18 p2544 N90-24520
In-band amplitude dispersion on a microwave link
20 p2846 N90-26189

RECEPTORS (PHYSIOLOGY)
NT BARORECEPTORS
NT GRAVIRECEPTORS
NT OTOLITH ORGANS
NT PHOTORECEPTORS
Transduction of nanovolt signals: Limits of electric-field detection
[AD-A219214] 16 p2312 N90-23177

RECHARGING
Preliminary study of rechargeable lithium cells for space applications
10 p1334 N90-17717

RECIPROCAL THEOREMS
On the reciprocity of state vectors in boundary value models
[AD-A214104] 08 p1115 N90-16458
Vector fields, linear spaces and tensors in physics. Part 3: Tensor analysis and its applications
[INPE-5000-MD/41] 11 p1561 N90-18997

RECIPROCATING ENGINES
U PISTON ENGINES

RECIPROCATION
Feasibility analysis of reciprocating magnetic heat pumps
[NASA-CR-186205] 07 p0927 N90-15363
Vertically reciprocating auger
[NASA-CR-182822] 18 p2535 N90-24458

RECIPROCITY THEOREM
Electromagnetic inverse scattering of buried objects
[ETN-90-97216] 20 p2856 N90-26242
Theory of planar near-field measurement
[FEL-89-B273] 22 p3244 N90-28395

RECIRCULATION
U CIRCULATION

RECIRCULATIVE FLUID FLOW
Characterization of nonpremixed turbulent bluff-body burner flames
[PB89-229447] 04 p0469 N90-12689
Theoretical investigation of the stabilization of a diffusion flame above a recirculation region
[ESA-TT-1149] 11 p1484 N90-18543
Continuous hydroponic wheat production using a recirculating system
[NASA-TM-102784] 11 p1538 N90-18853
Composite reduced Navier Stokes procedures for flow problems with strong pressure interactions
[AD-A219621] 17 p2403 N90-23687

RECLAMATION
NT GAS RECOVERY
NT MATERIALS RECOVERY
NT NUCLEAR FUEL REPROCESSING
NT SOLVOLYSIS
NT WATER RECLAMATION
Refurbishment of one-person regenerative air revitalization system
[NASA-CR-183757] 05 p0675 N90-13934

RECOGNITION
NT CHARACTER RECOGNITION
NT PATTERN RECOGNITION
NT SPEECH RECOGNITION
NT TARGET RECOGNITION
NT TIMBER IDENTIFICATION
Synaptic plasticity and memory formation
[AD-A211368] 03 p0379 N90-12158
A Conference on Three-Dimensional Representation held in University of Minnesota on 24-26 May 1989
[AD-A211630] 03 p0406 N90-12324
A validation of the proposed NATO standard method to determine target acquisition distances with image intensifiers
[IZF-1988-8] 04 p0554 N90-13230
Recognition and distinction of clouds, snow, and ice using AVHRR data
08 p1092 N90-16322
Development of a performance-based test of gaze capability: A threshold approach
[AD-A214675] 09 p1259 N90-17301
Stimulus familiarity determines recognition strategy for novel 3-D objects
[AD-A215274] 09 p1260 N90-17305
Improved processes for ultrasonic object recognition in robotics
[ETN-90-95362] 12 p1672 N90-19604
On the verification of hypothesized matches in model-based recognition
[AD-A214718] 12 p1699 N90-19759
Edge recognition using image-processing hardware
[OUEL-1777/89] 15 p2148 N90-22271
Implementing the Canny edge recognizer with datacube image-processing hardware
[OUEL-1786/89] 15 p2148 N90-22272
Automatic recognition of tractability in inference relations
[AD-A223698] 24 p3538 N90-30003

RECOIL IONS
Synchrotron-radiation experiments with recoil ions
[DE89-017579] 03 p0402 N90-12301

RECOIL PROTONS
A study of recoil protons in ultra-relativistic nucleus-nucleus collisions
[LUIP-8907] 06 p0838 N90-14873

RECOMBINATION COEFFICIENT
Hydrogen sulfide effect on hydrogen entry into iron: A mechanistic study
[AD-A216214] 10 p1354 N90-17854
Mechanistic model for catalytic recombination during aerobraking maneuvers
[NASA-CR-185611] 14 p1932 N90-21059

RECOMBINATION REACTIONS
NT ATOMIC RECOMBINATION
NT ELECTRON RECOMBINATION
NT ELECTRON-ION RECOMBINATION
NT HYDROGEN RECOMBINATIONS
NT ION RECOMBINATION
NT OXYGEN RECOMBINATION
NT RADIATIVE RECOMBINATION
Gas dynamical processes in the theory of galaxy formation
02 p0294 N90-11673
Calorimetric measurements on electrochemical cells with Pd-D cathodes
[DE90-002198] 06 p0805 N90-14685
Generation of H-, H2v(double prime), and H atoms by H2+ and H3+ ions incident upon barium surfaces
[DE90-005549] 09 p1280 N90-17423
A preliminary investigation of cold fusion by electrolysis of heavy water
[DE90-004383] 09 p1285 N90-17447
Electron production, electron attachment, and charge recombination process in high pressure gas discharges
[AD-A216301] 10 p1434 N90-18274
Isotope exchange in oxide-containing catalyst
[NASA-CASE-LAR-13542-2-SB]
13 p1769 N90-20154
Termolecular associations of ions in gases, recombination and electron-atom collisions
[AD-A217678] 13 p1883 N90-20805
Mechanistic model for catalytic recombination during aerobraking maneuvers
[NASA-CR-185611] 14 p1932 N90-21059
Atomic processes in high temperature plasmas
[DE90-008873] 14 p2028 N90-21632
Experimental evaluation of chemical cleaning processes for high-lifetime silicon processing
[DE90-009332] 16 p2226 N90-22699
The effects of different diffusion sources on silicon solar cell recombination properties
[DE90-011235] 19 p2710 N90-25426
Application of InAlAs/GaAs superlattice alloys to GaAs solar cells
[DE90-013070] 20 p2881 N90-26389
Non-premixed turbulent CO/H2 flames at local extinction conditions
21 p2975 N90-26907
Modeling of carbon monoxide oxidation kinetics over NASA carbon dioxide laser catalysts
[NASA-CR-186356] 22 p3155 N90-27885
Emitter and base recombination parameters in solar cells: Measurement process and dependence on temperature and injection
[ETN-90-97305] 22 p3196 N90-28138

RECOMMENDATIONS
Toward an understanding of global change: Initial priorities for US contributions to the International Geosphere-Biosphere Program
[NASA-CR-185873] 04 p0516 N90-12980
Remote measurement of ice thickness on the shuttle external tank surface
[NASA-TM-102667] 18 p2555 N90-24584
Program plan: International aircraft operator data base
[IAR-90-1] 19 p2763 N90-25697

RECOMPRESSION
U COMPRESSING

RECONNAISSANCE
NT AERIAL RECONNAISSANCE
NT AIRBORNE INTEGRATED RECONNAISSANCE SYSTEM
Solar radiation in Linkoeping (Sweden): Variations over half a year in irradiance and spectral composition in the interval 400-1000 nm
[FOA-C-30521-3.1] 02 p0250 N90-11417
Automated search techniques applied to optical payloads in unmanned air vehicles
08 p1026 N90-15931
Development of the agricultural information system. Characteristics and results of the Distrito Federal model
[INPE-4940-PRE/1430] 11 p1524 N90-18773
Design of a natural laminar flow airfoil for an unmanned aircraft
[PD-CF-9004] 14 p1916 N90-20975
Activities of the division of surveillance and seeker systems
[FOA-C-30549] 19 p2684 N90-25269
Space-based wide area surveillance system studies
21 p3068 N90-27444
Space-base multispectral imagery: Current and future applications and implications to the United States Army
[AD-A224046] 23 p3343 N90-28894

RECONNAISSANCE AIRCRAFT
NT U-2 AIRCRAFT
Pilotless airplanes
[AD-A211719] 03 p0305 N90-11734
Global Sentry: NASA/USRA high altitude reconnaissance aircraft design, volume 2
[NASA-CR-186820-VOL-2] 20 p2807 N90-25971

RECONNAISSANCE SPACECRAFT
A model for comparing game theory and artificial intelligence decision making processes
[AD-A215418] 09 p1271 N90-17369

RECONSTRUCTION
Type reconstruction with first-class polymorphic values
[AD-A210833] 01 p0106 N90-10605
Quantitative methods for waves in space plasmas
[PB89-210256] 02 p0280 N90-11599
High precision rocket attitude reconstruction using star sensor and magnetometer data
05 p0659 N90-13844
Fatigue analysis and reconstruction of helicopter load spectra
06 p0739 N90-14304
Application of adaptive least-squares algorithm to multi-element array signal reconstruction
12 p1644 N90-19448
Morphological sampling
[CWI-AM-R8913] 17 p2480 N90-24044

RECORDING
NT DATA RECORDING
NT DATA SMOOTHING
NT MAGNETIC RECORDING
Test-retest reliability of oxford Medilog 9000 sleep recording and SS-90-3 sleep stage scoring
|AD-A211165| 02 p0254 N90-11440
Noise floors of subnanosecond transient recording systems
|DE90-002339| 12 p1666 N90-19571
Multi-user facility for high performance optical recording of brain activity (DURIP)
|AD-A223491| 24 p3498 N90-29768
A review of manganin gauge technology for measurements in the gigapascal range
|MRL-TR-90-5| 24 p3541 N90-30026
Comparison of electro-optic diagnostic systems
|DE90-015619| 24 p3546 N90-30056
RECORDING INSTRUMENTS
NT BATHYTHERMOGRAPHS
NT FLIGHT LOAD RECORDERS
NT FLIGHT RECORDERS
NT PLOTTERS
NT SEISMOGRAPHS
NT VIDEO TAPE RECORDERS
NT WEATHER DATA RECORDERS
NT X-Y PLOTTERS
Effective waveform recorder evaluation procedures
|DE90-005197| 10 p1387 N90-18027
Comparisons of the recording instruments. Description of the difference-plots 21 p3022 N90-27181
Catalog of strong motion stations in Eastern North America
|PB90-251984| 24 p3490 N90-29722
RECORDS
NT VIDEO DISKS
RECORDS MANAGEMENT
Space operations: NASA is not properly safeguarding valuable data from past missions
|GAO/IMTEC-90-1| 20 p2936 N90-26704
Past, present and future: Aircraft integrated monitoring systems: An ever-developing technology 22 p3103 N90-27618
RECOVERABILITY
Flight crew aiding for recovery from subsystem failures
|NASA-CR-181905| 12 p1696 N90-19741
RECOVERABLE LAUNCH VEHICLES
Cost optimisation of reusable aerospaceplane transportation systems 09 p1175 N90-16803
Optimum ascent performance of winged two-stage vehicles 09 p1177 N90-16816
Are reusable boosters cost-effective 09 p1179 N90-16834
RECOVERABLE SATELLITES
U RECOVERABLE SPACECRAFT
RECOVERABLE SPACECRAFT
NT AEROSPACE PLANES
NT ASTRO VEHICLE
NT ATLANTIS (ORBITER)
NT BURAN SPACE SHUTTLE
NT CHALLENGER (ORBITER)
NT COLUMBIA (ORBITER)
NT HERMES MANNED SPACEPLANE
NT HOTOL LAUNCH VEHICLE
NT MARS (MANNED REUSABLE SPACECRAFT)
NT REUSABLE SPACECRAFT
NT SPACE SHUTTLE ORBITERS
NT SPACE SHUTTLES
The Spartan 1 mission
|NASA-TM-101887| 01 p0015 N90-10077
Orbit recovery of a low Earth orbiter from GPS and ground tracking stations
|FFI-89/7012| 17 p2361 N90-23446
RECOVERY
Energy management and recovery 08 p1032 N90-15962
Stall and recovery in multistage axial flow compressors 11 p1464 N90-18429
RECOVERY VEHICLES
Preliminary design of the Shuttle-C avionics recovery system
|NASA-CR-186230| 06 p0730 N90-14258
Project EGRESS: Earthbound guaranteed reentry from space station. The design of an assured crew recovery vehicle for the space station
|NASA-CR-186657| 19 p2664 N90-25162
RECREATION
Sensations of temperature and humidity during intermittent exercise and the influence of underwear knit structure
|AD-A215285| 09 p1252 N90-17266
RECRYSTALLIZATION
Containerless Processing of Metals: Undercooling and Solidification
|DLR-MITT-89-15| 05 p0625 N90-13645
Use of computer simulations to analyze limitations of kinetic models for recrystallization
|DE90-003618| 08 p1130 N90-16548
The concept of axial-symmetry constraint and its significance in recrystallization
|DE90-003620| 08 p1131 N90-16549
Softening mechanisms and microstructural instabilities during high temperature, low cycle fatigue of Ni, Ni3Al, and their metal matrix composites
|DE90-006487| 11 p1487 N90-18557
Microstructural simulations of dynamic recrystallization
|DE90-007504| 12 p1722 N90-19895
Computer simulation of recrystallization in the presence of second phase particles
|DE90-007531| 12 p1723 N90-19896
Identification of defects in SOI (Silicon-On-Insulator) wafers
|DE90-006020| 13 p1895 N90-20879
Behavior of Al-Mg alloys in hot working and superplasticity
|DE90-015193| 23 p3310 N90-28723
The roles of strain and reheating interval in continuous recrystallization during the thermomechanical processing by warm rolling of an Al-Mg alloy
|AD-A223673| 24 p3449 N90-29479
RECTANGLES
Finding squares and rectangles in sets of points
|RUU-CS-89-10| 18 p2601 N90-24806
An input-size/output-size trade-off in the time-complexity of rectilinear hidden surface removal
|RUU-CS-89-24| 18 p2602 N90-24814
RECTANGULAR COORDINATES
U CARTESIAN COORDINATES
RECTANGULAR PANELS
Eccentricity effects of square cutouts on the natural frequencies and mode shapes of curved rectangular composite panels
|AD-A216410| 10 p1350 N90-17831
RECTANGULAR PLANFORMS
NT RECTANGULAR PANELS
NT RECTANGULAR PLATES
NT RECTANGULAR WINGS
Effect of blade planform variation on a small-scale hovering rotor
|NASA-TM-4146| 06 p0717 N90-14186
RECTANGULAR PLATES
Natural frequencies of singly-curved laminated plates with simply-supported edges
|ESDU-89011| 03 p0359 N90-12052
Finite element analysis of laminated composite plates 06 p0737 N90-14291
The effect of elastic boundary conditions on the dynamic response of rectangular plates
|NASA-CR-186059| 14 p1990 N90-21405
Fourier series methods for plates and shells with cracks and inclusions 14 p1990 N90-21406
Review of formulae for the buckling of simply-supported, orthotropic plates under shear load, including transverse shear effects
|PB90-167073| 14 p1994 N90-21429
Flat plate vibration analysis experimental and numerical fillet study
|AD-A218789| 16 p2247 N90-22818
Postbuckling response of long thick isotropic plates loaded in compression including higher order transverse shearing effects
|NASA-TM-4199| 22 p3190 N90-28100
Buckling and postbuckling behavior of compression-loaded isotropic plates with cutouts
|NASA-TP-3024| 23 p3337 N90-28859
A nonlinear finite element formulation for the large displacement analysis of plates 23 p3338 N90-28867
RECTANGULAR WAVEGUIDES
Rectangular-to-circular waveguide transitions for high-power circular overmoded waveguides
|AD-A213925| 07 p0924 N90-15349
A new rectangular waveguide to coplanar waveguide transition
|NASA-TM-102477| 14 p1966 N90-21263
Analysis of a TM01 circular to TE10 rectangular waveguide mode converter
|AD-A224566| 24 p3464 N90-29568
RECTANGULAR WINGS
Modeling the wake as a continuous vortex sheet in a potential-flow solution using vortex panels
|AD-A216220| 10 p1385 N90-18016
Effects of spoiler surfaces on the aeroelastic behavior of a low-aspect-ratio rectangular wing
|NASA-TM-102622| 22 p3115 N90-27700
RECTENNAS
Vacuum microelectronics for beam power and rectennas 01 p0028 N90-10146
Millimeter-wave/infrared rectenna development at Georgia Tech 01 p0028 N90-10147
Antenna technology for beamed space-power 01 p0028 N90-10149
Technical options for high average power free electron milimeter-wave and laser devices 01 p0029 N90-10151
Millimeter wavelength rectenna development 15 p2060 N90-21797
Lunar orbiting microwave beam power system
|NASA-TM-103211| 19 p2667 N90-25173
Analysis of a Mars-stationary orbiting microwave power transmission system
|NASA-TM-101344| 20 p2843 N90-26172
RECTIFICATION
NT GEOMETRIC RECTIFICATION (IMAGERY)
Millimeter-wave/infrared rectenna development at Georgia Tech 01 p0028 N90-10147
Applications of remote sensing to studies of oceanic upper mixed layer dynamics 15 p2122 N90-22137
RECTIFIER ANTENNAS
U RECTENNAS
RECTIFIERS
NT AVALANCHE DIODES
NT IGNITRONS
NT SILICON CONTROLLED RECTIFIERS
NT THYRATRONS
NT THYRISTORS
A linearly controlled direct-current power source for high-current inductive loads in a magnetic suspension wind tunnel
|NASA-TM-4198| 19 p2692 N90-25319
A model of the synchronous machine with rectifier, especially for control purposes
|EUT-89-E-215| 20 p2858 N90-26256
A possibility to incorporate saturation in the simple, global model of a synchronous machine with rectifier
|EUT-89-E-225| 20 p2858 N90-26258
RECUPERATORS
U REGENERATORS
RECURSION FORMULAS
U RECURSIVE FUNCTIONS
RECURSIVE FUNCTIONS
Quotient-difference type generalizations of the power method and their analysis
|NASA-TM-102361| 01 p0112 N90-10635
A special case of second-order strictness analysis
|AD-A210829| 01 p0114 N90-10656
Mathematical equivalence in a primitive Ella
|RSRE-MEMO-4225| 04 p0531 N90-13066
Proving total correctness of recursive procedures
|CWI-CS-R8904| 04 p0532 N90-13075
Characterizing termination of logic problems with level mappings
|CWI-CS-R8912| 04 p0532 N90-13077
A recursive algorithm for computing the frequency response of a class of nonlinear difference equation models
|RR-354| 04 p0539 N90-13123
Identification of impulsive interference channels
|AD-A213154| 05 p0688 N90-14009
Membership-set parameter estimation via optimal bounding ellipsoids
|AD-A213807| 07 p0984 N90-15685
Maintaining bridge-connected and biconnected components on-line
|AD-A215107| 13 p1875 N90-20754
Adaptive control of a flexible manipulator with unknown changing loads 15 p2152 N90-22293
A decoupled recursive approach for constrained flexible multibody system dynamics 16 p2289 N90-23042
Naturalness of polymorphism
|CS-8916| 16 p2305 N90-23134
Inverting the flow of computation
|TR-89-10| 17 p2450 N90-23971
Counting and reporting intersections in arrangements of line segments
|RUU-CS-89-12| 18 p2601 N90-24808
A parallel recursive prediction error algorithm for training layered neural networks
|RR-373| 19 p2748 N90-25617
A comparison of the backpropagation and recursive prediction error algorithms for training neural networks
|RR-379| 19 p2748 N90-25620
Large sets of block designs
|ETN-90-97212| 20 p2918 N90-26602
Distributed transitive closure computations: The disconnection set approach
|REPT-90-014| 22 p3259 N90-28459
Evaluating recursive queries in distributed databases
|REPT-90-015| 22 p3260 N90-28460
Recursive least-squares learning algorithms for neural networks
|DE90-014926| 23 p3380 N90-29096
Recursive multibody dynamics and discrete-time optimal control 24 p3513 N90-29860
Recursive Newton-Euler formulation of manipulator dynamics 24 p3513 N90-29862

RECYCLING
Managing the waste stream: Background information for planning source separation programs
[PB90-100223] 07 p0956 N90-15530
Recycling waste-paper 18 p2514 N90-24359
Electrochemical control of iodine disinfectant for space transportation system and space station potable water 18 p2629 N90-24981

RED ARCS
Stable auroral red arc occurrences detected by the Pacific Northwest Laboratory photometer network: A decade of observations, 1978 - 1988
[DE90-004994] 09 p1298 N90-17522

RED BLOOD CELLS
U ERYTHROCYTES

RED GIANT STARS
NT CARBON STARS
Structural experiments of planetary nebulae: Charge-coupled devices, image reduction under MIDAS, information representation, and development of an evolution classification for PN's
[ETN-90-95736] 12 p1744 N90-20026
Astronomical observations of solid phase carbon 21 p3089 N90-27566
The shock process and light element production in supernovae envelopes
[NASA-CR-182854] 22 p3262 N90-28471

RED SHIFT
New statistical approaches to galaxy clustering 02 p0294 N90-11674
Cosmological observations in an inhomogeneous universe
[DE90-733096] 09 p1299 N90-17528
Near infrared (1-4 micron) spectroscopy of SN1987A 11 p1584 N90-19133
Near infrared spectroscopy of active galaxies 11 p1586 N90-19143
H-alpha emission lines in high redshift quasars 11 p1587 N90-19149
A comparison of void distributions in Abell cluster catalogue with numerical simulations
[DE90-610640] 11 p1590 N90-19173
A new interpretation of the feature of SiO maser spectra associated with M-type star
[DE90-610641] 11 p1590 N90-19174
The large scale structure of the universe in pancake models of galaxy formation 14 p2040 N90-21701
Horizon problem in cosmological models with non zero
[DE90-613367] 14 p2042 N90-21708
Search for rapidly star forming galaxies at high redshift 15 p2181 N90-22465
Extended optical emission in 3CR radio galaxies 15 p2193 N90-22523
Spectroscopic observations of high redshift QSOs: Galaxies and the intergalactic medium at early epochs 16 p2330 N90-23280
Kinematic Weyl space-time models
[ETN-90-96508] 18 p2627 N90-24971
X ray spectra of OVV QSOs 19 p2787 N90-25863
Ultrasoft components in X ray-selected AGN 19 p2787 N90-25864
The dependence of the soft X ray spectral slope with radio property, luminosity, and redshift, for a large sample of AGN from the Einstein IPC data base 19 p2789 N90-25876
Periodicity of redshift distribution in a T-3 universe
[FERMILAB-PUB-90/26-A] 22 p3262 N90-28475

REDOX CELLS
Interfacial systems for photochemical energy conversion
[DE90-003181] 07 p0953 N90-15514

REDUCED GRAVITY
Concepts for microgravity experiments utilizing gloveboxes
[NASA-TM-100378] 02 p0209 N90-11195
Nonintrusive inertial vibration isolation technology for microgravity space experiments
[NASA-TM-102386] 03 p0334 N90-11901
Biology in microgravity: A guide for experimenters
[ESA-TM-02] 04 p0482 N90-12769
Protein crystal growth in low gravity
[NASA-CR-186082] 04 p0483 N90-12770
An investigation of flame spread over shallow liquid pools in microgravity and nonair environments
[NASA-TM-102425] 05 p0630 N90-13680
User needs, benefits, and integration of robotic systems in a space station laboratory
[NASA-CR-185150] 05 p0651 N90-13794
The Norwegian balloon and sounding rocket program 1989-1992 05 p0656 N90-13829
The Swedish sounding rocket and balloon program 05 p0657 N90-13830
The German scientific balloon and sounding rocket program 05 p0657 N90-13831
Watchfulness and attention during weightlessness simulations: Use of computerized psychometric tests
[REPT-89-TOU-3-1045] 05 p0674 N90-13928
Response of lymphocytes to a mitogenic stimulus during spaceflight 05 p0677 N90-13942
Polarity establishment, morphogenesis, and cultured plant cells in space 05 p0677 N90-13943
How to detect when cells in space perceive gravity 05 p0678 N90-13946
Effects of microgravity on growth hormone concentration and distribution in plants 05 p0678 N90-13947
Free swimming organisms: Microgravity as an investigative tool 05 p0678 N90-13949
Gravity and animal embryos 05 p0678 N90-13951
Human factors issues in performing life science experiments in a 0-G environment 05 p0679 N90-13952
Do the design concepts used for the space flight hardware directly affect cell structure and/or cell function ground based simulations 05 p0679 N90-13953
Model system studies with a phase separated membrane bioreactor 05 p0679 N90-13954
Design challenges for space bioreactors 05 p0679 N90-13955
Fermentation and oxygen transfer in microgravity 05 p0679 N90-13956
Countermeasures to microgravity 05 p0680 N90-13957
Flight software development for the isothermal dendritic growth experiment
[NASA-TM-102412] 05 p0685 N90-13988
Partial gravity habitat study: With application to lunar base design
[NASA-CR-186048] 06 p0732 N90-14267
Materials processing in low gravity
[NASA-CR-183733] 06 p0755 N90-14397
Thermocapillary migration of liquid droplets in a temperature gradient in a density matched system
[NASA-CR-185178] 06 p0776 N90-14512
Engineering sciences design. Design and implementation of components for a bioregenerative system for growing higher order plants in space
[NASA-CR-186056] 06 p0819 N90-14761
Bridgman crystal growth
[NASA-CR-186204] 07 p0997 N90-15766
Experiment facilities for materials and fluid sciences embarked on Eureca-1
[ESA-SP-1118] 08 p1053 N90-16088
Experiment facilities for materials and fluid sciences embarked on Spacelab
[ESA-SP-1120] 08 p1053 N90-16089
Data compression for the microgravity experiments 08 p1074 N90-16212
Design manual for microgravity two-phase flow and heat transfer
[AD-A214937] 09 p1201 N90-16957
Combustion Experiments During KC-135 Parabolic Flights
[ESA-SP-1113] 09 p1201 N90-16958
Premixed flames in microgravity 09 p1201 N90-16959
Flow field observation of a hot He-CO2 jet in microgravity 09 p1201 N90-16960
Measurements of mean and fluctuating temperature in microgravity 09 p1201 N90-16961
Electric field-induced flame convection in the absence of gravity 09 p1202 N90-16962
Droplet vaporisation and combustion in microgravity 09 p1202 N90-16963
Polymer group microgravity combustion experiment 09 p1202 N90-16964
Heterogeneous combustion processes under microgravity conditions 09 p1202 N90-16965
A comparison of European and American microgravity combustion experimental techniques 09 p1202 N90-16966
An engineering approach to two-phase flow modeling in reduced gravity
[DE90-005539] 09 p1202 N90-16967
NASA Laser Light Scattering Advanced Technology Development Workshop, 1988
[NASA-CP-10033] 09 p1221 N90-17085
Maximum likelihood techniques in QELS 09 p1222 N90-17091
Improved optics for laser light scattering 09 p1222 N90-17092
Light scattering instrumentation for micro gravity research 09 p1223 N90-17096
Theory of microemulsions in a gravitational field 09 p1224 N90-17099
Proposed uses of laser light scattering instruments for polymerization studies 09 p1224 N90-17100
Polymer solution phase separation: Microgravity simulation 09 p1224 N90-17101
Protein crystal growth in microgravity 09 p1224 N90-17102
The 1988-1989 NASA space/gravitational biology accomplishments
[NASA-TM-4160] 09 p1250 N90-17251
Fire safety applications for spacecraft 10 p1314 N90-17595
Non-contact temperature measurement requirements of ground-based research and flight programs at JPL 10 p1362 N90-17895
Microgravity noncontact temperature requirements at NASA Lewis Research Center 10 p1362 N90-17897
Non-contact temperature measurements in support of microgravity combustion experiments 10 p1363 N90-17900
Signal processing applied to photothermal techniques for materials characterization 10 p1364 N90-17902
IR optical fiber-based noncontact pyrometer for drop tube instrumentation 10 p1365 N90-17909
Polymeric materials science in the microgravity environment 10 p1365 N90-17913
Non-Contact Temperature Requirements (NCTM) for drop and bubble physics 10 p1366 N90-17918
Materials thermal and thermoradiative properties/characterization technology 10 p1367 N90-17925
A new approach to active vibration isolation for microgravity space experiments
[NASA-TM-102470] 10 p1368 N90-17929
Zero-gravity vortex vent and PVT gaging system 11 p1475 N90-18486
Investigation of methods to produce a uniform cloud of fuel particles in a flame tube
[NASA-TM-102376] 11 p1505 N90-18665
Payload vibration isolation in a microgravity environment
[NASA-CR-186191] 11 p1518 N90-18744
Techniques for studying the effects of microgravity on model particle/cell systems 12 p1640 N90-19424
Secondary arm coarsening and microsegregation in superalloy PWA-1480 single crystals: Effect of low gravity
[NASA-TM-102445] 13 p1776 N90-20194
Instantaneously generated foam and its applicability to reduced gravity
[NASA-CR-185208] 13 p1784 N90-20237
German microgravity program and flight opportunities 13 p1784 N90-20239
User center and assitance 13 p1784 N90-20240
Systems with a miscibility gap in the liquid state 13 p1785 N90-20245
Molding solidification 13 p1785 N90-20246
Microgravity conditions of a space vehicle 13 p1785 N90-20247
Diffusion and germ formation in glasses 13 p1786 N90-20250
The NASA, Marshall Space Flight Center drop tube user's manual
[NASA-TM-100392] 13 p1786 N90-20251
Microgravity Science and Application Program tasks, 1989 revision
[NASA-TM-4191] 13 p1786 N90-20252
Design and test of a compact optics system for the pool boiling experiment
[NASA-TM-102530] 13 p1786 N90-20253
Space truss zero gravity dynamics 14 p1937 N90-21087
Microgravity science and applications bibliography, 1989 revision
[NASA-TM-4192] 14 p1957 N90-21207
Critical point wetting drop tower experiment
[NASA-CR-186513] 14 p1957 N90-21208
Apparatus for mixing solutions in low gravity environments
[NASA-CASE-MFS-26047-1] 14 p1958 N90-21209
Acoustic convective system
[NASA-CASE-NPO-17278-1-CU] 14 p1959 N90-21215
Microgravity acoustic mixing for particle cloud combustors
[NASA-CR-185159] 14 p2023 N90-21600
The vibro-acoustic mapping of low gravity trajectories on a Learjet aircraft
[NASA-TM-103103] 15 p2045 N90-21723
Development and integration of the capillary pumped loop GAS and Hitchhiker flight experiments
[NASA-TM-100756] 15 p2059 N90-21790
Issues in development, evaluation, and use of the NASA Preflight Adaptation Trainer (PAT)
[NASA-CR-185608] 15 p2137 N90-22212
Microgravity, the space application of the 21st century. Challenges, constraints, and strategies
[REPT-892-430-105] 16 p2226 N90-22696
Technical accomplishments of the NASA Lewis Research Center, 1989
[NASA-TM-102296] 17 p2486 N90-24220

Experiences with and error handling in a knowledge base assisted system for payload experiment automation
18 p2504 N90-24306
Progress in the design of a microgravity facility for in-orbit experiments 18 p2540 N90-24496
Design and manufacturing of an APTF to test fluid behaviour in microgravity environment
18 p2541 N90-24506
National Aeronautics and Space Administration (NASA)/American Society for Engineering Education (ASEE) Summer Faculty Fellowship Program-1989, volume 2
[NASA-CR-185601-VOL-2] 18 p2630 N90-24985
The effects of simulated hypogravity on murine bone marrow cells 18 p2631 N90-24989
Conservation of body calcium by increased dietary intake of potassium: A potential measure to reduce the osteoporosis process during prolonged exposure to microgravity 18 p2631 N90-24993
A study of concept options for the evolution of Space Station Freedom
[NASA-TM-102675] 19 p2663 N90-25154
Microgravity as a tool in developmental biology
[ESA-SP-1123] 19 p2680 N90-25239
Microgravity and mammalian cells
19 p2680 N90-25240
Epidermal Growth Factor (EGF) induced signal transduction in A431 cells is sensitive to gravity
19 p2680 N90-25241
Microgravity effects on insect development and aging
19 p2680 N90-25243
Experimental control of axis polarity in amphibian embryos 19 p2680 N90-25244
The role of gravity in bird development
19 p2681 N90-25246
An in-vitro technique to study bone metabolism in developing mouse long bone rudiments under microgravity and compression 19 p2681 N90-25248
Simulation of the inversion of amphibian eggs in a gravitational field using hollow glass spheres
19 p2681 N90-25251
A global approach for using kinematic redundancy to minimize base reactions of manipulators
[NASA-CR-186825] 19 p2725 N90-25499
A proposal to demonstrate production of salad crops in the space station mockup facility with particular attention to space, energy, and labor constraints
[NASA-CR-186811] 19 p2725 N90-25500
Fluid Phase Separation (FPS) experiment for flight on a space shuttle Get Away Special (GAS) canister
[NASA-CR-186830] 20 p2841 N90-26161
New findings and instrumentation from the NASA Lewis microgravity facilities
[NASA-TM-103189] 20 p2842 N90-26163
Bubble, Drop and Particle Unit (BDPU): A multi-user microgravity facility
[IAF-89-431] 20 p2842 N90-26164
Low-gravity fluid physics: A program overview
[NASA-TM-103215] 20 p2861 N90-26273
The US Experiments Flown on the Soviet Biosatellite Cosmos 1887
[NASA-TM-102254] 20 p2891 N90-26452
Effects of microgravity on rat muscle
20 p2891 N90-26453
Effects of microgravity on rat bone, cartilage and connective tissues 20 p2891 N90-26454
Experiment K-6-03. Gravity and skeletal growth, part 1. Part 2: Morphology and histochemistry of bone cells and vasculature of the tibia; Part 3: Nuclear volume analysis of osteoblast histogenesis in periodontal ligament cells; Part 4: Intervertebral disc swelling pressure associated with microgravity 20 p2892 N90-26457
Experiment K-6-04. Trace element balance in rats during spaceflight 20 p2892 N90-26458
Experiment K-6-05. The maturaton of bone and dentin matrices in rats flown on Cosmos 1887
20 p2893 N90-26459
Experiment K-6-06. Morphometric and EM analyses of tibial epiphyseal plates from Cosmos 1887 rats
20 p2893 N90-26460
Experiment K-6-08. Biochemical and histochemical observations of vastus medialis
20 p2893 N90-26462
Experiment K-6-12. Morphometric studies of atrial or granules and hepatocytes. Part 1: Morphometric study of the liver; Part 2: The atrial granular accumulations
20 p2894 N90-26466
Experiment K-6-13. Morphological and biochemical examination of heart tissue. Part 1: Effects of microgravity on the myocardial fine structure of rats flown on Cosmos 1887. Ultrastructure studies. Part 2: Cellular distribution of cyclic ampdependent protein kinase regulatory subunits in heart muscle of rats flown on Cosmos 1887
20 p2894 N90-26467
Experiment K-6-17. Structural changes and cell turnover in the rats small intestine induced by spaceflight
20 p2895 N90-26470
Experiment K-6-19. Pineal physiology in microgravity: Relation to rat gonadal function
20 p2895 N90-26472
Experiment K-6-20. The effect of spaceflight on pituitary oxytocin and vasopressin content of rats
20 p2896 N90-26473
Experiment K-6-21. Effect of microgravity on 1) metabolic enzymes of type 1 and type 2 muscle fibers and on 2) metabolic enzymes, neutransmitter amino acids, and neurotransmitter associated enzymes in motor and somatosensory cerebral cortex. Part 1: Metabolic enzymes of individual muscle fibers; part 2: metabolic enzymes of hippocampus and spinal cord 20 p2896 N90-26474
Experiment K-6-22. Growth hormone regulation, synthesis and secretion in microgravity. Part 1: Somatotroph physiology. Part 2: Immunohistochemical analysis of hypothalamic hormones. Part 3: Plasma analysis 20 p2896 N90-26475
Protein crystal growth in low gravity
[NASA-CR-186243] 20 p2929 N90-26663
Robot dynamics in reduced gravity environment
21 p3049 N90-27333
Research opportunities on the Space Station
21 p3092 N90-27578
Reaction-compensation technology for microgravity laboratory robots
[NASA-TM-103271] 22 p3183 N90-28062
Microgravity science and applications: Apparatus and facilities
[NASA-TM-101892] 23 p3285 N90-28588
Containerless low gravity processing of glass forming and immiscible alloys
[NASA-CR-186999] 23 p3316 N90-28747
Development and approach to low-frequency microgravity isolation systems
[NASA-TP-2984] 23 p3317 N90-28754
Design of a CO2 laser power control system for a Spacelab microgravity experiment
[NASA-TM-103112] 23 p3331 N90-28833
Cardiovascular deconditioning of cosmonauts: Role, importance and applications of the lower body negative pressure
[ETN-90-97507] 23 p3355 N90-28964
Fluid and electrolyte homeostasis during spaceflight: Elucidation of mechanisms in a primate
[NASA-CR-177548] 23 p3378 N90-29085
Microgravitation experiments in space: Compatibility with interfering dynamic influences 23 p3392 N90-29162
Influence of convection on microstructure
[NASA-CR-186506] 24 p3448 N90-29470
Renal response to seven days of lower body positive pressure in the squirrel monkey
[NASA-CR-183355] 24 p3497 N90-29761
Experimental study on two-dimensional free-flying robot satellite model 24 p3519 N90-29896

REDUCTION (CHEMISTRY)
NT DEOXIDIZING
NT HYDROGENATION
Solvent effects on the kinetics of electroreduction of Cu(I) at mercury
[AD-A209423] 01 p0038 N90-10211
In-situ spectroscopic studies of transition metal macrocycles as catalysts for the electrochemical reduction of oxygen
[PB89-219273] 03 p0321 N90-11826
Mechanisms of CO2 reduction metal and metal modified semiconductor electrodes
[AD-A213169] 04 p0473 N90-12712
Pentafluorothio polynitroaliphatic explosives
[AD-D014221] 06 p0753 N90-14383
New electronic materials and CO2 reduction
[AD-A214679] 09 p1191 N90-16899
Perfluorinated ligands in organometallic chemistry
[AD-A216415] 11 p1476 N90-18493
Techno-economic assessment of a carbothermic alumina reduction process
[DE90-007018] 13 p1772 N90-20170
O2 reduction at the IFC orbiter fuel cell O2 electrode
[NASA-TM-102580] 14 p2001 N90-21469
Characterization study of polycrystalline tin oxide surfaces before and after reduction in CO
18 p2559 N90-24601
Analysis of Pt/SnO(sub x) during catalysis of CO oxidation 18 p2560 N90-24607
Cyclic voltammetry at a rotating disk, electroreduction of nitrate in acidic nickel solutions, and frequency-response analysis of porous electrodes
[DE90-015317] 24 p3447 N90-29466
Chemical stabilization of laser dyes
[AD-A224219] 24 p3473 N90-29627

REDUCTION (MATHEMATICS)
U OPTIMIZATION

REDUNDANCY
Redundancies and don't cares in sequential logic synthesis
[AD-A211931] 03 p0343 N90-11956
Optical arithmetic logic using the modified signed-digit redundant number representation
[AD-D014176] 03 p0384 N90-12186
Base reaction optimization of redundant manipulators for space applications
[NASA-CR-186274] 07 p0941 N90-15447
Study on advanced information processing system
[NASA-CR-186342] 10 p1415 N90-18154
A perspective of software reuse
[AD-A216911] 11 p1546 N90-18901
A new approach to solve the kinematics resolution of a redundant robot
[DE90-010213] 14 p1988 N90-21397
Relatchable launch restraint mechanism for deployable booms 15 p2114 N90-22091
The art of fault-tolerant system reliability modeling
[NASA-TM-102623] 15 p2152 N90-22292
An inverse kinematics algorithm for a highly redundant variable-geometry-truss manipulator
16 p2288 N90-23033
An experimental evaluation of software redundancy as a strategy for improving reliability
[NASA-TM-102613] 17 p2448 N90-23958
A formal mechanism for determining redundancy and irrelevance in Hypertext views
[TR-89-9] 17 p2450 N90-23970
Space shuttle avionics system
[NASA-SP-504] 19 p2664 N90-25160
A global approach for using kinematic redundancy to minimize base reactions of manipulators
[NASA-CR-186825] 19 p2725 N90-25499
Method and apparatus for configuration control of redundant robots
[NASA-CASE-NPO-17801-1-CU]
21 p3010 N90-27110
Resolution of seven-axis manipulator redundancy: A heuristic issue 21 p3049 N90-27331
Combat aircraft control requirements
23 p3271 N90-28515
Motion coordination for mobile robots in unstructured environments
[PB90-199498] 23 p3332 N90-28837
A new approach to global control of redundant manipulators 23 p3363 N90-29002
Cartesian control of redundant robots
23 p3363 N90-29004
Kinematics, controls, and path planning results for a redundant manipulator 23 p3363 N90-29005
Control of intelligent robots in space
23 p3365 N90-29013
Multiple cooperating manipulators: The case of kinematically redundant arms 23 p3371 N90-29046
Preliminary study of a serial-parallel redundant manipulator 23 p3371 N90-29048
A single wafer bit-sliced convolver: An optimum statistical solution for the implementation of redundancy
[REPT-89-019] 24 p3466 N90-29584
Techniques for developing a system safety risk assessment model
[AD-A223477] 24 p3477 N90-29654
Redundant sensorized arm+hand system for space telerobotized manipulation 24 p3502 N90-29792
Redundancy of space manipulator on free-flying vehicle and its nonholonomic path planning
24 p3502 N90-29797
Redundancy in sensors, control and planning of a robotic system for space telerobotics 24 p3511 N90-29847
Robotic control of the seven-degree-of-freedom NASA laboratory telerobotic manipulator
24 p3515 N90-29870
Comparison of joint space versus task force load distribution optimization for a multiarm manipulator system 24 p3515 N90-29873

REDUNDANCY ENCODING
Research in mathematics and computer science: Calculation of the probability of undetected error for certain error detection codes, phase 1
[AD-A210302] 01 p0115 N90-10664
Computer-Aided Design for Built-In-Test (CADBIT). Volume 2: BIT Library
[AD-A215738] 09 p1268 N90-17354
Channel selection and control procedures in an automatic HF system 20 p2847 N90-26193
Conception of a reconfigurable microprocessor
[ETN-90-97248] 20 p2904 N90-26517
Multi-sensory perception of a geometrical structure of a scene
[ETN-90-97245] 20 p2915 N90-26587
Short encodings of evolving structures
[AD-A223641] 24 p3527 N90-29944

REDUNDANT COMPONENTS
Study for optimization of redundant vane-type flow-direction sensing systems and numerical analysis for design of the systems
[NAL-TM-571] 02 p0155 N90-10890
Jam resistant fluid power actuator for ballistic-damage tolerant redundant cylinder assemblies
[AD-D014360] 12 p1671 N90-19600
Kinematically redundant arm formulations for coordinated multiple arm implementations
19 p2736 N90-25551
Computer support for conducting supportability trade-offs in a team setting
[AD-A222002] 22 p3237 N90-28355
Reliability analysis of maintained structural system vulnerable to fatigue and fracture
23 p3338 N90-28868

REDUNDANT STRUCTURES
U REDUNDANT COMPONENTS

REELS
Mechanical evaluation of the differential drum concept for optical fiber pay-out
[AD-A214149] 07 p0993 N90-15740

REENTRY
NT HYPERSONIC REENTRY
NT SPACECRAFT REENTRY
NT UNCONTROLLED REENTRY (SPACECRAFT)
Re-entry hazards and cosmos 1900
[FOA-C-30535-9.4] 05 p0613 N90-13583
Thermal protection systems for reentry and hypersonic flight
[ESA-TT-1179] 19 p2667 N90-25177
Autonomous propulsion system requirements for placement of an STS (Space Transportation System) external tank in low Earth orbit
[PB90-183302] 22 p3133 N90-27777

REENTRY BODIES
U REENTRY VEHICLES

REENTRY EFFECTS
Modifications to the aerotherm charring material thermal response and ablation program (CMA) for carbon ablation analysis
[AD-A211069] 02 p0195 N90-11115
Analytical formulation for the interaction problem of dynamic reentry, and effects due to flexibility and vibration in an aerospace vehicle
[INPE-4963-TDL/392] 11 p1467 N90-18448

REENTRY GLIDERS
U LIFTING REENTRY VEHICLES

REENTRY SHIELDING
Debris/ice/TPS assessment and photographic analysis for Shuttle Mission STS-28R
[NASA-TM-102152] 01 p0016 N90-10079
Aeronautical aspects of Hermes re-entry: Question marks and prospects 09 p1178 N90-16822
SIMOUN: An optimized supersonic high temperature wind tunnel for testing construction materials to be used on the spaceplane
[REPT-892-430-111] 16 p2203 N90-22572

REENTRY TRAJECTORIES
Aeronautical aspects of Hermes re-entry: Question marks and prospects 09 p1178 N90-16822
Using the method of matched asymptotic expansions, analytically investigate the three-dimensional, atmosphere entry problem
[AD-A216287] 11 p1468 N90-18451
Reentry trajectory optimization and control
22 p3127 N90-27746
Hermes emergency reentry trajectories consequences on the Ariane 5 trajectories 22 p3127 N90-27747
Ascent and descent optimizations of an air-breathing launch vehicle 22 p3130 N90-27761

REENTRY VEHICLES
NT AEROSPACE PLANES
NT ASTRO VEHICLE
NT ATLANTIS (ORBITER)
NT BURAN SPACE SHUTTLE
NT CHALLENGER (ORBITER)
NT COLUMBIA (ORBITER)
NT HERMES MANNED SPACEPLANE
NT HOTOL LAUNCH VEHICLE
NT LIFTING REENTRY VEHICLES
NT MANEUVERABLE REENTRY BODIES
NT MARS (MANNED REUSABLE SPACECRAFT)
NT RECOVERABLE SPACECRAFT
NT REUSABLE SPACECRAFT
NT SINGLE STAGE TO ORBIT VEHICLES
NT SPACE SHUTTLE ORBITERS
NT SPACE SHUTTLES
Comparison of laser and neutral particle beam discrimination
[DE89-017786] 03 p0353 N90-12018
Preliminary design of the Shuttle-C avionics recovery system
[NASA-CR-186230] 06 p0730 N90-14258
Performance integration of a reusable launch vehicle with hybrid airbreathing rocket propulsion
09 p1177 N90-16820
Verification of aerothermodynamic codes by means of a winged experimental re-entry vehicle
09 p1180 N90-16842
User's guide to OPUS (Optimal Preferential Utility and Strategies)
[AD-A214384] 10 p1424 N90-18217
Three-dimensional structural analyses of reentry vehicles
[DE90-006278] 12 p1615 N90-19291
Lidar measurements of the optical propagation environment 15 p2084 N90-21930
Earth-to-orbit vehicle providing a reusable orbital stage
[NASA-CASE-LAR-13486-1] 16 p2206 N90-22584
Mission of LARVE 18 p2489 N90-24229
PLATO: A European plateform orbiter concept
[MBB-UO-0061/89-PUB] 19 p2652 N90-25095
Preliminary subsystem designs for the Assured Crew Return Vehicle (ACRV), volume 1
[NASA-CR-186677-VOL-1] 20 p2818 N90-26039
Flight mechanics applications for tethers in space: Cooperative Italian-US programs
22 p3131 N90-27770
Theoretical investigation of non-equilibrium chemistry and optical radiation in hypersonic flow fields
[NASA-CR-186335] 24 p3417 N90-29300

REFERENCE STARS
A statistical study of radio-source structure effects on astrometric very long baseline interferometry observations 04 p0485 N90-12788
The Hipparcos Mission. Prelaunch status. Volume 2: The input catalog
[ESA-SP-1111-VOL-2] 05 p0606 N90-13529
Successive iterations of the input catalog
05 p0607 N90-13534
Standard stars and photometric calibration
05 p0607 N90-13539
The choice of stars in open clusters
05 p0608 N90-13542
The choice of stars in the Magellanic clouds
05 p0608 N90-13543
The catalogs produced by the Inca consortium
05 p0608 N90-13546
The Hipparcos Mission. Prelaunch status. Volume 3: The data reductions
[ESA-SP-1111-VOL-3] 05 p0609 N90-13548
General and numerical approach to the sphere solution in FAST 05 p0610 N90-13555
The sphere solution and astrometric parameter determination in NDAC 05 p0610 N90-13557
Tycho astrometry 05 p0610 N90-13559
The Tycho input catalog 05 p0612 N90-13575
Experiments towards a global sphere solution
05 p0612 N90-13576

REFERENCES (STANDARDS)
U STANDARDS

REFINING
Influence of grain refining on the casting, physical, mechanical, and electrochemical properties of technical aluminum
[ETN-89-94661] 02 p0199 N90-11135
Investigation of commercial Al-Ti and Al-Ti-B master alloys and development of a new grain refining agent based on carbides for aluminum and aluminum alloys
[ETN-89-94663] 02 p0199 N90-11136
Empirical analysis and refinement of expert system knowledge bases
[AD-A213240] 05 p0707 N90-14143
Method for refining microstructures on prealloyed titanium powder compacts
[AD-D014280] 08 p1043 N90-16030
Building an environment model using depth information 23 p3374 N90-29064

REFLECTANCE
NT BIDIRECTIONAL REFLECTANCE
NT SPECTRAL REFLECTANCE
The measurement of infrared spectra of dense ceramics by specular reflectance spectroscopy
[AD-A210609] 01 p0051 N90-10291
Image-based terrain modeling with thematic mapper applied to resolving the limit of Holocene Lake expansion in the Great Salt Lake Desert, Utah, part 1
[NASA-CR-185913] 01 p0082 N90-10465
Surface reflection: Physical and geometrical perspectives
[AD-A210592] 01 p0124 N90-10710
Experimental investigations of transport and optical properties of 3-5 quantum well structures grown via molecular beam epitaxy under optimal growth conditions
[AD-A210269] 01 p0132 N90-10758
Spectral-domain analysis of finite frequency selective surfaces
[AD-A211669] 03 p0339 N90-11932
Development and evaluation of an instrument for rapid electroreflectance of semiconductor materials
[AD-A211690] 03 p0414 N90-12376
Hahn-Banach type theorems for dual semigroups
[CWI-AM-R8903] 04 p0543 N90-13149
Frequency agile synthetic aperture radar
[AD-D014235] 06 p0765 N90-14451
X ray reflectivity study of SiO2 on Si
[DE90-001326] 06 p0851 N90-14943
REFLECT: A computer program for the x ray reflectivity of bent perfect crystals
[DE90-001266] 06 p0851 N90-14946
From primal sketches to the recovery of intensity and reflectance representations 08 p1074 N90-16216
Reflectometers
[AD-D014249] 08 p1122 N90-16499
Light-trapping concentrator cells
[DE90-004988] 09 p1242 N90-17205
Method and apparatus for characterizing reflected ultrasonic pulses
[NASA-CASE-LAR-13966-1] 09 p1278 N90-17408
Evaluation of platinum silicide and indium antimonide as detector materials for space-based remote sensing in the 3.0-to-5.0 micrometer wavelength band
[AD-A216182] 10 p1354 N90-17853
Reflectance modulation with electrochromic Li(sub x)WO(3) films
[DE90-004571] 10 p1435 N90-18279
Unfurlable, continuous-surface reflector concept
12 p1609 N90-19257
Glancing angle XAFS (X ray Absorption Fine Structure) and x ray reflectivity studies of transition-metal/aluminum interfaces
[DE90-005575] 12 p1627 N90-19353
Doppler radar with multiphase modulation of transmitted and reflected signal
[NASA-CASE-MSC-18808-1] 13 p1791 N90-20280
Simple reflection holography
[DE90-008309] 13 p1805 N90-20359
High-efficiency silicon concentrator solar cell research
[DE90-008040] 13 p1827 N90-20490
An estimation of rainfall amounts using radar-derived Z-R relationships
[AD-A217950] 13 p1845 N90-20591
Observation of nonlinear reflectivity from InSb surface and optical switching application
[AD-A217184] 13 p1887 N90-20826
The measurement of surface reflectivity at millimetre wavelengths
[MRL-TN-559] 14 p1960 N90-21222
An assessment of the potential of continuous-wave ranging for measuring the distance to a highly reflective, infinite sheet
[NASA-TM-101680] 14 p1969 N90-21279
Fiber optic void fraction sensor
[DE90-009124] 14 p1983 N90-21386
Absolute multilayer characterization at high spatial resolution via real-time soft x ray imaging
[DE90-009181] 14 p1984 N90-21371
Digital processing of TM/LANDSAT data in monitoring interior water
[INPE-4956-PRE/1533] 14 p1997 N90-21448
Radar scatterometry and polarimetry at 220 GHz
15 p2085 N90-21935
Measurement of the reflectance ratio of natural light in the sea
[IOS-265] 15 p2135 N90-22199
The intensity dependent spread model and color constancy 15 p2140 N90-22228
Image segmentation with detection of highlights and inter-reflections using color
[AD-A218710] 16 p2317 N90-23213
Photoreflectance for in-situ characterization of MOCVD growth of semiconductors under micro-gravity conditions
[NASA-CR-186600] 17 p2383 N90-23576
Initiation and propagation of thunderstorm mesocyclones 17 p2428 N90-23838
Evolution of light domain walls interacting with dark matter, part 1
[NASA-CR-181123] 17 p2485 N90-24211
Surface enrichment and evaporation in a polymer mixture of long and short chains
[DE90-010073] 18 p2529 N90-24429
Implementation of reflectance models in operational AVHRR radiation budget processing
[NOAA-TR-NESDIS-49] 18 p2578 N90-24688
Optical properties monitor: Experiment definition phase
[NASA-CR-4293] 19 p2666 N90-25170
A room-temperature, laser diode-pumped, Q-switched, 2 micron, thulium-doped, solid state laser
[AD-D014527] 19 p2695 N90-25334
Mode-medium instability and its correction with a Gaussian reflectivity mirror
[NASA-TP-3023] 19 p2758 N90-25673

Estimation of the impulse response of a broadband mobile radio channel in suburbia at 910 MHz
20 p2846 N90-26187
The 27-28 October 1986 FIRE IFO Cirrus case study: Comparison of radiative transfer theory with observations by satellite and aircraft
| NASA-TM-103468 | 20 p2890 N90-26446
The 27-28 October 1986 FIRE IFO cirrus case study: Cirrus parameter relationships derived from satellite and lidar data
| NASA-TM-103469 | 20 p2890 N90-26447
Implementation of sensor and control designs for bioregenerative systems
| NASA-CR-186655 | 20 p2897 N90-26479
Modeling and measurement of tree canopy reflectance
| MITT-66 | 21 p3018 N90-27162
Cloud reflectance characteristics in the presence of variable Dimethylsulfide (DMS) sources
| AD-A222806 | 21 p3024 N90-27197
Annular slot antenna radiating into lossy material
| NPL-DITC-152/89 | 22 p3165 N90-27945
Mesoscale variability of free tropospheric humidity near San Nicolas Island during FIRE
22 p3214 N90-28234
Reflectivities of uniform and broken stratiform clouds: An update
22 p3215 N90-28236
Observed cloud reflectivities and liquid water paths: An update
22 p3215 N90-28237
Direct and remote sensing observations of the effects of ships on clouds
22 p3218 N90-28252
Interpretation of cirrus cloud properties using coincident satellite and lidar data during the FIRE cirrus IFO
22 p3223 N90-28276
Thermal imaging assessment
| AD-A224400 | 24 p3460 N90-29542
Two terminal CuInSe2 based cascade cells
| DE90-000363 | 24 p3485 N90-29697
Effect of retardation on the reflectance properties of the metallic Fibonacci quasi-superlattice
| DE90-627316 | 24 p3551 N90-30091

REFLECTED RADIATION
U REFLECTED WAVES

REFLECTED RAYS
U REFLECTED WAVES

REFLECTED WAVES
Angle estimation in a multipath environment with an eight element linear array operating at 10.5 GHz
| FEL-1989-15 | 04 p0491 N90-12826
The physical optics approximation in the near-field region
| FEL-1989-100 | 04 p0555 N90-13234
Corrections for non-ideal effects in reflected shock waves at low Mach numbers
| DE90-002192 | 06 p0721 N90-14208
Statistics of a reflected laser beam in the turbulent atmosphere (path correlation)
| PB90-113994 | 08 p1082 N90-16261
On multiple edge diffraction and multiple reflections of microwaves over terrain
| AD-A216418 | 10 p1377 N90-17985
Multiwavelength pyrometry to correct for reflected radiation
| NASA-TM-102578 | 17 p2407 N90-23714

REFLECTING TELESCOPES
NT LARGE DEPLOYABLE REFLECTOR
System and performance analysis of a low density actively controlled mirror for astronomic observation
02 p0178 N90-11002
An approach to optical structures control
05 p0595 N90-13456
A space qualified thermal imaging system using a Pt Si detector array
10 p1367 N90-17921
Telescope considered as a very high gain antenna
| ETN-90-96614 | 17 p2473 N90-24138
Advanced multilayer x ray optics
| DE90-008228 | 18 p2616 N90-24902
Research and facilities handbook 1989
| ISSN-0267-6281 | 19 p2784 N90-25840

REFLECTION
NT MACH REFLECTION
NT OPTICAL REFLECTION
NT RETROREFLECTION
NT SIGNAL REFLECTION
NT SPECULAR REFLECTION
NT SPREAD REFLECTION
NT ULTRAVIOLET REFLECTION
NT WAVE REFLECTION
Attenuated total reflection FTIR spectroscopy for measuring interfacial reaction kinetics at silica surfaces
| AD-A210314 | 01 p0041 N90-10224
Energy dependent transport problem with generalized boundary conditions
| DE89-617843 | 01 p0118 N90-10676
Surface reflection: Physical and geometrical perspectives
| AD-A210592 | 01 p0124 N90-10710
Eigensolutions for the reflection problem involving the interface of two chiral half spaces
| PB89-221592 | 03 p0338 N90-11926
A guide for estimating potential energy savings from increased solar reflectance of a low-sloped roof
| DE90-003720 | 07 p0955 N90-15526
Measurement of reflection and impedance in a beam by the structural intensity technique
| DE90-728212 | 08 p1088 N90-16299
Reflection technique for thermal mapping of semiconductors
| AD-D014263 | 08 p1129 N90-16541
Principles and formulation of solar reflecting and low infrared emitting coatings for defence use
| MRL-TR-89-2 | 10 p1358 N90-17874
On the scale of diffusion lengths observable by neutron reflection: Application to polymers
| DE90-005645 | 10 p1358 N90-17878
Multilayer optical elements for generation and analysis of circularly polarized x rays
| DE90-006103 | 10 p1430 N90-18250
The propagation of time harmonic Rayleigh-Lamb waves in a bimaterial plate
| AD-A216834 | 11 p1519 N90-18749
Some ray tracing problems related to circles and ellipses
| AD-A219306 | 16 p2318 N90-23217
The 27-28 October 1986 FIRE cirrus case study: Meteorology and clouds
22 p3223 N90-28280
Casimir effect in a D-dimensional flat spacetime and the cut-off method
| DE90-627177 | 23 p3390 N90-29151

REFLECTION COEFFICIENT
U REFLECTANCE

REFLECTION NEBULAE
Small grains in reflection nebulae: A study of diffuse interstellar bands, elemental depletions and infrared flux
02 p0293 N90-11672
Polycyclic aromatic hydrocarbons in the infrared spectra of IRAS sources
11 p1581 N90-19105
IRCAM observations of the Reipurth 50 IR source
11 p1583 N90-19119

REFLECTIVITY
U REFLECTANCE

REFLECTOMETERS
NT MICROWAVE REFLECTOMETERS
Reflectometers
| AD-D014249 | 08 p1122 N90-16499

REFLECTOR ANTENNAS
NT PARABOLIC ANTENNAS
Analysis and test of a 16-foot radial rib reflector developmental model
| NASA-TM-101648 | 01 p0080 N90-10457
Test results on conceptual models of the large deployable antenna for mobile communications satellites
02 p0185 N90-11050
ESA-D: An integrated software for antenna design and analysis
02 p0185 N90-11052
A comparison of reflector antenna designs for wide-angle scanning
12 p1610 N90-19264
Reflector surface distortion analysis techniques (thermal distortion analysis of antennas in space)
12 p1611 N90-19267
Mesh surfaces for reflector applications
12 p1611 N90-19268
Aperture taper determination for the half-scale accurate antenna reflector
| NASA-CR-185215 | 14 p1969 N90-21282
Dual-shaped offset reflector antenna designs from solutions of the geometrical optics first-order partial differential equations
15 p2076 N90-21887
Radiometric tests on wet and dry antenna reflector surface panels
15 p2076 N90-21890
Dynamics and control of tethered antennas/reflectors in orbit
| AD-A219316 | 16 p2207 N90-22594
Feasibility study of a synthesis procedure for array feeds to improve radiation performance of large distorted reflector antennas
| NASA-CR-186641 | 20 p2851 N90-26213

REFLECTORS
NT PARABOLIC REFLECTORS
NT PARABOLOID MIRRORS
NT RADAR CORNER REFLECTORS
NT RETROREFLECTORS
NT SOLAR COLLECTORS
NT SOLAR REFLECTORS
NT WIGGLER MAGNETS
Real-time sensing of optical alignment
05 p0599 N90-13479
Assembly considerations for large reflectors
05 p0599 N90-13480
Advances in large inflatable reflectors
12 p1609 N90-19258
Reflector surface distortion analysis techniques (thermal distortion analysis of antennas in space)
12 p1611 N90-19267
Mesh surfaces for reflector applications
12 p1611 N90-19268
Precision segmented reflector, figure verification sensor
12 p1611 N90-19272
A method for determination of control pixels for LANSAT using a reflector
| INPE-4884-PRE/1491 | 12 p1677 N90-19632
ASCIE: An integrated experiment to study CSI in large segmented optical systems
14 p1936 N90-21082
Preliminary design approach for large high precision segmented reflectors
| NASA-TM-102605 | 14 p1938 N90-21096
Power transmission device
| AD-D014430 | 14 p1969 N90-21281
A soft actuation system for segmented reflector articulation and isolation
15 p2113 N90-22084
Solar Concentrator Advanced Development Program
| NASA-CR-185173 | 16 p2250 N90-22834
Reflection oscillators employing series resonant crystals'
| NASA-CASE-GSC-13173-1 | 17 p2394 N90-23635
Structures for remotely deployable precision antennas
| NASA-CR-182065 | 20 p2822 N90-26061
New core design for use with precision composite reflectors
| NASA-CASE-NPO-17858-1-CU |
21 p2970 N90-26880
An x ray source for lithography
| AD-D014596 | 24 p3473 N90-29630

REFLEXES
NT VESTIBULAR NYSTAGMUS
Factor analytic reduction of the carotid-cardiac baroreflex parameters
08 p1155 N90-16693
Development of a performance-based test of gaze capability: A threshold approach
| AD-A214675 | 09 p1259 N90-17301

REFORESTATION
Contribution of deforestation to atmospheric CO2 and reforestation as an option to control CO2
| DE89-017255 | 04 p0516 N90-12979
Monitoring of reforested areas through digital analysis of TM data
| INPE-4930-PRE/1420 | 11 p1522 N90-18764
Project Floval: Correction of relief effects in eucalyptus reforestration
| INPE-4814-RPE/590 | 11 p1525 N90-18777
Evaluation of TM/LANDSAT and HRV/SPOT data in the identification of reforested areas in the Mogi-Guacu (SP) region
| INPE-4874-PRE/1485 | 13 p1819 N90-20442

REFRACTED RADIATION
U REFRACTED WAVES

REFRACTED RAYS
U REFRACTED WAVES

REFRACTED WAVES
Computations of the refraction of a plane shock wave at a slow-fast gas interface
| DE89-016508 | 02 p0220 N90-11258
Nonlinear acoustics: Reflection and refraction, propagation in a periodic waveguide, scattering of sound by sound and ellipsoidal focusing
| AD-A211224 | 02 p0271 N90-11550
Evidence for self-refraction in a convergence zone: NPE (Nonlinear progressive wave equation) model results
| AD-A218546 | 16 p2259 N90-22879
Image amplification in photoreactive crystals and utilization in optical reaction systems
| ETN-90-97285 | 24 p3546 N90-30059

REFRACTING TELESCOPES
Hybrid diffractive-refractive telescope
| AD-A219241 | 16 p2318 N90-23216

REFRACTION
NT ATMOSPHERIC REFRACTION
NT BIREFRINGENCE
Predicted and measured boundary layer refraction for advanced turboprop propeller noise
| NASA-TM-102365 | 09 p1279 N90-17413
A numerical study of shock wave refraction at a CO2/CH4 interface
| DE90-005997 | 10 p1386 N90-18022
Laser line transport with refraction
| DE90-008683 | 13 p1808 N90-20382
A temperature-dependent regular infrared band model for absorption and dispersion
15 p2083 N90-21927
Specification for environmental measurements to assess radar sensors
| AD-A219127 | 16 p2250 N90-22833
Seismic anisotropy and large-scale porosity in the ocean floor
| AD-A220453 | 17 p2431 N90-23849

Refractive error analysis in the interferometric measurement of 2-D density fields containing strong gradients
[LR-616] 20 p2927 N90-26655
Characteristics of pushbroom scanning type radiometer utilizing linear sensors
[NAL-TR-1024] 24 p3472 N90-29625
REFRACTIVE INDEX
U REFRACTIVITY
REFRACTIVITY
Observations of spherical-wave scintillation in strong refractive-index turbulence
[PB89-124747] 01 p0062 N90-10355
Laboratory measurements of microwave and millimeter-wave properties of planetary atmospheric constituents
[NASA-CR-185914] 01 p0141 N90-10815
Calculation of the refractive index change in dissociating shocked benzene
[DE89-017737] 03 p0322 N90-11833
Small-radius bending loss in single-mode fibers
[AD-A211822] 03 p0405 N90-12323
Recent flow visualization studies in the 0.3-m TCT
04 p0442 N90-12528
Engineer's Refractive Effects Prediction System (EREPS) 06 p0758 N90-14411
Analysis of propagation in an inhomogeneous atmosphere in the horizontal and vertical direction using the parabolic equation method 06 p0760 N90-14421
Propagation modeling for some horizontally varying tropospheric ducts 06 p0760 N90-14422
Assessment of anomalous propagation predictions using minisonde refractivity data and the parabolic equation method 06 p0760 N90-14424
A one-dimensional shipboard model for forecasting refractive effects in the planetary boundary layer
06 p0764 N90-14442
Optical solitons in liquid crystals
[DE90-000694] 07 p0991 N90-15728
A technique for the generation of range-height-angle charts
[AD-A214534] 09 p1204 N90-16979
Reactive atmosphere processing of BaTiO3 and origins of its photorefractive effect
[AD-A215034] 09 p1289 N90-17475
Low elevation angle KU-band satellite measurements at Austin, Texas 10 p1373 N90-17959
Measurement of gas intensity at high dynamic pressures
[ISL-CO-204/89] 11 p1507 N90-18680
A simulation of optical propagation through atmospheric turbulence using two-dimensional Fourier transform techniques
[AD-A216776] 11 p1586 N90-19013
Thermal modulation of light beams
[AD-D014322] 12 p1713 N90-19840
Information reconstruction from speckle interferograms
[ETN-90-95918] 12 p1729 N90-19939
An ellipsometric measurement of optical properties for InP surfaces
[AD-A217185] 13 p1887 N90-20827
Refractive index profiles of thermally grown and chemically vapor deposited films on silicon
[AD-A217187] 13 p1893 N90-20865
Crystallography, spectroscopic analysis, and lasing properties of Nd3+:Y3Sc2Al3O12
[AD-A217792] 13 p1897 N90-20891
Millimetric, infrared, and optical propagation studies over a 500 m path 15 p2080 N90-21913
Modeling of optically and IR effective atmospheric turbulence 15 p2082 N90-21923
Effect of atmospheric turbulence on electro-optical systems 15 p2086 N90-21940
An algorithm and computer program for the calculation of envelope curves
[PB90-155409] 15 p2145 N90-22254
Optical properties of zinc selenide grown using molecular beam deposition techniques
[RSRE-MEMO-4269] 15 p2174 N90-22423
A scattering center based numerical simulation of small scale atmospheric turbulence 16 p2312 N90-23179
Modeling of thermal lensing in side and end-pumped finite solid-state laser rods
[NASA-CR-4300] 17 p2407 N90-23716
Photorefractive damage mechanisms in electro-optic materials
[AD-A219786] 17 p2476 N90-24157
Optical techniques for determination of normal shock position in supersonic flows for aerospace applications
[NASA-TM-103201] 19 p2693 N90-25323
Satellite material contaminant optical properties
19 p2732 N90-25529
Laboratory measurements of microwave and millimeter-wave properties of planetary constituents
20 p2943 N90-26745
Structural and optical properties of DMP-128 holograms during environmental testing
[AD-A221691] 21 p3007 N90-27094
Ionospheric heating with oblique waves. Volume 2: Applications to high-frequency radio propagation
[AD-A223111] 21 p3025 N90-27202
Radio refractivity profiles deduced from lidar measurements
[AD-A221727] 21 p3026 N90-27208
Four techniques to measure complex refractive indices of liquids and solids at carbon dioxide laser wavelengths in the infrared spectral region
[AD-A222007] 22 p3180 N90-28043
Spectral absorption of marine stratocumulus clouds derived from in situ cloud radiation measurements
22 p3215 N90-28238
Compact 4-D optical neural network architecture
[AD-A222160] 22 p3241 N90-28379
Design and performance of a long, over-water microwave radio link
[PB90-207994] 23 p3318 N90-28758
REFRACTORIES
Refractory solids in chondrites and comets: How similar 08 p1148 N90-16654
Ceramic matrix composites, new high performance materials 11 p1477 N90-18500
Radiative heat transfer
[PB90-247602] 23 p3327 N90-28813
REFRACTORY COATINGS
Superconducting ceramics in the Bi1.5SrCaCu2O sub x system by melt quenching technique
[NASA-CR-185139] 02 p0281 N90-11606
Continuous preparation of a thin refractory carbide deposit on the surface of carbon fibers: Characterization of the C/SiC fiber 11 p1477 N90-18501
Metallaboranes as precursors to metallic glasses
[AD-A216946] 11 p1490 N90-18577
REFRACTORY MATERIALS
NT CHROMIUM
NT CHROMIUM ISOTOPES
NT IRIDIUM
NT MOLYBDENUM
NT MOLYBDENUM ALLOYS
NT NIOBIUM
NT NIOBIUM ALLOYS
NT NIOBIUM ISOTOPES
NT REFRACTORIES
NT REFRACTORY METAL ALLOYS
NT REFRACTORY METALS
NT TANTALUM
NT TUNGSTEN
NT TUNGSTEN ALLOYS
Tribological properties of ceramic/Ti3Al-Nb sliding couples for use as candidate seal materials to 700 deg C
[NASA-TM-102401] 04 p0464 N90-12658
Tribological properties of PM212: A high-temperature, self-lubricating, powder metallurgy composite
[NASA-TM-102355] 04 p0465 N90-12659
Graduate fellowships in the field of hard magnetic materials
[AD-A212303] 04 p0477 N90-12733
Surfaces and interfaces of ceramic materials
[AD-A212417] 05 p0627 N90-13657
Thermodynamic properties of some metal oxide-zirconia systems
[NASA-TM-102351] 05 p0628 N90-13666
High-temperature corrosion of heat exchanger materials
[DE90-001963] 06 p0748 N90-14352
A novel heat resistant blend produced by compositional quenching: A thermoplastic polyimide impact modified with a fluoroelastomer
[AD-A213724] 07 p0912 N90-15273
Rapid solidification processing of composites
[AD-A215175] 09 p1187 N90-16875
International Conference on Materials and Mechanisms of Superconductivity: High Temperature Superconductors
[AD-A215343] 09 p1290 N90-17480
Analysis of biaxial stress fields in plates cracking at elevated temperatures
[AD-A216271] 10 p1397 N90-18077
High quality tunnel junction devices using high T(sub c) superconductors
[AD-D014329] 10 p1435 N90-18283
Materials processing of diamond: Etching, doping by ion implantation and contact formation
[AD-A216530] 10 p1438 N90-18301
The processing and mechanical properties of high temperature/high performance composites. Book 3, section 2: Strength and fracture resistance, part
[AD-A216143] 11 p1478 N90-18508
Investigation of the processes controlling the flame generation of refractory materials
[DE90-007564] 12 p1624 N90-19333
Heat-resistant and anticorrosive paint
[DE90-006077] 12 p1630 N90-19369
Symposium on High Temperature and Materials Chemistry
[DE90-008047] 13 p1768 N90-20148
Determination of fundamental thermodynamic properties of constituent materials and performance screening of candidate systems
[AD-A218089] 13 p1769 N90-20153
An investigation of the mechanisms of solid state powder reaction in the combustion synthesis and sintering of high temperature materials
[DE90-007880] 13 p1777 N90-20198
Titanium aluminides: Processing, properties and potential
[AERE-R-13198] 14 p1949 N90-21158
Boron-containing organosilane polymers and ceramic materials thereof
[NASA-CASE-ARC-11649-2-SB] 14 p1952 N90-21177
Attachment of lead wires to thin film thermocouples mounted on high temperature materials using the parallel gap welding process
[NASA-TM-102442] 14 p1983 N90-21361
Approximate analysis for the formation of adiabatic shear bands
[AD-A218751] 16 p2221 N90-22670
Recent advances in nondestructive evaluation made possible by novel uses of video systems
[NASA-TM-102491] 16 p2244 N90-22801
Ultrafine microstructure composites prepared by chemical vapor deposition
[AD-A219650] 17 p2369 N90-23484
Recent implementations on ceramic composites and thermostructural materials
[REPT-892-430-106] 17 p2370 N90-23489
Lightweight ceramic insulation and method
[NASA-CASE-MSC-20782-1] 17 p2382 N90-23566
Development of high performance beta-SiC field-effect transistors
[AD-A218392] 17 p2394 N90-23637
Theory and experimental technique for nondestructive evaluation of ceramic composites
[NASA-TM-102561] 17 p2414 N90-23754
Technical accomplishments of the NASA Lewis Research Center, 1989
[NASA-TM-102296] 17 p2486 N90-24220
State of the art and future prospects for high temperature composites
[REPT-892-430-125] 18 p2517 N90-24375
Development of a design methodology for high temperature cyclic applications of materials which experience cyclic softening
[DE90-006722] 19 p2674 N90-25205
High-temperature materials. Coating, welding, and service tests
[VTT-RR-645] 19 p2675 N90-25214
Metal matrix composites and powder processing for aero-engine applications
[PNR90617] 20 p2828 N90-26087
Densification studies of refractory materials using Hot Isostatic Pressing (HIP) and tantalum containment
[DE90-013481] 20 p2833 N90-26114
Development of ceramic hybrid combustor: Design and combustion test results
[DE90-503442] 20 p2839 N90-26149
A silver-bearing, High-Temperature, Superconducting (HTS) paint
[AD-A221616] 21 p3084 N90-27539
High temperature ceramic superconductors
[AD-A221743] 21 p3084 N90-27540
United States Air Force research initiation program for 1988, volume 2
[AD-A223124] 21 p3102 N90-27614
Processability and high temperature behavior of emerging aerospace alloys
[AD-A224285] 24 p3448 N90-29475
The stress and temperature dependence of creep in an Al-2.0 wt percent Li alloy
[AD-A223676] 24 p3449 N90-29480
REFRACTORY METAL ALLOYS
NT MOLYBDENUM ALLOYS
NT NIOBIUM ALLOYS
NT TUNGSTEN ALLOYS
Material technology challenges in space transportation
09 p1179 N90-16836
REFRACTORY METALS
NT CHROMIUM
NT CHROMIUM ISOTOPES
NT IRIDIUM
NT MOLYBDENUM
NT NIOBIUM
NT NIOBIUM ISOTOPES
NT TANTALUM
NT TUNGSTEN

An investigation of the irradiation swelling mechanisms in refractory metals at high temperatures
[AD-A211406] 04 p0474 N90-12719
Spall strength measurements on shockloaded refractory metals
[DE90-000839] 06 p0747 N90-14345
Thermally stable metal/GaAs contacts
[DE90-002122] 07 p0998 N90-15774
High temperature aluminum-base alloy
[AD-D014270] 08 p1043 N90-16028
One step HIP canning of powder metallurgy composites
[NASA-CASE-LEW-14719-1] 17 p2370 N90-23493

REFRASIL (TRADEMARK)
U FIBERS
U SILICON DIOXIDE

REFRIGERANTS
Absorption fluids data survey: 1989 update
[DE90-003985] 08 p1096 N90-16346
Thermal control system corrosion study
[NASA-TM-102220] 14 p1971 N90-21294
An experimental evaluation of two nonazeotropic refrigerant mixtures in a water-to-water breadboard heat pump
[DE90-009016] 14 p1973 N90-21305
Experimental performance of ozone-safe alternative refrigerants: Experimental performance comparisons of R32, R125, R143a, R218, R134a, R152a, R124, R142b, RC318 and R143 in a refrigeration circuit
[DE90-009227] 15 p2073 N90-21876
Thermodynamic calculations for mixtures of environmentally safe refrigerants using the Lee-Kesler-Ploecker equation of state
[DE90-010493] 18 p2542 N90-24509
Boiling/evaporative heat transfer from spheres in packed-bed thermal energy storage units
[DE90-012023] 19 p2711 N90-25430

REFRIGERATING
Development of a low noise 10 K J-T refrigeration system
[AD-A213347] 04 p0484 N90-12779
Feasibility of cool storage systems in refrigeration
[DE90-728179] 08 p1054 N90-16093
Intermittent Solar Ammonia Absorption Cycle (ISAAC) refrigeration for lesser developed countries
[DE90-006700] 11 p1496 N90-18610
A progress report on using bolometers cooled by adiabatic demagnetization refrigeration
14 p1976 N90-21318
A theoretical and experimental investigation of an absorption refrigeration system for application with solar energy units
16 p2226 N90-22697

REFRIGERATING MACHINERY
NT REFRIGERATORS
Recent advances in magnetic heat pump technology
[DE89-013289] 07 p0928 N90-15370
Upcoming planetary missions and the applicability of high temperature superconductor bolometers
22 p3140 N90-27811

REFRIGERATORS
Design and calibration of an electrodynamic driver for the Space Thermoacoustic Refrigerator (STAR)
[AD-A212022] 03 p0335 N90-11906
Development of a low noise 10 K J-T refrigeration system
[AD-A213347] 04 p0484 N90-12779
A closed-cycle refrigerator for cooling maser amplifiers below 4 Kelvin 04 p0487 N90-12797
Cryogenics for LDR 05 p0598 N90-13471
An algorithm for control volume analysis of cryogenic systems
[AD-A213394] 05 p0631 N90-13683
Thermal design of a 10-kW helium refrigerator
[DE90-701785] 06 p0756 N90-14403
Feasibility of cool storage systems in refrigeration
[DE90-728179] 08 p1054 N90-16093
Evaluation of industrial magnetic heat pump/refrigerator concepts that utilize superconducting magnets
[DE90-008093] 13 p1787 N90-20258
A 100 micro Kelvin bolometer system for SIRTF
14 p1976 N90-21317
Multicomponent gas sorption Joule-Thomson refrigerator
[NASA-CASE-NPO-17569-1-CU]
20 p2844 N90-26176
Spacecraft thermal control design data, volume 5. Section R: Cryogenic cooling. Section S: Existing satellites
[ESA-PSS-03-108-ISSUE-1-VOL-5]
22 p3132 N90-27772

REFUELING
NT AIR TO AIR REFUELING
Experimental evaluation of impedance control for robotic aircraft refueling
[AD-A215532] 09 p1167 N90-16755
Application of railgun principle to high-velocity hydrogen pellet injection for magnetic fusion reactor refueling
[DE90-008281] 13 p1761 N90-20109
Advanced space transportation technologies
18 p2645 N90-25061
Engineering test results for the Moog Single Line Disconnect
[NASA-TM-100755] 22 p3132 N90-27776

REGENERATION (ENGINEERING)
Refurbishment of one-person regenerative air revitalization system
[NASA-CR-183757] 05 p0675 N90-13934
New heating and cooling technology: Regenerative heat pump according to the Vuilleumier principle
[DE90-002701] 06 p0807 N90-14699
Publications of the NASA Controlled Ecological Life Support System (CELSS) Program, 1979-1989
[NASA-CR-4297] 15 p2051 N90-21754
A comparison between experiment and simulation for concept VIC regenerative liquid propellant guns. Part 1: 30 mm
[AD-A218556] 16 p2225 N90-22692
Regenerative Cu La zeolite supported desulfurizing sorbents
[NASA-CASE-NPO-17480-1-CU]
20 p2830 N90-26098

REGENERATION (PHYSIOLOGY)
Lens and limb regeneration in newt during and after 13-day long spaceflight 19 p2681 N90-25252
Implementation of sensor and control designs for bioregenerative systems
[NASA-CR-186655] 20 p2897 N90-26479

REGENERATIVE COOLING
Thermodynamic transport properties of nitrogen tetroxide in hypercritical conditions for regenerative cooling of a rocket engine. Volume 1: Tests
[ETN-89-94975] 01 p0134 N90-10773
Thermodynamic transport properties of nitrogen tetroxide in hypercritical conditions for regenerative cooling of a rocket engine. Volume 2: Appendices
[ETN-89-94977] 01 p0134 N90-10774
Thermal protection systems for reentry and hypersonic flight
[DLR-MITT-89-14] 05 p0613 N90-13577
Feasibility analysis of reciprocating magnetic heat pumps
[NASA-CR-186205] 07 p0927 N90-15363
Spacecraft thermal control design data, volume 4
[ESA-PSS-03-108-ISSUE-1-VOL-4]
11 p1469 N90-18458
Development and fabrication of structural components for a scramjet engine
[NASA-CR-181945] 13 p1757 N90-20088

REGENERATIVE CYCLES
U REGENERATION (ENGINEERING)

REGENERATIVE FEEDBACK
U POSITIVE FEEDBACK

REGENERATIVE FUEL CELLS
Rechargeable lithium/polymer cathode batteries
[AD-A210978] 01 p0062 N90-10354
The fuel cell in space: Yesterday, today and tomorrow
[NASA-TM-102366] 03 p0318 N90-11804
Regenerative fuel cell systems for project pathfinder
10 p1333 N90-17708
European regenerative fuel cell technology for space use 10 p1333 N90-17709
Simulation of regenerative fuel cell systems including thermal control 10 p1333 N90-17711
Solid polymer electrolyte water electrolysis as a mean of energy storage for space applications
10 p1334 N90-17713
Preliminary study of rechargeable lithium cells for space applications 10 p1334 N90-17717
Integrated regenerative fuel cell experimental evaluation
[NASA-CR-185183] 11 p1530 N90-18808
Viscosity, density and conductivity of ImCl(HCl) sub 1.3
[AD-A218902] 16 p2216 N90-22641
The chemical effects of the Martian environment on power system component materials: A theoretical approach
[NASA-TM-103203] 20 p2825 N90-26074
Modeling and optimization of a regenerative fuel cell system using the ASPEN process simulator
[NASA-TM-103210] 20 p2882 N90-26396
A solar power system for an early Mars expedition
[NASA-TM-103219] 22 p3243 N90-28393

REGENERATORS
Gas turbine regenerators: A method for selecting the optimum plate-finned surface pair for minimum core volume
[AD-A213430] 07 p0930 N90-15382
Generation of ultrashort laser pulses from neodymium glass oscillator and regenerative amplifier
14 p1984 N90-21373

REGGE POLES
Simplicial lattices in classical and quantum gravity: Mathematical structure and application
10 p1439 N90-18304

REGIONAL PLANNING
NT URBAN PLANNING
The application of remote sensing techniques for regional planning, environmental studies, and environment maintenance
[BCRS-89-16] 18 p2574 N90-24667

REGIONS
NT AMAZON REGION (SOUTH AMERICA)
NT ANTARCTIC REGIONS
NT ARCTIC REGIONS
NT AURORAL ZONES
NT BRILLOUIN ZONES
NT D REGION
NT E REGION
NT EQUATORIAL REGIONS
NT F REGION
NT F 2 REGION
NT FRESNEL REGION
NT HABITATS
NT NULL ZONES
NT POLAR REGIONS
NT ROSS ICE SHELF
NT SOUTHEAST ASIA
NT SPORADIC E LAYER
NT TEMPERATE REGIONS
NT TROPICAL REGIONS
Sensitivity of ecological landscapes and regions to global climatic change
[PB90-120072] 12 p1684 N90-19674

REGISTERS (COMPUTERS)
NT ACCUMULATORS (COMPUTERS)
Cache for multi-threaded processors on a split-transaction bus
[AD-A216404] 10 p1415 N90-18156
Atomic snapshots of shared memory
[AD-A222765] 20 p2904 N90-26520

REGOLITH
Metamorphism of cosmic dust: Processing from circumstellar outflows to the cometary regolith
08 p1146 N90-16641
Petrographic working model of the Rosetta sampling and modelling subgroup for a comet nucleus
12 p1738 N90-19992
Erosional development of bedrock spur and gully topography in the Valles Marineris, Mars
[NASA-CR-180655] 17 p2424 N90-23813
Lunar regolith bagging system
[NASA-CR-186683] 19 p2677 N90-25223
Lunar regolith bagging system
[NASA-CR-186652] 19 p2677 N90-25224

REGRESSION (STATISTICS)
U REGRESSION ANALYSIS

REGRESSION ANALYSIS
NT REGRESSION COEFFICIENTS
Improved estimation of the disturbance variance in a linear regression model
[AD-A210272] 01 p0112 N90-10641
Asymptotic robustness in regression and autoregression based on Lindeberg conditions
[AD-A210725] 01 p0114 N90-10654
Advances in regression: Use of models in spectroscopic data analysis
[AD-A210541] 01 p0116 N90-10665
Forecasting contracting workload
[AD-A211935] 03 p0416 N90-12387
Estimating the relationships between the state of the art of technology and production cost for the US aircraft
[AD-A212127] 04 p0437 N90-12495
On the application of modified stepwise regression for the estimation of aircraft stability and control parameters
[REPT-8905] 05 p0583 N90-13400
Measuring of the complete stiffness matrix for anisotropic laminated materials
[DLR-MITT-89-11] 05 p0618 N90-13606
Measuring of the complete stiffness matrix for anisotropic laminated materials
[DLR-MITT-89-12] 05 p0618 N90-13607
Precipitation distributions associated with cyclones originating over the Gulf of Mexico and surrounding coastal regions
[AD-A213644] 07 p0963 N90-15569
Traction modeling of military lubricants
[AD-A213866] 09 p1230 N90-17139
Nonparametric estimation of reliability and related functions
[AD-A215138] 09 p1234 N90-17160
Distribution and seasonal variations of diffuse fraction
[DE90-601303] 09 p1246 N90-17228
A general method of using prior information in a simultaneous equation system
[NOAA-TR-NESDIS-47] 10 p1423 N90-18209

On detecting influential data and selecting regression variables
|AD-A216387| 10 p1423 N90-18213
TVI: A mathematical model for global estimation of Brazilian cerrado phytomass
|INPE-4836-PRE/1465| 11 p1521 N90-18759
Can the square law be validated
|DE90-007112| 11 p1553 N90-18945
Satellite imagery for water quality assessment in coastal regions
|INPE-4891-PRE/1492| 12 p1678 N90-19636
High resolution radar target modeling using ARMA (Autoregressive Moving Average) models
|AD-A218212| 13 p1791 N90-20278
Slepian models and regression approximations in crossing and extreme value theory
|AD-A218338| 13 p1879 N90-20779
Review and statistical analysis of the ultrasonic velocity method for estimating the porosity fraction in polycrystalline materials
|NASA-TM-102501-REV| 14 p1989 N90-21402
Performance evaluation of MSS/LANDSAT data in the estimation of fluvial channel width
|INPE-4906-PRE/1507| 14 p2000 N90-21463
The observed three-dimensional structure of baroclinic waves in the Northern Hemisphere winter as revealed in a linear regression analysis 15 p2128 N90-22167
Orthogonal distance regression
|PB90-151747| 15 p2160 N90-22336
Relationship between flexibility of closure and success in pilot night vision sensor system training
|AD-A221439| 16 p2261 N90-22890
Differential Loran-C using three secondary stations
|AD-A219573| 17 p2350 N90-23381
Model order determination methods for autoregressive radio direction finding techniques
|AD-A220707| 17 p2350 N90-23384
Application of the lagged-averaged technique to tropical cyclone track predictions
|AD-A218389| 17 p2425 N90-23819
M-estimators in linear models with long range dependent errors
|AD-A219921| 17 p2461 N90-24053
Mean square error behavior for prediction in linear regression models
|AD-A219988| 17 p2466 N90-24092
Non-linear systems identification using radial basis functions
|RR-378| 19 p2751 N90-25635
Variance reduction for quantile estimates in simulations via nonlinear controls
|AD-A222653| 20 p2916 N90-26590
Asymptotic optimality of the fast randomized versions of GCV and C(sub L) in ridge regression and regularization
|IMAG-RR-793-M| 20 p2918 N90-26606
A study of the asymptotic properties of least square estimators for multiple phase regression problems
|ETN-90-97244| 20 p2921 N90-26620
Nonlinear modeling of time series using Multivariate Adaptive Regression Splines (MARS)
|AD-A222710| 20 p2921 N90-26623
Radio refractivity profiles deduced from lidar measurements
|AD-A221727| 21 p3026 N90-27208
ROBFIT: A code for the analysis of histogram spectra with nonlinear regression and robust estimation
|AD-A221527| 21 p3055 N90-27369
STATLIB: NSWC library of statistical programs and subroutines
|AD-A221538| 21 p3055 N90-27370
Trend analysis of total ozone data
24 p3486 N90-29703

REGRESSION COEFFICIENTS
An estimation of rainfall amounts using radar-derived Z-R relationships
|AD-A217950| 13 p1845 N90-20591
Mean square error behavior for prediction in linear regression models
|AD-A219988| 17 p2466 N90-24092
Non-linear systems identification using radial basis functions
|RR-378| 19 p2751 N90-25635
Reversed residuals in autoregressive time series analysis
|AD-A222711| 20 p2921 N90-26624
Radio refractivity profiles deduced from lidar measurements
|AD-A221727| 21 p3026 N90-27208

REGULARITY
On smallest nonhamiltonian regular rough graphs
|MEMO-788| 05 p0687 N90-14003
Hidden regularity for a strongly nonlinear wave equation
|DE90-600742| 08 p1116 N90-16465

REGULATION
U CONTROL

REGULATIONS
Castings Airworthiness
|AGARD-R-762| 01 p0042 N90-10231
The question of the casting factor
01 p0043 N90-10238
Manual of regulations and procedures for federal radio frequency management, May 1986 edition: Revisions for January 1989
|PB89-193791| 01 p0056 N90-10320
Domestic technology transfer program regulation
|PB89-195374| 01 p0137 N90-10793
Review of the ESA fracture control policy
02 p0182 N90-11029
Consumer Ozone Protection Act of 1989
|S-HRG-101-377| 06 p0809 N90-14708
International aspects of restrictions of ozone-depleting substances
|DE90-001813| 07 p0957 N90-15534
Diesel starting system monitor: Prototype development
|DE90-004425| 08 p1084 N90-16276
Fire hardening of an aircraft passenger cabin
10 p1315 N90-17606
Advanced materials for interior and equipment related to fire safety in aviation 10 p1316 N90-17608
New materials for civil aircraft furnishing
10 p1316 N90-17609
Flammability testing of aircraft cabin materials
10 p1316 N90-17611
The research program at the Civil Aeromedical Institute concerning protective breathing equipment for use by crew and passengers in an aviation smoke/fume environment
10 p1317 N90-17616
High-Explosives Applications Facility (HEAF)
|DE90-008122| 13 p1787 N90-20257
A guide to performing and documenting safety analyses
|DE90-008688| 13 p1788 N90-20261
Information management systems for integrating the technical data and regulatory requirements of environmental restoration activities
|DE90-008622| 13 p1831 N90-20511
Development of a consolidated environmental data base
|DE90-009419| 17 p2479 N90-24177
Problems related to aircraft noise in Switzerland
18 p2611 N90-24871
The new US flight recorder regulations
22 p3106 N90-27642
System reliability optimization of aircraft wings
23 p3275 N90-28536
Tests for aircraft interior materials in fire accident
|LR-622| 24 p3423 N90-29337
Success of EPA's stratospheric ozone engineering research
|PB90-246265| 24 p3487 N90-29706

REGULATORS
NT AUTOMATIC FREQUENCY CONTROL
NT CURRENT REGULATORS
NT FLOW REGULATORS
NT FREQUENCY CONTROL
NT PRESSURE REGULATORS
NT SPEED REGULATORS
NT THERMOSTATS
NT VOLTAGE REGULATORS
ERIS: Engineering Resource Information System
|AD-A213357| 05 p0707 N90-14144
Dispelling the North American acid rain clouds: Developing a framework for political consensus through the identification of elite viewpoints, volumes 1 and 2
09 p1243 N90-17213
The subsystem regulator, the next generation in satellite regulated power conditioning 10 p1331 N90-17690
Optimization of sensors and actuators positioning aimed at obtaining reduced models for the synthesis of optimal control regulators of flexible structures
|INPE-4760-TDL/348| 11 p1468 N90-18450
A learning regulator for the plane longitudinal movement
|ETN-90-95381| 13 p1864 N90-20695
Adaptive control methods for mechanical manipulators: A comparative study
|AD-A219965| 17 p2413 N90-23749
Monitoring and control of spacecraft systems using procedural reasoning 19 p2731 N90-25524

REGULATORY MECHANISMS (BIOLOGY)
The pituitary growth hormone cell in space
05 p0676 N90-13941
The trials and tribulations of RAF defence mechanism testing 09 p1257 N90-17291
Neurocontrol systems and wing-fluid interactions underlying dragonfly flight 12 p1606 N90-19240
Elevated central venous pressure: A consequence of exercise training-induced hypervolemia
|NASA-TM-102965| 13 p1850 N90-20617
Epidermal Growth Factor (EGF) induced signal transduction in A431 cells is sensitive to gravity
19 p2680 N90-25241
Regulation of erythropoiesis in rats during space flight
|NASA-CR-177537| 23 p3378 N90-29086

REHEATING
U HEATING

REIGNITION
U IGNITION

REINFORCED PLASTICS
NT CARBON FIBER REINFORCED PLASTICS
NT GLASS FIBER REINFORCED PLASTICS
The creep behavior of an aramide fiber reinforced wound tow-strap
|LR-546| 12 p1620 N90-19312
Modelling of the impact response of fibre-reinforced composites
|OUEL-1784/89| 15 p2065 N90-21827
Mechanical testing of selected engineering plastics
|DE90-008186| 16 p2222 N90-22673
Study of failure processes in fiber reinforced composites using acoustic emission techniques
22 p3188 N90-28090

REINFORCED PLATES
Innovative design of composite structures: The use of curvilinear fiber format in structural design of composites
|NASA-CR-186406| 12 p1620 N90-19308

REINFORCEMENT (STRUCTURES)
Compact reinforced composite basic principles
|CBL-41| 11 p1480 N90-18520
High-strength concrete development through 25 years
|CBL-REPRINT-17| 11 p1492 N90-18589
Introduction to compact reinforced composite
|CBL-REPRINT-5| 19 p2673 N90-25199

REINFORCING FIBERS
NT BORON FIBERS
NT CARBON FIBERS
Field repair of composite materials in Army service: Planning for the future
|AD-A210732| 01 p0035 N90-10190
A study of the impact of a ball bearing on a long fiber composite plate with a carbon matrix, part 2
|ETCA-88-R-088-PT-2| 04 p0467 N90-12673
Oxide ceramic fibers by the sol-gel methods
|AD-A211315| 04 p0478 N90-12742
Rolling of ARALL laminates (an alternative method for post-stretching ARALL laminates)
|LR-560| 04 p0484 N90-12778
Fiber reinforced cementitious composites technology
|PB89-227813| 05 p0619 N90-13608
Method for stabilization of pan-based carbon fibers
|AD-D014228| 06 p0736 N90-14288
Metal matrix composites with long inorganic fibers
07 p0901 N90-15206
Metal matrix composites: A promising alternative to conventional alloys 07 p0901 N90-15208
Effects of moisture on composite materials
09 p1185 N90-16866
Studies on deformation and fracture of viscoelastic composite materials
|AD-A216095| 10 p1348 N90-17819
Mechanical behavior of whisker reinforced ceramics
|DE90-008758| 13 p1781 N90-20224
Reinforcement-matrix interface effects in metal matrix composites
|MRL-TN-562| 14 p1943 N90-21120
Seamless metal-clad fiber-reinforced organic matrix composite structures and process for their manufacture
|NASA-CASE-LAR-13562-1| 19 p2672 N90-25196
Development of ceramic fiber type combustor: Improvement of combustor and combustion test results
|DE90-503441| 20 p2839 N90-26148
Time temperature relations during rubber forming continuous fiber reinforced thermoplastics
|LR-620| 20 p2840 N90-26151
The 1990 Gordon Research Conference on Composites
|AD-A222849| 21 p2971 N90-26886
A study on carbon Fiber (long fiber) reinforced copper matrix composite
|AD-A221584| 21 p2972 N90-26891
Inorganic composite materials in Japan: Status and trends
|PB90-174392| 22 p3135 N90-27789
Reinforcing fibers and technology development for resin composites. Consequences for aircraft structures
|FOA-C-20777-2.5| 22 p3154 N90-27883
Study of failure processes in fiber reinforced composites using acoustic emission techniques
22 p3188 N90-28090
Creep and creep rupture of strongly reinforced metallic composites
|NASA-CR-185286| 22 p3192 N90-28110
Ceramic matrix composites in simulated SSME environments 23 p3298 N90-28655

Is there anything of practical value hidden amongst the composite toughening theories. A Jim Mueller prospective
[DE90-014905] 23 p3301 N90-28673
Evaluation of ARALL-4: An aramid fiber reinforced aluminum
[AD-A223502] 24 p3443 N90-29443
Development of dual fiber reinforced glass matrix composites for structural space based applications
[AD-A223801] 24 p3444 N90-29446
Interlaminar shear tests on continuous fiber reinforced thermoplastics: The effects of rubber forming
[LR-621] 24 p3444 N90-29451

REINFORCING MATERIALS
A design assessment for metallic pressure vessels circumferentially reinforced with a pre-tensioned high-specific-strength anisotropic composite overwind
[AD-A209108] 01 p0079 N90-10453
The application of cast SiC/Al to rotary engine components
[NASA-CR-179610] 05 p0581 N90-13385
Toughening of a particulate-reinforced/ceramic-matrix composite
[AD-A213180] 05 p0618 N90-13604
Carbon fiber reinforced metal matrix composites
[AD-D014245] 06 p0737 N90-14289
Composite activities at Lawrence Livermore National Laboratory
[DE90-002979] 07 p0891 N90-15149
Vibration damping composition suitable for outer space temperature variations
[AD-D014288] 08 p1088 N90-16296
Metal matrix composite: Strengthening mechanisms
[AD-A214843] 09 p1186 N90-16871
The processing and mechanical properties of high temperature/high performance composites. Book 4, section 3: Flow and creep strength
[AD-A216144] 10 p1349 N90-17822
Instrumented impact testing of fabric-reinforced composite materials
[AD-A216764] 11 p1479 N90-18513
Thermal analysis of polymer composites
[AD-A216947] 11 p1490 N90-18578
Jam resistant fluid power actuator for ballistic-damage tolerant redundant cylinder assemblies
[AD-D014360] 12 p1671 N90-19600
Introduction to compact reinforced composite
[CBL-REPRINT-5] 19 p2673 N90-25199
Crack bridging processes in toughened ceramics
[DE90-011650] 19 p2678 N90-25231
The 1990 Gordon Research Conference on Composites
[AD-A222849] 21 p2971 N90-26886
Theory of ceramic/zirconia composites: Toughening, strengthening, and synergism
[AD-A222931] 21 p2985 N90-26961
Evaluation of several micromechanics models for discontinuously reinforced metal matrix composites
[NASA-TM-102719] 23 p3339 N90-28872
Rheology of filler rubber: Silica-silicone
[AD-A223600] 24 p3455 N90-29511

REJECTION
A real-time rejection circuit to automatically reject multiple interfering hopping signals while passing a lower level desired signal
[AD-D014424] 14 p1965 N90-21251

RELATIVISTIC EFFECTS
String models for ultrarelativistic heavy ion collisions: Lund model versus color exchange models
[DE88-015856] 06 p0840 N90-14881
Gravitational radiation as a test of relativistic gravity 12 p1730 N90-19941
Applied general relativity 12 p1731 N90-19950
The gravity probe B relativity gyroscope program 12 p1732 N90-19960
Icarus lander 12 p1733 N90-19964
Small Mercury Relativity Orbiter 12 p1733 N90-19965
String dynamics in curved space-time revisited
[DE90-612796] 14 p2035 N90-21674
Relativistic corrections to He-3 photodisintegration sum rules
[NOTA-INTERNA-942] 16 p2315 N90-23197
Accretion onto neutron stars: Radiative transfer in a strong gravitational field 19 p2776 N90-25784
Relativistic light bending near neutron stars 19 p2779 N90-25810
Relativistic effects in low energy nucleon-nucleon scattering
[CEBAF-PR-89-025] 21 p3075 N90-27483

RELATIVISTIC ELECTRON BEAMS
The behavior of beams of relativistic non-thermal electrons under the influence of collisions and synchrotron losses
[NASA-CR-185983] 03 p0401 N90-12298
Electron beam propagation through a magnetic wiggler with random field errors
[AD-A212705] 04 p0498 N90-12867
Intense REB (Relativistic Electron Beam) transport in a weakly magnetized plasma
[DE90-002978] 07 p0994 N90-15749
Collective ion acceleration in high current relativistic electron beams
[DE90-008328] 13 p1886 N90-20821
Experimental demonstration of an electromagnetically pumped free-electron laser with cyclotron harmonic idlers
[AD-A218830] 17 p2408 N90-23719
Millimeter-wave gyroklystron amplifier experiment using a relativistic electron beam
[AD-A221209] 18 p2548 N90-24544
Relativistic klystron amplifiers driven by modulated intense relativistic electron beams
[AD-A221075] 18 p2607 N90-24849

RELATIVISTIC PARTICLES
NT RELATIVISTIC ELECTRON BEAMS
Global and local fluctuations in multiplicity and transverse energy for central ultra-relativistic heavy-ion interactions
[LUIP-8903] 02 p0272 N90-11555
Substructural dependence of the multiparticle production in relativistic heavy-ion interactions
[LUIP-8904] 07 p0989 N90-15716
High energy phenomena during solar flares
[INPE-4961-TDL/390] 14 p2043 N90-21713
Fragmentation of relativistic heavy nuclei with application to cosmic ray propagation 14 p2043 N90-21716

RELATIVISTIC PLASMAS
The dynamics of electrons in very intense lasers
[DE90-007246] 11 p1516 N90-18729
A continuous plasma final focus
[DE90-006096] 11 p1568 N90-19024
Ultrarelativistic envelope solitons in electron-positron plasma of the pulsar magnetosphere
[DE90-613289] 14 p1967 N90-21264
Relativistic stimulated Brillouin and Raman scattering in a laser-produced plasma
[DE90-613123] 14 p2028 N90-21627
Relativistic processes in active galactic nuclei 14 p2040 N90-21698
Iron K-shell lines from relativistic accretion disks 19 p2766 N90-25714

RELATIVISTIC THEORY
Elements of a relativistic microscopic theory of hadronic matter in equilibrium and non-equilibrium
[KVI-796] 04 p0552 N90-13218
Scale transformations, the energy-momentum tensor, and the equation of state
[DE90-005372] 10 p1440 N90-18308

RELATIVITY
Corrections to the thin wall approximation in general relativity
[NASA-CR-186078] 04 p0562 N90-13274
Some aspects of curvature in general relativity 05 p0704 N90-14122
On thick domain walls in general relativity
[NASA-CR-185926] 05 p0704 N90-14124
Black-hole decay and topological stability in quantum gravity
[DE89-618785] 06 p0863 N90-15017
Classical approach to higher-derivative gravity
[DE89-631649] 06 p0864 N90-15019
An exact solution for a thick domain wall in general relativity
[NASA-CR-185013] 07 p1006 N90-15826
Study of primitive universe in the Bianchi 9 model
[DE89-635903] 08 p1134 N90-16572
Universe as a topological defect in a higher-dimensional Einstein-Yang-Mills theory
[DE90-719507] 08 p1135 N90-16578
Simplicial lattices in classical and quantum gravity: Mathematical structure and application 10 p1439 N90-18304
Dimensional transition of the universe
[DE90-741461] 12 p1724 N90-19910
Causal boundary construction for space-times of the general relativity theory
[ETN-90-95357] 12 p1725 N90-19915
Relativistic Gravitational Experiments in Space
[NASA-CP-3046] 12 p1730 N90-19940
Gravitational radiation as a test of relativistic gravity 12 p1730 N90-19941
Gravitational radiation from rotating gravitational collapse 12 p1730 N90-19944
Experimental constraints on metric and non-metric theories of gravity 12 p1730 N90-19946
Gravitational consequences of modern field theories 12 p1730 N90-19947
Toward higher order tests of the gravitational interaction 12 p1731 N90-19948
Applied general relativity 12 p1731 N90-19950
General relativistic x ray (UV) polarization rotations as a quantitative test for black holes 12 p1732 N90-19957
The gravity probe B relativity gyroscope program 12 p1732 N90-19960
LAGEOS 3 and the gravitomagnetic field 12 p1733 N90-19961
The Stanford equivalence principle program 12 p1733 N90-19963
Icarus lander 12 p1733 N90-19964
Small Mercury Relativity Orbiter 12 p1733 N90-19965
Gravitational experiments on a solar probe mission: Scientific objectives and technology considerations 12 p1733 N90-19966
Optical interferometers for tests of relativistic gravity in space 12 p1734 N90-19967
New tests with old data 12 p1734 N90-19968
A review of atomic clock technology, the performance capability of present spaceborne and terrestrial atomic clocks, and a look toward the future 12 p1735 N90-19972
Improved ranging systems 12 p1735 N90-19973
Inertial corrections by dynamic estimation 12 p1735 N90-19976
Once more about the sizes of fast-moving objects
[DE90-615204] 14 p2022 N90-21592
The gravitational lens effect and its optical equivalents
[DE90-612767] 14 p2035 N90-21673
The synergism of analytic and numerical techniques in general relativity: Calculation of radiative spacetimes 15 p2174 N90-22425
Numerical investigations of nonlinear behavior in the Einstein equations 15 p2175 N90-22427
Multipole moments in general relativity and dynamical perturbations of black-hole magnetospheres 15 p2190 N90-22509
Background connection: A necessary object in general relativity
[DE90-620463] 16 p2325 N90-23258
Kinematic Weyl space-time models
[ETN-90-96508] 18 p2627 N90-24971
Unexpected properties of the centrifugal force
[DE90-627197] 23 p3392 N90-29164
Rotating neutron stars and the equation of state of dense matter
[DE90-014185] 23 p3410 N90-29269
Effects and control of the correlation properties of light sources
[AD-A224539] 24 p3545 N90-30049
A new vector-tensor theory and higher-dimensional cosmology
[DE90-507990] 24 p3555 N90-30117
Information loss down a black hole
[DE90-627482] 24 p3562 N90-30154

RELAXATION (MECHANICS)
NT SPIN-LATTICE RELAXATION
NT STRESS RELAXATION

RELAXATION METHOD (MATHEMATICS)
Upwind discretization of the steady Navier-Stokes equations
[CWI-NM-R8810] 04 p0502 N90-12891
Iterative methods for linear complementary and related problems
[AD-A212848] 04 p0534 N90-13089
On a rate of convergence of the multiknapsack value function
[CWI-MS-R8812] 04 p0542 N90-13144
Group-kinetic theory and modeling of atmospheric turbulence
[NASA-CR-183776] 06 p0813 N90-14728
An upwind-biased, point-implicit relaxation algorithm for viscous, compressible perfect-gas flows
[NASA-TP-2953] 09 p1214 N90-17042
A monotone surrogate algorithm for the 0-1 Multiknapsack problem
[INPE-4933-PRE/1423] 10 p1417 N90-18169
An exact algorithm for the problem of p-medians
[INPE-4924-TDL/384] 11 p1544 N90-18885
Multigrid accelerated relaxation solution of transonic full potential flow equation
[PD-CF-8942] 14 p1910 N90-20951
Convergence acceleration of upwind relaxation methods for the Navier-Stokes equations 15 p2092 N90-21973
Object detection using structural matching
[INPE-4954-PRE/1532] 15 p2159 N90-22333
A line relaxation smoother for the multigrid solution of the Boussinesq equations
[REPT-89-68] 17 p2458 N90-24027
NSFLEX: An implicit relaxation method for the Navier-Stokes equations for a wide range of Mach numbers
[MBB-FE-122/S/PUB-366] 19 p2651 N90-25086

RELAXATION OSCILLATORS
Delay test generation for synchronous sequential circuits
[AD-A211917] 05 p0634 N90-13697
RELAXATION TIME
Solvent dynamical effects in electron transfer: Evaluation of electronic matrix coupling elements for metallocene self-exchange reactions
[AD-A210306] 01 p0121 N90-10692
Dynamics of micellar oligomeric and monomeric sodium 10-undecenoate
[AD-A222570] 20 p2830 N90-26099
RELEASING
Pressure sensitive release device
[AD-D014220] 06 p0792 N90-14610
Releasable clamping apparatus
[NASA-CASE-MFS-28192-1] 09 p1233 N90-17154
Double swivel toggle release
[NASA-CASE-MSC-21436-1] 14 p1987 N90-21390
Analysis and test interaction in the development of a hold down and release mechanism
18 p2539 N90-24489
A spring-actuated spin and eject device for interplanetary missions 18 p2540 N90-24493
RELIABILITY
NT AIRCRAFT RELIABILITY
NT CIRCUIT RELIABILITY
NT COMPONENT RELIABILITY
NT SPACECRAFT RELIABILITY
NT STRUCTURAL RELIABILITY
Methodology of developing a combined environmental stress schedule for reliability growth testing
[AD-A211053] 02 p0231 N90-11326
Applications of the hybrid automated reliability predictor: Revised edition
[NASA-TP-2760-REV] 02 p0257 N90-11454
Experiments in fault tolerant software reliability
[NASA-CR-185927] 02 p0258 N90-11460
The RB199: An in-service success
[PNR90544] 03 p0307 N90-11746
The effect of incentives on the reliability and validity of cognitive speed tests
[AD-A211346] 03 p0383 N90-12181
A unified framework for simulating Markovian models of highly dependable systems
[AD-A212164] 03 p0396 N90-12267
On the precision and reliability of GPS networks computed using the double difference observable
[ETN-89-95719] 04 p0449 N90-12571
Software fault tolerance
[RSRE-MEMO-4237] 04 p0450 N90-12575
LORAN C stability integrity assurance
[AD-A212663] 05 p0577 N90-13364
A new view of weapon system reliability and maintainability
[AD-A213281] 05 p0580 N90-13382
A new view of weapon system reliability and maintainability: Executive summary
[AD-A213282] 05 p0580 N90-13383
Product assurance 05 p0605 N90-13522
Flight motor set 360L001 (STS-26R). Volume 5: Nozzle component
[NASA-CR-183771] 05 p0615 N90-13588
Electronic warfare: Reliable equipment needed to test Air Force's electronic warfare systems
[AD-A212952] 05 p0632 N90-13687
Operational activity in France and a new method of balloon temperature piloting 05 p0660 N90-13857
Sol-gel processing science using a Sol-Gel Optics Research Facility (SGORF)
[AD-A213056] 05 p0699 N90-14095
AGARD Highlights 89/2 06 p0717 N90-14184
Review of the Aerospace Safety Advisory Panel report for NASA fiscal year 1990 authorization
[GPO-24-234] 06 p0722 N90-14213
From small beginnings... The story of ESRO's sounding rocket programme in celebration of the twenty-fifth anniversary of the first ESRO sounding rocket launch
[ESA-BR-60] 08 p1038 N90-15999
Fault tree analysis: A tool for battery safety and reliability studies
[DE90-002582] 08 p1086 N90-16287
Software dependability growth characterization, modeling and evaluation
[LAAS-89320] 08 p1112 N90-16437
Complex availability problems solved with simulation
[DE89-012610] 08 p1116 N90-16459
On some problems in reliability theory
09 p1233 N90-17155
Statistical theory of reliability
[AD-A215320] 09 p1234 N90-17161
Project management in successful reliability and maintainability improvement programs
[AD-A215424] 09 p1234 N90-17162
Stochastic models in reliability
[AD-A215479] 09 p1234 N90-17163
R/M/T (Reliability, Maintainability, and Testability) design for fault tolerance, technical manager's design implementation guide
[AD-A215531] 09 p1234 N90-17164
RADC fault tolerant system reliability evaluation facility
[AD-A215298] 09 p1267 N90-17348
VHSIC/VHSIC-Like reliability prediction modeling
[AD-A214601] 09 p1288 N90-17468
The Hermes power system 10 p1330 N90-17682
Measurement and computer simulation of antennas on ships and aircraft for results of operational reliability
10 p1369 N90-17936
RADC reliability engineer's TOOLKIT
[AD-A215977] 10 p1394 N90-18058
Application of Bayesian reliability concepts to cruise missile electronic components
[AD-A216208] 10 p1394 N90-18059
Multitarget tracking by single sensor: Analysis of the main approaches developed in this area
[ESA-TT-1171] 11 p1500 N90-18633
Reliability studies of ceramic capacitors
[AD-A216763] 11 p1501 N90-18643
A test method for measuring corona inception voltage for transducer autotransformers
[AD-A216818] 11 p1502 N90-18646
Reliability assessment using finite element techniques
[AD-A216907] 11 p1502 N90-18647
Lithium ambient-temperature battery reliability
[DE90-005758] 11 p1502 N90-18650
Deceit: A flexible distributed file system
[NASA-CR-186402] 11 p1544 N90-18891
Optimum selection procedures in multi-stage screening, reliability, and time
[AD-A216811] 11 p1553 N90-18942
A nonparametric software reliability growth model
[NASA-CR-186438] 12 p1700 N90-19764
Theory and applications of belief functions
[AD-A217092] 12 p1702 N90-19774
Fault simulator evaluation
[AD-A217782] 13 p1796 N90-20308
Research in reliability, availability and maintainability for complex failure systems
[AD-A217744] 13 p1813 N90-20415
Development of microcomputer-based mental acuity tests for repeated-measures studies
[NASA-CR-185607] 14 p2010 N90-21521
Evaluation of a prototype lighted ball marker for powerline obstructions
[DOT/FAA/CT-TN90/12] 15 p2055 N90-21774
Regional wind energy assessment
[DE90-009439] 15 p2123 N90-22143
IAPSA 2 small-scale system specification
[NASA-CR-182006] 17 p2467 N90-24103
The Army/Air Force RAMCAD (Reliability And Maintainability Computer-Aided Design) program
[AD-A220923] 18 p2593 N90-24753
A Bayesian approach to reliability and confidence
18 p2628 N90-24974
Hardware and software reliability estimation using simulations
[NASA-CR-186637] 19 p2741 N90-25580
Space operations: NASA efforts to develop and deploy advanced spacecraft computers. Report to the Chairman, Subcommittee on Space Science and Applications, Committee on Science, Space, and Technology, House of Representatives
[GAO/IMTEC-89-17] 19 p2742 N90-25582
Multi-version software reliability through fault-avoidance and fault-tolerance
[NASA-CR-186502] 19 p2742 N90-25584
NASA project status reports: Congressional requirements can be met, but reliability must be ensured
[GAO/NSIAD-90-40] 20 p2843 N90-26169
A new technique in the global reliability of cyclic communications network
[NASA-TM-103479] 20 p2851 N90-26214
Electronic warfare technology: Trends and visions
[AD-A223034] 20 p2856 N90-26246
Statistical analysis of a software reliability model
[IMAG-RR-781-M] 20 p2874 N90-26352
A Bayesian proportional model for software reliability
[IMAG-RR-795-M] 20 p2874 N90-26353
Interim qualification tests and procedures for terrestrial photovoltaic thin-film flat-plate modules
[DE90-000354] 20 p2881 N90-26392
Preliminary designs for 25 kWe advanced Stirling conversion systems for dish electric applications
[NASA-TM-103188] 20 p2940 N90-26729
Magnetic flux leakage versus ultrasonic correlation
[AD-A222112] 21 p3071 N90-27462
Inspection reliability 22 p3184 N90-28072
DEPEND: A design environment for prediction and evaluation of system dependability
[NASA-CR-186890] 22 p3189 N90-28094
Improving software reusability by program specialization: A case study
[REPT-90-011] 22 p3240 N90-28374
STOVL fighter propulsion reliability, maintainability, and supportability characterization
[AD-A224221] 23 p3282 N90-28574
Methods for multisource data analysis in remote sensing
[NASA-CR-187005] 23 p3343 N90-28890
Reliability and performance of friction measuring tires and friction equipment correlation
[AD-A223694] 24 p3436 N90-29408
Systems reliability and inference: Summary of accomplishments 1988-1990
[AD-A224433] 24 p3477 N90-29653
Performance monitoring, fault detection, fault localization design guidance
[AD-A223619] 24 p3478 N90-29655
External information sources and aerospace R/D: The use and importance of technical reports by US Aerospace engineers and scientists
[NASA-TM-101232] 24 p3558 N90-30132
RELIABILITY ANALYSIS
Evaluation of tests and design factors
02 p0176 N90-10987
QM-8 field joint protection system, volume 7
[NASA-CR-183748] 05 p0614 N90-13586
Sufficiency and necessity in reliability modeling
[NASA-CR-186119] 05 p0635 N90-13706
Reliability analysis of the space station freedom electrical power system
[AD-A214105] 07 p0886 N90-15126
An iterative Bayes procedure for reliability assessment
[DE90-002106] 07 p0944 N90-15466
Validation of an exponentially decreasing failure rate software reliability model
[AD-A215546] 09 p1235 N90-17165
VHSIC/VHSIC-Like reliability prediction modeling
[AD-A214601] 09 p1288 N90-17468
Recalibrating software reliability models
[NASA-CR-186407] 12 p1700 N90-19763
A nonparametric software reliability growth model
[NASA-CR-186438] 12 p1700 N90-19764
Product assurance technology for procuring reliable, radiation-hard, custom LSI/VLSI electronics
[NASA-CR-185954] 13 p1791 N90-20281
Probabilistic finite elements: Applications to fracture and fatigue 15 p2121 N90-22134
The art of fault-tolerant system reliability modeling
[NASA-TM-102623] 15 p2152 N90-22292
Study and sizing of bonded joints in space structures
[REPT-892-430-124] 16 p2207 N90-22591
A numerical and analytical study of normal stresses and pressure differences in non-Newtonian creeping flows
16 p2234 N90-22749
Correlation/validation of finite element code analyses for vibration assessment of avionic equipment
[AD-A220393] 17 p2353 N90-23398
Reliability model generator specification
[NASA-CR-182005] 19 p2752 N90-25638
Extension of a noninteractive reliability model for ceramic matrix composites
[NASA-CR-185267] 20 p2838 N90-26142
Reliability analysis of continuous fiber composite laminates
[NASA-CR-185265] 20 p2878 N90-26372
Assessment and demonstration of the capabilities of NDI processes, equipment, and personnel
22 p3184 N90-28071
Reliability growth modeling analysis of the space shuttle main engines based upon the Weibull process
[NASA-TM-103511] 22 p3189 N90-28098
Ceramics Analysis and Reliability Evaluation of Structures (CARES). Users and programmers manual
[NASA-TP-2916] 22 p3190 N90-28099
Reliability analysis of a structural ceramic combustion chamber
[NASA-TM-103264] 22 p3192 N90-28112
Reliability analysis of maintained structural system vulnerable to fatigue and fracture
23 p3338 N90-28868
Formal design and verification of a reliable computing platform for real-time control. Phase 1: Results
[NASA-TM-102716] 24 p3530 N90-29965
RELIABILITY CONTROL
U QUALITY CONTROL
U RELIABILITY ENGINEERING
RELIABILITY ENGINEERING
Development and applications of reliability and maintainability design criteria in military aircraft
[ETN-89-95208] 04 p0452 N90-12591
Flanged joints of aeroengines
[PNR90594] 04 p0455 N90-12609
Aviation Engine Test Facilities (AETF) fire protection study
[AD-A211483] 04 p0483 N90-12777

Telerobotic control for teams of semi-autonomous agents, phase 1
[AD-A211648] 04 p0526 N90-13037
Laboratory test methodology for evaluating the effects of electromagnetic disturbances on fault-tolerant control systems
[NASA-TM-101665] 05 p0695 N90-14061
A tutorial on software reliability engineering
[DE89-012368] 06 p0830 N90-14828
How robust are distributed systems
[NASA-CR-186242] 06 p0832 N90-14837
Financial and commercial issues: A customer's perspective 09 p1174 N90-16794
Basic research in reliability for real systems
[AD-A214536] 09 p1234 N90-17158
Knowledge-based fault detection and analysis for robots: First results for the ROTEX robots
[ESA-TT-1150] 11 p1518 N90-18742
Component selection, procurement and control for ESA space systems
[ESA-PSS-01-60-ISSUE-2] 11 p1574 N90-19062
Reliability testing of the Hughes temperature controlled 1/4 watt split cycle cryogenic cooler (HD-1045 (V)/UA)
[AD-A216696] 12 p1641 N90-19426
Approximate evaluation of reliability and related quantities via perturbation techniques
[AD-A218340] 13 p1814 N90-20417
SPOT 4 space magnetic recorder mechanisms 15 p2112 N90-22082
Development of the CLAES instrument aperture door system 15 p2112 N90-22083
Excess noise, anomalous effects and reliability of high frequency devices (Schottky diodes, MESFET and HEMT)
[LAAS-89-394] 16 p2231 N90-22728
Design considerations for precision and reliability in space mechanisms 18 p2536 N90-24463
Rocket combustion chamber life-enhancing design concepts
[NASA-CR-185257] 19 p2669 N90-25183
NDT in aerospace: The next decade (1990's)
[PNR90628] 20 p2874 N90-26348
LASER: A Layout Sensitivity Explorer. Report and user's manual
[EUT-89-E-216] 20 p2908 N90-26545
Proceedings of Workshop on Reliability in Computational Mechanics
[AD-A221694] 21 p3065 N90-27426
United States Air Force research initiation program for 1988, volume 4
[AD-A223126] 21 p3102 N90-27616
Adjustable speed drive applications guidebook
[DE90-014151] 23 p3321 N90-28780
Smart microsensors for high temperature applications, phase 1
[AD-A224151] 23 p3330 N90-28828
Development of an all solid state 6 kHz pulse generator for driving free electron laser amplifiers
[AD-A224105] 24 p3463 N90-29561
VLSI design for reliability
[AD-A224264] 24 p3463 N90-29562
Analysis and synthesis of robust data structures
[AD-A224568] 24 p3558 N90-30131

RELIC RADIATION
Gamma ray cosmology: The extra galactic gamma spectrum and methods to detect the underlying source 16 p2337 N90-23321

RELIEF MAPS
Topographic map reading
[AD-A211269] 02 p0236 N90-11340
Land suitability maps and appropriate land use: An approach using SGI and satellite imagery
[INPE-4827-PRE/1458] 11 p1521 N90-18761
Development of the agricultural information system. Characteristics and results of the Distrito Federal model
[INPE-4940-PRE/1430] 11 p1524 N90-18773
Perspective revision of systematic mapping through orbital imagery
[INPE-4817-PRE/1453] 11 p1524 N90-18775
Satellite radar altimetry over ice. Volume 4: Users' guide for Antarctica elevation data from Seasat
[NASA-RP-1233-VOL-4] 13 p1840 N90-20564
Satellite-map position estimation for the Mars rover 23 p3375 N90-29069

RELIEVING
NT STRESS RELIEVING

RELUCTANCE
The reflectivity method
[REPT-90-004] 22 p3211 N90-28216

RELUCTIVITY
U RELUCTANCE

REMAGNETIZATION
U MAGNETIZATION

REMELTING
U MELTING

REMOTE CONSOLES
Remote use of an Electron Beam Tester (EBT)
[IMAG-RR-760-I] 08 p1077 N90-16233

REMOTE CONTROL
Remote control missile model test 01 p0013 N90-10063
NASA/NBS (National Aeronautics and Space Administration/National Bureau of Standards) standard reference model for telerobot control system architecture (NASREM)
[NASA-CR-185078] 02 p0228 N90-11310
Land vehicle teleoperation under conditions of reduced video resolution
[DE89-016925] 02 p0231 N90-11324
Spoken commands control robot that handles radioactive materials
[DE89-012632] 02 p0262 N90-11488
Pilotless airplanes
[AD-A211719] 03 p0305 N90-11734
Guidance and Control Panel Symposium on Guidance and Control of Unmanned Air Vehicles
[AGARD-AR-260] 04 p0458 N90-12623
Spark camera annotation and control system for the BRL (Ballistic Research Laboratory) Transonic Range Facility
[AD-A212266] 04 p0459 N90-12633
Assembly considerations for large reflectors 05 p0599 N90-13480
Performance evaluation of a six-axis generalized force-reflecting teleoperator
[NASA-CR-186106] 05 p0651 N90-13796
X.2 limited flight test plan
[AD-A214412] 07 p0880 N90-15099
A versatile stepping motor controller for systems with many motors
[DE90-001556] 07 p0921 N90-15327
SIMON (SuperIntelligent Mobile Observing Navigator): A high-reliability robot for a radiation environment
[DE90-003888] 07 p0943 N90-15460
Digital system for monitoring and controlling remote processes
[DE90-003935] 08 p1054 N90-16094
Connectionist model-based stereo vision for telerobotics 08 p1076 N90-16224
Remote use of an Electron Beam Tester (EBT)
[IMAG-RR-760-I] 08 p1077 N90-16233
Remote Manipulator System (RMS)-based Controls-Structures Interaction (CSI) flight experiment feasibility study
[NASA-CR-181952] 09 p1230 N90-17136
Electronically Variable Pressure Regulator (EVPR) 11 p1474 N90-18484
A human factors testbed for ground-vehicle telerobotics research
[DE90-006618] 12 p1697 N90-19746
The design and implementation of a position measuring system for a remotely controlled video camera
[AD-A218077] 13 p1805 N90-20362
Microwave Landing System (MLS) remote monitoring subsystem/remote maintenance monitoring system
[DOT/FAA/PS-89/2] 15 p2050 N90-21749
A new six-degree-of-freedom force-reflecting hand controller for space telerobotics 15 p2113 N90-22089
A flexible teleoperation test bed for human factors experimentation 18 p2503 N90-24304
Mechanical design engineering. NASA/university advanced design program: Lunar Bulk Material Transport Vehicle
[NASA-CR-184926] 18 p2534 N90-24455
Telepresence for space: The state of the concept 19 p2731 N90-25526
The telerobot testbed: An architecture for remote servicing 19 p2734 N90-25538
Visualization of three dimensional data 19 p2736 N90-25553
Remote operation of an orbital maneuvering vehicle in simulated docking maneuvers 19 p2736 N90-25554
Human factors issues in telerobotic systems for Space Station Freedom servicing 19 p2737 N90-25556
The application of NASREM to remote robot control 19 p2738 N90-25563
Test bed experiments for various telerobotic system characteristics and configurations 19 p2740 N90-25572
Lunar articulated remote transportation system
[NASA-CR-186817-VOL-1] 20 p2871 N90-26332
Creature co-op: Achieving robust remote operations with a community of low-cost robots 21 p3044 N90-27303
Multiple arm manipulation
[PB90-199506] 22 p3182 N90-28056
Remote atmospheric profiling systems for tropospheric monitoring
[PB90-216789] 23 p3349 N90-28927
A neural network for controlling the configuration of frame structure with elastic members 23 p3368 N90-29034
Plan recognition for space telerobotics 23 p3369 N90-29036
Tele-autonomous systems: New methods for projecting and coordinating intelligent action at a distance 24 p3502 N90-29794
Robotic tele-existence 24 p3502 N90-29796
Telepresence system development for application to the control of remote robotic systems 24 p3503 N90-29799
The 3D model control of image processing 24 p3503 N90-29800
Control strategies for a telerobot 24 p3504 N90-29808
Autonomous sensor-based dual-arm satellite grappling 24 p3504 N90-29809
A design strategy for autonomous systems 24 p3506 N90-29818
Learning in tele-autonomous systems using Soar 24 p3506 N90-29819
Design of a structural and functional hierarchy for planning and control of telerobotic systems 24 p3506 N90-29820
ROTEX-TRIIFEX: Proposal for a joint FRG-USA telerobotic flight experiment 24 p3510 N90-29842
Force-reflective teleoperated system with shared and compliant control capabilities 24 p3510 N90-29845
Global models: Robot sensing, control, and sensory-motor skills 24 p3511 N90-29849
The laboratory telerobotic manipulator program 24 p3515 N90-29869
System architectures for telerobotic research 24 p3515 N90-29872
Performance constraints and compensation for teleoperation with delay 24 p3517 N90-29881
Flight telerobotic servicer control from the Orbiter 24 p3517 N90-29882
Teleoperation experiments with a Utah/MIT hand and a VPL DataGlove 24 p3517 N90-29883
The JPL telerobotic Manipulator Control and Mechanization (MCM) subsystem 24 p3519 N90-29892
The astronaut and the banana peel: An EVA retriever scenario 24 p3519 N90-29897
Next generation space robot 24 p3520 N90-29899

REMOTE HANDLING
Telescience Testbed Pilot Program
[NASA-CR-184594] 02 p0257 N90-11455
Spoken commands control robot that handles radioactive materials
[DE89-012632] 02 p0262 N90-11488

REMOTE MANIPULATOR SYSTEM
Simulation of shuttle flight control system structural interaction with RMS deployed payloads 01 p0020 N90-10100
Independent Orbiter Assessment (IOA): Analysis of the remote manipulator system
[NASA-CR-185585] 02 p0164 N90-10926
Independent Orbiter Assessment (IOA): Analysis of the electrical power distribution and control/remote manipulator system subsystem
[NASA-CR-185526] 02 p0166 N90-10936
Independent Orbiter Assessment (IOA): CIL issues resolution report, volume 2
[NASA-CR-185524-VOL-2] 02 p0170 N90-10955
Independent Orbiter Assessment (IOA): Assessment of the remote manipulator system FMEA/CIL
[NASA-CR-185592] 02 p0171 N90-10964
Independent Orbiter Assessment (IOA): Assessment of the EPD and C/remote manipulator system FMEA/CIL
[NASA-CR-185583] 02 p0172 N90-10965
Remote Manipulator System (RMS)-based Controls-Structures Interaction (CSI) flight experiment feasibility study
[NASA-CR-181952] 09 p1230 N90-17136
A complete description of robot manipulator dynamics based on Lagrangian mechanics
[DE90-741467] 12 p1672 N90-19603
Prototype part task trainer: A remote manipulator system simulator 13 p1860 N90-20672
The development of the Canadian Mobile Servicing System Kinematic Simulation Facility 13 p1861 N90-20676
Development of a multipurpose hand controller for JEMRMS 15 p2113 N90-22087
The resupply interface mechanism RMS compatibility test 15 p2113 N90-22090
Multi-axis control of telemanipulators 16 p2271 N90-22943
Space station dynamics, attitude control and momentum management 16 p2287 N90-23029
Robotics program at the NASA Goddard Space Flight Center 18 p2500 N90-24285

Servicing test facility: A hardware simulator for telerobotic in-orbit servicing 18 p2501 N90-24287
Advanced robotics for the on-orbit servicing 18 p2501 N90-24289
The SPIDER robotic system 18 p2501 N90-24291
The Hermes robot arm teleoperation and control concept 18 p2503 N90-24301
Telerobotic architecture for an on-orbit servicer 18 p2503 N90-24302
Teleoperation of a force controlled robot manipulator without force feedback to a human operator 18 p2503 N90-24305
The bi-arm servicer: A multimission concept and a technological model for space robotics 18 p2504 N90-24307
A fast 3-D object recognition algorithm for the vision system of a special-purpose dexterous manipulator 24 p3503 N90-29803
Control strategies for a telerobot 24 p3504 N90-29808
Optimal payload rate limit algorithm for zero-G manipulators 24 p3513 N90-29858
Preshaping command inputs to reduce telerobotic system oscillations 24 p3517 N90-29880
Shuttle remote manipulator system mission preparation and operations 24 p3521 N90-29909
A comparison of the Shuttle remote manipulator system and the Space Station Freedom mobile servicing center 24 p3522 N90-29910
Dexterous manipulator flight demonstration 24 p3522 N90-29911

REMOTE REGIONS
NT ANTARCTIC REGIONS
NT ARCTIC REGIONS

REMOTE SENSING
Remote sensing techniques of the Wave Propagation Laboratory for the measurement of supercooled liquid water: Applications to aircraft icing
[PB89-208102] 02 p0148 N90-10842
Airborne gamma radiation snow water equivalent and soil moisture measurements and satellite areal extent of snow cover measuerments: A user's guide, version 3.0
[PB89-177877] 02 p0235 N90-11338
ANIMA: Image analyzer applied to remote sensing
[INPE-4766-PRE/1435] 02 p0256 N90-11447
Telescience Testbed Pilot Program
[NASA-CR-184594] 02 p0257 N90-11455
NASA/MSFC FY88 Global Scale Atmospheric Processes Research Program Review
[NASA-TM-100357] 03 p0360 N90-12059
Low level remote sensing: The Doppler Radar wind profiler 03 p0361 N90-12067
Remote sensing data acquisition, analysis and archival
[PB89-142566] 03 p0365 N90-12085
Earth resources: A continuing bibliography with indexes (issue 63)
[NASA-SP-7041(63)] 03 p0366 N90-12091
UV ionospheric remote sensing with the polar BEAR satellite
[AD-A211359] 03 p0372 N90-12127
A new generation of atmospheric tracers: The biological connection
[AD-A212285] 04 p0517 N90-12983
Spectrometer technology recommendations 05 p0597 N90-13468
Summaries of the thematic conferences on remote sensing for exploration geology
[NASA-CR-185321] 05 p0664 N90-13880
Global stratospheric change: Requirements for a Very-High-Altitude Aircraft for Atmospheric Research
[NASA-CP-10041] 06 p0723 N90-14220
The importance of environmental data 06 p0757 N90-14406
The use of broadcast signals for passive sensing in automated HF communication systems 06 p0762 N90-14433
Remote sensing of the aerosol scattering coefficient with a multi-field-of view lidar 06 p0763 N90-14437
An investigation of satellite sounding products for the remote sensing of the surface energy balance and soil moisture
[NASA-CR-186073] 06 p0801 N90-14664
Remote sensing of atmospheric water vapour by pressure modulation radiometry 06 p0802 N90-14667
A measurement of hydroxyl in the daytime mesosphere 06 p0814 N90-14732
RAIDS: An orbiting observatory for ionospheric remote sensing from space
[AD-A213717] 07 p0949 N90-15494
Laboratory of Space Technology
[PB90-110651] 08 p1033 N90-15967
Cloud phase discrimination by near-infrared remote sensing 08 p1090 N90-16310
Science plan for the Alaska SAR facility program. Phase 1: Data from the first European sensing satellite, ERS-1
[NASA-CR-185028] 08 p1091 N90-16312
Proceedings of the 5th User Seminar of the German Remote Sensing Data Center of the DFVLR
[DFVLR-MITT-89-04] 08 p1092 N90-16318
Introduction to the framework and tasks of the DFD --- German Remote Sensing Data Center (DFD) 08 p1092 N90-16319
Attempt to draw conclusions concerning the geological subsoil from the vegetation using digital image processing of TM data 08 p1093 N90-16329
Utilization of remote sensing in geoscientific development and projects 08 p1094 N90-16334
Use of remote sensing data for land and building statistics 08 p1094 N90-16335
Use of remote sensing in operational inventory and monitoring agricultural and forestry tasks 08 p1094 N90-16336
Statistical information system for cultivation of the soil. Use of remote sensing in official statistics 08 p1095 N90-16338
X ray spectrophotometric remote sensing of diffuse auroral ionization
[SD-TR-89-09] 08 p1139 N90-16599
The collection of non-conus aircraft icing data along with an identification of the geographical areas of potential severe icing and a study of a method of remote determining atmospheric icing data
[AD-A215055] 09 p1162 N90-16724
Multibeam radar altimetry: Spaceborne feasibiity and airborne experimentation
[AD-A215152] 09 p1207 N90-16995
Active and passive remote sensing of ice
[AD-A214863] 09 p1241 N90-17199
Analysis of significant weather on meso-alpha scales using conventional and remotely sensed data: Exploratory studies
[AD-A214563] 09 p1248 N90-17238
Evaluation of platinum silicide and indium antimonide as detector materials for space-based remote sensing in the 3.0-to-5.0 micrometer wavelength band
[AD-A216182] 10 p1354 N90-17853
Remote sensing of evaporation ducts for Naval warfare
[AD-A214849] 10 p1374 N90-17965
Study of alteration covers of part of the Sao Paulo State through remote sensing data
[INPE-4849-TDL/364] 10 p1399 N90-18086
The use of photographs for identification and analysis of urban residential sectors, with planning views
[INPE-4788-PRE/1448] 10 p1399 N90-18087
Remote sensing in agriculture: Basic concepts, methodology and applications
[INPE-4806-MD/39] 10 p1399 N90-18088
International course in remote sensing ONU/INPE, Brazil
[INPE-4802-NTE/288] 10 p1399 N90-18089
Remote sensing: Environmental effects of surface films
[AD-A216190] 10 p1400 N90-18094
The employment of SITIM-150 as an instructional objective for training in remote sensing
[INPE-4833-PRE/1463] 10 p1440 N90-18310
Major themes in the future of solar-terrestrial science 10 p1445 N90-18337
Multiparameter scatterometer for remote sensing (RADSER). Project Scatter: State-of-the-art and future applications
[INPE-4871-PRE/1482] 11 p1511 N90-18701
Orbital remote sensing in the decade of the nineties: New approaches and challenges in geology
[INPE-4838-PRE/1467] 11 p1521 N90-18758
Remote sensing applied to the monitoring of mineral extraction in the proximity of urban areas: Pros and cons
[INPE-4867-PRE/1478] 11 p1522 N90-18766
Remote sensing applied to vegetation as subsidized in municipal planning
[INPE-4908-PRE/1509] 11 p1523 N90-18770
ERS-1 European remote sensing satellite: A new tool for global environmental monitoring in the 1990's
[ESA-BR-36] 11 p1526 N90-18782
On the applicability of CAESAR for the remote sensing of bottom depth and bottom composition of shallow waters: A model study
[BCRS-89-13] 11 p1526 N90-18783
Erosion monitoring using remote sensing, part 2
[BCRS-89-15] 11 p1526 N90-18785
Remote sensing and run-off modelling in the Lake Victoria Basin, Kenya
[BCRS-89-19] 11 p1526 N90-18788
Remote sensing for the classification and quantification of vegetation in Spring staging areas of Brent geese on the Frisian Islands (Netherlands)
[BCRS-89-27] 11 p1527 N90-18790
Remote sensing of interior water: Perspectives
[INPE-4875-PRE/1486] 11 p1531 N90-18815
Earth Science Geostationary Platform Technology
[NASA-CP-3040] 12 p1608 N90-19249
Large space antenna concepts for ESGP 12 p1608 N90-19253
Remote Attitude Measurement Sensor (RAMS) 12 p1611 N90-19271
Definition study of Laser Experimental Active Fluorsensor (LEAF)
[BCRS-88-18] 12 p1668 N90-19582
Areas of aquatic macrophytes classified through vegetative indexes extracted from LANDSAT/TM imagery
[INPE-4880-PRE/1489] 12 p1677 N90-19633
Development of software routines for remote sensing digital image processing
[ETN-90-95452] 12 p1679 N90-19640
Possible applications of remote sensing satellite pictures for the water quality management of the Frisian lakes, Netherlands
[BCRS-88-17] 12 p1679 N90-19641
Possible applications of remote sensing in the preparatory phase of a land management project
[BCRS-88-19] 12 p1679 N90-19642
Technical and administrative feasibility of microlight remote sensing applications for river boards
[BCRS-89-01] 12 p1679 N90-19643
Segmentation of Side-Looking Airborne Radar (SLAR) images using a priori knowledge
[BCRS-89-03] 12 p1679 N90-19644
Activities report in remote sensing
[ETN-90-95472] 12 p1680 N90-19647
Hypotheses testing of watershed/landscape dynamics in northern Alaska using digital analysis
[DE90-006721] 13 p1820 N90-20450
Progress in the Determination of the Earth's Gravity Field
[NASA-CR-185721] 13 p1831 N90-20513
A system for analysis and interpretation of lineaments in remote sensing images
[INPE-4893-PRE/1494] 13 p1840 N90-20565
Programme of the International Training Course on Remote Sensing for African Specialists
[INPE-4878-NTE/290] 14 p1995 N90-21435
Shade images of forested areas obtained from LANDSAT MSS data
[NASA-TM-102939] 14 p1995 N90-21436
Remote sensing applied to sea water quality researches in coastal regions: A review
[INPE-4935-PRE/1425] 14 p1995 N90-21438
Geobotanical remote sensing: A review
[INPE-5026-PRE/1565] 14 p1996 N90-21440
Survey of land use through remote sensing
[INPE-5032-MD/042] 14 p1996 N90-21443
Analysis and modelling of spatial data proposal of a system for CBERS
[INPE-4911-PRE/1512] 14 p1997 N90-21445
Project CANASATE: Remote sensing applied to sugar cane crop survey
[INPE-4902-PRE/1503] 14 p1997 N90-21446
Monitoring vegetation of Brazil: Potentialities of multi-sensors approach
[INPE-4993-PRE/1555] 14 p1998 N90-21451
Evolution of remote sensing applied to vegetation and forest at INPE
[INPE-4970-PRE/1538] 14 p1998 N90-21452
Introduction of digital image processing by remote sensors applied to geology
[INPE-5023-RPE/616] 14 p1999 N90-21456
Regional remote sensing laboratory
[INPE-4922-PRE/1519] 14 p2001 N90-21465
Use of microwave satellite data to study variations in rainfall over the Indian Ocean
[NASA-CR-186408] 14 p2007 N90-21501
Modelling UV-visible radiation observed from space 15 p2085 N90-21937
Applications of remote sensing to studies of oceanic upper mixed layer dynamics 15 p2122 N90-22137
Field reports on radiometric campaigns of soybeans in the Federal district: Safra 88/89
[INPE-5021-RPE/615] 15 p2122 N90-22139
Mission to planet Earth 15 p2125 N90-22153
HCl Vapor Characterization and Detection. JANNAF Safety and Environmental Protection Subcommittee Workshop
[AD-A216252] 16 p2208 N90-22596
Measurement of HCl by near-infrared diode laser absorption 16 p2209 N90-22601
A laboratory comparison of field techniques for measurement of the liquid water fraction of snow
[AD-A219587] 17 p2417 N90-23774
Guided boundary detection in a digital image using dynamic programming
[ETN-90-96688] 17 p2419 N90-23782

Vision of the Remote Sensing Management Commission on the ESA long term Earth observation program
[BCRS-89-11] 17 p2419 N90-23785
Ocean variability from crossover differences derived from altimeter measurements
[ETN-90-96695] 17 p2431 N90-23852
The biogeochemistry of metal cycling
[NASA-CR-4295] 17 p2439 N90-23897
Remote optical sensing
[AD-A220780] 17 p2473 N90-24136
Development of cost-effective standards for Earth observation spacecraft 18 p2501 N90-24292
Remote measurement of ice thickness on the shuttle external tank surface
[NASA-TM-102667] 18 p2555 N90-24584
Development of remote sensing techniques for the investigation of neotectonic activity, eastern transverse ranges and vicinity, southern California 18 p2573 N90-24662
Use of high-dimensional spectral data to evaluate organic matter, reflectance relationships in soils
[NASA-CR-186650] 18 p2574 N90-24665
The application of remote sensing techniques for regional planning, environmental studies, and environment maintenance
[BCRS-89-16] 18 p2574 N90-24667
Modelling and synergism: Optical and microwave remote sensing. Partial report 1: Preliminary study
[BCRS-89-23] 18 p2575 N90-24668
The use of remote sensing for the localization of seepage near the Twenthe canal, Netherlands
[BCRS-89-30] 18 p2575 N90-24669
CAESAR: Performance and first evaluation of application possibilities
[BCRS-89-06] 19 p2705 N90-25393
Mapping and monitoring land use and land degradation in part of East Kalimantan, Indonesia, using aerospace remote sensing techniques: A SPOT case study
[BCRS-88-16B] 19 p2705 N90-25394
MARS (Monitoring Agro-ecological Resources with Remote sensing and Simulation) definition study: Results of the preparatory phase
[REPT-17] 19 p2706 N90-25395
Seasonal LAI in slash pine estimated with LANDSAT TM
[NASA-TM-102278] 19 p2706 N90-25397
Remote Sensing and the Earth's Environment
[ESA-SP-301] 19 p2706 N90-25398
Remote sensing for better understanding of the system Earth 19 p2706 N90-25399
Ocean colour: Methods, technologies, applications 19 p2707 N90-25406
Snow and land ice in the climate system: Research problems and possibilities of remote sensing 19 p2707 N90-25407
Snow cover mapping and snowmelt runoff simulations on microcomputers 19 p2707 N90-25408
Inventory and monitoring of extended forest lands by remote sensing 19 p2708 N90-25409
Geocoded spaceborne SAR products for geological applications 19 p2708 N90-25410
Solid Earth, gravity field and environment 19 p2708 N90-25412
Operational satellite environmental monitoring for food security by FAO: The ARTEMIS system 19 p2708 N90-25413
Vegetation stress monitoring by fluorescence 19 p2708 N90-25414
Land application of imaging spectrometry 19 p2708 N90-25415
Future developments of remote sensing systems: Data management and processing 19 p2709 N90-25416
The Telecommunications and Data Acquisition Report
[NASA-CR-186852] 20 p2852 N90-26217
Solid-state lasers for coherent communication and remote sensing
[NASA-CR-186634] 20 p2866 N90-26306
HIRIS performance study
[NASA-CR-186649] 20 p2878 N90-26375
Practical applications of remote sensing technology
[NASA-CR-186810] 20 p2879 N90-26377
Classification regions in remote sensing imagery utilizing spatial characteristics
[INPE-4913-PRE/1514] 20 p2879 N90-26381
Remote sensing of Earth terrain
[NASA-CR-186888] 20 p2880 N90-26382
Information sciences experiment system 21 p3015 N90-27142
Basic data requirements for microwave radiometer systems 21 p3015 N90-27143
Data analysis techniques 21 p3017 N90-27151
Applications of ISES for geology 21 p3017 N90-27154
Applications of ISES for the atmospheric sciences 21 p3017 N90-27155
Applications of ISES for vegetation and land use 21 p3018 N90-27158
Applications of ISES for snow, ice, and sea state 21 p3018 N90-27159
Applications of ISES for instrument science 21 p3018 N90-27161
Analysis of cirrus optical properties with data from NASA ER2 High-resolution Interferometer Sounder (HIS)
[NASA-CR-186365] 21 p3030 N90-27227
Sources of cloud nuclei and development of remote sensing techniques for cloud parameters
[AD-A222464] 21 p3031 N90-27233
Tactical oceanography from space: The next decade 21 p3068 N90-27442
Airborne CO2 Doppler lidar for wind shear detection 22 p3106 N90-27640
Workshop minutes on Remote Sensing of Hydrocarbons and Toxic Pollutants
[PB90-186370] 22 p3194 N90-28127
Remote sensing of the ocean surface with C- and Ku-band airborne scatterometers 22 p3195 N90-28129
Lidar cloud studies for FIRE and ECLIPS
[NASA-CR-186384] 22 p3211 N90-28214
FIRE Science Results 1989
[NASA-CP-3079] 22 p3213 N90-28224
Direct and remote sensing observations of the effects of ships on clouds 22 p3218 N90-28252
Size, duration, and rate of growth of nocturnal lightning events appearing on space shuttle video tapes
[NASA-CR-4313] 22 p3229 N90-28310
Concurrent Image Processing Executive (CIPE). Volume 1: Design overview
[NASA-CR-186853] 22 p3236 N90-28348
Comparison of methods of space color transformations for enhancement of colored images
[INPE-4977-PRE/1542] 23 p3341 N90-28881
On-line object feature extraction for multispectral scene representation
[NASA-CR-187006] 23 p3342 N90-28888
A method of classification for multisource data in remote sensing based on interval-valued probabilities
[NASA-CR-187007] 23 p3343 N90-28889
Methods for multisource data analysis in remote sensing
[NASA-CR-187005] 23 p3343 N90-28890
Study of anomalies in transition vegetation in Alto Xingo-NT, through remote sensing techniques
[INPE-4601-TDL/334] 23 p3343 N90-28891
Remote atmospheric profiling systems for tropospheric monitoring
[PB90-216789] 23 p3349 N90-28927
Gravity wave initiated convection
[NASA-CR-186868] 23 p3350 N90-28933
Detection of ocean inner waves by synthetic aperture radar: Observations at Gibraltar pass
[ETN-90-97477] 23 p3353 N90-28953
Proceedings of the NASA Conference on Space Telerobotics, volume 1
[NASA-CR-186856] 23 p3362 N90-29000
Non-contact contour gage
[DE90-014672] 24 p3475 N90-29642
The skin temperature of mountain slopes and the determination of the sensible heat flux
[DLR-FB-90-07] 24 p3495 N90-29754

REMOTE SENSORS

NT THEMATIC MAPPERS (LANDSAT)
Some significant results from testing a Remote Multiplexing Unit (RMU) for temperature-induced errors
[DE89-009432] 01 p0073 N90-10421
Satellite Data Processing System (SDPS) users manual V1.0
[NASA-CR-183054] 01 p0082 N90-10468
Study of high frequency water vapor absorption parameters
[AD-A210676] 02 p0194 N90-11108
A remote sensor to monitor combustion products using a tunable acousto-optic filter 02 p0223 N90-11275
Improved pattern recognition techniques for real time operation
[AD-A211395] 03 p0324 N90-11840
Earth resources: A continuing bibliography with indexes (issue 63)
[NASA-SP-7041(63)] 03 p0366 N90-12091
Investigation of atmospheric emissions in ultraviolet, vacuum ultraviolet, and extreme ultraviolet wavelength
[AD-A212169] 03 p0371 N90-12123
The development of a high response aerodynamic wedge probe and use on a high-speed research compressor
[PNR90598] 04 p0456 N90-12613
The detectors 05 p0604 N90-13507
A rough transform technique for extracting lead features from sea ice imagery
[AD-A212758] 06 p0801 N90-14666
RAIDS: An orbiting observatory for ionospheric remote sensing from space
[AD-A213717] 07 p0949 N90-15494
Development of the RAIDS (Remote Atmospheric and Ionospheric Detector System) extreme ultraviolet wedge and strip detector
[AD-A213730] 07 p0949 N90-15495
Liquid level measurement system for analog and digital readout
[AD-D014297] 08 p1076 N90-16227
Trajectory-capture cell instrumentation for measurement of dust particle mass, velocity and trajectory, and particle capture 08 p1146 N90-16644
Analysis of significant weather on meso-alpha scales using conventional and remotely sensed data: Exploratory studies
[AD-A214563] 09 p1248 N90-17238
The 15th Transducer Workshop --- for telemetry applications
[AD-A215515] 10 p1327 N90-17665
Evaluation of platinum silicide and indium antimonide as detector materials for space-based remote sensing in the 3.0-to-5.0 micrometer wavelength band
[AD-A216182] 10 p1354 N90-17853
Remote sensing of evaporation ducts for Naval warfare
[AD-A214849] 10 p1374 N90-17965
Remote sensing: Environmental effects of surface films
[AD-A216190] 10 p1400 N90-18094
An application of ocean wave-current refraction to the gulf stream using SEASAT SAR data
[AD-A216769] 11 p1537 N90-18851
Analysis of tectonic movements utilizing remote sensor products in the Southern Espinhaco (SE) region
[INPE-4830-PRE/1451] 12 p1690 N90-19708
Correlation of atmospheric optical turbulence and meteorological measurements
[AD-A218019] 13 p1842 N90-20576
The receiving system of a dual dye lidar to study molecular and aerosol densities at the base of the stratosphere
[AD-A218286] 13 p1843 N90-20581
MEGALIDAR proof-of-concept demonstration
[AD-A218787] 16 p2255 N90-22858
An analysis of the characteristics of atmospheric profiles obtained with the High resolution Interferometer Sounder (HIS) 24 p3488 N90-29716
A global approach to image texture analysis
[AD-A223532] 24 p3527 N90-29941

REMOTELY PILOTED VEHICLES

Robot vehicle video image compression, phase 1
[AD-A210974] 01 p0110 N90-10626
Land vehicle teleoperation under conditions of reduced video resolution
[DE89-016925] 02 p0231 N90-11324
The design of an airfoil for a high-altitude, long-endurance remotely piloted vehicle 04 p0445 N90-12545
Guidance and Control Panel Symposium on Guidance and Control of Unmanned Air Vehicles
[AGARD-AR-260] 04 p0458 N90-12623
Telerobotic control for teams of semi-autonomous agents, phase 1
[AD-A211648] 04 p0526 N90-13037
Guidance and Control of Unmanned Air Vehicles
[AGARD-CP-436] 08 p1025 N90-15924
Synthesis of control law, on a RPV, in order to minimize the number of sensors 08 p1025 N90-15925
Mirach 100 flight control system 08 p1025 N90-15926
Unmanned air vehicles payloads and sensors 08 p1026 N90-15930
Automated search techniques applied to optical payloads in unmanned air vehicles 08 p1026 N90-15931
An intelligence-driven RPV mission planner 08 p1027 N90-15932
Technology and evaluation of unmanned air vehicles 08 p1027 N90-15934
Navigation and guidance testing of the Lockheed/US Army Aquila remotely piloted vehicle 08 p1027 N90-15935
Aerodynamic analysis of a US Navy and Marine Corps unmanned air vehicle
[AD-A218282] 13 p1755 N90-20077
The MANTA: An RPV design to investigate forces and moments on a lifting surface
[NASA-CR-186227] 14 p1915 N90-20971
MMW SAR on RPV for battlefield surveillance 14 p1961 N90-21231
Preliminary design of a long-endurance Mars aircraft
[NASA-CR-185243] 15 p2052 N90-21763
Initial flight test of half-scale unmanned air vehicle
[AD-A219584] 17 p2351 N90-23388

Static wind-tunnel and radio-controlled flight test investigation of a remotely piloted vehicle having a delta wing planform
[NASA-TM-4200] 18 p2491 N90-24238
The Stealth biplane: A proposal in response to a low Reynolds Number station keeping mission
[NASA-CR-186680] 19 p2658 N90-25127
The Penguin: A low Reynolds number powered glider for station keeping missions
[NASA-CR-186667] 19 p2658 N90-25129
The FX/90: A proposal in response to a low Reynolds Number station keeping mission
[NASA-CR-186665] 19 p2659 N90-25131
The Screem-J4D: A proposal in response to a low Reynolds number station keeping mission
[NASA-CR-186664] 20 p2807 N90-25968
Literature concerning control and display technology applicable to the Orbital Maneuvering Vehicle (OMV)
[NASA-CR-186790] 20 p2820 N90-26048
The SKY SHARK: An RPV designed to investigate the pressure distribution on a lifting surface
[NASA-CR-186222] 21 p2959 N90-26824
The DELTA MONSTER: An RPV designed to investigate the aerodynamics of a delta wing platform
[NASA-CR-186226] 24 p3431 N90-29381

REMOVAL
Autonomous space processor for orbital debris
[NASA-CR-186043] 03 p0311 N90-11770
Environmental, health, and CFC substitution aspects of the ozone depletion issue
[DE90-004404] 08 p1099 N90-16363
Ultrasonic assisted paint removal method
[AD-D014264] 08 p1119 N90-16479
The future of aircraft paint removal methods
[AD-A214946] 09 p1197 N90-16936
Robots for aircraft coatings removal: Parameters and requirements
[DE90-009429] 15 p2106 N90-22048
Design of a rotary stepped auger for a lunar environment
[NASA-CR-184919] 17 p2384 N90-23577
Proof of principal for staircase auger chip removal theory
[NASA-CR-184934] 17 p2385 N90-23583
Autonomous space processor for orbital debris
[NASA-CR-186691] 20 p2820 N90-26044
Mechanical paint removal techniques for aircraft structures
[NIAR-90-12] 20 p2842 N90-26166
Assembly via disassembly: A case in machine perceptual development
[NASA-CR-186867] 20 p2900 N90-26497

REMS
U RAPID EYE MOVEMENT STATE

RENAL FUNCTION
Cardiovascular, renal, electrolyte, and hormonal changes in man during gravitational stress, weightlessness, and simulated weightlessness: Lower body positive pressure applied by the antigravity suit
[NASA-TM-102232] 04 p0522 N90-13013
Renal response to seven days of lower body positive pressure in the squirrel monkey
[NASA-CR-183355] 24 p3497 N90-29761

RENDEZVOUS
NT ORBITAL RENDEZVOUS
NT SPACE RENDEZVOUS

RENDEZVOUS GUIDANCE
Hermes rendezvous and navigation system
18 p2504 N90-24308
On-board expert system for manned rendezvous operation assistance 18 p2504 N90-24309

RENORMALIZATION GROUP METHODS
Trajectories of renormalization group flows on the phase diagram of N=2 superconformal field theories
[DE90-627212] 23 p3391 N90-29154
Criticality of the three-state chiral clock model: A renormalisation group study
[DE90-627321] 23 p3400 N90-29212
A generalised Hubbard Hamiltonian: Influence of temperature and fractality
[DE90-627322] 23 p3400 N90-29213
Z(6) model: Criticality and break-collape method
[DE90-627323] 23 p3401 N90-29214
Susceptibility of the Potts model in an hierarchical lattice: Renormalisation group approach
[DE90-627324] 23 p3401 N90-29215

REPAIRING
U MAINTENANCE

REPEATERS
Feasibility of millimeter-accuracy geodetic positioning and vehicle tracking with repeater satellites
[AD-A214755] 09 p1182 N90-16854
Measured effects of repeater jamming on direct-sequence spread spectrum receivers that use envelope detectors
[AD-A222231] 21 p2996 N90-27032

REPETITION
Effectiveness of progressive resistance training for increasing maximal repetitive lifting capacity
[AD-A215286] 09 p1252 N90-17267

REPLACING
ASIC (Application Specific Integrated Circuit) replacement for an SSI (Small Scale Integrated) component design: A case study
[DE89-013494] 02 p0215 N90-11232
Scientific justification and development plan for a mid-sized jet research aircraft
[PB89-208995] 03 p0305 N90-11731
What should be done with those noisy old aircraft
[PNR90562] 04 p0452 N90-12593
The telerobot testbed: An architecture for remote servicing 19 p2734 N90-25538
Preparing software conversion studies
[PB90-235623] 23 p3381 N90-29099

REPLICAS
Replica scaling analysis of interfaces in random media
[PREPRINT-713] 16 p2312 N90-23174

REPORTS
NT CONGRESSIONAL REPORTS
NT POSTLAUNCH REPORTS
NT PRESIDENTIAL REPORTS
NASA scientific and technical publications: A catalog of special publications, reference publications, conference publications, and technical papers, 1988
[NASA-SP-7063(03)] 01 p0136 N90-10782
A summary of 30 years of space launches
[AERONOMICA-ACTA-F-39-1989] 05 p0585 N90-13411
Reports of planetary astronomy, 1986
[NASA-TM-100776] 08 p1138 N90-16596
Focus 88: The activities of the European Space Agency
[ESA-BR-43] 08 p1157 N90-16706
Activities report in remote sensing
[ETN-90-95472] 12 p1680 N90-19647
A compendium of sources of fracture toughness and fatigue crack growth data for metallic alloys, part 4
[NASA-TM-102646] 14 p1950 N90-21164
Hermes preparatory programme: Fluidynamics studies. Activities performed by the Italian researchers
[DLC/COP-HER-TN-002] 17 p2363 N90-23453
Activities report of the Netherlands Space Research Organization
[ETN-90-96927] 18 p2636 N90-25021
NASA project status reports: Congressional requirements can be met, but reliability must be ensured
[GAO/NSIAD-90-40] 20 p2843 N90-26189
Activities report of the Institute of Sound and Vibration Research
[ETN-90-97604] 24 p3565 N90-30170

REPRESENTATIONS
Representations of the twisted SU(2) quantum group and some q-hypergeometric orthogonal polynomials
[CWI-PM-R8809] 04 p0541 N90-13140
Transformations and representations of nonlinear systems
[MEMO-776] 04 p0544 N90-13164
Principles and algorithms for causal reasoning with uncertainty
[AD-A214248] 07 p0977 N90-15644
Quantum si(2) enveloping algebra and representations of braid group
[DE90-607044] 09 p1275 N90-17389
A uniform representation scheme for freeform geometric modeling
[REPT-89-70] 17 p2458 N90-24028
Formal groups and differential equations
[ETN-90-96924] 18 p2603 N90-24825

REPRODUCTION (BIOLOGY)
Gravity and animal embryos 05 p0678 N90-13951
Microgravity effects on insect development and aging
19 p2680 N90-25243
Automatic experiment container for fertilisation of frog eggs in space: A multi-purpose piece of classified space hardware 19 p2681 N90-25249
The influence of a sounding rocket flight on sexual activation in Chlamydomonas gametes
19 p2681 N90-25250

REPRODUCTION (COPYING)
Copyright and home copying: Technology challenges the law
[PB90-151309] 21 p3086 N90-27547

REPRODUCTIVE SYSTEMS
NT TESTES

REPUBLIC MILITARY AIRCRAFT
U MILITARY AIRCRAFT

REPUBLIC OF CHINA
U TAIWAN

REQUIREMENTS
Casting factors imposed by the French regulation for foundry castings used in military aircraft
01 p0042 N90-10233
Key structures mechanical issues of the European Space Station and platform program Columbus
02 p0188 N90-11072
Methodology of developing a combined environmental stress schedule for reliability growth testing
[AD-A211053] 02 p0231 N90-11326
Conceptual design of liquid droplet radiator shuttle-attached experiment technical requirements document
[NASA-CR-185165] 03 p0318 N90-11806
Meeting review: The Second NCAR (National Center for Atmospheric Research) Research Aircraft Fleet Workshop
[PB89-200901] 03 p0369 N90-12113
Requirements specification with Petri nets using the cube tool methodology
[AD-A212190] 04 p0492 N90-12829
Integrated G-suit/immersion suit
[AD-A212989] 06 p0821 N90-14774
MANPRINT methods monograph: Aiding the development of manned system performance criteria
[AD-A213543] 07 p0968 N90-15593
A structured connectionist approach to direct inferences and figurative adjective-noun combinations
[AD-A214326] 07 p0978 N90-15649
Ultra high performance, highly reliable, numeric intensive processors and systems
[AD-A214100] 07 p0980 N90-15659
Pulsed plasma mission endurance test
[AD-A213462] 08 p1037 N90-15993
Fire hardening of aircraft through upgrades of materials and designs 10 p1315 N90-17605
Suggestions for designers of navy electronic equipment, 1989 edition, revision B
[AD-A215961] 10 p1380 N90-17998
KAPSE Interface Team (KIT) public report, volume 8, part 2
[AD-A215840] 10 p1419 N90-18178
Technology development, demonstration, and orbital support requirements for manned lunar and Mars missions
[NASA-TM-101666] 10 p1447 N90-18350
Development of a mass averaging temperature probe
11 p1461 N90-18418
Parkes radio science system design and testing for Voyager Neptune encounter 12 p1645 N90-19451
Requirements of IR space astronomy
14 p1975 N90-21314
Visual behavior in the F-15 simulator for air-to-air combat
[AD-A218648] 16 p2262 N90-22893
Navigation requirements: What they are and where they come from 17 p2358 N90-23422
Comparison of navigation systems
17 p2360 N90-23438
Nonlinear dynamics and control of flexible structures
[AD-A218476] 17 p2386 N90-23589
A study of the technology required for advanced vertical take-off aircraft
[ETN-90-96786] 18 p2497 N90-24268
Technology requirements for on-orbit servicing of spacecraft 18 p2506 N90-24321
Electronics principles inventory, Sheppard Technical Training Center
[AD-A219935] 18 p2547 N90-24534
A study of concept options for the evolution of Space Station Freedom
[NASA-TM-102675] 19 p2663 N90-25154
Knowledge-Based Systems (KBS) development standards: A maintenance perspective
19 p2739 N90-25570
Technical guide on documentation requirements for open market contract acquisitions of information resources
[NASA-TM-102650] 19 p2762 N90-25695
Program plan: International aircraft operator data base
[IAR-90-1] 19 p2763 N90-25697
A real-time optical 3D tracker for head-mounted display systems
[AD-A222747] 20 p2902 N90-26508
Cognitive requirements for aircraft navigation
[NASA-CR-186933] 21 p2955 N90-26804
Speech Analysis and Synthesis and Man-Machine Speech Communications for Air Operations
[AGARD-LS-170] 21 p2992 N90-27006
IRDS prototyping with applications to the representation of EA/RA models
[NASA-CR-186066] 21 p3039 N90-27273
Emerging technologies in electronics and their measurement needs, second edition
[PB90-188087] 23 p3320 N90-28773
Survey of formal specification techniques for reactive systems
[AD-A223741] 24 p3538 N90-30005

RESCUE OPERATIONS
Modeling, simulation, and analyses of attitude control for the Crew/Equipment Retriever (CER) proposed for space station
[AD-A208140] 01 p0025 N90-10125
Statistical models for the optimal estimation of oceanic fields
[AD-A211786] 03 p0377 N90-12149
Crew Safety and Rescue in Space: An International Approach
[ESA-SP-300] 08 p1034 N90-15974
Safety and rescue during STS operations
08 p1034 N90-15975
Assured crew return capability architecture
08 p1034 N90-15977
On the selection of crewmember rescue means for manned space launch systems
08 p1035 N90-15978
Crew safety and rescue aids
08 p1035 N90-15980
NASDA's approach to the interoperability of safety and rescue in space 08 p1035 N90-15981
TALON and CRADLE: Systems for the rescue of tumbling spacecraft and astronauts, a preliminary design
09 p1181 N90-16847
Aircraft internal fires 10 p1313 N90-17593
Frequency assignments for HFDF receivers in a search and rescue network
[AD-A220529] 17 p2390 N90-23610
Sweep width determination for HU-25B airborne radars: Life raft and recreational boat targets
[AD-A221362] 18 p2545 N90-24524
Technology for an intelligent, free-flying robot for crew and equipment retrieval in space
19 p2738 N90-25564
Mariners Weather Log, volume 33, number 4, Fall 1989
[PB90-146853] 20 p2890 N90-26445

RESEARCH
NT DYNAMIC PROGRAMMING
NT HIGH TEMPERATURE RESEARCH
NT LINEAR PROGRAMMING
NT MARKET RESEARCH
NT NONLINEAR PROGRAMMING
NT NUCLEAR RESEARCH
NT QUADRATIC PROGRAMMING
National register of research projects, 1986/87. Part 2B: Natural sciences: Physical, engineering and related sciences (new projects)
[DE89-015033] 01 p0143 N90-10826
Technology applications bulletins
[DE89-017454] 02 p0288 N90-11651
A history of West European rocketry and space research
[AD-A211191] 02 p0297 N90-11690
Development and use of a tribology research-in-progress database
[PB89-228274] 03 p0417 N90-12396
National Science Foundation
04 p0569 N90-13320
Summary of research academic departments, 1987-1988
[AD-A213252] 05 p0716 N90-14183
Chronology of KSC and KSC related events for 1988
[NASA-TM-101915] 06 p0867 N90-15040
The kind of mathematics involved in applied superconductivity research
[DE90-003706] 07 p1002 N90-15798
Activities report of the Institute of Interplanetary Stellar Physics
[IFSI-88-22] 10 p1445 N90-18339
Scientific activity programs for 1988-1990
[IFSI-88-23] 10 p1445 N90-18340
Materials Science Programs, fiscal year 1989
[DE90-008169] 13 p1765 N90-20131
Micro SAINT programs for numerical methods of integration and differential equations
[AD-A218097] 13 p1878 N90-20772
The Advanced Communications Technology Satellite (ACTS) capabilities for serving science
[NASA-CR-186584] 15 p2059 N90-21789
The Clemson University, university research initiative program in discrete mathematics and computational analysis
[AD-A220103] 17 p2461 N90-24055
United States Naval Academy summary of Research, Academic Departments, 1989-1990
[AD-A221219] 19 p2800 N90-25929
The 1990 Gordon Research Conference on Composites
[AD-A222849] 21 p2971 N90-26886
Research proposal
[AD-A221453] 21 p3085 N90-27545
Reports of planetary geology and geophysics program, 1989
[NASA-TM-4210] 21 p3100 N90-27606
United States Air Force research initiation program for 1988, volume 1
[AD-A223123] 21 p3101 N90-27613
United States Air Force research initiation program for 1988, volume 2
[AD-A223124] 21 p3102 N90-27614
United States Air Force research initiation program for 1988, volume 3
[AD-A223125] 21 p3102 N90-27615
United States Air Force research initiation program for 1988, volume 4
[AD-A223126] 21 p3102 N90-27616
Assuring both quality and creativity in basic research
[DE90-011489] 22 p3256 N90-28435
NSF Tokyo reports. Twenty-one new areas added for support under Monbusho's priority research area grants
[PB90-199589] 22 p3265 N90-28488
Japanese molecular biology 1990: An update
[PB90-188707] 23 p3354 N90-28958

RESEARCH AIRCRAFT
NT B-70 AIRCRAFT
NT U-2 AIRCRAFT
NT X-15 AIRCRAFT
STOVL aircraft simulation for integrated flight and propulsion control research
[NASA-TM-102419] 05 p0581 N90-13389
Longitudinal stability and control characteristics of the Quiet Short-Haul Research Aircraft (QSRA)
[NASA-TP-2965] 10 p1322 N90-17639
An improved airborne wind measurement technique for the NAE (National Aeronautical Establishment) Twin Otter
[AD-A217978] 13 p1842 N90-20575
Aerosol separator for use in aircraft
[PB90-142217] 15 p2125 N90-22155
Lateral-directional stability and control characteristics of the Quiet Short-Haul Research Aircraft (QSRA)
[NASA-TM-102250] 17 p2356 N90-23413
Experimental aerothermodynamic research of hypersonic aircraft
[NASA-CR-186903] 20 p2804 N90-25954
Technology development: Future use of NASA's large format camera is uncertain
[GAO/NSIAD-90-142] 20 p2865 N90-26298
An automated calibration laboratory for flight research instrumentation: Requirements and a proposed design approach
[NASA-TM-101719] 20 p2912 N90-26564
Aerodynamic parameters of High-Angle-of attack Research Vehicle (HARV) estimated from flight data
[NASA-TM-102592] 23 p3283 N90-28578
A knowledge-based system design/information tool
[NASA-CR-4316] 23 p3389 N90-29143
Procedure for calibrating fly-by-wire control chains of the flying testbed ATTAS
[DLR-MITT-90-02] 24 p3435 N90-29401
The signals of an ice warning device in dependence on total water content and normalized icing degree
[ESA-TT-1207] 24 p3484 N90-29692

RESEARCH AND DEVELOPMENT
Japanese structural ceramics research and development 01 p0048 N90-10272
Domestic technology transfer program regulation
[PB89-195374] 01 p0137 N90-10793
On the development of a basic flight test capability and some related research projects
02 p0155 N90-10885
Ariane 5 structural design and development
02 p0186 N90-11057
SDM challenges for space station
02 p0186 N90-11059
The Swedish defense research needs: For surveillance and seeker applications
[FOA-C-30520-3.3] 02 p0298 N90-11691
Inorganic composite materials in Japan: Status and trends
[PB89-230015] 03 p0319 N90-11810
An optimum trajectory planner for robot manipulators in joint-space and under physical constraints
[RR-349] 03 p0355 N90-12029
Twenty-five years of service, 1962-1987: Proceedings of the Air Force Studies Board Symposium on Air Force Research and Development, November 16, 1987
[PB89-198915] 03 p0415 N90-12384
Federal funds for research and development: Fiscal years 1986, 1987, and 1988. Volume 36: Detailed statistical tables
[PB89-223523] 03 p0419 N90-12407
Federal funds for research and development. Fiscal years 1987, 1988, and 1989. Volume 37: Detailed statistical tables
[PB89-223531] 03 p0419 N90-12408
The NASA experience in aeronautical R and D: Three case studies with analysis
[AD-A211486] 04 p0437 N90-12496
Acquisition and recording an AMX A/C. Aeritalia experience and present trends
[ETN-89-95217] 04 p0454 N90-12598
Gas turbine performance analysis
[PNR90599] 04 p0456 N90-12614
National Aeronautics and Space Administration
04 p0563 N90-13282
Fiscal year 1990 authorization request and budget estimates for the National Aeronautics and Space Administration
[GPO-96-945] 04 p0563 N90-13283
The 1990 National Aeronautics and Space Administration Authorization
[GPO-98-466] 04 p0563 N90-13285
National Aeronautics and Space Administration
04 p0564 N90-13287
National Aeronautics and Space Administration Authorization Act, fiscal year 1990
[S-REPT-101-157] 04 p0564 N90-13288
National Aeronautics and Space Administration Authorization Act, fiscal year 1990
[S-REPT-101-157] 04 p0564 N90-13289
NASA technology applications
[GPO-99-412] 04 p0564 N90-13290
Research and Technology annual report, 1988
[NASA-TM-101070] 04 p0569 N90-13319
European space technology: Celebrating twenty-five years of research and development
[ESA-BR-55] 04 p0569 N90-13322
Small business innovation research: Program solicitation
[NASA-TM-101869] 05 p0705 N90-14126
National Aeronautics and Space Administration Multiyear Authorization Act of 1989
05 p0709 N90-14148
National Aeronautics and Space Administration authorization
[S-HRG-101-348] 05 p0709 N90-14149
Centers for the commercial development of space
[NASA-PAM-525] 05 p0709 N90-14151
NASA commercial programs
[NASA-TM-101853] 05 p0709 N90-14152
AGARD Highlights 89/2 06 p0717 N90-14184
Challenges in processing for polymer composites
[DE90-002224] 06 p0752 N90-14376
Science and technology resources in US industry: Surveys of science resources series, 1975-1986
[PB90-107194] 06 p0756 N90-14401
Eurolaser CO2 laser
[ETN-90-95907] 06 p0787 N90-14582
NORDA's pattern analysis laboratory: Current contributions to naval mapping, charting, and geodesy
[AD-A212731] 06 p0801 N90-14665
Automation and robotics in construction: Japanese research and development
[AD-A214170] 07 p0942 N90-15456
Structural dynamics division research and technology accomplishments for FY 1989 and plans for FY 1990
[NASA-TM-101683] 08 p1019 N90-15894
Other cryogenic wind tunnel projects
08 p1029 N90-15948
Metal vaporisers: Bicentennial series of five historical monographs
[ISBN-0-642-13584-3] 08 p1052 N90-16081
The first year's work of race project 1036 WTDM broadband customer premises network
[BBC-RD-1989/6] 08 p1055 N90-16097
The development of over-the-horizon radar in Australia
[ISBN-0-642-13561-4] 08 p1055 N90-16099
Eurolaser definition phase, solid state lasers working group: Active medium, laser active crystals
[ETN-90-95899] 08 p1083 N90-16266
National program plan for electric vehicle battery research and development: Technical plan
[DE90-002023] 08 p1083 N90-16269
Project summaries
[PB90-103987] 08 p1118 N90-16472
Research and technology, 1989: Langley Research Center
[NASA-TM-4150] 08 p1157 N90-16703
The liquid rocket booster and its potential for the STS
09 p1179 N90-16833
The DLR technology programme on space transportation 09 p1180 N90-16841
Temperature profiles in high gradient furnaces
10 p1362 N90-17896
Office of Industrial Programs research in progress
[DE90-002100] 10 p1440 N90-18311
An analysis of the impacts of computer-based information systems on research and development organizations
[AD-A216283] 10 p1442 N90-18324
An exploration of benefits from NASA Spinoff
10 p1443 N90-18325
Development of a mass averaging temperature probe
11 p1461 N90-18418

The DFVLR 3-m x 3-m low speed wind tunnel (NWG) in Goettingen
[ESA-TT-1156] 11 p1465 N90-18436
Study on the measures to promote the use of photovoltaic power generating system overseas
[DE90-742056] 11 p1530 N90-18807
Calendar of selected aeronautical and space meetings
[AGARD-CAL-90/1] 11 p1574 N90-19060
Research Reports: 1989 NASA/ASEE Summer Faculty Fellowship Program
[NASA-CR-183837] 12 p1634 N90-19390
The Telecommunications and Data Acquisition Report
[NASA-CR-185033] 12 p1642 N90-19434
National Action Plan on Superconductivity Research and Development
[PB89-138512] 12 p1720 N90-19883
Science and technology report and outlook, 1985-1988
[PB90-115270] 12 p1727 N90-19926
Design and development activities on the candidate sample acquisition system for the Rosetta mission
12 p1738 N90-19993
Activities report of the Institute for Communication Technology
[ETN-90-95383] 12 p1747 N90-20043
Research and development quality assurance planning
[DE90-003687] 13 p1813 N90-20413
Ultra-high brightness laser research at LLNL (Lawrence Livermore National Laboratory)
[DE90-008366] 13 p1896 N90-20885
Middle management of research
[NASA-TM-102417] 13 p1899 N90-20901
A requirement for Australian research: Access to big science facilities, a report by the Australian National Committee for Crystallography
[DE90-614784] 14 p1930 N90-21048
Goes I-M and beyond: Science requirements and technology challenges 14 p1934 N90-21067
Research and Technology
[NASA-TM-102161] 14 p2044 N90-21721
Solid fuel combustion chamber
[LR-562] 15 p2068 N90-21846
Pre-study laser bathymetry
[BCRS-89-26] 15 p2134 N90-22198
Technologies for electronic transfer of information: The present state and trends in Japan
15 p2177 N90-22443
Applications to the aerospace and defense R and D community: The DOD computer-aided acquisition and logistics support (CALS) initiative
15 p2179 N90-22453
International science and technology policies: Testimony before the Subcommittee on International Scientific Cooperation, Committee on Science, Space, and Technology, United States House of Representatives
[DE90-009416] 15 p2181 N90-22463
Research and Technology Objectives and Plans Summary (RTOPS)
[NASA-TM-89662] 15 p2194 N90-22528
Microgravity, the space application of the 21st century. Challenges, constraints, and strategies
[REPT-892-430-105] 16 p2226 N90-22696
The automation management to support research and development 16 p2277 N90-22978
JPRS report: Science and technology. USSR: Physics and mathematics
[JPRS-UPM-89-001] 16 p2310 N90-23162
Research and applications of metallic superlattices, high T(sub c) superconductors, x ray optics, and compact synchrotrons 16 p2311 N90-23170
Hypersonic aerodynamics of spacecraft
[DLC-EST-TD-032] 17 p2346 N90-23361
Project Longshot: A mission to Alpha Centauri
[NASA-CR-186052] 17 p2357 N90-23417
Implementation of location programmes
17 p2360 N90-23440
Hermes preparatory programme: Fluidynamics studies. Activities performed by the Italian researchers
[DLC/COP-HER-TN-002] 17 p2363 N90-23453
Consortium for materials development in space
[NASA-CR-186534] 17 p2383 N90-23575
Small business innovation research program solicitation: Closing date July 16, 1990
[NASA-TM-101798] 17 p2479 N90-24173
Activities report of the Division of Informations Systems (FOA 37)
[FOA-C-30552-3.4] 17 p2480 N90-24178
Language in action
[ITLI-LP-89-04] 17 p2480 N90-24182
National patterns of research and development resources: 1989
[NSF-89-308] 17 p2486 N90-24218
Research and technology 1989
[NASA-TM-100369] 17 p2486 N90-24219
Langley aerospace test highlights, 1989
[NASA-TM-102631] 17 p2487 N90-24221
Activities report of the Joint Research Centre
[EUR-12305-EN] 17 p2487 N90-24222
NASA/GSFC split-rail parallel gripper
18 p2507 N90-24328
National Educators' Workshop: Update 1989 Standard Experiments in Engineering Materials Science and Technology
[NASA-CP-3074] 18 p2513 N90-24350
Departments of Veterans Affairs and Housing and Urban Development, and Independent Agencies Appropriations for Fiscal Year 1990, part 2
[S-HRG-101-345-PT-2] 18 p2636 N90-25017
Activities report of the Netherlands Space Research Organization
[ETN-90-96927] 18 p2636 N90-25021
A study of concept options for the evolution of Space Station Freedom
[NASA-TM-102675] 19 p2663 N90-25154
Technology transfer: US and foreign participation in R and D at Federal laboratories
[GAO/RCED-88-203BR] 19 p2764 N90-25706
Technology transfer: Implementation status of the Federal Technology Transfer Act of 1986. Report to Congressional requesters
[GAO/RCED-89-154] 19 p2764 N90-25707
Research at NASA's NFAC wind tunnels
[NASA-TM-102827] 20 p2801 N90-25933
Wright Research and Development Center test facilities handbook
[AD-A222582] 20 p2815 N90-26020
Hydrogen Energy Coordinating Committee summary of DOE hydrogen programs for FY 1988
[DOE/CE-0242] 21 p2989 N90-26989
Departments of Veterans Affairs and Housing and Urban Development, and independent agencies appropriations for 1991. Part 4: National Aeronautics and Space Administration
[GPO-30-861] 21 p3088 N90-27561
Independent research and independent exploratory development programs
[AD-A222690] 21 p3101 N90-27612
R and D aspects of the future operational concept of the BFS 22 p3112 N90-27679
PHARE: Concept and programme
22 p3114 N90-27690
Integration of flight management and air traffic management systems
[RAE-TM-FM-41] 22 p3114 N90-27693
Double sided silicon strip detectors
[MPI-PAE/EXP-EL-217] 22 p3176 N90-28036
Management of information in a research and development agency 22 p3257 N90-28442
NASA's educational programs
22 p3258 N90-28447
Legal ramifications of intellectual property
22 p3258 N90-28448
NSF Tokyo reports. The 1989 survey of research and development in Japan
[PB90-199340] 22 p3265 N90-28487
Scientific Colloquium in Honor of Prof. Dr. Rer. Nat. Hermann L. Jordan
[ESA-TT-1101] 23 p3391 N90-29159
Federal support to universities, colleges, and selected nonprofit institutions: Fiscal year 1988 (detailed statistical tables)
[PB90-226887] 23 p3404 N90-29236
Federal R and D funding by budget function: Fiscal years 1989-1991
[PB90-226879] 23 p3404 N90-29237
State science and technology indicators: An exploratory profile and analysis
[PB90-246711] 23 p3408 N90-29259
JPRS report: Science and technology. USSR: Earth sciences
[JPRS-UES-90-004] 24 p3483 N90-29688
JPRS report: Science and technology. USSR: Earth sciences
[JPRS-UES-90-003] 24 p3483 N90-29689
JPRS Report: Science and technology. USSR: Life sciences
[JPRS-ULS-90-007] 24 p3497 N90-29762
JPRS report: Science and technology. USSR: Life sciences
[JPRS-ULS-90-004] 24 p3497 N90-29763
Telerobotic activities at Johnson Space Center
24 p3516 N90-29875
NASA authorization, 1991, volume 2
[GPO-32-196] 24 p3559 N90-30138
Activities report of the Space Science Department
[ESA-SP-1126] 24 p3560 N90-30142
Activities report of the European Space Agency
[ISSN-0258-025X] 24 p3565 N90-30169
Activities report of the Institute of Sound and Vibration Research
[ETN-90-97604] 24 p3565 N90-30170

RESEARCH FACILITIES

NTES laser facility for physics experiments: Building 381 high bay option
[DE89-014326] 01 p0074 N90-10428
Research and test facilities for development of technologies and experiments with commercial applications
[NASA-TM-101789] 02 p0159 N90-10909
Physiographic and geological setting of the Coastal Engineering Research Center's field research facility
[AD-A210772] 02 p0238 N90-11356
National Center For Atmospheric Research annual report, fiscal year 1988
[PB89-208987] 02 p0252 N90-11428
AFRAPT (Air Force Research in Aero Propulsion Technology) Trainee Program
[AD-A211540] 03 p0307 N90-11744
Basic aerodynamic research facility for comparative studies of flow diagnostic techniques
04 p0441 N90-12526
Research and Technology annual report, 1988
[NASA-TM-101070] 04 p0569 N90-13319
The pituitary growth hormone cell in space
05 p0676 N90-13941
Sol-gel processing science using a Sol-Gel Optics Research Facility (SGORF)
[AD-A213056] 05 p0699 N90-14095
Centers for the commercial development of space
[NASA-PAM-525] 05 p0709 N90-14151
NRL (Naval Research Laboratory) Review
[AD-A212886] 05 p0716 N90-14182
Johnson Space Center software reuse activity
06 p0825 N90-14796
Chronology of KSC and KSC related events for 1988
[NASA-TM-101915] 06 p0867 N90-15040
Hypersonic nozzle design
[NASA-CR-186261] 07 p0876 N90-15077
NTES (Nuclear Test and Experimental Sciences) program laser facility for physics experiments Building 391 High Bay Option
[DE90-001795] 07 p0935 N90-15411
Magnetic mirror confinement concepts system studies
[DE90-003667] 07 p0995 N90-15753
A burst compression and expansion technique for variable-rate users in satellite-switched TDMA networks
[NASA-TM-102414] 08 p1035 N90-15983
Conceptual design for the space station Freedom modular combustion facility
[NASA-TM-102037] 08 p1053 N90-16087
Experiment facilities for materials and fluid sciences embarked on Eureca-1
[ESA-SP-1118] 08 p1053 N90-16088
Experiment facilities for materials and fluid sciences embarked on Spacelab
[ESA-SP-1120] 08 p1053 N90-16089
Computational fluid dynamics
[NASA-TM-102922] 09 p1216 N90-17052
RADC fault tolerant system reliability evaluation facility
[AD-A215298] 09 p1267 N90-17348
Activities report of the Institute of Interplanetary Stellar Physics
[IFSI-89-8] 09 p1298 N90-17520
Report on scientific activity and funds management for 1988
[IFSI-89-9] 09 p1298 N90-17521
X ray spectra produced by NaF implosions
[AD-A215803] 10 p1429 N90-18243
Compressor performance tests in the compressor research facility 11 p1463 N90-18428
Research equipment
[AD-A216515] 11 p1552 N90-18937
High power, high frequency component test facility
[NASA-TM-102500] 12 p1650 N90-19484
Relevance of laboratory studies to comets
12 p1743 N90-20023
Microgravity Science and Application Program tasks, 1989 revision
[NASA-TM-4191] 13 p1786 N90-20252
Proceedings of the 13th International Congress on Instrumentation in Aerospace Simulation Facilities
[EOARD-LR-89-069] 14 p1929 N90-21046
A survey of experiments and experimental facilities for active control of flexible structures
14 p1936 N90-21079
Cosmic Dust Collection Facility: Scientific objectives and programmatic relations
[NASA-TM-102160] 14 p1939 N90-21098
Microgravity science and applications bibliography, 1989 revision
[NASA-TM-4192] 14 p1957 N90-21207
Aeropropulsion facilities configuration control: Procedures manual
[NASA-TM-102541] 14 p1989 N90-21399

Activities and operations of the Advanced Computing Research Facility
[DE90-007957] 14 p2017 N90-21559
Research and Technology
[NASA-TM-102161] 14 p2044 N90-21721
Research in biological separations and cell culture
[NASA-CR-172060] 15 p2135 N90-22202
Hybrid vision activities at NASA Johnson Space Center 15 p2139 N90-22225
Hypersonic aerodynamics of spacecraft
[DLC-EST-TD-032] 17 p2346 N90-23361
NASA Lewis icing research tunnel user manual
[NASA-TM-102319] 17 p2355 N90-23407
A test matrix sequencer for research test facility automation
[NASA-TM-103108] 17 p2357 N90-23416
Data quality analysis at the National Transonic Facility
[NASA-CR-4303] 17 p2448 N90-23957
The Clemson University, university research initiative program in discrete mathematics and computational analysis
[AD-A220103] 17 p2461 N90-24055
Development of a consolidated environmental data base
[DE90-009419] 17 p2479 N90-24177
Technical accomplishments of the NASA Lewis Research Center, 1989
[NASA-TM-102296] 17 p2486 N90-24220
Langley aerospace test highlights, 1989
[NASA-TM-102631] 17 p2487 N90-24221
Activities report of the Joint Research Centre
[EUR-12305-EN] 17 p2487 N90-24222
MIT (Massachusetts Institute of Technology) short-wavelength laser project
[DE90-008975] 18 p2562 N90-24619
National Aeronautics and Space Administration (NASA)/American Society for Engineering Education (ASEE) Summer Faculty Fellowship Program-1989, volume 2
[NASA-CR-185601-VOL-2] 18 p2630 N90-24985
Artificial intelligence within AFSC 19 p2727 N90-25504
Spacecraft contamination programs within the Air Force Systems Command Laboratories 19 p2727 N90-25507
Research and facilities handbook 1989
[ISSN-0267-6281] 19 p2784 N90-25840
United States Naval Academy summary of Research, Academic Departments, 1989-1990
[AD-A221219] 19 p2800 N90-25929
New findings and instrumentation from the NASA Lewis microgravity facilities
[NASA-TM-103189] 20 p2842 N90-26163
Structural Mechanics Division research and technology plans for FY 1990 and accomplishments for FY 1989
[NASA-TM-102654] 20 p2876 N90-26361
Structural dynamics branch research and accomplishments
[NASA-TM-102488] 20 p2878 N90-26373
Genesis lunar outpost criteria and design
[NASA-CR-186831] 20 p2901 N90-26499
Experience in developing an improved ground-level test capability 22 p3120 N90-27720
NSF Tokyo reports. The 1989 survey of research and development in Japan
[PB90-199340] 22 p3265 N90-28487
Dynamic ground effects 23 p3275 N90-28531
Study of ground effects on flying scaled models 23 p3275 N90-28532
Microgravity science and applications: Apparatus and facilities
[NASA-TM-101892] 23 p3285 N90-28588

RESEARCH MANAGEMENT
Coordination of mesoscale meteorological research between ASL and European groups
[AD-A210902] 01 p0089 N90-10508
Army Science Conference Proceedings (16th) held in Fort Monroe, Virginia on 25-27 October 1988: Addenda
[AD-A210235] 01 p0143 N90-10827
National Climate Program five-year plan, 1989-1993
[PB89-207369] 02 p0252 N90-11426
Toward a national research network
[PB89-198709] 02 p0287 N90-11644
Ozone Research Program (German contribution to climate and atmosphere research)
[REPT-46-88] 03 p0369 N90-12111
The NASA experience in aeronautical R and D: Three case studies with analysis
[AD-A211486] 04 p0437 N90-12496
The integration of structured and formal methods
[RSRE-MEMO-4293] 04 p0531 N90-13068
Research on heating, instabilities, turbulence and RF emission from electric field dominated plasmas
[AD-A212122] 04 p0557 N90-13243
A new view of weapon system reliability and maintainability: Executive summary
[AD-A213282] 05 p0580 N90-13383
The HERMES development program 08 p1071 N90-16199
Focus 88: The activities of the European Space Agency
[ESA-BR-43] 08 p1157 N90-16706
Field of solar physics: Review and recommendations for ground-based solar research
[PB90-115684] 09 p1300 N90-17533
Total quality management: An application in a research and development laboratory
[AD-A215808] 10 p1440 N90-18312
The Pathfinder chemical transfer propulsion program 11 p1471 N90-18471
Research in reliability, availability and maintainability for complex failure systems
[AD-A217744] 13 p1813 N90-20415
Middle management of research
[NASA-TM-102417] 13 p1899 N90-20901
Reorganization of the German space administration. Foundation of DARA
[REPT-16/89] 13 p1899 N90-20902
Research and Technology Objectives and Plans Summary (RTOPS)
[NASA-TM-89662] 15 p2194 N90-22528
Aircraft technology management and the related significance of the supercomputer 16 p2277 N90-22975
Space Station Freedom media handbook
[NASA-TM-102901] 17 p2364 N90-23460
MTS high temperature testing system
[AD-A219613] 17 p2369 N90-23483
Center for Analysis of Heterogeneous and Nonlinear Media
[AD-A219627] 17 p2403 N90-23688
Vision of the Remote Sensing Management Commission on the ESA long term Earth observation program
[BCRS-89-11] 17 p2419 N90-23785
Strategic implementation plan
[NASA-TM-102907] 17 p2433 N90-23861
Interdisciplinary research: Promoting collaboration between the life sciences and medicine and the physical sciences and engineering 17 p2478 N90-24171
Small business innovation research program solicitation: Closing date July 16, 1990
[NASA-TM-101798] 17 p2479 N90-24173
Activities report of the Joint Research Centre
[EUR-12305-EN] 17 p2487 N90-24222
A research program in computer technology
[AD-A221184] 19 p2746 N90-25606
The Federal Aviation Administration plan for research, engineering and development. Volume 1: Program plan
[AD-A221263] 19 p2800 N90-25930
The Federal Aviation Administration plan for research, engineering and development. Volume 2: Project descriptions
[AD-A221264] 19 p2800 N90-25931
Research proposal
[AD-A221453] 21 p3085 N90-27545
Federal Aviation Administration small business innovation research 5-year project summaries
[AD-A221590] 21 p3086 N90-27546
Independent research and independent exploratory development programs
[AD-A222690] 21 p3101 N90-27612
Strategies of computer-based instructional design: A review of guidelines and empirical research
[AD-A224038] 23 p3383 N90-29112
Federal R and D funding by budget function: Fiscal years 1989-1991
[PB90-226879] 23 p3404 N90-29237
How can research and development leadtime be reduced
[AD-A224063] 23 p3404 N90-29240

RESEARCH PROJECTS
Research highlights of the NMC (National Meteorological Center) Development Division: 1987-1988
[PB89-206478] 01 p0088 N90-10501
Assessment of space power related measurement requirements of the Strategic Defense Initiative
[PB89-209357] 02 p0236 N90-11343
National Center For Atmospheric Research annual report, fiscal year 1988
[PB89-208987] 02 p0252 N90-11428
Toward a national research network
[PB89-198709] 02 p0287 N90-11644
The Knowledge Representation Project
[AD-A211288] 02 p0288 N90-11650
The StarLite project
[AD-A214193] 07 p0977 N90-15642
Science and technology report and outlook, 1985-1988
[PB90-115270] 12 p1727 N90-19926

RESEARCH VEHICLES
Research in knowledge-based vision techniques for the Autonomous Land Vehicle Program
[AD-A213440] 07 p0942 N90-15453
Singular perturbation analysis of AOTV-related trajectory optimization problems
[NASA-CR-186202] 08 p1027 N90-15936
Validation of the F-18 high alpha research vehicle flight control and avionics systems modifications
[NASA-TM-101723] 23 p3276 N90-28542
Aerodynamic parameters of High-Angle-of attack Research Vehicle (HARV) estimated from flight data
[NASA-TM-102692] 23 p3283 N90-28578

RESERVOIRS
Analysis of a model and sequential numerical method for thermal reservoir simulation
[DE89-015117] 01 p0067 N90-10384
Eutrophication assessment through remote sensing techniques
[INPE-4932-PRE/1422] 10 p1398 N90-18083
Erosion monitoring using remote sensing, part 2
[BCRS-89-15] 11 p1526 N90-18785
Remote sensing of interior water: Perspectives
[INPE-4875-PRE/1486] 11 p1531 N90-18815
Areas of aquatic macrophytes classified through vegetative indexes extracted from LANDSAT/TM imagery
[INPE-4880-PRE/1489] 12 p1677 N90-19633
Predicting effects of global climate change on reservoir water quality and fish habitat
[DE90-003674] 12 p1689 N90-19704
Monitoring of agrocattle-raising projects through visual/digital analysis of LANDSAT-TM imagery south of Para state
[INPE-4982-PRE/1542] 14 p1996 N90-21442
Thermal decay of an initially hot isothermal water body with application to thermal energy storage
[DE90-614742] 14 p2035 N90-21675
A modified Ubbelohde viscometer with improved dilution characteristics
[NIAR-90-16] 19 p2693 N90-25326

RESIDENTIAL AREAS
The use of photographs for identification and analysis of urban residential sectors, with planning views
[INPE-4788-PRE/1448] 10 p1399 N90-18087

RESIDENTIAL ENERGY
An assessment of technology for self-powered gas appliances: A GATC (Gas Appliance Technology Center)
[PB89-219265] 03 p0354 N90-12026
Performance predictions for passive solar water heating systems. Report 1: Performance monitoring to validate site-specific estimates of passive solar water heaters. Report 2: Laboratory report. Passive solar water heater tests
[DE90-002879] 10 p1401 N90-18096
Energy technology R and D and the greenhouse effect
[DE90-001339] 10 p1406 N90-18107

RESIDUAL STRENGTH
Evaluation of repeated impact damage in composite structures 12 p1619 N90-19303
Relevance of impacter shape to nonvisible damage and residual tensile strength of a thick graphite/epoxy laminate
[NASA-TM-102599] 14 p1943 N90-21122
Boeing/NASA composite components flight service evaluation
[NASA-CR-181898] 16 p2210 N90-22609
Summary of a study to determine low-velocity impact damage and residual tension strength for a thick graphite/epoxy motor case
[NASA-TM-102678] 19 p2702 N90-25374

RESIDUAL STRESS
Ceramic components in machines, Cologne and Aachen, West Germany; Maastricht, The Netherlands and Brussels, Belgium
[DE89-015831] 01 p0047 N90-10264
Finite element analysis of cure-induced residual stress in composite materials 02 p0190 N90-11084
Influence of core-shell grains on the internal stress state and permittivity response of zirconia modified barium titanate
[AD-A211245] 02 p0202 N90-11153
Questions from the Willmarth Workshop on New Directions in Research on Turbulent Wall-Layer Structures
[AD-A211282] 02 p0221 N90-11264
The Meta-Lax method of stress reduction in welds
[DE89-016437] 02 p0230 N90-11321
Thermomechanical contact phenomena and wear of sliding components
[AD-A211290] 03 p0355 N90-12028
Autofrettage-stress distribution under load and retained stresses after depressurization
[AD-A212090] 03 p0358 N90-12048

Fatigue fracture in the presence of shot peening residual stresses: Initiation, propagation, and relaxation phenomena 06 p0797 N90-14644
A theoretical investigation of the column behavior of cold-formed square hollow sections
[PB89-225981] 06 p0797 N90-14645
Reduction of residual stress and distortion in HY100 and HY130 high strength steels during welding
[AD-A213532] 07 p0905 N90-15231
Analysis of biaxial stress fields in plates cracking at elevated temperatures
[AD-A216271] 10 p1397 N90-18077
Investigation of collapse characteristics of cylindrical composite panels with large cutouts
[AD-A216378] 10 p1397 N90-18079
Residual stresses: A review of their measurement and interpretation using x ray diffraction
[AERE-R-13005] 13 p1815 N90-20423
Barkhausen noise analysis and ferromagnetic materials
[AD-A217989] 13 p1881 N90-20792
Use of unbalanced laminates as a screening method for microcracking
[NASA-TM-102517] 14 p1944 N90-21124
Fiber pushout test: A three-dimensional finite element computational simulation
[NASA-TM-102565] 14 p1945 N90-21131
Optimal fabrication processes for unidirectional metal-matrix composites: A computational simulation
[NASA-TM-102559] 14 p1947 N90-21143
Problems associated with residual and mismatch stresses in thin film structures 14 p1990 N90-21407
Determination of internal strains in high-temperature superconductor composites by intense pulsed neutron source
[DE90-007799] 14 p2033 N90-21884
Residual stresses in laminated thermoplastic matrix composites 15 p2063 N90-21815
Elastic stability and nonlinear behavior of imperfect shells with initial stresses 15 p2110 N90-22070
Axisymmetric and cylindrically orthotropic analysis of filament winding 16 p2246 N90-22811
Nondestructive measurement of residual stresses in aircraft transparencies
[AD-A218680] 17 p2415 N90-23762
Calculations of welding stresses and deformations by means of finite element method
[VTT-RR-648] 19 p2703 N90-25382
Resistivity, adhesive strength, and residual stress measurements of thin film metallizations on single crystal quartz
[DE90-011902] 20 p2837 N90-26135
Residual stresses measurements by means of x ray diffraction on electron beam welded joints and laser hardened surfaces
[ETN-90-97269] 20 p2877 N90-26371
High performance brittle matrices and brittle matrix composites, book 2
[AD-A223274] 24 p3443 N90-29441
Prediction and control of processing-induced residual stresses in composites. Part 2: AS4/PEEK composite
[AD-A223696] 24 p3443 N90-29445

RESIDUES
Standard method for measurement of nonvolatile residue on surfaces
[AD-A213324] 04 p0474 N90-12714
Thermal control system corrosion study
[NASA-TM-102220] 14 p1971 N90-21294

RESIN BONDING
A lightweight solid polymer electrolyte fuel cell with stack power density of 3 kW/lb (7 kW/kg)
[AD-A211542] 03 p0367 N90-12098
Molybdenum disulfide-molybdenum oxide lubricants
[AD-D014253] 08 p1048 N90-16059
Investigation of the techniques for the analysis of composite structures: Analysis and representation of the static and dynamic behavior of glued metal insert assemblies
[IMFL-89-44] 22 p3153 N90-27878

RESIN MATRIX COMPOSITES
NT GRAPHITE-EPOXY COMPOSITES
Crack propagation failure of carbon/resin composites
[ONERA-RT-45/7086-M] 04 p0467 N90-12677
Mechanical behavior of carbon/resin composites under delamination and cracking of transverse layers
[ONERA-RT-46/7086-M] 04 p0467 N90-12678
Textural and structural organization of the heat treated polymers: Mechanical properties relationships
[ETN-89-95711] 04 p0478 N90-12744
Review of polyarylacetylene matrices for thin-walled composites
[AD-A214921] 09 p1186 N90-16872
Enhanced bonding of fiber reinforcements to thermoset resins 11 p1476 N90-18496
Utilization of thermometric methods for the testing of carbon reinforced plastics
[ETN-90-96076] 12 p1621 N90-19314
Pultrusion process development for long space boom model
[NASA-TM-4017] 16 p2214 N90-22628
Composite curing: A new process
[REPT-892-430-114] 17 p2370 N90-23490
Demonstration centers for fiber reinforced materials
[REPT-45/89] 17 p2370 N90-23495
Development of a graphite/bismaleimide leading edge for the F-111 (EF-111A) horizontal stabilizer
21 p2956 N90-26809
Factors influencing the mode I interlaminar fracture resistance of toughened matrix composites
23 p3300 N90-28668
Thermal analysis of bismaleimide matrix resins
[DE90-016283] 24 p3457 N90-29523

RESINS
NT ACRYLIC RESINS
NT ADDITION RESINS
NT EPOXY RESINS
NT KEVLAR (TRADEMARK)
NT NYLON (TRADEMARK)
NT PEEK
NT PHENOLIC EPOXY RESINS
NT PHENOLIC RESINS
NT POLYAMIDE RESINS
NT POLYESTER RESINS
NT POLYIMIDE RESINS
NT POLYMETHYL METHACRYLATE
NT POLYURETHANE RESINS
NT SILICONE RESINS
NT SYNTHETIC RESINS
NT THERMOPLASTIC FILMS
NT THERMOPLASTIC RESINS
NT THERMOSETTING RESINS
NT VINYL COPOLYMERS
Composite activities at Lawrence Livermore National Laboratory
[DE90-002979] 07 p0891 N90-15149
A cure process model for resin transfer molding of advanced composites
[NASA-CR-186247] 09 p1185 N90-16867
Principles and formulation of solar reflecting and low infrared emitting coatings for defence use
[MRL-TR-89-2] 10 p1358 N90-17874
Rheological tests of Rigidite 5245 using the cone-plate and parallel plates method
[DT-310/88] 11 p1485 N90-18544
Thermal analysis of Acetylene Terminated Sulfone (ATS) resin
[AD-A220775] 17 p2381 N90-23558
Monocoque structure for the SKITTER three-legged walker
[NASA-CR-184635] 18 p2534 N90-24454
Characterization of the creep compliances J22 and J66 of orthotropic composites with PEEK and epoxy matrices using the nonlinear viscoelastic response of the neat resins
[MBB-Z-0258/89-PUB] 19 p2650 N90-25082
Elevator tab assembly producibility study
[IAR-89-16] 19 p2659 N90-25133
Pre-concentration method for inductively coupled plasma-mass spectrometry
[PB90-181348] 19 p2673 N90-25202
A tough high performance composite matrix
[NASA-CASE-LAR-14338-1] 21 p2970 N90-26881
Polyarylacetylene resin composites
[AD-A221507] 21 p2972 N90-26890
Elastomers and other organic composites
[AD-A222772] 21 p2984 N90-26958
Factors influencing the mode I interlaminar fracture resistance of toughened matrix composites
23 p3300 N90-28668

RESISTANCE HEATING
Battery actuation of NITINOL at sub-zero temperatures
[AD-A211254] 02 p0216 N90-11237
Joule heating and runaway electron acceleration in a solar flare 03 p0432 N90-12478
Actions of magnetospheres on planetary atmospheres
[IRF-SR-203] 17 p2486 N90-24215
Thermal analyses of power subsystem components
[NASA-CR-186314] 24 p3474 N90-29637

RESISTIVITY
U ELECTRICAL RESISTIVITY

RESISTOJET ENGINES
A numerical technique for analysis of resistojet nozzle flow 06 p0775 N90-14506
Analysis of the use of a methane propellant in a biowaste resistojet
[AD-A220475] 17 p2367 N90-23473

RESISTOJETS
U RESISTOJET ENGINES

RESISTORS
NT THERMISTORS
Microsensor and pattern recognition techniques in hydrazine detection 02 p0206 N90-11177
Energy ratings for metal oxide varistors under repetitively pulsed operation
[DE90-002353] 06 p0770 N90-14480

RESOLUTION
NT ANGULAR RESOLUTION
NT HIGH RESOLUTION
NT IMAGE RESOLUTION
NT RADAR RESOLUTION
NT RADIOMETRIC RESOLUTION
NT SPATIAL RESOLUTION
NT SPECTRAL RESOLUTION
NT TEMPORAL RESOLUTION
Measurement resolution of noise directivity patterns from acoustic flight tests
[NASA-TM-4134] 01 p0118 N90-10679
Completeness of resolution by transfinite induction
[CWI-CS-R8837] 02 p0260 N90-11473
Parallel inference based on delta processing
[CWI-CS-R8846] 02 p0261 N90-11482
Power spectral estimation algorithms
[NASA-CR-186189] 06 p0828 N90-14812
Flashlight radar: A three-dimensional imaging radar
[AD-A213439] 07 p0918 N90-15307
The lidar experiment at Andoya, Norway, during the Summer of 1988
[BONN-IR-89-16] 08 p1058 N90-16117
Phase ambiguity resolution for offset QPSK modulation systems
[NASA-CASE-NPO-17853-1-CU]
09 p1204 N90-16975
A Bayesian derivation of an iterative autofocus/super-resolution algorithm
[RSRE-MEMO-4337] 22 p3239 N90-28371
Image fusion through multi-resolution contrast decomposition
[IZF-1989-19] 22 p3247 N90-28412

RESOLUTION CELL
Temporal statistics of low-angle ground clutter
[AD-A220816] 17 p2391 N90-23621
Down-range imaging of radar targets
[AD-A221084] 18 p2544 N90-24521

RESOLVERS
On a generalization of the resolvent condition in the Kreiss matrix theorem
[TW-89-08] 18 p2603 N90-24827

RESOLVING POWER
U RESOLUTION

RESONANCE
NT BARYON RESONANCE
NT CYCLOTRON RESONANCE
NT ELECTRON PARAMAGNETIC RESONANCE
NT MAGNETIC RESONANCE
NT MICROWAVE RESONANCE
NT NUCLEAR MAGNETIC RESONANCE
NT NUCLEAR QUADRUPOLE RESONANCE
NT ORBITAL RESONANCES (CELESTIAL MECHANICS)
NT PLASMA RESONANCE
NT PROTON MAGNETIC RESONANCE
NT PROTON RESONANCE
NT RESONANT VIBRATION
NT SPIN RESONANCE
Density of states in a resonant tunneling structure
[AD-A209508] 01 p0128 N90-10731
Nonlinear optical studies of resonant systems
[AD-A211032] 02 p0227 N90-11301
Resonance effect on the oscillator distribution function
[DE89-630105] 02 p0271 N90-11548
Resonant quasiparticle-ion scattering in anisotropic superfluid (3)He
[PB89-221618] 03 p0413 N90-12369
Evaluation of 15th- and 30th-order geopotential harmonic coefficients from 26 resonant satellite orbits
[RAE-TR-88045] 04 p0461 N90-12640
Orbit determination and analysis for Cosmos 236 at 15th-order resonance
[RAE-TR-88058] 04 p0461 N90-12641
Measurements of bubble properties using a multi-frequency sound field
[AD-A212591] 04 p0551 N90-13211
Dynamics of an M-level atom interacting with cavity fields: Properties of photon statistics
[AD-A211321] 04 p0552 N90-13213
Study of the hydroxyl radical by DRASC resonance in a high pressure flame --- Diffusion Raman Anti-Stokes Coherence (DRASC)
[ONERA-RS-53/7131-PY] 05 p0622 N90-13632
Ring source/force excitation of axisymmetric shell structure
[ARE-TM(UHA)-88519] 05 p0698 N90-14085

Elastic impurity scattering in double-barrier resonant tunneling structures
[AD-A212850] 05 p0702 N90-14110
Resonance enhanced Raman studies of as-grown and laser-processed HgCdTe
[AD-A213855] 08 p1129 N90-16540
Resonances in low-energy positron-alkali scattering 11 p1560 N90-18992
Positron-molecule bound states and positive ion production 11 p1561 N90-18994
Transient and sustained resonance in very slowly varying oscillatory Hamiltonian systems with application to free-electron lasers
[DE90-005984] 12 p1666 N90-19574
Parametric resonance in horizontal axis wind turbines 14 p1912 N90-20962
Hopf bifurcation with nonsemisimple 1:1 resonance e
[MEMO-808] 15 p2161 N90-22347
Bifurcational aspects of parametric resonance
[W-8904] 16 p2231 N90-22730
Sustained resonance in very slowly varying oscillatory Hamiltonian systems
[DE90-010422] 18 p2598 N90-24783
New electronic states of NH and ND observed by resonance enhanced multiphoton ionization spectroscopy 20 p2945 N90-26760
UV and VUV spectroscopy and photochemistry of small molecules in a supersonic jet 20 p2947 N90-26771
Local and global resonances in heated 2-D jets
[AD-A221671] 21 p3005 N90-27079
Preliminary results on noncollocated torque control of space robot actuators 23 p3373 N90-29057
Spectral structure and generation mechanism of ducted VLF whistler mode sideband waves 24 p3489 N90-29720
Adiabatic invariance and transient resonance in very slowly varying oscillatory Hamiltonian systems
[DE90-016118] 24 p3538 N90-30007
Medium energy nuclear physics research
[DE90-015852] 24 p3544 N90-30042

RESONANCE FLUORESCENCE
A measurement of hydroxyl in the daytime mesosphere 06 p0814 N90-14732
The 2.7/4.3 micron CO2 branching ratio measurement
[AD-A215952] 11 p1534 N90-18830
Molecular dynamics and spectroscopy at gas-solid interfaces
[AD-A217743] 13 p1885 N90-20813
Decay rate and resonance fluorescence spectrum of a molecule near a composite material surface
[AD-A219692] 19 p2671 N90-25192
Rate constant for reaction of atomic hydrogen with germane 20 p2947 N90-26768

RESONANCE RADIATION
U RESONANCE FLUORESCENCE

RESONANCE SCATTERING
Spatial characteristics of airglow and solar scatter radiance from the earth's atmosphere
[AD-A211358] 03 p0372 N90-12126
Narrow one-channel resonances and their manifestation in the pure elastic scattering of unpolarized particles
[DE89-632177] 06 p0839 N90-14876
Positron-alkali atom scattering 11 p1556 N90-18958
Inelastic scattering of positrons with sodium 11 p1556 N90-18961

RESONANCE TESTING
A new vision to model the parallel resonant converter 10 p1336 N90-17727
Vibration test procedures for orbiter sidewall-mounted payloads, phase 2
[AD-A220774] 20 p2818 N90-26038

RESONANT CAVITIES
U CAVITY RESONATORS

RESONANT FREQUENCIES
Natural frequencies of singly-curved laminated plates with simply-supported edges
[ESDU-89011] 03 p0359 N90-12052
Measurements of bubble properties using a multi-frequency sound field
[AD-A212591] 04 p0551 N90-13211
Mobility power flow analysis of an L-shaped plate structure subjected to acoustic excitation
[NASA-CR-186130] 05 p0655 N90-13817
Structural response measurements and predictions for the SANDIA 34-meter test bed
[DE90-002575] 07 p0955 N90-15524
Conformation, orientation and interaction in molecular monolayers: A surface second harmonic and sum frequency generation study
[DE90-003108] 08 p1128 N90-16536
Theoretical analysis of microwave and millimeter wave integrated circuits based on magnetic films
[AD-A214772] 09 p1211 N90-17021
Eccentricity effects of square cutouts on the natural frequencies and mode shapes of curved rectangular composite panels
[AD-A216410] 10 p1350 N90-17831
Radio interference in the near-earth environment
[NASA-CR-180479] 11 p1498 N90-18623
Performance and modeling of superconducting ring resonators at millimeter-wave frequencies
[NASA-TM-102526] 11 p1500 N90-18634
Investigation of SSME alternate high pressure fuel turbopump lift-off seal fluid and structural dynamic interaction 12 p1636 N90-19400
Design and implementation of a flexible robot
[AD-A216453] 12 p1671 N90-19601
Complex demodulation for bearing fault detection
[AD-A218367] 13 p1812 N90-20407
Modal interactions in shell dynamics 13 p1814 N90-20418
Perturbation solutions in D* for buckling, vibration, and static loading of specially orthotropic plates 13 p1814 N90-20419
Active control of the forced and transient response of a finite beam
[NASA-CR-181957] 13 p1816 N90-20430
Experimental feasibility of investigating acoustic waves in Couette flow with entropy and pressure gradients
[NASA-TM-102621] 13 p1882 N90-20795
Software to characterize tuning fork resonators used in the Quartz Digital Accelerometer
[DE90-007913] 14 p1983 N90-21363
The effect of elastic boundary conditions on the dynamic response of rectangular plates
[NASA-CR-186059] 14 p1990 N90-21405
Integrated modeling and analysis of a space-truss article
[NASA-TM-102615] 14 p1991 N90-21412
Identification of XV-15 aeroelastic modes using frequency-domain methods
[NASA-TM-101021] 15 p2051 N90-21756
Probabilistic analysis of bladed turbine disks and the effect of mistuning
[NASA-TM-102564] 15 p2072 N90-21871
Optimum design of structures under shock and vibration environment 15 p2110 N90-22067
Dynamic response of a complex encapsulated electronic assembly subjected to a severe shock environment
[DE90-007689] 15 p2118 N90-22114
Differential equation based method for accurate approximations in optimization
[NASA-TM-102639] 16 p2200 N90-22558
Model reduction for flexible spacecraft with clustered natural frequencies 16 p2291 N90-23054
Multibody dynamics: Modeling component flexibility with fixed, free, loaded, constraint, and residual modes 16 p2295 N90-23072
Structural modeling for control design (articulated multibody component representation) 16 p2296 N90-23077
Mini-mast dynamic analysis using the truss-beam model 16 p2297 N90-23087
Shaping radiation pattern of excimer laser by means of controllable intracavity mirror 16 p2310 N90-23166
Numerical studies of the active control of sound transmission through double partitions
[ISVR-TR-183] 16 p2313 N90-23181
Structural behavior of composites with progressive fracture
[NASA-TM-102370] 17 p2368 N90-23477
Reflection oscillators employing series resonant crystals'
[NASA-CASE-GSC-13173-1] 17 p2394 N90-23635
Statistical techniques for designing a decoupled controller to be robust to model and sensor noise
[AD-A220476] 17 p2412 N90-23745
Finite element formulations for coupled fluid/structure eigenvalue analysis
[AD-A220793] 17 p2416 N90-23766
A comparison of the K-pulse and E-pulse techniques for aspect independent radar target identification
[AD-A220172] 18 p2542 N90-24511
Review of probabilistic analysis of dynamic response of systems with random parameters
[NASA-CR-186171] 18 p2568 N90-24636
Random vibration analysis of space flight hardware using NASTRAN 18 p2570 N90-24645
Dynamic analysis of space-related linear and non-linear structures
[NASA-TM-103490] 19 p2667 N90-25174
On the natural frequencies of a short circular cylinder, including the effects of entrained mass
[LR-602] 19 p2704 N90-25383
Vibration test procedures for orbiter sidewall-mounted payloads, phase 1
[AD-A220773] 20 p2818 N90-26037
Approximate natural damped frequencies of a finite viscous floating-zone under zero-gravity condition
[LRT-WE-9-FB-8(1988)] 21 p2990 N90-26995
Oscillatory response of a liquid column to counter rotational excitation
[LRT-WE-9-FB-12(1989)] 21 p3006 N90-27088
Numerical simulations of flowfields in a central-dump ramjet combustor. 3: Effects of chemistry
[AD-A224145] 23 p3282 N90-28573
A vector diagram approach to shaping inputs for vibration reduction
[AD-A223724] 24 p3480 N90-29671
Investigation of a heat driven thermoacoustic prime mover
[AD-A223928] 24 p3484 N90-29694

RESONANT TUNNELING
Density of states in a resonant tunneling structure
[AD-A209508] 01 p0128 N90-10731
Submillimeter quantum electronics
[AD-A210439] 01 p0132 N90-10762
Dwell time and average local speed in a resonant tunneling structure
[AD-A210566] 01 p0133 N90-10764
Resonant-tunneling oscillators and multipliers for submillimeter receivers 05 p0597 N90-13467
Elastic impurity scattering in double-barrier resonant tunneling structures
[AD-A212850] 05 p0702 N90-14110
Density of electronic states in a biased resonant tunneling structure
[AD-A215735] 09 p1291 N90-17486
Quantum-confined hole states in double-barrier resonant tunneling structures
[AD-A221342] 18 p2623 N90-24946

RESONANT VIBRATION
An improved beam model for the vibrations of rotor blades 02 p0232 N90-11333
Propagation of sound in vibrationally excited nitrogen and hydrogen gas mixtures
[AD-A213002] 05 p0696 N90-14073
Piezoelectric ceramic modeling and characterization at high levels of mechanical activity
[ISAL-89-0030] 08 p1051 N90-16074
Transition state spectroscopy of hydrogen transfer reactions
[AD-A215041] 09 p1191 N90-16901
Response of structures to atmospheric turbulence. Response to across-wind turbulence components
[ESDU-89049] 09 p1239 N90-17191
Performance of a 500 watt Nd:GGG zigzag slab oscillator
[DE90-006263] 11 p1503 N90-18657
Forcing function effects on rotor row unsteady aerodynamic response in a multistage compressor 16 p2196 N90-22536
Vibration test procedures for orbiter sidewall-mounted payloads, phase 2
[AD-A220774] 20 p2818 N90-26038
Non-linear axial vibrations of a cylindrical liquid column in zero-gravity
[LRT-WE-9-FB-4(1989)] 21 p2991 N90-26997
Response of differently axial-excited spinning liquid columns
[LRT-WE-9-FB-16(1989)] 21 p3006 N90-27091

RESONATORS
NT CAVITY RESONATORS
NT HELMHOLTZ RESONATORS
NT MULTIMODE RESONATORS
NT OPTICAL RESONATORS
Bulk acoustic waves resonators made of amorphous materials
[NOTE-TECHNIQUE-1989-4] 04 p0550 N90-13199
Theoretical analysis of microwave and millimeter wave integrated circuits based on magnetic films
[AD-A214772] 09 p1211 N90-17021
Quartz crystal resonator mass loading
[AD-A215199] 09 p1212 N90-17028
Bulk acoustic wave resonators made of amorphous materials
[ONERA-NT-1989-4] 09 p1279 N90-17416
Performance and modeling of superconducting ring resonators at millimeter-wave frequencies
[NASA-TM-102526] 11 p1500 N90-18634
Resonator modes in high gain free electron lasers
[DE90-006098] 11 p1514 N90-18720
Temperature compensated crystal oscillator (TCXO) with improved temperature compensation
[AD-D014334] 12 p1650 N90-19482
Finite element analysis of a quartz rotation sensor
[DE90-006959] 12 p1664 N90-19562
Generation of intensive UV laser radiation and utilization in high resolution spectroscopy of SO2
[ETN-90-95361] 12 p1668 N90-19581
Nine-year aging behavior of the ceramic flatpack resonator
[DE90-008044] 13 p1813 N90-20412

Software to characterize tuning fork resonators used in the Quartz Digital Accelerometer
[DE90-007913] 14 p1983 N90-21363
Temperature and coupling behavior of resonators and transducers of lithium tetraborate driven by lateral and thickness fields
[AD-A219548] 17 p2395 N90-23644
Phase locking of two HIQ resonators
[AD-A221123] 18 p2563 N90-24627

RESOURCE ALLOCATION
Electrophysiological studies of visual attention and resource allocation
[AD-A212287] 04 p0525 N90-13030
The 0-1 multiknapsack problem: Heuristic and reduction methods
[INPE-4894-PRE/1495] 12 p1704 N90-19782
Resource Allocation Planning Helper (RALPH): Lessons learned 15 p2152 N90-22296
Automated electric power management and control for Space Station Freedom
[NASA-TM-103151] 16 p2304 N90-23125
Resource allocation using constraint propagation 21 p3040 N90-27278

RESOURCES
NT AQUIFERS
NT COAL
NT CRUDE OIL
NT EARTH RESOURCES
NT EXTRATERRESTRIAL RESOURCES
NT FORESTS
NT FOSSIL FUELS
NT GEOTHERMAL RESOURCES
NT GEYSERS
NT GLACIERS
NT ICEBERGS
NT KEROGEN
NT LAND ICE
NT NATURAL GAS
NT PEAT
NT RAIN FORESTS
NT WATER RESOURCES
On modeling resources in multiprocessor systems
[MEMO-INF-88-33] 04 p0535 N90-13095
The DOD Gateway Information System: Operational prototype and transition period 1987-1988
[AD-A213044] 05 p0707 N90-14141

RESOURCES MANAGEMENT
NT FOREST MANAGEMENT
NT LAND MANAGEMENT
NT REFORESTATION
Decision-aid design factors in connection with HF communication and emitter location disciplines 06 p0758 N90-14413
Global natural resource monitoring and assessment
[DE90-001294] 06 p0802 N90-14671
The role of order in distributed programs
[NASA-CR-186252] 06 p0830 N90-14826
Cockpit resource management: A selected annotated bibliography
[AD-A214272] 07 p0969 N90-15594
FY 1989 update to the Information Resources Management review plan
[DE90-004185] 08 p1138 N90-16593
Improper use of economic analysis in materiel cost comparison studies
[AD-A214888] 09 p1297 N90-17518
International course in remote sensing ONU/INPE, Brazil
[INPE-4802-NTE/288] 10 p1399 N90-18089
Supporting tools of solar-terrestrial science 10 p1444 N90-18331
LANDSAT Thematic Mapper for hydrogeological mapping in Egypt
[BCRS-89-28] 11 p1527 N90-18791
Remote sensing of interior water: Perspectives
[INPE-4875-PRE/1486] 11 p1531 N90-18815
Development of an Ada programming support environment database SEAD (Software Engineering and Ada Database) administration manual
[NASA-CR-186064] 12 p1699 N90-19757
Synthesis and analysis of 25 years (1961-1986) of INPE/SRE activities related to the vegetation/forest area
[INPE-4969-RPE/604] 13 p1819 N90-20446
Global Warming: A Northwest Perspective
[DE90-008140] 13 p1830 N90-20505
Regional wind energy assessment
[DE90-009439] 15 p2123 N90-22143
The effects of climate change on energy planning and operations in the Pacific Northwest. Volume 2: Technical background
[DE90-009465] 17 p2425 N90-23817
Interdisciplinary research: Promoting collaboration between the life sciences and medicine and the physical sciences and engineering 17 p2478 N90-24171
Manual and computer-aided materials selection for industrial production: An exercise in decision making 18 p2516 N90-24368
Managing parallelism and resources in scientific dataflow programs
[AD-A221398] 18 p2635 N90-25010
Geoscience and a Lunar Base: A Comprehensive Plan for Lunar Exploration
[NASA-CP-3070] 18 p2638 N90-25030
SERI solar radiation resource assessment project
[DE90-000307] 19 p2711 N90-25428
OMS FDIR: Initial prototyping 19 p2738 N90-25562
Tools for distributed application management
[NASA-CR-186646] 19 p2762 N90-25692
Information resources management, 1984-1989: A bibliography with indexes
[NASA-SP-7079] 21 p3086 N90-27548
Chasing a specter: Risk management for global environmental change
[DE90-014455] 23 p3347 N90-28917
Global Climate Change: Seeking a Global Consensus
[S-HRG-101-842] 24 p3486 N90-29704
Effects of increased CO2 on forest response
[DE90-015406] 24 p3487 N90-29706
The technology transfer process: Background for the national energy strategy
[DE90-015301] 24 p3559 N90-30139

RESPIRATION
NT HIGH ALTITUDE BREATHING
NT PRESSURE BREATHING
Managing human exposure and health risks: An integrated approach and the role of uncertainty
[DE89-008611] 01 p0092 N90-10525
Measurement of respiratory air temperatures and calculation of respiratory heat loss when working at various ambient temperatures
[AD-A210378] 01 p0093 N90-10529
Synergistic effects of nitrogen dioxide and carbon dioxide following acute inhalation exposures in rats
[PB89-214779] 03 p0377 N90-12150
Short-term bioassays may be useful in evaluating fiber/whisker hazards
[DE90-003707] 08 p1104 N90-16393
The investigation of particulate matter in the lungs of smoke inhalation death victims 10 p1317 N90-17617
Regulation of nitrogen uptake and assimilation: Effects of nitrogen source, root-zone pH, and aerial CO2 concentration on growth and productivity of soybeans
[NASA-CR-177546] 10 p1413 N90-18147
Evaluation of the Scott aviation portable protective breathing device for contaminant leakage as prescribed by FAA Action Notice A-8150.2. Phase 1: Original tests of the portable protective breathing device. Phase 2: Tests of the redesigned portable protective breathing device
[AD-A216799] 12 p1601 N90-19214
A review of the literature on the toxicity of rare-earth metals as it pertains to the engineering demonstration system surrogate testing
[DE90-008049] 13 p1851 N90-20620
Carbon dioxide and water exchange rates by a wheat crop in NASA's biomass production chamber: Results from an 86-day study (January to April 1989)
[NASA-TM-102788] 19 p2716 N90-25453

RESPIRATORY DISEASES
The investigation of particulate matter in the lungs of smoke inhalation death victims 10 p1317 N90-17617

RESPIRATORY RATE
ELF (Extremely Low Frequency) communications system ecological monitoring program: Slime mold studies
[AD-A218623] 16 p2229 N90-22715

RESPIRATORY SYSTEM
NT LUNGS

RESPONDERS
U TRANSPONDERS

RESPONSE BIAS
An approximation for the response time of an open CP-disk system
[MEMO-COSOR-89-19] 16 p2327 N90-23266

RESPONSE TIME (COMPUTERS)
Performance evaluations of a parallel and expandable database computer: The multi-backend database computer
[AD-A212761] 04 p0528 N90-13046
Multiple crossbar network: Integrated supercomputing framework
[DE89-012614] 06 p0831 N90-14831
Alternative representations for database responses 07 p1009 N90-15847
New optimization techniques in database access and maintenance 08 p1137 N90-16586
Bounded-time fault-tolerant rule-based systems 15 p2157 N90-22318
Multigrid acceleration of transonic flow computations
[ENSM-8024] 16 p2237 N90-22760
Cognitive efficiency considerations for good graphic design
[AD-A218976] 16 p2263 N90-22899
Sojourn times in queueing networks
[CWI-BS-R8916] 17 p2467 N90-24102

RESPONSES
NT DYNAMIC RESPONSE
NT HEMODYNAMIC RESPONSES
NT MODAL RESPONSE
NT PHYSIOLOGICAL RESPONSES
NT TRANSIENT RESPONSE
Stimulus-response compatibility in spatial precuing and symbolic identification: Effects of coding practice, retention, and transfer
[AD-A210745] 02 p0255 N90-11443
Effect of extraneous color-coded targets on identification of targets on CRT displays
[AD-A219473] 17 p2436 N90-23879
Extreme quantile estimation in binary response models
[AD-A220150] 17 p2466 N90-24093

REST
NT BED REST
Use of self-induced hypnosis to modify thermal balance during cold water immersion
[AD-A216156] 10 p1412 N90-18140

RESTORATION
Optimal focal-plane restoration 08 p1073 N90-16207
Image gathering and coding for digital restoration: Information efficiency and visual quality 08 p1073 N90-16211
Projection techniques for image restoration 09 p1263 N90-17322
Event-train restoration via backpropagation neural networks
[AD-A216308] 10 p1420 N90-18189
Information management systems for integrating the technical data and regulatory requirements of environmental restoration activities
[DE90-008622] 13 p1831 N90-20511
Data analysis techniques 21 p3017 N90-27151
Improvement of the detail reconnaissance in radiographic irradiation images by digital image restoration
[ETN-90-97311] 22 p3189 N90-28096

RESTRAINTS
U CONSTRAINTS

RETARDANTS
NT FLAME RETARDANTS

RETARDING ION MASS SPECTROMETERS
U MASS SPECTROMETERS

RETENTION (PSYCHOLOGY)
Individual differences in associative learning and forgetting
[AD-A212765] 04 p0526 N90-13034
A long-term retention advantage for spatial information learned naturally and in the laboratory
[AD-A218268] 13 p1855 N90-20644
Automatic information processing and high performance skills: Application to training
[AD-A221709] 21 p3036 N90-27259
Automatic information processing and high performance skills: Acquisition, transfer, and retention
[AD-A221744] 21 p3036 N90-27260

RETICLES
NT WIRE GRID LENSES
Comparison of oculometer and head-fixed reticle with voice or switch and touch panel for data entry on a generic tactical air combat display
[AD-A217231] 13 p1855 N90-20646

RETINA
NT FOVEA
Treatment of laser-induced retinal injuries
[AD-A210284] 01 p0092 N90-10526
Role of retinocortical processing in spatial vision
[AD-A210995] 05 p0672 N90-13918
Image processing by Intensity-Dependent Spread (IDS) 08 p1074 N90-16215
Design principles of the LVT-2 model laser instrument for the measurement of visual characteristics
[AD-A214951] 09 p1228 N90-17124
Biological applications and effects of optical masers
[AD-A217910] 13 p1808 N90-20385
Detection acuity in the peripheral retina
[AD-A218183] 13 p1853 N90-20632
Filling in the retinal image 15 p2140 N90-22229
A3I visibility modeling project 15 p2140 N90-22230
A study of low level laser retinal damage
[AD-A218919] 16 p2261 N90-22887
Laser retinal effects: Electrophysiological determination in visual cortical cells of monkeys and cats
[AD-A218937] 16 p2261 N90-22888

A note on the statistics of laser speckle
[AD-A222408] 21 p3009 N90-27103
RETINAL ADAPTATION
NT DARK ADAPTATION
NT LIGHT ADAPTATION
RETINAL IMAGES
Neural networks for data compression and invariant image recognition 08 p1075 N90-16219
Paradoxical monocular stereopsis and perspective vergence 16 p2267 N90-22922
Exocentric direction judgements in computer-generated displays and actual scenes 16 p2270 N90-22936
Interactions of form and orientation 16 p2274 N90-22958
RETIREMENT FOR CAUSE
Retirement for cause of the F100 engine 21 p2957 N90-26813
A general discussion of the retirement for cause inspection system 21 p2957 N90-26814
Critical inspection of high performance turbine engine components: The RFC concept 22 p3185 N90-28073
Assessment and improvement of aeroengine disc structural integrity 24 p3433 N90-29392
RETORC (TORPEDOES)
U TORPEDOES
RETRACTABLE EQUIPMENT
Pivotal mono wing cruise missile with wing deployment and fastener mechanism
[AD-D014191] 04 p0452 N90-12594
SFU solar array 10 p1340 N90-17761
Design of a telescoping tube system for access and handling equipment 15 p2116 N90-22102
RETRACTABLE LANDING GEAR
U LANDING GEAR
U RETRACTABLE EQUIPMENT
RETRIEVAL
NT DATA RETRIEVAL
NT INFORMATION RETRIEVAL
NT PAYLOAD RETRIEVAL (STS)
RETROFITTING
What should be done with those noisy old aircraft
[PNR90562] 04 p0452 N90-12593
Aircraft modifications cost analysis. Volume 1: Overview of the study
[AD-A220764] 19 p2649 N90-25074
RETROREFLECTION
Turbulence effects for retroreflection
[FOA-C-30523-3.1] 02 p0276 N90-11575
RETROREFLECTORS
Defense to laser light irradiation
[AD-D014286] 08 p1036 N90-15984
Remote Attitude Measurement Sensor (RAMS) 12 p1611 N90-19271
Evaluation of scintillometer
[FOA-C-30546-3.1] 18 p2555 N90-24578
Equal path, phase shifting, sample point interferometer for monitoring the configuration of surfaces
[NASA-CASE-NPO-17913-1-CU] 21 p3076 N90-27488
RETURN TO EARTH SPACE FLIGHT
Advanced manned launch systems 09 p1175 N90-16797
Rosetta/CNSR altimeter and sounding radar 12 p1741 N90-20009
First impressions of the comet drilling problem 12 p1743 N90-20021
Relevance of laboratory studies to comets 12 p1743 N90-20023
Winged cargo return vehicle. Volume 1: Conceptual design
[NASA-CR-186823] 20 p2821 N90-26050
REUSABLE HEAT SHIELDING
Acousto-optic signature analysis for inspection of the orbiter thermal protection tile bonds
[DE90-013089] 20 p2819 N90-26043
REUSABLE LAUNCH VEHICLES
NT HOTOL LAUNCH VEHICLE
NT SINGLE STAGE TO ORBIT VEHICLES
U.S.S.R. space transportation systems 09 p1176 N90-16806
Mission-dependent selection of propulsion systems for reusable launch vehicles 09 p1177 N90-16815
Progress in airbreathing combined engines for future European launcher 09 p1177 N90-16817
Saenger propulsion system options 09 p1177 N90-16818
Performance integration of a reusable launch vehicle with hybrid airbreathing rocket propulsion 09 p1177 N90-16820
REUSABLE ROCKET ENGINES
Are reusable boosters cost-effective 09 p1179 N90-16834
The Pathfinder chemical transfer propulsion program 11 p1471 N90-18471
Probabilistic modeling for simulation of aerodynamic uncertainties in propulsion systems
[NASA-TM-102472] 14 p1927 N90-21036
A real time neural net estimator of fatigue life
[NASA-TM-103117] 14 p2018 N90-21564
Earth-to-orbit vehicle providing a reusable orbital stage
[NASA-CASE-LAR-13486-1] 16 p2206 N90-22584
Advanced Earth-to-orbit propulsion technology program overview: Impact of civil space technology initiative 23 p3290 N90-28612
REUSABLE SPACECRAFT
NT AEROSPACE PLANES
NT ATLANTIS (ORBITER)
NT BURAN SPACE SHUTTLE
NT CHALLENGER (ORBITER)
NT COLUMBIA (ORBITER)
NT HERMES MANNED SPACEPLANE
NT HOTOL LAUNCH VEHICLE
NT MARS (MANNED REUSABLE SPACECRAFT)
NT SINGLE STAGE TO ORBIT VEHICLES
NT SPACE SHUTTLE ORBITERS
NT SPACE SHUTTLES
Aerospace vehicle design, spacecraft section. Volume 1: Project Groups 3-5
[NASA-CR-186053] 06 p0731 N90-14263
Aerospace vehicle design, spacecraft section. Volume 1: Project Groups 3-5
[NASA-CR-186054] 06 p0731 N90-14264
Advanced manned launch systems 09 p1175 N90-16797
REUSE
Reusable navigation module 09 p1165 N90-16742
Reusable high-temperature heat pipes and heat pipe panels
[NASA-CASE-LAR-13761-1] 13 p1799 N90-20323
A tool for aiding in the reuse of software
[INPE-4981-PRE/1545] 16 p2298 N90-23091
Improving software reusability by program specialization: A case study
[REPT-90-011] 22 p3240 N90-28374
The effect of software reusability on information theory based software metrics
[AD-A224472] 24 p3526 N90-29936
REVENUE
Proceedings of a workshop on Future Airport Passenger Terminals
[PB90-213620] 23 p3284 N90-28580
REVERBERATION
Problems in nonlinear acoustics: Scattering of sound by sound, parametric receiving arrays, nonlinear effects in asymmetric sound beams and pulsed finite amplitude sound beams
[AD-A211756] 04 p0550 N90-13200
Numerical simulation of acoustic scatter from subsurface bubble clouds
[AD-A217068] 12 p1710 N90-19822
Temporal response of coupled one-dimensional dynamic systems
[AD-A222375] 21 p3073 N90-27470
Large aperture acoustic arrays in support of reverberation studies
[AD-A224002] 23 p3393 N90-29168
Angle sample variance of azimuthally spread scattering processes, using a two-element array
[AD-A223572] 24 p3542 N90-30034
REVERSE FIELD PINCH
Observations of azimuthal asymmetry for certain FRC operating regimes
[DE89-015300] 01 p0126 N90-10721
The Reversed-Field-Pinch (RFP) fusion neutron source: A conceptual design
[DE89-015297] 02 p0276 N90-11577
Quality assurance and quality control for the Compact Physics Research Facility (CPRF) and ZTH experiment
[DE90-002352] 06 p0796 N90-14636
Theoretical reversed field pinch studies
[DE90-002114] 06 p0848 N90-14929
End-on soft x ray imaging of Field-Reversed Configurations (FRCs) on the Field-Reversal-C (FRX-C)/Large Scale Modification (LSM) experiment
[DE90-004863] 08 p1082 N90-16260
First results from the MST (Madison Symmetric Torus) reversed field pinch
[DE90-005743] 10 p1433 N90-18268
The lower hybrid drift instability and the evolution of plasma gradients
[DE90-006521] 11 p1568 N90-19021
Rigorous upper bounds for turbulent transport in bounded systems: Passive advection and reversed-field pinches 15 p2168 N90-22390
REVERSE TIME
U REACTION TIME
REVERSING
Aerodynamic and propulsive control development of the STOL and maneuver technology demonstrator 23 p3271 N90-28514
Inflight thrust vectoring: A further degree of freedom in the aerodynamic/flight mechanical design of modern fighter aircraft 23 p3274 N90-28528
REVISIONS
Ada 9X project report. Revision request report
[AD-A213503] 07 p0975 N90-15629
Maintenance = reuse-oriented software development
[NASA-CR-186455] 14 p2012 N90-21531
Guide to RMS-literature
[REPT-89-52] 15 p2158 N90-22326
Evaluation of optical storage technology for decision support databases 15 p2176 N90-22436
Space Shuttle, NASA's major changes to flight hardware: Fact sheet for the Chairman, Committee on Science, Space, and Technology, House of Representatives
[GAO/NSIAD-88-173FS] 15 p2181 N90-22461
Aircraft modifications cost analysis. Volume 1: Overview of the study
[AD-A220764] 19 p2649 N90-25074
A modified Ubbelohde viscometer with improved dilution characteristics
[NIAR-90-16] 19 p2693 N90-25326
Space Shuttle 2 advanced space transportation system. Volume 1: Executive summary
[NASA-CR-185952] 21 p2965 N90-26853
Space Shuttle 2 advanced space transportation system, volume 2
[NASA-CR-185953] 21 p2965 N90-26854
Preparing software conversion studies
[PB90-235623] 23 p3381 N90-29099
REVOLUTION (MOTION)
U REVOLVING
REVOLVING
COBE nonspinning attitude propagation 05 p0587 N90-13418
REYNOLDS EQUATION
Numerical modeling of supersonic turbulent reacting free shear layers 06 p0719 N90-14197
An introduction to turbulence models 22 p3173 N90-28004
REYNOLDS LAW
U REYNOLDS EQUATION
REYNOLDS NUMBER
NT HIGH REYNOLDS NUMBER
NT LOW REYNOLDS NUMBER
Analysis of experimental data for CAST 10-2/DOA 2 supercritical airfoil at low Reynolds numbers and application to high Reynolds number flow
[AD-A211654] 05 p0571 N90-13326
Introduction to cryogenic wind tunnels 08 p1028 N90-15940
Numerical analysis of nonstationary fluid flow (a survey)
[PREPRINT-492] 08 p1065 N90-16159
An experimental study of the effect of streamwise vortices on unsteady turbulent boundary-layer separation 09 p1215 N90-17045
CAST-10-2/DOA 2 Airfoil Studies Workshop Results
[NASA-CP-3052] 10 p1323 N90-17647
Comparison of conventional and adaptive wall wind tunnel results with regard to Reynolds number effects 10 p1323 N90-17649
High Reynolds number tests of the CAST-10-2/DOA 2 transonic airfoil at ambient and cryogenic temper ature conditions 10 p1324 N90-17650
Investigation of CAST-10-2/DOA 2 airfoil in NAE high Reynolds number two-dimensional test facility 10 p1324 N90-17654
Carrier wing profile in nonstationary current
[ETN-90-95368] 12 p1600 N90-19208
Theoretical and experimental examination of the beginning of turbulence in a heated laminar conduit flow
[ETN-90-95369] 12 p1660 N90-19541
Wind tunnel design of heat island turbulent boundary layer
[IHW-ET/50] 12 p1660 N90-19542
Navier-Stokes analysis of turbine blade heat transfer
[NASA-TM-102496] 14 p1972 N90-21300
Computations of a horseshoe vortex around an endwall-mounted cylinder 17 p2400 N90-23673
The effects of Reynolds number, rotor incidence angle, and surface roughness on the heat transfer distribution in a large-scale turbine rotor passage
[NASA-CR-183891] 17 p2410 N90-23731
The gun tunnel of the Brunswick Institute for Fluid Mechanics: Current development status 18 p2489 N90-24227
Coherent structures, chaos and the role of modern dynamics in turbulent shear flows
[AD-A220884] 18 p2552 N90-24562
A linear-eddy model of turbulent shear layer mixing 21 p2974 N90-26904
Hypersonic Arbitrary-Body Aerodynamics (HABA) for conceptual design
[DE90-014750] 23 p3268 N90-28495

Wind tunnel investigation of periodic vortex separation from rough surface circular cylinders by means of acoustic measurements
[ESA-TT-1092] 23 p3268 N90-28499
Two-dimensional wind tunnel test and comparison with calculations for a 15.2 percent thick airfoil section for wind turbines
[FFA-TN-1990-16] 23 p3269 N90-28501
An experimental investigation of a single and multiphase confined coaxial jet 23 p3324 N90-28796

REYNOLDS STRESS
The structure of Reynolds stress in the near wall region of a turbulent pipe flow 02 p0218 N90-11247
Wall-layer eruptions in turbulent flows
[NASA-TM-102362] 02 p0219 N90-11250
Questions from the Willmarth Workshop on New Directions in Research on Turbulent Wall-Layer Structures
[AD-A211282] 02 p0221 N90-11264
A review of quasi-coherent structures in a numerically simulated turbulent boundary layer
[NASA-TM-102191] 05 p0638 N90-13723
Turbulence modeling and implementation in Navier-Stokes solvers 05 p0641 N90-13742
The structure of supersonic turbulent boundary layers subjected to concave surface curvature 08 p1017 N90-15883
An experimental study of the effect of streamwise vortices on unsteady turbulent boundary-layer separation 09 p1215 N90-17045
Measurement of velocity profiles and Reynolds stresses on an oscillating airfoil 11 p1463 N90-18427
Application of a Reynolds stress turbulence model to the compressible shear layer
[NASA-CR-182002] 12 p1660 N90-19537
Analytical methods for the development of Reynolds stress closures in turbulence
[NASA-CR-182017] 12 p1660 N90-19538
Secondary flows and Reynolds stress distributions downstream of a turbine cascade at different expansion ratios 14 p1923 N90-21015
A theoretical investigation of gravity-wave-generated stress and vorticity in the planetary boundary layer 15 p2191 N90-22512
Reynolds stress closure in jet flows using instability wave modeling 16 p2196 N90-22534
Computational simulation of transition to turbulence through inverse modeling 18 p2647 N90-25067
Near-wall modeling of compressible turbulent flows
[NASA-CR-186961] 22 p3109 N90-27658

RF-8 AIRCRAFT
U F-8 AIRCRAFT

RH-2 HELICOPTER
U UH-1 HELICOPTER

RHEA (ASTRONOMY)
Geology of coronae and domal structures on Venus and models of their origin 15 p2191 N90-22513

RHEOELECTRICAL SIMULATION
Evolution equation simulation of semiconductor lasers under a pulsed regime
[TELECOM-PARIS-89-D-010] 18 p2563 N90-24625
Simulation of the electrical and thermal behavior of gapless metal oxide surge arresters under AC-operation condition
[ETN-90-97309] 20 p2859 N90-26262

RHEOENCEPHALOGRAPHY
Rheoencephalography in simulated aviation environmental stress
[AD-A221150] 18 p2584 N90-24716

RHEOLOGY
A graph-theoretical approach to block-copolymer complexes. Part 3: Loops and cycles
[MEMO-778-PT-3] 04 p0479 N90-12750
Quadratic dynamical systems describing shear flow of non-Newtonian fluids
[AD-A212892] 05 p0638 N90-13720
Analysis of new phenomena in shear flow of non-Newtonian fluids
[AD-A212893] 05 p0638 N90-13721
Comments on ER (Electrorheological) fluid rheology
[DE90-002892] 07 p0894 N90-15166
Gelled propellant flow: Boundary layer theory for power-law fluids in a converging planar channel
[DE90-000923] 07 p0927 N90-15365
Determination of flow-regime boundaries for cohesive particles
[DE90-001405] 07 p0928 N90-15369
Advanced study in solid transport: Rheological behavior of dense suspension
[DE90-003369] 07 p0947 N90-15483
Non Newtonian gravity creeping flow
[DE90-600816] 07 p1006 N90-15828
Interdisciplinary research in viscoelasticity and rheology
[AD-A213630] 08 p1063 N90-16145
Traction modeling of military lubricants
[AD-A213856] 09 p1230 N90-17139
Model filled polymers 3. Rheological behavior of polystyrene containing crosslinked polystyrene beads
[AD-A215867] 11 p1489 N90-18567
A study on deformation and break-up of dispersed particles in elongational flow
[ETN-90-96268] 11 p1508 N90-18684
Elastic recovery and polymer-polymer interactions
[AD-A217085] 12 p1633 N90-19384
Calculation of nonlinear viscoelastic processes for plastic layer textile membranes
[ETN-90-95868] 12 p1675 N90-19622
Determination of flow-regime boundaries for cohesive particles
[DE90-007425] 13 p1800 N90-20332
A method for measuring the material moduli of granular materials: Flow in an orthogonal rheometer
[DE90-007160] 13 p1801 N90-20339
Tribological properties of boric acid and boric acid forming surfaces. Part 1: Crystal chemistry and self-lubricating mechanism of boric acid
[DE90-005665] 13 p1811 N90-20401
Nicalon/siliconoxycarbide ceramic composites
[NASA-TM-102563] 14 p1945 N90-21133
Determinations of molecular weight and molecular weight distribution of high polymers by the rheological properties
[NASA-CR-186450] 14 p1953 N90-21180
Experimental and analytical investigations of granular materials: Shear flow and convective heat transfer 15 p2091 N90-21968
Rheology of injection mould filling with DMCs
[NPL-DMA(A)-196] 16 p2222 N90-22675
Rheological and mechanical characteristics of poly-p-phenylene terephthalamide/nylon molecular and particulate composites
[AD-A219562] 17 p2368 N90-23482
Development of a device for surface tension measurement and phenomenological rheology
[ECL-89-12] 17 p2382 N90-23568
The effect of thermal damage on the mechanical properties of polymer regrinds 18 p2515 N90-24363
Rheology and microstructure of concentrated suspensions
[DE90-009976] 18 p2520 N90-24391
Theoretical studies of non-Newtonian and Newtonian fluid flow through porous media
[DE90-011610] 18 p2554 N90-24576
Elastomers and other organic composites
[AD-A222772] 21 p2984 N90-26958
Computational Fluid Dynamics for Industrial Flows
[VKI-LS-1990-04] 22 p3173 N90-28001
POLYFLOW theoretical background 22 p3173 N90-28005
Rheometer strain and strain-rate errors
[DE90-013845] 23 p3329 N90-28824
Rheology of filler rubber: Silica-silicone
[AD-A223600] 24 p3455 N90-29511
Effect of particulate fillers on the rheology of polymer melts
[AD-A223601] 24 p3455 N90-29512
Proceedings of damping '89. Volume 1: Pages AAB-1 through DCD-11
[AD-A223431] 24 p3479 N90-29664

RHEOMETERS
A method for measuring the material moduli of granular materials: Flow in an orthogonal rheometer
[DE90-007160] 13 p1801 N90-20339
Development of a device for surface tension measurement and phenomenological rheology
[ECL-89-12] 17 p2382 N90-23568
Rheometer strain and strain-rate errors
[DE90-013845] 23 p3329 N90-28824

RHODIUM
Luminescence in applied magnetic fields
[AD-A211551] 03 p0399 N90-12287

RHODIUM COMPOUNDS
NMR evidence for a planar arene intermediate in the electron-transfer induced eta 6 to eta 4 hapticity change of a rhodium arene complex
[AD-A210211] 01 p0033 N90-10177
Monomers, polymers and transition metal complexes based upon carboranes
[AD-A210226] 01 p0040 N90-10221
Thermodynamics, kinetics, and interface morphologies of phase formation reactions between metals and Gallium Arsenide: Bulk vs thin-film studies
[DE89-016469] 02 p0284 N90-11621
Antiferromagnetism and enhanced heat in CeM2Sn (M = Ni, Ir, Cu, Rh, Pd, and Pt
[DE90-014924] 23 p3399 N90-29206

RHOMBOIDS
Bistatic radar cross section of a perfectly conducting rhombus-shaped flat plate
[AD-A223418] 24 p3460 N90-29546

RHYTHM (BIOLOGY)
NT CIRCADIAN RHYTHMS
USSR Space Life Sciences Digest, issue 22
[NASA-CR-3922(26)] 03 p0378 N90-12153
A laboratory study of the effects of diet and bright light countermeasures to jet lag
[AD-A220146] 17 p2435 N90-23875
The 1989 Gordon Research Conference on Chronobiology
[AD-A221972] 22 p3231 N90-28322
Electrocardiogram of military aircraft pilots measured during real flight missions: Study of the variability of the cardiac rhythm in correlation with working stress
[ETN-90-97453] 22 p3231 N90-28324

RIBBON PARACHUTES
Performance and quality of a wing type parachute: Parametric analysis
[REPT-88-19] 03 p0302 N90-11710
An experimental investigation of wall-interference effects for parachutes in closed wind tunnels
[DE90-001802] 07 p0875 N90-15076

RIBBONS
Scintillating fiber ribbon - tungsten calorimeter
[DE89-016705] 03 p0350 N90-12001
Evolution of the EPR procedure for polycrystalline Si ribbon drawing for photovoltaic cell manufacturing
[ISAL-89-0027] 05 p0665 N90-13888
Analysis of a high harmonic rectangular gyrotron using ribbon beams 15 p2061 N90-21801

RIBLETS
Effect of riblets on flow separation from a cylinder and an airfoil in subsonic flow
[AD-A216197] 10 p1309 N90-17574
Drag reduction by longitudinal riblets on the surface of a streamwise aligned body of revolution
[MPIS-MITT-92] 12 p1600 N90-19210

RIBONUCLEIC ACIDS
Biomedical studies with the free electron laser
[AD-A208927] 01 p0091 N90-10519
Exposure of human cells to electromagnetic fields
[AD-A219377] 16 p2261 N90-22889

RIBS (SUPPORTS)
Large-diameter geostationary millimeter wavelength antenna concept 12 p1609 N90-19254
Design of a low-frequency (5-20 GHz), 15-meter-diameter passive radiometer for geostationary earth science platforms 12 p1609 N90-19255

RICCATI EQUATION
The singular H infinity control problem with dynamic measurement feedback
[MEMO-COSOR-89-14] 05 p0687 N90-14000
The algebraic Riccati equation and singular optimal control
[MEMO-COSOR-88-31] 05 p0690 N90-14028
The algebraic Riccati equation and singular optimal control
[MEMO-COSOR-89-11] 08 p1117 N90-16467
Direct multivariable adaptive controller with application to wing flutter 10 p1322 N90-17642
A comparison between the propagators method and the decomposition method for nonlinear equations
[DE90-005783] 12 p1704 N90-19781
On the continuous dependence with respect to sampling of the linear quadratic regulator problem for distributed parameter systems
[NASA-CR-182012] 14 p2018 N90-21566
On a fallacious conjecture about the stabilizability properties of solutions of the Riccati difference equation
[REPT-89-007] 16 p2305 N90-23132
The discrete time H infinity control problem: The full-information case
[MEMO-COSOR-89-25] 17 p2455 N90-24003
Completion of the squares in the finite horizon H infinity control problem by measurement feedback
[MEMO-COSOR-89-27] 17 p2455 N90-24004
Numerical conformal mapping and applications
[AD-A219789] 17 p2457 N90-24019
Linear-quadratic problems and the Riccati equation
[MEMO-COSOR-89-26] 17 p2459 N90-24037
On equations of motion on complex Grassman manifold
[DE90-628369] 24 p3537 N90-29999

RICHARDSON-DUSHMAN EQUATION
U TEMPERATURE EFFECTS
U THERMIONIC EMISSION

RIDGES
Coronae on Venus observations and models of origin 03 p0427 N90-12449

RIDING QUALITY
Canard versus aft-tail ride qualities performance and pilot command response 07 p0871 N90-15053
Human factors: The human interface with aircraft interiors
[NIAR-90-18] 20 p2900 N90-26496

RIEMANN INTEGRAL
U MEASURE AND INTEGRATION

RIEMANN MANIFOLD
On the differentiable manifold of fixed order stable linear systems
[REPT-88-89] 03 p0394 N90-12250
A (2+1)-dimensional pure gravity for an arbitrary closed initial surface
[DE90-701754] 07 p1007 N90-15829
Harmonic mappings into manifolds with boundary
[DE90-606961] 09 p1277 N90-17402
Superconformal algebra on meromorphic vector fields with three poles on super-Riemann sphere
[DE90-610423] 12 p1706 N90-19796
Quantum field theory on higher-genus Riemann surfaces
[DE90-741469] 12 p1725 N90-19912
Extension of the Krichever-Novikov algebra in the closed string theory
[DE90-612746] 14 p2020 N90-21578
Multipole moments in general relativity and dynamical perturbations of black-hole magnetospheres
15 p2190 N90-22509
Effective action for induced gravity on a 2-dimensional manifold
[PREPRINT-712] 16 p2311 N90-23173
Quantum mechanics in Riemannian space-time
[DE90-620448] 16 p2325 N90-23257
Beltrami algebra and symmetry of Beltrami equation on Riemann surfaces
[DE90-627157] 23 p3388 N90-29135
On an isospectrality question over compact Riemann surfaces
[DE90-627163] 23 p3390 N90-29147
A corollary to Kodaira-Spencer's theorem on continuity of eigenvalues
[DE90-627164] 23 p3390 N90-29148
Geometrical properties of an internal local octonionic space in a non-Riemannian manifold
[DE90-627175] 23 p3390 N90-29149
Dirac's equation as a geodesic in Riemann space
[DE90-627194] 23 p3390 N90-29152
Superconformal algebra and central extension of meromorphic vector fields with multipoles on super-Riemann sphere
[DE90-627211] 23 p3390 N90-29153
Anyons and Chern-Simons theory on compact spaces of finite genus
[DE90-627216] 23 p3391 N90-29157

RIEMANN PROBLEM
U CAUCHY PROBLEM

RIEMANN SPACE
U RIEMANN MANIFOLD

RIEMANN SPHERE
U RIEMANN MANIFOLD

RIEMANN WAVES
Basic research on methods of calculating supersonic and hypersonic flow
[ONERA-RSF-19/1123-AY-234A]
04 p0448 N90-12565

RIFT VALLEYS
U VALLEYS

RIFTS
U GEOLOGICAL FAULTS

RIGID BODIES
U RIGID STRUCTURES

RIGID ROTORS
A technique for the prediction of aerodynamics and aeroelasticity of rotor blades 05 p0579 N90-13377
The effects of structural flap-lag and pitch-lag coupling on soft inplane hingeless rotor stability in hover
[NASA-TP-3002] 23 p3269 N90-28503

RIGID ROTORS (PLASMA PHYSICS)
NT PLASMA PHYSICS

RIGID STRUCTURES
NT RIGID ROTORS
NT RIGID WINGS
Lumped mass formulations for modeling flexible body systems 01 p0019 N90-10091
Dynamic robot models using the Manutec r3 as an example
[ESA-TT-1132] 04 p0458 N90-12626
Extension to Eulers's theorem to n-dimensional spaces 05 p0589 N90-13431
On the motion of compliantly-connected rigid bodies in contact. Part 1: The motion prediction problem
[AD-A214135] 07 p0948 N90-15489
Dynamic interactions and globally optimal maneuver of distributed systems 09 p1236 N90-17172
Equations of motion of slung load systems with results for dual lift
[NASA-TM-102246] 10 p1322 N90-17641
Time and frequency-domain identification and verification of BO-105 dynamic models
[AD-A216828] 11 p1456 N90-18389
Detection of potential space station control/structure interaction with CO-ST-IN 14 p1935 N90-21074
Direct inversion of rigid-body rotational dynamics
[NASA-TM-102798] 15 p2055 N90-21773
Nonlinear strain-displacement relations and flexible multibody dynamics 16 p2284 N90-23014
Dynamic analysis of flexible multibody structures
18 p2642 N90-25048
Direct drive robotic hand
[NASA-CASE-NPO-17917-1-CU]
20 p2872 N90-26339
Flexible structure control and rigid body dynamics
22 p3129 N90-27757
Very low height drop test. Conditioning and tandem dropping of two loads conditioned in two PC6 platforms assembled by rigid structures
[REPT-89/07] 22 p3193 N90-28116
Very low height drop test. Conditioning and tandem dropping of two loads conditioned in two PC6 platforms assembled by one PD9 platform and rigid structures
[REPT-89/04] 22 p3193 N90-28117
A nonlinear finite element formulation for the large displacement analysis of plates
23 p3338 N90-28867
How to push a block along a wall
24 p3511 N90-29848

RIGID WINGS
COCOMAT: A Computer Aided Engineering (CAE) system for composite structures design
[NLR-MP-87078-U] 12 p1699 N90-19756

RILLS
U VALLEYS

RING LASERS
Performance of zig-zag slab regenerative ring amplifier laser system
[DE90-006995] 13 p1806 N90-20371
Dynamics and instabilities in homogeneously broadened lasers
[AD-A218427] 16 p2241 N90-22786
Laser gyros and field diagnostics
[AD-A220832] 17 p2406 N90-23709
Vertical emitting, ring geometry, ultra-low threshold, and ultra-high speed quantum well lasers for optical interconnect
[AD-A219946] 17 p2409 N90-23727
Stability of laser oscillator systems
18 p2641 N90-25045
Vertical emitting, ring geometry, ultra-low threshold, and ultra-high speed quantum well lasers for optical interconnect
[AD-A222932] 21 p3008 N90-27098
Ring laser gyro principles and techniques
24 p3426 N90-29352
Use of a three-axis monolithic ring laser gyro and digital signal processor in an inertial sensor element
24 p3426 N90-29354
Ring laser gyro marine inertial navigation systems
24 p3426 N90-29355
Novel approaches to sensitivity enhancement of ring laser gyros
[AD-A224335] 24 p3471 N90-29617

RING STRUCTURES
NT RING WINGS
Analysis of composite ring of compression test data
[DE90-004468] 09 p1239 N90-17194
Expanding ring joint
[AD-D014398] 14 p1986 N90-21384

RING WINGS
Steady and unsteady potential flow around thin annular wings and engines with simulation of jet engine flow
[DFVLR-FB-89-18] 03 p0302 N90-11711

RINGS
Hyperbolic Hjelmslev groups
[ETN-90-97298] 24 p3538 N90-30009

RINGS (MATHEMATICS)
Minimal prime ideals in semigroups without nilpotent elements
[DE90-606957] 10 p1423 N90-18207

RIOMETERS
On the relation between the electron content of the ionospheric D-region, variations of the riometer absorption, and the H-component of the geomagnetic field
22 p3210 N90-28208

RIPPLES
Electrical test of gyrotron coil
[INPE-4929-RPE/596] 09 p1214 N90-17041
On the temperature of surfaces
10 p1366 N90-17917
Dynamic and photometric evolutionary models of tidal tails and ripples 18 p2637 N90-25024
Erosion mechanisms in composite materials and ripple formation mechanism in erosion
[IAR-89-4-PT-1] 20 p2826 N90-26078
Erosion mechanisms in composite materials and ripple formation mechanism in erosion
[IAR-89-4-PT-2] 20 p2826 N90-26079
Applications of ripple analysis in hydro-acoustics
[ETN-90-97015] 22 p3244 N90-28397

RISK
Managing human exposure and health risks: An integrated approach and the role of uncertainty
[DE89-008611] 01 p0092 N90-10525
Review of the Aerospace Safety Advisory Panel report for NASA fiscal year 1990 authorization
[GPO-24-234] 06 p0722 N90-14213
Battery technology assessment and R and D plan
[DE90-002007] 06 p0772 N90-14489
Biological effects of hyperthermia and potential risk associated with ultrasonic exposure
[PB89-100702] 06 p0820 N90-14768
Elicitation of natural language representations of uncertainty using computer technology
[DE90-001416] 07 p0972 N90-15611
Risk assessment and its application to flight safety analysis
[DE90-004985] 09 p1161 N90-16722
Environmental quality and occupational health Special Emphasis Area Plan (SEAP)
[AD-A214738] 09 p1251 N90-17259
Definition of a management information system to support performance risk assessment
[AD-A215464] 09 p1297 N90-17516
Fire safety in civil aviation 10 p1312 N90-17586
VULCAIN: An expert system dedicated to fire risk analysis within complex industrial environments
10 p1314 N90-17599
Probability of failure and risk assessment of propulsion structural components 11 p1471 N90-18470
Risk analysis: Fundamental concepts, regulatory toxicology, and relative comparisons from radiation biology
[DE90-002466] 11 p1538 N90-18856
Safety Status Report for the Ulysses mission. Book 1: Risk analysis. General purpose heat source radioisotope thermoelectric generator program
[DE90-006826] 12 p1614 N90-19282
The pollution hazard assessment system: Documentation and users manual
[AD-A217108] 12 p1689 N90-19706
Simulator sickness in the CH-47 (Chinook) flight simulator
[AD-A218214] 13 p1853 N90-20634
Final safety analysis report for the Ulysses Mission
[DE90-008690] 14 p1940 N90-21106
Kinematic and kinetic analyses of drop landings
14 p2010 N90-21517
Final environmental impact statement for the Galileo Mission (Tier 2)
[NASA-TM-102925] 15 p2124 N90-22147
Computer vision techniques for rotorcraft low altitude flight 15 p2142 N90-22237
Kalman filter based range estimation for autonomous navigation using imaging sensors
15 p2142 N90-22238
Financing of large space transportation projects: Research on the financial project for the SSPS
[ILR-MITT-228(1989)] 17 p2363 N90-23456
Pilot decision-making training
[AD-A221349] 18 p2585 N90-24720
Progressive cervical osteoarthritis in high performance aircraft pilots 19 p2718 N90-25465
Space program: Space debris a potential threat to Space Station and shuttle
[GAO/IMTEC-90-18] 20 p2815 N90-26024
Space Propulsion Hazards Analysis Manual (SPHAM), volume 1
[AD-A219607] 21 p2969 N90-26874
Space Propulsion Hazards Analysis Manual (SPHAM), volume 2
[AD-A219608] 21 p2969 N90-26875
Block 6: The future DMSP space systems
21 p3068 N90-27443
Chasing a specter: Risk management for global environmental change
[DE90-014455] 23 p3347 N90-28917
Techniques for developing a system safety risk assessment model
[AD-A223477] 24 p3477 N90-29654
Preliminary hazard analysis in design application to EVA space suit
[ETN-90-97585] 24 p3523 N90-29918
For the definition of two person zero sum games
[ETN-90-97294] 24 p3541 N90-30022

RIVER BASINS
Erosion monitoring using remote sensing, part 2
[BCRS-89-15] 11 p1526 N90-18785

RIVERS
NT MISSISSIPPI RIVER (US)
Estimation of time to maximum supercooling during dynamic frazil ice formation
[AD-A212204] 04 p0471 N90-12699
Summary of 1987 and 1988 manatee aerial surveys at Kennedy Space Center
[NASA-TM-102783] 06 p0802 N90-14669

Position fixing by detection of roads and rivers
09 p1163 N90-16733
Quantification of structural field data in the Rio Grande do Norte basin and neighborhood
[INPE-4821-RPE/591] 11 p1533 N90-18826
Analysis of water quality parameters of the Piaui River (SE), Brazil, through field and TM/LANDSAT sensor data
[INPE-4918-PRE/1417] 14 p1998 N90-21453
Evaluation of the mangrove areas of the Rio Piaui (SE) through remote sensing
[INPE-4909-PRE/1510] 14 p1998 N90-21454
Performance evaluation of MSS/LANDSAT data in the estimation of fluvial channel width
[INPE-4906-PRE/1507] 14 p2000 N90-21463
Fundamental studies on hydrology, hydraulics and geometry of river networks
[AD-A218662] 16 p2250 N90-22830
Accuracy and precision of GOES data collection platforms for temperature measurements
[AD-A218798] 16 p2250 N90-22832
A study of mesoscale acid deposition in the lower Ohio River Valley 16 p2253 N90-22848
Activities report of the Hydraulics Research Laboratory
[ETN-90-96568] 19 p2687 N90-25281
Velocity distribution in a gravel-bed flume; for steady and unsteady flow 19 p2687 N90-25283
Grain-size distribution and armoring in gravel-bed rivers: A case study 19 p2687 N90-25285
Vertically averaged spectral model for tidal circulation in estuaries. Part 1: Model formulation
[PB90-181678] 22 p3230 N90-28319

RIVETED JOINTS
Bearing tests in Ti-6Al-4V plates made using superplastic forming
[INFORME-I-357/89] 10 p1396 N90-18068

RIVETS
Fastener design manual
[NASA-RP-1228] 11 p1517 N90-18740
Modeling growth of fatigue cracks which originate at rivet holes 18 p2645 N90-25060
Neural networks for detecting defects in aircraft structures
[IAR-90-4] 20 p2873 N90-26345

RNA
U RIBONUCLEIC ACIDS

ROADS
NT HIGHWAYS
Improving snow roads and airstrips in Antarctica
[AD-A211588] 03 p0335 N90-11907
Why stochastic modeling is essential in analyzing interdicted transportation network performance
[AD-A213140] 05 p0688 N90-14007
Position fixing by detection of roads and rivers
09 p1163 N90-16733
Monitoring of agrocattle-raising projects through visual/digital analysis of LANDSAT-TM imagery south of Para state
[INPE-4982-PRE/1542] 14 p1998 N90-21442
Inventory of program packages related to the project SIMONA
[ETN-90-96397] 15 p2148 N90-22270
Geographic information system: Coded data of agrocattle-raising projects in the Amazon
[INPE-4978-PRE/1543] 15 p2180 N90-22457
Conceptual design and analysis of roads and road construction machinery for initial lunar base operations
[NASA-CR-186673] 18 p2535 N90-24459
Color image processing for navigation: Two road trackers
[AD-A222667] 20 p2916 N90-26591
Guidance document for selecting antiskid materials applied to ice- and snow-covered roadways
[PB90-183658] 21 p2983 N90-26950

ROBOT ARMS
Manipulation strategies for massive space payloads
[NASA-CR-186081] 06 p0728 N90-14247
Controller design for a robotic manipulator
06 p0792 N90-14615
Control of mechanical manipulators
07 p0938 N90-15432
Feasibility study of using industrial robot for ultrasound testing
[DE90-002977] 07 p0943 N90-15461
Gaze controls with interactions and delays
[AD-A214286] 07 p0981 N90-15667
A knowledge-based machine vision system for space station automation 08 p1075 N90-16221
On-line estimation of mechanical nonlinearities in compliant two-link robot manipulators
08 p1085 N90-16280
Dynamic modeling of flexible bodies in multibody systems 09 p1229 N90-17134
Pareto optimization design techniques for the AFIT (Air Force Institute of Technology)/AAMRL (Armstrong Aeronautical Medical Research Laboratory) anthropomorphic robotic manipulator
[AD-A216178] 10 p1414 N90-18150
Kinematic control of robotic manipulators with multiple interchangeable wrists 12 p1670 N90-19592
Dynamics and control of robot manipulators with closed-kinematic chain mechanism
12 p1671 N90-19598
A complete description of robot manipulator dynamics based on Lagrangian mechanics
[DE90-741467] 12 p1672 N90-19603
Development of a passive robot-controlled reaction arm 13 p1809 N90-20389
Graphical programming and the use of simulation for space-based manipulators 13 p1861 N90-20674
End point control of flexible manipulators
[AD-A217319] 14 p1986 N90-21383
Development of a dynamic modeling technique and its application to the analysis and control of a high-precision robotic manipulator 14 p1987 N90-21391
Application of optimization in design and motion control of robot manipulators 14 p1988 N90-21393
Perturbation techniques in the dynamics and control of flexible manipulators
[OUEL-1772/89] 15 p2107 N90-22053
The JPL/KSC telerobotic inspection demonstration
15 p2155 N90-22312
An order (n) algorithm for the dynamics simulation of robotic systems 16 p2279 N90-22990
Recursive linearization of multibody dynamics equations of motion 16 p2280 N90-22993
A robot arm simulation with a shared memory multiprocessor machine 16 p2283 N90-23008
An inverse kinematics algorithm for a highly redundant variable-geometry-truss manipulator
16 p2288 N90-23033
On trajectory generation for flexible space crane: Inverse dynamics analysis by LATDYN 16 p2288 N90-23037
Parallel conjugate gradient algorithms for manipulator dynamic simulation 16 p2290 N90-23045
Man-in-the-control-loop simulation of manipulators
16 p2293 N90-23063
HERA and EVA co-operation scenarios
18 p2502 N90-24299
The Hermes robot arm teleoperation and control concept 18 p2503 N90-24301
HERA teleoperation test facility
18 p2503 N90-24303
The bi-arm servicer: A multimission concept and a technological model for space robotics
18 p2504 N90-24307
Simulation and ground-based testing of ORU-handling with a bi-arm robot 18 p2505 N90-24317
The real-time Hermes robot arm simulator: HSF-P
18 p2506 N90-24319
The Hermes robot arm: System description
18 p2507 N90-24327
Dynamic modeling and control of a flexible arm holding a non-rigid payload 18 p2507 N90-24331
Self-contained robotic arm manipulator
[NASA-CR-184925] 19 p2696 N90-25342
Out-reach in-space technology experiments program: Control of flexible robot manipulators in zero gravity, experiment definition phase
[NASA-CR-183849] 19 p2696 N90-25343
Design of a versatile, teleoperable, towable lifting machine with robotic capabilities for use in NASA's lunar base operations
[NASA-CR-186688] 19 p2697 N90-25345
Robot vibration control using inertial damping forces
[NASA-CR-186808] 19 p2698 N90-25352
Smart hands for the EVA retriever
19 p2736 N90-25550
Kinematically redundant arm formulations for coordinated multiple arm implementations
19 p2736 N90-25551
Numerical approach of collision avoidance and optimal control on robotic manipulators
19 p2736 N90-25552
A laboratory breadboard system for dual-arm teleoperation 19 p2740 N90-25573
Trajectory planning and control of a 6 DOF manipulator with Stewart platform-based mechanism
[NASA-CR-186813] 19 p2747 N90-25610
A parallel Newton-Euler formulation for fast dynamic simulation of robot manipulators
[RR-368] 19 p2748 N90-25614
Control strategy for cooperating disparate manipulators
[NASA-CR-186809] 20 p2870 N90-26328
Design of a lunar transportation system, volume 2
[NASA-CR-186833-VOL-2] 20 p2871 N90-26333
Direct drive robotic hand
[NASA-CASE-NPO-17917-1-CU]
20 p2872 N90-26339
Grasping with mechanical intelligence
[NASA-CR-186864] 20 p2900 N90-26498
Beam rider for an Articulated Robot Manipulator (ARM) accurate positioning of long flexible manipulators
[NASA-CR-185151] 20 p2914 N90-26581
A real-time robot arm collision detection system
[NASA-CR-185878] 20 p2915 N90-26582
Multi-sensory perception of a geometrical structure of a scene
[ETN-90-97245] 20 p2915 N90-26587
Method and apparatus for configuration control of redundant robots
[NASA-CASE-NPO-17801-1-CU]
21 p3010 N90-27110
Robot dynamics in reduced gravity environment
21 p3049 N90-27333
Development, implementation, and validation of control algorithms for the dual-arm robotic manipulation of a single object
[AD-A222502] 21 p3060 N90-27402
Multiple arm manipulation
[PB90-199506] 22 p3182 N90-28056
Reaction-compensation technology for microgravity laboratory robots
[NASA-TM-103271] 22 p3183 N90-28062
Motion coordination for a mobile manipulator system
[PB90-203076] 23 p3332 N90-28839
Modularity in robotic systems
23 p3365 N90-29014
A fast lightstripe rangefinding system with smart VLSI sensor 23 p3366 N90-29019
Grasp planning under uncertainty
23 p3370 N90-29041
Preliminary study of a serial-parallel redundant manipulator 23 p3371 N90-29048
The JPL telerobot operator control station. Part 1: Hardware 23 p3371 N90-29049
The JPL telerobot operator control station. Part 2: Software 23 p3371 N90-29050
Performance evaluation of a 6 axis high fidelity generalized force reflecting teleoperator
23 p3372 N90-29052
Human machine interaction via the transfer of power and information signals 23 p3372 N90-29054
Experiences with the JPL telerobot testbed: Issues and insights 23 p3373 N90-29059
The KALI multi-arm robot programming and control environment 23 p3373 N90-29060
Modeling, design, and control of flexible manipulator arms: Status and trends 24 p3500 N90-29782
Dynamical modeling of serial manipulators with flexible links and joints using the method of kinematic influence
24 p3500 N90-29783
Technology and task parameters relating to the effectiveness of the bracing strategy
24 p3500 N90-29785
Manipulators with flexible links: A simple model and experiments 24 p3501 N90-29786
Experiments in identification and control of flexible-link manipulators 24 p3501 N90-29787
Autonomous dexterous end-effectors for space robotics 24 p3501 N90-29788
Design and control of a multi-fingered robot hand provided with tactile feedback 24 p3501 N90-29789
Force/torque and tactile sensors for sensor-based manipulator control 24 p3501 N90-29791
Telepresence system development for application to the control of remote robotic systems
24 p3503 N90-29799
The 3D model control of image processing
24 p3503 N90-29800
Use of 3D vision for fine robot motion
24 p3503 N90-29804
Control strategies for a telerobot
24 p3504 N90-29808
Autonomous sensor-based dual-arm satellite grappling
24 p3504 N90-29809
Stability analysis of multiple-robot control systems
24 p3505 N90-29811
Time optimal movement of cooperating robots
24 p3505 N90-29815
Learning in tele-autonomous systems using Soar
24 p3506 N90-29819
Design of a structural and functional hierarchy for planning and control of telerobotic systems
24 p3506 N90-29820
Research and development activities at the Goddard Space Flight Center for the flight telerobotic servicer project 24 p3507 N90-29824
Test and validation for robot arm control dynamics simulation 24 p3507 N90-29826
Graphic overlays in high-precision teleoperation: Current and future work at JPL 24 p3508 N90-29827

Proceedings of the NASA Conference on Space Telerobotics, volume 4
[NASA-CR-186859] 24 p3508 N90-29830
An improved adaptive control for repetitive motion of robots 24 p3508 N90-29831
Model based manipulator control 24 p3509 N90-29833
A discrete decentralized variable structure robotic controller 24 p3509 N90-29835
The JAU-JPL anthropomorphic telerobot 24 p3509 N90-29838
A procedure concept for local reflex control of grasping 24 p3509 N90-29839
Sensor-based fine telemanipulation for space robotics 24 p3510 N90-29841
ROTEX-TRIIFEX: Proposal for a joint FRG-USA telerobotic flight experiment 24 p3510 N90-29842
Test and training simulator for ground-based teleoperated in-orbit servicing 24 p3510 N90-29843
Force-reflective teleoperated system with shared and compliant control capabilities 24 p3510 N90-29845
Redundancy in sensors, control and planning of a robotic system for space telerobotics 24 p3511 N90-29847
The effects of gear reduction on robot dynamics 24 p3513 N90-29861
Recursive Newton-Euler formulation of manipulator dynamics 24 p3513 N90-29862
Kinematic sensitivity of robot manipulators 24 p3513 N90-29863
The laboratory telerobotic manipulator program 24 p3515 N90-29869
Robotic control of the seven-degree-of-freedom NASA laboratory telerobotic manipulator 24 p3515 N90-29870
The control of space manipulators subject to spacecraft attitude control saturation limits 24 p3515 N90-29871
Comparison of joint space versus task force load distribution optimization for a multiarm manipulator system 24 p3515 N90-29873
Proceedings of the NASA Conference on Space Telerobotics, volume 5
[NASA-CR-186860] 24 p3516 N90-29874
Application of recursive manipulator dynamics to hybrid software/hardware simulation 24 p3516 N90-29876
Kinematics and control algorithm development and simulation for a redundant two-arm robotic manipulator system 24 p3516 N90-29877
Inverse dynamics of a 3 degree of freedom spatial flexible manipulator 24 p3516 N90-29878
A control approach for robots with flexible links and rigid end-effectors 24 p3516 N90-29879
Teleoperation experiments with a Utah/MIT hand and a VPL DataGlove 24 p3517 N90-29883
Integration of a sensor based multiple robot environment for space applications: The Johnson Space Center Teleoperator Branch Robotics Laboratory 24 p3518 N90-29890
On discrete control of nonlinear systems with applications to robotics 24 p3519 N90-29893
Flight experiments in telerobotics-Orbiter middeck concept 24 p3519 N90-29895
Experimental study on two-dimensional free-flying robot satellite model 24 p3519 N90-29896
Computed torque control of a free-flying cooperat ing-arm robot 24 p3520 N90-29898
Computer simulation and design of a three degree-of-freedom shoulder module 24 p3520 N90-29902
A collision avoidance system for a spaceplane manipulator arm 24 p3521 N90-29903

ROBOT CONTROL

Simulation and control problems in elastic robots 01 p0020 N90-10098
Flexible robot control: Modeling and experiments 01 p0021 N90-10104
Experimental validation of flexible robot arm modeling and control 01 p0023 N90-10113
The role of sensor directed, model based control in robotics
[DE89-014133] 01 p0077 N90-10442
Optimized resolved rate control of seven-degree-of-freedom Laboratory Telerobotic Manipulator (LTM) with application to three-dimensional graphics simulation
[NASA-TP-2938] 01 p0109 N90-10618
NASA/NBS (National Aeronautics and Space Administration/National Bureau of Standards) standard reference model for telerobot control system architecture (NASREM)
[NASA-CR-185078] 02 p0228 N90-11310
Modeling and simulation of spatial robotic manipulators with flexible links and joint drives for control strategies implementation and evaluation 02 p0228 N90-11311
Spoken commands control robot that handles radioactive materials
[DE89-012632] 02 p0262 N90-11488
Robot inverse dynamics computation via VLSI distributed architectures
[RR-350] 03 p0390 N90-12223
Telerobotic control for teams of semi-autonomous agents, phase 1
[AD-A211648] 04 p0526 N90-13037
Arc current control of a robotic welding system: Modeling and control system design
[AD-A213150] 05 p0650 N90-13788
Kinematics and control of manipulation robots
[WTHD-187] 05 p0652 N90-13803
Controller design for a robotic manipulator 06 p0792 N90-14615
Expert system control of a six-legged walking telerobot
[DE90-004661] 08 p1086 N90-16285
Mathematical model for adaptive control system of ASEA robot at Kennedy Space Center 08 p1157 N90-16701
Experimental evaluation of impedance control for robotic aircraft refueling
[AD-A215532] 09 p1167 N90-16755
Multiple model adaptive estimation techniques for adaptive model-based robot control
[AD-A215742] 09 p1231 N90-17146
Payload invariant control via neural networks: Development and experimental evaluation
[AD-A215740] 09 p1260 N90-17306
Learning-based position control of a closed-kinematic chain robot end-effector
[NASA-CR-186283] 10 p1391 N90-18043
A colony architecture for an artificial creature
[AD-A216802] 11 p1549 N90-18918
Kinematic control of robotic manipulators with multiple interchangeable wrists 12 p1670 N90-19592
Experiments in end-point control of a flexible robot with a mini-manipulator 12 p1671 N90-19596
Dynamics and control of robot manipulators with closed-kinematic chain mechanism 12 p1671 N90-19598
Design and implementation of a flexible robot
[AD-A216453] 12 p1671 N90-19601
A complete description of robot manipulator dynamics based on Lagrangian mechanics
[DE90-741467] 12 p1672 N90-19603
Development of a passive robot-controlled reaction arm 13 p1809 N90-20389
Resolved motion rate and resolved acceleration servo-control of wheeled mobile robots
[DE90-002585] 13 p1811 N90-20399
Design of a telerobotic controller with joint torque sensors
[DE90-008753] 13 p1812 N90-20404
Control system design of the third flexible joint of PUMA 560 robot
[AD-A218075] 13 p1812 N90-20405
End point control of flexible manipulators
[AD-A217319] 14 p1986 N90-21383
Development of a dynamic modeling technique and its application to the analysis and control of a high-precision robotic manipulator 14 p1987 N90-21391
Application of optimization in design and motion control of robot manipulators 14 p1988 N90-21393
Adaptive learning fuzzy control of a mobile robot
[DE90-759898] 14 p2018 N90-21562
Nonlinear stability analysis and control of dynamical robotic systems 15 p2104 N90-22037
A new six-degree-of-freedom force-reflecting hand controller for space telerobotics 15 p2113 N90-22089
Instrumentation and robotic image processing using top-down model control 15 p2142 N90-22239
Plan execution control and architecture for mobile robots
[LAAS-89-371] 16 p2243 N90-22793
Characterization of robotics parallel algorithms and mapping onto a reconfigurable SIMD machine 16 p2289 N90-23039
Distributed neural control of a hexapod walking vehicle 16 p2293 N90-23061
Experimental adaptive control of a hydraulic robot 16 p2303 N90-23121
Control of randomly sampled robotic systems
[AD-A218948] 16 p2309 N90-23157
Adaptive control methods for mechanical manipulators: A comparative study
[AD-A219965] 17 p2413 N90-23749
The Hermes robot arm teleoperation and control concept 18 p2503 N90-24301
Teleoperation of a force controlled robot manipulator without force feedback to a human operator 18 p2503 N90-24305
NASREM: A functional architecture for control of the flight telerobotic servicer 18 p2506 N90-24325
Adaptive control of visually guided grasping in neural networks
[AD-A221387] 18 p2597 N90-24780
Out-reach in-space technology experiments program: Control of flexible robot manipulators in zero gravity, experiment definition phase
[NASA-CR-183849] 19 p2696 N90-25343
Robot vibration control using inertial damping forces
[NASA-CR-186808] 19 p2698 N90-25352
A task control architecture for autonomous robots 19 p2735 N90-25546
Numerical approach of collision avoidance and optimal control on robotic manipulators 19 p2736 N90-25552
The application of NASREM to remote robot control 19 p2738 N90-25563
The JPL telerobot operator control station: Operational experiences 19 p2738 N90-25565
Computer-aided design of advanced control algorithms for industrial robotics: An overview of ESPRIT project SACODY
[REPT-81-DT-89-47] 19 p2744 N90-25596
Adaptive robot control using artificial neural networks: An application in the theory of cognition
[RR-374] 19 p2748 N90-25618
Space station definitions, design, and development. Task 5: Multiple arm telerobot coordination and control: Manipulator design methodology
[NASA-CR-182043] 20 p2914 N90-26577
Method and apparatus for configuration control of redundant robots
[NASA-CASE-NPO-17801-1-CU] 21 p3010 N90-27110
Special purpose parallel computer architecture for real-time control and simulation in robotic applications
[NASA-CASE-NPO-17629-1-CU] 21 p3038 N90-27268
A vision-based telerobotic control station 21 p3046 N90-27311
Development, implementation, and validation of control algorithms for the dual-arm robotic manipulation of a single object
[AD-A222502] 21 p3060 N90-27402
Solutions to the frictional dynamics problem and the reciprocal variable feedback methodology for design and control of robot mechanisms 23 p3333 N90-28846
Tele-Autonomous control involving contact --- object localization
[NASA-CR-187004] 23 p3335 N90-28854
Cartesian control of redundant robots 23 p3363 N90-29004
Control of intelligent robots in space 23 p3365 N90-29013
Multi-layer neural networks for robot control 23 p3368 N90-29031
A design philosophy for multi-layer neural networks with applications to robot control 23 p3368 N90-29033
The JPL telerobot operator control station. Part 1: Hardware 23 p3371 N90-29049
The JPL telerobot operator control station. Part 2: Software 23 p3371 N90-29050
Preliminary results on noncollocated torque control of space robot actuators 23 p3373 N90-29057
Portable Dextrous Force Feedback Master for robot telemanipulation (PDMFF) 23 p3373 N90-29058
The KALI multi-arm robot programming and control environment 23 p3373 N90-29060
Design and control of a multi-fingered robot hand provided with tactile feedback 24 p3501 N90-29789
Telepresence system development for application to the control of remote robotic systems 24 p3503 N90-29799
Control strategies for a telerobot 24 p3504 N90-29808
Stability analysis of multiple-robot control systems 24 p3505 N90-29811
Controlling multiple manipulators using RIPS 24 p3505 N90-29814
Design of a structural and functional hierarchy for planning and control of telerobotic systems 24 p3506 N90-29820
Test and validation for robot arm control dynamics simulation 24 p3507 N90-29826
Use of graphics in decision aids for telerobotic control: (Parts 5-8 of an 8-part MIT progress report) 24 p3508 N90-29829
An improved adaptive control for repetitive motion of robots 24 p3508 N90-29831
Direct adaptive control of a PUMA 560 industrial robot 24 p3508 N90-29832
Model based manipulator control 24 p3509 N90-29833
Discrete-time adaptive control of robot manipulators 24 p3509 N90-29834

A discrete decentralized variable structure robotic controller 24 p3509 N90-29835
A procedure concept for local reflex control of grasping 24 p3509 N90-29839
Force-reflective teleoperated system with shared and compliant control capabilities 24 p3510 N90-29845
Redundancy in sensors, control and planning of a robotic system for space telerobotics 24 p3511 N90-29847
Global models: Robot sensing, control, and sensory-motor skills 24 p3511 N90-29849
RCTS: A flexible environment for sensor integration and control of robot systems; the distributed processing approach 24 p3512 N90-29852
Real-time cartesian force feedback control of a teleoperated robot 24 p3513 N90-29857
Robotic control of the seven-degree-of-freedom NASA laboratory telerobotic manipulator 24 p3515 N90-29870
Kinematics and control algorithm development and simulation for a redundant two-arm robotic manipulator system 24 p3516 N90-29877
A control approach for robots with flexible links and rigid end-effectors 24 p3516 N90-29879
Flight telerobotic servicer control from the Orbiter 24 p3517 N90-29882
Multi-level manual and autonomous control superposition for intelligent telerobot 24 p3518 N90-29888
An alternative control structure for telerobotics 24 p3518 N90-29889
Requirements for implementing real-time control functional modules on a hierarchical parallel pipelined system 24 p3518 N90-29891
The JPL telerobotic Manipulator Control and Mechanization (MCM) subsystem 24 p3519 N90-29892
On discrete control of nonlinear systems with applications to robotics 24 p3519 N90-29893
Computed torque control of a free-flying cooperating-arm robot 24 p3520 N90-29898
Distributed communications and control network for robotic mining 24 p3520 N90-29901

ROBOT DYNAMICS
Applications of artificial intelligence to space station and automated software techniques: High level robot command language
[NASA-CR-182997] 05 p0686 N90-13991
Centralized and decentralized Kalman filter techniques for tracking, navigation, and control
[AD-A214245] 07 p0878 N90-15091
SIMON (SuperIntelligent Mobile Observing Navigator): A high-reliability robot for a radiation environment
[DE90-003888] 07 p0943 N90-15460
Mathematical model for adaptive control system of ASEA robot at Kennedy Space Center 08 p1157 N90-16701
Method and apparatus for positioning a robotic end effector
[NASA-CASE-MSC-21476-1] 09 p1230 N90-17137
On the kinematic behavior of robots while executing general robot level commands
[PB90-120965] 11 p1517 N90-18735
An approach centered in production rules for a partition of environment and planning in a visual navigation system (SNV)
[INPE-4813-TDL/360] 11 p1517 N90-18737
Kinematic control of robotic manipulators with multiple interchangeable wrists 12 p1670 N90-19592
Application of optimization in design and motion control of robot manipulators 14 p1988 N90-21393
Determination of joint drives for stable end-effector motion in flexible robotic systems 16 p2288 N90-23034
The real-time Hermes robot arm simulator: HSF-P 18 p2506 N90-24319
A three fingered multijointed gripper as a working tool for experimental use 18 p2507 N90-24329
Smart hands for the EVA retriever 19 p2736 N90-25550
Kinematically redundant arm formulations for coordinated multiple arm implementations 19 p2736 N90-25551
A parallel Newton-Euler formulation for fast dynamic simulation of robot manipulators
[RR-368] 19 p2748 N90-25614
Adaptive robot control using artificial neural networks: An application in the theory of cognition
[RR-374] 19 p2748 N90-25618
An inverse dynamic method yielding flexible manipulator state trajectories
[NASA-CR-186807] 20 p2870 N90-26329
Assembly via disassembly: A case in machine perceptual development
[NASA-CR-186867] 20 p2900 N90-26497
Method and apparatus for configuration control of redundant robots
[NASA-CASE-NPO-17801-1-CU] 21 p3010 N90-27110
Resolution of seven-axis manipulator redundancy: A heuristic issue 21 p3049 N90-27331
Robot dynamics in reduced gravity environment 21 p3049 N90-27333
Robotic space simulation integration of vision algorithms into an orbital operations simulation
[NASA-CR-185934] 21 p3059 N90-27395
Reaction-compensation technology for microgravity laboratory robots
[NASA-TM-103271] 22 p3183 N90-28062
Motion coordination for mobile robots in unstructured environments
[PB90-199498] 23 p3332 N90-28837
Motion coordination for a mobile manipulator system
[PB90-203076] 23 p3332 N90-28839
Dynamic interaction of multiple autonomous mobile robots 23 p3333 N90-28844
Experiments in the dynamic and strategic control of cooperating manipulators 23 p3333 N90-28845
Solutions to the frictional dynamics problem and the reciprocal variable feedback methodology for design and control of robot mechanisms 23 p3333 N90-28846
Tele-Autonomous control involving contact --- object localization
[NASA-CR-187004] 23 p3335 N90-28854
Magnetostrictive direct drive motors
[NASA-CR-186895] 23 p3335 N90-28855
Proceedings of the NASA Conference on Space Telerobotics, volume 1
[NASA-CR-186856] 23 p3362 N90-29000
A new approach to global control of redundant manipulators 23 p3363 N90-29002
Kinematic functions for the 7 DOF robotics research arm 23 p3363 N90-29003
A complete analytical solution for the inverse instantaneous kinematics of a spherical-revolute-spherical (7R) redundant manipulator 23 p3363 N90-29006
Adjustable impedance, force feedback and command language aids for telerobotics (parts 1-4 of an 8-part MIT progress report) 23 p3363 N90-29007
A laser tracking dynamic robot metrolpgy instrument 23 p3366 N90-29021
Map learning with indistinguishable locations 23 p3367 N90-29025
Three-dimensional motor schema based navigation 23 p3367 N90-29026
Exploiting map plans as resources for action 23 p3367 N90-29028
Grasp planning under uncertainty 23 p3370 N90-29041
Efficient mapping algorithms for scheduling robot inverse dynamics computation on a multiprocessor system 23 p3375 N90-29071
Planning robot actions under position and shape uncertainty 23 p3376 N90-29073
Technology and task parameters relating to the effectiveness of the bracing strategy 24 p3500 N90-29785
Autonomous dexterous end-effectors for space robotics 24 p3501 N90-29788
Redundant sensorized arm+hand system for space telerobotized manipulation 24 p3502 N90-29792
Impedance hand controllers for increasing efficiency in teleoperations 24 p3502 N90-29793
Tele-autonomous systems: New methods for projecting and coordinating intelligent action at a distance 24 p3502 N90-29794
Redundancy of space manipulator on free-flying vehicle and its nonholonomic path planning 24 p3502 N90-29797
Guidance algorithms for a free-flying space robot 24 p3503 N90-29798
Use of 3D vision for fine robot motion 24 p3503 N90-29804
An improved adaptive control for repetitive motion of robots 24 p3508 N90-29831
Direct adaptive control of a PUMA 560 industrial robot 24 p3508 N90-29832
Model based manipulator control 24 p3509 N90-29833
Discrete-time adaptive control of robot manipulators 24 p3509 N90-29834
A discrete decentralized variable structure robotic controller 24 p3509 N90-29835
Construction and demonstration of a 9-string 6 DOF force reflecting joystick for telerobotics 24 p3509 N90-29836
Response to reflected-force feedback to fingers in teleoperations 24 p3509 N90-29837
The JAU-JPL anthropomorphic telerobot 24 p3509 N90-29838
A procedure concept for local reflex control of grasping 24 p3509 N90-29839
Performance limitations of bilateral force reflection imposed by operator dynamic characteristics 24 p3510 N90-29840
Sensor-based fine telemanipulation for space robotics 24 p3510 N90-29841
ROTEX-TRIIFEX: Proposal for a joint FRG-USA telerobotic flight experiment 24 p3510 N90-29842
Concept synthesis of an equipment manipulation and transportation system EMATS 24 p3510 N90-29844
Force-reflective teleoperated system with shared and compliant control capabilities 24 p3510 N90-29845
How to push a block along a wall 24 p3511 N90-29848
Linear analysis of a force reflective teleoperator 24 p3513 N90-29856
Recursive multibody dynamics and discrete-time optimal control 24 p3513 N90-29860
The effects of gear reduction on robot dynamics 24 p3513 N90-29861
Recursive Newton-Euler formulation of manipulator dynamics 24 p3513 N90-29862
Kinematic sensitivity of robot manipulators 24 p3513 N90-29863
Efficient conjugate gradient algorithms for computation of the manipulator forward dynamics 24 p3514 N90-29864
Determining robot actions for tasks requiring sensor interaction 24 p3514 N90-29868
Robotic control of the seven-degree-of-freedom NASA laboratory telerobotic manipulator 24 p3515 N90-29870
The control of space manipulators subject to spacecraft attitude control saturation limits 24 p3515 N90-29871
Application of recursive manipulator dynamics to hybrid software/hardware simulation 24 p3516 N90-29876
Kinematics and control algorithm development and simulation for a redundant two-arm robotic manipulator system 24 p3516 N90-29877
Inverse dynamics of a 3 degree of freedom spatial flexible manipulator 24 p3516 N90-29878
A control approach for robots with flexible links and rigid end-effectors 24 p3516 N90-29879
Teleoperation experiments with a Utah/MIT hand and a VPL DataGlove 24 p3517 N90-29883
An alternative control structure for telerobotics 24 p3518 N90-29889
On discrete control of nonlinear systems with applications to robotics 24 p3519 N90-29893
A spatial operator algebra for manipulator modeling and control 24 p3519 N90-29894
Flight experiments in telerobotics-Orbiter middeck concept 24 p3519 N90-29895
Experimental study on two-dimensional free-flying robot satellite model 24 p3519 N90-29896
The astronaut and the banana peel: An EVA retriever scenario 24 p3519 N90-29897
Computed torque control of a free-flying cooperating-arm robot 24 p3520 N90-29898
Computer simulation and design of a three degree-of-freedom shoulder module 24 p3520 N90-29902
Dexterous manipulator flight demonstration 24 p3522 N90-29911
An intelligent, free-flying robot 24 p3522 N90-29912

ROBOT FINGERS
U END EFFECTORS

ROBOT HANDS
U END EFFECTORS

ROBOT MOTION
U ROBOT DYNAMICS

ROBOT SENSORS
Sensor integration using concurrent computing on-board the ORNL mobile robot
[DE89-006740] 07 p0939 N90-15436
Multiplexed robotic tactile sensor fabricated from polyvinylidene fluoride film
[AD-A215354] 09 p1231 N90-17145
The procedure safety system 15 p2155 N90-22311
Smart hands for the EVA retriever 19 p2736 N90-25550
Multi-sensory perception of a geometrical structure of a scene
[ETN-90-97245] 20 p2915 N90-26587
Dynamic interaction of multiple autonomous mobile robots 23 p3333 N90-28844
Real-time edge tracking using a tactile sensor 23 p3367 N90-29023
Reflexive obstacle avoidance for kinematically-redundant manipulators 23 p3371 N90-29047

Force/torque and tactile sensors for sensor-based manipulator control 24 p3501 N90-29791
A procedure concept for local reflex control of grasping 24 p3509 N90-29839
Sensor-based fine telemanipulation for space robotics 24 p3510 N90-29841
ROTEX-TRIIFEX: Proposal for a joint FRG-USA telerobotic flight experiment 24 p3510 N90-29842
Information management in an integrated space telerobot 24 p3511 N90-29846
Redundancy in sensors, control and planning of a robotic system for space telerobotics 24 p3511 N90-29847
The 3-D vision system integrated dexterous hand 24 p3511 N90-29850
RCTS: A flexible environment for sensor integration and control of robot systems; the distributed processing approach 24 p3512 N90-29852
Using multiple sensors for printed circuit board insertion 24 p3514 N90-29867
Determining robot actions for tasks requiring sensor interaction 24 p3514 N90-29868
Robotic control of the seven-degree-of-freedom NASA laboratory telerobotic manipulator 24 p3515 N90-29870
System architectures for telerobotic research 24 p3515 N90-29872
Integration of a sensor based multiple robot environment for space applications: The Johnson Space Center Teleoperator Branch Robotics Laboratory 24 p3518 N90-29890
Dexterous manipulator flight demonstration 24 p3522 N90-29911

ROBOTICS
NT TELEROBOTICS
Flexible robot control: Modeling and experiments 01 p0021 N90-10104
Experimental validation of flexible robot arm modeling and control 01 p0023 N90-10113
A robotic electrical and tensile testing system for diodes [DE89-014012] 01 p0073 N90-10417
Adaptive machine vision [AD-A208130] 01 p0076 N90-10436
An adaptive controller for enhancing operator performance during teleoperation [NASA-CR-183445] 01 p0077 N90-10438
The role of sensor directed, model based control in robotics [DE89-014133] 01 p0077 N90-10442
A new approach to control single-link flexible arms. Part 1: Modelling and identification in the presence of joint friction [AD-A210590] 01 p0078 N90-10445
Interchangeable end effector tools utilized on the protoflight manipulator arm [NASA-CR-179374] 01 p0078 N90-10447
Advancing automation and robotics technology for the space station Freedom and for the US economy [NASA-TM-101561] 01 p0102 N90-10577
Optimized resolved rate control of seven-degree-of-freedom Laboratory Telerobotic Manipulator (LTM) with application to three-dimensional graphics simulation [NASA-TP-2938] 01 p0109 N90-10618
Robotic vehicle message format [AD-A210996] 01 p0110 N90-10627
Modeling and simulation of spatial robotic manipulators with flexible links and joint drives for control strategies implementation and evaluation 02 p0228 N90-11311
Using computer design and simulation to improve manufacturing productivity, report period 1, 2 and 3 [AD-A210255] 02 p0258 N90-11462
Autonomous space processor for orbital debris [NASA-CR-186043] 03 p0311 N90-11770
A distributed pipelined architecture of the recursive Lagrangian equations of motion for robot manipulators with VLSI implementation --- VLSI (very large scale integration) [RR-353] 03 p0344 N90-11966
An optimum trajectory planner for robot manipulators in joint-space and under physical constraints [RR-349] 03 p0355 N90-12029
On the complexity analysis of the coriolis and centripetal effects of a 6 DOF robot manipulator --- Degrees of Freedom (DOF) [RR-344] 03 p0355 N90-12030
The dynamic performance of robot manipulators under different operating conditions [RR-345] 03 p0355 N90-12031
Three dimensional object recognition employing combined visual and tactile sensing [PB89-219489] 03 p0382 N90-12176
Design mechanism for interactive graphics mechanism design [PB89-219513] 03 p0387 N90-12202
A language for assembly instructions [REPT-88-90] 03 p0388 N90-12209
Distributed VLSI architecture for fast Jacobian and inverse Jacobian formulations [RR-346] 03 p0390 N90-12218
Navigation of robotic systems [DE89-017507] 03 p0390 N90-12219
Robot inverse dynamics computation via VLSI distributed architectures [RR-350] 03 p0390 N90-12223
Fast forward dynamics algorithm for robot arms using multiprocessing [RR-367] 03 p0391 N90-12225
Dynamic robot models using the Manutec r3 as an example [ESA-TT-1132] 04 p0458 N90-12626
A robot which will investigate the condition of underground pipe [PB89-230650] 04 p0508 N90-12928
Squirt: The prototypical mobile robot for autonomous graduate students [AD-A212337] 04 p0510 N90-12941
Development of an integrated mobile robot system at CMU (Carnegie-Mellon University) [AD-A212555] 04 p0510 N90-12944
Telerobotic control for teams of semi-autonomous agents, phase 1 [AD-A211648] 04 p0526 N90-13037
What is the balance sheet for investment in automated manufacturing [CETIM-105490] 04 p0532 N90-13071
An on-line distributed minimum-time trajectory generator for intelligent robot manipulators [RR-358] 04 p0536 N90-13102
Identification of robot dynamics: A parallel processing approach [RR-361] 04 p0537 N90-13103
Real-time robot motion: The VLSI implementation via transputers [RR-364] 04 p0537 N90-13104
Spatial data structures for robotic vehicle route planning [AD-A212806] 04 p0538 N90-13111
Research in computer vision for autonomous systems [AD-A212420] 04 p0555 N90-13235
Adaptive strategies for controls of flexible arms [NASA-CR-185868] 05 p0649 N90-13783
Arc current control of a robotic welding system: Modeling and control system design [AD-A213150] 05 p0650 N90-13788
Design and control of a two-degree-of-freedom lightweight flexible arm [AD-A213335] 05 p0650 N90-13790
A new approach to control single-link flexible arms. Part 3: Adaptive control of the tip position with payload changes [AD-A213337] 05 p0650 N90-13792
User needs, benefits, and integration of robotic systems in a space station laboratory [NASA-CR-185150] 05 p0651 N90-13794
Performance evaluation of a six-axis generalized force-reflecting teleoperator [NASA-CR-186106] 05 p0651 N90-13796
Applications of artificial intelligence to space station and automated software techniques: High level robot command language [NASA-CR-182997] 05 p0686 N90-13991
The space station tethered elevator system [NASA-CR-186051] 06 p0732 N90-14265
Results of the manipulator test test stand study: Comparison of manipulators and evaluation of equipment items [DE90-000977] 06 p0794 N90-14625
French technological progress in the field of robotics and teleoperation [DE90-001590] 06 p0794 N90-14626
Robotic vision system [AD-D014246] 06 p0832 N90-14838
Programmable near-infrared ranging system [AD-D014237] 06 p0843 N90-14903
M.I.N.G., Mars Investment for a New Generation: Robotic construction of a permanently manned Mars base [NASA-CR-186224] 06 p0865 N90-15028
CIS-lunar space infrastructure lunar technologies: Executive summary [NASA-CR-186220] 06 p0865 N90-15029
Autonomous land navigation in a structured environment [DE90-001625] 07 p0878 N90-15087
New approach to the inverse problem of six-link manipulators via the optimization technique [DE90-710044] 07 p0940 N90-15441
Spatial dynamics of deformable multibody systems with variable kinematic structure [AD-A214098] 07 p0942 N90-15455
Vision in dynamic environments [AD-A213434] 07 p0967 N90-15587
Visual Information Processing for Television and Telerobotics [NASA-CP-3053] 08 p1072 N90-16204
Connectionist model-based stereo vision for telerobotics 08 p1076 N90-16224
Expert system control of a six-legged walking telerobot [DE90-004661] 08 p1086 N90-16285
Interpretation of CAD (Computer Aided Design) models through IGES (Initial Graphics Exchange Specification) interface [PB90-121294] 08 p1112 N90-16441
Plant features measurements for robotics 08 p1156 N90-16695
Off-line robot programming and graphical verification of path planning 08 p1156 N90-16699
Mathematical model for adaptive control system of ASEA robot at Kennedy Space Center 08 p1157 N90-16701
Experimental evaluation of impedance control for robotic aircraft refueling [AD-A215532] 09 p1167 N90-16755
Power system modeling for a six legged walking vehicle 09 p1221 N90-17083
Multiplexed robotic tactile sensor fabricated from polyvinylidene fluoride film [AD-A215354] 09 p1231 N90-17145
Multiple model adaptive estimation techniques for adaptive model-based robot control [AD-A215742] 09 p1231 N90-17146
Payload invariant control via neural networks: Development and experimental evaluation [AD-A215740] 09 p1260 N90-17306
A vision system for robotic inspection and manipulation [DE90-005412] 09 p1283 N90-17440
A computer simulation study of a sensor-based heuristic navigation for three-dimensional rough terrain with obstacles [AD-A215115] 10 p1318 N90-17622
Learning-based position control of a closed-kinematic chain robot end-effector [NASA-CR-186283] 10 p1391 N90-18043
Rapid prototyping of tools [AD-A215956] 10 p1392 N90-18050
Pareto optimization design techniques for the AFIT (Air Force Institute of Technology)/AAMRL (Armstrong Aeronautical Medical Research Laboratory) anthropomorphic robotic manipulator [AD-A216178] 10 p1414 N90-18150
Advancing automation and robotics technology for the Space Station Freedom and for the US economy [NASA-TM-101691] 10 p1414 N90-18151
Hypercube expert system shell-applying production parallelism [AD-A215762] 10 p1418 N90-18173
High-Level Vision and Planning Workshop Proceedings [AD-A215982] 10 p1420 N90-18188
Visual servoing for autonomous aircraft refueling [AD-A216042] 11 p1455 N90-18386
Space orientation and orbital technology [ISBN-3-89100-015-4] 11 p1465 N90-18437
Superfluid helium orbital resupply coupling 11 p1475 N90-18488
The manufacturing procedures for composite materials, automation, and robotization [ETN-90-96232] 11 p1482 N90-18528
Advancing automation and robotics technology for the Space Station Freedom and for the US economy: Submitted to the United States Congress [NASA-TM-101647] 12 p1613 N90-19279
Kinematic control of robotic manipulators with multiple interchangeable wrists 12 p1670 N90-19592
Advanced control schemes and kinematic analysis for a kinematically redundant 7 DOF manipulator [NASA-CR-186175] 12 p1671 N90-19599
Improved processes for ultrasonic object recognition in robotics [ETN-90-95362] 12 p1672 N90-19604
Extending terrestrial mobile robotics to a proposed lunar base [DE89-016179] 12 p1672 N90-19606
A human factors testbed for ground-vehicle telerobotics research [DE90-006618] 12 p1697 N90-19746
Design of a high angle of attack robotic sting mount for tests in a low speed wind tunnel [AD-A218105] 13 p1759 N90-20099
The CMU Reconfigurable Modular Manipulator System [CMU-RI-TR-88-7] 13 p1809 N90-20388
Knowledge-based robotic grasping [DE90-007216] 13 p1811 N90-20402

Gripping device
[NASA-CASE-MSC-21365-1] 13 p1812 N90-20408
The use of graphics in the design of the human-telerobot interface 13 p1860 N90-20670
Robust planning and control using neural networks
[AD-A217216] 13 p1872 N90-20732
Artificial Intelligence (AI) Center of Excellence at the University of Pennsylvania
[AD-A217393] 13 p1874 N90-20743
Robotic mobility system: Road following algorithms
[AD-A218107] 13 p1874 N90-20748
Controlled multibody dynamics simulation for large space structures 14 p1934 N90-21068
Application of optimization in design and motion control of robot manipulators 14 p1988 N90-21393
Adaptive learning fuzzy control of a mobile robot
[DE90-759898] 14 p2018 N90-21562
Small business innovation research. Abstracts of 1988 phase 1 awards
[NASA-TM-102991] 14 p2036 N90-21680
Robust control of flexible structures 15 p2058 N90-21784
A robotically constructed production and supply base on Phobos
[NASA-CR-186234] 15 p2073 N90-21872
Nonlinear stability analysis and control of dynamical robotic systems 15 p2104 N90-22037
An alternative method to solving the kinematics of a redundant robot
[DE90-006892] 15 p2106 N90-22045
A new six-degree-of-freedom force-reflecting hand controller for space telerobotics 15 p2113 N90-22089
Development of cable drive systems for an automated assembly project 15 p2116 N90-22105
Instrumentation and robotic image processing using top-down model control 15 p2142 N90-22239
Space environment robot vision system 15 p2143 N90-22245
The procedure safety system 15 p2155 N90-22311
The JPL/KSC telerobotic inspection demonstration 15 p2155 N90-22312
The role of automation and robotics in the Lunar-Based Chemical Analysis Laboratory
[DE90-009401] 15 p2192 N90-22516
NASA Information Sciences and Human Factors Program
[NASA-TM-4190] 15 p2194 N90-22529
An assessment of multibody simulation tools for articulated spacecraft 16 p2279 N90-22988
Spatial operator algebra framework for multibody system dynamics 16 p2279 N90-22989
An order (n) algorithm for the dynamics simulation of robotic systems 16 p2279 N90-22990
Systematic generation of multibody equations of motion suitable for recursive and parallel manipulation 16 p2280 N90-22992
An innovations approach to decoupling of multibody dynamics and control 16 p2280 N90-22994
Efficient dynamic simulation for multiple chain robotic mechanisms 16 p2280 N90-22995
A robot arm simulation with a shared memory multiprocessor machine 16 p2283 N90-23008
Computational dynamics for robotics systems using a non-strict computational approach 16 p2283 N90-23011
Optimum control forces for multibody systems with intermittent motion 16 p2284 N90-23016
Development of efficient computer program for dynamic simulation of telerobotic manipulation 16 p2284 N90-23017
Explicit modeling of composite plates and beams in the dynamics of multibody systems 16 p2285 N90-23019
Modeling of control forces for kinematical constraints in the dynamics of multibody systems: A new approach 16 p2287 N90-23031
Characterization of robotics parallel algorithms and mapping onto a reconfigurable SIMD machine 16 p2289 N90-23039
Control of randomly sampled robotic systems
[AD-A218948] 16 p2309 N90-23157
Lunar crane hook
[NASA-CR-184921] 17 p2384 N90-23579
Lunar rated fasteners
[NASA-CR-182856] 17 p2411 N90-23737
Adaptive control methods for mechanical manipulators: A comparative study
[AD-A219965] 17 p2413 N90-23749
Advancing automation and robotics technology for the Space Station Freedom and for the US economy
[NASA-TM-102668] 17 p2439 N90-23899
Efficient motion planning for an L-shaped object
[RUU-CS-88-38] 17 p2463 N90-24073
Second European In-Orbit Operations Technology Symposium
[ESA-SP-297] 18 p2499 N90-24280
Toward the development of COSMO-LAB 18 p2500 N90-24281
Robotics program at the NASA Goddard Space Flight Center 18 p2500 N90-24285
Servicing test facility: A hardware simulator for telerobotic in-orbit servicing 18 p2501 N90-24287
Advanced robotics for the on-orbit servicing 18 p2501 N90-24289
In-orbit operations research and development program of the Toulouse Space Center 18 p2501 N90-24290
The SPIDER robotic system 18 p2501 N90-24291
Hierarchy of on-orbit servicing interfaces 18 p2502 N90-24294
Perspective features of internal automation and robotics for supporting Columbus attached laboratory payload operations 18 p2502 N90-24297
Telerobotic application to EVA 18 p2502 N90-24298
Robot-based equipment manipulation and transportation for the Columbus free flying laboratory 18 p2503 N90-24300
A flexible teleoperation test bed for human factors experimentation 18 p2503 N90-24304
Robotic simulation support to systems development 18 p2505 N90-24315
ROSED: Robotic Servicing Demonstrator 18 p2505 N90-24318
Orbital Replacement Units (ORUs) design considerations 18 p2506 N90-24320
Technology requirements for on-orbit servicing of spacecraft 18 p2506 N90-24321
Satellite servicer system flight demonstration program 18 p2506 N90-24322
Interconnecting devices conceived for in-orbit operations 18 p2506 N90-24323
Development of a fully automated fluid resupply interface system 18 p2506 N90-24324
Fourth European Space Mechanisms and Tribology Symposium
[ESA-SP-299] 18 p2535 N90-24462
Shape memory alloys for robot grippers and mechanical hands 18 p2536 N90-24466
A compact joint for the ROTEX manipulator 18 p2536 N90-24467
Optical calculation of correlation filters for a robotic vision system 18 p2630 N90-24986
Self-contained robotic arm manipulator
[NASA-CR-184925] 19 p2696 N90-25342
Design of a versatile, teleoperable, towable lifting machine with robotic capabilities for use in NASA's lunar base operations
[NASA-CR-186688] 19 p2697 N90-25345
Active perception and exploratory robotics
[MS-CIS-89-65] 19 p2726 N90-25501
Third Annual Workshop on Space Operations Automation and Robotics (SOAR 1989)
[NASA-CP-3059] 19 p2727 N90-25503
Mobile transporter path planning 19 p2727 N90-25505
SDIO robotics in space applications 19 p2729 N90-25514
Telepresence for space: The state of the concept 19 p2731 N90-25526
Telepresence and Space Station Freedom workstation operations 19 p2731 N90-25527
The Flight Telerobotic Servicer (FTS) NASA's first operational robotic system 19 p2733 N90-25537
The telerobot testbed: An architecture for remote servicing 19 p2734 N90-25538
Space environments and their effects on space automation and robotics 19 p2735 N90-25543
A task control architecture for autonomous robots 19 p2735 N90-25546
Smart hands for the EVA retriever 19 p2736 N90-25550
Kinematically redundant arm formulations for coordinated multiple arm implementations 19 p2736 N90-25551
Numerical approach of collision avoidance and optimal control on robotic manipulators 19 p2736 N90-25552
Visualization of three dimensional data 19 p2736 N90-25553
A helmet mounted display to adapt the telerobotic environment to human vision 19 p2737 N90-25555
Human factors issues in telerobotic systems for Space Station Freedom servicing 19 p2737 N90-25556
The application of NASREM to remote robot control 19 p2738 N90-25563
Technology for an intelligent, free-flying robot for crew and equipment retrieval in space 19 p2738 N90-25564
The JPL telerobot operator control station: Operational experiences 19 p2738 N90-25565
Test bed experiments for various telerobotic system characteristics and configurations 19 p2740 N90-25572
Lunar deep drill apparatus
[NASA-CR-182756] 20 p2869 N90-26322
Twilight zones and cornerstones: A gnat robot double feature
[AD-A220026] 20 p2870 N90-26326
Power saw
[NASA-CASE-MSC-21469-1] 20 p2872 N90-26340
Robotic-aided system for inspection of aging aircraft
[NIAR-90-9] 20 p2873 N90-26346
Grasping with mechanical intelligence
[NASA-CR-186864] 20 p2900 N90-26498
Neural networks for real-time sensory data processing and sensorimotor control
[AD-A223096] 20 p2916 N90-26592
Development of an integrated mobile robot system at Carnegie-Mellon University
[AD-A222494] 21 p3011 N90-27119
Special purpose parallel computer architecture for real-time control and simulation in robotic applications
[NASA-CASE-NPO-17629-1-CU] 21 p3038 N90-27268
Fifth Conference on Artificial Intelligence for Space Applications
[NASA-CP-3073] 21 p3040 N90-27275
Agent independent task planning 21 p3040 N90-27276
Artificial intelligence in the materials processing laboratory 21 p3041 N90-27283
Simulation-based intelligent robotic agent for Space Station Freedom 21 p3043 N90-27298
Space station advanced automation 21 p3044 N90-27300
A vision-based telerobotic control station 21 p3046 N90-27311
The real-time learning mechanism of the Scientific Research Associates Advanced Robotic System (SRAARS) 21 p3046 N90-27312
Robot dynamics in reduced gravity environment 21 p3049 N90-27333
A programming environment for parallel vision algorithms
[AD-A221486] 21 p3055 N90-27368
ARMTRAK: A domain for the unified study of natural language, planning, and active vision
[AD-A221701] 21 p3056 N90-27373
Development, implementation, and validation of control algorithms for the dual-arm robotic manipulation of a single object
[AD-A222502] 21 p3060 N90-27402
The challenge of assembling a space station in orbit 22 p3130 N90-27763
Towards an understanding of camera fixation
[PB90-160342] 22 p3177 N90-28027
Video-rate visual servoing for robots
[AD-A218711] 22 p3181 N90-28052
Advanced robotics for Air Force operations
[PB90-157009] 22 p3182 N90-28055
Multiple arm manipulation
[PB90-199506] 22 p3182 N90-28056
Robotic and automatic welding development at the Marshall Space Flight Center 23 p3298 N90-28656
Motion coordination for mobile robots in unstructured environments
[PB90-199498] 23 p3332 N90-28837
Motion coordination for a mobile manipulator system
[PB90-203076] 23 p3332 N90-28839
DOE/NIST Workshop on Common Architectures for Robotic Systems
[PB90-216839] 23 p3332 N90-28840
Experiments in the dynamic and strategic control of cooperating manipulators 23 p3333 N90-28845
Solutions to the frictional dynamics problem and the reciprocal variable feedback methodology for design and control of robot mechanisms 23 p3333 N90-28846
Proceedings of the NASA Conference on Space Telerobotics, volume 1
[NASA-CR-186856] 23 p3362 N90-29000
A 17 degree of freedom anthropomorphic manipulator 23 p3362 N90-29001
Kinematic functions for the 7 DOF robotics research arm 23 p3363 N90-29003
A complete analytical solution for the inverse instantaneous kinematics of a spherical-revolute-spherical (7R) redundant manipulator 23 p3363 N90-29006
Adjustable impedance, force feedback and command language aids for telerobotics (parts 1-4 of an 8-part MIT progress report) 23 p3363 N90-29007
Measurement of hand dynamics in a microsurgery environment: Preliminary data in the design of a bimanual telemicro-operation test bed 23 p3364 N90-29010

Development of a flexible test-bed for robotics, telemanipulation and servicing research
23 p3364 N90-29012
Control of intelligent robots in space
23 p3365 N90-29013
Modularity in robotic systems
23 p3365 N90-29014
A system architecture for a planetary rover
23 p3365 N90-29015
The NASA/OAST telerobot testbed architecture
23 p3365 N90-29016
Formulation of design guidelines for automated robotic assembly in outerspace
23 p3365 N90-29017
Automation and robotics technology for intelligent mining systems
23 p3366 N90-29018
A fast lightstripe rangefinding system with smart VLSI sensor
23 p3366 N90-29019
Computational neural learning formalisms for manipulator inverse kinematics
23 p3368 N90-29030
A neural network for controlling the configuration of frame structure with elastic members
23 p3368 N90-29034
Plan recognition for space telerobotics
23 p3369 N90-29036
Proceedings of the NASA Conference on Space Telerobotics, volume 2
[NASA-CR-186857]
23 p3370 N90-29044
Reflexive obstacle avoidance for kinematically-redundant manipulators
23 p3371 N90-29047
Preliminary study of a serial-parallel redundant manipulator
23 p3371 N90-29048
The JPL telerobot operator control station. Part 1: Hardware
23 p3371 N90-29049
The JPL telerobot operator control station. Part 2: Software
23 p3371 N90-29050
Design of a monitor and simulation terminal (master) for space station telerobotics and telescience
23 p3372 N90-29051
Performance evaluation of a 6 axis high fidelity generalized force reflecting teleoperator
23 p3372 N90-29052
Implementation and design of a teleoperation system based on a VMEBUS/68020 pipelined architecture
23 p3372 N90-29053
Human machine interaction via the transfer of power and information signals
23 p3372 N90-29054
Trajectory generation of space telerobots
23 p3372 N90-29055
On the simulation of space based manipulators with contact
23 p3373 N90-29056
Experiences with the JPL telerobot testbed: Issues and insights
23 p3373 N90-29059
The KALI multi-arm robot programming and control environment
23 p3373 N90-29060
Perceptual telerobotics
23 p3374 N90-29063
Planetary rover technology development requirements
23 p3375 N90-29067
Robotic sampling system for an unmanned Mars mission
23 p3375 N90-29070
Organising geometric computations for space telerobotics
23 p3376 N90-29074
A tesselated probabilistic representation for spatial robot perception and navigation
23 p3376 N90-29075
Integrating planning and reactive control
23 p3377 N90-29077
Integrating planning, execution, and learning
23 p3377 N90-29079
A hardware/software environment to support R/D in intelligent machines and mobile robotic systems
[DE90-014458]
23 p3385 N90-29119
Concept for a reference model Architecture for Real-Time Intelligent Control Systems (ARTICS)
[PB90-220286]
24 p3475 N90-29638
Robots, systems, and flexible automation
[DE90-015802]
24 p3476 N90-29649
Proceedings of the NASA Conference on Space Telerobotics, volume 3
[NASA-CR-186858]
24 p3500 N90-29780
The flight telerobotic servicer: NASA's first operational space robot
24 p3500 N90-29781
Modeling, design, and control of flexible manipulator arms: Status and trends
24 p3500 N90-29782
Capture of free-flying payloads with flexible space manipulators
24 p3500 N90-29784
Traction-drive force transmission for telerobotic joints
24 p3501 N90-29790
An advanced telerobotic system for shuttle payload changeout room processing applications
24 p3502 N90-29795
Robotic tele-existence
24 p3502 N90-29796
Telepresence system development for application to the control of remote robotic systems
24 p3503 N90-29799
The 3D model control of image processing
24 p3503 N90-29800
Weighted feature selection criteria for visual servoing of a telerobot
24 p3503 N90-29801
Telerobotic workstation design aid
24 p3504 N90-29805
Space robotic system for proximity operations
24 p3504 N90-29806
THREAD: A programming environment for interactive planning-level robotics applications
24 p3505 N90-29810
Experiments in cooperative manipulation: A system perspective
24 p3505 N90-29812
Controlling multiple manipulators using RIPS
24 p3505 N90-29814
Design of a structural and functional hierarchy for planning and control of telerobotic systems
24 p3506 N90-29820
The flight telerobotic servicer project: A technical overview
24 p3506 N90-29821
The flight telerobotic servicer Tinman concept: System design drivers and task analysis
24 p3506 N90-29822
The flight telerobotic servicer: From functional architecture to computer architecture
24 p3507 N90-29823
Research and development activities at the Goddard Space Flight Center for the flight telerobotic servicer project
24 p3507 N90-29824
The Goddard Space Flight Center (GSFC) robotics technology testbed
24 p3507 N90-29825
Use of graphics in decision aids for telerobotic control: (Parts 5-8 of an 8-part MIT progress report)
24 p3508 N90-29829
Proceedings of the NASA Conference on Space Telerobotics, volume 4
[NASA-CR-186859]
24 p3508 N90-29830
Global models: Robot sensing, control, and sensory-motor skills
24 p3511 N90-29849
A layered abduction model of perception: Integrating bottom-up and top-down processing in a multi-sense agent
24 p3512 N90-29851
Vehicle path-planning in three dimensions using optics analogs for optimizing visibility and energy cost
24 p3512 N90-29853
Vacuum mechatronics
24 p3512 N90-29854
Uniform task level definitions for robotic system performance comparisons
24 p3512 N90-29855
On the stability of robotic systems with random communication rates
24 p3514 N90-29865
Precedence relationship representations of mechanical assembly sequences
24 p3514 N90-29866
Proceedings of the NASA Conference on Space Telerobotics, volume 5
[NASA-CR-186860]
24 p3516 N90-29874
Telerobotic activities at Johnson Space Center
24 p3516 N90-29875
Integration of a sensor based multiple robot environment for space applications: The Johnson Space Center Teleoperator Branch Robotics Laboratory
24 p3518 N90-29890
An efficient temporal logic for robotic task planning
24 p3521 N90-29906
Approach to telerobot computing architecture
[NASA-CR-186993]
24 p3534 N90-29984

ROBOTS

Proceedings of the Workshop on Computational Aspects in the Control of Flexible Systems, part 1
[NASA-TM-101578-PT-1]
01 p0017 N90-10080
Simulation and control problems in elastic robots
01 p0020 N90-10098
Proceedings of the Workshop on Computational Aspects in the Control of Flexible Systems, part 2
[NASA-TM-101578-PT-2]
01 p0021 N90-10103
Flexible robot control: Modeling and experiments
01 p0021 N90-10104
Experimental validation of flexible robot arm modeling and control
01 p0023 N90-10113
Shape control of high degree-of-freedom variable geometry trusses
01 p0024 N90-10122
Analysis and construction of contact and tactile sensors
[DE89-013992]
01 p0072 N90-10416
The role of sensor directed, model based control in robotics
[DE89-014133]
01 p0077 N90-10442
Autonomous mobile robot research using the HERMIES-3 robot
[DE89-015916]
01 p0078 N90-10443
The 1988 year end report for road following at Carnegie-Mellon
[NASA-CR-185967]
01 p0078 N90-10446
Robot vehicle video image compression, phase 1
[AD-A210974]
01 p0110 N90-10626
NASA/NBS (National Aeronautics and Space Administration/National Bureau of Standards) standard reference model for telerobot control system architecture (NASREM)
[NASA-CR-185078]
02 p0228 N90-11310
The 3D-POLY: A robot vision system for recognizing objects in occluded environments
02 p0229 N90-11313
Rethinking synthesis of fine-motion strategies
[DE89-016671]
02 p0230 N90-11322
Spoken commands control robot that handles radioactive materials
[DE89-012632]
02 p0262 N90-11488
Magnetically levitated micro-robotics
02 p0270 N90-11542
Autonomous space processor for orbital debris
[NASA-CR-188043]
03 p0311 N90-11770
Navigation of robotic systems
[DE89-017507]
03 p0390 N90-12219
A survey of camera error sources in machine vision systems
[DE89-014072]
03 p0405 N90-12318
Dynamic robot models using the Manutec r3 as an example
[ESA-TT-1132]
04 p0458 N90-12626
Squirt: The prototypical mobile robot for autonomous graduate students
[AD-A212337]
04 p0510 N90-12941
Development of an integrated mobile robot system at CMU (Carnegie-Mellon University)
[AD-A212555]
04 p0510 N90-12944
Identification of robot dynamics: A parallel processing approach
[RR-361]
04 p0537 N90-13103
Conceptual dependency theory and robot programming
[REPT-89-20]
04 p0537 N90-13106
Design and control of a two-degree-of-freedom lightweight flexible arm
[AD-A213335]
05 p0650 N90-13790
A new approach to control single-link flexible arms. Part 3: Adaptive control of the tip position with payload changes
[AD-A213337]
05 p0650 N90-13792
Image segmentation for the stereoscopic vision of a mobile robot
[ONERA-RT-1/3692-SY]
05 p0652 N90-13800
Kinematics and control of manipulation robots
[WTHD-187]
05 p0652 N90-13803
French technological progress in the field of robotics and teleoperation
[DE90-001590]
06 p0794 N90-14626
Non-linear vibrations, stability, and dynamics of structures and mechanisms
[AD-A212152]
06 p0796 N90-14639
Robotic vision system
[AD-D014246]
06 p0832 N90-14838
Centralized and decentralized Kalman filter techniques for tracking, navigation, and control
[AD-A214245]
07 p0878 N90-15091
ROBOCAL (Robotic Calorimetry): An automated NDA (Nondestructive Assay) calorimetry and gamma isotopic system
[DE90-003217]
07 p0894 N90-15168
Development of a robotics system for automated chemical analysis of sediment, sludges, and soils
[DE90-003637]
07 p0895 N90-15170
Lunar construction utility vehicle
[NASA-CR-186231]
07 p0939 N90-15435
Sensor integration using concurrent computing on-board the ORNL mobile robot
[DE89-008740]
07 p0939 N90-15436
Research in knowledge-based vision techniques for the Autonomous Land Vehicle Program
[AD-A213440]
07 p0942 N90-15453
Feasibility study of using industrial robot for ultrasound testing
[DE90-002977]
07 p0943 N90-15461
Design and implementation of two concurrent multi-sensor integration algorithms for mobile robots
[DE90-003041]
07 p0981 N90-15663
Gaze controls with interactions and delays
[AD-A214286]
07 p0981 N90-15667
A note on the maximum size of a rectilinear maze
[AD-A214445]
07 p0982 N90-15668
Bilateral force reflection for teleoperators with masters and slaves with dissimilar and possibly redundant kinematics
[DE90-004392]
08 p1061 N90-16132
Visual Information Processing for Television and Telerobotics
[NASA-CP-3053]
08 p1072 N90-16204
Examples of robots and teleoperators at the Savannah River Site
[DE90-004659]
08 p1086 N90-16284

Expert system control of a six-legged walking telerobot
[DE90-004661] 08 p1086 N90-16285
Off-line robot programming and graphical verification of path planning 08 p1156 N90-16699
Mathematical model for adaptive control system of ASEA robot at Kennedy Space Center 08 p1157 N90-16701
Method and apparatus for positioning a robotic end effector
[NASA-CASE-MSC-21476-1] 09 p1230 N90-17137
Applications of a fingertip sensor for the Salisbury robot hand
[DE90-005002] 09 p1231 N90-17142
Classification and simulation of single and multi-degree-of-freedom motions
[AD-A214925] 09 p1231 N90-17143
Job planning and execution monitoring for a human-robot symbiotic system
[DE90-004464] 09 p1261 N90-17315
Vision-based navigation and parallel computing
[AD-A214481] 09 p1264 N90-17327
A vision system for robotic inspection and manipulation
[DE90-005412] 09 p1283 N90-17440
Learning-based position control of a closed-kinematic chain robot end-effector
[NASA-CR-186283] 10 p1391 N90-18043
Development of an integrated mobile robot system at Carnegie Mellon University: June 1988
[AD-A215955] 10 p1392 N90-18049
High-Level Vision and Planning Workshop Proceedings
[AD-A215982] 10 p1420 N90-18188
Visual navigation: Constructing and utilizing simple maps of an indoor environment
[AD-A216761] 11 p1455 N90-18382
Robot crane technology program
[PB90-111667] 11 p1516 N90-18734
On the kinematic behavior of robots while executing general robot level commands
[PB90-120965] 11 p1517 N90-18735
Knowledge-based fault detection and analysis for robots: First results for the ROTEX robots
[ESA-TT-1150] 11 p1518 N90-18742
Teleoperator servoloop tuning using an expert system
[DE90-005674] 11 p1542 N90-18876
RALPH: An automatic Robot Assembly Language Programmer: An overview
[PB90-120973] 11 p1548 N90-18912
A colony architecture for an artificial creature
[AD-A216802] 11 p1549 N90-18918
Architecture for a human-robot symbiotic system
[DE90-005670] 11 p1550 N90-18921
Multibody modeling and verification 12 p1640 N90-19422
Experiments in end-point control of a flexible robot with a mini-manipulator 12 p1671 N90-19596
Advanced control schemes and kinematic analysis for a kinematically redundant 7 DOF manipulator
[NASA-CR-186175] 12 p1671 N90-19599
Design and implementation of a flexible robot
[AD-A216453] 12 p1671 N90-19601
A complete description of robot manipulator dynamics based on Lagrangian mechanics
[DE90-741467] 12 p1672 N90-19603
Extending terrestrial mobile robotics to a proposed lunar base
[DE89-016179] 12 p1672 N90-19606
An approach to elemental task learning
[DE90-006614] 12 p1697 N90-19745
A human factors testbed for ground-vehicle telerobotics research
[DE90-006618] 12 p1697 N90-19746
Parallel neural net path-planner on hypercube and transputer
[DE90-006324] 12 p1703 N90-19777
Nonlinear continuum mechanics and applied analysis
[AD-A213629] 12 p1709 N90-19812
Multi-dimensional LADAR tracking and adaptive grasping for spaceborne assembly of SDI (Strategic Defense Initiative) platforms
[AD-A218236] 13 p1791 N90-20279
Estimation of modeled object pose from monocular images
[DE90-001678] 13 p1804 N90-20354
The CMU Reconfigurable Modular Manipulator System
[CMU-RI-TR-88-7] 13 p1809 N90-20388
Concept formation and generalization based on experimentation by an autonomous mobile robot
[DE90-001731] 13 p1810 N90-20395
Robot navigation research using the HERMIES mobile robot
[DE90-001952] 13 p1810 N90-20396
Robust performance of multiple tasks by a mobile robot
[DE90-001953] 13 p1811 N90-20397
Swing-free movement of simply suspended objects employing parameter estimation
[DE90-002238] 13 p1811 N90-20398
Resolved motion rate and resolved acceleration servo-control of wheeled mobile robots
[DE90-002585] 13 p1811 N90-20399
Knowledge-based robotic grasping
[DE90-007216] 13 p1811 N90-20402
Dynamic damping control: Implementation issues and simulation results
[DE90-007687] 13 p1812 N90-20403
Design of a telerobotic controller with joint torque sensors
[DE90-008753] 13 p1812 N90-20404
Control system design of the third flexible joint of PUMA 560 robot
[AD-A218075] 13 p1812 N90-20405
Parameter-scheduled trajectory planning for suppression of coupled horizontal and vertical vibrations in a flexible rod
[DE90-002313] 13 p1817 N90-20435
Graphical programming and the use of simulation for space-based manipulators 13 p1861 N90-20674
Using an instrumented manikin for Space Station Freedom analysis 13 p1861 N90-20675
RIPE: An object-oriented Robot Independent Programming Environment
[DE90-008501] 13 p1866 N90-20707
Robust planning and control using neural networks
[AD-A217216] 13 p1872 N90-20732
Boundary equations of configuration obstacles for manipulators
[DE90-002101] 13 p1874 N90-20745
Location recognition using stereo vision
[AD-A218218] 13 p1875 N90-20752
A solution level indicator system
[DE90-007939] 14 p1948 N90-21151
Modeling elastomer displacements for tactile sensing applications
[DE90-007959] 14 p1984 N90-21370
End point control of flexible manipulators
[AD-A217319] 14 p1986 N90-21383
A new approach to solve the kinematics resolution of a redundant robot
[DE90-010213] 14 p1988 N90-21397
The development of computational algorithms for manipulator inverse kinematics
[DE90-759877] 14 p2017 N90-21561
Adaptive learning fuzzy control of a mobile robot
[DE90-759898] 14 p2018 N90-21562
A robotically constructed production and supply base on Phobos
[NASA-CR-186234] 15 p2073 N90-21872
Definition of large components assembled on-orbit and robot compatible mechanical joints
[NASA-TM-100395] 15 p2105 N90-22043
Trajectory generation for car-like robots
[DE90-008407] 15 p2106 N90-22047
Robots for aircraft coatings removal: Parameters and requirements
[DE90-009429] 15 p2106 N90-22048
The Shock and Vibration Digest, volume 21, no. 3 15 p2109 N90-22064
A robot end effector exchange mechanism for space applications 15 p2113 N90-22088
Vision Science and Technology at NASA: Results of a Workshop
[NASA-TM-102214-REV-1] 15 p2138 N90-22216
Vision science and technology for supervised intelligent space robots 15 p2139 N90-22221
Algorithms and architectures for robot vision 15 p2141 N90-22236
Ames vision group research overview 15 p2143 N90-22242
Space environment robot vision system 15 p2143 N90-22245
Self-calibration of robot-sensor system 15 p2144 N90-22246
International science and technology policies: Testimony before the Subcommittee on International Scientific Cooperation, Committee on Science, Space, and Technology, United States House of Representatives
[DE90-009416] 15 p2161 N90-22463
The role of automation and robotics in the Lunar-Based Chemical Analysis Laboratory
[DE90-009401] 15 p2192 N90-22516
Plan execution control and architecture for mobile robots
[LAAS-89-371] 16 p2243 N90-22793
Telepresence, time delay, and adaptation 16 p2271 N90-22944
An order (n) algorithm for the dynamics simulation of robotic systems 16 p2279 N90-22990
Aspects of efficient and reliable multibody system simulation 16 p2279 N90-22991
An innovations approach to decoupling of multibody dynamics and control 16 p2280 N90-22994
Efficient dynamic simulation for multiple chain robotic mechanisms 16 p2280 N90-22995
Computational dynamics for robotics systems using a non-strict computational approach 16 p2283 N90-23011
Development of efficient computer program for dynamic simulation of telerobotic manipulation 16 p2284 N90-23017
Experimental adaptive control of a hydraulic robot 16 p2303 N90-23121
SKITTER/implement mechanical interface
[NASA-CR-184920] 17 p2384 N90-23578
Tubular space truss structure for SKITTER 2 robot
[NASA-CR-184922] 17 p2384 N90-23580
Lunar robotic maintenance module
[NASA-CR-183071] 17 p2411 N90-23735
Rod gripper, changer, and storage system
[NASA-CR-183154] 17 p2411 N90-23739
Lunar stone saw
[NASA-CR-182438] 17 p2412 N90-23741
Adaptive control methods for mechanical manipulators: A comparative study
[AD-A219965] 17 p2413 N90-23749
Conceptual dependency graphs and DJ
[REPT-89-62] 17 p2445 N90-23933
Second European In-Orbit Operations Technology Symposium
[ESA-SP-297] 18 p2499 N90-24280
Toward the development of COSMO-LAB 18 p2500 N90-24281
Telerobotic application to EVA 18 p2502 N90-24298
Hermes rendezvous and navigation system 18 p2504 N90-24308
NASREM: A functional architecture for control of the flight telerobotic servicer 18 p2506 N90-24325
NASA/GSFC split-rail parallel gripper 18 p2507 N90-24328
A three fingered multijointed gripper as a working tool for experimental use 18 p2507 N90-24329
Dynamics and control of free-flying inspection and maintenance vehicle with manipulators 18 p2508 N90-24332
Flexible test bed for space telepresence and telemanipulation research 18 p2508 N90-24334
Self-contained robotic arm manipulator
[NASA-CR-184925] 19 p2696 N90-25342
Third Annual Workshop on Space Operations Automation and Robotics (SOAR 1989)
[NASA-CP-3059] 19 p2727 N90-25503
Telepresence for space: The state of the concept 19 p2731 N90-25526
The human factors of workstation telepresence 19 p2732 N90-25528
The Flight Telerobotic Servicer (FTS) NASA's first operational robotic system 19 p2733 N90-25537
The telerobot testbed: An architecture for remote servicing 19 p2734 N90-25538
A task control architecture for autonomous robots 19 p2735 N90-25546
Numerical approach of collision avoidance and optimal control on robotic manipulators 19 p2736 N90-25552
The application of NASREM to remote robot control 19 p2738 N90-25563
Technology for an intelligent, free-flying robot for crew and equipment retrieval in space 19 p2738 N90-25564
The JPL telerobot operator control station: Operational experiences 19 p2738 N90-25565
A laboratory breadboard system for dual-arm teleoperation 19 p2740 N90-25573
Computer-aided design of advanced control algorithms for industrial robotics: An overview of ESPRIT project SACODY
[REPT-81-DT-89-47] 19 p2744 N90-25596
Twilight zones and cornerstones: A gnat robot double feature
[AD-A220026] 20 p2870 N90-26326
Design and construction of a wall-climbing robot
[NIAR-90-20] 20 p2870 N90-26327
Control strategy for cooperating disparate manipulators
[NASA-CR-186809] 20 p2870 N90-26328
University of Maryland walking robot: A design project for undergraduate students
[NASA-CR-186839] 20 p2870 N90-26331
Robotic-aided system for inspection of aging aircraft
[NIAR-90-9] 20 p2873 N90-26346

Space station definitions, design, and development. Task 5: Multiple arm telerobot coordination and control: Manipulator design methodology
[NASA-CR-182043] 20 p2914 N90-26577
Verification-correction of a program for including uncertainties in the robot automatic programming
[ETN-90-97246] 20 p2915 N90-26588
Method and apparatus for configuration control of redundant robots
[NASA-CASE-NPO-17801-1-CU] 21 p3010 N90-27110
Development of an integrated mobile robot system at Carnegie-Mellon University
[AD-A222494] 21 p3011 N90-27119
Creature co-op: Achieving robust remote operations with a community of low-cost robots 21 p3044 N90-27303
The real-time learning mechanism of the Scientific Research Associates Advanced Robotic System (SRAARS) 21 p3046 N90-27312
The sixth generation robot in space 21 p3049 N90-27332
ARMTRAK: A domain for the unified study of natural language, planning, and active vision
[AD-A221701] 21 p3056 N90-27373
In-space construction and dynamics of large space structures 22 p3130 N90-27764
Flexible space-based robot modelling and real-time simulation 22 p3131 N90-27769
Advanced robotics for Air Force operations
[PB90-157009] 22 p3182 N90-28055
Reaction-compensation technology for microgravity laboratory robots
[NASA-TM-103271] 22 p3183 N90-28062
Local spatial frequency analysis for computer vision
[NASA-CR-186990] 22 p3237 N90-28356
Motion coordination for mobile robots in unstructured environments
[PB90-199498] 23 p3332 N90-28837
Motion coordination for a mobile manipulator system
[PB90-203076] 23 p3332 N90-28839
DOE/NIST Workshop on Common Architectures for Robotic Systems
[PB90-216839] 23 p3332 N90-28840
Dynamic interaction of multiple autonomous mobile robots 23 p3333 N90-28844
Experiments in the dynamic and strategic control of cooperating manipulators 23 p3333 N90-28845
Solutions to the frictional dynamics problem and the reciprocal variable feedback methodology for design and control of robot mechanisms 23 p3333 N90-28846
Treatment of systematic errors 2: Fusion of ultrasound and visual sensor data
[DE90-014780] 23 p3334 N90-28850
ROSES, a Robot Operating System Expert Scheduler: Methodological framework
[DE90-014782] 23 p3334 N90-28851
Proceedings of the NASA Conference on Space Telerobotics, volume 1
[NASA-CR-186856] 23 p3362 N90-29000
A 17 degree of freedom anthropomorphic manipulator 23 p3362 N90-29001
Cartesian control of redundant robots 23 p3363 N90-29004
Adjustable impedance, force feedback and command language aids for telerobotics (parts 1-4 of an 8-part MIT progress report) 23 p3363 N90-29007
Development of a flexible test-bed for robotics, telemanipulation and servicing research 23 p3364 N90-29012
Control of intelligent robots in space 23 p3365 N90-29013
Modularity in robotic systems 23 p3365 N90-29014
The NASA/OAST telerobot testbed architecture 23 p3365 N90-29016
Formulation of design guidelines for automated robotic assembly in outerspace 23 p3365 N90-29017
Methods and strategies of object localization 23 p3366 N90-29020
A laser tracking dynamic robot metrology instrument 23 p3366 N90-29021
Robot Acting on Moving Bodies (RAMBO): Interaction with tumbling objects 23 p3366 N90-29022
Three-dimensional motor schema based navigation 23 p3367 N90-29026
Periodic gaits for the CMU ambler 23 p3367 N90-29027
Exploiting map plans as resources for action 23 p3367 N90-29028
Learned navigation in unknown terrains: A retraction method 23 p3368 N90-29029
Multi-layer neural networks for robot control 23 p3368 N90-29031
A design philosophy for multi-layer neural networks with applications to robot control 23 p3368 N90-29033
Plan recognition for space telerobotics 23 p3369 N90-29036
Causal simulation and sensor planning in predictive monitoring 23 p3369 N90-29037
A Boltzmann machine for the organization of intelligent machines 23 p3370 N90-29040
Grasp planning under uncertainty 23 p3370 N90-29041
Reflexive obstacle avoidance for kinematically-redundant manipulators 23 p3371 N90-29047
The JPL telerobot operator control station. Part 1: Hardware 23 p3371 N90-29049
The JPL telerobot operator control station. Part 2: Software 23 p3371 N90-29050
Design of a monitor and simulation terminal (master) for space station telerobotics and telescience 23 p3372 N90-29051
Performance evaluation of a 6 axis high fidelity generalized force reflecting teleoperator 23 p3372 N90-29052
Implementation and design of a teleoperation system based on a VMEBUS/68020 pipelined architecture 23 p3372 N90-29053
Human machine interaction via the transfer of power and information signals 23 p3372 N90-29054
Trajectory generation of space telerobots 23 p3372 N90-29055
On the simulation of space based manipulators with contact 23 p3373 N90-29056
Preliminary results on noncollocated torque control of space robot actuators 23 p3373 N90-29057
Portable Dextrous Force Feedback Master for robot telemanipulation (PDMFF) 23 p3373 N90-29058
Experiences with the JPL telerobot testbed: Issues and insights 23 p3373 N90-29059
The KALI multi-arm robot programming and control environment 23 p3373 N90-29060
How do robots take two parts apart 23 p3374 N90-29061
Techniques and potential capabilities of multi-resolutional information (knowledge) processing 23 p3374 N90-29062
Perceptual telerobotics 23 p3374 N90-29063
Building an environment model using depth information 23 p3374 N90-29064
HERMIES-3: A step toward autonomous mobility, manipulation, and perception 23 p3374 N90-29065
Rice-obot 1: An intelligent autonomous mobile robot 23 p3375 N90-29068
Satellite-map position estimation for the Mars rover 23 p3375 N90-29069
Planning robot actions under position and shape uncertainty 23 p3376 N90-29073
A tesselated probabilistic representation for spatial robot perception and navigation 23 p3376 N90-29075
Integrating planning, execution, and learning 23 p3377 N90-29079
A hardware/software environment to support R/D in intelligent machines and mobile robotic systems
[DE90-014458] 23 p3385 N90-29119
Robots, systems, and flexible automation
[DE90-015802] 24 p3476 N90-29649
Technology and task parameters relating to the effectiveness of the bracing strategy 24 p3500 N90-29785
Modeling and sensory feedback control for space manipulators 24 p3504 N90-29807
On the manipulability of dual cooperative robots 24 p3505 N90-29813
A design strategy for autonomous systems 24 p3506 N90-29818
Direct adaptive control of a PUMA 560 industrial robot 24 p3508 N90-29832
RCTS: A flexible environment for sensor integration and control of robot systems; the distributed processing approach 24 p3512 N90-29852
Real-time cartesian force feedback control of a teleoperated robot 24 p3513 N90-29857
Assembly of objects with not fully predefined shapes 24 p3513 N90-29859
Using multiple sensors for printed circuit board insertion 24 p3514 N90-29867
Instruction dialogues: Teaching new skills to a robot 24 p3517 N90-29884
Interset: A natural language interface for teleoperated robotic assembly of the EASE space structure 24 p3517 N90-29885
Establishing viable task domains for telerobot demonstrations 24 p3518 N90-29886
Requirements for implementing real-time control functional modules on a hierarchical parallel pipelined system 24 p3518 N90-29891
Next generation space robot 24 p3520 N90-29899
The indexed time table approach for planning and acting 24 p3521 N90-29907
Approach to telerobot computing architecture
[NASA-CR-186993] 24 p3534 N90-29984

ROBUSTNESS (MATHEMATICS)

Adaptive robust control 01 p0109 N90-10620
Asymptotic robustness in regression and autoregression based on Lindeberg conditions
[AD-A210725] 01 p0114 N90-10654
Performance and robustness of adaptive controllers for linear stochastic systems 02 p0261 N90-11485
Robust control design for flight control
[AD-A211957] 03 p0309 N90-11756
Adaptive feedback linearization: Stability and robustness
[PB89-219497] 03 p0390 N90-12220
A paradigm for robust geometric algorithms
[AD-A214324] 07 p0978 N90-15647
Intelligent landmarks recognition in satellites images 09 p1165 N90-16741
Robustness of a moving-bank multiple model adaptive controller for a large space structure
[AD-A215670] 09 p1183 N90-16859
Robustness of controllers designed using Galerkin type approximations
[NASA-CR-181986] 10 p1395 N90-18063
Contribution to the study of stability robustness of nonlinear multivariable regulators
[INPE-4801-TDL/356] 11 p1554 N90-18950
Stabilized determination of geopotential coefficients by the mixed hom-BLUP approach 13 p1832 N90-20520
Robust adaptive nonlinear control under extended matching conditions
[AD-A217684] 13 p1874 N90-20744
Application of stochastic robustness to aircraft control systems 14 p1908 N90-20936
Stochastic robustness of linear control systems 14 p1908 N90-20941
Robust control of flexible structures 15 p2058 N90-21784
Multivariate analysis of launcher guidance robustness
[REPT-892-422-105] 16 p2205 N90-22581
A survey on the structured singular value 16 p2281 N90-22998
Algorithms for computing the multivariable stability margin 16 p2281 N90-22999
Robustness analysis for real parametric uncertainty 16 p2281 N90-23000
Modern CACSD using the Robust-Control Toolbox 16 p2286 N90-23024
A methodology for formulating a minimal uncertainty model for robust control system design and analysis 16 p2287 N90-23028
Multivariable frequency weighted model order reduction for control synthesis
[AIAA-89-3558] 16 p2292 N90-23060
Robust adaptive control: Stability and asymptotic performance
[AD-A219259] 16 p2304 N90-23127
Sharing memory robustly in message-passing systems
[AD-A219923] 17 p2447 N90-23950
Dynamic stabilization of large flexible space structures
[ETN-90-96926] 18 p2511 N90-24344
Robust controller designs for second-order dynamic system: A virtual passive approach
[NASA-TM-102666] 19 p2701 N90-25369
Robustness evaluation of H2 and H(infinity) control theory as applied to a transport aircraft
[AD-A222795] 20 p2814 N90-26018
On controller choice for robust sliding mode performance
[MATHS-REPT-A-107] 20 p2872 N90-26337
Direct drive robotic hand
[NASA-CASE-NPO-17917-1-CU] 20 p2872 N90-26339
Intergration of system identification and robust controller designs for flexible structures in space
[NASA-TM-102695] 20 p2876 N90-26362
On the robust stability of MIMO linear feedback systems
[EUT-88-E-212] 20 p2915 N90-26585
Robustness, diagnostics, computing, and graphics in statistics
[AD-A222888] 21 p3052 N90-27349
ROBFIT: A code for the analysis of histogram spectra with nonlinear regression and robust estimation
[AD-A221527] 21 p3055 N90-27369
Robust eigensystem assignment for second-order estimators
[NASA-TM-102696] 22 p3191 N90-28103
Robust circle and sphere fitting by least squares
[NPL-DITC-153/89] 22 p3243 N90-28389
Robust controller design by contraction of a pole region
[ESA-TT-1042] 23 p3384 N90-29118

SuperCHIEF: A modified CHIEF (Combined Helmholz Integral Equation Formulation) method
[DE90-014744] 23 p3387 N90-29123
Robust design of LQG controllers 24 p3475 N90-29639
Analysis and synthesis of robust data structures
[AD-A224568] 24 p3558 N90-30131

ROCK MECHANICS
A casting and imaging technique for determining void geometry and relative permeability behavior of a single fracture specimen
[DE90-009192] 14 p1989 N90-21403
The effects of tortuosity on flow through a natural fracture
[DE90-009193] 15 p2129 N90-22172
Coupled behavior of rock joints
[DE90-009222] 15 p2129 N90-22174
Geothermal energy program summary
[DE89-009486] 16 p2251 N90-22838

ROCKET BOOSTERS
U BOOSTER ROCKET ENGINES

ROCKET CHAMBERS
U THRUST CHAMBERS

ROCKET ENGINE CASES
Flight set 360T004 (STS-30) insulation component, interim release, volume 3
[NASA-CR-183746] 01 p0031 N90-10169
Systems tunnel linear shaped charge lightning strike
[NASA-CR-183832] 05 p0584 N90-13404
JPS heater and sensor lightning qualification
[NASA-CR-183830] 06 p0779 N90-14530
Advanced composite polar boss
[AD-D014287] 08 p1037 N90-15994
Burst pressure prediction of metallic/fibre reinforced rocket motor cases using an elasto-plastic instability analysis
[RARDE-1/89] 08 p1038 N90-15997
Qualification of the RSRM case membrane case-to-insulation bondline inspection using the Thiokol Corporation ultrasonic RSRM bondline inspection system
[NASA-CR-183940] 16 p2209 N90-22602
Qualification of the RSRM field joint CF case-to-insulation bondline inspection using the Thiokol Corporation ultrasonic RSRM bondline inspection system
[NASA-CR-183931] 16 p2242 N90-22788
Summary of a study to determine low-velocity impact damage and residual tension strength for a thick graphite/epoxy motor case
[NASA-TM-102678] 19 p2702 N90-25374

ROCKET ENGINE CONTROL
High precision rocket attitude reconstruction using star sensor and magnetometer data 05 p0659 N90-13844
Liquid Rocket Booster (LRB) for the Space Transportion System (STS) systems study. Appendix D: Trade study summary for the liquid rocket booster
[NASA-CR-183790-APP-D] 23 p3289 N90-28604

ROCKET ENGINE DESIGN
Liquid rocket booster study. Volume 2, book 5, appendix 9: LRB alternate applications and evolutionary growth
[NASA-CR-183604] 01 p0026 N90-10134
Liquid rocket booster study. Volume 2, book 4, appendices 6-8: Reports of Rocketdyne, Pratt and Whitney, and TRW
[NASA-CR-183603] 01 p0027 N90-10135
A rocket engine design expert system
[NASA-TM-102373] 01 p0032 N90-10172
Thermodynamic transport properties of nitrogen tetroxide in hypercritical conditions for regenerative cooling of a rocket engine. Volume 1: Tests
[ETN-89-94975] 01 p0134 N90-10773
Thermodynamic transport properties of nitrogen tetroxide in hypercritical conditions for regenerative cooling of a rocket engine. Volume 2: Appendices
[ETN-89-94977] 01 p0134 N90-10774
Progress in airbreathing combined engines for future European launcher 09 p1177 N90-16817
Saenger propulsion system options 09 p1177 N90-16818
Parametric assessment of propulsion system mass for airbreathing launcher configurations 09 p1177 N90-16819
Transient pressure test article test program 11 p1470 N90-18463
Effect of correlation on multi-engine rocket propulsion systems 11 p1471 N90-18467
The Pathfinder chemical transfer propulsion program 11 p1471 N90-18471
Feasibility demonstration of a 445N high-performance rocket engine 11 p1473 N90-18481
Dual-fuel, dual-mode rocket engine
[NASA-CASE-LAR-13773-1] 12 p1617 N90-19298
Low power arcjet performance
[NASA-TM-103260] 23 p3298 N90-28657
High power arcjet
[NASA-CR-183086] 23 p3298 N90-28658

ROCKET ENGINES
NT ADVANCED SOLID ROCKET MOTOR (STS)
NT APOGEE BOOST MOTORS
NT ARC JET ENGINES
NT ASROC ENGINE
NT BOOSTER ROCKET ENGINES
NT DUCTED ROCKET ENGINES
NT ELECTRIC ROCKET ENGINES
NT ELECTROTHERMAL ENGINES
NT HYBRID PROPELLANT ROCKET ENGINES
NT HYDROGEN OXYGEN ENGINES
NT ION ENGINES
NT LIQUID PROPELLANT ROCKET ENGINES
NT MERCURY ION ENGINES
NT MICROROCKET ENGINES
NT NUCLEAR ENGINE FOR ROCKET VEHICLES
NT NUCLEAR ROCKET ENGINES
NT ORBIT MANEUVERING ENGINE (SPACE SHUTTLE)
NT OXYGEN-HYDROCARBON ROCKET ENGINES
NT RESISTOJET ENGINES
NT REUSABLE ROCKET ENGINES
NT SOLID PROPELLANT ROCKET ENGINES
NT SPACE SHUTTLE BOOSTERS
NT SPACE SHUTTLE MAIN ENGINE
NT UPPER STAGE ROCKET ENGINES
Evaluation of rocket motor exhaust and liner combustion by-products
[AD-A210747] 02 p0189 N90-11083
Independent Orbiter Assessment (IOA): Assessment of the reaction control system, volume 1
[NASA-CR-185543-VOL-1] 03 p0316 N90-11793
Independent Orbiter Assessment (IOA): Assessment of the reaction control system, volume 2
[NASA-CR-185543-VOL-2] 03 p0316 N90-11794
Independent Orbiter Assessment (IOA): Assessment of the reaction control system, volume 3
[NASA-CR-185543-VOL-3] 03 p0316 N90-11795
Independent Orbiter Assessment (IOA): Assessment of the reaction control system, volume 4
[NASA-CR-185543-VOL-4] 03 p0316 N90-11796
Independent Orbiter Assessment (IOA): Assessment of the reaction control system, volume 5
[NASA-CR-185543-VOL-5] 03 p0316 N90-11797
Apollo lightcraft project
[NASA-CR-186055] 04 p0464 N90-12655
QM-8 field joint protection system, volume 7
[NASA-CR-183748] 05 p0614 N90-13586
Gas flows in rocket motors, volume 1
[AD-A213348] 05 p0615 N90-13591
Swiss scientific balloon and sounding rocket experiments 1987-1989 05 p0656 N90-13827
AGARD Highlights 89/2 06 p0717 N90-14184
Extended temperature range rocket injector
[NASA-CASE-LEW-14846-1] 07 p0887 N90-15130
Development of an integrated BEM approach for hot fluid structure interaction
[NASA-CR-186214] 07 p0927 N90-15364
Vulcain engine development status 09 p1176 N90-16810
Mission-dependent selection of propulsion systems for reusable launch vehicles 09 p1177 N90-16815
Effects of scaling on the performance of magnetoplasmadynamic thrusters
[AD-A215690] 09 p1184 N90-16863
Thermal modelling of various thermal barrier coatings in a high heat flux rocket engine
[NASA-TM-102418] 09 p1193 N90-16911
Plume flowfield analysis of the shuttle primary Reaction Control System (RCS) rocket engine
[NASA-CR-186315] 10 p1329 N90-17676
The 1989 JANNAF Propulsion Meeting, volume 1
[CPIA-PUBL-515-VOL-1] 11 p1470 N90-18462
Effect of correlation on multi-engine rocket propulsion systems 11 p1471 N90-18467
AFOSR/ONR (Air Force Office of Scientific Research/Office of Naval Research) Contractors' Meeting on Combustion Rocket Propulsion Diagnostics of Reacting Flow
[AD-A216094] 11 p1476 N90-18491
Proceedings of a contractors meeting on Combustion Rocket Propulsion Diagnostics of Reacting Flow
[AD-A216445] 12 p1617 N90-19297
Spacecraft escape 13 p1753 N90-20066
Stress analysis of rocket motors with viscoelastic propellant by a mixed finite element model 14 p1941 N90-21112
Hybrid propulsion technology program. Volume 1: Conceptional design package
[NASA-CR-183953] 15 p2060 N90-21793
Hybrid propulsion technology program. Volume 2: Technology definition package
[NASA-CR-183954] 15 p2060 N90-21794
Experimental evaluation of a tuned electromagnetic damper for vibration control of cryogenic turbopump rotors
[NASA-TP-3005] 17 p2354 N90-23403
Rocket engine failure detection using system identification techiques
[NASA-CR-185259] 19 p2664 N90-25159
A comparison of analytical results for 20 K LOX/hydrogen instabilities
[NASA-TM-103166] 19 p2670 N90-25186
The jet engine: 1932
[ISBN-3-922010-49-0] 19 p2670 N90-25189
Gaseous optical contamination of the spacecraft environment: A review 19 p2730 N90-25519
Hard start problem of the apogee engine for the ETS-6
[DE90-505525] 20 p2825 N90-26072
QM-8 final performance evaluation report: SEALS, volume 4
[NASA-CR-183958] 20 p2869 N90-26324
Advanced launch vehicle configurations and performance trades 22 p3126 N90-27744
Effects of friction and end losses on MHD thruster efficiency
[DE90-013673] 23 p3289 N90-28608
Data base for crack growth properties of materials 23 p3296 N90-28647
A planar rocket motor model for visualization of violent reaction due to fragment impact
[AD-A224273] 24 p3441 N90-29431
Combustion characteristics of oxygen/hydrogen high pressure preburners for staged combustion cycle rocket engine
[NAL-TR-1044] 24 p3441 N90-29434
Effects of thruster firings on the shuttle environment 1: Neutral gas composition
[AD-A224404] 24 p3487 N90-29707

ROCKET EXHAUST
X-ray spectroscopy of the SSME plume
[NASA-CR-185308] 01 p0031 N90-10168
Evaluation of rocket motor exhaust and liner combustion by-products
[AD-A210747] 02 p0189 N90-11083
Modelling of satellite control thruster plumes 05 p0613 N90-13578
Measurement of optical radiations in spacecraft environments
[AD-A213814] 07 p0950 N90-15497
A field study of solid rocket exhaust impacts on the near-field environment
[NASA-TM-4172] 10 p1405 N90-18102
Spacecraft optical contamination environment
[AD-A218088] 13 p1889 N90-20838
HCl Vapor Characterization and Detection. JANNAF Safety and Environmental Protection Subcommittee Workshop
[AD-A216252] 16 p2208 N90-22596
Gaseous optical contamination of the spacecraft environment: A review 19 p2730 N90-25519
Spectroscopic study of combustion diagnostics on hydroxyl radicals
[NASA-CR-186998] 23 p3305 N90-28694

ROCKET FLIGHT
BEAR electrostatic analyzer: Flight results
[DE90-006511] 11 p1498 N90-18625

ROCKET LAUNCHERS
US commercial launcher summary 09 p1174 N90-16793
Conceptual work ;t Aerospatiale on air-breathing and non-air-breathing recoverable launchers
[REPT-892-422-104] 17 p2362 N90-23450

ROCKET LAUNCHING
NT LIFTOFF (LAUNCHING)
NT LUNAR LAUNCH
NT ORBITAL LAUNCHING
Tracking flares
[ISBN-0-642-13583-5] 08 p1052 N90-16080
Modeling the near acoustic field of a rocket during launch 08 p1156 N90-16694
A new stress routine for the Projectile Design Analysis System (PRODAS)
[AD-A220564] 17 p2346 N90-23357
On the simulation test for the relative motion of separated sub-boosters on M-3S2 with nearly half a model vehicle ST-735 and their motion analyses using inertial sensors output
[ISAS-635] 17 p2366 N90-23471
Computer tomography of thermal batteries and other closed systems
[AD-A218379] 17 p2419 N90-23787

ROCKET LININGS
Cooling of rocket thrust chambers with liquid oxygen
[NASA-TM-103146] 18 p2210 N90-22605

ROCKET MOTOR CASES
U ROCKET ENGINE CASES

ROCKET NOZZLES
Flight set 360T004 (STS-30) insulation component, interim release, volume 3
[NASA-CR-183746] 01 p0031 N90-10169
Three-dimensional, two-phase, transonic, canted nozzle flows
[AD-A211528] 03 p0347 N90-11984
RSRM nozzle fixed housing cooldown test
[NASA-CR-183741] 05 p0614 N90-13587
Gas flows in rocket motors. Volume 3, appendix D: Computer code listings
[AD-A213350] 05 p0616 N90-13593
Advanced composite polar boss
[AD-D014287] 08 p1037 N90-15994
Hypersonic nozzle/afterbody performance at low Mach numbers
[AD-A216223] 10 p1309 N90-17575
Heating rates in a High Energy Propulsion System (HEPS) Orbital Transfer Vehicle (OTV)
[AD-A214354] 10 p1360 N90-17888
Cold flow determination of the internal flow environment around the submerged TVC nozzle for the space shuttle SRM 11 p1470 N90-18465
Flight motor set 360L002 (STS-27R). Volume 5: Nozzle component
[NASA-CR-183945] 15 p2062 N90-21811
Shelf life extension for the lot AAE nozzle severance LSCs
[NASA-CR-183878] 15 p2062 N90-21813
Characterization of plasma flow through magnetic nozzles
[AD-A221044] 18 p2617 N90-24905
TRANSTRAIN: A program to compute strain transformations in composite materials
[NASA-TM-103509] 22 p3153 N90-27877
Computer code for the prediction of nozzle admittance 23 p3293 N90-28630

ROCKET OXIDIZERS
A surface coupled flamelet approach to dynamic response in heterogeneous propellant combustion 06 p0739 N90-14302
Gelled propellant flow: Boundary layer theory for power-law fluids in a converging planar channel
[DE90-000923] 07 p0927 N90-15365
Investigation of the phase stabilizing effect of 4 percent potassium fluoride on ammonium nitrate
[AD-A215313] 11 p1494 N90-18599
Hard start problem of the apogee engine for the ETS-6
[DE90-505525] 20 p2825 N90-26072

ROCKET PLANES
NT X-15 AIRCRAFT

ROCKET PROPELLANT TANKS
U PROPELLANT TANKS

ROCKET PROPELLANTS
NT CRYOGENIC ROCKET PROPELLANTS
NT DOUBLE BASE ROCKET PROPELLANTS
NT GASEOUS ROCKET PROPELLANTS
NT GELLED ROCKET PROPELLANTS
NT HYPERGOLIC ROCKET PROPELLANTS
NT LIQUID ROCKET PROPELLANTS
NT METAL PROPELLANTS
NT MONOPROPELLANTS
NT NITRAMINE PROPELLANTS
NT RP-1 ROCKET PROPELLANTS
NT SLURRY PROPELLANTS
NT SLUSH HYDROGEN
NT SOLID ROCKET PROPELLANTS
NT TATB
Atomic hydrogen as a launch vehicle propellant
[NASA-TM-102459] 06 p0735 N90-14284
Propellant trends in advanced rocket propulsion 09 p1179 N90-16838
Booster propulsion/vehicle impact study, 2
[NASA-CR-179313] 10 p1346 N90-17809
The measurement, modeling, and prediction of traction for rocket propellant 1
[NASA-CR-185186] 12 p1633 N90-19386
Research programs in aeronautical engineering, solid state physics, and materials science at Technion-Israel Institute of Technology, Haifa, Israel
[EOARD-LR-89-068] 14 p2044 N90-21720
Experimental studies on energy storage
[AD-A219032] 16 p2252 N90-22845
Tripropellant combustion process 23 p3293 N90-28631
Summary of booster propulsion/vehicle impact study results 23 p3294 N90-28635

ROCKET PROPELLED SLEDS
Evaluation of rocket motor exhaust and liner combustion by-products
[AD-A210747] 02 p0189 N90-11083

ROCKET SONDES
U SOUNDING ROCKETS

ROCKET SOUNDING
Solar X-ray Astronomy Sounding Rocket Program
[NASA-CR-183447] 01 p0138 N90-10796

ROCKET TEST FACILITIES
Static test deflector for Ariane-5 SRM: Technical design and economical choice 09 p1176 N90-16812
Low thrust rocket test facility
[NASA-TM-103206] 19 p2663 N90-25158

ROCKET THRUST
Laboratory simulation of the effect of rocket thrust on a precessing space vehicle
[NASA-CR-186681] 19 p2669 N90-25182
Advanced tube-bundle rocket thrust chamber
[NASA-TM-103139] 19 p2670 N90-25185
The 30-kW ammonia arcjet technology
[NASA-CR-186850] 19 p2670 N90-25190
Flight motor set 360L001 (STS-26R). Volume 1: System overview, revision A
[NASA-CR-183995] 22 p3133 N90-27778

ROCKET VEHICLES
NT ARIANE LAUNCH VEHICLE
NT ARIES SOUNDING ROCKET
NT MULTISTAGE ROCKET VEHICLES
NT PAYLOAD ASSIST MODULE
NT PEGASUS AIR-LAUNCHED BOOSTER
NT SKYLARK ROCKET VEHICLE
NT SOUNDING ROCKETS
NT TITAN LAUNCH VEHICLES
NT X-15 AIRCRAFT
Rocket-triggered lightning strikes and forest fire ignition 08 p1155 N90-16890

ROCKET-BORNE INSTRUMENTS
Design of scientific payloads and components
[AD-A211819] 03 p0351 N90-12005
Rocket studies of the lower ionosphere
[NASA-CR-186187] 06 p0814 N90-14735
Metal vaporisers: Bicentennial series of five historical monographs
[ISBN-0-642-13584-3] 08 p1052 N90-16081

ROCKETS
A history of West European rocketry and space research
[AD-A211191] 02 p0297 N90-11690

ROCKS
NT BASALT
NT BEDROCK
NT COAL
NT GNEISS
NT IGNEOUS ROCKS
NT LIMESTONE
NT LUNAR ROCKS
NT OBSIDIAN
NT REGOLITH
NT SHALES
Evaluation of selection techniques for multispectral bands employed in the discrimination of carbonatic rocks
[INPE-4850-TDL/365] 11 p1522 N90-18765
Using image analysis to determine petrophysical properties of reservoir rocks
[DE90-000222] 12 p1680 N90-19649
P-T condition to deformation from fluid inclusions in mylonites
[NASA-CR-186377] 12 p1690 N90-19710
Hot dry rock geothermal energy: A renewable energy resource that is ready for development now
[DE90-007509] 13 p1826 N90-20485
Characterization of linear structures from remote sensing data; Espinhaco Meridional (MG) sierra
[INPE-4905-PRE/1506] 14 p1997 N90-21449
The pressure dilation of a deep, jointed region of the earth
[DE90-007537] 15 p2128 N90-22170
Coupled behavior of rock joints
[DE90-009222] 15 p2129 N90-22174
Robotic sampling system for an unmanned Mars mission 23 p3375 N90-29070

ROCKY MOUNTAINS (NORTH AMERICA)
Inverted surface troughs accompanying Rocky Mountain lee-side cyclogenesis 06 p0816 N90-14745

RODENTS
NT MICE
NT RATS
The rodent research animal holding facility as a barrier to environmental contamination
[NASA-TM-102237] 03 p0378 N90-12151
Experiment K-6-10. Effects of zero gravity on myofibril protein content and isomyosin distribution in rodent skeletal muscle 20 p2894 N90-26464

RODS
Wave-mode coordinate analysis of L junction in LSS
[AD-A211116] 02 p0176 N90-10984
Fe-Ni-Cr alloys for coatings and electroforms
[PB89-195846] 03 p0325 N90-11849
Effects of dislocation substructure and prestrain on fracture behavior in aluminum and steel alloys 06 p0745 N90-14334
Elastic stress concentration factors. Geometric discontinuities in rods and tubes of isotropic materials
[ESDU-89048] 09 p1239 N90-17192
Critical current density and transition temperature measurements of Y-Ba-Cu-O rods
[AD-A216695] 12 p1719 N90-19875
Finite element models to predict the structural response of 120-mm sabot/rods during launch
[DE90-007497] 13 p1817 N90-20436
Computer simulations and experiments to study the fracture of rods by flying plates
[DE90-008308] 13 p1817 N90-20437
Modeling of thermal lensing in side and end-pumped finite solid-state laser rods
[NASA-CR-4300] 17 p2407 N90-23716
Numerical simulation of semi-infinite target penetration by continuous and segmented rods
[AD-A219437] 17 p2412 N90-23743
A cable-rigidized 3D pantograph 18 p2538 N90-24484
Low velocity impact analysis with NASTRAN 18 p2570 N90-24647
Plate rods and leaf springs with hybrid structure: Cross section optimization following different target criteria
[ILR-MITT-227(1989)] 20 p2877 N90-26366
Nylon and teflon scribe effect on NBR to Chemlok 233 and NBR to NBR bond interfaces
[NASA-CR-184004] 22 p3189 N90-28095
Static and dynamic characterization of the ATR 72 rods made of Ti 10.2.3 titanium alloy
[REPT-49-238] 23 p3310 N90-28722
Fractographic analysis of fatigue failures of airframe equipment parts: Examples of a rod end housing and a rod end cap
[NAL-TR-1047] 24 p3483 N90-29686

ROENTGEN SATELLITE
U ROSAT MISSION

ROGALLO WINGS
U FLEXIBLE WINGS
U FOLDING STRUCTURES

ROLL
Prediction of dynamic derivatives 01 p0012 N90-10055
Micro-miniature roll rate sensor
[AD-A214778] 09 p1225 N90-17107

ROLL CONTROL
U LATERAL CONTROL

ROLL FORMING
A study of the hot workability of Al-8.5 wt pct Mg alloys for armor plate applications
[AD-A211680] 03 p0329 N90-11868
Optimizing superplastic response in navalite, a lithium containing aluminum-magnesium alloy
[AD-A216552] 12 p1626 N90-19346
Structures instabilities in filament liquid crystals
[ETN-90-95916] 12 p1721 N90-19888
Crown and shape control in the rolling of thin, wide plates
[ETN-90-96946] 17 p2378 N90-23539
Processing and characterization of high strength, high ductility Hadfield steel
[AD-A221769] 21 p2982 N90-26947
The roles of strain and reheating interval in continuous recrystallization during the thermomechanical processing by warm rolling of an Al-Mg alloy
[AD-A223673] 24 p3449 N90-29479

ROLLER BEARINGS
Film thickness in lubricated Hertzian contacts. Part 2: Point contacts
[ESDU-89045] 09 p1232 N90-17148
Non-linear dynamic analysis of geared systems, part 2
[NASA-CR-180495] 17 p2410 N90-23732
Modification of the SHABERTH bearing code to incorporate RP-1 and a discussion of the traction model
[NASA-TP-3017] 22 p3183 N90-28066
Pratt and Whitney cryogenic turbopump bearing experience 23 p3292 N90-28624

ROLLERS
Fully articulated four-point-bend loading fixture
[NASA-CASE-LEW-14776-1] 07 p0940 N90-15445
Heat engine based on shape memory alloys
[AD-D014400] 14 p1988 N90-21385

ROLLING
Rolling of ARALL laminates (an alternative method for post-stretching ARALL laminates)
[LR-560] 04 p0484 N90-12778
Production and processing of Cu-Cr-Nb alloys
[NASA-TM-102495] 08 p1047 N90-16053
Unfurlable, continuous-surface reflector concept 12 p1609 N90-19257
Elastic and viscoelastic analysis of two multiply layered cylinders rolling over each other with Coulomb friction
[REPT-89-50] 15 p2107 N90-22051

Fabricating vanadium sheet to improve symmetry of drawn parts
[DE90-011253] 19 p2682 N90-25257

ROLLING CONTACT LOADS
Three-dimensional viscoelastic bodies in steady state frictional rolling contact with generalization to Knothe rolling
[REPT-89-23] 03 p0355 N90-12032
Tire modeling by finite elements 06 p0792 N90-14614
Rolling contact fatigue of surface modified 440C using a 'Ge-Polymet' type disc rod test rig
[NASA-TM-100390] 13 p1777 N90-20200
On the application of similarity laws to a scaled railway bogie model
[DLR-FB-90-06] 23 p3335 N90-26853

ROLLING MOMENTS
A video-based experimental investigation of wing rock
[AD-A218244] 13 p1755 N90-20075
A video-based experimental investigation of wing rock 15 p2054 N90-21771

ROLLUP SOLAR ARRAYS
U SOLAR ARRAYS

ROM DEVICES
U READ-ONLY MEMORY DEVICES

ROOFS
A guide for estimating potential energy savings from increased solar reflectance of a low-sloped roof
[DE90-003720] 07 p0955 N90-15526

ROOM TEMPERATURE
Crystal and magnetic structure of Er(2)(Co(sub x)Fe(sub 1-x))(17) compounds
[DE90-004928] 10 p1436 N90-18288
Comparison of solar pumped Nd:YAG and Nd:Cr:GSGG lasers at liquid nitrogen and room temperature
[DLR-FB-89-41] 16 p2240 N90-22781

ROOMS
NT CLEAN ROOMS
Space station wardroom habitability and equipment study
[NASA-CR-4246] 09 p1260 N90-17308

ROOT-MEAN-SQUARE ERRORS
Minimum attainable RMS attitude error using co-located rate sensors 16 p2288 N90-23038

ROOTS OF EQUATIONS
An algorithm for finding characteristic roots of quasi-triangular Markov chains
[AD-A215490] 10 p1421 N90-18196

ROSAT MISSION
On the nature of low-luminosity Be/X ray binaries 19 p2780 N90-25816
Fast classification of ROSAT sources on objective prism plates 19 p2788 N90-25871

ROSS ICE SHELF
Airfields on antarctic glacier ice
[AD-A217638] 13 p1759 N90-20097
On the effectiveness of the production of antarctic bottom water in the Weddell and Ross Seas
[AD-A218873] 16 p2259 N90-22880

ROSSBY WAVES
U PLANETARY WAVES

ROTARY DRIVES
U MECHANICAL DRIVES

ROTARY ENGINES
The application of cast SiC/Al to rotary engine components
[NASA-CR-179610] 05 p0581 N90-13385
Analysis of rotary engine combustion processes based on unsteady, three-dimensional computations
[NASA-TM-102469] 05 p0642 N90-13749
Performance of a supercharged direct-injection stratified-charge rotary combustion engine
[NASA-TM-103105] 20 p2809 N90-25982
Computational experience with a three-dimensional rotary engine combustion model
[NASA-TM-103104] 20 p2861 N90-26275

ROTARY GYROSCOPES
A new kind of heterodyne fiber-optic gyroscope
[AD-A213953] 07 p0933 N90-15404
Laser gyros and field diagnostics
[AD-A220832] 17 p2406 N90-23709

ROTARY STABILITY
NT GYROSCOPIC STABILITY
Equilibrium solutions of a spherical pendulum with rotating point of suspension and friction
[ESA-TT-1139] 03 p0400 N90-12288
Vortex dynamics
[AD-A212119] 04 p0499 N90-12877
Investigation of liquid sloshing in spin-stabilized satellites
[AD-A214730] 09 p1182 N90-16853
Active stabilization of aeromechanical systems
[AD-A216629] 11 p1506 N90-18672
Stability regimes in a rotating quadrupole focusing accelerator
[AD-A219513] 16 p2317 N90-23209

ROTARY WING AIRCRAFT
NT AH-1G HELICOPTER
NT AH-64 HELICOPTER
NT CH-47 HELICOPTER
NT H-53 HELICOPTER
NT HELICOPTERS
NT LIGHT HELICOPTERS
NT MILITARY HELICOPTERS
NT TILT ROTOR AIRCRAFT
NT UH-1 HELICOPTER
NT UH-60A HELICOPTER
NT XV-15 AIRCRAFT
Integrated multidisciplinary optimization of rotorcraft: A plan for development
[NASA-TM-101617] 04 p0450 N90-12580
General approach and scope --- rotor blade design optimization 04 p0451 N90-12581
Validation of the procedures --- integrated multidisciplinary optimization of rotorcraft 04 p0451 N90-12587
Appendix: Results obtained to date --- integrated multidisciplinary optimization of rotorcraft 04 p0451 N90-12588
NASA's program on icing research and technology 07 p0873 N90-15062
A survey of nonuniform inflow models for rotorcraft flight dynamics and control applications
[NASA-TM-102219] 08 p1028 N90-15938
Compendium of abstracts and viewgraphs.
[AD-A217189] 13 p1767 N90-20140
Stereopsis cueing effects on hover-in-turbulence performance in a simulated rotorcraft
[NASA-TP-2980] 14 p1921 N90-21004
Transmission research activities at NASA Lewis Research Center
[NASA-TM-103132] 14 p1988 N90-21394
Development and application of a generalized dynamic wake theory for lifting rotors 15 p2046 N90-21731
Quiet mode for nonlinear rotor models
[NASA-TM-102236] 15 p2051 N90-21758
Assessment of High Temperature Superconducting (HTS) electric motors for rotorcraft propulsion
[NASA-CR-185222] 15 p2052 N90-21761
Passive navigation using image irradiance tracking 15 p2141 N90-22232
Computer vision techniques for rotorcraft low altitude flight 15 p2142 N90-22237
Kalman filter based range estimation for autonomous navigation using imaging sensors 15 p2142 N90-22238
Extension of a three-dimensional viscous wing flow analysis
[NASA-CR-182023] 17 p2344 N90-23348
TRENDS: The aeronautical post-test database management system
[NASA-TM-101025] 19 p2662 N90-25149
AGARD highlights 90/1 20 p2951 N90-26788
The Second ARO Workshop on Rotorcraft Interactional Aerodynamics
[AD-A223310] 24 p3418 N90-29304

ROTARY WINGS
NT LIFTING ROTORS
NT RIGID ROTORS
NT TILTING ROTORS
Integrated multidisciplinary design optimization of rotorcraft
[NASA-TM-101642] 02 p0155 N90-10889
Rotor blade aerodynamic design 04 p0451 N90-12582
Rotor blade dynamic design 04 p0451 N90-12583
Rotor blade structural design 04 p0451 N90-12584
Acoustic design considerations: Review of rotor acoustic sources 04 p0451 N90-12585
Airframe design considerations: Overview --- rotor design optimization 04 p0451 N90-12586
Appendix: Results obtained to date --- integrated multidisciplinary optimization of rotorcraft 04 p0451 N90-12588
Euler equation solutions applied to a helicopter rotor in forward moving flight
[ONERA-RSF-32/1285-AY-346A] 04 p0452 N90-12592
RAN (Royal Australian Navy) vibration analysis system operator's guide
[AD-A212441] 04 p0453 N90-12596
An experimental investigation of the interaction between a model rotor and airframe in forward flight 06 p0723 N90-14219
Effects of aeroelastic tailoring on anisotropic composite material beam models of helicopter blades
[AD-A213478] 07 p0879 N90-15095
An examination of helicopter rotor load calculations
[AD-A214295] 07 p0880 N90-15098
Calculation of the flow field of a multiblade helicopter rotor using a Euler method including the wake 08 p1069 N90-16189
The response of helicopter rotors to vibratory airload
[AD-A215678] 09 p1167 N90-16758
Prediction of rotor blade-vortex interaction noise from 2-D aerodynamic calculations and measurements
[ISL-CO-243/88] 11 p1451 N90-18365
Performance of an optimized rotor blade at off-design flight conditions
[NASA-CR-4288] 12 p1603 N90-19226
Unsteady free-wake viscous aerodynamic analysis of helicopter rotors
[AD-A217166] 13 p1750 N90-20048
Analysis of small-scale rotor hover performance data
[NASA-TM-102271] 13 p1799 N90-20325
Performance data from a wind-tunnel test of two main-rotor blade designs for a utility-class helicopter
[NASA-TM-4183] 14 p1916 N90-20974
ROSAR (Helicopter-Rotor based Synthetic Aperture Radar) 14 p1961 N90-21229
Airloads, wakes, and aeroelasticity
[NASA-CR-177551] 15 p2048 N90-21738
Aerodynamic characteristics of two rotorcraft airfoils designed for application to the inboard region of a main rotor blade
[NASA-TP-3009] 18 p2491 N90-24239
HPLC analysis of helicopter rotor blade materials
[AD-A221121] 18 p2497 N90-24270
Scenario 2000
[MBB-UD-500/89-PUB] 19 p2652 N90-25092
Rotorcraft aeromechanical stability-methodology assessment. Phase 2: Workshop
[NASA-TM-102272] 21 p2955 N90-26800
Development of a method to design helicopter rotors
[REPT-100-30-03] 21 p2960 N90-26830
Applications of digital image processing in testing and evaluation of composite materials
[AD-A222939] 21 p2971 N90-26887
The acoustic results of a United Technologies scale model helicopter rotor tested at DNW
[NASA-TM-101879] 21 p3073 N90-27471
Theoretical studies carried out in 1988 on helicopter rotor noise under subsonic conditions
[ONERA-RS-82/5094-PY] 22 p3245 N90-28402
Solution of Euler equations applied to a rotor of a helicopter in steady flight
[ONERA-RSF-1/3731-AY-002A] 23 p3269 N90-28500
The effects of structural flap-lag and pitch-lag coupling on soft inplane hingeless rotor stability in hover
[NASA-TP-3002] 23 p3269 N90-28503
An enhanced integrated aerodynamic load/dynamic optimization procedure for helicopter rotor blades
[NASA-CR-4326] 24 p3432 N90-29383

ROTATING
U ROTATION

ROTATING BODIES
NT COMPRESSOR ROTORS
NT FLYWHEELS
NT HELICOPTER TAIL ROTORS
NT IMPELLERS
NT LIFTING ROTORS
NT PUMP IMPELLERS
NT RIGID ROTORS
NT ROTARY WINGS
NT ROTATING CYLINDERS
NT ROTATING DISKS
NT ROTATING SPHERES
NT ROTORS
NT TILTING ROTORS
NT TURBINE WHEELS
Computation of fluid flow and heat transfer in rotating disc-systems 09 p1215 N90-17044
Condensation fluid dynamics and heat transfer on rotating spherical surfaces in a microgravitational field
[DE90-005540] 11 p1495 N90-18607
The interaction of a supersonic streamwise vortex and a normal shock wave 18 p2491 N90-24241
Feasibility of a synthetic aperture Radar with Rotative Antennas (ROSAR)
[MBB-S/PUB-0385] 19 p2651 N90-25088
Rotating-unbalanced-mass devices for scanning balloon-borne experiments, free-flying spacecraft, and space shuttle/space station experiments
[NASA-TP-3030] 19 p2682 N90-25255

ROTATING CYLINDERS
The thermal stability between rotating cylinders in a radially symmetrical gravitational field
[DE89-618548] 02 p0287 N90-11638
On the thermal stability of flow of a radiating two-component plasma in a porous medium between two rotating cylinders
[DE89-636426] 06 p0847 N90-14928

Enhancement of mass transfer to a rotating cylinder electrode by inert particles suspended in the electrolyte
[DE90-008054] 13 p1771 N90-20165

Rheology and microstructure of concentrated suspensions
[DE90-009976] 18 p2520 N90-24391

On the spatial eigenvalue approach to high Reynolds number flow in a rotating and nutating cylinder
[AD-A221710] 21 p3005 N90-27081

Response of a liquid bridge with rotationally excited bottom
[LRT-WE-9-FB-13(1989)] 21 p3006 N90-27089

ROTATING DISKS

Electrostatically suspended rotor for angular encoder
[NASA-CASE-MFS-28294-1] 01 p0054 N90-10310

A theoretical study of ingress for shrouded rotating disk systems with radial outflow
[PNR90586] 04 p0455 N90-12607

The effects of trace anions on the voltammetry of single crystal gold surfaces
[AD-A211886] 04 p0558 N90-13254

Numerical investigations of heat transfer and flow rates in rotating cavities. Simulation of the movement generated by wall temperature gradients, by source-sink mass flows or by the differential rotation of the walls, under the influence or coriolis and centrifugal forces
[ETN-90-96253] 11 p1510 N90-18695

Numerical and experimental analysis of a thin liquid film on a rotating disk related to development of a spacecraft absorption cooling system
[NASA-CR-183457] 12 p1657 N90-19523

Generation of circumferential velocity contours associated with pulsed point suction on a rotating disk
18 p2646 N90-25065

ROTATING FLUIDS

NT ROTATING LIQUIDS

On the interaction of stationary crossflow vortices and Tollmien-Schlichting waves in the boundary layer on a rotating disc
[NASA-CR-181859] 01 p0002 N90-10007

Symmetry breaking bifurcations and the growth of chaos in a rotating fluid
[AD-A210969] 01 p0072 N90-10411

On the computation of normal modes of a rotating, viscous, incompressible fluid with a capillary free boundary
[REPT-89-01] 03 p0348 N90-11989

Flare-in texture in rotating superfluid (3)He-B
[PB89-218994] 03 p0412 N90-12368

Response of a rotating finite annular liquid layer to axial excitation
[LRT-WE-9-FB-15(1988)] 08 p1053 N90-16090

Laboratory studies of isolated eddies in a rotating fluid
[AD-A213903] 08 p1063 N90-16146

Superflow induced phase transition in the axial vortex-free texture of rotating superfluid He-3-B
[PB90-110388] 08 p1127 N90-16531

Theoretical study of the flow in a rotating channel. Experimental study through flow visualization in a curved channel 14 p1926 N90-21032

Semigeostrophic flow over orography in a stratified rotating atmosphere 15 p2127 N90-22163

Response of a viscous liquid column to pitching- and roll-excitation in zero-gravity environment
[LRT-WE-9-FB-10(1989)] 21 p2991 N90-27000

Response of a spinning liquid column to axial excitation
[LRT-WE-9-FB-10(1988)] 21 p3006 N90-27085

Liquid sloshing response in a spinning container due to axial excitation
[LRT-WE-9-FB-9(1989)] 21 p3006 N90-27087

Experimental study of the effects of rotation on the homogeneous turbulence. Comparison with the EDQNM model
[ONERA-RSF-11/1145-AY-166A] 22 p3176 N90-28025

ROTATING GENERATORS

NT AC GENERATORS
NT DYNAMOMETERS
NT HOMOPOLAR GENERATORS
NT TURBOGENERATORS

A software-based controller for generation of synchronized pulses for use with rotating machinery
[DE89-016672] 06 p0770 N90-14477

ROTATING LIQUIDS

Investigation of liquid sloshing in spin-stabilized satellites
[AD-A214730] 09 p1182 N90-16853

Response of differently axially excited viscous liquid bridges in zero-gravity
[LRT-WE-9-FB-14(1989)] 21 p2991 N90-27001

Response of a liquid column with respect to oscillatory rotational top- and bottom excitation
[LRT-WE-9-FB-8(1989)] 21 p3006 N90-27086

Oscillatory response of a liquid column to counter rotational excitation
[LRT-WE-9-FB-12(1989)] 21 p3006 N90-27088

Response of a liquid bridge with rotationally excited bottom
[LRT-WE-9-FB-13(1989)] 21 p3006 N90-27089

Response of a viscous liquid column to various pitch-excitations
[LRT-WE-9-FB-15(1989)] 21 p3006 N90-27090

Response of differently axial-excited spinning liquid columns
[LRT-WE-9-FB-16(1989)] 21 p3006 N90-27091

Effects of low bond number liquid motions on spacecraft attitude 22 p3131 N90-27768

ROTATING PLASMAS

Toroidal rotation retardation and ion anomalous transport by drift waves in a tokamak
[DE89-634427] 06 p0844 N90-14913

Study on rotating plasma with submillimeter laser interferometer
[DE90-615387] 14 p2027 N90-21623

ROTATING SHAFTS

NT TURBOSHAFTS

Vibration transmission through rolling element bearings in geared rotor system, part 1
[NASA-CR-186093] 04 p0509 N90-12936

Analysis of unsteady heat transfer by natural convection in a two-dimensional square cavity using a high order finite-volume method 12 p1657 N90-19521

A fiber optic sensor for noncontact measurement of shaft speed, torque, and power
[NASA-TM-102481] 14 p1983 N90-21360

Practical nonlinear simulation of rotating machinery dynamics with application to turbine blade rubbing
15 p2104 N90-22038

The Shock and Vibration Digest, volume 21, no. 3
15 p2109 N90-22064

Rotor-to-stationary element rub-related vibration phenomena in rotating machinery: Literature survey
15 p2109 N90-22065

Active lag angle device
[AD-D014538] 20 p2857 N90-26249

Cryogenic anti-friction bearing with inner race
[NASA-CASE-MFS-28384-1] 21 p3010 N90-27112

ROTATING SPHERES

Equilibrium solutions of a spherical pendulum with rotating point of suspension and friction
[ESA-TT-1139] 03 p0400 N90-12288

ROTATING STALLS

Stage effects on stalling and recovery of a high-speed 10-stage axial-flow compressor
04 p0454 N90-12600

Computational and experimental investigations of rotating stall in compressor cascades
16 p2201 N90-22565

An investigation of the three-dimensional flow field in a centrifugal compressor 16 p2235 N90-22751

ROTATING VEHICLES

U ROTATING BODIES
U VEHICLES

ROTATION

NT COUNTER ROTATION
NT EARTH ROTATION
NT MOLECULAR ROTATION
NT MUON SPIN ROTATION
NT SATELLITE ROTATION
NT SOLAR ROTATION
NT STELLAR ROTATION

Similarity solutions that give rise to hyperbolicity and change of type in steady flow of a viscoelastic fluid
[AD-A210920] 01 p0072 N90-10410

An algorithm for the systematic disturbance of optimal rotational solutions
[NASA-TM-101089] 01 p0102 N90-10575

A super element for multibody dynamics
02 p0178 N90-11004

Acoustic controlled rotation and orientation
[NASA-CASE-NPO-16995-1-CU] 03 p0400 N90-12289

Rotational and vibrational nonequilibrium effects in rarefied, hypersonic flow
[NASA-CR-182559] 04 p0437 N90-12498

Cross-axis synchronous flow through coil planet centrifuge for large-scale preparative countercurrent chromatography
[PB89-200174] 04 p0468 N90-12682

Experimental study of homogeneous turbulence submitted to rotational effects
[ONERA-RSF-10/1145-AY-164A] 04 p0502 N90-12894

A device to extract energy from water waves
[REPT-89-34] 04 p0516 N90-12978

Extension to Eulers's theorem to n-dimensional spaces 05 p0589 N90-13431

Rotation of the photospheric magnetic fields: A north-south asymmetry
[NASA-CR-186159] 05 p0715 N90-14177

Expert system for fault diagnostics of rotating machines
[DE89-766980] 06 p0793 N90-14621

The dynamics of simulated convective storms in hurricane environments 06 p0816 N90-14747

A study of the effects of Rotating Frame Turbulence (RFT) on helicopter flight mechanics
07 p0872 N90-15058

The role of attention in visual processing
[AD-A214158] 07 p0967 N90-15588

Some computational properties of rotation representations
[AD-A213888] 07 p0981 N90-15665

Mechanical evaluation of the differential drum concept for optical fiber pay-out
[AD-A214149] 07 p0993 N90-15740

Rotating Doppler frequency shifter
[AD-D014279] 08 p1118 N90-16475

TALON and CRADLE: Systems for the rescue of tumbling spacecraft and astronauts, a preliminary design
09 p1181 N90-16847

Micro-miniature roll rate sensor
[AD-A214778] 09 p1225 N90-17107

Static and rotational aerodynamic data from 0 deg to 90 deg angle of attack for a series of basic and altered forebody shapes
[AD-A216582] 11 p1451 N90-18361

Review of component defects, their relationship to manufacturing process, and their effect on materials behaviour (for critical rotating parts)
11 p1458 N90-18399

Techniques for studying the effects of microgravity on model particle/cell systems 12 p1640 N90-19424

Finite element analysis of a quartz rotation sensor
[DE90-006959] 12 p1664 N90-19562

Fluid dynamics analysis of a rotating axisymmetric part using FIDAP
[DE90-008733] 13 p1802 N90-20340

Apparatus for mixing solutions in low gravity environments
[NASA-CASE-MFS-26047-1] 14 p1958 N90-21209

Heat engine based on shape memory alloys
[AD-D014400] 14 p1986 N90-21385

Direct formulation of a 4-node hybrid shell element with rotational degrees of freedom
[NASA-CR-4262] 14 p1991 N90-21411

Experimental investigation of the effect of cavitation on the rotordynamic forces on a whirling centrifugal pump impeller 15 p2105 N90-22039

Wind instability as a possible cause of the spiral structure formation in the gaseous subsystem of galaxies with the circular magnetic field
[DE90-618944] 15 p2190 N90-22507

Atmospheric autorotating imaging device
[NASA-CASE-NPO-17390-1-CU] 16 p2238 N90-22769

Direction of movement effects under transformed visual/motor mappings 16 p2272 N90-22947

Multi-flexible-body dynamics capturing motion-induced stiffness 16 p2284 N90-23013

Counterrotating cores in elliptical galaxies
16 p2332 N90-23288

Conceptual design of a Moving Belt Radiator (MBR) shuttle-attached experiment
[NASA-CR-185169] 17 p2367 N90-23474

The impacts of Ginga results on QPO models
19 p2770 N90-25744

An unsteady lifting surface method for single rotation propellers
[NASA-CR-4302] 20 p2802 N90-25940

Rotating-unbalanced-mass devices and methods for scanning balloon-borne-experiments, free-flying spacecraft, and space shuttle/space station attached experiments
[NASA-CASE-MFS-28425-1] 20 p2866 N90-26304

Experimental investigation of the hydrodynamic forces on the shroud of a centrifugal pump impeller
[NASA-CR-186952] 21 p3009 N90-27108

Rotationally actuated prosthetic helping hand
[NASA-CASE-MFS-28426-1] 21 p3036 N90-27261

Magnetic forces in high-T(sub c) superconducting bearings 22 p3137 N90-27799

Faraday rotation mapping of mercury cadmium telluride
[AD-A224278] 23 p3311 N90-28729

A nonlinear finite element formulation for the large displacement analysis of plates
23 p3338 N90-28867

Situational awareness and vestibular stimulation: The influence of whole-body rotation upon task performance
[IZF-1989-14] 23 p3361 N90-28994

Robot Acting on Moving Bodies (RAMBO): Interaction with tumbling objects 23 p3366 N90-29022

ROTATIONAL FLOW
U FLUID FLOW
U VORTICES
ROTATIONAL SPECTRA
High resolution spectroscopy in the microwave and far infrared 20 p2943 N90-26746
Microwave spectra of van der Waals complexes of importance in planetary atmospheres 20 p2944 N90-26752
ROTONS
Quasi-diffusion between phonon and roton gases in two- and three-dimensional liquid helium
[AD-A210565] 02 p0192 N90-11096
Particle detection via rotons in helium-4 superfluid
[DE90-005417] 10 p1448 N90-18354
Coherent state in the roton region of superfluid helium-4
[DE90-610677] 12 p1720 N90-19882
Wigner symbols, quantum dynamics, and the kicked rotator
[AD-A224024] 23 p3403 N90-29234
ROTOR AERODYNAMICS
An investigation of counterrotating tip vortex interaction
[NASA-CR-185135] 02 p0271 N90-11549
Prediction of unsteady blade surface pressures on an advanced propeller at an angle of attack
[NASA-TM-102374] 04 p0447 N90-12560
Integrated multidisciplinary optimization of rotorcraft: A plan for development
[NASA-TM-101617] 04 p0450 N90-12580
General approach and scope — rotor blade design optimization 04 p0451 N90-12581
Rotor blade aerodynamic design 04 p0451 N90-12582
Influence of vane sweep on rotor-stator interaction noise 05 p0571 N90-13325
Computation of flow fields around propellers and hovering rotors based on the solution of the Euler equations
[DLR-FB-89-37] 05 p0572 N90-13333
Finite difference techniques and rotor blade aeroelastic partial differential equations with quasisteady aerodynamics 07 p0875 N90-15075
Measurement and prediction of propeller blade surface pressure distributions 14 p1912 N90-20961
The Shock and Vibration Digest, volume 21, no. 2 15 p2109 N90-22059
Forcing function effects on rotor row unsteady aerodynamic response in a multistage compressor 16 p2196 N90-22536
Experimental performance and acoustic investigation of modern, counterrotating blade concepts
[NASA-CR-185158] 17 p2352 N90-23393
Aerodynamic performance of a 0.27-scale model of an AH-64 helicopter with baseline and alternate rotor blade sets
[NASA-TM-4201] 18 p2491 N90-24237
The acoustic results of a United Technologies scale model helicopter rotor tested at DNW
[NASA-TM-101879] 21 p3073 N90-27471
Analysis of heliport environmental data, Intracoastal City
[DOT/FAA/CT-TN89/43] 23 p3284 N90-28584
ROTOR BLADES
Application of a two-dimensional unsteady viscous analysis code to a supersonic throughflow fan stage
[NASA-TM-4141] 05 p0581 N90-13387
Effect of blade planform variation on a small-scale hovering rotor
[NASA-TM-4146] 06 p0717 N90-14186
Analysis of the rotor tip leakage flow with tip cooling air ejection 14 p1926 N90-21029
Towards a unified analysis methodology for composite rotor blades 15 p2046 N90-21730
Extension-torsion coupling behavior of advanced composite tilt-rotor blades 18 p2644 N90-25057
Synthesis of individual rotor blade control system for gust alleviation
[NASA-TM-101886] 20 p2807 N90-25972
ROTOR BLADES (TURBOMACHINERY)
Laser anemometer measurements in a transonic axial-flow fan rotor
[NASA-TP-2879] 02 p0218 N90-11245
An improved beam model for the vibrations of rotor blades 02 p0232 N90-11333
Review and analysis of the DNW/Model 360 rotor acoustic data base
[NASA-TM-102253] 03 p0299 N90-11692
An investigation of end-wall vortex cavitation in a high Reynolds number axial-flow pump
[AD-A211426] 03 p0347 N90-11982
WISPER: A standardized fatigue load sequence for HAWT-blades
[NLR-MP-88029-U] 03 p0359 N90-12055
Airframe structural dynamic considerations in rotor design optimization
[NASA-TM-101646] 03 p0360 N90-12057
Numerical simulation of unsteady rotational flow over propfan configurations
[NASA-CR-186037] 04 p0438 N90-12500
Dynamic tip clearance measurements in axial flow compressors
[PNR90597] 04 p0456 N90-12612
Blading design for multi-storage HP compressor
[PNR90602] 04 p0456 N90-12616
An analysis of the viscous flow through a compact radial turbine by the average passage approach
[NASA-TM-102471] 06 p0720 N90-14206
A study of the effects of Rotating Frame Turbulence (RFT) on helicopter flight mechanics 07 p0872 N90-15058
Wake interaction effects on the transition process on turbine blades
[AD-A214492] 09 p1168 N90-16759
Study of the blade/vortice interaction on a one-blade rotor during forward flight (incompressible, non viscous fluid)
[ISL-R-115/88] 11 p1456 N90-18391
Design guidance to minimize unsteady forces in turbomachines 11 p1460 N90-18411
Unsteady blade loads due to wake influence 11 p1460 N90-18413
Gust response analysis for cascades operating in nonuniform mean flows 11 p1461 N90-18415
Blade row interaction effects on compressor measurements 11 p1462 N90-18419
Modelling unsteady transition and its effects on profile loss 11 p1462 N90-18423
Experimental investigation of the influence of rotor wakes on the development of the profile boundary layer and the performance of an annular compressor cascade 11 p1463 N90-18425
Digital determination of the three dimensional flow in turbomachines with the S1-S2 current function process
[ITSM-MITT-30] 12 p1605 N90-19236
An inverse method for the design of turbomachine blades 14 p1918 N90-20988
Experimental and numerical study on basic phenomena of secondary flows in turbines 14 p1923 N90-21014
Measurement of the flow field in the blade passage and side-wall region of a plane turbine cascade 14 p1924 N90-21019
Effects of secondary flow on heat transfer in rotating passages 14 p1926 N90-21031
Forcing function effects on rotor row unsteady aerodynamic response in a multistage compressor 16 p2196 N90-22536
Fluid dynamic and acoustic experiments on turbomachine rotors subject to variable flow conditions
[AD-A220298] 18 p2552 N90-24565
Theoretical studies carried out in 1988 on helicopter rotor noise under subsonic conditions
[ONERA-RS-82/5094-PY] 22 p3245 N90-28402
Measurement of the steady surface pressure distribution on a single rotation large scale advanced prop-fan blade at Mach numbers from 0.03 to 0.78
[NASA-CR-182124] 23 p3278 N90-28552
Flow coupling between a rotor and a stator in turbomachinery
[AD-A223882] 23 p3282 N90-28572
Analysis of heliport environmental data, Intracoastal City
[DOT/FAA/CT-TN89/43] 23 p3284 N90-28584
Turbomachinery rotor forces
[NASA-CR-183779] 23 p3334 N90-28852
Nonlinear static and dynamic modeling of composite rotor blades including warping effects 24 p3431 N90-29382
Investigation of fluid dynamic performance of LE-7 liquid oxygen pump
[NAL-TR-1020] 24 p3476 N90-29650
ROTOR DISKS
U TURBINE WHEELS
ROTOR DYNAMICS
Integrated multidisciplinary optimization of rotorcraft: A plan for development
[NASA-TM-101617] 04 p0450 N90-12580
General approach and scope — rotor blade design optimization 04 p0451 N90-12581
Rotor blade aerodynamic design 04 p0451 N90-12582
Rotor blade dynamic design 04 p0451 N90-12583
Application of the joined wing to tiltrotor aircraft
[NASA-CR-177543] 07 p0879 N90-15093
A method for the early detection of instabilities in rotordynamics
[NASA-CR-186307] 09 p1170 N90-16769
Gear noise, vibration, and diagnostic studies at NASA Lewis Research Center
[NASA-TM-102435] 10 p1390 N90-18041
A study of the effects of disk flexibility on the rotordynamics of the space shuttle main engine turbo-pumps 12 p1636 N90-19401
Rotordynamic analysis with shell elements for the transfer matrix method
[AD-A217455] 13 p1817 N90-20434
Design of a helicopter automatic flight control system using adaptive control 14 p1928 N90-21040
Internal rotor friction instability
[NASA-CR-183942] 14 p1988 N90-21395
Quiet mode for nonlinear rotor models
[NASA-TM-102236] 15 p2051 N90-21758
Probabilistic analysis of bladed turbine disks and the effect of mistuning
[NASA-TM-102564] 15 p2072 N90-21871
Experimental investigation of the effect of cavitation on the rotordynamic forces on a whirling centrifugal pump impeller 15 p2105 N90-22039
Elements of active vibration control for rotating machinery
[NASA-TM-102368] 16 p2227 N90-22703
Experimental performance and acoustic investigation of modern, counterrotating blade concepts
[NASA-CR-185158] 17 p2352 N90-23393
The applicability of simple helicopter models for flight mechanics studies
[ETN-90-96962] 20 p2808 N90-25975
Experimental investigation of the hydrodynamic forces on the shroud of a centrifugal pump impeller
[NASA-CR-186952] 21 p3009 N90-27108
Turbomachinery rotor forces
[NASA-CR-183779] 23 p3334 N90-28852
Correlation of AH-1G airframe flight vibration data with a coupled rotor-fuselage analysis
[NASA-CR-181974] 23 p3338 N90-28865
Rotordynamic properties of high pressure seals: An experimental approach 24 p3475 N90-29640
ROTOR HUBS
U HUBS
U ROTORS
ROTOR SPEED
Experimental evaluation of a tuned electromagnetic damper for vibration control of cryogenic turbopump rotors
[NASA-TP-3005] 17 p2354 N90-23403
ROTORCRAFT
U ROTARY WING AIRCRAFT
ROTORCRAFT AIRCRAFT
Integrated multidisciplinary design optimization of rotorcraft
[NASA-TM-101642] 02 p0155 N90-10889
Aerodynamic characteristics of two rotorcraft airfoils designed for application to the inboard region of a main rotor blade
[NASA-TP-3009] 18 p2491 N90-24239
ROTORDYNAMICS
U ROTOR DYNAMICS
ROTORS
NT COMPRESSOR ROTORS
NT FLYWHEELS
NT HELICOPTER TAIL ROTORS
NT IMPELLERS
NT LIFTING ROTORS
NT PUMP IMPELLERS
NT RIGID ROTORS
NT ROTARY WINGS
NT TILTING ROTORS
NT TURBINE WHEELS
Improved silicon carbide for advanced heat engines
[NASA-CR-180831] 01 p0051 N90-10293
An experimental investigation of helicopter rotor hub fairing drag characteristics
[NASA-TM-102182] 03 p0300 N90-11701
User's guide for a personal computer model of turbulence at a wind turbine rotor
[DE89-017753] 03 p0366 N90-12095
Large-scale Advanced Prop-fan (LAP) static rotor test report
[NASA-CR-180848] 04 p0457 N90-12617
Vibration transmission through rolling element bearings in geared rotor system, part 1
[NASA-CR-186093] 04 p0509 N90-12936
Influence of vane sweep on rotor-stator interaction noise 05 p0571 N90-13325
The application of cast SiC/Al to rotary engine components
[NASA-CR-179610] 05 p0581 N90-13385
Elasticity effects on cavitation in a squeeze film damper undergoing noncentered circular whirl
[NASA-TM-102392] 05 p0649 N90-13786
Effect of blade planform variation on a small-scale hovering rotor
[NASA-TM-4146] 06 p0717 N90-14186
Transient response of flexible rotor-bearing systems subjected to combined unbalance and ground excitations 06 p0792 N90-14616

Prediction of stochastic blade loads for three-bladed, rigid-hub rotors
[DE89-009508] 07 p0954 N90-15520
Dynamic analysis of geared rotors by finite elements
[NASA-TM-102349] 08 p1086 N90-16286
Wake interaction effects on the transition process on turbine blades
[AD-A214492] 09 p1168 N90-16759
Three-dimensional viscous rotor flow calculations using a viscous-inviscid interaction approach
[NASA-TM-102235] 12 p1599 N90-19204
Calculation and optimization of rotor start process
[ETN-90-95894] 12 p1604 N90-19229
A study of the effects of disk flexibility on the rotordynamics of the space shuttle main engine turbo-pumps 12 p1636 N90-19401
Theoretical and experimental studies of a brushless disk rotor motor with permanent magnetic excitation and gap windings
[ETN-90-96056] 12 p1655 N90-19512
Analysis of small-scale rotor hover performance data
[NASA-TM-102271] 13 p1799 N90-20325
A comparison of two-and three-dimensional S809 airfoil properties for rough and smooth HAWT (Horizontal-Axis Wind Tunnel) rotor operation
[DE89-009512] 13 p1827 N90-20492
Noise of a simulated installed model counterrotation propeller at angle-of-attack and takeoff/approach conditions
[NASA-TM-102440] 13 p1881 N90-20794
Statistics on aircraft gas turbine engine rotor failures that occurred in US commercial aviation during 1986
[DOT/FAA/CT-89/30] 14 p1922 N90-21008
Internal rotor friction instability
[NASA-CR-183942] 14 p1988 N90-21395
The Shock and Vibration Digest, volume 21, no. 2 15 p2109 N90-22059
The Shock and Vibration Digest, volume 21, no. 3 15 p2109 N90-22064
Rotor-to-stationary element rub-related vibration phenomena in rotating machinery: Literature survey 15 p2109 N90-22065
Aerodynamics of a full-scale, non rotating wind turbine blade under natural wind conditions
[RISOE-M-2768] 15 p2123 N90-22144
Rotor loading on a three-bladed wind turbine 15 p2123 N90-22145
Application of a dynamic stall model to rotor trim and aeroelastic response 16 p2200 N90-22556
Computational and experimental investigations of rotating stall in compressor cascades 16 p2201 N90-22565
Experimental evaluation of a tuned electromagnetic damper for vibration control of cryogenic turbopump rotors
[NASA-TP-3005] 17 p2354 N90-23403
The effects of Reynolds number, rotor incidence angle, and surface roughness on the heat transfer distribution in a large-scale turbine rotor passage
[NASA-CR-183891] 17 p2410 N90-23731
Rotary-Jet thrust augmentor with jet-flapped blades 18 p2492 N90-24243
Coupled rotor-body equations of motion hover flight
[NASA-CR-186710] 19 p2655 N90-25111
An unsteady lifting surface method for single rotation propellers
[NASA-CR-4302] 20 p2802 N90-25940
Two-dimensional Euler and Navier-Stokes Time accurate simulations of fan rotor flows
[NASA-TM-102402] 20 p2803 N90-25948
Development of creep-fatigue damage detection method of rotor steel by ultrasonic wave measurement
[DE90-503792] 20 p2877 N90-26365
Velocity measurements on a lifting rotor/airframe configuration in low speed forward flight 21 p2953 N90-26790
Experimental investigation of the hydrodynamic forces on the shroud of a centrifugal pump impeller
[NASA-CR-186952] 21 p3009 N90-27108
Dynamics of multistage gear transmission with effects of gearbox vibrations
[NASA-TM-103109] 22 p3182 N90-28060
Flow coupling between a rotor and a stator in turbomachinery
[AD-A223882] 23 p3282 N90-28572
An enhanced integrated aerodynamic load/dynamic optimization procedure for helicopter rotor blades
[NASA-CR-4326] 24 p3432 N90-29383
Noncontact measurement of rotating blade vibrations
[NAL-TR-1033] 24 p3483 N90-29687

ROUGHNESS
NT SEA ROUGHNESS
NT SURFACE ROUGHNESS
Investigation of rough elastohydrodynamic contact
[ISAL-89-0029] 08 p1085 N90-16281
Flatness and roughness metrological tests on the WRA flight unit receiver box and ACPB canister of the RETE experiment
[IFSI-88-20] 10 p1368 N90-17928
The joint effect of surface microtopography and near-surface structure on microcontact conditions
[DE90-006494] 11 p1493 N90-18591

ROUTES
Route data representation for ATC simulation experiments
[RSRE-MEMO-4133] 04 p0450 N90-12576
A 2d-1 lower bound 2-layer knock-knee channel routing
[AD-A211948] 04 p0495 N90-12847
Spatial data structures for robotic vehicle route planning
[AD-A212806] 04 p0538 N90-13111
A structural factoring approach for analyzing probabilistic networks 07 p0986 N90-15697
Position fixing by detection of roads and rivers 09 p1163 N90-16733
Three-dimensional route planning for a cruise missile for minimal detection by observer
[AD-A218336] 13 p1880 N90-20787
Simulator evaluation of the final approach spacing tool
[NASA-TM-102807] 17 p2348 N90-23374
Detecting black holes in packet-radio networks (SRNTN-56)
[AD-A219636] 17 p2389 N90-23604
IFR aircraft handled forecast by air route traffic control center: Fiscal years 1990 to 2005
[AD-A220312] 18 p2496 N90-24263
FAA/NASA En Route Noise Symposium
[NASA-CP-3067] 18 p2608 N90-24853
Proposed definition of the term en route in en route aircraft noise 18 p2608 N90-24854
PTA en route noise measurements 18 p2608 N90-24855
En route noise: NASA propfan test aircraft (corrected data - simplified procedure)
[DOT-TSC-FA953-LR4] 18 p2608 N90-24856
En route noise: NASA propfan test aircraft (calculated source noise
[DOT-TSC-FA953-LR5] 18 p2609 N90-24857
En route noise of turboprop aircraft and their acceptability: Report of tests 18 p2609 N90-24858
En route noise of two turboprop aircraft
[DLR-MITT-89-18] 18 p2609 N90-24859
Sound propagation elements in evaluation of en route noise of advanced turbofan aircraft 18 p2609 N90-24861
When propfans cruise, will LDN 65 fly 18 p2610 N90-24864
Agenda toward the development of a rational noise descriptor system relevant to human annoyance by en route aircraft noise 18 p2610 N90-24866
Social survey findings on en route noise annoyance issues 18 p2610 N90-24868
Predicting the audibility and annoyance of unducted fan engines 18 p2610 N90-24869
En route noise annoyance laboratory test: Preliminary results 18 p2611 N90-24870
Problems related to aircraft noise in Switzerland 18 p2611 N90-24871
Mobile transporter path planning 19 p2727 N90-25505
A comparison of two neural network schemes for navigation 19 p2733 N90-25536
Adaptive fault-tolerant routing in hypercube multicomputers
[NASA-CR-186781] 20 p2903 N90-26513
Finding minimum width for single-layer channel routing in linear time
[AD-A221876] 21 p3002 N90-27062

ROVING VEHICLES
NT LUNAR ROVING VEHICLES
Laser-powered Martian rover 01 p0029 N90-10157
A computer simulation study of a sensor-based heuristic navigation for three-dimensional rough terrain with obstacles
[AD-A215115] 10 p1318 N90-17622
United States planetary rover status: 1989
[NASA-CR-186843] 19 p2698 N90-25353
A task control architecture for autonomous robots 19 p2735 N90-25546
Planning for execution monitoring on a planetary rover 19 p2735 N90-25548
Evaluation of off-road terrain with static stereo and monoscopic displays 19 p2740 N90-25575
University of Maryland walking robot: A design project for undergraduate students
[NASA-CR-186839] 20 p2870 N90-26331
Autoplan: A self-processing network model for an extended blocks world planning environment
[NASA-CR-186733] 20 p2905 N90-26526
Nuclear power systems for lunar and Mars exploration
[NASA-TM-103168] 21 p2969 N90-26873
A system architecture for a planetary rover 23 p3365 N90-29015
Planetary rover technology development requirements 23 p3375 N90-29067
Satellite-map position estimation for the Mars rover 23 p3375 N90-29069
A survey of planning and scheduling research at the NASA Ames Research Center 23 p3376 N90-29076

RP-1 ROCKET PROPELLANTS
Liquid rocket booster study. Volume 2, book 1
[NASA-CR-183600] 01 p0026 N90-10133
Modification of the SHABERTH bearing code to incorporate RP-1 and a discussion of the traction model
[NASA-TP-3017] 22 p3183 N90-28066
Heavy hydrocarbon main injector technology 23 p3294 N90-28633

RPV
U REMOTELY PILOTED VEHICLES

RUBBER
NT CHLOROPRENE RESINS
NT ELASTOMERS
NT LATEX
NT SYNTHETIC RUBBERS
NT VITON RUBBER (TRADEMARK)
NT VULCANIZED ELASTOMERS
Evaluation of a neoprene latex modified SAMI (Stress Absorbing Membrane Interlayer)
[PB89-226435] 05 p0628 N90-13665
A novel heat resistant blend produced by compositional quenching: A thermoplastic polyimide impact modified with a fluoroelastomer
[AD-A213724] 07 p0912 N90-15273
Blow-out of rubber blocks due to internal heating
[AD-A215730] 09 p1198 N90-16943
Internal failures in model elastomeric composites
[AD-A215923] 10 p1348 N90-17818
Thermal crystallization of polytetrahydrofuran networks
[AD-A215336] 10 p1436 N90-18285
Runaway rubber removal
[AD-A218349] 13 p1759 N90-20100
Rubberlike elasticity experiment 18 p2515 N90-24362
Quantitative confirmation of diffusion-limited oxidation theories
[DE90-012997] 20 p2838 N90-26143
Model studies of the effect of surface roughness and mechanical interlocking on adhesion
[AD-A222402] 21 p2987 N90-26977
Toughening of SAN copolymers by an SAN emulsion grafted rubber
[AD-A224213] 24 p3453 N90-29502
Rheology of filler rubber: Silica-silicone
[AD-A223600] 24 p3455 N90-29511

RUBIDIUM
Elastic scattering of e- and e+ from Rb and Cd 11 p1556 N90-18960
Positron-rubidium scattering 11 p1556 N90-18964

RUBY
Spin-lattice relaxation and the calculation of gain, pump power, and noise temperature in ruby 04 p0486 N90-12790

RUBY LASERS
Laser probing non-cylindrical Z-pinch in near-isolator region of a discharged chamber
[DE89-632018] 06 p0844 N90-14912

RUDDERS
NT AERIAL RUDDERS
Independent Orbiter Assessment (IOA): Analysis of the rudder/speed brake subsystem
[NASA-CR-185560] 02 p0161 N90-10916
Hinge moment coefficient derivatives for trailing-edge controls on wings at subsonic speeds
[ESDU-89009] 06 p0726 N90-14239
Prediction of forces and moments for flight vehicle control effectors. Part 1: Validation of methods for predicting hypersonic vehicle controls forces and moments
[NASA-CR-186571] 15 p2047 N90-21734

RULES
NT FLIGHT RULES
NT INSTRUMENT FLIGHT RULES
NT PHASE RULE
NT SUM RULES

RUN TIME (COMPUTERS)
Efficiency and capabilities of multi-body simulations 01 p0019 N90-10095
Performance evaluation of the Scheme86 and HP precision architectures
[AD-A209418] 01 p0102 N90-10578
A multiprocessor architecture using modular arithmetic for very high precision computation
[AD-A208154] 01 p0102 N90-10579

Ada (trademark) projects at NASA. Runtime environment issues and recommendations
[NASA-CR-183435] 01 p0103 N90-10583
Solving 3D block bidiagonal linear systems on vector computers
[CWI-NM-R8819] 04 p0530 N90-13061
The cellular approach: A new method to speed up simulated annealing for macro placement
[MEMO-COSOR-88-29] 05 p0683 N90-13980
An efficient UNICOS run-time system for functional programs on a CRAY X-MP
[DE89-016603] 07 p0972 N90-15610
Systolic algorithms for imaging from space
[AD-A213870] 07 p0987 N90-15701
CPU timing routines for a CONVEX C220 computer system
[NASA-CR-181950] 08 p1110 N90-16424
Two adaptive techniques let progressive refinement outperform the traditional radiosity algorithm
[AD-A215174] 09 p1267 N90-17347
Database creation and/or reorganization over multiple database backends
[AD-A214939] 09 p1296 N90-17513
Finding minimum-cost flows by double scaling
[AD-A214498] 10 p1416 N90-18159
Distributed simulation, no special tools required
15 p2150 N90-22281
Performance of gigabit FDDI
15 p2150 N90-22283
Distributed simulation of network protocols
15 p2150 N90-22284
Extensibility and limitations of FDDI
15 p2151 N90-22286
The preprocessed doacross loop
[NASA-CR-182056] 16 p2276 N90-22972
Faster simulation plots 16 p2295 N90-23071
The Durra application debugger/monitor
[AD-A219290] 16 p2301 N90-23111
Hartstone: Synthetic benchmark requirements for hard real-time applications
[AD-A219326] 17 p2442 N90-23917
A fast, preconditioned conjugate gradient Toeplitz solver
[NASA-CR-180367] 18 p2589 N90-24731
Sensitivity analysis of transputer workfarm topologies
[AD-A219821] 18 p2595 N90-24766
Execution time supports for adaptive scientific algorithms on distributed memory machines
[NASA-CR-182052] 19 p2741 N90-25578
Multi-version software reliability through fault-avoidance and fault-tolerance
[NASA-CR-186502] 19 p2742 N90-25584
A parallel Newton-Euler formulation for fast dynamic simulation of robot manipulators
[RR-368] 19 p2748 N90-25614
Run-time parallelization and scheduling of loops
[NASA-CR-182039] 20 p2902 N90-26509
Combining zero Doppler filter calculations with MTI filter calculations to increase computational speed
[AD-A222468] 21 p2997 N90-27034
ROSES, a Robot Operating System Expert Scheduler: Methodological framework
[DE90-014782] 23 p3334 N90-28851

RUNGE-KUTTA METHOD
Variable step iteration of high-order Runge-Kutta methods on parallel computers
[CWI-NM-R8817] 02 p0260 N90-11476
Note on explicit parallel multistep Runge-Kutta methods
[CWI-NM-R8814] 02 p0268 N90-11529
On the equivalence of BS-stability and B-consistency
[CWI-NM-R8815] 02 p0268 N90-11530
An algebraic characterization of B-convergent Runge-Kutta methods
[CWI-NM-R8901] 04 p0541 N90-13133
Increasing the real stability boundary of explicit methods
[CWI-NM-R8902] 04 p0541 N90-13134
Inviscid 2D solutions on unstructured, adaptive grids
05 p0640 N90-13737
A one equation turbulence model for transonic airfoils
06 p0719 N90-14199
Conical Euler solution for a highly-swept delta wing undergoing wing-rock motion
[NASA-TM-102609] 12 p1600 N90-19211
A video-based experimental investigation of wing rock
[AD-A218244] 13 p1755 N90-20075
On spurious steady-state solutions of explicit Runge-Kutta schemes
[NASA-TM-102819] 15 p2160 N90-22340
The theta-methods in the numerical solution of delay differential equations
[TW-89-03] 15 p2161 N90-22349
Stability criteria in the numerical solution of initial value problems
[TW-89-05] 15 p2162 N90-22351
Contractivity in the maximum norm for Runge-Kutta methods
[TW-89-06] 15 p2162 N90-22352
Stability analysis of numerical methods for delay differential equations
[TW-89-09] 15 p2162 N90-22353
A computer code for the prediction of aerodynamic characteristics of lifting airfoils at transonic speed
[DLC-EST-TN-030] 17 p2346 N90-23359
Block Runge-Kutta methods on parallel computers
[CWI-NM-R8906] 17 p2452 N90-23982
Block Runge-Kutta methods
[CWI-NM-R8913] 17 p2452 N90-23983
Convergence properties of the Runge-Kutta-Chebyshev method
[CWI-NM-R8907] 17 p2459 N90-24038
Contractivity of Runge-Kutta methods
[TW-89-12] 17 p2464 N90-24079
Embedded diagonally implicit Runge-Kutta algorithms on parallel computers
[CWI-NM-R8912] 18 p2595 N90-24765
Two-dimensional Euler and Navier-Stokes Time accurate simulations of fan rotor flows
[NASA-TM-102402] 20 p2803 N90-25948
Numerical experiments on the accuracy of ENO and modified ENO schemes
[NASA-CR-182083] 23 p3387 N90-29128

RUNOFFS
U DRAINAGE

RUNWAY CONDITIONS
Evaluation of two transport aircraft and several ground test vehicle friction measurements obtained for various runway surface types and conditions. A summary of test results from joint FAA/NASA Runway Friction Program
[NASA-TP-2917] 08 p1021 N90-15902

RUNWAY LIGHTS
Helicopter Visual Segment Approach Lighting System (HALS)
[ACD-330] 02 p0150 N90-10856
Modified touchdown zone lighting
[DOT/FAA/CT-TN89/70] 14 p1929 N90-21042

RUNWAYS
Definition of research needs to address airport pavement distress in cold regions
[DOT/FAA/DS-89/13] 02 p0157 N90-10896
Improving snow roads and airstrips in Antarctica
[AD-A211588] 03 p0335 N90-11907
Ice runways near the South Pole
[AD-A211606] 03 p0335 N90-11908
Analytical and experimental study of runway runoff with wind effects
[PTI-8948] 04 p0458 N90-12627
Design temperatures for flexible airfield pavement design
[AD-A214141] 07 p0884 N90-15115
Crew emergency return vehicle autoland feasibility study
[NASA-CR-181940] 08 p1028 N90-15937
Dallas/Fort Worth simulation. Volume 2: Appendixes D, E, and F
[AD-A216613] 11 p1454 N90-18380
Airfields on antarctic glacier ice
[AD-A217638] 13 p1759 N90-20097
Runaway rubber removal
[AD-A218349] 13 p1759 N90-20100
Modified touchdown zone lighting
[DOT/FAA/CT-TN89/70] 14 p1929 N90-21042
Criteria for coal tar seal coats on airport pavements. Volume 2: Laboratory and field studies
[AD-A220167] 18 p2498 N90-24277
Taxiway sign effectiveness under reduced visibility conditions
[DOT/FAA/CT-TN90/20] 19 p2662 N90-25150
An overview of the joint FAA/NASA aircraft/ground runway friction program
[NASA-TM-103486] 20 p2805 N90-25957
Atlanta tower simulation, volume 1
[DOT/FAA/CT-TN89/27-VOL-1]
21 p2961 N90-26835
Atlanta tower simulation. Volume 2: Appendixes
[DOT/FAA/CT-TN89/27-VOL-2]
21 p2961 N90-26836
Development and testing of rapid repair methods for war damaged runways
[AD-A223970] 23 p3285 N90-28586
The potential for an extra runway at Heathrow: A preliminary feasibility study
[TT-9007] 24 p3435 N90-29403
Estimation of power spectral density of runway roughness
[NAL-TR-1037] 24 p3437 N90-29411
AutoPAVER: A software package for automated pavement evaluation
[AD-A224176] 24 p3458 N90-29531

RUPTURING
Fully articulated four-point-bend loading fixture
[NASA-CASE-LEW-14776-1] 07 p0940 N90-15445
Recent implementations on ceramic composites and thermostructural materials
[REPT-892-430-106] 17 p2370 N90-23489
State of the art and future prospects for high temperature composites
[REPT-892-430-125] 18 p2517 N90-24375
Fatigue testing apparatus
[AD-D014544] 22 p3192 N90-28108
Influence of diesel engine exposure on the rupture strength of silicon nitride and partially stabilized zirconia
[DE90-014759] 23 p3334 N90-28849

RURAL AREAS
Development and use of a passive technique for measuring nitrogen dioxide in the background atmosphere 16 p2331 N90-23285

RUTHENIUM
Electrochemical parameterization of metal complex redox potentials, using the ruthenium(III)/ruthenium(II) couple to generate a ligand electrochemical series
[AD-A214439] 08 p1041 N90-16015
Spectroscopic evidence for carbon-carbon bonding in carbide layers on metals
[AD-A216726] 11 p1479 N90-18512
Mechanistic studies of the CO-oxidation reaction on catalysts for use in long-life CO2 lasers
18 p2558 N90-24596
A viologen/ruthenium oxide-based microelectrochemical diode with pH-dependent current-voltage characteristics
[AD-A221961] 21 p3000 N90-27052
Structure of metal overlayers by low energy alkali ion scattering: Cu/Ru(0001) and Sn/Pt(111)
[DE90-014453] 23 p3310 N90-28718

RUTHENIUM COMPOUNDS
Advanced double layer capacitor
[AD-A211977] 04 p0469 N90-12688
Catalysts for ultrahigh current density oxygen cathodes for space fuel cell applications
[NASA-CR-180650] 16 p2251 N90-22835

RUTILE
Deformation and microstructure of rutile
[DE90-614113] 14 p2032 N90-21654
Epitaxy of TiO2 thin film on sapphire by MOCVDVD
[DE90-010054] 18 p2618 N90-24915
Ilmenite exsolution schemes in Apollo-17 high-Ti basalts
[DE90-011992] 21 p2976 N90-26912

RYDBERG SERIES
Determination of hyperfine structures and Rydberg convergence limits of selected optical transitions in Nb-93 using resonance ionization spectroscopy
[PB90-110719] 08 p1122 N90-16498

S

S BAND
U SUPERHIGH FREQUENCIES
U ULTRAHIGH FREQUENCIES

S GLASS
Erosion mechanisms in composite materials and ripple formation mechanism in erosion
[IAR-89-4-PT-1] 20 p2826 N90-26078
Damage tolerance of woven graphite-epoxy buffer strip panels
[NASA-TM-102702] 22 p3192 N90-28114

S MATRIX THEORY
On the construction of the scattering matrix for locally-noncommutative interactions of relativistic fields
[DE89-630138] 02 p0287 N90-11640
A well conditioned formulation for the analysis of multi-layered frequency selective surfaces using a cascaded matrix approach, revised
[RSRE-MEMO-4289-REV] 04 p0496 N90-12858
Narrow one-channel resonances and their manifestation in the pure elastic scattering of unpolarized particles
[DE89-632177] 06 p0839 N90-14876
A new technique for simulating composite material. Task 2: Analytical solutions with Generalized Impedance Boundary Conditions (GIBCs)
[NASA-CR-186249] 07 p0890 N90-15146
Recognition and analysis of aircraft targets by radar, using structural pattern representations derived from polarimetric signatures 15 p2074 N90-21879
Radar scatterometry and polarimetry at 220 GHz
15 p2085 N90-21935
Predissimilarities, prefilters, and ultrametrics on an arbitrary set
[IMAG-RR-970-M] 20 p2918 N90-26603
Theory of planar near-field measurement
[FEL-89-B273] 22 p3244 N90-28395

S WAVES
NT SH WAVES

Destabilization of supersonic free shear layers by parametric excitation using Mach waves generated by a wavy wall
[AD-A219655] 17 p2345 N90-23352
Improved transverse crack detection in composites
[NASA-TM-103261] 22 p3153 N90-27875

S-A-W DEVICES
U SURFACE ACOUSTIC WAVE DEVICES

S-27 SATELLITE
U ALOUETTE 1 SATELLITE

S-66 SATELLITE
U BEACON EXPLORER A

SABOT PROJECTILES
Finite element models to predict the structural response of 120-mm sabot/rods during launch
[DE90-007497] 13 p1817 N90-20436
A new stress routine for the Projectile Design Analysis System (PRODAS)
[AD-A220564] 17 p2346 N90-23357

SABRE AIRCRAFT
U F-86 AIRCRAFT

SACCADIC EYE MOVEMENTS
Separate visual representations for perception and for visually guided behavior 16 p2269 N90-22931
DURIP-Instrumentation for recording and analyzing multiple input/output saccadic eye movement neurosensory control
[AD-A219905] 17 p2435 N90-23871

SACCHARIDES
U CARBOHYDRATES

SADDLE POINTS
A study of the asymptotic behavior of linear difference equations with polynomial coefficients
[IMAG-RR-743-M] 03 p0395 N90-12254
Energy barriers in SK spin-glass model
[PREPRINT-665] 05 p0704 N90-14119
Asymptotic expansions of an integral containing a phase function with three saddle points
[CWI-AM-R8922] 18 p2599 N90-24793

SADDLES
Quadratic systems with three saddles and one antisaddle
[REPT-89-80] 17 p2458 N90-24033

SAFETY
NT AEROSPACE SAFETY
NT AIRCRAFT SAFETY
NT FLIGHT SAFETY
NT INDUSTRIAL SAFETY
NT REACTOR SAFETY
A severe human ESD (Electrostatic Discharge) model for safety and high reliability system qualification testing
[DE89-016177] 02 p0216 N90-11233
User's manual for the ride motion simulator
[AD-A212855] 05 p0584 N90-13402
Aircraft/airport compatibility: Some strategic, tactical, and operational issues
[TT-8902] 05 p0585 N90-13409
Battery technology assessment and R and D plan
[DE90-002007] 06 p0772 N90-14489
Biological effects of hyperthermia and potential risk associated with ultrasonic exposure
[PB89-100702] 06 p0820 N90-14768
Evaluation of the improved OV-ID anti-icing system, phase 2
[AD-A213928] 07 p0877 N90-15083
X.2 limited flight test plan
[AD-A214412] 07 p0880 N90-15099
Safety evaluation report for Galileo: Volume 1
[DE90-003086] 07 p0886 N90-15122
Safety evaluation report for Galileo, volume 2
[DE90-003087] 07 p0886 N90-15123
Aircraft accident report: Delta Air Lines, Inc., Boeing 727-232, N473DA, Dallas-Fort Worth International Airport, Texas, August 31, 1988
[PB89-910406] 08 p1019 N90-15895
Cryogenic engineering and materials 08 p1030 N90-15949
Safety and cryogenic wind tunnels 08 p1032 N90-15960
Energy management and recovery 08 p1032 N90-15962
Environmental, health, and safety concerns associated with nonpetroleum fuel use in US transportation
[DE90-004367] 08 p1099 N90-16362
Analysis of hydraulic fluids and lubricating oils for the formation of Trimethylolpropane Phosphate (TMP-P)
[AD-A215188] 09 p1198 N90-16939
Guidelines for safe human exposure to impact acceleration, update A
[AD-A215287] 09 p1253 N90-17268
Investigation and characteristics of major fire-related accidents in civil air transports over the past ten years 10 p1311 N90-17582
A review of UK civil aviation fire and cabin safety research 10 p1312 N90-17587
Advanced materials for interior and equipment related to fire safety in aviation 10 p1316 N90-17608
The importance of pathophysiological parameters in fire modelling of aircraft accidents 10 p1317 N90-17618
Safety evaluation of infrared lamp power output for oculometer eye/head tracker system
[AD-A215809] 10 p1411 N90-18138
RF modal quantity gaging 11 p1474 N90-18483
Superfluid helium orbital resupply coupling 11 p1475 N90-18488
Safety analysis for the Galileo light-weight radioisotope heater unit
[DE90-007147] 11 p1566 N90-19009
Safety Status Report for the Ulysses mission. Book 1: Risk analysis. General purpose heat source radioisotope thermoelectric generator program
[DE90-006826] 12 p1614 N90-19282
Safety status report for the Ulysses mission. Book 2: Risk analysis. General purpose heat source radioisotope thermoelectric generator program
[DE90-006827] 12 p1614 N90-19283
Safety Status Report for the Ulysses mission. Book 2: Accident analysis-appendices. General purpose heat source radioisotope thermoelectric generator program
[DE90-006830] 12 p1614 N90-19286
High-Explosives Applications Facility (HEAF)
[DE90-008122] 13 p1787 N90-20257
A guide to performing and documenting safety analyses
[DE90-008687] 13 p1788 N90-20260
A guide to performing and documenting safety analyses
[DE90-008688] 13 p1788 N90-20261
Software quality assurance and software safety in the biomed control system
[DE90-008072] 13 p1866 N90-20706
Final safety analysis report for the Ulysses Mission. Volume 2: Accident model document-appendices
[DE90-008695] 14 p1940 N90-21104
Final safety analysis report for the Ulysses Mission
[DE90-008690] 14 p1940 N90-21106
Final safety analysis report for the Ulysses mission. Volume 1: Reference design document
[DE90-008693] 14 p1940 N90-21107
Final (Tier 1) environmental impact statement for the Galileo and Ulysses Missions
[NASA-TM-102917] 15 p2056 N90-21779
The procedure safety system 15 p2155 N90-22311
General purpose heat source radioisotope thermoelectric generator program. Book 1: Accident analysis
[REPT-90SDS4202-BK-1] 15 p2166 N90-22379
HCl Vapor Characterization and Detection. JANNAF Safety and Environmental Protection Subcommittee Workshop
[AD-A216252] 16 p2208 N90-22596
Preliminary Subsystem Designs for the Assured Crew Return Vehicle (ACRV), volumes 1-3
[NASA-CR-186662] 17 p2363 N90-23455
Design of an autonomous teleoperated cargo transporting vehicle for lunar base operations
[NASA-CR-186686] 18 p2565 N90-24633
Advanced space transportation technologies 18 p2645 N90-25061
Biofidelity of a dummy's neck during automobile collision testing 19 p2721 N90-25477
Hazard classification testing of liquid propellants
[AD-A222070] 21 p2990 N90-26990
SP-100 design, safety, and testing
[DE90-012643] 21 p3075 N90-27484
Cosmic bombardment 2: Intercepting the bomblets cost-efficiently
[DE90-010401] 21 p3098 N90-27601
New aspects in aircraft inspection using eddy current methods 22 p3187 N90-28085
Human factors and safety considerations of night vision systems flight
[USAARL-89-12] 22 p3233 N90-28332
Space program safety: Funding for NASA's safety organizations should be centralized
[GAO/NSIAD-90-187] 22 p3255 N90-28434
Procedures for DOE-Navy exchange and approval of engineering information and material management required for production of W88-0/Mk5 RBA (reentry body assembly)
[DE90-014763] 23 p3287 N90-28595
Guidelines for pressure vessel safety assessment
[PB90-219619] 23 p3316 N90-28749
The nuclear battery
[DE90-630400] 24 p3462 N90-29559

SAFETY DEVICES
NT AIR BAG RESTRAINT DEVICES
NT EJECTION SEATS
NT ESCAPE CAPSULES
NT HELMETS
NT SEAT BELTS
Aircraft cabin fire suppression by means of an interior water spray system
[CAA-PAPER-88014] 03 p0303 N90-11719
Error detection in data processing devices by means of residue codes
[ETN-90-95370] 12 p1701 N90-19767
Maritime safety information in the year 2000: Listen up, Navy, the times they are a changin'
[AD-A220563] 17 p2390 N90-23611
Helmet-mounted head restraint
[AD-D014536] 20 p2899 N90-26491

SAFETY FACTORS
US Air Force certification of castings 01 p0042 N90-10232
Evaluation of tests and design factors 02 p0176 N90-10987
Safety considerations for sodium-sulfur batteries for electric vehicles
[DE89-017682] 03 p0342 N90-11949
Advanced spacecraft fire safety: Proposed projects and program plan
[NASA-CR-185147] 04 p0462 N90-12645
A transformational method for verifying safety properties in real time systems
[AD-A211925] 04 p0529 N90-13051
The United States Air Force approach to all-weather testing 07 p0870 N90-15047
Safety and rescue during STS operations 08 p1034 N90-15975
Assured crew return capability architecture 08 p1034 N90-15977
Crew safety and rescue aids 08 p1035 N90-15980
NASDA's approach to the interoperability of safety and rescue in space 08 p1035 N90-15981
MANPRINT (Manpower and Personnel Integration) evaluation: AN/TRC-170 digital troposcatter radio system
[AD-A211799] 08 p1055 N90-16100
The SMITE approach to security
[RSRE-89014] 08 p1106 N90-16404
Risk assessment and its application to flight safety analysis
[DE90-004985] 09 p1161 N90-16722
Hermes space vehicle: Safety considerations 09 p1178 N90-16825
Aircraft Fire Safety
[AGARD-CP-467] 10 p1311 N90-17581
Safety Status Report for the Ulysses mission. Book 1: Accident analysis. General purpose heat source radiosotope thermoelectric generator program
[DE90-006829] 12 p1614 N90-19285
Magnetic turbulence versus safety factor in the Tokapole 2 tokamak 15 p2168 N90-22391
Health management system for rocket engines
[NASA-CR-185223] 17 p2383 N90-23574
Lack of behavioral effects of high-peak-power microwave pulses from an axially extracted virtual cathode oscillator
[AD-A220779] 17 p2391 N90-23618
Aviation safety: Conditions within the air traffic control work force. Fact sheet for congressional requesters
[GAO/RCED-89-113FS] 20 p2805 N90-25958
Multimegawatt space nuclear power supply, phase 1. Volume 3: Annotated outline of preliminary safety assessment D180-30619-7
[DE90-012432] 20 p2926 N90-26646
Preliminary hazard analysis in design application to EVA space suit
[ETN-90-97585] 24 p3523 N90-29918

SAFETY MANAGEMENT
Derivation of improved load transformation matrices for launchers-spacecraft coupled analysis, and direct computation of margins of safety 02 p0188 N90-11077
UK airmisses involving commercial air transport
[CAA-2/88] 03 p0303 N90-11718
Product assurance 05 p0605 N90-13522
The US space station and its electric power system
[NASA-TM-101974] 05 p0616 N90-13596
Review of the Aerospace Safety Advisory Panel report for NASA fiscal year 1990 authorization
[GPO-24-234] 06 p0722 N90-14213
Risk-based fire safety experiment definition for manned spacecraft
[NASA-CR-183835] 06 p0731 N90-14262
Hermes space vehicle: Safety considerations 09 p1178 N90-16825
Aircraft fire safety: Learning from past accidents 10 p1312 N90-17584

Development of improved fire safety standards adopted by the Federal Aviation Administration
10 p1312 N90-17585
Fire safety in civil aviation 10 p1312 N90-17586
Objectives and results of cabin fire research in Germany 10 p1312 N90-17588
Fire safety applications for spacecraft
10 p1314 N90-17595
Forced and natural venting of aircraft cabin fires: A numerical simulation 10 p1314 N90-17597
Hot surface ignition studies of aviation fluids
10 p1314 N90-17600
The stability of fuel fires 10 p1315 N90-17601
Fire hardening of aircraft through upgrades of materials and designs 10 p1315 N90-17605
Heat release rate measurement for evaluating the flammability of aircraft materials
10 p1316 N90-17610
Brake performance of the McDonnell Douglas DC-10-30/40 during high speed, high energy rejected takeoffs
[PB90-917004] 14 p1920 N90-21000
Minutes of the 23rd Eplosives Safety Seminar, volume 2
[AD-A218265] 14 p1959 N90-21214
Aviation security: Corrective actions underway, but better inspection guidance still needed. Report to the Chairwoman, Government Activities and Transportation Subcommittee, Committee on Government Operations, House of Representatives
[GAO/RCED-88-160] 17 p2347 N90-23367
Life management planning 22 p3118 N90-27709
Minimal sleep to maintain performance: Search for sleep quantum in sustained operations
[AD-A223815] 24 p3498 N90-29770
Preliminary hazard analysis in design application to EVA space suit
[ETN-90-97585] 24 p3523 N90-29918

SAGE SATELLITE
The interpretation of SAGE 2 ozone measurements in the lower mesosphere 15 p2124 N90-22149
SAGE 3: A visible wavelength limb sounder
21 p3016 N90-27147

SAGITTARIUS CONSTELLATION
The Sagittarius B2 molecular cloud: An extreme case of a galactic center giant molecular cloud
15 p2187 N90-22493

SAGNAC EFFECT
Ring laser gyro principles and techniques
24 p3426 N90-29352

SAHARA DESERT (AFRICA)
Dust clouds from African dust storms in 1986-1987 as observed by Meteosat 21 p3029 N90-27222

SAILPLANES
U GLIDERS

SAILS
NT SOLAR SAILS

SALINITY
Chesapeake Bay surface salinities, 1951-88
[PB89-194583] 01 p0090 N90-10513
Semi-monthly temperature and geopotential anomaly in the upper 500 meters along the Oahu-Farallon Islands great circle from November 15, 1967 through December 15, 1979
[AD-A210640] 01 p0091 N90-10518
Utilization of LANDSAT-5 and NOAA-9 satellite imagery in the identification of physical-chemical parameters of the water in the Guanabara Bay
[INPE-4761-TDL/349] 13 p1819 N90-20445
Analysis of water quality parameters of the Piaui River (SE), Brazil, through field and TM/LANDSAT sensor data
[INPE-4918-PRE/1417] 14 p1998 N90-21453
MECCA program documentation
[NOAA-TR-NESDIS-46] 14 p2003 N90-21477
Ross Sea oceanographic data, 1983-1987: USCGC GLACIER, January-February 1983; USCGC POLAR SEA, January-February 1984; USCGC POLAR STAR, February 1984; USCGC POLAR SEA, February 1987
[PB90-243932] 23 p3354 N90-28955

SALMONELLA
The sensory transduction pathways in bacterial chemotaxis 05 p0677 N90-13944

SAMPLED DATA SYSTEMS
On the stability of robotic systems with random communication rates 24 p3514 N90-29865

SAMPLERS
Field evaluation of a passive sampling device for hydrazines in ambient air
[NASA-TM-103456] 18 p2578 N90-24686
Laboratory and field evaluations of extrasensitive sulfur dioxide and nitrogen dioxide analyzers for acid deposition monitoring
[PB90-201062] 22 p3199 N90-28153

SAMPLES
NT MARS SURFACE SAMPLES
Multi-sample functional statistical data analysis
[AD-A210992] 01 p0117 N90-10673
Techniques for recovery of shock-loaded samples
[DE89-016881] 02 p0233 N90-11337
Thermal perturbation of comet samples during their acquisition 12 p1741 N90-20008
Analysis of methods to determine emissivity for ground surface targets in the spectral band 8 to 14 microns
[INPE-4984-TDL/394] 13 p1820 N90-20447
Robotic sampling system for an unmanned Mars mission 23 p3375 N90-29070

SAMPLING
NT AIR SAMPLING
NT CORE SAMPLING
NT DATA SAMPLING
NT PARTICULATE SAMPLING
NT RANDOM SAMPLING
Method and apparatus for determining time, direction and composition of impacting space particles
[NASA-CASE-LAR-13392-1-CU]
01 p0026 N90-10132
Asymptotic robustness in regression and autoregression based on Lindeberg conditions
[AD-A210725] 01 p0114 N90-10654
Selection of the best with a preliminary test for two-parameter exponential distributions
[AD-A210275] 01 p0115 N90-10662
A technique to correlate fractography with NDE (Non-Destructive Evaluation) of small samples
[DE89-016904] 02 p0231 N90-11325
Alias-free Wigner distribution function and complex ambiguity function for discrete-time samples
[AD-A211050] 02 p0269 N90-11533
Estimated UV clutter levels at 10-100 meter sensor pixel resolution extrapolated from recent polar bear measurements
[AD-A211357] 03 p0372 N90-12125
Surface, interface, and bulk properties of high T(sub c) superconductors
[AD-A211490] 03 p0413 N90-12373
Multiparameter radar estimation of raindrop size distribution
[AD-A212410] 04 p0521 N90-13007
Asymptotic expansions for two-stage rank tests
[MEMO-773] 04 p0544 N90-13161
Interpretation and manipulation of Edgeworth expansions
[MEMO-775] 04 p0544 N90-13163
Illustration of Bayesian inference in normal data models using Gibbs sampling
[AD-A212630] 04 p0547 N90-13187
Identification of impulsive interference channels
[AD-A213154] 05 p0688 N90-14009
The fluid mechanics of filters
06 p0773 N90-14499
Environmental surveillance data
[DE90-001275] 07 p0956 N90-15532
Linear digital imaging system fidelity analysis
08 p1072 N90-16205
Analysis of organic compounds in returned comet nucleus samples 08 p1142 N90-16617
Candidate sample acquisition systems for the Rosetta
08 p1145 N90-16635
Methods for the mineralogical and textural analysis of comet nucleus samples 08 p1147 N90-16648
High-pressure promoted combustion chamber
[NASA-CASE-MSC-21470-1] 09 p1170 N90-16771
Chemical effect of fuel composition changes on emissions from a DI Diesel engine
[DE90-004486] 09 p1232 N90-17151
Sampling scattered data onto rectangular grids for volume visualization
[AD-A215533] 09 p1274 N90-17384
Statistics of a chi-square random variable obtained from independent Gaussian samples with a non-zero mean and arbitrary variance
[AD-A214477] 09 p1275 N90-17392
Estimation in a discrete tail rate family of recapture sampling models
[NASA-CR-180452] 10 p1421 N90-18197
Multistage forest volume estimation using a sampling system with probability variables
[INPE-4897-PRE/1498] 11 p1523 N90-18769
Adaptive state estimation and sampling rate analysis for invariant linear dynamic systems in time
[INPE-4960-TDL/389] 11 p1554 N90-18951
Exploiting surface observations of cloudiness for globalscale nephanalyses 12 p1692 N90-19719
A technique for convolving unequally spaced samples using fast Fourier transforms
[DE90-006466] 12 p1707 N90-19802
Spatial imaging using confocal Fabry-Perot interferometers
[DE90-008363] 13 p1807 N90-20378
Utilization of LANDSAT-5 and NOAA-9 satellite imagery in the identification of physical-chemical parameters of the water in the Guanabara Bay
[INPE-4761-TDL/349] 13 p1819 N90-20445
Underwater physiography of the continental shelf of Rio Grande do Norte visible through satellite imagery
[INPE-4964-TDL/392] 13 p1820 N90-20448
The electronic properties of high (Tc) superconductors probed by positron annihilation
[DE90-008354] 13 p1896 N90-20883
On the continuous dependence with respect to sampling of the linear quadratic regulator problem for distributed parameter systems
[NASA-CR-182012] 14 p2018 N90-21566
Aerosol separator for use in aircraft
[PB90-142217] 15 p2125 N90-22155
Sampling and noise in vision networks
15 p2138 N90-22217
Networks for image acquisition, processing and display 15 p2138 N90-22218
Development and use of a passive technique for measuring nitrogen dioxide in the background atmosphere 16 p2331 N90-23285
COS-B gamma ray sources beyond the predicted diffuse emission 16 p2335 N90-23308
Morphological sampling
[CWI-AM-R8913] 17 p2460 N90-24044
Sample size for correlation estimates
[AD-A219810] 17 p2465 N90-24085
More about general saddlepoint approximations
[AD-A221217] 18 p2604 N90-24832
Multiwavelength constraints on gamma-ray burst sources 18 p2639 N90-25032
Optical characterization of clouds of fine liquid-nitrogen particles
[NASA-TM-103208] 20 p2865 N90-26299
Analysis of acid precipitation samples collected by state agencies: January to December 1988
[PB90-191784] 22 p3198 N90-28151
Intercomparisons of GOES-derived cloud parameters and surface observations over San Nicolas Island
22 p3214 N90-28229
A computerized data-base system for land-use and land-cover data collected at ground-water sampling sites in the pilot national water-quality assessment program
[PB90-181868] 22 p3258 N90-28453
A system architecture for a planetary rover
23 p3365 N90-29015
A fast lightstripe rangefinding system with smart VLSI sensor 23 p3366 N90-29019
Robotic sampling system for an unmanned Mars mission 23 p3375 N90-29070
An improved method for choosing sampling points for the inspection of complex surfaces in a computer-aided manufacturing environment 23 p3380 N90-29093
Atmospheric methane data for the period 1983-1985 from the NOAA/GMCC global cooperative flask sampling network
[PB90-208588] 24 p3486 N90-29701
The Surface Air Sampling Program
[DE90-014873] 24 p3487 N90-29711
Trapezoidal stratified Monte Carlo integration
[AD-A223565] 24 p3540 N90-30021

SAMPLING DEVICES
U SAMPLERS

SAN ANDREAS FAULT
Strain accumulation and surface deformation along the San Andreas, California
[NASA-CR-185893] 05 p0666 N90-13894

SAN MARCO SATELLITES
A model of the perturbed spinning motion of the San Marco 5th spacecraft 22 p3129 N90-27755

SANDS
Numerical simulation of hydrazine transport in a sandy soil 02 p0205 N90-11172
Diagnostic study of atmosphere-terrain interaction leading to the formation of dust clouds and poor visibilities over near east desert areas
[AD-A211243] 02 p0239 N90-11358
Guidance document for selecting antiskid materials applied to ice- and snow-covered roadways
[PB90-183658] 21 p2983 N90-26950

SANDWICH CONSTRUCTION
U SANDWICH STRUCTURES

SANDWICH STRUCTURES
Transverse shear stiffness of composite and sandwich finite elements 02 p0182 N90-11034
The 2.5D- and 3D-fabrics for delamination resistant composite laminates and sandwich structures
02 p0186 N90-11063
Crack propagation failure of carbon/resin composites
[ONERA-RT-45/7096-M] 04 p0467 N90-12677
Computer-controlled ion beam sputter-deposition of superconducting oxide films
[AD-A213921] 07 p1004 N90-15812

Open-mode delamination stress concentrations in horseshoe and elliptic composite curved bars subjected to end forces
[NASA-TM-4164] 08 p1039 N90-16004
Bird impact tests on asymmetric sandwich structures made in Kevlar 49
[CEAT-NT-10/S/83-5] 09 p1162 N90-16727
Bird impact tests on curved structures of the type Sandwich-Kevlar-Nida for normal and angular shooting
[CEAT-NT-10/S/83-4] 09 p1162 N90-16728
A study of the structural efficiency of fluted core graphite-epoxy panels
[NASA-TM-101681] 10 p1396 N90-18070
Low-energy impact resistance of graphite-epoxy plates and ALS honeycomb sandwich panels
12 p1637 N90-19405
Stress analysis and minimum weight design of honeycomb sandwich plates 14 p1992 N90-21418
Wave receptance analysis of vibrating beams and stiffened plates 14 p1993 N90-21419
New core design for use with precision composite reflectors
[NASA-CASE-NPO-17858-1-CU]
21 p2970 N90-26880
Manufacturing and mechanical properties of new textile fiber preforms for structural sandwich applications
[MBB-Z-0296-90-PUB] 21 p2972 N90-26895
An examination of impact damage in glass-phenolic and aluminum honeycomb core composite panels
[NASA-TP-3042] 22 p3153 N90-27876
A low cost shadow moire device for the nondestructive evaluation of impact damage in composite laminates
[AD-A223451] 24 p3443 N90-29442
Proceedings of Damping '89. Volume 3: Pages ICA-1 through KDC-15
[AD-A223433] 24 p3479 N90-29666

SAPPHIRE
Preparation, structure and properties of VO(sub x) and TiO2 thin films by MOCVD
[DE90-003566] 07 p1001 N90-15793
High efficiency flashlamp-pumped titanium: Sapphire laser
[AD-A217596] 13 p1806 N90-20367
Flash-pumped titanium laser
[AD-A217599] 13 p1806 N90-20368
CVD diamond films for tribological applications
[AD-A220265] 17 p2413 N90-23750
Epitaxy of TiO2 thin film on sapphire by MOCVDVD
[DE90-010054] 18 p2618 N90-24915
Titanium-doped sapphire lasers with high energy pumping
[RSRE-MEMO-4290] 22 p3181 N90-28050
Thermal shock tests
[ETCA-89-R-163] 22 p3193 N90-28120
Special purpose spatial light modulators
[AD-A223794] 24 p3545 N90-30052

SARCOMA
U CANCER

SARGASSO SEA
The trace metal geochemistry of suspended oceanic particulate matter
[AD-A218604] 17 p2429 N90-23839

SARSAT
Location systems: ARGOS, SARSAT
17 p2359 N90-23430

SAS-D
U IUE

SATAN (SENSOR)
U TERRAIN ANALYSIS

SATELLITE ALTIMETRY
Regional height determination using gravimetric and topographical data
[UH-156] 08 p1091 N90-16315
Progress in the development of high degree potential coefficient models 13 p1832 N90-20516
Gravity field of the Western Weddell Sea: Comparison of airborne gravity and Geosat derived gravity
13 p1833 N90-20526
Performance of FFT methods in local gravity field modelling 13 p1835 N90-20537
The geoid in Kenya 13 p1836 N90-20542
Analysis of altimetry over inland seas
[NASA-TM-100729] 13 p1840 N90-20566
A free surface Bryan-Cox-Semtner model
[IOS-270] 15 p2135 N90-22201
Determination of the general ocean circulation using satellite altimetry from a simultaneous solution for the Earth's gravity field 16 p2203 N90-22569
The role of orbit errors in processing of satellite altimeter data
[ETN-90-96699] 16 p2204 N90-22575
Surface topography of the Greenland Ice Sheet from satellite radar altimetry
[NASA-SP-503] 16 p2253 N90-22850
The DORIS system 17 p2359 N90-23431
Ocean variability from crossover differences derived from altimeter measurements
[ETN-90-96695] 17 p2431 N90-23852
The determination of the orbit of the Japanese satellite Ajisai and the GEM-T1 and GEM-T2 gravity field models
[NASA-TM-100763] 19 p2714 N90-25443

SATELLITE ANTENNAS
Test results on conceptual models of the large deployable antenna for mobile communications satellites
02 p0185 N90-11050
ESA-D: An integrated software for antenna design and analysis 02 p0185 N90-11052
Proceedings of the 1988 Antenna Applications Symposium, volume 1
[AD-A211396] 03 p0338 N90-11928
Proceedings of the Antenna Applications Symposium, volume 2
[AD-A213815] 07 p0919 N90-15313
A space-fed local oscillator for spaceborne phased arrays
[AD-A216526] 10 p1328 N90-17673
Power conditioning for active array SAR antennas
10 p1338 N90-17744
Mesh surfaces for reflector applications
12 p1611 N90-19268
Antennas for 20/30 GHz and beyond
12 p1611 N90-19269
The effect of mechanical deformation on the radiation patterns of large space-based arrays
[AD-A219288] 16 p2230 N90-22719

SATELLITE ATMOSPHERES
NT LUNAR ATMOSPHERE
Ion bombardment of Io and Mercury
02 p0296 N90-11682
IR spectroscopy of planets and satellites; Venus, Mars, giant planets, and Titan 11 p1578 N90-19085

SATELLITE ATTITUDE CONTROL
Flight Mechanics/Estimation Theory Symposium, 1989
[NASA-CP-3050] 05 p0586 N90-13413
Autonomous spacecraft attitude control using magnetic torquing only 05 p0586 N90-13415
Simulation of spacecraft attitude dynamics using TREETOPS and model-specific computer Codes
05 p0587 N90-13419
Orbit and attitude determination results during launch support operations for SBS-5
[PAPER-7] 05 p0587 N90-13420
GOES I/M image navigation and registration
05 p0588 N90-13422
Temperature dependence of attitude sensor coalignments on the Solar Maximum Mission (SMM)
05 p0588 N90-13426
True covariance simulation of the EUVE update filter
05 p0589 N90-13427
A gyroscope calibration analysis for the Gamma Ray Observatory (GRO) 05 p0589 N90-13428
Extended Kalman filter for attitude estimation of the earth radiation budget satellite 05 p0590 N90-13433
Launch and early orbit 05 p0606 N90-13524
The in-orbit initialization phase
05 p0606 N90-13525
On-ground attitude determination
05 p0609 N90-13552
The great circle reductions 05 p0609 N90-13553
Great circle interactions: Attitude smoothing and grid-step inconsistencies 05 p0609 N90-13554
Modelling of satellite control thruster plumes
05 p0613 N90-13578
Choice of a differential method for the attitude restitution in dynamic unbalance
[CNES-CT/DTI/MS/CM/290] 05 p0613 N90-13582
Self-tuning control techniques, implicit and explicit, with parameter estimation in Kalman filters, applied to artificial satellite attitude
[INPE-4857-TDL/368] 12 p1613 N90-19276
Attitude and spin rate control of a spinning satellite using geomagnetic field
[INPE-4818-NTE/289] 12 p1613 N90-19277
Orbit control strategy for a constellation of three satellites in tundra orbits
[AAS-89-411] 17 p2361 N90-23445
Orbit control for a regional navigation system based on tundra orbit
[AIAA-89-3619] 17 p2365 N90-23466
ISO attitude and orbit control subsystem
[REPT-892-440-104] 17 p2366 N90-23467
A three axis attitude control of a satellite
[NASDA-TR-22] 24 p3439 N90-29421

SATELLITE ATTITUDE DISTURBANCE
U ATTITUDE STABILITY
U SPACECRAFT STABILITY

SATELLITE CAPTURE
U SPACECRAFT RECOVERY

SATELLITE COMMUNICATION
Effects of rain attenuation on satellite EHF (Extremely High Frequency) communications in the US
[AD-A210517] 01 p0057 N90-10325
Adaptive antenna arrays for satellite communication
[NASA-CR-185989] 04 p0485 N90-12784
Satellite range delay simulator for a matrix-switched time division multiple-access network simulator
[NASA-TM-102407] 04 p0489 N90-12813
Design and performance of an on-satellite laser diagnostic system for a free space optical heterodyne frequency-shift-keyed communication system
[AD-A211986] 04 p0505 N90-12915
Wider horizons: Potential contributions by space systems to socio-economic advancement in developing countries
[ESA-SP-1106] 04 p0562 N90-13276
The role of the ground segment
05 p0606 N90-13527
The use of digital signal processing in satellite communication 05 p0631 N90-13684
SLCSAT (Submarine Laser Communication Satellite) communication system design study
[AD-A213403] 07 p0917 N90-15304
A signal realization data base generated by the multiple phase-screen method
[AD-A214004] 07 p1010 N90-15852
Tactical UK military satellite ground terminals: A research and development review
[RSRE-MEMO-4262] 08 p1033 N90-15972
X-band atmospheric attenuation for an Earth terminal measurement system
[PB90-100736] 08 p1056 N90-16101
Helsinki University of Technology Radio Laboratory
[PB90-110677] 08 p1056 N90-16102
The European space effort: An integral part of the construction of Europe 09 p1180 N90-16845
Feasibility of millimeter-accuracy geodetic positioning and vehicle tracking with repeater satellites
[AD-A214755] 09 p1182 N90-16854
An approach to the development of software for computer-aided design of satellite communications receivers for operation in scintillating channels
[AD-A215299] 09 p1267 N90-17349
Proceedings of the Thirteenth NASA Propagation Experimenters Meeting (NAPEX 13)
[NASA-CR-186062] 10 p1371 N90-17945
Japanese propagation experiments with ETS-5
10 p1372 N90-17951
Plan of advanced satellite communication experiments using ETS-6 10 p1372 N90-17952
Recent achievements of OPEX
10 p1373 N90-17961
US Activity with the OLYMPUS satellite
10 p1374 N90-17964
Performance measurements for a laboratory-simulated 30/20 GHz communication satellite transponder
[NASA-TM-102424] 10 p1376 N90-17977
PRPSIM: A FORTRAN code to calculate properties of radio wave propagation in a structured ionized medium. Volume 2: Theory and models
[AD-A216299] 10 p1377 N90-17983
Rate compatible punctured codes, their use in military satellite communication systems
[AD-A216723] 11 p1497 N90-18619
Large antenna measurement and compensation techniques 12 p1610 N90-19263
Error control techniques for satellite and space communications
[NASA-CR-186221] 13 p1788 N90-20263
First-order intensity statistics for non-Rayleigh fading
[AD-A217572] 13 p1841 N90-20569
NASA's Advanced Communications Technology Satellite (ACTS): Will it benefit commercial/military satellites
[AD-A217710] 14 p1939 N90-21100
Small business innovation research. Abstracts of 1988 phase 1 awards
[NASA-TM-102991] 14 p2036 N90-21680
Small business innovation research. Abstracts of completed 1987 phase 1 projects
[NASA-TM-101797] 14 p2036 N90-21681
Prospects for integration of satellite communications, navigation and monitoring functions
17 p2360 N90-23439
NASA 60 GHz intersatellite communication link definition study. Addendum A: Mixed baseband and IF signals
[NASA-CR-186337] 17 p2387 N90-23593
NASA 60 GHz intersatellite communication link definition study. Baseline document
[NASA-CR-186339] 17 p2387 N90-23594
NASA 60 GHz intersatellite links definition study. Final Review
[NASA-CR-186338] 17 p2387 N90-23595

Applicability of Asynchronous Transfer Mode (ATM) techniques to satellite communications systems
[MBB-UK-0059-89-PUB] 17 p2392 N90-23625
System analysis of a tactical multi-satellite communication system
[AD-A220344] 18 p2510 N90-24343
Utilization of higher frequencies for satellite communications: Determination of atmospheric effects using experiments and models
[DLR-FB-89-46] 18 p2544 N90-24518
Conceptual definition of a high voltage power supply test facility
[NASA-CR-185216] 19 p2666 N90-25172
Texstar: The all-Texas educational satellite system
[NASA-CR-186654] 20 p2820 N90-26045
System factors to be considered in assessing propagation effects on modern digital satellite communications systems 20 p2850 N90-26208
Mobile satellite communications for civil aviation
[NLR-MP-88066-U] 20 p2855 N90-26238
Software set-up for data processing of depolarization due to rain and ice crystals in the Olympus project
[EUT-89-E-218] 20 p2855 N90-26240
Tactical applications of the UHF satellite communications system 21 p3070 N90-27451
The post-2000 MILSATCOM architecture 21 p3070 N90-27452
Lightweight EHF communications satellites 21 p3070 N90-27453
Tactical EHF satellite communications for NATO employing non-geostationary orbits 21 p3070 N90-27454
Rain-fade simulation and power augmentation for satellite communication systems
[NASA-TM-103134] 23 p3319 N90-28768
Satellite Constellation Orbit Evaluation (SCORE) program
[AD-A223531] 24 p3438 N90-29417
Jamming performance of frequency-hopped communication systems with nonuniform hopping distributions
[AD-A223419] 24 p3461 N90-29547

SATELLITE CONFIGURATIONS
Pulsed plasma mission endurance test
[AD-A213462] 08 p1037 N90-15993
The Italian approach to small satellites for low cost access to space developments
[ETN-90-96552] 16 p2206 N90-22587
Low cost station keeping maneuvers for a small-satellites constellation in tundra orbits
[ETN-90-96553] 16 p2206 N90-22588

SATELLITE CONTROL
NT SATELLITE ATTITUDE CONTROL
Control and stability of a spinning symmetric satellite in an elliptical orbit
[AD-A216284] 10 p1328 N90-17672
Drag-free satellite control 12 p1735 N90-19974
Orbit acquisition and control strategy for small satellites in inclined eccentric orbits
[ETN-90-96551] 16 p2203 N90-22573
Military space operations: Shuttle and satellite computer systems do not meet performance objectives
[GAO/IMTEC-88-7] 18 p2635 N90-25014
Fluid-loop reaction system
[NASA-CASE-NPO-17204-1-CU] 20 p2864 N90-26292

SATELLITE DEFENSE
U SPACECRAFT DEFENSE

SATELLITE DESIGN
Telescope structure for cryogenic application 02 p0180 N90-11019
Development of the large spacecraft structure 02 p0180 N90-11020
The service module structure of the IOS spacecraft development and qualification program 02 p0181 N90-11021
Petite Amateur Navy Satellite (PANSAT)
[NASA-CR-186049] 03 p0317 N90-11800
Acceleration tests of the ACPB canister flight unit from RETE experiment
[IFSI-89-2] 10 p1328 N90-17669
Vibration tests of the ACPB canister flight unit of the RETE experiment, integrated with the tests of the booms from R. Piaggio
[IFSI-89-11] 10 p1328 N90-17670
Structural design of the Telecom 2 solar array 10 p1343 N90-17786
The ITALSAT solar array 10 p1343 N90-17787
The electrical design of solar arrays for communication satellites 10 p1344 N90-17792
Space orientation and orbital technology
[ISBN-3-89100-015-4] 11 p1485 N90-18437
Perspective features of the tethered systems for space applications
[ETN-90-97279] 20 p2822 N90-26059

SATELLITE DOPPLER POSITIONING
General principles of radionavigation: Space mapping 17 p2358 N90-23423
Location and navigation technology: Putting theory into practice 17 p2358 N90-23424
Location systems: ARGOS, SARSAT 17 p2359 N90-23430
Comparison of location systems 17 p2360 N90-23437

SATELLITE DRAG
Orbital mechanics: A learning tool on the main frame
[AD-A218799] 16 p2204 N90-22576

SATELLITE GROUND SUPPORT
Space operations: NASA's communications support for Earth orbiting spacecraft. Report to Chairman, Subcommittee on Space Science and Applications, Committee on Science, Space and Technology, House of Representatives
[GAO/IMTEC-89-41] 20 p2851 N90-26215

SATELLITE IMAGERY
A compilation of digitized satellite imagery of the Gulf Stream (1982, 1983, and 1985)
[AD-A210243] 01 p0082 N90-10467
Analysis of forest fire smoke using satellite imagery
[AD-A210657] 02 p0236 N90-11339
Definition of imaging performance for satellite surveillance, models, and simulations
[FOA-C-30493-9.4] 02 p0236 N90-11341
Ionospheric Structure and Variability on a Global Scale and Interactions with Atmosphere and Magnetosphere
[AGARD-CP-441] 02 p0239 N90-11361
The middle and high latitude ionosphere at approximately 550 km altitude 02 p0242 N90-11374
North-south tropical F2 layer asymmetry at west AFrican and Pacific longitudes 02 p0247 N90-11398
Composited local area forecast techniques
[AD-A210802] 02 p0253 N90-11432
Phoebe: A preliminary control network and rotational elements
[NASA-CR-185716] 02 p0295 N90-11680
NASA/MSFC FY88 Global Scale Atmospheric Processes Research Program Review
[NASA-TM-100357] 03 p0360 N90-12059
Application of dynamical systems theory to global weather phenomena revealed by satellite imagery 03 p0361 N90-12063
The effect of latent heat release on synoptic-to-planetary wave interactions and its implication for satellite observations: Theoretical modeling 03 p0362 N90-12073
Use of satellite data and modeling to asses the influence of stratospheric processes on the troposphere 03 p0363 N90-12075
Characteristics, distribution and geologic/terrain associations of small dome-like hills on Venus 03 p0422 N90-12425
Removing stripes in GOES (Geostationary Operational Environmental Satellites) images by matching empirical distribution functions
[PB89-213359] 04 p0514 N90-12968
A hybrid architecture for feature labelling of oceanographic satellite images
[AD-A212236] 04 p0515 N90-12975
Meteorological Satellite Center Technical Note, no. 18, 1989
[MSC-TN-18] 04 p0519 N90-12997
Cloud cover determination in polar regions from satellite imagery
[NASA-CR-186096] 04 p0520 N90-13003
GOES I/M image navigation and registration 05 p0588 N90-13422
Proximity effects on adjacent and multiple stars 05 p0607 N90-13533
Modeling of the Hipparcos optical system 05 p0612 N90-13572
ALIS: An Auroral Large Imaging System in northern Scandinavia 05 p0663 N90-13877
Senegalese land surface change analysis and biophysical parameter estimation using NOAA AVHRR spectral data
[NASA-CR-186120] 05 p0664 N90-13883
The use of a deformation model for sampling digitalized stereoscopic images
[IMAG-RR-753-I] 05 p0664 N90-13884
Estimation of rain rate using spatial and multichannel coherence: Analysis of SSM/I data 05 p0670 N90-13905
Algorithm for atmospheric corrections of aircraft and satellite imagery
[NASA-TM-100751] 05 p0683 N90-13976
Normal points: Compression of satellite laser ranging data
[ETN-90-96008] 05 p0707 N90-14145
Image processing of LANDSAT MSS data for buried valley detection in northern Indiana 06 p0802 N90-14668
Synoptic scale tropical waves in multichannel satellite radiance data 06 p0816 N90-14745
Ice floe identification in satellite images using mathematical morphology and clustering about principal curves
[AD-A213854] 08 p1090 N90-16311
Quantitative evaluation of object-changes in multitemporal AGRISAR imagery
[FIM-195] 08 p1091 N90-16314
Evaluation of digital classification results of summer cultivation in a test area in the Parana-Ano state harvest 1986-1987
[INPE-4828-PRE/1459] 10 p1399 N90-18085
Study of alteration covers of part of the Sao Paulo State through remote sensing data
[INPE-4849-TDL/364] 10 p1399 N90-18086
Remote sensing in agriculture: Basic concepts, methodology and applications
[INPE-4806-MD/39] 10 p1399 N90-18088
LANDSAT-TM and agrometeorological data in the wheat crop yield estimation at the farm level
[INPE-4842-PRE/1471] 10 p1400 N90-18091
TVI: A mathematical model for global estimation of Brazilian cerrado phytomass
[INPE-4836-PRE/1465] 11 p1521 N90-18759
Land suitability maps and appropriate land use: An approach using SGI and satellite imagery
[INPE-4827-PRE/1458] 11 p1521 N90-18761
Evaluation of two methods for acquisition of training statistics for digital analysis of areas prepared for plowing
[INPE-4901-PRE/1502] 11 p1522 N90-18763
Multistage forest volume estimation using a sampling system with probability variables
[INPE-4897-PRE/1498] 11 p1523 N90-18769
Development of the agricultural information system. Characteristics and results of the Distrito Federal model
[INPE-4940-PRE/1430] 11 p1524 N90-18773
Perspective revision of systematic mapping through orbital imagery
[INPE-4817-PRE/1453] 11 p1524 N90-18775
Physiognomy of vegetation cover in the PNPM identified through the TM/LANDSAT sensor: A multitemporal analysis
[INPE-4834-PRE/1464] 11 p1525 N90-18776
Project Floval: Correction of relief effects in eucalyptus reforestration
[INPE-4814-RPE/590] 11 p1525 N90-18777
Classification of high resolution imagery using texture attributes
[INPE-4888-TDL/379] 11 p1525 N90-18778
Improvement of classification results from satellite imagery to update and differentiate land use classes on topographic maps
[BCRS-89-17] 11 p1526 N90-18786
SPOT for landscape: Development of a method for the use of SPOT pictures for the updating of the data base scale of the landscape
[BCRS-89-18] 11 p1526 N90-18787
Remote sensing and run-off modelling in the Lake Victoria Basin, Kenya
[BCRS-89-19] 11 p1526 N90-18788
Geological structure of the State of Rio de Janeiro viewed through MSS LANDSAT imagery
[INPE-4826-PRE/1457] 11 p1533 N90-18825
Areas of aquatic macrophytes classified through vegetative indexes extracted from LANDSAT/TM imagery
[INPE-4880-PRE/1489] 12 p1677 N90-19633
Availability of multitemporal LANDSAT data accompanying the variation of water surfaces in the program area of Careiro PDRI/AM
[INPE-4896-PRE/1496] 12 p1677 N90-19634
Satellite imagery for water quality assessment in coastal regions
[INPE-4891-PRE/1492] 12 p1678 N90-19636
The potential of combined use of satellite data with topographic TM information for manual/visual and digital updating of land use
[NLR-MP-88021-U] 12 p1678 N90-19639
Possible applications of remote sensing satellite pictures for the water quality management of the Frisian lakes, Netherlands
[BCRS-88-17] 12 p1679 N90-19641
Activities report in remote sensing
[ETN-90-95472] 12 p1680 N90-19647
Real time environment monitoring using data from METEOSAT and NOAA imaging satellites
[NLR-MP-87070-U] 12 p1684 N90-19672
Cyclogeneses and extratropical cyclones in the south-southeast region of Brazil and its influence in time
[INPE-4812-TDL/359] 12 p1693 N90-19722
An observational study of squall lines in the Amazon
[INPE-4865-TDL/376] 12 p1693 N90-19723

Utilization of LANDSAT-5 and NOAA-9 satellite imagery in the identification of physical-chemical parameters of the water in the Guanabara Bay
[INPE-4761-TDL/349] 13 p1819 N90-20445
Underwater physiography of the continental shelf of Rio Grande do Norte visible through satellite imagery
[INPE-4964-TDL/392] 13 p1820 N90-20448
Methods for local gravity field approximation
13 p1834 N90-20532
Derivation of kinematic fields using wind profiler data from the 1985 pre-storm experiment
[AD-A217952] 13 p1845 N90-20592
Forecasting 24 and 48 hour intensity changes, for northwestern Pacific tropical cyclones, using satellite imagery
[AD-A218174] 13 p1846 N90-20597
Correlation of AVHRR imagery with sub-surface features in California current
[AD-A218184] 13 p1848 N90-20607
Shade images of forested areas obtained from LANDSAT MSS data
[NASA-TM-102939] 14 p1995 N90-21436
Results of the Gondwana Project: An example of intercontinental geologic correlation utilizing LANDSAT imagery
[INPE-4870-PRE/1481] 14 p1995 N90-21437
Wheat yield estimation at the farm level using LANDSAT TM and agrometeorological data
[INPE-5017-RPE/611] 14 p1996 N90-21439
Monitoring of agrocattle-raising projects through visual/digital analysis of LANDSAT-TM imagery south of Para state
[INPE-4982-PRE/1542] 14 p1996 N90-21442
A knowledge-based information based for crop area estimation
[INPE-4990-PRE/1555] 14 p1996 N90-21444
Analysis of water quality parameters of the Piaui River (SE), Brazil, through field and TM/LANDSAT sensor data
[INPE-4918-PRE/1417] 14 p1998 N90-21453
Evaluation of the mangrove areas of the Rio Piaui (SE) through remote sensing
[INPE-4909-PRE/1510] 14 p1998 N90-21454
Introduction of digital image processing by remote sensors applied to geology
[INPE-5023-RPE/616] 14 p1999 N90-21456
Multitemporal analysis of LANDSAT/TM digital imagery in the detection of areas affected by caterpillar (sibine fusca) attack in the dende (elais guineensis) palm plantation
[INPE-4979-PRE/1544] 14 p1999 N90-21457
Evaluation of classification performance and proportion estimate of the sugar cane crop through PROCEDURE-INPE utilizing LANDSAT data
[INPE-4899-PRE/1500] 14 p1999 N90-21458
Subsystem TM Precision: Progress and perspective
[INPE-5006-PRE/1563] 14 p2000 N90-21461
Possible use of satellite data for flood plain mapping
[INPE-4968-PRE/1537] 14 p2000 N90-21462
Performance evaluation of morphological edge detectors
[INPE-4975-PRE/1540] 14 p2000 N90-21464
Modelling UV-visible radiation observed from space
15 p2085 N90-21937
Satellite image analysis using neural networks
15 p2157 N90-22321
A case for archaeological reconnaissance of the Cabo Catoche-Porvenir region of the northeastern Yucatan Peninsula
[NASA-TM-102248] 16 p2249 N90-22827
Tropical squall lines of the Arizona monsoon
16 p2257 N90-22867
The analysis of polar clouds from AVHRR satellite data using pattern recognition techniques
[NASA-CR-183300] 16 p2257 N90-22868
Topographic mapping from SPOT satellite imagery
[ETN-90-96689] 17 p2418 N90-23777
Atmospheric correction of satellite pictures in the framework of the project Friese Fronten
[BCRS-89-12] 17 p2419 N90-23786
Astronaut's guide to terrestrial impact craters
[NASA-TM-102902] 17 p2421 N90-23798
Tropical cyclones, 1989: Central north Pacific
[PB90-182536] 17 p2428 N90-23836
Multifrequency observations of Cyg X-2: X ray observations with Ginga 17 p2482 N90-24192
Contributions of the X Ray Astronomy Group of the Max-Planck-Institut fuer Extraterrestrische Physik
[MPE-PREPRINT-165] 17 p2482 N90-24196
Development of remote sensing techniques for the investigation of neotectonic activity, eastern transverse ranges and vicinity, southern California
18 p2573 N90-24662
Ecological study of peat landforms in Canada and Alaska
[NASA-CR-184923] 19 p2705 N90-25391
Multisensor monitoring of deforestation in the Guinea Highlands of West Africa
[NASA-CR-186709] 19 p2706 N90-25396
Seasonal LAI in slash pine estimated with LANDSAT TM
[NASA-TM-102278] 19 p2706 N90-25397
Research programs: Meteorological prediction. Oceanic processes. Climate and global change monitoring. Satellite instrumentation and calibration
19 p2714 N90-25447
EXOSAT observation of the pulsar PSR 1509-58
19 p2782 N90-25829
Practical applications of remote sensing technology
[NASA-CR-186810] 20 p2879 N90-26377
The main products and their distribution of FY-1 meteorological satellite
[AD-A221582] 21 p2967 N90-26865
Dust clouds Kosa from the east Asian dust storms in 1982-1988 as observed by the GMS satellite
21 p3028 N90-27214
Distribution and movement of smokes from forest fires that occurred along the boundary of the People's Republic of China and the USSR on April-May 1987
21 p3028 N90-27216
Investigation into position accuracy of typhoon center determined on GMS imagery 21 p3028 N90-27217
The test for automatic neph-analysis chart
21 p3029 N90-27219
Dust clouds from African dust storms in 1986-1987 as observed by Meteosat 21 p3029 N90-27222
Tactical applications of Defense Meteorological Satellite Program (DMSP) environmental data
21 p3067 N90-27439
Block 6: The future DMSP space systems
21 p3068 N90-27443
Space-based wide area surveillance system studies
21 p3068 N90-27444
Integration of multispectral SPOT imagery and panchromatic aerial photography for study in urban land use
[INPE-4967-PRE/1536] 22 p3194 N90-28125
Large-scale variability in marine stratocumulus clouds defined from simultaneous aircraft and satellite measurements 22 p3213 N90-28226
Observed cloud reflectivities and liquid water paths: An update 22 p3215 N90-28237
Properties of cirrus from multispectral AVHRR imagery data 22 p3223 N90-28277
Regional conditions during the 25 October 1986 FIRE cirrus/altocumulus case study 22 p3225 N90-28287
Instability bursts associated with Extratropical Cyclone Systems (ECSs) and a forecast index of 3 to 12 hour heavy precipitation
[NOAA-TM-NESDIS-30] 22 p3228 N90-28309
Digital geometric correction for MSS-LANDSAT imagery
[INPE-4627-PRE/1345] 23 p3342 N90-28886
Study of anomalies in transition vegetation in Alto Xingo-NT, through remote sensing techniques
[INPE-4601-TDL/334] 23 p3343 N90-28891
INPE geographic data base
[INPE-4636-PRE/1348] 23 p3407 N90-29253
Satellite image atlas of glaciers of the world: Irian Jaya, Indonesia, and New Zealand
[PB90-230095] 24 p3483 N90-29691

SATELLITE INSTRUMENTS

Atomic velocity distributions out of hydrogen maser dissociators
[AD-A219500] 17 p2408 N90-23721
Characterization of the surfaces of platinum/tin oxide based catalysts by Fourier transform spectroscopy (FTIR) 18 p2643 N90-25054
Conceptual design study for Infrared Limb Experiment (IRLE)
[NASA-CR-186950] 21 p2968 N90-26869

SATELLITE LAUNCHING

U SPACECRAFT LAUNCHING

SATELLITE LIFETIME

Arcjet nozzle design impacts
11 p1473 N90-18478
A proposed change to the NASA strategy for servicing space assets 18 p2500 N90-24282

SATELLITE MANEUVERS

U SPACECRAFT MANEUVERS

SATELLITE NAVIGATION SYSTEMS

High accuracy coordinate determination using the global positioning system 02 p0150 N90-10858
Carin and GPS: The combination of dead reckoning, map matching and satellite navigation in a hybrid automobile navigation system
[ETN-90-95451] 12 p1602 N90-19220
Location and Navigation Satellite Systems
[ISBN-2-85-428-242-6] 17 p2358 N90-23420
Navigation requirements: What they are and where they come from 17 p2358 N90-23422
Location and navigation technology: Putting theory into practice 17 p2358 N90-23424
Measurement errors 17 p2359 N90-23426
Reference frames: Orbitography
17 p2359 N90-23427
Signal processing: Kalman filtering
17 p2359 N90-23428
Back to the stars 17 p2359 N90-23429
Location systems: ARGOS, SARSAT
17 p2359 N90-23430
The GEOSTAR location and messaging system
17 p2360 N90-23435
LOCSTAR: A satellite radiodetermination system for Europe 17 p2360 N90-23436
Comparison of location systems
17 p2360 N90-23437
Comparison of navigation systems
17 p2360 N90-23438
Prospects for integration of satellite communications, navigation and monitoring functions
17 p2360 N90-23439
Implementation of location programmes
17 p2360 N90-23440
Navigation programmes: Financial and institutional aspects 17 p2361 N90-23441
Autonomous low earth orbit navigation
[REPT-892-440-101] 17 p2364 N90-23458
The 2-D and 3-D characterizations of GPS navigation service 24 p3425 N90-29348
Satellite navigation systems for land vehicles
24 p3430 N90-29376

SATELLITE NETWORKS

NT ARGOS SYSTEM

Wideband connectivity and support for Cronus cluster at USAF Electronic Systems Division
[AD-A210749] 02 p0212 N90-11215
Satellite range delay simulator for a matrix-switched time division multiple-access network simulator
[NASA-TM-102407] 04 p0489 N90-12813
Geodetic network adjustment using GPS triple difference observations and a priori stochastic information
[TR-1-1987] 05 p0577 N90-13367
World Weather Watch. Global observing system-satellite sub-system. Information on meteorological and other environmental satellites, second edition
[WMO-411-ED-2] 08 p1103 N90-16386
Broadcast file distribution on packet satellite networks
15 p2079 N90-21906
Electronic Transfer of Information and its Impact on Aerospace and Defence Research and Development
[AGARD-CP-466] 15 p2177 N90-22440
Document delivery via ISDN or satellite networks
15 p2178 N90-22446
Location and Navigation Satellite Systems
[ISBN-2-85-428-242-6] 17 p2358 N90-23420
NASA 60 GHz intersatellite communication link definition study. Addendum A: Mixed baseband and IF signals
[NASA-CR-186337] 17 p2387 N90-23593
NASA 60 GHz intersatellite communication link definition study. Baseline document
[NASA-CR-186339] 17 p2387 N90-23594
NASA 60 GHz intersatellite links definition study. Final Review
[NASA-CR-186338] 17 p2387 N90-23595
Applicability of Asynchronous Transfer Mode (ATM) techniques to satellite communications systems
[MBB-UK-0059-89-PUB] 17 p2392 N90-23625
Stand-alone terrestrial and satellite networks for nationwide interoperation of broadband networks
[PB90-172404] 22 p3164 N90-27942

SATELLITE OBSERVATION

A case study evaluation of satellite-derived rainfall estimates and their application to numerical model precipitation forecast verification
[PB89-194591] 01 p0088 N90-10499
Airborne gamma radiation snow water equivalent and soil moisture measurements and satellite areal extent of snow cover measuerments: A user's guide, version 3.0
[PB89-177877] 02 p0235 N90-11338
Composited local area forecast techniques
[AD-A210802] 02 p0253 N90-11432
Comparison of the LOWTRAN 7 code and S3-4 satellite measurements of UV radiance
[AD-A211356] 03 p0372 N90-12124
UV ionospheric remote sensing with the polar BEAR satellite
[AD-A211359] 03 p0372 N90-12127
Coronae on Venus observations and models of origin
03 p0427 N90-12449
Interplanetary energetic particle observations of the March 1989 events 03 p0434 N90-12484
Tropospheric influences on satellite-Earth paths and their determination by means of radar measurements
[ESA-TT-1143] 04 p0460 N90-12639

Design and tests of simple, inexpensive optical beacon for use on small satellites
[AD-A213325] 04 p0555 N90-13238
Test network Delft
[ETN-90-96009] 05 p0577 N90-13365
Geodetic network adjustment using GPS triple difference observations and a priori stochastic information
[TR-1-1987] 05 p0577 N90-13367
Precision of semi-geometrically determined SLR baselines vs. site occupation time
[ETN-90-96007] 05 p0665 N90-13885
Three dimensional analysis of the structure of the atmosphere in polar environments by vertical satellite sounding. Interest for the meteorological forecasts at high latitudes
[ETN-90-95506] 05 p0671 N90-13911
Rainfall estimation over Africa using satellite data
06 p0815 N90-14742
Geosat/ERM altimeter data analysis for the determination of global oceanic mesoscale variability
07 p0949 N90-15492
Science plan for the Alaska SAR facility program. Phase 1: Data from the first European sensing satellite, ERS-1
[NASA-CR-185028] 08 p1091 N90-16312
Use of remote sensing data for land and building statistics 08 p1094 N90-16335
Support of hydrological models calculations by satellite data 08 p1094 N90-16337
Scientific investigations of the Space Research Group
[ISBN-0-642-13252-6] 08 p1138 N90-16595
Enhanced satellite geodesy through the addition of a pseudorange observable
[AD-A214987] 09 p1241 N90-17200
Observing systems simulation experiments: Their role in meteorology
[AD-A215705] 09 p1248 N90-17243
Investigation of the observability of a satellite cluster in a near circular orbit
[AD-A216224] 10 p1326 N90-17662
The Australian experiment with ETS-V
10 p1372 N90-17949
Airborne observations of the infrared emission bands
11 p1580 N90-19101
Polycyclic aromatic hydrocarbons in the infrared spectra of IRAS sources 11 p1581 N90-19105
Coherent radar measurement of ocean currents from geostationary orbit 12 p1609 N90-19259
Self-tuning control techniques, implicit and explicit, with parameter estimation in Kalman filters, applied to artificial satellite attitude
[INPE-4857-TDL/368] 12 p1613 N90-19276
Exploiting surface observations of cloudiness for globalscale nephanalyses 12 p1692 N90-19719
Analysis of an observation of the x ray astronomy satellite EXOSAT at the low mass x ray binary star system GX5-1
[ETN-90-95828] 12 p1747 N90-20042
An improved model for the Earth's gravity field
13 p1832 N90-20515
FFT-local gravimetric geoid computation
13 p1835 N90-20536
A discussion of observation model, error sources and signal size for spaceborne gravitational gradiometry
13 p1839 N90-20557
EXOSAT observations of Seyfert type galaxies
13 p1901 N90-20910
Goes I-M and beyond: Science requirements and technology challenges 14 p1934 N90-21067
Investigations into the properties, conditions, and effects of the ionosphere
[AD-A217807] 14 p2005 N90-21489
A case for archaeological reconnaissance of the Cabo Catoche-Porvenir region of the northeastern Yucatan Peninsula
[NASA-TM-102248] 16 p2249 N90-22827
Anderson Mesa, Arizona as a site for an optical interferometric array 16 p2330 N90-23281
Development of cost-effective standards for Earth observation spacecraft 18 p2501 N90-24292
The use of satellite pictures of the Ysselmeer region (Netherlands). Optimization of the use of LANDSAT for water quality applications in the Ysselmeer region
[BCRS-89-31] 18 p2575 N90-24670
Satellite orbit determination and gravity field recovery from satellite-to-satellite tracking
[LR-605] 19 p2663 N90-25157
Electron populations above the nightside auroral oval during magnetic quiet times
[IRF-PREPRINT-116] 19 p2714 N90-25445
Ginga observations of X ray pulsars
19 p2766 N90-25718
Ginga observations of QPO 19 p2769 N90-25739
The impacts of Ginga results on QPO models
19 p2770 N90-25744
Ginga observations of SS 433
19 p2776 N90-25789
New X ray pulsars discovered with the Ginga satellite
19 p2777 N90-25795
Properties of circumstellar matter in GX301-2 observed by Tenma 19 p2778 N90-25798
Ginga observations of dipping low mass X ray binaries
19 p2781 N90-25821
Constraints on the SS433 system from the Ginga observations 19 p2784 N90-25838
Ginga observations of the X ray spectra of AGN
19 p2786 N90-25854
Signposts to the future 19 p2788 N90-25867
The 27-28 October 1986 FIRE IFO cirrus case study: Cirrus parameter relationships derived from satellite and lidar data
[NASA-TM-103469] 20 p2890 N90-26447
Estimation of convective rain volumes utilizing the are-time-integral technique
[NASA-CR-186814] 20 p2890 N90-26449
Laboratory studies, analysis, and interpretation of the spectra of hydrocarbons present in planetary atmospheres including cyanoacetylene, acetylene, propane, and ethane 20 p2943 N90-26748
The main products and their distribution of FY-1 meteorological satellite
[AD-A221582] 21 p2967 N90-26865
The global positioning system: A new tool for tectonic studies 21 p3014 N90-27137
Downwelled longwave surface irradiance data from five sites for the FIRE/SRB Wisconsin Experiment from October 12 through November 2, 1986
[NASA-TM-102597] 21 p3030 N90-27225
Analysis of cirrus optical properties with data from NASA ER2 High-resolution Interferometer Sounder (HIS)
[NASA-CR-186365] 21 p3030 N90-27227
Comparison of satellite derived dynamical quantities in the stratosphere of the Southern Hemisphere
22 p3210 N90-28210
Lidar cloud studies for FIRE and ECLIPS
[NASA-CR-186384] 22 p3211 N90-28214
Large-scale variability in marine stratocumulus clouds defined from simultaneous aircraft and satellite measurements 22 p3213 N90-28226
On estimating scale invariance in stratocumulus cloud fields 22 p3213 N90-28227
Intercomparisons of GOES-derived cloud parameters and surface observations over San Nicolas Island
22 p3214 N90-28229
Stratocumulus cloud height variations determined from surface and satellite observations
22 p3214 N90-28230
July 16, 1987 revisited: Lessons for modelers
22 p3214 N90-28232
Reflectivities of uniform and broken stratiform clouds: An update 22 p3215 N90-28236
Spectral absorption of marine stratocumulus clouds derived from in situ cloud radiation measurements
22 p3215 N90-28238
Cloud optical parameters as derived from the multispectral cloud radiometer 22 p3215 N90-28239
Satellite-derived cloud and radiation fields over the marine stratocumulus IFO 22 p3216 N90-28240
Direct and remote sensing observations of the effects of ships on clouds 22 p3216 N90-28252
A cloudiness transition in a marine boundary layer
22 p3219 N90-28259
FIRE aircraft observations of horizontal and vertical transport in marine stratocumulus
22 p3220 N90-28261
A comparison of ISCCP and FIRE satellite cloud parameters 22 p3221 N90-28267
Comparison of satellite based cloud retrieval methods for cirrus and stratocumulus 22 p3221 N90-28268
ETO lidar studies of cirrostratus altocumulogenitus: Another role for supercooled liquid water in cirrus cloud formation 22 p3221 N90-28269
Impact of cirrus on the surface radiative environment at the FIRE ETLA Palisades, NY site
22 p3221 N90-28270
Seasonal and interannual changes in cirrus
22 p3222 N90-28272
Relationship between the longwave cloud radiative forcing at the surface and the top of the atmosphere
22 p3222 N90-28273
Summary of results and conclusions based on analysis of volume imaging and high spectral resolution lidar data acquired during FIRE phase 1, part 1
22 p3223 N90-28278
Moisture and heat budgets of a cirrus cloud from aircraft measurements during FIRE 22 p3223 N90-28279
Satellite-derived cloud fields during the FIRE cirrus IFO case study 22 p3223 N90-28281
Comparison of surface-derived and ISCCP cloud optical properties 22 p3224 N90-28282
A system for recording physical properties of clouds
22 p3227 N90-28301
Intercomparison of standard resolution and high resolution TOVS soundings with radiosonde, lidar, and surface temperature/humidity data
22 p3228 N90-28306
Study of the ocean tides by the assimilation of marigraphic and altimetric satellite data in a hydrodynamic model
[ETN-90-97460] 22 p3231 N90-28320
Satellite measurements of magnetospheric Poynting flux
[AD-A224391] 24 p3490 N90-29724

SATELLITE ORBIT CALCULATION

U ORBIT CALCULATION

SATELLITE ORBITS

NT GEOSYNCHRONOUS ORBITS

NT POLAR ORBITS

On analytic modeling of lunar perturbations of artificial satellites of the earth
[AD-A210440] 01 p0016 N90-10078
Evaluation of 15th- and 30th-order geopotential harmonic coefficients from 26 resonant satellite orbits
[RAE-TR-88045] 04 p0461 N90-12640
Orbit determination and analysis for Cosmos 236 at 15th-order resonance
[RAE-TR-88058] 04 p0461 N90-12641
On mean elements for satellite orbits perturbed by the zonal harmonics of the geopotential
[AD-A212322] 04 p0461 N90-12642
The GEM-T2 gravitational model
[NASA-TM-100746] 04 p0517 N90-12984
Orbit and attitude determination results during launch support operations for SBS-5
[PAPER-7] 05 p0587 N90-13420
Automation of orbit determination functions for National Aeronautics and Space Administration (NASA)-supported satellite missions 05 p0590 N90-13434
Overview of the Hipparcos satellite
05 p0603 N90-13502
Re-entry hazards and cosmos 1900
[FOA-C-30535-9.4] 05 p0613 N90-13583
Precision of semi-geometrically determined SLR baselines vs. site occupation time
[ETN-90-96007] 05 p0665 N90-13885
Application of heuristic satellite plan synthesis algorithms to requirements of the WARC-88 allotment plan
[NASA-TM-102479] 06 p0835 N90-14856
On mean elements for satellite orbits perturbed by the zonal harmonics of the geopotential
[RAE-TM-SPACE-371] 08 p1033 N90-15971
Simulation of shading in synthetic surfaces
[INPE-4869-PRE/1480] 10 p1326 N90-17660
Satellite motion around an oblate planet: A perturbation solution for all orbital parameters
[AD-A216176] 10 p1326 N90-17661
Accuracy of global positioning system broadcast orbits for relative surveys
[PB90-125428] 12 p1602 N90-19218
Orbit acquisition and control strategy for small satellites in inclined eccentric orbits
[ETN-90-96551] 16 p2203 N90-22573
The role of orbit errors in processing of satellite altimeter data
[ETN-90-96699] 16 p2204 N90-22575
Satellite motion in axi-symmetric gravitational field. Part 2: Perturbations due to an arbitrary J(sub l)
[RAE-TR-89022] 16 p2206 N90-22586
Low cost station keeping maneuvers for a small-satellites constellation in tundra orbits
[ETN-90-96553] 16 p2206 N90-22588
Satellite orbitography 17 p2359 N90-23432
Archimedes mission aspects
[ETN-90-96556] 17 p2361 N90-23442
Orbit control strategy for a constellation of three satellites in tundra orbits
[AAS-89-411] 17 p2361 N90-23445
Orbit control for a regional navigation system based on tundra orbit
[AIAA-89-3619] 17 p2365 N90-23466
ISO attitude and orbit control subsystem
[REPT-892-440-104] 17 p2366 N90-23467
Land mobile communications from non geostationary orbits (review of Archimedes ESA study)
[REPT-892-440-106] 17 p2392 N90-23624
Theoretical principles of the FHP-GA trajectory calculation program
[FB-10-89] 19 p2663 N90-25156
Impact of satellite altimetric data on the numerical simulation of the general oceanic currents: Sensitivity to orbit parameters
[ETN-90-97461] 22 p3231 N90-28321
Satellite Constellation Orbit Evaluation (SCORE) program
[AD-A223531] 24 p3438 N90-29417

Satellite motion in an axi-symmetric gravitational field. Part 1: Perturbations due to J2 (second order) and J3
[RAE-TR-88068] 24 p3440 N90-29429

SATELLITE ORIENTATION
Choice of a differential method for the attitude restitution in dynamic unbalance
[CNES-CT/DTI/MS/CM/290] 05 p0613 N90-13582
Control and stability of a spinning symmetric satellite in an elliptical orbit
[AD-A216284] 10 p1328 N90-17672
Spacecraft attitude impacts on COLD-SAT non-vacuum jacketed LH2 supply tank thermal performance
[NASA-TM-103158] 16 p2207 N90-22592
Polar BEAR UV imaging of airglow and aurora-image processing and results
[AD-A219480] 17 p2422 N90-23802

SATELLITE PERTURBATION
An autonomous orbit determination system for earth satellites
[AD-A215671] 09 p1172 N90-16779
Satellite motion around an oblate planet: A perturbation solution for all orbital parameters
[AD-A216176] 10 p1326 N90-17661
Spatial registration of TIROS-N weather satellite data
[AD-A216041] 11 p1536 N90-18841

SATELLITE POWER TRANSMISSION
Second Beamed Space-Power Workshop
[NASA-CP-3037] 01 p0027 N90-10140
Power beaming options 01 p0027 N90-10142
Power from space for use on earth: An emerging global option 01 p0028 N90-10144
History and status of beamed power technology and applications at 2.45 Gigahertz 01 p0029 N90-10150
Overview of microwave concepts 01 p0029 N90-10155
Power for the moon: Is microwave power beaming an option? 01 p0030 N90-10158

SATELLITE RENDEZVOUS
U ORBITAL RENDEZVOUS

SATELLITE REPAIR
U ORBITAL SERVICING

SATELLITE ROTATION
Attitude and spin rate control of a spinning satellite using geomagnetic field
[INPE-4818-NTE/289] 12 p1613 N90-19277
Concurrent processing simulation of the space station 16 p2289 N90-23041

SATELLITE SOLAR ENERGY CONVERSION
Power from space for use on earth: An emerging global option 01 p0028 N90-10144
New energy conversion techniques in space, applicable to propulsion
[AIAA-79-1338] 01 p0028 N90-10145
Technical options for high average power free electron milimeter-wave and laser devices 01 p0029 N90-10151
Laser energy conversion 01 p0029 N90-10152
The modular power subsystem 10 p1332 N90-17700
On-orbit demonstration of GaAs solar cell and panel technologies 10 p1339 N90-17751
Structural and operational aspects of the concentrating SARA-Louver solar generator 10 p1340 N90-17760
SFU solar array 10 p1340 N90-17761
The GSR3: A new approach for solar array deployments 10 p1340 N90-17762
Deployment simulation for the third generation solar arrays GSR3 10 p1340 N90-17763
A low cost anticharging connection system for solar generators and its application on ASPERA solar array 10 p1341 N90-17765
In-orbit performance of CS-3a spacecraft GaAs solar array 10 p1346 N90-17804

SATELLITE SOUNDING
Meteorological rocket observations
[PB89-168769] 02 p0250 N90-11419
Direct statistical thermal wind estimation procedure
[AD-A211256] 02 p0253 N90-11433
Three dimensional analysis of the structure of the atmosphere in polar environments by vertical satellite sounding. Interest for the meteorological forecasts at high latitudes
[ETN-90-95506] 05 p0671 N90-13911
An investigation of satellite sounding products for the remote sensing of the surface energy balance and soil moisture
[NASA-CR-186073] 06 p0801 N90-14664
Synoptic scale tropical waves in multichannel satellite radiance data 06 p0816 N90-14745
Mesoscale analysis by numerical modelling coupled with satellite-based sounding 08 p1100 N90-16370
Intercomparison of standard resolution and high resolution TOVS soundings with radiosonde, lidar, and surface temperature/humidity data 22 p3228 N90-28306

SATELLITE SURFACES
NT LUNAR SURFACE
Optical constraints of kerogen from 0.15 to 40 microns: Comparison with meteoritic organics 20 p2948 N90-26776

SATELLITE TELEVISION
Beamforming devices and feed structures for a DBS flat-plate antenna
[BBC-RD-1989/12] 17 p2386 N90-23592

SATELLITE TEMPERATURE
Spacecraft attitude impacts on COLD-SAT non-vacuum jacketed LH2 supply tank thermal performance
[NASA-TM-103158] 16 p2207 N90-22592

SATELLITE TRACKING
NT SATELLITE-TO-SATELLITE TRACKING
The GEM-T2 gravitational model
[NASA-TM-100746] 04 p0517 N90-12984
Optimum data weighting and error calibration for estimation of gravitational parameters
[NASA-TM-100737] 04 p0517 N90-12985
Analytical derivation and verification of zero-gyro control for the IUE satellite
[NASA-TM-100748] 05 p0645 N90-13767
Application of heuristic satellite plan synthesis algorithms to requirements of the WARC-88 allotment plan
[NASA-TM-102479] 06 p0835 N90-14856
Ground-based deep-space LADAR for satellite detection: A parametric study
[AD-A215673] 09 p1228 N90-17126
Advanced tracking systems design and analysis
[NASA-CR-183459] 10 p1376 N90-17976
A satellite simulation program
[AD-A218079] 13 p1764 N90-20124
Gravity field determination and error assessment techniques 13 p1832 N90-20517
An improved error assessment for the GEM-T1 gravitational model 13 p1832 N90-20518
GPS-aided gravimetry at 30 km altitude from a balloon-borne platform 13 p1834 N90-20530
Geographically correlated orbit error 13 p1838 N90-20551
Local gravity disturbance estimation from multiple-high-single-low satellite-to-satellite tracking 13 p1839 N90-20555
Satellite-to-satellite tracking experiment for global gravity field mapping 13 p1839 N90-20556
Orbit recovery of a low Earth orbiter from GPS and ground tracking stations
[FFI-89/7012] 17 p2361 N90-23446
A reduced-dynamic technique for precise orbit determination 20 p2852 N90-26219
Tracking performance of a combined Costas/AFC-loop under noisy Rayleigh/Rician channel conditions with additive Gaussian noise jamming
[ETN-90-96964] 20 p2855 N90-26237
Integration of GPS and strapdown inertial subsystems into a single unit 24 p3423 N90-29340

SATELLITE TRANSMISSION
Error control techniques for satellite and space communications
[NASA-CR-182751] 05 p0631 N90-13685
LMSS drive simulator for multipath propagation 10 p1372 N90-17950
Japanese propagation experiments with ETS-5 10 p1372 N90-17951
Plan of advanced satellite communication experiments using ETS-6 10 p1372 N90-17952
A CCIR aeronautical mobile satellite report 10 p1372 N90-17954
Performance measurements for a laboratory-simulated 30/20 GHz communication satellite transponder
[NASA-TM-102424] 10 p1376 N90-17977
Effects of amplitude distortions and IF equalization on satellite communication system bit-error rate performance
[NASA-TM-102415] 12 p1645 N90-19454
Numerical Arc Segmentation Algorithm for a Radio Conference-NASARC (version 4.0) technical manual
[NASA-TM-101453] 13 p1788 N90-20264
Diode laser satellite systems for beamed power transmission
[NASA-TP-2992] 18 p2556 N90-24585
EINMUF: An HF MUF, FOT, LUF prediction program
[AD-A221577] 21 p3055 N90-27371
Rain-fade simulation and power augmentation for satellite communication systems
[NASA-TM-103134] 23 p3319 N90-28768

SATELLITE-BORNE INSTRUMENTS
NT ADVANCED VERY HIGH RESOLUTION RADIOMETER
NT TOTAL OZONE MAPPING SPECTROMETER
The solar activity measurements experiments (SAMEX) for improved scientific understanding of solar activity
[NASA-TM-100372] 06 p0867 N90-15036
PROTEL: Design, fabrication, calibration, testing, and satellite integration of a proton telescope
[AD-A214564] 09 p1183 N90-16861
Life test programme of ERS-1 AMI-high power amplifier 10 p1330 N90-17684
The MECB data collecting satellite power supply subsystem 10 p1332 N90-17699
The modular power subsystem 10 p1332 N90-17700
Mathematical modelling and expert system for battery management 10 p1332 N90-17703
High resolution analysis of satellite gradiometry 13 p1840 N90-20561
The mm-wave region propagation experiments by satellite 15 p2081 N90-21916
Complementary information from mm-wave-, infrared-, and gamma ray astronomy 16 p2334 N90-23299
Models of the external source contribution to magnetospheric magnetic fields for CRRES data analysis
[AD-A221059] 18 p2580 N90-24697
Calibration of the visible and near-infrared channels of the LANDSAT-5 Thematic Mapper using high-altitude aircraft measurements
[NASA-TM-102185] 21 p3015 N90-27138

SATELLITE-BORNE PHOTOGRAPHY
Satellite image sequences for motion analysis and change detection 08 p1092 N90-16323
Preliminary experiences with a novel method for the determination of displacement vector fields and satellite image sequences 08 p1093 N90-16324
Analysis of significant weather on meso-alpha scales using conventional and remotely sensed data: Exploratory studies
[AD-A214563] 09 p1248 N90-17238
Forecasters handbook for Central America and adjacent waters
[AD-A216752] 11 p1536 N90-18845
Forecasting 24 and 48 hour intensity changes, for northwestern Pacific tropical cyclones, using satellite imagery
[AD-A218174] 13 p1846 N90-20597
Environmental measurements and analysis: Arctic acoustics experiments in the marginal ice zone
[AD-A220509] 18 p2582 N90-24708
Cloud reflectance characteristics in the presence of variable Dimethylsulfide (DMS) sources
[AD-A222806] 21 p3024 N90-27197

SATELLITE-BORNE RADAR
Development of a traveling wave tube for the project X-SAR. Construction and testing of a breadboard model
[ETN-90-95900] 05 p0636 N90-13713
Programmable generation of linear frequency modulated pulses 14 p1961 N90-21232
Analysis and test interaction in the development of a hold down and release mechanism 18 p2539 N90-24489

SATELLITE-TO-SATELLITE TRACKING
Satellite orbit determination and gravity field recovery from satellite-to-satellite tracking
[LR-605] 19 p2663 N90-25157

SATURABLE REACTORS
Investigations into the use of dielectric coatings in magnetic switches
[DE90-014331] 23 p3321 N90-28776

SATURATED HYDROCARBONS
U ALKANES

SATURATION
Thermophysical properties of isopropyl alcohol. Part 1: The ideal gas and the saturated liquid and vapour
[ESDU-89017-PT-1] 06 p0738 N90-14297
Thermophysical properties of isopropyl alcohol. Part 2: Thermodynamic properties at elevated pressures
[ESDU-89020-PT-2] 06 p0739 N90-14300

SATURN (PLANET)
Auroral ultraviolet darkening on the outer planets 15 p2192 N90-22518
High resolution, low temperature photoabsorption cross-section of C2H2 with application to Saturn's atmosphere 20 p2945 N90-26757
Carbon in the outer solar system 21 p3096 N90-27593

SATURN ATMOSPHERE
Investigation of the Saturn dust environment from the analysis of energetic charged particle measurements
[NASA-CR-186727] 20 p2950 N90-26784

SATURN RINGS
Waves in Saturn's rings probed by radio occultation 15 p2191 N90-22511

SATURN SATELLITES
NT IAPETUS
NT PHOEBE
NT RHEA (ASTRONOMY)
NT TITAN

Laboratory studies of the interaction of ions with condensed gases: Planetary applications
20 p2949 N90-26778

SAVANNAHS
U GRASSLANDS

SAWS
Lunar stone saw
[NASA-CR-182438] 17 p2412 N90-23741

SAWTOOTH WAVEFORMS
First results from the MST (Madison Symmetric Torus) reversed field pinch
[DE90-005743] 10 p1433 N90-18268

SCALAR MAGNETIC CHARGE
U MAGNETIC CHARGE DENSITY

SCALARS
Scalar fields versus black holes
[DE89-611967] 03 p0420 N90-12413
Scalar transport in turbulent shear flows
05 p0640 N90-13734
On the application of subcell resolution to conservation laws with stiff source terms
[NASA-TM-102384] 06 p0833 N90-14844
An exact solution for a thick domain wall in general relativity
[NASA-CR-185013] 07 p1006 N90-15826
Nonlocality and stochastic quantization of field theory
[DE89-633913] 07 p1007 N90-15833
Non-Fourier computer generated holography for 3-D display
[AD-A215369] 09 p1225 N90-17109
An entropy-based approach to nonlinear stability
[NASA-TM-101086] 09 p1272 N90-17376
A kinetic equation with kinetic entropy functions for scalar conservation laws
[NASA-CR-181985] 09 p1277 N90-17401
Self similar solutions of the second kind of nonlinear diffusion-type equations
[DE90-606953] 10 p1422 N90-18204
Potential theory of radiation 12 p1635 N90-19395
Simulation of radar scattering from rough surfaces
[AD-A217841] 13 p1790 N90-20275
Cell averaging Chebyshev methods for hyperbolic problems
[NASA-CR-182028] 13 p1877 N90-20768
The dynamics of scalar fields in the early universe
14 p2039 N90-21696
Soft inflation
[NASA-CR-186593] 15 p2190 N90-22506
The multifractal nature of turbulence
16 p2235 N90-22752
Evaluation and representation of two and three dimensional data fields from optical stream measurements
[MPIS-18/1989] 17 p2474 N90-24143
Scalar dissipation measurements in the developing region of a jet 21 p2976 N90-26909
The spatial scalar structure of premixed turbulent stagnation point flames
[DE90-014189] 23 p3303 N90-28686
Casimir effect in a D-dimensional flat spacetime and the cut-off method
[DE90-627177] 23 p3390 N90-29151
Quantum gravity in two dimensions and the SL(2,R) current algebra
[DE90-627215] 23 p3391 N90-29156
On the infrared behaviour of some non-Minkowskian quantum fields 23 p3410 N90-29273
Ray traced scalar fields with shaded polygonal output
[DE90-011023] 24 p3529 N90-29955

SCALE (CORROSION)
Polypeptide inhibitors of mineral scaling and corrosion
[AD-A210507] 01 p0041 N90-10225
A review of the effects of microalloying constituents on the formation and breakdown of protective oxide scales on high-temperature alloys at temperatures below 700 C
[DE90-001277] 07 p0902 N90-15216
Experimental evaluation of new alloy coatings
[AD-A214922] 09 p1194 N90-16916
Study of adherent oxide scales
[AD-A215189] 09 p1198 N90-16940
Improved high temperature oxidation behavior of alloys by ion implantation
[AERE-R-13309] 16 p2217 N90-22650
High temperature surface interactions: Overview
23 p3306 N90-28699
Scale adherence effects in oxidation and sulfidation
23 p3307 N90-28703

SCALE EFFECT
Scaling study for SP-100 reactor technology
[NASA-TM-897140] 08 p1122 N90-16496
Effects of scaling on the performance of magnetoplasmadynamic thrusters
[AD-A215690] 09 p1184 N90-16863
An electrical model for plasma armature voltage
[DE90-007530] 12 p1718 N90-19866
Scaling effects in the static and dynamic response of graphite-epoxy beam-columns
[NASA-TM-102697] 20 p2876 N90-26363
Terrain visual cue analysis for simulating low-level flight: A multidimensional scaling approach
[AD-A223564] 24 p3436 N90-29407
Scale effects in steady-state friction
[DE90-012943] 24 p3476 N90-29647

SCALE HEIGHT
An analysis of the Palomar-Green subdwarfs and white dwarfs 23 p3409 N90-29263

SCALE MODELS
The spinning of aircraft: A discussion of spin prediction techniques including a chronological bibliography
[ARL-AERO-R-177] 02 p0155 N90-10888
Demonstration epicyclic gearbox
[PNR90567] 04 p0508 N90-12932
Application of two-point closures to subgrid scale modeling for homogeneous, 3D turbulence
05 p0640 N90-13732
Electromagnetic scale models using emulsions
[AD-A214855] 09 p1211 N90-17022
Engine inlet distortion in a 9.2 percent scale vectored thrust STOVL model in ground effect
[NASA-TM-102358] 10 p1307 N90-17561
Measurement and computer simulation of antennas on ships and aircraft for results of operational reliability
10 p1369 N90-17936
Automation of an RCS (Radar Cross Section) measurement system and its application to investigate the electromagnetic scattering from scale model aircraft canopies
[AD-A215741] 10 p1375 N90-17970
Lightning surge characteristics of transmission towers. Lightning surge characteristics of 15-meter-high scale model tower
[DE89-782322] 12 p1692 N90-19721
A new stress routine for the Projectile Design Analysis System (PRODAS)
[AD-A220564] 17 p2346 N90-23357
Expansion and orthogonalization of measured modes for structure identification 18 p2647 N90-25068
Wind tunnel study of wake downwash behind A 6 percent scale model B1-B aircraft
[DE90-011783] 20 p2802 N90-25941
Measurement of velocity and temperature profiles at the exit plane of a tubular gas turbine combustor
[DE90-505519] 20 p2809 N90-25983
Scaling effects in the static and dynamic response of graphite-epoxy beam-columns
[NASA-TM-102697] 20 p2876 N90-26363
The scalability of OTR (Out-of-core Thermionic Reactor) space nuclear power systems
[DE90-013553] 21 p3075 N90-27485

SCALERS
Double-periodic wormholes in theories with global symmetries
[DE90-719575] 08 p1136 N90-16581

SCALING LAWS
Scaling and modeling of turbulent suspension flows
01 p0069 N90-10393
Scaling in a non Abelian string network
[ROM1F-89-676] 05 p0695 N90-14066
Configurational statistics of strings, fractals and polymer physics. Part 2: Non Abelian strings
[ROM1F-89-680-PT-2] 05 p0696 N90-14067
String correlations and galaxies formation
[ROM1F-89-677] 05 p0713 N90-14170
Non Abelian string correlations and galaxies formation
[ROM1F-89-678] 05 p0714 N90-14171
Des Cloizeaux's law for strings and galaxies formation. Part 1: Abelian configurations
[ROM1F-89-681-PT-1] 05 p0714 N90-14172
A continuous plasma final focus
[DE90-006096] 11 p1568 N90-19024
On the application of similarity laws to a scaled railway bogie model
[DLR-FB-90-06] 23 p3335 N90-28853

SCANDIUM
Cryogenic mechanical properties of low density superplastic Al-Mg-Sc alloys
[DE90-002120] 07 p0904 N90-15222

SCANNER PROJECT
Multi-application scanning mechanism
18 p2537 N90-24473

SCANNERS
NT COASTAL ZONE COLOR SCANNER
NT INFRARED SCANNERS
NT MULTISPECTRAL BAND SCANNERS
NT OCEAN COLOR SCANNER
NT OPTICAL SCANNERS
NT THEMATIC MAPPERS (LANDSAT)
NT ULTRASONIC SCANNERS
Vehicle antenna for the mobile satellite experiment
[NASA-CR-186109] 06 p0733 N90-14271
Qualification of the RSRM case membrane case-to-insulation bondline inspection using the Thiokol Corporation ultrasonic RSRM bondline inspection system
[NASA-CR-183940] 16 p2209 N90-22602
Atmospheric autorotating imaging device
[NASA-CASE-NPO-17390-1-CU]
16 p2238 N90-22769
Qualification of the RSRM field joint CF case-to-insulation bondline inspection using the Thiokol Corporation ultrasonic RSRM bondline inspection system
[NASA-CR-183931] 16 p2242 N90-22788
Volumetric visualization of 3D data
16 p2275 N90-22964
Multi-application scanning mechanism
18 p2537 N90-24473
The feasibility of detecting corrosion in electric fuzes using the thermal transient technique
[AD-A221385] 18 p2549 N90-24547
Failure of the ERBE scanner instrument aboard NOAA 10 spacecraft and results of failure analysis
[NASA-TM-102661] 19 p2694 N90-25328
DoD-University research instrumentation program, FY 1986/FY 1987
[AD-A222578] 20 p2859 N90-26263
Optical characterization of clouds of fine liquid-nitrogen particles
[NASA-TM-103208] 20 p2865 N90-26299
Spatial conductivity measurements on high T(sub c) superconducting films 22 p3148 N90-27849

SCANNING
NT FREQUENCY SCANNING
NT PANORAMIC SCANNING
NT RADAR SCANNING
NT RASTER SCANNING
Synthesis and physical properties of poly(perfluoroalkylether) urethanes
[AD-A210500] 01 p0050 N90-10287
The 1988 year end report for road following at Carnegie-Mellon
[NASA-CR-185967] 01 p0078 N90-10446
Active participation in highly automated systems: Turning the wrong stuff into the right stuff
[AD-A210218] 01 p0101 N90-10572
Online support for the intellectual activity of browsing
01 p0136 N90-10784
HDTV displays: Subjective effects of scanning standards and domestic picture sizes
[BBC-RD-1989/9] 02 p0211 N90-11208
Two VAX-PASCAL terminal interface modules for visualizing scanning and parsing
[MEMO-INF-89-17] 02 p0259 N90-11470
Programmable near-infrared ranging system
[AD-D014237] 06 p0843 N90-14903
Scannable millimeter wave arrays, volume 1
[AD-A213895] 07 p0924 N90-15347
Scannable millimeter wave arrays, volume 2
[AD-A213896] 07 p0924 N90-15348
Development of a performance-based test of gaze capability: A threshold approach
[AD-A214675] 09 p1259 N90-17301
Multi-application scanning mechanism
18 p2537 N90-24473
Cockpit Ocular Recording System (CORS)
[NASA-CR-4281] 21 p3033 N90-27244

SCANNING DEVICES
U SCANNERS

SCANNING LASER ACOUSTIC MICROSCOPE (SLAM)
U ACOUSTIC MICROSCOPES

SCANNING TUNNELING MICROSCOPY
Scanning tunneling microscopy etching of micrometer level features on p-type GaAs
[AD-A209216] 01 p0058 N90-10328
Scanning tunneling microscope studies of surface defects
[AD-A214121] 08 p1130 N90-16543
Characterization of biopolymer surfaces using scanning microscopies
[AD-A216572] 11 p1490 N90-18572
Design and calibration of a vacuum compatible scanning tunneling microscope
[NASA-TM-102514] 13 p1804 N90-20353
Imaging and spectroscopy of small molecules by scanning tunneling microscopy
[AD-A222572] 20 p2924 N90-26641
Kinetic pathway in Stranski-Krastanov growth of Ge on Si(001)
[AD-A224324] 24 p3445 N90-29456
Scanning tunneling microscopy studies of chemisorbed layers on metal surfaces
[DE90-015623] 24 p3450 N90-29486
Microscopic aspects of the initial stages of epitaxial growth. A scanning tunneling microscopy study
[AD-A224325] 24 p3551 N90-30094

Scanning tunneling microscopy of semiconductor surfaces
[AD-A223339] 24 p3552 N90-30095

SCAR PROGRAM
U SUPERSONIC CRUISE AIRCRAFT RESEARCH

SCARS (GEOLOGY)
U EROSION

SCAT
U SUPERSONIC COMMERCIAL AIR TRANSPORT

SCATHA SATELLITE
SCATHA (Spacecraft Charging at High Altitudes) atlas data base, volume 1
[AD-A214204] 07 p0886 N90-15127
SCATHA (Spacecraft Charging At High Altitudes) atlas data base, volume 2
[AD-A214205] 07 p0887 N90-15128
The importance of adiabatic variations in trapped particle distributions observed by the SCATHA satellite
[AD-A220859] 17 p2423 N90-23806
A survey of equatorial magnetospheric wave activity between 5 and 8 R(sub E)
[AD-A220137] 17 p2424 N90-23812

SCATTER PROPAGATION
NT IONOSPHERIC F-SCATTER PROPAGATION
Preliminary investigation of Faraday rotation effects and description of polarization measurements on the AFGL high latitude meteor scatter test bed
[AD-A211298] 04 p0488 N90-12806
Forward scatter propagation path loss testing using surrogate terrain in the 100 to 1500 MHz region
06 p0760 N90-14425
First-order intensity statistics for non-Rayleigh fading
[AD-A217572] 13 p1841 N90-20569
Laboratory studies of acoustic scattering from the underside of sea ice
[AD-A221333] 19 p2753 N90-25644
Observations of plasma structure freezing scale at equatorial latitudes
[AD-A222529] 21 p3026 N90-27207

SCATTERERS
U SCATTERING

SCATTERING
NT ACOUSTIC SCATTERING
NT ATMOSPHERIC SCATTERING
NT BACKSCATTERING
NT COHERENT SCATTERING
NT COMPTON EFFECT
NT ELASTIC SCATTERING
NT ELECTROMAGNETIC SCATTERING
NT ELECTRON RUNAWAY (PLASMA PHYSICS)
NT ELECTRON SCATTERING
NT FORWARD SCATTERING
NT HALOS
NT INCOHERENT SCATTERING
NT INELASTIC SCATTERING
NT INVERSE SCATTERING
NT ION SCATTERING
NT IONOSPHERIC F-SCATTER PROPAGATION
NT LIGHT SCATTERING
NT MICROWAVE SCATTERING
NT MIE SCATTERING
NT NEUTRON SCATTERING
NT NUCLEAR SCATTERING
NT NUCLEON-NUCLEON SCATTERING
NT RADAR SCATTERING
NT RAMAN SPECTRA
NT RAYLEIGH SCATTERING
NT RESONANCE SCATTERING
NT REVERBERATION
NT THOMSON SCATTERING
NT TROPOSPHERIC SCATTERING
NT WAVE SCATTERING
NT X RAY SCATTERING
X-ray and gamma-ray spectroscopy of solids under pressure
[DE89-017271] 02 p0196 N90-11118
Nonprincipal-plane scattering from flat plates: Second-order and corner diffraction and pattern control of horn antennas
[NASA-CR-185485] 02 p0211 N90-11205
Part A: Nonprincipal-plane scattering from flat plates: Second-order and corner diffractions
02 p0211 N90-11206
Calculation of transient response from time-harmonic spectrum
[AD-A211972] 03 p0393 N90-12241
Internal Magnus effects in superfluid 3He-A
[PB89-212617] 03 p0410 N90-12351
Superconductivity and magnetic scattering in the Nd(sub 2-x)Ce(sub x)CuO(sub 4-delta)
[DE89-016524] 03 p0410 N90-12354
Analysis of carbon fiber's x ray microscopic structure
[AD-A212215] 04 p0480 N90-12752
Problems in nonlinear acoustics: Scattering of sound by sound, parametric receiving arrays, nonlinear effects in asymmetric sound beams and pulsed finite amplitude sound beams
[AD-A211756] 04 p0550 N90-13200
Nonpotential scattering for the density matrix and quantum gravity
[PREPRINT-688] 05 p0697 N90-14080
TROPO: A technique for predicting propagation and modem performance of digital troposcatter systems
06 p0764 N90-14444
Dynamical structure of liquid and amorphous metals
[DE90-003805] 07 p0905 N90-15229
Progress in LTE and non-LTE transport calculations
[DE90-003394] 07 p0997 N90-15764
Isotope driven critical scattering and phase separation from mixtures of deuterated and protonated polymers
[DE90-003976] 08 p1051 N90-16076
High-frequency asymptotic methods for analyzing the EM scattering by open-ended waveguide cavities
[NASA-CR-186244] 08 p1056 N90-16103
Sampling scattered data onto rectangular grids for volume visualization
[AD-A215533] 09 p1274 N90-17384
An analysis of scatter decomposition
[NASA-CR-181978] 09 p1276 N90-17396
Investigation of multiple scattering in aqueous suspensions of non-absorbing polystrene microspheres using spectrophotometry
[BCRS-89-09] 11 p1485 N90-18549
The extended equivalent source technique with underdetermined sources
[DE90-006989] 11 p1499 N90-18627
Transport effects and spectroscopy of defects in microstructures
[AD-A216718] 11 p1570 N90-19036
Correlation-induced changes of spectra
[AD-A217087] 12 p1669 N90-19591
Multiple versus single scattering of terrestrial infrared longwave radiation in an aerosol-laden planetary boundary layer
[AD-A217709] 13 p1790 N90-20272
Laser-induced shock waves effects in materials
[DE90-007626] 13 p1807 N90-20379
Laser line transport with refraction
[DE90-008683] 13 p1808 N90-20382
Scattering sources: A spherical harmonics expansion
[DE90-008724] 13 p1867 N90-20711
Fiber optic void fraction sensor
[DE90-009124] 14 p1983 N90-21366
Relativistic stimulated Brillouin and Raman scattering in a laser-produced plasma
[DE90-613123] 14 p2028 N90-21627
The solution of scattering and radiation problems for complex configurations based on 3-D grid and patch models 15 p2096 N90-21997
Elastodynamic scattering and transmission problems in three dimensions by the boundary integral equation method 15 p2111 N90-22077
Current drive in a supernova
15 p2187 N90-22491
An examination of the full-wave method for rough surface scattering
[AD-A218664] 16 p2308 N90-23155
A scattering center based numerical simulation of small scale atmospheric turbulence 16 p2312 N90-23179
Optical properties of novel GaAs-based semiconductors 16 p2321 N90-23235
VLA and VLBI angular broadening measurements: The distribution of interstellar scattering at low Galactic latitudes 16 p2330 N90-23279
Radar detection during scintillation
[AD-A220099] 17 p2393 N90-23630
Theory and experimental technique for nondestructive evaluation of ceramic composites
[NASA-TM-102561] 17 p2414 N90-23754
A comparison of the K-pulse and E-pulse techniques for aspect independent radar target identification
[AD-A220172] 18 p2542 N90-24511
Coupled BE/FE/BE approach for scattering from fluid-filled structures 18 p2570 N90-24649
Electromigration in metallic microstructures
[AD-A221208] 18 p2622 N90-24942
The effects of urban air pollution on solar radiation
[DE89-009455] 19 p2712 N90-25438
Automated angular momentum recoupling algebra
[DE90-011988] 19 p2750 N90-25626
Scattering from coated structures and antenna pattern control using impedance surfaces, part A/B
[NASA-CR-186871] 20 p2854 N90-26233
The 27-28 October 1986 FIRE IFO cirrus case study: Cirrus parameter relationships derived from satellite and lidar data
[NASA-TM-103469] 20 p2890 N90-26447
Non-destructive characterization of polymer/metal interphases using surface-enhanced Raman scattering
[AD-A222490] 21 p2988 N90-26980
Atmospherically induced optical contamination from orbiting thrusters
[AD-A223112] 21 p3021 N90-27174
Symmetry breaking oxygen displacement in superconducting oxides
[DE90-013670] 21 p3081 N90-27520
Wideband impedance transformer for UHF power transistor time domain waveform measurement system
[PB90-210642] 22 p3167 N90-27962
Front range lidar, aircraft, and balloon experiment
[PB90-225301] 22 p3212 N90-28218
Analysis of ER-2 radiometer and lidar observations from the 1987 marine stratus experiment
22 p3216 N90-28241
New approach to HF channel modeling and simulation. Part 2: Stochastic model
[PB90-200338] 23 p3317 N90-28755
Investigation of particulate formation during diesel spray combustion
[DE90-012682] 24 p3446 N90-29464
Radar clutter via ray methods
[AD-A223796] 24 p3462 N90-29553
Theoretical and experimental comparison of infrared and visible laser scattering from a variety of surface types
[RSRE-MEMO-4348] 24 p3474 N90-29636
Subpicosecond Raman study of hot electrons and hot phonons in GaAs
[DE90-015634] 24 p3553 N90-30106
Study of hot carrier relaxation in quantum wells by subpicosecond Raman scattering
[DE90-015635] 24 p3554 N90-30107
A comparative first principles study of phase stability in Ni-Ti and Ni-Al alloys around equiatomic composition
[DE90-016477] 24 p3554 N90-30111

SCATTERING AMPLITUDE
On the domain of string perturbation theory
[DE90-600759] 08 p1135 N90-16575

SCATTERING COEFFICIENTS
Remote sensing of the aerosol scattering coefficient with a multi-field-of view lidar 06 p0763 N90-14437
Anomalous absorption by atmospheric water vapor and stabilized water fogs in the infrared and CM-wave regions
[AD-A214202] 07 p0964 N90-15572
Lidar technique for adjusting aerosol model number densities to existing conditions
[AD-A213846] 08 p1101 N90-16374
Some problems in oceanic radiative transfer
[AD-A215935] 10 p1410 N90-18131
Scattering from coated structures and antenna pattern control using impedance surfaces, part A/B
[NASA-CR-186871] 20 p2854 N90-26233

SCATTERING CROSS SECTIONS
Spin fluctuations and excitations in a 2D xy-ferromagnet: CoCl2 in graphite
[DE89-017600] 02 p0196 N90-11119
Investigations into the influence of the state functions on the cross sections of the direct p,gamma reactions at energies in the 100 keV range, and project of a cascade accelerator for the measurement of the p,gamma capture cross sections
[ETN-89-94662] 02 p0273 N90-11561
Pacific marine radar sea scatter experimental results
[AD-A211593] 03 p0339 N90-11931
An explicit partition of the fusion-like cross section
[KVI-797] 04 p0553 N90-13225
A new technique for simulating composite material. Task 2: Analytical solutions with Generalized Impedance Boundary Conditions (GIBCs)
[NASA-CR-186249] 07 p0890 N90-15146
Research on acoustical scattering, diffraction catastrophes, optics of bubbles, acoustical phase conjugation, and wake of an oscillating circular cylinder
[AD-A214168] 07 p0989 N90-15711
Studies of elastic scattering and cross sections of the C-12 + Si-28 system
[DE89-635990] 08 p1120 N90-16486
Heavy ion inelastic scattering with a 4(pi) gamma detector
[DE90-002709] 08 p1120 N90-16488
Neutrino oscillations: An essay in honor of Felix Boehm
[DE90-003223] 08 p1121 N90-16491
A database of fragmentation cross section measurements applicable to cosmic ray propagation calculations
[NASA-CR-186328] 08 p1153 N90-16681
Surface-enhanced Raman scattering
[AD-A215976] 10 p1353 N90-17849
Annihilation in Gases and Galaxies
[NASA-CP-3058] 11 p1555 N90-18957
Positron-alkali atom scattering
11 p1556 N90-18958

Scattering of positrons and electrons by alkali atoms
11 p1556 N90-18959
Positron collisions with alkali-metal atoms
11 p1556 N90-18962
Inelastic collisions of positrons with one-valence-electron targets 11 p1556 N90-18963
Positron-rubidium scattering 11 p1556 N90-18964
Positronium formation in Ss state in e+-Li scattering
11 p1557 N90-18967
New parameter-free polarization potentials in low-energy positron collisions 11 p1557 N90-18968
The calculation of the contributions to low energy e+H2 scattering from sigma u+ and Pion u symmetries using the Kohn variational method 11 p1557 N90-18969
Ab initio R-matrix calculations of e+-molecule scattering 11 p1557 N90-18970
Positron excitation of neon 11 p1558 N90-18973
Positron-inert gas differential elastic scattering
11 p1558 N90-18974
Differential elastic scattering cross sections for 54.9eV positrons incident on helium 11 p1558 N90-18975
Total cross sections for positrons scattered elastically from helium based on new measurements of total ionization cross sections 11 p1558 N90-18976
Low-energy scattering of electrons and positrons in liquids 11 p1559 N90-18981
Anitproton-matter interactions in antiproton applications 11 p1560 N90-18989
Search for resonances in positron-atom systems
11 p1560 N90-18991
Positronium formation in e+ plus H- collisions
11 p1561 N90-18993
Theoretical studies in nuclear physics
[DE90-005981] 11 p1565 N90-19005
Measurement of the space potential of a high-temperature plasma by fast atomic beam scattering on an ion probe beam
[DE90-006118] 11 p1567 N90-19020
The electron momentum-transfer cross sections of tungsten, silicon, and silicon dioxide at energies from 0.1 to 10,000 eV
[DE90-009041] 12 p1712 N90-19833
Large-angle elastic and inelastic scattering of Pi+ and Pi- from Si28 and Ca40
[AD-A218163] 13 p1885 N90-20818
Thomson scattering in a magnetic field
14 p2040 N90-21699
Chopper for neutrinos and antineutrinos
[AD-A218402] 17 p2471 N90-24124
On the explanation of anomalies in inelastic neutron scattering by high-T(sub c) superconductors
[DE90-620561] 17 p2475 N90-24149
Electron-impact spectroscopy
20 p2949 N90-26779
Non-destructive characterization of polymer/metal interphases using surface-enhanced Raman scattering
[AD-A222490] 21 p2988 N90-26980
Backscatter enhancement in scattering from rough surfaces
[AD-A223110] 21 p2995 N90-27024
Theoretical studies of time-of-flight and atom and molecular surface collision
[AD-A221705] 21 p3075 N90-27480
Summary of results and conclusions based on analysis of volume imaging and high spectral resolution lidar data acquired during FIRE phase 1, part 2
22 p3227 N90-28300
A Bayesian derivation of an iterative autofocus/super-resolution algorithm
[RSRE-MEMO-4337] 22 p3239 N90-28371

SCATTERING FUNCTIONS
Generalized random phase approximation for multicomponent polymer systems
[DE90-613691] 14 p1955 N90-21194
The 27-28 October 1986 FIRE IFO Cirrus case study: Comparison of radiative transfer theory with observations by satellite and aircraft
[NASA-TM-103468] 20 p2890 N90-26446
New approach to HF channel modeling and simulation. Part 2: Stochastic model
[PB90-200338] 23 p3317 N90-28755
Angle sample variance of azimuthally spread scattering processes, using a two-element array
[AD-A223572] 24 p3542 N90-30034

SCATTERING MATRIX
U S MATRIX THEORY

SCATTEROMETERS
Investigation of the properties of radar backscatter from sea ice
[AD-A212808] 04 p0493 N90-12838
Multiparameter scatterometer for remote sensing (RADSER). Project Scatter: State-of-the-art and future applications
[INPE-4871-PRE/1482] 11 p1511 N90-18701
Radar scatterometry and polarimetry at 220 GHz
15 p2085 N90-21935
Modifications of the DUTSCAT system
[BCRS-89-33] 18 p2555 N90-24582
Dependence of radar backscatter on the energetics of the air-sea interface
[AD-A221966] 21 p2996 N90-27028
A day-to-day comparison study of Seasat scatterometer winds with winds observed from islands in the tropical Pacific
[NASA-CR-186696] 22 p3212 N90-28223

SCAVENGING
Development of an atmospheric diffusion model in fog (1). Literature review of scavenging process by precipitation
[DE89-782318] 12 p1685 N90-19676
Numerical modeling of atmospheric growth processes
[REPT-70] 12 p1693 N90-19726

SCENE ANALYSIS
Knowledge-based machine vision systems for space station automation
[NASA-CR-185710] 01 p0025 N90-10124
The 1988 year end report for road following at Carnegie-Mellon
[NASA-CR-185967] 01 p0078 N90-10446
Senegalese land surface change analysis and biophysical parameter estimation using NOAA AVHRR spectral data
[NASA-CR-186120] 05 p0664 N90-13883
A logic for the pixel assignment step of imagery classification predicated on class structure
07 p0949 N90-15493
Optical neural nets for scene analysis
[AD-A213986] 07 p0976 N90-15637
High compression image and image sequence coding
08 p1074 N90-16214
A knowledge-based machine vision system for space station automation 08 p1075 N90-16221
Alvey MMI007. Object identification from 2D images: The RSRE contribution
[RSRE-MEMO-4277] 08 p1110 N90-16428
Exocentric direction judgements in computer-generated displays and actual scenes 16 p2270 N90-22936
Optical neural nets for scene analysis
[AD-A220657] 17 p2472 N90-24135
Analysis of camera movement based on a sequence of images
[TELECOM-PARIS-89-D-008] 18 p2616 N90-24901
Ocean feature recognition using genetic algorithms with fuzzy fitness functions (GA/F3)
19 p2740 N90-25576
Extensions of algebraic image operators: An approach to model-based vision 19 p2741 N90-25577
Multi-sensory perception of a geometrical structure of a scene
[ETN-90-97245] 20 p2915 N90-26587
Dynamic monocular machine vision and applications of dynamic monocular machine vision
[LRT-WE-13-FB-88-3] 21 p3061 N90-27406
On-line object feature extraction for multispectral scene representation
[NASA-CR-187006] 23 p3342 N90-28888
Terrain visual cue analysis for simulating low-level flight: A multidimensional scaling approach
[AD-A223564] 24 p3436 N90-29407
Direct estimation of structure and motion from multiple frames
[AD-A223903] 24 p3534 N90-29985

SCF
U SELF CONSISTENT FIELDS

SCHEDULES
QUEST/Ada: Query utility environment for software testing of Ada
[NASA-CR-186121] 06 p0823 N90-14787
Calendar of selected aeronautical and space meetings
[AGARD-CAL-90/1] 11 p1574 N90-19060
Marshall Avionics Testbed System (MAST)
12 p1639 N90-19417
Priority arbitration with busses
[AD-A216392] 12 p1704 N90-19784
Space exploration: NASA's deep space missions are experiencing long delays
[GAO/NSIAD-88-128BR] 18 p2635 N90-25015
Space exploration: Cost, schedule, and performance of NASA's Mars Observer Mission. Fact sheet for the Chairman, Subcommittee on Science, Technology, and Space, Committee on Commerce, Science, and Transportation, US Senate
[GAO/NSIAD-88-137FS] 20 p2815 N90-26021
Space exploration: Cost, schedule, and performance of NASA's Magellan Mission to Venus. Fact sheet for the Chairman, Subcommittee on Science, Technology, and Space, Committee on Commerce, Science, and Transportation, US Senate
[GAO/NSIAD-88-130FS] 20 p2815 N90-26022
Space exploration: Cost, schedule, and performance of NASA's Ulysses Mission to the Sun. Fact sheet for the Chairman, Subcommittee on Science, Technology, and Space, Committee on Commerce, Science, and Transportation, US Senate
[GAO/NSIAD-88-129FS] 20 p2815 N90-26023
A technology assessment of alternative communications systems for the space exploration initiative
[NASA-TM-103243] 22 p3125 N90-27736
Focus of attention in an activity-based scheduler
23 p3369 N90-29039

SCHEDULING
NT PREDICTION ANALYSIS TECHNIQUES
Effective resource utilization for multiprocessor join execution
[DE89-016303] 01 p0105 N90-10595
Application of a hybrid generation/utility assessment heuristic to a class of scheduling problems
[NASA-TM-102367] 01 p0117 N90-10674
Processing rate sensitivities of a heterogeneous multiprocessor
[PB89-229017] 03 p0387 N90-12201
Scheduling sporadic and aperiodic events in a hard real-time system
[AD-A211344] 03 p0387 N90-12205
Algorithm development for SDI weapons system allocation
[AD-A212973] 04 p0534 N90-13090
Ada task scheduling: A focused Ada investigation
[NASA-CR-186072] 05 p0682 N90-13967
Elementary and middle school science improvement project
[NASA-CR-183768] 05 p0705 N90-14125
Payload crew utilization for spacelab missions
[NASA-TP-2976] 06 p0730 N90-14256
Simulating the scheduling of parallel supercomputer applications
[DE90-003604] 07 p0979 N90-15655
Automated observation scheduling for the VLT
[NASA-CR-186282] 07 p1012 N90-15861
Artificial intelligence approaches to astronomical observation scheduling
[NASA-CR-186277] 07 p1012 N90-15862
Automated telescope scheduling
[NASA-CR-186279] 07 p1012 N90-15863
Piloted simulation of a ground-based time-control concept for air traffic control
[NASA-TM-101085] 08 p1020 N90-15898
Dynamically allocating sets of fine-grained processors to running computations 08 p1114 N90-16447
International conference management
08 p1136 N90-16583
Experiences with knowledge-base and large database integration
[DE90-000686] 08 p1137 N90-16591
A planning and scheduling lexicon
[NASA-CR-186061] 09 p1171 N90-16777
Concurrency control for transactions with priorities
[NASA-CR-186268] 09 p1263 N90-17323
Technology maturity assessment methodology SDIO systems SETA
[AD-A214571] 09 p1294 N90-17501
Determination of the underlying task scheduling algorithm for and Ada runtime system
[AD-A215880] 11 p1544 N90-18890
Speculative computation in multilisp
[AD-A216579] 11 p1575 N90-19067
Real-time concurrency control and transaction scheduling
[AD-A218162] 13 p1901 N90-20909
Investigation of air transportation technology at the Massachusetts Institute of Technology, 1988-1989
14 p1905 N90-20922
Time and truth in plans 14 p1906 N90-20930
The 1990 Goddard Conference on Space Applications of Artificial Intelligence
[NASA-CP-3068] 15 p2152 N90-22294
The application of connectionism to query planning/scheduling in intelligent user interfaces
15 p2152 N90-22295
The role of artificial intelligence techniques in scheduling systems 15 p2152 N90-22297
PLAN-IT-2: The next generation planning and scheduling tool 15 p2153 N90-22298
An approach to rescheduling activities based on determination of priority and disruptivity
15 p2153 N90-22299
Space communications scheduler: A rule-based approach to adaptive deadline scheduling
15 p2153 N90-22300
SURE (Science User Resource Expert): A science planning and scheduling assistant for a resource based environment 15 p2153 N90-22302
Managing temporal relations 15 p2154 N90-22304
System control of an autonomous planetary mobile spacecraft 15 p2155 N90-22313

Electric power scheduling: A distributed problem-solving approac'.
[NASA-TM-103149] 15 p2157 N90-22323
An expert system for simulating electric loads aboard Space Station Freedom
[NASA-TM-103150] 15 p2158 N90-22325
Parallel processing of real-time dynamic systems simulation on OSCAR (Optimally SCheduled Advanced multiprocessoR) 16 p2282 N90-23006
Analysis of sequencing and scheduling methods for arrival traffic
[NASA-TM-102795] 17 p2348 N90-23373
Sequencing and scheduling: Algorithms and complexity
[CWI-BS-R8909] 17 p2446 N90-23942
Scheduling around a small common due date
[CWI-BS-R8914] 17 p2446 N90-23943
Probabilistic analysis of the minimum weighted flowtime scheduling problem
[CWI-BS-R8913] 17 p2466 N90-24091
Priority inversion and its prevention
[AD-A218613] 17 p2467 N90-24101
Minimum loss scheduling
[MEMO-821] 18 p2600 N90-24796
MARS, an AI-based Mission Activities and Resource Scheduler
[MBB-0060/89-PUB] 19 p2650 N90-25083
Automated control of hierarchical systems using value-driven methods 19 p2735 N90-25547
Investigation of automated task learning, decomposition and scheduling
[NASA-CR-186791] 20 p2899 N90-26488
Run-time parallelization and scheduling of loops
[NASA-CR-182039] 20 p2902 N90-26509
Evaluation of a decomposition approach for real-time scheduling using a Stochastic model
[AD-A222726] 20 p2921 N90-26625
Spike: Artificial intelligence scheduling for Hubble space telescope 21 p3040 N90-27277
Real-time adaptive aircraft scheduling
[NASA-CR-177558] 22 p3110 N90-27669
ROSES, a Robot Operating System Expert Scheduler: Methodological framework
[DE90-014782] 23 p3334 N90-28851
State-based scheduling: An architecture for telescope observation scheduling 23 p3369 N90-29038
Focus of attention in an activity-based scheduler 23 p3369 N90-29039
Approximation algorithms for planning and control 23 p3370 N90-29042
Efficient mapping algorithms for scheduling robot inverse dynamics computation on a multiprocessor system 23 p3375 N90-29071
Inertial navigation system simulator program: Top-level design
[AD-A223762] 24 p3431 N90-29379
A new momentum management controller for the space station
[NASA-CR-187265] 24 p3440 N90-29425
Reflections on the relationship between artificial intelligence and operations research 24 p3506 N90-29816

SCHEMATICS
U CIRCUIT DIAGRAMS

SCHIFF BASES
U IMINES

SCHLIEREN PHOTOGRAPHY
An investigation of flow structure, mixing and chemical reaction in combusting turbulent flows
[AD-A216739] 11 p1483 N90-18538
Investigation of the vortex flow over a sharp-edged delta wing in the transonic speed regime
[LR-594] 19 p2656 N90-25115
Flow visualization of dynamic stall on an oscillating airfoil
[AD-A222202] 21 p2954 N90-26797
Cavity aeroacoustics
[AD-A223853] 24 p3418 N90-29307

SCHMIDT CAMERAS
Galactical ultra wide angle Schmidt system 18 p2536 N90-24468

SCHMIDT NUMBER
A linear-eddy model of turbulent shear layer mixing 21 p2974 N90-26904

SCHMIDT TELESCOPES
Overview of the Hipparcos payload 05 p0603 N90-13503
The telescope mirrors 05 p0603 N90-13504
The baffles 05 p0604 N90-13509
Research and facilities handbook 1989
[ISSN-0267-6281] 19 p2784 N90-25840

SCHOOLS
Elementary and middle school science improvement project
[NASA-CR-183768] 05 p0705 N90-14125
Laser Technology Center
[PB90-115387] 12 p1665 N90-19564
The United States Air Force School of Aerospace Medicine: Special report
[AD-A217740] 13 p1851 N90-20622
ONR (Office of Naval Research) summer scholars for the 1989 PREFACE Program
[AD-A217746] 13 p1903 N90-20919
Launching a dream: A teachers guide to a simulated space shuttle mission
[NASA-TM-89715] 20 p2934 N90-26693

SCHOTTKY BARRIER DIODES
U SCHOTTKY DIODES

SCHOTTKY DIODES
Laterally stacked Schottky diodes for infrared sensor applications
[NASA-CASE-NPO-17426-1-CU] 01 p0058 N90-10329
Design, construction and test of a frequency doubler for 183 GHz
[PB89-212591] 03 p0341 N90-11944
Method of sensitizing PB-Salt epitaxial films for Schottky diodes
[AD-D014244] 06 p0850 N90-14937
High-efficiency Schottky-Varactor frequency multipliers at millimeter waves
[PB90-110701] 09 p1209 N90-17007
Deep level transient spectroscopy in resistive layers
[DE90-008349] 13 p1772 N90-20169
Infrared ground-based astronomy with the Hughes 256 X 256 PtSi array 14 p1978 N90-21331
Excess noise, anomalous effects and reliability of high frequency devices (Schottky diodes, MESFET and HEMT)
[LAAS-89-394] 16 p2231 N90-22728
Continued development and characterization of doped layers, contacts, and associated electronic devices in silicon carbide
[AD-A219211] 16 p2232 N90-22737
Investigation of Schottky barriers
[AD-A218422] 16 p2323 N90-23247
Development of a six port network analysis tool for the 1 to 18 GHz bandwidth range
[TELECOM-PARIS-89-D-015] 18 p2545 N90-24527
Photoelectron spectroscopy at limit surfaces of semiconductors with rare Earth and alkali metals
[ETN-90-97322] 22 p3249 N90-28427

SCHOTTKY EFFECT
U WORK FUNCTIONS

SCHROEDINGER EQUATION
Some exact solutions of the three-identical-particle problem with S-wave inverse square potentials
[DE89-618402] 02 p0267 N90-11524
On some stochastic properties of the infinitely dimensional Hamiltonian systems of classical mechanics
[DE89-618403] 02 p0267 N90-11525
The supersonic anisotropic collapse of Langmuir waves 06 p0783 N90-14550
Spectral properties of one dimensional quasi-crystals
[PREPRINT-659] 06 p0850 N90-14938
Nonlinear modulational stability and propagation of an electromagnetic pulse in a two-component, neutral plasma
[AD-A215131] 09 p1207 N90-16994
On the quantum inverse problem for a new type of nonlinear Schroedinger equation for Alfven waves in plasma
[DE90-607469] 10 p1431 N90-18259
Direct and inverse scattering problem associated with the elliptic Sinh-Gordon equation
[AD-A216455] 11 p1551 N90-18931
Local supersymmetry in non-relativistic systems
[DE90-612751] 14 p2034 N90-21670
A posterior stochastic equation for quantum Brownian motion
[PREPRINT-715] 16 p2315 N90-23194
Identifying decohering paths in closed quantum systems
[NASA-CR-182853] 19 p2761 N90-25690

SCHUMANN-RUNGE BANDS
New calculations of photodissociation cross-sections in the O2 Schumann-Runge system 05 p0657 N90-13834

SCHWARTZ INEQUALITY
Formation of design envelope criterion in terms of deterministic spectral procedure
[RAE-TM-SS-9] 20 p2804 N90-25953

SCHWARZSCHILD METRIC
Scalar fields versus black holes
[DE89-611967] 03 p0420 N90-12413
On quantum effects near a black hole singularity
[DE90-600754] 08 p1151 N90-16668
Vector fields, linear spaces and tensors in physics. Part 3: Tensor analysis and its applications
[INPE-5000-MD/41] 11 p1561 N90-18997
Perturbations of test mass motion in the Schwarzschild spacetime using the method of Hamilton and Jacobi 11 p1577 N90-19083
A comment on anisotropic spheres admitting one parameter group of conformal motions
[DE90-627195] 23 p3403 N90-29230

SCIENCE
Summary of research academic departments, 1987-1988
[AD-A213252] 05 p0716 N90-14183

SCIENTIFIC SATELLITES
NT ASTRONOMICAL SATELLITES
NT ATS
NT COSMIC BACKGROUND EXPLORER SATELLITE
NT ENVIRONMENTAL RESEARCH SATELLITES
NT EXOSAT SATELLITE
NT EXPLORER SATELLITES
NT EXPLORER 20 SATELLITE
NT EXPLORER 31 SATELLITE
NT EXTREME ULTRAVIOLET EXPLORER SATELLITE
NT GAMMA RAY OBSERVATORY
NT GEOPOTENTIAL RESEARCH MISSION
NT HUBBLE SPACE TELESCOPE
NT INTERNATIONAL SUN EARTH EXPLORER 3
NT LARGE DEPLOYABLE REFLECTOR
NT LONG DURATION EXPOSURE FACILITY
NT SPACE INFRARED TELESCOPE FACILITY
NT X RAY ASTROPHYSICS FACILITY
Report on ESA's scientific satellites
[ESA-SP-1110] 04 p0463 N90-12649
Spacecraft attitude impacts on COLD-SAT non-vacuum jacketed LH2 supply tank thermal performance
[NASA-TM-103158] 16 p2207 N90-22592
Conceptual design study for Infrared Limb Experiment (IRLE)
[NASA-CR-186950] 21 p2968 N90-26869

SCIENTISTS
Higher education for science and technology: A background paper
[PB89-191290] 02 p0287 N90-11642
Space flight (selected articles)
[AD-A212068] 03 p0311 N90-11769
Science and technology resources in US industry: Surveys of science resources series, 1975-1986
[PB90-107194] 06 p0756 N90-14401
Technical communications in aeronautics: Results of an exploratory study. An analysis of profit managers' and nonprofit managers' responses
[NASA-TM-101626] 07 p1009 N90-15848
Reports of planetary astronomy, 1986
[NASA-TM-100776] 08 p1138 N90-16596
European network of interest in the measurement and analysis of mean sea levels from tide gauge records
[PB90-151929] 15 p2134 N90-22196
Interdisciplinary research: Promoting collaboration between the life sciences and medicine and the physical sciences and engineering 17 p2478 N90-24171
Qualitative and quantitative reasoning about thermodynamics
[NASA-CR-186788] 20 p2933 N90-26689
Federal Scientists and Engineers: 1988. (Detailed statistical tables)
[PB90-226895] 22 p3256 N90-28437

SCINTILLATION
Observations of spherical-wave scintillation in strong refractive-index turbulence
[PB89-124747] 01 p0062 N90-10355
A liquid xenon imaging telescope for 1-30 MeV gamma-ray astrophysics
[NASA-CR-185999] 02 p0291 N90-11662
Scintillating fiber ribbon - tungsten calorimeter
[DE89-016705] 03 p0350 N90-12001
Probability density function of optical scintillations (scintillation distribution)
[PB89-103912] 06 p0843 N90-14906
A CCIR aeronautical mobile satellite report 10 p1372 N90-17954
First-order intensity statistics for non-Rayleigh fading
[AD-A217572] 13 p1841 N90-20569
Scintillation of millimeter-wave intensity and phase caused by turbulence and precipitation 15 p2080 N90-21912
The mm-wave region propagation experiments by satellite 15 p2081 N90-21916
Preliminary results of the peak experiment. ALTAIR deep-space measurements
[AD-A218622] 16 p2229 N90-22714
Radar detection during scintillation
[AD-A220099] 17 p2393 N90-23630
Amplitude and phase scintillation and ionospheric irregularities at sub-auroral latitudes
[AD-A222861] 21 p3025 N90-27198
Predictions of radiation backgrounds for GRO/OSSE
[RAE-TM-SPACE-372] 23 p3414 N90-29293

The effects on antenna-filtered scintillation parameters of non-zero antenna pointing angles
[AD-A223840] 24 p3462 N90-29554
Ionospheric irregularities: Source, structure, plasma processes and effects on sensor systems
[AD-A223908] 24 p3490 N90-29723
An assessment of the application of in situ ion-density data from DMSP to modeling of transionospheric scintillation
[AD-A222695] 24 p3491 N90-29730

SCINTILLATION COUNTERS
Gamma radiation background measurements from Spacelab 2
[NASA-CR-183782] 02 p0297 N90-11689
Radioactivity induced in gamma-ray spectrometers
[RAE-TM-SPACE-363] 04 p0569 N90-13317
The determination of the muon content of EAS from Cygnus X-3 05 p0715 N90-14179
A large detector for cosmic ray abundance and energy measurements 06 p0867 N90-15037
First results from the MACRO (Monopole, Astrophysics, Cosmic Ray Observatory) detector at the Gran Sasso Laboratory
[DE90-003243] 07 p1011 N90-15858
A low-threshold EAS (Extensive-Air-Shower) array for gamma-ray astronomy at Los Alamos
[DE89-016780] 08 p1139 N90-16600
Status of the expansion of the CYGNUS array at Los Alamos
[DE89-016781] 08 p1139 N90-16601
Performance of a coincidence based blood activity monitor
[DE90-006105] 11 p1540 N90-18865
Conception of an automatic measurement installation for spatial resolution detectors
[ETN-90-95732] 12 p1729 N90-19935
Mercuric iodide room temperature gamma-ray detectors
[NASA-TM-103318] 13 p1804 N90-20357
Development of intrinsic IPT scintillator
[DE90-007906] 14 p1984 N90-21367
Evaluation of scintillometer
[FOA-C-30546-3.1] 18 p2555 N90-24578
Methodology investigation calibration and quality control for new meteorological instrumentation, part 1
[AD-A221407] 18 p2582 N90-24706
Astronomy at ultra-high energies: Results from the CYGNUS experiment
[DE90-011979] 20 p2940 N90-26732
An assessment of the application of in situ ion-density data from DMSP to modeling of transionospheric scintillation
[AD-A224392] 24 p3490 N90-29725
Detector to study low-flex hard x ray/gamma ray sources
[UT-HE-90/08] 24 p3564 N90-30164

SCINTILLATORS
U SCINTILLATION COUNTERS

SCINTILLOMETERS
U SCINTILLATION COUNTERS

SCISSION
U CLEAVAGE

SCOOPS
Ramjet and ramrocket propulsion systems for missiles 21 p2973 N90-26897

SCORING
Test-retest reliability of oxford Medilog 9000 sleep recording and SS-90-3 sleep stage scoring
[AD-A211165] 02 p0254 N90-11440
Formula scoring: Basic theory and applications
[AD-A218368] 17 p2465 N90-24083
Nylon and teflon scribe effect on NBR to Chemlok 233 and NBR to NBR bond interfaces
[NASA-CR-184004] 22 p3189 N90-28095

SCOUT PROJECT
TOPAS preparation study: Summary representation of the study results
[OHB-TN-TOP-011/87] 12 p1607 N90-19244

SCR (RECTIFIERS)
U SILICON CONTROLLED RECTIFIERS

SCRAMJET ENGINES
U SUPERSONIC COMBUSTION RAMJET ENGINES

SCRAMJETS
U SUPERSONIC COMBUSTION RAMJET ENGINES

SCREWS
A feasibility study of hydrogen dosage estimation in screw threads submitted to surface electrolytic treatment
[CETIM-110110] 04 p0476 N90-12730
Small screw study: Fastener tensile strength and optimum thread depth
[DE90-005001] 09 p1231 N90-17141
Data and conclusions from tests on small screws
[DE90-007500] 15 p2106 N90-22048

SCRIBING
U SCORING

SCRUBBING
U WASHING

SCUTUM CONSTELLATION
Pulsations of delta Scuti stars
[DE90-003213] 08 p1139 N90-16598

SDV
U SHUTTLE DERIVED VEHICLES

SEA BREEZE
Verification study of a three-dimensional local scale atmospheric model PHYSIC at seacoast region
[DE90-719560] 08 p1102 N90-16384
An analysis of diurnal wind variability in the Santa Barbara Channel from SODAR measurements
[AD-A215769] 10 p1408 N90-18121
Report on meteorological assessment of Bald Hills incidents, phase 1
[AD-A216201] 10 p1408 N90-18123
Sea breeze: Induced mesoscale systems and severe weather
[NASA-CR-186367] 19 p2715 N90-25450
Vandenberg Boundary Layer Survey (VBLS): Results
[AD-A222517] 21 p3031 N90-27234

SEA ICE
NT ICE FLOES
NT ICEBERGS
The sea ice margins: A summary of physical phenomena
[PB89-212328] 02 p0253 N90-11436
Remote sensing data acquisition, analysis and archival
[PB89-142566] 03 p0365 N90-12085
Investigation of the properties of radar backscatter from sea ice
[AD-A212808] 04 p0493 N90-12838
The Regional Polar Ice Prediction System, Berents Sea (RPIPS-B): A technical description
[AD-A213159] 04 p0522 N90-13012
A rough transform technique for extracting lead features from sea ice imagery
[AD-A212758] 06 p0801 N90-14666
Airborne electromagnetic sensing of sea ice thickness
[AD-A214460] 09 p1240 N90-17198
Active and passive remote sensing of ice
[AD-A214863] 09 p1241 N90-17199
The Polar Ice Prediction System: A sea ice forecasting system
[AD-A214600] 09 p1249 N90-17246
Measurement of fluctuations in the tilt of Arctic ice at the CEAREX Oceanography Camp: Experiment review, data catalog, and preliminary results
[AD-A215059] 09 p1249 N90-17249
Satellite radar altimetry over ice. Volume 1: Processing and corrections of Seasat data over Greenland
[NASA-RP-1233-VOL-1] 13 p1840 N90-20562
Motion detection in astronomical and ice floe images 15 p2140 N90-22231
SeaRISE: A Multidisciplinary Research Initiative to Predict Rapid Changes in Global Sea Level Caused by Collapse of Marine Ice Sheets
[NASA-CP-3075] 16 p2249 N90-22824
A laboratory investigation into microwave backscattering from sea ice
[NASA-CR-186621] 18 p2542 N90-24510
Environmental measurements and analysis: Arctic acoustics experiments in the marginal ice zone
[AD-A220509] 18 p2582 N90-24708
A laboratory investigation into microwave backscattering from sea ice
[NASA-CR-186357] 19 p2705 N90-25390
Laboratory studies of acoustic scattering from the underside of sea ice
[AD-A221333] 19 p2753 N90-25644
Spatial cross-correlation of Antarctic Sea ice and seabed topography
[NASA-CR-186815] 20 p2891 N90-26451
Ross Sea oceanographic data, 1983-1987: USCGC GLACIER, January-February 1983; USCGC POLAR SEA, January-February 1984; USCGC POLAR STAR, February 1984; USCGC POLAR SEA, February 1987
[PB90-243932] 23 p3354 N90-28955
A global approach to image texture analysis
[AD-A223532] 24 p3527 N90-29941

SEA LAUNCHING
Kestrel 3 Program
[DE90-001796] 06 p0721 N90-14209
Elastomeric impulse energy storage and transfer system
[AD-D014223] 06 p0730 N90-14255

SEA LEVEL
Global lake-level variations from 18,000 to 0 years ago: A palaeoclimate analysis
[DE90-000998] 07 p0956 N90-15531
Status of a nonlinear water surge model in February 1988
[KNMI-WR-88-03] 12 p1695 N90-19735
European network of interest in the measurement and analysis of mean sea levels from tide gauge records
[PB90-151929] 15 p2134 N90-22196
SeaRISE: A Multidisciplinary Research Initiative to Predict Rapid Changes in Global Sea Level Caused by Collapse of Marine Ice Sheets
[NASA-CP-3075] 16 p2249 N90-22824
Considerations concerning the determination of the most desirable height for sea dikes
[W-8905] 17 p2431 N90-23853
The integration of GPS heights into the Australian height datum 19 p2705 N90-25392

SEA ROUGHNESS
Laser altimeter for use over the ocean
[AD-A211252] 02 p0224 N90-11286
A linearized surface condition in low speed hydrodynamics
[REPT-89-04] 04 p0501 N90-12885

SEA STATES
Pacific marine radar sea scatter experimental results
[AD-A211593] 03 p0339 N90-11931
ERS-1 European remote sensing satellite: A new tool for global environmental monitoring in the 1990's
[ESA-BR-36] 11 p1526 N90-18782
Ocean variability from crossover differences derived from altimeter measurements
[ETN-90-96695] 17 p2431 N90-23852
Observations of seafloor ambient noise with an ocean bottom seismometer array
[AD-A220159] 17 p2432 N90-23858
Applications of ISES for snow, ice, and sea state 21 p3018 N90-27159
Measuring the vertical directional spectra caused by sea surface sound
[AD-A223883] 23 p3354 N90-28957

SEA SURFACE TEMPERATURE
Atlas of tropical sea surface temperature and surface winds
[PB89-223598] 04 p0521 N90-13009
Airborne FLIR detection of surface targets 06 p0759 N90-14416
Sea surface temperature fields derived from aircraft and ship observations during FASINEX 1986
[AD-A215727] 09 p1250 N90-17250
On the relationship between water vapor over the oceans and sea surface temperature
[NASA-CR-186199] 10 p1409 N90-18127
The effects of abrupt topography on ocean currents as sensed by satellite remote sensing
[AD-A214123] 10 p1409 N90-18128
Effects of heating/cooling on changes in sea surface temperature: Consequences for computation of surface advection from satellite images
[AD-A214125] 10 p1409 N90-18129
Intertropical Convergence Zone (ITCZ) and its relationship with the precipitation of the north-northeast Brazilian region
[INPE-4887-TDL/378] 11 p1535 N90-18839
Applications of remote sensing to studies of oceanic upper mixed layer dynamics 15 p2122 N90-22137
The relationship between the buoyancy of near-surface air and the potential temperature of the tropopause 15 p2128 N90-22165
Monthly surface thermal forcing in the tropical Pacific from 1980 to 1983
[NASA-CR-183033] 16 p2259 N90-22877
A stratocumulus thermodynamic analysis: July 5 case study 22 p3217 N90-28245
Stratus: An interactive steady state mixed layer model for personal computers 22 p3219 N90-28255
Turbulent statistics in the vicinity of an SST front: A north wind case, FASINEX February 16, 1986 22 p3221 N90-28266

SEA WATER
Corrosion rates of structural materials on the ocean floor
[DE89-015211] 02 p0197 N90-11123
Long endurance underwater power system
[AD-A211386] 03 p0366 N90-12096
The biocorrosion of copper by biopolymers as examined in situ, in real time FT-IR/CIR/ATR in conjunction with pre and post XPS/AES
[DE90-002086] 06 p0747 N90-14348
Sea surface temperature fields derived from aircraft and ship observations during FASINEX 1986
[AD-A215727] 09 p1250 N90-17250
Remote sensing of evaporation ducts for Naval warfare
[AD-A214849] 10 p1374 N90-17965
The effects of abrupt topography on ocean currents as sensed by satellite remote sensing
[AD-A214123] 10 p1409 N90-18128
Experiments on oxygen desorption from surface warm seawater under Open-Cycle Ocean Thermal Energy Conversion (OC-OTEC) conditions
[DE90-000308] 12 p1683 N90-19666

Remote sensing applied to sea water quality researches in coastal regions: A review
[INPE-4935-PRE/1425] 14 p1995 N90-21438
Measurement of the reflectance ratio of natural light in the sea
[IOS-265] 15 p2135 N90-22199
The trace metal geochemistry of suspended oceanic particulate matter
[AD-A218604] 17 p2429 N90-23839
Trace metal sources for the atlantic inflow to the Mediterranean Sea
[AD-A218607] 17 p2429 N90-23842

SEALANTS
U SEALERS

SEALERS
The effect of primer age on adhesion of polysulphide sealant 08 p1022 N90-15909
Improved performance polysulfide based sealant 08 p1022 N90-15910
Fuel resistant coatings for metal and composite fuel tanks 08 p1022 N90-15911
Effect of temperature on the storage life of polysulfide aircraft sealants
[MRL-TR-89-31] 12 p1629 N90-19364
The corrosion protection of 6061-T6 aluminum by a polyurethane-sealed anodized coat
[NASA-TM-100394] 14 p1955 N90-21191
Seal requirements in rocket propulsion
[ETN-90-96611] 16 p2205 N90-22580
UNICOAT: Development of a primer/topcoat and flexible primer for aluminum
[AD-A221803] 21 p2989 N90-26986

SEALING
NT SELF SEALING
Apparatus and method for monitoring pressure leaks from a sealed system
[AD-D014168] 03 p0349 N90-11995
A theoretical study of ingress for shrouded rotating disk systems with radial outflow
[PNR90586] 04 p0455 N90-12607
Flanged joints of aeroengines
[PNR90594] 04 p0455 N90-12609
Advanced actuation systems development, volume 1
[AD-A213334] 04 p0458 N90-12624
Development and testing of a contactless static/dynamic shaft seal with little sealing gas requirement
[KFK-4599] 05 p0652 N90-13802
High temperature, flexible, thermal barrier seal
[NASA-CASE-LEW-14672-1] 07 p0940 N90-15444
Integral fuel tank sealing practice at British Aerospace (Kingston) 08 p1021 N90-15905
The repair of aircraft integral fuel tanks in the RAF: A user's view of fuel tank technology 08 p1022 N90-15908
Fuel resistant coatings for metal and composite fuel tanks 08 p1022 N90-15911
Spray sealing: A breakthrough in integral fuel tank sealing technology 08 p1022 N90-15912
Design philosophy and construction techniques for integral fuselage fuel tanks 08 p1023 N90-15913
Integral fuel tank certification and test methods 08 p1023 N90-15916
Sealing L-alloys/FeS(x) cells for a bipolar battery
[DE90-004887] 09 p1214 N90-17040
Flight set 360T004 (STS-30)
[NASA-CR-183927] 15 p2106 N90-22049
Seal requirements in rocket propulsion
[ETN-90-96611] 16 p2205 N90-22580
High temperature flexible seal
[NASA-CASE-LEW-14695-1] 17 p2413 N90-23751
Flight set 360L001 (STS-26) igniter, post flight
[NASA-CR-183957] 20 p2870 N90-26325
Igniter adapter-to-igniter chamber deflection test
[NASA-CR-184002] 22 p3133 N90-27780
Flight set 360H005 (STS-28) seals, volume 4
[NASA-CR-183904] 22 p3181 N90-28051

SEALS (STOPPERS)
NT GASKETS
NT HERMETIC SEALS
NT O RING SEALS
NT PACKINGS (SEALS)
NT PLUGS
Independent Orbiter Assessment (IOA): Assessment of the mechanical actuation subsystem, volume 1
[NASA-CR-185527-VOL-1] 02 p0169 N90-10952
Independent Orbiter Assessment (IOA): Assessment of the mechanical actuation subsystem, volume 2
[NASA-CR-185527-VOL-2] 02 p0169 N90-10953
Sliding seal materials for low heat rejection engines
[NASA-CR-182262] 03 p0331 N90-11882
A theoretical study of ingress for shrouded rotating disk systems with radial outflow
[PNR90586] 04 p0455 N90-12607
Sodium/sulfur post-test analysis at ANL
[DE90-001911] 06 p0771 N90-14488
On the selection of materials for cryogenic seals and the testing of their performance 08 p1156 N90-16696
Polycarbonate article with chemical resistant coating
[NASA-CASE-MSC-21503-1] 09 p1195 N90-16925
Investigation of SSME alternate high pressure fuel turbopump lift-off seal fluid and structural dynamic interaction 12 p1636 N90-19400
Thiokol/Wasatch installation evaluation of the redesigned field joint protection system (concepts 1 and 3)
[NASA-CR-183860] 13 p1765 N90-20127
The development of ultraviolet-ozone cleaning as a production process in the packaging of integrated circuits
[DE90-007960] 14 p1959 N90-21220
High temperature flexible seal
[NASA-CASE-LEW-14695-1] 17 p2413 N90-23751
Experimental investigation of the hydrodynamic forces on the shroud of a centrifugal pump impeller
[NASA-CR-186952] 21 p3009 N90-27108
Rotordynamic properties of high pressure seals: An experimental approach 24 p3475 N90-29640

SEARCH AND RESCUE SATELLITE
U SARSAT

SEARCH FOR EXTRATERRESTRIAL INTELLIGENCE
U PROJECT SETI

SEARCH PROFILES
A comparative evaluation and analysis of end-user search performance in an academic environment 07 p1009 N90-15845
Alternative representations for database responses 07 p1009 N90-15847
A hybrid model for document retrieval systems 10 p1441 N90-18315
Space communications scheduler: A rule-based approach to adaptive deadline scheduling 15 p2153 N90-22300
The EISI (Elemental and Interplanar Spacing Index) index: A search/match tool for electron diffraction phase analysis
[DE90-010832] 20 p2830 N90-26097

SEARCH RADAR
NT OVER-THE-HORIZON RADAR
ASR-9 weather channel test report
[AD-A211749] 03 p0339 N90-11934
Sweep width determination for HU-25B airborne radars: Life raft and recreational boat targets
[AD-A221362] 18 p2545 N90-24524

SEARCHING
NT SEARCH PROFILES
String Search
[PB89-195986] 01 p0104 N90-10593
Online support for the intellectual activity of browsing 01 p0136 N90-10784
Filling or outlining shapes with color: The effects on a visual search task
[AD-A211067] 02 p0255 N90-11444
Effects of type of responding on memory/visual search: Responding just yes or just no can lead to inflexible performance
[AD-A212764] 04 p0526 N90-13033
Novel graph searching methods for image analysis
[AD-A213065] 05 p0682 N90-13971
A note on the maximum size of a rectilinear maze
[AD-A214445] 07 p0982 N90-15668
Fine tuning your search output: Word processors, desktop publishing, electronic mail, databases, and beyond
[DE90-005192] 09 p1297 N90-17517
The formation and use of knowledge structures in problem solving domains
[AD-A216512] 11 p1552 N90-18936
MEXP: A programming tool for the CESAR programmable systolic array multiprocessor
[FFI-89/7020] 19 p2744 N90-25598
A topological image matcher
[OUEL-1798/89] 19 p2744 N90-25600
DEB: A Diagnostic Experience Browser using similarity networks 21 p3048 N90-27329
Advanced retrieval assistance for the DGIS gateway
[AD-A221592] 21 p3087 N90-27558
Attention, imagery, and memory: A neuromagnetic investigation
[AD-A224560] 24 p3499 N90-29775
Unique binary search tree representations and equality-testing of sets and sequences
[AD-A223643] 24 p3537 N90-30002
Textual regularities applicable to full text searching: The case of family history literature 24 p3557 N90-30125

SEAS
NT BALTIC SEA
NT BARENTS SEA
NT BEAUFORT SEA (NORTH AMERICA)
NT BERING SEA
NT BLACK SEA
NT CARIBBEAN SEA
NT CASPIAN SEA
NT MEDITERRANEAN SEA
NT NORTH SEA
Investigation of the properties of radar backscatter from sea ice
[AD-A212808] 04 p0493 N90-12838
A statistical model of the infrared signature of a wind roughened sea
[AD-A214531] 09 p1249 N90-17245
User's guide: Programs for processing altimeter data over inland seas
[NASA-TM-100730] 13 p1841 N90-20572
Calculation of IR propagation statistics in the eastern Atlantic for surveillance system performance assessment 15 p2085 N90-21938

SEASAT PROGRAM
Investigation of the backscatter behavior of selected test areas in two geocoded SEASAT-SAR scenes in greater Bonn (Fed. Republic of Germany) 08 p1094 N90-16331

SEASAT SATELLITES
Parallel algorithm for determining motion vectors in ice floe images by matching edge features 08 p1114 N90-16451
An application of ocean wave-current refraction to the gulf stream using SEASAT SAR data
[AD-A216769] 11 p1537 N90-18851
Satellite radar altimetry over ice. Volume 1: Processing and corrections of Seasat data over Greenland
[NASA-RP-1233-VOL-1] 13 p1840 N90-20562
Satellite radar altimetry over ice. Volume 2: Users' guide for Greenland elevation data from Seasat
[NASA-RP-1233-VOL-2] 13 p1840 N90-20563
Satellite radar altimetry over ice. Volume 4: Users' guide for Antarctica elevation data from Seasat
[NASA-RP-1233-VOL-4] 13 p1840 N90-20564
A day-to-day comparison study of Seasat scatterometer winds with winds observed from islands in the tropical Pacific
[NASA-CR-186696] 22 p3212 N90-28223

SEASONAL VARIATIONS
U ANNUAL VARIATIONS

SEASONS
NT SPRING (SEASON)
NT SUMMER
NT WINTER
The effects of seasonal and latitudinal earth infrared radiance variations on ERBS attitude control 05 p0586 N90-13414
Summary of 1989 Atlantic tropical cyclone activity and seasonal forecast verification 06 p0815 N90-14743
Seasonal LAI in slash pine estimated with LANDSAT TM
[NASA-TM-102278] 19 p2706 N90-25397
Measurements of CH4, N2O, CO, H2O and O3 in the middle atmosphere by the ATMOS experiment on Spacelab 3
[NASA-TM-103476] 20 p2883 N90-26400

SEAT BELTS
Risk of cervical injury in real and simulated accidents 19 p2721 N90-25475
Biodynamic simulations of an aircraft pilot/passenger in various crash environments
[NIAR-90-6] 20 p2900 N90-26494
Human factors: The human interface with aircraft interiors
[NIAR-90-18] 20 p2900 N90-26496

SEATS
NT EJECTION SEATS
Preliminary fire extinguishing tests with handheld bottles: A comparison of extinguishing compounds
[DOT/FAA/CT-TN89/60] 10 p1368 N90-17930
The application of a non-linear least squares method to predicting seat transmissibility
[ISVR-TR-173] 16 p2275 N90-22967
Operational effects on crashworthy seat attenuators
[AD-A221148] 18 p2495 N90-24259
Biodynamic simulations of an aircraft pilot/passenger in various crash environments
[NIAR-90-6] 20 p2900 N90-26494
Human factors: The human interface with aircraft interiors
[NIAR-90-18] 20 p2900 N90-26496
A review of research and development in crashworthiness of general aviation aircraft: Seats, restraints and floor structures
[AD-A221557] 22 p3115 N90-27698
Military aircrew seating: A human factors engineering approach
[AD-A218049] 23 p3362 N90-28999
A human factors engineering approach to the development and dynamic evaluation of a prototype aircrew seat for military aircraft
[AD-A218283] 24 p3500 N90-29779

SECONDARY BATTERIES
U STORAGE BATTERIES
SECONDARY COSMIC RAYS
LEAP: A balloon-borne search for low-energy cosmic ray antiprotons 07 p1015 N90-15878
SECONDARY EMISSION
Plasma-anode electron gun research
[AD-A211547] 03 p0312 N90-11773
Secondary electron emission characteristics of molybdenum-masked, ion-textured OFHC copper
[NASA-TP-2967] 07 p0902 N90-15211
Technology of fast spark gaps
[AD-A214199] 07 p0925 N90-15353
A voltage contrast detector with double channel energy analyzer in a scanning electron microscope
[ISBN-90-6275-568-2] 19 p2694 N90-25330
Pulsed field sample neutralization
[DE90-015131] 24 p3445 N90-29452
SECONDARY FLOW
Basic studies of the unsteady flow past high angle of attack airfoils
[AD-A210252] 01 p0002 N90-10008
Research on acoustical scattering, diffraction catastrophes, optics of bubbles, acoustical phase conjugation, and wake of an oscillating circular cylinder
[AD-A214168] 07 p0989 N90-15711
Secondary Flows in Turbomachines
[AGARD-CP-469] 14 p1922 N90-21009
Secondary flows and radial mixing predictions in axial compressors 14 p1922 N90-21010
The effects of compressor endwall flow on airfoil incidence and deviation 14 p1922 N90-21011
A study on secondary flow and spanwise mixing in axial flow compressors 14 p1923 N90-21012
Experimental and numerical study on basic phenomena of secondary flows in turbines 14 p1923 N90-21014
Secondary flows and Reynolds stress distributions downstream of a turbine cascade at different expansion ratios 14 p1923 N90-21015
An investigation of secondary flows in nozzle guide vanes 14 p1923 N90-21016
Secondary flow predictions for a transonic nozzle guide vane 14 p1924 N90-21017
Secondary flow in a turbine guide vane with low aspect ratio 14 p1924 N90-21018
Measurement of the flow field in the blade passage and side-wall region of a plane turbine cascade 14 p1924 N90-21019
Calculation of the three dimensional turbulent flow in a linear turbine blade 14 p1924 N90-21021
Calculation of the secondary flow in an axial turbine 14 p1924 N90-21022
Generation and decay of secondary flows and their impact on aerodynamic performance of modern turbomachinery components 14 p1925 N90-21023
Secondary flow calculations for axial and radial compressors 14 p1925 N90-21024
Research on cascade secondary and tip-leakage flows: Periodicity and surface flow visualization 14 p1925 N90-21026
Losses in the tip-leakage flow of a planar cascade of turbine blades 14 p1925 N90-21027
Computational prediction and measurement of the flow in axial turbine cascades and stages 14 p1925 N90-21028
Detailed heat transfer measurements in nozzle guide vane passages in linear and annular cascades in the presence of secondary flows 14 p1926 N90-21030
Effects of secondary flow on heat transfer in rotating passages 14 p1926 N90-21031
Theoretical study of the flow in a rotating channel. Experimental study through flow visualization in a curved channel 14 p1926 N90-21032
The effect of secondary flow on the redistribution of the total temperature field downstream of a stationary turbine cascade 14 p1926 N90-21033
Effect of suction on controlling the secondary instability of boundary layers
[NASA-CR-4306] 18 p2552 N90-24566
Decay of secondary flow and the associated loss variation downstream of an annual turbine stator cascade
[DE90-505520] 20 p2809 N90-25984
Measurement of terms and parameters in turbulent models
[NASA-CR-183993] 20 p2860 N90-26271
Heat exchanger with oscillating flow
[NASA-CASE-LAR-14033-1] 21 p3004 N90-27072
Free shear layer and swirl flow heat transfer enhancement
[PB90-228123] 23 p3325 N90-28798
Secondary flow in presence of wall jets: Incorporation of compression effects in a quasi-elliptic Navier-Stokes calculation code
[ETN-90-97559] 24 p3469 N90-29602
SECONDARY RADAR
Aircraft Reply and Interference Environment Simulator (ARIES) hardware principles of operation. Volume 2: Appendixes
[DOT/FAA/CT-TN88/4-2] 04 p0484 N90-12781
Aircraft Reply and Interference Environment Simulator (ARIES) hardware principles of operation, volume 1
[DOT/FAA/CT-TN88/4-1] 04 p0484 N90-12782
Experimental measurements in secondary radar field: Conception and first results
[ETN-90-95074] 12 p1648 N90-19471
SECONDARY WAVES
U S WAVES
SECRETIONS
NT CORTICOSTEROIDS
NT HORMONES
NT INSULIN
NT PITUITARY HORMONES
NT PROSTAGLANDINS
NT SWEAT
Experiment K-6-20. The effect of spaceflight on pituitary oxytocin and vasopressin content of rats 20 p2896 N90-26473
Experiment K-6-22. Growth hormone regulation, synthesis and secretion in microgravity. Part 1: Somatotroph physiology. Part 2: Immunohistochemical analysis of hypothalamic hormones. Part 3: Plasma analysis 20 p2896 N90-26475
SECULAR PERTURBATION
U LONG TERM EFFECTS
SECURITY
NT AIRPORT SECURITY
NT COMPUTER INFORMATION SECURITY
Analysis of damaged components from DOE security helicopter N7EG
[DE90-004488] 09 p1162 N90-16729
COCOM (Coordinating Committee for Multilateral Exports), technology transfer and its impact on national security
[AD-A214569] 09 p1297 N90-17519
Photochromic papers or films for noncopyable documents
[DE90-004006] 10 p1441 N90-18316
A paradoxical result in unconditionally secure authentication codes, and an explanation
[DE90-008529] 13 p1867 N90-20710
Automating security monitoring and analysis for Space Station Freedom's electric power system
[NASA-TM-103148] 15 p2158 N90-22324
Space operations: NASA is not properly safeguarding valuable data from past missions
[GAO/IMTEC-90-1] 20 p2936 N90-26704
The application of SAW devices in expanded frequency spectrum communications
[AD-A222958] 21 p2994 N90-27021
SEDIMENT TRANSPORT
Saltation thresholds and entrainment of fine particles at Earth and Martian pressures
[NASA-TM-102193] 06 p0860 N90-14997
Saltation and suspension of particulate matter in air
[AD-A213618] 07 p0960 N90-15552
SEDIMENTARY ROCKS
NT COAL
NT LIMESTONE
NT SHALES
SEDIMENTS
NT SANDS
A search for layering in the oceanic crust
[PB89-198220] 01 p0090 N90-10514
Development of a robotics system for automated chemical analysis of sediment, sludges, and soils
[DE90-003637] 07 p0895 N90-15170
Predicting the performance of ceramic filters by the use of silt density index
[DE90-001316] 07 p0909 N90-15256
Molecular dynamics simulation of sedimentation using the monotonic Lagrangian grid
[AD-A215099] 10 p1427 N90-18236
Erosion monitoring using remote sensing, part 2
[BCRS-89-15] 11 p1526 N90-18785
Analysis of tectonic movements utilizing remote sensor products in the Southern Espinhaco (SE) region
[INPE-4830-PRE/1451] 12 p1690 N90-19708
Hydrodynamic interactions and transport coefficients in a suspension of spherical particles
[DE90-008301] 13 p1801 N90-20336
Gaithersburg Nike control and launch area preliminary assessment/site inspection, Gaithersburg, Maryland
[AD-A217791] 14 p2003 N90-21482
The 5th International symposium on palaeolimnology
[AD-A219244] 20 p2887 N90-26431
Production of jet fuels from coal-derived liquids. Volume 13: Evaluation of storage and thermal stability of jet fuels derived from coal liquids
[AD-A224576] 24 p3457 N90-29527
SEEBECK COEFFICIENT
U SEEBECK EFFECT
SEEBECK EFFECT
Superconductivity and magnetic scattering in the Nd(sub 2-x)Ce(sub x)CuO(sub 4-delta)
[DE89-016524] 03 p0410 N90-12354
Preliminary investigation into the effect of high temperature thermal anneals on the figure of merit of silicon germanium alloys
[AD-A218573] 17 p2375 N90-23527
SEEDING (INOCULATION)
U INOCULATION
SEEDS
Laser velocimeter seed particle sizing by the whisker particle collector and laser aerosol spectrometer methods
[PB90-111287] 09 p1224 N90-17103
Implementation of sensor and control designs for bioregenerative systems
[NASA-CR-186655] 20 p2897 N90-26479
Proximate composition of seed and biomass from soybean plants grown at different carbon monoxide (CO2) concentrations
[NASA-TM-103496] 20 p2897 N90-26480
SEEKERS
U HOMING DEVICES
SEEPAGE
The use of remote sensing for the localization of seepage near the Twenthe canal, Netherlands
[BCRS-89-30] 18 p2575 N90-24669
SEGMENTS
On transonic flow over segmented slotted wind tunnel wall with mass transfer 02 p0294 N90-11676
Coherent phasing of segmented mirrors 05 p0598 N90-13474
Precision segmented reflector, figure verification sensor 12 p1611 N90-19272
Parallel distributed networks for image smoothing and segmentation in analog VSLI
[AD-A216780] 12 p1651 N90-19491
Segmentation of Side-Looking Airborne Radar (SLAR) images using a priori knowledge
[BCRS-89-03] 12 p1679 N90-19644
Numerical Arc Segmentation Algorithm for a Radio Conference-NASARC (version 4.0) technical manual
[NASA-TM-101453] 13 p1788 N90-20264
ASCIE: An integrated experiment to study CSI in large segmented optical systems 14 p1936 N90-21082
Ray shooting, implicit point location, and related queries in arrangements of segments
[RUU-CS-89-11] 18 p2601 N90-24807
Counting and reporting intersections in arrangements of line segments
[RUU-CS-89-12] 18 p2601 N90-24808
Storing line segments in partition trees
[RUU-CS-89-17] 18 p2601 N90-24811
Equal path, phase shifting, sample point interferometer for monitoring the configuration of surfaces
[NASA-CASE-NPO-17913-1-CU] 21 p3076 N90-27488
SEGREGATION
U SEPARATION
SEISMIC ENERGY
Regional studies with broadband data
[AD-A219215] 16 p2256 N90-22861
Observations of seafloor ambient noise with an ocean bottom seismometer array
[AD-A220159] 17 p2432 N90-23858
Regional phase propagation in three dimensionally heterogeneous media
[AD-A223279] 24 p3491 N90-29731
SEISMIC WAVES
NT LOVE WAVES
NT RAYLEIGH WAVES
A search for layering in the oceanic crust
[PB89-198220] 01 p0090 N90-10514
Institute of Geophysics and Planetary Physics, 1988
[DE89-014363] 01 p0137 N90-10794
Wind/seismic comparisons for upgrading existing structures
[DE89-016055] 03 p0357 N90-12044
Hydrophone investigations of earthquakes and explosion generated high-frequency seismic phases
[AD-A212055] 03 p0371 N90-12122
Seismic wave attenuation and yield determination at regional distances
[AD-A211548] 03 p0372 N90-12128
ULF/VLF (0.001 to 50 Hz) Seismo-Acoustic Noise in the Ocean
[AD-A212942] 05 p0671 N90-13913
Determination of Q as a function of depth and tectonic province
[AD-A213805] 07 p0960 N90-15554

Theoretical models of earthquake phenomena and the physical significance of seismic moment tensor expansions
[AD-A213813] 07 p0961 N90-15556
A multichannel processing approach to real time network detection, phase association, and threshold monitoring
[AD-A213940] 07 p0980 N90-15657
A numerical and theoretical study of seismic wave diffraction in complex geologic structure
[AD-A218209] 14 p2005 N90-21490
Effects of single fractures on seismic wave propagation
[DE90-009191] 15 p2129 N90-22171
Propagation and attenuation of Lg waves in South America
[AD-A218853] 16 p2255 N90-22859
Regional studies with broadband data
[AD-A219215] 16 p2256 N90-22861
Seismic wave propagation, attenuation and scattering over regional distances
[AD-A219358] 16 p2256 N90-22862
Measurements of high frequency seismic waves
[AD-A219370] 16 p2256 N90-22863
Analysis of regional phases using three-component data
[AD-A219482] 17 p2422 N90-23803
The composition and physical properties of the Earth's mantle and core 18 p2579 N90-24689
Broadband studies of seismic sources at regional and teleseismic distances using advanced time series analysis methods
[AD-A223113] 22 p3211 N90-28215
The reflectivity method
[REPT-90-004] 22 p3211 N90-28216
Investigation of the dynamic buckling of liquid-filled tanks 24 p3478 N90-29660
Regional phase propagation in three dimensionally heterogeneous media
[AD-A223279] 24 p3491 N90-29731
Elastic interfaces
[REPT-90-003] 24 p3493 N90-29742

SEISMOGRAMS
Calculation of 3-dimensional synthetic seismograms on the connection machine
[AD-A218472] 16 p2255 N90-22857

SEISMOGRAPHS
Observations of seafloor ambient noise with an ocean bottom seismometer array
[AD-A220159] 17 p2432 N90-23858
The reflectivity method
[REPT-90-004] 22 p3211 N90-28216

SEISMOLOGY
NT HELIOSEISMOLOGY
Hydrophone investigations of earthquakes and explosion generated high-frequency seismic phases
[AD-A212055] 03 p0371 N90-12122
ULF/VLF (0.001 to 50 Hz) Seismo-Acoustic Noise in the Ocean
[AD-A212942] 05 p0671 N90-13913
Theoretical models of earthquake phenomena and the physical significance of seismic moment tensor expansions
[AD-A213813] 07 p0961 N90-15556
Calculation of source and structure parameters at regional and teleseismic distances
[AD-A214297] 07 p0961 N90-15558
Summaries of physical research in the geosciences
[DE90-004993] 08 p1090 N90-16309
Proceedings of the 79th SEGJ Conference
[DE89-760006] 08 p1157 N90-16704
Self-similar growth of three-dimensional fault
[DE90-608162] 10 p1407 N90-18112
The interpretation of crustal dynamics data in terms of plate interactions and active tectonics of the Anatolian plate and surrounding regions in the Middle East
[NASA-CR-186200] 11 p1533 N90-18824
Seismic characterization of fracture properties
[DE90-007759] 13 p1841 N90-20570
Damage characteristics of time domain histories
[DE90-008787] 13 p1842 N90-20573
The effects of structure and source complexity on waveforms: Crustal structure of Tibet and the recovery of complex seismic sources
[AD-A218202] 13 p1843 N90-20579
A numerical and theoretical study of seismic wave diffraction in complex geologic structure
[AD-A218209] 14 p2005 N90-21490
Effects of single fractures on seismic wave propagation
[DE90-009191] 15 p2129 N90-22171
Temporal attributes of the ambient seismo-acoustic environment: La Junta, Colorado
[AD-A219369] 16 p2249 N90-22825
Seismic wave propagation, attenuation and scattering over regional distances
[AD-A219358] 16 p2256 N90-22862
Measurements of high frequency seismic waves
[AD-A219370] 16 p2256 N90-22863
Analysis of regional phases using three-component data
[AD-A219482] 17 p2422 N90-23803
ULF/VLF ocean bottom seismo-acoustics
[AD-A218810] 17 p2429 N90-23843
The composition and physical properties of the Earth's mantle and core 18 p2579 N90-24689
Proceedings of the 21st Joint Meeting of the US-Japan Cooperative Program in Natural Resources Panel Wind and Seismic Effects
[PB90-186826] 21 p3030 N90-27226
The reflectivity method
[REPT-90-004] 22 p3211 N90-28216
Catalog of strong motion stations in Eastern North America
[PB90-251984] 24 p3490 N90-29722

SEISMOMETERS
U SEISMOGRAPHS

SELECTION
NT PERSONNEL SELECTION
NT PILOT SELECTION
NT SITE SELECTION
Likelihood cross-validation bandwidth selection for nonparametric kernel density estimators
[REPT-89-10] 03 p0398 N90-12279
Stellar content of the input catalog 05 p0607 N90-13535
The choice of stars in open clusters 05 p0608 N90-13542
The choice of stars in the Magellanic clouds 05 p0608 N90-13543
The activity selection problem: A network and game theoretic approach
[MEMO-794] 05 p0694 N90-14056
Evaluation of selection techniques for multispectral bands employed in the discrimination of carbonatic rocks
[INPE-4850-TDL/365] 11 p1522 N90-18765
Optimum selection procedures in multi-stage screening, reliability, and time
[AD-A216811] 11 p1553 N90-18942
Material selection and design: An expert system approach
[PNR90611] 20 p2908 N90-26544
Space projects: Improvements needed in selecting future projects for private financing
[GAO/NSIAD-90-147] 22 p3256 N90-28439

SELECTIVE DISSEMINATION OF INFORMATION
DOD (Department of Defense) Freedom of Information Act Program (incorporating changes 1 and 2)
[PB90-104753] 06 p0859 N90-14993
The SMITE approach to security
[RSRE-89014] 08 p1106 N90-16404
Technology transfer: US and foreign participation in R and D at Federal laboratories
[GAO/RCED-88-203BR] 19 p2764 N90-25706
Energy data base: Subject categories and scope
[DE90-009212] 20 p2936 N90-26706
Helping America compete: The role of Federal scientific and technical information
[OTA-CIT-454] 21 p3086 N90-27549

SELECTIVE FADING
Digital radio link: Controlled simulator for frequency selective fading
[FOA-C-30527-3.5] 19 p2683 N90-25259
An experimental medium speed wideband modem 20 p2847 N90-26194
Combined effects of fast and selective fading on performance of PSK and MSK with coherent detection 20 p2849 N90-26204

SELECTIVE SURFACES
Spectral-domain analysis of finite frequency selective surfaces
[AD-A211669] 03 p0339 N90-11932
A well conditioned formulation for the analysis of multi-layered frequency selective surfaces using a cascaded matrix approach, revised
[RSRE-MEMO-4289-REV] 04 p0496 N90-12858

SELECTIVITY
Successive iterations of the input catalog 05 p0607 N90-13534
Correlations between surface structure and catalytic activity/selectivity
[DE90-003755] 07 p0896 N90-15181

SELENIDES
NT COPPER SELENIDES
NT ZINC SELENIDES

SELENIUM
CuInSe2 and CdTe: Scale-up for manufacturing
[DE89-009503] 13 p1827 N90-20489

SELENIUM COMPOUNDS
NT COPPER SELENIDES
NT ZINC SELENIDES
Phase equilibrium and crystal growth studies on AgGaSe2 and related nonlinear optical materials
[AD-A213650] 07 p1003 N90-15809
New electrically conducting solids based on nickel(II) - bis(1,3-dithiole-2-thione-4,5-diselenolate)
[DE90-003788] 08 p1042 N90-16020

SELF ADAPTIVE CONTROL SYSTEMS
Adaptive structures to meet future requirements for large precision structures 02 p0178 N90-11001
Adaptive control methods for mechanical manipulators: A comparative study
[AD-A219965] 17 p2413 N90-23749
Adaptive control of visually guided grasping in neural networks
[AD-A221387] 18 p2597 N90-24780

SELF ALIGNMENT
Demonstration epicyclic gearbox
[PNR90567] 04 p0508 N90-12932
Method of making self-aligned GaAs/AlGaAs FET's
[AD-D014229] 06 p0849 N90-14935
Structural and operational aspects of the concentrating SARA-Louver solar generator 10 p1340 N90-17760

SELF CONSISTENT FIELDS
A diagnostic for determining the quality of single-reference electron correlation methods 02 p0272 N90-11554
A self-consistent model of the most common nightglow emissions 05 p0660 N90-13853
A diagnostic for determining the quality of single-reference electron correlation methods
[NASA-TM-101929] 06 p0838 N90-14874
Relativistic self-consistent field studies of atoms and molecules
[AD-A214101] 07 p0991 N90-15724
Large scale calculations of the structure and dynamics of dense matter
[DE90-003654] 07 p0991 N90-15726
A self-consistent theory of radial transport of field-aligned current by microturbulence
[DE90-007920] 14 p2028 N90-21631

SELF DEPLOYING SPACE STATIONS
U SPACE STATIONS

SELF DIFFUSION (SOLID STATE)
Molecular dynamics simulations of grain-boundary diffusion for varying tilt angle geometries
[DE90-012919] 20 p2930 N90-26669

SELF EXCITATION
The behavior of matter under nonequilibrium conditions: Fundamental aspects and applications
[DE90-002522] 07 p0892 N90-15157

SELF FOCUSING
A Bayesian derivation of an iterative autofocus/super-resolution algorithm
[RSRE-MEMO-4337] 22 p3239 N90-28371

SELF INDUCED VIBRATION
NT SUBSONIC FLUTTER
NT TRANSONIC FLUTTER

SELF LUBRICATING MATERIALS
Tribological properties of PM212: A high-temperature, self-lubricating, powder metallurgy composite
[NASA-TM-102355] 04 p0465 N90-12659
Characterization of self-lubricating surface materials
[CETIM-108060] 04 p0479 N90-12749
Friction and wear of glassy carbon in sliding contact, revision 1
[DE90-000743] 06 p0750 N90-14365
Self-lubricating surfaces by ion beam processing
[AD-A222489] 21 p3011 N90-27118

SELF LUBRICATION
Self-lubricating polymer composites and polymer transfer film lubrication for space applications
[NASA-TM-102492] 15 p2071 N90-21862
Development of improved self lubricating cages for SSME HPOTP bearings 23 p3292 N90-28623

SELF ORGANIZING SYSTEMS
Can perceptrons find Lyapunov functions: An algorithmic approach to systems stability
[RR-365] 03 p0391 N90-12224
Self-organizing semantic maps
[PB89-212609] 04 p0529 N90-13049
User interaction with self-learning systems
[AD-A214280] 08 p1105 N90-16395
Guide to RMS-literature
[REPT-89-52] 15 p2158 N90-22326
Improving upon standard pattern classification algorithms by implementing them as multi-layer perceptrons
[AD-A220046] 17 p2447 N90-23954
A sum rule satisfied by optimized feed-forward layered networks
[RSRE-MEMO-4341] 20 p2914 N90-26579
On networks, optimized feature extraction, and the Bayes decision
[RSRE-MEMO-4342] 20 p2914 N90-26580

Conference on The Perception of Structure Program and Abstracts
[AD-A222437] 22 p3232 N90-28328
Selective learning algorithm for certain types of learning failure in multilayer perceptrons
[AD-A223982] 23 p3362 N90-28998

SELF PROPAGATION
Control of titanium diboride SHS reactions by inert dilutions and mechanical constraint
[AD-A214378] 10 p1357 N90-17870

SELF REGULATING
U AUTOMATIC CONTROL

SELF REPAIRING DEVICES
Flight-testing of the self-repairing flight control system using the F-15 highly integrated digital electronic control flight research facility
[NASA-TM-101725] 19 p2661 N90-25144

SELF SEALING
Spray sealing: A breakthrough in integral fuel tank sealing technology 08 p1022 N90-15912

SELF SUBTRACTION HOLOGRAPHY
U HOLOGRAPHIC SUBTRACTION

SELF TESTS
Built in test of folded PLAs
[IMAG-RR-758-I] 08 p1061 N90-16134
Navigation experiment NAVEX: The self-test delay times in the D1 Spacelab mission
[ESA-TT-1176] 11 p1467 N90-18446
Knowledge-based fault detection and analysis for robots: First results for the ROTEX robots
[ESA-TT-1150] 11 p1518 N90-18742
Advanced modulation technology development for earth station demodulator applications. Coded modulation system development
[NASA-CR-185149] 13 p1789 N90-20270
Smart built-in test 19 p2728 N90-25512
Self-checking on-line testable static RAM
[NASA-CASE-NPO-17939-1-CU] 20 p2904 N90-26518

SELSYNS (TRADEMARK)
U SERVOMOTORS

SEMANTICS
Determinism yields (event structure isomorphism equals step sequence equivalence)
[CWI-CS-R8839] 02 p0263 N90-11492
Computer generation of a tutorial dialogue
[AD-A211976] 03 p0380 N90-12162
Taxonomic syntax for first order inference
[AD-A211618] 03 p0390 N90-12221
Some techniques for anaphora resolution in algebraic linguistics
[REPT-89-28] 03 p0396 N90-12265
DOD Gateway Information System (DGIS) common command language: A retrospective on the introduction of prolog as the development tool
[AD-A211941] 03 p0418 N90-12400
Self-organizing semantic maps
[PB89-212609] 04 p0529 N90-13049
A simple definition for parallel composition of prime event structures
[CWI-CS-R8903] 04 p0532 N90-13074
Semantics and consistency of rule-based expert systems
[CWI-CS-R8824] 04 p0543 N90-13153
Database interfaces on NASA's heterogeneous distributed database system
[NASA-CR-185420] 05 p0706 N90-14133
Architecture and language for a layered relational database 05 p0707 N90-14146
An overview of lynx
[AD-A213714] 07 p0975 N90-15631
A structured connectionist approach to direct inferences and figurative adjective-noun combinations
[AD-A214326] 07 p0978 N90-15649
Complexity of human language comprehension
[AD-A214591] 09 p1258 N90-17299
KAPSE Interface Team (KIT) public report, volume 8, part 2
[AD-A215840] 10 p1419 N90-18178
Should a function continue
[AD-A216406] 11 p1551 N90-18929
The expression of syntagmatic relationships in frame-based indexing 12 p1726 N90-19917
Deceit: A flexible distributed file system
[NASA-CR-186412] 12 p1726 N90-19923
An introduction to Montague grammar
[REPT-89-46] 15 p2147 N90-22266
Some remarks on treatment of be in Montague's PTQ --- Proper Treatment of Quantification (PTQ)
[REPT-89-40] 15 p2147 N90-22267
Using expert systems to implement a semantic data model of a large mass storage system 15 p2156 N90-22315
Knowledge-based semantic query processing: An optimal transformation approach 15 p2176 N90-22437
Connectionism and compositional semantics
[AD-A219029] 16 p2264 N90-22904
Durra: A task-level description language reference manual, version 2
[AD-A219293] 16 p2301 N90-23114
Syntax, semantics, and pragmatism: An integrated focus based on textual linguistic knowledge
[INPE-4992-PRE/1554] 16 p2326 N90-23262
Natural language syntax and first order inference
[AD-A219944] 17 p2447 N90-23951
The semantics of TRIDL
[TR-89-17] 17 p2450 N90-23973
The fine-structure of categorial semantics
[ITLI-LP-89-01] 17 p2464 N90-24075
Dynamic predicate logic: Towards a compositional, non-representational semantics of discourse
[ITLI-LP-89-02] 17 p2464 N90-24076
The semantics of data flow diagrams
[TR-89-16] 17 p2480 N90-24181
Ocean feature recognition using genetic algorithms with fuzzy fitness functions (GA/F3)
19 p2740 N90-25576
Disconnected actions: An asynchronous extension to a nested atomic action system
[AD-A221937] 21 p3053 N90-27356
A user modelling approach for computer-based critiquing
[AD-A224042] 23 p3379 N90-29088
The SPECIALIST: Natural language processing system
[PB90-240029] 23 p3381 N90-29098
Inference engine for expert systems
[INPE-4565-PRE/1306] 23 p3382 N90-29104
Efficiency and effectiveness of deep structure-based subject indexing languages: PRECIS vs. DSIS 23 p3406 N90-29248
Formal semantics of SQL queries
[REPT-89-069] 24 p3531 N90-29973

SEMICIRCULAR CANALS
Vestibular responses and motion sickness during pitch, roll, and yaw sinusoidal whole-body oscillation
[AD-A223898] 24 p3497 N90-29787

SEMICONDUCTING FILMS
Beam assisted fabrication of 3-5/Si monolithic devices
[AD-A212046] 03 p0412 N90-12367
Optical modulators based on polymers
[EP-PATENT-0-294-061-A1] 05 p0700 N90-14099
Structural instabilities, impurities, and defects in electronic materials
[AD-A215384] 09 p1290 N90-17481
Hydrogenated amorphous and microcrystalline silicon deposited from silane-hydrogen mixtures
[ETN-90-96267] 11 p1493 N90-18590
Superconducting and semiconducting thin films of La(sub 123) and Y(sub 123) and their superlattices
[DE90-009565] 15 p2173 N90-22416
Scanning laser photocurrent spectroscopy of electrochemically grown bismuth sulphide films
[AERE-M-3709] 16 p2217 N90-22649

SEMICONDUCTOR DEVICES
NT AVALANCHE DIODES
NT BIPOLAR TRANSISTORS
NT CHARGE COUPLED DEVICES
NT CHARGE FLOW DEVICES
NT CHARGE INJECTION DEVICES
NT CMOS
NT FIELD EFFECT TRANSISTORS
NT GALLIUM ARSENIDE LASERS
NT HETEROJUNCTION DEVICES
NT HIGH ELECTRON MOBILITY TRANSISTORS
NT ITO (SEMICONDUCTORS)
NT JFET
NT JUNCTION DIODES
NT JUNCTION TRANSISTORS
NT LIGHT EMITTING DIODES
NT METAL OXIDE SEMICONDUCTORS
NT MIM (SEMICONDUCTORS)
NT MIS (SEMICONDUCTORS)
NT MODFETS
NT MOM (SEMICONDUCTORS)
NT PHOTODIODES
NT PHOTOTRANSISTORS
NT PHOTOVOLTAIC CELLS
NT SCHOTTKY DIODES
NT SEMICONDUCTOR LASERS
NT SILICON CONTROLLED RECTIFIERS
NT SILICON TRANSISTORS
NT SOI (SEMICONDUCTORS)
NT SOLAR CELLS
NT SOS (SEMICONDUCTORS)
NT THERMISTORS
NT THYRISTORS
NT TRANSFERRED ELECTRON DEVICES
NT TRANSISTORS
NT VARACTOR DIODES
NT VARISTORS
Scanning tunneling microscopy etching of micrometer level features on p-type GaAs
[AD-A209216] 01 p0058 N90-10328
Proceedings of the Polycrystalline Thin Film Program Meeting
[DE89-009457] 02 p0237 N90-11348
Pulsed-power switching for inertial confinement fusion with light ion beams
[DE89-016810] 02 p0279 N90-11595
European Solid State Device Research Conference (18th) ESSDERC 88 held in Montpellier, France on 13-16 September 1988
[AD-A210618] 04 p0558 N90-13250
Fundamental quantum 1/f noise in ultrasmall semiconductor devices and their optimal design principles
[AD-A211947] 05 p0702 N90-14107
Manufacturing and characterization of insulator-germanium structures
[ECL-88-13] 05 p0703 N90-14115
Study of surface uniformity of semiconductors 3 to 5 by photoluminescence imagery
[ECL-88-15] 05 p0703 N90-14116
Photoelectrochemical behavior of type n of GaAs in concentrated iodide media and realization of an experimental device
[ECL-88-18] 05 p0703 N90-14117
The effects of heavy particle radiation on semiconductor devices
[DE90-001679] 06 p0854 N90-14962
RF transistor thermal/electrical characterization
[DE90-001427] 07 p0920 N90-15326
Avalanche photoconductive switching
[DE90-002980] 07 p0922 N90-15337
Picosecond photoconductivity using a graded bandgap Al(x)Ga(1-x)As active detecting layer
[DE90-003452] 07 p1000 N90-15786
Very low energy ignition of pyrotechnics using a Semiconductor Bridge (SCB)
[DE90-002645] 08 p1052 N90-16082
Theory of the electronic and optical properties of semiconductor heterostructures
[AD-A214132] 08 p1130 N90-16544
Testing and data path redesign of a high speed, 16-point Winograd Fourier transform processor
[AD-A215661] 09 p1213 N90-17036
Research on amorphous silicon based thin film photovoltaic devices. Phase 2: Research on stable high-efficiency, large area amorphous silicon based submodules
[DE89-009515] 09 p1243 N90-17209
Growth of epitaxical SiC layers onto on- and off-axis 6H-SiC substrates by ion beam deposition
[DE90-004236] 09 p1287 N90-17459
Proceedings of the conference on Hot Carriers in Semiconductors
[AD-A215544] 09 p1291 N90-17482
Discretization of the steady state semiconductor device equations
[AD-A215807] 10 p1438 N90-18298
An overview of radiation-induced interface traps in MOS (Metal-Oxide Semiconductor) structures
[AD-A216101] 10 p1438 N90-18299
DANCIR (device and circuit simulator): A three dimensional steady-state semiconductor device simulator
[DE90-006370] 11 p1504 N90-18658
Utilization criteria for transistors of diverse technology in pulse inverters with high switching frequency
[ETN-90-95359] 12 p1653 N90-19500
Silicon carbide semiconductor device fabrication and characterization
[NASA-CR-186354] 12 p1719 N90-19873
Digital capacity transient spectroscopy of deep structure defects in III-V-Semiconductor structures
[ETN-90-96057] 12 p1722 N90-19890
Self-consistant calculation of point and pair structure defects in silicium
[ETN-90-96059] 12 p1722 N90-19891
Contact formation on (Hg,Cd) Te
[AD-A217088] 12 p1723 N90-19900
Summary report of the Summer Conference of the DARPA-Materials Research Council
[AD-A217380] 13 p1767 N90-20143
An electron-beam controlled semiconductor switch
[AD-A217181] 13 p1793 N90-20288
A new thermal sensor for x ray microcalorimetry
[DE90-008547] 13 p1805 N90-20360
Nonlinear systems of partial differential equations
[AD-A217581] 13 p1877 N90-20761
CCST (Center for Compound Semiconductor Technology) research briefs
[DE90-007782] 13 p1895 N90-20874
Germanium Blocked Impurity Band (BIB) detectors 14 p1976 N90-21321

New surface atomic structures for column 5 overlayers on the (110) surfaces of 3-5 compound semiconductors
[DE90-009003] 14 p2033 N90-21663
An assessment of the hardness of miniature vacuum tubes to high-voltage transients
[DE90-009541] 15 p2089 N90-21956
Lateral spreading of Au contacts on InP
[NASA-TM-103133] 16 p2252 N90-22843
Electronic theory of solids, surfaces, interfaces, and clusters 16 p2320 N90-23230
Nonlinear multigrid applied to a 1D stationary semiconductor model
[CWI-NM-R8905] 17 p2398 N90-23659
Interdigitated back contact silicon solar cell analysis and design recommendations for space use
[AD-A220414] 17 p2420 N90-23790
Experiments on liquid immersion natural convection cooling of leadless chip carriers mounted on ceramic substrate
[AD-A219893] 17 p2478 N90-24167
Multichip packaging technology with laser-patterned interconnects
[DE90-010743] 18 p2549 N90-24552
Development of a point-contact solar cell using high-volume processing techniques
[DE90-010330] 18 p2577 N90-24683
Light-millimeter wave interactions in semiconductor devices
[AD-A221214] 18 p2623 N90-24943
High frequency, frequency multiplier using parallel gunn diodes
[AD-D014523] 19 p2685 N90-25275
Polycrystalline thin film cadmium telluride n-i-p solar cells
[DE90-000351] 21 p3019 N90-27167
Integration of picosecond GaAs photoconductive devices with silicon circuits for optical clocking and interconnects
[DE90-012096] 21 p3080 N90-27512
Method of forming three-dimensional semiconductor structures
[NASA-CASE-NPO-17835-1-CU] 21 p3081 N90-27518
Defects associated with the incorporation of germanium in gallium arsenide
[AD-A222953] 21 p3082 N90-27527
High-temperature deformation of silicon
[DE90-013628] 22 p3160 N90-27919
Electronic and photonic power applications
[DE90-015567] 24 p3485 N90-29698

SEMICONDUCTOR DIODES
NT AVALANCHE DIODES
NT GUNN DIODES
NT JUNCTION DIODES
NT LIGHT EMITTING DIODES
NT PHOTODIODES
NT SCHOTTKY DIODES
NT VARACTOR DIODES
A robotic electrical and tensile testing system for diodes
[DE89-014012] 01 p0073 N90-10417
Dwell time and average local speed in a resonant tunneling structure
[AD-A210566] 01 p0133 N90-10764
Channelized coplanar waveguide pin-diode switches
[NASA-TM-102289] 03 p0341 N90-11943
Analysis of loss mechanisms in polycrystalline thin-film solar cells
[DE89-009454] 03 p0366 N90-12093
Power semiconductor devices for space nuclear power systems
[DE90-001178] 07 p1005 N90-15819
Optical flow measuring method using diode lasers, phase coupled arrays, and high frequency pulsed diode lasers 08 p1067 N90-16176
Laser cooling of neutral atoms
[AD-A214440] 09 p1279 N90-17418
CIC type thin diode for solar array 10 p1344 N90-17788
Characterization and development report for the SA3124, a 15-volt zener diode
[DE90-005711] 10 p1379 N90-17993
High speed imaging with a tapped solid state sensor
[DE90-006116] 11 p1511 N90-18702
Ignition of HMX (cyclotetramethylenetetranitramine) using low energy laser diodes
[DE90-007637] 12 p1624 N90-19334
Noise floors of subnanosecond transient recording systems
[DE90-002339] 12 p1666 N90-19571
High power semiconductor laser arrays by metalorganic chemical vapor deposition 13 p1805 N90-20363
Crystallography, spectroscopic analysis, and lasing properties of Nd3+:Y3Sc2Al3O12
[AD-A217792] 13 p1897 N90-20891
Millimeter wavelength rectenna development 15 p2060 N90-21797
Linear laser diode arrays for improvement in optical disk recording for space stations
[NASA-CR-4322] 22 p3180 N90-28047
Luminescence from electroformed metal-isolator-metal-structures
[ETN-90-97295] 22 p3249 N90-28425
Evaluation of a potential Wave Division Multiplexer (WDM) for use in the IRSTD
[AD-A223945] 24 p3463 N90-29560
Innovative techniques for the production of low cost 2D laser diode arrays
[AD-A223575] 24 p3474 N90-29632

SEMICONDUCTOR JUNCTIONS
NT HETEROJUNCTIONS
NT HOMOJUNCTIONS
NT N-P-N JUNCTIONS
NT P-I-N JUNCTIONS
NT P-N JUNCTIONS
NT P-N-P-N JUNCTIONS
NT SILICON JUNCTIONS
Dielectric spectroscopy of semiconductors
[AD-A211989] 04 p0559 N90-13255
GaAs gate dynamic memory technology
[AD-A212387] 04 p0560 N90-13266
Research on high-efficiency, multiple-gap, multijunction, amorphous-silicon-based alloy thin-film solar cells
[DE89-009444] 06 p0803 N90-14673
Research on stable high-efficiency, large area, amorphous silicon-based solar cells, phase 2
[DE89-009491] 09 p1242 N90-17208
Edge geometry superconducting tunnel junctions utilizing an NbN/MgO/NbN thin film structure
[NASA-CASE-NPO-17812-1-CU] 09 p1286 N90-17456
Direct implantation process development and characterization in advanced Hg(1)-(x)Cd(x) Te EPI layers
[AD-A219133] 16 p2324 N90-23252
A viologen/ruthenium oxide-based microelectrochemical diode with pH-dependent current-voltage characteristics
[AD-A221961] 21 p3000 N90-27052

SEMICONDUCTOR LASERS
NT GALLIUM ARSENIDE LASERS
Laser diode array and transmission optics 01 p0030 N90-10163
Efficient nonlinear conversion of laser diode pumped miniature solid state laser sources
[AD-A210708] 01 p0075 N90-10433
Automation of fiber-optic pigtailing process: Laser welding demonstration program
[AD-A210351] 01 p0123 N90-10707
Properties of devices prepared with epitaxial layers on InP
[AD-A210304] 01 p0132 N90-10759
Laser dynamics: The system dynamics and network theory of optoelectronic integrated circuit design 02 p0226 N90-11296
Semiconductor quantum well lasers and related optoelectronic devices on silicon, III-V
[AD-A210758] 02 p0227 N90-11299
Development of microstructured DH diode lasers and detectors for the near and medium IR spectral domain using molecular beam epitaxy
[IPM-15/1988] 03 p0354 N90-12023
Design and performance of an on-satellite laser diagnostic system for a free space optical heterodyne frequency-shift-keyed communication system
[AD-A211986] 04 p0505 N90-12915
Tunable Solid State Lasers conference edition: Tunable Solid State Lasers Topical Meeting
[AD-A212292] 04 p0506 N90-12920
Optical communication with semiconductor laser diode
[NASA-CR-185886] 05 p0647 N90-13770
Monolithic laser diode structure for microwave generation
[AD-D014210] 06 p0782 N90-14543
Qualification of diode foil materials for excimer lasers
[DE90-000602] 06 p0789 N90-14593
SLCSAT (Submarine Laser Communication Satellite) communication system design study
[AD-A213403] 07 p0917 N90-15304
Fiber optic sensing system
[NASA-CASE-LEW-14795-1] 07 p0992 N90-15733
Optical flow measuring method using diode lasers, phase coupled arrays, and high frequency pulsed diode lasers 08 p1067 N90-16176
Distance measurement using laser diodes
[ETN-90-96144] 08 p1082 N90-16264
Laser cooling of neutral atoms
[AD-A214440] 09 p1279 N90-17418
JSEP (Joint Services Electronics Program)
[AD-A215051] 09 p1290 N90-17476
Development of a solar-powered infrared injection laser microminiature transmitting system
[DE90-005672] 10 p1389 N90-18034
Direct detection optical intersatellite link at 220 Mbps using AlGaAs laser diode and silicon APD with 4-ary PPM signaling
[NASA-CR-186380] 12 p1646 N90-19460
Time resolved gain/loss studies under low and high power loading for the XeF C-A transition
[DE90-007506] 12 p1655 N90-19517
The III-V semiconductor quantum well lasers and related optoelectronic devices on silicon
[AD-A216980] 12 p1666 N90-19570
Experimental results of aging and thermal effects in high-power laser diodes
[DE90-005955] 12 p1666 N90-19573
Noise behavior of semiconductor lasers by optic feedback
[ETN-90-95728] 12 p1668 N90-19583
High power semiconductor laser arrays by metalorganic chemical vapor deposition 13 p1805 N90-20363
Development of mid-infrared solid state lasers for spaceborne lidar
[NASA-CR-185095] 15 p2103 N90-22031
Linear, nonlinear, and tunable guided wave modes for high-power (GaAl)As semiconductor lasers 15 p2104 N90-22036
An acousto-optic image correlator with a throughput rate of 1000 templates per second
[DE90-009323] 15 p2144 N90-22249
Measurement of HCl by near-infrared diode laser absorption 16 p2209 N90-22601
Ignition testing of low-energy laser diode ignited components
[DE90-009968] 16 p2214 N90-22630
SILEX Beacon equipment
[ETN-90-96613] 17 p2409 N90-23726
Spectral properties of a 1.3-micrometers InGaAsP diode laser under modulation
[AD-A220066] 17 p2409 N90-23729
Diode laser satellite systems for beamed power transmission
[NASA-TP-2992] 18 p2556 N90-24585
Monitoring of catalyst performance in CO2 lasers using frequency modulation spectroscopy with diode lasers 18 p2561 N90-24614
High-order mode dependencies in gain-guided twin-stripe laser diode arrays
[AD-A220868] 18 p2562 N90-24617
Evolution equation simulation of semiconductor lasers under a pulsed regime
[TELECOM-PARIS-89-D-010] 18 p2563 N90-24625
Diode laser-pumped solid-state lasers: A breakthrough in modern laser technology
[MBB-Z-0276/89-PUB] 19 p2649 N90-25077
Monolithic arrays of grating-surface-emitting diode lasers and quantum well modulators for optical communications
[NASA-CR-186772] 19 p2758 N90-25674
Apparatus for the efficient wavelength conversion of laser radiation
[AD-D014506] 20 p2866 N90-26305
A compact, high-powered Far-Infrared (FIR) laser
[DE90-009996] 20 p2867 N90-26312
High resolution infrared spectroscopy of planetary molecules using diode lasers and Fourier transform spectrometers 20 p2943 N90-26747
Diode laser pumped single mode 1.3 microns Nd:YALO microlaser
[AD-A223036] 21 p3008 N90-27100
Laser diode pumped, erbium-doped, solid state laser with high slope efficiency
[AD-D014482] 22 p3179 N90-28040
Linear laser diode arrays for improvement in optical disk recording for space stations
[NASA-CR-4322] 22 p3180 N90-28047
The III-V semiconductor quantum well lasers and related optoelectronic devices on silicon
[AD-A224120] 23 p3331 N90-28835
Development and evaluation of hermetic laser diode ignited pyrotechnic components
[DE90-015745] 24 p3458 N90-29529
Innovative techniques for the production of low cost 2D laser diode arrays
[AD-A223575] 24 p3474 N90-29632
Finite difference modeling of laser diode ignited components
[DE90-015652] 24 p3474 N90-29635
Comparison of electro-optic diagnostic systems
[DE90-015619] 24 p3546 N90-30056

SEMICONDUCTOR PLASMAS
Reactive ion etching of sputtered silicon carbide and tungsten thin films for device applications
[AD-A211711] 03 p0325 N90-11847

SEMICONDUCTORS (MATERIALS)
NT ACCEPTOR MATERIALS
NT AMORPHOUS SEMICONDUCTORS
NT AMORPHOUS SILICON
NT CMOS
NT DONOR MATERIALS
NT ITO (SEMICONDUCTORS)
NT METAL OXIDE SEMICONDUCTORS
NT MIM (SEMICONDUCTORS)
NT MIS (SEMICONDUCTORS)
NT MOM (SEMICONDUCTORS)
NT N-TYPE SEMICONDUCTORS
NT P-TYPE SEMICONDUCTORS
NT PHOTOCONDUCTORS
NT SOS (SEMICONDUCTORS)
NT SUPERLATTICES

Photoreflectance study of boron ion-implanted (100) cadmium telluride
[SD-TR-88-89] 01 p0053 N90-10300

Density of states in a resonant tunneling structure
[AD-A209508] 01 p0128 N90-10731

Ordered structures and metastable alloys grown by OMVPE
[DE89-016370] 01 p0129 N90-10744

Effects of coherent scattering on infrared absorption in doped semiconductors
[AD-A210224] 01 p0131 N90-10756

The growth of gallium nitride films via the innovative technique of atomic layer epitaxy
[AD-A210380] 01 p0132 N90-10760

Study of disorder and strain in semiconductor heterostructures and superlattices by Raman scattering 02 p0280 N90-11601

International workshop on Beam Injection Assessment of Defects in Semiconductors
[AD-A210842] 02 p0283 N90-11617

Reactive ion etching of sputtered silicon carbide and tungsten thin films for device applications
[AD-A211711] 03 p0325 N90-11847

Application of dimensional analysis to statistical process modeling
[AD-A211881] 03 p0335 N90-11905

Infrared detector array
[AD-D014170] 03 p0350 N90-11997

Construction of a picosecond laser system for the investigation of semiconductors using nonlinear optical methods
[ETN-89-94664] 03 p0352 N90-12013

Niobium and niobium nitride contacts on semiconducting material
[AD-D014177] 03 p0409 N90-12347

Electrolitic deposited ohmic contacts on III-V compound semiconductors: A review
[PB89-217400] 03 p0410 N90-12350

Ultra high speed compound semiconductors and real time signal processing
[AD-A211394] 03 p0413 N90-12372

Development and evaluation of an instrument for rapid electroreflectance of semiconductor materials
[AD-A211690] 03 p0414 N90-12376

Mechanisms of CO2 reduction metal and metal modified semiconductor electrodes
[AD-A213169] 04 p0473 N90-12712

Thin-film integrated injection logic
[AD-D014190] 04 p0497 N90-12860

RF and dc desensitized electroexplosive device
[AD-D014206] 04 p0497 N90-12862

High speed quantum-well optoelectronic devices by MBE
[AD-A212585] 04 p0555 N90-13237

Structural and electrical properties of thin films and superlattices composed of II-VI semiconductors 04 p0558 N90-13249

Semiconductor measurement technology: A software program for aiding the analysis of ellipsometric measurements, simple models
[PB89-235923] 04 p0560 N90-13261

Interstitial formation, non-equilibrium and macroscopic processes in mercury cadmium telluride
[AD-A212412] 04 p0561 N90-13267

Electrochemical study of the etching of III to V semiconductors
[ETN-90-96015] 05 p0623 N90-13633

Joint Services Electronics Program
[AD-A213015] 05 p0634 N90-13699

Ultrafast processes and spectroscopy with free electron lasers
[AD-A212889] 05 p0647 N90-13773

Reorganization free energy for electron transfers at liquid-liquid and dielectric semiconductor-liquid interfaces
[AD-A212985] 05 p0703 N90-14111

GaAs and GaAs:In: Influence of surface treatments and characterization of homogeneity by photoluminescent imagery
[ECL-88-24] 05 p0704 N90-14118

Towards ab initio calculation of electron energies in semiconductors
[ETN-90-96016] 05 p0704 N90-14121

Electrical properties of materials for high temperature strain gage applications
[NASA-CR-186192] 06 p0780 N90-14534

Photovoltaic Measurements and Performance Branch
[DE89-009500] 06 p0807 N90-14695

Method of making self-aligned GaAs/AlGaAs FET's
[AD-D014229] 06 p0849 N90-14935

Multiband photoconductive detector based on layered semiconductor quantum wells
[AD-D014232] 06 p0849 N90-14936

Ion beam processing of advanced electronic materials
[DE89-017342] 06 p0851 N90-14944

X ray studies of strain, interface, and impurity in semiconductors
[DE90-001525] 06 p0851 N90-14947

Research on GaAs quantum-coupled structures that can be used as electron devices
[AD-A214015] 07 p0924 N90-15350

Interfacial systems for photochemical energy conversion
[DE90-003181] 07 p0953 N90-15514

Photochemical solar energy conversion utilizing semiconductors localized in membrane mimetic systems
[DE90-003450] 07 p0953 N90-15515

Proceedings of the Latin American Conference on the Applications of the Moessbauer Effect
[DE90-600819] 07 p1002 N90-15803

Epitaxial iron films
[AD-A213551] 07 p1003 N90-15807

Interface phonons in semiconductor double heterostructures
[AD-A213732] 07 p1003 N90-15810

Innovative optoelectronic materials and structures using OMVPE
[AD-A214192] 07 p1004 N90-15815

Slow positron defect profiling of silicon epilayers
[DE90-003958] 08 p1087 N90-16288

Resonance enhanced Raman studies of as-grown and laser-processed HgCdTe
[AD-A213855] 08 p1129 N90-16540

Reflection technique for thermal mapping of semiconductors
[AD-D014263] 08 p1129 N90-16541

Group 2 cubic fluorides as dielectrics for III-V compound semiconductors
[AD-A214096] 08 p1129 N90-16542

Improvement of impulse breakdown strength of an XLPE cable by modifing semiconducting layer
[DE90-734942] 09 p1287 N90-17463

Growth characteristics and electronic behavior of ultrathin epitaxial metallizations
[AD-A214794] 09 p1289 N90-17474

Method of producing a thin silicon-on-insulator layer
[AD-D014330] 09 p1290 N90-17478

Excited state lifetime measurements of ytterbium in indium phosphide
[AD-A215709] 09 p1291 N90-17483

Selective excitation luminescence and photoluminescence investigations of ytterbium doped InP GaAs and AlGaAs
[AD-A215713] 09 p1291 N90-17485

Electron-beam induced damage in thin insulating films on compound semiconductors
[NASA-CR-185177] 10 p1378 N90-17987

Magnetoplasma oscillations of the wave-guided type in semiconductor superlattices
[DE90-607260] 10 p1431 N90-18258

Electron scattering by native defects in uniformly and modulation doped semiconductor structures
[DE90-006084] 10 p1437 N90-18295

Simulation and quantification of high-resolution Z-contrast imaging of semiconductor interfaces
[DE90-006159] 10 p1438 N90-18297

Microconvective heating of granular explosives by a semiconductor bridge
[DE90-005710] 11 p1484 N90-18541

State of the art in semiconductor detectors
[DE90-005567] 11 p1512 N90-18706

Luminescence of lanthanides and actinides implanted into binary III-V semiconductors and AlGaAs
[AD-A215759] 11 p1569 N90-19031

Proceedings of the 6th Conference on Hot Carriers in Semiconductors
[AD-A215978] 11 p1569 N90-19032

Crystal growth and mechanical properties of semiconductor alloys
[AD-A216697] 11 p1570 N90-19035

Structure and vibrational excitations of reconstructed semiconductor surfaces
[DE90-006589] 11 p1571 N90-19044

Crystallographic and magnetic properties of (C6 D11 ND3)CuBr3 and (Zn(1-x)Mn(x))3As2: A neutron scattering study
[ECN-219] 11 p1573 N90-19055

Low threshold current implanted-planar-buried-heterostructure, graded-index, separate-confinement-heterostructure GaAs-AlGaAs laser
[DE90-002579] 12 p1666 N90-19572

Solid State Photovoltaic Research Branch
[DE89-009463] 12 p1682 N90-19660

Passivating layer for III-V semiconductor materials
[AD-D014321] 12 p1719 N90-19872

A simple model for the determination of L(sub 0), D and tau in a semiconductor and their temperature dependence
[DE90-610564] 12 p1720 N90-19879

CCST (Center for Compound Semiconductor Technology) research briefs
[DE90-006446] 12 p1721 N90-19887

Ion mixing and surface modification in metal-semiconductor systems
[DE90-007557] 12 p1723 N90-19897

Contact formation on (Hg,Cd) Te
[AD-A217088] 12 p1723 N90-19900

Polymer liquid crystals with side chain discogens
[AD-A218013] 13 p1782 N90-20228

Research investigation directed toward extending the useful range of the electromagnetic spectrum
[AD-A217460] 13 p1789 N90-20267

An electron-beam controlled semiconductor switch
[AD-A217181] 13 p1793 N90-20288

Joint Services Electronics Program research in electronics
[AD-A217745] 13 p1796 N90-20307

An ellipsometric measurement of optical properties for InP surfaces
[AD-A217185] 13 p1887 N90-20827

Workshop on the Physics and Chemistry of Mercury Cadmium Telluride and Related II-VI compounds
[AD-A217496] 13 p1894 N90-20867

CCST (Center for Compound Semiconductor Technology) research briefs
[DE90-007782] 13 p1895 N90-20874

Theoretical and experimental study of solid phase miscibility gaps in III/V quaternary alloys
[DE90-008430] 13 p1895 N90-20877

Coupled magnetoplasmon-phonon modes at the surface of a semi-infinite semiconductor superlattice
[DE90-612904] 14 p2031 N90-21647

High voltage/high resolution studies of metal and semiconductor interfaces
[DE90-009065] 14 p2032 N90-21656

New surface atomic structures for column 5 overlayers on the (110) surfaces of 3-5 compound semiconductors
[DE90-009003] 14 p2033 N90-21663

An investigation of narrow-bandgap semiconductors: Devices, circuits, and systems 15 p2171 N90-22406

Positron trapping in semiconductors
[PB90-165606] 15 p2172 N90-22410

Report on the fifth workshop on synchrotron x ray lithography
[DE90-007903] 15 p2172 N90-22411

Optical bistability in semiconducting material 15 p2174 N90-22424

Reactions of laser-generated free radicals at semiconductor surfaces
[AD-A218552] 16 p2232 N90-22733

Improvement study of iron disilicide thermoelectric materials
[AD-A218946] 16 p2252 N90-22844

Acoustoelectronic interaction of surface waves in GaAs-InGaAs superlattices 16 p2310 N90-23163

Superconducting and normal compounds: Some high field/high pressure effects 16 p2320 N90-23229

Optical properties of novel GaAs-based semiconductors 16 p2321 N90-23235

Investigation of Schottky barriers
[AD-A218422] 16 p2323 N90-23247

Measurement of localized deep levels and wafer non-uniformities at 3-5 semiconductor heterojunctions
[AD-A218547] 16 p2323 N90-23248

Nonreciprocal components in the 140 and 220 GHz bands utilizing magnetoplasmons on semiconducting substrates
[AD-A219136] 16 p2324 N90-23253

Preliminary evaluation of a small wearable display
[AD-A219867] 17 p2350 N90-23385

Preliminary investigation into the effect of high temperature thermal anneals on the figure of merit of silicon germanium alloys
[AD-A218573] 17 p2375 N90-23527

Photoreflectance for in-situ characterization of MOCVD growth of semiconductors under micro-gravity conditions
[NASA-CR-186600] 17 p2383 N90-23576

Ultra high-speed compound semiconductors and real time signal processing
[AD-A220721] 17 p2396 N90-23651
Joint services electronics program: Electronics research at the University of Texas at Austin
[AD-A220834] 17 p2397 N90-23655
Fellowship in physics/modern optics and quantum electronics
[AD-A218772] 17 p2469 N90-24111
Theoretical studies of photochemical methods for semiconductor etching
[AD-A218475] 17 p2475 N90-24151
Fundamental and applied aspects of defect engineering in G2As; EL2 and other nonstoichiometric defects
[AD-A218597] 17 p2475 N90-24152
Diluted magnetic semiconductors
[AD-A220444] 17 p2476 N90-24159
Preparation and properties of iron doped II-VI chalcogenides
[AD-A220802] 17 p2477 N90-24163
Hot carrier in subpicosecond photoconductive experiments
[AD-A219874] 17 p2477 N90-24166
Report of research activity at the Research Laboratory of Electronics 17 p2486 N90-24217
Development of an all silicon integrated optical modulator for high speed data communications and sensor applications
[AD-A220270] 18 p2547 N90-24535
Studies of chemistry and diffusion on silicon and gallium arsenide surfaces using laser-induced thermal desorption
[AD-A220946] 18 p2547 N90-24539
Microscopic theory of non-linear phenomena in semiconductor superlattices
[AD-A221106] 18 p2622 N90-24941
Synthesis of large area, monocrystalline TiC as a substrate for heteroepitaxial growth of beta-SiC
[AD-A221392] 18 p2623 N90-24948
Atomic scale imaging of the structure and chemistry of semiconductor interfaces
[DE90-011321] 18 p2626 N90-24965
Neutron and gamma irradiation effects on power semiconductor switches
[NASA-TM-103200] 19 p2686 N90-25278
An analysis of the contact sintering process in III-V solar cells
[NASA-TM-103179] 19 p2709 N90-25420
PH3 surface chemistry on Si(111)-(7x7): A study by Auger spectroscopy and electron stimulated desorption methods
[AD-A221508] 21 p2979 N90-26929
Materials for high-density electronic packaging and interconnection
[NASA-CR-186934] 21 p3000 N90-27049
Fundamental electron transfer processes at the single crystal semiconductor/liquid interface
[DE90-011438] 21 p3079 N90-27508
The column-by-column compositional mapping at semiconductor interfaces using Z-contrast STEM
[DE90-012594] 21 p3081 N90-27516
Measurement of deep levels at InGaAs(P)/InP heterojunctions
[AD-A222890] 21 p3082 N90-27526
Electron-phonon interaction and transport in artificially made semiconductor microstructures
[AD-A223061] 21 p3082 N90-27529
Molecular beam epitaxial growth, characterization, and devices of modulated semiconductor structures
[AD-A221545] 21 p3084 N90-27538
In-situ integrated processing and characterization of thin films of high temperature superconductors, dielectrics and semiconductors by MOCVD 22 p3148 N90-27851
Incoherent imaging of materials structure and composition by Z-contrast stem
[DE90-012789] 22 p3155 N90-27888
Center for Electronics and Electrical Engineering technical progress bulletin covering center programs, July to September 1989, with 1990 CEEE events calender
[PB90-188095] 22 p3167 N90-27959
Fifteenth International Conference on X Ray and Inner-Shell Processes
[DE90-013024] 23 p3393 N90-29170
Semiconductor measurement technology: A software program for aiding the analysis of ellipsometric measurements, simple spectroscopic models
[PB90-216847] 23 p3398 N90-29201
Semiconductor measurement technology. EPROP: An interactive FORTRAN program for computing selected electronic properties of Gallium Arsenide and Silicon
[PB90-222738] 23 p3399 N90-29203
New real space correlated-basis-functions approach for the electron correlations of the semiconductor inversion layer
[DE90-627315] 24 p3551 N90-30090
Effect of retardation on the reflectance properties of the metallic Fibonacci quasi-superlattice
[DE90-627316] 24 p3551 N90-30091
Theory of electronic states and formations energies of defect complexes, interstitial defects, and crystal growth in semiconductors
[AD-A224069] 24 p3551 N90-30093
Scanning tunneling microscopy of semiconductor surfaces
[AD-A223339] 24 p3552 N90-30095
Nonlinear optical studies of the optical and electronic properties of semiconductor heterostructures
[AD-A223408] 24 p3552 N90-30096
The II-VI semiconductor superlattices
[AD-A223748] 24 p3553 N90-30101

SEMIMETALS
U METALLOIDS

SEMISPAN MODELS
Experimental and theoretical aerodynamic characteristics of a high-lift semispan wing model
[NASA-TP-2990] 13 p1749 N90-20046

SENDERS
U TRANSMITTERS

SENSE ORGANS
NT BARORECEPTORS
NT CORNEA
NT EAR
NT EYE (ANATOMY)
NT FOVEA
NT GRAVIRECEPTORS
NT OTOLITH ORGANS
NT PHOTORECEPTORS
NT RETINA
NT SEMICIRCULAR CANALS
NT VESTIBULES

SENSES
U SENSORY PERCEPTION

SENSIBILITY
U SENSITIVITY

SENSING
U DETECTION

SENSITIVITY
NT IMPACT RESISTANCE
NT LIGHT ADAPTATION
NT PHOTOSENSITIVITY
NT PHOTOTROPISM
NT PROPELLANT SENSITIVITY
NT RADIATION TOLERANCE
NT SPECTRAL SENSITIVITY
Test of EED (Electro-Explosive Devices). Part 3: Statistical aspects on the estimation of sensitivity
[FOA-C-20749-2.3-PT-3] 02 p0209 N90-11194
HPW (High Power Microwave) testing of electronic components
[DE89-016682] 02 p0217 N90-11241
Ion detector on the basis of microchannel plates for a high-sensitive mass spectrometer
[DE89-620335] 02 p0225 N90-11291
Sensitivity relationships in energetic materials
[DE89-016967] 03 p0333 N90-11897
Sensitivity of a regional oxidant model to variations in climate parameters, volume 1 and 2
[PB89-224943] 04 p0516 N90-12981
Quantitative AES and XPS: Determination of the electron spectrometer transmission function and the detector sensitivity energy dependencies for the production of true electron emission spectra in AES and XPS
[NPL-DMA(A)-194] 05 p0623 N90-13634
Quench sensitivity in Al-Cu-Li alloys
[AD-A213055] 05 p0624 N90-13639
Effect of spatial resolution on apparent sensitivity to initial conditions of a decaying flow as it becomes turbulent
[NASA-TM-102377] 05 p0638 N90-13719
Discussion of factors affecting the sensitivity of IR imaging sensors, particularly focal plane mosaic arrays --- staring mosaic arrays
[FOA-C-30536-3.1] 05 p0700 N90-14101
An investigation of the sensitization behavior of Fe-Mn-Cr austenitic steels
[DE90-002719] 07 p0904 N90-15226
More efficient sensitivity testing
[DE90-002639] 07 p0916 N90-15298
Preliminary investigation of parameter sensitivities for atmospheric entry and aerobraking at Mars
[NASA-TM-101607] 10 p1327 N90-17667
Computational aspects of sensitivity calculations in linear transient structural analysis
[NASA-TM-4156] 12 p1673 N90-19610
Sensitivity of ecological landscapes and regions to global climatic change
[PB90-120072] 12 p1684 N90-19674
Preparation, characterisation and cookoff behaviour of booster compositions prepared from RDX and acrylic or ethylene-vinyl acetate dispersions
[MRL-TR-89-44] 14 p1957 N90-21203
Overcoming the Bellman's curse of dimensionality in large optimization problems
[NASA-TM-102662] 17 p2352 N90-23391
Stability and stability sensitivity by periodically time dependent systems: Hill versus Floquet
[ILR-MITT-221(1989)] 17 p2463 N90-24071
Sensitivity analysis with a simple charging code
[RAE-TM-SPACE-374] 20 p2929 N90-26662
Measuring sensitivities and orthogonalities of magnetometer sensors in the Nurmijarvi coil hut 21 p3022 N90-27180
A study of the sensitivity of an imaging telescope (GRITS) for high energy gamma-ray astronomy
[NASA-CR-186921] 22 p3261 N90-28468
Kinematic sensitivity of robot manipulators 24 p3513 N90-29863

SENSITIZING
Method of sensitizing PB-Salt epitaxial films for Schottky diodes
[AD-D014244] 06 p0850 N90-14937
A study of the relation between grain boundary type and sensitisation in a partially-sensitised AISI 304 stainless steel using electron back-scattering patterns
[AERE-R-13327] 16 p2321 N90-23234

SENSORIMOTOR PERFORMANCE
NT PSYCHOMOTOR PERFORMANCE
Age-related changes in human posture control: Motor coordination tests
[NASA-CR-185855] 03 p0383 N90-12178
Telepresence, time delay, and adaptation 16 p2271 N90-22944
A commentary on perception-action relationships in spatial display instruments 16 p2272 N90-22950
Adaptive control of visually guided grasping in neural networks
[AD-A221387] 18 p2597 N90-24780
Experiment K-6-18. Study of muscarinic and gaba (benzodiazepine) receptors in the sensory-motor cortex, hippcampus and spinal code 20 p2895 N90-26471

SENSORS
A program to improve performance of AFGL (Air Force Geophysical Laboratory) automated present weather observing sensors
[AD-A207669] 01 p0087 N90-10495
Devices and procedures for the calibration of sensors and measurement: Systems of the flight test support system ATTAS
[DFVLR-MITT-89-06] 03 p0351 N90-12007
Software development for avionics SSME control and diagnostics
[NASA-CR-184894] 05 p0681 N90-13964
Implementing fault-tolerant sensors
[NASA-CR-186269] 09 p1225 N90-17105

SENSORY DISCRIMINATION
NT TACTILE DISCRIMINATION
NT VISUAL DISCRIMINATION
Auditory spectro-temporal pattern analysis
[AD-A218416] 16 p2313 N90-23184

SENSORY FEEDBACK
Paradoxical monocular stereopsis and perspective vergence 16 p2267 N90-22922
Seeing by exploring 16 p2268 N90-22923
Adapting to variable prismatic displacement 16 p2271 N90-22945
Sensory conflict in motion sickness: An observer theory approach 16 p2273 N90-22957
Voluntary presetting of the vestibular ocular reflex permits gaze stabilization despite perturbation of fast head movements 16 p2274 N90-22960
The human factors of workstation telepresence 19 p2732 N90-25528
Robotic tele-existence 24 p3502 N90-29796
Modeling and sensory feedback control for space manipulators 24 p3504 N90-29807

SENSORY PERCEPTION
NT AUDITORY PERCEPTION
NT CONSCIOUSNESS
NT KINESTHESIA
NT OLFACTORY PERCEPTION
NT PAIN
NT PROPRIOCEPTION
NT SPACE PERCEPTION
NT TACTILE DISCRIMINATION
NT TASTE
NT TOUCH
NT VERTICAL PERCEPTION
NT VISUAL DISCRIMINATION
NT VISUAL PERCEPTION
Sound Localization by Human Observers symposium proceedings
[AD-A212877] 04 p0524 N90-13026
A comparison of two subject-controlled attitude measures during somatogravic illusion exposure
[AD-A212528] 04 p0525 N90-13031
Three stages and two systems of visual processing
[AD-A212670] 04 p0525 N90-13032

Spatial tests for aviators
[IZF-1988-15] 04 p0527 N90-13041
Simulator induced sickness in the CP-140 (Aurora) flight deck simulator
[AD-A213096] 05 p0673 N90-13923
The characteristics of physiological responses and tolerance evaluation of pressure breathing
[AD-A214991] 09 p1252 N90-17262
Sensations of temperature and humidity during intermittent exercise and the influence of underwear knit structure
[AD-A215285] 09 p1252 N90-17266
Use of self-induced hypnosis to modify thermal balance during cold water immersion
[AD-A216156] 10 p1412 N90-18140
Computing with neural maps: Application to perceptual and cognitive functions
[AD-A216689] 10 p1412 N90-18143
Visual navigation: Constructing and utilizing simple maps of an indoor environment
[AD-A216761] 11 p1455 N90-18382
A colony architecture for an artificial creature
[AD-A216802] 11 p1549 N90-18918
Stochastic interactive activation and the effect of context on perception
[AD-A218929] 16 p2262 N90-22898
Transduction of nanovolt signals: Limits of electric-field detection
[AD-A219214] 16 p2312 N90-23177
Dynamical modifications to the head, load factors from additional weight 19 p2720 N90-25472
Multi-sensory perception of a geometrical structure of a scene
[ETN-90-97245] 20 p2915 N90-26587
Neural networks for real-time sensory data processing and sensorimotor control
[AD-A223096] 20 p2916 N90-26592
Situational Awareness in Aerospace Operations
[AGARD-CP-478] 23 p3357 N90-28972
A methodology for the objective measurement of pilot situation awareness 23 p3357 N90-28974
Situational Awareness Rating Technique (SART): The development of a tool for aircrew systems design 23 p3357 N90-28975
Performance-based measures of merit for tactical situation awareness 23 p3358 N90-28976
Evaluation of the Situational Awareness Rating Technique (SART) as a tool for aircrew systems design 23 p3358 N90-28977
Attention gradients in situation awareness 23 p3358 N90-28978
Workload induced spatio-temporal distortions and safety of flight: An investigation of cognitive intrusions in perceptual processes 23 p3360 N90-28986
Loss of alertness and consciousness from pilot position during long range flight 23 p3360 N90-28990
Situational awareness and vestibular stimulation: The influence of whole-body rotation upon task performance
[IZF-1989-14] 23 p3361 N90-28994
Cognition versus sensation: A paradigm for reorientation
[IZF-1989-20] 23 p3361 N90-28995
The 3D model control of image processing 24 p3503 N90-29800

SENSORY STIMULATION
Free swimming organisms: Microgravity as an investigative tool 05 p0678 N90-13949
Non-linear analysis of visual cortical neurons
[AD-A221543] 21 p3034 N90-27250

SENTENCES
NT WORDS (LANGUAGE)
Dual task performance with LPC (Linear Predictive Coding) degraded speech in a sentence verification task
[AD-A214298] 07 p0920 N90-15320

SENTINEL SYSTEM
Sentinel satellite positional precision derived from the NAVSTAR global positioning system
[AD-A211876] 03 p0303 N90-11720

SEO (INDIAN SPACECRAFT)
U INDIAN SPACECRAFT

SEPARATED FLOW
NT BOUNDARY LAYER SEPARATION
Basic studies of the unsteady flow past high angle of attack airfoils
[AD-A210252] 01 p0002 N90-10008
The three-dimensional vortex sheet structure on delta wings 01 p0064 N90-10367
Simultaneous detection of separation and transition in surface shear layers 01 p0064 N90-10368
Bifurcations in Poiseuille flow and wall turbulence 01 p0065 N90-10370
Numerically determined transition in separated internal flow 01 p0065 N90-10374
Flow visualization techniques for flight research 02 p0153 N90-10878
The structure of separated flow regions occurring near the leading edge of airfoils - including transition
[NASA-CR-185853] 03 p0299 N90-11695
Numerical analysis, scientific computing and fundamental studies of fluid mechanics
[DE89-017554] 03 p0346 N90-11975
A one equation turbulence model for transonic airfoils 06 p0719 N90-14199
Asymptotic analysis of performance of membrane modules for gas separations
[DE90-000699] 06 p0742 N90-14316
A direct-inverse method for transonic and separated flows about airfoils
[NASA-CR-4270] 07 p0875 N90-15072
Flows with Separation
[DGLR-PAPERS-88-05] 08 p1066 N90-16169
An interactive method for the flow calculation of airfoils with local separation regions 08 p1069 N90-16190
Calculation of the flap profile flows with separation based on coupled potential and boundary layer solutions 08 p1069 N90-16191
Inverse solutions for boundary layers with separation or close to separation under locally infinite swept wing conditions 08 p1070 N90-16192
Periodically unsteady effects on profiles, induced by separation 08 p1070 N90-16196
Determination of the heat transfer coefficients in separated flows using an infrared camera 08 p1081 N90-16257
Reacting flows 10 p1309 N90-17573
Unsteady viscous calculation method for cascades with leading edge induced separation 11 p1459 N90-18408
Numerical solution of 3D Navier-Stokes equations with upwind implicit schemes
[NASA-TM-101656] 12 p1600 N90-19205
Method and apparatus for detecting laminar flow separation and reattachment
[NASA-CASE-LAR-13952-1-SB] 12 p1659 N90-19534
Unsteady three-dimensional marginal separation, including breakdown
[NASA-TM-102525] 13 p1801 N90-20337
Experimental investigation of the mechanisms underlying vortex kinematics in unsteady separated flows
[AD-A217889] 13 p1802 N90-20346
Measurement of the flow field in the blade passage and side-wall region of a plane turbine cascade 14 p1924 N90-21019
Navier-Stokes analysis of turbine blade heat transfer
[NASA-TM-102496] 14 p1972 N90-21300
Control of flow separation and mixing by aerodynamic excitation
[NASA-TM-103131] 15 p2047 N90-21733
Numerical investigation of some control methods for 3-D turbulent interactions due to sharp fins 15 p2053 N90-21764
Numerical investigation of separated transonic turbulent flows with a multiple-time-scale turbulence model
[NASA-TM-102499] 15 p2090 N90-21962
Bifurcations in viscous flow fields. On the genesis and development of topologically complicated separated flow structures
[PB90-167156] 15 p2099 N90-22012
Unsteady separated flows produced by complex harmonic motions: Investigation of wing-flow interactions elicited by a mechanical model simulating dragonfly wing kinematics 15 p2100 N90-22018
Three-dimensional separated flow prediction on fusiform body using Euler and boundary layer methods 16 p2234 N90-22745
A study of supermanuever aerodynamics
[AD-A218378] 17 p2344 N90-23349
Fluid dynamic mechanisms and interactions within separated flows
[AD-A219628] 17 p2403 N90-23689
Method of forming a multiple layer dielectric and a hot film sensor therewith
[NASA-CASE-LAR-13678-1] 17 p2478 N90-24168
Flow studies in impeller passages 18 p2551 N90-24558
Identification of aerodynamic models for maneuvering aircraft
[NASA-CR-186630] 20 p2802 N90-25943
Report of the Fluid Dynamics Panel Working Group 10 on calculation of 3D separate turbulent flows in boundary layer limit
[AGARD-AR-255] 20 p2862 N90-26280
Model tilt-rotor hover performance and surface pressure measurement
[AD-A222535] 21 p2959 N90-26827
The dynamics and control of fluctuating pressure loads in the reattachment region of a supersonic free shear layer
[NASA-CR-184943] 22 p3108 N90-27852
Wind tunnel investigation of periodic vortex separation from rough surface circular cylinders by means of acoustic measurements
[ESA-TT-1092] 23 p3268 N90-28499
The effect of rapid spoiler deployment on the transient forces on an aerofoil 23 p3274 N90-28527
A numerical study of the response of the laminar unsteady separated flow about a circular cylinder to changes of boundary conditions
[DLR-FB-90-10] 24 p3471 N90-29613

SEPARATION
On the simulation test for the relative motion of separated sub-boosters on M-3S2 with nearly half a model vehicle ST-735 and their motion analyses using inertial sensors output
[ISAS-635] 17 p2366 N90-23471
Studies on phosphorus segregation in austenite
[ISBN-952-90-1488-0] 18 p2526 N90-24417
Fluid Phase Separation (FPS) experiment for flight on a space shuttle Get Away Special (GAS) canister
[NASA-CR-186830] 20 p2841 N90-26161

SEPARATORS
NT AIR FILTERS
NT CLASSIFIERS
NT DUST COLLECTORS
NT ELECTROSTATIC PRECIPITATORS
NT FLUID FILTERS
NT PRECIPITATORS
NT SIEVES
Membrane and durability studies for the zinc/bromine battery
[DE89-016181] 07 p0920 N90-15324
Low cost filter development and control of permeability in high temperature, high pressure ceramic filter elements
[DE90-000403] 11 p1507 N90-18676
Vortex motion phase separator for zero gravity liquid transfer
[NASA-CASE-KSC-11387-1] 13 p1783 N90-20236
The application of Dow Chemical's perfluorinated membranes in proton-exchange membrane fuel cells 13 p1823 N90-20466
Zero-G phase detector and separator
[NASA-CASE-LEW-14844-1] 15 p2101 N90-22024
Research in biological separations and cell culture
[NASA-CR-172060] 15 p2135 N90-22202
Electrochemical synthesis of ultrathin film composite membranes
[AD-A219041] 16 p2216 N90-22643
Resistivity measurements of halide-salt/MgO separators for thermal cells
[DE90-009740] 18 p2550 N90-24553

SEQUENCING
National airspace system approach and departure sequencing operational concept
[NAS-SR-1322] 01 p0004 N90-10017
General decomposition of sequential machines: Relationships to state assignment
[AD-A208189] 01 p0102 N90-10580
Application of a hybrid generation/utility assessment heuristic to a class of scheduling problems
[NASA-TM-102367] 01 p0117 N90-10674
Numerical analysis of chaotic symbol sequences generated by parabolic and triangle maps of the interval
[MPIS-22/1987] 04 p0539 N90-13124
Direct computation of 3D shape invariants and the focus of expansion
[AD-A212386] 04 p0549 N90-13195
Test generation for highly sequential circuits
[AD-A211932] 05 p0634 N90-13698
Nomenclature for physical mapping of complex genomes
[DE89-015173] 06 p0859 N90-14994
Preliminary experiences with a novel method for the determination of displacement vector fields and satellite image sequences 08 p1093 N90-16324
A planning and scheduling lexicon
[NASA-CR-186061] 09 p1171 N90-16777
Classification of acousto-optic correlation signatures of spread spectrum signals using artificial neural networks
[AD-A215045] 09 p1206 N90-16992
Boolean minimization and algebraic factorization procedures for fully testable sequential machines
[AD-A216779] 11 p1553 N90-18940
Influence of the parameters: Charge order, sequence classification, partial sequential circuit, and process regularity of a working charge (Gaussian process) on the lifetime of a component made of 3.1354 T3 and 3.4377 T761
[ETN-90-95378] 12 p1653 N90-19503
Adaptive, asynchronous stochastic global optimization algorithms for sequential and parallel computation
[AD-A217093] 12 p1702 N90-19775
A unified approach to the synthesis of fully testable sequential machines
[AD-A217120] 13 p1863 N90-20687

Irredundant sequential machines via optimal logic synthesis
[AD-A217119] 13 p1873 N90-20742
Passive navigation using image irradiance tracking
15 p2141 N90-22232
Kalman filter based range estimation for autonomous navigation using imaging sensors
15 p2142 N90-22238
A CSP model for distributed control software design
[OUEL-1789/89] 15 p2148 N90-22273
Constraint-based evaluation of sequential procedures
15 p2153 N90-22301
Spacecraft command verification: The AI solution
15 p2154 N90-22307
Encoding sequential structure in simple recurrent networks
[AD-A218928] 16 p2278 N90-22984
Analysis of sequencing and scheduling methods for arrival traffic
[NASA-TM-102795] 17 p2348 N90-23373
Fatigue testing of glass fibre reinforced epoxy using the WISPER sequence
[FFA-TN-1989-45] 17 p2381 N90-23561
Sequencing and scheduling: Algorithms and complexity
[CWI-BS-R8909] 17 p2446 N90-23942
Designing distributed algorithms by means of formal sequentially phased reasoning
[TR-89-8] 17 p2449 N90-23969
An empirically derived figure of merit for the quality of overall task performance 18 p2644 N90-25058
CESAR sequencer
[FFI-89/7021] 19 p2744 N90-25599
Modular arithmetic and randomization for exact matroid problems: Extended abstract
[REPT-89-064] 19 p2751 N90-25628
Optimal synchronization of spread spectrum sequenced by nontransferable switching operators
20 p2845 N90-26183
Direct-sequence spread spectrum system
[AD-A223021] 20 p2856 N90-26245
MTP: An atomic multicast transport protocol
[NASA-CR-186716] 20 p2858 N90-26254
Causal distributed breakpoints
[AD-A222613] 20 p2921 N90-26622
Generation of animation sequences of three dimensional models
[NASA-CASE-MSC-21379-1-SB]
21 p3050 N90-27340
Efficient instruction sequencing with inline target insertion
[NASA-CR-185341] 21 p3052 N90-27348
Precedence relationship representations of mechanical assembly sequences 24 p3514 N90-29866
Handbook of data compression algorithms
[ESA-TM-06] 24 p3531 N90-29969
Unique binary search tree representations and equality-testing of sets and sequences
[AD-A223643] 24 p3537 N90-30002

SEQUENTIAL ANALYSIS

Sequential quadratic programming algorithms for optimization
[AD-A212800] 04 p0534 N90-13088
Domain of attraction of an operator between supremum and sum
[REPT-89-05] 04 p0539 N90-13119
Timing optimization of multi-phase sequential logic
[AD-A220836] 17 p2397 N90-23656
Designing distributed algorithms by means of formal sequentially phased reasoning
[TR-89-8] 17 p2449 N90-23969
Causal distributed breakpoints
[AD-A222103] 21 p3066 N90-27431

SEQUENTIAL COMPUTERS

General decomposition of sequential machines: Relationships to state assignment
[AD-A208189] 01 p0102 N90-10580
A CSP model for distributed control software design
[OUEL-1789/89] 15 p2148 N90-22273
The bit full-decomposition of sequential machines
[EUT-89-E-223] 20 p2904 N90-26516
The full-decomposition of sequential machines with the separate realization of the next-state and output functions
[EUT-89-E-222] 20 p2909 N90-26547
MINAS: An algorithm for systematic state assignment of sequential machines: Computational aspects and results
[EUT-89-E-217] 20 p2912 N90-26566

SEQUENTIAL CONTROL

An algebra for process creation
[CWI-CS-R8907] 04 p0543 N90-13155
Efficient on-line simulations of tree machines and multidimensional turing machines by random access machines
[AD-A213152] 05 p0680 N90-13960
Compiling scientific code using partial evaluation
[AD-A215087] 09 p1270 N90-17363
Long period pseudo random number sequence generator
[NASA-CASE-NPO-17241-1-CU]
17 p2394 N90-23636
A model of a path expression based operating system shell
[MEMO-INF-89-71] 17 p2440 N90-23906
Sequencing and scheduling: Algorithms and complexity
[CWI-BS-R8909] 17 p2446 N90-23942
Sequentiality in orthogonal term rewriting systems
[CWI-CS-R8932] 18 p2592 N90-24744
CESAR sequencer
[FFI-89/7021] 19 p2744 N90-25599

SERIES (MATHEMATICS)

NT ASYMPTOTIC SERIES
NT CAMPBELL-HAUSDORFF SERIES
NT COSINE SERIES
NT FOURIER SERIES
NT PADE APPROXIMATION
NT POWER SERIES
NT SINE SERIES
NT TAYLOR SERIES

Optimization of series expressions. Part 2: Over view of the theory and implementation
[AD-A219961] 17 p2447 N90-23952
Nonlinear systems, the Lie series, and the left shift operator: Application to nonlinear optimal control
[RR-376] 19 p2748 N90-25619
Strong consistency of the least squares estimator for a non-ergodic threshold autoregressive model
[IMAG-RR-791-M] 20 p2918 N90-26604
Reversed residuals in autoregressive time series analysis
[AD-A222711] 20 p2921 N90-26624

SERIES EXPANSION

On the coefficients of differentiated expansions of ultraspherical polynomials
[NASA-CR-181913] 01 p0112 N90-10637
Evaluation of integrals related to the Debye function
[DE89-016930] 02 p0264 N90-11499
Rational expansion for nonlinear input-output maps
[RR-348] 03 p0394 N90-12248
Asymptotic expansions for two-stage rank tests
[MEMO-773] 04 p0544 N90-13161
Interpretation and manipulation of Edgeworth expansions
[MEMO-775] 04 p0544 N90-13163
Using the method of matched asymptotic expansions, analytically investigate the three-dimensional, atmosphere entry problem
[AD-A216287] 11 p1468 N90-18451
Very accurate upward continuation to low heights in a test of non-Newtonian theory 13 p1837 N90-20548
Observer based compensators for nonlinear systems
[AD-A217426] 13 p1875 N90-20760
A modified Moebius inverse formula and its applications in physics
[DE90-612740] 14 p2022 N90-21594
Adaptive pattern recognition by mini-max neural networks as a part of an intelligent processor
15 p2156 N90-22317
Effect on relaxation on nonlinear waves in crystals
16 p2310 N90-23165
Asymptotic expansions of an integral containing a phase function with three saddle points
[CWI-AM-R8922] 18 p2599 N90-24793
Flow structures around non-hyperbolic singularities on the wall with one vanishing eigenvalue: A discussion of the flow structures and the unfoldings
[LR-586] 19 p2692 N90-25315
Calculation of the algebraic curves parameterization: Hamburger-Noether expansions
[IMAG-RR-798-M] 20 p2919 N90-26608
Application of discrete Fourier series to the finite element stress analysis of axi-symmetric solids
[PB90-231010] 23 p3339 N90-28870

SERUMS

Human serum albumin crystals and method of preparation
[NASA-CASE-MFS-28234-1] 13 p1850 N90-20616

SERVICE LIFE

Predictive aging of polymers
[NASA-CASE-NPO-17524-1-CU]
01 p0046 N90-10261
The RB199: An in-service success
[PNR90544] 03 p0307 N90-11746
In service life monitoring system using g-meter readings and mass configuration control
[ETN-89-95218] 03 p0356 N90-12035
Long endurance underwater power system
[AD-A211386] 03 p0366 N90-12096
Thermal barrier coating life prediction model development, phase 1
[NASA-CR-182230] 05 p0581 N90-13388
Crazing and degradation of flexure strength in acrylic plates as a function of time
[AD-A212835] 06 p0749 N90-14357
A nonlinear high temperature fracture mechanics basis for strainrange partitioning
[NASA-TM-4133] 06 p0797 N90-14642
Ceramic technology for advanced heat engines project
[DE90-001852] 07 p0908 N90-15251
Membrane and durability studies for the zinc/bromine battery
[DE89-016181] 07 p0920 N90-15324
Life evaluation of valve-regulated lead-acid batteries for load-leveling applications
[DE90-002188] 07 p0922 N90-15336
Niobium 1 percent zirconium/potassium and titanium/potassium life-test heat pipe design and testing
[DE90-002430] 07 p0954 N90-15522
Cycle-life improvement of Zn/NiOOH cells by the addition of Ca(OH)2 to the zinc electrode
[DE90-004040] 08 p1062 N90-16139
Application of high-rate cutting tools
[AD-A214644] 09 p1203 N90-16970
Statistical theory of reliability
[AD-A215320] 09 p1234 N90-17161
Status of the cycling tests performed with SAFT NiH2 cells dedicated to space applications
10 p1334 N90-17715
Low earth orbit nickel cadmium battery lifetime testing
10 p1334 N90-17716
In-orbit performance of CS-3a spacecraft GaAs solar array 10 p1346 N90-17804
Space radiation effects on electronics
[DE90-602874] 10 p1378 N90-17986
Changes in impedance of Ni electrodes upon standing and cycling
[NASA-TM-102438] 10 p1401 N90-18097
Full-scale birdstrike testing of in-service aged F-111 ADBIRT windshield transparencies
[AD-A218035] 13 p1754 N90-20069
Theory system reliability demonstration and burn-in design
[AD-A217775] 13 p1814 N90-20416
Flow in a forward swept centrifugal fan, volumes 1 and 2 14 p1912 N90-20959
Fracture and longevity of composite structures
[AD-A217827] 14 p1944 N90-21127
Aging and compatibility of TNF-doped Mylar
[DE90-008508] 14 p1954 N90-21186
Collapsible fabric tank testing
[AD-A217861] 14 p1987 N90-21388
Test results and flight experience of ball bearing momentum and reaction wheels
15 p2115 N90-22099
Design of a telescoping tube system for access and handling equipment 15 p2116 N90-22102
Boeing/NASA composite components flight service evaluation
[NASA-CR-181898] 16 p2210 N90-22609
National Airspace System (NAS) software life cycle management study
[AD-A221180] 19 p2657 N90-25122
Rocket combustion chamber life-enhancing design concepts
[NASA-CR-185257] 19 p2669 N90-25183
Study on application of ultrasonic wave measurement to creep-fatigue damage detection
[DE89-782317] 19 p2700 N90-25361
Characterization of impact damage in composites
21 p2957 N90-26811
Damage tolerance analysis for manned hypervelocity vehicles. Volume 2: Software user's manual
[AD-A222136] 21 p2959 N90-26826
B-1B improved windshield development. Volume 2: Magna analysis: Baseline and parametric
[AD-A221501] 21 p2960 N90-26828
Life evaluation of valve regulated lead-acid batteries for cycling applications
[DE90-013649] 21 p2999 N90-27044
Advanced algorithms design and implementation in on-board microprocessor systems for engine life usage monitoring 22 p3104 N90-27628
AGARD/SMP Review Damage Tolerance for Engine Structures. 3: Component Behaviour and Life Management
[AGARD-R-770] 22 p3117 N90-27704
AGARD damage tolerance concepts for engine structures Workshop 3, Component Behaviour and Life Management 22 p3117 N90-27705
Calculation of service life of turbomachine components 22 p3117 N90-27706
The role of component testing
22 p3117 N90-27707

The role of inflight engine condition monitoring on life cycle management of CF-18/F404 engine components
22 p3118 N90-27708
Life management planning 22 p3118 N90-27709
Evaluation of composite components on the Bell 206L and Sikorsky S-76 helicopters
[NASA-TM-4195] 22 p3135 N90-27787
Liquid lubrication in space
[NASA-RP-1240] 22 p3183 N90-28063
An ultrasonic system for in-service non-destructive inspection of composite structures
22 p3185 N90-28076
NASA Langley Research Center National Aero-Space Plane Mission simulation profile sets
[NASA-TM-102670] 23 p3276 N90-28541
Energy Efficient Engine (E3) combustion system component technology performance report
[NASA-CR-168274] 23 p3279 N90-28555
Probabilistic structural analysis methods development for SSME 23 p3291 N90-28616
Cryogenic, high speed, turbopump bearing cooling requirements 23 p3291 N90-28620
Bearing optimization for SSME HPOTP application
23 p3292 N90-28622
Development of improved self lubricating cages for SSME HPOTP bearings 23 p3292 N90-28623
Cage stability analysis for SSME HPOTP bearings
23 p3292 N90-28625
Comparison of two computer codes for crack growth analysis: NASCRAC versus NASA/FLAGRO
23 p3297 N90-28648
Probabilistic model for fracture mechanics service life analysis 23 p3297 N90-28650
Durability of thermal barrier coatings in a high heat flux environment 23 p3297 N90-28651
Study of meteorological processes important in the degradation of materials through surface temperature
[PB90-222720] 23 p3336 N90-28856
Development of testing and analysis methodology to assess the long term durability of polymeric composites at high temperatures
[NASA-TM-102714] 23 p3339 N90-28871
Development of the sodium/sulfur technology for energy storage
[DE90-014329] 23 p3344 N90-28899

SERVICE MODULES
The service module structure of the IOS spacecraft development and qualification program
02 p0181 N90-11021

SERVICES
NT MEDICAL SERVICES
NT METEOROLOGICAL SERVICES
Distributed user services for supercomputers
[NASA-CR-180370] 17 p2450 N90-23976

SERVOCONTROL
Control of plasma position in the CASTOR tokamak
[IPPCZ-284] 03 p0407 N90-12332
Results of the manipulator test test stand study: Comparison of manipulators and evaluation of equipment items
[DE90-000977] 06 p0794 N90-14625
Application of a buck-type MC2 regulated converter for a stepper motor control 10 p1335 N90-17722
Digital to position converter
[DIGEL-1984-4] 12 p1654 N90-19509
Bi-directional thruster development and test report
[NASA-CR-182013] 15 p2058 N90-21785
Equipment specifications for launcher guidance using multivariable frequency methods
[REPT-892-422-106] 16 p2205 N90-22582
Design, simulation, and testing of a field-oriented ac servo-drive using a TM5 32010 signal processor
[EMV-88-42] 17 p2397 N90-23658
Video-rate visual servoing for robots
[AD-A218711] 22 p3181 N90-28052
Short period control using angular acceleration feedback: Compensation for first lag servo
[NAL-TM-600] 24 p3435 N90-29399

SERVOMECHANISMS
NT SERVOMOTORS
Advanced actuation systems development, volume 1
[AD-A213334] 04 p0458 N90-12624
Advanced actuation systems development, volume 2
[AD-A213378] 05 p0583 N90-13398
Kinematics and control of manipulation robots
[WTHD-187] 05 p0652 N90-13803
Results of the manipulator test test stand study: Comparison of manipulators and evaluation of equipment items
[DE90-000977] 06 p0794 N90-14625
Automation and robotics in construction: Japanese research and development
[AD-A214170] 07 p0942 N90-15456
Feasibility study of using industrial robot for ultrasound testing
[DE90-002977] 07 p0943 N90-15461
Teleoperator servoloop tuning using an expert system
[DE90-005674] 11 p1542 N90-18876
Architecture for a human-robot symbiotic system
[DE90-005670] 11 p1550 N90-18921
Disturbance torque rejection properties of the NASA/JPL 70-meter antenna axis servos
12 p1644 N90-19450
Digital to position converter
[DIGEL-1984-4] 12 p1654 N90-19509
Resolved motion rate and resolved acceleration servo-control of wheeled mobile robots
[DE90-002585] 13 p1811 N90-20399
Design of a telerobotic controller with joint torque sensors
[DE90-008753] 13 p1812 N90-20404
Bi-directional thruster development and test report
[NASA-CR-182013] 15 p2058 N90-21785
Experimental adaptive control of a hydraulic robot
16 p2303 N90-23121
Design, simulation, and testing of a field-oriented ac servo-drive using a TM5 32010 signal processor
[EMV-88-42] 17 p2397 N90-23658
Modeling flexible aircraft for flight control design
[AD-A219123] 19 p2660 N90-25140
Multi-microprocessor control of a precision pan and tilt head
[RSRE-MEMO-4252] 19 p2747 N90-25613
Simulated dynamic response of a servovalve controlled hydraulic actuator
[NASA-TM-101644] 20 p2842 N90-26167
Video-rate visual servoing for robots
[AD-A218711] 22 p3181 N90-28052
Application of recursive manipulator dynamics to hybrid software/hardware simulation 24 p3516 N90-29876
A control approach for robots with flexible links and rigid end-effectors 24 p3516 N90-29879

SERVOMOTORS
Design and use of brushless dc motor without detent torque 18 p2539 N90-24491
Microcomputer for the digital regulation of permanent magnet-synchronous servomotors
[ETN-90-96507] 18 p2588 N90-24727

SERVOS
U SERVOMOTORS

SERVOSTABILITY CONTROL
U SERVOCONTROL

SET THEORY
NT EQUIVALENCE
On the expected complexity of the three-dimensional Voronoi diagram
[PB89-209332] 01 p0112 N90-10636
An axiomatic theory for partial functions
[MEMO-INF-89-22] 02 p0268 N90-11527
Extended basis set calculations of atomization energies: Comparison of isogyric and direct results
[AD-A212268] 04 p0471 N90-12702
A point in betaZ/Z not contained in a maximal orbit closure
[REPT-89-26] 04 p0540 N90-13127
Acceleration sets of planar manipulators. Part 2: Applications and experiments
[AD-A213336] 05 p0650 N90-13791
The algebraic Riccati equation and singular optimal control
[MEMO-COSOR-88-31] 05 p0690 N90-14028
Membership-set parameter estimation via optimal bounding ellipsoids
[AD-A213807] 07 p0984 N90-15685
The algebraic Riccati equation and singular optimal control
[MEMO-COSOR-89-11] 08 p1117 N90-16467
Fixed points of expansive analytic maps
[AD-A214356] 10 p1421 N90-18194
Deductive computer programming, revision
[AD-A219848] 17 p2446 N90-23946
Compound sets in mathematical programming modeling languages
[MEMO-834] 17 p2449 N90-23963
Cyclotomy and association schemes
[REPT-89-73] 17 p2458 N90-24030
Applications of dynamical systems theory to fractals: A study of cookie-cutter Cantor sets
[REPT-89-76] 17 p2458 N90-24032
A generalization of Ore's theorem involving neighborhood unions
[MEMO-825] 17 p2462 N90-24064
Associated distributions in the analysis of two-dimensional random walks
[CWI-BS-R8917] 17 p2466 N90-24095
Analogues of the Lebesgue density theorem for fractal sets of reals and integers
[REPT-89-88] 17 p2468 N90-24106
On the independence of B-splines on unordered knot sets
[MEMO-827] 18 p2600 N90-24800
Finding complete bipartite subgraphs in bipartite graphs
[RUU-CS-89-30] 18 p2602 N90-24815
The axiomatization of randomness
[ITLI-ML-89-06] 18 p2603 N90-24824
The Second Asilomar Workshop on Progress in Mathematical Programming
[AD-A221986] 21 p3053 N90-27358
Multi-Hilbertian spaces and their duals
[AD-A222344] 21 p3064 N90-27421

SETI
U PROJECT SETI

SEWAGE
NT SOLID WASTES
Investigation report of the investigation commission for interchange of heat pump technology in Europe
[DE89-782293] 11 p1505 N90-18666

SEX FACTOR
International application of the DLR test-system: First year of cooperation with IBERIA in pilot selection
[DLR-FB-90-05] 19 p2723 N90-25491
Content effects in mathematics problem solving
[AD-A222436] 21 p3065 N90-27423
Physiological reactions to heat stress; quantifying the effects of individual parameters
[IZF-1989-30] 22 p3232 N90-28326

SEX GLANDS
NT TESTES

SEYFERT GALAXIES
Spectropolarimetry, variability, and the taxonomy of active galactic nuclei 02 p0292 N90-11667
Radio and optical observations of nearby active galaxies 06 p0860 N90-15000
Ion-heated thermal Comptonization models and x ray spectral correlations in active galactic nuclei
[DE90-003597] 08 p1151 N90-16667
Nearly simultaneous optical, ultraviolet, and x ray observations of three PG quasars
[NASA-CR-186355] 12 p1728 N90-19932
Nuclear activity, morphology, and far infrared properties of spiral galaxies
[ETN-90-95373] 12 p1744 N90-20024
EXOSAT observations of Seyfert type galaxies
13 p1901 N90-20910
Spectrum formation in active galactic nuclei and Type 2 supernovae 15 p2187 N90-22490
Spectral evolution of active galactic nuclei Penrose Compton scattering processes and gamma ray emission from Seyfert galaxies 16 p2337 N90-23317
The high energy source 3C 273
16 p2337 N90-23318
Very low luminosity AGN 19 p2786 N90-25851
The complex X ray spectra of AGN
19 p2786 N90-25855
Complex X ray spectra and thick matter in Seyfert 1 galaxies 19 p2787 N90-25860
Hard X ray observations of active galaxies
19 p2789 N90-25874
The EUV spectral shape of the big-bump in HS1700+6416 and F9: A genuine difference between Seyfert's and QSO's 19 p2789 N90-25878
X ray spectral variability in Seyfert 1 galaxies
19 p2792 N90-25891
X ray polarization of the reprocessed emission from accretion disk in Seyfert galaxies
19 p2792 N90-25892
Effect of X ray spectra of Seyfert galaxies on the cosmic X ray background 19 p2792 N90-25896
The X ray spectrum of MCG-6-30-15
19 p2793 N90-25898
X ray spectrum and variability of MRK 509 as observed with EXOSAT and Ginga 19 p2794 N90-25904
Einstein SSS+MPC observations of Seyfert type galaxies 19 p2795 N90-25913

SFERICS
U ATMOSPHERICS

SGEMP
U SYSTEM GENERATED ELECTROMAGNETIC PULSES

SH WAVES
Scattering of waves by inclusions in a nonhomogeneous elastic half space solved by boundary element methods
[PB90-145699] 15 p2116 N90-22107
A 2-D analysis of particle velocity and stress of SH waves from a strip radiator. An experimental verification of both amplitude and phase using EMA transducers
[AERE-R-12600] 16 p2227 N90-22704
Propagation and attenuation of Lg waves in South America
[AD-A218853] 16 p2255 N90-22859

SHADES
Shutter mechanism for controlling the exposure of samples to solar radiation 18 p2540 N90-24498

SHADOWGRAPH PHOTOGRAPHY
NT SCHLIEREN PHOTOGRAPHY

Application of the wide-field shadowgraph technique to rotor wake visualization
[NASA-TM-102222] 03 p0300 N90-11700
Recent flow visualization studies in the 0.3-m TCT
04 p0442 N90-12528
Spark camera annotation and control system for the BRL (Ballistic Research Laboratory) Transonic Range Facility
[AD-A212266] 04 p0459 N90-12633
Improvement of ultrashort pulsed laser shadowgraph photography by means of optical filters
[ISL-CO-215/88] 04 p0504 N90-12906
X ray shadowscopy in implosion experiments
06 p0784 N90-14563
Optical techniques for determination of normal shock position in supersonic flows for aerospace applications
[NASA-TM-103201] 19 p2693 N90-25323

SHADOWGRAPHS
U SHADOWGRAPH PHOTOGRAPHY

SHADOWS
An anisotropic shadowband correction for parameterized sky conditions and geometry
[DE89-014916] 01 p0085 N90-10485
Simulation of shading in synthetic surfaces
[INPE-4869-PRE/1480] 10 p1326 N90-17660
Three-dimensional motion estimation using shading information in multiple frames
[AD-A216804] 11 p1549 N90-18919
Factors affecting the perception of transparent motion
15 p2141 N90-22233
Depth buffer shadow algorithms
[DE90-012070] 19 p2744 N90-25595

SHAFTS (MACHINE ELEMENTS)
NT ROTATING SHAFTS
NT TURBOSHAFTS
Magnetostrictive torque sensor
[AD-D014169] 03 p0349 N90-11996
The nature and control of skidding in lightly loaded intershaft bearings
[PNR90591] 04 p0508 N90-12933
Continuously variable gear drive transmission
[AD-D014268] 08 p1084 N90-16275
Phase control mechanism for wave energy conversion
[AD-D014354] 12 p1681 N90-19657
An applicational process for dynamic balancing of turbomachinery shafting
[NASA-TM-102537] 13 p1810 N90-20392
Parametric resonance in horizontal axis wind turbines
14 p1912 N90-20962
Assessment of High Temperature Superconducting (HTS) electric motors for rotorcraft propulsion
[NASA-CR-185222] 15 p2052 N90-21761
The development of a complementary expendable launch vehicle interface for an STS deployable payload
15 p2113 N90-22086
Thermal/structural analysis of the shaft-disk region of a fan drive system
[NASA-TM-101687] 16 p2245 N90-22807
Experimental evaluation of a tuned electromagnetic damper for vibration control of cryogenic turbopump rotors
[NASA-TP-3005] 17 p2354 N90-23403
Non-linear dynamic analysis of geared systems, part 2
[NASA-CR-180495] 17 p2410 N90-23732
Prediction of gear tooth separation in single-stage gear systems, using numerical techniques
[AD-A220442] 17 p2412 N90-23744
Bidirectional drive and brake mechanism
[NASA-CASE-MSC-21540-1] 20 p2872 N90-26342
Experimental investigation of the hydrodynamic forces on the shroud of a centrifugal pump impeller
[NASA-CR-186952] 21 p3009 N90-27108
Preliminary results on noncollocated torque control of space robot actuators 23 p3373 N90-29057
Integrated controls and health monitoring fiberoptic shaft monitor
[NASA-CR-185210] 24 p3472 N90-29622

SHAKERS
VIBRAFUGE: A combined environment testing facility-vibration testing on a centrifuge
[DE89-015120] 01 p0080 N90-10458
Two years experience with the ESTEC multishaker system 02 p0187 N90-11065
Tamaris: A new European facility for low frequency multi-axis vibration simulation 02 p0187 N90-11068
A new European vibration test facility for Ariane 4 class satellites 02 p0187 N90-11070

SHAKING
NT DITHERS
Force determination sensitivities study for full-scale helicopter ground vibration testing
[AD-A215983] 10 p1322 N90-17643

SHALE OIL
Determination of flow-regime boundaries for cohesive particles
[DE90-007425] 13 p1800 N90-20332

SHALES
Organic geochemical and tectonic evolution of the midcontinent rift system: Organic geochemistry and micropaleontology
[DE89-017561] 06 p0818 N90-14760

SHALLOW SHELLS
A C(Superscript)-Anisoparametric three-node shallow shell element for general shell analysis
[AD-A212094] 03 p0358 N90-12049

SHALLOW WATER
Semi-Lagrangian, semi-implicit solutions of the shallow water equations in one dimension
[AD-A212658] 04 p0503 N90-12902
Instability mechanisms in a barotropic atmosphere
[KNMI-WR-89-01] 04 p0520 N90-13001
On the applicability of CAESAR for the remote sensing of bottom depth and bottom composition of shallow waters: A model study
[BCRS-89-13] 11 p1526 N90-18783
A new stability criterion in the shallow-water system for two-dimensional coherent eddies in the atmosphere and oceans 15 p2130 N90-22176
Computational Fluid Dynamics, volume 1
[VKI-LS-1990-03-VOL-1] 22 p3171 N90-27989
Numerical methods for shallow water flow
22 p3172 N90-27992
Vertically averaged spectral model for tidal circulation in estuaries. Part 1: Model formulation
[PB90-181678] 22 p3230 N90-28319

SHANKS
U JOINTS (JUNCTIONS)

SHANNON INFORMATION THEORY
U INFORMATION THEORY

SHAPE CONTROL
Shape control of high degree-of-freedom variable geometry trusses 01 p0024 N90-10122
Screening actuator locations for static shape control
[NASA-CR-181970] 09 p1182 N90-16851
A difference scheme with autocontrol artificial viscosity to predict ablated nosetip shape
[AD-A216625] 11 p1468 N90-18452
Robust control of flexible structures
15 p2058 N90-21784
Passive shape control of space antennas with determinate truss support structures
15 p2087 N90-21949
Modeling and control of flexible vehicles in space
[AD-A219622] 17 p2365 N90-23465
Crown and shape control in the rolling of thin, wide plates
[ETN-90-96946] 17 p2378 N90-23539

SHAPE MEMORY ALLOYS
NT NITINOL ALLOYS
Heat engine based on shape memory alloys
[AD-D014400] 14 p1986 N90-21385
Development of shape memory metal as the actuator of a fail safe mechanism 15 p2112 N90-22081
US Army Research Office Workshop on Smart Materials, Structures and Mathematical Issues proceedings
[AD-A218528] 17 p2468 N90-24110
Shape memory alloys for robot grippers and mechanical hands 18 p2536 N90-24466

SHAPED CHARGES
Systems tunnel linear shaped charge lightning strike
[NASA-CR-183832] 05 p0584 N90-13404
Minutes of the 23rd Explosives Safety Seminar, volume 1
[AD-A218264] 14 p1958 N90-21213
SR90, strontium shaped-charge critical ionization velocity experiment
[NASA-CR-186501] 14 p2024 N90-21606
Shelf life extension for the lot AAE nozzle severance LSCs
[NASA-CR-183878] 15 p2062 N90-21813

SHAPES
NT CONVEXITY
NT FLATNESS
NT LINE SHAPE
NT T SHAPE
The measurement of infrared spectra of dense ceramics by specular reflectance spectroscopy
[AD-A210609] 01 p0051 N90-10291
Filling or outlining shapes with color: The effects on a visual search task
[AD-A211067] 02 p0255 N90-11444
Development of a VSAERO (Vortex Separation Aerodynamics) model of the F/A-18
[AD-A212442] 04 p0448 N90-12566
Direct computation of 3D shape invariants and the focus of expansion
[AD-A212386] 04 p0549 N90-13195
A renormalization group approach to image processing: A new computational method for three-dimensional shapes in robot vision, and the computation complexity of the cooling algorithms
[AD-A214247] 07 p0977 N90-15643
Shapes of star-gas waves in spiral galaxies
[NASA-CR-186289] 07 p1011 N90-15859
Stripline feed for a microstrip array of patch elements with teardrop shaped probes
[NASA-CASE-NPO-17548-1-CU]
08 p1056 N90-16104
The development of two-dimensional object identification techniques
[NASA-CR-186203] 08 p1107 N90-16408
Comments on comet shapes and aggregation processes 08 p1142 N90-16622
Screening actuator locations for static shape control
[NASA-CR-181970] 09 p1182 N90-16851
A finite element-boundary integral formulation for scattering by three-dimensional cavity-backed apertures
[NASA-CR-186332] 09 p1187 N90-16878
Measures of subjective variables in visual cognition
[AD-A215084] 09 p1259 N90-17303
Aggregate filter
[AD-A215029] 09 p1282 N90-17432
Shape from focus
[AD-A215959] 10 p1393 N90-18052
A user's manual for the method of moments Aircraft Modeling Code (AMC)
[NASA-CR-186371] 11 p1456 N90-18390
Parts of recognition
[AD-A217694] 13 p1868 N90-20714
A tool for automatic design of airfoils in different operating conditions 14 p1919 N90-20994
Optimization of aerodynamic designs using computational fluid dynamics 14 p1920 N90-20999
Supersonic nozzle design of arbitrary cross-section
14 p1927 N90-21035
Molecular theory of fluid phase equilibria
[PB90-131277] 15 p2066 N90-21832
The solution of scattering and radiation problems for complex configurations based on 3-D grid and patch models 15 p2096 N90-21997
Lightweight piston architecture
[NASA-CASE-LAR-13926-1] 15 p2105 N90-22042
Circularity measuring system: A shape gauge designed especially for use on large objects
15 p2116 N90-22104
Two-dimensional shape recognition using sparse distributed memory 15 p2140 N90-22227
Development of the methods and means of precise forming and geometry control of superconducting current-carrying element for the UNR pulsed dipoles
[DE90-620108] 15 p2173 N90-22419
The minimum drag profile in laminar flow: A numerical way 16 p2196 N90-22535
An experimental study of tip shape effects on the flutter of aft-swept, flat-plate wings
[NASA-TM-4180] 16 p2199 N90-22555
Exocentric direction judgements in computer-generated displays and actual scenes 16 p2270 N90-22936
Hand shaping: A paradigm for cognitive/motoric interaction
[AD-A219908] 17 p2437 N90-23885
Shape discrimination research using an IBM PC
[AD-A219993] 17 p2447 N90-23953
Computer-Aided Structural Engineering (CASE) project. User's guide: A Three-Dimensional Stability Analysis/Design Program (3DSAD). Report 2: General loads module
[AD-A220331] 18 p2591 N90-24742
A contribution to the economic, optimal dimensioning, and shaping of aircraft structures using a design model
[ETN-90-96966] 20 p2808 N90-25976
Feasibility study of a synthesis procedure for array feeds to improve radiation performance of large distorted reflector antennas
[NASA-CR-186641] 20 p2851 N90-26213
Curvature estimation in orientation selection
[AD-A221481] 21 p3034 N90-27249
An algorithm for automated surface modelling in unigraphics
[AD-A223219] 21 p3053 N90-27355
Organising geometric computations for space telerobotics 23 p3376 N90-29074
Tokamak plasma shape identification with a Legendre-Fourier expansion of the vacuum poloidal flux function in the toroidal coordinates
[DE90-508031] 24 p3548 N90-30068

SHARP LEADING EDGES
Numerical simulation of the laminar and turbulent three dimensional flow on a delta wing with sharp leading edge 08 p1069 N90-16186
Glancing shock-boundary layer interactions
10 p1309 N90-17571
A video-based experimental investigation of wing rock
[AD-A218244] 13 p1755 N90-20075
Experimental and numerical investigation of the vortex flow over a sharp edged delta wing; with and without sideslip
[PB90-167131] 14 p1913 N90-20964

SHATTERING
U FRAGMENTATION
SHEAR
Stability conditions for steady shearing. Stability conditions for simple shear under mixed thermal boundary conditions 04 p0499 N90-12873
SHEAR CREEP
Creep in shear of experimental solder joints
[DE90-007062] 11 p1520 N90-18753
SHEAR DISTURBANCES
U S WAVES
SHEAR FATIGUE
U SHEAR STRESS
SHEAR FLOW
Direct numerical simulation of turbulent free shear flows
[AD-A210161] 01 p0040 N90-10218
Fluid Dynamics of Three-Dimensional Turbulent Shear Flows and Transition
[AGARD-CP-438] 01 p0062 N90-10356
Turbulence modelling of three-dimensional shear flows 01 p0066 N90-10381
Dynamics and control of turbulent shear flows
[AD-A210396] 01 p0070 N90-10402
Analysis of spurt phenomena for a non-Newtonian fluid
[AD-A210560] 01 p0071 N90-10405
Chemical reactions in turbulent mixing flows
[AD-A211240] 02 p0220 N90-11263
Numerical experiments on transition control in wall-bounded shear flows 04 p0443 N90-12536
Three-dimensional shear flows: Analysis of the track and angle of incidence
[CERT-RTS-OA-31/5025-AYD] 04 p0501 N90-12888
A planar reacting shear layer system for the study of fluid dynamics-combustion interaction
[NASA-TM-102422] 05 p0582 N90-13393
Quadratic dynamical systems describing shear flow of non-Newtonian fluids
[AD-A212892] 05 p0638 N90-13720
Analysis of new phenomena in shear flow of non-Newtonian fluids
[AD-A212893] 05 p0638 N90-13721
Turbulent Shear Flows
[VKI-LS-1989-03] 05 p0640 N90-13730
An introduction via vorticity dynamics and statistical theory — turbulent shear flows 05 p0640 N90-13731
Scalar transport in turbulent shear flows 05 p0640 N90-13734
Large eddy simulation of homogeneous turbulence undergoing shear and thermal gradients. Application to one point closing models
[ECL-88-23] 05 p0643 N90-13754
New transient algorithms for non-Newtonian flows
[AD-A213494] 07 p0930 N90-15385
A method for measuring the material moduli of granular materials: Flow in an orthogonal rheometer
[DE90-007160] 13 p1801 N90-20339
The effect of viscosity on the resistive tearing mode with the presence of shear flow
[DE90-009340] 14 p1974 N90-21312
The extension of rapid distortion theory to stratified shear flows 14 p2005 N90-21491
Instabilities and vortex dynamics in shear flow of magnetized plasmas
[DE90-009448] 14 p2030 N90-21643
Control of flow separation and mixing by aerodynamic excitation
[NASA-TM-103131] 15 p2047 N90-21733
Experimental and analytical investigations of granular materials: Shear flow and convective heat transfer 15 p2091 N90-21968
Automated analysis of measured turbulent boundary flow
[PB90-147844] 15 p2092 N90-21970
Modern developments in shear flow control with swirl
[NASA-CR-186586] 15 p2097 N90-22000
Unsteady separated flows produced by complex harmonic motions: Investigation of wing-flow interactions elicited by a mechanical model simulating dragonfly wing kinematics 15 p2100 N90-22018
Semigeostrophic flow over orography in a stratified rotating atmosphere 15 p2127 N90-22163
Flow visualization in supersonic turbulent boundary layers 16 p2195 N90-22533
Analysis of velocity and temperature fluctuations in turbulent shear flows 16 p2233 N90-22744
Transactions of the Seventh Army Conference on Applied Mathematics and Computing
[AD-A219220] 16 p2309 N90-23160
Fluid dynamic mechanisms and interactions within separated flows
[AD-A219628] 17 p2403 N90-23689
The computation of turbulent thin shear flows associated with flow around multielement aerofoils 18 p2491 N90-24240
Rheology and microstructure of concentrated suspensions
[DE90-009976] 18 p2520 N90-24391
A theoretical analysis of the acoustic radiation from two-dimensional turbulent mixing layers 18 p2551 N90-24559
Coherent structures, chaos and the role of modern dynamics in turbulent shear flows
[AD-A220884] 18 p2552 N90-24562
Turbulization of shear flows in astrophysics 19 p2773 N90-25763
Direct numerical simulation of compressible free shear flows 21 p2974 N90-26901
Local and global resonances in heated 2-D jets
[AD-A221671] 21 p3005 N90-27079
Calculations of chemically reacting shear flows above solid fuels 22 p3162 N90-27930
Study of the origin of three dimensional structures in shear flows through external forcing
[AD-A221923] 22 p3170 N90-27980
Experimental study of homogeneous turbulence under rotation and deformation modes
[ONERA-RSF-12/1145-AY-170A] 22 p3176 N90-28023
Wind tunnel simulation of Antarctic snowdrifting
[PB90-184565] 22 p3212 N90-28222
Aerodynamics of bodies in shear flow 23 p3268 N90-28496
Cavity aeroacoustics
[AD-A223853] 24 p3418 N90-29307
Particle dispersion in a turbulent shear flow
[AD-A224327] 24 p3467 N90-29590
SHEAR LAYERS
Chemical reactions in turbulent mixing flows
[AD-A211240] 02 p0220 N90-11263
Questions from the Willmarth Workshop on New Directions in Research on Turbulent Wall-Layer Structures
[AD-A211282] 02 p0221 N90-11264
Control of turbulent mixing layers
[AD-A211413] 03 p0301 N90-11708
A planar reacting shear layer system for the study of fluid dynamics-combustion interaction
[NASA-TM-102422] 05 p0582 N90-13393
Field-effect spectroscopy of interface states
[AD-A212998] 05 p0703 N90-14112
Numerical modeling of supersonic turbulent reacting free shear layers 06 p0719 N90-14197
An experimental investigation of shear layer mixing in supersonic flows 06 p0775 N90-14508
Computation of broadband mixing noise from turbomachinery
[AD-A214448] 07 p0989 N90-15713
New mixing-length model for numerical solution of turbulent supersonic flows 09 p1216 N90-17048
Opportunities for improved understanding of supersonic and hypersonic flows 10 p1308 N90-17566
Numerical simulation of supersonic free shear layers
[AD-A216289] 10 p1310 N90-17579
Damage mechanisms and indenter size effects in cross plied carbon-carbon composites
[AD-A216413] 10 p1351 N90-17832
Response of a chemically reacting layer to streamwise vorticity
[NASA-TM-102288] 10 p1383 N90-18005
Numerical simulation of unstably stratified sheared flows
[DE90-005396] 10 p1384 N90-18008
Computational aerodynamics of ordered vortex flows
[ETN-90-96272] 11 p1452 N90-18368
Separation bubbles at high Reynolds number: Measurement and computation
[CUED/A-AERO/15] 12 p1657 N90-19525
Application of a Reynolds stress turbulence model to the compressible shear layer
[NASA-CR-182002] 12 p1660 N90-19537
Experimental study of validity of the unstationary Kutta condition, with high Strouhal numbers
[ETN-90-95914] 12 p1661 N90-19547
The effects of forcing on a single stream shear layer and its parent boundary layer
[NASA-CR-186529] 14 p1973 N90-21301
Control of flow separation and mixing by aerodynamic excitation
[NASA-TM-103131] 15 p2047 N90-21733
Destabilization of supersonic free shear layers by parametric excitation using Mach waves generated by a wavy wall
[AD-A219655] 17 p2345 N90-23352
The stability of two-dimensional wakes and shear-layers at high Mach numbers
[NASA-CR-182050] 17 p2401 N90-23678
Fluid dynamic mechanisms and interactions within separated flows
[AD-A219628] 17 p2403 N90-23689
Seismic anisotropy and large-scale porosity in the ocean floor
[AD-A220453] 17 p2431 N90-23849
A theoretical analysis of the acoustic radiation from two-dimensional turbulent mixing layers 18 p2551 N90-24559
Turbulence modeling in the SHALE code
[DE90-010354] 18 p2553 N90-24574
A linear-eddy model of turbulent shear layer mixing 21 p2974 N90-26904
Numerical investigation of the incompressible plane shear layer between two gases with different densities
[ETN-90-97315] 21 p3006 N90-27084
The dynamics and control of fluctuating pressure loads in the reattachment region of a supersonic free shear layer
[NASA-CR-184943] 22 p3108 N90-27652
Free shear layer and swirl flow heat transfer enhancement
[PB90-228123] 23 p3325 N90-28798
Numerical simulation of the formation of two-dimensional and three-dimensional structures in shear layers and wakes
[ESA-TT-1008] 23 p3325 N90-28802
Numerical simulation supersonic free shear layers
[AD-A223771] 24 p3418 N90-29306
Cavity aeroacoustics
[AD-A223853] 24 p3418 N90-29307
Numerical simulations of the structure of supersonic shear layers
[AD-A224164] 24 p3467 N90-29587
SHEAR PROPERTIES
NT SHEAR STRENGTH
Stability of discontinuous shearing motions of a non-Newtonian fluid
[AD-A210643] 01 p0071 N90-10406
Transverse shear stiffness of composite and sandwich finite elements 02 p0182 N90-11034
Shear fatigue testing and life prediction of fibre composites
[REPT-8519] 04 p0466 N90-12668
Identification of equivalent modulus of a composite beam from nonmodal vibratory tests
[ECL-89-001] 05 p0656 N90-13821
The structure and properties of liquid crystal polymers 06 p0749 N90-14356
Heat treatment investigation of 4330 vanadium-modified steel
[AD-A214290] 07 p0906 N90-15239
Two dimensional laminated shell theory including parabolic transverse shear
[AD-A213817] 07 p0948 N90-15487
Stress analysis of the Princeton Plasma Physics Laboratory 1/2- x 1/2-inch shear/compression test fixture
[DE90-004401] 08 p1124 N90-16512
Adhesive for composite bonding
[DE90-005683] 09 p1188 N90-16885
Investigation of collapse characteristics of cylindrical composite panels with large cutouts
[AD-A216378] 10 p1397 N90-18079
Model filled polymers 3. Rheological behavior of polystyrene containing crosslinked polystyrene beads
[AD-A215867] 11 p1489 N90-18567
Irradiation-induced amorphization and elastic shear instability in intermetallic compounds
[DE90-004845] 12 p1625 N90-19341
Failure mechanisms under complex loading of glass-reinforced polyester composites and their matrices: The effect of superposed hydrostatic pressures up to 300 MPa on axial tensile and compressive strengths, and in-plane shear properties of unidirtionally reinforced glass-polyester composites and the relevant polyesters 15 p2110 N90-22072
Coupled behavior of rock joints
[DE90-009222] 15 p2129 N90-22174
Approximate analysis for the formation of adiabatic shear bands
[AD-A218751] 16 p2221 N90-22670
Role of shear instability in ballistic penetration
[AD-A219186] 16 p2244 N90-22799
High resolution electron energy loss spectroscopy studies of chemisorbed species on metal surfaces
[AD-A222272] 21 p2978 N90-26922
Strength under various modes of deformation
[AD-A222412] 21 p3013 N90-27132
Aqueous solution properties of ampholytic ionomers
[AD-A222152] 22 p3156 N90-27890
Is there anything of practical value hidden amongst the composite toughening theories. A Jim Mueller prospective
[DE90-014905] 23 p3301 N90-28673

Interlaminar shear tests on continuous fiber reinforced thermoplastics: The effects of rubber forming
[LR-621] 24 p3444 N90-29451
Rheology of filler rubber: Silica-silicone
[AD-A223600] 24 p3455 N90-29511
The MTL Torsional Split-Hopkinson bar
[AD-A223278] 24 p3479 N90-29663

SHEAR STRAIN
Theoretical and experimental investigation of thin-walled aluminum panels under cyclic shear load
02 p0177 N90-10996
Shear strain localization phenomenon in viscoplastic materials 06 p0798 N90-14649
Observations of fine-scale vertical shear and strain in the upper ocean
[AD-A214476] 10 p1410 N90-18130
Creep in shear of experimental solder joints
[DE90-007062] 11 p1520 N90-18753
Two-dimensional surface strain measurement based on a variation of Yamaguchi's laser-speckle strain gauge
[NASA-TM-103162] 16 p2241 N90-22784
Strain softening in viscoelasticity of the rate type
[AD-A219915] 17 p2417 N90-23772

SHEAR STRENGTH
Behavior of the adhesive A2 submitted to mechanical traction
[CETIM-105290] 04 p0479 N90-12748
Effects of high rate shear on the microstructure and deformation and fracture behavior of two high strength steels
[AD-A214107] 08 p1044 N90-16032
Interfaces of organic matrices and graphite fiber composites: A review of the literature
[AD-A214504] 09 p1186 N90-16870
Adhesive for composite bonding
[DE90-005683] 09 p1188 N90-16885
Plasma modification of poly (p-phenylenebenzobisthiazole)
[AD-A215761] 10 p1433 N90-18272
The effect of fiber coatings on interfacial shear strength and the mechanical behavior of ceramic composites
[DE90-007574] 12 p1632 N90-19380
Fiber pushout test: A three-dimensional finite element computational simulation
[NASA-TM-102565] 14 p1945 N90-21131
Tensile and shear strength of adhesives
18 p2515 N90-24366
Influence of interfacial shear strength on the mechanical properties of SiC fiber reinforced reaction-bonded silicon nitride matrix composites
[NASA-TM-102462] 18 p2518 N90-24382
Study of the mechanical behavior of composites under complex stress systems
[ETN-90-97455] 22 p3154 N90-27879

SHEAR STRESS
NT TORSIONAL STRESS
Simultaneous detection of separation and transition in surface shear layers 01 p0064 N90-10368
Analysis of spurt phenomena for a non-Newtonian fluid
[AD-A210560] 01 p0071 N90-10405
Stability of discontinuous steady states in shearing motion of a non-Newtonian fluid
[AD-A210644] 01 p0071 N90-10407
Stress intensity factors and displacements for arc bend samples using collocation
[AD-A210404] 01 p0080 N90-10460
Manual for Program PSTRESS: Peel stress computation
[NASA-CR-178408] 03 p0321 N90-11822
Absolute determination of the wall shear stress by means of an interferometer
[DFVLR-FB-89-13] 03 p0349 N90-11991
Visualization of boundary layer transition zone movement on oscillating airfoils with shear-sensitive liquid-crystal coatings
[DE89-009570] 06 p0721 N90-14210
Shear strain localization phenomenon in viscoplastic materials 06 p0798 N90-14649
Transverse (through-the-thickness) shear stiffnesses of fibre reinforced composite laminated plates (computer program)
[ESDU-89013] 07 p0891 N90-15152
New transient algorithms for non-Newtonian flows
[AD-A213494] 07 p0930 N90-15385
The structure of supersonic turbulent boundary layers subjected to concave surface curvature
08 p1017 N90-15883
Colinear fluctuating wall shear stress and fluctuating pressure transducer
[AD-D014296] 08 p1076 N90-16226
Surface flow visualization with shear stress sensitivive liquid crystals
[DNW-WTI-88.039] 08 p1081 N90-16255
Velocity profile and wall shear stress measurements for a Large Eddy Break-Up (LEBU) device
[AD-A214958] 09 p1217 N90-17059
Simple shear tests of the FMI 23.5.06 adhesive cured at low pressure (12 PSI)
[INFORME-I-298/88] 10 p1357 N90-17871
Bearing tests in Ti-6Al-4V plates made using superplastic forming
[INFORME-I-357/89] 10 p1396 N90-18068
Turbulence structure of mixing swirling flows
[AD-A216628] 11 p1506 N90-18671
Method and apparatus for detecting laminar flow separation and reattachment
[NASA-CASE-LAR-13952-1-SB] 12 p1659 N90-19534
Application of a Reynolds stress turbulence model to the compressible shear layer
[NASA-CR-182002] 12 p1660 N90-19537
Interlaminar shear stress effects on the postbuckling response of graphite-epoxy panels
[NASA-TM-102626] 12 p1676 N90-19630
Development of a defect stream function, law of the wall/wake method for compressible turbulent boundary layers 15 p2100 N90-22019
Three-dimensional finite element formulations for thick and thin laminated plates 15 p2121 N90-22132
Large deformation analysis of laminated composite structures by a continuum-based shell element with transverse deformation 16 p2211 N90-22613
Pressure and shear stress measurement uncertainty for DARPA SUBOFF experiment
[AD-A219109] 16 p2243 N90-22798
A numerical study of basic coastal upwelling processes 16 p2259 N90-22878
Effect of constitutive modeling on the dynamic development of shear bands in viscoplastic materials
[AD-A220443] 17 p2416 N90-23765
Strain softening in viscoelasticity of the rate type
[AD-A219915] 17 p2417 N90-23772
A day in the life of a warm front
[AD-A220373] 17 p2426 N90-23826
Investigation of the effect of mechanical stress on cold fusion
[AD-A220123] 17 p2474 N90-24147
The yield and post-yield behavior of high-density polyethylene
[NASA-CR-186574] 19 p2676 N90-25219
Flow resistance and critical shear stress in steep channels 19 p2687 N90-25282
A suitable transverse shear stiffness definition for buckling of laminates and sandwich plates
[LR-603] 19 p2704 N90-25384
Creep and creep rupture of strongly reinforced metallic composites
[NASA-CR-185286] 22 p3192 N90-28110
Spectral measurements of the wall shear stress and wall pressure in a turbulent boundary layer: Theory
[AD-A224070] 24 p3466 N90-29586
The MTL Torsional Split-Hopkinson bar
[AD-A223278] 24 p3479 N90-29663

SHEAR WAVES
U S WAVES

SHEARING
Shear-induced inflation of coronal magnetic fields
[NASA-CR-186103] 05 p0715 N90-14178
Energy release rate analysis of interfacial cracks in composites 15 p2065 N90-21829
The mechanics of shear band formation in thermal viscoplastic materials at high rates of loading
15 p2120 N90-22128
Postbuckling response of long thick plates loaded in compression including higher order transverse shearing effects
[NASA-TM-102663] 19 p2700 N90-25363
Postbuckling response of long thick isotropic plates loaded in compression including higher order transverse shearing effects
[NASA-TM-4199] 22 p3190 N90-28100

SHEARING STRESS
U SHEAR STRESS

SHEATHS
NT PLASMA SHEATHS
Lunar drill footplate and casing
[NASA-CR-183153] 17 p2411 N90-23738

SHEET METAL
U METAL SHEETS

SHELL STABILITY
Buckling load analysis for imperfect cylindrical shells, part 1
[LR-543-PT-1] 05 p0656 N90-13823
Experiments on buckling and critical buckling. Behavior of carbon fiber reinforced plastic shells submitted to tensile stresses
[ETN-90-95382] 13 p1816 N90-20429
ANILISA: Computational module for Koiter's imperfection sensitivity theory
[LR-582] 15 p2119 N90-22119
Some kinematic relations of thin elastic shells
[LR-612] 19 p2704 N90-25388
Investigation of the dynamic buckling of liquid-filled tanks 24 p3478 N90-29660
Recent developments in shell stability analysis
[LR-633] 24 p3483 N90-29685

SHELL THEORY
A C(Superscript)-Anisoparametric three-node shallow shell element for general shell analysis
[AD-A212094] 03 p0358 N90-12049
Two dimensional laminated shell theory including parabolic transverse shear
[AD-A213817] 07 p0948 N90-15487
A review of the theory and methods for determining dynamic pulse buckling of cylindrical shells
[AD-A214764] 09 p1238 N90-17185
Scaling Z-pinch plasmas with atomic number for a given K-shell emission
[AD-A215703] 09 p1285 N90-17450
Modeling and analysis of the space shuttle nose-gear tire with semianalytic finite elements
[NASA-TP-2977] 12 p1670 N90-19595
Modal interactions in shell dynamics
13 p1814 N90-20418
Large deformation analysis of laminated composite structures by a continuum-based shell element with transverse deformation 16 p2211 N90-22613
Transverse vibrations of a composite cylindrical tube of circular cross section
[AD-A219227] 16 p2248 N90-22820
Some kinematic relations of thin elastic shells
[LR-612] 19 p2704 N90-25388
From Lie group transformation to the generalized Koiter initial postbuckling theory of perfect shells
[LR-613] 19 p2704 N90-25389
Error detection and control for nonlinear shell analysis
[NASA-TM-102723] 23 p3340 N90-28877

SHELLS (STRUCTURAL FORMS)
NT ANISOTROPIC SHELLS
NT CONICAL SHELLS
NT CORRUGATED SHELLS
NT CYLINDRICAL SHELLS
NT ELASTIC SHELLS
NT FLUID FILLED SHELLS
NT LIQUID FILLED SHELLS
NT METAL SHELLS
NT ORTHOTROPIC SHELLS
NT PERFORATED SHELLS
NT RADOMES
NT SHALLOW SHELLS
NT SPHERICAL SHELLS
NT THIN WALLED SHELLS
Hygrothermal deformations of composite shells
02 p0185 N90-11055
Buckling load analysis for imperfect cylindrical shells, part 1
[LR-543-PT-1] 05 p0656 N90-13823
Interface between MEDUSA and GIFTS for shell structures
[LR-553] 05 p0684 N90-13985
Two dimensional laminated shell theory including parabolic transverse shear
[AD-A213817] 07 p0948 N90-15487
Finite element investigation of a composite cylindrical shell under transverse load with through thickness shear and snapping
[AD-A216377] 10 p1397 N90-18078
Investigation of collapse characteristics of cylindrical composite panels with large cutouts
[AD-A216378] 10 p1397 N90-18079
Development of finite beam and shell elements for structures under great inelastic deformations
[ETN-90-95869] 12 p1675 N90-19623
Fourier series methods for plates and shells with cracks and inclusions 14 p1990 N90-21406
Direct formulation of a 4-node hybrid shell element with rotational degrees of freedom
[NASA-CR-4282] 14 p1991 N90-21411
Determination of stresses around cutouts in multilayered composite plate and shell structures
14 p1992 N90-21417
Elasto-plastic large deformation analysis of thin-walled structures
[PB90-164757] 14 p1994 N90-21426
Accuracy of the QUAD4 thick shell element
18 p2569 N90-24641
Incorporation of a progressive failure analysis method in the CSM testbed software system
18 p2640 N90-25036
From Lie group transformation to the generalized Koiter initial postbuckling theory of perfect shells
[LR-613] 19 p2704 N90-25389

Understanding silica binders
[PNR90625] 20 p2840 N90-26150
Recent developments in shell stability analysis
[LR-633] 24 p3483 N90-29685

SHELTERS
NT LUNAR SHELTERS
Design of an unmanned lunar cargo lander that reconfigures into a shelter for a habitation module or disassembles into parts useful to a permanent manned lunar base
[NASA-CR-186687] 17 p2363 N90-23454

SHIELDING
NT ELECTROMAGNETIC SHIELDING
NT HEAT SHIELDING
NT MAGNETIC SHIELDING
NT RADIATION SHIELDING
NT REENTRY SHIELDING
NT REUSABLE HEAT SHIELDING
NT SOLAR RADIATION SHIELDING
NT SPACECRAFT SHIELDING
The baffles 05 p0604 N90-13509
Effect of unshielded and shielded horn balances on hinge moment coefficients for controls at low speeds
[ESDU-89003-A] 06 p0726 N90-14238
On protection of Freedom's solar dynamic radiator from the orbital debris environment. Part 1: Preliminary analyses and testing
[NASA-TM-102458] 06 p0736 N90-14285
Nuclear weapon radiation effects on a space based interceptor weapon platform
[DE89-016258] 09 p1181 N90-16850
Effects of oblique impact on hypervelocity shield performance
[DE90-008936] 11 p1517 N90-18739
Technology evaluation for space station atmospheric leakage
[DE90-007844] 12 p1616 N90-19294
Trailer shield assembly for a welding torch
[NASA-CASE-MFS-29260-1] 12 p1672 N90-19602
Scaling of nonnuclear kinetic-energy antisatellites
[DE90-009758] 15 p2059 N90-21791
Fracture mechanics of monolithic ceramic materials under small scale microcracking conditions
15 p2070 N90-21860
Validation of shielding effectiveness of cables with pigtails
[AD-A220647] 17 p2396 N90-23650
Forward canopy feasibility and Thru-The-Canopy (TTC) ejection system study
[AD-A220360] 18 p2495 N90-24258
Effects of X radiation on the LAMPSHADE orbital debris satellite shield, 2
[DE90-008214] 18 p2510 N90-24341
Development of ceramic hybrid combustor: Design and combustion test results
[DE90-503442] 20 p2839 N90-26149
Electrode carrying wire for GTAW welding
[NASA-CASE-MFS-29491-1] 20 p2842 N90-26168
Rings of Earth detected by orbital debris radar
20 p2854 N90-26232
A closed form solution to HZE propagation
[NASA-TM-103482] 20 p2924 N90-26640
Hypervelocity impact shield
[NASA-CASE-MSC-21420-1] 21 p2966 N90-26858
Cosmic bombardment 2: Intercepting the bomblets cost-efficiently
[DE90-010401] 21 p3098 N90-27601
A YBCO RF-SQUID magnetometer and its applications 22 p3151 N90-27867
Improved meteorological measurements from buoys and ships (IMET): Preliminary comparison of solar radiation air temperature shields
[PB90-241928] 22 p3229 N90-28314

SHIELDS (GEOLOGY)
U BEDROCK

SHIP HULLS
Calculation of the odd and even integral components of the wave resistance Green's function
[AD-A212384] 04 p0503 N90-12900
Numerical evaluation of the far field wave pattern of the radiation Green's function
[AD-A212839] 04 p0546 N90-13176
A review of the theory and methods for determining dynamic pulse buckling of cylindrical shells
[AD-A214764] 09 p1238 N90-17185
Underwater connect and disconnect plug and receptacle
[AD-D014175] 21 p2998 N90-27039
Hydrodynamic skin-friction reduction
[NASA-CASE-LAR-14078-1-CU] 21 p3003 N90-27071

SHIPS
NT AIRCRAFT CARRIERS
NT SUBMARINES
Statistical models for the optimal estimation of oceanic fields
[AD-A211786] 03 p0377 N90-12149
Climatological data for the North Sea based on observations by voluntary observing ships over the period 1961-1980
[KNMI-WR-89-02] 04 p0520 N90-13002
Damping loss factor determination of glass and graphite fiber composites
[AD-A214535] 10 p1347 N90-17816
GTD/UTD: Brief history of successive development of theory and recent advances. Applications to antennas on ships and aircraft 10 p1370 N90-17939
Suboptimal period design for a maneuvering missile to evade tracking filters 12 p1650 N90-19479
The browse file of NASA/JPL quick-look radar images from the Loch Linnhe 1989 experiment
[NASA-CR-186855] 20 p2935 N90-26701
Direct and remote sensing observations of the effects of ships on clouds 22 p3218 N90-28252
Optical properties of marine stratocumulus clouds modified by ship track effluents
22 p3218 N90-28253
Automated system for meteorological analysis
[INPE-4586-TDL/332] 23 p3352 N90-28945

SHIPYARDS
The use of technology transfer centers by department of defense industrial facilities
[AD-A216663] 10 p1443 N90-18328

SHIVERING
NT DITHERS
The effects of nonselective and selective beta blockade upon nonshivering thermogenesis during an acute cold exposure in cold acclimated men
06 p0820 N90-14767

SHOCK (PHYSIOLOGY)
Parachute opening shocks during high speed ejections: Normalization 13 p1751 N90-20056

SHOCK ABSORBERS
Numerical analysis of nonlinear viscoelastic structures: Application to elastomers and rubber-like materials
02 p0180 N90-11013
Structural vibration and shock isolator
[AD-D014202] 04 p0509 N90-12940
Evaluation of shock isolation techniques for a piezoresistive accelerometer
[DE89-014496] 06 p0780 N90-14535
An introduction to shaker shock simulations
[DE90-003057] 08 p1088 N90-16296
The Shock and Vibration Digest, volume 22, no. 2
14 p2022 N90-21596

SHOCK DIFFUSERS
U DIFFUSERS
U SHOCK WAVE ATTENUATION

SHOCK DISCONTINUITY
Shock capturing by the spectral viscosity method
[NASA-CR-181920] 01 p0112 N90-10639
Inviscid dynamics of unstable shear layers
[AD-A222297] 21 p3004 N90-27077

SHOCK FRONTS
Radiative shocks with electron thermal conduction
02 p0293 N90-11670
Thermodynamic properties and hydrodynamic response of high-density high-temperature C H N O mixtures
[DE90-000836] 06 p0742 N90-14318
The instability and fragmentation of the envelope of supernova 1987A 06 p0862 N90-15011
Shapes of star-gas waves in spiral galaxies
[NASA-CR-186289] 07 p1011 N90-15859
Shock thickness measurements with laser beams
[MPIS-7/1989] 08 p1083 N90-16267
Numerical modelling of shocks in gases and metals
[MRL-RR-8-89] 12 p1658 N90-19528
The dynamic instability of adiabatic blastwaves
[NASA-CR-182498] 17 p2401 N90-23679
Molecular gas in S106: Morphology, kinematics, and chemistry of a star forming region
17 p2484 N90-24209
A study of non-uniqueness and instability for convex materials
[DE90-012060] 19 p2689 N90-25294
Optical techniques for determination of normal shock position in supersonic flows for aerospace applications
[NASA-TM-103201] 19 p2693 N90-25323

SHOCK HEATING
Shock dissociation of molecular fluids: A possibility of first-order phase change
[DE89-016647] 03 p0322 N90-11829
Thermal/structural analyses of several hydrogen-cooled leading-edge concepts for hypersonic flight vehicles
[NASA-TM-102391] 06 p0775 N90-14511

SHOCK LAYERS
Experimental research on swept shock Wave/Boundary layer interactions
[AD-A211744] 03 p0348 N90-11988
Demonstration of the feasibility of laser induced fluorescence for arc jet flow diagnostics
[NASA-CR-185595] 08 p1040 N90-16013
A numerical and experimental investigation of multiple shock wave/turbulent boundary layer interactions in a rectangular duct 08 p1062 N90-16141
Shock layer vacuum UV spectroscopy in an arc-jet wind tunnel
[NASA-TM-102258] 09 p1226 N90-17112
Unsteadiness of supersonic and hypersonic shock induced turbulent boundary layer separation
10 p1309 N90-17572
Geometric scale of interaction between moving shock and stationary thermal layer
[AD-A217769] 13 p1802 N90-20344
Domain decomposition for a boundary-value problem with a shock layer
[DE90-007857] 13 p1877 N90-20762
An approximate viscous shock layer method for calculating the hypersonic flow over blunt-nosed bodies
14 p1910 N90-20947
Numerical investigation of some control methods for 3-D turbulent interactions due to sharp fins
15 p2053 N90-21764
National Aeronautics and Space Administration (NASA)/American Society for Engineering Education (ASEE) Summer Faculty Fellowship Program-1989, volume 1
[NASA-CR-185601-VOL-1] 18 p2627 N90-24972
Temperature determination of shock layer using spectroscopic techniques 18 p2628 N90-24973
X rays from the accretion column of compact objects: A Monte Carlo study 19 p2775 N90-25777
Boundary layer and shock layer in hypersonic flows
[CERT-31/5005-22-DERAT] 22 p3110 N90-27664
Nonequilibrium radiation and chemistry models for aerocapture vehicle flowfields
[NASA-CR-186728] 22 p3169 N90-27973
Shock-layer bounds for a singularly perturbed equation
[NASA-CR-182080] 22 p3243 N90-28391
Gas-jet and tangent-slot film cooling tests of a 12.5 deg cone at Mach number of 6.7
[NASA-TP-2786] 23 p3326 N90-28806

SHOCK LOADS
NT BLAST LOADS
Dynamically compressed metals: Theory
[AD-A210741] 01 p0045 N90-10257
Shock compression and release in high-strength ceramics
[DE89-013995] 01 p0047 N90-10265
Induced shock loads during the separation of the Ariane 5 VEB structure 02 p0184 N90-11045
Techniques for recovery of shock-loaded samples
[DE89-016881] 02 p0233 N90-11337
Calculation of the refractive index change in dissociating shocked benzene
[DE89-017737] 03 p0322 N90-11833
VISAR wave profile measurements in supra-compressed HE
[DE89-017736] 03 p0346 N90-11976
Pyrotechnic shock structural response
04 p0483 N90-12774
Shock-induced solid state reactions and phase transitions: X ray profile studies on shock-modified Fe3O4 and ZrO2 powders
[DE90-000669] 06 p0741 N90-14315
Shock-induced defects and flux pinning in YBa2Cu3O sub 7-delta + Ag composites
[DE90-000827] 06 p0853 N90-14960
The 59th Shock and Vibration Symposium, volume 1
[AD-A214578] 09 p1238 N90-17183
The 59th Shock and Vibration Symposium, volume 4
[AD-A214581] 09 p1238 N90-17184
Shock compression of solids: A tutorial
[DE90-009185] 14 p2032 N90-21659
Slow shocks in coronal mass ejections
[NASA-CR-186578] 15 p2193 N90-22522
Wind tunnel tests of a 20-gore disk-gap-band parachute
[AD-A221326] 18 p2493 N90-24251
Nonlinear material response to very rapid energy deposition
[AD-A221932] 21 p2989 N90-26988
The response and failure mechanisms of circular metal and composite plates subjected to underwater shock loading
[AD-A222200] 21 p3013 N90-27131

SHOCK MEASURING INSTRUMENTS
Shock thickness measurements with laser beams
[MPIS-7/1989] 08 p1083 N90-16267
State-of-the-art of measuring ground shock and cratering phenomena 09 p1235 N90-17170

SHOCK RESISTANCE
NT IMPACT RESISTANCE

A review of the theory and methods for determining dynamic pulse buckling of cylindrical shells
[AD-A214764] 09 p1238 N90-17185
Shock initiation sensitivity of damaged TP-H1207C composite propellant
[DE90-008509] 14 p1957 N90-21205
Thermal shock and oxidation resistance of ceramic coatings 23 p3308 N90-28711

SHOCK SIMULATORS

Direct simulation Monte Carlo of shock reflexion on a wedge with boundary layer
[ISL-CO-245/88] 11 p1508 N90-18681
An optical study of the flow start-up process in four convergent-divergent nozzles
[AD-A222918] 21 p2963 N90-26846

SHOCK SPECTRA

EPIC-2 calculated impact loading histories of thin plates
[AD-A210557] 01 p0081 N90-10461
Design concepts for hardened communications structures
[AD-A221233] 19 p2683 N90-25260

SHOCK TESTS

Remarks on certain aspects of solid explosive detonation via small projectile impact
[AD-A210648] 01 p0054 N90-10307
Pressure induced resonance Raman effects in shocked carbon disulfide
[AD-A210665] 02 p0194 N90-11107
Using small scale tests to estimate the failure diameter of a propellant
[DE90-001166] 07 p0913 N90-15281
The 59th Shock and Vibration Symposium, volume 2
[AD-A214579] 10 p1395 N90-18065
Test component attachment effects on resonant plate pyrotechnic shock simulation
[DE90-006478] 12 p1662 N90-19551
Dynamic response of a complex encapsulated electronic assembly subjected to a severe shock environment
[DE90-007689] 15 p2118 N90-22114
An optical study of the flow start-up process in four convergent-divergent nozzles
[AD-A222918] 21 p2963 N90-26846

SHOCK TUBES

Jet-flow from shock tubes
[AD-A210651] 02 p0220 N90-11260
Preliminary report on the feasibility of high power Electronic Warfare (EW) using explosive energy sources
[MRL-TR-89-3] 04 p0483 N90-12775
Application of a copper vapour laser to investigation of shock and blade interaction in a shock tube
[PNR90578] 04 p0506 N90-12918
Corrections for non-ideal effects in reflected shock waves at low Mach numbers
[DE90-002192] 06 p0721 N90-14208
Shock tube ignition of octanes
[DE90-001167] 07 p0893 N90-15164
Rayleigh-Taylor instability in compressible fluids
[DE90-003027] 07 p0929 N90-15376
Investigation of heat transfer with film cooling to a flat plate in a shock tube
[AD-A216379] 10 p1386 N90-18019
A study on upstream moving pressure waves induced by vortex separation
[ISL-CO-203/88] 12 p1597 N90-19192
Numerical modelling of shocks in gases and metals
[MRL-RR-8-89] 12 p1658 N90-19528
SPHC (Smooth Particle Hydrodynamics Code) manual
[AD-A220743] 17 p2444 N90-23928
Short time Force and moment measurement System for shock tubes (SFS) for measuring times less than 10 ms 18 p2490 N90-24233
The effects of blast trauma (impulse noise) on hearing: A parametric study source 2
[AD-A221731] 21 p3035 N90-27253

SHOCK WAVE ATTENUATION

Spallation and dynamic fracture as an effect of laser induced shock waves in carbon based composite materials
[AD-A216540] 11 p1478 N90-18509
Measurement and visualization of the shock wave caused by the impact of a pulsed YAG laser in water
[REPT-892-430-113] 16 p2240 N90-22783

SHOCK WAVE GENERATORS

NT SHOCK TUBES

SHOCK WAVE INTERACTION

A study of the structure of highly swept shock wave turbulent boundary layer interactions
01 p0066 N90-10376
Experimental research on swept shock Wave/Boundary layer interactions
[AD-A211744] 03 p0348 N90-11988
Upwind discretization of the steady Navier-Stokes equations
[CWI-NM-R8810] 04 p0502 N90-12891
Enhanced resolution concepts in large scale scientific computing
[AD-A214095] 07 p0932 N90-15393
Flow separation in shock wave boundary layer interactions at hypersonic speeds
[NASA-CR-4274] 08 p1017 N90-15885
Automatic control of cryogenic wind tunnels
08 p1031 N90-15957
Anomalous waves in shock wave - fluid interface collisions
[AD-A213584] 08 p1062 N90-16144
Turbulent stripping of interstellar clouds by interaction with supernova remnants
[DE90-003622] 08 p1152 N90-16674
Spallation and dynamic fracture as an effect of laser induced shock waves in carbon based composite materials
[AD-A216540] 11 p1478 N90-18509
Infrared line emission from high-velocity outflows in star-forming regions 11 p1582 N90-19116
Interaction of an oblique shock wave with supersonic flow over a blunt body 12 p1598 N90-19197
Swept shock/boundary layer interaction experiments in support of CFD code validation
[NASA-CR-186397] 12 p1659 N90-19535
A time-accurate adaptive grid method and the numerical simulation of a shock-vortex interaction
[NASA-TP-2998] 14 p2011 N90-21524
Numerical investigation of separated transonic turbulent flows with a multiple-time-scale turbulence model
[NASA-TM-102499] 15 p2090 N90-21962
Computational modeling and validation for hypersonic inlets
[NASA-TM-103111] 15 p2099 N90-22011
Interactive calculation procedures for mixed compression inlets
[NASA-CR-186581] 20 p2801 N90-25934
The dynamics and control of fluctuating pressure loads in the reattachment region of a supersonic free shear layer
[NASA-CR-184943] 22 p3108 N90-27652

SHOCK WAVE PROFILES

A device to extract energy from water waves
[REPT-89-34] 04 p0516 N90-12978
Computation of nonequilibrium gas flow past blunt bodies
[PREPRINT-488] 05 p0644 N90-13757

SHOCK WAVE PROPAGATION

Sharp shock model for propagating detonation waves
[DE89-016772] 02 p0221 N90-11266
Impulse time-integral function and Lagrangian analysis
[DE89-016997] 02 p0221 N90-11268
Gas dynamical processes in the theory of galaxy formation 02 p0294 N90-11673
Shock-induced reaction in several liquids
[DE89-016594] 03 p0346 N90-11973
Propagation of detonation waves from an impact region
[DE90-001184] 06 p0776 N90-14515
Statistical model for particle-void deformation kinetics in granular materials during shock wave propagation
[DE89-017729] 07 p0946 N90-15476
A numerical study of shock wave refraction at a CO2/CH4 interface
[DE90-005997] 10 p1386 N90-18022
Coherent phase transformation under nonhydrostatic stress-wave loading
[DE90-005719] 10 p1396 N90-18072
Numerical model of bond strength measurements
[DE90-006000] 10 p1396 N90-18073
A study on upstream moving pressure waves induced by vortex separation
[ISL-CO-203/88] 12 p1597 N90-19192
Laser-induced shock waves effects in materials
[DE90-007626] 13 p1807 N90-20379
Nonlinear interaction of photons and phonons in electron-positron plasmas
[DE90-009341] 14 p2030 N90-21640
Measurement and visualization of the shock wave caused by the impact of a pulsed YAG laser in water
[REPT-892-430-113] 16 p2240 N90-22783
Evidence for self-refraction in a convergence zone: NPE (Nonlinear progressive wave equation) model results
[AD-A218546] 16 p2259 N90-22879

SHOCK WAVES

NT DETONATION WAVES
NT NORMAL SHOCK WAVES
NT OBLIQUE SHOCK WAVES
NT RIEMANN WAVES
NT SONIC BOOMS
A numerical method for solving transonic flow past aircraft in Cartesian coordinates
[NAL-TR-1008] 01 p0001 N90-10003
A composite velocity procedure for the three-dimensional reduced Navier-Stokes equations
01 p0069 N90-10396
Shock behavior of explosives about the C-J (Chapman-Juget) point
[DE89-007642] 01 p0070 N90-10400
Theoretical Hugoniot of liquid hydrogen fluoride
[DE89-016504] 02 p0193 N90-11099
Thermochemical model for shock-induced chemical reactions in porous thermite: The heat detonation model
[DE89-016528] 02 p0193 N90-11100
Experimental measurements of shock-induced vaporization in cadmium and lead
[DE89-016877] 02 p0194 N90-11103
Pressure induced resonance Raman effects in shocked carbon disulfide
[AD-A210665] 02 p0194 N90-11107
Shock-induced atomic-scale structure in metals
[DE89-016539] 02 p0197 N90-11124
The HEL (Hugoniot Elastic Limit) and rate-dependent yield behavior
[DE89-016981] 02 p0199 N90-11134
Behaviour of VF(sub 2)/VF(sub 3) piezoelectric copolymers under shock loading
[DE89-016538] 02 p0201 N90-11145
Characterizations of shock-loaded aluminum-infiltrated boron carbide cermets
[DE89-016773] 02 p0201 N90-11146
A shock initiation model for fine-grained hexanitrostilbene
[DE89-007641] 02 p0207 N90-11185
In-situ study of the chemically driven flow fields in initiating homogeneous and heterogeneous nitromethane explosives
[DE89-008415] 02 p0207 N90-11186
Crystal orientation effects in PETN explosive with 4 GPa shocks
[DE89-016996] 02 p0208 N90-11190
Shock initiation of LX-17 as a function of its initial temperature
[DE89-017730] 02 p0208 N90-11192
Method of characteristic studies for rotational flow downstream of a curved shock wave
02 p0219 N90-11252
Computations of the refraction of a plane shock wave at a slow-fast gas interface
[DE89-016508] 02 p0220 N90-11258
Shock induced dissociation of polyethylene
[DE89-016983] 02 p0221 N90-11267
Response of standardized PVDF piezoelectric polymer gauges to direct shock pressures between 8 and 32 GPa
[DE89-016811] 02 p0224 N90-11282
The Sandia standard for PVDF (Polyvinylidene Di-Fluoride) shock sensors
[DE89-016530] 02 p0225 N90-11287
Laser-driven miniature flyer plates for shock initiation of secondary explosives
[DE89-016587] 02 p0225 N90-11288
Gas-accelerated plate stability study
[DE89-016880] 02 p0225 N90-11289
Effects of shock-modification on superconductivity in Tl2Ca2Ba2Cu3Oy and Bi2CaSr2Cu2Ox
[DE89-017231] 02 p0285 N90-11629
Studying shocks in model astrophysical flows
[DE89-618786] 02 p0295 N90-11677
Equation-of-state data of synthetic Uranus
[DE89-016509] 02 p0296 N90-11683
Wave combustors for trans-atmospheric vehicles
[NASA-TM-102238] 03 p0307 N90-11742
Calculation of the refractive index change in dissociating shocked benzene
[DE89-017737] 03 p0322 N90-11833
A rate-dependent constitutive model for Be
[DE89-017755] 03 p0327 N90-11861
Simulation of glancing shock wave and boundary layer interaction
[NASA-TM-102233] 03 p0345 N90-11970
Characteristics of flyer impact for one-dimensional shock-wave study applications
[DE89-017887] 03 p0346 N90-11977
Experimental investigation of a planar shock wave over a double wedge
[AD-A211366] 03 p0347 N90-11981
Lagrangian analysis of MIV (Magnetic Impulse-Velocity) gauge experiments on PBX 9502 using the mass-displacement moment function
[DE89-016612] 03 p0350 N90-12000
Shock pressure determination in detonator wires
[DE89-017756] 03 p0350 N90-12002
Pulsed-laser-excited Raman spectra of shock compressed triaminotrinitrobenzene
[DE90-000668] 03 p0353 N90-12019
Interplanetary energetic particle observations of the March 1989 events 03 p0434 N90-12484
Hypersonic boundary layers. Viscous effects within the shock layer
[CERT-RSF-OA-25/5005-AYD] 04 p0438 N90-12502

Laser initiated ignition of liquid propellant
[AD-A212342] 04 p0482 N90-12766
The Shock and Vibration Digest, volume 21, no. 10
04 p0483 N90-12771
Pyrotechnic shock structural response
04 p0483 N90-12774
Corrections for non-ideal effects in reflected shock waves at low Mach numbers
[DE90-002192] 06 p0721 N90-14208
Solving the blow-by problem in a two-stage gun
[DE90-000842] 06 p0728 N90-14246
Particle size effects in the initiation of explosives containing reactive and nonreactive continuous phases
[DE90-000786] 06 p0754 N90-14390
CTH: A three-dimensional shock wave physics code
[DE89-016529] 06 p0779 N90-14528
Experimental study of the shock waves generated by high energy laser pulses 06 p0784 N90-14557
Microstructure induced by laser shock in an austenitic steel 06 p0784 N90-14558
Dynamic sintering of metallic powders by laser shock
06 p0784 N90-14559
Time integrated study of spectral emission in the X-UV domain at the outlet of a laser shock, at the back of single or double foil targets 06 p0784 N90-14561
Pressure sensitive release device
[AD-D014220] 06 p0792 N90-14610
Projectile impact Hugoniot parameters for selected materials
[DE90-000891] 06 p0793 N90-14618
Comparison of shock severity measures
[DE90-000790] 06 p0799 N90-14654
Implications and origins of shock structure in solids
[DE90-000846] 06 p0800 N90-14658
Superconducting and microstructural properties of shock-compacted high-T sub c oxide powders
[DE90-000823] 06 p0853 N90-14958
Effects of shock-induced defects on flux pinning in YBa2Cu3O(7-delta)
[DE90-000824] 06 p0853 N90-14959
Hugoniot measurements with the LLNL electric gun facility
[DE90-002809] 07 p0885 N90-15119
Shock-wave characterization of energetic booster-rocket propellant WAK-2 and its simulant UGS
[DE90-002633] 07 p0914 N90-15285
Rayleigh-Taylor instability in compressible fluids
[DE90-003027] 07 p0929 N90-15376
Characterizing transient vibrations using band limited moments
[DE90-000799] 07 p0945 N90-15473
Micron-thin Nb films recovered from Mbar shock pressures
[DE90-001509] 07 p0998 N90-15772
Shock-induced reaction synthesis of aluminides and silicides
[DE90-003948] 08 p1049 N90-16066
A numerical and experimental investigation of multiple shock wave/turbulent boundary layer interactions in a rectangular duct 08 p1062 N90-16141
Anomalous waves in shock wave - fluid interface collisions
[AD-A213584] 08 p1062 N90-16144
An introduction to shaker shock simulations
[DE90-003057] 08 p1088 N90-16298
Accretion shock geometries in the magnetic variables
[NASA-CR-186290] 08 p1150 N90-16864
The design of low inductance electrical circuits for slapper detonator systems
[AD-A214981] 09 p1212 N90-17024
Shock layer vacuum UV spectroscopy in an arc-jet wind tunnel
[NASA-TM-102258] 09 p1226 N90-17112
MHD (Magnetohydrodynamic) slow shocks in coronal and interplanetary space
[AD-A214725] 09 p1299 N90-17527
Study of continuum higher order closure models evaluated by a statistical theory of shock structure
10 p1303 N90-17538
Glancing shock-boundary layer interactions
10 p1309 N90-17571
Unsteadiness of supersonic and hypersonic shock induced turbulent boundary layer separation
10 p1309 N90-17572
Liquid transverse jets in compressible crossflows
10 p1385 N90-18012
Fluid transmission line dynamics for signals of finite amplitude
[AD-A215758] 10 p1385 N90-18014
Computing shock waves in turbulent mixing regions
[DE90-005096] 10 p1386 N90-18021
A numerical study of shock wave refraction at a CO2/CH4 interface
[DE90-005997] 10 p1386 N90-18022
Self-similar growth of three-dimensional fault
[DE90-608162] 10 p1407 N90-18112
Unsteady aerodynamic phenomena in a simulated wake and shock wave passing experiment
11 p1461 N90-18414
Time-dependent measurements on vibrating annular turbine cascades under various steady state conditions
11 p1463 N90-18424
Spallation and dynamic fracture as an effect of laser induced shock waves in carbon based composite materials
[AD-A216540] 11 p1478 N90-18509
Study of the dynamical behavior of copper in a shock wave
[ISL-R-123/88] 11 p1507 N90-18679
Direct simulation Monte Carlo of shock reflexion on a wedge with boundary layer
[ISL-CO-245/88] 11 p1508 N90-18681
Transient responses of coupled systems
[ONERA-RT-13/3596-RY-070-R]
11 p1509 N90-18687
Interaction between oblique-angled incident shock wave and turbulent boundary layer on a heated wall. Experimental results
[ONERA-RT-84/7078-AY] 11 p1509 N90-18688
Piezoelectric polymer PVDF shock gauge: State of the research art
[ISL-CO-207/89] 11 p1512 N90-18705
Infrared diagnostics of interstellar shocks
11 p1582 N90-19115
High-excitation lines of molecular hydrogen: A discriminant between shock models
11 p1582 N90-19118
Interaction of minor ions with fast and slow shocks
[NASA-CR-186372] 11 p1594 N90-19181
Calculation of excrescence drag magnification due to pressure gradient at high subsonic speeds
[ESDU-87004] 12 p1598 N90-19195
Numerical modelling of shocks in gases and metals
[MRL-RR-8-89] 12 p1658 N90-19528
Viscous shock profiles and primitive formulations
[NASA-CR-182029] 13 p1750 N90-20049
Numerical modeling of airblast
[AD-A217993] 13 p1803 N90-20347
Domain decomposition for a boundary-value problem with a shock layer
[DE90-007857] 13 p1877 N90-20762
Shock compression of solids: A tutorial
[DE90-009185] 14 p2032 N90-21659
The interaction between a plane shock wave and a cylindrical afterbody 15 p2046 N90-21728
Impact tolerant material
[NASA-CASE-LAR-12887-3] 15 p2064 N90-21822
Gamma rays from pulsar wind shock acceleration
16 p2336 N90-23311
Ultrafast laser investigation of a solid-state explosion
[AD-A218530] 17 p2408 N90-23718
HUGOFIT and HUGOPLOT: Computer codes for plane shock wave analysis with materials that have non-simple Hugoniots
[DE90-010284] 18 p2594 N90-24761
Short time-dynamometer system for shock wave channels
[MBB-UT-115/89-PUB] 19 p2651 N90-25084
Investigation of the vortex flow over a sharp-edged delta wing in the transonic speed regime
[LR-594] 19 p2656 N90-25115
Design concepts for hardened communications structures
[AD-A221233] 19 p2683 N90-25260
A study of non-uniqueness and instability for convex materials
[DE90-012060] 19 p2689 N90-25294
Optical techniques for determination of normal shock position in supersonic flows for aerospace applications
[NASA-TM-103201] 19 p2693 N90-25323
An adaptive finite element method for shock developing partial differential equation
[FFI-89/7014] 19 p2751 N90-25632
Linearly extended cyclotron emission regions in AM Herculis systems 19 p2775 N90-25778
Radiative shock oscillations in AM Her cataclysmic binaries 19 p2783 N90-25834
Variability in BL Lac objects: A schematic model
19 p2787 N90-25861
Experimental study on vortex and shock wave development on a 65 deg delta wing
[NLR-MP-88033-U] 20 p2804 N90-25950
The study of VF2/VF3 piezoelectric copolymeteres submitted to shocks
[ISL-CO-210/9] 20 p2931 N90-26679
Computational methods for problems in aerodynamics using parallel and vector architecture
[AD-A221979] 21 p2954 N90-26795
Nonlinear material response to very rapid energy deposition
[AD-A221932] 21 p2989 N90-26988
The effects of blast trauma (impulse noise) on hearing: A parametric study source 2
[AD-A221731] 21 p3035 N90-27253
Survival of carbon grains in shocks
21 p3090 N90-27567
Carbon stardust: From soot to diamonds
21 p3090 N90-27568
The dynamics and control of fluctuating pressure loads in the reattachment region of a supersonic free shear layer
[NASA-CR-184943] 22 p3108 N90-27652
Formation of shock waves in a transonic vortex-profile interaction
[MPIS-3/1990] 22 p3174 N90-28010
Finite-volume application of high order ENO schemes to multi-dimensional boundary-value problems
[NASA-CR-186917] 22 p3242 N90-28387
The shock process and light element production in supernovae envelopes
[NASA-CR-182854] 22 p3262 N90-28471
Investigation of plasma density bulge in front of Venus bow shock
[NASA-CR-186937] 22 p3262 N90-28476
Shock dynamics in the sub-nanometer femtosecond domain
[DE90-014390] 23 p3304 N90-28589
A plasma diagnostic study of two wind-blown shell nebulae: NGC 7635 and NGC 2359
23 p3410 N90-29271
Theoretical study of the interaction between an oblique shock wave and a turbulent boundary layer from a heated wall
[ONERA-RSF-87/7078/AY-100-A]
24 p3419 N90-29313

SHOES
Engineering specification and system design for CAD/CAM of custom shoes. Phase 5: UMC involvement (January 1, 1989 - June 30, 1989)
[NASA-CR-185838] 02 p0257 N90-11456
Engineering specification and system design for CAD/CAM of custom shoes: UMC project effort
[NASA-CR-186547] 15 p2145 N90-22255

SHORELINES
Comparison of analytical methods for calculation of wind loads
[NASA-TM-102782] 05 p0654 N90-13813
Aerial videotape survey of coastal Louisiana, 1986. Louisiana Barrier Island erosion and land loss study: 1986-1990
[PB90-194648] 22 p3195 N90-28128

SHORT CIRCUIT CURRENTS
A severe human ESD (Electrostatic Discharge) model for safety and high reliability system qualification testing
[DE89-016177] 02 p0216 N90-11233

SHORT CIRCUITS
Development of an expert system supporting short-circuit tests for circuit breakers
[DE89-760384] 01 p0059 N90-10334
Test generation for highly sequential circuits
[AD-A211932] 05 p0634 N90-13698
JPS heater and sensor lightning qualification
[NASA-CR-183830] 06 p0779 N90-14530
A study of loaded microstrip antennas and their applications to arrays
[AD-A214857] 09 p1205 N90-16985
Thermal switch disc for short circuit protection of batteries
[NASA-CASE-MSC-21428-1] 09 p1209 N90-17008

SHORT CRACKS
Fatigue growth and closure of short cracks
[AD-A210824] 01 p0081 N90-10462
A numerical study of plasticity induced closure in short cracks by the finite element method
[AD-A220471] 18 p2571 N90-24654
Fracture mechanics analysis for short cracks
[AD-A222170] 21 p3013 N90-27130

SHORT HAUL AIRCRAFT
NT A-300 AIRCRAFT
NT A-310 AIRCRAFT
NT A-320 AIRCRAFT
NT EUROPEAN AIRBUS
Longitudinal stability and control characteristics of the Quiet Short-Haul Research Aircraft (QSRA)
[NASA-TP-2965] 10 p1322 N90-17639
Lateral-directional stability and control characteristics of the Quiet Short-Haul Research Aircraft (QSRA)
[NASA-TM-102250] 17 p2356 N90-23413

SHORT TAKEOFF AIRCRAFT
Flight simulator evaluation of a head-down display
[NAL-TM-573] 02 p0157 N90-10898
Wind tunnel test of CAD USB-STOL semi-borne prototype
[NAL-TM-566] 03 p0299 N90-11696
Acoustic-thermal environment for USB flap structure. Report 1: Ground simulation test results
[NAL-TM-567] 03 p0300 N90-11697

STOVL propulsion system volume dynamics approximations
[NASA-TM-102397] 03 p0306 N90-11740
Low-speed wind-tunnel study of reaction control-jet effectiveness for hover and transition of a STOVL fighter concept
[NASA-TM-4147] 03 p0308 N90-11751
The NASA experience in aeronautical R and D: Three case studies with analysis
[AD-A211486] 04 p0437 N90-12496
Powered-lift aircraft technology
[NASA-SP-501] 04 p0452 N90-12589
Real-time simulation of an F110/STOVL turbofan engine
[NASA-TM-102409] 04 p0457 N90-12618
STOVL aircraft simulation for integrated flight and propulsion control research
[NASA-TM-102419] 05 p0581 N90-13389
Development of the triplex digital flight control system of the STOL research aircraft ASKA
[NAL-TR-1013] 10 p1322 N90-17640
Performance characteristics of a one-third-scale, vectorable ventral nozzle for SSTOVL aircraft
[NASA-TM-103120] 15 p2045 N90-21725
Dynamic ground-effect measurements on the F-15 STOL and Maneuver Technology Demonstrator (S/MTD) configuration
[NASA-TP-3000] 16 p2195 N90-22531
Aerodynamic and propulsive control development of the STOL and maneuver technology demonstrator
23 p3271 N90-28514

SHORT WAVE RADIATION
NT CENTIMETER WAVES
NT MICROWAVE EMISSION
NT MICROWAVES
NT MILLIMETER WAVES
NT SUBMILLIMETER WAVES
Shortwavelength coherent radiation: Generation and applications
[AD-A209847] 01 p0074 N90-10427
The ISO short wavelength spectrometer
11 p1589 N90-19162
Short wavelength laser/materials interactions
[AD-A218015] 13 p1808 N90-20386
Downward shortwave surface irradiance from 17 sites for the FIRE/SRB Wisconsin experiment
[NASA-TM-102596] 13 p1844 N90-20583
Forced scattering of electromagnetic waves on electron beam in periodically inhomogeneous plasma
[DE90-620705] 16 p2228 N90-22707
Atmospheric planetary waves induced by solar rotation 22 p3204 N90-28178
Anomalous decay of Langmuir turbulence. High power, high frequency radiation from beam-plasma interaactions
[AD-A224282] 24 p3547 N90-30065

SHORT WAVE RADIO TRANSMISSION
Oblique ionospheric heating and effects on radio propagation
[AD-A214756] 09 p1205 N90-16983
Telemetry and telecommand omnidirectional antenna in the short wave band
[ETN-90-96285] 11 p1499 N90-18631
Ionospheric heating with oblique waves. Volume 2: Applications to high-frequency radio propagation
[AD-A223111] 21 p3025 N90-27202
The probability of SWF occurrence in relation to solar activity 22 p3209 N90-28204

SHOT NOISE
LAWS simulation: Sampling strategies and wind computation algorithms 03 p0364 N90-12081
Noise variability in Cyg X-1 and Her X-1
17 p2483 N90-24200
Noise variability in Cyg X-1 and Her X-1
19 p2771 N90-25753

SHOT PEENING
Improvement in pre-constraint fatigue resistance of modular ferretic and bainitic steel by shot peening treatments
[CETIM-106370] 04 p0476 N90-12727
Fatigue fracture in the presence of shot peening residual stresses: Initiation, propagation, and relaxation phenomena 06 p0797 N90-14644
Scratches and shot peening effects on the fatigue life of aluminum-lithium alloys
[NIAR-90-15] 19 p2674 N90-25208
Surface condition effect on the fatigue behavior of aluminum lithium alloys
[NIAR-90-13] 19 p2674 N90-25209
Fretting fatigue strength of Ti-6Al-4V at room and elevated temperatures and ways of improving it
23 p3308 N90-28709

SHRINKAGE
Mechanical properties of silica coatings
[DE90-012721] 20 p2837 N90-26138

SHROUDED BODIES
U SHROUDS

SHROUDED PROPELLERS
A computer program for the prediction of nozzle-propeller performance
[LR-578] 15 p2048 N90-21740
Recent improvements in the scope and accuracy of the performance prediction of nozzle propellers
[LR-598] 15 p2048 N90-21742

SHROUDED TURBINES
Advanced Turbine Technology Applications Project (ATTAP)
[NASA-CR-185133] 01 p0008 N90-10036

SHROUDS
Experimental investigation of the hydrodynamic forces on the shroud of a centrifugal pump impeller
[NASA-CR-186952] 21 p3009 N90-27108

SHUNTS
U CIRCUITS

SHUTTLE BOOSTERS
U SPACE SHUTTLE BOOSTERS

SHUTTLE DERIVED VEHICLES
Main propulsion system test requirements for the two-engine Shuttle-C
[NASA-TM-100382] 06 p0735 N90-14282
Shuttle-C utilization for assembly of the rephased Freedom configuration
[NASA-TM-101658] 07 p0885 N90-15120
Round trip to orbit. Human spaceflight alternatives: Special report
[OTA-ISC-419] 08 p1033 N90-15966
US Space Shuttle evolution 09 p1178 N90-16829
Shuttle C: Heavy-lift vehicle of the 1990's
09 p1178 N90-16830
HOPE: Its concept and technical features
09 p1179 N90-16835

SHUTTLE GLOW
U SPACECRAFT GLOW

SHUTTLE IMAGING RADAR
Necessity and benefit of the X-SAR Space Shuttle experiment
[ESA-TT-1164] 08 p1057 N90-16112
Spaceborne radar observations: A guide for Magellan radar-image analysis
[NASA-CR-184998] 16 p2249 N90-22826

SHUTTLE ORBITERS
U SPACE SHUTTLE ORBITERS

SI
U INTERNATIONAL SYSTEM OF UNITS

SICKNESSES
NT ALTITUDE SICKNESS
NT DECOMPRESSION SICKNESS

SID (IONOSPHERIC DISTURBANCES)
U SUDDEN IONOSPHERIC DISTURBANCES

SIDE-LOOKING RADAR
Segmentation of Side-Looking Airborne Radar (SLAR) images using a priori knowledge
[BCRS-89-03] 12 p1679 N90-19644
The PHARUS project: Design of a polarimetric C-band SAR in the Netherlands 14 p1961 N90-21228
Sea bottom topography with X-band SLAR
[BCRS-89-25] 17 p2431 N90-23854
Sweep width determination for HU-25B airborne radars: Life raft and recreational boat targets
[AD-A221362] 18 p2545 N90-24524

SIDEBANDS
Spectral structure and generation mechanism of ducted VLF whistler mode sideband waves
24 p3489 N90-29720

SIDELOBE REDUCTION
Statistical density and amplitude tapered arrays
[RSRE-MEMO-4211] 04 p0490 N90-12818
Spatial array processing by the method CLEAN
[FEL-1989-144] 22 p3165 N90-27949

SIDELOBES
Performance analysis of large adaptive sidelobe canceller arrays with reused elements
[AD-A212888] 04 p0494 N90-12841
Large-aperture sparse array detector system for multiple emitter location
[AD-D014303] 07 p0925 N90-15355
Planar array antenna design analysis, volume 1
[AD-A215537] 09 p1207 N90-16999
Effects of additional interfering signals on adaptive array performance
[NASA-CR-186508] 13 p1790 N90-20271
Low-sidelobe phased array antenna characteristics using the planar near-field Scanning technique: Theory and experiment
[AD-A220611] 17 p2390 N90-23613
The performance of wavelets for data compression in selected military applications. Volume 2: Supplementary tables and graphs
[AD-A219231] 18 p2615 N90-24893
MUSE: A systolic array for adaptive nulling with 64 degrees of freedom, using Givens transformations and wafer scale integration
[AD-A223812] 24 p3529 N90-29953

SIDERITE METEORITES
U IRON METEORITES

SIDESLIP
Experimental and numerical investigation of the vortex flow over a sharp edged delta wing; with and without sideslip
[PB90-167131] 14 p1913 N90-20964
Sideslip-induced static pressure errors in flight-test measurements
[NASA-TM-102846] 22 p3116 N90-27702

SIDEWINDER MISSILES
Renewed aging control of adhesion of inhibitor on the gas generator charges for RB 24
[FOA-C-20780-2.1] 20 p2840 N90-26153

SIERRA NEVADA MOUNTAINS (CA)
Steady state model to determine lake resources at risk to acid deposition in the Sierra Nevada, California
[PB89-103995] 06 p0809 N90-14705
Characterization of cloud chemistry and frequency of canopy exposure to clouds in the Sierra Nevada
[PB89-104035] 06 p0817 N90-14753
Transport of atmospheric aerosols above the Sierra Nevada slopes
[PB90-120288] 12 p1685 N90-19675

SIEVES
Activation of methane by transition metal-substituted aluminophosphate molecular sieves
[DE90-005663] 12 p1624 N90-19331

SIGHT
U VISUAL PERCEPTION

SIGNAL ANALYSIS
NT CEPSTRAL ANALYSIS
Combustion-driven oscillation in large combustion systems for power generation 01 p0038 N90-10207
Infrared target detection: Signal and noise sensitivity analysis
[AD-A215707] 09 p1282 N90-17436
Analysis of the CUK converter in delta V mode by charge and flux balances 10 p1337 N90-17738
Unsteady two level models
[TELECOM-89-E-006] 10 p1375 N90-17973
Simulation of radar and radiometer signals remote sensing cometary surface and subsurface structures
12 p1740 N90-20005

SIGNAL ANALYZERS
The use of broadcast signals for passive sensing in automated HF communication systems
06 p0762 N90-14433
High resolution, wide band Chirp-Z signal analyzer
[AD-D014240] 06 p0768 N90-14465
Air Force Boom Event Analyzer Recorder (BEAR): Sysstem description
[AD-A218048] 13 p1882 N90-20800
Ridge regression processing
14 p1907 N90-20931
Feasibility study for the advanced one-dimensional high temperature optical strain measurement system, phase 3
[NASA-CR-185254] 19 p2693 N90-25324
A voltage contrast detector with double channel energy analyzer in a scanning electron microscope
[ISBN-90-6275-568-2] 19 p2694 N90-25330
Speech coding 21 p2992 N90-27009
Improved front-end analysis in the ARM system: Linear transformations of SRUbank
[RSRE-MEMO-4358] 22 p3166 N90-27953

SIGNAL DETECTION
NT CORRELATION DETECTION
Polarization matrices of lithium tetraborate
[AD-A210774] 02 p0195 N90-11112
In-situ cure monitoring of composites by fiber-optic molecular sensors
[AD-A211495] 03 p0320 N90-11817
Microwave signal detection using modulation of polymeric optical waveguides
[DE89-017545] 03 p0337 N90-11921
Analysis of two-pass Modified Hough Transform (MHT) technique for the detection of wake like signals
[AD-A211982] 03 p0338 N90-11924
Hydrophone investigations of earthquakes and explosion generated high-frequency seismic phases
[AD-A212055] 03 p0371 N90-12122
Binaural masking: An analysis of models
[AD-A211578] 03 p0381 N90-12168
The NASA SETI sky survey: Recent developments
04 p0488 N90-12804
Test procedures for the evaluation of helmet and headset mounted active noise reduction systems
[AD-A212991] 05 p0676 N90-13937
A portable ionosonde in support of reliable communications 06 p0762 N90-14431
Detection of a chirping electromagnetic signal
[DE90-002105] 06 p0766 N90-14457
High resolution Doppler lidar
[NASA-CR-183288] 06 p0781 N90-14542

Effective utilization of acoustic wave sensor responses: Simultaneous measurement of velocity and attenuation
[DE90-002580] 06 p0838 N90-14872
A multichannel processing approach to real time network detection, phase association, and threshold monitoring
[AD-A213940] 07 p0980 N90-15657
Beamforming pre-processors for high discrimination algorithms
[RSRE-MEMO-4304] 08 p1110 N90-16429
Results on the detection of signals in spherically invariant random noise
[AD-A214933] 09 p1206 N90-16988
Multiplexed robotic tactile sensor fabricated from polyvinylidene fluoride film
[AD-A215354] 09 p1231 N90-17145
Millimeter wave radar clutter program
[AD-A215772] 10 p1376 N90-17978
The effects of luminance boundaries on color perception
[AD-A216741] 11 p1539 N90-18860
Costas loop lock detection in the advanced receiver 12 p1643 N90-19441
Complex demodulation for bearing fault detection
[AD-A218367] 13 p1812 N90-20407
Fiber optic void fraction sensor
[DE90-009124] 14 p1983 N90-21366
Sampling and noise in vision networks 15 p2138 N90-22217
Preliminary results of the peak experiment. ALTAIR deep-space measurements
[AD-A218622] 16 p2229 N90-22714
Transduction of nanovolt signals: Limits of electric-field detection
[AD-A219214] 16 p2312 N90-23177
Neutrino signals from the powerful solar flare on September 29, 1989
[PREPRINT-721] 16 p2339 N90-23331
Research on statistical techniques for signal processing
[AD-A218811] 17 p2388 N90-23599
Computer-aided mathematical analysis of probability of intercept for ground-based communication intercept system
[AD-A219856] 17 p2392 N90-23627
A parametric detection approach using multichannel processes
[AD-A219328] 17 p2395 N90-23641
Mental lapses and event-related potentials
[AD-A219454] 17 p2436 N90-23878
Development of a hybrid adaptive beamformer
[AD-A219652] 17 p2471 N90-24128
Innovative techniques for high-resolution imaging and precision tracking
[AD-A221380] 18 p2616 N90-24899
Differential psychological analysis of a computer-based audio-visual test of vigilance
[ESA-TT-1136] 19 p2724 N90-25494
A two-telescope receiver design for deep space optical communications 20 p2853 N90-26226
Interaction of electromagnetic signals with particulate clouds
[AD-A222804] 20 p2856 N90-26244
A preliminary analysis of threshold signal detection in ambient and signal-dependent noise environments
[AD-A222089] 21 p2996 N90-27030
The effects of luminance boundaries on color perception
[AD-A221544] 21 p3034 N90-27251
The validation and application of a rotor acoustic prediction computer program
[NASA-TM-101794] 21 p3072 N90-27465
Lightweight, broadband, pulsed, frequency agile, self-screening jammer for airborne deployment
[AD-D014468] 22 p3163 N90-27937
Improved compact optical RF spectrum analyzer
[AD-D014481] 22 p3177 N90-28026
Broadband studies of seismic sources at regional and teleseismic distances using advanced time series analysis methods
[AD-A223113] 22 p3211 N90-28215
A reliable, maintenance-free oxygen sensor for aircraft using an oxygen-sensitive coating on potentiometric electrodes
[AD-A222696] 23 p3277 N90-28545
A compact real-time acousto-optic image correlator
[DE90-015564] 24 p3546 N90-30054

SIGNAL DETECTORS

Analysis of two-pass Modified Hough Transform (MHT) technique for the detection of wake like signals
[AD-A211982] 03 p0338 N90-11924
Fundamental studies of turbulent wall pressure fluctuations with applications to advanced acoustic sensor systems
[AD-A213041] 04 p0552 N90-13212
Effective utilization of acoustic wave sensor responses: Simultaneous measurement of velocity and attenuation
[DE90-002580] 06 p0838 N90-14872
Narrow band and wide angle hemispherical interference optical filter
[AD-D014238] 06 p0843 N90-14904
Large-aperture sparse array detector system for multiple emitter location
[AD-D014303] 07 p0925 N90-15355
Optical acoustic sensor using optical fiber
[DE89-901267] 07 p0992 N90-15730
Surface acoustic wave sensors and piezoelectric actuators for investigations of transitional and turbulent flows
[AD-A214889] 09 p1279 N90-17415
Method and apparatus for detecting laminar flow separation and reattachment
[NASA-CASE-LAR-13952-1-SB] 12 p1659 N90-19534
A real-time rejection circuit to automatically reject multiple interfering hopping signals while passing a lower level desired signal
[AD-D014424] 14 p1965 N90-21251
Passive stabilization of a fiber optic nonlinear interferometric sensor
[AD-D014438] 14 p2026 N90-21620
Model order determination methods for autoregressive radio direction finding techniques
[AD-A220707] 17 p2350 N90-23384
Observations of seafloor ambient noise with an ocean bottom seismometer array
[AD-A220159] 17 p2432 N90-23858
Development of a hybrid adaptive beamformer
[AD-A219652] 17 p2471 N90-24128
Interaction of electromagnetic signals with particulate clouds
[AD-A222804] 20 p2856 N90-26244
Measured effects of repeater jamming on direct-sequence spread spectrum receivers that use envelope detectors
[AD-A222231] 21 p2996 N90-27032
Apparatus and method for minimizing polarization-induced signal fading in an interferometric fiber-optic sensor using input-polarization control
[AD-D014492] 22 p3164 N90-27940

SIGNAL DISCRIMINATORS

U SIGNAL DETECTORS

SIGNAL DISTORTION

Proximity effects on adjacent and multiple stars 05 p0607 N90-13533
Baseband development system implementation
[AD-A213464] 07 p0918 N90-15309
A compact acoustic recorder
[AD-A213581] 07 p0933 N90-15403
Compression phenomena in hard-saturated microwave amplifiers
[AD-A214546] 09 p1204 N90-16980
Voice preprocessor for digital voice applications
[AD-A214726] 09 p1205 N90-16982
Optimization of the intermodulation performance of GaAs MESFET small-signal amplifiers
[AD-A215193] 09 p1212 N90-17026
Angle estimation in the presence of mainbeam interference
[AD-A216832] 11 p1498 N90-18621
Effects of amplitude distortions and IF equalization on satellite communication system bit-error rate performance
[NASA-TM-102415] 12 p1645 N90-19454
Active phase and amplitude modulator
[AD-D014318] 12 p1650 N90-19480
ULF/VLF ocean bottom seismo-acoustics
[AD-A218810] 17 p2429 N90-23843
Radio channel measurement and modelling for future mobile radio systems 20 p2845 N90-26184
Transient signal distortion and coupling in multilayer multiconductor MIC microstrips
[AD-A222989] 21 p3000 N90-27050
Experimental characterization of the effects of pneumatic tubing on unsteady pressure measurements
[NASA-TM-4171] 22 p3116 N90-27703
Investigation of a heat driven thermoacoustic prime mover
[AD-A223928] 24 p3484 N90-29694

SIGNAL ENCODING

NT AMPLITUDE MODULATION
NT DELTA MODULATION
NT DIFFERENTIAL PULSE CODE MODULATION
NT FREQUENCY MODULATION
NT FREQUENCY SHIFT KEYING
NT PHASE MODULATION
NT PHASE SHIFT KEYING
NT PULSE AMPLITUDE MODULATION
NT PULSE CODE MODULATION
NT PULSE DURATION MODULATION
NT PULSE MODULATION
NT PULSE POSITION MODULATION
Pin switch circuits instrument for microsecond velocity measurements
[AD-A210638] 01 p0074 N90-10426
Binary Gray codes and index systems
[REPT-89-29] 04 p0530 N90-13060
SLCSAT (Submarine Laser Communication Satellite) communication system design study
[AD-A213403] 07 p0917 N90-15304
Information capacity of dimension-limited channels
[AD-A215238] 09 p1207 N90-16996
Error detection and correction for a multiple frequency quaternary phase shift keyed signal
[AD-A215706] 09 p1208 N90-17003
Enhanced satellite geodesy through the addition of a pseudorange observable
[AD-A214987] 09 p1241 N90-17200
An approach to the development of software for computer-aided design of satellite communications receivers for operation in scintillating channels
[AD-A215299] 09 p1267 N90-17349
On linear structure and phase rotation invariant properties of block 2(sup l)-PSK modulation codes
[NASA-CR-186308] 12 p1641 N90-19429
Executive summary for the network assessment model
[AD-A218762] 16 p2229 N90-22718
Advanced Communication Processing Techniques
[AD-A223244] 21 p2996 N90-27027
Atmospherically induced optical contamination from orbiting thrusters
[AD-A223112] 21 p3021 N90-27174

SIGNAL FADEOUT

U SIGNAL FADING

SIGNAL FADING

NT SELECTIVE FADING
Digital radio link: Wave propagation investigations on a 13 GHz line-of-sight path
[PB89-213128] 04 p0485 N90-12785
Ground effects on multipath fading
[TELECOM-PARIS-88-E017] 04 p0489 N90-12812
Spread spectrum mobile radio communications
[AD-A213726] 07 p0918 N90-15311
Use of an HF active monitoring array in the presence of high level interference
[BBC-RD-1989/7] 08 p1055 N90-16096
Channel simulator upgrade to use field propagation data 10 p1372 N90-17948
The Australian experiment with ETS-V 10 p1372 N90-17949
LMSS modeling status report 10 p1372 N90-17953
A CCIR aeronautical mobile satellite report 10 p1372 N90-17954
ACTS propagation concerns, issues, and plans 10 p1374 N90-17963
Apparatus and method for minimizing polarization-induced signal fading in an interferometric fiber-optic sensor using input-polarization modulation
[AD-D014315] 12 p1642 N90-19430
Effects of amplitude distortions and IF equalization on satellite communication system bit-error rate performance
[NASA-TM-102415] 12 p1645 N90-19454
First-order intensity statistics for non-Rayleigh fading
[AD-A217572] 13 p1841 N90-20569
Understanding tropscatter propagation
[AD-A220969] 18 p2544 N90-24520
An overview of Canadian radio propagation/communications technologies research 20 p2844 N90-26179
A global common-user system for the provision of HF propagation data 20 p2845 N90-26180
Measurement and simulation of widespread mobile radio channel characteristics 20 p2846 N90-26186
In-band amplitude dispersion on a microwave link 20 p2846 N90-26189
Tracking performance of a combined Costas/AFC-loop under noisy Rayleigh/Rician channel conditions with additive Gaussian noise jamming
[ETN-90-98964] 20 p2855 N90-26237
Apparatus and method for minimizing polarization-induced signal fading in an interferometric fiber-optic sensor using input-polarization control
[AD-D014492] 22 p3164 N90-27940
The probability of SWF occurrence in relation to solar activity 22 p3209 N90-28204

SIGNAL GENERATORS

NT FREQUENCY SYNTHESIZERS
NT FUNCTION GENERATORS
Waveform generator signal processing software
[PB89-192660] 01 p0103 N90-10587
SINA: A test system for proximity fuses
[FEL-1989-101] 12 p1653 N90-19498

SIGNAL MEASUREMENT
Pin switch circuits instrument for microsecond velocity measurements
[AD-A210638] 01 p0074 N90-10426
Doppler statistics of ocean velocity variability
[AD-A211687] 03 p0377 N90-12148
Preliminary results of the peak experiment. ALTAIR deep-space measurements
[AD-A218622] 16 p2229 N90-22714
Test diagnostics of RF effects in integrated circuits
[AD-A219737] 17 p2396 N90-23648
Atmospherically induced optical contamination from orbiting thrusters
[AD-A223112] 21 p3021 N90-27174
SIGNAL MIXING
Single mode communication link
[AD-A219499] 17 p2388 N90-23601
SIGNAL PROCESSING
System identification for large space structures 01 p0025 N90-10126
Network of dedicated processors for finding lowest-cost map path
[NASA-CASE-NPO-17716-1-CU] 01 p0107 N90-10608
Fluctuating pressures measured beneath a high-temperature, turbulent boundary layer on a flat plate at Mach number of 5
[NASA-TP-2947] 01 p0118 N90-10680
Adaptive tracking of maneuvering targets based on IR image data 02 p0149 N90-10853
Analytic signals in the damping coefficient estimation 02 p0178 N90-11003
Polarization matrices of lithium tetraborate
[AD-A210774] 02 p0195 N90-11112
An experimental SMI adaptive antenna array for weak interfering signals
[NASA-CR-185976] 02 p0212 N90-11211
Simulations for computer centerline approach
[DOT/FAA/CT-TN89/41] 03 p0304 N90-11726
Improved pattern recognition techniques for real time operation
[AD-A211395] 03 p0324 N90-11840
Adaptive noise cancellation for a class of nonlinear 2R filter
[RR-351] 03 p0344 N90-11965
Aerosol backscatter studies supporting LAWS 03 p0363 N90-12079
On the communication complexity of solving a polynomial equation
[AD-A211945] 03 p0393 N90-12240
Linear (passive) and non-linear guided and studies in glass
[AD-A211693] 03 p0406 N90-12325
Ultra high speed compound semiconductors and real time signal processing
[AD-A211394] 03 p0413 N90-12372
Simulation of circuits adapted to signal processing
[TELECOM-PARIS-89-E001] 04 p0489 N90-12811
Specification of Viper1 in Z
[RSRE-MEMO-4195] 04 p0490 N90-12817
Specification of Viper2 in Z
[RSRE-MEMO-4217] 04 p0490 N90-12819
Progress in the identification of airborne radar targets
[AD-A212749] 04 p0493 N90-12835
Characterization of liquid crystal displays for optical signal processing applications
[AD-A212832] 04 p0505 N90-12910
Time-frequency factors in auditory perception
[AD-A211491] 04 p0523 N90-13016
Spectrometer technology recommendations 05 p0597 N90-13468
The use of digital signal processing in satellite communication 05 p0631 N90-13684
Efficient detection of small moving objects
[AD-A213314] 05 p0632 N90-13690
An experimental analysis of the waveguide modes in a high-gain free-electron laser amplifier 05 p0648 N90-13779
A counter gating circuit for acoustic emission monitoring of structures cracking under repetitive alternating loads
[ARL-MAT-TM-398] 05 p0653 N90-13808
PROPHET and future signal warfare decision aids 06 p0758 N90-14412
Hybrid PE-ray-mode formulation of high frequency propagation in a bilinear tropospheric surface duct 06 p0759 N90-14417
Design of a compensation filter for a quadratic phase communication channel 06 p0761 N90-14428
Improved reliability prediction for HF digital voice transmission 06 p0761 N90-14429
A modern trans-ionospheric propagation sensing system 06 p0761 N90-14430
A portable ionosonde in support of reliable communications 06 p0762 N90-14431
The use of broadcast signals for passive sensing in automated HF communication systems 06 p0762 N90-14433
Pattern recognition techniques applied to the NASA-ACTS order-wire problem 06 p0764 N90-14446
The characteristics of the HF radio channel and its influence on modern HF data communication system design 06 p0765 N90-14448
Frequency agile synthetic aperture radar
[AD-D014235] 06 p0765 N90-14451
Symmetric waveguide junction combiner
[AD-D014243] 06 p0768 N90-14466
Nondestructive evaluation of flaw clusters and thin layer interfaces 06 p0795 N90-14633
Synoptic scale tropical waves in multichannel satellite radiance data 06 p0816 N90-14745
The effects of clutter-rejection filtering on estimating weather spectrum parameters
[NASA-CR-186212] 06 p0817 N90-14754
JPL reuse program 06 p0825 N90-14795
Fly-by-light flight control system technology development plan
[NASA-CR-181953] 07 p0883 N90-15111
Flashlight radar: A three-dimensional imaging radar
[AD-A213439] 07 p0918 N90-15307
Baseband development system implementation
[AD-A213464] 07 p0918 N90-15309
Focal plane antenna array for millimeter waves
[AD-D014306] 07 p0920 N90-15322
Array signal processing: New techniques for direction finding and spectrum estimation
[AD-A213883] 07 p0924 N90-15345
Identification and quantification of synoptic structure in simulated TIROS N radiance soundings
[AD-A213729] 07 p0960 N90-15553
A signal processing language for coarse grain data flow multiprocessors
[AD-A213863] 07 p0976 N90-15635
Ultra high performance, highly reliable, numeric intensive processors and systems
[AD-A214100] 07 p0980 N90-15659
Membership-set parameter estimation via optimal bounding ellipsoids
[AD-A213807] 07 p0984 N90-15685
An improved toeplitz approximation method
[AD-A213994] 07 p0984 N90-15688
Research in optical interconnection techniques
[AD-A214028] 07 p0993 N90-15739
Research on materials and components for opto-electronic signal processing and computing
[AD-A213740] 07 p1003 N90-15811
A signal realization data base generated by the multiple phase-screen method
[AD-A214004] 07 p1010 N90-15852
Use of an HF active monitoring array in the presence of high level interference
[BBC-RD-1989/7] 08 p1055 N90-16096
Satellite broadcasting: Requirements for the receiving antenna
[BBC-RD-1989/5] 08 p1055 N90-16098
Method for eliminating self-screening noise jamming in radar systems
[AD-D014271] 08 p1056 N90-16105
Knowledge-based imaging-sensor fusion system 08 p1075 N90-16220
A programmable image compression system 08 p1076 N90-16222
Apparatus for imaging deep arterial and coronary lesions
[NASA-CASE-NPO-17439-1-CU] 08 p1104 N90-16391
Restoring force method and response estimation
[DE90-002394] 08 p1116 N90-16463
A computational and experimental study of steady and transient acoustic energy flow from a complex mechanical structure 08 p1119 N90-16478
High speed signal extraction using electro-optic techniques
[AD-A214446] 08 p1122 N90-16500
Phase ambiguity resolution for offset QPSK modulation systems
[NASA-CASE-NPO-17853-1-CU] 09 p1204 N90-16975
Knowledge based signal processing
[AD-A214864] 09 p1205 N90-16986
Information capacity of dimension-limited channels
[AD-A215238] 09 p1207 N90-16996
Information capacity of the stationary Gaussian channel
[AD-A215408] 09 p1207 N90-16998
Polarization matrices of quartz
[AD-A215198] 09 p1212 N90-17027
Testing and data path redesign of a high speed, 16-point Winograd Fourier transform processor
[AD-A215661] 09 p1213 N90-17036
Laser light scattering review 09 p1221 N90-17086
Method and apparatus for positioning a robotic end effector
[NASA-CASE-MSC-21476-1] 09 p1230 N90-17137
Integrated analytical evaluation and optimization of model parameters against preprocessed measurement data
[AD-A215518] 09 p1247 N90-17231
Phase space and path integral methods applied to direct and inverse ocean seismo-acoustic modeling
[AD-A214777] 09 p1249 N90-17247
Projection techniques for image restoration 09 p1263 N90-17322
Localization of multiple broadband targets in spherical coordinates via adaptive beamforming and non-linear estimation
[AD-A215714] 09 p1274 N90-17387
A Doppler centroid estimation algorithm for SAR systems optimized for the quasi-homogeneous source
[NASA-CR-186229] 09 p1275 N90-17391
Studies in statistical signal processing
[AD-A214490] 09 p1275 N90-17393
Method and apparatus for characterizing reflected ultrasonic pulses
[NASA-CASE-LAR-13966-1] 09 p1278 N90-17408
Surface acoustic wave sensors and piezoelectric actuators for investigations of transitional and turbulent flows
[AD-A214889] 09 p1279 N90-17415
JSEP (Joint Services Electronics Program)
[AD-A215051] 09 p1290 N90-17476
Optical Johnson noise thermometry 10 p1363 N90-17899
Signal processing applied to photothermal techniques for materials characterization 10 p1364 N90-17902
Some applications of model-based parameter estimation in computational electromagnetics 10 p1369 N90-17935
Antennas on land vehicles for improved communications 10 p1370 N90-17938
Field measurements in MSAT-X 10 p1371 N90-17947
Japanese propagation experiments with ETS-5 10 p1372 N90-17951
Polarization radar processing technology
[AD-A215242] 10 p1374 N90-17967
Evaluation of a delay-Doppler imaging algorithm based on the Wigner-Ville distribution
[AD-A215827] 10 p1377 N90-17980
Development of a small signal theory for the harmonic gyroklystron
[AD-A216274] 10 p1380 N90-17999
Effective waveform recorder evaluation procedures
[DE90-005197] 10 p1387 N90-18027
Z-grid signal conditioning system user's guide and technical reference
[AD-A215122] 10 p1395 N90-18067
Event-train restoration via backpropagation neural networks
[AD-A216308] 10 p1420 N90-18189
Neurobeamformer 2: Further exploration of adaptive beamforming via neural networks
[AD-A215118] 10 p1426 N90-18226
Efficient detection and signal parameter estimation with application to high dynamic GPS receiver
[NASA-CASE-NPO-17820-1-CU] 11 p1454 N90-18379
Applications of acousto-optical correlation devices in radar signal processing
[AD-A216624] 11 p1497 N90-18616
Multitarget tracking by single sensor: Analysis of the main approaches developed in this area
[ESA-TT-1171] 11 p1500 N90-18633
Signal processing device to control microwave output
[AD-A216931] 11 p1502 N90-18648
Adaptive state estimation and sampling rate analysis for invariant linear dynamic systems in time
[INPE-4960-TDL/389] 11 p1554 N90-18951
The Telecommunications and Data Acquisition Report
[NASA-CR-185033] 12 p1642 N90-19434
Microwave oscillator with reduced phase noise by negative feedback incorporating microwave signals with suppressed carrier 12 p1643 N90-19437
Effect of laser frequency noise on fiber-optic frequency reference distribution 12 p1643 N90-19438
Thermal coefficient of delay for various coaxial and fiber-optic cables 12 p1643 N90-19439
Performance of the all-digital data-transition tracking loop in the advanced receiver 12 p1643 N90-19440
Costas loop lock detection in the advanced receiver 12 p1643 N90-19441
Memory management in traceback Viterbi decoders 12 p1643 N90-19443
Application of adaptive least-squares algorithm to multi-element array signal reconstruction 12 p1644 N90-19448

The effects of sinusoidal interference on the second-order carrier tracking loop preceded by a bandpass limiter in the Block 4 receiver 12 p1644 N90-19449
Parkes radio science system design and testing for Voyager Neptune encounter 12 p1645 N90-19451
Signal processing
[DE90-006904] 12 p1647 N90-19464
General multidimensional scanning ratio transformation and its utilization for norm transformation of television signals
[ETN-90-96058] 12 p1648 N90-19470
Digital video: Studio signal processing
[BBC-RD-1989/14] 12 p1648 N90-19476
Applications of frequency and wavenumber nonlinear digital signal processing to nonlinear hydrodynamics research
[AD-A216259] 12 p1658 N90-19530
All-fiber SFPM (Stimulated Four Photon Mixing) amplifier
[AD-D014358] 12 p1713 N90-19841
Proximity operations concept design study, task 6
[NASA-CR-181971] 13 p1761 N90-20112
Tomographic processing of synthetic aperture radar signals for enhanced resolution
[AD-A217178] 13 p1789 N90-20265
The adaptive line enhancer applied to chirp detection
[DE90-006772] 13 p1789 N90-20268
Doppler radar with multiphase modulation of transmitted and reflected signal
[NASA-CASE-MSC-18808-1] 13 p1791 N90-20280
The design of high-performance circuits for digital signal processing
[AD-A217786] 13 p1796 N90-20309
Common-mode rejector for pulse power diagnostics
[AD-A218096] 13 p1798 N90-20316
The design and implementation of a position measuring system for a remotely controlled video camera
[AD-A218077] 13 p1805 N90-20362
A discussion of observation model, error sources and signal size for spaceborne gravitational gradiometry 13 p1839 N90-20557
(DURIP) Two-Processor Alliant FX/4 System
[AD-A217810] 13 p1864 N90-20692
An algorithm for efficient estimation of superimposed exponential signals
[AD-A217218] 13 p1865 N90-20698
ISLE (Image and Signal Processing LISP Environment) reference manual
[DE90-007858] 13 p1866 N90-20705
Spectral analytic methods for the estimation of number of signals and directions of arrival
[AD-A217219] 13 p1876 N90-20757
GaAs traveling-wave optical modulators using modulated coplanar electrodes with periodic cross-tie overlays
[AD-A217731] 13 p1888 N90-20835
Ridge regression processing 14 p1907 N90-20931
Magneto acoustic emission apparatus for testing materials for embrittlement
[NASA-CASE-LAR-13817-1] 14 p1951 N90-21170
Intensity to frequency conversion technique in intensity modulated fiber optic sensing systems
[NASA-TM-102562] 14 p1969 N90-21277
Cepstrum analysis and applications to computational fluid dynamic solutions 14 p1973 N90-21302
Strategies for concurrent processing of complex algorithms in data driven architectures
[NASA-CR-186515] 14 p2013 N90-21535
Microwave Landing System (MLS) multiple system design interoperability interface control report
[DOT/FAA/SA-89/2] 15 p2050 N90-21750
A functional description of the advanced receiver 15 p2076 N90-21891
Digital Doppler extraction demonstration with the advanced receiver 15 p2076 N90-21893
Mark 4-A DSCC (Magellan-era) telemetry system description 15 p2078 N90-21903
The mm-wave region propagation experiments by satellite 15 p2081 N90-21916
LOWTRAN 7: Status, review, and impact for short-to-long-wavelength infrared applications 15 p2081 N90-21917
Multiresolution and time-frequency representations of signals
[REPT-89-47] 15 p2087 N90-21946
Balanced bridge feedback control system
[NASA-CASE-NPO-17430-1-CU] 15 p2088 N90-21951
Zero-G phase detector and separator
[NASA-CASE-LEW-14844-1] 15 p2101 N90-22024
Calculating the time domain average of gear vibration data sampled at less than the Nyquist frequency
[OUEL-1768/89] 15 p2107 N90-22052
Sampling and noise in vision networks 15 p2138 N90-22217
An investigation of narrow-bandgap semiconductors: Devices, circuits, and systems 15 p2171 N90-22406
Infrared absorption gas sensor for the detection of HCl in launch vehicle exhaust clouds 16 p2209 N90-22600
Qualitative aspects of signal processing through dynamical neural networks
[PREPRINT-711] 16 p2228 N90-22709
Optical excisor modeling
[AD-A219338] 16 p2230 N90-22722
Field oriented control of induction motors
[NASA-TM-103154] 16 p2231 N90-22731
Quantitative surface temperature measurement using two-color thermographic phosphors and video equipment
[NASA-CASE-LAR-13740-1] 16 p2238 N90-22770
Intelligent signal processing techniques for multi-sensor surveillance systems
[AD-A218890] 16 p2262 N90-22895
Multimedia system control
[AD-A219392] 16 p2276 N90-22971
Statistical inference from sampled data
[AD-A218731] 16 p2309 N90-23156
Learning environment for neural networks and transient acoustics
[AD-A219000] 16 p2314 N90-23186
MLS mathematical model validation study using airborne MLS data from Midway Airport engineering flight tests, August 1988
[DOT/FAA/CT-TN90/2] 17 p2349 N90-23378
Signal processing: Kalman filtering 17 p2359 N90-23428
Characterisation of fatigue of aluminium alloys by acoustic emission. Part 1: Identification of source mechanism
[AERE-R-13302-PT-1] 17 p2375 N90-23522
Proceedings of the 12th Symposium on Signal and Image Processing English-Language Abstracts
[AD-A218806] 17 p2388 N90-23598
Research on statistical techniques for signal processing
[AD-A218811] 17 p2388 N90-23599
A theoretical model for airborne radars
[AD-A220735] 17 p2390 N90-23615
Spectral characteristics of low-angle radar ground clutter
[AD-A220817] 17 p2392 N90-23622
Temperature and coupling behavior of resonators and transducers of lithium tetraborate driven by lateral and thickness fields
[AD-A219548] 17 p2395 N90-23644
Ultra high-speed compound semiconductors and real time signal processing
[AD-A220721] 17 p2396 N90-23651
Design, simulation, and testing of a field-oriented ac servo-drive using a TM5 32010 signal processor
[EMV-88-42] 17 p2397 N90-23658
Neuromorphic optical signal processing and image understanding for automated target recognition
[AD-A219827] 17 p2437 N90-23884
Neural networks applied to signal processing
[AD-A219605] 17 p2454 N90-24000
US Army Research Office Workshop on Smart Materials, Structures and Mathematical Issues proceedings
[AD-A218528] 17 p2458 N90-24110
Periodic signatures for the detection of cosmic axions
[NASA-CR-186608] 17 p2470 N90-24122
Multiple beam optical processing
[AD-A219048] 17 p2471 N90-24129
Investigations of laterally coupled all optical switches and detectors on silica fibers
[AD-A220297] 17 p2473 N90-24142
Signal processing on finite groups
[AD-A221129] 18 p2544 N90-24523
Experimental high speed/power ratio ASIC designs using residue numbers
[AD-A220302] 18 p2591 N90-24741
Optical signal processing
[AD-A220332] 18 p2615 N90-24897
Rocket engine failure detection using system identification techiques
[NASA-CR-185259] 19 p2684 N90-25159
Conception and results of the DLR realtime azimuth processor for the E-SAR system
[ESA-TT-1184] 19 p2684 N90-25268
Activities of the division of surveillance and seeker systems
[FOA-C-30549] 19 p2684 N90-25269
Feasibility study for the advanced one-dimensional high temperature optical strain measurement system, phase 3
[NASA-CR-185254] 19 p2693 N90-25324
Three-dimensional laser velocimeter simultaneity detector
[NASA-CASE-ARC-11876-1] 19 p2696 N90-25340
Active perception and exploratory robotics
[MS-CIS-89-65] 19 p2726 N90-25501
New multi-level codes over GF(q)
[NASA-CR-186862] 19 p2744 N90-25594
Optical high-speed parallel backplane
[AD-D014504] 19 p2757 N90-25670
Optical motion detector detecting visible and near infrared light
[AD-D014515] 19 p2758 N90-25671
The disturbance processes on the data links of the mode-S air traffic control system
[ETN-90-96960] 20 p2806 N90-25965
A two-telescope receiver design for deep space optical communications 20 p2853 N90-26226
QPSK loop lock detection in the advanced receiver 20 p2854 N90-26230
Analysis and improved design considerations for airborne pulse Doppler radar signal processing in the detection of hazardous windshear
[NASA-CR-186792] 20 p2890 N90-26448
Assembly via disassembly: A case in machine perceptual development
[NASA-CR-186867] 20 p2900 N90-26497
Closed-loop autonomous docking system
[NASA-CASE-MFS-28421-1] 21 p2966 N90-26861
The speech signal 21 p2992 N90-27008
Speech coding 21 p2992 N90-27009
Speech processing standards 21 p2993 N90-27013
Multistage estimation of received carrier signal parameters under very high dynamic conditions of the receiver
[NASA-CASE-NPO-17911-1-CU] 21 p2994 N90-27016
Spread-spectrum communications in non-Gaussian channels
[AD-A222886] 21 p2994 N90-27019
Nonlinear real-time signal processing
[AD-A222889] 21 p2994 N90-27020
Two-dimensional signal processing and storage, and theory and applications of electromagnetic measurements
[AD-A222984] 21 p2995 N90-27022
Combining zero Doppler filter calculations with MTI filter calculations to increase computational speed
[AD-A222468] 21 p2997 N90-27034
Some thoughts on data processing 21 p3023 N90-27189
Integrated radiometric profiler for atmospheric humidity and temperature measurements
[AD-A221931] 21 p3032 N90-27237
Digital signal processing software packages for IBM-PC and IBM-PC with DSP-16
[AD-A221679] 21 p3056 N90-27372
Neural networks
[AD-A222110] 21 p3060 N90-27398
Optics and symbolic computing
[AD-A221443] 21 p3077 N90-27493
Development and testing of methodology for evaluating the performance of multi-input/multi-output digital control systems
[NASA-TM-102704] 22 p3115 N90-27699
Adaptive polarization diversity detection scheme for coherent communications and interferometric fiber sensors
[AD-D014479] 22 p3163 N90-27938
Utilizations of an acoustic surface wave-convolver for signal processing in the measurement and information techniques
[ETN-90-97319] 22 p3165 N90-27947
SAR processing methods
[FEL-1989-131] 22 p3165 N90-27948
Center for Electronics and Electrical Engineering technical progress bulletin covering center programs, July to September 1989, with 1990 CEEE events calender
[PB90-188095] 22 p3167 N90-27959
Study of failure processes in fiber reinforced composites using acoustic emission techniques 22 p3188 N90-28090
Methods for detecting low-frequency signals in the presence of strong winds
[AD-A223980] 23 p3320 N90-28769
Target detection in Gaussian noise using artificial neural systems
[AD-A223983] 23 p3320 N90-28770
Modular digital GPS receivers 24 p3424 N90-29346
The determination of PDOP (Position Dilution of Precision) in GPS 24 p3425 N90-29351
Use of a three-axis monolithic ring laser gyro and digital signal processor in an inertial sensor element 24 p3426 N90-29354
Distributed control architecture for CNI preprocessors 24 p3426 N90-29356
JTIDS relative navigation: Principles, architecture, and inertial mixing 24 p3426 N90-29357
Overview of Omega signal coverage 24 p3429 N90-29368

Satellite navigation systems for land vehicles
24 p3430 N90-29376
Two-dimensional signal processing and storage and theory and applications of electromagnetic measurements
[AD-A224239] 24 p3459 N90-29538
Neural networks and radar systems
[FEL-89-B65] 24 p3462 N90-29558
Performance analysis of subspace-based parameter estimation algorithms
[AD-A224523] 24 p3463 N90-29566
Detectors and signal processing for the speed measuring system 4-01
[FEL-1989-64] 24 p3472 N90-29623
Proceedings of the 17th Annual Gravity Gradiometer Conference
[AD-A223568] 24 p3492 N90-29735
A comparison of hardware implementations for low-level vision algorithms
[AD-A223699] 24 p3527 N90-29945
Adaptive, robust, high-resolution signal processing
[AD-A223728] 24 p3538 N90-30004
A review of manganin gauge technology for measurements in the gigapascal range
[MRL-TR-90-5] 24 p3541 N90-30026
Optical signal computing
[AD-A223624] 24 p3545 N90-30051

SIGNAL RECEPTION
NT SYMBOLS
NT TELEVISION RECEPTION
ILS/MLS comparison tests at Miami/Tamiami, Florida Airport
[ACD-330] 01 p0005 N90-10018
Accurate measurements of the total angle of arrival of HF skywaves 02 p0248 N90-11402
South Pacific OMEGA validation analysis
[AD-A215916] 10 p1319 N90-17624
ACTS propagation concerns, issues, and plans
10 p1374 N90-17963
DOA (Direction of Arrival) estimation by Eigendecomposition using single vector Lanczos' algorithm
[AD-A215802] 11 p1544 N90-18887
The effects of sinusoidal interference on the second-order carrier tracking loop preceded by a bandpass limiter in the Block 4 receiver 12 p1644 N90-19449
Planar integrated circuits for microwave transmission and reception
[AD-A217676] 12 p1656 N90-19520
Filter process for parasitic suppression for reception of spectrally separated emission signals
[ETN-90-96506] 18 p2545 N90-24526
Concept study for UHF T/R modules
[AD-A220281] 18 p2547 N90-24536
Experimental study of a digital mobile radio spread spectrum in an urban site 20 p2849 N90-26205
Report from GPS MANPACK tests in Spitsbergen area (Norway)
[FFI-90/7007] 22 p3114 N90-27692

SIGNAL REFLECTION
A search for layering in the oceanic crust
[PB89-198220] 01 p0090 N90-10514
ILS mathematical modeling study of the effects of proposed hangar construction at the Orlando International Airport, Runway 17R, Orlando, Florida
[DOT/FAA/CT-TN89/52] 03 p0310 N90-11762
A method to model fuze performance. Part 2: Calculation of target reflections with physical optics
[FEL-1989-21-PT-2] 04 p0491 N90-12822
Rotating Doppler frequency shifter
[AD-D014279] 08 p1118 N90-16475
A linear systems theory approach to the range-independent acoustic channel
[AD-A216551] 12 p1710 N90-19817
Cepstrum analysis and applications to computational fluid dynamic solutions 14 p1973 N90-21302

SIGNAL STABILIZATION
Passive stabilization of a fiber optic nonlinear interferometric sensor
[AD-D014438] 14 p2026 N90-21620

SIGNAL TO NOISE RATIOS
Analysis of two-pass Modified Hough Transform (MHT) technique for the detection of wake like signals
[AD-A211982] 03 p0338 N90-11924
Adaptive antenna arrays for satellite communication
[NASA-CR-185989] 04 p0485 N90-12784
A performance comparison between block interleaved and helically interleaved concatenated coding systems
04 p0486 N90-12792
Performance of the image statistics decoder in conjunction with the Goldstone-VLA array
04 p0487 N90-12796
Performance of the split-symbol moments SNR estimator in the presence of inter-symbol interference
04 p0487 N90-12799
Application of an optimal filter for inflatable sphere data processing 05 p0659 N90-13849
Coding capacity for a class of additive channels
[AD-A215054] 09 p1206 N90-16993
Error detection and correction for a multiple frequency quaternary phase shift keyed signal
[AD-A215706] 09 p1208 N90-17003
Infrared target detection: Signal and noise sensitivity analysis
[AD-A215707] 09 p1282 N90-17436
Staring focal plane array system modeling
[AD-A215712] 09 p1283 N90-17438
South Pacific OMEGA validation analysis
[AD-A215916] 10 p1319 N90-17624
Polarization radar processing technology
[AD-A215242] 10 p1374 N90-17967
Applications of acousto-optical correlation devices in radar signal processing
[AD-A216624] 11 p1497 N90-18616
Angle estimation in the presence of mainbeam interference
[AD-A216832] 11 p1498 N90-18621
DOA (Direction of Arrival) estimation by Eigendecomposition using single vector Lanczos' algorithm
[AD-A215802] 11 p1544 N90-18887
Hydrogen assay foil counting system
[DE90-007415] 12 p1624 N90-19332
A real-time signal combining system for Ka-band feed arrays using maximum-likelihood weight estimates
15 p2076 N90-21888
QPSK carrier-acquisition performance in the advanced receiver 2 15 p2076 N90-21892
Exact closed-form expressions for the performance of the split-symbol moments estimator of signal-to-noise ratio 15 p2077 N90-21894
Validity of the two-level model for Viterbi decoder gap-cycle performance 15 p2077 N90-21896
Simulation and analysis of a MFQPSK signal transmitted through an acoustic medium
[AD-A220345] 17 p2393 N90-23633
Statistical techniques for designing a decoupled controller to be robust to model and sensor noise
[AD-A220476] 17 p2412 N90-23745
A comparison of the K-pulse and E-pulse techniques for aspect independent radar target identification
[AD-A220172] 18 p2542 N90-24511
Filter process for parasitic suppression for reception of spectrally separated emission signals
[ETN-90-96506] 18 p2545 N90-24526
The soft X ray excess in Einstein quasar spectra
19 p2794 N90-25910
Direct drive robotic hand
[NASA-CASE-NPO-17917-1-CU]
20 p2872 N90-26339
HIRIS performance study
[NASA-CR-186649] 20 p2878 N90-26375
Obtaining consistent models of helicopter flight-data measurement errors using kinematic-compatibility and state-reconstruction methods
[AD-A222533] 21 p2954 N90-26799
Utilizations of an acoustic surface wave-convolver for signal processing in the measurement and information techniques
[ETN-90-97319] 22 p3165 N90-27947
Comparison of speech intelligibility in cockpit noise using SPH-4 flight helmet with and without active noise reduction
[NASA-CR-177564] 23 p3271 N90-28510
Methods for detecting low-frequency signals in the presence of strong winds
[AD-A223980] 23 p3320 N90-28769
Bandwidth and signal-to-noise ratio enhancement of the NPS transient electromagnetic scattering laboratory
[AD-A224144] 23 p3320 N90-28771
Noise performance of microchannel plate imaging systems
[DE90-015037] 23 p3322 N90-28785
Metallic line profiles of the AOV star Vega
[NASA-CR-186906] 23 p3408 N90-29261
High power oblique incidence HF ionospheric modification
[AD-A224402] 24 p3491 N90-29729

SIGNAL TRANSMISSION
NT CODE DIVISION MULTIPLE ACCESS
NT DATA TRANSMISSION
NT IONOSPHERIC F-SCATTER PROPAGATION
NT IONOSPHERIC PROPAGATION
NT MICROWAVE ATTENUATION
NT MICROWAVE TRANSMISSION
NT MULTIPATH TRANSMISSION
NT MULTIPLE ACCESS
NT PACKET TRANSMISSION
NT PCM TELEMETRY
NT RADAR TRANSMISSION
NT RADIO TELEMETRY
NT RADIO TRANSMISSION
NT SATELLITE TRANSMISSION
NT SHORT WAVE RADIO TRANSMISSION
NT TELEMETRY
NT TELEVISION TRANSMISSION
Omega system performance assessment
[AD-A210342] 01 p0056 N90-10322
Automatic communications channel interference monitoring
[RSRE-MEMO-4243] 04 p0491 N90-12820
Low-altitude millimeter-wave propagation in the evaporation duct
[AD-A214432] 08 p1057 N90-16108
Generalized pulse equations for through-transmission evaluation of arbitrary multilayered structures
[NASA-TM-100752] 09 p1278 N90-17407
Signal processing applied to photothermal techniques for materials characterization 10 p1364 N90-17902
Low elevation angle KU-band satellite measurements at Austin, Texas 10 p1373 N90-17959
Atmospheric transmission calculations for optical frequencies 10 p1373 N90-17960
Adaptive vibration control of vibration isolation mounts, using an LMS-based control algorithm
[AD-A214386] 10 p1394 N90-18061
Effect of laser frequency noise on fiber-optic frequency reference distribution 12 p1643 N90-19438
Doppler radar with multiphase modulation of transmitted and reflected signal
[NASA-CASE-MSC-18808-1] 13 p1791 N90-20280
HDTV bandwidth reduction using motion compensation and DATV
[BBC-RD-1989/10] 14 p1965 N90-21254
Simulation and analysis of a MFQPSK signal transmitted through an acoustic medium
[AD-A220345] 17 p2393 N90-23633
The speech signal 21 p2992 N90-27008
Overview of Omega signal coverage
24 p3429 N90-29368
Omega navigation signal characteristics
24 p3429 N90-29369
Graphic overlays in high-precision teleoperation: Current and future work at JPL 24 p3508 N90-29827

SIGNATURE ANALYSIS
Issues and approaches for electronic document approval and transmittal using digital signatures and text authentication: Prototype documentation
[DE90-003382] 08 p1058 N90-16119
Sonic boom signature data from cruciform microphone array experiments during the 1966-1967 EAFB national sonic boom evaluation program
[NASA-CR-182027] 14 p2024 N90-21605
Recognition and analysis of aircraft targets by radar, using structural pattern representations derived from polarimetric signatures 15 p2074 N90-21879
Gamma radiation from the Crab and Vela pulsars
16 p2334 N90-23303
Item identities and their related observables
[AD-A219559] 17 p2468 N90-24104
Periodic signatures for the detection of cosmic axions
[NASA-CR-186608] 17 p2470 N90-24122
Acousto-optic signature analysis for inspection of the orbiter thermal protection tile bonds
[DE90-013089] 20 p2819 N90-26043
Optical signatures of molecular particles via mass-selected cluster spectroscopy
20 p2949 N90-26780
The plasma wave signature of a 'magnetic hole' in the vicinity of the magnetopause
[NASA-CR-187027] 22 p3212 N90-28220
Direct and remote sensing observations of the effects of ships on clouds 22 p3218 N90-28252
Bandwidth and signal-to-noise ratio enhancement of the NPS transient electromagnetic scattering laboratory
[AD-A224144] 23 p3320 N90-28771

SIGNATURES
NT INFRARED SIGNATURES
NT MAGNETIC SIGNATURES
NT RADAR SIGNATURES
NT SPECTRAL SIGNATURES
Two counter-rotating vortices approaching a free surface in a viscous fluid
[AD-A210495] 01 p0070 N90-10404
Nuclear magnetic resonance signatures of nitrogen-containing compounds
[AD-A213375] 05 p0622 N90-13628
Periodic signatures for the detection of cosmic axions
[NASA-CR-186608] 17 p2470 N90-24122
Bayesian characterization and detection of rare binary signature events
[AD-A221116] 18 p2606 N90-24844
Can the chirality of the ISM be measured
21 p3095 N90-27590

SIGNS (SYMBOLS)
U SYMBOLS

SIGNS AND SYMPTOMS
NT EDEMA
Simulator sickness in the AH-1S (Cobra) flight simulator
[AD-A214562] 09 p1250 N90-17254
Human factors in the naval environment: A review of motion sickness and biodynamic problems
[AD-A214733] 09 p1251 N90-17258
Psychophysiological correlates of human adaptation in antarctica
[AD-A216679] 10 p1412 N90-18142
Acute oral toxicity of JA-2 solid propellant in ICR mice
[AD-A217264] 13 p1848 N90-20609
Acute oral toxicity of DIGL-RP solid propellant in ICR mice
[AD-A217711] 13 p1849 N90-20613
Acute oral toxicity of DIGL-RP solid propellant in Sprague-Dawley rats
[AD-A217712] 13 p1849 N90-20614
Simulator sickness in the CH-47 (Chinook) flight simulator
[AD-A218214] 13 p1853 N90-20634
What should athletes know about low body temperature (hypothermia)
[AD-A218316] 13 p1854 N90-20637
A laboratory study of the effects of diet and bright light countermeasures to jet lag
[AD-A220148] 17 p2435 N90-23875
Decompression sickness presenting as a viral syndrome
[AD-A223880] 23 p3356 N90-28967

SIKORSKY AIRCRAFT
NT H-53 HELICOPTER
NT UH-60A HELICOPTER

SIKORSKY S-65 HELICOPTER
U H-53 HELICOPTER

SILANES
X-ray lithography studies of polysilane using a laser plasma X-ray source
[DE89-015390] 01 p0047 N90-10266
New polymer precursors to boron and silicon nitrides
[AD-A210287] 01 p0049 N90-10279
Synthesis of inorganic polymers as glass precursors and for other uses. Preceramic block or graft copolymers as potential precursors to nanocomposite materials
[AD-A211978] 05 p0626 N90-13655
Band-to-band transitions in poly (phenyl methyl silane)
[DE90-003575] 07 p0990 N90-15720
Surface modification of steels and aluminum alloys to control corrosion and hydrogen embrittlement. Part 1: Chemical methods
[AD-A216272] 10 p1356 N90-17866
Composite for smoothing the surface of ceramic substrates
[DE90-004005] 11 p1488 N90-18565
Characterization and role of an elastomeric interphase within polyepoxy reinforced glass, both particulate and fibrous
[ISAL-89-0064] 16 p2222 N90-22676
Dehydrogenative polymerization of silanes to polysilanes: A monomeric copper(2) siloxide
[AD-A218550] 16 p2223 N90-22681
Reactions of silane in active nitrogen
[AD-A220371] 17 p2373 N90-23511
An investigation of the chemistry of silane coupling agents for adhesive bonding of aluminum
[AD-A220797] 17 p2381 N90-23560
One-dimensional sigma-conjugated polysilylenes: Science and technology
[DE90-012902] 20 p2839 N90-26146
Laser techniques for studying chemical vapor deposition
[DE90-012921] 20 p2967 N90-26311

SILICA
U SILICON DIOXIDE

SILICA GEL
Elastic properties of silica xerogels
[AD-A216528] 12 p1630 N90-19366
Surface structure and chemistry of high surface area silica gels
[DE90-007684] 15 p2071 N90-21885

SILICA GLASS
A new model for the structure of silica glass
[AD-A212972] 05 p0627 N90-13659
Bonding aerogels with polyurethanes
[DE90-003050] 07 p0910 N90-15258
Crystallization of nanocomposite glasses made by the SSG process
[AD-A214572] 09 p1197 N90-16933
Multicomponent glass surfaces structure and adsorption
[DE90-007179] 11 p1493 N90-18596

SILICATES
NT BERYL
NT KAOLINITE
NT YTTRIUM-ALUMINUM GARNET
NT YTTRIUM-IRON GARNET
NT ZEOLITES
Applications of NMR spectroscopy to the study of zeolite synthesis
[DE89-015226] 02 p0192 N90-11095
Irreversible phase transition and wave propagation in silicate geologic materials
[DE89-016031] 02 p0250 N90-11414
Pyrolytic production of ceramic composites from silicates
[ETCA-89-R-012] 04 p0479 N90-12746
Sulphur silicate interactions on the Jovian satellite Io
15 p2192 N90-22515
The effect of elevated gravity on the crystallization of the MFI zeolites, ZSM-5, and silicalite
16 p2320 N90-23231
Kinetics and structure of silicate sol-gels
[DE90-015702] 24 p3456 N90-29521

SILICIDES
NT DISILICIDES
Study of palladium and chromium silicides formation in liquid phase and in solid phase
[LAAS-89040] 04 p0470 N90-12695
Shock-induced reaction synthesis of aluminides and silicides
[DE90-003948] 08 p1049 N90-16066
Evaluation of platinum silicide and indium antimonide as detector materials for space-based remote sensing in the 3.0-to-5.0 micrometer wavelength band
[AD-A216182] 10 p1354 N90-17853
Dislocation behaviour in Ge(x)Si(1-x) epilayers on (001) Si
[DE90-007063] 11 p1572 N90-19051
Modified dislocation structures in Ge(x)Si(1-x) double epilayers on (001) Si
[DE90-007078] 11 p1572 N90-19052
Method of forming three-dimensional semiconductor structures
[NASA-CASE-NPO-17835-1-CU]
21 p3081 N90-27518
Alloy design of ordered intermetallics
[DE90-016031] 24 p3451 N90-29490

SILICON
NT AMORPHOUS SILICON
NT SILICON ISOTOPES
The effects of normal annealing cycles during IGFET fabrication on initial and radiation induced gate insulator defects
[AD-A210282] 01 p0049 N90-10278
Performance of the CAMEX64 silicon strip readout chip
[DE89-014015] 01 p0130 N90-10747
Methods to decrease defect density in GaAs/Si heteroepitaxy
[DE89-016306] 01 p0131 N90-10753
Effects of coherent scattering on infrared absorption in doped semiconductors
[AD-A210224] 01 p0131 N90-10756
Bias and oxide thickness dependence of trapped charge buildup in MOS devices
[AD-A210264] 01 p0131 N90-10757
A new semicustom integrated bipolar amplifier for silicon strip detectors
[DE89-015585] 02 p0215 N90-11229
A prototype silicon compiler in prolog
[AD-A210669] 02 p0257 N90-11452
Hydrogen-assisted thermal donor formation in silicon
[DE89-016809] 02 p0279 N90-11594
Ion beam annealing of Ga-implanted Si
[DE89-016857] 02 p0282 N90-11610
Transition metal catalyzed synthesis of organmetallic polymers
[AD-A212133] 04 p0478 N90-12740
Semiconductor measurement technology: Database for and statistical analysis of the interlaboratory determination of the conversion coefficient for the measurement of the interstitial oxygen content of silicon by infrared absorption
[PB89-221170] 04 p0558 N90-13253
The growth of epitaxial GaAs and GaAlAs on silicon substrates by OMVPE
[AD-A212873] 04 p0561 N90-13269
Silicon-etalon fiber-optic temperature sensor
[NASA-TM-102389] 05 p0580 N90-13381
Evolution of the EPR procedure for polycrystalline Si ribbon drawing for photovoltaic cell manufacturing
[ISAL-89-0027] 05 p0665 N90-13888
Elastic softening in nanocrystalline silicon
[DE90-002268] 06 p0752 N90-14377
Fabrication of NBN based electronic devices with silicon barriers
[AD-D014230] 06 p0767 N90-14463
Preparation, structure and properties of VO(sub x) and TiO2 thin films by MOCVD
[DE90-003566] 07 p1001 N90-15793
Theoretical studies of chemisorption and surface reactions on nickel and silicon
[DE90-004849] 08 p1047 N90-16050
Silicon-based coatings on niobium metal
[DE90-003651] 08 p1048 N90-16057
Pairs of chalcogen impurities in silicon
[DE89-635767] 08 p1049 N90-16063
Silicon membrane formation
[DE90-003022] 08 p1049 N90-16064
Slow positron defect profiling of silicon epilayers
[DE90-003958] 08 p1087 N90-16288
Heteroepitaxy of GaAs on Si: Methods to decrease the defect density in the epilayer
[DE90-004028] 08 p1131 N90-16551
Hydrogen desorption from the monohydride phase on Si(100)
[AD-A215237] 09 p1191 N90-16903
Silicon hybrid wafer scale integration interconnect evaluation
[AD-A215353] 09 p1212 N90-17031
A new approach for the utilization of electron paramagnetic resonance and an investigation of copper oxide superconductors
[AD-A213833] 09 p1277 N90-17404
Method of producing a thin silicon-on-insulator layer
[AD-D014330] 09 p1290 N90-17478
Pilot production of 70 micron thin silicon solar cells
10 p1343 N90-17780
Limits of efficiency of solar cells under AMO-spectrum illumination: Comparison between Si and GaAs cells
10 p1343 N90-17784
Interfacial chemistry of MoS2 films on Si
[AD-A216527] 11 p1482 N90-18532
Surface intermediates in thin film deposition on silicon
[AD-A216662] 11 p1483 N90-18534
Time-resolved measurements of solidification and undercooling in metals and alloys
[DE90-007074] 11 p1488 N90-18564
Research relating to crystalline silicon-film on a foreign substrate
[DE90-005720] 11 p1491 N90-18582
Integrated silicon flip-flop sensors
[ETN-90-96271] 11 p1503 N90-18654
The III-V semiconductor quantum well lasers and related optoelectronic devices on silicon
[AD-A216980] 12 p1666 N90-19570
Mechanisms of reactive etching
[AD-A217679] 13 p1770 N90-20160
Infrared absorption study of zinc-doped silicon
[DE90-007779] 13 p1771 N90-20164
Refractive index profiles of thermally grown and chemically vapor deposited films on silicon
[AD-A217187] 13 p1893 N90-20865
Proceedings of the Joint NOSC/NRL (Naval Ocean Systems Center/Naval Research Laboratory) InP Microwave/Millimeter Wave Technology Workshop
[AD-A218216] 14 p1966 N90-21259
Initial astronomical results with a new 5-14 micron Si:Ga 58x62 DRO array camera 14 p1978 N90-21334
Improved Si:As BIBIB (Back-Illuminated Blocked-Impurity-Band) hybrid arrays
14 p1981 N90-21349
Improvement of small-area, amorphous-silicon thin-film photovoltaics on polymer substrate
[DE90-000314] 14 p2002 N90-21472
Research on amorphous silicon-based thin film photovoltaic devices. Task B: Research on stable high efficiency large area, amorphous silicon-based submodules
[DE90-000320] 14 p2002 N90-21473
Theoretical studies of silicon chemistry
[AD-A219232] 16 p2225 N90-22690
Experimental evaluation of chemical cleaning processes for high-lifetime silicon processing
[DE90-009332] 16 p2226 N90-22699
Reactions of laser-generated free radicals at semiconductor surfaces
[AD-A218552] 16 p2232 N90-22733
Continued development and characterization of doped layers, contacts, and associated electronic devices in silicon carbide
[AD-A219211] 16 p2232 N90-22737
Passivation and gating of GaAs and Si surfaces using pseudomorphic structures
[AD-A219351] 16 p2325 N90-23256
Interdigitated back contact silicon solar cell analysis and design recommendations for space use
[AD-A220414] 17 p2420 N90-23790
Studies of chemistry and diffusion on silicon and gallium arsenide surfaces using laser-induced thermal desorption
[AD-A220946] 18 p2547 N90-24539

An examination of the 1-MeV equivalent silicon damage methodology
[DE90-007167] 18 p2614 N90-24888
Advanced methods for the micromachining of sensors
[MBB-Z-0281/88-PUB] 19 p2650 N90-25081
Composite materials with improved properties in compression: Synthesis of 3-methylene-1,1-Dichlorosilacyclobutane and 1,1-dichlorosilacyclopent-3-ene
[AD-A222615] 20 p2828 N90-26088
The catalytic synthesis of inorganic polymers for high temperature applications and as ceramic precursors
[AD-A222620] 20 p2840 N90-26156
Rapid thermal processing: A study of the silicon oxidation and of the implanted boron activation
[LAAS-90051] 20 p2932 N90-26681
Ni impurity effects on hydrogen surface chemistry and etching of Si(111)
[AD-A222083] 21 p2977 N90-26921
The adsorption and thermal decomposition of PH3 on Si(111)-(7x7)
[AD-A222417] 21 p2978 N90-26927
PH3 surface chemistry on Si(111)-(7x7): A study by Auger spectroscopy and electron stimulated desorption methods
[AD-A221508] 21 p2979 N90-26929
Silicon containing electroconductive polymers and structures made therefrom
[NASA-CASE-NPO-17826-1-CU] 21 p2983 N90-26952
Background effects in ESDIAD measurements on Si(111)-(7x7)
[AD-A222242] 21 p3001 N90-27056
Electronic and structural properties of Si10 cluster
[AD-A222429] 21 p3074 N90-27478
Method of forming three-dimensional semiconductor structures
[NASA-CASE-NPO-17835-1-CU] 21 p3081 N90-27518
The epitaxial growth of copper on the (111) surface of silicon
[DE90-013817] 21 p3082 N90-27523
High-temperature deformation of silicon
[DE90-013628] 22 p3160 N90-27919
Double sided silicon strip detectors
[MPI-PAE/EXP-EL-217] 22 p3178 N90-28036
A double-sided silicon strip detector with capacitive read out and a new method of integrated bias coupling 22 p3178 N90-28037
Readout of double sided silicon strip detectors with high intensity integrated electronics 22 p3179 N90-28038
New developments in double sided silicon strip detectors 22 p3179 N90-28039
The III-V semiconductor quantum well lasers and related optoelectronic devices on silicon
[AD-A224120] 23 p3331 N90-28835
Use of electron spectroscopies in the tribological evaluation of diamond films
[DE90-014421] 23 p3334 N90-28848
Research on high-efficiency, multiple-gap, multi-junction amorphous silicon-based alloy thin-film solar cells
[DE90-000338] 23 p3344 N90-28896
Semiconductor measurement technology. EPROP: An interactive FORTRAN program for computing selected electronic properties of Gallium Arsenide and Silicon
[PB90-222738] 23 p3399 N90-29203
Kinetic pathway in Stranski-Krastanov growth of Ge on Si(001)
[AD-A224324] 24 p3445 N90-29456
Microscopic aspects of the initial stages of epitaxial growth. A scanning tunneling microscopy study
[AD-A224325] 24 p3551 N90-30094
Integrated technology in MCT/GaAs and MCT/Si for medium and long wavelength infrared
[AD-A223557] 24 p3552 N90-30100

SILICON ALLOYS

Microstructure morphology and quality of Al-Si castings 01 p0043 N90-10244
Structure of amorphous silicon alloy films
[DE89-009441] 01 p0128 N90-10734
Spectral sensitivity of device power output for tandem a-Si alloy solar cells
[DE89-009421] 08 p1095 N90-16340
Experimental evaluation of new alloy coatings
[AD-A214922] 09 p1194 N90-16916
Characterization of the 6242 Si alloy. Centrifugal wheel in conventional forging
[REPT-NT-3967] 10 p1355 N90-17859
Research on high-efficiency, multi-gap, multi-junction amorphous silicon-based alloy thin-film solar cells
[DE89-009492] 10 p1402 N90-18101
Annealing group III-V compound doped silicon-germanium alloy for improved thermo-electric conversion efficiency
[NASA-CASE-NPO-17259-1-CU] 12 p1721 N90-19884
Erosion mechanisms in composite materials and ripple formation mechanism in erosion
[IAR-89-4-PT-2] 20 p2826 N90-26079

SILICON CARBIDES

Shock compression and release in high-strength ceramics
[DE89-013995] 01 p0047 N90-10265
Thermophysical properties of ceramics. Part 2: Development of specific-heat-measurement apparatus at high temperature
[DE89-760382] 01 p0047 N90-10268
Improved silicon carbide for advanced heat engines
[NASA-CR-180831] 01 p0051 N90-10293
Zirconia toughened SiC whisker reinforced alumina composites small business innovation research
[NASA-CR-179629] 01 p0052 N90-10294
Effect of thermal and cyclic loads on silicon carbide yarn reinforced glass matrix composites
[DE89-016554] 02 p0191 N90-11091
Hydrogen-silicon carbide interactions
[NASA-TM-102382] 02 p0200 N90-11144
Kinetics and mechanisms of primary and steady state creep in B- and Al-containing alpha silicon carbide
[AD-A210739] 02 p0283 N90-11616
Investigations into the infiltration kinetics, wettability, and interfacial bond strength of Al/SiC composites
[AD-A211924] 03 p0320 N90-11815
Reactive ion etching of sputtered silicon carbide and tungsten thin films for device applications
[AD-A211711] 03 p0325 N90-11847
Fatigue behavior of silicon carbide Whisker/Aluminum composite
[AD-A213094] 05 p0618 N90-13603
Toughening of a particulate-reinforced/ceramic-matrix composite
[AD-A213180] 05 p0618 N90-13604
Toughening mechanisms in ceramic composites
[PB89-235907] 05 p0626 N90-13656
Mechanisms in reactive ion etching of silicon carbide thin films
[AD-A213018] 05 p0634 N90-13700
Oxidation effects on the mechanical properties of SiC fiber-reinforced reaction-bonded silicon nitride matrix composites
[NASA-TM-102360] 06 p0736 N90-14287
Friction and wear of glassy carbon in sliding contact, revision 1
[DE90-000743] 06 p0750 N90-14365
The 7th International Conference on Ceramics
[DE90-002144] 06 p0752 N90-14374
Study of microcrystalline, silicon-carbon p-layers prepared by photo-CVD and glow discharge
[DE89-009438] 06 p0850 N90-14939
Fatigue properties of SiC/Al composites 07 p0889 N90-15138
Empirical and analytical determination of the fracture resistance of a TiB2 particle/SiC matrix composite
[NASA-TM-101940] 07 p0890 N90-15143
Effects of filament-matrix interfaces on the mechanical properties of SiC-reinforced Si3N4: A review
[DE90-001863] 07 p0890 N90-15144
Laser mixing of titanium on silicon carbide
[DE90-003216] 07 p0891 N90-15150
Potential applications of structural ceramic composites in gas turbines
[DE90-001273] 07 p0908 N90-15248
IEA/Annex 2 powder characterization cooperative program
[AD-A213540] 07 p0911 N90-15271
Analytical study on the decreasing method of thermal stress for ceramic gas turbines
[DE90-734934] 08 p1051 N90-16078
The 1MeV-electron irradiation induced defects in epitaxially grown 3C-SiC
[DE90-719574] 08 p1131 N90-16554
Extrusion of alumina-silicon carbide whisker composites
[DE90-004379] 09 p1186 N90-16869
Crystallization of nanocomposite glasses made by the SSG process
[AD-A214572] 09 p1197 N90-16933
Research on stable high-efficiency, large area, amorphous silicon-based solar cells, phase 2
[DE89-009491] 09 p1242 N90-17208
Growth of epitaxical SiC layers onto on- and off-axis 6H-SiC substrates by ion beam deposition
[DE90-004236] 09 p1287 N90-17459
The processing and mechanical properties of high temperature/high performance composites. Book 4, section 3: Flow and creep strength
[AD-A216144] 10 p1349 N90-17822
Third European Conference on Composite Materials
[EOARD-LR-89-050] 11 p1476 N90-18494
Silicon carbo-nitride ceramic matrix composites by polymer pyrolysis 11 p1477 N90-18499
Ceramic matrix composites, new high performance materials 11 p1477 N90-18500
Continuous preparation of a thin refractory carbide deposit on the surface of carbon fibers: Characterization of the C/SiC fiber 11 p1477 N90-18501
Sputter deposition of diffusion barrier coatings on SiC monofilaments for use in Ti-based composites 11 p1477 N90-18502
Laboratory for the processing and evaluation of inorganic matrix composites
[AD-A216881] 11 p1480 N90-18516
Application of artificial intelligence control to the vapor-liquid-solid silicon carbide whisker process
[DE90-007835] 11 p1480 N90-18519
Fundamental aspects of erosion and impact damage
[DE90-006640] 11 p1492 N90-18587
Heat treatment study of the SiC/Ti-15-3 composite system
[NASA-TP-2970] 12 p1618 N90-19302
Identification and development of optimum SiC whiskers for silicon nitride matrix composites
[DE90-006888] 12 p1621 N90-19315
Fracture strength analysis of silicon nitride and silicon carbide ceramics from an international cooperative research program
[DE90-005319] 12 p1630 N90-19368
Fabrication, phase transformation studies, and characterization of SiC-AlN-Al2OC ceramics
[DE90-006591] 12 p1631 N90-19371
The effect of fiber coatings on interfacial shear strength and the mechanical behavior of ceramic composites
[DE90-007574] 12 p1632 N90-19380
Light-scattering measurements of CVD (Chemical Vapor Deposition) silicon carbide
[DE90-007885] 12 p1632 N90-19382
Silicon carbide semiconductor device fabrication and characterization
[NASA-CR-186354] 12 p1719 N90-19873
Evaluation of thermal and mechanical loading effects on the structural behavior of a SiC/titanium composite
[NASA-TM-102536] 13 p1767 N90-20139
Synthesis of alumina-coated SiC whiskers for production of SiC whisker-reinforced alumina composite materials
[DE90-007778] 13 p1768 N90-20147
Characterization of ceramic matrix composites fabricated by chemical vapor infiltration
[DE90-008409] 13 p1768 N90-20149
The effect of the SiC/Al interface on matrix microstructure in 2xxx-SiCp metal matrix
[AERE-R-13591] 13 p1775 N90-20184
The ageing effect of the matrix-reinforcement interface on the ageing response of an aluminium 6061 alloy reinforced with 20vol percent SiC particulates
[AERE-R-13361] 13 p1776 N90-20193
Acoustic characterisation of an aluminium silicon carbide metal matrix composite
[AERE-R-13273] 14 p1943 N90-21121
Ductile alloy encapsulated ceramic armor development
[AD-A217632] 14 p1954 N90-21183
Investigation of the reaction kinetics between SiC fibers and selectively alloyed titanium matrix composites and determination of their mechanical properties 16 p2219 N90-22659
Inelastic response of metal matrix composites under biaxial loading 16 p2220 N90-22661
Continued development and characterization of doped layers, contacts, and associated electronic devices in silicon carbide
[AD-A219211] 16 p2232 N90-22737
Continued development and characterization of doped layers, contacts and associated electronic devices in silicon carbide
[AD-A219234] 16 p2232 N90-22738
Comparison between data generated from standard fracture toughness specimens and from nonstandard specimens made of a silicon carbide
[DE90-009621] 16 p2247 N90-22814
High temperature fatigue behavior of a SiC/Ti-24Al-11Nb composite
[NASA-TM-103157] 16 p2248 N90-22822
Thermomechanical properties of new composite materials SiC/glass-ceramic
[REPT-892-430-118] 17 p2370 N90-23491
Quality evaluation of coatings by automatic scratch testing
[AD-A219331] 17 p2379 N90-23548
Theory and experimental technique for nondestructive evaluation of ceramic composites
[NASA-TM-102561] 17 p2414 N90-23754
Influence of interfacial shear strength on the mechanical properties of SiC fiber reinforced reaction-bonded silicon nitride matrix composites
[NASA-TM-102462] 18 p2518 N90-24382

Electron microscopy of interfaces in silicon carbide whisker-reinforced alumina composites
[DE90-010439] 18 p2519 N90-24386
A particle-level numerical simulation of the dynamic consolidation of a metal matrix composite material
[DE90-010950] 18 p2519 N90-24387
Metal matrix composites from dynamic consolidation of powder mixtures
[DE90-010951] 18 p2519 N90-24388
Mechanical property characterization of fiber-reinforced SiC matrix composites
[DE90-011316] 18 p2520 N90-24390
The influence of ion implantation on the near-surface mechanical properties of ceramics
[DE90-010139] 18 p2531 N90-24444
Ceramic technology for advanced heat engines project data base
[DE90-011491] 18 p2532 N90-24448
SiC film deposited by pulsed excimer laser ablation
[DE90-010634] 18 p2622 N90-24938
Synthesis of large area, monocrystalline TiC as a substrate for heteroepitaxial growth of beta-SiC
[AD-A221392] 18 p2623 N90-24948
Fundamental studies and device development in beta silicon carbide
[AD-A219253] 19 p2676 N90-25220
Crack bridging processes in toughened ceramics
[DE90-011650] 19 p2678 N90-25231
Thermomechanical testing techniques for high-temparature composites: TMF behavior of SiC(SCS-6)/Ti-15-3
[NASA-TM-103171] 19 p2701 N90-25367
Vitreous joining of SiC fiber reinforced SiC composites
[DE90-012951] 20 p2827 N90-26081
Synthesis of high purity sinterable silicon carbide powder
[DE90-012029] 20 p2828 N90-26084
Investigation of thermo-mechanical effects in silicon carbide Whisker/Al alloy composites
[AD-A222635] 20 p2828 N90-26089
Evaluation of fracture strength properties of silicon carbide ceramics under cyclic/static axial loading at ultra-high temperature
[DE90-503402] 20 p2839 N90-26147
A study of the elastic properties of Al2O3 and Si3N4 matrix composites with SiC whisker reinforcement
[DE90-013674] 21 p2970 N90-26882
High temperature strength of SiC whisker-reinforced silicon nitride composites
[DE90-013822] 21 p2970 N90-26883
Study on failure modes of SiC fiber reinforced aluminum composite materials by AE method
[DE90-505518] 21 p2971 N90-26884
Interfacial studies of Chemical Vapor Infiltrated (CVI) ceramic matrix composites
[AD-A221867] 21 p2972 N90-26893
Study of the behavior of Al metallic matrix + SiC composite materials under fatigue tests
[ETCA-89-R-077] 22 p3154 N90-27881
Ascertaining the fracture toughness of ceramic materials by means of bending testpieces of various notch types at ambient and high temperatures
[ESA-TT-992] 23 p3312 N90-28733
Improved silicon carbide for advanced heat engines
[NASA-CR-182186] 23 p3313 N90-28735
The friction and wear of lubricated Si3N4/SiC(w) composites
[DE90-015790] 24 p3444 N90-29448
Microstructure of alpha-Al base matrix/SiC particulate composites
[DE90-014894] 24 p3444 N90-29449
Characterization of unnotched SCS-6/Ti-15-3 metal matrix composites at 650 C
[NASA-TM-102699] 24 p3444 N90-29450

SILICON COMPOUNDS
NT BERYL
NT DISILICIDES
NT KAOLINITE
NT ORGANIC SILICON COMPOUNDS
NT QUARTZ
NT SILANES
NT SILICATES
NT SILICIDES
NT SILICON CARBIDES
NT SILICON DIOXIDE
NT SILICON NITRIDES
NT SILICON OXIDES
NT YTTRIUM-ALUMINUM GARNET
NT YTTRIUM-IRON GARNET
NT ZEOLITES

Reactions of hydrogen chloride and boron trichloride with trimethylsilylamino groups
[AD-A209006] 01 p0038 N90-10209
Bonding in transition metal silyl dimers. Molecular orbital theory
[AD-A208269] 01 p0046 N90-10260
Y-Si-Al-O-N glass fibers
[AD-A211170] 02 p0190 N90-11088
Research on amorphous silicon-germanium alloys for tandem solar cells
[DE89-009436] 07 p0950 N90-15499
Fabrication of nanometer single crystal metallic CoSi2 structures on Si
[NASA-CASE-NPO-17736-1-CU] 09 p1286 N90-17455
Thermochemical data for silicon-containing species from ab initio electronic structure calculations
[DE90-011024] 24 p3446 N90-29463

SILICON CONTROLLED RECTIFIERS
Integrated technology in MCT/GaAs and MCT/Si for medium and long wavelength infrared
[AD-A223557] 24 p3552 N90-30100

SILICON DIOXIDE
NT QUARTZ

Attenuated total reflection FTIR spectroscopy for measuring interfacial reaction kinetics at silica surfaces
[AD-A210314] 01 p0041 N90-10224
Analysis of surface modified colloidal silicas
[DE89-015849] 01 p0047 N90-10267
Silicon dioxide deposition at 100 deg C using vacuum ultraviolet light
[TR-0088(3945-07)-6] 01 p0047 N90-10269
A diffuse reflectance infrared Fourier transform spectroscopic study of adsorbed hydrazines 02 p0205 N90-11170
NBS/BAM (National Bureau of Standards/Bundesanstalt fuer Materialprufung) 1986 Symposium on Advanced Ceramics
[PB89-229074] 04 p0479 N90-12747
Unified model of charge build up and annealing of oxide charge and interface states in SiO2 due to stress
[HMI-B-465] 05 p0704 N90-14120
X ray reflectivity study of SiO2 on Si
[DE90-001326] 06 p0851 N90-14943
Laser glass (1989)
[DE90-002754] 07 p0909 N90-15257
Characterization of B and N implanted fused silica
[DE90-004198] 08 p1050 N90-16069
Electron-beam induced damage in thin insulating films on compound semiconductors
[NASA-CR-185177] 10 p1378 N90-17987
Investigation of low temperature multilevel dielectrics for application for radiation tolerant, submicron-scaled IC technology
[AD-A216114] 10 p1433 N90-18273
The improved adhesion of organic polymers to silica and to aluminum metal with zirconium Schiff-base block copolymer coatings
[AD-A216669] 11 p1490 N90-18575
Elastic properties of silica xerogels
[AD-A216528] 12 p1630 N90-19366
Radiation-induced density changes and creep in surface layers of glass
[DE90-008112] 12 p1633 N90-19383
Growth and characterization of gallium (III) oxide films
[AD-A217568] 12 p1723 N90-19902
Mechanisms of reactive etching
[AD-A217679] 13 p1770 N90-20160
Hydrous metal oxide-supported catalysts. Part 1: Preparation chemistry and physical and chemical properties
[DE90-007607] 13 p1771 N90-20161
Interaction between implanted ions and intrinsic defects in silica
[DE90-006569] 13 p1892 N90-20858
In-situ differential reflectance study of the etching of SiO2 films
[AD-A217186] 13 p1893 N90-20864
On the stability of amorphous silica coatings for high temperature service
[AERE-R-13425] 14 p1953 N90-21179
Methods for improving the flowability of a percussion primer composition
[MRL-TR-89-32] 14 p1956 N90-21201
Polysiloxanes derived from the controlled hydrolysis of tetraethoxysilane as precursors to silica for use in ceramic processing
[NASA-TM-102489] 15 p2070 N90-21858
Fast acting optical beam deflection system
[AD-A220186] 17 p2473 N90-24141
Investigations of laterally coupled all optical switches and detectors on silica fibers
[AD-A220297] 17 p2473 N90-24142
Mechanical properties of silica coatings
[DE90-012721] 20 p2837 N90-26138
Fractal structure and fractal time in silica sol-gels
[DE90-013197] 20 p2838 N90-26144
Understanding silica binders
[PNR90625] 20 p2840 N90-26150
Surface acoustic wave filters in ZnO-SiO2-Si layered structures: Design, technology, and monolithic integration with electronic circuitry
[ETN-90-97218] 20 p2924 N90-26638
Measurements of energy dispersion at liquid-solid interfaces: Fluorescence quenching of pyrene bound to fumed silica
[AD-A222371] 21 p2978 N90-26926
Construction of a UV cell for micro-liquid chromatography
[PML-1989-B] 22 p3156 N90-27894
Damage resistant optical coatings prepared using high temperature, plasma chemical-vapor-deposition
[DE90-015042] 23 p3313 N90-28738
Rheology of filler rubber: Silica-silicone
[AD-A223600] 24 p3455 N90-29511
Effect of particulate fillers on the rheology of polymer melts
[AD-A223601] 24 p3455 N90-29512

SILICON FILMS
Characterization of diamond films by thermogravimetric analysis and infrared spectroscopy
[AD-A210564] 01 p0050 N90-10288
Self-assembled organic monolayer films
[AD-A212006] 03 p0323 N90-11838
Spectroscopic ellipsometry characterization of CVD deposition and doping of polysilicon multilayer structures
[RSRE-MEMO-4258] 04 p0466 N90-12671
Tunneling microscopy of superconductors and tunneling barriers
[AD-A212120] 04 p0559 N90-13257
Novel in situ spectroscopic ellipsometer for real time analysis of CVD diamond films
[AD-A213218] 05 p0644 N90-13762
Instability of a-Si:H/Ag interface at 150 deg C
[DE89-009419] 07 p0950 N90-15498
Plasma assisted chemical vapor deposition of diamond films
[AD-A214641] 09 p1197 N90-16934
Direct glassing of silicon solar cells 10 p1341 N90-17769
Hydrogenated amorphous silicon films prepared by glow discharge of disilane
[DE90-000309] 11 p1491 N90-18581
Preparation and characterization of alumina films prepared by a novel spray pyrolysis method
[AD-A217570] 12 p1625 N90-19339
In-situ differential reflectance study of the etching of SiO2 films
[AD-A217186] 13 p1893 N90-20864
Advanced gas phase reactor for growth of Ge sub x Si sub 1-x
[AD-A219012] 16 p2323 N90-23250
Reactions of silane in active nitrogen
[AD-A220371] 17 p2373 N90-23511
Diagnostics of glow discharges used to produce hydrogenated amorphous silicon films
[DE90-000329] 18 p2522 N90-24402

SILICON ISOTOPES
Thermal stability of the carbon-carbon bond in ethylene adsorbed on Si(100): An isotopic mixing study
[AD-A211591] 04 p0470 N90-12691
Studies of elastic scattering and cross sections of the C-12 + Si-28 system
[DE89-635990] 08 p1120 N90-16486
Large-angle elastic and inelastic scattering of Pi+ and Pi- from Si28 and Ca40
[AD-A218163] 13 p1885 N90-20818
Strangeness enhancement in 14.6 A GeV/c Si+Au interactions?
[DE90-008826] 14 p2026 N90-21616
Studies of central interactions of Si ions at 14.5 x A GeV/c in Au and Cu
[DE90-015095] 23 p3397 N90-29195

SILICON JUNCTIONS
Preparation and characterization of alumina films prepared by a novel spray pyrolysis method
[AD-A217570] 12 p1625 N90-19339
Tunneling microscopy of submonolayer adsorbates on Si3
[AD-A216985] 12 p1719 N90-19876

SILICON NITRIDES
Combining spontaneous molecular assembly with microfabrication to pattern surfaces: Selective binding of isonitriles to platinum microwires and characterization by electrochemistry and surface spectroscopy
[AD-A209528] 01 p0039 N90-10213
New polymer precursors to boron and silicon nitrides
[AD-A210287] 01 p0049 N90-10279
Low temperature processing of reaction sintered silicon nitride
[DE89-017455] 02 p0191 N90-11092
The Si(1-x)Nx Rugate
[AD-A211236] 02 p0275 N90-11572

Flexure strength of advanced ceramics: A round robin exercise
[AD-A212101] 03 p0332 N90-11889
Effects of hot corrosion on the room temperature strength of structural ceramics
[AD-A212568] 04 p0481 N90-12762
Oxidation effects on the mechanical properties of SiC fiber-reinforced reaction-bonded silicon nitride matrix composites
[NASA-TM-102360] 06 p0736 N90-14287
Strength and toughness of monolithic and composite silicon nitrides
[NASA-TM-102423] 06 p0751 N90-14368
Process monitoring using optical ultrasonic wave detection
[DE90-002021] 06 p0838 N90-14870
Effects of filament-matrix interfaces on the mechanical properties of SiC-reinforced Si3N4: A review
[DE90-001863] 07 p0890 N90-15144
Ceramic technology for advanced heat engines project
[DE90-001852] 07 p0908 N90-15251
IEA/Annex 2 powder characterization cooperative program
[AD-A213540] 07 p0911 N90-15271
Study of silicon nitride pH response to the fabrication of microelectronic sensors
[LAAS-89229] 08 p1042 N90-16023
Cyclic fatigue of hot-isostatic-pressed silicon nitride
[PB90-122649] 08 p1090 N90-16308
Chemical profiling of silicon nitride structures
[AD-A215643] 09 p1192 N90-16907
Electron-beam induced damage in thin insulating films on compound semiconductors
[NASA-CR-185177] 10 p1378 N90-17987
Silicon carbo-nitride ceramic matrix composites by polymer pyrolysis 11 p1477 N90-18499
Mechanical properties and microstructure of Si3N4-whisker-reinforced Si3N4 matrix composite
[DE90-005651] 11 p1480 N90-18518
Comparison of tension, compression, and flexure creep for alumina and silicon nitride ceramics
[DE90-006154] 11 p1492 N90-18586
Synthesis of high-purity sinterable silicon nitride powder
[DE90-007050] 11 p1493 N90-18593
Microstructural characterization of silicon nitride ceramics processed by pressureless sintering, overpressure sintering, and sinter/HIP
[DE90-007126] 11 p1493 N90-18594
Biaxial strength and stress rupture of hot-pressed silicon nitride
[AD-A216950] 11 p1519 N90-18750
Identification and development of optimum SiC whiskers for silicon nitride matrix composites
[DE90-006888] 12 p1621 N90-19315
Fracture strength analysis of silicon nitride and silicon carbide ceramics from an international cooperative research program
[DE90-005319] 12 p1630 N90-19368
Research advances in fine ceramics
[DE90-008983] 14 p1956 N90-21197
Matrix density effects on the mechanical properties of SiC/RBSN composites
[NASA-TM-103098] 15 p2065 N90-21826
On the design and development of a miniature ceramic gimbal bearing 15 p2115 N90-22100
Crack detection in silicon nitride by acoustic microscopy
[AERE-R-13196] 16 p2245 N90-22803
Reactions of silane in active nitrogen
[AD-A220371] 17 p2373 N90-23511
Fracture mechanism maps for advanced structural ceramics. Part 1: Methodology and hot-pressed silicon nitride results
[AD-A220428] 17 p2380 N90-23556
Theory and experimental technique for nondestructive evaluation of ceramic composites
[NASA-TM-102561] 17 p2414 N90-23754
Influence of interfacial shear strength on the mechanical properties of SiC fiber reinforced reaction-bonded silicon nitride matrix composites
[NASA-TM-102462] 18 p2518 N90-24382
Ceramic technology for advanced heat engines project data base
[DE90-011491] 18 p2532 N90-24448
Crack bridging processes in toughened ceramics
[DE90-011650] 19 p2678 N90-25231
The interaction of polymeric materials with ceramic surfaces with special reference to the behaviour of bioceramics 20 p2836 N90-26127
Tensile strength measurement techniques for structural ceramics
[DE90-012193] 20 p2837 N90-26136
Influence of the manufacturing conditions on the microstructure and mechanical properties of the silicon nitride
[ISAL-90-0008] 20 p2840 N90-26154
Polymeric aluminasilazane precursors for aluminosilicon nitride
[AD-A222755] 20 p2841 N90-26158
A study of the elastic properties of Al2O3 and Si3N4 matrix composites with SiC whisker reinforcement
[DE90-013674] 21 p2970 N90-26882
High temperature strength of SiC whisker-reinforced silicon nitride composites
[DE90-013822] 21 p2970 N90-26883
Self-lubricating surfaces by ion beam processing
[AD-A222489] 21 p3011 N90-27118
Reliability analysis of a structural ceramic combustion chamber
[NASA-TM-103264] 22 p3192 N90-28112
Microdamage to ceramic surfaces under sliding conditions 23 p3308 N90-28708
Ascertaining the fracture toughness of ceramic materials by means of bending testpieces of various notch types at ambient and high temperatures
[ESA-TT-992] 23 p3312 N90-28733
Influence of diesel engine exposure on the rupture strength of silicon nitride and partially stabilized zirconia
[DE90-014759] 23 p3334 N90-28849
The friction and wear of lubricated Si3N4/SiC(w) composites
[DE90-015790] 24 p3444 N90-29448

SILICON OXIDES
NT QUARTZ
NT SILICON DIOXIDE
Instability of the behavior of high resistivity silicon detectors due to the presence of oxide charges
[REPT-89-038] 04 p0559 N90-13260
SiO overcoating and polishing of CFRP telescope panels 05 p0599 N90-13478
Synthesis of inorganic polymers as glass precursors and for other uses. Preceramic block or graft copolymers as potential precursors to nanocomposite materials
[AD-A211978] 05 p0626 N90-13655
Ordered ceramic membranes
[DE89-017426] 06 p0750 N90-14364
A new interpretation of the feature of SiO maser spectra associated with M-type star
[DE90-610641] 11 p1590 N90-19174
Experimentally determined wear behavior of an Al2O3-SiC composite from 25 to 1200 C
[NASA-TM-102549] 13 p1765 N90-20130
SiO(x) precipitation: Defect density correlation with the n+ substrate resistivity
[DE90-005593] 13 p1895 N90-20878
Properties of films prepared from low surface area/density alumina-silica
[DE90-011048] 18 p2531 N90-24446
Mechanical properties of coatings and interfaces
[DE90-012726] 20 p2838 N90-26139

SILICON POLYMERS
NT SILICONE RESINS
NT SILICONES
NT SILOXANES
Characterization of 4/3 technology large-scale integrated circuit on polysilicon processes
[BDX-613-3971] 01 p0059 N90-10335
Structure/reactivity relationships of polysilazane preceramics
[AD-A212028] 03 p0332 N90-11888
Boron-containing organosilane polymers and ceramic materials thereof
[NASA-CASE-ARC-11649-2-SB] 14 p1952 N90-21177
Durable heat diaphragm from ordered polymer films
[AD-A220794] 17 p2381 N90-23559
One-dimensional sigma-conjugated polysilylenes: Science and technology
[DE90-012902] 20 p2839 N90-26146
Polymeric aluminasilazane precursors for aluminosilicon nitride
[AD-A222755] 20 p2841 N90-26158
Catalytic synthesis of polymethylsilsesquioxanes
[AD-A222643] 22 p3159 N90-27910

SILICON SOLAR CELLS
U SOLAR CELLS

SILICON TRANSISTORS
NT SOS (SEMICONDUCTORS)
A gate array structure for the efficient project of digital circuits: The unit cell array
[ETN-90-95364] 12 p1653 N90-19502
Integrated silicon flow sensors
[ETN-90-96906] 17 p2407 N90-23715

SILICON-ON-INSULATOR SEMICONDUCTORS
U SOI (SEMICONDUCTORS)

SILICON-ON-SAPPHIRE JUNCTIONS
U SOS (SEMICONDUCTORS)

SILICON-ON-SAPPHIRE SEMICONDUCTORS
U SOS (SEMICONDUCTORS)

SILICON-ON-SAPPHIRE TRANSISTORS
U SOS (SEMICONDUCTORS)

SILICONE RESINS
Rheology of filler rubber: Silica-silicone
[AD-A223600] 24 p3455 N90-29511

SILICONES
NT SILOXANES
Equilibrium swelling of elastomeric materials in solvent environments
[DE90-010164] 18 p2529 N90-24430

SILOXANES
Synthesis and high temperature chemistry of methylsilsesquioxane polymers produced by titanium catalyzed redistribution of methylhydridooligo- and polysiloxanes
[AD-A212000] 04 p0477 N90-12736
High temperature insulators
[AD-D014193] 04 p0479 N90-12751
Amperometric biosensors for glucose, lactate, and glycolate based on oxidases and redox-modified siloxane polymers
[DE90-002301] 06 p0781 N90-14541
Ceramic processing using inorganic polymers
[DE90-003638] 07 p0911 N90-15268
The structure of silica-polysiloxane composites and its effects on their elastomeric properties
[DE89-014768] 08 p1039 N90-16005
Synthesis of poly(dimethylsiloxane) - nylon 6 diblock copolymers
[AD-A216850] 12 p1630 N90-19367
Sol-gel derived polytitanosiloxane coatings
[DE90-004186] 13 p1779 N90-20210
X ray specular reflection studies of silicon coated by organic monolayers (alkylsiloxanes)
[AD-A217418] 13 p1779 N90-20213
Polysiloxanes derived from the controlled hydrolysis of tetraethoxysilane as precursors to silica for use in ceramic processing
[NASA-TM-102489] 15 p2070 N90-21858
Synthesis and characterization of aromatic polyester and polysiloxane containing block copolymers: Multiphase transparent atomic oxygen resistant damping materials, liquid crystal films, and toughening components of sol/gel glasses
[AD-A218871] 16 p2224 N90-22685
Novel side-chain liquid cyrstalline polymers
[AD-A221998] 22 p3159 N90-27911
Effect of particulate fillers on the rheology of polymer melts
[AD-A223601] 24 p3455 N90-29512

SILTS
U SEDIMENTS

SILVER
Multiple internal reflection Fourier transform infrared spectroscopy studies of thiocyanate adsorption on silver and gold
[AD-A210245] 01 p0041 N90-10223
Temperature dependent effects during Ag deposition on Cu(110)
[DE89-016987] 03 p0327 N90-11857
Silver composite cathodes for alkaline secondary batteries
[AD-D014227] 06 p0767 N90-14462
Silver-nickel composite cathodes for alkaline secondary batteries
[AD-D014231] 06 p0767 N90-14464
Shock-induced defects and flux pinning in YBa2Cu3O sub 7-delta + Ag composites
[DE90-000827] 06 p0853 N90-14960
Solid lubrication of ceramic surfaces by IAD (Ion-Assisted Deposition)-silver coatings for heat engine applications
[DE90-002860] 07 p0909 N90-15253
Instability of a-Si:H/Ag interface at 150 deg C
[DE89-009419] 07 p0950 N90-15498
Rapidity densities and their fluctuations in central 200 A GeV S32 interations with Au and Ag,Br nuclei
[LUIP-8905] 07 p0989 N90-15715
Long term creep strength of silver alloyed copper
[DE90-602367] 08 p1045 N90-16039
Adhesion of silver films to ion-bombarded alumina
[DE90-005642] 09 p1199 N90-16947
High-temperature deformation of YBa2Cu3O(7-delta) with Ag additions
[DE90-004884] 09 p1292 N90-17491
Surface-enhanced Raman scattering from model acrylic adhesive systems
[AD-A216117] 10 p1359 N90-17883
Polymerization of nitro compounds on silver surfaces during surface-enhanced Raman scattering
[AD-A216116] 11 p1489 N90-18569
Time-dependent failure of silver interlayer welds
[DE90-008015] 13 p1818 N90-20440

Surface-plasmon enhanced nonlinear photoelectric emission from thin silver films
[DE90-007676] 13 p1884 N90-20807
An investigation of the dislocation structure of the Ni/Ag phase boundary
[DE90-008428] 13 p1895 N90-20876
Determination of internal strains in high-temperature superconductor composites by intense pulsed neutron source
[DE90-007799] 14 p2033 N90-21664
Ambient-temperature creep failure of silver-aided diffusion bonds between steel
[DE90-010687] 18 p2527 N90-24420
Effect of film adhesion on tribological properties of silver-coated alumina
[DE90-010090] 18 p2564 N90-24632
Atomic structure of Ag/Ni interfaces
[DE90-010053] 18 p2618 N90-24914
Highly-textured thallium-barium-calcium-copper-oxide polycrystalline superconducting films on silver substrates
[DE90-011972] 18 p2627 N90-24970
Molecular structure of interphases between DGEBA/BTDA adhesives and silver substances using surface-enhanced Raman scattering
[AD-A222750] 20 p2841 N90-26157
SDIO/IST ultrashort wavelength laser: Novel experimental schemes for observing the Moessbauer effect in long-lived nuclear levels and nuclear coherent states
[AD-A222607] 20 p2868 N90-26316
Characterization of polymer interphases using surface-enhanced Raman scattering
[AD-A223103] 21 p2985 N90-26965
Characterization of model polyimide/silver interphases using surface-enhanced Raman scattering
[AD-A222488] 21 p2988 N90-26979
Self-lubricating surfaces by ion beam processing
[AD-A222489] 21 p3011 N90-27118
Hyperthermal atomic oxygen generator
[NASA-CR-186573] 22 p3155 N90-27889
Ion-beam-assisted deposition of silver films on zirconia ceramics for improved tribological behavior
[DE90-009706] 24 p3456 N90-29516
Adhesion of silver films to ion-bombarded zirconia
[DE90-010088] 24 p3456 N90-29517

SILVER COMPOUNDS
NT SILVER HALIDES
NT SILVER NITRATES
NT SILVER OXIDES
Phase equilibrium and crystal growth studies on AgGaSe2 and related nonlinear optical materials
[AD-A213650] 07 p1003 N90-15809
Fundamental studies of surface processes and trace analysis using solid electrodes
[AD-A216538] 11 p1483 N90-18533

SILVER HALIDES
Design and construction of systems for the single-crystals growth of ternary silver halides, alkali halides, and alkaline earth fluorides, and the dielectric investigation of silver halide
[ETN-89-94673] 02 p0286 N90-11632

SILVER NITRATES
Silver-nickel composite cathodes for alkaline secondary batteries
[AD-D014231] 06 p0767 N90-14464
Silver coated superconducting ceramic powder
[AD-D014300] 07 p0913 N90-15278

SILVER OXIDE ZINC BATTERIES
U SILVER ZINC BATTERIES

SILVER OXIDES
Electrochemical preparation of silver oxide electrodes having high thermal stability
[AD-D014224] 06 p0767 N90-14460

SILVER ZINC BATTERIES
Liquid Rocket Booster (LRB) for the Space Transportation System (STS) systems study. Appendix C: Battery report for the liquid rocket booster TVC actuators
[NASA-CR-183789-APP-C] 23 p3288 N90-28603

SIMD (COMPUTERS)
Evaluating local indirect addressing in SIMD proc essors
[NASA-CR-181845] 01 p0103 N90-10581
The 2nd Symposium on the Frontiers of Massively Parallel Computations
[NASA-TM-101918] 08 p1113 N90-16442
How to cluster in parallel with neural networks 08 p1113 N90-16443
Overview and extensions of a system for routing directed graphs on SIMD architectures 08 p1113 N90-16444
Sort computation 08 p1113 N90-16446
Scan line graphics generation on the massively parallel processor 08 p1114 N90-16450
Parallelizing the SDI ACCESS algorithm for the Connection Machine-2
[DE90-006382] 11 p1548 N90-18909
Massively-parallel computational fluid dynamics
[AD-A217732] 13 p1802 N90-20342
Characterization of robotics parallel algorithms and mapping onto a reconfigurable SIMD machine 16 p2289 N90-23039
Special purpose parallel computer architecture for real-time control and simulation in robotic applications
[NASA-CASE-NPO-17629-1-CU] 21 p3038 N90-27268

SIMICOR (IMAGE CORRELATOR)
U IMAGE CORRELATORS

SIMILARITIES
U ANALOGIES

SIMILARITY NUMBERS
On the application of similarity laws to a scaled railway bogie model
[DLR-FB-90-06] 23 p3335 N90-28853

SIMPLEX METHOD
Finite methods for a nonlinear allocation problem
[AD-A209719] 01 p0111 N90-10629
Linear programming tools for integer programming
[AD-A219013] 16 p2300 N90-23106
Frequency assignments for HFDF receivers in a search and rescue network
[AD-A220529] 17 p2390 N90-23610
A block-LU update for large-scale linear programming
[AD-A219849] 18 p2590 N90-24738

SIMPLIFICATION
Decomposition for optimal synthesis in a parallel computing environment 10 p1419 N90-18184
Two-dimensional surface strain measurement based on a variation of Yamaguchi's laser-speckle strain gauge
[NASA-TM-103162] 16 p2241 N90-22784
Multivariable frequency weighted model order reduction for control synthesis
[AIAA-89-3558] 16 p2292 N90-23060
On simplified analytical flutter clearance procedures for light aircraft
[DLR-FB-89-56] 18 p2498 N90-24276
Effects of simplifying assumptions on optimal trajectory estimation for a high-performance aircraft
[NASA-TM-101721] 19 p2661 N90-25142
Specification for HF Lowest Usable Frequency (LUF) model
[AD-A222114] 21 p2996 N90-27031

SIMULATED ALTITUDE
U ALTITUDE SIMULATION

SIMULATION
NT ACOUSTIC SIMULATION
NT ALTITUDE SIMULATION
NT ANALOG SIMULATION
NT ATMOSPHERIC ENTRY SIMULATION
NT COMPUTER SYSTEMS SIMULATION
NT COMPUTERIZED SIMULATION
NT CONTROL SIMULATION
NT DIGITAL SIMULATION
NT ENVIRONMENT SIMULATION
NT EXHAUST FLOW SIMULATION
NT FLIGHT SIMULATION
NT LANDING SIMULATION
NT MOTION SIMULATION
NT NEUTRAL BUOYANCY SIMULATION
NT RHEOELECTRICAL SIMULATION
NT SOLAR SIMULATION
NT SPACE ENVIRONMENT SIMULATION
NT SYSTEMS SIMULATION
NT THERMAL SIMULATION
NT WEIGHTLESSNESS SIMULATION
Basic studies of the unsteady flow past high angle of attack airfoils
[AD-A210252] 01 p0002 N90-10008
Study of the NO3 radical decomposition reaction and the N2O5 in equilibrium with NO3 + NO2 equilibrium constant
[PB89-208961] 01 p0085 N90-10480
Numerical simulations of a midlatitude squall line 01 p0087 N90-10497
Discrete-time conversion for simulating finite-horizon Markov processes
[AD-A210683] 01 p0116 N90-10666
Markov chain moment formulas for regenerative simulation
[AD-A210684] 01 p0116 N90-10667
Particle kinetic simulation of high altitude hypervelocity flight
[NASA-CR-186003] 02 p0147 N90-10840
Deployment simulation for 3rd generation solar array GSR3 02 p0188 N90-11074
Study of the application of automation to composites manufacture
[AD-A211049] 02 p0190 N90-11087
Atmospheric chemistry of the fuel hydrazines 02 p0203 N90-11158
Numerical simulation of hydrazine transport in a sandy soil 02 p0205 N90-11172
Simulation of synthetic aperture radar 1: Feature density and accuracy requirements
[AD-A211019] 02 p0213 N90-11218
Internal voltages and currents in well-shielded cylindrical objects due to simulated direct-strike lightning
[DE89-012664] 02 p0215 N90-11231
Modeling and simulation of spatial robotic manipulators with flexible links and joint drives for control strategies implementation and evaluation 02 p0228 N90-11311
A re-evaluation of fatigue threshold test procedures and the simulation and prediction of fatigue crack growth under conditions of low crack closure 02 p0231 N90-11328
Development of an approximate technique for the nonlinear random vibrations analysis of hysteretic systems 02 p0233 N90-11335
Definition of imaging performance for satellite surveillance, models, and simulations
[FOA-C-30493-9.4] 02 p0236 N90-11341
ANTHEM simulation of the early time magnetic field penetration of the plasma surrounding a high density Z-pinch
[DE89-016980] 02 p0277 N90-11585
A fully electromagnetic hybrid model for high density plasma simulations
[DE89-016771] 02 p0279 N90-11593
Computation of ramjet internal flowfields
[AD-A212001] 03 p0307 N90-11743
Evaluation of the near-wall k-epsilon turbulence model by comparison with direct simulations of turbulent channel flow
[AD-A212674] 04 p0503 N90-12903
A simulation study of the overdetermined geodetic boundary value problem using collocation
[AD-A211785] 04 p0518 N90-12990
Work-preserving emulations of fixed-connection networks
[AD-A211915] 04 p0535 N90-13093
Note on the convergence of simulated annealing algorithms
[MEMO-774] 04 p0544 N90-13162
LORAN C stability integrity assurance
[AD-A212663] 05 p0577 N90-13364
True covariance simulation of the EUVE update filter 05 p0589 N90-13427
Recovery of particle size distribution of ultrafine aerosols from diffusional decay measurements
[AD-A213006] 05 p0621 N90-13621
Simulation of the control characteristics of an axial piston pump and a flapper-nozzle valve combination 05 p0649 N90-13784
Air quality simulation model performance for one-hour averages
[PB89-233506] 05 p0665 N90-13890
The structural memory: A network model for human perception of serial objects
[CWI-CS-R8829] 05 p0675 N90-13930
SIMOGEN: An object-oriented language for simulation
[AD-A213129] 05 p0682 N90-13973
Why stochastic modeling is essential in analyzing interdicted transportation network performance
[AD-A213140] 05 p0688 N90-14007
Identification of impulsive interference channels
[AD-A213154] 05 p0688 N90-14009
Global optimization and simulated annealing
[MEMO-COSOR-88-21] 05 p0690 N90-14025
Analysis of three approaches to qualitative simulation
[MEMO-INF-89-32] 05 p0691 N90-14035
Evaluation of the indirect effects of lightning on a system: Double transfer function method
[RAE-TRANS-2172] 06 p0721 N90-14211
Design of a compensation filter for a quadratic phase communication channel 06 p0761 N90-14428
Thermocapillary migration of liquid droplets in a temperature gradient in a density matched system
[NASA-CR-185178] 06 p0776 N90-14512
Granular flow: Numerical simulation of dry granular flows and calculation of hydrodynamic interactions in suspensions
[DE89-017544] 06 p0777 N90-14518
Technology development program for an advanced microsheet glass concentrator
[NASA-TM-102406] 06 p0804 N90-14678
A model for the simulation of the ozone budget in the atmosphere under anthropogenic perturbation
[DE89-636294] 06 p0811 N90-14719
The dynamics of simulated convective storms in hurricane environments 06 p0816 N90-14747
Tuning of the OSCURS (Ocean Surface Current Simulations) numerical model to ocean surface measurements in the Gulf of Alaska
[PB89-103979] 06 p0818 N90-14759
Engineering sciences design. Design and implementation of components for a bioregenerative system for growing higher order plants in space
[NASA-CR-186056] 06 p0819 N90-14761

Path integral simulations of liquid helium
[DE90-001171] 06 p0836 N90-14862
Principal characteristics of lightning on aircraft
07 p0874 N90-15067
Using small scale tests to estimate the failure diameter of a propellant
[DE90-001166] 07 p0913 N90-15281
Network simulator definition
[AD-A213463] 07 p0918 N90-15308
Baseband development system implementation
[AD-A213464] 07 p0918 N90-15309
On the domain of dominance of the asymptotic elastodynamic crack-tip fields 07 p0944 N90-15468
Calculation of source and structure parameters at regional and teleseismic distances
[AD-A214297] 07 p0961 N90-15558
Molecular-dynamics study of the amorphization of CuTi
[DE90-003563] 07 p1001 N90-15791
Laboratory simulations of the solar wind-comet interactions 07 p1015 N90-15875
Hybrid LZW compression 08 p1076 N90-16223
Load-shortening behavior of an initially curved eccentrically loaded column
[NASA-TM-101643] 08 p1088 N90-16293
An introduction to shaker shock simulations
[DE90-003057] 08 p1088 N90-16298
Numerical simulation of creep crack growth experiments
[IWM-W-4/88] 08 p1089 N90-16303
Stochastic simulation of charged particle transport on the massively parallel processor
08 p1114 N90-16448
Complex availability problems solved with simulation
[DE89-012610] 08 p1116 N90-16459
Modifications of comet materials by the sublimation process: Results from simulation experiments
08 p1142 N90-16621
Radiation modification of cometary materials: Laboratory simulations 08 p1143 N90-16626
Thermal histories of the samples of two KOSI comet nucleus simulation experiments
08 p1147 N90-16645
Stochastic models in reliability
[AD-A215479] 09 p1234 N90-17163
Numerical modeling of the atmosphere with an isentropic vertical coordinate 09 p1246 N90-17226
EDISON Project
[AD-A214724] 09 p1265 N90-17338
Simulation of rough surface scattering in three-dimensions
[AD-A215171] 09 p1277 N90-17405
Variational problems in astrophysics
09 p1298 N90-17524
Simulation of shading in synthetic surfaces
[INPE-4869-PRE/1480] 10 p1326 N90-17660
The design and performance of a general purpose 57 kilowatt solar array simulator for current and future large spacecraft 10 p1330 N90-17685
LMSS modeling status report
10 p1372 N90-17953
Multiple symbol differential detection of uncoded and trellis coded MPSK
[NASA-CR-186288] 10 p1376 N90-17975
Finite element modeling and thermal simulations of transistor integrated circuits
[AD-A215928] 10 p1380 N90-17997
Scuffing modelling and experiments for heavily loaded elastohydrodynamic lubrication contacts
10 p1391 N90-18047
Estimation in a discrete tail rate family of recapture sampling models
[NASA-CR-180452] 10 p1421 N90-18197
Dallas/Fort Worth simulation. Volume 2: Appendixes D, E, and F
[AD-A216613] 11 p1454 N90-18380
Space-based radar simulation laboratory
[AD-A216722] 11 p1497 N90-18618
A self-organizing multiple-view representation of three-dimensional objects
[AD-A216711] 11 p1541 N90-18871
Log-based recovery in asynchronous distributed systems
[NASA-CR-186190] 11 p1550 N90-18924
Hamiltonian analysis and simulation of free electron lasers
[INPE-4785-TDL/351] 11 p1567 N90-19018
Simulation of thermal dynamics of a vaporizing coal-water droplet in a combustor
[DE90-005356] 12 p1621 N90-19317
Kalman estimation for SEDS measurements
12 p1634 N90-19393
Parallel distributed networks for image smoothing and segmentation in analog VSLI
[AD-A216780] 12 p1651 N90-19491
Test component attachment effects on resonant plate pyrotechnic shock simulation
[DE90-006478] 12 p1662 N90-19551
Regional climate change predictions from the Goddard Institute for Space Studies high resolution GCM
[NASA-CR-186375] 12 p1693 N90-19725
Simulation fidelity in lightning penetration studies
[DE90-006367] 12 p1694 N90-19731
Recalibrating software reliability models
[NASA-CR-186407] 12 p1700 N90-19763
Plasma simulation on magnetohydrodynamic time scales
[DE90-007490] 12 p1718 N90-19865
Microstructural simulations of dynamic recrystallization
[DE90-007504] 12 p1722 N90-19895
Physics and Mechanics of Cometary Materials
[ESA-SP-302] 12 p1738 N90-19989
Thermal conductivities and diffusivities of porous ice samples at low pressures and temperatures and possible modes of heat transfer in near surface layers of comets
12 p1739 N90-19999
Simulation of radar and radiometer signals remote sensing cometary surface and subsurface structures
12 p1740 N90-20005
CO2 depth profiles in cometary model substances of KOSI 12 p1742 N90-20014
Possible targeting of particle emission by mechanical stress and penetration of sublimating ice-dust-surfaces
12 p1742 N90-20016
Mechanical properties of fluffy agglomerates consisting of core-mantle-particles 12 p1743 N90-20019
Dynamics of crust formation and dust emission of comet nucleus analogues under isolation
12 p1743 N90-20020
Evaluation of 2090-T8E48 aluminum-lithium plates
[AD-A217262] 13 p1776 N90-20196
Computational simulation of damping in composite structures
[NASA-TM-102567] 13 p1817 N90-20432
Simulation of landscape disturbances and the effect of climatic change
[DE90-007565] 13 p1829 N90-20503
Design considerations for a space database
13 p1858 N90-20659
The Orbital Maneuvering Vehicle Training Facility visual system concept 13 p1863 N90-20684
Performance tradeoffs in multithreaded processors
[AD-A217123] 13 p1871 N90-20729
High-resolution acoustical imaging
13 p1881 N90-20793
Aperture taper determination for the half-scale accurate antenna reflector
[NASA-CR-185215] 14 p1969 N90-21282
Numerical simulations of the cloud-capped marine boundary layer 14 p2008 N90-21506
Finite element algorithms for hyperbolic conservation laws with forcing terms
[INPE-5024-RPE/617] 14 p2022 N90-21595
New spectral features of stratospheric trace gases
15 p2079 N90-21910
Millimetre-wave propagation in the evaporation duct
15 p2084 N90-21929
The interpretation of SAGE 2 ozone measurements in the lower mesosphere 15 p2124 N90-22149
The role of input weighting and bounding in the characteristic GPC method
[OUEL-1762/89] 15 p2158 N90-22328
An intelligent interface for the design of optimal control systems
[INPE-4917-PRE/1516] 15 p2159 N90-22332
Orthogonal distance regression
[PB90-151747] 15 p2160 N90-22336
Increased stuck-at fault coverage with reduced I(sub DDQ) test sets
[DE90-009509] 16 p2245 N90-22804
Low frequency Raman spectra of liquid water, a molecular dynamics simulation
[PREPRINT-698] 16 p2314 N90-23192
COS-B gamma ray sources beyond the predicted diffuse emission 16 p2335 N90-23308
On the simulation test for the relative motion of separated sub-boosters on M-3S2 with nearly half a model vehicle ST-735 and their motion analyses using inertial sensors output
[ISAS-635] 17 p2366 N90-23471
Object orientated simulation on transputer arrays using time warp
[AD-A219795] 17 p2389 N90-23607
Pulse-width dependent radiation effects on electronic components
[AD-A219517] 17 p2395 N90-23643
Circuit recognition of VLSI layouts
[AD-A219806] 17 p2396 N90-23649
Temperature evolution of single particle correlation functions of TIP4P water
[PREPRINT-694] 17 p2470 N90-24119
Three legged walking mobile platform: Kinematic and dynamic analysis and simulation
[NASA-CR-184929] 18 p2535 N90-24457
Fundamental limitations of qualitative simulation
[MEMO-INF-89-56] 18 p2600 N90-24802
Ground-simulation investigations of VTOL airworthiness criteria for terminal-area operations
[NASA-TM-102810] 19 p2660 N90-25141
Laboratory simulation of the effect of rocket thrust on a precessing space vehicle
[NASA-CR-186681] 19 p2669 N90-25182
The role of gravity on macrosegregation in alloys
[NASA-CR-186530] 19 p2679 N90-25238
Formation of design envelope criterion in terms of deterministic spectral procedure
[RAE-TM-SS-9] 20 p2804 N90-25953
Qualitative evaluation of a conformal velocity vector display for use at high angles-of-attack in fighter aircraft
[NASA-TM-102629] 20 p2809 N90-25981
Comparison of currents predicted by NASCAP/LEO model simulations with elementary Langmuir-type bare probe models for an insulated cable containing a single pinhole
[NASA-TM-102486] 20 p2821 N90-26054
An inverse dynamic method yielding flexible manipulator state trajectories
[NASA-CR-186807] 20 p2870 N90-26329
Biodynamic simulations of an aircraft pilot/passenger in various crash environments
[NIAR-90-6] 20 p2900 N90-26494
Canonical eigenvalues. Part 1: General theory
[AD-A222812] 20 p2920 N90-26617
Analysis of random drop for gateway congestion control
[NASA-CR-186736] 20 p2935 N90-26698
Payload training methodology study
[NASA-CR-183907] 21 p2964 N90-26849
Local design methodologies for a hierarchic control architecture
[AD-A222006] 21 p2966 N90-26862
Direct numerical simulation of compressible free shear flows 21 p2974 N90-26901
Simulation of synthetic aperture radar 4: Summary and recommendations
[AD-A221822] 21 p2997 N90-27038
Numerical method for calculating indoor airflows using a turbulence model
[PB90-162009] 21 p3003 N90-27067
Perspective transformation for wide-view sky scenes
[AD-A222694] 21 p3007 N90-27093
Microscopic modeling of tribological phenomena
[AD-A222049] 21 p3011 N90-27117
Practical issues in the complexity of neural networks
[AD-A221420] 21 p3058 N90-27389
On parallel hashing and integer sorting
[AD-A221569] 21 p3058 N90-27390
Queing networks with finite capacities
[AD-A221547] 21 p3065 N90-27425
The theory and simulation of plasmoid formation and propagation
[AD-A222048] 21 p3079 N90-27504
Laboratory simulation of interstellar grain chemistry and the production of complex organic molecules
21 p3092 N90-27580
Impact fracture experiments simulating interstellar grain-grain collisions 21 p3093 N90-27584
Reentry trajectory optimization and control
22 p3127 N90-27746
Hydrocarbon-fueled scramjet combustor component development tests 22 p3162 N90-27934
Higher order diffusion model for a bipolar transistor
[PB90-190901] 22 p3167 N90-27960
Vertical-velocity skewness in the marine stratus-topped boundary layer 22 p3220 N90-28262
Experimental fault characterization of a neural network
[NASA-CR-186885] 22 p3240 N90-28373
A flight dynamic model of aircraft spinning
[AR-005-600] 23 p3283 N90-28576
Overview on hot gas tests and molten salt corrosion experiments at the DLR 23 p3309 N90-28714
Genesis of bow echoes: A rear-inflow induced meso-convective structure
[PB90-209776] 23 p3349 N90-28926
A nonhydrostatic numerical model in sigma-coordinates and simulations of mesoscale phenomena
23 p3350 N90-28932
Design of a monitor and simulation terminal (master) for space station telerobotics and telescience
23 p3372 N90-29051
Comparison of joint space versus task force load distribution optimization for a multiarm manipulator system 24 p3515 N90-29873
Interset: A natural language interface for teleoperated robotic assembly of the EASE space structure
24 p3517 N90-29885

Temporal logics meet telerobotics
24 p3521 N90-29905
Shuttle remote manipulator system mission preparation and operations 24 p3521 N90-29909
Innovative uses of parallel computers
[AD-A223578] 24 p3533 N90-29980

SIMULATOR TRAINING
U TRAINING SIMULATORS

SIMULATORS
NT COCKPIT SIMULATORS
NT CONTROL SIMULATION
NT ENVIRONMENT SIMULATORS
NT FLIGHT SIMULATORS
NT MOTION SIMULATORS
NT SHOCK SIMULATORS
NT SOLAR SIMULATORS
NT SPACE SIMULATORS
NT TARGET SIMULATORS
NT TRAINING SIMULATORS
NT VERTICAL MOTION SIMULATORS
NT VIBRATION SIMULATORS
CONSOLE: A CAD tandem for optimization-based design interacting with user-supplied simulators
01 p0017 N90-10085
Consumer electronics testing to fast-rise EMP (Electromagnetic Pulse) VEMPS (Vertical Electromagnetic Pulse Simulator) 2 development
[AD-A210505] 01 p0057 N90-10323
A simulator for a hydrocarbon ramrocket fuel gas generator: First phase development
[AR-005-621] 02 p0189 N90-11080
Thin section casting program. Volume 2-A: Appendix to volume 2
[DE89-009032] 02 p0210 N90-11200
Human Operator Simulator (HOS) 4 user's guide
[AD-A212007] 03 p0310 N90-11763
Satellite-matrix-switched, time-division-multiple-access network simulator
[NASA-TP-2944] 03 p0336 N90-11915
Satellite range delay simulator for a matrix-switched time division multiple-access network simulator
[NASA-TM-102407] 04 p0489 N90-12813
Implementation issues in source coding
[NASA-CR-185327] 05 p0681 N90-13963
Acoustic-vortical-combustion interaction in a solid fuel ramjet simulator 06 p0726 N90-14234
Design of a bounded wave EMP (Electromagnetic Pulse) simulator
[AD-A214137] 07 p0919 N90-15316
XNUSIM: Graphical interface for a multiprocessor simulator
[AD-A214176] 07 p0971 N90-15606
Knowledge representations for the automatic generation of numerical simulators for PDEs
[DE89-008036] 07 p0972 N90-15615
Application of holography to behavior simulators
[ISL-R-111/88] 09 p1226 N90-17115
Channel simulator upgrade to use field propagation data 10 p1372 N90-17948
LMSS drive simulator for multipath propagation
10 p1372 N90-17950
Performance measurements for a laboratory-simulated 30/20 GHz communication satellite transponder
[NASA-TM-102424] 10 p1376 N90-17977
An Autonomous Platform Simulator (APS)
[AD-A215768] 10 p1392 N90-18048
Aurora upgrade. Volume 5: Machine monitoring and control system
[AD-A215963] 10 p1393 N90-18053
Space-based radar simulation laboratory
[AD-A216722] 11 p1497 N90-18618
Back swing phenomenon of synchronous generator. Study on ac-dc power system simulator tests
[DE89-782321] 11 p1500 N90-18635
SINA: A test system for proximity fuses
[FEL-1989-101] 12 p1653 N90-19498
Lessons learned in the transition to ADA from FORTRAN at NASA/Goddard
[NASA-CR-186458] 12 p1701 N90-19765
Ejection seat training of jet pilots and weapon system officers at the German Air Force School of Aviation Medicine 13 p1752 N90-20061
Fault simulator evaluation
[AD-A217782] 13 p1796 N90-20308
Design considerations for a space database
13 p1858 N90-20659
Prototype part task trainer: A remote manipulator system simulator 13 p1860 N90-20672
SES cupola interactive display design environment
13 p1862 N90-20679
Issues in visual support to real-time space system simulation solved in the Systems Engineering Simulator
13 p1862 N90-20680
History of visual systems in the Systems Engineering Simulator 13 p1862 N90-20681
Computer image generation: Reconfigurability as a strategy in high fidelity space applications
13 p1862 N90-20682
Real-time graphics for the Space Station Freedom cupola, developed in the Systems Engineering Simulator
13 p1862 N90-20683
Simulator comparison of thumball, thumb switch, and touch screen input concepts for interaction with a large screen cockpit display format
[NASA-TM-102587] 14 p1921 N90-21005
CSI technology validation on an LSS ground experiment facility 14 p1937 N90-21089
Lessons learned in the transition to Ada from FORTRAN at NASA/Goddard
[NASA-TM-103311] 14 p2014 N90-21538
Plasma contactor research, 1989
[NASA-CR-185212] 15 p2168 N90-22389
Design and construction of a packed column simulator operating under atmospheric and reduced pressure
[ISAL-89-60] 16 p2236 N90-22757
Numerical study of unsteady flows in large air-driven blast simulators with single and multiple drivers
[UTIAS-334] 17 p2405 N90-23699
FASTER: The Fault Tolerant Architecture Simulation Tool for Evaluating Reliability, introduction and applications
[AD-A219941] 17 p2414 N90-23755
A low NOx strategy for combusting high nitrogen content fuels
[PB90-155664] 19 p2712 N90-25435
A digital Meteor-Burst Communication (MBC) propagation path simulator 20 p2847 N90-26190
A novel communication network simulator
[AD-A223045] 20 p2857 N90-26248
Single-pass memory system evaluation for multiprogramming workloads
[NASA-CR-186553] 20 p2910 N90-26558
Research opportunities on the Space Station
21 p3092 N90-27578
NPL absorbed dose graphite calorimeter correction for the effect of the gaps around the core
[NPL-RSA(EXT)-12] 22 p3178 N90-28032
DEPEND: A design environment for prediction and evaluation of system dependability
[NASA-CR-186890] 22 p3189 N90-28094
DSIM: A distributed simulator
[NASA-CR-186880] 22 p3237 N90-28353
Transonic 3-D Euler analysis of flows around fanjet engine and TPS (Turbine Powered Simulator). Comparison with wind tunnel experiment, evaluation of TPS testing method and 3-D flow
[NAL-TR-1045] 24 p3421 N90-29327
Control of a Cossor CSP1250 ionospheric simulator in an automated HF test bed
[AD-A223446] 24 p3461 N90-29549

SIMULTANEOUS EQUATIONS
NUMVEC FORTRAN library manual chapter: Simultaneous linear equations
[CWI-NM-R8903] 04 p0541 N90-13135
A fast PC-based solver for simultaneous linear equations
[AD-A220190] 17 p2461 N90-24056
The application of the finite element method to an aerodynamic problem specific to propeller design
[LR-614] 19 p2656 N90-25116
A possibility to incorporate saturation in the simple, global model of a synchronous machine with rectifier
[EUT-89-E-225] 20 p2858 N90-26258

SIMULTANEOUS IMAGE CORRELATOR
U IMAGE CORRELATORS

SINE SERIES
Explicitly solvable complex Chebyshev approximation problems related to sine polynomials
[NASA-CR-181575] 17 p2455 N90-24007

SINE WAVES
Comparison of sine dwell and broadband methods for modal testing 02 p0181 N90-11025
The Si(1-x)Nx Rugate
[AD-A211236] 02 p0275 N90-11572
Application of a buck-type MC2 regulated converter for a stepper motor control 10 p1335 N90-17722
Adaptive frequency estimation by MUSIC (Multiple Signal Classification) method
[PB90-166794] 15 p2086 N90-21943
Serrodyning by means of a digital phase shifter
[AD-A219593] 17 p2396 N90-23646
Crash-impact behavior of graphite/epoxy composite sine wave webs 23 p3300 N90-28667

SINGLE CRYSTALS
The measurement of infrared spectra of dense ceramics by specular reflectance spectroscopy
[AD-A210609] 01 p0051 N90-10291
Magnetic correlations in high T(sub c) oxides in the superconducting state
[DE89-016421] 01 p0130 N90-10746
Defect structures preceding amorphization by ion irradiations in YBa2Cu3O(7-delta)
[DE89-016905] 02 p0282 N90-11612
Passage of ultrarelativistic electrons through real crystals
[DE89-618624] 02 p0282 N90-11613
Design and construction of systems for the single-crystals growth of ternary silver halides, alkali halides, and alkaline earth fluorides, and the dielectric investigation of silver halide
[ETN-89-94673] 02 p0286 N90-11632
Process for single crystal growth of high T(sub c) superconductors
[AD-D014167] 03 p0409 N90-12346
Field-assisted bonding of single crystal quartz
[DE89-015407] 03 p0410 N90-12353
Surface, interface, and bulk properties of high T(sub c) superconductors
[AD-A211490] 03 p0413 N90-12373
High temperature superconducting compounds
[AD-A211511] 03 p0413 N90-12374
The effects of trace anions on the voltammetry of single crystal gold surfaces
[AD-A211886] 04 p0558 N90-13254
Magnetic excitations in thulium metal
[DE90-002475] 06 p0855 N90-14970
The influence of the substrate surface on the nucleation and growth of superconducting thin films
[DE90-003649] 06 p0857 N90-14983
Micromechanics of an extrusion in high-cycle fatigue with creep
[AD-A213509] 07 p0947 N90-15485
Superconductivity and stoichiometry in Tl2Ca2Ba2Cu3O(x) single crystals
[DE90-003838] 07 p1002 N90-15801
Eurolaser. High power excimer laser: Optical crystals
[ETN-90-95901] 08 p1132 N90-16558
The effects of oxygen and strontium vacancies on the superconductivity of single crystals of Bi2Sr(2-x)CuO(6-y)
[DE90-004242] 08 p1133 N90-16561
A new approach for the utilization of electron paramagnetic resonance and an investigation of copper oxide superconductors
[AD-A213833] 09 p1277 N90-17404
Fabrication of nanometer single crystal metallic CoSi2 structures on Si
[NASA-CASE-NPO-17736-1-CU]
09 p1286 N90-17455
Oxidation and reduction of Bi2Sr1.85CuO(6-y) crystals
[DE90-004246] 09 p1287 N90-17460
Hardness-damage correlations in Ta implanted single crystal Ni3Al
[DE90-005270] 09 p1293 N90-17494
Epitaxial growth of Cr(011) on LiF(001)
[DE90-005635] 09 p1293 N90-17496
Experiments on large single crystals of the superconducting oxides YBa2Cu3O7, La sub 2-xBa sub xCuO4, and Bi-Ca-Sr-O
[AD-A215283] 10 p1435 N90-18284
Surface intermediates in thin film deposition on silicon
[AD-A216662] 11 p1483 N90-18534
Opto-Em and devices investigation
[AD-A215033] 12 p1709 N90-19814
Search for far infrared radiation from optically pumped defect modes
[AD-A216976] 12 p1714 N90-19843
The preparation and properties of iron doped II-VI chalcogenides
[AD-A217569] 12 p1724 N90-19903
Secondary arm coarsening and microsegregation in superalloy PWA-1480 single crystals: Effect of low gravity
[NASA-TM-102445] 13 p1776 N90-20194
Diamond: A high power optical material
[DE90-008941] 14 p1955 N90-21196
The effect of hydrogen and microstructure on the deformation and fracture behavior of a single crystal nickel-base superalloy
[NASA-CR-185219] 15 p2068 N90-21849
Single-crystal diffraction analysis of 2-(trimethylsilylethynyl) 4-nitro-N,N-dimethylaniline
[AD-A218955] 16 p2216 N90-22642
Single crystal NMR of high temperature superconductors 16 p2321 N90-23236
Optical spectroscopy of Ti(3+) doped YAlO3
[AD-A219043] 16 p2324 N90-23251
Preparation and properties of iron doped II-VI chalcogenides
[AD-A220802] 17 p2477 N90-24163
Microstructure of sputtered superconducting films of Bi2Sr2CaCu2O(x) made by low-temperature, in situ growth
[DE90-010067] 18 p2618 N90-24916

Magnetic and resistive measurements of the upper critical field in intwinned single crystals of YBa2Cu3O(7-delta)
[DE90-010083] 18 p2619 N90-24918
The defect structure of ion and neutron irradiated YBa2Cu3O(7-delta) single crystals
[DE90-010100] 18 p2619 N90-24920
Synthesis of large area, monocrystalline TiC as a substrate for heteroepitaxial growth of beta-SiC
[AD-A221392] 18 p2623 N90-24948
Hydrogen induced fracture characteristics of single crystal nickel-based superalloys
[NASA-CR-183992] 20 p2832 N90-26108
Resistivity, adhesive strength, and residual stress measurements of thin film metallizations on single crystal quartz
[DE90-011902] 20 p2837 N90-26135
SDIO/IST ultrashort wavelength laser: Novel experimental schemes for observing the Moessbauer effect in long-lived nuclear levels and nuclear coherent states
[AD-A222607] 20 p2868 N90-26316
Crystal growth and deformation behavior of TiAl aluminides
[DE90-012972] 20 p2930 N90-26671
Research on sputtering of ferroelectric thin films
[AD-A221792] 21 p2983 N90-26949
Application of microdesigned interfaces to studies of ceramic processing
[DE90-011633] 21 p2983 N90-26951
Fabrication of microwave guides using high Tc superconductors
[AD-A221560] 21 p3001 N90-27059
Fundamental electron transfer processes at the single crystal semiconductor/liquid interface
[DE90-011438] 21 p3079 N90-27508
Method of forming three-dimensional semiconductor structures
[NASA-CASE-NPO-17835-1-CU] 21 p3081 N90-27518
Preparation and magnetic measurements of single crystal Tl2Ba2CaCu2O8
[DE90-013657] 21 p3081 N90-27519
Impact fracture experiments simulating interstellar grain-grain collisions 21 p3093 N90-27584
Flux creep in Bi2Sr2CaCu2O8(sub +x) single crystals 22 p3136 N90-27794
Nonlogarithmic magnetization relaxation at the initial time intervals and magnetic field dependence of the flux creep rate in Bi2Sr2Ca(sub I)Cu2Ox single crystals 22 p3137 N90-27801
Measurement of H(sub c1) in a single crystal of YBa2Cu3O7 with low pinning 22 p3151 N90-27864
Hyperthermal atomic oxygen generator
[NASA-CR-186573] 22 p3155 N90-27889
High resolution technique and instrument for measuring lattice parameters in single crystals
[AD-D014549] 22 p3177 N90-28029
The fatigue damage behavior of a single crystal superalloy 23 p3296 N90-28644
Second order tensor finite element
[NASA-CR-184008] 23 p3386 N90-29122
Numerical and analytical study of nonlinear bifurcations associated with the morphological stability of two-dimensional single crystals
[PB90-209594] 23 p3398 N90-29200
Studies on crack mechanics
[AD-A223634] 24 p3480 N90-29670
Surface photovoltage spectroscopy of real n-type GaAs(110) surfaces
[DE90-627325] 24 p3551 N90-30092

SINGLE ENGINE AIRCRAFT
NT F-8 AIRCRAFT
NT F-16 AIRCRAFT
NT F-86 AIRCRAFT
NT F-104 AIRCRAFT

SINGLE EVENT UPSETS
A beam induced upset during the flight of the ECHO-7 rocket
[NASA-CR-186089] 03 p0309 N90-11755
Space radiation effects on electronics
[DE90-602874] 10 p1378 N90-17986
Burnout thresholds and cross section of power MOS transistors with heavy ions
[AD-A218998] 16 p2232 N90-22736
Real-time closed-loop simulation and upset evaluation of control systems in harsh electromagnetic environments 16 p2294 N90-23069
SEU characterization and design dependence of the SA3300 microprocessor
[DE90-007678] 18 p2589 N90-24728
Measurements of the single event upset environment in the upper atmosphere
[RAE-TM-SPACE-373] 23 p3351 N90-28934
An advanced single event upset tester
[AD-A223613] 24 p3564 N90-30163

SINGLE INPUT SINGLE OUTPUT SYSTEMS
U SISO (CONTROL SYSTEMS)

SINGLE INSTRUCTION MULTIPLE DATA STREAM
U SIMD (COMPUTERS)

SINGLE STAGE TO ORBIT VEHICLES
NT HOTOL LAUNCH VEHICLE
Rapid near-optimal trajectory generation and guidance law development for single-stage-to-orbit airbreathing vehicles
[NASA-CR-186299] 12 p1612 N90-19275
HOTOL structures and materials at British Aerospace, Warton, UK
[EOARD-LR-90-001] 14 p1921 N90-21001
Real time guidance and propulsion control for single-stage-to-orbit airbreathing vehicles 23 p3285 N90-28587
High/variable mixture ratio O2/H2 engine 23 p3295 N90-28638
High variable mixture ratio oxygen/hydrogen engine 23 p3295 N90-28640

SINGLE-PHASE FLOW
Selection of the energy-efficient enhancement geometry for single-phase turbulent flow inside tubes
[DE89-017690] 06 p0777 N90-14519

SINGULAR INTEGRAL EQUATIONS
Green's functions for the elastic annulus and their application to various crack problems 15 p2120 N90-22129

SINGULARITY (MATHEMATICS)
NT NAKED SINGULARITIES
A structured singular value approach to missile autopilot analysis 2 01 p0014 N90-10068
Singularity theory and N = 2 superconformal field theories
[DE89-016582] 02 p0269 N90-11538
The quadratic matrix inequality in singular H infinity control with state feedback
[MEMO-COSOR-89-03] 05 p0686 N90-13997
The totally singular linear quadratic problem with indefinite cost
[MEMO-COSOR-89-05] 05 p0687 N90-13998
The singular zero sum differential game with stability using H infinity control theory
[MEMO-COSOR-89-09] 05 p0687 N90-13999
The singular H infinity control problem with dynamic measurement feedback
[MEMO-COSOR-89-14] 05 p0687 N90-14000
Vector fields and gravity on the lattice
[DE89-633885] 06 p0836 N90-14860
Mixed singular linear elliptic equations
[DE90-600722] 07 p0982 N90-15674
Using the singularity-separating method to study how to decrease the pressure at the end of a tube
[PREPRINT-490] 08 p1065 N90-16158
Theory of singular Lagrangians
[DE90-600735] 08 p1115 N90-16456
On quantum effects near a black hole singularity
[DE90-600754] 08 p1151 N90-16668
The stress-driven redistribution of point defects in the vicinity of crack-like singularities
[AERE-R-12898] 13 p1815 N90-20424
Three-dimensional viscous flow structures from bifurcation of a degenerate singularity with three zero eigenvalues
[LR-572] 19 p2692 N90-25314
Flow structures around non-hyperbolic singularities on the wall with one vanishing eigenvalue: A discussion of the flow structures and the unfoldings
[LR-586] 19 p2692 N90-25315
Numerical treatment of shell crossing singularities in the spherically symmetric gravitational collapse
[ETN-90-96967] 20 p2917 N90-26598
Calculation of the algebraic curves parameterization: Hamburger-Noether expansions
[IMAG-RR-798-M] 20 p2919 N90-26608
Contribution to the study of differential equations and to the differences in the complex field
[ETN-90-97250] 20 p2919 N90-26612
Dichotomies for certain product measures and stable processes
[AD-A222568] 20 p2921 N90-26621
Resolution of seven-axis manipulator redundancy: A heuristic issue 21 p3049 N90-27331
Topology of singularities and phase diagram of N=2 superconformal field theories
[DE90-627213] 23 p3391 N90-29155

SINKS
NT HEAT SINKS
A network flow model for load balancing in circuit-switched multicomputers
[NASA-CR-182049] 17 p2451 N90-23977

SINKS (GEOLOGY)
U STRUCTURAL BASINS

SINTERED ALUMINUM POWDER
Kinetics and mechanisms of primary and steady state creep in B- and Al-containing alpha silicon carbide
[AD-A210739] 02 p0283 N90-11616

SINTERING
Ceramic processing of bulk high-T(sub c) superconductors
[DE89-015703] 01 p0128 N90-10736
Low temperature processing of reaction sintered silicon nitride
[DE89-017455] 02 p0191 N90-11092
Freeze-dried processing of tungsten heavy alloys
[DE89-015171] 02 p0197 N90-11122
Processing and characterization of alumina platelet-reinforced mullite composites
[DE90-000057] 03 p0320 N90-11814
Flexure strength of advanced ceramics: A round robin exercise
[AD-A212101] 03 p0332 N90-11889
Correlation between microstructure and magnetic properties of porous sintered iron and porous iron containing composites
[KFK-4522] 05 p0625 N90-13647
Dynamic sintering of metallic powders by laser shock 06 p0784 N90-14559
Process monitoring using optical ultrasonic wave detection
[DE90-002021] 06 p0838 N90-14870
Sintering studies on high field varistors
[DE90-002626] 07 p0926 N90-15359
Properties of high Tc superconducting oxides
[DE90-003792] 07 p1005 N90-15821
ZrO2 sintered compact and method for its production
[DE90-004125] 08 p1039 N90-16006
Synthesis of air-sinterable lanthanum chromite powders
[DE90-004681] 08 p1046 N90-16049
Sintering of a model nickel/alumina catalyst
[ETN-90-96270] 11 p1487 N90-18561
Microstructural characterization of silicon nitride ceramics processed by pressureless sintering, overpressure sintering, and sinter/HIP
[DE90-007126] 11 p1493 N90-18594
Crystallization behavior and properties of BaO-Al2O3-2SiO2 glass matrices
[NASA-CR-185209] 12 p1631 N90-19374
Magnetic hardening studies and novel techniques for preparation of high performance magnets
[AD-A217737] 13 p1881 N90-20790
Synthesis and properties of polycrystalline Tl2Ba2CaCu2O(x) and Tl2Ba2Ca2Cu3O(x)
[DE90-007528] 13 p1897 N90-20887
Development of planar geometry solid oxide fuel cell technology, phase 2
[PB90-131293] 14 p2001 N90-21467
Alternative materials for solid oxide fuel cells
[DE90-008615] 14 p2001 N90-21468
Institute for Materials Science and Engineering, nondestructive evaluation: Technical activities
[PB90-132739] 15 p2108 N90-22055
A low temperature calorimetric study of several high-T(sub c) superconductors 16 p2322 N90-23237
Fracture mechanism maps for advanced structural ceramics. Part 1: Methodology and hot-pressed silicon nitride results
[AD-A220428] 17 p2380 N90-23556
Influence of sinter technical limits for the manufacturing of oscillation strained pieces made of sinter steel
[LBF-FB-184(1989)] 18 p2526 N90-24413
Cation and anion tracer diffusion in YBa(sub 2)Cu(sub 3)O(sub 7-delta)
[DE90-009708] 18 p2620 N90-24927
Use of neutron diffraction in determining strains in high-temperature superconducting composites
[DE90-010404] 18 p2621 N90-24931
RF surface resistance measurements in the Pb-Bi-Sr-Ca-Cu-O system
[DE90-010412] 18 p2621 N90-24932
Rapid thermal processing of high temperature superconducting fiber
[NASA-CR-186803] 18 p2626 N90-24964
Processing polymeric powders 18 p2647 N90-25069
An analysis of the contact sintering process in III-V solar cells
[NASA-TM-103179] 19 p2709 N90-25420
Synthesis of high purity sinterable silicon carbide powder
[DE90-012029] 20 p2828 N90-26084
Real-time monitoring of ceramic sintering with laser ultrasonics
[DE90-012960] 20 p2838 N90-26140
Production of superconductor/carbon bicomponent fibers 22 p3138 N90-27805
Sintering of ceramics by laser irradiation
[ETCA-89-R-134] 22 p3161 N90-27926

Microstructure and impurity effects on tungsten heavy alloys
[AD-A224220] 23 p3311 N90-28728
Powder processing of aluminides
[DE90-015314] 24 p3444 N90-29447
Processing of nanocrystalline ceramics
[DE90-015700] 24 p3456 N90-29520

SINUSOIDS
U SINE WAVES

SIPHONING
Siphon flows in isolated magnetic flux tubes. 3: The equilibrium path of the flux tube arch
[NASA-CR-186297] 12 p1709 N90-19813

SIPHONS
A modified Ubbelohde viscometer with improved dilution characteristics
[NIAR-90-16] 19 p2693 N90-25326
Improved meteorological measurements from buoys and ships (IMET): Preliminary comparison of precipitation sensors
[PB90-241902] 22 p3229 N90-28316

SIR-A
U SHUTTLE IMAGING RADAR

SIR-B
U SHUTTLE IMAGING RADAR

SIRTF
U SPACE INFRARED TELESCOPE FACILITY

SIS (SUPERCONDUCTORS)
SIS (Superconductor-Insulator-Superconductor) mixer research
[AD-A211607] 03 p0414 N90-12375
Far-infrared heterodyne receivers
05 p0597 N90-13465
Advances in SIS receiver technology
05 p0597 N90-13466
Edge geometry superconducting tunnel junctions utilizing an NbN/MgO/NbN thin film structure
[NASA-CASE-NPO-17812-1-CU]
09 p1286 N90-17456
Construction of a 345 gigahertz receiver based on superconducting tunnel junctions
[AD-A218781] 16 p2232 N90-22735

SISO (CONTROL SYSTEMS)
Batch LCAP2-linear control analysis, version 2.0: User's manual
[AD-A211670] 04 p0461 N90-12643
Experiments in end-point control of a flexible robot with a mini-manipulator 12 p1671 N90-19596
An expert system to perform on-line controller tuning
[NASA-TM-103101] 17 p2453 N90-23991

SITE SELECTION
Ice runways near the South Pole
[AD-A211606] 03 p0335 N90-11908
Vision for the introduction of the wind power generation system. Survey on the prospective market, part 2
[DE89-910386] 12 p1680 N90-19651
Anderson Mesa, Arizona as a site for an optical interferometric array 16 p2330 N90-23281
An evaluation of three models designed for siting wind turbines in areas of complex terrain
[DE90-013625] 22 p3196 N90-28137
The National Geodetic Survey absolute gravity program
[PB90-156951] 22 p3211 N90-28212
The potential for an extra runway at Heathrow: A preliminary feasibility study
[TT-9007] 24 p3435 N90-29403

SITES
NT LANDING SITES
NT LAUNCHING PADS
NT LAUNCHING SITES
NT LUNAR LANDING SITES

SITTING POSITION
The application of a non-linear least squares method to predicting seat transmissibility
[ISVR-TR-173] 16 p2275 N90-22967

SIZE (DIMENSIONS)
NT GRAIN SIZE
Relationship of fragment size to normalized spall strength for materials
[DE90-004165] 09 p1231 N90-17140
Psychological studies of visual cortical function
[AD-A217029] 11 p1541 N90-18872
An interactive method for estimating hailstone size and convectively-driven wind gusts from forecast soundings
[AD-A218499] 16 p2258 N90-22871
PDWAP: A preliminary design and weights analysis program for aerospace vehicles
[AD-A222614] 20 p2808 N90-25979
Micromechanics of size effect in failure due to distributed cracking
[AD-A223211] 21 p3013 N90-27128

SIZE DETERMINATION
NT PRECIPITATION PARTICLE MEASUREMENT
Droplet sizing instrumentation used for icing research: Operation, calibration, and accuracy
[NASA-CR-182293] 03 p0350 N90-11999
Measurements of bubble properties using a multi-frequency sound field
[AD-A212591] 04 p0551 N90-13211
WPK: Solar array dimensioning tool
10 p1346 N90-17808
Dimensional analysis of structures using wrapping techniques
[REPT-892-430-119] 16 p2247 N90-22815

SIZE DISTRIBUTION
NT PARTICLE SIZE DISTRIBUTION
Further guide for the retrieval of dropsize distributions in water clouds with a ground-based clear-air-sensing Doppler radar
[PB89-196000] 03 p0336 N90-11911
Multiparameter radar estimation of raindrop size distribution
[AD-A212410] 04 p0521 N90-13007
The in-situ cometary particulate size distribution measured for one comet: P/Halley
08 p1145 N90-16637
Comparison of drop size distributions from two droplet sizing systems
[NASA-TM-102520] 09 p1232 N90-17147
Colloid and interface chemistry aspects of ceramics
[AD-A216715] 11 p1490 N90-18576
Inclusion of clouds and rain in atmospheric slant path calculations 15 p2083 N90-21925
Comparison test of droplet sizing instruments used in icing research
[DOT/FAA/CT-TN90/13] 19 p2693 N90-25322
A study of the spatial scales of discrete polar auroral arcs
[NASA-CR-186806] 19 p2714 N90-25444
Spectral absorption of marine stratocumulus clouds derived from in situ cloud radiation measurements
22 p3215 N90-28238
Supersaturation, droplet spectra, and turbulent mixing in clouds 22 p3217 N90-28249

SKELETON
U MUSCULOSKELETAL SYSTEM

SKEWNESS
Three-dimensional adaptive grids with limited skewness 15 p2095 N90-21987
M-estimators in linear models with long range dependent errors
[AD-A219921] 17 p2461 N90-24053
The one dimensional skewing problem
[RUU-CS-89-23] 18 p2596 N90-24769
Numerical solution for the velocity-derivative skewness of a low-Reynolds-number decaying Navier-Stokes flow
[NASA-TM-103186] 22 p3171 N90-27985
Vertical-velocity skewness in the marine stratus-topped boundary layer 22 p3220 N90-28262

SKIDDING
The nature and control of skidding in lightly loaded intershaft bearings
[PNR90591] 04 p0508 N90-12933

SKILLS
U ABILITIES

SKIN (ANATOMY)
Occupational safety considerations with hydrazine
02 p0207 N90-11182
DNA damage and repair in human skin: Pathways and questions
[DE90-015126] 23 p3356 N90-28966

SKIN (STRUCTURAL MEMBER)
Some new techniques for aircraft fuselage skin tests
[LR-547] 05 p0580 N90-13379
A dynamicist's view of fuel tank skin durability
08 p1023 N90-15915
The drum: Mechanical oscillators and acoustic radiators
[REPT-FB-01/88] 12 p1710 N90-19819
Future automotive materials: Evolution or revolution
18 p2516 N90-24370

SKIN FRICTION
NT AERODYNAMIC DRAG
NT FRICTION DRAG
NT SUPERSONIC DRAG
NT VISCOUS DRAG
Simultaneous detection of separation and transition in surface shear layers 01 p0064 N90-10368
Control and modification of turbulence
01 p0066 N90-10377
Lockheed laminar-flow control systems development and applications 04 p0438 N90-12506
Recent tests at Langley with a University of Tennessee Space Institute (UTSI) skin friction balance
04 p0441 N90-12527
Skin friction measurements with hot elements
05 p0574 N90-13345
A one equation turbulence model for transonic airfoils
06 p0719 N90-14199
Test techniques for cryogenic wind tunnels
08 p1030 N90-15952
Skin friction balance
[NASA-CASE-LAR-13710-1] 09 p1226 N90-17117
Skin friction measurements by laser interferometry in supersonic flows 10 p1306 N90-17557
Viscous three-dimensional analyses for nozzles for hypersonic propulsion
[NASA-CR-185197] 10 p1321 N90-17635
Hypersonic waverider configurations for trans-atmospheric vehicles
[AD-A217925] 13 p1755 N90-20074
A brief review of some mechanisms causing boundary layer transition at high speeds
[NASA-TM-102834] 20 p2803 N90-25945
Hydrodynamic skin-friction reduction
[NASA-CASE-LAR-14078-1-CU]
21 p3003 N90-27071
The effects of grid-generated turbulence on flat and concave turbulent boundary layers
23 p3324 N90-28797
Use of liquid crystals for qualitative and quantitative 2-D studies of transition and skin friction
[RAE-TM-AERO-2159] 23 p3325 N90-28800

SKIN TEMPERATURE (BIOLOGY)
The effects of nonselective and selective beta blockade upon nonshivering thermogenesis during an acute cold exposure in cold acclimated men
06 p0820 N90-14767
Effective calibration of heat flux transducers for experimental use
[AD-A218262] 13 p1853 N90-20636

SKIN TEMPERATURE (NON-BIOLOGICAL)
The skin temperature of mountain slopes and the determination of the sensible heat flux
[DLR-FB-90-07] 24 p3495 N90-29754

SKY
NT NIGHT SKY
Perspective transformation for wide-view sky scenes
[AD-A222694] 21 p3007 N90-27093

SKY BRIGHTNESS
The optical night sky at low surface brightness: High latitude dust and faint field galaxies
15 p2185 N90-22481

SKY RADIATION
NT AIRGLOW
NT GEOCORONAL EMISSIONS
NT NIGHTGLOW
Improved meteorological measurements from buoys and ships (IMET): Preliminary comparison of pyranometers
[PB90-241936] 22 p3229 N90-28315

SKY SURVEYS (ASTRONOMY)
MOXE: An X-ray all-sky monitor for Soviet Spectrum-X-Gamma Mission
[NASA-TM-101266] 02 p0223 N90-11280
The NASA SETI sky survey: Recent developments
04 p0488 N90-12804
The detectors 05 p0604 N90-13507
Successive iterations of the input catalog
05 p0607 N90-13534
Stellar content of the input catalog
05 p0607 N90-13535
Ground-based astrometric measurements
05 p0607 N90-13536
The compilation of astrometric data
05 p0607 N90-13537
Standard stars and photometric calibration
05 p0607 N90-13539
Double stars 05 p0608 N90-13540
The choice of stars in open clusters
05 p0608 N90-13542
The choice of stars in the Magellanic clouds
05 p0608 N90-13543
Minor planets and other solar system objects
05 p0608 N90-13545
The catalogs produced by the Inca consortium
05 p0608 N90-13546
The SIMBAD data base 05 p0608 N90-13547
Realtime tracking system for wide-field-of-view telescope
[DE90-001147] 06 p0843 N90-14908
The COBE cosmic 3 K anisotropy experiment: A gravity wave and cosmic string probe 12 p1732 N90-19959
An infrared sky model based on the IRAS point source data
[NASA-CR-177526] 23 p3409 N90-29265

SKY WAVES
NT WHISTLERS
Accurate measurements of the total angle of arrival of HF skywaves 02 p0248 N90-11402
Ionospheric limitations to the accuracy of SSL estimates of HF transmitter locations 02 p0248 N90-11403

SKYDROL (TRADEMARK)
Flammability of fire resistant, aircraft hydraulic fluid
[DOT/FAA/CT-TN90/19] 19 p2677 N90-25222

SKYLAB SPACE STATION (UNMANNED)
U SKYLAB 1
SKYLAB 1
Technical characteristics and functions of different types of space stations 20 p2937 N90-26712
SKYLARK
U SKYLARK ROCKET VEHICLE
SKYLARK ROCKET VEHICLE
The Skylark sounding rocket program and future launcher developments by British Aerospace (Space Systems) Ltd. 05 p0662 N90-13871
SL 1
U SKYLAB 1
SLABS
An analysis of the finite-differenced, even-parity discrete-ordinates equations in slab geometry
[DE90-006479] 15 p2160 N90-22337
Transient electromagnetic scattering on anisotropic media
[DE90-011802] 19 p2683 N90-25262
Electromagnetic scattering from two-dimensional thick material junctions
[NASA-CR-186468] 23 p3319 N90-28767
SLAGS
Evaluation of copper slag blast media for railcar maintenance
[NASA-CR-183744] 05 p0630 N90-13681
MHD channel development, part 4
[DE90-009552] 15 p2169 N90-22397
Laboratory simulation of the effect of rocket thrust on a precessing space vehicle
[NASA-CR-186681] 19 p2669 N90-25182
SLANT
U SLOPES
SLANT PERCEPTION
U SPACE PERCEPTION
SLEDS
NT ROCKET PROPELLED SLEDS
SLEEP
NT HYPNOSIS
NT INSOMNIA
Test-retest reliability of oxford Medilog 9000 sleep recording and SS-90-3 sleep stage scoring
[AD-A211165] 02 p0254 N90-11440
Cumulative airport noise exposure metrics: An assessment of evidence for time-of-day weightings, revision
[AD-A214878] 09 p1170 N90-16773
Pharmacological resetting of the circadian sleep-wake cycle effects of triazolam on reentrainment of circadian rhythms in a diurnal primate
[AD-A224227] 24 p3497 N90-29764
Minimal sleep to maintain performance: Search for sleep quantum in sustained operations
[AD-A223815] 24 p3498 N90-29770
SLEEP DEPRIVATION
Daytime sleepiness, performance, mood, nocturnal sleep: The effect of benzodiazepine and caffeine on their relationship
[AD-A210915] 01 p0093 N90-10533
Analyses of the predictability of noise-induced sleep disturbance
[AD-A220156] 17 p2435 N90-23876
Evaluation of physiological and psychological impairment of human performance in cold stressed subjects
[AD-A223635] 24 p3498 N90-29769
Minimal sleep to maintain performance: Search for sleep quantum in sustained operations
[AD-A223815] 24 p3498 N90-29770
SLENDER BODIES
Aerodynamic test and analysis of a slender generic missile configuration
[AD-A212522] 04 p0448 N90-12567
Improved tangent-cone method for the Aerodynamic Preliminary Analysis System (APAS) version of the hypersonic arbitrary-body program
[NASA-TM-4165] 08 p1018 N90-15890
Flutter of slender bodies under axial stress
[PB90-167024] 14 p1994 N90-21425
An experimental investigation of the physical mechanisms controlling the asymmetric flow past slender bodies at large angles of attack 15 p2053 N90-21767
The aerodynamic characteristics of power-law bodies in continuum and transitional hypersonic flow
[RAE-TM-AERO-2164] 16 p2196 N90-22537
Effects of flowfield turbulence on asymmetric vortices over a slender body
[AD-A224139] 23 p3328 N90-28819
Aerodynamic forces acting on a finite rectangular slender body
[NAL-TR-1035] 24 p3421 N90-29329
SLENDER WINGS
Effects of flowfield turbulence on asymmetric vortices over a slender body
[AD-A224139] 23 p3328 N90-28819
SLEWING
Use of the quasilinearization algorithm for the simulation of LSS slewing 01 p0022 N90-10110
Dynamics and control of flexible spacecraft during and after slewing maneuvers
[NASA-CR-186123] 06 p0733 N90-14270
NASA CSI suspension methods overview 14 p1936 N90-21080
The determination of maximum deep space station slew rates for a high Earth orbiter 15 p2075 N90-21882
Sliding control of pointing and tracking with operator spline estimation 16 p2281 N90-22997
Modeling and control of flexible space stations (slew maneuvers) 16 p2297 N90-23086
The dynamics and control of large flexible space structures - 13
[NASA-CR-186930] 23 p3286 N90-28591
SLIDING
Friction and wear of oxide-ceramic sliding against IN-718 nickel base alloy at 25 to 800 C in atmospheric air
[NASA-TM-102291] 01 p0046 N90-10262
Planar sliding of a rigid body with dry friction: Limit surfaces and dynamics of motion 02 p0229 N90-11314
Hybrid butterfly valve
[NASA-CASE-SSC-00004] 07 p0940 N90-15443
A procedure for force-balancing planar linkages using counterweights
[ESDU-89028] 07 p0940 N90-15446
Quick disconnect duct coupler
[AD-D014265] 08 p1084 N90-16274
The experimental evaluation and application of high-temperature solid lubricants
[NASA-TM-102476] 09 p1198 N90-16944
Low-noise nozzle valve
[NASA-CASE-MFS-28383-1] 09 p1216 N90-17051
A micromechanical viscoplastic stress-strain model with grain boundary sliding
[DE90-006013] 10 p1437 N90-18295
Nonlinear spline operator interpolation and sliding control of deformable maneuvering bodies 15 p2074 N90-21878
Sliding control of pointing and tracking with operator spline estimation 16 p2281 N90-22997
The experimental evaluation and application of high temperature solid lubricants 18 p2564 N90-24631
On conditions for the development of stable discrete-time sliding mode control systems
[MATHS-REPT-A-124] 19 p2747 N90-25612
On controller choice for robust sliding mode performance
[MATHS-REPT-A-107] 20 p2872 N90-26337
Influence of microslidings on the macroscopic behavior of composite textiles
[ETN-90-97459] 22 p3154 N90-27880
Microdamage to ceramic surfaces under sliding conditions 23 p3308 N90-28708
SLIDING FRICTION
Thermomechanical contact phenomena and wear of sliding components
[AD-A211290] 03 p0355 N90-12028
Tribological properties of ceramic/Ti3Al-Nb sliding couples for use as candidate seal materials to 700 deg C
[NASA-TM-102401] 04 p0464 N90-12658
Characterization of self-lubricating surface materials
[CETIM-108060] 04 p0479 N90-12749
Friction and wear of glassy carbon in sliding contact, revision 1
[DE90-000743] 06 p0750 N90-14365
Investigation of rough elastohydrodynamic contact
[ISAL-89-0029] 08 p1085 N90-16281
A quantitative analysis of slip phenomena along a dry contact surface between two bodies in comparison to interfacial crack propagation
[ISAL-89-0032] 08 p1089 N90-16304
The mechanism, measurement, and influence of properties on the galling of metals
[DE90-006533] 11 p1487 N90-18558
The joint effect of surface microtopography and near-surface structure on microcontact conditions
[DE90-006494] 11 p1493 N90-18591
Wear of gold-plated contacts: Microscopic aspects, role of oxygen 18 p2538 N90-24479
Wear transition surfaces for long-term wear effects
[DE90-011314] 19 p2698 N90-25351
Interfacial viscosity measurements of adsorbed monolayers on metal surfaces
[AD-A221689] 21 p2979 N90-26931
Friction microprobe studies of composite surfaces
[DE90-014224] 23 p3299 N90-28662
Scale effects in steady-state friction
[DE90-012943] 24 p3476 N90-29647
SLIP BANDS
U EDGE DISLOCATIONS
SLIP CASTING
Low cost filter development and control of permeability in high temperature, high pressure ceramic filter elements
[DE90-000403] 11 p1507 N90-18676
SLIPSTREAMS
NT PROPELLER SLIPSTREAMS
Prediction of two-dimensional time-dependent gasdynamic flows for hypersonic studies
[UTIAS-335] 20 p2801 N90-25935
SLITS
The modulating grid 05 p0803 N90-13505
Airborne sound insulation of slits, joints, and sealing stripes
[PB90-128976] 14 p2023 N90-21599
SLOPES
NT GLIDE PATHS
Calculated solar radiation incident upon slopes of different orientated surfaces in Finland
[FMI-MP-8] 03 p0370 N90-12116
Operational measures of central tendency
[DE89-016959] 03 p0392 N90-12234
Installed tailplane lift-curve slope at subsonic speeds
[ESDU-89029] 07 p0876 N90-15081
Visual slant underestimation 16 p2268 N90-22926
Flow resistance and critical shear stress in steep channels 19 p2687 N90-25282
SLOSHING
U LIQUID SLOSHING
SLOT ANTENNAS
Application of the moment method to the design of slotted waveguide array antennas 04 p0484 N90-12780
Wire grid modeling of the linear tapered slot antenna
[AD-A212977] 04 p0494 N90-12842
Annular slot antenna radiating into lossy material
[NPL-DITC-152/89] 22 p3165 N90-27945
SLOTS
NT WING SLOTS
A design procedure for a slotted waveguide with probe-fed slots radiating into plasma
[DE90-004168] 09 p1284 N90-17446
A numerical and analytical study of normal stresses and pressure differences in non-Newtonian creeping flows 16 p2234 N90-22749
A laser-induced fluorescence technique for measurement of slot-injected fluid concentration profiles in a plate turbulent boundary layer
[AD-A221388] 18 p2553 N90-24572
Resonant coupling through a slot to a loaded cylindrical cavity: Experimental results
[AD-A223000] 20 p2922 N90-26631
Gas-jet and tangent-slot film cooling tests of a 12.5 deg cone at Mach number of 6.7
[NASA-TP-2786] 23 p3326 N90-28806
SLOTTED ANTENNAS
U SLOT ANTENNAS
SLOTTED WIND TUNNELS
On transonic flow over segmented slotted wind tunnel wall with mass transfer 02 p0294 N90-11676
Slotted-wall research with disk and parachute models in a low-speed wind tunnel
[DE90-002989] 15 p2048 N90-21737
SLUDGE
Development of a robotics system for automated chemical analysis of sediment, sludges, and soils
[DE90-003637] 07 p0895 N90-15170
SLURRIES
The secondary slurry-zinc/air battery
[DE90-002600] 06 p0772 N90-14491
Optimum catalytic process for alcohol fuels from syngas
[DE90-007188] 11 p1495 N90-18604
Fluidization mechanisms in slurry flow
[DE90-006497] 11 p1509 N90-18691
An evaluation of ethylene-vinyl acetate copolymers as desensitizers for RDX in insensitive booster compositions prepared by slurry coating technology
[MRL-TR-89-33] 12 p1633 N90-19385
Turbulence in slurry pipe flow
[DE90-008940] 15 p2098 N90-22006
Subsonic combustor testing 20 p2811 N90-25997
Understanding silica binders
[PNR90625] 20 p2840 N90-26150
An experimental investigation of a single and multiphase confined coaxial jet 23 p3324 N90-28796
SLURRY PROPELLANTS
NT SLUSH HYDROGEN
Ignition and combustion characteristics of metallized propellants
[NASA-CR-186870] 21 p2976 N90-26911

SLUSH
Slush Hydrogen (SLH2) technology development for application to the National Aerospace Plane (NASP)
[NASA-TM-102315] 06 p0732 N90-14266
FLUSH: A tool for the design of slush hydrogen flow systems
[NASA-TM-102467] 10 p1361 N90-17890
SLUSH HYDROGEN
Background, current status, and prognosis of the ongoing slush hydrogen technology development program for the NASP
[NASA-TM-103220] 20 p2622 N90-26055
SMART STRUCTURES
Smart microsensors for high temperature applications, phase 1
[AD-A224151] 23 p3330 N90-28828
SMELL
U OLFACTORY PERCEPTION
SMOKE
Analysis of forest fire smoke using satellite imagery
[AD-A210657] 02 p0236 N90-11339
Flammability, smoke, and dry arc tracking tests of aircraft electrical wire insulations
[DOT/FAA/CT-89/21] 03 p0302 N90-11714
A smoke generator system for aerodynamic flight research
[NASA-TM-4137] 05 p0578 N90-13372
Evaluate and characterize mechanisms controlling transport, fate, and effects of army smokes in the aerosol wind tunnel: Transport, transformations, fate, and terrestrial ecological effects of hexachloroethane obscurant smokes
[DE90-002923] 07 p0957 N90-15536
Ambient flow studies and particulate collection measurements: A laminar flow, reduced entrainment electrostatic precipitator
[DE90-001457] 08 p1063 N90-16149
Visualization of gas flows using the smoke wire technique 08 p1079 N90-16242
Aircraft Fire Safety
[AGARD-CP-467] 10 p1311 N90-17581
Fire science and aircraft safety 10 p1314 N90-17596
Passenger behaviour in aircraft emergencies involving smoke and fire 10 p1317 N90-17613
Smokehoods donned quickly. The impact of donning smokehoods on evacuation times 10 p1317 N90-17614
The investigation of particulate matter in the lungs of smoke inhalation death victims 10 p1317 N90-17617
Experimental investigation of the mechanisms underlying vortex kinematics in unsteady separated flows
[AD-A217889] 13 p1802 N90-20346
Field evaluation of a passive sampling device for hydrazines in ambient air
[NASA-TM-103456] 18 p2578 N90-24686
Video photographic considerations for measuring the proximity of a probe aircraft with a smoke seeded trailing vortex
[NASA-TM-102691] 19 p2657 N90-25120
Meteorological Satellite Center Technical Note, no. 17, 1988
[ISSN-0388-9653] 21 p3028 N90-27213
Distribution and movement of smokes from forest fires that occurred along the boundary of the People's Republic of China and the USSR on April-May 1987 21 p3028 N90-27216
Evaluation of the wake effects on plume dispersion using video image analysis
[PB90-186354] 22 p3169 N90-27972
The reduction of smoke emissions from Allison T56 engines
[ARL-PROP-R-182] 23 p3277 N90-28547
Diffusion in the surface layer of the convective boundary layer
[AD-A224125] 23 p3349 N90-28924
Activities report for the IBDF-INPE project SEQE, year 1987
[INPE-4534-RPE/565] 23 p3415 N90-29298
SMOKE DETECTORS
Fire safety applications for spacecraft 10 p1314 N90-17595
SMOOTHING
NT DATA SMOOTHING
Inf-convolution splines
[IMAG-RR-749-M] 03 p0395 N90-12256
Estimating methods for counting process intensities: Non-parametric methods
[IMAG-RR-774-M] 06 p0834 N90-14848
Shapes of star-gas waves in spiral galaxies
[NASA-CR-186289] 07 p1011 N90-15859
Numerical analysis of nonstationary fluid flow (a survey)
[PREPRINT-492] 08 p1065 N90-16159
Image smoothing and differentiation with minimal-curvature filters
[AD-A215184] 09 p1273 N90-17382
Orbit determination of artificial Earth satellites through estmation techniques combined with state smoothing techniques
[INPE-4959-TDL/388] 11 p1465 N90-18440
Parallel distributed networks for image smoothing and segmentation in analog VSLI
[AD-A216780] 12 p1651 N90-19491
Spline function smoothing and differentiation of noisy data on a rectangular grid
[DE90-009319] 15 p2160 N90-22338
UD filtering and smoothing applied to orbit determination
[INPE-4966-PRE/1535] 15 p2189 N90-22501
An innovations approach to decoupling of multibody dynamics and control 16 p2280 N90-22994
Efficient smoothing for boundary value models
[AD-A218484] 17 p2456 N90-24014
A global approach for using kinematic redundancy to minimize base reactions of manipulators
[NASA-CR-186825] 19 p2725 N90-25499
SNATCHING
U SPACECRAFT RECOVERY
SNEAK CIRCUIT ANALYSIS
Sneak circuit analysis for the common man
[AD-A215275] 09 p1212 N90-17029
SNELLS LAW
Vehicle path-planning in three dimensions using optics analogs for optimizing visibility and energy cost 24 p3512 N90-29853
SNOW
A diffusion on a fractal state space
[AD-A213555] 07 p0988 N90-15707
Recognition and distinction of clouds, snow, and ice using AVHRR data 08 p1092 N90-16322
Optical measurement of precipitation
[AD-A214357] 10 p1407 N90-18116
Laboratory techniques for the characterisation of snow structures 12 p1741 N90-20007
Guidance document for selecting antiskid materials applied to ice- and snow-covered roadways
[PB90-183658] 21 p2983 N90-26950
Applications of ISES for snow, ice, and sea state 21 p3018 N90-27159
Wind tunnel simulation of Antarctic snowdrifting
[PB90-184565] 22 p3212 N90-28222
SNOW COVER
Airborne gamma radiation snow water equivalent and soil moisture measurements and satellite areal extent of snow cover measuerments: A user's guide, version 3.0
[PB89-177877] 02 p0235 N90-11338
A laboratory comparison of field techniques for measurement of the liquid water fraction of snow
[AD-A219587] 17 p2417 N90-23774
Snow and land ice in the climate system: Research problems and possibilities of remote sensing 19 p2707 N90-25407
Snow cover mapping and snowmelt runoff simulations on microcomputers 19 p2707 N90-25408
Physical parameterization of snow albedo for use in climate models
[PB90-167313] 19 p2712 N90-25433
SNOWPLOW EFFECT
U PLASMA DYNAMICS
SNOWSTORMS
Second National Winter Weather Workshop Conducted by the National Weather Service
[PB90-147414] 15 p2131 N90-22183
SOBOLEV SPACE
On the equation: Delta u+c=Ke(sup u)
[DE90-612741] 14 p2020 N90-21575
On approximation of nonlinear boundary integral equations for the combined method
[DE90-009784] 16 p2305 N90-23130
An H(m)sub 0 interpolation result
[AD-A219888] 17 p2461 N90-24051
SOCIAL FACTORS
NT ETHNIC FACTORS
Environmental impact assessment: Process and implementation
[DE90-004882] 10 p1406 N90-18109
Survey on the social and economic influences of wide-spreading heat-pump technology
[DE89-782294] 12 p1658 N90-19526
International application of the DLR test-system: First year of cooperation with IBERIA in pilot selection
[DLR-FB-90-05] 19 p2723 N90-25491
SOCIOLOGY
NT ETHNIC FACTORS
NT SOCIAL FACTORS
The astronomy of Andean myth: The history of a cosmology 02 p0291 N90-11660
US Forest Service and National Park Service Wilderness Aircraft Overflight Study: Sociological background and study plans 18 p2609 N90-24863
SODAR
An analysis of diurnal wind variability in the Santa Barbara Channel from SODAR measurements
[AD-A215769] 10 p1408 N90-18121
Methodology investigation calibration and quality control for new meteorological instrumentation, part 1
[AD-A221407] 18 p2582 N90-24706
SODIUM
NT LIQUID SODIUM
A new inexpensive electrochemical meter for oxygen in sodium coolant
[DE89-630802] 02 p0194 N90-11104
Diurnal variation of the sodium layer at polar latitudes in summer 05 p0662 N90-13869
Modeling of sodium/metal chloride batteries
[DE89-017685] 06 p0770 N90-14478
Inelastic scattering of positrons with sodium 11 p1556 N90-18961
Test results from a full-scale sodium reflux pool-boiler solar receiver
[DE90-003577] 12 p1684 N90-19671
Low temperature elastic and dielectric properties of incommensurate barium sodium niobate
[AD-A216969] 12 p1709 N90-19815
Determinations of photon spectra
[AD-A218003] 13 p1885 N90-20816
An evaluation of metal salts of 3-nitro-1,2,4-triazol-5-one (NTO) as potential primary explosives
[MRL-TN-563] 14 p1956 N90-21202
Conservation of body calcium by increased dietary intake of potassium: A potential measure to reduce the osteoporosis process during prolonged exposure to microgravity 18 p2631 N90-24993
Wind tunnel simulation of Antarctic snowdrifting
[PB90-184565] 22 p3212 N90-28222
SODIUM CARBONATES
Determination of optimum electrolyte composition for molten carbonate fuel cells
[DE90-000410] 09 p1243 N90-17210
SODIUM CHLORIDES
The effect of dissolved chlorine on the pitting behavior of 304L stainless steel in a 0.5 N NaCl solution
[AD-A213803] 07 p0905 N90-15234
NMR (Nuclear Magnetic Resonance) imaging development for the study of solids
[AD-A217073] 12 p1723 N90-19899
Direct sublimation of NaCl salt from carbon matrixes
[DE90-007927] 14 p1946 N90-21139
Ionic equilibrium between octahedral and tetrahedral complexes in liquid aluminium-sodium fluoride mixtures
[DE90-613690] 14 p1948 N90-21150
Development and applications of a coupled cavity sodium-chloride laser 15 p2102 N90-22029
Guidance document for selecting antiskid materials applied to ice- and snow-covered roadways
[PB90-183658] 21 p2983 N90-26950
SODIUM COMPOUNDS
NT CRYOLITE
NT SODIUM CARBONATES
NT SODIUM CHLORIDES
NT SODIUM FLUORIDES
NT SODIUM IODIDES
NT SODIUM SULFATES
Hydrous metal oxide-supported catalysts. Part 1: Preparation chemistry and physical and chemical properties
[DE90-007607] 13 p1771 N90-20161
SODIUM FLUORIDES
X ray spectra produced by NaF implosions
[AD-A215803] 10 p1429 N90-18243
Ionic equilibrium between octahedral and tetrahedral complexes in liquid aluminium-sodium fluoride mixtures
[DE90-613690] 14 p1948 N90-21150
SODIUM IODIDES
Particle transport simulation for spaceborne, NaI gamma-ray spectrometers
[AD-A205150] 04 p0564 N90-13292
The problem of dead layer in gamma ray burst spectra recorded with NaI or CsI crystals 19 p2776 N90-25787
SODIUM SULFATES
Effects of hot corrosion on the room temperature strength of structural ceramics
[AD-A212568] 04 p0481 N90-12762
The initiation of intergranular stress corrosion-cracking on sensitized stainless steel in dilute thiosulphate solutions
[AERE-R-13317] 16 p2217 N90-22648
SODIUM SULFUR BATTERIES
Safety considerations for sodium-sulfur batteries for electric vehicles
[DE89-017682] 03 p0342 N90-11949

Heat pipes for sodium-sulfur batteries
[AD-A212523] 04 p0497 N90-12865
Sodium/sulfur evaluation at SNL
[DE89-015846] 06 p0769 N90-14472
Sodium/sulfur post-test analysis at ANL
[DE90-001911] 06 p0771 N90-14488
Novel high-rate, all solid-state, sodium and lithium/organosulfur batteries
[DE90-001014] 07 p0920 N90-15325
Advanced rechargeable sodium batteries with novel cathodes 13 p1822 N90-20459
Sodium-sulfur battery flight experiment definition study 13 p1825 N90-20479
The INEL battery data base
[DE90-010914] 18 p2550 N90-24555
Development of the sodium/sulfur technology for energy storage
[DE90-014329] 23 p3344 N90-28899

SOFT LANDING SPACECRAFT
NT AEROSPACE PLANES
NT ASTRO VEHICLE
NT BURAN SPACE SHUTTLE
NT HOTOL LAUNCH VEHICLE
NT LUNAR LANDING MODULES
NT LUNAR MODULE

SOFTENING
Elastic softening in nanocrystalline silicon
[DE90-002268] 06 p0752 N90-14377
Softening mechanisms and microstructural instabilities during high temperature, low cycle fatigue of Ni, Ni3Al, and their metal matrix composites
[DE90-006487] 11 p1487 N90-18557
Development of a design methodology for high temperature cyclic applications of materials which experience cyclic softening
[DE90-006722] 19 p2674 N90-25205
Cyclic stress strain behavior of an austenitic stainless steel Polarit 778 under variable amplitude loading
[VTT-RR-647] 19 p2675 N90-25215

SOFTWARE (COMPUTERS)
U COMPUTER PROGRAMS
U COMPUTER SYSTEMS PROGRAMS

SOFTWARE ENGINEERING
NT ASSEMBLER ROUTINES
NT COMPUTER PROGRAMMING
NT LANGUAGE PROGRAMMING
NT LOGIC PROGRAMMING
NT MICROPROGRAMMING
NT MULTIPROGRAMMING
NT PARALLEL PROGRAMMING
NT SYMBOLIC PROGRAMMING
Proceedings of the Workshop on Computational Aspects in the Control of Flexible Systems, part 1
[NASA-TM-101578-PT-1] 01 p0017 N90-10080
Additional software developments wanted for modeling and control of flexible space systems 01 p0017 N90-10083
A comparison of software for the modeling and control of flexible systems 01 p0019 N90-10092
Control law synthesis and optimization software for large order aeroservoelastic systems 01 p0022 N90-10111
Structure flow diagram generator
[PB89-195978] 01 p0104 N90-10592
String Search
[PB89-195986] 01 p0104 N90-10593
Considerations for a design and operations knowledge support system for Space Station Freedom
[NASA-TM-102156] 02 p0256 N90-11451
Software configuration management: An overview
[PB89-193833] 02 p0258 N90-11458
Module algebra (revised version)
[CWI-CS-R8844-REV] 02 p0260 N90-11474
Transport systems research vehicle color display system operations manual
[NASA-TM-101577] 03 p0306 N90-11736
Requirements for multidisciplinary design of aerospace vehicles on high performance computers
[NASA-CR-181915] 03 p0384 N90-12183
Adoption of software engineering innovations in organizations
[AD-A211573] 03 p0387 N90-12206
Case study on rapid software prototyping and automated software generation: An inertial navigation system
[AD-A212272] 04 p0450 N90-12578
Telescience Testbed Pilot Program
[NASA-CR-184997] 04 p0528 N90-13047
Building a software package for solving large sparse nonlinear systems of equations
[AD-A211758] 04 p0529 N90-13055
LOTOS tools based on the Cornell synthesizer generator
[MEMO-INF-89-5] 04 p0530 N90-13062
A mapping for converting Mascot designs to Ada programs
[RSRE-MEMO-4244] 04 p0531 N90-13070
Software Engineering Exercise (SEE) guidelines
[AD-A212510] 04 p0534 N90-13085
Toward a formal model of the design and evolution of software
[AD-A212533] 04 p0534 N90-13087
Processing of undifferences GPS carrier beat phase measurements and adjustment computations
[TR-5-1988] 05 p0578 N90-13368
Definition of avionics concepts for a heavy lift cargo vehicle, appendix A
[NASA-CR-183817] 05 p0580 N90-13380
The development of a program analysis environment for Ada
[NASA-CR-185860] 05 p0681 N90-13962
Software development for avionics SSME control and diagnostics
[NASA-CR-184894] 05 p0681 N90-13964
Methodology for automating software systems. Task 1 of the foundations for automating software systems
[NASA-CR-180499] 05 p0681 N90-13965
Software engineering and Ada (Trademark) training: An implementation model for NASA
[NASA-CR-186071] 05 p0681 N90-13966
Ada task scheduling: A focused Ada investigation
[NASA-CR-186072] 05 p0682 N90-13967
The APROS software for process simulation and model development
[VTT-618] 05 p0684 N90-13987
Flight software development for the isothermal dendritic growth experiment
[NASA-TM-102412] 05 p0685 N90-13988
Applications of artificial intelligence to space station and automated software techniques: High level robot command language
[NASA-CR-182997] 05 p0686 N90-13991
Executive overview and introduction to the SMAP information system life-cycle and documentation standards
[NASA-TM-101765] 05 p0706 N90-14134
QUEST/Ada: Query utility environment for software testing of Ada
[NASA-CR-186121] 06 p0823 N90-14787
Software Reuse Issues
[NASA-CP-3057] 06 p0824 N90-14789
Knowledge-based reusable software synthesis system 06 p0824 N90-14791
Impact of domain analysis on reuse methods 06 p0824 N90-14792
Prototype software reuse environment at Goddard Space Flight Center 06 p0825 N90-14794
JPL reuse program 06 p0825 N90-14795
Johnson Space Center software reuse activity 06 p0825 N90-14796
Reuse research plans at Langley Research Center 06 p0825 N90-14797
Reuse at the Software Productivity Consortium 06 p0825 N90-14798
SSFP approach to software reuse 06 p0826 N90-14799
Level 2 software reuse study 06 p0826 N90-14800
An SSE approach to reusability 06 p0826 N90-14801
Support for life-cycle product reuse in NASA's SSE 06 p0826 N90-14802
Application of reusable software components at the SEI 06 p0826 N90-14804
Technology transfer in software engineering 06 p0827 N90-14805
AdaNET services 06 p0827 N90-14806
Advanced Software Development Workstation Project 06 p0827 N90-14807
Continuation of research in software for space operations support
[NASA-CR-186092] 06 p0827 N90-14808
Using object-oriented development to support prototyping
[DE90-000547] 06 p0829 N90-14821
A tutorial on software reliability engineering
[DE89-012368] 06 p0830 N90-14828
XNUSIM: Graphical interface for a multiprocessor simulator
[AD-A214176] 07 p0971 N90-15606
Transport modeling and advanced computer techniques
[DE90-001481] 07 p0972 N90-15612
Environment for failure region analysis: REACHER - a reachability condition derivation tool
[AD-A214183] 07 p0977 N90-15641
Using the singularity-separating method to study how to decrease the pressure at the end of a tube
[PREPRINT-490] 08 p1065 N90-16158
The Suprenum architecture and its application to computational fluid dynamics
[GMD-389] 08 p1065 N90-16161
The new programming
[RSRE-MEMO-4249] 08 p1110 N90-16425
Low-cost volumetric modeling
[CRIF-MC-85] 08 p1111 N90-16435
Software dependability growth characterization, modeling and evaluation
[LAAS-89320] 08 p1112 N90-16437
NASA/ASEE Summer Faculty Fellowship Program
[NASA-CR-166837] 08 p1154 N90-16686
Formalisms for user interface specification and design 08 p1155 N90-16687
Reusable navigation module 09 p1165 N90-16742
Spark source mass spectrometry software documentation and verification
[DE90-004463] 09 p1192 N90-16909
Supporting shared data structures on distributed memory architectures
[NASA-CR-181981] 09 p1262 N90-17318
Adapting software development policies to modern technology
[AD-A213991] 10 p1416 N90-18157
Raster Metafile and Raster Metafile Transiator
[NASA-TM-102588] 10 p1417 N90-18166
A system for execution of JSD requirements
[INPE-4915-TDL/381] 10 p1417 N90-18170
Logical architecture
[INPE-4792-RPE/585] 10 p1418 N90-18171
KAPSE Interface Team (KIT) public report, volume 7
[AD-A215838] 10 p1418 N90-18176
KAPSE Interface Team (KIT) public report, volume 8, part 1
[AD-A215839] 10 p1418 N90-18177
The implications of using integrated software support environment for design of guidance and control systems software
[AGARD-AR-229] 11 p1464 N90-18432
Vertical migration in operational system nucleus
[INPE-4879-RPE/593] 11 p1543 N90-18883
Technology assessment of software engineering
[AD-A216943] 11 p1546 N90-18902
Marshall Avionics Testbed System (MAST) 12 p1639 N90-19417
Design and architecture of fourth and fifth generation software engineering environments
[ETN-90-95365] 12 p1698 N90-19752
Development of an Ada programming support environment database SEAD (Software Engineering and Ada Database) administration manual
[NASA-CR-186064] 12 p1699 N90-19757
Recalibrating software reliability models
[NASA-CR-186407] 12 p1700 N90-19763
A nonparametric software reliability growth model
[NASA-CR-186438] 12 p1700 N90-19764
Software development: A paradigm for the future
[NASA-CR-186456] 12 p1701 N90-19766
Deceit: A flexible distributed file system
[NASA-CR-186412] 12 p1726 N90-19923
The Rapid Geodetic Survey System (RGSS) 13 p1834 N90-20528
Operational computer graphics in the flight dynamics environment 13 p1859 N90-20668
Software systems for modeling articulated figures 13 p1861 N90-20677
GCS plan for software aspects of certification
[NASA-CR-181972] 13 p1864 N90-20694
The HS6000/20 development system
[LINO-1989-6] 13 p1865 N90-20696
Using formal methods to develop a paradigm for software design
[DE90-005633] 13 p1866 N90-20703
Technical specifications requirements: Automated reasoning applications
[DE90-008799] 13 p1867 N90-20712
Research in programming languages and software engineering
[AD-A217765] 13 p1868 N90-20715
A review of the suitability of available Computer Aided Software Engineering (CASE) tools for the small software development environment
[AD-A218276] 13 p1870 N90-20726
Human centrifuge controller
[NAL-TM-SE-8901] 14 p1929 N90-21043
Numerical Arc Segmentation Algorithm for a Radio Conference (NASARC), version 4.0: User's manual
[NASA-TM-101454] 14 p1964 N90-21250
Human factors in fighter software development
[PD-CF-9003] 14 p2011 N90-21522
Maintenance = reuse-oriented software development
[NASA-CR-186455] 14 p2012 N90-21531
Integrating automated support for a software management cycle into the TAME system
[NASA-CR-186457] 14 p2013 N90-21532
Lessons learned in the transition to Ada from FORTRAN at NASA/Goddard
[NASA-TM-103311] 14 p2014 N90-21538

Toward a new CIM (Computer Integrated Manufacturing) architecture for Sandia Laboratories
[DE90-008677] 14 p2015 N90-21548
Improving a data-acquisition software system with abstract data type components
15 p2078 N90-21901
Software quality assurance: Towards a measurable quality improvement
[REPT-89-42] 15 p2147 N90-22264
A CSP model for distributed control software design
[OUEL-1789/89] 15 p2148 N90-22273
A study of caching in capability computers
[RSRE-89015] 15 p2149 N90-22276
The interactive digital video interface
16 p2271 N90-22941
The making of the mechanical universe
16 p2274 N90-22961
Object-oriented query languages: The notion and the issues
[REPT-89-054] 16 p2298 N90-23093
Comparative evaluations of four specification methods for real-time systems
[AD-A219187] 16 p2300 N90-23109
Version description and installation guide Kernel version 3.0
[AD-A219292] 16 p2301 N90-23113
Software techniques for non-von Neumann architectures
[AD-A220390] 17 p2440 N90-23902
A distributed program composition system
[NASA-CR-181568] 17 p2441 N90-23911
Evaluation methodology for software engineering
[AD-A218474] 17 p2441 N90-23913
Software maintenance on Airbus family
[REPT-892-111-101] 17 p2444 N90-23931
Some elementary questions on software quality control
[REPT-89-83] 17 p2445 N90-23939
Testing of elementary functions in Ada
[CWI-NM-R8909] 17 p2446 N90-23941
An experimental evaluation of software redundancy as a strategy for improving reliability
[NASA-TM-102613] 17 p2448 N90-23958
Concurrent Clean
[TR-89-18] 17 p2450 N90-23974
Fast casual multicast
[NASA-CR-186643] 17 p2462 N90-24059
Some issues related to simulation of the tracking and communications computer network
18 p2630 N90-24988
An approach to a real-time distribution system
19 p2733 N90-25535
GCS support/development system configuration document
[NASA-CR-182046] 19 p2743 N90-25589
Operations mission planner
[NASA-CR-186846] 19 p2747 N90-25611
Applying formal models and proofs to the verification of distributed systems
[IAR-89-7] 19 p2750 N90-25625
Technical evaluation report on the Guidance and Control Panel 49th Symposium on Fault Tolerant Design Concepts for Highly Integrated Flight Critical Guidance and Control Systems
[AGARD-AR-281] 20 p2813 N90-26012
Statistical analysis of a software reliability model
[IMAG-RR-781-M] 20 p2874 N90-26352
A Bayesian proportional model for software reliability
[IMAG-RR-795-M] 20 p2874 N90-26353
Practical applications of remote sensing technology
[NASA-CR-186810] 20 p2879 N90-26377
An expert system based software sizing tool, phase 2
[NASA-CR-186706] 20 p2905 N90-26525
Parallel processors and nonlinear structural dynamics algorithms and software
[NASA-CR-186755] 20 p2907 N90-26536
Documentation of program Tankplot
[FFI-89/7019] 20 p2908 N90-26541
Study of a class of non convex optimization algorithms: Implementation and applications
[ETN-90-97241] 20 p2909 N90-26552
VISTA (Vertical Integration of Science, Technology, and Applications) user interface software study
[DE90-010003] 20 p2936 N90-26707
Establishing a communications-intensive network to resolve artificial intelligence issues within NASA's Space Station Freedom research centers community
21 p3042 N90-27291
The integration of automated knowledge acquisition with computer-aided software engineering for space shuttle expert systems 21 p3045 N90-27307
Artificial Intelligence Software Engineering (AISE) model 21 p3045 N90-27309
An application generator for rapid prototyping of Ada real-time control software 21 p3046 N90-27316
Derivation of sorting programs
21 p3047 N90-27319
Inductive knowledge acquisition experience with commercial tools for space shuttle main engine testing
21 p3048 N90-27326
Automated unit-level testing with heuristic rules
21 p3049 N90-27335
Some software implementation of the functions sine and cosine
[DE90-010398] 21 p3050 N90-27339
Expert system in software engineering using Structured Analysis and Design Technique (SADT)
[AD-A223022] 21 p3052 N90-27351
Conceptual design of an integrated system for software systems design implementation and testing
[ETN-90-97318] 21 p3057 N90-27381
Rapid prototyping of formal specifications using Miranda
[NPL-DITC-150/89] 21 p3057 N90-27383
Start-up built-in test for the DISCUS fault tolerant, fly-by-wire computer system 22 p3104 N90-27625
Advanced algorithms design and implementation in on-board microprocessor systems for engine life usage monitoring 22 p3104 N90-27628
Economical graphics display system for flight simulation avionics
[NASA-CR-186886] 22 p3116 N90-27701
Concurrent Image Processing Executive (CIPE). Volume 2: Programmer's guide
[NASA-CR-186854] 22 p3236 N90-28349
Applications of X windows in astronautics: Status and prospects
[MBB-UO-0082-90-PUB] 22 p3238 N90-28365
Advanced transport operating system software upgrade: Flight management/flight controls software description
[NASA-CR-181936] 22 p3239 N90-28366
A conceptual framework for fighter flight control systems
[PD-CF-9009] 23 p3283 N90-28577
Data base for crack growth properties of materials
23 p3296 N90-28647
DOE/NIST Workshop on Common Architectures for Robotic Systems
[PB90-216839] 23 p3332 N90-28840
Experiments in the dynamic and strategic control of cooperating manipulators 23 p3333 N90-28845
The JPL telerobot operator control station. Part 2: Software 23 p3371 N90-29050
The KALI multi-arm robot programming and control environment 23 p3373 N90-29060
Preparing software conversion studies
[PB90-235623] 23 p3381 N90-29099
A stucture dependent software development on a relational basis: An integral approach
[ETN-90-97289] 23 p3381 N90-29101
Documenting the decision structure in software development
[NASA-CR-186865] 23 p3382 N90-29108
A knowledge-based system design/information tool
[NASA-CR-4316] 23 p3389 N90-29143
System software for Soviet computers
24 p3523 N90-29921
AHTO project: Software technology for open distributed processing
[PB90-190943] 24 p3524 N90-29923
Effects of parameter uncertainties on software development effort estimates
[AD-A223304] 24 p3526 N90-29938
Software development: A product life-cycle perspective
[AD-A223783] 24 p3528 N90-29952

SOFTWARE TOOLS

Computational controls for aerospace systems
01 p0017 N90-10082
CONSOLE: A CAD tandem for optimization-based design interacting with user-supplied simulators
01 p0017 N90-10085
Control/structure interaction methods for space station power systems 01 p0018 N90-10087
Modeling and control system design and analysis tools for flexible structures 01 p0018 N90-10090
String Search
[PB89-195986] 01 p0104 N90-10593
The applicability and limitations of expert system shells
[AD-A210801] 01 p0110 N90-10625
A distributed debugger for Amoeba
[CWI-CS-R8826] 02 p0257 N90-11453
Software configuration management: An overview
[PB89-193833] 02 p0258 N90-11458
Tools to aid in the development high-performance algorithms
[DE89-012395] 03 p0386 N90-12194
Software fault tolerance
[RSRE-MEMO-4237] 04 p0450 N90-12575
Automatic communications channel interference monitoring
[RSRE-MEMO-4243] 04 p0491 N90-12820
LOTOS tools based on the Cornell synthesizer generator
[MEMO-INF-89-5] 04 p0530 N90-13062
Truth maintenance systems and their implementation in PROLOG
[MEMO-INF-89-13] 04 p0531 N90-13064
User manual of the force structure model scenario editor SCENE
[FEL-1988-101] 04 p0531 N90-13069
Expert system for test program set fault candidate selection
[AD-A213336] 04 p0535 N90-13091
Test network Delft
[ETN-90-96009] 05 p0577 N90-13365
Computer-based tools for assisting air traffic controllers with arrivals flow management
[RSRE-88001] 05 p0577 N90-13366
Mission simulations 05 p0607 N90-13532
On the design of a computer-aided design system for digital circuits 05 p0633 N90-13695
Methodology for automating software systems. Task 1 of the foundations for automating software systems
[NASA-CR-180499] 05 p0681 N90-13965
The APROS software for process simulation and model development
[VTT-618] 05 p0684 N90-13987
Integrated computer-based tools to facilitate environmental monitoring, assessment, and restoration
[DE90-002732] 06 p0811 N90-14717
The effects of clutter-rejection filtering on estimating weather spectrum parameters
[NASA-CR-186212] 06 p0817 N90-14754
Software Reuse Issues
[NASA-CP-3057] 06 p0824 N90-14789
Classic-Ada(TM) 06 p0824 N90-14793
Prototype software reuse environment at Goddard Space Flight Center 06 p0825 N90-14794
Reuse research plans at Langley Research Center
06 p0825 N90-14797
SSFP approach to software reuse
06 p0826 N90-14799
Application of reusable software components at the SEI 06 p0826 N90-14804
Technology transfer in software engineering
06 p0827 N90-14805
Selecting and effectively using a computer aided software engineering tool
[DE89-017876] 06 p0828 N90-14815
Guidelines for evaluating energy analysis software
[AD-A214171] 07 p0976 N90-15640
Environment for failure region analysis: REACHER - a reachability condition derivation tool
[AD-A214183] 07 p0977 N90-15641
Young Investigator's Award and distributed self-adaptive databases
[AD-A214194] 07 p1010 N90-15854
The application of Z to the specification of air traffic control systems. 1: An initial specification of the radar processing activity
[RSRE-MEMO-4280] 08 p1020 N90-15900
The new programming
[RSRE-MEMO-4249] 08 p1110 N90-16425
A persistent heap for ALGOL 68
[RSRE-MEMO-4268] 08 p1110 N90-16427
Tool support for the production of high integrity software
[RSRE-89005] 08 p1111 N90-16433
A computer program to calculate the population numbers of multi-level species
[IFSI-89-15] 08 p1151 N90-16671
Parallel processing implementation of a flight controller 09 p1165 N90-16743
The performance implications of Ada in a MASCOT 3 design
[YM-5748-M304/2] 09 p1263 N90-17324
VULCAIN: An expert system dedicated to fire risk analysis within complex industrial environments
10 p1314 N90-17599
KAPSE Interface Team (KIT) public report, volume 8, part 2
[AD-A215840] 10 p1419 N90-18178
Aerodynamics of unsteady systems. Numerical study of potential flow/boundary layer coupling
[ETN-90-96257] 11 p1452 N90-18367
Ada-Linda preliminary report: Motivation, informal description, and examples
[AD-A216004] 11 p1545 N90-18892
. User manual for NEXT 1.2: NLR engineering X-pert system toolkit
[NLR-TR-87178-U] 11 p1547 N90-18905
A survey of performability modelling tools
[MEMO-INF-89-50] 11 p1547 N90-18907

Design and architecture of fourth and fifth generation software engineering environments
[ETN-90-95365] 12 p1698 N90-19752
TAE Plus: Transportable Applications Environment Plus tools for building graphic-oriented applications
13 p1856 N90-20652
Applications of graphics to support a testbed for autonomous space vehicle operations
13 p1858 N90-20661
The use of graphics in the design of the human-telerobot interface 13 p1860 N90-20670
Graphical programming and the use of simulation for space-based manipulators 13 p1861 N90-20674
Supercomputer environments
[AD-A217682] 13 p1863 N90-20689
A review of the suitability of available Computer Aided Software Engineering (CASE) tools for the small software development environment
[AD-A218276] 13 p1870 N90-20726
Fast causal multicast
[NASA-CR-186495] 14 p2013 N90-21533
Annotated bibliography of software engineering laboratory literature
[NASA-TM-103313] 14 p2013 N90-21536
Exploiting virtual synchrony in distributed systems
[NASA-CR-182855] 14 p2016 N90-21555
The ultimate CASE tool
[DE90-009351] 14 p2037 N90-21687
Distributed simulation, no special tools required
15 p2150 N90-22281
Resource Allocation Planning Helper (RALPH): Lessons learned 15 p2152 N90-22296
Orbital mechanics: A learning tool on the main frame
[AD-A218799] 16 p2204 N90-22576
A task-analytic approach to the automated design of information graphics
[AD-A219271] 16 p2265 N90-22912
The making of the mechanical universe
16 p2274 N90-22961
An assessment of multibody simulation tools for articulated spacecraft 16 p2279 N90-22988
Computational issue in the analysis of adaptive control systems 16 p2281 N90-23001
Overview of computational control research at UT Austin 16 p2291 N90-23051
ASTEC: Controls analysis for personal computers
16 p2291 N90-23052
A tool for aiding in the reuse of software
[INPE-4981-PRE/1545] 16 p2298 N90-23091
Reusing software components by specialization
[REPT-89-062] 16 p2298 N90-23094
Fault tolerant multiprocessing and development of tools
[AD-A219216] 16 p2301 N90-23110
ESPRIT 820:QUIC. QUIC toolkit demonstrator applications
[REPT-892-440-105] 17 p2386 N90-23590
A distributed program composition system
[NASA-CR-181568] 17 p2441 N90-23911
Tool support for VDM
[REPT-89-81] 17 p2445 N90-23938
Numerical optimization, system theoretic and software tools for the integrated design of flexible structures and their control systems
[AD-A219877] 17 p2447 N90-23949
A fast PC-based solver for simultaneous linear equations
[AD-A220190] 17 p2461 N90-24056
Computational tools for multi-linked flexible structures
[NASA-CR-186139] 17 p2462 N90-24058
Fast casual multicast
[NASA-CR-186643] 17 p2462 N90-24059
Distributed mission planning technology for Columbus
18 p2501 N90-24288
Flight support system servicing aid tool
18 p2501 N90-24293
Real time automatic programming
[AD-A220162] 18 p2591 N90-24740
Construction of an Ethernet model with the PROMISE simulation tool
[NLR-MP-88047-U] 18 p2593 N90-24757
CERC (Center for Energy Research Computation) report: Results of the CERC Project with recommendations for ANL (Argonne National Laboratory) institutional strategies in advanced scientific computing
[DE90-008238] 18 p2594 N90-24759
Graph structure model
[DE90-008945] 18 p2594 N90-24760
Tools for mapping environmental monitoring data
[PB90-129685] 19 p2712 N90-25432
SHAPA: An interactive software tool for protocol analysis applied to aircrew communications and workload
19 p2734 N90-25541
Execution time supports for adaptive scientific algorithms on distributed memory machines
[NASA-CR-182052] 19 p2741 N90-25576
Multi-version software reliability through fault-avoidance and fault-tolerance
[NASA-CR-186502] 19 p2742 N90-25584
Tools for distributed application management
[NASA-CR-186711] 19 p2742 N90-25586
A search for radio pulsars in globular clusters and transient X ray sources 19 p2772 N90-25755
Inference and control mechanisms in NEXT 2.0
[NLR-MP-88062-U] 20 p2844 N90-26175
ISIS and META projects
[NASA-CR-186645] 20 p2905 N90-26524
An expert system based software sizing tool, phase 2
[NASA-CR-186706] 20 p2905 N90-26525
SUPES version 2.1: A Software Utilities Package for the Engineering Sciences
[DE90-011763] 20 p2906 N90-26531
CAD/CAM reinforces the competitive edge of European mouldmakers
[CRIF-MC-88] 20 p2908 N90-26542
ATN design tool
[AD-A223030] 20 p2911 N90-26559
Communications network analysis tool
[AD-A222061] 21 p2996 N90-27029
Theoretical and computational aspects of turbulence
[AD-A221795] 21 p3005 N90-27083
ATS displays: A reasoning visualization tool for expert systems 21 p3042 N90-27290
Expert System Development Methodology (ESDM)
21 p3042 N90-27292
Design knowledge capture for a corporate memory facility 21 p3045 N90-27304
A plan for scientific visualization at ANL
[DE90-013565] 21 p3051 N90-27344
Knowledge based quality assurance tools
[AD-A223064] 21 p3053 N90-27353
Zadok user guide
[AD-A222071] 21 p3054 N90-27360
Rapid prototyping of formal specifications using Miranda
[NPL-DITC-150/89] 21 p3057 N90-27383
Debugging and analysis of large-scale parallel programs
[AD-A221678] 21 p3059 N90-27393
CUIS user's manual
[ESA-TM-03] 22 p3132 N90-27775
START: A module for image processing to IMAGE-BASE
[FOA-C-30551-8.3] 22 p3238 N90-28363
Improving software reusability by program specialization: A case study
[REPT-90-011] 22 p3240 N90-28374
Graph structure model
[DE90-014930] 23 p3381 N90-29097
A stucture dependent software development on a relational basis: An integral approach
[ETN-90-97289] 23 p3381 N90-29101
Software development tools
[PB90-250051] 23 p3381 N90-29103
Parallelization of a software relating to aerodynamics on MIMD type computers
[ONERA-RT-31/3479-CY] 23 p3384 N90-29114
Piecewise linear models of processor utilization
[DE90-014774] 23 p3384 N90-29115
Multi-disciplinary optimization of aeroservoelastic systems
[NASA-CR-185931] 24 p3432 N90-29385
Programming your way out of the past: ISIS and the META Project
[NASA-CR-186275] 24 p3524 N90-29922
MacRootLocus: A CAD design tool for feedback control systems
[AD-A223772] 24 p3528 N90-29951
ESTEC software catalogue
[ESA-SP-1133] 24 p3531 N90-29968
Supporting large scale applications on networks of workstations
[NASA-CR-186346] 24 p3532 N90-29975
Assessment System for Aircraft Noise (ASAN): Development of alpha-test prototype system software
[AD-A223770] 24 p3543 N90-30036

SOHO MISSION

The SOHO mission. Scientific and technical aspects of the instruments
[ESA-SP-1104] 04 p0566 N90-13302
SOHO: An observatory to study the solar interior and the solar atmosphere 04 p0566 N90-13303
GOLF: Global Oscillations at Low Frequencies for the SOHO mission 04 p0566 N90-13304
VIRGO: The solar monitor experiment on SOHO
04 p0567 N90-13305
SOI: The Solar Oscillations Imager on SOHO
04 p0567 N90-13306
EIT: Solar corona synoptic observations from SOHO with an Extreme-ultraviolet Imaging Telescope
04 p0567 N90-13309
UVCS: An Ultraviolet Coronagraph Spectrometer for SOHO 04 p0568 N90-13310
LASCO: A wide-field white light and spectrometric coronagraph for SOHO 04 p0568 N90-13311
SWAN: A study of solar wind anisotropies
04 p0568 N90-13312
CELIAS: Charge, element and isotope analysis system for SOHO 04 p0568 N90-13313
COSTEP: A comprehensive suprathermal and energetic particle analyzer for SOHO 04 p0568 N90-13314

SOI (SEMICONDUCTORS)

Epitaxial GaAs on SOI wafers
[AD-A209009] 01 p0127 N90-10729
Chemical profiling of silicon nitride structures
[AD-A215643] 09 p1192 N90-16907
Method of producing a thin silicon-on-insulator layer
[AD-D014330] 09 p1290 N90-17478
Radiation-hardened wafer scale integration
[AD-A217332] 13 p1793 N90-20290
Transient radiation hardened CMOS (Complementary Metal Oxide Semiconductor) operational amplifiers
[AD-A217972] 13 p1797 N90-20313
Identification of defects in SOI (Silicon-On-Insulator) wafers
[DE90-006020] 13 p1895 N90-20879

SOIL EROSION

Mechanics of aeolian processes: Soil erosion and dust production 12 p1638 N90-19410
Aerial videotape survey of coastal Louisiana, 1986. Louisiana Barrier Island erosion and land loss study: 1986-1990
[PB90-194648] 22 p3195 N90-28128

SOIL MAPPING

Physically-based parameterization of spatially variable soil and vegetation using satellite multispectral data
[NASA-CR-185957] 05 p0663 N90-13879
The use of a deformation model for sampling digitalized stereoscopic images
[IMAG-RR-753-I] 05 p0664 N90-13884
Land suitability maps and appropriate land use: An approach using SGI and satellite imagery
[INPE-4827-PRE/1458] 11 p1521 N90-18761
Mapping and monitoring land use and land degradation in part of East Kalimantan, Indonesia, using aerospace remote sensing techniques: A SPOT case study
[BCRS-88-16B] 19 p2705 N90-25394

SOIL MECHANICS

Proceedings of the 4th European Conference, volume 2
[AD-A216521] 14 p1986 N90-21382

SOIL MOISTURE

An investigation of satellite sounding products for the remote sensing of the surface energy balance and soil moisture
[NASA-CR-186073] 06 p0801 N90-14664
Multiparameter scatterometer for remote sensing (RADSER). Project Scatter: State-of-the-art and future applications
[INPE-4871-PRE/1482] 11 p1511 N90-18701

SOIL SCIENCE

The soil microbiology of hydrazines
02 p0205 N90-11171
Utilization of remote sensing in geoscientific development and projects 08 p1094 N90-16334
Statistical information system for cultivation of the soil. Use of remote sensing in official statistics
08 p1095 N90-16338
LANDSAT-TM and agrometeorological data in the wheat crop yield estimation at the farm level
[INPE-4842-PRE/1471] 10 p1400 N90-18091
Radiometric study of wheat and bean crops in three types of latossolo
[INPE-4843-PRE/1472] 11 p1523 N90-18767
Relationships between spectral parameters and agronomics of wheat and beam crops
[INPE-4791-RPE/584] 11 p1523 N90-18768
Spectral response of wheat and its relationship with agronomical prameters
[INPE-4950-RPE/599] 11 p1524 N90-18774
Relationship of radiometric field measurements of wheat in the Assis-Safra region, 1988
[INPE-4949-RPE/598] 13 p1819 N90-20443
Wheat productivity estimate through field radiometry
[INPE-4994-PRE/1556] 14 p2000 N90-21460
Scattering of waves by inclusions in a nonhomogeneous elastic half space solved by boundary element methods
[PB90-145699] 15 p2116 N90-22107
Spectral response of wheat and its relationship with agronomic variables in the tropical region
[INPE-5018-RPE/612] 15 p2122 N90-22138
Soil experiment
[NASA-CR-184927] 20 p2842 N90-26165

SOILS
NT ALLUVIUM
NT LUNAR DUST
NT LUNAR SOIL
NT PERMAFROST
NT SANDS
The Third Conference on the Environmental Chemistry of Hydrazine Fuels
[AD-A197632] 02 p0203 N90-11157
Hydrazine fate and transformation in natural waters and soils 02 p0204 N90-11165
Vibrational spectroscopic study of the kaolinite-hydrazine intercalation complex 02 p0204 N90-11166
The soil microbiology of hydrazines 02 p0205 N90-11171
Measurement of hydrazine contamination in soils 02 p0206 N90-11180
Global data bases on distribution, characteristics and methane emission of natural wetlands: Documentation of archived data tape
[NASA-TM-4153] 03 p0365 N90-12090
Image processing of LANDSAT MSS data for buried valley detection in northern Indiana 06 p0802 N90-14668
Development of a robotics system for automated chemical analysis of sediment, sludges, and soils
[DE90-003637] 07 p0895 N90-15170
Attempt to draw conclusions concerning the geological subsoil from the vegetation using digital image processing of TM data 08 p1093 N90-16329
Estimating water flow through a hillslope using the massively parallel processor 08 p1114 N90-16449
The pollution hazard assessment system: Documentation and users manual
[AD-A217108] 12 p1689 N90-19706
LANDSAT-5 data in the study of wheat and bean crops
[INPE-4746-RPE/580] 13 p1819 N90-20444
Analysis of methods to determine emissivity for ground surface targets in the spectral band 8 to 14 microns
[INPE-4984-TDL/394] 13 p1820 N90-20447
Air pollution-caused changes in photosynthesis: Effects on plant growth and rhizosphere functions
[DE90-007184] 13 p1829 N90-20501
Monitoring of agrocattle-raising projects through visual/digital analysis of LANDSAT-TM imagery south of Para state
[INPE-4982-PRE/1542] 14 p1996 N90-21442
Effects of Air Pollution on Western Forests
[PB90-131111] 14 p2003 N90-21481
Gaithersburg Nike control and launch area preliminary assessment/site inspection, Gaithersburg, Maryland
[AD-A217791] 14 p2003 N90-21482
Radon concentration over the Brazilian Amazon Basin during the wet season (Belem-Manaus GTE-ABLE-2B flight of April 24, 1987)
[INPE-4892-PRE/1493] 14 p2004 N90-21486
Scattering of waves by inclusions in a nonhomogeneous elastic half space solved by boundary element methods
[PB90-145699] 15 p2116 N90-22107
Use of high-dimensional spectral data to evaluate organic matter, reflectance relationships in soils
[NASA-CR-186650] 18 p2574 N90-24665
Ecological study of peat landforms in Canada and Alaska
[NASA-CR-184923] 19 p2705 N90-25391
Enhanced bioreclamation of jet fuels: A full-scale test at Eglin AFB, Florida
[AD-A222348] 21 p2990 N90-26992
Evaluation of the role of ozone, acid deposition, and other airborne pollutants in the forests of eastern North America
[PB90-184896] 22 p3197 N90-28140
Development and testing of rapid repair methods for war damaged runways
[AD-A223970] 23 p3285 N90-28586
Robotic sampling system for an unmanned Mars mission 23 p3375 N90-29070
Data Base Analyzer and Parameter Estimator (DBAPE) interactive computer program user's manual
[PB90-193053] 23 p3406 N90-29252

SOL-GEL PROCESSES
Fifth International Workshop on Glasses and Ceramics from Gels
[DE89-016899] 02 p0201 N90-11147
Synthesis of powder with gel technique
[FOA-C-20752-2.4(2.1)] 02 p0202 N90-11156
Linear (passive) and non-linear guided and studies in glass
[AD-A211693] 03 p0406 N90-12325
Synthesis and microstructure of highly oriented PbTiO3 thin films prepared by a sol-gel method
[AD-A211735] 03 p0414 N90-12377
Oxide ceramic fibers by the sol-gel methods
[AD-A211315] 04 p0478 N90-12742
Sol-gel processing science using a Sol-Gel Optics Research Facility (SGORF)
[AD-A213056] 05 p0699 N90-14095
Superconducting film fabrication by the sol-gel process
[DE90-002069] 07 p0909 N90-15252
High-temperature ceramic superconductors
[AD-A214251] 07 p1005 N90-15818
Development of low density silica aerogel as a capture medium for hyper-velocity particles
[NASA-CR-185930] 08 p1121 N90-16489
Advanced ceramics
[DE90-608004] 12 p1630 N90-19370
Sol-gel derived polytitanosiloxane coatings
[DE90-004186] 13 p1779 N90-20210
Synthesis and characterization of aromatic polyester and polysiloxane containing block copolymers: Multiphase transparent atomic oxygen resistant damping materials, liquid crystal films, and toughening components of sol/gel glasses
[AD-A218871] 16 p2224 N90-22685
Properties of films prepared from low surface area/density alumina-silica
[DE90-011048] 18 p2531 N90-24446
Sol-gel coating on acoustic wave devices: Thin film characterization and chemical sensor development
[DE90-012224] 19 p2679 N90-25235
Sol-gel processing for fiber optic applications
[DE90-012083] 19 p2758 N90-25675
Structure-property behavior of new organic-inorganic polymeric hybrid materials based on sol gel chemistry
[AD-A222168] 21 p2987 N90-26974
Preparation and characterization of thin films based on sol-gel technique and development of spectroscopic probe for film formation and characterization
[AD-A221762] 21 p2988 N90-26984
Kinetics and structure of silicate sol-gels
[DE90-015702] 24 p3456 N90-29521

SOLAR ACTIVITY
NT SOLAR FLARES
NT SOLAR PROMINENCES
NT SOLAR STORMS
NT SUNSPOTS
Solar-geophysical data number 532, December 1988. Part 1: Data for November, October 1988, and late data
[PB89-152086] 01 p0142 N90-10818
Solar-geophysical data number 533. Part 1: Data for December, November 1988, and late data
[PB89-162481] 01 p0142 N90-10820
Solar-geophysical data number 534, February 1989. Part 1: (Prompt reports). Data for January 1989, December 1988 and late data
[PB89-173041] 01 p0142 N90-10822
Long-term solar-terrestrial observations
[DE89-016318] 01 p0143 N90-10825
Meeting of intercosmos space physics group 02 p0158 N90-10902
Solar-geophysical data number 536, part 1. Data for March, Febuary 1989 and late data
[PB89-194716] 02 p0296 N90-11684
MHD (magnetohydrodynamic) modeling of solar and interplanetary processes
[PB89-215461] 03 p0420 N90-12416
Access to Max '91 information via computer networks 03 p0430 N90-12466
Solar-geophysical data number 537, May 1989. Part 2: Comprehensive Reports, data for Nov. 1988 and miscellaneous
[PB89-207401] 04 p0566 N90-13300
Solar-geophysical data number 538, June 1989. Part 1: (Prompt reports). Data for May, April 1989, and late data
[PB89-223838] 06 p0866 N90-15031
Solar-geophysical data number 540, August 1989. Part 1: (Prompt reports). Data for July, June 1989, and late data
[PB90-108572] 06 p0866 N90-15035
The solar activity measurements experiments (SAMEX) for improved scientific understanding of solar activity
[NASA-TM-100372] 08 p0867 N90-15036
Solar variability observed through changes in solar figure and mean diameter
[DE90-006600] 11 p1535 N90-18834
Solar-geophysical data number 541, September 1989. Part 1: (Prompt reports). Data for August, July 1989, and late data
[PB90-122763] 12 p1745 N90-20032
Solar cyclical trend study of the mid-latitude, quiet-time, meridional, neutral winds at winter solstice conditions
[AD-A217398] 13 p1841 N90-20568
A 154-day periodicity in the occurrence rate of proton flares
[NASA-CR-185826] 16 p2340 N90-23333
Solar UV variability 22 p3201 N90-28162

SOLAR ACTIVITY EFFECTS
Radio propagation conditions forecast above a low latitude region 02 p0247 N90-11400
User's guide to the Space Environment Services Center geophysical alert broadcasts
[PB89-194617] 02 p0249 N90-11411
Some of the terrestrial effects of AR 5395 03 p0433 N90-12482
Interplanetary energetic particle observations of the March 1989 events 03 p0434 N90-12484
Solar-geophysical data number 538, June 1989. Part 1: (Prompt reports). Data for May, April 1989, and late data
[PB89-223838] 06 p0866 N90-15031
Solar cycle effects on trapped energetic particles
[AD-A215028] 09 p1300 N90-17532
Estimates of galactic cosmic ray shielding requirements during solar minimum
[NASA-TM-4167] 09 p1300 N90-17535
On the antarctic ozone depletion during solar cycle 21
[NOTA-INTERNA-943] 16 p2253 N90-22849
The Pioneer Venus Orbiter: 11 years of data. A laboratory for atmospheres seminar talk
[NASA-TM-100761] 16 p2328 N90-23273
Proceedings of Workshop on Atmospheric Density and Aerodynamic Drag Models for Air Force Operations, volume 2
[AD-A220382] 17 p2345 N90-23356
Space exploration: Cost, schedule, and performance of NASA's Ulysses Mission to the Sun. Fact sheet for the Chairman, Subcommittee on Science, Technology, and Space, Committee on Commerce, Science, and Transportation, US Senate
[GAO/NSIAD-88-129FS] 20 p2815 N90-26023
Middle Atmosphere Program. Handbook for MAP, volume 29. Part 1: Extended Abstracts, International Symposium on Solar Activity Forcing of the Middle Atmosphere. Part 2: MASH Workshop
[NASA-CR-186005] 22 p3201 N90-28161
Effects of corpuscular radiation on weather and climate 22 p3201 N90-28164
The tropospheric response pattern to solar activity forcing 22 p3201 N90-28165
A review of the 11-year solar cycle, the QBO, and the atmosphere relationship 22 p3202 N90-28166
Seasonal variation of the 11 year solar cycle effect on the middle atmosphere: Role of the quasi biennial oscillation 22 p3202 N90-28167
Influence of solar activity on middle atmosphere associated with phases of equatorial quasi-biennial oscillation 22 p3202 N90-28168
Solar activity influence on climatic variations of stratosphere and mesosphere in mid-latitudes 22 p3202 N90-28169
The QBO and weak external forcing by solar activity: A three dimensional model study 22 p3203 N90-28171
Solar activity, the QBO, and tropospheric responses 22 p3203 N90-28172
A search for solar related changes in tropospheric weather 22 p3203 N90-28173
The mesospheric responses to short-term solar ultraviolet variability 22 p3204 N90-28174
Response of the middle atmosphere to solar UV and dynamical perturbations 22 p3204 N90-28175
Gases of the middle atmosphere and short-term solar radiation variations 22 p3204 N90-28177
Resonant Rossby waves and solar activity 22 p3205 N90-28179
On the relationship between the phases of 27-day total ozone and solar activity indices in different latitudinal zones 22 p3205 N90-28180
Total ozone time variations during the spring reversals in the high latitudinal stratosphere of the Northern Hemisphere during the 20th and 21st solar cycles 22 p3205 N90-28181
The vertical ozone distribution during maximum and minimum solar activity 22 p3205 N90-28182
Variation of D-region nitric-oxide density with solar activity and season at the dip equator 22 p3205 N90-28183
Physical mechanisms of solar activity effects in the middle atmosphere 22 p3206 N90-28185
Numerical simulation of the middle atmosphere chemical composition and temperature under changing solar conditions 22 p3206 N90-28186
An influence of solar activity on latitudinal distribution of atmospheric ozone and temperature in 2-D radiative-photochemical model 22 p3206 N90-28187
The effects of solar particle events on the middle atmosphere 22 p3206 N90-28189
A change of mesospheric ozone content under electron precipitation influence 22 p3207 N90-28191
Solar activity influence on cosmic ray penetration in the middle atmosphere 22 p3207 N90-28192

Effects of solar activity in the middle atmosphere dynamical regime over Eastern Siberia, USSR
22 p3207 N90-28195
Solar activity influences on atmospheric electricity and on some structures in the middle atmosphere
22 p3207 N90-28196
Relationship between solar activities and thunderstorm activities in the Beijing area and the northeast region of China 22 p3208 N90-28197
General overview of the solar activity effects on the lower ionosphere 22 p3208 N90-28198
Electron density profiles in the background of LF absorption during Forbush-decrease and PSE
22 p3208 N90-28199
Solar or meteorological control of lower ionospheric fluctuations (2-15 and 27 days) in middle latitudes
22 p3209 N90-28202
The 27-day versus 13.5-day variations in the solar Lyman-alpha radiation and the radio wave absorption in the lower ionosphere over Europe
22 p3209 N90-28203
The probability of SWF occurrence in relation to solar activity 22 p3209 N90-28204
The natural VLF emission as diagnostics and estimation means of the fluxes of solar x ray bursts
22 p3209 N90-28206
Ionospheric effects of the extreme solar activity of February 1986 22 p3210 N90-28207
A radio frequency user's guide to the space environment services center geophysical alert broadcasts
[PB90-240631] 23 p3351 N90-28935

SOLAR AND HELIOSPHERIC OBSERVATORY
U SOHO MISSION

SOLAR ARRAYS
NT SOLAR BLANKETS
Power beaming options 01 p0027 N90-10142
Applicability of the beamed power concept to lunar rovers, construction, mining, explorers and other mobile equipment 01 p0030 N90-10159
Earth orbit laser systems 01 p0030 N90-10162
Central electrical utility power for a satellite ring city in low earth orbit space 01 p0031 N90-10166
Acoustic response analysis in the low frequency domain 02 p0179 N90-11010
The third generation rigid solar array GSR3
02 p0180 N90-11017
Mathematical model and predictions for static and dynamic behavior of solar array structure
02 p0184 N90-11049
Space telescope solar array: Nonlinear test and analysis effects 02 p0185 N90-11051
Deployment simulation for 3rd generation solar array GSR3 02 p0188 N90-11074
STSA-Space Telescope solar array interconnectors: From simple approaches to complex modeling. A case study of the necessity of complex analysis
02 p0188 N90-11076
The Space Station Photovoltaic Panels Plasma Interaction Test Program: Test plan and results
[NASA-TM-102474] 05 p0613 N90-13581
Results of the 1989 NASA/JPL balloon flight solar cell calibration program
[NASA-CR-186114] 06 p0803 N90-14672
The design and performance of a general purpose 57 kilowatt solar array simulator for current and future large spacecraft 10 p1330 N90-17685
The spacebus power conditioning application to the Eutelsat 2 spacecraft 10 p1330 N90-17689
European Space Power, volume 2
[ESA-SP-294-VOL-2] 10 p1338 N90-17748
On-orbit demonstration of GaAs solar cell and panel technologies 10 p1339 N90-17751
Application of gallium arsenide solar cell arrays for long duration low earth orbit missions like Columbus
10 p1340 N90-17759
Structural and operational aspects of the concentrating SARA-Louver solar generator 10 p1340 N90-17760
SFU solar array 10 p1340 N90-17761
The GSR3: A new approach for solar array deployments 10 p1340 N90-17762
Deployment simulation for the third generation solar arrays GSR3 10 p1340 N90-17763
Solar array designs for Columbus elements
10 p1340 N90-17764
A low cost anticharging connection system for solar generators and its application on ASPERA solar array
10 p1341 N90-17765
The ISO solar generator: Solar cells and OSR mixed
10 p1341 N90-17767
Design development and qualification of a solar array with OSRs (SSM) bonded to the ISO spacecraft rigid sunshield 10 p1341 N90-17768
Direct glassing of silicon solar cells
10 p1341 N90-17769
Development of an aluminium solar cell interconnector technology 10 p1341 N90-17771
Manufacture and testing of a solar panel assembly comprising bifacial solar cells (AMOC-SPA)
10 p1342 N90-17773
NASA advanced space photovoltaic technology: Status, potential and future mission applications
10 p1342 N90-17775
The INMARSAT-2 solar generator panels
10 p1343 N90-17782
A pulsed solar simulator for electrical performance tests of space solar cells/arrays 10 p1343 N90-17783
Structural design of the Telecom 2 solar array
10 p1343 N90-17786
The ITALSAT solar array 10 p1343 N90-17787
CIC type thin diode for solar array
10 p1344 N90-17788
New models and techniques for predicting radiation effects on solar array performances
10 p1344 N90-17790
The electrical design of solar arrays for communication satellites 10 p1344 N90-17792
Assessment of in-orbit performance data of a bifacial flight experiment 10 p1344 N90-17793
SPOT 1 solar array: Three years in orbit performance evaluation 10 p1344 N90-17795
Design development, qualification, and flight production of an ATOX resistant flexible solar array for low earth orbit mission 10 p1344 N90-17796
The advanced photovoltaic solar array program
10 p1345 N90-17797
The solar array of Japanese solar observatory satellite Solar-A 10 p1345 N90-17798
Lightweight, low cost, thin silicon cell arrays
10 p1345 N90-17800
Solar arrays in the LEO-plasma environment: A model for leakage current phenomena deduced from experimental and theoretical studies
10 p1345 N90-17802
Review of synergistic environmental interactions: Guidelines for new testing approaches on future solar arrays 10 p1345 N90-17803
In-orbit performance of CS-3a spacecraft GaAs solar array 10 p1346 N90-17804
Simulation of micrometeoroid impacts by laser pulses
10 p1346 N90-17806
WPK: Solar array dimensioning tool
10 p1346 N90-17808
A transient plasticity study and low cycle fatigue analysis of the Space Station Freedom photovoltaic solar array blanket
[NASA-TM-102516] 12 p1674 N90-19617
Space mechanism of low velocity for an array of solar panels: Analysis and design of an experimental model; dimensions of bearings
[INPE-4859-TDL/370] 13 p1809 N90-20390
Controls, Astrophysics, and Structures Experiment in Space (CASES) 14 p1937 N90-21085
Recent results from advanced research on space solar cells at NASA
[NASA-TM-102485] 14 p1968 N90-21274
Infrared ground-based astronomy with the Hughes 256 X 256 PtSi array 14 p1978 N90-21331
Preliminary design of a long-endurance Mars aircraft
[NASA-CR-185243] 15 p2052 N90-21763
Photovoltaic power for Space Station Freedom
[NASA-TM-102569] 15 p2062 N90-21812
Analysis of thermal energy storage material with change-of-phase volumetric effects
[NASA-TM-102457] 15 p2092 N90-21974
Space Station Freedom solar array panels plasma interaction test facility
[NASA-TM-102475] 15 p2186 N90-22488
Mechanisms add foldability to ROSAT solar panels
18 p2538 N90-24483
Detachable interface mechanism
18 p2540 N90-24497
Dynamic analysis of space-related linear and non-linear structures
[NASA-TM-103490] 19 p2667 N90-25174
Performance of a self-aligning solar array tracking controller
[DE90-011184] 19 p2698 N90-25350
LEO high voltage solar array arcing response model, continuation 5
[NASA-CR-186505] 19 p2709 N90-25418
The photovoltaic concentrator initiative
[DE90-011228] 19 p2710 N90-25425
Solar array automation limitations
19 p2729 N90-25513
Discharge transient coupling in large space power systems 19 p2735 N90-25544
Interactions between the Space Station and the environment: A preliminary assessment of EMI
19 p2737 N90-25557
Solar array arcing in plasmas
19 p2737 N90-25558
Photovoltaic array space power plus diagnostics experiment 19 p2737 N90-25559
The chemical effects of the Martian environment on power system component materials: A theoretical approach
[NASA-TM-103203] 20 p2825 N90-26074
Analysis of a Mars-stationary orbiting microwave power transmission system
[NASA-TM-101344] 20 p2843 N90-26172
The natural VLF emission as diagnostics and estimation means of the fluxes of solar x ray bursts
22 p3209 N90-28206
A solar power system for an early Mars expedition
[NASA-TM-103219] 22 p3243 N90-28393

SOLAR ATMOSPHERE
The hard x rays and gamma-rays from solar flares
[NASA-CR-185982] 03 p0429 N90-12458
Investigation of active regions at high resolution by balloon flights of the Solar Optical Universal Polarimeter (SOUP) 03 p0434 N90-12487
SOHO: An observatory to study the solar interior and the solar atmosphere 04 p0566 N90-13303
EIT: Solar corona synoptic observations from SOHO with an Extreme-ultraviolet Imaging Telescope
04 p0567 N90-13309
CELIAS: Charge, element and isotope analysis system for SOHO 04 p0568 N90-13313
ERNE: Energetic and Relativistic Nuclei and Electron experiment 04 p0568 N90-13315
A high-resolution atlas of the infrared spectrum of the Sun and the Earth atmosphere from space: A compilation of ATMOS spectra of the region from 650 to 4800 cm (2.3 to 16 micron). Volume 1: The Sun
[NASA-RP-1224-VOL-1] 05 p0666 N90-13893
Rotation of the photospheric magnetic fields: A north-south asymmetry
[NASA-CR-186159] 05 p0715 N90-14177

SOLAR AZIMUTH
U AZIMUTH
U SOLAR POSITION

SOLAR BLANKETS
The advanced photovoltaic solar array program
10 p1345 N90-17797

SOLAR CELLS
Laser energy conversion 01 p0029 N90-10152
Laser-powered lunar base 01 p0029 N90-10156
High-efficiency CuInSe2 and CuInGaSe2 based cells and materials research
[DE89-009449] 01 p0083 N90-10471
Alternative fabrication techniques for high-efficiency CuInSe2 and CuInSe2-alloy films and cells
[DE89-009451] 01 p0083 N90-10474
Study of a gallium arsenide solar cell interconnector
02 p0182 N90-11033
CuInSe2 solar cell research by sputter deposition
[DE89-009450] 02 p0236 N90-11345
Laser grooved and polycrystalline silicon solar cell research
[DE89-015196] 02 p0237 N90-11347
Proceedings of the Polycrystalline Thin Film Program Meeting
[DE89-009457] 02 p0237 N90-11348
Novel thin-film CuInSe2 fabrication
[DE89-009440] 02 p0281 N90-11604
On-orbit annealing of gallium arsenide solar cell arrays
[AD-A212087] 03 p0334 N90-11900
Analysis of loss mechanisms in polycrystalline thin-film solar cells
[DE89-009454] 03 p0366 N90-12093
Graded bandgap solar cells
[AD-A211537] 03 p0367 N90-12097
The photovoltaic properties of an Al In As/InP heterojunctions grown by LPE method
[NASA-CR-185996] 05 p0665 N90-13886
Evolution of the EPR procedure for polycrystalline Si ribbon drawing for photovoltaic cell manufacturing
[ISAL-89-0027] 05 p0665 N90-13888
Results of the 1989 NASA/JPL balloon flight solar cell calibration program
[NASA-CR-186114] 06 p0803 N90-14672
Research on high-efficiency, multiple-gap, multijunction, amorphous-silicon-based alloy thin-film solar cells
[DE89-009444] 06 p0803 N90-14673
Preparation and properties of high deposition a-Si:H films and solar cells using disilane
[DE89-009467] 06 p0804 N90-14679
Thin film cadmium telluride, zinc telluride, and mercury zinc telluride solar cells
[DE89-009499] 06 p0804 N90-14681
Research on high-efficiency, single-junction, monolithic, thin-film amorphous silicon solar cells
[DE89-000846] 06 p0805 N90-14687
High-efficiency large-area CdTe modules
[DE89-009498] 06 p0806 N90-14689
Hydrogen radical enhanced growth of solar cells
[DE89-009497] 06 p0806 N90-14694

Photovoltaic Measurements and Performance Branch
[DE89-009500] 06 p0807 N90-14695
Study of microcrystalline, silicon-carbon p-layers prepared by photo-CVD and glow discharge
[DE89-009438] 06 p0850 N90-14939
Instability of a-Si:H/Ag interface at 150 deg C
[DE89-009419] 07 p0950 N90-15498
Research on amorphous silicon-germanium alloys for tandem solar cells
[DE89-009436] 07 p0950 N90-15499
Research on high-efficiency, single-junction, monolithic, thin-film amorphous silicon solar cells, phase 1
[DE89-009495] 07 p0951 N90-15502
Research on high-efficiency, single-junction, monolithic, thin-film amorphous silicon solar cells, phase 2
[DE89-009496] 07 p0951 N90-15503
US Polycrystalline Thin Film Solar Cells Program
[DE89-009506] 07 p0951 N90-15504
High-efficiency silicon concentrator solar cells for use with prismatic covers
[DE90-002644] 07 p0952 N90-15509
Characteristics of CMOS analog integrated structures using MOSIS (Metal Oxide Semiconductor Implementation System)
[DE90-001630] 07 p0998 N90-15773
The effect of annealing treatments on defect structure and diffusion lengths in n-type GaAs
[AD-A214215] 07 p1005 N90-15817
Spectral sensitivity of device power output for tandem a-Si alloy solar cells
[DE89-009421] 08 p1095 N90-16340
Radiation resistance of solar cells for space application. 1: Study on the irradiation procedure of electron beams
[DE90-719546] 08 p1096 N90-16349
Light-trapping concentrator cells
[DE90-004988] 09 p1242 N90-17205
High-efficiency copper ternary thin film solar cells
[DE89-009470] 09 p1242 N90-17207
Research on stable high-efficiency, large area, amorphous silicon-based solar cells, phase 2
[DE89-009491] 09 p1242 N90-17208
European Space Power, volume 2
[ESA-SP-294-VOL-2] 10 p1338 N90-17748
GaAs cells on Si substrates: A new challenge for space photovoltaic applications 10 p1339 N90-17750
On-orbit demonstration of GaAs solar cell and panel technologies 10 p1339 N90-17751
Advanced GaAs space solar cells by MOCVD technique 10 p1339 N90-17752
Fabrication of ultra thin GaAs and Ge substrates for high efficiency solar cells 10 p1339 N90-17753
GaAs solar cells with V-grooved emitters 10 p1339 N90-17754
GaAs space solar cells: Pilot production experience using a multi wafer infinite melt liquid phase epitaxy process 10 p1339 N90-17756
Radiation effects in ITO/InP solar cells 10 p1340 N90-17757
Indium phosphide solar cell research in the United States: Comparison with non-photovoltaic sources 10 p1340 N90-17758
Application of gallium arsenide solar cell arrays for long duration low earth orbit missions like Columbus 10 p1340 N90-17759
SFU solar array 10 p1340 N90-17761
Ultrasonic and parallel gap welding of GaAs solar cells, experimental and simulation results 10 p1341 N90-17766
Direct glassing of silicon solar cells 10 p1341 N90-17769
A concept of a pilot production plant for directly glassed silicon 10 p1341 N90-17770
Development of an aluminium solar cell interconnector technology 10 p1341 N90-17771
Assembly technology of GaAs solar cell 10 p1341 N90-17772
Temperature measurement during welding of solar cells and calibration of finite element models 10 p1342 N90-17774
NASA advanced space photovoltaic technology: Status, potential and future mission applications 10 p1342 N90-17775
Assessment of solar cell quality criteria 10 p1342 N90-17776
High-efficient solar cells for space application 10 p1342 N90-17777
Reduction of 50 micron thick solar cell weight by selective back contact silver plating 10 p1342 N90-17778
Assessment of bifacial silicon solar cells for space applications 10 p1342 N90-17779
Pilot production of 70 micron thin silicon solar cells 10 p1343 N90-17780
GaAs back point contact solar cell simulation 10 p1343 N90-17781
A pulsed solar simulator for electrical performance tests of space solar cells/arrays 10 p1343 N90-17783
Limits of efficiency of solar cells under AMO-spectrum illumination: Comparison between Si and GaAs cells 10 p1343 N90-17784
Solar cell coverglasses with enhanced thermal and mechanical properties 10 p1343 N90-17785
Investigations on hot spots effects in reverse biased spatial solar cells 10 p1344 N90-17789
New models and techniques for predicting radiation effects on solar array performances 10 p1344 N90-17790
Solar cell electrodynamic characteristics test equipment 10 p1344 N90-17791
The electrical design of solar arrays for communication satellites 10 p1344 N90-17792
On-orbit results of the LIPS 3/InP homojunction solar cell experiment 10 p1344 N90-17794
Lightweight, low cost, thin silicon cell arrays 10 p1345 N90-17800
Micrometeoroid impacts on silver bus bar targets at elevated voltages 10 p1346 N90-17805
Improved solar cells testing fixtures 10 p1346 N90-17807
Development of a solar-powered infrared injection laser microminiature transmitting system
[DE90-005672] 10 p1389 N90-18034
Research on high-efficiency, multi-gap, multi-junction amorphous silicon-based alloy thin-film solar cells
[DE89-009492] 10 p1402 N90-18101
International Summer School on Solid State Microbatteries
[AD-A213457] 10 p1434 N90-18277
Hydrogenated amorphous silicon films prepared by glow discharge of disilane
[DE90-000309] 11 p1491 N90-18581
Progress in thin film solar photovoltaic technologies
[DE89-009513] 11 p1527 N90-18792
Optimization of the reference parameters in the accompanying solar panel dynamics
[INPE-4795-PRE/1449] 11 p1528 N90-18798
Radiation-hard high-efficiency InP space solar cell development
[AD-A216857] 11 p1528 N90-18800
Chemical vapor deposition and photochemical vapor deposition of amorphous silicon photovoltaic devices
[DE89-009510] 11 p1529 N90-18803
Study on the measures to promote the use of photovoltaic power generating system overseas
[DE90-742056] 11 p1530 N90-18807
Study of the optimization of reference parameters to the dynamic constraints of solar panels
[INPE-4793-TDL/355] 12 p1681 N90-19656
Investigations of CuInSe2 thin films and contacts
[DE90-000301] 12 p1721 N90-19886
Space mechanism of low velocity for an array of solar panels: Analysis and design of an experimental model; dimensions of bearings
[INPE-4859-TDL/370] 13 p1809 N90-20390
Photovoltaic energy
[DE89-009473] 13 p1826 N90-20486
CuInSe2 and CdTe: Scale-up for manufacturing
[DE89-009503] 13 p1827 N90-20489
High-efficiency silicon concentrator solar cell research
[DE90-008040] 13 p1827 N90-20490
Perspectives on solar energy and the environment
[DE90-007680] 13 p1828 N90-20494
Enhanced ceria solid electrolyte fuel cell development. Reduction of electronic conductivity permits use of a solid ceria electrolyte in high efficiency high power density fuel cells at temperatures compatible with metallic cell hardware
[AD-A217840] 13 p1828 N90-20498
Recent results from advanced research on space solar cells at NASA
[NASA-TM-102485] 14 p1968 N90-21274
Peeled film GaAs solar cells for space power
[NASA-TM-103125] 14 p1970 N90-21287
Characterization and comparison of optically transparent conducting films
[DE90-000319] 14 p2033 N90-21660
Photovoltaic Program Branch
[DE90-000318] 15 p2123 N90-22142
Automating security monitoring and analysis for Space Station Freedom's electric power system
[NASA-TM-103148] 15 p2158 N90-22324
Space Station Freedom solar array panels plasma interaction test facility
[NASA-TM-102475] 15 p2186 N90-22488
High-efficiency silicon solar cells for a 22-sun line-focus module
[DE90-010242] 16 p2251 N90-22840
New directions in InP solar cell research
[NASA-TM-103160] 17 p2398 N90-23662
Interdigitated back contact silicon solar cell analysis and design recommendations for space use
[AD-A220414] 17 p2420 N90-23790
Radiation-hard-high-efficiency InP space solar cell development
[AD-A220500] 17 p2420 N90-23791
Diagnostics of glow discharges used to produce hydrogenated amorphous silicon films
[DE90-000329] 18 p2522 N90-24402
SERI photovoltaic subcontract reports: 1989 abstracts and document control information, March 1, 1987 to February 29, 1988
[DE90-000336] 18 p2577 N90-24682
Development of a point-contact solar cell using high-volume processing techniques
[DE90-010330] 18 p2577 N90-24683
Photovoltaic Energy Program summary. Volume 2: Research summaries
[DE89-009474] 19 p2710 N90-25422
Structural and electronic studies of a:SiGe:H alloys
[DE90-000313] 19 p2710 N90-25424
The effects of different diffusion sources on silicon solar cell recombination properties
[DE90-011235] 19 p2710 N90-25426
Research on design and fabrication of high-efficiency solar cells
[DE90-012010] 19 p2711 N90-25429
Discharge transient coupling in large space power systems 19 p2735 N90-25544
Solar array arcing in plasmas 19 p2737 N90-25558
Estimation of minority carrier diffusion lengths in InP/GaAs solar cells
[NASA-TM-103213] 20 p2824 N90-26069
Silicon concentrator solar cell development
[DE90-011782] 20 p2880 N90-26386
Dendritic web silicon photovoltaic cell research
[DE90-011786] 20 p2880 N90-26387
Application of InAlAs/GaAs superlattice alloys to GaAs solar cells
[DE90-013070] 20 p2881 N90-26389
Megawatt solar power systems for lunar surface operations
[NASA-CR-186509] 20 p2881 N90-26391
Development of a multi-purpose, pulsed-laser system for solar cell processing applications
[DE90-012181] 21 p3008 N90-27096
Recent technological advances in thin film solar cells
[DE90-000321] 21 p3019 N90-27165
Polycrystalline thin film cadmium telluride n-i-p solar cells
[DE90-000351] 21 p3019 N90-27167
Emitter and base recombination parameters in solar cells: Measurement process and dependence on temperature and injection
[ETN-90-97305] 22 p3196 N90-28138
Research on high-efficiency, multiple-gap, multi-junction amorphous silicon-based alloy thin-film solar cells
[DE90-000338] 23 p3344 N90-28896
Research on stable, large-area, amorphous silicon based submodules, phase 3
[DE90-000339] 23 p3399 N90-29204
Basic studies of 3-V high efficiency cell components
[DE90-000360] 24 p3484 N90-29696

SOLAR COLLECTORS

Structural concepts for very large (400-meter-diameter) solar concentrators 01 p0029 N90-10153
Analysis of the efficiency of a dielectric solar energy collector
[PB89-212716] 03 p0366 N90-12092
Conceptual design study of a 5 kilowatt solar dynamic Brayton power system using a dome Fresnel lens solar concentrator
[NASA-CR-185134] 06 p0735 N90-14281
Technology development program for an advanced microsheet glass concentrator
[NASA-TM-102406] 06 p0804 N90-14678
Chromatic dispersion compensation in a Fresnel lens by means of a diffraction grating
[DE90-004030] 08 p1123 N90-16506
Light-trapping concentrator cells
[DE90-004988] 09 p1242 N90-17205
Phase-Change Thermal Energy Storage
[DE89-009426] 11 p1529 N90-18801
Measuring flow properties of wicks for heat pipe solar receivers
[DE89-016537] 12 p1683 N90-19664
Radiative transport models for solar thermal receiver/reactors
[DE90-000303] 12 p1683 N90-19665
Status of stretched-membrane heliostats
[DE90-000801] 12 p1683 N90-19669
Evaluation of thermal cycling creep-fatigue damage for a molten salt receiver
[DE90-002907] 12 p1684 N90-19670

Test results from a full-scale sodium reflux pool-boiler solar receiver
[DE90-003577] 12 p1684 N90-19671
Solar thermal program summary, fiscal year 1989
[DE89-009475] 13 p1826 N90-20487
The effect of leveling coatings on the atomic oxygen durability of solar concentrator surfaces
[NASA-TM-102557] 14 p1941 N90-21110
Recent results from advanced research on space solar cells at NASA
[NASA-TM-102485] 14 p1968 N90-21274
Solar Concentrator Advanced Development Program
[NASA-CR-185173] 16 p2250 N90-22834
High-efficiency silicon solar cells for a 22-sun line-focus module
[DE90-010242] 16 p2251 N90-22840
A direct absorber reactor/receiver for solar thermal applications
[DE90-006280] 18 p2577 N90-24679
Dynamic analysis of space-related linear and non-linear structures
[NASA-TM-103490] 19 p2667 N90-25174
Megawatt solar power systems for lunar surface operations
[NASA-CR-186509] 20 p2881 N90-26391
Preliminary designs for 25 kWe advanced Stirling conversion systems for dish electric applications
[NASA-TM-103188] 20 p2940 N90-26729
Wind loads and local pressure distributions on parabolic dish solar collectors
[DE90-000328] 21 p3019 N90-27166
Some studies related to a new Hexagonal Compound Parabolic Concentrator (HCPC) as a secondary in tandem with a solar tower
[DLR-FB-90-12] 24 p3485 N90-29700

SOLAR CONSTANT
Solar variability observed through changes in solar figure and mean diameter
[DE90-006600] 11 p1535 N90-18834
Observed solar near UV variability: A contribution to variations of the solar constant
22 p3201 N90-28163

SOLAR CONVERTERS
U SOLAR GENERATORS

SOLAR COOLING
Solar buildings program summary. Volume 2: Research summaries
[DE89-009478] 11 p1530 N90-18810
Failure and degradation modes in selected solar materials: A review
[DE90-009075] 14 p2002 N90-21476
A theoretical and experimental investigation of an absorption refrigeration system for application with solar energy units 16 p2226 N90-22697

SOLAR CORONA
NT CORONAL HOLES
NT CORONAL LOOPS
Soft X-ray astronomy using grazing incidence optics
01 p0138 N90-10797
The design and evaluation of grazing incidence relay optics 01 p0138 N90-10799
The correspondence between small-scale coronal structures and the evolving solar magnetic field
01 p0138 N90-10800
MHD (magnetohydrodynamic) modeling of solar and interplanetary processes
[PB89-215461] 03 p0420 N90-12416
Heating and acceleration of coronal and chromospheric ions during solar flares 03 p0433 N90-12479
Chromospheric-coronal coupling during solar flares: Current systems and particle acceleration
03 p0433 N90-12480
The Owens Valley solar array
03 p0435 N90-12490
EIT: Solar corona synoptic observations from SOHO with an Extreme-ultraviolet Imaging Telescope
04 p0567 N90-13309
UVCS: An Ultraviolet Coronagraph Spectrometer for SOHO 04 p0568 N90-13310
Interplanetary dust close to the Sun (F corona): Its observation in the visible and infrared by a rocket-borne coronagraph 05 p0661 N90-13864
Shear-induced inflation of coronal magnetic fields
[NASA-CR-186103] 05 p0715 N90-14178
Solar nebula condensates and the composition of comets 08 p1144 N90-16634
MHD (Magnetohydrodynamic) slow shocks in coronal and interplanetary space
[AD-A214725] 09 p1299 N90-17527
Magnetic field generation by acoustic oscillations in solar atmosphere
[DE90-606054] 11 p1594 N90-19180
Spontaneous magnetic reconnection in a turbulent plasma 13 p1889 N90-20840
Cyclotron maser and plasma wave growth in magnetic loops
[NASA-CR-179862] 15 p2170 N90-22402
The large and small scale density structure in the solar corona 16 p2338 N90-23327
Vlasov-Maxwell equilibria of solar coronal loops
[DE90-015025] 23 p3414 N90-29289

SOLAR CORPUSCULAR RADIATION
NT SOLAR NEUTRINOS
NT SOLAR NEUTRONS
NT SOLAR PROTONS
ERNE: Energetic and Relativistic Nuclei and Electron experiment 04 p0568 N90-13315
Effects of corpuscular radiation on weather and climate 22 p3201 N90-28164
The effects of solar particle events on the middle atmosphere 22 p3206 N90-28189
Energy deposition of corpuscular radiation in the middle atmosphere 22 p3206 N90-28190
Solar activity influence on cosmic ray penetration in the middle atmosphere 22 p3207 N90-28192

SOLAR COSMIC RAYS
Solar-geophysical data number 532, December 1988. Part 1: Data for November, October 1988, and late data
[PB89-152086] 01 p0142 N90-10818
Solar-geophysical data number 533. Part 1: Data for December, November 1988, and late data
[PB89-162481] 01 p0142 N90-10820
Solar-geophysical data number 534, February 1989. Part 1: (Prompt reports). Data for January 1989, December 1988 and late data
[PB89-173041] 01 p0142 N90-10822
The onset of the solar active cycle 22
03 p0434 N90-12488
Simplified model for solar cosmic ray exposure in manned Earth orbital flights
[NASA-TM-4182] 14 p2043 N90-21715
Neutrino signals from the powerful solar flare on September 29, 1989
[PREPRINT-721] 16 p2339 N90-23331
Improved model for solar cosmic ray exposure in manned Earth orbital flights
[NASA-TP-2987] 18 p2639 N90-25031
Energy deposition of corpuscular radiation in the middle atmosphere 22 p3206 N90-28190
Solar cosmic ray effects in the lower ionosphere
22 p3208 N90-28201

SOLAR CYCLES
NT SUNSPOT CYCLE
Max '91 Workshop 2: Developments in Observations and Theory for Solar Cycle 22
[NASA-TM-101893] 03 p0429 N90-12459
When and where to look to observe major solar flares
03 p0430 N90-12465
Rotation of the photospheric magnetic fields: A north-south asymmetry
[NASA-CR-186159] 05 p0715 N90-14177
Solar cycle effects on trapped energetic particles
[AD-A215028] 09 p1300 N90-17532
Field of solar physics: Review and recommendations for ground-based solar research
[PB90-115684] 09 p1300 N90-17533
Intermittent Solar Ammonia Absorption Cycle (ISAAC) refrigeration for lesser developed countries
[DE90-006700] 11 p1496 N90-18610
Solar cyclical trend study of the mid-latitude, quiet-time, meridional, neutral winds at winter solstice conditions
[AD-A217398] 13 p1841 N90-20568
On the antarctic ozone depletion during solar cycle 21
[NOTA-INTERNA-943] 16 p2253 N90-22849
The large and small scale density structure in the solar corona 16 p2338 N90-23327
A 154-day periodicity in the occurrence rate of proton flares
[NASA-CR-185826] 16 p2340 N90-23333
Application of solar seismology to study of the convection zone
[AD-A221975] 21 p3101 N90-27610
Observed solar near UV variability: A contribution to variations of the solar constant
22 p3201 N90-28163
The tropospheric response pattern to solar activity forcing 22 p3201 N90-28165
A review of the 11-year solar cycle, the QBO, and the atmosphere relationship 22 p3202 N90-28166
Seasonal variation of the 11 year solar cycle effect on the middle atmosphere: Role of the quasi biennial oscillation 22 p3202 N90-28167
Influence of solar activity on middle atmosphere associated with phases of equatorial quasi-biennial oscillation 22 p3202 N90-28168
Solar activity influence on climatic variations of stratosphere and mesosphere in mid-latitudes
22 p3202 N90-28169
The planetary waves dynamics and interannual course of meteorological parameters of the high latitude stratosphere and mesosphere of the Northern and Southern Hemispheres during the 20th and 21st solar cycles and different phases of QBO
22 p3203 N90-28170
A search for solar related changes in tropospheric weather 22 p3203 N90-28173
Resonant Rossby waves and solar activity
22 p3205 N90-28179
On the relationship between the phases of 27-day total ozone and solar activity indices in different latitudinal zones 22 p3205 N90-28180
Total ozone time variations during the spring reversals in the high latitudinal stratosphere of the Northern Hemisphere during the 20th and 21st solar cycles
22 p3205 N90-28181
Physical mechanisms of solar activity effects in the middle atmosphere 22 p3206 N90-28185
Energy deposition of corpuscular radiation in the middle atmosphere 22 p3206 N90-28190
Ionospheric effects of the extreme solar activity of February 1986 22 p3210 N90-28207
Trend analysis of total ozone data
24 p3486 N90-29703

SOLAR DIAMETER
Solar variability observed through changes in solar figure and mean diameter
[DE90-006600] 11 p1535 N90-18834

SOLAR DISK
U SUN

SOLAR DYNAMIC POWER SYSTEMS
Conceptual design study of a 5 kilowatt solar dynamic Brayton power system using a dome Fresnel lens solar concentrator
[NASA-CR-185134] 06 p0735 N90-14281
A heat receiver design for solar dynamic space power systems
[NASA-TM-102473] 06 p0735 N90-14283
On protection of Freedom's solar dynamic radiator from the orbital debris environment. Part 1: Preliminary analyses and testing
[NASA-TM-102458] 06 p0736 N90-14285
Technology development program for an advanced microsheet glass concentrator
[NASA-TM-102406] 06 p0804 N90-14678
European Space Power, volume 1
[ESA-SP-294-VOL-1] 10 p1329 N90-17678
The 25 kWe spaceborne solar dynamic generator
10 p1331 N90-17696
Optimized sensible heat storage systems for application to solar dynamic power generation
10 p1334 N90-17719
Development of a high temperature storage unit for integration with solar dynamic systems
10 p1335 N90-17720
European Space Power, volume 2
[ESA-SP-294-VOL-2] 10 p1338 N90-17748
Hot filament technique for measuring the thermal conductivity of molten lithium fluoride
[NASA-TM-102506] 12 p1631 N90-19373
Mechanical properties of pure nickel alloys after long term exposures to LiOH and vacuum at 775 K
[NASA-TM-102403] 13 p1774 N90-20181
Model development in viscoplastic ratchetting
[NASA-TM-102509] 13 p1816 N90-20431
Photovoltaic power for Space Station Freedom
[NASA-TM-102569] 15 p2062 N90-21812
Solar energy for high temperature technology and applications
[ETN-90-97429] 23 p3345 N90-28902

SOLAR DYNAMICS
U HELIOSEISMOLOGY

SOLAR ENERGY
Power from space for use on earth: An emerging global option 01 p0028 N90-10144
Analysis of the efficiency of a dielectric solar energy collector
[PB89-212716] 03 p0366 N90-12092
Photovoltaic system research status
[DE89-016764] 03 p0366 N90-12094
Analysis of catalytically enhanced solar absorption chemical reactors: 1 - numerical model description
[DE89-014742] 07 p0951 N90-15505
Satellite thermal storage systems using metallic phase-change materials
[DE89-016872] 07 p0952 N90-15507
SERI (Solar Energy Research Institute) solar radiation resource assessment project
[DE89-009456] 08 p1097 N90-16352
Overview of photovoltaic and battery applications
[PB90-120536] 09 p1242 N90-17206

Study of the atmospheric emissions of OI wavelength 557.7 nm and O2 (0,0) wavelength 761.9 nm in the equatorial region utilizing measurement of photometer on-board a rocket
[INPE-4811-TDL/358] 11 p1533 N90-18827
Enhancement of processes for solar photocatalytic detoxification of water
[DE90-003949] 12 p1623 N90-19330
Solar and thermic utilization in high temperature area: Research and development
[ETN-90-96062] 12 p1682 N90-19663
Radiative transport models for solar thermal receiver/reactors
[DE90-000303] 12 p1683 N90-19665
Spectral solar radiation data base documentation
[DE89-009448] 12 p1745 N90-20033
Photovoltaic energy
[DE89-009473] 13 p1826 N90-20486
Solar thermal program summary, fiscal year 1989
[DE89-009475] 13 p1826 N90-20487
Design and demonstration of an improved stretched-membrane heliostat
[DE90-007904] 14 p2001 N90-21470
Ocean energy program summary. Volume 2: Research summaries
[DE89-009482] 18 p2576 N90-24677
A direct absorber reactor/receiver for solar thermal applications
[DE90-006280] 18 p2577 N90-24679
SERI photovoltaic subcontract reports: 1989 abstracts and document control information, March 1, 1987 to February 29, 1988
[DE90-000336] 18 p2577 N90-24682
Advanced solar-propelled cargo spacecraft for Mars missions
[NASA-CR-186218] 19 p2665 N90-25164
Energy storage for a lunar base by the reversible chemical reaction: CaO+H2O reversible reaction Ca(OH)2
[NASA-TM-103145] 19 p2709 N90-25419
The effects of urban air pollution on solar radiation
[DE89-009455] 19 p2712 N90-25438
The use of hydrogen in energy economy of Finland
[DE90-796180] 20 p2881 N90-26388
The potential of renewable energy
[DE90-000322] 21 p3019 N90-27163
Opportunities in solar energy research over the next decade
[DE90-012479] 21 p3019 N90-27164
Abstracts of 1989 Japan Solar Energy Society and Japan Wind Energy Association Joint Conference
[DE90-503616] 21 p3019 N90-27168
A solar power system for an early Mars expedition
[NASA-TM-103219] 22 p3243 N90-28393
Development of the sodium/sulfur technology for energy storage
[DE90-014329] 23 p3344 N90-28899
Solar energy for high temperature technology and applications
[ETN-90-97429] 23 p3345 N90-28902

SOLAR ENERGY ABSORBERS
Analysis of catalytically enhanced solar absorption chemical reactors. 2: Predicted characteristics of a 100 kW chemical reactor
[DE89-014743] 07 p0954 N90-15521
A direct absorber reactor/receiver for solar thermal applications
[DE90-006280] 18 p2577 N90-24679
Solar electricity and solar fuels
[DE90-796156] 22 p3196 N90-28135

SOLAR ENERGY CONVERSION
NT PHOTOTHERMAL CONVERSION
NT PHOTOVOLTAIC CONVERSION
Power beaming options 01 p0027 N90-10142
Laser-powered Martian rover 01 p0029 N90-10157
United States photovoltaic concentrator technology process and new program initiative
[DE89-013812] 01 p0083 N90-10475
Stretched-membrane heliostats for solar central-receiver power plants
[DE89-016034] 01 p0084 N90-10476
Photochemical solar energy conversion utilizing semiconductors localized in membrane mimetic systems
[DE90-003450] 07 p0953 N90-15515
The Solar Power Satellite (SPS): Progress so far 07 p1008 N90-15840
Lunar power system summary of studies for the lunar enterprise task force NASA-office of exploration 07 p1008 N90-15841
SERI (Solar Energy Research Institute) solar radiation resource assessment project
[DE89-009456] 08 p1097 N90-16352
Survey on energy conversion of CO2 gas. Approach to solution of CO2 gas problems
[DE90-742055] 10 p1352 N90-17843
Progress in thin film solar photovoltaic technologies
[DE89-009513] 11 p1527 N90-18792
Resource Assessment Project: User needs survey results
[DE89-009502] 11 p1529 N90-18802
Energy transfer and photochemistry in biomimetic solar conversion
[PB90-114562] 12 p1681 N90-19652
Direct absorption receiver
[DE90-000311] 12 p1683 N90-19667
Status of stretched-membrane heliostats
[DE90-000801] 12 p1683 N90-19669
High-efficiency silicon concentrator solar cell research
[DE90-008040] 13 p1827 N90-20490
Perspectives on solar energy and the environment
[DE90-007680] 13 p1828 N90-20494
Failure and degradation modes in selected solar materials: A review
[DE90-009075] 14 p2002 N90-21476
Photosynthetic water splitting, phase 2
[PB90-132671] 15 p2066 N90-21833
Electric power scheduling: A distributed problem-solving approach
[NASA-TM-103149] 15 p2157 N90-22323
A theoretical and experimental investigation of an absorption refrigeration system for application with solar energy units 16 p2226 N90-22697
Photovoltaic advanced research and development project: Solar radiation research
[DE90-000302] 16 p2251 N90-22839
The pressure loaded volumetric ceramic receiver
[DLR-MITT-89-17] 16 p2252 N90-22842
New generation power subsystems for satellites
[AD-A219540] 17 p2365 N90-23464
Photovoltaic Energy Program summary. Volume 2: Research summaries
[DE89-009474] 19 p2710 N90-25422
SERI solar radiation resource assessment project
[DE90-000307] 19 p2711 N90-25428
Solar electricity and solar fuels
[DE90-796156] 22 p3196 N90-28135
Solar energy for high temperature technology and applications
[ETN-90-97429] 23 p3345 N90-28902

SOLAR FLARES
Solar-geophysical data number 531, part 2. Data foor May 1988 and miscellaneous
[PB89-139950] 01 p0142 N90-10817
Solar-geophysical data number 532, December 1988. Part 1: Data for November, October 1988, and late data
[PB89-152086] 01 p0142 N90-10818
Solar-geophysical data number 532, December 1988. Part 2: Data for June 1988 and miscellaneous
[PB89-152094] 01 p0142 N90-10819
Solar-geophysical data number 533. Part 2: Data for July 1988 and miscellaneous
[PB89-162499] 01 p0142 N90-10821
Solar-geophysical data number 534, February 1989. Part 2: (Comprehensive reports). Data for August 1988 and miscellaneous
[PB89-173058] 01 p0143 N90-10823
Solar-geophysical data number 536, part 2. Data for October 1988 and miscellaneous
[PB89-194658] 01 p0143 N90-10824
Solar-terrestrial relations: Flare and solar wind effects 02 p0240 N90-11362
Solar-geophysical data number 536, part 1. Data for March, Febuary 1989 and late data
[PB89-194716] 02 p0296 N90-11684
Solar-geophysical data number 537, part 1. Data for April, March 1989 and late data
[PB89-207393] 02 p0296 N90-11685
The hard x rays and gamma-rays from solar flares
[NASA-CR-185982] 03 p0429 N90-12458
Max '91 Workshop 2: Developments in Observations and Theory for Solar Cycle 22
[NASA-TM-101893] 03 p0429 N90-12459
High energy flare physics group summary 03 p0429 N90-12460
Magnetograph group summary 03 p0429 N90-12461
Theory and modeling group 03 p0430 N90-12462
Scientific objectives of solar gamma-ray observations 03 p0430 N90-12463
The Gamma-Ray Observatory: An overview 03 p0430 N90-12464
When and where to look to observe major solar flares 03 p0430 N90-12465
Access to Max '91 information via computer networks 03 p0430 N90-12466
Capabilities of GRO/OSSE for observing solar flares 03 p0430 N90-12467
The solar gamma ray and neutron capabilities of COMPTEL on the Gamma Ray Observatory 03 p0431 N90-12468
The BATSE experiment on the Gamma Ray Observatory: Solar flare hard x ray and gamma-ray capabilities 03 p0431 N90-12469
The solar flare and cosmic gamma-ray burst experiment aboard the Ulysses spacecraft 03 p0431 N90-12470
VLA-Max '91 tests of high energy flare physics 03 p0431 N90-12471
First interferometric observations with arc-sec. resolution of solar radio bursts at millimeter wavelengths 03 p0431 N90-12472
Observational goals for Max '91 to identify the causative agent for impulsive bursts 03 p0431 N90-12473
Solar flare gamma-ray and hard x ray imaging with the GRID-on-a-balloon 03 p0432 N90-12474
The soft x ray telescope for Solar-A 03 p0432 N90-12475
Pre-pulses: Signature of a trigger process in short (less than 60 secs) solar hard x ray flares 03 p0432 N90-12476
Flare model sensitivity of the Balmer spectrum 03 p0432 N90-12477
Joule heating and runaway electron acceleration in a solar flare 03 p0432 N90-12478
Heating and acceleration of coronal and chromospheric ions during solar flares 03 p0433 N90-12479
Chromospheric-coronal coupling during solar flares: Current systems and particle acceleration 03 p0433 N90-12480
Some of the terrestrial effects of AR 5395 03 p0433 N90-12482
The 10.7-cm microwave observations of AR 5395 and related terrestrial effects 03 p0433 N90-12483
The SMM UV observations of Active Region 5395 03 p0434 N90-12485
Hard x ray highlights of AR 5395 03 p0434 N90-12486
An imaging vector magnetograph for the next solar maximum 03 p0435 N90-12489
The Owens Valley solar array 03 p0435 N90-12490
A high-speed digital camera system for the observation of rapid H-alpha fluctuations in solar flares 03 p0435 N90-12491
Solar-geophysical data number 537, May 1989. Part 2: Comprehensive Reports, data for Nov. 1988 and miscellaneous
[PB89-207401] 04 p0566 N90-13300
Berne solar observations
[REPT-55] 04 p0566 N90-13301
The SOHO mission. Scientific and technical aspects of the instruments
[ESA-SP-1104] 04 p0566 N90-13302
Solar-geophysical data number 538, June 1989. Part 1: (Prompt reports). Data for May, April 1989, and late data
[PB89-223838] 06 p0866 N90-15031
Solar-geophysical data number 538, June 1989. Part 2: (Comprehensive reports). Data for December 1988 and miscellaneous
[PB89-223846] 06 p0866 N90-15032
Solar-geophysical data number 539, July 1989. Part 1: (Prompt reports). Data for June, May 1989, and late data
[PB89-235451] 06 p0866 N90-15033
Solar-geophysical data number 539, July 1989. Part 2: (Comprehensive reports). Data for January 1989, and miscellaneous
[PB89-235469] 06 p0866 N90-15034
Solar-geophysical data number 540, August 1989. Part 1: (Prompt reports). Data for July, June 1989, and late data
[PB90-108572] 06 p0866 N90-15035
Solar-geophysical data number 540, August 1989. Part 2: (Comprehensive reports). Data for February 1989
[PB89-108598] 06 p0867 N90-15039
A simple model for the stellar analogy of compact solar flares
[DE90-003215] 07 p1015 N90-15877
Determination of solar flare accelerated ion angular distributions from SMM gamma ray and neutron measurements and determination of the He-3/H ratio in the solar photosphere from SMM gamma ray measurements
[NASA-CR-186038] 08 p1153 N90-16676
A study of the evolution of solar active regions for improving solar flare forecasts
[AD-A216325] 10 p1448 N90-18356
Radiation exposure for manned Mars surface missions
[NASA-TP-2979] 10 p1448 N90-18357
Solar-geophysical data number 541, September 1989. Part 2: (Comprehensive reports). Data for March 1989 and miscellaneous
[PB90-122755] 12 p1745 N90-20031
Solar-geophysical data number 541, September 1989. Part 1: (Prompt reports). Data for August, July 1989, and late data
[PB90-122763] 12 p1745 N90-20032

Reliability of equivalent sphere model in blood-forming organ dose estimation
[NASA-TM-4178] 12 p1746 N90-20036
Solar flares and dynamics of Langmuir waves in current-carrying plasmas
[IPPCZ-291] 14 p2042 N90-21710
Substorms: Their expansion and recovery phases
[DE90-008970] 14 p2042 N90-21712
High energy phenomena during solar flares
[INPE-4961-TDL/390] 14 p2043 N90-21713
Solar-geophysical data number 542, October 1989. Part 1: (Prompt reports). Data for September, August 1989, and late data
[PB90-148669] 15 p2193 N90-22520
Solar-geophysical data number 542, October 1989. Part 2: (Comprehensive reports). Data for April 1989 and miscellaneous
[PB90-148677] 15 p2193 N90-22521
What is learned from high energy bursts and flares
16 p2336 N90-23314
Numerical simulations of x rays and gamma rays from solar flares 16 p2339 N90-23330
Neutrino signals from the powerful solar flare on September 29, 1989
[PREPRINT-721] 16 p2339 N90-23331
Solar flares and magnetospheric particles: Investigations based upon the ONR-602 and ONR-604 experiments
[AD-A218844] 16 p2340 N90-23332
A 154-day periodicity in the occurrence rate of proton flares
[NASA-CR-185826] 16 p2340 N90-23333
Berne solar observations: Data for July to December 1989
[REPT-56] 19 p2797 N90-25924
The charged particle radiation environment for AXAF
[NASA-TM-100405] 20 p2942 N90-26741
Nonpotential magnetic fields at sites of gamma ray flares
[NASA-TM-103493] 20 p2950 N90-26785
Gases of the middle atmosphere and short-term solar radiation variations 22 p3204 N90-28177
The effects of solar particle events on the middle atmosphere 22 p3206 N90-28189
Relationship between solar activities and thunderstorm activities in the Beijing area and the northeast region of China 22 p3208 N90-28197
Solar or meteorological control of lower ionospheric fluctuations (2-15 and 27 days) in middle latitudes
22 p3209 N90-28202
The probability of SWF occurrence in relation to solar activity 22 p3209 N90-28204
Post-flare effects in the lower ionosphere of middle latitudes 22 p3209 N90-28205
Solar-geophysical data number 545, January 1990. Part 2 (Comprehensive reports). Data for July 1989 and miscellaneous
[PB90-182346] 22 p3263 N90-28480
Solar-geophysical data number 544, December 1989. Part 1 (Prompt reports). Data for November, October 1989, and late data
[PB90-171661] 22 p3263 N90-28481
Solar-geophysical data number 544, December 1989. Part 2 (Comprehensive reports). Data for June 1989 and miscellaneous
[PB90-171679] 22 p3264 N90-28482
Theoretical studies of proton beams in solar flare loops 23 p3413 N90-29286
Search for neutrino events in the Kamiokande-2 detector in correlation with the solar-flare activity in March 1989
[DE90-508085] 24 p3563 N90-30160

SOLAR FLUX
The correspondence between small-scale coronal structures and the evolving solar magnetic field
01 p0138 N90-10800
Solar UV variability 22 p3201 N90-28162
Observed solar near UV variability: A contribution to variations of the solar constant
22 p3201 N90-28163
A review of the 11-year solar cycle, the QBO, and the atmosphere relationship 22 p3202 N90-28166
Response of the middle atmosphere to solar UV and dynamical perturbations 22 p3204 N90-28175
Physical mechanisms of solar activity effects in the middle atmosphere 22 p3206 N90-28185
General overview of the solar activity effects on the lower ionosphere 22 p3208 N90-28198
Solar or meteorological control of lower ionospheric fluctuations (2-15 and 27 days) in middle latitudes
22 p3209 N90-28202
The 27-day versus 13.5-day variations in the solar Lyman-alpha radiation and the radio wave absorption in the lower ionosphere over Europe
22 p3209 N90-28203
The natural VLF emission as diagnostics and estimation means of the fluxes of solar x ray bursts
22 p3209 N90-28206
Relationship between the longwave cloud radiative forcing at the surface and the top of the atmosphere
22 p3222 N90-28273

SOLAR FLUX DENSITY
NT SOLAR CONSTANT
A solar extreme ultraviolet flux model
02 p0296 N90-11686
Prediction of the 10 cm solar flux index
05 p0662 N90-13872
Berne solar observations: Data for July to December 1989
[REPT-56] 19 p2797 N90-25924

SOLAR FURNACES
Solar thermal program summary. Volume 2: Research summaries
[DE89-009476] 18 p2576 N90-24674

SOLAR GENERATORS
NT SOLAR CELLS
NT SOLAR DYNAMIC POWER SYSTEMS
Power generation and distribution
05 p0604 N90-13515
European Space Power, volume 1
[ESA-SP-294-VOL-1] 10 p1329 N90-17678
Challenges for future space power systems
10 p1331 N90-17695
The 25 kWe spaceborne solar dynamic generator
10 p1331 N90-17696
Ga0.47In0.53As cells for GaAs-stacked photovoltaic tandems 10 p1338 N90-17749
Structural and operational aspects of the concentrating SARA-Louver solar generator 10 p1340 N90-17760
SFU solar array 10 p1340 N90-17761
A low cost anticharging connection system for solar generators and its application on ASPERA solar array
10 p1341 N90-17765
The ISO solar generator: Solar cells and OSR mixed
10 p1341 N90-17767
The INMARSAT-2 solar generator panels
10 p1343 N90-17782
Investigations on hot spots effects in reverse biased spatial solar cells 10 p1344 N90-17789
Photovoltaic energy
[DE89-009473] 13 p1826 N90-20486
Automating security monitoring and analysis for Space Station Freedom's electric power system
[NASA-TM-103148] 15 p2158 N90-22324
An analysis of space power system masses
[NASA-TM-103199] 19 p2669 N90-25184
Discharge transient coupling in large space power systems 19 p2735 N90-25544
Qualification of concentrating mirror systems with the HERMES measurement system and the HELIOS simulation program
[DLR-FB-89-51] 20 p2882 N90-26394
Some studies related to a new Hexagonal Compound Parabolic Concentrator (HCPC) as a secondary in tandem with a solar tower
[DLR-FB-90-12] 24 p3485 N90-29700

SOLAR GRAVITATION
Solar variability observed through changes in solar figure and mean diameter
[DE90-006600] 11 p1535 N90-18834
Gravitational experiments on a solar probe mission: Scientific objectives and technology considerations
12 p1733 N90-19966

SOLAR HEATING
SUMER: Solar Ultraviolet Measurements of Emitted Radiation 04 p0567 N90-13307
CDS: The Coronal Diagnostic Spectrometer
04 p0567 N90-13308
Performance predictions for passive solar water heating systems. Report 1: Performance monitoring to validate site-specific estimates of passive solar water heaters. Report 2: Laboratory report. Passive solar water heater tests
[DE90-002879] 10 p1401 N90-18096
Solar buildings program summary. Volume 2: Research summaries
[DE89-009478] 11 p1530 N90-18810
Pyranometry
[DWD-14] 12 p1682 N90-19661
Study of possible solar heating effects on thermosonde probes: Error analysis
[AD-A218116] 13 p1903 N90-20917
Failure and degradation modes in selected solar materials: A review
[DE90-009075] 14 p2002 N90-21476
Activities report in technical-physical research
[ETN-90-96771] 17 p2487 N90-24223

SOLAR HOUSES
Solar buildings program summary. Volume 2: Research summaries
[DE89-009478] 11 p1530 N90-18810

SOLAR INSTRUMENTS
High energy flare physics group summary
03 p0429 N90-12460
The solar activity measurements experiments (SAMEX) for improved scientific understanding of solar activity
[NASA-TM-100372] 06 p0867 N90-15036
A general-purpose balloon-borne pointing system for solar scientific instruments
[NASA-TP-3013] 14 p1959 N90-21219

SOLAR INTERIOR
SOHO: An observatory to study the solar interior and the solar atmosphere 04 p0566 N90-13303
GOLF: Global Oscillations at Low Frequencies for the SOHO mission 04 p0566 N90-13304
VIRGO: The solar monitor experiment on SOHO
04 p0567 N90-13305
A look on non-standard solar models
[SER-C-PREPUBL-FASC-40] 08 p1153 N90-16677
Field of solar physics: Review and recommendations for ground-based solar research
[PB90-115684] 09 p1300 N90-17533
Report from solar physics 10 p1445 N90-18335
Nonlinear multi-mode coupling of the solar gravity modes in a rotationally split multiplet 21 p3100 N90-27608

SOLAR LASERS
U SOLAR-PUMPED LASERS

SOLAR MAGNETIC FIELD
The correspondence between small-scale coronal structures and the evolving solar magnetic field
01 p0138 N90-10800
The observation of possible reconnection events in the boundary changes of solar coronal holes
01 p0138 N90-10801
Solar-geophysical data number 532, December 1988. Part 1: Data for November, October 1988, and late data
[PB89-152086] 01 p0142 N90-10818
Solar-geophysical data number 533. Part 1: Data for December, November 1988, and late data
[PB89-162481] 01 p0142 N90-10820
Solar-geophysical data number 534, February 1989. Part 1: (Prompt reports). Data for January 1989, December 1988 and late data
[PB89-173041] 01 p0142 N90-10822
Solar-geophysical data number 536, part 1. Data for March, February 1989 and late data
[PB89-194716] 02 p0296 N90-11684
Magnetograph group summary
03 p0429 N90-12461
Investigation of active regions at high resolution by balloon flights of the Solar Optical Universal Polarimeter (SOUP) 03 p0434 N90-12487
An imaging vector magnetograph for the next solar maximum 03 p0435 N90-12489
The Owens Valley solar array
03 p0435 N90-12490
The SOHO mission. Scientific and technical aspects of the instruments
[ESA-SP-1104] 04 p0566 N90-13302
GOLF: Global Oscillations at Low Frequencies for the SOHO mission 04 p0566 N90-13304
SOI: The Solar Oscillations Imager on SOHO
04 p0567 N90-13306
Rotation of the photospheric magnetic fields: A north-south asymmetry
[NASA-CR-186159] 05 p0715 N90-14177
Shear-induced inflation of coronal magnetic fields
[NASA-CR-186103] 05 p0715 N90-14178
Solar-geophysical data number 538, June 1989. Part 1: (Prompt reports). Data for May, April 1989, and late data
[PB89-223838] 06 p0866 N90-15031
Solar-geophysical data number 539, July 1989. Part 1: (Prompt reports). Data for June, May 1989, and late data
[PB89-235451] 06 p0866 N90-15033
Solar-geophysical data number 540, August 1989. Part 1: (Prompt reports). Data for July, June 1989, and late data
[PB90-108572] 06 p0866 N90-15035
The solar activity measurements experiments (SAMEX) for improved scientific understanding of solar activity
[NASA-TM-100372] 06 p0867 N90-15036
Report from solar physics 10 p1445 N90-18335
Magnetic field generation by acoustic oscillations in solar atmosphere
[DE90-606054] 11 p1594 N90-19180
Solar-geophysical data number 541, September 1989. Part 1: (Prompt reports). Data for August, July 1989, and late data
[PB90-122763] 12 p1745 N90-20032
Cyclotron maser and plasma wave growth in magnetic loops
[NASA-CR-179862] 15 p2170 N90-22402
Solar-geophysical data number 542, October 1989. Part 1: (Prompt reports). Data for September, August 1989, and late data
[PB90-148669] 15 p2193 N90-22520
Nonpotential magnetic fields at sites of gamma ray flares
[NASA-TM-103493] 20 p2950 N90-26785

Solar-geophysical data number 544, December 1989. Part 1 (Prompt reports). Data for November, October 1989, and late data
[PB90-171661] 22 p3263 N90-28481

SOLAR MAXIMUM MISSION
Capabilities of GRO/OSSE for observing solar flares 03 p0430 N90-12467
The BATSE experiment on the Gamma Ray Observatory: Solar flare hard x ray and gamma-ray capabilities 03 p0431 N90-12469
The solar flare and cosmic gamma-ray burst experiment aboard the Ulysses spacecraft 03 p0431 N90-12470
VLA-Max '91 tests of high energy flare physics 03 p0431 N90-12471
Observational goals for Max '91 to identify the causative agent for impulsive bursts 03 p0431 N90-12473
Solar flare gamma-ray and hard x ray imaging with the GRID-on-a-balloon 03 p0432 N90-12474
The SMM UV observations of Active Region 5395 03 p0434 N90-12485
Hard x ray highlights of AR 5395 03 p0434 N90-12486
A high-speed digital camera system for the observation of rapid H-alpha fluctuations in solar flares 03 p0435 N90-12491
Temperature dependence of attitude sensor coalignments on the Solar Maximum Mission (SMM) 05 p0588 N90-13426
Analysis of the flight dynamics of the Solar Maximum Mission (SMM) off-sun scientific pointing 05 p0590 N90-13432
MAX 1991. The active sun: A plan for pursuing the study of the active sun at the time of the next maximum in solar activity, January 1985
[NASA-CR-186125] 12 p1745 N90-20030

SOLAR NEBULA
U SOLAR CORONA

SOLAR NEIGHBORHOOD
Mass functions for eight galactic clusters in the solar neighborhood 08 p1150 N90-16660

SOLAR NEUTRINOS
Solar opacities constrained by solar neutrinos and solar oscillations
[DE89-016988] 02 p0297 N90-11687
Dark matter and the solar neutrino problem: Can particle physics provide a single solution
[DE90-001827] 06 p0864 N90-15024
Neutrino oscillations: An essay in honor of Felix Boehm
[DE90-003223] 08 p1121 N90-16491
BOREX: Solar neutrino experiment via weak neutral and charged currents in boron-11
[DE90-003790] 09 p1300 N90-17530
The GALLEX Project
[DE90-005573] 09 p1300 N90-17534
Solar variability observed through changes in solar figure and mean diameter
[DE90-006600] 11 p1535 N90-18834
The observed properties of the intermediate-degree gravity modes and their relevance to the solar neutrino paradox 15 p2193 N90-22519
Neutrino signals from the powerful solar flare on September 29, 1989
[PREPRINT-721] 16 p2339 N90-23331
Enrichment services for chromium isotopes for the GALLEX (gallium experiment) international collaboration experiment on solar neutrino flux
[DE90-014300] 23 p3413 N90-29285

SOLAR NEUTRONS
Scientific objectives of solar gamma-ray observations 03 p0430 N90-12463
The solar gamma ray and neutron capabilities of COMPTEL on the Gamma Ray Observatory 03 p0431 N90-12468
The ground-level cosmic-ray event of September 29, 1989 as recorded by the Rome detectors
[NOTA-INTERNA-944] 16 p2340 N90-23336

SOLAR NOISE
U SOLAR RADIO EMISSION

SOLAR OBSERVATORIES
High energy flare physics group summary 03 p0429 N90-12460
Investigation of active regions at high resolution by balloon flights of the Solar Optical Universal Polarimeter (SOUP) 03 p0434 N90-12487
Berne solar observations
[REPT-55] 04 p0566 N90-13301
The SOHO mission. Scientific and technical aspects of the instruments
[ESA-SP-1104] 04 p0566 N90-13302
SOHO: An observatory to study the solar interior and the solar atmosphere 04 p0566 N90-13303
LASCO: A wide-field white light and spectrometric coronagraph for SOHO 04 p0568 N90-13311
SWAN: A study of solar wind anisotropies 04 p0568 N90-13312
The solar activity measurements experiments (SAMEX) for improved scientific understanding of solar activity
[NASA-TM-100372] 06 p0867 N90-15036
The solar array of Japanese solar observatory satellite Solar-A 10 p1345 N90-17798
NASA Marshall Space Flight Center solar observatory report, January to December 1989
[NASA-TM-100404] 19 p2797 N90-25923
NASA Marshall Space Flight Center Solar Observatory report, January - June 1990
[NASA-TM-103512] 23 p3409 N90-29268

SOLAR OSCILLATIONS
Solar opacities constrained by solar neutrinos and solar oscillations
[DE89-016988] 02 p0297 N90-11687
GOLF: Global Oscillations at Low Frequencies for the SOHO mission 04 p0566 N90-13304
VIRGO: The solar monitor experiment on SOHO 04 p0567 N90-13305
SOI: The Solar Oscillations Imager on SOHO 04 p0567 N90-13306
Nonlinear multi-mode coupling of the solar gravity modes in a rotationally split multiplet 21 p3100 N90-27605
Middle Atmosphere Program. Handbook for MAP, volume 29. Part 1: Extended Abstracts, International Symposium on Solar Activity Forcing of the Middle Atmosphere. Part 2: MASH Workshop
[NASA-CR-186005] 22 p3201 N90-28161
The tropospheric response pattern to solar activity forcing 22 p3201 N90-28165
A review of the 11-year solar cycle, the QBO, and the atmosphere relationship 22 p3202 N90-28166
Seasonal variation of the 11 year solar cycle effect on the middle atmosphere: Role of the quasi biennial oscillation 22 p3202 N90-28167
Influence of solar activity on middle atmosphere associated with phases of equatorial quasi-biennial oscillation 22 p3202 N90-28168
The planetary waves dynamics and interannual course of meteorological parameters of the high latitude stratosphere and mesosphere of the Northern and Southern Hemispheres during the 20th and 21st solar cycles and different phases of QBO 22 p3203 N90-28170
The QBO and weak external forcing by solar activity: A three dimensional model study 22 p3203 N90-28171
Solar activity, the QBO, and tropospheric responses 22 p3203 N90-28172
Solar oscillation frequency and solar neutrino predictions
[DE90-014918] 23 p3413 N90-29288

SOLAR PHYSICS
Solar X-ray Astronomy Sounding Rocket Program
[NASA-CR-183447] 01 p0138 N90-10796
Solar-geophysical data number 537, part 1. Data for April, March 1989 and late data
[PB89-207393] 02 p0296 N90-11685
MHD (magnetohydrodynamic) modeling of solar and interplanetary processes
[PB89-215461] 03 p0420 N90-12416
The hard x rays and gamma-rays from solar flares
[NASA-CR-185982] 03 p0429 N90-12458
Max '91 Workshop 2: Developments in Observations and Theory for Solar Cycle 22
[NASA-TM-101893] 03 p0429 N90-12459
High energy flare physics group summary 03 p0429 N90-12460
Magnetograph group summary 03 p0429 N90-12461
Theory and modeling group 03 p0430 N90-12462
Scientific objectives of solar gamma-ray observations 03 p0430 N90-12463
The Gamma-Ray Observatory: An overview 03 p0430 N90-12464
VLA-Max '91 tests of high energy flare physics 03 p0431 N90-12471
Observational goals for Max '91 to identify the causative agent for impulsive bursts 03 p0431 N90-12473
Solar-geophysical data number 537, May 1989. Part 2: Comprehensive Reports, data for Nov. 1988 and miscellaneous
[PB89-207401] 04 p0566 N90-13300
SOHO: An observatory to study the solar interior and the solar atmosphere 04 p0566 N90-13303
An implementation plan for priorities in solar-system space physics
[NASA-CR-185375] 05 p0710 N90-14154
Analysis of coordinated observations of a giant stellar flare
[NASA-CR-185961] 05 p0715 N90-14176
An international discussion on research in solar and space physics 06 p0859 N90-14996
Solar-geophysical data number 539, July 1989. Part 2: (Comprehensive reports). Data for January 1989, and miscellaneous
[PB89-235469] 06 p0866 N90-15034
Field of solar physics: Review and recommendations for ground-based solar research
[PB90-115684] 09 p1300 N90-17533
Report from solar physics 10 p1445 N90-18335
MAX 1991. The active sun: A plan for pursuing the study of the active sun at the time of the next maximum in solar activity, January 1985
[NASA-CR-186125] 12 p1745 N90-20030
Solar-geophysical data number 541, September 1989. Part 2: (Comprehensive reports). Data for March 1989 and miscellaneous
[PB90-122755] 12 p1745 N90-20031
Solar-geophysical data number 541, September 1989. Part 1: (Prompt reports). Data for August, July 1989, and late data
[PB90-122763] 12 p1745 N90-20032
NSSDC data listing
[NASA-TM-102989] 15 p2180 N90-22456
Solar-geophysical data number 542, October 1989. Part 1: (Prompt reports). Data for September, August 1989, and late data
[PB90-148669] 15 p2193 N90-22520
Solar-geophysical data number 542, October 1989. Part 2: (Comprehensive reports). Data for April 1989 and miscellaneous
[PB90-148677] 15 p2193 N90-22521
Research and technology 1989
[NASA-TM-100389] 17 p2486 N90-24219
Eleventh European Cosmic Ray Symposium
[DE90-611424] 19 p2798 N90-25927
Application of solar seismology to study of the convection zone
[AD-A221975] 21 p3101 N90-27610
Solar-geophysical data number 545, January 1990. Part 2 (Comprehensive reports). Data for July 1989 and miscellaneous
[PB90-182346] 22 p3263 N90-28480
Solar-geophysical data number 544, December 1989. Part 1 (Prompt reports). Data for November, October 1989, and late data
[PB90-171661] 22 p3263 N90-28481
Solar-geophysical data number 544, December 1989. Part 2 (Comprehensive reports). Data for June 1989 and miscellaneous
[PB90-171679] 22 p3264 N90-28482
Data catalog series for space science and applications flight missions. Volume 5A: Descriptions of astronomy, astrophysics, and solar physics spacecraft and investigations. Volume 5B: Descriptions of data sets from astronomy, astrophysics, and solar physics spacecraft and investigations
[NASA-TM-101908] 24 p3437 N90-29413
The Ulysses data book: A summary of the technical elements of the Ulysses spacecraft and its scientific payload
[ESA-BR-65] 24 p3440 N90-29427
Activities report of the Space Science Department
[ESA-SP-1126] 24 p3560 N90-30142

SOLAR PLANETARY INTERACTIONS
NT SOLAR TERRESTRIAL INTERACTIONS
User's guide to the Space Environment Services Center geophysical alert broadcasts
[PB89-194617] 02 p0249 N90-11411
National Center For Atmospheric Research annual report, fiscal year 1988
[PB89-208987] 02 p0252 N90-11428
Solar-geophysical data number 537, May 1989. Part 2: Comprehensive Reports, data for Nov. 1988 and miscellaneous
[PB89-207401] 04 p0566 N90-13300
Actions of magnetospheres on planetary atmospheres
[IRF-SR-203] 17 p2486 N90-24215

SOLAR PLASMA (RADIATION)
U SOLAR WIND

SOLAR POSITION
Launch and early orbit 05 p0606 N90-13524
On airborne measurements of radiation from broken cloud fields
[MITT-67] 21 p3027 N90-27211

SOLAR POWER GENERATION
U SOLAR GENERATORS

SOLAR POWER SATELLITES
Second Beamed Space-Power Workshop
[NASA-CP-3037] 01 p0027 N90-10140
Power from space for use on earth: An emerging global option 01 p0028 N90-10144
New energy conversion techniques in space, applicable to propulsion
[AIAA-79-1338] 01 p0028 N90-10145
History and status of beamed power technology and applications at 2.45 Gigahertz 01 p0029 N90-10150

Technical options for high average power free electron milimeter-wave and laser devices
01 p0029 N90-10151
Laser-powered Martian rover
01 p0029 N90-10157
Applicability of the beamed power concept to lunar rovers, construction, mining, explorers and other mobile equipment
01 p0030 N90-10159
The Solar Power Satellite (SPS): Progress so far
07 p1008 N90-15840
Transportation and operations aspects of space energy systems
07 p1008 N90-15842
System analysis and project of a laser-moved spaceship
[ILR-MITT-232(1989)] 18 p2513 N90-24348
Lunar orbiting microwave beam power system
[NASA-TM-103211] 19 p2667 N90-25173

SOLAR POWER SOURCES
U SOLAR GENERATORS

SOLAR PROBES
Gravitational experiments on a solar probe mission: Scientific objectives and technology considerations
12 p1733 N90-19966

SOLAR PROMINENCES
Solar-geophysical data number 531, part 2. Data foor May 1988 and miscellaneous
[PB89-139950] 01 p0142 N90-10817
Solar-geophysical data number 532, December 1988. Part 2: Data for June 1988 and miscellaneous
[PB89-152094] 01 p0142 N90-10819
Solar-geophysical data number 533. Part 2: Data for July 1988 and miscellaneous
[PB89-162499] 01 p0142 N90-10821
Solar-geophysical data number 534, February 1989. Part 2: (Comprehensive reports). Data for August 1988 and miscellaneous
[PB89-173058] 01 p0143 N90-10823
Solar-geophysical data number 536, part 2. Data for October 1988 and miscellaneous
[PB89-194658] 01 p0143 N90-10824
Solar-geophysical data number 538, June 1989. Part 2: (Comprehensive reports). Data for December 1988 and miscellaneous
[PB89-223846] 06 p0866 N90-15032
Solar-geophysical data number 540, August 1989. Part 2: (Comprehensive reports). Data for February 1989
[PB89-108598] 06 p0867 N90-15039
Solar-geophysical data number 541, September 1989. Part 2: (Comprehensive reports). Data for March 1989 and miscellaneous
[PB90-122755] 12 p1745 N90-20031
Solar-geophysical data number 544, December 1989. Part 2 (Comprehensive reports). Data for June 1989 and miscellaneous
[PB90-171679] 22 p3264 N90-28482

SOLAR PROTONS
A 154-day periodicity in the occurrence rate of proton flares
[NASA-CR-185826] 16 p2340 N90-23333

SOLAR RADIATION
NT SOLAR CORPUSCULAR RADIATION
NT SOLAR COSMIC RAYS
NT SOLAR NEUTRINOS
NT SOLAR NEUTRONS
NT SOLAR PROTONS
NT SOLAR RADIO BURSTS
NT SOLAR RADIO EMISSION
NT SOLAR WIND
NT SOLAR X-RAYS
NT SUNLIGHT
NT TYPE 3 BURSTS
An anisotropic shadowband correction for parameterized sky conditions and geometry
[DE89-014916] 01 p0085 N90-10485
Geophysical monitoring for climatic change number 16
[PB89-159628] 01 p0087 N90-10494
Solar radiation in Linkoeping (Sweden): Variations over half a year in irradiance and spectral composition in the interval 400-1000 nm
[FOA-C-30521-3.1] 02 p0250 N90-11417
A solar extreme ultraviolet flux model
02 p0296 N90-11686
Photolysis of spacecraft contaminants
[AD-A211715] 03 p0317 N90-11801
Calculated solar radiation incident upon slopes of different orientated surfaces in Finland
[FMI-MP-8] 03 p0370 N90-12116
The SMM UV observations of Active Region 5395
03 p0434 N90-12485
The Owens Valley solar array
03 p0435 N90-12490
SUMER: Solar Ultraviolet Measurements of Emitted Radiation
04 p0567 N90-13307
Design and technical aspects of the Solly instrument
05 p0659 N90-13847
Observation of the solar Lyman-alpha line
05 p0662 N90-13868
Senegalese land surface change analysis and biophysical parameter estimation using NOAA AVHRR spectral data
[NASA-CR-186120] 05 p0664 N90-13883
Beyond the IDMY (International Daylighting Measurements Year): A network instrument for low-cost data acquisition
[DE90-002722] 06 p0815 N90-14740
Atlas of albedo and absorbed solar radiation derived from Nimbus 6 earth radiation budget data set, July 1975 to May 1978
[NASA-RP-1230] 06 p0815 N90-14741
Analysis of catalytically enhanced solar absorption chemical reactors: 1 - numerical model description
[DE89-014742] 07 p0951 N90-15505
A guide for estimating potential energy savings from increased solar reflectance of a low-sloped roof
[DE90-003720] 07 p0955 N90-15526
SERI (Solar Energy Research Institute) solar radiation resource assessment project
[DE89-009456] 08 p1097 N90-16352
Climatic summaries and documentation for the primary meteorological Station, H. J. Andrews Experimental Forest, 1972 to 1984
[PB90-104373] 08 p1102 N90-16382
A look on non-standard solar models
[SER-C-PREPUBL-FASC-40] 08 p1153 N90-16677
Galactic cosmic-ray modulation and solar-terrestrial relationships
[IFSI-88-17] 08 p1153 N90-16679
The 1989 National Convention Record IEE Japan, part 11
[DE89-910083] 09 p1210 N90-17014
Atlas of albedo and absorbed solar radiation derived from Nimbus 7 Earth radiation budget data set, November 1978 to October 1985
[NASA-RP-1231] 09 p1247 N90-17233
USSR Climate Handbook Number 27. Part 1: Solar radiation, radiation balance and sunshine
[AD-A215647] 09 p1248 N90-17242
Resource Assessment Project: User needs survey results
[DE89-009502] 11 p1529 N90-18802
Solar and thermic utilization in high temperature area: Research and development
[ETN-90-96062] 12 p1682 N90-19663
Solar-geophysical data number 541, September 1989. Part 2: (Comprehensive reports). Data for March 1989 and miscellaneous
[PB90-122755] 12 p1745 N90-20031
Spectral solar radiation data base documentation
[DE89-009448] 12 p1745 N90-20033
Developments in solar photocatalysis for destruction of organics in water
[DE90-007685] 13 p1771 N90-20162
Spectral solar radiation data base documentation, volume 1
[DE89-009447] 13 p1841 N90-20571
Determination of rates of reaction in the gas-phase in the troposphere: Theory and practice. 2: Rate of direct photoreaction: Screening-level test guideline-spectroscopic determination of the cross section and the maximum rate of direct photoreaction in sunlight
[PB90-146291] 15 p2125 N90-22156
JARE data reports, no. 140 (meteorology 21): Meteorological data at Asuka Camp, Antarctica in 1987
[ISSN-0075-3343] 15 p2132 N90-22188
Photovoltaic advanced research and development project: Solar radiation research
[DE90-000302] 16 p2251 N90-22839
Numerical simulations of x rays and gamma rays from solar flares
16 p2339 N90-23330
Effects of air temperature on atmospheric CO2-plant growth relationships
[DE90-010159] 17 p2420 N90-23793
Optical properties monitor: Experiment definition phase
[NASA-CR-4293] 19 p2666 N90-25170
SERI solar radiation resource assessment project
[DE90-000307] 19 p2711 N90-25428
The effects of urban air pollution on solar radiation
[DE89-009455] 19 p2712 N90-25438
Photodissociation of O2 in the stratosphere and mesosphere: A general parametrization of the Schumman-Runge Bands
20 p2887 N90-26427
SAGE 3: A visible wavelength limb sounder
21 p3016 N90-27147
Abstracts of 1989 Japan Solar Energy Society and Japan Wind Energy Association Joint Conference
[DE90-503616] 21 p3019 N90-27168
On airborne measurements of radiation from broken cloud fields
[MITT-67] 21 p3027 N90-27211
Application of solar seismology to study of the convection zone
[AD-A221975] 21 p3101 N90-27610
Solar electricity and solar fuels
[DE90-796156] 22 p3196 N90-28135
Solar UV variability
22 p3201 N90-28162
Gases of the middle atmosphere and short-term solar radiation variations
22 p3204 N90-28177
The 27-day versus 13.5-day variations in the solar Lyman-alpha radiation and the radio wave absorption in the lower ionosphere over Europe
22 p3209 N90-28203
Relationship between the longwave cloud radiative forcing at the surface and the top of the atmosphere
22 p3222 N90-28273
Improved meteorological measurements from buoys and ships (IMET): Preliminary comparison of solar radiation air temperature shields
[PB90-241928] 22 p3229 N90-28314
Improved meteorological measurements from buoys and ships (IMET): Preliminary comparison of pyranometers
[PB90-241936] 22 p3229 N90-28315
A manual for analysis of hemispherical canopy photography
[DE90-014718] 23 p3342 N90-28885
Natural and anthropogenic climate change
[DE90-015528] 23 p3348 N90-28923
Daily temperature, solar radiation, wind speed, cloud cover, and precipitation data recorded at the meteorological station for calendar years 1957--1988
[DE90-014399] 23 p3352 N90-28941
The Ulysses data book: A summary of the technical elements of the Ulysses spacecraft and its scientific payload
[ESA-BR-65] 24 p3440 N90-29427

SOLAR RADIATION SHIELDING
Design development and qualification of a solar array with OSRs (SSM) bonded to the ISO spacecraft rigid sunshield
10 p1341 N90-17768
Reliability of equivalent sphere model in blood-forming organ dose estimation
[NASA-TM-4178] 12 p1746 N90-20036
Shutter mechanism for controlling the exposure of samples to solar radiation
18 p2540 N90-24498

SOLAR RADIO BURSTS
NT TYPE 3 BURSTS
Solar-geophysical data number 531, part 2. Data foor May 1988 and miscellaneous
[PB89-139950] 01 p0142 N90-10817
Solar-geophysical data number 532, December 1988. Part 2: Data for June 1988 and miscellaneous
[PB89-152094] 01 p0142 N90-10819
Solar-geophysical data number 533. Part 2: Data for July 1988 and miscellaneous
[PB89-162499] 01 p0142 N90-10821
Solar-geophysical data number 534, February 1989. Part 2: (Comprehensive reports). Data for August 1988 and miscellaneous
[PB89-173058] 01 p0143 N90-10823
Solar-geophysical data number 536, part 2. Data for October 1988 and miscellaneous
[PB89-194658] 01 p0143 N90-10824
The solar gamma ray and neutron capabilities of COMPTEL on the Gamma Ray Observatory
03 p0431 N90-12468
First interferometric observations with arc-sec. resolution of solar radio bursts at millimeter wavelengths
03 p0431 N90-12472
Observational goals for Max '91 to identify the causative agent for impulsive bursts
03 p0431 N90-12473
Solar-geophysical data number 537, May 1989. Part 2: Comprehensive Reports, data for Nov. 1988 and miscellaneous
[PB89-207401] 04 p0566 N90-13300
Solar-geophysical data number 538, June 1989. Part 2: (Comprehensive reports). Data for December 1988 and miscellaneous
[PB89-223846] 06 p0866 N90-15032
Solar-geophysical data number 539, July 1989. Part 2: (Comprehensive reports). Data for January 1989, and miscellaneous
[PB89-235469] 06 p0866 N90-15034
Solar-geophysical data number 540, August 1989. Part 2: (Comprehensive reports). Data for February 1989
[PB89-108598] 06 p0867 N90-15039
Natural and man-made emissions at 1.0 to 5.6 MHz measured between 10 and 18 R sub E
[MPE-PREPRINT-146] 08 p1058 N90-16116
Solar-geophysical data number 541, September 1989. Part 2: (Comprehensive reports). Data for March 1989 and miscellaneous
[PB90-122755] 12 p1745 N90-20031
Solar-geophysical data number 542, October 1989. Part 2: (Comprehensive reports). Data for April 1989 and miscellaneous
[PB90-148677] 15 p2193 N90-22521

Neutrino signals from the powerful solar flare on September 29, 1989
[PREPRINT-721] 16 p2339 N90-23331
Solar-geophysical data number 545, January 1990. Part 2 (Comprehensive reports). Data for July 1989 and miscellaneous
[PB90-182346] 22 p3263 N90-28480
Solar-geophysical data number 544, December 1989. Part 2 (Comprehensive reports). Data for June 1989 and miscellaneous
[PB90-171679] 22 p3264 N90-28482
Alfven wave solitons and solar intermediate drift bursts
[MPE-PREPRINT-173] 23 p3413 N90-29287

SOLAR RADIO EMISSION
NT SOLAR RADIO BURSTS
NT TYPE 3 BURSTS
Solar-geophysical data number 532, December 1988. Part 1: Data for November, October 1988, and late data
[PB89-152086] 01 p0142 N90-10818
Solar-geophysical data number 533. Part 1: Data for December, November 1988, and late data
[PB89-162481] 01 p0142 N90-10820
Solar-geophysical data number 534, February 1989. Part 1: (Prompt reports). Data for January 1989, December 1988 and late data
[PB89-173041] 01 p0142 N90-10822
Solar-geophysical data number 536, part 1. Data for March, Febuary 1989 and late data
[PB89-194716] 02 p0296 N90-11684
Solar-geophysical data number 537, part 1. Data for April, March 1989 and late data
[PB89-207393] 02 p0296 N90-11685
Berne solar observations
[REPT-55] 04 p0566 N90-13301
Solar-geophysical data number 538, June 1989. Part 1: (Prompt reports). Data for May, April 1989, and late data
[PB89-223838] 06 p0866 N90-15031
Solar-geophysical data number 539, July 1989. Part 1: (Prompt reports). Data for June, May 1989, and late data
[PB89-235451] 06 p0866 N90-15033
Solar-geophysical data number 540, August 1989. Part 1: (Prompt reports). Data for July, June 1989, and late data
[PB90-108572] 06 p0866 N90-15035
Solar-geophysical data number 541, September 1989. Part 1: (Prompt reports). Data for August, July 1989, and late data
[PB90-122763] 12 p1745 N90-20032
Solar-geophysical data number 542, October 1989. Part 1: (Prompt reports). Data for September, August 1989, and late data
[PB90-148669] 15 p2193 N90-22520
Berne solar observations: Data for July to December 1989
[REPT-56] 19 p2797 N90-25924
Solar-geophysical data number 544, December 1989. Part 1 (Prompt reports). Data for November, October 1989, and late data
[PB90-171661] 22 p3263 N90-28481
Alfven wave solitons and solar intermediate drift bursts
[MPE-PREPRINT-173] 23 p3413 N90-29287

SOLAR RADIO WAVES
U SOLAR RADIO EMISSION

SOLAR RECEIVERS
U SOLAR COLLECTORS

SOLAR REFLECTORS
NT SOLAR COLLECTORS
LDR structural experiment definition
05 p0600 N90-13483
LDR structural technology activities at JPL
05 p0601 N90-13488
Enhancement of processes for solar photocatalytic detoxification of water
[DE90-003949] 12 p1623 N90-19330
Qualification of concentrating mirror systems with the HERMES measurement system and the HELIOS simulation program
[DLR-FB-89-51] 20 p2882 N90-26394

SOLAR ROTATION
Variational problems in astrophysics
09 p1298 N90-17524
Evolutionary models of the rotating sun and implications for other low mass stars 16 p2339 N90-23329
The QBO and weak external forcing by solar activity: A three dimensional model study
22 p3203 N90-28171
Stratospheric effects of solar ultraviolet variations on the solar rotation time scale 22 p3204 N90-28176
Atmospheric planetary waves induced by solar rotation 22 p3204 N90-28178
Solar or meteorological control of lower ionospheric fluctuations (2-15 and 27 days) in middle latitudes
22 p3209 N90-28202

SOLAR SAILS
Design of a solar sail mission to Mars
[NASA-CR-186045] 03 p0311 N90-11771

SOLAR SEA POWER PLANTS
Planning for hybrid-cycle OTEC experiments using the HMTSTA test facility at the Natural Energy Laboratory of Hawaii
[DE89-013278] 02 p0237 N90-11349
Ocean thermal energy conversion: An overview
[DE89-000838] 07 p0953 N90-15512
Ocean energy program summary
[DE89-009481] 16 p2251 N90-22836
Ocean energy program summary. Volume 2: Research summaries
[DE89-009482] 18 p2576 N90-24677

SOLAR SEISMOLOGY
U HELIOSEISMOLOGY

SOLAR SELECTIVE COATINGS
U SELECTIVE SURFACES

SOLAR SENSORS
Temperature dependence of attitude sensor coalignments on the Solar Maximum Mission (SMM)
05 p0588 N90-13426
Analytical derivation and verification of zero-gyro control for the IUE satellite
[NASA-TM-100748] 05 p0645 N90-13767
Study of possible solar heating effects on thermosonde probes: Error analysis
[AD-A218116] 13 p1903 N90-20917
Thermal and orbital analysis of Earth monitoring Sun-synchronous space experiments
[NASA-TM-101630] 19 p2666 N90-25168
High altitude balloon flight test of the GRAD experiment
[AD-A224398] 24 p3432 N90-29388

SOLAR SIMULATION
A pulsed solar simulator for electrical performance tests of space solar cells/arrays 10 p1343 N90-17783
The solar array design of the Vesta small bodies spacecraft 10 p1345 N90-17799
The synergism of analytic and numerical techniques in general relativity: Calculation of radiative spacetimes
15 p2174 N90-22425

SOLAR SIMULATORS
A pulsed solar simulator for electrical performance tests of space solar cells/arrays 10 p1343 N90-17783
Preliminary design of a pointer for movement of a solar simulator
[INPE-4864-TDL/375] 11 p1517 N90-18736
Direct solar-pumped iodine laser amplifier
[NASA-CR-186442] 15 p2103 N90-22030

SOLAR SPECTRA
Solar X-ray Astronomy Sounding Rocket Program
[NASA-CR-183447] 01 p0138 N90-10796
X-ray bright points and He I lambda 10830 dark points
01 p0139 N90-10802
Advances in photographic X-ray imaging for solar astronomy 01 p0139 N90-10803
Correspondence between solar fine-scale structures in the corona, transition region, and lower atmosphere from collaborative observations 01 p0139 N90-10804
The hard x rays and gamma-rays from solar flares
[NASA-CR-185982] 03 p0429 N90-12458
A high-speed digital camera system for the observation of rapid H-alpha fluctuations in solar flares
03 p0435 N90-12491
Solar-geophysical data number 538, June 1989. Part 1: (Prompt reports). Data for May, April 1989, and late data
[PB89-223838] 06 p0866 N90-15031
Solar-geophysical data number 540, August 1989. Part 1: (Prompt reports). Data for July, June 1989, and late data
[PB90-108572] 06 p0866 N90-15035
Far-ultraviolet spectroscopy of Comet Halley
12 p1736 N90-19979
Comet Halley: An optical continuum study
12 p1736 N90-19981
Berne solar observations: Data for July to December 1989
[REPT-56] 19 p2797 N90-25924
Resonant Rossby waves and solar activity
22 p3205 N90-28179

SOLAR SPECTROMETERS
The SOHO mission. Scientific and technical aspects of the instruments
[ESA-SP-1104] 04 p0566 N90-13302
VIRGO: The solar monitor experiment on SOHO
04 p0567 N90-13305
SUMER: Solar Ultraviolet Measurements of Emitted Radiation 04 p0567 N90-13307
CDS: The Coronal Diagnostic Spectrometer
04 p0567 N90-13308
UVCS: An Ultraviolet Coronagraph Spectrometer for SOHO 04 p0568 N90-13310
Design and technical aspects of the Solly instrument
05 p0659 N90-13847

SOLAR STORMS
The effects of solar particle events on the middle atmosphere 22 p3206 N90-28189

SOLAR STREAMS
U SOLAR CORPUSCULAR RADIATION

SOLAR SYSTEM
The German space science program
05 p0662 N90-13873
An implementation plan for priorities in solar-system space physics
[NASA-CR-185375] 05 p0710 N90-14154
JPRS Report: Science and technology. USSR: Space. Soviet space program to the year 2000
[JPRS-USP-89-008] 06 p0728 N90-14248
Non-equilibrium chemistry in the solar nebula and early solar system: Implications for the chemistry of comets
08 p1142 N90-16618
Publications of the Exobiology Program for 1988: A special bibliography
[NASA-TM-4169] 09 p1262 N90-17316
Detecting extended solar system structures with COBE (Cosmic Background Explorer)
[AD-A216380] 10 p1447 N90-18349
Pioneers 10 and 11 deep space missions
[NASA-TM-102269] 10 p1448 N90-18355
Infrared cometary spectroscopy
11 p1578 N90-19086
Human exploration mission studies
13 p1821 N90-20457
Cosmic Dust Collection Facility: Scientific objectives and programmatic relations
[NASA-TM-102160] 14 p1939 N90-21098
Research and Technology
[NASA-TM-102161] 14 p2044 N90-21721
Improving a data-acquisition software system with abstract data type components
15 p2078 N90-21901
Project Longshot: A mission to Alpha Centauri
[NASA-CR-186052] 17 p2357 N90-23417
Institute of Astronomy 17 p2481 N90-24190
Activities report of the Institute for Astronomy and Astrophysics
[MITT-10] 18 p2636 N90-25020
The Telecommunications and Data Acquisition Report
[NASA-CR-186852] 20 p2852 N90-26217
Preliminary error budget for an optical ranging system: Range, range rate, and differenced range observables
20 p2853 N90-26227
Reports of planetary astronomy, 1990
[NASA-TM-4205] 20 p2940 N90-26730
Submillimeter and millimeter observations of solar system objects
[NASA-CR-186636] 20 p2940 N90-26731
Absolute vacuum ultraviolet photoabsorption cross section studies of atomic and molecular species: Techniques and observational data
20 p2944 N90-26754
SIRTF: Probing the dark corners of the galaxy
21 p3091 N90-27577
The possible presence of interstellar PAHs in meteorites and interplanetary dust particles
21 p3092 N90-27579
Impact fracture experiments simulating interstellar grain-grain collisions 21 p3093 N90-27584
On diamond, graphitic and amorphous carbons in primitive extraterrestrial solar system materials
21 p3095 N90-27591
Carbon in the outer solar system
21 p3096 N90-27593

SOLAR TEMPERATURE
Solar opacities constrained by solar neutrinos and solar oscillations
[DE89-016988] 02 p0297 N90-11687

SOLAR TERRESTRIAL INTERACTIONS
Ionospheric Structure and Variability on a Global Scale and Interactions with Atmosphere and Magnetosphere
[AGARD-CP-441] 02 p0239 N90-11361
Solar-terrestrial relations: Flare and solar wind effects
02 p0240 N90-11362
Magnetospheric substorms as a signature of the solar terrestrial interaction 02 p0240 N90-11363
Stormtime coupling of the neutral and ionized upper atmosphere at middle latitudes
02 p0243 N90-11381
Coordinated multi-parameter measurements and predictions of the global-scale ionosphere
02 p0247 N90-11397
On the statistics of El Nino occurrences and the relationship of El Nino to volcanic and solar/geomagnetic activity
[NASA-TP-2948] 03 p0429 N90-12456
Some of the terrestrial effects of AR 5395
03 p0433 N90-12482

The 10.7-cm microwave observations of AR 5395 and related terrestrial effects 03 p0433 N90-12483
An implementation plan for priorities in solar-system space physics
[NASA-CR-185375] 05 p0710 N90-14154
Galactic cosmic-ray modulation and solar-terrestrial relationships
[IFSI-88-17] 08 p1153 N90-16679
Solar cycle effects on trapped energetic particles
[AD-A215028] 09 p1300 N90-17532
Solar-Terrestrial Science Strategy Workshop
[NASA-CP-3048] 10 p1444 N90-18329
Background of the workshop
10 p1444 N90-18330
Supporting tools of solar-terrestrial science
10 p1444 N90-18331
Report from magnetospheric science
10 p1444 N90-18334
Report from solar physics 10 p1445 N90-18335
Recommendations for the future
10 p1445 N90-18338
Orbital mechanics: A learning tool on the main frame
[AD-A218799] 16 p2204 N90-22576
Thermal and orbital analysis of Earth monitoring Sun-synchronous space experiments
[NASA-TM-101630] 19 p2666 N90-25168
Middle Atmosphere Program. Handbook for MAP, volume 29. Part 1: Extended Abstracts, International Symposium on Solar Activity Forcing of the Middle Atmosphere. Part 2: MASH Workshop
[NASA-CR-186005] 22 p3201 N90-28161
Observed solar near UV variability: A contribution to variations of the solar constant
22 p3201 N90-28163
The tropospheric response pattern to solar activity forcing 22 p3201 N90-28165
Seasonal variation of the 11 year solar cycle effect on the middle atmosphere: Role of the quasi biennial oscillation 22 p3202 N90-28167
The planetary waves dynamics and interannual course of meteorological parameters of the high latitude stratosphere and mesosphere of the Northern and Southern Hemispheres during the 20th and 21st solar cycles and different phases of QBO
22 p3203 N90-28170
The QBO and weak external forcing by solar activity: A three dimensional model study
22 p3203 N90-28171
Resonant Rossby waves and solar activity
22 p3205 N90-28179
On the relationship between the phases of 27-day total ozone and solar activity indices in different latitudinal zones 22 p3205 N90-28180
Solar activity influence on cosmic ray penetration in the middle atmosphere 22 p3207 N90-28192
Effects of solar activity in the middle atmosphere dynamical regime over Eastern Siberia, USSR
22 p3207 N90-28195
Solar activity influences on atmospheric electricity and on some structures in the middle atmosphere
22 p3207 N90-28196
Relationship between solar activities and thunderstorm activities in the Beijing area and the northeast region of China 22 p3208 N90-28197
General overview of the solar activity effects on the lower ionosphere 22 p3208 N90-28198
Electron density profiles in the background of LF absorption during Forbush-decrease and PSE
22 p3208 N90-28199
The probability of SWF occurrence in relation to solar activity 22 p3209 N90-28204
The natural VLF emission as diagnostics and estimation means of the fluxes of solar x ray bursts
22 p3209 N90-28206
Effects of energy, momentum and particle transport in the near-earth solar terrestrial system
[AD-A224393] 24 p3490 N90-29726
Some personal reminiscences. The ESRO-ESA space science story: Twenty-five years of European cooperation
[ESA-BR-66] 24 p3565 N90-30168

SOLAR THERMAL ELECTRIC POWER PLANTS

Phase-Change Thermal Energy Storage
[DE89-009426] 11 p1529 N90-18801
Solar thermal program summary, fiscal year 1989
[DE89-009475] 13 p1826 N90-20487
Solar thermal program summary. Volume 2: Research summaries
[DE89-009476] 18 p2576 N90-24674
Solar energy for high temperature technology and applications
[ETN-90-97429] 23 p3345 N90-28902

SOLAR WIND

Numerical simulation of the compressible Orszag-Tang vortex
[AD-A210465] 01 p0127 N90-10725
Solar-terrestrial relations: Flare and solar wind effects
02 p0240 N90-11362
Magnetospheric substorms as a signature of the solar terrestrial interaction 02 p0240 N90-11363
MHD (magnetohydrodynamic) modeling of solar and interplanetary processes
[PB89-215461] 03 p0420 N90-12416
SUMER: Solar Ultraviolet Measurements of Emitted Radiation 04 p0567 N90-13307
CDS: The Coronal Diagnostic Spectrometer
04 p0567 N90-13308
LASCO: A wide-field white light and spectrometric coronagraph for SOHO 04 p0568 N90-13311
CELIAS: Charge, element and isotope analysis system for SOHO 04 p0568 N90-13313
Solar-geophysical data number 538, June 1989. Part 2: (Comprehensive reports). Data for December 1988 and miscellaneous
[PB89-223846] 06 p0866 N90-15032
Solar-geophysical data number 540, August 1989. Part 2: (Comprehensive reports). Data for February 1989
[PB89-108598] 06 p0867 N90-15039
Laboratory simulations of the solar wind-comet interactions 07 p1015 N90-15875
Some properties of so-called magnetic cloud structures in the solar wind
[IFSI-88-16] 08 p1153 N90-16678
Interaction of minor ions with fast and slow shocks
[NASA-CR-186372] 11 p1594 N90-19181
Gravitational experiments on a solar probe mission: Scientific objectives and technology considerations
12 p1733 N90-19966
Disturbance structures and its magnetic field features in plasma comet tail
[DE90-610636] 12 p1737 N90-19986
The Advanced Composition Explorer
[DE90-006522] 12 p1737 N90-19987
The production and spatial distribution of neutral and ionized water vapor in Comet P/Halley
15 p2185 N90-22484
Solar activity, the QBO, and tropospheric responses
22 p3203 N90-28172
Solar wind and high energy particle effects in the middle atmosphere 22 p3206 N90-28188
Effects of solar activity in the middle atmosphere dynamical regime over Eastern Siberia, USSR
22 p3207 N90-28195
General overview of the solar activity effects on the lower ionosphere 22 p3208 N90-28198
The influence of IMF on the lower ionosphere plasma in high and middle latitudes 22 p3208 N90-28200
Interplanetary medium data book, supplement 4, 1985-1988
[NASA-TM-101867] 24 p3561 N90-30149

SOLAR WIND VELOCITY

The SOHO mission. Scientific and technical aspects of the instruments
[ESA-SP-1104] 04 p0566 N90-13302
SWAN: A study of solar wind anisotropies
04 p0568 N90-13312
The importance of adiabatic variations in trapped particle distributions observed by the SCATHA satellite
[AD-A220859] 17 p2423 N90-23806

SOLAR X-RAYS

The correspondence between small-scale coronal structures and the evolving solar magnetic field
01 p0138 N90-10800
Solar-geophysical data number 531, part 2. Data foor May 1988 and miscellaneous
[PB89-139950] 01 p0142 N90-10817
Solar-geophysical data number 532, December 1988. Part 2: Data for June 1988 and miscellaneous
[PB89-152094] 01 p0142 N90-10819
Solar-geophysical data number 533. Part 2: Data for July 1988 and miscellaneous
[PB89-162499] 01 p0142 N90-10821
Solar-geophysical data number 534, February 1989. Part 2: (Comprehensive reports). Data for August 1988 and miscellaneous
[PB89-173058] 01 p0143 N90-10823
Solar-geophysical data number 536, part 2. Data for October 1988 and miscellaneous
[PB89-194658] 01 p0143 N90-10824
The hard x rays and gamma-rays from solar flares
[NASA-CR-185982] 03 p0429 N90-12458
Pre-pulses: Signature of a trigger process in short (less than 60 secs) solar hard x ray flares
03 p0432 N90-12476
Joule heating and runaway electron acceleration in a solar flare 03 p0432 N90-12478
Chromospheric-coronal coupling during solar flares: Current systems and particle acceleration
03 p0433 N90-12480
Hard x ray highlights of AR 5395
03 p0434 N90-12486
A high-speed digital camera system for the observation of rapid H-alpha fluctuations in solar flares
03 p0435 N90-12491
Solar-geophysical data number 537, May 1989. Part 2: Comprehensive Reports, data for Nov. 1988 and miscellaneous
[PB89-207401] 04 p0566 N90-13300
Prediction of the 10 cm solar flux index
05 p0662 N90-13872
Solar-geophysical data number 538, June 1989. Part 2: (Comprehensive reports). Data for December 1988 and miscellaneous
[PB89-223846] 06 p0866 N90-15032
Solar-geophysical data number 539, July 1989. Part 2: (Comprehensive reports). Data for January 1989, and miscellaneous
[PB89-235469] 06 p0866 N90-15034
Solar-geophysical data number 540, August 1989. Part 2: (Comprehensive reports). Data for February 1989
[PB89-108598] 06 p0867 N90-15039
Solar-geophysical data number 541, September 1989. Part 2: (Comprehensive reports). Data for March 1989 and miscellaneous
[PB90-122755] 12 p1745 N90-20031
Numerical simulations of x rays and gamma rays from solar flares 16 p2339 N90-23330

SOLAR-PUMPED LASERS

Development of a solar-powered infrared injection laser microminiature transmitting system
[DE90-005672] 10 p1389 N90-18034
Free-Space Power Transmission
[NASA-CP-10016] 15 p2060 N90-21795
Solar-pumped laser for free space power transmission
15 p2061 N90-21804
Comparison of solar pumped Nd:YAG and Nd:Cr:GSGG lasers at liquid nitrogen and room temperature
[DLR-FB-89-41] 16 p2240 N90-22781
Advanced solar-propelled cargo spacecraft for Mars missions
[NASA-CR-186218] 19 p2665 N90-25164
Theoretical studies of solar pumped lasers
[NASA-CR-186712] 20 p2867 N90-26308
Potential of solar-simulator-pumped alexandrite lasers
[NASA-TM-102701] 22 p3180 N90-28046

SOLDERED JOINTS

Isothermal fatigue behavior of Sn-Pb solar joints
[DE90-003280] 07 p0943 N90-15484
Magellan/Galileo solder joint failure analysis and recommendations
[NASA-CR-186294] 09 p1233 N90-17157
Cyclic deformation of Sn-60 to Pb-40 solder joints during thermomechanical fatigue
[DE90-004197] 09 p1237 N90-17179
Creep in shear of experimental solder joints
[DE90-007062] 11 p1520 N90-18753
The metallurgical mechanisms of solder fatigue
[DE90-008390] 13 p1778 N90-20206
Computed tomography of electronics
[AD-A217976] 13 p1797 N90-20314
Compatibility of Au base thick films with solder alloys: Solid state growth of intermetallics
[DE90-009285] 14 p1952 N90-21175
Proceedings of the 14th Annual Electronics Manufacturing Seminar
[AD-A224276] 24 p3463 N90-29563

SOLDERING

NT ULTRASONIC SOLDERING
A method of soldering aluminum
[AD-D014226] 06 p0792 N90-14611
Automated convection soldering
[KCP-613-4005] 07 p0916 N90-15300

SOLDERS

The metallurgical mechanisms of solder fatigue
[DE90-008390] 13 p1778 N90-20206
Compatibility of Au base thick films with solder alloys: Solid state growth of intermetallics
[DE90-009285] 14 p1952 N90-21175

SOLENOIDS

A nonintrusive method for measuring the operating temperature of a solenoid-operated valve
[DE90-007576] 13 p1804 N90-20355

SOLID ARGON

U SOLIDIFIED GASES

SOLID CRYOGENS

Solid fiber Z-pinches: Cold-start computations
[DE89-016768] 02 p0279 N90-11592
Auger and x ray absorption studies of solid molecular oxygen
[DE90-003966] 07 p1006 N90-15825
Optical constants of solid methane
20 p2948 N90-26775

SOLID ELECTRODES

The effect of electrode configuration on arcjet performance
[NASA-TM-102346] 02 p0189 N90-11081

Metal transfer in gas metal arc welding
[AD-A213390] 05 p0624 N90-13642
Electrode development in monolithic solid oxide fuel cells
[DE90-001910] 06 p0805 N90-14684
Solid oxide fuel cells electrodes based on In(sub 2)O(sub 3)-PrO(sub 1.83)-ZrO(sub 2)
[DE90-002666] 06 p0806 N90-14691
Fundamental studies of surface processes and trace analysis using solid electrodes
[AD-A216538] 11 p1483 N90-18533
Electrochemical investigations of novel solid redox polymerization electrodes
[DE90-006087] 11 p1492 N90-18584
Lightweight solid polymer electrolyte fuel cell with stack power density of 3 kW/lb (7 kW/kg)
[AD-A223964] 23 p3345 N90-28905

SOLID ELECTROLYTES
Impedance studies of the cell Pt/Ag+ conducting glass/Ag beta-alumina/Pt
[AD-A209820] 01 p0038 N90-10210
Advanced double layer capacitor
[AD-A210510] 01 p0061 N90-10348
Long endurance underwater power system
[AD-A211386] 03 p0366 N90-12096
A lightweight solid polymer electrolyte fuel cell with stack power density of 3 kW/lb (7 kW/kg)
[AD-A211542] 03 p0367 N90-12098
Advanced double layer capacitor
[AD-A211977] 04 p0469 N90-12688
The multivalent beta'-aluminas
[AD-A212103] 04 p0478 N90-12738
Modeling of sodium/metal chloride batteries
[DE89-017685] 06 p0770 N90-14478
Proceedings of the First Annual Fuel Cells Contractors Review Meeting
[DE89-011699] 06 p0803 N90-14675
Interfacial effects in monolithic solid oxide fuel cells
[DE90-001914] 06 p0806 N90-14690
Solid State Division
[DE90-000979] 06 p0851 N90-14945
Novel high-rate, all solid-state, sodium and lithium/organosulfur batteries
[DE90-001014] 07 p0920 N90-15325
Solid-state electrolyte catalysis for methane and oxygen synthesis
[PB90-100231] 08 p1040 N90-16011
Development of planar geometry solid oxide fuel cells
[PB90-100769] 08 p1095 N90-16341
Patents on solid electrolyte fuel cells: Japan
[DE90-702639] 09 p1241 N90-17202
Patents on solid electrolyte fuel cells: US and Britain
[DE90-702640] 09 p1241 N90-17203
Patents on solid electrolyte fuel cells: West Germany, Netherlands and Sweden
[DE90-702641] 09 p1242 N90-17204
Solid polymer electrolyte water electrolysis as a mean of energy storage for space applications
10 p1334 N90-17713
Structural and fast ion transport properties of glassy and amorphous materials
[DE90-005587] 10 p1358 N90-17877
Application of polymer electrolytes to lithium batteries
[AD-A216038] 10 p1401 N90-18099
A lightweight solid polymer electrolyte fuel cell with stack power density of 3kW/lb (7 kW/kg)
[AD-A216253] 10 p1401 N90-18100
Advanced double layer capacitor
[AD-A217110] 12 p1656 N90-19518
The electrochemical generation of useful chemical species from lunar materials 13 p1822 N90-20461
Recent advances in solid polymer electrolyte fuel cell technology with low platinum loading electrodes
13 p1823 N90-20465
Hydrogen-oxygen proton-exchange membrane fuel cells and electrolyzers 13 p1823 N90-20467
Thermoelectric conversion with ion conductors
[AD-A217822] 13 p1828 N90-20497
Enhanced ceria solid electrolyte fuel cell development. Reduction of electronic conductivity permits use of a solid ceria electrolyte in high efficiency high power density fuel cells at temperatures compatible with metallic cell hardware
[AD-A217840] 13 p1828 N90-20498
Alternative materials for solid oxide fuel cells
[DE90-008615] 14 p2001 N90-21468
Advanced double layer capacitor
[AD-A219419] 16 p2233 N90-22741
Enhanced ceria solid electrolyte fuel cell development. Reduction of electronic conductivity permits use of a solid ceria electrolyte in high efficiency high power density fuel cells at temperatures compatible with metallic cell hardware
[AD-A219297] 16 p2253 N90-22846
NMR studies of polymeric solid electrolytes
[AD-A219833] 17 p2381 N90-23562
A lightweight solid polymer electrolyte fuel cell with stack power density of 3 kW/lb (7kW/kg)
[AD-A223068] 21 p3020 N90-27169
Use of microelectrode arrays to directly measure diffusion of ions in solid electrolytes: Physical diffusion of Ag(+) in a solid polymer electrolyte
[AD-A222026] 22 p3159 N90-27913
A high temperature molten salt thermal electrochemical cell
[AD-D014469] 22 p3195 N90-28131
Lightweight solid polymer electrolyte fuel cell with stack power density of 3 kW/lb (7 kW/kg)
[AD-A223964] 23 p3345 N90-28905
Electrochemical characteristics of acid electrolytes for fuel cells
[PB90-244385] 24 p3484 N90-29693
Advanced materials and electrochemical processes in high-temperature solid electrolytes
[DE90-015552] 24 p3553 N90-30104

SOLID LUBRICANTS
Ion-assisted deposition of high-temperature lubricious surfaces
[DE89-012397] 03 p0331 N90-11883
Structural studies of sputter-deposited MoS2 solid lubricant films
[AD-A212407] 04 p0481 N90-12759
Cold press lubrication: Fine tuning of the CETIM Forgelub test
[CETIM-105160] 04 p0509 N90-12938
Evaluation of newly formulated Dow Corning 321 dry film lubricant
[NASA-CR-183828] 05 p0627 N90-13661
Solid lubrication of ceramic surfaces by IAD (Ion-Assisted Deposition)-silver coatings for heat engine applications
[DE90-002860] 07 p0909 N90-15253
Molybdenum disulfide-molybdenum oxide lubricants
[AD-D014253] 08 p1048 N90-16059
The experimental evaluation and application of high-temperature solid lubricants
[NASA-TM-102476] 09 p1198 N90-18944
Effects of microstructure and adhesion on performance of sputter-deposited MoS2 solid lubricant coatings
[AD-A220900] 18 p2530 N90-24434
Tribological properties of PVD-applied MoS2 coatings used on space mechanisms 18 p2537 N90-24470
Thick and compact MoS2 coatings
18 p2541 N90-24501
The experimental evaluation and application of high temperature solid lubricants 18 p2564 N90-24631
Lubrication characteristics of rolling bearings lubricated by self-lubricating composite retainers. Part 1: Selection of bearings for Earth sensors
[NAL-TR-1019] 24 p3477 N90-29651
Friction, wear and electric characteristics of slip-ring brush materials for space applications. Part 1: Screening by pin-on-disk friction tests
[NAL-TR-1040] 24 p3478 N90-29657

SOLID MECHANICS
Proceedings of the Army Symposium on Solid Mechanics, 1989: Mechanics of Engineered Materials and Applications
[AD-A211954] 04 p0511 N90-12951
Element-by-element preconditioning techniques for large-scale, vectorized finite element analysis in nonlinear solid and structural mechanics 08 p1087 N90-16291
Compact scheme for systems of equations applied to fundamental problems of mechanics of continua
[NASA-CR-186494] 14 p1971 N90-21292
NASA-UVA light aerospace alloy and structures technology program
[NASA-CR-182607] 16 p2217 N90-22651
Symmetry and global bifurcation in nonlinear solid mechanics
[AD-A221981] 21 p3013 N90-27129

SOLID PHASES
Structure-property relationships as an aid in the rational design of (beta)-(ET)(sub 2)X organic superconductors
[DE89-016912] 03 p0410 N90-12356
Theoretical and experimental study of solid phase miscibility gaps in III/V quaternary alloys
[DE90-008430] 13 p1895 N90-20877
Optical constants of solid methane
20 p2948 N90-26775
Laboratory studies of the interaction of ions with condensed gases: Planetary applications
20 p2949 N90-26778

SOLID PROPELLANT COMBUSTION
NT SOLID PROPELLANT IGNITION
A theoretical model of double base propellant combustion
[ONERA-RTF-23/7128-EY] 05 p0629 N90-13672
A surface coupled flamelet approach to dynamic response in heterogeneous propellant combustion
06 p0739 N90-14302
Steady flow combustion model for solid-fuel ramjet projectiles
[BRL-TR-2987] 07 p0893 N90-15163
Spectral studies of solid propellant combustion. 2: Emission and absorption results for M-30 and HMX1 propellants
[AD-A213857] 07 p0915 N90-15292
Solid fuel combustion chamber, phase 10
[LR-536] 08 p1038 N90-16000
Solid fuel combustion chamber
[LR-555] 08 p1038 N90-16001
Application of the singularity-separating method to computing problems of solid-propellant combustion in a closed vessel
[PREPRINT-489] 08 p1053 N90-16086
On the direct simulation of vortex shedding
[LR-513] 15 p2048 N90-21743
The pyrolysis of polymethylmethacrylate during combustion in a solid fuel combustion chamber
[LR-531] 15 p2068 N90-21845
Solid fuel combustion chamber
[LR-562] 15 p2068 N90-21846
Solid fuel combustion chamber
[LR-591] 15 p2068 N90-21847
Temperature measurements through a solid-propellant combustion wave using imbedded fine wire thermocouples
[AD-A218642] 16 p2225 N90-22693
Implementation of image action plus software for image analysis of solid propellant combustion holograms
[AD-A219644] 17 p2372 N90-23508
Solid fuel combustion chamber
[LR-634] 24 p3441 N90-29433
Spectroscopy of propellant-related flames
[AD-A224068] 24 p3457 N90-29525
An experimental investigation of strand burning metallized solid propellants
[AD-A224074] 24 p3457 N90-29526

SOLID PROPELLANT IGNITION
Calculation of Einstein A coefficients and oscillator strengths for the A(perturbed)(2)A(1)-X(perturbed)(2)B(1) transition of NH(2)
[AD-A213837] 07 p0896 N90-15176
Workshop on ESD (Electrostatic Discharge) Ignition of Composite Solid Propellants
[AD-A216599] 17 p2382 N90-23569
Igniter adapter-to-igniter chamber deflection test
[NASA-CR-184002] 22 p3133 N90-27780
Flight motor set 360L008 (STS-32R). Volume 1: System overview
[NASA-CR-184010] 23 p3289 N90-28609

SOLID PROPELLANT ROCKET ENGINES
NT ADVANCED SOLID ROCKET MOTOR (STS)
NT APOGEE BOOST MOTORS
NT ASROC ENGINE
NT SPACE SHUTTLE BOOSTERS
Turbulent reacting flows in solid-propellant ducted rocket combustors 02 p0189 N90-11079
Three-dimensional, two-phase, transonic, canted nozzle flows
[AD-A211528] 03 p0347 N90-11984
RSRM-3 (360L003) ballistics/mass properties report
[NASA-CR-183716] 04 p0463 N90-12651
Ballistics/mass properties
[NASA-CR-183723] 04 p0463 N90-12652
A data acquisition and processing system for six component solid rocket motor testing
[AD-A212200] 04 p0464 N90-12657
Systems tunnel linear shaped charge lightning strike
[NASA-CR-183832] 05 p0584 N90-13404
Review of the Aerospace Safety Advisory Panel report for NASA fiscal year 1990 authorization
[GPO-24-234] 06 p0722 N90-14213
Flight set 360T004 (STS-30) field joint protection system, volume 7
[NASA-CR-183829] 06 p0735 N90-14280
A surface coupled flamelet approach to dynamic response in heterogeneous propellant combustion
06 p0739 N90-14302
Ariane-5 solid boosters stage development
09 p1176 N90-16811
Static test deflector for Ariane-5 SRM: Technical design and economical choice 09 p1176 N90-16812
Combustion instability in solid propellant rockets
[AD-A216740] 11 p1476 N90-18492
Thiokol/Wasatch installation evaluation of the redesigned field joint protection system (concepts 1 and 3)
[NASA-CR-183860] 13 p1765 N90-20127
Transportation monitoring unit qualification
[NASA-CR-183930] 14 p1932 N90-21060
Technical Evaluation Motor no. 5 (TEM-5)
[NASA-CR-183932] 14 p1942 N90-21117
Flight motor set 360L002 (STS-27R). Volume 5: Nozzle component
[NASA-CR-183945] 15 p2082 N90-21811

Shelf life extension for the lot AAE nozzle severance LSCs
[NASA-CR-183878] 15 p2062 N90-21813
Development of low thermal conductivity pan-based carbon fibers for solid rocket motor nozzle applications
15 p2063 N90-21818
Solid fuel combustion chamber
[LR-591] 15 p2068 N90-21847
Flight set 360T004 (STS-30)
[NASA-CR-183927] 15 p2106 N90-22049
Experimental study of mixing and combustion processes in a solid-propellant ducted rocket motor
17 p2367 N90-23472
Space shuttle: Changes to the solid rocket motor contract
[GAO/NSIAD-88-203] 18 p2636 N90-25016
Laboratory simulation of the effect of rocket thrust on a precessing space vehicle
[NASA-CR-186681] 19 p2669 N90-25182
Loads analysis and testing of flight configuration solid rocket motor outer boot ring segments
[NASA-TP-3028] 19 p2701 N90-25366
Space shuttle: Follow-up evaluation of NASA's solid rocket motor procurement. Report to the Chairman, Committee on Government Operations, House of Representatives
[GAO/NSIAD-89-89] 20 p2824 N90-26066
Flight motor set 360L007 (STS-33R)
[NASA-CR-183979] 20 p2824 N90-26067
Flight set 360L001 (STS-26) igniter, post flight
[NASA-CR-183957] 20 p2870 N90-26325
Flow induced nutation instability in spinning solid propellant rockets
[AD-A222504] 21 p2969 N90-26877
Flight motor set 360L001 (STS-26R). Volume 1: System overview, revision A
[NASA-CR-183995] 22 p3133 N90-27778
Igniter adapter-to-igniter chamber deflection test
[NASA-CR-184002] 22 p3133 N90-27780
Flight motor set 360L006 (STS-34). Volume 1: System overview
[NASA-CR-184007] 22 p3133 N90-27781
TRANSTRAIN: A program to compute strain transformations in composite materials
[NASA-TM-103509] 22 p3153 N90-27877
Evaluation of EDR-3 vibration, shock, temperature, and humidity recording unit
[NASA-CR-184006] 22 p3177 N90-28028
Flight set 360H005 (STS-28) seals, volume 4
[NASA-CR-183904] 22 p3181 N90-28051
Liquid Rocket Booster (LRB) for the Space Transportation System (STS) systems study. Appendix C: Battery report for the liquid rocket booster TVC actuators
[NASA-CR-183789-APP-C] 23 p3288 N90-28603

SOLID PROPELLANTS
NT COMPOSITE PROPELLANTS
NT DOUBLE BASE ROCKET PROPELLANTS
NT HMX
NT HTPB PROPELLANTS
NT METAL PROPELLANTS
NT NITRAMINE PROPELLANTS
NT PLASTIC PROPELLANTS
NT SOLID ROCKET PROPELLANTS
Laser propulsion to earth orbit. Has its time come?
01 p0028 N90-10143
Pulsed plasma mission endurance test
[AD-A213462] 08 p1037 N90-15993
Investigation into the feasibility of using solid fuel ramjets for high supersonic/low hypersonic tactical missiles
[AD-A214737] 09 p1168 N90-16761
Combustion instability in solid propellant rockets
[AD-A216740] 11 p1476 N90-18492
Acute oral toxicity of JA-2 solid propellant in ICR mice
[AD-A217264] 13 p1848 N90-20609
Acute oral toxicity of DIGL-RP solid propellant in ICR mice
[AD-A217711] 13 p1849 N90-20613
Acute oral toxicity of DIGL-RP solid propellant in Sprague-Dawley rats
[AD-A217712] 13 p1849 N90-20614
The modelling of heat and mass transfer near solid boundaries and comparison with experimental results
[PB90-167040] 14 p1974 N90-21310
HCl monitor
16 p2209 N90-22599
An evaluation of imbedded thermocouples as a solid-propellant combustion diagnostic
[AD-A219947] 17 p2406 N90-23711
The jet engine: 1932
[ISBN-3-922010-49-0] 19 p2670 N90-25189

SOLID ROCKET BOOSTERS (SPACE SHUTTLE)
U SPACE SHUTTLE BOOSTERS

SOLID ROCKET PROPELLANTS
NT DOUBLE BASE ROCKET PROPELLANTS
NT HMX
NT HTPB PROPELLANTS
NT METAL PROPELLANTS
HCl monitor, phase 2
[AD-A213572] 07 p0958 N90-15542
Solid fuel combustion chamber
[LR-562] 15 p2068 N90-21846
HCl Vapor Characterization and Detection. JANNAF Safety and Environmental Protection Subcommittee Workshop
[AD-A216252] 16 p2208 N90-22596
Workshop on ESD (Electrostatic Discharge) Ignition of Composite Solid Propellants
[AD-A218599] 17 p2382 N90-23569
Metallized fuel particle size study in a solid fuel ramjet
[AD-A220079] 18 p2533 N90-24451
Solid rocket propellant initiation via particle beam heating
[AD-A221900] 21 p2969 N90-26878
Atmospheric dispersion of solid and liquid rocket propellants
[AD-A221293] 21 p3020 N90-27173
An experimental investigation of strand burning metallized solid propellants
[AD-A224074] 24 p3457 N90-29526

SOLID ROTATION
U ROTATING BODIES

SOLID STATE
Computer simulations of polymer dynamics in the solid state
[DE89-010337] 01 p0048 N90-10275
Shock-induced solid state reactions and phase transitions: X ray profile studies on shock-modified Fe3O4 and ZrO2 powders
[DE90-000669] 06 p0741 N90-14315
Solid-state fluorescence above 1000 C: Application to high-temperature laser thermometry
[DE90-000728] 06 p0789 N90-14594
Solid State Division
[DE90-000979] 06 p0851 N90-14945
Solid-state phase equilibria in the ZnS-Ga2S3 system
[AD-A213944] 07 p0906 N90-15238
Novel high-rate, all solid-state, sodium and lithium/organosulfur batteries
[DE90-001014] 07 p0920 N90-15325
Solid state research
[AD-A213405] 07 p1003 N90-15806
Tritium and neutron measurements of a solid state cell
[DE90-003657] 07 p1005 N90-15820
Solid-state electrolyte catalysis for methane and oxygen synthesis
[PB90-100231] 08 p1040 N90-16011
Steep front impulse tests on a solid-state relay
[DE90-004243] 08 p1062 N90-16140
Solid state voltammetry and sensors in solids and gases
[DE90-003234] 08 p1129 N90-16538
Solid state, surface, and catalytic studies of oxides
[DE90-004850] 08 p1134 N90-16566
International Summer School on Solid State Microbatteries
[AD-A213457] 10 p1434 N90-18277
High speed imaging with a tapped solid state sensor
[DE90-006116] 11 p1511 N90-18702
Solid-state fluorescence above 1000 C: Application to high-temperature laser thermography
[DE90-006422] 11 p1514 N90-18721
Solid-state proton conductors
[DE90-007595] 11 p1531 N90-18812
Solid State Photovoltaic Research Branch
[DE89-009463] 12 p1682 N90-19660
Materials Science Programs, fiscal year 1989
[DE90-008169] 13 p1765 N90-20131
DURIP FTIR studies of solid state reaction dynamics
[AD-A217713] 13 p1773 N90-20174
An investigation of the mechanisms of solid state powder reaction in the combustion synthesis and sintering of high temperature materials
[DE90-007880] 13 p1777 N90-20198
Transistor and solid-state technology: A historical development
[AD-A218141] 13 p1798 N90-20317
The solid state photomultiplier: Status of photon counting beyond the near-infrared 14 p1976 N90-21319
Ternary reactions among polymer substrate-organohalogen-antimony oxides under pyrolytic, oxidative and flaming conditions
[PB90-154766] 15 p2071 N90-21861
Ultrafast laser investigation of a solid-state explosion
[AD-A218530] 17 p2408 N90-23718
Characterization of solid state bonding between Coors AD-999 alumina and niobium
[DE90-010653] 18 p2518 N90-24379
DURIP advanced polymer solid state NMR instrumentation
[AD-A221401] 18 p2531 N90-24440
Direct writing of microstructures for solid-state electronics
[AD-A220996] 18 p2535 N90-24460
A compact, high-powered Far-Infrared (FIR) laser
[DE90-009996] 20 p2867 N90-26312
Stibathiolanes: Synthesis, solid state structure, and solution behavior
[AD-A223255] 20 p2933 N90-26688
Fabrication of intermetallic compounds by solid state reaction of roll-bonded materials
[AD-A221960] 21 p2982 N90-26943
Solid state circuitry with optical data interfacing
[AD-D014548] 22 p3248 N90-28422

SOLID STATE DEVICES
NT AVALANCHE DIODES
NT BIPOLAR TRANSISTORS
NT CHARGE COUPLED DEVICES
NT CHARGE FLOW DEVICES
NT CHARGE INJECTION DEVICES
NT CMOS
NT FIELD EFFECT TRANSISTORS
NT GALLIUM ARSENIDE LASERS
NT HETEROJUNCTION DEVICES
NT HIGH ELECTRON MOBILITY TRANSISTORS
NT ITO (SEMICONDUCTORS)
NT JFET
NT JUNCTION DIODES
NT JUNCTION TRANSISTORS
NT LIGHT EMITTING DIODES
NT METAL OXIDE SEMICONDUCTORS
NT MIM (SEMICONDUCTORS)
NT MIS (SEMICONDUCTORS)
NT MODFETS
NT PHOTODIODES
NT PHOTOTRANSISTORS
NT PHOTOVOLTAIC CELLS
NT RUBY LASERS
NT SCHOTTKY DIODES
NT SEMICONDUCTOR DEVICES
NT SEMICONDUCTOR LASERS
NT SILICON CONTROLLED RECTIFIERS
NT SILICON TRANSISTORS
NT SIS (SUPERCONDUCTORS)
NT SOI (SEMICONDUCTORS)
NT SOLAR CELLS
NT SOLID STATE LASERS
NT SOS (SEMICONDUCTORS)
NT THERMISTORS
NT THYRISTORS
NT TRANSFERRED ELECTRON DEVICES
NT TRANSISTORS
NT VARACTOR DIODES
NT VARISTORS
NT YAG LASERS
Vacuum microelectronics for beam power and rectennas 01 p0028 N90-10146
Quantum 1/F noise in solid state devices in particular Hg1-(sub x)Cd(sub x)Te N(+)-P diodes
[AD-A209365] 01 p0128 N90-10730
Submillimeter quantum electronics
[AD-A210439] 01 p0132 N90-10762
A general-purpose computer program for the Volterra-series analysis of nonlinear microwave circuits
[AD-A210768] 02 p0216 N90-11236
Solid-State Sensor and Actuator
[AD-A211427] 03 p0344 N90-11961
SIS (Superconductor-Insulator-Superconductor) mixer research
[AD-A211607] 03 p0414 N90-12375
Joint Services Electronics Program
[AD-A212309] 04 p0497 N90-12864
Assessment of thin film batteries based on polymer electrolytes. Part 3: Specific energy versus specific power
[AD-A212141] 04 p0515 N90-12976
European Solid State Device Research Conference (18th) ESSDERC 88 held in Montpellier, France on 13-16 September 1988
[AD-A210618] 04 p0558 N90-13250
Contribution to the study of a self-protected static switch and its command strategy
[ECL-89-002] 05 p0636 N90-13711
A study of Inter-Injection-Locked phased arrays
[AD-A214097] 07 p0925 N90-15352
Solid state electrical switch employing materials with reversible phase transistors
[NASA-CASE-NPO-17621-1-CU] 09 p1209 N90-17010
Solid state microelectrochemical devices: Transistor and diode devices employing a solid polymer electrolyte
[AD-A214206] 09 p1211 N90-17019
The 120V 10A SSPC for the Columbus programme
10 p1330 N90-17683

Chemistry at clusters, microstructures and surfaces
[AD-A215842] 10 p1353 N90-17844
Application of polymer electrolytes to lithium batteries
[AD-A216038] 10 p1401 N90-18099
Automated visibility and cloud cover measurements with a solid-state imaging system
[AD-A216906] 12 p1693 N90-19724
Transistor and solid-state technology: A historical development
[AD-A218141] 13 p1798 N90-20317
Joint services electronics program: Electronics research at the University of Texas at Austin
[AD-A220834] 17 p2397 N90-23855
Solid state research
[NASA-CR-186699] 17 p2476 N90-24160
Solid state research
[NASA-CR-186700] 17 p2477 N90-24161
Characterization of a solid-state microelectrochemical diode employing a poly(vinyl alcohol)/phosphoric acid solid-state electrolyte: Rectification at junctions between WO3 and polyaniline
[AD-A222025] 21 p3000 N90-27054
A solid-state multiple-pass amplifier for diode pumped coherent laser radar systems
[AD-A222537] 21 p3009 N90-27104
Application of a rechargeable, small caliber railgun power supply
[AD-A224207] 24 p3438 N90-29418

SOLID STATE LASERS
NT GALLIUM ARSENIDE LASERS
NT RUBY LASERS
NT YAG LASERS
Earth orbit laser systems 01 p0030 N90-10162
A battery-powered, solid state magnetic compressor with applications for high PRF accelerators and lasers
[DE89-015770] 01 p0058 N90-10332
Efficient nonlinear conversion of laser diode pumped miniature solid state laser sources
[AD-A210708] 01 p0075 N90-10433
Nonlinear dynamics of broad-band lasers
[DE89-017442] 02 p0228 N90-11307
Tunable Solid State Lasers conference edition: Tunable Solid State Lasers Topical Meeting
[AD-A212292] 04 p0506 N90-12920
Advanced source development and applications. Laser-produced plasmas: A compact soft x ray source with high peak brightness
[AD-A212677] 04 p0557 N90-13245
Development of mid-infrared solid state lasers for spaceborne lidar
[NASA-CR-183290] 05 p0647 N90-13772
SLCSAT (Submarine Laser Communication Satellite) communication system design study
[AD-A213403] 07 p0917 N90-15304
The search for solid state fusion lasers
[DE89-012301] 07 p0934 N90-15410
SBS (Stimulated Brillouin Scattering) pulse distortion in multimode optical fibers: Preliminary results
[DE90-003023] 07 p0992 N90-15731
Eurolaser definition phase, solid state lasers working group: Active medium, laser active crystals
[ETN-90-95899] 08 p1083 N90-16266
Miniature instrumentation for laser light scattering experiments 09 p1222 N90-17088
Solid state lasers for use in non-contact temperature measurements 10 p1363 N90-17901
Properties and performance of the LiCaAlF6:Cr(3+) laser material
[DE90-007242] 11 p1516 N90-18728
Low threshold current implanted-planar-buried-heterostructure, graded-index, separate-confinement-heterostructure GaAs-AlGaAs laser
[DE90-002579] 12 p1666 N90-19572
Assessment of research needs for laser technologies applied to advanced spectroscopic methods
[DE90-007402] 12 p1669 N90-19588
CCST (Center for Compound Semiconductor Technology) research briefs
[DE90-006446] 12 p1721 N90-19887
Laser enhanced chemical reactions
[DE90-008273] 13 p1807 N90-20377
Contract crystal growth and fabrication services
[AD-A218327] 14 p2031 N90-21646
Progress in the material development of LiCaAlF(6):Cr(3+) laser crystals
[DE90-009542] 14 p2034 N90-21666
Development of mid-infrared solid state lasers for spaceborne lidar
[NASA-CR-185095] 15 p2103 N90-22031
Laser Program of the Lawrence Livermore National Laboratory
[DE90-008198] 16 p2240 N90-22779
Modeling of thermal lensing in side and end-pumped finite solid-state laser rods
[NASA-CR-4300] 17 p2407 N90-23716
An investigation of a mathematical model of an optically pumped Ti(3+):Al2O3 laser system
18 p2646 N90-25063
Diode laser-pumped solid-state lasers: A breakthrough in modern laser technology
[MBB-Z-0276/89-PUB] 19 p2649 N90-25077
A room-temperature, laser diode-pumped, Q-switched, 2 micron, thulium-doped, solid state laser
[AD-D014527] 19 p2695 N90-25334
Depletion mode pumping of solid state lasers
[DE90-012090] 19 p2696 N90-25339
Solid-state lasers for coherent communication and remote sensing
[NASA-CR-186834] 20 p2866 N90-26306
OASIS, LLNL version: Software maintenance manual
[DE90-013522] 20 p2868 N90-26313
Damage measurements on optical materials for use in high-peak-power lasers
[DE90-013489] 20 p2868 N90-26314
Chemical and laser sciences division
[DE90-013532] 21 p3101 N90-27611
Laser diode pumped, erbium-doped, solid state laser with high slope efficiency
[AD-D014482] 22 p3179 N90-28040
A tunable, continuous wave, thulium-doped, solid state laser cross-reference to related application
[AD-D014558] 22 p3180 N90-28045
New resonantly photo-pumped x ray laser scheme
[DE90-015044] 23 p3331 N90-28831

SOLID STATE PHYSICS
Superconducting ceramics in the Bi1.5SrCaCu2O sub x system by melt quenching technique
[NASA-CR-185139] 02 p0281 N90-11606
Spectral properties of one dimensional quasi-crystals
[PREPRINT-659] 06 p0850 N90-14938
The effect of annealing treatments on defect structure and diffusion lengths in n-type GaAs
[AD-A214215] 07 p1005 N90-15817
Timing optimization of multi-phase sequential logic
[AD-A220836] 17 p2397 N90-23656
Center for Space Microelectronics Technology 1988-1989 technical report
[NASA-CR-186849] 19 p2753 N90-25642

SOLID SURFACES
NT CRYSTAL SURFACES
Quantitative interpretation of auger lineshapes and electron/photon stimulated desorption
[AD-A211550] 03 p0324 N90-11842
Surface topography measurements over the 1 meter to 10 micrometer spatial period bandwidth
[DE90-003642] 08 p1122 N90-16501
Chemical structure and kinetics at liquid/solid interfaces
[AD-A222766] 20 p2831 N90-26105

SOLID SUSPENSIONS
Scaling and modeling of turbulent suspension flows
01 p0069 N90-10393
Turbulence kinetic energy equation for dilute suspensions 01 p0069 N90-10394
Fluid-particle interaction in solid-liquid two-phase grid turbulence 06 p0773 N90-14496
Advanced instrumentation for local measurement of gas-solid suspension flows
[DE90-008498] 17 p2400 N90-23671

SOLID WASTES
Managing the waste stream: Background information for planning source separation programs
[PB90-100223] 07 p0956 N90-15530

SOLID-SOLID INTERFACES
Influence of the fiber/matrix interface on damage development in CFRP 02 p0183 N90-11037
Numerical analysis of scattering by interface flaws
[AD-A212996] 05 p0654 N90-13810
Effects of filament-matrix interfaces on the mechanical properties of SiC-reinforced Si3N4: A review
[DE90-001863] 07 p0890 N90-15144
Energetics of BCC-FCC lattice deformation in iron
[AD-A213801] 07 p0905 N90-15233
Instability of a-Si:H/Ag interface at 150 deg C
[DE89-009419] 07 p0950 N90-15498
The influence of residual contamination on the structure and properties of metal/GaAs interfaces
[DE90-000549] 08 p1127 N90-16530
A new approach for the utilization of electron paramagnetic resonance and an investigation of copper oxide superconductors
[AD-A213833] 09 p1277 N90-17404
Point defects and interfaces in insulating solids
[AD-A214668] 09 p1289 N90-17471
Mechanical aspects of interfaces in high performance composites 10 p1347 N90-17812
Interfacial chemistry of MoS2 films on Si
[AD-A216527] 11 p1482 N90-18532
Colloid and interface chemistry aspects of ceramics
[AD-A216715] 11 p1490 N90-18576
Glancing angle XAFS (X ray Absorption Fine Structure) and x ray reflectivity studies of transition-metal/aluminum interfaces
[DE90-005575] 12 p1627 N90-19353
Molecular dynamics and spectroscopy at gas-solid interfaces
[AD-A217743] 13 p1885 N90-20813
Corrosion control through a better understanding of the metallic substrate/organic coating interface
[AD-A220432] 17 p2377 N90-23533
Atomic structure of Ag/Ni interfaces
[DE90-010053] 18 p2618 N90-24914
Quantum ballistic and adiabatic electron transport, studied with quantum point contacts
[ETN-90-97262] 20 p2889 N90-26440
Problems of enclosed crystal interfaces
[DE90-011594] 21 p3079 N90-27509
Influence of microslidings on the macroscopic behavior of composite textiles
[ETN-90-97459] 22 p3154 N90-27880
Lightweight solid polymer electrolyte fuel cell with stack power density of 3 kW/lb (7 kW/kg)
[AD-A223964] 23 p3345 N90-28905
Interface formation and percusory dynamics
[AD-A224128] 23 p3402 N90-29223

SOLIDIFICATION
NT DIRECTIONAL SOLIDIFICATION (CRYSTALS)
NT MELT SPINNING
Development of metastable processing paths for high temperature alloys
[AD-A210550] 01 p0045 N90-10254
Establishment and initial operation of a resource facility for RSR (Rapid Solidification Rate) processed alloys in pilot quantities
[AD-A210369] 01 p0050 N90-10283
Solidification front/viscous phase transitions, forward-backward heat equations
[AD-A211068] 02 p0195 N90-11114
Formation and modification of surface alloys by excimer laser melting and resolidification
[DE89-016968] 03 p0327 N90-11856
Kinetic processes in advanced alloys
[AD-A212049] 03 p0329 N90-11867
Superplastic forming and diffusion bonding of rapidly solidified, dispersion strengthened aluminum alloys for elevated temperature structural applications
[NASA-CR-181849] 04 p0474 N90-12718
Containerless Processing of Metals: Undercooling and Solidification
[DLR-MITT-89-15] 05 p0625 N90-13645
The effects of alloying and thermal factors on the solidification and mechanical properties of gray iron
[VTT-619] 05 p0625 N90-13651
High temperature aluminum-base alloy
[AD-D014270] 08 p1043 N90-16028
Rapid solidification processing of composites
[AD-A215175] 09 p1187 N90-16875
Evolution of structure and electrical properties during crystallization of rapidly solidified Bi4Ti3O12
[DE90-005221] 09 p1292 N90-17492
A fundamental understanding of the effect of alloying elements on the corrosion resistance of rapidly solidified Mg alloys
[AD-A216767] 11 p1486 N90-18553
Time-resolved measurements of solidification and undercooling in metals and alloys
[DE90-007074] 11 p1488 N90-18564
Pulsed laser-induced melting of intermediate Cu-Zn phases
[DE90-005404] 11 p1513 N90-18713
Rigid rod molecules as liquid crystal thermosets
[AD-A217573] 13 p1770 N90-20158
Secondary arm coarsening and microsegregation in superalloy PWA-1480 single crystals: Effect of low gravity
[NASA-TM-102445] 13 p1776 N90-20194
Center of Gravity: Metallic Solidification
[DFVLR-IB-333-89/3] 13 p1784 N90-20238
Principles of metallic solidification
13 p1784 N90-20241
Dynamics of the solidification front
13 p1785 N90-20243
Dispersion reinforced materials
13 p1785 N90-20244
Molding solidification 13 p1785 N90-20246
Method of preparing radially homogeneous mercury cadmium telluride crystals
[NASA-CASE-MFS-25786-2] 13 p1898 N90-20896
Shock compression of solids: A tutorial
[DE90-009185] 14 p2032 N90-21659
Undercooling and nucleation in rapid solidification rate metal powders using solid in solid emulsification
[AD-A218527] 17 p2375 N90-23526
Solidification of highly undercooled liquid droplets
[AD-A218776] 17 p2376 N90-23529

A study of the influence of alloying additions on the passivity of aluminium
[AD-A219630] 17 p2376 N90-23532
Solidification of dilute alloys under fluctuating residual gravity
[REPT-892-430-112] 17 p2377 N90-23535
The effects of cooling rate XD (trademark) TiAl weld microstructure
[DE90-011975] 18 p2528 N90-24427
Nucleation kinetics in undercooled, class-forming metallic melts
[ESA-TT-1186] 19 p2676 N90-25218
The role of gravity on macrosegregation in alloys
[NASA-CR-186530] 19 p2679 N90-25238
Effect of boron on intergranular hot cracking in Ni-Cr-Fe superalloys containing niobium
[NASA-CR-184038] 20 p2834 N90-26115
Formation of Titanium-boron surface alloys by excimer laser mixing
[DE90-013172] 20 p2834 N90-26118
Undercooling and solidification
[DLR-FB-90-020] 20 p2931 N90-26678
Solidification processing of alloys using an applied electric field
[NASA-CASE-MFS-26083-1-CU] 21 p2981 N90-26940
Algorithms to solve nonlinear time dependent problems of engineering and physics
[AD-A221463] 21 p3055 N90-27366
High temperature oxidation of Al-Li alloys 23 p3307 N90-28705
High performance brittle matrices and brittle matrix composites, book 1
[AD-A223273] 24 p3443 N90-29440
Influence of convection on microstructure
[NASA-CR-186506] 24 p3448 N90-29470
A welding metallurgy study of Hastelloy Alloys B-2 and W
[DE90-011910] 24 p3449 N90-29481
The influence of solidification rate on solute redistribution and second-phase formation in stainless steel alloys
[DE90-015189] 24 p3450 N90-29482
Single-phase solidification during rapid resolidification of stainless steel alloys
[DE90-015190] 24 p3450 N90-29483

SOLIDIFIED GASES
NT SOLID CRYOGENS
Auger and x ray absorption studies of solid molecular oxygen
[DE90-003966] 07 p1006 N90-15825
Optical constants of solid methane 20 p2948 N90-26775
Proceedings of the High Energy Density Materials Contractors Conference
[AD-A223793] 24 p3484 N90-29695
Experimental studies leading to energy storage. Spectroscopy and dynamics of polyatomic hydrogen in liquid, solid and gaseous hydrogen plasmas
[AD-A224343] 24 p3547 N90-30066

SOLIDS
NT SOLID CRYOGENS
NT SOLIDIFIED GASES
Hierarchical structure in polymeric solids and its influence on properties
[AD-A210918] 01 p0052 N90-10297
Radiationless transitions and excited-state absorption of low-field chromium complexes in solids
[AD-A210653] 02 p0194 N90-11105
X-ray and gamma-ray spectroscopy of solids under pressure
[DE89-017271] 02 p0196 N90-11118
Computer simulations of radiation damage in amorphous solids
[PB89-212682] 03 p0322 N90-11827
International seminar on the inelastic behavior of solids: Models and utilization
[DE89-017420] 03 p0327 N90-11858
A numerical laboratory for granular solids
[DE89-016367] 03 p0358 N90-12045
Granular flow: Numerical simulation of dry granular flows and calculation of hydrodynamic interactions in suspensions
[DE89-017544] 06 p0777 N90-14518
Implications and origins of shock structure in solids
[DE90-000846] 06 p0800 N90-14658
Wide-angle propagation in inhomogeneous fluids and elastic solids using perturbation methods 06 p0837 N90-14868
Direction-dependent stopping power and beam deflection in anisotropic solids
[DE90-001076] 06 p0840 N90-14883
Theoretical models of earthquake phenomena and the physical significance of seismic moment tensor expansions
[AD-A213813] 07 p0961 N90-15556
Refractory solids in chondrites and comets: How similar 08 p1148 N90-16654
The physical-organic chemistry of surfaces, and its relevance to molecular recognition
[AD-A215987] 10 p1354 N90-17850
Kinetic relations and the propagation of phase boundaries in solids
[AD-A215881] 11 p1519 N90-18747
Modern theory of magnetism
[DE90-007374] 11 p1561 N90-18998
Pressure induced superconductivity in elemental solids
[DE90-610664] 11 p1572 N90-19048
Elastic solutions in a semi-infinite solid with an ellipsoidal inclusion
[AD-A217063] 12 p1625 N90-19338
NMR (Nuclear Magnetic Resonance) imaging development for the study of solids
[AD-A217073] 12 p1723 N90-19899
A method for measuring the material moduli of granular materials: Flow in an orthogonal rheometer
[DE90-007160] 13 p1801 N90-20339
Pulsed laser photothermal spectroscopy of liquids and solids
[DE90-008642] 13 p1808 N90-20380
Utilization of LANDSAT-5 and NOAA-9 satellite imagery in the identification of physical-chemical parameters of the water in the Guanabara Bay
[INPE-4761-TDL/349] 13 p1819 N90-20445
Energy transfer between electrons and ions in collision cascades in solids
[AERE-R-13662] 13 p1883 N90-20801
High-resolution Brillouin gain spectroscopy in solids
[DE90-009475] 14 p1949 N90-21155
Laser velocimeter measurements of multiphase flow of solids
[DE90-007604] 14 p1974 N90-21311
Shock compression of solids: A tutorial
[DE90-009185] 14 p2032 N90-21659
Transient effects in Brillouin gain spectroscopy in solids
[DE90-009476] 15 p2067 N90-21839
High resolution stimulated Raman-Brillouin spectroscopy in gases and solids
[DE90-009535] 15 p2067 N90-21840
A spectral analysis approach to wave propagation in layered solids 15 p2120 N90-22131
A weak formulation for phase-change problems with bulk movement due to unequal densities
[DE90-009398] 15 p2163 N90-22361
Computations of weight functions in fracture mechanics 16 p2246 N90-22809
Electronic theory of solids, surfaces, interfaces, and clusters 16 p2320 N90-23230
Real space method of powder diffraction for non-periodic and nearly periodic materials
[DE90-010537] 18 p2621 N90-24935
Design and implementation of sensor systems for control of a closed-loop life support system
[NASA-CR-186675] 19 p2725 N90-25497
Symmetry and global bifurcation in nonlinear solid mechanics
[AD-A221981] 21 p3013 N90-27129
Ultrasensitive laser spectroscopy in solids: Statistical fine structure and single-molecule detection
[AD-A222391] 21 p3074 N90-27477
A continuum model for phase transformation in thermoelastic solids
[AD-A222353] 21 p3085 N90-27542
Astronomical observations of solid phase carbon 21 p3089 N90-27566
Four techniques to measure complex refractive indices of liquids and solids at carbon dioxide laser wavelengths in the infrared spectral region
[AD-A222007] 22 p3180 N90-28043
Mechanics of impact energy absorption
[PB90-190836] 22 p3190 N90-28101
Surface and defect excitations in covalently bonded solids
[AD-A221995] 23 p3303 N90-28682
Application of discrete Fourier series to the finite element stress analysis of axi-symmetric solids
[PB90-231010] 23 p3339 N90-28870

SOLIDS FLOW
Numerical modelling of shocks in gases and metals
[AD-A218586] 17 p2402 N90-23684
On the planar translation of two bodies in a uniform flow
[AD-A220143] 17 p2404 N90-23698
Lightweight solid polymer electrolyte fuel cell with stack power density of 3 kW/lb (7 kW/kg)
[AD-A223964] 23 p3345 N90-28905

SOLITARY WAVES
A straightforward method for finding implicit solitary wave solutions of nonlinear evolution and wave equations
[AD-A210561] 01 p0113 N90-10647
Davydov solutions at 300 Kelvin: The final search
[DE89-015248] 03 p0401 N90-12296
The initial-boundary value problem for the Davey-Stewartson 1 equation; how to generate and drive localized coherent structures in multidimensions
[PREPRINT-684] 05 p0643 N90-13756
Energy exchange of interacting solitons in multidimensions
[PREPRINT-662] 05 p0696 N90-14071
Optical solitons in liquid crystals
[DE90-000694] 07 p0991 N90-15728
Ultrarelativistic envelope solitons in electron-positron plasma of the pulsar magnetosphere
[DE90-613289] 14 p1967 N90-21264
Nonlinear interaction of photons and phonons in electron-positron plasmas
[DE90-009341] 14 p2030 N90-21640
Analysis of nonlinear internal waves observed by LANDSAT-TM
[PREPRINT-704] 16 p2249 N90-22828
Effect on relaxation on nonlinear waves in crystals 16 p2310 N90-23165
Alfven wave solitons and solar intermediate drift bursts
[MPE-PREPRINT-173] 23 p3413 N90-29287

SOLITONS
U SOLITARY WAVES

SOLSTICES
Relationship between the current and the width of the POGO electrojet during the solstices
[DE89-619725] 04 p0565 N90-13294
Solar cyclical trend study of the mid-latitude, quiet-time, meridional, neutral winds at winter solstice conditions
[AD-A217398] 13 p1841 N90-20568

SOLUBILITY
Mechanical properties, solubilities, and processabilities in the design of the first super-strong liquid-crystalline polymers
[DE89-009252] 01 p0048 N90-10273
Synthetic polypeptide composites for sensor applications
[AD-A210797] 01 p0052 N90-10296
A new method for the characterization of solutes and solvent phases using solvatochromic parameters
[AD-A211238] 02 p0196 N90-11116
Measurement and correlation of the solubility and diffusion coefficient for oxygen and chlorine in basic hydrogen peroxide
[AD-A212348] 04 p0472 N90-12703
Solid state voltammetry and sensors in solids and gases
[DE90-003234] 08 p1129 N90-16538
Systems with a miscibility gap in the liquid state 13 p1785 N90-20245
Advanced calcium thionyl chloride high power battery
[AD-A216685] 13 p1825 N90-20482
A systematic study of the effects of metal substitutions for Cu in YBa(sub 2) (Cu(sub 1-x) M(sub x)3 O(sub 7-rho), M=Fe, Co, Al, Ga, Cr, Ni, and Zn
[DE90-003957] 13 p1892 N90-20857
Theoretical and experimental study of solid phase miscibility gaps in III/V quaternary alloys
[DE90-008430] 13 p1895 N90-20877
Phase equilibrium of mixtures consisting of molecules with large size and shape differences (thermodynamic modeling of Supercritical Fluid Extraction and Retrograde Condensation, SFE/RC)
[PB90-131285] 14 p1947 N90-21146
A study of the influence of alloying additions on the passivity of aluminium
[AD-A219630] 17 p2376 N90-23532
Instabilities: Miscible and immiscible flows 19 p2689 N90-25298
Viscous fingering in porous media: A discussion of the small length scale cut-off 19 p2691 N90-25311
Passivation of high temperature superconductors
[NASA-CASE-NPO-17949-1-CU] 20 p2932 N90-26684
Solubility characteristics of a methacrylate copolymer
[AD-A222938] 21 p2985 N90-26962
Miscibility and phase behavior of poly (enaminonitrile)/PEO blends
[AD-A222255] 21 p2987 N90-26975

SOLUTES
Monte Carlo simulations of small solute/solvent clusters: Cluster properties and phase transitions
[AD-A209559] 01 p0119 N90-10684
A new method for the characterization of solutes and solvent phases using solvatochromic parameters
[AD-A211238] 02 p0196 N90-11116
The effect of electric field on attachment of electrons to solutes in liquid argon
[DE90-003969] 11 p1482 N90-18529
The influence of solidification rate on solute redistribution and second-phase formation in stainless steel alloys
[DE90-015189] 24 p3450 N90-29482

Single-phase solidification during rapid resolidification of stainless steel alloys
[DE90-015190] 24 p3450 N90-29483

SOLUTIONS
NT AIR
NT AQUEOUS SOLUTIONS
NT COMPRESSED AIR
NT DETONABLE GAS MIXTURES
NT GAS MIXTURES
NT HIGH TEMPERATURE AIR
NT NUCLEAR EMULSIONS
Stress in dilute suspensions 01 p0068 N90-10389
Wavefront propagation for reaction-diffusion systems of PDE
[AD-A210862] 02 p0265 N90-11510
The generalized van der Waals theory of pure fluids and mixtures
[DE90-000504] 06 p0740 N90-14307
Determination of iron in chromium plating and polishing solutions by atomic absorption spectrometry
[AD-A214467] 09 p1189 N90-16892
Determination of trivalent chromium ions in chromium plating solutions by ultraviolet-visible spectrophotometry
[AD-A215688] 10 p1351 N90-17837
Photoinduced electron transfer processes in homogeneous and microheterogeneous solutions
[DE90-006048] 10 p1352 N90-17842
The evaporation of sessile droplets. Part 1: Theoretical factors for a two-component system
[AD-A215946] 10 p1353 N90-17848
Minimum cycle covering and integer flows
[AD-A216546] 12 p1705 N90-19785
Generalized random phase approximation for multicomponent polymer systems
[DE90-613691] 14 p1955 N90-21194
Characterization of a thermally imidized soluble polyimide film
[NASA-TM-103484] 20 p2836 N90-26131
Microscopic models for electromagnetic wave propagation in highly dispersive media
[AD-A224382] 24 p3480 N90-29540

SOLVATION
Potential dependence of the elementary steps in the kinetics of electrode reactions involving amalgam formation
[AD-A209424] 01 p0038 N90-10212

SOLVENTS
NT TETRAHYDROFURAN
Solvent effects on the kinetics of electroreduction of Cu(I) at mercury
[AD-A209423] 01 p0038 N90-10211
Solvent relaxation in electron-transfer reactions: Comparisons between barrier-crossing dynamics in water and polar aprotic media
[AD-A210212] 01 p0040 N90-10220
Monte Carlo simulations of small solute/solvent clusters: Cluster properties and phase transitions
[AD-A209559] 01 p0119 N90-10684
Solvent effects on intervalence electron-transfer energies for biferrocene cations: Comparisons with molecular models of solvent reorganization
[AD-A210263] 01 p0120 N90-10691
Solvent dynamical effects in electron transfer: Evaluation of electronic matrix coupling elements for metallocene self-exchange reactions
[AD-A210306] 01 p0121 N90-10692
A new method for the characterization of solutes and solvent phases using solvatochromic parameters
[AD-A211238] 02 p0196 N90-11116
Cleaning of printed circuit assemblies with surface-mounted components
[DE89-013609] 03 p0341 N90-11945
Electrochemical cell for obtaining oxygen from carbon dioxide atmospheres
[NASA-CR-186225] 09 p1189 N90-16886
Improved performance in co-processing through fundamental and mechanistic studies in hydrogen transfer and catalysis
[DE90-004794] 10 p1352 N90-17839
Phase equilibrium of mixtures consisting of molecules with large size and shape differences (thermodynamic modeling of Supercritical Fluid Extraction and Retrograde Condensation, SFE/RC)
[PB90-131285] 14 p1947 N90-21146
Generalized random phase approximation for multicomponent polymer systems
[DE90-613691] 14 p1955 N90-21194
Acetylene terminated aspartimides and resins therefrom
[NASA-CASE-LAR-14188-1] 17 p2379 N90-23545
Equilibrium swelling of elastomeric materials in solvent environments
[DE90-010164] 18 p2529 N90-24430
Dynamical solvent effects on electron-transfer processes: Recent progress and perspectives
[AD-A222603] 20 p2830 N90-26101
Imide/arylene ether copolymers
[NASA-CASE-LAR-14159-1-CU] 21 p2983 N90-26953
Aromatic polyimides containing a dimethylsilane-linked dianhydride
[NASA-CASE-LAR-14198-1] 21 p2984 N90-26956
Solubility characteristics of a methacrylate copolymer
[AD-A222938] 21 p2985 N90-26962
Corrosion-inhibiting coating composition
[AD-D014546] 22 p3159 N90-27916
Processing of polymers using supercritical fluids
[AD-A223681] 24 p3455 N90-29514

SOLVOLYSIS
Enhanced oxidation and solovolysis reactions in chemically inert microheterogeneous systems
[AD-A210748] 02 p0195 N90-11110

SONAR
Doppler statistics of ocean velocity variability
[AD-A211687] 03 p0377 N90-12148
Sensor integration using concurrent computing on-board the ORNL mobile robot
[DE89-008740] 07 p0939 N90-15436
Observations of fine-scale vertical shear and strain in the upper ocean
[AD-A214476] 10 p1410 N90-18130
Visual navigation: Constructing and utilizing simple maps of an indoor environment
[AD-A216761] 11 p1455 N90-18382
Effect of extraneous color-coded targets on identification of targets on CRT displays
[AD-A219473] 17 p2436 N90-23879
A preliminary analysis of threshold signal detection in ambient and signal-dependent noise environments
[AD-A222089] 21 p2996 N90-27030
Spatial array processing by the method CLEAN
[FEL-1989-144] 22 p3165 N90-27949
Angle sample variance of azimuthally spread scattering processes, using a two-element array
[AD-A223572] 24 p3542 N90-30034

SONDES
NT IONOSONDES
NT RADIOSONDES
NT RAWINSONDES
The development of a high response aerodynamic wedge probe and use on a high-speed research compressor
[PNR90598] 04 p0456 N90-12613
PVDF contact probes
[VTT-RR-623] 20 p2857 N90-26253

SONIC ANEMOMETERS
Wind tunnel investigation of three sonic anemometers
[PB90-149808] 15 p2046 N90-21729
Methodology investigation calibration and quality control for new meteorological instrumentation, part 1
[AD-A221407] 18 p2582 N90-24706

SONIC BOOMS
Noise and sonic boom impact technology. Sonic boom damage to conventional structures
[AD-A213594] 09 p1237 N90-17178
Noise and sonic boom impact technology. Effects of aircraft noise and sonic booms on structures: An assessment of the current state-of-knowledge
[AD-A213919] 09 p1278 N90-17409
Noise and sonic boom impact technology. Initial development of an Assessment System for Aircraft Noise (ASAN). Volume 1: Executive summary
[AD-A214164] 09 p1278 N90-17410
Noise and sonic boom impact technology. Initial development of an Assessment System for Aircraft Noise (ASAN). Volume 2: System design strategy
[AD-A214454] 09 p1278 N90-17411
Noise and sonic boom impact technology. Initial development of an Assessment System for Aircraft Noise (ASAN). Volume 3: Technical description
[AD-A214455] 09 p1278 N90-17412
Air Force Boom Event Analyzer Recorder (BEAR): Sysstem description
[AD-A218048] 13 p1882 N90-20800
Sonic boom signature data from cruciform microphone array experiments during the 1966-1967 EAFB national sonic boom evaluation program
[NASA-CR-182027] 14 p2024 N90-21605
Assessment System for Aircraft Noise (ASAN) citation database. Volume 1: User's manual
[AD-A219175] 16 p2314 N90-23188
Assessment System for Aircraft Noise (ASAN) citation database. Volume 2: Database update manual
[AD-A219176] 16 p2314 N90-23189
Assessment System for Aircraft Noise (ASAN) citation database. Volume 3: New citation review procedures
[AD-A219177] 16 p2314 N90-23190
Summary of sonic boom rise times observed during FAA community response studies over a 6-month period in the Oklahoma City area
[NASA-CR-4277] 18 p2608 N90-24852
Vibration responses of two house structures during the Edwards Air Force Base phase of the national sonic boom program
[NASA-CR-182089] 23 p3393 N90-29169

SONIC FLOW
U TRANSONIC FLOW

SONIC SOLDERING
U ULTRASONIC SOLDERING

SONIC SPEED
U ACOUSTIC VELOCITY

SONOHOLOGRAPHY
U ACOUSTICAL HOLOGRAPHY

SOOT
Transport phenomena and interfacial kinetics in multiphase combustion systems
[AD-A212932] 05 p0621 N90-13620
Kinetics and mechanism of soot formation in hydrocarbon combustion
[NASA-CR-186162] 06 p0740 N90-14305
Combustor cooling aspects
[CIT/SME/VKI/RS/5] 20 p2810 N90-25989
Carbon deposition model for oxygen-hydrocarbon combustion. Task 6: Data analysis and formulation of an empirical model
[NASA-CR-183986] 20 p2829 N90-26095
Carbon stardust: From soot to diamonds
21 p3090 N90-27568
A unifying picture of gas-phase formation and growth of PAH (Polycyclic Aromatic Hydrocarbons), soot, diamond and graphite
21 p3091 N90-27575
An ionic mechanism of carbon formation in flames
21 p3093 N90-27582
Diamonds in detonation soot
21 p3094 N90-27585

SORBENTS
NT ADSORBENTS
High temperature interaction of SO2 with oxide sorbents
[DE90-000435] 11 p1485 N90-18545
Potential technology transfers of research on low-temperature carbon monoxide-oxygen recombination catalysts 18 p2562 N90-24616
Regenerative Cu La zeolite supported desulfurizing sorbents
[NASA-CASE-NPO-17480-1-CU]
20 p2830 N90-26098
Multicomponent gas sorption Joule-Thomson refrigerator
[NASA-CASE-NPO-17569-1-CU]
20 p2844 N90-26176

SORPTION
NT ADSORPTION
NT CHEMISORPTION
Numerical simulation of hydrazine transport in a sandy soil 02 p0205 N90-11172
CO2 diffusion and solubility in a Polystyrene/Polybutadiene block copolymer with highly oriented lamellar morphology
[AD-A217165] 13 p1779 N90-20211
Multicomponent gas sorption Joule-Thomson refrigerator
[NASA-CASE-NPO-17569-1-CU]
20 p2844 N90-26176
Diffusion of penetrants in polymers
[AD-A223217] 21 p2986 N90-26969

SORTING
U CLASSIFYING

SOS (SEMICONDUCTORS)
Precision materials characterization in the near millimeter and submillimeter wavelength range
[AD-A210655] 02 p0194 N90-11106
Parametric testing for the RSRE CMOS, silicon on sapphire process
[RSRE-MEMO-4369] 24 p3555 N90-30115

SOUND
U ACOUSTICS

SOUND ABSORPTION
U SOUND TRANSMISSION

SOUND AMPLIFICATION
Propagation of sound in vibrationally excited nitrogen and hydrogen gas mixtures
[AD-A213002] 05 p0696 N90-14073
A continued study of optical sound generation and amplification
[AD-A217640] 13 p1882 N90-20796

SOUND BARRIER
U ACOUSTIC VELOCITY

SOUND FIELDS
The theory and application of quadratic minimization in the active reduction of sound and vibration
01 p0119 N90-10682
Measurements of bubble properties using a multi-frequency sound field
[AD-A212591] 04 p0551 N90-13211

ULF/VLF (0.001 to 50 Hz) Seismo-Acoustic Noise in the Ocean
[AD-A212942] 05 p0671 N90-13913
Modeling the near acoustic field of a rocket during launch 08 p1156 N90-16694
Two dimensional modifications of Gaussian laser light bundles
[AD-A215207] 10 p1389 N90-13033
A linear systems theory approach to the range-independent acoustic channel
[AD-A216551] 12 p1710 N90-19817
Microgravity acoustic mixing for particle cloud combustors
[NASA-CR-185159] 14 p2023 N90-21600
The optical measurement of acoustic velocity fields 14 p2023 N90-21601
The radiation of sound from a propeller at angle of attack
[NASA-CR-4264] 14 p2023 N90-21602
Time-varying filter modelling and time-frequency characterisation of nonstationary sound fields due to a moving source 16 p2312 N90-23178
Contributions of individual structural modes to the scattered acoustic field
[AD-A219128] 16 p2314 N90-23187
Large aperture array measurements of the vertical ambient noise field
[AD-A220165] 17 p2432 N90-23859
Estimation of noise field directionality: Comparison with Fourier series method
[AD-A220366] 17 p2469 N90-24114
Coupled BE/FE/BE approach for scattering from fluid-filled structures 18 p2570 N90-24649
Experimental validation study of an analytical model of discrete frequency sound propagation in closed-test-section wind tunnels
[NASA-TM-102801] 19 p2754 N90-25647
Asymptotic modal analysis and statistical energy analysis
[NASA-CR-186732] 20 p2923 N90-26634

SOUND FREQUENCIES
U ACOUSTIC FREQUENCIES

SOUND GENERATORS
Dynamics of a class of vortex rings 07 p0926 N90-15362
Modeling the near acoustic field of a rocket during launch 08 p1156 N90-16694
A continued study of optical sound generation and amplification
[AD-A217640] 13 p1882 N90-20796
Acousto-ultrasonic nondestructive evaluation of materials using laser beam generation and detection
[NASA-CR-186694] 17 p2398 N90-23664
Experimental validation study of an analytical model of discrete frequency sound propagation in closed-test-section wind tunnels
[NASA-TM-102801] 19 p2754 N90-25647
Investigation of a heat driven thermoacoustic prime mover
[AD-A223928] 24 p3484 N90-29694

SOUND HOLOGRAPHY
U ACOUSTICAL HOLOGRAPHY

SOUND INTENSITY
NT ZERO SOUND
Effect of contralateral masking parameters on difference limen for intensity
[AD-A214169] 10 p1411 N90-18135

SOUND LOCALIZATION
Sound Localization by Human Observers symposium proceedings
[AD-A212877] 04 p0524 N90-13026
Perception of long-period complex sounds
[AD-A216743] 11 p1539 N90-18861
The simulation of localized sounds for improved situational awareness 23 p3359 N90-28984
The effects of acoustic orientation cues on instrument flight performance in a flight simulator 23 p3359 N90-28985

SOUND MEASUREMENT
U ACOUSTIC MEASUREMENT

SOUND PERCEPTION
U AUDITORY PERCEPTION

SOUND PRESSURE
Optical acoustic sensor using optical fiber
[DE89-901267] 07 p0992 N90-15730
Modeling the near acoustic field of a rocket during launch 08 p1156 N90-16694
Estimation of subsonic far-field jet-mixing noise from single-stream circular nozzles
[ESDU-89041] 09 p1161 N90-16721
Effect of contralateral masking parameters on difference limen for intensity
[AD-A214169] 10 p1411 N90-18135
Noise levels from a VSTOL aircraft measured at ground level and at 1.2 m above the ground
[NPL-RSA(EXT)-009] 11 p1562 N90-18999
The radiation of sound from a propeller at angle of attack
[NASA-CR-4264] 14 p2023 N90-21602
Free-field propagation of high intensity noise
[NASA-CR-186577] 14 p2024 N90-21604
Field calibration of two types of microphones in hyperbaric air
[AD-A219477] 17 p2395 N90-23642
Annoyance caused by advanced turboprop aircraft flyover noise: Counter-rotating-propeller configuration
[NASA-TP-3027] 23 p3392 N90-29166
Numerical pulse propagation studies using two classical ocean waveguide models
[AD-A224118] 24 p3542 N90-30033

SOUND PROPAGATION
NT VOICE
An investigation of the diffraction of an acoustic plane wave by a curved surface of finite impedance
[NASA-CR-186069] 04 p0550 N90-13204
Sound attenuation apparatus
[NASA-CASE-LAR-13968-1] 07 p0988 N90-15710
The calculation of overground sound propagation in the presence of wind and temperature gradients
[ESDU-89036] 07 p0989 N90-15714
A scattering center based numerical simulation of small scale atmospheric turbulence 16 p2312 N90-23179
Sound propagation elements in evaluation of en route noise of advanced turbofan aircraft 18 p2609 N90-24861
Experimental validation study of an analytical model of discrete frequency sound propagation in closed-test-section wind tunnels
[NASA-TM-102801] 19 p2754 N90-25647
Sound propagation through atmospheric turbulence: A literature summary
[RPI-MATH-184] 23 p3350 N90-28930

SOUND RANGING
Modified Newton-type methods for long-range target motion analysis
[FEL-1989-82] 04 p0551 N90-13208

SOUND TRANSDUCERS
NT ELECTROACOUSTIC TRANSDUCERS
NT HYDROPHONES
NT MICROPHONES

SOUND TRANSMISSION
IFD (Implicit Finite Difference): Interfaced with Harvard open ocean model forecasts
[AD-A210521] 01 p0090 N90-10517
Calculation of sound transmission through a cylindrical shell using ASKA acoustics 02 p0179 N90-11009
Sound Localization by Human Observers symposium proceedings
[AD-A212877] 04 p0524 N90-13026
UHB demonstrator interior noise control flight tests and analysis
[NASA-CR-181897] 04 p0549 N90-13198
Evaluation of speech intelligibility through a bone conduction stimulator
[AD-A212002] 05 p0673 N90-13919
Boundary element analysis of single and multidomain problems in acoustics 06 p0837 N90-14867
Sound attenuation apparatus
[NASA-CASE-LAR-13968-1] 07 p0988 N90-15710
Phase space and path integral methods applied to direct and inverse ocean seismo-acoustic modeling
[AD-A214777] 09 p1249 N90-17247
A linear systems theory approach to the range-independent acoustic channel
[AD-A216551] 12 p1710 N90-19817
The Shock and Vibration Digest, volume 21, no. 6 15 p2163 N90-22363
Noise transmission into propeller-driven airplanes 15 p2163 N90-22364
Numerical studies of the active control of sound transmission through double partitions
[ISVR-TR-183] 16 p2313 N90-23181
Noise reduction theory acoustic barrier construction
[CRIF-MC-87] 16 p2313 N90-23183
Finite element formulations for coupled fluid/structure eigenvalue analysis
[AD-A220793] 17 p2416 N90-23766
Analytic parabolic equation solutions
[AD-A218588] 17 p2456 N90-24015
Normal-mode and phase-integral methods for determining phase and group velocities in simple underwater acoustic ducts
[AD-A221393] 18 p2612 N90-24877
Tests of an ultra-light tunnel in the anechoic wind tunnel facility CEPRA 19
[ONERA-RF-20/7294-PH] 22 p3122 N90-27729

SOUND VELOCITY
U ACOUSTIC VELOCITY

SOUND WAVES
NT AERODYNAMIC NOISE
NT AIRCRAFT NOISE
NT BLADE SLAP NOISE
NT ENGINE NOISE
NT ION ACOUSTIC WAVES
NT JET AIRCRAFT NOISE
NT LAMB WAVES
NT NOISE (SOUND)
NT PROPELLER NOISE
NT SONIC BOOMS
NT THERMAL NOISE
Acoustic-vortex-chemical interactions in an idealized ramjet 01 p0037 N90-10206
The dynamics of circular plates with patch damping: A numerical and experimental study 02 p0232 N90-11329
Nonlinear acoustics: Reflection and refraction, propagation in a periodic waveguide, scattering of sound by sound and ellipsoidal focusing
[AD-A211224] 02 p0271 N90-11550
Application of sound and temperature to control boundary-layer transition 04 p0443 N90-12537
A frequency domain technique for improving sound field reproduction
[RAE-TM-MM-10] 04 p0551 N90-13205
Perceived urgency of warning signals determined using a forced choice pair comparison technique
[RAE-TM-MM-12] 04 p0551 N90-13206
Measurements of bubble properties using a multi-frequency sound field
[AD-A212591] 04 p0551 N90-13211
Ring source/force excitation of axisymmetric shell structure
[ARE-TM(UHA)-88519] 05 p0698 N90-14085
Effective utilization of acoustic wave sensor responses: Simultaneous measurement of velocity and attenuation
[DE90-002580] 06 p0838 N90-14872
A compact acoustic recorder
[AD-A213581] 07 p0933 N90-15403
Bulk wave characterization of high T(sub c) superconductors
[AD-A214030] 07 p1004 N90-15813
SAW (Surface Acoustic Wave) transducer with improved bus-bar design
[AD-D014250] 08 p1060 N90-16125
Measurement of reflection and impedance in a beam by the structural intensity technique
[DE90-728212] 08 p1088 N90-16299
A computational and experimental study of steady and transient acoustic energy flow from a complex mechanical structure 08 p1119 N90-16478
Bulk acoustic wave resonators made of amorphous materials
[ONERA-NT-1989-4] 09 p1279 N90-17416
Full field visualization of surface and bulk acoustic waves using heterodyne holographic interferometry
[AD-A214353] 10 p1387 N90-18023
Gear noise, vibration, and diagnostic studies at NASA Lewis Research Center
[NASA-TM-102435] 10 p1390 N90-18041
On categorizing sounds
[AD-A216417] 10 p1427 N90-18232
Magnetic field generation by acoustic oscillations in solar atmosphere
[DE90-606054] 11 p1594 N90-19180
Dynamics of a class of vortex rings
[NASA-TM-102257] 12 p1657 N90-19524
The drum: Mechanical oscillators and acoustic radiators
[REPT-FB-01/88] 12 p1710 N90-19819
Sandia National Laboratories' new high level acoustic test facility
[DE90-006810] 12 p1710 N90-19820
Modeling and classification of acoustic transients by speech recognition techniques
[AD-A218070] 13 p1791 N90-20277
Laser-induced shock waves effects in materials
[DE90-007626] 13 p1807 N90-20379
High-resolution acoustical imaging 13 p1881 N90-20793
Experimental feasibility of investigating acoustic waves in Couette flow with entropy and pressure gradients
[NASA-TM-102621] 13 p1882 N90-20795
A continued study of optical sound generation and amplification
[AD-A217640] 13 p1882 N90-20796
The measurements of thermoacoustic phenomena using thermoacoustic couples
[AD-A218018] 13 p1882 N90-20798
Rapidly quantifying the relative distention of a human bladder
[NASA-CASE-LAR-13901-1-NP] 14 p2010 N90-21519
Free-field propagation of high intensity noise
[NASA-CR-186577] 14 p2024 N90-21604
Impact tolerant material
[NASA-CASE-LAR-12887-3] 15 p2064 N90-21822
Propagation environments, effects, and decision aids 15 p2081 N90-21918

Boundary layer turbulence pulsed by acoustic waves
[ETN-90-96621] 16 p2236 N90-22759
Sound waves in weakly ionized gas
[DE90-620704] 16 p2313 N90-23180
Finite element formulations for coupled fluid/structure eigenvalue analysis
[AD-A220793] 17 p2416 N90-23766
In situ investigation of sea surface noise from a depth of one meter
[AD-A220158] 17 p2432 N90-23857
A theoretical analysis of the acoustic radiation from two-dimensional turbulent mixing layers
18 p2551 N90-24559
Solution of exterior acoustic problems by the boundary element method 18 p2611 N90-24874
Millimeter-wave acoustic transducers
[AD-A221402] 18 p2612 N90-24878
Sol-gel coating on acoustic wave devices: Thin film characterization and chemical sensor development
[DE90-012224] 19 p2679 N90-25235
Listening to turbulence: An example of scientific audiolization
[DE90-010637] 19 p2753 N90-25646
Surface wave characterization of high T(sub c) superconductors
[AD-A221077] 19 p2760 N90-25683
A preliminary study of the masking of wind turbine noise by ambient sound
[FFA-TN-1990-01] 20 p2923 N90-26636
Surface acoustic wave filters in ZnO-SiO2-Si layered structures: Design, technology, and monolithic integration with electronic circuitry
[ETN-90-97218] 20 p2924 N90-26638
Interaction of acoustic waves generated by coupled plate
[NASA-CR-186873] 21 p3072 N90-27464
An injective far-field pattern operator and inverse scattering problem in a finite depth ocean
[PB90-159294] 22 p3230 N90-28318
Acoustic confinement in the large hydrodynamic tunnel: Identification of the acoustic charateristics with a one-directional source
[REPT-8228-86] 22 p3244 N90-28399
Wind tunnel investigation of periodic vortex separation from rough surface circular cylinders by means of acoustic measurements
[ESA-TT-1092] 23 p3268 N90-28499
Combustion instability coupling with feed system acoustics 23 p3293 N90-28629
Definition of a near real time microbiological monitor for space vehicles
[NASA-CR-185599] 24 p3441 N90-29430
The computation and analysis of acoustic waves in transonic airfoil-vortex interactions
24 p3542 N90-30031
Study of the reflection of surface acoustic wave from a material discontinuity boundary using a perturbation method 24 p3542 N90-30032

SOUND-SOUND INTERACTIONS
Nonlinear acoustics: Reflection and refraction, propagation in a periodic waveguide, scattering of sound by sound and ellipsoidal focusing
[AD-A211224] 02 p0271 N90-11550

SOUNDERS
U SOUNDING

SOUNDING
NT ACOUSTIC SOUNDING
NT ATMOSPHERIC SOUNDING
NT BALLOON SOUNDING
NT ECHO SOUNDING
NT IONOSPHERIC SOUNDING
NT MICROWAVE SOUNDING
NT ROCKET SOUNDING
NT SATELLITE SOUNDING
Operational ozone monitoring with the Global Ozone Monitoring Radiometer (GOMR)
[PB90-114034] 08 p1098 N90-16359
Estimating sea ice thickness using time-of-flight data from impulse radar soundings
[AD-A218736] 16 p2250 N90-22831
SAGE 3: A visible wavelength limb sounder
21 p3016 N90-27147
Analysis of cirrus optical properties with data from NASA ER2 High-resolution Interferometer Sounder (HIS)
[NASA-CR-186365] 21 p3030 N90-27227

SOUNDING ROCKETS
NT ARIES SOUNDING ROCKET
NT SKYLARK ROCKET VEHICLE
Meteorological rocket observations
[PB89-168769] 02 p0250 N90-11419
A beam induced upset during the flight of the ECHO-7 rocket
[NASA-CR-186089] 03 p0309 N90-11755
Current limiting mechanisms in electron and ion beams experiments
[AD-A212295] 04 p0460 N90-12637
European Rocket and Balloon Programs and Related Research
[ESA-SP-291] 05 p0656 N90-13826
Swiss scientific balloon and sounding rocket experiments 1987-1989 05 p0656 N90-13827
The Norwegian balloon and sounding rocket program 1989-1992 05 p0656 N90-13829
The Swedish sounding rocket and balloon program
05 p0657 N90-13830
The German scientific balloon and sounding rocket program 05 p0657 N90-13831
The SN 1987A attitude control system
05 p0659 N90-13845
Design and technical aspects of the Solly instrument
05 p0659 N90-13847
Preliminary results of the rocket and scatter experiments ROSE: Measurements with the newly designed spherical probe 05 p0659 N90-13850
Andoya rocket range: New installations, future plans, and investments 05 p0661 N90-13859
Qualification of the 4th stage propulsor of the Brazilian launcher. SLV: A new sounding rocket
05 p0661 N90-13860
The Brazilian space program: Actual state of the art
05 p0661 N90-13861
Optical observations of interplanetary pick-up ions: The experiment Helly 05 p0661 N90-13863
The x ray mirror and the PSPC of the supernova-rocket-project 05 p0662 N90-13867
Esrange 05 p0663 N90-13876
A measurement of hydroxyl in the daytime mesosphere 06 p0814 N90-14732
Flight experiment hardware for sounding rocket investigations. Materials science and fluid sciences
[ESA-SP-1116] 08 p1038 N90-15998
From small beginnings... The story of ESRO's sounding rocket programme in celebration of the twenty-fifth anniversary of the first ESRO sounding rocket launch
[ESA-BR-60] 08 p1038 N90-15999
Preliminary results from the quadrupole probe on NEED-1
[FFI-89/7015] 19 p2714 N90-25446
Gaseous optical contamination of the spacecraft environment: A review 19 p2730 N90-25519

SOURCE PROGRAMS
Managing the waste stream: Background information for planning source separation programs
[PB90-100223] 07 p0956 N90-15530
High power millimeter wave source development program 15 p2061 N90-21805

SOUTH AMERICA
Connections between the circulation in altitude and convection over South America
[INPE-4923-TDL/383] 11 p1534 N90-18828
Cyclogeneses and extratropical cyclones in the south-southeast region of Brazil and its influence in time
[INPE-4812-TDL/359] 12 p1693 N90-19722
Evolution of finite amplitude baroclinic waves in the atmosphere and ocean
[INPE-4752-TDL/346] 12 p1695 N90-19733
Southern oscillation simulation in coupled ocean/atmosphere global climate models
15 p2131 N90-22181

SOUTHEAST ASIA
Re-analysis of data on the space radiation environment above southeast Asia
[AD-A224155] 24 p3564 N90-30162
Re-analysis of data on the space radiation environment above south-east Asia
[RAE-TR-89048] 24 p3565 N90-30166

SOUTHERN HEMISPHERE
NT ANTARCTIC REGIONS
NT ROSS ICE SHELF
Auroral and sub-auroral F-layer irregularity studies in the Northern and Southern Hemisphere during the equinox transition study September 16-26, 1984
02 p0246 N90-11393
Observational studies of low-frequency oscillations in the Southern Hemisphere 02 p0250 N90-11420
South Pole surface radiation balance measurements, April 1986 to February 1988
[PB89-224018] 04 p0519 N90-12993
Humidity local measurements in the middle atmosphere 05 p0657 N90-13833
Long duration balloon flights in the middle stratosphere 05 p0663 N90-13874
Study of peculiar galaxies in the Southern Hemisphere
[INPE-4810-TDL/357] 11 p1594 N90-19184
New water vapor masers in the Southern Hemisphere
[INPE-4844-PRE/1473] 14 p2037 N90-21689
VHE gamma ray emission from Southern Hemisphere X ray binaries 19 p2772 N90-25758
Comparison of satellite derived dynamical quantities in the stratosphere of the Southern Hemisphere
22 p3210 N90-28210
Vorticity balance study for a tropical region, during the Southern Hemisphere summer
[INPE-4634-TDL/336] 23 p3353 N90-28949
An observational study of the circulation in the Southern Hemisphere stratosphere 24 p3488 N90-29715

SOUTHERN OSCILLATION
Observational studies of low-frequency oscillations in the Southern Hemisphere 02 p0250 N90-11420
Southern oscillation in the OSU coupled upper ocean/atmosphere GCM
[DE90-008415] 13 p1844 N90-20588
Southern oscillation simulation in coupled ocean/atmosphere global climate models
15 p2131 N90-22181

SOVIET SATELLITES
NT COSMOS SATELLITES
NT MOLNIYA SATELLITES
Compendium of meteorological space programs, satellites, and experiments
[NASA-TM-102924] 12 p1607 N90-19243

SOVIET SPACECRAFT
NT BURAN SPACE SHUTTLE
NT MIR SPACE STATION
USSR and international cooperation in space
02 p0158 N90-10905
Manned spacecraft
[AD-A214218] 07 p0887 N90-15129
Glavkosmos U.S.S.R. and the basic objectives of its activity 09 p1174 N90-16788

SOVIET UNION
U U.S.S.R.

SOYBEANS
Spectral responses of soybeans and their relationship with agronomical parameters
[INPE-4832-PRE/1462] 10 p1398 N90-18084
Thermal remote sensing in the differentiation of soybean crops (glycine max (L.) merrill) submitted to water deficit
[INPE-4900-PRE/1501] 11 p1522 N90-18762
Field reports on radiometric campaigns of soybeans in the Federal district: Safra 88/89
[INPE-5021-RPE/615] 15 p2122 N90-22139
Proximate composition of seed and biomass from soybean plants grown at different carbon monoxide (CO_2) concentrations
[NASA-TM-103496] 20 p2897 N90-26480

SPACE ADAPTATION SYNDROME
Biology in microgravity: A guide for experimenters
[ESA-TM-02] 04 p0482 N90-12769
Cardiovascular, renal, electrolyte, and hormonal changes in man during gravitational stress, weightlessness, and simulated weightlessness: Lower body positive pressure applied by the antigravity suit
[NASA-TM-102232] 04 p0522 N90-13013
Preliminary study of pharmacological control of space disease
[ETN-90-95015] 05 p0674 N90-13927
Space adaptation syndrome induced by a long duration +3Gx centrifuge run
[AD-A218248] 14 p2010 N90-21518
Issues in development, evaluation, and use of the NASA Preflight Adaptation Trainer (PAT)
[NASA-CR-185608] 15 p2137 N90-22212
Regulation of erythropoiesis in rats during space flight
[NASA-CR-177537] 23 p3378 N90-29086

SPACE BASED RADAR
Space-based radar simulation laboratory
[AD-A216722] 11 p1497 N90-18618
Arrays for space applications
12 p1610 N90-19265
Development of a receiver for a space-based laser radar system
[AD-A215079] 12 p1665 N90-19566
High Resolution Air- and Spaceborne Radar
[AGARD-CP-459] 14 p1960 N90-21223
Concepts for high resolution space based SAR/ISAR systems: Preliminary design considerations
14 p1960 N90-21224
Trade-offs in a space based surveillance radar
14 p1960 N90-21225
Concept for a spaceborne Synthetic Aperture Radar (SAR) sensor based on active phased array technology
14 p1962 N90-21234
Design options for space-based radar systems
[ETN-90-96548] 16 p2228 N90-22710
Spaceborne radar observations: A guide for Magellan radar-image analysis
[NASA-CR-184998] 16 p2249 N90-22826
Radar detection during scintillation
[AD-A220099] 17 p2393 N90-23630
Kinetic and extraction measurements on 12C18O2
[AD-A220417] 17 p2472 N90-24133
Command and control in the age of space-based surveillance 21 p3069 N90-27445

SPACE BASES
NT LUNAR BASES
NT SPACE COLONIES

M.I.N.G., Mars Investment for a New Generation: Robotic construction of a permanently manned Mars base
[NASA-CR-186224] 06 p0865 N90-15028
A robotically constructed production and supply base on Phobos
[NASA-CR-186234] 15 p2073 N90-21872
Project WISH: The Emerald City
[NASA-CR-186692] 17 p2366 N90-23470

SPACE BIOLOGY
U EXOBIOLOGY

SPACE BUSES
U FERRY SPACECRAFT

SPACE CAPSULES
NT ESCAPE CAPSULES
Verification of aerothermodynamic codes by means of a winged experimental re-entry vehicle
09 p1180 N90-16842

SPACE CHARGE
Extraction induced emittance growth for negative ion sources
[DE89-017586] 02 p0273 N90-11559
A beam induced upset during the flight of the ECHO-7 rocket
[NASA-CR-186089] 03 p0309 N90-11755
Plasma-anode electron gun research
[AD-A211547] 03 p0312 N90-11773
DART: A simulation code for charged particle beams, revision 1
[DE89-016697] 03 p0404 N90-12312
Thermionic emission including both space charge and image forces
[AD-A212732] 04 p0498 N90-12869
Electron transport in heterojunction superlattices
[AD-A212366] 04 p0560 N90-13265
Intense REB (Relativistic Electron Beam) transport in a weakly magnetized plasma
[DE90-002978] 07 p0994 N90-15749
Stability of hollow beams in longitudinal phase space
[DE90-004284] 10 p1427 N90-18234
BEAR electrostatic analyzer: Flight results
[DE90-006511] 11 p1498 N90-18625
The dynamics of electrons in very intense lasers
[DE90-007246] 11 p1516 N90-18729
Identification and solution of a charging problem in a high-altitude detector
[DE90-008637] 12 p1616 N90-19296
Impedance characteristics of terawatt ion diodes
[DE90-006276] 12 p1652 N90-19494
Near contact phenomena and transient effects in far infrared photoconductors 14 p1976 N90-21316
Intense electron beam propagation across a magnetic field
[DE90-009993] 16 p2316 N90-23204
Measurement of plasma-neutralized super-vacuum currents in a gyrotron configuration
[AD-A218505] 16 p2316 N90-23207
Flight model discharge system
[AD-A220261] 18 p2510 N90-24342
Control of nonlinear space-charge emittance growth
[DE90-014752] 23 p3410 N90-29270

SPACE COLONIES
The first 1000 days of a future lunar base
[ILR-MITT-224] 08 p1033 N90-15970
The partnership: Space shuttle, space science, and space station
[NASA-TM-102900] 14 p1930 N90-21050
Greenhouse design for a Martian colony: Structural, solar collection and light distribution systems
[NASA-CR-186818] 20 p2901 N90-26501

SPACE COMMERCIALIZATION
Research and test facilities for development of technologies and experiments with commercial applications
[NASA-TM-101789] 02 p0159 N90-10909
Development of a shuttle recovery Commercial Materials Processing in Space (CMPS) program
[NASA-CR-183720] 05 p0630 N90-13678
Fundamental results from microgravity cell experiments with possible commericial applications
05 p0676 N90-13940
Centers for the commercial development of space
[NASA-PAM-525] 05 p0709 N90-14151
NASA commercial programs
[NASA-TM-101853] 05 p0709 N90-14152
Report of NASA Lunar Energy Enterprise Case Study Task Force
[NASA-TM-101652] 07 p1007 N90-15836
Report of the NASA lunar energy enterprise case study task force 07 p1008 N90-15837
Analysis of the financial factors governing the profitability of lunar helium-3 07 p1008 N90-15838
Transportation and operations aspects of space energy systems 07 p1008 N90-15842
The European long-term space plan: A basis for autonomy and cooperation 09 p1173 N90-16784
US commercial launcher summary
09 p1174 N90-16793
Financial and commercial issues: A customer's perspective 09 p1174 N90-16794
Launch insurance: Its role in the future development of commerce in space 09 p1174 N90-16795
Legal aspects of commercial space transportation
09 p1175 N90-16796
The European space effort: An integral part of the construction of Europe 09 p1180 N90-16845
Space Station Workshop: Commercial Missions and User Requirements
[NASA-TM-102912] 15 p2175 N90-22428
Aeronautics and space report of the President: 1987 activities 15 p2181 N90-22462
Microgravity, the space application of the 21st century. Challenges, constraints, and strategies
[REPT-892-430-105] 16 p2226 N90-22696
Space Station Freedom Pre-Workshop Session
[NASA-TM-102913] 17 p2479 N90-24172
Space manufacture: Protection and valuation of innovations from a users point of view
20 p2939 N90-26724
Space projects: Improvements needed in selecting future projects for private financing
[GAO/NSIAD-90-147] 22 p3256 N90-28439
Preliminary analysis of NASA commercialization initiatives
[PB90-202706] 23 p3407 N90-29257

SPACE COMMUNICATION
NT SATELLITE COMMUNICATION
NT SPACECRAFT COMMUNICATION
Telescience Testbed Pilot Program
[NASA-CR-184594] 02 p0257 N90-11455
The Telecommunications and Data Acquisition Report
[NASA-CR-185093] 04 p0485 N90-12786
Spread spectrum mobile radio communications
[AD-A213726] 07 p0918 N90-15311
On board cross support scenarios
[INPE-5005-PRE/1562] 14 p1967 N90-21268
Environmental projects, volume 11. Environmental assessment: Addition to operations building, Mars site
[NASA-CR-186449] 14 p2003 N90-21479
Environmental projects, volume 10. Environmental assessment: New 34-meter antenna at Apollo site
[NASA-CR-186448] 14 p2003 N90-21480
The Telecommunications and Data Acquisition Report
[NASA-CR-186479] 15 p2074 N90-21880
Mark 4-A DSCC (Magellan-era) telemetry system description 15 p2078 N90-21903
The mm-wave region propagation experiments by satellite 15 p2081 N90-21916
Performance analysis of CCSDS path service
[NASA-CR-180699] 17 p2364 N90-23457
Tactical applications of the UHF satellite communications system 21 p3070 N90-27451

SPACE COOLING (BUILDINGS)
Guidelines for evaluating energy analysis software
[AD-A214171] 07 p0976 N90-15640
Solar buildings program summary. Volume 2: Research summaries
[DE89-009478] 11 p1530 N90-18810
Advanced absorption technology development in the United States
[DE90-001336] 12 p1641 N90-19428

SPACE DEBRIS
Orbital debris research at NASA Johnson Space Center, 1986-1988
[NASA-TM-102155] 01 p0138 N90-10795
Autonomous space processor for orbital debris
[NASA-CR-186043] 03 p0311 N90-11770
The time evaluation of the number of space probes and debris at different orbit heights with a view to a future collision risk in space
[R-8718] 03 p0311 N90-11772
Report on orbital debris
[NASA-TM-101855] 04 p0460 N90-12635
Optical detection of space debris using a large achromatic coronagraph
[AD-A211362] 04 p0462 N90-12647
On protection of Freedom's solar dynamic radiator from the orbital debris environment. Part 1: Preliminary analyses and testing
[NASA-TM-102458] 06 p0736 N90-14285
Present and future risk of satellite and manned platforms collisions with other space objects and particles on earth orbits
[R-8841] 12 p1615 N90-19287
Present and future risk of collision of satellites and manned platforms with other space objects and particles in terrestrial orbit
[R-8840] 12 p1615 N90-19288
Satellites and debris in earth revolution orbits and first estimation of the collision probability
[R-8709] 12 p1615 N90-19289
Project for the European space organization in the area of space debris
[REPT-29/89] 12 p1615 N90-19290
Effects of X radiation on the LAMPSHADE orbital debris satellite shield, 2
[DE90-008214] 18 p2510 N90-24341
Space environments and their effects on space automation and robotics 19 p2735 N90-25543
Space program: Space debris a potential threat to Space Station and shuttle
[GAO/IMTEC-90-18] 20 p2815 N90-26024
Autonomous space processor for orbital debris
[NASA-CR-186691] 20 p2820 N90-26044
Rings of Earth detected by orbital debris radar
20 p2854 N90-26232
Semi-active orbital debris sweeper
[NASA-CASE-MSC-21534-1] 21 p2966 N90-26860
Final design for a comprehensive orbital debris management program
[NASA-CR-186674] 22 p3126 N90-27739

SPACE DENSITY
Theory of interacting plasmas in space
07 p0993 N90-15742

SPACE DETECTION AND TRACKING SYSTEM
Independent Orbiter Assessment (IOA): Assessment of the communication and tracking subsystem, volume 1
[NASA-CR-185528-VOL-1] 03 p0315 N90-11789
Independent Orbiter Assessment (IOA): Assessment of the communication and tracking subsystem, volume 2
[NASA-CR-185528-VOL-2] 03 p0315 N90-11790
Independent Orbiter Assessment (IOA): Assessment of the communication and tracking subsystem, volume 3
[NASA-CR-185528-VOL-3] 03 p0315 N90-11791

SPACE DIVERSITY
U RECEPTION DIVERSITY

SPACE ENVIRONMENT
U AEROSPACE ENVIRONMENTS

SPACE ENVIRONMENT SIMULATION
NT NEUTRAL BUOYANCY SIMULATION
NT WEIGHTLESSNESS SIMULATION
Space environment effects on carbon/epoxy materials
02 p0185 N90-11056
Droplet combustion experiment drop tower tests using models of the space flight apparatus
[NASA-TM-101472] 02 p0209 N90-11196
Watchfulness and attention during weightlessness simulations: Use of computerized psychometric tests
[REPT-89-TOU-3-1045] 05 p0674 N90-13928
Hollow-cathode experiments to support electrodynamic tether applications
[IFSI-89-5] 08 p1036 N90-15986
Electrical battery model for LEO application based on absolute instantaneous state of charge
10 p1332 N90-17702
The solar array design of the Vesta small bodies spacecraft 10 p1345 N90-17799
Outline of high voltage solar array experiment using SFU platform 10 p1345 N90-17801
Review of synergistic environmental interactions: Guidelines for new testing approaches on future solar arrays 10 p1345 N90-17803
Simulation of micrometeoroid impacts by laser pulses
10 p1348 N90-17806
Analysis of alternative concepts for transport systems on the Moon surface
[ETN-90-95727] 12 p1672 N90-19605
Space environment simulation of the SCD-01 satellite through heating plates
[INPE-4988-PRE/1550] 14 p1940 N90-21105
Interface tribology and space conditions
18 p2536 N90-24469
The advantages and limitations of sputtered molybdenum disulphide as a space lubricant
18 p2537 N90-24471
Investigation of lubrication characteristics of MoS2 films in space environment 18 p2537 N90-24472
Design and manufacturing of an APTF to test fluid behaviour in microgravity environment
18 p2541 N90-24506
Electrical connector for operation in space
18 p2541 N90-24507
Microgravity science and applications: Apparatus and facilities
[NASA-TM-101892] 23 p3285 N90-28588

SPACE ENVIRONMENTAL LUBRICATION
U SPACECRAFT LUBRICATION

SPACE ERECTABLE STRUCTURES
NT BEACON EXPLORER A
NT BEACON SATELLITES
NT INFLATABLE SPACECRAFT
Structural concepts for very large (400-meter-diameter) solar concentrators 01 p0029 N90-10153
A super element for multibody dynamics
02 p0178 N90-11004
Thermoelastic behavior of large space structures: Modeling and control 02 p0179 N90-11012

Assembly considerations for large reflectors
05 p0599 N90-13480
Hybrid deployable support truss designs for LDR
05 p0600 N90-13485
Joints in deployable space truss structures
05 p0601 N90-13489
Support trusses for large precision segmented reflectors: Preliminary design and analysis
[NASA-TM-101560] 11 p1468 N90-18453
Preliminary design approach for large high precision segmented reflectors
[NASA-TM-102605] 14 p1938 N90-21096
Heavily loaded joints for assembling aerobrake support trusses
[NASA-CR-181992] 14 p1939 N90-21099
In-orbit operations research and development program of the Toulouse Space Center 18 p2501 N90-24290
Mechanisms to assemble space structures in extravehicular environment 18 p2538 N90-24480
A cable-rigidized 3D pantograph
18 p2538 N90-24484
A sequentially deployable structure for space applications. Part 2: Engineering model manufacturing and testing 18 p2541 N90-24504
Inmarsat omni-antenna deployment mechanism
18 p2542 N90-24508
Utilization of space station, part 3
[NAL-TM-597-PT-3] 24 p3439 N90-29422
A lunar space station
[NASA-CR-186223] 24 p3563 N90-30158

SPACE EXPLORATION
Overview of laser concepts 01 p0029 N90-10154
A history of West European rocketry and space research
[AD-A211191] 02 p0297 N90-11690
A survey of permanently-manned lunar base concepts
[AD-A212575] 04 p0460 N90-12638
Space operations: Listing of NASA scientific missions, 1980-2000. Fact sheet for the Chairman, Subcommittee on Space Science and Applications, Committee on Science, Space, and Technology, House of Representatives
[AD-A213493] 07 p1016 N90-15881
Reports of planetary astronomy, 1986
[NASA-TM-100776] 08 p1138 N90-16596
Science exploration opportunities for manned missions to the Moon, Mars, Phobos, and an asteroid
[NASA-CR-186295] 09 p1171 N90-16776
Human exploration mission studies
13 p1821 N90-20457
Romans to Mars
[NASA-TM-103094] 16 p2342 N90-23339
Project Longshot: A mission to Alpha Centauri
[NASA-CR-186052] 17 p2357 N90-23417
Human exploration of space: A review of NASA's 90-day study and alternatives
[NASA-CR-186394] 17 p2357 N90-23418
International cooperation for Mars exploration and sample return
[NASA-CR-186511] 17 p2358 N90-23419
Space exploration: NASA's deep space missions are experiencing long delays
[GAO/NSIAD-88-128BR] 18 p2635 N90-25015
Mars in this decade: The great exploration
[DE90-011232] 19 p2797 N90-25920
Astronautics and Aeronautics, 1979-1984: A chronology
[NASA-SP-4024] 19 p2800 N90-25928
Space exploration: Cost, schedule, and performance of NASA's Mars Observer Mission. Fact sheet for the Chairman, Subcommittee on Science, Technology, and Space, Committee on Commerce, Science, and Transportation, US Senate
[GAO/NSIAD-88-137FS] 20 p2815 N90-26021
Space exploration: Cost, schedule, and performance of NASA's Magellan Mission to Venus. Fact sheet for the Chairman, Subcommittee on Science, Technology, and Space, Committee on Commerce, Science, and Transportation, US Senate
[GAO/NSIAD-88-130FS] 20 p2815 N90-26022
Space exploration: Cost, schedule, and performance of NASA's Ulysses Mission to the Sun. Fact sheet for the Chairman, Subcommittee on Science, Technology, and Space, Committee on Commerce, Science, and Transportation, US Senate
[GAO/NSIAD-88-129FS] 20 p2815 N90-26023
Space exploration: Cost, schedule, and performance of NASA's Galileo Mission to Jupiter. Fact sheet for the Chairman, Subcommittee on Science, Technology, and Space, Committee on Commerce, Science, and Transportation, US Senate
[GAO/NSIAD-88-138FS] 20 p2816 N90-26025
Possible applications of tethered systems to Mars exploration missions
[IAF-89-489] 20 p2822 N90-26060
Reports of planetary astronomy, 1990
[NASA-TM-4205] 20 p2940 N90-26730
Directory of research projects: Planetary geology and geophysics program
[NASA-TM-4211] 20 p2942 N90-26743
The lessons of Varsovian's reconnaissance
[NASA-TM-103207] 20 p2951 N90-26789
Nuclear power systems for lunar and Mars exploration
[NASA-TM-103168] 21 p2969 N90-26873
The real-time learning mechanism of the Scientific Research Associates Advanced Robotic System (SRAARS) 21 p3046 N90-27312
A technology assessment of alternative communications systems for the space exploration initiative
[NASA-TM-103243] 22 p3125 N90-27736
The flight telerobotic servicer: NASA's first operational space robot 24 p3500 N90-29781
Some personal reminiscences. The ESRO-ESA space science story: Twenty-five years of European cooperation
[ESA-BR-66] 24 p3565 N90-30168

SPACE FLIGHT
NT APOLLO 15 FLIGHT
NT INTERPLANETARY FLIGHT
NT LONG DURATION SPACE FLIGHT
NT LUNAR FLIGHT
NT MANNED SPACE FLIGHT
NT RETURN TO EARTH SPACE FLIGHT
NT SPACE SHUTTLE MISSION 41-G
NT SPACE SHUTTLE MISSION 51-J
NT SPACE SHUTTLE MISSION 51-L
NT SPACE SHUTTLE MISSION 61-A
NT SPACE SHUTTLE MISSION 61-B
NT SPACE SHUTTLE MISSION 61-C
NT SPACE SHUTTLE MISSION 61-E
NT SPACE SHUTTLE MISSIONS
Space flight (selected articles)
[AD-A212068] 03 p0311 N90-11769
Report on orbital debris
[NASA-TM-101855] 04 p0460 N90-12635
Sandia Satellite Program summary of operational procedures
[DE90-000892] 06 p0728 N90-14249
Design considerations for space flight hardware
[NASA-TM-102300] 06 p0734 N90-14275
A foundation for the design of an astronautics specification system based on dynamic motivation analysis
[ILR-MITT-220] 08 p1033 N90-15969
Safety Status Report for the Ulysses mission: Summary. General purpose heat source radioisotope thermoelectric generator program
[DE90-006828] 12 p1614 N90-19284
Working on the moon: The Apollo experience
[DE90-003662] 12 p1697 N90-19744
NSSDC data listing
[NASA-TM-102989] 15 p2180 N90-22456
Extraterrestrial life in the universe
[NASA-TM-102363] 15 p2181 N90-22464
Langley aerospace test highlights, 1989
[NASA-TM-102631] 17 p2487 N90-24221
Effects of microgravity on rat bone, cartilage and connective tissues 20 p2891 N90-26454
Experiment K-6-02. Biomedical, biochemical and morphological alterations of muscle and dense, fibrous connective tissues during 14 days of spaceflight
20 p2892 N90-26456
Experiment K-6-03. Gravity and skeletal growth, part 1. Part 2: Morphology and histochemistry of bone cells and vasculature of the tibia; Part 3: Nuclear volume analysis of osteoblast histogenesis in periodontal ligament cells; Part 4: Intervertebral disc swelling pressure associated with microgravity 20 p2892 N90-26457
Experiment K-6-04. Trace element balance in rats during spaceflight 20 p2892 N90-26458
Experiment K-6-05. The maturaton of bone and dentin matrices in rats flown on Cosmos 1887
20 p2893 N90-26459
Experiment K-6-06. Morphometric and EM analyses of tibial epiphyseal plates from Cosmos 1887 rats
20 p2893 N90-26460
Experiment K-6-07. Metabolic and morphologic properties of muscle fibers after spaceflight
20 p2893 N90-26461
Experiment K-6-09. Morphological and biochemical investigation of microgravity-induced nerve and muscle breakdown. Part 1: Investigation of nerve and muscle breakdown during spaceflight; Part 2: Biochemical analysis of EDL and PLT muscles 20 p2893 N90-26463
Experiment K-6-12. Morphometric studies of atrial or granules and hepatocytes. Part 1: Morphometric study of the liver; Part 2: The atrial granular accumulations
20 p2894 N90-26466
Experiment K-6-14. Hepatic function in rats after spaceflight 20 p2895 N90-26468
Experiment K-6-17. Structural changes and cell turnover in the rats small intestine induced by spaceflight
20 p2895 N90-26470
Experiment K-6-19. Pineal physiology in microgravity: Relation to rat gonadal function
20 p2895 N90-26472
Experiment K-6-20. The effect of spaceflight on pituitary oxytocin and vasopressin content of rats
20 p2896 N90-26473
Experiment K-6-23. Effect of spaceflight on levels and function of immune cells 20 p2897 N90-26476
Experiment K-6-27. Analysis of radiographs and biosamples from primate studies
20 p2897 N90-26478
Hydroelastic problems in space flight vehicles
[LRT-WE-9-FB-11(1989)] 21 p2967 N90-26868
Joint US/USSR study: Comparison of effects of horizontal and head-down bed rest
[NASA-TP-3037] 23 p3355 N90-28965
Regulation of erythropoiesis in rats during space flight
[NASA-CR-177537] 23 p3378 N90-29086
The flight telerobotic servicer project: A technical overview 24 p3506 N90-29821

SPACE FLIGHT STRESS
Exercise countermeasures for bed rest deconditioning
[NASA-TM-101045] 05 p0674 N90-13926
Research in human performance related to space: A compilation of three projects/proposals
18 p2629 N90-24983
Fluid and electrolyte homeostasis during spaceflight: Elucidation of mechanisms in a primate
[NASA-CR-177548] 23 p3378 N90-29085

SPACE FLIGHT TRACKING AND DATA NETWORK
Navigation experiment NAVEX: Data storage and processing
[DFVLR-MITT-89-09] 03 p0304 N90-11727
Navigation experiment NAVEX: The equipment delay times in the Spacelab mission D1
[DFVLR-MITT-89-10] 03 p0304 N90-11728
GPS network analysis: The influence of stochastic prior information of orbital elements on ground station position measures
[TR-4-1988] 08 p1020 N90-15901

SPACE FLIGHT TRAINING
Advanced manned space flight simulation and training: An investigation of simulation host computer system concepts
[NASA-CR-185998] 02 p0160 N90-10911

SPACE GLIDERS
U LIFTING REENTRY VEHICLES

SPACE GLOSSARIES
Space Station Freedom: List of acronyms
17 p2479 N90-24176

SPACE HABITATS
Measurement of the light flux density patterns from luminaires proposed as photon sources for photosynthesis during space travel
[NASA-CR-186124] 05 p0672 N90-13916
M.I.N.G., Mars Investment for a New Generation: Robotic construction of a permanently manned Mars base
[NASA-CR-186224] 06 p0865 N90-15028
Utilization of non-conventional systems for conversion of biomass to food components
[NASA-CR-177545] 07 p0968 N90-15591
Project WISH: The Emerald City
[NASA-CR-186692] 17 p2366 N90-23470
Automation in the Space Station module power management and distribution Breadboard
19 p2728 N90-25509
Space Station Freedom pressurized element interior design process
[NASA-CR-181297] 23 p3287 N90-28597
A lunar space station
[NASA-CR-186223] 24 p3563 N90-30158

SPACE HEATING (BUILDINGS)
Solar buildings program summary. Volume 2: Research summaries
[DE89-009478] 11 p1530 N90-18810

SPACE INDUSTRIALIZATION
NT SPACE MANUFACTURING
NT SPACE PROCESSING
Research and test facilities for development of technologies and experiments with commercial applications
[NASA-TM-101789] 02 p0159 N90-10909
A quasi-economic role for lunar science
[DE90-000679] 07 p1015 N90-15876
Space Station Freedom Pre-Workshop Session
[NASA-TM-102913] 17 p2479 N90-24172

SPACE INFRARED TELESCOPE FACILITY
Status of direct detector and array development
05 p0596 N90-13464
The infrared spectrograph during the SIRTF pre-definition phase
[NASA-CR-183234] 05 p0644 N90-13759

SOFIA (Stratospheric Observatory For Infrared Astronomy): A 3m class airborne telescope
05 p0659 N90-13846
Long-lived space observatories for astronomy and astrophysics
[NASA-CR-185373] 06 p0731 N90-14261
CCD TV focal plane guider development and comparison to SIRTF applications
[NASA-CR-185977] 06 p0842 N90-14900
BASG thermomechanical pump helium 2 transfer tests
[NASA-CR-177541] 14 p1939 N90-21097
Proceedings of the Third Infrared Detector Technology Workshop
[NASA-TM-102209] 14 p1975 N90-21313
A 100 micro Kelvin bolometer system for SIRTF
14 p1976 N90-21317
Ga:Ge array development 14 p1977 N90-21323
Study of advanced InSb arrays for SIRTF (Space Infrared Telescope Facility) 14 p1977 N90-21325
InSb DRO array characteristics
14 p1977 N90-21326
SIRTF in high earth orbit 14 p1980 N90-21345
Laboratory characterization of direct readout Si:Sb and Si:Ga infrared detector arrays 14 p1980 N90-21347
SIRTF: Probing the dark corners of the galaxy
21 p3091 N90-27577

SPACE LABORATORIES
NT LONG DURATION EXPOSURE FACILITY
NT MANNED ORBITAL LABORATORIES
NT SKYLAB 1
NT SPACELAB
User needs, benefits, and integration of robotic systems in a space station laboratory
[NASA-CR-185150] 05 p0651 N90-13794
Toward the development of COSMO-LAB
18 p2500 N90-24281
Planning for Space Station Freedom laboratory payload integration
[NASA-CR-186751] 20 p2820 N90-26047
Conceptual design study for Infrared Limb Experiment (IRLE)
[NASA-CR-186950] 21 p2968 N90-26869
Research opportunities on the Space Station
21 p3092 N90-27578

SPACE LAW
International treaties and active experiments in space
[AD-A219368] 16 p2328 N90-23272
Manned Space Stations: Legal Issues
[ESA-SP-305] 20 p2937 N90-26711
The US/International Space Station: Legal aspects of space objects and jurisdiction and control
20 p2937 N90-26713
Damage responsibility and liability in space stations
20 p2937 N90-26714
MIR: A Soviet Space Station. Some legal aspects of international cooperation 20 p2938 N90-26715
The International Space Station: The legal framework
20 p2938 N90-26716
The partnership concept and international management 20 p2938 N90-26717
The International Space Station: Conditions of access and use 20 p2938 N90-26718
Human work in space: The astronaut's legal status. Introduction 20 p2938 N90-26719
The manned national space station: International legal considerations 20 p2938 N90-26720
The astronauts' legal status: The International Space Station 20 p2938 N90-26721
Crossborder movements: Goods, personnel and technologies 20 p2939 N90-26722
Space Station intellectual property rights and US patent law 20 p2939 N90-26723
Space manufacture: Protection and valuation of innovations from a users point of view
20 p2939 N90-26724
Space law put to the test by the International Space Station 20 p2939 N90-26727

SPACE LOGISTICS
Superconducting magnets in space
[DE90-002671] 06 p0837 N90-14865
The international space transportation market: A European perspective 09 p1173 N90-16785
An exploration of issues related to future space logisticians
[AD-A215374] 09 p1276 N90-17397
The partnership: Space shuttle, space science, and space station
[NASA-TM-102900] 14 p1930 N90-21050
Lunar shelter
[ILR-MITT-233(1989)] 17 p2439 N90-23896
Long cycle pressurized logistics module: An Italian contribution to the Space Station Freedom logistics scenario
[IAF-89-083] 20 p2822 N90-26058

SPACE MAINTENANCE
Interchangeable end effector tools utilized on the protoflight manipulator arm
[NASA-CR-179374] 01 p0078 N90-10447
An exploration of issues related to future space logisticians
[AD-A215374] 09 p1276 N90-17397
Orbital servicing: Issue or answer
[AD-A217284] 12 p1616 N90-19295
The European EVA suit: An optimized tool for Hermes/MTFF in-orbit operations
18 p2502 N90-24296
EVA power tool prototype 18 p2538 N90-24482
Detachable interface mechanism
18 p2540 N90-24497
Columbus scientific airlock 18 p2541 N90-24503
SDIO robotics in space applications
19 p2729 N90-25514
Telepresence for space: The state of the concept
19 p2731 N90-25526
The Flight Telerobotic Servicer (FTS) NASA's first operational robotic system 19 p2733 N90-25537
The telerobot testbed: An architecture for remote servicing 19 p2734 N90-25538
Telerobotic workstation design aid
24 p3504 N90-29805

SPACE MANUFACTURING
Meeting of intercosmos space physics group
02 p0158 N90-10902
Materials processing in low gravity
[NASA-CR-183733] 06 p0755 N90-14397
The international space transportation market: A European perspective 09 p1173 N90-16785
Space Station Workshop: Commercial Missions and User Requirements
[NASA-TM-102912] 15 p2175 N90-22428
Consortium for materials development in space
[NASA-CR-186534] 17 p2383 N90-23575
Space Station Freedom Pre-Workshop Session
[NASA-TM-102913] 17 p2479 N90-24172
Space manufacture: Protection and valuation of innovations from a users point of view
20 p2939 N90-26724

SPACE MECHANICS
NT ASTRODYNAMICS
NT CELESTIAL MECHANICS
NT KEPLER LAWS
NT ORBITAL MECHANICS

SPACE MEDICINE
U AEROSPACE MEDICINE

SPACE MISSIONS
NT CASSINI MISSION
NT COMET RENDEZVOUS ASTEROID FLYBY MISSION
NT FLYBY MISSIONS
NT GIOTTO MISSION
NT GRAND TOURS
NT MANNED MARS MISSIONS
NT MARS SAMPLE RETURN MISSIONS
NT SOHO MISSION
NT SOLAR MAXIMUM MISSION
NT ULYSSES MISSION
JPRS Report: Science and Technology. USSR: Space
[JPRS-USP-89-007] 02 p0158 N90-10900
Soviet Mars program 02 p0158 N90-10903
USSR and international cooperation in space
02 p0158 N90-10905
Sagdeyev discusses space missions, policy, Mars plans 02 p0159 N90-10906
A summary of 30 years of space launches
[AERONOMICA-ACTA-F-39-1989]
05 p0585 N90-13411
Optical properties monitor: Experiment definition phase
[NASA-CR-183836] 05 p0699 N90-14092
An implementation plan for priorities in solar-system space physics
[NASA-CR-185375] 05 p0710 N90-14154
Continuation of research in software for space operations support
[NASA-CR-186092] 06 p0827 N90-14808
Physical process in MPD plasmas
[AD-A213679] 07 p0996 N90-15761
Space operations: Listing of NASA scientific missions, 1980-2000. Fact sheet for the Chairman, Subcommittee on Space Science and Applications, Committee on Science, Space, and Technology, House of Representatives
[AD-A213493] 07 p1016 N90-15881
NASDA's approach to the interoperability of safety and rescue in space 08 p1035 N90-15981
The European long-term space plan: A basis for autonomy and cooperation 09 p1173 N90-16784
Major themes in the future of solar-terrestrial science
10 p1445 N90-18337
Pioneers 10 and 11 deep space missions
[NASA-TM-102269] 10 p1448 N90-18355
A perspective on the use of storable propellants for future space vehicle propulsion
11 p1472 N90-18473
Structures for remotely deployable precision antennas
12 p1609 N90-19256
A survey of advanced battery systems for space applications 13 p1822 N90-20458
Advanced rechargeable sodium batteries with novel cathodes 13 p1822 N90-20459
Nuclear technology and the space exploration missions
[NASA-TM-103156] 16 p2253 N90-22847
Romans to Mars
[NASA-TM-103094] 16 p2342 N90-23339
Performance analysis of CCSDS path service
[NASA-CR-180699] 17 p2364 N90-23457
Robotic simulation support to systems development
18 p2505 N90-24315
Space exploration: NASA's deep space missions are experiencing long delays
[GAO/NSIAD-88-128BR] 18 p2635 N90-25015
National Aeronautics and Space Administration, 3 May 1989 18 p2636 N90-25019
Astronautics and Aeronautics, 1979-1984: A chronology
[NASA-SP-4024] 19 p2800 N90-25928
Proceedings of the Second Symposium on GPS Applications in space, volume 1
[AD-A219978] 20 p2806 N90-25962
Proceedings of the Second Symposium on GPS Applications in Space, volume 2
[AD-A219979] 20 p2806 N90-25963
Space exploration: Cost, schedule, and performance of NASA's Mars Observer Mission. Fact sheet for the Chairman, Subcommittee on Science, Technology, and Space, Committee on Commerce, Science, and Transportation, US Senate
[GAO/NSIAD-88-137FS] 20 p2815 N90-26021
Preliminary subsystem designs for the Assured Crew Return Vehicle (ACRV), volume 1
[NASA-CR-186677-VOL-1] 20 p2818 N90-26039
Project LOCOST: Laser or Chemical Hybrid Orbital Space Transport
[NASA-CR-186822] 20 p2819 N90-26042
Long-range planning cost model for support of future space missions by the deep space network
20 p2854 N90-26231
New observations of stratospheric N2O5
[NASA-TM-103478] 20 p2883 N90-26402
A diagnosis system using object-oriented fault tree models 21 p3046 N90-27313
Upcoming planetary missions and the applicability of high temperature superconductor bolometers
22 p3140 N90-27811
Liquid lubrication in space
[NASA-RP-1240] 22 p3183 N90-28063
Formulation of design guidelines for automated robotic assembly in outerspace 23 p3365 N90-29017
Data catalog series for space science and applications flight missions. Volume 5A: Descriptions of astronomy, astrophysics, and solar physics spacecraft and investigations. Volume 5B: Descriptions of data sets from astronomy, astrophysics, and solar physics spacecraft and investigations
[NASA-TM-101908] 24 p3437 N90-29413
Data catalog series for space science and applications flight flight missions. Volume 2B: Descriptions of data sets from geostationary and high-altitude scientific spacecraft and investigations
[NASA-TM-101909] 24 p3437 N90-29414
Data catalog series for space science and applications flight missions. Volume 1A: Descriptions of planetary and heliocentric spacecraft and investigations, second edition
[NASA-TM-101910] 24 p3438 N90-29415
Data catalog series for space science and applications flight missions. Volume 6: Master index volume
[NASA-TM-101913] 24 p3438 N90-29416
Data catalog series for space science and applications flight missions. Volume 4B: Descriptions of data sets from meteorological and terrestrial applications spacecraft and investigations
[NASA-TM-101880] 24 p3556 N90-30123
Data catalog series for space science and applications flight missions. Volume 3B: Descriptions of data sets from low- and medium-altitude scientific spacecraft and investigations
[NASA-TM-89680] 24 p3560 N90-30140
Data catalog series for space science and applications flight missions. Volume 1B: Descriptions of data sets from planetary and heliocentric spacecraft and investigations
[NASA-TM-89695] 24 p3561 N90-30148
A guide to the National Space Science Data Center
[NASA-TM-89637] 24 p3565 N90-30167

SPACE NAVIGATION
NT INTERPLANETARY NAVIGATION
Independent Orbiter Assessment (IOA): Analysis of the guidance, navigation, and control subsystem
[NASA-CR-185555] 02 p0162 N90-10920
Independent Orbiter Assessment (IOA): Assessment of the guidance, navigation, and control subsystem FMEA/CIL
[NASA-CR-185552] 03 p0314 N90-11784
GOES I/M image navigation and registration 05 p0588 N90-13422
Shuttle relative navigation of a tethered satellite mission with current on board software 05 p0588 N90-13423
Impact of tether cutting on onboard navigation during the Tethered Satellite Mission-1 05 p0588 N90-13424
Microgravity conditions of a space vehicle 13 p1785 N90-20247
Galileo Earth approach navigation using connected-element interferometer phase-delay tracking 15 p2075 N90-21884
Using connected-element interferometer phase-delay data for Magellan navigation in Venus orbit 15 p2075 N90-21885
Location and Navigation Satellite Systems
[ISBN-2-85-428-242-6] 17 p2358 N90-23420
General principles of radionavigation: Space mapping 17 p2358 N90-23423
Orbit control for a regional navigation system based on tundra orbit
[AIAA-89-3619] 17 p2365 N90-23466
Proceedings of the Second Symposium on GPS Applications in space, volume 1
[AD-A219978] 20 p2806 N90-25962
Applications of different design methodologies in navigation systems and development at JPL 20 p2852 N90-26221
Theoretical specifications of the trajectory estimation for a space navigation system with the function of guidance and control
[NAL-TR-1032] 24 p3439 N90-29420

SPACE OBSERVATIONS (FROM EARTH)
VLA observations of the coronal plasma
[NASA-CR-186540] 14 p2042 N90-21711

SPACE PERCEPTION
Visual motion perception
[AD-A210994] 03 p0379 N90-12160
Visual acuity and stereopsis with night vision goggles
[AD-A211552] 03 p0381 N90-12167
Discriminating rigid from nonrigid motion
[AD-A211794] 03 p0383 N90-12180
Distance and clearance perception using forward-looking, vehicular television systems
[DE89-014740] 03 p0405 N90-12319
A Conference on Three-Dimensional Representation held in University of Minnesota on 24-26 May 1989
[AD-A211630] 03 p0406 N90-12324
Visual processing of object velocity and acceleration
[AD-A216509] 11 p1539 N90-18858
The effects of linear acceleration on perception and nystagmus 15 p2136 N90-22209
Visual sensitivities and discriminations and their role in aviation
[AD-A219319] 16 p2266 N90-22917
Spatial constraints of stereopsis in video displays 16 p2267 N90-22920
Stereoscopic distance perception 16 p2267 N90-22921
Seeing by exploring 16 p2268 N90-22923
The perception of three-dimensionality across continuous surfaces 16 p2268 N90-22924
Perceiving environmental properties from motion information: Minimal conditions 16 p2268 N90-22925
Spatial vision within egocentric and exocentric frames of reference 16 p2268 N90-22928
Separate visual representations for perception and for visually guided behavior 16 p2269 N90-22931
How to reinforce perception of depth in single two-dimensional pictures 16 p2270 N90-22937
Spatial issues in user interface design from a graphic design perspective 16 p2270 N90-22939
Determination of depth-viewing volumes for stereo three-dimensional graphic displays
[NASA-TP-2999] 16 p2275 N90-22965
Disparity gradients and depth scaling
[AD-A218612] 17 p2453 N90-23992
The incremental validity of spatial and perceptual-psychomotor tests relative to the armed services vocational aptitude battery
[AD-A220903] 18 p2585 N90-24719
Segmentation before and after reconstruction of 3-D surfaces in depth imagery
[RR-788-I-IMAG-97-LIFIA] 20 p2909 N90-26551
Non-linear analysis of visual cortical neurons
[AD-A221543] 21 p3034 N90-27250
A real-time optical 6D tracker for head-mounted display systems
[AD-A222884] 21 p3036 N90-27262

SPACE PHOTOGRAPHY
U SPACEBORNE PHOTOGRAPHY

SPACE PLASMAS
NT SOLAR WIND
NT STELLAR WINDS
Computer simulation of plasma interactions near Titan 01 p0142 N90-10816
Quantitative methods for waves in space plasmas
[PB89-210256] 02 p0280 N90-11599
Can ion acceleration by double-cyclotron absorption produce O(+) ion conics
[IRF-PREPRINT-114] 02 p0280 N90-11600
Numerical study of the current sheet and PSBL in a magnetotail model
[NASA-CR-183289] 02 p0293 N90-11669
COSTEP: A comprehensive suprathermal and energetic particle analyzer for SOHO 04 p0568 N90-13314
Research in cosmic and gamma ray astrophysics
[NASA-CR-185451] 04 p0569 N90-13316
Particle simulations in magnetospheric plasmas
[NASA-CR-186238] 06 p0848 N90-14934
Solar-geophysical data number 539, July 1989. Part 2: (Comprehensive reports). Data for January 1989, and miscellaneous
[PB89-235469] 06 p0866 N90-15034
Theory of interacting plasmas in space 07 p0993 N90-15742
Simulation of radial expansion of an electron beam injected into a background plasma
[NASA-CR-186188] 07 p0994 N90-15743
The dynamics of dust in planetary magnetospheres 08 p1149 N90-16658
Outline of high voltage solar array experiment using SFU platform 10 p1345 N90-17801
Solar arrays in the LEO-plasma environment: A model for leakage current phenomena deduced from experimental and theoretical studies 10 p1345 N90-17802
Report from space plasma science 10 p1445 N90-18336
Particle simulations in magnetospheric plasmas
[AD-A216256] 11 p1534 N90-18831
Active probing of space plasmas
[AD-A216867] 12 p1716 N90-19855
VLA observations of the coronal plasma
[NASA-CR-186540] 14 p2042 N90-21711
Equilibrium and stability analysis of magnetospheric plasmas 15 p2057 N90-21782
The intrinsic stochasticity of near-integrable Hamiltonian systems
[IPPCZ-282] 15 p2167 N90-22386
Plasma contactor research, 1989
[NASA-CR-185212] 15 p2168 N90-22389
NSSDC data listing
[NASA-TM-102989] 15 p2180 N90-22456
Space Station Freedom solar array panels plasma interaction test facility
[NASA-TM-102475] 15 p2186 N90-22488
Solar-geophysical data number 542, October 1989. Part 2: (Comprehensive reports). Data for April 1989 and miscellaneous
[PB90-148677] 15 p2193 N90-22521
International treaties and active experiments in space
[AD-A219366] 16 p2328 N90-23272
Solar flares and magnetospheric particles: Investigations based upon the ONR-602 and ONR-604 experiments
[AD-A218844] 16 p2340 N90-23332
Evaluation of space plasma data: Effects upon spacecraft materials and predictions of hazardous conditions; polar ARCS
[AD-A219509] 17 p2474 N90-24145
Plasma interactions and effects for large systems 19 p2735 N90-25545
Solar array arcing in plasmas 19 p2737 N90-25558
The iron abundance gradient in the intracluster medium of Perseus: A galactic wind model. Application to other clusters 19 p2793 N90-25901
Solar-geophysical data number 544, December 1989. Part 2 (Comprehensive reports). Data for June 1989 and miscellaneous
[PB90-171679] 22 p3264 N90-28482

SPACE PLATFORMS
NT COLUMBUS SPACE STATION
NT EURECA (ESA)
NT LONG DURATION EXPOSURE FACILITY
NT MAN TENDED FREE FLYERS
NT SPACE STATION POLAR PLATFORMS
NT SYNCHRONOUS PLATFORMS
Input-output oriented computation algorithms for the control of large flexible structures 01 p0023 N90-10118
On the analysis and optimization of a platform manipulator 07 p0938 N90-15433
The effects of natural and enhanced Van Allen Belt radiation on a space based weapon platform
[DE89-016219] 08 p1154 N90-16685
A power system for ARTEP 10 p1331 N90-17694
Outline of high voltage solar array experiment using SFU platform 10 p1345 N90-17801
Tracking a hypersonic aircraft from a space platform
[AD-A216399] 10 p1377 N90-17984
Major themes in the future of solar-terrestrial science 10 p1445 N90-18337
Orbital fluid resupply assessment 11 p1475 N90-18487
Modeling and control of flexible space platforms with articulated payloads 14 p1935 N90-21073
PLATO: A European plateform orbiter concept
[MBB-UO-0061/89-PUB] 19 p2652 N90-25095
Trajectory planning and control of a 6 DOF manipulator with Stewart platform-based mechanism
[NASA-CR-186813] 19 p2747 N90-25610
Advanced propulsion for LEO and GEO platforms
[NASA-TM-103228] 22 p3134 N90-27785
Guidance algorithms for a free-flying space robot 24 p3503 N90-29798

SPACE POWER REACTORS
NT SPACE POWER UNIT REACTORS
A feasibility assessment of installation, operation and disposal options for nuclear reactor power system concepts for a NASA growth space station
[NASA-TM-89923] 01 p0032 N90-10174
Creep strength of niobium alloys, Nb-1%Zr and PWC-11
[NASA-TM-102390] 03 p0326 N90-11854
Electrical performance characteristics of high power converters for space power applications
[NASA-CR-185947] 06 p0734 N90-14279
Introductory testimony: Hearing on nuclear power in space
[DE90-001137] 06 p0842 N90-14897
A review of gas-cooled reactor concepts for SDI (Strategic Defense Initiative)
[DE89-016962] 06 p0842 N90-14898
Power semiconductor devices for space nuclear power systems
[DE90-001178] 07 p1005 N90-15819
Dynamics analyses of space power systems using the salt code
[DE90-002274] 08 p1038 N90-15995
The onset of boiling of the liquid alkali metals
[DE90-002276] 08 p1044 N90-16036
Low risk low powrr heat pipe/thermoelectric space power supply
[DE89-014817] 08 p1095 N90-16342
Scaling study for SP-100 reactor technology
[NASA-TM-897140] 08 p1122 N90-16496
Model-reference adaptive control applied to loadfollowing of a space-nuclear power system
[DE89-014561] 10 p1429 N90-18245
Space nuclear safety program
[DE90-006436] 11 p1565 N90-19007
Analysis and evaluation of ZPPR (Zero Power Physics Reactor) critical experiments for a 100 kilowatt-electric space reactor
[DE90-005634] 12 p1713 N90-19835
Prevention of significant deterioration application for approval to construct SP-100 Ground Engineering System Test Site
[DE90-007986] 15 p2166 N90-22381
Nuclear technology and the space exploration missions
[NASA-TM-103156] 16 p2253 N90-22847
Nuclear power in space
[GPO-23-835] 16 p2316 N90-23202
National emissions standards for hazardous air pollutants application for approval of construction SP-100 ground engineering system test site
[DE90-007985] 16 p2316 N90-23203
Gas production and behavior in the coolant of the SP-100 space nuclear power system
[DE90-010674] 18 p2614 N90-24890
TFE verification program
[DE90-008227] 18 p2614 N90-24891
High-temperature superconductors for space power transmission lines
[NASA-TM-103459] 18 p2624 N90-24952
Multimegawatt space nuclear power supply, phase 1. Volume 2: Phase 2 plan D180-30619-6
[DE90-012431] 20 p2925 N90-26645
Multimegawatt space nuclear power supply, phase 1. Volume 3: Annotated outline of preliminary safety assessment D180-30619-7
[DE90-012432] 20 p2926 N90-26646

Multimegawatt space nuclear power supply, phase 1. Supplement: D180-30619-8
[DE90-012433] 20 p2926 N90-26647
SP-100 design, safety, and testing
[DE90-012643] 21 p3075 N90-27484
The effects of atomic oxygen on the thermal emittance of high temperature radiator surfaces
[NASA-TM-103224] 23 p3301 N90-28670

SPACE POWER UNIT REACTORS
SP-100 power system conceptual design for lunar base applications
[NASA-TM-102090] 06 p0866 N90-15030

SPACE PROBES
NT GALILEO SPACECRAFT
NT GIOTTO MISSION
NT JUPITER PROBES
NT MAGELLAN SPACECRAFT (NASA)
NT MARS OBSERVER
NT PIONEER 10 SPACE PROBE
NT PIONEER 11 SPACE PROBE
NT SOLAR PROBES
NT VIKING LANDER SPACECRAFT
NT VOYAGER 1 SPACECRAFT
NT VOYAGER 2 SPACECRAFT
The time evaluation of the number of space probes and debris at different orbit heights with a view to a future collision risk in space
[R-8718] 03 p0311 N90-11772
Preliminary results of the rocket and scatter experiments ROSE: Measurements with the newly designed spherical probe 05 p0659 N90-13850
Active probing of space plasmas
[AD-A216867] 12 p1716 N90-19855
High stability radio links 12 p1734 N90-19970
A spring-actuated spin and eject device for interplanetary missions 18 p2540 N90-24493
NASA/USRA university advanced design program at the University of Illinois for the 1989-1990 academic year
[NASA-CR-186829] 20 p2821 N90-26049

SPACE PROCESSING
Space Station Freedom: A foothold on the future
[NASA-NP-107/10-88] 02 p0159 N90-10907
Concepts for microgravity experiments utilizing gloveboxes
[NASA-TM-100378] 02 p0209 N90-11195
On-orbit annealing of gallium arsenide solar cell arrays
[AD-A212087] 03 p0334 N90-11900
Development of a shuttle recovery Commercial Materials Processing in Space (CMPS) program
[NASA-CR-183720] 05 p0630 N90-13678
Materials processing in low gravity
[NASA-CR-183733] 06 p0755 N90-14397
Extravehicular activity welding experiment
[NASA-CR-183848] 06 p0791 N90-14608
Non-contact temperature measurement requirements of ground-based research and flight programs at JPL 10 p1362 N90-17895
Comments on containerless bulk crystal growth and epitaxy in space and on their implications regarding non-contact temperature measurements 10 p1365 N90-17911
Non-Contact Temperature Requirements (NCTM) for drop and bubble physics 10 p1366 N90-17918
Small business innovation research. Abstracts of 1988 phase 1 awards
[NASA-TM-102991] 14 p2036 N90-21680
Small business innovation research. Abstracts of completed 1987 phase 1 projects
[NASA-TM-101797] 14 p2036 N90-21681
Space Station Workshop: Commercial Missions and User Requirements
[NASA-TM-102912] 15 p2175 N90-22428
Solidification of dilute alloys under fluctuating residual gravity
[REPT-892-430-112] 17 p2377 N90-23535
Consortium for materials development in space
[NASA-CR-186534] 17 p2383 N90-23575
Space Station Freedom Pre-Workshop Session
[NASA-TM-102913] 17 p2479 N90-24172
Research and technology 1989
[NASA-TM-100369] 17 p2486 N90-24219
Fluid Phase Separation (FPS) experiment for flight on a space shuttle Get Away Special (GAS) canister
[NASA-CR-186830] 20 p2841 N90-26161
Noncontact measurement of high temperature using optical fiber sensors
[NASA-CR-186975] 23 p3329 N90-28825
Scientific Colloquium in Honor of Prof. Dr. Rer. Nat. Hermann L. Jordan
[ESA-TT-1101] 23 p3391 N90-29159
Microgravitation experiments in space: Compatibility with interfering dynamic influences 23 p3392 N90-29162
Influence of convection on microstructure
[NASA-CR-186506] 24 p3448 N90-29470
A lunar space station
[NASA-CR-186223] 24 p3563 N90-30158

SPACE PROGRAMS
NT BRAZILIAN SPACE PROGRAM
NT CHINESE SPACE PROGRAM
NT EUROPEAN SPACE PROGRAMS
NT FRENCH SPACE PROGRAM
NT GALILEO PROJECT
NT GEOGRAPHIC APPLICATIONS PROGRAM
NT INDIAN SPACE PROGRAM
NT ITALIAN SPACE PROGRAM
NT JAPANESE SPACE PROGRAM
NT MAGELLAN PROJECT (NASA)
NT NASA SPACE PROGRAMS
NT PIONEER PROJECT
NT PROJECT SETI
NT SCOUT PROJECT
NT SEASAT PROGRAM
NT SWEDISH SPACE PROGRAM
NT U.S.S.R. SPACE PROGRAM
NT VIKING MARS PROGRAM
NT VOYAGER PROJECT
Federal Radionavigation Plan, 1988
[PB89-163075] 02 p0148 N90-10846
Recommended changes in US military space policies and programs: A paper submitted to the Commission on Integrated Long-Term Strategy
[PB89-219364] 04 p0460 N90-12636
Development of a shuttle recovery Commercial Materials Processing in Space (CMPS) program
[NASA-CR-183720] 05 p0630 N90-13678
European Rocket and Balloon Programs and Related Research
[ESA-SP-291] 05 p0656 N90-13826
An international discussion on research in solar and space physics 06 p0859 N90-14996
Crew Safety and Rescue in Space: An International Approach
[ESA-SP-300] 08 p1034 N90-15974
Progress in Space Transportation
[ESA-SP-293] 09 p1173 N90-16782
Financial and commercial issues: A customer's perspective 09 p1174 N90-16794
Legal aspects of commercial space transportation 09 p1175 N90-16796
Comparison between horizontally launched air-breathing single and two-stage to orbit space vehicles 09 p1175 N90-16802
Purchase of technology 11 p1576 N90-19072
The bringing to market of the RF alert (a case study in technology transfer) 11 p1576 N90-19073
Compendium of meteorological space programs, satellites, and experiments
[NASA-TM-102924] 12 p1607 N90-19243
Antennas for 20/30 GHz and beyond 12 p1611 N90-19269
Development and application of nonflammable, high-temperature beta fibers
[NASA-TM-102158] 13 p1855 N90-20645
Reorganization of the German space administration. Foundation of DARA
[REPT-16/89] 13 p1899 N90-20902
Aeronautics and space report of the President: 1987 activities 15 p2181 N90-22462
The International Space University
[NASA-TM-103163] 16 p2209 N90-22604
Technical accomplishments of the NASA Lewis Research Center, 1989
[NASA-TM-102296] 17 p2486 N90-24220
Theoretical studies of solar pumped lasers
[NASA-CR-186712] 20 p2867 N90-26308
Space program safety: Funding for NASA's safety organizations should be centralized
[GAO/NSIAD-90-187] 22 p3255 N90-28434
Structured analysis of the applicability of A and R technologies in space programs
[MBB-UO-0084-90-PUB] 22 p3256 N90-28436
Impact of the whole national economy of defense spending and space in the US: A literature analysis
[ISSN-0342-0787] 22 p3260 N90-28464

SPACE RADIATION
U EXTRATERRESTRIAL RADIATION

SPACE RADIATORS
U SPACECRAFT RADIATORS

SPACE RENDEZVOUS
NT ORBITAL RENDEZVOUS
Active rendezvous between a low-earth orbit user spacecraft and the Space Transportation System (STS) shuttle 05 p0590 N90-13436
Crew Safety and Rescue in Space: An International Approach
[ESA-SP-300] 08 p1034 N90-15974
Systems interoperability approach Apollo/Soyuz test project 08 p1035 N90-15979
RVD scenari and interfaces between Hermes and space station 08 p1035 N90-15982
A homotopy approach to the solutions of minimum-fuel space-flight rendezvous problems 14 p1931 N90-21053
GPS navigational performance in space rendezvous operations 18 p2504 N90-24310
Satellite servicer system flight demonstration program 18 p2506 N90-24322
Genetic algorithm based fuzzy control of spacecraft autonomous rendezvous 21 p3041 N90-27281

SPACE SCIENCES
U AEROSPACE SCIENCES

SPACE SHUTTLE ASCENT STAGE
Flight Motor Set 360L003 (STS-29R)
[NASA-CR-183739-VOL-1] 01 p0031 N90-10170
Atmospheric environment for space shuttle (STS-29) launch
[NASA-TM-100376] 02 p0175 N90-10980
Atmospheric environment for space shuttle (STS-30) launch
[NASA-TM-100381] 02 p0175 N90-10981
On computations of the integrated space shuttle flowfield using overset grids
[NASA-CR-186927] 22 p3124 N90-27734
Atmospheric environment for Space Shuttle (STS-32) launch
[NASA-TM-100400] 23 p3346 N90-28912
Atmospheric environment for Space Shuttle (STS-31) launch
[NASA-TM-103508] 23 p3347 N90-28913
Atmospheric environment for space shuttle (STS-36) launch
[NASA-TM-100403] 23 p3347 N90-28914
Atmospheric environment for space shuttle (STS-34) launch
[NASA-TM-100396] 23 p3347 N90-28915

SPACE SHUTTLE BOOSTERS
NT ADVANCED SOLID ROCKET MOTOR (STS)
Flight set 360T004 (STS-30) insulation component, interim release, volume 3
[NASA-CR-183746] 01 p0031 N90-10169
Flight Motor Set 360L003 (STS-29R)
[NASA-CR-183739-VOL-1] 01 p0031 N90-10170
Generic system components of the Thiokol ultrasonic RSRM case-to-insulation bondline inspection system
[NASA-CR-183738] 01 p0031 N90-10171
Flight motor set 360L001 (STS-26R). (Reconstructed dynamic loads analysis)
[NASA-CR-183811] 04 p0464 N90-12656
Cable coupling lightning transient qualification
[NASA-CR-183826] 05 p0584 N90-13405
Development of a shuttle plume radiation heating indicator
[NASA-CR-183679] 05 p0614 N90-13584
RSRM nozzle fixed housing cooldown test
[NASA-CR-183741] 05 p0614 N90-13587
Qualification of improved joint heaters
[NASA-CR-183827] 05 p0616 N90-13594
SRB thermal environments
[NASA-CR-183801] 06 p0734 N90-14276
HCl monitor, phase 2
[AD-A213572] 07 p0958 N90-15542
Space shuttle solid rocket booster redesign and testing 09 p1175 N90-16804
The 1989 JANNAF Propulsion Meeting, volume 1
[CPIA-PUBL-515-VOL-1] 11 p1470 N90-18462
Transient pressure test article test program 11 p1470 N90-18463
Test data of flow field of shuttle SRM nozzle joint with bond defects, using unheated air 11 p1470 N90-18464
Cold flow determination of the internal flow environment around the submerged TVC nozzle for the space shuttle SRM 11 p1470 N90-18465
Technique for evaluating the erosive properties of ablative internal insulation materials 11 p1471 N90-18466
Aerospace Safety Advisory Panel
[NASA-TM-101748] 12 p1634 N90-19389
Development of inspection techniques for quantitatively measuring surface contamination on SRM hardware
[NASA-CR-183902] 12 p1673 N90-19608
Compendium of fracture mechanics problems
[NASA-TM-100393] 14 p1992 N90-21414
Space Shuttle, NASA's major changes to flight hardware: Fact sheet for the Chairman, Committee on Science, Space, and Technology, House of Representatives
[GAO/NSIAD-88-173FS] 15 p2181 N90-22461
Space shuttle: Changes to the solid rocket motor contract
[GAO/NSIAD-88-203] 18 p2636 N90-25016
QM-8 final performance evaluation report: SEALS, volume 4
[NASA-CR-183958] 20 p2869 N90-26324
Accuracy analysis of the space shuttle solid rocket motor profile measuring device
[NASA-TM-101131] 21 p2968 N90-26871

QM-6 final performance evaluation report igniter, volume 6
[NASA-CR-184001] 22 p3133 N90-27779
Liquid Rocket Booster (LRB) for the Space Transportation System (STS) systems study. Appendix C: Battery report for the liquid rocket booster TVC actuators
[NASA-CR-183789-APP-C] 23 p3288 N90-28603
Flight motor set 360L008 (STS-32R). Volume 1: System overview
[NASA-CR-184010] 23 p3289 N90-28609
Operational cost drivers 23 p3294 N90-28636

SPACE SHUTTLE MAIN ENGINE
X-ray spectroscopy of the SSME plume
[NASA-CR-185308] 01 p0031 N90-10168
Independent Orbiter Assessment (IOA): Analysis of the orbiter main propulsion system
[NASA-CR-185584] 02 p0164 N90-10927
Independent Orbiter Assessment (IOA): Assessment of the orbiter main propulsion system FMEA/CIL, volume 1
[NASA-CR-185559-VOL-1] 03 p0312 N90-11775
Independent Orbiter Assessment (IOA): Assessment of the main propulsion subsystem FMEA/CIL, volume 2
[NASA-CR-185559-VOL-2] 03 p0313 N90-11776
Independent Orbiter Assessment (IOA): Assessment of the main propulsion subsystem FMEA/CIL, volume 3
[NASA-CR-185559-VOL-3] 03 p0313 N90-11777
Independent Orbiter Assessment (IOA): Assessment of the main propulsion subsystem FMEA/CIL, volume 4
[NASA-CR-185559-VOL-4] 03 p0313 N90-11778
Computation of viscous incompressible flows
[NASA-TM-101090] 05 p0572 N90-13329
SSME LOX post flow analysis/fluid structure interaction. Volume 1: Flow analysis
[NASA-CR-183677] 05 p0637 N90-13715
SSME LOX post flow analysis/fluid structure interaction. Volume 2: Fluid structure interaction
[NASA-CR-183678] 05 p0637 N90-13716
Software development for avionics SSME control and diagnostics
[NASA-CR-184894] 05 p0681 N90-13964
The 59th Shock and Vibration Symposium, volume 3
[AD-A214580] 10 p1395 N90-18066
Experimental flow models for SSME flowfield characterization 11 p1471 N90-18469
Aerospace Safety Advisory Panel
[NASA-TM-101748] 12 p1634 N90-19389
A parametric heat transfer study for cryogenic ball bearings in SSME HPOTP 12 p1635 N90-19397
Investigation of SSME alternate high pressure fuel turbopump lift-off seal fluid and structural dynamic interaction 12 p1636 N90-19400
A study of the effects of disk flexibility on the rotordynamics of the space shuttle main engine turbo-pumps 12 p1636 N90-19401
Iterative procedures for space shuttle main engine performance models 12 p1639 N90-19416
Numerical simulation methods of incompressible flows and an application to the space shuttle main engine
[NASA-TM-100038] 13 p1800 N90-20333
A parallel architecture for real-time simulation
[AD-A218321] 13 p1873 N90-20741
Compendium of fracture mechanics problems
[NASA-TM-100393] 14 p1992 N90-21414
Framework for a space shuttle main engine health monitoring system
[NASA-CR-185224] 15 p2061 N90-21809
Space Shuttle, NASA's major changes to flight hardware: Fact sheet for the Chairman, Committee on Science, Space, and Technology, House of Representatives
[GAO/NSIAD-88-173FS] 15 p2181 N90-22481
Heat transfer and pressure measurements for the SSME fuel-side turbopump
[NASA-CR-184928] 17 p2355 N90-23405
Health management system for rocket engines
[NASA-CR-185223] 17 p2383 N90-23574
The effects of Reynolds number, rotor incidence angle, and surface roughness on the heat transfer distribution in a large-scale turbine rotor passage
[NASA-CR-183891] 17 p2410 N90-23731
Rocket combustion chamber life-enhancing design concepts
[NASA-CR-185257] 19 p2669 N90-25183
LOX manifold tee analysis
[NASA-CR-183994] 19 p2670 N90-25188
Digital filtering of plume emission spectra
[NASA-TM-103135] 20 p2824 N90-26070
Reusable rocket engine turbopump health monitoring system, part 3
[NASA-CR-182294] 20 p2869 N90-26320
The structural dynamics analysis of the main injector LOX inlet tee and its redesign
[NASA-CR-186764] 20 p2875 N90-26358
Space Shuttle 2 advanced space transportation system, volume 2
[NASA-CR-185953] 21 p2965 N90-26854
Object oriented fault diagnosis system for space shuttle main engine redlines 21 p3046 N90-27315
Inductive knowledge acquisition experience with commercial tools for space shuttle main engine testing 21 p3048 N90-27326
Multi-sensor analysis techniques for SSME safety monitoring
[NASA-CR-185260] 22 p3124 N90-27732
Reliability growth modeling analysis of the space shuttle main engines based upon the Weibull process
[NASA-TM-103511] 22 p3189 N90-28098
A comparison of single-cycle versus multiple-cycle proof testing strategies
[NASA-CR-4318] 22 p3193 N90-28115
The space transportation main engine phase A' study
[NASA-CR-179399] 23 p3290 N90-28610
Probabilistic structural analysis methods development for SSME 23 p3291 N90-28616
Determination of the SSME high pressure oxidizer turbopump bearing temperature 23 p3291 N90-28619
Cryogenic, high speed, turbopump bearing cooling requirements 23 p3291 N90-28620
Bearing optimization for SSME HPOTP application 23 p3292 N90-28622
Development of improved self lubricating cages for SSME HPOTP bearings 23 p3292 N90-28623
Cage stability analysis for SSME HPOTP bearings 23 p3292 N90-28625
Rocketdyne LOX bearing tester program 23 p3293 N90-28626
Structural response of SSME turbine blade airfoils 23 p3297 N90-28649
A failure diagnosis system based on a neural network classifier for the space shuttle main engine
[NASA-TM-103607] 23 p3299 N90-28659

SPACE SHUTTLE MISSION 41-G
Mission report on the Orbiter Camera Payload System (OCPS) Large Format Camera (LFC) and Attitude Reference System (ARS)
[NASA-CR-186273] 09 p1240 N90-17197

SPACE SHUTTLE MISSION 51-J
Debris/ice/TPS assessment and photographic analysis for Shuttle Mission STS-28R
[NASA-TM-102152] 01 p0016 N90-10079

SPACE SHUTTLE MISSION 51-L
GPHS-RTG response to Challenger type accident 19 p2665 N90-25163
Atmospheric environment for space shuttle (STS-33) launch
[NASA-TM-100399] 22 p3200 N90-28159

SPACE SHUTTLE MISSION 61-A
Atmospheric environment for space shuttle (STS-29) launch
[NASA-TM-100376] 02 p0175 N90-10980
Atmospheric environment for space shuttle (STS-30) launch
[NASA-TM-100381] 02 p0175 N90-10981

SPACE SHUTTLE MISSION 61-B
Atmospheric environment for Space Shuttle (STS-31) launch
[NASA-TM-103508] 23 p3347 N90-28913

SPACE SHUTTLE MISSION 61-C
Flight motor set 360L008 (STS-32R). Volume 1: System overview
[NASA-CR-184010] 23 p3289 N90-28609
Atmospheric environment for Space Shuttle (STS-32) launch
[NASA-TM-100400] 23 p3346 N90-28912

SPACE SHUTTLE MISSION 61-E
Debris/ice/TPS assessment and photographic analysis for Shuttle Mission STS-34
[NASA-TM-102153] 05 p0594 N90-13447
Atmospheric environment for space shuttle (STS-34) launch
[NASA-TM-100396] 23 p3347 N90-28915

SPACE SHUTTLE MISSIONS
NT SPACE SHUTTLE MISSION 41-G
NT SPACE SHUTTLE MISSION 51-J
NT SPACE SHUTTLE MISSION 51-L
NT SPACE SHUTTLE MISSION 61-A
NT SPACE SHUTTLE MISSION 61-B
NT SPACE SHUTTLE MISSION 61-C
NT SPACE SHUTTLE MISSION 61-E
Flight Motor Set 360L003 (STS-29R)
[NASA-CR-183739-VOL-1] 01 p0031 N90-10170
Shuttle Atlantis to deploy Galileo probe toward Jupiter
[NASA-TM-101888] 02 p0175 N90-10982
Shuttle relative navigation of a tethered satellite mission with current on board software 05 p0588 N90-13423
Syncom 4 deploy, LDEF retrieval highlight 10-day Columbia flight
[NASA-NEWS-RELEASE-89-180] 05 p0594 N90-13448
Get Away Special: The first ten years
[NASA-TM-102921] 09 p1171 N90-16775
Debris/ice/TPS assessment and photographic analysis for Shuttle Mission STS-33R
[NASA-TM-102785] 09 p1180 N90-16846
Major themes in the future of solar-terrestrial science 10 p1445 N90-18337
Aerospace Safety Advisory Panel
[NASA-TM-101748] 12 p1634 N90-19389
Seeing in a new light: Astro-1 teacher's guide with activities
[NASA-EP-274] 13 p1899 N90-20900
Launching a dream: A teachers guide to a simulated space shuttle mission
[NASA-TM-89715] 20 p2934 N90-26693
Atmospheric environment for space shuttle (STS-36) launch
[NASA-TM-100403] 23 p3347 N90-28914

SPACE SHUTTLE ORBITAL FLIGHT TESTS
U SPACE TRANSPORTATION SYSTEM FLIGHTS

SPACE SHUTTLE ORBITAL FLIGHTS
U SPACE TRANSPORTATION SYSTEM FLIGHTS

SPACE SHUTTLE ORBITER 099
U CHALLENGER (ORBITER)

SPACE SHUTTLE ORBITER 102
U COLUMBIA (ORBITER)

SPACE SHUTTLE ORBITER 104
U ATLANTIS (ORBITER)

SPACE SHUTTLE ORBITERS
NT ATLANTIS (ORBITER)
NT CHALLENGER (ORBITER)
NT COLUMBIA (ORBITER)
Independent Orbiter Assessment (IOA): Analysis of the manned maneuvering unit
[NASA-CR-185565] 02 p0161 N90-10913
Independent Orbiter Assessment (IOA): Assessment of the electrical power generation/fuel cell powerplant subsystem FMEA/CIL
[NASA-CR-185562] 02 p0161 N90-10914
Independent Orbiter Assessment (IOA): Analysis of the electrical power generation/fuel cell powerplant subsystem
[NASA-CR-185561] 02 p0161 N90-10915
Independent Orbiter Assessment (IOA): Analysis of the rudder/speed brake subsystem
[NASA-CR-185560] 02 p0161 N90-10916
Independent Orbiter Assessment (IOA): Assessment of the data processing system FMEA/CIL
[NASA-CR-185546] 02 p0162 N90-10917
Independent Orbiter Assessment (IOA): Analysis of the electrical power generation/power reactant storage and distribution subsystem
[NASA-CR-185556] 02 p0162 N90-10918
Independent Orbiter Assessment (IOA): Analysis of the orbital maneuvering system
[NASA-CR-185554] 02 p0162 N90-10919
Independent Orbiter Assessment (IOA): Analysis of the guidance, navigation, and control subsystem
[NASA-CR-185555] 02 p0162 N90-10920
Independent Orbiter Assessment (IOA): Analysis of the nose wheel steering subsystem
[NASA-CR-185548] 02 p0163 N90-10921
Independent Orbiter Assessment (IOA): FMEA/CIL instructions and ground rules
[NASA-CR-185551] 02 p0163 N90-10922
Independent Orbiter Assessment (IOA): Assessment of the electrical power generation/power reactant storage and distribution subsystem FMEA/CIL
[NASA-CR-185545] 02 p0163 N90-10923
Independent Orbiter Assessment (IOA): Analysis of the DPS subsystem
[NASA-CR-185549] 02 p0163 N90-10924
Independent Orbiter Assessment (IOA): Analysis of the atmospheric revitalization pressure control subsystem
[NASA-CR-185593] 02 p0163 N90-10925
Independent Orbiter Assessment (IOA): Analysis of the remote manipulator system
[NASA-CR-185585] 02 p0164 N90-10926
Independent Orbiter Assessment (IOA): Analysis of the orbiter main propulsion system
[NASA-CR-185584] 02 p0164 N90-10927
Independent Orbiter Assessment (IOA): Analysis of the instrumentation subsystem
[NASA-CR-185571] 02 p0164 N90-10928
Independent Orbiter Assessment (IOA): Analysis of the ascent thrust vector control actuator subsystem
[NASA-CR-185579] 02 p0164 N90-10929
Independent Orbiter Assessment (IOA): Analysis of the body flap subsystem
[NASA-CR-185574] 02 p0165 N90-10930
Independent Orbiter Assessment (IOA): Analysis of the auxiliary power unit
[NASA-CR-185568] 02 p0165 N90-10931
Independent Orbiter Assessment (IOA): Analysis of the backup flight system
[NASA-CR-185567] 02 p0165 N90-10932

Independent Orbiter Assessment (IOA): Analysis of the electrical power distribution and control/electrical power generation subsystem
[NASA-CR-185538] 02 p0165 N90-10933
Independent Orbiter Assessment (IOA): Analysis of the hydraulics/water spray boiler subsystem
[NASA-CR-185541] 02 p0165 N90-10934
Independent Orbiter Assessment (IOA): Analysis of the elevon subsystem
[NASA-CR-185576] 02 p0166 N90-10935
Independent Orbiter Assessment (IOA): Analysis of the electrical power distribution and control/remote manipulator system subsystem
[NASA-CR-185526] 02 p0166 N90-10936
Independent Orbiter Assessment (IOA): Analysis of the extravehicular mobility unit
[NASA-CR-185540] 02 p0166 N90-10937
Independent Orbiter Assessment (IOA): Analysis of the reaction control system, volume 1
[NASA-CR-185532-VOL-1] 02 p0166 N90-10938
Independent Orbiter Assessment (IOA): Analysis of the reaction control system, volume 2
[NASA-CR-185532-VOL-2] 02 p0167 N90-10939
Independent Orbiter Assessment (IOA): Analysis of the reaction control system, volume 3
[NASA-CR-185532-VOL-3] 02 p0167 N90-10940
Independent Orbiter Assessment (IOA): Analysis of the electrical power distribution and control subsystem, volume 1
[NASA-CR-185529-VOL-1] 02 p0167 N90-10941
Independent Orbiter Assessment (IOA): Analysis of the electrical power distribution and control subsystem, volume 2
[NASA-CR-185529-VOL-2] 02 p0167 N90-10942
Independent Orbiter Assessment (IOA): Analysis of the landing/deceleration subsystem
[NASA-CR-185569] 02 p0167 N90-10943
Independent Orbiter Assessment (IOA): Analysis of the mechanical actuation subsystem
[NASA-CR-185525] 02 p0168 N90-10944
Independent Orbiter Assessment (IOA): Analysis of the pyrotechnics subsystem
[NASA-CR-185530] 02 p0168 N90-10945
Independent Orbiter Assessment (IOA): Assessment of the pyrotechnics subsystem
[NASA-CR-185531] 02 p0168 N90-10946
Independent Orbiter Assessment (IOA): Assessment of the nose wheel steering subsystem
[NASA-CR-185533] 02 p0168 N90-10947
Independent Orbiter Assessment (IOA): Weibull analysis report
[NASA-CR-185534] 02 p0168 N90-10948
Independent Orbiter Assessment (IOA): Assessment of the purge, vent and drain subsystem
[NASA-CR-185535] 02 p0168 N90-10949
Independent Orbiter Assessment (IOA): Assessment of the extravehicular mobility unit, volume 1
[NASA-CR-185536-VOL-1] 02 p0169 N90-10950
Independent Orbiter Assessment (IOA): Assessment of the extravehicular mobility unit, volume 2
[NASA-CR-185536-VOL-2] 02 p0169 N90-10951
Independent Orbiter Assessment (IOA): Assessment of the mechanical actuation subsystem, volume 1
[NASA-CR-185527-VOL-1] 02 p0169 N90-10952
Independent Orbiter Assessment (IOA): Assessment of the mechanical actuation subsystem, volume 2
[NASA-CR-185527-VOL-2] 02 p0169 N90-10953
Independent Orbiter Assessment (IOA): CIL issues resolution report, volume 1
[NASA-CR-185524-VOL-1] 02 p0169 N90-10954
Independent Orbiter Assessment (IOA): CIL issues resolution report, volume 2
[NASA-CR-185524-VOL-2] 02 p0170 N90-10955
Independent Orbiter Assessment (IOA) CIL issues resolution report, volume 3
[NASA-CR-185524-VOL-3] 02 p0170 N90-10956
Independent Orbiter Assessment (IOA): Assessment of the atmospheric revitalization pressure control subsystem FMEA/CIL
[NASA-CR-185594] 02 p0170 N90-10957
Independent Orbiter Assessment (IOA): Analysis of the crew equipment subsystem
[NASA-CR-185591] 02 p0170 N90-10958
Independent Orbiter Assessment (IOA): Assessment of the ascent thrust vector control actuator subsystem FMEA/CIL
[NASA-CR-185590] 02 p0170 N90-10959
Independent Orbiter Assessment (IOA): FMEA/CIL assessment
[NASA-CR-185589] 02 p0170 N90-10960
Independent Orbiter Assessment (IOA): Assessment of the displays and controls subsystem
[NASA-CR-185588] 02 p0171 N90-10961
Independent Orbiter Assessment (IOA): Assessment of the Orbiter Experiment (OEX) subsystem
[NASA-CR-185587] 02 p0171 N90-10962
Independent Orbiter Assessment (IOA): Analysis of the Orbiter Experiment (OEX) subsystem
[NASA-CR-185586] 02 p0171 N90-10963
Independent Orbiter Assessment (IOA): Assessment of the remote manipulator system FMEA/CIL
[NASA-CR-185592] 02 p0171 N90-10964
Independent Orbiter Assessment (IOA): Assessment of the EPD and C/remote manipulator system FMEA/CIL
[NASA-CR-185583] 02 p0172 N90-10965
Independent Orbiter Assessment (IOA): Assessment of the landing/deceleration (LDG/DEC) subsystem FMEA/CIL
[NASA-CR-185570] 02 p0172 N90-10966
Independent Orbiter Assessment (IOA): Analysis of the communication and tracking subsystem
[NASA-CR-185582] 02 p0172 N90-10967
Independent Orbiter Assessment (IOA): Assessment of the body flap subsystem FMEA/CIL
[NASA-CR-185575] 02 p0172 N90-10968
Independent Orbiter Assessment (IOA): Analysis of the purge, vent and drain subsystem
[NASA-CR-185547] 02 p0172 N90-10969
Independent Orbiter Assessment (IOA): Assessment of the elevon actuator subsystem FMEA/CIL
[NASA-CR-185578] 02 p0173 N90-10970
Independent Orbiter Assessment (IOA): Assessment of the crew equipment subsystem
[NASA-CR-185577] 02 p0173 N90-10971
Independent Orbiter Assessment (IOA): Assessment of instrumental subsystem FMEA/CIL
[NASA-CR-185572] 02 p0173 N90-10972
Independent Orbiter Assessment (IOA): Assessment of the backup flight system FMEA/CIL
[NASA-CR-185566] 02 p0173 N90-10973
Independent Orbiter Assessment (IOA): Assessment of the manned maneuvering unit
[NASA-CR-185564] 02 p0173 N90-10974
Independent Orbiter Assessment (IOA): Assessment of the rudder/speed brake subsystem FMEA/CIL
[NASA-CR-185558] 02 p0174 N90-10975
Independent Orbiter Assessment (IOA): Assessment of the auxiliary power unit
[NASA-CR-185580] 02 p0174 N90-10976
Independent Orbiter Assessment (IOA): Assessment of the life support and airlock support systems, volume 1
[NASA-CR-185581-VOL-1] 02 p0174 N90-10977
Independent Orbiter Assessment (IOA): Assessment of the life support and airlock support systems, volume 2
[NASA-CR-185581-VOL-2] 02 p0174 N90-10978
Independent Orbiter Assessment (IOA): Assessment of the active thermal control system
[NASA-CR-185573] 02 p0174 N90-10979
Automated stress analysis of Shuttle orbiter thermal protection system 02 p0184 N90-11043
Independent Orbiter Assessment (IOA): Analysis of the displays and controls subsystem
[NASA-CR-185563] 03 p0312 N90-11774
Independent Orbiter Assessment (IOA): Assessment of the orbiter main propulsion system FMEA/CIL, volume 1
[NASA-CR-185559-VOL-1] 03 p0312 N90-11775
Independent Orbiter Assessment (IOA): Assessment of the main propulsion subsystem FMEA/CIL, volume 2
[NASA-CR-185559-VOL-2] 03 p0313 N90-11776
Independent Orbiter Assessment (IOA): Assessment of the main propulsion subsystem FMEA/CIL, volume 3
[NASA-CR-185559-VOL-3] 03 p0313 N90-11777
Independent Orbiter Assessment (IOA): Assessment of the main propulsion subsystem FMEA/CIL, volume 4
[NASA-CR-185559-VOL-4] 03 p0313 N90-11778
Independent Orbiter Assessment (IOA): Assessment of the electrical power distribution and control subsystem, volume 1
[NASA-CR-185557-VOL-1] 03 p0313 N90-11779
Independent Orbiter Assessment (IOA): Assessment of the electrical power distribution and control subsystem, volume 2
[NASA-CR-185557-VOL-2] 03 p0313 N90-11780
Independent Orbiter Assessment (IOA): Assessment of the electrical power distribution and control subsystem, volume 3
[NASA-CR-185557-VOL-3] 03 p0313 N90-11781
Independent Orbiter Assessment (IOA): Analysis of the active thermal control subsystem
[NASA-CR-185553] 03 p0314 N90-11782
Independent Orbiter Assessment (IOA): FMEA/CIL assessment
[NASA-CR-185550] 03 p0314 N90-11783
Independent Orbiter Assessment (IOA): Assessment of the guidance, navigation, and control subsystem FMEA/CIL
[NASA-CR-185552] 03 p0314 N90-11784
Independent Orbiter Assessment (IOA): Assessment of the Electrical Power Distribution and Control/Electrical Power Generation (EPD and C/EPG) FMEA/CIL
[NASA-CR-185542] 03 p0314 N90-11785
Independent Orbiter Assessment (IOA): Analysis of the life support and airlock support subsystems
[NASA-CR-185539] 03 p0314 N90-11786
Independent Orbiter Assessment (IOA): Assessment of the orbital maneuvering system FMEA/CIL, volume 1
[NASA-CR-185544-VOL-1] 03 p0315 N90-11787
Independent Orbiter Assessment (IOA): Assessment of the orbital maneuvering subsystem, volume 2
[NASA-CR-185544-VOL-2] 03 p0315 N90-11788
Independent Orbiter Assessment (IOA): Assessment of the communication and tracking subsystem, volume 1
[NASA-CR-185528-VOL-1] 03 p0315 N90-11789
Independent Orbiter Assessment (IOA): Assessment of the communication and tracking subsystem, volume 2
[NASA-CR-185528-VOL-2] 03 p0315 N90-11790
Independent Orbiter Assessment (IOA): Assessment of the communication and tracking subsystem, volume 3
[NASA-CR-185528-VOL-3] 03 p0315 N90-11791
Independent Orbiter Assessment (IOA): Assessment of the hydraulics/water spray boiler subsystem
[NASA-CR-185537] 03 p0316 N90-11792
Independent Orbiter Assessment (IOA): Assessment of the reaction control system, volume 1
[NASA-CR-185543-VOL-1] 03 p0316 N90-11793
Independent Orbiter Assessment (IOA): Assessment of the reaction control system, volume 2
[NASA-CR-185543-VOL-2] 03 p0316 N90-11794
Independent Orbiter Assessment (IOA): Assessment of the reaction control system, volume 3
[NASA-CR-185543-VOL-3] 03 p0316 N90-11795
Independent Orbiter Assessment (IOA): Assessment of the reaction control system, volume 4
[NASA-CR-185543-VOL-4] 03 p0316 N90-11796
Independent Orbiter Assessment (IOA): Assessment of the reaction control system, volume 5
[NASA-CR-185543-VOL-5] 03 p0316 N90-11797
Debris/ice/TPS assessment and photographic analysis for Shuttle Mission STS-34
[NASA-TM-102153] 05 p0594 N90-13447
Control of an experiment to measure acoustic noise in the space shuttle
[NPS62-89-022] 06 p0838 N90-14869
Conceptual design of a moving belt radiator shuttle-attached experiments: Technical requirement Document
[NASA-CR-185168] 08 p1038 N90-15996
Cooperative control of two active spacecraft during proximity operations
[NASA-CR-185596] 09 p1172 N90-16778
US Space Shuttle evolution 09 p1178 N90-16829
Orbital fluid resupply assessment
11 p1475 N90-18487
Aerospace Safety Advisory Panel
[NASA-TM-101748] 12 p1634 N90-19389
Modeling and analysis of the space shuttle nose-gear tire with semianalytic finite elements
[NASA-TP-2977] 12 p1670 N90-19595
Prediction of forces and moments for flight vehicle control effectors. Part 1: Validation of methods for predicting hypersonic vehicle controls forces and moments
[NASA-CR-186571] 15 p2047 N90-21734
Study to identify future cryogen payload elements/users for space shuttle launch during period 1990 to 2000
[NASA-CR-186311] 17 p2363 N90-23452
Utilization of Moire patterns as an orbital docking aid to space shuttle/Space Station Freedom
18 p2629 N90-24980
Monitoring and control of spacecraft systems using procedural reasoning 19 p2731 N90-25524
Orbiter utilization as an ACRV
[NASA-TM-102700] 20 p2817 N90-26032
Vibration test procedures for orbiter sidewall-mounted payloads, phase 1
[AD-A220773] 20 p2818 N90-26037
A model for a space shuttle safing and failure-detection expert 21 p3046 N90-27314
Flight mechanics applications for tethers in space: Cooperative Italian-US programs
22 p3131 N90-27770
Microgravity science and applications: Apparatus and facilities
[NASA-TM-101892] 23 p3285 N90-28588
Liquid Rocket Booster (LRB) for the Space Transportation System (STS) systems study. Appendix B: Liquid rocket booster acoustic and thermal environments
[NASA-CR-183788-APP-B] 23 p3288 N90-28602
In-flight investigation of shuttle tile pressure orifice installations
[NASA-TM-4219] 23 p3328 N90-28820
Thermal analyses of power subsystem components
[NASA-CR-186314] 24 p3474 N90-29637

SPACE SHUTTLE PAYLOADS

NT ASTRO MISSIONS (STS)
NT EARTH RADIATION BUDGET EXPERIMENT
NT GET AWAY SPECIALS (STS)

NT HALOGEN OCCULTATION EXPERIMENT
NT SPACELAB
NT X RAY ASTROPHYSICS FACILITY
The Spartan 1 mission
[NASA-TM-101887] 01 p0015 N90-10077
Shuttle Atlantis to deploy Galileo probe toward Jupiter
[NASA-TM-101888] 02 p0175 N90-10982
Conceptual design of liquid droplet radiator shuttle-attached experiment
[NASA-CR-185164] 03 p0318 N90-11805
Syncom 4 deploy, LDEF retrieval highlight 10-day Columbia flight
[NASA-NEWS-RELEASE-89-180] 05 p0594 N90-13448
Development of a shuttle recovery Commercial Materials Processing in Space (CMPS) program
[NASA-CR-183720] 05 p0630 N90-13678
Flight software development for the isothermal dendritic growth experiment
[NASA-TM-102412] 05 p0685 N90-13988
Main propulsion system test requirements for the two-engine Shuttle-C
[NASA-TM-100382] 06 p0735 N90-14282
United States space transportation survey 09 p1173 N90-16787
Shuttle C: Heavy-lift vehicle of the 1990's 09 p1178 N90-16830
Mission report on the Orbiter Camera Payload System (OCPS) Large Format Camera (LFC) and Attitude Reference System (ARS)
[NASA-CR-186273] 09 p1240 N90-17197
Development of an infrared imaging system for the surface tension driven convection experiment 10 p1367 N90-17922
Large antenna measurement and compensation techniques 12 p1610 N90-19263
Spacelab qualified infrared imager for microgravity science experiments
[NASA-TM-102503] 13 p1804 N90-20352
Animation graphic interface for the space shuttle onboard computer 13 p1859 N90-20667
VAPEPS user's reference manual, version 5.0
[NASA-CR-180781] 13 p1868 N90-20713
Spacecraft optical contamination environment
[AD-A218068] 13 p1889 N90-20838
The partnership: Space shuttle, space science, and space station
[NASA-TM-102900] 14 p1930 N90-21050
United States Air Force Academy get-away-special flexible beam experiment 14 p1937 N90-21088
UV spectrometer system AFGL 801 A HUP
[AD-A217805] 14 p2026 N90-21619
Impact of low gravity on water electrolysis operation
[NASA-CR-185521] 15 p2072 N90-21870
Space Station Workshop: Commercial Missions and User Requirements
[NASA-TM-102912] 15 p2175 N90-22428
Study to identify future cryogen payload elements/users for space shuttle launch during period 1990 to 2000
[NASA-CR-186311] 17 p2363 N90-23452
Precision pointing and locking capabilities combined by a linear actuator 18 p2537 N90-24475
Vibration test procedures for orbiter sidewall-mounted payloads, phase 1
[AD-A220773] 20 p2818 N90-26037
Vibration test procedures for orbiter sidewall-mounted payloads, phase 2
[AD-A220774] 20 p2818 N90-26038
Technology development: Future use of NASA's large format camera is uncertain
[GAO/NSIAD-90-142] 20 p2865 N90-26298
Dynamics and dynamics experiments in TSS-1 22 p3129 N90-27758
Regulation of erythropoiesis in rats during space flight
[NASA-CR-177537] 23 p3378 N90-29086
An advanced telerobotic system for shuttle payload changeout room processing applications 24 p3502 N90-29795

SPACE SHUTTLE SOLID ROCKET MOTORS
U SPACE SHUTTLE BOOSTERS

SPACE SHUTTLES
NT BURAN SPACE SHUTTLE
NT HERMES MANNED SPACEPLANE
Simulation of shuttle flight control system structural interaction with RMS deployed payloads 01 p0020 N90-10100
Liquid rocket booster study. Volume 1: Executive summary
[NASA-CR-183599] 01 p0027 N90-10137
Liquid rocket booster study. Volume 2, book 6, appendix 10: Vehicle systems effects
[NASA-CR-183605] 01 p0027 N90-10138
STS-GPS (Space Transportation System - Global Positioning System) tracking experiment for gravitation estimation: Feasibility study
[AD-A211265] 02 p0150 N90-10859
Landing tests for Buran shuttle with jet engine-equipped mock-up 02 p0158 N90-10904
Nonintrusive inertial vibration isolation technology for microgravity space experiments
[NASA-TM-102386] 03 p0334 N90-11901
Final Environmental Impact Statement for the Galileo Mission (Tier 2)
[NASA-TM-101825] 03 p0367 N90-12102
Active rendezvous between a low-earth orbit user spacecraft and the Space Transportation System (STS) shuttle 05 p0590 N90-13436
Tank pressure control experiment on the space shuttle
[NASA-TM-102313] 05 p0615 N90-13590
Preliminary design of the Shuttle-C avionics recovery system
[NASA-CR-186230] 06 p0730 N90-14258
Chronology of KSC and KSC related events for 1988
[NASA-TM-101915] 06 p0867 N90-15040
Measurement of optical radiations in spacecraft environments
[AD-A213814] 07 p0950 N90-15497
Safety and rescue during STS operations 08 p1034 N90-15975
New atmospheric turbulence model for shuttle applications
[NASA-TM-4168] 08 p1103 N90-16389
Artificial intelligence in process control: Knowledge base for the shuttle ECS model 08 p1156 N90-16697
United States space transportation survey 09 p1173 N90-16787
America's shuttle returns to space 09 p1174 N90-16792
Are reusable boosters cost-effective 09 p1179 N90-16834
A field study of solid rocket exhaust impacts on the near-field environment
[NASA-TM-4172] 10 p1405 N90-18102
Space shuttle RCS oxidizer leak repair for STS-26 11 p1474 N90-18485
Superfluid helium orbital resupply coupling 11 p1475 N90-18488
Technology update-89
[DE90-005813] 11 p1593 N90-19178
Safety Status Report for the Ulysses mission. Book 2: Accident analysis-appendices. General purpose heat source radioisotope thermoelectric generator program
[DE90-006830] 12 p1614 N90-19286
Radar transponder antenna pattern analysis for the space shuttle 12 p1638 N90-19414
Docking mechanism for spacecraft
[NASA-CASE-MSC-21386-1] 13 p1764 N90-20126
Graphics Technology in Space Applications (GTSA 1989)
[NASA-CP-3045] 13 p1856 N90-20651
The Real Time Display Builder (RTDB) 13 p1857 N90-20656
Onboard shuttle on-line software requirements system: Prototype 13 p1858 N90-20658
Tools for 3D scientific visualization in computational aerodynamics 13 p1858 N90-20660
Animation graphic interface for the space shuttle onboard computer 13 p1859 N90-20667
Seeing in a new light: Astro-1 teacher's guide with activities
[NASA-EP-274] 13 p1899 N90-20900
The partnership: Space shuttle, space science, and space station
[NASA-TM-102900] 14 p1930 N90-21050
Optimal trajectories for the aeroassisted flight experiment. Part 3: Formulation, results, and analysis
[NASA-CR-186165] 14 p1930 N90-21051
General purpose heat source radioisotope thermoelectric generator. Book 2: Accident analysis, appendices
[REPT-90SDS4202-BK-2] 15 p2166 N90-22380
Space Shuttle, NASA's major changes to flight hardware: Fact sheet for the Chairman, Committee on Science, Space, and Technology, House of Representatives
[GAO/NSIAD-88-173FS] 15 p2181 N90-22461
Debris/ice/TPS assessment and photographic analysis for Shuttle Mission STS-36
[NASA-TM-102789] 16 p2205 N90-22583
HCl monitor 16 p2209 N90-22599
Space shuttle: The future of the Vandenberg launch site needs to be determined
[GAO/NSIAD-88-158] 18 p2509 N90-24337
Remote measurement of ice thickness on the shuttle external tank surface
[NASA-TM-102667] 18 p2555 N90-24584
Space shuttle avionics system
[NASA-SP-504] 19 p2664 N90-25160
Rotating-unbalanced-mass devices for scanning balloon-borne experiments, free-flying spacecraft, and space shuttle/space station experiments
[NASA-TP-3030] 19 p2682 N90-25255
Atmospheric environment for space shuttle (STS-28) launch
[NASA-TM-100386] 19 p2715 N90-25452
Contamination of spacecraft by recontact of dumped liquids 19 p2728 N90-25508
ACES: Space shuttle flight software analysis expert system 19 p2739 N90-25571
Research at NASA's NFAC wind tunnels
[NASA-TM-102827] 20 p2801 N90-25933
Debris/ice/TPS assessment and photographic analysis for shuttle mission STS-31R
[NASA-TM-102790] 20 p2819 N90-26040
Acousto-optic signature analysis for inspection of the orbiter thermal protection tile bonds
[DE90-013089] 20 p2819 N90-26043
Winged cargo return vehicle. Volume 1: Conceptual design
[NASA-CR-186823] 20 p2821 N90-26050
The aerobraking space transfer vehicle
[NASA-CR-186819] 20 p2821 N90-26053
Flight motor set 360L007 (STS-33R)
[NASA-CR-183979] 20 p2824 N90-26067
Field experience in using laser acoustic sensing for inspection
[DE90-012954] 20 p2873 N90-26347
Space Shuttle 2 advanced space transportation system. Volume 1: Executive summary
[NASA-CR-185952] 21 p2965 N90-26853
Space Shuttle 2 advanced space transportation system, volume 2
[NASA-CR-185953] 21 p2965 N90-26854
The integration of automated knowledge acquisition with computer-aided software engineering for space shuttle expert systems 21 p3045 N90-27307
A model for a space shuttle safing and failure-detection expert 21 p3046 N90-27314
Debrix/ice/TPS assessment and photographic analysis of Shuttle Mission STS-32R
[NASA-TM-102787] 22 p3124 N90-27733
A transient response analysis of the space shuttle vehicle during liftoff
[NASA-TM-103505] 22 p3125 N90-27735
Space shuttle descent flight verification by simulation: A challenge in implementing flight control system robustness 22 p3127 N90-27748
The instrument pointing system: Precision attitude control in space 22 p3129 N90-27756
Flight motor set 360L001 (STS-26R). Volume 1: System overview, revision A
[NASA-CR-183995] 22 p3133 N90-27778
Flight motor set 360L006 (STS-34). Volume 1: System overview
[NASA-CR-184007] 22 p3133 N90-27781
Evaluation of EDR-3 vibration, shock, temperature, and humidity recording unit
[NASA-CR-184006] 22 p3177 N90-28028
Shuttle to Shuttle 2: Subsystem weight reduction potential (estimated 1992 technology readiness date)
[NASA-TM-89114] 23 p3286 N90-28589
Development and approach to low-frequency microgravity isolation systems
[NASA-TP-2984] 23 p3317 N90-28754
Re-analysis of data on the space radiation environment above south-east Asia
[RAE-TR-89048] 24 p3565 N90-30166

SPACE SIMULATORS
Thermal environmental tests on space simulation chamber
[DE90-000927] 06 p0729 N90-14251
Thermal histories of the samples of two KOSI comet nucleus simulation experiments 08 p1147 N90-16645
Mechanical and SEM analysis of artificial comet nucleus samples 08 p1148 N90-16650
OMV mission simulator 13 p1860 N90-20669
Issues in development, evaluation, and use of the NASA Preflight Adaptation Trainer (PAT)
[NASA-CR-185608] 15 p2137 N90-22212
An introductory guide preparing to use the ESTEC environmental test facilities
[ESA-TM-05] 24 p3438 N90-29419

SPACE STATION PAYLOADS
Space station RT and E utilization study
[NASA-CR-181707] 01 p0026 N90-10129
Science and applications on the space station: A strategic vision
[NASA-TM-101863] 05 p0601 N90-13493
Facilities for microgravity combustion research
[NASA-TM-102014] 05 p0630 N90-13679
Space station attached payload program support
[NASA-CR-183838] 06 p0733 N90-14274
Astrometric Telescope Facility isolation and pointing study
[NASA-CR-177473] 10 p1328 N90-17675
Recommendations for the future 10 p1445 N90-18338

Technology development, demonstration, and orbital support requirements for manned lunar and Mars missions
[NASA-TM-101666] 10 p1447 N90-18350
Space station Simulation Computer System (SCS) study for NASA/MSFC. Volume 1: Overview and summary
[NASA-CR-183840] 13 p1762 N90-20113
Vibration isolation versus vibration compensation on multiple payload platforms 14 p1933 N90-21066
Space Station Workshop: Commercial Missions and User Requirements
[NASA-TM-102912] 15 p2175 N90-22428
On-orbit operations of the Space Station Freedom attached payloads accommodations equipment 18 p2500 N90-24283
Robotics program at the NASA Goddard Space Flight Center 18 p2500 N90-24285
Perspective features of internal automation and robotics for supporting Columbus attached laboratory payload operations 18 p2502 N90-24297
Rotating-unbalanced-mass devices for scanning balloon-borne experiments, free-flying spacecraft, and space shuttle/space station experiments
[NASA-TP-3030] 19 p2682 N90-25255
Space Station attached payloads 21 p3015 N90-27141
Utilization of space station, part 3
[NAL-TM-597-PT-3] 24 p3439 N90-29422

SPACE STATION POLAR PLATFORMS
Key structures mechanical issues of the European Space Station and platform program Columbus 02 p0188 N90-11072
Science and applications on the space station: A strategic vision
[NASA-TM-101863] 05 p0601 N90-13493
Environmental constraints for polar platform design
[RAE-TR-89014] 09 p1181 N90-16849
Solar array designs for Columbus elements 10 p1340 N90-17764
Space Station Freedom solar array panels plasma interaction test facility
[NASA-TM-102475] 15 p2186 N90-22488
Future developments of remote sensing systems: Data management and processing 19 p2709 N90-25416

SPACE STATION POWER SUPPLIES
Space station RT and E utilization study
[NASA-CR-181707] 01 p0026 N90-10129
Space station systems: A bibliography with indexes (supplement 8)
[NASA-SP-7056(08)] 01 p0026 N90-10131
Beamed laser power in support of near-earth missions 01 p0031 N90-10167
A feasibility assessment of installation, operation and disposal options for nuclear reactor power system concepts for a NASA growth space station
[NASA-TM-89923] 01 p0032 N90-10174
Bidirectional power converter control electronics
[NASA-CR-175070] 01 p0032 N90-10175
Space station systems: A bibliography with indexes (supplement 9)
[NASA-SP-7056(09)] 05 p0613 N90-13580
The Space Station Photovoltaic Panels Plasma Interaction Test Program: Test plan and results
[NASA-TM-102474] 05 p0613 N90-13581
The US space station and its electric power system
[NASA-TM-101974] 05 p0616 N90-13596
Modeling of power electronic systems with EMTP
[NASA-TM-102375] 05 p0695 N90-14060
Reliability analysis of the space station freedom electrical power system
[AD-A214105] 07 p0886 N90-15126
The Columbus power system simulation programme 10 p1330 N90-17686
The 25 kWe spaceborne solar dynamic generator 10 p1331 N90-17696
CNES-CEA comparative evaluation study of various candidate 20 kWe space power systems 10 p1331 N90-17697
Space Station Freedom energy storage system design and development 10 p1332 N90-17701
Space Station Freedom electric power system availability study
[NASA-CR-185181] 13 p1763 N90-20120
Model development in viscoplastic ratchetting
[NASA-TM-102509] 13 p1816 N90-20431
Photovoltaic power for Space Station Freedom
[NASA-TM-102569] 15 p2062 N90-21812
Electric power scheduling: A distributed problem-solving approach
[NASA-TM-103149] 15 p2157 N90-22323
Space Station Freedom solar array panels plasma interaction test facility
[NASA-TM-102475] 15 p2186 N90-22488
Automated electric power management and control for Space Station Freedom
[NASA-TM-103151] 16 p2304 N90-23125
Project WISH: The Emerald City
[NASA-CR-186692] 17 p2366 N90-23470
Space station systems: A bibliography with indexes (supplement 10)
[NASA-SP-7056(10)] 19 p2666 N90-25171
Interactions between the Space Station and the environment: A preliminary assessment of EMI 19 p2737 N90-25557
A hybrid approach to space power control 21 p3043 N90-27293
A lunar space station
[NASA-CR-186223] 24 p3563 N90-30158

SPACE STATION PROPULSION
Space station systems: A bibliography with indexes (supplement 8)
[NASA-SP-7056(08)] 01 p0026 N90-10131
Space station systems: A bibliography with indexes (supplement 9)
[NASA-SP-7056(09)] 05 p0613 N90-13580
Project WISH: The Emerald City
[NASA-CR-186692] 17 p2366 N90-23470
Space station systems: A bibliography with indexes (supplement 10)
[NASA-SP-7056(10)] 19 p2666 N90-25171

SPACE STATION STRUCTURES
Space station systems: A bibliography with indexes (supplement 8)
[NASA-SP-7056(08)] 01 p0026 N90-10131
SDM challenges for space station 02 p0186 N90-11059
Space station systems: A bibliography with indexes (supplement 9)
[NASA-SP-7056(09)] 05 p0613 N90-13580
A modular habitation unit adapted for service in low earth and geostationary earth orbits
[ILR-MITT-217] 08 p1036 N90-15990
Concept design for Hermes docking/berthing mechanism 18 p2536 N90-24464
Mechanisms to assemble space structures in extravehicular environment 18 p2538 N90-24480
Space station systems: A bibliography with indexes (supplement 10)
[NASA-SP-7056(10)] 19 p2666 N90-25171
Perspective features of the tethered systems for space applications
[ETN-90-97279] 20 p2822 N90-26059
Overcenter collet space station truss fastener
[NASA-CASE-MSC-21504-1] 21 p2966 N90-26859
Space Station Freedom pressurized element interior design process
[NASA-CR-181297] 23 p3287 N90-28597
Utilization of space station, part 3
[NAL-TM-597-PT-3] 24 p3439 N90-29422
A lunar space station
[NASA-CR-186223] 24 p3563 N90-30158

SPACE STATIONS
NT COLUMBUS SPACE STATION
NT MAN TENDED FREE FLYERS
NT MIR SPACE STATION
NT ORBITING LUNAR STATIONS
NT SKYLAB 1
NT SPACE STATION POLAR PLATFORMS
Control/structure interaction methods for space station power systems 01 p0018 N90-10087
Explicit modeling and computational load distribution for concurrent processing simulation of the space station 01 p0020 N90-10096
Modeling and stabilization of large flexible space stations 01 p0024 N90-10120
Knowledge-based machine vision systems for space station automation
[NASA-CR-185710] 01 p0025 N90-10124
System identification for large space structures 01 p0025 N90-10126
Space station RT and E utilization study
[NASA-CR-181707] 01 p0026 N90-10129
Space station systems: A bibliography with indexes (supplement 8)
[NASA-SP-7056(08)] 01 p0026 N90-10131
Central electrical utility power for a satellite ring city in low earth orbit space 01 p0031 N90-10166
Beamed laser power in support of near-earth missions 01 p0031 N90-10167
Advancing automation and robotics technology for the space station Freedom and for the US economy
[NASA-TM-101561] 01 p0102 N90-10577
Orbital debris research at NASA Johnson Space Center, 1986-1988
[NASA-TM-102155] 01 p0138 N90-10795
Space Station Freedom: A foothold on the future
[NASA-NP-107/10-88] 02 p0159 N90-10907
Advanced manned space flight simulation and training: An investigation of simulation host computer system concepts
[NASA-CR-185998] 02 p0160 N90-10911
Evolutionary space station fluids management strategies
[NASA-CR-185137] 02 p0175 N90-10983
SDM challenges for space station 02 p0186 N90-11059
NASA/NBS (National Aeronautics and Space Administration/National Bureau of Standards) standard reference model for telerobot control system architecture (NASREM)
[NASA-CR-185078] 02 p0228 N90-11310
Considerations for a design and operations knowledge support system for Space Station Freedom
[NASA-TM-102156] 02 p0256 N90-11451
Docking system for spacecraft
[NASA-CASE-MSC-21327-1] 03 p0317 N90-11798
Advanced spacecraft fire safety: Proposed projects and program plan
[NASA-CR-185147] 04 p0462 N90-12645
Proposal for a zero-gravity toilet facility for the space station
[NASA-CR-183151] 04 p0526 N90-13036
Telescience Testbed Pilot Program
[NASA-CR-184997] 04 p0528 N90-13047
National Aeronautics and Space Administration 04 p0563 N90-13282
Fiscal year 1990 authorization request and budget estimates for the National Aeronautics and Space Administration
[GPO-96-945] 04 p0563 N90-13283
The 1990 National Aeronautics and Space Administration Authorization
[GPO-98-466] 04 p0563 N90-13285
National Aeronautics and Space Administration 04 p0564 N90-13287
National Aeronautics and Space Administration Authorization Act, fiscal year 1990
[S-REPT-101-157] 04 p0564 N90-13288
National Aeronautics and Space Administration Authorization Act, fiscal year 1990
[S-REPT-101-157] 04 p0564 N90-13289
Periodic-disturbance accommodating control of the space station for asymptotic momentum management 05 p0586 N90-13416
LDR structural experiment definition 05 p0600 N90-13483
Space station gas compressor technology study program, phase 1
[NASA-CR-183758] 05 p0601 N90-13491
Space Station Engineering Design Issues
[NASA-CR-185978] 05 p0601 N90-13492
Space station systems: A bibliography with indexes (supplement 9)
[NASA-SP-7056(09)] 05 p0613 N90-13580
User needs, benefits, and integration of robotic systems in a space station laboratory
[NASA-CR-185150] 05 p0651 N90-13794
Exercise countermeasures for bed rest deconditioning
[NASA-TM-101045] 05 p0674 N90-13926
Functional decor in the International Space Station: Body orientation cues and picture perception
[NASA-TM-102242] 05 p0675 N90-13931
National Aeronautics and Space Administration Multiyear Authorization Act of 1989 05 p0709 N90-14148
National Aeronautics and Space Administration authorization
[S-HRG-101-348] 05 p0709 N90-14149
Review of the Aerospace Safety Advisory Panel report for NASA fiscal year 1990 authorization
[GPO-24-234] 06 p0722 N90-14213
Aerospace vehicle design, spacecraft section. Volume 1: Project Groups 3-5
[NASA-CR-186053] 06 p0731 N90-14263
Aerospace vehicle design, spacecraft section. Volume 1: Project Groups 3-5
[NASA-CR-186054] 06 p0731 N90-14264
An image compression algorithm for a high-resolution digital still camera
[NASA-CR-185079] 06 p0780 N90-14532
Software Reuse Issues
[NASA-CP-3057] 06 p0824 N90-14789
SSFP approach to software reuse 06 p0826 N90-14799
Level 2 software reuse study 06 p0826 N90-14800
Support for life-cycle product reuse in NASA's SSE 06 p0826 N90-14802
Shuttle-C utilization for assembly of the rephased Freedom configuration
[NASA-TM-101658] 07 p0885 N90-15120
Reliability analysis of the space station freedom electrical power system
[AD-A214105] 07 p0886 N90-15126
Manned spacecraft
[AD-A214218] 07 p0887 N90-15129

Onorbit electron beam welding experiment definition
[NASA-CR-183847] 07 p0938 N90-15431
RVD scenari and interfaces between Hermes and space station 08 p1035 N90-15982
Conceptual design for the space station Freedom modular combustion facility
[NASA-TM-102037] 08 p1053 N90-16087
A knowledge-based machine vision system for space station automation 08 p1075 N90-16221
Remote Manipulator System (RMS)-based Controls-Structures Interaction (CSI) flight experiment feasibility study
[NASA-CR-181952] 09 p1230 N90-17136
Space station wardroom habitability and equipment study
[NASA-CR-4246] 09 p1260 N90-17308
Space station contamination control study: Internal combustion, phase 1
[NASA-CR-179323] 10 p1328 N90-17674
Preliminary evaluation of space station transmission line in a ring configuration
[NASA-TM-102461] 10 p1329 N90-17677
Japanese experiment module electrical power system 10 p1329 N90-17680
Non-contact temperature measurement requirements 10 p1363 N90-17898
Advancing automation and robotics technology for the Space Station Freedom and for the US economy
[NASA-TM-101691] 10 p1414 N90-18151
KAPSE Interface Team (KIT) public report, volume 8, part 2
[AD-A215840] 10 p1419 N90-18178
Process development and fabrication of space station type aluminum-clad graphite epoxy struts
[NASA-CR-181873] 11 p1488 N90-18454
Space station technology summary 11 p1474 N90-18482
Zero-gravity vortex vent and PVT gaging system 11 p1475 N90-18486
Orbital fluid resupply assessment 11 p1475 N90-18487
Payload vibration isolation in a microgravity environment
[NASA-CR-186191] 11 p1518 N90-18744
Development of an experimental space station model for structural dynamics research
[NASA-TM-102601] 11 p1519 N90-18751
Advancing automation and robotics technology for the Space Station Freedom and for the US economy: Submitted to the United States Congress
[NASA-TM-101647] 12 p1613 N90-19279
Technology evaluation for space station atmospheric leakage
[DE90-007844] 12 p1616 N90-19294
Aerospace Safety Advisory Panel
[NASA-TM-101748] 12 p1634 N90-19389
A transient plasticity study and low cycle fatigue analysis of the Space Station Freedom photovoltaic solar array blanket
[NASA-TM-102516] 12 p1674 N90-19617
Aerospace induction motor actuators driven from a 20-kHz power link
[NASA-TM-102482] 13 p1756 N90-20085
Proximity operations concept design study, task 6
[NASA-CR-181971] 13 p1761 N90-20112
Space station Simulation Computer System (SCS) study for NASA/MSFC. Volume 1: Overview and summary
[NASA-CR-183840] 13 p1762 N90-20113
Space station Simulation Computer System (SCS) study for NASA/MSFC. Volume 2: Concept document
[NASA-CR-183841] 13 p1762 N90-20114
Space station Simulation Computer System (SCS) study for NASA/MSFC. Volume 3: Refined conceptual design report
[NASA-CR-183842] 13 p1762 N90-20115
Space station Simulation Computer System (SCS) study for NASA/MSFC. Volume 4: Conceptual design report
[NASA-CR-183843] 13 p1762 N90-20116
Space station Simulation Computer System (SCS) study for NASA/MSFC. Volume 5: Study analysis report
[NASA-CR-183844] 13 p1763 N90-20117
Space station Simulation Computer System (SCS) study for NASA/MSFC. Volume 6: Study issues report
[NASA-CR-183845] 13 p1763 N90-20118
Space Station Freedom electric power system availability study
[NASA-CR-185181] 13 p1763 N90-20120
Docking mechanism for spacecraft
[NASA-CASE-MSC-21386-1] 13 p1764 N90-20126
Graphics Technology in Space Applications (GTSA 1989)
[NASA-CP-3045] 13 p1856 N90-20651
Space Station Freedom integrated fault model 13 p1860 N90-20673
Graphical programming and the use of simulation for space-based manipulators 13 p1861 N90-20674
Using an instrumented manikin for Space Station Freedom analysis 13 p1861 N90-20675
The development of the Canadian Mobile Servicing System Kinematic Simulation Facility 13 p1861 N90-20676
SES cupola interactive display design environment 13 p1862 N90-20679
Issues in visual support to real-time space system simulation solved in the Systems Engineering Simulator 13 p1862 N90-20680
Real-time graphics for the Space Station Freedom cupola, developed in the Systems Engineering Simulator 13 p1862 N90-20683
The partnership: Space shuttle, space science, and space station
[NASA-TM-102900] 14 p1930 N90-21050
Detection of potential space station control/structure interaction with CO-ST-IN 14 p1935 N90-21074
Cosmic Dust Collection Facility: Scientific objectives and programmatic relations
[NASA-TM-102160] 14 p1939 N90-21098
Thermal control system corrosion study
[NASA-TM-102220] 14 p1971 N90-21294
Photovoltaic power for Space Station Freedom
[NASA-TM-102569] 15 p2062 N90-21812
The determination of maximum deep space station slew rates for a high Earth orbiter 15 p2075 N90-21882
Automating security monitoring and analysis for Space Station Freedom's electric power system
[NASA-TM-103148] 15 p2158 N90-22324
An expert system for simulating electric loads aboard Space Station Freedom
[NASA-TM-103150] 15 p2158 N90-22325
Space Station Workshop: Commercial Missions and User Requirements
[NASA-TM-102912] 15 p2175 N90-22428
Aeronautics and space report of the President: 1987 activities 15 p2181 N90-22462
Space Station Freedom environmental control and life support system phase 3 simplified integrated test detailed report
[NASA-TM-4204] 16 p2207 N90-22593
Space station dynamics, attitude control and momentum management 16 p2287 N90-23029
Concurrent processing simulation of the space station 16 p2289 N90-23041
Overview of computational control research at UT Austin 16 p2291 N90-23051
Space Station Freedom media handbook
[NASA-TM-102901] 17 p2364 N90-23460
Project WISH: The Emerald City
[NASA-CR-186692] 17 p2366 N90-23470
Analysis of the use of a methane propellant in a biowaste resistojet
[AD-A220475] 17 p2367 N90-23473
Qualitative models for space system engineering
[NASA-CR-180682] 17 p2385 N90-23585
Advancing automation and robotics technology for the Space Station Freedom and for the US economy
[NASA-TM-102668] 17 p2439 N90-23899
Space Station Freedom Pre-Workshop Session
[NASA-TM-102913] 17 p2479 N90-24172
Space Station Freedom: List of acronyms 17 p2479 N90-24176
Robotics program at the NASA Goddard Space Flight Center 18 p2500 N90-24285
Evolution of EVA capabilities for space station construction and maintenance: Soviet and American experience 18 p2502 N90-24295
National Aeronautics and Space Administration (NASA)/American Society for Engineering Education (ASEE) Summer Faculty Fellowship Program-1989, volume 1
[NASA-CR-185601-VOL-1] 18 p2627 N90-24972
Effect of low air velocities on thermal homeostasis and comfort during exercise at space station operational temperature and humidity 18 p2628 N90-24975
Identifying atmospheric monitoring needs for Space Station Freedom 18 p2628 N90-24977
Utilization of Moire patterns as an orbital docking aid to space shuttle/Space Station Freedom 18 p2629 N90-24980
Electrochemical control of iodine disinfectant for space transportation system and space station potable water 18 p2629 N90-24981
Knowledge-based control of an adaptive interface 18 p2630 N90-24987
Some issues related to simulation of the tracking and communications computer network 18 p2630 N90-24988
Keeping the dream alive: Managing the Space Station Program, 1982 to 1986
[NASA-CR-4272] 18 p2633 N90-25000
Departments of Veterans Affairs and Housing and Urban Development, and Independent Agencies Appropriations for Fiscal Year 1990, part 2
[S-HRG-101-345-PT-2] 18 p2636 N90-25017
National Aeronautics and Space Administration, 2 May 1989 18 p2636 N90-25018
National Aeronautics and Space Administration, 3 May 1989 18 p2636 N90-25019
A study of concept options for the evolution of Space Station Freedom
[NASA-TM-102675] 19 p2663 N90-25154
Project EGRESS: Earthbound guaranteed reentry from space station. The design of an assured crew recovery vehicle for the space station
[NASA-CR-186657] 19 p2664 N90-25162
Space station based Microacceleration Experiment Platform
[NASA-CR-186659] 19 p2666 N90-25167
Space station systems: A bibliography with indexes (supplement 10)
[NASA-SP-7056(10)] 19 p2666 N90-25171
Conceptual definition of a high voltage power supply test facility
[NASA-CR-185216] 19 p2666 N90-25172
Dynamic analysis of space-related linear and non-linear structures
[NASA-TM-103490] 19 p2667 N90-25174
A design optimization process for Space Station Freedom
[NASA-CR-186851] 19 p2667 N90-25175
An analysis of space power system masses
[NASA-TM-103199] 19 p2669 N90-25184
Autonomous power expert system
[NASA-CR-185263] 19 p2670 N90-25187
Rotating-unbalanced-mass devices for scanning balloon-borne experiments, free-flying spacecraft, and space shuttle/space station experiments
[NASA-TP-3030] 19 p2682 N90-25255
A direct-interface, fusible heat sink for astronaut cooling
[NASA-TM-102835] 19 p2689 N90-25292
A proposal to demonstrate production of salad crops in the space station mockup facility with particular attention to space, energy, and labor constraints
[NASA-CR-186811] 19 p2725 N90-25500
Third Annual Workshop on Space Operations Automation and Robotics (SOAR 1989)
[NASA-CP-3059] 19 p2727 N90-25503
Mobile transporter path planning 19 p2727 N90-25505
SOAR 89: Space Station. Space suit test program 19 p2727 N90-25506
Automation in the Space Station module power management and distribution Breadboard 19 p2728 N90-25509
NASA systems autonomy demonstration project: Advanced automation demonstration of Space Station Freedom thermal control system 19 p2728 N90-25510
Solar array automation limitations 19 p2729 N90-25513
The use of PLAID in the Space Station Freedom viewing analysis 19 p2729 N90-25517
Spacecraft external molecular contamination analysis 19 p2730 N90-25520
Autonomous power expert fault diagnostic system for Space Station Freedom electrical power system testbed 19 p2730 N90-25521
The environmental control and life support system advanced automation project. Phase 1: Application evaluation 19 p2730 N90-25523
Telepresence and Space Station Freedom workstation operations 19 p2731 N90-25527
Process and information integration via hypermedia 19 p2733 N90-25534
The Flight Telerobotic Servicer (FTS) NASA's first operational robotic system 19 p2733 N90-25537
Discharge transient coupling in large space power systems 19 p2735 N90-25544
Plasma interactions and effects for large systems 19 p2735 N90-25545
Automated control of hierarchical systems using value-driven methods 19 p2735 N90-25547
Remote operation of an orbital maneuvering vehicle in simulated docking maneuvers 19 p2736 N90-25554
Interactions between the Space Station and the environment: A preliminary assessment of EMI 19 p2737 N90-25557
OMS FDIR: Initial prototyping 19 p2738 N90-25562
Technology for an intelligent, free-flying robot for crew and equipment retrieval in space 19 p2738 N90-25564

Space operations: NASA efforts to develop and deploy advanced spacecraft computers. Report to the Chairman, Subcommittee on Space Science and Applications, Committee on Science, Space, and Technology, House of Representatives
[GAO/IMTEC-89-17] 19 p2742 N90-25582
Design of a Lunar farside observatory
[NASA-CR-186671] 19 p2765 N90-25709
Project Exodus
[NASA-CR-186836] 20 p2816 N90-26026
National space test centers, Lewis research center facilities
[NASA-TM-103187] 20 p2817 N90-26030
Orbiter utilization as an ACRV
[NASA-TM-102700] 20 p2817 N90-26032
Preliminary subsystem designs for the Assured Crew Return Vehicle (ACRV), volume 1
[NASA-CR-186677-VOL-1] 20 p2818 N90-26039
Project LOCOST: Laser or Chemical Hybrid Orbital Space Transport
[NASA-CR-186822] 20 p2819 N90-26042
Planning for Space Station Freedom laboratory payload integration
[NASA-CR-186751] 20 p2820 N90-26047
Winged cargo return vehicle. Volume 1: Conceptual design
[NASA-CR-186823] 20 p2821 N90-26050
Biconic cargo return vehicle with an advanced recovery system. Volume 1: Conceptual design
[NASA-CR-186520] 20 p2821 N90-26052
Technology for large space systems: A bibliography with indexes (supplement 22)
[NASA-SP-7046(22)] 20 p2822 N90-26056
Long cycle pressurized logistics module: An Italian contribution to the Space Station Freedom logistics scenario
[IAF-89-083] 20 p2822 N90-26058
Two-dimensional model of a Space Station Freedom thermal energy storage canister
[NASA-TM-103124] 20 p2862 N90-26279
Rotating-unbalanced-mass devices and methods for scanning balloon-borne-experiments, free-flying spacecraft, and space shuttle/space station attached experiments
[NASA-CASE-MFS-28425-1] 20 p2866 N90-26304
Automation of closed environments in space for human comfort and safety
[NASA-CR-186834] 20 p2901 N90-26500
Space station definitions, design, and development. Task 5: Multiple arm telerobot coordination and control: Manipulator design methodology
[NASA-CR-182043] 20 p2914 N90-26577
Manned Space Stations: Legal Issues
[ESA-SP-305] 20 p2937 N90-26711
Technical characteristics and functions of different types of space stations 20 p2937 N90-26712
Human work in space: The astronaut's legal status. Introduction 20 p2938 N90-26719
The manned national space station: International legal considerations 20 p2938 N90-26720
Space Station attached payloads 21 p3015 N90-27141
Agent independent task planning 21 p3040 N90-27276
Departments of Veterans Affairs and Housing and Urban Development, and independent agencies appropriations for 1991. Part 4: National Aeronautics and Space Administration
[GPO-30-861] 21 p3088 N90-27561
Research opportunities on the Space Station 21 p3092 N90-27578
Hermes rendezvous with the space station 22 p3128 N90-27753
The instrument pointing system: Precision attitude control in space 22 p3129 N90-27756
The challenge of assembling a space station in orbit 22 p3130 N90-27763
A new method for a tethered system aided space station assembly 22 p3130 N90-27765
Space station contamination modeling
[NASA-CR-183871] 23 p3286 N90-28590
Development and approach to low-frequency microgravity isolation systems
[NASA-TP-2984] 23 p3317 N90-28754
Design of a monitor and simulation terminal (master) for space station telerobotics and telescience 23 p3372 N90-29051
Atmosphere and water quality monitoring on Space Station Freedom
[NASA-CR-186707] 23 p3378 N90-29084
Preliminary analysis of NASA commercialization initiatives
[PB90-202706] 23 p3407 N90-29257
Utilization of space station, part 3
[NAL-TM-597-PT-3] 24 p3439 N90-29422
A new momentum management controller for the space station
[NASA-CR-187265] 24 p3440 N90-29425
Definition of a near real time microbiological monitor for space vehicles
[NASA-CR-185599] 24 p3441 N90-29430

SPACE STORAGE
Evolutionary space station fluids management strategies
[NASA-CR-185137] 02 p0175 N90-10983

SPACE SUITS
NT EXTRAVEHICULAR MOBILITY UNITS
Independent Orbiter Assessment (IOA): Analysis of the extravehicular mobility unit
[NASA-CR-185540] 02 p0166 N90-10937
Independent Orbiter Assessment (IOA): Analysis of the crew equipment subsystem
[NASA-CR-185591] 02 p0170 N90-10958
Independent Orbiter Assessment (IOA): Assessment of the crew equipment subsystem
[NASA-CR-185577] 02 p0173 N90-10971
EVA space suit. General concepts of design and arrangement 08 p1034 N90-15976
ESA's space transportation programme 09 p1173 N90-16786
Suitport extra-vehicular access facility
[NASA-CASE-ARC-11635-1] 09 p1183 N90-16860
Cycle life machine for AX-5 space suit 15 p2112 N90-22080
AX-5 space suit bearing torque investigation 15 p2115 N90-22101
The European EVA suit: An optimized tool for Hermes/MTFF in-orbit operations 18 p2502 N90-24296
The European EVA spacesuit mechanisms 18 p2538 N90-24481
The use of underwater dynamometry to evaluate two space suits 18 p2632 N90-24995
Design of a device to remove lunar dust from space suits for the proposed lunar base
[NASA-CR-186679] 19 p2724 N90-25496
Hazards protection for space suits and spacecraft
[NASA-CASE-MSC-21366-1] 19 p2725 N90-25498
SOAR 89: Space Station. Space suit test program 19 p2727 N90-25506

SPACE SURVEILLANCE (SPACEBORNE)
Space-based radar simulation laboratory
[AD-A216722] 11 p1497 N90-18618

SPACE SYSTEMS ENGINEERING
U AEROSPACE ENGINEERING

SPACE TECHNOLOGY EXPERIMENTS
Laboratory of Space Technology
[PB90-110651] 08 p1033 N90-15967

SPACE TELESCOPE
U HUBBLE SPACE TELESCOPE

SPACE TEMPERATURE
Vibration damping composition suitable for outer space temperature variations
[AD-D014288] 08 p1088 N90-16296

SPACE TOOLS
Interchangeable end effector tools utilized on the protoflight manipulator arm
[NASA-CR-179374] 01 p0078 N90-10447
Lunar hand tools
[NASA-CR-184924] 17 p2384 N90-23581

SPACE TRANSPORTATION
NT ADVANCED LAUNCH SYSTEM (STS)
NT SPACE TRANSPORTATION SYSTEM
Low-earth-orbit to low-lunar-orbit laser freighter 01 p0030 N90-10160
Laser propulsion option 01 p0030 N90-10161
Laser thruster 01 p0030 N90-10164
A survey of permanently-manned lunar base concepts
[AD-A212575] 04 p0460 N90-12638
Round trip to orbit. Human spaceflight alternatives: Special report
[OTA-ISC-419] 08 p1033 N90-15966
Overview of Japan's current and future space transportation programmes 09 p1174 N90-16789
The German hypersonic technology programme 09 p1174 N90-16790
Glavkosmos operational space transportation systems 09 p1174 N90-16791
Progress in Saenger space transportation system definition 09 p1175 N90-16799
Comparison between horizontally launched air-breathing single and two-stage to orbit space vehicles 09 p1175 N90-16802
U.S.S.R. space transportation systems 09 p1176 N90-16806
Development status of Japan's new launch vehicle: H-2 rocket 09 p1176 N90-16807
Aerodynamic and structural design challenges of a reusable single stage to orbit air-breathing launch vehicle 09 p1177 N90-16814
Mission-dependent selection of propulsion systems for reusable launch vehicles 09 p1177 N90-16815
Progress in airbreathing combined engines for future European launcher 09 p1177 N90-16817
Views on the evolution of European space transport: The reference launcher concept EARL 2 09 p1179 N90-16831
HOPE: Its concept and technical features 09 p1179 N90-16835
Material technology challenges in space transportation 09 p1179 N90-16836
New materials and structural concepts for space transportation systems 09 p1179 N90-16837
The DLR technology programme on space transportation 09 p1180 N90-16841
A perspective on the use of storable propellants for future space vehicle propulsion 11 p1472 N90-18473
Research and Technology
[NASA-TM-102161] 14 p2044 N90-21721
Aeronautics and space report of the President: 1987 activities 15 p2181 N90-22462
US access to space: Launch vehicle choices for 1990 to 2010 16 p2205 N90-22579
Financing of large space transportation projects: Research on the financial project for the SSPS
[ILR-MITT-228(1989)] 17 p2363 N90-23456
Research and technology 1989
[NASA-TM-100369] 17 p2486 N90-24219
Neptune, 2000 plus: Concept of a heavy space freighter for the 21st century
[ILR-MITT-229(1989)] 18 p2509 N90-24338
System analysis and project of a laser-moved spaceship
[ILR-MITT-232(1989)] 18 p2513 N90-24348
Advanced space transportation technologies 18 p2645 N90-25061
Thermal protection systems for reentry and hypersonic flight
[ESA-TT-1179] 19 p2667 N90-25177
Space Transportation Avionics Technology Symposium. Volume 1: Executive summary
[NASA-CP-3081-VOL-1] 20 p2809 N90-25980
Space transportation: NASA has no firm need for increasingly costly orbital maneuvering vehicle
[GAO/NSIAD-90-192] 20 p2819 N90-26041
Flight control issues of the next generation space transportation launch vehicles 22 p3126 N90-27742
Development of the electric vehicle analyzer
[AD-A224201] 23 p3323 N90-28788
Preliminary analysis of NASA commercialization initiatives
[PB90-202706] 23 p3407 N90-29257
Numerical simulation of hypersonic viscous flow for the design of H-2 orbiting plane (HOPE)
[NAL-TR-1028] 24 p3422 N90-29330

SPACE TRANSPORTATION SYSTEM
NT ADVANCED LAUNCH SYSTEM (STS)
Liquid rocket booster study. Volume 2, book 2, appendix 1: Trades studies
[NASA-CR-183601] 01 p0027 N90-10136
Liquid rocket booster study. Volume 2, book 3, appendices 2-5: PPIP, transition plan, AMOS plan, and environmental analysis
[NASA-CR-183602] 01 p0027 N90-10139
STS-GPS (Space Transportation System - Global Positioning System) tracking experiment for gravitation estimation: Feasibility study
[AD-A211265] 02 p0150 N90-10859
STS payload design load evolution 02 p0176 N90-10989
National Aeronautics and Space Administration 04 p0563 N90-13282
Fiscal year 1990 authorization request and budget estimates for the National Aeronautics and Space Administration
[GPO-96-945] 04 p0563 N90-13283
The 1990 National Aeronautics and Space Administration Authorization
[GPO-98-466] 04 p0563 N90-13285
National Aeronautics and Space Administration Authorization Act, fiscal year 1990
[S-REPT-101-157] 04 p0564 N90-13288
National Aeronautics and Space Administration Authorization Act, fiscal year 1990
[S-REPT-101-157] 04 p0564 N90-13289
On the wings of a dream: The Space Shuttle
[NASA-EP-269] 05 p0593 N90-13446
National Aeronautics and Space Administration Multiyear Authorization Act of 1989 05 p0709 N90-14148
National Aeronautics and Space Administration authorization
[S-HRG-101-348] 05 p0709 N90-14149

Review of the Aerospace Safety Advisory Panel report for NASA fiscal year 1990 authorization
[GPO-24-234] 06 p0722 N90-14213
Flight set 360T004 (STS-30) field joint protection system, volume 7
[NASA-CR-183829] 06 p0735 N90-14280
Study of metal corrosion using ac impedance techniques in the STS launch environment
08 p1155 N90-16688
The international space transportation market: A European perspective 09 p1173 N90-16785
United States space transportation survey
09 p1173 N90-16787
French studies on advanced space transportation systems 09 p1175 N90-16798
A methodology for the concept definition of advanced space transportation systems 09 p1176 N90-16813
The liquid rocket booster and its potential for the STS
09 p1179 N90-16833
Mission report on the Orbiter Camera Payload System (OCPS) Large Format Camera (LFC) and Attitude Reference System (ARS)
[NASA-CR-186273] 09 p1240 N90-17197
Aerospace Safety Advisory Panel
[NASA-TM-101748] 12 p1634 N90-19389
An all electronic transportation system from LEO to GEO and beyond 15 p2060 N90-21796
General purpose heat source radioisotope thermoelectric generator. Book 2: Accident analysis, appendices
[REPT-90SDS4202-BK-2] 15 p2166 N90-22380
Study to identify future cryogen payload elements/users for space shuttle launch during period 1990 to 2000
[NASA-CR-186311] 17 p2363 N90-23452
Conceptual design of a Moving Belt Radiator (MBR) shuttle-attached experiment
[NASA-CR-185169] 17 p2367 N90-23474
Operations considerations in Space Station Freedom assembly 18 p2500 N90-24284
Random vibration analysis of space flight hardware using NASTRAN 18 p2570 N90-24645
Electrochemical control of iodine disinfectant for space transportation system and space station potable water
18 p2629 N90-24981
The use of underwater dynamometry to evaluate two space suits 18 p2632 N90-24995
Departments of Veterans Affairs and Housing and Urban Development, and Independent Agencies Appropriations for Fiscal Year 1990, part 2
[S-HRG-101-345-PT-2] 18 p2636 N90-25017
Flight set 360L001 (STS-26) igniter, post flight
[NASA-CR-183957] 20 p2870 N90-26325
Space Shuttle 2 advanced space transportation system. Volume 1: Executive summary
[NASA-CR-185952] 21 p2965 N90-26853
Space Shuttle 2 advanced space transportation system, volume 2
[NASA-CR-185953] 21 p2965 N90-26854
Departments of Veterans Affairs and Housing and Urban Development, and independent agencies appropriations for 1991. Part 4: National Aeronautics and Space Administration
[GPO-30-861] 21 p3088 N90-27561
Optimal trajectories for Saenger-type vehicles
22 p3129 N90-27760
Autonomous propulsion system requirements for placement of an STS (Space Transportation System) external tank in low Earth orbit
[PB90-183302] 22 p3133 N90-27777
Liquid Rocket Booster (LRB) for the Space Transportation System (STS) systems study. Volume 1: Executive summary
[NASA-CR-183822] 23 p3288 N90-28599
Liquid Rocket Booster (LRB) for the Space Transportation System (STS) systems study, volume 2
[NASA-CR-183786] 23 p3288 N90-28600
Liquid Rocket Booster (LRB) for the Space Transportation System (STS) systems study. Appendix A: Stress analysis report for the pump-fed and pressure-fed liquid rocket booster
[NASA-CR-183787-APP-A] 23 p3288 N90-28601
Liquid Rocket Booster (LRB) for the Space Transportation System (STS) systems study. Appendix B: Liquid rocket booster acoustic and thermal environments
[NASA-CR-183788-APP-B] 23 p3288 N90-28602
Liquid Rocket Booster (LRB) for the Space Transportation System (STS) systems study. Appendix C: Battery report for the liquid rocket booster TVC actuators
[NASA-CR-183789-APP-C] 23 p3288 N90-28603
Liquid Rocket Booster (LRB) for the Space Transportion System (STS) systems study. Appendix D: Trade study summary for the liquid rocket booster
[NASA-CR-183790-APP-D] 23 p3289 N90-28604
Liquid Rocket Booster (LRB) for the Space Transportation System (STS) systems study. Appendix E: Pressure-fed booster test bed for the liquid rocket booster study
[NASA-CR-183791-APP-E] 23 p3289 N90-28605
Liquid Rocket Booster (LRB) for the Space Transportation System (STS) systems study. Appendix F: Performance and trajectory for ALS/LRB launch vehicles
[NASA-CR-183792-APP-F] 23 p3289 N90-28606
Liquid Rocket Booster (LRB) for the Space Transportation System (STS) systems study. Appendix G: LRB for the STS system study level 2 requirements, revision 1
[NASA-CR-183793-APP-G] 23 p3289 N90-28607
The space transportation main engine phase A' study
[NASA-CR-179399] 23 p3290 N90-28610
Advanced Earth-to-orbit propulsion technology program overview: Impact of civil space technology initiative
23 p3290 N90-28612
Shuttle remote manipulator system mission preparation and operations 24 p3521 N90-29909

SPACE TRANSPORTATION SYSTEM FLIGHTS
Independent Orbiter Assessment (IOA): Analysis of the active thermal control subsystem
[NASA-CR-185553] 03 p0314 N90-11782
Debris/ice/TPS assessment and photographic analysis for Shuttle Mission STS-33R
[NASA-TM-102785] 09 p1180 N90-16846
Aerospace Safety Advisory Panel
[NASA-TM-101748] 12 p1634 N90-19389
Large screen display for the Mission Control Center
13 p1858 N90-20662
Final environmental impact statement for the Galileo Mission (Tier 2)
[NASA-TM-102925] 15 p2124 N90-22147
Debris/ice/TPS assessment and photographic analysis for Shuttle Mission STS-36
[NASA-TM-102789] 16 p2205 N90-22583
Overview on the Hermes in-orbit control system
[MBB-UK-0056/89-PUB] 19 p2652 N90-25094
Process and information integration via hypermedia
19 p2733 N90-25534
Debris/ice/TPS assessment and photographic analysis for shuttle mission STS-31R
[NASA-TM-102790] 20 p2819 N90-26040
Flight motor set 360L007 (STS-33R)
[NASA-CR-183979] 20 p2824 N90-26067
Debrix/ice/TPS assessment and photographic analysis of Shuttle Mission STS-32R
[NASA-TM-102787] 22 p3124 N90-27733
Space shuttle descent flight verification by simulation: A challenge in implementing flight control system robustness 22 p3127 N90-27748
Flight motor set 360L001 (STS-26R). Volume 1: System overview, revision A
[NASA-CR-183995] 22 p3133 N90-27778
Flight motor set 360L006 (STS-34). Volume 1: System overview
[NASA-CR-184007] 22 p3133 N90-27781

SPACE TUGS
Space transportation: NASA has no firm need for increasingly costly orbital maneuvering vehicle
[GAO/NSIAD-90-192] 20 p2819 N90-26041

SPACE VEHICLE CHECKOUT PROGRAM
Hermes ground operation concepts
09 p1178 N90-16826

SPACE VEHICLE CONTROL
U SPACECRAFT CONTROL

SPACE WEAPONS
Assessment of space power related measurement requirements of the Strategic Defense Initiative
[PB89-209357] 02 p0236 N90-11343
A review of gas-cooled reactor concepts for SDI (Strategic Defense Initiative)
[DE89-016962] 06 p0842 N90-14898
Prospects for space arms control
[DE90-003392] 07 p0987 N90-15700
The effects of natural and enhanced Van Allen Belt radiation on a space based weapon platform
[DE89-016219] 08 p1154 N90-16685
A new method for power generation and distribution in outer space
[DE90-005571] 09 p1243 N90-17211
Defending against a space blockade: CADRE paper
[AD-A215681] 09 p1276 N90-17398
United States Department of Energy stategic defense initiative: New and innovative concepts program
[DE90-005006] 09 p1276 N90-17399
Survivability and effectiveness of near-term strategic defense
[DE90-005805] 11 p1555 N90-18955
Assessing the morality of using the space environment as a platform for weapons
[AD-A217348] 13 p1879 N90-20780
The thrust and parry of the SIOP (Single Integrated Operational Plan) and SDI
[AD-A217617] 13 p1880 N90-20784
SDI (Strategic Defense Initiative): Is its future past
[DE90-008016] 13 p1880 N90-20785
Role of free-electron lasers in strategic defense
[DE90-008028] 13 p1880 N90-20786
Zenith Star: A structural control challenge
14 p1933 N90-21064
Scaling of nonnuclear kinetic-energy antisatellites
[DE90-009758] 15 p2059 N90-21791
Nonlinear dynamics and control of flexible structures
[AD-A218476] 17 p2386 N90-23589
Guidance and targeting for the strategic target system
[DE90-005239] 20 p2817 N90-26031
ASATs vs Brilliant Pebbles
[DE90-010348] 20 p2922 N90-26626
Thermal management of an accelerator system in space
[DE90-013153] 20 p2922 N90-26627
Multimegawatt space nuclear power supply, phase 1. Volume 2: Phase 2 plan D180-30619-6
[DE90-012431] 20 p2925 N90-26645
Multimegawatt space nuclear power supply, phase 1. Volume 3: Annotated outline of preliminary safety assessment D180-30619-7
[DE90-012432] 20 p2926 N90-26646
Multimegawatt space nuclear power supply, phase 1. Supplement: D180-30619-8
[DE90-012433] 20 p2926 N90-26647
Space test range
[AD-A223259] 21 p2964 N90-26850
Department of Energy Strategic Defense Initiative programs: Potential programmatic and facility impacts due to a prospective defense and space treaty
[DE90-012717] 21 p3067 N90-27437

SPACE-TIME CONTINUUM
U RELATIVITY

SPACE-TIME FUNCTIONS
Are there causal vacuum solutions with the symmetries of the Goedel universe in higher-derivative gravity
[DE89-611966] 01 p0134 N90-10770
On the construction of the scattering matrix for locally-noncommutative interactions of relativistic fields
[DE89-630138] 02 p0287 N90-11640
Scalar fields versus black holes
[DE89-611967] 03 p0420 N90-12413
Index formulas for generalized Wiener-Hopf operators and Boson-Fermion correspondence in 2N dimensions
[CWI-PM-R8811] 04 p0542 N90-13141
Strings, p-branes and Skyrmions in curved space
04 p0565 N90-13293
Some aspects of curvature in general relativity
05 p0704 N90-14122
Quantum fields in cosmological space-times: A soluble example
[DE89-618837] 08 p1150 N90-16662
New spacetime superalgebras and their Kac-Moody extension
[DE90-606949] 10 p1422 N90-18201
Cubic interaction in conformal theory of integer higher-spin fields in four dimensional space-time
[DE90-607095] 10 p1425 N90-18220
Concepts and experiments on space-time chaos
[ETN-90-96255] 11 p1508 N90-18683
Perturbations of test mass motion in the Schwarzschild spacetime using the method of Hamilton and Jacobi
11 p1577 N90-19083
Propagation of electromagnetic waves in multidimensional homogeneous cosmologies
[DE90-610474] 12 p1647 N90-19462
Causal boundary construction for space-times of the general relativity theory
[ETN-90-95357] 12 p1725 N90-19915
Toward higher order tests of the gravitational interaction 12 p1731 N90-19948
Applied general relativity 12 p1731 N90-19950
High stability radio links 12 p1734 N90-19970
Theoretical investigations in elementary particle physics
[DE90-007178] 13 p1883 N90-20802
Characteristics consequences of space-time coordinate relativization
[DE90-615201] 14 p2034 N90-21668
Conserved conformal currents in curved space-time
[DE90-612766] 14 p2034 N90-21672
String dynamics in curved space-time revisited
[DE90-612796] 14 p2035 N90-21674
Propagation of transient acoustic waves in porous media
[ETN-90-96401] 15 p2099 N90-22015
Computer simulation of time-dependent spherically symmetric spacetimes containing radiating fluids: Formalism and code tests 15 p2185 N90-22483
Quantum mechanics in Riemannian space-time
[DE90-620448] 16 p2325 N90-23257

Anisotropic inflation 16 p2331 N90-23286
Kinematic Weyl space-time models
[ETN-90-96508] 18 p2627 N90-24971
The structure of random discrete spacetime
[NASA-CR-182841] 22 p3255 N90-28429
Geometrical properties of an internal local octonionic space in a non-Riemannian manifold
[DE90-627175] 23 p3390 N90-29149
Casimir effect in a D-dimensional flat spacetime and the cut-off method
[DE90-627177] 23 p3390 N90-29151
A comment on anisotropic spheres admitting one parameter group of conformal motions
[DE90-627195] 23 p3403 N90-29230

SPACE-TIME METRIC
U SPACE-TIME FUNCTIONS

SPACEBORNE ASTRONOMY
Project Radioastron 02 p0158 N90-10901
The Voyager Neptune travel guide
[NASA-CR-186108] 05 p0585 N90-13412
Interplanetary dust close to the Sun (F corona): Its observation in the visible and infrared by a rocket-borne coronagraph 05 p0661 N90-13864
Long-lived space observatories for astronomy and astrophysics
[NASA-CR-185373] 06 p0731 N90-14261
Herbig Ae/Be stars: Fine structure far-infrared lines 11 p1584 N90-19126
Seeing in a new light: Astro-1 teacher's guide with activities
[NASA-EP-274] 13 p1899 N90-20900
Proceedings of the Third Infrared Detector Technology Workshop
[NASA-TM-102209] 14 p1975 N90-21313
Stressed Ge:Ga photoconductors for space-based astronomy. (Is there life beyond 120 micron) 14 p1975 N90-21315
Design considerations for precision and reliability in space mechanisms 18 p2536 N90-24463
A long look back: ESA's faint object camera. The story of the faint object camera, one of ESA's contributions to the Hubble space telescope
[ESA-BR-67] 19 p2784 N90-25839
Predictions of radiation backgrounds for GRO/OSSE
[RAE-TM-SPACE-372] 23 p3414 N90-29293

SPACEBORNE EXPERIMENTS
Space Station Freedom: A foothold on the future
[NASA-NP-107/10-88] 02 p0159 N90-10907
Shuttle Atlantis to deploy Galileo probe toward Jupiter
[NASA-TM-101888] 02 p0175 N90-10982
Concepts for microgravity experiments utilizing gloveboxes
[NASA-TM-100378] 02 p0209 N90-11195
Droplet combustion experiment drop tower tests using models of the space flight apparatus
[NASA-TM-101472] 02 p0209 N90-11196
Petite Amateur Navy Satellite (PANSAT)
[NASA-CR-186049] 03 p0317 N90-11800
Nonintrusive inertial vibration isolation technology for microgravity space experiments
[NASA-TM-102386] 03 p0334 N90-11901
The BATSE experiment on the Gamma Ray Observatory: Solar flare hard x ray and gamma-ray capabilities 03 p0431 N90-12469
Current limiting mechanisms in electron and ion beams experiments
[AD-A212295] 04 p0460 N90-12637
Biology in microgravity: A guide for experimenters
[ESA-TM-02] 04 p0482 N90-12769
Syncom 4 deploy, LDEF retrieval highlight 10-day Columbia flight
[NASA-NEWS-RELEASE-89-180] 05 p0594 N90-13448
Science and applications on the space station: A strategic vision
[NASA-TM-101863] 05 p0601 N90-13493
The Norwegian balloon and sounding rocket program 1989-1992 05 p0656 N90-13829
The DYANA campaign 1990 05 p0662 N90-13870
Cells in Space
[NASA-CP-10034] 05 p0676 N90-13939
The pituitary growth hormone cell in space 05 p0676 N90-13941
Response of lymphocytes to a mitogenic stimulus during spaceflight 05 p0677 N90-13942
How to detect when cells in space perceive gravity 05 p0678 N90-13946
Gravity and animal embryos 05 p0678 N90-13951
Design challenges for space bioreactors 05 p0679 N90-13955
Shuttle Laser Technology Experiment Facility (LTEF)-to-airplane lasercom experiment: Airplane considerations
[NASA-TM-100749] 06 p0731 N90-14260
Design considerations for space flight hardware
[NASA-TM-102300] 06 p0734 N90-14275
Extravehicular activity welding experiment
[NASA-CR-183848] 06 p0791 N90-14608
Flight experiment hardware for sounding rocket investigations. Materials science and fluid sciences
[ESA-SP-1116] 08 p1038 N90-15998
Experiment facilities for materials and fluid sciences embarked on Spacelab
[ESA-SP-1120] 08 p1053 N90-16089
Get Away Special: The first ten years
[NASA-TM-102921] 09 p1171 N90-16775
Critical fluid light scattering 09 p1222 N90-17087
Light scattering instrumentation for micro gravity research 09 p1223 N90-17096
Outline of high voltage solar array experiment using SFU platform 10 p1345 N90-17801
Development of an infrared imaging system for the surface tension driven convection experiment 10 p1367 N90-17922
A new approach to active vibration isolation for microgravity space experiments
[NASA-TM-102470] 10 p1368 N90-17929
Solar-Terrestrial Science Strategy Workshop
[NASA-CP-3048] 10 p1444 N90-18329
Background of the workshop 10 p1444 N90-18330
Navigation experiment NAVEX data storage and processing
[ESA-TT-1175] 11 p1467 N90-18445
Navigation experiment NAVEX: The self-test delay times in the D1 Spacelab mission
[ESA-TT-1176] 11 p1467 N90-18446
Investigation of methods to produce a uniform cloud of fuel particles in a flame tube
[NASA-TM-102376] 11 p1505 N90-18665
Synchronization of the ground station atomic clocks using three weighted transportable cesium time standards in the Navex navigation experiment
[ESA-TT-1153] 11 p1512 N90-18711
Compendium of meteorological space programs, satellites, and experiments
[NASA-TM-102924] 12 p1607 N90-19243
Relativistic Gravitational Experiments in Space
[NASA-CP-3046] 12 p1730 N90-19940
Optical interferometers for tests of relativistic gravity in space 12 p1734 N90-19967
A discussion of observation model, error sources and signal size for spaceborne gravitational gradiometry 13 p1839 N90-20557
The GRADIO spaceborne gravity gradiometer: Development and accommodation 13 p1840 N90-20560
A spaceborne optical interferometer: The JPL CSI mission focus 14 p1933 N90-21063
Tests of the Rockwell Si:As Back-Illuminated Blocked-Impurity Band (BIBIB) detectors 14 p1981 N90-21350
Impact of low gravity on water electrolysis operation
[NASA-CR-185521] 15 p2072 N90-21870
An expert system for simulating electric loads aboard Space Station Freedom
[NASA-TM-103150] 15 p2158 N90-22325
Space Station Workshop: Commercial Missions and User Requirements
[NASA-TM-102912] 15 p2175 N90-22428
Spacecraft attitude impacts on COLD-SAT non-vacuum jacketed LH2 supply tank thermal performance
[NASA-TM-103158] 16 p2207 N90-22592
Study to identify future cryogen payload elements/users for space shuttle launch during period 1990 to 2000
[NASA-CR-186311] 17 p2363 N90-23452
Consortium for materials development in space
[NASA-CR-186534] 17 p2383 N90-23575
Progress in the design of a microgravity facility for in-orbit experiments 18 p2540 N90-24496
Shutter mechanism for controlling the exposure of samples to solar radiation 18 p2540 N90-24498
Mechanism for deployment and retraction of biological samples 18 p2540 N90-24499
Hemispherical pointing mechanism 18 p2541 N90-24502
Thermal and orbital analysis of Earth monitoring Sun-synchronous space experiments
[NASA-TM-101630] 19 p2686 N90-25168
Microgravity as a tool in developmental biology
[ESA-SP-1123] 19 p2680 N90-25239
The first seven minutes of a Zenopus egg fertilised on a sounding rocket in space 19 p2680 N90-25245
The effect of clinostat rotation on plant protoplasts 19 p2681 N90-25247
An in-vitro technique to study bone metabolism in developing mouse long bone rudiments under microgravity and compression 19 p2681 N90-25248
Automatic experiment container for fertilisation of frog eggs in space: A multi-purpose piece of classified space hardware 19 p2681 N90-25249
The influence of a sounding rocket flight on sexual activation in Chlamydomonas gametes 19 p2681 N90-25250
Simulation of the inversion of amphibian eggs in a gravitational field using hollow glass spheres 19 p2681 N90-25251
Lens and limb regeneration in newt during and after 13-day long spaceflight 19 p2681 N90-25252
Rotating-unbalanced-mass devices for scanning balloon-borne experiments, free-flying spacecraft, and space shuttle/space station experiments
[NASA-TP-3030] 19 p2682 N90-25255
An expert system to advise astronauts during experiments: The protocol manager module 19 p2730 N90-25522
Small helium-cooled infrared telescope experiment for Spacelab-2 (IRT)
[NASA-CR-183983] 19 p2765 N90-25708
Observations of black hole candidates with the Mir-Kvant HEXE 19 p2774 N90-25774
High energy X ray observations of GX 1+4 with HEXE 19 p2779 N90-25808
Hard X ray observations of AGN 19 p2791 N90-25889
Proceedings of the LDEF Materials Data Analysis Workshop
[NASA-CP-10046] 20 p2826 N90-26075
The US Experiments Flown on the Soviet Biosatellite Cosmos 1887
[NASA-TM-102254] 20 p2891 N90-26452
Experiment K-6-24, K-6-25, K-6-26. Radiation dosimetry and spectrometry 20 p2897 N90-26477
Production activities in space: The problems of protection 20 p2939 N90-26725
Possible solutions 20 p2939 N90-26726
Radars in space 21 p3015 N90-27144
Applications of ISES for snow, ice, and sea state 21 p3018 N90-27159
Flight mechanics applications for tethers in space: Cooperative Italian-US programs 22 p3131 N90-27770
Microgravity science and applications: Apparatus and facilities
[NASA-TM-101892] 23 p3285 N90-28588
Development and approach to low-frequency microgravity isolation systems
[NASA-TP-2984] 23 p3317 N90-28754
Design of a CO2 laser power control system for a Spacelab microgravity experiment
[NASA-TM-103112] 23 p3331 N90-28833
Microgravitation experiments in space: Compatibility with interfering dynamic influences 23 p3392 N90-29162
Pointing control system for the Teal Ruby experiment 24 p3429 N90-29370
The Ulysses data book: A summary of the technical elements of the Ulysses spacecraft and its scientific payload
[ESA-BR-65] 24 p3440 N90-29427
Characteristics of pushbroom scanning type radiometer utilizing linear sensors
[NAL-TR-1024] 24 p3472 N90-29625

SPACEBORNE LASERS
The recovery of orbital and geophysical parameters using a spaceborne laser ranging system 02 p0226 N90-11294
Laser sounding from space: Report of the ESA Technology Working Group on Space Laser Sounding and Ranging
[ESA-SP-1108] 03 p0354 N90-12024
Outline on the future Italian transportable laser ranging station
[CISE-4845] 05 p0649 N90-13782
Normal points: Compression of satellite laser ranging data
[ETN-90-96008] 05 p0707 N90-14145
Laser intersatellite transmission experiment spatial acquisition, tracking, and pointing system
[AD-A215934] 10 p1389 N90-18036
Development of a receiver for a space-based laser radar system
[AD-A215079] 12 p1665 N90-19566
Frequency stable high power lasers in space 12 p1734 N90-19969
Zenith Star: A structural control challenge 14 p1933 N90-21064
Solar-pumped laser for free space power transmission 15 p2061 N90-21804
Stability of laser oscillator systems 18 p2641 N90-25045

SPACEBORNE PHOTOGRAPHY
NT SATELLITE-BORNE PHOTOGRAPHY
Technology development: Future use of NASA's large format camera is uncertain
[GAO/NSIAD-90-142] 20 p2865 N90-26298

Mesoscale Lightning Experiment (MLE): A view of lightning as seen from space during the STS-26 mission
[NASA-TM-103513] 23 p3353 N90-28951

SPACEBORNE TELESCOPES
NT HUBBLE SPACE TELESCOPE
NT INFRARED SPACE OBSERVATORY (ISO)
NT LARGE DEPLOYABLE REFLECTOR
NT SPACE INFRARED TELESCOPE FACILITY
NT STARLAB
NT X RAY ASTROPHYSICS FACILITY

Project Radioastron 02 p0158 N90-10901
The x ray mirror and the PSPC of the supernova-rocket-project 05 p0662 N90-13867
Astrometric Telescope Facility isolation and pointing study
[NASA-CR-177473] 10 p1328 N90-17675
Requirements of IR space astronomy 14 p1975 N90-21314
Small helium-cooled infrared telescope experiment for Spacelab-2 (IRT)
[NASA-CR-183983] 19 p2765 N90-25708

SPACECRAFT ANTENNAS
Ka-band MMIC beam steered transmitter array 04 p0488 N90-12803
Dynamics and control of flexible spacecraft during and after slewing maneuvers
[NASA-CR-186123] 06 p0733 N90-14270
Large space antenna concepts for ESGP 12 p1608 N90-19253
Mesh surfaces for reflector applications 12 p1611 N90-19268
Antennas for 20/30 GHz and beyond 12 p1611 N90-19269
Discrete-time control of a spacecraft with retargetable flexible antennas 13 p1763 N90-20119
Discrete-time control of a spacecraft with retargetable flexible antennas
[AD-A218345] 13 p1764 N90-20125
Control of large space structures
[AD-A221216] 18 p2511 N90-24345
A Communications Antenna Pointing System (CAPS): A modular approach 18 p2537 N90-24474

SPACECRAFT CABIN ATMOSPHERES
Independent Orbiter Assessment (IOA): Analysis of the atmospheric revitalization pressure control subsystem
[NASA-CR-185593] 02 p0163 N90-10925
Refurbishment of one-person regenerative air revitalization system
[NASA-CR-183757] 05 p0675 N90-13934

SPACECRAFT CABINS
Suitport extra-vehicular access facility
[NASA-CASE-ARC-11635-1] 09 p1183 N90-16860

SPACECRAFT CHARGING
Current limiting mechanisms in electron and ion beams experiments
[AD-A212295] 04 p0460 N90-12637
Strategic characteristics of Dynamics Explorer 1 retarding ion mass spectrometer and the consequences for core plasma measurements
[AD-A214013] 07 p0886 N90-15125
SCATHA (Spacecraft Charging at High Altitudes) atlas data base, volume 1
[AD-A214204] 07 p0886 N90-15127
SCATHA (Spacecraft Charging At High Altitudes) atlas data base, volume 2
[AD-A214205] 07 p0887 N90-15128
Environmental constraints for polar platform design
[RAE-TR-89014] 09 p1181 N90-16849
Spacecraft environmental anomalies handbook
[NASA-CR-186331] 09 p1182 N90-16852
Integrated analytical evaluation and optimization of model parameters against preprocessed measurement data
[AD-A215518] 09 p1247 N90-17231
PIC code modeling of spacecraft charging potential during electron beam injection into a background of neutral gas and plasma, part 1
[NASA-CR-186602] 15 p2059 N90-21792
Flight model discharge system
[AD-A220261] 18 p2510 N90-24342
Plasma interactions and effects for large systems 19 p2735 N90-25545
Comparison of currents predicted by NASCAP/LEO model simulations with elementary Langmuir-type bare probe models for an insulated cable containing a single pinhole
[NASA-TM-102486] 20 p2821 N90-28054
Sensitivity analysis with a simple charging code
[RAE-TM-SPACE-374] 20 p2929 N90-26662
Spacecraft charging effects
[RAE-TM-SPACE-375] 23 p3287 N90-28594

SPACECRAFT COMMUNICATION
NT SATELLITE COMMUNICATION
Space station RT and E utilization study
[NASA-CR-181707] 01 p0026 N90-10129
Design of a solar sail mission to Mars
[NASA-CR-186045] 03 p0311 N90-11771
Independent Orbiter Assessment (IOA): Assessment of the communication and tracking subsystem, volume 1
[NASA-CR-185528-VOL-1] 03 p0315 N90-11789
Independent Orbiter Assessment (IOA): Assessment of the communication and tracking subsystem, volume 2
[NASA-CR-185528-VOL-2] 03 p0315 N90-11790
Independent Orbiter Assessment (IOA): Assessment of the communication and tracking subsystem, volume 3
[NASA-CR-185528-VOL-3] 03 p0315 N90-11791
Aerospace vehicle design, spacecraft section. Volume 1: Project Groups 3-5
[NASA-CR-186054] 06 p0731 N90-14264
A planning and scheduling lexicon
[NASA-CR-186061] 09 p1171 N90-16777
Packet telemetry standard
[ESA-PSS-04-106-ISSUE-1] 11 p1467 N90-18447
The Telecommunications and Data Acquisition Report
[NASA-CR-185033] 12 p1642 N90-19434
Effects of amplitude distortions and IF equalization on satellite communication system bit-error rate performance
[NASA-TM-102415] 12 p1645 N90-19454
A space-based optical communication system utilizing fiber optics
[AD-A217333] 13 p1887 N90-20828
The Advanced Communications Technology Satellite (ACTS) capabilities for serving science
[NASA-CR-186584] 15 p2059 N90-21789
CLEAR: Automating control centers with expert system technology 19 p2733 N90-25533
Design of a monitor and simulation terminal (master) for space station telerobotics and telescience 23 p3372 N90-29051

SPACECRAFT COMPONENTS
NT COMMAND SERVICE MODULES
NT LUNAR LANDING MODULES
NT LUNAR MODULE
NT SERVICE MODULES
NT SPACECRAFT CABINS
NT SPACECRAFT DOCKING MODULES
NT SPACECRAFT MODULES
Materials for engine applications above 3000 deg F: An overview
[NASA-TM-100169] 01 p0034 N90-10188
Evaluation of titanium castings for aerospace components 01 p0043 N90-10237
Independent Orbiter Assessment (IOA): FMEA/CIL assessment
[NASA-CR-185589] 02 p0170 N90-10960
The use of damage characterization for life prediction methodologies 02 p0185 N90-11053
Independent Orbiter Assessment (IOA): Analysis of the life support and airlock support subsystems
[NASA-CR-185539] 03 p0314 N90-11786
Docking system for spacecraft
[NASA-CASE-MSC-21327-1] 03 p0317 N90-11798
European space technology: Celebrating twenty-five years of research and development
[ESA-BR-55] 04 p0569 N90-13322
Electrical testing 05 p0605 N90-13520
Instrumentation for a facility for the test, analysis and active control of spacecraft truss structures
[AD-A213655] 07 p0886 N90-15124
A strategy for concurrent product and process design of aerospace components
[DE90-002926] 07 p0916 N90-15299
Satellite thermal storage systems using metallic phase-change materials
[DE89-016872] 07 p0952 N90-15507
Nuclear weapon radiation effects on a space based interceptor weapon platform
[DE89-016258] 09 p1181 N90-16850
Sensitivity of space system availability predictions to underlying component reliability estimates
[AD-A215535] 09 p1183 N90-16858
Acceleration tests of the ACPB canister flight unit from RETE experiment
[IFSI-89-2] 10 p1328 N90-17669
Vibration tests of the ACPB canister flight unit of the RETE experiment, integrated with the tests of the booms from R. Piaggio
[IFSI-89-11] 10 p1328 N90-17670
Flatness and roughness metrological tests on the WRA flight unit receiver box and ACPB canister of the RETE experiment
[IFSI-88-20] 10 p1368 N90-17928
Component selection, procurement and control for ESA space systems
[ESA-PSS-01-60-ISSUE-2] 11 p1574 N90-19062
Short wavelength laser/materials interactions
[AD-A218015] 13 p1808 N90-20386
Theory of filtering and control with application to control of large space structures
[AD-A219936] 17 p2366 N90-23468
Plasma interactions and effects for large systems 19 p2735 N90-25545
Spacecraft thermal control design data. Volume 8: Index
[ESA-PSS-03-108-ISSUE-1-VOL-6] 22 p3132 N90-27773
Transformational part-count in layered octahedral-tetrahedral truss configurations
[NASA-TM-102635] 23 p3287 N90-28598
A comparison of single-cycle versus multi-cycle proof testing strategies 23 p3296 N90-28646
Utilization of space station, part 3
[NAL-TM-597-PT-3] 24 p3439 N90-29422
Proceedings of damping '89. Volume 2: Pages FAA-1 through IBD-15
[AD-A223432] 24 p3479 N90-29665

SPACECRAFT COMPUTERS
U AIRBORNE/SPACEBORNE COMPUTERS

SPACECRAFT CONFIGURATIONS
NT SATELLITE CONFIGURATIONS
NT SPACE SHUTTLE ASCENT STAGE
Dynamic substructuring for modular analysis and testing 02 p0180 N90-11015
NASA/USRA advanced space design program: The laser powered interorbital vehicle
[NASA-CR-186044] 04 p0462 N90-12646
Aerospace vehicle design, spacecraft section. Volume 1: Project Groups 3-5
[NASA-CR-186053] 06 p0731 N90-14263
Aerospace vehicle design, spacecraft section. Volume 1: Project Groups 3-5
[NASA-CR-186054] 06 p0731 N90-14264
French studies on advanced space transportation systems 09 p1175 N90-16798
Ariane-5 upper stage EPS 09 p1176 N90-16809
Sensor and actuator selection for fault-tolerant control of flexible structures
[AD-A217384] 13 p1817 N90-20433
Global nonlinear optimization of spacecraft protective structures design
[NASA-TM-100387] 14 p1938 N90-21095
Analyzing spacecraft configurations through specialization and default reasoning 15 p2155 N90-22308
Modeling and control of flexible space stations (slew maneuvers) 16 p2297 N90-23086
Operations considerations in Space Station Freedom assembly 18 p2500 N90-24284
Ion thrusters and spacecraft configuration
[RAE-TM-SPACE-206] 19 p2682 N90-25253
Space exploration: Cost, schedule, and performance of NASA's Mars Observer Mission. Fact sheet for the Chairman, Subcommittee on Science, Technology, and Space, Committee on Commerce, Science, and Transportation, US Senate
[GAO/NSIAD-88-137FS] 20 p2815 N90-26021
Space Shuttle 2 advanced space transportation system, volume 2
[NASA-CR-185953] 21 p2965 N90-26854
Shuttle to Shuttle 2: Subsystem weight reduction potential (estimated 1992 technology readiness date)
[NASA-TM-89114] 23 p3286 N90-28589
The space transportation main engine phase A' study
[NASA-CR-179399] 23 p3290 N90-28610

SPACECRAFT CONSTRUCTION MATERIALS
Conference on Aerospace Transparent Materials and Enclosures (15th) 16-20 January 1989. Volume 2: Sessions 6-9
[AD-A210201] 01 p0006 N90-10024
Liquid infiltrated C/SiC: An alternative material for hot space structures 02 p0182 N90-11030
Material properties of 2219-T851 aluminum alloy plasma welded compared to TIG welding 02 p0182 N90-11032
Development of graphite-magnesium composites for space applications 02 p0185 N90-11054
Space environment effects on carbon/epoxy materials 02 p0185 N90-11056
Axial compression buckling test on the H-2 launch vehicle satellite fairing structural element prototype (aluminum surface plate/aluminum honeycomb sandwiched curved surface plate)
[NAL-TM-563] 03 p0356 N90-12039
Manned spacecraft
[AD-A214218] 07 p0887 N90-15129
Progress in Space Transportation
[ESA-SP-293] 09 p1173 N90-16782
Material technology challenges in space transportation 09 p1179 N90-16836
New materials and structural concepts for space transportation systems 09 p1179 N90-16837
Composites design handbook for space structure applications
[ESA-PSS-03-1101-ISSUE-1-REV-1] 11 p1469 N90-18459

The determination of offgassing products from materials and assembled articles to be used in a manned space vehicle crew compartment
[ESA-PSS-01-729-ISSUE-1] 11 p1469 N90-18461
State of the art and future prospects for high temperature composites 11 p1477 N90-18498
HOTOL structures and materials at British Aerospace, Warton, UK
[EOARD-LR-90-001] 14 p1921 N90-21001
Ultrasonic and radiographic evaluation of advanced aerospace materials: Ceramic composites
[NASA-TM-102540] 14 p1989 N90-21401
Qualification test rationale for measuring the resistance of equipment to pyrotechnic shock
[REPT-892-430-117] 16 p2207 N90-22590
Production of a variety of shapes using wrapping and draping techniques
[REPT-892-430-122] 16 p2213 N90-22625
Evaluation of joints bonded with elastoplastic adhesives
[REPT-892-430-120] 16 p2247 N90-22816
Materials and processes for spacecraft: The ESTEC approach
[ESA-STM-244] 19 p2667 N90-25176
Plasma interactions and effects for large systems 19 p2735 N90-25545
Proceedings of the LDEF Materials Data Analysis Workshop
[NASA-CP-10046] 20 p2826 N90-26075
Materials and structures for 2000 and beyond: An attempted forecast by the DLR Materials and Structures Department
[ESA-TT-1154-REV] 20 p2843 N90-26173
Experiment K-6-24, K-6-25, K-6-26. Radiation dosimetry and spectrometry 20 p2897 N90-26477
The effects of space radiation on thin films of YBa2Cu3O(sub 7-x) 22 p3147 N90-27845
Shuttle to Shuttle 2: Subsystem weight reduction potential (estimated 1992 technology readiness date)
[NASA-TM-89114] 23 p3286 N90-28589

SPACECRAFT CONTAMINATION
Photolysis of spacecraft contaminants
[AD-A211715] 03 p0317 N90-11801
The rodent research animal holding facility as a barrier to environmental contamination
[NASA-TM-102237] 03 p0378 N90-12151
Standard method for measurement of nonvolatile residue on surfaces
[AD-A213324] 04 p0474 N90-12714
Measurement of optical radiations in spacecraft environments
[AD-A213814] 07 p0950 N90-15497
Space station contamination control study: Internal combustion, phase 1
[NASA-CR-179323] 10 p1328 N90-17674
Spacecraft optical contamination environment
[AD-A216088] 13 p1889 N90-20838
Space station contamination study: Assessment of contaminant spectral brightness
[NASA-CR-186173] 19 p2666 N90-25169
Third Annual Workshop on Space Operations Automation and Robotics (SOAR 1989)
[NASA-CP-3059] 19 p2727 N90-25503
Spacecraft contamination programs within the Air Force Systems Command Laboratories 19 p2727 N90-25507
Spacecraft external molecular contamination analysis 19 p2730 N90-25520
Satellite material contaminant optical properties 19 p2732 N90-25529
Laboratory investigations: Low Earth orbit environment chemistry with spacecraft surfaces 19 p2732 N90-25531
Atmospherically induced optical contamination from orbiting thrusters
[AD-A223112] 21 p3021 N90-27174
Space station contamination modeling
[NASA-CR-183871] 23 p3286 N90-28590
Effects of thruster firings on the shuttle environment 1: Neutral gas composition
[AD-A224404] 24 p3487 N90-29707

SPACECRAFT CONTROL
NT SATELLITE ATTITUDE CONTROL
NT SATELLITE CONTROL
Computational controls for aerospace systems 01 p0017 N90-10082
Additional software developments wanted for modeling and control of flexible space systems 01 p0017 N90-10083
Flexible structure control experiments using a real-time workstation for computer-aided control engineering 01 p0017 N90-10084
Control/structure interaction methods for space station power systems 01 p0018 N90-10087
Simulation of shuttle flight control system structural interaction with RMS deployed payloads 01 p0020 N90-10100
Optical processing for distributed sensors in control of flexible spacecraft 01 p0021 N90-10102
Input-output oriented computation algorithms for the control of large flexible structures 01 p0023 N90-10118
Space station RT and E utilization study
[NASA-CR-181707] 01 p0026 N90-10129
Independent Orbiter Assessment (IOA): Analysis of the guidance, navigation, and control subsystem
[NASA-CR-185555] 02 p0162 N90-10920
Independent Orbiter Assessment (IOA): Analysis of the backup flight system
[NASA-CR-185567] 02 p0165 N90-10932
Independent Orbiter Assessment (IOA): Assessment of the rudder/speed brake subsystem FMEA/CIL
[NASA-CR-185558] 02 p0174 N90-10975
Use of Lanczos vectors in structural dynamics 02 p0179 N90-11011
Thermoelastic behavior of large space structures: Modeling and control 02 p0179 N90-11012
Guaranteed cost control of flexible space structures 02 p0287 N90-11643
Independent Orbiter Assessment (IOA): Analysis of the displays and controls subsystem
[NASA-CR-185563] 03 p0312 N90-11774
Periodic-disturbance accommodating control of the space station for asymptotic momentum management 05 p0586 N90-13416
Simultaneous quaternion estimation (QUEST) and bias determination 05 p0587 N90-13417
Spacecraft attitude determination using the earth's magnetic field 05 p0589 N90-13429
Analysis of the flight dynamics of the Solar Maximum Mission (SMM) off-sun scientific pointing 05 p0590 N90-13432
Optimal trajectories for the aeroassisted flight experiment, 1988-89
[NASA-CR-186132] 05 p0592 N90-13443
The dynamics and control of large flexible space structures - 12, supplement 11
[NASA-CR-185966] 05 p0602 N90-13494
Dynamics and control of flexible spacecraft during and after slewing maneuvers
[NASA-CR-186123] 06 p0733 N90-14270
Instrumentation for a facility for the test, analysis and active control of spacecraft truss structures
[AD-A213855] 07 p0886 N90-15124
Pulsed plasma mission endurance test
[AD-A213462] 08 p1037 N90-15993
Assessment of visual function in aerospace medicine
[BMVG-FBWM-89-5] 08 p1105 N90-16397
Cooperative control of two active spacecraft during proximity operations
[NASA-CR-185596] 09 p1172 N90-16778
Overview of the Hermes in-orbit control system 09 p1178 N90-16824
Configuration management and control for ESA space systems
[ESA-PSS-01-11-ISSUE-1] 11 p1574 N90-19061
Magnetic suspension railway systems based on space technology 11 p1577 N90-19081
Advanced topics in structural dynamics: The maneuver of flexible spacecraft, and on-off decentralized control of flexible structures 12 p1612 N90-19274
Discrete-time control of a spacecraft with retargetable flexible antennas
[AD-A218345] 13 p1764 N90-20125
Sensor and actuator selection for fault-tolerant control of flexible structures
[AD-A217384] 13 p1817 N90-20433
Applications of graphics to support a testbed for autonomous space vehicle operations 13 p1858 N90-20661
GCS plan for software aspects of certification
[NASA-CR-181972] 13 p1864 N90-20694
Direct inversion of rigid-body rotational dynamics
[NASA-TM-102798] 15 p2055 N90-21773
A dynamic motion simulator for future European docking systems 15 p2113 N90-22085
Spacecraft command verification: The AI solution 15 p2154 N90-22307
System control of an autonomous planetary mobile spacecraft 15 p2155 N90-22313
Automated procedure execution for space vehicle autonomous control 15 p2156 N90-22314
Approximate optimal guidance schemes for atmospheric orbital maneuvering 16 p2206 N90-22585
Proceedings of the 3rd Annual Conference on Aerospace Computational Control, volume 1
[NASA-CR-186446] 16 p2279 N90-22987
New multivariable capabilities of the INCA program 16 p2290 N90-23049
The use of real-time, hardware-in-the-loop simulation in the design and development of the new Hughes HS601 spacecraft attitude control system 16 p2293 N90-23065
Multibody dynamics: Modeling component flexibility with fixed, free, loaded, constraint, and residual modes 16 p2295 N90-23072
Issues in CSI analysis for large scale systems 16 p2296 N90-23076
Modeling and control of flexible vehicles in space
[AD-A219622] 17 p2365 N90-23465
Investigations on docking and berthing dynamics 18 p2504 N90-24312
Control of large space structures
[AD-A221216] 18 p2511 N90-24345
Overview on the Hermes in-orbit control system
[MBB-UK-0056/89-PUB] 19 p2652 N90-25094
Monitoring and control of spacecraft systems using procedural reasoning 19 p2731 N90-25524
The Screem-J4D: A proposal in response to a low Reynolds number station keeping mission
[NASA-CR-186664] 20 p2807 N90-25968
Guidance and control strategies for aerospace vehicles
[NASA-CR-186878] 20 p2814 N90-26013
Space Shuttle 2 advanced space transportation system, volume 2
[NASA-CR-185953] 21 p2965 N90-26854
Local design methodologies for a hierarchic control architecture
[AD-A222006] 21 p2966 N90-26862
Control of orbiting large space structural systems with discrete time observational data and random measurement noise
[AD-A222476] 21 p2967 N90-26863
The instrument pointing system: Precision attitude control in space 22 p3129 N90-27756
Effects of low bond number liquid motions on spacecraft attitude 22 p3131 N90-27768
The control of space manipulators subject to spacecraft attitude control saturation limits 24 p3515 N90-29871
Performance constraints and compensation for teleoperation with delay 24 p3517 N90-29881

SPACECRAFT DEFENSE
Defense to laser light irradiation
[AD-D014286] 08 p1036 N90-15984
Bayesian characterization and detection of rare binary signature events
[AD-A221116] 18 p2606 N90-24844

SPACECRAFT DESIGN
NT SATELLITE DESIGN
NASA'S controls-structures interaction program 01 p0017 N90-10081
Computational controls for aerospace systems 01 p0017 N90-10082
Orbital debris research at NASA Johnson Space Center, 1986-1988
[NASA-TM-102155] 01 p0138 N90-10795
Flight testing and flight research: From the age of the tower jumper to the age of the astronaut 02 p0154 N90-10882
Qualification by simulation: Dream or reality 02 p0177 N90-10990
Experimental identification of modal momentum coefficients and modal identity parameters of the FLECS structure 02 p0177 N90-10991
Experiences using a major FEM package interactively for spacecraft applications 02 p0179 N90-11008
Numerical treatment of the thermo-structural-dynamic problems: The interpolation techniques 02 p0180 N90-11016
Modeling of liquid sloshing effects in multibody systems 02 p0181 N90-11023
Comparison of sine dwell and broadband methods for modal testing 02 p0181 N90-11025
Thermal and structural analysis of Hermes 02 p0186 N90-11058
Exploitation of data management facilities for finite element analysis in aerospace structural engineering applications 02 p0188 N90-11078
Project AENEAS: A feasibility study for crew emergency return vehicle
[PB89-217020] 03 p0317 N90-11799
Requirements for multidisciplinary design of aerospace vehicles on high performance computers
[NASA-CR-181915] 03 p0384 N90-12183
Report on orbital debris
[NASA-TM-101855] 04 p0460 N90-12635
NASA/USRA advanced space design program: The laser powered interorbital vehicle
[NASA-CR-186044] 04 p0462 N90-12646
Apollo lightcraft project
[NASA-CR-186055] 04 p0464 N90-12655

Lifetime predictions for the Solar Maximum Mission (SMM) and San Marco spacecraft
05 p0591 N90-13440
Preliminary design document: Ground based testbed for avionics systems
[NASA-CR-183821] 06 p0725 N90-14231
Aerospace vehicle design, spacecraft section. Volume 1: Project Groups 3-5
[NASA-CR-186053] 06 p0731 N90-14263
Aerospace vehicle design, spacecraft section. Volume 1: Project Groups 3-5
[NASA-CR-186054] 06 p0731 N90-14264
The space station tethered elevator system
[NASA-CR-186051] 06 p0732 N90-14265
Project Argo: The design and analysis of an all-propulsive and an aeroassisted version of a manned space transportation vehicle
[NASA-CR-186047] 06 p0732 N90-14266
Design considerations for space flight hardware
[NASA-TM-102300] 06 p0734 N90-14275
Main propulsion system test requirements for the two-engine Shuttle-C
[NASA-TM-100382] 06 p0735 N90-14282
Shuttle-C utilization for assembly of the rephased Freedom configuration
[NASA-TM-101658] 07 p0885 N90-15120
A strategy for concurrent product and process design of aerospace components
[DE90-002926] 07 p0916 N90-15299
Crew emergency return vehicle autoland feasibility study
[NASA-CR-181940] 08 p1028 N90-15937
Round trip to orbit. Human spaceflight alternatives: Special report
[OTA-ISC-419] 08 p1033 N90-15966
NASDA's approach to the interoperability of safety and rescue in space 08 p1035 N90-15981
The Gevaltig: An inertial fusion powered manned spacecraft design for outer solar system missions
[NASA-CR-185163] 08 p1036 N90-15985
A two-stage earth-to-orbit transport with translating oblique wings for booster recovery
[NASA-CASE-LAR-14156-1] 09 p1173 N90-16781
Overview of Japan's current and future space transportation programmes 09 p1174 N90-16789
Glavkosmos operational space transportation systems 09 p1174 N90-16791
French studies on advanced space transportation systems 09 p1175 N90-16798
National aero-spaceplane status and plans 09 p1175 N90-16801
U.S.S.R. space transportation systems 09 p1176 N90-16806
Development status of Japan's new launch vehicle: H-2 rocket 09 p1176 N90-16807
Ariane-5 upper stage EPS 09 p1176 N90-16809
A methodology for the concept definition of advanced space transportation systems 09 p1176 N90-16813
The Hermes system: Its design objectives and solutions 09 p1177 N90-16821
Hermes propulsion system 09 p1178 N90-16823
Views on the evolution of European space transport: The reference launcher concept EARL 2
09 p1179 N90-16831
HOPE: Its concept and technical features
09 p1179 N90-16835
An assessment of potential markets for small satellites
[NASA-TM-101943] 09 p1181 N90-16848
Magellan/Galileo solder joint failure analysis and recommendations
[NASA-CR-186294] 09 p1233 N90-17157
Supersonic aerodynamic characteristics of a proposed Assured Crew Return Capability (ACRC) lifting-body configuration
[NASA-TM-4136] 10 p1307 N90-17560
The Columbus power system simulation programme
10 p1330 N90-17686
The solar array design of the Vesta small bodies spacecraft 10 p1345 N90-17799
Spacecraft thermal control design data, volume 1
[ESA-PSS-03-108-ISSUE-1-VOL-1]
11 p1468 N90-18455
Spacecraft thermal control design data, volume 2
[ESA-PSS-03-108-ISSUE-1-VOL-2]
11 p1469 N90-18456
Spacecraft thermal control design data, volume 3
[ESA-PSS-03-108-ISSUE-1-VOL-3]
11 p1469 N90-18457
Spacecraft thermal control design data, volume 4
[ESA-PSS-03-108-ISSUE-1-VOL-4]
11 p1469 N90-18458
Composites design handbook for space structure applications
[ESA-PSS-03-1101-ISSUE-1-REV-1]
11 p1469 N90-18459
Operational requirements and the geostationary platform 12 p1608 N90-19250
Implications of Advanced Technologies for Air and Spacecraft Escape
[AGARD-CP-472] 13 p1751 N90-20054
Using an instrumented manikin for Space Station Freedom analysis 13 p1861 N90-20675
The partnership: Space shuttle, space science, and space station
[NASA-TM-102900] 14 p1930 N90-21050
Zenith Star: A structural control challenge
14 p1933 N90-21064
Proceedings of the 3rd Annual Conference on Aerospace Computational Control, volume 1
[NASA-CR-186446] 16 p2279 N90-22987
Concurrent processing simulation of the space station
16 p2289 N90-23041
Implementation of generalized optimality criteria in a multidisciplinary environment 16 p2290 N90-23048
Control/structure interaction design methodology
16 p2291 N90-23053
Design considerations for precision and reliability in space mechanisms 18 p2536 N90-24463
Design of an autonomous teleoperated cargo transporting vehicle for lunar base operations
[NASA-CR-186686] 18 p2565 N90-24633
Overview on the Hermes in-orbit control system
[MBB-UK-0056/89-PUB] 19 p2652 N90-25094
PLATO: A European plateform orbiter concept
[MBB-UO-0061/89-PUB] 19 p2652 N90-25095
Ion thrusters and spacecraft configuration
[RAE-TM-SPACE-206] 19 p2682 N90-25253
United States planetary rover status: 1989
[NASA-CR-186843] 19 p2698 N90-25353
The use of PLAID in the Space Station Freedom viewing analysis 19 p2729 N90-25517
Space operations: NASA efforts to develop and deploy advanced spacecraft computers. Report to the Chairman, Subcommittee on Space Science and Applications, Committee on Science, Space, and Technology, House of Representatives
[GAO/IMTEC-89-17] 19 p2742 N90-25582
Assembly vs. direct launch of transfer vehicles
[NASA-TM-102686] 19 p2797 N90-25921
Autonomous space processor for orbital debris
[NASA-CR-186691] 20 p2820 N90-26044
NASA/USRA university advanced design program at the Univeraity of Illinois for the 1989-1990 academic year
[NASA-CR-186829] 20 p2821 N90-26049
The aerobraking space transfer vehicle
[NASA-CR-186819] 20 p2821 N90-26053
Long cycle pressurized logistics module: An Italian contribution to the Space Station Freedom logistics scenario
[IAF-89-083] 20 p2822 N90-26058
Fluid-loop reaction system
[NASA-CASE-NPO-17204-1-CU]
20 p2864 N90-26292
Structural dynamics branch research and accomplishments
[NASA-TM-102488] 20 p2878 N90-26373
Microspacecraft and Earth observation: Electrical field (ELF) measurement project
[NASA-CR-186821] 20 p2888 N90-26436
Space station definitions, design, and development. Task 5: Multiple arm telerobot coordination and control: Manipulator design methodology
[NASA-CR-182043] 20 p2914 N90-26577
Space Shuttle 2 advanced space transportation system, volume 2
[NASA-CR-185953] 21 p2965 N90-26854
Galileo: Earth avoidance study report
[NASA-CR-186424] 22 p3123 N90-27730
Affordable spacecraft: Design and launch alternatives. Background paper 22 p3125 N90-27737
Ascent and descent optimizations of an air-breathing launch vehicle 22 p3130 N90-27761
Global optimization of air breathing launch vehicle trajectories 22 p3130 N90-27762
Spacecraft thermal control design data. Volume 6: Index
[ESA-PSS-03-108-ISSUE-1-VOL-6]
22 p3132 N90-27773
Shuttle to Shuttle 2: Subsystem weight reduction potential (estimated 1992 technology readiness date)
[NASA-TM-89114] 23 p3286 N90-28589
A lunar space station
[NASA-CR-186223] 24 p3563 N90-30158

SPACECRAFT DOCKING

Docking system for spacecraft
[NASA-CASE-MSC-21327-1] 03 p0317 N90-11798
Active rendezvous between a low-earth orbit user spacecraft and the Space Transportation System (STS) shuttle 05 p0590 N90-13436
Crew Safety and Rescue in Space: An International Approach
[ESA-SP-300] 08 p1034 N90-15974
Systems interoperability approach Apollo/Soyuz test project 08 p1035 N90-15979
RVD scenari and interfaces between Hermes and space station 08 p1035 N90-15982
Supersonic aerodynamic characteristics of a proposed Assured Crew Return Capability (ACRC) lifting-body configuration
[NASA-TM-4136] 10 p1307 N90-17560
Yaw rate control of an air bearing vehicle
12 p1639 N90-19420
Docking mechanism for spacecraft
[NASA-CASE-MSC-21386-1] 13 p1764 N90-20126
Animation graphic interface for the space shuttle onboard computer 13 p1859 N90-20667
OMV mission simulator 13 p1860 N90-20669
A dynamic motion simulator for future European docking systems 15 p2113 N90-22085
The resupply interface mechanism RMS compatibility test 15 p2113 N90-22090
Orbital Maneuvering Vehicle (OMV) three-point docking latch 15 p2114 N90-22094
Computer vision research at Marshall Space Flight Center 15 p2142 N90-22240
OMV (Orbital Maneuvering Vehicle) payload support concept for Pegasus boosted payloads
[AD-A218371] 17 p2365 N90-23463
DDTF improvements for more accurate space docking simulation 18 p2504 N90-24311
Investigations on docking and berthing dynamics
18 p2504 N90-24312
Docking berthing systems: Functions and simulation
18 p2505 N90-24313
Satellite servicer system flight demonstration program
18 p2506 N90-24322
Concept design for Hermes docking/berthing mechanism 18 p2536 N90-24464
Utilization of Moire patterns as an orbital docking aid to space shuttle/Space Station Freedom
18 p2629 N90-24980
Remote operation of an orbital maneuvering vehicle in simulated docking maneuvers 19 p2736 N90-25554
Biconic cargo return vehicle with an advanced recovery system. Volume 1: Conceptual design
[NASA-CR-186520] 20 p2821 N90-26052
Closed-loop autonomous docking system
[NASA-CASE-MFS-28421-1] 21 p2966 N90-26861
Hermes rendezvous with the space station
22 p3128 N90-27753

SPACECRAFT DOCKING MODULES

Concept design for Hermes docking/berthing mechanism 18 p2536 N90-24464

SPACECRAFT ELECTRONIC EQUIPMENT

Evaluation test of CCD area sensor for star sensor
[NAL-TM-570] 02 p0274 N90-11566
CRRES (Combined Release and Radiation Effects Satellite) SPACERAD plasma wave experiment
[AD-A210791] 02 p0278 N90-11587
Payload electronics and mechanisms
05 p0604 N90-13508
Space radiation effects on electronics
[DE90-602874] 10 p1378 N90-17986
Heavy ion tests on programmable VLSI
[ETN-90-97254] 20 p2822 N90-26057

SPACECRAFT ENVIRONMENTS

Space Station Freedom: A foothold on the future
[NASA-NP-107/10-88] 02 p0159 N90-10907
Independent Orbiter Assessment (IOA): Assessment of the life support and airlock support systems, volume 1
[NASA-CR-185581-VOL-1] 02 p0174 N90-10977
Independent Orbiter Assessment (IOA): Assessment of the life support and airlock support systems, volume 2
[NASA-CR-185581-VOL-2] 02 p0174 N90-10978
Partial gravity habitat study: With application to lunar base design
[NASA-CR-186048] 06 p0732 N90-14267
Exploring the living universe: A strategy for space life sciences
[NASA-TM-101891] 06 p0822 N90-14778
SCATHA (Spacecraft Charging at High Altitudes) atlas data base, volume 1
[AD-A214204] 07 p0886 N90-15127
SCATHA (Spacecraft Charging At High Altitudes) atlas data base, volume 2
[AD-A214205] 07 p0887 N90-15128
Measurement of optical radiations in spacecraft environments
[AD-A213814] 07 p0950 N90-15497
A modular habitation unit adapted for service in low earth and geostationary earth orbits
[ILR-MITT-217] 08 p1036 N90-15990
Study of metal corrosion using ac impedance techniques in the STS launch environment
08 p1155 N90-16688

Artificial intelligence in process control: Knowledge base for the shuttle ECS model 08 p1156 N90-16697
The 1988-1989 NASA space/gravitational biology accomplishments
[NASA-TM-4160] 09 p1250 N90-17251
Solar cycle effects on trapped energetic particles
[AD-A215028] 09 p1300 N90-17532
The determination of offgassing products from materials and assembled articles to be used in a manned space vehicle crew compartment
[ESA-PSS-01-729-ISSUE-1] 11 p1469 N90-18461
Design and operation of an inert gas facility for thermoelectric generator storage
[DE90-007146] 11 p1565 N90-19008
Knowledge representation in space flight operations 13 p1857 N90-20655
Spacecraft optical contamination environment
[AD-A218088] 13 p1889 N90-20838
Stressed Ge:Ga photoconductors for space-based astronomy. (Is there life beyond 120 micron) 14 p1975 N90-21315
Gaseous optical contamination of the spacecraft environment: A review 19 p2730 N90-25519
The environmental control and life support system advanced automation project. Phase 1: Application evaluation 19 p2730 N90-25523
Space station contamination modeling
[NASA-CR-183871] 23 p3286 N90-28590
Space Station Freedom pressurized element interior design process
[NASA-CR-181297] 23 p3287 N90-28597
Electrochemical incineration of wastes
[NASA-CR-187033] 23 p3317 N90-28753
Atmosphere and water quality monitoring on Space Station Freedom
[NASA-CR-186707] 23 p3378 N90-29084

SPACECRAFT EQUIPMENT
NT SPACECRAFT ELECTRONIC EQUIPMENT
Space station RT and E utilization study
[NASA-CR-181707] 01 p0026 N90-10129
Radioactivity induced in gamma-ray spectrometers
[RAE-TM-SPACE-363] 04 p0569 N90-13317
Overview of the Hipparcos payload 05 p0603 N90-13503
Space station wardroom habitability and equipment study
[NASA-CR-4246] 09 p1260 N90-17308
System safety requirements for ESA space systems and associated equipment
[ESA-PSS-01-40-ISSUE-2] 11 p1469 N90-18460
Acoustic convective system
[NASA-CASE-NPO-17278-1-CU] 14 p1959 N90-21215
On-orbit operations of the Space Station Freedom attached payloads accommodations equipment 18 p2500 N90-24283

SPACECRAFT GLOW
Space environments and their effects on space automation and robotics 19 p2735 N90-25543

SPACECRAFT GUIDANCE
Computational controls for aerospace systems 01 p0017 N90-10082
Independent Orbiter Assessment (IOA): Analysis of the guidance, navigation, and control subsystem
[NASA-CR-185555] 02 p0162 N90-10920
Evaluation test of CCD area sensor for star sensor
[NAL-TM-570] 02 p0274 N90-11566
Independent Orbiter Assessment (IOA): Assessment of the guidance, navigation, and control subsystem FMEA/CIL
[NASA-CR-185552] 03 p0314 N90-11784
Trajectory optimization and guidance for an aerospace plane
[NASA-CR-185884] 05 p0578 N90-13369
Optimal trajectories for the aeroassisted flight experiment, 1988-89
[NASA-CR-186132] 05 p0592 N90-13443
Rapid near-optimal trajectory generation and guidance law development for single-stage-to-orbit airbreathing vehicles
[NASA-CR-186299] 12 p1612 N90-19275
GCS plan for software aspects of certification
[NASA-CR-181972] 13 p1864 N90-20694
Multivariate analysis of launcher guidance robustness
[REPT-892-422-105] 16 p2205 N90-22581
Hermes rendezvous and navigation system 18 p2504 N90-24308
Investigations on docking and berthing dynamics 18 p2504 N90-24312

SPACECRAFT INSTRUMENTS
NT SATELLITE INSTRUMENTS
Independent Orbiter Assessment (IOA): Assessment of the Orbiter Experiment (OEX) subsystem
[NASA-CR-185587] 02 p0171 N90-10962
Independent Orbiter Assessment (IOA): Analysis of the Orbiter Experiment (OEX) subsystem
[NASA-CR-185586] 02 p0171 N90-10963
Independent Orbiter Assessment (IOA): Analysis of the communication and tracking subsystem
[NASA-CR-185582] 02 p0172 N90-10967
Independent Orbiter Assessment (IOA): Assessment of instrumental subsystem FMEA/CIL
[NASA-CR-185572] 02 p0173 N90-10972
Evaluation test of CCD area sensor for star sensor
[NAL-TM-570] 02 p0274 N90-11566
Independent Orbiter Assessment (IOA): Analysis of the displays and controls subsystem
[NASA-CR-185563] 03 p0312 N90-11774
The Gamma-Ray Observatory: An overview 03 p0430 N90-12464
Radioactivity induced in gamma-ray spectrometers
[RAE-TM-SPACE-363] 04 p0569 N90-13317
The Voyager Neptune travel guide
[NASA-CR-186108] 05 p0585 N90-13412
GRADIO: An error analysis of the spaceborne gravity gradiometer
[ETN-90-96010] 05 p0667 N90-13901
Proceedings of the Second Noncontact Temperature Measurement Workshop
[NASA-CR-181289] 10 p1362 N90-17894
Non-contact temperature measurement requirements of ground-based research and flight programs at JPL 10 p1362 N90-17895
Microgravity noncontact temperature requirements at NASA Lewis Research Center 10 p1362 N90-17897
Identification and solution of a charging problem in a high-altitude detector
[DE90-008637] 12 p1616 N90-19296
Multi-application scanning mechanism 18 p2537 N90-24473
Microspacecraft and Earth observation: Electrical field (ELF) measurement project
[NASA-CR-186821] 20 p2888 N90-26436

SPACECRAFT LANDING
NT LUNAR LANDING
NT MARS LANDING
Landing tests for Buran shuttle with jet engine-equipped mock-up 02 p0158 N90-10904
Independent Orbiter Assessment (IOA): Analysis of the nose wheel steering subsystem
[NASA-CR-185548] 02 p0163 N90-10921
Independent Orbiter Assessment (IOA): Assessment of the landing/deceleration (LDG/DEC) subsystem FMEA/CIL
[NASA-CR-185570] 02 p0172 N90-10966
Space Shuttle 2 advanced space transportation system. Volume 1: Executive summary
[NASA-CR-185952] 21 p2965 N90-26853

SPACECRAFT LAUNCHING
NT LIFTOFF (LAUNCHING)
The Spartan 1 mission
[NASA-TM-101887] 01 p0015 N90-10077
Flight-mechanical environment on Ariane launch vehicle payloads 02 p0184 N90-11048
Computation of generalized modal loads in an acoustic field define by a distribution of correlated pressures
[NASA-CR-186041] 03 p0358 N90-12047
Final Environmental Impact Statement for the Galileo Mission (Tier 2)
[NASA-TM-101825] 03 p0367 N90-12102
A summary of 30 years of space launches
[AERONOMICA-ACTA-F-39-1989] 05 p0585 N90-13411
Launch and early orbit 05 p0606 N90-13524
The Brazilian space program: Actual state of the art 05 p0661 N90-13861
An in-flight technique for wind measurement in support of the space shuttle program
[NASA-TM-4154] 06 p0724 N90-14224
Draft Environmental Impact Statement for the Ulysses Mission (Tier 2)
[NASA-TM-102903] 06 p0812 N90-14727
The international space transportation market: A European perspective 09 p1173 N90-16785
Advanced manned launch systems 09 p1175 N90-16797
Ariane-5 solid boosters stage development 09 p1176 N90-16811
A field study of solid rocket exhaust impacts on the near-field environment
[NASA-TM-4172] 10 p1405 N90-18102
Space shuttle RCS oxidizer leak repair for STS-26 11 p1474 N90-18485
Superfluid helium orbital resupply coupling 11 p1475 N90-18488
Geostationary earth science platform concepts 12 p1608 N90-19252
LACE flight dynamics experiment 14 p1937 N90-21086
Advanced Launch System (ALS): Electrical actuation and power systems improve operability and cost picture
[NASA-TM-102547] 14 p1968 N90-21271
Final (Tier 1) environmental impact statement for the Galileo and Ulysses Missions
[NASA-TM-102917] 15 p2056 N90-21779
Final environmental impact statement for the Galileo Mission (Tier 2)
[NASA-TM-102925] 15 p2124 N90-22147
Draft environmental impact statement for the Galileo Mission (Tier 2)
[NASA-TM-102926] 15 p2124 N90-22148
Final Environmental Impact Statement for the Ulysses Mission (Tier 2)
[NASA-TM-101104] 15 p2126 N90-22162
General purpose heat source radioisotope thermoelectric generator program. Book 1: Accident analysis
[REPT-90SDS4202-BK-1] 15 p2166 N90-22379
General purpose heat source radioisotope thermoelectric generator. Book 2: Accident analysis, appendices
[REPT-90SDS4202-BK-2] 15 p2166 N90-22380
Orbit acquisition and control strategy for small satellites in inclined eccentric orbits
[ETN-90-96551] 16 p2203 N90-22573
US access to space: Launch vehicle choices for 1990 to 2010 16 p2205 N90-22579
Operations considerations in Space Station Freedom assembly 18 p2500 N90-24284
Atmospheric environment for space shuttle (STS-28) launch
[NASA-TM-100386] 19 p2715 N90-25452
Trajectory optimization for an asymmetric launch vehicle
[NASA-CR-185630] 20 p2817 N90-26033
Report of the Defense Science Board 1989 summer study on national space launch strategy
[AD-A222419] 21 p2963 N90-26848
Space Shuttle 2 advanced space transportation system. Volume 1: Executive summary
[NASA-CR-185952] 21 p2965 N90-26853
Affordable spacecraft: Design and launch alternatives. Background paper
[PB90-203225] 22 p3126 N90-27740
Space Vehicle Flight Mechanics
[AGARD-CP-489] 22 p3126 N90-27741
Advanced launch vehicle configurations and performance trades 22 p3126 N90-27744
Possible trajectory profiles to achieve the geostationary orbit without any drift phase 22 p3127 N90-27745
Hermes emergency reentry trajectories consequences on the Ariane 5 trajectories 22 p3127 N90-27747
Atmospheric environment for space shuttle (STS-33) launch
[NASA-TM-100399] 22 p3200 N90-28159
Flight motor set 360L008 (STS-32R). Volume 1: System overview
[NASA-CR-184010] 23 p3289 N90-28609
Atmospheric environment for Space Shuttle (STS-32) launch
[NASA-TM-100400] 23 p3346 N90-28912
Atmospheric environment for Space Shuttle (STS-31) launch
[NASA-TM-103508] 23 p3347 N90-28913
Atmospheric environment for space shuttle (STS-36) launch
[NASA-TM-100403] 23 p3347 N90-28914
Atmospheric environment for space shuttle (STS-34) launch
[NASA-TM-100396] 23 p3347 N90-28915

SPACECRAFT LUBRICATION
Tribological properties of PVD-applied MoS2 coatings used on space mechanisms 18 p2537 N90-24470
The advantages and limitations of sputtered molybdenum disulphide as a space lubricant 18 p2537 N90-24471
Investigation of lubrication characteristics of MoS2 films in space environment 18 p2537 N90-24472
Study of ball bearings for space use 18 p2537 N90-24477
Modification of the SHABERTH bearing code to incorporate RP-1 and a discussion of the traction model
[NASA-TP-3017] 22 p3183 N90-28066

SPACECRAFT MAINTENANCE
Magellan/Galileo solder joint failure analysis and recommendations
[NASA-CR-186294] 09 p1233 N90-17157
The development of the Canadian Mobile Servicing System Kinematic Simulation Facility 13 p1861 N90-20676
Second European In-Orbit Operations Technology Symposium
[ESA-SP-297] 18 p2499 N90-24280
A proposed change to the NASA strategy for servicing space assets 18 p2500 N90-24282

Advanced robotics for the on-orbit servicing
18 p2501 N90-24289
In-orbit operations research and development program of the Toulouse Space Center 18 p2501 N90-24290
The SPIDER robotic system 18 p2501 N90-24291
Hierarchy of on-orbit servicing interfaces
18 p2502 N90-24294
Evolution of EVA capabilities for space station construction and maintenance: Soviet and American experience 18 p2502 N90-24295
HERA and EVA co-operation scenarios
18 p2502 N90-24299
Robot-based equipment manipulation and transportation for the Columbus free flying laboratory
18 p2503 N90-24300
Orbital Replacement Units (ORUs) design considerations 18 p2506 N90-24320
Satellite servicer system flight demonstration program
18 p2506 N90-24322
An Earth orbiting satellite service and repair facility
[NASA-CR-186669] 19 p2665 N90-25166
SDIO robotics in space applications
19 p2729 N90-25514
Engineering test results for the Moog Single Line Disconnect
[NASA-TM-100755] 22 p3132 N90-27776

SPACECRAFT MANEUVERS
NT ORBITAL MANEUVERS
Independent Orbiter Assessment (IOA): Analysis of the reaction control system, volume 1
[NASA-CR-185532-VOL-1] 02 p0166 N90-10938
Independent Orbiter Assessment (IOA): Assessment of the reaction control system, volume 1
[NASA-CR-185543-VOL-1] 03 p0316 N90-11793
Independent Orbiter Assessment (IOA): Assessment of the reaction control system, volume 2
[NASA-CR-185543-VOL-2] 03 p0316 N90-11794
Independent Orbiter Assessment (IOA): Assessment of the reaction control system, volume 3
[NASA-CR-185543-VOL-3] 03 p0316 N90-11795
Independent Orbiter Assessment (IOA): Assessment of the reaction control system, volume 4
[NASA-CR-185543-VOL-4] 03 p0316 N90-11796
Independent Orbiter Assessment (IOA): Assessment of the reaction control system, volume 5
[NASA-CR-185543-VOL-5] 03 p0316 N90-11797
Analysis of the flight dynamics of the Solar Maximum Mission (SMM) off-sun scientific pointing
05 p0590 N90-13432
Cooperative control of two active spacecraft during proximity operations
[NASA-CR-185596] 09 p1172 N90-16778
Use of random Martian atmosphere to evaluate potential entry guidance schemes
[NASA-TM-102606] 13 p1764 N90-20122
Suboptimal and hybrid numerical solution schemes for orbit transfer manoeuvres
[INPE-4991-PRE/1556] 14 p1931 N90-21054
Attitude control modes for the MECB remote sensing satellites
[INPE-4755-PRE/1427] 14 p1938 N90-21094
Analysis, selection, and implementation of procedures which approve optimal artificial satellite maneuvers
[INPE-5003-TDL/397] 15 p2058 N90-21786
Accurate nonlinear control for satellites using reaction wheels
[INPE-4983-PRE/1546] 15 p2059 N90-21787
Low cost station keeping maneuvers for a small-satellites constellation in tundra orbits
[ETN-90-96553] 16 p2206 N90-22588
Interactive orbital proximity operations planning system 16 p2273 N90-22953
Concurrent processing simulation of the space station
16 p2289 N90-23041
Modeling and control of flexible space stations (slew maneuvers) 16 p2297 N90-23086
The dynamics and control of large flexible space structures - 13
[NASA-CR-186930] 23 p3286 N90-28591

SPACECRAFT MODELS
Landing tests for Buran shuttle with jet engine-equipped mock-up 02 p0158 N90-10904
Spacecraft Structures and Mechanical Testing
[ESA-SP-289] 02 p0176 N90-10986
Thermoelastic behavior of large space structures: Modeling and control 02 p0179 N90-11012
Artificial intelligence in process control: Knowledge base for the shuttle ECS model 08 p1156 N90-16697
Development and use of data analysis procedures for the CRRES (Combined Release and Radiation Effects Satellite) payloads AFGL-701-2/Dosimeter and AFGL-701-4/Fluxmeter and application of the data analysis results to improve the static and dynamic models of the Earth's radiation belts
[AD-A215953] 10 p1447 N90-18348
A theory of control for infinite dimensional systems with application to large scale space structures
[AD-A219937] 17 p2366 N90-23469
On the simulation test for the relative motion of separated sub-boosters on M-3S2 with nearly half a model vehicle ST-735 and their motion analyses using inertial sensors output
[ISAS-635] 17 p2366 N90-23471
A transient response analysis of the space shuttle vehicle during liftoff
[NASA-TM-103505] 22 p3125 N90-27735

SPACECRAFT MODULES
NT COMMAND SERVICE MODULES
NT LUNAR LANDING MODULES
NT LUNAR MODULE
Space station wardroom habitability and equipment study
[NASA-CR-4246] 09 p1260 N90-17308
Project SPARC: Space-based aeroassisted reusable craft
[NASA-CR-186816] 20 p2821 N90-26051
Long cycle pressurized logistics module: An Italian contribution to the Space Station Freedom logistics scenario
[IAF-89-083] 20 p2822 N90-26058

SPACECRAFT MOTION
Lumped mass formulations for modeling flexible body systems 01 p0019 N90-10091
Enhanced element-specific modal formulations for flexible multibody dynamics 01 p0019 N90-10094
Advanced topics in structural dynamics: The maneuver of flexible spacecraft, and on-off decentralized control of flexible structures 12 p1612 N90-19274
Spacecraft attitude dynamics: Evolution and current challenges 22 p3128 N90-27754
A model of the perturbed spinning motion of the San Marco 5th spacecraft 22 p3129 N90-27755

SPACECRAFT ORBITAL ASSEMBLY
U ORBITAL ASSEMBLY

SPACECRAFT ORBITS
NT GEOSYNCHRONOUS ORBITS
NT POLAR ORBITS
NT SATELLITE ORBITS
NT TRANSFER ORBITS
An analytic development of orbit determination for a distant, planetary orbiter 04 p0485 N90-12787
Spacecraft Orbit Design and Analysis (SODA), version 1.0 user's guide
[NASA-CR-181932] 04 p0529 N90-13050
The attitude and orbit control system
05 p0605 N90-13516
The in-orbit initialization phase
05 p0606 N90-13525
SCATHA (Spacecraft Charging at High Altitudes) atlas data base, volume 1
[AD-A214204] 07 p0886 N90-15127
Space operations: NASA's communications support for Earth orbiting spacecraft. Report to Chairman, Subcommittee on Space Science and Applications, Committee on Science, Space and Technology, House of Representatives
[GAO/IMTEC-89-41] 20 p2851 N90-26215
Control of orbiting large space structural systems with discrete time observational data and random measurement noise
[AD-A222476] 21 p2967 N90-28863
Atmospherically induced optical contamination from orbiting thrusters
[AD-A223112] 21 p3021 N90-27174
Space station contamination modeling
[NASA-CR-183871] 23 p3286 N90-28590

SPACECRAFT PERFORMANCE
Independent Orbiter Assessment (IOA): FMEA/CIL instructions and ground rules
[NASA-CR-185551] 02 p0163 N90-10922
Glavkosmos operational space transportation systems
09 p1174 N90-16791
Automated procedure execution for space vehicle autonomous control 15 p2156 N90-22314

SPACECRAFT POWER SUPPLIES
Second Beamed Space-Power Workshop
[NASA-CP-3037] 01 p0027 N90-10140
Overview of microwave concepts
01 p0029 N90-10155
Central electrical utility power for a satellite ring city in low earth orbit space 01 p0031 N90-10166
Circuit level modeling of inductive elements
[DE89-015122] 01 p0032 N90-10173
Independent Orbiter Assessment (IOA): Assessment of the electrical power generation/fuel cell powerplant subsystem FMEA/CIL
[NASA-CR-185562] 02 p0161 N90-10914
Independent Orbiter Assessment (IOA): Analysis of the electrical power generation/fuel cell powerplant subsystem
[NASA-CR-185561] 02 p0161 N90-10915
Independent Orbiter Assessment (IOA): Analysis of the electrical power generation/power reactant storage and distribution subsystem
[NASA-CR-185556] 02 p0162 N90-10918
Independent Orbiter Assessment (IOA): Analysis of the orbital maneuvering system
[NASA-CR-185554] 02 p0162 N90-10919
Independent Orbiter Assessment (IOA): Assessment of the electrical power generation/power reactant storage and distribution subsystem FMEA/CIL
[NASA-CR-185545] 02 p0163 N90-10923
Independent Orbiter Assessment (IOA): Analysis of the electrical power distribution and control/electrical power generation subsystem
[NASA-CR-185538] 02 p0165 N90-10933
Independent Orbiter Assessment (IOA): Analysis of the electrical power distribution and control/remote manipulator system subsystem
[NASA-CR-185526] 02 p0166 N90-10936
Independent Orbiter Assessment (IOA): Analysis of the reaction control system, volume 2
[NASA-CR-185532-VOL-2] 02 p0167 N90-10939
Independent Orbiter Assessment (IOA): Analysis of the reaction control system, volume 3
[NASA-CR-185532-VOL-3] 02 p0167 N90-10940
Independent Orbiter Assessment (IOA): Analysis of the electrical power distribution and control subsystem, volume 1
[NASA-CR-185529-VOL-1] 02 p0167 N90-10941
Independent Orbiter Assessment (IOA): Analysis of the electrical power distribution and control subsystem, volume 2
[NASA-CR-185529-VOL-2] 02 p0167 N90-10942
Independent Orbiter Assessment (IOA): CIL issues resolution report, volume 2
[NASA-CR-185524-VOL-2] 02 p0170 N90-10955
Independent Orbiter Assessment (IOA): Assessment of the auxiliary power unit
[NASA-CR-185580] 02 p0174 N90-10976
Independent Orbiter Assessment (IOA): Assessment of the electrical power distribution and control subsystem, volume 1
[NASA-CR-185557-VOL-1] 03 p0313 N90-11779
Independent Orbiter Assessment (IOA): Assessment of the electrical power distribution and control subsystem, volume 2
[NASA-CR-185557-VOL-2] 03 p0313 N90-11780
Independent Orbiter Assessment (IOA): Assessment of the electrical power distribution and control subsystem, volume 3
[NASA-CR-185557-VOL-3] 03 p0313 N90-11781
Independent Orbiter Assessment (IOA): Assessment of the Electrical Power Distribution and Control/Electrical Power Generation (EPD and C/EPG) FMEA/CIL
[NASA-CR-185542] 03 p0314 N90-11785
Independent Orbiter Assessment (IOA): Assessment of the reaction control system, volume 1
[NASA-CR-185543-VOL-1] 03 p0316 N90-11793
Independent Orbiter Assessment (IOA): Assessment of the reaction control system, volume 2
[NASA-CR-185543-VOL-2] 03 p0316 N90-11794
Independent Orbiter Assessment (IOA): Assessment of the reaction control system, volume 3
[NASA-CR-185543-VOL-3] 03 p0316 N90-11795
Independent Orbiter Assessment (IOA): Assessment of the reaction control system, volume 4
[NASA-CR-185543-VOL-4] 03 p0316 N90-11796
Independent Orbiter Assessment (IOA): Assessment of the reaction control system, volume 5
[NASA-CR-185543-VOL-5] 03 p0316 N90-11797
The fuel cell in space: Yesterday, today and tomorrow
[NASA-TM-102366] 03 p0318 N90-11804
Analysis and simulation of dynamics of spacecraft power systems 04 p0463 N90-12653
The fault monitoring and diagnosis knowledge-based system for space power systems: AMPERES, phase 1
[NASA-CR-185486] 04 p0464 N90-12654
Airborne/spaceborne pulsed power source
[AD-A211762] 04 p0495 N90-12850
Power generation and distribution
05 p0604 N90-13515
Electrical performance characteristics of high power converters for space power applications
[NASA-CR-185947] 06 p0734 N90-14279
A heat receiver design for solar dynamic space power systems
[NASA-TM-102473] 06 p0735 N90-14283
Draft Environmental Impact Statement for the Ulysses Mission (Tier 2)
[NASA-TM-102903] 06 p0812 N90-14727
Introductory testimony: Hearing on nuclear power in space
[DE90-001137] 06 p0842 N90-14897
Safety evaluation report for Galileo, volume 2
[DE90-003087] 07 p0886 N90-15123

Tuned-circuit Johnson noise thermometry
[DE89-016221] 07 p0925 N90-15356
Conceptual design of a moving belt radiator shuttle-attached experiments: Technical requirement Document
[NASA-CR-185168] 08 p1038 N90-15996
Solar cycle effects on trapped energetic particles
[AD-A215028] 09 p1300 N90-17532
European Space Power, volume 1
[ESA-SP-294-VOL-1] 10 p1329 N90-17678
Japanese experiment module electrical power system 10 p1329 N90-17680
Toward an electrical power utility for space exploration 10 p1329 N90-17681
The Hermes power system 10 p1330 N90-17682
The spacebus power conditioning application to the Eutelsat 2 spacecraft 10 p1330 N90-17689
The subsystem regulator, the next generation in satellite regulated power conditioning 10 p1331 N90-17690
Autonomous electrical power supply subsystem for the Vesta mission 10 p1331 N90-17692
On the development of the power sources for the Ulysses and Galileo missions 10 p1331 N90-17693
A power system for ARTEP 10 p1331 N90-17694
Challenges for future space power systems 10 p1331 N90-17695
CNES-CEA comparative evaluation study of various candidate 20 kWe space power systems 10 p1331 N90-17697
Design considerations and lessons learned on the European retrievable carrier 10 p1332 N90-17698
The MECB data collecting satellite power supply subsystem 10 p1332 N90-17699
The modular power subsystem 10 p1332 N90-17700
Advanced space power PEM fuel cell systems 10 p1333 N90-17707
European regenerative fuel cell technology for space use 10 p1333 N90-17709
Solid polymer electrolyte water electrolysis as a mean of energy storage for space applications 10 p1334 N90-17713
Nickel hydrogen cell design for space applications 10 p1334 N90-17714
Status of the cycling tests performed with SAFT NiH2 cells dedicated to space applications 10 p1334 N90-17715
Preliminary study of rechargeable lithium cells for space applications 10 p1334 N90-17717
A lithium sulphur dioxide cell for deep space applications 10 p1334 N90-17718
Magnetic coupled current sensing techniques for spacecraft power systems 10 p1335 N90-17725
Power processing unit for 20mN-class ion engine system 10 p1336 N90-17732
Analysis and design of a HV dc/dc series resonant converter using a multi-stage voltage multiplier 10 p1338 N90-17746
European Space Power, volume 2
[ESA-SP-294-VOL-2] 10 p1338 N90-17748
The ISO solar generator: Solar cells and OSR mixed 10 p1341 N90-17767
Assessment of bifacial silicon solar cells for space applications 10 p1342 N90-17779
CIC type thin diode for solar array 10 p1344 N90-17788
The advanced photovoltaic solar array program 10 p1345 N90-17797
Model-reference adaptive control applied to loadfollowing of a space-nuclear power system
[DE89-014561] 10 p1429 N90-18245
Design and operation of an inert gas facility for thermoelectric generator storage
[DE90-007146] 11 p1565 N90-19008
Safety Status Report for the Ulysses mission. Book 1: Accident analysis. General purpose heat source radioisotope thermoelectric generator program
[DE90-006829] 12 p1614 N90-19285
Hot filament technique for measuring the thermal conductivity of molten lithium fluoride
[NASA-TM-102506] 12 p1631 N90-19373
High power, high frequency component test facility
[NASA-TM-102500] 12 p1650 N90-19484
Space Electrochemical Research and Technology (SERT), 1989
[NASA-CP-3056] 13 p1821 N90-20454
Overview of battery usage in NASA/GSFC LEO and GEOspacecrafts 13 p1821 N90-20455
The importance of batteries in unmanned missions 13 p1821 N90-20456
Monolithic solid oxide fuel cell development 13 p1822 N90-20460
A new concept for high-cycle-life LEO: Rechargeable MnO2-hydrogen 13 p1822 N90-20462
Multi-mission Ni-H2 battery cells for the 1990's 13 p1825 N90-20477
Sodium-sulfur battery flight experiment definition study 13 p1825 N90-20479
A comparative study of electric power distribution systems for spacecraft
[NASA-CR-186531] 14 p1942 N90-21113
Recent Stirling engine loss-understanding results
[NASA-TM-103122] 14 p1942 N90-21114
Recent results from advanced research on space solar cells at NASA
[NASA-TM-102485] 14 p1968 N90-21274
Peeled film GaAs solar cells for space power
[NASA-TM-103125] 14 p1970 N90-21287
Space power generation and distribution
[DE90-008676] 14 p2002 N90-21474
Small business innovation research. Abstracts of completed 1987 phase 1 projects
[NASA-TM-101797] 14 p2036 N90-21681
Effect of LEO cycling on 125 Ah advanced design IPV nickel-hydrogen battery cells
[NASA-TM-103128] 15 p2061 N90-21808
Draft environmental impact statement for the Galileo Mission (Tier 2)
[NASA-TM-102926] 15 p2124 N90-22148
Final Environmental Impact Statement for the Ulysses Mission (Tier 2)
[NASA-TM-101104] 15 p2126 N90-22162
Automating security monitoring and analysis for Space Station Freedom's electric power system
[NASA-TM-103148] 15 p2158 N90-22324
Programmatic status of NASA's CSTI high capacity power Stirling space power converter program
[NASA-TM-103142] 16 p2210 N90-22606
Nuclear power in space
[GPO-23-835] 16 p2316 N90-23202
Technical accomplishments of the NASA Lewis Research Center, 1989
[NASA-TM-102296] 17 p2486 N90-24220
Conceptual definition of a high voltage power supply test facility
[NASA-CR-185216] 19 p2666 N90-25172
An analysis of space power system masses
[NASA-TM-103199] 19 p2669 N90-25184
Automation in the Space Station module power management and distribution Breadboard 19 p2728 N90-25509
Solar array automation limitations 19 p2729 N90-25513
Autonomous power expert fault diagnostic system for Space Station Freedom electrical power system testbed 19 p2730 N90-25521
Discharge transient coupling in large space power systems 19 p2735 N90-25544
Photovoltaic array space power plus diagnostics experiment 19 p2737 N90-25559
The aerobraking space transfer vehicle
[NASA-CR-186819] 20 p2821 N90-26053
The chemical effects of the Martian environment on power system component materials: A theoretical approach
[NASA-TM-103203] 20 p2825 N90-26074
NASA aerospace flight battery systems program
[NASA-TM-103237] 20 p2882 N90-26397
Multimegawatt space nuclear power supply, phase 1. Volume 2: Phase 2 plan D180-30619-6
[DE90-012431] 20 p2925 N90-26645
Multimegawatt space nuclear power supply, phase 1. Volume 3: Annotated outline of preliminary safety assessment D180-30619-7
[DE90-012432] 20 p2926 N90-26646
Two-phase heat transport systems for spacecraft scaling with respect to gravity
[NLR-TP-89127-U] 21 p2965 N90-26857
Nuclear power systems for lunar and Mars exploration
[NASA-TM-103168] 21 p2969 N90-26873
The scalability of OTR (Out-of-core Thermionic Reactor) space nuclear power systems
[DE90-013553] 21 p3075 N90-27485
Hubble space telescope six-battery test bed
[NASA-TM-103506] 22 p3124 N90-27731
Electrical characterization of a Mapham inverter using pulse testing techniques
[NASA-TM-103254] 22 p3134 N90-27784
Liquid Rocket Booster (LRB) for the Space Transportation System (STS) systems study. Appendix C: Battery report for the liquid rocket booster TVC actuators
[NASA-CR-183789-APP-C] 23 p3288 N90-28603
Thermal analyses of power subsystem components
[NASA-CR-186314] 24 p3474 N90-29637

SPACECRAFT PRELAUNCH TESTS
U SPACE VEHICLE CHECKOUT PROGRAM

SPACECRAFT PROPULSION
NT ELECTROMAGNETIC PROPULSION
NT ION PROPULSION
NT MATTER-ANTIMATTER PROPULSION
NT PLASMA PROPULSION

Liquid rocket booster study. Volume 1: Executive summary
[NASA-CR-183599] 01 p0027 N90-10137
Second Beamed Space-Power Workshop
[NASA-CP-3037] 01 p0027 N90-10140
Overview of microwave concepts 01 p0029 N90-10155
Microwave beam power 01 p0030 N90-10165
Independent Orbiter Assessment (IOA) CIL issues resolution report, volume 3
[NASA-CR-185524-VOL-3] 02 p0170 N90-10956
The effect of electrode configuration on arcjet performance
[NASA-TM-102346] 02 p0189 N90-11081
Independent Orbiter Assessment (IOA): Assessment of the orbiter main propulsion system FMEA/CIL, volume 1
[NASA-CR-185559-VOL-1] 03 p0312 N90-11775
Independent Orbiter Assessment (IOA): Assessment of the main propulsion subsystem FMEA/CIL, volume 2
[NASA-CR-185559-VOL-2] 03 p0313 N90-11776
Independent Orbiter Assessment (IOA): Assessment of the main propulsion subsystem FMEA/CIL, volume 3
[NASA-CR-185559-VOL-3] 03 p0313 N90-11777
Independent Orbiter Assessment (IOA): Assessment of the main propulsion subsystem FMEA/CIL, volume 4
[NASA-CR-185559-VOL-4] 03 p0313 N90-11778
Independent Orbiter Assessment (IOA): Assessment of the reaction control system, volume 1
[NASA-CR-185543-VOL-1] 03 p0316 N90-11793
Independent Orbiter Assessment (IOA): Assessment of the reaction control system, volume 2
[NASA-CR-185543-VOL-2] 03 p0316 N90-11794
Independent Orbiter Assessment (IOA): Assessment of the reaction control system, volume 3
[NASA-CR-185543-VOL-3] 03 p0316 N90-11795
Independent Orbiter Assessment (IOA): Assessment of the reaction control system, volume 4
[NASA-CR-185543-VOL-4] 03 p0316 N90-11796
Independent Orbiter Assessment (IOA): Assessment of the reaction control system, volume 5
[NASA-CR-185543-VOL-5] 03 p0316 N90-11797
Apollo lightcraft project
[NASA-CR-186055] 04 p0464 N90-12655
Thin-film sensors for reusable space propulsion systems
[NASA-TM-102383] 05 p0616 N90-13595
Project Argo: The design and analysis of an all-propulsive and an aeroassisted version of a manned space transportation vehicle
[NASA-CR-186047] 06 p0732 N90-14266
Design of a thrust stand for high power electric propulsion devices
[NASA-TM-102372] 08 p1037 N90-15992
French studies on advanced space transportation systems 09 p1175 N90-16798
Hermes propulsion system 09 p1178 N90-16823
Propellant trends in advanced rocket propulsion 09 p1179 N90-16838
The Pathfinder chemical transfer propulsion program 11 p1471 N90-18471
Advanced APS impacts on vehicle payloads 11 p1472 N90-18472
Electric propulsion options for 10 kW class earth-space missions 11 p1472 N90-18474
Test facility and preliminary performance of a 100 kW class MPD thruster 11 p1472 N90-18476
Feasibility demonstration of a 445N high-performance rocket engine 11 p1473 N90-18481
Space station technology summary 11 p1474 N90-18482
Viability study of ionic microthruster tests on MECB satellite
[INPE-4973-RPE/605] 11 p1475 N90-18490
Rapid near-optimal trajectory generation and guidance law development for single-stage-to-orbit airbreathing vehicles
[NASA-CR-186299] 12 p1612 N90-19275
Monostable electrovalve
[INPE-4928-RPE/595] 12 p1651 N90-19487
Advanced launch vehicle propulsion at the NASA Lewis Research Center
[NASA-TM-103096] 13 p1761 N90-20110
Experimental proposition aboard the second data collecting satellite-SCD 2 of the MECB
[INPE-4980-RPE/606] 13 p1765 N90-20128
A radiological assessment of nuclear power and propulsion operations near Space Station Freedom
[NASA-CR-185185] 14 p1941 N90-21108
Small business innovation research. Abstracts of 1988 phase 1 awards
[NASA-TM-102991] 14 p2036 N90-21680
Small business innovation research. Abstracts of completed 1987 phase 1 projects
[NASA-TM-101797] 14 p2036 N90-21681

Transport properties of plasmas in microwave electrothermal thrusters
[AD-A219408] 16 p2320 N90-23228
Analysis of the use of a methane propellant in a biowaste resistojet
[AD-A220475] 17 p2367 N90-23473
The 30-kW ammonia arcjet technology
[NASA-CR-186850] 19 p2670 N90-25190
National space test centers, Lewis research center facilities
[NASA-TM-103187] 20 p2817 N90-26030
NASA/USRA university advanced design program at the University of Illinois for the 1989-1990 academic year
[NASA-CR-186829] 20 p2821 N90-26049
Advanced propulsion concepts
[NASA-CR-185920] 21 p2969 N90-26872
Low power arcjet performance
[NASA-TM-103280] 23 p3298 N90-28657
AFOSR/ONR Contractors' Meeting on Combustion Rocket Propulsion Diagnostics of Reacting Flow
[AD-A224411] 24 p3441 N90-29432

SPACECRAFT RADIATORS

Total hemispherical emittance measured at high temperatures by the calorimetric method
[NASA-TM-102322] 01 p0054 N90-10309
Design of ceramic fabric heat pipe with water working fluid
[DE89-016565] 02 p0221 N90-11265
Conceptual design of liquid droplet radiator shuttle-attached experiment
[NASA-CR-185164] 03 p0318 N90-11805
Conceptual design of liquid droplet radiator shuttle-attached experiment technical requirements document
[NASA-CR-185165] 03 p0318 N90-11806
An improved algorithm for the modeling of vapor flow in heat pipes
[NASA-CR-185179] 05 p0642 N90-13748
On protection of Freedom's solar dynamic radiator from the orbital debris environment. Part 1: Preliminary analyses and testing
[NASA-TM-102458] 06 p0736 N90-14285
Conceptual design of a moving belt radiator shuttle-attached experiments: Technical requirement Document
[NASA-CR-185168] 08 p1038 N90-15996
Expandable radiator
[AD-D014258] 08 p1063 N90-16147
Spacecraft thermal control design data, volume 3
[ESA-PSS-03-108-ISSUE-1-VOL-3] 11 p1469 N90-18457
Condensation fluid dynamics and heat transfer on rotating spherical surfaces in a microgravitational field
[DE90-005540] 11 p1495 N90-18607
Conceptual design of a Moving Belt Radiator (MBR) shuttle-attached experiment
[NASA-CR-185169] 17 p2367 N90-23474

SPACECRAFT RECOVERY

Syncom 4 deploy, LDEF retrieval highlight 10-day Columbia flight
[NASA-NEWS-RELEASE-89-180] 05 p0594 N90-13448
Preliminary design of the Shuttle-C avionics recovery system
[NASA-CR-186230] 06 p0730 N90-14258
Preliminary Subsystem Designs for the Assured Crew Return Vehicle (ACRV), volumes 1-3
[NASA-CR-186662] 17 p2363 N90-23455

SPACECRAFT REENTRY

NT UNCONTROLLED REENTRY (SPACECRAFT)
Guidance and control strategies for aerospace vehicles
[NASA-CR-186878] 20 p2814 N90-26013

SPACECRAFT RELIABILITY

Liquid rocket booster study. Volume 2, book 2, appendix 1: Trades studies
[NASA-CR-183601] 01 p0027 N90-10136
Independent Orbiter Assessment (IOA): Analysis of the manned maneuvering unit
[NASA-CR-185565] 02 p0161 N90-10913
Independent Orbiter Assessment (IOA): Assessment of the electrical power generation/fuel cell powerplant subsystem FMEA/CIL
[NASA-CR-185562] 02 p0161 N90-10914
Independent Orbiter Assessment (IOA): Analysis of the electrical power generation/fuel cell powerplant subsystem
[NASA-CR-185561] 02 p0161 N90-10915
Independent Orbiter Assessment (IOA): Analysis of the rudder/speed brake subsystem
[NASA-CR-185560] 02 p0161 N90-10916
Independent Orbiter Assessment (IOA): Assessment of the data processing system FMEA/CIL
[NASA-CR-185546] 02 p0162 N90-10917
Independent Orbiter Assessment (IOA): Analysis of the electrical power generation/power reactant storage and distribution subsystem
[NASA-CR-185556] 02 p0162 N90-10918
Independent Orbiter Assessment (IOA): Analysis of the orbital maneuvering system
[NASA-CR-185554] 02 p0162 N90-10919
Independent Orbiter Assessment (IOA): Analysis of the nose wheel steering subsystem
[NASA-CR-185548] 02 p0163 N90-10921
Independent Orbiter Assessment (IOA): FMEA/CIL instructions and ground rules
[NASA-CR-185551] 02 p0163 N90-10922
Independent Orbiter Assessment (IOA): Assessment of the electrical power generation/power reactant storage and distribution subsystem FMEA/CIL
[NASA-CR-185545] 02 p0163 N90-10923
Independent Orbiter Assessment (IOA): Analysis of the DPS subsystem
[NASA-CR-185549] 02 p0163 N90-10924
Independent Orbiter Assessment (IOA): Analysis of the atmospheric revitalization pressure control subsystem
[NASA-CR-185593] 02 p0163 N90-10925
Independent Orbiter Assessment (IOA): Analysis of the remote manipulator system
[NASA-CR-185585] 02 p0164 N90-10926
Independent Orbiter Assessment (IOA): Analysis of the instrumentation subsystem
[NASA-CR-185571] 02 p0164 N90-10928
Independent Orbiter Assessment (IOA): Analysis of the ascent thrust vector control actuator subsystem
[NASA-CR-185579] 02 p0164 N90-10929
Independent Orbiter Assessment (IOA): Analysis of the body flap subsystem
[NASA-CR-185574] 02 p0165 N90-10930
Independent Orbiter Assessment (IOA): Analysis of the auxiliary power unit
[NASA-CR-185568] 02 p0165 N90-10931
Independent Orbiter Assessment (IOA): Analysis of the backup flight system
[NASA-CR-185567] 02 p0165 N90-10932
Independent Orbiter Assessment (IOA): Analysis of the electrical power distribution and control/electrical power generation subsystem
[NASA-CR-185538] 02 p0165 N90-10933
Independent Orbiter Assessment (IOA): Analysis of the hydraulics/water spray boiler subsystem
[NASA-CR-185541] 02 p0165 N90-10934
Independent Orbiter Assessment (IOA): Analysis of the elevon subsystem
[NASA-CR-185576] 02 p0166 N90-10935
Independent Orbiter Assessment (IOA): Analysis of the electrical power distribution and control/remote manipulator system subsystem
[NASA-CR-185526] 02 p0166 N90-10936
Independent Orbiter Assessment (IOA): Analysis of the extravehicular mobility unit
[NASA-CR-185540] 02 p0166 N90-10937
Independent Orbiter Assessment (IOA): Analysis of the reaction control system, volume 1
[NASA-CR-185532-VOL-1] 02 p0166 N90-10938
Independent Orbiter Assessment (IOA): Analysis of the reaction control system, volume 2
[NASA-CR-185532-VOL-2] 02 p0167 N90-10939
Independent Orbiter Assessment (IOA): Analysis of the reaction control system, volume 3
[NASA-CR-185532-VOL-3] 02 p0167 N90-10940
Independent Orbiter Assessment (IOA): Analysis of the electrical power distribution and control subsystem, volume 1
[NASA-CR-185529-VOL-1] 02 p0167 N90-10941
Independent Orbiter Assessment (IOA): Analysis of the electrical power distribution and control subsystem, volume 2
[NASA-CR-185529-VOL-2] 02 p0167 N90-10942
Independent Orbiter Assessment (IOA): Analysis of the landing/deceleration subsystem
[NASA-CR-185569] 02 p0167 N90-10943
Independent Orbiter Assessment (IOA): Analysis of the mechanical actuation subsystem
[NASA-CR-185525] 02 p0168 N90-10944
Independent Orbiter Assessment (IOA): Analysis of the pyrotechnics subsystem
[NASA-CR-185530] 02 p0168 N90-10945
Independent Orbiter Assessment (IOA): Assessment of the pyrotechnics subsystem
[NASA-CR-185531] 02 p0168 N90-10946
Independent Orbiter Assessment (IOA): Assessment of the nose wheel steering subsystem
[NASA-CR-185533] 02 p0168 N90-10947
Independent Orbiter Assessment (IOA): Weibull analysis report
[NASA-CR-185534] 02 p0168 N90-10948
Independent Orbiter Assessment (IOA): Assessment of the purge, vent and drain subsystem
[NASA-CR-185535] 02 p0168 N90-10949
Independent Orbiter Assessment (IOA): Assessment of the extravehicular mobility unit, volume 1
[NASA-CR-185536-VOL-1] 02 p0169 N90-10950
Independent Orbiter Assessment (IOA): Assessment of the extravehicular mobility unit, volume 2
[NASA-CR-185536-VOL-2] 02 p0169 N90-10951
Independent Orbiter Assessment (IOA): Assessment of the mechanical actuation subsystem, volume 1
[NASA-CR-185527-VOL-1] 02 p0169 N90-10952
Independent Orbiter Assessment (IOA): Assessment of the mechanical actuation subsystem, volume 2
[NASA-CR-185527-VOL-2] 02 p0169 N90-10953
Independent Orbiter Assessment (IOA): CIL issues resolution report, volume 2
[NASA-CR-185524-VOL-2] 02 p0170 N90-10955
Independent Orbiter Assessment (IOA) CIL issues resolution report, volume 3
[NASA-CR-185524-VOL-3] 02 p0170 N90-10956
Independent Orbiter Assessment (IOA): Assessment of the atmospheric revitalization pressure control subsystem FMEA/CIL
[NASA-CR-185594] 02 p0170 N90-10957
Independent Orbiter Assessment (IOA): Analysis of the crew equipment subsystem
[NASA-CR-185591] 02 p0170 N90-10958
Independent Orbiter Assessment (IOA): Assessment of the ascent thrust vector control actuator subsystem FMEA/CIL
[NASA-CR-185590] 02 p0170 N90-10959
Independent Orbiter Assessment (IOA): FMEA/CIL assessment
[NASA-CR-185589] 02 p0170 N90-10960
Independent Orbiter Assessment (IOA): Assessment of the displays and controls subsystem
[NASA-CR-185588] 02 p0171 N90-10961
Independent Orbiter Assessment (IOA): Assessment of the Orbiter Experiment (OEX) subsystem
[NASA-CR-185587] 02 p0171 N90-10962
Independent Orbiter Assessment (IOA): Analysis of the Orbiter Experiment (OEX) subsystem
[NASA-CR-185586] 02 p0171 N90-10963
Independent Orbiter Assessment (IOA): Assessment of the remote manipulator system FMEA/CIL
[NASA-CR-185592] 02 p0171 N90-10964
Independent Orbiter Assessment (IOA): Assessment of the EPD and C/remote manipulator system FMEA/CIL
[NASA-CR-185583] 02 p0172 N90-10965
Independent Orbiter Assessment (IOA): Assessment of the landing/deceleration (LDG/DEC) subsystem FMEA/CIL
[NASA-CR-185570] 02 p0172 N90-10966
Independent Orbiter Assessment (IOA): Analysis of the communication and tracking subsystem
[NASA-CR-185582] 02 p0172 N90-10967
Independent Orbiter Assessment (IOA): Assessment of the body flap subsystem FMEA/CIL
[NASA-CR-185575] 02 p0172 N90-10968
Independent Orbiter Assessment (IOA): Analysis of the purge, vent and drain subsystem
[NASA-CR-185547] 02 p0172 N90-10969
Independent Orbiter Assessment (IOA): Assessment of the elevon actuator subsystem FMEA/CIL
[NASA-CR-185578] 02 p0173 N90-10970
Independent Orbiter Assessment (IOA): Assessment of the crew equipment subsystem
[NASA-CR-185577] 02 p0173 N90-10971
Independent Orbiter Assessment (IOA): Assessment of instrumental subsystem FMEA/CIL
[NASA-CR-185572] 02 p0173 N90-10972
Independent Orbiter Assessment (IOA): Assessment of the backup flight system FMEA/CIL
[NASA-CR-185566] 02 p0173 N90-10973
Independent Orbiter Assessment (IOA): Assessment of the manned maneuvering unit
[NASA-CR-185564] 02 p0173 N90-10974
Independent Orbiter Assessment (IOA): Assessment of the rudder/speed brake subsystem FMEA/CIL
[NASA-CR-185558] 02 p0174 N90-10975
Independent Orbiter Assessment (IOA): Assessment of the auxiliary power unit
[NASA-CR-185580] 02 p0174 N90-10976
Independent Orbiter Assessment (IOA): Assessment of the life support and airlock support systems, volume 1
[NASA-CR-185581-VOL-1] 02 p0174 N90-10977
Independent Orbiter Assessment (IOA): Assessment of the life support and airlock support systems, volume 2
[NASA-CR-185581-VOL-2] 02 p0174 N90-10978
Independent Orbiter Assessment (IOA): Assessment of the active thermal control system
[NASA-CR-185573] 02 p0174 N90-10979
Independent Orbiter Assessment (IOA): Analysis of the displays and controls subsystem
[NASA-CR-185563] 03 p0312 N90-11774
Independent Orbiter Assessment (IOA): Assessment of the orbiter main propulsion system FMEA/CIL, volume 1
[NASA-CR-185559-VOL-1] 03 p0312 N90-11775

Independent Orbiter Assessment (IOA): Assessment of the main propulsion subsystem FMEA/CIL, volume 2
[NASA-CR-185559-VOL-2] 03 p0313 N90-11776
Independent Orbiter Assessment (IOA): Assessment of the main propulsion subsystem FMEA/CIL, volume 3
[NASA-CR-185559-VOL-3] 03 p0313 N90-11777
Independent Orbiter Assessment (IOA): Assessment of the main propulsion subsystem FMEA/CIL, volume 4
[NASA-CR-185559-VOL-4] 03 p0313 N90-11778
Independent Orbiter Assessment (IOA): Assessment of the electrical power distribution and control subsystem, volume 1
[NASA-CR-185557-VOL-1] 03 p0313 N90-11779
Independent Orbiter Assessment (IOA): Assessment of the electrical power distribution and control subsystem, volume 2
[NASA-CR-185557-VOL-2] 03 p0313 N90-11780
Independent Orbiter Assessment (IOA): Assessment of the electrical power distribution and control subsystem, volume 3
[NASA-CR-185557-VOL-3] 03 p0313 N90-11781
Independent Orbiter Assessment (IOA): Analysis of the active thermal control subsystem
[NASA-CR-185553] 03 p0314 N90-11782
Independent Orbiter Assessment (IOA): FMEA/CIL assessment
[NASA-CR-185550] 03 p0314 N90-11783
Independent Orbiter Assessment (IOA): Assessment of the guidance, navigation, and control subsystem FMEA/CIL
[NASA-CR-185552] 03 p0314 N90-11784
Independent Orbiter Assessment (IOA): Assessment of the Electrical Power Distribution and Control/Electrical Power Generation (EPD and C/EPG) FMEA/CIL
[NASA-CR-185542] 03 p0314 N90-11785
Independent Orbiter Assessment (IOA): Analysis of the life support and airlock support subsystems
[NASA-CR-185539] 03 p0314 N90-11786
Independent Orbiter Assessment (IOA): Assessment of the orbital maneuvering system FMEA/CIL, volume 1
[NASA-CR-185544-VOL-1] 03 p0315 N90-11787
Independent Orbiter Assessment (IOA): Assessment of the orbital maneuvering subsystem, volume 2
[NASA-CR-185544-VOL-2] 03 p0315 N90-11788
Independent Orbiter Assessment (IOA): Assessment of the communication and tracking subsystem, volume 1
[NASA-CR-185528-VOL-1] 03 p0315 N90-11789
Independent Orbiter Assessment (IOA): Assessment of the communication and tracking subsystem, volume 2
[NASA-CR-185528-VOL-2] 03 p0315 N90-11790
Independent Orbiter Assessment (IOA): Assessment of the communication and tracking subsystem, volume 3
[NASA-CR-185528-VOL-3] 03 p0315 N90-11791
Independent Orbiter Assessment (IOA): Assessment of the hydraulics/water spray boiler subsystem
[NASA-CR-185537] 03 p0316 N90-11792
Independent Orbiter Assessment (IOA): Assessment of the reaction control system, volume 1
[NASA-CR-185543-VOL-1] 03 p0316 N90-11793
Independent Orbiter Assessment (IOA): Assessment of the reaction control system, volume 2
[NASA-CR-185543-VOL-2] 03 p0316 N90-11794
Independent Orbiter Assessment (IOA): Assessment of the reaction control system, volume 3
[NASA-CR-185543-VOL-3] 03 p0316 N90-11795
Independent Orbiter Assessment (IOA): Assessment of the reaction control system, volume 4
[NASA-CR-185543-VOL-4] 03 p0316 N90-11796
Independent Orbiter Assessment (IOA): Assessment of the reaction control system, volume 5
[NASA-CR-185543-VOL-5] 03 p0316 N90-11797
Sensitivity of space system availability predictions to underlying component reliability estimates
[AD-A215535] 09 p1183 N90-16858

SPACECRAFT RENDEZVOUS
U SPACE RENDEZVOUS

SPACECRAFT SENSORS
U SPACECRAFT INSTRUMENTS

SPACECRAFT SHIELDING
Preliminary design of a large tetrahedral truss/hexagonal heatshield panel aerobrake
[NASA-TM-101612] 01 p0025 N90-10127
Orbital debris research at NASA Johnson Space Center, 1986-1988
[NASA-TM-102155] 01 p0138 N90-10795
Report on orbital debris
[NASA-TM-101855] 04 p0460 N90-12635
Debris/ice/TPS assessment and photographic analysis for Shuttle Mission STS-34
[NASA-TM-102153] 05 p0594 N90-13447
Stand-off shields for hypervelocity particles
[DE89-016182] 07 p0939 N90-15437
Material responses to incident x rays
[DE89-015366] 08 p1089 N90-16305
Design development and qualification of a solar array with OSRs (SSM) bonded to the ISO spacecraft rigid sunshield 10 p1341 N90-17768
Spacecraft thermal control design data, volume 2
[ESA-PSS-03-108-ISSUE-1-VOL-2] 11 p1469 N90-18456

SPACECRAFT STABILITY
Flight motor set 360L001 (STS-26R). (Reconstructed dynamic loads analysis)
[NASA-CR-183811] 04 p0464 N90-12656
The dynamics and control of large flexible space structures - 12, supplement 11
[NASA-CR-185966] 05 p0602 N90-13494
Baseline experiment for active control of structural vibrations
[AD-A216194] 10 p1397 N90-18076
Design and development of a spacecraft stability boom 18 p2540 N90-24494
The Screem-J4D: A proposal in response to a low Reynolds number station keeping mission
[NASA-CR-186664] 20 p2807 N90-25968
Increasing the margin of stability of arbitrarily finite modes of flexible large space structures with damping
[AD-A221742] 21 p2967 N90-26867
Hydroelastic problems in space flight vehicles
[LRT-WE-9-FB-11(1989)] 21 p2967 N90-26868
Flow induced nutation instability in spinning solid propellant rockets
[AD-A222504] 21 p2969 N90-26877

SPACECRAFT STRUCTURES
Hierarchical damage tolerant controllers for smart structures
[AD-A209422] 01 p0005 N90-10022
NASA'S controls-structures interaction program 01 p0017 N90-10081
Flexible structure control experiments using a real-time workstation for computer-aided control engineering 01 p0017 N90-10084
Explicit modeling and computational load distribution for concurrent processing simulation of the space station 01 p0020 N90-10096
Spacecraft Structures and Mechanical Testing
[ESA-SP-289] 02 p0176 N90-10986
Updating of finite element model by means of normal mode parameters 02 p0177 N90-10992
Reduction of dynamic response of spacecraft structures and payloads 02 p0178 N90-11000
Acoustic response analysis in the low frequency domain 02 p0179 N90-11010
Advances in design and testing of spacecraft structures 02 p0180 N90-11018
Development of the large spacecraft structure 02 p0180 N90-11020
Modal analysis of space structures with the Ibrahim Time Domain method 02 p0181 N90-11026
Transient vibration testing of spacecraft structures. Experience with multiaxial base motion and combined base motion and point force excitation 02 p0183 N90-11039
Transient tests for spacecraft structures 02 p0183 N90-11040
Multi-axis transient testing: Experimental investigations 02 p0184 N90-11042
A new aspect for the use of thin walled beams as shell stiffeners of spacecraft structures 02 p0184 N90-11046
New data handling system (MDH) for mechanical tests at ESTEC 02 p0187 N90-11066
Exploitation of data management facilities for finite element analysis in aerospace structural engineering applications 02 p0188 N90-11078
Basic research on processing of ceramics for space structures
[AD-A205954] 02 p0199 N90-11139
The Hipparcos Mission. Prelaunch status. Volume 1: The Hipparcos satellite
[ESA-SP-1111-VOL-1] 05 p0603 N90-13499
The payload structure 05 p0604 N90-13510
The spacecraft structure 05 p0604 N90-13512
Instrumentation for a facility for the test, analysis and active control of spacecraft truss structures
[AD-A213655] 07 p0886 N90-15124
Base reaction optimization of redundant manipulators for space applications
[NASA-CR-186274] 07 p0941 N90-15447
Radiation of plasma waves from large space structures in low earth orbit
[AD-A215062] 09 p1182 N90-16856
The 59th Shock and Vibration Symposium, volume 4
[AD-A214581] 09 p1238 N90-17184
Aiming control: Theory and applications to dynamic control of space structures
[AD-A217877] 13 p1764 N90-20123
PACOSS program status and results 14 p1933 N90-21065
Global nonlinear optimization of spacecraft protective structures design
[NASA-TM-100387] 14 p1938 N90-21095
Study and sizing of bonded joints in space structures
[REPT-892-430-124] 16 p2207 N90-22591
Pultrusion process development for long space boom model
[NASA-TM-4017] 16 p2214 N90-22628
Explicit modeling of composite plates and beams in the dynamics of multibody systems 16 p2285 N90-23019
Dynamic analysis of flexible mechanical systems using LATDYN 16 p2296 N90-23080
Dynamic analysis of space-related linear and non-linear structures
[NASA-TM-103490] 19 p2667 N90-25174
Design and implementation of robust decentralized control laws for the ACES structure at Marshall Space Flight Center
[NASA-CR-4310] 20 p2820 N90-26046
Materials and structures for 2000 and beyond: An attempted forecast by the DLR Materials and Structures Department
[ESA-TT-1154-REV] 20 p2843 N90-26173
Computational methods for problems in aerodynamics using parallel and vector architecture
[AD-A221979] 21 p2954 N90-26795
Aiming control: Theory and applications to dynamic control of space structures
[AD-A221532] 21 p2967 N90-26864
Guidelines for threaded fasteners
[ESA-PSS-03-208-ISSUE-1] 22 p3182 N90-28061
Transformational part-count in layered octahedral-tetrahedral truss configurations
[NASA-TM-102635] 23 p3287 N90-28598

SPACECRAFT TELEVISION
NT SATELLITE TELEVISION

SPACECRAFT TEMPERATURE
Independent Orbiter Assessment (IOA): Analysis of the electrical power distribution and control/electrical power generation subsystem
[NASA-CR-185538] 02 p0165 N90-10933
Independent Orbiter Assessment (IOA): Assessment of the active thermal control system
[NASA-CR-185573] 02 p0174 N90-10979
Temperature dependence of attitude sensor coalignments on the Solar Maximum Mission (SMM) 05 p0588 N90-13426
Spacecraft thermal control design data, volume 1
[ESA-PSS-03-108-ISSUE-1-VOL-1] 11 p1468 N90-18455
Spacecraft thermal control design data, volume 2
[ESA-PSS-03-108-ISSUE-1-VOL-2] 11 p1469 N90-18456
Spacecraft thermal control design data, volume 3
[ESA-PSS-03-108-ISSUE-1-VOL-3] 11 p1469 N90-18457
Spacecraft thermal control design data, volume 4
[ESA-PSS-03-108-ISSUE-1-VOL-4] 11 p1469 N90-18458
NASA systems autonomy demonstration project: Advanced automation demonstration of Space Station Freedom thermal control system 19 p2728 N90-25510
Spacecraft thermal control design data, volume 5. Section R: Cryogenic cooling. Section S: Existing satellites
[ESA-PSS-03-108-ISSUE-1-VOL-5] 22 p3132 N90-27772
Spacecraft thermal control design data. Volume 6: Index
[ESA-PSS-03-108-ISSUE-1-VOL-6] 22 p3132 N90-27773

SPACECRAFT TRACKING
NT SATELLITE TRACKING
NT SATELLITE-TO-SATELLITE TRACKING
Independent Orbiter Assessment (IOA) CIL issues resolution report, volume 3
[NASA-CR-185524-VOL-3] 02 p0170 N90-10956
Independent Orbiter Assessment (IOA): Assessment of the communication and tracking subsystem, volume 1
[NASA-CR-185528-VOL-1] 03 p0315 N90-11789
Independent Orbiter Assessment (IOA): Assessment of the communication and tracking subsystem, volume 2
[NASA-CR-185528-VOL-2] 03 p0315 N90-11790
Independent Orbiter Assessment (IOA): Assessment of the communication and tracking subsystem, volume 3
[NASA-CR-185528-VOL-3] 03 p0315 N90-11791
The Telecommunications and Data Acquisition Report
[NASA-CR-185093] 04 p0485 N90-12786
Automation of orbit determination functions for National Aeronautics and Space Administration (NASA)-supported satellite missions 05 p0590 N90-13434
Optimum data weighting and error calibration for estimation of gravitational parameters 05 p0591 N90-13437

Shuttle Laser Technology Experiment Facility (LTEF)-to-airplane lasercom experiment: Airplane considerations
[NASA-TM-100749] 06 p0731 N90-14260
Tracking a hypersonic aircraft from a space platform
[AD-A216399] 10 p1377 N90-17984
Efficient detection and signal parameter estimation with application to high dynamic GPS receiver
[NASA-CASE-NPO-17820-1-CU] 11 p1454 N90-18379
Precise estimation of tropospheric path delays with GPS techniques 15 p2074 N90-21881
The determination of maximum deep space station slew rates for a high Earth orbiter 15 p2075 N90-21882
Galileo Earth approach navigation using connected-element interferometer phase-delay tracking 15 p2075 N90-21884
Digital Doppler extraction demonstration with the advanced receiver 15 p2076 N90-21893
Goldstone intracomplex connected element interferometry 20 p2852 N90-26218

SPACECRAFT TRAJECTORIES
NT EARTH-MOON TRAJECTORIES
NT INTERPLANETARY TRAJECTORIES
On mean elements for satellite orbits perturbed by the zonal harmonics of the geopotential
[AD-A212322] 04 p0461 N90-12642
Three-dimensional shear flows: Analysis of the track and angle of incidence
[CERT-RTS-OA-31/5025-AYD] 04 p0501 N90-12888
Automation of orbit determination functions for National Aeronautics and Space Administration (NASA)-supported satellite missions 05 p0590 N90-13434
Calculation of double-lunar swingby trajectories: I. Keplerian foundation 05 p0590 N90-13435
The controllability of the aeroassist flight experiment atmospheric skip trajectory 05 p0591 N90-13438
Cooperative control of two active spacecraft during proximity operations
[NASA-CR-185596] 09 p1172 N90-16778
Orbit determination of artificial Earth satellites through estmation techniques combined with state smoothing techniques
[INPE-4959-TDL/388] 11 p1465 N90-18440
Rapid near-optimal trajectory generation and guidance law development for single-stage-to-orbit airbreathing vehicles
[NASA-CR-186299] 12 p1612 N90-19275
Icarus lander 12 p1733 N90-19964
A satellite simulation program
[AD-A218079] 13 p1764 N90-20124
Galileo Earth approach navigation using connected-element interferometer phase-delay tracking 15 p2075 N90-21884
The influence of the gas surface interaction on spacecraft orbital motion 17 p2365 N90-23461
Possible trajectory profiles to achieve the geostationary orbit without any drift phase 22 p3127 N90-27745
An introduction to space trajectories 22 p3127 N90-27749
Optimization of the deployment of a pair of satellites in inclined eccentric geosynchronous orbits 22 p3128 N90-27751
Noncoplanar orbit transfer optimization for an aeroassisted sortie vehicle 22 p3128 N90-27752

SPACECREWS
Independent Orbiter Assessment (IOA): Analysis of the extravehicular mobility unit
[NASA-CR-185540] 02 p0166 N90-10937
Independent Orbiter Assessment (IOA): Analysis of the crew equipment subsystem
[NASA-CR-185591] 02 p0170 N90-10958
Independent Orbiter Assessment (IOA): Assessment of the crew equipment subsystem
[NASA-CR-185577] 02 p0173 N90-10971
Project AENEAS: A feasibility study for crew emergency return vehicle
[PB89-217020] 03 p0317 N90-11799
Functional decor in the International Space Station: Body orientation cues and picture perception
[NASA-TM-102242] 05 p0675 N90-13931
Payload crew utilization for spacelab missions
[NASA-TP-2976] 06 p0730 N90-14256
The first 1000 days of a future lunar base
[ILR-MITT-224] 08 p1033 N90-15970
Crew Safety and Rescue in Space: An International Approach
[ESA-SP-300] 08 p1034 N90-15974
Assured crew return capability architecture 08 p1034 N90-15977
On the selection of crewmember rescue means for manned space launch systems 08 p1035 N90-15978
Crew safety and rescue aids 08 p1035 N90-15980
Requirements for protective pressure suits for the Hermes spacecrew 13 p1753 N90-20065
Space station Simulation Computer System (SCS) study for NASA/MSFC. Volume 6: Study issues report
[NASA-CR-183845] 13 p1763 N90-20118
A radiological assessment of nuclear power and propulsion operations near Space Station Freedom
[NASA-CR-185185] 14 p1941 N90-21108
Perspective features of internal automation and robotics for supporting Columbus attached laboratory payload operations 18 p2502 N90-24297
Effect of fluid countermeasures of varying osmolarity on cardiovascular responses to orthostatic stress 18 p2628 N90-24978
Overtraining and exercise motivation: A research prospectus 18 p2629 N90-24982
MARS, an AI-based Mission Activities and Resource Scheduler
[MBB-0060/89-PUB] 19 p2650 N90-25083
Project EGRESS: Earthbound guaranteed reentry from space station. The design of an assured crew recovery vehicle for the space station
[NASA-CR-186657] 19 p2664 N90-25162
Technology for an intelligent, free-flying robot for crew and equipment retrieval in space 19 p2738 N90-25564

SPACELAB
Gamma radiation background measurements from Spacelab 2
[NASA-CR-183782] 02 p0297 N90-11689
Navigation experiment NAVEX: The equipment delay times in the Spacelab mission D1
[DFVLR-MITT-89-10] 03 p0304 N90-11728
Spacelab system analysis Marshall Avionics System Testbed (MAST)
[NASA-CR-183804] 03 p0317 N90-11802
Pre- and postflight postural control of the D1 Spacelab mission astronauts examined with a tilting room
[IZF-1988-25] 04 p0527 N90-13039
Experiment facilities for materials and fluid sciences embarked on Spacelab
[ESA-SP-1120] 08 p1053 N90-16089
Structural characterization of Spacelab
[ETN-90-95214] 08 p1087 N90-16289
Non-contact temperature measurement requirements 10 p1363 N90-17898
Fusion furnaces for Spacelab 13 p1785 N90-20248
Spacelab qualified infrared imager for microgravity science experiments
[NASA-TM-102503] 13 p1804 N90-20352
An in-vitro technique to study bone metabolism in developing mouse long bone rudiments under microgravity and compression 19 p2681 N90-25248
Small helium-cooled infrared telescope experiment for Spacelab-2 (IRT)
[NASA-CR-183983] 19 p2765 N90-25708
New observations of stratospheric N2O5
[NASA-TM-103478] 20 p2883 N90-26402
Microgravity science and applications: Apparatus and facilities
[NASA-TM-101892] 23 p3285 N90-28588

SPACELAB PAYLOADS
NT GEOPHYSICAL FLUID FLOW CELLS
Gamma radiation background measurements from Spacelab 2
[NASA-CR-183782] 02 p0297 N90-11689
Refurbishment and modification of the Metric Camera (RMK) for reflight on EOM-1 Spacelab mission
[ETN-90-96284] 11 p1512 N90-18710
Knowledge-based fault detection and analysis for robots: First results for the ROTEX robots
[ESA-TT-1150] 11 p1518 N90-18742
Random vibration analysis of space flight hardware using NASTRAN 18 p2570 N90-24645
Bubble, Drop and Particle Unit (BDPU): A multi-user microgravity facility
[IAF-89-431] 20 p2842 N90-26164

SPACELAB UV-OPTICAL TELESCOPE FACILITY
U STARLAB

SPACERS
Critical inspection of high performance turbine engine components: The RFC concept 22 p3185 N90-28073

SPACETENNAS
Feasibility study of a synthesis procedure for array feeds to improve radiation performance of large distorted reflector antennas
[NASA-CR-186641] 20 p2851 N90-26213
Tropospheric wind profiling using radar interferometry: A feasibility study of a compact mobile system
[PB90-217068] 23 p3351 N90-28939

SPACING
NT AIRCRAFT APPROACH SPACING
Primary arm spacing in directionally solidified Pb-10 wt percent Sn alloys
[NASA-CR-185190] 06 p0756 N90-14398
Interplanar spacing for various phases in austenitic stainless steels
[DE90-602350] 08 p1045 N90-16038
Blade row interaction effects on compressor measurements 11 p1462 N90-18419
Production of diffraction gratings using holographic interferometry
[DE90-612841] 14 p1983 N90-21362
Three-dimensional structure of plane mixing layers 17 p2344 N90-23347
Simulator evaluation of the final approach spacing tool
[NASA-TM-102807] 17 p2348 N90-23374

SPADATS (TRACKING SYSTEM)
U SPACE DETECTION AND TRACKING SYSTEM

SPALLATION
Deformation behavior of SiC/2014 Al metal-matrix composite
[AD-A212095] 03 p0320 N90-11816
Shock-wave characterization of energetic booster-rocket propellant WAK-2 and its simulant UGS
[DE90-002633] 07 p0914 N90-15285
Proceedings of the specialists' meeting on physics and engineering of fission and spallation
[DE90-719706] 08 p1125 N90-16519
Spallation and dynamic fracture as an effect of laser induced shock waves in carbon based composite materials
[AD-A216540] 11 p1478 N90-18509
Spallation of oxide scales from 20 percent Cr/25 percent Ni/Nb stainless steel
[AERE-R-13464] 13 p1775 N90-20189
Scale adherence effects in oxidation and sulfidation 23 p3307 N90-28703

SPALLING
Microstructural effects on spall fracture in 1008 steel
[DE89-016770] 02 p0198 N90-11131
Spall resistance of alumina
[AD-A213213] 04 p0477 N90-12735
Thermal barrier coating life prediction model development, phase 1
[NASA-CR-182230] 05 p0581 N90-13388
Spall strength measurements on shockloaded refractory metals
[DE90-000839] 06 p0747 N90-14345

SPANLOADER AIRCRAFT
Design of a spanloader cargo aircraft
[NASA-CR-186046] 06 p0722 N90-14216

SPARK DISCHARGES
U ELECTRIC SPARKS

SPARK GAPS
An empirical formula for gas switch breakdown delay
[DE89-017233] 03 p0342 N90-11947
Technology of fast spark gaps
[AD-A214199] 07 p0925 N90-15353
Study on lightning parameters in the light of long gap discharge phenomena
[DE90-734987] 09 p1248 N90-17237

SPARK IGNITION
Cold starting a neat methanol (M100) vehicle with long duration spark ignition
[PB89-230692] 06 p0792 N90-14613
Modeling of knock in spark-ignition engines
[DE90-010875] 22 p3182 N90-28058
Evaluation of a hybrid kinetics/mixing-controlled combustion model for turbulent premixed and diffusion combustion using KIVA-2
[NASA-TM-103196] 23 p3323 N90-28792

SPARK MACHINING
Electrode/workpiece combinations
[DE90-003919] 08 p1054 N90-16095

SPARK SHADOWGRAPH PHOTOGRAPHY
U SHADOWGRAPH PHOTOGRAPHY

SPARKS
NT ELECTRIC SPARKS
Spark source mass spectrometry software documentation and verification
[DE90-004463] 09 p1192 N90-16909
Electronic precipitator control
[NASA-CASE-LAR-13273-2] 13 p1798 N90-20320
Development of a spark assisted direct injection multifuel diesel engine especially for alcohol fuels
[ACTA-POLYTEC-SCAND-ME-94] 17 p2412 N90-23747

SPARTAN SATELLITES
The Spartan 1 mission
[NASA-TM-101887] 01 p0015 N90-10077

SPATIAL DEPENDENCIES
Spatial fluctuations in the diffuse X ray background 19 p2785 N90-25845

SPATIAL DISTRIBUTION
NT STAR DISTRIBUTION

Evaluation of the North Atlantic seasonal nitrogen model, version 2
[DE89-016157] 01 p0090 N90-10515
Solvent dynamical effects in electron transfer: Predicted influences of electron coupling upon the rate-dielectric friction dependence
[AD-A210193] 01 p0120 N90-10690
Spatial and temporal short range total cloud cover estimation by metric analysis of composite imagery 02 p0251 N90-11423
Doppler statistics of ocean velocity variability
[AD-A211687] 03 p0377 N90-12148
Visual motion perception
[AD-A210994] 03 p0379 N90-12160
Eye movements and spatial pattern vision
[AD-A211650] 03 p0381 N90-12169
Survey of the CLUSE main experiment Grand-CLUSE, May 1 - June 15, 1988 --- Humidity Exchange Over the Sea (HEXOS) experiment
[FEL-1988-43] 04 p0518 N90-12991
Spatial data structures for robotic vehicle route planning
[AD-A212806] 04 p0538 N90-13111
A statistical analysis of spatial point patterns, a case study
[CWI-MS-R8813] 04 p0547 N90-13180
Liquid and solid ion plasmas
[AD-A212415] 04 p0557 N90-13244
Successive iterations of the input catalog 05 p0607 N90-13534
Study of the hydroxyl radical by DRASC resonance in a high pressure flame --- Diffusion Raman Anti-Stokes Coherence (DRASC)
[ONERA-RS-53/7131-PY] 05 p0622 N90-13632
The relationship between subjective and objective measures of simulator-induced ataxia
[AD-A213095] 05 p0673 N90-13922
Data structures for the representation and manipulation of polyhedrons
[IMAG-RR-772-M] 05 p0692 N90-14042
Spatial evolution of nonlinear acoustic mode instabilities on hypersonic boundary layers
[NASA-TM-102431] 06 p0777 N90-14517
Frequency distributions of heavy rainstorms in Illinois
[PB90-100215] 06 p0816 N90-14748
The radar-based short term prediction of the time-space evolution of rain fields
[AD-A213802] 07 p0918 N90-15312
Spatial dynamics of deformable multibody systems with variable kinematic structure
[AD-A214098] 07 p0942 N90-15455
Global distribution of total cloud cover and cloud type amounts over the ocean
[DE90-003187] 07 p0964 N90-15574
Measures of subjective variables in visual cognition
[AD-A215084] 09 p1259 N90-17303
Proximity compatibility and information display: The effects of space and color on the analysis of aircraft stall conditions
[AD-A214488] 09 p1260 N90-17309
Two dimensional modifications of Gaussian laser light bundles
[AD-A215207] 10 p1389 N90-18033
Laser intersatellite transmission experiment spatial acquisition, tracking, and pointing system
[AD-A215934] 10 p1389 N90-18036
Computing with neural maps: Application to perceptual and cognitive functions
[AD-A216689] 10 p1412 N90-18143
Numerical simulation of non-inductive current drive for tokamak plasmas with time-varying electron temperatures
[DE90-733144] 10 p1432 N90-18264
An investigation of flow structure, mixing and chemical reaction in combusting turbulent flows
[AD-A216739] 11 p1483 N90-18538
A colony architecture for an artificial creature
[AD-A216802] 11 p1549 N90-18918
Zodiacal dust bands: Their relation to asteroid families
[AD-A216025] 11 p1590 N90-19170
Monte Carlo models and analysis of galactic disk gamma-ray burst distributions 12 p1636 N90-19403
Use of environmental monitoring data in evaluation of atmospheric modeling results
[DE90-008607] 13 p1831 N90-20510
Parts of recognition
[AD-A217694] 13 p1868 N90-20714
The production and spatial distribution of neutral and ionized water vapor in Comet P/Halley 15 p2185 N90-22484
Quantitative characterization of spatial distribution of particles in materials: Application to materials processing 16 p2219 N90-22660
Skewering the universe with QSO lines of sight: Lyman alpha clouds as probes of large scale structure 16 p2329 N90-23278
Development and use of a passive technique for measuring nitrogen dioxide in the background atmosphere 16 p2331 N90-23285
A survey of equatorial magnetospheric wave activity between 5 and 8 R(sub E)
[AD-A220137] 17 p2424 N90-23812
Vertical directionality measurements of ambient noise in the NE Pacific
[AD-A220007] 17 p2432 N90-23856
Estimation of noise field directionality: Comparison with Fourier series method
[AD-A220366] 17 p2469 N90-24114
A range-dependent analysis of acoustic transmission across a cold filament in the California current
[AD-A220175] 18 p2583 N90-24709
Cloud field classification based on textural features 18 p2646 N90-25066
Selective metallization of carbonyl-containing polymer films
[AD-D014526] 19 p2678 N90-25230
A study of the spatial scales of discrete polar auroral arcs
[NASA-CR-186806] 19 p2714 N90-25444
Electron populations above the nightside auroral oval during magnetic quiet times
[IRF-PREPRINT-116] 19 p2714 N90-25445
On the spatial eigenvalue approach to high Reynolds number flow in a rotating and nutating cylinder
[AD-A221710] 21 p3005 N90-27081
Structural and optical properties of DMP-128 holograms during environmental testing
[AD-A221691] 21 p3007 N90-27094
Distribution and movement of smokes from forest fires that occurred along the boundary of the People's Republic of China and the USSR on April-May 1987 21 p3028 N90-27216
Curvature estimation in orientation selection
[AD-A221481] 21 p3034 N90-27249
Spatial array processing by the method CLEAN
[FEL-1989-144] 22 p3165 N90-27949
Study of the origin of three dimensional structures in shear flows through external forcing
[AD-A221923] 22 p3170 N90-27980
Local spatial frequency analysis for computer vision
[NASA-CR-186990] 22 p3237 N90-28356
Compact 4-D optical neural network architecture
[AD-A222160] 22 p3241 N90-28379
Mode competition in the quasioptical gyrotron
[AD-A222181] 23 p3329 N90-28823
Meteorological conditions over the North Atlantic Ocean during GCE/CASE/WATOX
[PB90-252032] 24 p3494 N90-29747
Effects and control of the correlation properties of light sources
[AD-A224539] 24 p3545 N90-30049
Special purpose spatial light modulators
[AD-A223794] 24 p3545 N90-30052

SPATIAL FILTERING
Temporal and spatial filtering remedies for dispersion in electromagnetic particle codes
[DE89-017534] 03 p0408 N90-12337
Spatiotemporal characteristics of visual localization, phase 2
[AD-A212934] 05 p0674 N90-13929
Neural networks for data compression and invariant image recognition 08 p1075 N90-16219
Texture segmentation using localized spatial filtering
[AD-A218064] 13 p1869 N90-20722

SPATIAL ISOTROPY
U ISOTROPY
U SPATIAL DISTRIBUTION

SPATIAL MARCHING
Supersonic flow computations over aerospace configurations using an Euler marching solver
[NASA-CR-4085] 01 p0003 N90-10012

SPATIAL ORIENTATION
U ATTITUDE (INCLINATION)

SPATIAL RESOLUTION
Land vehicle teleoperation under conditions of reduced video resolution
[DE89-016925] 02 p0231 N90-11324
Estimated UV clutter levels at 10-100 meter sensor pixel resolution extrapolated from recent polar bear measurements
[AD-A211357] 03 p0372 N90-12125
Effect of spatial resolution on apparent sensitivity to initial conditions of a decaying flow as it becomes turbulent
[NASA-TM-102377] 05 p0638 N90-13719
Role of retinocortical processing in spatial vision
[AD-A210995] 05 p0672 N90-13918
Temporally and spatially resolved flow in a two-stage axial compressor. Part 2: Computational assessment
[NASA-TM-102273] 06 p0726 N90-14236
X ray microimaging for the life sciences
[DE90-002613] 06 p0819 N90-14766
Image enhancement using the IRAS (Infrared Astronomy Satellite) survey data
[AD-A213811] 07 p0950 N90-15496
Context dependent anti-aliasing image reconstruction 08 p1073 N90-16209
Context dependent prediction and category encoding for DPCM image compression 08 p1073 N90-16210
The determination of subscale structures in thermal images 08 p1093 N90-16330
Multibeam radar altimetry: Spaceborne feasibility and airborne experimentation
[AD-A215152] 09 p1207 N90-16995
Broadband incoherent imaging using multiple aperture optics
[AD-A215708] 09 p1282 N90-17437
Fracture analysis through photographic imagery of low spatial resolution: A contribution to the study of tectonic evoluation of the Araripe Plateau region
[INPE-4876-PRE/1487] 11 p1520 N90-18756
Perspective revision of systematic mapping through orbital imagery
[INPE-4817-PRE/1453] 11 p1524 N90-18775
The effects of luminance boundaries on color perception
[AD-A216741] 11 p1539 N90-18860
Three-dimensional motion estimation using shading information in multiple frames
[AD-A216804] 11 p1549 N90-18919
Spatially high-resolution flame diagnosis by means of spontaneous Raman spectroscopy
[ETN-90-95870] 12 p1623 N90-19328
Conception of an automatic measurement installation for spatial resolution detectors
[ETN-90-95732] 12 p1729 N90-19935
Space telescope searches for black holes in galactic nuclei 12 p1732 N90-19958
Simulation of radar and radiometer signals remote sensing cometary surface and subsurface structures 12 p1740 N90-20005
Capabilities of bistatic synthetic aperture radar for covert battlefield surveillance 14 p1961 N90-21230
Concept for a spaceborne Synthetic Aperture Radar (SAR) sensor based on active phased array technology 14 p1962 N90-21234
A solution for real time motion compensation for SAR without using inertial navigation systems 14 p1962 N90-21236
A fast ISAR-imaging process and its inherent degrading effects on image quality 14 p1963 N90-21239
Radar target image by ISAR case study 14 p1963 N90-21242
Absolute multilayer characterization at high spatial resolution via real-time soft x ray imaging
[DE90-009181] 14 p1984 N90-21371
Some recent applications of laser ultrasound to the characterisation of materials
[AERE-R-13438] 14 p1985 N90-21374
Spaceborne radar observations: A guide for Magellan radar-image analysis
[NASA-CR-184998] 16 p2249 N90-22826
Spatial Displays and Spatial Instruments
[NASA-CP-10032] 16 p2267 N90-22918
Spatial constraints of stereopsis in video displays 16 p2267 N90-22920
Visual slant underestimation 16 p2268 N90-22926
The photo-colorimetric space as a medium for the representation of spatial data 16 p2268 N90-22927
Spatial vision within egocentric and exocentric frames of reference 16 p2268 N90-22928
On the efficacy of cinema, or what the visual system did not evolve to do 16 p2269 N90-22934
The perception of geometrical structure from congruence 16 p2270 N90-22935
Interactive displays in medical art 16 p2271 N90-22940
Perception-action relationships reconsidered in light of spatial display instruments 16 p2272 N90-22949
A commentary on perception-action relationships in spatial display instruments 16 p2272 N90-22950
Spatial displays as a means to increase pilot situational awareness 16 p2272 N90-22951
Interactions of form and orientation 16 p2274 N90-22958
Optical, gravitational, and kinesthetic determinants of judged eye level 16 p2274 N90-22959
Wide-angle display developments by computer graphics 16 p2275 N90-22963
High spatial resolution isotopic CO and CS observations of M17 SW: The clumpy structure of the molecular cloud core
[MPE-PREPRINT-161] 16 p2330 N90-23283
Polar BEAR UV imaging of airglow and aurora-image processing and results
[AD-A219480] 17 p2422 N90-23802
Data analysis of a two-lidar experiment
[AD-A220289] 17 p2428 N90-23834

Cloud field classification based on textural features
18 p2646 N90-25066
Spatial and spectral features of soft diffuse X ray background seen by the Einstein observatory
19 p2792 N90-25895
Integration of multispectral SPOT imagery and panchromatic aerial photography for study in urban land use
[INPE-4967-PRE/1536] 22 p3194 N90-28125
Comparison of satellite based cloud retrieval methods for cirrus and stratocumulus 22 p3221 N90-28268
Spatial scales of cirrus cloud properties
22 p3222 N90-28275
Preliminary simulations of the large-scale environment during the FIRE cirrus IFO 22 p3225 N90-28290
Spatial interferometry in optical astronomy
[NASA-RP-1245] 22 p3262 N90-28470
Spatial disorientation incidents in the RNLAF F16 and F5 aircraft and suggestions for prevention
23 p3357 N90-28973
Attention gradients in situation awareness
23 p3358 N90-28978
The three-dimensional structure of visual attention and its implications for display design
23 p3359 N90-28980
Workload induced spatio-temporal distortions and safety of flight: An investigation of cognitive intrusions in perceptual processes 23 p3360 N90-28986
Head-mounted spatial instruments II: Synthetic reality or impossible dream 24 p3508 N90-29828

SPECIES DIFFUSION
Unsteady diffusion from a hemispherical pit
[NPL-DMA(A)-190] 04 p0553 N90-13220

SPECIFIC GRAVITY
U DENSITY (MASS/VOLUME)

SPECIFIC HEAT
Thermophysical properties of ceramics. Part 2: Development of specific-heat-measurement apparatus at high temperature
[DE89-760382] 01 p0047 N90-10268
Studies of novel superconductors
[DE89-016744] 02 p0282 N90-11609
Heat capacities of 1-methyl-3-ethylimidazolium chloride-aluminum chloride molten salts
[AD-A212790] 04 p0472 N90-12707
Summary physical data tables: Alkanes
[ESDU-PD3] 07 p0893 N90-15162
Thermal conductivity of gaseous aliphatic hydrocarbons. Part 1: Alkanes
[ESDU-89035-PT-1] 07 p0897 N90-15183
On the free carrier-negative U center interacting model for the high-T(sub c) oxide superconductor
[DE89-635908] 07 p0998 N90-15775
Effect of manganese additions on the physical and superconducting properties of Nb-46.5Ti
[DE90-005393] 10 p1436 N90-18290
Low temperature specific heat and magnetic susceptibility of NbTi and NbTiMn alloys
[DE90-005390] 11 p1486 N90-18552
Heat capacities of solid polymers (The Advanced THermal Analysis System, ATHAS)
[DE90-007130] 11 p1493 N90-18595
Specific heat and critical fluctuations in anisotropic high-T(sub c) oxide superconductors
[DE90-613394] 14 p2031 N90-21651
The Chemkin Thermodynamic Data Base
[DE90-007953] 14 p2035 N90-21676
The thermo-mechanical behavior of cometary nuclei
14 p2041 N90-21703
Compression molded polyurethane block copolymers. 1: Thermal and thermomechanical properties
[AD-A220068] 18 p2529 N90-24431
Research on high-specific-heat dielectrics
[AD-A221215] 18 p2623 N90-24944
Low-temperature specific heat measurements on metals: Application to high-T(sub c) superconductors
[DE90-011612] 18 p2626 N90-24966
Searching for heavy fermion materials in Ce intermetallic compounds
[DE90-011809] 20 p2834 N90-26116
Estimation of liquid heat capacities. 1: Review and evaluation of Missenard method
[AD-A224161] 24 p3445 N90-29454

SPECIFIC IMPULSE
Energy deposition in low power coaxial plasma thrusters 06 p0844 N90-14911
The 30-kW ammonia arcjet technology
[NASA-CR-186850] 19 p2670 N90-25190

SPECIFICATIONS
NT AIRCRAFT SPECIFICATIONS
NT EQUIPMENT SPECIFICATIONS
NT FUNCTIONAL DESIGN SPECIFICATIONS
Dependency-directed localization of software bugs
[AD-A210837] 01 p0106 N90-10606
A verification exercise relating to specification styles in LOTOS
[MEMO-INF-89-18] 02 p0259 N90-11471
Advanced light source master oscillator
[DE90-000123] 03 p0342 N90-11953
CALS (Computer-aided Acquisition and Logistic Support) Test Network information exchange: User's manual
[DE89-016700] 03 p0418 N90-12399
Requirements specification with Petri nets using the cube tool methodology
[AD-A212190] 04 p0492 N90-12829
An implementation-oriented specification of the TUMULT communication primitives
[MEMO-INF-88-34] 04 p0536 N90-13096
Multi-level specification and verification of real-time software
[AD-A213227] 05 p0683 N90-13975
ERIS: Engineering Resource Information System
[AD-A213357] 05 p0707 N90-14144
Markets for high-speed intercity Maglev technology: A systems analysis approach
[DE89-017683] 06 p0794 N90-14623
A graphically oriented specification language for automatic code generation. GRASP/Ada: A Graphical Representation of Algorithms, Structure, and Processes for Ada, phase 1
[NASA-CR-183212] 06 p0828 N90-14813
National airspace system: Airport movement area control operational concept
[WP-89W00181] 07 p0878 N90-15086
Sizing and selection of batteries for stand-alone photovoltaic systems
[DE90-002990] 08 p1060 N90-16129
Eurolaser definition phase: A comparison of high power lasers available
[ETN-90-96061] 08 p1083 N90-16268
Design of JT-60U ICRF launcher
[DE90-733145] 10 p1326 N90-17663
A system for execution of JSD requirements
[INPE-4915-TDL/381] 10 p1417 N90-18170
The determination of offgassing products from materials and assembled articles to be used in a manned space vehicle crew compartment
[ESA-PSS-01-729-ISSUE-1] 11 p1469 N90-18461
A battery data base for electric vehicle applications
[DE90-007085] 11 p1503 N90-18655
An interactive system applied to the linear quadratic problem
[INPE-4945-TDL/386] 11 p1548 N90-18913
A digital HDTV recorder using a cluster of four D1 DVTRs
[BBC-RD-1989/13] 12 p1649 N90-19477
Design considerations in achieving 1 MW CW operation with a whispering-gallery-mode gyrotron
[DE90-007283] 12 p1663 N90-19557
Progress in the CW operation of a 140 GHz gyrotron
[DE90-007382] 12 p1663 N90-19558
An equational language for specifying, querying, and updating database domains
[PB90-124694] 12 p1726 N90-19918
Pyrotechnic device technology
[DE90-007683] 13 p1783 N90-20234
Technical specifications requirements: Automated reasoning applications
[DE90-008799] 13 p1867 N90-20712
A locally constrained parallel activation model for diagnostic reasoning
[AD-A217808] 13 p1874 N90-20747
CCST (Center for Compound Semiconductor Technology) research briefs
[DE90-007782] 13 p1895 N90-20874
Equipment specifications for launcher guidance using multivariable frequency methods
[REPT-892-422-106] 16 p2205 N90-22582
The GPS-NAVSTAR location and navigation system
17 p2359 N90-23433
Gamma Ray Observatory (GRO) dynamics simulator requirements and mathematical specifications, revision 1
[NASA-CR-183465] 17 p2362 N90-23447
Automatic runtime consistency checking and debugging of formally specified programs
[AD-A218855] 17 p2442 N90-23916
Gemini2: A second generation layout validation program
[AD-A220731] 17 p2444 N90-23926
Specification modules in LOTOS
[MEMO-INF-89-46] 17 p2449 N90-23965
IAPSA 2 small-scale system specification
[NASA-CR-182006] 17 p2467 N90-24103
A compact joint for the ROTEX manipulator
18 p2536 N90-24467
Space shuttle avionics system
[NASA-SP-504] 19 p2664 N90-25160
Reliability model generator specification
[NASA-CR-182005] 19 p2752 N90-25638
The conceptual task model: A specification technique between requirements engineering and program development
[TR-89-15] 19 p2762 N90-25694
Vibration test procedures for orbiter sidewall-mounted payloads, phase 2
[AD-A220774] 20 p2818 N90-26038
Software requirements: Guidance and control software development specification
[NASA-CR-182058] 20 p2906 N90-26527
The rationale and specification of the ELLA graphics systems
[RSRE-89017] 20 p2909 N90-26548
Multimegawatt space nuclear power supply, phase 1. Supplement: D180-30619-8
[DE90-012433] 20 p2926 N90-26647
IRDS prototyping with applications to the representation of EA/RA models
[NASA-CR-186066] 21 p3039 N90-27273
Flight motor set 360L006 (STS-34). Volume 1: System overview
[NASA-CR-184007] 22 p3133 N90-27781
In-service inspection of composite components on aircraft at depot and field levels
22 p3186 N90-28078
A model parametric real-time logic
[REPT-90-010] 22 p3241 N90-28381
Procedures for DOE-Navy exchange and approval of engineering information and material management required for production of W88-0/Mk5 RBA (reentry body assembly)
[DE90-014763] 23 p3287 N90-28595
Specifications, tolerances, and other technical requirements for weighing and measuring devices as adopted by the 74th National Conference on Weights and Measures, 1989 (1990 edition)
[PB90-184961] 23 p3316 N90-28748
Adjustable speed drive applications guidebook
[DE90-014151] 23 p3321 N90-28780
Quality function deployment as a mechanism for process characterization and control
[DE90-014755] 23 p3337 N90-28857
Survey of formal specification techniques for reactive systems
[AD-A223741] 24 p3538 N90-30005

SPECIMEN GEOMETRY
Fatigue behavior of specimens under compression load spectra
[ETN-89-95207] 04 p0512 N90-12954
Observations of fatigue crack initiation and damage growth in notched titanium matrix composites
[NASA-TM-101688] 10 p1347 N90-17815
Tensile mechanical properties in flat specimens of 7150-T7751
[INFORME-I-296/88] 10 p1356 N90-17860
Thermo-oxidative stability studies of PMR-15 polymer matrix composites reinforced with various fibers
[NASA-TM-102439] 12 p1620 N90-19310

SPECIMENS
Method of radiographic inspection of wooden members
[NASA-CASE-LAR-13724-1] 17 p2414 N90-23756

SPECKLE INTERFEROMETRY
Speckle interferometry for high resolution pictures of astronomical objects
[ETN-90-95827] 12 p1729 N90-19936
Information reconstruction from speckle interferograms
[ETN-90-95918] 12 p1729 N90-19939
Experimental validation of extended image reconstruction using bispectral speckle interferometry
[DE90-008545] 13 p1772 N90-20171
Preliminary results on two-dimensional interferometry of HL Tau
14 p1979 N90-21335
Super-diffraction limited measurements through the turbulent atmosphere by speckle interferometry
[AD-A221227] 18 p2581 N90-24699
Coherent optical techniques for industrial inspection
[PNR90605] 20 p2927 N90-26654
Spatial interferometry in optical astronomy
[NASA-RP-1245] 22 p3262 N90-28470
Bispectral-based optimization algorithms for speckle imaging
[DE90-015610] 24 p3529 N90-29957

SPECKLE PATTERNS
Practical systems for speckle velocimetry
05 p0574 N90-13341
Development of interferometric and holographic techniques in fluid mechanics
[ISL-CO-227/88] 09 p1218 N90-17068
An optical white light speckle process in forward dispersion for measurement of the velocity field in free convective currents
[ETN-90-95913] 12 p1661 N90-19546

Two-dimensional surface strain measurement based on a variation of Yamaguchi's laser-speckle strain gauge
[NASA-TM-103162] 16 p2241 N90-22784
A note on the statistics of laser speckle
[AD-A222408] 21 p3009 N90-27103
High resolution optical imaging through the atmosphere
[AD-A221913] 21 p3097 N90-27599
Progress in high temperature speckle-shift strain measurement system
[NASA-TM-103255] 22 p3177 N90-28031

SPECTRA
NT ABSORPTION SPECTRA
NT ATOMIC SPECTRA
NT BALMER SERIES
NT CONTINUOUS SPECTRA
NT ELECTROMAGNETIC SPECTRA
NT ELECTRONIC SPECTRA
NT EMISSION SPECTRA
NT ENERGY SPECTRA
NT FRAUNHOFER LINES
NT GAMMA RAY SPECTRA
NT H ALPHA LINE
NT H BETA LINE
NT H LINES
NT INFRARED SPECTRA
NT K LINES
NT LINE SPECTRA
NT LYMAN SPECTRA
NT MASS SPECTRA
NT MICROWAVE SPECTRA
NT MOLECULAR SPECTRA
NT NEUTRON SPECTRA
NT NOISE SPECTRA
NT OXYGEN SPECTRA
NT PLASMA SPECTRA
NT POWER SPECTRA
NT RADIATION SPECTRA
NT RADIO SPECTRA
NT RAMAN SPECTRA
NT ROTATIONAL SPECTRA
NT RYDBERG SERIES
NT SCHUMANN-RUNGE BANDS
NT SHOCK SPECTRA
NT SOLAR SPECTRA
NT SPECTRAL BANDS
NT STELLAR SPECTRA
NT UBV SPECTRA
NT ULTRAVIOLET SPECTRA
NT VIBRATIONAL SPECTRA
NT VISIBLE SPECTRUM
NT X RAY SPECTRA
On the photoemission spectrum and optical gap in La2CuO4
[DE89-015281] 02 p0281 N90-11605
Spectral-domain analysis of finite frequency selective surfaces
[AD-A211669] 03 p0339 N90-11932
Fluctuations in transverse energy and multiplicity, energy densities, and neutral pion spectra in nucleus-nucleus collisions at 200 GeV/nucleon
[DE89-017583] 03 p0402 N90-12302
Spectral study of a compressible isotropic turbulence
[ECL-88-16] 05 p0643 N90-13753
The grand unified photon spectrum: A coherent view of the diffuse extragalactic background radiation
[NASA-CR-186077] 05 p0715 N90-14180
Fatigue analysis and reconstruction of helicopter load spectra 06 p0739 N90-14304
Array signal processing: New techniques for direction finding and spectrum estimation
[AD-A213883] 07 p0924 N90-15345
Stable supermembrane vacuum with a discrete spectrum
[DE89-635722] 07 p0962 N90-15561
Studies of quantitative methods for imaging from scattered fields
[AD-A214047] 07 p0976 N90-15638
Wind speed dependence of acoustic ambient vertical directional spectra at high frequency
[AD-A214293] 07 p0989 N90-15712
Soft modes, freezing, and nonlinear response of a dipolar glass
[DE90-003647] 08 p1051 N90-16075
Transition state spectroscopy of hydrogen transfer reactions
[AD-A215041] 09 p1191 N90-16901
Simulation of rough surface scattering in three-dimensions
[AD-A215171] 09 p1277 N90-17405
Report on the multicolor pyrometry session at the Second NASA Non-Contact Temperature-Measurement Workshop 10 p1367 N90-17926
Numerical simulations of coherent structures in a jet flame with a noncircular cross section
[AD-A216710] 11 p1483 N90-18535
Reliability studies of ceramic capacitors
[AD-A216763] 11 p1501 N90-18643
Metal alkoxides: Models for metal oxides. Alkoxide ligands in early transition metal organometallic chemistry
[DE90-007523] 13 p1894 N90-20869
Modified tight-binding approximation and electron-phonon spectral function for transition metals
[DE90-614022] 14 p1950 N90-21166
Radar RFI at Goldstone DSS 12 and DSS 16 15 p2078 N90-21900
Spectral response of wheat and its relationship with agronomic variables in the tropical region
[INPE-5018-RPE/612] 15 p2122 N90-22138
An algorithm and computer program for the calculation of envelope curves
[PB90-155409] 15 p2145 N90-22254
Turbulence spectral widths view angle independence as observed by Doppler radar
[AD-A219169] 16 p2199 N90-22550
ISS and TPD study of the adsorption and interaction of CO and H2 on polycrystalline Pt 18 p2559 N90-24602
A study of the spatial scales of discrete polar auroral arcs
[NASA-CR-186806] 19 p2714 N90-25444
Annual and interannual variations of Earth-emitted radiation based on a 10-year data set
[NASA-TM-103465] 20 p2887 N90-26432
Probing the possibility of a C-12/C-13 galactic abundance gradient 21 p3094 N90-27586
Measuring the vertical directional spectra caused by sea surface sound
[AD-A223883] 23 p3354 N90-28957
Supercritical fluid chromatography/supersonic jet spectroscopy
[DE90-015220] 24 p3447 N90-29465
IUE-ULDA access guide no. 2. International Ultraviolet Explorer-Uniform Low Dispersion Archive: Comets
[ESA-SP-1134] 24 p3563 N90-30157

SPECTRAL ABSORPTION
U ABSORPTION SPECTRA

SPECTRAL ANALYSIS
U SPECTRUM ANALYSIS

SPECTRAL BANDS
NT ABSORPTION SPECTRA
NT FRAUNHOFER LINES
NT SCHUMANN-RUNGE BANDS
Growth and characterization of materials for tunable lasers in the near infrared spectral region
[NASA-CR-185832] 03 p0352 N90-12009
Evaluating CO, CO2 and H2O concentration by partial integration of absorption band spectra
[ISL-R-110/88] 09 p1244 N90-17219
Photoelectron spectroscopic study of the interaction of thin Fe films with the MoS2(0001) surface
[AD-A214348] 10 p1351 N90-17836
Analysis of methods to determine emissivity for ground surface targets in the spectral band 8 to 14 microns
[INPE-4984-TDL/394] 13 p1820 N90-20447
New spectral features of stratospheric trace gases 15 p2079 N90-21910
Computation of broad spectral band electro-optical system transmittance response characteristics to military smokes and obscurants using field test data from transmissometer system measurements 15 p2086 N90-21939
The calculation of infrared limb emission by ozone in the terrestrial middle atmosphere 15 p2125 N90-22151
Spectral feature design in high dimensional multispectral data
[NASA-CR-186647] 18 p2574 N90-24664
Multiwavelength observations of BL Lacertae 19 p2791 N90-25886
X ray variability of active galactic nuclei 19 p2795 N90-25914
Analysis of cirrus optical properties with data from NASA ER2 High-resolution Interferometer Sounder (HIS)
[NASA-CR-186365] 21 p3030 N90-27227
Laboratory simulation of interstellar grain chemistry and the production of complex organic molecules 21 p3092 N90-27580
Radiative properties of cirrus clouds inferred from broadband measurements during FIRE 22 p3226 N90-28295
Peak analysis in gas chromatography and the development of new stationary phases for anion chromatography
[DE90-014428] 23 p3304 N90-28687
Study of anomalies in transition vegetation in Alto Xingo-NT, through remote sensing techniques
[INPE-4601-TDL/334] 23 p3343 N90-28891
Metallic line profiles of the AOV star Vega
[NASA-CR-186906] 23 p3408 N90-29261

SPECTRAL CORRELATION
Reexamination of data from the asteroid/meteoroid detector
[NASA-CR-185997] 05 p0714 N90-14175
Statistics of two-color laser beam propagation in the turbulent atmosphere (spectral correlation)
[PB89-236699] 06 p0787 N90-14581
Ion-heated thermal Comptonization models and x ray spectral correlations in active galactic nuclei
[DE90-003597] 08 p1151 N90-16667
Correlations between X ray luminosity and pulse shape as well as spectral shape in binary X ray pulsars 19 p2773 N90-25767
Ion-heated thermal comptonization models and X ray spectral correlations in active galactic nuclei 19 p2790 N90-25880
X ray spectral variability in Seyfert 1 galaxies 19 p2792 N90-25891

SPECTRAL EMISSION
Theory of atomic spectral emission intensity
[IRF-PREPRINT-110] 02 p0287 N90-11641
A solar extreme ultraviolet flux model 02 p0296 N90-11686
The ratio to X-ray spectral shape and variability of blazars 02 p0297 N90-11688
Proceedings of a workshop on Higher-Order Spectral Analysis
[AD-A215849] 10 p1353 N90-17845
Spectral emissivities and optical constants of electromagnetically levitated liquid metals as functions of temperature and wavelength 10 p1364 N90-17907
Measurement of spectral emissivity by Fourier transform infrared spectrometer
[DE89-782319] 11 p1510 N90-18698
Power spectral densities for selected digital phase-continuous MFSK (M-ary Frequency Shift Keying) emissions
[PB90-129990] 12 p1647 N90-19463
Non-random uncertainties in the calibration of protection-level secondary standards
[NPL-RS(EXT)-110] 15 p2166 N90-22378
Filter process for parasitic suppression for reception of spectrally separated emission signals
[ETN-90-96506] 18 p2545 N90-24526

SPECTRAL ENERGY DISTRIBUTION
UV observations of NGC 205
[NASA-CR-185975] 02 p0291 N90-11661
Pacific marine radar sea scatter experimental results
[AD-A211593] 03 p0339 N90-11931
Search for rapidly star forming galaxies at high redshift 15 p2181 N90-22465
Spectral characteristics of low-angle radar ground clutter
[AD-A220817] 17 p2392 N90-23622
Evolution equation simulation of semiconductor lasers under a pulsed regime
[TELECOM-PARIS-89-D-010] 18 p2563 N90-24625
The high-energy properties of X ray pulsars 19 p2767 N90-25719
Ultrasensitive laser spectroscopy in solids: Statistical fine structure and single-molecule detection
[AD-A222391] 21 p3074 N90-27477
The effects on antenna-filtered scintillation parameters of non-zero antenna pointing angles
[AD-A223840] 24 p3462 N90-29554

SPECTRAL LINE WIDTH
GRIS observations of the Galactic Center 11 p1559 N90-18982
Dust in planetary nebulae: IRSPEC observations in the 3.0 micron-3.8 micron range 11 p1584 N90-19132
Tunable XeCl-laser featuring high spectral luminance 16 p2311 N90-23167
A search for additional parameters in the infrared luminosity/21 cm line-width relation for spiral galaxies in clusters of galaxies 16 p2328 N90-23274
Evolution equation simulation of semiconductor lasers under a pulsed regime
[TELECOM-PARIS-89-D-010] 18 p2563 N90-24625
Optical FeII emission and the BLR structure in QSOs 19 p2793 N90-25899
Neutral column density and soft excesses in active galactic nuclei 19 p2794 N90-25908
Quantitative spectroscopy of x ray laser plasmas in pulsed power devices
[AD-A221964] 21 p3078 N90-27501

SPECTRAL LINES
U LINE SPECTRA

SPECTRAL METHODS
On the coefficients of differentiated expansions of ultraspherical polynomials
[NASA-CR-181913] 01 p0112 N90-10637
Shock capturing by the spectral viscosity method
[NASA-CR-181920] 01 p0112 N90-10639
A conforming spectral collocation strategy for Stokes flow through a channel contraction
[NASA-CR-181912] 02 p0263 N90-11495

Convergence results for pseudospectral approximations of hyperbolic systems by a penalty type boundary treatment
[NASA-CR-181929] 03 p0391 N90-12230
Modified Chebyshev pseudospectral method with O(N exp -1) time step restriction
[NASA-CR-181958] 06 p0834 N90-14848
Finite word length considerations in high resolution spectral estimation
[AD-A214684] 09 p1273 N90-17377
Spectral multi-domain approximation of the Navier-Stokes equations in curved complex geometries
[ONERA-NT-1987-2] 11 p1508 N90-18685
DOA (Direction of Arrival) estimation by Eigendecomposition using single vector Lanczos' algorithm
[AD-A215802] 11 p1544 N90-18867
Conforming Chebyshev spectral collocation methods for the solution of laminar flow in a constricted channel
[NASA-CR-182011] 12 p1660 N90-19539
Spectral simulation of unsteady compressible flow past a circular cylinder
[NASA-CR-182030] 13 p1750 N90-20050
Unsteady three-dimensional marginal separation, including breakdown
[NASA-TM-102525] 13 p1801 N90-20337
Spectral analytic methods for the estimation of number of signals and directions of arrival
[AD-A217219] 13 p1876 N90-20757
Fourier analysis of finite element preconditioned collocation schemes
[NASA-CR-182040] 16 p2304 N90-23128
Numerical study of the onset of instability in the flow past a sphere 17 p2400 N90-23672
The CFL condition for spectral approximations to hyperbolic initial-boundary value problems
[NASA-CR-182053] 18 p2604 N90-24833
Using implicit ODE methods with iterative linear equation solvers in spectral methods
[FFI-89/7017] 19 p2751 N90-25633
Calculation of unsteady two dimensional viscous incompressible flows by spectral methods
[ETN-90-97449] 22 p3175 N90-28015
Experimental study of homogeneous turbulence under rotation and deformation modes
[ONERA-RSF-12/1145-AY-170A] 22 p3176 N90-28023
Experimental study of the effects of rotation on the homogeneous turbulence. Comparison with the EDQNM model
[ONERA-RSF-11/1145-AY-166A] 22 p3176 N90-28025

SPECTRAL NOISE
U WHITE NOISE

SPECTRAL REFLECTANCE
Photoreflectance study of boron ion-implanted (100) cadmium telluride
[SD-TR-88-89] 01 p0053 N90-10300
Spatial characterization of acid rain stress in Canadian Shield Lakes
[NASA-CR-183446] 01 p0084 N90-10479
Physically-based parameterization of spatially variable soil and vegetation using satellite multispectral data
[NASA-CR-185957] 05 p0663 N90-13879
Cloud phase discrimination by near-infrared remote sensing 08 p1090 N90-16310
Relationships between the aerial biomass from ground layers of cerrado and its spectral reflectance
[INPE-4848-PRE/1477] 11 p1521 N90-18760
In-situ differential reflectance study of the etching of SiO2 films
[AD-A217186] 13 p1893 N90-20864
Development of remote sensing techniques for the investigation of neotectonic activity, eastern transverse ranges and vicinity, southern California 18 p2573 N90-24662
Spectral feature design in high dimensional multispectral data
[NASA-CR-186647] 18 p2574 N90-24664
Use of high-dimensional spectral data to evaluate organic matter, reflectance relationships in soils
[NASA-CR-186650] 18 p2574 N90-24665
The 27-28 October 1986 FIRE IFO cirrus case study: Comparison of satellite and aircraft derived particle size 22 p3224 N90-28285

SPECTRAL RESOLUTION
As observational and theoretical investigation of stellar flares 06 p0862 N90-15012
On the range resolution of point targets with FMCW radar systems
[DLR-FB-89-47] 11 p1499 N90-18629
IRAS LRS spectra of extended objects: The Crab nebula 11 p1581 N90-19107
High resolution infrared spectroscopy of symbiotic stars 11 p1583 N90-19125
Isophot-S, a low resolution 2.5 to 12 microns spectrometer for ISO 11 p1589 N90-19167
A solution for real time motion compensation for SAR without using inertial navigation systems 14 p1962 N90-21236
Cirrus cloud optical properties measured with the University of Wisconsin high spectral resolution and volume imaging lidars 15 p2084 N90-21932
The super-gratings: How to improve the limiting resolution of grating spectrometers
[PREPRINT-695] 16 p2204 N90-22577
Spectral feature design in high dimensional multispectral data
[NASA-CR-186647] 18 p2574 N90-24664
Use of high-dimensional spectral data to evaluate organic matter, reflectance relationships in soils
[NASA-CR-186650] 18 p2574 N90-24665
The problem of dead layer in gamma ray burst spectra recorded with NaI or CsI crystals 19 p2776 N90-25787
Simulations of high-resolution X ray spectra of AGNs 19 p2791 N90-25885
Spatial and spectral features of soft diffuse X ray background seen by the Einstein observatory 19 p2792 N90-25895
Spectroscopy of AGNs with Xspect/Sodart in 1993 19 p2794 N90-25909
The interstellar D1 line at high resolution
[NASA-CR-184915] 20 p2941 N90-26737
Summary of results and conclusions based on analysis of volume imaging and high spectral resolution lidar data acquired during FIRE phase 1, part 1 22 p3223 N90-28278
Summary of results and conclusions based on analysis of volume imaging and high spectral resolution lidar data acquired during FIRE phase 1, part 2 22 p3227 N90-28300
A laser spectrometer and wavemeter for pulsed lasers
[NASA-CR-181731] 23 p3331 N90-28832
Infrared spectroscopic measurements on planetary atmospheric gases 23 p3412 N90-29283
An analysis of the characteristics of atmospheric profiles obtained with the High resolution Interferometer Sounder (HIS) 24 p3488 N90-29716

SPECTRAL SENSITIVITY
In-situ cure monitoring of composites by fiber-optic molecular sensors
[AD-A211495] 03 p0320 N90-11817
Spectral sensitivity of device power output for tandem a-Si alloy solar cells
[DE89-009421] 08 p1095 N90-16340
In-situ differential reflectance study of the etching of SiO2 films
[AD-A217186] 13 p1893 N90-20864
Emitter and base recombination parameters in solar cells: Measurement process and dependence on temperature and injection
[ETN-90-97305] 22 p3196 N90-28138
High power oblique incidence HF ionospheric modification
[AD-A224402] 24 p3491 N90-29729

SPECTRAL SIGNATURES
Flare model sensitivity of the Balmer spectrum 03 p0432 N90-12477
Use of the Egret instrument in studies of the origin of the cosmic radiation. 2: Spectral signatures of discrete cosmic-ray sources
[DE90-003595] 08 p1154 N90-16682
Evaluation of two methods for acquisition of training statistics for digital analysis of areas prepared for plowing
[INPE-4901-PRE/1502] 11 p1522 N90-18763
The infrared spectral signature of star formation 11 p1582 N90-19114
Inventory and monitoring of extended forest lands by remote sensing 19 p2708 N90-25409
Spectral signatures of X ray photoionized nebulae 19 p2778 N90-25800
Ultrasoft components in X ray-selected AGN 19 p2787 N90-25864
Long term multi-frequency study of 3C 273 19 p2790 N90-25879
A search for iron features in the EXOSAT spectral survey sources 19 p2791 N90-25887
Spatial and spectral features of soft diffuse X ray background seen by the Einstein observatory 19 p2792 N90-25895
Optical signatures of molecular particles via mass-selected cluster spectroscopy 20 p2949 N90-26780
The plasma wave signature of a 'magnetic hole' in the vicinity of the magnetopause
[NASA-CR-187027] 22 p3212 N90-28220

SPECTRAL THEORY
Theory of atomic spectral emission intensity
[IRF-PREPRINT-110] 02 p0287 N90-11641
Proceedings of the Focused Research Program on Spectral Theory and Boundary Value Problems. Volume 4: Nonlinear Differential Equations
[DE90-000920] 06 p0822 N90-14780
Design of a large angular aperture TeO2 acousto-optic tunable filter
[AD-A213999] 07 p0993 N90-15738
Polarization radar processing technology
[AD-A215242] 10 p1374 N90-17967
X ray spectra produced by NaF implosions
[AD-A215803] 10 p1429 N90-18243
Correlation-induced changes of spectra
[AD-A217087] 12 p1669 N90-19591
US Navy hindcast spectral ocean wave model climatic atlas: Mediterranean Sea
[AD-A219755] 17 p2426 N90-23825
Spectral transport model for turbulence
[DE90-011265] 19 p2689 N90-25295
Broadband studies of seismic sources at regional and teleseismic distances using advanced time series analysis methods
[AD-A223113] 22 p3211 N90-28215
On the dynamic and thermodynamic structures of marine stratocumulus 22 p3216 N90-28244
Modification of the background flow by roll vortices 22 p3219 N90-28258
Planetary-scale flow on a two-layer beta-plane channel model with topography 23 p3350 N90-28931

SPECTROGRAMS
New Voyager radio spectrograms of Uranus
[NASA-CR-180381] 23 p3412 N90-29284

SPECTROGRAPHS
Assessment of research needs for laser technologies applied to advanced spectrographic methods
[DE90-001154] 06 p0788 N90-14587
X ray spectra produced by NaF implosions
[AD-A215803] 10 p1429 N90-18243
Quantum yield of photocathodes in far and extreme ultraviolet wavelength area
[ETN-90-95731] 12 p1654 N90-19505
The microchannel plate camera as a detector at high resolution spectrographs: Experiments for velocity distribution in planetary nebulae
[ETN-90-95733] 12 p1664 N90-19560
SIRTF in high earth orbit 14 p1980 N90-21345
Monolithic Optical Programmable Spectrograph (MOPS)
[AD-D014502] 19 p2757 N90-25669

SPECTROMETERS
NT GAMMA RAY SPECTROMETERS
NT IMAGING SPECTROMETERS
NT INFRARED SPECTROMETERS
NT LASER SPECTROMETERS
NT MASS SPECTROMETERS
NT NEUTRON SPECTROMETERS
NT SOLAR SPECTROMETERS
NT TIME OF FLIGHT SPECTROMETERS
NT TOTAL OZONE MAPPING SPECTROMETER
NT ULTRAVIOLET SPECTROMETERS
Droplet sizing instrumentation used for icing research: Operation, calibration, and accuracy
[NASA-CR-182293] 03 p0350 N90-11999
Electron cyclotron emission and absorption experiment on the CASTOR tokamak
[IPPCZ-285] 03 p0407 N90-12331
Spectrometer technology recommendations 05 p0597 N90-13488
Three-meter balloon-borne telescope 05 p0601 N90-13490
Capillary electrophoresis ionization-mass spectrometry and tandem mass spectrometry
[DE90-002664] 07 p0892 N90-15158
Design of a large superconducting spectrometer magnet
[DE90-719505] 08 p1131 N90-16553
Determination of iron in chromium plating and polishing solutions by atomic absorption spectrometry
[AD-A214467] 09 p1189 N90-16892
Spectroscopic techniques for the analysis of CdTe substrates used for the growth of HgCdTe
[AD-A214545] 09 p1288 N90-17466
Linear Variable Differential Transformer (LVDT) with conditioner for the control of stepping motor drivers (part of the sliding-foil follower system of the Emin spectrometers)
[DIGEL-1989-9] 11 p1504 N90-18660
Optimization of digital filters for a short-scan interferometer
[AD-A217997] 13 p1798 N90-20315
AFGL ten micron mosaic array spectrometer: Recent results 14 p1978 N90-21333
Design and status of the detector block for the ISO-SWS 14 p1980 N90-21341
Status of the isophot detector development 14 p1980 N90-21342
ISO/LWS: Detector status 14 p1980 N90-21343

Development of the CLAES instrument aperture door system 15 p2112 N90-22083
Improved crystal bending techniques applied to the LLNL dual-arm Johann mounting x ray spectrometer
[DE90-009528] 15 p2173 N90-22415
The super-gratings: How to improve the limiting resolution of grating spectrometers
[PREPRINT-695] 16 p2204 N90-22577
Interstellar HCN, HNC and HCO+: Stability experiments with acoustooptic spectrometers
[ETN-90-96495] 18 p2638 N90-25028
Comparison test of droplet sizing instruments used in icing research
[DOT/FAA/CT-TN90/13] 19 p2693 N90-25322
A voltage contrast detector with double channel energy analyzer in a scanning electron microscope
[ISBN-90-6275-568-2] 19 p2694 N90-25330
Einstein SSS+MPC observations of Seyfert type galaxies 19 p2795 N90-25913
Experiment K-6-24, K-6-25, K-6-26. Radiation dosimetry and spectrometry 20 p2897 N90-26477
High resolution infrared spectroscopy of planetary molecules using diode lasers and Fourier transform spectrometers 20 p2943 N90-26747
Planar waveguide spectrometer
[DE90-016308] 24 p3546 N90-30057

SPECTROMETRY
U SPECTROMETERS

SPECTROPHOTOMETERS
Optical instrumentation support for the airborne ionospheric observatory
[AD-A218207] 13 p1889 N90-20839
Reports from the German Meteorological Service. No. 179: Development, realization and functioning of lidar to evaluate the atmospheric ozone profile
[ISBN-3-88148-252-0] 18 p2578 N90-24685

SPECTROPHOTOMETRY
NT STELLAR SPECTROPHOTOMETRY
Laboratory analyses of micron-sized solid grains: Experimental techniques and recent results 08 p1141 N90-16616
Determination of trivalent chromium ions in chromium plating solutions by ultraviolet-visible spectrophotometry
[AD-A215688] 10 p1351 N90-17837
Investigation of multiple scattering in aqueous suspensions of non-absorbing polystrene microspheres using spectrophotometry
[BCRS-89-09] 11 p1485 N90-18549
Study of rifampicin fixation on plasma proteins by derivative spectrophotometry
[CERMA-89-25] 11 p1540 N90-18866
Spectrophotometry of dust with Isophot 11 p1589 N90-19164
Hot OH and CN: Evidence for organic molecules close to the nucleus of comet Halley 12 p1742 N90-20012
Study of new technique of solid combustible materials to determination of volatile elements by flame atomic absorption spectrophotometry
[DE90-612907] 14 p1947 N90-21147
Spectrally selective tinoxide and indiumoxide coatings
[ISBN-90-9003138-3] 17 p2382 N90-23567

SPECTROPOLARIMETERS
U POLARIMETERS

SPECTRORADIOMETERS
Performance parameter characterisation of various types of IR single element detectors 11 p1588 N90-19161
Workshop minutes on Remote Sensing of Hydrocarbons and Toxic Pollutants
[PB90-186370] 22 p3194 N90-28127

SPECTROSCOPES
U SPECTROMETERS

SPECTROSCOPIC ANALYSIS
Advances in regression: Use of models in spectroscopic data analysis
[AD-A210541] 01 p0116 N90-10665
Laboratory measurements of microwave and millimeter-wave properties of planetary atmospheric constituents
[NASA-CR-185914] 01 p0141 N90-10815
A diffuse reflectance infrared Fourier transform spectroscopic study of adsorbed hydrazines 02 p0205 N90-11170
Hardening mechanisms and analysis of the structure of the TGDDM/DDS epoxy resin system (tetraglycidyl-4,4' diaminodiphenylmethane/4,4' diaminodiphenylsulfone)
[NOTE-TECHNIQUE-1988-8] 04 p0465 N90-12662
Spectroscopic ellipsometry characterization of CVD deposition and doping of polysilicon multilayer structures
[RSRE-MEMO-4258] 04 p0466 N90-12671
Improved method for determination of helium-4 in helium-3 by mass spectrometry
[PB89-201404] 04 p0469 N90-12686
Study of the hydroxyl radical by DRASC resonance in a high pressure flame --- Diffusion Raman Anti-Stokes Coherence (DRASC)
[ONERA-RS-53/7131-PY] 05 p0622 N90-13632
Computational studies of structural and transport properties of amorphous solids
[ETN-90-96027] 05 p0628 N90-13664
Novel in situ spectroscopic ellipsometer for real time analysis of CVD diamond films
[AD-A213218] 05 p0644 N90-13762
Combined capillary electrophoresis and electrospray ionization mass spectrometry
[DE90-001903] 06 p0743 N90-14322
Photovoltaic Measurements and Performance Branch
[DE89-009500] 06 p0807 N90-14695
ICP/AES (Inductively Coupled Plasma/Atomic Emission Spectroscopy): A modern analytical tool
[DE90-003822] 07 p0997 N90-15765
Carbon-13 nuclear magnetic resonance of heterocyclic salts and its precursors
[DE89-635768] 08 p1041 N90-16016
Workshop on Analysis of Returned Comet Nucleus Samples
[NASA-CR-184821] 08 p1140 N90-16607
Analytical study of comet nucleus samples 08 p1140 N90-16608
The origin, composition and history of cometary ices from spectroscopic studies 08 p1140 N90-16609
Laboratory analyses of micron-sized solid grains: Experimental techniques and recent results 08 p1141 N90-16616
Sulfur compounds in comets 08 p1143 N90-16627
Organic chemistry of cometary dust as derived from PUMA 1 data 08 p1143 N90-16628
Composition of dust from Comet P/Halley: The mineral fraction 08 p1144 N90-16631
Handling and analysis of ices in cryostats and glove boxes in view of cometary samples 08 p1146 N90-16643
Methods for the mineralogical and textural analysis of comet nucleus samples 08 p1147 N90-16648
Electron Spin Resonance (ESR) studies of returned comet nucleus samples 08 p1148 N90-16651
The measurement of trace elements in interplanetary dust and cometary particles by ultra-high sensitivity INAA 08 p1149 N90-16656
Raman spectroscopic analysis of impregnated cathodes
[AD-A214559] 09 p1190 N90-16895
Determination of trivalent chromium ions in chromium plating solutions by ultraviolet-visible spectrophotometry
[AD-A215688] 10 p1351 N90-17837
Application of high performance liquid chromatography/mass spectrometry to environmental analysis
[PB90-116963] 11 p1531 N90-18814
Crystallography, spectroscopic analysis, and lasing properties of Nd3+:Y3Sc2Al3O12
[AD-A217792] 13 p1897 N90-20891
Continued investigations of new concepts for improved spectrochemical analysis
[AD-A219403] 16 p2216 N90-22644
Characterization of Monel alloys by x ray fluorescence technique
[DE90-617175] 16 p2221 N90-22665
Method and apparatus for determining optical absorption and emission characteristics of a crystal or non-crystalline fiber
[NASA-CASE-LAR-13963-1] 17 p2475 N90-24150
Surface and interface studies by Auger electron spectroscopy
[ETN-90-96948] 18 p2522 N90-24398
Laboratory measurements of microwave and millimeter-wave properties of planetary constituents 20 p2943 N90-26745
On diamond, graphitic and amorphous carbons in primitive extraterrestrial solar system materials 21 p3095 N90-27591
Novel numerical analysis method for the study of convolution equations in appearance potential spectroscopy
[ETN-90-97288] 23 p3400 N90-29210

SPECTROSCOPIC TELESCOPES
Hybrid diffractive-refractive telescope
[AD-A219241] 16 p2318 N90-23216
Advanced multilayer x ray optics
[DE90-008228] 18 p2616 N90-24902
Variable magnification variable dispersion glancing incidence imaging x ray spectroscopic telescope
[NASA-CASE-MFS-28013-3] 21 p3096 N90-27594
Bispectral-based optimization algorithms for speckle imaging
[DE90-015610] 24 p3529 N90-29957
XMM space telescope: Development plan for the lightweight replicated x ray gratings
[DE90-015620] 24 p3546 N90-30055

SPECTROSCOPY
NT ABSORPTION SPECTROSCOPY
NT ASTRONOMICAL SPECTROSCOPY
NT AUGER SPECTROSCOPY
NT ELECTRON SPECTROSCOPY
NT FLAME SPECTROSCOPY
NT GAS SPECTROSCOPY
NT INFRARED SPECTROSCOPY
NT LASER SPECTROSCOPY
NT MAGNETIC SPECTROSCOPY
NT MASS SPECTROSCOPY
NT MOLECULAR SPECTROSCOPY
NT OPTICAL EMISSION SPECTROSCOPY
NT OPTOGALVANIC SPECTROSCOPY
NT PHOTOACOUSTIC SPECTROSCOPY
NT PHOTOELECTRON SPECTROSCOPY
NT RAMAN SPECTROSCOPY
NT SPECTROPHOTOMETRY
NT SPECTROSCOPIC ANALYSIS
NT STELLAR SPECTROPHOTOMETRY
NT ULTRASONIC SPECTROSCOPY
NT ULTRAVIOLET SPECTROSCOPY
NT VACUUM SPECTROSCOPY
NT X RAY SPECTROSCOPY
Advances in regression: Use of models in spectroscopic data analysis
[AD-A210541] 01 p0116 N90-10665
Lithium compensation of GaAs
[DE89-616080] 01 p0129 N90-10740
Applications of NMR spectroscopy to the study of zeolite synthesis
[DE89-015226] 02 p0192 N90-11095
A diffuse reflectance infrared Fourier transform spectroscopic study of adsorbed hydrazines 02 p0205 N90-11170
The theory of ac impedance of rough electrode-electrolyte interfaces
[DE89-017474] 02 p0217 N90-11243
Positron annihilation studies of interpenetrating polymer networks
[AD-A212162] 03 p0332 N90-11890
The national synchrotron light source and its applications
[DE89-017605] 03 p0405 N90-12320
Dielectric spectroscopy of semiconductors
[AD-A211989] 04 p0559 N90-13255
Ultrafast processes and spectroscopy with free electron lasers
[AD-A212889] 05 p0647 N90-13773
Field-effect spectroscopy of interface states
[AD-A212998] 05 p0703 N90-14112
Supercritical fluid chromatography/supersonic jet spectroscopy
[DE90-001378] 06 p0740 N90-14308
Non-linear optical studies of adsorbates: Spectroscopy and dynamics
[DE90-001543] 06 p0741 N90-14312
Spectral properties of one dimensional quasi-crystals
[PREPRINT-659] 06 p0850 N90-14938
Compensation for peak shifts and variable background responses in fluorescence spectroscopy
[DE90-001102] 07 p0892 N90-15154
First International Symposium on Electrochemical Impedance Spectroscopy. Extended abstracts
[AD-A214406] 07 p0925 N90-15354
Outlier detection in multivariate calibration
[DE90-001502] 07 p0982 N90-15672
Spectroscopic and laser properties of Cr:LiCaAlF6 and Cr:LiSrAlF6 crystals
[DE90-000783] 07 p0998 N90-15770
The origin, composition and history of cometary ices from spectroscopic studies 08 p1140 N90-16609
Spectrophotometric observations of comet P/Giacobini-Zinner 08 p1144 N90-16630
Transition state spectroscopy of hydrogen transfer reactions
[AD-A215041] 09 p1191 N90-16901
NASA Laser Light Scattering Advanced Technology Development Workshop, 1988
[NASA-CP-10033] 09 p1221 N90-17085
Enhanced resolution particle size distributions by multiple angle photon correlation spectroscopy 09 p1223 N90-17094
Spectral characteristics of arc-heated low density plasma flows (IV) air and N2-CO2 mixture plasmas
[NAL-TR-1012] 09 p1285 N90-17451
Spectroscopic techniques for the analysis of CdTe substrates used for the growth of HgCdTe
[AD-A214545] 09 p1288 N90-17466
Fluorescence and elastic scattering from laser dye-filled capillaries
[AD-A217026] 11 p1484 N90-18540

Transport effects and spectroscopy of defects in microstructures
[AD-A216718] 11 p1570 N90-19036
Correlation-induced changes of spectra
[AD-A217087] 12 p1669 N90-19591
FOMA: A Fast Optical Multichannel Analyzer
[DE90-004093] 12 p1713 N90-19839
Digital capacity transient spectroscopy of deep structure defects in III-V-Semiconductor structures
[ETN-90-96057] 12 p1722 N90-19890
Chemical and electrochemical studies in ionic liquids
[AD-A217742] 13 p1773 N90-20175
Positron annihilation spectroscopy: A nondestructive, submicroscopic characterization technique for structural polymers
[AD-A217748] 13 p1782 N90-20226
An electrochemical and spectroscopic study of electrode processes
[AD-A217261] 13 p1793 N90-20289
Structural comparison of nickel electrodes and precursor phases 13 p1824 N90-20472
The application of electrochemical impedance spectroscopy for characterizing the degradation of Ni(OH)2/NiOOH electrodes 13 p1824 N90-20474
Time-resolved spectroscopy of nonequilibrium ionization in laser-produced plasmas
[DE90-008663] 13 p1891 N90-20854
High-resolution Brillouin gain spectroscopy in solids
[DE90-009475] 14 p1949 N90-21155
Introduction to the Infrared Space Observatory (ISO) 14 p1979 N90-21340
Transient effects in Brillouin gain spectroscopy in solids
[DE90-009476] 15 p2067 N90-21839
High resolution stimulated Raman-Brillouin spectroscopy in gases and solids
[DE90-009535] 15 p2067 N90-21840
Brillouin gain spectroscopy in glasses and crystals
[DE90-009536] 15 p2067 N90-21841
Institute for Materials Science and Engineering, nondestructive evaluation: Technical activities
[PB90-132739] 15 p2108 N90-22055
Linear and nonlinear electrical response of condensed matter: Ionic, dielectric, and mixed-conduction materials
[AD-A218771] 16 p2215 N90-22639
Continued investigations of new concepts for improved spectrochemical analysis
[AD-A219403] 16 p2216 N90-22644
Spectroscopic observations of high redshift QSOs: Galaxies and the intergalactic medium at early epochs 16 p2330 N90-23280
ISS and TPD study of the adsorption and interaction of CO and H2 on polycrystalline Pt 18 p2559 N90-24602
X ray optics
[AD-A221218] 18 p2616 N90-24898
Fast plasma mixing: A new excitation method for CW gas lasers
[AD-A220290] 18 p2617 N90-24904
SiC film deposited by pulsed excimer laser ablation
[DE90-010634] 18 p2622 N90-24938
Temperature determination of shock layer using spectroscopic techniques 18 p2628 N90-24973
Characterization of the surfaces of platinum/tin oxide based catalysts by Fourier transform spectroscopy (FTIR) 18 p2643 N90-25054
Traps for neutral atoms
[AD-A221331] 19 p2754 N90-25649
Preliminary plume characteristics of an arcjet thruster
[NASA-TM-103241] 20 p2825 N90-26071
Measurements of CH4, N2O, CO, H2O and O3 in the middle atmosphere by the ATMOS experiment on Spacelab 3
[NASA-TM-103476] 20 p2883 N90-26400
First International Conference on Laboratory Research for Planetary Atmospheres
[NASA-CP-3077] 20 p2942 N90-26744
High resolution spectroscopy in the microwave and far infrared 20 p2943 N90-26746
Electron-impact spectroscopy 20 p2949 N90-26779
Optical signatures of molecular particles via mass-selected cluster spectroscopy 20 p2949 N90-26780
Advanced optical diagnostics in hypersonic research 21 p2975 N90-26905
Phase-sensitive optical detection of ballistic phonon pulses using frequency-modulation spectroscopy and persistent spectral holes
[AD-A221521] 21 p2979 N90-26930
Description of SAFIRE for ISES 21 p3016 N90-27148
SIRTF: Probing the dark corners of the galaxy 21 p3091 N90-27577
Dynamics of fluids in bulk and near a vertical wall: Studied by photoncorrelation spectroscopy
[PB90-200452] 22 p3169 N90-27976
Semiconductor measurement technology: A software program for aiding the analysis of ellipsometric measurements, simple spectroscopic models
[PB90-216847] 23 p3398 N90-29201
Supercritical fluid chromatography/supersonic jet spectroscopy
[DE90-015220] 24 p3447 N90-29465
Kinetics and structure of silicate sol-gels
[DE90-015702] 24 p3456 N90-29521
Planar waveguide spectrometer
[DE90-016308] 24 p3546 N90-30057
Surface photovoltage spectroscopy of real n-type GaAs(110) surfaces
[DE90-627325] 24 p3551 N90-30092

SPECTRUM ANALYSIS
NT CEPSTRAL ANALYSIS
NT FLAME SPECTROSCOPY
NT MAXIMUM ENTROPY METHOD
Low ppb level detection of toxic compounds with a fully automated CO2 laser photoacoustic detector 02 p0206 N90-11181
Solar radiation in Linkoeping (Sweden): Variations over half a year in irradiance and spectral composition in the interval 400-1000 nm
[FOA-C-30521-3.1] 02 p0250 N90-11417
Quantitative methods for waves in space plasmas
[PB89-210256] 02 p0280 N90-11599
Theory of atomic spectral emission intensity
[IRF-PREPRINT-110] 02 p0287 N90-11641
Rocket and satellite observations of the local interstellar medium 02 p0292 N90-11668
Calculation of transient response from time-harmonic spectrum
[AD-A211972] 03 p0393 N90-12241
Infrared spectrometry of aerosols
[AD-A213303] 04 p0473 N90-12713
The NASA SETI sky survey: Recent developments 04 p0488 N90-12804
Spectral study of a compressible isotropic turbulence
[ECL-86-16] 05 p0643 N90-13753
Neutral air turbulence in the middle and upper atmosphere observed during the MAC/EPSILON campaign 05 p0660 N90-13855
Archival research on absorption lines in violently star-forming galaxies
[NASA-CR-185960] 05 p0712 N90-14163
Spectral contents readout of birefringent sensor
[NASA-CR-179444] 06 p0843 N90-14905
Experimental determination of the fluid velocity by spectral analysis of temperature fluctuations
[DE89-636430] 07 p0928 N90-15372
Experimental investigation of a three-dimensional wake. Part 2: Spectral and turbulent energy analysis
[ONERA-RT-32/5025-AYD-PT-2] 08 p1018 N90-15887
Natural and man-made emissions at 1.0 to 5.6 MHz measured between 10 and 18 R sub E
[MPE-PREPRINT-146] 08 p1058 N90-16116
Spectroscopic diagnostics of high temperature plasmas
[DE90-003912] 08 p1126 N90-16522
Measurement of fluctuations in the tilt of Arctic ice at the CEAREX Oceanography Camp: Experiment review, data catalog, and preliminary results
[AD-A215059] 09 p1249 N90-17249
Transmission micro-grids for shift analysis of x ray frequencies
[MPE-216] 09 p1283 N90-17439
Spectral characteristics of arc-heated low density plasma flows (IV) air and N2-CO2 mixture plasmas
[NAL-TR-1012] 09 p1285 N90-17451
Proceedings of a workshop on Higher-Order Spectral Analysis
[AD-A215849] 10 p1353 N90-17845
An analysis of diurnal wind variability in the Santa Barbara Channel from SODAR measurements
[AD-A215769] 10 p1408 N90-18121
Doppler spectra from incoherent backscatter: Principles and examples for application for POLDIRAD
[DLR-FB-89-48] 11 p1499 N90-18630
Relationships between spectral parameters and agronomics of wheat and beam crops
[INPE-4791-RPE/584] 11 p1523 N90-18768
Spectral response of wheat and its relationship with agronomical prameters
[INPE-4950-RPE/599] 11 p1524 N90-18774
IR spectroscopy of planets and satellites; Venus, Mars, giant planets, and Titan 11 p1578 N90-19085
Interpretation of the 10 micron and 20 micron absorption bands in comets, the interstellar medium, and in an external galaxy 11 p1579 N90-19093
Spectropolarimetry as a diagnostic of the interstellar medium 11 p1579 N90-19096
The infrared spectral signature of star formation 11 p1582 N90-19114
Infrared spectroscopy of supernova 1987A 11 p1583 N90-19124
Herbig Ae/Be stars: Fine structure far-infrared lines 11 p1584 N90-19126
CO infrared bands in atmospheres of long-period variables 11 p1584 N90-19128
Measurement system of spectral irradiance in the near infrared 11 p1588 N90-19160
Far-ultraviolet spectroscopy of Comet Halley 12 p1736 N90-19979
Spectral simulation of unsteady compressible flow past a circular cylinder
[NASA-CR-182030] 13 p1750 N90-20050
Modeling and classification of acoustic transients by speech recognition techniques
[AD-A218070] 13 p1791 N90-20277
Spectral analyses of satellite geopotential missions 13 p1838 N90-20552
Spectral analytic methods for the estimation of number of signals and directions of arrival
[AD-A217219] 13 p1876 N90-20757
Wheat productivity estimate through field radiometry
[INPE-4994-PRE/1556] 14 p2000 N90-21460
New spectral features of stratospheric trace gases 15 p2079 N90-21910
A spectral analysis approach to wave propagation in layered solids 15 p2120 N90-22131
Analysis of gamma squared Velorum photometry from the South Pole 15 p2183 N90-22472
Fast spectroscopic variations on rapidly-rotating, cool dwarfs. 3: Masses of circumstellar absorbing clouds on AB Doradus
[NASA-CR-186563] 15 p2184 N90-22479
Spectral plane quasars, spectral turn-over, and frequency atlas
[INPE-5011-TDL/399] 16 p2329 N90-23277
Spectral determinations for discrete sources with EGRET 16 p2336 N90-23312
Gamma ray bursts: Current status of observations and theory 16 p2336 N90-23313
COMPTEL observations of active galactic nuclei 16 p2337 N90-23319
Spectral measurements of the cosmic microwave background 16 p2340 N90-23334
An intensity expression organising spectral line intensity data
[IRF-SR-202] 17 p2373 N90-23513
Contributions of the X Ray Astronomy Group of the Max-Planck-Institut fuer Extraterrestrische Physik
[MPE-PREPRINT-165] 17 p2482 N90-24196
Observations of black hole candidates with the Mir-Kvant HEXE 17 p2483 N90-24198
The role of comptonisation in energy spectra of standard QPO-sources 17 p2484 N90-24205
Dynamics of bulk and surface-adsorbed polyacrylates
[AD-A221046] 18 p2530 N90-24437
Evolution equation simulation of semiconductor lasers under a pulsed regime
[TELECOM-PARIS-89-D-010] 18 p2563 N90-24625
Development of remote sensing techniques for the investigation of neotectonic activity, eastern transverse ranges and vicinity, southern California 18 p2573 N90-24662
Use of high-dimensional spectral data to evaluate organic matter, reflectance relationships in soils
[NASA-CR-186650] 18 p2574 N90-24665
Optical signal processing
[AD-A220332] 18 p2615 N90-24897
Temperature determination of shock layer using spectroscopic techniques 18 p2628 N90-24973
Synthetic spectra of accretion disks in DQ Her binaries
[NASA-CR-186837] 18 p2638 N90-25029
The X ray absorption spectra of massive X ray binaries 19 p2766 N90-25716
Spectral variability of LMC X-4 19 p2766 N90-25717
XB 1905+00: A very compact low-mass X ray binary viewed at low inclination 19 p2773 N90-25765
Is KO Vel (E1013-477) an intermediate polar 19 p2773 N90-25766
Variability of the X ray sources in M31 19 p2773 N90-25768
The X ray dip source 4U 1624-49 19 p2776 N90-25786
EXOSAT observations of the pulse profile of Her X-1 during intermediate intensity states in a 35-day cycle in 1985 19 p2776 N90-25788
Hard X ray pulses from Vela X-1 19 p2777 N90-25791
The optical light curve of Cygnus X-1 19 p2778 N90-25801
Search of the optical counterpart of the X rays source 1H 0521+373 19 p2780 N90-25815

Self-consistent Comptonised models for the spectra of low mass X ray binaries 19 p2780 N90-25817
The 3A1954+319: A possible supergiant X ray binary 19 p2782 N90-25830
The complex X ray spectra of AGN 19 p2786 N90-25855
Ultrasoft components in X ray-selected AGN 19 p2787 N90-25864
A search for iron features in the EXOSAT spectral survey sources 19 p2791 N90-25887
X ray spectral variability in Seyfert 1 galaxies 19 p2792 N90-25891
The X ray spectrum of MCG-6-30-15 19 p2793 N90-25898
Comparing measurements of AGN X ray spectra with the shape of the diffuse X ray background spectrum 19 p2793 N90-25902
The soft X ray excess in Einstein quasar spectra 19 p2794 N90-25910
X ray spectral index variability in NGC 4151 19 p2795 N90-25911
High resolution spectroscopy in the microwave and far infrared 20 p2943 N90-26746
ROBFIT: A code for the analysis of histogram spectra with nonlinear regression and robust estimation [AD-A221527] 21 p3055 N90-27369
Raman spectroscopic studies of carbon in extra-terrestrial materials 21 p3095 N90-27589
Improved compact optical RF spectrum analyzer [AD-D014481] 22 p3177 N90-28026
Turbulence spectra of the FIRE stratocumulus-topped boundary layers 22 p3217 N90-28246
Supersaturation, droplet spectra, and turbulent mixing in clouds 22 p3217 N90-28249
Observations of anthropogenic cloud condensation nuclei 22 p3218 N90-28251
X ray spectra of cataclysmic variables [NASA-CR-187002] 23 p3412 N90-29280
Integrating rule-based and neural-net techniques for spectral analysis [AD-A223517] 24 p3446 N90-29462
Technique for the measurement of noise of the flow associated to the small wave numbers of the turbulence spectra [ETN-90-97558] 24 p3469 N90-29601
Spectral structure and generation mechanism of ducted VLF whistler mode sideband waves 24 p3489 N90-29720

SPECULAR REFLECTION
The measurement of infrared spectra of dense ceramics by specular reflectance spectroscopy [AD-A210609] 01 p0051 N90-10291
Analysis of two-pass Modified Hough Transform (MHT) technique for the detection of wake like signals [AD-A211982] 03 p0338 N90-11924
Speckle imaging through the atmosphere [AD-A214652] 09 p1281 N90-17428
Positronium reflection and positronium beams 11 p1559 N90-18980
X ray specular reflection studies of silicon coated by organic monolayers (alkylsiloxanes) [AD-A217418] 13 p1779 N90-20213
Simple reflection holography [DE90-008309] 13 p1805 N90-20359
The effect of leveling coatings on the atomic oxygen durability of solar concentrator surfaces [NASA-TM-102557] 14 p1941 N90-21110
The measurement of surface reflectivity at millimetre wavelengths [MRL-TN-559] 14 p1960 N90-21222
Agile multiple aperture imager receiver development [AD-A218956] 16 p2318 N90-23215
Analysis of phase retrieval in active imaging [AD-A221080] 18 p2563 N90-24626
Near-angle scattering and binary optics [AD-A224140] 23 p3396 N90-29186

SPEECH
NT ARTICULATION (SPEECH)
NT CONVERSATION
NT PHONEMES
NT PHONETICS
NT WORDS (LANGUAGE)
Computer programs for measuring variations in speech [AD-A211126] 02 p0259 N90-11467
Dual task performance with LPC (Linear Predictive Coding) degraded speech in a sentence verification task [AD-A214298] 07 p0920 N90-15320
DURIP: Computational modeling of cognitive processes [AD-A219934] 17 p2437 N90-23886
Speech processing standards 21 p2993 N90-27013

SPEECH BASEBAND COMPRESSION
A narrowband tactical communication system for the VHF and UHF mobile radio bands 20 p2847 N90-26192

SPEECH DISCRIMINATION
U SPEECH RECOGNITION

SPEECH RECOGNITION
Phase 2 testing and evaluation of low data rate voice CODEC equipment [ACD-330-PHASE-2] 01 p0055 N90-10315
Attention and vigilance in speech perception [AD-A210493] 01 p0095 N90-10539
Scientific and technical report voice activated gun turrent control [AD-A210350] 01 p0110 N90-10623
Computer programs for measuring variations in speech [AD-A211126] 02 p0259 N90-11467
Spoken commands control robot that handles radioactive materials [DE89-012632] 02 p0262 N90-11488
The effects of hearing protectors on speech communication and the perception of warning signals [AD-A212521] 04 p0492 N90-12832
Shape instabilities of plate-like structures. 1: Experimental observations in heavily cold worked in situ composites [AD-A212251] 04 p0523 N90-13021
Application of active noise reduction for hearing protection and speech intelligibility improvement [IZF-1988-21] 04 p0527 N90-13042
Explicit modelling of state duration correlations in hidden Markov models --- speech recognition [RSRE-MEMO-4152] 04 p0546 N90-13178
Speech reception in quiet and in noisy conditions by individuals with noise-induced hearing loss in relation to their audiogram [IZF-1989-11] 05 p0633 N90-13692
Evaluation of speech intelligibility through a bone conduction stimulator [AD-A212002] 05 p0673 N90-13919
Voice preprocessor for digital voice applications [AD-A214726] 09 p1205 N90-16982
Checklist reading problems in airplanes equipped with speech recognition systems [ILR-MITT-223(1989)] 09 p1261 N90-17314
Research and development in natural language understanding as part of the Strategic Computing Program [AD-A214586] 09 p1264 N90-17330
Research and development in natural language understanding as part of the Strategic Computing Program [AD-A214587] 09 p1264 N90-17331
Connected digit recognition in a multilingual environment [AD-A196150] 10 p1371 N90-17942
Speech synthesis: From segmental synthesis to acoustic rules, using temporal decomposition [TELECOM-88-E-019] 10 p1375 N90-17972
Perception of long-period complex sounds [AD-A216743] 11 p1539 N90-18861
Knowledge-based extensible natural language interface technology program [AD-A216664] 11 p1545 N90-18897
Modeling and classification of acoustic transients by speech recognition techniques [AD-A218070] 13 p1791 N90-20277
Investigation of air transportation technology at the Massachusetts Institute of Technology, 1988-1989 14 p1905 N90-20922
Automatic speech recognition in air traffic control 14 p1905 N90-20923
A connectionist implementation of cognitive phonology [AD-A219095] 16 p2264 N90-22906
Adaptive Resonance Theory 1 [AD-A219044] 16 p2304 N90-23126
A neural network based speech recognition system [AD-A219794] 17 p2389 N90-23606
Perception of complex auditory patterns [AD-A219626] 17 p2434 N90-23867
Northeast Artificial Intelligence Consortium. Volume 4. Distributed AI for communications network management [AD-A218717] 17 p2453 N90-23994
Evaluation of speech recognizers for use in advanced combat helicopter crew station research and development [NASA-CR-177547] 18 p2496 N90-24265
Automatic speech recognition in air-ground data link 18 p2640 N90-25037
Experiments in variable frame rate analysis for speech recognition [RSRE-MEMO-4330] 19 p2683 N90-25264
Speech Analysis and Synthesis and Man-Machine Speech Communications for Air Operations [AGARD-LS-170] 21 p2992 N90-27006
Overview of requirements and networks for voice communications and speech processing 21 p2992 N90-27007
The speech signal 21 p2992 N90-27008
Current methods of digital speech processing 21 p2993 N90-27010
Speech recognition based on pattern recognition techniques 21 p2993 N90-27011
Quality evaluation of speech processing systems 21 p2993 N90-27012
Application of audio/speech recognition for military applications 21 p2993 N90-27014
The development of the time-delayed neural network architecture [AD-A221540] 21 p3061 N90-27403
Further experiments in variable frame rate analysis for speech recognition [RSRE-MEMO-4336] 22 p3165 N90-27951
Triphone clustering in the ARM system [RSRE-MEMO-4357] 22 p3166 N90-27952
Improved front-end analysis in the ARM system: Linear transformations of SRUbank [RSRE-MEMO-4358] 22 p3166 N90-27953
Experiments with grand variance in the ARM continuous speech recognition system [RSRE-MEMO-4359] 22 p3166 N90-27954
Studies in automatic speech recognition and its application in aerospace 23 p3318 N90-28759
IEEE Conference on Neural Information Processing Systems, Natural and Synthetic [AD-A223611] 24 p3461 N90-29552

SPEECHES
U LECTURES

SPEED
U VELOCITY

SPEED CONTROL
Independent Orbiter Assessment (IOA): Analysis of the rudder/speed brake subsystem [NASA-CR-185560] 02 p0161 N90-10916
Adjustable speed drive study, part 1 [DE89-017654] 03 p0342 N90-11948
Adjustable speed drive study, June 1985 to September 1988. Part 2: Appendices [DE90-002771] 07 p0922 N90-15332
Coordinate transformation for an asynchronous, machine, and time discretization of a state observer [EMV-88-30] 17 p2397 N90-23657
Design, simulation, and testing of a field-oriented ac servo-drive using a TMS 32010 signal processor [EMV-88-42] 17 p2397 N90-23658
Optimal payload rate limit algorithm for zero-G manipulators 24 p3513 N90-29858

SPEED INDICATORS
NT TACHOMETERS
Detectors and signal processing for the speed measuring system 4-01 [FEL-1989-64] 24 p3472 N90-29623

SPEED REGULATION
U SPEED CONTROL

SPEED REGULATORS
Adjustable speed drive study, June 1985 to September 1988. Part 2: Appendices [DE90-002771] 07 p0922 N90-15332
Continuously variable gear drive transmission [AD-D014268] 08 p1084 N90-16275

SPEEDOMETERS
U SPEED INDICATORS

SPENT FUELS
MHD seed recovery and regeneration [DE89-002711] 01 p0125 N90-10715

SPERMATOCYTES
U GAMETOCYTES

SPERMATOZOA
Experiment K-6-16. Morphological examination of rat testes. The effect of Cosmos 1887 flight on spermatogonial population and testosterone level in rat testes 20 p2895 N90-26489

SPHERES
NT CELESTIAL SPHERE
NT ROTATING SPHERES
DMC (Distinct Motion Code): A rigid body motion code for determining the interaction of multiple spherical particles [DE89-016929] 02 p0270 N90-11543
Parametric study of power absorption from electromagnetic waves by small ferrite spheres [NASA-TP-2949] 03 p0399 N90-12282
A kernel approach to estimation of the sphere radius density in Wicksell's corpuscle problem [CWI-MS-R8809] 04 p0542 N90-13142
Single particle friction tests with cellulose acetate sphere samples [DE89-017537] 06 p0793 N90-14622
Study of flow around a sphere in a hydraulic test tunnel [CERT-1/2313/MES] 08 p1064 N90-16156

Multigrid methods for two- and three-dimensional Poisson-type equations on the sphere
[GMD-391] 08 p1117 N90-16468
Surface topography measurements over the 1 meter to 10 micrometer spatial period bandwidth
[DE90-003642] 08 p1122 N90-16501
Underwater acoustic scattering from spherical particulates and bubbles
[AD-A214827] 09 p1279 N90-17414
Process for making a noble metal on tin oxide catalyst
[NASA-CASE-LAR-13741-1-SB] 13 p1774 N90-20180
Mass transfer from a sphere in an oscillating flow with zero mean velocity
[NASA-TM-102566] 13 p1801 N90-20338
A remark on the Kelvin transform and a non-linear partial differential equation
[PB90-165622] 14 p2021 N90-21589
Numerical study of the onset of instability in the flow past a sphere 17 p2400 N90-23672
Rheology and microstructure of concentrated suspensions
[DE90-009976] 18 p2520 N90-24391
A preliminary design of interior structure and foundation of an inflatable lunar habitat 18 p2633 N90-24999
Boiling/evaporative heat transfer from spheres in packed-bed thermal energy storage units
[DE90-012023] 19 p2711 N90-25430
Full vector wave calculation of photonic band structures in face-centered cubic dielectric media
[AD-A222616] 20 p2933 N90-26686
Down-to-earth studies of carbon clusters 21 p3091 N90-27573
Quasi-static analysis of scattering from a chiral sphere
[PB90-189135] 22 p3164 N90-27943
Planning 3-D collision-free paths using spheres 23 p3367 N90-29024
Superconformal algebra and central extension of meromorphic vector fields with multipoles on super-Riemann sphere
[DE90-627211] 23 p3390 N90-29153
A comment on anisotropic spheres admitting one parameter group of conformal motions
[DE90-627195] 23 p3403 N90-29230

SPHERICAL COORDINATES
Particle simulation in curvilinear coordinate systems
[DE89-016727] 02 p0277 N90-11583
Localization of multiple broadband targets in spherical coordinates via adaptive beamforming and non-linear estimation
[AD-A215714] 09 p1274 N90-17387

SPHERICAL HARMONICS
On the coefficients of differentiated expansions of ultraspherical polynomials
[NASA-CR-181913] 01 p0112 N90-10637
Processing of DMSP magnetic data and its use in geomagnetic field modeling
[NASA-TM-100750] 03 p0370 N90-12115
Gravitational model improvement at the Goddard Space Flight Center 13 p1831 N90-20514
Stabilized determination of geopotential coefficients by the mixed hom-BLUP approach 13 p1832 N90-20520
Precise solution for a finite set of spherical coefficients from equiangular gridded data 13 p1833 N90-20522
Modeling of the Earth's gravity field using the New Global Earth Model (NEWGEM) 13 p1833 N90-20523
Downward continuation of the free-air gravity anomalies to the ellipsoid using the gradient solution and terrain correction: An attempt of global numerical computations 13 p1836 N90-20541
Spectral analyses of satellite geopotential missions 13 p1838 N90-20552
The GRADIO spaceborne gravity gradiometer: Development and accommodation 13 p1840 N90-20560
High resolution analysis of satellite gradiometry 13 p1840 N90-20561
Scattering sources: A spherical harmonics expansion
[DE90-008724] 13 p1867 N90-20711

SPHERICAL PLASMAS
Numerical simulation of the preheating by x rays in spherical plasmas 06 p0784 N90-14564

SPHERICAL SHELLS
Ring source/force excitation of axisymmetric shell structure
[ARE-TM(UHA)-88519] 05 p0698 N90-14085
Steady state temperatures and thermal stresses in a spherical or cylindrical laminated shell
[ESDU-89027] 12 p1674 N90-19612
The microwave permeability of conducting spherical shells
[AD-A220746] 17 p2369 N90-23485
Multi-element spherical shell generation
[NASA-CASE-NPO-17203-1-CU] 17 p2405 N90-23700
Coupled BE/FE/BE approach for scattering from fluid-filled structures 18 p2570 N90-24649
A numerical investigation of thermal convection in highly viscous spherical shells with applications to mantle dynamics in the Earth and other terrestrial planets 18 p2579 N90-24691
A preliminary design of interior structure and foundation of an inflatable lunar habitat 18 p2633 N90-24999
Natural melting within a spherical shell
[NASA-TM-102822] 20 p2861 N90-26274

SPHERICAL WAVES
Observations of spherical-wave scintillation in strong refractive-index turbulence
[PB89-124747] 01 p0062 N90-10355

SPHEROIDS
NT PROLATE SPHEROIDS

SPHEROMAKS
Design of a spheromak compressor driven by high explosives
[DE90-003652] 08 p1086 N90-16283
Recent progress on the HESS (High Explosive Spheromak Source) experiment
[DE90-003218] 08 p1125 N90-16520
Progress with small, high-magnetic-field spheromaks in CTX
[DE90-003395] 08 p1127 N90-16527
MHD stable high beta spheromak equilibrium
[DE90-004873] 08 p1127 N90-16529
The impedance of energy efficiency of a coaxial magnetized plasma source used for spheromak formation and sustainment
[DE90-003220] 13 p1889 N90-20841
Advances in spheromak understanding and parameters
[DE90-012052] 19 p2759 N90-25678

SPILLING
Water-tunnel investigation of concepts for alleviation of adverse inlet spillage interactions with external stores
[NASA-TM-4181] 12 p1599 N90-19199

SPIN
NT ELECTRON CAPTURE
NT ELECTRON SPIN
NT ISOTOPIC SPIN
NT NUCLEAR SPIN
NT PARTICLE SPIN
NT SPIN-ORBIT INTERACTIONS
NT SPIN-SPIN COUPLING
The spinning of aircraft: A discussion of spin prediction techniques including a chronological bibliography
[ARL-AERO-R-177] 02 p0155 N90-10888
COBE nonspinning attitude propagation 05 p0587 N90-13418
Cubic interaction in conformal theory of integer higher-spin fields in four dimensional space-time
[DE90-607095] 10 p1425 N90-18220

SPIN DECOUPLING
Control and stability of a spinning symmetric satellite in an elliptical orbit
[AD-A216284] 10 p1328 N90-17672

SPIN DYNAMICS
Spin fluctuations and excitations in a 2D xy-ferromagnet: CoCl2 in graphite
[DE89-017600] 02 p0196 N90-11119
Neutron scattering studies of amorphous Invar alloys
[DE89-016868] 02 p0197 N90-11126
Spin-orbit relaxation rates of Bi(6p(3)) 2D(3/2) following photolysis of Bi(CH3)3 at lambda = 193 nm
[AD-A211792] 03 p0402 N90-12303
Electronic and ionic transport in polymers
[AD-A213410] 07 p0911 N90-15270
Two-dimensional magnetic phase transition of ultrathin iron films on Pd(100)
[DE90-003555] 07 p1000 N90-15788
Electrochemical parameterization of metal complex redox potentials, using the ruthenium(III)/ruthenium(II) couple to generate a ligand electrochemical series
[AD-A214439] 08 p1041 N90-16015
Investigation of liquid sloshing in spin-stabilized satellites
[AD-A214730] 09 p1182 N90-16853
International Conference on Materials and Mechanisms of Superconductivity: High Temperature Superconductors
[AD-A215343] 09 p1290 N90-17480
Computational fluid dynamics method for low Reynolds number flow in a precessing/spinning, liquid filled cylinder with rounded endcaps
[AD-A216997] 12 p1659 N90-19531
F-15B high angle-of-attack phenomena and spin prediction using bifurcation analysis
[AD-A217366] 13 p1754 N90-20073
Interior fluid dynamics of liquid-filled projectiles
[AD-A217630] 13 p1800 N90-20330
Direct inversion of rigid-body rotational dynamics
[NASA-TM-102798] 15 p2055 N90-21773
Generalized killing equations and symmetries of spinning space
[NIKHEF-H/89-8] 15 p2165 N90-22375
Side moment exerted by a spinning, coning, highly viscous liquid payload
[AD-A218746] 16 p2237 N90-22763
Miniaturization of flight deflection measurement system
[NASA-CASE-LAR-13628-1] 17 p2406 N90-23707
Novel numerical algorithms for sensing, discrimination, and control
[AD-A220805] 17 p2444 N90-23929
Transverse- and zero-field muon SR investigation of magnetism and superconductivity in (Y(1-x)Pr(x)Ba2Cu3O7)
[DE90-010597] 18 p2624 N90-24953
A model of the perturbed spinning motion of the San Marco 5th spacecraft 22 p3129 N90-27755
Dynamics of the iron spins in superconducting YBa2(Cu(1-x)Fe(x))O7 22 p3143 N90-27825
Magnetic correlations in La(2-x)Sr(x)CuO4 from NQR relaxation and specific heat 22 p3143 N90-27827

SPIN EXCHANGE
Studies of ultrathin magnetic films and particle-surface interactions with spin-sensitive electron spectroscopies
[DE89-016741] 02 p0273 N90-11556

SPIN GLASS
Energy barriers in SK spin-glass model
[PREPRINT-665] 05 p0704 N90-14119

SPIN RESONANCE
Search for resonances in positron-atom systems 11 p1560 N90-18991

SPIN STABILIZATION
Stall/spin/flight simulation
[DOT/FAA/CT-88/28] 03 p0310 N90-11765
Orbit and attitude determination results during launch support operations for SBS-5
[PAPER-7] 05 p0587 N90-13420
Investigation of liquid sloshing in spin-stabilized satellites
[AD-A214730] 09 p1182 N90-16853
Attitude and spin rate control of a spinning satellite using geomagnetic field
[INPE-4818-NTE/289] 12 p1613 N90-19277
Computational fluid dynamics method for low Reynolds number flow in a precessing/spinning, liquid filled cylinder with rounded endcaps
[AD-A216997] 12 p1659 N90-19531
Design and development of a spacecraft stability boom 18 p2540 N90-24494

SPIN TESTS
Fracture and three dimensional stress analyses of 7075 aluminum projectile components under spin and inertia load
[AD-A210986] 01 p0081 N90-10463
Measurements of pressures on the tail and aft fuselage of an airplane model during rotary motions at spin attitudes
[NASA-TP-2939] 02 p0145 N90-10829
The spinning of aircraft: A discussion of spin prediction techniques including a chronological bibliography
[ARL-AERO-R-177] 02 p0155 N90-10888

SPIN WAVES
U MAGNONS

SPIN-LATTICE RELAXATION
Spin-lattice relaxation and the calculation of gain, pump power, and noise temperature in ruby 04 p0486 N90-12790
Copper and oxygen NMR studies on the magnetic properties of YBa2Cu3O(7-y)
[DE90-007889] 13 p1893 N90-20863
Single crystal NMR of high temperature superconductors 16 p2321 N90-23236
A (mu)SR-investigation of the mixed state of the high-Tc superconductor HoBa2Cu3O7-delta
[DE90-620802] 16 p2322 N90-23241
Investigation of YBa2Cu3O(7-sigma) by NMR and construction of an ultra low temperature cryostat 24 p3550 N90-30088

SPIN-ORBIT INTERACTIONS
NT ELECTRON CAPTURE
Spin-orbit relaxation rates of Bi(6p(3)) 2D(3/2) following photolysis of Bi(CH3)3 at lambda = 193 nm
[AD-A211792] 03 p0402 N90-12303
An effective He-3 nucleon force for the He-3, t) charge exchange reaction
[KVI-813] 16 p2315 N90-23198

SPIN-SPIN COUPLING
Computational modeling of pi-conjugated polyradicals
[AD-A210573] 01 p0113 N90-10648
Positron-rubidium scattering 11 p1556 N90-18964

SPINAL CORD
Biomedical influences on spinal cord function
[AD-A210311] 01 p0092 N90-10527

Temperature regulation during upper body exercise: Able bodied and spinal cord injured
[AD-A215130] 09 p1252 N90-17264

SPINE
NT VERTEBRAE
A survey of cervical pain in pilots of a Belgian F-16 Air Defence Wing 19 p2718 N90-25462
Radiological investigation of the vertebral column of candidates for military flying training the the Royal Norwegian Air Force 19 p2718 N90-25463
Data analysis in cervical trauma 19 p2718 N90-25464
Electronystagmographic findings following cervical injuries 19 p2718 N90-25466
Aircrew neck injuries: A new, or an existing, misunderstood phenomenon 19 p2719 N90-25467
Flexion, extension and lateral bending responses of the cervical spine 19 p2719 N90-25468
Analysis of the biomechanic and ergonomic aspects of the cervical spine under load 19 p2719 N90-25470
Effects of head mounted devices on head-neck dynamic response to +G(sub z) accelerations 19 p2720 N90-25471
A computer simulation model for studying cervical spine injury prevention 19 p2721 N90-25476

SPINEL
Precipitation and transformation toughening of Al-Mg signals
[ETN-89-94675] 02 p0199 N90-11138
Corrosion testing of candidates for the alkaline fuel cell cathode 13 p1824 N90-20471
Research on high-specific-heat dielectrics
[AD-A221215] 18 p2623 N90-24944

SPINOR GROUPS
Reduction of the Dirac equation to the Dirac-Kaehler equation
[DE89-630111] 02 p0270 N90-11541

SPIRAL GALAXIES
NT ANDROMEDA GALAXY
NT BARRED GALAXIES
NT MILKY WAY GALAXY
Shapes of star-gas waves in spiral galaxies
[NASA-CR-186289] 07 p1011 N90-15859
Infrared properties of five spiral galaxies 11 p1587 N90-19154
Nuclear activity, morphology, and far infrared properties of spiral galaxies
[ETN-90-95373] 12 p1744 N90-20024
M51's spiral structure
[DE90-007624] 13 p1903 N90-20916
The molecular cloud content of early type galaxies. 2: A molecular ring in NGC 404
[PB90-124348] 14 p2039 N90-21695
The distribution of molecular clouds in spiral galaxies 15 p2186 N90-22489
Wind instability as a possible cause of the spiral structure formation in the gaseous subsystem of galaxies with the circular magnetic field
[DE90-618944] 15 p2190 N90-22507
A search for additional parameters in the infrared luminosity/21 cm line-width relation for spiral galaxies in clusters of galaxies 16 p2328 N90-23274
VLA and VLBI angular broadening measurements: The distribution of interstellar scattering at low Galactic latitudes 16 p2330 N90-23279
Disk mass densities in edge-on spiral galaxies 21 p3097 N90-27600
Star formation and the distribution of HI and infrared emission in M51
[NASA-CR-186928] 23 p3408 N90-29262

SPIRAL WRAPPING
Polymerization of composites
[REPT-892-430-102] 16 p2213 N90-22621
The surprising possibilities of wrapping
[REPT-892-430-108] 16 p2213 N90-22624

SPLEEN
Experiment K-6-23. Effect of spaceflight on levels and function of immune cells 20 p2897 N90-26476

SPLINE FUNCTIONS
Global/local stress analysis of composite structures
[NASA-TM-101640] 01 p0080 N90-10456
An interactive program for constrained spline approximation of numerical data
[DE89-016674] 02 p0267 N90-11520
Inf-convolution splines
[IMAG-RR-749-M] 03 p0395 N90-12256
Splines and equations of nonlinear parameters
[IMAG-RR-750-M] 03 p0395 N90-12257
Multivariable divided difference and B-splines
[MEMO-772] 04 p0544 N90-13160
On new methods for computing with multivariate B-splines
[MEMO-783] 04 p0547 N90-13183
Smooth track generation for target motion analysis
[FEL-1989-83] 04 p0555 N90-13233
On the recurrence relation for multivariate B-splines with respect to dimension
[MEMO-786] 05 p0689 N90-14017
Practice of bivariate quadratic simplicial splines
[MEMO-800] 05 p0691 N90-14034
A tensor product b-spline method for 3D multi-block elliptic grid generation
[DE89-017440] 06 p0836 N90-14859
An executive system for modeling with rational b-splines
[AD-A213460] 07 p0974 N90-15627
Quasi interpolants and approximation power of multivariate splines
[AD-A213535] 07 p0983 N90-15678
Use of beta-splines for digital elevation modeling
[INPE-4941-PRE/1431] 10 p1400 N90-18093
A tensor product B-spline method for numerical grid generation
[DE90-005979] 12 p1705 N90-19792
The basis spline method and associated techniques
[DE90-008403] 13 p1877 N90-20763
GRID2D/3D: A computer program for generating grid systems in complex-shaped two- and three-dimensional spatial domains. Part 1: Theory and method
[NASA-TM-102453] 15 p2147 N90-22262
Spline function smoothing and differentiation of noisy data on a rectangular grid
[DE90-009319] 15 p2160 N90-22338
The approximation of a composite Bezier cubic curve by a composite Bezier quadratic curve
[NPL-DITC-147/89] 15 p2162 N90-22354
The use of local polynomial approximations in a knot-placement strategy for least squares spline fitting
[NPL-DITC-148/89] 15 p2162 N90-22355
Sliding control of pointing and tracking with operator spline estimation 16 p2281 N90-22997
Transactions of the Seventh Army Conference on Applied Mathematics and Computing
[AD-A219220] 16 p2309 N90-23160
Extrapolation of missile flight lines
[ETN-90-96494] 18 p2508 N90-24336
On computational aspects of simplicial splines
[MEMO-818] 18 p2600 N90-24795
Bivariate simplicial splines in finite element computations
[MEMO-823] 18 p2600 N90-24797
On the independence of B-splines on unordered knot sets
[MEMO-827] 18 p2600 N90-24800
G2-continuity in homogeneous co-ordinates
[MATHS-REPT-A-110] 20 p2917 N90-26599
Rational cubics with G2-continuity
[MATHS-REPT-A-113] 20 p2918 N90-26601
Asymptotic optimality of the fast randomized versions of GCV and C(sub L) in ridge regression and regularization
[IMAG-RR-793-M] 20 p2918 N90-26606
Nonlinear modeling of time series using Multivariate Adaptive Regression Splines (MARS)
[AD-A222710] 20 p2921 N90-26623
A study of terrain following systems and the creation of flight paths for terrain following vehicles
[FOA-C-20774-2.5] 22 p3114 N90-27691

SPLINES
On two polynomial spaces associated with a box spline
[AD-A210559] 01 p0113 N90-10646
Application of Lagrangian blending functions for grid generation around airplane geometries
[NASA-CR-186318] 08 p1018 N90-15891
Thin-plate spline quadrature of geodetic integrals 13 p1836 N90-20539
Internal rotor friction instability
[NASA-CR-183942] 14 p1988 N90-21395
Nonlinear spline operator interpolation and sliding control of deformable maneuvering bodies 15 p2074 N90-21878
Multi-grid and B(ox)-splines
[MEMO-828] 18 p2600 N90-24801

SPLITS (GEOLOGY)
U GEOLOGICAL FAULTS

SPLITTING
Microwave spectra of van der Waals complexes of importance in planetary atmospheres 20 p2944 N90-26752

SPOILERS
Boeing/NASA composite components flight service evaluation
[NASA-CR-181898] 16 p2210 N90-22609
Effects of spoiler surfaces on the aeroelastic behavior of a low-aspect-ratio rectangular wing
[NASA-TM-102622] 22 p3115 N90-27700
The effect of rapid spoiler deployment on the transient forces on an aerofoil 23 p3274 N90-28527

SPONTANEOUS COMBUSTION
Devices and methods for in-situ combustion ignition
[DE89-000766] 06 p0740 N90-14309

SPONTANEOUS EMISSION
Comprehensive, nonintercepting electron-beam diagnostics using spontaneous emission
[DE90-003211] 07 p0935 N90-15414
Atomic processes in plasmas under ultra-intense laser irradiation
[DE90-003221] 08 p1126 N90-16521
A simple model for amplified spontaneous emission in dyes
[DE90-007249] 11 p1516 N90-18730
Amplified spontaneous emission measurements on the aurora large-aperture module
[DE90-004841] 13 p1806 N90-20369
Three-dimensional simulations of the generation of one Angstrom radiation by a self-amplified spontaneous emission free-electron laser
[DE90-015032] 23 p3330 N90-28830

SPORADIC E LAYER
Enhanced electron density layers in the high-latitude lower ionosphere 05 p0657 N90-13832

SPORES
Particle resuspension and associated coherent structures in a turbulent boundary layer 09 p1245 N90-17224
In vitro photoreactivation of transforming DNA of bacillus subtilis spores after irradiation with UV light
[DLR-FB-89-45] 18 p2583 N90-24710

SPOT (FRENCH SATELLITE)
SPOT after two years in operation: An appraisal of results and a review of selected applications 08 p1093 N90-16326
SPOT 1 solar array: Three years in orbit performance evaluation 10 p1344 N90-17795
SPOT for landscape: Development of a method for the use of SPOT pictures for the updating of the data base scale of the landscape
[BCRS-89-18] 11 p1526 N90-18787
SPOT 4 space magnetic recorder mechanisms 15 p2112 N90-22082
The DORIS system 17 p2359 N90-23431
Topographic mapping from SPOT satellite imagery
[ETN-90-96689] 17 p2418 N90-23777
Operational digital land use map 1:50,000; investigation of a multiple automatic classification based on SPOT and LANDSAT Thematic Mapper satellite pictures
[BCRS-89-10] 17 p2419 N90-23784
SPOT 4 magnetic tape recorder mechanisms 18 p2540 N90-24500

SPRAY CHARACTERISTICS
Combustion characteristics of sprays
[AD-A213651] 07 p0895 N90-15173
Dense-spray properties: Structure and turbulence modulation
[AD-A213671] 07 p0931 N90-15387
Subsonic combustor testing 20 p2811 N90-25997

SPRAYED COATINGS
Evaluation of newly formulated Dow Corning 321 dry film lubricant
[NASA-CR-183828] 05 p0627 N90-13661
Thermal modelling of various thermal barrier coatings in a high heat flux rocket engine
[NASA-TM-102418] 09 p1193 N90-16911
Evaluation of abrasion-resistant metallized coatings for civil works applications
[AD-A221078] 18 p2530 N90-24438
Study of the structure of ZrO2-Al2O3 plasma sprayed coatings
[ETCA-89-R-078] 22 p3161 N90-27924
Characteristics required for thermal barriers of zirconium oxide-yttrium compounds obtained by plasma spraying. Morphological analysis by x ray diffraction
[ETCA-89-R-113] 22 p3161 N90-27925

SPRAYED PROTECTIVE COATINGS
U PROTECTIVE COATINGS
U SPRAYED COATINGS

SPRAYERS
Theory of droplet. Part 1: Renormalized laws of droplet vaporization in non-dilute sprays 01 p0068 N90-10390
Independent Orbiter Assessment (IOA): Analysis of the hydraulics/water spray boiler subsystem
[NASA-CR-185541] 02 p0165 N90-10934
Continuing studies of liquid propellant drops in hot, high-pressure environments
[AD-A212265] 04 p0482 N90-12765
Two dimensional orifice array, monodisperse drop source, phase 1
[AD-A211319] 04 p0500 N90-12881
Survey of the CLUSE main experiment Grand-CLUSE, May 1 - June 15, 1988 --- Humidity Exchange Over the Sea (HEXOS) experiment
[FEL-1988-43] 04 p0518 N90-12991

High power density spray cooling
[AD-A213575] 07 p0930 N90-15386
Spray sealing: A breakthrough in integral fuel tank sealing technology 08 p1022 N90-15912
Aircraft internal fires 10 p1313 N90-17593
A field study of solid rocket exhaust impacts on the near-field environment
[NASA-TM-4172] 10 p1405 N90-18102
Effects of turbulence mixing, variable properties, and vaporization on spray droplet combustion
[NASA-CR-186463] 12 p1623 N90-19326
Preparation and characterization of alumina films prepared by a novel spray pyrolysis method
[AD-A217570] 12 p1625 N90-19339
Growth and characterization of gallium (III) oxide films
[AD-A217568] 12 p1723 N90-19902
Spray deposition: A fundamental study of droplet impingement, spreading and consolidation
[AD-A217202] 13 p1787 N90-20255
The accelerated cooling in GTS plate mill
[ETN-90-97019] 19 p2682 N90-25256
Liquid fueled ramjet combustion instability: Acoustical and vortical interactions with burning sprays
[AD-A222752] 20 p2831 N90-26104
Critical evaluation of Jet-A spray combustion using propane chemical kinetics in gas turbine combustion simulated by KIVA-2
[NASA-TM-103173] 20 p2843 N90-26170
The preparation of ACEL thin films
[AD-A222919] 21 p2999 N90-27048
M-52 spray booth qualification test
[NASA-CR-184003] 22 p3122 N90-27727
Analyses of spray and droplet ignition for pure and multicomponent fuels 23 p3304 N90-28688

SPRAYING
NT ARC SPRAYING
NT METAL SPRAYING
NT PLASMA SPRAYING
On the question of spray effects 12 p1687 N90-19691

SPRAYING APPARATUS
U SPRAYERS

SPRAYS
U SPRAYERS

SPREAD F
Auroral and sub-auroral interaction at the F region ionosphere
[AD-A213284] 05 p0666 N90-13896

SPREAD REFLECTION
A note on the statistics of laser speckle
[AD-A222408] 21 p3009 N90-27103

SPREAD SPECTRUM TRANSMISSION
Performance of four rake modems over the non-disturbed wideband HF channel
[AD-A211589] 03 p0339 N90-11930
Improving the quality of a spread-spectrum radiomobile link 06 p0761 N90-14426
Spread spectrum mobile radio communications
[AD-A213726] 07 p0918 N90-15311
Performance of cellular frequency-hopped spread-spectrum radio networks
[AD-A214480] 09 p1204 N90-16978
Classification of acousto-optic correlation signatures of spread spectrum signals using artificial neural networks
[AD-A215045] 09 p1206 N90-16992
Signal processing applied to photothermal techniques for materials characterization 10 p1364 N90-17902
Packet radio networks under dynamic jamming
[AD-A217094] 12 p1648 N90-19475
Joint Services Electronics Program research in electronics
[AD-A217745] 13 p1796 N90-20307
Location and navigation technology: Putting theory into practice 17 p2358 N90-23424
Joint tactical anti-jam communications: A systems approach
[AD-A219592] 17 p2388 N90-23602
Throughput and delay characteristics for a slow-frequency hopped aircraft-to-aircraft packet radio network
[AD-A220525] 17 p2389 N90-23609
Filter process for parasitic suppression for reception of spectrally separated emission signals
[ETN-90-96506] 18 p2545 N90-24526
Propagation Effects and Circuit Performance of Modern Military Radio Systems with Particular Emphasis on Those Employing Bandspreading
[AGARD-CP-442] 20 p2844 N90-26178
An overview of Canadian radio propagation/communications technologies research 20 p2844 N90-26179
Optimal synchronization of spread spectrum sequenced by nontransferable switching operators 20 p2845 N90-26183
CORA: A direct sequence spread spectrum radio for voice and data 20 p2848 N90-26195
Minimization of the cost of information transfer in HF spread spectrum transmission 20 p2848 N90-26198
Synchronization of frequency shift transmission and the effect of oversampling 20 p2848 N90-26200
HF spread spectrum, an audit of the power requirements and LPI vulnerability 20 p2849 N90-26203
Experimental study of a digital mobile radio spread spectrum in an urban site 20 p2849 N90-26205
Direct-sequence spread spectrum system
[AD-A223021] 20 p2856 N90-26245
Dynamic jamming of networks
[AD-A223044] 20 p2856 N90-26247
A novel communication network simulator
[AD-A223045] 20 p2857 N90-26248
Spread-spectrum communications in non-Gaussian channels
[AD-A222886] 21 p2994 N90-27019
Measured effects of repeater jamming on direct-sequence spread spectrum receivers that use envelope detectors
[AD-A222231] 21 p2996 N90-27032
PLRS: A new spread spectrum position location reporting system 24 p3427 N90-29358
IEEE Conference on Neural Information Processing Systems, Natural and Synthetic
[AD-A223611] 24 p3461 N90-29552

SPREADING
Microcomputer enhanced optical investigation of spreading and evaporative processes in ultra thin films
[DE90-006323] 11 p1492 N90-18585
Spray deposition: A fundamental study of droplet impingement, spreading and consolidation
[AD-A217202] 13 p1787 N90-20255

SPRING (SEASON)
Subjective uses of wind profiler data in warm season analysis and forecasting: Wind profiler training manual number 3
[PB89-223333] 04 p0520 N90-13004

SPRINGS (ELASTIC)
Numerical calculations of the collapse of a cavity in the vicinity of a compliant wall
[AD-A210489] 01 p0070 N90-10403
A spring-actuated spin and eject device for interplanetary missions 18 p2540 N90-24493
Plate rods and leaf springs with hybrid structure: Cross section optimization following different target criteria
[ILR-MITT-227(1989)] 20 p2877 N90-26366
Minimum weight design of a leaf spring tapered in thickness and width for the Hubble Space Telescope-space support equipment
[NASA-TM-4233] 23 p3340 N90-28879

SPUR (REACTORS)
U SPACE POWER UNIT REACTORS

SPUTTERING
NT MAGNETRON SPUTTERING
Alternative fabrication techniques for high-efficiency CuInSe2 and CuInSe2-alloy films and cells
[DE89-009451] 01 p0083 N90-10474
Ion implantation of two titanium alloys
[DE89-016958] 02 p0198 N90-11133
CuInSe2 solar cell research by sputter deposition
[DE89-009450] 02 p0236 N90-11345
Characterization and in situ testing of diamond films
[DE90-003155] 07 p0911 N90-15265
Near-surface sputtered particle transport for an oblique incidence magnetic field plasma
[DE90-004422] 07 p0996 N90-15758
Partial reduction of re-oxidation processing of Y-Ba-Cu-O sputtered thin films
[DE90-003655] 07 p0999 N90-15782
Orientation of rf-sputter-deposited MoS2 films
[ATR-89(4752)-1] 07 p1000 N90-15784
Computer-controlled ion beam sputter-deposition of superconducting oxide films
[AD-A213921] 07 p1004 N90-15812
Lithium cobalt oxide thin film and its electrochromism
[DE90-004570] 08 p1133 N90-16564
Artificially structured superconductors
[DE90-004851] 08 p1134 N90-16567
The use of BaF2 buffer layers for the sputter-deposition of TlCaBaCuO thin-film superconductors
[DE90-004859] 09 p1292 N90-17490
Materials processing of diamond: Etching, doping by ion implantation and contact formation
[AD-A216530] 10 p1438 N90-18301
Sputter deposition of diffusion barrier coatings on SiC monofilaments for use in Ti-based composites 11 p1477 N90-18502
Particle emission by oblique ion bombardment of gold
[ETN-90-95825] 12 p1711 N90-19827
Silicon carbide semiconductor device fabrication and characterization
[NASA-CR-186354] 12 p1719 N90-19873
Rolling contact fatigue of surface modified 440C using a 'Ge-Polymet' type disc rod test rig
[NASA-TM-100390] 13 p1777 N90-20200
Physical sputtering of metallic systems by charged-particle impact
[DE90-007803] 13 p1777 N90-20201
Reactive sputtering of molybdenum
[DE90-008307] 13 p1778 N90-20204
A unified integrated model for sputter coating uniformity
[DE90-008322] 13 p1778 N90-20205
XPS studies of doped polypyrrole films
[AD-A219424] 17 p2379 N90-23550
Power density effects in the physical and chemical properties of sputtered diamond-like carbon thin films
[DE90-011587] 18 p2532 N90-24450
The advantages and limitations of sputtered molybdenum disulphide as a space lubricant 18 p2537 N90-24471
Tribology of MoS2: Effect of film thickness 18 p2541 N90-24505
Multichip packaging technology with laser-patterned interconnects
[DE90-010743] 18 p2549 N90-24552
Microstructure of sputtered superconducting films of Bi2Sr2CaCu2O(x) made by low-temperature, in situ growth
[DE90-010067] 18 p2618 N90-24916
Sputtered superconducting films of Bi2Sr2CaCu2O(x) made by low-temperature, in-situ growth
[DE90-010092] 18 p2619 N90-24919
Computer-controlled ion beam sputter deposition of multicomponent oxides
[DE90-010544] 18 p2619 N90-24923
Studies on ion scattering and sputtering processes in ion beam sputter-deposition of high Tc superconducting films: The optimization of deposition parameters
[DE90-010538] 18 p2621 N90-24936
Studies on ion scattering and sputtering processes relevant to ion beam sputter deposition of multicomponent thin films
[DE90-010071] 20 p2931 N90-26675
Study of the polyoxymethylene and its sputtered fragments: Implications for comets 20 p2949 N90-26781
Photon sputtering of H2O ices: A preliminary report 20 p2949 N90-26783
The preparation of ACEL thin films
[AD-A222919] 21 p2999 N90-27048
Microstructures and properties of superconducting Y-Er-BaCu-O thin films obtained from disordered Y-Er-BaF2-Cu films 22 p3147 N90-27848
Adhesion of silver films to ion-bombarded zirconia
[DE90-010088] 24 p3456 N90-29517
Ion-beam mixing of Fe/B layers for tribological applications
[DE90-010091] 24 p3456 N90-29518

SQUALLS
Numerical simulations of a midlatitude squall line 01 p0087 N90-10497
Disturbances in the Arizona Monsoon 03 p0362 N90-12071
An observational study of squall lines in the Amazon
[INPE-4865-TDL/376] 12 p1693 N90-19723
A case study of cloud-to-ground lightning during the GALE program 15 p2132 N90-22185
Tropical squall lines of the Arizona monsoon 16 p2257 N90-22887
Case study on Pre-Typhoon Active Convective Clouds (PTACC) 21 p3029 N90-27220

SQUARE WELLS
The generalized van der Waals theory of pure fluids and mixtures
[DE90-000504] 06 p0740 N90-14307

SQUARES (MATHEMATICS)
Finding squares and rectangles in sets of points
[RUU-CS-89-10] 18 p2601 N90-24806

SQUEEZE FILMS
Elasticity effects on cavitation in a squeeze film damper undergoing noncentered circular whirl
[NASA-TM-102392] 05 p0649 N90-13786
Some problems in hydrodynamic lubrication 09 p1229 N90-17133
Current research in cavitating fluid films
[NASA-TM-103184] 23 p3323 N90-28791

SQUEEZED STATES (QUANTUM THEORY)
Multisqueezing of mechanical states and back-action evasion measurements
[IFSI-89-6] 08 p1123 N90-16504

SQUEEZING
U COMPRESSING

SQUID (DETECTORS)
Construction of a SQUID magnetometer for investigation of screening properties of high-T(sub c) superconductors
[FOA-C-20765-2.2] 05 p0645 N90-13768
Analysis of an R-SQUID noise thermometer
[VTT-PUBL-54] 05 p0645 N90-13769
Superconducting gravity gradiometer and a test of inverse square law 12 p1735 N90-19975

Scaling behaviour of relaxation dependencies in metaloxide superconductors 22 p3138 N90-27802
Navy superconductivity efforts 22 p3145 N90-27837

SR (REACTORS)
U SATURABLE REACTORS
SRB (SOLID ROCKET BOOSTERS)
U SPACE SHUTTLE BOOSTERS
STABILITY
NT ACOUSTIC INSTABILITY
NT AERODYNAMIC STABILITY
NT AIRCRAFT STABILITY
NT ATTITUDE STABILITY
NT BAROCLINIC INSTABILITY
NT BOUNDARY LAYER STABILITY
NT COMBUSTION STABILITY
NT CONTROL STABILITY
NT DIMENSIONAL STABILITY
NT DIRECTIONAL STABILITY
NT DYNAMIC STABILITY
NT FLAME STABILITY
NT FLOW STABILITY
NT FREQUENCY STABILITY
NT GOERTLER INSTABILITY
NT GYROSCOPIC STABILITY
NT HOVERING STABILITY
NT LATERAL STABILITY
NT LONGITUDINAL STABILITY
NT LOW SPEED STABILITY
NT MAGNETOHYDRODYNAMIC STABILITY
NT MAGNETOSPHERIC INSTABILITY
NT MOTION STABILITY
NT ROTARY STABILITY
NT SHELL STABILITY
NT SPACECRAFT STABILITY
NT STATIC STABILITY
NT STORAGE STABILITY
NT STRUCTURAL STABILITY
NT SURFACE STABILITY
NT SYSTEMS STABILITY
NT THERMAL STABILITY
Stability of discontinuous shearing motions of a non-Newtonian fluid
[AD-A210643] 01 p0071 N90-10406
Tangent map analysis of the beam-beam interaction
[DE89-015857] 01 p0120 N90-10689
Gas-accelerated plate stability study
[DE89-016880] 02 p0225 N90-11289
Stability requirements of RF linac-driven free-electron lasers
[DE89-016609] 02 p0227 N90-11303
An extension of Cochran's test for homogeneity of variances
[AD-A211054] 02 p0269 N90-11534
On the differentiable manifold of fixed order stable linear systems
[REPT-88-89] 03 p0394 N90-12250
Fast sampling and stability of nonlinear sampled-data systems. Part 1: Existence theorems
[RR-340-PT-1] 03 p0398 N90-12276
Slow sampling and stability of nonlinear sampled-data systems
[RR-342] 03 p0398 N90-12277
Stable summability and approximation theory
[AD-A211379] 04 p0539 N90-13118
Increasing the real stability boundary of explicit methods
[CWI-NM-R8902] 04 p0541 N90-13134
Instability of the behavior of high resistivity silicon detectors due to the presence of oxide charges
[REPT-89-038] 04 p0559 N90-13260
LORAN C stability integrity assurance
[AD-A212663] 05 p0577 N90-13364
Synchrotron-betatron parametric instability in free-electron lasers
[AD-A213373] 05 p0648 N90-13777
The singular zero sum differential game with stability using H infinity control theory
[MEMO-COSOR-89-09] 05 p0687 N90-13999
Stabilizability and detectability of discrete-time time-varying systems
[MEMO-COSOR-88-16] 05 p0690 N90-14023
Continuity properties of one-parameter families of linear-quadratic problems without stability
[MEMO-COSOR-88-17] 05 p0690 N90-14024
On the output-stabilizable subspace
[MEMO-COSOR-88-27] 05 p0690 N90-14027
Another approach to the local disturbance decoupling problem with stability for nonlinear systems
[MEMO-799] 05 p0691 N90-14033
On stability of queueing models of local area networks with slotted ring protocols
[MEMO-795] 05 p0694 N90-14057
Optical properties monitor: Experiment definition phase
[NASA-CR-183836] 05 p0699 N90-14092
Superplasticity: An overview 06 p0743 N90-14326
Stability and dynamics of constrained flexible multibody systems 06 p0791 N90-14609
Block predictor (low order) corrector methods to solve ordinary differential equations on parallel computers
[IMAG-RR-757-M] 06 p0834 N90-14845
Stability of numerical solutions for stratified two-phase flow
[DE90-701646] 07 p0929 N90-15370
Stable supermembrane vacuum with a discrete spectrum
[DE89-635722] 07 p0962 N90-15561
Stability and fragmentation of ejecta in hypervelocity impact
[DE90-004087] 08 p1085 N90-16278
Mechanics of iron, its stability and phase transformation
[DE89-636210] 09 p1193 N90-16913
An entropy-based approach to nonlinear stability
[NASA-TM-101086] 09 p1272 N90-17376
Supersonic aerodynamic characteristics of a proposed Assured Crew Return Capability (ACRC) lifting-body configuration
[NASA-TM-4136] 10 p1307 N90-17560
The stability of fuel fires 10 p1315 N90-17601
Low NO(x) potential of gas turbine engines
[NASA-TM-102452] 10 p1321 N90-17636
Direct multivariable adaptive controller with application to wing flutter 10 p1322 N90-17642
Solid state lasers for use in non-contact temperature measurements 10 p1363 N90-17901
The effect of the virtual mass force term on the stability of transient two-phase flow analysis
[DE90-733142] 10 p1384 N90-18010
Dynamics of column stability with partial end restraints
[NASA-TM-101651] 10 p1396 N90-18069
Nonlinear optical processes in one-dimensional polymers
[AD-A216103] 11 p1489 N90-18568
Strongly coupled one-dimensional system and the polymer
[AD-A216330] 11 p1489 N90-18571
Contribution to the study of stability robustness of nonlinear multivariable regulators
[INPE-4801-TDL/356] 11 p1554 N90-18950
Thermo-oxidative stability studies of PMR-15 polymer matrix composites reinforced with various fibers
[NASA-TM-102439] 12 p1620 N90-19310
Contact formation on (Hg,Cd) Te
[AD-A217088] 12 p1723 N90-19900
Development of an ejection seat specification for a new fighter aircraft 13 p1751 N90-20057
Electronic structure, alloy phase stability, and phase diagrams
[DE90-008306] 13 p1778 N90-20203
Elastic-plastic instability of plane frames 14 p1992 N90-21415
On the stability of a certain difference scheme
[PB90-165614] 14 p2021 N90-21588
Verification of Klett's method by comparison of lidar and transmissometer measurements 15 p2084 N90-21933
Inverse problems of heat conduction 15 p2091 N90-21969
Instabilities and subharmonic resonances of subsonic heated round jets, volume 2
[NASA-CR-186058] 15 p2100 N90-22017
Long term intensity stability of Auger electron spectrometers: Instructions for the interlaboratory comparison
[NPL-DMM(A)-1] 15 p2102 N90-22027
High power CO2 laser instability and its corrections 15 p2102 N90-22028
Nonlinear stability analysis and control of dynamical robotic systems 15 p2104 N90-22037
Orthogonal distance regression
[PB90-151747] 15 p2160 N90-22336
Stability criteria in the numerical solution of initial value problems
[TW-89-05] 15 p2162 N90-22351
Stability of compactification during inflation
[NASA-CR-186597] 15 p2189 N90-22502
A theoretical investigation of gravity-wave-generated stress and vorticity in the planetary boundary layer 15 p2191 N90-22512
Semianalytic study of high-eccentricity orbit stability and evolution 16 p2204 N90-22574
Measurement of HCl by near-infrared diode laser absorption 16 p2209 N90-22601
The effects of zinc addition on the environmental stability of Al-Li alloys 16 p2219 N90-22657
Side moment exerted by a spinning, coning, highly viscous liquid payload
[AD-A218746] 16 p2237 N90-22763
Algorithms for computing the multivariable stability margin 16 p2281 N90-22999
Determination of joint drives for stable end-effector motion in flexible robotic systems 16 p2288 N90-23034
On a fallacious conjecture about the stabilizability properties of solutions of the Riccati difference equation
[REPT-89-007] 16 p2305 N90-23132
Thermal phenomena in high-Tc thin film superconductors 16 p2321 N90-23233
Instability-related delamination growth of embedded and edge delaminations
[NASA-TM-100655] 17 p2370 N90-23494
Solidification of highly undercooled liquid droplets
[AD-A218776] 17 p2376 N90-23529
Controlled crack growth specimen for brittle systems
[NASA-TM-103126] 17 p2378 N90-23543
Diffusion in the thermal degradation of NC base propellants
[AD-A219831] 17 p2383 N90-23572
Reflection oscillators employing series resonant crystals'
[NASA-CASE-GSC-13173-1] 17 p2394 N90-23635
Convergence properties of the Runge-Kutta-Chebyshev method
[CWI-NM-R8907] 17 p2459 N90-24038
Stability and stability sensitivity by periodically time dependent systems: Hill versus Floquet
[ILR-MITT-221(1989)] 17 p2463 N90-24071
Observation of a magic number in the ion distribution of ethene clusters
[AD-A219837] 18 p2521 N90-24393
A first principles examination of phase stability in FCC-based ordered Ni-V alloys
[DE90-010635] 18 p2525 N90-24411
New liquid cathode electrolytes in high rate cells
[AD-A219822] 18 p2546 N90-24531
Stability and error estimates for sinc interpolation
[CWI-AM-R8914] 18 p2599 N90-24790
Phase stability in the Al(6-x)Cu(x)Zr2 system for 0 less than x less than 1.0
[DE90-010620] 18 p2620 N90-24925
An investigation of a mathematical model of an optically pumped Ti(3+):Al2O3 laser system 18 p2646 N90-25063
Design of a versatile, teleoperable, towable lifting machine with robotic capabilities for use in NASA's lunar base operations
[NASA-CR-186688] 19 p2697 N90-25345
Experimental observations and finite element analysis of the initiation of fiber microbuckling in notched composite laminates
[NASA-CR-186207] 19 p2699 N90-25359
Active perception and exploratory robotics
[MS-CIS-89-65] 19 p2726 N90-25501
A control problem for Burgers' equation with bounded input/output
[NASA-CR-182062] 19 p2747 N90-25608
On the linear and nonlinear stability of non-parallel flow 21 p3002 N90-27065
Adjustable choke for fluids nozzle
[NASA-CASE-NPO-17625-1-CU] 21 p3003 N90-27070
The dynamics of orbital maneuvering: Design and evaluation of a visual display aid for human controllers 22 p3131 N90-27767
Effects of low bond number liquid motions on spacecraft attitude 22 p3131 N90-27768
Energetics and crystal chemistry of Huddlesden-Popper type structures in high T(sub c) ceramic superconductors 22 p3141 N90-27814
Laboratory experiments on stability and entrainment of oceanic stratocumulus. Part 1: Instability experiment 22 p3220 N90-28263
Laboratory experiments on stability and entrainment of oceanic stratocumulus. Part 2: Entrainment experiment 22 p3220 N90-28264
The October 27-28, 1986, FIRE cirrus case study: Cloud microstructure 22 p3224 N90-28283
Fretting wear and fretting fatigue at temperatures up to 600 C 23 p3307 N90-28706
Ion divergence and the stability of magnetically insulated diodes
[DE90-014565] 23 p3321 N90-28777
Teleoperator comfort and psychometric stability: Criteria for limiting master-controller forces of operation and feedback during telemanipulation 23 p3364 N90-29009
Computational neural learning formalisms for manipulator inverse kinematics 23 p3368 N90-29030
Electron acoustic and magnetoacoustic modes in a magnetized beam plasma system
[DE90-627473] 23 p3398 N90-29199
Numerical and analytical study of nonlinear bifurcations associated with the morphological stability of two-dimensional single crystals
[PB90-209594] 23 p3398 N90-29200

Theoretical studies of proton beams in solar flare loops 23 p3413 N90-29286
An instability theorem for a certain sixth order differential equation
[DE90-627150] 24 p3536 N90-29990
Effect of a crystal-melt interface on Taylor-Vortex flow with buoyancy
[PB90-244401] 24 p3551 N90-30089

STABILITY AUGMENTATION
Structural stability augmentation system design using BODEDIRECT: A quick and accurate approach 01 p0023 N90-10116
Output model-following control synthesis for an oblique-wing aircraft
[NASA-TM-100454] 12 p1606 N90-19241
Lateral-directional stability and control characteristics of the Quiet Short-Haul Research Aircraft (QSRA)
[NASA-TM-102250] 17 p2356 N90-23413
Short period control using angular acceleration feedback: Compensation for first lag servo
[NAL-TM-600] 24 p3435 N90-29399

STABILITY DERIVATIVES
NT PITCHING MOMENTS
NT ROLLING MOMENTS
NT YAWING MOMENTS
Analysis of flight data from a High-Incidence Research Model by system identification methods
[NASA-TP-2940] 01 p0015 N90-10074
The active flexible wing aeroservoelastic wind-tunnel test program 01 p0024 N90-10119
Stability and control derivatives of the De Havilland DHC-2 BEAVER aircraft
[PB89-217525] 03 p0309 N90-11754
A functional expansion and stability for nonlinear input-output maps
[RR-359] 04 p0539 N90-13121
Dynamic derivatives of missiles and fighter-type configurations at high angles of attack 10 p1306 N90-17554
Computational fluid dynamics method for low Reynolds number flow in a precessing/spinning, liquid filled cylinder with rounded endcaps
[AD-A216997] 12 p1659 N90-19531
The influence of the gas surface interaction on spacecraft orbital motion 17 p2365 N90-23461
Aerodynamic interferences of in-flight thrust reversers in ground effect 23 p3274 N90-28529

STABILITY TESTS
NT FLIGHT STABILITY TESTS
NT WIND TUNNEL STABILITY TESTS
A contribution to the stability analysis of large space structures 02 p0177 N90-10997
Performance and quality of a wing type parachute: Parametric analysis
[REPT-88-19] 03 p0302 N90-11710
The effect of the virtual mass force term on the stability of transient two-phase flow analysis
[DE90-733142] 10 p1384 N90-18010
Microcalometric studies of gun propellant KKR 8
[FOA-C-20770-2.1] 11 p1495 N90-18606
A learning regulator for the plane longitudinal movement
[ETN-90-95381] 13 p1864 N90-20695
Computation of nonequilibrium chemically reacting flows in hypersonic flow field 14 p1911 N90-20954
Numerical study of the onset of instability in the flow past a sphere 17 p2400 N90-23672
The role of gravity on macrosegregation in alloys
[NASA-CR-186530] 19 p2679 N90-25238
Robust controller designs for second-order dynamic system: A virtual passive approach
[NASA-TM-102666] 19 p2701 N90-25369
Adaptive node movement in finite-difference solutions of partial differential equations with applications to gasdynamics, part 2
[UTIAS-333-PT-2] 19 p2750 N90-25623
Aerodynamic control design: Experience and results at Aermacchi 23 p3272 N90-28518
Improved meteorological measurements from buoys and ships (IMET): Preliminary report on barometric pressure sensors
[PB90-242116] 24 p3494 N90-29748

STABILIZATION
NT SIGNAL STABILIZATION
NT SPIN STABILIZATION
NT THREE AXIS STABILIZATION
Regulation of nonlinear and generalized linear systems
[AD-A207725] 01 p0109 N90-10619
Realization theoretic solution of two analytic matrix equations with applications to stabilization of infinite-dimensional systems
[AD-A211118] 02 p0265 N90-11512
The output-stabilizable subspace and linear optimal control
[MEMO-COSOR-89-15] 05 p0687 N90-14001
Investigation of the phase stabilizing effect of potassium fluoride on ammonium nitrate
[AD-A213042] 06 p0753 N90-14381
The stability of fuel fires 10 p1315 N90-17601
Dynamics and stabilization of materials possessing high energy content
[AD-A216320] 11 p1489 N90-18570
Control and stabilization of linear and nonlinear distributed systems
[AD-A216446] 11 p1547 N90-18908
Escape systems research at RAE 13 p1751 N90-20058
Controllable propulsion for escape systems control 13 p1753 N90-20064
Spacecraft escape 13 p1753 N90-20066
Digital-flutter-suppression-system investigations for the active flexible wing wind-tunnel model
[NASA-TM-102618] 13 p1758 N90-20093
Stabilized determination of geopotential coefficients by the mixed hom-BLUP approach 13 p1832 N90-20520
Stabilization of high (Tc) superconductivity in cadmium sulfide
[DE90-008249] 13 p1896 N90-20881
CSI sensing and control: Analytical and experimental results 14 p1936 N90-21083
The extension of rapid distortion theory to stratified shear flows 14 p2005 N90-21491
Accurate nonlinear control for satellites using reaction wheels
[INPE-4963-PRE/1546] 15 p2059 N90-21787
Modelling and control of a balloon borne stabilized platform 17 p2355 N90-23408
The effect of catalysts on gas-phase hydrocarbon ignition
[AD-A218775] 17 p2371 N90-23499
Modeling and experimental studies of oxide covered metal surfaces
[DE90-009961] 17 p2375 N90-23525
Compensatability and optimal compensation of systems with stochastic parameters
[REPT-89-61] 17 p2457 N90-24024
Calculation of the aeroelastic blade stabilization with linearized process
[MITT-87-01] 18 p2497 N90-24272
Dynamic stabilization of large flexible space structures
[ETN-90-96926] 18 p2511 N90-24344
Increasing the margin of stability of arbitrarily finite modes of flexible large space structures with damping
[AD-A221742] 21 p2967 N90-26867
Experience in developing an improved design of experiment (lessons learned) 22 p3120 N90-27718
The instrument pointing system: Precision attitude control in space 22 p3129 N90-27756
A new method for a tethered system aided space station assembly 22 p3130 N90-27765
Oxygen stabilization induced enhancement in J(sub c) and T(sub c) of superconducting oxides 22 p3137 N90-27800
Hydrocarbon-fueled scramjet combustor component development tests 22 p3162 N90-27934
Development and testing of rapid repair methods for war damaged runways
[AD-A223970] 23 p3285 N90-28586
Stabilization of Taylor-Couette flow due to time-periodic outer cylinder oscillation
[PB90-219130] 23 p3323 N90-28790
Chemical stabilization of laser dyes
[AD-A224219] 24 p3473 N90-29627

STABILIZED PLATFORMS
Modelling and control of a balloon borne stabilized platform 17 p2355 N90-23408
Galactical ultra wide angle Schmidt system 18 p2536 N90-24468
The large wheel actuator LDR 100-0: Development status and test results 18 p2539 N90-24487

STABILIZERS (FLUID DYNAMICS)
NT HORIZONTAL TAIL SURFACES
Evaluation of a damaged F/A-18 horizontal stabilator
[AD-A212573] 04 p0453 N90-12597
Cost effectiveness of composite materials on the F-15 and F-16 aircrafts
[AD-A216353] 10 p1320 N90-17631
The MANTA: An RPV design to investigate forces and moments on a lifting surface
[NASA-CR-186227] 14 p1915 N90-20971
DRAG-n-FLY: A proposal in response to a low Reynolds number station keeping mission
[NASA-CR-186666] 19 p2658 N90-25130
Development of a graphite/bismaleimide leading edge for the F-111 (EF-111A) horizontal stabilizer 21 p2956 N90-26809
A sensor stabilization/tracking system for unmanned air vehicles
[AD-A224008] 23 p3283 N90-28579

STABLE OSCILLATIONS
Deep traps and sidegating in GaAs devices
[AD-A210740] 01 p0133 N90-10765

STACKING FAULT ENERGY
Determination of the gaseous hydrogen ductile-brittle transition in copper-nickel alloys
[NASA-TM-86494] 04 p0474 N90-12715
The lithium concentration dependence of creep in binary aluminum-lithium alloys
[AD-A218706] 16 p2221 N90-22668

STACKING FAULTS
U CRYSTAL DEFECTS

STACKS
Theoretical analysis of microwave and millimeter wave integrated circuits based on magnetic films
[AD-A214772] 09 p1211 N90-17021
Failure analysis of woven hybrid composite using a finite element method
[OUEL-1791/89] 15 p2065 N90-21828

STAGE SEPARATION
Independent Orbiter Assessment (IOA): Analysis of the electrical power distribution and control subsystem, volume 1
[NASA-CR-185529-VOL-1] 02 p0167 N90-10941
Computation of transient three-dimensional interstage flowfields using the arbitrary Lagrangian-Eulerian method 02 p0219 N90-11253
Comparison between horizontally launched air-breathing single and two-stage to orbit space vehicles 09 p1175 N90-16802
The development of a complementary expendable launch vehicle interface for an STS deployable payload 15 p2113 N90-22086
Qualification test rationale for measuring the resistance of equipment to pyrotechnic shock
[REPT-892-430-117] 16 p2207 N90-22590

STAGING (ROCKETS)
U STAGE SEPARATION

STAGNATION FLOW
On catalytic recombination rates in hypersonic stagnation heat transfer 05 p0573 N90-13338
Vorticity amplification in nonorthogonal stagnation flow 08 p1064 N90-16152

STAGNATION POINT
Theory of stagnation point heat transfer in dissociated air 05 p0573 N90-13337
A tomographic study of premixed turbulent stagnation point flames
[DE90-002462] 07 p0892 N90-15156
Shock layer vacuum UV spectroscopy in an arc-jet wind tunnel
[NASA-TM-102258] 09 p1226 N90-17112
An experimental and theoretical investigation of the flow over plane delta wings with supersonic leading edges
[LR-588] 19 p2655 N90-25114
The spatial scalar structure of premixed turbulent stagnation point flames
[DE90-014189] 23 p3303 N90-28686
Real-time aerodynamic heating and surface temperature calculations for hypersonic flight simulation
[NASA-TM-4222] 23 p3327 N90-28815

STAGNATION PRESSURE
Jet-flow from shock tubes
[AD-A210651] 02 p0220 N90-11260
An experimental, analytical, and computational investigation of turbomachinery rotor flow fields 07 p0926 N90-15360

STAGNATION REGION
U STAGNATION POINT

STAGNATION TEMPERATURE
Spectral characteristics of arc-heated low density plasma flows (IV) air and N2-CO2 mixture plasmas
[NAL-TR-1012] 09 p1285 N90-17451

STAINLESS STEELS
NT AUSTENITIC STAINLESS STEELS
NT FERRITIC STAINLESS STEELS
NT MARTENSITIC STAINLESS STEELS
Gaussmeter determination of 302 stainless steel material condition
[BDX-613-3941] 01 p0044 N90-10249
Grain boundary chemistry in irradiated stainless steel and its influence on environmental degradation
[DE89-016827] 02 p0197 N90-11125
Compositional analysis of steels by X-ray fluorescence spectrometry
[DE89-630803] 02 p0198 N90-11129
Rapid heating tensile tests of high-energy-rate-forged 316L stainless steel charged with hydrogen and tritium
[DE89-017869] 04 p0474 N90-12717
Advances and future directions in superplastic materials 06 p0744 N90-14328
An evaluation of electrochemical potentiokinetic reactivation techniques for in-service measurements on Type 304 stainless steel
[DE89-017859] 06 p0746 N90-14340

Rapid heating tensile tests of hydrogen-charged high-energy-rate-forged 316L stainless steel
[DE90-000591] 06 p0746 N90-14342
The 4.2 K fracture toughness of 304 stainless steel in a magnetic field
[DE90-002083] 06 p0747 N90-14347
Embrittlement of laboratory- and reactor-aged CF-3, CF-8, and CF-8M duplex stainless steels
[DE90-002777] 06 p0748 N90-14354
The feasibility of welding of irradiated materials
[DE90-002200] 06 p0795 N90-14631
Failure probability estimate of Type 304 stainless steel piping
[DE90-000659] 06 p0796 N90-14635
Helium-induced weld cracking in irradiated 304 stainless steel
[DE90-001312] 07 p0903 N90-15219
Accelerated aging embrittlement of cast duplex stainless steel: Activation energy for extrapolation
[DE90-001773] 07 p0903 N90-15221
The effect of dissolved chlorine on the pitting behavior of 304L stainless steel in a 0.5 N NaCl solution
[AD-A213803] 07 p0905 N90-15234
The effect of dissolved ozone on the corrosion behavior of Cu-30 Ni and 304L stainless steel in 0.5 N NaCl solutions
[AD-A213804] 07 p0906 N90-15235
Cast stainless steel aging: Mechanisms and predictions
[DE90-003772] 07 p0907 N90-15241
Experience with J testing of 304/308 stainless steel weldment
[DE90-002046] 07 p0946 N90-15478
Stainless steel passivity
[AD-A214108] 08 p1044 N90-16033
Irradiation creep and swelling of annealed type 304L stainless steel at approximately 390 C and high neutron fluence
[DE90-004521] 08 p1046 N90-16047
Failure probability estimate of Type 304 stainless steel piping
[DE90-003896] 11 p1486 N90-18550
Mitigation of stress corrosion cracking of AISI 304 stainless steel in oxygenated water at 289 C by organic species at low concentration
[DE90-005631] 12 p1628 N90-19354
Ageing effects in welded cast CF3 stainless steel
[AERE-R-13559] 13 p1775 N90-20188
Spallation of oxide scales from 20 percent Cr/25 percent Ni/Nb stainless steel
[AERE-R-13464] 13 p1775 N90-20189
A STEM study of changing grain boundary chemistry during the sensitisation of AISI 304 stainless steel
[AERE-R-13418] 14 p1949 N90-21157
Current fluctuations associated with localised corrosion: Mechanistic studies of the early stages of pitting and stress corrosion cracking of stainless steel
[AERE-R-13531] 14 p1950 N90-21159
Mathematical modelling of intergranular attack in stainless steels: A preliminary study
[AERE-M-3698] 14 p1950 N90-21160
Materials for ultra-high vacuum
[DE90-007908] 14 p1959 N90-21217
On-line assessment of weld quality using ultrasonics
[AERE-R-13401] 14 p1989 N90-21398
The effect of aging at 343 C on type 308 stainless steel weldments
[DE90-009232] 15 p2069 N90-21853
VAMAS project on variable weld penetration: Surface tension of the steels
[NPL-DMA(A)-188] 15 p2070 N90-21856
The initiation of intergranular stress corrosion-cracking on sensitized stainless steel in dilute thiosulphate solutions
[AERE-R-13317] 16 p2217 N90-22648
Hydrogenation of stainless steels implanted with nitrogen
[DE90-617397] 16 p2221 N90-22666
Fracture toughness and fatigue crack initiation tests of welded precipitation-hardening stainless steel
[AD-A218745] 16 p2221 N90-22669
A study of the relation between grain boundary type and sensitisation in a partially-sensitised AISI 304 stainless steel using electron back-scattering patterns
[AERE-R-13327] 16 p2321 N90-23234
Fracture-tough, corrosion-resistant bearing steels
[NASA-CR-186796] 19 p2675 N90-25213
Oxidation and sulfidation of Type 310S stainless steel at elevated temperatures
[DE90-010149] 20 p2832 N90-26109
Materials studies for magnetic fusion energy applications at low temperatures, volume 12
[PB90-157553] 22 p3248 N90-28417
Thermogravimetry-mass spectrometry analysis of gas bubbles in molten glass
[DE90-014116] 23 p3303 N90-28684
Tensile behavior of borated stainless steels, phase 1
[DE90-014368] 23 p3309 N90-28717
The influence of solidification rate on solute redistribution and second-phase formation in stainless steel alloys
[DE90-015189] 24 p3450 N90-29482
Single-phase solidification during rapid resolidification of stainless steel alloys
[DE90-015190] 24 p3450 N90-29483

STALLING
Computation of viscous aerodynamic characteristics of 2-D airfoils for helicopter applications
[NLR-MP-88052-U] 20 p2804 N90-25951

STANDARD DEVIATION
Turbulence spectral widths view angle independence as observed by Doppler radar
[AD-A219169] 16 p2199 N90-22550
An empirically derived figure of merit for the quality of overall task performance 18 p2644 N90-25058

STANDARDIZATION
NT COMMONALITY
Response of standardized PVDF piezoelectric polymer gauges to direct shock pressures between 8 and 32 GPa
[DE89-016811] 02 p0224 N90-11282
Directory of International and Regional Organizations Conducting Standards-Related Activities, May 1989
[PB89-221147] 04 p0483 N90-12776
Interpretation and manipulation of Edgeworth expansions
[MEMO-775] 04 p0544 N90-13163
Transferring data objects: A focused Ada investigation
[NASA-CR-186065] 06 p0823 N90-14786
Terminology strategies for international information exchange
[AD-A214147] 07 p1010 N90-15853
Standardized tests for research with environmental stressors: The AGARD STRES battery 09 p1258 N90-17295
DoD manual for standard data elements
[AD-A216441] 11 p1575 N90-19066
Proceedings of the Advisory Committee on Standardization of Carbon-Phenolic Test Methods and Specifications
[NASA-CR-186478] 15 p2063 N90-21817
Knowledge-Based Systems (KBS) development standards: A maintenance perspective 19 p2739 N90-25570
VISTA (Vertical Integration of Science, Technology, and Applications) user interface software study
[DE90-010003] 20 p2936 N90-26707
Aviation acoustical noise measurement
[AD-A222014] 21 p3073 N90-27469
Solid state space harmonic amplifier
[AD-D014455] 22 p3166 N90-27955
Crossroads of Information Technology Standards
[PB90-239732] 23 p3406 N90-29251

STANDARDS
NT FREQUENCY STANDARDS
Castings Airworthiness
[AGARD-R-762] 01 p0042 N90-10231
Quality control of castings 01 p0043 N90-10239
The creation of quality: New directions in the production of aeronautics castings 01 p0043 N90-10241
Intrinsic damage and strength criteria for advanced composite laminates in space applications 02 p0187 N90-11071
Calibration and de-embedding of microwave measurements using any combination of one- or two-port standards
[PB89-212674] 03 p0337 N90-11916
Comparison of I2-stabilized HE-NE lasers
[PB89-219844] 03 p0352 N90-12014
WISPER: A standardized fatigue load sequence for HAWT-blades
[NLR-MP-88029-U] 03 p0359 N90-12055
Review of the national ambient air quality standards for lead: Exposure analysis methodology and validation
[PB89-207914] 03 p0368 N90-12104
CALS (Computer-aided Acquisition and Logistic Support) Test Network information exchange: User's manual
[DE89-016700] 03 p0418 N90-12399
Introduction to the Mil-Std-1553B serial multiplex data bus
[RAE-TM-MM-9] 03 p0418 N90-12405
Directory of International and Regional Organizations Conducting Standards-Related Activities, May 1989
[PB89-221147] 04 p0483 N90-12776
A formatting style for typesetting and distributing draft international standards
[NPL-DITC-143/89] 04 p0530 N90-13059
Publications of the National Institute of Standards and Technology, 1988 catalog
[PB89-218382] 04 p0563 N90-13279
Considerations about the acceptance inspection of HS fasteners intended for controlled tightening
[CRIF-MT-175] 05 p0653 N90-13806
Executive overview and introduction to the SMAP information system life-cycle and documentation standards
[NASA-TM-101765] 05 p0706 N90-14134
Information system life-cycle and documentation standards, volume 1
[NASA-TM-101856] 05 p0706 N90-14135
Management plan documentation standard and Data Item Descriptions (DID). Volume of the information system life-cycle and documentation standards, volume 2
[NASA-TM-101857] 05 p0706 N90-14136
Product specification documentation standard and Data Item Descriptions (DID). Volume of the information system life-cycle and documentation standards, volume 3
[NASA-TM-101858] 05 p0706 N90-14137
Assurance specification documentation standard and Data Item Descriptions (DID). Volume of the information system life-cycle and documentation standards, volume 4
[NASA-TM-101859] 05 p0706 N90-14138
Management control and status reports documentation standard and Data Item Descriptions (DID). Volume of the information system life-cycle and documentation standards, volume 5
[NASA-TM-101860] 05 p0706 N90-14139
Calibration curves for some standard Gap Tests
[DE89-016599] 06 p0754 N90-14389
Results of the 1989 NASA/JPL balloon flight solar cell calibration program
[NASA-CR-186114] 06 p0803 N90-14672
Nomenclature for physical mapping of complex genomes
[DE89-015173] 06 p0859 N90-14994
An expert system for quality assurance (a.k.a.) QA Express
[DE90-003887] 07 p0944 N90-15467
FRAG requirements for control of fatigue testing
[RAE-TM-MAT/STR-1130] 08 p1089 N90-16300
Changes in the volt, ohm, and temperature and long range impact of using the Josephson voltage standard
[DE90-004493] 09 p1214 N90-17039
Environmental quality and occupational health Special Emphasis Area Plan (SEAP)
[AD-A214738] 09 p1251 N90-17259
Aircraft Fire Safety
[AGARD-CP-467] 10 p1311 N90-17581
Development of improved fire safety standards adopted by the Federal Aviation Administration 10 p1312 N90-17585
New aircraft cabin and cargo flammability standards for transport category aircraft 10 p1312 N90-17589
Suggestions for designers of navy electronic equipment, 1989 edition, revision B
[AD-A215961] 10 p1380 N90-17998
Packet telemetry standard
[ESA-PSS-04-106-ISSUE-1] 11 p1467 N90-18447
The Uniform Engine Test Programme
[AGARD-AR-248] 12 p1604 N90-19232
Nine-year aging behavior of the ceramic flatpack resonator
[DE90-008044] 13 p1813 N90-20412
Terrestrial gravity instrumentation in the 20th Century: A brief review 13 p1834 N90-20527
The laminar flow element: Its use as a flow standard
[PB90-129677] 15 p2126 N90-22157
Comparison between data generated from standard fracture toughness specimens and from nonstandard specimens made of a silicon carbide
[DE90-009621] 16 p2247 N90-22814
Data exchange strategy. Part 1: Review of digital data exchange technology
[AD-A218506] 16 p2327 N90-23267
Model for predicting the effects of laser exposures and eye protection on vision
[AD-A219697] 17 p2434 N90-23868
Dazzling glare: Protection criteria versus visual performance
[AD-A219676] 17 p2438 N90-23889
Development of a consolidated environmental data base
[DE90-009419] 17 p2479 N90-24177
Development of cost-effective standards for Earth observation spacecraft 18 p2501 N90-24292
Thermodynamic calculations for mixtures of environmentally safe refrigerants using the Lee-Kesler-Ploecker equation of state
[DE90-010493] 18 p2542 N90-24509
The effect of noise-abatement profiles on noise immissions and human annoyance underneath a subsequent climbpath 18 p2610 N90-24865
Agenda toward the development of a rational noise descriptor system relevant to human annoyance by en route aircraft noise 18 p2610 N90-24866
A model for a knowledge-based system's life cycle 19 p2739 N90-25569

NASA project status reports: Congressional requirements can be met, but reliability must be ensured
[GAO/NSIAD-90-40] 20 p2843 N90-26169
International standards for text preparation and interchange
[DE90-011868] 20 p2935 N90-26699
Speech processing standards
21 p2993 N90-27013
Authors guide to the publishing procedures at Defence Research Establishment Suffield
[AD-A223101] 21 p3087 N90-27554
NIST (National Institute of Standards and Technology) serial holdings, 1990 edition
[PB90-183245] 22 p3163 N90-27936
Improved meteorological measurements from buoys and ships (IMET): Preliminary conventions from buoys and standards data and file formats
[PB90-241910] 22 p3229 N90-28312
Development of standards for superconductors
[PB90-196536] 22 p3248 N90-28418
Liquid Rocket Booster (LRB) for the Space Transportation System (STS) systems study. Appendix G: LRB for the STS system study level 2 requirements, revision 1
[NASA-CR-183793-APP-G] 23 p3289 N90-28607
Specifications, tolerances, and other technical requirements for weighing and measuring devices as adopted by the 74th National Conference on Weights and Measures, 1989 (1990 edition)
[PB90-184961] 23 p3316 N90-28748
Goverment's role in standards-related activities: Analysis of comments
[PB90-215534] 23 p3404 N90-29239
Microscopic models for electromagnetic wave propagation in highly dispersive media
[AD-A224382] 24 p3460 N90-29540
Radar receiver procedures
[AD-A224399] 24 p3460 N90-29541

STANDING WAVES
Dynamics of nucleation at electrochemical interfaces via surface EXAFS and standing wave measurements
[AD-A210733] 02 p0195 N90-11109
Influence of RF-parameters on beam lifetime
[NIKHEF-K/AMPS/89-06] 05 p0699 N90-14091
The measurements of thermoacoustic phenomena using thermoacoustic couples
[AD-A218018] 13 p1882 N90-20798
Probing interfacial structure and composition with x ray standing waves
[AD-A223071] 21 p2977 N90-26916
Variable length-scale studies at interfaces with X ray standing waves
[AD-A223043] 21 p3004 N90-27075

STANDS
U SUPPORTS

STANNIDES
NT NIOBIUM STANNIDES
Molecular beam epitaxial growth, characterization, and devices of modulated semiconductor structures
[AD-A221545] 21 p3084 N90-27538

STAR CATALOGS
U ASTRONOMICAL CATALOGS

STAR CLUSTERS
NT GLOBULAR CLUSTERS
NT OPEN CLUSTERS
NT PLEIADES CLUSTER
Effects of main-sequence mass loss on the turnoff ages of population 1 clusters
[DE89-016755] 03 p0421 N90-12417
The Hipparcos Mission. Prelaunch status. Volume 2: The input catalog
[ESA-SP-1111-VOL-2] 05 p0606 N90-13529
The choice of stars in open clusters
05 p0608 N90-13542
Equation of state and opacity of dense plasmas
[DE90-002223] 06 p0847 N90-14926
Mass functions for eight galactic clusters in the solar neighborhood 08 p1150 N90-16660
Interactions of massive stars with the interstellar medium: Bow shocks and superbubbles
15 p2186 N90-22485
The association of supernovae with regions of recent star formation in late-type galaxies
15 p2188 N90-22497
The dynamical evolution of dense clusters of compact stars 16 p2331 N90-23287
Evolutionary models of the rotating sun and implications for other low mass stars 16 p2339 N90-23329
The low mass X ray binaries in the LMC
19 p2768 N90-25730
EXOSAT deep exposure of the LMC X-4 region
19 p2780 N90-25814
A hard X ray observation of the Coma Cluster
19 p2789 N90-25875

STAR DISTRIBUTION
Infrared spectroscopy of star formation in galaxies: Extreme conditions and very short time scales
11 p1586 N90-19147
Fifth fundamental catalogue (FK5). Part 1: The basic fundamental stars
[REPT-32(1988)-PT-1] 16 p2330 N90-23282
Globular cluster X ray binaries
19 p2768 N90-25729
The Z/atoll classification 19 p2769 N90-25740
Moving out of the galaxy: Future prospects for X Ray binaries studies 19 p2770 N90-25746
TTM-Kvant observations of the galactic plane
19 p2783 N90-25836
Population properties of AGN in the soft X-ray band
19 p2784 N90-25844

STAR FIELDS
U STAR DISTRIBUTION

STAR FORMATION
UV observations of NGC 205
[NASA-CR-185975] 02 p0291 N90-11661
The stability of magnetohydrodynamic shock waves in molecular clouds 02 p0292 N90-11665
Gas dynamical processes in the theory of galaxy formation 02 p0294 N90-11673
Orion B: Anatomy of a star-forming region
05 p0710 N90-14155
Very high resolution radio observations of molecular cloud cores 06 p0863 N90-15013
Outflows in high mass star-forming regions
08 p1149 N90-16657
Infrared Spectroscopy in Astronomy
[ESA-SP-290] 11 p1578 N90-19084
The infrared spectral signature of star formation
11 p1582 N90-19114
Infrared line emission from high-velocity outflows in star-forming regions 11 p1582 N90-19116
Far-infrared spectroscopy of galaxies
11 p1586 N90-19146
Infrared spectroscopy of star formation in galaxies: Extreme conditions and very short time scales
11 p1586 N90-19147
A search for the CO feature in active galactic nuclei
11 p1587 N90-19151
Fluorescent molecular hydrogen emission from star-forming galaxies 11 p1588 N90-19155
H53-alpha emission from M82
11 p1588 N90-19156
Accretion flows in high mass star formation
[DE90-007251] 12 p1744 N90-20027
Small scale structures and density of star-forming regions 14 p2041 N90-21706
A theoretical scenario for the dynamics of formation and early evolution of globular clusters in galaxies
15 p2187 N90-22494
The association of supernovae with regions of recent star formation in late-type galaxies
15 p2188 N90-22497
Molecular gas in S106: Morphology, kinematics, and chemistry of a star forming region
17 p2484 N90-24209
Dynamic and photometric evolutionary models of tidal tails and ripples 18 p2637 N90-25024
Neutron star formation in low-mass binary systems
19 p2778 N90-25797
Accretion induced collapse and field decay
19 p2783 N90-25833
Active star-forming galaxies in the X ray foreground
19 p2785 N90-25848
Radio loud far-infrared galaxies
[DE90-012993] 20 p2950 N90-26786
A site for the astrophysical gamma ray process
[DE90-013473] 20 p2950 N90-26787
Star formation and the distribution of HI and infrared emission in M51
[NASA-CR-186928] 23 p3408 N90-29262
The formation of globular clusters
23 p3410 N90-29272

STAR FORMATION RATE
Search for rapidly star forming galaxies at high redshift 15 p2181 N90-22465
Dynamic and photometric evolutionary models of tidal tails and ripples 18 p2637 N90-25024
Radiation-driven evolution and statistics of low-mass X ray binaries 19 p2770 N90-25745
The evolution of horizontal branch stars and the calibration of globular cluster ages
24 p3562 N90-30152

STAR TRACKERS
NT CCD STAR TRACKER
Temperature dependence of attitude sensor coalignments on the Solar Maximum Mission (SMM)
05 p0588 N90-13426
Operating principle 05 p0603 N90-13500
The modulating grid 05 p0603 N90-13505
The detectors 05 p0604 N90-13507
The SN 1987A attitude control system
05 p0659 N90-13845
Remote Attitude Measurement Sensor (RAMS)
12 p1611 N90-19271
Automated star pattern recognition
16 p2211 N90-22612

STAR TRACKING
U STAR TRACKERS

STARBURST GALAXIES
Near-infrared spectroscopy of starburst and interacting galaxies 11 p1586 N90-19144
Infrared spectroscopy of star formation in galaxies: Extreme conditions and very short time scales
11 p1586 N90-19147
The strengths of the 2.3 micron CO band in luminous interacting and merging galaxies
11 p1587 N90-19148
Evolutionary synthesis of the far-infrared emission in starburst galaxies 11 p1587 N90-19152
Near infrared spectroscopy and spectroscopic imaging of NGC253 11 p1588 N90-19159
The interstellar medium of a starburst galaxy; millimeter interferometric observations of M82
16 p2329 N90-23276
Contributions of discrete sources to the X ray background 19 p2785 N90-25847

STARCHES
Research and development on enhanced degradable plastics
[AD-A217180] 13 p1779 N90-20212

STARFIGHTER AIRCRAFT
U F-104 AIRCRAFT

STARK EFFECT
Stark and Zeeman effects on laser cooling of positronium 11 p1560 N90-18986
High resolution stimulated Raman-Brillouin spectroscopy in gases and solids
[DE90-009535] 15 p2067 N90-21840
Fellowship in physics/modern optics and quantum electronics
[AD-A218772] 17 p2469 N90-24111
Anomalous decay of Langmuir turbulence. High power, high frequency radiation from beam-plasma interactions
[AD-A224282] 24 p3547 N90-30065
Lectures in plasma diagnostics
[DE90-015825] 24 p3550 N90-30086

STARLAB
A space qualified thermal imaging system using a Pt Si detector array 10 p1367 N90-17921

STARLIFTER AIRCRAFT
U C-141 AIRCRAFT

STARS
NT A STARS
NT ASYMPTOTIC GIANT BRANCH STARS
NT B STARS
NT BINARY STARS
NT BLACK HOLES (ASTRONOMY)
NT BLUE STARS
NT BROWN DWARF STARS
NT CARBON STARS
NT CATACLYSMIC VARIABLES
NT CEPHEID VARIABLES
NT COOL STARS
NT DOUBLE STARS
NT DWARF NOVAE
NT DWARF STARS
NT EARLY STARS
NT ECLIPSING BINARY STARS
NT F STARS
NT FLARE STARS
NT G STARS
NT GIANT STARS
NT HERCULES NOVA
NT HORIZONTAL BRANCH STARS
NT HOT STARS
NT INFRARED STARS
NT K STARS
NT LATE STARS
NT M STARS
NT MAGNETIC STARS
NT MAIN SEQUENCE STARS
NT METALLIC STARS
NT MIRA VARIABLES
NT NEUTRON STARS
NT NOVAE
NT O STARS
NT PRE-MAIN SEQUENCE STARS
NT PROTOSTARS
NT PULSARS
NT RADIO STARS
NT RED GIANT STARS
NT REFERENCE STARS
NT SUBDWARF STARS
NT SUN
NT SUPERGIANT STARS
NT SUPERNOVA 1987A

NT SUPERNOVAE
NT SYMBIOTIC STARS
NT T TAURI STARS
NT TRIPLE STARS
NT VARIABLE STARS
NT WHITE DWARF STARS
NT WOLF-RAYET STARS
NT X RAY BINARIES
NT X RAY STARS
From scientific proposals to the Inca data base
05 p0606 N90-13530
The Inca data base 05 p0607 N90-13531
The compilation of astrometric data
05 p0607 N90-13537
Study of modern instrumentation and methods for astronomic positioning in the field
[AD-A213217] 05 p0710 N90-14157
Infrared Spectroscopy in Astronomy
[ESA-SP-290] 11 p1578 N90-19084
Signature objects: Preliminaries for the satellite project HIPPARCOS/TYCHO
[ETN-90-95730] 12 p1729 N90-19934
Preliminary results on two-dimensional interferometry of HL Tau 14 p1979 N90-21335
The Al-26(rho, gamma)Si-27 reaction: Stellar origins of galactic Al-26 15 p2188 N90-22498
Institute of Astronomy 17 p2481 N90-24190
Large scale structure and microwave background anisotropies in cosmological models and stellar photometry techniques with the wide field/planetary camera of the Hubble space telescope
18 p2637 N90-25023
Research and facilities handbook 1989
[ISSN-0267-6281] 19 p2784 N90-25840
Astronomy at ultra-high energies: Results from the CYGNUS experiment
[DE90-011979] 20 p2940 N90-26732
Carbon chemistry in dense molecular clouds: Theory and observational constraints 21 p3090 N90-27571
On planetary nebulae as sources of carbon dust: Infrared emission from planetary nebulae of the galactic halo
21 p3093 N90-27583
Formation of hydrogen line and continuum emission in young stellar objects 24 p3562 N90-30150

STARSPOTS
NT SUNSPOTS

STARTERS
The dc arc weld starter
[DE90-014679] 24 p3475 N90-29641

STARTING
NT AIR START
Studies on the startup transients and performance of a gas loaded sodium heat pipe
[AD-A211880] 03 p0414 N90-12379
Calculation and optimization of rotor start process
[ETN-90-95894] 12 p1604 N90-19229

STATE EQUATIONS
U EQUATIONS OF STATE

STATE ESTIMATION
An analytic development of orbit determination for a distant, planetary orbiter 04 p0485 N90-12787
Viscoplasticity: A thermodynamic formulation
[NASA-TM-102388] 06 p0797 N90-14640
Parameter estimation of linear systems in the presence of process noise using the maximum liklihood method
[ESDU-89032] 07 p0985 N90-15693
System identification and filtering of nonlinear controlled Markov processes by canonical variate analysis
[AD-A214873] 09 p1273 N90-17381
Autonomous orbit determination using GPS
[INPE-4815-TDL/361] 11 p1466 N90-18442
Adaptive state estimation and sampling rate analysis for invariant linear dynamic systems in time
[INPE-4960-TDL/389] 11 p1554 N90-18951
Physical models of cometary nuclei: A review
12 p1738 N90-19991
Flight path reconstruction using extended Kalman filtering techniques
[PD-FC-9001] 14 p1915 N90-20970
Experimental and theoretical investigation of optimal control methods with model reduction
14 p1928 N90-21039
Direct inversion of rigid-body rotational dynamics
[NASA-TM-102798] 15 p2055 N90-21773
Robust modelling of sampled systems for time delay estimation
[REPT-89-047] 16 p2298 N90-23092
Estimating short-period dynamics using an extended Kalman filter
[NASA-TM-101722] 17 p2352 N90-23392
Simulation and interdisciplinary design methodology for control-structure interaction systems
17 p2385 N90-23584
MINAS: An algorithm for systematic state assignment of sequential machines: Computational aspects and results
[EUT-89-E-217] 20 p2912 N90-26566
H-infinity control: An exploratory study
[EUT-88-E-211] 20 p2915 N90-26584
Robust eigensystem assignment for second-order estimators
[NASA-TM-102696] 22 p3191 N90-28103
State estimation for systems moving through random fields 24 p3429 N90-29373

STATE VECTORS
On the reciprocity of state vectors in boundary value models
[AD-A214104] 08 p1115 N90-16458
Investigation of the observability of a satellite cluster in a near circular orbit
[AD-A216224] 10 p1326 N90-17662
GPS navigational performance in space rendezvous operations 18 p2504 N90-24310
Optimal control law phenomena in certain adaptive second-order observation systems
[AD-A224274] 24 p3534 N90-29986

STATIC AERODYNAMIC CHARACTERISTICS
Prediction of the aerodynamic stability of missiles
01 p0012 N90-10052
Prediction of tactical missile dynamics
01 p0012 N90-10056

STATIC CHARACTERISTICS
NT STATIC AERODYNAMIC CHARACTERISTICS
The effects of foreplanes on the static and dynamic characteristics of a combat aircraft model
23 p3273 N90-28520
Static and dynamic characterization of the ATR 72 rods made of Ti 10.2.3 titanium alloy
[REPT-49-238] 23 p3310 N90-28722

STATIC DEFORMATION
Significance of norms and completeness in variational based methods 16 p2296 N90-23078

STATIC ELECTRICITY
Cable coupling lightning transient qualification
[NASA-CR-183826] 05 p0584 N90-13405
The 1989 National Convention Record IEE Japan, part 7
[DE89-910080] 09 p1210 N90-17012
A new vision to model the parallel resonant converter
10 p1336 N90-17727
Passivating layer for III-V semiconductor materials
[AD-D014321] 12 p1719 N90-19872
Nonlocal free energy density functional approximations for the electrical double layer; comparison with Monte Carlo results for 2:1 salt
[AD-A220911] 18 p2521 N90-24395

STATIC LOADS
Design of a custom load cell for a precision assembly application
[DE90-004439] 07 p0923 N90-15340
Perturbation solutions in D* for buckling, vibration, and static loading of specially orthotropic plates
13 p1814 N90-20419
Fracture toughness and crack growth of Zerodur
[NASA-TM-4185] 14 p1954 N90-21187
Development of ultrasonic nondestructive methods for defect and damage characterization in composite materials 15 p2063 N90-21816
Investigation of the effect of mechanical stress on cold fusion
[AD-A220123] 17 p2474 N90-24147
Analysis of shell-type structures subjected to time-dependent mechanical and thermal loading
[NASA-CR-185077] 18 p2571 N90-24653
Agusta methodology for pitch link loads prediction in preliminary design phase
[ETN-90-97270] 20 p2808 N90-25978
Evaluation of fracture strength properties of silicon carbide ceramics under cyclic/static axial loading at ultra-high temperature
[DE90-503402] 20 p2839 N90-26147
Scaling effects in the static and dynamic response of graphite-epoxy beam-columns
[NASA-TM-102697] 20 p2876 N90-26363

STATIC MODELS
Experimental flow models for SSME flowfield characterization 11 p1471 N90-18469
The contour model architecture and assembly language
[AD-A217114] 13 p1865 N90-20697
Dynamic constraints networks
[AD-A219778] 17 p2457 N90-24018
Evaluation of magnetospheric internal magnetic field models and existing software
[AD-A221816] 21 p3027 N90-27210
Investigation of the techniques for the analysis of composite structures: Analysis and representation of the static and dynamic behavior of glued metal insert assemblies
[IMFL-89-44] 22 p3153 N90-27878

STATIC PRESSURE
NT HYDROSTATIC PRESSURE
The measurement of boundary layers on a compressor blade in cascade. Volume 2: Data tables
[NASA-CR-185118-VOL-2] 01 p0009 N90-10039
Static pressure distribution in an angular channel with helicoidal wire
[DE89-636474] 07 p0928 N90-15374
Pressure losses in flow through a sudden contraction of duct area
[ESDU-89040] 09 p1220 N90-17077
Turbulence structure of mixing swirling flows
[AD-A216628] 11 p1506 N90-18671
Study of the turbulent boundary layer on an afterbody
[TM-EA-8901] 12 p1601 N90-19212
The interaction of a supersonic streamwise vortex and a normal shock wave 18 p2491 N90-24241
Evaluation of water cooled supersonic temperature and pressure probes for application to 2000 F flows
[NASA-TM-102612] 19 p2753 N90-25645
Sideslip-induced static pressure errors in flight-test measurements
[NASA-TM-102846] 22 p3116 N90-27702

STATIC STABILITY
NT DIMENSIONAL STABILITY
NT SHELL STABILITY
NT STRUCTURAL STABILITY
Airworthiness and flight characteristics test of the UH-60A Black Hawk helicopter equipped with the XM-139 multiple mine dispensing system (VOLCANO)
[AD-A210271] 01 p0006 N90-10025
Combustor influence on fighter engine operability
01 p0035 N90-10193
Aerodynamic test and analysis of a slender generic missile configuration
[AD-A212522] 04 p0448 N90-12567
Material instabilities in solids
[AD-A218451] 16 p2247 N90-22817
DRAG-n-FLY: A proposal in response to a low Reynolds number station keeping mission
[NASA-CR-186666] 19 p2658 N90-25130
Low-speed wind tunnel investigation of the static stability and control characteristics of an advanced turboprop configuration with the propellers placed over the tail
[NASA-CR-186900] 20 p2814 N90-26017
Soil stabilization mat for lunar launch/landing site
[NASA-CR-186690] 20 p2836 N90-26128

STATIC TESTS
Static aeroelastic analysis for generic configuration aircraft
[NASA-TM-89423] 01 p0009 N90-10042
Delamination tests under static compression loading
02 p0186 N90-11061
Static tensile and tensile creep testing of four boron nitride coated ceramic fibers at elevated temperatures
[NASA-CR-184999] 03 p0318 N90-11807
Large-scale Advanced Prop-fan (LAP) static rotor test report
[NASA-CR-180848] 04 p0457 N90-12617
Static and free-vibrational response of semi-circular graphite-epoxy frames with thin-walled open sections
[NASA-CR-186097] 05 p0617 N90-13600
Space shuttle Production Verification Motor 1 (PV-1) static fire
[NASA-CR-183784] 08 p1037 N90-15991
Results of aircraft open-loop tests of an experimental magnetic leader cable system for guidance during roll-out and turnoff
[NASA-TM-4135] 09 p1169 N90-16767
Static investigation of a two-dimensional convergent-divergent exhaust nozzle with multiaxis thrust-vectoring capability
[NASA-TP-2973] 12 p1597 N90-19193
Static strength and damage tolerance tests on the Fokker 100 airframe
[NLR-MP-88023-U] 12 p1604 N90-19228
Floor pull test of a transport airframe section
[DOT/FAA/CT-TN88/14] 13 p1754 N90-20072
Thiokol/Wasatch installation evaluation of the redesigned field joint protection system (concepts 1 and 3)
[NASA-CR-183860] 13 p1765 N90-20127
Technical Evaluation Motor no. 5 (TEM-5)
[NASA-CR-183932] 14 p1942 N90-21117
QM-8 final performance evaluation report: SEALS, volume 4
[NASA-CR-183958] 20 p2869 N90-26324
Scaling effects in the static and dynamic response of graphite-epoxy beam-columns
[NASA-TM-102697] 20 p2876 N90-26363

QM-6 final performance evaluation report igniter, volume 6
[NASA-CR-184001] 22 p3133 N90-27779
Nonlinear modeling of joint dominated structures
[NASA-CR-4324] 24 p3439 N90-29423
Evaluation of static and fatigue properties of thin sheets of 8090-T8 aluminum-lithium alloy and observation of its fracture surfaces
[NAL-TR-1039] 24 p3453 N90-29499

STATICS
NT ELECTROSTATICS
NT HYDROSTATICS
ASR-9 weather channel test report
[AD-A211749] 03 p0339 N90-11934

STATIONKEEPING
Pulsed plasma mission endurance test
[AD-A213462] 08 p1037 N90-15993
Orbit control strategy for a constellation of three satellites in tundra orbits
[AAS-89-411] 17 p2361 N90-23445
Project Dawdler: A proposal in response to a low Reynolds number station keeping mission
[NASA-CR-186668] 19 p2658 N90-25128
The Penguin: A low Reynolds number powered glider for station keeping missions
[NASA-CR-186667] 19 p2658 N90-25129
DRAG-n-FLY: A proposal in response to a low Reynolds number station keeping mission
[NASA-CR-186666] 19 p2658 N90-25130
The FX/90: A proposal in response to a low Reynolds Number station keeping mission
[NASA-CR-186665] 19 p2659 N90-25131
Development of a computer model to predict platform station keeping requirements in the Gulf of Mexico using remote sensing data
[NASA-CR-186678] 19 p2663 N90-25155
T4A thruster starting sequences and the design of an electromagnetic sequencer for cyclic life tests
[RAE-TR-77042] 19 p2669 N90-25179
The Screem-J4D: A proposal in response to a low Reynolds number station keeping mission
[NASA-CR-186664] 20 p2807 N90-25968

STATIONS
NT AUTOMATIC WEATHER STATIONS
NT COLUMBUS SPACE STATION
NT CREW WORKSTATIONS
NT EARTH TERMINALS
NT GLOBAL TRACKING NETWORK
NT GROUND STATIONS
NT INTEGRATED MISSION CONTROL CENTER
NT MAN TENDED FREE FLYERS
NT MIR SPACE STATION
NT ORBITING LUNAR STATIONS
NT PAYLOAD STATIONS
NT POLYSTATION DOPPLER TRACKING SYSTEM
NT SKYLAB 1
NT SPACE DETECTION AND TRACKING SYSTEM
NT SPACE STATION POLAR PLATFORMS
NT SPACE STATIONS
NT TRACKING STATIONS
NT WEATHER STATIONS
NT WORKSTATIONS
Catalog of strong motion stations in Eastern North America
[PB90-251984] 24 p3490 N90-29722

STATISTICAL ANALYSIS
NT AMPLITUDE DISTRIBUTION ANALYSIS
NT ANALYSIS OF VARIANCE
NT BIVARIATE ANALYSIS
NT CORRELATION COEFFICIENTS
NT COVARIANCE
NT DISCRIMINANT ANALYSIS (STATISTICS)
NT FACTOR ANALYSIS
NT GOODNESS OF FIT
NT LIKELIHOOD RATIO
NT MAXWELL-BOLTZMANN DENSITY FUNCTION
NT MULTIVARIATE STATISTICAL ANALYSIS
NT NONPARAMETRIC STATISTICS
NT NORMAL DENSITY FUNCTIONS
NT ORTHOGONALITY
NT POISSON DENSITY FUNCTIONS
NT PROBABILITY DENSITY FUNCTIONS
NT PROBABILITY DISTRIBUTION FUNCTIONS
NT QUANTILES
NT RANK TESTS
NT RAYLEIGH DISTRIBUTION
NT REGRESSION ANALYSIS
NT REGRESSION COEFFICIENTS
NT SEQUENTIAL ANALYSIS
NT STANDARD DEVIATION
NT STATISTICAL CORRELATION
NT STATISTICAL DECISION THEORY
NT STATISTICAL TESTS
NT VARIANCE (STATISTICS)
NT WEIBULL DENSITY FUNCTIONS
Statistical modeling of electrical components
[BDX-613-3939] 01 p0059 N90-10336
The computation and use of the asymptotic covariance matrix for measurement error models
[PB89-215321] 01 p0115 N90-10659
On lower confidence for PCS in truncated location parameter models
[AD-A210274] 01 p0115 N90-10661
Computational and statistical issues in discrete-event simulation
[AD-A210743] 01 p0116 N90-10668
Analytical study of mistuning/friction/aerodynamics interaction in a bladed disk assembly
[AD-A211139] 02 p0156 N90-10893
Development of an approximate technique for the nonlinear random vibrations analysis of hysteretic systems 02 p0233 N90-11335
Joint VHF coherent radar and oblique sounder observations for short term ionosphere forecasting 02 p0247 N90-11399
Spatial and temporal short range total cloud cover estimation by metric analysis of composite imagery 02 p0251 N90-11423
Direct statistical thermal wind estimation procedure
[AD-A211256] 02 p0253 N90-11433
Procedures for separations within batches of values, 1. The orderly tool kit and some heuristics
[AD-A210652] 02 p0268 N90-11531
Boundary kernel estimation of the two sample comparison density function
[AD-A210757] 02 p0268 N90-11532
Infrared backscattering 03 p0364 N90-12083
A statistical intercomparison of temperature and precipitation predicted by four general circulation models with historical data
[DE89-017785] 03 p0369 N90-12108
Statistical models for the optimal estimation of oceanic fields
[AD-A211786] 03 p0377 N90-12149
Visual acuity and stereopsis with night vision goggles
[AD-A211552] 03 p0381 N90-12167
Federal funds for research and development: Fiscal years 1986, 1987, and 1988. Volume 36: Detailed statistical tables
[PB89-223523] 03 p0419 N90-12407
Federal funds for research and development. Fiscal years 1987, 1988, and 1989. Volume 37: Detailed statistical tables
[PB89-223531] 03 p0419 N90-12408
On the analysis of line profile variations: A statistical approach 03 p0420 N90-12412
Performance of the split-symbol moments SNR estimator in the presence of inter-symbol interference 04 p0487 N90-12799
Vibration transmission through rolling element bearings in geared rotor system, part 1
[NASA-CR-186093] 04 p0509 N90-12936
A real-time wind model using digital data from aircraft
[RSRE-MEMO-4309] 04 p0521 N90-13005
Catalog of absolutely calibrated, range normalized, wideband, electric field waveforms from located lightning flashes in Florida: July 24 and August 14, 1985 data
[AD-A212708] 04 p0521 N90-13008
Atlas of tropical sea surface temperature and surface winds
[PB89-223598] 04 p0521 N90-13009
Parallel and deterministic algorithms from MRF (Markov Random Fields): Surface reconstruction and integration
[AD-A212457] 04 p0533 N90-13084
Berry-Esseen rates and bootstrap results for generalized L-statistics
[CWI-MS-R8808] 04 p0546 N90-13179
A statistical analysis of spatial point patterns, a case study
[CWI-MS-R8813] 04 p0547 N90-13180
Stochastic process models in device physics
[AD-A212284] 04 p0547 N90-13185
The shape of the probability density function of short-term concentration fluctuations of plumes in the atmospheric boundary layer
[AD-A212632] 04 p0548 N90-13188
Semiconductor measurement technology: Database for and statistical analysis of the interlaboratory determination of the conversion coefficient for the measurement of the interstitial oxygen content of silicon by infrared absorption
[PB89-221170] 04 p0558 N90-13253
Study of the engine bird ingestion experience of the Boeing 737 aircraft
[DOT/FAA/CT-89/16] 05 p0576 N90-13360
An introduction via vorticity dynamics and statistical theory --- turbulent shear flows 05 p0640 N90-13731
Expected supernovae rates and gravitational waves detection
[NOTA-INTERNA-933] 05 p0713 N90-14166
Des Cloizeaux's law for strings and galaxies formation. Part 1: Abelian configurations
[ROM1F-89-681-PT-1] 05 p0714 N90-14172
Modelling UHF propagation for frequency assignment in radio relay networks 06 p0764 N90-14445
Statistics of two-color laser beam propagation in the turbulent atmosphere (spectral correlation)
[PB89-236699] 06 p0787 N90-14581
An initial look at the dynamics of the microscale flow field within a large wind farm in response to variations in the natural inflow
[DE89-009501] 06 p0804 N90-14682
Frequency distributions of heavy rainstorms in Illinois
[PB90-100215] 06 p0816 N90-14748
Measurements of horizontal visibility in the lowest 300 m over Northern Germany 07 p0872 N90-15059
The radar-based short term prediction of the time-space evolution of rain fields
[AD-A213802] 07 p0918 N90-15312
Statistical model for particle-void deformation kinetics in granular materials during shock wave propagation
[DE89-017729] 07 p0946 N90-15476
Observational study of the macroscopic behavior of moist-convective processes 07 p0959 N90-15547
Flux parameterization techniques in the atmospheric surface layer 07 p0959 N90-15548
Developmental versions of FORTRAN/77 routines for the design and analysis of mixture experiments
[DE90-003513] 07 p0974 N90-15624
Two basic partial orderings for distributions derived from Schur functions and majorization
[AD-A213703] 07 p0984 N90-15682
Likelihood ratio derivative estimators for stochastic systems
[AD-A213787] 07 p0984 N90-15684
Use of remote sensing data for land and building statistics 08 p1094 N90-16335
Statistical information system for cultivation of the soil. Use of remote sensing in official statistics 08 p1095 N90-16338
Risk assessment and its application to flight safety analysis
[DE90-004985] 09 p1161 N90-16722
CRC (Coordinating Research Council) octane number requirement survey 1988
[AD-A214845] 09 p1200 N90-16954
Information capacity of dimension-limited channels
[AD-A215238] 09 p1207 N90-16996
On some problems in reliability theory 09 p1233 N90-17155
Eddy current test for bolts
[AD-A214829] 09 p1234 N90-17159
Statistical theory of reliability
[AD-A215320] 09 p1234 N90-17161
A statistical study of the surface accuracy of a planar truss beam
[NASA-TM-4161] 09 p1235 N90-17171
A statistical model of the infrared signature of a wind roughened sea
[AD-A214531] 09 p1249 N90-17245
A Doppler centroid estimation algorithm for SAR systems optimized for the quasi-homogeneous source
[NASA-CR-186229] 09 p1275 N90-17391
Studies in statistical signal processing
[AD-A214490] 09 p1275 N90-17393
Three position estimation procedures
[AD-A214992] 09 p1276 N90-17395
Infrared target detection: Signal and noise sensitivity analysis
[AD-A215707] 09 p1282 N90-17436
Variational problems in astrophysics 09 p1298 N90-17524
Study of continuum higher order closure models evaluated by a statistical theory of shock structure 10 p1303 N90-17538
Aircraft fires: A study of transport accidents from 1975 to the present 10 p1311 N90-17583
Objectives and results of cabin fire research in Germany 10 p1312 N90-17588
Adaptive processor emulation development
[AD-A214392] 10 p1371 N90-17944
Rain core structure statistics derived from radar and disdrometer measurements in the mid-Atlantic coast of the US 10 p1373 N90-17956
Radiometric observations at 20.6, 31.65, and 90.0 GHz: Continuing studies 10 p1373 N90-17958
Eutrophication assessment through remote sensing techniques
[INPE-4932-PRE/1422] 10 p1398 N90-18083
Evaluation of digital classification results of summer cultivation in a test area in the Parana-Ano state harvest 1986-1987
[INPE-4828-PRE/1459] 10 p1399 N90-18085
Surface observation climatic summaries
[AD-A215786] 10 p1408 N90-18122

Estimation in a discrete tail rate family of recapture sampling models
[NASA-CR-180452] 10 p1421 N90-18197
Proceedings of a research workshop on Nonlinear Time Series Analysis and Applications
[AD-A216541] 10 p1423 N90-18214
A study of the evolution of solar active regions for improving solar flare forecasts
[AD-A216325] 10 p1448 N90-18356
Multistage forest volume estimation using a sampling system with probability variables
[INPE-4897-PRE/1498] 11 p1523 N90-18769
The patterns of fracture and the conditioning tectonics in the region of the Quadrilatero Ferrifero and part of the Migmatitic-Gnanulitic Complex in Minas Gerais (Brazil)
[INPE-4895-PRE/1496] 11 p1534 N90-18829
An integrated vision on methodologies and environments for modeling and simulation assisted by computer
[INPE-4861-TDL/372] 11 p1544 N90-18886
A comparison of void distributions in Abell cluster catalogue with numerical simulations
[DE90-610640] 11 p1590 N90-19173
Kalman estimation for SEDS measurements
12 p1634 N90-19393
Photon statistical limitations for daytime optical tracking 12 p1643 N90-19442
The NASA digital VGH program. Exploration of methods and final results. Volume 3: B 727 data 1978-1980: 1765 hours
[NASA-CR-181909-VOL-3] 13 p1756 N90-20082
The NASA digital VGH program: Exploration of methods and final results. Volume 4: B 747 data 1978-1980, 1689 hours
[NASA-CR-181909-VOL-4] 13 p1756 N90-20083
The NASA digital VGH program: Exploration of methods and final results. Volume 5: DC 10 data 1981-1982, 129 hours
[NASA-CR-181909-VOL-5] 13 p1756 N90-20084
Statistical equipment modeling for VLSI manufacturing
[DE90-008527] 13 p1795 N90-20304
Optimization of digital filters for a short-scan interferometer
[AD-A217997] 13 p1798 N90-20315
Methods for local gravity field approximation
13 p1834 N90-20532
VAPEPS user's reference manual, version 5.0
[NASA-CR-180781] 13 p1868 N90-20713
Local moduli of continuity of some classes of Gaussian processes
[AD-A217692] 13 p1879 N90-20778
Slepian models and regression approximations in crossing and extreme value theory
[AD-A218338] 13 p1879 N90-20779
Fundamental studies of photon statistics
[AD-A217825] 13 p1888 N90-20836
Ridge regression processing
14 p1907 N90-20931
Annual review of aircraft accident data: US general aviation calendar year 1987
[PB90-138066] 14 p1913 N90-20966
Statistics on aircraft gas turbine engine rotor failures that occurred in US commercial aviation during 1986
[DOT/FAA/CT-89/30] 14 p1922 N90-21008
Quality at a glance
[AD-A217297] 14 p1989 N90-21400
Review and statistical analysis of the ultrasonic velocity method for estimating the porosity fraction in polycrystalline materials
[NASA-TM-102501-REV] 14 p1989 N90-21402
Project CANASATE: Remote sensing applied to sugar cane crop survey
[INPE-4902-PRE/1503] 14 p1997 N90-21446
Performance evaluation of MSS/LANDSAT data in the estimation of fluvial channel width
[INPE-4906-PRE/1507] 14 p2000 N90-21463
An outline for the analysis of wave induced bottom pressure fluctuations
[MRL-TN-558] 14 p2008 N90-21510
SIGNIF: A C function to compute significant digits
[DE90-009242] 14 p2015 N90-21550
STORM: A statistical object representation model
[DE90-009048] 14 p2036 N90-21686
Molecular theory of fluid phase equilibria
[PB90-131277] 15 p2066 N90-21832
A real-time signal combining system for Ka-band feed arrays using maximum-likelihood weight estimates
15 p2076 N90-21888
Exact closed-form expressions for the performance of the split-symbol moments estimator of signal-to-noise ratio 15 p2077 N90-21894
Millimetric, infrared, and optical propagation studies over a 500 m path 15 p2080 N90-21913
Adaptive frequency estimation by MUSIC (Multiple Signal Classification) method
[PB90-166794] 15 p2086 N90-21943
Inverse problems of heat conduction
15 p2091 N90-21969
Orthogonal distance regression
[PB90-151747] 15 p2160 N90-22336
An investigation of the generation and radiation of aerodynamic noise in real piping systems
15 p2164 N90-22368
The MHD structure of an open magnetotail boundary
15 p2168 N90-22388
Managing Federal information resources
[PB90-100173] 15 p2175 N90-22429
A study of mesoscale acid deposition in the lower Ohio River Valley 16 p2253 N90-22848
Graphics equipment for data analysis
[AD-A218983] 16 p2278 N90-22985
Two barriers problem for continuously differentiable processes
[AD-A218564] 16 p2312 N90-23176
Looking at large data sets using binned data plots
[DE90-008206] 16 p2326 N90-23263
The diffuse galactic gamma ray emission
16 p2333 N90-23296
Research on statistical techniques for signal processing
[AD-A218811] 17 p2388 N90-23599
Second moment models of turbulence: Complex or stratified flow
[ECL-90-02] 17 p2405 N90-23703
The chemical and structural properties of sea ice in the southern Beaufort Sea
[AD-A219746] 17 p2418 N90-23776
Cloud volume statistics for southern Sweden
[CM-77] 17 p2427 N90-23830
A comparison of lightning network data with surface weather observations
[AD-A220003] 17 p2427 N90-23832
The application of kriging in the statistical analysis of anthropometric data, volume 1
[AD-A220613] 17 p2438 N90-23891
The application of kriging in the statistical analysis of anthropometric data, volume 2
[AD-A220614] 17 p2438 N90-23892
Adaptive control of a system with periodic dynamics: Application of an impulse response method to the helicopter vibration problem 17 p2453 N90-23990
Computational tools for multi-linked flexible structures
[NASA-CR-186139] 17 p2462 N90-24058
Bayesian learning
[NASA-CR-181528] 17 p2465 N90-24082
Formula scoring: Basic theory and applications
[AD-A218368] 17 p2465 N90-24083
The Trickett-Welch Solution to the Behrens-Fisher problem applied to one-sided tolerance limits for random effects model
[AD-A220416] 17 p2465 N90-24086
On a class of N-dimensional associated random walks and the hitting point identity
[CWI-BS-R8911] 17 p2466 N90-24090
Experiments and other methods for developing expertise with design of experiments in a classroom setting
18 p2516 N90-24367
More about general saddlepoint approximations
[AD-A221217] 18 p2604 N90-24832
G exchangeability and the construction of distribution-free statistics 18 p2605 N90-24837
On the statistical analysis of growth
[ETN-90-96923] 18 p2606 N90-24841
Bayesian characterization and detection of rare binary signature events
[AD-A221116] 18 p2606 N90-24844
A white noise theory of infinite dimensional calculus
[AD-A221253] 18 p2607 N90-24850
The effect of random variations of radiosonde data on the predicted FLIR performance calculated by the program UFLR
[AD-A220034] 18 p2615 N90-24896
A Bayesian approach to reliability and confidence
18 p2628 N90-24974
Evaluating Statistical Process Control (SPC) techniques and computing the uncertainty of force calibrations
18 p2631 N90-24992
Multiwavelength constraints on gamma-ray burst sources 18 p2639 N90-25032
Cloud field classification based on textural features
18 p2646 N90-25066
Study of the engine bird ingestion experience of the Boeing 737 aircraft (October 1986 to September 1988)
[DOT/FAA/CT-89/29] 19 p2656 N90-25119
Anthropogenic sources of NO(x), SO()x, CO, and CH4: Geographical distribution
[AERONOMICA-ACTA-A-353-1990]
19 p2713 N90-25440
An atlas of ECMWF analyses (1980-1987). Part 2: Second moment quantities
[NASA-TM-100762-PT-2] 19 p2715 N90-25451
Data analysis in cervical trauma
19 p2718 N90-25464
Modeling and synthesis of multicomputer interconnection networks
[NASA-CR-186619] 19 p2746 N90-25604
Handbook of uncertainty methodology for engine testing at Pyestock (England)
[RAE-TM-P-1179] 20 p2812 N90-26007
Viking data analysis
[AD-A222609] 20 p2823 N90-26062
Statistical treatment of slow strain rate data for assessment of hydrogen embrittlement in low alloy high strength steel
[ARL-MAT-R-122] 20 p2832 N90-26106
Broadband analysis of ground wave propagation at a50 to 400 MHz 20 p2846 N90-26185
Application of inertial instruments for DSN antenna pointing and tracking 20 p2853 N90-26224
Statistical analysis of a software reliability model
[IMAG-RR-781-M] 20 p2874 N90-26352
A Bayesian proportional model for software reliability
[IMAG-RR-795-M] 20 p2874 N90-26353
Analysis and improved design considerations for airborne pulse Doppler radar signal processing in the detection of hazardous windshear
[NASA-CR-186792] 20 p2890 N90-26448
Computer architecture evaluation for structural dynamics computations: Project summary
[NASA-CR-186137] 20 p2903 N90-26512
Estimating the parameters of a sporadically observed queue
[DE90-012903] 20 p2917 N90-26596
Power flow analysis of two coupled plates with arbitrary characteristics
[NASA-CR-182033] 20 p2923 N90-26632
Asymptotic modal analysis and statistical energy analysis
[NASA-CR-186732] 20 p2923 N90-26634
Multistage estimation of received carrier signal parameters under very high dynamic conditions of the receiver
[NASA-CASE-NPO-17911-1-CU]
21 p2994 N90-27016
Robustness, diagnostics, computing, and graphics in statistics
[AD-A222888] 21 p3052 N90-27349
Active control of aerothermoelastic effects for a conceptual hypersonic aircraft
[NASA-TM-102713] 22 p3122 N90-27725
Progress and challenges in modeling turbulent aerodynamic flows
[NASA-TM-102811] 22 p3170 N90-27981
Analysis of marine stratocumulus clearing events during FIRE 22 p3220 N90-28260
Federal Scientists and Engineers: 1988. (Detailed statistical tables)
[PB90-226895] 22 p3256 N90-28437
Line identification studies using traditional techniques and wavelength coincidence statistics
[NASA-CR-186901] 22 p3261 N90-28467
Quasar pairs and quasar's peculiar velocity
[FERMILAB-PUB-90/25-A] 22 p3262 N90-28474
Development of acceptance plans for airport pavement materials. Volume 1: Development
[DOT/FAA/RD-90/15] 23 p3284 N90-28581
Phoenix data analysis and numerical simulation
[AD-A224226] 23 p3320 N90-28772
Methods for multisource data analysis in remote sensing
[NASA-CR-187005] 23 p3343 N90-28890
A conceptual weather-type classification procedure for the Philadelphia, Pennsylvania area
[PB90-231705] 23 p3352 N90-28944
Autoregressive-moving average models for texture classification
[INPE-4987-PRE/1549] 23 p3380 N90-29092
Estimation of individual coupling loss factors in a multi-subsystem
[ISVR-TR-184] 23 p3389 N90-29141
Prediction, control, and decision-making aspects for chaotic systems
[DE90-014452] 23 p3402 N90-29224
Data Base Analyzer and Parameter Estimator (DBAPE) interactive computer program user's manual
[PB90-193053] 23 p3406 N90-29252
UK airmisses involving commercial air transport: May - August 1989
[ISSN-0951-6301] 24 p3422 N90-29335
A single wafer bit-sliced convolver: An optimum statistical solution for the implementation of redundancy
[REPT-89-019] 24 p3466 N90-29584
Counter-current flow limitation in thin rectangular channels
[DE90-015124] 24 p3469 N90-29599
Time series, statistics, and information
[AD-A224317] 24 p3540 N90-30018

Effects and control of the correlation properties of light sources
[AD-A224539] 24 p3545 N90-30049

STATISTICAL COMMUNICATION THEORY
U COMMUNICATION THEORY

STATISTICAL CORRELATION
New statistical approaches to galaxy clustering 02 p0294 N90-11674
Index formulas for generalized Wiener-Hopf operators and Boson-Fermion correspondence in 2N dimensions
[CWI-PM-R8811] 04 p0542 N90-13141
Statistics of a reflected laser beam in the turbulent atmosphere (path correlation)
[PB90-113994] 08 p1082 N90-16261
Additive evaluation criteria for aircraft noise 18 p2610 N90-24867
Influence of solar activity on middle atmosphere associated with phases of equatorial quasi-biennial oscillation 22 p3202 N90-28168
System reliability optimization of aircraft wings 23 p3275 N90-28536

STATISTICAL DECISION THEORY
Classification techniques for quantum-limited and classical-intensity images
[AD-A218693] 16 p2317 N90-23212

STATISTICAL DISTRIBUTIONS
NT BRIGHTNESS DISTRIBUTION
NT PROBABILITY DISTRIBUTION FUNCTIONS
NT RAYLEIGH DISTRIBUTION
Asymptotic robustness in regression and autoregression based on Lindeberg conditions
[AD-A210725] 01 p0114 N90-10654
Selection of the best with a preliminary test for two-parameter exponential distributions
[AD-A210275] 01 p0115 N90-10662
A unified approach to estimating tail behavior
[AD-A210961] 01 p0117 N90-10672
Multi-sample functional statistical data analysis
[AD-A210992] 01 p0117 N90-10673
Frequency distributions and hydroclimatic characteristics of heavy rainstorms in Illinois
[PB89-203988] 02 p0252 N90-11427
Procedures for separations within batches of values, 1. The orderly tool kit and some heuristics
[AD-A210652] 02 p0268 N90-11531
A semiparametric model for citation counts
[CWI-MS-R8814] 04 p0542 N90-13145
A statistical analysis of spatial point patterns, a case study
[CWI-MS-R8813] 04 p0547 N90-13180
Self-decomposable distributions and branching processes
[MEMO-COSOR-89-06] 05 p0693 N90-14052
Note on Urbanik's class L(sub n) --- self-decomposability of functions
[MEMO-COSOR-89-07] 05 p0694 N90-14053
Reverse self-decomposability --- for characteristic functions
[MEMO-COSOR-89-08] 05 p0694 N90-14054
Frequency distributions of heavy rainstorms in Illinois
[PB90-100215] 06 p0816 N90-14748
Precipitation distributions associated with cyclones originating over the Gulf of Mexico and surrounding coastal regions
[AD-A213644] 07 p0963 N90-15569
Recurrence and ergodicity for exponential family state-space models
[AD-A213466] 07 p0983 N90-15677
Thermal and statistical properties of nuclei and nuclear systems
[DE90-000183] 07 p0990 N90-15717
Application of Bayesian reliability concepts to cruise missile electronic components
[AD-A216208] 10 p1394 N90-18059
Maxwellian cascade model
[DE90-004389] 10 p1427 N90-18235
Automated viability and cloud cover measurements with a solid-state imaging system
[AD-A216906] 12 p1693 N90-19724
Geology, distribution of hot springs and hydrothermal alteration zones of major geothermal areas in Japan
[DE90-753026] 13 p1820 N90-20451
On metric entropy, Vapnik-Chervonenkis dimension, and learnability for a class of distributions
[AD-A217331] 13 p1876 N90-20759
Clustering and uniqueness in mathematical models of percolation phenomena
[ETN-90-96400] 15 p2163 N90-22358
Characterizing exponential distributions via conditional independence
[AD-A219255] 16 p2309 N90-23158
Gamma rays from active galactic nuclei 16 p2337 N90-23316
Temporal statistics of low-angle ground clutter
[AD-A220816] 17 p2391 N90-23621
Approximate interval estimation methods for the reliability of systems using component data with exponential and Weibull distributions
[AD-A219857] 17 p2460 N90-24048
Applications of non-parametric density estimation
[AD-A220206] 17 p2466 N90-24094
Associated distributions in the analysis of two-dimensional random walks
[CWI-BS-R8917] 17 p2466 N90-24095
Belief networks in plausible reasoning
[CWI-CS-R8927] 17 p2467 N90-24098
Some observations for the pigeon hole principle
[RUU-CS-88-39] 19 p2750 N90-25624
A trend analysis of women who hold Federal Aviation Administration certificates: Relationship to the representation of women in collegiate aviation faculty ranks
[IAR-90-3] 19 p2762 N90-25691
Constitutive laws for discrete velocity models of gas (continued)
[ETN-90-97451] 22 p3175 N90-28016
Cloud top entrainment instability and cloud top distributions 22 p3214 N90-28231
Autoregressive-moving average models for texture classification
[INPE-4987-PRE/1549] 23 p3380 N90-29092
Techniques for autonomous GPS integrity monitoring 24 p3424 N90-29345
Barotropic mechanisms associated with tropical plume formation 24 p3489 N90-29719
Effects of parameter uncertainties on software development effort estimates
[AD-A223304] 24 p3526 N90-29938
Classical and Bayes-P subset selection procedures for double exponential populations
[AD-A223830] 24 p3538 N90-30006

STATISTICAL MECHANICS
Theory of atomic spectral emission intensity
[IRF-PREPRINT-110] 02 p0287 N90-11641
A graph-theoretical approach to block-copolymer complexes. Part 3: Loops and cycles
[MEMO-778-PT-3] 04 p0479 N90-12750
Statistical mechanics of strings and topology
[ROM1F-89-683] 05 p0696 N90-14068
Where is an object before you look at it
[NOTA-INTERNA-935] 05 p0704 N90-14123
Estimating departure times from traffic counts using dynamic assignment
[DE89-016259] 07 p0979 N90-15653
Outlier detection in multivariate calibration
[DE90-001502] 07 p0982 N90-15672
Brownian trail rectified
[DE90-003339] 07 p0988 N90-15706
Equation of state of partially-ionized dense plasmas
[DE90-005246] 09 p1286 N90-17452
Statistical mechanical models for liquid and amorphous structure in covalently bonded systems
[DE90-607233] 10 p1428 N90-18240
Replica scaling analysis of interfaces in random media
[PREPRINT-713] 16 p2312 N90-23174
Ultrafast laser investigation of a solid-state explosion
[AD-A218530] 17 p2408 N90-23718
Report of research activity at the Research Laboratory of Electronics 17 p2486 N90-24217
Hydrogen in palladium alloys: Experiments, models and simulations
[PB90-200429] 22 p3156 N90-27896
Reduced distribution functions and nonequilibrium thermodynamics of single component fluids
[PB90-189119] 22 p3254 N90-28428
Statement of research objectives and summary of research efforts
[RLE-PR-132] 23 p3415 N90-29295

STATISTICAL MOMENTS
U DISTRIBUTION MOMENTS

STATISTICAL PROBABILITY
U PROBABILITY THEORY

STATISTICAL TESTS
NT RANK TESTS
A unified view of infinitesimal perturbation analysis and likelihood ratios
[AD-A210682] 01 p0114 N90-10652
Number of test samples needed to obtain a desired Bayesian confidence interval for a proportion
[AD-A208157] 01 p0115 N90-10658
Selection of the best with a preliminary test for two-parameter exponential distributions
[AD-A210275] 01 p0115 N90-10662
Multi-sample functional statistical data analysis
[AD-A210992] 01 p0117 N90-10673
Comparison of sine dwell and broadband methods for modal testing 02 p0181 N90-11025
Utilization of the generalized likelihood ratio test for the suppression of systematic errors in noisy systems
[ETN-89-94656] 02 p0214 N90-11225
Two enhancements of the logarithmic least-squares method for analyzing subjective comparisons
[AD-A211192] 02 p0266 N90-11514
An extension of Cochran's test for homogeneity of variances
[AD-A211054] 02 p0269 N90-11534
Computer problems in goodness-of-fit
[AD-A211411] 03 p0397 N90-12268
On the asymptotic optimality of certain empirical Bayes simultaneous testing procedures
[AD-A211649] 03 p0397 N90-12270
Accuracy and characteristics of the Hipparcos catalog 05 p0611 N90-13566
An evaluation of trend detection techniques for use in water quality monitoring programs
[PB89-100058] 06 p0808 N90-14702
More efficient sensitivity testing
[DE90-002639] 07 p0916 N90-15298
Basic research in reliability for real systems
[AD-A214536] 09 p1234 N90-17158
A review of circadian effects on selected human information processing tasks
[AD-A214673] 09 p1251 N90-17256
Statistics of a chi-square random variable obtained from independent Gaussian samples with a non-zero mean and arbitrary variance
[AD-A214477] 09 p1275 N90-17392
Approximate interval estimation methods for the reliability of systems using component data with exponential and Weibull distributions
[AD-A219857] 17 p2460 N90-24048
A hypothesis test of cumulative sums of multinomial parameters
[AD-A221466] 21 p3067 N90-27434
Unification of statistical methods for continuous and discrete data
[AD-A224307] 24 p3540 N90-30017

STATISTICAL WEATHER FORECASTING
Application of the lagged-averaged technique to tropical cyclone track predictions
[AD-A218389] 17 p2425 N90-23819
A study of the effect of synoptic scale processes in GCM modelling
[NASA-CR-184804] 21 p3021 N90-27175

STATISTICS
Interpretation and manipulation of Edgeworth expansions
[MEMO-775] 04 p0544 N90-13163

STATOR BLADES
Application of a copper vapour laser to investigation of shock and blade interaction in a shock tube
[PNR90578] 04 p0506 N90-12918
Off-design loss measurements in a compressor cascade
[AD-A220094] 18 p2552 N90-24564

STATORS
Dynamic analysis of rotors under interference rubs 02 p0229 N90-11312
High gain flux compression generator fabrication issues
[DE89-017888] 03 p0342 N90-11951
Influence of vane sweep on rotor-stator interaction noise 05 p0571 N90-13325
Design of a high-gain flux-compression generator
[DE90-002795] 07 p0922 N90-15333
Aerodynamic study on forced vibrations on stator rows of axial compressors 11 p1460 N90-18412
Blade row interaction effects on compressor measurements 11 p1462 N90-18419
The numerical simulation of multistage turbomachinery flows 14 p1925 N90-21025
The effect of secondary flow on the redistribution of the total temperature field downstream of a stationary turbine cascade 14 p1926 N90-21033
Analytical and experimental study of high phase order induction motors
[NASA-CR-186580] 15 p2088 N90-21952
Rotor-to-stationary element rub-related vibration phenomena in rotating machinery: Literature survey 15 p2109 N90-22065
Decay of secondary flow and the associated loss variation downstream of an annual turbine stator cascade
[DE90-505520] 20 p2809 N90-25984
Prediction and measurement of rotor blade/stator vane dynamic characteristics of a modern aero-engine axial compressor
[PNR90667] 20 p2812 N90-26002
Flow coupling between a rotor and a stator in turbomachinery
[AD-A223882] 23 p3282 N90-28572

STEADY FLOW
NT COUETTE FLOW
NT HARTMANN FLOW

Similarity solutions that give rise to hyperbolicity and change of type in steady flow of a viscoelastic fluid
[AD-A210920] 01 p0072 N90-10410
Steady and unsteady potential flow around thin annular wings and engines with simulation of jet engine flow
[DFVLR-FB-89-18] 03 p0302 N90-11711
Numerical algorithms for steady and unsteady incompressible Navier-Stokes equations
[NASA-CR-186039] 04 p0437 N90-12499
Additions and corrections to SUPER: A program for calculating steady and oscillatory supersonic flow over a thin wing, tail plane and fin
[AD-A211771] 04 p0438 N90-12501
Unsteady three-dimensional thin-layer Navier Stokes solutions on dynamic blocked grids
[AD-A212377] 04 p0503 N90-12899
Generalized similarity solutions for three dimensional, laminar, steady, compressible boundary layer flows on swept profile cylinders
[DLR-FB-89-34] 05 p0639 N90-13725
Computational investigation of incompressible airfoil flows at high angles of attack
[AD-A205885] 06 p0720 N90-14201
Steady flow combustion model for solid-fuel ramjet projectiles
[BRL-TR-2987] 07 p0893 N90-15163
Irreversible processes from reversible mechanics
[DE90-001057] 07 p0927 N90-15368
An improvement of convection fidelity in Euler calculations 09 p1159 N90-16709
Oblique impact of two cylinders in a uniform flow
[AD-A215933] 10 p1385 N90-18015
Carrier wing profile in nonstationary current
[ETN-90-95368] 12 p1600 N90-19208
Unsteady three-dimensional marginal separation, including breakdown
[NASA-TM-102525] 13 p1801 N90-20337
Convergence acceleration of hypersonic flow calculations: A nonlinear relaxation factor 14 p1911 N90-20957
ULTRA-SHARP nonoscillatory convection schemes for high-speed steady multidimensional flow
[NASA-TM-102568] 14 p2019 N90-21570
Prediction of length scales in a Mach reflection flowfield 15 p2089 N90-21959
Numerical study of the onset of instability in the flow past a sphere 17 p2400 N90-23672
A lifting surface method for the calculation of steady and unsteady, incompressible propeller aerodynamics
[ESA-TT-1151] 19 p2655 N90-25113
Velocity distribution in a gravel-bed flume; for steady and unsteady flow 19 p2687 N90-25283
Analysis and mitigation of numerical dissipation in inviscid and viscid computation of vortex-dominated flows
[NASA-CR-186887] 20 p2862 N90-26281
Adaptation for unsteady flow 21 p2963 N90-26845
Efficient solution of the steady Euler equations with a centered implicit method 22 p3173 N90-27999
Prediction of subsonic vortex shedding from forebodies with chines
[NASA-CR-4323] 23 p3268 N90-28494
Regular and chaotic motion of uniform elliptical vortices in external linear time dependent velocity fields 23 p3268 N90-28497
Solution of Euler equations applied to a rotor of a helicopter in steady flight
[ONERA-RSF-1/3731-AY-002A] 23 p3269 N90-28500

STEADY STATE
Capillary effects in steady-state flow in heterogeneous cores
[DE89-000758] 01 p0070 N90-10399
Stability of discontinuous shearing motions of a non-Newtonian fluid
[AD-A210643] 01 p0071 N90-10406
Stability of discontinuous steady states in shearing motion of a non-Newtonian fluid
[AD-A210644] 01 p0071 N90-10407
Computational and statistical issues in discrete-event simulation
[AD-A210743] 01 p0116 N90-10668
Deep traps and sidegating in GaAs devices
[AD-A210740] 01 p0133 N90-10765
Stochastic optimization by simulation: Some experiments with a simple steady-state queue
[AD-A210762] 02 p0265 N90-11508
Dynamics of baroclinic wave systems 03 p0362 N90-12072
Small sample theory for steady state confidence intervals
[AD-A212097] 03 p0393 N90-12242
Elements of a relativistic microscopic theory of hadronic matter in equilibrium and non-equilibrium
[KVI-796] 04 p0552 N90-13218
Euler and Navier-Stokes computations for two-dimensional geometries using unstructured meshes
[NASA-CR-181977] 08 p1019 N90-15893
A computational and experimental study of steady and transient acoustic energy flow from a complex mechanical structure 08 p1119 N90-16478
PWM converter topologies 10 p1335 N90-17721
Finite element modeling and thermal simulations of transistor integrated circuits
[AD-A215928] 10 p1380 N90-17997
Steady-state and transient Zener parameters in viscoplasticity: Drag strength versus yield strength
[NASA-TM-102487] 10 p1395 N90-18064
Discretization of the steady state semiconductor device equations
[AD-A215807] 10 p1438 N90-18298
Compressor performance tests in the compressor research facility 11 p1463 N90-18428
Investigation of methods to produce a uniform cloud of fuel particles in a flame tube
[NASA-TM-102376] 11 p1505 N90-18665
The microwave background in steady-state cosmology 11 p1587 N90-19150
Steady state temperatures and thermal stresses in a spherical or cylindrical laminated shell
[ESDU-89027] 12 p1674 N90-19612
Plasma centrifuge with vacuum arc discharge applied to the separation of stable isotopes
[INPE-4925-TDL/385] 12 p1716 N90-19854
On spurious steady-state solutions of explicit Runge-Kutta schemes
[NASA-TM-102819] 15 p2160 N90-22340
Nonlinear internal gravity wave critical layers 17 p2422 N90-23801
Behaviour in the large of numerical solutions to one-dimensional nonlinear viscoelasticity by continuous time Galerkin methods
[AD-A220197] 17 p2461 N90-24057
Predicting switched-bias response from steady-state irradiations
[DE90-006770] 18 p2624 N90-24950
Numerical solutions to steady-state problems with discontinuities
[AD-A222205] 21 p3064 N90-27418
Comparison of altitude test cell results 22 p3119 N90-27715
Calculation of the combustion distribution in a liquid-fuel ramjet 22 p3162 N90-27931
Stratus: An interactive steady state mixed layer model for personal computers 22 p3219 N90-28255
Unsteady aerodynamics of controls 23 p3273 N90-28525
Radiative heat transfer
[PB90-247602] 23 p3327 N90-28813
Planetary-scale flow on a two-layer beta-plane channel model with topography 23 p3350 N90-28931
Multigrid for hypersonic inviscid flows
[NASA-CR-182082] 23 p3387 N90-29125
Scale effects in steady-state friction
[DE90-012943] 24 p3476 N90-29647

STEADY STATE CREEP
Kinetics and mechanisms of primary and steady state creep in B- and Al-containing alpha silicon carbide
[AD-A210739] 02 p0283 N90-11616
Three-dimensional viscoelastic bodies in steady state frictional rolling contact with generalization to Knothe rolling
[REPT-89-23] 03 p0355 N90-12032

STEADY STATE FLOW
U EQUILIBRIUM FLOW

STEAM
Steam cooled rich-burn combustor liner
[NASA-CASE-LEW-13609-1] 03 p0321 N90-11824
Experimental investigation of condensation of steam in the presence of noncondensable gases for open-cycle surface condensers
[DE90-003552] 08 p1097 N90-16353

STEAM FLOW
Experimental investigation of condensation of steam in the presence of noncondensable gases for open-cycle surface condensers
[DE90-003552] 08 p1097 N90-16353

STEAM GENERATORS
U BOILERS

STEAM TURBINES
Aerodynamic superposition principle in vibrating turbine cascades 11 p1460 N90-18410
Phase-Change Thermal Energy Storage
[DE89-009426] 11 p1529 N90-18801
Innovative turbine concepts for open-cycle OTEC (Ocean Thermal Energy Conversion)
[DE90-000315] 13 p1827 N90-20493
Research and development of advanced gas turbine
[DE90-503377] 20 p2871 N90-26335

STEEL STRUCTURES
Plastic bending tests of cold-formed rectangular hollow sections
[PB90-124611] 12 p1674 N90-19613
Fatigue crack monitoring from initiation to through cracking in welded thick steel sections
[ARE-TM(UHS)-90203] 22 p3194 N90-28122
Multiaxial fatigue criterion for 2-1/4 Cr-1 Mo steel for use in high-temperature structural design
[DE90-016039] 24 p3452 N90-29491

STEELS
NT AUSTENITIC STAINLESS STEELS
NT BAINITIC STEEL
NT CARBON STEELS
NT CHROMIUM STEELS
NT FERRITIC STAINLESS STEELS
NT HIGH STRENGTH STEELS
NT LOW CARBON STEELS
NT MARAGING STEELS
NT MARTENSITIC STAINLESS STEELS
NT NICKEL STEELS
NT STAINLESS STEELS
Properties of HY-100 for naval construction
[MRL-R-1149] 01 p0044 N90-10247
Delayed failure of silver-aided diffusion welds between steel
[DE89-016652] 01 p0045 N90-10252
Investigation of the pyrometallurgical, physical and mechanical behavior of weld metal
[AD-A211114] 01 p0046 N90-10258
Development of a semiquantitative corrosion monitor
[AD-A208132] 01 p0072 N90-10414
Micromechanisms of surface friction in zinc electrogalvanized steel sheets
[DE89-011819] 01 p0077 N90-10440
Thin section casting program. Volume 1: Executive summary and overview
[DE89-009030] 02 p0209 N90-11198
Thin section casting program. Volume 2: Horizontal TSC (Thin-Section Casting) approach
[DE89-009031] 02 p0210 N90-11199
Thin section casting program. Volume 3: Vertical TSC (Thin-Section Casting) approach
[DE89-009033] 02 p0210 N90-11201
Thin section casting program. Volume 4: Static cast product bending, straightening, and rolling
[DE89-009034] 02 p0210 N90-11202
Thin section casting program. Volume 5: Westinghouse MHD Project
[DE89-009035] 02 p0210 N90-11203
Fe-Ni-Cr alloys for coatings and electroforms
[PB89-195846] 03 p0325 N90-11849
Creep and fracture behavior of heat resistant steels in characteristic cases of variable fatigue loading
[ETN-89-94671] 03 p0326 N90-11855
Coating galvanized steel
[AD-A211775] 03 p0329 N90-11869
An experimental and analytical program to develop crack tip fracture criteria
[AD-A211565] 03 p0359 N90-12051
Fatigue testing of welded steel assemblies with or without finishing treatments
[CETIM-107900] 04 p0513 N90-12961
Experimental and numerical investigations of the crack arrest behavior of steels and cast iron materials
[MPA-TWB-88-03] 05 p0623 N90-13635
A finite strip method for the elastic-plastic large displacement analysis of thin-walled and cold-formed steel sections
[PB89-226021] 06 p0798 N90-14647
On-line system to measure magnetic characteristics of steel samples
[DE89-633443] 06 p0836 N90-14861
The effects of Mo2C morphology and strain distribution on the fatigue properties of Fe-C-Mo dual-phase steels 07 p0901 N90-15210
Guide to the selection of surface treatments for the improvement of fatigue strength of steels
[ESDU-89031] 07 p0907 N90-15245
On the domain of dominance of the asymptotic elastodynamic crack-tip fields 07 p0944 N90-15468
Experiences with three-point bending test specimens for determining the crack-arrest fracture toughness K(sub Ia) in low-alloy steel
[DE90-004120] 08 p1089 N90-16306
Investigation into the effect of fibre size on the tribological behaviour of semi-metallic brake material 09 p1185 N90-16864
Fractographic analysis of long rod penetrator-armor ceramic interactions
[AD-A215172] 09 p1197 N90-16938
Application of high-rate cutting tools
[AD-A214644] 09 p1203 N90-16970
Tellurium embrittlement of type 316 steel
[AERE-R-13440] 13 p1776 N90-20192

Design and processing of strong-tough microcomposite steels
[DE90-007764] 13 p1777 N90-20197
Evaluation of material homogeneity as a function of thickness of low-alloy ferritic steel
[DE90-008069] 13 p1777 N90-20202
Corrosion behavior of mild steel in high pH aqueous media
[PB90-131152] 14 p1950 N90-21162
Magneto acoustic emission apparatus for testing materials for embrittlement
[NASA-CASE-LAR-13817-1] 14 p1951 N90-21170
Structural fatigue in the 34-meter HA-Dec antennas 15 p2078 N90-21902
About the effect of loading sequence on the fatigue life of notched specimens made from steel and aluminum alloys
[LBF-FB-186(1989)] 18 p2526 N90-24414
Fracture-tough, corrosion-resistant bearing steels
[NASA-CR-186796] 19 p2675 N90-25213
Residual stresses measurements by means of x ray diffraction on electron beam welded joints and laser hardened surfaces
[ETN-90-97269] 20 p2877 N90-26371
Microstructural development in HSLA-100 steel weld metals
[AD-A222105] 21 p2982 N90-26944
Evaluation of EA-934NA with 2.5 percent Cab-O-Sil
[NASA-CR-184005] 22 p3158 N90-27909
Investigation of the effects of acid deposition on materials
[PB90-158973] 22 p3197 N90-28143
Determination of the NDT temperature and Charpy V-notch impact properties of AAR TC128 grades B steel and A 8XX grade B steel
[PB90-207804] 23 p3309 N90-28716
Study of meteorological processes important in the degradation of materials through surface temperature
[PB90-222720] 23 p3336 N90-28856
Operation and calibration of MRL permeameter for measurement of DC magnetic properties of materials under stress
[MRL-TN-574] 23 p3338 N90-28863
Mechanical properties and fracture toughness of AAR-TC128 Grade B steel and a micro-alloyed, control-rolled steel, A 8XX grade B, from -80F to +73F
[PB90-207796] 24 p3448 N90-29471
Multiaxial fatigue criterion for 2-1/4 Cr-1 Mo steel for use in high-temperature structural design
[DE90-016039] 24 p3452 N90-29491

STEEP GRADIENT AIRCRAFT
U V/STOL AIRCRAFT

STEEPNESS
U SLOPES

STEERABLE ANTENNAS
Automated Steerable Nulling Antenna Processor (SNAP) model
[PB89-231740] 04 p0509 N90-12937
Discrete-time control of a spacecraft with retargetable flexible antennas 13 p1763 N90-20119
Effects of additional interfering signals on adaptive array performance
[NASA-CR-186508] 13 p1790 N90-20271
Guidance and control techniques for airborne transfer alignment and SAR motion compensation 24 p3429 N90-29372

STEERING
Independent Orbiter Assessment (IOA): Analysis of the nose wheel steering subsystem
[NASA-CR-185548] 02 p0163 N90-10921
Independent Orbiter Assessment (IOA): Analysis of the landing/deceleration subsystem
[NASA-CR-185569] 02 p0167 N90-10943
Independent Orbiter Assessment (IOA): Assessment of the nose wheel steering subsystem
[NASA-CR-185533] 02 p0168 N90-10947
Independent Orbiter Assessment (IOA): CIL issues resolution report, volume 2
[NASA-CR-185524-VOL-2] 02 p0170 N90-10955
Ka-band MMIC beam steered transmitter array 04 p0488 N90-12803
Guidance, steering, load relief and control of an asymmetric launch vehicle
[NASA-CR-185598] 06 p0730 N90-14257
Vehicle antenna for the mobile satellite experiment
[NASA-CR-186109] 06 p0733 N90-14271
Large angle off-axis beam steering of a phased telescope array
[AD-D014269] 08 p1060 N90-16127
Development of an integrated mobile robot system at Carnegie Mellon University: June 1988
[AD-A215955] 10 p1392 N90-18049
Structures for remotely deployable precision antennas 12 p1609 N90-19256
Structures for remotely deployable precision antennas
[NASA-CR-182065] 20 p2822 N90-26061
Closed-loop autonomous docking system
[NASA-CASE-MFS-28421-1] 21 p2966 N90-26861
A sensor stabilization/tracking system for unmanned air vehicles
[AD-A224008] 23 p3283 N90-28579

STELLAR (STAR TRACKER)
U CCD STAR TRACKER

STELLAR ACTIVITY
NT SOLAR ACTIVITY
NT SOLAR FLARES
NT SOLAR PROMINENCES
NT SOLAR STORMS
NT STELLAR FLARES
NT SUNSPOTS
The soft gamma ray bursts detected with the APEX experiment: Evidence for a persistent SGR-like activity 19 p2771 N90-25748
UBVRI-photopolarimetry and the X ray dips of V471 Tau 19 p2775 N90-25781
On the nature of the 1980 outburst of the Be/X ray binary A0535+26=HDE 245770 19 p2778 N90-25803

STELLAR ATMOSPHERES
NT CHROMOSPHERE
NT SOLAR ATMOSPHERE
Ultraviolet properties of hot stars in globular clusters 06 p0862 N90-15007
FGK stars and T Tauri stars: Monograph series on nonthermal phenomena in stellar atmospheres
[NASA-SP-502] 10 p1446 N90-18344
CO infrared bands in atmospheres of long-period variables 11 p1584 N90-19128
IR spectrophotometry of bright carbon stars 11 p1584 N90-19131
A storage process of the magnetic energy results from the unsteady plasma flow field in the space active regions and stellar atmosphere
[DE90-610638] 12 p1717 N90-19858
O-star parameters from line profiles of wind-blanketed model atmospheres 12 p1736 N90-19982
Model atmospheres for novae during the early stages
[NASA-CR-180498] 14 p2038 N90-21694
Coronae and winds around accretion discs 19 p2774 N90-25771
X ray burster spectra in the state of the persistent flux level. Two temperature models of the neutron star atmosphere 19 p2782 N90-25824
Astronomical observations of solid phase carbon 21 p3089 N90-27566
Metallic line profiles of the AOV star Vega
[NASA-CR-186906] 23 p3408 N90-29261

STELLAR COLOR
Mark-3 interferometer
[AD-A213155] 04 p0505 N90-12911
New developments in stellar ages and modelling of Pop. I stars
[SER-C-PREPUBL-FASC-41] 08 p1151 N90-16669
The evolution and geometry of the outer parts of the small Magellanic cloud 14 p2040 N90-21697
The association of supernovae with regions of recent star formation in late-type galaxies 15 p2188 N90-22497
Super-diffraction limited measurements through the turbulent atmosphere by speckle interferometry
[AD-A221227] 18 p2581 N90-24699
Near-infrared speckle observations of T Tauri stars and a multi-wavelength study of the prototype star T Tauri 23 p3409 N90-29264
Nova LMC (Large Magellanic Cloud) 1990 no. 1: The first extragalactic neon nova
[NASA-CR-180409] 23 p3411 N90-29276
An observational study of disk-population globular clusters 24 p3560 N90-30145

STELLAR COMPOSITION
The mass distribution in the galactic centre estimated from OH/IR stars
[PB89-154884] 02 p0291 N90-11663
Mathematical method for the study and teaching of stellar and protostellar structure 02 p0292 N90-11666
O-star parameters from line profiles of wind-blanketed model atmospheres 12 p1736 N90-19982
A comparison of photospheric and circumstellar (HCN)/(CO)-ratios for bright carbon stars
[PB90-151101] 15 p2184 N90-22477
Upper limits on Co-57 abundance in SN1987A according to the Kvant data 19 p2769 N90-25735
Astronomical observations of solid phase carbon 21 p3089 N90-27566

STELLAR CORONAS
NT CORONAL HOLES
NT CORONAL LOOPS
NT SOLAR CORONA
Accretion disks in low-mass X ray binaries 19 p2768 N90-25726
Coronae and winds around accretion discs 19 p2774 N90-25771

STELLAR DOPPLER SHIFT
U DOPPLER EFFECT
U EXTRATERRESTRIAL RADIATION

STELLAR ENVELOPES
The winds of high luminosity late-type bright stars
[NASA-CR-182961] 05 p0712 N90-14160
Properties of evolved star circumstellar grains 06 p0861 N90-15003
Metamorphism of cosmic dust: Processing from circumstellar outflows to the cometary regolith 08 p1146 N90-16641
Unidentified infrared features in proto-planetary nebulae 11 p1584 N90-19130
IR spectrophotometry of bright carbon stars 11 p1584 N90-19131
Observations of 40-70 micron bands of ice in IRAS 09371+1212 and other stars 11 p1585 N90-19134
JCMT observations of the circumstellar envelope IRC+10216 11 p1585 N90-19138
Infrared heterodyne spectroscopy of polyatomic molecules in circumstellar envelopes 12 p1736 N90-19980
Cometary bodies in the circumstellar disk around beta Pictoris 12 p1741 N90-20010
A theoretical study of circumstellar dust around Ae/Be stars 14 p2040 N90-21700
A comparison of photospheric and circumstellar (HCN)/(CO)-ratios for bright carbon stars
[PB90-151101] 15 p2184 N90-22477
Photometric monitoring of early type emission line stars 15 p2184 N90-22478
Fast spectroscopic variations on rapidly-rotating, cool dwarfs. 3: Masses of circumstellar absorbing clouds on AB Doradus
[NASA-CR-186563] 15 p2184 N90-22479
Herbig-Haro objects and stellar jets 15 p2186 N90-22487
Investigation of the late stages of stellar evolution: Mass loss from evolved stars 15 p2187 N90-22492
Molecular studies of dense cores 17 p2484 N90-24207
UBVRI-photopolarimetry and the X ray dips of V471 Tau 19 p2775 N90-25781
Properties of circumstellar matter in GX301-2 observed by Tenma 19 p2778 N90-25798
Carbon chemistry of circumstellar envelopes 21 p3090 N90-27570
The formation and structure of circumstellar and interstellar dust 21 p3091 N90-27576
Near-infrared speckle observations of T Tauri stars and a multi-wavelength study of the prototype star T Tauri 23 p3409 N90-29264

STELLAR EVOLUTION
NT STAR FORMATION
NT STELLAR MASS ACCRETION
IRAS observations of the extended galactic objects Cas A and W80 02 p0290 N90-11657
Mathematical method for the study and teaching of stellar and protostellar structure 02 p0292 N90-11666
Effects of main-sequence mass loss on the turnoff ages of globular clusters
[DE89-016784] 02 p0295 N90-11678
Particle physics and cosmology using stellar evolution theory
[DE89-017529] 03 p0421 N90-12418
Properties of evolved star circumstellar grains 06 p0861 N90-15003
Meteoritic basalts
[NASA-CR-185949] 06 p0861 N90-15004
Ultraviolet properties of hot stars in globular clusters 06 p0862 N90-15007
The instability and fragmentation of the envelope of supernova 1987A 06 p0862 N90-15011
Pulsations of delta Scuti stars
[DE90-003213] 08 p1139 N90-16598
New developments in stellar ages and modelling of Pop. I stars
[SER-C-PREPUBL-FASC-41] 08 p1151 N90-16669
A look on non-standard solar models
[SER-C-PREPUBL-FASC-40] 08 p1153 N90-16677
Infrared spectroscopy of supernova 1987A 11 p1583 N90-19124
Unidentified infrared features in proto-planetary nebulae 11 p1584 N90-19130
Carbon monoxide in supernova 1987A 11 p1585 N90-19135
Detection of SN1986j in NGC891 at millimetre wavelengths 11 p1585 N90-19137
Photometry of variable AFGL sources
[AD-A216938] 11 p1594 N90-19185
Multi-wavelength observations of novae in outburst
[DE90-008934] 14 p2038 N90-21692

Evolutionary effects in B stars
14 p2041 N90-21704
Physics of systems containing neutron stars
[NASA-CR-186002] 15 p2182 N90-22467
Investigation of the late stages of stellar evolution: Mass loss from evolved stars 15 p2187 N90-22492
Topological defects in extended inflation
[NASA-CR-186594] 15 p2190 N90-22505
Soft inflation
[NASA-CR-186593] 15 p2190 N90-22506
Evolutionary models of the rotating sun and implications for other low mass stars 16 p2339 N90-23329
The decay of neutron star magnetic fields
19 p2769 N90-25737
Radiation-driven evolution and statistics of low-mass X ray binaries 19 p2770 N90-25745
Exploding neutron stars near the minimum mass: The total energy release 19 p2774 N90-25769
Nonlinear phenomena in accretion disks: Possibility for observational verification 19 p2775 N90-25779
On the nature of low-luminosity Be/X ray binaries
19 p2780 N90-25816
On the problem of the supernova expansion law in the large Magellanic cloud 19 p2781 N90-25818
New results of numerical simulations of X ray binaries evolution 19 p2782 N90-25828
Carbon chemistry in dense molecular clouds: Theory and observational constraints 21 p3090 N90-27571
Quasars in galaxy cluster environments
22 p3263 N90-28477
Cepheid masses for models with enhanced opacities
[DE90-014919] 23 p3409 N90-29266
Nonradial instability strips for post-AGB stars
[DE90-014922] 23 p3411 N90-29278
An observational study of disk-population globular clusters 24 p3560 N90-30145
The evolution of horizontal branch stars and the calibration of globular cluster ages
24 p3562 N90-30152

STELLAR FIELDS
U STAR DISTRIBUTION

STELLAR FLARES
NT SOLAR FLARES
Analysis of coordinated observations of a giant stellar flare
[NASA-CR-185961] 05 p0715 N90-14176
As observational and theoretical investigation of stellar flares 06 p0862 N90-15012
Flare stars at radio wavelengths
[NASA-CR-186539] 14 p2044 N90-21719
Contributions of the X Ray Astronomy Group of the Max-Planck-Institut fuer Extraterrestrische Physik
[MPE-PREPRINT-165] 17 p2482 N90-24196
Spectral variability of LMC X-4
17 p2483 N90-24204
The behaviour of SS433 and Cygnus X-3 at low frequency 19 p2772 N90-25756
Hard X ray pulses from Vela X-1
19 p2777 N90-25791
On the nature of the 1980 outburst of the Be/X ray binary A0535+26=HDE 245770
19 p2778 N90-25803
A multi-wavelength campaign to observe Scorpius X-1: Preliminary results from the X ray data
19 p2783 N90-25835
A magnetic flare model for X ray variability in AGN
19 p2794 N90-25907

STELLAR GRAVITATION
NT SOLAR GRAVITATION
Nuclear driving of stellar oscillations and their coupling to convection 10 p1446 N90-18345
O-star parameters from line profiles of wind-blanketed model atmospheres 12 p1736 N90-19982

STELLAR INTERIORS
NT SOLAR INTERIOR
Abundance differences among G and K giants
17 p2484 N90-24208
Exploding neutron stars near the minimum mass: The total energy release 19 p2774 N90-25769

STELLAR LUMINOSITY
The winds of high luminosity late-type bright stars
[NASA-CR-182961] 05 p0712 N90-14160
Studies of elementary particles: Proposal
[DE90-001120] 06 p0839 N90-14879
Theory of wide-angle photometry from standard stars
[NASA-CR-185964] 06 p0860 N90-14999
On the mass to light ratios of dwarf spheroidal galaxies
[DE90-610645] 11 p1591 N90-19175
Signature objects: Preliminaries for the satellite project HIPPARCOS/TYCHO
[ETN-90-95730] 12 p1729 N90-19934
Origin of pulsed emission from the young supernova remnant SN 1987A
[CAL-377] 15 p2182 N90-22469
Gamma rays, cosmic rays, and local molecular clouds
15 p2193 N90-22524
Ultraviolet and infrared studies of Be stars
16 p2329 N90-23275
Gamma radiation from radio pulsars
16 p2334 N90-23302
Molecular studies of dense cores
17 p2484 N90-24207
Super-diffraction limited measurements through the turbulent atmosphere by speckle interferometry
[AD-A221227] 18 p2581 N90-24699
Be/X ray binaries 19 p2766 N90-25715
Time-dependent two dimensional radiation hydrodynamics of accreting matter onto highly magnetized neutron stars 19 p2767 N90-25722
XB 1905+00: A very compact low-mass X ray binary viewed at low inclination 19 p2773 N90-25765
Correlations between X ray luminosity and pulse shape as well as spectral shape in binary X ray pulsars
19 p2773 N90-25767
Be/X ray sources 19 p2776 N90-25785
The X ray dip source 4U 1624-49
19 p2776 N90-25786
High energy X ray observations of GX 1+4 with HEXE
19 p2779 N90-25808
On the nature of low-luminosity Be/X ray binaries
19 p2780 N90-25816
New results of numerical simulations of X ray binaries evolution 19 p2782 N90-25828
The spectra (2 to 10 keV) of high luminosity quasars
19 p2786 N90-25852
Pure luminosity evolution and the AGN contribution to the X ray background 19 p2790 N90-25883
Detection of emission lines from the secondary star in IX Vel (=CPD-48 deg 1577)
[MPE-PREPRINT-172] 22 p3265 N90-28485
Nova LMC (Large Magellanic Cloud) 1990 no. 1: The first extragalactic neon nova
[NASA-CR-180409] 23 p3411 N90-29276
Quantifying the FIR interaction enhancement in paired galaxies
[DE90-627485] 23 p3412 N90-29281
Formation of hydrogen line and continuum emission in young stellar objects 24 p3562 N90-30150
The evolution of horizontal branch stars and the calibration of globular cluster ages
24 p3562 N90-30152

STELLAR MAGNETIC FIELDS
NT SOLAR MAGNETIC FIELD
Magnetic fields in late-type dwarfs: Preliminary results from a multiline approach
[SER-C-PREPUB-FASC-31] 12 p1728 N90-19928
Accretion flows in high mass star formation
[DE90-007251] 12 p1744 N90-20027
Physics of systems containing neutron stars
[NASA-CR-186002] 15 p2182 N90-22467
Synthetic spectra of accretion disks in DQ Her binaries
[NASA-CR-186837] 18 p2638 N90-25029
Cyclotron absorption in gamma ray bursts seen with Ginga 19 p2769 N90-25736
The decay of neutron star magnetic fields
19 p2769 N90-25737
Three dimensional accretion disk simulation with external magnetic field 19 p2772 N90-25754
Accretion induced collapse and field decay
19 p2783 N90-25833
A magnetic flare model for X ray variability in AGN
19 p2794 N90-25907

STELLAR MAGNETOSPHERES
NT PULSAR MAGNETOSPHERES
Gamma ray bursts from magnetospheric plasma oscillations 19 p2779 N90-25805

STELLAR MAGNITUDE
Proximity effects on adjacent and multiple stars
05 p0607 N90-13533
Recent advances in the studies of the nova outburst
[DE90-008936] 14 p2038 N90-21691
The evolution and geometry of the outer parts of the small Magellanic cloud 14 p2040 N90-21697
Fifth fundamental catalogue (FK5). Part 1: The basic fundamental stars
[REPT-32(1988)-PT-1] 16 p2330 N90-23282
An analysis of the Palomar-Green subdwarfs and white dwarfs 23 p3409 N90-29263
An observational study of disk-population globular clusters 24 p3560 N90-30145

STELLAR MASS
Theoretical statistics of zero-age cataclysmic variables
01 p0141 N90-10810
The mass distribution in the galactic centre estimated from OH/IR stars
[PB89-154884] 02 p0291 N90-11663
Effects of main-sequence mass loss on the turnoff ages of globular clusters
[DE89-016784] 02 p0295 N90-11678
Pulsars lost and found: The second Princeton-Arecibo millisecond pulsar search 07 p1013 N90-15865
Mass functions for eight galactic clusters in the solar neighborhood 08 p1150 N90-16660
Annihilation physics of exotic galactic dark matter particles 11 p1559 N90-18984
Nearly simultaneous optical, ultraviolet, and x ray observations of three PG quasars
[NASA-CR-186355] 12 p1728 N90-19932
Discovery of low mass objects in Taurus
14 p1978 N90-21329
Small scale structures and density of star-forming regions 14 p2041 N90-21706
Does mass accretion lead to field decay in neutron stars
[CAL-394] 15 p2182 N90-22470
Investigation of the late stages of stellar evolution: Mass loss from evolved stars 15 p2187 N90-22492
The association of supernovae with regions of recent star formation in late-type galaxies
15 p2188 N90-22497
Evolutionary models of the rotating sun and implications for other low mass stars 16 p2339 N90-23329
Radiation-driven evolution of low-mass x ray binaries
18 p2637 N90-25022
Optical observations of LMXB AC211(M15): Solving the puzzle 19 p2768 N90-25731
The possible X ray triple 4U2129+47 (=V1727 Cygni)
19 p2768 N90-25732
Radiation-driven evolution and statistics of low-mass X ray binaries 19 p2770 N90-25745
XB 1905+00: A very compact low-mass X ray binary viewed at low inclination 19 p2773 N90-25765
The accretion disk in the galactic center: An independent indication for a massive central object
19 p2790 N90-25881
Pulsations of the white dwarf component in V471 tauri-like binaries
[DE90-014921] 23 p3409 N90-29267
A plasma diagnostic study of two wind-blown shell nebulae: NGC 7635 and NGC 2359
23 p3410 N90-29271
Nova LMC (Large Magellanic Cloud) 1990 no. 1: The first extragalactic neon nova
[NASA-CR-180409] 23 p3411 N90-29276
Nonradial instability strips for post-AGB stars
[DE90-014922] 23 p3411 N90-29278

STELLAR MASS ACCRETION
Accretion shock geometries in the magnetic variables
[NASA-CR-186290] 08 p1150 N90-16664
Thermal pair cloud models of MeV gamma ray emissions from Cygnus X-1 and the Galactic Center
[DE90-001168] 09 p1301 N90-17536
Accretion flows in high mass star formation
[DE90-007251] 12 p1744 N90-20027
Observations of Cygnus X-2 with IUE: Ultraviolet results from a multiwavelength campaign
17 p2482 N90-24193
The 23rd ESLAB Symposium on Two Topics in X Ray Astronomy. Volume 1: X Ray Binaries
[ESA-SP-296-VOL-1] 19 p2765 N90-25711
Iron K-shell lines from relativistic accretion disks
19 p2766 N90-25714
QPOs and preferred time scales in the variability of X ray pulsars 19 p2767 N90-25721
Time-dependent two dimensional radiation hydrodynamics of accreting matter onto highly magnetized neutron stars 19 p2767 N90-25722
Super-critical accretion in Cir X-1
19 p2767 N90-25725
Accretion disks in low-mass X ray binaries
19 p2768 N90-25726
Radiation-driven evolution and statistics of low-mass X ray binaries 19 p2770 N90-25745
On the viscosity in accretion disks
19 p2774 N90-25775
Accretion onto neutron stars: Radiative transfer in a strong gravitational field 19 p2776 N90-25784
Be/X ray sources 19 p2776 N90-25785
Hard X rays with a power law spectrum from a neutron star accreting through the relativistic gap
19 p2777 N90-25793
Neutron star formation in low-mass binary systems
19 p2778 N90-25797
Simulation of the boundary layer in accretion disks with the SPH method 19 p2779 N90-25807
Accretion induced collapse and field decay
19 p2783 N90-25833

STELLAR MASS EJECTION
MHD (Magnetohydrodynamic) slow shocks in coronal and interplanetary space
[AD-A214725] 09 p1299 N90-17527
Infrared diagnostics of interstellar shocks
11 p1582 N90-19115
Neon novae, recurrent novae, and type I supernovae
[DE90-003188] 12 p1728 N90-19931

Slow shocks in coronal mass ejections
[NASA-CR-186578] 15 p2193 N90-22522
X ray observations of SS433 and its jets
19 p2769 N90-25734
Exploration of jet physics with some applications to SS 433 19 p2777 N90-25794
A shell ejection model for optical light variations in Be stars: Application to Be/X ray binaries
19 p2779 N90-25804
Ionization effects in the radiative driving of stellar winds in massive X ray binary systems
19 p2781 N90-25823
The formation and structure of circumstellar and interstellar dust 21 p3091 N90-27576
Solar-geophysical data number 545, January 1990. Part 2 (Comprehensive reports). Data for July 1989 and miscellaneous
[PB90-182346] 22 p3263 N90-28480

STELLAR MODELS
The instability and fragmentation of the envelope of supernova 1987A 06 p0862 N90-15011
As observational and theoretical investigation of stellar flares 06 p0862 N90-15012
Perturbation methods for the calculation of gravitational waves from slightly non-spherical spacetimes with applications to stellar core collapse
06 p0863 N90-15015
Accretion shock geometries in the magnetic variables
[NASA-CR-186290] 08 p1150 N90-16664
New developments in stellar ages and modelling of Pop. I stars
[SER-C-PREPUBL-FASC-41] 08 p1151 N90-16669
A look on non-standard solar models
[SER-C-PREPUBL-FASC-40] 08 p1153 N90-16677
Carbon monoxide in supernova 1987A
11 p1585 N90-19135
O-star parameters from line profiles of wind-blanketed model atmospheres 12 p1736 N90-19982
Model calculations for dynamic development of planetary nebulae
[ETN-90-95734] 12 p1744 N90-20025
Multi-wavelength observations of novae in outburst
[DE90-008934] 14 p2038 N90-21692
Small scale structures and density of star-forming regions 14 p2041 N90-21706
Modelling late-time atmospheres of supernovae
15 p2189 N90-22500
Gamma ray pulsars: Models and observations
16 p2335 N90-23304
The illusive Geminga: What is it
16 p2335 N90-23307
A unified model of accretion flows and X ray emission in low mass X ray binary systems
19 p2770 N90-25742
The impacts of Ginga results on QPO models
19 p2770 N90-25744
X ray nova GS 2000+25 = Nova Vul 1988: X ray and optical light curves, spectra, and model
19 p2772 N90-25757
Unusual counterparts of the soft X ray transients 4U 1543-47 and 4U 2129+47 in quiescence: Interlopers or third stars 19 p2773 N90-25764
Exploding neutron stars near the minimum mass: The total energy release 19 p2774 N90-25769
On the viscosity in accretion disks
19 p2774 N90-25775
X rays from the accretion column of compact objects: A Monte Carlo study 19 p2775 N90-25777
Linearly extended cyclotron emission regions in AM Herculis systems 19 p2775 N90-25778
A theory of the rapid burster (MXB1730-335)
19 p2775 N90-25782
Hard X rays with a power law spectrum from a neutron star accreting through the relativistic gap
19 p2777 N90-25793
Exploration of jet physics with some applications to SS 433 19 p2777 N90-25794
New X ray pulsars discovered with the Ginga satellite
19 p2777 N90-25795
Long period variations in high mass X ray binaries and their possible relationship with SU UMa stars
19 p2777 N90-25796
A shell ejection model for optical light variations in Be stars: Application to Be/X ray binaries
19 p2779 N90-25804
X ray burster spectra in the state of the persistent flux level. Two temperature models of the neutron star atmosphere 19 p2782 N90-25824
Radiative shock oscillations in AM Her cataclysmic binaries 19 p2783 N90-25834
Constraints on the SS433 system from the Ginga observations 19 p2784 N90-25838
Reacceleration of pairs in compact sources
19 p2787 N90-25859
Variability in BL Lac objects: A schematic model
19 p2787 N90-25861
Detailed non-LTE calculations of the iron emission from NGC 1068 19 p2788 N90-25872
Electron positron pair winds and the Eddington limit
19 p2791 N90-25888
X ray spectral index variability in NGC 4151
19 p2795 N90-25911
Cepheid masses for models with enhanced opacities
[DE90-014919] 23 p3409 N90-29266
The evolution of horizontal branch stars and the calibration of globular cluster ages
24 p3562 N90-30152

STELLAR MOTIONS
NT SOLAR OSCILLATIONS
NT SOLAR ROTATION
NT STELLAR ORBITS
NT STELLAR OSCILLATIONS
NT STELLAR ROTATION
Ground-based astrometric measurements
05 p0607 N90-13536
Stellar kinematics in the galactic centre
11 p1586 N90-19141

STELLAR ORBITS
Fifth fundamental catalogue (FK5). Part 1: The basic fundamental stars
[REPT-32(1988)-PT-1] 16 p2330 N90-23282
Ginga observations of X ray pulsars
19 p2766 N90-25718
Superhumps in accretion disks
19 p2768 N90-25728
The possible X ray triple 4U2129+47 (=V1727 Cygni)
19 p2768 N90-25732
X ray observations of SS433 and its jets
19 p2769 N90-25734
VHE gamma ray emission from Southern Hemisphere X ray binaries 19 p2772 N90-25758

STELLAR OSCILLATIONS
NT SOLAR OSCILLATIONS
Nuclear driving of stellar oscillations and their coupling to convection 10 p1446 N90-18345
Physics of systems containing neutron stars
[NASA-CR-186002] 15 p2182 N90-22467
Does SN 1987A contain a rapidly vibrating neutron star
[CAL-371] 15 p2182 N90-22468
QPOs and preferred time scales in the variability of X ray pulsars 19 p2767 N90-25721
Ginga observations of QPO 19 p2769 N90-25739
QPO from the rapid burster 19 p2770 N90-25741
A unified model of accretion flows and X ray emission in low mass X ray binary systems
19 p2770 N90-25742
QPOs from black-hole candidates
19 p2770 N90-25743
The impacts of Ginga results on QPO models
19 p2770 N90-25744
Detection of 2.93 ms pulsations in Sco X-1
19 p2774 N90-25772
Einstein SSS and MPC observations of Aql X-1 and 4U1820-30 19 p2777 N90-25790
Methods for probing quasi-periodic oscillations on short time scales 19 p2780 N90-25811
The role of comptonisation in energy spectra of standard QPO-sources 19 p2781 N90-25820
A multi-wavelength campaign to observe Scorpius X-1: Preliminary results from the X ray data
19 p2783 N90-25835
Pulsations of the white dwarf component in V471 tauri-like binaries
[DE90-014921] 23 p3409 N90-29267

STELLAR PARALLAX
Analysis of the image dissector tube data
05 p0609 N90-13550
Analysis of the star mapper data
05 p0609 N90-13551
On-ground attitude determination
05 p0609 N90-13552
Astrometric parameter determination in FAST
05 p0610 N90-13556
Signature objects: Preliminaries for the satellite project HIPPARCOS/TYCHO
[ETN-90-95730] 12 p1729 N90-19934

STELLAR PHYSICS
NT SOLAR PHYSICS
The mass distribution in the galactic centre estimated from OH/IR stars
[PB89-154884] 02 p0291 N90-11663
The South African Astronomical Observatory
[NASA-CR-186258] 07 p1011 N90-15856
Some properties of so-called magnetic cloud structures in the solar wind
[IFSI-88-16] 08 p1153 N90-16678
The 23rd ESLAB Symposium on Two Topics in X Ray Astronomy. Volume 1: X Ray Binaries
[ESA-SP-296-VOL-1] 19 p2765 N90-25711
A theory of the rapid burster (MXB1730-335)
19 p2775 N90-25782
Ionization effects in the radiative driving of stellar winds in massive X ray binary systems
19 p2781 N90-25823
Kappa effect pulsational instability for hot extreme helium stars
[DE90-014920] 23 p3411 N90-29277
Pulsations of B star models by an opacity mechanism
[DE90-014923] 23 p3412 N90-29279

STELLAR RADIATION
NT STELLAR WINDS
Analysis of coordinated observations of a giant stellar flare
[NASA-CR-185961] 05 p0715 N90-14176
Theory of wide-angle photometry from standard stars
[NASA-CR-185964] 06 p0860 N90-14999
The instability and fragmentation of the envelope of supernova 1987A 06 p0862 N90-15011
Perturbation methods for the calculation of gravitational waves from slightly non-spherical spacetimes with applications to stellar core collapse
06 p0863 N90-15015
IUE-ULDA access guide number 1: International Ultraviolet Explorer-Uniform Low Dispersion Archive. Dwarf novae and nova-like stars
[ESA-SP-1114] 08 p1152 N90-16672
Herbig Ae/Be stars: Fine structure far-infrared lines
11 p1584 N90-19126
Soft x ray emission from classical novae in outburst
[DE90-006480] 11 p1595 N90-19187
The inter-outburst behavior of cataclysmic variables
[NASA-CR-186374] 13 p1902 N90-20914
Does SN 1987A contain a rapidly vibrating neutron star
[CAL-371] 15 p2182 N90-22468
The bright X ray transient GS2023+338 (=V404 Cyg) in optical outburst and decline 19 p2767 N90-25724
Radiation-driven evolution and statistics of low-mass X ray binaries 19 p2770 N90-25745
The soft gamma ray bursts detected with the APEX experiment: Evidence for a persistent SGR-like activity
19 p2771 N90-25748
Hard X ray observations of galactic sources
19 p2771 N90-25752
VHE gamma ray emission from Southern Hemisphere X ray binaries 19 p2772 N90-25758
Orbitally modulated VHE gamma rays from Cen X-3
19 p2780 N90-25812
Radiative shock oscillations in AM Her cataclysmic binaries 19 p2783 N90-25834
Hard X ray observations of AGN
19 p2791 N90-25889
United States Air Force research initiation program for 1988, volume 2
[AD-A223124] 21 p3102 N90-27614

STELLAR ROTATION
NT SOLAR ROTATION
Phoebe: A preliminary control network and rotational elements
[NASA-CR-185716] 02 p0295 N90-11680
Thomson scattering in a magnetic field
14 p2040 N90-21699
The emission lines in the ultra-violet spectrum of Beta Lyrae 15 p2183 N90-22474
Ultraviolet and infrared studies of Be stars
16 p2329 N90-23275
What is learned from high energy bursts and flares
16 p2336 N90-23314
Evolutionary models of the rotating sun and implications for other low mass stars 16 p2339 N90-23329
X ray timing and spectral measurements of the X ray pulsar 4U 1538-52 19 p2774 N90-25770
Detection of 2.93 ms pulsations in Sco X-1
19 p2774 N90-25772
Rotating neutron stars and the equation of state of dense matter
[DE90-014185] 23 p3410 N90-29269
Investigation of x ray variability in highly active cool stars
[NASA-CR-183853] 24 p3560 N90-30143

STELLAR SPECTRA
NT SOLAR SPECTRA
The ratio to X-ray spectral shape and variability of blazars 02 p0297 N90-11688
On the analysis of line profile variations: A statistical approach 03 p0420 N90-12412
The softest Einstein AGN (Active Galactic Nuclei)
[DE89-009389] 06 p0864 N90-15020
The environment of young stellar objects studied by high-resolution infrared spectroscopy
11 p1583 N90-19120
High resolution infrared spectroscopy of symbiotic stars 11 p1583 N90-19125
Detection of SN1986j in NGC891 at millimetre wavelengths 11 p1585 N90-19137

A new interpretation of the feature of SiO maser spectra associated with M-type star
[DE90-610641] 11 p1590 N90-19174
Magnetic fields in late-type dwarfs: Preliminary results from a multiline approach
[SER-C-PREPUB-FASC-31] 12 p1728 N90-19928
Infrared heterodyne spectroscopy of polyatomic molecules in circumstellar envelopes 12 p1736 N90-19980
O-star parameters from line profiles of wind-blanketed model atmospheres 12 p1736 N90-19982
AFGL ten micron mosaic array spectrometer: Recent results 14 p1978 N90-21333
Preliminary results on two-dimensional interferometry of HL Tau 14 p1979 N90-21335
Fast spectroscopic variations on rapidly-rotating, cool dwarfs. 3: Masses of circumstellar absorbing clouds on AB Doradus
[NASA-CR-186563] 15 p2184 N90-22479
Multifrequency observations of Cyg X-2: X ray observations with Ginga 17 p2482 N90-24192
Observations of Cygnus X-2 with IUE: Ultraviolet results from a multiwavelength campaign 17 p2482 N90-24193
Radio observations of the x ray binary Cygnus X-2 17 p2482 N90-24195
Black holes in X ray binaries: X ray properties of the galactic black hole candidates 19 p2765 N90-25712
The X ray spectrum of Nova Vul 1988. Mir-Kvant data 19 p2766 N90-25713
The X ray absorption spectra of massive X ray binaries 19 p2766 N90-25716
Time-dependent two dimensional radiation hydrodynamics of accreting matter onto highly magnetized neutron stars 19 p2767 N90-25722
The bright X ray transient GS2023+338 (=V404 Cyg) in optical outburst and decline 19 p2767 N90-25724
Super-critical accretion in Cir X-1 19 p2767 N90-25725
X ray observations of SS433 and its jets 19 p2769 N90-25734
Non-thermal radio emission of X ray binaries 19 p2769 N90-25738
X ray timing and spectral measurements of the X ray pulsar 4U 1538-52 19 p2774 N90-25770
Linearly extended cyclotron emission regions in AM Herculis systems 19 p2775 N90-25778
The X ray dip source 4U 1624-49 19 p2776 N90-25786
Ginga observations of SS 433 19 p2776 N90-25789
Hard X ray pulses from Vela X-1 19 p2777 N90-25791
Hard X rays with a power law spectrum from a neutron star accreting through the relativistic gap 19 p2777 N90-25793
Is the hard tail of X rays from GX339-4 a Compton scattering component 19 p2779 N90-25806
Orbitally modulated VHE gamma rays from Cen X-3 19 p2780 N90-25812
EXOSAT deep exposure of the LMC X-4 region 19 p2780 N90-25814
Self-consistent Comptonised models for the spectra of low mass X ray binaries 19 p2780 N90-25817
The pulsed light curve of Vela X-1 19 p2781 N90-25819
A multi-wavelength campaign to observe Scorpius X-1: Preliminary results from the X ray data 19 p2783 N90-25835
Hard X ray observations of active galaxies 19 p2789 N90-25874
The EUV spectral shape of the big-bump in HS1700+6416 and F9: A genuine difference between Seyfert's and QSO's 19 p2789 N90-25878
The X ray time variability of NGC 6814 revisited 19 p2790 N90-25882
Line identification studies using traditional techniques and wavelength coincidence statistics
[NASA-CR-186901] 22 p3261 N90-28467
Strong associated C 4 absorption in low redshift quasars
[NASA-CR-186936] 22 p3262 N90-28469
Quasars in galaxy cluster environments 22 p3263 N90-28477
Metallic line profiles of the AOV star Vega
[NASA-CR-186906] 23 p3408 N90-29261
X ray spectra of cataclysmic variables
[NASA-CR-187002] 23 p3412 N90-29280
Monte Carlo simulation of complex spectra for opacity calculations
[DE90-015198] 24 p3561 N90-30147

STELLAR SPECTROPHOTOMETRY
New ground-based photometric measurements 05 p0607 N90-13538
Standard stars and photometric calibration 05 p0607 N90-13539
Double stars 05 p0608 N90-13540
Variable stars 05 p0608 N90-13541
Theory of wide-angle photometry from standard stars
[NASA-CR-185964] 06 p0860 N90-14999
Infrared spectroscopy and imaging of supernova remnants 11 p1580 N90-19104
IR spectrophotometry of bright carbon stars 11 p1584 N90-19131
Photometric monitoring of early type emission line stars 15 p2184 N90-22478
The bright X ray transient GS2023+338 (=V404 Cyg) in optical outburst and decline 19 p2767 N90-25724
BBXRT observations of X ray binaries 19 p2778 N90-25802
Metallic line profiles of the AOV star Vega
[NASA-CR-186906] 23 p3408 N90-29261

STELLAR STRUCTURE
Mathematical method for the study and teaching of stellar and protostellar structure 02 p0292 N90-11666
The mass of the Coma cluster 15 p2188 N90-22496

STELLAR SYSTEMS
Be/X ray sources 19 p2776 N90-25785
Nonlinear multi-mode coupling of the solar gravity modes in a rotationally split multiplet 21 p3100 N90-27608

STELLAR TEMPERATURE
O-star parameters from line profiles of wind-blanketed model atmospheres 12 p1736 N90-19982
The ratio of neutral hydrogen to neutral helium in the local interstellar medium 15 p2189 N90-22499
Ultraviolet and infrared studies of Be stars 16 p2329 N90-23275
X ray burster spectra in the state of the persistent flux level. Two temperature models of the neutron star atmosphere 19 p2782 N90-25824
The Tempel 2 dust trail
[AD-A224395] 24 p3562 N90-30153

STELLAR WINDS
The winds of high luminosity late-type bright stars
[NASA-CR-182961] 05 p0712 N90-14160
Very high resolution radio observations of molecular cloud cores 06 p0863 N90-15013
A source of observational constraints on the structure of Wolf-Rayet winds
[DE90-001236] 06 p0864 N90-15023
Outflows in high mass star-forming regions 08 p1149 N90-16657
Predictions of infrared recombinations lines in stellar winds of hot stars 11 p1585 N90-19136
O-star parameters from line profiles of wind-blanketed model atmospheres 12 p1736 N90-19982
Interactions of massive stars with the interstellar medium: Bow shocks and superbubbles 15 p2186 N90-22485
Wind instability as a possible cause of the spiral structure formation in the gaseous subsystem of galaxies with the circular magnetic field
[DE90-618944] 15 p2190 N90-22507
The effect of a stellar wind on an expanding H II region 16 p2333 N90-23292
Be/X ray binaries 19 p2766 N90-25715
The X ray absorption spectra of massive X ray binaries 19 p2766 N90-25716
Coronae and winds around accretion discs 19 p2774 N90-25771
On the problem of the supernova expansion law in the large Magellanic cloud 19 p2781 N90-25818
Ionization effects in the radiative driving of stellar winds in massive X ray binary systems 19 p2781 N90-25823
A plasma diagnostic study of two wind-blown shell nebulae: NGC 7635 and NGC 2359 23 p3410 N90-29271

STELLARATORS
Stellarator transport theory
[DE89-016371] 03 p0406 N90-12328
Theoretical plasma physics
[DE90-000009] 03 p0408 N90-12341
Experiments on linear high beta helical axis stellarators to study simulated toroidal effects and Alfven-wave heating
[DE90-001704] 07 p0994 N90-15745
The 17th AINSE Plasma Physics Conference: Conference handbook
[DE90-600936] 07 p0996 N90-15759
ATF-2 studies
[DE90-004380] 08 p1124 N90-16510
Near-term directions in the world stellarator program
[DE90-004381] 08 p1124 N90-16511
Dissipative trapped electron modes in ell equals 2 torsatrons
[DE90-004919] 10 p1431 N90-18256
The ANU (Australian National University) Heliac Program
[DE90-006620] 13 p1890 N90-20843
Transition from resistive-g to eta-i driven turbulence in stellarator systems
[DE90-009382] 14 p2030 N90-21641
Numerical methods for the problem of the free-boundary plasma equilibrium in a stellarator (torsatron)
[DE90-620580] 16 p2319 N90-23223
Activities report of the Institute for Plasma Research
[ETN-90-96467] 16 p2319 N90-23225
Formation of magnetic islands due to field perturbations in toroidal stellarators
[DE90-012132] 19 p2759 N90-25679
Stability regimes in a helical quadrupole focusing accelerator: Theory and simulation
[AD-A221755] 21 p3079 N90-27507
Formation of magnetic islands due to field perturbations in toroidal stellarator configurations
[DE90-014789] 23 p3397 N90-29191
Stellarator status, 1989
[DE90-014791] 23 p3397 N90-29192

STEP FAULTS
U GEOLOGICAL FAULTS

STEP FUNCTIONS
Long steps with the logarithmic penalty barrier function in linear programming
[REPT-89-44] 15 p2147 N90-22265
On the use of stability regions in the numerical analysis of stability value problems
[TW-89-07] 18 p2603 N90-24826

STEPPING MOTORS
A versatile stepping motor controller for systems with many motors
[DE90-001556] 07 p0921 N90-15327
Application of a buck-type MC2 regulated converter for a stepper motor control 10 p1335 N90-17722
Linear Variable Differential Transformer (LVDT) with conditioner for the control of stepping motor drivers (part of the sliding-foil follower system of the Emin spectrometers)
[DIGEL-1989-9] 11 p1504 N90-18660
Further development of the cryogenic Fabry-Perot interchange mechanism for ISO LWS 18 p2539 N90-24492

STEREOCHEMISTRY
Composite materials with improved properties in compression. Appendix 1: Cyclopropanation of poly(1-methyl 1-phenyl 1-sila-cis-pent-3-ene). Synthesis and characterization of poly(1-methyl 3,4-methylene-1-phenyl 1-sila-cis-pent-3-ene)
[AD-A221494] 21 p2971 N90-26889
Magnetic resonance elucidation of molecule/macromolecule interaction stereochemistry
[AD-A221444] 21 p2979 N90-26928

STEREOGRAPHY
U STEREOPHOTOGRAPHY

STEREOPHOTOGRAPHY
The use of a deformation model for sampling digitalized stereoscopic images
[IMAG-RR-753-I] 05 p0664 N90-13884
Mission report on the Orbiter Camera Payload System (OCPS) Large Format Camera (LFC) and Attitude Reference System (ARS)
[NASA-CR-186273] 09 p1240 N90-17197
Technical and administrative feasibility of microlight remote sensing applications for river boards
[BCRS-89-01] 12 p1679 N90-19643
Survey of instrumental methods for the determination of the high frequency wave spectrum
[IOS-267] 15 p2135 N90-22200
Real-time stereo-microradiography
[AD-A218433] 16 p2245 N90-22805
Topographic mapping from SPOT satellite imagery
[ETN-90-96689] 17 p2418 N90-23777

STEREOSCOPIC PHOTOGRAPHY
U STEREOPHOTOGRAPHY

STEREOSCOPIC VISION
Connectionist model-based stereo vision for telerobotics 08 p1076 N90-16224
Stereo feature matching in disparity space
[AD-A218170] 13 p1875 N90-20751
Location recognition using stereo vision
[AD-A218218] 13 p1875 N90-20752
Space environment robot vision system 15 p2143 N90-22245
Spatial constraints of stereopsis in video displays 16 p2267 N90-22920
Stereoscopic distance perception 16 p2267 N90-22921
Paradoxical monocular stereopsis and perspective vergence 16 p2267 N90-22922
The perception of three-dimensionality across continuous surfaces 16 p2268 N90-22924
Perceiving environmental properties from motion information: Minimal conditions 16 p2268 N90-22925
How to reinforce perception of depth in single two-dimensional pictures 16 p2270 N90-22937

Visual enhancements in pick-and-place tasks: Human operators controlling a simulated cylindrical manipulator
16 p2271 N90-22946
Development of a stereo 3-D pictorial primary flight display
16 p2273 N90-22955
Determination of depth-viewing volumes for stereo three-dimensional graphic displays
[NASA-TP-2999] 16 p2275 N90-22965
Supervisory controlled telemanipulation and vision systems for inspection and maintenance operations
18 p2508 N90-24333
Telepresence and Space Station Freedom workstation operations
19 p2731 N90-25527
The interaction of chromostereopsis and stereopsis in stereoscopic CRT (Cathode Ray Tubes) displays
[AD-A217906] 23 p3277 N90-28544
Trinocular stereovision using figural continuity, dealing with curved objects
24 p3503 N90-29802
Use of 3D vision for fine robot motion
24 p3503 N90-29804

STEREOSCOPY
NT STEREOPHOTOGRAPHY
Low-cost three-dimensional stereoscopic display technique for computer-aided design
[DE89-011635] 01 p0104 N90-10594
Low-cost three-dimensional stereoscopic display technique for computer-aided design
[DE89-017732] 03 p0386 N90-12196
Parallel implementation and evaluation of motion estimation system algorithms on a distributed memory multiprocessor using knowledge based mappings
[NASA-CR-185984] 03 p0389 N90-12213
Novel techniques for data decomposition and load balancing for parallel processing of vision systems: implementation and evaluation using a motion estimation system
[NASA-CR-185991] 03 p0389 N90-12214

STERILIZATION
Factors affecting practical application of food irradiation
[DE90-631277] 24 p3522 N90-29914

STERNS
U AFTERBODIES

STEROIDS
NT CORTICOSTEROIDS
NT PROSTAGLANDINS

STIFF STRUCTURES
U RIGID STRUCTURES

STIFFENING
A new aspect for the use of thin walled beams as shell stiffeners of spacecraft structures
02 p0184 N90-11046
Acoustic radiation of cylindrical shells, with stiffening finishing and coated with masking materials
[ISAL-89-0035] 10 p1426 N90-18227
Structural analysis and optimum design of geodesically stiffened composite panels
[NASA-CR-186944] 23 p3337 N90-28862

STIFFNESS
Transverse shear stiffness of composite and sandwich finite elements
02 p0182 N90-11034
Field-effect spectroscopy of interface states
[AD-A212998] 05 p0703 N90-14112
Finite element analysis of frictional contact problems
06 p0792 N90-14612
Transverse (through-the-thickness) shear stiffnesses of fibre reinforced composite laminated plates (computer program)
[ESDU-89013] 07 p0891 N90-15152
Current status of the application of conventional aluminium-lithium alloys and the potential for future developments
07 p0900 N90-15203
Some problems in hydrodynamic lubrication
09 p1229 N90-17133
Dynamic modeling of flexible bodies in multibody systems
09 p1229 N90-17134
Integrated force method versus displacement method for finite element analysis
[NASA-TP-2937] 10 p1398 N90-18081
A global approach for the identification of structural connection properties
[NASA-TM-102502] 11 p1518 N90-18745
Evaluation of repeated impact damage in composite structures
12 p1619 N90-19303
Wave receptance analysis of vibrating beams and stiffened plates
14 p1993 N90-21419
In-situ fracture stiffness determination
[DE90-009202] 15 p2129 N90-22173
Multi-flexible-body dynamics capturing motion-induced stiffness
16 p2284 N90-23013
An approach for relating the results of quantitative nondestructive evaluation to intrinsic properties of high-performance materials
[NASA-CR-186484] 19 p2699 N90-25355
Loads analysis and testing of flight configuration solid rocket motor outer boot ring segments
[NASA-TP-3028] 19 p2701 N90-25366
A suitable transverse shear stiffness definition for buckling of laminates and sandwich plates
[LR-603] 19 p2704 N90-25384
Buckling and postbuckling behavior of compression-loaded isotropic plates with cutouts
[NASA-TP-3024] 23 p3337 N90-28859

STIFFNESS MATRIX
Parametric identification of conservative self adjoint structures
02 p0177 N90-10994
On the equivalence of BS-stability and B-consistency
[CWI-NM-R8815] 02 p0268 N90-11530
An algebraic characterization of B-convergent Runge-Kutta methods
[CWI-NM-R8901] 04 p0541 N90-13133
Measuring of the complete stiffness matrix for anisotropic laminated materials
[DLR-MITT-89-11] 05 p0618 N90-13606
Measuring of the complete stiffness matrix for anisotropic laminated materials
[DLR-MITT-89-12] 05 p0618 N90-13607
A study of incremental-iterative strategies for nonlinear analyses
[PB89-226005] 06 p0798 N90-14646
Mesh refinement in finite element analysis by minimization of the stiffness matrix trace
[NASA-CR-185170] 07 p0938 N90-15434
Dynamic structural analysis using boundary element techniques
[AD-A222943] 21 p3012 N90-27126

STILBENE
Polymer liquid crystals with side chain discogens
[AD-A218013] 13 p1782 N90-20228
Nonlinear optical responses and laser damage thresholds of films of a polarized stilbene side chain liquid crystal polymer and a phthalocyanine
[AD-A219462] 17 p2408 N90-23720

STIMULANTS
NT ATROPINE
NT CAFFEINE
The sensory transduction pathways in bacterial chemotaxis
05 p0677 N90-13944

STIMULATED EMISSION
Research on sliding spark preionization in a TEA CO2 laser
[ISL-R-113/88] 11 p1516 N90-18732
High intensity laser beam interactions with single droplets
15 p2083 N90-21924
Pulsed-discharge carbon dioxide lasers
18 p2556 N90-24587

STIMULATED EMISSION DEVICES
NT AIRBORNE LASERS
NT ARGON LASERS
NT ATMOSPHERIC LASERS
NT CARBON DIOXIDE LASERS
NT CARBON LASERS
NT CARBON MONOXIDE LASERS
NT CHEMICAL LASERS
NT CONTINUOUS WAVE LASERS
NT DISTRIBUTED FEEDBACK LASERS
NT DYE LASERS
NT EXCIMER LASERS
NT FREE ELECTRON LASERS
NT GALLIUM ARSENIDE LASERS
NT GAMMA RAY LASERS
NT GAS LASERS
NT GASDYNAMIC LASERS
NT GLASS LASERS
NT HELIUM-NEON LASERS
NT HF LASERS
NT HIGH POWER LASERS
NT HYDROGEN MASERS
NT INFRARED LASERS
NT INJECTION LASERS
NT INTERSTELLAR MASERS
NT IODINE LASERS
NT KRYPTON FLUORIDE LASERS
NT LASERS
NT MASERS
NT METAL VAPOR LASERS
NT NEODYMIUM LASERS
NT NOVA LASER SYSTEM
NT NUCLEAR PUMPED LASERS
NT ORGANIC LASERS
NT PULSED LASERS
NT Q SWITCHED LASERS
NT RAMAN LASERS
NT RARE GAS-HALIDE LASERS
NT RING LASERS
NT RUBY LASERS
NT SEMICONDUCTOR LASERS
NT SOLAR-PUMPED LASERS
NT SOLID STATE LASERS
NT SPACEBORNE LASERS
NT TEA LASERS
NT TRAVELING WAVE MASERS
NT TUNABLE LASERS
NT ULTRASHORT PULSED LASERS
NT ULTRAVIOLET LASERS
NT WATER MASERS
NT WAVEGUIDE LASERS
NT X RAY LASERS
NT XENON CHLORIDE LASERS
NT XENON FLUORIDE LASERS
NT YAG LASERS

STIMULATION
NT AUDITORY STIMULI
NT SENSORY STIMULATION
Stimulus-response compatibility in spatial precuing and symbolic identification: Effects of coding practice, retention, and transfer
[AD-A210745] 02 p0255 N90-11443
Evaluation of speech intelligibility through a bone conduction stimulator
[AD-A212002] 05 p0673 N90-13919
CW (Continuous Wave) stimulated Brillouin scattering of long-pulse chemical laser beams
[AD-A216409] 10 p1390 N90-18039
Beam combining of excimer lasers by stimulated Raman scattering
[AD-A222973] 21 p3008 N90-27099
Situational awareness and vestibular stimulation: The influence of whole-body rotation upon task performance
[IZF-1989-14] 23 p3361 N90-28994

STIMULI
Models of mental functioning
[AD-A210456] 01 p0094 N90-10538

STIRLING CYCLE
Dynamic characteristics concerned in the design of a free-piston Stirling engine/magnetic coupling/compressor system
[DE89-015981] 02 p0230 N90-11317
System design and performance prediction of a free-piston Stirling engine/magnetic coupling/compressor assembly in a gas residential heat pump
[DE89-016070] 06 p0807 N90-14696
SP-100 power system conceptual design for lunar base applications
[NASA-TM-102090] 06 p0866 N90-15030
Phase 1 supplemental development of a kinematic Stirling/Rankine commercial gas-fired heat pump system
[PB90-129974] 13 p1825 N90-20483
Recent Stirling engine loss-understanding results
[NASA-TM-103122] 14 p1942 N90-21114
Preliminary designs for 25 kWe advanced Stirling conversion systems for dish electric applications
[NASA-TM-103188] 20 p2940 N90-26729

STIRLING ENGINES
Laser-powered lunar base
01 p0029 N90-10156
An experimental investigation of transition in oscillating pipe flow
02 p0218 N90-11249
Free-Piston Stirling Engine magnetically coupled heat pump: Critical component evaluation
[DE89-015646] 02 p0229 N90-11316
Automotive Stirling engine development program
[NASA-CR-180839] 02 p0289 N90-11654
SP-100 power system conceptual design for lunar base applications
[NASA-TM-102090] 06 p0866 N90-15030
Development of free-piston Stirling engine performance and optimization codes based on Martini simulation technique
[NASA-CR-182210] 10 p1443 N90-18326
Identification of a cast iron alloy containing nonstrategic elements
[NASA-CR-185174] 11 p1487 N90-18559
Stirling engine technologies in Japan
[DE89-782296] 11 p1528 N90-18795
Recent Stirling engine loss-understanding results
[NASA-TM-103122] 14 p1942 N90-21114
Programmatic status of NASA's CSTI high capacity power Stirling space power converter program
[NASA-TM-103142] 16 p2210 N90-22606
Preliminary designs for 25 kWe advanced Stirling conversion systems for dish electric applications
[NASA-TM-103188] 20 p2940 N90-26729
Evaluation of the STM4-120 kinematic Stirling engine
[DE90-013836] 23 p3344 N90-28897
Performance measurements and energy balance of an SPS V160 Stirling motor at the German Aerospace Research Establishment
[DLR-MITT-90-03] 23 p3345 N90-28903
Automotive Stirling engine development program
[NASA-CR-180840] 23 p3408 N90-29260

STOCHASTIC PROCESSES
NT MARKOV CHAINS
NT MARKOV PROCESSES
NT RANDOM PROCESSES
NT RANDOM WALK

A comparison of wind turbulence simulation models for stochastic loads analysis for horizontal-axis wind turbines
[DE89-009442] 01 p0083 N90-10473
Stochastic control theory, nonlinear structural mechanics and applied combinatorics
[AD-A209042] 01 p0114 N90-10657
Stochastic quantization
[AD-A210942] 01 p0117 N90-10671
Radon transform analysis of a probabilistic method for image generation
[AD-A207814] 01 p0123 N90-10702
Performance and robustness of adaptive controllers for linear stochastic systems 02 p0261 N90-11485
Stochastic optimization by simulation: Some experiments with a simple steady-state queue
[AD-A210762] 02 p0265 N90-11508
Stochastic flows in networks
[AD-A211209] 02 p0266 N90-11515
On some stochastic properties of the infinitely dimensional Hamiltonian systems of classical mechanics
[DE89-618403] 02 p0267 N90-11525
Seismic wave attenuation and yield determination at regional distances
[AD-A211548] 03 p0372 N90-12128
Doppler statistics of ocean velocity variability
[AD-A211687] 03 p0377 N90-12148
Statistical density and amplitude tapered arrays
[RSRE-MEMO-4211] 04 p0490 N90-12818
Free-field response from inclined body waves in viscoelastic random medium
[REPT-88-99] 04 p0499 N90-12876
A semiparametric model for citation counts
[CWI-MS-R8814] 04 p0542 N90-13145
Stochastic process models in device physics
[AD-A212284] 04 p0547 N90-13185
Monte Carlo (importance) sampling within a Benders' decomposition algorithm for stochastic linear programs
[AD-A212854] 04 p0548 N90-13189
Fellowships in information and stochastic systems
[AD-A212385] 04 p0563 N90-13280
Test network Delft
[ETN-90-96009] 05 p0577 N90-13365
An autopilot design methodology for bank-to-turn missiles
[AD-A213379] 05 p0583 N90-13399
Stochastic modelling of EM scattering from foliage
[AD-A213118] 05 p0632 N90-13689
First-order Bragg SAR imagery of Kelvin wakes and moving internal wave fields
[AD-A213361] 05 p0633 N90-13691
Why stochastic modeling is essential in analyzing interdicted transportation network performance
[AD-A213140] 05 p0688 N90-14007
Large deviation estimates in the stochastic quantization of phi sub 2 exp 4
[PREPRINT-686] 05 p0693 N90-14050
Optimal stochastic modeling and control of flexible structures
[AD-A212347] 06 p0733 N90-14269
A two dimensional power spectral estimate for some nonstationary processes
[NASA-CR-186100] 06 p0833 N90-14843
Prediction of stochastic blade loads for three-bladed, rigid-hub rotors
[DE89-009508] 07 p0954 N90-15520
The parallel decomposition of linear programs
[DE90-003538] 07 p0974 N90-15625
Two basic partial orderings for distributions derived from Schur functions and majorization
[AD-A213703] 07 p0984 N90-15682
Optimization of stochastic systems via simulation
[AD-A214011] 07 p0985 N90-15689
Numerical methods for parabolic equations and inequalities in very high dimensions
[AD-A214102] 07 p0985 N90-15690
A structural factoring approach for analyzing probabilistic networks 07 p0986 N90-15697
Nonlocality and stochastic quantization of field theory
[DE89-633913] 07 p1007 N90-15833
The Eighteenth Conference on Stochastic Processes and their Applications
[AD-A212301] 08 p1040 N90-16010
Integrated geodetic network analysis with stochastic prior information about the gravity field and reference ellipsoid
[SER-C-351] 08 p1091 N90-16317
Stochastic simulation of charged particle transport on the massively parallel processor 08 p1114 N90-16448
Stochastic action of dynamical systems on curved manifolds. The isokinetic developing map on trajectories
[PREPRINT-666] 08 p1117 N90-16466
Optimal step sizes in semi-stochastic approximation procedures
[ETN-90-95888] 08 p1117 N90-16469
Langmuir wave interaction with ion-sound one. Part 1: Stochastic effects
[DE90-603368] 08 p1118 N90-16474
Nonparametric estimation of trends in linear stochastic systems
[AD-A213741] 09 p1272 N90-17374
Absolute continuity and mutual information for Gaussian mixtures
[AD-A215185] 09 p1274 N90-17383
Unsteady two level models
[TELECOM-89-E-006] 10 p1375 N90-17973
Segmentation of topographic profiles of the seafloor based on a self-affine model
[AD-A215938] 10 p1410 N90-18132
Nonprocedural implementation of mathematical programming algorithms
[AD-A216039] 10 p1419 N90-18179
Stochastic adaptive control and estimation enhancement
[AD-A215486] 10 p1420 N90-18187
User's guide to OPUS (Optimal Preferential Utility and Strategies)
[AD-A214384] 10 p1424 N90-18217
Evaluation of influences of errors involved in orbit propagation of artiificial satellites
[INPE-4962-TDL/391] 11 p1466 N90-18441
Parallel distributed networks for image smoothing and segmentation in analog VSLI
[AD-A216780] 12 p1651 N90-19491
Implementation of a finite element process for the Euler equations of the gas dynamics
[PREPRINT-500] 12 p1661 N90-19545
Adaptive, asynchronous stochastic global optimization algorithms for sequential and parallel computation
[AD-A217093] 12 p1702 N90-19775
Optimal iteration steps by stochastic approximation processes for the solution of optimization problems with twice differentiable functions
[ETN-90-95887] 12 p1708 N90-19809
On the Langevin equation for stochastic quantization of gravity
[DE90-750024] 12 p1725 N90-19914
Stochastic approach to the initiation of pitting corrosion
[AERE-R-13348] 13 p1775 N90-20190
On the existence of local times: A geometric study
[AD-A218337] 13 p1879 N90-20776
Homogeneous chaos, p-forms, scaling and the feynman integral
[AD-A218339] 13 p1879 N90-20777
Slepian models and regression approximations in crossing and extreme value theory
[AD-A218338] 13 p1879 N90-20779
Application of stochastic robustness to aircraft control systems 14 p1908 N90-20936
Stochastic robustness of linear control systems 14 p1908 N90-20941
Effective techniques for the identification and accommodation of disturbances 14 p1934 N90-21072
Quadratic Hadamard Memories 1
[AD-A217224] 14 p2013 N90-21534
Homogeneous dilute turbulent particle-laden water flows 15 p2090 N90-21965
Vibration analysis of systems with random parametric excitations 15 p2109 N90-22060
The Shock and Vibration Digest, volume 22, no. 1 15 p2111 N90-22073
An approach to rescheduling activities based on determination of priority and disruptivity 15 p2153 N90-22299
The intrinsic stochasticity of near-integrable Hamiltonian systems
[IPPCZ-282] 15 p2167 N90-22386
A new stochastic model of turbulent dispersion in the convective planetary boundary layer and the results of the Atterbury-87 field study 16 p2254 N90-22853
Stochastic interactive activation and the effect of context on perception
[AD-A218929] 16 p2262 N90-22898
Parallel and vector computation for stochastic optimal control applications 16 p2282 N90-23007
Modern CACSD using the Robust-Control Toolbox 16 p2286 N90-23024
Periodic ARMA models: Optimal prediction and minimum-phase condition
[REPT-89-006] 16 p2305 N90-23131
Stochastic processes as Fourier integrals and dilation of vector measures
[AD-A219413] 16 p2308 N90-23150
Transactions of the Seventh Army Conference on Applied Mathematics and Computing
[AD-A219220] 16 p2309 N90-23160
Rigorous analysis of low temperature stochastic Ising models: Metastability and exponential approach to equilibrium
[PREPRINT-720] 16 p2312 N90-23175
A posterior stochastic equation for quantum Brownian motion
[PREPRINT-715] 16 p2315 N90-23194
A passive homing missile guidance law based on new target maneuver models
[AD-A220419] 17 p2356 N90-23411
A theory of control for infinite dimensional systems with application to large scale space structures
[AD-A219937] 17 p2366 N90-23469
The cost of conservative synchronization in parallel discrete event simulations
[NASA-CR-182034] 17 p2441 N90-23912
Comparison of selection procedures and validation of criterion used in selection of significant control variates of a simulation model
[AD-A220459] 17 p2443 N90-23921
Stochastic adaptive control and estimation enhancement
[AD-A219629] 17 p2454 N90-24001
An averaging result for random differential equations
[AD-A220364] 17 p2457 N90-24021
Compensatability and optimal compensation of systems with stochastic parameters
[REPT-89-61] 17 p2457 N90-24024
An asymmetric shortest queue problem
[MEMO-COSOR-89-22] 17 p2459 N90-24035
Bounding separable recourse functions with limited distribution information
[AD-A219504] 17 p2465 N90-24084
Stochastics realization problems
[CWI-BS-R8920] 17 p2467 N90-24097
Evaluation of Stochastic models for estimating the persistence probability of cloud-free lines-of-sight
[AD-A220283] 18 p2581 N90-24702
Cloud field classification based on textural features 18 p2646 N90-25066
The proposal of a high-level stochastic Petri net
[REPT-90-005] 19 p2752 N90-25637
Closed-form solution of decomposable stochastic models
[NASA-TM-103466] 20 p2920 N90-26619
Dichotomies for certain product measures and stable processes
[AD-A222568] 20 p2921 N90-26621
Evaluation of a decomposition approach for real-time scheduling using a Stochastic model
[AD-A222726] 20 p2921 N90-26625
A linear-eddy model of turbulent shear layer mixing 21 p2974 N90-26904
Stochastic structural dynamics for aerospace applications
[AD-A221517] 21 p3013 N90-27133
Construction of dynamic stochastic simulation models using knowledge-based techniques 21 p3047 N90-27322
Identification techniques for nonlinear differential equations of motion
[AD-A220695] 21 p3062 N90-27407
Statistical methodologies for non-Gaussian noisy environments
[AD-A222137] 21 p3066 N90-27433
Computation of efficient solutions of discretely distributed stochastic optimization problems
[ETN-90-97330] 21 p3067 N90-27436
BRS invariant stochastic quantization of Einstein gravity
[DE90-791126] 21 p3085 N90-27541
Stochastic dynamic programming for reservoir optimal control: Dense discretization and inflow correlation assumption made possible by parallel computing
[REPT-89-056] 22 p3238 N90-28360
Genetic algorithms: The state of the art and some research proposals
[REPT-89-058] 22 p3241 N90-28380
Matrix generators for production of equally distributed pseudorandom vectors
[ETN-90-97291] 22 p3243 N90-28390
New approach to HF channel modeling and simulation. Part 2: Stochastic model
[PB90-200338] 23 p3317 N90-28755
Simulation of INPE's printed circuit laboratory production line
[INPE-4556-TDL/331] 23 p3322 N90-28784
Study of meteorological processes important in the degradation of materials through surface temperature
[PB90-222720] 23 p3336 N90-28856
Learning in stochastic neural networks for constraint satisfaction problems 23 p3377 N90-29078
Regional phase propagation in three dimensionally heterogeneous media
[AD-A223279] 24 p3491 N90-29731

Geophysical turbulence research at NCAR
[AD-A223361] 24 p3492 N90-29732
Optimal control law phenomena in certain adaptive second-order observation systems
[AD-A224274] 24 p3534 N90-29986
Propagation of chaos and the McKean-Vlasov equation in duals of nuclear spaces
[AD-A224431] 24 p3543 N90-30039
Stochastic properties of the plasma wave heating map
[DE90-508077] 24 p3548 N90-30070

STOICHIOMETRY
Method for growing patterned thin films of superconductors
[AD-D014195] 04 p0560 N90-13262
Application of neutron diffraction NDE to high-temperature superconducting composites
[DE90-002184] 06 p0738 N90-14295
Oxygen stoichiometry, structural transitions, and thermodynamic behavior of the YBa2Cu3O(x) system
[DE89-017694] 06 p0852 N90-14951
Superconductivity and stoichiometry in Tl2Ca2Ba2Cu3O(x) single crystals
[DE90-003838] 07 p1002 N90-15801
La(sub 2)MO(sub 4 + delta) (M = Cu, Ni, Co): Phase separation and superconductivity resulting from excess oxygen defects
[DE90-001988] 08 p1128 N90-16534
Lithium cobalt oxide thin film and its electrochromism
[DE90-004570] 08 p1133 N90-16564
Spectroscopic techniques for the analysis of CdTe substrates used for the growth of HgCdTe
[AD-A214545] 09 p1288 N90-17466
Optical waveguide fabrication by stoichiometric implantation of Ti and O into LiNbO3
[DE90-004238] 09 p1292 N90-17488
Research in energetic compounds
[AD-A214106] 10 p1360 N90-17887
High temperature chemistry of oxide superconductors
[DE90-007821] 13 p1895 N90-20875
Energy beam treatment for improved adhesion of coatings to surfaces
[AD-D014449] 14 p1954 N90-21190
Influence of the deposition conditions on radiofrequency magnetron sputtered MoS2 films
[NASA-TP-2994] 14 p1958 N90-21210
A low NOx strategy for combusting high nitrogen content fuels
[PB90-155664] 19 p2712 N90-25435
High temperature x ray diffraction and Landau theory investigations of order-disorder transition in defect NaCl-type solids
[DE90-011807] 20 p2930 N90-26673
MBE growth technology for high quality strained III-V layers
[NASA-CASE-NPO-17723-1-CU] 20 p2932 N90-26685
Four-step kinetics for methane and implications for turbulent combustion 21 p2975 N90-26906
Ignition and combustion characteristics of metallized propellants
[NASA-CR-186870] 21 p2976 N90-26911
Growth of III-V films by control of MBE growth front stoichiometry
[NASA-CASE-NPO-17724-1-CU] 21 p3081 N90-27517
Method of forming three-dimensional semiconductor structures
[NASA-CASE-NPO-17835-1-CU] 21 p3081 N90-27518
Rapid annealing of iron implanted Hg(1-x)Cd(x)Te
[AD-A222777] 21 p3082 N90-27524
Optimal trajectories for Saenger-type vehicles 22 p3129 N90-27760
Effect of shock pressure on the structure and superconducting properties of Y-Ba-Cu-O in explosively fabricated bulk metal-matrix composites 22 p3138 N90-27804
Effect of oxygen stoichiometry on T(sub c) of Bi-based superconductors 22 p3142 N90-27818
Study of local structure and magnetism in high-T(sub c) copper oxide superconductors 22 p3143 N90-27824
An investigation of solid-fuel, dual-mode combustion ramjets 22 p3162 N90-27933
Reflection Mass Spectrometry (REMS) during 3/5 MBE
[DE90-014568] 23 p3304 N90-28690
Synthesis and structural chemistry of Au(III)-substituted Ba2YCu3O(7-delta)
[NASA-TM-103292] 23 p3305 N90-28696
A design tool utilizing stoichiometric structure for the analysis of biochemical reaction networks
[AD-A223873] 23 p3355 N90-28961

STOKES FLOW
A conforming spectral collocation strategy for Stokes flow through a channel contraction
[NASA-CR-181912] 02 p0263 N90-11495
Extrapolation techniques for finite element approximations of Stokes and Navier-Stokes flow over a backward facing step
[PREPRINT-499] 08 p1065 N90-16160
Finite element approximations of the stokes flow problem based upon various variational principles
[DE90-608612] 12 p1659 N90-19533
Plane Stokes flow driven by capillarity on a free surface: Overview and status
[DE90-009186] 15 p2098 N90-22008
Plane Stokes flow driven by capillarity on a free surface: Overview and status
[DE90-009290] 15 p2098 N90-22009
A finite difference treatment of Stokes-type flows: Preliminary report
[NASA-CR-186480] 22 p3168 N90-27970

STOKES THEOREM (VECTOR CALCULUS)
A multidomain spectral collocation method for the Stokes problem
[NASA-CR-181876] 03 p0396 N90-12266

STOL AIRCRAFT
U SHORT TAKEOFF AIRCRAFT

STONES (ROCKS)
U ROCKS

STONY METEORITES
NT ACHONDRITES
NT ALLENDE METEORITE
NT CARBONACEOUS CHONDRITES
NT CARBONACEOUS METEORITES
NT CHONDRITES
NT MURCHISON METEORITE

STOPPING
On the smooth fit boundary conditions in the optimal stopping problem for semimartingales
[CWI-MS-R8819] 04 p0542 N90-13147
Stopping rules for a class of random methods for detecting necessary linear inequality constraints
[MEMO-777] 05 p0683 N90-13977
On the safe approximation of PROLOG programs
[CWI-CS-R8913] 05 p0683 N90-13978
Epoxy-resin cable terminations
[AD-A213789] 07 p0942 N90-15454
Brake performance of the McDonnell Douglas DC-10-30/40 during high speed, high energy rejected takeoffs
[PB90-917004] 14 p1920 N90-21000
Use of Ni63 overvoltage gap switches in the flight termination systems on boosters launched from US Army Kwajalein Atoll (USAKA)
[AD-A223866] 23 p3299 N90-28661
Laser beam stop
[AD-D014595] 24 p3473 N90-29629

STOPPING POWER
Interaction of low-energy electrons and positrons with condensed matter: Stopping powers and inelastic mean free paths from optical data
[DE90-001001] 06 p0840 N90-14882
Direction-dependent stopping power and beam deflection in anisotropic solids
[DE90-001076] 06 p0840 N90-14883
Stopping power for protons in Al for the whole range of velocities
[DE90-008558] 13 p1884 N90-20810

STORABLE PROPELLANTS
Experimental study on the stability of small rocket engines with storable liquid propellants 01 p0036 N90-10196
A perspective on the use of storable propellants for future space vehicle propulsion 11 p1472 N90-18473

STORAGE
Annual operating plan for fiscal year 1990 for chemical/hydrogen energy systems program
[DE90-003964] 07 p0955 N90-15527
Environmental Projects. Volume 9: Construction of hazardous materials storage facilities
[NASA-CR-186296] 09 p1244 N90-17216

STORAGE BATTERIES
NT LEAD ACID BATTERIES
NT NICKEL CADMIUM BATTERIES
NT NICKEL HYDROGEN BATTERIES
NT NICKEL ZINC BATTERIES
NT SILVER ZINC BATTERIES
NT ZINC-BROMIDE BATTERIES
Rechargeable lithium/polymer cathode batteries
[AD-A210978] 01 p0062 N90-10354
Advanced calcium-thionyl chloride high-power battery
[AD-A211856] 04 p0495 N90-12846
The use of lithium batteries in biomedical devices
[AD-A212187] 04 p0497 N90-12863
Assessment of thin film batteries based on polymer electrolytes. Part 3: Specific energy versus specific power
[AD-A212141] 04 p0515 N90-12976
Silver composite cathodes for alkaline secondary batteries
[AD-D014227] 06 p0767 N90-14462
Silver-nickel composite cathodes for alkaline secondary batteries
[AD-D014231] 06 p0767 N90-14464
The secondary slurry-zinc/air battery
[DE90-002600] 06 p0772 N90-14491
Application of ac impedance method for diagnosis of lithium secondary battery degradation. Preliminary study with AA size Li/MoS2 cells
[DE90-702474] 08 p1061 N90-16137
Evaluation of a prototype lithium molybdenum disulfide secondary battery for load conditioner: Characteristics and performance of 70Wh class BC cell
[DE90-702460] 09 p1210 N90-17016
Outlook for new energies. Secondary batteries
[DE90-734946] 09 p1210 N90-17017
Thermal study of battery charge control by temperature derivative reduction 10 p1332 N90-17704
International Summer School on Solid State Microbatteries
[AD-A213457] 10 p1434 N90-18277
Feasibility of a super high energy density battery of the Li/BrF3 electrochemical system
[AD-A216794] 11 p1502 N90-18644
Life-cycle cost comparisons of advanced storage batteries and fuel cells for utility, stand-alone, and electric vehicle applications
[DE90-008090] 13 p1794 N90-20298
A survey of advanced battery systems for space applications 13 p1822 N90-20458
The electrochemical generation of useful chemical species from lunar materials 13 p1822 N90-20461
A new concept for high-cycle-life LEO: Rechargeable MnO2-hydrogen 13 p1822 N90-20462
Photovoltaic power for Space Station Freedom
[NASA-TM-102569] 15 p2062 N90-21812
Storage battery operation technique of photovoltaic system to prevent the imbalance of state of charge
[DE90-503032] 20 p2858 N90-26255

STORAGE RINGS (PARTICLE ACCELERATORS)
X-ray lithography sources: A review
[DE89-017610] 02 p0271 N90-11547
Advanced light source master oscillator
[DE90-000123] 03 p0342 N90-11953
The national synchrotron light source and its applications
[DE89-017605] 03 p0405 N90-12320
Influence of RF-parameters on beam lifetime
[NIKHEF-K/AMPS/89-06] 05 p0699 N90-14091
NIKHEF-K contributions to the 1989 Particle Accelerator Conference
[NIKHEF/AMPS/89/03] 06 p0841 N90-14891
The Amsterdam pulse stretcher project (AmPS) 06 p0841 N90-14892
Optics of the Amsterdam pulse stretcher (AmPS) 06 p0841 N90-14893
Modification of MEA modulator-klystron units enabling short pulse injection into a pulse-stretcher ring 06 p0841 N90-14894
Performance and modification of the MEA RF drive system 06 p0842 N90-14895
To construct a linac/storage ring FEL facility
[AD-A214620] 09 p1211 N90-17020
Instability investigation for storage mode. Microwave instability (single-bunch instability)
[NIKHEF-K/AMPS/89/05] 11 p1499 N90-18628
Biomedical applications of synchrotron x ray microscopy
[DE90-004957] 11 p1540 N90-18867
On storage rings for short wavelength FELs
[DE90-009059] 14 p1985 N90-21379
Exclusive production of p, p-, pi, and pi- in photon photon collisions
[NIKHEF-H/89-9] 15 p2165 N90-22376
A beauty factory using an SRF linac and a storage ring
[CEBAF-PR-89-017] 20 p2925 N90-26644
Activities report of the Werner-Heisenberg Institute for Physics, Munich, Federal Republic of Germany
[ISSN-0173-6256] 21 p3075 N90-27481
Status of the advanced light source
[DE90-015636] 23 p3395 N90-29185
Technical activities 1989, Electron and Optical Physics Division
[PB90-207267] 23 p3415 N90-29296

STORAGE STABILITY
Advanced calcium-thionyl chloride high-power battery
[AD-A211856] 04 p0495 N90-12846

Investigation of the phase stabilizing effect of 4 percent potassium fluoride on ammonium nitrate
[AD-A215313] 11 p1494 N90-18599
Instability investigation for storage mode. Microwave instability (single-bunch instability)
[NIKHEF-K/AMPS/89/05] 11 p1499 N90-18626
Effect of temperature on the storage life of polysulfide aircraft sealants
[MRL-TR-89-31] 12 p1629 N90-19364
Nickel-hydrogen capacity loss on storage 13 p1825 N90-20478
Shelf life extension for the lot AAE nozzle severance LSCs
[NASA-CR-183878] 15 p2062 N90-21813
Method and apparatus for assessing distillate fuel stability by oxygen overpressure
[AD-D014499] 19 p2679 N90-25237

STORAGE TANKS
Fluid-structure interaction effects in tank structures due to sloshing and hydrodynamic ram: Coupled Lagangian-Eulerian simulations 02 p0181 N90-11022
Modeling of liquid sloshing effects in multibody systems 02 p0181 N90-11023
Hydrazine fate and transformation in natural waters and soils 02 p0204 N90-11165
The strength-toughness combination of the aluminum-lithium alloys 2090 and 2091 at cryogenic temperatures
[DE90-001425] 06 p0746 N90-14338
An experimental and analytical examination of stratified thermal storage 09 p1215 N90-17046
Zero-gravity vortex vent and PVT gaging system 11 p1475 N90-18486
System for venting gas from a liquid storage tank
[NASA-CASE-MSC-21253-1] 13 p1787 N90-20254
Collapsible fabric tank testing
[AD-A217861] 14 p1987 N90-21388
Spacecraft attitude impacts on COLD-SAT non-vacuum jacketed LH2 supply tank thermal performance
[NASA-TM-103158] 16 p2207 N90-22592
Design of cryogenic tanks for launch vehicles 16 p2220 N90-22662
Numerical investigation of the thermal stratification in cryogenic tanks subjected to wall heat flux
[NASA-TM-103194] 22 p3171 N90-27984
Guidelines for pressure vessel safety assessment
[PB90-219619] 23 p3316 N90-28749
Study and analysis of leaking underground storage tank remediation techniques incorporated in states in EPA Region 6
[PB90-214834] 23 p3333 N90-28847

STORE RELEASE
U EXTERNAL STORE SEPARATION

STORM DAMAGE
Extreme hurricanes in the nineteenth century
[PB89-201305] 01 p0087 N90-10498

STORM SUPPRESSION
ASR-9 weather channel test report
[AD-A211749] 03 p0339 N90-11934

STORM SURGES
Coastal field data collection program. Hurricane Gilbert storm surge data
[AD-A218752] 17 p2426 N90-23823
Proceedings of the 21st Joint Meeting of the US-Japan Cooperative Program in Natural Resources Panel Wind and Seismic Effects
[PB90-186826] 21 p3030 N90-27226

STORMS
NT CYCLONES
NT DUST STORMS
NT HAILSTORMS
NT HURRICANES
NT IONOSPHERIC STORMS
NT MAGNETIC STORMS
NT MICROBURSTS (METEOROLOGY)
NT POLAR SUBSTORMS
NT RAINSTORMS
NT SNOWSTORMS
NT SOLAR STORMS
NT STORMS (METEOROLOGY)
NT SUDDEN IONOSPHERIC DISTURBANCES
NT THUNDERSTORMS
NT TORNADOES
NT TROPICAL STORMS
NT TYPHOONS
Catalog of absolutely calibrated, range normalized, wideband, electric field waveforms from located lightning flashes in Florida: July 24 and August 14, 1985 data
[AD-A212708] 04 p0521 N90-13008
Application of a mass-consistent wind model to chinook windstorms
[AD-A213622] 07 p0963 N90-15568
Coastal frontogenesis and associated severe weather on 13 March 1986 (GALE IOP 13)
[AD-A217708] 13 p1845 N90-20590
A sub-cloud layer vorticity budget analysis for two microburst-producing storms from jaws dual-Doppler data
[AD-A218180] 13 p1847 N90-20599
Tropopause undulations and the development of extratropical cyclones 15 p2132 N90-22186
Large aperture array measurements of the vertical ambient noise field
[AD-A220165] 17 p2432 N90-23859
The instability mechanism of synoptic-scale eddies 22 p3211 N90-28217

STORMS (METEOROLOGY)
NT CYCLONES
NT DUST STORMS
NT HAILSTORMS
NT HURRICANES
NT MICROBURSTS (METEOROLOGY)
NT POLAR SUBSTORMS
NT RAINSTORMS
NT SNOWSTORMS
NT THUNDERSTORMS
NT TORNADOES
NT TROPICAL STORMS
NT TYPHOONS
National Severe Storms Laboratory, fiscal year 1988
[PB89-156145] 01 p0087 N90-10493
Numerical simulations of a midlatitude squall line 01 p0087 N90-10497
Extreme hurricanes in the nineteenth century
[PB89-201305] 01 p0087 N90-10498
Vertical distribution of pollutants in the presence of convective storms
[DE90-002590] 07 p0960 N90-15549
Diagnostic and kinematic fields associated with curved and straight jet streaks using a two-layer primitive equation model 08 p1100 N90-16371
Analysis of GALE (Genesis of Atlantic Lows Experiment) data
[AD-A217182] 13 p1844 N90-20584
Gravity wave initiated convection
[NASA-CR-186868] 23 p3350 N90-28933

STOVL AIRCRAFT
U V/STOL AIRCRAFT

STRAIGHT WINGS
U RECTANGULAR WINGS

STRAIN AGING
U PRECIPITATION HARDENING

STRAIN DISTRIBUTION
The effects of Mo2C morphology and strain distribution on the fatigue properties of Fe-C-Mo dual-phase steels 07 p0901 N90-15210
Nonlinear strain-displacement relations for thin axisymmetric shells
[PB89-226013] 07 p0945 N90-15470
Mechanical strain isolator mount
[NASA-CASE-LAR-13580-1] 08 p1084 N90-16272
Strain induced amorphization of aluminium by manganese implantation
[DE90-607259] 10 p1356 N90-17863
Modeling the pressure-strain correlation of turbulence: An invariant dynamical systems approach
[NASA-CR-181979] 10 p1383 N90-18003
A 4-node assumed-stress hybrid shell element with rotational degrees of freedom
[NASA-CR-4279] 13 p1815 N90-20422
Direct formulation of a 4-node hybrid shell element with rotational degrees of freedom
[NASA-CR-4282] 14 p1991 N90-21411
Finite element elastic-plastic-creep and cyclic life analysis of a cowl lip
[NASA-TM-102342] 16 p2246 N90-22808
Finite element analysis of structural components using viscoplastic models with application to a cowl lip problem
[NASA-CR-185189] 17 p2416 N90-23769
A photoelastic analysis of the strain field around impact damage in a graphite fibre reinforced panel subjected to compression loads
[FFA-TN-1989-48] 19 p2703 N90-25379
Analysis of strain relaxation in Au/Ni multilayers by x ray diffraction
[IAR-89-25] 20 p2875 N90-26357
Variational formulation and finite element implementation of Pagano's theory of laminated plates 24 p3442 N90-29437

STRAIN ENERGY METHODS
Spallation of oxide scales from 20 percent Cr/25 percent Ni/Nb stainless steel
[AERE-R-13464] 13 p1775 N90-20189
A numerical micromechanics analysis of the mechanical properties of a plain weave composite
[OUEL-1760/89] 19 p2673 N90-25201

STRAIN ENERGY RELEASE RATE
Analysis of delamination growth 02 p0183 N90-11036
Effects of T-tabs and large deflections in DCB specimen tests
[NASA-TM-101677] 09 p1186 N90-16868
Fatigue delamination onset prediction in tapered composite laminates
[NASA-TM-101673] 09 p1236 N90-17177
Combined effect of matrix cracking and stress-free edge on delamination
[NASA-TM-102591] 14 p1944 N90-21126
Delamination failure in a unidirectional curved composite laminate
[NASA-CR-182018] 14 p1993 N90-21421
Energy release rate analysis of interfacial cracks in composites 15 p2065 N90-21829
Strain energy release rate analysis of delamination in a tapered laminate subjected to tension load
[NASA-TM-102592] 20 p2826 N90-26076

STRAIN FATIGUE
U FATIGUE (MATERIALS)

STRAIN GAGE BALANCES
A FORTRAN program for the calculation of the calibration coefficients of a six-component strain gauge balance
[AD-A210375] 01 p0105 N90-10599
Development of a multi-component internal strain-gauge balance for model tests in a cryogenic wind tunnel
[NLR-TR-88157-U] 04 p0459 N90-12628
Experience with strain-gage balances for cryogenic wind tunnels 08 p1031 N90-15958
Cryogenic balances for the US NTF 08 p1031 N90-15959
Analysis of a six-component, flow-through, strain-gage, force balance used for hypersonic wind tunnel models with scramjet exhaust flow simulation
[NASA-CR-186585] 15 p2055 N90-21775
A microprocessor controlled strain gauge calibration module
[AR-005-579] 23 p3329 N90-28821

STRAIN GAGES
Development of a multi-component internal strain-gauge balance for model tests in a cryogenic wind tunnel
[NLR-TR-88157-U] 04 p0459 N90-12628
Optical techniques for in-plane strain analysis in an industrial environment
[PNR90601] 04 p0512 N90-12957
Plasma separation process: Magnet move to Oak Ridge National Laboratory
[DE89-017457] 04 p0556 N90-13242
High temperature capacitive strain gage
[NASA-CR-4266] 05 p0644 N90-13760
Development and characterization of PdCr temperature-compensated wire resistance strain gage
[NASA-CR-185153] 05 p0644 N90-13761
Electrical properties of materials for high temperature strain gage applications
[NASA-CR-186192] 06 p0780 N90-14534
The Shock and Vibration Digest, volume 21, no. 9 09 p1235 N90-17168
State-of-the-art of measuring ground shock and cratering phenomena 09 p1235 N90-17170
Instrumentation of pendulum impactor using metal foil strain gauges
[PB90-122656] 10 p1387 N90-18024
Aerodynamic testing of a rotating wind turbine blade
[DE90-000312] 11 p1451 N90-18362
Small strain gage applications 2
[DE90-008312] 15 p2102 N90-22026
Two-dimensional surface strain measurement based on a variation of Yamaguchi's laser-speckle strain gauge
[NASA-TM-103162] 16 p2241 N90-22784
Composite integrity monitoring
[AD-A220813] 17 p2369 N90-23487
A resistance strain gage with repeatable and cancellable apparent strain for use to 800 C
[NASA-CR-185256] 20 p2823 N90-26063

STRAIN HARDENING
Delayed failure of silver-aided diffusion welds between steel
[DE89-016652] 01 p0045 N90-10252
Strain aging in tungsten-heavy alloys
[AD-A211166] 01 p0046 N90-10259
The 4.2 K fracture toughness of 304 stainless steel in a magnetic field
[DE90-002083] 06 p0747 N90-14347
Viscoplasticity: A thermodynamic formulation
[NASA-TM-102388] 06 p0797 N90-14640
Shear strain localization phenomenon in viscoplastic materials 06 p0798 N90-14649
Approximate methods for dynamic plastic deformation of structures
[DE90-002214] 06 p0800 N90-14660
Steady-state and transient Zener parameters in viscoplasticity: Drag strength versus yield strength
[NASA-TM-102487] 10 p1395 N90-18064

Strengthening mechanisms of tungsten powder reinforced uranium
[DE90-009331] 14 p1947 N90-21144
A viscoplastic model with application to LiF-22 percent CaF2 hypereutectic salt
[NASA-TM-103181] 17 p2417 N90-23770
A vectroized elastic/plastic power law hardening material model including Lueders strain
[DE90-010172] 18 p2572 N90-24655
Processing and characterization of high strength, high ductility Hadfield steel
[AD-A221769] 21 p2982 N90-26947
Engineering fracture mechanics
[AD-A222699] 21 p3012 N90-27123
Studies on crack mechanics
[AD-A223634] 24 p3480 N90-29670
A method for modeling kinematic hardening and cyclic strain effects
[ONERA-RT-77/1765-RY-089-R] 24 p3481 N90-29677

STRAIN MEASUREMENT
An interferometric strain-displacement measurement system
[NASA-TM-101638] 01 p0080 N90-10454
Optical techniques for in-plane strain analysis in an industrial environment
[PNR90601] 04 p0512 N90-12957
Spectral contents readout of birefringent sensor
[NASA-CR-179444] 06 p0843 N90-14905
Measuring strain in carbon fibre composite laminates using the Raman optomechanical strain gauge 11 p1477 N90-18503
Strain and dynamic measurements using fiber optic sensors embedded into graphite/epoxy tubes 14 p1937 N90-21090
Two-dimensional surface strain measurement based on a variation of Yamaguchi's laser-speckle strain gauge
[NASA-TM-103162] 16 p2241 N90-22784
Non destructive testing of composite structures using embedded optical fibers: A mechanical interaction model
[ETN-90-97016] 18 p2573 N90-24661
Intelligent composites containing measuring fibre optic networks for continuous self diagnosis
[ETN-90-97018] 19 p2673 N90-25200
Feasibility study for the advanced one-dimensional high temperature optical strain measurement system, phase 3
[NASA-CR-185254] 19 p2693 N90-25324
Progress in high temperature speckle-shift strain measurement system
[NASA-TM-103255] 22 p3177 N90-28031

STRAIN RATE
Delayed failure of silver-aided diffusion welds between steel
[DE89-016652] 01 p0045 N90-10252
Analysis of spurt phenomena for a non-Newtonian fluid
[AD-A210560] 01 p0071 N90-10405
Stability of discontinuous shearing motions of a non-Newtonian fluid
[AD-A210643] 01 p0071 N90-10406
The HEL (Hugoniot Elastic Limit) and rate-dependent yield behavior
[DE89-016981] 02 p0199 N90-11134
Characterizations of shock-loaded aluminum-infiltrated boron carbide cermets
[DE89-016773] 02 p0201 N90-11146
An evaluation of the Chaboche and Bodner-Partom viscoplastic constitutive theories for strain rate sensitive materials 02 p0232 N90-11330
Strain and density dependent valence-band masses in InGaAs/GaAs and GaAs/GaAsP strained-layer structures
[DE89-016882] 02 p0285 N90-11627
Deformation behavior of SiC/2014 Al metal-matrix composite
[AD-A212095] 03 p0320 N90-11816
Deformation and defects in Laves-phase intermetallic compounds
[DE89-017798] 03 p0328 N90-11862
Mechanism for shear band formation in the high strain rate torsion test
[PB89-215370] 03 p0356 N90-12038
An approach to low temperature high strain rate superplasticity in aluminum alloy 2090
[AD-A212271] 04 p0476 N90-12731
Anomalous strain rate dependence of the serrated flow in Ni-H and Ni-C-H alloys
[AD-A213244] 05 p0624 N90-13641
A slow strain-rate tensile testing machine
[ARL-MAT-TM-399] 05 p0645 N90-13764
The Fourth Oxford International Conference on the Mechanical Properties of Materials at High Rates of Strain
[AD-A212293] 05 p0653 N90-13809
Shear strain localization phenomenon in viscoplastic materials 06 p0798 N90-14649
New transient algorithms for non-Newtonian flows
[AD-A213494] 07 p0930 N90-15385
Irradiation creep and swelling of annealed type 304L stainless steel at approximately 390 C and high neutron fluence
[DE90-004521] 08 p1046 N90-16047
Fatigue life estimates for helicopter loading spectra
[NASA-CR-181941] 08 p1088 N90-16294
Cyclic deformation of Sn-60 to Pb-40 solder joints during thermomechanical fatigue
[DE90-004197] 09 p1237 N90-17179
A summary of the Bodner-Stouffer constitutive model
[AD-A214532] 09 p1237 N90-17182
Hydrogen embrittlement of titanium and its alloys
[DE90-602366] 10 p1355 N90-17858
A micromechanical viscoplastic stress-strain model with grain boundary sliding
[DE90-006013] 10 p1437 N90-18295
An objective time-integration procedure for isotropic rate-independent and rate-dependent elastic-plastic constitutive equations
[PB90-121245] 11 p1550 N90-18925
The mechanics of shear band formation in thermal viscoplastic materials at high rates of loading 15 p2120 N90-22128
Statistical treatment of slow strain rate data for assessment of hydrogen embrittlement in low alloy high strength steel
[ARL-MAT-R-122] 20 p2832 N90-26106
Load-point compliance for the arc bend-arc support fracture toughness specimen
[AD-A221618] 21 p3014 N90-27134
Methodology of the fatigue under shocks. Experimental results: 7075 T6 and 35 NCD16
[ETCA-89-R-140] 22 p3157 N90-27901
Inelastic analysis of laminated composites 23 p3301 N90-28669
Rheometer strain and strain-rate errors
[DE90-013845] 23 p3329 N90-28824
Processability and high temperature behavior of emerging aerospace alloys
[AD-A224285] 24 p3448 N90-29475
The MTL Torsional Split-Hopkinson bar
[AD-A223278] 24 p3479 N90-29663

STRAIN SOFTENING
U PLASTIC DEFORMATION

STRAITS
Comparison of circulation obtained through the trajectory of a drifting buoy tracked by satellite and hydrographic data in the Bransfield Strait
[INPE-4946-TDL/387] 11 p1537 N90-18850

STRAKES
VLA missile development and high angle of attack behavior 10 p1305 N90-17553
Actuated forebody strakes
[NASA-CASE-LAR-13983-1] 17 p2352 N90-23390
Development of non-conventional control methods for high angle of attack flight using vortex manipulation 23 p3273 N90-28522

STRANDS
Design of coupled or uncoupled multifilamentary SSC-type strands with almost zero retained magnetization at fields near 0.3 T
[DE90-005391] 08 p1047 N90-16052
Convergent strand array liquid pumping system
[NASA-CASE-NPO-17301-1-CU] 17 p2385 N90-23587

STRANGE ATTRACTORS
Chaotic transients, higher dimensional phenomena, and coupled ordinary differential equations
[DE90-006641] 12 p1706 N90-19794
Coherent structures, chaos and the role of modern dynamics in turbulent shear flows
[AD-A220884] 18 p2552 N90-24562

STRANGENESS
Strangeness enhancement in 14.6 A GeV/c Si+Au interactions?
[DE90-008826] 14 p2026 N90-21616
Fast pulsars, strange stars: An opportunity in radio astronomy
[DE90-015630] 24 p3563 N90-30155

STRAPDOWN INERTIAL GUIDANCE
Hybrid angular velocity reference system for the investigation of dynamic properties of strapdown gryos
[DFVLR-FB-89-25] 04 p0450 N90-12577
RTSIN1: A model of a strapdown INS on a two-axis rate table
[AD-A212406] 04 p0450 N90-12579
SINS1: A model of a strapdown inertial navigation system
[AD-A215495] 09 p1166 N90-16749
The Fourteenth Biennial Guidance Test Symposium, volume 1
[AD-A216925] 11 p1455 N90-18383
Development of a standardized three axis sensor for inertial data achievement for future flight rule systems
[ETN-90-96075] 12 p1604 N90-19231
Integration of GPS and strapdown inertial subsystems into a single unit 24 p3423 N90-29340
Kalman filter formulations for transfer alignment of strapdown inertial units 24 p3424 N90-29342
Integration of GPS/INS with partitioned filters 24 p3425 N90-29347
Integrated strapdown avionics for precision guided vehicles 24 p3427 N90-29361
Integrated navigation/flight control for future high performance aircraft 24 p3427 N90-29362
Fault Detection and Isolation (FDI) techniques for guidance and control systems 24 p3428 N90-29366
Guidance and control techniques for airborne transfer alignment and SAR motion compensation 24 p3429 N90-29372

STRAPS
The creep behavior of an aramide fiber reinforced wound tow-strap
[LR-546] 12 p1620 N90-19312
Aircraft crash survival design guide. Volume 4: Aircraft seats, restraints, litters, and cockpit/cabin delethalization
[AD-A218437] 16 p2198 N90-22548
Helmet-mounted head restraint
[AD-D014536] 20 p2899 N90-26491

STRATA
NT SUBSTRATES
Concentric layer ramjet fuel
[AD-D014443] 14 p1941 N90-21111
Electromagnetic inverse profiling of stratified media
[ETN-90-96402] 15 p2087 N90-21947

STRATEGIC MATERIALS
Identification of a cast iron alloy containing nonstrategic elements
[NASA-CR-185174] 11 p1487 N90-18559

STRATEGY
Comparison of DPCM prediction strategies for high-quality digital television bit-rate reduction
[BBC-RD-1989/8] 01 p0056 N90-10318
An analytical hierarchy process approach to establish the systems analyst's knowledge base for selecting an information requirements determination strategy 01 p0136 N90-10785
Operating principle 05 p0603 N90-13500
Electronic warfare: Reliable equipment needed to test Air Force's electronic warfare systems
[AD-A212952] 05 p0632 N90-13687
The processes of scientific research: The strategy of experimentation 06 p0824 N90-14788
Concerning advanced architectures for strategic defense
[DE90-001894] 06 p0836 N90-14857
Federal scientific and technical information in an electronic age: Opportunities and challenges
[PB90-114414] 09 p1295 N90-17505
Fire hardening of aircraft through upgrades of materials and designs 10 p1315 N90-17605
Solar-Terrestrial Science Strategy Workshop
[NASA-CP-3048] 10 p1444 N90-18329
Background of the workshop 10 p1444 N90-18330
Recommendations for the future 10 p1445 N90-18338
Remote sensing applied to vegetation as subsidized in municipal planning
[INPE-4908-PRE/1509] 11 p1523 N90-18770
Survivability and effectiveness of near-term strategic defense
[DE90-005805] 11 p1555 N90-18955
Investigations into a new algorithm for calculating H infinity optimal controllers 12 p1637 N90-19406
Strategies for high efficiency operation of the E-beam excited atomic xenon laser using high-power and high-energy loading
[DE90-005196] 13 p1806 N90-20370
Space in warfare
[AD-A217527] 13 p1879 N90-20782
Controller reduction for effective interdisciplinary design of active structures 14 p1935 N90-21077
Microgravity, the space application of the 21st century. Challenges, constraints, and strategies
[REPT-892-430-105] 16 p2226 N90-22696
Data exchange strategy. Part 1: Review of digital data exchange technology
[AD-A218506] 16 p2327 N90-23267
Object orientated simulation on transputer arrays using time warp
[AD-A219795] 17 p2389 N90-23607
An experimental evaluation of software redundancy as a strategy for improving reliability
[NASA-TM-102613] 17 p2448 N90-23958
Optical computing strategies
[AD-A219433] 17 p2472 N90-24131

From where they look to what they think: Determining controller cognitive strategies from oculometer scanning data 18 p2641 N90-25041
Multisensor monitoring of deforestation in the Guinea Highlands of West Africa [NASA-CR-186709] 19 p2706 N90-25396
Prevalence of G-induced cervical injury in US Air Force pilots 19 p2717 N90-25460
Testing of 3-D models in 2-D adaptive wall test sections 21 p2962 N90-26842
Possible trajectory profiles to achieve the geostationary orbit without any drift phase 22 p3127 N90-27745
Congestion-reduction and service-restoration strategies for telecommunication networks [PB90-207938] 22 p3164 N90-27944
Studies in automatic speech recognition and its application in aerospace 23 p3318 N90-28759
Methods and strategies of object localization 23 p3366 N90-29020
Map learning with indistinguishable locations 23 p3367 N90-29025
How do robots take two parts apart 23 p3374 N90-29061
Search strategies for computer-stored information: A microcomputer tutorial 24 p3557 N90-30126

STRATIFICATION
NT ATMOSPHERIC STRATIFICATION
NT INTERCALATION
An experimental and analytical examination of stratified thermal storage 09 p1215 N90-17046
The extension of rapid distortion theory to stratified shear flows 14 p2005 N90-21491
Stratified ocean mixing [AD-A219233] 16 p2259 N90-22881
Arithmetic classification of perfect models of stratified programs (extended version) [CWI-CS-R8928] 17 p2462 N90-24063
Experiments with unsteady, free surface, three-dimensional vortices in a thermally stable, stratified fluid [AD-A222088] 21 p2954 N90-26796
A numerical study of the role of meso beta and meso gamma scale vertical exchange processes in the evolution of upper tropospheric frontal systems [AD-A222057] 21 p3031 N90-27230
Numerical investigation of the thermal stratification in cryogenic tanks subjected to wall heat flux [NASA-TM-103194] 22 p3171 N90-27984
Laboratory experiments on stability and entrainment of oceanic stratocumulus. Part 2: Entrainment experiment 22 p3220 N90-28264

STRATIFIED FLOW
The interaction and variation of waves and turbulence from MST radar data [AD-A212849] 05 p0670 N90-13906
Stability of numerical solutions for stratified two-phase flow [DE90-701646] 07 p0929 N90-15379
Experiments with unsteady, free surface, three-dimensional vortices in a thermally stable, stratified fluid [AD-A222088] 21 p2954 N90-26796

STRATIFIED LAYERS
U STRATA

STRATIGRAPHY
Three ages of Venus 03 p0428 N90-12453
Organic geochemical and tectonic evolution of the midcontinent rift system: Organic geochemistry and micropaleontology [DE89-017561] 06 p0818 N90-14760
Physical models of cometary nuclei: A review 12 p1738 N90-19991
Petrographic working model of the Rosetta sampling and modelling subgroup for a comet nucleus 12 p1738 N90-19992
Dynamics of crust formation and dust emission of comet nucleus analogues under isolation 12 p1743 N90-20020

STRATOCUMULUS CLOUDS
Stratiform clouds and their interaction with atmospheric motions 03 p0360 N90-12060
The chemistry and dynamics of marine stratocumulus 08 p1102 N90-16381
A modeling study of the cloud-topped marine boundary layer [AD-A218103] 13 p1846 N90-20594
FIRE Science Results 1989 [NASA-CP-3079] 22 p3213 N90-28224
Comparative climatology of four marine stratocumulus regimes 22 p3213 N90-28225
Large-scale variability in marine stratocumulus clouds defined from simultaneous aircraft and satellite measurements 22 p3213 N90-28226
On estimating scale invariance in stratocumulus cloud fields 22 p3213 N90-28227
Inhomogeneities of stratocumulus liquid water 22 p3213 N90-28228
Intercomparisons of GOES-derived cloud parameters and surface observations over San Nicolas Island 22 p3214 N90-28229
Stratocumulus cloud height variations determined from surface and satellite observations 22 p3214 N90-28230
July 16, 1987 revisited: Lessons for modelers 22 p3214 N90-28232
An eight-month climatology of marine stratocumulus cloud fraction, albedo, and integrated liquid water 22 p3214 N90-28233
Reflectivities of uniform and broken stratiform clouds: An update 22 p3215 N90-28236
Spectral absorption of marine stratocumulus clouds derived from in situ cloud radiation measurements 22 p3215 N90-28238
Cloud optical parameters as derived from the multispectral cloud radiometer 22 p3215 N90-28239
Satellite-derived cloud and radiation fields over the marine stratocumulus IFO 22 p3216 N90-28240
The radiation budget of stratocumulus clouds measured by tethered balloon instrumentation: Variability of flux measurements 22 p3216 N90-28242
Structural analysis of stratocumulus convection 22 p3216 N90-28243
On the dynamic and thermodynamic structures of marine stratocumulus 22 p3216 N90-28244
A stratocumulus thermodynamic analysis: July 5 case study 22 p3217 N90-28245
Turbulence structure in clear and cloudy regions of the 7 July 1987 Electra mission 22 p3217 N90-28247
Diurnal variation in the turbulent structure of the cloudy marine boundary layer during FIRE 1987 22 p3217 N90-28248
The influence of continental sources of aerosols on the marine stratocumulus during FIRE IFO-1 22 p3218 N90-28250
Optical properties of marine stratocumulus clouds modified by ship track effluents 22 p3218 N90-28253
A unified view of convective transports by stratocumulus clouds, shallow cumulus clouds, and deep convection 22 p3219 N90-28254
A case study of cumulus formation beneath a stratocumulus sheet: Its structure and effect on boundary layer budgets 22 p3219 N90-28256
A cloudiness transition in a marine boundary layer 22 p3219 N90-28259
Analysis of marine stratocumulus clearing events during FIRE 22 p3220 N90-28260
FIRE aircraft observations of horizontal and vertical transport in marine stratocumulus 22 p3220 N90-28261
Laboratory experiments on stability and entrainment of oceanic stratocumulus. Part 1: Instability experiment 22 p3220 N90-28263
Laboratory experiments on stability and entrainment of oceanic stratocumulus. Part 2: Entrainment experiment 22 p3220 N90-28264
A comparison of ISCCP and FIRE satellite cloud parameters 22 p3221 N90-28267
Comparison of satellite based cloud retrieval methods for cirrus and stratocumulus 22 p3221 N90-28268
Radiative diffusivity factors in cirrus and stratocumulus clouds: Application to two-stream models 22 p3226 N90-28293
Physically-based general circulation model parameterization of clouds and their radiative interaction 22 p3228 N90-28308

STRATOFORTRESS AIRCRAFT
U B-52 AIRCRAFT

STRATOPAUSE
Remote sensing of atmospheric water vapour by pressure modulation radiometry 06 p0802 N90-14667

STRATOSPHERE
NT OZONOSPHERE
NT STRATOPAUSE
Paper 1. Impact of volcanic aerosols on stratospheric chemistry. Paper 2. O2 (1 sigma g +) and O2 (1 delta g) in the H + O2 reaction system. Paper 3. Barotropic instability of zonal jets on Mars, Earth and Venus 01 p0084 N90-10477
Stratospheric ozone depletion [PB89-207476] 02 p0238 N90-11354
Two-Dimensional Intercomparison of Stratospheric Models [NASA-CP-3042] 02 p0248 N90-11405
Report on the 2-D Model Intercomparison Workshop held January 11-16, 1987 in Fort Myers Beach, Florida, chapter 2 02 p0248 N90-11406
Report of the 1988 2-D Intercomparison Workshop, chapter 3 02 p0248 N90-11407
Model documentation, chapter 4 02 p0249 N90-11408
Lidar observations of the stratospheric aerosol: Boulder, Colorado, 1985 to 1987 [PB89-203871] 02 p0251 N90-11425
Studies of baroclinic instability in the presence of surface topography and stratospheric ozone 03 p0361 N90-12068
Use of satellite data and modeling to asses the influence of stratospheric processes on the troposphere 03 p0363 N90-12075
Humidity local measurements in the middle atmosphere 05 p0657 N90-13833
SOFIA (Stratospheric Observatory For Infrared Astronomy): A 3m class airborne telescope 05 p0659 N90-13846
A double focusing mass-spectrometer for simultaneous ion measurements in the stratosphere 05 p0659 N90-13848
Operational activity in France and a new method of balloon temperature piloting 05 p0660 N90-13857
Long duration balloon flights in the middle stratosphere 05 p0663 N90-13874
Observations of stratospheric HCl: 1975-1985 [AERONOMICA-ACTA-A-349-1989] 05 p0666 N90-13892
The interaction and variation of waves and turbulence from MST radar data [AD-A212849] 05 p0670 N90-13906
Meteorological atlas of the Northern Hemisphere lower stratosphere for January and February 1989 during the Airborne Arctic Stratospheric Expedition [NASA-TM-4145] 05 p0671 N90-13908
Global stratospheric change: Requirements for a Very-High-Altitude Aircraft for Atmospheric Research [NASA-CP-10041] 06 p0723 N90-14220
Remote sensing of atmospheric water vapour by pressure modulation radiometry 06 p0802 N90-14667
The retrieval of the concentrations of nitric oxide and nitrogen dioxide from satellite solar occultation measurements at sunset and sunrise 06 p0814 N90-14733
Extraterrestrial halogen and sulfur content of the stratosphere [DE89-017623] 06 p0815 N90-14738
Environmental, health, and CFC substitution aspects of the ozone depletion issue [DE90-004404] 08 p1099 N90-16363
The effect of orographic forcing on the mean flow of the stratosphere 08 p1099 N90-16367
A double focussing mass-spectrometer for simultaneous ion measurements in the stratosphere [AERONOMICA-ACTA-A-350-1989] 08 p1102 N90-16379
Numerical modeling of the atmosphere with an isentropic vertical coordinate 09 p1246 N90-17226
Nimbus 7 solar backscatter ultraviolet (SBUV) ozone products user's guide [NASA-RP-1234] 09 p1246 N90-17227
The receiving system of a dual dye lidar to study molecular and aerosol densities at the base of the stratosphere [AD-A218286] 13 p1843 N90-20581
New spectral features of stratospheric trace gases 15 p2079 N90-21910
Opportunities for US-USSR cooperation in the investigation of Arctic stratospheric ozone 15 p2125 N90-22154
Forecast of Atlantic seasonal hurricane activity for 1990 15 p2134 N90-22194
Gravity wave and turbulence studies using a high-resolution ST radar [AD-A218877] 16 p2255 N90-22860
Effects of solar ultraviolet radiation on biogeochemical dynamics in aquatic environments [AD-A221119] 18 p2578 N90-24687
IR transition moments and collisional dynamics of vibrationally excited OH radicals via time-resolved laser absorption spectroscopy [AD-A221005] 18 p2580 N90-24696
New observations of stratospheric N2O5 [NASA-TM-103478] 20 p2883 N90-26402
Stratospheric chemistry 20 p2886 N90-26424
Photodissociation of O2 in the stratosphere and mesosphere: A general parametrization of the Schumman-Runge Bands 20 p2887 N90-26427
Laboratory measurements and methane photochemistry modeling 20 p2947 N90-26770
Conceptual design study for Infrared Limb Experiment (IRLE) [NASA-CR-186950] 21 p2968 N90-26869
Crossed-microwave-beam air ionization laboratory experiments [DE90-012056] 21 p3024 N90-27195

Lidar observations of stratospheric aerosols in 1988
[PB90-180670] 22 p3198 N90-28145
Subjective-probability-based scenarios for uncertain input parameters: Stratospheric ozone depletion
[N-3140-EPA/JMO/RC] 22 p3199 N90-28157
Solar activity influence on climatic variations of stratosphere and mesosphere in mid-latitudes
22 p3202 N90-28169
The planetary waves dynamics and interannual course of meteorological parameters of the high latitude stratosphere and mesosphere of the Northern and Southern Hemispheres during the 20th and 21st solar cycles and different phases of QBO
22 p3203 N90-28170
Stratospheric effects of solar ultraviolet variations on the solar rotation time scale 22 p3204 N90-28176
Total ozone time variations during the spring reversals in the high latitudinal stratosphere of the Northern Hemisphere during the 20th and 21st solar cycles
22 p3205 N90-28181
Diurnal and temporal variation of UV-flux and its dependence on stratospheric ozone
22 p3205 N90-28184
Solar activity influences on atmospheric electricity and on some structures in the middle atmosphere
22 p3207 N90-28196
Comparison of satellite derived dynamical quantities in the stratosphere of the Southern Hemisphere
22 p3210 N90-28210
An observational study of the circulation in the Southern Hemisphere stratosphere 24 p3488 N90-29715
Measurements of the high altitude infrared characteristics of the atmosphere
[AD-A224401] 24 p3491 N90-29728

STRATOSPHERIC AEROSOL & GAS EXPERIMENT
U SAGE SATELLITE

STRATOSPHERIC WARMING
Greenhouse gases: Changing the global climate
[DE90-002788] 07 p0957 N90-15535
The effect of orographic forcing on the mean flow of the stratosphere 08 p1099 N90-16367
An observational study of the circulation in the Southern Hemisphere stratosphere 24 p3488 N90-29715

STRATOTANKER AIRCRAFT
U C-135 AIRCRAFT

STRATUS CLOUDS
Optical transmission through clouds
[AD-A214765] 09 p1248 N90-17240
Reflectivities of uniform and broken stratiform clouds: An update 22 p3215 N90-28236
Cloud optical parameters as derived from the multispectral cloud radiometer 22 p3215 N90-28239
Analysis of ER-2 radiometer and lidar observations from the 1987 marine stratus experiment
22 p3216 N90-28241
Direct and remote sensing observations of the effects of ships on clouds 22 p3218 N90-28252
FIRE aircraft observations of horizontal and vertical transport in marine stratocumulus
22 p3220 N90-28261
Vertical-velocity skewness in the marine stratus-topped boundary layer 22 p3220 N90-28262

STREAK CAMERAS
Interferometry and high speed photography of laser-driven flyer plates
[DE89-016990] 02 p0225 N90-11290
A microchannel plate intensified, subnanosecond, X-ray imaging camera
[DE89-017781] 03 p0350 N90-12003
Noise floors of subnanosecond transient recording systems
[DE90-002339] 12 p1666 N90-19571
Evaluation of dynamic range for LLNL streak cameras using high contrast pulses and pulse podiatry on the Nova laser system
[DE90-015203] 24 p3472 N90-29620
Long-term flat-field behavior in LLNL streak cameras: Preliminary results
[DE90-015615] 24 p3472 N90-29621

STREAK PHOTOGRAPHY
Air breakdown photography in the picosecond domain
[DE89-016775] 03 p0322 N90-11830

STREAM FUNCTIONS (FLUIDS)
A conforming spectral collocation strategy for Stokes flow through a channel contraction
[NASA-CR-181912] 02 p0263 N90-11495
Development of a defect stream function, law of the wall/wake method for compressible turbulent boundary layers
[NASA-CR-4286] 11 p1507 N90-18675

STREAMLINE FLOW
U LAMINAR FLOW

STREAMLINED BODIES
NT FAIRINGS

STREAMLINING
Streamlining algorithms for complete adaptation
21 p2962 N90-26841
The streamline diffusion finite element method for compressible and incompressible fluid flow
22 p3172 N90-27991
Three-dimensional model testing in the transonic self-streamlining wind tunnel 23 p3284 N90-28583

STREAMS
NT GAS STREAMS
Evaluation and representation of two and three dimensional data fields from optical stream measurements
[MPIS-18/1989] 17 p2474 N90-24143
Prediction of episodic acidification in Maryland coastal plain streams
[PB90-194978] 22 p3199 N90-28152

STRENGTH OF MATERIALS
U MECHANICAL PROPERTIES

STRESS (PHYSIOLOGY)
NT ACCELERATION STRESSES (PHYSIOLOGY)
Control of thermoregulatory sweating during exercise in the heat
[AD-A206001] 01 p0092 N90-10523
Heatstroke pathophysiology: The energy depletion model
[AD-A212156] 03 p0380 N90-12164
Microcomputer-based tests for repeated-measures: Metric properties and predictive validities
[NASA-CR-185517] 03 p0382 N90-12174
A menu of self-administered microcomputer-based neurotoxicology tests
[NASA-CR-185518] 03 p0382 N90-12175
Prediction of thermal stress casualties
[AD-A212356] 04 p0523 N90-13022
Effects of serial wet-dry-wet cold exposure: Thermal balance, physical activity, and cognitive performance
[AD-A212704] 04 p0524 N90-13025
The effects of noise on performance
[AD-A212519] 04 p0551 N90-13209
Adaptation and resistance of ecosystems to stress
[AD-A212999] 05 p0665 N90-13889
Potential for reduction of decompression sickness by prebreathing with 100 percent oxygen while exercising
[AD-A213449] 07 p0966 N90-15581
The effects of foveal load on peripheral sensitivity in the visual field
[AD-A214872] 09 p1251 N90-17260
Sensations of temperature and humidity during intermittent exercise and the influence of underwear knit structure
[AD-A215285] 09 p1252 N90-17266
Workshop on the Effects of Combined Fire Products on Human Physiological and Psychological Performance
[AD-A215465] 09 p1253 N90-17270
Human Behaviour in High Stress Situations in Aerospace Operations
[AGARD-CP-458] 09 p1254 N90-17275
Reactions to emergency situations in actual and simulated flight 09 p1255 N90-17283
Peripheral nervous velocity of conduction in fighter pilots 09 p1256 N90-17287
Standardized tests for research with environmental stressors: The AGARD STRES battery
09 p1258 N90-17295
Windblast protection for advanced ejection seats
13 p1752 N90-20063
Field assessment of wet bulb globe temperature: Present and future
[AD-A218224] 13 p1853 N90-20635
Effective calibration of heat flux transducers for experimental use
[AD-A218262] 13 p1853 N90-20636
Comparison of light duty gloves with natural and synthetic materials under wet and dry conditions
[AD-A218119] 13 p1856 N90-20649
Biological effects of ELF (Extremely-Low-Frequency) electric and magnetic fields
[DE90-008634] 14 p2009 N90-21514
ELF (Extremely Low Frequency) communications system ecological monitoring program: Slime mold studies
[AD-A218623] 16 p2229 N90-22715
Strategies to sustain and enhance performance in stressful environments
[AD-A221224] 18 p2583 N90-24711
Prevalence of G-induced cervical injury in US Air Force pilots 19 p2717 N90-25460
The integration of complex information from auditory and visual channels under stress
[AD-A222686] 21 p3033 N90-27245
Evaluation of physiological and psychological impairment of human performance in cold stressed subjects
[AD-A223635] 24 p3498 N90-29769
Optimism and cardiovascular reactivity to psychological and cold pressor stress
[AD-A223818] 24 p3498 N90-29771

STRESS (PSYCHOLOGY)
Study of the behavioral and biological effects of high intensity 60 Hz electric fields
[DE89-015528] 02 p0254 N90-11438
Computer programs for measuring variations in speech
[AD-A211126] 02 p0259 N90-11467
Workshop on the Effects of Combined Fire Products on Human Physiological and Psychological Performance
[AD-A215465] 09 p1253 N90-17270
Human Behaviour in High Stress Situations in Aerospace Operations
[AGARD-CP-458] 09 p1254 N90-17275
Causes of aircrew error in the Royal Air Force
09 p1254 N90-17276
Psychological reactions of pilots involved in accidents in the Swedish Air Force 09 p1254 N90-17279
Expertise, stress, and pilot judgment
09 p1255 N90-17284
Stress and performance during a simulated flight in a F-16 simulator 09 p1256 N90-17285
Activation: Positive and negative effects of the alarm system in the brain 09 p1257 N90-17290
The trials and tribulations of RAF defence mechanism testing 09 p1257 N90-17291
Standardized tests for research with environmental stressors: The AGARD STRES battery
09 p1258 N90-17295
Information gathering and decisionmaking under stress
[AD-A218233] 13 p1854 N90-20643
Motor and cognitive performance do not change during a ten-week submarine patrol
[AD-A218639] 16 p2276 N90-22969
Development of a meta-analytic technique to assess stress effects
[AD-A220468] 19 p2723 N90-25487
Study of the application of a stress reactivity test in personnel selection
[DLR-FB-89-54] 19 p2723 N90-25489
Evaluation of physiological and psychological impairment of human performance in cold stressed subjects
[AD-A223635] 24 p3498 N90-29769
Optimism and cardiovascular reactivity to psychological and cold pressor stress
[AD-A223818] 24 p3498 N90-29771
Coping strategies and mood during cold weather training
[AD-A223915] 24 p3498 N90-29773

STRESS ANALYSIS
NT BOUNDARY ELEMENT METHOD
Analysis of results from wind tunnel tests of inlets for an advanced turboprop nacelle installation
[NASA-CR-174937] 01 p0003 N90-10011
Casting airworthiness joint European civil authorities view-point 01 p0042 N90-10234
Analysis of spurt phenomena for a non-Newtonian fluid
[AD-A210560] 01 p0071 N90-10405
Limit analysis of welded tee end connections for hollow tubes
[PB89-191647] 01 p0079 N90-10452
A design assessment for metallic pressure vessels circumferentially reinforced with a pre-tensioned high-specific-strength anisotropic composite overwind
[AD-A209108] 01 p0079 N90-10453
Global/local stress analysis of composite structures
[NASA-TM-101640] 01 p0080 N90-10456
Fracture and three dimensional stress analyses of 7075 aluminum projectile components under spin and inertia load
[AD-A210986] 01 p0081 N90-10463
Transverse shear stiffness of composite and sandwich finite elements 02 p0182 N90-11034
Automated stress analysis of Shuttle orbiter thermal protection system 02 p0184 N90-11043
Advances in instrumentation for experimental stress and vibration analysis and its applications
02 p0187 N90-11069
Finite element analysis of cure-induced residual stress in composite materials 02 p0190 N90-11084
Methodology of developing a combined environmental stress schedule for reliability growth testing
[AD-A211053] 02 p0231 N90-11326
A finite element formulation for inelastic plates and shells based on a mixed variational principle
02 p0233 N90-11334
Study of disorder and strain in semiconductor heterostructures and superlattices by Raman scattering
02 p0280 N90-11601

Mechanism for shear band formation in the high strain rate torsion test
[PB89-215370] 03 p0356 N90-12038
Rotor blade structural design
04 p0451 N90-12584
Optical fibre witnesses of fatigue damage in composite materials 04 p0465 N90-12660
Multilayer theory for delamination analysis of a composite curved bar subjected to end forces and end moments
[NASA-TM-4139] 04 p0466 N90-12669
Stress waves through projectile joints and interfaces
[AD-A212201] 04 p0513 N90-12963
The effect of a rigid elliptical inclusion on a straight crack
[AD-A212263] 04 p0513 N90-12965
Probabilistic finite element analysis of dynamic structural response
[AD-A213249] 05 p0650 N90-13789
Stress intensity factors for cracking metal structures under rapid thermal loading. Volume 2: Theoretical background
[AD-A213297] 05 p0654 N90-13812
Mean stress and the exhaustion of fatigue-damage resistance
[NASA-TM-101311] 05 p0655 N90-13819
Application of fracture mechanics and half-cycle method to the prediction of fatigue life of B-52 aircraft pylon components
[NASA-TM-88277] 05 p0655 N90-13820
Design and evaluation of a new biaxial testing method for sheet material (SUPERBAT)
[LR-548] 05 p0656 N90-13824
Parametric studies to determine the effect of compliant layers on metal matrix composite systems
[NASA-TM-102465] 06 p0737 N90-14294
Numerical and empirical verification of the stress state in a ceramic, button-head, tensile specimen
[DE90-001645] 06 p0752 N90-14375
Further studies of transverse stress effects in cable-in-conduit conductors
[DE90-001517] 06 p0771 N90-14484
The stress analysis of thin-walled screwed tubular joints 06 p0796 N90-14637
Flexural and torsional-flexural buckling of thin-walled open section struts
[ESDU-89007] 06 p0797 N90-14643
Magnetotransport studies of epitaxial Cr thin films
[DE90-001930] 06 p0856 N90-14975
Toughening behavior and interfacial properties of fiber-reinforced ceramic composites
[DE89-015351] 07 p0913 N90-15279
Nonlinear viscous waves produced by an impulsively moving plate
[AD-A214014] 07 p0932 N90-15392
Investigation of loads generated by temperature transients in pipes
[DE89-636433] 07 p0932 N90-15395
Burst pressure prediction of metallic/fibre reinforced rocket motor cases using an elasto-plastic instability analysis
[RARDE-1/89] 08 p1038 N90-15997
Stress analysis of the Princeton Plasma Physics Laboratory 1/2- x 1/2-inch shear/compression test fixture
[DE90-004401] 08 p1124 N90-16512
Design of a large superconducting spectrometer magnet
[DE90-719505] 08 p1131 N90-16553
Further development and limited flight testing of the CycloCrane
[AD-A215519] 09 p1167 N90-16754
Stress analysis in pressure vessels by mixed finite element methods taking into account shear deformation
[DE90-606755] 09 p1233 N90-17152
A summary of the Bodner-Stouffer constitutive model
[AD-A214532] 09 p1237 N90-17182
Elastic-plastic analysis of a thick-walled composite tube subjected to internal pressure
[AD-A215258] 09 p1238 N90-17187
Three-dimensional stress analysis of plain weave composites
[NASA-TM-101672] 10 p1347 N90-17813
Analysis of biaxial stress fields in plates cracking at elevated temperatures
[AD-A216271] 10 p1397 N90-18077
Investigation of collapse characteristics of cylindrical composite panels with large cutouts
[AD-A216378] 10 p1397 N90-18079
Theory and verification of the fiber composite damage model implemented in DYNA3D
[AD-A216600] 11 p1479 N90-18511
Development of a progressive failure model for strength of laminated composite structure
[AD-A216966] 11 p1480 N90-18517
Computational and experimental of railgun structural performance
[DE90-006418] 12 p1607 N90-19247
Three-dimensional structural analyses of reentry vehicles
[DE90-006278] 12 p1615 N90-19291
Fracture strength analysis of silicon nitride and silicon carbide ceramics from an international cooperative research program
[DE90-005319] 12 p1630 N90-19368
Radiation-induced density changes and creep in surface layers of glass
[DE90-008112] 12 p1633 N90-19383
Anode plasma formation as a possible mechanism for an electrical stress limit in cold cathode diodes
[DE90-007503] 12 p1655 N90-19516
Application of a Reynolds stress turbulence model to the compressible shear layer
[NASA-CR-182002] 12 p1660 N90-19537
Analytical methods for the development of Reynolds stress closures in turbulence
[NASA-CR-182017] 12 p1660 N90-19538
Use of chaotic and random vibrations to generate high frequency test inputs. Part 2: Chaotic vibrations
[DE90-007153] 12 p1676 N90-19627
Use of chaotic and random vibrations to generate high frequency test inputs
[DE90-007412] 12 p1676 N90-19628
Tunneling microscopy of submonolayer adsorbates on Si3
[AD-A216985] 12 p1719 N90-19876
Through-thickness strain response of thick composites in compression
[AD-A217233] 13 p1767 N90-20141
Optimization of laminated composite plates
[AD-A217621] 13 p1768 N90-20146
Model development in viscoplastic ratchetting
[NASA-TM-102509] 13 p1816 N90-20431
Innovative turbine concepts for open-cycle OTEC (Ocean Thermal Energy Conversion)
[DE90-000315] 13 p1827 N90-20493
Stress analysis of rocket motors with viscoelastic propellant by a mixed finite element model
14 p1941 N90-21112
Micromechanics analysis of space simulated thermal deformations and stresses in continuous fiber reinforced composites
[NASA-TM-102633] 14 p1946 N90-21140
Fourier series methods for plates and shells with cracks and inclusions 14 p1990 N90-21406
Determination of stresses around cutouts in multilayered composite plate and shell structures
14 p1992 N90-21417
Stress analysis and minimum weight design of honeycomb sandwich plates 14 p1992 N90-21418
Elasto-plastic large deformation analysis of thin-walled structures
[PB90-164757] 14 p1994 N90-21426
Design and demonstration of an improved stretched-membrane heliostat
[DE90-007904] 14 p2001 N90-21470
Strength in notched and impact-damaged laminates
15 p2064 N90-21820
Fracture toughness and tensile properties of alloy HT9 in thin sections under high neutron fluences
[DE90-008386] 15 p2069 N90-21851
A stress-strength interference approach to fast and delayed fracture reliability analysis for ceramic components 15 p2070 N90-21859
Data and conclusions from tests on small screws
[DE90-007500] 15 p2106 N90-22046
Dynamic response of a complex encapsulated electronic assembly subjected to a severe shock environment
[DE90-007689] 15 p2118 N90-22114
Continued research on the strain to failure of thick-walled cylinders subjected to internal pressure
[DE90-008952] 15 p2118 N90-22115
The computational structural mechanics testbed data library description
[NASA-TM-100645-REV-1] 15 p2121 N90-22135
Impact damage in graphite/epoxy laminates: Damage characterization, acoustic emission, and finite element simulation, volumes 1 and 2 16 p2211 N90-22610
High temperature ceramic-tubed reformer
[DE90-009617] 16 p2236 N90-22755
The behaviour of mechanically fastened joints in composite structures 16 p2242 N90-22789
Comparison between data generated from standard fracture toughness specimens and from nonstandard specimens made of a silicon carbide
[DE90-009621] 16 p2247 N90-22814
A new stress routine for the Projectile Design Analysis System (PRODAS)
[AD-A220564] 17 p2346 N90-23357
Composite integrity monitoring
[AD-A220813] 17 p2369 N90-23487
Precision laser cutting
[DE90-009949] 17 p2407 N90-23717
Prediction of gear tooth separation in single-stage gear systems, using numerical techniques
[AD-A220442] 17 p2412 N90-23744
The computation of turbulent thin shear flows associated with flow around multielement aerofoils
18 p2491 N90-24240
Accuracy improvements in finite element stress analysis 18 p2571 N90-24851
Structural zooming research and development of an interactive computer graphical interface for stress analysis of cracks 18 p2641 N90-25042
Fatigue analysis of mini-mast space truss
18 p2643 N90-25052
Comparison of two computer codes for crack growth analysis: NASCRAC Versus NASA/FLAGRO
[NASA-TM-100383] 19 p2700 N90-25360
Calculations of welding stresses and deformations by means of finite element method
[VTT-RR-648] 19 p2703 N90-25382
From Lie group transformation to the generalized Koiter initial postbuckling theory of perfect shells
[LR-613] 19 p2704 N90-25389
Strain energy release rate analysis of delamination in a tapered laminate subjected to tension load
[NASA-TM-102592] 20 p2826 N90-26076
High temperature multiaxiale creep testing of Nimonic 115
[RAE-TM-P-1182] 20 p2835 N90-26122
Determination of the stress distributions in a ceramic: Tensile specimen using numerical techniques
[NASA-TM-101914] 20 p2837 N90-26132
Calculation of 3D turbulent jets in crossflow with a multigrid method and a second-moment closure model
[NASA-TM-103159] 20 p2862 N90-26282
Design of ceramic components with the NASA/CARES computer program
[NASA-TM-102369] 20 p2875 N90-26359
Static and fatigue strength of an adhesive bonded CFRP butt-strap joint: The effects of stacking sequence and temperature
[NLR-TR-88036-U] 20 p2877 N90-26370
Application of damage tolerance
21 p2958 N90-26817
Photoelasticity: A cost effective design tool
21 p2958 N90-26819
An interdisciplinary approach to the predictive modeling of structural adhesive bonding
[AD-A221703] 21 p2988 N90-26982
Load-point compliance for the arc bend-arc support fracture toughness specimen
[AD-A221618] 21 p3014 N90-27134
Improved computational strategy for predicting the response of complex systems
[AD-A221661] 21 p3014 N90-27135
Influence of microslidings on the macroscopic behavior of composite textiles
[ETN-90-97459] 22 p3154 N90-27880
Calculation of temperature distribution in various turbine blades using a boundary-fitted coordinate transformation method 23 p3278 N90-28550
Development of a thickness design procedure for stabilized layers under rigid airfield pavements
[DOT/FAA/RD-90/22] 23 p3284 N90-28582
Liquid Rocket Booster (LRB) for the Space Transportation System (STS) systems study. Appendix A: Stress analysis report for the pump-fed and pressure-fed liquid rocket booster
[NASA-CR-183787-APP-A] 23 p3288 N90-28601
Liquid Rocket Booster (LRB) for the Space Transportation System (STS) systems study. Appendix E: Pressure-fed booster test bed for the liquid rocket booster study
[NASA-CR-183791-APP-E] 23 p3289 N90-28605
Blade tip rubbing stress prediction
23 p3290 N90-28615
Constitutive and life modeling of single crystal blade alloys for root attachment analysis
23 p3296 N90-28643
Mechanical behavior of thick, curved, laminated composites 23 p3299 N90-28664
Application of discrete Fourier series to the finite element stress analysis of axi-symmetric solids
[PB90-231010] 23 p3339 N90-28870
Mechanical property measurement of polycrystalline diamond films
[AD-A224037] 23 p3402 N90-29222
Assessment and improvement of aeroengine disc structural integrity 24 p3433 N90-29392
Variational formulation and finite element implementation of Pagano's theory of laminated plates
24 p3442 N90-29437
Interlaminar shear tests on continuous fiber reinforced thermoplastics: The effects of rubber forming
[LR-621] 24 p3444 N90-29451

On a generalized laminate theory with application to bending, vibration, and delamination buckling in composite laminates 24 p3478 N90-29659

STRESS CALCULATIONS
U STRESS ANALYSIS

STRESS CONCENTRATION
Interlaminar stress concentration in fiber composites [ETN-89-94670] 03 p0319 N90-11809
Autofrettage-stress distribution under load and retained stresses after depressurization [AD-A212090] 03 p0358 N90-12048
On the domain of dominance of the asymptotic elastodynamic crack-tip fields 07 p0944 N90-15468
Open-mode delamination stress concentrations in horseshoe and elliptic composite curved bars subjected to end forces [NASA-TM-4164] 08 p1039 N90-16004
Elastic stress concentration factors. Geometric discontinuities in rods and tubes of isotropic materials [ESDU-89048] 09 p1239 N90-17192
The effect of loading on the laser ablation of graphite/epoxy composite material [AD-A216209] 10 p1349 N90-17826
Effect of a single overload upon fatigue crack growth in an aluminum-lithium alloy [AD-A216183] 10 p1356 N90-17865
Oxygen concentrations on surfaces of carbon fibers [AD-A217724] 13 p1769 N90-20152
Determination of stresses around cutouts in multilayered composite plate and shell structures 14 p1992 N90-21417
Fracture mechanics assessment of a cracked 16-inch inner diameter 1945 vintage-jacketed pressure vessel [AD-A219135] 16 p2248 N90-22819
The effects of slip character and crack closure on the growth of small fatigue cracks in titanium-aluminium alloys [AD-A220714] 17 p2377 N90-23534
Wide range stress intensity factor and crack-mouth-opening displacement expressions suitable for short crack fracture testing with arc bend-chord support samples [AD-A218395] 17 p2415 N90-23761
The stress intensity factor and stress concentration for a finite plate with a single crack emanating from a hole [LR-607] 19 p2704 N90-25385
A finite width plate with a single crack at the edge of a central hole. The K-value of the crack and sigma peak at the other side of the hole [LR-608] 19 p2704 N90-25386
The blunt notch behaviour of metal laminates: ARALL and GLARE [LR-617] 20 p2877 N90-26368
Fracture mechanics analysis for short cracks [AD-A222170] 21 p3013 N90-27130

STRESS CORROSION
NT STRESS CORROSION CRACKING
Contribution to the transcrystalline stress crack corrosion of austenite chromium-nickel steels [ETN-89-94665] 02 p0199 N90-11137
Mechanical property characterization of VascoMax T-300 [AD-A212950] 05 p0623 N90-13637
Corrosion and stress corrosion of aluminium-lithium alloys 07 p0898 N90-15190
Fabrication of test-articles from Al-Li 2091 for Fokker 100 07 p0899 N90-15196
An investigation of the sensitization behavior of Fe-Mn-Cr austenitic steels [DE90-002719] 07 p0904 N90-15226
Interplanar spacing for various phases in austenitic stainless steels [DE90-602350] 08 p1045 N90-16038
Biaxial strength and stress rupture of hot-pressed silicon nitride [AD-A216950] 11 p1519 N90-18750
Mitigation of stress corrosion cracking of AISI 304 stainless steel in oxygenated water at 289 C by organic species at low concentration [DE90-005631] 12 p1628 N90-19354
Evaluation of 2090-T8E48 aluminum-lithium plates [AD-A217262] 13 p1776 N90-20196
The stress corrosion performance of diffusion bonded nickel base alloys [DE90-008130] 13 p1777 N90-20199
Grain boundary chemistry effects on irradiation-assisted stress corrosion cracking [DE90-008623] 14 p1951 N90-21167
Measurements and mechanisms of localized aqueous corrosion in aluminum-lithium alloys 16 p2219 N90-22656
Irradiation assisted stress corrosion cracking [DE90-010629] 18 p2572 N90-24656
Fracture-tough, corrosion-resistant bearing steels [NASA-CR-186796] 19 p2675 N90-25213
Surface chemistry and structural effects in the stress corrosion of glass and ceramic materials [AD-A223305] 24 p3454 N90-29507

STRESS CORROSION CRACKING
Grain boundary chemistry in irradiated stainless steel and its influence on environmental degradation [DE89-016827] 02 p0197 N90-11125
Deformation induced microstructural and microchemical changes during thermomechanical treatment [DE89-017266] 02 p0197 N90-11127
Failure modes and mechanisms in nickel alloys: Primarily austenitic stainless steel [DE89-016823] 02 p0198 N90-11132
Contribution to the transcrystalline stress crack corrosion of austenite chromium-nickel steels [ETN-89-94665] 02 p0199 N90-11137
An evaluation of electrochemical potentiokinetic reactivation techniques for in-service measurements on Type 304 stainless steel [DE89-017859] 06 p0746 N90-14340
Acoustic emission during intergranular stress corrosion cracking [DE90-002894] 06 p0749 N90-14355
Failure probability estimate of Type 304 stainless steel piping [DE90-000659] 06 p0796 N90-14635
Corrosion and stress corrosion of aluminium-lithium alloys 07 p0898 N90-15190
Fabrication of test-articles from Al-Li 2091 for Fokker 100 07 p0899 N90-15196
Analysis of some fracture mechanics test procedures for defence research applications [MRL-TR-89-11] 09 p1236 N90-17175
Failure probability estimate of Type 304 stainless steel piping [DE90-003896] 11 p1486 N90-18550
Evaluation of radiation-induced sensitization using electrochemical potentiokinetic reactivation technique for austenitic stainless steels [DE90-002708] 12 p1627 N90-19352
Mitigation of stress corrosion cracking of AISI 304 stainless steel in oxygenated water at 289 C by organic species at low concentration [DE90-005631] 12 p1628 N90-19354
Evaluation of 2090-T8E48 aluminum-lithium plates [AD-A217262] 13 p1776 N90-20196
The stress corrosion performance of diffusion bonded nickel base alloys [DE90-008130] 13 p1777 N90-20199
A corrosion fatigue/stress corrosion testing facility at Materials Research Laboratory [MRL-TN-568] 14 p1929 N90-21044
A STEM study of changing grain boundary chemistry during the sensitisation of AISI 304 stainless steel [AERE-R-13418] 14 p1949 N90-21157
Current fluctuations associated with localised corrosion: Mechanistic studies of the early stages of pitting and stress corrosion cracking of stainless steel [AERE-R-13531] 14 p1950 N90-21159
Grain boundary chemistry effects on irradiation-assisted stress corrosion cracking [DE90-008623] 14 p1951 N90-21167
The initiation of intergranular stress corrosion-cracking on sensitized stainless steel in dilute thiosulphate solutions [AERE-R-13317] 16 p2217 N90-22648
The effects of zinc addition on the environmental stability of Al-Li alloys 16 p2219 N90-22657
Irradiation assisted stress corrosion cracking [DE90-010629] 18 p2572 N90-24656
Measurement of localized corrosion using current density mapping [DE90-015086] 23 p3310 N90-28721
Surface chemistry and structural effects in the stress corrosion of glass and ceramic materials [AD-A223305] 24 p3454 N90-29507

STRESS CYCLES
Porosity and crack initiation during low cycle fatigue [AD-A210989] 01 p0081 N90-10464
Methodology of developing a combined environmental stress schedule for reliability growth testing [AD-A211053] 02 p0231 N90-11326
Peak identification techniques 21 p2959 N90-26822
Prediction and control of processing-induced residual stresses in composites. Part 2: AS4/PEEK composite [AD-A223696] 24 p3443 N90-29445

STRESS DISTRIBUTION
NT STRESS CONCENTRATION
Stress in dilute suspensions 01 p0068 N90-10389
Multi-axis transient testing: Experimental investigations 02 p0184 N90-11042
Three-dimensional analysis of surface crack-Hertzian stress field interaction [NASA-CR-4254] 02 p0232 N90-11332
Autofrettage-stress distribution under load and retained stresses after depressurization [AD-A212090] 03 p0358 N90-12048
Stress distribution and topography of Tellus Regio, Venus 03 p0428 N90-12452
The effect of hydrogen charging on the mechanical properties of aluminum alloy 2090 [DE90-000129] 06 p0746 N90-14341
A global ocean wind stress climatology based on ECMWF (European Centre for Medium Range Weather Forecasts) analyses [PB90-109968] 06 p0817 N90-14752
A study of impact damage in composite laminates 07 p0888 N90-15137
Development of a rate independent plasticity theory for general cyclic loading 07 p0945 N90-15471
Three-dimensional stress analysis of plain weave composites [NASA-TM-101672] 10 p1347 N90-17813
Innovative design of composite structures: The use of curvilinear fiber format in structural design of composites [NASA-CR-186406] 12 p1620 N90-19308
Interlaminar shear stress effects on the postbuckling response of graphite-epoxy panels [NASA-TM-102626] 12 p1678 N90-19630
A 4-node assumed-stress hybrid shell element with rotational degrees of freedom [NASA-CR-4279] 13 p1815 N90-20422
Residual stresses: A review of their measurement and interpretation using x ray diffraction [AERE-R-13005] 13 p1815 N90-20423
The stress-driven redistribution of point defects in the vicinity of crack-like singularities [AERE-R-12898] 13 p1815 N90-20424
Stress field near crack tip: An experimental evaluation of the three dimensional variation [AD-A217878] 13 p1818 N90-20441
Secondary flows and Reynolds stress distributions downstream of a turbine cascade at different expansion ratios 14 p1923 N90-21015
Direct formulation of a 4-node hybrid shell element with rotational degrees of freedom [NASA-CR-4282] 14 p1991 N90-21411
Residual stresses in laminated thermoplastic matrix composites 15 p2063 N90-21815
Elastic and viscoelastic analysis of two multiply layered cylinders rolling over each other with Coulomb friction [REPT-89-50] 15 p2107 N90-22051
Contact mechanics for three-dimensional geometries 15 p2111 N90-22076
Graphs of the state of stress at rounded corners [MEMT-1] 15 p2119 N90-22122
The stress field due to an edge dislocation and some fracture problems for a three-phase composite cylinder model 15 p2120 N90-22126
Analysis of a finite two-dimensional solid with an inclined crack and a rigid inclusion 15 p2120 N90-22127
An investigation into the foundations of elastic-plastic fracture mechanics 15 p2120 N90-22130
Internal fractures in model elastomeric composites 15 p2121 N90-22133
Finite element elastic-plastic-creep and cyclic life analysis of a cowl lip [NASA-TM-102342] 16 p2246 N90-22808
Axisymmetric and cylindrically orthotropic analysis of filament winding 16 p2246 N90-22811
Theoretical analysis and pressure distribution of thin-walled metal inverbuckle energy absorbing tubes 17 p2414 N90-23758
Finite element analysis of structural components using viscoplastic models with application to a cowl lip problem [NASA-CR-185189] 17 p2416 N90-23769
Stress fields in composite materials by means of a nonclassical approach 18 p2517 N90-24372
Calculations of welding stresses and deformations by means of finite element method [VTT-RR-648] 19 p2703 N90-25382
A suitable transverse shear stiffness definition for buckling of laminates and sandwich plates [LR-603] 19 p2704 N90-25384
Damage states in laminated composite three-point bend specimens: An experimental-analytical correlation study [NASA-TM-101800] 20 p2827 N90-26083
Determination of the stress distributions in a ceramic: Tensile specimen using numerical techniques [NASA-TM-101914] 20 p2837 N90-26132
Residual stresses measurements by means of x ray diffraction on electron beam welded joints and laser hardened surfaces [ETN-90-97269] 20 p2877 N90-26371
A framework to correlate a/W ratio effects on elastic-plastic fracture toughness (J (sub c)) [AD-A222822] 21 p3012 N90-27125

Computer-aided design of high-contact-ratio gears for minimum dynamic load and stress
[NASA-TM-103275] 22 p3183 N90-28065
A hybrid-stress finite element for linear anisotropic elasticity 23 p3290 N90-28614
Studies on crack mechanics
[AD-A223634] 24 p3480 N90-29670
An investigation of crack-tip stress field criteria for predicting cleavage-crack initiation
[DE90-015597] 24 p3480 N90-29672

STRESS FIELDS
U STRESS DISTRIBUTION

STRESS FUNCTIONS
Postbuckling response of long thick plates loaded in compression including higher order transverse shearing effects
[NASA-TM-102663] 19 p2700 N90-25363
Postbuckling response of long thick isotropic plates loaded in compression including higher order transverse shearing effects
[NASA-TM-4199] 22 p3190 N90-28100

STRESS INTENSITY FACTORS
Stress intensity factors and displacements for arc bend samples using collocation
[AD-A210404] 01 p0080 N90-10460
A re-evaluation of fatigue threshold test procedures and the simulation and prediction of fatigue crack growth under conditions of low crack closure 02 p0231 N90-11328
Three-dimensional analysis of surface crack-Hertzian stress field interaction
[NASA-CR-4254] 02 p0232 N90-11332
Fatigue behavior of specimens under compression load spectra
[ETN-89-95207] 04 p0512 N90-12954
Unilateral contact analysis of a crack with friction. Applications
[ETN-89-95511] 04 p0512 N90-12956
The effect of a rigid elliptical inclusion on a straight crack
[AD-A212263] 04 p0513 N90-12965
Stress intensity factors for cracking metal structures under rapid thermal loading. Volume 2: Theoretical background
[AD-A213297] 05 p0654 N90-13812
Unified model of charge build up and annealing of oxide charge and interface states in SiO2 due to stress
[HMI-B-465] 05 p0704 N90-14120
Critical and subcritical crack-growth behavior along toughened ceramic/metal interfaces 07 p0889 N90-15140
On the domain of dominance of the asymptotic elastodynamic crack-tip fields 07 p0944 N90-15468
Failure analysis of a missile locking hook from the F-14 jet
[AD-A214995] 09 p1194 N90-16917
Fatigue crack propagation rates for titanium alloy sheet
[ESDU-89051] 09 p1201 N90-16956
Analysis of some fracture mechanics test procedures for defence research applications
[MRL-TR-89-11] 09 p1236 N90-17175
Crack propagation from artificial defects in typical engine disk materials; interpretation of experimental results by means of 3D J integral 11 p1458 N90-18401
Fatigue crack initiation and small crack growth in several airframe alloys
[NASA-TM-102598] 11 p1518 N90-18746
Fatigue crack growth in martensitic 2 1/4Cr-1Mo steel at elevated temperatures
[AERE-R-13524] 13 p1776 N90-20191
Through-the-thickness fatigue crack closure behavior in an aluminum alloy
[NASA-TM-102590] 13 p1816 N90-20427
Fracture of sandwiched composites 14 p1946 N90-21136
Fatigue crack growth from narrow-band Gaussian spectrum loading in 6063 aluminum alloy
[DE90-008957] 14 p1952 N90-21173
Nonlinear fracture mechanics using semicircular specimens and tension-softening behavior 15 p2116 N90-22108
Fatigue crack growth in unidirectional metal matrix composite
[NASA-TM-103102] 15 p2118 N90-22117
The stress field due to an edge dislocation and some fracture problems for a three-phase composite cylinder model 15 p2120 N90-22126
Analysis of a finite two-dimensional solid with an inclined crack and a rigid inclusion 15 p2120 N90-22127
Probablistic finite elements: Applications to fracture and fatigue 15 p2121 N90-22134
Elevated temperature crack growth in aluminum alloys: Tensile deformation of 2618 and FVS0812 aluminum alloys 16 p2218 N90-22654
Wide range stress intensity factor and crack-mouth-opening displacement expressions suitable for short crack fracture testing with arc bend-chord support samples
[AD-A218395] 17 p2415 N90-23761
Mechanistic modeling of corrosion fatigue crack growth of steels in aqueous solutions 18 p2524 N90-24404
Corrosion fatigue crack propagation in metals
[NASA-CR-4301] 18 p2524 N90-24405
Stress intensity factors for arbitrary two-dimensional crack problems involving crack face loadings
[FFA-TN-1990-10] 19 p2703 N90-25380
Weight functions and stress intensity factors for mode 1 cracks in arbitrary 2D geometries under general crack surface loading
[FFA-TN-1990-17] 19 p2703 N90-25381
The stress intensity factor and stress concentration for a finite plate with a single crack emanating from a hole
[LR-607] 19 p2704 N90-25385
A finite width plate with a single crack at the edge of a central hole. The K-value of the crack and sigma peak at the other side of the hole
[LR-608] 19 p2704 N90-25386
The blunt notch behaviour of metal laminates: ARALL and GLARE
[LR-617] 20 p2877 N90-26368
Fracture mechanics analysis for short cracks
[AD-A222170] 21 p3013 N90-27130
Use of acoustic emission for continuous surveillance of aircraft structures 22 p3188 N90-28092
Damage tolerance of the fighter aircraft 37 Viggen. Part 1: Analytical assessment
[FFA-TN-1990-12-PT-1] 23 p3276 N90-28538
An investigation of hole-edge crack problem by a combined complex variable and least square method
[LR-626] 24 p3482 N90-29679
Fatigue, static tensile strength and stress corrosion of aircraft materials and structures. Part 1: Text
[LR-630-PT-1-REV] 24 p3482 N90-29682
Fatigue, static tensile strength and stress corrosion of aircraft materials and structures. Part 2: Figures
[LR-630-PT-2] 24 p3482 N90-29683

STRESS MEASUREMENT
NT X RAY STRESS MEASUREMENT
The Sandia standard for PVDF (Polyvinylidene Di-Fluoride) shock sensors
[DE89-016530] 02 p0225 N90-11287
Spectral contents readout of birefringent sensor
[NASA-CR-179444] 06 p0843 N90-14905
Turbine blade data acquisition system user's guide
[AD-A214986] 09 p1169 N90-16763
Turbine blade data acquisition system software reference
[AD-A215134] 09 p1169 N90-16764
Turbine blade data acquisition system technical reference
[AD-A215135] 09 p1169 N90-16765
Z-grid signal conditioning system user's guide and technical reference
[AD-A215122] 10 p1395 N90-18067
A 2-D analysis of particle velocity and stress of SH waves from a strip radiator. An experimental verification of both amplitude and phase using EMA transducers
[AERE-R-12600] 16 p2227 N90-22704
Nondestructive measurement of residual stresses in aircraft transparencies
[AD-A218680] 17 p2415 N90-23762
Smart built-in test 19 p2728 N90-25512
Resistivity, adhesive strength, and residual stress measurements of thin film metallizations on single crystal quartz
[DE90-011902] 20 p2837 N90-26135
Mechanical property measurement of polycrystalline diamond films
[AD-A224037] 23 p3402 N90-29222
Evaluation of plane-of-light noninterference stress measurement systems for measuring bladed disk vibrations
[AD-A223487] 24 p3479 N90-29667

STRESS PROPAGATION
Instability-related delamination growth of embedded and edge delaminations
[NASA-TM-100655] 17 p2370 N90-23494
Theory of stress transfer in a cross-ply laminate containing a parallel array of transverse cracks
[NPL-DMA(A)-189] 22 p3192 N90-28109

STRESS RATIO
Fatigue growth and closure of short cracks
[AD-A210824] 01 p0081 N90-10462
Fatigue crack propagation rates for titanium alloy sheet
[ESDU-89051] 09 p1201 N90-16956

STRESS RELAXATION
Derivation of improved load transformation matrices for launchers-spacecraft coupled analysis, and direct computation of margins of safety 02 p0188 N90-11077
The Meta-Lax method of stress reduction in welds
[DE89-016437] 02 p0230 N90-11321
Fatigue fracture in the presence of shot peening residual stresses: Initiation, propagation, and relaxation phenomena 06 p0797 N90-14644
Residual stresses in laminated thermoplastic matrix composites 15 p2063 N90-21815
The analysis of stress relaxation on indentation of a rigid punch into a viscoelastic sheet of finite thickness
[NPL-DMA(A)-193] 15 p2162 N90-22357
Analysis of strain relaxation in Au/Ni multilayers by x ray diffraction
[IAR-89-25] 20 p2875 N90-26357
A viscoelastic material model for computing stresses in glass
[DE90-014851] 24 p3481 N90-29673

STRESS RELIEVING
Study of a gallium arsenide solar cell interconnector 02 p0182 N90-11033
Steam cooled rich-burn combustor liner
[NASA-CASE-LEW-13609-1] 03 p0321 N90-11824

STRESS RUPTURE STRENGTH
U CREEP RUPTURE STRENGTH

STRESS TENSORS
State-of-the-art of measuring ground shock and cratering phenomena 09 p1235 N90-17170
Rectangular subsonic jet flow field measurements
[NASA-CR-181925] 14 p2023 N90-21598

STRESS WAVES
Stress waves through projectile joints and interfaces
[AD-A212201] 04 p0513 N90-12963
Coherent phase transformation under nonhydrostatic stress-wave loading
[DE90-005719] 10 p1396 N90-18072
A spectral analysis approach to wave propagation in layered solids 15 p2120 N90-22131
HYPUF upgrade
[AD-A218400] 17 p2379 N90-23547
Acousto-ultrasonic nondestructive evaluation of materials using laser beam generation and detection
[NASA-CR-186694] 17 p2398 N90-23664

STRESS-STRAIN DIAGRAMS
Mechanical testing of selected engineering plastics
[DE90-008186] 16 p2222 N90-22673
Inelastic analysis of laminated composites 23 p3301 N90-28669

STRESS-STRAIN RELATIONSHIPS
Fatigue crack initiation mechanics of metal aircraft structures
[AD-A210567] 01 p0045 N90-10255
Anomalous strain rate dependence of the serrated flow in Ni-H and Ni-C-H alloys
[AD-A213244] 05 p0624 N90-13641
The Fourth Oxford International Conference on the Mechanical Properties of Materials at High Rates of Strain
[AD-A212293] 05 p0653 N90-13809
A theoretical investigation of the column behavior of cold-formed square hollow sections
[PB89-225981] 06 p0797 N90-14645
A finite strip method for the elastic-plastic large displacement analysis of thin-walled and cold-formed steel sections
[PB89-226021] 06 p0798 N90-14647
Mechanical behavior of laminated composites at elevated temperatures 07 p0889 N90-15141
A simple shell element formulation for large-scale elastoplastic analysis
[DE89-015452] 07 p0946 N90-15475
Mechanical evaluation of the differential drum concept for optical fiber pay-out
[AD-A214149] 07 p0993 N90-15740
Improved solution techniques for the eigenstructure of fractional order systems
[AD-A213844] 08 p1088 N90-16295
Construction of inelastic stress-strain curves from minimal materials data (computer program)
[ESDU-89052] 09 p1239 N90-17189
Investigation of failure modes in a ceramic composite under off-axis loading
[AD-A216133] 10 p1348 N90-17820
A study of failure characteristics in thermoplastic composite laminates due to an eccentric circular discontinuity
[AD-A216226] 10 p1349 N90-17827
A study of near tip phenomena for cracks in a particulate composite 10 p1395 N90-18062
A micromechanical viscoplastic stress-strain model with grain boundary sliding
[DE90-006013] 10 p1437 N90-18295

Improved computational fluid dynamics for continuum hypersonic flow
[AD-A216981] 11 p1506 N90-18674
Demonstration of capabilities of high temperature composites analyzer code HITCAN
[NASA-TM-102560] 12 p1676 N90-19629
Optimization of fracture resistance in composites
[AD-A217431] 13 p1768 N90-20144
Element-specific modal formulations for large-displacement multibody dynamics
14 p1934 N90-21069
Nicalon/siliconoxycarbide ceramic composites
[NASA-TM-102563] 14 p1945 N90-21133
Modeling elastomer displacements for tactile sensing applications
[DE90-007959] 14 p1984 N90-21370
Three-dimensional fatigue crack closure behavior of metals 15 p2070 N90-21857
Coordinate systems for plastic yield surfaces stress and strain space theories
[PB90-164765] 15 p2117 N90-22110
High-temperature deformation of mechanically-alloyed aluminum IN90211 16 p2216 N90-22645
Inelastic response of metal matrix composites under biaxial loading 16 p2220 N90-22661
The lithium concentration dependence of creep in binary aluminum-lithium alloys
[AD-A218706] 16 p2221 N90-22668
The microstructural basis of damping in high damping alloys
[AD-A219572] 16 p2248 N90-22821
Finite element analysis of structural components using viscoplastic models with application to a cowl lip problem
[NASA-CR-185189] 17 p2416 N90-23769
A viscoplastic model with application to LiF-22 percent CaF2 hypereutectic salt
[NASA-TM-103181] 17 p2417 N90-23770
Development of a design methodology for high temperature cyclic applications of materials which experience cyclic softening
[DE90-006722] 19 p2674 N90-25205
Cyclic stress strain behavior of an austenitic stainless steel Polarit 778 under variable amplitude loading
[VTT-RR-647] 19 p2675 N90-25215
Investigation of the mechanical properties of superconducting coils
[DE90-012020] 19 p2761 N90-25689
Processing and characterization of high strength, high ductility Hadfield steel
[AD-A221769] 21 p2982 N90-26947
High-temperature deformation of silicon
[DE90-013628] 22 p3160 N90-27919
Inelastic analysis of laminated composites
23 p3301 N90-28659
Characterization of unnotched SCS-6/Ti-15-3 metal matrix composites at 650 C
[NASA-TM-102699] 24 p3444 N90-29450
The MTL Torsional Split-Hopkinson bar
[AD-A223278] 24 p3479 N90-29663

STRESSES
NT AXIAL STRESS
NT CRITICAL LOADING
NT PLANE STRESS
NT RESIDUAL STRESS
NT REYNOLDS STRESS
NT SHEAR STRESS
NT TENSILE STRESS
NT THERMAL STRESSES
NT TORSIONAL STRESS
NT VIBRATIONAL STRESS

Two stage gear tooth dynamics program
[NASA-CR-185110] 01 p0077 N90-10437
Effects of stress on judgment and decision making in dynamic tasks
[AD-A210605] 01 p0135 N90-10781
The HEL (Hugoniot Elastic Limit) and rate-dependent yield behavior
[DE89-016981] 02 p0199 N90-11134
Impulse time-integral function and Lagrangian analysis
[DE89-016997] 02 p0221 N90-11268
The Sandia standard for PVDF (Polyvinylidene Di-Fluoride) shock sensors
[DE89-016530] 02 p0225 N90-11287
Plasma separation process: Magnet move to Oak Ridge National Laboratory
[DE89-017457] 04 p0556 N90-13242
A generalized thermomechanical constitutive model for metal matrix composites with plastic strain and damage
06 p0737 N90-14293
High speed transfer switch with 50 kA and 50 kV ratings
[DE90-002448] 06 p0770 N90-14481
Thin films under chemical stress
[DE90-003754] 07 p0947 N90-15484
Structural response measurements and predictions for the SANDIA 34-meter test bed
[DE90-002575] 07 p0955 N90-15524
Mechanical evaluation of the differential drum concept for optical fiber pay-out
[AD-A214149] 07 p0993 N90-15740
An investigation of mechanical behavior of crystalline solids
[DE90-003530] 07 p1000 N90-15787
Material responses to incident x rays
[DE89-015366] 08 p1089 N90-16305
Metal matrix composite: Strengthening mechanisms
[AD-A214843] 09 p1186 N90-16871
High modulus coatings
[AD-A215448] 09 p1198 N90-16941
Coherent phase transformation under nonhydrostatic stress-wave loading
[DE90-005719] 10 p1396 N90-18072
A method for measuring the material moduli of granular materials: Flow in an orthogonal rheometer
[DE90-007160] 13 p1801 N90-20339
Seismic characterization of fracture properties
[DE90-007759] 13 p1841 N90-20570
Stressed Ge:Ga photoconductors for space-based astronomy. (Is there life beyond 120 micron)
14 p1975 N90-21315
Influence of linear profile modification and loading conditions on the dynamic tooth load and stress of high contact ratio gears
[NASA-TM-103136] 16 p2243 N90-22796
Stress versus temperature dependent activation energies in creep
[NASA-TM-103192] 17 p2417 N90-23773
A vectroized elastic/plastic power law hardening material model including Lueders strain
[DE90-010172] 18 p2572 N90-24655
Development and application of an optimization procedure for space and aircraft structures
[MBB-FW-522/S/PUB-383] 19 p2650 N90-25078
Development of a design methodology for high temperature cyclic applications of materials which experience cyclic softening
[DE90-006722] 19 p2674 N90-25205
Determination of the stress distributions in a ceramic: Tensile specimen using numerical techniques
[NASA-TM-101914] 20 p2837 N90-26132
Dynamic properties of porous B4C
[AD-A222650] 21 p2985 N90-26960
High-temperature deformation of silicon
[DE90-013628] 22 p3160 N90-27919
A theoretical investigation into the inelastic behavior of metal-matrix composites
[AD-A223973] 23 p3302 N90-28677
The stress and temperature dependence of creep in an Al-2.0 wt percent Li alloy
[AD-A223676] 24 p3449 N90-29480
Multiaxial fatigue criterion for 2-1/4 Cr-1 Mo steel for use in high-temperature structural design
[DE90-016039] 24 p3452 N90-29491
The MTL Torsional Split-Hopkinson bar
[AD-A223278] 24 p3479 N90-29663
A viscoelastic material model for computing stresses in glass
[DE90-014851] 24 p3481 N90-29673

STRETCHING
Effects of flame stretch on the propagation, extinction, and stability of premixed flames
06 p0739 N90-14301
NIKHEF-K contributions to the 1989 Particle Accelerator Conference
[NIKHEF/AMPS/89/03] 06 p0841 N90-14891
The Amsterdam pulse stretcher project (AmPS)
06 p0841 N90-14892
Optics of the Amsterdam pulse stretcher (AmPS)
06 p0841 N90-14893
Modification of MEA modulator-klystron units enabling short pulse injection into a pulse-stretcher ring
06 p0841 N90-14894

STRIATION
Free surface scars and striations
[AD-A212429] 04 p0503 N90-12901

STRING THEORY
Research program in theoretical high energy physics
[DE89-013963] 01 p0121 N90-10695
General covariance and strings
[DE89-016505] 02 p0286 N90-11633
Three level constraints on conformal field theories and string models
[DE89-016942] 02 p0286 N90-11634
Operator product coefficients in non-diagonal conformal field theories
[PB89-216873] 03 p0399 N90-12283
Bordered surfaces, off-shell amplitudes, sewing, and string field theory
[DE90-000006] 03 p0414 N90-12378
Cosmic strings and ultra-high energy cosmic rays
[NASA-CR-185924] 03 p0435 N90-12492
More on the super WZW theory
[NIKHEF-H/88-11] 04 p0562 N90-13273
Strings, p-branes and Skyrmions in curved space
04 p0565 N90-13293
Evolution of domain walls in the early universe
[NASA-CR-186076] 04 p0565 N90-13297
Small scale structure on cosmic strings
[NASA-CR-186075] 04 p0565 N90-13298
Cosmic strings and baryon decay catalysis
[NASA-CR-186074] 04 p0566 N90-13299
Scaling in a non Abelian string network
[ROM1F-89-676] 05 p0695 N90-14066
Configurational statistics of strings, fractals and polymer physics. Part 2: Non Abelian strings
[ROM1F-89-680-PT-2] 05 p0696 N90-14067
Statistical mechanics of strings and topology
[ROM1F-89-683] 05 p0696 N90-14068
Observational physics of mirror world
[NASA-CR-185923] 05 p0697 N90-14076
String correlations and galaxies formation
[ROM1F-89-677] 05 p0713 N90-14170
Non Abelian string correlations and galaxies formation
[ROM1F-89-678] 05 p0714 N90-14171
Des Cloizeaux's law for strings and galaxies formation. Part 1: Abelian configurations
[ROM1F-89-681-PT-1] 05 p0714 N90-14172
Des Cloizeaux's law for strings and galaxies formation. Part 2: Non Abelian configurations
[ROM1F-89-682-PT-2] 05 p0714 N90-14173
Hamiltonian flows, SU(infinity), SO(infinity), USp(infinity), and strings
[DE90-001987] 06 p0835 N90-14851
String models for ultrarelativistic heavy ion collisions: Lund model versus color exchange models
[DE88-015856] 06 p0840 N90-14881
The dynamics of domain walls and strings
[NASA-CR-186255] 07 p1007 N90-15832
Small scale structure on cosmic strings
[DE90-003128] 07 p1013 N90-15867
The off-shell closed strings as the topological open membranes: Dynamical transmutation of world sheet dimension
[DE89-635721] 08 p1134 N90-16571
On the domain of string perturbation theory
[DE90-600759] 08 p1135 N90-16575
An estimation of the one-loop mass shifts in open superstring theory
[DE90-719578] 08 p1136 N90-16582
Research in theoretical physics
[DE90-005605] 09 p1294 N90-17500
Research program in elementary particle theory
[DE90-005600] 10 p1428 N90-18241
BRS current and related anomalies in two-dimensional gravity and string theories
[DE90-733095] 10 p1440 N90-18307
Superconformal algebra on meromorphic vector fields with three poles on super-Riemann sphere
[DE90-610423] 12 p1706 N90-19796
Research accomplishments and future goals in particle physics
[DE90-007296] 12 p1712 N90-19830
Construction of four-dimensional open superstrings
[DE90-006484] 12 p1724 N90-19908
Reparametrization BRS cohomology in two-dimensional gravity and non-critical string theories
[DE90-741468] 12 p1725 N90-19911
Gravitational consequences of modern field theories
12 p1730 N90-19947
The COBE cosmic 3 K anisotropy experiment: A gravity wave and cosmic string probe 12 p1732 N90-19959
Cosmic string in compactified gauge theory
[DE90-741463] 12 p1738 N90-19988
Superstring field theory
[DE90-007694] 13 p1899 N90-20897
Extension of the constraints algebra for the closed string with the fixed topology world sheet
[DE90-612745] 14 p2020 N90-21577
Extension of the Krichever-Novikov algebra in the closed string theory
[DE90-612746] 14 p2020 N90-21578
Rings
[DE90-009035] 14 p2025 N90-21613
String dynamics in curved space-time revisited
[DE90-612796] 14 p2035 N90-21674
Gravitational couplings of the inflation in extended inflation
[NASA-CR-186595] 15 p2190 N90-22504
Topological defects in extended inflation
[NASA-CR-186594] 15 p2190 N90-22505
Ultrahigh-energy particle flux from cosmic strings
[NASA-CR-186592] 15 p2194 N90-22525
A general low-harmonic cosmic string and its self-intersection and fragmentation
16 p2331 N90-23284

Classical theory of radiating strings
[NASA-CR-186607] 17 p2485 N90-24214
Cosmic strings and baryon decay
[NASA-CR-182842] 19 p2754 N90-25651
A research program in theoretical high energy physics
[DE90-013322] 20 p2926 N90-26648
Comment on high resolution simulations of cosmic strings. 1: Network evoloution
[NASA-CR-186606] 20 p2941 N90-26734
A research program in physics of the early universe
[DE90-013319] 20 p2942 N90-26742
Proceedings of workshop on Dark Matter and the Structure of the Universe
[DE90-791308] 21 p3098 N90-27602
Biased clustering in a universe with hot dark matter and cosmic string
[FERMILAB-PUB-90/23-A] 22 p3262 N90-28473
Effective actions for bosonic topological defects
[NASA-CR-187271] 24 p3544 N90-30041
Introductory lectures on conformal field theory and strings
[DE90-627219] 24 p3556 N90-30120

STRINGS
General covariance and strings
[DE89-016505] 02 p0286 N90-11633

STRIP TRANSMISSION LINES
NT MICROSTRIP TRANSMISSION LINES
Dielectric covered microstrip patch antennas
[AD-A211577] 03 p0344 N90-11963
Investigation of broadband microstrip antenna structures for application in monolithic millimeter wave arrays
[AD-A213856] 07 p0923 N90-15344
A study of loaded microstrip antennas and their applications to arrays
[AD-A214857] 09 p1205 N90-16985
Theoretical analysis of microwave and millimeter wave integrated circuits based on magnetic films
[AD-A214772] 09 p1211 N90-17021
Rigorous calculations of lumped electrical parameters for a microstrip interdigitated electrode structure
[AD-A215337] 10 p1378 N90-17989
Discontinuous-taper directional coupler
[AD-D014324] 12 p1650 N90-19481
Internal transmission line filter element
[AD-D014353] 12 p1651 N90-19489
Experimental investigations on channelized coplanar waveguide
[NASA-TM-102494] 13 p1792 N90-20286
The 4th Annual Review of Progress in Applied Computational Electromagnetics
[AD-A217912] 14 p1966 N90-21257
Joint services electronics program
[AD-A220815] 17 p2397 N90-23654
Characteristic impedances and loss data for a common stripline pickup geometry
[CEBAF-PR-89-038] 19 p2755 N90-25656
Transient signal distortion and coupling in multilayer multiconductor MIC microstrips
[AD-A222989] 21 p3000 N90-27050
Solid state space harmonic amplifier
[AD-D014455] 22 p3166 N90-27955
Coupled strip line circuit
[AD-D014487] 22 p3166 N90-27956

STRIPPING
The future of aircraft paint removal methods
[AD-A214946] 09 p1197 N90-16936

STRONG INTERACTIONS (FIELD THEORY)
Lattice fields and strong interactions
[DE89-015099] 01 p0135 N90-10777
The ultimate structure of matter: The high energy physics program from the 1950s through the 1980s
[DE90-005682] 12 p1713 N90-19836

STRONGLY COUPLED PLASMAS
Dynamically compressed metals: Theory
[AD-A210741] 01 p0045 N90-10257
Studies of a strongly coupled plasma produced in a capillary discharge
[DE89-016611] 02 p0277 N90-11581
Properties of strongly coupled multi-ionic plasmas
[DE89-017782] 03 p0408 N90-12339
The measurement of transport properties in strongly coupled plasmas
[DE90-003451] 07 p0996 N90-15755
High growth rate diamond synthesis in a large area atmospheric pressure inductively coupled plasma
[AD-A216090] 11 p1567 N90-19019
Electrical resistivity of strongly coupled plasmas in intense fields
[DE90-002236] 12 p1717 N90-19861
Nonlinear stability in fluid and plasma dynamics
[AD-A217735] 13 p1892 N90-20856
Center of excellence in theoretical geoplasma research
[AD-A215035] 14 p2005 N90-21488
Development of an all silicon integrated optical modulator for high speed data communications and sensor applications
[AD-A220270] 18 p2547 N90-24535
Viking data analysis
[AD-A222609] 20 p2823 N90-26062
The near-Earth orbital environment coupling to its energy sources
[AD-A222435] 21 p3026 N90-27206

STRONTIUM
The effects of oxygen and strontium vacancies on the superconductivity of single crystals of Bi2Sr(2-x)CuO(6-y)
[DE90-004242] 08 p1133 N90-16561
SR90, strontium shaped-charge critical ionization velocity experiment
[NASA-CR-186501] 14 p2024 N90-21606
Aligned bismuth, strontium, calcium cuprate coatings on polycrystalline substrates
[AD-D014522] 19 p2678 N90-25229
Superconductivity in the Sn-Ba-Sr-Y-Cu-O system
22 p3151 N90-27863
High T(sub c) copper-oxide superconductors
[AD-D014483] 22 p3247 N90-28416

STRONTIUM COMPOUNDS
NT STRONTIUM FLUORIDES
Bi-Sr-Ca-Cu-O superconducting ceramics
[DE89-636225] 06 p0855 N90-14972
The influence of the substrate surface on the nucleation and growth of superconducting thin films
[DE90-003649] 06 p0857 N90-14983
Spectroscopic and laser properties of Cr:LiCaAlF6 and Cr:LiSrAlF6 crystals
[DE90-000783] 07 p0998 N90-15770
Microstructures of Y123 films on SrTiO3, LaGaO3, and LaAlO3
[DE90-003367] 08 p1129 N90-16537
Synthesis of Bi-Sr-Ca-Cu oxide superconductor by solution technique
[DE90-008707] 13 p1897 N90-20888
On the explanation of anomalies in inelastic neutron scattering by high-T(sub c) superconductors
[DE90-620561] 17 p2475 N90-24149
In-situ growth of superconducting films of Bi-Sr-Ca-Cu-O using magnetron sputtering
[DE90-011161] 18 p2626 N90-24962
Flux creep in Bi2Sr2CaCu2O8(sub +x) single crystals
22 p3136 N90-27794
Magnetic properties of the 110K superconducting phase in Pb-doped Bi-Sr-Ca-Cu-O thin films
22 p3151 N90-27868
Optical and microwave detection using Bi-Sr-Ca-Cu-O thin films
22 p3152 N90-27870

STRONTIUM FLUORIDES
Spectroscopy of laser properties of Nd(3+)-doped CaF2, SrF2, and BaF2
[DE90-012086] 19 p2695 N90-25337

STROUHAL NUMBER
Experimental study of validity of the unstationary Kutta condition, with high Strouhal numbers
[ETN-90-95914] 12 p1661 N90-19547

STRUCTURAL ANALYSIS
NT DYNAMIC STRUCTURAL ANALYSIS
NT ENERGY METHODS
NT EQUILIBRIUM METHODS
NT FLUTTER ANALYSIS
NT MATRIX METHODS
NT STRAIN ENERGY METHODS
SSME Alternate Turbopump Development Program: Design verification specification for high-pressure fuel turbopump
[NASA-CR-183676] 01 p0008 N90-10033
Static aeroelastic analysis for generic configuration aircraft
[NASA-TM-89423] 01 p0009 N90-10042
Aeroelastic analysis of missile control surfaces with structural non-linearity 01 p0015 N90-10071
Control/structure interaction methods for space station power systems 01 p0018 N90-10087
Modeling and control system design and analysis tools for flexible structures 01 p0018 N90-10090
Lumped mass formulations for modeling flexible body systems 01 p0019 N90-10091
Efficiency and capabilities of multi-body simulations
01 p0019 N90-10095
Simulation of flexible structures with impact: Experimental validation 01 p0020 N90-10097
Linearized flexibility models in multibody dynamics and control 01 p0020 N90-10099
Composite Blade Structural Analyzer (COBSTRAN) theoretical/programmer's manual
[NASA-TM-101958] 01 p0033 N90-10181
Structure-mechanical property relationships in ion implanted ceramics
[DE89-010129] 01 p0048 N90-10274
The MHOST finite element program: 3-D inelastic analysis methods for hot section components. Volume 2: User's manual
[NASA-CR-182235-VOL-2] 01 p0079 N90-10450
Design guide for predicting nonlinear random response (including snap-through) of buckled plates
[NASA-CR-181877] 01 p0118 N90-10681
Spacecraft Structures and Mechanical Testing
[ESA-SP-289] 02 p0176 N90-10986
Parametric identification of conservative self adjoint structures 02 p0177 N90-10994
Overview of actual buckling calculation methods for space vehicle structures 02 p0177 N90-10995
Theoretical and experimental investigation of thin-walled aluminum panels under cyclic shear load
02 p0177 N90-10996
A contribution to the stability analysis of large space structures 02 p0177 N90-10997
Adaptive structures to meet future requirements for large precision structures 02 p0178 N90-11001
Acoustic response analysis in the low frequency domain 02 p0179 N90-11010
Dynamic substructuring for modular analysis and testing 02 p0180 N90-11015
Advances in design and testing of spacecraft structures 02 p0180 N90-11018
Modal analysis of fluid-structure systems by parallel subspace iteration 02 p0181 N90-11024
Modal analysis of space structures with the Ibrahim Time Domain method 02 p0181 N90-11026
A direct two response approach for updating analytical dynamic models of structures with emphasis on uniqueness 02 p0182 N90-11028
Thermal and structural analysis of Hermes
02 p0186 N90-11058
Derivation of improved load transformation matrices for launchers-spacecraft coupled analysis, and direct computation of margins of safety
02 p0188 N90-11077
Computational aspects of sensitivity calculations in linear transient structural analysis 02 p0231 N90-11327
Development of an approximate technique for the nonlinear random vibrations analysis of hysteretic systems 02 p0233 N90-11335
An analytical and experimental study of the elastodynamic response characteristics of planar linkage mechanism with bearing clearances
02 p0233 N90-11336
New computing systems and their impact on structural analysis and design
[NASA-CR-185831] 02 p0257 N90-11457
Estimation on nonlinear damping in second order distributed parameter systems
[NASA-CR-181890] 02 p0263 N90-11494
Fractographic and microstructural analysis of fatigue crack growth in a Ti-6Al-4V fan disc forging
[NLR-MP-88028-U] 03 p0330 N90-11877
Flexure strength of advanced ceramics: A round robin exercise
[AD-A212101] 03 p0332 N90-11889
Wind/seismic comparisons for upgrading existing structures
[DE89-016055] 03 p0357 N90-12044
Numerical solution of acoustic-structure interaction problems
[AD-A211505] 03 p0400 N90-12293
Integrated multidisciplinary optimization of rotorcraft: A plan for development
[NASA-TM-101617] 04 p0450 N90-12580
General approach and scope --- rotor blade design optimization 04 p0451 N90-12581
Rotor blade aerodynamic design
04 p0451 N90-12582
Rotor blade structural design
04 p0451 N90-12584
Validation of the procedures --- integrated multidisciplinary optimization of rotorcraft
04 p0451 N90-12587
Appendix: Results obtained to date --- integrated multidisciplinary optimization of rotorcraft
04 p0451 N90-12588
Evaluation of a damaged F/A-18 horizontal stabilator
[AD-A212573] 04 p0453 N90-12597
SSME structural dynamic model development
[NASA-CR-183671] 04 p0463 N90-12650
Influence of the structure of epoxy network models on the volumetric, mechanical and viscoelastic properties
[ISAL-89-0024] 04 p0466 N90-12666
Structural studies of sputter-deposited MoS2 solid lubricant films
[AD-A212407] 04 p0481 N90-12759
Effects of hot corrosion on the room temperature strength of structural ceramics
[AD-A212568] 04 p0481 N90-12762

A center for advanced electrical and structural polymers
[AD-A212853] 04 p0482 N90-12764
Structural vibration and shock isolator
[AD-D014202] 04 p0509 N90-12940
Proceedings of the Army Symposium on Solid Mechanics, 1989: Mechanics of Engineered Materials and Applications
[AD-A211954] 04 p0511 N90-12951
Multilevel optimization with system Optsys
[FFA-TN-1988-60] 04 p0512 N90-12953
A mechanical power flow capability for the finite element code NASTRAN
[AD-A212202] 04 p0513 N90-12964
Analysis of the non-planar response of a cantilever, with the aid of computerized symbolic manipulation
[AD-A212421] 04 p0545 N90-13172
Structural and electrical properties of thin films and superlattices composed of II-VI semiconductors
04 p0558 N90-13249
Constitutive modeling for isotropic materials (HOST)
[NASA-CR-179522] 05 p0582 N90-13390
Constitutive modeling for isotropic materials (HOST)
[NASA-CR-174718] 05 p0582 N90-13391
Composite panel development at JPL
05 p0595 N90-13458
Control of optical systems 05 p0600 N90-13484
Hybrid deployable support truss designs for LDR
05 p0600 N90-13485
Effects of joints in truss structures
05 p0600 N90-13486
RSRM nozzle fixed housing cooldown test
[NASA-CR-183741] 05 p0614 N90-13587
Measuring of the complete stiffness matrix for anisotropic laminated materials
[DLR-MITT-89-11] 05 p0618 N90-13606
Measuring of the complete stiffness matrix for anisotropic laminated materials
[DLR-MITT-89-12] 05 p0618 N90-13607
Fiber reinforced cementitious composites technology
[PB89-227813] 05 p0619 N90-13608
Magneto-elastic interactions in conducting structures in transient magnetic fields 05 p0632 N90-13686
Probabilistic finite element analysis of dynamic structural response
[AD-A213249] 05 p0650 N90-13789
Mobility power flow analysis of an L-shaped plate structure subjected to acoustic excitation
[NASA-CR-186130] 05 p0655 N90-13817
A theoretical investigation of the column behavior of cold-formed square hollow sections
[PB89-225981] 06 p0797 N90-14645
A study of incremental-iterative strategies for nonlinear analyses
[PB89-226005] 06 p0798 N90-14646
Verification of the NIKE3D structural analysis code by comparison against the analytic solution for a spherical cavity under a far-field uniaxial stress
[DE90-000929] 06 p0799 N90-14653
Control of the variable speed generator on the Sandia 34-metre vertical axis wind turbine
[DE90-000803] 06 p0803 N90-14674
An examination of helicopter rotor load calculations
[AD-A214295] 07 p0880 N90-15098
Instrumentation for a facility for the test, analysis and active control of spacecraft truss structures
[AD-A213655] 07 p0886 N90-15124
Solution of potential flow past an elastic body using the boundary element technique
[AD-A213843] 07 p0931 N90-15390
Modifications of the Penn State Boundary Layer Research Facility for boundary layer/structure interaction experimental research
[AD-A213874] 07 p0931 N90-15391
Proceedings of the 1988 Structural Integrity Program Conference
[AD-A213545] 07 p0947 N90-15486
Structural response measurements and predictions for the SANDIA 34-meter test bed
[DE90-002575] 07 p0955 N90-15524
Structural analysis of zirconium-aluminum plasma deposits
[ETCA-89-R-073] 08 p1046 N90-16045
Interdisciplinary research in viscoelasticity and rheology
[AD-A213630] 08 p1063 N90-16145
Element-by-element preconditioning techniques for large-scale, vectorized finite element analysis in nonlinear solid and structural mechanics 08 p1087 N90-16291
Load-shortening behavior of an initially curved eccentrically loaded column
[NASA-TM-101643] 08 p1088 N90-16293
Measurement of reflection and impedance in a beam by the structural intensity technique
[DE90-726212] 08 p1088 N90-16299
Physical models for supersonic turbulent boundary layer structure
[AD-A215284] 09 p1160 N90-16716
Turbine blade data acquisition system software reference
[AD-A215134] 09 p1169 N90-16764
Turbine blade data acquisition system technical reference
[AD-A215135] 09 p1169 N90-16765
High-order mixture homogenization of fiber-reinforced composites
[AD-A215247] 09 p1187 N90-16876
Dynamic interactions and globally optimal maneuver of distributed systems 09 p1236 N90-17172
Noise and sonic boom impact technology. Sonic boom damage to conventional structures
[AD-A213594] 09 p1237 N90-17178
Compatibility conditions of structural mechanics for finite element analysis
[NASA-TM-102413] 09 p1237 N90-17180
Structural vibration and shock isolation in a high pressure environment
[AD-D014311] 09 p1238 N90-17186
Noise and sonic boom impact technology. Effects of aircraft noise and sonic booms on structures: An assessment of the current state-of-knowledge
[AD-A213919] 09 p1278 N90-17409
Integrated force method versus displacement method for finite element analysis
[NASA-TP-2937] 10 p1398 N90-18081
POS2D: A graphic program for analysing axisymmetric and two-dimensional structures
[DE90-608884] 10 p1417 N90-18168
Support trusses for large precision segmented reflectors: Preliminary design and analysis
[NASA-TM-101560] 11 p1468 N90-18453
Probability of failure and risk assessment of propulsion structural components 11 p1471 N90-18470
Hydrogenated amorphous and microcrystalline silicon deposited from silane-hydrogen mixtures
[ETN-90-96267] 11 p1493 N90-18590
Computational and experimental of railgun structural performance
[DE90-006418] 12 p1607 N90-19247
Integrated control/structure optimization by multilevel decomposition
[NASA-TM-102619] 12 p1613 N90-19281
Three-dimensional structural analyses of reentry vehicles
[DE90-006278] 12 p1615 N90-19291
An experimental study of the aeroelastic behaviour of two parallel interfering circular cylinders
12 p1673 N90-19609
Computational aspects of sensitivity calculations in linear transient structural analysis
[NASA-TM-4156] 12 p1673 N90-19610
PATRAN-STAGS translator (PATSTAGS)
[NASA-TM-100388] 12 p1674 N90-19616
A transient plasticity study and low cycle fatigue analysis of the Space Station Freedom photovoltaic solar array blanket
[NASA-TM-102516] 12 p1674 N90-19617
Digital treatment of elastic-plastic structures by means of quadratic optimization processes from the finite element method
[ETN-90-95823] 12 p1675 N90-19621
COCOMAT: A Computer Aided Engineering (CAE) system for composite structures design
[NLR-MP-87078-U] 12 p1699 N90-19756
Analysis of flow-, thermal-, and structural-interaction of hypersonic structures subjected to severe aerodynamic heating
[AD-A217882] 13 p1750 N90-20053
Extended x ray absorption fine structure analysis applied to composite materials
[DE90-008575] 13 p1769 N90-20150
An electrochemical and spectroscopic study of electrode processes
[AD-A217261] 13 p1793 N90-20289
Comparison of two matrix data structures for advanced CSM testbed applications
[NASA-CR-181951] 13 p1815 N90-20421
A 4-node assumed-stress hybrid shell element with rotational degrees of freedom
[NASA-CR-4279] 13 p1815 N90-20422
Limitations and applications of fracture assessment with R6
[AERE-R-13012] 13 p1815 N90-20425
Evaluation of an adaptive unstructured remeshing technique for integrated fluid-thermal-structural analysis
[NASA-TM-102611] 13 p1815 N90-20426
Automated finite element modeling and simulation
13 p1875 N90-20753
The role of structural analysis in airworthiness certification
[BR112064] 14 p1915 N90-20972
Computer-aided structural optimisation of aircraft structures
[BR112837] 14 p1915 N90-20973
Zenith Star: A structural control challenge
14 p1933 N90-21064
A distributed finite-element modeling and control approach for large flexible structures
14 p1934 N90-21071
Mechanics of interface fracture
14 p1990 N90-21408
The computational structural mechanics testbed generic structural-element processor manual
[NASA-CR-181728] 14 p1991 N90-21410
Direct formulation of a 4-node hybrid shell element with rotational degrees of freedom
[NASA-CR-4282] 14 p1991 N90-21411
Integrated modeling and analysis of a space-truss article
[NASA-TM-102615] 14 p1991 N90-21412
The Shock and Vibration Digest, volume 22, no. 2
14 p2022 N90-21596
Research programs in aeronautical engineering, solid state physics, and materials science at Technion-Israel Institute of Technology, Haifa, Israel
[EOARD-LR-89-068] 14 p2044 N90-21720
Towards a unified analysis methodology for composite rotor blades 15 p2046 N90-21730
Computational simulation of structural fracture in fiber composites
[NASA-TM-102505] 15 p2064 N90-21821
Surface structure and chemistry of high surface area silica gels
[DE90-007684] 15 p2071 N90-21865
Review of analysis methods for mechanically fastened joints in composites
[LR-599] 15 p2107 N90-22050
The Shock and Vibration Digest, volume 21, no. 8
15 p2110 N90-22068
Recent progress in the dynamic plastic behavior of structures, part 5 15 p2110 N90-22069
The Shock and Vibration Digest, volume 22, no. 1
15 p2111 N90-22073
Scattering of waves by inclusions in a nonhomogeneous elastic half space solved by boundary element methods
[PB90-145699] 15 p2116 N90-22107
Free wave propagation in orthogonally stiffened cylinders 15 p2119 N90-22124
The computational structural mechanics testbed data library description
[NASA-TM-100645-REV-1] 15 p2121 N90-22135
Graphically-oriented nonlinear analysis of statically loaded plane frames on microcomputers
[PB90-165945] 15 p2144 N90-22248
Large deformation analysis of laminated composite structures by a continuum-based shell element with transverse deformation 16 p2211 N90-22613
Probabilistic structural analysis of aerospace components using NESSUS
[NASA-TM-102324] 16 p2248 N90-22823
Solar Concentrator Advanced Development Program
[NASA-CR-185173] 16 p2250 N90-22834
Spatial operator algebra framework for multibody system dynamics 16 p2279 N90-22989
A unifying framework for rigid multibody dynamics and serial and parallel computational issues
16 p2283 N90-23009
A decoupled recursive approach for constrained flexible multibody system dynamics 16 p2289 N90-23042
Model reduction for flexible spacecraft with clustered natural frequencies 16 p2291 N90-23054
OPTICON: Pro-Matlab software for large order controlled structure design 16 p2292 N90-23058
Structural behavior of composites with progressive fracture
[NASA-TM-102370] 17 p2368 N90-23477
Soluble polysilanes: A new class of radiation sensitive O2-RIE resistant polymers for use in microlithography
[AD-A219476] 17 p2379 N90-23551
Fracture mechanism maps for advanced structural ceramics. Part 1: Methodology and hot-pressed silicon nitride results
[AD-A220428] 17 p2380 N90-23556
Simulation and interdisciplinary design methodology for control-structure interaction systems
17 p2385 N90-23584
Nonlinear dynamics and control of flexible structures
[AD-A218476] 17 p2386 N90-23589
Lunar rated fasteners
[NASA-CR-182856] 17 p2411 N90-23737
Application of finite-element-based solution technologies for viscoplastic structural analyses
[NASA-CR-185196] 17 p2414 N90-23757
Finite element formulations for coupled fluid/structure eigenvalue analysis
[AD-A220793] 17 p2416 N90-23766

STARS: An integrated general-purpose finite element structural, aeroelastic, and aeroservoelastic analysis computer program
[NASA-TM-101709] 17 p2416 N90-23768
Finite element analysis of structural components using viscoplastic models with application to a cowl lip problem
[NASA-CR-185189] 17 p2416 N90-23769
The chemical and structural properties of sea ice in the southern Beaufort Sea
[AD-A219746] 17 p2418 N90-23776
Cumulative reports and publications through December 31, 1989
[NASA-CR-182041] 17 p2439 N90-23898
Design of finite element systems for parallel computers 17 p2450 N90-23975
Development of damped metal matrix composites for advanced structural applications
[AD-A219864] 18 p2518 N90-24380
Morphological and structural characterization of the spinodal decomposition of Fe-Cr alloys
[DE90-010496] 18 p2526 N90-24418
Eighteenth NASTRAN (R) Users' Colloquium
[NASA-CP-3069] 18 p2568 N90-24637
A NASTRAN trainer for dynamics 18 p2569 N90-24638
Accuracy of the QUAD4 thick shell element 18 p2569 N90-24641
Eigenvalue computations with the QUAD4 consistent-mass matrix 18 p2569 N90-24642
Transitioning of power flow in beam models with bends 18 p2570 N90-24648
Monitoring of Ritz modal generation 18 p2571 N90-24650
Computational methods and plasticity
[PB90-167917] 18 p2571 N90-24652
Analysis of shell-type structures subjected to time-dependent mechanical and thermal loading
[NASA-CR-185077] 18 p2571 N90-24653
Understanding our genetic inheritance. The US Human genome project: The first five years, FY 1991-1995
[DE90-008240] 18 p2584 N90-24718
Computer-Aided Structural Engineering (CASE) project. User's guide: A Three-Dimensional Stability Analysis/Design Program (3DSAD). Report 2: General loads module
[AD-A220331] 18 p2591 N90-24742
Development of a postprocessing and 3D graphical imaging facility
[AD-A221212] 18 p2593 N90-24755
Incorporation of a progressive failure analysis method in the CSM testbed software system 18 p2640 N90-25036
Dynamic analysis of flexible multibody structures 18 p2642 N90-25048
Hybrid analysis: Coupling of the finite element method with analytical approaches
[MBB-UO-0048/89-PUB] 19 p2650 N90-25079
Flexion, extension and lateral bending responses of the cervical spine 19 p2719 N90-25468
ICASE semiannual report, April 1 - September 30, 1989
[NASA-CR-181988] 19 p2727 N90-25502
Multiprocessor architecture: Synthesis and evaluation
[NASA-CR-186618] 19 p2741 N90-25579
Structural analysis and optimization of a propfan blade using a finite element method
[DLR-FB-90-01] 20 p2812 N90-26006
Biconic cargo return vehicle with an advanced recovery system. Volume 1: Conceptual design
[NASA-CR-186520] 20 p2821 N90-26052
Integrated support structure
[NASA-CR-186835] 20 p2841 N90-26162
Structured electrode interfaces
[AD-A222763] 20 p2859 N90-26265
Design of ceramic components with the NASA/CARES computer program
[NASA-TM-102369] 20 p2875 N90-26359
Structural Mechanics Division research and technology plans for FY 1990 and accomplishments for FY 1989
[NASA-TM-102654] 20 p2876 N90-26361
Research conducted at the Institute for Computer Applications in Science and Engineering in applied mathematics, numerical analysis, and computer science
[NASA-CR-182057] 20 p2903 N90-26510
Peak identification techniques 21 p2959 N90-26822
Evaluation of energy absorption of new concepts of aircraft composite subfloor intersections
[NASA-TP-2951] 21 p2959 N90-26823
Supersonic jet studies of benzyl alcohols: Minimum energy conformations and torsional motion
[AD-A221815] 21 p2980 N90-26934
Advanced processing and properties of high performance alloys
[AD-A221776] 21 p2983 N90-26948
An interdisciplinary approach to the predictive modeling of structural adhesive bonding
[AD-A221703] 21 p2988 N90-26982
Modal interaction in postbuckled plates. Theory
[NASA-TP-2943] 21 p3012 N90-27121
Stochastic structural dynamics for aerospace applications
[AD-A221517] 21 p3013 N90-27133
The composite load spectra project 21 p3047 N90-27323
Interaction of acoustic waves generated by coupled plate
[NASA-CR-186873] 21 p3072 N90-27464
Electronic and structural properties of Si10 cluster
[AD-A222429] 21 p3074 N90-27478
Study of the structure of the vortices created by the drag of a natched edge by thermal tracing
[IMFL-89-26] 22 p3109 N90-27660
Integration of externally carried weapon systems with military helicopters
[AGARD-AR-247] 22 p3115 N90-27696
Thermal-distortion analysis of an antenna strongback for geostationary high-frequency microwave applications
[NASA-TP-3016] 22 p3125 N90-27738
Flexible structure control and rigid body dynamics 22 p3129 N90-27757
Investigation of the techniques for the analysis of composite structures: Analysis and representation of the static and dynamic behavior of glued metal insert assemblies
[IMFL-89-44] 22 p3153 N90-27878
Assessment and demonstration of the capabilities of NDI processes, equipment, and personnel 22 p3184 N90-28071
Ceramics Analysis and Reliability Evaluation of Structures (CARES). Users and programmers manual
[NASA-TP-2916] 22 p3190 N90-28099
Postbuckling response of long thick isotropic plates loaded in compression including higher order transverse shearing effects
[NASA-TM-4199] 22 p3190 N90-28100
Mechanics of impact energy absorption
[PB90-190836] 22 p3190 N90-28101
Graphically-oriented linear analysis of plane frames subjected to complex loadings on microcomputers
[PB90-173279] 22 p3190 N90-28102
A comparison of single-cycle versus multiple-cycle proof testing strategies
[NASA-CR-4318] 22 p3193 N90-28115
The radiation budget of stratocumulus clouds measured by tethered balloon instrumentation: Variability of flux measurements 22 p3216 N90-28242
Liquid Rocket Booster (LRB) for the Space Transportation System (STS) systems study. Appendix E: Pressure-fed booster test bed for the liquid rocket booster study
[NASA-CR-183791-APP-E] 23 p3289 N90-28605
Probabilistic structural analysis methods development for SSME 23 p3291 N90-28616
Development of an integrated BEM for hot fluid-structure interaction 23 p3291 N90-28617
Structural response of SSME turbine blade airfoils 23 p3297 N90-28649
Probabilistic model for fracture mechanics service life analysis 23 p3297 N90-28650
Inelastic analysis of laminated composites 23 p3301 N90-28669
Structure of metal overlayers by low energy alkali ion scattering: Cu/Ru(0001) and Sn/Pt(111)
[DE90-014453] 23 p3310 N90-28718
Simulation of INPE's printed circuit laboratory production line
[INPE-4556-TDL/331] 23 p3322 N90-28784
Structural analysis and optimum design of geodesically stiffened composite panels
[NASA-CR-186944] 23 p3337 N90-28862
Torsional effects in structures subjected to strong ground motion
[PB90-226960] 23 p3339 N90-28869
Analysis of vibrational power transmission through a beam system including a flexible section
[ISVR-TR-176] 23 p3340 N90-28875
Error detection and control for nonlinear shell analysis
[NASA-TM-102723] 23 p3340 N90-28877
Human factors model concerning the man-machine interface of mining crewstations 23 p3364 N90-29011
Second order tensor finite element
[NASA-CR-184008] 23 p3386 N90-29122
Generalized Advanced Propeller Analysis System (GAPAS). Volume 2: Computer program user manual
[NASA-CR-185277] 24 p3434 N90-29394
Structural testing and analytical research of turbine components
[AD-A223516] 24 p3434 N90-29396
Development of dual fiber reinforced glass matrix composites for structural space based applications
[AD-A223801] 24 p3444 N90-29446
Proceedings of damping '89. Volume 2: Pages FAA-1 through IBD-15
[AD-A223432] 24 p3479 N90-29665
Spatial structure of particle-orbit loss regions in l=2 helical systems
[DE90-508080] 24 p3548 N90-30073

STRUCTURAL BASINS

NT GREAT BASIN (US)
NT RIVER BASINS
NT WATERSHEDS
Late quaternary geomorphology of the Great Salt Lake region, Utah, and other hydrographically closed basins in the western United States: A summary of observations
[NASA-CR-185912] 05 p0663 N90-13878
Radon concentration over the Brazilian Amazon Basin during the wet season (Belem-Manaus GTE-ABLE-2B flight of April 24, 1987)
[INPE-4892-PRE/1493] 14 p2004 N90-21486

STRUCTURAL BEAMS

U BEAMS (SUPPORTS)

STRUCTURAL DESIGN

Large scale prop-fan structural design study. Volume 1: Initial concepts
[NASA-CR-174992] 01 p0010 N90-10043
Large scale prop-fan structural design study. Volume 2: Preliminary design of SR-7
[NASA-CR-174993] 01 p0010 N90-10044
Royal Aerospace Establishment: No place for a castings factor 01 p0042 N90-10235
Application of formal optimization techniques in thermal/structural design of a heat-pipe-cooled panel for a hypersonic vehicle
[NASA-TM-89131] 01 p0071 N90-10409
Analysis and test of a 16-foot radial rib reflector developmental model
[NASA-TM-101648] 01 p0080 N90-10457
Design of grazing incidence monochromators involving unconventional gratings
[DE89-016341] 01 p0123 N90-10704
A lunar far-side very low frequency array
[NASA-CP-3039] 01 p0139 N90-10805
Conceptual design of a synchronous Mars telecommunications satellite
[NASA-TP-2942] 01 p0141 N90-10814
Environmental testing: An approach to more cost efficiency 02 p0176 N90-10988
Reduction of dynamic response of spacecraft structures and payloads 02 p0178 N90-11000
Employment of modal survey methodologies in dynamic analysis procedures 02 p0179 N90-11006
Integration of analytical and test software for optimal structural design under dynamic loads 02 p0179 N90-11007
Experiences using a major FEM package interactively for spacecraft applications 02 p0179 N90-11008
Advances in design and testing of spacecraft structures 02 p0180 N90-11018
Development of the large spacecraft structure 02 p0180 N90-11020
Ariane 5 structural design and development 02 p0186 N90-11057
SDM challenges for space station 02 p0186 N90-11059
Key structures mechanical issues of the European Space Station and platform program Columbus 02 p0188 N90-11072
New computing systems and their impact on structural analysis and design
[NASA-CR-185831] 02 p0257 N90-11457
Aspects of the development of a 1-5 micron infrared camera for astronomy 02 p0290 N90-11656
The fuel cell in space: Yesterday, today and tomorrow
[NASA-TM-102366] 03 p0318 N90-11804
Application of process integration to utilities, combined heat and power, and heat pumps
[ESDU-89001] 03 p0335 N90-11909
Integrated multidisciplinary optimization of rotorcraft: A plan for development
[NASA-TM-101617] 04 p0450 N90-12580
General approach and scope --- rotor blade design optimization 04 p0451 N90-12581
Rotor blade aerodynamic design 04 p0451 N90-12582
Rotor blade dynamic design 04 p0451 N90-12583
Rotor blade structural design 04 p0451 N90-12584
Acoustic design considerations: Review of rotor acoustic sources 04 p0451 N90-12585
Airframe design considerations: Overview --- rotor design optimization 04 p0451 N90-12586
Appendix: Results obtained to date --- integrated multidisciplinary optimization of rotorcraft 04 p0451 N90-12588

Scaling of an 85 GHz gyrotron to operate at 94 GHz
[AD-A212756] 04 p0504 N90-12909
Efficient methods for integrated structural-aerodynamic wing optimum design 05 p0579 N90-13376
Development of an advanced fan blade containment system
[DOT/FAA/CT-89/20] 05 p0581 N90-13386
Aeroelastic control of composite lifting surfaces: Integrated aeroelastic control optimization 05 p0583 N90-13396
Cryogenic systems for the large deployable reflector 05 p0597 N90-13470
LDR structural technology activities at JPL 05 p0601 N90-13488
Joints in deployable space truss structures 05 p0601 N90-13489
Space Station Engineering Design Issues
[NASA-CR-185978] 05 p0601 N90-13492
Kinematics and control of manipulation robots
[WTHD-187] 05 p0652 N90-13803
Design and demonstration of heat pipe cooling for NASP and evaluation of heating methods at high heating rates
[DE89-016995] 06 p0724 N90-14227
Preliminary design document: Ground based testbed for avionics systems
[NASA-CR-183821] 06 p0725 N90-14231
Sandia Satellite Program summary of operational procedures
[DE90-000892] 06 p0728 N90-14249
Mechanisms of wear in structural ceramic materials 06 p0749 N90-14360
Technology development program for an advanced microsheet glass concentrator
[NASA-TM-102406] 06 p0804 N90-14678
The interference of flightmechanical control laws with those of load alleviation and its influence on structural design 07 p0871 N90-15054
Design and calibration of an in-stack, low-pressure impactor
[AD-A213531] 07 p0882 N90-15105
Design of a custom load cell for a precision assembly application
[DE90-004439] 07 p0923 N90-15340
NOISE: A nonlinear optimization induction free-electron laser systems engineering code
[DE90-004438] 07 p0936 N90-15420
On the analysis and optimization of a platform manipulator 07 p0938 N90-15433
Hybrid butterfly valve
[NASA-CASE-SSC-00004] 07 p0940 N90-15443
Pipeline vibrations. Fluid transients in non-rigid, unbranched planar piping systems
[ESDU-89030] 07 p0948 N90-15491
Design philosophy and construction techniques for integral fuselage fuel tanks 08 p1023 N90-15913
Unmanned air vehicles payloads and sensors 08 p1026 N90-15930
Special Course on Advances in Cryogenic Wind Tunnel Technology
[AGARD-R-774] 08 p1028 N90-15939
The European Transonic Windtunnel (ETW) 08 p1029 N90-15945
The cryogenic Ludwieg tube tunnel at Goettingen 08 p1029 N90-15947
Design of a thrust stand for high power electric propulsion devices
[NASA-TM-102372] 08 p1037 N90-15992
Tracking flares
[ISBN-0-642-13583-5] 08 p1052 N90-16080
Metal vaporisers: Bicentennial series of five historical monographs
[ISBN-0-642-13584-3] 08 p1052 N90-16081
Conceptual design for the space station Freedom modular combustion facility
[NASA-TM-102037] 08 p1053 N90-16087
Organic cathode for a secondary battery
[NASA-CASE-NPO-17604-1-CU] 08 p1059 N90-16124
Sizing and selection of batteries for stand-alone photovoltaic systems
[DE90-002990] 08 p1060 N90-16129
MHD stable high beta spheromak equilibrium
[DE90-004873] 08 p1127 N90-16529
Design of a large superconducting spectrometer magnet
[DE90-719505] 08 p1131 N90-16553
High-pressure promoted combustion chamber
[NASA-CASE-MSC-21470-1] 09 p1170 N90-16771
Aerodynamic and structural design challenges of a reusable single stage to orbit air-breathing launch vehicle 09 p1177 N90-16814
Suitport extra-vehicular access facility
[NASA-CASE-ARC-11635-1] 09 p1183 N90-16860
Thermal switch disc for short circuit protection of batteries
[NASA-CASE-MSC-21428-1] 09 p1209 N90-17008
Noncontact temperature pattern measuring device
[NASA-CASE-NPO-17824-1-CU] 09 p1229 N90-17132
Dynamic modeling of flexible bodies in multibody systems 09 p1229 N90-17134
Mechanized fluid connector and assembly tool system
[NASA-CASE-MSC-21434-1] 09 p1230 N90-17138
Releasable clamping apparatus
[NASA-CASE-MFS-28192-1] 09 p1233 N90-17154
Bio-reactor chamber
[NASA-CASE-MSC-20929-1] 09 p1250 N90-17252
Advanced materials for interior and equipment related to fire safety in aviation 10 p1316 N90-17608
Design of JT-60U ICRF launcher
[DE90-733145] 10 p1326 N90-17663
The design and performance of a general purpose 57 kilowatt solar array simulator for current and future large spacecraft 10 p1330 N90-17685
Structural design of the Telecom 2 solar array 10 p1343 N90-17786
Design development, qualification, and flight production of an ATOX resistant flexible solar array for low earth orbit mission 10 p1344 N90-17796
The solar array of Japanese solar observatory satellite Solar-A 10 p1345 N90-17798
The solar array design of the Vesta small bodies spacecraft 10 p1345 N90-17799
Lightweight transformer demonstration
[DE90-001470] 10 p1379 N90-17991
First pump limiter experiments in TORE SUPRA
[DE90-004968] 10 p1432 N90-18266
Design guidance to minimize unsteady forces in turbomachines 11 p1460 N90-18411
Composites design handbook for space structure applications
[ESA-PSS-03-1101-ISSUE-1-REV-1] 11 p1469 N90-18459
Probability of failure and risk assessment of propulsion structural components 11 p1471 N90-18470
Small displacement, long life on-orbit compressor design and fabrication 11 p1475 N90-18489
Structures and materials technology for hypersonic aerospacecraft
[NASA-TM-102583] 11 p1519 N90-18752
X-29A aircraft structural loads flight testing
[NASA-TM-101715] 12 p1603 N90-19225
Aeroservoelasticity
[NASA-TM-102620] 12 p1603 N90-19227
Unfurlable, continuous-surface reflector concept 12 p1609 N90-19257
ROCOPT: A user friendly interactive code to optimize rocket structural components 12 p1639 N90-19415
Frequency response of electrochemical cells 12 p1639 N90-19419
Design considerations in achieving 1 MW CW operation with a whispering-gallery-mode gyrotron
[DE90-007283] 12 p1663 N90-19557
Computational aspects of sensitivity calculations in linear transient structural analysis
[NASA-TM-4156] 12 p1673 N90-19610
Development and fabrication of structural components for a scramjet engine
[NASA-CR-181945] 13 p1757 N90-20088
Design and performance of a multi-stage cylindrical reconnection launcher
[DE90-007820] 13 p1761 N90-20108
A progress report on the Livermore Miniature Vacuum Tube Project
[DE90-008302] 13 p1794 N90-20299
Space mechanism of low velocity for an array of solar panels: Analysis and design of an experimental model; dimensions of bearings
[INPE-4859-TDL/370] 13 p1809 N90-20390
Computational Methods for Aerodynamic Design (Inverse) and Optimization
[AGARD-CP-463] 14 p1916 N90-20976
Progress in inverse design and optimization in aerodynamics 14 p1916 N90-20977
Inverse design of airfoil contours: Constraints, numerical method, and applications 14 p1917 N90-20980
An intensive procedure for the design of pressure-specified three-dimensional configurations at subsonic and supersonic speeds by means of a higher-order panel method 14 p1917 N90-20982
An inverse method for the design of turbomachine blades 14 p1918 N90-20988
Application of an inverse method to the design of a radial inflow turbine 14 p1918 N90-20989
Aerodynamic optimization by simultaneously updating flow variables and design parameters 14 p1918 N90-20991
Calculation of the secondary flow in an axial turbine 14 p1924 N90-21022
Generation and decay of secondary flows and their impact on aerodynamic performance of modern turbomachinery components 14 p1925 N90-21023
Effects of secondary flow on heat transfer in rotating passages 14 p1926 N90-21031
NASA/DOD Controls-Structures Interaction Technology 1989
[NASA-CP-3041] 14 p1933 N90-21062
Vibration isolation versus vibration compensation on multiple payload platforms 14 p1933 N90-21066
Element-specific modal formulations for large-displacement multibody dynamics 14 p1934 N90-21069
Modeling and control of flexible space platforms with articulated payloads 14 p1935 N90-21073
Detection of potential space station control/structure interaction with CO-ST-IN 14 p1935 N90-21074
Optimization of the structural and control system for LSS with reduced-order model 14 p1935 N90-21075
Computational architecture for integrated controls and structures design 14 p1935 N90-21076
Controller reduction for effective interdisciplinary design of active structures 14 p1935 N90-21077
Recent experience in simultaneous control-structure optimization 14 p1936 N90-21078
A survey of experiments and experimental facilities for active control of flexible structures 14 p1936 N90-21079
NASA CSI suspension methods overview 14 p1936 N90-21080
ASCIE: An integrated experiment to study CSI in large segmented optical systems 14 p1936 N90-21082
CSI sensing and control: Analytical and experimental results 14 p1936 N90-21083
Experimental evaluation of active-member control of precision structures 14 p1936 N90-21084
Controls, Astrophysics, and Structures Experiment in Space (CASES) 14 p1937 N90-21085
LACE flight dynamics experiment 14 p1937 N90-21086
CSI technology validation on an LSS ground experiment facility 14 p1937 N90-21089
Initial operational capability of the ASTREX large space structures test bed 14 p1938 N90-21091
In-house experiments in large space structures at the Air Force Wright Aeronautical Laboratories Flight Dynamics Laboratory 14 p1938 N90-21092
Preliminary design approach for large high precision segmented reflectors
[NASA-TM-102605] 14 p1938 N90-21096
Multi-objective shape and material optimization of composite structures including damping
[NASA-TM-102579] 14 p1945 N90-21132
Structural tailoring of select fiber composite structures
[NASA-TM-102484] 14 p1946 N90-21137
Review of the state of the technology for joining ceramics for high-temperature structural applications
[DE90-009224] 14 p1956 N90-21199
Development of a fracture analysis technique for use with a general-purpose finite element program 14 p1992 N90-21416
The 10-100 kW submillimeter gyrotron 15 p2061 N90-21803
An experimental study of tip shape effects on the flutter of aft-swept, flat-plate wings
[NASA-TM-4180] 16 p2199 N90-22555
Differential equation based method for accurate approximations in optimization
[NASA-TM-102639] 16 p2200 N90-22558
Limiting performance based structural and control optimization for large vibrating structures 16 p2202 N90-22568
Design of cryogenic tanks for launch vehicles 16 p2220 N90-22662
A disturbance based control/structure design algorithm 16 p2282 N90-23003
Combined control-structure optimization 16 p2282 N90-23005
Implementation of generalized optimality criteria in a multidisciplinary environment 16 p2290 N90-23048
Aircraft drawings index 17 p2343 N90-23340
Correlation/validation of finite element code analyses for vibration assessment of avionic equipment
[AD-A220393] 17 p2353 N90-23398
Tubular space truss structure for SKITTER 2 robot
[NASA-CR-184922] 17 p2384 N90-23580
Soil Transport Implement
[NASA-CR-184931] 17 p2385 N90-23582
Simulation and interdisciplinary design methodology for control-structure interaction systems 17 p2385 N90-23584
Qualitative models for space system engineering
[NASA-CR-180682] 17 p2385 N90-23585
Cable suspended windmill
[NASA-CASE-LAR-13434-1] 17 p2412 N90-23742
Application of finite-element-based solution technologies for viscoplastic structural analyses
[NASA-CR-185196] 17 p2414 N90-23757

Guide for the use of intergraph randmicas structural software for Computer-Aided Design and Drafting(CADD)
[AD-A220624] 17 p2443 N90-23924
Development of damped metal matrix composites for advanced structural applications
[AD-A219864] 18 p2518 N90-24380
Simplified design procedures for fiber composite structural components/joints
[NASA-TM-103113] 18 p2519 N90-24384
Abrasion resistant coatings on plastics 18 p2529 N90-24428
Concept design for Hermes docking/berthing mechanism 18 p2536 N90-24464
Obtaining an equivalent beam 18 p2570 N90-24646
Photovoltaic concentrator technology development
[DE90-011479] 18 p2577 N90-24684
A preliminary design of interior structure and foundation of an inflatable lunar habitat 18 p2633 N90-24999
Modeling growth of fatigue cracks which originate at rivet holes 18 p2645 N90-25060
Flexural fatigue life prediction of closed hat-section using materially nonlinear axial fatigue characteristics 18 p2645 N90-25062
The Penguin: A low Reynolds number powered glider for station keeping missions
[NASA-CR-186667] 19 p2658 N90-25129
Dynamic analysis of space-related linear and non-linear structures
[NASA-TM-103490] 19 p2667 N90-25174
Design of a versatile, teleoperable, towable lifting machine with robotic capabilities for use in NASA's lunar base operations
[NASA-CR-186688] 19 p2697 N90-25345
Innovative design of composite structures: Axisymmetric deformations of unsymmetrically laminated cylinders loaded in axial compression
[NASA-CR-186635] 19 p2700 N90-25364
Behavior of composite/metal aircraft structural elements and components under crash type loads: What are they telling us
[NASA-TM-102681] 19 p2701 N90-25368
Structures for remotely deployable precision antennas
[NASA-CR-182065] 20 p2822 N90-26061
Micro coring apparatus
[NASA-CR-183072] 20 p2869 N90-26321
QM-8 final performance evaluation report: SEALS, volume 4
[NASA-CR-183958] 20 p2869 N90-26324
Design and construction of a wall-climbing robot
[NIAR-90-20] 20 p2870 N90-26327
Advanced Turbine Technology Applications Project (ATTAP)
[NASA-CR-185240] 20 p2939 N90-26728
An expert system advisor for damage repair of composite wing skins (repairman) 21 p2956 N90-26810
Improved high power/high frequency inductor
[NASA-CASE-NPO-17830-1-CU] 21 p2998 N90-27042
Space Station attached payloads 21 p3015 N90-27141
Airport pavement drainage
[DOT/FAA/RD-90/24] 22 p3122 N90-27728
The dynamics of orbital maneuvering: Design and evaluation of a visual display aid for human controllers 22 p3131 N90-27767
TRANSTRAIN: A program to compute strain transformations in composite materials
[NASA-TM-103509] 22 p3153 N90-27877
Lateral buckling of short I-beams under cyclic loading
[PB90-213653] 22 p3191 N90-28104
Sandia's CONCEPT-90 photovoltaic concentrator module
[DE90-012243] 22 p3196 N90-28134
Study of ground effects on flying scaled models 23 p3275 N90-28532
Measurement of the steady surface pressure distribution on a single rotation large scale advanced prop-fan blade at Mach numbers from 0.03 to 0.78
[NASA-CR-182124] 23 p3278 N90-28552
Operational cost drivers 23 p3294 N90-28636
Design optimization of gas generator hybrid propulsion boosters
[NASA-CR-181096] 23 p3299 N90-28660
Formulation of design guidelines for automated robotic assembly in outerspace 23 p3365 N90-29017
Multi-disciplinary optimization of aeroservoelastic systems
[NASA-CR-185931] 24 p3432 N90-29385
WingDesign: Program for the structural design of a wing cross-section
[LR-627] 24 p3433 N90-29390
Structural testing and analytical research of turbine components
[AD-A223516] 24 p3434 N90-29396
Multiaxial fatigue criterion for 2-1/4 Cr-1 Mo steel for use in high-temperature structural design
[DE90-016039] 24 p3452 N90-29491

STRUCTURAL DESIGN CRITERIA

Analysis of results from wind tunnel tests of inlets for an advanced turboprop nacelle installation
[NASA-CR-174937] 01 p0003 N90-10011
Preliminary design of a large tetrahedral truss/hexagonal heatshield panel aerobrake
[NASA-TM-101612] 01 p0025 N90-10127
Design guide for predicting nonlinear random response (including snap-through) of buckled plates
[NASA-CR-181877] 01 p0118 N90-10681
Evaluation of tests and design factors 02 p0176 N90-10987
Transient tests for spacecraft structures 02 p0183 N90-11040
Multi-axis transient testing: Experimental investigations 02 p0184 N90-11042
Development and applications of reliability and maintainability design criteria in military aircraft
[ETN-89-95208] 04 p0452 N90-12591
Project, implementation, and utilization of composite structures
[ETN-89-95209] 04 p0466 N90-12665
Point of view of a civil aircraft manufacturer on Al-Li alloy 07 p0899 N90-15200
Uses and properties of Al-Li on the new EH101 helicopter 07 p0900 N90-15201
Analytical study on the decreasing method of thermal stress for ceramic gas turbines
[DE90-734934] 08 p1051 N90-16078
Semi-empirical transition criteria for the design of laminar profiles 08 p1067 N90-16174
Development of transition criteria on the basis of e to the N power for three dimensional wing boundary layers 08 p1067 N90-16179
The solar array of Japanese solar observatory satellite Solar-A 10 p1345 N90-17798
Improved solar cells testing fixtures 10 p1346 N90-17807
Structures and materials technology for hypersonic aerospacecraft
[NASA-TM-102583] 11 p1519 N90-18752
Conceptual design and analysis of roads and road construction machinery for initial lunar base operations
[NASA-CR-186673] 18 p2535 N90-24459
Diode laser satellite systems for beamed power transmission
[NASA-TP-2992] 18 p2556 N90-24585

STRUCTURAL DYNAMICS

U DYNAMIC STRUCTURAL ANALYSIS

STRUCTURAL ENGINEERING

CONSOLE: A CAD tandem for optimization-based design interacting with user-supplied simulators 01 p0017 N90-10085
Control/structure interaction methods for space station power systems 01 p0018 N90-10087
The development of an expert system for the creative design of mechanisms
[AD-A211115] 01 p0110 N90-10628
Exploitation of data management facilities for finite element analysis in aerospace structural engineering applications 02 p0188 N90-11078
The use of Lanczos's method to solve the large generalized symmetric definite eigenvalue problem
[NASA-CR-181914] 03 p0385 N90-12193
Designing and designing knowledge in engineering and architecture
[PB89-219521] 03 p0415 N90-12383
The adhesive bonding of thermoplastic composites
[AD-A213358] 05 p0618 N90-13605
Automation and robotics in construction: Japanese research and development
[AD-A214170] 07 p0942 N90-15456
Aircraft fuel tank construction and testing experience 08 p1021 N90-15907
Noise and sonic boom impact technology. Effects of aircraft noise and sonic booms on structures: An assessment of the current state-of-knowledge
[AD-A213919] 09 p1278 N90-17409
Structures and materials technology for hypersonic aerospacecraft
[NASA-TM-102583] 11 p1519 N90-18752
COCOMAT: A Computer Aided Engineering (CAE) system for composite structures design
[NLR-MP-87078-U] 12 p1699 N90-19756
Parallel methods for solving nonlinear block bordered systems of equations
[AD-A217062] 12 p1707 N90-19806
Initial operational capability of the ASTREX large space structures test bed 14 p1938 N90-21091
The Shock and Vibration Digest, volume 21, no. 1 15 p2109 N90-22061
Recent advances in structural control 15 p2109 N90-22062
The Shock and Vibration Digest, volume 21, no. 7 15 p2110 N90-22066
Optimum design of structures under shock and vibration environment 15 p2110 N90-22067
The Shock and Vibration Digest, volume 21, no. 8 15 p2110 N90-22068
Aircraft crash survival design guide. Volume 3: Aircraft structural crash resistance
[AD-A218436] 16 p2198 N90-22547
NASA-UVA light aerospace alloy and structures technology program
[NASA-CR-182607] 16 p2217 N90-22651
Guide for the use of intergraph randmicas structural software for Computer-Aided Design and Drafting(CADD)
[AD-A220624] 17 p2443 N90-23924
Computer-Aided Structural Engineering (CASE) project. User's guide: A Three-Dimensional Stability Analysis/Design Program (3DSAD). Report 2: General loads module
[AD-A220331] 18 p2591 N90-24742
The application of engineering ceramics in gas turbines
[PNR90676] 20 p2812 N90-26005
Technology for large space systems: A bibliography with indexes (supplement 22)
[NASA-SP-7046(22)] 20 p2822 N90-26056
The use of Lanczo's method to solve the large generalized symmetric Eigenvalue problem in parallel
[NASA-CR-182072] 20 p2907 N90-26533
Construction of geological and geotechnical information database
[DE90-503417] 20 p2936 N90-26708
Conjugate gradient methods for constrained least squares problems
[AD-A222706] 21 p3063 N90-27411
Integrated structural/control design via multiobjective optimization
[AD-A223088] 21 p3071 N90-27459
Index of USACERL publications, October 1984-December 1989
[AD-A221644] 21 p3088 N90-27559
Guidelines for threaded fasteners
[ESA-PSS-03-208-ISSUE-1] 22 p3182 N90-28061
Wind tunnel simulation of Antarctic snowdrifting
[PB90-184565] 22 p3212 N90-28222
Statement of research objectives and summary of research efforts
[RLE-PR-132] 23 p3415 N90-29295
Computer-Aided Structural Engineering (CASE) project: Investigation and design of U-frame structures using program CUFRBC. Volume A: Program criteria and documentation
[AD-A224387] 24 p3525 N90-29934

STRUCTURAL FAILURE

Composite Blade Structural Analyzer (COBSTRAN) theoretical/programmer's manual
[NASA-TM-101958] 01 p0033 N90-10181
Estimating the time to fatigue failure of mooring cables
[PB89-220677] 04 p0511 N90-12946
Proceedings of the 1988 Structural Integrity Program Conference
[AD-A213545] 07 p0947 N90-15486
Biaxial strength and stress rupture of hot-pressed silicon nitride
[AD-A216950] 11 p1519 N90-18750
Limitations and applications of fracture assessment with R6
[AERE-R-13012] 13 p1815 N90-20425
NASA airframe structural integrity program
[NASA-TM-102637] 14 p1993 N90-21422
An evaluation of the pressure proof test concept for thin sheet 2024-T3
[NASA-TM-101675] 14 p1994 N90-21424
Advances in optimal active control techniques for aerospace systems; application to aircraft active landing gear 15 p2054 N90-21769
Deformation-induced structural developments of ultra-high molecular weight polyethylene
[ETN-90-96899] 18 p2529 N90-24432
Advanced buckling analyses of beams with arbitrary cross sections
[ISBN-90-9002808-0] 18 p2572 N90-24659
Development of a finite element based delamination analysis for laminates subject to extension, bending, and torsion 18 p2642 N90-25049
Integrated support structure
[NASA-CR-186835] 20 p2841 N90-26162
Proceedings of the 1987 Aircraft/Engine Structural Integrity Program (ASIP/ENSIP) Conference
[AD-A198037] 21 p2956 N90-26807
Lessons learned from the T-46A durability and damage tolerance program 21 p2957 N90-26812
Automated analysis of MXU-553 flight data 21 p2958 N90-26821

Evaluation of energy absorption of new concepts of aircraft composite subfloor intersections
[NASA-TP-2951] 21 p2959 N90-26823
Modal interaction in postbuckled plates. Theory
[NASA-TP-2943] 21 p3012 N90-27121
TRANSTRAIN: A program to compute strain transformations in composite materials
[NASA-TM-103509] 22 p3153 N90-27877
The role of NDI in the certification of turbine engine components 22 p3184 N90-28069
Development of an automated ultrasonic inspection system for composite structure on in-service aircraft 22 p3186 N90-28079
Reliability analysis of a structural ceramic combustion chamber
[NASA-TM-103264] 22 p3192 N90-28112
Assessment and improvement of aeroengine disc structural integrity 24 p3433 N90-29392

STRUCTURAL FATIGUE
U FATIGUE (MATERIALS)

STRUCTURAL MATERIALS
U CONSTRUCTION MATERIALS

STRUCTURAL MEMBERS
NT ANISOTROPIC PLATES
NT BEAMS (SUPPORTS)
NT BOX BEAMS
NT CANTILEVER BEAMS
NT CIRCULAR PLATES
NT CORRUGATED PLATES
NT CURVED BEAMS
NT ELASTIC PLATES
NT END PLATES
NT FLAT PLATES
NT I BEAMS
NT MEMBRANE STRUCTURES
NT METAL PLATES
NT ORTHOTROPIC PLATES
NT PERFORATED PLATES
NT PLATES (STRUCTURAL MEMBERS)
NT RECTANGULAR PLATES
NT REINFORCED PLATES
NT SKIN (STRUCTURAL MEMBER)
NT STRAKES
NT STRUTS
NT TIMOSHENKO BEAMS
NT TRUSSES
NT WING PANELS
Structural problems of accurate inflatable surfaces 02 p0184 N90-11044
Life of concentrated contacts in the mixed EHD and boundary film regimes
[AD-A216673] 11 p1517 N90-18738
Heat engine based on shape memory alloys
[AD-D014400] 14 p1986 N90-21385
Structural fatigue in the 34-meter HA-Dec antennas 15 p2078 N90-21902
A cable-rigidized 3D pantograph 18 p2538 N90-24484
Design of an autonomous teleoperated cargo transporting vehicle for lunar base operations
[NASA-CR-186686] 18 p2565 N90-24633

STRUCTURAL PROPERTIES (GEOLOGY)
Coronae on Venus observations and models of origin 03 p0427 N90-12449
Fracture analysis through photographic imagery of low spatial resolution: A contribution to the study of tectonic evoluation of the Araripe Plateau region
[INPE-4876-PRE/1487] 11 p1520 N90-18756
Evaluation of selection techniques for multispectral bands employed in the discrimination of carbonatic rocks
[INPE-4850-TDL/365] 11 p1522 N90-18765
Geological structure of the State of Rio de Janeiro viewed through MSS LANDSAT imagery
[INPE-4826-PRE/1457] 11 p1533 N90-18825
Quantification of structural field data in the Rio Grande do Norte basin and neighborhood
[INPE-4821-RPE/591] 11 p1533 N90-18826
Analysis of photogeologic lineaments in the Ithacare (BA) region: A proposed methodology
[INPE-4855-PRE/1478] 12 p1677 N90-19635
Analysis of tectonic movements utilizing remote sensor products in the Southern Espinhaco (SE) region
[INPE-4830-PRE/1451] 12 p1690 N90-19708
Comets: Dirty snowballs or icy dirtballs 12 p1739 N90-19994
Laboratory techniques for the characterisation of snow structures 12 p1741 N90-20007
Underwater physiography of the continental shelf of Rio Grande do Norte visible through satellite imagery
[INPE-4964-TDL/392] 13 p1820 N90-20448
A system for analysis and interpretation of lineaments in remote sensing images
[INPE-4893-PRE/1494] 13 p1840 N90-20565
The effects of structure and source complexity on waveforms: Crustal structure of Tibet and the recovery of complex seismic sources
[AD-A218202] 13 p1843 N90-20579
Characterization of linear structures from remote sensing data; Espinhaco Meridional (MG) sierra
[INPE-4905-PRE/1506] 14 p1997 N90-21449
Geology of Espinhaco Meridional, including the Quadrilatero Ferrifero: Integration through remote sensing data
[INPE-4904-PRE/1505] 14 p1998 N90-21450
A numerical and theoretical study of seismic wave diffraction in complex geologic structure
[AD-A218209] 14 p2005 N90-21490
Geology of coronae and domal structures on Venus and models of their origin 15 p2191 N90-22513
A numerical investigation of thermal convection in highly viscous spherical shells with applications to mantle dynamics in the Earth and other terrestrial planets 18 p2579 N90-24691
Characterization of porous media: Pore level 19 p2690 N90-25303
Characterization of porous media: Field level 19 p2690 N90-25304
Geologic interpretation of gravity anomalies
[AD-A222910] 21 p3025 N90-27199

STRUCTURAL RELIABILITY
Evaluation of tests and design factors 02 p0176 N90-10987
The Fourth Oxford International Conference on the Mechanical Properties of Materials at High Rates of Strain
[AD-A212293] 05 p0653 N90-13809
Proceedings of the 1988 Structural Integrity Program Conference
[AD-A213545] 07 p0947 N90-15486
Analysis of whisker-toughened ceramic components: A design engineer's viewpoint
[NASA-TM-102333] 11 p1478 N90-18504
Boeing/NASA composite components flight service evaluation
[NASA-CR-181898] 16 p2210 N90-22609
Correlation/validation of finite element code analyses for vibration assessment of avionic equipment
[AD-A220393] 17 p2353 N90-23398
Lunar rated fasteners
[NASA-CR-182656] 17 p2411 N90-23737
An aluminum quality breakthrough for aircraft structural reliability 21 p2957 N90-26816
Computational investigation of local material strength and toughness on crack growth
[AD-A223189] 21 p3012 N90-27127
Multichannel on-board load and fatigue monitoring 22 p3103 N90-27621
Reliability analysis of maintained structural system vulnerable to fatigue and fracture 23 p3338 N90-28868
Reliability study of TWT output RF window
[AD-A223688] 24 p3465 N90-29574

STRUCTURAL RIGIDITY
U STRUCTURAL STABILITY

STRUCTURAL STABILITY
NT SHELL STABILITY
Modeling and stabilization of large flexible space stations 01 p0024 N90-10120
Theoretical and experimental investigation of thin-walled aluminum panels under cyclic shear load 02 p0177 N90-10996
A contribution to the stability analysis of large space structures 02 p0177 N90-10997
Wind/seismic comparisons for upgrading existing structures
[DE89-016055] 03 p0357 N90-12044
Development of a VSAERO (Vortex Separation Aerodynamics) model of the F/A-18
[AD-A212442] 04 p0448 N90-12566
Flight motor set 360L001 (STS-26R). (Reconstructed dynamic loads analysis)
[NASA-CR-183811] 04 p0464 N90-12656
Performance effects of tie-truss modifications for a 70-meter centerline beam waveguide antenna 04 p0486 N90-12791
Space telescope pointing control 05 p0595 N90-13454
Comparison of analytical methods for calculation of wind loads
[NASA-TM-102782] 05 p0654 N90-13813
Analysis and testing of axial compression in imperfect slender truss struts
[NASA-TM-4174] 08 p1087 N90-16292
Structural stability of heat treated W/B4C multilayers
[DE90-005322] 09 p1188 N90-16884
Fatigue delamination onset prediction in tapered composite laminates
[NASA-TM-101673] 09 p1236 N90-17177
Boundary walls, fences and hoardings: Mean and peak wind loads and overturning moments
[ESDU-89050] 09 p1239 N90-17190
Fatigue of aluminium alloy joints with various fastener systems. Low load transfer
[ESDU-89046] 09 p1239 N90-17193
Baseline experiment for active control of structural vibrations
[AD-A216194] 10 p1397 N90-18076
Integrated force method versus displacement method for finite element analysis
[NASA-TP-2937] 10 p1398 N90-18081
Study of vortex arrays induced artificially and from centrifugal instabilities
[AD-A216499] 11 p1506 N90-18669
Active stabilization of aeromechanical systems
[AD-A216629] 11 p1506 N90-18672
Structures instabilities in filament liquid crystals
[ETN-90-95916] 12 p1721 N90-19888
Floor pull test of a transport airframe section
[DOT/FAA/CT-TN88/14] 13 p1754 N90-20072
Limitations and applications of fracture assessment with R6
[AERE-R-13012] 13 p1815 N90-20425
Initial operational capability of the ASTREX large space structures test bed 14 p1938 N90-21091
Fatigue crack growth predictions for variable-amplitude and spectrum loading
[LR-526] 15 p2118 N90-22118
OPTICON: Pro-Matlab software for large order controlled structure design 16 p2292 N90-23058
Multivariable frequency weighted model order reduction for control synthesis
[AIAA-89-3558] 16 p2292 N90-23060
Structural modeling for control design (articulated multibody component representation) 16 p2296 N90-23077
Feasibility study for a microwave-powered ozone sniffer aircraft
[NASA-CR-186660] 17 p2353 N90-23397
Computer-Aided Structural Engineering (CASE) project. User's guide: A Three-Dimensional Stability Analysis/Design Program (3DSAD). Report 2: General loads module
[AD-A220331] 18 p2591 N90-24742
Increasing the margin of stability of arbitrarily finite modes of flexible large space structures with damping
[AD-A221742] 21 p2967 N90-26867
Structural and optical properties of DMP-128 holograms during environmental testing
[AD-A221691] 21 p3007 N90-27094
Computational investigation of local material strength and toughness on crack growth
[AD-A223189] 21 p3012 N90-27127
The effect of reinforcement stability on composition redistribution in cast aluminum metal matrix composites
[DE90-012469] 22 p3135 N90-27791
Parametrical retiming of vibrational models of structures
[ONERA-RT-9/3313-RY-080-R] 22 p3194 N90-28121
Surface chemistry and structural effects in the stress corrosion of glass and ceramic materials
[AD-A223305] 24 p3454 N90-29507

STRUCTURAL STRAIN
Analysis of delamination growth 02 p0183 N90-11036
Evaluation of a damaged F/A-18 horizontal stabilator
[AD-A212573] 04 p0453 N90-12597
Strain accumulation and surface deformation along the San Andreas, California
[NASA-CR-185893] 05 p0666 N90-13894
Wind-excited behavior of structures, 5 09 p1235 N90-17169
Elastic buckling of imperfect cylindrical shells containing granular solids
[PB90-110362] 09 p1236 N90-17174
Through-thickness strain response of thick composites in compression
[AD-A217233] 13 p1767 N90-20141
A continuum model for phase transformation in thermoelastic solids
[AD-A222353] 21 p3085 N90-27542

STRUCTURAL VIBRATION
NT BENDING VIBRATION
NT FLUTTER
NT LINEAR VIBRATION
NT SUBSONIC FLUTTER
NT TORSIONAL VIBRATION
NT TRANSONIC FLUTTER
Flexible structure control experiments using a real-time workstation for computer-aided control engineering 01 p0017 N90-10084
A performance comparison of integration algorithms in simulating flexible structures 01 p0021 N90-10101

Modifying high-order aeroelastic math model of a jet transport using maximum likelihood estimation
01 p0021 N90-10106
Aircraft modal supression system: Existing design approach and its shortcomings
01 p0023 N90-10115
Modeling and stabilization of large flexible space stations 01 p0024 N90-10120
Thermoelastic behavior of large space structures: Modeling and control 02 p0179 N90-11012
Evaluation of dispersive behavior in periodic structures by discrete Fourier transform 02 p0180 N90-11014
Computational aspects of sensitivity calculations in linear transient structural analysis 02 p0231 N90-11327
Development of an approximate technique for the nonlinear random vibrations analysis of hysteretic systems 02 p0233 N90-11335
An analytical and experimental study of the elastodynamic response characteristics of planar linkage mechanism with bearing clearances
02 p0233 N90-11336
Problems related to the acquisition, processing and utilization of the modal parameters measured in flight tests in order to obtain the full envelope for flutter
[ETN-89-95210] 03 p0305 N90-11735
Investigation of difficult component effects on finite element model vibration prediction for the Bell AH-1G helicopter. Volume 1: Ground vibration test results
[NASA-CR-181916-VOL-1] 03 p0360 N90-12058
Airframe design considerations: Overview --- rotor design optimization 04 p0451 N90-12586
The Shock and Vibration Digest, volume 21, no. 10
04 p0483 N90-12771
Pyrotechnic shock structural response
04 p0483 N90-12774
Vibration transmission through rolling element bearings in geared rotor system, part 1
[NASA-CR-186093] 04 p0509 N90-12936
Plasma separation process: Magnet move to Oak Ridge National Laboratory
[DE89-017457] 04 p0556 N90-13242
Pointing control for LDR 05 p0595 N90-13453
Static and free-vibrational response of semi-circular graphite-epoxy frames with thin-walled open sections
[NASA-CR-186097] 05 p0617 N90-13600
Probabilistic finite element analysis of dynamic structural response
[AD-A213249] 05 p0650 N90-13789
Investigation of difficult component effects on finite element model vibration prediction for the Bell AG-1G helicopter. Volume 2: Correlation results
[NASA-CR-181916-VOL-2] 05 p0654 N90-13814
Measurement of damping of graphite epoxy composite materials and structural joints
[NASA-CR-183802] 06 p0736 N90-14286
Non-linear vibrations, stability, and dynamics of structures and mechanisms
[AD-A212152] 06 p0796 N90-14639
Evaluation of analysis techniques for low frequency interior noise and vibration of commercial aircraft
[NASA-CR-181851] 06 p0837 N90-14866
Active control system for gust load allevation and structural damping 07 p0871 N90-15056
Effect of modal truncation on derivatives of closed-loop damping ratios in structural control
07 p0882 N90-15109
Measurement of reflection and impedance in a beam by the structural intensity technique
[DE90-728212] 08 p1088 N90-16299
The Shock and Vibration Digest, volume 21, no. 9
09 p1235 N90-17168
Wind-excited behavior of structures, 5
09 p1235 N90-17169
Structural vibration and shock isolation in a high pressure environment
[AD-D014311] 09 p1238 N90-17186
Parametric version of structural vibration models
[ONERA-RT-9/3313-RY-080-R]
09 p1238 N90-17188
Force determination sensitivities study for full-scale helicopter ground vibration testing
[AD-A215983] 10 p1322 N90-17643
Baseline experiment for active control of structural vibrations
[AD-A216194] 10 p1397 N90-18076
Analytical formulation for the interaction problem of dynamic reentry, and effects due to flexibility and vibration in an aerospace vehicle
[INPE-4963-TDL/392] 11 p1467 N90-18448
A study of the vibrational transmission through flanged joints
[ISVR-TR-181] 11 p1520 N90-18755
Helicopter flight vibration of large transportation containers: A case for testing tailoring
[DE90-007429] 12 p1601 N90-19215
Modified independent modal space control of flexible structures 12 p1671 N90-19597
Active control of the forced and transient response of a finite beam
[NASA-CR-181957] 13 p1816 N90-20430
Computational simulation of damping in composite structures
[NASA-TM-102567] 13 p1817 N90-20432
PACOSS program status and results
14 p1933 N90-21065
Nonlinear and distributed parameter models of the mini-mast truss 14 p1934 N90-21070
The effect of elastic boundary conditions on the dynamic response of rectangular plates
[NASA-CR-186059] 14 p1990 N90-21405
Exhaust environment measurements of a turbofan engine equipped with an afterburner and 2D nozzle
[NASA-CR-4289] 15 p2052 N90-21760
Robust control of flexible structures
15 p2058 N90-21784
The Shock and Vibration Digest, volume 21, no. 2
15 p2109 N90-22059
Vibration analysis of systems with random parametric excitations 15 p2109 N90-22060
The Shock and Vibration Digest, volume 21, no. 1
15 p2109 N90-22061
A review of approximate methods for determining the vibrational modes of membranes
15 p2109 N90-22063
The Shock and Vibration Digest, volume 21, no. 7
15 p2110 N90-22066
Optimum design of structures under shock and vibration environment 15 p2110 N90-22067
The Shock and Vibration Digest, volume 21, no. 8
15 p2110 N90-22068
The Shock and Vibration Digest, volume 22, no. 1
15 p2111 N90-22073
Stable response of damped mechanical systems, 4
15 p2111 N90-22074
The Shock and Vibration Digest, volume 21, no. 6
15 p2163 N90-22363
Limiting performance based structural and control optimization for large vibrating structures
16 p2202 N90-22568
Robust control of vibration in flexible structures
16 p2241 N90-22787
Dynamic substructuring by the boundary flexibility vector method of component mode synthesis
[NASA-CR-182445] 16 p2247 N90-22813
Flat plate vibration analysis experimental and numerical fillet study
[AD-A218789] 16 p2247 N90-22818
Contributions of individual structural modes to the scattered acoustic field
[AD-A219128] 16 p2314 N90-23187
Experimental determination of material damping using vibration analyzer 18 p2514 N90-24358
Eighteenth NASTRAN (R) Users' Colloquium
[NASA-CP-3069] 18 p2568 N90-24637
Transitioning of power flow in beam models with bends 18 p2570 N90-24648
Control structure interaction instrumentation
[AD-A221375] 19 p2693 N90-25320
Calculation of flight vibration levels of the AH-1G helicopter and correlation with existing flight vibration measurements
[NASA-CR-182031] 19 p2702 N90-25375
Power flow analysis of two coupled plates with arbitrary characteristics
[NASA-CR-182033] 20 p2923 N90-26632
Creating a VAPEPS database: A VAPEPS tutorial
[NASA-CR-186629] 20 p2936 N90-26705
Static and free-vibrational response of semi-circular graphite-epoxy frames with thin-walled open sections
[NASA-CR-4287] 21 p3012 N90-27122
Improved computational strategy for predicting the response of complex systems
[AD-A221661] 21 p3014 N90-27135
Interaction of acoustic waves generated by coupled plate
[NASA-CR-186873] 21 p3072 N90-27464
Active control of flexible structures
23 p3282 N90-28575
Analysis of vibrational power transmission through a beam system including a flexible section
[ISVR-TR-176] 23 p3340 N90-28875
A vector diagram approach to shaping inputs for vibration reduction
[AD-A223724] 24 p3480 N90-29671
Preshaping command inputs to reduce telerobotic system oscillations 24 p3517 N90-29880

STRUCTURAL WEIGHT
Scaling study for SP-100 reactor technology
[NASA-TM-897140] 08 p1122 N90-16496
A space-fed local oscillator for spaceborne phased arrays
[AD-A216526] 10 p1328 N90-17673
ROCOPT: A user friendly interactive code to optimize rocket structural components 12 p1639 N90-19415
Earth-orbiting resonant-mass gravitational wave detectors 12 p1731 N90-19954
Electrochemical impregnation and cycle life of lightweight nickel electrodes for nickel-hydrogen cells
[NASA-TM-103140] 15 p2068 N90-21844
AVION: A detailed report on the preliminary design of a 79-passenger, high-efficiency, commercial transport aircraft
[NASA-CR-186663] 17 p2353 N90-23395
A preliminary design of interior structure and foundation of an inflatable lunar habitat 18 p2633 N90-24999

STRUTS
Plasma separation process: Magnet move to Oak Ridge National Laboratory
[DE89-017457] 04 p0556 N90-13242
Flexural and torsional-flexural buckling of thin-walled open section struts
[ESDU-89007] 06 p0797 N90-14643
Analysis and testing of axial compression in imperfect slender truss struts
[NASA-TM-4174] 08 p1087 N90-16292
Process development and fabrication of space station type aluminum-clad graphite epoxy struts
[NASA-CR-181873] 11 p1468 N90-18454
Heavily loaded joints for assembling aerobrake support trusses
[NASA-CR-181992] 14 p1939 N90-21099
An experimental investigation of support strut interference on a three-percent fighter model at high angles of attack
[AD-A219793] 17 p2345 N90-23353
Strut-node joint conjugates for the assembly of semi-permanent or reusable truss structures
18 p2640 N90-25039
Installation and pretest analysis of DARPA suboff model in the DTRC anechoic wind tunnel
[AD-A221497] 21 p2955 N90-26801
Transformational part-count in layered octahedral-tetrahedral truss configurations
[NASA-TM-102635] 23 p3287 N90-28598
Nonlinear modeling of joint dominated structures
[NASA-CR-4324] 24 p3439 N90-29423

STS
U SPACE TRANSPORTATION SYSTEM

STUDENTS
Higher education for science and technology: A background paper
[PB89-191290] 02 p0287 N90-11642
AFRAPT (Air Force Research in Aero Propulsion Technology) Trainee Program
[AD-A211540] 03 p0307 N90-11744
Computer generation of a tutorial dialogue
[AD-A211976] 03 p0380 N90-12162
Vestibular examination of motion sick student pilots
[IZF-1988-22] 12 p1696 N90-19738
A long-term retention advantage for spatial information learned naturally and in the laboratory
[AD-A218268] 13 p1855 N90-20644
The International Space University
[NASA-TM-103163] 16 p2209 N90-22604
The Clemson University, university research initiative program in discrete mathematics and computational analysis
[AD-A220103] 17 p2461 N90-24055
A study of effects of instructional modes in a sequence of computer-assisted instruction lessons, with an introduction to computer-aided diagnosis of arithmetic errors 18 p2589 N90-24730
The development of expertise on an intelligent tutoring system 18 p2630 N90-24984
Winged cargo return vehicle. Volume 1: Conceptual design
[NASA-CR-186823] 20 p2821 N90-26050

STYRENES
NT POLYSTYRENE
Initiation precursors and initiators in laser-induced copolymerization of styrene and maleic anhydride in acetone
[NASA-TM-4166] 10 p1346 N90-17810
Density profile of terminally adsorbed polymers
[AD-A220897] 18 p2529 N90-24433
Toughening of SAN copolymers by an SAN emulsion grafted rubber
[AD-A224213] 24 p3453 N90-29502

SUBCIRCUITS
U CIRCUITS

SUBDUCTION (GEOLOGY)
Stored mafic/ultramafic crust and early Archean mantle depletion
[NASA-CR-186460] 12 p1691 N90-19715

SUBDWARF STARS
A high galactic latitude survey of far ultraviolet excess objects 15 p2183 N90-22473
An analysis of the Palomar-Green subdwarfs and white dwarfs 23 p3409 N90-29263
SUBGRAVITY
U REDUCED GRAVITY
SUBGROUPS
A point in betaZ/Z not contained in a maximal orbit closure
[REPT-89-26] 04 p0540 N90-13127
On distance-transitive graphs and involutions
[CWI-PM-R8808] 05 p0691 N90-14037
The algebraic Riccati equation and singular optimal control
[MEMO-COSOR-89-11] 08 p1117 N90-16467
A number-theoretic approach to subgroups of dihedral groups
[AD-A222857] 21 p3063 N90-27413
SUBJECTS
Medical subject headings: Annotated alphabetic list, 1990
[PB90-100009] 14 p2036 N90-21683
Permuted medical subject headings, 1990
[PB90-100025] 14 p2036 N90-21684
SUBLATTICES
U LATTICES (MATHEMATICS)
U SUBGROUPS
SUBLAYERS
U SUBSTRATES
SUBLIMATION
Human body regional convective heat transfer determination using sublimating naphthalene disks
[AD-A212170] 03 p0380 N90-12165
The use of sublimation methods for the recognition of transition at low speed 08 p1080 N90-16251
Modifications of comet materials by the sublimation process: Results from simulation experiments
08 p1142 N90-16621
Direct sublimation of NaCl salt from carbon matrixes
[DE90-007927] 14 p1946 N90-21139
SUBMARINES
Elastomeric impulse energy storage and transfer system
[AD-D014223] 06 p0730 N90-14255
SLCSAT (Submarine Laser Communication Satellite) communication system design study
[AD-A213403] 07 p0917 N90-15304
A review of the theory and methods for determining dynamic pulse buckling of cylindrical shells
[AD-A214764] 09 p1238 N90-17185
Design of a high power density, permanent magnet, axial gap dc motor
[DE90-005449] 12 p1655 N90-19514
Control of submersible vortex flows
[NASA-TM-102693] 23 p3267 N90-28493
SUBMERGED BODIES
NT DIVING (UNDERWATER)
Heat transfer to a stationary and moving sphere immersed in a fluidized bed 06 p0774 N90-14503
Methods of perturbation theory as a means for interactive design from bodies in a flow
[ETN-90-96502] 18 p2553 N90-24573
SUBMILLIMETER WAVES
Submillimeter quantum electronics
[AD-A210439] 01 p0132 N90-10762
Precision materials characterization in the near millimeter and submillimeter wavelength range
[AD-A210655] 02 p0194 N90-11106
The excess flux in the cosmic submillimeter background radiation and the primordial deuterium abundance
[NASA-CR-186312] 08 p1154 N90-16683
The James Clerk Maxwell telescope
11 p1589 N90-19166
Conference digest: Thirteenth International Conference on Infrared and Millimeter Waves, volume 1039
[AD-A217343] 13 p1793 N90-20291
Study on rotating plasma with submillimeter laser interferometer
[DE90-615387] 14 p2027 N90-21623
The 10-100 kW submillimeter gyrotron
15 p2061 N90-21803
The Sagittarius B2 molecular cloud: An extreme case of a galactic center giant molecular cloud
15 p2187 N90-22493
Construction of a 345 gigahertz receiver based on superconducting tunnel junctions
[AD-A218781] 16 p2232 N90-22735
Microwigglers for submillimeter wavelength free-electron lasers
[AD-A220185] 17 p2409 N90-23730
Submillimeter and millimeter observations of solar system objects
[NASA-CR-186636] 20 p2940 N90-26731
SUBMINIATURIZATION
Electrical resistance measurements of connector-panel interfaces
[AD-A221431] 21 p3001 N90-27057
SUBREFLECTORS
DSS 15, 45, and 65 34-meter high efficiency antenna radio frequency performance enhancement by tilt added to the subreflector during elevation angle changes
20 p2854 N90-26229
SUBROUTINE LIBRARIES (COMPUTERS)
Extended memory library for AFOS (Automation of Field Operations and Services) applications
[PB89-230858] 05 p0708 N90-14147
Basic mathematical function libraries for scientific computation
[NASA-TM-102256] 08 p1110 N90-16423
STATLIB: NSWC library of statistical programs and subroutines
[AD-A221538] 21 p3055 N90-27370
SUBROUTINES
Batch LCAP2-linear control analysis, version 2.0: User's manual
[AD-A211670] 04 p0461 N90-12643
FORTRAN subroutines for the evaluation of the confluent hypergeometric functions
[AD-A213308] 05 p0689 N90-14012
SINS1: A model of a strapdown inertial navigation system
[AD-A215495] 09 p1166 N90-16749
Symbol manipulation and applied mathematics
[AD-A214702] 09 p1273 N90-17378
Hypercluster parallel processing library user's manual
[NASA-CR-185231] 14 p2016 N90-21552
Solution of exterior acoustic problems by the boundary element method 18 p2611 N90-24874
The implementation of the graphics of program EAGLE: A numerical grid generation code on NASA Langley SNS computer system 18 p2642 N90-25050
EINMUF: An HF MUF, FOT, LUF prediction program
[AD-A221577] 21 p3055 N90-27371
Automated system for meteorological analysis
[INPE-4586-TDL/332] 23 p3352 N90-28945
Software development tools
[PB90-250051] 23 p3381 N90-29103
Semiconductor measurement technology: A software program for aiding the analysis of ellipsometric measurements, simple spectroscopic models
[PB90-216847] 23 p3398 N90-29201
SUBSETS (MATHEMATICS)
U SET THEORY
SUBSIDENCE
The above-inversion moisture structure observed during FIRE 22 p3215 N90-28235
SUBSONIC AIRCRAFT
Lockheed laminar-flow control systems development and applications 04 p0438 N90-12506
Preliminary results from a subsonic high angle-of-attack flush airdata sensing (HI-FADS) system: Design, calibration, and flight test evaluation
[NASA-TM-101713] 09 p1168 N90-16758
Life cycle cost in the conceptual design of subsonic commercial aircraft, volumes 1 and 2
23 p3275 N90-28535
High-speed civil transport study: Special factors
[NASA-CR-181881] 23 p3276 N90-28537
SUBSONIC FLOW
Rectangular subsonic jet flow field measurements
[NASA-CR-185962] 02 p0219 N90-11255
Computation of ramjet internal flowfields
[AD-A212001] 03 p0307 N90-11743
Flow quality measurements in compressible subsonic flows 04 p0441 N90-12521
CFD methods for drag prediction and analysis currently in use in UK
[RAE-TM-AERO-2146] 04 p0448 N90-12563
Upwind discretization of the steady Navier-Stokes equations
[CWI-NM-R8810] 04 p0502 N90-12891
Multigrid solution method for the Euler equations
[PB89-219463] 04 p0539 N90-13116
Effect of suction and cooling on the stability of subsonic and supersonic boundary layers
05 p0642 N90-13745
An alternative derivation for an integral equation for linearized subsonic flow over a wing
[AD-A214140] 07 p0876 N90-15079
Effect of riblets on flow separation from a cylinder and an airfoil in subsonic flow
[AD-A216197] 10 p1309 N90-17574
Chemical reactions in turbulent mixing flows
[AD-A216273] 10 p1355 N90-17856
A study on upstream moving pressure waves induced by vortex separation
[ISL-CO-203/88] 12 p1597 N90-19192
Digital determination of the three dimensional flow in turbomachines with the S1-S2 current function process
[ITSM-MITT-30] 12 p1605 N90-19236
Application of a three-dimensional Navier-Stokes model for a subsonic jet in a crossflow
13 p1749 N90-20045
A matrix-free locally-implicit scheme for Navier-Stokes equations
[AD-A218298] 13 p1803 N90-20349
Subsonic and transonic blade design by means of analysis codes 14 p1917 N90-20985
Numerical optimization of target pressure distributions for subsonic and transonic airfoil design
14 p1919 N90-20993
Subsonic flutter analysis using MSC/NASTRAN
[PB90-166786] 14 p1928 N90-21041
Rectangular subsonic jet flow field measurements
[NASA-CR-181925] 14 p2023 N90-21598
Instabilities and subharmonic resonances of subsonic heated round jets, volume 2
[NASA-CR-186058] 15 p2100 N90-22017
Estimation of extra drag force on a circular cylinder due to the presence of solid particles in subsonic compressible flow
[AD-A218635] 16 p2197 N90-22542
The 3-D composite velocity solutions for subsonic/transonic flow over forebodies and afterbodies
[AD-A220370] 17 p2345 N90-23354
STARS: An integrated general-purpose finite element structural, aeroelastic, and aeroservoelastic analysis computer program
[NASA-TM-101709] 17 p2416 N90-23768
Effects of forebody geometry on subsonic boundary-layer stability
[NASA-CR-4314] 20 p2802 N90-25939
Subsonic combustor flow modeling: State of the art of CFD techniques for reacting and combusting flow
20 p2810 N90-25991
Flame extinction in compressible flow
21 p2973 N90-26899
Extrapolation procedures at outflow boundaries for the Navier-Stokes equations
[FFA-TN-1990-23] 23 p3327 N90-28811
SUBSONIC FLUTTER
Subsonic flutter analysis using MSC/NASTRAN
[PB90-166786] 14 p1928 N90-21041
SUBSONIC SPEED
Hinge moment coefficient derivatives for trailing-edge controls on wings at subsonic speeds
[ESDU-89009] 06 p0726 N90-14239
Installed tailplane lift-curve slope at subsonic speeds
[ESDU-89029] 07 p0876 N90-15081
The maximum lift coefficient of plain wings at subsonic speeds
[ESDU-89034] 07 p0876 N90-15082
Body effect on wing angle of attack and pitching moment at zero lift at low speeds
[ESDU-89042] 09 p1167 N90-16757
An intensive procedure for the design of pressure-specified three-dimensional configurations at subsonic and supersonic speeds by means of a higher-order panel method 14 p1917 N90-20982
AVION: A detailed report on the preliminary design of a 79-passenger, high-efficiency, commercial transport aircraft
[NASA-CR-186663] 17 p2353 N90-23395
Flow unsteadiness effects on boundary layers
[NASA-CR-186067] 18 p2550 N90-24557
Gas Turbine Combustion, volume 2
[VKI-LS-1990-02-VOL-2] 20 p2811 N90-25995
Three-dimensional cavity flow fields at subsonic and transonic speeds
[NASA-TM-4209] 22 p3107 N90-27650
Theoretical studies carried out in 1988 on helicopter rotor noise under subsonic conditions
[ONERA-RS-82/5094-PY] 22 p3245 N90-28402
An investigation of the inviscid spatial instability of compressible mixing layers
[AD-A223776] 24 p3468 N90-29596
SUBSONIC WIND TUNNELS
The aerodynamic experimental center of Aeritalia: Combat aircraft group
[ETN-89-95213] 03 p0311 N90-11766
A data acquisition parallel bus for wind tunnels at ARL (Aeronautical Research Laboratory)
[AD-A218052] 13 p1759 N90-20098
The Langley 14- by 22-foot subsonic tunnel: Description, flow characteristics, and guide for users
[NASA-TP-3008] 22 p3107 N90-27649
Dynamic ground effects 23 p3275 N90-28531
SUBSTANCES
U MATERIALS
SUBSTITUTES
Re-engine with the Rolls-Royce Tay 670, the route to significant noise reduction
[PNR90585] 04 p0455 N90-12606

The substitution of IVD (Ion Vapor Deposition) aluminum for cadmium
[AD-A215633] 09 p1195 N90-16921
A systematic study of the effects of metal substitutions for Cu in YBa(sub 2) (Cu(sub 1-x) M(sub x)3 O(sub 7-rho), M=Fe, Co, Al, Ga, Cr, Ni, and Zn
[DE90-003957] 13 p1892 N90-20857
Studies of iron impurities in YxPr1-xBa2Cu3O7-delta 22 p3151 N90-27865

SUBSTITUTION
U SUBSTITUTES

SUBSTRATES
Characterization of GaAs/Si/GaAs heterointerfaces
[DE89-016302] 01 p0131 N90-10752
Method of modifying the dielectric properties of an organic polymer film
[AD-D014171] 03 p0330 N90-11879
A SAW Slanted Array Correlator (SAC) with separate amplitude compensation channel
[AD-D014174] 03 p0336 N90-11914
Infrared detector array
[AD-D014170] 03 p0350 N90-11997
Structure and properties of polymer interphases
[AD-A212796] 04 p0481 N90-12763
Method for growing patterned thin films of superconductors
[AD-D014195] 04 p0560 N90-13262
The growth of epitaxial GaAs and GaAlAs on silicon substrates by OMVPE
[AD-A212873] 04 p0561 N90-13269
Method for fabricating thin film metallic meshes for use as Fabry-Perot interferometer elements, filters and other devices
[AD-D014236] 06 p0779 N90-14529
The influence of the substrate surface on the nucleation and growth of superconducting thin films
[DE90-003649] 06 p0857 N90-14983
Improved performance polysulfide based sealant 08 p1022 N90-15910
Heteroepitaxy of GaAs on Si: Methods to decrease the defect density in the epilayer
[DE90-004028] 08 p1131 N90-16551
Spectroscopic techniques for the analysis of CdTe substrates used for the growth of HgCdTe
[AD-A214545] 09 p1288 N90-17466
The growth of epitaxial GaAs and GaAlAs on silicon substrates by OMVPE
[AD-A214642] 09 p1288 N90-17469
Epitaxial growth of Cr(011) on LiF(001)
[DE90-005635] 09 p1293 N90-17496
Research relating to crystalline silicon-film on a foreign substrate
[DE90-005720] 11 p1491 N90-18582
Pulsed laser deposition of high T(sub c) superconducting thin films
[AD-A216507] 11 p1569 N90-19034
The III-V semiconductor quantum well lasers and related optoelectronic devices on silicon
[AD-A216980] 12 p1666 N90-19570
A method of estimating temperature profiles and chemical differentiation in the near surface layers of porous comet nuclei: First results for comet P/Churyumov-Gerasimenko 12 p1742 N90-20013
Process for making a noble metal on tin oxide catalyst
[NASA-CASE-LAR-13741-1-SB] 13 p1774 N90-20180
Wetting of metallic carbides by non-reactive liquid metals
[AERE-M-3759] 13 p1775 N90-20185
Refractive index profiles of thermally grown and chemically vapor deposited films on silicon
[AD-A217187] 13 p1893 N90-20865
Proceedings of the Joint NOSC/NRL (Naval Ocean Systems Center/Naval Research Laboratory) InP Microwave/Millimeter Wave Technology Workshop
[AD-A218216] 14 p1966 N90-21259
Alternating gradient photodetector
[NASA-CASE-NPO-17235-1-CU] 14 p1982 N90-21358
Improvement of small-area, amorphous-silicon thin-film photovoltaics on polymer substrate
[DE90-000314] 14 p2002 N90-21472
Dynamic response of a complex encapsulated electronic assembly subjected to a severe shock environment
[DE90-007689] 15 p2118 N90-22114
Growth and patterning of laser ablated superconducting YBa2Cu3O7 films on LaAlO3 substrates
[NASA-TM-102436] 15 p2173 N90-22421
Development of a unique laboratory standard indium gallium arsenide detector for the 500 to 1700 micron spectral region, phase 2
[NASA-CR-180482] 16 p2238 N90-22767
Optical properties of novel GaAs-based semiconductors 16 p2321 N90-23235
Nonreciprocal components in the 140 and 220 GHz bands utilizing magnetoplasmons on semiconducting substrates
[AD-A219136] 16 p2324 N90-23253
New directions in InP solar cell research
[NASA-TM-103160] 17 p2398 N90-23662
Development of damped metal matrix composites for advanced structural applications
[AD-A219864] 18 p2518 N90-24380
Proof of principle study of thickness measurements using characteristic x ray line ratio techniques
[AD-A221113] 18 p2535 N90-24461
Microstructure of sputtered superconducting films of Bi2Sr2CaCu2O(x) made by low-temperature, in situ growth
[DE90-010067] 18 p2618 N90-24916
Highly-textured thallium-barium-calcium-copper-oxide polycrystalline superconducting films on silver substrates
[DE90-011972] 18 p2627 N90-24970
Microstructures of superconducting YBa2Cu3O(7-x) thin films
[DE90-011976] 19 p2761 N90-25688
Molecular structure of interphases between DGEBA/BTDA adhesives and silver substances using surface-enhanced Raman scattering
[AD-A222750] 20 p2841 N90-26157
MBE growth technology for high quality strained III-V layers
[NASA-CASE-NPO-17723-1-CU] 20 p2932 N90-26685
Laser induced surface chemical epitaxy
[AD-A222082] 21 p2977 N90-26920
Characterization of polymer interphases using surface-enhanced Raman scattering
[AD-A223103] 21 p2985 N90-26965
Nature and origin of interstellar diamond from the Allende CV3 meteorite 21 p3092 N90-27581
Laser ablated high T(sub c) superconducting thin YBa2Cu3O(7-x) films on substrates suitable for microwave applications 22 p3139 N90-27808
Corrosion-inhibiting coating composition
[AD-D014546] 22 p3159 N90-27916
Adhesion of silver films to ion-bombarded zirconia
[DE90-010088] 24 p3456 N90-29517
Ion-beam mixing of Fe/B layers for tribological applications
[DE90-010091] 24 p3456 N90-29518

SUBSTRUCTURES
Structural problems of accurate inflatable surfaces 02 p0184 N90-11044
The spacecraft structure 05 p0604 N90-13512
Effects of dislocation substructure and prestrain on fracture behavior in aluminum and steel alloys 06 p0745 N90-14334
Design philosophy and construction techniques for integral fuselage fuel tanks 08 p1023 N90-15913
Substructural controller synthesis 16 p2292 N90-23055
Unique failure behavior of metal/composite aircraft structural components under crash type loads
[NASA-TM-102679] 18 p2572 N90-24660
Evaluation of energy absorption of new concepts of aircraft composite subfloor intersections
[NASA-TP-2951] 21 p2959 N90-26823
Interaction of acoustic waves generated by coupled plate
[NASA-CR-186873] 21 p3072 N90-27464
Progress in the detection of cracks under installed fasteners using eddy currents 22 p3186 N90-28081

SUBTROPICAL REGIONS
U TEMPERATE REGIONS
U TROPICAL REGIONS

SUBZERO TEMPERATURE
Battery actuation of NITINOL at sub-zero temperatures
[AD-A211254] 02 p0216 N90-11237

SUCTION
Numerical experiments on transition control in wall-bounded shear flows 04 p0443 N90-12536
Effect of suction and cooling on the stability of subsonic and supersonic boundary layers 05 p0642 N90-13745
Simulated-airline-service flight tests of laminar-flow control with perforated-surface suction system
[NASA-TP-2966] 10 p1319 N90-17627
Time-dependent measurements on vibrating annular turbine cascades under various steady state conditions 11 p1463 N90-18424
Method for maintaining precise suction strip porosities
[NASA-CASE-LAR-13638-1] 12 p1641 N90-19427
Effect of suction on controlling the secondary instability of boundary layers
[NASA-CR-4306] 18 p2552 N90-24566
Generation of circumferential velocity contours associated with pulsed point suction on a rotating disk 18 p2646 N90-25065

SUD AVIATION AIRCRAFT
NT CONCORDE AIRCRAFT

SUDAN
Central Sudan surface wind data and climate characteristic
[KNMI-WR-88-01] 04 p0520 N90-13000

SUDDEN IONOSPHERIC DISTURBANCES
Solar-geophysical data number 533. Part 1: Data for December, November 1988, and late data
[PB89-162481] 01 p0142 N90-10820
Solar-geophysical data number 534, February 1989. Part 1: (Prompt reports). Data for January 1989, December 1988 and late data
[PB89-173041] 01 p0142 N90-10822
User's guide to the Space Environment Services Center geophysical alert broadcasts
[PB89-194617] 02 p0249 N90-11411
Solar-geophysical data number 536, part 1. Data for March, Febuary 1989 and late data
[PB89-194716] 02 p0296 N90-11684
Solar-geophysical data number 538, June 1989. Part 1: (Prompt reports). Data for May, April 1989, and late data
[PB89-223838] 06 p0866 N90-15031
Solar-geophysical data number 539, July 1989. Part 1: (Prompt reports). Data for June, May 1989, and late data
[PB89-235451] 06 p0866 N90-15033
Solar-geophysical data number 540, August 1989. Part 1: (Prompt reports). Data for July, June 1989, and late data
[PB90-108572] 06 p0866 N90-15035
Solar-geophysical data number 544, December 1989. Part 1 (Prompt reports). Data for November, October 1989, and late data
[PB90-171661] 22 p3263 N90-28481

SUDDEN STORM COMMENCEMENTS
Solar-geophysical data number 536, part 1. Data for March, Febuary 1989 and late data
[PB89-194716] 02 p0296 N90-11684
Solar-geophysical data number 538, June 1989. Part 1: (Prompt reports). Data for May, April 1989, and late data
[PB89-223838] 06 p0866 N90-15031

SUGAR CANE
Agricultural yield estimation of sugarcane based on agrometeorological-spectral model
[INPE-5016-RPE/610] 14 p1996 N90-21441
Project CANASATE: Remote sensing applied to sugar cane crop survey
[INPE-4902-PRE/1503] 14 p1997 N90-21446
Evaluation of classification performance and proportion estimate of the sugar cane crop through PROCEDURE-INPE utilizing LANDSAT data
[INPE-4899-PRE/1500] 14 p1999 N90-21458

SUGARS
NT GLUCOSE

SUITS
NT EXTRAVEHICULAR MOBILITY UNITS
NT PRESSURE SUITS
NT SPACE SUITS

SULFATES
NT LITHIUM SULFATES
NT SODIUM SULFATES
High temperature chemistry of complex vaporization/decomposition processes
[DE89-016559] 06 p0740 N90-14306
Thermal expansion of LATGS crystals
[DE89-636239] 08 p1130 N90-16546
Chemical composition of precipitation and wet/dry deposition of sulfur compounds around the coastal area
[DE89-782324] 12 p1685 N90-19677
Effects of cholinergic drugs on exercise performance and simple reaction time of rhesus monkeys
[AD-A219455] 17 p2433 N90-23862

SULFATION
High temperature interaction of SO2 with oxide sorbents
[DE90-000435] 11 p1485 N90-18545

SULFIDATION
High-temperature oxidation and sulfidation of Fe-20Cr-16Ni-4Al-1Y2O3 oxide-dispersion-strengthened alloy
[DE90-007897] 14 p1951 N90-21168
Oxidation and sulfidation of Type 310S stainless steel at elevated temperatures
[DE90-010149] 20 p2832 N90-26109
Oxidation, sulfidation, and hot corrosion: Mechanisms and interrelationships 23 p3307 N90-28702
Scale adherence effects in oxidation and sulfidation 23 p3307 N90-28703

SULFIDES
NT BISMUTH SULFIDES
NT CADMIUM SULFIDES
NT CALCIUM SULFIDES
NT CARBON DISULFIDE
NT DISULFIDES

NT HYDROGEN SULFIDE
NT MOLYBDENUM DISULFIDES
NT MOLYBDENUM SULFIDES
NT POLYSULFIDES
NT ZINC SULFIDES
Fifth International Workshop on Glasses and Ceramics from Gels
[DE89-016899] 02 p0201 N90-11147
Molybdenum disulfide-molybdenum oxide lubricants
[AD-D014253] 08 p1048 N90-16059
Researches on amorphous perovskite
[DE89-900733] 08 p1128 N90-16535
Preparation, properties, and development of calcium lanthanum sulfide as an 8- to 12-micrometer transmitting ceramic
[AD-A220200] 17 p2382 N90-23565
SULFONATES
Comparison of carboxylated and sulfonated model polyurethane ionomers
[AD-A210438] 01 p0050 N90-10284
Nonlinear optical processes in one-dimensional polymers
[AD-A216103] 11 p1489 N90-18568
SULFONES
Thermal analysis of Acetylene Terminated Sulfone (ATS) resin
[AD-A220775] 17 p2381 N90-23558
SULFONIC ACID
Electrochemical evaluation of new fluorosulfonic and fluorophosphonic acids as fuel cell electrolytes
[DE90-016626] 24 p3485 N90-29699
SULFUR
Properties of F-34 (JP-8) fuel for 1988
[AD-A210188] 01 p0053 N90-10303
An electroformed nickel-sulfur alloy for a nose cone
[DE90-000666] 06 p0745 N90-14337
Extraterrestrial halogen and sulfur content of the stratosphere
[DE89-017623] 06 p0815 N90-14738
Mobility of sulfur in thermally altered meteorites
06 p0862 N90-15010
Study of adherent oxide scales
[AD-A215189] 09 p1198 N90-16940
Sulphur silicate interactions on the Jovian satellite Io
15 p2192 N90-22515
Phytoplankton and its contribution to the atmospheric sulfur budget of northern Europe
20 p2885 N90-26417
High resistivity Al(x)Ga(1-x) As(y)Sb(1-y) epitaxial layers by sulfur compensation doping
[DE90-012228] 22 p3248 N90-28419
Investigation of the effects of microalloy constituents, surface treatment and oxidation conditions on the development and breakdown of protective oxide scales
[DE90-015710] 24 p3451 N90-29488
Meteorological conditions over the North Atlantic Ocean during GCE/CASE/WATOX
[PB90-252032] 24 p3494 N90-29747
SULFUR COMPOUNDS
NT BISMUTH SULFIDES
NT CADMIUM SULFIDES
NT CALCIUM SULFIDES
NT CARBON DISULFIDE
NT DISULFIDES
NT HYDROGEN SULFIDE
NT LITHIUM SULFATES
NT MOLYBDENUM DISULFIDES
NT MOLYBDENUM SULFIDES
NT ORGANIC SULFUR COMPOUNDS
NT POLYSULFIDES
NT SODIUM SULFATES
NT SULFATES
NT SULFIDES
NT SULFONATES
NT SULFONES
NT SULFUR DIOXIDES
NT SULFUR FLUORIDES
NT SULFUR OXIDES
NT SULFURIC ACID
NT THIOLS
NT ZINC SULFIDES
Advanced calcium-thionyl chloride high-power battery
[AD-A211856] 04 p0495 N90-12846
Studies of organo phosphorus-, nitrogen-, and sulfur-containing molecules
[AD-A213518] 07 p0888 N90-15135
Sulfur compounds in comets
08 p1143 N90-16627
High spatial resolution isotopic CO and CS observations of M17 SW: The clumpy structure of the molecular cloud core
[MPE-PREPRINT-161] 18 p2330 N90-23283
The effect of carbon type and processing on high rate thionyl chloride cathode collectors
[AD-A219823] 18 p2546 N90-24532
Results from global tropospheric sulphur simulations
20 p2885 N90-26413
Phytoplankton and its contribution to the atmospheric sulfur budget of northern Europe
20 p2885 N90-26417
SULFUR DIOXIDES
Electrochemistry in near-critical and supercritical fluids. Part 7: SO2
[AD-A208207] 01 p0039 N90-10214
Micrometeorological investigation of surface exchange of trace gases: A case study
[PB89-208375] 02 p0249 N90-11412
Computational solution of chemistry problems
[NASA-CR-186000] 05 p0620 N90-13618
Air quality simulation model performance for one-hour averages
[PB89-233506] 05 p0665 N90-13890
Profile measurements of sulfur dioxide, nitrogen oxides, and nitric acid deposition velocities in California's south coast air basin
[PB90-104001] 06 p0808 N90-14703
The continuous crystallization of sulfur formed by the liquid-phase reaction of hydrogen sulfide and sulfur dioxide
[DE90-003991] 08 p1041 N90-16018
A lithium sulphur dioxide cell for deep space applications 10 p1334 N90-17718
High temperature interaction of SO2 with oxide sorbents
[DE90-000435] 11 p1485 N90-18545
Generation of intensive UV laser radiation and utilization in high resolution spectroscopy of SO2
[ETN-90-95361] 12 p1668 N90-19581
Estimation of the distribution of SO2 and NOX emission in Europe 12 p1688 N90-19699
Ultraviolet observations of the atmosphere of Io and the plasma torus 12 p1728 N90-19929
Transformation and deposition of airborne gaseous and particulate pollutants during transport over the Baltic Sea
[PUBL-AIR-QUALITY-5] 14 p2003 N90-21478
Deposition to the Baltic Sea 20 p2884 N90-26404
Verification and improvement of the EMEP model for long-range transport and deposition of pollutants
20 p2884 N90-26405
Laboratory and field evaluations of extrasensitive sulfur dioxide and nitrogen dioxide analyzers for acid deposition monitoring
[PB90-201062] 22 p3199 N90-28153
Preliminary exposure study to determine the effects of acid deposition on coated steel substrates
[PB90-201799] 23 p3309 N90-28715
SULFUR FLUORIDES
Dissociation and vibrational relaxation of XeF by various collision partners
[AD-A210769] 02 p0227 N90-11300
Measurement of the p, v, T behavior under microgram conditions
[ETN-90-95906] 08 p1065 N90-16162
Wick-type liquid-metal combustion
[AD-A216019] 11 p1482 N90-18530
The dielectric behavior of sulfur hexafluoride submitted to rapid transitory overvoltages
[ECL-89-16] 17 p2374 N90-23520
Research for electric energy systems
[DE90-014221] 23 p3321 N90-28775
SULFUR OXIDES
NT SULFUR DIOXIDES
Acid deposition
[DE90-003959] 07 p0958 N90-15544
Time and spatially dependent estimates of pollutant trace gas emissions and their effect on tropospheric ozone 09 p1243 N90-17212
Reactions of N2A3 sigma u + and candidates for short wavelengths lasers
[DE90-009514] 15 p2103 N90-22033
Anthropogenic sources of NO(x), SO()x, CO, and CH4: Geographical distribution
[AERONOMICA-ACTA-A-353-1990] 19 p2713 N90-25440
Acid deposition: No such thing as a free launch
[DE90-015085] 23 p3348 N90-28920
SULFURIC ACID
Venus volcanism: Rate estimates from laboratory studies of sulfur gas-solid reactions 03 p0422 N90-12428
Steady state model to determine lake resources at risk to acid deposition in the Sierra Nevada, California
[PB89-103995] 06 p0809 N90-14705
Assessment of the theory and hypotheses of the acidification of watersheds
[DE90-005528] 10 p1406 N90-18111
SUM RULES
Existence of Bose-Einstein condensation in one and two dimensions
[DE89-635910] 09 p1294 N90-17498
Relativistic corrections to He-3 photodisintegration sum rules
[NOTA-INTERNA-942] 16 p2315 N90-23197
Identifying decohering paths in closed quantum systems
[NASA-CR-182853] 19 p2761 N90-25690
A sum rule satisfied by optimized feed-forward layered networks
[RSRE-MEMO-4341] 20 p2914 N90-26579
SUMMARIES
NT ABSTRACTS
NT PRELAUNCH SUMMARIES
A summary of 30 years of space launches
[AERONOMICA-ACTA-F-39-1989] 05 p0585 N90-13411
SUMMER
Subjective uses of wind profiler data in warm season analysis and forecasting: Wind profiler training manual number 3
[PB89-223333] 04 p0520 N90-13004
Observation of wind corners in the middle atmosphere over Andenes (69 N) during winter 1983/84, summer 1987 and summer 1988 05 p0657 N90-13836
Evaluation of digital classification results of summer cultivation in a test area in the Parans-Ano state harvest 1986-1987
[INPE-4828-PRE/1459] 10 p1399 N90-18085
Controlling Summer Heat Islands: Proceedings
[DE90-008075] 13 p1830 N90-20508
Vorticity balance study for a tropical region, during the Southern Hemisphere summer
[INPE-4634-TDL/336] 23 p3353 N90-28949
SUMS
Tail triviality for sums of stationary random variables
[CWI-MS-R8810] 04 p0542 N90-13143
A hypothesis test of cumulative sums of multinomial parameters
[AD-A221466] 21 p3067 N90-27434
SUN
Long-term solar-terrestrial observations
[DE89-016318] 01 p0143 N90-10825
Investigation of active regions at high resolution by balloon flights of the Solar Optical Universal Polarimeter (SOUP) 03 p0434 N90-12487
Astophysical opacities at LLNL
[DE90-003599] 07 p1014 N90-15872
Report from solar physics 10 p1445 N90-18335
Major themes in the future of solar-terrestrial science
10 p1445 N90-18337
Pioneers 10 and 11 deep space missions
[NASA-TM-102269] 10 p1448 N90-18355
Some considerations on cohesive forces in sun-grazing comets 12 p1742 N90-20015
Distributed earth model/orbiter simulation
13 p1860 N90-20671
Evolutionary models of the rotating sun and implications for other low mass stars 16 p2339 N90-23329
Institute of Astronomy 17 p2481 N90-24190
Sunspot prediction using neural networks
19 p2737 N90-25560
U. radio emission from quiescent filaments
[NASA-CR-186538] 19 p2797 N90-25922
Space exploration: Cost, schedule, and performance of NASA's Ulysses Mission to the Sun. Fact sheet for the Chairman, Subcommittee on Science, Technology, and Space, Committee on Commerce, Science, and Transportation, US Senate
[GAO/NSIAD-88-129FS] 20 p2815 N90-26023
Application of solar seismology to study of the convection zone
[AD-A221975] 21 p3101 N90-27610
Solar-geophysical data number 545, January 1990. Part 2 (Comprehensive reports). Data for July 1989 and miscellaneous
[PB90-182346] 22 p3263 N90-28480
Solar-geophysical data number 544, December 1989. Part 2 (Comprehensive reports). Data for June 1989 and miscellaneous
[PB90-171679] 22 p3264 N90-28482
Solar oscillation frequency and solar neutrino predictions
[DE90-014918] 23 p3413 N90-29288
SUN SENSORS
U SOLAR SENSORS
SUNLIGHT
A measurement of hydroxyl in the daytime mesosphere 06 p0814 N90-14732
Determination of rates of reaction in the gas-phase in the troposphere: Theory and practice. 2: Rate of direct photoreaction: Screening-level test guideline-spectroscopic determination of the cross section and the maximum rate of direct photoreaction in sunlight
[PB90-146291] 15 p2125 N90-22156
Field evaluation of a passive sampling device for hydrazines in ambient air
[NASA-TM-103456] 18 p2578 N90-24686

Sunlight diffusing tent for lunar worksite
[NASA-CR-186651] 19 p2677 N90-25225
Gaseous optical contamination of the spacecraft environment: A review 19 p2730 N90-25519
SUNRISE
The retrieval of the concentrations of nitric oxide and nitrogen dioxide from satellite solar occultation measurements at sunset and sunrise 06 p0814 N90-14733
Tidal and lunar data for Point Mugu, San Nicolas Island, and the Barking Sands Area during 1990
[AD-A214828] 09 p1249 N90-17248
SUNSET
The retrieval of the concentrations of nitric oxide and nitrogen dioxide from satellite solar occultation measurements at sunset and sunrise 06 p0814 N90-14733
Tidal and lunar data for Point Mugu, San Nicolas Island, and the Barking Sands Area during 1990
[AD-A214828] 09 p1249 N90-17248
SUNSPOT CYCLE
The onset of the solar active cycle 22 03 p0434 N90-12488
Ionospheric effects of the extreme solar activity of February 1986 22 p3210 N90-28207
SUNSPOTS
Solar-geophysical data number 537, part 1. Data for April, March 1989 and late data
[PB89-207393] 02 p0296 N90-11685
The onset of the solar active cycle 22 03 p0434 N90-12488
Correlative analyses for geomagnetic indices, cosmic-ray intensities and sunspot numbers recorded since 1937
[IFSI-89-4] 08 p1151 N90-16670
Sunspot prediction using neural networks 19 p2737 N90-25560
SUPERALLOYS
U HEAT RESISTANT ALLOYS
SUPERCHARGERS
Low cost Brayton engine for gas-fired cogeneration system, phase 1
[PB90-127457] 12 p1681 N90-19655
A simulation code for turbocompound diesel engines
[IAR-89-26] 19 p2697 N90-25348
SUPERCHARGING
U SUPERCHARGERS
SUPERCOMPUTERS
NT CRAY COMPUTERS
Proceedings of the 2nd International Conference on Vector and Parallel Computing
[AD-A209401] 01 p0103 N90-10585
Applications of parallel supercomputers: Scientific results and computer science lessons
[DE89-016385] 01 p0107 N90-10611
An integrated distributed processing interface for supercomputers and workstations
[DE89-016769] 02 p0260 N90-11478
Solving three dimensional block bidiagonal linear systems on vector computers
[REPT-89-14] 04 p0530 N90-13056
Solving 3D block bidiagonal linear systems on vector computers
[CWI-NM-R8819] 04 p0530 N90-13061
VLSI theory and parallel supercomputing
[AD-A214035] 07 p0925 N90-15351
LLNL's plan for a prototype circuit switch, a potential gigabit LAN of the future
[DE90-003614] 07 p0969 N90-15597
Transport modeling and advanced computer techniques
[DE90-001481] 07 p0972 N90-15612
The components of scientific visualization
[DE90-001992] 07 p0972 N90-15614
Simulating the scheduling of parallel supercomputer applications
[DE90-003604] 07 p0979 N90-15655
Performance characterization of the Convex C-240 computer system
[DE90-006425] 11 p1543 N90-18879
Cedar project: Original goals and progress to date
[DE90-006761] 11 p1543 N90-18880
Dynamic reconfiguration and link fault tolerance in a transputer network
[AD-A215105] 12 p1642 N90-19433
Supercomputer applications for materials science: Ordering effects of hydrogen in palladium
[DE90-004664] 12 p1718 N90-19870
An improved error assessment for the GEM-T1 gravitational model 13 p1832 N90-20518
Tools for 3D scientific visualization in computational aerodynamics 13 p1858 N90-20660
Efficient utilization of graphics technology for space animation 13 p1859 N90-20663
Supercomputer environments
[AD-A217682] 13 p1863 N90-20689
Computer Science and Technology Board
[DE90-008292] 13 p1864 N90-20690
High performance computing and networking for science
[PB90-131228] 14 p2011 N90-21526
Supercomputers need super arithmetic
[PB90-130253] 15 p2145 N90-22252
Supercomputer and Technology
[NLR-PUB-8801] 16 p2277 N90-22974
Aircraft technology management and the related significance of the supercomputer 16 p2277 N90-22975
Numerical flow simulation and supercomputers: More than a digital wind tunnel 16 p2277 N90-22976
The use of supercomputers for the design and analysis of constructions 16 p2277 N90-22977
Access to supercomputers 16 p2277 N90-22979
Strategy of supercomputer development 16 p2278 N90-22981
Parallel and vector computation for stochastic optimal control applications 16 p2282 N90-23007
Proceedings of the NATO Advanced Workshop on Supercomputing
[AD-A218508] 16 p2299 N90-23102
Interconnection networks for highly parallel supercomputing architectures
[REPT-89-053] 16 p2302 N90-23118
ONR Far East Scientific Information Bulletin, Volume 13, No. 4
[ONRFE-SCI-INFO-BULL-13(4)88] 16 p2311 N90-23168
Current Japanese supercomputers for computational fluid dynamics applications 16 p2311 N90-23172
Multiprocessing on supercomputers for computational aerodynamics
[NASA-TM-102806] 17 p2347 N90-23366
Distributed user services for supercomputers
[NASA-CR-180370] 17 p2450 N90-23976
Informatics aspects of large flow calculations on the SX-2 supercomputer
[NLR-MP-88037-U] 20 p2864 N90-26290
Superconcurrent processing: A dynamic approach to heterogeneous parallelism
[AD-A222798] 20 p2914 N90-26576
Supercomputer workstation communication
[AD-A222466] 21 p3039 N90-27272
Critical problems in very large scale computer systems
[AD-A221603] 21 p3058 N90-27391
Parallel algorithms for computer vision
[AD-A221871] 21 p3059 N90-27394
SUPERCONDUCTING FILMS
Study of deposition of YBa2Cu3O7-x on cubic zirconia
[NASA-TM-102350] 01 p0128 N90-10737
Effect of annealing conditions on the structural and superconducting properties of Y-Ba-Cu-O films
[AD-A211308] 03 p0413 N90-12371
Microwave microstrip resonator measurements of Y1Ba2Cu3O(7-x) and Bi2Sr2Ca1Cu2O(8-y) thin films
[NASA-TM-102159] 05 p0635 N90-13704
Ion beam analysis and modification of thin-film, high-temperature superconductors
[DE90-000918] 06 p0850 N90-14941
The influence of the substrate surface on the nucleation and growth of superconducting thin films
[DE90-003649] 06 p0857 N90-14983
Superconducting film fabrication by the sol-gel process
[DE90-002069] 07 p0909 N90-15252
Partial reduction of re-oxidation processing of Y-Ba-Cu-O sputtered thin films
[DE90-003655] 07 p0999 N90-15782
Ion-irradiation effects in Tl2Ca2Ba2Cu3O10 superconductors
[DE90-003840] 07 p1002 N90-15802
Microstructures of Y123 films on SrTiO3, LaGaO3, and LaAlO3
[DE90-003367] 08 p1129 N90-16537
Electrical transport dissipation effects in epitaxial Y1Ba2Cu3O(7-x) thin films
[DE90-004301] 09 p1287 N90-17461
The use of BaF2 buffer layers for the sputter-deposition of TlCaBaCuO thin-film superconductors
[DE90-004859] 09 p1292 N90-17490
Influence of ion beam mixing on the growth of high temperature oxide superconducting thin film
[DE90-004837] 10 p1435 N90-18280
High temperature superconductivity
[AD-A215491] 10 p1436 N90-18286
Long laser-pulse method of producing Y-Ba-Cu-O superconducting films
[DE90-005202] 10 p1436 N90-18289
Pulsed laser deposition of high T(sub c) superconducting thin films
[AD-A216507] 11 p1569 N90-19034
In situ growth of epitaxial superconducting YBa2Cu3O(7-x) films on insulating semiconducting and ferroelectric K(Ta, Nb)O3 by pulsed laser ablation
[DE90-006588] 11 p1571 N90-19043
In situ growth of high quality epitaxial YBa2Cu3O(7-x) thin films at moderate temperatures by pulsed laser ablation
[DE90-006629] 11 p1571 N90-19045
Laser mass spectrometric studies of high temperature superconductor ablation
[DE90-006518] 12 p1668 N90-19585
Oxygenation and possible etching of high T(sub c) superconducting films by oxygen plasma
[DE90-004956] 12 p1719 N90-19871
Characterization of ground state neutral and ion transport during laser ablation of 1:2:3 superconductors by transient optical absorption spectroscopy
[DE90-006623] 12 p1720 N90-19878
Millimeter wave surface resistance of RBa2Cu3O(7-delta) (R = Y,Eu,Dy,Sm,Er) superconductors
[NASA-TM-102571] 13 p1897 N90-20886
JETC (Japanese Technology Evaluation Center) Panel Report on High Temperature Superconductivity in Japan
[NASA-CR-180413] 15 p2172 N90-22409
Pulsed laser processing of high temperature superconducting thin films
[DE90-008928] 15 p2172 N90-22413
Superconducting and semiconducting thin films of La(sub 123) and Y(sub 123) and their superlattices
[DE90-009565] 15 p2173 N90-22416
In-situ pulsed laser deposition of high-T(sub c) YBa(sub 2)Cu(sub 3)O(sub 7) superconducting thin films on (100) LaAlO3 substrates
[DE90-009861] 15 p2173 N90-22418
Growth and patterning of laser ablated superconducting YBa2Cu3O7 films on LaAlO3 substrates
[NASA-TM-102436] 15 p2173 N90-22421
Photoresponse of YBa2Cu3O(7-delta) granular and epitaxial superconducting thin films
[NASA-TM-103144] 16 p2231 N90-22732
ONR Far East Scientific Information Bulletin, Volume 13, No. 4
[ONRFE-SCI-INFO-BULL-13(4)88] 16 p2311 N90-23168
High temperature superconducting thin films in Japan 16 p2311 N90-23169
The onset of superconductivity in two-dimensional disordered systems 16 p2321 N90-23232
Thermal phenomena in high-Tc thin film superconductors 16 p2321 N90-23233
Electrical transport through tunnel barriers and thin dielectric layers and physical properties of the high Tc oxide superconductors
[AD-A219860] 17 p2477 N90-24165
Microstructure of sputtered superconducting films of Bi2Sr2CaCu2O(x) made by low-temperature, in situ growth
[DE90-010067] 18 p2618 N90-24916
Sputtered superconducting films of Bi2Sr2CaCu2O(x) made by low-temperature, in-situ growth
[DE90-010092] 18 p2619 N90-24919
Conference on the Science and Technology of Thin-Film Superconductors
[DE90-000326] 18 p2620 N90-24926
Studies on ion scattering and sputtering processes in ion beam sputter-deposition of high Tc superconducting films: The optimization of deposition parameters
[DE90-010538] 18 p2621 N90-24936
Superconducting thin films of YBaCu oxides prepared by MOCVD
[DE90-011109] 18 p2625 N90-24961
In-situ growth of superconducting films of Bi-Sr-Ca-Cu-O using magnetron sputtering
[DE90-011161] 18 p2626 N90-24962
Preparation and properties of superconducting thin films by excimer laser ablation
[DE90-011929] 18 p2626 N90-24967
Highly-textured thallium-barium-calcium-copper-oxide polycrystalline superconducting films on silver substrates
[DE90-011972] 18 p2627 N90-24970
Sequentially evaporated thin film YBa2Cu3O(7-x) superconducting microwave ring resonator
[NASA-TM-103180] 19 p2685 N90-25273
Formation of high Tc superconducting films by organometallic chemical vapor deposition
[AD-D014498] 19 p2760 N90-25682
Microstructures of superconducting YBa2Cu3O(7-x) thin films
[DE90-011976] 19 p2761 N90-25688
Studies on ion scattering and sputtering processes relevant to ion beam sputter deposition of multicomponent thin films
[DE90-010071] 20 p2931 N90-26675

Ellipsometric study of YBa2Cu3O(7-x) laser ablated and co-evaporated films
[NASA-TM-103223] 20 p2932 N90-26682
Pulsed laser deposition of high (Tc) superconducting thin films: Present and future
[DE90-011950] 21 p3080 N90-27511
Laser ablated high T(sub c) superconducting thin YBa2Cu3O(7-x) films on substrates suitable for microwave applications 22 p3139 N90-27808
The effect of temperature cycling typical of low earth orbit satellites on thin films of YBa2Cu3O(7-x) 22 p3140 N90-27812
Kinetics and thermodynamics of ceramic/metal interface reactions related to high T(sub c) superconducting applications 22 p3141 N90-27815
Critical currents and high temperature superconductors 22 p3142 N90-27823
Superconducting film on metallic wire 22 p3146 N90-27840
Microwave conductivity of laser ablated YBaCuO superconducting films and its relation to microstrip transmission line 22 p3147 N90-27844
The effects of space radiation on thin films of YBa2Cu3O(sub 7-x) 22 p3147 N90-27845
Spatial conductivity measurements on high T(sub c) superconducting films 22 p3148 N90-27849
In-situ integrated processing and characterization of thin films of high temperature superconductors, dielectrics and semiconductors by MOCVD 22 p3148 N90-27851
XES studies of density of states of high temperature superconductors 22 p3150 N90-27859
Magnetic properties of the 110K superconducting phase in Pb-doped Bi-Sr-Ca-Cu-O thin films 22 p3151 N90-27868
Optical and microwave detection using Bi-Sr-Ca-Cu-O thin films 22 p3152 N90-27870

SUPERCONDUCTING MAGNETS
A compact X-ray lithography lattice using superferric magnets
[DE89-013947] 01 p0127 N90-10728
The effect of twins on critical currents of high Tc superconductors
[AD-A210988] 01 p0133 N90-10768
A solution to nonlinearity problems
[DE89-016975] 02 p0270 N90-11544
X-ray lithography sources: A review
[DE89-017610] 02 p0271 N90-11547
Propagation of normal zones of finite size in large, composite superconductors
[DE89-016866] 02 p0282 N90-11611
The characterization of Nb3Sn superconductors for use in magnets of 19 T and greater
[DE89-017758] 03 p0412 N90-12364
Surface cooled, vacuum impregnated superconducting magnet systems: Design, construction, applications
[ETN-90-96014] 05 p0696 N90-14072
Superconducting magnets in space
[DE90-002671] 06 p0837 N90-14885
Applications of superconductor technologies to transportation
[DE90-000856] 06 p0853 N90-14961
Retractable gas cooled leads for ASTROMAG
[DE90-002679] 07 p0921 N90-15331
Feasibility analysis of reciprocating magnetic heat pumps
[NASA-CR-186205] 07 p0927 N90-15363
Recent advances in magnetic heat pump technology
[DE89-013289] 07 p0928 N90-15370
Design of a large superconducting spectrometer magnet
[DE90-719505] 08 p1131 N90-16553
Acoustic emission diagnostic techniques for high-field high current-density super inducting poles
[DE90-007400] 11 p1562 N90-19000
Evaluation of industrial magnetic heat pump/refrigerator concepts that utilize superconducting magnets
[DE90-008093] 13 p1787 N90-20258
The design of a large aperture high field dipole
[DE90-007910] 14 p1970 N90-21285
Heat leak measurements in superconducting dipole magnet supports
[DE90-620109] 15 p2173 N90-22420
Superconducting permanent magnets
[AD-A218944] 18 p2618 N90-24912
Use of high-temperature superconductors in superconducting magnetic energy power sources
[DE90-011119] 19 p2761 N90-25686
Parametric design studies of toroidal magnetic energy storage units
[DE90-013086] 20 p2881 N90-26390
Materials studies for magnetic fusion energy applications at low temperatures, volume 12
[PB90-157553] 22 p3248 N90-28417

SUPERCONDUCTING POWER TRANSMISSION
Silver coated superconducting ceramic powder
[AD-D014300] 07 p0913 N90-15278
Processing YBa2Cu3O(x) wires in O3/O2
[DE90-003570] 07 p1001 N90-15794
Conceptual design of high Tc superconducting power cable and its economic evaluation
[DE90-734940] 09 p1287 N90-17452

SUPERCONDUCTING QUANTUM INTERFEROMETERS
U SQUID (DETECTORS)

SUPERCONDUCTING SUPER COLLIDER
New tools for the simulation and design of calorimeters
[DE89-016323] 02 p0223 N90-11281
Thermal conduction of SSC (Superconducting Super Collider) wire
[DE89-016710] 03 p0319 N90-11811
Exotic Higgs production at e+e- colliders
[PREPRINT-671] 05 p0698 N90-14088
Recent developments of gigatron technology
[DE90-001067] 06 p0769 N90-14474
The 17.1-GHz free-electron laser as a microwave source for TeV colliders
[DE90-001506] 07 p0934 N90-15406
Properties and design of multifilamentary NbTi composite superconductors
[DE90-004904] 08 p1134 N90-16569
Megawatt-klystron amplifiers in L-band
[DE90-004864] 10 p1379 N90-17992
Acoustic emission diagnostic techniques for high-field high current-density super inducting poles
[DE90-007400] 11 p1562 N90-19000
The design of a large aperture high field dipole
[DE90-007910] 14 p1970 N90-21285
High energy physics at Tufts University
[DE90-014664] 23 p3394 N90-29174

SUPERCONDUCTIVITY
NT KONDO EFFECT
Measuring the shielding effectiveness of superconductive composites
[DE89-015164] 01 p0033 N90-10180
Mott transition: Low-energy excitations and superconductivity
[DE89-617778] 01 p0129 N90-10741
Superconductivity from valence fluctuations with finite U
[DE89-015302] 01 p0129 N90-10742
Critical magnetic fields (H(sub c2), H(sub c1)) and kappa in YBa2(Cu0.98M0.02)3O(7+delta), M=Ni, Al, and Cu
[DE89-016412] 01 p0130 N90-10745
Structural aspects of the phase separation in La2CuO4.032
[DE89-016183] 01 p0130 N90-10751
Superconducting ceramics in the Bi1.5SrCaCu2O sub x system by melt quenching technique
[NASA-CR-185139] 02 p0281 N90-11606
Adaptation of the theory of superconductivity to the behavior of oxides
[DE89-016518] 02 p0282 N90-11608
Physics and materials science of high temperature superconductors
[AD-A211246] 02 p0283 N90-11619
Origins of high-temperature superconductivity in the new copper oxide based ceramic superconductors
[DE89-016543] 02 p0284 N90-11622
Effects of shock-modification on superconductivity in Tl2Ca2Ba2Cu3Oy and Bi2CaSr2Cu2Ox
[DE89-017231] 02 p0285 N90-11629
Neutron scattering experiments on high-temperature superconducting materials: Foreign trip report, September 13, 1988--October 4, 1988
[DE89-017451] 02 p0285 N90-11630
Thermal conduction of SSC (Superconducting Super Collider) wire
[DE89-016710] 03 p0319 N90-11811
Characterization of the Structure and Chemistry of Defects in Materials: Proceedings, volume 138
[DE89-014796] 03 p0410 N90-12352
Superconductivity and magnetic scattering in the Nd(sub 2-x)Ce(sub x)CuO(sub 4-delta)
[DE89-016524] 03 p0410 N90-12354
Structure-property relationships as an aid in the rational design of (beta)-(ET)(sub 2)X organic superconductors
[DE89-016912] 03 p0410 N90-12356
Anomalous ion-channeling behavior across the superconducting transition in high-T(sub c) materials
[DE89-017677] 03 p0411 N90-12360
High temperature superconducting compounds
[AD-A211511] 03 p0413 N90-12374
Resistivity measurements of superconducting materials
[PB89-225700] 04 p0496 N90-12856
Synthesis and characterization of new low-dimensional metal complex conductors
[AD-A213189] 04 p0498 N90-12871
Fractional charging and reentrance in granular superconductors 04 p0557 N90-13248
Composite vs constituent particle aspects of hole motion in the CuO2 plane
[DE89-618864] 04 p0558 N90-13251
Tunneling microscopy of superconductors and tunneling barriers
[AD-A212120] 04 p0559 N90-13257
Method for growing patterned thin films of superconductors
[AD-D014195] 04 p0560 N90-13262
Synthesis and study of materials for superconducting electronics
[AD-A212966] 04 p0561 N90-13270
Surfaces and interfaces of ceramic materials
[AD-A212417] 05 p0627 N90-13657
Joint Services Electronics Program
[AD-A213015] 05 p0634 N90-13699
Theory of strongly fluctuating superconductivity
[DE90-001073] 06 p0850 N90-14942
Solid State Division
[DE90-000979] 06 p0851 N90-14945
X ray studies of strain, interface, and impurity in semiconductors
[DE90-001525] 06 p0851 N90-14947
Development of a real time monitor for superconductive thin film preparation
[DE89-017772] 06 p0852 N90-14952
Superconductivity from finite-U valence fluctuations
[DE90-000603] 06 p0852 N90-14954
A simple figure of merit for high temperature superconducting switches
[DE90-000610] 06 p0852 N90-14955
Muon SR investigation of magnetism and superconductivity in (Y(1-x)Pr(x))Ba2Cu3O7
[DE90-000689] 06 p0852 N90-14956
Superconducting and microstructural properties of shock-compacted high-T sub c oxide powders
[DE90-000823] 06 p0853 N90-14958
Applications of superconductor technologies to transportation
[DE90-000856] 06 p0853 N90-14961
Charge transfer and bond lengths in YBa2Cu(sub 3-x)M(sub x)O(sub 6+y)
[DE90-002241] 06 p0854 N90-14966
Powder neutron diffraction study of the structural phase diagram of the Ba(sub 1-x)K(sub x)BiO3 system
[DE90-002264] 06 p0854 N90-14967
RF superconductivity research and development at Los Alamos National Laboratory
[DE90-002440] 06 p0855 N90-14969
A model of the isotope effect of the oxide superconductor
[DE89-635907] 06 p0855 N90-14971
Macroscopic persistent currents in high temperature ceramic superconductors
[DE89-636232] 06 p0855 N90-14973
Anisotropy of oxygen tracer diffusion in YBa2Cu3O7-delta single crystals
[DE90-001931] 06 p0856 N90-14979
Superconducting gravity gradiometer mission. Volume 1: Study team executive summary
[NASA-TM-4091-VOL-1] 07 p0959 N90-15545
Phonons and charge-transfer excitations in HTS superconductors
[DE89-016616] 07 p0997 N90-15768
Tunneling spectroscopy and the electron-phonon interaction in Ba(1-x)K(x)BiO3
[DE90-002842] 07 p0999 N90-15776
The possible occurrence of multi-phase behavior in the high T(sub c) superconductor YBa2Cu3O(sub x)
[DE90-002999] 07 p0999 N90-15777
Synthesis conductivity, and x ray photoelectron spectrum of Bi2Sr2Cu(sub 7+x). A new ternary bismuth-oxide system exhibiting metallic conductivity
[DE90-003010] 07 p0999 N90-15778
Further studies on possible coexistence of antiferromagnetism and superconductivity in 2D Heisenberg model
[DE90-601082] 07 p1000 N90-15783
Magnetic and electronic correlations in YBa2Cu3O(sub 6+x)
[DE89-017604] 07 p1000 N90-15785
Magnetic mechanisms of high temperature superconductivity
[DE90-003625] 07 p1001 N90-15796
The kind of mathematics involved in applied superconductivity research
[DE90-003706] 07 p1002 N90-15798
Magnetic flux pinning in YBa2Cu3O7 films
[DE90-003709] 07 p1002 N90-15799
Superconductivity and stoichiometry in Tl2Ca2Ba2Cu3O(x) single crystals
[DE90-003838] 07 p1002 N90-15801
Cu-O chains in YBa2Cu3O(7-delta) and the phonon mechanism of high-Tc superconductivity
[DE90-603502] 07 p1003 N90-15805

Bulk wave characterization of high T(sub c) superconductors
[AD-A214030] 07 p1004 N90-15813
Properties of high Tc superconducting oxides
[DE90-003792] 07 p1005 N90-15821
Effects of non-linearity in the variation of pinning potential with current-density on magnetic flux creep in high and low T(sub c) superconductors
[DE90-003952] 07 p1005 N90-15822
Atomic scale structure of twin boundary in Y-Ba-Cu-O superconductors
[DE90-003955] 07 p1006 N90-15823
The fabrication of YBa2Cu3O7 thin films by thermal coevaporation in oxygen
[DE90-003960] 07 p1006 N90-15824
Rotational magnetic processes in YB2Cu3O7
[DE90-000541] 08 p1128 N90-16533
La(sub 2)MO(sub 4 + delta) (M = Cu, Ni, Co): Phase separation and superconductivity resulting from excess oxygen defects
[DE90-001988] 08 p1128 N90-16534
Structure-property correlations in the design of organic metals and superconductors: An overview
[DE90-003794] 08 p1131 N90-16550
B-Factory Final Focus System using superconducting quadrupoles
[DE90-004432] 08 p1131 N90-16552
Neutron experiments on high-temperature superconductors
[DE90-003978] 08 p1132 N90-16559
Magnetic interactions in Sn-119 substituted for Cu in antiferromagnetic and superconducting lamellar cuprates
[DE90-003661] 08 p1132 N90-16560
The effects of oxygen and strontium vacancies on the superconductivity of single crystals of Bi2Sr(2-x)CuO(6-y)
[DE90-004242] 08 p1133 N90-16561
Physical properties of Bi2Sr2CuO6, the semiconducting phase, structurally distinct from the n = 1 Bi-cuprate superconductor
[DE90-004299] 08 p1133 N90-16563
High temperature neutron diffraction study of the formation reaction of bismuth superconductors
[DE90-004883] 08 p1134 N90-16568
Magnetic studies of proximity-effect coupling in a very closely spaced fine-filament NbTi/CuMn composite superconductor
[DE90-005387] 08 p1134 N90-16570
New electronic materials and CO2 reduction
[AD-A214679] 09 p1191 N90-16899
The 1989 National Convention Record IEE Japan, part 7
[DE89-910080] 09 p1210 N90-17012
Oxidation and reduction of Bi2Sr1.85CuO(6-y) crystals
[DE90-004246] 09 p1287 N90-17460
Review of new energy. Superconductivity
[DE90-734947] 09 p1287 N90-17464
Superconducting Bi1.5Pb0.5Sr2Ca2Cu3O(x) ceramics by rapid melt quenching and glass crystallization
[NASA-CR-185184] 09 p1288 N90-17465
International Conference on Materials and Mechanisms of Superconductivity: High Temperature Superconductors
[AD-A215343] 09 p1290 N90-17480
Flux flow, pinning, and resistive behavior in superconducting networks
[DE90-005242] 09 p1293 N90-17493
Development of a superconducting six-axis accelerometer
[AD-A215948] 10 p1319 N90-17625
Developmental condition and technical problems on electric insulation for super-conducting electric power machine
[DE90-741973] 10 p1379 N90-17994
Experiments on large single crystals of the superconducting oxides YBa2Cu3O7, La sub 2-xBa sub xCuO4, and Bi-Ca-Sr-O
[AD-A215283] 10 p1435 N90-18284
High temperature superconductivity
[AD-A215491] 10 p1436 N90-18286
Anisotropy and dimensionality in untwinned crystals of YBa2Cu3O(7-delta)
[DE90-004890] 10 p1436 N90-18287
Long laser-pulse method of producing Y-Ba-Cu-O superconducting films
[DE90-005202] 10 p1436 N90-18289
Effect of manganese additions on the physical and superconducting properties of Nb-46.5Ti
[DE90-005393] 10 p1436 N90-18290
Chemistry of the doping mechanism in Ba(1-x)K(x)BiO3 and La2CuO(sub 4 + delta) oxide superconductors
[DE90-005640] 10 p1437 N90-18293
Microwave radiation absorption by Ho(Y)-Ba-Cu-O superconducting ceramics
[DE90-610665] 11 p1492 N90-18588
Performance and modeling of superconducting ring resonators at millimeter-wave frequencies
[NASA-TM-102526] 11 p1500 N90-18634
Mechanical disturbances in high-performance superconducting dipoles
[DE90-006237] 11 p1570 N90-19040
Pressure induced superconductivity in elemental solids
[DE90-610664] 11 p1572 N90-19048
Spectral functions from Quantum Monte Carlo
[DE90-004870] 11 p1572 N90-19050
Superconducting materials
[DE90-007419] 11 p1573 N90-19054
Superconductivity in Ba(1-x)BiO3
[DE90-003781] 12 p1718 N90-19869
BCS (Bardeen-Cooper-Schrieffer) primer: A guide to computational methods in superconductivity theory
[AD-A216393] 12 p1719 N90-19874
Critical current density and transition temperature measurements of Y-Ba-Cu-O rods
[AD-A216695] 12 p1719 N90-19875
National Action Plan on Superconductivity Research and Development
[PB89-138512] 12 p1720 N90-19883
Neutron scattering measurements of the magnetic excitations of high-temperature superconducting materials
[DE90-006567] 12 p1721 N90-19885
Materials Science Programs, fiscal year 1989
[DE90-008169] 13 p1765 N90-20131
Processing, fabrication, characterization and device demonstration of high temperature superconducting ceramics
[AD-A218330] 13 p1782 N90-20231
Superconductive microprobes for eddy current evaluation of materials
[AD-A217776] 13 p1805 N90-20361
High resolution transmission electron microscopy study of defect structures in mixed-phase YBaCuO
[DE90-007767] 13 p1894 N90-20873
Stabilization of high (Tc) superconductivity in cadmium sulfide
[DE90-008249] 13 p1896 N90-20881
Millimeter wave surface resistance of RBa2Cu3O(7-delta) (R=Y,Eu,Dy,Sm,Er) superconductors
[NASA-TM-102571] 13 p1897 N90-20886
Technology assessment of superconductivity
[AD-A217697] 13 p1897 N90-20889
Modified tight-binding approximation and electron-phonon spectral function for transition metals
[DE90-614022] 14 p1950 N90-21166
JPRS report: Science and technology. USSR: Physics and mathematics
[JPRS-UPM-90-002] 14 p2022 N90-21593
Chern-Simons superconductivity at finite temperature
[DE90-613393] 14 p2031 N90-21650
On the substitution of Sr ions at Y sites in YB(suba2)Cu3O(sub7-d)
[DE90-613395] 14 p2031 N90-21652
Thermogravimetric analysis of Nd(2-x)Ce(x)CuO(4-delta)
[DE90-009184] 14 p2032 N90-21658
Some global problems in gauge theories (variations on a theme of Aharonov and Bohm)
[DE90-009034] 14 p2035 N90-21678
A superconducting quenchgun for delivering lunar derived oxygen to lunar orbit
[NASA-CR-185161] 15 p2061 N90-21806
Transport and relaxation properties in anisotropic superconductors 15 p2170 N90-22403
JETC (Japanese Technology Evaluation Center) Panel Report on High Temperature Superconductivity in Japan
[NASA-CR-180413] 15 p2172 N90-22409
Development of the methods and means of precise forming and geometry control of superconducting current-carrying element for the UNR pulsed dipoles
[DE90-620108] 15 p2173 N90-22419
Growth and patterning of laser ablated superconducting YBa2Cu3O7 films on LaAlO3 substrates
[NASA-TM-102436] 15 p2173 N90-22421
International science and technology policies: Testimony before the Subcommittee on International Scientific Cooperation, Committee on Science, Space, and Technology, United States House of Representatives
[DE90-009416] 15 p2181 N90-22463
Photoresponse of YBa2Cu3O(7-delta) granular and epitaxial superconducting thin films
[NASA-TM-103144] 16 p2231 N90-22732
The onset of superconductivity in two-dimensional disordered systems 16 p2321 N90-23232
A low temperature calorimetric study of several high-T(sub c) superconductors 16 p2322 N90-23237
High temperature superconductivity
[AD-A219483] 17 p2476 N90-24155
Effects of large doses of high energy electrons on a YBa2Cu3O6(+)delta high temperature superconductor
[AD-A220423] 17 p2476 N90-24158
Chemical and crystallographic phase behavior in the Ba(1-x)K(x)BiO3 system
[DE90-010072] 18 p2618 N90-24917
Use of neutron diffraction in determining strains in high-temperature superconducting composites
[DE90-010404] 18 p2621 N90-24931
The effect of magnetic field on the critical current density of bulk superconducting wires
[DE90-010458] 18 p2621 N90-24934
Transverse- and zero-field muon SR investigation of magnetism and superconductivity in (Y(1-x)Pr(x)Ba2Cu3O7)
[DE90-010597] 18 p2624 N90-24953
Effect of Cu(2+) magnetic moments on the superconductivity of YBa2Cu3O7: The origin of the linear term in the specific heat; the volume fraction of superconductivity
[DE90-011214] 18 p2626 N90-24963
Rapid thermal processing of high temperature superconducting fiber
[NASA-CR-186803] 18 p2626 N90-24964
Low-temperature specific heat measurements on metals: Application to high-T(sub c) superconductors
[DE90-011612] 18 p2626 N90-24966
Sequentially evaporated thin film YBa2Cu3O(7-x) superconducting microwave ring resonator
[NASA-TM-103180] 19 p2685 N90-25273
Center for Space Microelectronics Technology 1988-1989 technical report
[NASA-CR-186849] 19 p2753 N90-25642
Status of the CEBAF injector
[CEBAF-PR-89-027] 19 p2755 N90-25655
The CEBAF instrumentation and control system
[CEBAF-PR-89-037] 19 p2755 N90-25657
Design of CEBAF's RF separator and results of cold tests
[CEBAF-PR-89-021] 19 p2756 N90-25658
On using a superconducting linac to drive a short wavelength FEL
[CEBAF-PR-89-019] 19 p2756 N90-25660
Requirements for longitudinal HOM damping in superconducting recirculating linacs
[CEBAF-PR-89-018] 19 p2756 N90-25662
Impedance and wakefields beyond cutoff
[CEBAF-PR-89-016] 19 p2756 N90-25663
Suitability of electrodeposition processes for high temperature superconductors
[IAR-89-22] 19 p2760 N90-25685
Superconductivity in nonsymmetric epitaxial YBa2Cu3O(sub 7-delta)-PrBa2Cu3O(sub 7-delta) superlattices grown by pulsed laser ablation
[DE90-011637] 19 p2761 N90-25687
Investigation of the mechanical properties of superconducting coils
[DE90-012020] 19 p2761 N90-25689
A beauty factory using an SRF linac and a storage ring
[CEBAF-PR-89-017] 20 p2925 N90-26644
Passivation of high temperature superconductors
[NASA-CASE-NPO-17949-1-CU] 20 p2932 N90-26684
Physics and techniques for the investigation of the properties of ultra small systems
[AD-A221985] 21 p3071 N90-27461
Flux motion effects in Tl-Ca-Ba-Cu-O thin films
[DE90-012176] 21 p3080 N90-27514
Symmetry breaking oxygen displacement in superconducting oxides
[DE90-013670] 21 p3081 N90-27520
High temperature superconductivity applications for electronic warfare and microwave systems
[AD-A222972] 21 p3082 N90-27528
Fabrication of composite high temperature superconductor wires from Ag/YBa2Cu3O(sub x) powder produced by AgNO3 decomposition
[AD-A221936] 21 p3083 N90-27532
A silver-bearing, High-Temperature, Superconducting (HTS) paint
[AD-A221616] 21 p3084 N90-27539
The superconducting state of the high-transition temperature superconductors: Experimental basis 22 p3136 N90-27793
Oxygen stabilization induced enhancement in J(sub c) and T(sub c) of superconducting oxides 22 p3137 N90-27800
Scaling behaviour of relaxation dependencies in metaloxide superconductors 22 p3138 N90-27802
Effect of shock pressure on the structure and superconducting properties of Y-Ba-Cu-O in explosively fabricated bulk metal-matrix composites 22 p3138 N90-27804
High-T(sub c) squid application in medicine and geophysics 22 p3139 N90-27806

Oxide superconductors under magnetic field
22 p3139 N90-27807
Perspectives on high temperature superconducting electronics
22 p3139 N90-27810
Preparation and characteristics of superconducting cuprate thin films: Nd(2-x)Ce(x)CuO4 and substituted Bi-system
22 p3140 N90-27813
Ternary and quaternary oxides of Bi, Sr, and Cu
22 p3141 N90-27817
Phenomenological theory of the normal and superconductive states of Cu-O and Bi-O metals
22 p3142 N90-27819
Dynamics of the iron spins in superconducting YBa2(Cu(1-x)Fe(x))O7
22 p3143 N90-27825
A systematic study of superconductivity in BiPb(Sn)-Sb Sr-Ca-Cu-O systems
22 p3144 N90-27831
Structure and superconducting properties of ((Ln(1-x)Ln*(x) 1/2 (Ba(1-y)Sr(y) 1/3 Ce 1/6) 8Cu6O(z)
22 p3144 N90-27833
Progress of research of high-T(sub c) superconductors
22 p3145 N90-27835
The NASA high temperature superconductivity program
22 p3145 N90-27836
Navy superconductivity efforts
22 p3145 N90-27837
Low frequency electrical noise across contacts between a normal conductor and superconducting bulk YBa2Cu3O7
22 p3146 N90-27841
Electronic state and superconductivity of YBa2Cu3-xO7-y (M=Al,Zn and Sn) systems
22 p3146 N90-27842
A technique to measure the thermal diffusivity of high T(sub c) superconductors
22 p3147 N90-27846
Superconductivity in 2-2-3 Y2Ba2Cu3O(sub 8+ delta)
22 p3147 N90-27847
Microstructures and properties of superconducting Y-Er-BaCu-O thin films obtained from disordered Y-Er-BaF2-Cu films
22 p3147 N90-27848
Spatial conductivity measurements on high T(sub c) superconducting films
22 p3148 N90-27849
Composite superconducting wires obtained by high-rate tinning in molten Bi-Pb-Sr-Ca-Cu-O system
22 p3148 N90-27850
In-situ integrated processing and characterization of thin films of high temperature superconductors, dielectrics and semiconductors by MOCVD
22 p3148 N90-27851
Localization effects in radiationally disordered high-temperature superconductors: Theoretical interpretation
22 p3148 N90-27853
Coupled bipolarons and optical phonons as a model for high-T(sub c) superconductors
22 p3149 N90-27854
Synthesis of Y1Ba2Cu3O(sub x) superconducting powders by intermediate phase reaction
22 p3149 N90-27855
Electron energy spectrum and magnetic interactions in high-T(sub c) superconductors
22 p3149 N90-27857
Processing Bi-Pb-Sr-Ca-Cu-O superconductors from amorphous state
22 p3150 N90-27860
The relation between ferroelasticity and superconductivity
22 p3150 N90-27861
Novel superconducting phases of Tl-based compounds
22 p3150 N90-27862
Superconductivity in the Sn-Ba-Sr-Y-Cu-O system
22 p3151 N90-27863
Studies of iron impurities in YxPr1-xBa2Cu3O7-delta
22 p3151 N90-27865
Study of the superconducting properties of the Bi-Ca-Sr-Cu-O system
22 p3151 N90-27866
A YBCO RF-SQUID magnetometer and its applications
22 p3151 N90-27867
Magnetic properties of the 110K superconducting phase in Pb-doped Bi-Sr-Ca-Cu-O thin films
22 p3151 N90-27868
Optical and microwave detection using Bi-Sr-Ca-Cu-O thin films
22 p3152 N90-27870
In Situ deposition of YBCO high-T(sub c) superconducting thin films by MOCVD and PE-MOCVD
22 p3152 N90-27871
Development of standards for superconductors
[PB90-196536] 22 p3248 N90-28418
Survey of superconductors for energy applications
[DE90-796181] 22 p3248 N90-28420
Thermogravimetry-mass spectrometry analysis of gas bubbles in molten glass
[DE90-014116] 23 p3303 N90-28684
High temperature superconducting thin film microwave circuits: Fabrication, characterization, and applications
[NASA-TM-103235] 23 p3322 N90-28786
Superconductivity in mixed boson-fermion systems
[DE90-627491] 23 p3401 N90-29216
Parity violation and superconductivity in doped Mott insulators
[DE90-627493] 23 p3401 N90-29217
Performance test plan for variable-speed ac superconducting motor
[DE90-016208] 24 p3465 N90-29579
Practical superconductor development for electrical power applications
[DE90-014836] 24 p3554 N90-30109
Superconductivity and information exchange
[DE90-015767] 24 p3554 N90-30110

SUPERCONDUCTOR INSULATOR SUPERCONDUCTORS
U SIS (SUPERCONDUCTORS)

SUPERCONDUCTORS
NT HIGH TEMPERATURE SUPERCONDUCTORS
Measuring the shielding effectiveness of superconductive composites
[DE89-015164] 01 p0033 N90-10180
New electrodynamic and electrostatic models with applications to antenna theory, superconductor slots, and lasers
01 p0055 N90-10316
Composite ceramic superconducting wires for electric motor applications
[AD-A210345] 01 p0060 N90-10346
Ceramic processing of bulk high-T(sub c) superconductors
[DE89-015703] 01 p0128 N90-10736
Mixed-valent and heavy fermions and related systems
[DE89-016335] 01 p0129 N90-10743
Critical magnetic fields (H(sub c2), H(sub c1)) and kappa in YBa2(Cu0.98M0.02)3O(7+delta), M=Ni, Al, and Cu
[DE89-016412] 01 p0130 N90-10745
X-ray and gamma-ray spectroscopy of solids under pressure
[DE89-017271] 02 p0196 N90-11118
A study of the tribological and surface micromechanical properties of YBa2Cu3O7-x
[DE89-015680] 02 p0281 N90-11607
Propagation of normal zones of finite size in large, composite superconductors
[DE89-016866] 02 p0282 N90-11611
Rational design of high-current cable-in-conduit superconductors
[DE89-016867] 02 p0284 N90-11626
Quantitative interpretation of auger lineshapes and electron/photon stimulated desorption
[AD-A211550] 03 p0324 N90-11842
Process for single crystal growth of high T(sub c) superconductors
[AD-D014167] 03 p0409 N90-12346
Structure-property relationships as an aid in the rational design of (beta)-(ET)(sub 2)X organic superconductors
[DE89-016912] 03 p0410 N90-12356
Electron-positron momentum distribution measurements of high-T(sub c) superconductors and related systems
[DE89-017538] 03 p0411 N90-12358
The characterization of Nb3Sn superconductors for use in magnets of 19 T and greater
[DE89-017758] 03 p0412 N90-12364
Fractional charging and reentrance in granular superconductors
04 p0557 N90-13248
Tunneling microscopy of superconductors and tunneling barriers
[AD-A212120] 04 p0559 N90-13257
Method for growing patterned thin films of superconductors
[AD-D014195] 04 p0560 N90-13262
Synthesis and study of materials for superconducting electronics
[AD-A212966] 04 p0561 N90-13270
Joint Services Electronics Program
[AD-A213015] 05 p0634 N90-13699
The formation of metal-oxygen species at low temperatures
[DE90-002298] 06 p0743 N90-14323
The 7th International Conference on Ceramics
[DE90-002144] 06 p0752 N90-14374
Studies of neutral and ion transport during laser ablation of 1:2:3 superconductors by optical absorption spectroscopy
[DE90-001968] 06 p0790 N90-14604
Use of superconducting plates and shells to deflect magnetic noise fields: Application to MEG
[DE89-012592] 06 p0803 N90-14676
Photovoltaic Measurements and Performance Branch
[DE89-009500] 06 p0807 N90-14695
Program CICC flow and heat transfer in Cable-In-Conduit Conductors
[DE90-001519] 06 p0829 N90-14818
Solid State Division
[DE90-000979] 06 p0851 N90-14945
Superconductivity from finite-U valence fluctuations
[DE90-000603] 06 p0852 N90-14954
Muon SR investigation of magnetism and superconductivity in (Y(1-x)Pr(x))Ba2Cu3O7
[DE90-000689] 06 p0852 N90-14956
Superconducting and microstructural properties of shock-compacted high-T sub c oxide powders
[DE90-000823] 06 p0853 N90-14958
Shock-induced defects and flux pinning in YBa2Cu3O sub 7-delta + Ag composites
[DE90-000827] 06 p0853 N90-14960
Applications of superconductor technologies to transportation
[DE90-000856] 06 p0853 N90-14961
Dissipation measurement in high T(sub c) superconductors with electromagnetic probes
[DE90-002058] 06 p0854 N90-14963
The effect of composition and processing on high T(sub c) superconductors containing bismuth
[DE90-002203] 06 p0854 N90-14965
A model of the isotope effect of the oxide superconductor
[DE89-635907] 06 p0855 N90-14971
Bi-Sr-Ca-Cu-O superconducting ceramics
[DE89-636225] 06 p0855 N90-14972
Microstructure and electrical properties of bulk high-T(sub c) superconductors
[DE90-001762] 06 p0855 N90-14974
Improved performance of low-T(sub c) superconductors for detection of minimum-ionizing particles
[DE90-001985] 06 p0856 N90-14976
New organic synthetic metals derived from BEDT-TTF, Ni(dsit)2 and BEDO-TTF
[DE90-003793] 07 p0907 N90-15242
Fabrication of superconductor coils
[DE90-003571] 07 p0922 N90-15338
Phonons and charge-transfer excitations in HTS superconductors
[DE89-016616] 07 p0997 N90-15768
On the free carrier-negative U center interacting model for the high-T(sub c) oxide superconductor
[DE89-635908] 07 p0998 N90-15775
The possible occurrence of multi-phase behavior in the high T(sub c) superconductor YBa2Cu3O(sub x)
[DE90-002999] 07 p0999 N90-15777
Processing and fabrication of YBa2Cu4O8 and YBa2Cu4O8/YBa2Cu3O(x) composites
[DE90-003559] 07 p1001 N90-15789
Cation disordering in the Tl-2122 superconductors
[DE90-003579] 07 p1001 N90-15795
X ray absorption studies of YBa2Cu3O(6+x), La(2-x)Sr(x)CuO4, and Nd(2-x)Ce(x)CuO4
[DE90-003640] 07 p1002 N90-15797
On functional integral representations in the lower Hubbard band based on generalized coherent states
[DE90-602936] 07 p1003 N90-15804
Computer-controlled ion beam sputter-deposition of superconducting oxide films
[AD-A213921] 07 p1004 N90-15812
Properties of high Tc superconducting oxides
[DE90-003792] 07 p1005 N90-15821
Effects of non-linearity in the variation of pinning potential with current-density on magnetic flux creep in high and low T(sub c) superconductors
[DE90-003952] 07 p1005 N90-15822
Atomic scale structure of twin boundary in Y-Ba-Cu-O superconductors
[DE90-003955] 07 p1006 N90-15823
Design of coupled or uncoupled multifilamentary SSC-type strands with almost zero retained magnetization at fields near 0.3 T
[DE90-005391] 08 p1047 N90-16052
Researches on amorphous perovskite
[DE89-900733] 08 p1128 N90-16535
Magnetic interactions in Sn-119 substituted for Cu in antiferromagnetic and superconducting lamellar cuprates
[DE90-003661] 08 p1132 N90-16560
Physical properties of Bi2Sr2CuO6, the semiconducting phase, structurally distinct from the n = 1 Bi-cuprate superconductor
[DE90-004299] 08 p1133 N90-16563
Electron beam induced oxygen in YBa2Cu3O(7-x) superconductors
[DE90-004839] 08 p1133 N90-16565
Properties and design of multifilamentary NbTi composite superconductors
[DE90-004904] 08 p1134 N90-16569
Magnetic studies of proximity-effect coupling in a very closely spaced fine-filament NbTi/CuMn composite superconductor
[DE90-005387] 08 p1134 N90-16570
Method of forming low cost, formable High T(subc) superconducting wire
[NASA-CASE-LEW-14676-2] 09 p1286 N90-17454
Normal state electronic structure and the superconducting energy gap in HTSC's as determined from photoemission spectroscopy
[DE90-004857] 09 p1292 N90-17489
High-temperature deformation of YBa2Cu3O(7-delta) with Ag additions
[DE90-004884] 09 p1292 N90-17491

Development of a superconducting six-axis accelerometer
[AD-A215948] 10 p1319 N90-17625
Performance of superconductive oxides as cathodes for lithium rechargeable batteries
[AD-A216030] 10 p1401 N90-18098
Structural, magnetic and electrical properties of La(sub 2-x) Ba(sub x) NiO4
[AD-A214347] 10 p1434 N90-18278
Thermal conductivity of quasi-one dimensional conductors
[DE90-004844] 10 p1435 N90-18281
Experiments on large single crystals of the superconducting oxides YBa2Cu3O7, La sub 2-xBa sub xCuO4, and Bi-Ca-Sr-O
[AD-A215283] 10 p1435 N90-18284
Hyper- and hypobaric processing of Tl-Ba-Ca-Cu-O superconductors
[DE90-005637] 10 p1437 N90-18292
Chemistry of the doping mechanism in Ba(1-x)K(x)BiO3 and La2CuO(sub 4 + delta) oxide superconductors
[DE90-005640] 10 p1437 N90-18293
Pulsed laser deposition of high T(sub c) superconducting thin films
[AD-A216507] 11 p1569 N90-19034
Understanding electronegative effects in core-level electron spectroscopies; application to the high temperature superconductors
[AD-A216728] 11 p1570 N90-19037
Superconducting materials
[DE90-007419] 11 p1573 N90-19054
Laser surface interactions of high-(Tc) superconductors
[DE90-006894] 12 p1669 N90-19587
BCS (Bardeen-Cooper-Schrieffer) primer: A guide to computational methods in superconductivity theory
[AD-A216393] 12 p1719 N90-19874
Critical current density and transition temperature measurements of Y-Ba-Cu-O rods
[AD-A216695] 12 p1719 N90-19875
On dissipative states in narrow current-carrying superconducting filaments
[ETN-90-95915] 12 p1721 N90-19889
FWP executive summaries: Basic energy sciences materials sciences programs
[DE90-006373] 12 p1722 N90-19893
Symposium on High Temperature and Materials Chemistry
[DE90-008047] 13 p1768 N90-20148
Processing, fabrication, characterization and device demonstration of high temperature superconducting ceramics
[AD-A218330] 13 p1782 N90-20231
Superconductive microprobes for eddy current evaluation of materials
[AD-A217776] 13 p1805 N90-20361
Ultra-high brightness laser research at LLNL (Lawrence Livermore National Laboratory)
[DE90-008366] 13 p1896 N90-20885
Millimeter wave surface resistance of RBa2Cu3O(7-delta) (R=Y,Eu,Dy,Sm,Er) superconductors
[NASA-TM-102571] 13 p1897 N90-20886
Synthesis and properties of polycrystalline Tl2Ba2CaCu2O(x) and Tl2Ba2Ca2Cu3O(x)
[DE90-007528] 13 p1897 N90-20887
Synthesis of Bi-Sr-Ca-Cu oxide superconductor by solution technique
[DE90-008707] 13 p1897 N90-20888
Technology assessment of superconductivity
[AD-A217697] 13 p1897 N90-20889
Deformation processing of YBa2Cu3O(sub x)
[DE90-007795] 14 p2030 N90-21644
Toughened YBa2Cu3O(sub x)/ZrO2 composites
[DE90-007796] 14 p2031 N90-21645
Specific heat and critical fluctuations in anisotropic high-T(sub c) oxide superconductors
[DE90-613394] 14 p2031 N90-21651
Shock compression of solids: A tutorial
[DE90-009185] 14 p2032 N90-21659
Transport and relaxation properties in anisotropic superconductors 15 p2170 N90-22403
Transport properties of anisotropic superconductors 15 p2170 N90-22404
Construction of a 345 gigahertz receiver based on superconducting tunnel junctions
[AD-A218781] 16 p2232 N90-22735
Excitation of hypersound at boundary between Type-2 superconductor and a concentrated paramagnetic compound 16 p2310 N90-23164
A low temperature calorimetric study of several high-T(sub c) superconductors 16 p2322 N90-23237
Influence of high energy radiation on critical parameters of superconducting ceramics YBa2Cu3O7
[DE90-620562] 16 p2322 N90-23239
Reply to coupled S- and D-wave states in the thorium-doped heavy-fermion superconducting UBe13 by H. Pleiner and H. R. Brand
[AD-A220843] 17 p2477 N90-24164
Superconducting permanent magnets
[AD-A218944] 18 p2618 N90-24912
The use of curium as a rare Earth substitute in high T(sub c)-related compounds
[DE90-009724] 18 p2620 N90-24928
RF surface resistance measurements in the Pb-Bi-Sr-Ca-Cu-O system
[DE90-010412] 18 p2621 N90-24932
Synthesis of ceramic superconductors under low oxygen pressure
[DE90-010415] 18 p2621 N90-24933
Pressure in the study of organic superconductors
[DE90-011049] 18 p2625 N90-24959
Sequentially evaporated thin film YBa2Cu3O(7-x) superconducting microwave ring resonator
[NASA-TM-103180] 19 p2685 N90-25273
Formation of high Tc superconducting films by organometallic chemical vapor deposition
[AD-D014498] 19 p2760 N90-25682
Experiments on superconductor imaging surface magnetometry
[DE90-008925] 20 p2929 N90-26665
Characterization of NbTi multifilamentary superconducting wires
[DE90-626245] 20 p2930 N90-26672
Composite ceramic superconducting wires for electric motor applications
[AD-A222085] 21 p3001 N90-27055
Physics and techniques for the investigation of the properties of ultra small systems
[AD-A221985] 21 p3071 N90-27461
Symmetry breaking oxygen displacement in superconducting oxides
[DE90-013670] 21 p3081 N90-27520
Characterization of superconducting materials with muon spin rotation
[DE90-013755] 21 p3081 N90-27522
High temperature superconductivity applications for electronic warfare and microwave systems
[AD-A222972] 21 p3082 N90-27528
The 1990 Gordon Research Conference on Crystal Growth
[AD-A223218] 21 p3083 N90-27531
Pinning, flow and plastic deformation of flux vortices in high T(sub c) superconductors 22 p3136 N90-27796
Scaling behaviour of relaxation dependencies in metaloxide superconductors 22 p3138 N90-27802
Production of superconductor/carbon bicomponent fibers 22 p3138 N90-27805
High-T(sub c) squid application in medicine and geophysics 22 p3139 N90-27806
Oxide superconductors under magnetic field 22 p3139 N90-27807
Ternary and quaternary oxides of Bi, Sr, and Cu 22 p3141 N90-27817
Plastic superconductor bearings any size, any shape, 77 k and up 22 p3145 N90-27838
Low frequency electrical noise across contacts between a normal conductor and superconducting bulk YBa2Cu3O7 22 p3146 N90-27841
The effects of space radiation on thin films of YBa2Cu3O(sub 7-x) 22 p3147 N90-27845
A technique to measure the thermal diffusivity of high T(sub c) superconductors 22 p3147 N90-27846
Superconductivity in 2-2-3 Y2Ba2Cu3O(sub 8+ delta) 22 p3147 N90-27847
Grain orientation studies in superconductors 22 p3148 N90-27852
Spin bipolaron in the framework of emery model for high-T(sub c) copper oxide superconductors 22 p3149 N90-27856
Processing Bi-Pb-Sr-Ca-Cu-O superconductors from amorphous state 22 p3150 N90-27860
Superconductivity in the Sn-Ba-Sr-Y-Cu-O system 22 p3151 N90-27863
Comparative study of flux pinning flux creep and critical currents between YBaCuO crystals with and without Y2BaCuO5 inclusions 22 p3152 N90-27869
Digital beam position regulation of the superconducting accelerator at Darmstadt
[ETN-90-97293] 22 p3246 N90-28406
Development of standards for superconductors
[PB90-196536] 22 p3248 N90-28418
Survey of superconductors for energy applications
[DE90-796181] 22 p3248 N90-28420
Analysis of three-dimensional eddy current field. Application to calculation of magnetic screening effect of the damper system in a model superconducting generator
[DE90-507869] 23 p3321 N90-28779
High temperature superconducting thin film microwave circuits: Fabrication, characterization, and applications
[NASA-TM-103235] 23 p3322 N90-28786
Dynamical information for Fe doped YBa2Cu3O7 superconducting oxides obtained from high temperature Moessbauer studies
[DE90-627871] 23 p3401 N90-29218
Synthesis and property evaluation of Y-Ba2-Cu3-O(6+x) superconductors
[AD-A223494] 24 p3552 N90-30098

SUPERCOOLING

NT CRYOGENIC COOLING
Remote sensing techniques of the Wave Propagation Laboratory for the measurement of supercooled liquid water: Applications to aircraft icing
[PB89-208102] 02 p0148 N90-10842
Estimation of time to maximum supercooling during dynamic frazil ice formation
[AD-A212204] 04 p0471 N90-12699
Time-resolved measurements of solidification and undercooling in metals and alloys
[DE90-007074] 11 p1488 N90-18564
Principles of metallic solidification 13 p1784 N90-20241
Supercooling and germ formation 13 p1784 N90-20242
Infrared fiber-optical temperature sensor
[AD-D014519] 19 p2693 N90-25321
Traps for neutral atoms
[AD-A221331] 19 p2754 N90-25649
Undercooling and solidification
[DLR-FB-90-020] 20 p2931 N90-26678
ETO lidar studies of cirrostratus altocumulogenitus: Another role for supercooled liquid water in cirrus cloud formation 22 p3221 N90-28269

SUPERCRITICAL AIRFOILS

NT SUPERCRITICAL WINGS
A study of high-lift airfoils at high Reynolds numbers in the Langley low-turbulence pressure tunnel
[NASA-TM-89125] 01 p0001 N90-10002
A direct-inverse method for transonic and separated flows about airfoils
[NASA-CR-4270] 07 p0875 N90-15072
NASA supercritical airfoils: A matrix of family-related airfoils
[NASA-TP-2969] 09 p1159 N90-16710
Comparison of conventional and adaptive wall wind tunnel results with regard to Reynolds number effects 10 p1323 N90-17649
Experience with some repeat tests on the 9 inch chord CAST-10-2/DOA 2 airfoil model in the Langley 0.3-m TCT adaptive wall test section 10 p1325 N90-17657
Aerodynamic design techniques at DLR Institute for Design Aerodynamics 14 p1916 N90-20979

SUPERCRITICAL FLOW

Analysis of experimental data for CAST 10-2/DOA 2 supercritical airfoil at low Reynolds numbers and application to high Reynolds number flow
[AD-A211654] 05 p0571 N90-13326
Calculation of turbulent choppy flow mixing
[ETN-90-95929] 08 p1065 N90-16165
Aerofoil design techniques 14 p1916 N90-20978
Inverse design of airfoil contours: Constraints, numerical method, and applications 14 p1917 N90-20980
Inverse computation of transonic internal flows with application for multi-point-design of supercritical compressor blades 14 p1918 N90-20987
Limits of adaptation, residual interferences 21 p2963 N90-26844

SUPERCRITICAL FLUIDS

Electrochemistry in near-critical and supercritical fluids. Part 7: SO2
[AD-A208207] 01 p0039 N90-10214
Evaluation of supercritical cryogen storage and transfer systems for future NASA missions
[NASA-TM-102394] 02 p0160 N90-10912
Thermophysical properties of supercritical fluids and fluid mixtures
[DE89-016568] 02 p0193 N90-11102
Research and Development Opportunities in Supercritical Fluid Technology
[DE89-015320] 04 p0469 N90-12684
Supercritical fluid chromatography/supersonic jet spectroscopy
[DE90-001378] 06 p0740 N90-14308
Electrochemistry in near-critical and supercritical fluids. 8: Methyl viologen, decamethylferrocene, Os(bpy)3(sup 2+) and ferrocene in acetonitrile and the effect of pressure on diffusion coefficients under supercritical conditions
[AD-A213407] 07 p0895 N90-15172
Thermodynamic properties of supercritical mixtures
[DE90-006720] 12 p1724 N90-19909

Phase equilibrium of mixtures consisting of molecules with large size and shape differences (thermodynamic modeling of Supercritical Fluid Extraction and Retrograde Condensation, SFE/RC)
[PB90-131285] 14 p1947 N90-21146
Supercritical fluid chromatography/supersonic jet spectroscopy
[DE90-015220] 24 p3447 N90-29465
Processing of polymers using supercritical fluids
[AD-A223681] 24 p3455 N90-29514

SUPERCRITICAL PRESSURES
Electrochemistry in near-critical and supercritical fluids. 8: Methyl viologen, decamethylferrocene, Os(bpy)3(sup 2+) and ferrocene in acetonitrile and the effect of pressure on diffusion coefficients under supercritical conditions
[AD-A213407] 07 p0895 N90-15172

SUPERCRITICAL WINGS
Results of LFC experiment on slotted swept supercritical airfoil in Langley's 8-foot transonic pressure tunnel
04 p0442 N90-12531
Boundary-layer stability analysis of Langley Research Center 8-foot LFC experimental data
04 p0442 N90-12532

SUPERFLUID FLOW
U SUPERFLUIDITY

SUPERFLUIDITY
Internal Magnus effects in superfluid 3He-A
[PB89-212617] 03 p0410 N90-12351
Flare-in texture in rotating superfluid (3)He-B
[PB89-218994] 03 p0412 N90-12368
Resonant quasiparticle-ion scattering in anisotropic superfluid (3)He
[PB89-221618] 03 p0413 N90-12369
Collective-mode spectroscopy of textures in superfluid (3)He-B
[PB89-221634] 03 p0413 N90-12370
Symmetry breaking phenomena in liquid Helium-4
[DE89-618886] 04 p0469 N90-12685
Persistent current, NMR, and ion transmission experiments in rotating He-3 superfluids --- Nuclear Magnetic Resonance (NMR)
[ISBN-952-90056-1-X] 04 p0553 N90-13221
Superfluid phase slippage in (3)He-B flow through a narrow channel
[PB89-218986] 04 p0559 N90-13258
Construction of the rotating cryostat ROTA2, its use for zero sound experiments in (3)He-B, and calculations of ion mobility in (3)He-A and (3)He-P
[ISBN-052-90091-3-5] 05 p0645 N90-13765
Path integral simulations of liquid helium
[DE90-001171] 06 p0836 N90-14862
Superflow induced phase transition in the axial vortex-free texture of rotating superfluid He-3-B
[PB90-110388] 08 p1127 N90-16531
Design and testing of a superfluid liquid helium cooling loop
[NASA-CR-182776] 09 p1216 N90-17050
Research and development of a helium-4 based solar neutrino detector
[DE90-005416] 10 p1447 N90-18353
Particle detection via rotons in helium-4 superfluid
[DE90-005417] 10 p1448 N90-18354
Superfluid helium orbital resupply coupling
11 p1475 N90-18488
Bose condensate in superfluid (sup 4)He and momentum distributions by deep inelastic scattering
[DE90-007541] 12 p1712 N90-19832
Nucleation of vortices in superfluid helium-4
[DE90-610675] 12 p1720 N90-19880
Goldstone excitation and symmetry breaking mechanism in superfluid He-4
[DE90-610676] 12 p1720 N90-19881
Coherent state in the roton region of superfluid helium-4
[DE90-610677] 12 p1720 N90-19882
Nonlinear acoustic interactions in superfluid helium
15 p2164 N90-22367
Spacecraft thermal control design data, volume 5. Section R: Cryogenic cooling. Section S: Existing satellites
[ESA-PSS-03-108-ISSUE-1-VOL-5]
22 p3132 N90-27772
Thermophysical properties of Helium-4 from 0.8 to 1500 K with pressures to 2000 MPa
[NASA-CR-186992] 23 p3303 N90-28681

SUPERGIANT STARS
Properties of evolved star circumstellar grains
06 p0861 N90-15003
The 3A1954+319: A possible supergiant X ray binary
19 p2782 N90-25830

SUPERGRAVITY
N=1,2 supergravities in 2+1 dimensions as Chern-Simons theories
[DE89-612006] 01 p0134 N90-10771
D=3 Chern-Simons action, supergravity and quantization
[DE89-617530] 01 p0134 N90-10775
Two dimensional conformal supergravity and critical behavior
[DE89-611968] 03 p0420 N90-12414
Physics with ultra-low energy antiprotons
[DE90-002397] 06 p0840 N90-14888
Cubic interaction in conformal theory of integer higher-spin fields in four dimensional space-time
[DE90-607095] 10 p1425 N90-18220
N=2 supergravity in superspace and the BRS symmetry
[DE90-607062] 10 p1439 N90-18305
BRS current and related anomalies in two-dimensional gravity and string theories
[DE90-733095] 10 p1440 N90-18307
Theoretical investigations in elementary particle physics
[DE90-007178] 13 p1883 N90-20802
Quantization of the N = 2m simple supergravity in d = 2 + 1
[DE90-612765] 14 p2034 N90-21671

SUPERHEATING
Aerosol heating and vaporization of high-flux laser beams
[DE90-003471] 07 p0937 N90-15428
The onset of boiling of the liquid alkali metals
[DE90-002276] 08 p1044 N90-16036

SUPERHETERODYNE RECEIVERS
Calculation, optimization and comparison of optical transmission systems with superheterodyne reception
[ETN-89-94651] 02 p0214 N90-11224
Far-infrared heterodyne receivers
05 p0597 N90-13465
Advances in SIS receiver technology
05 p0597 N90-13466

SUPERHIGH FREQUENCIES
The effectiveness of adaptive PRF (Pulse Repetition Frequency) selection in minimizing range obscuration in the TDWR (Terminal Doppler Weather Radar) system
[AD-A211267] 02 p0213 N90-11222
Geology of Southern Guinevere Planitia, Venus, based on analyses of Goldstone radar data
03 p0422 N90-12424
DSN 70-meter antenna microwave optics design and performance improvements. Part 2: Comparison with measurements
04 p0487 N90-12800
X-band atmospheric attenuation for an Earth terminal measurement system
[PB90-100736] 08 p1056 N90-16101
Proceedings of the Thirteenth NASA Propagation Experimenters Meeting (NAPEX 13)
[NASA-CR-186062] 10 p1371 N90-17945
Wideband S band transmitter
[AD-A217620] 13 p1794 N90-20295
Radiometric tests on wet and dry antenna reflector surface panels
15 p2076 N90-21890
Temporal statistics of low-angle ground clutter
[AD-A220816] 17 p2391 N90-23621
Spectral characteristics of low-angle radar ground clutter
[AD-A220817] 17 p2392 N90-23622
Design and performance analysis of the DSS-13 beam waveguide antenna
20 p2853 N90-26225
Remote sensing of the ocean surface with C- and Ku-band airborne scatterometers
22 p3195 N90-28129

SUPERHYBRID MATERIALS
NT GRAPHITE-EPOXY COMPOSITES

SUPERIMPOSITION (MATHEMATICS)
U SUPERPOSITION (MATHEMATICS)

SUPERLATTICES
Methods to decrease defect density in GaAs/Si heteroepitaxy
[DE89-016306] 01 p0131 N90-10753
Intergranular and interphase boundaries in ceramics
[DE89-016969] 02 p0202 N90-11154
Adaptation of the theory of superconductivity to the behavior of oxides
[DE89-016518] 02 p0282 N90-11608
Strain and density dependent valence-band masses in InGaAs/GaAs and GaAs/GaAsP strained-layer structures
[DE89-016882] 02 p0285 N90-11627
Short period multilayers: Interface dominated structures
[DE89-017536] 03 p0319 N90-11812
Structural and electrical properties of thin films and superlattices composed of II-VI semiconductors
04 p0558 N90-13249
Electron transport in heterojunction superlattices
[AD-A212366] 04 p0560 N90-13265
Elastic softening in nanocrystalline silicon
[DE90-002268] 06 p0752 N90-14377
Magnetic and electrical properties
[DE90-002183] 06 p0856 N90-14977
Heteroepitaxy of GaAs on Si: Methods to decrease the defect density in the epilayer
[DE90-004028] 08 p1131 N90-16551
Fundamental issues in heteroepitaxy (condensed from the DOE panel report)
[DE90-003980] 08 p1132 N90-16555
Artificially structured superconductors
[DE90-004851] 08 p1134 N90-16567
Tailorable infrared sensing device with strain layer superlattice structure
[NASA-CASE-NPO-16617-2-CU]
09 p1227 N90-17118
Electronic properties of GaAs-(Al,Ga)As quasiperiodic
[AD-A214704] 09 p1289 N90-17472
Magnetoplasma oscillations of the wave-guided type in semiconductor superlattices
[DE90-607260] 10 p1431 N90-18258
Current status of InAsSb strained layer superlattice infrared detectors: Demonstration of a high detectivity, 10 micron photodiode
[DE90-000800] 10 p1434 N90-18276
Crystal growth and mechanical properties of semiconductor alloys
[AD-A216697] 11 p1570 N90-19035
Studies of the structure and properties of organic monolayers, multilayers and superlattices
[DE90-008330] 13 p1765 N90-20129
CCST (Center for Compound Semiconductor Technology) research briefs
[DE90-007782] 13 p1895 N90-20874
Coupled magnetoplasmon-phonon modes at the surface of a semi-infinite semiconductor superlattice
[DE90-612904] 14 p2031 N90-21647
Microstructure of Au/Nb multilayers
[DE90-008722] 14 p2033 N90-21662
Superconducting and semiconducting thin films of La(sub 123) and Y(sub 123) and their superlattices
[DE90-009565] 15 p2173 N90-22416
Acoustoelectronic interaction of surface waves in GaAs-InGaAs superlattices
16 p2310 N90-23163
ONR Far East Scientific Information Bulletin, Volume 13, No. 4
[ONRFE-SCI-INFO-BULL-13(4)88]
16 p2311 N90-23168
Research and applications of metallic superlattices, high T(sub c) superconductors, x ray optics, and compact synchrotrons
16 p2311 N90-23170
Electronic theory of solids, surfaces, interfaces, and clusters
16 p2320 N90-23230
HREM defects in GaAs/Ga(1-x)In(x)As strained layer superlattices
[DE90-010610] 18 p2620 N90-24924
Microscopic theory of non-linear phenomena in semiconductor superlattices
[AD-A221106] 18 p2622 N90-24941
Chlorine reactive-ion-beam etching of InSb and InAs0.15Sb0.85/InSb strained-layer-superlattices
[DE90-010848] 18 p2625 N90-24958
Superconductivity in nonsymmetric epitaxial YBa2Cu3O(sub 7-delta)-PrBa2Cu3O(sub 7-delta) superlattices grown by pulsed laser ablation
[DE90-011637] 19 p2761 N90-25687
Investigation on the MBE growth and properties of AlGaInAs/InP and InGaAs-InAlAs superlattices
[DE90-012248] 21 p3080 N90-27515
The column-by-column compositional mapping at semiconductor interfaces using Z-contrast STEM
[DE90-012594] 21 p3081 N90-27516
An EPR methodology for measuring the London penetration depth for the ceramic superconductors
22 p3143 N90-27828
The III-V semiconductor quantum well lasers and related optoelectronic devices on silicon
[AD-A224120] 23 p3331 N90-28835
Radiation effects in InAsSb strained-layer superlattice photodiodes induced by dose-rate and transient x ray environments
[DE90-015000] 23 p3400 N90-29208
Dynamical properties of two-dimensional Josephson junction arrays
[AD-A223965] 23 p3402 N90-29221
New real space correlated-basis-functions approach for the electron correlations of the semiconductor inversion layer
[DE90-627315] 24 p3551 N90-30090
Effect of retardation on the reflectance properties of the metallic Fibonacci quasi-superlattice
[DE90-627316] 24 p3551 N90-30091
.The II-VI semiconductor superlattices
[AD-A223748] 24 p3553 N90-30101

SUPERNOVA REMNANTS
IRAS observations of the extended galactic objects Cas A and W80
02 p0290 N90-11657

Nonequilibrium ionization in supernova remnants: The case of Tycho
[MPE-PREPRINT-153] 04 p0565 N90-13295
Detectable gravitational waves by supernova SN 1987 A pulsar relic
[PREPRINT-658] 05 p0714 N90-14174
A study of the infrared emission of galactic supernova remnants 06 p0861 N90-15006
Pulsars lost and found: The second Princeton-Arecibo millisecond pulsar search 07 p1013 N90-15865
Turbulent stripping of interstellar clouds by interaction with supernova remnants
[DE90-003622] 08 p1152 N90-16674
Radio continuum maps at 22 GHz of the H II regions RCW57 and W49
[INPE-4767-TDL/353] 10 p1446 N90-18343
Strange-quark-matter stars
[DE90-006102] 10 p1446 N90-18347
Infrared spectroscopy and imaging of supernova remnants 11 p1580 N90-19104
Near infrared spectroscopy of the supernova remnant RCW103 11 p1581 N90-19109
The evolution of the supernova remnant IC 443 15 p2186 N90-22486
Radio pulsar timing observations for GRO 16 p2334 N90-23301
What can gamma rays tell us about binary x ray sources and SNR's 16 p2336 N90-23310
Gamma rays from pulsar wind shock acceleration 16 p2336 N90-23311
Ginga observations of SS 433 19 p2776 N90-25789
Exploration of jet physics with some applications to SS 433 19 p2777 N90-25794
On the problem of the supernova expansion law in the large Magellanic cloud 19 p2781 N90-25818
EXOSAT observation of the pulsar PSR 1509-58 19 p2782 N90-25829
Gamma ray evidence for cosmic ray sources 23 p3414 N90-29292

SUPERNOVA 1987A

Astrophysical and cosmological constraints to neutrino properties
[NASA-CR-185031] 01 p0140 N90-10809
The SN 1987A attitude control system 05 p0659 N90-13845
Project Supernova 1987 05 p0662 N90-13866
SN 1987: A telemetry decoding system 05 p0663 N90-13875
Correlation among gravitational wave and neutrino detectors data during SN1987A
[NOTA-INTERNA-932] 05 p0713 N90-14165
The instability and fragmentation of the envelope of supernova 1987A 06 p0862 N90-15011
Strange-quark-matter stars
[DE90-006102] 10 p1446 N90-18347
Infrared spectroscopy of supernova 1987A 11 p1583 N90-19124
Near infrared (1-4 micron) spectroscopy of SN1987A 11 p1584 N90-19133
Carbon monoxide in supernova 1987A 11 p1585 N90-19135
Does SN 1987A contain a rapidly vibrating neutron star
[CAL-371] 15 p2182 N90-22468
Origin of pulsed emission from the young supernova remnant SN 1987A
[CAL-377] 15 p2182 N90-22469
Modelling late-time atmospheres of supernovae 15 p2189 N90-22500
Contributions of the X Ray Astronomy Group of the Max-Planck-Institut fuer Extraterrestrische Physik
[MPE-PREPRINT-165] 17 p2482 N90-24196
Mir-Kvant-Hexe hard x ray light curve of SN 1987A 17 p2482 N90-24197
Fast pulsars, strange stars
[DE90-011631] 19 p2765 N90-25710
Upper limits on Co-57 abundance in SN1987A according to the Kvant data 19 p2769 N90-25735
Mir-Kvant-HEXE hard X ray light curve of SN 1987A 19 p2775 N90-25776
X ray observations of the LMC field by the TTM instrument onboard the Kvant module: November 1988 to June 1989 19 p2782 N90-25825

SUPERNOVAE

NT SUPERNOVA 1987A
Research program in theoretical high energy physics
[DE89-013963] 01 p0121 N90-10695
The interaction of supernovae and pulsars with the circumstellar environment 02 p0293 N90-11671
Expected supernovae rates and gravitational waves detection
[NOTA-INTERNA-933] 05 p0713 N90-14166
Detectable gravitational waves by supernova SN 1987 A pulsar relic
[PREPRINT-658] 05 p0714 N90-14174
Perturbation methods for the calculation of gravitational waves from slightly non-spherical spacetimes with applications to stellar core collapse 06 p0863 N90-15015
Supernovae, compact stars, and nuclear physics
[DE90-002682] 06 p0864 N90-15022
The disk-halo connection and the nature of the interstellar medium
[NASA-CR-186286] 07 p1012 N90-15860
Search for proton decay and supernova neutrino bursts with a lunar base neutron detector
[DE90-607644] 10 p1448 N90-18358
Theoretical and experimental high energy physics
[DE90-006168] 11 p1565 N90-19006
IR line emission from supernovae in molecular clouds 11 p1580 N90-19102
Detection of SN1986j in NGC891 at millimetre wavelengths 11 p1585 N90-19137
Neon novae, recurrent novae, and type I supernovae
[DE90-003188] 12 p1728 N90-19931
Interactions of massive stars with the interstellar medium: Bow shocks and superbubbles 15 p2186 N90-22485
Spectrum formation in active galactic nuclei and Type 2 supernovae 15 p2187 N90-22490
Current drive in a supernova 15 p2187 N90-22491
The association of supernovae with regions of recent star formation in late-type galaxies 15 p2188 N90-22497
The dynamic instability of adiabatic blastwaves
[NASA-CR-182498] 17 p2401 N90-23679
A site for the astrophysical gamma ray process
[DE90-013473] 20 p2950 N90-26787
Survival of carbon grains in shocks 21 p3090 N90-27567
Nature and origin of interstellar diamond from the Allende CV3 meteorite 21 p3092 N90-27581
The shock process and light element production in supernovae envelopes
[NASA-CR-182854] 22 p3262 N90-28471
A historical supernova's lower limit to the galactic stellar-collapse rate
[FERMILAB-PUB-90/24-A] 22 p3262 N90-28472
Prospects for nuclear astrophysics with intense radioactive ion beams
[DE90-015616] 24 p3544 N90-30044

SUPERPLASTICITY

Application of superplastically formed and diffusion bonded aluminum to a laminar flow control leading edge
[NASA-CR-178316] 01 p0007 N90-10030
Deformation of Ti-6Al-4V bar and extrusion under superplastic forming conditions
[RAE-TM-MAT/STR-1110] 03 p0330 N90-11875
Deformation of extruded titanium alloys under superplastic conditions
[RAE-TM-MAT/STR-1111] 03 p0330 N90-11876
Deformation of electron beam welded Ti-6Al-4V alloy sheet under superplastic conditions
[RAE-TM-MAT/STR-1109] 03 p0359 N90-12053
Effect of superplastic deformation on the surface roughness of sheet
[RAE-TM-MAT/STR-1112] 03 p0359 N90-12054
Superplastic forming and diffusion bonding of rapidly solidified, dispersion strengthened aluminum alloys for elevated temperature structural applications
[NASA-CR-181849] 04 p0474 N90-12718
An approach to low temperature high strain rate superplasticity in aluminum alloy 2090
[AD-A212271] 04 p0476 N90-12731
Superplasticity
[AGARD-LS-168] 06 p0743 N90-14325
Superplasticity: An overview 06 p0743 N90-14326
Superplastic sheet forming 06 p0743 N90-14327
Advances and future directions in superplastic materials 06 p0744 N90-14328
Cavitation and superplasticity 06 p0744 N90-14329
Diffusion bonding of metals 06 p0744 N90-14330
The mechanical properties of superplastically formed titanium and aluminium alloys 06 p0744 N90-14331
Designing for superplastic alloys 06 p0744 N90-14332
The manufacture of superplastic alloys 06 p0745 N90-14333
Aluminum lithium alloys for Navy aircraft 07 p0898 N90-15193
Superplastic performance and properties of the Lital Alloys 07 p0899 N90-15199
Cryogenic mechanical properties of low density superplastic Al-Mg-Sc alloys
[DE90-002120] 07 p0904 N90-15222
Bearing tests in Ti-6Al-4V plates made using superplastic forming
[INFORME-I-357/89] 10 p1396 N90-18068
Processing and elevated temperature ductility of aluminum alloy 7475
[AD-A216840] 11 p1486 N90-18554
Optimizing superplastic response in navalite, a lithium containing aluminum-magnesium alloy
[AD-A216552] 12 p1626 N90-19346
High-temperature deformation of mechanically-alloyed aluminum IN90211 16 p2216 N90-22645
Elevated temperature crack growth in aluminum alloys: Tensile deformation of 2618 and FVS0812 aluminum alloys 16 p2218 N90-22654
Design of cryogenic tanks for launch vehicles 16 p2220 N90-22662
Ultrahigh carbon steels and their laminates
[AD-A218780] 17 p2376 N90-23530
Processing and properties of advanced aluminum alloys
[AD-A221292] 18 p2526 N90-24416
Behavior of Al-Mg alloys in hot working and superplasticity
[DE90-015193] 23 p3310 N90-28723
Processability and high temperature behavior of emerging aerospace alloys
[AD-A224285] 24 p3448 N90-29475
The roles of strain and reheating interval in continuous recrystallization during the thermomechanical processing by warm rolling of an Al-Mg alloy
[AD-A223673] 24 p3449 N90-29479

SUPERPOSITION (MATHEMATICS)

Aerodynamic superposition principle in vibrating turbine cascades 11 p1460 N90-18410

SUPERSATURATION

Supersaturation, droplet spectra, and turbulent mixing in clouds 22 p3217 N90-28249
Mechanism of habit change for atmospheric ice crystal growth 24 p3489 N90-29717
Rates of vertical mixing, gas exchange, and new productions: Estimates from seasonal gas cycles in the upper ocean near Bermuda
[PB90-244781] 24 p3496 N90-29758

SUPERSONIC AIRCRAFT

NT B-58 AIRCRAFT
NT B-70 AIRCRAFT
NT CONCORDE AIRCRAFT
NT F-4 AIRCRAFT
NT F-8 AIRCRAFT
NT F-14 AIRCRAFT
NT F-15 AIRCRAFT
NT F-16 AIRCRAFT
NT F-17 AIRCRAFT
NT F-104 AIRCRAFT
NT F-111 AIRCRAFT
NT SUPERSONIC COMMERCIAL AIR TRANSPORT
NT SUPERSONIC TRANSPORTS
NT X-15 AIRCRAFT
A supersonic through-flow fan engine airframe integration study
[NASA-CR-185140] 01 p0001 N90-10004
Determination of the minimum energy conformation of alkyl substituted pyrazines
[AD-A216974] 11 p1484 N90-18539
Passive venting technique for shallow cavities
[NASA-CASE-LAR-14031-1] 13 p1755 N90-20079
Preliminary design of a supersonic Short Takeoff and Vertical Landing (STOVL) fighter aircraft
[NASA-CR-186670] 17 p2352 N90-23394
Convex models of malfunction diagnosis in high performance aircraft
[AD-A218514] 19 p2649 N90-25073
Prevalence of G-induced cervical injury in US Air Force pilots 19 p2717 N90-25460
Interactive calculation procedures for mixed compression inlets
[NASA-CR-186581] 20 p2801 N90-25934
High-speed civil transport study: Special factors
[NASA-CR-181881] 23 p3276 N90-28537

SUPERSONIC BOUNDARY LAYERS

Stability of a supersonic boundary layer along a swept leading edge 01 p0063 N90-10359
Supersonic laminar-flow control 04 p0446 N90-12554
Supersonic boundary-layer transition on the LaRC F-106 and the DFRF F-15 aircraft. Part 1: Transition measurements and stability analysis 04 p0447 N90-12558
Supersonic boundary-layer transition on the LaRC F-106 and the DFRF F-15 aircraft. Part 2: Aerodynamic predictions 04 p0447 N90-12559
Numerical study of three-dimensional spatial instability of a supersonic flat plate boundary layer
[NASA-CR-181931] 04 p0499 N90-12874
Effect of suction and cooling on the stability of subsonic and supersonic boundary layers 05 p0642 N90-13745
Stability of a supersonic boundary layer on a sharp cone at a small angle of attack 06 p0775 N90-14510

The structure of supersonic turbulent boundary layers subjected to concave surface curvature
08 p1017 N90-15883
Physical models for supersonic turbulent boundary layer structure
[AD-A215284] 09 p1160 N90-16716
Flow visualization in supersonic turbulent boundary layers 16 p2195 N90-22533

SUPERSONIC COMBUSTION
Computation of ramjet internal flowfields
[AD-A212001] 03 p0307 N90-11743
The next generation supersonic transport engine: Critical issues
[PNR90576] 04 p0455 N90-12605
Numerical solutions of the complete Navier-Stokes equations
[NASA-CR-186102] 05 p0642 N90-13747
Numerical modeling of supersonic turbulent reacting free shear layers 06 p0719 N90-14197
Investigation into the feasibility of using solid fuel ramjets for high supersonic/low hypersonic tactical missiles
[AD-A214737] 09 p1168 N90-16761
Hypersonic nozzle/afterbody performance at low Mach numbers
[AD-A216223] 10 p1309 N90-17575
Supersonic combustor modeling
20 p2810 N90-25992
Supersonic reacting internal flow fields
[NASA-TM-103480] 20 p2829 N90-26094
Ramjet and ramrocket propulsion systems for missiles
21 p2973 N90-26897
Flame extinction in compressible flow
21 p2973 N90-26899
Raman scattering measurements using UV excimer lasers 21 p2974 N90-26902
Concentration, temperature, and density in a hydrogen-air flame by excimer-induced Raman scattering 21 p2974 N90-26903
Turbulent reacting flows and supersonic combustion
[AD-A221793] 21 p2979 N90-26933
The 26th JANNAF Combustion Meeting, volume 1
[CPIA-PUBL-529-VOL-1] 22 p3161 N90-27927
Photo-sensitized ignition of hydrogen/oxygen mixtures for hypersonic flight vehicles 22 p3163 N90-27935

SUPERSONIC COMBUSTION RAMJET ENGINES
Cycle analysis of scramjet engines
[NAL-TR-1002] 01 p0008 N90-10035
Effects of low-frequency instabilities on the operation of Ramjet air inlets 01 p0036 N90-10198
Computation of ramjet internal flowfields
[AD-A212001] 03 p0307 N90-11743
Numerical modeling of supersonic turbulent reacting free shear layers 06 p0719 N90-14197
RAMSCRAM: A flexible ramjet/scramjet engine simulation program
[NASA-TM-102451] 06 p0726 N90-14235
Spatially-resolved, nonintrusive measurements in a nonreacting scramjet combustor using laser-induced iodine fluorescence 07 p0881 N90-15103
Investigation into the feasibility of using solid fuel ramjets for high supersonic/low hypersonic tactical missiles
[AD-A214737] 09 p1168 N90-16761
Hypersonic nozzle/afterbody performance at low Mach numbers
[AD-A216223] 10 p1309 N90-17575
Development and fabrication of structural components for a scramjet engine
[NASA-CR-181945] 13 p1757 N90-20088
Performance of an aero-space plane propulsion nozzle 14 p1926 N90-21034
Transatmospheric vehicle research
[NASA-CR-186705] 20 p2807 N90-25970
Supersonic combustor modeling
20 p2810 N90-25992
Gas Turbine Combustion, volume 2
[VKI-LS-1990-02-VOL-2] 20 p2811 N90-25995
Supersonic reacting internal flow fields
[NASA-TM-103480] 20 p2829 N90-26094
Modeling of supersonic reacting flow fields
21 p2973 N90-26898
Flame extinction in compressible flow
21 p2973 N90-26899
Hydrocarbon-fueled scramjet combustor component development tests 22 p3182 N90-27934
Real time guidance and propulsion control for single-stage-to-orbit airbreathing vehicles
23 p3285 N90-28587
Numerical simulation supersonic free shear layers
[AD-A223771] 24 p3418 N90-29306
A comparison of scramjet engine performances of various cycles
[NAL-TR-1042] 24 p3434 N90-29397
Analysis of scramjet engine characteristics
[NAL-TR-1041] 24 p3434 N90-29398
AFOSR/ONR Contractors' Meeting on Combustion Rocket Propulsion Diagnostics of Reacting Flow
[AD-A224411] 24 p3441 N90-29432

SUPERSONIC COMMERCIAL AIR TRANSPORT
The next generation supersonic transport engine: Critical issues
[PNR90576] 04 p0455 N90-12605

SUPERSONIC COMPRESSORS
A method for the prediction of supersonic compressor blade performance
[CUED/A-TURBO/TR-126] 10 p1321 N90-17634

SUPERSONIC CRUISE AIRCRAFT RESEARCH
A supersonic through-flow fan engine airframe integration study
[NASA-CR-185140] 01 p0001 N90-10004
Study of high-speed civil transports
[NASA-CR-4235] 05 p0578 N90-13370

SUPERSONIC DIFFUSERS
Experimental investigation of a chemical laser cavity flowfield
[AD-A216398] 10 p1390 N90-18038

SUPERSONIC DRAG
CFD methods for drag prediction and analysis currently in use in UK
[RAE-TM-AERO-2146] 04 p0448 N90-12563
Influence of friction and separation phenomena on the dynamic blade loading of transonic turbine cascades
[MITT-88-04] 12 p1605 N90-19235
Projectile supersonic drag characteristics
[AD-A224217] 23 p3270 N90-28506

SUPERSONIC FLIGHT
RAMSCRAM: A flexible ramjet/scramjet engine simulation program
[NASA-TM-102451] 06 p0726 N90-14235
Noise and sonic boom impact technology. Sonic boom damage to conventional structures
[AD-A213594] 09 p1237 N90-17178
External flow computations for a finned 60mm ramjet in steady supersonic flight
[AD-A216998] 12 p1605 N90-19233
An aerodynamic tradeoff study of the scissor wing configuration
[NASA-CR-186576] 14 p1913 N90-20965
Thermal structures: Four decades of progress
[NASA-CR-186698] 22 p3191 N90-28105

SUPERSONIC FLOW
Supersonic flow computations over aerospace configurations using an Euler marching solver
[NASA-CR-4085] 01 p0003 N90-10012
New test techniques to evaluate near field effects for supersonic store carriage and separation
01 p0013 N90-10062
A parallel numerical simulation for supersonic flows using zonal overlapped grids and local time steps for common and distributed memory multiprocessors
[DE89-015252] 02 p0147 N90-10839
Additions and corrections to SUPER: A program for calculating steady and oscillatory supersonic flow over a thin wing, tail plane and fin
[AD-A211771] 04 p0438 N90-12501
The effects of wall surface defects on boundary-layer transition in quiet and noisy supersonic flow
04 p0448 N90-12556
Basic research on methods of calculating supersonic and hypersonic flow
[ONERA-RSF-19/1123-AY-234A]
04 p0448 N90-12565
Upwind discretization of the steady Navier-Stokes equations
[CWI-NM-R8810] 04 p0502 N90-12891
Multigrid solution method for the Euler equations
[PB89-219463] 04 p0539 N90-13116
Hot and cold wire applications in supersonic flows: Introductory notes 05 p0574 N90-13343
Laser applications in supersonic unsteady flow
05 p0574 N90-13344
Computation of Navier-Stokes equations for three-dimensional flow separation
[NASA-TM-102266] 05 p0575 N90-13353
Application of a two-dimensional unsteady viscous analysis code to a supersonic throughflow fan stage
[NASA-TM-4141] 05 p0581 N90-13387
Generation of iodine monofluoride in a supersonic multipurpose flowtube facility
[AD-A213082] 05 p0647 N90-13774
A computational analysis of the transonic flow field of two-dimensional minimum length nozzles
06 p0718 N90-14194
Supercritical fluid chromatography/supersonic jet spectroscopy
[DE90-001378] 06 p0740 N90-14308
An experimental investigation of shear layer mixing in supersonic flows 06 p0775 N90-14508
The supersonic anisotropic collapse of Langmuir waves 06 p0783 N90-14550
Explicit and implicit calculations of turbulent cavity flows with and without yaw angle
[NASA-CR-186293] 07 p0929 N90-15381
An algebraic turbulence model for flow separation caused by forward and backward facing steps
[AD-A213800] 07 p0931 N90-15389
A numerical and experimental investigation of multiple shock wave/turbulent boundary layer interactions in a rectangular duct 08 p1062 N90-16141
Calculation of two and three dimensional super and hypersonic flows by solving the Euler equations
08 p1070 N90-16197
Lecture notes on supersonic molecular beam sources
[MPIS-20/1988] 08 p1121 N90-16494
Development and application of oxygen flow tagging for velocity measurements and flow visualization in turbulent three-dimensional supersonic flows
[AD-A214491] 09 p1160 N90-16715
Physical models for supersonic turbulent boundary layer structure
[AD-A215284] 09 p1160 N90-16716
Measurement of the aerodynamical coefficients related to square section models defined by resemblance to the normalized models AGARD HB1 and HB2 in supersonic flow. Part 2: Incidence up to 25 deg
[ISL-R-108/88-PT-2] 09 p1161 N90-16718
New mixing-length model for numerical solution of turbulent supersonic flows 09 p1216 N90-17048
Skin friction measurements by laser interferometry in supersonic flows 10 p1306 N90-17557
Special Course on Three-Dimensional Supersonic/Hypersonic Flows Including Separation
[AGARD-R-764] 10 p1308 N90-17565
Opportunities for improved understanding of supersonic and hypersonic flows 10 p1308 N90-17566
Numerical simulation of supersonic free shear layers
[AD-A216289] 10 p1310 N90-17579
Development of an alternative concentration probe calibration method
[AD-A216245] 10 p1388 N90-18031
Experimental investigation of a chemical laser cavity flowfield
[AD-A216398] 10 p1390 N90-18038
The inviscid stability of supersonic flow past a sharp cone
[NASA-CR-181996] 11 p1451 N90-18363
Experiments on the unsteady flow in a supersonic compressor stage 11 p1462 N90-18422
Interaction between oblique-angled incident shock wave and turbulent boundary layer on a heated wall. Experimental results
[ONERA-RT-84/7078-AY] 11 p1509 N90-18688
Interaction of an oblique shock wave with supersonic flow over a blunt body 12 p1598 N90-19197
Numerical simulations of supersonic flow through oscillating cascade sections
[NASA-TM-103100] 13 p1750 N90-20051
Compression pylon
[NASA-CASE-LAR-13777-1] 13 p1755 N90-20078
A two-dimensional unsteady analysis for transonic and supersonic cascade flows 14 p1911 N90-20955
Exhaust nozzles for propulsion systems with emphasis on supersonic cruise aircraft
[NASA-RP-1235] 14 p1927 N90-21037
A quasi-Lagrangian moving grid technique for investigating compressible flows
14 p1972 N90-21298
Prediction of length scales in a Mach reflection flowfield 15 p2089 N90-21959
The effects of compressibility on a supersonic mixing layer
[AD-A219315] 16 p2197 N90-22543
Supersonic flow computations for an ASTOVL aircraft configuration, phase 2, part 2
[NASA-CR-4284] 16 p2234 N90-22746
STARS: An integrated general-purpose finite element structural, aeroelastic, and aeroservoelastic analysis computer program
[NASA-TM-101709] 17 p2416 N90-23768
A review of instability and noise propagation in supersonic flows
[NASA-CR-186800] 19 p2655 N90-25112
An experimental and theoretical investigation of the flow over plane delta wings with supersonic leading edges
[LR-588] 19 p2655 N90-25114
Optical techniques for determination of normal shock position in supersonic flows for aerospace applications
[NASA-TM-103201] 19 p2693 N90-25323
Supersonic reacting internal flow fields
[NASA-TM-103480] 20 p2829 N90-26094
UV and VUV spectroscopy and photochemistry of small molecules in a supersonic jet 20 p2947 N90-26771
Summary of Discussions at the Eleventh Meeting of the Sandia Cooperative Group on the Aerothermochemistry of Turbulent Combustion
[DE89-001846] 21 p2973 N90-26896

Modeling of supersonic reacting flow fields
21 p2973 N90-26898
Flame extinction in compressible flow
21 p2973 N90-26899
Development of Planar Laser-Induced Fluorescence (PLIF) techniques for supersonic flows
21 p2974 N90-26900
Turbulent reacting flows and supersonic combustion
[AD-A221793] 21 p2979 N90-26933
The dynamics and control of fluctuating pressure loads in the reattachment region of a supersonic free shear layer
[NASA-CR-184943] 22 p3108 N90-27652
Study of the compressibility effects on the turbulence of supersonic drags
[ETN-90-97448] 22 p3109 N90-27661
Experimental study on the vortices generated by the body of a missile during flight. Part 1: Laminar boundary layer
[ONERA-RT-40/1147-AY-130A-PT-1]
22 p3110 N90-27665
Progress and challenges in modeling turbulent aerodynamic flows
[NASA-TM-102811] 22 p3170 N90-27981
Supersonic/hypersonic aerodynamics and heat transfer for projectile design using viscous-inviscid interaction
[AD-A224354] 24 p3418 N90-29303
Numerical simulation supersonic free shear layers
[AD-A223771] 24 p3418 N90-29306
Thermal transfers in unsteady compressible inviscid flow
[ETN-90-97557] 24 p3419 N90-29311
Theoretical study of the interaction between an oblique shock wave and a turbulent boundary layer from a heated wall
[ONERA-RSF-87/7078/AY-100-A]
24 p3419 N90-29313

SUPERSONIC FLOW INLETS
U SUPERSONIC INLETS

SUPERSONIC INLETS
A method for the prediction of supersonic compressor blade performance
[CUED/A-TURBO/TR-126] 10 p1321 N90-17634
Comparison of 3-D viscous flow computations of Mach 5 inlet with experimental data
[NASA-TM-102518] 13 p1757 N90-20090
Numerical simulations of the structure of supersonic shear layers
[AD-A224164] 24 p3467 N90-29587

SUPERSONIC JET FLOW
Characterization of tetrahydrogen via state-selected excitation of H2
[AD-A216239] 10 p1355 N90-17855
Chemical reactions in turbulent mixing flows
[AD-A216273] 10 p1355 N90-17856
Tomographic investigations of weakly perturbed supersonic free jets
[MPIS-MITT-91] 12 p1600 N90-19209
A review of instability and noise propagation in supersonic flows
[NASA-CR-186600] 19 p2655 N90-25112
Evaluation of water cooled supersonic temperature and pressure probes for application to 2000 F flows
[NASA-TM-102612] 19 p2753 N90-25645

SUPERSONIC NOZZLES
Gas flows in rocket motors, volume 1
[AD-A213348] 05 p0615 N90-13591
Supersonic nozzle design of arbitrary cross-section
14 p1927 N90-21035
Exhaust nozzles for propulsion systems with emphasis on supersonic cruise aircraft
[NASA-RP-1235] 14 p1927 N90-21037
Supersonic wind tunnel nozzles: A selected, annotated bibliography to aid in the development of quiet wind tunnel technology
[NASA-CR-4294] 20 p2814 N90-26019

SUPERSONIC SPEED
High temperature VSCF (Variable Speed Constant Frequency) generator system
[AD-A210823] 01 p0061 N90-10351
A numerical and experimental investigation of multiple shock wave/turbulent boundary layer interactions in a rectanular duct 08 p1062 N90-16141
Supersonic aerodynamic characteristics of a proposed Assured Crew Return Capability (ACRC) lifting-body configuration
[NASA-TM-4136] 10 p1307 N90-17560
Axial flow in corners at supersonic and hypersonic speeds 10 p1308 N90-17570
Hypersonic nozzle/afterbody performance at low Mach numbers
[AD-A216223] 10 p1309 N90-17575
A study of flows over highly-swept wings designed for maneuver at supersonic speeds
[AD-A216837] 12 p1599 N90-19202
An intensive procedure for the design of pressure-specified three-dimensional configurations at subsonic and supersonic speeds by means of a higher-order panel method 14 p1917 N90-20982
High speed commercial transport fuels considerations and research needs
[NASA-TM-102535] 15 p2072 N90-21869
Nonaxisymmetric body, supersonic, inviscid dynamic derivative prediction
[AD-A220839] 17 p2346 N90-23358
High speed civil transport
[NASA-TM-186661] 17 p2353 N90-23396
Projectile supersonic drag characteristics
[AD-A224217] 23 p3270 N90-28506

SUPERSONIC TEST APPARATUS
Laser induced fluorescence: Practical applications
24 p3421 N90-29323

SUPERSONIC TRANSPORTS
NT CONCORDE AIRCRAFT
NT SUPERSONIC COMMERCIAL AIR TRANSPORT
Revolutionary opportunities for materials and structures study
[NASA-CR-179642] 01 p0034 N90-10184
Study of high-speed civil transports
[NASA-CR-4235] 05 p0578 N90-13370
Supersonic through-flow fan engine and aircraft mission performance
[NASA-TM-102304] 14 p1927 N90-21038
Application of laminar flow control to supersonic transport configurations
[NASA-CR-181917] 20 p2803 N90-25944
The aerodynamic design of the oblique flying wing supersonic transport
[NASA-CR-177552] 23 p3276 N90-28540
Measurements of the single event upset environment in the upper atmosphere
[RAE-TM-SPACE-373] 23 p3351 N90-28934

SUPERSONIC TURBINES
Revolutionary opportunities for materials and structures study
[NASA-CR-179642] 01 p0034 N90-10184
Aerodynamic and heat transfer measurements on blading for a high rim-speed transonic turbine
[RAE-TM-P-1151] 08 p1024 N90-15920
Influence of friction and separation phenomena on the dynamic blade loading of transonic turbine cascades
[MITT-88-04] 12 p1605 N90-19235
Supersonic through-flow fan engine and aircraft mission performance
[NASA-TM-102304] 14 p1927 N90-21038

SUPERSONIC WIND TUNNELS
Design and fabrication requirements for low noise supersonic/hypersonic wind tunnels
04 p0446 N90-12555
Volumetric analysis by spontaneous Raman diffusion in a supersonic wind tunnel
[ISL-R-109/88] 04 p0448 N90-12564
Comparison of 3-D viscous flow computations of Mach 5 inlet with experimental data
[NASA-TM-102518] 13 p1757 N90-20090
DURIP optical equipment for high-speed viscous-inviscid interaction research
[AD-A217772] 13 p1802 N90-20345
SIMOUN: An optimized supersonic high temperature wind tunnel for testing construction materials to be used on the spaceplane
[REPT-892-430-111] 16 p2203 N90-22572
Euler analysis comparison with LDV data for an advanced counter-rotation propfan at cruise
[NASA-TM-103249] 20 p2803 N90-25946
Supersonic wind tunnel nozzles: A selected, annotated bibliography to aid in the development of quiet wind tunnel technology
[NASA-CR-4294] 20 p2814 N90-26019

SUPERSONICS
Aerodynamic development perspective for traffic aeroplanes
[DGLR-89-141] 18 p2495 N90-24260
Integral-equation methods in steady and unsteady subsonic, transonic and supersonic aerodynamics for interdisciplinary design
[NASA-TM-102677] 19 p2655 N90-25110
Hydrocarbon-fueled scramjet combustor component development tests 22 p3162 N90-27934

SUPERSTRING THEORY
U STRING THEORY

SUPERSYMMETRY
N=1,2 supergravities in 2+1 dimensions as Chern-Simons theories
[DE89-612006] 01 p0134 N90-10771
Superfiled formulation of Chern-Simons supersymmetry
[DE89-618459] 02 p0286 N90-11636
Two dimensional conformal supergravity and critical behavior
[DE89-611968] 03 p0420 N90-12414
Strings, p-branes and Skyrmions in curved space
04 p0565 N90-13293
Supersymmetric dark matter above the W mass
[NASA-CR-186168] 06 p0863 N90-15016
Modular invariants for theta-functions with characteristics and the twisted N=2 superconformal and SU(2) Kac-Moody algebras
[DE89-635701] 07 p0982 N90-15671
Lefschetz trace formula and BRST
[DE89-635705] 07 p1007 N90-15835
Are gravitons windows to higher dimensions
[DE90-600756] 08 p1101 N90-16376
New spacetime superalgebras and their Kac-Moody extension
[DE90-606949] 10 p1422 N90-18201
Construction of second constant of motion for two dimensional classical super systems
[DE90-607046] 10 p1423 N90-18208
N=2 supergravity in superspace and the BRS symmetry
[DE90-607062] 10 p1439 N90-18305
BRS current and related anomalies in two-dimensional gravity and string theories
[DE90-733095] 10 p1440 N90-18307
Superconformal algebra on meromorphic vector fields with three poles on super-Riemann sphere
[DE90-610423] 12 p1706 N90-19796
Construction of four-dimensional open superstrings
[DE90-006484] 12 p1724 N90-19908
The N = 2 superconformal algebras on hyperelliptic surfaces and their Coulomb gas realization
[DE90-612790] 14 p2020 N90-21581
Local supersymmetry in non-relativistic systems
[DE90-612751] 14 p2034 N90-21670
Generalized killing equations and symmetries of spinning space
[NIKHEF-H/89-8] 15 p2165 N90-22375
Higher order equations of motion
[DE90-627522] 24 p3543 N90-30038

SUPPLYING
Aerospace vehicle design, spacecraft section. Volume 1: Project Groups 3-5
[NASA-CR-186053] 06 p0731 N90-14263
Aerospace vehicle design, spacecraft section. Volume 1: Project Groups 3-5
[NASA-CR-186054] 06 p0731 N90-14264

SUPPORT INTERFERENCE
Wind tunnel investigation of three sonic anemometers
[PB90-149808] 15 p2046 N90-21729
An experimental investigation of support strut interference on a three-percent fighter model at high angles of attack
[AD-A219793] 17 p2345 N90-23353
Subsonic sting interference on the aerodynamic characteristics of a family of slanted-base ogive-cylinders
[NASA-CR-4299] 18 p2492 N90-24242

SUPPORT SYSTEMS
NT CLOSED ECOLOGICAL SYSTEMS
NT EMERGENCY LIFE SUSTAINING SYSTEMS
NT GROUND OPERATIONAL SUPPORT SYSTEM
NT GROUND SUPPORT SYSTEMS
NT LIFE SUPPORT SYSTEMS
Space station RT and E utilization study
[NASA-CR-181707] 01 p0026 N90-10129
Wideband connectivity and support for Cronus cluster at USAF Electronic Systems Division
[AD-A210749] 02 p0212 N90-11215
Considerations for a design and operations knowledge support system for Space Station Freedom
[NASA-TM-102156] 02 p0256 N90-11451
Human factors aspects of decision support systems
06 p0757 N90-14408
The Tactical Environmental Support System (TESS(3))
06 p0757 N90-14409
Load-shortening behavior of an initially curved eccentrically loaded column
[NASA-TM-101643] 08 p1088 N90-16293
Advances in navigation support systems based on operational pilot's heuristics 09 p1164 N90-16737
Technology development, demonstration, and orbital support requirements for manned lunar and Mars missions
[NASA-TM-101666] 10 p1447 N90-18350
Using object-oriented analysis techniques to support system testing
[DE90-009540] 16 p2226 N90-22700
NASA Lewis icing research tunnel user manual
[NASA-TM-102319] 17 p2355 N90-23407
A decision support system for control and automation of dynamical processes
[AD-A219501] 17 p2454 N90-23995
Flight support system servicing aid tool
18 p2501 N90-24293
Explanation of Bayesian conditioning for decision support systems 18 p2633 N90-25002

GCS support/development system configuration document
[NASA-CR-182046] 19 p2743 N90-25589
Terrapin technologies manned Mars mission proposal
[NASA-CR-186838] 20 p2816 N90-26027
Earth Sciences Requirements for the Information Sciences Experiment System
[NASA-CP-3072] 21 p3015 N90-27140

SUPPORTS
NT PYLONS
Wind tunnel support system effects on a fighter aircraft model at Mach numbers from 0.6 to 2.0
[AD-A210614] 01 p0002 N90-10010
Design and performance of an optical mount using cross-flexure pivots
[DE89-017551] 04 p0508 N90-12929
Mechanical strain isolator mount
[NASA-CASE-LAR-13580-1] 08 p1084 N90-16272
Investigation of the effects of external supports on manual lifting
[PB90-103367] 09 p1260 N90-17307
Design of a high angle of attack robotic sting mount for tests in a low speed wind tunnel
[AD-A218105] 13 p1759 N90-20099
Tensile film clamps and mounting block for the rheovibron and autovibron viscoelastometer
[NASA-CASE-LAR-13696-1] 13 p1812 N90-20409
Vibration isolation versus vibration compensation on multiple payload platforms 14 p1933 N90-21066
Heat leak measurements in superconducting dipole magnet supports
[DE90-620109] 15 p2173 N90-22420
Progress in the design of a microgravity facility for in-orbit experiments 18 p2540 N90-24496
A global approach for using kinematic redundancy to minimize base reactions of manipulators
[NASA-CR-186825] 19 p2725 N90-25499
Load-point compliance for the arc bend-arc support fracture toughness specimen
[AD-A221618] 21 p3014 N90-27134
Rotationally actuated prosthetic helping hand
[NASA-CASE-MFS-28426-1] 21 p3036 N90-27261
Elastomeric mount for thrust bearing shoe
[AD-D014465] 22 p3181 N90-28054
Sting-support interference on afterbody drag at transonic speeds
[NAL-TM-EA-8902] 23 p3267 N90-28492

SUPPRESSORS
Experimental investigation to suppress flow-induced pressure oscillations in open cavities
[AD-A216285] 10 p1310 N90-17578
Characterization and development report for the SA3274-1 and SA3274-2 transient voltage suppressors
[DE90-005712] 11 p1502 N90-18649

SURFACE ACOUSTIC WAVE DEVICES
A SAW Slanted Array Correlator (SAC) with separate amplitude compensation channel
[AD-D014174] 03 p0336 N90-11914
Improving the quality of a spread-spectrum radiomobile link 06 p0761 N90-14426
SAW (Surface Acoustic Wave) transducer with improved bus-bar design
[AD-D014250] 08 p1060 N90-16125
Surface acoustic wave sensors and piezoelectric actuators for investigations of transitional and turbulent flows
[AD-A214889] 09 p1279 N90-17415
Surface acoustic wave filters in ZnO-SiO2-Si layered structures: Design, technology, and monolithic integration with electronic circuitry
[ETN-90-97218] 20 p2924 N90-26638
The application of SAW devices in expanded frequency spectrum communications
[AD-A222958] 21 p2994 N90-27021
Utilizations of an acoustic surface wave-convolver for signal processing in the measurement and information techniques
[ETN-90-97319] 22 p3165 N90-27947

SURFACE COOLING
Studies of gas turbine heat transfer airfoil surfaces and end-wall cooling effects
[AD-A212451] 04 p0457 N90-12620
Surface-cooling effects on compressible boundary-layer instability
[NASA-CR-182003] 14 p1971 N90-21290
Ablative cooling of aerodynamically heated radomes
[AD-D014426] 14 p1971 N90-21293
Experiments on liquid immersion natural convection cooling of leadless chip carriers mounted on ceramic substrate
[AD-A219893] 17 p2478 N90-24167

SURFACE CRACKS
Definition of research needs to address airport pavement distress in cold regions
[DOT/FAA/DS-89/13] 02 p0157 N90-10896
Three-dimensional analysis of surface crack-Hertzian stress field interaction
[NASA-CR-4254] 02 p0232 N90-11332
Biaxial flexing of a fiber-reinforced aluminum composite
[AD-A212742] 04 p0468 N90-12681
Crazing and degradation of flexure strength in acrylic plates as a function of time
[AD-A212835] 06 p0749 N90-14357
BAM: German Federal Institute for Materials Research and Testing, Berlin
[DE90-004293] 08 p1090 N90-16307
Failure analysis of a missile locking hook from the F-14 jet
[AD-A214995] 09 p1194 N90-16917
Internal failures in model elastomeric composites
[AD-A215923] 10 p1348 N90-17818
Plasma and ion fluorination for chemical hardening of synthetic rubbers
[AD-A216388] 10 p1360 N90-17885
Material instabilities in solids
[AD-A218451] 16 p2247 N90-22817
The effects of slip character and crack closure on the growth of small fatigue cracks in titanium-aluminium alloys
[AD-A220714] 17 p2377 N90-23534
Mechanics of necking, crazing, and crack growth in polymers 17 p2378 N90-23540
Fracture behavior of surface modified ceramics
[DE90-011552] 18 p2532 N90-24449
Applications of an acoustic-emission data-acquisition workstation: 2
[DE90-010941] 18 p2612 N90-24880
Fracture toughness of polyimide films
[NASA-TM-103473] 20 p2836 N90-26130
Fracture mechanics analysis for short cracks
[AD-A222170] 21 p3013 N90-27130
Metallurgical analysis of leaking tray packs
[AD-A223157] 22 p3157 N90-27899
Study of a method for measuring the dimensions of cracks on the surface of ceramics by Rayleigh waves
[ETCA-89-R-024] 22 p3160 N90-27922
Characterization by ultrasonic tests of ceramics submitted to thermal shocks: Influence of several parameters on the crack dimensioning
[ETCA-89-R-060] 22 p3160 N90-27923
The ACR-program for automatic finite element model generation for part through cracks
[DE90-631545] 24 p3479 N90-29662

SURFACE DEFECTS
Structural problems of accurate inflatable surfaces 02 p0184 N90-11044
The effects of wall surface defects on boundary-layer transition in quiet and noisy supersonic flow 04 p0446 N90-12556
Surfaces and interfaces of ceramic materials
[AD-A212417] 05 p0627 N90-13657
Study of surface uniformity of semiconductors 3 to 5 by photoluminescence imagery
[ECL-88-15] 05 p0703 N90-14116
Structure-property relationships in surface-modified ceramics. NATO Advanced Science Institutes, series E: Applied Sciences, volume 170
[AD-A212939] 06 p0749 N90-14359
Scanning tunneling microscope studies of surface defects
[AD-A214121] 08 p1130 N90-16543
Crack detection in silicon nitride by acoustic microscopy
[AERE-R-13196] 16 p2245 N90-22803
Negative electron affinity for infrared detection
[AD-A218816] 17 p2395 N90-23639
Surface and interface studies by Auger electron spectroscopy
[ETN-90-96948] 18 p2522 N90-24398
Surface defects and chemistry on the SnO2(110) surface 18 p2559 N90-24603
Scratches and shot peening effects on the fatigue life of aluminum-lithium alloys
[NIAR-90-15] 19 p2674 N90-25208
Surface condition effect on the fatigue behavior of aluminum lithium alloys
[NIAR-90-13] 19 p2674 N90-25209
Theoretical studies of time-of-flight and atom and molecular surface collision
[AD-A221705] 21 p3075 N90-27480
New aspects in aircraft inspection using eddy current methods 22 p3187 N90-28085
A comparison of single-cycle versus multiple-cycle proof testing strategies
[NASA-CR-4318] 22 p3193 N90-28115
Surface and defect excitations in covalently bonded solids
[AD-A221995] 23 p3303 N90-28682
Light scattering from surface and sub-surface defects
[DE90-016311] 24 p3546 N90-30058

SURFACE DIFFUSION
Isotopic selectivity of surface diffusion: An activated diffusion model
[DE90-003473] 07 p0894 N90-15169
Investigation of applications of diamond film
[AD-A216104] 10 p1368 N90-17931
Studies of chemistry and diffusion on silicon and gallium arsenide surfaces using laser-induced thermal desorption
[AD-A220946] 18 p2547 N90-24539
In situ analysis of CO during chemisorption and oxidation on graphite: Supported Pt by FTIR-microspectrometry 18 p2559 N90-24605
Diffusion in the surface layer of the convective boundary layer
[AD-A224125] 23 p3349 N90-28924

SURFACE DISTORTION
Optical techniques for in-plane strain analysis in an industrial environment
[PNR90601] 04 p0512 N90-12957
Interferometric surface distortion detector
[AD-D014211] 06 p0842 N90-14901
Reflector surface distortion analysis techniques (thermal distortion analysis of antennas in space) 12 p1611 N90-19267
Curvature-dependent parametrization of curves and surfaces
[CS-8915] 16 p2299 N90-23100
Minimizing distortion and internal forces in truss structures by simulated annealing 18 p2644 N90-25055

SURFACE ENERGY
An investigation of satellite sounding products for the remote sensing of the surface energy balance and soil moisture
[NASA-CR-186073] 06 p0801 N90-14664
Measurements of energy dispersion at liquid-solid interfaces: Fluorescence quenching of pyrene bound to fumed silica
[AD-A222371] 21 p2978 N90-26926
Mechanism of habit change for atmospheric ice crystal growth 24 p3489 N90-29717

SURFACE FINISHING
Advances in the technology of titanium castings 01 p0043 N90-10243
Adhesion of encapsulating elastomer to polyolefin sleeve
[BDX-613-3985] 01 p0048 N90-10271
Formation and modification of surface alloys by excimer laser melting and resolidification
[DE89-016968] 03 p0327 N90-11856
Coating galvanized steel
[AD-A211775] 03 p0329 N90-11869
Design and fabrication requirements for low noise supersonic/hypersonic wind tunnels 04 p0446 N90-12555
Surface treatments of carbon fibers in an organic environment. Finite element analysis of pull-out tests
[ONERA-RT-7/3549-M] 04 p0471 N90-12698
The quality of vacuum deposited surface treatments
[CETIM-107040] 04 p0476 N90-12729
A feasibility study of hydrogen dosage estimation in screw threads submitted to surface electrolytic treatment
[CETIM-110110] 04 p0476 N90-12730
Lightweight composite reflector panels 05 p0596 N90-13462
Evaluation of copper slag blast media for railcar maintenance
[NASA-CR-183744] 05 p0630 N90-13681
GaAs and GaAs:In: Influence of surface treatments and characterization of homogeneity by photoluminescent imagery
[ECL-88-24] 05 p0704 N90-14118
Influence of hole surface finish, cyclic frequency and spectrum severity on the fatigue behavior of thick section aluminum alloy pin joints
[ARL-STRUC-R-430] 06 p0745 N90-14336
The influence of the substrate surface on the nucleation and growth of superconducting thin films
[DE90-003649] 06 p0857 N90-14983
Guide to the selection of surface treatments for the improvement of fatigue strength of steels
[ESDU-89031] 07 p0907 N90-15245
Characterization and in situ testing of diamond films
[DE90-003155] 07 p0911 N90-15265
Physical chemical characterization of the surface of carbon fibers: Test report
[REPT-49-740/F] 09 p1188 N90-16881
Microporous structure with layered interstitial surface treatment, and method and apparatus for preparation thereof
[NASA-CASE-MSC-21487-1] 09 p1189 N90-16887
Failure analysis of a missile locking hook from the F-14 jet
[AD-A214995] 09 p1194 N90-16917

Compound for metallic surface treatment
[DE90-004121] 09 p1196 N90-16927
Advanced tribological coatings for high specific strength alloys
[AD-A214061] 09 p1196 N90-16930
An Auger electron spectroscopy study of surface-preparation contaminants
[NASA-TP-2972] 09 p1203 N90-16968
Full surface interferometric testing of grazing incidence mirrors
[AD-A213590] 09 p1281 N90-17425
Flatness and roughness metrological tests on the WRA flight unit receiver box and ACPB canister of the RETE experiment
[IFSI-88-20] 10 p1368 N90-17928
Composite for smoothing the surface of ceramic substrates
[DE90-004005] 11 p1488 N90-18565
Crystal preparation at LBL, 1976 to 1986
[DE90-007754] 13 p1894 N90-20871
Institute for Materials Science and Engineering, nondestructive evaluation: Technical activities
[PB90-132739] 15 p2108 N90-22055
Machining of new materials at Aerospatiale
[REPT-892-430-104] 16 p2213 N90-22622
High resistance bolts: Test trials for plated bolts
[CRIF-MT-178] 17 p2413 N90-23748
Ultra precision machining
[AD-A222422] 21 p2991 N90-27003
Influence of a surface finishing on the fatigue behavior of a 32CDV13 steel
[ETCA-89-R-164] 22 p3157 N90-27902
Surface reactions of the TA6V titanium alloy under laser irradiation
[ETCA-90-R-012] 22 p3158 N90-27904
Electrochemical surface finishing using amino-substrates on carbon fibers in organic media. Effects of the finishing on the mechanical properties of carbon-epoxy composites
[ONERA-RT-9/3549-M] 23 p3301 N90-28672
Fretting fatigue strength of Ti-6Al-4V at room and elevated temperatures and ways of improving it
23 p3308 N90-28709

SURFACE INTERACTIONS
U SURFACE REACTIONS

SURFACE LAYERS
NT MONOMOLECULAR FILMS
Attenuated total reflection FTIR spectroscopy for measuring interfacial reaction kinetics at silica surfaces
[AD-A210314] 01 p0041 N90-10224
Thin-film integrated injection logic
[AD-D014190] 04 p0497 N90-12860
Flux parameterization techniques in the atmospheric surface layer 07 p0959 N90-15548
Specification for evaporation duct height calculations
[AD-A213841] 07 p0964 N90-15570
Modifications of comet materials by the sublimation process: Results from simulation experiments
08 p1142 N90-16621
Morphology and compositional differentiation of the surface of comets 08 p1143 N90-16624
Radiation modification of cometary materials: Laboratory simulations 08 p1143 N90-16626
Internal failures in model elastomeric composites
[AD-A215923] 10 p1348 N90-17818
Pulsed laser deposition of high T(sub c) superconducting thin films
[AD-A216507] 11 p1569 N90-19034
Preparation and characterization of alumina films prepared by a novel spray pyrolysis method
[AD-A217570] 12 p1625 N90-19339
Radiation-induced density changes and creep in surface layers of glass
[DE90-008112] 12 p1633 N90-19383
A method of estimating temperature profiles and chemical differentiation in the near surface layers of porous comet nuclei: First results for comet P/Churyumov-Gerasimenko 12 p1742 N90-20013
A numerical study of basic coastal upwelling processes 16 p2259 N90-22878
A study of the surface layers at an air-water interface
[AD-A219378] 16 p2260 N90-22882
Microstructure of thin films
[AD-A219262] 16 p2324 N90-23255
Picosecond laser pulse interactions with metallic and semiconducting surfaces
[AD-A219680] 17 p2408 N90-23723
On the G1 smooth connection between triangular Bernstein-Bezier patches. Part 1: Around and N-patch corner
[TELECOM-PARIS-89-D-012] 18 p2575 N90-24671
On the G1 smooth connection between triangular Bernstein-Bezier patches. Part 2: In a piecewise representation
[TELECOM-PARIS-89-D-013] 18 p2575 N90-24672
A nonlocal free energy density functional approximation for the electrical double layer
[AD-A220664] 18 p2607 N90-24848
Surface reconstruction based on critical contours in a multi-image context
[RR-784-I-IMAG-94-LIFIA] 20 p2880 N90-26383
Exact results for the structured liquid-solid interface
[AD-A222762] 20 p2922 N90-26630
Structure and dynamics of water at the Pt (111) interface: Molecular dynamics study
[AD-A222628] 20 p2933 N90-26687
Interfacial viscosity measurements of adsorbed monolayers on metal surfaces
[AD-A221689] 21 p2979 N90-26931
Boundary layer parameterization for use in a limited area forecast model 21 p3029 N90-27224
Coupled strip line circuit
[AD-D014487] 22 p3166 N90-27956
Calculation of surface free three dimensional flows
[ONERA-RSF-5/4368-AY-002A] 22 p3176 N90-28022
High temperature oxidation of Al-Li alloys
23 p3307 N90-28705

SURFACE NAVIGATION
Federal Radionavigation Plan, 1988
[PB89-163075] 02 p0148 N90-10846
Effects of the advanced map interpretation and terrain analysis course on contour-level navigation performance
[AD-A212163] 03 p0304 N90-11723
Distance and clearance perception using forward-looking, vehicular television systems
[DE89-014740] 03 p0405 N90-12319
Problem-dependent transformations of 3D terrain elevation maps into cost precursor maps
[PB89-218127] 04 p0514 N90-12969
Spatial data structures for robotic vehicle route planning
[AD-A212806] 04 p0538 N90-13111
Autonomous land navigation in a structured environment
[DE90-001625] 07 p0878 N90-15087
Planning minimum-energy paths in an off-road environment with anisotropic traversal costs and motion constraints
[AD-A214181] 07 p0942 N90-15457
A computer simulation study of a sensor-based heuristic navigation for three-dimensional rough terrain with obstacles
[AD-A215115] 10 p1318 N90-17622
Carin and GPS: The combination of dead reckoning, map matching and satellite navigation in a hybrid automobile navigation system
[ETN-90-95451] 12 p1602 N90-19220
M1A2 adjunct analysis (POSNOV volume)
[AD-A218802] 16 p2199 N90-22553
Back to the stars 17 p2359 N90-23429
Maritime safety information in the year 2000: Listen up, Navy, the times they are a changin'
[AD-A220563] 17 p2390 N90-23611
Planning for execution monitoring on a planetary rover
19 p2735 N90-25548
Investigations of monopulse-assisted radio location systems for the safety of surface traffic
[ETN-90-97324] 21 p2956 N90-26806
Rice-obot 1: An intelligent autonomous mobile robot
23 p3375 N90-29068
A tesselated probabilistic representation for spatial robot perception and navigation 23 p3376 N90-29075
Combining LORAN and GPS: The best of both worlds
24 p3424 N90-29343
An Ada-based marine radar simulator for collision avoidance training
[ETN-90-97611] 24 p3531 N90-29970

SURFACE NOISE INTERACTIONS
Boundary layer turbulence pulsed by acoustic waves
[ETN-90-96621] 16 p2236 N90-22759
The validation and application of a rotor acoustic prediction computer program
[NASA-TM-101794] 21 p3072 N90-27465

SURFACE PRESSURE
U PRESSURE

SURFACE PROPERTIES
NT ADHESION
NT COEFFICIENT OF FRICTION
NT INTERFACIAL TENSION
NT SKIN TEMPERATURE (NON-BIOLOGICAL)
NT SPECTRAL REFLECTANCE
NT SURFACE CRACKS
NT SURFACE DEFECTS
NT SURFACE ENERGY
NT SURFACE ROUGHNESS
NT SURFACE STABILITY
NT SURFACE TEMPERATURE
NT WALL TEMPERATURE
Analysis of surface modified colloidal silicas
[DE89-015849] 01 p0047 N90-10267
Synthesis and physical properties of poly(perfluoroalkylether) urethanes
[AD-A210500] 01 p0050 N90-10287
Epitaxial GaAs on SOI wafers
[AD-A209009] 01 p0127 N90-10729
Reactive ion etching of SiC thin films by mixtures of fluorinated gases and oxygen
[AD-A211046] 02 p0195 N90-11113
A study of the tribological and surface micromechanical properties of YBa2Cu3O7-x
[DE89-015680] 02 p0281 N90-11607
Formation and modification of surface alloys by excimer laser melting and resolidification
[DE89-016968] 03 p0327 N90-11856
Spectral-domain analysis of finite frequency selective surfaces
[AD-A211669] 03 p0339 N90-11932
RF performance of polycrystalline high-T(sub c) superconductors
[DE89-017671] 03 p0411 N90-12359
Surface, interface, and bulk properties of high T(sub c) superconductors
[AD-A211490] 03 p0413 N90-12373
Venus surface properties deduced from radar and radiometry 03 p0423 N90-12431
Characterization of self-lubricating surface materials
[CETIM-108060] 04 p0479 N90-12749
Seminars of Applied Physics, Materials Physics and Biomedical Engineering, 1989
[PB89-218572] 04 p0548 N90-13192
Workshop on Recent Progress in Surface and Volume Scattering
[AD-A212455] 04 p0555 N90-13236
Coherent phasing of segmented mirrors
05 p0598 N90-13474
Characterization of surfaces cut with a laser beam and thermal model of the process
[ISAL-89-0008] 05 p0648 N90-13780
Senegalese land surface change analysis and biophysical parameter estimation using NOAA AVHRR spectral data
[NASA-CR-186120] 05 p0664 N90-13883
Study of surface uniformity of semiconductors 3 to 5 by photoluminescence imagery
[ECL-88-15] 05 p0703 N90-14116
Non-linear optical studies of adsorbates: Spectroscopy and dynamics
[DE90-001543] 06 p0741 N90-14312
Superplasticity: An overview 06 p0743 N90-14326
Solid State Division
[DE90-000979] 06 p0851 N90-14945
Surface magneto-optical studies of ultrathin ferromagnetic films
[DE90-002199] 06 p0856 N90-14980
A numerical model for the axisymmetric equilibrium shape of drops in uniform motion: Effects of external flow, electric field and surface charge
07 p0874 N90-15071
Correlations between surface structure and catalytic activity/selectivity
[DE90-003755] 07 p0896 N90-15181
Studies of the adsorption/desorption behavior of explosive-like molecules
[DE90-001867] 07 p0913 N90-15283
A coning motion apparatus for hydrodynamic model testing in a non-planar cross-flow
[AD-A213431] 07 p0930 N90-15383
Laser-induced surface ablation and optical damage of ZnS crystals caused by single- and multiple-pulse laser-irradiation
[DE90-003807] 07 p0936 N90-15419
Fractal dimension of the fractured surface of materials
[DE89-635764] 07 p0946 N90-15477
Resultant forces and moments in completely restrained plates subjected to a recovery temperature varying linearly with time
[ESDU-89024] 07 p0947 N90-15480
Orientation of rf-sputter-deposited MoS2 films
[ATR-89(4752)-1] 07 p1000 N90-15784
Selectivity of the reactions of oxygenates on transition metal surfaces
[DE90-003911] 08 p1045 N90-16040
Theoretical studies of chemisorption and surface reactions on nickel and silicon
[DE90-004849] 08 p1047 N90-16050
Structure-property relationships in ion-beam surface-modified ceramics: Theory and applications
[AD-A212785] 08 p1047 N90-16054
Diblock copolymers at surfaces
[DE90-005406] 08 p1051 N90-16079
The influence of residual contamination on the structure and properties of metal/GaAs interfaces
[DE90-000549] 08 p1127 N90-16530
Theory of the dissociation dynamics of small molecules on metal surfaces: Finite temperature studies
[DE90-005217] 09 p1195 N90-16923

Basic studies on separative glass
[DE90-702436] 09 p1196 N90-16928
Arcjet cathode phenomena 11 p1473 N90-18477
Structure and reactivity of model thin film catalysts
[DE90-007365] 11 p1485 N90-18546
Characterization of biopolymer surfaces using scanning microscopies
[AD-A216572] 11 p1490 N90-18572
The joint effect of surface microtopography and near-surface structure on microcontact conditions
[DE90-006494] 11 p1493 N90-18591
Multicomponent glass surfaces structure and adsorption
[DE90-007179] 11 p1493 N90-18596
Evaluating a glass surface produced by ductile grinding
[DE90-006782] 11 p1496 N90-18608
Coherent radar measurement of ocean currents from geostationary orbit 12 p1609 N90-19259
International conference on Surface Modification of Metals by Ion Beams
[AD-A215872] 12 p1626 N90-19345
Modification of surface mechanical properties of high-chromium tool steel by carbon-implanted codeposited Fe-Ti films
[DE90-007502] 12 p1628 N90-19358
Light-scattering measurements of CVD (Chemical Vapor Deposition) silicon carbide
[DE90-007885] 12 p1632 N90-19382
Single antenna interferometry
[DE90-008120] 12 p1648 N90-19474
Three-dimensional Fe analysis of the surface distribution in notched compact samples of 20 MnMoNi 55
[W-1/89] 12 p1676 N90-19625
Passivating layer for III-V semiconductor materials
[AD-D014321] 12 p1719 N90-19872
Investigations of CuInSe2 thin films and contacts
[DE90-000301] 12 p1721 N90-19886
The effects of gradients on boundary stability
[DE90-007428] 12 p1722 N90-19894
Petrographic working model of the Rosetta sampling and modelling subgroup for a comet nucleus 12 p1738 N90-19992
Laboratory studies of cometary ice analogues 12 p1739 N90-19997
Simulation of radar and radiometer signals remote sensing cometary surface and subsurface structures 12 p1740 N90-20005
Dynamics of crust formation and dust emission of comet nucleus analogues under isolation 12 p1743 N90-20020
Studies of the structure and properties of organic monolayers, multilayers and superlattices
[DE90-008330] 13 p1765 N90-20129
Oxygen concentrations on surfaces of carbon fibers
[AD-A217724] 13 p1769 N90-20152
Rolling contact fatigue of surface modified 440C using a 'Ge-Polymet' type disc rod test rig
[NASA-TM-100390] 13 p1777 N90-20200
Ceramic oxide thin film formation utilizing biological processes
[DE90-008599] 13 p1781 N90-20225
Design and calibration of a vacuum compatible scanning tunneling microscope
[NASA-TM-102514] 13 p1804 N90-20353
Magnetic properties of surfaces and interfaces
[DE90-007348] 13 p1880 N90-20789
An ellipsometric measurement of optical properties for InP surfaces
[AD-A217185] 13 p1887 N90-20827
Low energy ion generator
[DE90-759905] 14 p1955 N90-21195
The measurement of surface reflectivity at millimetre wavelengths
[MRL-TN-559] 14 p1960 N90-21222
Depth-averaged equations for turbulent free-surface flow
[PB90-184781] 14 p1974 N90-21308
Modeling elastomer displacements for tactile sensing applications
[DE90-007959] 14 p1984 N90-21370
Absolute multilayer characterization at high spatial resolution via real-time soft x ray imaging
[DE90-009181] 14 p1984 N90-21371
Surface structure and chemistry of high surface area silica gels
[DE90-007684] 15 p2071 N90-21865
Inverse problems of heat conduction 15 p2091 N90-21969
Computerized inspection of gear tooth surfaces
[NASA-TM-102395] 15 p2107 N90-22054
The effects of tortuosity on flow through a natural fracture
[DE90-009193] 15 p2129 N90-22172
Scanning laser photocurrent spectroscopy of electrochemically grown bismuth sulphide films
[AERE-M-3709] 16 p2217 N90-22649
Time-resolved surface structural study by picosecond reflection high-energy electron diffraction
[AD-A218417] 16 p2228 N90-22712
Surface physics instrumentation
[AD-A220460] 17 p2373 N90-23512
Subsurface hardening and flow of aluminum during the incubation period of solid particle erosion
[DE90-010141] 18 p2525 N90-24409
Surface enrichment and evaporation in a polymer mixture of long and short chains
[DE90-010073] 18 p2529 N90-24429
Effects of microstructure and adhesion on performance of sputter-deposited MoS2 solid lubricant coatings
[AD-A220900] 18 p2530 N90-24434
Fluid dynamic and acoustic experiments on turbomachine rotors subject to variable flow conditions
[AD-A220298] 18 p2552 N90-24565
Effect of film adhesion on tribological properties of silver-coated alumina
[DE90-010090] 18 p2564 N90-24632
RF surface resistance measurements in the Pb-Bi-Sr-Ca-Cu-O system
[DE90-010412] 18 p2621 N90-24932
Adlayer physics
[AD-A221064] 19 p2673 N90-25203
Surface dilation and fluid-dynamical behaviour of Newtonian liquids in an overflowing cylinder. 1: Pure liquids
[LR-601] 19 p2692 N90-25317
Wear transition surfaces for long-term wear effects
[DE90-011314] 19 p2698 N90-25351
Scanning electron microscopy by photovoltage contrast imaging
[AD-D014517] 19 p2760 N90-25684
Molecular structure of interphases between DGEBA/BTDA adhesives and silver substances using surface-enhanced Raman scattering
[AD-A222750] 20 p2841 N90-26157
Surface reconstruction based on critical contours in a multi-image context
[RR-784-I-IMAG-94-LIFIA] 20 p2880 N90-26383
Exact results for the structured liquid-solid interface
[AD-A222762] 20 p2922 N90-26630
Laboratory studies of the interaction of ions with condensed gases: Planetary applications 20 p2949 N90-26778
Interfacial viscosity measurements of adsorbed monolayers on metal surfaces
[AD-A221689] 21 p2979 N90-26931
The thermal radiative properties of metals at high temperature
[DE90-012468] 21 p2981 N90-26938
An interdisciplinary approach to the predictive modeling of structural adhesive bonding
[AD-A221703] 21 p2988 N90-26982
Surface property improvement in titanium alloy gas turbine components through ion implantation 23 p3309 N90-28713
Structure of metal overlayers by low energy alkali ion scattering: Cu/Ru(0001) and Sn/Pt(111)
[DE90-014453] 23 p3310 N90-28718
Technical bibliography of high performance polyethylene fibers
[SNPE-NT-106/89/GTR/RP/NP] 23 p3313 N90-28736
Surface effect for test piece on flexural test of carbon fiber reinforced plastic laminates
[NAL-TM-601] 24 p3442 N90-29436
On hydrogen chemisorption on metals: The electron correlation effects
[DE90-627318] 24 p3448 N90-29473
Thermal imaging assessment
[AD-A224400] 24 p3460 N90-29542
Theoretical and experimental comparison of infrared and visible laser scattering from a variety of surface types
[RSRE-MEMO-4348] 24 p3474 N90-29636
Scanning tunneling microscopy of semiconductor surfaces
[AD-A223339] 24 p3552 N90-30095

SURFACE REACTIONS

The structure determination of molecular adsorbates with large unit cells or lattice-gas disorder on metal surfaces
[AD-A210926] 01 p0042 N90-10230
Dynamics of nucleation at electrochemical interfaces via surface EXAFS and standing wave measurements
[AD-A210733] 02 p0195 N90-11109
Surface-catalyzed air oxidation of hydrazines: Environmental chamber studies 02 p0203 N90-11159
Vibrational spectroscopic study of the kaolinite-hydrazine intercalation complex 02 p0204 N90-11166
Surface-catalyzed air oxidation reactions of hydrazines: Tubular reactor studies 02 p0204 N90-11167
A diffuse reflectance infrared Fourier transform spectroscopic study of adsorbed hydrazines 02 p0205 N90-11170
Self-assembled organic monolayer films
[AD-A212006] 03 p0323 N90-11838
Synaptic plasticity and memory formation
[AD-A211368] 03 p0379 N90-12158
Studies of organo phosphorus-, nitrogen-, and sulfur-containing molecules
[AD-A213518] 07 p0888 N90-15135
Interfacial systems for photochemical energy conversion
[DE90-003181] 07 p0953 N90-15514
Theoretical studies of chemisorption and surface reactions on nickel and silicon
[DE90-004849] 08 p1047 N90-16050
Theory of the dissociation dynamics of small molecules on metal surfaces: Finite temperature studies
[DE90-005217] 09 p1195 N90-16923
Chemistry at clusters, microstructures and surfaces
[AD-A215842] 10 p1353 N90-17844
The evaporation of sessile droplets. Part 1: Theoretical factors for a two-component system
[AD-A215946] 10 p1353 N90-17848
Surface-enhanced Raman scattering
[AD-A215976] 10 p1353 N90-17849
The physical-organic chemistry of surfaces, and its relevance to molecular recognition
[AD-A215987] 10 p1354 N90-17850
Interactions of molecules with surfaces
[DE90-005337] 10 p1428 N90-18237
Surface intermediates in thin film deposition on silicon
[AD-A216662] 11 p1483 N90-18534
Polymerization of nitro compounds on silver surfaces during surface-enhanced Raman scattering
[AD-A216116] 11 p1489 N90-18569
Aeolian removal of dust from photovoltaic surfaces on Mars
[NASA-TM-102507] 12 p1617 N90-19299
Development of inspection techniques for quantitatively measuring surface contamination on SRM hardware
[NASA-CR-183902] 12 p1673 N90-19608
Improved high temperature oxidation behavior of alloys by ion implantation
[AERE-R-13309] 16 p2217 N90-22650
Time-resolved surface structural study by picosecond reflection high-energy electron diffraction
[AD-A218417] 16 p2228 N90-22712
Reactions of laser-generated free radicals at semiconductor surfaces
[AD-A218552] 16 p2232 N90-22733
Quantitative surface temperature measurement using two-color thermographic phosphors and video equipment
[NASA-CASE-LAR-13740-1] 16 p2238 N90-22770
The influence of the gas surface interaction on spacecraft orbital motion 17 p2365 N90-23461
The effect of catalysts on gas-phase hydrocarbon ignition
[AD-A218775] 17 p2371 N90-23499
An examination of the relationship between SERS intensities and surface concentration for pyridine adsorbed at the gold/aqueous solution interface
[AD-A219520] 17 p2372 N90-23505
Instrumentation for surface reaction dynamics
[AD-A218608] 17 p2406 N90-23708
Mechanistic modeling of corrosion fatigue crack growth of steels in aqueous solutions 18 p2524 N90-24404
Dynamics of bulk and surface-adsorbed polyacrylates
[AD-A221046] 18 p2530 N90-24437
Studies of chemistry and diffusion on silicon and gallium arsenide surfaces using laser-induced thermal desorption
[AD-A220946] 18 p2547 N90-24539
Surface defects and chemistry on the SnO2(110) surface 18 p2559 N90-24603
In situ analysis of CO during chemisorption and oxidation on graphite: Supported Pt by FTIR-microspectrometry 18 p2559 N90-24605
Analysis of Pt/SnO(sub x) during catalysis of CO oxidation 18 p2560 N90-24607
Monoenergetic positron beam studies of near-surface phenomena
[ETN-90-96947] 18 p2613 N90-24887
Oxide thermal stability on gamma titanium aluminide
[DE90-012054] 19 p2678 N90-25232
Field-induced surface chemistry of NO
[AD-A223007] 21 p2977 N90-26915
Laser induced surface chemical epitaxy
[AD-A222082] 21 p2977 N90-26920
Ni impurity effects on hydrogen surface chemistry and etching of Si(111)
[AD-A222083] 21 p2977 N90-26921

High resolution electron energy loss spectroscopy studies of chemisorbed species on metal surfaces
[AD-A222272] 21 p2978 N90-26922
The adsorption and thermal decomposition of PH3 on Si(111)-(7x7)
[AD-A222417] 21 p2978 N90-26927
PH3 surface chemistry on Si(111)-(7x7): A study by Auger spectroscopy and electron stimulated desorption methods
[AD-A221508] 21 p2979 N90-26929
Surface reactions in the space environment
[AD-A221767] 21 p2979 N90-26932
Background effects in ESDIAD measurements on Si(111)-(7x7)
[AD-A222242] 21 p3001 N90-27056
Microscopic modeling of tribological phenomena
[AD-A222049] 21 p3011 N90-27117
AMSAHTS 1990: Advances in Materials Science and Applications of High Temperature Superconductors
[NASA-CP-10043] 22 p3136 N90-27792
Laser surface interactions of high-T(sub c) superconductors 22 p3139 N90-27809
Experimental and kinetic modeling of acid/base redox reactions over metal oxide catalysts
[DE90-013835] 22 p3156 N90-27893
Regression and combustion characteristics of boron containing fuels for solid fuel ramjets 22 p3161 N90-27928
Theoretical investigation of gas-surface interactions
[NASA-CR-186881] 22 p3245 N90-28403
High Temperature Surface Interactions
[AGARD-CP-461] 23 p3306 N90-28698
High temperature surface interactions: Overview 23 p3306 N90-28699
Oxidation, sulfidation, and hot corrosion: Mechanisms and interrelationships 23 p3307 N90-28702
Surface chemistry and structural effects in the stress corrosion of glass and ceramic materials
[AD-A223305] 24 p3454 N90-29507

SURFACE ROUGHNESS
Surface reflection: Physical and geometrical perspectives
[AD-A210592] 01 p0124 N90-10710
Numerical solutions of turbulent flow with heat transfer over rough surfaces 02 p0218 N90-11246
An experimental study of surface roughness effects on turbulent boundary layer flow and heat transfer
[AD-A212099] 03 p0347 N90-11980
Effect of superplastic deformation on the surface roughness of sheet
[RAE-TM-MAT/STR-1112] 03 p0359 N90-12054
Effect of roughness on the stability of boundary layers 04 p0440 N90-12518
Recent tests at Langley with a University of Tennessee Space Institute (UTSI) skin friction balance 04 p0441 N90-12527
Effect of pipe roughness on orifice flow measurement
[PB89-231484] 04 p0500 N90-12880
Convective heat transfer measurements from a NACA 0012 airfoil in flight and in the NASA Lewis Icing Research Tunnel
[NASA-TM-102448] 05 p0642 N90-13750
X ray reflectivity study of SiO2 on Si
[DE90-001326] 06 p0851 N90-14943
Surface roughening of Ge(001) during 200 eV Xe ion bombardment and Ge molecular beam epitaxy
[DE90-000674] 07 p0998 N90-15769
Surface topography measurements over the 1 meter to 10 micrometer spatial period bandwidth
[DE90-003642] 08 p1122 N90-16501
Scanning tunneling microscope studies of surface defects
[AD-A214121] 08 p1130 N90-16543
A statistical model of the infrared signature of a wind roughened sea
[AD-A214531] 09 p1249 N90-17245
Simulation of rough surface scattering in three-dimensions
[AD-A215171] 09 p1277 N90-17405
Shape from focus
[AD-A215959] 10 p1393 N90-18052
Heat transfer measurements from a NACA 0012 airfoil in flight and in the NASA Lewis icing research tunnel
[NASA-CR-4278] 12 p1599 N90-19203
Numerical simulation of acoustic scatter from subsurface bubble clouds
[AD-A217068] 12 p1710 N90-19822
Simulation of radar scattering from rough surfaces
[AD-A217841] 13 p1790 N90-20275
Investigation of surface water behavior during glaze ice accretion 14 p1906 N90-20927
Bearing elastohydrodynamic lubrication: A complex calculation made simple
[NASA-TM-102575] 15 p2105 N90-22041
Surface roughness and the physical properties of fractures
[DE90-006046] 15 p2128 N90-22169
An examination of the full-wave method for rough surface scattering
[AD-A218664] 16 p2308 N90-23155
Full surface interferometric testing of grazing incidence mirrors
[AD-A219394] 16 p2318 N90-23218
Millimeter - wave radar scattering from terrain: Data handbook
[AD-A220770] 17 p2391 N90-23617
The effects of Reynolds number, rotor incidence angle, and surface roughness on the heat transfer distribution in a large-scale turbine rotor passage
[NASA-CR-183891] 17 p2410 N90-23731
On the receptivity problem for Goertler vortices: Vortex motions induced by wall roughness
[NASA-CR-182036] 19 p2654 N90-25109
Mechanical paint removal techniques for aircraft structures
[IAR-89-23] 19 p2682 N90-25254
Laser ultrasonic measurements on ceramic materials with rough surfaces
[DE90-012961] 20 p2838 N90-26141
Model studies of the effect of surface roughness and mechanical interlocking on adhesion
[AD-A222402] 21 p2987 N90-26977
Backscatter enhancement in scattering from rough surfaces
[AD-A223110] 21 p2995 N90-27024
A note on the statistics of laser speckle
[AD-A222408] 21 p3009 N90-27103
Investigations of polarized light scattering from rough surfaces
[AD-A221943] 21 p3076 N90-27491
Simple graphical descriptions of natural land profiles and the application of fractal and sub-fractal models to them
[RSRE-MEMO-4305] 22 p3195 N90-28130
Wind tunnel investigation of periodic vortex separation from rough surface circular cylinders by means of acoustic measurements
[ESA-TT-1092] 23 p3268 N90-28499
Friction microprobe studies of composite surfaces
[DE90-014224] 23 p3299 N90-28662
Large aperture acoustic arrays in support of reverberation studies
[AD-A224002] 23 p3393 N90-29168
Near-angle scattering and binary optics
[AD-A224140] 23 p3396 N90-29186
Estimation of power spectral density of runway roughness
[NAL-TR-1037] 24 p3437 N90-29411
The investigation and production of titanium-tantalum junctions diffusion bonded at high temperature (855 C to 920 C): The influence of temperature, time pressure and roughness on the mechanical properties, and the optimisation of the bonded conditions
[BR114894] 24 p3476 N90-29646

SURFACE ROUGHNESS EFFECTS
An experimental study of surface roughness effects on turbulent boundary layer flow and heat transfer
[AD-A212099] 03 p0347 N90-11980
The effects of wall surface defects on boundary-layer transition in quiet and noisy supersonic flow 04 p0446 N90-12556
Some problems in hydrodynamic lubrication 09 p1229 N90-17133
Scuffing modelling and experiments for heavily loaded elastohydrodynamic lubrication contacts 10 p1391 N90-18047
Modeling of surface roughness effects on glaze ice accretion 14 p1905 N90-20925
Grain-size distribution and armoring in gravel-bed rivers: A case study 19 p2687 N90-25285
Model studies of the effect of surface roughness and mechanical interlocking on adhesion
[AD-A222402] 21 p2987 N90-26977

SURFACE STABILITY
Deep traps and sidegating in GaAs devices
[AD-A210740] 01 p0133 N90-10765
Ion beam modification of metals: Mechanical properties and structure
[AD-A214701] 09 p1194 N90-16915

SURFACE TEMPERATURE
NT SKIN TEMPERATURE (NON-BIOLOGICAL)
NT WALL TEMPERATURE
Crau 1987: The KNMI contribution --- KNMI (Royal Netherlands Meteorological Institute)
[KNMI-TR-110] 03 p0375 N90-12140
Description of a software library for the calculation of surface fluxes
[KNMI-TR-112] 03 p0375 N90-12141
The thermal behavior of natural backgrounds and its prediction by means of numerical models 06 p0762 N90-14436
Numerical investigation of transition control of a flat plate boundary layer 07 p0926 N90-15361
Antarctic surface temperature and pressure data
[DE90-000971] 07 p0963 N90-15565
Mesoscale analysis by numerical modelling coupled with satellite-based sounding 08 p1100 N90-16370
Low speed flowfield characterization by infrared measurements of surface temperatures 10 p1306 N90-17556
A multicolor imaging pyrometer 10 p1364 N90-17905
On the temperature of surfaces 10 p1366 N90-17917
Development of an infrared imaging system for the surface tension driven convection experiment 10 p1367 N90-17922
Remote sensing of evaporation ducts for Naval warfare
[AD-A214849] 10 p1374 N90-17965
Spacecraft thermal control design data, volume 1
[ESA-PSS-03-108-ISSUE-1-VOL-1] 11 p1468 N90-18455
Design and test of a compact optics system for the pool boiling experiment
[NASA-TM-102530] 13 p1786 N90-20253
Analysis of methods to determine emissivity for ground surface targets in the spectral band 8 to 14 microns
[INPE-4984-TDL/394] 13 p1820 N90-20447
An intercomparison of general circulation model predictions of regional climate change
[DE90-008325] 13 p1845 N90-20589
Thermal radiation characteristics of nonisothermal cylindrical enclosures using a numerical ray tracing technique
[NASA-TM-102527] 14 p1972 N90-21296
Sulphur silicate interactions on the Jovian satellite Io 15 p2192 N90-22515
Multiwavelength pyrometry to correct for reflected radiation
[NASA-TM-102578] 17 p2407 N90-23714
Measuring and modeling near-surface reflected and emitted radiation fluxes at the FIFE site
[NASA-CR-180953] 20 p2879 N90-26378
Vandenberg Boundary Layer Survey (VBLS): Results
[AD-A222517] 21 p3031 N90-27234
Stratocumulus cloud height variations determined from surface and satellite observations 22 p3214 N90-28230
Determination of the SSME high pressure oxidizer turbopump bearing temperature 23 p3291 N90-28619
Transient cooling of a hot surface by droplets evaporation
[PB90-227968] 23 p3325 N90-28799
Real-time aerodynamic heating and surface temperature calculations for hypersonic flight simulation
[NASA-TM-4222] 23 p3327 N90-28815
Study of meteorological processes important in the degradation of materials through surface temperature
[PB90-222720] 23 p3336 N90-28856
Thermographic phosphor technique 24 p3421 N90-29324

SURFACE TENSION
U INTERFACIAL TENSION

SURFACE TO AIR MISSILES
Experience gained in the improvement of the Aspide aerodynamic configuration for the surface to air role 01 p0015 N90-10072
Laser techniques for ground to air applications
[FOA-C-30524-3.1] 02 p0228 N90-11309
Flowfield effects of launch on a vertically-launched missile
[AD-A214468] 09 p1160 N90-16714
Missile Aerodynamics: NEAR Conference on Missile Aerodynamics
[ISBN-0-9620629-1-X] 10 p1303 N90-17540
The use of lateral jet control at Aerospatiale 10 p1305 N90-17551
Design of a robust controller for an unstable nonminimum phase guided missile
[AD-A216147] 10 p1323 N90-17645
Flowfield measurements in the wake of a missile at high angle of attack
[AD-A219645] 17 p2345 N90-23351
Optimizing ECM techniques against monopulse acquisition and tracking radars
[AD-A220036] 17 p2393 N90-23629

SURFACE TO SURFACE MISSILES
NT ANTITANK MISSILES
NT CRUISE MISSILES
NT INTERCONTINENTAL BALLISTIC MISSILES
Present and future US and Soviet chemical missiles and chemical rocket projectiles
[AD-A212199] 04 p0461 N90-12644

SURFACE TREATMENT
NT SURFACE FINISHING

Effect of surface oxygen on adhesion of carbon fiber-reinforced composites
[AD-A220777] 17 p2369 N90-23486

SURFACE VEHICLES
NT AIRCRAFT CARRIERS
NT AUTOMOBILES
NT BOATS
NT ELECTRIC AUTOMOBILES
NT ELECTRIC HYBRID VEHICLES
NT ELECTRIC MOTOR VEHICLES
NT LUNAR ROVING VEHICLES
NT LUNAR SURFACE VEHICLES
NT MAGNETIC LEVITATION VEHICLES
NT MOTOR VEHICLES
NT ROCKET PROPELLED SLEDS
NT ROVING VEHICLES
NT TANKS (COMBAT VEHICLES)
NT TRACKED VEHICLES
NT TRANSPORTER
NT TRUCKS
NT WALKING MACHINES
Land vehicle teleoperation under conditions of reduced video resolution
[DE89-016925] 02 p0231 N90-11324
Vision-based navigation for autonomous ground vehicles
[AD-A211584] 03 p0304 N90-11725
Problem-dependent transformations of 3D terrain elevation maps into cost precursor maps
[PB89-218127] 04 p0514 N90-12969
Computer oriented methods of multibody dynamics for application in vehicle technology
[DFVLR-FB-89-17] 04 p0533 N90-13080
Research in knowledge-based vision techniques for the Autonomous Land Vehicle Program
[AD-A213440] 07 p0942 N90-15453
Articulated suspension system
[NASA-CASE-NPO-17354-1-CU] 09 p1233 N90-17153
An Autonomous Platform Simulator (APS)
[AD-A215768] 10 p1392 N90-18048
Development of an integrated mobile robot system at Carnegie Mellon University: June 1988
[AD-A215955] 10 p1392 N90-18049
A human factors testbed for ground-vehicle telerobotics research
[DE90-006618] 12 p1697 N90-19746
Robotic mobility system: Road following algorithms
[AD-A218107] 13 p1874 N90-20748
Proceedings of the 4th European Conference, volume 2
[AD-A216521] 14 p1986 N90-21382
Three legged walking mobile platform: Kinematic and dynamic analysis and simulation
[NASA-CR-184929] 18 p2535 N90-24457
Lunar articulated remote transportation system
[NASA-CR-186817-VOL-1] 20 p2871 N90-26332
Development of an integrated mobile robot system at Carnegie-Mellon University
[AD-A222494] 21 p3011 N90-27119
The flight telerobotic servicer: NASA's first operational space robot 24 p3500 N90-29781

SURFACE WATER
Assessment of the theory and hypotheses of the acidification of watersheds
[DE90-005528] 10 p1406 N90-18111
Utilization of LANDSAT-5 and NOAA-9 satellite imagery in the identification of physical-chemical parameters of the water in the Guanabara Bay
[INPE-4761-TDL/349] 13 p1819 N90-20445
Investigation of surface water behavior during glaze ice accretion 14 p1906 N90-20927
Analysis of water quality parameters of the Piaui River (SE), Brazil, through field and TM/LANDSAT sensor data
[INPE-4918-PRE/1417] 14 p1998 N90-21453

SURFACE WAVES
NT BAROCLINIC WAVES
NT CAPILLARY WAVES
NT ELECTROMAGNETIC SURFACE WAVES
NT GRAVITY WAVES
NT RIPPLES
Surface wave ray tracing and Ms:yield determination in a laterally heterogeneous earth
[AD-A210241] 01 p0090 N90-10516
Dynamics of nucleation at electrochemical interfaces via surface EXAFS and standing wave measurements
[AD-A210733] 02 p0195 N90-11109
Investigations of Eurasian seismic sources and upper mantle structure
[AD-A211806] 03 p0371 N90-12120
Seismic wave attenuation and yield determination at regional distances
[AD-A211548] 03 p0372 N90-12128
Similarity relations of wind waves in finite depth
[PB89-198113] 03 p0376 N90-12144
A linearized surface condition in low speed hydrodynamics
[REPT-89-04] 04 p0501 N90-12885
Surface current and wave modulation measurements over bottom topography: A comparison with theory
[AD-A212469] 04 p0522 N90-13011
A numerical study of rain-induced surface gravity wave attenuation
[AD-A212762] 04 p0549 N90-13197
Magnetostatic wave device characterization by Brillouin light scattering
[AD-A213798] 09 p1281 N90-17426
Green's functions for a theoretical model of an aperture fed stacked-patch microstrip antenna
[AD-A216280] 12 p1645 N90-19455
An outline for the analysis of wave induced bottom pressure fluctuations
[MRL-TN-558] 14 p2008 N90-21510
Interaction of a turbulent round jet with the free surface 15 p2090 N90-21964
Polarization coupling in the acousto-optic interaction of surface waves 15 p2164 N90-22365
Acoustoelectronic interaction of surface waves in GaAs-InGaAs superlattices 16 p2310 N90-23163
Nonreciprocal components in the 140 and 220 GHz bands utilizing magnetoplasmons on semiconducting substrates
[AD-A219136] 16 p2324 N90-23253
The Gauss beam method for surface waves. Theory and utilization for a lateral heterogeneous spheric Earth
[ETN-90-96492] 18 p2580 N90-24695
Finite amplitude surface waves in cooled plasmas with smeared interface
[DE90-611308] 18 p2617 N90-24909
Surface wave characterization of high T(sub c) superconductors
[AD-A221077] 19 p2760 N90-25683
Study of a method for measuring the dimensions of cracks on the surface of ceramics by Rayleigh waves
[ETCA-89-R-024] 22 p3160 N90-27922
Magnetostatic wave transducers, resonators and dispersion control
[AD-A223437] 24 p3464 N90-29571
Research in nonlinear water waves
[AD-A224065] 24 p3496 N90-29759
Study of the reflection of surface acoustic wave from a material discontinuity boundary using a perturbation method 24 p3542 N90-30032

SURFACE-ACTIVE AGENTS
U SURFACTANTS

SURFACES
Free surface scars and striations
[AD-A212429] 04 p0503 N90-12901
Damage evaluation from surface displacement data 07 p0944 N90-15489
Material responses to incident x rays
[DE89-015366] 08 p1089 N90-16305
Stochastic action of dynamical systems on curved manifolds. The isokinetic developing map on trajectories
[PREPRINT-566] 08 p1117 N90-16486
Theory of gearing
[NASA-RP-1212] 12 p1670 N90-19593
Coordinate systems for plastic yield surfaces stress and strain space theories
[PB90-164765] 15 p2117 N90-22110
The curvature of conjugate profiles in points of contract
[MEMO-COSOR-89-18] 16 p2243 N90-22795
Formation of Titanium-boron surface alloys by excimer laser mixing
[DE90-013172] 20 p2834 N90-26118
An improved method for choosing sampling points for the inspection of complex surfaces in a computer-aided manufacturing environment 23 p3380 N90-29093

SURFACTANTS
Chemical and photochemical reactivity in microemulsions and waterless microemulsions
[AD-A211776] 04 p0470 N90-12692
An evaluation of ethylene-vinyl acetate copolymers as desensitizers for RDX in insensitive booster compositions prepared by slurry coating technology
[MRL-TR-89-33] 12 p1633 N90-19385
Dynamics of micellar oligomeric and monomeric sodium 10-undecenoate
[AD-A222570] 20 p2830 N90-26099

SURGEONS
NT FLIGHT SURGEONS

SURGERY
Laser-produced plasmas in medicine
[DE90-007623] 13 p1891 N90-20849
Laser diode pumped, erbium-doped, solid state laser with high slope efficiency
[AD-D014482] 22 p3179 N90-28040
Measurement of hand dynamics in a microsurgery environment: Preliminary data in the design of a bimanual telemicro-operation test bed 23 p3364 N90-29010

SURGES
Deep traps and sidegating in GaAs devices
[AD-A210740] 01 p0133 N90-10765
Lightning and surge protection of photovoltaic installations: Two case histories, Vulcano and Kythnos
[PB89-229058] 03 p0374 N90-12135
Studies on the startup transients and performance of a gas loaded sodium heat pipe
[AD-A211880] 03 p0414 N90-12379
Transient fault behavior in a microprocessor: A case study
[NASA-CR-186240] 10 p1320 N90-17633
Lightning surge characteristics of transmission towers. Lightning surge characteristics of 15-meter-high scale model tower
[DE89-782322] 12 p1692 N90-19721
Deep level transient spectroscopy in resistive layers
[DE90-008349] 13 p1772 N90-20169
An experimental study of fault propagation in a jet-engine controller
[NASA-CR-181335] 17 p2354 N90-23401
Transient pulse monitor
[AD-A220353] 18 p2508 N90-24335
A new transient X ray burst source near GX 1+4 19 p2782 N90-25826
L-SWITCH: A PC program for computing transient voltages and currents during switching off three-phase inductances
[EUT-89-E-221] 20 p2858 N90-26257
Simulation of the electrical and thermal behavior of gapless metal oxide surge arresters under AC-operation condition
[ETN-90-97309] 20 p2859 N90-26262

SURVEILLANCE
NT SPACE SURVEILLANCE (SPACEBORNE)
Fiber optic technique for surveillance and control of mine fields
[FOA-C-30526-3.1] 02 p0225 N90-11293
The Swedish defense research needs: For surveillance and seeker applications
[FOA-C-30520-3.3] 02 p0298 N90-11691
Rotorcraft low altitude CNS benefit/cost analysis: Rotorcraft operations data
[DOT/FAA/DS-89/9] 03 p0419 N90-12406
Mode S data link trials, 10-11 January 1989
[RSRE-MEMO-4267] 04 p0490 N90-12815
Control outside of independent surveillance coverage operational concept
[AD-A214163] 07 p0878 N90-15090
Geotechnical instrumentation
[PB89-198675] 07 p0933 N90-15398
Electro-optic sensors for surveillance and target acquisition 08 p1026 N90-15929
Tomographic processing of synthetic aperture radar signals for enhanced resolution
[AD-A217178] 13 p1789 N90-20265
MMW SAR on RPV for battlefield surveillance 14 p1961 N90-21231
Calculation of IR propagation statistics in the eastern Atlantic for surveillance system performance assessment 15 p2085 N90-21938
Intelligent signal processing techniques for multi-sensor surveillance systems
[AD-A218890] 16 p2262 N90-22695
Aviation security: Corrective actions underway, but better inspection guidance still needed. Report to the Chairwoman, Government Activities and Transportation Subcommittee, Committee on Government Operations, House of Representatives
[GAO/RCED-88-160] 17 p2347 N90-23367
Computer-aided mathematical analysis of probability of intercept for ground-based communication intercept system
[AD-A219856] 17 p2392 N90-23627
Characteristics of the IAEA correlation monitor material for surveillance programmes
[VTT-RR-639] 19 p2682 N90-25258
Activities of the division of surveillance and seeker systems
[FOA-C-30549] 19 p2684 N90-25269
Optical motion detector detecting visible and near infrared light
[AD-D014515] 19 p2758 N90-25671
Space-based wide area surveillance system studies 21 p3068 N90-27444
Command and control in the age of space-based surveillance 21 p3069 N90-27445
An assessment of the application of in situ ion-density data from DMSP to modeling of transionospheric scintillation
[AD-A222695] 24 p3491 N90-29730

SURVEILLANCE RADAR
NT AIRBORNE SURVEILLANCE RADAR
NT MULTISTATIC RADAR
ASR-9 weather channel test report
[AD-A211749] 03 p0339 N90-11934

Aircraft Reply and Interference Environment Simulator (ARIES) hardware principles of operation. Volume 2: Appendixes
[DOT/FAA/CT-TN88/4-2] 04 p0484 N90-12781
Aircraft Reply and Interference Environment Simulator (ARIES) hardware principles of operation, volume 1
[DOT/FAA/CT-TN88/4-1] 04 p0484 N90-12782
Fine resolution errors in secondary surveillance radar altitude reporting amongst aircraft transmitting the conspicuity codes 4321 and 4322
[RSRE-88004] 04 p0490 N90-12816
Multitarget tracking by single sensor: Analysis of the main approaches developed in this area
[ESA-TT-1171] 11 p1500 N90-18633
Experimental measurements in secondary radar field: Conception and first results
[ETN-90-96074] 12 p1648 N90-19471
High Resolution Air- and Spaceborne Radar
[AGARD-CP-459] 14 p1960 N90-21223
Trade-offs in a space based surveillance radar
14 p1960 N90-21225
Vertical ozone probing with lidar
20 p2885 N90-26416

SURVEYING
U SURVEYS

SURVEYS
NT GEODETIC SURVEYS
NT GEOLOGICAL SURVEYS
NT SKY SURVEYS (ASTRONOMY)
Laser anemometer measurements in a transonic axial-flow fan rotor
[NASA-TP-2879] 02 p0218 N90-11245
Ice runways near the South Pole
[AD-A211606] 03 p0335 N90-11908
Characterization of self-lubricating surface materials
[CETIM-108060] 04 p0479 N90-12749
A survey of the current state-of-the-art in high-energy-product permanent magnets
[AD-A211761] 04 p0549 N90-13193
Summary of 1987 and 1988 manatee aerial surveys at Kennedy Space Center
[NASA-TM-102783] 06 p0802 N90-14669
Image enhancement using the IRAS (Infrared Astronomy Satellite) survey data
[AD-A213811] 07 p0950 N90-15496
A survey of nonuniform inflow models for rotorcraft flight dynamics and control applications
[NASA-TM-102219] 08 p1028 N90-15938
Absorption fluids data survey: 1989 update
[DE90-003985] 08 p1096 N90-16346
CRC (Coordinating Research Council) octane number requirement survey 1988
[AD-A214845] 09 p1200 N90-16954
High pressure waterjet cutting industrial needs survey
[AD-A214952] 10 p1368 N90-17927
Investigation of applications of diamond film
[AD-A216104] 10 p1368 N90-17931
A selective survey of computational electromagnetics for antenna applications 10 p1369 N90-17933
Measuring Day-Night Noise Levels (DNL) using the metrosonics db-310 sound level analyzer (Dosimeter)
[AD-A215757] 10 p1427 N90-18230
Resource Assessment Project: User needs survey results
[DE89-009502] 11 p1529 N90-18802
Survey on the social and economic influences of wide-spreading heat-pump technology
[DE89-782294] 12 p1658 N90-19526
Survey on the possibility of introducing new energy to regional development plans
[DE89-782627] 12 p1681 N90-19654
Synthesis and analysis of 25 years (1961-1986) of INPE/SRE activities related to the vegetation/forest area
[INPE-4969-RPE/604] 13 p1819 N90-20446
A survey of advanced battery systems for space applications 13 p1822 N90-20458
Synopsis of early field test results from the gravity gradiometer survey system 13 p1833 N90-20525
The Rapid Geodetic Survey System (RGSS)
13 p1834 N90-20528
First year's results and field experience with the latest JILA absolute gravimeter 13 p1834 N90-20529
Treatment of geodetic leveling in the integrated geodesy approach 13 p1837 N90-20546
A survey of experiments and experimental facilities for active control of flexible structures
14 p1936 N90-21079
Survey of land use through remote sensing
[INPE-5032-MD/042] 14 p1996 N90-21443
Project CANASATE: Remote sensing applied to sugar cane crop survey
[INPE-4902-PRE/1503] 14 p1997 N90-21446
Evolution of remote sensing applied to vegetation and forest at INPE
[INPE-4970-PRE/1538] 14 p1998 N90-21452
The molecular cloud content of early type galaxies. 2: A molecular ring in NGC 404
[PB90-124348] 14 p2039 N90-21695
A survey of the maritime-aerosol data collected at South Uist and the implications for the LOWTRAN maritime aerosol model 15 p2079 N90-21908
Search for rapidly star forming galaxies at high redshift 15 p2181 N90-22465
A high galactic latitude survey of far ultraviolet excess objects 15 p2183 N90-22473
An astrophysics data program investigation of cluster evolution
[NASA-CR-181296] 15 p2191 N90-22510
US Coast guard radionavigation system user survey
[AD-A218480] 17 p2349 N90-23380
Determination of tide heights from airborne bathymetric data
[AD-A220412] 17 p2430 N90-23848
Social survey findings on en route noise annoyance issues 18 p2610 N90-24868
An aircraft noise study in Norway
18 p2611 N90-24872
A systematic approach to training: A training needs assessment 18 p2645 N90-25059
SERI solar radiation resource assessment project
[DE90-000307] 19 p2711 N90-25428
A survey of cervical pain in pilots of a Belgian F-16 Air Defence Wing 19 p2718 N90-25462
The Einstein All-Sky IPC slew survey
19 p2787 N90-25865
Aviation safety: Conditions within the air traffic control work force. Fact sheet for congressional requesters
[GAO/RCED-89-113FS] 20 p2805 N90-25958
Aviation safety: Serious problems continue to trouble the air traffic control work force. Report to congressional requesters
[GAO/RCED-89-112] 20 p2805 N90-25959
Facilities involved in adaptive wall research
21 p2962 N90-26840
Vandenberg Boundary Layer Survey (VBLS): Results
[AD-A222517] 21 p3031 N90-27234
Copyright and home copying: Technology challenges the law
[PB90-151309] 21 p3086 N90-27547
Comparison of overstory canopy cover estimates on forest survey plots
[PB90-159484] 22 p3194 N90-28126
Aerial videotape survey of coastal Louisiana, 1986. Louisiana Barrier Island erosion and land loss study: 1986-1990
[PB90-194648] 22 p3195 N90-28128
Circulation and property distributions in the Central Bering Sea, Spring, 1988
[PB90-155847] 22 p3230 N90-28317
Implications of the IRAS data for galactic gamma-ray astronomy and EGRET
[NASA-TM-103452] 22 p3261 N90-28466
Severe thunderstorm forecasting: An operational review
[PB90-215484] 23 p3353 N90-28948
Scientists, engineers, and technicians in nonmanufacturing industries: 1987. (Detailed statistical tables)
[PB90-226903] 23 p3404 N90-29235
An analysis of the Palomar-Green subdwarfs and white dwarfs 23 p3409 N90-29263
QTA (QUESTIONNAIRE-TASK-ANALYSIS): An electronic tool for job/task analysis
[DE90-008944] 24 p3499 N90-29778

SURVIVAL
The human factors relating to escape and survival from helicopters ditching in water
[AGARD-AG-305(E)] 05 p0576 N90-13358
Aircraft fires: A study of transport accidents from 1975 to the present 10 p1311 N90-17583
Alterations in the metabolic and sympathetic response to cold exposure after cold air acclimation
[AD-A216817] 10 p1412 N90-18144
Implications of Advanced Technologies for Air and Spacecraft Escape
[AGARD-CP-472] 13 p1751 N90-20054
Aircraft crash survival design guide. Volume 1: Design criteria and checklists
[AD-A218434] 16 p2198 N90-22545
Aircraft crash survival design guide. Volume 4: Aircraft seats, restraints, litters, and cockpit/cabin delethalization
[AD-A218437] 16 p2198 N90-22548
Aircraft crash survival design guide. Volume 5: Aircraft postcrash survival
[AD-A218438] 16 p2198 N90-22549
Lunar shelter
[ILR-MITT-233(1989)] 17 p2439 N90-23896
An analysis of requirements for a P-3 windshear training program
[AD-A222577] 20 p2805 N90-25960

SUSCEPTIBILITY (MAGNETISM)
U MAGNETIC PERMEABILITY

SUSPENDING (HANGING)
NT MAGNETIC SUSPENSION
Electrostatically suspended rotor for angular encoder
[NASA-CASE-MFS-28294-1] 01 p0054 N90-10310
Equilibrium solutions of a spherical pendulum with rotating point of suspension and friction
[ESA-TT-1139] 03 p0400 N90-12288
Equations of motion of slung load systems with results for dual lift
[NASA-TM-102246] 10 p1322 N90-17641
Swing-free movement of simply suspended objects employing parameter estimation
[DE90-002238] 13 p1811 N90-20398
An air-bearing weight offload system for ground test of heavy LSS structures 14 p1936 N90-21081
Hanging drop crystal growth apparatus and method
[NASA-CASE-MFS-28206-1-SB] 16 p2322 N90-23242
Cable suspended windmill
[NASA-CASE-LAR-13434-1] 17 p2412 N90-23742
Suspension mechanism and method
[NASA-CASE-LAR-14142-1] 21 p3011 N90-27116
Suspension systems for ground testing large space structures
[NASA-CR-4325] 24 p3439 N90-29424

SUSPENDING (MIXING)
Advanced study in solid transport: Rheological behavior of dense suspension
[DE90-003369] 07 p0947 N90-15483
Saltation and suspension of particulate matter in air
[AD-A213618] 07 p0960 N90-15552
Enhancement of mass transfer to a rotating cylinder electrode by inert particles suspended in the electrolyte
[DE90-008054] 13 p1771 N90-20165
A simple multicomponent fluid theory with accurate physics
[DE90-006537] 13 p1801 N90-20334
Hydrodynamic interactions and transport coefficients in a suspension of spherical particles
[DE90-008301] 13 p1801 N90-20336

SUSPENSION SYSTEMS (VEHICLES)
Planning systems for autonomous legged vehicles
[AD-A214242] 07 p0942 N90-15458
Articulated suspension system
[NASA-CASE-NPO-17354-1-CU] 09 p1233 N90-17153
NASA CSI suspension methods overview
14 p1936 N90-21080

SWAMPS
U MARSHLANDS

SWARMING
Time-resolved swarm studies in gases with emphasis on electron detachment and ion conversion
[ISBN-90-9003013-1] 18 p2613 N90-24883

SWEAT
Adjustment and validation of the mathematical prediction model for sweat rate, heart rate, and body temperature under outdoor conditions
[AD-A222599] 20 p2898 N90-26486
Generation rates and chemical compositions of waste streams in a typical crewed space habitat
[NASA-TM-102799] 22 p3233 N90-28333

SWEAT COOLING
Control of thermoregulatory sweating during exercise in the heat
[AD-A206001] 01 p0092 N90-10523
Temperature regulation during upper body exercise: Able bodied and spinal cord injured
[AD-A215130] 09 p1252 N90-17264

SWEATING
U PERSPIRATION

SWEDEN
Cloud volume statistics for southern Sweden
[CM-77] 17 p2427 N90-23830
Activities report of the Division of Informations Systems (FOA 37)
[FOA-C-30552-3.4] 17 p2480 N90-24178

SWEDISH SPACE PROGRAM
The Swedish sounding rocket and balloon program
05 p0657 N90-13830

SWEEP ANGLE
NT LEADING EDGE SWEEP
A study of the structure of highly swept shock wave turbulent boundary layer interactions
01 p0066 N90-10376
Trailing-edge sweep and three-dimensional vortex interactions in jets and mixing layers
01 p0066 N90-10379
Computational design of low aspect ratio wing-winglet configurations for transonic wind-tunnel tests
[NASA-CR-181939] 10 p1303 N90-17539

SWEEP EFFECT
Design of the low-speed NLF(1)-0414F and the high-speed HSNLF(1)-0213 airfoils with high-lift systems
04 p0444 N90-12540
Experimental and theoretical investigation of boundary-layer instability mechanisms on a swept leading edge at Mach 3.5
04 p0447 N90-12557
SWEEPBACK
NT LEADING EDGE SWEEP
SWELLING
Irradiation creep and swelling of annealed type 304L stainless steel at approximately 390 C and high neutron fluence
[DE90-004521] 08 p1046 N90-16047
Equilibrium swelling of elastomeric materials in solvent environments
[DE90-010164] 18 p2529 N90-24430
Swelling of neutron irradiated vanadium alloys
[DE90-015294] 24 p3448 N90-29472
Tensile behavior and swelling of ternary austenitic alloys irradiated in different neutron spectra
[DE90-015295] 24 p3450 N90-29485
SWEPT FORWARD WINGS
An in-flight investigation of ground effect on a forward-swept wing airplane
[NASA-TM-101708] 06 p0720 N90-14202
Applications of modern control theory synthesis to a super-augmented aircraft
[AD-A215431] 09 p1167 N90-16753
X-29A aircraft structural loads flight testing
[NASA-TM-101715] 12 p1603 N90-19225
A look at tomorrow today 23 p3273 N90-28524
An in-flight investigation of ground effect on a forward-swept wing airplane 23 p3275 N90-28533
SWEPT WINGS
NT DELTA WINGS
NT SWEPT FORWARD WINGS
NT SWEPTBACK WINGS
Experimental study of transition and leading edge contamination on swept wings 01 p0063 N90-10362
A three-dimensional linear stability approach to transition on wings at incidence 01 p0065 N90-10373
A European collaborative investigation of the three-dimensional turbulent shear layers of a swept wing
01 p0066 N90-10380
Boundary-layer stability analysis of Langley Research Center 8-foot LFC experimental data
04 p0442 N90-12532
Theoretical methods and design studies for NLF and HLFC swept wings at subsonic and supersonic speeds
04 p0443 N90-12535
Experimental and theoretical investigation of boundary-layer instability mechanisms on a swept leading edge at Mach 3.5
04 p0447 N90-12557
Improvements in the formulations and numerical solution of the Euler problem for swept wings
[RAE-TM-AERO-2139] 04 p0447 N90-12562
Generalized similarity solutions for three dimensional, laminar, steady, compressible boundary layer flows on swept profile cylinders
[DLR-FB-89-34] 05 p0639 N90-13725
Navier-Stokes simulation of the crossflow instability in swept-wing flows
[NASA-CR-186122] 05 p0641 N90-13744
Experimental transonic flutter characteristics of two 72 deg-sweep delta-wing models
[NASA-TM-101659] 06 p0720 N90-14205
Experiments on the laminar-turbulent transition on swept wings 08 p1066 N90-16170
The precise calculation of the inviscid leading edge flow on a laminar airfoil using simple methods and verification by measurements on the TLF pilot model
08 p1068 N90-16180
A study of flows over highly-swept wings designed for maneuver at supersonic speeds
[AD-A216837] 12 p1599 N90-19202
Output model-following control synthesis for an oblique-wing aircraft
[NASA-TM-100454] 12 p1606 N90-19241
Swept wing ice accretion modeling
[NASA-TM-103114] 15 p2046 N90-21727
The steady and time-dependent aerodynamic characteristics of a combat aircraft with a delta or swept canard 23 p3274 N90-28526
SWEPTBACK WINGS
NT DELTA WINGS
Aeroelastic characteristics of aircraft with circulation control wings 13 p1754 N90-20070
An experimental study of tip shape effects on the flutter of aft-swept, flat-plate wings
[NASA-TM-4180] 16 p2199 N90-22555
SWIMMING
Free swimming organisms: Microgravity as an investigative tool 05 p0678 N90-13949
SWINGBY TECHNIQUE
Calculation of double-lunar swingby trajectories: I. Keplerian foundation 05 p0590 N90-13435
SWIRLING
Calculation on film preparation and film motion of a swirl atomizer
[ESA-TT-1096] 03 p0348 N90-11990
Swirl-stabilized flames: Fluid dynamics, mixing, and flame stability limits 08 p1040 N90-16009
Turbulence structure of mixing swirling flows
[AD-A216628] 11 p1506 N90-18671
Analytic solutions for the decay of turbulent swirling flow in a cylinder
[DE90-005744] 11 p1507 N90-18677
Vortex motion phase separator for zero gravity liquid transfer
[NASA-CASE-KSC-11387-1] 13 p1783 N90-20236
Numerical simulation of vortex breakdown
14 p1970 N90-21288
Modern developments in shear flow control with swirl
[NASA-CR-186586] 15 p2097 N90-22000
Unsteady group behavior of droplet clouds in swirling flows 16 p2233 N90-22743
Swirl coaxial injector element characterization for booster engines 23 p3294 N90-28632
SWIRLING WAKES
U TURBULENT WAKES
SWITCHES
NT ELECTRIC RELAYS
NT ELECTRIC SWITCHES
NT SWITCHING CIRCUITS
NT THERMOSTATS
Analysis of the performance of gallium arsenide photoavalanche switches
[DE89-015774] 01 p0129 N90-10739
Independent Orbiter Assessment (IOA): Analysis of the backup flight system
[NASA-CR-185567] 02 p0165 N90-10932
ANTHEM simulation of plasma opening switches
[DE89-016617] 02 p0217 N90-11239
An empirical formula for gas switch breakdown delay
[DE89-017233] 03 p0342 N90-11947
Superconducting switch program
[AD-A211580] 03 p0344 N90-11964
Experimental investigation of a fast-acting exploding metallic foil opening switch
[DE90-001051] 06 p0770 N90-14479
High speed transfer switch with 50 kA and 50 kV ratings
[DE90-002448] 06 p0770 N90-14481
A simple figure of merit for high temperature superconducting switches
[DE90-000610] 06 p0852 N90-14955
Single fluid simulations of plasma openings switch behavior
[DE90-002643] 07 p0921 N90-15330
Portable digital pressure indicator for calibrating magnetic tape recorders
[NASA-TM-101650] 07 p0933 N90-15401
Command operated liquid metal opening switch
[AD-D014262] 08 p1060 N90-16126
Thermal switch disc for short circuit protection of batteries
[NASA-CASE-MSC-21428-1] 09 p1209 N90-17008
Solid state electrical switch employing materials with reversible phase transistors
[NASA-CASE-NPO-17621-1-CU]
09 p1209 N90-17010
Analysis and evaluation of technical data on the photochromic and non-linear optical properties of materials
[AD-A216124] 10 p1431 N90-18254
Coating possibilities for magnetic switches
[DE90-006536] 11 p1504 N90-18659
Magnetohydrodynamic modeling of plasma opening switches and gas puff plasmas
[DE90-005825] 11 p1569 N90-19028
Fast optical switch and limiter using quantum size effect in metal grain composites
[AD-D014332] 12 p1619 N90-19305
Modeling A circuit switched multiprocessor interconnect
[AD-A217122] 12 p1656 N90-19519
Dynamics of plasma injection along magnetic field lines in the PBFA 2 (Particle Beam Fusion Accelerator 2) plasma opening switch
[DE90-006751] 12 p1717 N90-19862
Interaction of switch actuation on tracking with a four-axis flight control (cross-coupling)
[AD-A217981] 13 p1758 N90-20095
Electron-impact ionization and electron attachment cross sections of radicals important in transient gaseous discharges
[AD-A217510] 13 p1806 N90-20386
New methods in plasma simulation
[DE90-007507] 13 p1890 N90-20847
Simulator comparison of thumball, thumb switch, and touch screen input concepts for interaction with a large screen cockpit display format
[NASA-TM-102587] 14 p1921 N90-21005
Definition of a design methodology and study of the driving and protection functions of a smart power switch
[LAAS-89-330] 16 p2231 N90-22727
Long period pseudo random number sequence generator
[NASA-CASE-NPO-17241-1-CU]
17 p2394 N90-23636
Advanced guided wave electro-optical switches
[AD-A219784] 17 p2472 N90-24132
Investigations of laterally coupled all optical switches and detectors on silica fibers
[AD-A220297] 17 p2473 N90-24142
Neutron and gamma irradiation effects on power semiconductor switches
[NASA-TM-103200] 19 p2686 N90-25278
Performance of a self-aligning solar array tracking controller
[DE90-011184] 19 p2698 N90-25350
Integrated optics interdigitated-electrode switches
[AD-A223245] 21 p3076 N90-27490
Use of Ni63 overvoltage gap switches in the flight termination systems on boosters launched from US Army Kwajalein Atoll (USAKA)
[AD-A223866] 23 p3299 N90-28661
Investigations into the use of dielectric coatings in magnetic switches
[DE90-014331] 23 p3321 N90-28776
Modeling tape-wound magnetic switches
[DE90-015121] 23 p3322 N90-28782
SWITCHING
NT BEAM SWITCHING
NT MAGNETIC SWITCHING
NT MICROWAVE SWITCHING
NT OPTICAL SWITCHING
NT PACKET SWITCHING
Use of depletion edge translation for high-speed modulation and switching of lightwaves
[AD-A211186] 01 p0124 N90-10713
Switched power workshop: Introduction and summary
[DE90-000036] 03 p0342 N90-11952
Apparatus for cooling electronic components in aircraft
[AD-D014207] 05 p0579 N90-13373
Studies of structure and switching dynamics in ferroelectric crystal and liquid crystal thin films
[AD-A212650] 05 p0702 N90-14109
Avalanche photoconductive switching
[DE90-002980] 07 p0922 N90-15337
Efficient interconnection schemes for VLSI and parallel computation
[AD-A216405] 10 p1420 N90-18185
Induction motor control
[NASA-TM-102533] 12 p1605 N90-19234
Fast optical switch and limiter using quantum size effect in metal grain composites
[AD-D014332] 12 p1619 N90-19305
Modeling A circuit switched multiprocessor interconnect
[AD-A217122] 12 p1656 N90-19519
Optical Bistability, 1988
[AD-A217681] 13 p1888 N90-20832
Long period pseudo random number sequence generator
[NASA-CASE-NPO-17241-1-CU]
17 p2394 N90-23636
DURIP: Instrumentation for laser switched power LINAC
[AD-A222629] 20 p2868 N90-26318
Lyapunov-based control for switched power converters
[AD-A221974] 21 p3000 N90-27053
A computer for low contest-switch time
[AD-A222883] 21 p3038 N90-27269
SWITCHING CIRCUITS
Commercial high current ignitron development
[DE89-015077] 01 p0058 N90-10331
Pin switch circuits instrument for microsecond velocity measurements
[AD-A210638] 01 p0074 N90-10426
A contribution to the synthesis of communication switching systems with decentralized control using modular components
[ETN-89-94660] 02 p0214 N90-11226
Pulsed-power switching for inertial confinement fusion with light ion beams
[DE89-016810] 02 p0279 N90-11595
Launched electrons in plasma opening switches
[DE89-016886] 02 p0279 N90-11596
Power up modification for video switcher microprocessor interface for sensor system processing system
[AD-A211543] 03 p0344 N90-11962

Subnanosecond linear GaAs photoconductive switching, revision 1
[DE89-017739] 03 p0412 N90-12363
Contribution to the study of a self-protected static switch and its command strategy
[ECL-89-002] 05 p0636 N90-13711
A prototype microprocessor based audiometer for use by the CF (Canadian Forces) medical services for periodic hearing tests
[AD-A212990] 05 p0673 N90-13921
Studies of structure and switching dynamics in ferroelectric crystal and liquid crystal thin films
[AD-A212650] 05 p0702 N90-14109
Characterization of two MMIC GaAs switch matrices at microwave frequencies
[NASA-TM-102449] 06 p0733 N90-14273
High power density dc/dc converter: Selection of converter topology
[NASA-CR-186129] 06 p0768 N90-14467
Inductive store opening switch and tests for energy transfer to a load
[DE90-002818] 06 p0770 N90-14482
A cost effective battery bank for I(sup 2)T testing and evaluation of electrical switchgear
[DE90-002350] 06 p0772 N90-14490
LLNL's plan for a prototype circuit switch, a potential gigabit LAN of the future
[DE90-003614] 07 p0969 N90-15597
Programs for control of an analog-signal switching network
[DE90-003645] 07 p0974 N90-15626
Theoretical and computational studies of magnetic insulation and other plasma-opening-switch phenomena
[DE90-004421] 07 p0996 N90-15757
A physical and numerical study of the turn-off behavior of bipolar power transistors
[LAAS-89185] 08 p1061 N90-16136
The 120V 20A PWM switch for applications in high power distribution 10 p1335 N90-17724
Techniques for high frequency power conversion 10 p1336 N90-17729
Dynamical model of series-resonant converter with peak capacitor voltage predictor and switching frequency control 10 p1336 N90-17730
Power diode switching behavior
[ETN-90-95363] 12 p1653 N90-19501
An electron-beam controlled semiconductor switch
[AD-A217181] 13 p1793 N90-20288
Laser controlled semiconductor armature for electromagnetic launchers
[AD-D014435] 14 p1931 N90-21055
NASA's Advanced Communications Technology Satellite (ACTS): Will it benefit commercial/military satellites
[AD-A217710] 14 p1939 N90-21100
An assessment of the hardness of miniature vacuum tubes to high-voltage transients
[DE90-009541] 15 p2089 N90-21956
Optical shutter switching matrix
[NASA-CASE-KSC-11392-1] 15 p2167 N90-22383
Definition of a design methodology and study of the driving and protection functions of a smart power switch
[LAAS-89-330] 16 p2231 N90-22727
A network flow model for load balancing in circuit-switched multicomputers
[NASA-CR-182049] 17 p2451 N90-23977
Controling, cabling and protection of GTO thyristors in pulse inverters
[ETN-90-96500] 18 p2549 N90-24548
Generalized averaging method for power conversion circuits
[AD-A221977] 21 p3020 N90-27171
L-SWITCH: A PC-program for computing transient voltages and currents during switching off three-phase inductances
[PB90-191412] 22 p3167 N90-27961
Interconnection networks and parallel processing
[FEL-1989-112] 22 p3240 N90-28376

SWITCHING ELEMENTS
U SWITCHING CIRCUITS

SWITZERLAND
Problems related to aircraft noise in Switzerland 18 p2611 N90-24871
Trend analysis of total ozone data 24 p3486 N90-29703

SWIVELS
Double swivel toggle release
[NASA-CASE-MSC-21436-1] 14 p1987 N90-21390
Performance characteristics of a one-third-scale, vectorable ventral nozzle for SSTOVL aircraft
[NASA-TM-103120] 15 p2045 N90-21725

SYMBIOSIS
Computer symbiosis: Emergence of symbiotic behavior through evolution
[DE89-015247] 02 p0256 N90-11450
Job planning and execution monitoring for a human-robot symbiotic system
[DE90-004464] 09 p1261 N90-17315

SYMBIOTIC STARS
Infrared spectroscopy of novae and related objects 11 p1583 N90-19123
High resolution infrared spectroscopy of symbiotic stars 11 p1583 N90-19125

SYMBOLIC PROGRAMMING
On the efficient exploitation of speculation under data flow paradigms of control
[AD-A214112] 08 p1115 N90-16455
Knowledge based signal processing
[AD-A214864] 09 p1205 N90-16986
Symbol manipulation and applied mathematics
[AD-A214702] 09 p1273 N90-17378
Hypercube expert system shell-applying production parallelism
[AD-A215762] 10 p1418 N90-18173
An investigation of the locality of memory accesses during symbolic program execution
[AD-A218168] 13 p1875 N90-20750
Rules and maps in connectionist symbol processing
[AD-A219028] 16 p2264 N90-22903
An engineering approach to automatic programming 21 p3046 N90-27317
Optics and symbolic computing
[AD-A221443] 21 p3077 N90-27493
Optical symbolic processor for expert system execution
[AD-A224284] 24 p3525 N90-29931
Optical signal computing
[AD-A223624] 24 p3545 N90-30051

SYMBOLS
Stimulus-response compatibility in spatial precuing and symbolic identification: Effects of coding practice, retention, and transfer
[AD-A210745] 02 p0255 N90-11443
Frame synchronization methods based on channel symbol measurements 04 p0486 N90-12795
Performance of the split-symbol moments SNR estimator in the presence of inter-symbol interference 04 p0487 N90-12799
Numerical analysis of chaotic symbol sequences generated by parabolic and triangle maps of the interval
[MPIS-22/1987] 04 p0539 N90-13124
Development of the AH-64 display symbology training module
[AD-A213456] 07 p0968 N90-15592
MASC: Multiprocessor architecture for symbolic processing
[AD-A213504] 07 p0979 N90-15656
Symbol manipulation and applied mathematics
[AD-A214702] 09 p1273 N90-17378
Multiple symbol differential detection of uncoded and trellis coded MPSK
[NASA-CR-186288] 10 p1376 N90-17975
Exact closed-form expressions for the performance of the split-symbol moments estimator of signal-to-noise ratio 15 p2077 N90-21894
Technologies for electronic transfer of information: The present state and trends in Japan 15 p2177 N90-22443
Taxiway sign effectiveness under reduced visibility conditions
[DOT/FAA/CT-TN90/20] 19 p2662 N90-25150
Development of a methodology for icon evaluation
[NPL-DITC-159/90] 22 p3235 N90-28345
Wigner symbols, quantum dynamics, and the kicked rotator
[AD-A224024] 23 p3403 N90-29234

SYMMETRICAL BODIES
NT AXISYMMETRIC BODIES
NT BODIES OF REVOLUTION
NT CELESTIAL SPHERE
NT CONICAL BODIES
NT CYLINDRICAL BODIES
NT ELLIPSOIDS
NT FAIRINGS
NT ROTATING CYLINDERS
NT ROTATING SPHERES
NT SPHERES
NT TORUSES
A numeric analysis of incompressible, viscous flow around a symmetrical body of revolution
[ISL-CO-215/87] 08 p1064 N90-16157

SYMMETRY
NT BROKEN SYMMETRY
NT SUPERSYMMETRY
Moduli spaces and topological quantum field theories
[DE89-016943] 02 p0287 N90-11639
The algebraic Riccati equation and singular optimal control
[MEMO-COSOR-88-31] 05 p0690 N90-14028
R-matrices and higher Poisson brackets for integrable systems
[PREPRINT-669] 05 p0696 N90-14069
SL(2,R) current algebra in two-dimensional conformal quantum gravity
[DE90-600755] 07 p0983 N90-15675
Double-periodic wormholes in theories with global symmetries
[DE90-719575] 08 p1136 N90-16581
Vortex cores and vortex breakdown
[AD-A215266] 09 p1218 N90-17062
Factoring symmetric indefinite matrices on high-performance architectures
[NASA-CR-181982] 10 p1421 N90-18195
Cubic interaction in conformal theory of integer higher-spin fields in four dimensional space-time
[DE90-607095] 10 p1425 N90-18220
Electronic energies for Neon dimer dication radiative charge transfer
[AD-A215817] 10 p1429 N90-18244
Particle theory and cosmology
[DE90-005338] 10 p1446 N90-18346
New aspects in bifurcation with symmetry
[AD-A216506] 11 p1552 N90-18935
Dynamics of a class of vortex rings
[NASA-TM-102257] 12 p1657 N90-19524
Apparatus and method for locating the axis of symmetry (center of circular cross section) of three dimensional objects
[AD-D014407] 14 p1982 N90-21354
The production and spatial distribution of neutral and ionized water vapor in Comet P/Halley 15 p2185 N90-22484
Spaceborne radar observations: A guide for Magellan radar-image analysis
[NASA-CR-184998] 16 p2249 N90-22826
Non-symmetric double well and Euclidean functional integral
[PREPRINT-709] 16 p2305 N90-23133
Feasibility for EGRET detection of antimatter concentrations in the universe 16 p2338 N90-23323
Parallel computation of supersonic flows using a three-dimensional, zonal, Navier-Stokes code
[AD-A218824] 17 p2344 N90-23350
Discrete mathematics for communication systems
[AD-A220430] 17 p2457 N90-24022
Skew-symmetric matrices in classical mechanics
[MEMO-COSOR-89-23] 17 p2459 N90-24036
M-estimators in linear models with long range dependent errors
[AD-A219921] 17 p2461 N90-24053
Fabricating vanadium sheet to improve symmetry of drawn parts
[DE90-011253] 19 p2682 N90-25257
Liquid fueled ramjet combustion instability: Acoustical and vortical interactions with burning sprays
[AD-A222752] 20 p2831 N90-26104
Transient signal distortion and coupling in multilayer multiconductor MIC microstrips
[AD-A222989] 21 p3000 N90-27050
Symmetry and global bifurcation in nonlinear solid mechanics
[AD-A221981] 21 p3013 N90-27129
Can the chirality of the ISM be measured 21 p3095 N90-27590
Ternary and quaternary oxides of Bi, Sr, and Cu 22 p3141 N90-27817
Numerical simulations of flowfields in a central-dump ramjet combustor. 3: Effects of chemistry
[AD-A224145] 23 p3282 N90-28573
Beltrami algebra and symmetry of Beltrami equation on Riemann surfaces
[DE90-627157] 23 p3388 N90-29135
On the zeta-function regularization of chiral Jacobians for singular Dirac operators
[DE90-627176] 23 p3390 N90-29150
Twisted crystals: Propagation, genesis, and relationships with optical activity and molecular symmetry (excerpts)
[DE90-014259] 23 p3399 N90-29205
Symmetrical layered thin film edge field-emitter-array and method for its production
[AD-D014594] 24 p3464 N90-29569
Symmetry and island structure of the standard map
[DE90-508076] 24 p3548 N90-30069

SYMMETRY BREAKING
U BROKEN SYMMETRY

SYMPATHETIC NERVOUS SYSTEM
A program for the study of skeletal muscle catabolism following physical trauma
[AD-A216569] 11 p1539 N90-18859
Effects of cholinergic drugs on exercise performance and simple reaction time of rhesus monkeys
[AD-A219455] 17 p2433 N90-23862

SYMPATHOMIMETICS
U ADRENERGICS

SYMPOSIA
U CONFERENCES
SYMPTOMS
U SIGNS AND SYMPTOMS
SYNAPSES
Synaptic plasticity and memory formation
[AD-A211368] 03 p0379 N90-12158
Fear-potentiated startle as a model system for analyzing learning and memory
[AD-A212131] 04 p0525 N90-13029
Analog hardware for delta-backpropagation neural networks
[NASA-CASE-NPO-17564-1-CU] 09 p1204 N90-16974
SYNCHRONISM
NT BIT SYNCHRONIZATION
NT FREQUENCY SYNCHRONIZATION
Synchrony with empty process — the algebra of synchronous processes
[CWI-CS-R8832] 02 p0261 N90-11481
Asynchronous integration of ordinary differential equations on multiprocessors
[DE89-014169] 02 p0263 N90-11493
Studies on predicting the resynchronization of the circadian system after transmedian flights
[DFVLR-FB-89-10] 03 p0382 N90-12172
Sequential searching in multidimensional monotone arrays
[AD-A211938] 03 p0384 N90-12188
Adaptive backoff synchronization techniques
[AD-A213966] 07 p0980 N90-15658
Using mappings to prove timing properties
[AD-A213967] 07 p0981 N90-15666
Periodic phase adjustment distributed clock synchronization in the hard realtime environment
[AD-A213842] 07 p0988 N90-15708
A burst compression and expansion technique for variable-rate users in satellite-switched TDMA networks
[NASA-TM-102414] 08 p1035 N90-15983
Parallel asynchronous systems and image processing algorithms 08 p1075 N90-16218
Multisqueezing of mechanical states and back-action evasion measurements
[IFSI-89-6] 08 p1123 N90-16504
Synchronization of the ground station atomic clocks using three weighted transportable cesium time standards in the Navex navigation experiment
[ESA-TT-1153] 11 p1512 N90-18711
Log-based recovery in asynchronous distributed systems
[NASA-CR-186190] 11 p1550 N90-18924
Priority arbitration with busses
[AD-A216392] 12 p1704 N90-19784
Preliminary results of the peak experiment. ALTAIR deep-space measurements
[AD-A218622] 16 p2229 N90-22714
Hand shaping: A paradigm for cognitive/motoric interaction
[AD-A219908] 17 p2437 N90-23885
The cost of conservative synchronization in parallel discrete event simulations
[NASA-CR-182034] 17 p2441 N90-23912
Sharing memory robustly in message-passing systems
[AD-A219923] 17 p2447 N90-23950
Constraint-oriented specification in a constructive formal description technique
[MEMO-INF-89-44] 17 p2463 N90-24070
Implementation of an I-structure memory controller
[AD-A221397] 18 p2588 N90-24726
Synchronously parallel Boltzmann machines: A mathematical model
[MEMO-COSOR-89-21] 18 p2590 N90-24732
CESAR sequencer
[FFI-89/7021] 19 p2744 N90-25599
Direct-sequence spread spectrum system
[AD-A223021] 20 p2856 N90-26245
MTP: An atomic multicast transport protocol
[NASA-CR-186716] 20 p2858 N90-26254
A model of the synchronous machine with rectifier, especially for control purposes
[EUT-89-E-215] 20 p2858 N90-26256
A possibility to incorporate saturation in the simple, global model of a synchronous machine with rectifier
[EUT-89-E-225] 20 p2858 N90-26258
Knowledge and inhibition in asynchronous distributed systems
[TR-90-1139] 20 p2935 N90-26703
Fact system: A standardizing modelization processing for concurrent systems
[ETN-90-97286] 24 p3533 N90-29982
SYNCHRONIZATION
U SYNCHRONISM
SYNCHRONIZED OSCILLATORS
Laser activities 06 p0786 N90-14576
Tunable CW single-frequency source for injection seeding 2-micrometer lasers
[AD-A223979] 23 p3331 N90-28834
SYNCHRONOUS COMMUNICATION SATELLITES
U SYNCOM SATELLITES
SYNCHRONOUS DETECTORS
U CORRELATORS
SYNCHRONOUS MOTORS
Induction motor control
[NASA-TM-102533] 12 p1605 N90-19234
Design and use of high speed synchronous motor running in aggressive liquids 18 p2538 N90-24478
Microcomputer for the digital regulation of permanent magnet-synchronous servomotors
[ETN-90-96507] 18 p2588 N90-24727
SYNCHRONOUS PLATFORMS
Earth Science Geostationary Platform Technology
[NASA-CP-3040] 12 p1608 N90-19249
Operational requirements and the geostationary platform 12 p1608 N90-19250
Science requirements for passive microwave sensors on earth science geostationary platforms 12 p1608 N90-19251
Geostationary earth science platform concepts 12 p1608 N90-19252
Large space antenna concepts for ESGP 12 p1608 N90-19253
Design of a low-frequency (5-20 GHz), 15-meter-diameter passive radiometer for geostationary earth science platforms 12 p1609 N90-19255
Structures for remotely deployable precision antennas 12 p1609 N90-19256
Coherent radar measurement of ocean currents from geostationary orbit 12 p1609 N90-19259
Rain radars for earth science geostationary platforms: Some possibilities 12 p1610 N90-19262
An Earth orbiting satellite service and repair facility
[NASA-CR-186669] 19 p2665 N90-25166
Texstar: The all-Texas educational satellite system
[NASA-CR-186654] 20 p2820 N90-26045
Dust clouds Kosa from the east Asian dust storms in 1982-1988 as observed by the GMS satellite 21 p3028 N90-27214
Reproduction of GMS IR calibration table 21 p3028 N90-27215
Distribution and movement of smokes from forest fires that occurred along the boundary of the People's Republic of China and the USSR on April-May 1987 21 p3028 N90-27216
Behavior of dust clouds from Australian dust storms in 1982-1983 as observed by the GMS 21 p3029 N90-27221
Thermal-distortion analysis of an antenna strongback for geostationary high-frequency microwave applications
[NASA-TP-3016] 22 p3125 N90-27738
Orbit computation 22 p3128 N90-27750
SYNCHRONOUS SATELLITES
NT GOES SATELLITES
NT GOES 4
NT SYNCOM SATELLITES
Inexpensive global location and tracking systems using geostationary satellites
[AD-A213025] 05 p0602 N90-13498
SCATHA (Spacecraft Charging at High Altitudes) atlas data base, volume 1
[AD-A214204] 07 p0886 N90-15127
Spacecraft environmental anomalies handbook
[NASA-CR-186331] 09 p1182 N90-16852
The INMARSAT-2 solar generator panels 10 p1343 N90-17782
Tracking a hypersonic aircraft from a space platform
[AD-A216399] 10 p1377 N90-17984
Orbital maneuvers optimization for station acquisition of geostationary satellites. Deterministic and stochastic approaches
[LAAS-89-359] 16 p2206 N90-22589
Flight model discharge system
[AD-A220261] 18 p2510 N90-24342
Optimization of the deployment of a pair of satellites in inclined eccentric geosynchronous orbits 22 p3128 N90-27751
A three axis attitude control of a satellite
[NASDA-TR-22] 24 p3439 N90-29421
Satellite motion in an axi-symmetric gravitational field. Part 1: Perturbations due to J2 (second order) and J3
[RAE-TR-88068] 24 p3440 N90-29429
SYNCHROTRON RADIATION
Research in X-ray optics with the ultimate aim of constructing a synchrotron radiation pumped soft X-ray lithium laser
[DE89-016788] 02 p0227 N90-11304
Synchrotron radiation, free electron laser, and nuclear structure
[DE89-017352] 02 p0228 N90-11306
X-ray lithography sources: A review
[DE89-017610] 02 p0271 N90-11547
The behavior of beams of relativistic non-thermal electrons under the influence of collisions and synchrotron losses
[NASA-CR-185983] 03 p0401 N90-12298
Synchrotron-radiation experiments with recoil ions
[DE89-017579] 03 p0402 N90-12301
The national synchrotron light source and its applications
[DE89-017605] 03 p0405 N90-12320
Center for X Ray Optics, 1988
[DE90-003300] 07 p0992 N90-15732
Non-destructive trace element microanalysis of as-received cometary nucleus samples using synchrotron x ray fluorescence 08 p1147 N90-16649
Fluorescence from photoexcitation of Cl2 at 50 to 105 nm
[NASA-CR-186206] 09 p1189 N90-16888
To construct a linac/storage ring FEL facility
[AD-A214620] 09 p1211 N90-17020
Biomedical applications of synchrotron x ray microscopy
[DE90-004957] 11 p1540 N90-18867
A continuous plasma final focus
[DE90-006096] 11 p1568 N90-19024
X ray microimaging by diffractive techniques
[DE90-008444] 13 p1804 N90-20356
Design of D-3 He commercial tokamak
[DE90-008252] 13 p1891 N90-20852
A requirement for Australian research: Access to big science facilities, a report by the Australian National Committee for Crystallography
[DE90-614784] 14 p1930 N90-21048
Origin of pulsed emission from the young supernova remnant SN 1987A
[CAL-377] 15 p2182 N90-22469
Impedance and wakefields beyond cutoff
[CEBAF-PR-89-016] 19 p2756 N90-25663
Probing interfacial structure and composition with x ray standing waves
[AD-A223071] 21 p2977 N90-26916
Variable length-scale studies at interfaces with X ray standing waves
[AD-A223043] 21 p3004 N90-27075
Identification of tetragonal and cubic structures of zirconia
[AD-A222373] 21 p3083 N90-27535
Status of the advanced light source
[DE90-015636] 23 p3395 N90-29185
Effects and control of the correlation properties of light sources
[AD-A224539] 24 p3545 N90-30049
SYNCHROTRONS
NT STORAGE RINGS (PARTICLE ACCELERATORS)
A compact X-ray lithography lattice using superferric magnets
[DE89-013947] 01 p0127 N90-10728
A solution to nonlinearity problems
[DE89-016975] 02 p0270 N90-11544
Bunch length in internal target mode
[NIKHEF-AMPS/89/04] 04 p0496 N90-12854
Synchrotron-betatron parametric instability in free-electron lasers
[AD-A213373] 05 p0648 N90-13777
A Scanning Photoelectron Microscope (SPEM) at the National Synchrotron Light Source (NSLS)
[DE90-001551] 06 p0780 N90-14537
Trace element abundance determinations by Synchrotron X Ray Fluorescence (SXRF) on returned comet nucleus mineral grains 08 p1142 N90-16619
Report on the fifth workshop on synchrotron x ray lithography
[DE90-007903] 15 p2172 N90-22411
Research and applications of metallic superlattices, high T(sub c) superconductors, x ray optics, and compact synchrotrons 16 p2311 N90-23170
Technical activities 1989, Electron and Optical Physics Division
[PB90-207267] 23 p3415 N90-29296
SYNCOM SATELLITES
Syncom 4 deploy, LDEF retrieval highlight 10-day Columbia flight
[NASA-NEWS-RELEASE-89-180] 05 p0594 N90-13448
SYNDROMES
U SIGNS AND SYMPTOMS
SYNOPTIC MEASUREMENT
EIT: Solar corona synoptic observations from SOHO with an Extreme-ultraviolet Imaging Telescope 04 p0567 N90-13309
SYNOPTIC METEOROLOGY
Research highlights of the NMC (National Meteorological Center) Development Division: 1987-1988
[PB89-206478] 01 p0088 N90-10501
Synoptic/planetary-scale interactions and blocking over the North Atlantic Ocean 03 p0360 N90-12061

Tropical Pacific moisture variability
03 p0362 N90-12070
The effect of latent heat release on synoptic-to-planetary wave interactions and its implication for satellite observations: Theoretical modeling
03 p0362 N90-12073
Cloud cover determination in polar regions from satellite imagery
[NASA-CR-186096] 04 p0520 N90-13003
The identification of terrain-induced circulations using principal components
[DE90-001991] 06 p0815 N90-14739
The development of a spatial synoptic climatological index for environmental analysis
06 p0816 N90-14744
Synoptic scale tropical waves in multichannel satellite radiance data 06 p0816 N90-14745
Workshop on synoptic meteorology instruction
[PB90-109950] 06 p0817 N90-14751
The role of an upstream cyclone and corresponding synoptic/planetary-scale interactions during the development of a blocking anticyclone
08 p1150 N90-16659
Colloquium on Synoptic Meteorology
[PB90-121112] 12 p1692 N90-19720
An atlas of ECMWF analyses (1980-1987). Part 2: Second moment quantities
[NASA-TM-100762-PT-2] 19 p2715 N90-25451
A study of the effect of synoptic scale processes in GCM modelling
[NASA-CR-184804] 21 p3021 N90-27175
The instability mechanism of synoptic-scale eddies
22 p3211 N90-28217
The 27-28 October 1986 FIRE cirrus case study: Meteorology and clouds 22 p3223 N90-28280
Atmospheric environment for Space Shuttle (STS-32) launch
[NASA-TM-100400] 23 p3346 N90-28912
Atmospheric environment for Space Shuttle (STS-31) launch
[NASA-TM-103508] 23 p3347 N90-28913
Atmospheric environment for space shuttle (STS-36) launch
[NASA-TM-100403] 23 p3347 N90-28914
Atmospheric environment for space shuttle (STS-34) launch
[NASA-TM-100396] 23 p3347 N90-28915

SYNTAX
NT SENTENCES
NT WORDS (LANGUAGE)
Computer generation of a tutorial dialogue
[AD-A211976] 03 p0380 N90-12162
Taxonomic syntax for first order inference
[AD-A211618] 03 p0390 N90-12221
DOD Gateway Information System (DGIS) common command language: A retrospective on the introduction of prolog as the development tool
[AD-A211941] 03 p0418 N90-12400
A table-driven approach to fast context-free parsing
[AD-A212210] 04 p0533 N90-13082
Database interfaces on NASA's heterogeneous distributed database system
[NASA-CR-185420] 05 p0706 N90-14133
Knowledge based text generation
[AD-A214273] 07 p0977 N90-15645
An introduction to Montague grammar
[REPT-89-46] 15 p2147 N90-22266
Some remarks on treatment of be in Montague's PTQ --- Proper Treatment of Quantification (PTQ)
[REPT-89-40] 15 p2147 N90-22267
Knowledge structure representation and automated updates in intelligent information management systems
15 p2156 N90-22316
Durra: A task-level description language reference manual, version 2
[AD-A219293] 16 p2301 N90-23114
Syntax, semantics, and pragmatism: An integrated focus based on textual linguistic knowledge
[INPE-4992-PRE/1554] 16 p2326 N90-23262
Natural language syntax and first order inference
[AD-A219944] 17 p2447 N90-23951
Dynamic predicate logic: Towards a compositional, non-representational semantics of discourse
[ITLI-LP-89-02] 17 p2464 N90-24076
Design of a specification language by abstract syntax engineering
[CWI-CS-R8934] 18 p2599 N90-24789
Current methods of digital speech processing
21 p2993 N90-27010
Zadok user guide
[AD-A222071] 21 p3054 N90-27360
The SPECIALIST: Natural language processing system
[PB90-240029] 23 p3381 N90-29098
Formal semantics of SQL queries
[REPT-89-069] 24 p3531 N90-29973

SYNTHESIS (CHEMISTRY)
NT COPOLYMERIZATION
NT DIMERIZATION
NT POLYMERIZATION
International Conference on Organometallic Chemistry (13th) held in Torino, Europe on 4-9 September 1988: Abstracts
[AD-A210617] 01 p0033 N90-10178
Measuring the shielding effectiveness of superconductive composites
[DE89-015164] 01 p0033 N90-10180
Raman spectroscopic study of the rare earth sesquisulfides
[AD-A210610] 01 p0041 N90-10226
Metal-assisted syntheses of boranes and carboranes
[AD-A210728] 01 p0041 N90-10227
The synthesis and structure of novel antimony thiametallacycles
[AD-A210888] 01 p0042 N90-10229
Analysis of surface modified colloidal silicas
[DE89-015849] 01 p0047 N90-10267
New polymer precursors to boron and silicon nitrides
[AD-A210287] 01 p0049 N90-10279
Control of synthetic peptide tertiary structure
[AD-A210339] 01 p0049 N90-10281
Comparison of carboxylated and sulfonated model polyurethane ionomers
[AD-A210438] 01 p0050 N90-10284
Synthesis and interfacial properties of new generation polyurethane systems
[AD-A210446] 01 p0050 N90-10286
Monolayer formation characteristics of novel organic molecules with nonlinear optically active moieties
[AD-A210496] 01 p0121 N90-10693
Synthesis and chemistry of strained and conjugated fluorocarbons
[AD-A211633] 03 p0324 N90-11844
Suppression of side chain crystallization and transformation of monotropic mesophases into enantiotropic mesophases by copolymerization of the parent polymers' monomer pairs containing constitutional isomeric mesogenic side groups
[AD-A209066] 03 p0330 N90-11878
Boron analogues of amino acids and derivatives
[AD-A211311] 03 p0379 N90-12157
Structure-property relationships as an aid in the rational design of (beta)-(ET)(sub 2)X organic superconductors
[DE89-016912] 03 p0410 N90-12356
Synthesis and microstructure of highly oriented PbTiO3 thin films prepared by a sol-gel method
[AD-A211735] 03 p0414 N90-12377
Electrically conducting organic materials: Design, synthesis and characterization
[AD-A212214] 04 p0471 N90-12700
The multivalent beta'-aluminas
[AD-A212103] 04 p0478 N90-12738
Transition metal catalyzed synthesis of organmetallic polymers
[AD-A212133] 04 p0478 N90-12740
Synthesis and crystallization behavior of fluoride glasses
[AD-A212142] 04 p0478 N90-12741
The chemistry of hexaazatriphenylene hexanitrile, a polyfunctional heterocycle with potential utility in the formulation of thermostable polymers
[AD-A212353] 04 p0480 N90-12757
Synthesis and characterization of new low-dimensional metal complex conductors
[AD-A213189] 04 p0498 N90-12871
Synthesis and properties of NdNiO(3) prepared by low temperature methods
[AD-A212117] 04 p0559 N90-13256
Synthesis and study of materials for superconducting electronics
[AD-A212966] 04 p0561 N90-13270
Computer synthesis of ceramic preforms for molten-metal infiltration
[DE90-000826] 06 p0751 N90-14370
Pentafluorothio polynitroaliphatic explosives
[AD-D014221] 06 p0753 N90-14383
Novel polyimide compositions based on 4,4': Isophthaloyldiphthalic anaydride (IDPA)
[NASA-CASE-LAR-14194-1] 07 p0890 N90-15148
Wet spinning of solid polyamic acid fibers
[NASA-CASE-LAR-14162-1] 07 p0910 N90-15259
Polyimides with carbonyl and ether connecting groups between the aromatic rings
[NASA-CASE-LAR-14001-1] 07 p0910 N90-15260
Optical properties and laser damage measurements of inorganic polymer films
[DE90-003633] 07 p0911 N90-15267
Survey on synthesis technologies of methanol as an alternative fuel
[DE89-901303] 07 p0914 N90-15284
Inorganic halogen oxidizers
[AD-A213990] 07 p0915 N90-15294
Solid-state electrolyte catalysis for methane and oxygen synthesis
[PB90-100231] 08 p1040 N90-16011
Carbon-13 nuclear magnetic resonance of heterocyclic salts and its precursors
[DE89-635768] 08 p1041 N90-16016
Synthesis of air-sinterable lanthanum chromite powders
[DE90-004681] 08 p1046 N90-16049
Silicon-based coatings on niobium metal
[DE90-003651] 08 p1048 N90-16057
Copolymers for drag reduction in marine propulsion: New molecular structures with enhanced effectiveness
[AD-A214444] 08 p1049 N90-16062
Shock-induced reaction synthesis of aluminides and silicides
[DE90-003948] 08 p1049 N90-16066
Synthesis of tetrafluorohydrazine
[AD-D014281] 08 p1052 N90-16083
High temperature neutron diffraction study of the formation reaction of bismuth superconductors
[DE90-004883] 08 p1134 N90-16568
Electrochemical cell for obtaining oxygen from carbon dioxide atmospheres
[NASA-CR-186225] 09 p1189 N90-16886
Microporous structure with layered interstitial surface treatment, and method and apparatus for preparation thereof
[NASA-CASE-MSC-21487-1] 09 p1189 N90-16887
Highly reduced carbene complexes: Formation of an alkoxymalonate by coupling of carbon dioxide with the nucleophilic carbene in Cr(CO4)=C(OMe)Ph2(-)
[AD-A215132] 09 p1191 N90-16902
LARC-IA: A flexible backbone polyimide
[NASA-TM-102586] 09 p1196 N90-16926
Copolyimide with a combination of flexibilizing groups
[NASA-CASE-LAR-13821-1] 09 p1199 N90-16950
The processing and mechanical properties of high temperature/high performance composites. Book 1, section 1: Coatings and interfaces
[AD-A216141] 10 p1348 N90-17821
Control of titanium diboride SHS reactions by inert dilutions and mechanical constraint
[AD-A214378] 10 p1357 N90-17870
Synthesis of high-purity sinterable silicon nitride powder
[DE90-007050] 11 p1493 N90-18593
Optimum catalytic process for alcohol fuels from syngas
[DE90-005290] 11 p1494 N90-18600
High growth rate diamond synthesis in a large area atmospheric pressure inductively coupled plasma
[AD-A216090] 11 p1567 N90-19019
New Condensation polyimides containing 1,1,1-triaryl-2,2,2-trifluoroethane structures
[NASA-CASE-LEW-14346-1] 12 p1618 N90-19300
Synthesis and chemistry of unsaturated metal nitrogen compounds
[AD-A216550] 12 p1622 N90-19321
FWP executive summaries: Basic energy sciences materials sciences programs
[DE90-006373] 12 p1722 N90-19893
Preparation and properties of the system Cu(x)Pd(1-x)O (0 less than or equal to x less than or equal to 0.175)
[AD-A217567] 12 p1723 N90-19901
The 1-((diorganooxyphosphonyl)-methyl)-2,4- and -2,6-diamido benzenes
[NASA-CASE-ARC-11425-4] 13 p1766 N90-20133
Analytical electron microscopy of catalyst preparations
[DE90-008699] 13 p1773 N90-20173
Process for making a noble metal on tin oxide catalyst
[NASA-CASE-LAR-13741-1-SB] 13 p1774 N90-20180
An investigation of the mechanisms of solid state powder reaction in the combustion synthesis and sintering of high temperature materials
[DE90-007880] 13 p1777 N90-20198
Human serum albumin crystals and method of preparation
[NASA-CASE-MFS-28234-1] 13 p1850 N90-20616
Development of gamma-emitting, receptor-binding radiotracers for imaging the brain and pancreas
[DE90-008314] 13 p1851 N90-20621
Synthesis and properties of polycrystalline Tl2Ba2CaCu2O(x) and Tl2Ba2Ca2Cu3O(x)
[DE90-007528] 13 p1897 N90-20887
Synthesis of Bi-Sr-Ca-Cu oxide superconductor by solution technique
[DE90-008707] 13 p1897 N90-20888
Bis(4-(3,4-dimethylenepyrrolidyl)-phenyl) methane
[NASA-CASE-LAR-13965-1-CU] 14 p1942 N90-21118
Apparatus for mixing solutions in low gravity environments
[NASA-CASE-MFS-26047-1] 14 p1958 N90-21209

Method of making a long life high current density cathode from tungsten and iridium powders using a quarternary compound as the impregnant
[AD-D014425] 14 p1958 N90-21211
Alternative materials for solid oxide fuel cells
[DE90-008615] 14 p2001 N90-21468
Method of making a cathode from tungsten powder
[AD-D014434] 15 p2069 N90-21850
Polysiloxanes derived from the controlled hydrolysis of tetraethoxysilane as precursors to silica for use in ceramic processing
[NASA-TM-102489] 15 p2070 N90-21858
Preparation and characterization of Cu2ZnGeS(4-y)Se(y)
[AD-A217469] 15 p2171 N90-22407
The first example of an organogallium compound containing a Ga-Te bond: Synthesis, properties, and molecular structure of ((Me3CCH2)2GaTeph)2
[AD-A219258] 16 p2210 N90-22608
Synthesis and properties of a thermotropic copolyester based on 4,4 prime-dihydroxy-a,a prime-dimethylbenzalazine
[AD-A218803] 16 p2223 N90-22682
Synthesis and characterization of aromatic polyester and polysiloxane containing block copolymers: Multiphase transparent atomic oxygen resistant damping materials, liquid crystal films, and toughening components of sol/gel glasses
[AD-A218871] 16 p2224 N90-22685
Experimental studies on energy storage
[AD-A219032] 16 p2252 N90-22845
Substituted 1,1,1-triaryl-2,2,2-trifluoroethanes and processes for their synthesis
[NASA-CASE-LEW-14345-2] 17 p2371 N90-23497
Acetylene terminated aspartimides and resins therefrom
[NASA-CASE-LAR-14188-1] 17 p2379 N90-23545
Process for lowering the dielectric constant of polyimides using diamic acid additives
[NASA-CASE-LAR-13902-1] 17 p2379 N90-23546
NMR studies of polymeric solid electrolytes
[AD-A219833] 17 p2381 N90-23562
Preparation, properties, and development of calcium lanthanum sulfide as an 8- to 12-micrometer transmitting ceramic
[AD-A220200] 17 p2382 N90-23565
Second order non-linear optical polyphosphazenes
[AD-A219868] 18 p2615 N90-24895
Synthesis of large area, monocrystalline TiC as a substrate for heteroepitaxial growth of beta-SiC
[AD-A221392] 18 p2623 N90-24948
Practical superconductor development for electrical power applications
[DE90-010262] 18 p2625 N90-24957
Computed structures of polyimides model compounds
[NASA-TM-101674] 19 p2672 N90-25195
Preparation of ultra-pure metal halides
[AD-D014529] 19 p2674 N90-25204
Preparation and characterization of properties of oxynitride glasses and fibers
[AD-A221334] 19 p2677 N90-25227
Synthesis of high purity sinterable silicon carbide powder
[DE90-012029] 20 p2828 N90-26084
Composite materials with improved properties in compression: Synthesis of 3-methylene-1,1-Dichlorosilacyclobutane and 1,1-dichlorosilacyclopent-3-ene
[AD-A222615] 20 p2828 N90-26088
Condensation polyimides
[NASA-TM-103467] 20 p2836 N90-26129
Stibathiolanes: Synthesis, solid state structure, and solution behavior
[AD-A223255] 20 p2933 N90-26688
Composite materials with improved properties in compression. Appendix 1: Cyclopropanation of poly(1-methyl 1-phenyl 1-sila-cis-pent-3-ene). Synthesis and characterization of poly(1-methyl 3,4-methylene-1-phenyl 1-sila-cis-pent-3-ene)
[AD-A221494] 21 p2971 N90-26889
The synthesis and structure of stibaindoles
[AD-A222990] 21 p2976 N90-26914
Synthesis, structure, electric, and magnetic properties of CaNiN
[AD-A222273] 21 p2978 N90-26923
Imide/arylene ether copolymers
[NASA-CASE-LAR-14159-1-CU] 21 p2983 N90-26953
Polyimidazoles via aromatic nucleophilic displacement
[NASA-CASE-LAR-14145-1] 21 p2983 N90-26954
Aromatic polyimides containing a dimethylsilane-linked dianhydride
[NASA-CASE-LAR-14198-1] 21 p2984 N90-26956
Elastomers and other organic composites
[AD-A222772] 21 p2984 N90-26958
Synthesis of energetic single phase and multi-phase polymers
[AD-A222491] 21 p2988 N90-26981
Preparation and magnetic measurements of single crystal Tl2Ba2CaCu2O8
[DE90-013657] 21 p3081 N90-27519
Synthesis, structure, and properties of Ca2ZnN2
[AD-A222012] 21 p3083 N90-27533
Composite materials with improved properties in compression: Synthesis and dimerization 2,3-dimethyl-5-silaspiro(4.4)nona-2,7-diene
[AD-A222552] 22 p3156 N90-27892
Catalytic synthesis of polymethylsilsesquioxanes
[AD-A222643] 22 p3159 N90-27910
Novel side-chain liquid cyrstalline polymers
[AD-A221998] 22 p3159 N90-27911
A study of catalysts and mechanisms in synthesis reactions
[DE90-015064] 23 p3304 N90-28691
Synthesis and structural chemistry of Au(III)-substituted Ba2YCu3O(7-delta)
[NASA-TM-103292] 23 p3305 N90-28696
A new low density, high porosity lithium hydride-beryllium hydride foam
[DE90-015150] 23 p3313 N90-28739
Novel macrocyclic carriers for proton-coupled liquid membrane transport
[DE90-015529] 24 p3445 N90-29453
Pyrromethene-BF2 complexes as laser dyes
[AD-A223562] 24 p3473 N90-29631
Synthesis and property evaluation of Y-Ba2-Cu3-O(6+x) superconductors
[AD-A223494] 24 p3552 N90-30098

SYNTHETIC APERTURE RADAR

NT SIDE-LOOKING RADAR

The development of mission-specific advanced inertially-based avionics system
02 p0149 N90-10851
A high precision gravity compensation system for the deployment test of the ERS-1 SAR antenna
02 p0183 N90-11038
Simulation of synthetic aperture radar 1: Feature density and accuracy requirements
[AD-A211019] 02 p0213 N90-11218
Aircraft SAR simulation Sargen 1.0
[FEL-1989-44] 04 p0491 N90-12823
Conception and results of the DLR realtime azimuth processor for the E-SAR system
[DLR-FB-89-30] 04 p0492 N90-12827
First-order Bragg SAR imagery of Kelvin wakes and moving internal wave fields
[AD-A213361] 05 p0633 N90-13691
Development of a traveling wave tube for the project X-SAR. Construction and testing of a breadboard model
[ETN-90-95900] 05 p0636 N90-13713
Frequency agile synthetic aperture radar
[AD-D014235] 06 p0765 N90-14451
Polarimetric SAR antenna characterization
[AD-A213438] 07 p0917 N90-15306
Necessity and benefit of the X-SAR Space Shuttle experiment
[ESA-TT-1164] 08 p1057 N90-16112
Science plan for the Alaska SAR facility program. Phase 1: Data from the first European sensing satellite, ERS-1
[NASA-CR-185028] 08 p1091 N90-16312
Investigation of the backscatter behavior of selected test areas in two geocoded SEASAT-SAR scenes in greater Bonn (Fed. Republic of Germany)
08 p1094 N90-16331
Investigation of the topographic components of the image content of radar pictures
08 p1094 N90-16332
Parallel algorithm for determining motion vectors in ice floe images by matching edge features
08 p1114 N90-16451
The development of an airborne synthetic aperture radar motion compensation system 09 p1165 N90-16745
Simulation of synthetic aperture radar 2: Simulating SAR (Synthetic Aperture Radar) using the advanced visual technology system
[AD-A213659] 09 p1204 N90-16976
Target classification using SAR (Synthetic Aperture Radar) polarimetric data
[AD-A215672] 09 p1208 N90-17002
Active and passive remote sensing of ice
[AD-A214863] 09 p1241 N90-17199
A Doppler centroid estimation algorithm for SAR systems optimized for the quasi-homogeneous source
[NASA-CR-186229] 09 p1275 N90-17391
Power conditioning for active array SAR antennas
10 p1338 N90-17744
Fractal geometry segmentation of polarimetric synthetic aperture radar images
[AD-A216278] 10 p1377 N90-17982
Synthetic aperture radar imagery of airports and surrounding areas: Archived SAR data
[NASA-CR-4275] 11 p1453 N90-18371
Synthetic aperture radar imagery of airports and surrounding areas: Philadelphia Airport
[NASA-CR-4280] 11 p1453 N90-18372
Simulation of synthetic aperture radar 3: Evaluation of prototype digital feature analysis data
[AD-A216750] 11 p1498 N90-18620
An application of ocean wave-current refraction to the gulf stream using SEASAT SAR data
[AD-A216769] 11 p1537 N90-18851
Activities report in German aerospace
[ISSN-0070-3966] 11 p1595 N90-19189
Rosetta/CNSR altimeter and sounding radar
12 p1741 N90-20009
Tomographic processing of synthetic aperture radar signals for enhanced resolution
[AD-A217178] 13 p1789 N90-20265
High Resolution Air- and Spaceborne Radar
[AGARD-CP-459] 14 p1960 N90-21223
Concepts for high resolution space based SAR/ISAR systems: Preliminary design considerations
14 p1960 N90-21224
Trade-offs in a space based surveillance radar
14 p1960 N90-21225
Application of superresolution methods for airborne radar 14 p1961 N90-21227
ROSAR (Helicopter-Rotor based Synthetic Aperture Radar) 14 p1961 N90-21229
Capabilities of bistatic synthetic aperture radar for covert battlefield surveillance 14 p1961 N90-21230
Real-time adaptive radiometric correction for imaging radars systems 14 p1962 N90-21233
Concept for a spaceborne Synthetic Aperture Radar (SAR) sensor based on active phased array technology
14 p1962 N90-21234
A motion compensation study for the PHARUS project
14 p1962 N90-21235
A solution for real time motion compensation for SAR without using inertial navigation systems
14 p1962 N90-21236
SAR and ISAR imagery of marine targets
14 p1962 N90-21237
Problems in ISAR processing with range resolution by stepped frequency bursts 14 p1962 N90-21238
A fast ISAR-imaging process and its inherent degrading effects on image quality 14 p1963 N90-21239
Radar observations of a formation of two fighters: A case study for ISAR imaging 14 p1963 N90-21240
The 1D-ISAR imaging of manoeuvering aircraft
14 p1963 N90-21241
Radar target image by ISAR case study
14 p1963 N90-21242
Concept and results of the DLR realtime SAR processor 14 p1963 N90-21244
Image simulation of geometric targets for synthetic aperture radar 14 p1964 N90-21245
SAR image coding 14 p1964 N90-21246
Using connected-element interferometer phase-delay data for Magellan navigation in Venus orbit
15 p2075 N90-21885
Spaceborne radar observations: A guide for Magellan radar-image analysis
[NASA-CR-184998] 16 p2249 N90-22826
Sea bottom topography with X-band SLAR
[BCRS-89-25] 17 p2431 N90-23854
Synthetic aperture radar imagery of airports and surrounding areas: Denver Stapleton International Airport
[NASA-CR-4305] 18 p2495 N90-24257
Analysis and test interaction in the development of a hold down and release mechanism
18 p2539 N90-24489
Automated segmentation and extraction of area terrain features from radar imagery
[AD-A221096] 18 p2544 N90-24522
Feasibility of a synthetic aperture Radar with Rotative Antennas (ROSAR)
[MBB-S/PUB-0385] 19 p2651 N90-25088
Concepts for high resolution space based SAR/ISAR systems
[MBB-UK-0057/89-PUB] 19 p2652 N90-25096
Geocoded spaceborne SAR products for geological applications 19 p2708 N90-25410
The browse file of NASA/JPL quick-look radar images from the Loch Linnhe 1989 experiment
[NASA-CR-186855] 20 p2935 N90-26701
Simulation of synthetic aperture radar 4: Summary and recommendations
[AD-A221822] 21 p2997 N90-27038
SAR processing methods
[FEL-1989-131] 22 p3165 N90-27948
A Bayesian derivation of an iterative autofocus/super-resolution algorithm
[RSRE-MEMO-4337] 22 p3239 N90-28371

Detection of ocean inner waves by synthetic aperture radar: Observations at Gibraltar pass
[ETN-90-97477] 23 p3353 N90-28953
Guidance and control techniques for airborne transfer alignment and SAR motion compensation
24 p3429 N90-29372
Detection and analysis of wind fronts and current shear in digital SAR images
[FFI-89/7016] 24 p3495 N90-29755

SYNTHETIC APERTURES
MERLIN and VLBI observations of the radio galaxy Virgo A 06 p0860 N90-15001
Broadband incoherent imaging using multiple aperture optics
[AD-A215708] 09 p1282 N90-17437
Science requirements for passive microwave sensors on earth science geostationary platforms
12 p1608 N90-19251
Synthetic Aperture Interferometric Radiometer (SAIR)
12 p1610 N90-19261
Shaping the insonifying pulse to optimise B-scans obtained in austenite
[AERE-R-13518] 13 p1775 N90-20187
Diffraction-limited imaging on the 200-inch telescope
15 p2183 N90-22475

SYNTHETIC FIBERS
NT CERAMIC FIBERS
NT GLASS FIBERS
NT NYLON (TRADEMARK)
NT RAYON
Synthesis and properties of a thermotropic copolyester based on 4,4 prime-dihydroxy-a,a prime-dimethylbenzalazine
[AD-A218803] 16 p2223 N90-22682
Processing of thermotropic liquid crystalline polymers and their blends
[AD-A218804] 16 p2223 N90-22683
Laboratory evaluation of two new high-performance polyester batting insulation materials
[AD-A222291] 21 p2987 N90-26976
Compressive strength of rigid-rod polymer fibers
[AD-A221886] 21 p2989 N90-26987

SYNTHETIC FUELS
Environmental quality and the shift to alternative fuels: Progress and interim findings of a Department of Energy study of transition in vehicular power systems
[DE90-002178] 06 p0810 N90-14716
Survey on synthesis technologies of methanol as an alternative fuel
[DE89-901303] 07 p0914 N90-15284
The Third Pacific Basin Biofuels Workshop: Proceedings
[DE90-002523] 07 p0953 N90-15513
Biomass fuels in the developing countries: An overview
[DE90-002616] 09 p1241 N90-17201
Optimum catalytic process for alcohol fuels from syngas
[DE90-005290] 11 p1494 N90-18600
Alternative fuels R/D needs: Program directions
[DE90-007053] 11 p1495 N90-18603
Optimum catalytic process for alcohol fuels from syngas
[DE90-007188] 11 p1495 N90-18604
Design and operation of an outdoor microalgae test facility
[DE89-009493] 13 p1848 N90-20608
Biofuels program summary. Volume 2: Research summaries
[DE89-009484] 18 p2576 N90-24678
Analysis of the T63-A-700 engine used in alcohol turbine fuel extender test
[DOT/FAA/CT-TN90/18] 23 p3278 N90-28549
Production of jet fuels from coal-derived liquids. Volume 13: Evaluation of storage and thermal stability of jet fuels derived from coal liquids
[AD-A224576] 24 p3457 N90-29527

SYNTHETIC METALS
New organic synthetic metals derived from BEDT-TTF, Ni(dsit)2 and BEDO-TTF
[DE90-003793] 07 p0907 N90-15242

SYNTHETIC RESINS
NT ACRYLIC RESINS
NT ADDITION RESINS
NT EPOXY RESINS
NT KEVLAR (TRADEMARK)
NT NYLON (TRADEMARK)
NT PEEK
NT PHENOLIC EPOXY RESINS
NT PHENOLIC RESINS
NT POLYAMIDE RESINS
NT POLYESTER RESINS
NT POLYMETHYL METHACRYLATE
NT THERMOPLASTIC FILMS
NT THERMOPLASTIC RESINS
NT THERMOSETTING RESINS
NT VINYL COPOLYMERS
Nonlinear optics and organic materials
[AD-A210570] 01 p0124 N90-10709
A literature survey of inherently conducting polymers
[FOA-C-20763-2.4] 05 p0628 N90-13668
Acetylene terminated aspartimides and resins therefrom
[NASA-CASE-LAR-14188-1] 17 p2379 N90-23545
Non-destructive characterization of polymer/metal interphases using surface-enhanced Raman scattering
[AD-A222490] 21 p2988 N90-26980

SYNTHETIC RUBBERS
NT CHLOROPRENE RESINS
NT ELASTOMERS
NT VITON RUBBER (TRADEMARK)
NT VULCANIZED ELASTOMERS
Effects of tacky mat contamination on bond degradation for Chemlok/liner and NBR/liner bonds
[NASA-CR-183742] 05 p0626 N90-13653
Plasma and ion fluorination for chemical hardening of synthetic rubbers
[AD-A216388] 10 p1360 N90-17885
Nylon and teflon scribe effect on NBR to Chemlok 233 and NBR to NBR bond interfaces
[NASA-CR-184004] 22 p3189 N90-28095

SYSTEM EFFECTIVENESS
Director, Operational Test and Evaluation report FY-88
[AD-A206784] 01 p0135 N90-10778
Air Combat Environment Test and Evaluation Facility (ACETEF) 02 p0154 N90-10883
Transport systems research vehicle color display system operations manual
[NASA-TM-101577] 03 p0306 N90-11736
Characterization and cycle tests of lightweight nickel electrodes
[NASA-TM-102399] 04 p0470 N90-12696
A new view of weapon system reliability and maintainability: Executive summary
[AD-A213282] 05 p0580 N90-13383
The 25-KVA amorphous metal-core transformer developmental test report
[AD-A215444] 09 p1213 N90-17035
Validity of empirical studies of information system effectiveness
[AD-A214474] 09 p1295 N90-17507
Hydride heat pumps for upgrading spacecraft waste heat 10 p1385 N90-18013
Total quality management: An application in a research and development laboratory
[AD-A215808] 10 p1440 N90-18312
Evaluation of VHF intercept and direction finding systems
[AD-A219805] 17 p2350 N90-23382
Conceptual design for aerospace vehicles
18 p2641 N90-25043
Expanded damage test facilities at LLNL
[DE90-011466] 19 p2695 N90-25336
Bermuda ionosonde tests in support of OTH-B
[NASA-TM-89359] 19 p2713 N90-25442
Development of a meta-analytic technique to assess stress effects
[AD-A220468] 19 p2723 N90-25487
Queing networks with finite capacities
[AD-A221547] 21 p3065 N90-27425

SYSTEM FAILURES
Independent Orbiter Assessment (IOA): FMEA/CIL assessment
[NASA-CR-185589] 02 p0170 N90-10960
Independent Orbiter Assessment (IOA): Assessment of the body flap subsystem FMEA/CIL
[NASA-CR-185575] 02 p0172 N90-10968
Independent Orbiter Assessment (IOA): Assessment of the elevon actuator subsystem FMEA/CIL
[NASA-CR-185578] 02 p0173 N90-10970
Independent Orbiter Assessment (IOA): Analysis of the life support and airlock support subsystems
[NASA-CR-185539] 03 p0314 N90-11786
Sufficiency and necessity in reliability modeling
[NASA-CR-186119] 05 p0635 N90-13706
Electrical breakdown in vacuum
[DE90-001623] 06 p0771 N90-14485
A tutorial on software reliability engineering
[DE89-012368] 06 p0830 N90-14828
VHSIC/VHSIC-Like reliability prediction modeling
[AD-A214601] 09 p1288 N90-17468
Flight crew aiding for recovery from subsystem failures
[NASA-CR-181905] 12 p1696 N90-19741
Reliability importance measures and their calculation
[DE90-620391] 15 p2108 N90-22057
A methodology for knowledge-based restructurable control to accommodate system failures
15 p2109 N90-22058
NASA ground terminal communication equipment automated fault isolation expert systems
15 p2154 N90-22305
User's guide to the 1.6 x 2.0 square m high speed wind tunnel HST, part 1
[ETN-90-96772] 17 p2357 N90-23414
NASA systems autonomy demonstration project: Advanced automation demonstration of Space Station Freedom thermal control system
19 p2728 N90-25510
StarPlan: A model-based diagnostic system for spacecraft 19 p2728 N90-25511
Smart built-in test 19 p2728 N90-25512
Monitoring and control of spacecraft systems using procedural reasoning 19 p2731 N90-25524
Artificial intelligence for multi-mission planetary operations 19 p2732 N90-25532
CLEAR: Automating control centers with expert system technology 19 p2733 N90-25533
System reliability optimization of aircraft wings
23 p3275 N90-28536
Reliable communication in the presence of failures
[NASA-CR-183046] 24 p3533 N90-29977

SYSTEM GENERATED ELECTROMAGNETIC PULSES
A beam induced upset during the flight of the ECHO-7 rocket
[NASA-CR-186089] 03 p0309 N90-11755

SYSTEM IDENTIFICATION
System identification for large space structures
01 p0025 N90-10126
Adaptive noise cancellation for a class of nonlinear 2R filter
[RR-351] 03 p0344 N90-11965
Orthogonal least squares methods and their application to nonlinear system identification
[RR-343] 03 p0395 N90-12259
Fuzzy logic and the generalized modus ponens
[REPT-88-92] 03 p0397 N90-12274
Control of optical systems 05 p0600 N90-13484
LDR structural technology activities at JPL
05 p0601 N90-13488
Stabilizability and detectability of discrete-time time-varying systems
[MEMO-COSOR-88-16] 05 p0690 N90-14023
On the output-stabilizable subspace
[MEMO-COSOR-88-27] 05 p0690 N90-14027
An intelligent tool for the design of presentations: A system identification study
[AD-A215770] 10 p1418 N90-18174
System properties from frequency response functions, part 1
[ISVR-TR-166-PT-1] 11 p1520 N90-18754
CSI sensing and control: Analytical and experimental results 14 p1936 N90-21083
In-house experiments in large space structures at the Air Force Wright Aeronautical Laboratories Flight Dynamics Laboratory 14 p1938 N90-21092
Application of neural nets to system identification and bifurcation analysis of real world experimental data
[DE90-007539] 14 p2017 N90-21558
Adaptive control of a flexible manipulator with unknown changing loads 15 p2152 N90-22293
Rocket engine failure detection using system identification techiques
[NASA-CR-185259] 19 p2684 N90-25159
Intergration of system identification and robust controller designs for flexible structures in space
[NASA-TM-102695] 20 p2876 N90-26362
AGARD highlights 90/1 20 p2951 N90-26788
Adaptive time series analysis using predictive inference and entropy
[AD-A222337] 21 p2997 N90-27033
Robust adaptive control: Handling the excitation problem 22 p3241 N90-28382

SYSTEMS ANALYSIS
NT SYSTEM IDENTIFICATION
Modal analysis of fluid-structure systems by parallel subspace iteration 02 p0181 N90-11024
Comparison of phase resonance, mode separation, and driven-base modal identification methods applied to the FLECS test structure 02 p0181 N90-11027
New data handling system (MDH) for mechanical tests at ESTEC 02 p0187 N90-11066
Laser dynamics: The system dynamics and network theory of optoelectronic integrated circuit design
02 p0226 N90-11296
Systems analysis considerations in artificial intelligence/expert systems technology applications
[DE89-016847] 02 p0262 N90-11490
A survey of research methods to study design
[AD-A211213] 02 p0262 N90-11491
Spacelab system analysis Marshall Avionics System Testbed (MAST)
[NASA-CR-183804] 03 p0317 N90-11802

On the complexity analysis of the coriolis and centripetal effects of a 6 DOF robot manipulator — Degrees of Freedom (DOF)
[RR-344] 03 p0355 N90-12030
Non linear vibrations in a drive train when coupled to constant torque and constant power loads
[PNR90593] 04 p0508 N90-12934
The integration of structured and formal methods
[RSRE-MEMO-4293] 04 p0531 N90-13068
Variational and asymptotic methods in open and closed waveguide analysis
[REPT-34] 04 p0554 N90-13229
Semiconductor measurement technology: A software program for aiding the analysis of ellipsometric measurements, simple models
[PB89-235923] 04 p0560 N90-13261
Spacelab system analysis: The modified free access protocol: An access protocol for communication systems with periodic and Poisson traffic
[NASA-CR-183805] 05 p0602 N90-13497
Research on the controllability of integrated circuits by means of electron beams
[ETN-90-95710] 05 p0636 N90-13708
Micro-based fact collection tool user's manual
[NASA-CR-180414] 05 p0684 N90-13981
An artificial intelligence approach to analog system diagnosis
[AD-A213135] 05 p0686 N90-13992
Analysis of three approaches to qualitative simulation
[MEMO-INF-89-32] 05 p0691 N90-14035
On a new integrable Hamiltonian system with nearest neighbors interaction
[PREPRINT-667] 05 p0692 N90-14043
Nucleon polarizabilities in the constituent quark model
[NOTA-INTERNA-936] 05 p0698 N90-14082
Empirical analysis and refinement of expert system knowledge bases
[AD-A213240] 05 p0707 N90-14143
Review of the Aerospace Safety Advisory Panel report for NASA fiscal year 1990 authorization
[GPO-24-234] 06 p0722 N90-14213
Preliminary design document: Ground based testbed for avionics systems
[NASA-CR-183821] 06 p0725 N90-14231
Mathematical techniques for system realization and identification
[AD-A212088] 06 p0833 N90-14841
Solution bias in complex systems modeling
[DE90-002001] 06 p0836 N90-14858
Ocean thermal energy conversion: An overview
[DE89-000838] 07 p0953 N90-15512
A simulation model for dynamic system availability analysis
[AD-A213499] 07 p0974 N90-15628
A structured connectionist approach to direct inferences and figurative adjective-noun combinations
[AD-A214326] 07 p0978 N90-15649
A UK perspective on the uniform engine test programme
[RAE-TM-P-1172] 08 p1025 N90-15922
Dynamics analyses of space power systems using the salt code
[DE90-002274] 08 p1038 N90-15995
Linear digital imaging system fidelity analysis
08 p1072 N90-16205
Two possible configurations for the top-hat electrostatic analyzer: A numerical study
[IFSI-88-18] 08 p1077 N90-16229
Fault tree analysis: A tool for battery safety and reliability studies
[DE90-002582] 08 p1086 N90-16287
Appearance analysis from CAD models
[IMAG-RR-756-I-IMAG-88-LIFIA]
08 p1111 N90-16434
Assessment of ground-coupled heat pumps
[DE90-003977] 09 p1220 N90-17079
RADC fault tolerant system reliability evaluation facility
[AD-A215298] 09 p1267 N90-17348
A specification and analysis of the IEEE (Institute of Electrical and Electronic Engineers) token ring protocol
[AD-A214567] 09 p1269 N90-17359
Chaos and turbulence
[AD-A215310] 09 p1294 N90-17499
Definition of a management information system to support performance risk assessment
[AD-A215464] 09 p1297 N90-17516
Analysis of power bus topologies used in telecommunications satellites 10 p1331 N90-17691
Advanced tracking systems design and analysis
[NASA-CR-183459] 10 p1376 N90-17976
A fractional calculus model of aeroelasticity
[AD-A216244] 10 p1423 N90-18212
Impact of uncertainty and diagnosticity on classification of multidimensional data with integral and separable displays of system status
[AD-A215966] 10 p1424 N90-18215
Airborne radar systems specialist, AFSC 118X2
[AD-A215450] 11 p1496 N90-18611
A linear systems theory approach to the range-independent acoustic channel
[AD-A216551] 12 p1710 N90-19817
A guide to performing and documenting safety analyses
[DE90-008688] 13 p1788 N90-20261
Using formal methods to develop a paradigm for software design
[DE90-005633] 13 p1866 N90-20703
Detection of potential space station control/structure interaction with CO-ST-IN 14 p1935 N90-21074
Computation of broad spectral band electro-optical system transmittance response characteristics to military smokes and obscurants using field test data from transmissometer system measurements
15 p2086 N90-21939
Insights into complex human performance
[DE90-006957] 15 p2137 N90-22214
An introduction to selected structured methods
[RSRE-MEMO-4294] 15 p2148 N90-22275
Electric power scheduling: A distributed problem-solving approach
[NASA-TM-103149] 15 p2157 N90-22323
Performance analysis of Aloha networks with power capture and near/far effect
[AD-A218739] 16 p2229 N90-22717
Helicopter Airborne Laser Positioning System (HALPS)
[NASA-TM-102814] 17 p2354 N90-23399
Nonflammable hydraulic power system for tactical aircraft. Volume 1: Aircraft system definition, design and analysis
[AD-A218493] 17 p2356 N90-23409
Prospects for integration of satellite communications, navigation and monitoring functions
17 p2360 N90-23439
Joint tactical anti-jam communications: A systems approach
[AD-A219592] 17 p2388 N90-23602
Symbolic reasoning in model-based diagnosis: Efficient and effective information processing
[MEMO-INF-89-03] 17 p2452 N90-23984
Space shuttle: The future of the Vandenberg launch site needs to be determined
[GAO/NSIAD-88-158] 18 p2509 N90-24337
System analysis of a tactical multi-satellite communication system
[AD-A220344] 18 p2510 N90-24343
A survey of human factors methodologies and models for improving the maintainability design of emerging Army aviation systems
[AD-A221159] 18 p2586 N90-24724
Military space operations: Shuttle and satellite computer systems do not meet performance objectives
[GAO/IMTEC-88-7] 18 p2635 N90-25014
SEDS experiment design definition
[NASA-CR-183909] 19 p2665 N90-25165
A design optimization process for Space Station Freedom
[NASA-CR-186851] 19 p2667 N90-25175
Artificial intelligence for multi-mission planetary operations 19 p2732 N90-25532
Behavioral networks as a model for intelligent agents
19 p2738 N90-25561
ACES: Space shuttle flight software analysis expert system 19 p2739 N90-25571
The interpretation of nonlinear frequency response functions
[RR-375] 19 p2753 N90-25643
The Federal Aviation Administration plan for research, engineering and development. Volume 2: Project descriptions
[AD-A221264] 19 p2800 N90-25931
Single-pass memory system evaluation for multiprogramming workloads
[NASA-CR-186553] 20 p2910 N90-26558
The integration of automated knowledge acquisition with computer-aided software engineering for space shuttle expert systems 21 p3045 N90-27307
Construction of dynamic stochastic simulation models using knowledge-based techniques
21 p3047 N90-27322
Integrated structural/control design via multiobjective optimization
[AD-A223088] 21 p3071 N90-27459
Observer or direct inversion 22 p3103 N90-27622
Knowledge based diagnosis of jet engines under consideration of model based methods
22 p3105 N90-27631
Spacecraft attitude dynamics: Evolution and current challenges 22 p3128 N90-27754
Experimental fault characterization of a neural network
[NASA-CR-186885] 22 p3240 N90-28373
Liquid Rocket Booster (LRB) for the Space Transportation System (STS) systems study. Appendix G: LRB for the STS system study level 2 requirements, revision 1
[NASA-CR-183793-APP-G] 23 p3289 N90-28607
A vector diagram approach to shaping inputs for vibration reduction
[AD-A223724] 24 p3480 N90-29671
RCTS: A flexible environment for sensor integration and control of robot systems; the distributed processing approach 24 p3512 N90-29852
Survey of formal specification techniques for reactive systems
[AD-A223741] 24 p3538 N90-30005

SYSTEMS COMPATIBILITY

Cockpit lighting compatibility with image intensification night imaging systems: Issues and answers
[AD-A210503] 01 p0006 N90-10028

SYSTEMS DESIGN

U SYSTEMS ENGINEERING

SYSTEMS ENGINEERING

NT COMPUTER SYSTEMS DESIGN
NT CONTROL SYSTEMS DESIGN

An appraisal of a number of power assessment procedures being proposed for use in Chinook-Lycoming T55 engine
[AD-A210482] 01 p0009 N90-10041
Investigations of thrust vector control for high-alpha pitchover 01 p0014 N90-10067
NASA'S controls-structures interaction program
01 p0017 N90-10081
Flexible structure control experiments using a real-time workstation for computer-aided control engineering
01 p0017 N90-10084
CONSOLE: A CAD tandem for optimization-based design interacting with user-supplied simulators
01 p0017 N90-10085
Control/structure interaction methods for space station power systems 01 p0018 N90-10087
Approximate simulation model for analysis and optimization in engineering system design
[NASA-TM-101616] 01 p0054 N90-10308
Aerospace system unified life cycle engineering producibility measurement issues
[AD-A210937] 01 p0106 N90-10607
An analytical hierarchy process approach to establish the systems analyst's knowledge base for selecting an information requirements determination strategy
01 p0136 N90-10785
Kalman Filter Integration of Modern Guidance and Navigation Systems
[AGARD-LS-166] 02 p0148 N90-10847
Design of a Kalman filter for transfer alignment
02 p0149 N90-10848
Development of the integrated all-weather navigation system for Tornado 02 p0149 N90-10849
A high performance airborne INS/GPS Integrated Navigation System 02 p0149 N90-10850
The development of mission-specific advanced inertially-based avionics system
02 p0149 N90-10851
Flight Test Techniques
[AGARD-CP-452] 02 p0151 N90-10860
Flight test techniques adopted by Avions Marcel Dassault-Breguet Aviation 02 p0152 N90-10867
Identification Friend, Foe or Neutral Joint Test
02 p0154 N90-10881
On the development of a basic flight test capability and some related research projects
02 p0155 N90-10885
Independent Orbiter Assessment (IOA): FMEA/CIL assessment
[NASA-CR-185589] 02 p0170 N90-10960
The third generation rigid solar array GSR3
02 p0180 N90-11017
Dynamic characteristics concerned in the design of a free-piston Stirling engine/magnetic coupling/compressor system
[DE89-015981] 02 p0230 N90-11317
Methodology of developing a combined environmental stress schedule for reliability growth testing
[AD-A211053] 02 p0231 N90-11326
Considerations for a design and operations knowledge support system for Space Station Freedom
[NASA-TM-102156] 02 p0256 N90-11451
Engineering specification and system design for CAD/CAM of custom shoes. Phase 5: UMC involvement (January 1, 1989 - June 30, 1989)
[NASA-CR-185838] 02 p0257 N90-11456
A survey of research methods to study design
[AD-A211213] 02 p0262 N90-11491
A design methodology for self-tuning control of systems with inherent conflicts
[PB89-219505] 03 p0344 N90-11960

Requirements for multidisciplinary design of aerospace vehicles on high performance computers
[NASA-CR-181915] 03 p0384 N90-12183
DOD Gateway Information System (DGIS) common command language: A retrospective on the introduction of prolog as the development tool
[AD-A211941] 03 p0418 N90-12400
Advanced actuation systems development, volume 1
[AD-A213334] 04 p0458 N90-12624
Development of a low noise 10 K J-T refrigeration system
[AD-A213347] 04 p0484 N90-12779
Performance evaluations of a parallel and expandable database computer: The multi-backend database computer
[AD-A212761] 04 p0528 N90-13046
A transformational method for verifying safety properties in real time systems
[AD-A211925] 04 p0529 N90-13051
Building a software package for solving large sparse nonlinear systems of equations
[AD-A211758] 04 p0529 N90-13055
Toward a formal model of the design and evolution of software
[AD-A212533] 04 p0534 N90-13087
International Conference on Operator Theory: Advances and applications
[AD-A212341] 04 p0545 N90-13170
Discretization and model reduction for a class of nonlinear systems 05 p0583 N90-13397
Advanced actuation systems development, volume 2
[AD-A213378] 05 p0583 N90-13398
Space Station Engineering Design Issues
[NASA-CR-185978] 05 p0601 N90-13492
The Hipparcos Mission. Prelaunch status. Volume 1: The Hipparcos satellite
[ESA-SP-1111-VOL-1] 05 p0603 N90-13499
The payload structure 05 p0604 N90-13510
The spacecraft structure 05 p0604 N90-13512
Resistive fuses: Analog hardware for detecting discontinuities in early vision
[AD-A211891] 05 p0634 N90-13696
On control of manipulators
[ISBN-90-9002789-0] 05 p0652 N90-13804
The problem of automation: Inappropriate feedback and interaction, not overautomation
[NASA-CR-186126] 05 p0686 N90-13994
On the output-stabilizable subspace
[MEMO-COSOR-88-27] 05 p0690 N90-14027
Preliminary design document: Ground based testbed for avionics systems
[NASA-CR-183821] 06 p0725 N90-14231
Sandia Satellite Program summary of operational procedures
[DE90-000892] 06 p0728 N90-14249
The space station tethered elevator system
[NASA-CR-186051] 06 p0732 N90-14265
Propagation assessment and tactical decision aids 06 p0757 N90-14407
A communications system with an adaptive multi-functional architecture 06 p0759 N90-14415
Controller design for a robotic manipulator 06 p0792 N90-14615
Exploring the living universe: A strategy for space life sciences
[NASA-TM-101891] 06 p0822 N90-14778
Reuse research plans at Langley Research Center 06 p0825 N90-14797
Application of reusable software components at the SEI 06 p0826 N90-14804
A dynamic systems engineering methodology research study. Phase 2: Evaluating methodologies, tools, and techniques for applicability to NASA's systems projects
[NASA-CR-181319] 06 p0857 N90-14985
NOISE: A nonlinear optimization induction free-electron laser systems engineering code
[DE90-004438] 07 p0936 N90-15420
Young Investigator's Award and distributed self-adaptive databases
[AD-A214194] 07 p1010 N90-15854
Advances in techniques and technologies for air vehicle navigation and guidance
[AGARD-AR-276] 08 p1020 N90-15899
Guidance and Control of Unmanned Air Vehicles
[AGARD-CP-436] 08 p1025 N90-15924
Mirach 100 flight control system 08 p1025 N90-15926
An electronic pressure profile display system for aeronautic test facilities
[NASA-TM-102478] 08 p1032 N90-15964
MANPRINT (Manpower and Personnel Integration) evaluation: AN/TRC-170 digital troposcatter radio system
[AD-A211799] 08 p1055 N90-16100
Miniature GPS-based guidance package 09 p1163 N90-16736
A method for the early detection of instabilities in rotordynamics
[NASA-CR-186307] 09 p1170 N90-16769
Progress in airbreathing combined engines for future European launcher 09 p1177 N90-16817
Decision-analytic approach to rule-based expert system development using GPS (Global Positioning System) as the model
[AD-A216179] 10 p1319 N90-17626
Advanced tracking systems design and analysis
[NASA-CR-183459] 10 p1376 N90-17976
Expert systems development methodology
[AD-A216892] 10 p1421 N90-18191
Structured analysis tool interface to the strategic defense initiative architecture dataflow modeling technique
[AD-A216281] 10 p1424 N90-18218
National airspace system plan: Facilities, equipment, associated development and other capital needs
[AD-A215882] 11 p1453 N90-18373
Design of a new control system for hovercrafts
[ETN-90-96230] 11 p1465 N90-18435
System safety requirements for ESA space systems and associated equipment
[ESA-PSS-01-40-ISSUE-2] 11 p1469 N90-18460
Back swing phenomenon of synchronous generator. Study on ac-dc power system simulator tests
[DE89-782321] 11 p1500 N90-18635
Optimal planning method of underground distribution system, part 2. Application to various types of system configurations
[DE89-782323] 11 p1500 N90-18636
Integrated silicon flip-flop sensors
[ETN-90-96271] 11 p1503 N90-18654
User manual for NEXT 1.2: NLR engineering X-pert system toolkit
[NLR-TR-87178-U] 11 p1547 N90-18905
Augmenting and updating NASA spacelink electronic information system 12 p1634 N90-19392
Parkes radio science system design and testing for Voyager Neptune encounter 12 p1645 N90-19451
Aspects of VHF radars illustrated by the example of an experimental system
[REPT-1-89] 12 p1647 N90-19468
Flight crew aiding for recovery from subsystem failures
[NASA-CR-181905] 12 p1696 N90-19741
Generic distributed systems model
[AD-A217078] 12 p1702 N90-19773
Potential role of avionics in escape systems 13 p1752 N90-20060
Proximity operations concept design study, task 6
[NASA-CR-181971] 13 p1761 N90-20112
Space station Simulation Computer System (SCS) study for NASA/MSFC. Volume 2: Concept document
[NASA-CR-183841] 13 p1762 N90-20114
A linear filtering technique for removal of low-frequency noise
[DE90-006183] 13 p1794 N90-20296
The CMU Reconfigurable Modular Manipulator System
[CMU-RI-TR-88-7] 13 p1809 N90-20388
Operational computer graphics in the flight dynamics environment 13 p1859 N90-20668
Space Station Freedom integrated fault model 13 p1860 N90-20673
SES cupola interactive display design environment 13 p1862 N90-20679
Issues in visual support to real-time space system simulation solved in the Systems Engineering Simulator 13 p1862 N90-20680
History of visual systems in the Systems Engineering Simulator 13 p1862 N90-20681
Computer image generation: Reconfigurability as a strategy in high fidelity space applications 13 p1862 N90-20682
Real-time graphics for the Space Station Freedom cupola, developed in the Systems Engineering Simulator 13 p1862 N90-20683
The Orbital Maneuvering Vehicle Training Facility visual system concept 13 p1863 N90-20684
Design decision making with multiple interacting criteria and varying relative weights
[AD-A218027] 13 p1869 N90-20721
Towards SDS (Strategic Defense System) testing and evaluation: A collection of relevant topics
[AD-A217610] 13 p1880 N90-20783
NASA/DOD Controls-Structures Interaction Technology 1989
[NASA-CP-3041] 14 p1933 N90-21062
Software verification and validation: Its role in computer assurance and its relationship with software project management standards
[PB90-111691] 14 p2012 N90-21530
Evolution of Ada technology in the flight dynamics area: Implementation/testing phase analysis
[NASA-TM-103310] 14 p2014 N90-21539
An all electronic transportation system from LEO to GEO and beyond 15 p2060 N90-21796
Solar-pumped laser for free space power transmission 15 p2061 N90-21804
Progression of damage and fracture in composites under dynamic loading
[NASA-TM-103118] 15 p2065 N90-21825
Vibration analysis of systems with random parametric excitations 15 p2109 N90-22060
Understanding the computing system domain of advanced computing with microcomputers
[DE90-009825] 15 p2145 N90-22251
Design options for space-based radar systems
[ETN-90-96548] 16 p2228 N90-22710
Component model reduction via the projection and assembly method 16 p2295 N90-23073
MLS mathematical model validation study using airborne MLS data from Midway Airport engineering flight tests, August 1988
[DOT/FAA/CT-TN90/2] 17 p2349 N90-23378
Location systems: ARGOS, SARSAT 17 p2359 N90-23430
Assessment of fundamental materials needs for Thick Thermal Barrier Coatings (TTBC's) for truck diesel engines
[NASA-TM-103130] 17 p2377 N90-23536
Qualitative models for space system engineering
[NASA-CR-180682] 17 p2385 N90-23585
Convergent strand array liquid pumping system
[NASA-CASE-NPO-17301-1-CU] 17 p2385 N90-23587
Design, simulation, and testing of a field-oriented ac servo-drive using a TM5 32010 signal processor
[EMV-88-42] 17 p2397 N90-23658
Numerical optimization, system theoretic and software tools for the integrated design of flexible structures and their control systems
[AD-A219877] 17 p2447 N90-23949
A comparison of a relational and nested-relational IDEF0 data model
[AD-A220147] 17 p2448 N90-23956
On the structure at infinity of a structured system
[CWI-BS-R8918] 17 p2468 N90-24108
Development of a hybrid adaptive beamformer
[AD-A219652] 17 p2471 N90-24128
Conceptual design and analysis of roads and road construction machinery for initial lunar base operations
[NASA-CR-186673] 18 p2535 N90-24459
Design and use of high speed synchronous motor running in aggressive liquids 18 p2538 N90-24478
Understanding tropscatter propagation
[AD-A220969] 18 p2544 N90-24520
Modifications of the DUTSCAT system
[BCRS-89-33] 18 p2555 N90-24582
The Army/Air Force RAMCAD (Reliability And Maintainability Computer-Aided Design) program
[AD-A220923] 18 p2593 N90-24753
Evaluating Statistical Process Control (SPC) techniques and computing the uncertainty of force calibrations 18 p2631 N90-24992
Incorporation of a progressive failure analysis method in the CSM testbed software system 18 p2640 N90-25036
Space shuttle avionics system
[NASA-SP-504] 19 p2664 N90-25160
Analog electronic control differential transmitter
[AD-D014508] 19 p2685 N90-25272
System development and early biological tests in NASA's biomass production chamber
[NASA-TM-103494] 19 p2716 N90-25456
Omni-directional human head-neck response
[SAE-861893] 19 p2721 N90-25478
Knowledge representation to support reasoning based on multiple models 19 p2731 N90-25525
A comparison of two neural network schemes for navigation 19 p2733 N90-25536
Test bed experiments for various telerobotic system characteristics and configurations 19 p2740 N90-25572
GCS support/development system configuration document
[NASA-CR-182046] 19 p2743 N90-25589
RF control system development at CEBAF
[CEBAF-PR-89-026] 19 p2755 N90-25653
The conceptual task model: A specification technique between requirements engineering and program development
[TR-89-15] 19 p2762 N90-25694
Enroute flight planning: The design of cooperative planning systems
[NASA-CR-186797] 20 p2806 N90-25964
National space test centers, Lewis research center facilities
[NASA-TM-103187] 20 p2817 N90-26030
A novel multireceiver communications system configuration based on optimal estimation theory
[NASA-CR-186847] 20 p2851 N90-26216

Applications of different design methodologies in navigation systems and development at JPL
20 p2852 N90-26221
Low-gravity fluid physics: A program overview
[NASA-TM-103215] 20 p2861 N90-26273
Automation of closed environments in space for human comfort and safety
[NASA-CR-186834] 20 p2901 N90-26500
Innovative design systems: Where are we, and where do we go from here
[AD-A222586] 20 p2910 N90-26556
Cost effective technology
[PNR90664] 21 p2991 N90-27002
Electric vehicle battery R/D in the context of a propulsion system
[DE90-013667] 21 p2999 N90-27046
Compiling knowledge-based systems from KEE to Ada
21 p3049 N90-27334
Potential new tactical applications of the Global Positioning System (GPS) 21 p3069 N90-27449
Systems engineering management guide
[AD-A223168] 21 p3085 N90-27544
Interim status and recommendations for the Engineering Information System (EIS) program
[AD-A222060] 21 p3087 N90-27555
Observer or direct inversion 22 p3103 N90-27622
Aircraft lightning protection handbook
[AD-A222716] 22 p3110 N90-27668
Experimental study towards a future airport ground movement simulator 22 p3113 N90-27687
DEPEND: A design environment for prediction and evaluation of system dependability
[NASA-CR-186890] 22 p3189 N90-28094
Improved meteorological measurements from buoys and ships (IMET): Preliminary conventions from buoys and standards data and file formats
[PB90-241910] 22 p3229 N90-28312
System reliability optimization of aircraft wings
23 p3275 N90-28536
Design and realization of a two stage C-band low noise amplifier
[FEL-89-B265] 23 p3322 N90-28783
Evaluation of the Situational Awareness Rating Technique (SART) as a tool for aircrew systems design
23 p3358 N90-28977
The JPL telerobot operator control station. Part 1: Hardware 23 p3371 N90-29049
Designing intelligent computer aided instruction systems with integrated knowledge representation schemes
[AD-A224178] 23 p3383 N90-29113
A knowledge-based system design/information tool
[NASA-CR-4316] 23 p3389 N90-29143
Flight test engineering with the ATTAS
23 p3391 N90-29160
Electro-optics engineering support for the integrated launch and recovery television surveillance system
[AD-A223450] 24 p3436 N90-29406
Techniques for developing a system safety risk assessment model
[AD-A223477] 24 p3477 N90-29654
Telerobotic workstation design aid
24 p3504 N90-29805
Computer-aided engineering environment for controlled mechanical systems
[AD-A223551] 24 p3527 N90-29942
Working implementation agreements for open systems interconnection protocols
[PB90-197948] 24 p3557 N90-30127

SYSTEMS INTEGRATION

Liquid rocket booster study. Volume 2, book 3, appendices 2-5: PPIP, transition plan, AMOS plan, and environmental analysis
[NASA-CR-183602] 01 p0027 N90-10139
Planning an Integrated On-line Library System (IOLS)
[AD-A209406] 01 p0136 N90-10783
Kalman Filter Integration of Modern Guidance and Navigation Systems
[AGARD-LS-166] 02 p0148 N90-10847
A high performance airborne INS/GPS Integrated Navigation System 02 p0149 N90-10850
The development of mission-specific advanced inertially-based avionics system
02 p0149 N90-10851
Development of a marine integrated navigation system
02 p0149 N90-10852
Flight Test Techniques
[AGARD-CP-452] 02 p0151 N90-10860
Real-time flight test analysis and display techniques for the X-29A aircraft 02 p0152 N90-10866
Flight test techniques adopted by Avions Marcel Dassault-Breguet Aviation 02 p0152 N90-10867
Lessons learned from the integration of flight systems
02 p0153 N90-10874
Planning for hybrid-cycle OTEC experiments using the HMTSTA test facility at the Natural Energy Laboratory of Hawaii
[DE89-013278] 02 p0237 N90-11349
Parallel architectures and parallel algorithms for integrated vision systems
[NASA-CR-185990] 03 p0389 N90-12215
STOVL aircraft simulation for integrated flight and propulsion control research
[NASA-TM-102419] 05 p0581 N90-13389
Space station gas compressor technology study program, phase 1
[NASA-CR-183758] 05 p0601 N90-13491
User needs, benefits, and integration of robotic systems in a space station laboratory
[NASA-CR-185150] 05 p0651 N90-13794
Engineering sciences design. Design and implementation of components for a bioregenerative system for growing higher order plants in space
[NASA-CR-186056] 06 p0819 N90-14761
SSFP approach to software reuse
06 p0826 N90-14799
Developing integrated parametric planning models for budgeting and managing complex projects
[NASA-CR-186006] 06 p0857 N90-14986
Integration of a gated microchannel plate detector into the Nova laser system
[DE90-002981] 07 p0935 N90-15413
A burst compression and expansion technique for variable-rate users in satellite-switched TDMA networks
[NASA-TM-102414] 08 p1035 N90-15983
Experiences with knowledge-base and large database integration
[DE90-000686] 08 p1137 N90-16591
Integrated flight guidance system using differential-GPS for landing approach guidance 09 p1163 N90-16735
Miniature GPS-based guidance package
09 p1163 N90-16736
R/M/T (Reliability, Maintainability, and Testability) design for fault tolerance, technical manager's design implementation guide
[AD-A215531] 09 p1234 N90-17164
Antenna installation on aircraft: Theory and practice
10 p1371 N90-17941
Performance measurements for a laboratory-simulated 30/20 GHz communication satellite transponder
[NASA-TM-102424] 10 p1376 N90-17977
The implications of using integrated software support environment for design of guidance and control systems software
[AGARD-AR-229] 11 p1464 N90-18432
Integrated regenerative fuel cell experimental evaluation
[NASA-CR-185183] 11 p1530 N90-18808
An integrated vision on methodologies and environments for modeling and simulation assisted by computer
[INPE-4861-TDL/372] 11 p1544 N90-18886
Highly accurate navigation: Integration of navigation and geodesic methods
[SFB-228] 12 p1602 N90-19221
Big Viterbi Decoder (BVD) results for (7,1/2) convolutional code 12 p1644 N90-19446
Experimental proposition aboard the second data collecting satellite-SCD 2 of the MECB
[INPE-4980-RPE/606] 13 p1765 N90-20128
Flexible automatic discrete parts assembly
[AD-A217401] 13 p1787 N90-20256
The Real Time Display Builder (RTDB)
13 p1857 N90-20656
ASCIE: An integrated experiment to study CSI in large segmented optical systems 14 p1936 N90-21082
An introduction to selected structured methods
[RSRE-MEMO-4294] 15 p2148 N90-22275
Minimum attainable RMS attitude error using co-located rate sensors 16 p2288 N90-23038
Preliminary design of a supersonic Short Takeoff and Vertical Landing (STOVL) fighter aircraft
[NASA-CR-186670] 17 p2352 N90-23394
Continued development and analysis of a new extended Kalman filter for the Completely Integrated Reference Instrumentation System (CIRIS)
[AD-A220106] 17 p2354 N90-23400
Space shuttle avionics system
[NASA-SP-504] 19 p2664 N90-25160
NASA systems autonomy demonstration project: Advanced automation demonstration of Space Station Freedom thermal control system
19 p2728 N90-25510
Process and information integration via hypermedia
19 p2733 N90-25534
Test bed experiments for various telerobotic system characteristics and configurations
19 p2740 N90-25572
Technical evaluation report on the Guidance and Control Panel 49th Symposium on Fault Tolerant Design Concepts for Highly Integrated Flight Critical Guidance and Control Systems
[AGARD-AR-281] 20 p2813 N90-26012
Intergration of system identification and robust controller designs for flexible structures in space
[NASA-TM-102695] 20 p2876 N90-26362
A knowledge-based approach to configuration layout, justification, and documentation
21 p3041 N90-27286
Robotic space simulation integration of vision algorithms into an orbital operations simulation
[NASA-CR-185934] 21 p3059 N90-27395
Aircraft Integrated Monitoring Systems
[DLR-MITT-90-04] 22 p3103 N90-27617
Performance assessment of MIL-STD-1553B on the avionic systems demonstrator rig of British Aerospace
22 p3104 N90-27624
Knowledge based diagnosis of jet engines under consideration of model based methods
22 p3105 N90-27631
New features of JAL's ground station
22 p3105 N90-27633
Reconfigurable integrated system architecture for future monitoring systems 22 p3106 N90-27638
PHARE: Concept and programme
22 p3114 N90-27690
Congestion-reduction and service-restoration strategies for telecommunication networks
[PB90-207838] 22 p3164 N90-27944
A look at tomorrow today 23 p3273 N90-28524
Description of the primary flight display and flight guidance system logic in the NASA B-737 transport systems research vehicle
[NASA-TM-102710] 23 p3277 N90-28546
Propulsion system-flight control integration and optimization: Flight evaluation and technology transition
[NASA-TM-4207] 23 p3278 N90-28551
Experiences with the JPL telerobot testbed: Issues and insights 23 p3373 N90-29059
Information management directions: The integration challenge
[PB90-219866] 23 p3405 N90-29245
Integration of GPS and strapdown inertial subsystems into a single unit 24 p3423 N90-29340
The integration of multiple avionic sensors and technologies for future military helicopters
24 p3424 N90-29344
Integration of GPS/INS with partitioned filters
24 p3425 N90-29347
Integrated strapdown avionics for precision guided vehicles 24 p3427 N90-29361
Integrated navigation/flight control for future high performance aircraft 24 p3427 N90-29362
A low cost inertial/GPS integrated approach to land navigation 24 p3430 N90-29374
An integrated system for land navigation
24 p3430 N90-29377

SYSTEMS MANAGEMENT

Planning an Integrated On-line Library System (IOLS)
[AD-A209406] 01 p0136 N90-10783
Information system life-cycle and documentation standards, volume 1
[NASA-TM-101856] 05 p0706 N90-14135
Management plan documentation standard and Data Item Descriptions (DID). Volume of the information system life-cycle and documentation standards, volume 2
[NASA-TM-101857] 05 p0706 N90-14136
Product specification documentation standard and Data Item Descriptions (DID). Volume of the information system life-cycle and documentation standards, volume 3
[NASA-TM-101858] 05 p0706 N90-14137
Impact of domain analysis on reuse methods
06 p0824 N90-14792
A dynamic systems engineering methodology research study. Phase 2: Evaluating methodologies, tools, and techniques for applicability to NASA's systems projects
[NASA-CR-181319] 06 p0857 N90-14985
America's shuttle returns to space
09 p1174 N90-16792
The global positioning system
[AD-A217266] 12 p1602 N90-19222
Making real-time reactive systems reliable
[NASA-CR-186642] 20 p2873 N90-26344
Space station advanced automation
21 p3044 N90-27300
Purchase of computer equipment: Justification and cost appraisal
[RSRE-89023] 22 p3256 N90-28438

SYSTEMS SIMULATION

Approximate simulation model for analysis and optimization in engineering system design
[NASA-TM-101616] 01 p0054 N90-10308
A super element for multibody dynamics
02 p0178 N90-11004

Induced shock loads during the separation of the Ariane 5 VEB structure
02 p0184 N90-11045

MSP: Modeling of concurrent processes. Version 1.00 General introduction and directions for use
[REPT-88-88] 02 p0260 N90-11477

An accurate timing model for fault simulation in MOS circuits
[AD-A213153] 05 p0635 N90-13702

Efficient on-line simulations of tree machines and multidimensional turing machines by random access machines
[AD-A213152] 05 p0680 N90-13960

Definition of avionics concepts for a heavy lift cargo vehicle. Volume 1: Executive summary
[NASA-CR-183818] 06 p0725 N90-14229

Definition of avionics concepts for a heavy lift cargo vehicle, volume 2
[NASA-CR-183819] 06 p0725 N90-14230

Simulation of synthetic aperture radar 2: Simulating SAR (Synthetic Aperture Radar) using the advanced visual technology system
[AD-A213659] 09 p1204 N90-16976

Observing systems simulation experiments: Their role in meteorology
[AD-A215705] 09 p1248 N90-17243

Optimized sensible heat storage systems for application to solar dynamic power generation
10 p1334 N90-17719

Deployment simulation for the third generation solar arrays GSR3
10 p1340 N90-17763

Graphics Technology in Space Applications (GTSA 1989)
[NASA-CP-3045] 13 p1856 N90-20651

Issues in visual support to real-time space system simulation solved in the Systems Engineering Simulator
13 p1862 N90-20680

History of visual systems in the Systems Engineering Simulator
13 p1862 N90-20681

Computer image generation: Reconfigurability as a strategy in high fidelity space applications
13 p1862 N90-20682

Probabilistic modeling for simulation of aerodynamic uncertainties in propulsion systems
[NASA-TM-102472] 14 p1927 N90-21036

Parallel processing of real-time dynamic systems simulation on OSCAR (Optimally SCheduled Advanced multiprocessoR)
16 p2282 N90-23006

A new scheme for identification and control
[EUT-88-E-213] 20 p2915 N90-26586

Algorithms and evaluation for regulation of linear, time-independent difference systems under position value limitation
[ETN-90-97308] 22 p3238 N90-28364

Workshop on Low Level Flight Training
[AGARD-AR-288] 24 p3436 N90-29404

SYSTEMS STABILITY

Can perceptrons find Lyapunov functions: An algorithmic approach to systems stability
[RR-365] 03 p0391 N90-12224

Nonlinear systems and Kolmogorov's representation theorem
[RR-363] 04 p0508 N90-12931

Uniform stability for time-varying infinite-dimensional discrete linear systems
[DE89-635712] 08 p1116 N90-16460

System properties from frequency response functions, part 1
[ISVR-TR-166-PT-1] 11 p1520 N90-18754

A priori results in linear-quadratic optimal control theory (extended version)
[MEMO-COSOR-89-17] 16 p2304 N90-23124

On conditions for the development of stable discrete-time sliding mode control systems
[MATHS-REPT-A-124] 19 p2747 N90-25612

The stability of differential systems with delay
[RR-377] 21 p3062 N90-27408

SYSTOLIC ARRAYS

A virtual zero-time, monolithic systolic sorting array
[DE90-001000] 12 p1698 N90-19753

MEXP: A programming tool for the CESAR programmable systolic array multiprocessor
[FFI-89/7020] 19 p2744 N90-25598

Parallel algorithm for distributed memory computers (applications to matricial algorithms)
[ETN-90-97252] 20 p2913 N90-26573

MUSE: A systolic array for adaptive nulling with 64 degrees of freedom, using Givens transformations and wafer scale integration
[AD-A223812] 24 p3529 N90-29953

T

T SHAPE

The structural dynamics analysis of the main injector LOX inlet tee and its redesign
[NASA-CR-186764] 20 p2875 N90-26358

T TAURI STARS

FGK stars and T Tauri stars: Monograph series on nonthermal phenomena in stellar atmospheres
[NASA-SP-502] 10 p1446 N90-18344

Near-infrared speckle observations of T Tauri stars and a multi-wavelength study of the prototype star T Tauri
23 p3409 N90-29264

TABLES (DATA)

The 1984 direct strike lightning data, part 2
[NASA-TM-87690-PT-2] 01 p0089 N90-10506

The 1984 direct strike lightning data, part 3
[NASA-TM-87690-PT-3] 01 p0089 N90-10507

Federal funds for research and development: Fiscal years 1986, 1987, and 1988. Volume 36: Detailed statistical tables
[PB89-223523] 03 p0419 N90-12407

Federal funds for research and development. Fiscal years 1987, 1988, and 1989. Volume 37: Detailed statistical tables
[PB89-223531] 03 p0419 N90-12408

Tables for the thermophysical properties of methane
[PB89-222608] 04 p0469 N90-12690

Berne solar observations
[REPT-55] 04 p0566 N90-13301

Thermophysical properties of isopropyl alcohol. Part 2: Thermodynamic properties at elevated pressures
[ESDU-89020-PT-2] 06 p0739 N90-14300

Airborne electromagnetic sensing of sea ice thickness
[AD-A214460] 09 p1240 N90-17198

Tidal and lunar data for Point Mugu, San Nicolas Island, and the Barking Sands Area during 1990
[AD-A214828] 09 p1249 N90-17248

Model designation of military aerospace vehicles
[PB90-206301] 22 p3107 N90-27646

Analysis of acid precipitation samples collected by state agencies: January to December 1988
[PB90-191784] 22 p3198 N90-28151

World jet airplane inventory at year-end 1989
[PB90-207218] 23 p3267 N90-28489

Industrial patent activity in the US. Part 2: Alphabetical listing by company, 1969-1989
[PB90-214412] 23 p3405 N90-29246

Brorfelde Geomagnetic Observatory: Magnetic results, 1987
[ISBN-87-7478-297-5] 24 p3496 N90-29756

TABS (CONTROL SURFACES)

Effects of T-tabs and large deflections in DCB specimen tests
[NASA-TM-101677] 09 p1186 N90-16868

Elevator tab assembly producibility study
[IAR-89-16] 19 p2659 N90-25133

TABULATING

U TABULATION PROCESSES

TABULATION PROCESSES

Gridded environmental data compaction: An investigation
[AD-A210580] 02 p0252 N90-11430

UEDIT: A full-scale, scrollable APL2 spreadsheet input/output editor
[AD-A222712] 20 p2910 N90-26557

TACHOMETERS

A simple fiber optic autocorrelation tachometer
[ETN-90-96146] 08 p1077 N90-16228

TACTICS

Communications Data Base (CDB), phase 3 (with software documentation)
[AD-A210540] 01 p0137 N90-10789

Propagation-based decision aids in the U.S. Navy
06 p0757 N90-14410

Engineer's Refractive Effects Prediction System (EREPS)
06 p0758 N90-14411

Brain activity during tactical decision-making. Part 3: Relationships between probe-evoked potentials, simulation performance, and on-job performance
[AD-A217207] 13 p1854 N90-20638

Computer vision techniques for rotorcraft low altitude flight
15 p2142 N90-22237

TACTILE DISCRIMINATION

Analysis and construction of contact and tactile sensors
[DE89-013992] 01 p0072 N90-10416

Force/torque and tactile sensors for sensor-based manipulator control
24 p3501 N90-29791

TACTILE SENSATION

U TOUCH

TAGGING

U MARKING

TAIL ASSEMBLIES

Measurements of pressures on the tail and aft fuselage of an airplane model during rotary motions at spin attitudes
[NASA-TP-2939] 02 p0145 N90-10829

Additions and corrections to SUPER: A program for calculating steady and oscillatory supersonic flow over a thin wing, tail plane and fin
[AD-A211771] 04 p0438 N90-12501

Canard versus aft-tail ride qualities performance and pilot command response
07 p0871 N90-15053

Assessment of computational prediction of tail buffeting
[NASA-TM-101613] 08 p1018 N90-15886

An experimental investigation of support strut interference on a three-percent fighter model at high angles of attack
[AD-A219793] 17 p2345 N90-23353

Effect of tail size reductions on longitudinal aerodynamic characteristics of a three surface F-15 model with nonaxisymmetric nozzles
[NASA-TP-3036] 20 p2802 N90-25938

TAIL MOUNTINGS

U TAIL ASSEMBLIES

TAIL PLANES

U HORIZONTAL TAIL SURFACES

TAIL ROTORS

NT HELICOPTER TAIL ROTORS

TAIL SURFACES

NT HORIZONTAL TAIL SURFACES

TAILLESS AIRCRAFT

NT B-58 AIRCRAFT

TAILS (ASSEMBLIES)

U TAIL ASSEMBLIES

TAIWAN

Determination of mean gravity anomalies in the Taiwan Island
13 p1837 N90-20547

TAKEOFF

NT VERTICAL TAKEOFF

The 1987 survey of track keeping and altitudes on Heathrow and Gatwick standard instrument departure routes (DAY)
[CAA-PAPER-88010] 03 p0305 N90-11729

Airplane takeoff and landing performance monitoring system
[NASA-CASE-LAR-13734-1-CU]
13 p1758 N90-20096

Brake performance of the McDonnell Douglas DC-10-30/40 during high speed, high energy rejected takeoffs
[PB90-917004] 14 p1920 N90-21000

HOTOL structures and materials at British Aerospace, Warton, UK
[EOARD-LR-90-001] 14 p1921 N90-21001

Optimization and guidance of flight trajectories in the presence of windshear
[NASA-CR-186163] 15 p2049 N90-21747

En route noise annoyance laboratory test: Preliminary results
18 p2611 N90-24870

A quantitative technique to estimate microburst wind shear hazard to aircraft
18 p2640 N90-25040

Replication of NASPAC Dallas/Fort Worth study
[DOT/FAA/CT-TN90/26] 19 p2657 N90-25123

An accurate numerical technique for determining flight test rate gyroscope biases prior to takeoff
[AD-A220987] 19 p2660 N90-25138

An overview of the joint FAA/NASA aircraft/ground runway friction program
[NASA-TM-103486] 20 p2805 N90-25957

BASEOPS default profiles for civil aircraft
[AD-A223161] 21 p2959 N90-26825

Vibration responses of two house structures during the Edwards Air Force Base phase of the national sonic boom program
[NASA-CR-182089] 23 p3393 N90-29169

TALKING

NT WORDS (LANGUAGE)

TANDEM MIRRORS

Magnetic mirror confinement concepts system studies
[DE90-003667] 07 p0995 N90-15753

Thermal barrier research
[DE90-009213] 16 p2319 N90-23221

TANDEM ROTOR HELICOPTERS

NT CH-47 HELICOPTER

TANGENTS

Tangent map analysis of the beam-beam interaction
[DE89-015857] 01 p0120 N90-10689

TANK GEOMETRY

Small amplitude liquid oscillations in a rectangular container under zero-gravity
[LRT-WE-9-FB-2(1989)] 08 p1066 N90-16167

TANKER AIRCRAFT

Developing air tanker performance guidelines
[PB90-183765] 22 p3114 N90-27695

TANKS (COMBAT VEHICLES)
Vehicle acceleration and fuel consumption when operated on JP-8 fuel
[AD-A216275] 10 p1393 N90-18055
M1A2 adjunct analysis (POSNOV volume)
[AD-A218802] 16 p2199 N90-22553
Motion sickness, visual displays, and armored vehicle design
[AD-A222678] 20 p2902 N90-26506

TANKS (CONTAINERS)
NT CYLINDRICAL TANKS
NT EXTERNAL TANKS
NT FUEL TANKS
NT PROPELLANT TANKS
NT STORAGE TANKS
On the computation of normal modes of a rotating, viscous, incompressible fluid with a capillary free boundary
[REPT-89-01] 03 p0348 N90-11989
Tensile behavior of cylindrical pressure tanks in fiber assembling + metal hybrid structure
[ILR-MITT-213] 12 p1675 N90-19818
Design and manufacturing of an APTF to test fluid behaviour in microgravity environment
18 p2541 N90-24506
Hydroelastic problems in space flight vehicles
[LRT-WE-9-FB-11(1989)] 21 p2967 N90-26868
Nonlinear axisymmetric free vibrations of a liquid in a cylindrical tank with an elastic bottom
[LRT-WE-9-FB-17(1989)] 21 p3006 N90-27092

TANTALUM
Exploratory study of niobium, titanium, zirconium and tantalum aluminides
[AD-A210658] 02 p0283 N90-11615
Hardness-damage correlations in Ta implanted single crystal NiAl
[DE90-005270] 09 p1293 N90-17494
Ta and Nb reinforced MoSi2
[DE90-010596] 18 p2517 N90-24377
Densification studies of refractory materials using Hot Isostatic Pressing (HIP) and tantalum containment
[DE90-013481] 20 p2833 N90-26114
The investigation and production of titanium-tantalum junctions diffusion bonded at high temperature (855 C to 920 C): The influence of temperature, time pressure and roughness on the mechanical properties, and the optimisation of the bonded conditions
[BR114894] 24 p3476 N90-29646

TANTALUM COMPOUNDS
NT TANTALUM OXIDES
Thermal conductivity of quasi-one dimensional conductors
[DE90-004844] 10 p1435 N90-18281

TANTALUM OXIDES
Synthetic polypeptide composites for sensor applications
[AD-A210797] 01 p0052 N90-10296
Microstructure of thin films
[AD-A219262] 16 p2324 N90-23255

TAPE RECORDERS
NT VIDEO TAPE RECORDERS
Portable digital pressure indicator for calibrating magnetic tape recorders
[NASA-TM-101650] 07 p0933 N90-15401
A compact acoustic recorder
[AD-A213581] 07 p0933 N90-15403
SPOT 4 space magnetic recorder mechanisms
15 p2112 N90-22082

TAPER
U TAPERING

TAPERED WINGS
U SWEPT WINGS

TAPERING
Properties of density tapered arrays
[RSRE-MEMO-4210] 04 p0489 N90-12810
Statistical density and amplitude tapered arrays
[RSRE-MEMO-4211] 04 p0490 N90-12818
Wire grid modeling of the linear tapered slot antenna
[AD-A212977] 04 p0494 N90-12842
Discontinuous-taper directional coupler
[AD-D014324] 12 p1650 N90-19481
Aperture taper determination for the half-scale accurate antenna reflector
[NASA-CR-185215] 14 p1969 N90-21282

TAPES
High density tape casting system
[NASA-CASE-NPO-16901-1-CU]
12 p1640 N90-19425

TARE (DATA REDUCTION)
U DATA REDUCTION

TARGET ACQUISITION
Adaptive tracking of maneuvering targets based on IR image data 02 p0149 N90-10853
Guidance and Control Panel Symposium on Guidance and Control of Unmanned Air Vehicles
[AGARD-AR-260] 04 p0458 N90-12623
Dedicated tracking of crossing targets with a phased array monopulse radar
[FEL-1988-95] 04 p0491 N90-12821
A method to model fuze performance. Part 2: Calculation of target reflections with physical optics
[FEL-1989-21-PT-2] 04 p0491 N90-12822
Modified Newton-type methods for long-range target motion analysis
[FEL-1989-82] 04 p0551 N90-13208
A validation of the proposed NATO standard method to determine target acquisition distances with image intensifiers
[IZF-1988-8] 04 p0554 N90-13230
Smooth track generation for target motion analysis
[FEL-1989-83] 04 p0555 N90-13233
Airborne FLIR detection of surface targets
06 p0759 N90-14416
Guidance and Control of Unmanned Air Vehicles
[AGARD-CP-436] 08 p1025 N90-15924
Electro-optic sensors for surveillance and target acquisition 08 p1026 N90-15929
Automated search techniques applied to optical payloads in unmanned air vehicles
08 p1026 N90-15931
Terrain-aided navigation and target acquisition on the AFTI/F-16 09 p1166 N90-16747
Long term integration for radar detection of small targets in clutter 09 p1203 N90-16972
Survey of ERIM approaches applicable to semi-automatic target detection and cueing for multispectral and multisensor exploitation
[AD-A214241] 09 p1258 N90-17296
A Doppler centroid estimation algorithm for SAR systems optimized for the quasi-homogeneous source
[NASA-CR-186229] 09 p1275 N90-17391
Laser intersatellite transmission experiment spatial acquisition, tracking, and pointing system
[AD-A215934] 10 p1389 N90-18036
Visual target detection and recognition
[DE90-006903] 11 p1567 N90-19015
ROSAR (Helicopter-Rotor based Synthetic Aperture Radar) 14 p1961 N90-21229
MMW SAR on RPV for battlefield surveillance
14 p1961 N90-21231
SAR and ISAR imagery of marine targets
14 p1962 N90-21237
Radar target image by ISAR case study
14 p1963 N90-21242
Tracking in uncertain environments
[RAE-TM-AW-121] 16 p2261 N90-22891
Optimizing ECM techniques against monopulse acquisition and tracking radars
[AD-A220036] 17 p2393 N90-23629
Target selection in anti-tank helicopter operations: Relative weight of cues in target evaluation judgements
[FOA-C-50072-5.2] 17 p2436 N90-23881
Target selection in anti-tank operations: Effects of experience
[FOA-C-50073-5.2] 17 p2436 N90-23882
Mode of presentation of cues in policy capturing: A comparison between verbal and pictorial presentation of targets in judgement of probability to fire
[FOA-C-50074-5.2] 17 p2436 N90-23883
Application of frequency interpolation to acoustic-structure interaction problems
[AD-A219330] 17 p2469 N90-24113
On the relation between various levels of target acquisition
[IZF-1989-38] 19 p2724 N90-25492
PHIND, an analytical model to predict target acquisition distance with image intensifiers
[IZF-1989-45] 19 p2724 N90-25493
Guidance and targeting for the strategic target system
[DE90-005239] 20 p2817 N90-26031
Target acquisition probability as a function of distance, calculated with PHIND
[IZF-1989-46] 22 p3244 N90-28394
Target detection in Gaussian noise using artificial neural systems
[AD-A223983] 23 p3320 N90-28770
Target acquisition under load factors: Advantages and disadvantages of a helmet mounted sight
23 p3359 N90-28983
Tracking performance and influence of field of view
23 p3360 N90-28988
Investigation method for AA-proximity fuses
[FEL-89-A194] 24 p3459 N90-29535
Airborne target detection, acquisition, and tracking devices
[AD-A223852] 24 p3462 N90-29555

TARGET DRONE AIRCRAFT
Pilotless airplanes
[AD-A211719] 03 p0305 N90-11734

TARGET PENETRATION
U TERMINAL BALLISTICS

TARGET RECOGNITION
Tracking performance evaluation
[AD-A210499] 01 p0095 N90-10540
Progress in the identification of airborne radar targets
[AD-A212749] 04 p0493 N90-12835
Research in computer vision for autonomous systems
[AD-A212420] 04 p0555 N90-13235
Efficient detection of small moving objects
[AD-A213314] 05 p0632 N90-13690
Compensatory tracking in disturbance tasks and target following tasks. The influence of cockpit motion on performance and control behavior
[LR-511] 05 p0675 N90-13933
High resolution imaging by phase retrieval and discrimination using speckle, volume 1
[AD-A214243] 07 p0919 N90-15317
Research in knowledge-based vision techniques for the Autonomous Land Vehicle Program
[AD-A213440] 07 p0942 N90-15453
Mirach 100 flight control system
08 p1025 N90-15926
Target classification using SAR (Synthetic Aperture Radar) polarimetric data
[AD-A215672] 09 p1208 N90-17002
Survey of ERIM approaches applicable to semi-automatic target detection and cueing for multispectral and multisensor exploitation
[AD-A214241] 09 p1258 N90-17296
Development of advanced WTA algorithms for parallel processing
[AD-A214874] 09 p1266 N90-17341
A genetic adaptive system for image understanding and learning research
[AD-A214810] 09 p1271 N90-17367
Localization of multiple broadband targets in spherical coordinates via adaptive beamforming and non-linear estimation
[AD-A215714] 09 p1274 N90-17387
Gabor transforms for forward looking infrared image segmentation
[AD-A215046] 09 p1282 N90-17433
Infrared target detection: Signal and noise sensitivity analysis
[AD-A215707] 09 p1282 N90-17436
Neurobeamformer 2: Further exploration of adaptive beamforming via neural networks
[AD-A215118] 10 p1426 N90-18226
Psychological studies of visual cortical function
[AD-A217029] 11 p1541 N90-18872
A simulation of optical propagation through atmospheric turbulence using two-dimensional Fourier transform techniques
[AD-A216776] 11 p1566 N90-19013
ARGUS/LLNL IR camera calibration and characterization
[AD-A217076] 12 p1664 N90-19563
Processing infrared images for target detection: A literature study
[IZF-1988-12] 12 p1715 N90-19847
Multi-dimensional LADAR tracking and adaptive grasping for spaceborne assembly of SDI (Strategic Defense Initiative) platforms
[AD-A218236] 13 p1791 N90-20279
Algorithms for optimal processing of polarimetric radar data
[AD-A217330] 13 p1876 N90-20758
Modification, testing, and calibration of infrared search and target designator hardware received from NSWC
[AD-A217920] 13 p1889 N90-20837
High Resolution Air- and Spaceborne Radar
[AGARD-CP-459] 14 p1960 N90-21223
Automatic classification of images
[AD-D014437] 14 p1966 N90-21260
The effect of windscreen bows and HUD pitch ladder format on pilot performance during simulated flight
[AD-A218139] 14 p2011 N90-21523
Recognition and analysis of aircraft targets by radar, using structural pattern representations derived from polarimetric signatures 15 p2074 N90-21879
Intelligent signal processing techniques for multi-sensor surveillance systems
[AD-A218890] 16 p2262 N90-22895
Spectral characteristics of low-angle radar ground clutter
[AD-A220817] 17 p2392 N90-23622
Joint services electronics program
[AD-A220815] 17 p2397 N90-23654
Mental lapses and event-related potentials
[AD-A219454] 17 p2436 N90-23878
Effect of extraneous color-coded targets on identification of targets on CRT displays
[AD-A219473] 17 p2436 N90-23879
Analysis of the accuracy of a proposed target motion analysis procedure
[AD-A219481] 17 p2436 N90-23880

Neuromorphic optical signal processing and image understanding for automated target recognition
[AD-A219827] 17 p2437 N90-23884
A PC-based imaging system for the Naval Postgraduate School Infrared Search and Target Designation (NPS-IRSTD) system
[AD-A220109] 17 p2448 N90-23955
A comparison of the K-pulse and E-pulse techniques for aspect independent radar target identification
[AD-A220172] 18 p2542 N90-24511
Sweep width determination for HU-25B airborne radars: Life raft and recreational boat targets
[AD-A221362] 18 p2545 N90-24524
The target pursuit of Giotto camera
[ETN-90-96496] 18 p2555 N90-24581
On the relation between various levels of target acquisition
[IZF-1989-38] 19 p2724 N90-25492
PHIND, an analytical model to predict target acquisition distance with image intensifiers
[IZF-1989-45] 19 p2724 N90-25493
Acousto-optical localization of speed maneuvering flight targets
[FB-11-89] 19 p2758 N90-25676
High resolution exponential modeling of fully polarized radar returns
[AD-A221432] 21 p2997 N90-27036
Target signature modeling and bistatic scattering measurement studies
[NASA-CR-186611] 23 p3319 N90-28766
Target detection in Gaussian noise using artificial neural systems
[AD-A223983] 23 p3320 N90-28770
Modeling and reconstruction algorithms for detection, location, and identification of subsurface anomalies
[AD-A224358] 24 p3459 N90-29539
Airborne target detection, acquisition, and tracking devices
[AD-A223852] 24 p3462 N90-29555
Evaluation of a potential Wave Division Multiplexer (WDM) for use in the IRSTD
[AD-A223945] 24 p3463 N90-29560

TARGET SIMULATORS
Smooth track generation for target motion analysis
[FEL-1989-83] 04 p0555 N90-13233
A homing missile guidance law based on new target maneuver models
[AD-A220392] 17 p2356 N90-23410

TARGET THICKNESS
Studies in penetration mechanics
[AD-A210713] 01 p0079 N90-10448
Effects of parametric variations of complex targets on damage from projectile impact
[DE90-003214] 07 p0941 N90-15450

TARGETS
NT LASER TARGETS
NT PARTICLE ACCELERATOR TARGETS
NT RADAR TARGETS
EPIC-2 calculated impact loading histories of thin plates
[AD-A210557] 01 p0081 N90-10461
Tests of gating algorithms for tracking of multiple objects. Part 1: Theory, requirements and performance measures
[AD-A210519] 01 p0113 N90-10644
Evaluation of integrals related to the Debye function
[DE89-016930] 02 p0264 N90-11499
Acceleration of thin foil targets using fiber-coupled optical pulses
[DE89-016526] 02 p0275 N90-11569
Visual acuity and stereopsis with night vision goggles
[AD-A211552] 03 p0381 N90-12167
Analytical derivation and verification of zero-gyro control for the IUE satellite
[NASA-TM-100748] 05 p0645 N90-13767
Spatiotemporal characteristics of visual localization, phase 2
[AD-A212934] 05 p0674 N90-13929
Some quick and efficient methods for bearing-only target motion analysis
[IMAG-RR-762-M] 05 p0693 N90-14049
MF/HF multistatic mid-ocean radar experiments in support of SWOTHR (Surface-Wave Over-The-Horizon Radar)
[AD-A213830] 07 p0919 N90-15314
Effects of parametric variations of complex targets on damage from projectile impact
[DE90-003214] 07 p0941 N90-15450
Evaluation of a simple algorithm for estimating infrared signatures from multi-pixel to sub-pixel targets applied to AGA thermovision imagery
[AD-A214103] 07 p0976 N90-15639
Guidance and control considerations for a maneuvering aerial target system 09 p1165 N90-16746
Fractographic analysis of long rod penetrator-armor ceramic interactions
[AD-A215172] 09 p1197 N90-16938
Survey of ERIM approaches applicable to semi-automatic target detection and cueing for multispectral and multisensor exploitation
[AD-A214241] 09 p1258 N90-17296
A covariant multiple scattering series for elastic projectile-target scattering
[NASA-TM-101942] 09 p1279 N90-17417
Aggregate filter
[AD-A215029] 09 p1282 N90-17432
Enhanced tracking of ballistic targets using forward looking infrared measurements with active target illumination
[AD-A215422] 09 p1282 N90-17434
On multiple edge diffraction and multiple reflections of microwaves over terrain
[AD-A216418] 10 p1377 N90-17985
Spallation and dynamic fracture as an effect of laser induced shock waves in carbon based composite materials
[AD-A216540] 11 p1478 N90-18509
Analysis of methods to determine emissivity for ground surface targets in the spectral band 8 to 14 microns
[INPE-4984-TDL/394] 13 p1820 N90-20447
Determination of Li-Al alloy extent in tubular aluminum elements by small source neutron radiology
[DE90-009142] 14 p1952 N90-21174
Image simulation of geometric targets for synthetic aperture radar 14 p1964 N90-21245
Optimal and near-optimal medium range air-to-air missile guidance against maneuvering targets
15 p2053 N90-21766
A homing missile guidance law based on new target maneuver models
[AD-A220392] 17 p2356 N90-23410
A passive homing missile guidance law based on new target maneuver models
[AD-A220419] 17 p2356 N90-23411
Analysis of the accuracy of a proposed target motion analysis procedure
[AD-A219481] 17 p2436 N90-23880
IR and millimeter waves: Properties, models, and examples of ground target applications
[FOA-C-30541-3.3] 18 p2543 N90-24516
Low velocity impact analysis with NASTRAN
18 p2570 N90-24647
Bayesian characterization and detection of rare binary signature events
[AD-A221116] 18 p2606 N90-24844
The effect of random variations of radiosonde data on the predicted FLIR performance calculated by the program UFLR
[AD-A220034] 18 p2615 N90-24896
Proceedings of symposium on Production and Target Interaction of Particle Beam
[IPPJ-900] 18 p2616 N90-24903
Explanation of Bayesian conditioning for decision support systems 18 p2633 N90-25002
Extensions of algebraic image operators: An approach to model-based vision 19 p2741 N90-25577
Multi-microprocessor control of a precision pan and tilt head
[RSRE-MEMO-4252] 19 p2747 N90-25613
Acousto-optical localization of speed maneuvering flight targets
[FB-11-89] 19 p2758 N90-25676
Qualitative evaluation of a conformal velocity vector display for use at high angles-of-attack in fighter aircraft
[NASA-TM-102629] 20 p2809 N90-25981
The variably trimmed mean CFAR detector for nonhomogeneous background
[AD-A222801] 20 p2856 N90-26243
Multiple target tracking in a wide-field-of-view camera system
[DE90-013488] 20 p2865 N90-26300
A preliminary analysis of threshold signal detection in ambient and signal-dependent noise environments
[AD-A222089] 21 p2996 N90-27030
Noise adaptation and correlated maneuver gating of an extended Kalman filter
[AD-A221713] 21 p3001 N90-27060
Space-based wide area surveillance system studies
21 p3068 N90-27444
Airborne target detection, acquisition, and tracking devices
[AD-A223852] 24 p3462 N90-29555
A 94 GHz transmissometer
[AD-A223309] 24 p3471 N90-29618

TARS
Criteria for coal tar seal coats on airport pavements. Volume 2: Laboratory and field studies
[AD-A220167] 18 p2498 N90-24277

TASK COMPLEXITY
Effects of miniature CRT (Cathode Ray Tube) location upon primary and secondary task performances
[AD-A210223] 01 p0101 N90-10573
Payload crew utilization for spacelab missions
[NASA-TP-2976] 06 p0730 N90-14256
Prediction of success in flight training by single- and dual-task performance 09 p1257 N90-17293
Subjective Workload Assessment Technique (SWAT): A user's guide
[AD-A215405] 09 p1261 N90-17312
Aiding the decision maker: Perceptual and cognitive issues at the human-machine interface
[AD-A217862] 13 p1855 N90-20648
Cognitive efficiency considerations for good graphic design
[AD-A218976] 16 p2263 N90-22899
What makes some problems hard: Explorations in the problem space of difficulty
[AD-A219002] 16 p2263 N90-22901
TOM: Test of multiple task performance, user manual
[DLR-FB-89-60] 19 p2723 N90-25490
Performance-based workload assessment: Allocation strategy and added task sensitivity
19 p2734 N90-25539
Maintaining spatial orientation awareness
23 p3361 N90-28993
Uniform task level definitions for robotic system performance comparisons 24 p3512 N90-29855

TASK PLANNING (ROBOTICS)
Agent independent task planning
21 p3040 N90-27276
An efficient temporal logic for robotic task planning
24 p3521 N90-29906

TASKS
NT VISUAL TASKS
Models of mental functioning
[AD-A210456] 01 p0094 N90-10538
Differences in writers initial task representations
[AD-A210433] 01 p0136 N90-10788
Ada task scheduling: A focused Ada investigation
[NASA-CR-186072] 05 p0682 N90-13967
Human factors aspects of decision support systems
06 p0757 N90-14408
Task-oriented display design: Concept and example
[NASA-TM-101685] 07 p0881 N90-15101
Dual task performance with LPC (Linear Predictive Coding) degraded speech in a sentence verification task
[AD-A214298] 07 p0920 N90-15320
MANPRINT methods monograph: Aiding the development of manned system performance criteria
[AD-A213543] 07 p0968 N90-15593
FAA air traffic control operations concepts. Volume 7: ATCT (Airport Traffic Control Towers) tower controllers
[AD-A210455] 09 p1163 N90-16730
Further development and limited flight testing of the CycloCrane
[AD-A215519] 09 p1167 N90-16754
Effectiveness of progressive resistance training for increasing maximal repetitive lifting capacity
[AD-A215286] 09 p1252 N90-17267
An analysis of scatter decomposition
[NASA-CR-181978] 09 p1276 N90-17396
An approach to elemental task learning
[DE90-006614] 12 p1697 N90-19745
Human task animation from performance models and natural language input 13 p1861 N90-20678
Adding a dimension: Time as a factor in the generalizability of predictive relationships
[AD-A219679] 17 p2438 N90-23890
A parallel algorithm for global routing
[NASA-CR-186152] 17 p2448 N90-23959
From where they look to what they think: Determining controller cognitive strategies from oculometer scanning data 18 p2641 N90-25041
An empirically derived figure of merit for the quality of overall task performance 18 p2644 N90-25058
Performance-based workload assessment: Allocation strategy and added task sensitivity
19 p2734 N90-25539
Conceptual task modeling
[TR-89-14] 19 p2762 N90-25693
The conceptual task model: A specification technique between requirements engineering and program development
[TR-89-15] 19 p2762 N90-25694
Design and construction of a wall-climbing robot
[NIAR-90-20] 20 p2870 N90-26327
Investigation of automated task learning, decomposition and scheduling
[NASA-CR-186791] 20 p2899 N90-26488
The integration of complex information from auditory and visual channels under stress
[AD-A222686] 21 p3033 N90-27245
Focus of attention in an activity-based scheduler
23 p3369 N90-29039
Ability and metacognitive determinants of skill acquisition and transfer
[AD-A224569] 24 p3499 N90-29776

QTA (QUESTIONNAIRE-TASK-ANALYSIS): An electronic tool for job/task analysis
[DE90-008944] 24 p3499 N90-29778
Uniform task level definitions for robotic system performance comparisons 24 p3512 N90-29855
Assembly of objects with not fully predefined shapes 24 p3513 N90-29859
Precedence relationship representations of mechanical assembly sequences 24 p3514 N90-29866
Determining robot actions for tasks requiring sensor interaction 24 p3514 N90-29868
Visual processing: Implications for helmet mounted displays
[AD-A223488] 24 p3522 N90-29916

TASTE
Integration of neurobiological and computational analyses of the neural network essentials for conditioned taste aversions
[AD-A210228] 01 p0094 N90-10537
Utilization of non-conventional systems for conversion of biomass to food components
[NASA-CR-177545] 07 p0968 N90-15591

TATB
Shock initiation of LX-17 as a function of its initial temperature
[DE89-017730] 02 p0208 N90-11192
Pulsed-laser-excited Raman spectra of shock compressed triaminotrinitrobenzene
[DE90-000668] 03 p0353 N90-12019
A future for LLNL (Lawrence Livermore National Laboratory) research in composite high explosives
[DE90-004442] 07 p0915 N90-15290
Condensed phase kinetic deuterium isotope effects in high energy phenomena: Mechanistic investigations and relationships
[AD-A217161] 13 p1770 N90-20156
Study of the induction time in isothermal decomposition of explosives
[DE90-014906] 23 p3315 N90-28745

TAXIING
Results of aircraft open-loop tests of an experimental magnetic leader cable system for guidance during roll-out and turnoff
[NASA-TM-4135] 09 p1169 N90-16767

TAXONOMY
Taxonomic syntax for first order inference
[AD-A211618] 03 p0390 N90-12221
Message handling in the post-2000 era: Executive summary
[AD-A219983] 17 p2393 N90-23628
Multiple inheritance and exceptions in frame systems
[CMI-CS-R8931] 18 p2591 N90-24743
Flora and threatened and endangered plants of John F. Kennedy Space Center, Florida
[NASA-TM-102791] 23 p3349 N90-28925

TAYLOR INSTABILITY
The dynamic instability of adiabatic blastwaves
[NASA-CR-182498] 17 p2401 N90-23679
Turbulence modeling in the SHALE code
[DE90-010354] 18 p2553 N90-24574
Experimental study of the Taylor-Goertler instability
[ETN-90-97447] 22 p3175 N90-28014

TAYLOR SERIES
The fast Gauss transform
[AD-A211287] 02 p0266 N90-11517
Tensor methods for unconstrained optimization using second derivatives
[AD-A213642] 07 p0983 N90-15681
Modeling the gate I/V characteristic of a GaAs MESFET for Volterra-series analysis
[AD-A215314] 09 p1212 N90-17030
PROTEUS two-dimensional Navier-Stokes computer code, version 1.0. Volume 3: Programmer's reference
[NASA-TM-102553] 14 p1974 N90-21307

TAYLOR THEOREM
U TAYLOR SERIES

TAYLOR-GOERTLER INSTABILITY
U GOERTLER INSTABILITY

TDMA
U TIME DIVISION MULTIPLE ACCESS

TDR SATELLITES
Advanced tracking systems design and analysis
[NASA-CR-183459] 10 p1376 N90-17976
OMV mission simulator 13 p1860 N90-20669
CLEAR: Automating control centers with expert system technology 19 p2733 N90-25533
Space operations: NASA's communications support for Earth orbiting spacecraft. Report to Chairman, Subcommittee on Space Science and Applications, Committee on Science, Space and Technology, House of Representatives
[GAO/IMTEC-89-41] 20 p2851 N90-26215
ATDRS payload technology research and development
[NASA-TM-103256] 23 p3287 N90-28596

TEA LASERS
Research on sliding spark preionization in a TEA CO2 laser
[ISL-R-113/88] 11 p1516 N90-18732
Contributions to the development of SLM TEA CO2 laser sources for high resolution molecular spectroscopy 16 p2240 N90-22778
Phillips CO-oxidation catalyts for long-lived CO2 lasers: Activity and initial characterization studies 18 p2557 N90-24592
Synthesis, characterization and evaluation of CO-oxidation catalysts for high repetition rate CO2 TEA lasers 18 p2557 N90-24593

TEACHERS
U INSTRUCTORS

TEACHING
U EDUCATION

TEAMS
Personality factors in flight operations. Volume 1: Leader characteristics and crew performance in a full-mission air transport simulation
[NASA-TM-102259] 17 p2348 N90-23370
Effect of organizational structure on performance of decision making teams
[AD-A223160] 20 p2934 N90-26697

TEARING
Effect of oxygen on the tear strength of elastomers
[AD-A215845] 10 p1359 N90-17879
Inclusion of unstable ductile tearing and extrapolated crack-arrest toughness data in PWR vessel integrity assessment
[DE90-009427] 15 p2118 N90-22116

TEARING MODES (PLASMAS)
Spontaneous magnetic reconnection in a turbulent plasma 13 p1889 N90-20840
The effect of viscosity on the resistive tearing mode with the presence of shear flow
[DE90-009340] 14 p1974 N90-21312
MHD modes driven by anomalous electron viscosity and their role in fast sawtooth crashes
[DE90-009311] 14 p2029 N90-21639
Resonant MHD modes with toroidal coupling
[DE90-010077] 16 p2319 N90-23222
Nonlinear tearing mode: Rutherford regime and global characteristics
[DE90-015003] 23 p3397 N90-29193

TECHNICAL WRITING
Differences in writers initial task representations
[AD-A210433] 01 p0136 N90-10788
Technical communications in aeronautics: Results of an exploratory study. An analysis of managers' and nonmanagers' responses
[NASA-TM-101625] 02 p0288 N90-11647
Planning in writing: The cognition of a constructive process
[AD-A210434] 02 p0288 N90-11648
Source hierarchy list. Volume 1: A through D
[AD-A216050] 10 p1442 N90-18321
Source hierarchy list. Volume 2: E through N
[AD-A216051] 10 p1442 N90-18322
A compendium of sources of fracture toughness and fatigue crack growth data for metallic alloys, part 4
[NASA-TM-102646] 14 p1950 N90-21164
Grammar, punctuation, and capitalization: A handbook for technical writers and editors
[NASA-SP-7084] 20 p2937 N90-26710
Technical writing for software engineers
[AD-A223872] 23 p3382 N90-29109

TECHNOLOGICAL FORECASTING
NT DELPHI METHOD (FORECASTING)
NT PROFILE METHOD (FORECASTING)
Future military powerplants --- fighter aircraft engines
[PNR90554] 03 p0308 N90-11749
A vision of the future: The new engine technology
[PNR90566] 04 p0455 N90-12603
The next generation supersonic transport engine: Critical issues
[PNR90576] 04 p0455 N90-12605
Material requirements for future aeroengines
[PNR90595] 04 p0456 N90-12610
Composite materials for future aeroengines
[PNR90584] 04 p0466 N90-12667
The future of non ferrous metals in aerospace engines
[PNR90572] 04 p0475 N90-12720
Establishment of the Innovative Technology Utilization Center at West Virginia University
[PB90-114711] 08 p1138 N90-16594
Aeronautical aspects of Hermes re-entry: Question marks and prospects 09 p1178 N90-16822
Propellant trends in advanced rocket propulsion 09 p1179 N90-16838
Critical problems in very large scale computer systems
[AD-A215190] 09 p1270 N90-17365
Toward an electrical power utility for space exploration 10 p1329 N90-17681
Challenges for future space power systems 10 p1331 N90-17695
NASA advanced space photovoltaic technology: Status, potential and future mission applications 10 p1342 N90-17775
Adapting software development policies to modern technology
[AD-A213391] 10 p1416 N90-18157
Space orientation and orbital technology
[ISBN-3-89100-015-4] 11 p1465 N90-18437
Long term planning for space flight activities within the DFVLR
[DFVLR-IB-303-88/2] 11 p1465 N90-18438
Methodology panel 11 p1576 N90-19076
An integrative research review of the relationship between technology and structure: A meta-analytic synthesis
[AD-A218115] 13 p1899 N90-20903
Experimental aeroelasticity history, status and future in brief
[NASA-TM-102651] 14 p1930 N90-21047
NASA's Advanced Communications Technology Satellite (ACTS): Will it benefit commercial/military satellites
[AD-A217710] 14 p1939 N90-21100
Back to the stars 17 p2359 N90-23429
Satellite orbitography 17 p2359 N90-23432
Materials and processes for spacecraft: The ESTEC approach
[ESA-STM-244] 19 p2667 N90-25176
Materials and structures for 2000 and beyond: An attempted forecast by the DLR Materials and Structures Department
[ESA-TT-1154-REV] 20 p2843 N90-26173
The integration of multiple avionic sensors and technologies for future military helicopters 24 p3424 N90-29344

TECHNOLOGIES
NT BIOTECHNOLOGY
NT ENERGY TECHNOLOGY
NT GEOTHERMAL TECHNOLOGY
NT MARINE TECHNOLOGY
NT MILITARY TECHNOLOGY
NT REACTOR TECHNOLOGY
Publications of the National Institute of Standards and Technology, 1988 catalog
[PB89-218382] 04 p0563 N90-13279
Technology transfer to the United States: The MIT (Massachusetts Institute of Technology) Japan Science and Technology Program. A background paper of OTA's (Office of Technology Assessment's) assessment on technology, innovation, and US trade
[PB89-224711] 04 p0564 N90-13291
Advancing automation and robotics technology for the Space Station Freedom and for the US economy
[NASA-TM-101691] 10 p1414 N90-18151
An integrative research review of the relationship between technology and structure: A meta-analytic synthesis
[AD-A218115] 13 p1899 N90-20903
ONR (Office of Naval Research) summer scholars for the 1989 PREFACE Program
[AD-A217746] 13 p1903 N90-20919
Goes I-M and beyond: Science requirements and technology challenges 14 p1934 N90-21067
International science and technology policies: Testimony before the Subcommittee on International Scientific Cooperation, Committee on Science, Space, and Technology, United States House of Representatives
[DE90-009416] 15 p2181 N90-22463
JPRS report: Science and technology. USSR: Physics and mathematics
[JPRS-UPM-89-001] 16 p2310 N90-23162
Hypersonic aerodynamics of spacecraft
[DLC-EST-TD-032] 17 p2346 N90-23361
National Educators' Workshop: Update 1989 Standard Experiments in Engineering Materials Science and Technology
[NASA-CP-3074] 18 p2513 N90-24350
Preparing technicians for engineering materials technology 18 p2516 N90-24369
Project TTA-79: Summary project report
[ETN-90-96773] 19 p2661 N90-25146
Critical connections: Communication for the future
[PB90-182742] 21 p2992 N90-27005
NIST (National Institute of Standards and Technology) serial holdings, 1990 edition
[PB90-183245] 22 p3163 N90-27936
Federal support to universities, colleges, and selected nonprofit institutions: Fiscal year 1988 (detailed statistical tables)
[PB90-226887] 23 p3404 N90-29236
Goverment's role in standards-related activities: Analysis of comments
[PB90-215534] 23 p3404 N90-29239

State science and technology indicators: An exploratory profile and analysis
[PB90-246711] 23 p3408 N90-29259

TECHNOLOGY ASSESSMENT

Large scale prop-fan structural design study. Volume 1: Initial concepts
[NASA-CR-174992] 01 p0010 N90-10043
Large scale prop-fan structural design study. Volume 2: Preliminary design of SR-7
[NASA-CR-174993] 01 p0010 N90-10044
Castings, from theory to practical application 01 p0042 N90-10236
Japanese structural ceramics research and development 01 p0048 N90-10272
Advanced Turbine Technology Applications Program, (ATTAP)
[DE89-016067] 02 p0230 N90-11318
An assessment of technology for self-powered gas appliances: A GATC (Gas Appliance Technology Center)
[PB89-219265] 03 p0354 N90-12026
Estimating the relationships between the state of the art of technology and production cost for the US aircraft
[AD-A212127] 04 p0437 N90-12495
LFC: A maturing concept
[DOUGLAS-PAPER-7878] 04 p0438 N90-12505
Ultrastructure processing and characterization of polymers
[AD-A211460] 04 p0478 N90-12743
A survey of the current state-of-the-art in high-energy-product permanent magnets
[AD-A211761] 04 p0549 N90-13193
Research on heating, instabilities, turbulence and RF emission from electric field dominated plasmas
[AD-A212122] 04 p0557 N90-13243
LORAN C stability integrity assurance
[AD-A212663] 05 p0577 N90-13364
Study of high-speed civil transports
[NASA-CR-4235] 05 p0578 N90-13370
Introduction to the report of the Asilomar 3 LDR workshop 05 p0594 N90-13450
Preliminary experiments on filament winding nylon impregnated glass fibers (FIT)
[LR-545] 05 p0628 N90-13669
Propagation assessment and tactical decision aids 06 p0757 N90-14407
Battery technology assessment and R and D plan
[DE90-002007] 06 p0772 N90-14489
Assessment of research needs for laser technologies applied to advanced spectrographic methods
[DE90-001154] 06 p0788 N90-14587
French technological progress in the field of robotics and teleoperation
[DE90-001590] 06 p0794 N90-14626
Applications of superconductor technologies to transportation
[DE90-000856] 06 p0853 N90-14961
Accessing Japanese technical information: A group of essays extracted from the NTIS (National Technical Information Service) Directory of Japanese Technical Resources in the United States for 1987 and 1988
[PB90-100165] 06 p0858 N90-14992
Proceedings of the Antenna Applications Symposium, volume 2
[AD-A213815] 07 p0919 N90-15313
Ocean thermal energy conversion: An overview
[DE89-000838] 07 p0953 N90-15512
Introduction to D-He(3) fusion reactors 07 p1008 N90-15839
The Solar Power Satellite (SPS): Progress so far 07 p1008 N90-15840
Importance of helium-3 for the future 07 p1009 N90-15843
Technology and evaluation of unmanned air vehicles 08 p1027 N90-15934
Assessment of battery technologies for electric vehicles, volume 1
[DE90-002049] 08 p1059 N90-16122
National program plan for electric vehicle battery research and development: Technical plan
[DE90-002023] 08 p1083 N90-16269
SERI (Solar Energy Research Institute) solar radiation resource assessment project
[DE89-009456] 08 p1097 N90-16352
Project summaries
[PB90-103987] 08 p1118 N90-16472
Changes in the volt, ohm, and temperature and long range impact of using the Josephson voltage standard
[DE90-004493] 09 p1214 N90-17039
Technology maturity assessment methodology SDIO systems SETA
[AD-A214571] 09 p1294 N90-17501
Federal scientific and technical information in an electronic age: Opportunities and challenges
[PB90-114414] 09 p1295 N90-17505
Regenerative fuel cell systems for project pathfinder 10 p1333 N90-17708
Numerical simulation of unstably stratified sheared flows
[DE90-005396] 10 p1384 N90-18008
Technology assessment of computer languages
[AD-A216940] 10 p1419 N90-18182
Technology assessment of operating systems
[AD-A216893] 10 p1421 N90-18192
Solar-Terrestrial Science Strategy Workshop
[NASA-CP-3048] 10 p1444 N90-18329
Background of the workshop 10 p1444 N90-18330
Rheological tests of Rigidite 5245 using the cone-plate and parallel plates method
[DT-310/88] 11 p1485 N90-18544
Technology assessment of software engineering
[AD-A216943] 11 p1546 N90-18902
Mechanical disturbances in high-performance superconducting dipoles
[DE90-006237] 11 p1570 N90-19040
Advanced ceramics
[DE90-608004] 12 p1630 N90-19370
High throughput data communication system
[AD-D014342] 12 p1642 N90-19432
Assessment of research needs for laser technologies applied to advanced spectroscopic methods
[DE90-007402] 12 p1669 N90-19588
Solid State Photovoltaic Research Branch
[DE89-009463] 12 p1682 N90-19660
A preliminary analysis of US CO2 emissions reduction potential from energy conservation and the substitution of natural gas for coal in the period to 2010
[DOE/NBB-0085] 12 p1684 N90-19673
High speed modem
[AD-D014319] 12 p1698 N90-19750
Science and technology report and outlook, 1985-1988
[PB90-115270] 12 p1727 N90-19926
First impressions of the comet drilling problem 12 p1743 N90-20021
Pyrotechnic device technology
[DE90-007683] 13 p1783 N90-20234
Technology assessment of video teleconferencing
[AD-A217318] 13 p1789 N90-20266
Exploratory battery technology development and testing report for 1988
[DE90-007996] 13 p1794 N90-20297
Solar thermal program summary, fiscal year 1989
[DE89-009475] 13 p1826 N90-20487
Assessment of crew workload measurement methods, techniques and procedures. Volume 1: Process, methods and results
[AD-A217699] 13 p1855 N90-20647
Technology assessment of superconductivity
[AD-A217697] 13 p1897 N90-20889
Review of the state of the technology for joining ceramics for high-temperature structural applications
[DE90-009224] 14 p1956 N90-21199
High performance computing and networking for science
[PB90-131228] 14 p2011 N90-21526
An all electronic transportation system from LEO to GEO and beyond 15 p2060 N90-21796
Aging characteristics of Li/SO(sub 2) cells
[NASA-CR-180432] 15 p2088 N90-21954
Trajectory generation for car-like robots
[DE90-008407] 15 p2106 N90-22047
Low order FIR and IIR filters in dynamic vision
[OUEL-1785/89] 15 p2167 N90-22384
Japanese magnetic confinement fusion research 15 p2169 N90-22392
JETC (Japanese Technology Evaluation Center) Panel Report on High Temperature Superconductivity in Japan
[NASA-CR-180413] 15 p2172 N90-22409
US access to space: Launch vehicle choices for 1990 to 2010 16 p2205 N90-22579
The Department of Defense critical technologies plan for the Committees on Armed Services United States Congress
[AD-A219300] 16 p2227 N90-22702
An assessment of second-generation stretched-membrane mirror modules
[DE90-010243] 16 p2252 N90-22841
Application of high-temperature superconducting thin-film devices to electro-optical and electronic warfare systems
[AD-A218805] 16 p2323 N90-23249
Quantum non-demolition stroboscopic observables and multipumping back-action evasion schemes
[PREPRINT-699] 16 p2326 N90-23260
Are quantum measurements on macroscopic bodies feasible
[PREPRINT-700] 16 p2326 N90-23261
Romans to Mars
[NASA-TM-103094] 16 p2342 N90-23339
Preliminary design of a supersonic Short Takeoff and Vertical Landing (STOVL) fighter aircraft
[NASA-CR-186670] 17 p2352 N90-23394
Project Longshot: A mission to Alpha Centauri
[NASA-CR-186052] 17 p2357 N90-23417
Human exploration of space: A review of NASA's 90-day study and alternatives
[NASA-CR-186394] 17 p2357 N90-23418
Artificial dielectrics
[AD-A219671] 17 p2389 N90-23605
Applicability of Asynchronous Transfer Mode (ATM) techniques to satellite communications systems
[MBB-UK-0059-89-PUB] 17 p2392 N90-23625
A viewpoint on the contribution of expert systems of logistics
[REPT-892-320-101] 17 p2454 N90-24002
Material evaluation of optical fibers and payout bobbins: An overview
[AD-A220104] 17 p2473 N90-24140
A study of the technology required for advanced vertical take-off aircraft
[ETN-90-96786] 18 p2497 N90-24268
Technology requirements for on-orbit servicing of spacecraft 18 p2506 N90-24321
Workshop on III-V Integrated Optoelectronics
[AD-A218759] 18 p2546 N90-24529
Solar thermal program summary. Volume 2: Research summaries
[DE89-009476] 18 p2576 N90-24674
Ocean energy program summary. Volume 2: Research summaries
[DE89-009482] 18 p2576 N90-24677
Summary results of an assessment of research projects in the national photovoltaics program
[DE90-008222] 18 p2577 N90-24680
Photovoltaic measurements and performance branch
[DE90-000324] 18 p2577 N90-24681
Photovoltaic concentrator technology development
[DE90-011479] 18 p2577 N90-24684
Lecture notes on flight simulation techniques
[LR-596] 19 p2662 N90-25153
Integrated controls and health monitoring for chemical transfer propulsion
[NASA-TM-103185] 19 p2668 N90-25178
Outlook for ceramics in heat engines, 1990 - 2010: A technical and economic assessment based on a worldwide Delphi survey
[DE90-011262] 19 p2679 N90-25234
The photovoltaic concentrator initiative
[DE90-011228] 19 p2710 N90-25425
SERI solar radiation resource assessment project
[DE90-000307] 19 p2711 N90-25428
Comparative assessment of world research efforts on magnetic confinement fusion 19 p2759 N90-25680
Autonomous space processor for orbital debris
[NASA-CR-186691] 20 p2820 N90-26044
Tensile strength measurement techniques for structural ceramics
[DE90-012193] 20 p2837 N90-26136
Figure of merit studies of beam power concepts for advanced space exploration
[NASA-CR-186720] 20 p2854 N90-26234
Electronic warfare technology: Trends and visions
[AD-A223034] 20 p2856 N90-26246
VISTA (Vertical Integration of Science, Technology, and Applications) user interface software study
[DE90-010003] 20 p2936 N90-26707
Prototyping an in-house business intelligence database
[PNR90665] 20 p2937 N90-26709
The lessons of Varsovian's reconnaissance
[NASA-TM-103207] 20 p2951 N90-26789
Critical connections: Communication for the future
[PB90-182742] 21 p2992 N90-27005
Onboard processor technology review 21 p3017 N90-27152
Evaluation of correlations between meteorological measurements and observations of lightning activity using artificial neural systems
[AD-A222659] 21 p3030 N90-27229
The post-2000 MILSATCOM architecture 21 p3070 N90-27452
Airport pavement drainage
[DOT/FAA/RD-90/24] 22 p3122 N90-27728
A technology assessment of alternative communications systems for the space exploration initiative
[NASA-TM-103243] 22 p3125 N90-27736
Structured analysis of the applicability of A and R technologies in space programs
[MBB-UO-0084-90-PUB] 22 p3256 N90-28436
Energy efficient engine program technology benefit/cost study. Volume 1: Executive summary
[NASA-CR-174766-VOL-1] 23 p3280 N90-28564
Measurement Techniques for Hypersonic Flows
[VKI-LS-1990-05] 24 p3419 N90-29314

The 2-D and 3-D characterizations of GPS navigation service
24 p3425 N90-29348
ECS: Sixth year in orbit
[ESA-BR-70] 24 p3440 N90-29428
System software for Soviet computers
24 p3523 N90-29921

TECHNOLOGY TRANSFER
NT AEROSPACE TECHNOLOGY TRANSFER
Domestic technology transfer program regulation
[PB89-195374] 01 p0137 N90-10793
Toward a national research network
[PB89-198709] 02 p0287 N90-11644
Globalization of Technology: International Perspectives. Proceedings of the 6th Convocation of the Council of Academies of Engineering and Technological Sciences
[PB89-198840] 02 p0288 N90-11645
Technology applications bulletins
[DE89-017454] 02 p0288 N90-11651
The transfer and diffusion of new technologies: A review of the economics literature
[DE89-015671] 02 p0290 N90-11655
Adoption of software engineering innovations in organizations
[AD-A211573] 03 p0387 N90-12206
Development and use of a tribology research-in-progress database
[PB89-228274] 03 p0417 N90-12396
Technology transfer to the United States: The MIT (Massachusetts Institute of Technology) Japan Science and Technology Program. A background paper of OTA's (Office of Technology Assessment's) assessment on technology, innovation, and US trade
[PB89-224711] 04 p0564 N90-13291
Centers for the commercial development of space
[NASA-PAM-525] 05 p0709 N90-14151
NASA commercial programs
[NASA-TM-101853] 05 p0709 N90-14152
Technology transfer in software engineering
06 p0827 N90-14805
Accessing Japanese technical information: A group of essays extracted from the NTIS (National Technical Information Service) Directory of Japanese Technical Resources in the United States for 1987 and 1988
[PB90-100165] 06 p0858 N90-14992
DOD (Department of Defense) Freedom of Information Act Program (incorporating changes 1 and 2)
[PB90-104753] 06 p0859 N90-14993
Point of view of a civil aircraft manufacturer on Al-Li alloy
07 p0899 N90-15200
Research in mathematics and computer science at Argonne
[DE90-000975] 07 p0969 N90-15595
Establishment of the Innovative Technology Utilization Center at West Virginia University
[PB90-114711] 08 p1138 N90-16594
United States Department of Energy stategic defense initiative: New and innovative concepts program
[DE90-005006] 09 p1276 N90-17399
Federal scientific and technical information in an electronic age: Opportunities and challenges
[PB90-114414] 09 p1295 N90-17505
COCOM (Coordinating Committee for Multilateral Exports), technology transfer and its impact on national security
[AD-A214569] 09 p1297 N90-17519
Technology transfer and the FSX: Effects on the United States/Japanese relationship
[AD-A216348] 10 p1443 N90-18327
The use of technology transfer centers by department of defense industrial facilities
[AD-A216863] 10 p1443 N90-18328
Long term planning for space flight activities within the DFVLR
[DFVLR-IB-303-88/2] 11 p1465 N90-18438
Transfer of heat pump technology
[DE90-007373] 11 p1509 N90-18693
Programs in Renewable Energy
[DE89-009489] 11 p1530 N90-18809
Report of the First Annual Airborne Weapons Training Technology Review
[DE90-007189] 12 p1697 N90-19747
Programme of the International Training Course on Remote Sensing for African Specialists
[INPE-4878-NTE/290] 14 p1995 N90-21435
Regional remote sensing laboratory
[INPE-4922-PRE/1519] 14 p2001 N90-21465
Toward a new CIM (Computer Integrated Manufacturing) architecture for Sandia Laboratories
[DE90-008677] 14 p2015 N90-21548
Advanced manufacturing technology: A Department of Energy technology transfer initiative
[DE90-008601] 14 p2037 N90-21688
How to get it: A guide to defense-related information resources
[AD-A201600] 15 p2176 N90-22433
International science and technology policies: Testimony before the Subcommittee on International Scientific Cooperation, Committee on Science, Space, and Technology, United States House of Representatives
[DE90-009416] 15 p2181 N90-22463
ONR Far East Scientific Information Bulletin, Volume 13, No. 4
[ONRFE-SCI-INFO-BULL-13(4)88]
16 p2311 N90-23168
Potential technology transfers of research on low-temperature carbon monoxide-oxygen recombination catalysts
18 p2562 N90-24616
Crystalline photovoltaic cell research, status, and future direction
[DE90-011478] 19 p2710 N90-25427
NASA's experience in the international exchange of scientific and technical information in the aerospace field
[NASA-TM-103093] 19 p2764 N90-25704
Technology transfer: US and foreign participation in R and D at Federal laboratories
[GAO/RCED-88-203BR] 19 p2764 N90-25706
Technology transfer: Implementation status of the Federal Technology Transfer Act of 1986. Report to Congressional requesters
[GAO/RCED-89-154] 19 p2764 N90-25707
International standards for text preparation and interchange
[DE90-011868] 20 p2935 N90-26699
Electric and hybrid vehicles program
[DE90-013560] 21 p2998 N90-27043
Applications of ISES for meteorology
21 p3018 N90-27160
Establishing a communications-intensive network to resolve artificial intelligence issues within NASA's Space Station Freedom research centers community
21 p3042 N90-27291
The role of the US government technical report in aeronautics: An exploratory study
[NASA-TM-893470] 21 p3087 N90-27553
Technology utilization: Managing the transfer of NASA aerospace technology to other industries
22 p3257 N90-28446
Legal ramifications of intellectual property
22 p3258 N90-28448
Transferring building energy technologies by linking government and private-sector programs
[DE90-000346] 23 p3408 N90-29258
State science and technology indicators: An exploratory profile and analysis
[PB90-246711] 23 p3408 N90-29259
Diagnostic development and support of MHD test facilities
[DE90-015403] 24 p3550 N90-30083
Superconductivity and information exchange
[DE90-015767] 24 p3554 N90-30110
The technology transfer process: Background for the national energy strategy
[DE90-015301] 24 p3559 N90-30139

TECHNOLOGY UTILIZATION
Advanced Turbine Technology Applications Program, (ATTAP)
[DE89-016067] 02 p0230 N90-11318
Systems analysis considerations in artificial intelligence/expert systems technology applications
[DE89-016847] 02 p0262 N90-11490
Globalization of Technology: International Perspectives. Proceedings of the 6th Convocation of the Council of Academies of Engineering and Technological Sciences
[PB89-198840] 02 p0288 N90-11645
Technology applications bulletins
[DE89-017454] 02 p0288 N90-11651
Research and Development Opportunities in Supercritical Fluid Technology
[DE89-015320] 04 p0469 N90-12684
Proceedings of the 10 May 1989 Antiproton Technology Workshop: Addendum
[AD-A212804] 04 p0554 N90-13227
NASA technology applications
[GPO-99-412] 04 p0564 N90-13290
European space technology: Celebrating twenty-five years of research and development
[ESA-BR-55] 04 p0569 N90-13322
Aircraft propulsion: Leading the way in aviation
[LR-532] 05 p0583 N90-13395
Large heavy duty balloons in Europe
05 p0661 N90-13858
Centers for the commercial development of space
[NASA-PAM-525] 05 p0709 N90-14151
NASA commercial programs
[NASA-TM-101853] 05 p0709 N90-14152
Base reaction optimization of redundant manipulators for space applications
[NASA-CR-186274] 07 p0941 N90-15447
Establishment of the Innovative Technology Utilization Center at West Virginia University
[PB90-114711] 08 p1138 N90-16594
Research and technology, 1989: Langley Research Center
[NASA-TM-4150] 08 p1157 N90-16703
An exploration of benefits from NASA Spinoff
10 p1443 N90-18325
The DFVLR 3-m x 3-m low speed wind tunnel (NWG) in Goettingen
[ESA-TT-1156] 11 p1465 N90-18436
Technology development and circuit design for a parallel laser programmable floating point application specific processor
[AD-A215870] 11 p1500 N90-18637
Promotion of European Space Technology Transfer
[ESA-SP-1122] 11 p1575 N90-19068
ESA project to promote and assist technology transfer by industry
11 p1576 N90-19069
Space technology transfers in Europe
11 p1576 N90-19070
DTE and space technology transfer
11 p1576 N90-19071
Purchase of technology
11 p1576 N90-19072
The bringing to market of the RF alert (a case study in technology transfer)
11 p1576 N90-19073
French approach to space technology transfer
11 p1576 N90-19074
Introductory remarks for the panel discussions on technology transfer
11 p1576 N90-19075
Methodology panel
11 p1576 N90-19076
Problems on transfer of space technology to non-space areas and solutions: Legal aspects
11 p1577 N90-19077
Identification of and response to market demand
11 p1577 N90-19078
The improvement of technology transfer from space to industry
11 p1577 N90-19079
Internal technology transfer
11 p1577 N90-19080
Magnetic suspension railway systems based on space technology
11 p1577 N90-19081
An example of technology transfer by Aerospatiale: Fire protection materials
11 p1577 N90-19082
Large-diameter geostationary millimeter wavelength antenna concept
12 p1609 N90-19254
Arrays for space applications
12 p1610 N90-19265
Antennas for 20/30 GHz and beyond
12 p1611 N90-19269
Multibody modeling and verification
12 p1640 N90-19422
First direct observation of FEL (Free-Electron Laser) from lambda=20 to 45 microns
[DE90-007508] 12 p1669 N90-19589
Possible applications of remote sensing in the preparatory phase of a land management project
[BCRS-88-19] 12 p1679 N90-19642
Induction-type metal detector with increased scanning area capability
[NASA-CASE-KSC-11386-1] 15 p2101 N90-22023
Information technology applications: A British Aerospace Military Aircraft Ltd view
15 p2180 N90-22455
Impact of meteorology on the agricultural sector: Compilation and analysis of projects
[INPE-4846-PRE/1475] 16 p2257 N90-22866
Application of high-temperature superconducting thin-film devices to electro-optical and electronic warfare systems
[AD-A218805] 16 p2323 N90-23249
User's guide to the 1.6 x 2.0 square m high speed wind tunnel HST, part 1
[ETN-90-96772] 17 p2357 N90-23414
Material evaluation of optical fibers and payout bobbins: An overview
[AD-A220104] 17 p2473 N90-24140
Materials and structures for 2000 and beyond: An attempted forecast by the DLR Materials and Structures Department
[ESA-TT-1154-REV] 20 p2843 N90-26173
Theoretical studies of solar pumped lasers
[NASA-CR-186712] 20 p2867 N90-26308
Advanced Turbine Technology Applications Project (ATTAP)
[NASA-CR-185240] 20 p2939 N90-26728
Preliminary designs for 25 kWe advanced Stirling conversion systems for dish electric applications
[NASA-TM-103188] 20 p2940 N90-26729
Fluid Dynamics Panel Working Group 12 on Adaptive Wind Tunnel Walls: Technology and Applications
[AGARD-AR-269] 21 p2961 N90-26838
Intelligent tutoring systems for space applications
21 p3048 N90-27324
AMSAHTS 1990: Advances in Materials Science and Applications of High Temperature Superconductors
[NASA-CP-10043] 22 p3136 N90-27792
Navy superconductivity efforts
22 p3145 N90-27837

Government Information Quarterly. Volume 7, no. 2: National Aeronautics and Space Administration Scientific and Technical Information Programs. Special issue
[ISSN-0740-624X] 22 p3257 N90-28440
Introduction to National Aeronautics and Space Administration's scientific and technical information programs 22 p3257 N90-28441
Technology utilization: Managing the transfer of NASA aerospace technology to other industries 22 p3257 N90-28446
An introductory guide preparing to use the ESTEC environmental test facilities
[ESA-TM-05] 24 p3438 N90-29419
Friction, wear and electric characteristics of slip-ring brush materials for space applications. Part 1: Screening by pin-on-disk friction tests
[NAL-TR-1040] 24 p3478 N90-29657
Integration of a sensor based multiple robot environment for space applications: The Johnson Space Center Teleoperator Branch Robotics Laboratory 24 p3518 N90-29890

TECTONIC MOVEMENT
U TECTONICS

TECTONICS
Tessera terrain: Characteristics and models of origin 03 p0422 N90-12426
Tectonism on Venus: A review 03 p0425 N90-12440
Venus: Mantle convection, hotspots, and tectonics 03 p0426 N90-12442
Lakshmi Planum: A distinctive highland volcanic province 03 p0426 N90-12444
Crustal deformation: Earth vs Venus 03 p0427 N90-12450
Eastern Ishtar Terra: Tectonic evolution derived from recognized features 03 p0428 N90-12451
Organic geochemical and tectonic evolution of the midcontinent rift system: Organic geochemistry and micropaleontology
[DE89-017561] 06 p0818 N90-14760
Determination of Q as a function of depth and tectonic province
[AD-A213805] 07 p0960 N90-15554
Evolution of overlapping spreading centers: A Sea Mark 2 investigation
[AD-A214278] 07 p0965 N90-15576
Tectonic history of the terrestrial planets
[NASA-CR-186309] 09 p1246 N90-17229
Fracture analysis through photographic imagery of low spatial resolution: A contribution to the study of tectonic evoluation of the Araripe Plateau region
[INPE-4876-PRE/1487] 11 p1520 N90-18756
The interpretation of crustal dynamics data in terms of plate interactions and active tectonics of the Anatolian plate and surrounding regions in the Middle East
[NASA-CR-186200] 11 p1533 N90-18824
Geological structure of the State of Rio de Janeiro viewed through MSS LANDSAT imagery
[INPE-4826-PRE/1457] 11 p1533 N90-18825
The patterns of fracture and the conditioning tectonics in the region of the Quadrilatero Ferrifero and part of the Migmatitic-Gnanulitic Complex in Minas Gerais (Brazil)
[INPE-4895-PRE/1496] 11 p1534 N90-18829
Analysis of tectonic movements utilizing remote sensor products in the Southern Espinhaco (SE) region
[INPE-4830-PRE/1451] 12 p1690 N90-19708
P-T condition fo deformation from fluid inclusions in mylonites
[NASA-CR-186377] 12 p1690 N90-19710
Development and testing of a universally implementable recording aligning system
[SER-C-349] 12 p1691 N90-19716
The effects of structure and source complexity on waveforms: Crustal structure of Tibet and the recovery of complex seismic sources
[AD-A218202] 13 p1843 N90-20579
Characterization of linear structures from remote sensing data; Espinhaco Meridional (MG) sierra
[INPE-4905-PRE/1506] 14 p1997 N90-21449
Geology of Espinhaco Meridional, including the Quadrilatero Ferrifero: Integration through remote sensing data
[INPE-4904-PRE/1505] 14 p1998 N90-21450
Contribution for the study of the evolution of part of the Espinhaco supergroup and its foundation through fracture analysis
[INPE-4907-PRE/1508] 14 p1999 N90-21459
Geology of coronae and domal structures on Venus and models of their origin 15 p2191 N90-22513
The Very Long Baseline Interferometry (VLBI) functional model and the relation with tectonic motions
[ETN-90-96694] 17 p2424 N90-23814
Development of remote sensing techniques for the investigation of neotectonic activity, eastern transverse ranges and vicinity, southern California 18 p2573 N90-24662
The Gauss beam method for surface waves. Theory and utilization for a lateral heterogeneous sphenic Earth
[ETN-90-96492] 18 p2580 N90-24695
The global positioning system: A new tool for tectonic studies 21 p3014 N90-27137
MEVTV Workshop on Early Tectonic and Volcanic Evolution of Mars
[NASA-CR-186098] 21 p3021 N90-27176
Evolution of overlapping spreading centers: A SeaMARC 2 investigation
[AD-A223102] 21 p3025 N90-27200
MEVTV Workshop on Tectonic Features on Mars
[NASA-CR-186143] 21 p3100 N90-27609
NASA geodynamics program: Bibliography
[NASA-TM-4220] 22 p3194 N90-28123
Some aspects of the structure and evolution of oceanic spreading centers 24 p3496 N90-29757

TED
U TRANSFERRED ELECTRON DEVICES

TEDLAR (TRADEMARK)
U POLYVINYL FLUORIDE

TEE
U T SHAPE

TEFLON (TRADEMARK)
Thermodynamic and fluid mechanic analysis of rapid pressurization in a dead-end tube 18 p2631 N90-24990
M-52 spray booth qualification test
[NASA-CR-184003] 22 p3122 N90-27727
Nylon and teflon scribe effect on NBR to Chemlok 233 and NBR to NBR bond interfaces
[NASA-CR-184004] 22 p3189 N90-28095

TELECHIRICS
U REMOTE HANDLING

TELECOMMUNICATION
NT AIRCRAFT COMMUNICATION
NT BROADCASTING
NT CLOSED CIRCUIT TELEVISION
NT CODE DIVISION MULTIPLE ACCESS
NT COLOR TELEVISION
NT COMMUNICATION
NT DATA LINKS
NT DEFENSE COMMUNICATIONS SYSTEM (DCS)
NT ELECTRONIC MAIL
NT GROUND-AIR-GROUND COMMUNICATION
NT MULTICHANNEL COMMUNICATION
NT MULTIPLE ACCESS
NT OPTICAL COMMUNICATION
NT PACKET TRANSMISSION
NT PCM TELEMETRY
NT PULSE COMMUNICATION
NT RADIO COMMUNICATION
NT RADIO RELAY SYSTEMS
NT RADIO TELEMETRY
NT SATELLITE COMMUNICATION
NT SATELLITE TELEVISION
NT SPACE COMMUNICATION
NT SPACECRAFT ANTENNAS
NT SPACECRAFT COMMUNICATION
NT TELEMETRY
NT TELEPHONY
NT TIME DIVISION MULTIPLE ACCESS
NT UNDERWATER COMMUNICATION
NT VIDEO COMMUNICATION
NT VOICE COMMUNICATION
NT WIDEBAND COMMUNICATION
ELF (Extremely Low Frequency) Communications System Ecological Monitoring Program: Electromagnetic field measurements and engineering support, 1988
[AD-A210200] 01 p0056 N90-10321
SINCGARS (Single-Channel Ground/Airborne Radio System) operator performance decay
[AD-A210716] 01 p0057 N90-10326
Active participation in highly automated systems: Turning the wrong stuff into the right stuff
[AD-A210218] 01 p0101 N90-10572
Communications Data Base (CDB), phase 3 (with software documentation)
[AD-A210540] 01 p0137 N90-10789
Deep null antennas and their applications to tactical VHF radio communications
[AD-A210656] 02 p0212 N90-11214
World Weather Watch: Implementation
[WMO-714] 03 p0375 N90-12139
The J-Machine: A fine grain concurrent computer
[AD-A211909] 03 p0384 N90-12187
Requirements specification with Petri nets using the cube tool methodology
[AD-A212190] 04 p0492 N90-12829
Removal of noise from noise-degraded speech signals
[AD-A212876] 04 p0493 N90-12840
Data handling and telecommunications 05 p0604 N90-13514
Optical communication with semiconductor laser diode
[NASA-CR-185886] 05 p0647 N90-13770
A communications system with an adaptive multi-functional architecture 06 p0759 N90-14415
A portable ionosonde in support of reliable communications 06 p0762 N90-14431
The use of broadcast signals for passive sensing in automated HF communication systems 06 p0762 N90-14433
Communication Overview Program (COP) 06 p0762 N90-14435
AdaNET services 06 p0827 N90-14806
Publications of the Jet Propulsion Laboratory, 1988
[NASA-CR-185956] 06 p0859 N90-14995
A burst compression and expansion technique for variable-rate users in satellite-switched TDMA networks
[NASA-TM-102414] 08 p1035 N90-15983
MT's algorithm: A new algorithm to search for the optimum set of modulation indices for simultaneous range, command, and telemetry
[NASA-CR-186259] 08 p1057 N90-16110
USAF/GL meteor scatter data analysis program: A user's guide
[AD-A214988] 09 p1206 N90-16989
Information capacity of dimension-limited channels
[AD-A215238] 09 p1207 N90-16996
An approach to the development of software for computer-aided design of satellite communications receivers for operation in scintillating channels
[AD-A215299] 09 p1267 N90-17349
A specification and analysis of the IEEE (Institute of Electrical and Electronic Engineers) token ring protocol
[AD-A214567] 09 p1269 N90-17359
ELF (Extremely Low Frequency) communications system ecological monitoring program: Summary of 1988 progress
[AD-A216153] 10 p1377 N90-17981
Event-train restoration via backpropagation neural networks
[AD-A216308] 10 p1420 N90-18189
Integrated IMA (Information Mission Areas) IC (Information Center) guide
[AD-A216944] 11 p1547 N90-18903
High throughput data communication system
[AD-D014342] 12 p1642 N90-19432
The Telecommunications and Data Acquisition Report
[NASA-CR-186479] 15 p2074 N90-21880
Atmospheric Propagation in the UV, Visible, IR, and mm-Wave Region and Related Systems Aspects
[AGARD-CP-454] 15 p2079 N90-21907
Electronic Transfer of Information and its Impact on Aerospace and Defence Research and Development
[AGARD-CP-466] 15 p2177 N90-22440
Technologies for electronic transfer of information: The present state and trends in Europe 15 p2177 N90-22441
Innovations in telecommunications networks 15 p2178 N90-22444
Electronic mail systems 15 p2179 N90-22451
Computer conferencing: Minds meeting anywhere anytime 15 p2179 N90-22452
The RACE (research and development in advanced technologies for Europe) program: A 1989 update
[AD-A218509] 16 p2228 N90-22713
Object orientated simulation on transputer arrays using time warp
[AD-A219795] 17 p2389 N90-23607
Maritime safety information in the year 2000: Listen up, Navy, the times they are a changin'
[AD-A220563] 17 p2390 N90-23611
Engineer's Refractive Effects Prediction System (EREPS), revision 2.0
[AD-A220742] 17 p2391 N90-23616
Computer-aided mathematical analysis of probability of intercept for ground-based communication intercept system
[AD-A219856] 17 p2392 N90-23627
System analysis of a tactical multi-satellite communication system
[AD-A220344] 18 p2510 N90-24343
Wave propagation over sea: Tropospheric effects on communication, radar, and ESM systems; proposal for a measuring programme
[FOA-C-30544-8.3] 18 p2543 N90-24517
Design of a Lunar farside observatory
[NASA-CR-186671] 19 p2765 N90-25709
A novel multireceiver communications system configuration based on optimal estimation theory
[NASA-CR-186847] 20 p2851 N90-26216
The Telecommunications and Data Acquisition Report
[NASA-CR-186852] 20 p2852 N90-26217
Critical connections: Communication for the future
[PB90-182742] 21 p2992 N90-27005
Quality evaluation of speech processing systems 21 p2993 N90-27012
The application of SAW devices in expanded frequency spectrum communications
[AD-A222958] 21 p2994 N90-27021

Advanced Communication Processing Techniques
[AD-A223244] 21 p2996 N90-27027
Measured effects of repeater jamming on direct-sequence spread spectrum receivers that use envelope detectors
[AD-A222231] 21 p2996 N90-27032
Meteor burst communications systems
[AD-A221675] 21 p2997 N90-27037
Brief state-of-the-art review on optical communications for the NASA ISES workshop 21 p3017 N90-27153
Tactical uses of the DSCS 3 communications system 21 p3069 N90-27450
The post-2000 MILSATCOM architecture 21 p3070 N90-27452
A technology assessment of alternative communications systems for the space exploration initiative
[NASA-TM-103243] 22 p3125 N90-27736
Congestion-reduction and service-restoration strategies for telecommunication networks
[PB90-207838] 22 p3164 N90-27944
Report of the Invitational Workshop on Data Integrity
[PB90-148123] 22 p3240 N90-28372
Requirements for implementing real-time control functional modules on a hierarchical parallel pipelined system 24 p3518 N90-29891

TELECONFERENCING
Technology assessment of video teleconferencing
[AD-A217318] 13 p1789 N90-20266

TELECONNECTIONS (METEOROLOGY)
A search for solar related changes in tropospheric weather 22 p3203 N90-28173

TELEMETERS
U TELEMETRY

TELEMETRY
NT PCM TELEMETRY
NT RADIO TELEMETRY
Analysis of flutter tests with the use of a telemetry system 02 p0152 N90-10871
Flight test instrumentation and data processing at British Aerospace, Warton, U.K. 02 p0155 N90-10887
Type-specific dynamic measurements on wind turbines at the test site Schnittlingen (Germany, F.R.)
[DFVLR-MITT-88-31] 03 p0367 N90-12099
Performance of the image statistics decoder in conjunction with the Goldstone-VLA array 04 p0487 N90-12796
Radar and sensor array design planning for a naval missile testing center. Artificial intelligence applications
[ETCA-88-R-099] 04 p0537 N90-13108
The role of the ground segment 05 p0606 N90-13527
The interface with the data reduction consortia 05 p0606 N90-13528
SN 1987: A telemetry decoding system 05 p0663 N90-13875
SAND DEVIL: A digital video link for telemetry applications
[DE90-001879] 06 p0730 N90-14259
A rough transform technique for extracting lead features from sea ice imagery
[AD-A212758] 06 p0801 N90-14666
X.2 limited flight test plan
[AD-A214412] 07 p0880 N90-15099
Identification and quantification of synoptic structure in simulated TIROS N radiance soundings
[AD-A213729] 07 p0960 N90-15553
MT's algorithm: A new algorithm to search for the optimum set of modulation indices for simultaneous range, command, and telemetry
[NASA-CR-186259] 08 p1057 N90-16110
Delta 181 sensor module command center
[AD-A214868] 09 p1182 N90-16855
The 15th Transducer Workshop — for telemetry applications
[AD-A215515] 10 p1327 N90-17665
Near real time VHF telemetry of near shore oceanographic data
[AD-A215756] 10 p1327 N90-17666
SHARP: A multi-mission artificial intelligence system for spacecraft telemetry monitoring and diagnosis
[NASA-CR-186285] 11 p1467 N90-18444
Packet telemetry standard
[ESA-PSS-04-106-ISSUE-1] 11 p1467 N90-18447
Telemetry and telecommand omnidirectional antenna in the short wave band
[ETN-90-96285] 11 p1499 N90-18831
PC-based PCM (Pulse Code Modulation) telemetry data reduction system hardware
[DE90-000316] 12 p1612 N90-19273
Kalman estimation for SEDS measurements 12 p1634 N90-19393
The Real Time Display Builder (RTDB) 13 p1857 N90-20656
Operational computer graphics in the flight dynamics environment 13 p1859 N90-20668
VLSI single-chip (255,223) Reed-Solomon encoder with interleaver
[NASA-CASE-NPO-17280-1-CU] 14 p1933 N90-21061
Subsystem TM Precision: Progress and perspective
[INPE-5006-PRE/1563] 14 p2000 N90-21461
Environmental projects, volume 11. Environmental assessment: Addition to operations building, Mars site
[NASA-CR-186449] 14 p2003 N90-21479
Digital Doppler extraction demonstration with the advanced receiver 15 p2076 N90-21893
Mark 4-A DSCC (Magellan-era) telemetry system description 15 p2078 N90-21903
An 8.4-GHz dual-maser front-end system for Parkes reimplementation 15 p2078 N90-21905
Preliminary results of the peak experiment. ALTAIR deep-space measurements
[AD-A218622] 16 p2229 N90-22714
Performance analysis of CCSDS path service
[NASA-CR-180699] 17 p2364 N90-23457
A low-cost PC-based telemetry data-reduction system
[DE90-000330] 18 p2509 N90-24339
New approach for the thin layer manufacturing: The wafer telemetry system
[MBB-UE-0004/89-PUB] 19 p2653 N90-25102
StarPlan: A model-based diagnostic system for spacecraft 19 p2728 N90-25511
Artificial intelligence for multi-mission planetary operations 19 p2732 N90-25532
Preliminary error budget for an optical ranging system: Range, range rate, and differenced range observables 20 p2853 N90-26227
Special test and evaluation methods used for a nine-axis accelerometer
[PB90-209578] 23 p3329 N90-28822
A system architecture for a planetary rover 23 p3365 N90-29015
A personal computer-based, multitasking data acquisition system
[NASA-TM-4232] 23 p3382 N90-29107
Database development for the DMSP experiments
[AD-A224346] 24 p3557 N90-30129

TELEOPERATOR MANEUVERING SYSTEM
U TELEOPERATORS

TELEOPERATORS
An adaptive controller for enhancing operator performance during teleoperation
[NASA-CR-183445] 01 p0077 N90-10438
Interchangeable end effector tools utilized on the protoflight manipulator arm
[NASA-CR-179374] 01 p0078 N90-10447
NASA/NBS (National Aeronautics and Space Administration/National Bureau of Standards) standard reference model for telerobot control system architecture (NASREM)
[NASA-CR-185078] 02 p0228 N90-11310
Land vehicle teleoperation under conditions of reduced video resolution
[DE89-016925] 02 p0231 N90-11324
Telescience Testbed Pilot Program
[NASA-CR-184594] 02 p0257 N90-11455
Distance and clearance perception using forward-looking, vehicular television systems
[DE89-014740] 03 p0405 N90-12319
Telerobotic control for teams of semi-autonomous agents, phase 1
[AD-A211648] 04 p0526 N90-13037
Performance evaluation of a six-axis generalized force-reflecting teleoperator
[NASA-CR-186106] 05 p0651 N90-13796
The SN 1987A attitude control system 05 p0659 N90-13845
French technological progress in the field of robotics and teleoperation
[DE90-001590] 06 p0794 N90-14626
Architectural study of the design and operation of advanced force feedback manual controllers
[NASA-CR-185948] 07 p0981 N90-15664
Bilateral force reflection for teleoperators with masters and slaves with dissimilar and possibly redundant kinematics
[DE90-004392] 08 p1061 N90-16132
Visual Information Processing for Television and Telerobotics
[NASA-CP-3053] 08 p1072 N90-16204
Connectionist model-based stereo vision for telerobotics 08 p1076 N90-16224
Examples of robots and teleoperators at the Savannah River Site
[DE90-004659] 08 p1086 N90-16284
Teleoperator servoloop tuning using an expert system
[DE90-005674] 11 p1542 N90-18876
Design and implementation of a flexible robot
[AD-A216453] 12 p1671 N90-19601
Extending terrestrial mobile robotics to a proposed lunar base
[DE89-016179] 12 p1672 N90-19606
Multi-dimensional LADAR tracking and adaptive grasping for spaceborne assembly of SDI (Strategic Defense Initiative) platforms
[AD-A218236] 13 p1791 N90-20279
Design of a telerobotic controller with joint torque sensors
[DE90-008753] 13 p1812 N90-20404
Graphics Technology in Space Applications (GTSA 1989)
[NASA-CP-3045] 13 p1856 N90-20651
The use of graphics in the design of the human-telerobot interface 13 p1860 N90-20670
Mars in this century: The Olympia Project
[DE90-008356] 14 p2042 N90-21709
A new six-degree-of-freedom force-reflecting hand controller for space telerobotics 15 p2113 N90-22089
Development of cable drive systems for an automated assembly project 15 p2116 N90-22105
Hybrid vision activities at NASA Johnson Space Center 15 p2139 N90-22225
Instrumentation and robotic image processing using top-down model control 15 p2142 N90-22239
Computer vision research at Marshall Space Flight Center 15 p2142 N90-22240
The JPL/KSC telerobotic inspection demonstration 15 p2155 N90-22312
Multi-axis control of telemanipulators 16 p2271 N90-22943
Telepresence, time delay, and adaptation 16 p2271 N90-22944
Visual enhancements in pick-and-place tasks: Human operators controlling a simulated cylindrical manipulator 16 p2271 N90-22946
Displays for telemanipulation 16 p2272 N90-22948
Experiences in teleoperation of land vehicles 16 p2273 N90-22954
Development of efficient computer program for dynamic simulation of telerobotic manipulation 16 p2284 N90-23017
Robotics program at the NASA Goddard Space Flight Center 18 p2500 N90-24285
Servicing test facility: A hardware simulator for telerobotic in-orbit servicing 18 p2501 N90-24287
Flight support system servicing aid tool 18 p2501 N90-24293
Hierarchy of on-orbit servicing interfaces 18 p2502 N90-24294
Telerobotic application to EVA 18 p2502 N90-24298
Robot-based equipment manipulation and transportation for the Columbus free flying laboratory 18 p2503 N90-24300
Telerobotic architecture for an on-orbit servicer 18 p2503 N90-24302
HERA teleoperation test facility 18 p2503 N90-24303
A flexible teleoperation test bed for human factors experimentation 18 p2503 N90-24304
Teleoperation of a force controlled robot manipulator without force feedback to a human operator 18 p2503 N90-24305
Experiences with and error handling in a knowledge base assisted system for payload experiment automation 18 p2504 N90-24306
The bi-arm servicer: A multimission concept and a technological model for space robotics 18 p2504 N90-24307
Robotic simulation support to systems development 18 p2505 N90-24315
Satellite servicer system flight demonstration program 18 p2506 N90-24322
NASREM: A functional architecture for control of the flight telerobotic servicer 18 p2506 N90-24325
Supervisory controlled telemanipulation and vision systems for inspection and maintenance operations 18 p2508 N90-24333
Flexible test bed for space telepresence and telemanipulation research 18 p2508 N90-24334
Design of an autonomous teleoperated cargo transporting vehicle for lunar base operations
[NASA-CR-186686] 18 p2565 N90-24633
Design of a versatile, teleoperable, towable lifting machine with robotic capabilities for use in NASA's lunar base operations
[NASA-CR-186688] 19 p2697 N90-25345
Third Annual Workshop on Space Operations Automation and Robotics (SOAR 1989)
[NASA-CP-3059] 19 p2727 N90-25503
SDIO robotics in space applications 19 p2729 N90-25514

Telepresence for space: The state of the concept
19 p2731 N90-25526
Telepresence and Space Station Freedom workstation operations 19 p2731 N90-25527
The human factors of workstation telepresence
19 p2732 N90-25528
The Flight Telerobotic Servicer (FTS) NASA's first operational robotic system 19 p2733 N90-25537
The telerobot testbed: An architecture for remote servicing 19 p2734 N90-25538
Impact of end effector technology on telemanipulation performance 19 p2736 N90-25549
Visualization of three dimensional data
19 p2736 N90-25553
A helmet mounted display to adapt the telerobotic environment to human vision 19 p2737 N90-25555
Human factors issues in telerobotic systems for Space Station Freedom servicing 19 p2737 N90-25556
The application of NASREM to remote robot control
19 p2738 N90-25563
The JPL telerobot operator control station: Operational experiences 19 p2738 N90-25565
Test bed experiments for various telerobotic system characteristics and configurations
19 p2740 N90-25572
A laboratory breadboard system for dual-arm teleoperation 19 p2740 N90-25573
Space station definitions, design, and development. Task 5: Multiple arm telerobot coordination and control: Manipulator design methodology
[NASA-CR-182043] 20 p2914 N90-26577
Robot dynamics in reduced gravity environment
21 p3049 N90-27333
Tele-Autonomous control involving contact — object localization
[NASA-CR-187004] 23 p3335 N90-28854
Adjustable impedance, force feedback and command language aids for telerobotics (parts 1-4 of an 8-part MIT progress report) 23 p3363 N90-29007
Variable force and visual feedback effects on teleoperator man/machine performance
23 p3364 N90-29008
Teleoperator comfort and psychometric stability: Criteria for limiting master-controller forces of operation and feedback during telemanipulation
23 p3364 N90-29009
Development of a flexible test-bed for robotics, telemanipulation and servicing research
23 p3364 N90-29012
The NASA/OAST telerobot testbed architecture
23 p3365 N90-29016
Exploiting map plans as resources for action
23 p3367 N90-29028
A neural network for controlling the configuration of frame structure with elastic members
23 p3368 N90-29034
Plan recognition for space telerobotics
23 p3369 N90-29036
The JPL telerobot operator control station. Part 1: Hardware 23 p3371 N90-29049
The JPL telerobot operator control station. Part 2: Software 23 p3371 N90-29050
Design of a monitor and simulation terminal (master) for space station telerobotics and telescience
23 p3372 N90-29051
Performance evaluation of a 6 axis high fidelity generalized force reflecting teleoperator
23 p3372 N90-29052
Implementation and design of a teleoperation system based on a VMEBUS/68020 pipelined architecture
23 p3372 N90-29053
Trajectory generation of space telerobots
23 p3372 N90-29055
Portable Dextrous Force Feedback Master for robot telemanipulation (PDMFF) 23 p3373 N90-29058
Experiences with the JPL telerobot testbed: Issues and insights 23 p3373 N90-29059
The KALI multi-arm robot programming and control environment 23 p3373 N90-29060
Perceptual telerobotics 23 p3374 N90-29063
Organising geometric computations for space telerobotics 23 p3376 N90-29074
Proceedings of the NASA Conference on Space Telerobotics, volume 3
[NASA-CR-186858] 24 p3500 N90-29780
The flight telerobotic servicer: NASA's first operational space robot 24 p3500 N90-29781
Traction-drive force transmission for telerobotic joints
24 p3501 N90-29790
Redundant sensorized arm+hand system for space telerobotized manipulation 24 p3502 N90-29792
Impedance hand controllers for increasing efficiency in teleoperations 24 p3502 N90-29793
Tele-autonomous systems: New methods for projecting and coordinating intelligent action at a distance
24 p3502 N90-29794
An advanced telerobotic system for shuttle payload changeout room processing applications
24 p3502 N90-29795
Robotic tele-existence 24 p3502 N90-29796
Telepresence system development for application to the control of remote robotic systems
24 p3503 N90-29799
Weighted feature selection criteria for visual servoing of a telerobot 24 p3503 N90-29801
A fast 3-D object recognition algorithm for the vision system of a special-purpose dexterous manipulator
24 p3503 N90-29803
Telerobotic workstation design aid
24 p3504 N90-29805
Space robotic system for proximity operations
24 p3504 N90-29806
Control strategies for a telerobot
24 p3504 N90-29808
Learning in tele-autonomous systems using Soar
24 p3506 N90-29819
Design of a structural and functional hierarchy for planning and control of telerobotic systems
24 p3506 N90-29820
The flight telerobotic servicer project: A technical overview 24 p3506 N90-29821
The flight telerobotic servicer Tinman concept: System design drivers and task analysis
24 p3506 N90-29822
The flight telerobotic servicer: From functional architecture to computer architecture
24 p3507 N90-29823
Research and development activities at the Goddard Space Flight Center for the flight telerobotic servicer project 24 p3507 N90-29824
The Goddard Space Flight Center (GSFC) robotics technology testbed 24 p3507 N90-29825
Test and validation for robot arm control dynamics simulation 24 p3507 N90-29826
Graphic overlays in high-precision teleoperation: Current and future work at JPL 24 p3508 N90-29827
Use of graphics in decision aids for telerobotic control: (Parts 5-8 of an 8-part MIT progress report)
24 p3508 N90-29829
Proceedings of the NASA Conference on Space Telerobotics, volume 4
[NASA-CR-186859] 24 p3508 N90-29830
Construction and demonstration of a 9-string 6 DOF force reflecting joystick for telerobotics
24 p3509 N90-29836
Response to reflected-force feedback to fingers in teleoperations 24 p3509 N90-29837
The JAU-JPL anthropomorphic telerobot
24 p3509 N90-29838
Performance limitations of bilateral force reflection imposed by operator dynamic characteristics
24 p3510 N90-29840
Sensor-based fine telemanipulation for space robotics
24 p3510 N90-29841
ROTEX-TRIIFEX: Proposal for a joint FRG-USA telerobotic flight experiment 24 p3510 N90-29842
Test and training simulator for ground-based teleoperated in-orbit servicing 24 p3510 N90-29843
Concept synthesis of an equipment manipulation and transportation system EMATS 24 p3510 N90-29844
Force-reflective teleoperated system with shared and compliant control capabilities 24 p3510 N90-29845
Information management in an integrated space telerobot 24 p3511 N90-29846
Redundancy in sensors, control and planning of a robotic system for space telerobotics 24 p3511 N90-29847
Linear analysis of a force reflective teleoperator
24 p3513 N90-29856
Real-time cartesian force feedback control of a teleoperated robot 24 p3513 N90-29857
Optimal payload rate limit algorithm for zero-G manipulators 24 p3513 N90-29858
The laboratory telerobotic manipulator program
24 p3515 N90-29869
Robotic control of the seven-degree-of-freedom NASA laboratory telerobotic manipulator
24 p3515 N90-29870
System architectures for telerobotic research
24 p3515 N90-29872
Proceedings of the NASA Conference on Space Telerobotics, volume 5
[NASA-CR-186860] 24 p3516 N90-29874
Telerobotic activities at Johnson Space Center
24 p3516 N90-29875
A control approach for robots with flexible links and rigid end-effectors 24 p3516 N90-29879
Preshaping command inputs to reduce telerobotic system oscillations 24 p3517 N90-29880
Performance constraints and compensation for teleoperation with delay 24 p3517 N90-29881
Flight telerobotic servicer control from the Orbiter
24 p3517 N90-29882
Teleoperation experiments with a Utah/MIT hand and a VPL DataGlove 24 p3517 N90-29883
Interset: A natural language interface for teleoperated robotic assembly of the EASE space structure
24 p3517 N90-29885
Establishing viable task domains for telerobot demonstrations 24 p3518 N90-29886
The telerobot workstation testbed for the shuttle aft flight deck: A project plan for integrating human factors into system design 24 p3518 N90-29887
An alternative control structure for telerobotics
24 p3518 N90-29889
Integration of a sensor based multiple robot environment for space applications: The Johnson Space Center Teleoperator Branch Robotics Laboratory
24 p3518 N90-29890
The JPL telerobotic Manipulator Control and Mechanization (MCM) subsystem
24 p3519 N90-29892
Flight experiments in telerobotics-Orbiter midbeck concept 24 p3519 N90-29895
The astronaut and the banana peel: An EVA retriever scenario 24 p3519 N90-29897
Next generation space robot
24 p3520 N90-29899
Distributed communications and control network for robotic mining 24 p3520 N90-29901
Temporal logics meet telerobotics
24 p3521 N90-29905
An intelligent, free-flying robot
24 p3522 N90-29912
Approach to telerobot computing architecture
[NASA-CR-186993] 24 p3534 N90-29984

TELEPHONES

Triphone clustering in the ARM system
[RSRE-MEMO-4357] 22 p3166 N90-27952

TELEPHONY

Feasibility of graphics voice telephones for the post 2000 era
[FEL-1988-26] 03 p0340 N90-11937
Removal of noise from noise-degraded speech signals
[AD-A212876] 04 p0493 N90-12840
On the privacy problems involved in allowing access to computers via the public telephone system
[RSRE-88006] 07 p0917 N90-15303
Proceedings of the 38th International Wire and Cable Symposium
[AD-A216023] 11 p1501 N90-18638

TELEROBOTICS

Optimized resolved rate control of seven-degree-of-freedom Laboratory Telerobotic Manipulator (LTM) with application to three-dimensional graphics simulation
[NASA-TP-2938] 01 p0109 N90-10618
NASA/NBS (National Aeronautics and Space Administration/National Bureau of Standards) standard reference model for telerobot control system architecture (NASREM)
[NASA-CR-185078] 02 p0228 N90-11310
Telerobotic control for teams of semi-autonomous agents, phase 1
[AD-A211648] 04 p0526 N90-13037
Visual Information Processing for Television and Telerobotics
[NASA-CP-3053] 08 p1072 N90-16204
Connectionist model-based stereo vision for telerobotics 08 p1076 N90-16224
Examples of robots and teleoperators at the Savannah River Site
[DE90-004659] 08 p1086 N90-16284
Expert system control of a six-legged walking telerobot
[DE90-004661] 08 p1086 N90-16285
A human factors testbed for ground-vehicle telerobotics research
[DE90-006618] 12 p1697 N90-19746
Design of a telerobotic controller with joint torque sensors
[DE90-008753] 13 p1812 N90-20404
The use of graphics in the design of the human-telerobot interface 13 p1860 N90-20670
A new six-degree-of-freedom force-reflecting hand controller for space telerobotics
15 p2113 N90-22089
The JPL/KSC telerobotic inspection demonstration
15 p2155 N90-22312
Development of efficient computer program for dynamic simulation of telerobotic manipulation
16 p2284 N90-23017
Servicing test facility: A hardware simulator for telerobotic in-orbit servicing 18 p2501 N90-24287
Telerobotic application to EVA
18 p2502 N90-24298
Telerobotic architecture for an on-orbit servicer
18 p2503 N90-24302

NASREM: A functional architecture for control of the flight telerobotic servicer 18 p2506 N90-24325
The Flight Telerobotic Servicer (FTS) NASA's first operational robotic system 19 p2733 N90-25537
The telerobot testbed: An architecture for remote servicing 19 p2734 N90-25538
A helmet mounted display to adapt the telerobotic environment to human vision 19 p2737 N90-25555
Human factors issues in telerobotic systems for Space Station Freedom servicing 19 p2737 N90-25556
The JPL telerobot operator control station: Operational experiences 19 p2738 N90-25565
Test bed experiments for various telerobotic system characteristics and configurations 19 p2740 N90-25572
Space station definitions, design, and development. Task 5: Multiple arm telerobot coordination and control: Manipulator design methodology [NASA-CR-182043] 20 p2914 N90-26577
A vision-based telerobotic control station 21 p3046 N90-27311
Proceedings of the NASA Conference on Space Telerobotics, volume 1 [NASA-CR-186856] 23 p3362 N90-29000
Adjustable impedance, force feedback and command language aids for telerobotics (parts 1-4 of an 8-part MIT progress report) 23 p3363 N90-29007
The NASA/OAST telerobot testbed architecture 23 p3365 N90-29016
Plan recognition for space telerobotics 23 p3369 N90-29036
Proceedings of the NASA Conference on Space Telerobotics, volume 2 [NASA-CR-186857] 23 p3370 N90-29044
The JPL telerobot operator control station. Part 1: Hardware 23 p3371 N90-29049
The JPL telerobot operator control station. Part 2: Software 23 p3371 N90-29050
Design of a monitor and simulation terminal (master) for space station telerobotics and teleascience 23 p3372 N90-29051
Trajectory generation of space telerobots 23 p3372 N90-29055
Experiences with the JPL telerobot testbed: Issues and insights 23 p3373 N90-29059
Perceptual telerobotics 23 p3374 N90-29063
Organising geometric computations for space telerobotics 23 p3376 N90-29074
Proceedings of the NASA Conference on Space Telerobotics, volume 3 [NASA-CR-186858] 24 p3500 N90-29780
The flight telerobotic servicer: NASA's first operational space robot 24 p3500 N90-29781
Traction-drive force transmission for telerobotic joints 24 p3501 N90-29790
Redundant sensorized arm+hand system for space telerobotized manipulation 24 p3502 N90-29792
An advanced telerobotic system for shuttle payload changeout room processing applications 24 p3502 N90-29795
Weighted feature selection criteria for visual servoing of a telerobot 24 p3503 N90-29801
Telerobotic workstation design aid 24 p3504 N90-29805
Control strategies for a telerobot 24 p3504 N90-29806
Design of a structural and functional hierarchy for planning and control of telerobotic systems 24 p3506 N90-29820
The flight telerobotic servicer project: A technical overview 24 p3506 N90-29821
The flight telerobotic servicer Tinman concept: System design drivers and task analysis 24 p3506 N90-29822
The flight telerobotic servicer: From functional architecture to computer architecture 24 p3507 N90-29823
Research and development activities at the Goddard Space Flight Center for the flight telerobotic servicer project 24 p3507 N90-29824
Use of graphics in decision aids for telerobotic control: (Parts 5-8 of an 8-part MIT progress report) 24 p3508 N90-29829
Proceedings of the NASA Conference on Space Telerobotics, volume 4 [NASA-CR-186859] 24 p3508 N90-29830
Construction and demonstration of a 9-string 6 DOF force reflecting joystick for telerobotics 24 p3509 N90-29836
The JAU-JPL anthropomorphic telerobot 24 p3509 N90-29838
ROTEX-TRIIFEX: Proposal for a joint FRG-USA telerobotic flight experiment 24 p3510 N90-29842
Information management in an integrated space telerobot 24 p3511 N90-29846
Redundancy in sensors, control and planning of a robotic system for space telerobotics 24 p3511 N90-29847
The laboratory telerobotic manipulator program 24 p3515 N90-29869
Robotic control of the seven-degree-of-freedom NASA laboratory telerobotic manipulator 24 p3515 N90-29870
System architectures for telerobotic research 24 p3515 N90-29872
Proceedings of the NASA Conference on Space Telerobotics, volume 5 [NASA-CR-186860] 24 p3516 N90-29874
Telerobotic activities at Johnson Space Center 24 p3516 N90-29875
Preshaping command inputs to reduce telerobotic system oscillations 24 p3517 N90-29880
Flight telerobotic servicer control from the Orbiter 24 p3517 N90-29882
Establishing viable task domains for telerobot demonstrations 24 p3518 N90-29886
The telerobot workstation testbed for the shuttle aft flight deck: A project plan for integrating human factors into system design 24 p3518 N90-29887
Multi-level manual and autonomous control superposition for intelligent telerobot 24 p3518 N90-29888
An alternative control structure for telerobotics 24 p3518 N90-29889
Integration of a sensor based multiple robot environment for space applications: The Johnson Space Center Teleoperator Branch Robotics Laboratory 24 p3518 N90-29890
The JPL telerobotic Manipulator Control and Mechanization (MCM) subsystem 24 p3519 N90-29892
Flight experiments in telerobotics-Orbiter middeck concept 24 p3519 N90-29895
Temporal logics meet telerobotics 24 p3521 N90-29905
Approach to telerobot computing architecture [NASA-CR-186993] 24 p3534 N90-29984

TELESCOPES
NT GAMMA RAY TELESCOPES
NT GRAZING INCIDENCE TELESCOPES
NT HUBBLE SPACE TELESCOPE
NT INFRARED SPACE OBSERVATORY (ISO)
NT INFRARED TELESCOPES
NT LARGE DEPLOYABLE REFLECTOR
NT PARTICLE TELESCOPES
NT PYROHELIOMETERS
NT RADIO TELESCOPES
NT REFLECTING TELESCOPES
NT REFRACTING TELESCOPES
NT SCHMIDT TELESCOPES
NT SPACE INFRARED TELESCOPE FACILITY
NT SPACEBORNE TELESCOPES
NT SPECTROSCOPIC TELESCOPES
NT STARLAB
NT ULTRAVIOLET TELESCOPES
NT VERY LARGE ARRAY (VLA)
NT X RAY ASTROPHYSICS FACILITY
NT X RAY TELESCOPES

Astrometric telescope facility. Preliminary systems definition study. Volume 3: Cost estimate [NASA-TM-89429-VOL-3] 01 p0140 N90-10808
A liquid xenon imaging telescope for 1-30 MeV gamma-ray astrophysics [NASA-CR-185999] 02 p0291 N90-11662
An imaging vector magnetograph for the next solar maximum 03 p0435 N90-12489
A laboratory verification sensor 05 p0599 N90-13477
SiO overcoating and polishing of CFRP telescope panels 05 p0599 N90-13478
Three-meter balloon-borne telescope 05 p0601 N90-13490
SOFIA (Stratospheric Observatory For Infrared Astronomy): A 3m class airborne telescope 05 p0659 N90-13846
Realtime tracking system for wide-field-of-view telescope [DE90-001147] 06 p0843 N90-14908
Design of incoherent imaging arrays [DE90-000861] 06 p0844 N90-14909
Evidence for anomalous cosmic ray hydrogen 06 p0861 N90-15005
Large angle off-axis beam steering of a phased telescope array [AD-D014269] 08 p1060 N90-16127
Recent leak telescope development [DE90-004101] 09 p1225 N90-17106
Speckle imaging through the atmosphere [AD-A214652] 09 p1281 N90-17428
Broadband incoherent imaging using multiple aperture optics [AD-A215708] 09 p1282 N90-17437
Laser diffraction particle sizing: Instrument probe volume relocation and elongation [NASA-TM-102512] 10 p1387 N90-18025
JCMT observations of the circumstellar envelope IRC+10216 11 p1585 N90-19138
The James Clerk Maxwell telescope 11 p1589 N90-19166
Imaging Germanium Telescope Array for Gamma-Rays (IGETAGRAY) [DE90-006994] 11 p1595 N90-19188
Placement of multiple apertures for imaging telescopes [DE90-006991] 13 p1888 N90-20833
Design and performance analysis of adaptive optical telescopes using laser guide stars [AD-A218025] 13 p1902 N90-20913
Experimental evaluation of active-member control of precision structures 14 p1936 N90-21084
Initial astronomical results with a new 5-14 micron Si:Ga 58x62 DRO array camera 14 p1978 N90-21334
Introduction to the Infrared Space Observatory (ISO) 14 p1979 N90-21340
SOFIA: Stratospheric Observatory for Infrared Astronomy 14 p1980 N90-21346
A soft actuation system for segmented reflector articulation and isolation 15 p2113 N90-22084
Diffraction-limited imaging on the 200-inch telescope 15 p2183 N90-22475
NASA Marshall Space Flight Center solar observatory report, January to December 1989 [NASA-TM-100404] 19 p2797 N90-25923
A two-telescope receiver design for deep space optical communications 20 p2853 N90-26226
Carbon chemistry of circumstellar envelopes 21 p3090 N90-27570
Wind lidar for BEST [CNES-NT-125] 23 p3353 N90-28947
NASA Marshall Space Flight Center Solar Observatory report, January - June 1990 [NASA-TM-103512] 23 p3409 N90-29268

TELESCOPING STRUCTURES
U FOLDING STRUCTURES

TELETYPEWRITERS
An introduction to high frequency radioteletype systems [PB90-145533] 14 p1965 N90-21252

TELEVISION CAMERAS
Distance and clearance perception using forward-looking, vehicular television systems [DE89-014740] 03 p0405 N90-12319
CCD TV focal plane guider development and comparison to SIRTF applications [NASA-CR-185977] 06 p0842 N90-14900
Use of the Xybion ISG-camera in the RETRA-1000 TV-Holography unit [AD-A219842] 18 p2554 N90-24577
The use of PLAID in the Space Station Freedom viewing analysis 19 p2729 N90-25517

TELEVISION EQUIPMENT
NT IMAGE DISSECTOR TUBES
NT TELEVISION CAMERAS

TELEVISION RECEPTION
General multidimensional scanning ratio transformation and its utilization for norm transformation of television signals [ETN-90-96058] 12 p1648 N90-19470

TELEVISION SYSTEMS
NT CLOSED CIRCUIT TELEVISION
NT COLOR TELEVISION
NT SATELLITE TELEVISION

HDTV displays: Subjective effects of scanning standards and domestic picture sizes [BBC-RD-1989/9] 02 p0211 N90-11208
Television systems with enhanced image quality for new broadband channels [ETN-89-94622] 03 p0340 N90-11936
Distance and clearance perception using forward-looking, vehicular television systems [DE89-014740] 03 p0405 N90-12319
Theoretical and material studies of thin-film electroluminescent devices [NASA-CR-186104] 06 p0768 N90-14468
Visual Information Processing for Television and Telerobotics [NASA-CP-3053] 08 p1072 N90-16204
Contribution to the study of design methods for numerical filters with finite pulse response and applications to image processing [TELECOM-89-E-007] 10 p1376 N90-17974
HDTV bandwidth reduction using motion compensation and DATV [BBC-RD-1989/10] 14 p1965 N90-21254
Prediction of VHF/UHF mobile reception in urban areas: Comparison with measurements in London [BBC-RD-1989/11] 14 p1965 N90-21255

Experiences in teleoperation of land vehicles
16 p2273 N90-22954
Demo of three ways to use a computer to assist in lab
18 p2515 N90-24364
HDTV: A chance to enhance television colorimetry
[BBC-RD-1990/2] 18 p2543 N90-24515
PC-based closed-circuit television system
[DE90-013366] 21 p2994 N90-27017
Stenopic radiography: A non-destructive test without contact 22 p3187 N90-28086

TELEVISION TRANSMISSION
Comparison of DPCM prediction strategies for high-quality digital television bit-rate reduction
[BBC-RD-1989/8] 01 p0056 N90-10318
Satellite broadcasting: Requirements for the receiving antenna
[BBC-RD-1989/5] 08 p1055 N90-16098

TELLEGEN THEORY
U NETWORK ANALYSIS
U NETWORK SYNTHESIS

TELLURIDES
NT CADMIUM TELLURIDES
NT LEAD TELLURIDES
NT MERCURY TELLURIDES
NT TIN TELLURIDES
NT ZINC TELLURIDES

TELLURIUM
NT TELLURIUM ISOTOPES
Tellurium embrittlement of type 316 steel
[AERE-R-13440] 13 p1776 N90-20192
The first example of an organogallium compound containing a Ga-Te bond: Synthesis, properties, and molecular structure of ((Me3CCH2)2GaTeph)2
[AD-A219258] 16 p2210 N90-22608
Laser induced surface chemical epitaxy
[AD-A222082] 21 p2977 N90-26920

TELLURIUM COMPOUNDS
NT CADMIUM TELLURIDES
NT LEAD TELLURIDES
NT MERCURY TELLURIDES
NT TIN TELLURIDES
NT ZINC TELLURIDES
Design of a large angular aperture TeO2 acousto-optic tunable filter
[AD-A213999] 07 p0993 N90-15738

TELLURIUM ISOTOPES
Tellurium-118/antimony-118 generator
[DE89-015225] 01 p0122 N90-10698

TELLURIUM 119
U TELLURIUM ISOTOPES

TEMPER (METALLURGY)
Gaussmeter determination of 302 stainless steel material condition
[BDX-613-3941] 01 p0044 N90-10249
The effect of manganese on the onset of the stage 2 reaction in an austempered ductile iron matrix
[DE90-011804] 20 p2834 N90-26119

TEMPERATE REGIONS
Precipitation mechanisms in tropical and midlatitude convective clouds 14 p2008 N90-21507
Tropical-extratropical interaction in a model atmosphere 17 p2422 N90-23800
Barotropic mechanisms associated with tropical plume formation 24 p3489 N90-29719

TEMPERATURE
NT AMBIENT TEMPERATURE
NT ATMOSPHERIC TEMPERATURE
NT BODY TEMPERATURE
NT BRIGHTNESS TEMPERATURE
NT COMBUSTION TEMPERATURE
NT CRITICAL TEMPERATURE
NT CRYOGENIC TEMPERATURE
NT FLAME TEMPERATURE
NT GAS TEMPERATURE
NT GLASS TRANSITION TEMPERATURE
NT HIGH TEMPERATURE
NT IGNITION TEMPERATURE
NT INLET TEMPERATURE
NT ION TEMPERATURE
NT LOW TEMPERATURE
NT NOISE TEMPERATURE
NT OCEAN TEMPERATURE
NT OPERATING TEMPERATURE
NT PLANETARY TEMPERATURE
NT PLASMA TEMPERATURE
NT ROOM TEMPERATURE
NT SATELLITE TEMPERATURE
NT SEA SURFACE TEMPERATURE
NT SKIN TEMPERATURE (BIOLOGY)
NT SKIN TEMPERATURE (NON-BIOLOGICAL)
NT SOLAR TEMPERATURE
NT SPACE TEMPERATURE
NT STAGNATION TEMPERATURE
NT STELLAR TEMPERATURE
NT SUBZERO TEMPERATURE
NT SURFACE TEMPERATURE
NT TRANSITION TEMPERATURE
NT WALL TEMPERATURE
NT WATER TEMPERATURE
Modeling the temperature rise at the tip of a fast crack
[AD-A212418] 04 p0514 N90-12966
Comparison of protective breathing equipment performance at ground level and 8,000 feet altitude using parameters prescribed by portions of FAA action notice A-8150.2
[AD-A212852] 06 p0821 N90-14773
The GIT model: An atmospheric boundary layer model along a trajectory
[FOA-E-40039-3.2] 18 p2579 N90-24693
Thermal comptonization in accretion disks
19 p2791 N90-25890
Fabrication of intermetallic compounds by solid state reaction of roll-bonded materials
[AD-A221960] 21 p2982 N90-26943

TEMPERATURE COMPENSATION
Temperature compensated crystal oscillator (TCXO) with improved temperature compensation
[AD-D014334] 12 p1650 N90-19482

TEMPERATURE CONTROL
Method and apparatus for maintaining thermal control in plasma conditions
[NASA-CASE-MFS-28368-1] 01 p0125 N90-10717
Independent Orbiter Assessment (IOA): Analysis of the electrical power distribution and control/electrical power generation subsystem
[NASA-CR-185538] 02 p0165 N90-10933
Independent Orbiter Assessment (IOA): CIL issues resolution report, volume 1
[NASA-CR-185524-VOL-1] 02 p0169 N90-10954
Independent Orbiter Assessment (IOA): Assessment of the active thermal control system
[NASA-CR-185573] 02 p0174 N90-10979
Design of a solar sail mission to Mars
[NASA-CR-186045] 03 p0311 N90-11771
Independent Orbiter Assessment (IOA): Analysis of the active thermal control subsystem
[NASA-CR-185553] 03 p0314 N90-11782
Modelling and control of a diffusion/LPCVD furnace
[REPT-88-97] 03 p0336 N90-11910
Phase change material for spacecraft thermal management
[AD-A211404] 04 p0462 N90-12648
Heat pipes for sodium-sulfur batteries
[AD-A212523] 04 p0497 N90-12865
Payload thermal control 05 p0604 N90-13511
Spacecraft thermal control 05 p0604 N90-13513
Simulation of regenerative fuel cell systems including thermal control 10 p1333 N90-17711
Non-contact true temperature measurements in the microgravity environment 10 p1364 N90-17906
Temperature control and calibration issues in the growth, processing and characterization of electronic materials
10 p1365 N90-17914
Combustion process science and technology
10 p1366 N90-17916
Dynamic response for thermal control and measurement and fast radiation thermometry
10 p1367 N90-17924
Spacecraft thermal control design data, volume 1
[ESA-PSS-03-108-ISSUE-1-VOL-1]
11 p1468 N90-18455
Spacecraft thermal control design data, volume 2
[ESA-PSS-03-108-ISSUE-1-VOL-2]
11 p1469 N90-18456
Spacecraft thermal control design data, volume 3
[ESA-PSS-03-108-ISSUE-1-VOL-3]
11 p1469 N90-18457
Spacecraft thermal control design data, volume 4
[ESA-PSS-03-108-ISSUE-1-VOL-4]
11 p1469 N90-18458
Condensation fluid dynamics and heat transfer on rotating spherical surfaces in a microgravitational field
[DE90-005540] 11 p1495 N90-18607
Temperature compensated crystal oscillator (TCXO) with improved temperature compensation
[AD-D014334] 12 p1650 N90-19482
Development of the blackbody probe type pyrometer, part 1. Experimental study on the fundamental characteristics
[DE89-782288] 12 p1663 N90-19553
Modification, testing, and calibration of infrared search and target designator hardware received from NSWC
[AD-A217920] 13 p1889 N90-20837
Space environment simulation of the SCD-01 satellite through heating plates
[INPE-4988-PRE/1550] 14 p1940 N90-21105
Thermal control system corrosion study
[NASA-TM-102220] 14 p1971 N90-21294
Development and integration of the capillary pumped loop GAS and Hitchhiker flight experiments
[NASA-TM-100756] 15 p2059 N90-21790
Computer controlled cryogenic temperature controller
[AD-A218785] 16 p2227 N90-22701
Design and implementation of sensor systems for control of a closed-loop life support system
[NASA-CR-186675] 19 p2725 N90-25497
NASA systems autonomy demonstration project: Advanced automation demonstration of Space Station Freedom thermal control system
19 p2728 N90-25510
Thermal management of an accelerator system in space
[DE90-013153] 20 p2922 N90-26627
Spacecraft thermal control design data, volume 5. Section R: Cryogenic cooling. Section S: Existing satellites
[ESA-PSS-03-108-ISSUE-1-VOL-5]
22 p3132 N90-27772
Spacecraft thermal control design data. Volume 6: Index
[ESA-PSS-03-108-ISSUE-1-VOL-6]
22 p3132 N90-27773
A cost-effective realization of environmental temperature control
[DE90-011651] 24 p3458 N90-29532
Thermal analyses of power subsystem components
[NASA-CR-186314] 24 p3474 N90-29637

TEMPERATURE DEPENDENCE
Theoretical Hugoniot of liquid hydrogen fluoride
[DE89-016504] 02 p0193 N90-11099
Thermal expansion and phase transformation studies on some materials by high temperature X-ray powder diffractometry
[DE89-631032] 02 p0198 N90-11130
Temperature dependent effects during Ag deposition on Cu(110)
[DE89-016987] 03 p0327 N90-11857
Temperature dependence of positron diffusion in cubic metals
[PB89-222020] 04 p0475 N90-12722
Temperature dependence of attitude sensor coalignments on the Solar Maximum Mission (SMM)
05 p0588 N90-13426
Ultraviolet absorption cross-sections of bromoform in the temperature range 295-240 K
[AERONOMICA-ACTA-A-348-1989]
05 p0622 N90-13630
Flux pinning and microstructure in YBa2Cu3O7
[DE90-001562] 06 p0851 N90-14948
Accelerated aging embrittlement of cast duplex stainless steel: Activation energy for extrapolation
[DE90-001773] 07 p0903 N90-15221
Navigation experiment NAVEX: The self-test delay times in the D1 Spacelab mission
[ESA-TT-1176] 11 p1467 N90-18446
Temperature dependence of photon-gated persistent spectral hole-burning for the meso-tetra-p-tolyl Zn-tetrabenzoporphyrin/chloroform system in poly(methylmethacrylate)
[AD-A216086] 11 p1482 N90-18531
Microwave radiation absorption by Ho(Y)-Ba-Cu-O superconducting ceramics
[DE90-610665] 11 p1492 N90-18588
Strong source heat transfer simulations based on a GalerKin/gradient least squares method
[DE90-608613] 11 p1507 N90-18678
A simple model for the determination of L(sub 0), D and tau in a semiconductor and their temperature dependence
[DE90-610564] 12 p1720 N90-19879
Ultrastructure processing of ordered polymers
[AD-A218331] 13 p1783 N90-20232
Modeling the temperature dependence of the thermal conductivity of aluminum nitride
[DE90-009428] 14 p1949 N90-21154
O2 reduction at the IFC orbiter fuel cell O2 electrode
[NASA-TM-102580] 14 p2001 N90-21469
Chern-Simons superconductivity at finite temperature
[DE90-613393] 14 p2031 N90-21650
Detailed mechanism for oxidation of benzene
[NASA-TM-102443] 15 p2067 N90-21842
A temperature-dependent regular infrared band model for absorption and dispersion 15 p2083 N90-21927
Evaluating thermographic phosphors in an operating turbine engine
[DE90-004874] 15 p2105 N90-22044
Optical bistability in semiconducting material
15 p2174 N90-22424
High-temperature deformation of mechanically-alloyed aluminum IN90211 16 p2216 N90-22645
A (mu)SR-investigation of the mixed state of the high-Tc superconductor HoBa2Cu3O7-delta
[DE90-620802] 16 p2322 N90-23241
Stress versus temperature dependent activation energies in creep
[NASA-TM-103192] 17 p2417 N90-23773

Stability projections for high temperature superconductors
[AD-A218945] 18 p2618 N90-24913
Weak-beam electron microscopy of dislocation splitting in TiAl: Relationship to plasticity
[ESA-TT-1159] 19 p2676 N90-25217
Photodissociation of NO2: Influence of photolysis wavelength and temperature dependence on product formation 20 p2887 N90-26426
Infrared line parameters at low temperatures relevant to planetary atmospheres 20 p2944 N90-26753
PH3 surface chemistry on Si(111)-(7x7): A study by Auger spectroscopy and electron stimulated desorption methods
[AD-A221508] 21 p2979 N90-26929
The stability of the martensitic phases in Cu-Zn-Al at an electron concentration of 1.534
[DE90-628628] 23 p3311 N90-28727
Proceedings of a discussion meeting on Thermodynamics of Alloys
[AD-A224336] 24 p3449 N90-29476
The stress and temperature dependence of creep in an Al-2.0 wt percent Li alloy
[AD-A223676] 24 p3449 N90-29480

TEMPERATURE DIFFERENCES
U TEMPERATURE GRADIENTS

TEMPERATURE DISTRIBUTION
Cryogenic free jets
[ESA-TT-1128] 03 p0311 N90-11767
Dimensional reduction at high temperature revisited
[KVI-791] 04 p0549 N90-13194
Payload electronics and mechanisms
05 p0604 N90-13508
Payload thermal control 05 p0604 N90-13511
Modelling of the effects of the equatorial electrojet on its environment
[DE89-636296] 06 p0811 N90-14720
Inverted surface troughs accompanying Rocky Mountain lee-side cyclogenesis 06 p0816 N90-14746
Temperatures in plates subjected to a recovery temperature varying linearly with time
[ESDU-89023] 07 p1007 N90-15831
Two-Dimensional Measuring Techniques
[DGLR-PAPERS-88-04] 08 p1078 N90-16236
Simultaneous determination of temperature and velocity fields in a thermal convection flow with non-enclosed liquid crystal tracers 08 p1078 N90-16239
Sea surface temperature fields derived from aircraft and ship observations during FASINEX 1986
[AD-A215727] 09 p1250 N90-17250
A multicolor imaging pyrometer
10 p1364 N90-17905
Development of an infrared imaging system for the surface tension driven convection experiment
10 p1367 N90-17922
Heat transfer definitions and equations
[ESDU-89022] 12 p1657 N90-19522
Information on the use of data items on hot structures
[ESDU-89021] 12 p1674 N90-19611
An analytic model of axisymmetric mantle plume due to thermal and chemical diffusion
[NASA-CR-186461] 12 p1691 N90-19714
Temperatures in plates subjected to a sudden increase in recovery temperature
[ESDU-89026] 12 p1724 N90-19904
Thermal perturbation of comet samples during their acquisition 12 p1741 N90-20008
Design and test of a compact optics system for the pool boiling experiment
[NASA-TM-102530] 13 p1786 N90-20253
Structure and dynamics of the Arizona monsoon boundary
[AD-A217378] 13 p1844 N90-20586
The effect of secondary flow on the redistribution of the total temperature field downstream of a stationary turbine cascade 14 p1926 N90-21033
MECCA program documentation
[NOAA-TR-NESDIS-46] 14 p2003 N90-21477
Inverse problems of heat conduction
15 p2091 N90-21969
Three-dimensional analysis on flow and temperature distributions for aircraft fuel thermal stability
[AD-A219651] 17 p2383 N90-23571
The effects of Reynolds number, rotor incidence angle, and surface roughness on the heat transfer distribution in a large-scale turbine rotor passage
[NASA-CR-183891] 17 p2410 N90-23731
Temperature evolution of single particle correlation functions of TIP4P water
[PREPRINT-694] 17 p2470 N90-24119
High-temperature creep under a nonuniform temperature distribution
[ATR-88(3728-02)-1] 19 p2702 N90-25373
Calculations of welding stresses and deformations by means of finite element method
[VTT-RR-648] 19 p2703 N90-25382
Temperature and OH concentrations in a solid propellant flame using absorption techniques
[AD-A222591] 20 p2830 N90-26100
Disk mass densities in edge-on spiral galaxies
21 p3097 N90-27600
Numerical investigation of the thermal stratification in cryogenic tanks subjected to wall heat flux
[NASA-TM-103194] 22 p3171 N90-27984
Stratocumulus cloud height variations determined from surface and satellite observations
22 p3214 N90-28230
Calculation of temperature distribution in various turbine blades using a boundary-fitted coordinate transformation method 23 p3278 N90-28550
Transient cooling of a hot surface by droplets evaporation
[PB90-227968] 23 p3325 N90-28799
Frequency response of a thermocouple wire: Effects of axial conduction
[NASA-CR-180454] 23 p3330 N90-28827
Theoretical studies of proton beams in solar flare loops 23 p3413 N90-29286
Calculation of turbulent air streams in driver cabs
[ETN-90-97320] 24 p3419 N90-29310

TEMPERATURE EFFECTS
Hygrothermal effects on the complex moduli of composite laminates 01 p0033 N90-10182
New structural materials
[AD-A209425] 01 p0044 N90-10246
Predictive aging of polymers
[NASA-CASE-NPO-17524-1-CU]
01 p0046 N90-10261
Some significant results from testing a Remote Multiplexing Unit (RMU) for temperature-induced errors
[DE89-009432] 01 p0073 N90-10421
Accelerated aging of metal matrix composites
02 p0190 N90-11085
Effect of thermal and cyclic loads on silicon carbide yarn reinforced glass matrix composites
[DE89-016554] 02 p0191 N90-11091
Shock initiation of LX-17 as a function of its initial temperature
[DE89-017730] 02 p0208 N90-11192
Efficient numerical method for computation of thermohydrodynamics of laminar lubricating films
[NASA-CR-185136] 02 p0219 N90-11256
Interannual variability of temperature in the upper layer of the North Pacific eastern boundary region, 1971-1987
[PB89-190227] 02 p0253 N90-11434
Hydrogen-assisted thermal donor formation in silicon
[DE89-016809] 02 p0279 N90-11594
Superconducting ceramics in the Bi1.5SrCaCu2O sub x system by melt quenching technique
[NASA-CR-185139] 02 p0281 N90-11606
Effects of a heat cycle on material strength
[NAL-TM-562] 03 p0306 N90-11737
Carbon fiber reinforced glass matrix composites for structural space based applications
[AD-A211682] 03 p0320 N90-11818
Phase behavior of pure and mixed systems at high pressure
[DE89-017734] 03 p0322 N90-11832
Elevated temperature aluminum-titanium alloy by powder metallurgy process
[AD-D014165] 03 p0326 N90-11852
The effects of temperature on fatigue crack propagation in 310 austenitic stainless steel
[DE90-000136] 03 p0328 N90-11865
New mechanism for toughening ceramic materials
[AD-A211651] 03 p0332 N90-11892
Sensitivity relationships in energetic materials
[DE89-016967] 03 p0333 N90-11897
Davydov solutions at 300 Kelvin: The final search
[DE89-015248] 03 p0401 N90-12296
Lifetime of singlet oxygen in aqueous hydrogen peroxide (BHP)
[AD-A211545] 03 p0403 N90-12306
The characterization of Nb3Sn superconductors for use in magnets of 19 T and greater
[DE89-017758] 03 p0412 N90-12364
Effect of annealing conditions on the structural and superconducting properties of Y-Ba-Cu-O films
[AD-A211308] 03 p0413 N90-12371
Application of sound and temperature to control boundary-layer transition 04 p0443 N90-12537
Nonlinear theories concerning laminated composites under compression with delamination
[ONERA-RT-19/3542-RY-081-R]
04 p0467 N90-12672
Thermophysical properties of benzene. Part 1: The ideal gas and the saturated liquid and vapour
[ESDU-89002-PT-1] 04 p0470 N90-12693
Temperature effects in shock consolidation of metal powders
[DE89-016782] 04 p0474 N90-12716
Behavior of the adhesive A2 submitted to mechanical traction
[CETIM-105290] 04 p0479 N90-12748
Heat exhaustion
[AD-A212128] 04 p0522 N90-13014
Large Deployable Reflector (LDR) thermal characteristics 05 p0596 N90-13460
Mechanical and thermal testing
05 p0605 N90-13521
QM-8 field joint protection system, volume 7
[NASA-CR-183748] 05 p0614 N90-13586
Thermal barrier coatings for gas turbine and diesel engines
[NASA-TM-102408] 05 p0623 N90-13636
The effects of alloying and thermal factors on the solidification and mechanical properties of gray iron
[VTT-619] 05 p0625 N90-13651
Effect of suction and cooling on the stability of subsonic and supersonic boundary layers
05 p0642 N90-13745
Cryogenic temperature effects on sting-balance deflections in the National Transonic Facility
[NASA-TM-4157] 06 p0727 N90-14244
Thermophysical properties of isopropyl alcohol. Part 1: The ideal gas and the saturated liquid and vapour
[ESDU-89017-PT-1] 06 p0738 N90-14297
The thermally induced gas-phase reactions of methane and oxygen: A comparison of experimental and computational results
[DE90-000785] 06 p0742 N90-14317
Superplastic sheet forming 06 p0743 N90-14327
The metallurgical determinants of toughness as cryogenic temperature
[DE90-002331] 06 p0748 N90-14351
Strength and toughness of monolithic and composite silicon nitrides
[NASA-TM-102423] 06 p0751 N90-14368
Airborne FLIR detection of surface targets
06 p0759 N90-14416
The thermal behavior of natural backgrounds and its prediction by means of numerical models
06 p0762 N90-14436
Effects of composition and age hardening on precious metal electrical contacts
[DE88-008791] 06 p0769 N90-14476
Pipe and bend erosion by pneumatic transport of solids at high temperature
[DE89-015741] 06 p0778 N90-14524
Shear strain localization phenomenon in viscoplastic materials 06 p0798 N90-14649
Low-temperature conversion of high-moisture biomass: Continuous reactor system results
[DE90-000984] 06 p0805 N90-14683
Calorimetric measurements on electrochemical cells with Pd-D cathodes
[DE90-002198] 06 p0805 N90-14685
Microstructural evolution of martensitic steels during fast neutron irradiation
[DE89-016231] 07 p0902 N90-15212
Nickel beryllides and their properties
[DE90-001736] 07 p0903 N90-15220
Solid lubrication of ceramic surfaces by IAD (Ion-Assisted Deposition)-silver coatings for heat engine applications
[DE90-002860] 07 p0909 N90-15253
Studies of the adsorption/desorption behavior of explosive-like molecules
[DE90-001867] 07 p0913 N90-15283
Investigation of loads generated by temperature transients in pipes
[DE89-636433] 07 p0932 N90-15395
Innovative optoelectronic materials and structures using OMVPE
[AD-A214192] 07 p1004 N90-15815
Power semiconductor devices for space nuclear power systems
[DE90-001178] 07 p1005 N90-15819
Cryogenic engineering and materials
08 p1030 N90-15949
The use of hypervelocity launchers to explore previously inaccessible states of matter
[DE90-004088] 08 p1034 N90-15973
ZrO2 sintered compact and method for its production
[DE90-004125] 08 p1039 N90-16006
Development of a diamond insulator for thermionic applications
[DE90-002849] 08 p1048 N90-16055
Silicon membrane formation
[DE90-003022] 08 p1049 N90-16064
Thermodynamic analysis of chemical stability of ceramic materials in hydrogen-containing atmospheres at high temperatures
[NASA-CR-4271] 08 p1050 N90-16072

Magnetic penetration depth and intragrain critical current density in gain-aligned Tl2Ca2Ba2Cu3O10 superconductor
[DE90-004245] 08 p1133 N90-16562
Mechanical and SEM analysis of artificial comet nucleus samples 08 p1148 N90-16650
Effects of heat treatment on microstructure and flexural properties of unidirectional carbon-carbon composites
[AD-A214985] 09 p1186 N90-16873
Raman spectroscopic analysis of impregnated cathodes
[AD-A214559] 09 p1190 N90-16895
Thermal modelling of various thermal barrier coatings in a high heat flux rocket engine
[NASA-TM-102418] 09 p1193 N90-16911
Crystallization of nanocomposite glasses made by the SSG process
[AD-A214572] 09 p1197 N90-16933
Diffusion and processing of YBa2Cu3O(x)
[DE90-003569] 09 p1286 N90-17457
Oxidation and reduction of Bi2Sr1.85CuO(6-y) crystals
[DE90-004246] 09 p1287 N90-17460
High-temperature deformation of YBa2Cu3O(7-delta) with Ag additions
[DE90-004884] 09 p1292 N90-17491
Time development of convection flow patterns in aircraft cabins under post-crash fire exposure 10 p1314 N90-17598
Effects of elevated temperatures and thermal cycling on ceramic composite materials
[AD-A216242] 10 p1350 N90-17828
Environmental embrittlement: A major cause for low ductility of ordered intermetallics
[DE90-006161] 10 p1356 N90-17864
Structure and properties of resorcinol-formaldehyde gels
[DE90-005201] 10 p1358 N90-17876
Continuous gas exchange measurements using individual fascicle cuvettes: The tubule system
[DE90-004932] 10 p1405 N90-18105
Influence of ion beam mixing on the growth of high temperature oxide superconducting thin film
[DE90-004837] 10 p1435 N90-18280
Structural study of thermo-hardenable matrices. Deformation processes of composite matrices as a function of their molecular structure
[ONERA-RT-10/3521-M] 11 p1481 N90-18522
Comparison between the damage modes of thermo-hardenable and thermo-plastic composite matrices
[ONERA-RT-47/7086-M] 11 p1481 N90-18523
Calculation of mechanical properties variations depending on matrix parameters in a composite, as a function of the test temperature
[DT-311/88] 11 p1481 N90-18526
High temperature interaction of SO2 with oxide sorbents
[DE90-000435] 11 p1485 N90-18545
Thermal remote sensing in the differentiation of soybean crops (glycine max (L.) merrill) submitted to water deficit
[INPE-4900-PRE/1501] 11 p1522 N90-18762
In situ growth of high quality epitaxial YBa2Cu3O(7-x) thin films at moderate temperatures by pulsed laser ablation
[DE90-006629] 11 p1571 N90-19045
Effect of temperature on the storage life of polysulfide aircraft sealants
[MRL-TR-89-31] 12 p1629 N90-19364
Alternate film dielectric materials
[DE90-007213] 12 p1632 N90-19378
A parametric heat transfer study for cryogenic ball bearings in SSME HPOTP 12 p1635 N90-19397
Thermal coefficient of delay for various coaxial and fiber-optic cables 12 p1643 N90-19439
Experimental results of aging and thermal effects in high-power laser diodes
[DE90-005955] 12 p1666 N90-19573
Ion mixing and surface modification in metal-semiconductor systems
[DE90-007557] 12 p1723 N90-19897
Physical processes in cometary ices inferred from laboratory studies 12 p1739 N90-19996
Laboratory studies of cometary ice analogues 12 p1739 N90-19997
Thermal perturbation of comet samples during their acquisition 12 p1741 N90-20008
Evaluation of thermal and mechanical loading effects on the structural behavior of a SiC/titanium composite
[NASA-TM-102536] 13 p1767 N90-20139
Fundamental aspects of and failure modes in high-temperature composites
[NASA-TM-102558] 13 p1769 N90-20151
Experimental investigation of the thermocapillary migration of water droplets in butylbenzoate
[MPIS-14/1988] 13 p1770 N90-20155
Effect of heat treatment on the fracture toughness transition properties of an A508 class 3 steel
[AERE-R-13548] 13 p1774 N90-20182
Hydrogen, thermal ageing and the role of carbides in fatigue of a high strength steel
[AERE-R-13599] 13 p1774 N90-20183
Fluorinated diamond thin films for tribological applications
[AD-A217452] 13 p1779 N90-20214
Tensile fracture toughness of ceramic materials: Effects of dynamic loading and elevated temperatures
[DE90-008329] 13 p1781 N90-20223
The effect of moisture absorption in clothing on the human heat balance
[AD-A217899] 13 p1852 N90-20626
Study of possible solar heating effects on thermosonde probes: Error analysis
[AD-A218116] 13 p1903 N90-20917
Transportation monitoring unit qualification
[NASA-CR-183930] 14 p1932 N90-21060
LaRC TPI 1500 series polymers
[NASA-CR-181899] 14 p1945 N90-21129
Micromechanics analysis of space simulated thermal deformations and stresses in continuous fiber reinforced composites
[NASA-TM-102633] 14 p1946 N90-21140
Optimal fabrication processes for unidirectional metal-matrix composites: A computational simulation
[NASA-TM-102559] 14 p1947 N90-21143
A STEM study of changing grain boundary chemistry during the sensitisation of AISI 304 stainless steel
[AERE-R-13418] 14 p1949 N90-21157
Titanium aluminides: Processing, properties and potential
[AERE-R-13198] 14 p1949 N90-21158
On the stability of amorphous silica coatings for high temperature service
[AERE-R-13425] 14 p1953 N90-21179
Research advances in fine ceramics
[DE90-008983] 14 p1956 N90-21197
Pressure rig for repetitive casting
[NASA-CASE-LAR-14050-1] 14 p1959 N90-21216
Deformation and microstructure of rutile
[DE90-614113] 14 p2032 N90-21654
Thermogravimetric analysis of Nd(2-x)Ce(x)CuO(4-delta)
[DE90-009184] 14 p2032 N90-21658
Analysis of a six-component, flow-through, strain-gage, force balance used for hypersonic wind tunnel models with scramjet exhaust flow simulation
[NASA-CR-186585] 15 p2055 N90-21775
METCAN verification status
[NASA-TM-103119] 15 p2064 N90-21824
The temperature variation of hydrogen diffusion coefficients in metal alloys
[NASA-TM-100397] 15 p2067 N90-21836
Development of shape memory metal as the actuator of a fail safe mechanism 15 p2112 N90-22081
Deformation and fracture of thin sheet aluminum-lithium alloys: The effect of cryogenic temperatures 16 p2218 N90-22655
Low temperature degradation of Y-TZP materials
[AD-A218841] 16 p2223 N90-22684
Methods for evaluation of thermally induced reactions in liquid propellants
[AD-A218750] 16 p2225 N90-22694
High-efficiency silicon solar cells for a 22-sun line-focus module
[DE90-010242] 16 p2251 N90-22840
Preliminary investigation into the effect of high temperature thermal anneals on the figure of merit of silicon germanium alloys
[AD-A218573] 17 p2375 N90-23527
Dynamic mechanical analysis of polymeric materials 18 p2513 N90-24353
Resistivity measurements of halide-salt/MgO separators for thermal cells
[DE90-009740] 18 p2550 N90-24553
Effect of pretreatment on a platinized tin oxide catalyst used for low-temperature CO-oxidation 18 p2558 N90-24599
High-temperature superconductors for space power transmission lines
[NASA-TM-103459] 18 p2624 N90-24952
Development of a design methodology for high temperature cyclic applications of materials which experience cyclic softening
[DE90-006722] 19 p2674 N90-25205
Oxidation characteristics of Ti-14Al-21Nb ingot alloy
[NASA-TP-3012] 19 p2674 N90-25206
High-temperature materials. Coating, welding, and service tests
[VTT-RR-645] 19 p2675 N90-25214
TEM, positron lifetime, and hardness measurements of irradiated, cold-worked, and annealed Zr-1 percent Nb
[VTT-RR-650] 19 p2676 N90-25216
High-temperature creep under a nonuniform temperature distribution
[ATR-88(3728-02)-1] 19 p2702 N90-25373
Ion-heated thermal comptonization models and X ray spectral correlations in active galactic nuclei 19 p2790 N90-25880
Extension of a noninteractive reliability model for ceramic matrix composites
[NASA-CR-185267] 20 p2838 N90-26142
Fluid Phase Separation (FPS) experiment for flight on a space shuttle Get Away Special (GAS) canister
[NASA-CR-186830] 20 p2841 N90-26161
Influence of thermal conditioning media on Charpy specimen test temperature
[DE90-012784] 20 p2875 N90-26360
Static and fatigue strength of an adhesive bonded CFRP butt-strap joint: The effects of stacking sequence and temperature
[NLR-TR-88036-U] 20 p2877 N90-26370
The role of heat transfer during reactive-ion etching of polymer films
[AD-A222072] 21 p2977 N90-26919
Research on sputtering of ferroelectric thin films
[AD-A221792] 21 p2983 N90-26949
Miscibility and phase behavior of poly (enaminonitrile)/PEO blends
[AD-A222255] 21 p2987 N90-26975
Life evaluation of valve regulated lead-acid batteries for cycling applications
[DE90-013649] 21 p2999 N90-27044
Calculation of service life of turbomachine components 22 p3117 N90-27706
The effect of temperature cycling typical of low earth orbit satellites on thin films of YBa2Cu3O(7-x) 22 p3140 N90-27812
Thermal response of large area high temperature superconducting YBaCuO infrared bolometer 22 p3146 N90-27839
Elementary characterization of the pre-impregnated carbon/epoxy NCHR 914/155/34 percent-T300F from Brochier after the technical note CEAT number 1/M/87
[CEAT-PV-M7/6211] 22 p3154 N90-27884
Evaluation of EA-934NA with 2.5 percent Cab-O-Sil
[NASA-CR-184005] 22 p3158 N90-27909
A study of mixed convection in large baffled rectangular chambers with and without internal heat sources
[AD-A223158] 22 p3169 N90-27977
On the dynamic and thermodynamic structures of marine stratocumulus 22 p3216 N90-28244
Double layer effects on the enthalpy of activation of heterogeneous electron transfer reactions
[AD-A221934] 22 p3245 N90-28404
Liquid Rocket Booster (LRB) for the Space Transportation System (STS) systems study. Appendix B: Liquid rocket booster acoustic and thermal environments
[NASA-CR-183788-APP-B] 23 p3288 N90-28602
High temperature fatigue behavior of Haynes 188 23 p3295 N90-28642
Durability of thermal barrier coatings in a high heat flux environment 23 p3297 N90-28651
Vacuum application of thermal barrier plasma coatings 23 p3298 N90-28653
Dissipation of mechanical work and temperature rise in AS4/PEEK thermoplastic composite
[NASA-CR-186893] 23 p3302 N90-28678
High Temperature Surface Interactions
[AGARD-CP-461] 23 p3306 N90-28698
Fretting wear and fretting fatigue at temperatures up to 600 C 23 p3307 N90-28706
Fretting fatigue strength of Ti-6Al-4V at room and elevated temperatures and ways of improving it 23 p3308 N90-28709
High-temperature deformation and microstructural analysis for Si3N4-Sc2O3
[NASA-TM-103239] 23 p3314 N90-28740
Radiative heat transfer
[PB90-247602] 23 p3327 N90-28813
Frequency response of a thermocouple wire: Effects of axial conduction
[NASA-CR-180454] 23 p3330 N90-28827
Influence of diesel engine exposure on the rupture strength of silicon nitride and partially stabilized zirconia
[DE90-014759] 23 p3334 N90-28849
UV-induced degradation of the Si-SiO2 interface: Applications to the point contact solar cell
[DE90-013843] 23 p3344 N90-28898
Numerical and analytical study of nonlinear bifurcations associated with the morphological stability of two-dimensional single crystals
[PB90-209594] 23 p3398 N90-29200
A generalised Hubbard Hamiltonian: Influence of temperature and fractality
[DE90-627322] 23 p3400 N90-29213
Prediction and control of processing-induced residual stresses in composites. Part 2: AS4/PEEK composite
[AD-A223696] 24 p3443 N90-29445

Characterization of unnotched SCS-6/Ti-15-3 metal matrix composites at 650 C
[NASA-TM-102699] 24 p3444 N90-29450
Isotopic tailoring and other techniques used to study helium effects in austenitic alloys
[DE90-016344] 24 p3452 N90-29495
The investigation and production of titanium-tantalum junctions diffusion bonded at high temperature (855 C to 920 C): The influence of temperature, time pressure and roughness on the mechanical properties, and the optimisation of the bonded conditions
[BR114894] 24 p3476 N90-29646
A viscoelastic material model for computing stresses in glass
[DE90-014851] 24 p3481 N90-29673
Mechanism of habit change for atmospheric ice crystal growth 24 p3489 N90-29717

TEMPERATURE FIELDS
U TEMPERATURE DISTRIBUTION

TEMPERATURE GRADIENTS
NT THERMOCLINES
A seasonal isotherm depth climatology for the eastern tropical Pacific
[PB89-193577] 01 p0090 N90-10512
Ion temperature gradient instability
[DE89-016574] 02 p0277 N90-11580
Fast and objective MRTD measurement
[FEL-1988-24] 03 p0351 N90-12006
The 4th US Army Workshop on Low Heat Rejection Engines
[AD-A212379] 04 p0510 N90-12943
Thermocapillary migration of liquid droplets in a temperature gradient in a density matched system
[NASA-CR-185178] 06 p0776 N90-14512
Simultaneous multipoint measurements of density gradients and temperature in a flame
[DE90-001719] 07 p0892 N90-15155
Experimental determination of the fluid velocity by spectral analysis of temperature fluctuations
[DE89-636430] 07 p0928 N90-15372
Ocean thermal energy conversion: An overview
[DE89-000838] 07 p0953 N90-15512
The calculation of overground sound propagation in the presence of wind and temperature gradients
[ESDU-89036] 07 p0989 N90-15714
Measurements of heat-transfer coefficients in the interaction regions between oblique shock waves and turbulent boundary layers with a multi-layered thin film heat transfer gauge
[DE90-004123] 09 p1216 N90-17054
Analysis of significant weather on meso-alpha scales using conventional and remotely sensed data: Exploratory studies
[AD-A214563] 09 p1248 N90-17238
Staring focal plane array system modeling
[AD-A215712] 09 p1283 N90-17438
Carbon black/polyethylene composites for PTC (Positive Temperature Coefficient) thermistor applications
[AD-A215988] 12 p1619 N90-19307
Heat transfer definitions and equations
[ESDU-89022] 12 p1657 N90-19522
A method of estimating temperature profiles and chemical differentiation in the near surface layers of porous comet nuclei: First results for comet P/Churyumov-Gerasimenko 12 p1742 N90-20013
Experimental feasibility of investigating acoustic waves in Couette flow with entropy and pressure gradients
[NASA-TM-102621] 13 p1882 N90-20795
The measurements of thermoacoustic phenomena using thermoacoustic couples
[AD-A218018] 13 p1882 N90-20798
Thermomechanical deformation testing and modeling in the presence of metallurgical instabilities
[NASA-CR-185188] 14 p1993 N90-21420
TOODEE: A two-dimensional, time-dependent heat conduction program
[DE90-009631] 15 p2099 N90-22010
Scattered-light scanner measurements of cryogenic liquid-jet breakup
[NASA-TM-102432] 15 p2101 N90-22021
Linear, nonlinear, and tunable guided wave modes for high-power (GaAl)As semiconductor lasers
15 p2104 N90-22036
Effect of a crystal-melt interface on Taylor-vortex flow
[NASA-CR-186512] 15 p2171 N90-22408
Ocean energy program summary
[DE89-009481] 16 p2251 N90-22836
Activation uniformity dependence of undoped semi-insulating GaAs on post-implant annealing conditions
[ETN-90-96549] 16 p2323 N90-23246
Temperature and coupling behavior of resonators and transducers of lithium tetraborate driven by lateral and thickness fields
[AD-A219548] 17 p2395 N90-23644
Temperature-gradient instability induced by conducting end walls
[DE90-014334] 23 p3396 N90-29188
Investigation of a heat driven thermoacoustic prime mover
[AD-A223928] 24 p3484 N90-29694

TEMPERATURE INDICATORS
U INDICATING INSTRUMENTS
U TEMPERATURE MEASURING INSTRUMENTS

TEMPERATURE INSTRUMENTS
U TEMPERATURE MEASURING INSTRUMENTS

TEMPERATURE INVERSIONS
An aircraft investigation of a convective boundary layer over Lake Michigan
[AD-A218175] 13 p1846 N90-20598
Infrared propagation in the air-sea boundary layer
15 p2083 N90-21926
Inverse problems of heat conduction
15 p2091 N90-21969

TEMPERATURE MEASUREMENT
Three-in-one gage
[NASA-CR-183714] 01 p0072 N90-10413
Thin film thermocouples for high temperature measurement
[PB89-209290] 01 p0073 N90-10420
Some significant results from testing a Remote Multiplexing Unit (RMU) for temperature-induced errors
[DE89-009432] 01 p0073 N90-10421
NIST (National Institute of Standards and Technology) measurement services: The calibration of thermocouples and thermocouple materials
[PB89-209340] 02 p0222 N90-11274
A remote sensor to monitor combustion products using a tunable acousto-optic filter 02 p0223 N90-11275
Infrared temperature measurement with automatic consideration of emissivity
[ESA-TT-1131] 03 p0351 N90-12008
Center for Electronics and Electrical Engineering technical publication announcements covering Center programs, January-March 1989 with 1989 CEEE events calendar
[PB89-228308] 03 p0418 N90-12402
Payload thermal control 05 p0604 N90-13511
Spacecraft thermal control 05 p0604 N90-13513
Evidence for accurate temperatures from the inflatable falling sphere 05 p0657 N90-13835
Near-mesopause temperatures at 69 N latitude in late summer 05 p0658 N90-13837
Resonance cone diagnostics in the mid-latitude ionosphere 05 p0658 N90-13840
Operational activity in France and a new method of balloon temperature piloting 05 p0660 N90-13857
Simultaneous multipoint measurements of density gradients and temperature in a flame
[DE90-001719] 07 p0892 N90-15155
Surface thermometry of energetic materials by laser-induced fluorescence
[AD-A214423] 07 p0916 N90-15297
Tuned-circuit Johnson noise thermometry
[DE89-016221] 07 p0925 N90-15356
Pulsed EMAT (Electromagnetic Acoustic Transducer) acoustic measurements on a horizontal continuous caster for internal temperature determination
[DE90-002735] 07 p0988 N90-15709
Thickness, velocity, and temperature measurements in falling liquid films
[DE90-004290] 08 p1063 N90-16151
Modeling a self-calibrating thermocouple for use in a smart temperature measurement system
[DE90-003697] 08 p1081 N90-16259
Upper atmosphere research
[ISBN-0-642-13582-7] 08 p1100 N90-16368
Measurement of the speed and temperature of ignition gases
[ISL-CO-246/88] 09 p1192 N90-16908
Noncontact temperature pattern measuring device
[NASA-CASE-NPO-17824-1-CU] 09 p1229 N90-17132
Low speed flowfield characterization by infrared measurements of surface temperatures
10 p1306 N90-17556
Temperature measurement during welding of solar cells and calibration of finite element models
10 p1342 N90-17774
Proceedings of the Second Noncontact Temperature Measurement Workshop
[NASA-CR-181289] 10 p1362 N90-17894
Non-contact temperature measurement requirements of ground-based research and flight programs at JPL
10 p1362 N90-17895
Temperature profiles in high gradient furnaces
10 p1362 N90-17896
Non-contact temperature measurement requirements
10 p1363 N90-17898
Optical Johnson noise thermometry
10 p1363 N90-17899
Non-contact temperature measurements in support of microgravity combustion experiments
10 p1363 N90-17900
Solid state lasers for use in non-contact temperature measurements 10 p1363 N90-17901
Radiation thermometry at NIST: An update of services and research activities 10 p1364 N90-17903
A multicolor imaging pyrometer
10 p1364 N90-17905
Non-contact true temperature measurements in the microgravity environment 10 p1364 N90-17906
A potential nuclear magnetic resonance imaging approach for noncontact temperature measurement
10 p1364 N90-17908
Use of anomolous thermal imaging effects for multi-mode systems control during crystal growth
10 p1365 N90-17910
Comments on containerless bulk crystal growth and epitaxy in space and on their implications regarding non-contact temperature measurements
10 p1365 N90-17911
Non-contact temperature measurement of a falling drop 10 p1365 N90-17912
Temperature control and calibration issues in the growth, processing and characterization of electronic materials
10 p1365 N90-17914
Combustion process science and technology
10 p1366 N90-17916
NCTM workshop splinter session, IR thermal measurement instruments 10 p1367 N90-17923
Dynamic response for thermal control and measurement and fast radiation thermometry
10 p1367 N90-17924
Materials thermal and thermoradiative properties/characterization technology
10 p1367 N90-17925
Report on the multicolor pyrometry session at the Second NASA Non-Contact Temperature-Measurement Workshop 10 p1367 N90-17926
Simultaneous observations of the emissions OI (5577), O2A(0.1), NaD(5893) and OH(9.4) and the rotational temperatures TO2 and TOH in the upper atmosphere
[INPE-4851-TDL/366] 10 p1407 N90-18113
An atlas of ECMWF analyses (1980-1987). Part 1: First moment quantities
[NASA-TM-100747-PT-1] 10 p1408 N90-18120
Interactions of molecules with surfaces
[DE90-005337] 10 p1428 N90-18237
Thermal analysis of polymer composites
[AD-A216947] 11 p1490 N90-18578
Solid-state fluorescence above 1000 C: Application to high-temperature laser thermography
[DE90-006422] 11 p1514 N90-18721
Preliminary comparison of temperature soundings obtained from simultaneous radiometric, radio-acoustic, and rawinsonde measurements
[PB90-119835] 11 p1535 N90-18838
Transient heat transfer measurements on a flat plate in turbulent flow using an electrical analog
[AD-A216286] 11 p1573 N90-19057
Utilization of thermometric methods for the testing of carbon reinforced plastics
[ETN-90-96076] 12 p1621 N90-19314
Drifting buoy data from Western Tropical Pacific for the period February 1, 1986 through February 28, 1989
[PB90-113978] 12 p1695 N90-19732
Critical current density and transition temperature measurements of Y-Ba-Cu-O rods
[AD-A216695] 12 p1719 N90-19875
Spacelab qualified infrared imager for microgravity science experiments
[NASA-TM-102503] 13 p1804 N90-20352
A nonintrusive method for measuring the operating temperature of a solenoid-operated valve
[DE90-007576] 13 p1804 N90-20355
Applications of microwave radiometric measurements to infer tropical cyclone intensity and strength
[AD-A218273] 13 p1847 N90-20600
Analysis of water quality parameters of the Piaui River (SE), Brazil, through field and TM/LANDSAT sensor data
[INPE-4918-PRE/1417] 14 p1998 N90-21453
Inverse problems of heat conduction
15 p2091 N90-21969
Uncertainty evaluation in an automated high temperature environmental simulation oven
[REPT-892-430-103] 16 p2203 N90-22571
Temperature measurements through a solid-propellant combustion wave using imbedded fine wire thermocouples
[AD-A218642] 16 p2225 N90-22693
Analysis of velocity and temperature fluctuations in turbulent shear flows 16 p2233 N90-22744

Quantitative surface temperature measurement using two-color thermographic phosphors and video equipment
[NASA-CASE-LAR-13740-1] 16 p2238 N90-22770
Accuracy and precision of GOES data collection platforms for temperature measurements
[AD-A218798] 16 p2250 N90-22832
Multiwavelength pyrometry to correct for reflected radiation
[NASA-TM-102578] 17 p2407 N90-23714
Integrated silicon flow sensors
[ETN-90-96906] 17 p2407 N90-23715
Environmental measurements and analysis: Arctic acoustics experiments in the marginal ice zone
[AD-A220509] 18 p2582 N90-24708
National Aeronautics and Space Administration (NASA)/American Society for Engineering Education (ASEE) Summer Faculty Fellowship Program-1989, volume 1
[NASA-CR-185601-VOL-1] 18 p2627 N90-24972
Temperature determination of shock layer using spectroscopic techniques 18 p2628 N90-24973
Intelligent composites containing measuring fibre optic networks for continuous self diagnosis
[ETN-90-97018] 19 p2673 N90-25200
Infrared fiber-optical temperature sensor
[AD-D014519] 19 p2693 N90-25321
Feasibility study for the advanced one-dimensional high temperature optical strain measurement system, phase 3
[NASA-CR-185254] 19 p2693 N90-25324
Evaluation of water cooled supersonic temperature and pressure probes for application to 2000 F flows
[NASA-TM-102612] 19 p2753 N90-25645
Vapor pressures of acetylene at low temperatures 20 p2949 N90-26777
Concentration, temperature, and density in a hydrogen-air flame by excimer-induced Raman scattering 21 p2974 N90-26903
Integrated radiometric profiler for atmospheric humidity and temperature measurements
[AD-A221931] 21 p3032 N90-27237
A technique to measure the thermal diffusivity of high T(sub c) superconductors 22 p3147 N90-27846
Evaluation of EDR-3 vibration, shock, temperature, and humidity recording unit
[NASA-CR-184006] 22 p3177 N90-28028
Improved meteorological measurements from buoys and ships (IMET): Preliminary comparison of solar radiation air temperature shields
[PB90-241928] 22 p3229 N90-28314
Gas-jet and tangent-slot film cooling tests of a 12.5 deg cone at Mach number of 6.7
[NASA-TP-2786] 23 p3326 N90-28806
Noncontact measurement of high temperature using optical fiber sensors
[NASA-CR-186975] 23 p3329 N90-28825
Wind lidar for BEST
[CNES-NT-125] 23 p3353 N90-28947
Feasibility of the temperature measurements in hypersonic flow by multibeam coherent Raman anti-Stokes scattering
[ONERA-RF-56/7131-PY] 24 p3419 N90-29312
Measurement Techniques for Hypersonic Flows
[VKI-LS-1990-05] 24 p3419 N90-29314
CARS spectroscopy and applications 24 p3420 N90-29321
Thermographic phosphor technique 24 p3421 N90-29324
Infrared thermography 24 p3421 N90-29325
Recommended practices for measurement of gas path pressures and temperatures for performance assessment of aircraft turbine engines and components
[AGARD-AR-245] 24 p3433 N90-29393

TEMPERATURE MEASURING INSTRUMENTS
NT BATHYTHERMOGRAPHS
NT PNEUMATIC PROBES
NT PYROMETERS
NT RADIATION PYROMETERS
NT TEMPERATURE PROBES
NT THERMOMETERS
Low speed hot and cold wire techniques for unsteady flow 05 p0574 N90-13342
Silicon-etalon fiber-optic temperature sensor
[NASA-TM-102389] 05 p0580 N90-13381
A feasibility study for using CARS in temperature and volumetric measurement as a function of time
[ISL-CO-223/88] 09 p1226 N90-17116
Development of a mass averaging temperature probe 11 p1461 N90-18418

TEMPERATURE PROBES
NT PNEUMATIC PROBES
Development of an automated probe for thermal conductivity measurements
[PB89-209324] 01 p0073 N90-10419
NIST (National Institute of Standards and Technology) measurement services: The calibration of thermocouples and thermocouple materials
[PB89-209340] 02 p0222 N90-11274
Evaluation of water cooled supersonic temperature and pressure probes for application to 2000 F flows
[NASA-TM-102612] 19 p2753 N90-25645
A reliable, maintenance-free oxygen sensor for aircraft using an oxygen-sensitive coating on potentiometric electrodes
[AD-A222696] 23 p3277 N90-28545

TEMPERATURE PROFILES
Direct statistical thermal wind estimation procedure
[AD-A211256] 02 p0253 N90-11433
Disturbances in the Arizona Monsoon 03 p0362 N90-12071
Phase change material for spacecraft thermal management
[AD-A211404] 04 p0462 N90-12648
Retrieval of atomic oxygen and temperature in the thermosphere. Part 1: Feasibility of an experiment based on the spectrally resolved 147 micrometer limb emission
[AD-A211987] 04 p0517 N90-12986
Near-mesopause temperatures at 69 N latitude in late summer 05 p0658 N90-13837
Thermal histories of the samples of two KOSI comet nucleus simulation experiments 08 p1147 N90-16645
Measurements of mean and fluctuating temperature in microgravity 09 p1201 N90-16961
Temperature profiles in high gradient furnaces 10 p1362 N90-17896
Microwave brightness temperature and its relation to atmospheric general circulation features
[AD-A218312] 13 p1847 N90-20603
The observed properties of the intermediate-degree gravity modes and their relevance to the solar neutrino paradox 15 p2193 N90-22519
Temperature measurements through a solid-propellant combustion wave using imbedded fine wire thermocouples
[AD-A218642] 16 p2225 N90-22693
Atmospheric turbulence measurements in support of adaptive optics technology
[AD-A220445] 17 p2423 N90-23805
Study of seasonal variation of mixing phenomena in the hypolimnion of Lake Geneva (Switzerland) 19 p2688 N90-25287
Measurement of velocity and temperature profiles at the exit plane of a tubular gas turbine combustor
[DE90-505519] 20 p2809 N90-25983
Resonant coupling through a slot to a loaded cylindrical cavity: Experimental results
[AD-A223000] 20 p2922 N90-26631
Description of SAFIRE for ISES 21 p3016 N90-27148
Integrated radiometric profiler for atmospheric humidity and temperature measurements
[AD-A221931] 21 p3032 N90-27237
Solar activity, the QBO, and tropospheric responses 22 p3203 N90-28172
Airborne lidar/radiometric measurements of cirrus cloud parameters and their application to LOWTRAN radiance evaluations 22 p3227 N90-28298
An investigation of the inviscid spatial instability of compressible mixing layers
[AD-A223776] 24 p3468 N90-29596

TEMPERATURE RATIO
An investigation of the inviscid spatial instability of compressible mixing layers
[AD-A223776] 24 p3468 N90-29596

TEMPERATURE SENSORS
NT THERMISTORS
Independent Orbiter Assessment (IOA): Assessment of the Orbiter Experiment (OEX) subsystem
[NASA-CR-185587] 02 p0171 N90-10962
Solid state lasers for use in non-contact temperature measurements 10 p1363 N90-17901
Infrared fiber-optical temperature sensor
[AD-D014519] 19 p2693 N90-25321
Smart microsensors for high temperature applications, phase 1
[AD-A224151] 23 p3330 N90-28828

TEMPERING
Austempered ductile iron data base: A cooperative program between industry and the Trade Adjustment Assistance Program of the Department of Commerce
[PB90-115569] 12 p1626 N90-19343
Microstructural development in HSLA-100 steel weld metals
[AD-A222105] 21 p2982 N90-26944

TEMPLATES
Database interfaces on NASA's heterogeneous distributed database system
[NASA-CR-185420] 05 p0706 N90-14133
Using template/hotwire cutting to demonstrate moldless composite fabrication 18 p2515 N90-24361
Explanation of Bayesian conditioning for decision support systems 18 p2633 N90-25002
Method of insetting predesigned disbond areas into composite laminates
[NASA-CASE-LAR-13225-1] 19 p2672 N90-25197

TEMPORAL DISTRIBUTION
Spatial and temporal short range total cloud cover estimation by metric analysis of composite imagery 02 p0251 N90-11423
A study of the temporal stability of multiple cell vortices
[NASA-CR-4261] 03 p0345 N90-11968
Time-weighted accumulations ap(tau) and Kp(tau)
[RAE-TR-88050] 03 p0421 N90-12422
The M/G/1 processor sharing queue as the almost sure limit of feedback queues
[REPT-89-32] 04 p0528 N90-13044
The discrete-time single-server queueing model
[MEMO-780] 04 p0544 N90-13165
A range-dependent analysis of acoustic transmission across a cold filament in the California current
[AD-A220175] 18 p2583 N90-24709
Solar UV variability 22 p3201 N90-28162
Diurnal and temporal variation of UV-flux and its dependence on stratospheric ozone 22 p3205 N90-28184

TEMPORAL RESOLUTION
Land vehicle teleoperation under conditions of reduced video resolution
[DE89-016925] 02 p0231 N90-11324
Temporally and spatially resolved flow in a two-stage axial compressor. Part 2: Computational assessment
[NASA-TM-102273] 06 p0726 N90-14236
Excited state lifetime measurements of ytterbium in indium phosphide
[AD-A215709] 09 p1291 N90-17483
Physiognomy of vegetation cover in the PNPM identified through the TM/LANDSAT sensor: A multitemporal analysis
[INPE-4834-PRE/1464] 11 p1525 N90-18776
Three-dimensional motion estimation using shading information in multiple frames
[AD-A216804] 11 p1549 N90-18919
Time resolved gain/loss studies under low and high power loading for the XeF C-A transition
[DE90-007506] 12 p1655 N90-19517
Some recent applications of laser ultrasound to the characterisation of materials
[AERE-R-13438] 14 p1985 N90-21374
Evaluation of the mangrove areas of the Rio Piaui (SE) through remote sensing
[INPE-4909-PRE/1510] 14 p1998 N90-21454
Multitemporal analysis of LANDSAT/TM digital imagery in the detection of areas affected by caterpillar (sibine fusca) attack in the dende (elais guineensis) palm plantation
[INPE-4979-PRE/1544] 14 p1999 N90-21457
Time-resolved surface structural study by picosecond reflection high-energy electron diffraction
[AD-A218417] 16 p2228 N90-22712
Preliminary simulations of the large-scale environment during the FIRE cirrus IFO 22 p3225 N90-28290
Workload induced spatio-temporal distortions and safety of flight: An investigation of cognitive intrusions in perceptual processes 23 p3360 N90-28966

TENSILE CREEP
Delayed failure of silver-aided diffusion welds between steel
[DE89-016652] 01 p0045 N90-10252
Static tensile and tensile creep testing of four boron nitride coated ceramic fibers at elevated temperatures
[NASA-CR-184999] 03 p0318 N90-11807
Creep behavior of alloys based on TiAl containing TiB2 and TiN particulates
[DE90-006489] 12 p1628 N90-19355
Deformation and fracture of TiAl + W at elevated temperatures
[DE90-006490] 12 p1628 N90-19356
Time-dependent failure of silver-interlayer diffusion bonds between non-deforming base-metals
[DE90-006925] 12 p1628 N90-19357
Improved toughness alloys based on titanium aluminides
[AD-A218149] 13 p1778 N90-20208
Ambient-temperature creep failure of silver-aided diffusion bonds between steel
[DE90-010687] 18 p2527 N90-24420
Evaluation of advanced austenitic alloys relative to alloy design criteria for steam service. Part 1: Lean stainless steel
[DE90-014785] 23 p3310 N90-28720

TENSILE DEFORMATION

Biaxial flexing of a fiber-reinforced aluminum composite
[AD-A212742] 04 p0468 N90-12681

Deformation and fracture of TiAl + W at elevated temperatures
[DE90-006490] 12 p1628 N90-19356

Time-dependent failure of silver-interlayer diffusion bonds between non-deforming base-metals
[DE90-006925] 12 p1628 N90-19357

Laser-induced shock waves effects in materials
[DE90-007626] 13 p1807 N90-20379

Continued research on the strain to failure of thick-walled cylinders subjected to internal pressure
[DE90-008952] 15 p2118 N90-22115

Elevated temperature crack growth in aluminum alloys: Tensile deformation of 2618 and FVS0812 aluminum alloys 16 p2218 N90-22654

TENSILE PROPERTIES

Mechanical properties, solubilities, and processabilities in the design of the first super-strong liquid-crystalline polymers
[DE89-009252] 01 p0048 N90-10273

Rapid heating tensile tests of high-energy-rate-forged 316L stainless steel charged with hydrogen and tritium
[DE89-017869] 04 p0474 N90-12717

Fiber reinforced cementitious composites technology
[PB89-227813] 05 p0619 N90-13608

Mechanical property characterization of VascoMax T-300
[AD-A212950] 05 p0623 N90-13637

Spall strength measurements on shockloaded refractory metals
[DE90-000839] 06 p0747 N90-14345

Effects of precipitate distribution on 293 K and 77 K properties of 2090-T81 weldments
[DE90-002332] 06 p0747 N90-14349

The structure and properties of liquid crystal polymers 06 p0749 N90-14356

Predictive aging of elastomers in air: The importance of understanding diffusion-limited oxidation effects
[DE90-001385] 06 p0751 N90-14372

Qualification of diode foil materials for excimer lasers
[DE90-000602] 06 p0789 N90-14593

Heat treatment investigation of 4330 vanadium-modified steel
[AD-A214290] 07 p0906 N90-15239

Small screw study: Fastener tensile strength and optimum thread depth
[DE90-005001] 09 p1231 N90-17141

Impact damage tolerance of composite cylindrical panels
[AD-A216401] 10 p1350 N90-17830

Tensile mechanical properties in flat specimens of 7150-T7751
[INFORME-I-296/88] 10 p1356 N90-17860

Environmental embrittlement: A major cause for low ductility of ordered intermetallics
[DE90-006161] 10 p1356 N90-17864

Preliminary evaluation of the strength of pin-joints in laminated composite materials
[DE90-006353] 11 p1481 N90-18524

Ageing effects in welded cast CF3 stainless steel
[AERE-R-13559] 13 p1775 N90-20188

The ageing effect of the matrix-reinforcement interface on the ageing response of an aluminium 6061 alloy reinforced with 20vol percent SiC particulates
[AERE-R-13361] 13 p1776 N90-20193

Evaluation of 2090-T8E48 aluminum-lithium plates
[AD-A217262] 13 p1776 N90-20196

Tensile film clamps and mounting block for the rheovibron and autovibron viscoelastometer
[NASA-CASE-LAR-13696-1] 13 p1812 N90-20409

The effects of a nearby subsequent fusion weld on the properties of an inertia friction weld
[DE90-007972] 14 p1988 N90-21396

Fracture toughness and tensile properties of alloy HT9 in thin sections under high neutron fluences
[DE90-008386] 15 p2069 N90-21851

Data and conclusions from tests on small screws
[DE90-007500] 15 p2106 N90-22046

Elevated temperature crack growth in advanced powder metallurgy aluminum alloys 16 p2218 N90-22653

Vanadium alloys with improved resistance to helium embrittlement
[DE90-009811] 17 p2375 N90-23524

Characterization of solid state bonding between Coors AD-999 alumina and niobium
[DE90-010653] 18 p2518 N90-24379

Development of damped metal matrix composites for advanced structural applications
[AD-A219864] 18 p2518 N90-24380

A vectroized elastic/plastic power law hardening material model including Lueders strain
[DE90-010172] 18 p2572 N90-24655

The influence of microstructure on the tensile behavior of an aluminum metal matrix composite
[NASA-TM-102694] 20 p2827 N90-26082

Compendium of material test results on HY-130 and Ti-3Al2V metals in support of United States navy programs
[DE90-011754] 20 p2833 N90-26112

Fracture toughness and failure mechanisms in commercial 2091 Al-Li sheet at cryogenic temperatures
[AD-A222803] 20 p2835 N90-26125

Imide/arylene ether copolymers
[NASA-CASE-LAR-14159-1-CU] 21 p2983 N90-26953

Study of the microstructure of a titanium alloy (6246) for turbomachine compressors
[ETN-90-97450] 22 p3157 N90-27900

Evaluations of new polyimide films for flexible circuit applications at EG and G Mound Applied Technologies
[DE90-014117] 23 p3312 N90-28731

Evaluation of ARALL-4: An aramid fiber reinforced aluminum
[AD-A223502] 24 p3443 N90-29443

Mechanical properties and fracture toughness of AAR-TC128 Grade B steel and a micro-alloyed, control-rolled steel, A 8XX grade B, from -80F to +73F
[PB90-207796] 24 p3448 N90-29471

Tensile behavior and swelling of ternary austenitic alloys irradiated in different neutron spectra
[DE90-015295] 24 p3450 N90-29485

Alloy design of ordered intermetallics
[DE90-016031] 24 p3451 N90-29490

The use of automated ball indentation testing to measure flow properties and estimate fracture toughness in metallic materials
[DE90-015797] 24 p3452 N90-29493

The effect of helium on microstructural evolution in austenitic steels as determined by spectral tailoring experiments
[DE90-016360] 24 p3452 N90-29496

TENSILE STRENGTH

Effects of a heat cycle on material strength
[NAL-TM-562] 03 p0306 N90-11737

Contamination removal using various solvents and methodologies
[NASA-CR-183747] 05 p0626 N90-13652

The strength-toughness combination of the aluminum-lithium alloys 2090 and 2091 at cryogenic temperatures
[DE90-001425] 06 p0746 N90-14338

The effect of hydrogen charging on the mechanical properties of aluminum alloy 2090
[DE90-000129] 06 p0748 N90-14341

The mechanisms of dispersion strengthening and fracture in Al-based XD (TM) alloys
[NASA-CR-4276] 09 p1187 N90-16879

Development of a progressive failure model for strength of laminated composite structure
[AD-A216966] 11 p1480 N90-18517

Fluorinated graphite fibers as a new engineering material: Promises and challenges
[NASA-TM-102511] 12 p1618 N90-19301

Heat treatment study of the SiC/Ti-15-3 composite system
[NASA-TP-2970] 12 p1618 N90-19302

Evaluation of repeated impact damage in composite structures 12 p1619 N90-19303

Time-dependent failure of silver-interlayer diffusion bonds between non-deforming base-metals
[DE90-006925] 12 p1628 N90-19357

Tensile behavior of cylindrical pressure tanks in fiber assembling + metal hybrid structure
[ILR-MITT-213] 12 p1675 N90-19618

Some considerations on cohesive forces in sun-grazing comets 12 p1742 N90-20015

Mechanical properties of pure nickel alloys after long term exposures to LiOH and vacuum at 775 K
[NASA-TM-102403] 13 p1774 N90-20181

Tensile fracture toughness of ceramic materials: Effects of dynamic loading and elevated temperatures
[DE90-008329] 13 p1781 N90-20223

Relevance of impacter shape to nonvisible damage and residual tensile strength of a thick graphite/epoxy laminate
[NASA-TM-102599] 14 p1943 N90-21122

Strength in notched and impact-damaged laminates 15 p2064 N90-21820

Matrix density effects on the mechanical properties of SiC/RBSN composites
[NASA-TM-103098] 15 p2065 N90-21826

The effect of aging at 343 C on type 308 stainless steel weldments
[DE90-009232] 15 p2069 N90-21853

Nonlinear fracture mechanics using semicircular specimens and tension-softening behavior 15 p2116 N90-22108

Rheological and mechanical characteristics of poly-p-phenylene terephthalamide/nylon molecular and particulate composites
[AD-A219562] 17 p2368 N90-23482

Tensile and shear strength of adhesives 18 p2515 N90-24366

Application of high performance metals in gas turbine engines
[PNR90640] 20 p2811 N90-25999

The effect of manganese on the onset of the stage 2 reaction in an austempered ductile iron matrix
[DE90-011804] 20 p2834 N90-26119

The interaction of polymeric materials with ceramic surfaces with special reference to the behaviour of bioceramics 20 p2836 N90-26127

Tensile strength measurement techniques for structural ceramics
[DE90-012193] 20 p2837 N90-26136

Strength under various modes of deformation
[AD-A222412] 21 p3013 N90-27132

Strengthening in heavily cold worked Cu-20 vol. percent Fe in situ composites
[DE90-011741] 22 p3135 N90-27790

Study of the mechanical behavior of composites under complex stress systems
[ETN-90-97455] 22 p3154 N90-27879

Evaluation of EA-934NA with 2.5 percent Cab-O-Sil
[NASA-CR-184005] 22 p3158 N90-27909

Behavior of aramid/epoxy wounded tubes under uniaxial and biaxial loading
[ETCA-89-R-150] 23 p3339 N90-28873

Development of dual fiber reinforced glass matrix composites for structural space based applications
[AD-A223801] 24 p3444 N90-29446

Effects of low Chromium(3) concentration in electrodeposition of low contraction chromium
[AD-A223338] 24 p3449 N90-29477

Fatigue, static tensile strength and stress corrosion of aircraft materials and structures. Part 1: Text
[LR-630-PT-1-REV] 24 p3482 N90-29682

Fatigue, static tensile strength and stress corrosion of aircraft materials and structures. Part 2: Figures
[LR-630-PT-2] 24 p3482 N90-29683

TENSILE STRESS

Martensite transformation in NiTi alloys induced by tensile stress pulses
[DE90-001832] 06 p0747 N90-14346

The behavior of a composite material in compression
[AD-A216324] 10 p1350 N90-17829

Practical calculation of the liveload of carbon fiber reinforced plastics by the finite element method
[ETN-90-95867] 12 p1620 N90-19311

Ultrastructure processing of ordered polymers
[AD-A218331] 13 p1783 N90-20232

Experiments on buckling and critical buckling. Behavior of carbon fiber reinforced plastic shells submitted to tensile stresses
[ETN-90-95382] 13 p1816 N90-20429

Modelling of the impact response of fibre-reinforced composites
[OUEL-1784/89] 15 p2065 N90-21827

Mechanical testing of selected engineering plastics
[DE90-008186] 16 p2222 N90-22673

Investigation of the effect of mechanical stress on cold fusion
[AD-A220123] 17 p2474 N90-24147

Study of the mechanical behavior of composites under complex stress systems
[ETN-90-97455] 22 p3154 N90-27879

Microstructure: Property correlation --- multiaxial fatigue damage evolution in waspaloy
[NASA-CR-180406] 23 p3340 N90-28880

Processability and high temperature behavior of emerging aerospace alloys
[AD-A224285] 24 p3448 N90-29475

TENSILE TESTS

A robotic electrical and tensile testing system for diodes
[DE89-014012] 01 p0073 N90-10417

Mechanics of the crack path formation
[NASA-CR-185143] 01 p0080 N90-10455

Influence of the fiber/matrix interface on damage development in CFRP 02 p0183 N90-11037

Worked-in holes in three-dimensional reinforced composites 02 p0186 N90-11060

Static tensile and tensile creep testing of four boron nitride coated ceramic fibers at elevated temperatures
[NASA-CR-184999] 03 p0318 N90-11807

Constitutive modeling for isotropic materials (HOST)
[NASA-CR-179522] 05 p0582 N90-13390

A slow strain-rate tensile testing machine
[ARL-MAT-TM-399] 05 p0645 N90-13764

Epoxy-resin cable terminations
[AD-A213789] 07 p0942 N90-15454

Fatigue and impact strength of diffusion bonded titanium alloy joints
[RAE-TM-MAT/STR-1123] 08 p1045 N90-16043
Fracture toughness of ferritic alloys at very high neutron exposures
[DE90-004519] 08 p1046 N90-16046
Interfacial studies in fiber-reinforced thermoplastic-matrix composites
15 p2062 N90-21814
Failure analysis of woven hybrid composite using a finite element method
[OUEL-1791/89] 15 p2065 N90-21828
Deformation and fracture of aluminum-lithium alloys: The effect of dissolved hydrogen 16 p2219 N90-22658
The assessment of metal fiber reinforced polymeric composites 18 p2514 N90-24357
M-52 spray booth qualification test
[NASA-CR-184003] 22 p3122 N90-27727
Plane strain fracture toughness test procedures for particulate metal matrix composites
[NPL-DMM(A)-3] 22 p3153 N90-27873
Investigation of the techniques for the analysis of composite structures: Analysis and representation of the static and dynamic behavior of glued metal insert assemblies
[IMFL-89-44] 22 p3153 N90-27878
Tensile behavior of borated stainless steels, phase 1
[DE90-014368] 23 p3309 N90-28717
Static and dynamic characterization of the ATR 72 rods made of Ti 10.2.3 titanium alloy
[REPT-49-238] 23 p3310 N90-28722

TENSOR ANALYSIS
Nonlinear adjustment with or without constraints, applicable to geodetic models
[AD-A210820] 02 p0265 N90-11509
Tensor methods for unconstrained optimization using second derivatives
[AD-A213642] 07 p0983 N90-15681
Nijenhuis tensor and integrable models
[DE90-001403] 07 p0987 N90-15702
Vector fields, linear spaces and tensors in physics. Part 3: Tensor analysis and its applications
[INPE-5000-MD/41] 11 p1561 N90-18997
A new class of exact solutions of the vacuum quadratic Poincare gauge field theory
[MATHS-REPT-A-119] 20 p2933 N90-26691

TENSOR FIELDS
U TENSORS

TENSORS
NT STRESS TENSORS
A tensor product b-spline method for 3D multi-block elliptic grid generation
[DE89-017440] 06 p0836 N90-14859
Nijenhuis tensor and integrable models
[DE90-001403] 07 p0987 N90-15702
Domain decomposition with local mesh refinement
[AD-A215806] 10 p1418 N90-18175
Scale transformations, the energy-momentum tensor, and the equation of state
[DE90-005372] 10 p1440 N90-18308
Vector fields, linear spaces and tensors in physics. Part 3: Tensor analysis and its applications
[INPE-5000-MD/41] 11 p1561 N90-18997
A tensor product B-spline method for numerical grid generation
[DE90-005979] 12 p1705 N90-19792
The generally covariant representation of energy-momentum pseudotensor of gravitational field
[DE90-615203] 14 p2034 N90-21669
New algorithms for one-loop integrals
[NIKHEF-H/89-17] 15 p2148 N90-22268
Effective action for induced gravity on a 2-dimensional manifold
[PREPRINT-712] 16 p2311 N90-23173
On null tratorial torsion in vacuum quadratic Poincare gauge field theory
[MATHS-REPT-A-111] 19 p2751 N90-25630
Application of symbolic computations to the constitutive modeling of structural materials
[NASA-TM-103225] 20 p2876 N90-26364
Implementation of algorithms used in calculating the tensor product of matrices on a distributed memory machine
[IMAG-RR-786-I] 20 p2913 N90-26572
A new class of exact solutions of the vacuum quadratic Poincare gauge field theory
[MATHS-REPT-A-119] 20 p2933 N90-26691
On trivector torsion in vacuum quadratic Poincare gauge field theory
[MATHS-REPT-A-121] 20 p2933 N90-26692
Second order tensor finite element
[NASA-CR-184008] 23 p3386 N90-29122
On the relation between the absolute parallelism spaces and spaces having a GL(4) connection
[DE90-627222] 23 p3403 N90-29232
On the infrared behaviour of some non-Minkowskian quantum fields 23 p3410 N90-29273
The f2 dominance of the energy-momentum tensor
[DE90-508027] 24 p3460 N90-29544
A new vector-tensor theory and higher-dimensional cosmology
[DE90-507990] 24 p3555 N90-30117

TERBIUM
Terbium-dysprosium magnetostrictive high power transducers
[AD-D014509] 19 p2753 N90-25641

TERBIUM COMPOUNDS
An explicit partition of the fusion-like cross section
[KVI-797] 04 p0553 N90-13225

TEREPHTHALATE
NT POLYETHYLENE TEREPHTHALATE
A model for long-term creep and the effects of physical ageing in poly (butylene terephthalate)
[NPL-DMA(A)-182] 03 p0333 N90-11895

TERMINAL BALLISTICS
Alternative test methodology for ballistic performance ranking of armor ceramics
[AD-A210587] 01 p0051 N90-10290
Studies in penetration mechanics
[AD-A210713] 01 p0079 N90-10448
EPIC-2 calculated impact loading histories of thin plates
[AD-A210557] 01 p0081 N90-10461
MESA 3-D calculations of armor penetration by projectiles with combined obliquity and yaw
[DE89-015265] 07 p0939 N90-15438
Fragmentation statistics from Eulerian hydrocode calculations
[DE90-002906] 07 p0941 N90-15449
Fractographic analysis of long rod penetrator-armor ceramic interactions
[AD-A215172] 09 p1197 N90-16938
Effects of oblique impact on hypervelocity shield performance
[DE90-006936] 11 p1517 N90-18739
Jam resistant fluid power actuator for ballistic-damage tolerant redundant cylinder assemblies
[AD-D014360] 12 p1671 N90-19600
Evaluation of 2090-T8E48 aluminum-lithium plates
[AD-A217262] 13 p1776 N90-20196
Role of shear instability in ballistic penetration
[AD-A219186] 16 p2244 N90-22799
Large-scale simulations of monolithic and segmented projectiles impacting spaced armor
[AD-A219374] 16 p2244 N90-22800
Numerical simulation of semi-infinite target penetration by continuous and segmented rods
[AD-A219437] 17 p2412 N90-23743

TERMINAL FACILITIES
FAA air traffic activity: Fiscal year 1988
[AD-A211338] 04 p0449 N90-12570

TERMINAL GUIDANCE
NT LASER GUIDANCE
Navigation up-date using radar mapping: Assessment and optimisation simulation tool
08 p1026 N90-15928

TERMINATING
U STOPPING

TERMINOLOGY
Terminology strategies for international information exchange
[AD-A214147] 07 p1010 N90-15853
NASA Thesaurus supplement: A four part cumulative supplement to the 1988 edition of the NASA Thesaurus (supplement 3)
[NASA-SP-7064-SUPPL-3] 15 p2177 N90-22438
Quick guide of the essential concepts used in optical digital data disk technology 17 p2479 N90-24175

TERMS
CRISP (Computer Retrieval of Information on Scientific Projects) thesaurus, fiscal year 1990
[PB90-138652] 12 p1726 N90-19922
Medical subject headings: Annotated alphabetic list, 1990
[PB90-100009] 14 p2036 N90-21683
Permuted medical subject headings, 1990
[PB90-100025] 14 p2036 N90-21684
A dictionary of acquisition and contracting terms
[AD-A221681] 21 p3088 N90-27560
A glossary of terms, definitions, acronyms, and abbreviations related to the National Airspace System
[DOT/FAA/CT-TN89/53] 23 p3406 N90-29249

TERNARY ALLOYS
Tensile behavior and swelling of ternary austenitic alloys irradiated in different neutron spectra
[DE90-015295] 24 p3450 N90-29485

TERNARY SYSTEMS
Design and construction of systems for the single-crystals growth of ternary silver halides, alkali halides, and alkaline earth fluorides, and the dielectric investigation of silver halide
[ETN-89-94673] 02 p0286 N90-11632
Process for single crystal growth of high T(sub c) superconductors
[AD-D014167] 03 p0409 N90-12348
Ternary reciprocal system of lithium and potassium fluorides and bromides
[DE90-004938] 10 p1352 N90-17840
Synthesis, structure, and properties of a new ternary metal nitride, Ca3CrN3
[AD-A222274] 21 p2978 N90-26924
Synthesis, structure, and properties of Ca2ZnN2
[AD-A222012] 21 p3083 N90-27533
Ternary and quaternary oxides of Bi, Sr, and Cu
22 p3141 N90-27817

TERNARY SYSTEMS (DIGITAL)
U DIGITAL SYSTEMS

TERPENES
NT AZULENE
The diurnal ozone cycle in a coniferous forest: The importance of meteorology and chemistry
[CM-75] 17 p2421 N90-23795
Measurements of monoterpenes in a coniferous forest
20 p2886 N90-26421
Terpene concentrations and emissions in a Scots pine forest 20 p2886 N90-26422

TERRACES (LANDFORMS)
Fracture analysis through photographic imagery of low spatial resolution: A contribution to the study of tectonic evoluation of the Araripe Plateau region
[INPE-4876-PRE/1487] 11 p1520 N90-18756

TERRADYNAMICS
Clotho Tessera, Venus: A fragment of Fortuna Tessera 03 p0425 N90-12439

TERRAIN
Thermal radiation from terrain: Measurements and first results
[FOA-C-30525-3.1] 02 p0236 N90-11342
Diagnostic study of atmosphere-terrain interaction leading to the formation of dust clouds and poor visibilities over near east desert areas
[AD-A211243] 02 p0239 N90-11358
Tessera terrain: Characteristics and models of origin
03 p0422 N90-12426
Radar scattering from desert terrains, Pisgah/Lavic Region, California: Implications for Magellan
03 p0426 N90-12443
Problem-dependent transformations of 3D terrain elevation maps into cost precursor maps
[PB89-218127] 04 p0514 N90-12969
Forward scatter propagation path loss testing using surrogate terrain in the 100 to 1500 MHz region
06 p0760 N90-14425
Low level range coverage performance prediction for VHF radar 06 p0763 N90-14439
The identification of terrain-induced circulations using principal components
[DE90-001991] 06 p0815 N90-14739
Measurements of horizontal visibility in the lowest 300 m over Northern Germany 07 p0872 N90-15059
Parallel algorithms for interactive manipulation of digital terrain models 08 p1113 N90-16445
Evaluation of the use of flat terrain models versus complex terrain screening models in estimating pollutant transport and deposition in complex terrain
[DE90-005271] 09 p1245 N90-17223
Development of an automatic ground collision avoidance system using a digital terrain database
[AD-A216247] 10 p1318 N90-17621
A computer simulation study of a sensor-based heuristic navigation for three-dimensional rough terrain with obstacles
[AD-A215115] 10 p1318 N90-17622
On multiple edge diffraction and multiple reflections of microwaves over terrain
[AD-A216418] 10 p1377 N90-17985
An Autonomous Platform Simulator (APS)
[AD-A215768] 10 p1392 N90-18048
Study of alteration covers of part of the Sao Paulo State through remote sensing data
[INPE-4849-TDL/364] 10 p1399 N90-18086
Project Floval: Correction of relief effects in eucalyptus reforestration
[INPE-4814-RPE/590] 11 p1525 N90-18777
An evaluation of an airborne laser profiling system for high precision terrain mapping
[AD-A217025] 11 p1525 N90-18780
SPOT for landscape: Development of a method for the use of SPOT pictures for the updating of the data base scale of the landscape
[BCRS-89-18] 11 p1526 N90-18787

Heli/SITAN: A terrain referenced navigation algorithm for helicopters
[DE90-005193] 12 p1602 N90-19217
A method for determination of control pixels for LANSAT using a reflector
[INPE-4884-PRE/1491] 12 p1677 N90-19632
Visibility problems in numerical models of terrain
[INPE-4921-TDL/382] 12 p1726 N90-19919
A split-and-merge method for creating polygonal homogeneous-vegetation regions from digitized terrain data
[AD-A218080] 13 p1821 N90-20453
Simulation of landscape disturbances and the effect of climatic change
[DE90-007565] 13 p1829 N90-20503
The use of high-resolution terrain data in gravity field prediction 13 p1835 N90-20533
Proceedings of the 4th European Conference, volume 2
[AD-A216521] 14 p1986 N90-21382
Millimeter-wave bistatic scattering by terrain 15 p2085 N90-21936
Optimal helicopter trajectory planning for terrain following flight
[NASA-CR-186470] 17 p2349 N90-23376
Millimeter - wave radar scattering from terrain: Data handbook
[AD-A220770] 17 p2391 N90-23617
Automated segmentation and extraction of area terrain features from radar imagery
[AD-A221096] 18 p2544 N90-24522
Planning for execution monitoring on a planetary rover 19 p2735 N90-25548
Evaluation of off-road terrain with static stereo and monoscopic displays 19 p2740 N90-25575
Remote sensing of Earth terrain
[NASA-CR-186686] 20 p2880 N90-26382
Vandenberg Boundary Layer Survey (VBLS): Results
[AD-A222517] 21 p3031 N90-27234
Simple graphical descriptions of natural land profiles and the application of fractal and sub-fractal models to them
[RSRE-MEMO-4305] 22 p3195 N90-28130
An evaluation of three models designed for siting wind turbines in areas of complex terrain
[DE90-013625] 22 p3196 N90-28137
Wind tunnel simulation of Antarctic snowdrifting
[PB90-184565] 22 p3212 N90-28222
Multiband imaging systems
[AD-A223969] 23 p3343 N90-28893
Learned navigation in unknown terrains: A retraction method 23 p3368 N90-29029
First results in terrain mapping for a roving planetary explorer 23 p3375 N90-29066

TERRAIN ANALYSIS
Image-based terrain modeling with thematic mapper applied to resolving the limit of Holocene Lake expansion in the Great Salt Lake Desert, Utah, part 1
[NASA-CR-185913] 01 p0082 N90-10465
ONR/NORDA Workshop on Terrain Analysis and Quantitative Geomorphology
[AD-A210464] 01 p0086 N90-10489
Flight testing of the Tornado Terrain Following System 02 p0153 N90-10875
Effects of the advanced map interpretation and terrain analysis course on contour-level navigation performance
[AD-A212163] 03 p0304 N90-11723
Visualization of high-resolution digital terrain
[AD-A212149] 04 p0515 N90-12971
Spatial data structures for robotic vehicle route planning
[AD-A212806] 04 p0538 N90-13111
Reflection indicatrices of natural surfaces for AVHRR channels 1 and 2
[DLR-MITT-89-16] 05 p0664 N90-13882
Advances in techniques and technologies for air vehicle navigation and guidance
[AGARD-AR-276] 08 p1020 N90-15899
Recent developments in TERPROM 09 p1163 N90-16732
Terrain-aided navigation and target acquisition on the AFTI/F-16 09 p1166 N90-16747
Active and passive remote sensing of ice
[AD-A214863] 09 p1241 N90-17199
An evaluation of an airborne laser profiling system for high precision terrain mapping
[AD-A217025] 11 p1525 N90-18780
Fourier transform methods in local gravity modeling 13 p1836 N90-20538
Three-dimensional route planning for a cruise missile for minimal detection by observer
[AD-A218336] 13 p1880 N90-20787
Generation of triangular form models in a microcomputer environment
[INPE-4974-PRE/1539] 14 p1997 N90-21447
Digital terrain elevation data compact disk-read only memory prototype evaluation
[AD-A218545] 17 p2442 N90-23915
Reflection indicatrices of natural surfaces for AVHRR channels 1 and 2
[ESA-TT-1192] 19 p2709 N90-25417
Technical evaluation report on the Guidance and Control Panel 49th Symposium on Fault Tolerant Design Concepts for Highly Integrated Flight Critical Guidance and Control Systems
[AGARD-AR-281] 20 p2813 N90-26012
Improving the geometric fidelity of imaging systems employing sensor arrays
[NASA-CASE-NPO-17970-1-CU] 20 p2880 N90-26384
The production potential of wind power in Finland
[DE90-796157] 22 p3196 N90-28138
Description of the MARC measuring system
[FEL-89-B170] 23 p3342 N90-28887
Survivable penetration 24 p3428 N90-29363
A land navigation demonstration vehicle with a color map display for tactical use 24 p3430 N90-29375
Terrain visual cue analysis for simulating low-level flight: A multidimensional scaling approach
[AD-A223564] 24 p3436 N90-29407

TERRAIN FOLLOWING AIRCRAFT
Model-based method for terrain-following display design
[AD-A219302] 16 p2201 N90-22563
Application of optimal tracking methods to aircraft terrain following
[AD-A221099] 18 p2496 N90-24264
A study of terrain following systems and the creation of flight paths for terrain following vehicles
[FOA-C-20774-2.5] 22 p3114 N90-27691

TERRESTRIAL MAGNETISM
U GEOMAGNETISM

TERRESTRIAL PLANETS
NT EARTH (PLANET)
NT MARS (PLANET)
NT MERCURY (PLANET)
NT VENUS (PLANET)
Tectonic history of the terrestrial planets
[NASA-CR-186309] 09 p1246 N90-17229
Large impact events and atmospheric evolution on the terrestrial planets 12 p1744 N90-20028

TERRESTRIAL RADIATION
South Pole surface radiation balance measurements, April 1986 to February 1988
[PB89-224018] 04 p0519 N90-12993
Impact of cirrus on the surface radiative environment at the FIRE ETLA Palisades, NY site 22 p3221 N90-28270

TEST BEDS
U TEST STANDS

TEST CHAMBERS
NT ANECHOIC CHAMBERS
NT HYPERBARIC CHAMBERS
NT PRESSURE CHAMBERS
NT VACUUM CHAMBERS
The Environmental Test Centre at ESTEC (an overview) 02 p0187 N90-11064
An atmospheric pressure flow reactor: Gas phase kinetics and mechanism in tropospheric conditions without wall effects 02 p0203 N90-11160
The behavior of hydrazine vapor in an environmental chamber under simulated atmospheric conditions 02 p0203 N90-11161
Modeling of hydrazine surface interactions in environmental reaction chambers 02 p0203 N90-11162
Surface-catalyzed air oxidation reactions of hydrazines: Tubular reactor studies 02 p0204 N90-11167
Performance evaluation of the Puritan-Bennett crew-member portable protective breathing device as prescribed by portions of FAA action notice A-8150.2
[AD-A211113] 06 p0821 N90-14772
The NASA Langley 0.3-meter transonic cryogenic tunnel 08 p1028 N90-15941
Numerical study of unsteady flows in large air-driven blast simulators with single and multiple drivers
[UTIAS-334] 17 p2405 N90-23699
Self-calibrating apparatus to find dynamic compressibility of organic solids
[AD-A219780] 17 p2415 N90-23763
The behaviour of the L3 muon chambers in a magnetic field
[ETN-90-96920] 18 p2613 N90-24884
Research at NASA's NFAC wind tunnels
[NASA-TM-102827] 20 p2801 N90-25933
The aims and history of adaptive wall wind tunnels 21 p2962 N90-26839
Analysis and design of modifications for improved performance of the AFIT radar cross section measurement chamber
[AD-A223352] 24 p3460 N90-29545

TEST EQUIPMENT
Ignitability test method and apparatus
[NASA-CASE-LAR-13996-1-SB] 07 p0893 N90-15161
Solar cell electrodynamic characteristics test equipment 10 p1344 N90-17791
Control structure interaction instrumentation
[AD-A221375] 19 p2693 N90-25320
Using embedded microcontrollers in radar test equipment
[DE90-014997] 23 p3319 N90-28763
Test and training simulator for ground-based teleoperated in-orbit servicing 24 p3510 N90-29843
The laboratory telerobotic manipulator program 24 p3515 N90-29869
The telerobot workstation testbed for the shuttle aft flight deck: A project plan for integrating human factors into system design 24 p3518 N90-29887
Next generation space robot 24 p3520 N90-29899

TEST FACILITIES
NT ANECHOIC CHAMBERS
NT BALLISTIC RANGES
NT CRYOGENIC WIND TUNNELS
NT ENGINE TESTING LABORATORIES
NT HOTSHOT WIND TUNNELS
NT HYDRAULIC TEST TUNNELS
NT HYPERSONIC WIND TUNNELS
NT HYPERVELOCITY WIND TUNNELS
NT LOW DENSITY WIND TUNNELS
NT LOW SPEED WIND TUNNELS
NT PLASMA JET WIND TUNNELS
NT ROCKET TEST FACILITIES
NT SLOTTED WIND TUNNELS
NT SUBSONIC WIND TUNNELS
NT SUPERSONIC WIND TUNNELS
NT TEST RANGES
NT TEST STANDS
NT TRANSONIC WIND TUNNELS
NT TRISONIC WIND TUNNELS
NT WIND TUNNELS
The aerospace energy systems laboratory: Hardware and software implementation
[NASA-TM-101706] 01 p0107 N90-10610
Astrometric telescope facility. Preliminary systems definition study. Volume 3: Cost estimate
[NASA-TM-89429-VOL-3] 01 p0140 N90-10808
US Navy principal site testing concept and the F-18 02 p0151 N90-10861
The Air Force Flight Test Center Flight Test Safety Program 02 p0153 N90-10872
Air Combat Environment Test and Evaluation Facility (ACETEF) 02 p0154 N90-10883
Flight simulation test facility: Function and specification of the simulator cockpit system
[NAL-TM-577] 02 p0157 N90-10899
Research and test facilities for development of technologies and experiments with commercial applications
[NASA-TM-101789] 02 p0159 N90-10909
Spacecraft Structures and Mechanical Testing
[ESA-SP-289] 02 p0176 N90-10986
Comparison of phase resonance, mode separation, and driven-base modal identification methods applied to the FLECS test structure 02 p0181 N90-11027
Development of a thermoacoustic test facility 02 p0183 N90-11041
Space environment effects on carbon/epoxy materials 02 p0185 N90-11056
The Environmental Test Centre at ESTEC (an overview) 02 p0187 N90-11064
Two years experience with the ESTEC multishaker system 02 p0187 N90-11065
New data handling system (MDH) for mechanical tests at ESTEC 02 p0187 N90-11066
The large European Acoustic Facility at ESTEC 02 p0187 N90-11067
Tamaris: A new European facility for low frequency multi-axis vibration simulation 02 p0187 N90-11068
A new European vibration test facility for Ariane 4 class satellites 02 p0187 N90-11070
Spacelab system analysis Marshall Avionics System Testbed (MAST)
[NASA-CR-183804] 03 p0317 N90-11802
The fault monitoring and diagnosis knowledge-based system for space power systems: AMPERES, phase 1
[NASA-CR-185486] 04 p0464 N90-12654
Dynamic testing techniques and applications for an aeroelastic rotor test facility 05 p0584 N90-13406
Definition of avionics concepts for a heavy lift cargo vehicle. Volume 1: Executive summary
[NASA-CR-183818] 06 p0725 N90-14229
Definition of avionics concepts for a heavy lift cargo vehicle, volume 2
[NASA-CR-183819] 06 p0725 N90-14230

Thermal environmental tests on space simulation chamber
[DE90-000927] 06 p0729 N90-14251
Flame acceleration studies in the MINIFLAME facility
[DE90-000041] 06 p0740 N90-14310
VIBRAFUGE: Combined vibration and centrifuge testing
[DE90-001091] 07 p0884 N90-15114
Hugoniot measurements with the LLNL electric gun facility
[DE90-002809] 07 p0885 N90-15119
Instrumentation for a facility for the test, analysis and active control of spacecraft truss structures
[AD-A213655] 07 p0886 N90-15124
NTES (Nuclear Test and Experimental Sciences) program laser facility for physics experiments Building 391 High Bay Option
[DE90-001795] 07 p0935 N90-15411
The design and performance of a general purpose 57 kilowatt solar array simulator for current and future large spacecraft 10 p1330 N90-17685
Simulation of the dynamic environment for missile component testing: Demonstration
[AD-A216979] 11 p1466 N90-18443
Preliminary design of a pointer for movement of a solar simulator
[INPE-4864-TDL/375] 11 p1517 N90-18736
Resource Assessment Project: User needs survey results
[DE89-009502] 11 p1529 N90-18802
Thermal vacuum life test facility for radioisotope thermoelectric generators
[DE90-007148] 11 p1566 N90-19010
The Uniform Engine Test Programme
[AGARD-AR-248] 12 p1604 N90-19232
Marshall Avionics Testbed System (MAST)
12 p1639 N90-19417
Sandia National Laboratories' new high level acoustic test facility
[DE90-006810] 12 p1710 N90-19820
Relevance of laboratory studies to comets
12 p1743 N90-20023
High-Explosives Applications Facility (HEAF)
[DE90-008122] 13 p1787 N90-20257
Nine-year aging behavior of the ceramic flatpack resonator
[DE90-008044] 13 p1813 N90-20412
Diagnostic development and support of MHD (Magnetohydrodynamics) test facilities
[DE90-004969] 13 p1890 N90-20845
A corrosion fatigue/stress corrosion testing facility at Materials Research Laboratory
[MRL-TN-568] 14 p1929 N90-21044
Liquid Transfer Cryogenic Test Facility: Initial hydrogen and nitrogen no-vent fill data
[NASA-TM-102572] 14 p1972 N90-21295
A dynamic motion simulator for future European docking systems 15 p2113 N90-22085
Prevention of significant deterioration application for approval to construct SP-100 Ground Engineering System Test Site
[DE90-007986] 15 p2166 N90-22381
MHD channel development, part 4
[DE90-009552] 15 p2169 N90-22397
Design and construction of a packed column simulator operating under atmospheric and reduced pressure
[ISAL-89-60] 16 p2236 N90-22757
National emissions standards for hazardous air pollutants application for approval of construction SP-100 ground engineering system test site
[DE90-007985] 16 p2316 N90-23203
A test matrix sequencer for research test facility automation
[NASA-TM-103108] 17 p2357 N90-23416
Servicing test facility: A hardware simulator for telerobotic in-orbit servicing 18 p2501 N90-24287
HERA teleoperation test facility
18 p2503 N90-24303
A flexible teleoperation test bed for human factors experimentation 18 p2503 N90-24304
DDTF improvements for more accurate space docking simulation 18 p2504 N90-24311
Groundbased simulations of in-orbit operations
18 p2505 N90-24314
Simulation and ground-based testing of ORU-handling with a bi-arm robot 18 p2505 N90-24317
ROSED: Robotic Servicing Demonstrator
18 p2505 N90-24318
Flexible test bed for space telepresence and telemanipulation research 18 p2508 N90-24334
Solar thermal program summary. Volume 2: Research summaries
[DE89-009476] 18 p2576 N90-24674
Rome air development center cryo test facility
[AD-A220067] 19 p2662 N90-25147
High-temperature test facility at the NASA Lewis engine components research laboratory
[NASA-TM-103143] 19 p2662 N90-25151
Conceptual definition of a high voltage power supply test facility
[NASA-CR-185216] 19 p2666 N90-25172
Expanded damage test facilities at LLNL
[DE90-011466] 19 p2695 N90-25336
Use of the TACL system at CEBAF for control of the cryogenic test facility
[CEBAF-PR-89-024] 19 p2755 N90-25652
Comparative assessment of world research efforts on magnetic confinement fusion 19 p2759 N90-25680
Wright Research and Development Center test facilities handbook
[AD-A222582] 20 p2815 N90-26020
National space test centers, Lewis research center facilities
[NASA-TM-103187] 20 p2817 N90-26030
High temperature multiaxiale creep testing of Nimonic 115
[RAE-TM-P-1182] 20 p2835 N90-26122
Bringing aircraft noise testing down to Earth
[PNR90642] 20 p2924 N90-26637
Facilities for improving evaluations of electromagnetic susceptibilities of weapon systems and electronic equipment
[PB90-155862] 21 p2961 N90-26837
SP-100 design, safety, and testing
[DE90-012643] 21 p3075 N90-27484
Design of the UETP experiment
22 p3118 N90-27712
Comparison of altitude test cell results
22 p3119 N90-27715
Comparison of ground-level test cells and ground-level to altitude test cells 22 p3119 N90-27716
General test plan 22 p3120 N90-27721
Requirements for long-life operation of inert gas hollow cathodes: Preliminary report
[NASA-TM-103242] 22 p3134 N90-27783
Source emission test of gas turbine engine test facility, Kelly AFB, TX
[AD-A223869] 23 p3282 N90-28571
Oxygen/hydrogen technology test bed status update
23 p3290 N90-28613
Flight test engineering with the ATTAS
23 p3391 N90-29160
An introductory guide preparing to use the ESTEC environmental test facilities
[ESA-TM-05] 24 p3438 N90-29419
Test and training simulator for ground-based teleoperated in-orbit servicing 24 p3510 N90-29843
Diagnostic development and support of MHD test facilities
[DE90-015403] 24 p3550 N90-30083

TEST FIRING
QM-8 field joint protection system, volume 7
[NASA-CR-183748] 05 p0614 N90-13586
Space shuttle Production Verification Motor 1 (PV-1) static fire
[NASA-CR-183784] 08 p1037 N90-15991
Vulcain engine development status
09 p1176 N90-16810
Technique for evaluating the erosive properties of ablative internal insulation materials
11 p1471 N90-18466
Technical Evaluation Motor no. 5 (TEM-5)
[NASA-CR-183932] 14 p1942 N90-21117
A comparison between experiment and simulation for concept VIC regenerative liquid propellant guns. Part 1: 30 mm
[AD-A218556] 16 p2225 N90-22692
First Vulcain engine test results
[MBB-UK-0054/88-PUB] 19 p2652 N90-25093
Rocket engine failure detection using system identification techiques
[NASA-CR-185259] 19 p2664 N90-25159
Supersonic combustor testing
20 p2811 N90-25998
Ceramic matrix composites in simulated SSME environments 23 p3298 N90-28655

TEST PATTERN GENERATORS
Built-in generation for CMOS circuits
[IMAG-RR-736-I] 04 p0496 N90-12855
Design for testability of stuck-open and stack-on CMOS combinatorial circuits
[REPT-89-044] 16 p2230 N90-22725
Contribution to CMOS integrated circuit tests: Study of the stuck-on and stuck-open fault tests
[ETN-90-97256] 20 p2859 N90-26261

TEST PILOTS
Voice measures of workload in the advanced flight deck: Additional studies
[NASA-CR-4258] 17 p2437 N90-23887

TEST RANGES
NT BALLISTIC RANGES
The psychology of computer displays in the modern mission control center
[NASA-TM-100451] 15 p2137 N90-22213
Development of an optimized compact test range
[MBB-0053/88-PUB] 19 p2651 N90-25085
Space test range
[AD-A223259] 21 p2964 N90-26850

TEST STANDS
Design of a thrust stand for high power electric propulsion devices
[NASA-TM-102372] 08 p1037 N90-15992
The 120 VDC test bed for Columbus power system
10 p1329 N90-17679
Feasibility demonstration of a 445N high-performance rocket engine 11 p1473 N90-18481
Analysis of small-scale rotor hover performance data
[NASA-TM-102271] 13 p1799 N90-20325
Experimental identification of helicopter engine dynamics from closed loop data
22 p3104 N90-27627
Energy Efficient Engine acoustic supporting technology report
[NASA-CR-174834] 23 p3279 N90-28557
Liquid Rocket Booster (LRB) for the Space Transportation System (STS) systems study. Appendix E: Pressure-fed booster test bed for the liquid rocket booster study
[NASA-CR-183791-APP-E] 23 p3289 N90-28605
Development of a flexible test-bed for robotics, telemanipulation and servicing research
23 p3364 N90-29012
The NASA/OAST telerobot testbed architecture
23 p3365 N90-29016
Control of a Cossor CSP1250 ionospheric simulator in an automated HF test bed
[AD-A223446] 24 p3461 N90-29549

TEST VEHICLES
NT FLIGHT TEST VEHICLES
An Autonomous Platform Simulator (APS)
[AD-A215768] 10 p1392 N90-18048
Vehicle acceleration and fuel consumption when operated on JP-8 fuel
[AD-A216275] 10 p1393 N90-18055

TESTERS
U TEST EQUIPMENT

TESTES
Experiment K-6-16. Morphological examination of rat testes. The effect of Cosmos 1887 flight on spermatogonial population and testosterone level in rat testes
20 p2895 N90-26469

TESTING MACHINES
U TEST EQUIPMENT

TESTING TIME
VLSI integrated circuit tests
[IMAG-RR-763-I] 08 p1061 N90-16135

TETHERED BALLOONS
The radiation budget of stratocumulus clouds measured by tethered balloon instrumentation: Variability of flux measurements 22 p3216 N90-28242
Structural analysis of stratocumulus convection
22 p3216 N90-28243

TETHERED SATELLITES
Aeritalia Space Systems Group, Turin, Italy
[EOARD-LR-89-041] 02 p0159 N90-10908
Shuttle relative navigation of a tethered satellite mission with current on board software
05 p0588 N90-13423
Impact of tether cutting on onboard navigation during the Tethered Satellite Mission-1
05 p0588 N90-13424
Shuttle tethered operations: The effect on orbital trajectory and inertial navigation
05 p0588 N90-13425
Hollow-cathode experiments to support electrodynamic tether applications
[IFSI-89-5] 08 p1036 N90-15986
Electrical characteristics measurements for the TSS-1 satellite painting
[IFSI-89-7] 08 p1036 N90-15987
RETE experiment activity at the TSS-1 POCC
[IFSI-89-12] 08 p1036 N90-15988
Kalman estimation for SEDS measurements
12 p1634 N90-19393
A vectorized algorithm for 3D dynamics of a tethered satellite 12 p1640 N90-19423
Perspective features of the tethered systems for space applications
[ETN-90-97279] 20 p2822 N90-26059
Possible applications of tethered systems to Mars exploration missions
[IAF-89-489] 20 p2822 N90-26060
Dynamics and dynamics experiments in TSS-1
22 p3129 N90-27758
Flight mechanics applications for tethers in space: Cooperative Italian-US programs
22 p3131 N90-27770

TETHERING
The space station tethered elevator system
[NASA-CR-186051] 06 p0732 N90-14265
Kalman estimation for SEDS measurements
12 p1634 N90-19393
Dynamics and control of tethered antennas/reflectors in orbit
[AD-A219316] 16 p2207 N90-22594
SEDS experiment design definition
[NASA-CR-183909] 19 p2665 N90-25165
Perspective features of the tethered systems for space applications
[ETN-90-97279] 20 p2822 N90-26059
Possible applications of tethered systems to Mars exploration missions
[IAF-89-489] 20 p2822 N90-26060
Dynamics and dynamics experiments in TSS-1
22 p3129 N90-27758
A new method for a tethered system aided space station assembly 22 p3130 N90-27765
Flight mechanics applications for tethers in space: Cooperative Italian-US programs
22 p3131 N90-27770

TETHERLINES
Impact of tether cutting on onboard navigation during the Tethered Satellite Mission-1
05 p0588 N90-13424
Modeling and control of the rapid deployment of towed airborne devices 07 p0879 N90-15092
Radiation of plasma waves from large space structures in low earth orbit
[AD-A215062] 09 p1182 N90-16856
A new method for a tethered system aided space station assembly 22 p3130 N90-27765
Flight mechanics applications for tethers in space: Cooperative Italian-US programs
22 p3131 N90-27770

TETRACHLOROMETHANE
U CARBON TETRACHLORIDE

TETRAFLUOROHYDRAZINE
Synthesis of tetrafluorohydrazine
[AD-D014281] 08 p1052 N90-16083

TETRAGONS
NT RECTANGLES
NT RHOMBOIDS
NT SQUARES (MATHEMATICS)
NT TRAPEZOIDS

TETRAHEDRONS
Component count and preliminary assembly considerations for large space truss structures
[NASA-TM-102604] 13 p1763 N90-20121
Ionic equilibrium between octahedral and tetrahedral complexes in liquid aluminium-sodium fluoride mixtures
[DE90-613690] 14 p1948 N90-21150
Unstructured mesh generation by a generalized Delaunay algorithm 15 p2096 N90-21995
The tetrahedral wedge attachment mechanism
18 p2539 N90-24490
Parallelization of an annealing simulation applied to improving tetrahedric grids
[IMAG-RR-796-M] 20 p2913 N90-26570

TETRAHYDROFURAN
Thermal crystallization of polytetrahydrofuran networks
[AD-A215336] 10 p1436 N90-18285

TETRANITROTETRAZACYCLOOCTANE
U HMX

TEXAS
Texstar: The all-Texas educational satellite system
[NASA-CR-186654] 20 p2820 N90-26045

TEXTBOOKS
Missile aerodynamics
[ISBN-0-9620629-0-1] 18 p2490 N90-24236
Rhetorical structure theory and text analysis
[AD-A222655] 20 p2941 N90-26733

TEXTILES
NT COTTON FIBERS
NT RAYON
RTM user's guide
[NASA-CR-186091] 04 p0531 N90-13065
Calculation of nonlinear viscoelastic processes for plastic layer textile membranes
[ETN-90-95868] 12 p1675 N90-19622
Manufacturing and mechanical properties of new textile fiber preforms for structural sandwich applications
[MBB-Z-0296-90-PUB] 21 p2972 N90-26895
Influence of microslidings on the macroscopic behavior of composite textiles
[ETN-90-97459] 22 p3154 N90-27880

TEXTS
Differences in writers initial task representations
[AD-A210433] 01 p0136 N90-10788
The design and implementation of an intelligent interface for information retrieval 06 p0858 N90-14991
Knowledge based text generation
[AD-A214273] 07 p0977 N90-15645
Approaches to the planning of coherent text
[AD-A216463] 11 p1545 N90-18895
Desk top publishing: What you need to know
15 p2178 N90-22449
Electronic publishing with Standard Generalized Markup Language (SGML) 15 p2179 N90-22450
The rationale and specification of the ELLA graphics systems
[RSRE-89017] 20 p2909 N90-26548
The speech signal 21 p2992 N90-27008
Current methods of digital speech processing
21 p2993 N90-27010
Further research on heading in text
[AD-A221511] 21 p3087 N90-27557
The SPECIALIST: Natural language processing system
[PB90-240029] 23 p3381 N90-29098
Textual regularities applicable to full text searching: The case of family history literature
24 p3557 N90-30125

TEXTURES
Radon transform analysis of a probabilistic method for image generation
[AD-A207814] 01 p0123 N90-10702
Collective-mode spectroscopy of textures in superfluid (3)He-B
[PB89-221634] 03 p0413 N90-12370
Development of texture analysis and its applications to titanium aero engine components
[PNR90561] 04 p0454 N90-12602
Textural and structural organization of the heat treated polymers: Mechanical properties relationships
[ETN-89-95711] 04 p0478 N90-12744
Methods for the mineralogical and textural analysis of comet nucleus samples 08 p1147 N90-16648
Shape from focus
[AD-A215959] 10 p1393 N90-18052
Study of alteration covers of part of the Sao Paulo State through remote sensing data
[INPE-4849-TDL/364] 10 p1399 N90-18086
Classification of high resolution imagery using texture attributes
[INPE-4888-TDL/379] 11 p1525 N90-18778
Visual processing in texture segregation
[AD-A216539] 12 p1696 N90-19737
Texture segmentation using localized spatial filtering
[AD-A218064] 13 p1869 N90-20722
Characterization of linear structures from remote sensing data; Espinhaco Meridional (MG) sierra
[INPE-4905-PRE/1506] 14 p1997 N90-21449
Gravitational effects of global textures
[NASA-CR-186596] 15 p2189 N90-22503
Cloud field classification based on textural features
18 p2646 N90-25066
Texture of materials by time-of-flight neutron diffraction
[DE90-008968] 20 p2830 N90-26096
Pattern classification of textura by moment and distance autocorrelation function
[INPE-4976-PRE/1541] 20 p2879 N90-26379
Classification regions in remote sensing imagery utilizing spatial characteristics
[INPE-4913-PRE/1514] 20 p2879 N90-26381
Detecting perceptual groupings in textures by continuity considerations 21 p3045 N90-27310
Autoregressive-moving average models for texture classification
[INPE-4987-PRE/1549] 23 p3380 N90-29092
A global approach to image texture analysis
[AD-A223532] 24 p3527 N90-29941

TFX AIRCRAFT
U F-111 AIRCRAFT

THAILAND
Applied atmospheric resources research program in Thailand
[PB89-235402] 05 p0668 N90-13903

THALAMUS
Extrathalamic modulation of cortical function
[AD-A211044] 01 p0094 N90-10535

THALLIUM
Novel superconducting phases of Tl-based compounds 22 p3150 N90-27862
High T(sub c) copper-oxide superconductors
[AD-D014483] 22 p3247 N90-28416

THALLIUM COMPOUNDS
Cation disordering in the Tl-2122 superconductors
[DE90-003579] 07 p1001 N90-15795
Hyper- and hypobaric processing of Tl-Ba-Ca-Cu-O superconductors
[DE90-005637] 10 p1437 N90-18292
Highly-textured thallium-barium-calcium-copper-oxide polycrystalline superconducting films on silver substrates
[DE90-011972] 18 p2627 N90-24970
Preparation and magnetic measurements of single crystal Tl2Ba2CaCu2O8
[DE90-013657] 21 p3081 N90-27519
An explanation for the rise in T(sub c) in the Tl- and Bi-based high temperature superconductors
22 p3142 N90-27822
Magnetism and superconductivity of some Tl-Cu oxides 22 p3143 N90-27829

THAWING
U MELTING

THEMATIC MAPPERS (LANDSAT)
Image-based terrain modeling with thematic mapper applied to resolving the limit of Holocene Lake expansion in the Great Salt Lake Desert, Utah, part 1
[NASA-CR-185913] 01 p0082 N90-10465
Spatial characterization of acid rain stress in Canadian Shield Lakes
[NASA-CR-183446] 01 p0084 N90-10479
Investigation of the usefulness of LANDSAT 5 thematic mapper data for mapping forest disease
[DFVLR-FB-89-06] 03 p0365 N90-12088
Signature analysis and classification of pine of different vitality classes using airborne thematic mapper data
[DFVLR-FB-89-07] 03 p0365 N90-12089
An attempt to draw conclusions from the vegetation to the geological underground in the area of Amberg (Germany, F.R.) by means of digital image processing of TM data
[DFVLR-FB-89-24] 04 p0515 N90-12974
Computer-aided boundary delineation of agricultural lands
[NASA-TM-102243] 08 p1091 N90-16313
Image segmentation by iterative parallel region growing with application to data compression and image analysis
08 p1114 N90-16452
Improvement of classification results from satellite imagery to update and differentiate land use classes on topographic maps
[BCRS-89-17] 11 p1526 N90-18786
LANDSAT Thematic Mapper for hydrogeological mapping in Egypt
[BCRS-89-28] 11 p1527 N90-18791
The potential of combined use of satellite data with topographic TM information for manual/visual and digital updating of land use
[NLR-MP-88021-U] 12 p1678 N90-19639
Analysis of nonlinear internal waves observed by LANDSAT-TM
[PREPRINT-704] 16 p2249 N90-22828
Operational digital land use map 1:50,000; investigation of a multiple automatic classification based on SPOT and LANDSAT Thematic Mapper satellite pictures
[BCRS-89-10] 17 p2419 N90-23784
Atmospheric correction of satellite pictures in the framework of the project Friese Fronten
[BCRS-89-12] 17 p2419 N90-23786
The use of satellite pictures of the Ysselmeer region (Netherlands). Optimization of the use of LANDSAT for water quality applications in the Ysselmeer region
[BCRS-89-31] 18 p2575 N90-24670
MARS (Monitoring Agro-ecological Resources with Remote sensing and Simulation) definition study: Results of the preparatory phase
[REPT-17] 19 p2706 N90-25395
Seasonal LAI in slash pine estimated with LANDSAT TM
[NASA-TM-102278] 19 p2706 N90-25397
Calibration of the visible and near-infrared channels of the LANDSAT-5 Thematic Mapper using high-altitude aircraft measurements
[NASA-TM-102185] 21 p3015 N90-27138

THEMATIC MAPPING
Investigation of the usefulness of LANDSAT 5 thematic mapper data for mapping forest disease
[DFVLR-FB-89-06] 03 p0365 N90-12088
Signature analysis and classification of pine of different vitality classes using airborne thematic mapper data
[DFVLR-FB-89-07] 03 p0365 N90-12089
An attempt to draw conclusions from the vegetation to the geological underground in the area of Amberg (Germany, F.R.) by means of digital image processing of TM data
[DFVLR-FB-89-24] 04 p0515 N90-12974
Overview of the Hipparcos payload
05 p0603 N90-13503
The detectors 05 p0604 N90-13507
Standard stars and photometric calibration
05 p0607 N90-13539
Analysis of the star mapper data
05 p0609 N90-13551
Photometry: Main mission and Tycho
05 p0610 N90-13560
Experiments towards a global sphere solution
05 p0612 N90-13576
Summaries of the thematic conferences on remote sensing for exploration geology
[NASA-CR-185321] 05 p0664 N90-13880

The use of LANDSAT-TM data for the management of pine forestations in central Chile
[DLR-FB-89-44] 05 p0664 N90-13881
The visible channel of OMEGA-VIMS
[IFSI-89-14] 08 p1077 N90-16231
Forest mapping Nuerenberg German national forest with special emphasis on the spectral reflection behavior of pine trees 08 p1093 N90-16328
Attempt to draw conclusions concerning the geological subsoil from the vegetation using digital image processing of TM data 08 p1093 N90-16329
TM land use classification of a region. Utilization for planning and statistics 08 p1095 N90-16339
Eutrophication assessment through remote sensing techniques
[INPE-4932-PRE/1422] 10 p1398 N90-18083
Study of alteration covers of part of the Sao Paulo State through remote sensing data
[INPE-4849-TDL/364] 10 p1399 N90-18086
Monitoring of reforested areas through digital analysis of TM data
[INPE-4930-PRE/1420] 11 p1522 N90-18764
Evaluation of selection techniques for multispectral bands employed in the discrimination of carbonatic rocks
[INPE-4850-TDL/365] 11 p1522 N90-18765
Radiometric study of wheat and bean crops in three types of latossolo
[INPE-4843-PRE/1472] 11 p1523 N90-18767
Relationships between spectral parameters and agronomics of wheat and beam crops
[INPE-4791-RPE/584] 11 p1523 N90-18768
Remote sensing applied to vegetation as subsidized in municipal planning
[INPE-4908-PRE/1509] 11 p1523 N90-18770
Evaluation of TM/LANDSAT and HRV/SPOT data in reforested areas
[INPE-4575-RPE/567] 11 p1524 N90-18772
Perspective revision of systematic mapping through orbital imagery
[INPE-4817-PRE/1453] 11 p1524 N90-18775
Physiognomy of vegetation cover in the PNPM identified through the TM/LANDSAT sensor: A multitemporal analysis
[INPE-4834-PRE/1464] 11 p1525 N90-18776
Project Floval: Correction of relief effects in eucalyptus reforestration
[INPE-4814-RPE/590] 11 p1525 N90-18777
On the applicability of CAESAR for the remote sensing of bottom depth and bottom composition of shallow waters: A model study
[BCRS-89-13] 11 p1526 N90-18783
LANDSAT Thematic Mapper for hydrogeological mapping in Egypt
[BCRS-89-28] 11 p1527 N90-18791
Quantification of structural field data in the Rio Grande do Norte basin and neighborhood
[INPE-4821-RPE/591] 11 p1533 N90-18826
Areas of aquatic macrophytes classified through vegetative indexes extracted from LANDSAT/TM imagery
[INPE-4880-PRE/1489] 12 p1677 N90-19633
Thematic coupling between digital images and geographic information systems
[ETN-90-95723] 12 p1679 N90-19646
Evaluation of TM/LANDSAT and HRV/SPOT data in the identification of reforested areas in the Mogi-Guacu (SP) region
[INPE-4874-PRE/1485] 13 p1819 N90-20442
Utilization of LANDSAT-5 and NOAA-9 satellite imagery in the identification of physical-chemical parameters of the water in the Guanabara Bay
[INPE-4761-TDL/349] 13 p1819 N90-20445
Geobotanical remote sensing: A review
[INPE-5026-PRE/1565] 14 p1996 N90-21440
Survey of land use through remote sensing
[INPE-5032-MD/042] 14 p1996 N90-21443
Digital processing of TM/LANDSAT data in monitoring interior water
[INPE-4956-PRE/1533] 14 p1997 N90-21448
Analysis of water quality parameters of the Piaui River (SE), Brazil, through field and TM/LANDSAT sensor data
[INPE-4918-PRE/1417] 14 p1998 N90-21453
Evaluation of the mangrove areas of the Rio Piaui (SE) through remote sensing
[INPE-4909-PRE/1510] 14 p1998 N90-21454
Evaluation of classification performance and proportion estimate of the sugar cane crop through PROCEDURE-INPE utilizing LANDSAT data
[INPE-4899-PRE/1500] 14 p1999 N90-21458
Performance evaluation of morphological edge detectors
[INPE-4975-PRE/1540] 14 p2000 N90-21464
A case for archaeological reconnaissance of the Cabo Catoche-Porvenir region of the northeastern Yucatan Peninsula
[NASA-TM-102248] 16 p2249 N90-22827
Sea bottom topography with X-band SLAR
[BCRS-89-25] 17 p2431 N90-23854
Multisensor monitoring of deforestation in the Guinea Highlands of West Africa
[NASA-CR-186709] 19 p2706 N90-25396
Atmospheric correction of thematic mapping measurements about seabeds of the German Bay
[GKSS-89/E/47] 20 p2816 N90-26029
INPE geographic data base
[INPE-4636-PRE/1348] 23 p3407 N90-29253

THEODOLITES
Experiences with modern absolute instruments 21 p3022 N90-27183

THEOREM PROVING
Parallel inference based on delta processing
[CWI-CS-R8846] 02 p0261 N90-11482
A dynamic proof of the Frobenius-Perron theorem for Metzler matrices
[AD-A211839] 03 p0392 N90-12235
Smooth linearization of hyperbolic fixed points without resonance conditions
[REPT-89-03] 03 p0394 N90-12251
Generalizations of Laguerre polynomials
[REPT-89-25] 03 p0396 N90-12263
A generalization of Moak's q-Laguerre polynomials
[REPT-89-21] 04 p0540 N90-13126
Well posedness of triples of operators (in the sense of linear systems theory)
[TW-292] 04 p0545 N90-13168
Linear groups and distance-transitive graphs
[CWI-PM-R8805] 05 p0691 N90-14036
On distance-transitive graphs and involutions
[CWI-PM-R8808] 05 p0691 N90-14037
A comparison result and elliptic equations involving subcritical exponents
[DE90-001772] 06 p0834 N90-14850
On pure radical in semigroups with zero
[DE90-606954] 10 p1422 N90-18205
Note on p-semisimple BCI-algebras
[DE90-606955] 10 p1423 N90-18206
Panconnectivity of locally connected K(1,3)-free graphs
[AD-A216548] 12 p1705 N90-19786
OTTER (Organized Techniques for Theorem-proving and Effective Research) 2.0 users guide
[DE90-007978] 14 p2018 N90-21563
A proof of the isoenergetic KAM: Theorem from the ordinary one
[W-8906] 16 p2305 N90-23136
Deductive computer programming, revision
[AD-A219848] 17 p2446 N90-23946
Fixed point theory in multiply ordered spaces
[REPT-89-74] 17 p2458 N90-24031
Short proofs on multicommodity flows and cuts
[CWI-BS-R8922] 17 p2462 N90-24061
A generalization of Ore's theorem involving neighborhood unions
[MEMO-825] 17 p2462 N90-24064
Intensional Lambek calculi: Theory and application
[ITLI-LP-89-06] 17 p2464 N90-24078
On a class of generalized orthogonal polynomials with real zeros
[MEMO-826] 18 p2600 N90-24799
Explicit fixed points for interpretability logic
[ITLI-ML-89-01] 18 p2603 N90-24820
Extending the lambda calculus with surjective pairing is conservative
[ITLI-ML-89-02] 18 p2603 N90-24821
Applications of cone theory to boundary value problems
[AD-A220939] 18 p2603 N90-24828
The Knuth-Bendix completion algorithm and its specification in Z
[RSRE-MEMO-4323] 19 p2745 N90-25601
Generalization in the presence of free variables: A mechanically-checked correctness proof for one algorithm
[AD-A222681] 21 p3051 N90-27346
Non-interactive zero knowledge
[AD-A222698] 21 p3052 N90-27347
Proving Boolean equivalence with Prolog
[AD-A221766] 21 p3065 N90-27427
Study of an environment using formal reasoning. DILOG: State of the art and prototype
[CERT-1/334300-DERI] 22 p3239 N90-28368
Weighted norm inequalities for Riemann-Liouville fractional integral
[DE90-627153] 23 p3388 N90-29132
On comparable L(sup p)-norms of subadditive functions on topological groups
[DE90-627154] 23 p3390 N90-29146
A corollary to Kodaira-Spencer's theorem on continuity of eigenvalues
[DE90-627164] 23 p3390 N90-29148
Oscillatory and nonoscillatory behaviour of solutions of an equation alternately of retarded and advanced type
[DE90-627159] 24 p3536 N90-29993
Tail and quantile estimation for strongly mixing stationary sequences
[AD-A223472] 24 p3540 N90-30019

THEOREMS
NT BAYES THEOREM
NT BERNOULLI THEOREM
NT DUALITY THEOREM
NT EXISTENCE THEOREMS
NT FLOQUET THEOREM
NT GAUSS-MARKOV THEOREM
NT LEBESGUE THEOREM
NT POYNTING THEOREM
NT RECIPROCAL THEOREMS
NT RECIPROCITY THEOREM
NT STOKES THEOREM (VECTOR CALCULUS)
NT UNIQUENESS THEOREM
An approximate max-flow min-cut theorem for uniform multicommodity flow problems with applications to approximation algorithms
[AD-A211908] 03 p0386 N90-12198
Taxonomic syntax for first order inference
[AD-A211618] 03 p0390 N90-12221
The realization of input-output maps using bialgebras
[NASA-CR-185362] 03 p0391 N90-12228
Hahn-Banach type theorems for dual semigroups
[CWI-AM-R8903] 04 p0543 N90-13149
Strong moderate deviation theorems for m-dependent random variables
[AD-A212618] 04 p0546 N90-13173
Smoothed limit theorems for equilibrium processes
[AD-A212321] 04 p0547 N90-13186
Extension to Eulers's theorem to n-dimensional spaces 05 p0589 N90-13431
A new model for the structure of silica glass
[AD-A212972] 05 p0627 N90-13659
The totally singular linear quadratic problem with indefinite cost
[MEMO-COSOR-89-05] 05 p0687 N90-13998
Inductive reasoning and Kolmogorov complexity (preliminary version)
[CWI-CS-R8915] 05 p0695 N90-14062
A basic theorem of complementarity for the generalized variational-like inequality problem
[DE90-003102] 07 p0973 N90-15620
On the sum of two maximal monotone operators
[REPT-89-31] 07 p0982 N90-15669
Strong large deviation and local limit theorems
[AD-A213610] 07 p0986 N90-15698
Mathematical methods of Physics 6: Integral transformation
[INPE-4807-MD/40] 11 p1551 N90-18926
Strong moderate deviation theorems
[MEMO-804] 11 p1555 N90-18954
Euler's theorem for polynomials
[AD-A218148] 13 p1878 N90-20774
The intrinsic stochasticity of near-integrable Hamiltonian systems
[IPPCZ-282] 15 p2167 N90-22386
On the early history of intuitionistic logic
[ITLI-LP-89-04] 17 p2440 N90-23900
On models for propositional dynamic logic
[RUU-CS-89-3] 17 p2460 N90-24046
Two-dimensional modal logics for relational algebras and temporal logic of intervals
[ITLI-LP-89-03] 17 p2464 N90-24077
Intensional Lambek calculi: Theory and application
[ITLI-LP-89-06] 17 p2464 N90-24078
Affine polar spaces
[CWI-AM-R8909] 17 p2468 N90-24107
Computational methods and plasticity
[PB90-167917] 18 p2571 N90-24652
A Lyapunov bound for solutions of Poisson's equation
[AD-A220223] 18 p2599 N90-24787
Explicit fixed points for interpretability logic
[ITLI-ML-89-01] 18 p2603 N90-24820
Extending the lambda calculus with surjective pairing is conservative
[ITLI-ML-89-02] 18 p2603 N90-24821
Rosser orderings and free variables
[ITLI-ML-89-03] 18 p2603 N90-24822
Sigma-completeness and bounded arithmetic
[ITLI-ML-89-05] 18 p2603 N90-24823
Applications of cone theory to boundary value problems
[AD-A220939] 18 p2603 N90-24828
Around three lemmas in Hamiltonian graph theory
[MEMO-816] 18 p2606 N90-24846
Kharitonov's theorem: Generalizations and algorithms 18 p2646 N90-25064

On comparable L(sup p)-norms of subadditive functions on topological groups
[DE90-627154] 23 p3390 N90-29146
A corollary to Kodaira-Spencer's theorem on continuity of eigenvalues
[DE90-627164] 23 p3390 N90-29148
On Einsteinian 4-submanifolds in E(sup 6)
[DE90-627149] 23 p3402 N90-29226
An instability theorem for a certain sixth order differential equation
[DE90-627150] 24 p3536 N90-29990

THEORETICAL PHYSICS
NT NEWTON THEORY
NT QUANTUM THEORY
Studies of elementary particles
[DE89-014859] 01 p0119 N90-10685
Research program in theoretical high energy physics
[DE89-013963] 01 p0121 N90-10695
A theoretical high energy physics program
[DE89-012685] 01 p0121 N90-10696
Theoretical atomic physics for fusion
[DE89-017363] 02 p0274 N90-11563
Theoretical plasma physics
[DE90-000009] 03 p0408 N90-12341
Aspects of the physics of the standard model
[PREPRINT-670] 05 p0698 N90-14087
A theoretical perspective on neutrino physics
[DE90-000759] 06 p0839 N90-14878
Theory of interacting plasmas in space 07 p0993 N90-15742
Some theoretical aspects of cold fusion: A report
[DE90-601098] 08 p1125 N90-16514
Proceedings of the 23rd Annual Seminar on Theoretical Physics
[DE90-601827] 08 p1135 N90-16577
Research in theoretical physics
[DE90-005605] 09 p1294 N90-17500
Research in theoretical nuclear physics
[DE90-006063] 10 p1440 N90-18309
Mathematical methods of Physics 6: Integral transformation
[INPE-4807-MD/40] 11 p1551 N90-18926
Theoretical studies in nuclear physics
[DE90-005981] 11 p1565 N90-19005
Theoretical and experimental high energy physics
[DE90-006168] 11 p1565 N90-19006
Research accomplishments and future goals in particle physics
[DE90-007296] 12 p1712 N90-19830
Experimental and theoretical high energy physics
[DE90-005974] 12 p1712 N90-19834
Studies of high energy phenomena using muons
[DE90-008272] 13 p1886 N90-20820
The Inevitable Universe: Parker-Rhodes' peculiar mixture of ontology and physics
[DE90-006453] 13 p1902 N90-20915
Periodic solutions for Hamiltonian systems in a nonconvex potential well
[DE90-612752] 14 p2020 N90-21580
Reply to coupled S- and D-wave states in the thorium-doped heavy-fermion superconducting UBe13 by H. Pleiner and H. R. Brand
[AD-A220843] 17 p2477 N90-24164
An instability theorem for a certain sixth order differential equation
[DE90-627150] 24 p3536 N90-29990
Periodic solutions of certain fifth order differential equations
[DE90-627160] 24 p3536 N90-29994

THEORIES
Trace theory --- concurrent processing
[MEMO-INF-89-16] 04 p0536 N90-13100

THERAPY
NT CHEMOTHERAPY
NT RADIATION THERAPY
Radio frequency (13.56 MHz) energy enhances rewarming from mild hypothermia
[AD-A212703] 04 p0524 N90-13024
Biological effects of hyperthermia and potential risk associated with ultrasonic exposure
[PB89-100702] 06 p0820 N90-14768
A laboratory study of the effects of diet and bright light countermeasures to jet lag
[AD-A220148] 17 p2435 N90-23875
Decompression sickness presenting as a viral syndrome
[AD-A223880] 23 p3356 N90-28967

THERMAL ABSORPTION
NT POLAR CAP ABSORPTION
Radiationless transitions and excited-state absorption of low-field chromium complexes in solids
[AD-A210653] 02 p0194 N90-11105
Piezoelectric and pyroelectric effects of a crystalline polymer 18 p2515 N90-24360

THERMAL AGITATION
U THERMAL ENERGY

THERMAL ANALYSIS
Thermal and structural analysis of Hermes 02 p0186 N90-11058
Low temperature processing of reaction sintered silicon nitride
[DE89-017455] 02 p0191 N90-11092
Prediction of the thermal environment and thermal response of simple panels exposed to radiant heat
[NASA-TM-101660] 03 p0400 N90-12292
A theoretical method for the mechanical calculation of heat exchangers with sliding heads, phase 1 study
[CETIM-110240-PHASE-1] 04 p0502 N90-12896
Large Deployable Reflector (LDR) thermal characteristics 05 p0596 N90-13460
Feature modeling: The incorporation of a front and eddy map into optimum interpolation-based thermal analysis
[AD-A213253] 05 p0672 N90-13914
Thermal design of a 10-kW helium refrigerator
[DE90-701785] 06 p0756 N90-14403
Simultaneous thermal analysis techniques for characterization of energetic materials
[DE90-003028] 07 p0914 N90-15289
Thermal analysis of fixed and tilting pad journal bearings including cross-film viscosity variations and deformations 07 p0937 N90-15429
Thermal and chemical processing of the outermost layer of cometary nuclei 08 p1141 N90-16614
Acquisition of analytical instruments for combustion research
[AD-A214495] 09 p1190 N90-16893
Optimum element density studies for finite-element thermal analysis of hypersonic aircraft structures
[NASA-TM-4163] 09 p1219 N90-17074
Phase properties of the rapid cooled palladium-silicon alloy in the concentration range 40 to 58 at. percent Si
[DE90-719525] 09 p1284 N90-17444
Spacecraft thermal control design data, volume 4
[ESA-PSS-03-108-ISSUE-1-VOL-4] 11 p1469 N90-18458
Thermal analysis of polymer composites
[AD-A216947] 11 p1490 N90-18578
Heat capacities of solid polymers (The Advanced THermal Analysis System, ATHAS)
[DE90-007130] 11 p1493 N90-18595
Reflector surface distortion analysis techniques (thermal distortion analysis of antennas in space) 12 p1611 N90-19267
Evaluation of an adaptive unstructured remeshing technique for integrated fluid-thermal-structural analysis
[NASA-TM-102611] 13 p1815 N90-20426
The influence of large, cold objects on engulfing fire environments
[DE90-003342] 15 p2073 N90-21875
Spacecraft attitude impacts on COLD-SAT non-vacuum jacketed LH2 supply tank thermal performance
[NASA-TM-103158] 16 p2207 N90-22592
Solar Concentrator Advanced Development Program
[NASA-CR-185173] 16 p2250 N90-22834
Thermal analysis of Acetylene Terminated Sulfone (ATS) resin
[AD-A220775] 17 p2381 N90-23558
The origin of multiple melting in polyurethane block copolymers
[AD-A220050] 17 p2381 N90-23563
Dynamic mechanical analysis of polymeric materials 18 p2513 N90-24353
Personal Computer (PC) thermal analyzer
[AD-A221325] 18 p2548 N90-24548
Direct conversion technology
[NASA-CR-186795] 18 p2576 N90-24675
Thermal and phase analysis of YBa2Cu3O(7-x) powder compacts with organic acid additives
[DE90-010142] 18 p2620 N90-24930
Synthesis of ceramic superconductors under low oxygen pressure
[DE90-010415] 18 p2621 N90-24933
Improved processing of ceramic superconductors
[DE90-009721] 18 p2624 N90-24951
Thermal and orbital analysis of Earth monitoring Sun-synchronous space experiments
[NASA-TM-101630] 19 p2666 N90-25168
Flight motor set 360L007 (STS-33R)
[NASA-CR-183979] 20 p2824 N90-26067
New discharge pumping method for CO2 lasers
[AD-A220898] 20 p2866 N90-26307
Thermal analysis of heat pipe radiators with a rectangular groove wick structure
[AD-A222952] 21 p3004 N90-27074
Thermal response of large area high temperature superconducting YBaCuO infrared bolometer 22 p3146 N90-27839
Engine testing of thermographic phosphors
[DE90-013269] 22 p3182 N90-28059
Thermal analysis of thermal barrier coatings in a high heat flux environment 23 p3297 N90-28652
Finite element analysis of coupled thermoelasticity
[PB90-201211] 23 p3337 N90-28860
A welding metallurgy study of Hastelloy Alloys B-2 and W
[DE90-011910] 24 p3449 N90-29481
Thermal analysis of bismaleimide matrix resins
[DE90-016283] 24 p3457 N90-29523
Thermal analyses of power subsystem components
[NASA-CR-186314] 24 p3474 N90-29637
High resolution transmission electron microscopy of aluminophosphates
[DE90-015632] 24 p3553 N90-30105

THERMAL BARRIERS (PLASMA CONTROL)
Thermal barrier research
[DE90-009213] 16 p2319 N90-23221
Characteristics required for thermal barriers of zirconium oxide-yttrium compounds obtained by plasma spraying. Morphological analysis by x ray diffraction
[ETCA-89-R-113] 22 p3161 N90-27925

THERMAL BATTERIES
Pyrotechnic ignition studies using a gun tunnel
[DE89-012496] 01 p0060 N90-10341
Computer tomography of thermal batteries and other closed systems
[AD-A218379] 17 p2419 N90-23787
Resistivity measurements of halide-salt/MgO separators for thermal cells
[DE90-009740] 18 p2550 N90-24553

THERMAL BLOOMING
Effect of a random wind field on thermal blooming instabilities
[DE90-007241] 11 p1532 N90-18823
Narrow-bandwidth unstable laser resonator
[AD-D014362] 12 p1665 N90-19568
Linear theory of thermal blooming in turbulence
[DE90-007243] 12 p1667 N90-19579
Turbulent mixing effects in models of thermal blooming
[DE90-007245] 12 p1667 N90-19580
Atmospheric thermal blooming and beam clearing by aerosol vaporization
[DE90-006271] 12 p1690 N90-19711
Nonlinear optics in thin films
[AD-A217336] 13 p1887 N90-20829

THERMAL BOUNDARY LAYER
Geometric scale of interaction between moving shock and stationary thermal layer
[AD-A217769] 13 p1802 N90-20344
Spectral measurements of the wall shear stress and wall pressure in a turbulent boundary layer: Theory
[AD-A224070] 24 p3466 N90-29586

THERMAL BUCKLING
Experimental and computational study of the viscoplastic response of high temperature structures 16 p2220 N90-22663

THERMAL COMFORT
National Aeronautics and Space Administration (NASA)/American Society for Engineering Education (ASEE) Summer Faculty Fellowship Program-1989, volume 1
[NASA-CR-185601-VOL-1] 18 p2627 N90-24972
Effect of low air velocities on thermal homeostasis and comfort during exercise at space station operational temperature and humidity 18 p2628 N90-24975

THERMAL CONDUCTIVITY
On the effective transport properties of composite materials 02 p0190 N90-11086
Program for high speed computation of physical properties of propellants and combustion gas of an LH2/LOX rocket engine
[NAL-TM-564] 03 p0318 N90-11803
Thermal conduction of SSC (Superconducting Super Collider) wire
[DE89-016710] 03 p0319 N90-11811
RF performance of polycrystalline high-T(sub c) superconductors
[DE89-017671] 03 p0411 N90-12359
Development and evaluation of an instrument for rapid electroreflectance of semiconductor materials
[AD-A211690] 03 p0414 N90-12376
Metal transfer in gas metal arc welding
[AD-A213390] 05 p0624 N90-13642
Thermal/structural analyses of several hydrogen-cooled leading-edge concepts for hypersonic flight vehicles
[NASA-TM-102391] 06 p0775 N90-14511
Summary physical data tables: Alkanes
[ESDU-PD3] 07 p0893 N90-15162
On the choice of trial function in theoretical calculations of the thermal conductivity
[DE90-001733] 07 p0897 N90-15182
Thermal conductivity of gaseous aliphatic hydrocarbons. Part 1: Alkanes
[ESDU-89035-PT-1] 07 p0897 N90-15183
Short fibre and particulate reinforced metal matrix composites 07 p0901 N90-15207

Laser-induced surface ablation and optical damage of ZnS crystals caused by single- and multiple-pulse laser-irradiation
[DE90-003807] 07 p0936 N90-15419
Selection of phase-change and containment materials for thermal energy storage
[NASA-CR-186228] 07 p0952 N90-15506
Satellite thermal storage systems using metallic phase-change materials
[DE89-016872] 07 p0952 N90-15507
Physical process in MPD plasmas
[AD-A213679] 07 p0996 N90-15761
The physical properties of microcellular composite foams
[DE90-003658] 08 p1048 N90-16058
Analytical study on the decreasing method of thermal stress for ceramic gas turbines
[DE90-734934] 08 p1051 N90-16078
Thermal histories of the samples of two KOSI comet nucleus simulation experiments
08 p1147 N90-16645
Thermal modelling of various thermal barrier coatings in a high heat flux rocket engine
[NASA-TM-102418] 09 p1193 N90-16911
Capillary flow properties of mesh wicks
[AD-A214769] 09 p1217 N90-17057
The effect of loading on the laser ablation of graphite/epoxy composite material
[AD-A216209] 10 p1349 N90-17826
Thermal conductivity of quasi-one dimensional conductors
[DE90-004844] 10 p1435 N90-18281
Hot filament technique for measuring the thermal conductivity of molten lithium fluoride
[NASA-TM-102506] 12 p1631 N90-19373
Heat transfer definitions and equations
[ESDU-89022] 12 p1657 N90-19522
Experiments of thermoconvection in a cubic cell
[MPIS-6/1989] 12 p1661 N90-19544
Thermal conductivities and diffusivities of porous ice samples at low pressures and temperatures and possible modes of heat transfer in near surface layers of comets
12 p1739 N90-19999
The thermal response of generic objects in JP-4 pool fires
[DE90-008503] 13 p1788 N90-20259
Core cooling studies at LLNL (Lawrence Livermore National Laboratory) and Sandia
[DE90-008303] 13 p1795 N90-20300
Area Over Length (AOL): A program for the calculation of effective two-dimensional thermal conductance through an arbitrarily shaped region
[DE90-008005] 13 p1801 N90-20335
A nonintrusive method for measuring the operating temperature of a solenoid-operated valve
[DE90-007576] 13 p1804 N90-20355
High temperature chemistry of oxide superconductors
[DE90-007821] 13 p1895 N90-20875
An experimental investigation of the thermal conductivity of porous adsorbents
[AD-A217854] 13 p1899 N90-20899
Modeling the temperature dependence of the thermal conductivity of aluminum nitride
[DE90-009428] 14 p1949 N90-21154
An experimental evaluation of two nonazeotropic refrigerant mixtures in a water-to-water breadboard heat pump
[DE90-009016] 14 p1973 N90-21305
Nonoptimal entropy generation by heat transfer in cryogenic domain
[DE90-007544] 14 p2034 N90-21667
The thermo-mechanical behavior of cometary nuclei
14 p2041 N90-21703
Experimental determination of thermal conductance in bolted joint impact in satellites
[INPE-4989-PRE/1551] 15 p2059 N90-21788
Development of low thermal conductivity pan-based carbon fibers for solid rocket motor nozzle applications
15 p2063 N90-21818
TOODEE: A two-dimensional, time-dependent heat conduction program
[DE90-009631] 15 p2099 N90-22010
Low temperature properties of amorphous solids
15 p2171 N90-22405
Heat leak measurements in superconducting dipole magnet supports
[DE90-620109] 15 p2173 N90-22420
Approximate analysis for the formation of adiabatic shear bands
[AD-A218751] 16 p2221 N90-22670
Thermal phenomena in high-Tc thin film superconductors 16 p2321 N90-23233
Preparation, properties, and development of calcium lanthanum sulfide as an 8- to 12-micrometer transmitting ceramic
[AD-A220200] 17 p2382 N90-23565
An evaluation of imbedded thermocouples as a solid-propellant combustion diagnostic
[AD-A219947] 17 p2406 N90-23711
National Educators' Workshop: Update 1989 Standard Experiments in Engineering Materials Science and Technology
[NASA-CP-3074] 18 p2513 N90-24350
Thermal conductivity of metals
18 p2514 N90-24356
Multichip packaging technology with laser-patterned interconnects
[DE90-010743] 18 p2549 N90-24552
Heat and fluid flow within the Earth's crust: In situ measurements and mathematical models
18 p2579 N90-24690
Thermal response of large area high temperature superconducting YBaCuO infrared bolometer
22 p3146 N90-27839
Thermophysical properties of Helium-4 from 0.8 to 1500 K with pressures to 2000 MPa
[NASA-CR-186992] 23 p3303 N90-28681
Investigations into the use of dielectric coatings in magnetic switches
[DE90-014331] 23 p3321 N90-28776
Transient cooling of a hot surface by droplets evaporation
[PB90-227968] 23 p3325 N90-28799
Frequency response of a thermocouple wire: Effects of axial conduction
[NASA-CR-180454] 23 p3330 N90-28827

THERMAL CONDUCTIVITY GAGES
Development of an automated probe for thermal conductivity measurements
[PB89-209324] 01 p0073 N90-10419
Interlaboratory comparison of two types of line-source thermal-conductivity apparatus measuring five insulating materials
[PB89-218325] 02 p0200 N90-11142

THERMAL CONDUCTORS
Radiative shocks with electron thermal conduction
02 p0293 N90-11670

THERMAL CONTROL COATINGS
Heat transfer to throat tubes in a square-chambered rocket engine at the NASA Lewis Research Center
[NASA-TM-102336] 02 p0189 N90-11082
Thermal barrier coating life prediction model development, phase 1
[NASA-CR-182230] 05 p0581 N90-13388
Thermal barrier coatings for gas turbine and diesel engines
[NASA-TM-102408] 05 p0623 N90-13636
Electrical characteristics measurements for the TSS-1 satellite painting
[IFSI-89-7] 08 p1036 N90-15987
Thermal modelling of various thermal barrier coatings in a high heat flux rocket engine
[NASA-TM-102418] 09 p1193 N90-16911
Spacecraft thermal control design data, volume 2
[ESA-PSS-03-108-ISSUE-1-VOL-2]
11 p1469 N90-18456
Assessment of fundamental materials needs for Thick Thermal Barrier Coatings (TTBC's) for truck diesel engines
[NASA-TM-103130] 17 p2377 N90-23536
Spectrally selective tinoxide and indiumoxide coatings
[ISBN-90-9003138-3] 17 p2382 N90-23567
Durability of thermal barrier coatings in a high heat flux environment 23 p3297 N90-28651
Thermal analysis of thermal barrier coatings in a high heat flux environment 23 p3297 N90-28652
Vacuum application of thermal barrier plasma coatings
23 p3298 N90-28653
Application of advanced coating techniques to rocket engine components 23 p3298 N90-28654
Molten salt induced high temperature degradation of thermal barrier coatings 23 p3307 N90-28704
Effect of protective coatings on mechanical properties of superalloys 23 p3308 N90-28707
High temperature protective coatings: Recent trends
23 p3308 N90-28710
Thermal shock and oxidation resistance of ceramic coatings 23 p3308 N90-28711

THERMAL CONVECTION
U FREE CONVECTION

THERMAL CURRENTS
U CONVECTIVE FLOW

THERMAL CYCLING TESTS
Cyclic deformation of Sn-60 to Pb-40 solder joints during thermomechanical fatigue
[DE90-004197] 09 p1237 N90-17179
Investigation of the failure modes in a metal matrix composite under thermal cycling
[AD-A216195] 10 p1349 N90-17825
Effects of elevated temperatures and thermal cycling on ceramic composite materials
[AD-A216242] 10 p1350 N90-17828
Evaluation of thermal cycling creep-fatigue damage for a molten salt receiver
[DE90-002907] 12 p1684 N90-19670
NRL hybrid reliability. Physics of failure initial study
[AD-A217986] 13 p1898 N90-20893
Use of unbalanced laminates as a screening method for microcracking
[NASA-TM-102517] 14 p1944 N90-21124
The effect of temperature cycling typical of low earth orbit satellites on thin films of YBa2Cu3O(7-x)
22 p3140 N90-27812
The stress and temperature dependence of creep in an Al-2.0 wt percent Li alloy
[AD-A223676] 24 p3449 N90-29480

THERMAL DECOMPOSITION
NT PYROLYSIS
Flammability, smoke, and dry arc tracking tests of aircraft electrical wire insulations
[DOT/FAA/CT-89/21] 03 p0302 N90-11714
Properties and thermal decomposition of the double salts of uranyl nitrate-ammonium nitrate
[DE89-004909] 07 p0914 N90-15287
Blow-out of rubber blocks due to internal heating
[AD-A215730] 09 p1198 N90-16943
Determination of the thermal stability of perfluoroalkylethers
[NASA-TM-102493] 10 p1358 N90-17875
The adsorption and thermal decomposition of PH3 on Si(111)-(7x7)
[AD-A222417] 21 p2978 N90-26927
Development of a mathematical model for the thermal decomposition of aviation fuels
[AD-A221673] 21 p2990 N90-26994
Toxicity of thermolysis products from the materials of airplane cockpits
[CEAT-PV-M6/5924/02] 22 p3156 N90-27895
Toxicological aspects of fire onboard aircrafts: Role of the pressurization and ventilation in the cockpit
[ETN-90-97452] 22 p3233 N90-28335

THERMAL DEFOCUSING
U THERMAL BLOOMING

THERMAL DEGRADATION
Aging of CFRP due to longterm storage in heated air
[ESA-TT-1124] 03 p0333 N90-11893
Hardening and toughening of ZnS-Ga2S3 ceramics by solid-state reactions
[AD-A213875] 07 p0912 N90-15276
Thermal stability of jet fuel
[DE90-002760] 07 p0914 N90-15288
Characterization of the thermal degradation of selected energetic materials and mixtures by Rapid-Scan Fourier Transform Infrared (RSFTIR) spectroscopy
[AD-A214411] 07 p0916 N90-15296
Arcjet cathode phenomena 11 p1473 N90-18477
Design and operation of an inert gas facility for thermoelectric generator storage
[DE90-007146] 11 p1585 N90-19008
Thermal vacuum life test facility for radioisotope thermoelectric generators
[DE90-007148] 11 p1566 N90-19010
Experimental results of aging and thermal effects in high-power laser diodes
[DE90-005955] 12 p1686 N90-19573
Study of possible solar heating effects on thermosonde probes: Error analysis
[AD-A218116] 13 p1903 N90-20917
Boron-containing organosilane polymers and ceramic materials thereof
[NASA-CASE-ARC-11649-2-SB]
14 p1952 N90-21177
Low temperature degradation of Y-TZP materials
[AD-A218841] 16 p2223 N90-22684
Thermal analysis of Acetylene Terminated Sulfone (ATS) resin
[AD-A220775] 17 p2381 N90-23558
Diffusion in the thermal degradation of NC base propellants
[AD-A219831] 17 p2383 N90-23572
The effect of thermal damage on the mechanical properties of polymer regrinds 18 p2515 N90-24363
Study of an impact on organic matrix and long fibers composite plates (thermal aspect)
[ETCA-89-R-155] 22 p3154 N90-27882
UV-induced degradation of the Si-SiO2 interface: Applications to the point contact solar cell
[DE90-013843] 23 p3344 N90-28898

THERMAL DIFFUSION
Quasi-diffusion between phonon and roton gases in two- and three-dimensional liquid helium
[AD-A210565] 02 p0192 N90-11096
Some new algorithms for boundary value problems in smooth particle hydrodynamics
[AD-A211728] 03 p0348 N90-11987
Numerical study of diffusion jet flames
12 p1621 N90-19318

An analytic model of axisymmetric mantle plume due to thermal and chemical diffusion
[NASA-CR-186461] 12 p1691 N90-19714
THERMAL DIFFUSIVITY
A study of runaway electron confinement and theory of neoclassical MHD turbulence
[DE89-016728] 02 p0277 N90-11584
Heat transfer definitions and equations
[ESDU-89022] 12 p1657 N90-19522
Thermal conductivities and diffusivities of porous ice samples at low pressures and temperatures and possible modes of heat transfer in near surface layers of comets
12 p1739 N90-19999
Difference in electron thermal diffusivity and profile between interior and exterior of TFTR L-mode plasmas
[DE90-007479] 13 p1890 N90-20846
An extended diffusive model for calculating thermal diffusivity from single monopole tokamak heat pulse propagation
[DE90-007958] 14 p2029 N90-21637
Flow boiling with enhancement devices for cold plate coolant channel design
[NASA-CR-186358] 15 p2089 N90-21961
Heat sink effects on weld bead: VPPA process
[NASA-CR-186723] 19 p2697 N90-25349
A technique to measure the thermal diffusivity of high T(sub c) superconductors 22 p3147 N90-27846
THERMAL EFFECTS
U TEMPERATURE EFFECTS
THERMAL EFFICIENCY
U THERMODYNAMIC EFFICIENCY
THERMAL EMISSION
NT THERMIONIC EMISSION
Electron cyclotron emission and absorption experiment on the CASTOR tokamak
[IPPCZ-285] 03 p0407 N90-12331
Evaluation of a damaged F/A-18 horizontal stabilator
[AD-A212573] 04 p0453 N90-12597
Selective excitation luminescence and photoluminescence investigations of ytterbium doped InP, GaAs and AlGaAs
[AD-A215713] 09 p1291 N90-17485
Thermal pair cloud models of MeV gamma ray emissions from Cygnus X-1 and the Galactic Center
[DE90-001168] 09 p1301 N90-17536
Applications of remote sensing to studies of oceanic upper mixed layer dynamics 15 p2122 N90-22137
Spectrally selective tinoxide and indiumoxide coatings
[ISBN-90-9003136-3] 17 p2382 N90-23567
THERMAL ENERGY
High resolution X-ray spectroscopy using germanium microcalorimeters
[DE89-017784] 03 p0351 N90-12004
Analysis of the efficiency of a dielectric solar energy collector
[PB89-212716] 03 p0366 N90-12092
Heat pipe and thermal energy storage and corrosion studies (1988)
[AD-A212655] 04 p0472 N90-12706
A heat receiver design for solar dynamic space power systems
[NASA-TM-102473] 06 p0735 N90-14283
Thermal energy storage
[DE90-000953] 07 p0950 N90-15500
Selection of phase-change and containment materials for thermal energy storage
[NASA-CR-186228] 07 p0952 N90-15506
Satellite thermal storage systems using metallic phase-change materials
[DE89-016872] 07 p0952 N90-15507
Generation of axial and lateral magnetic fields in laser produced plasmas
[DE90-607470] 10 p1432 N90-18260
Phase-Change Thermal Energy Storage
[DE89-009426] 11 p1529 N90-18801
Ion and electron interactions at thermal and suprathermal energies
[AD-A216905] 12 p1622 N90-19323
Direct absorption receiver
[DE90-000311] 12 p1683 N90-19667
An analytic model of axisymmetric mantle plume due to thermal and chemical diffusion
[NASA-CR-186461] 12 p1691 N90-19714
Flow boiling with enhancement devices for cold plate coolant channel design
[NASA-CR-186358] 15 p2089 N90-21961
Conceptual design of a Moving Belt Radiator (MBR) shuttle-attached experiment
[NASA-CR-185169] 17 p2367 N90-23474
Thermal conductivity of metals
18 p2514 N90-24356
Direct conversion technology
[NASA-CR-186795] 18 p2576 N90-24675
Boiling/evaporative heat transfer from spheres in packed-bed thermal energy storage units
[DE90-012023] 19 p2711 N90-25430
Solar energy for high temperature technology and applications
[ETN-90-97429] 23 p3345 N90-28902
THERMAL ENERGY STORAGE
U HEAT STORAGE
THERMAL ENVIRONMENTS
Acoustic-thermal environment for USB flap structure. Report 1: Ground simulation test results
[NAL-TM-567] 03 p0300 N90-11697
SRB thermal environments
[NASA-CR-183801] 06 p0734 N90-14276
Arcjet thruster research and technology. Phase 1: Executive summary
[NASA-CR-182106] 06 p0734 N90-14278
Hydrogen, thermal ageing and the role of carbides in fatigue of a high strength steel
[AERE-R-13599] 13 p1774 N90-20183
Correlation/validation of finite element code analyses for vibration assessment of avionic equipment
[AD-A220393] 17 p2353 N90-23398
Thermal-distortion analysis of an antenna strongback for geostationary high-frequency microwave applications
[NASA-TP-3016] 22 p3125 N90-27738
Liquid Rocket Booster (LRB) for the Space Transportation System (STS) systems study. Appendix B: Liquid rocket booster acoustic and thermal environments
[NASA-CR-183788-APP-B] 23 p3288 N90-28602
THERMAL EXPANSION
Thermal expansion and phase transformation studies on some materials by high temperature X-ray powder diffractometry
[DE89-631032] 02 p0198 N90-11130
Status of Gr/glass composites technology at UTOS
05 p0596 N90-13459
Advanced composite materials for precision segmented reflectors 05 p0596 N90-13461
Short fibre and particulate reinforced metal matrix composites 07 p0901 N90-15207
Thermal expansion of LATGS crystals
[DE89-636239] 08 p1130 N90-16546
Metal matrix composite: Strengthening mechanisms
[AD-A214843] 09 p1186 N90-16871
Coefficients of thermal expansion for a carbon-carbon composite
[DE90-004484] 09 p1188 N90-16883
Electrochemical cell for obtaining oxygen from carbon dioxide atmospheres
[NASA-CR-186225] 09 p1189 N90-16886
Magellan/Galileo solder joint failure analysis and recommendations
[NASA-CR-186294] 09 p1233 N90-17157
Fluorinated graphite fibers as a new engineering material: Promises and challenges
[NASA-TM-102511] 12 p1618 N90-19301
Crystallization behavior and properties of BaO-Al2O3-2SiO2 glass matrices
[NASA-CR-185209] 12 p1631 N90-19374
Use of unbalanced laminates as a screening method for microcracking
[NASA-TM-102517] 14 p1944 N90-21124
Modeling the temperature dependence of the thermal conductivity of aluminum nitride
[DE90-009428] 14 p1949 N90-21154
The thermo-mechanical behavior of cometary nuclei
14 p2041 N90-21703
Thermomechanical properties of polymeric materials and related stresses
[NASA-TM-100758] 15 p2071 N90-21864
Thermomechanically-induced convective motion and natural convection in confined gaseous helium subjected to boundary heating 15 p2089 N90-21960
Thermomechanical properties of new composite materials SiC/glass-ceramic
[REPT-892-430-118] 17 p2370 N90-23491
Preparation, properties, and development of calcium lanthanum sulfide as an 8- to 12-micrometer transmitting ceramic
[AD-A220200] 17 p2382 N90-23565
The composition and physical properties of the Earth's mantle and core 18 p2579 N90-24689
Seamless metal-clad fiber-reinforced organic matrix composite structures and process for their manufacture
[NASA-CASE-LAR-13562-1] 19 p2672 N90-25196
A cost-effective realization of environmental temperature control
[DE90-011651] 24 p3458 N90-29532
THERMAL FATIGUE
Acoustic-thermal environment for USB flap structure. Report 1: Ground simulation test results
[NAL-TM-567] 03 p0300 N90-11697
The 4th US Army Workshop on Low Heat Rejection Engines
[AD-A212379] 04 p0510 N90-12943
Thermal fatigue durability for advanced propulsion materials
[NASA-TM-102348] 06 p0797 N90-14641
Thermal mechanical fatigue of coated blade materials
[AD-A214258] 07 p0882 N90-15107
Isothermal fatigue behavior of Sn-Pb solar joints
[DE90-003280] 07 p0943 N90-15464
Cryogenic engineering and materials
08 p1030 N90-15949
Softening mechanisms and microstructural instabilities during high temperature, low cycle fatigue of Ni, Ni3Al, and their metal matrix composites
[DE90-006487] 11 p1487 N90-18557
Creep in shear of experimental solder joints
[DE90-007062] 11 p1520 N90-18753
An attempt of improving high-temperature fatigue properties of Ni-Cr-W superalloys in HTGR helium
[DE90-741482] 12 p1627 N90-19350
The metallurgical mechanisms of solder fatigue
[DE90-008390] 13 p1778 N90-20206
High temperature fatigue behavior of tungsten copper composites
[NASA-TM-102404] 14 p1948 N90-21138
High temperature fatigue behavior of a SiC/Ti-24Al-11Nb composite
[NASA-TM-103157] 16 p2248 N90-22822
Damage tolerance analysis for manned hypervelocity vehicles. Volume 1: Final technical report
[AD-A221970] 22 p3191 N90-28106
High temperature fatigue behavior of Haynes 188
23 p3295 N90-28642
Structural response of SSME turbine blade airfoils
23 p3297 N90-28649
Evaluation of high temperature protective coatings for gas turbine engines under simulated service conditions
23 p3309 N90-28712
Characterization of unnotched SCS-6/Ti-15-3 metal matrix composites at 650 C
[NASA-TM-102699] 24 p3444 N90-29450
A viscoelastic material model for computing stresses in glass
[DE90-014851] 24 p3481 N90-29673
THERMAL GRAVIMETRY
U THERMOGRAVIMETRY
THERMAL INSTABILITY
Direct and inverse scattering problem associated with the elliptic Sinh-Gordon equation
[AD-A216455] 11 p1551 N90-18931
Measurement of the stimulated thermal Rayleigh scattering instability
[DE90-007849] 13 p1807 N90-20376
The formation of globular clusters
23 p3410 N90-29272
THERMAL INSULATION
Flight set 360T004 (STS-30) insulation component, interim release, volume 3
[NASA-CR-183746] 01 p0031 N90-10169
Composite multilayer insulations for thermal protection of aerospace vehicles
[NASA-TM-101071] 01 p0034 N90-10183
The Kryo-Kanal Koeln (KKK): Description of the tunnel conversion. Thermal insulation, instrumentation, operational experience, test results and operating costs
08 p1029 N90-15943
Investigation of ablation phenomena using IR thermography in a hypersonic wind tunnel
08 p1081 N90-16258
Federal roles to realize national energy-efficiency opportunities in the 1990s
[DE90-004410] 08 p1096 N90-16348
Insulation, compressibility and absorbency of dry suit undergarments
[AD-A215944] 10 p1414 N90-18149
Spacecraft thermal control design data, volume 2
[ESA-PSS-03-108-ISSUE-1-VOL-2]
11 p1469 N90-18456
Information on the use of data items on hot structures
[ESDU-89021] 12 p1674 N90-19611
Temperatures in plates subjected to a sudden increase in recovery temperature
[ESDU-89026] 12 p1724 N90-19904
Control of surface melting and ablation in electromagnetic launchers via the magnetic vapor shielding mechanism
[AD-A219035] 16 p2204 N90-22578
Thermal/structural analysis of the shaft-disk region of a fan drive system
[NASA-TM-101687] 16 p2245 N90-22807
Lightweight ceramic insulation and method
[NASA-CASE-MSC-20782-1] 17 p2382 N90-23566
Space plane model for visual measurement of aerodynamic heating
[DE90-505514] 20 p2803 N90-25949
Laboratory evaluation of two new high-performance polyester batting insulation materials
[AD-A222291] 21 p2987 N90-26976
Physical characteristics of clothing materials with regard to heat transport
[IZF-1989-10] 22 p3233 N90-28336

THERMAL MAPPING
Thermal radiation from terrain: Measurements and first results
[FOA-C-30525-3.1] 02 p0236 N90-11342
Fast and objective MRTD measurement
[FEL-1988-24] 03 p0351 N90-12006
The determination of subscale structures in thermal images 08 p1093 N90-16330
Reflection technique for thermal mapping of semiconductors
[AD-D014263] 08 p1129 N90-16541
Staring focal plane array system modeling
[AD-A215712] 09 p1283 N90-17438
Infrared thermal imaging figures of merit 10 p1364 N90-17904
A multicolor imaging pyrometer 10 p1364 N90-17905
Use of anomolous thermal imaging effects for multi-mode systems control during crystal growth 10 p1365 N90-17910
Non-contact temperature measurement of a falling drop 10 p1365 N90-17912
A space qualified thermal imaging system using a Pt Si detector array 10 p1367 N90-17921
NCTM workshop splinter session, IR thermal measurement instruments 10 p1367 N90-17923
Boundary estimation problems arising in thermal tomography
[NASA-CR-181964] 10 p1421 N90-18193
Thermal remote sensing in the differentiation of soybean crops (glycine max (L.) merrill) submitted to water deficit
[INPE-4900-PRE/1501] 11 p1522 N90-18762
Interrelationship of spatial and radiometric resolution in the thermal infrared band
[INPE-4860-TDL/371] 11 p1523 N90-18771
Infrared spectroscopy of dust 11 p1579 N90-19094
ARGUS/LLNL IR camera calibration and characterization
[AD-A217076] 12 p1664 N90-19563
Human factors and safety considerations of night vision systems flight using thermal imaging systems
[AD-A223226] 21 p3037 N90-27263
Thermal imaging assessment
[AD-A224400] 24 p3460 N90-29542

THERMAL NOISE
Advanced Doppler tracking experiments 12 p1731 N90-19951
Analysis of radiometer calibration effects with TOUCHSTONE
[NASA-CR-186476] 13 p1792 N90-20284

THERMAL PLASMAS
Thermal loads on tokamak plasma facing components during normal operation and disruptions
[DE90-000794] 06 p0846 N90-14919
The 10th Gordon Research Conference on Plasma Chemistry
[AD-A215161] 09 p1285 N90-17449
Report from ionospheric science 10 p1444 N90-18333
High growth rate diamond synthesis in a large area atmospheric pressure inductively coupled plasma
[AD-A216090] 11 p1567 N90-19019
The 41st Annual Gaseous Electronics Conference
[AD-A214540] 12 p1715 N90-19851
Relativistic processes in active galactic nuclei 14 p2040 N90-21698

THERMAL POWER
U TURBOGENERATORS

THERMAL PROPERTIES
U THERMODYNAMIC PROPERTIES

THERMAL PROTECTION
Composite multilayer insulations for thermal protection of aerospace vehicles
[NASA-TM-101071] 01 p0034 N90-10183
Automated stress analysis of Shuttle orbiter thermal protection system 02 p0184 N90-11043
Thermal and structural analysis of Hermes 02 p0186 N90-11058
Effects of serial wet-dry-wet cold exposure: Thermal balance, physical activity, and cognitive performance
[AD-A212704] 04 p0524 N90-13025
Debris/ice/TPS assessment and photographic analysis for Shuttle Mission STS-34
[NASA-TM-102153] 05 p0594 N90-13447
Thermal protection systems for reentry and hypersonic flight
[DLR-MITT-89-14] 05 p0613 N90-13577
QM-8 field joint protection system, volume 7
[NASA-CR-183748] 05 p0614 N90-13586
Static test deflector for Ariane-5 SRM: Technical design and economical choice 09 p1176 N90-16812
Debris/ice/TPS assessment and photographic analysis for Shuttle Mission STS-33R
[NASA-TM-102785] 09 p1180 N90-16846
Polycarbonate article with chemical resistant coating
[NASA-CASE-MSC-21503-1] 09 p1195 N90-16925
Thermal switch disc for short circuit protection of batteries
[NASA-CASE-MSC-21428-1] 09 p1209 N90-17008
Spacecraft thermal control design data, volume 1
[ESA-PSS-03-108-ISSUE-1-VOL-1] 11 p1468 N90-18455
An example of technology transfer by Aerospatiale: Fire protection materials 11 p1577 N90-19082
Development and fabrication of structural components for a scramjet engine
[NASA-CR-181945] 13 p1757 N90-20088
SIMOUN: An optimized supersonic high temperature wind tunnel for testing construction materials to be used on the spaceplane
[REPT-892-430-111] 16 p2203 N90-22572
Debris/ice/TPS assessment and photographic analysis for Shuttle Mission STS-36
[NASA-TM-102789] 16 p2205 N90-22583
The position of carbon/carbon composites among high temperature composites
[REPT-892-430-126] 16 p2213 N90-22626
Preliminary Subsystem Designs for the Assured Crew Return Vehicle (ACRV), volumes 1-3
[NASA-CR-186662] 17 p2363 N90-23455
Aerodynamic pressure and heating-rate distributions in tile gaps around chine regions with pressure gradients at a Mach number of 6.6
[NASA-TP-2988] 17 p2400 N90-23670
Field management of accidental hypothermia during diving
[AD-A219560] 17 p2434 N90-23866
Design of a thermal and micrometeorite protection system for an unmanned lunar cargo lander
[NASA-CR-186682] 19 p2664 N90-25161
Thermal protection systems for reentry and hypersonic flight
[ESA-TT-1179] 19 p2667 N90-25177
Acousto-optic signature analysis for inspection of the orbiter thermal protection tile bonds
[DE90-013089] 20 p2819 N90-26043
The aerobraking space transfer vehicle
[NASA-CR-186819] 20 p2821 N90-26053
A computational study of the effectiveness of coating materials for KE projectile fins subjected to the combined effects of inbore and aerodynamic heating
[AD-A222595] 20 p2840 N90-26155
Flight set 360L001 (STS-26) igniter, post flight
[NASA-CR-183957] 20 p2870 N90-26325
Field experience in using laser acoustic sensing for inspection
[DE90-012954] 20 p2873 N90-26347
Debrix/ice/TPS assessment and photographic analysis of Shuttle Mission STS-32R
[NASA-TM-102787] 22 p3124 N90-27733
Flight motor set 360L001 (STS-26R). Volume 1: System overview, revision A
[NASA-CR-183995] 22 p3133 N90-27778
Design and evaluation of candidate pressure distribution and air data system tile penetration for the aeroassist flight experiment
[NASA-CR-4312] 24 p3471 N90-29615

THERMAL RADIATION
NT BLACK BODY RADIATION
Thermal radiation from terrain: Measurements and first results
[FOA-C-30525-3.1] 02 p0236 N90-11342
Interaction of radiation with matter: Atomic collision processes occurring in the presence of radiation fields
[AD-A213112] 05 p0697 N90-14078
The thermal behavior of natural backgrounds and its prediction by means of numerical models 06 p0762 N90-14436
An experimental investigation of the thermal conductivity of porous adsorbents
[AD-A217854] 13 p1899 N90-20899
Thermal radiation characteristics of nonisothermal cylindrical enclosures using a numerical ray tracing technique
[NASA-TM-102527] 14 p1972 N90-21296
Heat engine based on shape memory alloys
[AD-D014400] 14 p1986 N90-21385
Principles of the radiosity method for canopy reflectance modeling
[DE90-008943] 14 p2001 N90-21466
An evaluation of imbedded thermocouples as a solid-propellant combustion diagnostic
[AD-A219947] 17 p2406 N90-23711
Retention index monitoring of volatile organic compounds using thermal desorption gas chromatography
[AD-A221117] 18 p2521 N90-24397
Studies of chemistry and diffusion on silicon and gallium arsenide surfaces using laser-induced thermal desorption
[AD-A220948] 18 p2547 N90-24539
Exploding neutron stars near the minimum mass: The total energy release 19 p2774 N90-25769
X ray emission from relativistic jets in AGNs and statistical implications 19 p2792 N90-25893
Variability of the continuum emission of GQ Comae 19 p2793 N90-25903
The thermal radiative properties of metals at high temperature
[DE90-012468] 21 p2981 N90-26938
Experimental study of the optical constants of metals at high temperatures
[DE90-014732] 23 p3310 N90-28719

THERMAL RESISTANCE
Creep strength of niobium alloys, Nb-1%Zr and PWC-11
[NASA-TM-102390] 03 p0326 N90-11854
Mechanical and thermal testing 05 p0605 N90-13521
Steady state temperatures and thermal stresses in a spherical or cylindrical laminated shell
[ESDU-89027] 12 p1674 N90-19612
Finite element analysis of structural components using viscoplastic models with application to a cowl lip problem
[NASA-CR-185189] 17 p2416 N90-23769
Thermal shock tests
[ETCA-89-R-163] 22 p3193 N90-28120
NASA Langley Research Center National Aero-Space Plane Mission simulation profile sets
[NASA-TM-102670] 23 p3276 N90-28541

THERMAL RESOURCES
NT GEOTHERMAL RESOURCES
NT GEYSERS

THERMAL SHIELDING
U HEAT SHIELDING

THERMAL SHOCK
Analytical study on the decreasing method of thermal stress for ceramic gas turbines
[DE90-734934] 08 p1051 N90-16078
Extrusion of alumina-silicon carbide whisker composites
[DE90-004379] 09 p1186 N90-16869
Characterization by ultrasonic tests of ceramics submitted to thermal shocks: Influence of several parameters on the crack dimensioning
[ETCA-89-R-060] 22 p3160 N90-27923
Thermal shock tests
[ETCA-89-R-163] 22 p3193 N90-28120
Durability of thermal barrier coatings in a high heat flux environment 23 p3297 N90-28651
Vacuum application of thermal barrier plasma coatings 23 p3298 N90-28653
Ceramic matrix composites in simulated SSME environments 23 p3298 N90-28655
Thermal shock and oxidation resistance of ceramic coatings 23 p3308 N90-28711

THERMAL SIMULATION
Analysis of a model and sequential numerical method for thermal reservoir simulation
[DE89-015117] 01 p0067 N90-10384
Acoustic-thermal environment for USB flap structure. Report 1: Ground simulation test results
[NAL-TM-567] 03 p0300 N90-11697
Thermal environmental tests on space simulation chamber
[DE90-000927] 06 p0729 N90-14251
Thermal study of battery charge control by temperature derivative reduction 10 p1332 N90-17704
The ground testing of nickel hydrogen batteries prior to launch 10 p1333 N90-17705
Simulation of regenerative fuel cell systems including thermal control 10 p1333 N90-17711
Optimized sensible heat storage systems for application to solar dynamic power generation 10 p1334 N90-17719
Finite element modeling and thermal simulations of transistor integrated circuits
[AD-A215928] 10 p1380 N90-17997
Uncertainty evaluation in an automated high temperature environmental simulation oven
[REPT-892-430-103] 16 p2203 N90-22571
Natural convection liquid immersion cooling of high density columns of discrete heat sources in a vertical channel
[AD-A218388] 17 p2402 N90-23681
Simulation of the electrical and thermal behavior of gapless metal oxide surge arresters under AC-operation condition
[ETN-90-97309] 20 p2859 N90-26262

THERMAL SINKS
U HEAT SINKS

THERMAL STABILITY
Space structures concepts and materials
[NASA-CR-183727] 01 p0025 N90-10128
Mechanics of damping for fiber composite laminates including hygro-thermal effects
[NASA-TM-102329] 01 p0034 N90-10185
The thermal stability between rotating cylinders in a radially symmetrical gravitational field
[DE89-618548] 02 p0287 N90-11638
Sensitivity relationships in energetic materials
[DE89-016967] 03 p0333 N90-11897
Thermal stability of the carbon-carbon bond in ethylene adsorbed on Si(100): An isotopic mixing study
[AD-A211591] 04 p0470 N90-12691
High temperature insulators
[AD-D014193] 04 p0479 N90-12751
The chemistry of hexaazatriphenylene hexanitrile, a polyfunctional heterocycle with potential utility in the formulation of thermostable polymers
[AD-A212353] 04 p0480 N90-12757
Report of the Asilomar 3 LDR Workshop
[NASA-CR-184656] 05 p0594 N90-13449
Status of Gr/glass composites technology at UTOS
05 p0596 N90-13459
Advanced composite materials for precision segmented reflectors 05 p0596 N90-13461
Payload thermal control 05 p0604 N90-13511
Spacecraft thermal control 05 p0604 N90-13513
Method for stabilization of pan-based carbon fibers
[AD-D014228] 06 p0736 N90-14288
Temperature stable ceramic dielectric compositions
[AD-D014209] 06 p0749 N90-14358
The 3F condensation polyimides: Review and update
[NASA-TM-102353] 06 p0750 N90-14363
Pentafluorothio polynitroaliphatic explosives
[AD-D014221] 06 p0753 N90-14383
Thermal stability of jet fuel
[DE90-001160] 06 p0753 N90-14385
Study of new materials for gun propellant formulations
[DE89-015285] 06 p0754 N90-14388
Electrochemical preparation of silver oxide electrodes having high thermal stability
[AD-D014224] 06 p0767 N90-14460
Practical superconductor development for electrical power applications
[DE90-001804] 06 p0771 N90-14487
On the thermal stability of flow of a radiating two-component plasma in a porous medium between two rotating cylinders
[DE89-636426] 06 p0847 N90-14928
A novel heat resistant blend produced by compositional quenching: A thermoplastic polyimide impact modified with a fluoroelastomer
[AD-A213724] 07 p0912 N90-15273
Thermal stability of jet fuel
[DE90-002760] 07 p0914 N90-15288
Characterization of the thermal degradation of selected energetic materials and mixtures by Rapid-Scan Fourier Transform Infrared (RSFTIR) spectroscopy
[AD-A214411] 07 p0916 N90-15296
Instability of a-Si:H/Ag interface at 150 deg C
[DE89-009419] 07 p0950 N90-15498
Physical process in MPD plasmas
[AD-A213679] 07 p0996 N90-15761
Thermally stable metal/GaAs contacts
[DE90-002122] 07 p0998 N90-15774
Studies of the structure and properties of amorphous a-Zr76Fe24Hx
[AD-A214646] 09 p1190 N90-16897
Phase stability of a manganese-stabilized low-activation martensitic steel
[DE90-004114] 09 p1193 N90-16914
Determination of the thermal stability of perfluoroalkylethers
[NASA-TM-102493] 10 p1358 N90-17875
Thermal analysis of polymer composites
[AD-A216947] 11 p1490 N90-18578
Thermo-oxidative stability studies of PMR-15 polymer matrix composites reinforced with various fibers
[NASA-TM-102439] 12 p1620 N90-19310
An evaluation of ethylene-vinyl acetate copolymers as desensitizers for RDX in insensitive booster compositions prepared by slurry coating technology
[MRL-TR-89-33] 12 p1633 N90-19385
Stable isotope studies of cometary analogue materials
12 p1740 N90-20001
Ring expansion and equilibration in organophosphazenes, and the relationship to polymerization
[AD-A218234] 13 p1782 N90-20230
Energy beam treatment for improved adhesion of coatings to surfaces
[AD-D014449] 14 p1954 N90-21190
High speed commercial transport fuels considerations and research needs
[NASA-TM-102535] 15 p2072 N90-21889
Seal requirements in rocket propulsion
[ETN-90-96611] 16 p2205 N90-22580
Elevated temperature crack growth in advanced powder metallurgy aluminum alloys 16 p2218 N90-22653
Methods for evaluation of thermally induced reactions in liquid propellants
[AD-A218750] 16 p2225 N90-22694
Thermal phenomena in high-Tc thin film superconductors 16 p2321 N90-23233
Thermal analysis of Acetylene Terminated Sulfone (ATS) resin
[AD-A220775] 17 p2381 N90-23558
Three-dimensional analysis on flow and temperature distributions for aircraft fuel thermal stability
[AD-A219651] 17 p2383 N90-23571
Stability projections for high temperature superconductors
[AD-A218945] 18 p2618 N90-24913
Morphological control of inter-penetrating polymer networks 18 p2642 N90-25046
Optical properties monitor: Experiment definition phase
[NASA-CR-4293] 19 p2666 N90-25170
Oxide thermal stability on gamma titanium aluminide
[DE90-012054] 19 p2678 N90-25232
Composite materials with improved properties in compression: Copolymerization of 1,1-dimethyl-1-Silacyclopent-3-ene and 1,1-diphenyl-1-Silacyclopent-3-ene. Characterization of copolymer microstructures by H1, C13, and Si29 NMR spectroscopy
[AD-A221686] 21 p2972 N90-26892
Cryogenic, high speed, turbopump bearing cooling requirements 23 p3291 N90-28620
Theoretical investigations and attempted synthesis of organic magnetic polymers and oligomers
[AD-A223409] 24 p3455 N90-29509

THERMAL STRESSES
Effects of a heat cycle on material strength
[NAL-TM-562] 03 p0306 N90-11737
The 4th US Army Workshop on Low Heat Rejection Engines
[AD-A212379] 04 p0510 N90-12943
Prediction of thermal stress casualties
[AD-A212356] 04 p0523 N90-13022
Stress intensity factors for cracking metal structures under rapid thermal loading. Volume 2: Theoretical background
[AD-A213297] 05 p0654 N90-13812
Thermal/structural analyses of several hydrogen-cooled leading-edge concepts for hypersonic flight vehicles
[NASA-TM-102391] 06 p0775 N90-14511
Thermal stresses in unrestrained plates subjected to a recovery temperature varying linearly with time
[ESDU-89025] 07 p0947 N90-15481
Analytical study on the decreasing method of thermal stress for ceramic gas turbines
[DE90-734934] 08 p1051 N90-16078
Optimum element density studies for finite-element thermal analysis of hypersonic aircraft structures
[NASA-TM-4163] 09 p1219 N90-17074
Shock-shock boundary layer interactions
10 p1308 N90-17569
Investigations on hot spots effects in reverse biased spatial solar cells 10 p1344 N90-17789
Investigation of the failure modes in a metal matrix composite under thermal cycling
[AD-A216195] 10 p1349 N90-17825
Analysis of biaxial stress fields in plates cracking at elevated temperatures
[AD-A216271] 10 p1397 N90-18077
Steady state temperatures and thermal stresses in a spherical or cylindrical laminated shell
[ESDU-89027] 12 p1674 N90-19612
Optimization of fracture resistance in composites
[AD-A217431] 13 p1768 N90-20144
Magnetic vapor shield mechanism for protection of material surfaces exposed to high heat load
[AD-A217667] 13 p1780 N90-20217
Fiber pushout test: A three-dimensional finite element computational simulation
[NASA-TM-102565] 14 p1945 N90-21131
Micromechanics analysis of space simulated thermal deformations and stresses in continuous fiber reinforced composites
[NASA-TM-102633] 14 p1946 N90-21140
Optimal fabrication processes for unidirectional metal-matrix composites: A computational simulation
[NASA-TM-102559] 14 p1947 N90-21143
The thermo-mechanical behavior of cometary nuclei
14 p2041 N90-21703
Thermomechanical properties of polymeric materials and related stresses
[NASA-TM-100758] 15 p2071 N90-21864
SPOT 4 space magnetic recorder mechanisms
15 p2112 N90-22082
Computations of weight functions in fracture mechanics 16 p2246 N90-22809
Activation uniformity dependence of undoped semi-insulating GaAs on post-implant annealing conditions
[ETN-90-96549] 16 p2323 N90-23246
Theory of stress transfer in a cross-ply laminate containing a parallel array of transverse cracks
[NPL-DMA(A)-189] 22 p3192 N90-28109
Calculation of temperature distribution in various turbine blades using a boundary-fitted coordinate transformation method 23 p3278 N90-28550
Reliability study of TWT output RF window
[AD-A223688] 24 p3465 N90-29574

THERMAL VACUUM TESTS
On-ground photometric calibration
05 p0605 N90-13523
Thermal vacuum life test facility for radioisotope thermoelectric generators
[DE90-007148] 11 p1566 N90-19010
Space Station Freedom solar array panels plasma interaction test facility
[NASA-TM-102475] 15 p2186 N90-22488

THERMALIZATION (ENERGY ABSORPTION)
The 25 kWe spaceborne solar dynamic generator
10 p1331 N90-17696

THERMIONIC CATHODES
Thermionic emission including both space charge and image forces
[AD-A212732] 04 p0498 N90-12869
Raman spectroscopic analysis of impregnated cathodes
[AD-A214559] 09 p1190 N90-16895

THERMIONIC CONVERSION SYSTEMS
U THERMIONIC POWER GENERATION

THERMIONIC CONVERTERS
NT SOLAR BLANKETS
True asymptotic plasma-sheath matching with an asymptotically correct collisional presheath
[AD-A212857] 05 p0701 N90-14104
Development of a diamond insulator for thermionic applications
[DE90-002849] 08 p1048 N90-16055
Final safety analysis report for the Ulysses mission. Volume 1: Reference design document
[DE90-008693] 14 p1940 N90-21107
The scalability of OTR (Out-of-core Thermionic Reactor) space nuclear power systems
[DE90-013553] 21 p3075 N90-27485

THERMIONIC DIODES
A 2-MeV microwave thermionic gun
[DE89-015640] 04 p0494 N90-12844
Impedance characteristics of terawatt ion diodes
[DE90-006276] 12 p1652 N90-19494

THERMIONIC EMISSION
Thermionic emission including both space charge and image forces
[AD-A212732] 04 p0498 N90-12869
Thermionic gun control system for the CEBAF injector
[CEBAF-PR-89-028] 19 p2755 N90-25654

THERMIONIC POWER GENERATION
True asymptotic plasma-sheath matching with an asymptotically correct collisional presheath
[AD-A212857] 05 p0701 N90-14104

THERMIONIC REACTORS
U ION ENGINES
U NUCLEAR ROCKET ENGINES

THERMISTORS
Development of an automated probe for thermal conductivity measurements
[PB89-209324] 01 p0073 N90-10419
Carbon black/polyethylene composites for PTC (Positive Temperature Coefficient) thermistor applications
[AD-A215988] 12 p1619 N90-19307
Evaluation of a thermistor power measurement system for use on the NPL antenna extrapolation range
[NPL-DES-89] 24 p3466 N90-29583

THERMITES
Thermochemical model for shock-induced chemical reactions in porous thermite: The heat detonation model
[DE89-016528] 02 p0193 N90-11100
An effective low-profile thermite torch
[DE90-015746] 24 p3459 N90-29534

THERMOCHEMICAL PROPERTIES
NT HEAT OF COMBUSTION
NT HEAT OF FORMATION
NT LATENT HEAT
SGTE data for pure elements
[NPL-DMA(A)-195] 15 p2181 N90-22460

THERMOCHEMISTRY
NT AEROTHERMOCHEMISTRY
NT COMBUSTION CHEMISTRY
A thermochemical analysis of proposed working fluids for electrothermal guns
[AD-A210661] 02 p0159 N90-10910

Hydrogen-silicon carbide interactions
[NASA-TM-102382] 02 p0200 N90-11144
Thermodynamic principles of the process of the effect of electromagnetic fields on a polymer melt
[AD-A210698] 02 p0201 N90-11149
Molecular dynamics study of the primitive model of 1-3 electrolyte studies
[AD-A211653] 03 p0325 N90-11846
Positron annihilation studies of interpenetrating polymer networks
[AD-A212162] 03 p0332 N90-11890
Laser probe vaporization/oxidation testing of high temperature composites
[AD-A211410] 04 p0465 N90-12663
Evaluation of selected computer models for modeling pyrotechnic and propellant devices
[AD-A213003] 05 p0629 N90-13671
Thermochemical calculations with inert compounds
[FOA-C-20759-2.1] 05 p0630 N90-13677
CANOES 2: Dynamics of atmospheric infrared thermochemical excitation, volume 3
[AD-A213343] 05 p0667 N90-13899
Method for fabricating thin film metallic meshes for use as Fabry-Perot interferometer elements, filters and other devices
[AD-D014236] 06 p0779 N90-14529
High temperature chemistry of aromatic hydrocarbons
[DE90-003664] 07 p0888 N90-15133
Guide to the selection of surface treatments for the improvement of fatigue strength of steels
[ESDU-89031] 07 p0907 N90-15245
Reacting flows 10 p1309 N90-17573
Determination of fundamental thermodynamic properties of constituent materials and performance screening of candidate systems
[AD-A218089] 13 p1769 N90-20153
Condensed phase kinetic deuterium isotope effects in high energy phenomena: Mechanistic investigations and relationships
[AD-A217161] 13 p1770 N90-20156
Testing of an advanced thermochemical conversion reactor system
[DE90-007989] 15 p2123 N90-22141
Development of high performance beta-SiC field-effect transistors
[AD-A218392] 17 p2394 N90-23637
An orthotropic theory of viscoplasticity based on overstress for thermomechanical deformation and its application to laminated metal matrix composites
17 p2415 N90-23759
Energy storage for a lunar base by the reversible chemical reaction: CaO+H2O reversible reaction Ca(OH)2
[NASA-TM-103145] 19 p2709 N90-25419
Kinetics and thermochemistry of polyatomic free radicals: New results and new understandings
20 p2946 N90-26764
The applications of chemical thermodynamics and chemical kinetics to planetary atmospheres research
20 p2948 N90-26773
Thermochemical data for silicon-containing species from ab initio electronic structure calculations
[DE90-011024] 24 p3446 N90-29463

THERMOCHROMATIC MATERIALS
Unsteady heat transfer measurement using thermochromatic liquid crystals as temperature indicators 08 p1081 N90-16254
CO2 depth profiles in cometary model substances of KOSI 12 p1742 N90-20014

THERMOCLINES
An experimental and analytical examination of stratified thermal storage 09 p1215 N90-17046
Study of seasonal variation of mixing phenomena in the hypolimnion of Lake Geneva (Switzerland)
19 p2688 N90-25287
On the fine-scale mixing in the metalimnion and the seasonal thermocline of the Leman (Lake Geneva, Switzerland) 19 p2688 N90-25288
Rates of vertical mixing, gas exchange, and new productions: Estimates from seasonal gas cycles in the upper ocean near Bermuda
[PB90-244781] 24 p3496 N90-29758

THERMOCOUPLES
Thin film thermocouples for high temperature measurement
[PB89-209290] 01 p0073 N90-10420
NIST (National Institute of Standards and Technology) measurement services: The calibration of thermocouples and thermocouple materials
[PB89-209340] 02 p0222 N90-11274
Using self-calibrating thermocouples in industry
[DE89-013539] 02 p0223 N90-11278
Thin-film sensors for reusable space propulsion systems
[NASA-TM-102383] 05 p0616 N90-13595
Modeling a self-calibrating thermocouple for use in a smart temperature measurement system
[DE90-003697] 08 p1081 N90-16259
Attachment of lead wires to thin film thermocouples mounted on high temperature materials using the parallel gap welding process
[NASA-TM-102442] 14 p1983 N90-21361
Temperature measurements through a solid-propellant combustion wave using imbedded fine wire thermocouples
[AD-A218642] 16 p2225 N90-22693
An evaluation of imbedded thermocouples as a solid-propellant combustion diagnostic
[AD-A219947] 17 p2406 N90-23711
A technique to measure the thermal diffusivity of high T(sub c) superconductors 22 p3147 N90-27846
Frequency response of a thermocouple wire: Effects of axial conduction
[NASA-CR-180454] 23 p3330 N90-28827

THERMODYNAMIC COUPLING
A model of the isotope effect of the oxide superconductor
[DE89-635907] 06 p0855 N90-14971
The measurements of thermoacoustic phenomena using thermoacoustic couples
[AD-A218018] 13 p1882 N90-20798

THERMODYNAMIC CYCLES
NT BRAYTON CYCLE
NT RANKINE CYCLE
NT STIRLING CYCLE
Cycle analysis of scramjet engines
[NAL-TR-1002] 01 p0008 N90-10035
Cycle analysis for helicopter gas turbine engines
[RAE-TM-P-1154] 08 p1025 N90-15921
Mechano-caloric cooling device
[NASA-CR-186316] 12 p1662 N90-19552
Preliminary design of a supersonic Short Takeoff and Vertical Landing (STOVL) fighter aircraft
[NASA-CR-186670] 17 p2352 N90-23394
Qualitative models for space system engineering
[NASA-CR-180682] 17 p2385 N90-23585
Qualitative and quantitative reasoning about thermodynamics
[NASA-CR-186788] 20 p2933 N90-26689
Open cycle heat pump development for local resource use. Phase 2: District heating case study analysis
[DE90-011123] 23 p3345 N90-28904
A comparison of scramjet engine performances of various cycles
[NAL-TR-1042] 24 p3434 N90-29397

THERMODYNAMIC EFFICIENCY
Theoretical and experimental research on a millimeter-wavelength free-electron laser
[AD-A213321] 04 p0507 N90-12925
Annual summary of basic research in thermoacoustic heat transport
[AD-A214185] 07 p1007 N90-15834
Study of the effect of ceramics gas turbine development
[DE90-702638] 09 p1196 N90-16929
A theoretical and experimental investigation of an absorption refrigeration system for application with solar energy units 16 p2226 N90-22697
Research and development of advanced gas turbine
[DE90-503377] 20 p2871 N90-26335
Laboratory study of ion-neutral collisions at suprathermal energies
[AD-A222117] 21 p3074 N90-27475
Overview on hot gas tests and molten salt corrosion experiments at the DLR 23 p3309 N90-28714
Study of a 1-Hz hypocycloidal pinch (HCP) pump for production of ultraviolet lasers
[AD-A224091] 24 p3547 N90-30064

THERMODYNAMIC EQUILIBRIUM
Global existence and asymptotic stability for a nonlinear integrodifferential equation modeling heat flow
[AD-A210647] 01 p0071 N90-10408
Balance equations for ionospheric plasmas with different partial temperatures 02 p0240 N90-11364
Vapor-liquid equilibrium of binary mixtures in the extended critical region. Part 1: Thermodynamic model
[PB89-218374] 04 p0469 N90-12687
Unitarity limits on the mass and radius of dark matter particles
[NASA-CR-186079] 05 p0713 N90-14164
RAMSCRAM: A flexible ramjet/scramjet engine simulation program
[NASA-TM-102451] 06 p0726 N90-14235
Progress in LTE and non-LTE transport calculations
[DE90-003394] 07 p0997 N90-15764
Phase equilibrium and crystal growth studies on AgGaSe2 and related nonlinear optical materials
[AD-A213650] 07 p1003 N90-15809
Critical fluid light scattering 09 p1222 N90-17087
Phase properties of the rapid cooled palladium-silicon alloy in the concentration range 40 to 58 at. percent Si
[DE90-719525] 09 p1284 N90-17444
Measurement of spectral emissivity by Fourier transform infrared spectrometer
[DE89-782319] 11 p1510 N90-18898
The free energy principle, negative energy modes, and stability
[DE90-005368] 11 p1573 N90-19056
Vapor-liquid equilibria for complex mixtures with special emphasis on the critical region
[PB90-130345] 12 p1622 N90-19324
Longitudinal traveling waves bifurcating from Vlasov plasma equilibria 12 p1715 N90-19850
Theory of defect process: Basic issues in quantitative understanding
[AERE-R-13661] 13 p1892 N90-20860
Phase equilibria and solution thermodynamics of bismuth-lead alloys
[PB90-138421] 14 p1950 N90-21163
The dynamics of scalar fields in the early universe
14 p2039 N90-21696
Toward quantum corrections in black hole thermodynamics 14 p2040 N90-21702
The calculation of infrared limb emission by ozone in the terrestrial middle atmosphere
15 p2125 N90-22151
Computer simulation of time-dependent spherically symmetric spacetimes containing radiating fluids: Formalism and code tests 15 p2185 N90-22483
Baryogenesis in extended inflation. 2: Baryogenesis via primordial black holes
[NASA-CR-182843] 20 p2941 N90-26735
Dynamics of fluids in bulk and near a vertical wall: Studied by photoncorrelation spectroscopy
[PB90-200452] 22 p3169 N90-27976
Research on the structural and electronic properties of defects in amorphous silicon
[DE90-000342] 23 p3312 N90-28730
Semiconductor measurement technology. EPROP: An interactive FORTRAN program for computing selected electronic properties of Gallium Arsenide and Silicon
[PB90-222738] 23 p3399 N90-29203

THERMODYNAMIC PROPERTIES
NT CRITICAL POINT
NT CRITICAL PRESSURE
NT CRITICAL TEMPERATURE
NT EMISSIVITY
NT ENTHALPY
NT ENTROPY
NT FREE ENERGY
NT GIBBS FREE ENERGY
NT HEAT OF COMBUSTION
NT HEAT OF FORMATION
NT LATENT HEAT
NT MELTING POINTS
NT PYROELECTRICITY
NT SPECIFIC HEAT
NT SUPERCRITICAL PRESSURES
NT SURFACE ENERGY
NT THERMAL CONDUCTIVITY
NT THERMAL DIFFUSION
NT THERMAL DIFFUSIVITY
NT THERMAL EXPANSION
NT THERMAL INSTABILITY
NT THERMAL STABILITY
NT THERMOCHEMICAL PROPERTIES
NT THERMOPHYSICAL PROPERTIES
NT VAPOR PRESSURE
NT VOLATILITY
Dynamically compressed metals: Theory
[AD-A210741] 01 p0045 N90-10257
Study of the NO3 radical decomposition reaction and the N2O5 in equilibrium with NO3 + NO2 equilibrium constant
[PB89-208961] 01 p0085 N90-10480
Thermoregulatory responses to intermittent exercise are influenced by knit structure of underwear
[AD-A209087] 01 p0095 N90-10541
Thermodynamic transport properties of nitrogen tetroxide in hypercritical conditions for regenerative cooling of a rocket engine. Volume 1: Tests
[ETN-89-94975] 01 p0134 N90-10773
Thermodynamic transport properties of nitrogen tetroxide in hypercritical conditions for regenerative cooling of a rocket engine. Volume 2: Appendices
[ETN-89-94977] 01 p0134 N90-10774
Interlaboratory comparison of two types of line-source thermal-conductivity apparatus measuring five insulating materials
[PB89-218325] 02 p0200 N90-11142
Consequence of condensed-phase formation in transient burning of TiHx/KClO in a closed system
[DE89-013922] 02 p0208 N90-11188

Efficient numerical method for computation of thermohydrodynamics of laminar lubricating films
[NASA-CR-185136] 02 p0219 N90-11256
Direct statistical thermal wind estimation procedure
[AD-A211256] 02 p0253 N90-11433
Physics and materials science of high temperature superconductors
[AD-A211246] 02 p0283 N90-11619
Analysis of opposed jet hydrogen-air counter flow diffusion flame
[NASA-CR-182366] 03 p0321 N90-11825
Application of process integration to utilities, combined heat and power, and heat pumps
[ESDU-89001] 03 p0335 N90-11909
Thermal model for double-drift IMPATT diodes on diamond heat sinks
[AD-A211746] 03 p0415 N90-12380
A critical assessment of thermodynamic and phase diagram data for the Ga-In system
[NPL-DMA(A)-174] 03 p0415 N90-12382
Flare model sensitivity of the Balmer spectrum 03 p0432 N90-12477
Heat pipe and thermal energy storage and corrosion studies (1988)
[AD-A212655] 04 p0472 N90-12706
Effects of hot corrosion on the room temperature strength of structural ceramics
[AD-A212568] 04 p0481 N90-12762
Thermal initiation of confined primary explosives with a proton beam
[AD-A212954] 04 p0482 N90-12767
A survey of the current state-of-the-art in high-energy-product permanent magnets
[AD-A211761] 04 p0549 N90-13193
Synthesis and properties of NdNiO(3) prepared by low temperature methods
[AD-A212117] 04 p0559 N90-13256
The application of cast SiC/Al to rotary engine components
[NASA-CR-179610] 05 p0581 N90-13385
Large Deployable Reflector (LDR) thermal characteristics 05 p0596 N90-13460
Low temperature optical testing of CFRP telescope panels 05 p0596 N90-13463
Thin-film sensors for reusable space propulsion systems
[NASA-TM-102383] 05 p0616 N90-13595
Thermodynamic properties of some metal oxide-zirconia systems
[NASA-TM-102351] 05 p0628 N90-13666
Efficient real gas Navier-Stokes computations of high speed flows using an LU scheme
[NASA-TM-102429] 06 p0720 N90-14203
High temperature chemistry of complex vaporization/decomposition processes
[DE89-016559] 06 p0740 N90-14306
Thermodynamic properties and hydrodynamic response of high-density high-temperature C H N O mixtures
[DE90-000836] 06 p0742 N90-14318
Earth Sciences Division annual report 1988
[DE90-002617] 06 p0801 N90-14663
Oxygen stoichiometry, structural transitions, and thermodynamic behavior of the YBa2Cu3O(x) system
[DE89-017694] 06 p0852 N90-14951
A model of the thermal and electrical properties of cosmic dust particles 06 p0863 N90-15014
Properties of aluminum-uranium alloys
[DE90-003889] 07 p0907 N90-15243
Surface thermometry of energetic materials by laser-induced fluorescence
[AD-A214423] 07 p0916 N90-15297
RF transistor thermal/electrical characterization
[DE90-001427] 07 p0920 N90-15326
A high spatial resolution study of the thermospheric response to a discrete auroral arc
[NASA-TM-102904] 07 p0961 N90-15559
Thermal and statistical properties of nuclei and nuclear systems
[DE90-000183] 07 p0990 N90-15717
Reflection technique for thermal mapping of semiconductors
[AD-D014263] 08 p1129 N90-16541
Thermodynamic studies on the ferroelectric phase transition in neutron irradiated (Li(sub x)K(1-x))2SO4 crystals at high temperature
[DE89-635786] 08 p1130 N90-16545
Estimation of thermodynamic properties of alloys from phase diagram and other loose boundary conditions
[DE90-719511] 08 p1135 N90-16579
Thermal characteristics of power MOS-FETS. Results obtained with the IRF-250 10 p1330 N90-17688
Solar cell coverglasses with enhanced thermal and mechanical properties 10 p1343 N90-17785
Prediction of high temperature metal matrix composite ply properties
[NASA-TM-102490] 10 p1348 N90-17817
Effects of elevated temperatures and thermal cycling on ceramic composite materials
[AD-A216242] 10 p1350 N90-17828
A preliminary assessment of 3-Nitro-1,2,4-Triazol-5-One (NTO) as an insensitive high explosive
[AD-A215063] 10 p1360 N90-17889
Materials thermal and thermoradiative properties/characterization technology 10 p1367 N90-17925
Finite element modeling and thermal simulations of transistor integrated circuits
[AD-A215928] 10 p1380 N90-17997
Reliability assessment using finite element techniques
[AD-A216907] 11 p1502 N90-18647
Spectroscopy and physico-chemistry of CO:H2O and CO2:H2O ices 11 p1581 N90-19111
A transient plasticity study and low cycle fatigue analysis of the Space Station Freedom photovoltaic solar array blanket
[NASA-TM-102516] 12 p1674 N90-19617
An observational study of squall lines in the Amazon
[INPE-4865-TDL/376] 12 p1693 N90-19723
Thermal modulation of light beams
[AD-D014322] 12 p1713 N90-19840
Thermodynamic properties of supercritical mixtures
[DE90-006720] 12 p1724 N90-19909
Determination of fundamental thermodynamic properties of constituent materials and performance screening of candidate systems
[AD-A218089] 13 p1769 N90-20153
Condensed phase kinetic deuterium isotope effects in high energy phenomena: Mechanistic investigations and relationships
[AD-A217161] 13 p1770 N90-20156
Electronic structure, alloy phase stability, and phase diagrams
[DE90-008306] 13 p1778 N90-20203
The measurements of thermoacoustic phenomena using thermoacoustic couples
[AD-A218018] 13 p1882 N90-20798
Investigation of surface water behavior during glaze ice accretion 14 p1906 N90-20927
Phase equilibrium of mixtures consisting of molecules with large size and shape differences (thermodynamic modeling of Supercritical Fluid Extraction and Retrograde Condensation, SFE/RC)
[PB90-131285] 14 p1947 N90-21146
Computer codes for the evaluation of thermodynamic properties, transport properties, and equilibrium constants of an 11-species air model
[NASA-TM-102602] 14 p1972 N90-21297
High power, high sensitivity microwave calorimeter
[AD-D014427] 14 p1982 N90-21355
Development of low thermal conductivity pan-based carbon fibers for solid rocket motor nozzle applications 15 p2063 N90-21818
Inverse problems of heat conduction 15 p2091 N90-21969
Displacement flow and deuteron drag in a metal: A path towards cold fusion
[PREPRINT-703] 16 p2320 N90-23227
Critical behavior of the thermal power near the metal-insulator transition
[PREPRINT-714] 16 p2323 N90-23244
The effect of catalysts on gas-phase hydrocarbon ignition
[AD-A218775] 17 p2371 N90-23499
Combined effect of isotopic substitution, temperature, and magnetic field on the lifetimes of triplet biradicals
[AD-A219711] 17 p2372 N90-23509
Preliminary investigation into the effect of high temperature thermal anneals on the figure of merit of silicon germanium alloys
[AD-A218573] 17 p2375 N90-23527
The origin of multiple melting in polyurethane block copolymers
[AD-A220050] 17 p2381 N90-23563
The feasibility of detecting corrosion in electric fuzes using the thermal transient technique
[AD-A221385] 18 p2549 N90-24547
Heat and fluid flow within the Earth's crust: In situ measurements and mathematical models 18 p2579 N90-24690
Atmospheric environment for space shuttle (STS-28) launch
[NASA-TM-100386] 19 p2715 N90-25452
Isothermal compressibility of SPC/E water
[AD-A222723] 20 p2925 N90-26643
Mathematical simulation of heat exchanges and thermoelastic constraints in Czochralski crystal growth
[ETN-90-97242] 20 p2931 N90-26680
The thermal radiative properties of metals at high temperature
[DE90-012468] 21 p2981 N90-26938
Molecular dynamics of physical aging processes in polymer glasses (experiment and theory)
[AD-A222848] 21 p2984 N90-26959
A review of reaction rates and thermodynamic and transport properties for an 11-species air model for chemical and thermal nonequilibrium calculations to 30000 K
[NASA-RP-1232] 21 p3002 N90-27064
Physics and techniques for the investigation of the properties of ultra small systems
[AD-A221985] 21 p3071 N90-27461
AMSAHTS 1990: Advances in Materials Science and Applications of High Temperature Superconductors
[NASA-CP-10043] 22 p3136 N90-27792
Kinetics and thermodynamics of ceramic/metal interface reactions related to high T(sub c) superconducting applications 22 p3141 N90-27815
Thermal and electric properties of Nd(1.85)Ce(0.15)CuO(4-y) and Pr(1.85)Ce(0.15)CuO(4-y) 22 p3141 N90-27816
Development of polysilsesquioxane composites
[NASA-CR-180263] 22 p3152 N90-27872
Atmospheric environment for space shuttle (STS-33) launch
[NASA-TM-100399] 22 p3200 N90-28159
FIRE Science Results 1989
[NASA-CP-3079] 22 p3213 N90-28224
The above-inversion moisture structure observed during FIRE 22 p3215 N90-28235
On the dynamic and thermodynamic structures of marine stratocumulus 22 p3216 N90-28244
Modification of the background flow by roll vortices 22 p3219 N90-28258
Calculation of clothing insulation and vapour resistance
[IZF-1989-49] 22 p3234 N90-28338
Phase diagram and thermodynamic data for the Am-Pu system
[NPL-DMM(A)-5] 22 p3255 N90-28431
Fuels research, volume 1
[DE90-015393] 23 p3305 N90-28695
Organic polyradical models for organic magnetic materials
[AD-A223691] 24 p3442 N90-29435
Statistically designed study of the variables and parameters of carbon dioxide equations of state
[DE90-016196] 24 p3447 N90-29467
Investigation of weld bead cooling rate during startup of gas metal arc welding
[AD-A223567] 24 p3449 N90-29478
The stress and temperature dependence of creep in an Al-2.0 wt percent Li alloy
[AD-A223676] 24 p3449 N90-29480
Piezoelectric and electrostrictive materials for transducer applications, volume 2
[AD-A223561] 24 p3480 N90-29669

THERMODYNAMICS
NT AEROTHERMODYNAMICS
NT COMBUSTION PHYSICS
NT NONEQUILIBRIUM THERMODYNAMICS
Hierarchical structure in polymeric solids and its influence on properties
[AD-A210918] 01 p0052 N90-10297
Ordered structures and metastable alloys grown by OMVPE
[DE89-016370] 01 p0129 N90-10744
Solidification front/viscous phase transitions, forward-backward heat equations
[AD-A211068] 02 p0195 N90-11114
Thermodynamic principles of the process of the effect of electromagnetic fields on a polymer melt
[AD-A210698] 02 p0201 N90-11149
A shock initiation model for fine-grained hexanitrostilbene
[DE89-007641] 02 p0207 N90-11185
Thermodynamics, kinetics, and interface morphologies of phase formation reactions between metals and Gallium Arsenide: Bulk vs thin-film studies
[DE89-016469] 02 p0284 N90-11621
An open-loop transient thermodynamic model of the Cougar turbojet
[AD-A211774] 03 p0307 N90-11745
Fuel cells for vehicle propulsion applications: A thermodynamic systems analysis
[DE89-017689] 03 p0342 N90-11950
Thermomechanical contact phenomena and wear of sliding components
[AD-A211290] 03 p0355 N90-12028
Studies on the startup transients and performance of a gas loaded sodium heat pipe
[AD-A211880] 03 p0414 N90-12379
An introduction to effectiveness: NTU relationships
[ESDU-89016] 03 p0415 N90-12381
A generalized thermomechanical constitutive model for metal matrix composites with plastic strain and damage 06 p0737 N90-14293

Structure-property relationships in surface-modified ceramics. NATO Advanced Science Institutes, series E: Applied Sciences, volume 170
[AD-A212939] 06 p0749 N90-14359

Hypervelocity impact calculations using CTH: Case studies
[DE90-002891] 06 p0795 N90-14632

Viscoplasticity: A thermodynamic formulation
[NASA-TM-102388] 06 p0797 N90-14640

Thermal fatigue durability for advanced propulsion materials
[NASA-TM-102348] 06 p0797 N90-14641

New heating and cooling technology: Regenerative heat pump according to the Vuilleumier principle
[DE90-002701] 06 p0807 N90-14699

Algorithmic randomness, physical entropy, measurements, and the second law
[DE90-002413] 06 p0830 N90-14823

A study of variable geometry in advanced gas turbines
07 p0881 N90-15104

Irreversible processes from reversible mechanics
[DE90-001057] 07 p0927 N90-15368

On the free carrier-negative U center interacting model for the high-T(sub c) oxide superconductor
[DE89-635908] 07 p0998 N90-15775

The use of hypervelocity launchers to explore previously inaccessible states of matter
[DE90-004098] 08 p1034 N90-15973

Thermodynamic analysis of chemical stability of ceramic materials in hydrogen-containing atmospheres at high temperatures
[NASA-CR-4271] 08 p1050 N90-16072

Modeling a self-calibrating thermocouple for use in a smart temperature measurement system
[DE90-003697] 08 p1081 N90-16259

Numerical predictions of local entropy generation for an impinging jet
[DE90-004671] 09 p1220 N90-17081

A numerical study of the formation of mesoscale convective complexes 09 p1245 N90-17225

An entropy-based approach to nonlinear stability
[NASA-TM-101086] 09 p1272 N90-17376

Multi-dimensional discrete ordinates solutions to combined mode radiation heat transfer problems and their application to a free-falling particle, direct absorption solar receiver
[DE90-004987] 09 p1300 N90-17531

Hydrogen energy coordinating committee: Summary of DOE hydrogen programs
[DE90-004480] 10 p1361 N90-17891

Colliding natural convection boundary layer flow in a rectangular enclosure
[DE90-005397] 10 p1384 N90-18009

Hydride heat pumps for upgrading spacecraft waste heat 10 p1385 N90-18013

Coherent phase transformation under nonhydrostatic stress-wave loading
[DE90-005719] 10 p1396 N90-18072

Processing and elevated temperature ductility of aluminum alloy 7475
[AD-A216840] 11 p1486 N90-18554

Control of phase structure in polymer blends
[AD-A217034] 11 p1491 N90-18580

Summer Study Program in Geophysical Fluid Dynamics: The Influence of Convection on Large-Scale Circulations, 1988
[AD-A216024] 11 p1535 N90-18840

Thermodynamics of systems with very many components phase equilibrium
[DE90-007345] 11 p1573 N90-19059

Demonstration of capabilities of high temperature composites analyzer code HITCAN
[NASA-TM-102560] 12 p1676 N90-19629

Linear free energy relations for multielectron transfer kinetics: A brief look at the Bronsted/Tafel analogy
[AD-A215078] 12 p1710 N90-19823

Thermal infrared scene simulation
[DE90-006900] 12 p1714 N90-19845

Theory of field reversed configurations
[DE90-006702] 12 p1717 N90-19860

The renormalization group and lattice QCD
[DE90-004860] 12 p1724 N90-19905

Evaluation of thermal and mechanical loading effects on the structural behavior of a SiC/titanium composite
[NASA-TM-102536] 13 p1767 N90-20139

Techno-economic assessment of a carbothermic alumina reduction process
[DE90-007018] 13 p1772 N90-20170

A unified integrated model for sputter coating uniformity
[DE90-008322] 13 p1778 N90-20205

Core cooling studies at LLNL (Lawrence Livermore National Laboratory) and Sandia
[DE90-008303] 13 p1795 N90-20300

A nonintrusive method for measuring the operating temperature of a solenoid-operated valve
[DE90-007576] 13 p1804 N90-20355

A technical and economic evaluation of oxygen-enriched combustion in diesel engines using water-emulsified fuels
[DE90-008095] 13 p1810 N90-20394

Analysis of methods to determine emissivity for ground surface targets in the spectral band 8 to 14 microns
[INPE-4984-TDL/394] 13 p1820 N90-20447

Coastal frontogenesis and associated severe weather on 13 March 1986 (GALE IOP 13)
[AD-A217708] 13 p1845 N90-20590

A case study of a quasi-stationary tropical convective line
[AD-A218325] 13 p1847 N90-20604

Theoretical and experimental study of solid phase miscibility gaps in III/V quaternary alloys
[DE90-008430] 13 p1895 N90-20877

BASG thermomechanical pump helium 2 transfer tests
[NASA-CR-177541] 14 p1939 N90-21097

High temperature fatigue behavior of tungsten copper composites
[NASA-TM-102404] 14 p1946 N90-21138

Phase equilibrium of mixtures consisting of molecules with large size and shape differences (thermodynamic modeling of Supercritical Fluid Extraction and Retrograde Condensation, SFE/RC)
[PB90-131285] 14 p1947 N90-21146

Ice-making heat exchanger evaluation and test plan
[DE90-008824] 14 p1959 N90-21218

An experimental evaluation of two nonazeotropic refrigerant mixtures in a water-to-water breadboard heat pump
[DE90-009016] 14 p1973 N90-21305

Thermal decay of an initially hot isothermal water body with application to thermal energy storage
[DE90-614742] 14 p2035 N90-21675

The Chemkin Thermodynamic Data Base
[DE90-007953] 14 p2035 N90-21676

The thermo-mechanical behavior of cometary nuclei
14 p2041 N90-21703

Molecular theory of fluid phase equilibria
[PB90-131277] 15 p2066 N90-21832

Thermomechanical properties of polymeric materials and related stresses
[NASA-TM-100758] 15 p2071 N90-21864

TOODEE: A two-dimensional, time-dependent heat conduction program
[DE90-009631] 15 p2099 N90-22010

Heat-transfer regimes in nuclear-reactor-pumped gas lasers
[DE90-002904] 15 p2103 N90-22032

The mechanics of shear band formation in thermal viscoplastic materials at high rates of loading
15 p2120 N90-22128

The relationship between the buoyancy of near-surface air and the potential temperature of the tropopause
15 p2128 N90-22165

Characteristics of cumulus bandclouds off the east coast of Hawaii 15 p2130 N90-22178

Overview of current bulk and thick film high temperature superconductor processing strategies
[DE90-008949] 15 p2172 N90-22414

A galaxy formation cookbook: Recipes and utensils
15 p2190 N90-22508

The HCl/aerosol problem 16 p2208 N90-22597

Inelastic response of metal matrix composites under biaxial loading 16 p2220 N90-22661

High temperature ceramic-tubed reformer
[DE90-009617] 16 p2236 N90-22755

Geothermal energy program summary
[DE89-009485] 16 p2251 N90-22837

An orthotropic theory of viscoplasticity based on overstress for thermomechanical deformation and its application to laminated metal matrix composites
17 p2415 N90-23759

Strain softening in viscoelasticity of the rate type
[AD-A219915] 17 p2417 N90-23772

Examination of microburst development in Colorado thunderstorm for the 5 August 1982 case
[AD-A218478] 17 p2425 N90-23820

Observation of a magic number in the ion distribution of ethene clusters
[AD-A219837] 18 p2521 N90-24393

Compression molded polyurethane block copolymers. 1: Thermal and thermomechanical properties
[AD-A220068] 18 p2529 N90-24431

Thermodynamic calculations for mixtures of environmentally safe refrigerants using the Lee-Kesler-Ploecker equation of state
[DE90-010493] 18 p2542 N90-24509

Ocean energy program summary. Volume 2: Research summaries
[DE89-009482] 18 p2576 N90-24677

Preconditioned time-differencing for the parallel solution of the heat equation
[DE90-010636] 18 p2590 N90-24737

Improved processing of ceramic superconductors
[DE90-009721] 18 p2624 N90-24951

National Aeronautics and Space Administration (NASA)/American Society for Engineering Education (ASEE) Summer Faculty Fellowship Program-1989, volume 2
[NASA-CR-185601-VOL-2] 18 p2630 N90-24985

Thermodynamic and fluid mechanic analysis of rapid pressurization in a dead-end tube
18 p2631 N90-24990

Thermomechanical testing techniques for high-temperature composites: TMF behavior of SiC(SCS-6)/Ti-15-3
[NASA-TM-103171] 19 p2701 N90-25367

Performance of a supercharged direct-injection stratified-charge rotary combustion engine
[NASA-TM-103105] 20 p2809 N90-25982

Investigation of thermo-mechanical effects in silicon carbide Whisker/Al alloy composites
[AD-A222635] 20 p2828 N90-26089

Code enhancements and validation of GASP
[NPS-PAPER-44] 20 p2861 N90-26277

Isothermal compressibility of SPC/E water
[AD-A222723] 20 p2925 N90-26643

Qualitative and quantitative reasoning about thermodynamics
[NASA-CR-186788] 20 p2933 N90-26689

A lattice gas model for thermohydrodynamics
[DE90-011964] 20 p2933 N90-26690

First International Conference on Laboratory Research for Planetary Atmospheres
[NASA-CP-3077] 20 p2942 N90-26744

Liquid-vapor equilibrium of multicomponent cryogenic systems 20 p2948 N90-26774

Substitution principle theory for compressible flows
21 p2953 N90-26791

Concentration, temperature, and density in a hydrogen-air flame by excimer-induced Raman scattering 21 p2974 N90-26903

The role of heat transfer during reactive-ion etching of polymer films
[AD-A222072] 21 p2977 N90-26919

The thermal radiative properties of metals at high temperature
[DE90-012468] 21 p2981 N90-26938

Determination of the heat dissipated from a specimen undergoing cyclic plasticity by a hybrid numerical/experimental method
[AD-A221575] 21 p2982 N90-26946

A continuum model for phase transformation in thermoelastic solids
[AD-A222353] 21 p3085 N90-27542

Electronic and molecular structure of carbon grains
21 p3091 N90-27574

Experimental and kinetic modeling of acid/base redox reactions over metal oxide catalysts
[DE90-013835] 22 p3156 N90-27893

Hydrocarbon-fueled scramjet combustor component development tests 22 p3162 N90-27934

Numerical investigation of the thermal stratification in cryogenic tanks subjected to wall heat flux
[NASA-TM-103194] 22 p3171 N90-27984

Noncontact laser thermomechanical nondestructive evaluation for advanced coatings
22 p3187 N90-28087

A stratocumulus thermodynamic analysis: July 5 case study 22 p3217 N90-28245

Stratus: An interactive steady state mixed layer model for personal computers 22 p3219 N90-28255

The 27-28 October 1986 FIRE cirrus case study: Meteorology and clouds 22 p3223 N90-28280

Theoretical thermodynamics: Equation of state and perturbation studies
[PB90-199332] 22 p3255 N90-28430

Molten salt induced high temperature degradation of thermal barrier coatings 23 p3307 N90-28704

Thermodynamics and structure of liquid alkali metals from the charged-hard-sphere reference fluid
[DE90-627792] 23 p3311 N90-28725

Genesis of bow echoes: A rear-inflow induced meso-convective structure
[PB90-209776] 23 p3349 N90-28926

Viscous causal cosmologies
[DE90-627487] 23 p3412 N90-29282

Estimation of liquid heat capacities. 1: Review and evaluation of Missenard method
[AD-A224161] 24 p3445 N90-29454

Proceedings of a discussion meeting on Thermodynamics of Alloys
[AD-A224336] 24 p3449 N90-29476

The roles of strain and reheating interval in continuous recrystallization during the thermomechanical processing by warm rolling of an Al-Mg alloy
[AD-A223673] 24 p3449 N90-29479
Investigation of the effects of microalloy constituents, surface treatment and oxidation conditions on the development and breakdown of protective oxide scales
[DE90-015710] 24 p3451 N90-29488
Ion-beam-assisted deposition of silver films on zirconia ceramics for improved tribological behavior
[DE90-009706] 24 p3456 N90-29516
The worldwide ionospheric data base
[NASA-TM-101823] 24 p3488 N90-29714
Three-dimensional numerical study of thunderstorm downdrafts and associated outflow boundaries
24 p3494 N90-29746

THERMOELASTICITY
NT AEROTHERMOELASTICITY
Thermoelastic behavior of large space structures: Modeling and control 02 p0179 N90-11012
A thermoelastic transversely isotropic thick walled cylinder/disk application: An analytical solution and study
[NASA-TM-102320] 04 p0511 N90-12950
Thermoelastic response of an epoxy
[AD-A215639] 09 p1198 N90-16942
Analysis of biaxial stress fields in plates cracking at elevated temperatures
[AD-A216271] 10 p1397 N90-18077
An approximation theory for the identification of linear thermoelastic systems
[NASA-CR-182015] 13 p1877 N90-20764
Residual stresses in laminated thermoplastic matrix composites 15 p2063 N90-21815
Axisymmetric and cylindrically orthotropic analysis of filament winding 16 p2246 N90-22811
Approximation in LQG control of a thermoelastic rod 16 p2297 N90-23084
Approximations of thermoelastic and viscoelastic control systems
[NASA-CR-182054] 18 p2604 N90-24834
A continuum model for phase transformation in thermoelastic solids
[AD-A222353] 21 p3085 N90-27542
Finite element analysis of coupled thermoelasticity
[PB90-201211] 23 p3337 N90-28860
Application of the complex variable solution to some problems in linear elastic materials with voids
24 p3478 N90-29658

THERMOELECTRIC CONVERSION SYSTEMS
U THERMOELECTRIC POWER GENERATION

THERMOELECTRIC COOLING
Design and calibration of an electrodynamic driver for the Space Thermoacoustic Refrigerator (STAR)
[AD-A212022] 03 p0335 N90-11906

THERMOELECTRIC GENERATORS
NT SOLAR SEA POWER PLANTS
Draft Environmental Impact Statement for the Ulysses Mission (Tier 2)
[NASA-TM-102903] 06 p0812 N90-14727
Safety evaluation report for Galileo: Volume 1
[DE90-003086] 07 p0886 N90-15122
Safety evaluation report for Galileo, volume 2
[DE90-003087] 07 p0886 N90-15123
On the development of the power sources for the Ulysses and Galileo missions 10 p1331 N90-17693
Design and operation of an inert gas facility for thermoelectric generator storage
[DE90-007146] 11 p1565 N90-19008
Thermal vacuum life test facility for radioisotope thermoelectric generators
[DE90-007148] 11 p1566 N90-19010
Safety Status Report for the Ulysses mission. Book 1: Risk analysis. General purpose heat source radioisotope thermoelectric generator program
[DE90-006826] 12 p1614 N90-19282
Safety status report for the Ulysses mission. Book 2: Risk analysis. General purpose heat source radioisotope thermoelectric generator program
[DE90-006827] 12 p1614 N90-19283
Safety Status Report for the Ulysses mission: Summary. General purpose heat source radioisotope thermoelectric generator program
[DE90-006828] 12 p1614 N90-19284
Final Safety Analysis Report for the Ulysses Mission. Volume 3 (Book 1): Nuclear risk analysis document
[DE90-008691] 14 p1939 N90-21101
Final safety analysis report for the Ulysses mission. Volume 2 (Book 1): Accident model document
[DE90-008694] 14 p1940 N90-21103
Final safety analysis report for the Ulysses Mission
[DE90-008690] 14 p1940 N90-21106
Final environmental impact statement for the Galileo Mission (Tier 2)
[NASA-TM-102925] 15 p2124 N90-22147
Draft environmental impact statement for the Galileo Mission (Tier 2)
[NASA-TM-102926] 15 p2124 N90-22148
Final Environmental Impact Statement for the Ulysses Mission (Tier 2)
[NASA-TM-101104] 15 p2126 N90-22162
General purpose heat source radioisotope thermoelectric generator program. Book 1: Accident analysis
[REPT-90SDS4202-BK-1] 15 p2166 N90-22379
General purpose heat source radioisotope thermoelectric generator. Book 2: Accident analysis, appendices
[REPT-90SDS4202-BK-2] 15 p2166 N90-22380
GPHS-RTG response to Challenger type accident
19 p2665 N90-25163

THERMOELECTRIC MATERIALS
Improvement study of iron disilicide thermoelectric materials
[AD-A218946] 16 p2252 N90-22844

THERMOELECTRIC POWER GENERATION
Low risk low power heat pipe/thermoelectric space power supply
[DE89-014817] 08 p1095 N90-16342
Thermoelectric conversion with ion conductors
[AD-A217822] 13 p1828 N90-20497
Improvement study of iron disilicide thermoelectric materials
[AD-A218946] 16 p2252 N90-22844

THERMOELECTRICITY
A thermochemical analysis of proposed working fluids for electrothermal guns
[AD-A210661] 02 p0159 N90-10910
Annealing group III-V compound doped silicon-germanium alloy for improved thermo-electric conversion efficiency
[NASA-CASE-NPO-17259-1-CU]
12 p1721 N90-19884
Transport and relaxation properties in anisotropic superconductors 15 p2170 N90-22403
Preliminary investigation into the effect of high temperature thermal anneals on the figure of merit of silicon germanium alloys
[AD-A218573] 17 p2375 N90-23527
Pressure dependence of thermoelectric power of high T(sub c) 123 compound
[PD-MT-9001] 20 p2829 N90-26092
Thermal and electric properties of Nd(1.85)Ce(0.15)CuO(4-y) and Pr(1.85)Ce(0.15)CuO(4-y)
22 p3141 N90-27816

THERMOGRAMS
U RECORDING INSTRUMENTS
U TEMPERATURE MEASURING INSTRUMENTS

THERMOGRAPHY
NDE (Non-Destructive Evaluation) publications, 1985
[PB89-229025] 03 p0356 N90-12036
Readout and signal conditioning for a linear pyroelectric array
[RSRE-MEMO-4102] 04 p0504 N90-12905
Enhancement of infrared thermographic imagery: Local smoothing and time-based interpolation
[ONERA-RT-8/7254-SN] 04 p0555 N90-13232
Investigation of ablation phenomena using IR thermography in a hypersonic wind tunnel
08 p1081 N90-16258
Analysis of biaxial stress fields in plates cracking at elevated temperatures
[AD-A216271] 10 p1397 N90-18077
Boundary estimation problems arising in thermal tomography
[NASA-CR-181964] 10 p1421 N90-18193
Evaluating thermographic phosphors in an operating turbine engine
[DE90-004874] 15 p2105 N90-22044
Engine testing of thermographic phosphors
[DE90-013269] 22 p3182 N90-28059
The application of infrared thermography to the nondestructive testing of composite materials
22 p3187 N90-28084
Image fusion through multi-resolution contrast decomposition
[IZF-1989-19] 22 p3247 N90-28412
Transient cooling of a hot surface by droplets evaporation
[PB90-227968] 23 p3325 N90-28799
Thermographic phosphor technique
24 p3421 N90-29324
Infrared thermography 24 p3421 N90-29325
Studies of surface heat transfer in an arc-heated wind tunnel
[NAL-TR-1048] 24 p3437 N90-29410

THERMOGRAVIMETRY
Characterization of diamond films by thermogravimetric analysis and infrared spectroscopy
[AD-A210564] 01 p0050 N90-10288
Structure/reactivity relationships of polysilazane preceramics
[AD-A212028] 03 p0332 N90-11888
Improved Thermo-Oxidative-Deposition screening tests for turbine lubricants
[AD-A217795] 14 p1954 N90-21188
Thermogravimetric analysis of Nd(2-x)Ce(x)CuO(4-delta)
[DE90-009184] 14 p2032 N90-21658
Thermogravimetry-mass spectrometry analysis of gas bubbles in molten glass
[DE90-014116] 23 p3303 N90-28684

THERMOHYDRAULICS
Doubly-fluted tubes and enhanced tubes in confined crossflow
[PB89-217921] 03 p0345 N90-11971
Use of the linear variate method of Monte Carlo for estimating uncertainty in thermal-hydraulic codes
[DE89-017871] 07 p0985 N90-15694
Thermohydraulics of a heat dissipating debris bed
19 p2691 N90-25310
Two-phase heat transport systems for spacecraft scaling with respect to gravity
[NLR-TP-89127-U] 21 p2965 N90-26857

THERMOLUMINESCENCE
Laser detection and discrimination system
[AD-D014301] 07 p0937 N90-15426

THERMOMAGNADYHAMICS
U THERMOMAGNETIC EFFECTS

THERMOMAGNETIC EFFECTS
Direct conversion technology
[NASA-CR-186795] 18 p2576 N90-24675

THERMOMAGNETISM
U THERMOMAGNETIC EFFECTS

THERMOMECHANICAL TREATMENT
NT HOT ISOSTATIC PRESSING
NT HOT PRESSING
Deformation induced microstructural and microchemical changes during thermomechanical treatment
[DE89-017266] 02 p0197 N90-11127
Aluminum lithium alloys for Navy aircraft
07 p0898 N90-15193
Superplastic performance and properties of the Lital Alloys 07 p0899 N90-15199
Characterization of the 6242 Si alloy. Centrifugal wheel in conventional forging
[REPT-NT-3967] 10 p1355 N90-17859
Thermomechanically-induced convective motion and natural convection in confined gaseous helium subjected to boundary heating 15 p2089 N90-21960
Study and sizing of bonded joints in space structures
[REPT-892-430-124] 16 p2207 N90-22591
The accelerated cooling in GTS plate mill
[ETN-90-97019] 19 p2682 N90-25256
The roles of strain and reheating interval in continuous recrystallization during the thermomechanical processing by warm rolling of an Al-Mg alloy
[AD-A223673] 24 p3449 N90-29479

THERMOMECHANICS
U THERMODYNAMICS

THERMOMETERS
Analysis of an R-SQUID noise thermometer
[VTT-PUBL-54] 05 p0645 N90-13769
Solid-state fluorescence above 1000 C: Application to high-temperature laser thermometry
[DE90-000728] 06 p0789 N90-14594
Measurements of heat-transfer coefficients in the interaction regions between oblique shock waves and turbulent bounuary layers with a multi-layered thin film heat transfer gauge
[DE90-004123] 09 p1216 N90-17054
Radiation thermometry at NIST: An update of services and research activities 10 p1364 N90-17903
Computer controlled cryogenic temperature controller
[AD-A218785] 16 p2227 N90-22701

THERMOMETRY
U TEMPERATURE MEASUREMENT

THERMONUCLEAR EXPLOSIONS
Exploding neutron stars near the minimum mass: The total energy release 19 p2774 N90-25769

THERMONUCLEAR PROPULSION
U NUCLEAR PROPULSION

THERMONUCLEAR REACTIONS
NT CONTROLLED FUSION
NT NUCLEAR FUSION
On the utility and ubiquity of atomic collision physics
[DE89-015356] 01 p0119 N90-10686
Ignition and burn criteria for D3He tokamak and spherical torus reactors
[DE89-015059] 01 p0125 N90-10716
Massachusetts Institute of Technology Plasma Fusion Center
[DE89-016050] 01 p0126 N90-10723
Highlights of papers presented at the workshop on Cold Fusion Phenomena
[DE89-016956] 03 p0407 N90-12334

A preliminary investigation of cold fusion by electrolysis of heavy water
[DE90-004383] 09 p1285 N90-17447
Cold fusion research
[DE90-005611] 10 p1433 N90-18267
Neon novae, recurrent novae, and type I supernovae
[DE90-003188] 12 p1728 N90-19931
US-Japan Workshop on Atomic Collisions in Solids: Abstracts of lectures
[DE90-008979] 14 p2025 N90-21611
Fusion burn dynamics in Dense Z-Pinch (DZP)
[DE90-007976] 14 p2029 N90-21638
Ignition and burn control characteristics of thermonuclear plasmas
[DE90-015385] 23 p3398 N90-29197

THERMOPHYSICAL PROPERTIES
NT CRITICAL POINT
NT CRITICAL PRESSURE
NT CRITICAL TEMPERATURE
NT EMISSIVITY
NT LATENT HEAT
NT MELTING POINTS
NT PYROELECTRICITY
NT SPECIFIC HEAT
NT SUPERCRITICAL PRESSURES
NT THERMAL CONDUCTIVITY
NT THERMAL DIFFUSION
NT THERMAL DIFFUSIVITY
NT THERMAL STABILITY
NT VAPOR PRESSURE
NT VOLATILITY

Thermophysical properties of ceramics. Part 2: Development of specific-heat-measurement apparatus at high temperature
[DE89-760382] 01 p0047 N90-10268
Development of an automated probe for thermal conductivity measurements
[PB89-209324] 01 p0073 N90-10419
Finite element analysis of cure-induced residual stress in composite materials 02 p0190 N90-11084
Low temperature properties of glasses 02 p0200 N90-11141
Interlaboratory comparison of two types of line-source thermal-conductivity apparatus measuring five insulating materials
[PB89-218325] 02 p0200 N90-11142
Mechanism for shear band formation in the high strain rate torsion test
[PB89-215370] 03 p0356 N90-12038
Tables for the thermophysical properties of methane
[PB89-222608] 04 p0469 N90-12690
Thermophysical properties of benzene. Part 2: Thermodynamic properties at elevated pressures
[ESDU-89003-PT-2] 04 p0470 N90-12694
Study of palladium and chromium silicides formation in liquid phase and in solid phase
[LAAS-89040] 04 p0470 N90-12695
Thermophysical properties of buta-1,3-diene
[ESDU-89005] 05 p0620 N90-13619
Beam collector and output window for a 35 GHz 100 kW gyrotron
[INPE-4958-RPE/603] 11 p1511 N90-18699
Effect of casting procedures and diesel engine environment on the behavior of aluminum titanate
[AD-A223079] 20 p2835 N90-26126
Critical evaluation of Jet-A spray combustion using propane chemical kinetics in gas turbine combustion simulated by KIVA-2
[NASA-TM-103173] 20 p2843 N90-26170

THERMOPHYSICS
U THERMODYNAMICS

THERMOPLASTIC FILMS
A capacitive technique for real-time monitoring polymer coating thickness on carbon filaments during prepregging process
[NASA-TM-101682] 06 p0780 N90-14533

THERMOPLASTIC RESINS
NT PEEK
NT THERMOPLASTIC FILMS
Interfacial adsorption and crystallization of polycarbonate in carbon fiber composites
[AD-A211230] 02 p0191 N90-11090
Synthesis of energetic single phase and multi-phase polymers
[AD-A212539] 04 p0481 N90-12761
The adhesive bonding of thermoplastic composites
[AD-A213358] 05 p0618 N90-13605
Impact tests on aluminum 2024 T3, aramid and glass reinforced aluminum laminates and thermoplastic composites
[LR-534] 05 p0619 N90-13613
Crosslinkable polymer
[GB-PATENT-2-205-846-A] 05 p0628 N90-13663
A novel heat resistant blend produced by compositional quenching: A thermoplastic polyimide impact modified with a fluoroelastomer
[AD-A213724] 07 p0912 N90-15273
Vibration damping composition suitable for outer space temperature variations
[AD-D014288] 08 p1088 N90-16296
Interfaces of organic matrices and graphite fiber composites: A review of the literature
[AD-A214504] 09 p1186 N90-16870
A study of failure characteristics in thermoplastic composite laminates due to an eccentric circular discontinuity
[AD-A216226] 10 p1349 N90-17827
Comparison between the damage modes of thermo-hardenable and thermo-plastic composite matrices
[ONERA-RT-47/7086-M] 11 p1481 N90-18523
Determinations of molecular weight and molecular weight distribution of high polymers by the rheological properties
[NASA-CR-186450] 14 p1953 N90-21180
Mechanics of necking, crazing, and crack growth in polymers 17 p2378 N90-23540
Industrial plastics waste: Identification and segregation 18 p2513 N90-24351
Time temperature relations during rubber forming continuous fiber reinforced thermoplastics
[LR-620] 20 p2840 N90-26151
Synthesis of energetic single phase and multi-phase polymers
[AD-A222491] 21 p2988 N90-26981
A characterization of V-391/H46-8B, A toughened BMI prepreg system produced by US Polymeric
[AD-A221772] 21 p2989 N90-26985
Transcrystalline morphology in carbon fibre composites with thermoplastic matrix and its influence on the mechanical properties
[FOA-C-20783-2.1] 22 p3248 N90-28423
Some studies of the vibration welding of thermoplastics 23 p3332 N90-28842
Prediction and control of processing-induced residual stresses in composites. Part 2: AS4/PEEK composite
[AD-A223696] 24 p3443 N90-29445
Interlaminar shear tests on continuous fiber reinforced thermoplastics: The effects of rubber forming
[LR-621] 24 p3444 N90-29451
Solid-state N15 NMR of N15-labeled nylon 6 and nylon 11
[AD-A223271] 24 p3446 N90-29459

THERMOPLASTICITY
Stability conditions for steady shearing. Stability conditions for simple shear under mixed thermal boundary conditions 04 p0499 N90-12873
The adhesive bonding of thermoplastic composites
[AD-A213358] 05 p0618 N90-13605
A novel heat resistant blend produced by compositional quenching: A thermoplastic polyimide impact modified with a fluoroelastomer
[AD-A213724] 07 p0912 N90-15273
LARC-IA: A flexible backbone polyimide
[NASA-TM-102586] 09 p1196 N90-16926
A study of failure characteristics in thermoplastic composite laminates due to an eccentric circular discontinuity
[AD-A216226] 10 p1349 N90-17827
Residual stresses in laminated thermoplastic matrix composites 15 p2063 N90-21815
Ply cracking in composite laminates 17 p2368 N90-23478
An elastic/viscoplastic constitutive model for fiber-reinforced thermoplastic composites 18 p2516 N90-24371
Processing polymeric powders 18 p2647 N90-25069
The yield and post-yield behavior of high-density polyethylene
[NASA-CR-186574] 19 p2676 N90-25219
Fractography of composite delamination
[NASA-CR-181965] 19 p2702 N90-25372
Fracture toughness of polyimide films
[NASA-TM-103473] 20 p2836 N90-26130
A tough high performance composite matrix
[NASA-CASE-LAR-14338-1] 21 p2970 N90-26881
A tough performance simultaneous semi-interpenetrating polymer network
[NASA-CASE-LAR-14339-1] 21 p2984 N90-26955
Dissipation of mechanical work and temperature rise in AS4/PEEK thermoplastic composite
[NASA-CR-186893] 23 p3302 N90-28678
A constitutive model for AS4/PEEK thermoplastic composites under cyclic loading
[NASA-CR-180393] 23 p3302 N90-28679

THERMOREGULATION
Control of thermoregulatory sweating during exercise in the heat
[AD-A206001] 01 p0092 N90-10523
Thermoregulatory responses to intermittent exercise are influenced by knit structure of underwear
[AD-A209087] 01 p0095 N90-10541
Measurement of mechanical work and energy expenditure in running and bicycling 05 p0675 N90-13935
The effects of nonselective and selective beta blockade upon nonshivering thermogenesis during an acute cold exposure in cold acclimated men 06 p0820 N90-14767
Temperature regulation during upper body exercise: Able bodied and spinal cord injured
[AD-A215130] 09 p1252 N90-17264
Sensations of temperature and humidity during intermittent exercise and the influence of underwear knit structure
[AD-A215285] 09 p1252 N90-17266
Use of self-induced hypnosis to modify thermal balance during cold water immersion
[AD-A216156] 10 p1412 N90-18140
Influence of theobromine on heat production and body temperatures in cold-exposed humans: A preliminary report
[AD-A217203] 13 p1850 N90-20618
The effect of moisture absorption in clothing on the human heat balance
[AD-A217899] 13 p1852 N90-20626
Hydration effects on human physiology and exercise-heat performance
[AD-A217969] 13 p1852 N90-20629
Field management of accidental hypothermia during diving
[AD-A219560] 17 p2434 N90-23866
Work enhancement and thermal changes during intermittent work in cool water after carbohydrate loading
[AD-A222877] 21 p3034 N90-27247

THERMOSETTING RESINS
NT EPOXY RESINS
NT KEVLAR (TRADEMARK)
NT NYLON (TRADEMARK)
NT PHENOLIC EPOXY RESINS
NT PHENOLIC RESINS
NT POLYAMIDE RESINS
Study of the application of automation to composites manufacture
[AD-A211049] 02 p0190 N90-11087
RTM user's guide
[NASA-CR-186091] 04 p0531 N90-13065
Cellular thermosetting fluorodiepoxide polymers
[NASA-CASE-GSC-13008-2] 09 p1199 N90-16949
Fundamental studies of time-dependent response and fracture of cross-linked polymers
[AD-A216694] 10 p1360 N90-17886
Enhanced bonding of fiber reinforcements to thermoset resins 11 p1476 N90-18496

THERMOSPHERE
Seasonal and geomagnetic response of the thermosphere and ionosphere 02 p0243 N90-11380
Ionosphere-thermosphere coupling at high latitudes: Aspect angle dependence of non-thermal plasmas 02 p0244 N90-11382
Calculation of the temperature and velocity vector of the neutral gas using EISCAT CP3-data 02 p0244 N90-11384
Retrieval of atomic oxygen and temperature in the thermosphere. Part 2: Feasibility of an experiment based on limb emission in the OI lines
[AD-A211807] 03 p0371 N90-12121
Spatial characteristics of airglow and solar scatter radiance from the earth's atmosphere
[AD-A211358] 03 p0372 N90-12126
Retrieval of atomic oxygen and temperature in the thermosphere. Part 1: Feasibility of an experiment based on the spectrally resolved 147 micrometer limb emission
[AD-A211987] 04 p0517 N90-12986
Neutral air turbulence in the middle and upper atmosphere observed during the MAC/EPSILON campaign 05 p0660 N90-13855
A high spatial resolution study of the thermospheric response to a discrete auroral arc
[NASA-TM-102904] 07 p0961 N90-15559
Report from upper atmospheric science 10 p1444 N90-18332
USU center of excellence in theory and analysis of the geo-plasma environment
[AD-A217736] 13 p1759 N90-20101
Low latitude F-region dynamical processes from atomic oxygen nightglow emissions
[INPE-4999-PRE/1561] 14 p2006 N90-21494

A study of gravity wave variability, saturation, and turbulence generation in the mesosphere and lower thermosphere
[AD-A220018] 17 p2424 N90-23810
Ion neutral gas coupling in the polar atmosphere: Use of EISCAT for the calculation of thermospheric parameters
[ETN-90-96490] 18 p2580 N90-24694
Current status of SHARC, the strategic high altitude radiance code, and description of its new auroral module
[AD-A221068] 18 p2580 N90-24698
Conceptual design study for Infrared Limb Experiment (IRLE)
[NASA-CR-186950] 21 p2968 N90-26869
Absolute wind measurements in the lower thermosphere of Venus using infrared heterodyne spectroscopy
[NASA-CR-4290] 21 p3100 N90-27605
Solar wind and high energy particle effects in the middle atmosphere 22 p3206 N90-28188
Lower thermosphere (80-100 km) dynamics response to solar and geomagnetic activity: Overview 22 p3207 N90-28194
A new calculation of the radiative cooling by carbon dioxide in the middle atmosphere and the lower thermosphere 22 p3210 N90-28211
Atmospheric structure and variability
[AD-A223439] 24 p3492 N90-29734

THERMOSTABILITY
U THERMAL STABILITY

THERMOSTATS
Measurement of the p, v, T behavior under microgram conditions
[ETN-90-95906] 08 p1065 N90-16162

THERMOTROPISM
U ANISOTROPY
U TEMPERATURE EFFECTS

THESAURI
Terminology strategies for international information exchange
[AD-A214147] 07 p1010 N90-15853
CRISP (Computer Retrieval of Information on Scientific Projects) thesauras, fiscal year 1990
[PB90-138652] 12 p1726 N90-19922
NASA Thesaurus supplement: A four part cumulative supplement to the 1988 edition of the NASA Thesaurus (supplement 3)
[NASA-SP-7064-SUPPL-3] 15 p2177 N90-22438
The NATO thesaurus project
[NASA-CR-186931] 21 p3087 N90-27552

THETA PINCH
Initial results from FRC (Field-Reversed Configuration) compression experiments on FRX-C/LSM
[DE90-003390] 07 p0995 N90-15754
Microfluctuations of plasma density in a theta-pinch and spatial coherency of a probing laser beam
[DE90-603347] 07 p0996 N90-15760

THICK FILMS
The 120V 10A SSPC for the Columbus programme 10 p1330 N90-17683
Compatibility of Au base thick films with solder alloys: Solid state growth of intermetallics
[DE90-009285] 14 p1952 N90-21175
Overview of current bulk and thick film high temperature superconductor processing strategies
[DE90-008949] 15 p2172 N90-22414
Scanning laser photocurrent spectroscopy of electrochemically grown bismuth sulphide films
[AERE-M-3709] 16 p2217 N90-22649
Spatial conductivity measurements on high T(sub c) superconducting films 22 p3148 N90-27849

THICK PLATES
Finite element analysis of laminated composite plates 06 p0737 N90-14291
Crazing and degradation of flexure strength in acrylic plates as a function of time
[AD-A212835] 06 p0749 N90-14357
Resultant forces and moments in completely restrained plates subjected to a recovery temperature varying linearly with time
[ESDU-89024] 07 p0947 N90-15480
Thermal stresses in unrestrained plates subjected to a recovery temperature varying linearly with time
[ESDU-89025] 07 p0947 N90-15481
Temperatures in plates subjected to a recovery temperature varying linearly with time
[ESDU-89023] 07 p1007 N90-15831
Information on the use of data items on hot structures
[ESDU-89021] 12 p1674 N90-19611
Temperatures in plates subjected to a sudden increase in recovery temperature
[ESDU-89026] 12 p1724 N90-19904
Through-thickness strain response of thick composites in compression
[AD-A217233] 13 p1767 N90-20141
Three-dimensional finite element formulations for thick and thin laminated plates 15 p2121 N90-22132
Accuracy of the QUAD4 thick shell element 18 p2569 N90-24641
Postbuckling response of long thick plates loaded in compression including higher order transverse shearing effects
[NASA-TM-102663] 19 p2700 N90-25363
Postbuckling response of long thick isotropic plates loaded in compression including higher order transverse shearing effects
[NASA-TM-4199] 22 p3190 N90-28100

THICK WALLS
A thermoelastic transversely isotropic thick walled cylinder/disk application: An analytical solution and study
[NASA-TM-102320] 04 p0511 N90-12950
Elastic-plastic analysis of a thick-walled composite tube subjected to internal pressure
[AD-A215258] 09 p1238 N90-17187
Calculation of thick wall fiber binders for rotor components of modern helicopters
[MBB-UD-554/84-PUB] 19 p2660 N90-25137

THICKNESS
Alternative test methodology for ballistic performance ranking of armor ceramics
[AD-A210587] 01 p0051 N90-10290
Bias and oxide thickness dependence of trapped charge buildup in MOS devices
[AD-A210264] 01 p0131 N90-10757
Measuring the thickness of austenitic weld deposits on carbon steel walls using a magnetic method
[DE89-635446] 06 p0794 N90-14628
Thickness, velocity, and temperature measurements in falling liquid films
[DE90-004290] 08 p1063 N90-16151
Application of x ray fluorescence method to measuring thickness of galvanic coatings and measures of improving sensitivity of such measurings
[DE89-633351] 09 p1233 N90-17156
Airborne electromagnetic sensing of sea ice thickness
[AD-A214460] 09 p1240 N90-17198
Assembly technology of GaAs solar cell 10 p1341 N90-17772
Optimization of laminated composite plates
[AD-A217621] 13 p1768 N90-20146
Evaluation of material homogeneity as a function of thickness of low-alloy ferritic steel
[DE90-008069] 13 p1777 N90-20202
Through-the-thickness fatigue crack closure behavior in an aluminum alloy
[NASA-TM-102590] 13 p1816 N90-20427
Ultrasonic techniques for aircraft ice accretion measurement 14 p1906 N90-20926
Estimating sea ice thickness using time-of-flight data from impulse radar soundings
[AD-A218736] 16 p2250 N90-22831
Assessment of fundamental materials needs for Thick Thermal Barrier Coatings (TTBC's) for truck diesel engines
[NASA-TM-103130] 17 p2377 N90-23536
Remote measurement of ice thickness on the shuttle external tank surface
[NASA-TM-102667] 18 p2555 N90-24584
Minimum weight design of a leaf spring tapered in thickness and width for the Hubble Space Telescope-space support equipment
[NASA-TM-4233] 23 p3340 N90-28879
Nondestructive material characterization
[DE90-015176] 24 p3477 N90-29652

THICKNESS RATIO
Proof of principle study of thickness measurements using characteristic x ray line ratio techniques
[AD-A221113] 18 p2535 N90-24461

THIN AIRFOILS
NT THIN WINGS
Some recent developments in materials and techniques for model fabrication 08 p1031 N90-15955

THIN FILMS
NT FERROMAGNETIC FILMS
NT MONOMOLECULAR FILMS
Raman characterization of high temperature materials using an imaging detector
[DE89-016308] 01 p0040 N90-10219
Silicon dioxide deposition at 100 deg C using vacuum ultraviolet light
[TR-0088(3945-07)-6] 01 p0047 N90-10269
Characterization of diamond films by thermogravimetric analysis and infrared spectroscopy
[AD-A210564] 01 p0050 N90-10288
Thin film thermocouples for high temperature measurement
[PB89-209290] 01 p0073 N90-10420
Alternative fabrication techniques for high-efficiency CuInSe2 and CuInSe2-alloy films and cells
[DE89-009451] 01 p0083 N90-10474
Analytic theory for the selection of Saffman-Taylor fingers in the presence of thin film effects
[NASA-CR-181910] 01 p0118 N90-10677
Second-order nonlinear optical devices in poled polymers
[DE89-015842] 01 p0123 N90-10703
Optical dispersion relations for diamondlike carbon films
[NASA-TM-102356] 01 p0129 N90-10738
Morphological aspects of the friction of hot-filament-grown diamond thin films
[DE89-015986] 01 p0130 N90-10750
Reactive ion etching of SiC thin films by mixtures of fluorinated gases and oxygen
[AD-A211046] 02 p0195 N90-11113
Capacitive behavior in conducting polymers: The ac impedance and quartz crystal microbalance studies
[AD-A210754] 02 p0201 N90-11150
Cell performance of ultra-thin polymer cathode system: Theoretical energy and power density projections
[AD-A210786] 02 p0202 N90-11151
Intergranular and interphase boundaries in ceramics
[DE89-016969] 02 p0202 N90-11154
Efficient numerical method for computation of thermohydrodynamics of laminar lubricating films
[NASA-CR-185136] 02 p0219 N90-11256
CuInSe2 solar cell research by sputter deposition
[DE89-009450] 02 p0236 N90-11345
Proceedings of the Polycrystalline Thin Film Program Meeting
[DE89-009457] 02 p0237 N90-11348
Diamondlike carbon coatings for optical systems
[AD-A211255] 02 p0276 N90-11573
Novel thin-film CuInSe2 fabrication
[DE89-009440] 02 p0281 N90-11604
Physics and materials science of high temperature superconductors
[AD-A211246] 02 p0283 N90-11619
Thermodynamics, kinetics, and interface morphologies of phase formation reactions between metals and Gallium Arsenide: Bulk vs thin-film studies
[DE89-016469] 02 p0284 N90-11621
Reactive ion etching of sputtered silicon carbide and tungsten thin films for device applications
[AD-A211711] 03 p0325 N90-11847
Temperature dependent effects during Ag deposition on Cu(110)
[DE89-016987] 03 p0327 N90-11857
Method of modifying the dielectric properties of an organic polymer film
[AD-D014171] 03 p0330 N90-11879
Plasma-deposited amorphous hydrogenated carbon films and their tribological properties
[NASA-TM-102379] 03 p0331 N90-11880
Vanadium dioxide protective devices
[AD-A212018] 03 p0332 N90-11887
Microwave signal detection using modulation of polymeric optical waveguides
[DE89-017545] 03 p0337 N90-11921
Assessment of thin film batteries based on polymer electrolytes. Part 1: Energy density
[AD-A212111] 03 p0343 N90-11958
Analysis of loss mechanisms in polycrystalline thin-film solar cells
[DE89-009454] 03 p0366 N90-12093
Thin film magnetic memory elements
[AD-D014177] 03 p0398 N90-12281
Characterizations of electrical properties of highT(sub c) superconducting materials
[NASA-TM-100380] 03 p0409 N90-12345
Field-assisted bonding of single crystal quartz
[DE89-015407] 03 p0410 N90-12353
Ion beam deposition of epitaxial germanium and gallium arsenide layers
[DE89-017439] 03 p0411 N90-12357
Synthesis and microstructure of highly oriented PbTiO3 thin films prepared by a sol-gel method
[AD-A211735] 03 p0414 N90-12377
Spectroscopic ellipsometry characterization of CVD deposition and doping of polysilicon multilayer structures
[RSRE-MEMO-4258] 04 p0466 N90-12671
Thermal stability of the carbon-carbon bond in ethylene adsorbed on Si(100): An isotopic mixing study
[AD-A211591] 04 p0470 N90-12691
Metallo-organic decomposition process for dielectric films
[AD-A211590] 04 p0495 N90-12849
Thin-film integrated injection logic
[AD-D014190] 04 p0497 N90-12860
Laser Induced Damage in Optical Materials: 1987
[PB89-221162] 04 p0505 N90-12913
Assessment of thin film batteries based on polymer electrolytes. Part 3: Specific energy versus specific power
[AD-A212141] 04 p0515 N90-12976

High speed quantum-well optoelectronic devices by MBE
[AD-A212585] 04 p0555 N90-13237
Structural and electrical properties of thin films and superlattices composed of II-VI semiconductors 04 p0558 N90-13249
Method for growing patterned thin films of superconductors
[AD-D014195] 04 p0560 N90-13262
Synthesis and study of materials for superconducting electronics
[AD-A212966] 04 p0561 N90-13270
Growth and characterization of zinc sulfide films by conversion of zinc oxide films with H2S
[AD-A213345] 04 p0561 N90-13271
Thin-film sensors for reusable space propulsion systems
[NASA-TM-102383] 05 p0616 N90-13595
Evaluation of newly formulated Dow Corning 321 dry film lubricant
[NASA-CR-183828] 05 p0627 N90-13661
Microwave microstrip resonator measurements of Y1Ba2Cu3O(7-x) and Bi2Sr2Ca1Cu2O(8-y) thin films
[NASA-TM-102159] 05 p0635 N90-13704
Studies of structure and switching dynamics in ferroelectric crystal and liquid crystal thin films
[AD-A212650] 05 p0702 N90-14109
The biocorrosion of copper by biopolymers as examined in situ, in real time FT-IR/CIR/ATR in conjunction with pre and post XPS/AES
[DE90-002086] 06 p0747 N90-14348
Fast transit gas- and condensed-phase chemistry of energetic materials
[DE90-001656] 06 p0755 N90-14395
Theoretical and material studies of thin-film electroluminescent devices
[NASA-CR-186104] 06 p0768 N90-14468
Practical superconductor development for electrical power applications
[DE90-001804] 06 p0771 N90-14487
Method for fabricating thin film metallic meshes for use as Fabry-Perot interferometer elements, filters and other devices
[AD-D014236] 06 p0779 N90-14529
Research on high-efficiency, multiple-gap, multijunction, amorphous-silicon-based alloy thin-film solar cells
[DE89-009444] 06 p0803 N90-14673
Preparation and properties of high deposition a-Si:H films and solar cells using disilane
[DE89-009467] 06 p0804 N90-14679
Thin film cadmium telluride, zinc telluride, and mercury zinc telluride solar cells
[DE89-009499] 06 p0804 N90-14681
Research on high-efficiency, single-junction, monolithic, thin-film amorphous silicon solar cells
[DE89-000846] 06 p0805 N90-14687
Photovoltaic Measurements and Performance Branch
[DE89-009500] 06 p0807 N90-14695
Static and dynamic magnetization properties of Y1Ba2Cu3O(sub z) thin films
[DE89-017584] 06 p0850 N90-14940
Ion beam analysis and modification of thin-film, high-temperature superconductors
[DE90-000918] 06 p0850 N90-14941
X ray reflectivity study of SiO2 on Si
[DE90-001326] 06 p0851 N90-14943
Solid State Division
[DE90-000979] 06 p0851 N90-14945
Development of a real time monitor for superconductive thin film preparation
[DE89-017772] 06 p0852 N90-14952
Magnetotransport studies of epitaxial Cr thin films
[DE90-001930] 06 p0856 N90-14975
Magnetic and electrical properties
[DE90-002183] 06 p0856 N90-14977
The influence of the substrate surface on the nucleation and growth of superconducting thin films
[DE90-003649] 06 p0857 N90-14983
Electronic materials high-T(sub c) superconductivity polymers and composites structural materials surface science and catalysts industry participation
[NASA-CR-186063] 07 p0890 N90-15145
Superconducting film fabrication by the sol-gel process
[DE90-002069] 07 p0909 N90-15252
Characterization and in situ testing of diamond films
[DE90-003155] 07 p0911 N90-15265
Optical properties and laser damage measurements of inorganic polymer films
[DE90-003633] 07 p0911 N90-15267
New devices using ferroelectric thin films
[DE90-000789] 07 p0921 N90-15328
Analysis of an elastohydrodynamic lubricated point contact: User's manual
[AD-A214257] 07 p0943 N90-15459
Thin films under chemical stress
[DE90-003754] 07 p0947 N90-15484
Research on high-efficiency, single-junction, monolithic, thin-film amorphous silicon solar cells, phase 1
[DE89-009495] 07 p0951 N90-15502
Research on high-efficiency, single-junction, monolithic, thin-film amorphous silicon solar cells, phase 2
[DE89-009496] 07 p0951 N90-15503
US Polycrystalline Thin Film Solar Cells Program
[DE89-009506] 07 p0951 N90-15504
Phonons and charge-transfer excitations in HTS superconductors
[DE89-016616] 07 p0997 N90-15768
Micron-thin Nb films recovered from Mbar shock pressures
[DE90-001509] 07 p0998 N90-15772
Partial reduction of re-oxidation processing of Y-Ba-Cu-O sputtered thin films
[DE90-003655] 07 p0999 N90-15782
Orientation of rf-sputter-deposited MoS2 films
[ATR-89(4752)-1] 07 p1000 N90-15784
Two-dimensional magnetic phase transition of ultrathin iron films on Pd(100)
[DE90-003555] 07 p1000 N90-15788
Characterization of MOCVD (Metal Organic Chemical Vapor Deposition) grown epitaxial ceramic oxide thin films
[DE90-003561] 07 p1001 N90-15790
Preparation, structure and properties of VO(sub x) and TiO2 thin films by MOCVD
[DE90-003566] 07 p1001 N90-15793
Magnetic flux pinning in YBa2Cu3O7 films
[DE90-003709] 07 p1002 N90-15799
Computer-controlled ion beam sputter-deposition of superconducting oxide films
[AD-A213921] 07 p1004 N90-15812
High-temperature ceramic superconductors
[AD-A214251] 07 p1005 N90-15818
The fabrication of YBa2Cu3O7 thin films by thermal coevaporation in oxygen
[DE90-003960] 07 p1006 N90-15824
Solid state voltammetry and sensors in solids and gases
[DE90-003234] 08 p1129 N90-16538
Lithium cobalt oxide thin film and its electrochromism
[DE90-004570] 08 p1133 N90-16564
Artificially structured superconductors
[DE90-004851] 08 p1134 N90-16567
Plasma assisted chemical vapor deposition of diamond films
[AD-A214641] 09 p1197 N90-16934
Adhesion of silver films to ion-bombarded alumina
[DE90-005642] 09 p1199 N90-16947
Rotary absorption heat pump sensitivity analysis
[DE90-002877] 09 p1216 N90-17053
Measurements of heat-transfer coefficients in the interaction regions between oblique shock waves and turbulent boundary layers with a multi-layered thin film heat transfer gauge
[DE90-004123] 09 p1216 N90-17054
High-efficiency copper ternary thin film solar cells
[DE89-009470] 09 p1242 N90-17207
Research on amorphous silicon based thin film photovoltaic devices. Phase 2: Research on stable high-efficiency, large area amorphous silicon based submodules
[DE89-009515] 09 p1243 N90-17209
Edge geometry superconducting tunnel junctions utilizing an NbN/MgO/NbN thin film structure
[NASA-CASE-NPO-17812-1-CU] 09 p1286 N90-17456
Electrical transport dissipation effects in epitaxial Y1Ba2Cu3O(7-x) thin films
[DE90-004301] 09 p1287 N90-17461
Interfacial and thin film chemistry in electron device fabrication
[AD-A214784] 09 p1289 N90-17473
Growth characteristics and electronic behavior of ultrathin epitaxial metallizations
[AD-A214794] 09 p1289 N90-17474
Method of producing a thin silicon-on-insulator layer
[AD-D014330] 09 p1290 N90-17478
Effects of O2 ion bombardment of Y-BaCu-oxide during thin film growth
[DE90-005315] 09 p1293 N90-17495
Epitaxial growth of Cr(011) on LiF(001)
[DE90-005635] 09 p1293 N90-17496
Mechanical aspects of interfaces in high performance composites 10 p1347 N90-17812
Photoelectron spectroscopic study of the interaction of thin Fe films with the MoS2(0001) surface
[AD-A214348] 10 p1351 N90-17836
Strain induced amorphization of aluminium by manganese implantation
[DE90-607259] 10 p1356 N90-17863
Computer simulation of electromigration in thin films
[AD-A216382] 10 p1357 N90-17867
Electron-beam induced damage in thin insulating films on compound semiconductors
[NASA-CR-185177] 10 p1378 N90-17987
Remote sensing: Environmental effects of surface films
[AD-A216190] 10 p1400 N90-18094
Research on high-efficiency, multi-gap, multi-junction amorphous silicon-based alloy thin-film solar cells
[DE89-009492] 10 p1402 N90-18101
Chemical activation of molecules by metals: Experimental studies of electron distributions and bonding
[DE90-005371] 10 p1428 N90-18238
Develop techniques for ion implantation of PLZT for adaptive optics
[AD-A216005] 10 p1431 N90-18253
Investigation of low temperature multilevel dielectrics for application for radiation tolerant, submicron-scaled IC technology
[AD-A216114] 10 p1433 N90-18273
Reflectance modulation with electrochromic Li(sub x)WO(3) films
[DE90-004571] 10 p1435 N90-18279
High temperature superconductivity
[AD-A215491] 10 p1436 N90-18286
Materials processing of diamond: Etching, doping by ion implantation and contact formation
[AD-A216530] 10 p1438 N90-18301
Interfacial chemistry of MoS2 films on Si
[AD-A216527] 11 p1482 N90-18532
Surface intermediates in thin film deposition on silicon
[AD-A216662] 11 p1483 N90-18534
Structure and reactivity of model thin film catalysts
[DE90-007365] 11 p1485 N90-18546
Perforated monolayers
[DE90-005469] 11 p1488 N90-18566
Metallaboranes as precursors to metallic glasses
[AD-A216946] 11 p1490 N90-18577
Hydrogenated amorphous silicon films prepared by glow discharge of disilane
[DE90-000309] 11 p1491 N90-18581
Research relating to crystalline silicon-film on a foreign substrate
[DE90-005720] 11 p1491 N90-18582
Microcomputer enhanced optical investigation of spreading and evaporative processes in ultra thin films
[DE90-006323] 11 p1492 N90-18585
Cell performance of ultra-thin polymer cathode systems. Part 1: Anion intercalating polymer cathode
[AD-A216037] 11 p1501 N90-18639
Progress in thin film solar photovoltaic technologies
[DE89-009513] 11 p1527 N90-18792
Chemical vapor deposition and photochemical vapor deposition of amorphous silicon photovoltaic devices
[DE89-009510] 11 p1529 N90-18803
Pulsed laser deposition of high T(sub c) superconducting thin films
[AD-A216507] 11 p1569 N90-19034
Structure and vibrational excitations of reconstructed semiconductor surfaces
[DE90-006589] 11 p1571 N90-19044
In situ growth of high quality epitaxial YBa2Cu3O(7-x) thin films at moderate temperatures by pulsed laser ablation
[DE90-006629] 11 p1571 N90-19045
Preparation and characterization of alumina films prepared by a novel spray pyrolysis method
[AD-A217570] 12 p1625 N90-19339
Nanolayer reactions in aluminum-metal interfaces
[DE90-004955] 12 p1626 N90-19342
Glancing angle XAFS (X ray Absorption Fine Structure) and x ray reflectivity studies of transition-metal/aluminum interfaces
[DE90-005575] 12 p1627 N90-19353
Transmission and reflection studies of thin films in the vacuum ultraviolet 12 p1638 N90-19412
High density tape casting system
[NASA-CASE-NPO-16901-1-CU] 12 p1640 N90-19425
Numerical and experimental analysis of a thin liquid film on a rotating disk related to development of a spacecraft absorption cooling system
[NASA-CR-183457] 12 p1657 N90-19523
Laser mass spectrometric studies of high temperature superconductor ablation
[DE90-006518] 12 p1668 N90-19585
Heteroepitaxial growth of germanium films by supersonic free jet chemical beam epitaxy
[DE90-006621] 12 p1720 N90-19877
Characterization of ground state neutral and ion transport during laser ablation of 1:2:3 superconductors by transient optical absorption spectroscopy
[DE90-006623] 12 p1720 N90-19878

Investigations of CuInSe2 thin films and contacts
[DE90-000301] 12 p1721 N90-19886
Growth and characterization of gallium (III) oxide films
[AD-A217568] 12 p1723 N90-19902
Studies of the structure and properties of organic monolayers, multilayers and superlattices
[DE90-008330] 13 p1765 N90-20129
Symposium on High Temperature and Materials Chemistry
[DE90-008047] 13 p1768 N90-20148
Mechanisms of reactive etching
[AD-A217679] 13 p1770 N90-20160
Hydrous metal oxide-supported catalysts. Part 1: Preparation chemistry and physical and chemical properties
[DE90-007607] 13 p1771 N90-20161
Deep level transient spectroscopy in resistive layers
[DE90-008349] 13 p1772 N90-20169
Infrared and X ray photoelectron spectroscopy studies of the polyimide/metal interface
[AD-A218249] 13 p1773 N90-20179
Reactive sputtering of molybdenum
[DE90-008307] 13 p1778 N90-20204
X ray specular reflection studies of silicon coated by organic monolayers (alkylsiloxanes)
[AD-A217418] 13 p1779 N90-20213
Fluorinated diamond thin films for tribological applications
[AD-A217452] 13 p1779 N90-20214
Ceramic oxide thin film formation utilizing biological processes
[DE90-008599] 13 p1781 N90-20225
Polymer liquid crystals with side chain discogens
[AD-A218013] 13 p1782 N90-20226
All-solid-state thin-film rechargeable lithium batteries using solid redox polymerization electrodes
[DE90-008665] 13 p1796 N90-20306
CuInSe2 and CdTe: Scale-up for manufacturing
[DE89-009503] 13 p1827 N90-20489
Dielectric composite thin films
[AD-A217940] 13 p1881 N90-20791
Surface-plasmon enhanced nonlinear photoelectric emission from thin silver films
[DE90-007676] 13 p1884 N90-20807
An ellipsometric measurement of optical properties for InP surfaces
[AD-A217185] 13 p1887 N90-20827
Nonlinear optics in thin films
[AD-A217336] 13 p1887 N90-20829
Chemically prepared PZT films doped with niobium
[DE90-006811] 13 p1892 N90-20859
Refractive index profiles of thermally grown and chemically vapor deposited films on silicon
[AD-A217187] 13 p1893 N90-20865
Molecular organization and electrical properties of mixed Langmuir-Blodgett multilayer thin films of polypyrrole
[DE90-007627] 13 p1894 N90-20870
Millimeter wave surface resistance of RBa2Cu3O(7-delta) (R=Y,Eu,Dy,Sm,Er) superconductors
[NASA-TM-102571] 13 p1897 N90-20886
Growth, characterization and device development in monocrystalline diamond films
[AD-A218211] 13 p1898 N90-20895
The effect of leveling coatings on the atomic oxygen durability of solar concentrator surfaces
[NASA-TM-102557] 14 p1941 N90-21110
Magnetron sputtered boron films and Ti/B multilayer structures
[DE90-009190] 14 p1948 N90-21153
Influence of the deposition conditions on radiofrequency magnetron sputtered MoS2 films
[NASA-TP-2994] 14 p1958 N90-21210
Peeled film GaAs solar cells for space power
[NASA-TM-103125] 14 p1970 N90-21287
Attachment of lead wires to thin film thermocouples mounted on high temperature materials using the parallel gap welding process
[NASA-TM-102442] 14 p1983 N90-21361
Problems associated with residual and mismatch stresses in thin film structures 14 p1990 N90-21407
Improvement of small-area, amorphous-silicon thin-film photovoltaics on polymer substrate
[DE90-000314] 14 p2002 N90-21472
Research on amorphous silicon-based thin film photovoltaic devices. Task B: Research on stable high efficiency large area, amorphous silicon-based submodules
[DE90-000320] 14 p2002 N90-21473
Inelastic electron scattering from surfaces
[DE90-009365] 14 p2025 N90-21614
Shock compression of solids: A tutorial
[DE90-009185] 14 p2032 N90-21659
Characterization and comparison of optically transparent conducting films
[DE90-000319] 14 p2033 N90-21660
Microstructure of Au/Nb multilayers
[DE90-008722] 14 p2033 N90-21662
New flexible circuit material evaluation
[DE90-008313] 15 p2071 N90-21866
Photovoltaic Program Branch
[DE90-000318] 15 p2123 N90-22142
Pulsed laser processing of high temperature superconducting thin films
[DE90-008928] 15 p2172 N90-22413
Superconducting and semiconducting thin films of La(sub 123) and Y(sub 123) and their superlattices
[DE90-009565] 15 p2173 N90-22416
In-situ pulsed laser deposition of high-T(sub c) YBa(sub 2)Cu(sub 3)O(sub 7) superconducting thin films on (100) LaAlO3 substrates
[DE90-009861] 15 p2173 N90-22418
Growth and patterning of laser ablated superconducting YBa2Cu3O7 films on LaAlO3 substrates
[NASA-TM-102436] 15 p2173 N90-22421
Electrochemical synthesis of ultrathin film composite membranes
[AD-A219041] 16 p2216 N90-22643
Scanning laser photocurrent spectroscopy of electrochemically grown bismuth sulphide films
[AERE-M-3709] 16 p2217 N90-22649
Photoresponse of YBa2Cu3O(7-delta) granular and epitaxial superconducting thin films
[NASA-TM-103144] 16 p2231 N90-22732
Continued development and characterization of doped layers, contacts and associated electronic devices in silicon carbide
[AD-A219234] 16 p2232 N90-22738
High temperature superconducting thin films in Japan 16 p2311 N90-23169
Thermal phenomena in high-Tc thin film superconductors 16 p2321 N90-23233
Measurement of localized deep levels and wafer non-uniformities at 3-5 semiconductor heterojunctions
[AD-A218547] 16 p2323 N90-23248
Application of high-temperature superconducting thin-film devices to electro-optical and electronic warfare systems
[AD-A218805] 16 p2323 N90-23249
Microstructure of thin films
[AD-A219262] 16 p2324 N90-23255
Reactions of silane in active nitrogen
[AD-A220371] 17 p2373 N90-23511
Surface and interface studies by Auger electron spectroscopy
[ETN-90-96948] 18 p2522 N90-24398
Vibrational and optical properties of amorphous metals
[DE90-011427] 18 p2522 N90-24403
Grain growth and phase formation in ion irradiated/annealed thin Ni-Al alloys films
[DE90-010409] 18 p2525 N90-24407
Properties of films prepared from low surface area/density alumina-silica
[DE90-011048] 18 p2531 N90-24446
Power density effects in the physical and chemical properties of sputtered diamond-like carbon thin films
[DE90-011587] 18 p2532 N90-24450
Proof of principle study of thickness measurements using characteristic x ray line ratio techniques
[AD-A221113] 18 p2595 N90-24461
The advantages and limitations of sputtered molybdenum disulphide as a space lubricant 18 p2537 N90-24471
In-situ topographical imaging of electrode surfaces using high resolution phase-measurement interferometric microscopy
[AD-A221021] 18 p2548 N90-24542
Multichip packaging technology with laser-patterned interconnects
[DE90-010743] 18 p2549 N90-24552
Effect of film adhesion on tribological properties of silver-coated alumina
[DE90-010090] 18 p2564 N90-24632
Tribological and mechanical properties of Fe/Ti multilayered films
[DE90-011949] 18 p2565 N90-24635
Summary results of an assessment of research projects in the national photovoltaics program
[DE90-008222] 18 p2577 N90-24680
Novel pulsed plasma treatment and coating process: Multilayer structures for optical computing applications
[AD-A220737] 18 p2615 N90-24894
Second order non-linear optical polyphosphazenes
[AD-A219868] 18 p2615 N90-24895
Epitaxy of TiO2 thin film on sapphire by MOCVDVD
[DE90-010054] 18 p2618 N90-24915
Deposition of electrooptic thin films
[DE90-010543] 18 p2619 N90-24922
Computer-controlled ion beam sputter deposition of multicomponent oxides
[DE90-010544] 18 p2619 N90-24923
Conference on the Science and Technology of Thin-Film Superconductors
[DE90-000326] 18 p2620 N90-24926
The catalytic reactivity of thin film crystal surfaces
[DE90-010579] 18 p2622 N90-24937
SiC film deposited by pulsed excimer laser ablation
[DE90-010634] 18 p2622 N90-24938
Electromigration in metallic microstructures
[AD-A221208] 18 p2622 N90-24942
Superconducting thin films of YBaCu oxides prepared by MOCVD
[DE90-011109] 18 p2625 N90-24961
Preparation and properties of superconducting thin films by excimer laser ablation
[DE90-011929] 18 p2626 N90-24967
New approach for the thin layer manufacturing: The wafer telemetry system
[MBB-UE-0004/89-PUB] 19 p2653 N90-25102
Adlayer physics
[AD-A221064] 19 p2673 N90-25203
Sol-gel coating on acoustic wave devices: Thin film characterization and chemical sensor development
[DE90-012224] 19 p2679 N90-25235
Sequentially evaporated thin film YBa2Cu3O(7-x) superconducting microwave ring resonator
[NASA-TM-103180] 19 p2685 N90-25273
Design and fabrication of high damage threshold turning mirrors for the Nova laser
[DE90-012703] 19 p2696 N90-25341
Microstructures of superconducting YBa2Cu3O(7-x) thin films
[DE90-011976] 19 p2761 N90-25688
Resistivity, adhesive strength, and residual stress measurements of thin film metallizations on single crystal quartz
[DE90-011902] 20 p2837 N90-26135
Selective electrocatalysis of anodic oxygen-transfer reactions at chemically modified, thin-film lead dioxide electrodes
[DE90-011747] 20 p2857 N90-26252
Interim qualification tests and procedures for terrestrial photovoltaic thin-film flat-plate modules
[DE90-000354] 20 p2881 N90-26392
Large, orientation-dependent enhancements of critical currents in Y1Ba2Cu3O(7-x) epitaxial thin films: Evidence for intrinsic flux pinning
[DE90-009424] 20 p2929 N90-26666
Studies on ion scattering and sputtering processes relevant to ion beam sputter deposition of multicomponent thin films
[DE90-010071] 20 p2931 N90-26675
Vacuum deposition by pulsed laser radiation: Plasma composition, deposition techniques, and thin film properties
[ETN-90-97263] 20 p2931 N90-26677
Laser induced surface chemical epitaxy
[AD-A222082] 21 p2977 N90-26920
Research on sputtering of ferroelectric thin films
[AD-A221792] 21 p2983 N90-26949
Characterization of polymer interphases using surface-enhanced Raman scattering
[AD-A223103] 21 p2985 N90-26965
Preparation and characterization of thin films based on sol-gel technique and development of spectroscopic probe for film formation and characterization
[AD-A221762] 21 p2988 N90-26984
The preparation of ACEL thin films
[AD-A222919] 21 p2999 N90-27048
Self-lubricating surfaces by ion beam processing
[AD-A222489] 21 p3011 N90-27118
Recent technological advances in thin film solar cells
[DE90-000321] 21 p3019 N90-27165
Polycrystalline thin film cadmium telluride n-i-p solar cells
[DE90-000351] 21 p3019 N90-27167
Pulsed laser deposition of high (Tc) superconducting thin films: Present and future
[DE90-011950] 21 p3080 N90-27511
Flux motion effects in Tl-Ca-Ba-Cu-O thin films
[DE90-012176] 21 p3080 N90-27514
Fracture-EXAFS: A new method for the study of interfaces in thin films and polycrystalline materials
[DE90-013736] 21 p3081 N90-27521
Laser ablated high T(sub c) superconducting thin YBa2Cu3O(7-x) films on substrates suitable for microwave applications 22 p3139 N90-27808
The effect of temperature cycling typical of low earth orbit satellites on thin films of YBa2Cu3O(7-x) 22 p3140 N90-27812
Preparation and characteristics of superconducting cuprate thin films: Nd(2-x)Ce(x)CuO4 and substituted Bi-system 22 p3140 N90-27813
Critical currents and high temperature superconductors 22 p3142 N90-27823
The effects of space radiation on thin films of YBa2Cu3O(sub 7-x) 22 p3147 N90-27845

Microstructures and properties of superconducting Y-Er-BaCu-O thin films obtained from disordered Y-Er-BaF2-Cu films 22 p3147 N90-27848
Spatial conductivity measurements on high T(sub c) superconducting films 22 p3148 N90-27849
In-situ integrated processing and characterization of thin films of high temperature superconductors, dielectrics and semiconductors by MOCVD 22 p3148 N90-27851
XES studies of density of states of high temperature superconductors 22 p3150 N90-27859
A YBCO RF-SQUID magnetometer and its applications 22 p3151 N90-27867
Magnetic properties of the 110K superconducting phase in Pb-doped Bi-Sr-Ca-Cu-O thin films 22 p3151 N90-27868
Optical and microwave detection using Bi-Sr-Ca-Cu-O thin films 22 p3152 N90-27870
In Situ deposition of YBCO high-T(sub c) superconducting thin films by MOCVD and PE-MOCVD 22 p3152 N90-27871
Experimental and kinetic modeling of acid/base redox reactions over metal oxide catalysts [DE90-013835] 22 p3156 N90-27893
A reliable, maintenance-free oxygen sensor for aircraft using an oxygen-sensitive coating on potentiometric electrodes [AD-A222696] 23 p3277 N90-28545
High temperature superconducting thin film microwave circuits: Fabrication, characterization, and applications [NASA-TM-103235] 23 p3322 N90-28786
Use of electron spectroscopies in the tribological evaluation of diamond films [DE90-014421] 23 p3334 N90-28848
Mechanical properties testing of diamond and diamond-like films by ultra-low load indentation [DE90-014456] 23 p3337 N90-28861
Research on high-efficiency, multiple-gap, multi-junction amorphous silicon-based alloy thin-film solar cells [DE90-000338] 23 p3344 N90-28896
Research on stable, large-area, amorphous silicon based submodules, phase 3 [DE90-000339] 23 p3399 N90-29204
Dynamical properties of two-dimensional Josephson junction arrays [AD-A223965] 23 p3402 N90-29221
Mechanical property measurement of polycrystalline diamond films [AD-A224037] 23 p3402 N90-29222
Symmetrical layered thin film edge field-emitter-array and method for its production [AD-D014594] 24 p3464 N90-29569
Piezoelectric and electrostrictive materials for transducer applications, volume 1 [AD-A223560] 24 p3480 N90-29668
Transmission electron microscopy study of ICB Al on Ge and Si(001) substrates [DE90-015299] 24 p3553 N90-30103

THIN PLATES

EPIC-2 calculated impact loading histories of thin plates [AD-A210557] 01 p0081 N90-10461
Natural frequencies of singly-curved laminated plates with simply-supported edges [ESDU-89011] 03 p0359 N90-12052
The relationship between the mechanical properties of materials after press forming and their in-service properties [CETIM-101530] 04 p0475 N90-12723
An investigation on combined extension and bending of thin sheets with a central crack [LR-561] 04 p0512 N90-12958
Increased fragility of deep pressed thin plates [CETIM-13-Y-313] 04 p0513 N90-12962
Pilot production of 70 micron thin silicon solar cells 10 p1343 N90-17780
Turbulent boundary layer pressure field-induced vibrations in a thin flexible plate under water 10 p1383 N90-18002
Thin-plate spline quadrature of geodetic integrals 13 p1836 N90-20539
Three-dimensional finite element formulations for thick and thin laminated plates 15 p2121 N90-22132
Crown and shape control in the rolling of thin, wide plates [ETN-90-96946] 17 p2378 N90-23539
Modeling of composite beams and plates for static and dynamic analysis [NASA-CR-186459] 20 p2874 N90-26354
The response and failure mechanisms of circular metal and composite plates subjected to underwater shock loading [AD-A222200] 21 p3013 N90-27131

THIN WALLED SHELLS

Theoretical and experimental investigation of thin-walled aluminum panels under cyclic shear load 02 p0177 N90-10996
Equilibrium and stability in composite thin shell 02 p0178 N90-10998
General buckling tests with thin-walled shells [DLR-MITT-89-13] 05 p0655 N90-13816
Nonlinear strain-displacement relations for thin axisymmetric shells [PB89-226013] 07 p0945 N90-15470
Compressive behavior of laminated composite structures 14 p1945 N90-21134
UNIVIMP: A universal instrument for the survey of initial imperfections of thin-walled shells [PB90-167065] 14 p1984 N90-21369
Elastic stability and nonlinear behavior of imperfect shells with initial stresses 15 p2110 N90-22070
Interactions of massive stars with the interstellar medium: Bow shocks and superbubbles 15 p2186 N90-22485
Coupled BE/FE/BE approach for scattering from fluid-filled structures 18 p2570 N90-24649
Static and free-vibrational response of semi-circular graphite-epoxy frames with thin-walled open sections [NASA-CR-4287] 21 p3012 N90-27122

THIN WALLS

Thin walled cast high-strength structural parts 01 p0043 N90-10242
A new aspect for the use of thin walled beams as shell stiffeners of spacecraft structures 02 p0184 N90-11046
Mechanism for shear band formation in the high strain rate torsion test [PB89-215370] 03 p0356 N90-12038
Corrections to the thin wall approximation in general relativity [NASA-CR-186078] 04 p0562 N90-13274
The stress analysis of thin-walled screwed tubular joints 06 p0796 N90-14637
A finite strip method for the elastic-plastic large displacement analysis of thin-walled and cold-formed steel sections [PB89-226021] 06 p0798 N90-14647
Review of polyarylacetylene matrices for thin-walled composites [AD-A214921] 09 p1186 N90-16872
The elastic-plastic behavior of composite materials 16 p2212 N90-22615
Theoretical analysis and pressure distribution of thin-walled metal inverbuckle energy absorbing tubes 17 p2414 N90-23758
Free vibrations of thin-walled semicircular graphite-epoxy composite frames [NASA-TM-102680] 19 p2701 N90-25365
The effect of local thinning on the remaining life of superheater tubes [VTT-RR-631] 19 p2703 N90-25377

THIN WINGS

Additions and corrections to SUPER: A program for calculating steady and oscillatory supersonic flow over a thin wing, tail plane and fin [AD-A211771] 04 p0438 N90-12501
Chordwise loading and camber for two-dimensional thin sections [AD-A213318] 04 p0448 N90-12568
Wind tunnel tests of the influence of aerofoil thickness on the normal force and pitching moment of two slender wings at transonic and supersonic Mach numbers [ESA-TT-1129] 08 p1018 N90-15889

THINNERS

U SOLVENTS

THIOLS

Multiple internal reflection Fourier transform infrared spectroscopy studies of thiocyanate adsorption on silver and gold [AD-A210245] 01 p0041 N90-10223

THIXOTROPIC PROPELLANTS

U GELLED ROCKET PROPELLANTS

THOMSON EFFECT

U THERMOELECTRICITY

THOMSON SCATTERING

A 13-point Thomson scattering system for JFT-2M plasma [DE90-733140] 10 p1432 N90-18263
Thomson scattering in a magnetic field 14 p2040 N90-21699

THORIUM COMPOUNDS

Dynamics of plasma injection along magnetic field lines in the PBFA 2 (Particle Beam Fusion Accelerator 2) plasma opening switch [DE90-006751] 12 p1717 N90-19862

THORON

U RADON ISOTOPES

THREADS

A feasibility study of hydrogen dosage estimation in screw threads submitted to surface electrolytic treatment [CETIM-110110] 04 p0476 N90-12730
The stress analysis of thin-walled screwed tubular joints 06 p0796 N90-14637
Threaded joint design for composites [DE90-005553] 11 p1478 N90-18506
Fastener design manual [NASA-RP-1228] 11 p1517 N90-18740
Investigation into the mechanism of polymer thread drag reduction [AD-A217492] 13 p1800 N90-20329
Guidelines for threaded fasteners [ESA-PSS-03-208-ISSUE-1] 22 p3182 N90-28061

THREAT EVALUATION

UK airmisses involving commercial air transport, May-August 1988 [ISSN-0951-6301] 03 p0303 N90-11717
Target selection in anti-tank helicopter operations: Relative weight of cues in target evaluation judgements [FOA-C-50072-5.2] 17 p2436 N90-23881
Target selection in anti-tank operations: Effects of experience [FOA-C-50073-5.2] 17 p2436 N90-23882
Mode of presentation of cues in policy capturing: A comparison between verbal and pictorial presentation of targets in judgement of probability to fire [FOA-C-50074-5.2] 17 p2436 N90-23883

THREE AXIS STABILIZATION

Analysis of the star mapper data 05 p0609 N90-13551
Operational requirements and the geostationary platform 12 p1608 N90-19250
Determination of the implementation of the 3-axis attitude motion simulator digital position controller 12 p1638 N90-19409
Attitude control modes for the MECB remote sensing satellites [INPE-4755-PRE/1427] 14 p1938 N90-21094
A general-purpose balloon-borne pointing system for solar scientific instruments [NASA-TP-3013] 14 p1959 N90-21219
Galactical ultra wide angle Schmidt system 18 p2536 N90-24468
A three axis attitude control of a satellite [NASDA-TR-22] 24 p3439 N90-29421

THREE DIMENSIONAL BODIES

Three-dimensional viscoelastic bodies in steady state frictional rolling contact with generalization to Knothe rolling [REPT-89-23] 03 p0355 N90-12032
Comparison of integral and finite-difference methods for predicting the turbulent boundary layer on axisymmetric bodies [ARE-TM(UHA)-88512] 05 p0643 N90-13752
Tire modeling by finite elements 06 p0792 N90-14614
Appearance analysis from CAD models [IMAG-RR-756-I-IMAG-88-LIFIA] 08 p1111 N90-16434
Apparatus and method for locating the axis of symmetry (center of circular cross section) of three dimensional objects [AD-D014407] 14 p1982 N90-21354
Volumetric visualization of 3D data 16 p2275 N90-22964
A time-marching method to calculate unsteady airloads on three-dimensional wings. Part 1: Linearized formulation [DLR-FB-89-58] 18 p2494 N90-24254
A time-marching method for calculating unsteady airloads on three-dimentional wings. Part 2: Full-potential formulation [DLR-FB-89-59] 18 p2494 N90-24255
Segmentation before and after reconstruction of 3-D surfaces in depth imagery [RR-788-I-IMAG-97-LIFIA] 20 p2909 N90-26551

THREE DIMENSIONAL BOUNDARY LAYER

Stability and transition of three-dimensional boundary layers 01 p0062 N90-10357
Three-dimensional boundary layer transition on a concave surface 01 p0064 N90-10365
Curvature effects on the stability of three-dimensional laminar boundary layers 01 p0064 N90-10366
Experimental study of instability modes in a three-dimensional boundary layer 01 p0064 N90-10369
Primary and secondary stability analysis applied to the DFVLR-transition swept-plate experiment 01 p0065 N90-10371
Numerical investigation of transition in 3D boundary layers 01 p0065 N90-10372
A three-dimensional linear stability approach to transition on wings at incidence 01 p0065 N90-10373
A European collaborative investigation of the three-dimensional turbulent shear layers of a swept wing 01 p0066 N90-10380
Numerical solutions of the compressible 3-D boundary-layer equations for aerospace configurations with emphasis on LFC 04 p0443 N90-12534

Numerical simulation of transition in three-dimensional boundary layers
[DLR-FB-89-12] 05 p0639 N90-13728
Numerical investigation of transition control of a flat plate boundary layer 07 p0926 N90-15361
Method for the primary stability analysis of the three dimensional, compressible boundary layer flows 08 p1066 N90-16171
An efficient solver of the Eigenvalue problem of the linear stability equations for three dimensional, compressible boundary-layer flows 08 p1066 N90-16172
Numerical simulation of the nonlinear evolution of a perturbation in a three dimensional boundary layer 08 p1067 N90-16173
Development of transition criteria on the basis of e to the N power for three dimensional wing boundary layers 08 p1067 N90-16179
Effects of controlled three-dimensional perturbations on boundary layer transition
[AD-A215080] 10 p1384 N90-18011
Numerical investigation of some control methods for 3-D turbulent interactions due to sharp fins 15 p2053 N90-21764
Local mode smoothing analysis for various incomplete factorization iterative methods in three dimensions
[REPT-89-38] 15 p2147 N90-22263
Three-dimensional separated flow prediction on fusiform body using Euler and boundary layer methods 16 p2234 N90-22745
Experimental study of a three-dimensional shear-driven turbulent boundary layer with streamwise adverse pressure gradient 17 p2399 N90-23669
Advanced instrumentation for local measurement of gas-solid suspension flows
[DE90-008498] 17 p2400 N90-23671
Concerning the interaction of non-stationary cross-flow vortices in a three-dimensional boundary layer
[NASA-CR-182037] 18 p2492 N90-24245
Generation of circumferential velocity contours associated with pulsed point suction on a rotating disk 18 p2646 N90-25065
Simulation of the boundary layer in accretion disks with the SPH method 19 p2779 N90-25807
Report of the Fluid Dynamics Panel Working Group 10 on calculation of 3D separate turbulent flows in boundary layer limit
[AGARD-AR-255] 20 p2862 N90-26280
Study of the flow around the prototype of A300: Results of the third test campaign at F2 and comparison with calculations
[CERT-33/5025-29-DERAT] 22 p3109 N90-27663
Numerical simulations of blade-vortex interactions and lifting hovering rotor flows
[AD-A224238] 24 p3417 N90-29302

THREE DIMENSIONAL COMPOSITES
Worked-in holes in three-dimensional reinforced composites 02 p0186 N90-11060
Theory and verification of the fiber composite damage model implemented in DYNA3D
[AD-A216600] 11 p1479 N90-18511
Through-thickness strain response of thick composites in compression
[AD-A217233] 13 p1767 N90-20141
The 3-D composite velocity solutions for subsonic/transonic flow over forebodies and afterbodies
[AD-A220370] 17 p2345 N90-23354
Stress fields in composite materials by means of a nonclassical approach 18 p2517 N90-24372
Reinforcing fibers and technology development for resin composites. Consequences for aircraft structures
[FOA-C-20777-2.5] 22 p3154 N90-27683

THREE DIMENSIONAL FLOW
NT KARMAN-BODEWADT FLOW
NT SECONDARY FLOW
Boost-phase discrimination research activities
[NASA-TM-101889] 01 p0032 N90-10176
Fluid Dynamics of Three-Dimensional Turbulent Shear Flows and Transition
[AGARD-CP-438] 01 p0062 N90-10356
Numerical solution of three-dimensional unsteady flows: Application to instability problems 01 p0065 N90-10375
Trailing-edge sweep and three-dimensional vortex interactions in jets and mixing layers 01 p0066 N90-10379
Turbulence modelling of three-dimensional shear flows 01 p0066 N90-10381
A composite velocity procedure for the three-dimensional reduced Navier-Stokes equations 01 p0069 N90-10396
A computational/experimental study of the flow around a body of revolution at angle of attack
[NASA-TM-88329] 02 p0219 N90-11254
Three component laser Doppler measurements in an axisymmetric jet
[NASA-CR-181908] 03 p0300 N90-11702
Simulation of glancing shock wave and boundary layer interaction
[NASA-TM-102233] 03 p0345 N90-11970
Near-wall, three-dimensional turbulence measurements: A challenge for laser velocimetry
[NASA-TM-102252] 03 p0346 N90-11978
Three-dimensional, two-phase, transonic, canted nozzle flows
[AD-A211528] 03 p0347 N90-11984
Numerical study of three-dimensional spatial instability of a supersonic flat plate boundary layer
[NASA-CR-181931] 04 p0499 N90-12874
Three-dimensional shear flows: Analysis of the track and angle of incidence
[CERT-RTS-OA-31/5025-AYD] 04 p0501 N90-12888
Multigrid calculations of 3-D turbulent viscous flows
[NASA-CR-185154] 05 p0571 N90-13323
Computation of viscous incompressible flows
[NASA-TM-101090] 05 p0572 N90-13329
Block-structured solution of three-dimensional transonic flows using parallel processing
[AD-A212851] 05 p0572 N90-13330
Measurement Techniques in Aerodynamics
[VKI-LS-1989-05] 05 p0573 N90-13339
Practical systems for speckle velocimetry 05 p0574 N90-13341
Recent progress in research pertaining to estimates of gas-side heat transfer in an aircraft gas turbine
[NASA-TM-102460] 05 p0582 N90-13394
A three-dimensional potential flow analysis of dynamic fluid forces acting on a whirling centrifugal impeller bounded by a volute 05 p0637 N90-13717
Calculation of flow fields by the solution of the Euler equations using an extended finite volume discretization scheme
[DLR-FB-89-38] 05 p0639 N90-13729
Application of two-point closures to subgrid scale modeling for homogeneous, 3D turbulence 05 p0640 N90-13732
Inviscid 3D solution methods 05 p0640 N90-13736
Pressure correction calculation procedures for 3D viscous flow 05 p0641 N90-13738
Three D flows in turbine blade rows 05 p0641 N90-13739
Model and computation of three-dimensional turbulent jets in a crossflow
[ECL-89-007] 05 p0643 N90-13755
On the topology of three-dimensional viscous flow structures near a plane wall. A classification and non-hyperbolic singularities on the wall
[LR-541] 05 p0644 N90-13758
Numerical investigations in three-dimensional internal flows
[NASA-CR-186068] 06 p0718 N90-14189
A note concerning the onset of three dimensionality and time dependence in Goertler vortices
[NASA-CR-181956] 06 p0718 N90-14193
Advanced 3-D CFD algorithm for turbomachinery 06 p0725 N90-14233
A dynamic multiblock approach to solving the unsteady Euler equations about complex configurations 06 p0773 N90-14497
Comparative study of the vorticity field in turbulent flows: Theory, experiments, and computations
[DE90-001399] 06 p0776 N90-14516
Explicit and implicit calculations of turbulent cavity flows with and without yaw angle
[NASA-CR-186293] 07 p0929 N90-15381
An experimental study of the time-dependent behavior of the appendage-body junction vortex
[AD-A213465] 07 p0930 N90-15384
Adaptive local grid refinement for the compressible 3-D Euler equations
[FFA-TN-1989-40] 08 p1064 N90-16155
Visualization of 2 and 3 dimensional flows
[REPT-1] 08 p1065 N90-16164
Numerical simulation of the laminar and turbulent three dimensional flow on a delta wing with sharp leading edge 08 p1069 N90-16186
A finite volume calculation method for three dimensional, complex flows 08 p1070 N90-16195
Calculation of two and three dimensional super and hypersonic flows by solving the Euler equations 08 p1070 N90-16197
Coded trajectories for the investigation of strongly unsteady flow fields 08 p1078 N90-16240
Development and application of oxygen flow tagging for velocity measurements and flow visualization in turbulent three-dimensional supersonic flows
[AD-A214491] 09 p1160 N90-16715
An upwind-biased, point-implicit relaxation algorithm for viscous, compressible perfect-gas flows
[NASA-TP-2953] 09 p1214 N90-17042
Formation of a pair of turbulent layers in the region of a flow around an axisymmetric body with an incidence angle
[ISL-R-130/87] 09 p1219 N90-17070
Formation of turbulent layers in the separated region around a body with polygonal cross section at large incidence and rolling
[ISL-R-101/88] 09 p1219 N90-17071
Study for the dissipative structures geometry in three dimensional developed turbulence
[ETN-90-96102] 09 p1219 N90-17072
Special Course on Three-Dimensional Supersonic/Hypersonic Flows Including Separation
[AGARD-R-764] 10 p1308 N90-17565
Numerical simulation of supersonic free shear layers
[AD-A216289] 10 p1310 N90-17579
Comparison of two- and three-dimensional Navier-Stokes solutions with NASA experimental data for CAST-10 airfoil 10 p1325 N90-17658
Numerical simulation of three-dimensional unsteady flows in turbomachines 11 p1481 N90-18417
A simple algebraic grid adaptation scheme with applications to two- and three-dimensional flow problems
[NASA-TM-102446] 11 p1505 N90-18667
Contribution to the study of three-dimensional separation in turbulent incompressible flow
[ESA-TT-1169] 11 p1510 N90-18697
Doppler lidar working group report
[ESA-SP-1112] 11 p1537 N90-18848
Three-dimensional viscous rotor flow calculations using a viscous-inviscid interaction approach
[NASA-TM-102235] 12 p1599 N90-19204
Tomographic investigations of weakly perturbed supersonic free jets
[MPIS-MITT-91] 12 p1600 N90-19209
Digital determination of the three dimensional flow in turbomachines with the S1-S2 current function process
[ITSM-MITT-30] 12 p1605 N90-19236
On total variation diminishing schemes for transonic turbulent flow computation 14 p1909 N90-20945
Secondary Flows in Turbomachines
[AGARD-CP-469] 14 p1922 N90-21009
Parabolized calculations of turbulent three dimensional flows in a turbine duct 14 p1923 N90-21013
Experimental and numerical study on basic phenomena of secondary flows in turbines 14 p1923 N90-21014
An investigation of secondary flows in nozzle guide vanes 14 p1923 N90-21016
Measurement of the flow field in the blade passage and side-wall region of a plane turbine cascade 14 p1924 N90-21019
Centrifugal impeller geometry and its influence on secondary flows 14 p1924 N90-21020
Calculation of the three dimensional turbulent flow in a linear turbine blade 14 p1924 N90-21021
Generation and decay of secondary flows and their impact on aerodynamic performance of modern turbomachinery components 14 p1925 N90-21023
Swept wing ice accretion modeling
[NASA-TM-103114] 15 p2046 N90-21727
Effective methods of controlling a junction vortex system in an incompressible, three-dimensional, turbulent flow 15 p2047 N90-21732
Extension of a three-dimensional viscous wing flow analysis user's manual: VISTA 3-D code
[NASA-CR-182024] 16 p2197 N90-22538
Investigation of advanced counterrotation blade configuration concepts for high speed turboprop systems, task 1: Ducted propfan analysis
[NASA-CR-185217] 16 p2202 N90-22567
Three-dimensional separated flow prediction on fusiform body using Euler and boundary layer methods 16 p2234 N90-22745
An investigation of the three-dimensional flow field in a centrifugal compressor 16 p2235 N90-22751
Extension of a three-dimensional viscous wing flow analysis
[NASA-CR-182023] 17 p2344 N90-23348
Parallel computation of supersonic flows using a three-dimensional, zonal, Navier-Stokes code
[AD-A218824] 17 p2344 N90-23350
Three-dimensional analysis on flow and temperature distributions for aircraft fuel thermal stability
[AD-A219651] 17 p2383 N90-23571
Topology of three-dimensional, variable density flows
[NASA-CR-186622] 17 p2402 N90-23683
Composite reduced Navier Stokes procedures for flow problems with strong pressure interactions
[AD-A219621] 17 p2403 N90-23687
Evaluation and representation of two and three dimensional data fields from optical stream measurements
[MPIS-18/1989] 17 p2474 N90-24143

Computational modeling of three-dimensional compressible leading edge vortices
[AD-A221022] 18 p2553 N90-24569
Three-dimensional viscous flow structures from bifurcation of a degenerate singularity with three zero eigenvalues
[LR-572] 19 p2692 N90-25314
Three-dimensional laser velocimeter simultaneity detector
[NASA-CASE-ARC-11876-1] 19 p2696 N90-25340
Numerical analysis of three-dimensional particle-laden flow equations
[IAR-90-2] 20 p2860 N90-26268
A fully implicit ADI method for quasi three-dimensional flows through straight blade rows
[ETN-90-96965] 20 p2863 N90-26283
The effect of a three-dimensional source on the flow through a channel with square cross section
[LR-512] 20 p2863 N90-26289
Informatics aspects of large flow calculations on the SX-2 supercomputer
[NLR-MP-88037-U] 20 p2864 N90-26290
Experiments with unsteady, free surface, three-dimensional vortices in a thermally stable, stratified fluid
[AD-A222088] 21 p2954 N90-26796
An approximate method for calculating three-dimensional inviscid hypersonic flow fields
[NASA-TP-3018] 21 p3002 N90-27066
Numerical interactive grid generation for 3-D flow calculations
[NLR-MP-88055-U] 21 p3003 N90-27069
Three-dimensional cavity flow fields at subsonic and transonic speeds
[NASA-TM-4209] 22 p3107 N90-27650
On computations of the integrated space shuttle flowfield using overset grids
[NASA-CR-186927] 22 p3124 N90-27734
Numerical investigation of laminar-turbulent transition in a flat plate wake
[AD-A222462] 22 p3170 N90-27978
Study of the origin of three dimensional structures in shear flows through external forcing
[AD-A221923] 22 p3170 N90-27980
Implicit solution of three-dimensional internal turbulent flows
[NASA-TM-103099] 22 p3170 N90-27982
The discretization of the three dimensional boundary layer equations
[ETN-90-97292] 22 p3171 N90-27987
Solution of the Orr-Sommerfeld equation for three dimensional incompressible flow using Galerkin method and Chebichev polynomials: The COCIP code
[CERT-46/5618-34-DERAT] 22 p3176 N90-28021
Calculation of surface free three dimensional flows
[ONERA-RSF-5/4368-AY-002A] 22 p3176 N90-28022
Oscillatory convection
[ESA-TT-890] 23 p3325 N90-28801
Numerical simulation of the formation of two-dimensional and three-dimensional structures in shear layers and wakes
[ESA-TT-1008] 23 p3325 N90-28802
Experimental investigations on the stability and transition of three-dimensional boundary layers
[ESA-TT-1026] 23 p3325 N90-28803
Numerical simulation supersonic free shear layers
[AD-A223771] 24 p3418 N90-29306
Transonic 3-D Euler analysis of flows around fanjet engine and TPS (Turbine Powered Simulator). Comparison with wind tunnel experiment, evaluation of TPS testing method and 3-D flow
[NAL-TR-1045] 24 p3421 N90-29327
An investigation of the inviscid spatial instability of compressible mixing layers
[AD-A223776] 24 p3468 N90-29596
Three dimensional studies of helical equilibria and magnetic surface breaking due to the finite beta effect
[DE90-508078] 24 p3548 N90-30071

THREE DIMENSIONAL MODELS

Numerical investigation of the effects of longitudinal vortices on the onset of transition in a flat plate boundary layer 01 p0063 N90-10363
Bifurcations in Poiseuille flow and wall turbulence 01 p0065 N90-10370
Numerical investigation of transition in 3D boundary layers 01 p0065 N90-10372
A study of the structure of highly swept shock wave turbulent boundary layer interactions 01 p0066 N90-10376
The 3D-POLY: A robot vision system for recognizing objects in occluded environments 02 p0229 N90-11313
Modelling ionospheric density structures 02 p0242 N90-11375
Analytical studies of three-dimensional combustion processes
[AD-A211903] 03 p0323 N90-11837
A cell-centered multigrid method for three-dimensional anisotropic-diffusion and interface problems
[REPT-89-35] 04 p0540 N90-13128
Placing mirrors in grids
[CWI-CS-R8906] 04 p0543 N90-13154
Navier-Stokes simulation of the crossflow instability in swept-wing flows
[NASA-CR-186122] 05 p0641 N90-13744
Interface between MEDUSA and GIFTS for shell structures
[LR-553] 05 p0684 N90-13985
An analysis of the viscous flow through a compact radial turbine by the average passage approach
[NASA-TM-102471] 06 p0720 N90-14206
Mechanical properties and morphology of oriented polymer blends 06 p0750 N90-14361
Development of a three-dimensional local scale atmospheric model with turbulence closure model
[DE90-710045] 07 p0960 N90-15551
Experimental investigation of a three-dimensional wake. Part 2: Spectral and turbulent energy analysis
[ONERA-RT-32/5025-AYD-PT-2] 08 p1018 N90-15887
The cryogenic induction tunnel T2 at Toulouse 08 p1029 N90-15946
Verification study of a three-dimensional local scale atmospheric model PHYSIC at seacoast region
[DE90-719560] 08 p1102 N90-16384
Design of a large superconducting spectrometer magnet
[DE90-719505] 08 p1131 N90-16553
Non-Fourier computer generated holography for 3-D display
[AD-A215369] 09 p1225 N90-17109
Three-dimensional simulation of free-electron laser harmonics with FRED
[DE90-005253] 09 p1229 N90-17130
Computer perception of three-dimensional objects
[AD-A215058] 09 p1267 N90-17345
Flux flow, pinning, and resistive behavior in superconducting networks
[DE90-005242] 09 p1293 N90-17493
Forced and natural venting of aircraft cabin fires: A numerical simulation 10 p1314 N90-17597
Response of a chemically reacting layer to streamwise vorticity
[NASA-TM-102288] 10 p1383 N90-18005
Three-dimensional coculture process
[NASA-CASE-MSC-21560-1] 11 p1538 N90-18852
Recognizing three-dimensional objects without the use of models
[AD-A216766] 11 p1540 N90-18862
Application of a three-dimensional Navier-Stokes model for a subsonic jet in a crossflow 13 p1749 N90-20045
Unsteady three-dimensional marginal separation, including breakdown
[NASA-TM-102525] 13 p1801 N90-20337
Finite element models to predict the structural response of 120-mm sabot/rods during launch
[DE90-007497] 13 p1817 N90-20436
Distributed earth model/orbiter simulation 13 p1860 N90-20671
Recent advances in 3D finite difference mesh generation using the BRL-CAD package
[DE90-007854] 13 p1866 N90-20704
A fast collocation method for transonic airfoil design 14 p1917 N90-20984
Numerical method for designing 3D turbomachinery blade rows 14 p1918 N90-20990
Supersonic nozzle design of arbitrary cross-section 14 p1927 N90-21035
Swept wing ice accretion modeling
[NASA-TM-103114] 15 p2046 N90-21727
Three-dimensional simulation of vortex breakdown
[NASA-TM-102664] 15 p2049 N90-21744
General structured grid generation systems 15 p2093 N90-21977
Grid patching approaches for complex three-dimensional configurations 15 p2094 N90-21985
The solution of scattering and radiation problems for complex configurations based on 3-D grid and patch models 15 p2096 N90-21997
Contact mechanics for three-dimensional geometries 15 p2111 N90-22076
On three-dimensional scaling and consistent truncation of global atmospheric models 15 p2127 N90-22164
Hail growth in a highly-glaciated central high plains multi-cellular hailstorm 15 p2131 N90-22184
Frontal structure in a mesoscale model 15 p2132 N90-22187
Three-dimensional simulations of simple electron drift wave turbulence in tokamak geometry
[DE90-009581] 15 p2169 N90-22398
A numerical study of basic coastal upwelling processes 16 p2259 N90-22878
Introducing the VRT gas turbine combustor
[NASA-TM-103176] 17 p2386 N90-23591
Rotary-Jet thrust augmentor with jet-flapped blades 18 p2492 N90-24243
Metal matrix composites microfracture: Computational simulation
[NASA-TM-103153] 18 p2518 N90-24383
A numerical investigation of thermal convection in highly viscous spherical shells with applications to mantle dynamics in the Earth and other terrestrial planets 18 p2579 N90-24691
Self-similar Langmuir collapse
[DE90-611310] 18 p2617 N90-24911
A few modeling and rendering techniques for computer graphics and their implementation on ultra hardware 18 p2640 N90-25038
A 3D visualization system for molecular structures 18 p2641 N90-25044
Development of a finite element based delamination analysis for laminates subject to extension, bending, and torsion 18 p2642 N90-25049
Small helium-cooled infrared telescope experiment for Spacelab-2 (IRT)
[NASA-CR-183983] 19 p2765 N90-25708
Three dimensional accretion disk simulation with external magnetic field 19 p2772 N90-25754
Computational experience with a three-dimensional rotary engine combustion model
[NASA-TM-103104] 20 p2861 N90-26275
Fluid Dynamics Panel Working Group 12 on Adaptive Wind Tunnel Walls: Technology and Applications
[AGARD-AR-269] 21 p2961 N90-26838
Testing of 3-D models in 2-D adaptive wall test sections 21 p2962 N90-26842
Limits of adaptation, residual interferences 21 p2963 N90-26844
Generation of animation sequences of three dimensional models
[NASA-CASE-MSC-21379-1-SB] 21 p3050 N90-27340
The QBO and weak external forcing by solar activity: A three dimensional model study 22 p3203 N90-28171
Parallelization of implicit finite difference schemes in computational fluid dynamics
[NASA-CR-182081] 22 p3243 N90-28392
Three-dimensional model testing in the transonic self-streamlining wind tunnel 23 p3284 N90-28583
Three-dimensional simulations of the generation of one Angstrom radiation by a self-amplified spontaneous emission free-electron laser
[DE90-015032] 23 p3330 N90-28830
Building an environment model using depth information 23 p3374 N90-29064
A package for 3-D unstructured grid generation, finite-element flow solution and flow field visualization
[NASA-CR-182090] 24 p3419 N90-29309
Comparison of crack closure result obtained by 3D elastic-plastic FEM and modified Dugdale model
[FFA-TN-1990-18] 24 p3481 N90-29675
Three-dimensional numerical study of thunderstorm downdrafts and associated outflow boundaries 24 p3494 N90-29746
The 3D model control of image processing 24 p3503 N90-29800

THREE DIMENSIONAL MOTION

NT KARMAN-BODEWADT FLOW
NT SECONDARY FLOW
NT THREE DIMENSIONAL FLOW
A Conference on Three-Dimensional Representation held in University of Minnesota on 24-26 May 1989
[AD-A211630] 03 p0406 N90-12324
Vision in dynamic environments
[AD-A213434] 07 p0967 N90-15587
The perceptual buildup of three-dimensional structure from motion
[AD-A214640] 09 p1259 N90-17300
Three-dimensional motion estimation using shading information in multiple frames
[AD-A216804] 11 p1549 N90-18919
A vectorized algorithm for 3D dynamics of a tethered satellite 12 p1640 N90-19423
Towards an understanding of camera fixation
[PB90-160342] 22 p3177 N90-28027
The dynamics and control of large flexible space structures - 13
[NASA-CR-186930] 23 p3286 N90-28591

THRESHOLD CURRENTS

Current protections modelisation in a buck cell 10 p1335 N90-17723

Low threshold current implanted-planar-buried-heterostructure, graded-index, separate-confinement-heterostructure GaAs-AlGaAs laser
[DE90-002579] 12 p1666 N90-19572
Subthreshold technique for fixed and interface trapped charge separation in irradiated MOSFETs
[AD-A221861] 21 p3001 N90-27061

THRESHOLD GATES
Subthreshold technique for fixed and interface trapped charge separation in irradiated MOSFETs
[AD-A221861] 21 p3001 N90-27061

THRESHOLD SHIFT
U THRESHOLDS

THRESHOLD VOLTAGE
High energy neutron irradiation effects in GaAs modulation-Doped Field Effect Transistors (MODFETS): Threshold voltage
[AD-A210502] 01 p0132 N90-10763
Strong-inversion model of threshold voltage in modulation doped field effect transistors: The role of unintentional acceptors
[AD-A212750] 04 p0498 N90-12870

THRESHOLDS
Ignition testing of low-energy laser diode ignited components
[DE90-009968] 16 p2214 N90-22630

THROATS
Heat transfer to throat tubes in a square-chambered rocket engine at the NASA Lewis Research Center
[NASA-TM-102336] 02 p0189 N90-11082
Supersonic nozzle design of arbitrary cross-section
14 p1927 N90-21035

THRUST
NT JET THRUST
NT LOW THRUST
NT ROCKET THRUST
NT VARIABLE THRUST
Effect of pylon wake with and without pylon blowing on propeller thrust
[NASA-TM-4162] 06 p0718 N90-14190
Energy deposition in low power coaxial plasma thrusters 06 p0844 N90-14911
Design of a thrust stand for high power electric propulsion devices
[NASA-TM-102372] 08 p1037 N90-15992
Pulsed plasma mission endurance test
[AD-A213462] 08 p1037 N90-15993
Engine inlet distortion in a 9.2 percent scale vectored thrust STOVL model in ground effect
[NASA-TM-102358] 10 p1307 N90-17561
Optimal control of an aircraft flying through a downburst 15 p2053 N90-21765
Hybrid propulsion technology program. Volume 1: Conceptional design package
[NASA-CR-183953] 15 p2060 N90-21793
Hybrid propulsion technology program. Volume 2: Technology definition package
[NASA-CR-183954] 15 p2060 N90-21794
A modeling technique for STOVL ejector and volume dynamics
[NASA-TM-103167] 16 p2202 N90-22566
Fundamental hydrodynamics research
[AD-A219179] 16 p2238 N90-22766
Evaluation of various thrust calculation techniques on an F404 engine
[NASA-TP-3001] 19 p2659 N90-25134
Low thrust rocket test facility
[NASA-TM-103206] 19 p2663 N90-25158
Geometric effects in applied-field MPD thrusters
[NASA-TM-103259] 22 p3134 N90-27782
Elastomeric mount for thrust bearing shoe
[AD-D014465] 22 p3181 N90-28054

THRUST AUGMENTATION
Characteristics of combustion driven pressure oscillations in advanced turbo-fan engines with afterburner 01 p0035 N90-10194
Rotary-Jet thrust augmentor with jet-flapped blades
18 p2492 N90-24243

THRUST BEARINGS
Elastomeric mount for thrust bearing shoe
[AD-D014465] 22 p3181 N90-28054

THRUST CHAMBER PRESSURE
Swirl coaxial injector element characterization for booster engines 23 p3294 N90-28632
Heavy hydrocarbon main injector technology
23 p3294 N90-28633

THRUST CHAMBERS
A rocket engine design expert system
[NASA-TM-102373] 01 p0032 N90-10172
Feasibility demonstration of a 445N high-performance rocket engine 11 p1473 N90-18481
Cooling of rocket thrust chambers with liquid oxygen
[NASA-TM-103146] 16 p2210 N90-22605
Combustor design and analysis using the Rocket Combustor Interactive Design (ROCCID) methodology
[NASA-TM-103165] 18 p2513 N90-24349
Advanced tube-bundle rocket thrust chamber
[NASA-TM-103139] 19 p2670 N90-25185

THRUST CONTROL
NT THRUST VECTOR CONTROL
Plume shape optimization of small attitude control thrusters with respect to impingement and thrust
[ISL-CO-220/88] 08 p1064 N90-16153
Performance of an optimized rotor blade at off-design flight conditions
[NASA-CR-4288] 12 p1603 N90-19226
A comparison of time-optimal interception trajectories for the F-8 and F-15
[NASA-CR-186300] 15 p2050 N90-21753
Guidance and control strategies for aerospace vehicles
[NASA-CR-186878] 20 p2814 N90-26013
High power arcjet
[NASA-CR-183086] 23 p3298 N90-28658

THRUST FAULTS
U GEOLOGICAL FAULTS

THRUST LOADS
Lubrication characteristics of rolling bearings lubricated by self-lubricating composite retainers. Part 1: Selection of bearings for Earth sensors
[NAL-TR-1019] 24 p3477 N90-29651

THRUST MEASUREMENT
Measurement effects on the calculation of in-flight thrust for an F404 turbofan engine
[NASA-TM-4140] 03 p0307 N90-11741
Arcjet nozzle design impacts
11 p1473 N90-18478

THRUST POWER
U THRUST

THRUST REVERSAL
Aerodynamic interferences of in-flight thrust reversers in ground effect 23 p3274 N90-28529
Dynamic ground effects 23 p3275 N90-28531

THRUST VECTOR CONTROL
Investigations of thrust vector control for high-alpha pitchover 01 p0014 N90-10067
Independent Orbiter Assessment (IOA): Analysis of the ascent thrust vector control actuator subsystem
[NASA-CR-185579] 02 p0164 N90-10329
Independent Orbiter Assessment (IOA): Assessment of the ascent thrust vector control actuator subsystem FMEA/CIL
[NASA-CR-185590] 02 p0170 N90-10959
Aerodynamics of thrust vectoring
[NASA-CR-185074] 05 p0575 N90-13354
An experimental investigation of thrust vectoring two-dimensional convergent-divergent nozzles installed in a twin-engine fighter model at high angles of attack
[NASA-TM-4155] 08 p1017 N90-15884
Static investigation of a two-dimensional convergent-divergent exhaust nozzle with multiaxis thrust-vectoring capability
[NASA-TP-2973] 12 p1597 N90-19193
Internal performance of two nozzles utilizing gimbal concepts for thrust vectoring
[NASA-TP-2991] 12 p1599 N90-19200
Spacecraft escape 13 p1753 N90-20066
Electromechanical actuation for thrust vector control applications
[NASA-TM-102548] 14 p1968 N90-21272
Aerodynamics of Combat Aircraft Controls and of Ground Effects
[AGARD-CP-465] 23 p3271 N90-28513
Aerodynamic and propulsive control development of the STOL and maneuver technology demonstrator
23 p3271 N90-28514
Inflight thrust vectoring: A further degree of freedom in the aerodynamic/flight mechanical design of modern fighter aircraft 23 p3274 N90-28528

THRUSTORS
Bi-directional thruster development and test report
[NASA-CR-182013] 15 p2058 N90-21785

THULIUM
Magnetic excitations in thulium metal
[DE90-002475] 06 p0855 N90-14970
A room-temperature, laser diode-pumped, Q-switched, 2 micron, thulium-doped, solid state laser
[AD-D014527] 19 p2695 N90-25334
A tunable, continuous wave, thulium-doped, solid state laser cross-reference to related application
[AD-D014558] 22 p3180 N90-28045

THUNDERSTORMS
Forecasting convection with the AFOS (Automation of Field Operations and Services) data analysis programs. (ADAP-version 2.0) (AFOS data analysis programs-version 2.0)
[PB89-145940] 01 p0086 N90-10492
A collection of papers related to heavy precipitation forecasting
[PB89-230833] 05 p0671 N90-13910
Report on meteorological assessment of Bald Hills incidents, phase 1
[AD-A216201] 10 p1408 N90-18123
The 1985 and 1986 direct strike lightning data, part 1
[NASA-TM-100533-PT-1] 10 p1409 N90-18125
The 1985 and 1986 direct strike lightning data, part 2
[NASA-TM-100533-PT-2] 10 p1409 N90-18126
Characterization of thunderstorm induced Maxwell current densities in the middle atmosphere
12 p1634 N90-19391
Forecasting the tornadic intensities of thunderstorms by multivariate techniques
[AD-A218284] 13 p1847 N90-20602
A case study of a quasi-stationary tropical convective line
[AD-A218325] 13 p1847 N90-20604
A case study of cloud-to-ground lightning during the GALE program 15 p2132 N90-22185
Turbulence spectral widths view angle independence as observed by Doppler radar
[AD-A219169] 16 p2199 N90-22550
Tropical squall lines of the Arizona monsoon
16 p2257 N90-22867
A study of turbulence near thunderstorm tops
[NASA-CR-186620] 16 p2258 N90-22870
Examination of microburst development in Colorado thunderstorm for the 5 August 1982 case
[AD-A218478] 17 p2425 N90-23820
A comparison of lightning network data with surface weather observations
[AD-A220003] 17 p2427 N90-23832
Initiation and propagation of thunderstorm mesocyclones 17 p2428 N90-23838
Aureole lidar: Ground based measurement
[AD-A223207] 21 p3008 N90-27101
Relationship between solar activities and thunderstorm activities in the Beijing area and the northeast region of China 22 p3208 N90-28197
Severe thunderstorm cases of July 1988 through June 1989
[PB90-226424] 22 p3229 N90-28311
An investigation of forcing mechanisms during a surprise tornadic thunderstorm
[PB90-216805] 23 p3352 N90-28940
Severe thunderstorm forecasting: An operational review
[PB90-215484] 23 p3353 N90-28948
On the dynamics of severe thunderstorms
[DE90-627922] 23 p3353 N90-28950
Mesoscale Lightning Experiment (MLE): A view of lightning as seen from space during the STS-26 mission
[NASA-TM-103513] 23 p3353 N90-28951
A global model of thunderstorm electricity and the prediction of whistler duct formation
24 p3493 N90-29744
Three-dimensional numerical study of thunderstorm downdrafts and associated outflow boundaries
24 p3494 N90-29746

THYRATRONS
An analysis of the anomalous high-current cathode emission in pseudospark and back-of-the-cathode lighted thyratron switches
[AD-A215328] 10 p1378 N90-17988

THYRISTORS
NT SILICON CONTROLLED RECTIFIERS
Power semiconductor devices for space nuclear power systems
[DE90-001178] 07 p1005 N90-15819
A GaAs p-n-p-n thyristor model
[DE90-005757] 11 p1570 N90-19039
Controling, cabling and protection of GTO thyristors in pulse inverters
[ETN-90-96500] 18 p2549 N90-24548
A new technique for hardening optically-triggered thyristors
[DE90-006769] 18 p2549 N90-24550

TIBIA
Experiment K-6-27. Analysis of radiographs and biosamples from primate studies
20 p2897 N90-26478

TIDAL OSCILLATION
U TIDES

TIDES
NT ATMOSPHERIC TIDES
NT EARTH TIDES
Tidal and lunar data for Point Mugu, San Nicolas Island, and the Barking Sands Area during 1990
[AD-A214828] 09 p1249 N90-17248
Status of a nonlinear water surge model in February 1988
[KNMI-WR-88-03] 12 p1695 N90-19735

Analysis of water quality parameters of the Piaui River (SE), Brazil, through field and TM/LANDSAT sensor data
[INPE-4918-PRE/1417] 14 p1998 N90-21453
MECCA program documentation
[NOAA-TR-NESDIS-46] 14 p2003 N90-21477
A free surface Bryan-Cox-Semtner model
[IOS-270] 15 p2135 N90-22201
Determination of tide heights from airborne bathymetric data
[AD-A220412] 17 p2430 N90-23848
Dynamic and photometric evolutionary models of tidal tails and ripples 18 p2637 N90-25024
The integration of GPS heights into the Australian height datum 19 p2705 N90-25392
The effect of tidal friction between galaxies on the formation and development of galactic clusters in the expanding universe
[ETN-90-97314] 21 p3098 N90-27603
Vertically averaged spectral model for tidal circulation in estuaries. Part 1: Model formulation
[PB90-181678] 22 p3230 N90-28319

TIG WELDING
U GAS TUNGSTEN ARC WELDING

TIGHTNESS
Pressure air tightness tests of laminated panels for wing leading edge heat shields
[INFORME-I-377/89] 10 p1358 N90-17873
High resistance bolts: Test trials for plated bolts
[CRIF-MT-178] 17 p2413 N90-23748

TILES
Automated stress analysis of Shuttle orbiter thermal protection system 02 p0184 N90-11043
Low cost processing routes leading to high-performance ceramic tiles
[AD-A219034] 16 p2224 N90-22688
Aerodynamic pressure and heating-rate distributions in tile gaps around chine regions with pressure gradients at a Mach number of 6.6
[NASA-TP-2988] 17 p2400 N90-23670
Acousto-optic signature analysis for inspection of the orbiter thermal protection tile bonds
[DE90-013089] 20 p2819 N90-26043
Field experience in using laser acoustic sensing for inspection
[DE90-012954] 20 p2873 N90-26347
In-flight investigation of shuttle tile pressure orifice installations
[NASA-TM-4219] 23 p3328 N90-28820
Design and evaluation of candidate pressure distribution and air data system tile penetration for the aeroassist flight experiment
[NASA-CR-4312] 24 p3471 N90-29615

TILT
U ATTITUDE (INCLINATION)

TILT ROTOR AIRCRAFT
NT XV-15 AIRCRAFT
Application of the wide-field shadowgraph technique to rotor wake visualization
[NASA-TM-102222] 03 p0300 N90-11700
A CFD study of tilt rotor flowfields
[NASA-CR-186116] 05 p0575 N90-13349
Preliminary design of four aircraft to service the California Corridor in the year 2010: The California Condor, California Sky-Hopper, high capacity short range transport tilt rotor aircraft needed to simplify intercity transportation
[NASA-CR-186232] 06 p0724 N90-14226
An early overview of tiltrotor aircraft characteristics and pilot procedures in civil transport applications
[DOT/FAA/DS-89/37] 14 p1921 N90-21003
The influence of contract type in program execution/V-22 Osprey: A case study
[AD-A220011] 17 p2484 N90-24206
Extension-torsion coupling behavior of advanced composite tilt-rotor blades 18 p2644 N90-25057
Ground-simulation investigations of VTOL airworthiness criteria for terminal-area operations
[NASA-TM-102810] 19 p2660 N90-25141
Model tilt-rotor hover performance and surface pressure measurement
[AD-A222535] 21 p2959 N90-26827
FAA Rotorcraft Research, Engineering, and Development Bibliography 1962-1989
[AD-A224256] 24 p3417 N90-29299

TILTING
U ATTITUDE (INCLINATION)

TILTING ROTORS
Application of the wide-field shadowgraph technique to rotor wake visualization
[NASA-TM-102222] 03 p0300 N90-11700
A CFD study of tilt rotor flowfields
[NASA-CR-186116] 05 p0575 N90-13349
Identification of XV-15 aeroelastic modes using frequency-domain methods
[NASA-TM-101021] 15 p2051 N90-21756
An approach for design and analysis of composite rotor blades
[AD-A219257] 19 p2657 N90-25125

TILTMETERS
Measurement of fluctuations in the tilt of Arctic ice at the CEAREX Oceanography Camp: Experiment review, data catalog, and preliminary results
[AD-A215059] 09 p1249 N90-17249
An electronic spirit level tilt sensor
[ETN-90-96697] 17 p2406 N90-23710

TIMBER IDENTIFICATION
Inventory and monitoring of extended forest lands by remote sensing 19 p2708 N90-25409

TIMBER INVENTORY
Investigation of the usefulness of LANDSAT 5 thematic mapper data for mapping forest disease
[DFVLR-FB-89-06] 03 p0365 N90-12088
Inventory and monitoring of extended forest lands by remote sensing 19 p2708 N90-25409

TIMBER VIGOR
Signature analysis and classification of pine of different vitality classes using airborne thematic mapper data
[DFVLR-FB-89-07] 03 p0365 N90-12089

TIME
NT ACCESS TIME
NT DOWNTIME
NT EPHEMERIS TIME
NT FLIGHT TIME
NT MTBF
NT REACTION TIME
NT RELAXATION TIME
NT RESPONSE TIME (COMPUTERS)
NT TESTING TIME
NT TRANSIT TIME
NT UNIVERSAL TIME
Northeast Artificial Intelligence Consortium annual report for 1987. Volume 7, part A: Time oriented problem solving
[AD-A210331] 01 p0110 N90-10622
Time-frequency factors in auditory perception
[AD-A211491] 04 p0523 N90-13016
Fatigue, pilot deviations and time of day
[NASA-CR-185369] 04 p0526 N90-13035
The discrete-time single-server queueing model
[MEMO-780] 04 p0544 N90-13165
An accurate timing model for fault simulation in MOS circuits
[AD-A213153] 05 p0635 N90-13702
Using mappings to prove timing properties
[AD-A213967] 07 p0981 N90-15666
Periodic phase adjustment distributed clock synchronization in the hard realtime environment
[AD-A213842] 07 p0988 N90-15708
Uniform stability for time-varying infinite-dimensional discrete linear systems
[DE89-635712] 08 p1116 N90-16460
Apparatus for using a time interval counter to measure frequency stability
[NASA-CASE-NPO-17325-1-CU] 09 p1208 N90-17005
Pulsar timing and gravitational waves 12 p1732 N90-19955
Time and truth in plans 14 p1906 N90-20930
String dynamics in curved space-time revisited
[DE90-612796] 14 p2035 N90-21674
Time-varying filter modelling and time-frequency characterisation of nonstationary sound fields due to a moving source 16 p2312 N90-23178
Differential Loran-C using three secondary stations
[AD-A219573] 17 p2350 N90-23381
Adding a dimension: Time as a factor in the generalizability of predictive relationships
[AD-A219679] 17 p2438 N90-23890
Item identities and their related observables
[AD-A219559] 17 p2468 N90-24104
How can research and development leadtime be reduced
[AD-A224063] 23 p3404 N90-29240

TIME DELAY
U TIME LAG

TIME DEPENDENCE
An assessment of robustness of flight control systems based on variable structure techniques 02 p0157 N90-10895
Studies of time-dependent polar cap convection patterns 02 p0251 N90-11421
Development of a numerical solution to the time dependent kinetic equation 03 p0433 N90-12481
Time-domain Green function corresponding to a time-harmonic point source in complex space
[PB89-218846] 04 p0539 N90-13117
A moving-grid interface for systems of one-dimensional time-dependent partial differential equations
[CWI-NM-R8904] 04 p0541 N90-13136
Unsteady diffusion from a hemispherical pit
[NPL-DMA(A)-190] 04 p0553 N90-13220
A note concerning the onset of three dimensionality and time dependence in Goertler vortices
[NASA-CR-181956] 06 p0718 N90-14193
Crazing and degradation of flexure strength in acrylic plates as a function of time
[AD-A212835] 06 p0749 N90-14357
General exact solution for homogeneous time-dependent self-gravitating perfect fluids
[DE89-618425] 06 p0776 N90-14514
Nonlinear quantum effects in the Maser model: A large N scaling behaviour
[DE89-631631] 06 p0787 N90-14584
Numerical simulation of the unsteady two-dimensional flow in a time-dependent doubly-connected domain 07 p0875 N90-15073
Time-dependent free convection in liquid metals
[DE90-000957] 07 p0927 N90-15366
Time-dependent free convection in low Prandtl number fluids
[DE90-003053] 07 p0929 N90-15377
An experimental study of the time-dependent behavior of the appendage-body junction vortex
[AD-A213465] 07 p0930 N90-15384
Uniform stability for time-varying infinite-dimensional discrete linear systems
[DE89-635712] 08 p1116 N90-16460
A solution method for the time-dependent Navier-Stokes equations for laminar, incompressible flow
[FFA-146] 09 p1219 N90-17075
Time and spatially dependent estimates of pollutant trace gas emissions and their effect on tropospheric ozone 09 p1243 N90-17212
On scattering by time-dependent potentials: The 2-D case
[DE89-635708] 09 p1275 N90-17390
First results from the MST (Madison Symmetric Torus) reversed field pinch
[DE90-005743] 10 p1433 N90-18268
A numerical solution of the time-dependent Boltzmann equation
[AD-A216397] 10 p1434 N90-18275
Time-dependent measurements on vibrating annular turbine cascades under various steady state conditions 11 p1463 N90-18424
Time-dependent failure of silver-interlayer diffusion bonds between non-deforming base-metals
[DE90-006925] 12 p1628 N90-19357
Simulation of global Kr-85 and (14)CO2 distribution by means of a time-dependent, two dimensional model of the atmosphere
[ETN-90-95376] 12 p1689 N90-19702
Time-dependent failure of silver interlayer welds
[DE90-008015] 13 p1818 N90-20440
Plane Stokes flow driven by capillarity on a free surface: Overview and status
[DE90-009290] 15 p2098 N90-22009
Computer simulation of time-dependent spherically symmetric spacetimes containing radiating fluids: Formalism and code tests 15 p2185 N90-22483
Molecular evolution in astrophysical environments 16 p2332 N90-23291
Vertical directionality measurements of ambient noise in the NE Pacific
[AD-A220007] 17 p2432 N90-23856
Analysis of shell-type structures subjected to time-dependent mechanical and thermal loading
[NASA-CR-185077] 18 p2571 N90-24653
Development of a postprocessing and 3D graphical imaging facility
[AD-A221212] 18 p2593 N90-24755
Time-dependent density-functional theory
[AD-A220993] 18 p2604 N90-24829
Extended inflation from higher dimensional theories
[NASA-CR-180549] 19 p2796 N90-25916
Prediction of two-dimensional time-dependent gasdynamic flows for hypersonic studies
[UTIAS-335] 20 p2801 N90-25935
Experiments on initial behaviour of corona generated with electrical pulses superimposed on DC bias
[EUT-89-E-226] 20 p2858 N90-26259
Algorithms to solve nonlinear time dependent problems of engineering and physics
[AD-A221463] 21 p3055 N90-27368
Regular and chaotic motion of uniform elliptical vortices in external linear time dependent velocity fields 23 p3268 N90-28497
The steady and time-dependent aerodynamic characteristics of a combat aircraft with a delta or swept canard 23 p3274 N90-28526
Time-based competition for competitive advantage: An information technology perspective
[AD-A224474] 23 p3407 N90-29255

TIME DISCRIMINATION
Multiresolution and time-frequency representations of signals
[REPT-89-47] 15 p2087 N90-21946

Visual sensitivities and discriminations and their role in aviation
[AD-A219319] 16 p2266 N90-22917

TIME DIVISION MULTIPLE ACCESS
Satellite-matrix-switched, time-division-multiple-access network simulator
[NASA-TP-2944] 03 p0336 N90-11915
Satellite range delay simulator for a matrix-switched time division multiple-access network simulator
[NASA-TM-102407] 04 p0489 N90-12813
Characterization of two MMIC GaAs switch matrices at microwave frequencies
[NASA-TM-102449] 06 p0733 N90-14273
A burst compression and expansion technique for variable-rate users in satellite-switched TDMA networks
[NASA-TM-102414] 08 p1035 N90-15983
PLRS: A new spread spectrum position location reporting system 24 p3427 N90-29358

TIME DIVISION MULTIPLEXING
The first year's work of race project 1036 WTDM broadband customer premises network
[BBC-RD-1989/6] 08 p1055 N90-16097

TIME FUNCTIONS
Time-weighted accumulations ap(tau) and Kp(tau)
[RAE-TR-88050] 03 p0421 N90-12422
Berry-Esseen rates and bootstrap results for generalized L-statistics
[CWI-MS-R8808] 04 p0546 N90-13179
Excess transit time as a function of burst current in an exploding bridgewire detonator
[DE90-007168] 11 p1512 N90-18708
Series reversion/inversion of Lambert's time function
[AD-A216243] 12 p1607 N90-19245

TIME LAG
Frequency agile synthetic aperture radar
[AD-D014235] 06 p0765 N90-14451
Precise estimation of tropospheric path delays with GPS techniques 15 p2074 N90-21881
Telepresence, time delay, and adaptation 16 p2271 N90-22944
Robust modelling of sampled systems for time delay estimation
[REPT-89-047] 16 p2298 N90-23092
Application of the lagged-averaged technique to tropical cyclone track predictions
[AD-A218389] 17 p2425 N90-23819
Space operations: NASA efforts to develop and deploy advanced spacecraft computers. Report to the Chairman, Subcommittee on Space Science and Applications, Committee on Science, Space, and Technology, House of Representatives
[GAO/IMTEC-89-17] 19 p2742 N90-25582
QPOs from black-hole candidates 19 p2770 N90-25743
Is the hard tail of X rays from GX339-4 a Compton scattering component 19 p2779 N90-25806
Model following control system design: Preliminary ATTAS in-flight simulation test results
[PD-FC-9003] 20 p2813 N90-26010
The development of the time-delayed neural network architecture
[AD-A221540] 21 p3061 N90-27403
Control and estimation for aerospace applications with system time delays 24 p3428 N90-29367
Graphic overlays in high-precision teleoperation: Current and future work at JPL 24 p3508 N90-29827
Performance constraints and compensation for teleoperation with delay 24 p3517 N90-29881

TIME MARCHING
A parallel numerical simulation for supersonic flows using zonal overlapped grids and local time steps for common and distributed memory multiprocessors
[DE89-015252] 02 p0147 N90-10839
Derivation of synthetic mission profiles from electric vehicle field data
[DE89-011125] 06 p0793 N90-14620
Group implicit concurrent algorithms in nonlinear structural dynamics
[NASA-CR-185950] 06 p0796 N90-14638
Modified Chebyshev pseudospectral method with O(N exp -1) time step restriction
[NASA-CR-181958] 06 p0834 N90-14848
Extension of a streamwise upwind algorithm to a moving grid system
[NASA-TM-102800] 15 p2048 N90-21739
Application of a dynamic stall model to rotor trim and aeroelastic response 16 p2200 N90-22556
Three-dimensional separated flow prediction on fusiform body using Euler and boundary layer methods 16 p2234 N90-22745
A parallel structure transient response algorithm using independent substructure response computation 16 p2290 N90-23044
Reduced order models for nonlinear aerodynamics 18 p2492 N90-24244
A time-marching method to calculate unsteady airloads on three-dimensional wings. Part 1: Linearized formulation
[DLR-FB-89-58] 18 p2494 N90-24254
A time-marching method for calculating unsteady airloads on thrse-dimentional wings. Part 2: Full-potential formulation
[DLR-FB-89-59] 18 p2494 N90-24255
Tailoring explicit time-marching schemes to improve convergence characteristics 22 p3172 N90-27997

TIME MEASUREMENT
Time and frequency in geodesy measuring methods
[SER-C-337] 03 p0365 N90-12087
Stable Kalman filters for processing clock measurement data 04 p0487 N90-12801
An analysis of the time variation of the frequency response of the LMS adaptive line enhancer
[ISVR-TR-175] 08 p1058 N90-16115
Navigation experiment NAVEX data storage and processing
[ESA-TT-1175] 11 p1467 N90-18445
Synchronization of the ground station atomic clocks using three weighted transportable cesium time standards in the Navex navigation experiment
[ESA-TT-1153] 11 p1512 N90-18711
Thermal coefficient of delay for various coaxial and fiber-optic cables 12 p1643 N90-19439
X ray timing observations and gravitational physics 12 p1732 N90-19956
A review of atomic clock technology, the performance capability of present spaceborne and terrestrial atomic clocks, and a look toward the future 12 p1735 N90-19972
Frequency domain techniques for analyzing picosecond optical pulses
[AD-A218856] 16 p2318 N90-23214
Radio pulsar timing observations for GRO 16 p2334 N90-23301
Photoreflectance for in-situ characterization of MOCVD growth of semiconductors under micro-gravity conditions
[NASA-CR-186600] 17 p2383 N90-23576
Short time Force and moment measurement System for shock tubes (SFS) for measuring times less than 10 ms 18 p2490 N90-24233
An empirically derived figure of merit for the quality of overall task performance 18 p2644 N90-25058
Timing analysis of binary X ray pulsars observed by HEAO 1 19 p2781 N90-25822
Wideband impedance transformer for UHF power transistor time domain waveform measurement system
[PB90-210642] 22 p3167 N90-27962

TIME MEASURING INSTRUMENTS
NT ATOMIC CLOCKS
NT AUTONOMOUS SPACECRAFT CLOCKS
NT CLOCKS
NT TIMING DEVICES

TIME OF FLIGHT SPECTROMETERS
CELIAS: Charge, element and isotope analysis system for SOHO 04 p0568 N90-13313
Low energy neutral particle energy analyser by time of flight method
[DE90-719529] 08 p1125 N90-16517
Nuclear interactions of high energy heavy ions and applications in astrophysics
[DE90-006691] 12 p1737 N90-19984
Estimating sea ice thickness using time-of-flight data from impulse radar soundings
[AD-A218736] 16 p2250 N90-22831

TIME OPTIMAL CONTROL
Sequential design of experiments with physically based models 23
[AD-A211918] 03 p0393 N90-12239
The cellular approach: A new method to speed up simulated annealing for macro placement
[MEMO-COSOR-88-29] 05 p0663 N90-13980
Optimal control of aero-assisted orbit transfer vehicles 06 p0727 N90-14241
Control and stabilization of linear and nonlinear distributed systems
[AD-A216446] 11 p1547 N90-18908
A real time, FEM based optimal control algorithm and its implementation using parallel processing hardware (transistors) in a microprocessor environment 16 p2294 N90-23066
The discrete time H infinity control problem: The full-information case
[MEMO-COSOR-89-25] 17 p2455 N90-24003
On output deadbeat control of discrete-time multivariable systems
[MATHS-REPT-A-122] 20 p2915 N90-26583

TIME SERIES ANALYSIS
Method and apparatus for determining time, direction and composition of impacting space particles
[NASA-CASE-LAR-13392-1-CU] 01 p0026 N90-10132
Are ozone exceedance rates decreasing. Comment on extreme value analysis of environmental time-series: An application to trend detection in ground-level ozone
[AD-A211029] 02 p0239 N90-11357
Task analysis of the UH-60 mission and decision rules for developing a UH-60 workload prediction model. Volume 1: Summary report
[AD-A210763] 02 p0255 N90-11446
Fast sampling and stability of nonlinear sampled data systems. Part 2: Sampling rate estimations
[RR-341] 03 p0397 N90-12271
Modeling and analysis of nonlinear time series
[RR-355] 03 p0397 N90-12272
On the analysis of line profile variations: A statistical approach 03 p0420 N90-12412
Tail triviality for sums of stationary random variables
[CWI-MS-R8810] 04 p0542 N90-13143
Turbulent wind at the equatorial segment of an operating Darrieus wind turbine blade
[DE90-002672] 06 p0807 N90-14698
Parametric identification of discrete time series models for structural response prediction 07 p0945 N90-15472
Higher order crossings from a parametric family of linear filters
[AD-A213427] 07 p0983 N90-15676
Recurrence and ergodicity for exponential family state-space models
[AD-A213466] 07 p0983 N90-15677
An exploratory analysis of motion sickness data: A time series approach
[AD-A215534] 09 p1253 N90-17271
Segmentation of topographic profiles of the seafloor based on a self-affine model
[AD-A215938] 10 p1410 N90-18132
Proceedings of a research workshop on Nonlinear Time Series Analysis and Applications
[AD-A216541] 10 p1423 N90-18214
Optimum selection procedures in multi-stage screening, reliability, and time
[AD-A216811] 11 p1553 N90-18942
Damage characteristics of time domain histories
[DE90-008787] 13 p1842 N90-20573
Application of neural nets to system identification and bifurcation analysis of real world experimental data
[DE90-007539] 14 p2017 N90-21558
The observed three-dimensional structure of baroclinic waves in the Northern Hemisphere winter as revealed in a linear regression analysis 15 p2128 N90-22167
Finite element formulations for coupled fluid/structure eigenvalue analysis
[AD-A220793] 17 p2416 N90-23766
A numerical study of wind forcing in the eastern boundary current system off Portugal
[AD-A219596] 17 p2430 N90-23847
Bayesian characterization and detection of rare binary signature events
[AD-A221116] 18 p2606 N90-24844
Rocket engine failure detection using system identification techiques
[NASA-CR-185259] 19 p2664 N90-25159
An atlas of ECMWF analyses (1980-1987). Part 2: Second moment quantities
[NASA-TM-100762-PT-2] 19 p2715 N90-25451
Long timescale X ray variability in AGN 19 p2788 N90-25868
Nonlinear modeling of time series using Multivariate Adaptive Regression Splines (MARS)
[AD-A222710] 20 p2921 N90-26623
Reversed residuals in autoregressive time series analysis
[AD-A222711] 20 p2921 N90-26624
Adaptive time series analysis using predictive inference and entropy
[AD-A222337] 21 p2997 N90-27033
Some thoughts on data processing 21 p3023 N90-27189
Statistical methodologies for non-Gaussian noisy environments
[AD-A222137] 21 p3066 N90-27433
Broadband studies of seismic sources at regional and teleseismic distances using advanced time series analysis methods
[AD-A223113] 22 p3211 N90-28215
Comparative climatology of four marine stratocumulus regimes 22 p3213 N90-28225
Time series, statistics, and information
[AD-A224317] 24 p3540 N90-30018

TIME SHARING
Shared memory versus message passing architectures: An application based study
[AD-A210312] 01 p0108 N90-10615
The M/G/1 processor sharing queue as the almost sure limit of feedback queues
[REPT-89-32] 04 p0528 N90-13044

Waiting times in polling systems with Markovian server routing
[CWI-BS-R8905] 05 p0685 N90-13989
Workloads and waiting times in single-server systems with multiple customer classes
[CWI-BS-R8906] 05 p0689 N90-14020
Simple appoximations for second moment characteristics of the sojurn time in the M/G/1 processor sharing queue
[CWI-BS-R8907] 05 p0694 N90-14055
The implementation of a coherent memory abstraction on a NUMA (Non-Uniform Memory Access) multiprocessor: Experiences with PLATINUM (Platform for Investigating Non-Uniform Memory)
[AD-A213909] 07 p0970 N90-15600
Memory management for large-scale NUMA (Non-Uniform Memory Access) multiprocessors
[AD-A213910] 07 p0970 N90-15601
An overview of PLATINUM: A Platform for Investiga ting Non-Uniform Memory (preliminary version)
[AD-A213911] 07 p0970 N90-15602
Evolution of an operating system for large-scale shared-memory multiprocessors
[AD-A213912] 07 p0970 N90-15603
A data acquisition parallel bus for wind tunnels at ARL (Aeronautical Research Laboratory)
[AD-A218052] 13 p1759 N90-20098
Use of optical storage devices as shared resources in local area networks
[AD-A219198] 16 p2327 N90-23269
Sharing memory robustly in message-passing systems
[AD-A219923] 17 p2447 N90-23950
Parallel execution of LISP programs
[AD-A219623] 17 p2451 N90-23978
Atomic snapshots of shared memory
[AD-A222765] 20 p2904 N90-26520
Parallel performance of domain-decomposed preconditioned Krylov methods for PDEs with adaptive refinement
[AD-A222339] 21 p3064 N90-27420

TIME SIGNALS
Navigation experiment NAVEX: The self-test delay times in the D1 Spacelab mission
[ESA-TT-1176] 11 p1467 N90-18446
Synchronization of the ground station atomic clocks using three weighted transportable cesium time standards in the Navex navigation experiment
[ESA-TT-1153] 11 p1512 N90-18711
A real-time rejection circuit to automatically reject multiple interfering hopping signals while passing a lower level desired signal
[AD-D014424] 14 p1965 N90-21251

TIME TEMPERATURE PARAMETER
Aging of CFRP due to longterm storage in heated air
[ESA-TT-1124] 03 p0333 N90-11893
Gravimetric measurements of materials outgassing applied to graphite-epoxy laminates
[NASA-TM-100753] 05 p0619 N90-13609
A cure process model for resin transfer molding of advanced composites
[NASA-CR-186247] 09 p1185 N90-16867
Time temperature relations during rubber forming continuous fiber reinforced thermoplastics
[LR-620] 20 p2840 N90-26151

TIMERS
U TIMING DEVICES

TIMING
U TIME MEASUREMENT

TIMING DEVICES
Precision timing and interlocks systems for FEL (Free-Electron Laser) heating experiments on MTX (Microwave Tokamak Experiment)
[DE90-000833] 06 p0847 N90-14923
The RAP unit: A remote autoranging picoammeter
[DE90-007711] 14 p1982 N90-21357

TIMOSHENKO BEAMS
Wave-mode coordinate analysis of L junction in LSS
[AD-A211116] 02 p0176 N90-10984
A new aspect for the use of thin walled beams as shell stiffeners of spacecraft structures
02 p0184 N90-11046
An improved beam model for the vibrations of rotor blades 02 p0232 N90-11333
Parametric version of structural vibration models
[ONERA-RT-9/3313-RY-080-R]
09 p1238 N90-17188
An experimental system for measuring the wavenumber-frequency response of Timoshenko beams
[AD-A222569] 20 p2878 N90-26374
Parametrical retiming of vibrational models of structures
[ONERA-RT-9/3313-RY-080-R]
22 p3194 N90-28121

TIN
NT TIN ISOTOPES
Noncontacting laser ultrasonic generation and detection at the surface of molten metal
[DE90-002020] 06 p0791 N90-14605
The effect of H2O and pretreatment on the activity of a Pt/SnO2 catalyst 18 p2558 N90-24597
Effect of pretreatment on a platinized tin oxide catalyst used for low-temperature CO-oxidation
18 p2558 N90-24599
Tin doping of InSb grown by MOCVD using tetraethyltin
[DE90-009727] 18 p2620 N90-24929
Superconductivity in the Sn-Ba-Sr-Y-Cu-O system
22 p3151 N90-27863
Structure of metal overlayers by low energy alkali ion scattering: Cu/Ru(0001) and Sn/Pt(111)
[DE90-014453] 23 p3310 N90-28718

TIN ALLOYS
Primary arm spacing in directionally solidified Pb-10 wt percent Sn alloys
[NASA-CR-185190] 06 p0756 N90-14398
Isothermal fatigue behavior of Sn-Pb solar joints
[DE90-003280] 07 p0943 N90-15464

TIN COMPOUNDS
NT NIOBIUM STANNIDES
NT STANNIDES
NT TIN OXIDES
NT TIN TELLURIDES
Photochemically-driven biomimetic oxidation of alkanes and olefins
[DE89-011536] 02 p0193 N90-11097
The characterization of Nb3Sn superconductors for use in magnets of 19 T and greater
[DE89-017758] 03 p0412 N90-12364
Investigation of optical nonlinearities, conductivity and magnetism in organometallic materials
[AD-A218548] 16 p2317 N90-23211
Antiferromagnetism and enhanced heat in CeM2Sn (M = Ni, Ir, Cu, Rh, Pd, and Pt
[DE90-014924] 23 p3399 N90-29206

TIN ISOTOPES
Cyclic deformation of Sn-60 to Pb-40 solder joints during thermomechanical fatigue
[DE90-004197] 09 p1237 N90-17179
Study of Sn-116 via neutron pickup and proton stripping reactions
[KVI-814] 16 p2315 N90-23199

TIN OXIDES
Research on high-efficiency, single-junction, monolithic, thin-film amorphous silicon solar cells
[DE89-000846] 06 p0805 N90-14687
Process for making a noble metal on tin oxide catalyst
[NASA-CASE-LAR-13741-1-SB]
13 p1774 N90-20180
Characterization and comparison of optically transparent conducting films
[DE90-000319] 14 p2033 N90-21660
Spectrally selective tinoxide and indiumoxide coatings
[ISBN-90-9003138-3] 17 p2382 N90-23567
Pt/SnO2-based CO-oxidation catalysts for long-life closed-cycle CO2 lasers 18 p2556 N90-24589
The oxidation of carbon monoxide using tin oxide based catalysts 18 p2557 N90-24590
Mechanistic studies of the CO-oxidation reaction on catalysts for use in long-life CO2 lasers
18 p2558 N90-24596
Effect of pretreatment on a platinized tin oxide catalyst used for low-temperature CO-oxidation
18 p2558 N90-24599
Platinized tin oxide catalysts for CO2 lasers: Effects of pretreatment 18 p2559 N90-24600
Characterization study of polycrystalline tin oxide surfaces before and after reduction in CO
18 p2559 N90-24601
Surface defects and chemistry on the SnO2(110) surface 18 p2559 N90-24603
Review of model sensor studies on Pd/SnO2(110) surfaces 18 p2559 N90-24604
Analysis of Pt/SnO(sub x) during catalysis of CO oxidation 18 p2560 N90-24607
Characterization of the surfaces of platinum/tin oxide based catalysts by Fourier Transform Infrared Spectroscopy (FTIR) 18 p2560 N90-24608
Chemisorption studies of Pt/SnO2 catalysts
18 p2560 N90-24609
Characterization of the surfaces of platinum/tin oxide based catalysts by Fourier transform spectroscopy (FTIR) 18 p2643 N90-25054

TIN TELLURIDES
Bridgman crystal growth
[NASA-CR-186204] 07 p0997 N90-15766

TIP SPEED
En route noise of turboprop aircraft and their acceptability: Report of tests 18 p2609 N90-24858

TIPS
NT BLADE TIPS
NT CRACK TIPS
NT NOSE TIPS
NT WING TIPS

TIRES
NT AIRCRAFT TIRES
Tire modeling by finite elements
06 p0792 N90-14814
An overview of the joint FAA/NASA aircraft/ground runway friction program
[NASA-TM-103486] 20 p2805 N90-25957

TIROS N SERIES SATELLITES
Spatial registration of TIROS-N weather satellite data
[AD-A216041] 11 p1536 N90-18841

TIROS SATELLITES
NT ITOS SATELLITES
NT TIROS N SERIES SATELLITES
RAIDS: An orbiting observatory for ionospheric remote sensing from space
[AD-A213717] 07 p0949 N90-15494

TISSUES (BIOLOGY)
NT ADIPOSE TISSUES
Electroporation: Theory of basic mechanisms
[AD-A210196] 01 p0091 N90-10520
Membrane fusion: The role of polyphosphatidylinositol
[AD-A211289] 03 p0379 N90-12156
Investigation of resonant ac-dc magnetic field effects
[AD-A211612] 03 p0379 N90-12159
Biology in microgravity: A guide for experimenters
[ESA-TM-02] 04 p0482 N90-12769
Apparatus for imaging deep arterial and coronary lesions
[NASA-CASE-NPO-17439-1-CU]
08 p1104 N90-16391
Three-dimensional coculture process
[NASA-CASE-MSC-21560-1] 11 p1538 N90-18852
Accurate determination of the complex permittivity of biological tissue at 90 GHz, 70 GHz, and over a broad band around 35 GHz
[AD-A222062] 21 p3033 N90-27240

TITAN
Computer simulation of plasma interactions near Titan
01 p0142 N90-10816
Reports of workshops on Probe Measurements of Particles and Radiation in the Atmosphere of Titan
[NASA-TM-102218] 19 p2797 N90-25919
Role of the methylene amidogen (H2CN) radical in the atmospheres of Titan and Jupiter
20 p2947 N90-26769
Liquid-vapor equilibrium of multicomponent cryogenic systems 20 p2948 N90-26774

TITAN LAUNCH VEHICLES
Draft environmental impact statement for the Galileo Mission (Tier 2)
[NASA-TM-102926] 15 p2124 N90-22148
Atmospheric dispersion of solid and liquid rocket propellants
[AD-A221293] 21 p3020 N90-27173

TITANATES
NT BARIUM TITANATES
NT ILMENITE
NT LEAD TITANATES
NT LEAD ZIRCONATE TITANATES
NT PEROVSKITES
NT PIEZOELECTRIC CERAMICS
Heat treatment study of the SiC/Ti-15-3 composite system
[NASA-TP-2970] 12 p1618 N90-19302
Effect of casting procedures and diesel engine environment on the behavior of aluminum titanate
[AD-A223079] 20 p2835 N90-26126

TITANIA
Synthesis, characterization and evaluation of CO-oxidation catalysts for high repetition rate CO2 TEA lasers 18 p2557 N90-24593

TITANIUM
Powder morphology effects in the ignition of titanium-based pyrotechnics
[DE89-017229] 02 p0208 N90-11191
Exploratory study of niobium, titanium, zirconium and tantalum aluminides
[AD-A210658] 02 p0283 N90-11615
Development of texture analysis and its applications to titanium aero engine components
[PNR90561] 04 p0454 N90-12602
Synthesis and high temperature chemistry of methylsilsesquioxane polymers produced by titanium catalyzed redistribution of methylhydridooligo- and polysiloxanes
[AD-A212000] 04 p0477 N90-12736
Wear-resistant coated object
[EP-PATENT-0-289-173-A1] 05 p0624 N90-13643
Development of a titanium/boron blending process
[DE90-001450] 06 p0754 N90-14386

Laser mixing of titanium on silicon carbide
[DE90-003216] 07 p0891 N90-15150
Epoxy-resin cable terminations
[AD-A213789] 07 p0942 N90-15454
Optical waveguide fabrication by stoichiometric implantation of Ti and O into LiNbO3
[DE90-004238] 09 p1292 N90-17488
Observations of fatigue crack initiation and damage growth in notched titanium matrix composites
[NASA-TM-101688] 10 p1347 N90-17815
Develop techniques for ion implantation of PLZT for adaptive optics
[AD-A216005] 10 p1431 N90-18253
High efficiency flashlamp-pumped titanium: Sapphire laser
[AD-A217598] 13 p1806 N90-20367
Flash-pumped titanium laser
[AD-A217599] 13 p1806 N90-20368
L shell XANES (X ray Absorption Near Edge Structure) for solid metals: Ti, V, Cr, Fe, Ni, Cu
[DE90-008043] 13 p1896 N90-20880
Titanium aluminides: Processing, properties and potential
[AERE-R-13198] 14 p1949 N90-21158
Effects of titanium on some surface properties of nitride ceramics
[AERE-R-13566] 14 p1953 N90-21178
Investigation of the reaction kinetics between SiC fibers and selectively alloyed titanium matrix composites and determination of their mechanical properties
16 p2219 N90-22659
Inelastic response of metal matrix composites under biaxial loading 16 p2220 N90-22661
Investigation of the effect of mechanical stress on cold fusion
[AD-A220123] 17 p2474 N90-24147
Tribological and mechanical properties of Fe/Ti multilayered films
[DE90-011949] 18 p2565 N90-24635
Au-Ge-Ni-Ti ohmic contacts on gallium arsenide
[DE90-011064] 18 p2625 N90-24960
Characterization of NbTi multifilamentary superconducting wires
[DE90-626245] 20 p2930 N90-26672
Ilmenite exsolution schemes in Apollo-17 high-Ti basalts
[DE90-011992] 21 p2976 N90-26912
Fabrication of intermetallic compounds by solid state reaction of roll-bonded materials
[AD-A221960] 21 p2982 N90-26943
Titanium-doped sapphire lasers with high energy pumping
[RSRE-MEMO-4290] 22 p3181 N90-28050
On hydrogen chemisorption on metals: The electron correlation effects
[DE90-627318] 24 p3448 N90-29473
Recent progress in electronic structure calculations for defects in metals
[DE90-016323] 24 p3452 N90-29494
Fundamental studies on intermetallic compounds
[ONERA-RT-4/1855-M] 24 p3453 N90-29497
The investigation and production of titanium-tantalum junctions diffusion bonded at high temperature (855 C to 920 C): The influence of temperature, time pressure and roughness on the mechanical properties, and the optimisation of the bonded conditions
[BR114894] 24 p3476 N90-29646

TITANIUM ALLOYS
NT NITINOL ALLOYS
Evaluation of titanium castings for aerospace components 01 p0043 N90-10237
Advances in the technology of titanium castings
01 p0043 N90-10243
Emittance, catalysis, and dynamic oxidation of Ti-14Al-21Nb
[NASA-TP-2955] 01 p0044 N90-10248
Influence of microstructure and microdamage processes on fracture at high loading rates
[AD-A210307] 01 p0045 N90-10253
Ion implantation of two titanium alloys
[DE89-016958] 02 p0198 N90-11133
Elevated temperature aluminum-titanium alloy by powder metallurgy process
[AD-D014165] 03 p0326 N90-11852
Deformation of Ti-6Al-4V bar and extrusion under superplastic forming conditions
[RAE-TM-MAT/STR-1110] 03 p0330 N90-11875
Deformation of extruded titanium alloys under superplastic conditions
[RAE-TM-MAT/STR-1111] 03 p0330 N90-11876
Deformation of electron beam welded Ti-6Al-4V alloy sheet under superplastic conditions
[RAE-TM-MAT/STR-1109] 03 p0359 N90-12053
Tribological properties of ceramic/Ti3Al-Nb sliding couples for use as candidate seal materials to 700 deg C
[NASA-TM-102401] 04 p0464 N90-12658
Potential difference applied to the measurement of small fatigue crack growth at notches in Ti-6Al-4V
[FFA-TN-1989-09] 04 p0512 N90-12952
The effect of composition and aging treatment on the microstructure and mechanical properties of aluminum-lithium-titanium alloys
[AD-A213144] 05 p0624 N90-13640
Threshold for fatigue crack propagation
[DLR-FB-89-33] 05 p0655 N90-13815
The mechanical properties of superplastically formed titanium and aluminium alloys 06 p0744 N90-14331
The manufacture of superplastic alloys
06 p0745 N90-14333
Martensite transformation in NiTi alloys induced by tensile stress pulses
[DE90-001832] 06 p0747 N90-14346
Method to produce titanium alloy articles with high fatigue and fracture resistance
[AD-D014278] 08 p1043 N90-16029
Method for refining microstructures on prealloyed titanium powder compacts
[AD-D014280] 08 p1043 N90-16030
Method of marking titanium alloy articles having distinct microstructural regions corresponding to high creep and fatigue resistance
[AD-D014283] 08 p1043 N90-16031
Fundamental studies of beta phase decomposition modes in titanium alloys
[AD-A214424] 08 p1044 N90-16035
Microstructural explanation for irradiation embrittlement of V-15Cr-5Ti
[DE90-004112] 08 p1045 N90-16041
Fatigue and impact strength of diffusion bonded titanium alloy joints
[RAE-TM-MAT/STR-1123] 08 p1045 N90-16043
Effect of carbon on ion beam mixing of Fe-Ti bilayers
[DE90-003650] 08 p1048 N90-16056
Magnetic penetration depth and intragrain critical current density in gain-aligned Tl2Ca2Ba2Cu3O10 superconductor
[DE90-004245] 08 p1133 N90-16562
Properties and design of multifilamentary NbTi composite superconductors
[DE90-004904] 08 p1134 N90-16569
The effects of hydrogen embrittlement of titanium
08 p1156 N90-16698
Advanced tribological coatings for high specific strength alloys
[AD-A214061] 09 p1196 N90-16930
Fatigue crack propagation rates for titanium alloy sheet
[ESDU-89051] 09 p1201 N90-16956
Hydrogen embrittlement of titanium and its alloys
[DE90-602366] 10 p1355 N90-17858
Characterization of the 6242 Si alloy. Centrifugal wheel in conventional forging
[REPT-NT-3967] 10 p1355 N90-17859
Bearing tests in Ti-6Al-4V plates made using superplastic forming
[INFORME-I-357/89] 10 p1396 N90-18068
Effect of manganese additions on the physical and superconducting properties of Nb-46.5Ti
[DE90-005393] 10 p1436 N90-18290
Low temperature specific heat and magnetic susceptibility of NbTi and NbTiMn alloys
[DE90-005390] 11 p1486 N90-18552
Ac loss measurements of two multifilamentary NbTi composite strands
[DE90-005388] 12 p1619 N90-19304
Deformation and fracture of TiAl + W at elevated temperatures
[DE90-006490] 12 p1628 N90-19356
Improved toughness alloys based on titanium aluminides
[AD-A218149] 13 p1778 N90-20208
Surface characterization of hydrogen charged and uncharged alpha-2 and gamma titanium aluminide alloys using AES and REELS
[NASA-CR-186561] 14 p1951 N90-21171
Fatigue crack growth investigation of a Ti-6Al-4V forging under complex loading conditions: NATO/AGARD supplemental engine disk program
[AD-A220239] 17 p2377 N90-23538
The effects of cooling rate XD (trademark) TiAl weld microstructure
[DE90-011975] 18 p2528 N90-24427
Oxidation characteristics of Ti-14Al-21Nb ingot alloy
[NASA-TP-3012] 19 p2674 N90-25206
Deformation and fracture behavior of TiAl
[DE90-012212] 19 p2675 N90-25212
Weak-beam electron microscopy of dislocation splitting in TiAl: Relationship to plasticity
[ESA-TT-1159] 19 p2676 N90-25217
Application of high performance metals in gas turbine engines
[PNR90640] 20 p2811 N90-25999
Compendium of material test results on HY-130 and Ti-3Al2V metals in support of United States navy programs
[DE90-011754] 20 p2833 N90-26112
Formation of Titanium-boron surface alloys by excimer laser mixing
[DE90-013172] 20 p2834 N90-26118
Small crack growth and its influence in near alpha-titanium alloys
[RAE-TM-P-1171] 20 p2835 N90-26121
Structures and mechanical properties of near-beta titanium alloys TiV10Fe2Al3 and TiV10Cu3Al3
[ONERA-NT-1989-3] 20 p2835 N90-26123
Crystal growth and deformation behavior of TiAl aluminides
[DE90-012972] 20 p2930 N90-26671
Advanced processing and properties of high performance alloys
[AD-A221776] 21 p2983 N90-26948
Study of the microstructure of a titanium alloy (6246) for turbomachine compressors
[ETN-90-97450] 22 p3157 N90-27900
Surface reactions of the TA6V titanium alloy under laser irradiation
[ETCA-90-R-012] 22 p3158 N90-27904
Fretting fatigue strength of Ti-6Al-4V at room and elevated temperatures and ways of improving it
23 p3308 N90-28709
Surface property improvement in titanium alloy gas turbine components through ion implantation
23 p3309 N90-28713
Static and dynamic characterization of the ATR 72 rods made of Ti 10.2.3 titanium alloy
[REPT-49-238] 23 p3310 N90-28722
Crack layer analysis of fatigue fracture of a beta titanium alloy 23 p3338 N90-28864
The use of automated ball indentation testing to measure flow properties and estimate fracture toughness in metallic materials
[DE90-015797] 24 p3452 N90-29493
Realization of equipment for manufacturing titanium alloy electrodes for first step melting
[ONERA-RT-15/3578-M] 24 p3453 N90-29498

TITANIUM BORIDES
New structural materials
[AD-A209425] 01 p0044 N90-10246
Shock compression and release in high-strength ceramics
[DE89-013995] 01 p0047 N90-10265
Toughening of a particulate-reinforced/ceramic-matrix composite
[AD-A213180] 05 p0618 N90-13604
Empirical and analytical determination of the fracture resistance of a TiB2 particle/SiC matrix composite
[NASA-TM-101940] 07 p0890 N90-15143
Control of titanium diboride SHS reactions by inert dilutions and mechanical constraint
[AD-A214378] 10 p1357 N90-17870
Low cost processing routes leading to high-performance ceramic tiles
[AD-A219034] 16 p2224 N90-22688
Quality evaluation of coatings by automatic scratch testing
[AD-A219331] 17 p2379 N90-23548
The mechanical properties of Cu/TiB2 multilayer structures
[DE90-010608] 18 p2517 N90-24378
Titanium-boron mixtures as variable heat sources
[DE90-009729] 18 p2522 N90-24401
Microstructure and stability of TiB2 and Cu multilayers
[DE90-011955] 18 p2627 N90-24968

TITANIUM CARBIDES
Investigation of commercial Al-Ti and Al-Ti-B master alloys and development of a new grain refining agent based on carbides for aluminum and aluminum alloys
[ETN-89-94663] 02 p0199 N90-11136
Laser mixing of titanium on silicon carbide
[DE90-003216] 07 p0891 N90-15150
Synthesis of large area, monocrystalline TiC as a substrate for heteroepitaxial growth of beta-SiC
[AD-A221392] 18 p2623 N90-24948

TITANIUM CHLORIDES
TiCl4 as a source of TiO2 particles for laser anemometry measurements in hot gas
[NASA-TM-102581] 13 p1805 N90-20358

TITANIUM COMPOUNDS
NT BARIUM TITANATES
NT ILMENITE
NT LEAD TITANATES
NT LEAD ZIRCONATE TITANATES

NT PEROVSKITES
NT PIEZOELECTRIC CERAMICS
NT RUTILE
NT TITANATES
NT TITANIUM BORIDES
NT TITANIUM CARBIDES
NT TITANIUM CHLORIDES
NT TITANIUM NITRIDES
NT TITANIUM OXIDES

Consequence of condensed-phase formation in transient burning of TiHx/KClO in a closed system
[DE89-013922] 02 p0208 N90-11188

Lithium polymer electrolyte battery, electrochemical behavior of cathode materials
[AD-A210755] 02 p0216 N90-11235

Heat treatment of pulsed Nd: YAG laser welds in a Ti-14.8 wt pct Al-21.3 wt pct Nb titanium aluminide
[DE90-003484] 07 p0905 N90-15228

Development of a reliable fabrication technique to produce intermetallic compounds
[AD-A215004] 09 p1194 N90-16918

Creep behavior of alloys based on TiAl containing TiB2 and TiN particulates
[DE90-006489] 12 p1628 N90-19355

Sol-gel derived polytitanosiloxane coatings
[DE90-004186] 13 p1779 N90-20210

Optical spectroscopy of Ti(3+) doped YAlO3
[AD-A219043] 16 p2324 N90-23251

TITANIUM DIOXIDE
U TITANIUM OXIDES

TITANIUM NITRIDES
Wear-resistant coated object
[EP-PATENT-0-289-173-A1] 05 p0624 N90-13643

Effects of titanium on some surface properties of nitride ceramics
[AERE-R-13566] 14 p1953 N90-21178

Quality evaluation of coatings by automatic scratch testing
[AD-A219331] 17 p2379 N90-23548

TITANIUM OXIDES
NT ILMENITE
NT RUTILE

Basic research on processing of ceramics for space structures
[AD-A205954] 02 p0199 N90-11139

Ordered ceramic membranes
[DE89-017426] 06 p0750 N90-14364

Processing and properties of nanophase oxides
[DE90-003826] 07 p0895 N90-15171

Research on high-efficiency, single-junction, monolithic, thin-film amorphous silicon solar cells, phase 1
[DE89-009495] 07 p0951 N90-15502

Characterization of MOCVD (Metal Organic Chemical Vapor Deposition) grown epitaxial ceramic oxide thin films
[DE90-003561] 07 p1001 N90-15790

Preparation, structure and properties of VO(sub x) and TiO2 thin films by MOCVD
[DE90-003566] 07 p1001 N90-15793

Microstructures of Y123 films on SrTiO3, LaGaO3, and LaAlO3
[DE90-003367] 08 p1129 N90-16537

Evolution of structure and electrical properties during crystallization of rapidly solidified Bi4Ti3O12
[DE90-005221] 09 p1292 N90-17492

Studies of photochemically and electrochemically driven electron transport in zeolites
[DE90-007659] 12 p1624 N90-19335

Hydrous metal oxide-supported catalysts. Part 2: Catalytic properties and applications
[DE90-008098] 12 p1625 N90-19336

Diffraction studies of the structure of glasses and liquids
[DE90-007662] 12 p1632 N90-19381

Zirconia-based electrodes for solid oxide fuel cells
[DE90-000462] 12 p1655 N90-19513

TiCl4 as a source of TiO2 particles for laser anemometry measurements in hot gas
[NASA-TM-102581] 13 p1805 N90-20358

Center for surface radiation damage studies
[AD-A218452] 16 p2222 N90-22678

Ceramic epitaxial films and multilayers prepared by MOCVD
[DE90-011090] 18 p2532 N90-24447

An investigation of a mathematical model of an optically pumped Ti(3+):Al2O3 laser system
18 p2646 N90-25063

Processing of nanocrystalline ceramics
[DE90-015700] 24 p3456 N90-29520

TITRATION
Calorimetry, activity, and micro-FTIR analysis of CO chemisorption, titration, and oxidation on supported Pt
18 p2560 N90-24606

TNT (TRINITROTOLUENE)
U TRINITROTOLUENE

TOILETS
Proposal for a zero-gravity toilet facility for the space station
[NASA-CR-183151] 04 p0526 N90-13036

TOKAMAK DEVICES
Ignition and burn criteria for D3He tokamak and spherical torus reactors
[DE89-015059] 01 p0125 N90-10716

Kinetic effects in Alfven wave heating. Part 2: Propagation and absorption with a single minority species
[DE89-016619] 01 p0126 N90-10724

Theory of high-n toroidicity-induced shear Alfven eigenmode in tokamaks
[DE89-016726] 02 p0277 N90-11582

A study of runaway electron confinement and theory of neoclassical MHD turbulence
[DE89-016728] 02 p0277 N90-11584

Projections for a steady-state tokamak reactor based on ITER
[DE89-016678] 02 p0278 N90-11589

Electron cyclotron emission and absorption experiment on the CASTOR tokamak
[IPPCZ-285] 03 p0407 N90-12331

Control of plasma position in the CASTOR tokamak
[IPPCZ-284] 03 p0407 N90-12332

Microwave Tokamak Experiment (MTX) ohmic heating system
[DE89-017892] 03 p0408 N90-12340

Effect of the length of the multijunction grill on its lower hybrid current drive efficiency
[IPPCZ-283] 04 p0556 N90-13240

On optimization of the multijunction grill for the lower hybrid current drive
[IPPCZ-280] 04 p0556 N90-13241

Acceleration of small, light projectiles (including hydrogen isotopes) to high speeds using a two-stage light gas gun
[DE90-002479] 06 p0729 N90-14253

Modeling of runaway electron damage for the design of tokamak plasma facing components
[DE90-000847] 06 p0845 N90-14914

Thermal loads on tokamak plasma facing components during normal operation and disruptions
[DE90-000794] 06 p0846 N90-14919

Microwave Tokamak Experiment (MTX) first year of operation and future plans
[DE90-000817] 06 p0846 N90-14920

Microwave Transport Systems for the MTX (Microwave Tokamak Experiment)
[DE90-000821] 06 p0846 N90-14921

MTX (Microwave Tokamak Experiment)/ELF (Electron Laser Facility) 2 microwave power measurements and calibration for the 2-GW, 140-GHz, ELF 2 Free Electron Laser (FEL)
[DE90-000825] 06 p0846 N90-14922

Precision timing and interlocks systems for FEL (Free-Electron Laser) heating experiments on MTX (Microwave Tokamak Experiment)
[DE90-000833] 06 p0847 N90-14923

Microwave Tokamak Experiment: An overview of the construction and checkout phase
[DE90-000834] 06 p0847 N90-14924

Stability of the Global Alfven Eigenmode in the presence of fusion alpha particles in an ignited tokamak plasma
[DE89-016618] 06 p0848 N90-14930

Computation of electromagnetic effects in a tokamak due to a plasma disruption
[DE90-001764] 06 p0848 N90-14931

Practical aspects of a 2-D edge-plasma model
[DE90-002995] 06 p0848 N90-14932

Fundamental studies of fusion plasmas
[DE90-002343] 06 p0848 N90-14933

Upgrade plans to handle 30 to 40 Mbytes of data for D3-D
[DE90-003291] 07 p0995 N90-15750

Design of DIII-D advanced divertor
[DE90-003343] 07 p0995 N90-15752

Magnetic mirror confinement concepts system studies
[DE90-003667] 07 p0995 N90-15753

Destabilization of tokamak pressure-gradient driven instabilities by energetic alpha populations
[DE90-003716] 07 p0996 N90-15756

The 17th AINSE Plasma Physics Conference: Conference handbook
[DE90-600936] 07 p0996 N90-15759

Introduction to D-He(3) fusion reactors
07 p1008 N90-15839

Data file management in the D3-D data acquisition and analysis computer systems
[DE90-003289] 07 p1010 N90-15850

Initial deuterium confinement studies in DIII-D tokamak: DIII-D milestone report number 58
[DE90-003942] 08 p1124 N90-16509

Modeling energy output of inertial storage devices for the DIII-D tokamak
[DE90-004096] 08 p1126 N90-16524

Electron assisted glow discharges for conditioning fusion tokamak devices
[DE90-004104] 09 p1284 N90-17445

Design of a microwave calorimeter for the microwave tokamak experiment
[DE90-004486] 10 p1387 N90-18026

Microwave free-electron laser applications for electron cyclotron heating of plasmas
[DE90-005203] 10 p1431 N90-18257

Numerical simulation of non-inductive current drive for tokamak plasmas with time-varying electron temperatures
[DE90-733144] 10 p1432 N90-18264

The rapid inward diffusion of cold ions in tokamaks and their effect on ion transport
[DE90-006863] 11 p1568 N90-19022

Thermonuclear instability of global-type shear Alfven modes
[DE90-007087] 11 p1568 N90-19026

On 140 GHz microwave FEL experiments using ELF-2
[DE90-006764] 12 p1667 N90-19576

FOMA: A Fast Optical Multichannel Analyzer
[DE90-004093] 12 p1713 N90-19839

Computation of coupling elements between waveguides and modes for large launching structures
[IPPCZ-290] 13 p1890 N90-20842

Enhanced pinch effect due to electrostatic potential
[DE90-007088] 13 p1890 N90-20844

High elongation plasmas
[DE90-007575] 13 p1891 N90-20848

Materials and selection criteria analysis for the compact ignition tokamak toroidal field coil turn-to-turn insulation system: Photographic summary oflaboratory testing
[DE90-008020] 13 p1891 N90-20850

Particle transport in pellet fueled JET (Jet European Torus) plasmas
[DE90-008077] 13 p1891 N90-20851

Design of D-3 He commercial tokamak
[DE90-008252] 13 p1891 N90-20852

Numerical code AEOLUS-E1 for analysing free-boundary resistive MHD mode
[DE90-759903] 14 p2028 N90-21630

West European magnetic confinement fusion research
14 p2029 N90-21634

Applied plasma physics
[DE90-007932] 14 p2029 N90-21635

An extended diffusive model for calculating thermal diffusivity from single monopole tokamak heat pulse propagation
[DE90-007958] 14 p2029 N90-21637

Magnetic turbulence versus safety factor in the Tokapole 2 tokamak
15 p2168 N90-22391

Three-dimensional simulations of simple electron drift wave turbulence in tokamak geometry
[DE90-009581] 15 p2169 N90-22398

Resonant MHD modes with toroidal coupling
[DE90-010077] 16 p2319 N90-23222

The beta limit in the DIII-D tokamak
[DE90-011896] 19 p2759 N90-25677

Comparative assessment of world research efforts on magnetic confinement fusion 19 p2759 N90-25680

Proceedings of the US-Japan Fusion Cooperation Program Exchange P148 Workshop on Advanced Current Drive Concepts
[IPPJ-REV-4] 21 p3078 N90-27498

A study on the heating and diagnostic of a tokamak plasma by electromagnetic waves of the electron cyclotron range of frequencies
[DE90-791312] 21 p3078 N90-27499

Combined electron cyclotron ray tracing and transport code studies in the compact ignition tokamak
[DE90-014097] 23 p3396 N90-29189

Nonlinear tearing mode: Rutherford regime and global characteristics
[DE90-015003] 23 p3397 N90-29193

Ignition and burn control characteristics of thermonuclear plasmas
[DE90-015385] 23 p3398 N90-29197

TSC (Tokamak Simulation Code) simulations of Alcator C-MOD discharges 3: Study of axisymmetric stability
[DE90-015386] 23 p3398 N90-29198

Tokamak plasma shape identification with a Legendre-Fourier expansion of the vacuum poloidal flux function in the toroidal coordinates
[DE90-508031] 24 p3548 N90-30068

A model of peaked density profile and inward pinch in tokamaks
[DE90-508079] 24 p3548 N90-30072

Structure of magnetic field in tokamaks
[DE90-628904] 24 p3549 N90-30075

Magnetic surfaces in tokamaks
[DE90-628905] 24 p3549 N90-30076

Fundamental studies of fusion plasmas
[DE90-015732] 24 p3549 N90-30080

TOLERANCES (MECHANICS)
NT IMPACT TOLERANCES
Casting airworthiness joint European civil authorities view-point 01 p0042 N90-10234
Advances in the technology of titanium castings 01 p0043 N90-10243
Relating tolerances and kinematic behavior
[AD-A211125] 01 p0055 N90-10311
Adaptive structures to meet future requirements for large precision structures 02 p0178 N90-11001
Dynamic tip clearance measurements in axial flow compressors
[PNR90597] 04 p0456 N90-12612
Point of view of a civil aircraft manufacturer on Al-Li alloy 07 p0899 N90-15200
Overview on radiation effects in electronics
[DE90-000841] 07 p0926 N90-15357
FRAG requirements for control of fatigue testing
[RAE-TM-MAT/STR-1130] 08 p1089 N90-16300
Impact damage tolerance of composite cylindrical panels
[AD-A216401] 10 p1350 N90-17830
AGARD/SMP Review: Damage Tolerance for Engine Structures. 2: Defects and Quantitative Materials Behaviour — conference
[AGARD-R-769] 11 p1457 N90-18396
The damage tolerance of disc materials: Metallurgical factors; relationship with processing parameters 11 p1458 N90-18398
Future technology requirements (related to defects and quantitative material behavior to aid in implementation of damage tolerance for design of engine structures) 11 p1459 N90-18403
Static strength and damage tolerance tests on the Fokker 100 airframe
[NLR-MP-88023-U] 12 p1604 N90-19228
Solar Concentrator Advanced Development Program
[NASA-CR-185173] 16 p2250 N90-22834
The Trickett-Welch Solution to the Behrens-Fisher problem applied to one-sided tolerance limits for random effects model
[AD-A220416] 17 p2485 N90-24086
Damage tolerance demonstration for A310-300 CFRP components
[MBB-UT-012/89-PUB] 19 p2652 N90-25091
Lessons learned for composite aircraft structures qualification 21 p2956 N90-26808
Lessons learned from the T-46A durability and damage tolerance program 21 p2957 N90-26812
Application of damage tolerance 21 p2958 N90-26817
Individual Helicopter Tracking Program (IHTP) for the MH-53J helicopter 21 p2958 N90-26818
Damage tolerance analysis for manned hypervelocity vehicles. Volume 2: Software user's manual
[AD-A222136] 21 p2959 N90-26826
A tough performance simultaneous semi-interpenetrating polymer network
[NASA-CASE-LAR-14339-1] 21 p2984 N90-26955
AGARD/SMP Review Damage Tolerance for Engine Structures. 3: Component Behaviour and Life Management
[AGARD-R-770] 22 p3117 N90-27704
AGARD damage tolerance concepts for engine structures Workshop 3, Component Behaviour and Life Management 22 p3117 N90-27705
A Protection And Detection Surface (PADS) for damage tolerance
[NASA-TP-3011] 22 p3135 N90-27788
Damage tolerance analysis for manned hypervelocity vehicles. Volume 1: Final technical report
[AD-A221970] 22 p3191 N90-28106
Damage tolerance of woven graphite-epoxy buffer strip panels
[NASA-TM-102702] 22 p3192 N90-28114

TOLERANCES (PHYSIOLOGY)
NT ACCELERATION TOLERANCE
NT COLD TOLERANCE
NT HEAT TOLERANCE
NT HUMAN TOLERANCES
NT RADIATION TOLERANCE
Evaluation of rocket motor exhaust and liner combustion by-products
[AD-A210747] 02 p0189 N90-11083
Effects of serial wet-dry-wet cold exposure: Thermal balance, physical activity, and cognitive performance
[AD-A212704] 04 p0524 N90-13025
The effects of noise on performance
[AD-A212519] 04 p0551 N90-13209
Generation of free radicals during cold injury and rewarming
[AD-A213088] 05 p0672 N90-13915
Evaluation of two objective measures of effective auditory stimulus level
[AD-A214669] 09 p1250 N90-17255
The effects of foveal load on peripheral sensitivity in the visual field
[AD-A214872] 09 p1251 N90-17260
The characteristics of physiological responses and tolerance evaluation of pressure breathing
[AD-A214991] 09 p1252 N90-17262
Guidelines for safe human exposure to impact acceleration, update A
[AD-A215287] 09 p1253 N90-17268
Alterations in the metabolic and sympathetic response to cold exposure after cold air acclimation
[AD-A216817] 10 p1412 N90-18144
The pollution hazard assessment system: Documentation and users manual
[AD-A217108] 12 p1689 N90-19706
Metabolism, seizures, and blood flow in brain following organophosphate exposure: Mechanisms of action and possible therapeutic agents
[AD-A217098] 12 p1696 N90-19740
A comparison of the mechanisms of cold- and microgravity-induced fluid loss
[AD-A218098] 13 p1852 N90-20631
Aircraft crash survival design guide. Volume 2: Aircraft design crash impact conditions and human tolerance
[AD-A218435] 16 p2198 N90-22545
Lack of behavioral effects of high-peak-power microwave pulses from an axially extracted virtual cathode oscillator
[AD-A220779] 17 p2391 N90-23618
Laser eye protection
[AD-A219659] 17 p2408 N90-23722
Updating a dosage-effect relationship for the prevalence of annoyance due to general transportation noise
[AD-A219416] 17 p2421 N90-23794
Dazzling glare: Protection criteria versus visual performance
[AD-A219676] 17 p2438 N90-23889
Mechanisms of microwave induced damage in biologic materials
[AD-A222454] 21 p3033 N90-27242
A human factors engineering approach to the development and dynamic evaluation of a prototype aircrew seat for military aircraft
[AD-A218283] 24 p3500 N90-29779

TOLLMIEN-SCHLICHTING WAVES
On the interaction of stationary crossflow vortices and Tollmien-Schlichting waves in the boundary layer on a rotating disc
[NASA-CR-181859] 01 p0002 N90-10007
Near-planar TS waves and longitudinal vortices in channel flow: Nonlinear interaction and focusing
[NASA-CR-181928] 03 p0300 N90-11698
Long-range LFC transport 04 p0439 N90-12508
Interaction of Tollmien-Schlichting waves and Goertler vortices 04 p0440 N90-12515
Boundary-layer receptivity and laminar-flow airfoil design 04 p0440 N90-12516
Effect of roughness on the stability of boundary layers 04 p0440 N90-12518
Predicted and hot-film measured Tollmien-Schlichting wave characteristics 04 p0441 N90-12523
Sensitivity of LFC techniques in the non-linear regime 04 p0442 N90-12533
Design and test of an NLF wing glove for the variable-sweep transition flight experiment 04 p0444 N90-12544
Multiple paths to subharmonic laminar breakdown in a boundary layer
[NASA-CR-181948] 05 p0638 N90-13722
TS - Dean interactions in curved channel flow
[NASA-CR-181983] 10 p1306 N90-17559
Surface-cooling effects on compressible boundary-layer instability
[NASA-CR-182003] 14 p1971 N90-21290
Experimental investigation of Tollmien-Schlichting instability and transition in similar boundary layer flow in an adverse pressure gradient (Hartree beta = -0.14)
[LR-604] 19 p2692 N90-25318

TOLUENE
Nonlinear optical processes in one-dimensional polymers
[AD-A216103] 11 p1489 N90-18568

TOMOGRAPHY
NT COMPUTER AIDED TOMOGRAPHY
Ceramic components in machines, Cologne and Aachen, West Germany; Maastricht, The Netherlands and Brussels, Belgium
[DE89-015631] 01 p0047 N90-10264
Tellurium-118/antimony-118 generator
[DE89-015225] 01 p0122 N90-10698
Tomographic imagery by multislot coding applied to x ray diagnostics of laser plasmas: Implementation of a direct electronic detection camera 06 p0787 N90-14579
A tomographic study of premixed turbulent stagnation point flames
[DE90-002462] 07 p0892 N90-15156
Phase space and path integral methods applied to direct and inverse ocean seismo-acoustic modeling
[AD-A214777] 09 p1249 N90-17247
Boundary estimation problems arising in thermal tomography
[NASA-CR-181964] 10 p1421 N90-18193
An application of ocean wave-current refraction to the gulf stream using SEASAT SAR data
[AD-A216769] 11 p1537 N90-18851
Inverse scattering and tomography
[AD-A216456] 11 p1551 N90-18932
Tomographic investigations of weakly perturbed supersonic free jets
[MPIS-MITT-91] 12 p1600 N90-19209
Tomographic processing of synthetic aperture radar signals for enhanced resolution
[AD-A217178] 13 p1789 N90-20265
Three-dimensional medical image analysis using local dynamic algorithm selection on a multiple-instruction, multiple-data architecture
[AD-A218024] 13 p1852 N90-20630
An initial comparison between two 3-D x ray CT algorithms for characterizing
[DE90-013656] 21 p2984 N90-26957
Geophysical diffraction tomography: A complementary remote sensing technique for hazardous waste site characterization
[DE90-013025] 23 p3341 N90-28882

TOMS
U TOTAL OZONE MAPPING SPECTROMETER

TONOMETRY
U PRESSURE MEASUREMENT

TOOLING
Low cost tooling material and process for graphite and Kevlar composites
[NASA-CR-179427] 10 p1351 N90-17834
Development and fabrication of structural components for a scramjet engine
[NASA-CR-181945] 13 p1757 N90-20088
NASA/GSFC split-rail parallel gripper 18 p2507 N90-24328

TOOLS
NT BORING MACHINES
NT DRILL BITS
NT GRINDING MACHINES
NT MACHINE TOOLS
NT MILLING MACHINES
NT SAWS
NT SPACE TOOLS
Adjustable depth gage
[NASA-CASE-LEW-14880-1] 01 p0072 N90-10415
Case tool evaluation system
[DE90-003698] 08 p1108 N90-16413
Mechanized fluid connector and assembly tool system
[NASA-CASE-MSC-21434-1] 09 p1230 N90-17138
Rapid prototyping of tools
[AD-A215956] 10 p1392 N90-18050
Report on the fifth workshop on synchrotron x ray lithography
[DE90-007903] 15 p2172 N90-22411
SKITTER/implement mechanical interface
[NASA-CR-184920] 17 p2384 N90-23578
Lunar hand tools
[NASA-CR-184924] 17 p2384 N90-23581
EVA power tool prototype 18 p2538 N90-24482
Modeling strength data for CREW CHIEF 19 p2729 N90-25516
The challenge of assembling a space station in orbit 22 p3130 N90-27763
Power beam technology at Los Alamos: A review of research and development activities
[DE90-009002] 22 p3182 N90-28057

TOPEX
Error modeling of bias-type parameters for TOPEX orbit determination 07 p0884 N90-15117
Refinement of Earth's gravity field with Topex GPS measurements 13 p1838 N90-20553

TOPOGRAPHY
NT LUNAR TOPOGRAPHY
NT TERRAIN
Topographic map reading
[AD-A211269] 02 p0236 N90-11340
The astronomy of Andean myth: The history of a cosmology 02 p0291 N90-11660
Geology of Southern Guinevere Planitia, Venus, based on analyses of Goldstone radar data 03 p0422 N90-12424
Contrasting landform perception with varied radar illumination geometries and at simulated resolutions of Venera and Magellan 03 p0423 N90-12430
Stress distribution and topography of Tellus Regio, Venus 03 p0428 N90-12452

Semi-Lagrangian, semi-implicit solutions of the shallow water equations in one dimension
[AD-A212658] 04 p0503 N90-12902
Surface current and wave modulation measurements over bottom topography: A comparison with theory
[AD-A212469] 04 p0522 N90-13011
Self-organizing semantic maps
[PB89-212609] 04 p0529 N90-13049
An investigation of the diffraction of an acoustic plane wave by a curved surface of finite impedance
[NASA-CR-186069] 04 p0550 N90-13204
Climatology of Lawrence Livermore National Laboratory
[DE90-000905] 06 p0818 N90-14756
Geosat/ERM altimeter data analysis for the determination of global oceanic mesoscale variability
07 p0949 N90-15492
Evolution of overlapping spreading centers: A Sea Mark 2 investigation
[AD-A214278] 07 p0965 N90-15576
Regional height determination using gravimetric and topographical data
[UH-156] 08 p1091 N90-16315
Investigation of the topographic components of the image content of radar pictures
08 p1094 N90-16332
Surface topography measurements over the 1 meter to 10 micrometer spatial period bandwidth
[DE90-003642] 08 p1122 N90-16501
Determination of the gravity disturbance on the earth's topographic surface from airborne gravity gradient data
[AD-A214596] 09 p1246 N90-17230
Simulation of shading in synthetic surfaces
[INPE-4869-PRE/1480] 10 p1326 N90-17660
The effects of abrupt topography on ocean currents as sensed by satellite remote sensing
[AD-A214123] 10 p1409 N90-18128
Segmentation of topographic profiles of the seafloor based on a self-affine model
[AD-A215938] 10 p1410 N90-18132
Land suitability maps and appropriate land use: An approach using SGI and satellite imagery
[INPE-4827-PRE/1458] 11 p1521 N90-18761
Perspective revision of systematic mapping through orbital imagery
[INPE-4817-PRE/1453] 11 p1524 N90-18775
Improvement of classification results from satellite imagery to update and differentiate land use classes on topographic maps
[BCRS-89-17] 11 p1526 N90-18786
SPOT for landscape: Development of a method for the use of SPOT pictures for the updating of the data base scale of the landscape
[BCRS-89-18] 11 p1526 N90-18787
Quantification of structural field data in the Rio Grande do Norte basin and neighborhood
[INPE-4821-RPE/591] 11 p1533 N90-18826
Applications of FM-CW laser radar to antenna contour mapping 12 p1611 N90-19270
Analysis of photogeologic lineaments in the Ithacare (BA) region: A proposed methodology
[INPE-4855-PRE/1478] 12 p1677 N90-19635
The potential of combined use of satellite data with topographic TM information for manual/visual and digital updating of land use
[NLR-MP-88021-U] 12 p1678 N90-19639
Evolution of midplate hotspot swells: Numerical solutions
[NASA-CR-186462] 12 p1691 N90-19713
Digital production of perspective images
[SER-C-347] 12 p1701 N90-19768
Design and calibration of a vacuum compatible scanning tunneling microscope
[NASA-TM-102514] 13 p1804 N90-20353
Simulation of landscape disturbances and the effect of climatic change
[DE90-007565] 13 p1829 N90-20503
Gravitational model improvement at the Goddard Space Flight Center 13 p1831 N90-20514
Geopotential coefficient determination and the gravimetric boundary value problem: A new approach
13 p1833 N90-20521
First year's results and field experience with the latest JILA absolute gravimeter 13 p1834 N90-20529
Critique of the vertical gradient of gravity
13 p1834 N90-20531
The role of topography in geodetic gravity field modelling 13 p1835 N90-20534
High resolution analysis of satellite gradiometry
13 p1840 N90-20561
Evaluation of classification performance and proportion estimate of the sugar cane crop through PROCEDURE-INPE utilizing LANDSAT data
[INPE-4899-PRE/1500] 14 p1999 N90-21458
Performance evaluation of MSS/LANDSAT data in the estimation of fluvial channel width
[INPE-4906-PRE/1507] 14 p2000 N90-21463
Surface roughness and the physical properties of fractures
[DE90-006046] 15 p2128 N90-22169
Geographic information system: Coded data of agrocattle-raising projects in the Amazon
[INPE-4978-PRE/1543] 15 p2180 N90-22457
Geology of coronae and domal structures on Venus and models of their origin 15 p2191 N90-22513
Sulphur silicate interactions on the Jovian satellite Io
15 p2192 N90-22515
Determination of the general ocean circulation using satellite altimetry from a simultaneous solution for the Earth's gravity field 16 p2203 N90-22569
Surface topography of the Greenland Ice Sheet from satellite radar altimetry
[NASA-SP-503] 16 p2253 N90-22850
Topographic mapping from SPOT satellite imagery
[ETN-90-96689] 17 p2418 N90-23777
Erosional development of bedrock spur and gully topography in the Valles Marineris, Mars
[NASA-CR-180655] 17 p2424 N90-23813
Sea bottom topography with X-band SLAR
[BCRS-89-25] 17 p2431 N90-23854
In-situ topographical imaging of electrode surfaces using high resolution phase-measurement interferometric microscopy
[AD-A221021] 18 p2548 N90-24542
Heat and fluid flow within the Earth's crust: In situ measurements and mathematical models
18 p2579 N90-24690
A numerical investigation of thermal convection in highly viscous spherical shells with applications to mantle dynamics in the Earth and other terrestrial planets
18 p2579 N90-24691
Estimation of the impulse response of a broadband mobile radio channel in suburbia at 910 MHz
20 p2846 N90-26187
Spatial cross-correlation of Antarctic Sea ice and seabed topography
[NASA-CR-186815] 20 p2891 N90-26451
Evolution of overlapping spreading centers: A SeaMARC 2 investigation
[AD-A223102] 21 p3025 N90-27200
The role of the topography in gravity gradiometer reductions and in the solution of the geodetic boundary value problem using analytical downward continuation
[AD-A223107] 21 p3025 N90-27201
Vandenberg Boundary Layer Survey (VBLS): Results
[AD-A222517] 21 p3031 N90-27234
An evaluation of three models designed for siting wind turbines in areas of complex terrain
[DE90-013625] 22 p3196 N90-28137
Planetary-scale flow on a two-layer beta-plane channel model with topography 23 p3350 N90-28931
Near-angle scattering and binary optics
[AD-A224140] 23 p3396 N90-29186
INPE geographic data base
[INPE-4636-PRE/1348] 23 p3407 N90-29253
Asymptotic code vector density in topographic vector quantisers
[RSRE-MEMO-4392] 24 p3539 N90-30012

TOPOLOGY

NT FIXED POINTS (MATHEMATICS)
NT HOMOTOPY THEORY
NT INVARIANT IMBEDDINGS
NT LINKS (MATHEMATICS)
NT METRIC SPACE

Finding isolated zero points of complex polynomial mappings
[DE89-617523] 01 p0111 N90-10633
General action for topological quantum field theories
[DE89-618460] 02 p0286 N90-11637
Moduli spaces and topological quantum field theories
[DE89-016943] 02 p0287 N90-11639
A theory of networks for approximation and learning
[AD-A212359] 04 p0538 N90-13110
International Conference on Fixed Point Theory and Applications
[AD-A212369] 04 p0545 N90-13171
Julia-Fatou-Sullivan theory for real one-dimensional dynamics
[REPT-88-100] 04 p0548 N90-13190
On the topology of three-dimensional viscous flow structures near a plane wall. A classification and non-hyperbolic singularities on the wall
[LR-541] 05 p0644 N90-13758
Scaling in a non Abelian string network
[ROM1F-89-676] 05 p0695 N90-14066
Configurational statistics of strings, fractals and polymer physics. Part 2: Non Abelian strings
[ROM1F-89-680-PT-2] 05 p0696 N90-14067
Statistical mechanics of strings and topology
[ROM1F-89-683] 05 p0696 N90-14068
Some aspects of curvature in general relativity
05 p0704 N90-14122
On thick domain walls in general relativity
[NASA-CR-185926] 05 p0704 N90-14124
Spatial dynamics of deformable multibody systems with variable kinematic structure
[AD-A214098] 07 p0942 N90-15455
A (2+1)-dimensional pure gravity for an arbitrary closed initial surface
[DE90-701754] 07 p1007 N90-15829
Abelian gauge theory in topologically non-trivial space
[DE90-710100] 07 p1007 N90-15830
Harmonic mappings into manifolds with boundary
[DE90-606961] 09 p1277 N90-17402
Analysis of power bus topologies used in telecommunications satellites 10 p1331 N90-17691
PWM converter topologies 10 p1335 N90-17721
An assessment of the use of resonant-mode topologies for high frequency power conversion
10 p1335 N90-17726
Modelling the buck-type converter transient response with pulsating load 10 p1337 N90-17740
On the approximative normal values of multivalued operators in topological vector space
[DE90-610430] 12 p1707 N90-19800
Linearized analysis of (2+1)-dimensional Einstein-Maxwell theory
[DE90-741470] 12 p1725 N90-19913
Extension of the constraints algebra for the closed string with the fixed topology world sheet
[DE90-612745] 14 p2020 N90-21577
Fusion algebra and fusing matrices
[DE90-612798] 14 p2021 N90-21583
Algebraic block-structured grid generation based on a macro-block concept 15 p2093 N90-21978
Multiblock topology specification and grid generation for complete aircraft configurations
15 p2094 N90-21986
Bifurcations in viscous flow fields. On the genesis and development of topologically complicated separated flow structures
[PB90-167156] 15 p2099 N90-22012
Preference numbers and funnel dimension
[REPT-89-57] 15 p2161 N90-22346
Experimental study of vortex ring interaction with a free surface 16 p2233 N90-22742
Computational chaos in massively parallel neural networks 16 p2283 N90-23012
Topology of three-dimensional, variable density flows
[NASA-CR-186622] 17 p2402 N90-23683
Topological classification of structurally stable quadratic systems without limit cycles
[REPT-89-66] 17 p2457 N90-24025
A uniform representation scheme for freeform geometric modeling
[REPT-89-70] 17 p2458 N90-24028
Fixed point theory in multiply ordered spaces
[REPT-89-74] 17 p2458 N90-24031
Reflexivity, the dual Radon-Nykodym property, and continuity of adjoint semigroups
[CWI-AM-R8908] 17 p2460 N90-24042
On the G1 smooth connection between triangular Bernstein-Bezier patches. Part 1: Around and N-patch corner
[TELECOM-PARIS-89-D-012] 18 p2575 N90-24671
On the G1 smooth connection between triangular Bernstein-Bezier patches. Part 2: In a piecewise representation
[TELECOM-PARIS-89-D-013] 18 p2575 N90-24672
Free-form surface modelling using tensor product Bezier patches: A review with new solutions
[TELECOM-PARIS-89-D-014] 18 p2575 N90-24673
Sensitivity analysis of transputer workfarm topologies
[AD-A219821] 18 p2595 N90-24766
A topological image matcher
[OUEL-1798/89] 19 p2744 N90-25600
Optical high-speed parallel backplane
[AD-D014504] 19 p2757 N90-25670
Hierarchical structure of polygonal data for spatial analysis and representation of cartographical data
[INPE-4986-PRE/1548] 20 p2879 N90-26380
Predissimilarities, prefilters, and ultrametrics on an arbitrary set
[IMAG-RR-970-M] 20 p2918 N90-26603
Generation and improvement of meshes for finite elements methods in two and three dimensions
[ETN-90-97249] 20 p2919 N90-26611
Integrated structural/control design via multiobjective optimization
[AD-A223088] 21 p3071 N90-27459
Periodicity of redshift distribution in a T-3 universe
[FERMILAB-PUB-90/26-A] 22 p3262 N90-28475
Beltrami algebra and symmetry of Beltrami equation on Riemann surfaces
[DE90-627157] 23 p3388 N90-29135

On comparable L(sup p)-norms of subadditive functions on topological groups
[DE90-627154] 23 p3390 N90-29146
On an isospectrality question over compact Riemann surfaces
[DE90-627163] 23 p3390 N90-29147
Topology of singularities and phase diagram of N=2 superconformal field theories
[DE90-627213] 23 p3391 N90-29155
Effective actions for bosonic topological defects
[NASA-CR-187271] 24 p3544 N90-30041

TORCHES
Internal wire guide for GTAW welding
[NASA-CASE-MFS-29489-1] 17 p2385 N90-23586
Electrode carrying wire for GTAW welding
[NASA-CASE-MFS-29491-1] 20 p2842 N90-26168
An effective low-profile thermite torch
[DE90-015746] 24 p3459 N90-29534

TORNADO AIRCRAFT
U MRCA AIRCRAFT

TORNADOES
Forecasting the tornadic intensities of thunderstorms by multivariate techniques
[AD-A216284] 13 p1847 N90-20602
Severe local storm warning verification: 1989
[PB90-248592] 22 p3229 N90-28313
An investigation of forcing mechanisms during a surprise tornadic thunderstorm
[PB90-216805] 23 p3352 N90-28940
Program on development of basic understanding of severe weather phenomena
[PB90-226564] 23 p3352 N90-28943
Observations of tornadoes and wall clouds with a portable FM-CW Doppler radar: 1989--1990 results
[DE90-013152] 24 p3495 N90-29752

TOROIDAL PLASMAS
Theory of high-n toroidicity-induced shear Alfven eigenmode in tokamaks
[DE89-016726] 02 p0277 N90-11582
Particle simulation in curvilinear coordinate systems
[DE89-016727] 02 p0277 N90-11583
Compact torus configurations with high frequency driven currents
[ETN-89-94674] 02 p0280 N90-11598
Anisotropy of electron distributions related to the anisotropy and polarization of the continuous emitted x rays 06 p0785 N90-14566
Toroidal rotation retardation and ion anomalous transport by drift waves in a tokamak
[DE89-634427] 06 p0844 N90-14913
Thermal loads on tokamak plasma facing components during normal operation and disruptions
[DE90-000794] 06 p0846 N90-14919
Computation of electromagnetic effects in a tokamak due to a plasma disruption
[DE90-001764] 06 p0848 N90-14931
Practical aspects of a 2-D edge-plasma model
[DE90-002995] 06 p0848 N90-14932
Experiments on linear high beta helical axis stellarators to study simulated toroidal effects and Alfven-wave heating
[DE90-001704] 07 p0994 N90-15745
Studies of plasma performance and transport in the Advanced Toroidal Facility (ATF)
[DE90-001737] 07 p0994 N90-15746
Toroidal magnetic fields in terms of field-line invariants
[DE89-016610] 08 p1123 N90-16507
Design of a microwave calorimeter for the microwave tokamak experiment
[DE90-004486] 10 p1387 N90-18026
Dissipative trapped electron modes in ell equals 2 torsatrons
[DE90-004919] 10 p1431 N90-18256
Overview of recent results from the Advanced Toroidal Facility
[DE90-005673] 12 p1716 N90-19853
Anomalous transport in toroidal plasmas
[DE90-006549] 12 p1717 N90-19859
Ultraviolet observations of the atmosphere of Io and the plasma torus 12 p1728 N90-19929
Materials and selection criteria analysis for the compact ignition tokamak toroidal field coil turn-to-turn insulation system: Photographic summary oflaboratory testing
[DE90-008020] 13 p1891 N90-20850
Impurity control in toroidal devices
[DE90-618585] 15 p2170 N90-22399
Resonant MHD modes with toroidal coupling
[DE90-010077] 16 p2319 N90-23222
Combined electron cyclotron ray tracing and transport code studies in the compact ignition tokamak
[DE90-014097] 23 p3396 N90-29189
Resonant MHD modes with toroidal coupling
[DE90-015185] 23 p3397 N90-29196

TOROIDAL WHEELS
Structural problems of accurate inflatable surfaces 02 p0184 N90-11044

TOROIDS
Toroid monitor
[DIGEL-1989-8] 11 p1504 N90-18663
Parametric design studies of toroidal magnetic energy storage units
[DE90-013086] 20 p2881 N90-26390
Confinement of nonneutral plasma in unconventional geometries
[DE90-013048] 20 p2928 N90-26659
Compact toroid research
[DE90-016123] 24 p3550 N90-30087

TORPEDOES
Real time image enhancement during underwater recovery operations
[AD-A213139] 05 p0700 N90-14097

TORQUE
Magnetostrictive torque sensor
[AD-D014169] 03 p0349 N90-11996
Non linear vibrations in a drive train when coupled to constant torque and constant power loads
[PNR90593] 04 p0508 N90-12934
Autonomous spacecraft attitude control using magnetic torquing only 05 p0586 N90-13415
Continuously variable gear drive transmission
[AD-D014268] 08 p1084 N90-16275
Electronically Variable Pressure Regulator (EVPR) 11 p1474 N90-18484
Back swing phenomenon of synchronous generator. Study on ac-dc power system simulator tests
[DE89-782321] 11 p1500 N90-18635
Disturbance torque rejection properties of the NASA/JPL 70-meter antenna axis servos 12 p1644 N90-19450
Space mechanism of low velocity for an array of solar panels: Analysis and design of an experimental model; dimensions of bearings
[INPE-4859-TDL/370] 13 p1809 N90-20390
Design of a telerobotic controller with joint torque sensors
[DE90-008753] 13 p1812 N90-20404
Design of a digital model following controller of reaction wheel torques
[INPE-4753-PRE/1425] 14 p1938 N90-21093
A fiber optic sensor for noncontact measurement of shaft speed, torque, and power
[NASA-TM-102481] 14 p1983 N90-21360
AX-5 space suit bearing torque investigation 15 p2115 N90-22101
Lunar hand tools
[NASA-CR-184924] 17 p2384 N90-23581
Direct drive robotic hand
[NASA-CASE-NPO-17917-1-CU] 20 p2872 N90-26339
Investigation of maximum achievable body torque for a walking machine with friction cone constraints
[PB90-203175] 23 p3332 N90-28838
Performance evaluation of a 6 axis high fidelity generalized force reflecting teleoperator 23 p3372 N90-29052
Preliminary results on noncollocated torque control of space robot actuators 23 p3373 N90-29057
Force/torque and tactile sensors for sensor-based manipulator control 24 p3501 N90-29791
Stability analysis of multiple-robot control systems 24 p3505 N90-29811
Time optimal movement of cooperating robots 24 p3505 N90-29815

TORQUE MEASURING APPARATUS
U TORQUEMETERS

TORQUE MOTORS
Design and use of brushless dc motor without detent torque 18 p2539 N90-24491
Active lag angle device
[AD-D014538] 20 p2857 N90-26249
Magnetostrictive direct drive motors
[NASA-CR-186895] 23 p3335 N90-28855

TORQUEMETERS
A fiber optic sensor for noncontact measurement of shaft speed, torque, and power
[NASA-TM-102481] 14 p1983 N90-21360

TORSION
Deformation behavior of SiC/2014 Al metal-matrix composite
[AD-A212095] 03 p0320 N90-11816
Initial test results for the mini-mast 05 p0600 N90-13482
Flexural and torsional-flexural buckling of thin-walled open section struts
[ESDU-89007] 06 p0797 N90-14843
Elastic stress concentration factors. Geometric discontinuities in rods and tubes of isotropic materials
[ESDU-89048] 09 p1239 N90-17192
Positioning control of highest accuracy for very dynamic coupled system
[ETN-90-95893] 12 p1701 N90-19769
Constitutive data acquisition and modelling in aluminium 2014 alloy
[AERE-R-13651] 13 p1775 N90-20186
On free products of torsion free abelian groups
[AD-A218146] 13 p1878 N90-20773
Parametric resonance in horizontal axis wind turbines 14 p1912 N90-20962
Rotor loading on a three-bladed wind turbine 15 p2123 N90-22145
Diesel engine condition monitoring: Laser-based diagnostic techniques 17 p2410 N90-23733
Transitioning of power flow in beam models with bends 18 p2570 N90-24648
On the performance of algorithms for large-scale bound constrained problems
[DE90-010084] 18 p2590 N90-24736
Development of a finite element based delamination analysis for laminates subject to extension, bending, and torsion 18 p2642 N90-25049
On null tratorial torsion in vacuum quadratic Poincare gauge field theory
[MATHS-REPT-A-111] 19 p2751 N90-25630
On trivector torsion in vacuum quadratic Poincare gauge field theory
[MATHS-REPT-A-121] 20 p2933 N90-26692
Supersonic jet studies of benzyl alcohols: Minimum energy conformations and torsional motion
[AD-A221815] 21 p2980 N90-26934
Torsional effects in structures subjected to strong ground motion
[PB90-226960] 23 p3339 N90-28869
The MTL Torsional Split-Hopkinson bar
[AD-A223278] 24 p3479 N90-29663

TORSIONAL STRESS
Mechanism for shear band formation in the high strain rate torsion test
[PB89-215370] 03 p0356 N90-12038
Effect of constitutive modeling on the dynamic development of shear bands in viscoplastic materials
[AD-A220443] 17 p2416 N90-23765
Agusta methodology for pitch link loads prediction in preliminary design phase
[ETN-90-97270] 20 p2808 N90-25978
Microstructure: Property correlation --- multiaxial fatigue damage evolution in waspaloy
[NASA-CR-180406] 23 p3340 N90-28880

TORSIONAL VIBRATION
The response of helicopter rotors to vibratory airload
[AD-A215678] 09 p1167 N90-16756
Diesel engine condition monitoring: Laser-based diagnostic techniques 17 p2410 N90-23733
Dynamics of multistage gear transmission with effects of gearbox vibrations
[NASA-TM-103109] 22 p3182 N90-28060

TORUSES
Non Abelian string correlations and galaxies formation
[ROM1F-89-678] 05 p0714 N90-14171
Plasma diagnostics generated in the Compact Torus of UNICAMP
[INPE-4862-RPE/593] 10 p1433 N90-18271
Hopf bifurcation with nonsemisimple 1:1 resonance e
[MEMO-808] 15 p2161 N90-22347
Studies of Io's atmosphere and plasma torus 16 p2338 N90-23326
Distributed computing on transitive networks: The torus
[RUU-CS-88-31] 18 p2634 N90-25007

TOTAL OZONE MAPPING SPECTROMETER
Nimbus-7 TOMS Antarctic ozone atlas: August through November, 1989
[NASA-RP-1237] 17 p2428 N90-23837

TOTAL VARIATION DIMINISHING SCHEMES
U TVD SCHEMES

TOUCH
NT TACTILE DISCRIMINATION
Three dimensional object recognition employing combined visual and tactile sensing
[PB89-219489] 03 p0382 N90-12176
Modeling elastomer displacements for tactile sensing applications
[DE90-007959] 14 p1984 N90-21370
Telepresence for space: The state of the concept 19 p2731 N90-25526
Human machine interaction via the transfer of power and information signals 23 p3372 N90-29054

TOUCHDOWN
Modified touchdown zone lighting
[DOT/FAA/CT-TN89/70] 14 p1929 N90-21042

TOUGHNESS
Deformation behavior of SiC/2014 Al metal-matrix composite
[AD-A212095] 03 p0320 N90-11816
Toughening of a particulate-reinforced/ceramic-matrix composite
[AD-A213180] 05 p0618 N90-13604

The metallurgical determinants of toughness as cryogenic temperature
[DE90-002331] 06 p0748 N90-14351
Hardening and toughening of ZnS-Ga2S3 ceramics by solid-state reactions
[AD-A213875] 07 p0912 N90-15276
Fracture toughness of ferritic alloys at very high neutron exposures
[DE90-004519] 08 p1046 N90-16048
Mechanics of interface fracture
14 p1990 N90-21408
Inclusion of unstable ductile tearing and extrapolated crack-arrest toughness data in PWR vessel integrity assessment
[DE90-009427] 15 p2118 N90-22116
Microcracking and toughness of ceramic-fiber/ceramic-matrix composites under high temperature
[AD-A218516] 16 p2223 N90-22680
Thermomechanical properties of new composite materials SiC/glass-ceramic
[REPT-892-430-118] 17 p2370 N90-23491
Fracture toughness and failure mechanisms in commercial 2091 Al-Li sheet at cryogenic temperatures
[AD-A222803] 20 p2835 N90-26125
Theory of ceramic/zirconia composites: Toughening, strengthening, and synergism
[AD-A222931] 21 p2985 N90-26961
A characterization of V-391/H46-8B, A toughened BMI prepreg system produced by US Polymeric
[AD-A221772] 21 p2989 N90-26985
Computational investigation of local material strength and toughness on crack growth
[AD-A223189] 21 p3012 N90-27127
Study of a method for measuring the dimensions of cracks on the surface of ceramics by Rayleigh waves
[ETCA-89-R-024] 22 p3160 N90-27922
Factors influencing the mode I interlaminar fracture resistance of toughened matrix composites
23 p3300 N90-28668
Electrochemical surface finishing using amino-substrates on carbon fibers in organic media. Effects of the finishing on the mechanical properties of carbon-epoxy composites
[ONERA-RT-9/3549-M] 23 p3301 N90-28672
Is there anything of practical value hidden amongst the composite toughening theories. A Jim Mueller prospective
[DE90-014905] 23 p3301 N90-28673
Static and dynamic characterization of the ATR 72 rods made of Ti 10.2.3 titanium alloy
[REPT-49-238] 23 p3310 N90-28722
High performance brittle matrices and brittle matrix composites, book 2
[AD-A223274] 24 p3443 N90-29441
Mechanical properties and fracture toughness of AAR-TC128 Grade B steel and a micro-alloyed, control-rolled steel, A 8XX grade B, from -80F to +73F
[PB90-207796] 24 p3448 N90-29471
Toughening of SAN copolymers by an SAN emulsion grafted rubber
[AD-A224213] 24 p3453 N90-29502

TOWED BODIES
Modeling and control of the rapid deployment of towed airborne devices 07 p0879 N90-15092
Modeling towed cable system dynamics
[AD-A223610] 24 p3476 N90-29644

TOWED TARGETS
U TARGETS
U TOWED BODIES

TOWERS
NT AIRPORT TOWERS
Rotor loading on a three-bladed wind turbine
15 p2123 N90-22145
Design of a versatile, teleoperable, towable lifting machine with robotic capabilities for use in NASA's lunar base operations
[NASA-CR-186688] 19 p2697 N90-25345
Design and performance of a long, over-water microwave radio link
[PB90-207994] 23 p3318 N90-28758

TOWING
Modeling towed cable system dynamics
[AD-A223610] 24 p3476 N90-29644

TOWNSEND DISCHARGE
NT GAS DISCHARGES

TOXIC HAZARDS
The Third Conference on the Environmental Chemistry of Hydrazine Fuels
[AD-A197632] 02 p0203 N90-11157
The soil microbiology of hydrazines
02 p0205 N90-11171
Fuel neutralization by ozone oxidation
02 p0206 N90-11176
Low ppb level detection of toxic compounds with a fully automated CO2 laser photoacoustic detector
02 p0206 N90-11181
Occupational safety considerations with hydrazine
02 p0207 N90-11182
Aircraft cabin fire suppression by means of an interior water spray system
[CAA-PAPER-88014] 03 p0303 N90-11719
Analysis of hydraulic fluids and lubricating oils for the formation of Trimethylolpropane Phosphate (TMP-P)
[AD-A215188] 09 p1198 N90-16939
Environmental Projects. Volume 9: Construction of hazardous materials storage facilities
[NASA-CR-186295] 09 p1244 N90-17216
Aircraft Fire Safety
[AGARD-CP-467] 10 p1311 N90-17581
Modelling time to incapacitation and death from toxic and physical hazards in aircraft fires
10 p1318 N90-17619
Daytime wind valleys adjacent to the Great Salt Lake
[DE90-008991] 15 p2133 N90-22190
The acute, delayed neurotoxicity evaluation of two jet engine oil formulations
[AD-A222018] 21 p2986 N90-26972
Compiling air toxics emission inventories, 2nd edition
[PB90-185422] 22 p3198 N90-28148

TOXICITY
Heterogeneous catalysts in water
[AD-A210742] 01 p0041 N90-10228
Organic explosives and related compounds. Environmental and health considerations
[AD-A210554] 01 p0054 N90-10306
A matrix-isolation FT-IR study of hydrazine
02 p0204 N90-11168
Effects of atmospheric mix and toxic fumes on military performance
[PB89-223630] 04 p0522 N90-13015
Recovery of particle size distribution of ultrafine aerosols from diffusional decay measurements
[AD-A213006] 05 p0621 N90-13621
Novel carbamates, their production and their use as fuels additives
[EP-PATENT-0-298-636-A-1] 05 p0629 N90-13676
Adaptation and resistance of ecosystems to stress
[AD-A212999] 05 p0665 N90-13889
The substitution of IVD (Ion Vapor Deposition) aluminum for cadmium
[AD-A215633] 09 p1195 N90-16921
Environmental quality and occupational health Special Emphasis Area Plan (SEAP)
[AD-A214738] 09 p1251 N90-17259
Proceedings of the 17th Conference on Toxicology
[AD-A215076] 09 p1252 N90-17263
Workshop on the Effects of Combined Fire Products on Human Physiological and Psychological Performance
[AD-A215465] 09 p1253 N90-17270
Method for the evaluation of toxicity of combustion products from aircraft cabin materials: Analysis and results 10 p1316 N90-17612
Risk analysis: Fundamental concepts, regulatory toxicology, and relative comparisons from radiation biology
[DE90-002466] 11 p1538 N90-18856
Study of hydrazine metabolism and toxicity
[AD-A217103] 12 p1695 N90-19736
Development of a laser fluorosensor for the aircraft supported analysis of maritime toxic agents loads: Definition phase
[ETN-90-95320] 13 p1829 N90-20499
Acute oral toxicity of JA-2 solid propellant in ICR mice
[AD-A217264] 13 p1848 N90-20609
Acute oral toxicity of DIGL-RP solid propellant in ICR mice
[AD-A217711] 13 p1849 N90-20613
Acute oral toxicity of DIGL-RP solid propellant in Sprague-Dawley rats
[AD-A217712] 13 p1849 N90-20614
A review of the literature on the toxicity of rare-earth metals as it pertains to the engineering demonstration system surrogate testing
[DE90-008049] 13 p1851 N90-20620
Airliner cabin ozone: An updated review
[AD-A219264] 16 p2276 N90-22970
Bioluminescence for detection of trace compounds
[AD-A219435] 17 p2372 N90-23503
Southern California air quality study: Toxic air contaminants, task 1
[PB90-171570] 19 p2712 N90-25437
The global consequences of increasing tropospheric ozone concentrations
[NASA-TM-103477] 20 p2883 N90-26401
Space Propulsion Hazards Analysis Manual (SPHAM), volume 1
[AD-A219607] 21 p2969 N90-26874
Space Propulsion Hazards Analysis Manual (SPHAM), volume 2
[AD-A219608] 21 p2969 N90-26875
The acute, delayed neurotoxicity evaluation of two jet engine oil formulations
[AD-A222018] 21 p2986 N90-26972
Toxicity of thermolysis products from the materials of airplane cockpits
[CEAT-PV-M8/5924/02] 22 p3156 N90-27895
Workshop minutes on Remote Sensing of Hydrocarbons and Toxic Pollutants
[PB90-186370] 22 p3194 N90-28127
Toxicological aspects of fire onboard aircrafts: Role of the pressurization and ventilation in the cockpit
[ETN-90-97452] 22 p3233 N90-28335
Acid deposition: No such thing as a free launch
[DE90-015085] 23 p3348 N90-28920

TOXICOLOGY
Organic explosives and related compounds. Environmental and health considerations
[AD-A210554] 01 p0054 N90-10306
Microcomputer-based tests for repeated-measures: Metric properties and predictive validities
[NASA-CR-185517] 03 p0382 N90-12174
A menu of self-administered microcomputer-based neurotoxicology tests
[NASA-CR-185518] 03 p0382 N90-12175
Environmental quality and occupational health Special Emphasis Area Plan (SEAP)
[AD-A214738] 09 p1251 N90-17259
Proceedings of the 17th Conference on Toxicology
[AD-A215076] 09 p1252 N90-17263
Acute oral toxicity of JA-2 solid propellant in ICR mice
[AD-A217264] 13 p1848 N90-20609
JPRS report: Science and technology. USSR: Life sciences
[JPRS-ULS-90-002] 14 p1995 N90-21434
A study of mixed convection in large baffled rectangular chambers with and without internal heat sources
[AD-A223158] 22 p3169 N90-27977

TOXINS AND ANTITOXINS
Recovery of particle size distribution of ultrafine aerosols from diffusional decay measurements
[AD-A213006] 05 p0621 N90-13621
Mutagenic responses of some petroleum-base obscurants in the Ames test
[AD-A214201] 07 p0915 N90-15295

TRACE CONTAMINANTS
Potential effects of global climate change on the United States. Volume 1: Regional studies. Draft
[PB89-161053] 02 p0238 N90-11351
Evaluation and sensitivity analyses results of the MESOPUFF 2 model with CAPTEX (Cross-Appalachian Tracer Experiment) measurements
[PB89-198253] 03 p0368 N90-12103
Study of the electrical and optical properties of the vanadium and nickel impurities in GaAs
[ISAL-89-0028] 04 p0559 N90-13259
Methodology used for gas analysis and control of trace chemical contaminants at a hyperbaric facility. 1: Gas sampling
[AD-A216155] 10 p1325 N90-17859
Effects of solar ultraviolet radiation on biogeochemical dynamics in aquatic environments
[AD-A221119] 18 p2578 N90-24687
Space station contamination study: Assessment of contaminant spectral brightness
[NASA-CR-186173] 19 p2666 N90-25169
Generation rates and chemical compositions of waste streams in a typical crewed space habitat
[NASA-TM-102799] 22 p3233 N90-28333
Ozone for trace organic contaminant removal
[PB90-221680] 23 p3347 N90-28916

TRACE ELEMENTS
Micrometeorological investigation of surface exchange of trace gases: A case study
[PB89-208375] 02 p0249 N90-11412
A high-resolution atlas of the infrared spectrum of the Sun and the Earth atmosphere from space: A compilation of ATMOS spectra of the region from 650 to 4800 cm (2.3 to 16 micron). Volume 1: The Sun
[NASA-RP-1224-VOL-1] 05 p0666 N90-13893
Mobility of sulfur in thermally altered meteorites
06 p0862 N90-15010
Scientific linkages in global change
[PB90-112608] 08 p1098 N90-16356
Trace element abundance determinations by Synchrotron X Ray Fluorescence (SXRF) on returned comet nucleus mineral grains 08 p1142 N90-16619
Prompt Gamma Activation Analysis (PGAA): Technique of choice for nondestructive bulk analysis of returned comet samples 08 p1144 N90-16633
Non-destructive trace element microanalysis of as-received cometary nucleus samples using synchrotron x ray fluorescence 08 p1147 N90-16649

The measurement of trace elements in interplanetary dust and cometary particles by ultra-high sensitivity INAA
08 p1149 N90-16656
Bioluminescence for detection of trace compounds
[AD-A213458] 09 p1189 N90-16889
Technology update-89
[DE90-005813] 11 p1593 N90-19178
Geochemical survey on faults overland with alluvial deposits, part 1. Application for the Neodani and the Atera faults survey
[DE89-782326] 12 p1690 N90-19707
Development of gamma-emitting, receptor-binding radiotracers for imaging the brain and pancreas
[DE90-008314] 13 p1851 N90-20621
Study of new technique of solid combustible materials to determination of volatile elements by flame atomic absorption spectrophotometry
[DE90-612907] 14 p1947 N90-21147
Small scale structures and density of star-forming regions 14 p2041 N90-21706
New spectral features of stratospheric trace gases
15 p2079 N90-21910
Global distribution of organo-bromine gases
15 p2124 N90-22150
Trace metal sources for the atlantic inflow to the Mediterranean Sea
[AD-A218607] 17 p2429 N90-23842
Molecular studies of dense cores
17 p2484 N90-24207
Natural and anthropogenic components in bulk precipitation at Blidoe (archipelago of Stockholm, Sweden) 20 p2884 N90-26409
Experiment K-6-04. Trace element balance in rats during spaceflight 20 p2892 N90-26458
Estimating the spatial variability of trace gas deposition velocities
[PB90-208570] 23 p3349 N90-28928
Infrared spectroscopic measurements on planetary atmospheric gases 23 p3412 N90-29283

TRACKED VEHICLES
Computer oriented methods of multibody dynamics for application in vehicle technology
[DFVLR-FB-89-17] 04 p0533 N90-13080
Lunar construction utility vehicle
[NASA-CR-186231] 07 p0939 N90-15435
Design of an autonomous Lunar construction utility vehicle
[NASA-CR-186832] 20 p2870 N90-26330

TRACKING (POSITION)
NT CCD STAR TRACKER
NT COMPENSATORY TRACKING
NT INFRARED TRACKING
NT MISSILE TRACKING
NT OPTICAL TRACKING
NT POLYSTATION DOPPLER TRACKING SYSTEM
NT PURSUIT TRACKING
NT RADAR TRACKING
NT RADIO TRACKING
NT RANGE AND RANGE RATE TRACKING
NT SATELLITE TRACKING
NT SATELLITE-TO-SATELLITE TRACKING
NT SPACE DETECTION AND TRACKING SYSTEM
NT SPACECRAFT TRACKING
NT STAR TRACKERS
NT VIDEO LANDMARK ACQUISITION AND TRACKING
Alternative polar homing strategies
01 p0013 N90-10059
Tests of gating algorithms for tracking of multiple objects. Part 1: Theory, requirements and performance measures
[AD-A210519] 01 p0113 N90-10644
Kalman Filter Integration of Modern Guidance and Navigation Systems
[AGARD-LS-166] 02 p0148 N90-10847
Adaptive tracking of maneuvering targets based on IR image data 02 p0149 N90-10853
Passive trajectography by azimuth: Improvement of estimation quality 02 p0150 N90-10854
Independent Orbiter Assessment (IOA): Analysis of the communication and tracking subsystem
[NASA-CR-185582] 02 p0172 N90-10967
Analysis of forest fire smoke using satellite imagery
[AD-A210657] 02 p0238 N90-11339
The 1987 survey of track keeping and altitudes on Heathrow and Gatwick standard instrument departure routes (DAY)
[CAA-PAPER-88010] 03 p0305 N90-11729
Optimal observer motion for bearings-only localization and tracking 04 p0449 N90-12569
Dedicated tracking of crossing targets with a phased array monopulse radar
[FEL-1988-95] 04 p0491 N90-12821
Modified Newton-type methods for long-range target motion analysis
[FEL-1989-82] 04 p0551 N90-13208
Inexpensive global location and tracking systems using geostationary satellites
[AD-A213025] 05 p0602 N90-13498
Electronic warfare: Reliable equipment needed to test Air Force's electronic warfare systems
[AD-A212952] 05 p0632 N90-13687
Compensatory tracking in disturbance tasks and target following tasks. The influence of cockpit motion on performance and control behavior
[LR-511] 05 p0675 N90-13933
Realtime tracking system for wide-field-of-view telescope
[DE90-001147] 06 p0843 N90-14908
Research in knowledge-based vision techniques for the Autonomous Land Vehicle Program
[AD-A213440] 07 p0942 N90-15453
Analytical techniques for tracking filter implementation
08 p1021 N90-15903
Tracking flares
[ISBN-0-642-13583-5] 08 p1052 N90-16080
Estimation and control of nonlinear and hybrid systems with applications to air-to-air guidance
[AD-A214542] 09 p1170 N90-16770
Feasibility of millimeter-accuracy geodetic positioning and vehicle tracking with repeater satellites
[AD-A214755] 09 p1182 N90-16854
Method and apparatus for positioning a robotic end effector
[NASA-CASE-MSC-21476-1] 09 p1230 N90-17137
Payload invariant control via neural networks: Development and experimental evaluation
[AD-A215740] 09 p1260 N90-17306
Enhanced tracking of ballistic targets using forward looking infrared measurements with active target illumination
[AD-A215422] 09 p1282 N90-17434
Sensitivity of the peripheral vision to simulated aircraft ascent and descent 10 p1413 N90-18145
An evaluation of an airborne laser profiling system for high precision terrain mapping
[AD-A217025] 11 p1525 N90-18780
The Telecommunications and Data Acquisition Report
[NASA-CR-185033] 12 p1642 N90-19434
Performance of the all-digital data-transition tracking loop in the advanced receiver 12 p1643 N90-19440
An investigation of the transfer of monopulse tracking between two coherent point sources
[AD-A217007] 12 p1646 N90-19457
Interaction of switch actuation on tracking with a four-axis flight control (cross-coupling)
[AD-A217981] 13 p1758 N90-20095
High resolution analysis of satellite gradiometry
13 p1840 N90-20561
Implementation of midcourse tracking and correlation on massively parallel computers
[DE90-008166] 13 p1873 N90-20740
Tropical cyclone track predictability and the adjoint method of data assimilation
[AD-A218324] 14 p2007 N90-21505
Passive navigation using image irradiance tracking
15 p2141 N90-22232
Preliminary results of the peak experiment. ALTAIR deep-space measurements
[AD-A218622] 16 p2229 N90-22714
Visual behavior in the F-15 simulator for air-to-air combat
[AD-A218648] 16 p2262 N90-22893
Sliding control of pointing and tracking with operator spline estimation 16 p2281 N90-22997
A Kalman filter with smoothing for hurricane tracking and prediction
[AD-A220413] 17 p2426 N90-23827
Intersecting line segments, ray shooting, and other applications of geometric partitioning techniques
[RUU-CS-88-26] 18 p2601 N90-24804
Innovative techniques for high-resolution imaging and precision tracking
[AD-A221380] 18 p2616 N90-24899
A helmet mounted display to adapt the telerobotic environment to human vision 19 p2737 N90-25555
Adaptive tracking for complex systems using reduced-order models
[NASA-CR-183464] 19 p2747 N90-25609
Multi-microprocessor control of a precision pan and tilt head
[RSRE-MEMO-4252] 19 p2747 N90-25613
Application of inertial instruments for DSN antenna pointing and tracking 20 p2853 N90-26224
QPSK loop lock detection in the advanced receiver
20 p2854 N90-26230
Multiple target tracking in a wide-field-of-view camera system
[DE90-013488] 20 p2865 N90-26300
Eye tracking device for the measurement of flight performance in simulators
[AD-A220075] 20 p2898 N90-26484
A real-time optical 3D tracker for head-mounted display systems
[AD-A222747] 20 p2902 N90-26508
Communications and tracking expert systems study
[NASA-CR-185935] 21 p2992 N90-27004
Measured effects of repeater jamming on direct-sequence spread spectrum receivers that use envelope detectors
[AD-A222231] 21 p2996 N90-27032
Application of automatic method to estimating high-level cloud motion wind in operational system and the characteristics of the resultant wind vectors
21 p3028 N90-27218
Tracking a head-mounted display in a room-sized environment with head-mounted cameras
[AD-A222545] 21 p3037 N90-27266
Position finding and ground target direction finding by an aircraft with a gimballed video camera
[DLR-FB-89-62] 22 p3111 N90-27673
A sensor stabilization/tracking system for unmanned air vehicles
[AD-A224008] 23 p3283 N90-28579
Tracking performance and influence of field of view
23 p3360 N90-28986
Control and estimation for aerospace applications with system time delays 24 p3428 N90-29367
Airborne target detection, acquisition, and tracking devices
[AD-A223852] 24 p3462 N90-29555
Autonomous sensor-based dual-arm satellite grappling
24 p3504 N90-29809
IUE-ULDA access guide no. 2. International Ultraviolet Explorer-Uniform Low Dispersion Archive: Comets
[ESA-SP-1134] 24 p3563 N90-30157

TRACKING AND DATA RELAY SATELLITES
U TDR SATELLITES

TRACKING ANTENNAS
U DIRECTIONAL ANTENNAS

TRACKING FILTERS
Analytical techniques for tracking filter implementation
08 p1021 N90-15903
Design of a robust controller for an unstable nonminimum phase guided missile
[AD-A216147] 10 p1323 N90-17845
Multitarget tracking by single sensor: Analysis of the main approaches developed in this area
[ESA-TT-1171] 11 p1500 N90-18833
Suboptimal period design for a maneuvering missile to evade tracking filters 12 p1650 N90-19479
Tracking in uncertain environments
[RAE-TM-AW-121] 16 p2261 N90-22891

TRACKING NETWORKS
NT DEEP SPACE NETWORK
NT GLOBAL TRACKING NETWORK
NT POLYSTATION DOPPLER TRACKING SYSTEM
NT RADAR NETWORKS
NT SPACE DETECTION AND TRACKING SYSTEM
NT SPACE FLIGHT TRACKING AND DATA NETWORK
Automatic line network extraction from aerial imagery of urban areas through knowledge based image analysis
[AD-A222675] 20 p2880 N90-26385

TRACKING PROBLEM
Passive trajectography by azimuth: Improvement of estimation quality 02 p0150 N90-10854
Optimal observer motion for bearings-only localization and tracking 04 p0449 N90-12569
Investigations into a new algorithm for calculating H infinity optimal controllers 12 p1637 N90-19406
Iconic tracking algorithms for high energy physics using the TRAX-I massively parallel processor
[MPI-PAE/EXP.EL-216] 18 p2596 N90-24773
Cartesian control of redundant robots
23 p3363 N90-29004

TRACKING RADAR
Radar and sensor array design planning for a naval missile testing center. Artificial intelligence applications
[ETCA-88-R-099] 04 p0537 N90-13108
The application of Z to the specification of air traffic control systems. 1: An initial specification of the radar processing activity
[RSRE-MEMO-4280] 08 p1020 N90-15900
Multitarget tracking by single sensor: Analysis of the main approaches developed in this area
[ESA-TT-1171] 11 p1500 N90-18833

TRACKING STATIONS
NT GLOBAL TRACKING NETWORK
NT POLYSTATION DOPPLER TRACKING SYSTEM
NT SPACE DETECTION AND TRACKING SYSTEM
Navigation experiment NAVEX: Data storage and processing
[DFVLR-MITT-89-09] 03 p0304 N90-11727
Environmental Projects. Volume 9: Construction of hazardous materials storage facilities
[NASA-CR-186296] 09 p1244 N90-17216

Navigation experiment NAVEX data storage and processing
[ESA-TT-1175] 11 p1467 N90-18445

TRACKING STUDIES
U TRACKING (POSITION)

TRACTION
Stability conditions for steady shearing. Stability conditions for simple shear under mixed thermal boundary conditions 04 p0499 N90-12873
Articulated suspension system
[NASA-CASE-NPO-17354-1-CU] 09 p1233 N90-17153
The measurement, modeling, and prediction of traction for rocket propellant 1
[NASA-CR-185186] 12 p1633 N90-19386
Finite element analysis of elastic contact problems with friction 15 p2105 N90-22040
Traction-drive force transmission for telerobotic joints 24 p3501 N90-29790

TRACTORS
NT TRACKED VEHICLES

TRADEOFFS
Space station gas compressor technology study program, phase 1
[NASA-CR-183758] 05 p0601 N90-13491
Applications of FM-CW laser radar to antenna contour mapping 12 p1611 N90-19270
Performance tradeoffs in multithreaded processors
[AD-A217123] 13 p1871 N90-20729
Trade-offs in non-reversing diameter
[RUU-CS-89-22] 18 p2602 N90-24813
An input-size/output-size trade-off in the time-complexity of rectilinear hidden surface removal
[RUU-CS-89-24] 18 p2602 N90-24814
Knowledge and inhibition in asynchronous distributed systems
[TR-90-1139] 20 p2935 N90-26703
Computer support for conducting supportability trade-offs in a team setting
[AD-A222002] 22 p3237 N90-28355
Liquid Rocket Booster (LRB) for the Space Transportion System (STS) systems study. Appendix D: Trade study summary for the liquid rocket booster
[NASA-CR-183790-APP-D] 23 p3289 N90-28604

TRAFFIC
NT AIR TRAFFIC
Linkoeping's A.I. Consortium (LAIC) for plan guided systems. Review of the first 18 months
[FOA-C-30528-3.4] 02 p0269 N90-11537
Estimating departure times from traffic counts using dynamic assignment
[DE89-016259] 07 p0979 N90-15653
Adaptive backoff synchronization techniques
[AD-A213966] 07 p0980 N90-15658
Updating a dosage-effect relationship for the prevalence of annoyance due to general transportation noise
[AD-A219416] 17 p2421 N90-23794
Satellite navigation systems for land vehicles 24 p3430 N90-29376

TRAFFIC CONTROL
NT AIR TRAFFIC CONTROL
NT AUTOMATED EN ROUTE ATC
NT RADAR APPROACH CONTROL
Sensor system for automatic traffic recording in free area
[ETN-90-96493] 18 p2565 N90-24634
Observation of ship movement by aeroplane
[FFI-90/7001] 19 p2657 N90-25124
Investigations of monopulse-assisted radio location systems for the safety of surface traffic
[ETN-90-97324] 21 p2956 N90-26806

TRAILING EDGES
NT BLUNT TRAILING EDGES
Trailing-edge sweep and three-dimensional vortex interactions in jets and mixing layers 01 p0066 N90-10379
Hinge moment coefficient derivatives for trailing-edge controls on wings at subsonic speeds
[ESDU-89009] 06 p0726 N90-14239
Serrated trailing edges for improving lift and drag characteristics of lifting surfaces
[NASA-CASE-LAR-13870-1] 07 p0879 N90-15094
A wind tunnel study of a sting-mounted circulation control wing
[AD-A216248] 10 p1310 N90-17577
Calculation of excrescence drag magnification due to pressure gradient at high subsonic speeds
[ESDU-87004] 12 p1598 N90-19195
Euler code predicted separation at the airfoil trailing edge
[FFA-TN-1989-30] 17 p2346 N90-23364

TRAINEES
U STUDENTS

TRAINERS
U TRAINING DEVICES

TRAINING
U EDUCATION

TRAINING ANALYSIS
SINCGARS (Single-Channel Ground/Airborne Radio System) operator performance decay
[AD-A210716] 01 p0057 N90-10326
Higher education for science and technology: A background paper
[PB89-191290] 02 p0287 N90-11642
Where to from here. Future applications of mental models of complex performance
[DE90-002091] 07 p0967 N90-15586
Structural understanding in problem solving
[AD-A214776] 09 p1273 N90-17379
A comparison of microcomputer training methods and sources
[AD-A216349] 10 p1413 N90-18146
Evaluation of two methods for acquisition of training statistics for digital analysis of areas prepared for plowing
[INPE-4901-PRE/1502] 11 p1522 N90-18763
Symposium on air traffic control training for tomorrow's technology
[PB90-127325] 12 p1601 N90-19216
Laser Technology Center
[PB90-115387] 12 p1665 N90-19564
Pilot candidate selection
[AD-A217296] 12 p1696 N90-19742
Issues in development, evaluation, and use of the NASA Preflight Adaptation Trainer (PAT)
[NASA-CR-185608] 15 p2137 N90-22212
Guide for the use of intergraph randmicas structural software for Computer-Aided Design and Drafting(CADD)
[AD-A220624] 17 p2443 N90-23924
Preparing technicians for engineering materials technology 18 p2516 N90-24369
A systematic approach to training: A training needs assessment 18 p2645 N90-25059
Aircrew life support systems enhancement
[AD-A222626] 20 p2902 N90-26505
Payload training methodology study
[NASA-CR-183907] 21 p2964 N90-26849
The effects of training on errors of perceived direction in perspective displays
[NASA-TM-102792] 22 p3232 N90-28329
Human factors evaluation and validation criteria for quality training programs: Development, presentation, and assessment
[DE90-014724] 23 p3377 N90-29081
QTA (QUESTIONNAIRE-TASK-ANALYSIS): An electronic tool for job/task analysis
[DE90-008944] 24 p3499 N90-29778

TRAINING DEVICES
Subjective uses of wind profiler data in warm season analysis and forecasting: Wind profiler training manual number 3
[PB89-223333] 04 p0520 N90-13004
Development of the AH-64 display symbology training module
[AD-A213456] 07 p0968 N90-15592
Ejection seat training of jet pilots and weapon system officers at the German Air Force School of Aviation Medicine 13 p1752 N90-20061
Prototype part task trainer: A remote manipulator system simulator 13 p1860 N90-20672
Visions of visualization aids: Design philosophy and experimental results 15 p2138 N90-22220
Field-of-view assessment of low-level flight and an airdrop in the C-130 Weapon System Trainer (WST)
[AD-A218504] 16 p2200 N90-22559
A structure for maturing intelligent tutoring system student models 21 p3047 N90-27320

TRAINING EVALUATION
Higher education for science and technology: A background paper
[PB89-191290] 02 p0287 N90-11642
Backward transfer and skill acquisition in the AH-1 flight and weapons simulator
[AD-A213432] 09 p1170 N90-16772
Prediction of success in flight training by single- and dual-task performance 09 p1257 N90-17293
A comparison of microcomputer training methods and sources
[AD-A216349] 10 p1413 N90-18146
Airborne radar systems specialist, AFSC 118X2
[AD-A215450] 11 p1496 N90-18611
Schema-based theories of problem solving
[AD-A216717] 11 p1552 N90-18939
Report of the First Annual Airborne Weapons Training Technology Review
[DE90-007189] 12 p1697 N90-19747
An analysis of requirements for a P-3 windshear training program
[AD-A222577] 20 p2805 N90-25960
Payload training methodology study
[NASA-CR-183907] 21 p2964 N90-26849
Human factors research in aircrew performance and training
[AD-A221657] 21 p3037 N90-27267

TRAINING SIMULATORS
NT COCKPIT SIMULATORS
NT FLIGHT SIMULATORS
Cockpit resource management: A selected annotated bibliography
[AD-A214272] 07 p0969 N90-15594
Simulation of synthetic aperture radar 3: Evaluation of prototype digital feature analysis data
[AD-A216750] 11 p1498 N90-18620
Space station Simulation Computer System (SCS) study for NASA/MSFC. Volume 1: Overview and summary
[NASA-CR-183840] 13 p1762 N90-20113
Space station Simulation Computer System (SCS) study for NASA/MSFC. Volume 2: Concept document
[NASA-CR-183841] 13 p1762 N90-20114
Space station Simulation Computer System (SCS) study for NASA/MSFC. Volume 4: Conceptual design report
[NASA-CR-183843] 13 p1762 N90-20116
Space station Simulation Computer System (SCS) study for NASA/MSFC. Volume 5: Study analysis report
[NASA-CR-183844] 13 p1763 N90-20117
Space station Simulation Computer System (SCS) study for NASA/MSFC. Volume 6: Study issues report
[NASA-CR-183845] 13 p1763 N90-20118
Graphics Technology in Space Applications (GTSA 1989)
[NASA-CP-3045] 13 p1856 N90-20651
The Orbital Maneuvering Vehicle Training Facility visual system concept 13 p1863 N90-20684
Issues in development, evaluation, and use of the NASA Preflight Adaptation Trainer (PAT)
[NASA-CR-185608] 15 p2137 N90-22212
Pilot decision-making training
[AD-A221349] 18 p2585 N90-24720
An intelligent simulation training system 19 p2739 N90-25566
Functional description of a command and control language tutor 19 p2739 N90-25567
Experimental study towards a future airport ground movement simulator 22 p3113 N90-27687
Study improvement training facilities ground control air traffic controllers. Part 1: Alternative solutions and their consequences
[FEL-89-A257-PT-1] 24 p3431 N90-29380
Study improvement training facilities ground control air traffic controllers. Part 2: Functional analysis approach control trainer
[FEL-89-A280-PT-2] 24 p3436 N90-29409
Test and training simulator for ground-based teleoperated in-orbit servicing 24 p3510 N90-29843
An Ada-based marine radar simulator for collision avoidance training
[ETN-90-97611] 24 p3531 N90-29970

TRAJECTORIES
NT ASCENT TRAJECTORIES
NT BALLISTIC TRAJECTORIES
NT DESCENT TRAJECTORIES
NT EARTH-MOON TRAJECTORIES
NT ELECTRON TRAJECTORIES
NT INTERORBITAL TRAJECTORIES
NT INTERPLANETARY TRAJECTORIES
NT MIDCOURSE TRAJECTORIES
NT MISSILE TRAJECTORIES
NT MOLECULAR TRAJECTORIES
NT PARTICLE TRAJECTORIES
NT REENTRY TRAJECTORIES
NT SPACECRAFT TRAJECTORIES
The role of sensor directed, model based control in robotics
[DE89-014133] 01 p0077 N90-10442
The temporal development of collision cascades in the binary collision approximation
[DE89-015860] 01 p0122 N90-10699
Passive trajectography by azimuth: Improvement of estimation quality 02 p0150 N90-10854
Optimal and on-board near-optimal midcourse guidance 02 p0150 N90-10857
A polynomial method of approximate weighted centers for linear programming
[REPT-89-13] 03 p0388 N90-12210
Optimal trajectories for the aeroassisted flight experiment
[NASA-CR-186133] 06 p0729 N90-14250
Guidance, steering, load relief and control of an asymmetric launch vehicle
[NASA-CR-185598] 06 p0730 N90-14257
Aerobraking characteristics for several potential manned Mars entry vehicles
[NASA-TM-101669] 06 p0733 N90-14272
Geometric considerations for a waypoint guidance method
[DE90-001803] 07 p0878 N90-15088

Anharmonic betatron motion in free electron lasers
[DE90-001515] 07 p0934 N90-15407
MESA 3-D calculations of armor penetration by projectiles with combined obliquity and yaw
[DE89-015265] 07 p0939 N90-15438
Feasibility study of using industrial robot for ultrasound testing
[DE90-002977] 07 p0943 N90-15461
Singular perturbation analysis of AOTV-related trajectory optimization problems
[NASA-CR-186202] 08 p1027 N90-15936
Dissipation mechanism of the large-amplitude collective motion. Dynamical evolution of a collective bundle of trajectories in the TDHF phase space for a simple soluble model
[DE90-719557] 08 p1118 N90-16477
The dynamics of dust in planetary magnetospheres
08 p1149 N90-16658
Application of experimental techniques to store release problems 10 p1304 N90-17545
Generating optimally evasive MaRV trajectories
[DE90-004496] 10 p1328 N90-17671
Control and stability of a spinning symmetric satellite in an elliptical orbit
[AD-A216284] 10 p1328 N90-17672
Spatial registration of TIROS-N weather satellite data
[AD-A216041] 11 p1536 N90-18841
The EGS4 Code System: Solution of gamma-ray and electron transport problems
[DE90-008100] 12 p1713 N90-19838
Escape systems research at RAE
13 p1751 N90-20058
Swing-free movement of simply suspended objects employing parameter estimation
[DE90-002238] 13 p1811 N90-20398
Parameter-scheduled trajectory planning for suppression of coupled horizontal and vertical vibrations in a flexible rod
[DE90-002313] 13 p1817 N90-20435
Periodic trajectories for two-dimensional nonintegrable Hamiltonians
[DE90-006082] 13 p1877 N90-20765
Optimal trajectories for the aeroassisted flight experiment. Part 3: Formulation, results, and analysis
[NASA-CR-186165] 14 p1930 N90-21051
Optimization and guidance of flight trajectories in the presence of windshear
[NASA-CR-186163] 15 p2049 N90-21747
First-order weight corrections for real-time flight path management
[LR-580] 15 p2050 N90-21751
A comparison of time-optimal interception trajectories for the F-8 and F-15
[NASA-CR-186300] 15 p2050 N90-21753
Optimal trajectories for the aeroassisted flight experiment. Part 4: Data, tables, and graphs
[NASA-CR-186164] 15 p2056 N90-21780
UD filtering and smoothing applied to orbit determination
[INPE-4966-PRE/1535] 15 p2189 N90-22501
Approximate minimum-time trajectories for 2-link flexible manipulators 16 p2287 N90-23030
On trajectory generation for flexible space crane: Inverse dynamics analysis by LATDYN 16 p2288 N90-23037
An averaging result for random differential equations
[AD-A220364] 17 p2457 N90-24021
Neptune, 2000 plus: Concept of a heavy space freighter for the 21st century
[ILR-MITT-229(1989)] 18 p2509 N90-24338
Vortex-induced boundary-layer separation
18 p2551 N90-24560
Effects of simplifying assumptions on optimal trajectory estimation for a high-performance aircraft
[NASA-TM-101721] 19 p2661 N90-25142
Numerical approach of collision avoidance and optimal control on robotic manipulators
19 p2736 N90-25552
Adaptive tracking for complex systems using reduced-order models
[NASA-CR-183464] 19 p2747 N90-25609
An inverse dynamic method yielding flexible manipulator state trajectories
[NASA-CR-186807] 20 p2870 N90-26329
A user's manual for MCPRAM (Monte Carlo PReprocessor for AMEER) and for the fuze options in AMEER (Aero Mechanical Equation Evaluation Routines)
[DE90-013598] 21 p3051 N90-27345
Laboratory study of ion-neutral collisions at suprathermal energies
[AD-A222117] 21 p3074 N90-27475
Robot Acting on Moving Bodies (RAMBO): Interaction with tumbling objects 23 p3366 N90-29022
Multiple cooperating manipulators: The case of kinematically redundant arms 23 p3371 N90-29046
Trajectory generation of space telerobots
23 p3372 N90-29055
Trajectories of renormalization group flows on the phase diagram of N=2 superconformal field theories
[DE90-627212] 23 p3391 N90-29154
User's manual for the Trajectory Simulation and Analysis Program (TSAP)
[DE90-014850] 24 p3440 N90-29426
Long pulse diode experiments
[DE90-018218] 24 p3485 N90-29578
Windshear estimation along the trajectory of an aircraft 24 p3494 N90-29745
Database development for the DMSP experiments
[AD-A224346] 24 p3557 N90-30129

TRAJECTORY ANALYSIS
Design of a solar sail mission to Mars
[NASA-CR-186045] 03 p0311 N90-11771
A polynomial method of approximate weighted centers for linear programming
[REPT-89-13] 03 p0388 N90-12210
Shuttle relative navigation of a tethered satellite mission with current on board software
05 p0588 N90-13423
Impact of tether cutting on onboard navigation during the Tethered Satellite Mission-1
05 p0588 N90-13424
Some quick and efficient methods for bearing-only target motion analysis
[IMAG-RR-762-M] 05 p0693 N90-14049
Stochastic action of dynamical systems on curved manifolds. The isokinetic developing map on trajectories
[PREPRINT-666] 08 p1117 N90-16466
Use of random Martian atmosphere to evaluate potential entry guidance schemes
[NASA-TM-102606] 13 p1764 N90-20122
Reference frames: Orbitography
17 p2359 N90-23427
Acousto-optical localization of speed maneuvering flight targets
[FB-11-89] 19 p2758 N90-25676
Further development and application of an atmospheric chemistry trajectory model 20 p2884 N90-26408
Theoretical specifications of the trajectory estimation for a space navigation system with the function of guidance and control
[NAL-TR-1032] 24 p3439 N90-29420
User's manual for the Trajectory Simulation and Analysis Program (TSAP)
[DE90-014850] 24 p3440 N90-29426

TRAJECTORY CONTROL
NT TRAJECTORY OPTIMIZATION
Shuttle tethered operations: The effect on orbital trajectory and inertial navigation
05 p0588 N90-13425
Manipulation strategies for massive space payloads
[NASA-CR-186081] 06 p0728 N90-14247
Off-line robot programming and graphical verification of path planning 08 p1156 N90-16699
Payload invariant control via neural networks: Development and experimental evaluation
[AD-A215740] 09 p1260 N90-17306
Learning-based position control of a closed-kinematic chain robot end-effector
[NASA-CR-186283] 10 p1391 N90-18043
The CMU Reconfigurable Modular Manipulator System
[CMU-RI-TR-88-7] 13 p1809 N90-20388
Parameter-scheduled trajectory planning for suppression of coupled horizontal and vertical vibrations in a flexible rod
[DE90-002313] 13 p1817 N90-20435
On trajectory generation for flexible space crane: Inverse dynamics analysis by LATDYN 16 p2288 N90-23037
Optimal helicopter trajectory planning for terrain following flight
[NASA-CR-186470] 17 p2349 N90-23376
Mobile transporter path planning
19 p2727 N90-25505
Planning for execution monitoring on a planetary rover
19 p2735 N90-25548
Numerical approach of collision avoidance and optimal control on robotic manipulators
19 p2736 N90-25552
Trajectory planning and control of a 6 DOF manipulator with Stewart platform-based mechanism
[NASA-CR-186813] 19 p2747 N90-25610
Galileo: Earth avoidance study report
[NASA-CR-186424] 22 p3123 N90-27730
Reentry trajectory optimization and control
22 p3127 N90-27746
The dynamics of orbital maneuvering: Design and evaluation of a visual display aid for human controllers
22 p3131 N90-27767
Reaction-compensation technology for microgravity laboratory robots
[NASA-TM-103271] 22 p3183 N90-28062
Kinematics, controls, and path planning results for a redundant manipulator 23 p3363 N90-29005
Robot Acting on Moving Bodies (RAMBO): Interaction with tumbling objects 23 p3366 N90-29022
Planning 3-D collision-free paths using spheres
23 p3367 N90-29024
Grasp planning under uncertainty
23 p3370 N90-29041
Characterization and control of self-motions in redundant manipulators 23 p3370 N90-29045
Trajectory generation of space telerobots
23 p3372 N90-29055
Redundancy of space manipulator on free-flying vehicle and its nonholonomic path planning
24 p3502 N90-29797
Telepresence system development for application to the control of remote robotic systems
24 p3503 N90-29799
Test and validation for robot arm control dynamics simulation 24 p3507 N90-29826
An improved adaptive control for repetitive motion of robots 24 p3508 N90-29831
Vehicle path-planning in three dimensions using optics analogs for optimizing visibility and energy cost
24 p3512 N90-29853

TRAJECTORY MEASUREMENT
Tracking performance evaluation
[AD-A210499] 01 p0095 N90-10540
Radar and sensor array design planning for a naval missile testing center. Artificial intelligence applications
[ETCA-88-R-099] 04 p0537 N90-13108
Smooth track generation for target motion analysis
[FEL-1989-83] 04 p0555 N90-13233
Some quick and efficient methods for bearing-only target motion analysis
[IMAG-RR-762-M] 05 p0693 N90-14049
Trajectory-capture cell instrumentation for measurement of dust particle mass, velocity and trajectory, and particle capture 08 p1146 N90-16644
Comparison of circulation obtained through the trajectory of a drifting buoy tracked by satellite and hydrographic data in the Bransfield Strait
[INPE-4946-TDL/387] 11 p1537 N90-18850
Continued development and analysis of a new extended Kalman filter for the Completely Integrated Reference Instrumentation System (CIRIS)
[AD-A220106] 17 p2354 N90-23400
A laser tracking dynamic robot metrology instrument
23 p3366 N90-29021

TRAJECTORY OPTIMIZATION
Nonlinear maneuver autopilot for the F-15 aircraft
[NASA-CR-179442] 02 p0262 N90-11487
An optimum trajectory planner for robot manipulators in joint-space and under physical constraints
[RR-349] 03 p0355 N90-12029
Optimal observer motion for bearings-only localization and tracking 04 p0449 N90-12569
An on-line distributed minimum-time trajectory generator for intelligent robot manipulators
[RR-358] 04 p0536 N90-13102
Trajectory optimization and guidance for an aerospace plane
[NASA-CR-185884] 05 p0578 N90-13369
Shuttle tethered operations: The effect on orbital trajectory and inertial navigation
05 p0588 N90-13425
Optimal trajectories for the Aeroassisted Flight Experiment. Part 1: Equations of motion in an Earth-fixed system
[NASA-CR-186134] 05 p0592 N90-13441
Optimal trajectories for the Aeroassisted Flight Experiment. Part 2: Equations of motion in an inertial system
[NASA-CR-186135] 05 p0592 N90-13442
Optimal trajectories for the aeroassisted flight experiment, 1988-89
[NASA-CR-186132] 05 p0592 N90-13443
Guidance and Control strategies for aerospace vehicles
[NASA-CR-186195] 06 p0727 N90-14243
Optimal trajectories for the aeroassisted flight experiment
[NASA-CR-186133] 06 p0729 N90-14250
Guidance analysis of the aeroglide plane change maneuver as a turning point problem
[NASA-TM-101639] 07 p0883 N90-15110
Singular perturbation analysis of AOTV-related trajectory optimization problems
[NASA-CR-186202] 08 p1027 N90-15936
Efficient calculation of Ariane ascent trajectories with recursive quadratic programming
09 p1180 N90-16844
Preliminary investigation of parameter sensitivities for atmospheric entry and aerobraking at Mars
[NASA-TM-101607] 10 p1327 N90-17667

Pareto optimization design techniques for the AFIT (Air Force Institute of Technology)/AAMRL (Armstrong Aeronautical Medical Research Laboratory) anthropomorphic robotic manipulator
[AD-A216178] 10 p1414 N90-18150
Rapid near-optimal trajectory generation and guidance law development for single-stage-to-orbit airbreathing vehicles
[NASA-CR-186299] 12 p1612 N90-19275
Icarus lander 12 p1733 N90-19964
Optimal, impulsive, time-fixed orbital rendezvous and interception with path constraints
13 p1760 N90-20102
ETO (Earth-To-Orbit): A trajectory program for aerospace vehicles
[AD-A218157] 13 p1760 N90-20103
Trajectory optimization in the presence of constraints
[AD-A218271] 13 p1760 N90-20104
Three-dimensional route planning for a cruise missile for minimal detection by observer
[AD-A218336] 13 p1880 N90-20787
Optimal trajectories for the aeroassisted flight experiment. Part 3: Formulation, results, and analysis
[NASA-CR-186165] 14 p1930 N90-21051
An approach to on-board optimization of cruise at constant altitude
[LR-581] 15 p2050 N90-21752
Trajectory generation for car-like robots
[DE90-008407] 15 p2106 N90-22047
An algorithm for the solution of dynamic linear programs 16 p2286 N90-23026
A finite element based method for solution of optimal control problems 16 p2286 N90-23027
Solution of the optimal control problem using the software package STOMP
[MBB-FE-126/S/PUB-370] 19 p2651 N90-25087
Effects of simplifying assumptions on optimal trajectory estimation for a high-performance aircraft
[NASA-TM-101721] 19 p2661 N90-25142
Trajectory optimization for an asymmetric launch vehicle
[NASA-CR-185630] 20 p2817 N90-26033
The effect of interplanetary trajectory options on a manned Mars aerobrake configuration
[NASA-TP-3019] 20 p2818 N90-26036
Trajectory optimization of a bimodal nuclear powered spacecraft to Mars
[AD-A222974] 21 p2969 N90-26876
Galileo: Earth avoidance study report
[NASA-CR-186424] 22 p3123 N90-27730
Ascent and descent trajectory optimization of Ariane 5/Hermes 22 p3126 N90-27743
Reentry trajectory optimization and control
22 p3127 N90-27746
Hermes emergency reentry trajectories consequences on the Ariane 5 trajectories 22 p3127 N90-27747
Optimization of the deployment of a pair of satellites in inclined eccentric geosynchronous orbits
22 p3128 N90-27751
Noncoplanar orbit transfer optimization for an aeroassisted sortie vehicle 22 p3128 N90-27752
Optimal trajectories for Saenger-type vehicles
22 p3129 N90-27760
Ascent and descent optimizations of an air-breathing launch vehicle 22 p3130 N90-27761
Global optimization of air breathing launch vehicle trajectories 22 p3130 N90-27762
Real time guidance and propulsion control for single-stage-to-orbit airbreathing vehicles
23 p3285 N90-28587
Optimal trajectories for hypervelocity flight
24 p3430 N90-29378
Theoretical specifications of the trajectory estimation for a space navigation system with the function of guidance and control
[NAL-TR-1032] 24 p3439 N90-29420
Guidance algorithms for a free-flying space robot
24 p3503 N90-29798
Space robotic system for proximity operations
24 p3504 N90-29806
Vehicle path-planning in three dimensions using optics analogs for optimizing visibility and energy cost
24 p3512 N90-29853
Optimal payload rate limit algorithm for zero-G manipulators 24 p3513 N90-29858

TRAJECTORY PLANNING
Off-line robot programming and graphical verification of path planning 08 p1156 N90-16699
Parameter-scheduled trajectory planning for suppression of coupled horizontal and vertical vibrations in a flexible rod
[DE90-002313] 13 p1817 N90-20435
Optimal helicopter trajectory planning for terrain following flight
[NASA-CR-186470] 17 p2349 N90-23376
Mobile transporter path planning
19 p2727 N90-25505
Trajectory planning and control of a 6 DOF manipulator with Stewart platform-based mechanism
[NASA-CR-186813] 19 p2747 N90-25610
Kinematics, controls, and path planning results for a redundant manipulator 23 p3363 N90-29005
Redundancy of space manipulator on free-flying vehicle and its nonholonomic path planning
24 p3502 N90-29797
Vehicle path-planning in three dimensions using optics analogs for optimizing visibility and energy cost
24 p3512 N90-29853

TRANSATMOSPHERIC VEHICLES
Wave combustors for trans-atmospheric vehicles
[NASA-TM-102238] 03 p0307 N90-11742
Hypersonic waverider configurations for trans-atmospheric vehicles
[AD-A217925] 13 p1755 N90-20074
Transatmospheric vehicle research
[NASA-CR-186705] 20 p2807 N90-25970

TRANSCEIVERS
U TRANSMITTER RECEIVERS

TRANSCENDENTAL FUNCTIONS
NT COSINE SERIES
NT EXPONENTIAL FUNCTIONS
NT LOGARITHMS
NT PERIODIC FUNCTIONS
NT SINE SERIES
NT TANGENTS
NT TRIGONOMETRIC FUNCTIONS
Some remarks on solutions of Fermats last equation in terms of Wright's hypergeometric function
[AD-A218066] 13 p1878 N90-20771

TRANSCONDUCTANCE
The sensory transduction pathways in bacterial chemotaxis 05 p0677 N90-13944
Output performance of idealized microwave power amplifiers
[AD-A216797] 11 p1502 N90-18645

TRANSDUCERS
NT DIGITAL TRANSDUCERS
NT ELECTROACOUSTIC TRANSDUCERS
NT HYDROPHONES
NT IMAGE TRANSDUCERS
NT MICROPHONES
NT PIEZOELECTRIC GAGES
NT PIEZOELECTRIC TRANSDUCERS
NT PIEZORESISTIVE TRANSDUCERS
NT PRESSURE SENSORS
NT QUARTZ TRANSDUCERS
NT ULTRASONIC WAVE TRANSDUCERS
Performance of a broadbanded ultrasonic transducer with coaxially mounted, nondirectional receiver
[DE89-015838] 01 p0060 N90-10343
Method and apparatus to enhance the sensitivity of cylindrical magnetostrictive transducer to magnetic fields
[AD-D014218] 06 p0767 N90-14459
High power transducers
[AD-D014225] 06 p0767 N90-14461
SAW (Surface Acoustic Wave) transducer with improved bus-bar design
[AD-D014250] 08 p1060 N90-16125
Apparatus for imaging deep arterial and coronary lesions
[NASA-CASE-NPO-17439-1-CU]
08 p1104 N90-16391
The 15th Transducer Workshop --- for telemetry applications
[AD-A215515] 10 p1327 N90-17665
Integrated silicon flip-flop sensors
[ETN-90-96271] 11 p1503 N90-18654
Effective calibration of heat flux transducers for experimental use
[AD-A218262] 13 p1853 N90-20636
MHD channel development, part 2
[DE90-009550] 15 p2169 N90-22395
Aerodynamic pressure measurements on a rotating wind turbine blade
[DE90-000327] 18 p2494 N90-24256
Terbium-dysprosium magnetostrictive high power transducers
[AD-D014509] 19 p2753 N90-25641
A dual-wavelength passive homodyne detection unit for fiber-coupled white-light interferometers
[ETN-90-97036] 20 p2927 N90-26653
New inflight experiments to measure aerodynamics loads
[ETN-90-97276] 21 p2961 N90-26834
Method and apparatus for applying a mechanical force to surface
[NASA-CASE-LAR-14009-1] 21 p3011 N90-27115
An ultrasonic system for in-service non-destructive inspection of composite structures
22 p3185 N90-28076
Special test and evaluation methods used for a nine-axis accelerometer
[PB90-209578] 23 p3329 N90-28822
Preliminary results on noncollocated torque control of space robot actuators 23 p3373 N90-29057
Magnetostatic wave transducers, resonators and dispersion control
[AD-A223437] 24 p3464 N90-29571

TRANSFER
U TRANSFERRING

TRANSFER FUNCTIONS
NT MODULATION TRANSFER FUNCTION
Numerically efficient algorithm for model development of high-order systems 01 p0022 N90-10108
Transfer functions for nonlinear systems via Fourier-Borel transforms
[NASA-TM-100034] 02 p0145 N90-10828
A new approach to HF (High Frequency) channel modeling and simulation. Part 1: Deterministic model
[PB89-203962] 03 p0336 N90-11913
Batch LCAP2-linear control analysis, version 2.0: User's manual
[AD-A211670] 04 p0461 N90-12643
Wideband phase-locked angular modulator
04 p0487 N90-12798
Mathematical equivalence in a primitive Ella
[RSRE-MEMO-4225] 04 p0531 N90-13066
Well posedness of triples of operators (in the sense of linear systems theory)
[TW-292] 04 p0545 N90-13168
Evaluation of the indirect effects of lightning on a system: Double transfer function method
[RAE-TRANS-2172] 06 p0721 N90-14211
AcSim: Aircraft simulation program with application to flight profile generation
[AD-A212466] 06 p0723 N90-14217
Design of a compensation filter for a quadratic phase communication channel 06 p0761 N90-14428
Applications of a new exact solution of the Navier-Stokes equations to flow in pipes of varying width
06 p0774 N90-14504
Some easily analyzable convolutional codes
12 p1644 N90-19444
Shaping the insonifying pulse to optimise B-scans obtained in austenite
[AERE-R-13518] 13 p1775 N90-20187
Design and testing of a noninteracting control loop for the dynamically tuned dry gyro
[NAL-TR-1017] 13 p1803 N90-20350
The role of input weighting and bounding in the characteristic GPC method
[OUEL-1762/89] 15 p2158 N90-22328
A robust stability result for generalised predictive control
[OUEL-1773/89] 15 p2158 N90-22330
Frequency response modeling and control of flexible structures: Computational methods
16 p2285 N90-23021
Efficient computer algebra algorithms for polynomial matrices in control design 16 p2285 N90-23022
A methodology for formulating a minimal uncertainty model for robust control system design and analysis
16 p2287 N90-23028
Transfer matrices for multimode optical fiber systems
[AD-A218459] 16 p2317 N90-23210
On the structure at infinity of a structured system
[CWI-BS-R8918] 17 p2468 N90-24108
Current distribution in cylindrical porous electrodes
[DE90-009707] 18 p2546 N90-24530
Image of the angle by partially coherent lighting: Calculations and experiments
[ETN-90-96505] 18 p2616 N90-24900
Large scale structure and microwave background anisotropies in cosmological models and stellar photometry techniques with the wide field/planetary camera of the Hubble space telescope
18 p2637 N90-25023
System factors to be considered in assessing propagation effects on modern digital satellite communications systems 20 p2850 N90-26208
H-infinity control: An exploratory study
[EUT-88-E-211] 20 p2915 N90-26584
A new scheme for identification and control
[EUT-88-E-213] 20 p2915 N90-26586
Infrared thermography 24 p3421 N90-29325
A digital controller for active aeroelastic controls
[NAL-TR-1014] 24 p3435 N90-29402

TRANSFER OF TRAINING
Backward transfer and skill acquisition in the AH-1 flight and weapons simulator
[AD-A213432] 09 p1170 N90-16772
Automatic information processing and high performance skills: Application to training
[AD-A221709] 21 p3036 N90-27259

Automatic information processing and high performance skills: Acquisition, transfer, and retention
[AD-A221744] 21 p3036 N90-27260

TRANSFER ORBITS
GOES-I/M ascent maneuvers from transfer orbit to station 05 p0587 N90-13421
Optimal trajectories for the Aeroassisted Flight Experiment. Part 1: Equations of motion in an Earth-fixed system
[NASA-CR-186134] 05 p0592 N90-13441
Optimal trajectories for the Aeroassisted Flight Experiment. Part 2: Equations of motion in an inertial system
[NASA-CR-186135] 05 p0592 N90-13442
Optimal trajectories for the aeroassisted flight experiment, 1988-89
[NASA-CR-186132] 05 p0592 N90-13443
The apogee boost motor 05 p0605 N90-13517
Launch and early orbit 05 p0606 N90-13524
Optimal trajectories for the aeroassisted flight experiment
[NASA-CR-186133] 06 p0729 N90-14250
Series reversion/inversion of Lambert's time function
[AD-A216243] 12 p1607 N90-19245
Optimal trajectories for the aeroassisted flight experiment. Part 3: Formulation, results, and analysis
[NASA-CR-186165] 14 p1930 N90-21051
Suboptimal and hybrid numerical solution schemes for orbit transfer manoeuvres
[INPE-4991-PRE/1556] 14 p1931 N90-21054
An all electronic transportation system from LEO to GEO and beyond 15 p2060 N90-21796
Semianalytic study of high-eccentricity orbit stability and evolution 16 p2204 N90-22574
Investigations on docking and berthing dynamics 18 p2504 N90-24312
Guidance and control strategies for aerospace vehicles
[NASA-CR-186878] 20 p2814 N90-26013
Forbidden tangential orbit transfers between intersecting Keplerian orbits
[NASA-TP-3031] 20 p2816 N90-26028
IRIS system and future application to expandable launchers
[IAF-89-212] 20 p2818 N90-26035
Project SPARC: Space-based aeroassisted reusable craft
[NASA-CR-186816] 20 p2821 N90-26051
Noncoplanar orbit transfer optimization for an aeroassisted sortie vehicle 22 p3128 N90-27752
Advanced Earth-to-Orbit Propulsion Technology 1988, volume 1
[NASA-CP-3012-VOL-1] 23 p3290 N90-28611
Advanced Earth-to-orbit propulsion technology program overview: Impact of civil space technology initiative 23 p3290 N90-28612
Development of the electric vehicle analyzer
[AD-A224201] 23 p3323 N90-28788

TRANSFERRED ELECTRON DEVICES
Research on monolithic millimeter-wave devices
[AD-A215771] 10 p1379 N90-17996

TRANSFERRING
NT DROP TRANSFER
Effects of type of responding on memory/visual search: Responding just yes or just no can lead to inflexible performance
[AD-A212764] 04 p0526 N90-13033
Model system studies with a phase separated membrane bioreactor 05 p0679 N90-13954
Fermentation and oxygen transfer in microgravity 05 p0679 N90-13956
High speed transfer switch with 50 kA and 50 kV ratings
[DE90-002448] 06 p0770 N90-14481
Transition state spectroscopy of hydrogen transfer reactions
[AD-A215041] 09 p1191 N90-16901
An investigation of the transfer of monopulse tracking between two coherent point sources
[AD-A217007] 12 p1646 N90-19457
The aerobraking space transfer vehicle
[NASA-CR-186819] 20 p2821 N90-26053

TRANSFORM INTEGRALS
U INTEGRAL TRANSFORMATIONS

TRANSFORMATION TENSORS
U TENSORS

TRANSFORMATIONS (MATHEMATICS)
NT COORDINATE TRANSFORMATIONS
NT FAST FOURIER TRANSFORMATIONS
NT FOURIER TRANSFORMATION
NT HILBERT TRANSFORMATION
NT HOUSEHOLDER TRANSFORMATIONS
NT INTEGRAL TRANSFORMATIONS
NT LAPLACE TRANSFORMATION
NT LINEAR TRANSFORMATIONS
The fast Gauss transform
[AD-A211257] 02 p0266 N90-11517
A transformational method for verifying safety properties in real time systems
[AD-A211925] 04 p0529 N90-13051
Transformations and representations of nonlinear systems
[MEMO-776] 04 p0544 N90-13164
Program transformation with abstract relation algebras
[AD-A213270] 05 p0688 N90-14011
Description and manipulation of convex polygons using polarity
[IMAG-RR-771-M] 05 p0692 N90-14041
A helicopter flight path controller design via a nonlinear transformation technique 06 p0727 N90-14242
Gabor transforms for forward looking infrared image segmentation
[AD-A215046] 09 p1282 N90-17433
Optimal layout via Boolean satisfiability
[AD-A216777] 12 p1705 N90-19787
A remark on the Kelvin transform and a non-linear partial differential equation
[PB90-165622] 14 p2021 N90-21589
Efficient estimation in the Clayton-Cuzick model for survival data
[TW-88-06] 15 p2161 N90-22348
Naturalness of polymorphism
[CS-8916] 16 p2305 N90-23134
Processes and formalisms for unbounded choice
[CS-8917] 16 p2305 N90-23135
Optimization of series expressions. Part 2: Over view of the theory and implementation
[AD-A219961] 17 p2447 N90-23952
Inverting the flow of computation
[TR-89-10] 17 p2450 N90-23971
Optimization and optimality test for the max-cut problem
[MEMO-830] 17 p2463 N90-24066
A monotone complementarity problem in Hilbert space
[AD-A220819] 17 p2468 N90-24105
G exchangeability and the construction of distribution-free statistics 18 p2605 N90-24837
On two transformations in the generalized theory of linear systems
[MATHS-REPT-A-109] 19 p2751 N90-25629
All-optical device and method for remapping images
[AD-D014540] 19 p2758 N90-25672
Mathematical problem-solving transfer: The effects of cognitive load and attention a schema acquisition and rule automation 20 p2917 N90-26594
The system matrix characterisation of input-output equivalence
[MATHS-REPT-A-112] 20 p2918 N90-26600
Unification and disunification: Theory and applications
[ETN-90-97247] 20 p2919 N90-26610
Mobility studies in multiloop spatial linkages 20 p2922 N90-26628
Substitution principle theory for compressible flows 21 p2953 N90-26791
Comparison of methods of space color transformations for enhancement of colored images
[INPE-4977-PRE/1542] 23 p3341 N90-28881
Parallel algorithms for computation of the manipulator inertia matrix 23 p3376 N90-29072
On the relation between the absolute parallelism spaces and spaces having a GL(4) connection
[DE90-627222] 23 p3403 N90-29232
Recognition by linear combination of models
[AD-A224268] 24 p3525 N90-29929
New approaches to linear and nonlinear programming
[AD-A224328] 24 p3525 N90-29932
Short encodings of evolving structures
[AD-A223641] 24 p3527 N90-29944
A comparison of alternative families of transformations for variables constrained to lie on the interval (0,1)
[MATHS-REPT-A-126] 24 p3539 N90-30011
Transformation group methods in plasma physics
[DE90-628755] 24 p3548 N90-30074
On Dirac's conjecture for Hamiltonian systems with first and second class constraints
[DE90-627206] 24 p3555 N90-30116

TRANSFORMERS
NT VOLTAGE CONVERTERS (AC TO AC)
Circuit level modeling of inductive elements
[DE89-015122] 01 p0032 N90-10173
Electron beam welding: Model of high voltage bias transmission line and termination circuits
[DE89-016900] 02 p0230 N90-11323
Development of high frequency spice models for ferrite core inductors and transformers
[DE89-015121] 03 p0341 N90-11946
High power density dc/dc converter: Selection of converter topology
[NASA-CR-186129] 06 p0768 N90-14467
Computer controlled MHD power consolidation and pulse-generation system
[DE90-001224] 07 p0981 N90-15662
Analysis of the 60-Hz power system at KSC: The Orsino substation 08 p1155 N90-16692
The 25-KVA amorphous metal-core transformer developmental test report
[AD-A215444] 09 p1213 N90-17035
Analysis of the behaviour of a current-fed multi-stage voltage multiplier with capacitive output 10 p1338 N90-17745
Lightweight transformer demonstration
[DE90-001470] 10 p1379 N90-17991
Developmental condition and technical problems on electric insulation for super-conducting electric power machine
[DE90-741973] 10 p1379 N90-17994
A test method for measuring corona inception voltage for transducer autotransformers
[AD-A216818] 11 p1502 N90-18646
Linear Variable Differential Transformer (LVDT) with conditioner for the control of stepping motor drivers (part of the sliding-foil follower system of the Emin spectrometers)
[DIGEL-1989-9] 11 p1504 N90-18660
Toroid monitor
[DIGEL-1989-8] 11 p1504 N90-18663
Voltage source ac-to-dc converters for high-power transmitters 15 p2075 N90-21886
Optimization of a pulsed air core transformer for low impedance inductive ignition
[AD-A218748] 16 p2232 N90-22734
Study and simulation of the behavior of a high frequency transformer
[ECL-89-008] 17 p2399 N90-23667
Underwater connect and disconnect plug and receptacle
[AD-D014175] 21 p2998 N90-27039
A 6.4 kV pulse generator with transformers
[DIGEL-1989-1] 21 p3002 N90-27063
Wideband impedance transformer for UHF power transistor time domain waveform measurement system
[PB90-210642] 22 p3167 N90-27962

TRANSFORMS
U TRANSFORMATIONS (MATHEMATICS)

TRANSIENT HEATING
NT SHOCK HEATING
Transients in turbulent convective heat transfer to a flow of supercritical helium
[ETN-90-97217] 20 p2863 N90-26286

TRANSIENT LOADS
NT BLAST LOADS
NT GUST LOADS
NT IMPACT LOADS
NT SHOCK LOADS
Transient tests for spacecraft structures 02 p0183 N90-11040
Multi-axis transient testing: Experimental investigations 02 p0184 N90-11042
Reliability analysis of maintained structural system vulnerable to fatigue and fracture 23 p3338 N90-28868

TRANSIENT OSCILLATIONS
Analysis of new phenomena in shear flow of non-Newtonian fluids
[AD-A212893] 05 p0638 N90-13721
A contribution to the theory of transient conductor simulations
[ETN-90-95891] 12 p1654 N90-19511
The bright X ray transient GS2023+338 (=V404 Cyg) in optical outburst and decline 19 p2767 N90-25724
Unusual counterparts of the soft X ray transients 4U 1543-47 and 4U 2129+47 in quiescence: Interlopers or third stars 19 p2773 N90-25764

TRANSIENT PRESSURES
Transient pressure test article test program 11 p1470 N90-18463
Composite reduced Navier Stokes procedures for flow problems with strong pressure interactions
[AD-A219621] 17 p2403 N90-23687

TRANSIENT RESPONSE
Active control of the forced and transient response of a finite beam 03 p0357 N90-12040
Calculation of transient response from time-harmonic spectrum
[AD-A211972] 03 p0393 N90-12241
A transient response method for linear coupled substructures
[NASA-TP-2926] 05 p0592 N90-13444
Transient response of flexible rotor-bearing systems subjected to combined unbalance and ground excitations 06 p0792 N90-14616
Parametric identification of discrete time series models for structural response prediction 07 p0945 N90-15472

Modelling the buck-type converter transient response with pulsating load 10 p1337 N90-17740
Transient pressure test article test program 11 p1470 N90-18463
Transient responses of coupled systems [ONERA-RT-13/3596-RY-070-R] 11 p1509 N90-18687
Computational aspects of sensitivity calculations in linear transient structural analysis [NASA-TM-4156] 12 p1673 N90-19610
Active control of the forced and transient response of a finite beam [NASA-CR-181957] 13 p1816 N90-20430
Transient response of a cylindrical shell of finite length to transverse impact [OUEL-1780/89] 15 p2119 N90-22123
A parallel structure transient response algorithm using independent substructure response computation 16 p2290 N90-23044
Estimating short-period dynamics using an extended Kalman filter [NASA-TM-101722] 17 p2352 N90-23392
An experimental study of fault propagation in a jet-engine controller [NASA-CR-181335] 17 p2354 N90-23401
An expert system to perform on-line controller tuning [NASA-TM-103101] 17 p2453 N90-23991
Low velocity impact analysis with NASTRAN 18 p2570 N90-24647
Monitoring of Ritz modal generation 18 p2571 N90-24650
A transient response analysis of the space shuttle vehicle during liftoff [NASA-TM-103505] 22 p3125 N90-27735
Higher order diffusion model for a bipolar transistor [PB90-190901] 22 p3167 N90-27960
Bandwidth and signal-to-noise ratio enhancement of the NPS transient electromagnetic scattering laboratory [AD-A224144] 23 p3320 N90-28771
Analysis of dynamic transient response and postflutter behavior of super-maneuvering airplane [AD-A224126] 24 p3432 N90-29386

TRANSIENTS (SURGES)
U SURGES

TRANSISTOR CIRCUITS
GaAs gate dynamic memory technology [AD-A212387] 04 p0560 N90-13266
Finite element modeling and thermal simulations of transistor integrated circuits [AD-A215928] 10 p1380 N90-17997
Planar integrated circuits for microwave transmission and reception [AD-A217676] 12 p1656 N90-19520
Design for testability of stuck-open and stack-on CMOS combinatorial circuits [REPT-89-044] 16 p2230 N90-22725
Detection of bridging faults in DFCMOS combinational gates [REPT-89-060] 16 p2231 N90-22726
Predicting switched-bias response from steady-state irradiations [DE90-006770] 18 p2624 N90-24950

TRANSISTOR LOGIC
Thin-film integrated injection logic [AD-D014190] 04 p0497 N90-12860

TRANSISTORS
NT BIPOLAR TRANSISTORS
NT CHARGE FLOW DEVICES
NT FIELD EFFECT TRANSISTORS
NT HIGH ELECTRON MOBILITY TRANSISTORS
NT JFET
NT JUNCTION TRANSISTORS
NT MODFETS
NT PHOTOTRANSISTORS
NT SILICON TRANSISTORS
NT SOS (SEMICONDUCTORS)
RF transistor thermal/electrical characterization [DE90-001427] 07 p0920 N90-15326
Solid state microelectrochemical devices: Transistor and diode devices employing a solid polymer electrolyte [AD-A214206] 09 p1211 N90-17019
A GaAs p-n-p-n thyristor model [DE90-005757] 11 p1570 N90-19039
Utilization criteria for transistors of diverse technology in pulse inverters with high switching frequency [ETN-90-95359] 12 p1653 N90-19500
Measurement of proton induced radiation damage to CMOS transistors and pin diodes [DE90-007836] 13 p1792 N90-20283
Transistor and solid-state technology: A historical development [AD-A218141] 13 p1798 N90-20317
Flux motion effects in Tl-Ca-Ba-Cu-O thin films [DE90-012176] 21 p3080 N90-27514
In-situ integrated processing and characterization of thin films of high temperature superconductors, dielectrics and semiconductors by MOCVD 22 p3148 N90-27851

TRANSIT SATELLITES
An error sensitivity model for Doppler positioning using transit satellites [AD-A216724] 11 p1455 N90-18381

TRANSIT TIME
Generalized pulse equations for through-transmission evaluation of arbitrary multilayered structures [NASA-TM-100752] 09 p1278 N90-17407
Excess transit time as a function of burst current in an exploding bridgewire detonator [DE90-007168] 11 p1512 N90-18708
Transient photoconduction in doped polymers: Spatial and energetic disorder [ETN-90-95917] 12 p1631 N90-19376

TRANSITION FLIGHT
H-infinity based integrated flight-propulsion control design for a STOVL aircraft in transition flight [NASA-TM-103198] 20 p2813 N90-26011

TRANSITION FLOW
The laminar to slug flow transition in Hele-Shaw flow [DE90-000636] 06 p0777 N90-14521
Experiments on the laminar-turbulent transition on swept wings 08 p1066 N90-16170
Development of transition criteria on the basis of e to the N power for three dimensional wing boundary layers 08 p1067 N90-16179
The use of sublimation methods for the recognition of transition at low speed 08 p1080 N90-16251
European research on viscous flow (EuroVisc) [NLR-TP-89077-U] 15 p2099 N90-22014
Computational simulation of transition to turbulence through inverse modeling 18 p2647 N90-25067
Experimental investigation of Tollmien-Schlichting instability and transition in similar boundary layer flow in an adverse pressure gradient (Hartree beta = -0.14) [LR-604] 19 p2692 N90-25318

TRANSITION METALS
NT CADMIUM
NT CHROMIUM
NT CHROMIUM ISOTOPES
NT COBALT
NT COBALT ISOTOPES
NT COBALT 60
NT COPPER
NT COPPER ISOTOPES
NT GOLD
NT GOLD ISOTOPES
NT HAFNIUM
NT IRIDIUM
NT IRON
NT IRON ISOTOPES
NT MANGANESE
NT MANGANESE ISOTOPES
NT MERCURY (METAL)
NT MOLYBDENUM
NT NICKEL
NT NICKEL ISOTOPES
NT NIOBIUM
NT NIOBIUM ISOTOPES
NT PALLADIUM
NT PLATINUM
NT RHODIUM
NT RUTHENIUM
NT SCANDIUM
NT SILVER
NT TANTALUM
NT TITANIUM
NT TUNGSTEN
NT VANADIUM
NT YTTRIUM
NT ZINC
NT ZIRCONIUM
Metal-assisted syntheses of boranes and carboranes [AD-A210728] 01 p0041 N90-10227
Heterogeneous catalysts in water [AD-A210742] 01 p0041 N90-10228
Bonding in transition metal silyl dimers. Molecular orbital theory [AD-A208269] 01 p0046 N90-10260
In-situ spectroscopic studies of transition metal macrocycles as catalysts for the electrochemical reduction of oxygen [PB89-219273] 03 p0321 N90-11826
Electronic structure of transition metal alloys and intermetallics: Charge transfer and its implications for Moessbauer effect measurements [DE89-017603] 03 p0327 N90-11860
Transition metal catalyzed synthesis of organmetallic polymers [AD-A212133] 04 p0478 N90-12740
First-principles interatomic potentials in transition metals: Multi-ion interactions and their analytic representation [DE90-001990] 06 p0748 N90-14353
Electrical properties of materials for high temperature strain gage applications [NASA-CR-186192] 06 p0780 N90-14534
Host materials for transition-metal ions [AD-A213605] 07 p1003 N90-15808
Selectivity of the reactions of oxygenates on transition metal surfaces [DE90-003911] 08 p1045 N90-16040
Conductive polymers of transition-metal complexes coordinated by a Diamino-Dichalcogen-Benzene compound [AD-D014326] 12 p1629 N90-19360
Theoretical studies of electrons and electron transfer processes in fluids [DE90-008414] 17 p2470 N90-24117
First-principles interatomic potentials for transition metals and their surfaces [DE90-011233] 18 p2528 N90-24424
Formation of cubic Ll2 phases from Al3Ti and Al3Zr by transition metal substitutions for Al [DE90-012288] 20 p2834 N90-26117
Synthesis, structure, electric, and magnetic properties of CaNiN [AD-A222273] 21 p2978 N90-26823
Fundamental studies of strongly magnetic rare earth-transition metal alloys [DE90-012458] 21 p2980 N90-26937
Transition metal activation and functionalization of carbon-hydrogen bonds [DE90-015826] 24 p3451 N90-29489

TRANSITION POINTS
Design and fabrication requirements for low noise supersonic/hypersonic wind tunnels 04 p0446 N90-12555
Determination of the N-factor in the Brunswick (Federal Rep. of Germany) transonic wind tunnel using measurements of pressure distributions and transition points, and the Sally method 08 p1067 N90-16177

TRANSITION PRESSURE
Radiationless transitions and excited-state absorption of low-field chromium complexes in solids [AD-A210653] 02 p0194 N90-11105

TRANSITION PROBABILITIES
Further observations of rotationally excited far infrared OH16 and OH18 emission in Orion-KL: Tighter constraints on the nature of the emitting region [NASA-CR-186004] 05 p0710 N90-14156
Recombination lines of C I and N II in the interstellar medium 15 p2182 N90-22466
Critical behavior of the thermal power near the metal-insulator transition [PREPRINT-714] 16 p2323 N90-23244
Optical emissions from bombarding atmospheric gases with heavy ions [AD-A223544] 24 p3543 N90-30040

TRANSITION TEMPERATURE
Structural aspects of the phase separation in La2CuO4.032 [DE89-016183] 01 p0130 N90-10751
Studies of novel superconductors [DE89-016744] 02 p0282 N90-11609
New mechanism for toughening ceramic materials [AD-A211651] 03 p0332 N90-11892
Anomalous ion-channeling behavior across the superconducting transition in high-T(sub c) materials [DE89-017677] 03 p0411 N90-12360
Preparation and characterization of single phase Ba(1-x)KxBiO3 [DE89-017735] 03 p0411 N90-12362
The effect of composition and processing on high T(sub c) superconductors containing bismuth [DE90-002203] 06 p0854 N90-14965
Improved performance of low-T(sub c) superconductors for detection of minimum-ionizing particles [DE90-001985] 06 p0856 N90-14976
Optical solitons in liquid crystals [DE90-000694] 07 p0991 N90-15728
Linear electron-hole-electron pair model of high-temperature superconductivity in La(2-x)M(x)CuO4 and YBa2Cu3O(7-y): Part 2. Dependence of the superconducting transition temperatures on pressure and on hole concentration [DE90-003012] 07 p0999 N90-15779
Cation disordering in the Tl-2122 superconductors [DE90-003579] 07 p1001 N90-15795
Study of phase transformations liquid-solid-solid of ultrafine particles [ISAL-89-0019] 08 p1042 N90-16022
The modified Ginzburg-Landau theory for anisotropic high temperature superconductors [DE89-635909] 08 p1128 N90-16532

Structure-property correlations in the design of organic metals and superconductors: An overview
[DE90-003794] 08 p1131 N90-16550
High quality tunnel junction devices using high T(sub c) superconductors
[AD-D014329] 10 p1435 N90-18263
Calculation of mechanical properties variations depending on matrix parameters in a composite, as a function of the test temperature
[DT-311/88] 11 p1481 N90-16526
Pressure induced superconductivity in elemental solids
[DE90-610664] 11 p1572 N90-19048
On the substitution of Sr ions at Y sites in YB(suba2)Cu3O(sub7-d)
[DE90-613395] 14 p2031 N90-21652
The onset of superconductivity in two-dimensional disordered systems 16 p2321 N90-23232
Influence of high energy radiation on critical parameters of superconducting ceramics YBa2Cu3O7
[DE90-620562] 16 p2322 N90-23239
Irradiation effects on impact behavior of 12Cr-1MoVW and 2 1/4Cr-1Mo steels
[DE90-011075] 18 p2527 N90-24421
Preparation of high Tc superconducting ceramic materials of the Y-Ba-Cu-oxide type
[FOA-C-30550-3.2] 18 p2622 N90-24939
Pressure in the study of organic superconductors
[DE90-011049] 18 p2625 N90-24959
A systematic study of superconductivity in BiPb(Sn)-Sb Sr-Ca-Cu-O systems 22 p3144 N90-27831
Studies of iron impurities in YxPr1-xBa2Cu3O7-delta 22 p3151 N90-27865
Electron microscopy of transition-metal doped BiCaSrCuO
[DE90-014184] 23 p3398 N90-29202
Superconductivity in mixed boson-fermion systems
[DE90-627491] 23 p3401 N90-29216

TRANSITS
NT THEODOLITES

TRANSLATING
NT MACHINE TRANSLATION
Abstract grammars based on transductions
[MEMO-INF-89-7-REV] 04 p0531 N90-13063
PCI: A PATRAN-NASTRAN model translator 18 p2569 N90-24639
A generic interface between COSMIC/NASTRAN and PATRAN (R) 18 p2569 N90-24640

TRANSLATIONAL MOTION
NT KARMAN-BODEWADT FLOW
NT SECONDARY FLOW
NT THREE DIMENSIONAL FLOW
NT THREE DIMENSIONAL MOTION
Coherent phasing of segmented mirrors 05 p0598 N90-13474
Dynamic modeling of flexible bodies in multibody systems 09 p1229 N90-17134
The coupling effects of kinematics and flexibility on the Lagrangian dynamic formulation of open chain deformable links 16 p2284 N90-23018
Evaluation of nonlinear motion-drive algorithms for flight simulators
[UTIAS-TN-272] 19 p2662 N90-25148
A noncontacting motion monitoring system for an astronaut translation aid
[NASA-TM-102640] 19 p2693 N90-25325
Suspension mechanism and method
[NASA-CASE-LAR-14142-1] 21 p3011 N90-27116
Motion translator
[AD-D014452] 22 p3181 N90-28053

TRANSLUNAR SPACE
U INTERPLANETARY SPACE

TRANSMISSION
NT ACOUSTIC PROPAGATION
NT AERODYNAMIC HEAT TRANSFER
NT CODE DIVISION MULTIPLE ACCESS
NT CONDUCTIVE HEAT TRANSFER
NT CONVECTIVE HEAT TRANSFER
NT DATA TRANSMISSION
NT DEMULTIPLEXING
NT DIFFRACTION PROPAGATION
NT ELECTRIC POWER TRANSMISSION
NT ELECTROMAGNETIC WAVE TRANSMISSION
NT FREQUENCY DIVISION MULTIPLEXING
NT GROUND WAVE PROPAGATION
NT HALOS
NT HEAT TRANSFER
NT HEAT TRANSMISSION
NT IONOSPHERIC F-SCATTER PROPAGATION
NT IONOSPHERIC PROPAGATION
NT LAMINAR HEAT TRANSFER
NT LIGHT SCATTERING
NT LIGHT TRANSMISSION
NT MICROWAVE ATTENUATION
NT MICROWAVE TRANSMISSION
NT MULTIPATH TRANSMISSION
NT MULTIPLE ACCESS
NT MULTIPLEXING
NT PACKET TRANSMISSION
NT PCM TELEMETRY
NT RADAR TRANSMISSION
NT RADIATIVE HEAT TRANSFER
NT RADIO TELEMETRY
NT RADIO TRANSMISSION
NT SATELLITE TRANSMISSION
NT SCATTER PROPAGATION
NT SELF PROPAGATION
NT SHOCK WAVE PROPAGATION
NT SHORT WAVE RADIO TRANSMISSION
NT SIGNAL TRANSMISSION
NT SOUND TRANSMISSION
NT SPREAD SPECTRUM TRANSMISSION
NT STRESS PROPAGATION
NT TELEMETRY
NT TELEPHONY
NT TELEVISION TRANSMISSION
NT TIME DIVISION MULTIPLE ACCESS
NT TIME DIVISION MULTIPLEXING
NT TURBULENT HEAT TRANSFER
NT WAVE PROPAGATION
NT WAVELENGTH DIVISION MULTIPLEXING
Development of a solar-powered infrared injection laser microminiature transmitting system
[DE90-005672] 10 p1389 N90-18034
Conjugate field approaches for active array compensation 12 p1610 N90-19266
Concept study for UHF T/R modules
[AD-A220281] 18 p2547 N90-24536
Near-field gain of pyramidal horns from 18 to 40 GHz
[PB90-155854] 22 p3164 N90-27941

TRANSMISSION CIRCUITS
Studies of high power density, pico-second rise-time light activated semiconductor switch
[AD-A210549] 01 p0061 N90-10349
Electron beam welding: Model of high voltage bias transmission line and termination circuits
[DE89-016900] 02 p0230 N90-11323
Modeling of power electronic systems with EMTP
[NASA-TM-102375] 05 p0695 N90-14060
Investigation of tapered multiple microstrip lines for VLSI circuits
[AD-A217855] 13 p1797 N90-20310

TRANSMISSION EFFICIENCY
Multi-level bandwidth efficient block modulation codes
[NASA-CR-185484] 01 p0056 N90-10317
Omega system performance assessment
[AD-A210342] 01 p0056 N90-10322
Binary Gray codes and index systems
[REPT-89-29] 04 p0530 N90-13060
Dynamic workload modeling of high speed token rings in a metropolitan area network
[MEMO-INF-89-21] 05 p0694 N90-14059
Long pulse narrowband XeCl laser studies
[AD-A219774] 17 p2409 N90-23724
The distributed bit complexity of the ring: From the anonymous to the non-anonymous case
[RUU-CS-88-33] 17 p2452 N90-23988
Transmission, reflection, and radiation at junction planes of different open waveguides
[ISBN-90-9002864-1] 20 p2855 N90-26241
Optical transmission through a polarization preserving single mode optical fiber at two Ar(+) laser wavelengths
[NASA-TM-103475] 20 p2926 N90-26651
Evaluation of a potential Wave Division Multiplexer (WDM) for use in the IRSTD
[AD-A223945] 24 p3463 N90-29560

TRANSMISSION LINES
NT BEAM WAVEGUIDES
NT CIRCULAR WAVEGUIDES
NT COAXIAL CABLES
NT COMMUNICATION CABLES
NT FLUID TRANSMISSION LINES
NT MICROSTRIP TRANSMISSION LINES
NT OPTICAL FIBERS
NT OPTICAL WAVEGUIDES
NT PLASMAGUIDES
NT POWER LINES
NT RECTANGULAR WAVEGUIDES
NT STRIP TRANSMISSION LINES
NT UNDERGROUND TRANSMISSION LINES
NT WAVEGUIDES
Improved propagation models for discrete random media
[AD-A211085] 01 p0057 N90-10327
Electron beam welding: Model of high voltage bias transmission line and termination circuits
[DE89-016900] 02 p0230 N90-11323
Rational design of high-current cable-in-conduit superconductors
[DE89-016867] 02 p0284 N90-11626
High power, solid state RF pulse generators
[AD-D014172] 03 p0341 N90-11941
An empirical formula for gas switch breakdown delay
[DE89-017233] 03 p0342 N90-11947
JPS heater and sensor lightning qualification
[NASA-CR-183830] 06 p0779 N90-14530
Program CICC flow and heat transfer in Cable-In-Conduit Conductors
[DE90-001519] 06 p0829 N90-14818
Silver coated superconducting ceramic powder
[AD-D014300] 07 p0913 N90-15278
Laser communication system with wide band magnetostrictive modulation
[AD-D014302] 07 p0937 N90-15427
Processing YBa2Cu3O(x) wires in O3/O2
[DE90-003570] 07 p1001 N90-15794
Microwave screening on digital radio communication links due to multicircuit power transmission lines
[DE90-734950] 08 p1058 N90-16118
Theoretical and experimental investigation of axial power extraction from a magnetically insulated transmission line oscillator
[DE90-003486] 08 p1060 N90-16131
Silicon hybrid wafer scale integration interconnect evaluation
[AD-A215353] 09 p1212 N90-17031
Improvement of impulse breakdown strength of an XLPE cable by modifing semiconducting layer
[DE90-734942] 09 p1287 N90-17463
Preliminary evaluation of space station transmission line in a ring configuration
[NASA-TM-102461] 10 p1329 N90-17677
Fluid transmission line dynamics for signals of finite amplitude
[AD-A215758] 10 p1385 N90-18014
Proceedings of the 38th International Wire and Cable Symposium
[AD-A216023] 11 p1501 N90-18638
Design, implementation and test of an RS-232 compatible bi-directional, full duplex, fiber-optic interface with provision for hardware handshaking on a minimum of fiber-optic lines
[AD-A216504] 11 p1566 N90-19012
A contribution to the theory of transient conductor simulations
[ETN-90-95891] 12 p1654 N90-19511
Lightning surge characteristics of transmission towers. Lightning surge characteristics of 15-meter-high scale model tower
[DE89-782322] 12 p1692 N90-19721
All-fiber SFPM (Stimulated Four Photon Mixing) amplifier
[AD-D014358] 12 p1713 N90-19841
Technology assessment of video teleconferencing
[AD-A217318] 13 p1789 N90-20266
Microwave transmission line and method of modulating the phase of a signal passed through said line
[AD-D014457] 17 p2395 N90-23640
Very high frequency measurements of geometric factors in transmission line lead acid cells
[AD-A219463] 17 p2420 N90-23788
Optical links for microwave application
[AD-A220574] 17 p2472 N90-24134
Monolithic phase shifter study
[AD-A219859] 18 p2546 N90-24533
High-temperature superconductors for space power transmission lines
[NASA-TM-103459] 18 p2624 N90-24952
Packet radio network concepts for the Norwegian field army 20 p2850 N90-26206
DURIP: Instrumentation for laser switched power LINAC
[AD-A222629] 20 p2868 N90-26318
Transient signal distortion and coupling in multilayer multiconductor MIC microstrips
[AD-A222989] 21 p3000 N90-27050

TRANSMISSION LOSS
Handbook of radio wave propagation loss (100-20,000 MHz), part 2
[PB89-195473] 03 p0336 N90-11912
Modeling of diffraction reflection and clutter loss in UHF radio wave propagation
[FEL-1988-28] 03 p0340 N90-11938
Diffraction, chopping, and background subtraction for LDR 05 p0598 N90-13476
Rectangular-to-circular waveguide transitions for high-power circular overmoded waveguides
[AD-A213925] 07 p0924 N90-15349
Atmospheric transmission calculations for optical frequencies 10 p1373 N90-17960
Millimeter wave radar clutter program
[AD-A215772] 10 p1376 N90-17978
Programmable generation of linear frequency modulated pulses 14 p1961 N90-21232
Subsystem TM Precision: Progress and perspective
[INPE-5006-PRE/1563] 14 p2000 N90-21461
Evaporation duct effects at millimeter wavelengths 15 p2080 N90-21914

Report on STC/Technische Universiteit (TU) Delft Extremely High Frequency (EHF) radio relay study
15 p2081 N90-21915
The mm-wave region propagation experiments by satellite 15 p2081 N90-21916
Propagation environments, effects, and decision aids
15 p2081 N90-21918
Modeling millimeter-wave propagation effects in the atmosphere 15 p2082 N90-21922
A temperature-dependent regular infrared band model for absorption and dispersion 15 p2083 N90-21927
Radar scatterometry and polarimetry at 220 GHz
15 p2085 N90-21935
Calculation of IR propagation statistics in the eastern Atlantic for surveillance system performance assessment 15 p2085 N90-21938
An investigation of the generation and radiation of aerodynamic noise in real piping systems
15 p2164 N90-22368
Millimeter wave filter design with suspended stripline
[AD-A219582] 17 p2395 N90-23645
Advanced guided wave electro-optical switches
[AD-A219784] 17 p2472 N90-24132
Wave propagation over sea: Tropospheric effects on communication, radar, and ESM systems; proposal for a measuring programme
[FOA-C-30544-8.3] 18 p2543 N90-24517
Wideband characterization of forest propagation channels 20 p2846 N90-26188

TRANSMISSIONS (MACHINE ELEMENTS)
Demonstration epicyclic gearbox
[PNR90567] 04 p0508 N90-12932
Non linear vibrations in a drive train when coupled to constant torque and constant power loads
[PNR90593] 04 p0508 N90-12934
Assessment of worm gearing for helicopter transmissions
[NASA-TM-102441] 08 p1025 N90-15923
Continuously variable gear drive transmission
[AD-D014268] 08 p1084 N90-16275
Life of concentrated contacts in the mixed EHD and boundary film regimes
[AD-A216673] 11 p1517 N90-18738
A theory of quantitative inference for artifact sets applied to a mechanical design compiler
[AD-A216535] 11 p1545 N90-18896
Computer-aided design of flywheel transmission systems 14 p1988 N90-21392
Transmission research activities at NASA Lewis Research Center
[NASA-TM-103132] 14 p1988 N90-21394
Influence of linear profile modification and loading conditions on the dynamic tooth load and stress of high contact ratio gears
[NASA-TM-103136] 16 p2243 N90-22796
Non-linear dynamic analysis of geared systems, part 2
[NASA-CR-180495] 17 p2410 N90-23732
SPOT 4 magnetic tape recorder mechanisms
18 p2540 N90-24500
Efficiency study comparing two helicopter planetary reduction stages
[NASA-TM-103106] 20 p2871 N90-26334
Dynamics of multistage gear transmission with effects of gearbox vibrations
[NASA-TM-103109] 22 p3182 N90-28060

TRANSMISSIVITY
Atmospheric transmissivity update - 1988
[AD-A209130] 01 p0085 N90-10484
Probability density function of optical scintillations (scintillation distribution)
[PB89-103912] 06 p0843 N90-14906
A new method for measuring the transmissivity of aircraft transparencies
[AD-A216953] 12 p1714 N90-19842
Fabrication of low frequency structureborne vibration isolation mount
[AD-D014532] 19 p2697 N90-25346

TRANSMISSOMETERS
Verification of Klett's method by comparison of lidar and transmissometer measurements
15 p2084 N90-21933
A 94 GHz transmissometer
[AD-A223309] 24 p3471 N90-29618

TRANSMITTANCE
Solvent dynamical effects in electron transfer: Predicted influences of electron coupling upon the rate-dielectric friction dependence
[AD-A210193] 01 p0120 N90-10690
Density of states in a resonant tunneling structure
[AD-A209508] 01 p0128 N90-10731
Comments on the use of LOWTRAN in transmission calculations for sites with the ground elevated relative to sea level
[AD-A212724] 04 p0519 N90-12995
Description of SHARC: The Strategic High-Altitude Radiance Code
[AD-A213806] 07 p0961 N90-15555
Atmospheric transmittance determination from a two-angle measurement of radiance change
[AD-A213847] 08 p1101 N90-16375
Optical anti-aliasing filters
[AD-A215826] 10 p1430 N90-18251
Power transmission device
[AD-D014430] 14 p1969 N90-21281
Minimizing the effects of the atmosphere in the observation of ultraviolet radiation
15 p2080 N90-21911
LOWTRAN 7: Status, review, and impact for short-to-long-wavelength infrared applications
15 p2081 N90-21917
UV spectral simulations using LOWTRAN 7
15 p2083 N90-21928
Technique for selecting an aerosol model useful for infrared atmospheric transmittance calculations
15 p2085 N90-21934
Computation of broad spectral band electro-optical system transmittance response characteristics to military smokes and obscurants using field test data from transmissometer system measurements
15 p2086 N90-21939
Fast method for computing infrared transmission, computation examples 15 p2086 N90-21942
An algorithm and computer program for the calculation of envelope curves
[PB90-155409] 15 p2145 N90-22254
Preparation, properties, and development of calcium lanthanum sulfide as an 8- to 12-micrometer transmitting ceramic
[AD-A220200] 17 p2382 N90-23565
Single mode communication link
[AD-A219499] 17 p2388 N90-23601
Transmission of infrared radiation through the Australian atmosphere: Predictions using the LOWTRAN model
[AD-A220340] 17 p2428 N90-23835
Fast acting optical beam deflection system
[AD-A220186] 17 p2473 N90-24141
Characterizing microwave propagation using the AFGL microwave attenuation/transmittance/brightness temperature code
[AD-A220248] 18 p2543 N90-24513
Current status of SHARC, the strategic high altitude radiance code, and description of its new auroral module
[AD-A221068] 18 p2580 N90-24698
Satellite material contaminant optical properties
19 p2732 N90-25529
Analysis of cirrus optical properties with data from NASA ER2 High-resolution Interferometer Sounder (HIS)
[NASA-CR-186365] 21 p3030 N90-27227
A LOWTRAN7 sensitivity study in the 8-12 and 3-5 micron bands: Includes comparison with LOWTRAN6 results
[AD-A222094] 21 p3031 N90-27231
Dynamic consolidation of super hard materials
[AD-A224460] 24 p3454 N90-29505
Sounder update and field strength software modifications for Special Operations Radio Frequency Management System (SORFMS). Volume 1: Program descriptions and testing
[AD-A224510] 24 p3460 N90-29543

TRANSMITTER RECEIVERS
Inexpensive global location and tracking systems using geostationary satellites
[AD-A213025] 05 p0602 N90-13498
Specification for HF Maximum Usable Frequency (MUF) model
[AD-A214996] 09 p1206 N90-16990
Planar integrated circuits for microwave transmission and reception
[AD-A217676] 12 p1656 N90-19520
Equipment feasibility study: Very high frequency communication equipment (136-137 megahertz)
[DOT/FAA/CT-TN89/72] 20 p2850 N90-26210
Microprocessor chip incorporating optical signal coupling receiver
[AD-D014547] 22 p3167 N90-27964
Ground-based weather radar compatibility with digital radio-relay microwave systems
[PB90-206236] 23 p3318 N90-28756

TRANSMITTERS
NT EMERGENCY LOCATOR TRANSMITTERS
NT IONOSONDES
NT RADAR TRANSMITTERS
NT RADIO TRANSMITTERS
NT RADIOSONDES
NT RAWINSONDES
NT REPEATERS
NT TRANSMITTER RECEIVERS
Excitatory amino acids as transmitters in the brain
[AD-A210685] 01 p0093 N90-10532
Ionospheric limitations to the accuracy of SSL estimates of HF transmitter locations 02 p0248 N90-11403
Ka-band MMIC beam steered transmitter array
04 p0488 N90-12803
Direction-of-arrival calculations at VLF/LF (Very Low Frequency/Low Frequency)
[AD-A212620] 04 p0493 N90-12833
Optical communication with semiconductor laser diode
[NASA-CR-185886] 05 p0647 N90-13770
SLCSAT (Submarine Laser Communication Satellite) communication system design study
[AD-A213403] 07 p0917 N90-15304
Diffraction limited dichroic combiner diode laser
[AD-D014291] 08 p1082 N90-16263
Velocity matched optical transmitter
[AD-A217413] 13 p1887 N90-20830
Feasibility of using frequency offset on very high frequency air/ground voice channels
[DOT/FAA/CT-TN89/71] 14 p1964 N90-21248
Voltage source ac-to-dc converters for high-power transmitters 15 p2075 N90-21886
Simulation and analysis of a MFQPSK signal transmitted through an acoustic medium
[AD-A220345] 17 p2393 N90-23633
Lunar orbiting microwave beam power system
[NASA-TM-103211] 19 p2667 N90-25173
Analog electronic control differential transmitter
[AD-D014508] 19 p2685 N90-25272
Man-made noise in a military environment
20 p2847 N90-26191
Measured effects of repeater jamming on direct-sequence spread spectrum receivers that use envelope detectors
[AD-A222231] 21 p2996 N90-27032
Lightweight EHF communications satellites
21 p3070 N90-27453
Special test and evaluation methods used for a nine-axis accelerometer
[PB90-209578] 23 p3329 N90-28822
Radar clutter via ray methods
[AD-A223796] 24 p3462 N90-29553

TRANSONIC AIRCRAFT
U SUPERSONIC AIRCRAFT

TRANSONIC FLIGHT
A tool for automatic design of airfoils in different operating conditions 14 p1919 N90-20994

TRANSONIC FLOW
A numerical method for solving transonic flow past aircraft in Cartesian coordinates
[NAL-TR-1008] 01 p0001 N90-10003
Computation of transonic flow about stores
[AD-A210402] 01 p0002 N90-10009
Laser anemometer measurements in a transonic axial-flow fan rotor
[NASA-TP-2879] 02 p0218 N90-11245
Development of direct-inverse 3-D methods for applied transonic aerodynamic wing design and analysis
[NASA-CR-186036] 03 p0305 N90-11733
Three-dimensional, two-phase, transonic, canted nozzle flows
[AD-A211528] 03 p0347 N90-11984
Theoretical methods and design studies for NLF and HLFC swept wings at subsonic and supersonic speeds
04 p0443 N90-12535
Improvements in the formulations and numerical solution of the Euler problem for swept wings
[RAE-TM-AERO-2139] 04 p0447 N90-12582
Spark camera annotation and control system for the BRL (Ballistic Research Laboratory) Transonic Range Facility
[AD-A212266] 04 p0459 N90-12633
Solution of the thin-layer Navier-Stokes equations for laminar transonic flow
[PB89-221600] 04 p0500 N90-12879
Multigrid solution method for the Euler equations
[PB89-219453] 04 p0539 N90-13116
Block-structured solution of three-dimensional transonic flows using parallel processing
[AD-A212851] 05 p0572 N90-13330
Transonic Euler solutions on mutually interfering finned bodies
[AD-A213395] 05 p0572 N90-13331
A vapor generator for transonic flow visualization
[NASA-TM-101670] 05 p0584 N90-13403
A two-dimensional adaptive-wall test section with ventilated walls in the Ames 2- by 2-foot transonic wind tunnel
[NASA-TM-102207] 05 p0585 N90-13407
A computational analysis of the transonic flow field of two-dimensional minimum length nozzles
06 p0718 N90-14194
Navier-Stokes solutions of 2-D transonic flow over unconventional airfoils 06 p0719 N90-14195
Computation of unsteady transonic flow about airfoils in frequency domain using the full-potential equation
06 p0719 N90-14198

Three-dimensional solution-adaptive grid generation of composite configurations 06 p0775 N90-14509
Nonlinear phenomena in computational transonic aeroelasticity 07 p0874 N90-15070
A direct-inverse method for transonic and separated flows about airfoils
[NASA-CR-4270] 07 p0875 N90-15072
Personal computer study of finite-difference methods for the transonic small disturbance equation
[NASA-TM-102582] 08 p1019 N90-15892
Finite element calculations for transonic flows taking into account several far field boundary conditions 08 p1069 N90-16188
Digital image interpretation for optical flow measurement methods: System description and preliminary application examples 08 p1079 N90-16244
An improvement of convection fidelity in Euler calculations 09 p1159 N90-16709
Nonlinear transonic Wall-interference Assessment/Correction (WIAC) procedures and application to cast-10 airfoil results from the NASA 0.3-m TCT 8- by 24-inch Slotted Wall Test Section (SWTS) 10 p1323 N90-17648
High Reynolds number tests of the CAST-10-2/DOA 2 transonic airfoil at ambient and cryogenic temper ature conditions 10 p1324 N90-17650
Application of Jameson's type nonlinear artificial dissipation to the two-dimensional Navier-Stokes computation
[NAL-TR-1015T] 10 p1384 N90-18006
High-resolution Euler computations of unsteady transonic flows in cascades 11 p1462 N90-18420
Asymptotic analysis of transonic flow through oscillating cascades 11 p1462 N90-18421
Calibration of the sonic measuring and control cross section in the gas feed installation of the solid fuel combustion chamber
[LR-552] 12 p1661 N90-19548
A matrix-free locally-implicit scheme for Navier-Stokes equations
[AD-A218298] 13 p1803 N90-20349
On total variation diminishing schemes for transonic turbulent flow computation 14 p1909 N90-20945
Multigrid accelerated relaxation solution of transonic full potential flow equation
[PD-CF-8942] 14 p1910 N90-20951
A two-dimensional unsteady analysis for transonic and supersonic cascade flows 14 p1911 N90-20955
Subsonic and transonic blade design by means of analysis codes 14 p1917 N90-20985
Inverse computation of transonic internal flows with application for multi-point-design of supercritical compressor blades 14 p1918 N90-20987
Numerical optimization of target pressure distributions for subsonic and transonic airfoil design 14 p1919 N90-20993
Numerical optimization of wings in transonic flow 14 p1920 N90-20997
Secondary flow in a turbine guide vane with low aspect ratio 14 p1924 N90-21018
Numerical investigation of separated transonic turbulent flows with a multiple-time-scale turbulence model
[NASA-TM-102499] 15 p2090 N90-21962
A discussion on issues relating to multiblock grid generation 15 p2095 N90-21991
Investigation of advanced counterrotation blade configuration concepts for high speed turboprop systems, task 1: Ducted propfan analysis
[NASA-CR-185217] 16 p2202 N90-22567
Multigrid acceleration of transonic flow computations
[ENSM-8024] 16 p2237 N90-22760
The 3-D composite velocity solutions for subsonic/transonic flow over forebodies and afterbodies
[AD-A220370] 17 p2345 N90-23354
Code ETF-3D. Euler transonic flow: Theoretical manual
[DLC/FLU-INT-TN-005] 18 p2493 N90-24247
Code ETF-3D. Euler transonic flow: Validation manual
[DLC/FLU-INT-TN-007] 18 p2493 N90-24248
Transonic wing charge improvements by passive shock boundary layer interference control: Development status and prospects
[ETN-90-96463] 18 p2496 N90-24267
Integral-equation methods in steady and unsteady subsonic, transonic and supersonic aerodynamics for interdisciplinary design
[NASA-TM-102677] 19 p2655 N90-25110
Study of the compressibility effects on the turbulence of supersonic drags
[ETN-90-97448] 22 p3109 N90-27661
Progress and challenges in modeling turbulent aerodynamic flows
[NASA-TM-102811] 22 p3170 N90-27981
Formation of shock waves in a transonic vortex-profile interaction
[MPIS-3/1990] 22 p3174 N90-28010
Solution of Euler equations applied to a rotor of a helicopter in steady flight
[ONERA-RSF-1/3731-AY-002A] 23 p3269 N90-28500
Unsteady aerodynamics of controls 23 p3273 N90-28525
Some topics in computational transonic aerodynamics: Revision
[NAL-TR-1018T] 24 p3422 N90-29332
The computation and analysis of acoustic waves in transonic airfoil-vortex interactions 24 p3542 N90-30031

TRANSONIC FLUTTER
Experimental transonic flutter characteristics of two 72 deg-sweep delta-wing models
[NASA-TM-101659] 06 p0720 N90-14205
Effects of spoiler surfaces on the aeroelastic behavior of a low-aspect-ratio rectangular wing
[NASA-TM-102622] 22 p3115 N90-27700

TRANSONIC INLETS
U SUPERSONIC INLETS

TRANSONIC NOZZLES
Three-dimensional, two-phase, transonic, canted nozzle flows
[AD-A211528] 03 p0347 N90-11984

TRANSONIC SPEED
On transonic flow over segmented slotted wind tunnel wall with mass transfer 02 p0294 N90-11676
Wind tunnel tests of the influence of aerofoil thickness on the normal force and pitching moment of two slender wings at transonic and supersonic Mach numbers
[ESA-TT-1129] 08 p1018 N90-15889
Flow unsteadiness effects on boundary layers
[NASA-CR-186067] 18 p2550 N90-24557
Three-dimensional cavity flow fields at subsonic and transonic speeds
[NASA-TM-4209] 22 p3107 N90-27650
Sting-support interference on afterbody drag at transonic speeds
[NAL-TM-EA-8902] 23 p3267 N90-28492

TRANSONIC TURBINES
U SUPERSONIC TURBINES

TRANSONIC WIND TUNNELS
Basic aerodynamic research facility for comparative studies of flow diagnostic techniques 04 p0441 N90-12526
Residual interference assessment in adaptive wall wind tunnels
[NASA-CR-181896] 04 p0458 N90-12625
The design and development of an acoustic test section for the ARA transonic wind tunnel
[PNR90574] 04 p0550 N90-13202
Studies of the European transonic wind tunnel
[ONERA-RSF-12/0694-GY] 04 p0562 N90-13278
A two-dimensional adaptive-wall test section with ventilated walls in the Ames 2- by 2-foot transonic wind tunnel
[NASA-TM-102207] 05 p0585 N90-13407
Cryogenic temperature effects on sting-balance deflections in the National Transonic Facility
[NASA-TM-4157] 06 p0727 N90-14244
The NASA Langley 0.3-meter transonic cryogenic tunnel 08 p1028 N90-15941
The US National Transonic Facility, NTF 08 p1028 N90-15942
The European Transonic Windtunnel (ETW) 08 p1029 N90-15945
The cryogenic Ludwieg tube tunnel at Goettingen 08 p1029 N90-15947
Other cryogenic wind tunnel projects 08 p1029 N90-15948
Test techniques for cryogenic wind tunnels 08 p1030 N90-15952
Automatic control of cryogenic wind tunnels 08 p1031 N90-15957
Cryogenic balances for the US NTF 08 p1031 N90-15959
Safety and cryogenic wind tunnels 08 p1032 N90-15960
Determination of the N-factor in the Brunswick (Federal Rep. of Germany) transonic wind tunnel using measurements of pressure distributions and transition points, and the Sally method 08 p1067 N90-16177
Use of the film-of-oil technique for profile measurements in the Transonic Wind tunnel Brunswick (TWB) 08 p1080 N90-16252
An experimental AWTS process and comparisons of ONERA T2 and 0.3-m TCT AWTS data for the ONERA CAST-10 aerofoil 10 p1324 N90-17653
Half model tests on an ONERA calibration model in the transonic wind tunnel Goettingen, Federal Republic of Germany
[DLR-MITT-89-20] 11 p1452 N90-18370
New transonic test sections for the NAE 5 ft x 5 ft trisonic wind tunnel
[AD-A220933] 18 p2499 N90-24278
Investigation of the vortex flow over a sharp-edged delta wing in the transonic speed regime
[LR-594] 19 p2656 N90-25115
Effect of tail size reductions on longitudinal aerodynamic characteristics of a three surface F-15 model with nonaxisymmetric nozzles
[NASA-TP-3036] 20 p2802 N90-25938
Three-dimensional model testing in the transonic self-streamlining wind tunnel 23 p3284 N90-28583
Transonic 3-D Euler analysis of flows around fanjet engine and TPS (Turbine Powered Simulator). Comparison with wind tunnel experiment, evaluation of TPS testing method and 3-D flow
[NAL-TR-1045] 24 p3421 N90-29327

TRANSONICS
U TRANSONIC FLOW

TRANSPARENCE
Conference on Aerospace Transparent Materials and Enclosures (15th) 16-20 January 1989. Volume 2: Sessions 6-9
[AD-A210201] 01 p0006 N90-10024
Basic investigations of cutting machinability of inorganic glasses using single-point tools
[W-15/87] 02 p0210 N90-11204
An illustrated guide of optical characteristics of aircraft transparencies
[AD-A214565] 09 p1167 N90-16752
High modulus coatings
[AD-A215448] 09 p1198 N90-16941
A new method for measuring the transmissivity of aircraft transparencies
[AD-A216953] 12 p1714 N90-19842
Characterization and comparison of optically transparent conducting films
[DE90-000319] 14 p2033 N90-21660
High intensity laser beam interactions with single droplets 15 p2083 N90-21924
Factors affecting the perception of transparent motion 15 p2141 N90-22233
Modelling late-time atmospheres of supernovae 15 p2189 N90-22500
Synthesis and characterization of aromatic polyester and polysiloxane containing block copolymers: Multiphase transparent atomic oxygen resistant damping materials, liquid crystal films, and toughening components of sol/gel glasses
[AD-A218871] 16 p2224 N90-22685
Remote sounding through semi-transparent cirrus cloud 22 p3226 N90-28296
Large hydrodynamic tunnel: Calculation of the acoustic transparency of the jet stream
[REPT-89/115] 23 p3393 N90-29167

TRANSPARENT MATERIALS
U TRANSPARENCE

TRANSPIRATION
The utilization of an infrared imaging system as a cooling slot blockage detector in the inspection of a transpiration cooled nozzle
[NASA-TM-102608] 12 p1663 N90-19555
Transpiration cooling in hypersonic flight
[NASA-CR-186435] 13 p1750 N90-20052
Carbon dioxide and water exchange rates by a wheat crop in NASA's biomass production chamber: Results from an 86-day study (January to April 1989)
[NASA-TM-102788] 19 p2716 N90-25453
System development and early biological tests in NASA's biomass production chamber
[NASA-TM-103494] 19 p2716 N90-25456

TRANSPIRATION COOLING
U SWEAT COOLING

TRANSPONDERS
Performance measurements for a laboratory-simulated 30/20 GHz communication satellite transponder
[NASA-TM-102424] 10 p1376 N90-17977
An error sensitivity model for Doppler positioning using transit satellites
[AD-A216724] 11 p1455 N90-18381
Radar transponder antenna pattern analysis for the space shuttle 12 p1638 N90-19414
Navigation software for the MPL vertical line array
[AD-A220166] 17 p2432 N90-23860
Data link test and analysis system/ATCRBS transponder test system technical reference
[DOT/FAA/CT-TN90/7] 21 p2955 N90-26803

TRANSPORT AIRCRAFT
NT A-300 AIRCRAFT
NT A-310 AIRCRAFT
NT A-320 AIRCRAFT
NT BOEING 727 AIRCRAFT
NT BOEING 737 AIRCRAFT
NT BOEING 747 AIRCRAFT
NT BOEING 757 AIRCRAFT
NT C-5 AIRCRAFT
NT C-130 AIRCRAFT
NT C-135 AIRCRAFT
NT C-140 AIRCRAFT

NT C-141 AIRCRAFT
NT CARGO AIRCRAFT
NT CH-47 HELICOPTER
NT CONCORDE AIRCRAFT
NT DC 10 AIRCRAFT
NT DHC 2 AIRCRAFT
NT EUROPEAN AIRBUS
NT H-53 HELICOPTER
NT L-1011 AIRCRAFT
NT SHORT HAUL AIRCRAFT
NT SPANLOADER AIRCRAFT
NT TANKER AIRCRAFT
NT UH-60A HELICOPTER

Modifying high-order aeroelastic math model of a jet transport using maximum likelihood estimation
01 p0021 N90-10106

Development of pressure containment and damage tolerance technology for composite fuselage structures in large transport aircraft
[NASA-CR-3996] 01 p0034 N90-10186

Comparison of flying qualities derived from in-flight and ground-based simulators for a jet-transport airplane for the approach and landing pilot tasks
[NASA-TP-2962] 03 p0309 N90-11757

The aerodynamic experimental center of Aeritalia: Combat aircraft group
[ETN-89-95213] 03 p0311 N90-11766

Transport composite fuselage technology: Impact dynamics and acoustic transmission
[NASA-CR-4035] 03 p0321 N90-11821

Laminar flow: Challenge and potential
04 p0438 N90-12504

Lockheed laminar-flow control systems development and applications 04 p0438 N90-12506

Long-range LFC transport 04 p0439 N90-12508

Preliminary design of four aircraft to service the California Corridor in the year 2010: The California Condor, California Sky-Hopper, high capacity short range transport tilt rotor aircraft needed to simplify intercity transportation
[NASA-CR-186232] 06 p0724 N90-14226

Relative merits of reactive and forward-look detection for wind-shear encounters during landing approach for various microburst escape strategies
[NASA-TM-4158] 07 p0882 N90-15108

Evaluation of two transport aircraft and several ground test vehicle friction measurements obtained for various runway surface types and conditions. A summary of test results from joint FAA/NASA Runway Friction Program
[NASA-TP-2917] 08 p1021 N90-15902

Investigation and characteristics of major fire-related accidents in civil air transports over the past ten years
10 p1311 N90-17582

Development of improved fire safety standards adopted by the Federal Aviation Administration
10 p1312 N90-17585

New aircraft cabin and cargo flammability standards for transport category aircraft 10 p1312 N90-17589

Fire prevention in transport airplane passenger cabins
10 p1313 N90-17590

Characteristics of transport, aircraft fires measured by full-scale tests 10 p1313 N90-17591

Full-scale air transport category fuselage burnthrough tests
[DOT/FAA/CT-TN89/65] 14 p1913 N90-20967

Simulator comparison of thumball, thumb switch, and touch screen input concepts for interaction with a large screen cockpit display format
[NASA-TM-102587] 14 p1921 N90-21005

Civil air transport: A fresh look at power-by-wire and fly-by-light
[NASA-TM-102574] 14 p1969 N90-21283

An evaluation of the pressure proof test concept for thin sheet 2024-T3
[NASA-TM-101675] 14 p1994 N90-21424

High speed commercial transport fuels considerations and research needs
[NASA-TM-102535] 15 p2072 N90-21869

UK airmisses involving commercial air transport, January - April 1989
[ISSN-0951-6301] 16 p2197 N90-22544

Multilevel decomposition approach to the preliminary sizing of a transport aircraft wing
[NASA-CR-4296] 16 p2200 N90-22557

Fire hazards of aerosol cans in aircraft cargo compartments
[DOT/FAA/CT-89/32] 17 p2347 N90-23369

AVION: A detailed report on the preliminary design of a 79-passenger, high-efficiency, commercial transport aircraft
[NASA-CR-186663] 17 p2353 N90-23395

High speed civil transport
[NASA-CR-186661] 17 p2353 N90-23396

Research and development: Technical and scientific publications 1989
[ISSN-0931-9751] 19 p2649 N90-25075

Study of high-speed civil transports. Summary
[NASA-CR-4236] 20 p2806 N90-25966

Robustness evaluation of H2 and H(infinity) control theory as applied to a transport aircraft
[AD-A222795] 20 p2814 N90-26018

High-speed civil transport study: Special factors
[NASA-CR-181881] 23 p3276 N90-28537

Energy Efficient Engine: Flight propulsion system final design and analysis
[NASA-CR-168219] 23 p3279 N90-28558

TRANSPORT COEFFICIENTS
U TRANSPORT PROPERTIES

TRANSPORT PROPERTIES
NT DIFFUSION COEFFICIENT
NT EDDY VISCOSITY
NT ELECTRICAL RESISTIVITY
NT ELECTRON MOBILITY
NT GAS VISCOSITY
NT GASEOUS DIFFUSION
NT HOLE MOBILITY
NT IONIC MOBILITY
NT IONOSPHERIC CONDUCTIVITY
NT KONDO EFFECT
NT MAGNETORESISTIVITY
NT PHOTOCONDUCTIVITY
NT PLASMA CONDUCTIVITY
NT SUPERCONDUCTIVITY
NT THERMAL CONDUCTIVITY
NT THERMAL DIFFUSIVITY
NT VISCOSITY

Impedance analysis of ionic transport in polypyrrole-polyazulene copolymer and its charge-discharge characteristics
[AD-A210979] 01 p0052 N90-10299

Electroporation: Theory of basic mechanisms
[AD-A210196] 01 p0091 N90-10520

Experimental investigations of transport and optical properties of 3-5 quantum well structures grown via molecular beam epitaxy under optimal growth conditions
[AD-A210269] 01 p0132 N90-10758

Deep traps and sidegating in GaAs devices
[AD-A210740] 01 p0133 N90-10765

Thermodynamic transport properties of nitrogen tetroxide in hypercritical conditions for regenerative cooling of a rocket engine. Volume 1: Tests
[ETN-89-94975] 01 p0134 N90-10773

Thermodynamic transport properties of nitrogen tetroxide in hypercritical conditions for regenerative cooling of a rocket engine. Volume 2: Appendices
[ETN-89-94977] 01 p0134 N90-10774

On the effective transport properties of composite materials 02 p0190 N90-11086

Transport studies of conducting polymers
02 p0200 N90-11140

Electronic and ionic transport in polymers
[AD-A210654] 02 p0201 N90-11148

Capacitive behavior in conducting polymers: The ac impedance and quartz crystal microbalance studies
[AD-A210754] 02 p0201 N90-11150

Numerical simulation of hydrazine transport in a sandy soil 02 p0205 N90-11172

New secondary batteries utilizing electronically conductive polymer cathodes
[NASA-CR-185885] 02 p0215 N90-11227

A solution to nonlinearity problems
[DE89-016975] 02 p0270 N90-11544

Transport properties of thermally grown Cr2O3
[DE89-016703] 02 p0284 N90-11623

Analysis of opposed jet hydrogen-air counter flow diffusion flame
[NASA-CR-182366] 03 p0321 N90-11825

Effect of electrical double layer on transport limited currents at microelectrodes
[AD-A211586] 03 p0324 N90-11843

Flux-corrected transport algorithms for two-dimensional compressible magnetohydrodynamics
[AD-A212757] 04 p0557 N90-13246

Transport phenomena and interfacial kinetics in multiphase combustion systems
[AD-A212932] 05 p0621 N90-13620

Computational studies of structural and transport properties of amorphous solids
[ETN-90-96027] 05 p0628 N90-13664

Turbulent Shear Flows
[VKI-LS-1989-03] 05 p0640 N90-13730

Scalar transport in turbulent shear flows
05 p0640 N90-13734

Proceedings: US/FRG (Federal Republic of Germany) Workshop on Photochemical Ozone Problem and Its Control: US Experiences and the Situation in Europe
[PB89-233514] 05 p0666 N90-13891

Local error estimates for discontinuous solutions of nonlinear hyperbolic equations
[NASA-CR-181960] 06 p0834 N90-14847

Preparation and properties of icosahedral borides
[DE90-003574] 07 p0896 N90-15180

Electronic and ionic transport in polymers
[AD-A213410] 07 p0911 N90-15270

The measurement of transport properties in strongly coupled plasmas
[DE90-003451] 07 p0996 N90-15755

Near-surface sputtered particle transport for an oblique incidence magnetic field plasma
[DE90-004422] 07 p0996 N90-15758

Progress in LTE and non-LTE transport calculations
[DE90-003394] 07 p0997 N90-15764

La(sub 2)MO(sub 4 + delta) (M = Cu, Ni, Co): Phase separation and superconductivity resulting from excess oxygen defects
[DE90-001988] 08 p1128 N90-16534

NMR measurements of solvent self-diffusion coefficients in polymer solutions
[AD-A215276] 09 p1279 N90-17419

Electrical transport dissipation effects in epitaxial Y1Ba2Cu3O(7-x) thin films
[DE90-004301] 09 p1287 N90-17461

Reactive atmosphere processing of BaTiO3 and origins of its photorefractive effect
[AD-A215034] 09 p1289 N90-17475

Structural and fast ion transport properties of glassy and amorphous materials
[DE90-005587] 10 p1358 N90-17877

A numerical solution to the Boltzmann equation for use in calculating pumping rates in a CO2 discharge laser
[AD-A216376] 11 p1514 N90-18718

Magnetohydrodynamic modeling of plasma opening switches and gas puff plasmas
[DE90-005825] 11 p1569 N90-19028

Transport effects and spectroscopy of defects in microstructures
[AD-A216718] 11 p1570 N90-19036

The EGS4 Code System: Solution of gamma-ray and electron transport problems
[DE90-008100] 12 p1713 N90-19838

Characterization of ground state neutral and ion transport during laser ablation of 1:2:3 superconductors by transient optical absorption spectroscopy
[DE90-006623] 12 p1720 N90-19878

Electronic and ionic transport in processable conducting polymers
[AD-A218093] 13 p1782 N90-20229

Hydrodynamic interactions and transport coefficients in a suspension of spherical particles
[DE90-008301] 13 p1801 N90-20336

Computer codes for the evaluation of thermodynamic properties, transport properties, and equilibrium constants of an 11-species air model
[NASA-TM-102602] 14 p1972 N90-21297

Inventory of program packages related to the project SIMONA
[ETN-90-96397] 15 p2148 N90-22270

Transport and relaxation properties in anisotropic superconductors 15 p2170 N90-22403

Transport properties of anisotropic superconductors
15 p2170 N90-22404

The effect of catalysts on gas-phase hydrocarbon ignition
[AD-A218775] 17 p2371 N90-23499

Atmospheric transport and dispersion model hierarchy, part 2
[AD-A220138] 17 p2427 N90-23833

Hot carrier in subpicosecond photoconductive experiments
[AD-A219874] 17 p2477 N90-24166

Electronic and ionic transport in processable conducting polymers
[AD-A221045] 18 p2530 N90-24436

Spectral transport model for turbulence
[DE90-011265] 19 p2689 N90-25295

Modeling and Applications of Transport Phenomena in Porous Media, volume 1
[VKI-LS-1990-01-VOL-1] 19 p2689 N90-25296

Reaction and transport in porous media
19 p2690 N90-25300

Continuum approach and contaminant transport in ground water flows 19 p2690 N90-25301

Modeling and Applications of Transport Phenomena in Porous Media, volume 2
[VKI-LS-1990-01-VOL-2] 19 p2690 N90-25302

Characterization of fluids in porous media
19 p2690 N90-25305

Fingering in 2-D porous media: Experiments, network simulators and statistical models
19 p2691 N90-25308

Optical properties and transport properties of hydrogenated amorphous silicon
[ETN-90-97215] 20 p2927 N90-26656

Development of a mathematical model for the thermal decomposition of aviation fuels
[AD-A221673] 21 p2990 N90-26994

A review of reaction rates and thermodynamic and transport properties for an 11-species air model for chemical and thermal nonequilibrium calculations to 30000 K
[NASA-RP-1232] 21 p3002 N90-27064
Preparation and characteristics of superconducting cuprate thin films: Nd(2-x)Ce(x)CuO4 and substituted Bi-system 22 p3140 N90-27813
Phase compatibilities of YBa2Cu3O(9-delta) type structure in quintenary systems Y-Ba-Cu-O-X (impurity) 22 p3145 N90-27834
Electronic state and superconductivity of YBa2Cu3-xO7-y (M=Al,Zn and Sn) systems 22 p3146 N90-27842
Hyperthermal atomic oxygen generator
[NASA-CR-186573] 22 p3155 N90-27889
Reynolds stress and the physics of turbulent momentum transport
[AD-A224172] 24 p3467 N90-29588
Investigation of structure and transport processes in the high latitude ionospheric plasma using ground based and airborne digisondes
[AD-A224397] 24 p3491 N90-29727

TRANSPORT THEORY
NT MIXING LENGTH FLOW THEORY
Evaluation and sensitivity analyses results of the MESOPUFF 2 model with CAPTEX (Cross-Appalachian Tracer Experiment) measurements
[PB89-198253] 03 p0368 N90-12103
Stellarator transport theory
[DE89-016371] 03 p0406 N90-12328
A stochastic model for the calculation of multiple scattered lidar returns
[DLR-FB-89-36] 05 p0648 N90-13778
Efficient real gas Navier-Stokes computations of high speed flows using an LU scheme
[NASA-TM-102429] 06 p0720 N90-14203
The Delta-t transport protocol: Features and experience useful for high performance networks
[DE89-016542] 06 p0831 N90-14832
Fundamental studies of fusion plasmas
[DE90-002343] 06 p0848 N90-14933
Evaluate and characterize mechanisms controlling transport, fate, and effects of army smokes in the aerosol wind tunnel: Transport, transformations, fate, and terrestrial ecological effects of hexachloroethane obscurant smokes
[DE90-002923] 07 p0957 N90-15536
Transport modeling and advanced computer techniques
[DE90-001481] 07 p0972 N90-15612
Studies of plasma performance and transport in the Advanced Toroidal Facility (ATF)
[DE90-001737] 07 p0994 N90-15746
The neoclassical transport of toroidal momentum in tokamaks
[DE90-006864] 11 p1568 N90-19023
Anomalous transport in toroidal plasmas
[DE90-006549] 12 p1717 N90-19859
The numerical simulation of multistage turbomachinery flows 14 p1925 N90-21025
A self-consistent theory of radial transport of field-aligned current by microturbulence
[DE90-007920] 14 p2028 N90-21631
Transition from resistive-g to eta-i driven turbulence in stellarator systems
[DE90-009382] 14 p2030 N90-21641
Millimeter-wave bistatic scattering by terrain 15 p2085 N90-21936
Rigorous upper bounds for turbulent transport in bounded systems: Passive advection and reversed-field pinches 15 p2168 N90-22390
Towards a quantum pump of electric charges and currents
[AD-A221257] 18 p2607 N90-24851
Ensemble Monte Carlo simulation of electron transport in AlGaAs/GaAs heterostructures
[ISBN-90-9003048-4] 18 p2622 N90-24940
One dimensional heavy ion beam transport: Energy independent model
[NASA-CR-186722] 19 p2754 N90-25650
Lecture notes on incompressible flow and the finite element method
[DE90-014665] 23 p3326 N90-28805
Applied mathematics of transport theory
[DE90-014627] 23 p3387 N90-29126
Deterministic transport on an arbitrarily-connected grid
[DE90-015148] 23 p3388 N90-29131
Fundamental studies of fusion plasmas
[DE90-015732] 24 p3549 N90-30080

TRANSPORT VEHICLES
SKITTER/implement mechanical interface
[NASA-CR-184920] 17 p2384 N90-23578
Tubular space truss structure for SKITTER 2 robot
[NASA-CR-184922] 17 p2384 N90-23580
Two wheeled lunar dumptruck
[NASA-CR-182840] 17 p2410 N90-23734
Lunar material transport vehicle
[NASA-CR-185929] 18 p2534 N90-24456
Bidirectional drive and brake mechanism
[NASA-CASE-MSC-21540-1] 20 p2872 N90-26342
A method for the reduction of aerodynamic drag of road vehicles
[NASA-TM-102589] 22 p3108 N90-27656

TRANSPORTATION
NT ADVANCED LAUNCH SYSTEM (STS)
NT AIR TRANSPORTATION
NT MARINE TRANSPORTATION
NT RAIL TRANSPORTATION
NT RAPID TRANSIT SYSTEMS
NT SPACE TRANSPORTATION
NT SPACE TRANSPORTATION SYSTEM
NT URBAN TRANSPORTATION
Opportunities and prospects for Maglev in North America
[DE90-002190] 06 p0794 N90-14627
Applications of superconductor technologies to transportation
[DE90-000856] 06 p0853 N90-14961
An assessment and comparison of fuel cells for transportation applications
[DE90-001807] 07 p0952 N90-15508
Environmental, health, and safety concerns associated with nonpetroleum fuel use in US transportation
[DE90-004367] 08 p1099 N90-16362
Analysis of alternative concepts for transport systems on the Moon surface
[ETN-90-95727] 12 p1672 N90-19605
Transportation monitoring unit qualification
[NASA-CR-183930] 14 p1932 N90-21060
US Coast guard radionavigation system user survey
[AD-A218480] 17 p2349 N90-23380
Soil Transport Implement
[NASA-CR-184931] 17 p2385 N90-23582
A study of concept options for the evolution of Space Station Freedom
[NASA-TM-102675] 19 p2663 N90-25154
Biconic cargo return vehicle with an advanced recovery system. Volume 1: Conceptual design
[NASA-CR-186520] 20 p2821 N90-26052
Design of a lunar transportation system, volume 2
[NASA-CR-186833-VOL-2] 20 p2871 N90-26333

TRANSPORTATION ENERGY
Opportunities and prospects for Maglev in North America
[DE90-002190] 06 p0794 N90-14627
An approach for testing fuel-cell/battery hybrid power sources for bus applications
[DE90-002090] 08 p1083 N90-16270

TRANSPORTATION NETWORKS
Why stochastic modeling is essential in analyzing interdicted transportation network performance
[AD-A213140] 05 p0688 N90-14007
A Mars/Phobos transportation system
[NASA-CR-186217] 09 p1230 N90-17135

TRANSPORTER
Mobile transporter path planning 19 p2727 N90-25505

TRANSPUTERS
Parallel processing on transputer arrays for the recognition of objects in infrared images
[RSRE-MEMO-4197] 03 p0389 N90-12217
Real-time robot motion: The VLSI implementation via transputers
[RR-364] 04 p0537 N90-13104
A fault-tolerant software algorithm for a network of transputers
[AD-A213092] 05 p0682 N90-13972
Transient finite element computations on the transputer system
[NASA-CR-185199] 10 p1396 N90-18071
Dynamic reconfiguration and link fault tolerance in a transputer network
[AD-A215105] 12 p1642 N90-19433
Parallel neural net path-planner on hypercube and transputer
[DE90-006324] 12 p1703 N90-19777
Object orientated simulation on transputer arrays using time warp
[AD-A219795] 17 p2389 N90-23607
Sensitivity analysis of transputer workfarm topologies
[AD-A219821] 18 p2595 N90-24766

TRANSURANIUM ELEMENTS
NT AMERICIUM
NT CURIUM
NT PLUTONIUM

TRANSVERSE ACCELERATION
Center of excellence in theoretical geoplasma research
[AD-A215035] 14 p2005 N90-21488

TRANSVERSE OSCILLATION
Research on acoustical scattering, diffraction catastrophes, optics of bubbles, acoustical phase conjugation, and wake of an oscillating circular cylinder
[AD-A214168] 07 p0989 N90-15711
Dynamic analysis of geared rotors by finite elements
[NASA-TM-102349] 08 p1086 N90-16286
Transient response of a cylindrical shell of finite length to transverse impact
[OUEL-1780/89] 15 p2119 N90-22123
Transverse vibrations of a composite cylindrical tube of circular cross section
[AD-A219227] 16 p2248 N90-22820

TRANSVERSE VIBRATION
U TRANSVERSE OSCILLATION

TRANSVERSE WAVES
Elastic properties of silica xerogels
[AD-A216528] 12 p1630 N90-19366

TRANSVERSELY EXCITED ATMOSPHERIC LASERS
U TEA LASERS

TRAPATT DIODES
U AVALANCHE DIODES

TRAPEZOIDS
Trapezoidal crystal in the six beam implosion 06 p0786 N90-14577

TRAPPED MAGNETIC FIELDS
The importance of adiabatic variations in trapped particle distributions observed by the SCATHA satellite
[AD-A220859] 17 p2423 N90-23806

TRAPPED PARTICLES
NT RADIATION BELTS
Method and apparatus for determining time, direction and composition of impacting space particles
[NASA-CASE-LAR-13392-1-CU] 01 p0026 N90-10132
Bias and oxide thickness dependence of trapped charge buildup in MOS devices
[AD-A210264] 01 p0131 N90-10757
Hybrid particle-fluid approach to low-frequency turbulence in magnetically confined plasmas
[DE89-015904] 02 p0277 N90-11579
An apparatus for the electrodynamic containment of charged macroparticles 04 p0486 N90-12789
Solar cycle effects on trapped energetic particles
[AD-A215028] 09 p1300 N90-17532
Dissipative trapped electron modes in ell equals 2 torsatrons
[DE90-004919] 10 p1431 N90-18256
Langmuir wave interaction with ion acoustic wave
[DE90-615407] 14 p2027 N90-21624
Traps for neutral atoms
[AD-A221331] 19 p2754 N90-25649
Inhomogeneous electric field effects in a linear RF quadruple trap 20 p2853 N90-26222
A study of the influence of Hg(6(3)P2) population in a low-pressure discharge on mercury ion emission at 194.2 nm 20 p2853 N90-26223
NASA radiation belt models AP-8 and AE-8
[AD-A223660] 24 p3492 N90-29737

TRAPPING
NT CRYOTRAPPING
Laser surface interactions of high-(Tc) superconductors
[DE90-006894] 12 p1669 N90-19587
Positron trapping in semiconductors
[PB90-165606] 15 p2172 N90-22410
Axions and SN 1987A: Axion trapping
[NASA-CR-186604] 18 p2612 N90-24881
Inhomogeneous electric field effects in a linear RF quadruple trap 20 p2853 N90-26222
Re-analysis of data on the space radiation environment above south-east Asia
[RAE-TR-89048] 24 p3565 N90-30166

TRAPS
NT ION TRAPS (INSTRUMENTATION)
An overview of radiation-induced interface traps in MOS (Metal-Oxide Semiconductor) structures
[AD-A216101] 10 p1438 N90-18299

TRAVELING WAVE AMPLIFIERS
A brief description of traveling wave tubes
[FOA-C-30522-3.6] 02 p0217 N90-11244
Development of a traveling wave tube for the project X-SAR. Construction and testing of a breadboard model
[ETN-90-95900] 05 p0636 N90-13713
Theoretical studies of solar lasers and converters
[NASA-CR-186194] 06 p0787 N90-14583

TRAVELING WAVE MASERS
Ultralow noise performance of an 8.4-GHz maser-feedhorn system 15 p2076 N90-21889

TRAVELING WAVE MODULATION
Galactic cosmic-ray modulation and solar-terrestrial relationships
[IFSI-88-17] 08 p1153 N90-16679

GaAs traveling-wave optical modulators using modulated coplanar electrodes with periodic cross-tie overlays
[AD-A217731] 13 p1888 N90-20835

TRAVELING WAVE TUBES
NT BACKWARD WAVE TUBES
NT CARCINOTRONS
A brief description of traveling wave tubes
[FOA-C-30522-3.6] 02 p0217 N90-11244
Development of a traveling wave tube for the project X-SAR. Construction and testing of a breadboard model
[ETN-90-95900] 05 p0636 N90-13713
Gigatron: A new technology for microwave power devices
[DE90-001066] 06 p0771 N90-14483
Secondary electron emission characteristics of molybdenum-masked, ion-textured OFHC copper
[NASA-TP-2967] 07 p0902 N90-15211
A complete EPC simulation 10 p1337 N90-17741
Miniature traveling wave tube and method of making
[NASA-CASE-LEW-14520-1] 16 p2230 N90-22724
Serrodyning by means of a digital phase shifter
[AD-A219593] 17 p2396 N90-23646
Conceptual definition of a high voltage power supply test facility
[NASA-CR-185216] 19 p2666 N90-25172
Spent-beam refocusing analysis and multistage depressed collector design for a 75-W, 59- to 64-GHz coupled-cavity traveling-wave tube
[NASA-TP-3039] 22 p3167 N90-27965
Rain-fade simulation and power augmentation for satellite communication systems
[NASA-TM-103134] 23 p3319 N90-28768
Reliability study of TWT output RF window
[AD-A223688] 24 p3465 N90-29574

TRAVELING WAVES
NT SOLITARY WAVES
Atmospheric gravity waves in the auroral source region of TIDs, studied with the EISCAT CP2-data
02 p0244 N90-11387
Influence of RF-parameters on beam lifetime
[NIKHEF-K/AMPS/89-06] 05 p0699 N90-14091
Active stabilization of aeromechanical systems
[AD-A216629] 11 p1506 N90-18672
Longitudinal traveling waves bifurcating from Vlasov plasma equilibria 12 p1715 N90-19850
On the instability of Goertler vortices to nonlinear travelling waves
[NASA-CR-181994] 14 p1970 N90-21289
Implementation of an algorithm for travelling-wave-based directional detection
[EUT-89-E-214] 20 p2855 N90-26239
On travelling-wave-based protection of high-voltage networks
[ISBN-90-9002955-9] 20 p2858 N90-26260
On traveling wave solutions of a set of coupled Boussinesq-like equations
[DE90-013182] 20 p2917 N90-26597
Analysis of a TM01 circular to TE10 rectangular waveguide mode converter
[AD-A224566] 24 p3464 N90-29568
Research into traveling wave control in flexible structures
[AD-A224504] 24 p3479 N90-29661

TREADMILLS
Control of thermoregulatory sweating during exercise in the heat
[AD-A206001] 01 p0092 N90-10523
The predictability and efficiency of human walking: Metabolic, mechanical, and biophysical considerations
15 p2137 N90-22211
Physiological and perceptual responses to prolonged treadmill load carriage
[AD-A218910] 16 p2260 N90-22886
Physiological and perceptual responses to prolonged treadmill load carriage
[AD-A218809] 17 p2433 N90-23865

TREES (MATHEMATICS)
NT FAULT TREES
Automated model formulation for time-varying flexible structures 01 p0022 N90-10107
Three dimensional object recognition employing combined visual and tactile sensing
[PB89-219489] 03 p0382 N90-12176
Parallel graph contraction
[AD-A211916] 03 p0386 N90-12199
Dynamic embedding of trees in hypercubes with constant dilation and load
[AD-A211884] 03 p0392 N90-12236
Labeled trees and the efficient computation of derivations
[NASA-CR-185386] 04 p0538 N90-13113
Anaphoric trees and an extension of the model of anaphora resolution
[REPT-89-37] 04 p0540 N90-13130
Efficient on-line simulations of tree machines and multidimensional turing machines by random access machines
[AD-A213152] 05 p0680 N90-13960
Spanning trees of hypercubes with a maximum of sixteen peaks
[IMAG-RR-755-I] 08 p1107 N90-16406
Efficient algorithms for dilated mappings of binary trees
[NASA-CR-181980] 09 p1262 N90-17317
Binary space partitioning trees and their uses
13 p1857 N90-20657
Program inversion: More than fun
[CS-8903] 16 p2299 N90-23095
On linear time minor tests and depth first search
[RUU-CS-89-1] 17 p2446 N90-23944
Deductive computer programming, revision
[AD-A219848] 17 p2446 N90-23946
Designing distributed algorithms by means of formal sequentially phased reasoning
[TR-89-8] 17 p2449 N90-23969
Disjoint homotopic paths and trees in a planar graph
[CWI-BS-R8923] 17 p2462 N90-24062
Multiple inheritance and exceptions in frame systems
[CWI-CS-R8931] 18 p2591 N90-24743
Achromatic number is NP-complete for cographs and interval graphs
[RUU-CS-88-25] 18 p2600 N90-24803
Improved self-reduction algorithms for graphs with bounded tree width
[RUU-CS-88-29] 18 p2601 N90-24805
Concatenable structures for decomposable problems
[RUU-CS-89-16] 18 p2601 N90-24810
Storing line segments in partition trees
[RUU-CS-89-17] 18 p2601 N90-24811
Trade-offs in non-reversing diameter
[RUU-CS-89-22] 18 p2602 N90-24813
Automated angular momentum recoupling algebra
[DE90-011988] 19 p2750 N90-25626
Hopf-algebraic structure of combinatorial objects and differential operators
[NASA-CR-186360] 19 p2752 N90-25640
Large sets of block designs
[ETN-90-97212] 20 p2918 N90-26602
Combinatorial problems using a hypercube and Hamming graphs
[ETN-90-97240] 20 p2919 N90-26609
Unification and disunification: Theory and applications
[ETN-90-97247] 20 p2919 N90-26610
Using decision-tree classifier systems to extract knowledge from databases 21 p3048 N90-27328
Efficient algorithms for a class of partitioning problems
[NASA-CR-182073] 22 p3237 N90-28357
Trees, bialgebras and intrinsic numerical algorithms
[NASA-CR-187031] 24 p3524 N90-29925
Unique binary search tree representations and equality-testing of sets and sequences
[AD-A223643] 24 p3537 N90-30002

TREES (PLANTS)
NT CONIFERS
Nitrogen deposition to forest trees
[DE90-003285] 06 p0812 N90-14726
Forest mapping Nuerenberg German national forest with special emphasis on the spectral reflection behavior of pine trees 08 p1093 N90-16328
Continuous gas exchange measurements using individual fascicle cuvettes: The tubule system
[DE90-004932] 10 p1405 N90-18105
Shade images of forested areas obtained from LANDSAT MSS data
[NASA-TM-102939] 14 p1995 N90-21436
Evaluation of the role of ozone, acid deposition, and other airborne pollutants in the forests of eastern North America
[PB90-184896] 22 p3197 N90-28140

TREND ANALYSIS
Methods for trend analysis: Examples with problem/failure data 12 p1635 N90-19396
The application of kriging in the statistical analysis of anthropometric data, volume 2
[AD-A220614] 17 p2438 N90-23892
A trend analysis of women who hold Federal Aviation Administration certificates: Relationship to the representation of women in collegiate aviation faculty ranks
[IAR-90-3] 19 p2762 N90-25691
Trend analysis of total ozone data
24 p3486 N90-29703

TRENDS
Are ozone exceedance rates decreasing. Comment on extreme value analysis of environmental time-series: An application to trend detection in ground-level ozone
[AD-A211029] 02 p0239 N90-11357
The evolution of light alloys in the aerospace industry
[ETN-89-95216] 03 p0329 N90-11872
Diffusion bonding of metals 06 p0744 N90-14330
Fire resistance and breakdown of composite materials
10 p1316 N90-17607
Background of the workshop
10 p1444 N90-18330
Remote sensing applied to vegetation as subsidized in municipal planning
[INPE-4908-PRE/1509] 11 p1523 N90-18770
Heat sink effects on weld bead: VPPA process
12 p1639 N90-19418
Survey on the social and economic influences of wide-spreading heat-pump technology
[DE89-782294] 12 p1658 N90-19526
Analysis of photogeologic lineaments in the Ithacare (BA) region: A proposed methodology
[INPE-4855-PRE/1478] 12 p1677 N90-19635
Fighter escape system: The next step forward
13 p1752 N90-20059
Power conditioning techniques
[NASA-TM-102577] 13 p1795 N90-20301
Joint Japanese-American Workshop on Future Trends in Logic Programming
[DE90-008343] 13 p1867 N90-20709
Contribution for the study of the evolution of part of the Espinhaco supergroup and its foundation through fracture analysis
[INPE-4907-PRE/1508] 14 p1999 N90-21459
Electronic Transfer of Information and its Impact on Aerospace and Defence Research and Development
[AGARD-CP-466] 15 p2177 N90-22440
Technologies for electronic transfer of information: The present state and trends in Europe
15 p2177 N90-22441
Technologies for electronic transfer of information: The present state and trends in Japan
15 p2177 N90-22443
Megatendances 15 p2178 N90-22445
Geometric programming prediction of design trends for OMV protective structures
[NASA-TM-4206] 17 p2365 N90-23462
National patterns of research and development resources: 1989
[NSF-89-308] 17 p2486 N90-24218
Unique failure behavior of metal/composite aircraft structural components under crash type loads
[NASA-TM-102679] 18 p2572 N90-24660
The effect of aircraft size on cabin floor dynamic pulses
[DOT/FAA/CT-88/15] 19 p2659 N90-25136
Comparative assessment of world research efforts on magnetic confinement fusion 19 p2759 N90-25680
Estimating the cost of major ongoing cost plus hardware development programs
[NASA-TM-100401] 19 p2764 N90-25705
Technical evaluation report on the Guidance and Control Panel 49th Symposium on Fault Tolerant Design Concepts for Highly Integrated Flight Critical Guidance and Control Systems
[AGARD-AR-281] 20 p2813 N90-26012
Radars in space 21 p3015 N90-27144
Block 6: The future DMSP space systems
21 p3068 N90-27443
Active control of aerothermoelastic effects for a conceptual hypersonic aircraft
[NASA-TM-102713] 22 p3122 N90-27725
Impact of NDE-NDI methods on aircraft design, manufacture, and maintenance, from the fundamental point of view 22 p3189 N90-28093
Developments in test procedures for hot-salt corrosion of superalloys 23 p3306 N90-28700
High temperature protective coatings: Recent trends
23 p3308 N90-28710
National air quality and emissions trends report, 1988
[PB90-200114] 23 p3346 N90-28909
Trend analysis of total ozone data
24 p3486 N90-29703

TRIAMINOTRINITROBENZENE
U TATB

TRIANGLES
Triangle based TVD schemes for hyperbolic conservation laws
[NASA-CR-181984] 08 p1106 N90-16401
An improved technique for output-sensitive hidden surface removal
[RUU-CS-89-32] 18 p2602 N90-24817
The first order phase transition for six-state Potts model on two dimensional random triangle lattice
[DE90-627210] 23 p3389 N90-29140

TRIANGULAR WINGS
U DELTA WINGS

TRIANGULATION
Applications of artificial intelligence to digital photogrammetry 02 p0262 N90-11486
Asymptotically fast triangularization of matrices over rings
[DE90-003161] 08 p1117 N90-16471

Solving computer graphics problems through boolean combinations of polygons
[AD-A214788] 09 p1273 N90-17380
Generation of triangular form models in a microcomputer environment
[INPE-4974-PRE/1539] 14 p1997 N90-21447
Unstructured mesh generation by a generalized Delaunay algorithm 15 p2096 N90-21995
On the G1 smooth connection between triangular Bernstein-Bezier patches. Part 1: Around and N-patch corner
[TELECOM-PARIS-89-D-012] 18 p2575 N90-24671
On the G1 smooth connection between triangular Bernstein-Bezier patches. Part 2: In a piecewise representation
[TELECOM-PARIS-89-D-013] 18 p2575 N90-24672
Free-form surface modelling using tensor product Bezier patches: A review with new solutions
[TELECOM-PARIS-89-D-014] 18 p2575 N90-24673
Generation and improvement of meshes for finite elements methods in two and three dimensions
[ETN-90-97249] 20 p2919 N90-26611

TRIBOLOGY
Morphological aspects of the friction of hot-filament-grown diamond thin films
[DE89-015986] 01 p0130 N90-10750
A study of the tribological and surface micromechanical properties of YBa2Cu3O7-x
[DE89-015680] 02 p0281 N90-11607
Plasma-deposited amorphous hydrogenated carbon films and their tribological properties
[NASA-TM-102379] 03 p0331 N90-11880
Fundamental tribological properties of ion-beam-deposited boron nitride films
[NASA-TM-102088] 03 p0331 N90-11881
Development and use of a tribology research-in-progress database
[PB89-226274] 03 p0417 N90-12396
Tribological properties of ceramic/TiAl-Nb sliding couples for use as candidate seal materials to 700 deg C
[NASA-TM-102401] 04 p0464 N90-12658
Tribological properties of PM212: A high-temperature, self-lubricating, powder metallurgy composite
[NASA-TM-102355] 04 p0465 N90-12659
A new test machine for measuring friction and wear in controlled atmospheres to 1200 C
[NASA-TM-102405] 04 p0466 N90-12670
Structural studies of sputter-deposited MoS2 solid lubricant films
[AD-A212407] 04 p0481 N90-12759
Mechanisms of wear in structural ceramic materials 06 p0749 N90-14360
Characterization and in situ testing of diamond films
[DE90-003155] 07 p0911 N90-15265
Investigation into the effect of fibre size on the tribological behaviour of semi-metallic brake material 09 p1185 N90-16864
Advanced tribological coatings for high specific strength alloys
[AD-A214061] 09 p1196 N90-16930
The experimental evaluation and application of high-temperature solid lubricants
[NASA-TM-102476] 09 p1198 N90-16944
Adhesion of silver films to ion-bombarded alumina
[DE90-005642] 09 p1199 N90-16947
Film thickness in lubricated Hertzian contacts. Part 2: Point contacts
[ESDU-89045] 09 p1232 N90-17148
Friction in bearings
[ESDU-89044] 09 p1232 N90-17149
The application of a computer data acquisition system for a new high temperature tribometer
[NASA-TM-102508] 10 p1347 N90-17811
The joint effect of surface microtopography and near-surface structure on microcontact conditions
[DE90-006494] 11 p1493 N90-18591
Experimentally determined wear behavior of an Al2O3-SiC composite from 25 to 1200 C
[NASA-TM-102549] 13 p1765 N90-20130
Fluorinated diamond thin films for tribological applications
[AD-A217452] 13 p1779 N90-20214
Tribological properties of boric acid and boric-acid-forming surfaces. Part 2: Formation and self-lubrication mechanisms of boric acid films on boron- and boric-oxide-containing surfaces
[DE90-005632] 13 p1811 N90-20400
Tribological properties of boric acid and boric acid forming surfaces. Part 1: Crystal chemistry and self-lubricating mechanism of boric acid
[DE90-005665] 13 p1811 N90-20401
Studies of mechano-chemical interactions in the tribological behavior of materials
[NASA-TM-102545] 14 p1953 N90-21182
Self-lubricating polymer composites and polymer transfer film lubrication for space applications
[NASA-TM-102492] 15 p2071 N90-21862
The 24th Aerospace Mechanisms Symposium
[NASA-CP-3062] 15 p2112 N90-22079
Tribomaterial factors in space mechanism brake performance 15 p2114 N90-22096
An analytical study of tribochemical phases with colloidal additives. Contributions made by energy filtering electron microscopy
[ECL-89-009] 17 p2374 N90-23521
CVD diamond films for tribological applications
[AD-A220265] 17 p2413 N90-23750
The mechanical properties of Cu/TiB2 multilayer structures
[DE90-010608] 18 p2517 N90-24378
Fourth European Space Mechanisms and Tribology Symposium
[ESA-SP-299] 18 p2535 N90-24462
Interface tribology and space conditions 18 p2536 N90-24469
Tribological properties of PVD-applied MoS2 coatings used on space mechanisms 18 p2537 N90-24470
The advantages and limitations of sputtered molybdenum disulphide as a space lubricant 18 p2537 N90-24471
Wear of gold-plated contacts: Microscopic aspects, role of oxygen 18 p2538 N90-24479
Thick and compact MoS2 coatings 18 p2541 N90-24501
Tribology of MoS2: Effect of film thickness 18 p2541 N90-24505
The experimental evaluation and application of high temperature solid lubricants 18 p2564 N90-24631
Effect of film adhesion on tribological properties of silver-coated alumina
[DE90-010090] 18 p2564 N90-24632
Tribological and mechanical properties of Fe/Ti multilayered films
[DE90-011949] 18 p2565 N90-24635
Wear transition surfaces for long-term wear effects
[DE90-011314] 19 p2698 N90-25351
Microscopic modeling of tribological phenomena
[AD-A222049] 21 p3011 N90-27117
Friction microprobe studies of composite surfaces
[DE90-014224] 23 p3299 N90-28662
Fretting wear and fretting fatigue at temperatures up to 600 C 23 p3307 N90-28706
Microdamage to ceramic surfaces under sliding conditions 23 p3308 N90-28708
Use of electron spectroscopies in the tribological evaluation of diamond films
[DE90-014421] 23 p3334 N90-28848
Ion-beam-assisted deposition of silver films on zirconia ceramics for improved tribological behavior
[DE90-009706] 24 p3456 N90-29516
Adhesion of silver films to ion-bombarded zirconia
[DE90-010088] 24 p3456 N90-29517
Ion-beam mixing of Fe/B layers for tribological applications
[DE90-010091] 24 p3456 N90-29518
Wear of advanced ceramics: An overview
[DE90-012166] 24 p3456 N90-29519
Scale effects in steady-state friction
[DE90-012943] 24 p3476 N90-29647
Lubrication characteristics of rolling bearings lubricated by self-lubricating composite retainers. Part 1: Selection of bearings for Earth sensors
[NAL-TR-1019] 24 p3477 N90-29651

TRICHLORIDES
U CHLORIDES

TRIGGER CIRCUITS
Pressure sensitive release device
[AD-D014220] 06 p0792 N90-14610
First results from the MACRO (Monopole, Astrophysics, Cosmic Ray Observatory) detector at the Gran Sasso Laboratory
[DE90-003243] 07 p1011 N90-15858
CCST (Center for Compound Semiconductor Technology) research briefs
[DE90-006446] 12 p1721 N90-19887
A new technique for hardening optically-triggered thyristors
[DE90-006769] 18 p2549 N90-24550

TRIGGERS
U ACTUATORS

TRIGONOMETRIC FUNCTIONS
NT COSINE SERIES
NT SINE SERIES
NT TANGENTS
Transient response of a cylindrical shell of finite length to transverse impact
[OUEL-1780/89] 15 p2119 N90-22123

TRIGONOMETRY
Quantum si(2) enveloping algebra and representations of braid group
[DE90-607044] 09 p1275 N90-17389

TRIM (BALANCE)
U AERODYNAMIC BALANCE

TRIMERS
Effects of heat treatment on microstructure and flexural properties of unidirectional carbon-carbon composites
[AD-A214985] 09 p1186 N90-16873

TRIMETHYL COMPOUNDS
Reactions of hydrogen chloride and boron trichloride with trimethylsilylamino groups
[AD-A209006] 01 p0038 N90-10209

TRINITROTOLUENE
Free-expansion experiments and modeling in detonation: Chemistry and hydrodynamics on a laboratory scale
[DE89-007748] 01 p0053 N90-10302
Remarks on certain aspects of solid explosive detonation via small projectile impact
[AD-A210648] 01 p0054 N90-10307
Carbon in detonations
[DE89-016037] 02 p0208 N90-11189
Condensed phase kinetic deuterium isotope effects in high energy phenomena: Mechanistic investigations and relationships
[AD-A217161] 13 p1770 N90-20156

TRINITROTRIAZOCYCLOHEXANE
U RDX

TRIODES
Micro-cavity integrable vacuum diodes and triodes
[DE89-016649] 01 p0060 N90-10344
A progress report on the Livermore Miniature Vacuum Tube Project
[DE90-008302] 13 p1794 N90-20299

TRIPLE AXIS SPECTROMETERS
U NEUTRON SPECTROMETERS

TRIPLE STARS
Studies of the possible X ray triple 4U1915-05 19 p2768 N90-25727
The possible X ray triple 4U2129+47 (=V1727 Cygni) 19 p2768 N90-25732
Unusual counterparts of the soft X ray transients 4U 1543-47 and 4U 2129+47 in quiescence: Interlopers or third stars 19 p2773 N90-25764

TRIPLET EXCITATION
U ATOMIC ENERGY LEVELS

TRIPLET STATE
U ATOMIC ENERGY LEVELS

TRIPROPELLANTS
U LIQUID ROCKET PROPELLANTS

TRISONIC WIND TUNNELS
New transonic test sections for the NAE 5 ft x 5 ft trisonic wind tunnel
[AD-A220933] 18 p2499 N90-24278

TRITIUM
Ignition and burn criteria for D3He tokamak and spherical torus reactors
[DE89-015059] 01 p0125 N90-10716
Rapid heating tensile tests of high-energy-rate-forged 316L stainless steel charged with hydrogen and tritium
[DE89-017869] 04 p0474 N90-12717
Rapid heating tensile tests of hydrogen-charged high-energy-rate-forged 316L stainless steel
[DE90-000591] 06 p0748 N90-14342
Phases in lanthanum-nickel-aluminum intermetallic alloys
[DE90-000651] 06 p0746 N90-14343
Lawrence Livermore National Laboratory (LLNL) research on cold fusion
[DE90-000930] 06 p0845 N90-14915
Cold fusion: Alchemist's dream
[DE90-000865] 06 p0847 N90-14925
Tritium and neutron measurements of a solid state cell
[DE90-003657] 07 p1005 N90-15820
Cold fusion research
[DE90-005611] 10 p1433 N90-18267
Technology update-89
[DE90-005813] 11 p1593 N90-19178
Investigation of a simulated tritium plasma using Coherent Anti-Stokes Raman Spectroscopy (CARS)
[DE90-005696] 12 p1622 N90-19319
Few-body collisions in a weakly interacting Bose gas
[ETN-90-96893] 18 p2613 N90-24886
Mass spectrometric analysis of hydrogen isotopes in metals and metal hydrides
[DE90-014118] 23 p3303 N90-28685

TRITON
Neptune's Triton: A moon rich in dry ice and carbon
[NASA-CR-186298] 08 p1152 N90-16675

TRITONS
The effective (3)He-nucleon force in a microscopic DWBA approach to the (3)He,t charge exchange reaction --- Distorted Wave-Borne Approximation (DWBA)
[KVI-763] 05 p0697 N90-14077
TRIVALENT IONS
Determination of trivalent chromium ions in chromium plating solutions by ultraviolet-visible spectrophotometry
[AD-A215688] 10 p1351 N90-17837
TROCHOIDS
U PIVOTS
TROPICAL METEOROLOGY
A study of the impact of simulated satellite lidar wind observations
[AD-A210430] 01 p0086 N90-10488
A seasonal isotherm depth climatology for the eastern tropical Pacific
[PB89-193577] 01 p0090 N90-10512
Hurricane Research Division fiscal year 1988 programs, fiscal year 1989 projections
[PB89-152268] 02 p0250 N90-11418
Atlas of tropical sea surface temperature and surface winds
[PB89-223598] 04 p0521 N90-13009
Wind lidar for BEST
[CNES-NT-125] 23 p3353 N90-28947
TROPICAL REGIONS
NT AMAZON REGION (SOUTH AMERICA)
North-south tropical F2 layer asymmetry at west AFrican and Pacific longitudes 02 p0247 N90-11398
Synoptic scale tropical waves in multichannel satellite radiance data 06 p0816 N90-14745
Eutrophication assessment through remote sensing techniques
[INPE-4932-PRE/1422] 10 p1398 N90-18083
Spectral response of wheat and its relationship with agronomical prameters
[INPE-4950-RPE/599] 11 p1524 N90-18774
Photointerpretation with instruments for evaluation of environmental impact: Mata Atlantica in Cubata
[INPE-4910-PRE/1511] 11 p1531 N90-18817
Drifting buoy data from Western Tropical Pacific for the period February 1, 1986 through February 28, 1989
[PB90-113978] 12 p1695 N90-19732
Cloud types and the tropical Earth radiation budget, revised
[NASA-CR-180475] 13 p1843 N90-20582
A case study of a quasi-stationary tropical convective line
[AD-A218325] 13 p1847 N90-20604
Wheat productivity estimate through field radiometry
[INPE-4994-PRE/1556] 14 p2000 N90-21460
Low latitude F-region dynamical processes from atomic oxygen nightglow emissions
[INPE-4999-PRE/1561] 14 p2006 N90-21494
Precipitation mechanisms in tropical and midlatitude convective clouds 14 p2008 N90-21507
Spectral response of wheat and its relationship with agronomic variables in the tropical region
[INPE-5018-RPE/612] 15 p2122 N90-22138
The interpretation of SAGE 2 ozone measurements in the lower mesosphere 15 p2124 N90-22149
The relationship between the buoyancy of near-surface air and the potential temperature of the tropopause 15 p2128 N90-22165
Southern oscillation simulation in coupled ocean/atmosphere global climate models 15 p2131 N90-22181
Monthly surface thermal forcing in the tropical Pacific from 1980 to 1983
[NASA-CR-183033] 16 p2259 N90-22877
VLA and VLBI angular broadening measurements: The distribution of interstellar scattering at low Galactic latitudes 16 p2330 N90-23279
Tropical-extratropical interaction in a model atmosphere 17 p2422 N90-23800
An analytic/empirical model of the middle and low latitude ionosphere
[AD-A220004] 17 p2423 N90-23809
Tropical cyclones, 1989: Central north Pacific
[PB90-182536] 17 p2428 N90-23836
A day-to-day comparison study of Seasat scatterometer winds with winds observed from islands in the tropical Pacific
[NASA-CR-186696] 22 p3212 N90-28223
The above-inversion moisture structure observed during FIRE 22 p3215 N90-28235
Study of anomalies in transition vegetation in Alto Xingo-NT, through remote sensing techniques
[INPE-4601-TDL/334] 23 p3343 N90-28891
Vorticity balance study for a tropical region, during the Southern Hemisphere summer
[INPE-4634-TDL/336] 23 p3353 N90-28949
Barotropic mechanisms associated with tropical plume formation 24 p3489 N90-29719
TROPICAL STORMS
NT HURRICANES
NT TYPHOONS
Hurricane Research Division fiscal year 1988 programs, fiscal year 1989 projections
[PB89-152268] 02 p0250 N90-11418
Further research on dynamics of marine atmospheres in tropical cyclones
[AD-A213882] 07 p0964 N90-15571
ONR tropical cyclone motion research initiative: Data assimilation considerations for field experiment analyses
[AD-A215726] 09 p1248 N90-17244
The invertibility principle for a simple hurricane model
[AD-A218344] 13 p1848 N90-20605
Forecast of Atlantic seasonal hurricane activity for 1990 15 p2134 N90-22194
A description of tropical cyclone recurvature in terms of isentropic potential vorticity
[AD-A218482] 17 p2425 N90-23821
TROPICS
U TROPICAL REGIONS
TROPISM
NT GRAVITROPISM
TROPOPAUSE
The relationship between the buoyancy of near-surface air and the potential temperature of the tropopause 15 p2128 N90-22165
Tropopause undulations and the development of extratropical cyclones 15 p2132 N90-22186
TROPOSPHERE
NT TROPOPAUSE
An atmospheric pressure flow reactor: Gas phase kinetics and mechanism in tropospheric conditions without wall effects 02 p0203 N90-11160
Use of satellite data and modeling to asses the influence of stratospheric processes on the troposphere 03 p0363 N90-12075
Aerosol in the Pacific troposphere 03 p0363 N90-12078
Global tropospheric chemistry: Chemical fluexes in the global atmosphere
[NASA-CR-186090] 03 p0369 N90-12109
Physics of the tropospheric radiopropagation
[DE89-619726] 04 p0485 N90-12783
Zonal average cloud characteristics for global atmospheric chemistry modeling
[CM-76] 04 p0518 N90-12992
The interaction and variation of waves and turbulence from MST radar data
[AD-A212849] 05 p0670 N90-13906
Hybrid PE-ray-mode formulation of high frequency propagation in a bilinear tropospheric surface duct 06 p0759 N90-14417
The parabolic equation approach to predicting tropospheric propagation effects in operational environments 06 p0759 N90-14418
RPE: A parabolic equation radio assessment model 06 p0759 N90-14419
Propagation modeling for some horizontally varying tropospheric ducts 06 p0760 N90-14422
Assessment of anomalous propagation predictions using minisonde refractivity data and the parabolic equation method 06 p0760 N90-14424
An observational study of intramonthly quasi-periodicities in the Northern Hemisphere, extratropical geopotential height field 06 p0813 N90-14729
The chemistry and dynamics of marine stratocumulus 08 p1102 N90-16381
Time and spatially dependent estimates of pollutant trace gas emissions and their effect on tropospheric ozone 09 p1243 N90-17212
Numerical modeling of the atmosphere with an isentropic vertical coordinate 09 p1246 N90-17226
Tropospheric chemistry of natural hydrocarbons and energy-related pollutants: Biosphere/climate feedbacks
[DE90-005643] 11 p1532 N90-18820
Connections between the circulation in altitude and convection over South America
[INPE-4923-TDL/383] 11 p1534 N90-18828
Development and status of the EURAD project 12 p1686 N90-19681
The Chemical Transfer Model (CTM) of EURAD: Development status 12 p1686 N90-19683
The EURAD model in EUROTRAC 12 p1689 N90-19701
Source attribution for tropospheric ozone in the US
[DE90-007994] 14 p2004 N90-21484
Precise estimation of tropospheric path delays with GPS techniques 15 p2074 N90-21881
Lidar measurements of the optical propagation environment 15 p2084 N90-21930
Determination of rates of reaction in the gas-phase in the troposphere: Theory and practice. 2: Rate of direct photoreaction: Screening-level test guideline-spectroscopic determination of the cross section and the maximum rate of direct photoreaction in sunlight
[PB90-146291] 15 p2125 N90-22156
The sources and chemistry of late winter Arctic tropospheric aerosols
[PB90-131988] 15 p2126 N90-22158
An analysis of propagation in a surface duct over a periodically rough Earth
[AD-A220565] 17 p2390 N90-23612
Radar clutter via waveguide methods
[AD-A220237] 18 p2542 N90-24512
Global changes in tropospheric chemistry 19 p2708 N90-25411
Measurements of tropospheric nitric acid over the Western United States and Northeastern Pacific Ocean
[NASA-TM-103470] 20 p2883 N90-26399
The global consequences of increasing tropospheric ozone concentrations
[NASA-TM-103477] 20 p2883 N90-26401
Results from the IVL TOR Station at Roervik, Sweden. A contribution to the EURATRAC subproject TOR 20 p2885 N90-26415
Formation kinetics of N2O in the atmosphere 20 p2886 N90-26425
Tropospheric sounders 21 p3016 N90-27150
A numerical study of the role of meso beta and meso gamma scale vertical exchange processes in the evolution of upper tropospheric frontal systems
[AD-A222057] 21 p3031 N90-27230
The tropospheric response pattern to solar activity forcing 22 p3201 N90-28165
Solar activity, the QBO, and tropospheric responses 22 p3203 N90-28172
A search for solar related changes in tropospheric weather 22 p3203 N90-28173
Solar activity influences on atmospheric electricity and on some structures in the middle atmosphere 22 p3207 N90-28196
Front range lidar, aircraft, and balloon experiment
[PB90-225301] 22 p3212 N90-28218
Mesoscale variability of free tropospheric humidity near San Nicolas Island during FIRE 22 p3214 N90-28234
The October 27-28, 1986, FIRE cirrus case study: Cloud microstructure 22 p3224 N90-28283
The distribution of middle tropospheric carbon monoxide during early October 1984
[NASA-TM-103485] 23 p3346 N90-28906
Tropospheric nitrogen: The influence of anthropogenic sources on distributions and deposition, executive summary
[DE90-015401] 23 p3348 N90-28922
Remote atmospheric profiling systems for tropospheric monitoring
[PB90-216789] 23 p3349 N90-28927
Tropospheric wind profiling using radar interferometry: A feasibility study of a compact mobile system
[PB90-217068] 23 p3351 N90-28939
Tropospheric nitrogen: The influence of anthropogenic sources on distributions and deposition
[DE90-015408] 24 p3487 N90-29709
The Surface Air Sampling Program
[DE90-014873] 24 p3487 N90-29711
TROPOSPHERIC RADIATION
Tropospheric monitoring technology for gravity wave experiments 12 p1734 N90-19971
TROPOSPHERIC SCATTERING
Tropospheric influences on satellite-Earth paths and their determination by means of radar measurements
[ESA-TT-1143] 04 p0480 N90-12639
MANPRINT (Manpower and Personnel Integration) evaluation: AN/TRC-170 digital troposcatter radio system
[AD-A211799] 08 p1055 N90-16100
Measurement errors 17 p2359 N90-23426
Wave propagation over sea: Tropospheric effects on communication, radar, and ESM systems; proposal for a measuring programme
[FOA-C-30544-8.3] 18 p2543 N90-24517
Understanding tropscatter propagation
[AD-A220969] 18 p2544 N90-24520
Measurement and simulation of widespread mobile radio channel characteristics 20 p2848 N90-26186
TROPOSPHERIC WAVES
NT PLANETARY WAVES
TROUBLESHOOTING
U MAINTENANCE
TROUGHS
Inverted surface troughs accompanying Rocky Mountain lee-side cyclogenesis 06 p0816 N90-14746
Geology of coronae and domal structures on Venus and models of their origin 15 p2191 N90-22513

A case study of explosive cyclogenesis in the eastern Pacific Ocean 14 to 17 December 1987
[AD-A219543] 17 p2426 N90-23824

TRUCKS
DSEP (Dual Shaft Electric Propulsion) operation and maintenance manual for the NVH and TB-2 vehicles: Advanced Dual Shaft Electric Propulsion System technology development program
[DE89-017549] 03 p0420 N90-12411
Autonomous land navigation in a structured environment
[DE90-001625] 07 p0878 N90-15087
Development of an integrated mobile robot system at Carnegie Mellon University: June 1988
[AD-A215955] 10 p1392 N90-18049
LOCSTAR: A satellite radiodetermination system for Europe 17 p2360 N90-23436
Two wheeled lunar dumptruck
[NASA-CR-182840] 17 p2410 N90-23734
Lunar material transport vehicle
[NASA-CR-185929] 18 p2534 N90-24456
Hitching mechanism for lunar dump train
[NASA-CR-183034] 19 p2697 N90-25344
Engineering evaluation testing of the Soleq dual battery van
[DE90-012685] 19 p2698 N90-25354
Proof of principle model for a lunar dumptruck
[NASA-CR-182557] 20 p2869 N90-26323

TRUNCATION (MATHEMATICS)
U APPROXIMATION

TRUNCATION ERRORS
Evaluation of influences of errors involved in orbit propagation of artificial satellites
[INPE-4962-TDL/391] 11 p1466 N90-18441
Adaptive node movement in finite-difference solutions of partial differential equations with applications to gasdynamics, part 1
[UTIAS-333-PT-1] 19 p2750 N90-25622
Adaptive node movement in finite-difference solutions of partial differential equations with applications to gasdynamics, part 2
[UTIAS-333-PT-2] 19 p2750 N90-25623

TRUNKS (LINES)
U TRANSMISSION LINES

TRUNNIONS
U SHAFTS (MACHINE ELEMENTS)

TRUSSES
Shape control of high degree-of-freedom variable geometry trusses 01 p0024 N90-10122
Preliminary design of a large tetrahedral truss/hexagonal heatshield panel aerobrake
[NASA-TM-101612] 01 p0025 N90-10127
Space structures concepts and materials
[NASA-CR-183727] 01 p0025 N90-10128
Test results on conceptual models of the large deployable antenna for mobile communications satellites 02 p0185 N90-11050
Application of matrix correction methods on a plate and a truss structure
[NLR-MP-88042-U] 03 p0359 N90-12056
Performance effects of tie-truss modifications for a 70-meter centerline beam waveguide antenna 04 p0486 N90-12791
Initial test results for the mini-mast 05 p0600 N90-13482
LDR structural experiment definition 05 p0600 N90-13483
Hybrid deployable support truss designs for LDR 05 p0600 N90-13485
Effects of joints in truss structures 05 p0600 N90-13486
Joints in deployable space truss structures 05 p0601 N90-13489
Analysis and testing of axial compression in imperfect slender truss struts
[NASA-TM-4174] 08 p1087 N90-16292
A statistical study of the surface accuracy of a planar truss beam
[NASA-TM-4161] 09 p1235 N90-17171
Support trusses for large precision segmented reflectors: Preliminary design and analysis
[NASA-TM-101560] 11 p1468 N90-18453
Process development and fabrication of space station type aluminum-clad graphite epoxy struts
[NASA-CR-181873] 11 p1468 N90-18454
Component count and preliminary assembly considerations for large space truss structures
[NASA-TM-102604] 13 p1763 N90-20121
Nonlinear and distributed parameter models of the mini-mast truss 14 p1934 N90-21070
A distributed finite-element modeling and control approach for large flexible structures 14 p1934 N90-21071
An air-bearing weight offload system for ground test of heavy LSS structures 14 p1936 N90-21081
Experimental evaluation of active-member control of precision structures 14 p1936 N90-21084
Space truss zero gravity dynamics 14 p1937 N90-21087
In-house experiments in large space structures at the Air Force Wright Aeronautical Laboratories Flight Dynamics Laboratory 14 p1938 N90-21092
Heavily loaded joints for assembling aerobrake support trusses
[NASA-CR-181992] 14 p1939 N90-21099
Integrated modeling and analysis of a space-truss article
[NASA-TM-102615] 14 p1991 N90-21412
Passive shape control of space antennas with determinate truss support structures 15 p2087 N90-21949
Solar Concentrator Advanced Development Program
[NASA-CR-185173] 16 p2250 N90-22834
An inverse kinematics algorithm for a highly redundant variable-geometry-truss manipulator 16 p2288 N90-23033
Control of a flexible planar truss using proof mass actuators 16 p2288 N90-23035
Minimum attainable RMS attitude error using co-located rate sensors 16 p2288 N90-23038
Mini-mast dynamic analysis using the truss-beam model 16 p2297 N90-23087
Tubular space truss structure for SKITTER 2 robot
[NASA-CR-184922] 17 p2384 N90-23580
A cable-rigidized 3D pantograph 18 p2538 N90-24484
A sequentially deployable structure for space applications. Part 2: Engineering model manufacturing and testing 18 p2541 N90-24504
Strut-node joint conjugates for the assembly of semi-permanent or reusable truss structures 18 p2640 N90-25039
Fatigue analysis of mini-mast space truss 18 p2643 N90-25052
Minimizing distortion and internal forces in truss structures by simulated annealing 18 p2644 N90-25055
Expansion and orthogonalization of measured modes for structure identification 18 p2647 N90-25068
Dynamic analysis of space-related linear and non-linear structures
[NASA-TM-103490] 19 p2667 N90-25174
Control structure interaction instrumentation
[AD-A221375] 19 p2693 N90-25320
Overcenter collet space station truss fastener
[NASA-CASE-MSC-21504-1] 21 p2966 N90-26859
Quick connect coupling
[NASA-CASE-MSC-21539-1] 21 p3010 N90-27111
Stochastic structural dynamics for aerospace applications
[AD-A221517] 21 p3013 N90-27133
A new method for a tethered system aided space station assembly 22 p3130 N90-27765
Transformational part-count in layered octahedral-tetrahedral truss configurations
[NASA-TM-102635] 23 p3287 N90-28598
Nonlinear modeling of joint dominated structures
[NASA-CR-4324] 24 p3439 N90-29423

TRYPTOPHAN
Advanced biosensors for amino acid detection
[AD-A214029] 08 p1076 N90-16225

TSUNAMI WAVES
Proceedings of the 21st Joint Meeting of the US-Japan Cooperative Program in Natural Resources Panel Wind and Seismic Effects
[PB90-186826] 21 p3030 N90-27226

TUBE ANODES
Evaluation of a diffusion/trapping model for hydrogen ingress in high strength alloys
[AD-A215528] 09 p1194 N90-16920

TUBE CATHODES
NT PHOTOCATHODES
NT THERMIONIC CATHODES
An analysis of the anomalous high-current cathode emission in pseudospark and back-of-the-cathode lighted thyratron switches
[AD-A215326] 10 p1378 N90-17988

TUBE HEAT EXCHANGERS
A theoretical method for the mechanical calculation of heat exchangers with sliding heads, phase 1 study
[CETIM-110240-PHASE-1] 04 p0502 N90-12896
Laboratory study of the dynamic losses of a single speed, split system air-to-air heat pump having tube and plate fin heat exchangers, 1985 to 1986
[DE90-000970] 07 p0927 N90-15367
Eddy-current inspection of shuttle heat exchanger tube welds
[NASA-CR-186302] 07 p0943 N90-15462
The effect of local thinning on the remaining life of superheater tubes
[VTT-RR-631] 19 p2703 N90-25377

TUBING
U PIPES (TUBES)

TUMBLING MOTION
TALON and CRADLE: Systems for the rescue of tumbling spacecraft and astronauts, a preliminary design 09 p1181 N90-16847
Robot Acting on Moving Bodies (RAMBO): Interaction with tumbling objects 23 p3366 N90-29022

TUMORS
NT CANCER
Reciprocal relationships between the immune and central nervous system
[AD-A221259] 18 p2583 N90-24712

TUNABLE LASERS
Growth and characterization of materials for tunable lasers in the near infrared spectral region
[NASA-CR-185832] 03 p0352 N90-12009
Progress of research on water vapor lidar
[NASA-CR-185970] 03 p0352 N90-12011
Tunable Solid State Lasers conference edition: Tunable Solid State Lasers Topical Meeting
[AD-A212292] 04 p0506 N90-12920
Prospects for wavelength tunable lasers based on vacancy defects in alkaline-earth oxides
[DE90-001078] 06 p0789 N90-14592
Development of tunable excimer lasers
[AD-A213521] 07 p0936 N90-15421
Development of glass-ceramic lasers
[AD-A214146] 07 p0936 N90-15423
Computer simulation of laser plasma interaction
[DE90-002828] 07 p0994 N90-15748
Spectroscopic and laser properties of Cr:LiCaAlF6 and Cr:LiSrAlF6 crystals
[DE90-000783] 07 p0998 N90-15770
Absorption experiments on electron-beam pumped rare gases
[DE90-006504] 11 p1515 N90-18722
Tunable XeCl-laser featuring high spectral luminance 16 p2311 N90-23167
A tunable, continuous wave, thulium-doped, solid state laser cross-reference to related application
[AD-D014558] 22 p3180 N90-28045
Tunable CW single-frequency source for injection seeding 2-micrometer lasers
[AD-A223979] 23 p3331 N90-28834

TUNGSTEN
Reactive ion etching of sputtered silicon carbide and tungsten thin films for device applications
[AD-A211711] 03 p0325 N90-11847
Scintillating fiber ribbon - tungsten calorimeter
[DE89-016705] 03 p0350 N90-12001
Structural stability of heat treated W/B4C multilayers
[DE90-005322] 09 p1188 N90-16884
Raman spectroscopic analysis of impregnated cathodes
[AD-A214559] 09 p1190 N90-16895
Fractographic analysis of long rod penetrator-armor ceramic interactions
[AD-A215172] 09 p1197 N90-16938
Relationship of fragment size to normalized spall strength for materials
[DE90-004165] 09 p1231 N90-17140
Structure and reactivity of model thin film catalysts
[DE90-007365] 11 p1485 N90-18546
Method of making a long life high current density cathode from tungsten and iridium powders using a quarternary compound as the impregnant
[AD-D014425] 14 p1958 N90-21211
Method of making a cathode from tungsten powder
[AD-D014434] 15 p2069 N90-21850
Experimental study of the optical constants of metals at high temperatures
[DE90-014732] 23 p3310 N90-28719

TUNGSTEN ALLOYS
Strain aging in tungsten-heavy alloys
[AD-A211166] 01 p0046 N90-10259
Freeze-dried processing of tungsten heavy alloys
[DE89-015171] 02 p0197 N90-11122
Deformation and fracture of TiAl + W at elevated temperatures
[DE90-006490] 12 p1628 N90-19356
High temperature fatigue behavior of tungsten copper composites
[NASA-TM-102404] 14 p1946 N90-21138
Strengthening mechanisms of tungsten powder reinforced uranium
[DE90-009331] 14 p1947 N90-21144
Microstructure and impurity effects on tungsten heavy alloys
[AD-A224220] 23 p3311 N90-28728

TUNGSTEN CARBIDES
Friction and wear of tungsten carbides with nitrogen ion implants
[ECL-89-19] 17 p2371 N90-23496

TUNGSTEN COMPOUNDS
NT TUNGSTEN CARBIDES
NT TUNGSTEN OXIDES
TUNGSTEN INERT GAS WELDING
U GAS TUNGSTEN ARC WELDING
TUNGSTEN OXIDES
Model catalytic oxidation studies using supported monometallic and heterobimetallic oxides
[DE90-009984] 16 p2220 N90-22664
TUNING
Analytical study of mistuning/friction/aerodynamics interaction in a bladed disk assembly
[AD-A211139] 02 p0156 N90-10893
Effects of mistuning and matrix structure on the topology of frequency response curves
[NASA-TM-102290] 03 p0357 N90-12041
Airborne/spaceborne pulsed power source
[AD-A211762] 04 p0495 N90-12850
Advances in SIS receiver technology
05 p0597 N90-13466
The use of broadcast signals for passive sensing in automated HF communication systems
06 p0762 N90-14433
Software to characterize tuning fork resonators used in the Quartz Digital Accelerometer
[DE90-007913] 14 p1983 N90-21363
Design of sharp cutoff filters with low quality factors
[AD-A223130] 21 p3000 N90-27051
TUNNEL RESISTORS
U ELECTRON TUNNELING
U RESISTORS
TURBINE BLADES
Large scale prop-fan structural design study. Volume 1: Initial concepts
[NASA-CR-174992] 01 p0010 N90-10043
Large scale prop-fan structural design study. Volume 2: Preliminary design of SR-7
[NASA-CR-174993] 01 p0010 N90-10044
Analytical study of mistuning/friction/aerodynamics interaction in a bladed disk assembly
[AD-A211139] 02 p0156 N90-10893
Heat transfer to throat tubes in a square-chambered rocket engine at the NASA Lewis Research Center
[NASA-TM-102336] 02 p0189 N90-11082
Model 0A wind turbine generator FMEA
[NASA-TM-102378] 03 p0356 N90-12034
Effects of mistuning and matrix structure on the topology of frequency response curves
[NASA-TM-102290] 03 p0357 N90-12041
User's guide for a personal computer model of turbulence at a wind turbine rotor
[DE89-017753] 03 p0366 N90-12095
A computer integrated approach to dimensional inspection
[PNR90596] 04 p0456 N90-12611
Three D flows in turbine blade rows
05 p0641 N90-13739
Flows with tip leakage 05 p0641 N90-13740
Turbulent wind at the equatorial segment of an operating Darrieus wind turbine blade
[DE90-002672] 06 p0807 N90-14698
Inclusion of nonlinear aerodynamics in the FLAP code
[DE89-009507] 07 p0954 N90-15519
Prediction of stochastic blade loads for three-bladed, rigid-hub rotors
[DE89-009508] 07 p0954 N90-15520
Aerodynamic design and initial performance measurements for the SANDIA 34-metre diameter vertical-axis wind turbine
[DE90-002574] 07 p0955 N90-15523
Aerodynamic and heat transfer measurements on blading for a high rim-speed transonic turbine
[RAE-TM-P-1151] 08 p1024 N90-15920
The use of piezofoil sensors for the determination of the unsteady pressure distribution at the surface of a gas turbine blade 08 p1080 N90-16250
Performance predictions for an intermediate-sized VAWT based on performance of the 34-m VAWT test bed
[DE90-002835] 08 p1096 N90-16345
Wake interaction effects on the transition process on turbine blades
[AD-A214492] 09 p1168 N90-16759
Turbine blade data acquisition system user's guide
[AD-A214986] 09 p1169 N90-16763
Turbine blade data acquisition system software reference
[AD-A215134] 09 p1169 N90-16764
Turbine blade data acquisition system technical reference
[AD-A215135] 09 p1169 N90-16765
Turbulence scale effects on heat transfer in a linear turbine cascade
[AD-A216222] 10 p1321 N90-17637
Turbulence structure resulting from interaction between an embedded vortex and wall jet
[AD-A215702] 10 p1383 N90-18004
Aerodynamic testing of a rotating wind turbine blade
[DE90-000312] 11 p1451 N90-18362
A comparison of flutter calculations based on eigenvalue and energy method 11 p1459 N90-18406
Unsteady aerodynamic phenomena in a simulated wake and shock wave passing experiment
11 p1461 N90-18414
Time-dependent measurements on vibrating annular turbine cascades under various steady state conditions
11 p1463 N90-18424
Measurements of surface pressures on an operating vertical-axis wind turbine
[DE90-005722] 11 p1529 N90-18805
Influence of friction and separation phenomena on the dynamic blade loading of transonic turbine cascades
[MITT-88-04] 12 p1605 N90-19235
The influence of a wall function on turbine blade heat transfer prediction 12 p1640 N90-19421
Heat transfer near the entrance to a film cooling hole in a gas turbine blade
[AD-A217396] 13 p1757 N90-20089
A comparison of two-and three-dimensional S809 airfoil properties for rough and smooth HAWT (Horizontal-Axis Wind Tunnel) rotor operation
[DE89-009512] 13 p1827 N90-20492
Innovative turbine concepts for open-cycle OTEC (Ocean Thermal Energy Conversion)
[DE90-000315] 13 p1827 N90-20493
Subsonic and transonic blade design by means of analysis codes 14 p1917 N90-20985
Calculation of the three dimensional turbulent flow in a linear turbine blade 14 p1924 N90-21021
Calculation of the secondary flow in an axial turbine
14 p1924 N90-21022
Losses in the tip-leakage flow of a planar cascade of turbine blades 14 p1925 N90-21027
Navier-Stokes analysis of turbine blade heat transfer
[NASA-TM-102496] 14 p1972 N90-21300
Probabilistic analysis of bladed turbine disks and the effect of mistuning
[NASA-TM-102564] 15 p2072 N90-21871
Practical nonlinear simulation of rotating machinery dynamics with application to turbine blade rubbing
15 p2104 N90-22038
Aerodynamics of a full-scale, non rotating wind turbine blade under natural wind conditions
[RISOE-M-2768] 15 p2123 N90-22144
Probabilistic structural analysis of aerospace components using NESSUS
[NASA-TM-102324] 16 p2248 N90-22823
Heat transfer and pressure measurements for the SSME fuel-side turbopump
[NASA-CR-184928] 17 p2355 N90-23405
Aerodynamic pressure measurements on a rotating wind turbine blade
[DE90-000327] 18 p2494 N90-24256
Calculation of the aeroelastic blade stabilization with linearized process
[MITT-87-01] 18 p2497 N90-24272
Wind energy program summary. Volume 2: Research summaries
[DE89-009480] 19 p2710 N90-25423
Turbine blade heat transfer coefficient evaluation by modified version of STAN5. Comparison with experimental data
[ETN-90-97283] 20 p2813 N90-26008
Calculation of temperature distribution in various turbine blades using a boundary-fitted coordinate transformation method 23 p3278 N90-28550
Flow coupling between a rotor and a stator in turbomachinery
[AD-A223882] 23 p3282 N90-28572
Micromechanics of cyclic deformation in SSME turbopump blade materials 23 p3295 N90-28641
Constitutive and life modeling of single crystal blade alloys for root attachment analysis
23 p3296 N90-28643
Structural response of SSME turbine blade airfoils
23 p3297 N90-28649
Durability of thermal barrier coatings in a high heat flux environment 23 p3297 N90-28651
Thermal analysis of thermal barrier coatings in a high heat flux environment 23 p3297 N90-28652
Vacuum application of thermal barrier plasma coatings
23 p3298 N90-28653
Application of advanced coating techniques to rocket engine components 23 p3298 N90-28654
The effects of a compressor rebuild on gas turbine engine performance: Final results
23 p3306 N90-28701
Comparison of wind tunnel airfoil performance data with wind turbine blade data
[DE90-000343] 24 p3418 N90-29308
Further studies of turbulence structure resulting from interactions between embedded vortices and wall jets at high blowing ratios
[AD-A223296] 24 p3468 N90-29593
TURBINE ENGINES
NT GAS TURBINE ENGINES
NT JET ENGINES
NT RAMJET ENGINES
NT SUPERSONIC COMBUSTION RAMJET ENGINES
NT TURBOFAN ENGINES
NT TURBOJET ENGINES
NT TURBOPROP ENGINES
NT TURBORAMJET ENGINES
Dynamic instability characteristics of aircraft turbine engine combustors 01 p0036 N90-10195
A computer integrated approach to dimensional inspection
[PNR90596] 04 p0456 N90-12611
Advanced Turbine Technology Applications Project (ATTAP)
[NASA-CR-185109] 05 p0709 N90-14153
Fluid flow analysis of the SSME high pressure fuel and oxidizer turbine coolant systems
[NASA-CR-183736] 06 p0734 N90-14277
Aircraft performance enhancement with active compressor stabilization
[AD-A213652] 07 p0879 N90-15097
Characterization of chemicals on engine exhaust particles
[AD-A213566] 07 p0882 N90-15106
Improved Thermo-Oxidative-Deposition screening tests for turbine lubricants
[AD-A217795] 14 p1954 N90-21188
Effect of vane twist on the performance of dome swirlers for gas turbine airblast atomizers
[NASA-TM-103195] 19 p2688 N90-25289
The role of NDI in the certification of turbine engine components
[PNR90629] 20 p2874 N90-26349
Engine testing of thermographic phosphors
[DE90-013269] 22 p3182 N90-28059
Energy Efficient Engine: Flight propulsion system final design and analysis
[NASA-CR-168219] 23 p3279 N90-28558
Energy Efficient Engine core design and performance report
[NASA-CR-168069] 23 p3279 N90-28559
NASA/GE Energy Efficient Engine low pressure turbine scaled test vehicle performance report
[NASA-CR-168290] 23 p3280 N90-28563
TURBINE EXHAUST NOZZLES
Computational fluid dynamics 3-D analysis for advanced transonic turbine design
[ETN-90-97282] 20 p2864 N90-26291
Device for the dilution of hot exhaust jets
[ETN-90-97435] 22 p3120 N90-27723
TURBINE INSTRUMENTS
Combustion instrumentation 20 p2811 N90-25996
TURBINE PUMPS
SSME Alternate Turbopump Development Program: Design verification specification for high-pressure fuel turbopump
[NASA-CR-183676] 01 p0008 N90-10033
SSME structural dynamic model development
[NASA-CR-183671] 04 p0463 N90-12650
Cryostatless high temperature supercurrent bearings for rocket engine turbopumps
[NASA-CR-183807] 04 p0509 N90-12935
The 59th Shock and Vibration Symposium, volume 3
[AD-A214580] 10 p1395 N90-18066
A parametric heat transfer study for cryogenic ball bearings in SSME HPOTP 12 p1635 N90-19397
Investigation of SSME alternate high pressure fuel turbopump lift-off seal fluid and structural dynamic interaction 12 p1636 N90-19400
Probabilistic modeling for simulation of aerodynamic uncertainties in propulsion systems
[NASA-TM-102472] 14 p1927 N90-21036
Experimental evaluation of a tuned electromagnetic damper for vibration control of cryogenic turbopump rotors
[NASA-TP-3005] 17 p2354 N90-23403
Heat transfer and pressure measurements for the SSME fuel-side turbopump
[NASA-CR-184928] 17 p2355 N90-23405
The effects of Reynolds number, rotor incidence angle, and surface roughness on the heat transfer distribution in a large-scale turbine rotor passage
[NASA-CR-183891] 17 p2410 N90-23731
Reusable rocket engine turbopump health monitoring system, part 3
[NASA-CR-182294] 20 p2869 N90-26320
Evolution and use of combined mechanical and thermal codes for cryogenic turbopump bearings
23 p3291 N90-28618

Determination of the SSME high pressure oxidizer turbopump bearing temperature
23 p3291 N90-28619
Cryogenic, high speed, turbopump bearing cooling requirements
23 p3291 N90-28620
Pool boiling from rotating and stationary spheres in liquid nitrogen
23 p3292 N90-28621
Bearing optimization for SSME HPOTP application
23 p3292 N90-28622
Pratt and Whitney cryogenic turbopump bearing experience
23 p3292 N90-28624
Injector element characterization methodology
23 p3294 N90-28634
Micromechanics of cyclic deformation in SSME turbopump blade materials
23 p3295 N90-28641
Turbomachinery rotor forces
[NASA-CR-183779] 23 p3334 N90-28852

TURBINE WHEELS
Advanced technologies impact on compressor design and development: A perspective
[NASA-TM-102341] 02 p0156 N90-10891
Independent Orbiter Assessment (IOA): Weibull analysis report
[NASA-CR-185534] 02 p0168 N90-10948
Defects in monoblock cast turbine wheels
11 p1458 N90-18400
Probabilistic analysis of bladed turbine disks and the effect of mistuning
[NASA-TM-102564] 15 p2072 N90-21871

TURBINES
NT AXIAL FLOW TURBINES
NT GAS TURBINES
NT SHROUDED TURBINES
NT STEAM TURBINES
NT SUPERSONIC TURBINES
NT TWO STAGE TURBINES
NT WIND TURBINES
Advanced Turbine Technology Applications Program, (ATTAP)
[DE89-016067] 02 p0230 N90-11318
An analysis of the viscous flow through a compact radial turbine by the average passage approach
[NASA-TM-102471] 06 p0720 N90-14206
Turbulence scale effects on heat transfer in a linear turbine cascade
[AD-A216222] 10 p1321 N90-17637
Heat transfer and pressure measurements for the SSME fuel-side turbopump
[NASA-CR-184928] 17 p2355 N90-23405
A simulation code for turbocompound diesel engines
[IAR-89-26] 19 p2697 N90-25348
Decay of secondary flow and the associated loss variation downstream of an annual turbine stator cascade
[DE90-505520] 20 p2809 N90-25984
A heat transfer analysis for rough turbine airfoils
[AD-A221942] 21 p2960 N90-26831
Scandia-stabilized zirconia coating for composites
[AD-D014550] 22 p3160 N90-27917
Flow coupling between a rotor and a stator in turbomachinery
[AD-A223882] 23 p3282 N90-28572
Transonic 3-D Euler analysis of flows around fanjet engine and TPS (Turbine Powered Simulator). Comparison with wind tunnel experiment, evaluation of TPS testing method and 3-D flow
[NAL-TR-1045] 24 p3421 N90-29327

TURBOCHARGERS
U SUPERCHARGERS
U TURBOCOMPRESSORS

TURBOCOMPRESSORS
Improved silicon carbide for advanced heat engines
[NASA-CR-180831] 01 p0051 N90-10293
Dynamic analysis of rotors under interference rubs
02 p0229 N90-11312
Coatings for gas turbine compressors
[NLR-MP-88045-U] 03 p0308 N90-11750
The development of a high response aerodynamic wedge probe and use on a high-speed research compressor
[PNR90598] 04 p0456 N90-12613
Blading design for multi-storage HP compressor
[PNR90602] 04 p0456 N90-12616
Preliminary experience with high response pressure measurements in a multistage, high speed compressor
[RAE-TM-P-1141] 04 p0457 N90-12619
Review and evaluation of a turbomachinery throughflow finite element code
[AD-A213058] 05 p0650 N90-13787
Temporally and spatially resolved flow in a two-stage axial compressor. Part 2: Computational assessment
[NASA-TM-102273] 06 p0726 N90-14236
Performance of a highly-loaded HP compressor
[RAE-TM-P-1149] 08 p1024 N90-15919
Aerodynamic study on forced vibrations on stator rows of axial compressors
11 p1460 N90-18412
Numerical prediction of axial turbine stage aerodynamics
11 p1461 N90-18416
Stall and recovery in multistage axial flow compressors
11 p1464 N90-18429
Low cost Brayton engine for gas-fired cogeneration system, phase 1
[PB90-127457] 12 p1681 N90-19655
The effects of compressor endwall flow on airfoil incidence and deviation
14 p1922 N90-21011
A study on secondary flow and spanwise mixing in axial flow compressors
14 p1923 N90-21012
Secondary flow calculations for axial and radial compressors
14 p1925 N90-21024
Forcing function effects on rotor row unsteady aerodynamic response in a multistage compressor
16 p2196 N90-22536
Computational and experimental investigations of rotating stall in compressor cascades
16 p2201 N90-22565
A simulation code for turbocompound diesel engines
[IAR-89-26] 19 p2697 N90-25348
Application of high performance metals in gas turbine engines
[PNR90640] 20 p2811 N90-25999
Prediction and measurement of rotor blade/stator vane dynamic characteristics of a modern aero-engine axial compressor
[PNR90667] 20 p2812 N90-26002
Development of a software package for automatic data acquisition, analysis, and controls in an axial flow compressor test rig
[PD-PR-8910] 24 p3524 N90-29926

TURBOCONVERTERS
U TURBOGENERATORS

TURBOELECTRIC CONVERSION
U TURBOGENERATORS

TURBOFAN AIRCRAFT
NT BOEING 727 AIRCRAFT
NT BOEING 737 AIRCRAFT
NT BOEING 757 AIRCRAFT
NT C-141 AIRCRAFT
NT CONCORDE AIRCRAFT
NT F-111 AIRCRAFT
Sound propagation elements in evaluation of en route noise of advanced turbofan aircraft
18 p2609 N90-24861
Energy efficient engine program technology benefit/cost study. Volume 1: Executive summary
[NASA-CR-174766-VOL-1] 23 p3280 N90-28564
Energy efficient engine program technology benefit/cost study, volume 2
[NASA-CR-174766-VOL-2] 23 p3280 N90-28565

TURBOFAN ENGINES
PMR graphite engine duct development
[NASA-CR-182228] 01 p0008 N90-10037
Full scale technology demonstration of a modern counterrotating unducted fan engine concept: Component test
[NASA-CR-180868] 01 p0010 N90-10047
Full scale technology demonstration of a modern counterrotating unducted fan engine concept. Design report
[NASA-CR-180867] 01 p0010 N90-10048
Full scale technology demonstration of a modern counterrotating unducted fan engine concept. Engine test
[NASA-CR-180869] 01 p0011 N90-10049
New energy conversion techniques in space, applicable to propulsion
[AIAA-79-1338] 01 p0028 N90-10145
Characteristics of combustion driven pressure oscillations in advanced turbo-fan engines with afterburner
01 p0035 N90-10194
Advanced technologies impact on compressor design and development: A perspective
[NASA-TM-102341] 02 p0156 N90-10891
STOVL propulsion system volume dynamics approximations
[NASA-TM-102397] 03 p0306 N90-11740
Measurement effects on the calculation of in-flight thrust for an F404 turbofan engine
[NASA-TM-4140] 03 p0307 N90-11741
Near-field noise predictions of an aircraft in cruise
04 p0443 N90-12538
The 757 NLF glove flight test results
04 p0445 N90-12548
What should be done with those noisy old aircraft
[PNR90562] 04 p0452 N90-12593
Designing for reliable and low maintenance cost aero engines
[PNR90570] 04 p0455 N90-12604
Blading design for multi-storage HP compressor
[PNR90602] 04 p0456 N90-12616
Real-time simulation of an F110/STOVL turbofan engine
[NASA-TM-102409] 04 p0457 N90-12618
The commercial aircraft noise problem
[PNR90577] 04 p0550 N90-13203
Advanced detection, isolation, and accommodation of sensor failures in turbofan engines: Real-time microcomputer implementation
[NASA-TP-2925] 07 p0883 N90-15112
Altitude testing of the 2D V/STOL ADEN demonstrator on an F404 engine
[NASA-CR-174824] 10 p1321 N90-17638
In-line wear monitor
[AD-A217799] 13 p1757 N90-20091
Supersonic through-flow fan engine and aircraft mission performance
[NASA-TM-102304] 14 p1927 N90-21038
Exhaust environment measurements of a turbofan engine equipped with an afterburner and 2D nozzle
[NASA-CR-4289] 15 p2052 N90-21760
A/F32T-9 large turbo fan engine enclosed noise suppressor system (T-9 NSS), exterior far-field and interior noise, McConnell AFB, Kansas
[AD-A220535] 17 p2354 N90-23402
Design of a low cost short takeoff-vertical landing export fighter/attack aircraft
[NASA-CR-186658] 19 p2659 N90-25132
Effective optimal control of a fighter aircraft engine
23 p3277 N90-28548
Energy Efficient Engine combustor test hardware detailed design report
[NASA-CR-168301] 23 p3279 N90-28554
Energy Efficient Engine (E3) combustion system component technology performance report
[NASA-CR-168274] 23 p3279 N90-28555
Energy Efficient Engine acoustic supporting technology report
[NASA-CR-174834] 23 p3279 N90-28557
Energy Efficient Engine program advanced turbofan nacelle definition study
[NASA-CR-174942] 23 p3280 N90-28560
Energy Efficient Engine: Control system component performance report
[NASA-CR-174851] 23 p3280 N90-28562
Energy efficient engine program technology benefit/cost study. Volume 1: Executive summary
[NASA-CR-174766-VOL-1] 23 p3280 N90-28564
Energy efficient engine program technology benefit/cost study, volume 2
[NASA-CR-174766-VOL-2] 23 p3280 N90-28565

TURBOGENERATORS
Expert system for fault diagnostics of rotating machines
[DE89-766980] 06 p0793 N90-14621
The role of input weighting and bounding in the characteristic GPC method
[OUEL-1762/89] 15 p2158 N90-22328

TURBOJET AIRCRAFT
U JET AIRCRAFT

TURBOJET ENGINE CONTROL
An experimental study of fault propagation in a jet-engine controller
[NASA-CR-181335] 17 p2354 N90-23401

TURBOJET ENGINES
NT TURBOFAN ENGINES
NT TURBOPROP ENGINES
NT TURBORAMJET ENGINES
An open-loop transient thermodynamic model of the Couguar turbojet
[AD-A211774] 03 p0307 N90-11745
Experimental study of velocity fields and turbulence in a turbojet engine
[ISL-CO-231/88] 09 p1169 N90-16766
The implementation and operation of a variable-response electronic throttle control system for a TF-104G aircraft
[NASA-TM-101696] 13 p1756 N90-20086
On the use of external burning to reduce aerospace vehicle transonic drag
[NASA-TM-103107] 15 p2052 N90-21782
Turbulent combustion modeling for turbo-jet combustion chambers
20 p2811 N90-25993
Comparative Engine Performance Measurements
[AGARD-LS-169] 22 p3118 N90-27711
Comparison of ground-level test cells and ground-level to altitude test cells
22 p3119 N90-27716

TURBOMACHINE BLADES
NT COMPRESSOR BLADES
NT ROTOR BLADES (TURBOMACHINERY)
NT STATOR BLADES
NT TURBINE BLADES
Composite Blade Structural Analyzer (COBSTRAN) theoretical/programmer's manual
[NASA-TM-101958] 01 p0033 N90-10181
Advanced clearance control systems --- blade tips
[PNR90553] 04 p0454 N90-12601

Automation and extension of LDV (Laser-Doppler Velocimetry) measurements of off-design flow in a subsonic cascade wind tunnel
[AD-A216627] 11 p1506 N90-18670
Unsteady flow phenomena in turbomachines
[AD-A218370] 17 p2402 N90-23680

TURBOMACHINERY
NT AXIAL FLOW TURBINES
NT CENTRIFUGAL COMPRESSORS
NT CENTRIFUGAL PUMPS
NT GAS TURBINES
NT SHROUDED TURBINES
NT STEAM TURBINES
NT SUPERSONIC TURBINES
NT TURBINE PUMPS
NT TURBINES
NT TURBOCOMPRESSORS
NT TURBOGENERATORS
NT TWO STAGE TURBINES
NT WIND TURBINES
Data acquisition in aerodynamic research
05 p0574 N90-13340
Application of a two-dimensional unsteady viscous analysis code to a supersonic throughflow fan stage
[NASA-TM-4141] 05 p0581 N90-13387
Numerical Methods for Flows in Turbomachinery, volume 1
[VKI-LS-1989-06-VOL-1] 05 p0640 N90-13735
Numerical Methods for Flows in Turbomachinery, volume 2
[VKI-LS-1989-06-VOL-2] 05 p0641 N90-13741
Numerical methods for unsteady turbomachinery flow
05 p0641 N90-13743
Probabilistic finite element analysis of dynamic structural response
[AD-A213249] 05 p0650 N90-13789
An interactive grid generation procedure for axial and radial flow turbomachinery
[NASA-CR-185167] 05 p0682 N90-13968
Advanced 3-D CFD algorithm for turbomachinery
06 p0725 N90-14233
An experimental, analytical, and computational investigation of turbomachinery rotor flow fields
07 p0926 N90-15360
Computation of broadband mixing noise from turbomachinery
[AD-A214448] 07 p0989 N90-15713
Unsteady Aerodynamic Phenomena in Turbomachines
[AGARD-CP-468] 11 p1459 N90-18405
Numerical investigation of unsteady flow in oscillating turbine and compressor cascades
11 p1459 N90-18407
Numerical simulation of three-dimensional unsteady flows in turbomachines 11 p1461 N90-18417
Numerical investigations of heat transfer and flow rates in rotating cavities. Simulation of the movement generated by wall temperature gradients, by source-sink mass flows or by the differential rotation of the walls, under the influence or coriolis and centrifugal forces
[ETN-90-96253] 11 p1510 N90-18695
An applicational process for dynamic balancing of turbomachinery shafting
[NASA-TM-102537] 13 p1810 N90-20392
Rotordynamic analysis with shell elements for the transfer matrix method
[AD-A217455] 13 p1817 N90-20434
GRID2D/3D: A computer program for generating grid systems in complex-shaped two- and three-dimensional spatial domains. Part 2: User's manual and program listing
[NASA-TM-102454] 13 p1867 N90-20708
Computational Methods for Aerodynamic Design (Inverse) and Optimization
[AGARD-CP-463] 14 p1916 N90-20976
Numerical method for designing 3D turbomachinery blade rows 14 p1918 N90-20990
Secondary Flows in Turbomachines
[AGARD-CP-469] 14 p1922 N90-21009
Generation and decay of secondary flows and their impact on aerodynamic performance of modern turbomachinery components 14 p1925 N90-21023
The numerical simulation of multistage turbomachinery flows 14 p1925 N90-21025
Mesh generation for flow computation in turbomachine
15 p2094 N90-21981
Experimental investigation of the effect of cavitation on the rotordynamic forces on a whirling centrifugal pump impeller 15 p2105 N90-22039
The Shock and Vibration Digest, volume 21, no. 2
15 p2109 N90-22059
Fundamental hydrodynamics research
[AD-A219179] 16 p2238 N90-22766
A process for the measurement of the unsteady three dimensional stream vectors in turbomachines
[MITT-89-01] 17 p2405 N90-23702
Rotating flow in radial turbomachinery
[AD-A222885] 21 p3004 N90-27073
Calculation of service life of turbomachine components 22 p3117 N90-27706
Computer code for predicting coolant flow and heat transfer in turbomachinery
[NASA-TP-2985] 22 p3120 N90-27722
Turbulent thermal convection in rotating cavities, volume 1
[ETN-90-97433] 22 p3174 N90-28011
Turbulent thermal convection in rotating cavities, volume 2
[ETN-90-97434] 22 p3174 N90-28012

TURBOPROP AIRCRAFT
NT C-130 AIRCRAFT
P-180 AVANTI: Project and flight test program comprehensive overview 02 p0151 N90-10863
Low-speed wind-tunnel investigation of the flight dynamic characteristics of an advanced turboprop business/commuter aircraft configuration
[NASA-TP-2982] 12 p1606 N90-19239
Noise of a simulated installed model counterrotation propeller at angle-of-attack and takeoff/approach conditions
[NASA-TM-102440] 13 p1881 N90-20794
En route noise of turboprop aircraft and their acceptability: Report of tests 18 p2609 N90-24858
En route noise of two turboprop aircraft
[DLR-MITT-89-18] 18 p2609 N90-24859
High speed turboprop aeroacoustic study (counterrotation). Volume 1: Model development
[NASA-CR-185241] 20 p2923 N90-26633

TURBOPROP ENGINES
Large-scale Advanced Prop-fan (LAP) high speed wind tunnel test report
[NASA-CR-182125] 01 p0010 N90-10045
Full scale technology demonstration of a modern counterrotating unducted fan engine concept. Design report
[NASA-CR-180867] 01 p0010 N90-10048
Propfan Test Assessment (PTA)
[NASA-CR-185138] 03 p0306 N90-11739
UHB demonstrator interior noise control flight tests and analysis
[NASA-CR-181897] 04 p0549 N90-13198
User's guide to PMESH: A grid-generation program for single-rotation and counterrotation advanced turboprops
[NASA-CR-185156] 06 p0823 N90-14783
The Shock and Vibration Digest, volume 21, no. 6
15 p2163 N90-22363
Noise transmission into propeller-driven airplanes
15 p2163 N90-22364
Advanced gearbox technology
[NASA-CR-179625] 18 p2498 N90-24274

TURBOPUMPS
U TURBINE PUMPS

TURBORAMJET ENGINES
Progress in airbreathing combined engines for future European launcher 09 p1177 N90-16817
Saenger propulsion system options
09 p1177 N90-16818
Parametric assessment of propulsion system mass for airbreathing launcher configurations
09 p1177 N90-16819

TURBOROTORS
U TURBINE WHEELS

TURBOSHAFTS
Development and testing of a contactless static/dynamic shaft seal with little sealing gas requirement
[KFK-4599] 05 p0652 N90-13802
The development of a T53-L11 engine computer model
[AD-A214533] 09 p1168 N90-16760

TURBULENCE
NT ATMOSPHERIC TURBULENCE
NT CLEAR AIR TURBULENCE
NT GUSTS
NT HOMOGENEOUS TURBULENCE
NT ISOTROPIC TURBULENCE
NT LOW TURBULENCE
NT MAGNETOHYDRODYNAMIC TURBULENCE
NT PLASMA TURBULENCE
Observations of spherical-wave scintillation in strong refractive-index turbulence
[PB89-124747] 01 p0062 N90-10355
Bifurcations in Poiseuille flow and wall turbulence
01 p0065 N90-10370
Control and modification of turbulence
01 p0066 N90-10377
Turbulence management: Application aspects
01 p0066 N90-10378
A comparison of wind turbulence simulation models for stochastic loads analysis for horizontal-axis wind turbines
[DE89-009442] 01 p0083 N90-10473
Premixed turbulent flame propagation
[AD-A211489] 03 p0324 N90-11841
Computational methods for complex flowfields
[AD-A211485] 03 p0347 N90-11983
Low level remote sensing: Orographic winds
03 p0361 N90-12066
User's guide for a personal computer model of turbulence at a wind turbine rotor
[DE89-017753] 03 p0366 N90-12095
Coherency properties of strong Langmuir turbulence
[DE89-009290] 03 p0371 N90-12119
Experimental study of homogeneous turbulence submitted to rotational effects
[ONERA-RSF-10/1145-AY-164A]
04 p0502 N90-12894
Application of large eddy interaction model to a mixing layer
[NASA-CR-185123] 05 p0572 N90-13328
Two-dimensional analysis of two-phase reacting flow in a firing direct-injection diesel engine
[NASA-TM-102069] 05 p0582 N90-13392
Effect of spatial resolution on apparent sensitivity to initial conditions of a decaying flow as it becomes turbulent
[NASA-TM-102377] 05 p0638 N90-13719
Numerical modeling of supersonic turbulent reacting free shear layers 06 p0719 N90-14197
A one equation turbulence model for transonic airfoils
06 p0719 N90-14199
Fluid-particle interaction in solid-liquid two-phase grid turbulence 06 p0773 N90-14496
The analysis and modeling of dilatational terms in compressible turbulence
[NASA-CR-181959] 06 p0776 N90-14513
Aspects of field theory related to the Zakharov problem 06 p0783 N90-14551
Statistics of two-color laser beam propagation in the turbulent atmosphere (spectral correlation)
[PB89-236699] 06 p0787 N90-14581
An initial look at the dynamics of the microscale flow field within a large wind farm in response to variations in the natural inflow
[DE89-009501] 06 p0804 N90-14682
Convective boundary layer and modeling of dispersion
06 p0813 N90-14731
Systems for airborne wind and turbulence measurement 07 p0869 N90-15046
Influence of windshear, downdraft and turbulence on flight safety 07 p0870 N90-15048
Dense-spray properties: Structure and turbulence modulation
[AD-A213671] 07 p0931 N90-15387
Inclusion of nonlinear aerodynamics in the FLAP code
[DE89-009507] 07 p0954 N90-15519
Turbulence spectral widths view angle independence as observed by Doppler radar
[DOT/FAA/SA-89/2] 07 p0963 N90-15566
Specification for evaporation duct height calculations
[AD-A213841] 07 p0964 N90-15570
A numerical and experimental investigation of multiple shock wave/turbulent boundary layer interactions in a rectanular duct 08 p1062 N90-16141
Vorticity amplification in nonorthogonal stagnation flow
08 p1064 N90-16152
The response of the atmospheric convective boundary layer to surface inhomogeneities
08 p1100 N90-16369
Turbulent stripping of interstellar clouds by inieraction with supernova remnants
[DE90-003622] 08 p1152 N90-16674
Turbulent heat and momentum transfer in recirculating and impinging flows 09 p1215 N90-17043
Special Course on Three-Dimensional Supersonic/Hypersonic Flows Including Separation
[AGARD-R-764] 10 p1308 N90-17565
Some Navier-Stokes calculations for the CAST-10 airfoil 10 p1324 N90-17651
Anomalous particle diffusion through a magnetic picket fence
[INPE-4841-PRE/1470] 10 p1433 N90-18270
Fluidization mechanisms in slurry flow
[DE90-006497] 11 p1509 N90-18691
Vertical axis wind turbine turbulent response model. Part 2: Response of Sandia National laboratories' 34-meter VAWT with aeroelastic effects
[DE90-005721] 11 p1529 N90-18804
Carrier wing profile in nonstationary current
[ETN-90-95368] 12 p1600 N90-19208
Overview of recent results from the Advanced Toroidal Facility
[DE90-005673] 12 p1716 N90-19853
Mark 3 interferometer
[AD-A217188] 13 p1902 N90-20912
Stereopsis cueing effects on hover-in-turbulence performance in a simulated rotorcraft
[NASA-TP-2980] 14 p1921 N90-21004

LDV measurements and the flow analysis in the vortex region of a radial inflow turbine
14 p1922 N90-21007
Secondary flows and Reynolds stress distributions downstream of a turbine cascade at different expansion ratios 14 p1923 N90-21015
Numerical simulations of the cloud-capped marine boundary layer 14 p2008 N90-21506
A self-consistent theory of radial transport of field-aligned current by microturbulence
[DE90-007920] 14 p2028 N90-21631
Dynamics of cavitons in strong Langmuir turbulence
[DE90-008918] 14 p2029 N90-21633
Transition from resistive-g to eta-i driven turbulence in stellarator systems
[DE90-009382] 14 p2030 N90-21641
Numerical investigation of some control methods for 3-D turbulent interactions due to sharp fins
15 p2053 N90-21764
Studies on reactive flows 15 p2066 N90-21831
Fire propagation in concurrent flows
[PB90-151754] 15 p2066 N90-21834
Scintillation of millimeter-wave intensity and phase caused by turbulence and precipitation
15 p2080 N90-21912
Millimetre-wave propagation in the evaporation duct
15 p2084 N90-21929
Lidar measurement of concentration and turbulence in battlefield obscurants 15 p2084 N90-21931
An experimental investigation of mixing in buoyant flows 15 p2090 N90-21963
An investigation of turbulence structure in a low Reynolds number incompressible turbulent boundary layer
15 p2091 N90-21986
Experimental observations on transition to turbulence in confined coaxial jets and other boundary layer flows
[DE90-008939] 15 p2098 N90-22005
Turbulence in slurry pipe flow
[DE90-008940] 15 p2098 N90-22006
Scattered-light scanner measurements of cryogenic liquid-jet breakup
[NASA-TM-102432] 15 p2101 N90-22021
Regional wind energy assessment
[DE90-009439] 15 p2123 N90-22143
Rotor loading on a three-bladed wind turbine
15 p2123 N90-22145
Magnetic turbulence versus safety factor in the Tokapole 2 tokamak 15 p2168 N90-22391
Three-dimensional simulations of simple electron drift wave turbulence in tokamak geometry
[DE90-009581] 15 p2169 N90-22398
A three-year study of the OH masers in Orion-KL and a study of the (3,2) transition of ammonia
15 p2183 N90-22471
Fast spectroscopic variations on rapidly-rotating, cool dwarfs. 3: Masses of circumstellar absorbing clouds on AB Doradus
[NASA-CR-186563] 15 p2184 N90-22479
A theoretical scenario for the dynamics of formation and early evolution of globular clusters in galaxies
15 p2187 N90-22494
Turbulence spectral widths view angle independence as observed by Doppler radar
[AD-A219189] 16 p2199 N90-22550
The multifractal nature of turbulence
16 p2235 N90-22752
A new stochastic model of turbulent dispersion in the convective planetary boundary layer and the results of the Atterbury-87 field study 16 p2254 N90-22853
A numerical study of basic coastal upwelling processes 16 p2259 N90-22878
VLA and VLBI angular broadening measurements: The distribution of interstellar scattering at low Galactic latitudes 16 p2330 N90-23279
Extra compressibility terms for Favre-averaged two-equation models of inhomogeneous turbulent flows
[NASA-CR-177556] 17 p2405 N90-23701
A process for the measurement of the unsteady three dimensional stream vectors in turbomachines
[MITT-89-01] 17 p2405 N90-23702
Atmospheric turbulence measurements in support of adaptive optics technology
[AD-A220445] 17 p2423 N90-23805
A study of gravity wave variability, saturation, and turbulence generation in the mesosphere and lower thermosphere
[AD-A220018] 17 p2424 N90-23810
The interaction of a supersonic streamwise vortex and a normal shock wave 18 p2491 N90-24241
New transonic test sections for the NAE 5 ft x 5 ft trisonic wind tunnel
[AD-A220933] 18 p2499 N90-24278
The modeling of drop-containing turbulent eddies
[NASA-CR-186805] 18 p2553 N90-24570
Renormalized microscopic theory of fluctuations in inhomogeneous magnetized plasmas
[DE90-611307] 18 p2617 N90-24908
A computational efficient modelling of laminar separation bubbles
[NASA-CR-186729] 19 p2688 N90-25291
Spectral transport model for turbulence
[DE90-011265] 19 p2689 N90-25295
Listening to turbulence: An example of scientific audiolization
[DE90-010637] 19 p2753 N90-25646
Formation of design envelope criterion in terms of deterministic spectral procedure
[RAE-TM-SS-9] 20 p2804 N90-25953
A critical evaluation of two-equation models for near wall turbulence
[NASA-CR-182068] 20 p2860 N90-26270
Measurement of terms and parameters in turbulent models
[NASA-CR-183993] 20 p2860 N90-26271
Effect of initial conditions on the development of two-phase jets
[AD-A222621] 20 p2864 N90-26293
A linear-eddy model of turbulent shear layer mixing
21 p2974 N90-26904
Four-step kinetics for methane and implications for turbulent combustion 21 p2975 N90-26906
Non-premixed turbulent CO/H2 flames at local extinction conditions 21 p2975 N90-26907
Scalar dissipation measurements in the developing region of a jet 21 p2976 N90-26909
Theoretical and computational aspects of turbulence
[AD-A221795] 21 p3005 N90-27083
Aureole lidar: Ground based measurement
[AD-A223207] 21 p3008 N90-27101
An improved k-epsilon model for near-wall turbulence and comparison with direct numerical simulation
[NASA-TM-103221] 22 p3171 N90-27983
Turbulence spectra of the FIRE stratocumulus-topped boundary layers 22 p3217 N90-28246
Turbulence structure in clear and cloudy regions of the 7 July 1987 Electra mission 22 p3217 N90-28247
Diurnal variation in the turbulent structure of the cloudy marine boundary layer during FIRE 1987
22 p3217 N90-28248
The spatial scalar structure of premixed turbulent stagnation point flames
[DE90-014189] 23 p3303 N90-28686
An investigation of chaotic Kolmogorov flows
[NASA-CR-182079] 23 p3328 N90-28816
Diffusion in the surface layer of the convective boundary layer
[AD-A224125] 23 p3349 N90-28924
A nonhydrostatic numerical model in sigma-coordinates and simulations of mesoscale phenomena
23 p3350 N90-28932
An additive turbulent decomposition of the Navier-Stokes equations implemented on highly parallel computer systems
[AD-A223678] 24 p3468 N90-29595
Unstable phenomena in mechanical systems
[AD-A223640] 24 p3537 N90-30001

TURBULENCE EFFECTS
A study of high-lift airfoils at high Reynolds numbers in the Langley low-turbulence pressure tunnel
[NASA-TM-89125] 01 p0001 N90-10002
Convection of a pattern of vorticity through a reacting shock wave
[NASA-CR-181921] 01 p0102 N90-10576
Turbulence effects for retroreflection
[FOA-C-30523-3.1] 02 p0276 N90-11575
Effects on electromagnetic wave propagation and rocket vapor trails of intense turbulence generated by breaking internal gravity waves
[AD-A211755] 03 p0373 N90-12130
Experimental study of homogeneous turbulence submitted to rotational effects
[ONERA-RSF-10/1145-AY-164A]
04 p0502 N90-12894
Turbulence effects of aircraft flight dynamics and control 07 p0871 N90-15055
A study of the effects of Rotating Frame Turbulence (RFT) on helicopter flight mechanics
07 p0872 N90-15058
Flowfield effects of launch on a vertically-launched missile
[AD-A214468] 09 p1160 N90-16714
The Shock and Vibration Digest, volume 21, no. 9
09 p1235 N90-17168
Wind-excited behavior of structures, 5
09 p1235 N90-17169
Turbulence scale effects on heat transfer in a linear turbine cascade
[AD-A216222] 10 p1321 N90-17637
Effects of turbulence mixing, variable properties, and vaporization on spray droplet combustion
[NASA-CR-186463] 12 p1623 N90-19326
Separation bubbles at high Reynolds number: Measurement and computation
[CUED/A-AERO/15] 12 p1657 N90-19525
Spontaneous magnetic reconnection in a turbulent plasma 13 p1889 N90-20840
Control of flow separation and mixing by aerodynamic excitation
[NASA-TM-103131] 15 p2047 N90-21733
Rigorous upper bounds for turbulent transport in bounded systems: Passive advection and reversed-field pinches 15 p2168 N90-22390
Numerical investigation of turbulent flame sheets
[AD-A218553] 16 p2215 N90-22635
Numerical simulation of turbulent combustion using vortex methods
[AD-A219624] 17 p2372 N90-23507
Spatially accelerating flow in smooth open channel
19 p2687 N90-25284
Aircraft measurements of the turbulence structure in cirrus clouds
[ISSN-0069-5882] 20 p2890 N90-26450
Hydrodynamic skin-friction reduction
[NASA-CASE-LAR-14078-1-CU]
21 p3003 N90-27071
The effects of grid-generated turbulence on flat and concave turbulent boundary layers
23 p3324 N90-28797
Effects of flowfield turbulence on asymmetric vortices over a slender body
[AD-A224139] 23 p3328 N90-28819

TURBULENCE METERS
Preliminary experimental measurement of isoplanatic angle
[AD-A215828] 10 p1407 N90-18115

TURBULENCE MODELS
NT K-EPSILON TURBULENCE MODEL
Fluid Dynamics of Three-Dimensional Turbulent Shear Flows and Transition
[AGARD-CP-438] 01 p0052 N90-10356
A European collaborative investigation of the three-dimensional turbulent shear layers of a swept wing
01 p0066 N90-10380
Turbulence modelling of three-dimensional shear flows
01 p0066 N90-10381
Numerical simulation of turbulent plane channel flows
01 p0067 N90-10382
Scaling and modeling of turbulent suspension flows
01 p0069 N90-10393
Turbulence kinetic energy equation for dilute suspensions 01 p0069 N90-10394
A comparison of wind turbulence simulation models for stochastic loads analysis for horizontal-axis wind turbines
[DE89-009442] 01 p0083 N90-10473
Application of large eddy interaction model to a mixing layer
[NASA-CR-185123] 05 p0572 N90-13328
SSME LOX post flow analysis/fluid structure interaction. Volume 1: Flow analysis
[NASA-CR-183677] 05 p0637 N90-13715
Application of two-point closures to subgrid scale modeling for homogeneous, 3D turbulence
05 p0640 N90-13732
Numerical Methods for Flows in Turbomachinery, volume 2
[VKI-LS-1989-06-VOL-2] 05 p0641 N90-13741
Turbulence modeling and implementation in Navier-Stokes solvers 05 p0641 N90-13742
Numerical solutions of the complete Navier-Stokes equations
[NASA-CR-186102] 05 p0642 N90-13747
A one equation turbulence model for transonic airfoils
06 p0719 N90-14199
A one-dimensional shipboard model for forecasting refractive effects in the planetary boundary layer
06 p0764 N90-14442
Group-kinetic theory and modeling of atmospheric turbulence
[NASA-CR-183776] 06 p0813 N90-14728
Turbulence effects of aircraft flight dynamics and control 07 p0871 N90-15055
A study of the effects of Rotating Frame Turbulence (RFT) on helicopter flight mechanics
07 p0872 N90-15058
Explicit and implicit calculations of turbulent cavity flows with and without yaw angle
[NASA-CR-186293] 07 p0929 N90-15381
An algebraic turbulence model for flow separation caused by forward and backward facing steps
[AD-A213800] 07 p0931 N90-15389
Development of a three-dimensional local scale atmospheric model with turbulence closure model
[DE90-710045] 07 p0960 N90-15551

Euler and Navier-Stokes computations for two-dimensional geometries using unstructured meshes
[NASA-CR-181977] 08 p1019 N90-15893
Nonlinear wave coupling and clumps in drift wave turbulence theory
[DE90-004103] 08 p1063 N90-16150
Grid-independent wall layer turbulence model for complex flow calculations
[DE90-003500] 08 p1071 N90-16200
New atmospheric turbulence model for shuttle applications
[NASA-TM-4168] 08 p1103 N90-16389
Turbulent heat and momentum transfer in recirculating and impinging flows 09 p1215 N90-17043
Appendage flow computations using the INS3D computer code
[AD-A215689] 09 p1218 N90-17066
Large-eddy interaction model in the turbulent wake of a circular cylinder 10 p1307 N90-17563
Special Course on Three-Dimensional Supersonic/Hypersonic Flows Including Separation
[AGARD-R-764] 10 p1308 N90-17565
Turbulence models for compressive flows 10 p1308 N90-17568
Some Navier-Stokes calculations for the CAST-10 airfoil 10 p1324 N90-17651
Modeling the pressure-strain correlation of turbulence: An invariant dynamical systems approach
[NASA-CR-181979] 10 p1383 N90-18003
Turbulence structure of mixing swirling flows
[AD-A216628] 11 p1506 N90-18671
Numerical solution of 3D Navier-Stokes equations with upwind implicit schemes
[NASA-TM-101656] 12 p1600 N90-19205
The influence of a wall function on turbine blade heat transfer prediction 12 p1640 N90-19421
Application of a Reynolds stress turbulence model to the compressible shear layer
[NASA-CR-182002] 12 p1660 N90-19537
Comparison of 3-D viscous flow computations of Mach 5 inlet with experimental data
[NASA-TM-102518] 13 p1757 N90-20090
A study of low-dimensional models for the wall region of a turbulent boundary layer 13 p1798 N90-20321
An approximate viscous shock layer method for calculating the hypersonic flow over blunt-nosed bodies 14 p1910 N90-20947
An efficient airfoil design method using the Navier-Stokes equations 14 p1917 N90-20981
Centrifugal impeller geometry and its influence on secondary flows 14 p1924 N90-21020
PROTEUS two-dimensional Navier-Stokes computer code, version 1.0. Volume 1: Analysis description
[NASA-TM-102551] 14 p1973 N90-21303
A multiblock/multizone code (PAB 3D-v2) for the three-dimensional Navier-Stokes equations: Preliminary applications
[NASA-CR-182032] 15 p2049 N90-21745
Numerical investigation of separated transonic turbulent flows with a multiple-time-scale turbulence model
[NASA-TM-102499] 15 p2090 N90-21962
Computational modeling and validation for hypersonic inlets
[NASA-TM-103111] 15 p2099 N90-22011
Development of a defect stream function, law of the wall/wake method for compressible turbulent boundary layers 15 p2100 N90-22019
The analysis and simulation of compressible turbulence
[NASA-CR-181997] 16 p2197 N90-22539
Extension of a three-dimensional viscous wing flow analysis
[NASA-CR-182023] 17 p2344 N90-23348
The 3-D composite velocity solutions for subsonic/transonic flow over forebodies and afterbodies
[AD-A220370] 17 p2345 N90-23354
Experimental study of a three-dimensional shear-driven turbulent boundary layer with streamwise adverse pressure gradient 17 p2399 N90-23669
Algebraic turbulence modeling for unstructured and adaptive meshes
[NASA-CR-182035] 17 p2401 N90-23676
Extra compressibility terms for Favre-averaged two-equation models of inhomogeneous turbulent flows
[NASA-CR-177556] 17 p2405 N90-23701
Second moment models of turbulence: Complex or stratified flow
[ECL-90-02] 17 p2405 N90-23703
Modeling turbulent flow with mixed thermal convection transfer
[ECL-89-19] 17 p2405 N90-23704
Turbulence modeling in the SHALE code
[DE90-010354] 18 p2553 N90-24574
Computational simulation of transition to turbulence through inverse modeling 18 p2647 N90-25067
Turbulization of shear flows in astrophysics 19 p2773 N90-25763
An investigation into the numerical prediction of boundary layer transition using the K.Y. Chien turbulence model
[NASA-CR-185252] 20 p2860 N90-26269
Report of the Fluid Dynamics Panel Working Group 10 on calculation of 3D separate turbulent flows in boundary layer limit
[AGARD-AR-255] 20 p2862 N90-26280
Numerical method for calculating indoor airflows using a turbulence model
[PB90-162009] 21 p3003 N90-27067
A comparison of two central difference schemes for solving the Navier-Stokes equations
[NASA-TM-102815] 22 p3108 N90-27654
Boundary layer and shock layer in hypersonic flows
[CERT-31/5005-22-DERAT] 22 p3110 N90-27664
Implicit solution of three-dimensional internal turbulent flows
[NASA-TM-103099] 22 p3170 N90-27982
An introduction to turbulence models 22 p3173 N90-28004
FLUENT and FLUENT/BFC CFD computer programs 22 p3174 N90-28008
Experimental study of homogeneous turbulence under rotation and deformation modes
[ONERA-RSF-12/1145-AY-170A] 22 p3176 N90-28023
Numerical resolution of Navier-Stokes equations using several turbulence models and applications on turbomachines
[ETN-90-97478] 23 p3326 N90-28808
Development of turbulence models for the analysis of compressible or incompressible unsteady flow
[ETN-90-97486] 23 p3326 N90-28810
A boundary-layer transition model for the Navier-Stokes computation for a natural-laminar-flow airfoil
[NAL-TR-1038T] 24 p3421 N90-29328
Reynolds stress and the physics of turbulent momentum transport
[AD-A224172] 24 p3467 N90-29588
Technique for the measurement of noise of the flow associated to the small wave numbers of the turbulence spectra
[ETN-90-97558] 24 p3469 N90-29601

TURBULENT BOUNDARY LAYER

The measurement of boundary layers on a compressor blade in cascade. Volume 1: Experimental technique, analysis and results
[NASA-CR-185118-VOL-1] 01 p0009 N90-10038
A study of the structure of highly swept shock wave turbulent boundary layer interactions 01 p0066 N90-10376
Fluctuating pressures measured beneath a high-temperature, turbulent boundary layer on a flat plate at Mach number of 5
[NASA-TP-2947] 01 p0118 N90-10680
Wall-layer eruptions in turbulent flows
[NASA-TM-102362] 02 p0219 N90-11250
Near-wall, three-dimensional turbulence measurements: A challenge for laser velocimetry
[NASA-TM-102252] 03 p0346 N90-11978
An experimental study of surface roughness effects on turbulent boundary layer flow and heat transfer
[AD-A212099] 03 p0347 N90-11980
Experimental research on swept shock Wave/Boundary layer interactions
[AD-A211744] 03 p0348 N90-11988
Reduction of turbulent drag: Boundary layer manipulators
[CERT-RSF-OA-74/2259-AYD] 04 p0501 N90-12889
Multiple paths to subharmonic laminar breakdown in a boundary layer
[NASA-CR-181948] 05 p0638 N90-13722
A review of quasi-coherent structures in a numerically simulated turbulent boundary layer
[NASA-TM-102191] 05 p0638 N90-13723
Comparison of integral and finite-difference methods for predicting the turbulent boundary layer on axisymmetric bodies
[ARE-TM(UHA)-88512] 05 p0643 N90-13752
Numerical investigations in three-dimensional internal flows
[NASA-CR-186068] 06 p0718 N90-14189
An experimental study of the time-dependent behavior of the appendage-body junction vortex
[AD-A213465] 07 p0930 N90-15384
Modifications of the Penn State Boundary Layer Research Facility for boundary layer/structure interaction experimental research
[AD-A213874] 07 p0931 N90-15391
Further research on dynamics of marine atmospheres in tropical cyclones
[AD-A213882] 07 p0964 N90-15571
Computation of broadband mixing noise from turbomachinery
[AD-A214448] 07 p0989 N90-15713
The structure of supersonic turbulent boundary layers subjected to concave surface curvature 08 p1017 N90-15883
Flow separation in shock wave boundary layer interactions at hypersonic speeds
[NASA-CR-4274] 08 p1017 N90-15885
A numerical and experimental investigation of multiple shock wave/turbulent boundary layer interactions in a rectanular duct 08 p1062 N90-16141
Experiments on the laminar-turbulent transition on swept wings 08 p1066 N90-16170
An interactive method for the flow calculation of airfoils with local separation regions 08 p1069 N90-16190
Inverse solutions for boundary layers with separation or close to separation under locally infinite swept wing conditions 08 p1070 N90-16192
Development and application of oxygen flow tagging for velocity measurements and flow visualization in turbulent three-dimensional supersonic flows
[AD-A214491] 09 p1160 N90-16715
Physical models for supersonic turbulent boundary layer structure
[AD-A215284] 09 p1160 N90-16716
An experimental study of the effect of streamwise vortices on unsteady turbulent boundary-layer separation 09 p1215 N90-17045
New mixing-length model for numerical solution of turbulent supersonic flows 09 p1216 N90-17048
Measurements of heat-transfer coefficients in the interaction regions between oblique shock waves and turbulent boundary layers with a multi-layered thin film heat transfer gauge
[DE90-004123] 09 p1216 N90-17054
Velocity profile and wall shear stress measurements for a Large Eddy Break-Up (LEBU) device
[AD-A214958] 09 p1217 N90-17059
Effect of vortex circulation on injectant from a single film-cooling hole and a row of film-cooling holes in a turbulent boundary layer. Part 1: Injection beneath the vortex downwash
[AD-A215288] 09 p1218 N90-17063
Study of pressure sensors in hydrodynamic turbulent boundary layer
[ONERA-RF-17/7218-PY] 09 p1218 N90-17067
Formation of turbulent layers in the separated region around a body with polygonal cross section at large incidence and rolling
[ISL-R-101/88] 09 p1219 N90-17071
Particle resuspension and associated coherent structures in a turbulent boundary layer 09 p1245 N90-17224
A review of high-speed, convective, heat-transfer computation methods 10 p1305 N90-17548
Glancing shock-boundary layer interactions 10 p1309 N90-17571
Unsteadiness of supersonic and hypersonic shock induced turbulent boundary layer separation 10 p1309 N90-17572
Numerical studies on laminar-turbulent transition in boundary layers 10 p1383 N90-18001
Turbulent boundary layer pressure field-induced vibrations in a thin flexible plate under water 10 p1383 N90-18002
Turbulence structure resulting from interaction between an embedded vortex and wall jet
[AD-A215702] 10 p1383 N90-18004
Effects of controlled three-dimensional perturbations on boundary layer transition
[AD-A215080] 10 p1384 N90-18011
Study of vortex arrays induced artificially and from centrifugal instabilities
[AD-A216499] 11 p1506 N90-18669
Development of a defect stream function, law of the wall/wake method for compressible turbulent boundary layers
[NASA-CR-4286] 11 p1507 N90-18675
Interaction between oblique-angled incident shock wave and turbulent boundary layer on a heated wall. Experimental results
[ONERA-RT-84/7078-AY] 11 p1509 N90-18688
Study of the turbulent boundary layer on an afterbody
[TM-EA-8901] 12 p1601 N90-19212
Swept shock/boundary layer interaction experiments in support of CFD code validation
[NASA-CR-186397] 12 p1659 N90-19535
Wind tunnel design of heat island turbulent boundary layer
[IHW-ET/50] 12 p1660 N90-19542
Experimental examination of the development behavior of a gaseous body in a steady state and neutral layer turbulent sheet boundary layer with ground asperity
[ETN-90-96067] 12 p1682 N90-19549

A study of low-dimensional models for the wall region of a turbulent boundary layer 13 p1798 N90-20321
The effect of adverse pressure gradient on turbulent burst structure in low-Reynolds number equilibrium boundary layers
[AD-A217308] 13 p1799 N90-20327
Theoretical modeling studies of the marine planetary
[AD-A217200] 13 p1841 N90-20567
Correlation of atmospheric optical turbulence and meteorological measurements
[AD-A218019] 13 p1842 N90-20576
A modeling study of the cloud-topped marine boundary layer
[AD-A218103] 13 p1846 N90-20594
An aircraft investigation of a convective boundary layer over Lake Michigan
[AD-A218175] 13 p1846 N90-20598
A case study of a quasi-stationary tropical convective line
[AD-A218325] 13 p1847 N90-20604
Numerical investigation of separated transonic turbulent flows with a multiple-time-scale turbulence model
[NASA-TM-102499] 15 p2090 N90-21962
An investigation of turbulence structure in a low Reynolds number incompressible turbulent boundary layer
15 p2091 N90-21966
Automated analysis of measured turbulent boundary flow
[PB90-147844] 15 p2092 N90-21970
European research on viscous flow (EuroVisc)
[NLR-TP-89077-U] 15 p2099 N90-22014
Development of a defect stream function, law of the wall/wake method for compressible turbulent boundary layers 15 p2100 N90-22019
Flow visualization in supersonic turbulent boundary layers 16 p2195 N90-22533
Three-dimensional separated flow prediction on fusiform body using Euler and boundary layer methods
16 p2234 N90-22745
Boundary layer turbulence pulsed by acoustic waves
[ETN-90-96621] 16 p2236 N90-22759
Experimental study of a three-dimensional shear-driven turbulent boundary layer with streamwise adverse pressure gradient 17 p2399 N90-23669
Large eddy simulation of a fully turbulent plane channel flow
[VKI-TN-171] 17 p2404 N90-23693
The diurnal ozone cycle in a coniferous forest: The importance of meteorology and chemistry
[CM-75] 17 p2421 N90-23795
Interaction of the large eddy structure in the inner-half of a turbulent boundary layer 18 p2551 N90-24561
Coherent structures, chaos and the role of modern dynamics in turbulent shear flows
[AD-A220884] 18 p2552 N90-24562
A laser-induced fluorescence technique for measurement of slot-injected fluid concentration profiles in a plate turbulent boundary layer
[AD-A221388] 18 p2553 N90-24572
Simulation of the boundary layer in accretion disks with the SPH method 19 p2779 N90-25807
Interactive calculation procedures for mixed compression inlets
[NASA-CR-186581] 20 p2801 N90-25934
A critical evaluation of two-equation models for near wall turbulence
[NASA-CR-182068] 20 p2860 N90-26270
Report of the Fluid Dynamics Panel Working Group 10 on calculation of 3D separate turbulent flows in boundary layer limit
[AGARD-AR-255] 20 p2862 N90-26280
Vortex-induced boundary layer separation
[AD-A221564] 21 p3005 N90-27078
The dynamics and control of fluctuating pressure loads in the reattachment region of a supersonic free shear layer
[NASA-CR-184943] 22 p3108 N90-27652
Numerical investigation of laminar-turbulent transition in a flat plate wake
[AD-A222462] 22 p3170 N90-27978
Ultra-fast visualization of a turbulent boundary layer by a laser velocimeter
[IMFL-89-37] 22 p3181 N90-28048
Turbulence spectra of the FIRE stratocumulus-topped boundary layers 22 p3217 N90-28246
Phoenix data analysis and numerical simulation
[AD-A224226] 23 p3320 N90-28772
The effects of grid-generated turbulence on flat and concave turbulent boundary layers
23 p3324 N90-28797
Vortice-propeller interaction
[LIMSI-89-9] 23 p3326 N90-28809
Effect of vortex circulation on injectant from a single film-cooling hole and a row of film-cooling holes in a turbulent boundary layer. Part 2: Injection beneath the vortex upwash
[AD-A223894] 23 p3328 N90-28818
Theoretical study of the interaction between an oblique shock wave and a turbulent boundary layer from a heated wall
[ONERA-RSF-87/7078/AY-100-A]
24 p3419 N90-29313
Spectral measurements of the wall shear stress and wall pressure in a turbulent boundary layer: Theory
[AD-A224070] 24 p3466 N90-29586
Further studies of turbulence structure resulting from interactions between embedded vortices and wall jets at high blowing ratios
[AD-A223296] 24 p3468 N90-29593
Transition of the boundary layer
[DERAT-RSF-50/5018-37] 24 p3469 N90-29600
Technique for the measurement of noise of the flow associated to the small wave numbers of the turbulence spectra
[ETN-90-97558] 24 p3469 N90-29601

TURBULENT DIFFUSION

Application of large eddy interaction model to a mixing layer
[NASA-CR-185123] 05 p0572 N90-13328
Scalar transport in turbulent shear flows
05 p0640 N90-13734
An investigation of flow structure, mixing and chemical reaction in combusting turbulent flows
[AD-A216739] 11 p1483 N90-18538
Parabolized calculations of turbulent three dimensional flows in a turbine duct 14 p1923 N90-21013
The numerical simulation of multistage turbomachinery flows 14 p1925 N90-21025
A linear analysis of monsoon base states associated with banded convection 15 p2130 N90-22179
The diurnal ozone cycle in a coniferous forest: The importance of meteorology and chemistry
[CM-75] 17 p2421 N90-23795
The diurnal ozone cycle in a coniferous forest: The importance of meteorology and chemistry
20 p2886 N90-26423
A theoretical study of flow structure and radiation for multiphase turbulent diffusion flames
[AD-A222934] 21 p2976 N90-26913
Model of turbulent diffusion flames and nitric oxide generation
[PB90-155557] 22 p3155 N90-27886
Structure and radiation properties of turbulent diffusion flames
[PB90-216777] 22 p3155 N90-27887

TURBULENT FLOW

NT CAVITATION FLOW

Three-dimensional unsteady transonic viscous-inviscid interaction 01 p0001 N90-10005
Direct numerical simulation of turbulent free shear flows
[AD-A210161] 01 p0040 N90-10218
Fluid Dynamics of Three-Dimensional Turbulent Shear Flows and Transition
[AGARD-CP-438] 01 p0062 N90-10356
A European collaborative investigation of the three-dimensional turbulent shear layers of a swept wing
01 p0066 N90-10380
Numerical simulation of turbulent plane channel flows
01 p0067 N90-10382
Scaling and modeling of turbulent suspension flows
01 p0069 N90-10393
Dynamics and control of turbulent shear flows
[AD-A210396] 01 p0070 N90-10402
The suitability of diffusion and wind-field techniques for an emergency-response dispersion model
[PB89-190219] 01 p0085 N90-10481
Thermophysical properties of supercritical fluids and fluid mixtures
[DE89-016568] 02 p0193 N90-11102
Numerical solutions of turbulent flow with heat transfer over rough surfaces 02 p0218 N90-11246
The structure of Reynolds stress in the near wall region of a turbulent pipe flow 02 p0218 N90-11247
Wall-layer eruptions in turbulent flows
[NASA-TM-102362] 02 p0219 N90-11250
Cellular automata and massively parallel physics
[DE89-016506] 02 p0220 N90-11257
An experimental study of helicity and related properties in turbulent flows
[DE89-016785] 02 p0220 N90-11259
Chemical reactions in turbulent mixing flows
[AD-A211240] 02 p0220 N90-11263
Questions from the Willmarth Workshop on New Directions in Research on Turbulent Wall-Layer Structures
[AD-A211282] 02 p0221 N90-11264
Numerical simulation of turbulent flow downstream a sudden axisymmetric expansion
[FOA-C-20758-2.1] 02 p0222 N90-11272
Some implications of the isotropic momentarily frozen assumptions for the SPAN-MAT program
[NASA-CR-181937] 03 p0301 N90-11704
Control of turbulent mixing layers
[AD-A211413] 03 p0301 N90-11708
Doubly-fluted tubes and enhanced tubes in confined crossflow
[PB89-217921] 03 p0345 N90-11971
Near-wall, three-dimensional turbulence measurements: A challenge for laser velocimetry
[NASA-TM-102252] 03 p0346 N90-11978
An experimental study of surface roughness effects on turbulent boundary layer flow and heat transfer
[AD-A212099] 03 p0347 N90-11980
Investigation of turbulent flow in highly curved ducts with application to turbomachinery components
[NASA-CR-186060] 04 p0500 N90-12882
Transition in surface boundary layers
[CERT-RSF-OA-43/5018-AYD]
04 p0502 N90-12897
Semi-Lagrangian, semi-implicit solutions of the shallow water equations in one dimension
[AD-A212658] 04 p0503 N90-12902
Evaluation of the near-wall k-epsilon turbulence model by comparison with direct simulations of turbulent channel flow
[AD-A212674] 04 p0503 N90-12903
A numerical study of rain-induced surface gravity wave attenuation
[AD-A212762] 04 p0549 N90-13197
Fundamental studies of turbulent wall pressure fluctuations with applications to advanced acoustic sensor systems
[AD-A213041] 04 p0552 N90-13212
Multigrid calculations of 3-D turbulent viscous flows
[NASA-CR-185154] 05 p0571 N90-13323
Application of large eddy interaction model to a mixing layer
[NASA-CR-185123] 05 p0572 N90-13328
Reduction of profile drag by modifying the structure next to the wake area
[IMFL-88/35] 05 p0576 N90-13356
A planar reacting shear layer system for the study of fluid dynamics-combustion interaction
[NASA-TM-102422] 05 p0582 N90-13393
Effect of spatial resolution on apparent sensitivity to initial conditions of a decaying flow as it becomes turbulent
[NASA-TM-102377] 05 p0638 N90-13719
The influence of multiple hot-wire probe geometry on the results of measurements in turbulent flows
[DLR-FB-89-26] 05 p0639 N90-13724
Numerical simulation of transition in three-dimensional boundary layers
[DLR-FB-89-12] 05 p0639 N90-13726
Turbulent Shear Flows
[VKI-LS-1989-03] 05 p0640 N90-13730
An introduction via vorticity dynamics and statistical theory --- turbulent shear flows
05 p0640 N90-13731
Application of two-point closures to subgrid scale modeling for homogeneous, 3D turbulence
05 p0640 N90-13732
Coherent structures in a round jet
05 p0640 N90-13733
Scalar transport in turbulent shear flows
05 p0640 N90-13734
Turbulence modeling and implementation in Navier-Stokes solvers 05 p0641 N90-13742
Numerical solutions of the complete Navier-Stokes equations
[NASA-CR-186102] 05 p0642 N90-13747
Comparison of integral and finite-difference methods for predicting the turbulent boundary layer on axisymmetric bodies
[ARE-TM(UHA)-88512] 05 p0643 N90-13752
Spectral study of a compressible isotropic turbulence
[ECL-88-16] 05 p0643 N90-13753
Large eddy simulation of homogeneous turbulence undergoing shear and thermal gradients. Application to one point closing models
[ECL-88-23] 05 p0643 N90-13754
Model and computation of three-dimensional turbulent jets in a crossflow
[ECL-89-007] 05 p0643 N90-13755
A one equation turbulence model for transonic airfoils
06 p0719 N90-14199
Acoustic-vortical-combustion interaction in a solid fuel ramjet simulator 06 p0726 N90-14234
Embedded function methods for compressible high speed turbulent flow
[NASA-CR-186131] 06 p0773 N90-14498

Comparative study of the vorticity field in turbulent flows: Theory, experiments, and computations
[DE90-001399] 06 p0776 N90-14516
Selection of the energy-efficient enhancement geometry for single-phase turbulent flow inside tubes
[DE89-017690] 06 p0777 N90-14519
Simultaneous multipoint measurements of density gradients and temperature in a flame
[DE90-001719] 07 p0892 N90-15155
Combustion characteristics of sprays
[AD-A213651] 07 p0895 N90-15173
Explicit and implicit calculations of turbulent cavity flows with and without yaw angle
[NASA-CR-186293] 07 p0929 N90-15381
Assessment of computational prediction of tail buffeting
[NASA-TM-101613] 08 p1018 N90-15886
Calculation of turbulent choppy flow mixing
[ETN-90-95929] 08 p1065 N90-16165
Numerical simulation of the laminar and turbulent three dimensional flow on a delta wing with sharp leading edge 08 p1069 N90-16186
A finite volume calculation method for three dimensional, complex flows 08 p1070 N90-16195
Grid-independent wall layer turbulence model for complex flow calculations
[DE90-003500] 08 p1071 N90-16200
Colinear fluctuating wall shear stress and fluctuating pressure transducer
[AD-D014296] 08 p1076 N90-16226
Turbulent stripping of interstellar clouds by interaction with supernova remnants
[DE90-003622] 08 p1152 N90-16674
Development and application of oxygen flow tagging for velocity measurements and flow visualization in turbulent three-dimensional supersonic flows
[AD-A214491] 09 p1160 N90-16715
Development of flow visualization and nonintrusive velocity measurement in turbulent flow
[ETN-90-96077] 09 p1161 N90-16717
Experimental study of velocity fields and turbulence in a turbojet engine
[ISL-CO-231/88] 09 p1169 N90-16766
Computation of fluid flow and heat transfer in rotating disc-systems 09 p1215 N90-17044
New mixing-length model for numerical solution of turbulent supersonic flows 09 p1216 N90-17048
Influence of wall strain rate, polymer concentration, and channel height upon drag reduction and turbulent structure
[AD-A215378] 09 p1218 N90-17064
Theoretical and experimental approach of wave phenomena in free jets
[ISL-CO-247/88] 09 p1219 N90-17069
Formation of a pair of turbulent layers in the region of a flow around an axisymmetric body with an incidence angle
[ISL-R-130/87] 09 p1219 N90-17070
Study for the dissipative structures geometry in three dimensional developed turbulence
[ETN-90-96102] 09 p1219 N90-17072
Theoretical study of instabilities in vortices: Applications to hydrodynamics and magnetohydrodynamics
[ETN-90-96103] 09 p1219 N90-17073
Particle resuspension and associated coherent structures in a turbulent boundary layer 09 p1245 N90-17224
Surface acoustic wave sensors and piezoelectric actuators for investigations of transitional and turbulent flows
[AD-A214889] 09 p1279 N90-17415
Chaos and turbulence
[AD-A215310] 09 p1294 N90-17499
Turbulence scale effects on heat transfer in a linear turbine cascade
[AD-A216222] 10 p1321 N90-17637
Chemical reactions in turbulent mixing flows
[AD-A216273] 10 p1355 N90-17856
Modeling the pressure-strain correlation of turbulence: An invariant dynamical systems approach
[NASA-CR-181979] 10 p1383 N90-18003
Fluid transmission line dynamics for signals of finite amplitude
[AD-A215758] 10 p1385 N90-18014
Computing shock waves in turbulent mixing regions
[DE90-005996] 10 p1386 N90-18021
Direct numerical simulation of aerodynamic noise
[AD-A214122] 10 p1426 N90-18225
An investigation of flow structure, mixing and chemical reaction in combusting turbulent flows
[AD-A216739] 11 p1483 N90-18538
Turbulence structure of mixing swirling flows
[AD-A216628] 11 p1506 N90-18671
Analytic solutions for the decay of turbulent swirling flow in a cylinder
[DE90-005744] 11 p1507 N90-18677
Concepts and experiments on space-time chaos
[ETN-90-96255] 11 p1508 N90-18683
Numerical simulation of the incompressible inhomogeneous turbulence in a plane channel flow
[ONERA-NT-1988-5] 11 p1508 N90-18686
Contribution to the study of three-dimensional separation in turbulent incompressible flow
[ESA-TT-1169] 11 p1510 N90-18697
Vertical axis wind turbine turbulent response model. Part 2: Response of Sandia National laboratories' 34-meter VAWT with aeroelastic effects
[DE90-005721] 11 p1529 N90-18804
Transient heat transfer measurements on a flat plate in turbulent flow using an electrical analog
[AD-A216286] 11 p1573 N90-19057
Separation bubbles at high Reynolds number: Measurement and computation
[CUED/A-AERO/15] 12 p1657 N90-19525
Theoretical and experimental examination of the beginning of turbulence in a heated laminar conduit flow
[ETN-90-95369] 12 p1660 N90-19541
A review of models for the analysis of the injection of densely loaded flows into entrained flow gasifiers
[DE90-000453] 12 p1662 N90-19550
Linear theory of thermal blooming in turbulence
[DE90-007243] 12 p1667 N90-19579
A study of low-dimensional models for the wall region of a turbulent boundary layer 13 p1798 N90-20321
Nonintrusive optical measurements of turbulence and mixing in a stably stratified fluid 13 p1799 N90-20322
A numerical investigation of the compressible mixing layer
[AD-A217738] 13 p1802 N90-20343
Numerical modeling of airblast
[AD-A217993] 13 p1803 N90-20347
Flow visualization studies in a curved rectangular channel with 40 to 1 aspect ratio and a straight channel with bulk flow unsteadiness
[AD-A218020] 13 p1803 N90-20348
Correlation of atmospheric optical turbulence and meteorological measurements
[AD-A218019] 13 p1842 N90-20576
An aircraft investigation of a convective boundary layer over Lake Michigan
[AD-A218175] 13 p1846 N90-20598
The role of chaos in hemispheric process and attention
[AD-A217674] 13 p1854 N90-20639
On total variation diminishing schemes for transonic turbulent flow computation 14 p1909 N90-20945
Parabolized calculations of turbulent three dimensional flows in a turbine duct 14 p1923 N90-21013
Calculation of the three dimensional turbulent flow in a linear turbine blade 14 p1924 N90-21021
Effects of secondary flow on heat transfer in rotating passages 14 p1926 N90-21031
Depth-averaged equations for turbulent free-surface flow
[PB90-164781] 14 p1974 N90-21308
Numerical investigation of separated transonic turbulent flows with a multiple-time-scale turbulence model
[NASA-TM-102499] 15 p2090 N90-21962
Homogeneous dilute turbulent particle-laden water flows 15 p2090 N90-21965
Numerical study of laminar and turbulent flows past two-dimensional and axisymmetric bodies 15 p2100 N90-22020
The analysis and simulation of compressible turbulence
[NASA-CR-181997] 16 p2197 N90-22539
Analysis of velocity and temperature fluctuations in turbulent shear flows 16 p2233 N90-22744
Nonlinear bifurcation study of plane Poiseuille flow
[DLR-FB-89-42] 16 p2236 N90-22756
Holocinematography for studies of turbulent multiphase flow
[AD-A219130] 16 p2237 N90-22765
Stratified ocean mixing
[AD-A219233] 16 p2259 N90-22881
Premixed turbulent flame propagation
[AD-A219834] 17 p2373 N90-23515
Experimental study of a three-dimensional shear-driven turbulent boundary layer with streamwise adverse pressure gradient 17 p2399 N90-23669
Computations of a horseshoe vortex around an endwall-mounted cylinder 17 p2400 N90-23673
Algebraic turbulence modeling for unstructured and adaptive meshes
[NASA-CR-182035] 17 p2401 N90-23676
Second moment models of turbulence: Complex or stratified flow
[ECL-90-02] 17 p2405 N90-23703
Modeling turbulent flow with mixed thermal convection transfer
[ECL-89-19] 17 p2405 N90-23704
Test and evaluation of surf forecasting model
[AD-A219580] 17 p2430 N90-23845
The computation of turbulent thin shear flows associated with flow around multielement aerofoils 18 p2491 N90-24240
Interaction of the large eddy structure in the inner-half of a turbulent boundary layer 18 p2551 N90-24561
Coherent structures, chaos and the role of modern dynamics in turbulent shear flows
[AD-A220884] 18 p2552 N90-24562
Development of a postprocessing and 3D graphical imaging facility
[AD-A221212] 18 p2593 N90-24755
Turbulent combustion modeling for turbo-jet combustion chambers 20 p2811 N90-25993
Chemistry of combustion processes 20 p2811 N90-25994
An investigation into the numerical prediction of boundary layer transition using the K.Y. Chien turbulence model
[NASA-CR-185252] 20 p2860 N90-26269
Report of the Fluid Dynamics Panel Working Group 10 on calculation of 3D separate turbulent flows in boundary layer limit
[AGARD-AR-255] 20 p2862 N90-26280
Analysis of turbulent density fluctuations by means of spontaneous Raman diffusion
[ISL-R-103/89] 20 p2863 N90-26287
The finite analytic method and its applications. Volume 1: Laminar and turbulent flows past two-dimensional and axisymmetric bodies
[AD-A222787] 20 p2864 N90-26294
Effects of 2 Hz imposed bulk flow unsteadiness on laminar-turbulent transition in a straight channel
[AD-A223028] 20 p2864 N90-26295
Analysis of near-surface flow physics in a two-stage, 10 km/s, electromagnetic launcher
[DE90-013292] 21 p2964 N90-26852
A theoretical study of flow structure and radiation for multiphase turbulent diffusion flames
[AD-A222934] 21 p2976 N90-26913
Turbulent reacting flows and supersonic combustion
[AD-A221793] 21 p2979 N90-26933
Numerical method for calculating indoor airflows using a turbulence model
[PB90-162009] 21 p3003 N90-27067
Rotating flow in radial turbomachinery
[AD-A222885] 21 p3004 N90-27073
Three-dimensional structure of boundary layers in transition to turbulence
[AD-A223242] 21 p3004 N90-27076
Theoretical and computational aspects of turbulence
[AD-A221795] 21 p3005 N90-27083
Near-wall modelling of compressible turbulent flows
[NASA-CR-186961] 22 p3109 N90-27658
Study of the compressibility effects on the turbulence of supersonic drags
[ETN-90-97448] 22 p3109 N90-27661
Numerical investigation of laminar-turbulent transition in a flat plate wake
[AD-A222462] 22 p3170 N90-27978
Progress and challenges in modeling turbulent aerodynamic flows
[NASA-TM-102811] 22 p3170 N90-27981
Implicit solution of three-dimensional internal turbulent flows
[NASA-TM-103099] 22 p3170 N90-27982
Numerical solution for the velocity-derivative skewness of a low-Reynolds-number decaying Navier-Stokes flow
[NASA-TM-103186] 22 p3171 N90-27985
Computational Fluid Dynamics for Industrial Flows
[VKI-LS-1990-04] 22 p3173 N90-28001
A finite element method for turbulent incompressible flow 22 p3174 N90-28007
Modeling of near-wall turbulence
[NASA-TM-103222] 22 p3174 N90-28009
Turbulent thermal convection in rotating cavities, volume 1
[ETN-90-97433] 22 p3174 N90-28011
Turbulent thermal convection in rotating cavities, volume 2
[ETN-90-97434] 22 p3174 N90-28012
Numerical study of turbulence in the presence of walls
[ONERA-RSF-15/3419-AY-114A] 22 p3176 N90-28024
Wind tunnel simulation of Antarctic snowdrifting
[PB90-184565] 22 p3212 N90-28222
Vertical-velocity skewness in the marine stratus-topped boundary layer 22 p3220 N90-28262
Development of comprehensive numerical schemes for predicting evaporating gas-droplets flow processes of a liquid-fueled combustor
[NASA-CR-187018] 23 p3305 N90-28693
Numerical simulation of reactive turbulent flows
[ETN-90-97476] 23 p3326 N90-28807
Numeric fluid mechanics 23 p3392 N90-29161

Calculation of turbulent air streams in driver cabs
[ETN-90-97320] 24 p3419 N90-29310
AFOSR/ONR Contractors' Meeting on Combustion Rocket Propulsion Diagnostics of Reacting Flow
[AD-A224411] 24 p3441 N90-29432
Reynolds stress and the physics of turbulent momentum transport
[AD-A224172] 24 p3467 N90-29588
Direct numerical simulation of turbulent couette flow
[AD-A224287] 24 p3467 N90-29589
Particle dispersion in a turbulent shear flow
[AD-A224327] 24 p3467 N90-29590
Effects of 1 Hz imposed bulk flow unsteadiness on laminar/turbulent transition in a straight channel
[AD-A223396] 24 p3468 N90-29594
Solid particle erosion in turbulent flows past tube banks
[DE90-015711] 24 p3469 N90-29598

TURBULENT HEAT TRANSFER
An experimental study of surface roughness effects on turbulent boundary layer flow and heat transfer
[AD-A212099] 03 p0347 N90-11980
Coherent structures in a round jet
05 p0640 N90-13733
Physical models for supersonic turbulent boundary layer structure
[AD-A215264] 09 p1160 N90-16716
Computation of fluid flow and heat transfer in rotating disc-systems 09 p1215 N90-17044
Turbulence structure resulting from interaction between an embedded vortex and wall jet
[AD-A215702] 10 p1383 N90-18004
Investigation of heat transfer with film cooling to a flat plate in a shock tube
[AD-A216379] 10 p1386 N90-18019
Transient heat transfer measurements on a flat plate in turbulent flow using an electrical analog
[AD-A216286] 11 p1573 N90-19057
Analysis of unsteady heat transfer by natural convection in a two-dimensional square cavity using a high order finite-volume method 12 p1657 N90-19521
Turbulent mixing effects in models of thermal blooming
[DE90-007245] 12 p1667 N90-19580
Improved analytical capabilities for foil air bearings, phase 1
[AD-A218071] 14 p1987 N90-21389
Computer simulation of ionospheric radio frequency heating
[DE90-009478] 15 p2087 N90-21944
Thermal conductivity of metals
18 p2514 N90-24356
Turbine blade heat transfer coefficient evaluation by modified version of STAN5. Comparison with experimental data
[ETN-90-97283] 20 p2813 N90-26008
Transients in turbulent convective heat transfer to a flow of supercritical helium
[ETN-90-97217] 20 p2863 N90-26286
A numerical study of the role of meso beta and meso gamma scale vertical exchange processes in the evolution of upper tropospheric frontal systems
[AD-A222057] 21 p3031 N90-27230
Direct numerical simulation of turbulent couette flow
[AD-A224287] 24 p3467 N90-29589
Further studies of turbulence structure resulting from interactions between embedded vortices and wall jets at high blowing ratios
[AD-A223296] 24 p3468 N90-29593

TURBULENT JETS
A laser Doppler anemometry investigation of single-phase and particle-laden jet flows
[AD-A210660] 02 p0220 N90-11261
Chemical reactions in turbulent mixing flows
[AD-A211240] 02 p0220 N90-11263
Numerical modeling of supersonic turbulent reacting free shear layers 06 p0719 N90-14197
Impingement characteristics of heated plane turbulent jets 09 p1215 N90-17047
Numerical simulations of coherent structures in a jet flame with a noncircular cross section
[AD-A216710] 11 p1483 N90-18535
Interaction of a turbulent round jet with the free surface 15 p2090 N90-21964
Laser Doppler anemometry measurements of a confined turbulent water jet with a uniform background flow
15 p2092 N90-21971
Modern developments in shear flow control with swirl
[NASA-CR-186586] 15 p2097 N90-22000
Lagrangian model simulation of the turbulent transport of evaporating jet droplets 15 p2128 N90-22168
Reynolds stress closure in jet flows using instability wave modeling 16 p2196 N90-22534
Calculation of 3D turbulent jets in crossflow with a multigrid method and a second-moment closure model
[NASA-TM-103159] 20 p2862 N90-26282
PDF modeling of chemical nonequilibrium effects in turbulent nonpremixed jet flames
21 p2975 N90-26908
Model of turbulent diffusion flames and nitric oxide generation
[PB90-155557] 22 p3155 N90-27886
The entrainment rate for a row of turbulent jets
[NASA-CR-185278] 23 p3269 N90-28504
Structure in the near field of the transverse jet
[AD-A224502] 24 p3467 N90-29591
Further studies of turbulence structure resulting from interactions between embedded vortices and wall jets at high blowing ratios
[AD-A223296] 24 p3468 N90-29593

TURBULENT MIXING
Turbulent reacting flows in solid-propellant ducted rocket combustors 02 p0189 N90-11079
Chemical reactions in turbulent mixing flows
[AD-A211240] 02 p0220 N90-11263
Control of turbulent mixing layers
[AD-A211413] 03 p0301 N90-11708
Characterization of nonpremixed turbulent bluff-body burner flames
[PB89-229447] 04 p0489 N90-12689
Numerical solutions of the complete Navier-Stokes equations
[NASA-CR-186102] 05 p0642 N90-13747
Numerical modeling of supersonic turbulent reacting free shear layers 06 p0719 N90-14197
An experimental and theoretical study of the aeroacoustics of external-Coanda gas flares
06 p0773 N90-14495
Calculation of turbulent choppy flow mixing
[ETN-90-95929] 08 p1065 N90-16165
An experimental and analytical examination of stratified thermal storage 09 p1215 N90-17046
Chemical reactions in turbulent mixing flows
[AD-A216273] 10 p1355 N90-17856
Computing shock waves in turbulent mixing regions
[DE90-005996] 10 p1386 N90-18021
Turbulent mixing effects in models of thermal blooming
[DE90-007245] 12 p1667 N90-19580
Nonintrusive optical measurements of turbulence and mixing in a stably stratified fluid
13 p1799 N90-20322
DURIP optical equipment for high-speed viscous-inviscid interaction research
[AD-A217772] 13 p1802 N90-20345
Cloud hole-boring with long pulse CO2 lasers
[DE90-008946] 14 p1985 N90-21377
Stratified ocean mixing
[AD-A219233] 16 p2259 N90-22881
A theoretical analysis of the acoustic radiation from two-dimensional turbulent mixing layers
18 p2551 N90-24559
Summary of Discussions at the Eleventh Meeting of the Sandia Cooperative Group on the Aerothermochemistry of Turbulent Combustion
[DE89-001646] 21 p2973 N90-26896
Supersaturation, droplet spectra, and turbulent mixing in clouds 22 p3217 N90-28249

TURBULENT WAKES
NT PROPELLER SLIPSTREAMS
NT SLIPSTREAMS
Linear instability of supersonic plane wakes
[NASA-CR-181911] 02 p0146 N90-10833
The near-wake flow structure of wake-cylinder interaction and surface loading of cylinder
02 p0218 N90-11248
Effect of pylon wake with and without pylon blowing on propeller thrust
[NASA-TM-4162] 06 p0718 N90-14190
An experimental, analytical, and computational investigation of turbomachinery rotor flow fields
07 p0926 N90-15360
Computation of broadband mixing noise from turbomachinery
[AD-A214448] 07 p0989 N90-15713
Experimental investigation of a three-dimensional wake. Part 2: Spectral and turbulent energy analysis
[ONERA-RT-32/5025-AYD-PT-2]
08 p1018 N90-15887
An experimental investigation of viscous aspects of propeller blade flow 09 p1159 N90-16711
Flowfield effects of launch on a vertically-launched missile
[AD-A214468] 09 p1160 N90-16714
Large-eddy interaction model in the turbulent wake of a circular cylinder 10 p1307 N90-17563
Flowfield measurements in the wake of a missile at high angle of attack
[AD-A219645] 17 p2345 N90-23351
Fluid dynamic mechanisms and interactions within separated flows
[AD-A219628] 17 p2403 N90-23689
Local and global resonances in heated 2-D jets
[AD-A221671] 21 p3005 N90-27079
Laboratory experiments on stability and entrainment of oceanic stratocumulus. Part 1: Instability experiment
22 p3220 N90-28263
Effects of flowfield turbulence on asymmetric vortices over a slender body
[AD-A224139] 23 p3328 N90-28819

TURING MACHINES
General decomposition of sequential machines: Relationships to state assignment
[AD-A208189] 01 p0102 N90-10580
Efficient on-line simulations of tree machines and multidimensional turing machines by random access machines
[AD-A213152] 05 p0680 N90-13960
Optimum and heuristic algorithms for finite state machine decomposition and partitioning
[AD-A216778] 11 p1546 N90-18899
Boolean minimization and algebraic factorization procedures for fully testable sequential machines
[AD-A216779] 11 p1553 N90-18940
Computational complexity of random access models
[AD-A217685] 13 p1865 N90-20701

TURNING FLIGHT
Guidance analysis of the aeroglide plane change maneuver as a turning point problem
[NASA-TM-101639] 07 p0883 N90-15110
The SKY SHARK: An RPV designed to investigate the pressure distribution on a lifting surface
[NASA-CR-186222] 21 p2959 N90-26824

TVC (CONTROL)
U THRUST VECTOR CONTROL

TVD SCHEMES
Triangle based TVD schemes for hyperbolic conservation laws
[NASA-CR-181984] 08 p1106 N90-16401
An entropy-based approach to nonlinear stability
[NASA-TM-101086] 09 p1272 N90-17376
High-resolution Euler computations of unsteady transonic flows in cascades 11 p1462 N90-18420
On total variation diminishing schemes for transonic turbulent flow computation 14 p1909 N90-20945
Some aspects of Essentially Nonoscillatory (ENO) formulations for the Euler equations, part 3
[NASA-CR-4285] 14 p1910 N90-20949
ULTRA-SHARP nonoscillatory convection schemes for high-speed steady multidimensional flow
[NASA-TM-102568] 14 p2019 N90-21570
Numerical simulation of hypersonic flow around a space plane. Part 2: Application to high angles of attack flow
[NAL-TR-1011T] 15 p2045 N90-21726
Three-dimensional separated flow prediction on fusiform body using Euler and boundary layer methods
16 p2234 N90-22745
Prediction of two-dimensional time-dependent gasdynamic flows for hypersonic studies
[UTIAS-335] 20 p2801 N90-25935
On central-difference and upwind schemes
[NASA-CR-182061] 20 p2917 N90-26595

TWINNING
NT MECHANICAL TWINNING
The effect of twins on critical currents of high Tc superconductors
[AD-A210988] 01 p0133 N90-10768
Deformation and fracture of ordered intermetallic compounds
[DE90-007422] 11 p1488 N90-18563

TWISTING
Magnetostrictive torque sensor
[AD-D014169] 03 p0349 N90-11996
An approach for design and analysis of composite rotor blades
[AD-A219257] 19 p2657 N90-25125

TWO BODY ORBITS
U TWO BODY PROBLEM

TWO BODY PROBLEM
Series reversion/inversion of Lambert's time function
[AD-A216243] 12 p1607 N90-19245
Forbidden tangential orbit transfers between intersecting Keplerian orbits
[NASA-TP-3031] 20 p2816 N90-26028

TWO DIMENSIONAL BODIES
A scalar/vector potential solution for aerodynamic coefficients in wind shear 02 p0147 N90-10838
POS2D: A graphic program for analysing axisymmetric and two-dimensional structures
[DE90-608884] 10 p1417 N90-18168
Numerical study of laminar and turbulent flows past two-dimensional and axisymmetric bodies
15 p2100 N90-22020
Associated distributions in the analysis of two-dimensional random walks
[CWI-BS-R8917] 17 p2466 N90-24095

The finite analytic method and its applications. Volume 1: Laminar and turbulent flows past two-dimensional and axisymmetric bodies
[AD-A222787] 20 p2864 N90-26294
Aerodynamics of bodies in shear flow
23 p3268 N90-28496
A numerical calculation of hypersonic flow around blunt bodies using upwind difference scheme
[NAL-TR-1025] 24 p3422 N90-29331

TWO DIMENSIONAL BOUNDARY LAYER
Wall-layer eruptions in turbulent flows
[NASA-TM-102362] 02 p0219 N90-11250
The initial-boundary value problem for the Davey-Stewartson 1 equation; how to generate and drive localized coherent structures in multidimensions
[PREPRINT-684] 05 p0643 N90-13756
Application of a mass-consistent wind model to chinook windstorms
[AD-A213622] 07 p0963 N90-15568
Heat transfer near the entrance to a film cooling hole in a gas turbine blade
[AD-A217396] 13 p1757 N90-20089
Interaction of the large eddy structure in the inner-half of a turbulent boundary layer 18 p2551 N90-24561
Vortex-induced boundary layer separation
[AD-A221564] 21 p3005 N90-27078

TWO DIMENSIONAL FLOW
NT COUETTE FLOW
Two counter-rotating vortices approaching a free surface in a viscous fluid
[AD-A210495] 01 p0070 N90-10404
The upwind control volume scheme for unstructured triangular grids
[NASA-TM-101664] 03 p0301 N90-11703
Control of turbulent mixing layers
[AD-A211413] 03 p0301 N90-11708
Nonparallel stability of boundary layers
04 p0440 N90-12514
Design of the low-speed NLF(1)-0414F and the high-speed HSNLF(1)-0213 airfoils with high-lift systems
04 p0444 N90-12540
Wind tunnel results of the low-speed NLF(1)-0414F airfoil 04 p0444 N90-12541
Wind tunnel results of the high-speed NLF(1)-0213 airfoil 04 p0444 N90-12542
Measurement Techniques in Aerodynamics
[VKI-LS-1989-05] 05 p0573 N90-13339
Inviscid 2D solutions on unstructured, adaptive grids
05 p0640 N90-13737
Navier-Stokes solutions of 2-D transonic flow over unconventional airfoils 06 p0719 N90-14195
Computational investigation of incompressible airfoil flows at high angles of attack
[AD-A205885] 06 p0720 N90-14201
Multigrid solutions of elliptic fluid flow problems
06 p0775 N90-14507
Numerical simulation of the unsteady two-dimensional flow in a time-dependent doubly-connected domain
07 p0875 N90-15073
Visualization of 2 and 3 dimensional flows
[REPT-1] 08 p1065 N90-16164
Calculation of two and three dimensional super and hypersonic flows by solving the Euler equations
08 p1070 N90-16197
Two-Dimensional Measuring Techniques
[DGLR-PAPERS-88-04] 08 p1078 N90-16236
Coded trajectories for the investigation of strongly unsteady flow fields 08 p1078 N90-16240
Analysis of the measuring range and the accuracy of an existing particle image velocimetry system
08 p1080 N90-16247
Wake interaction effects on the transition process on turbine blades
[AD-A214492] 09 p1168 N90-16759
Comparison of two- and three-dimensional Navier-Stokes solutions with NASA experimental data for CAST-10 airfoil 10 p1325 N90-17658
Calculation of the unsteady two-dimensional, inviscid, compressible flow around a strongly cambered oscillating single blade 11 p1460 N90-18409
A simple algebraic grid adaptation scheme with applications to two- and three-dimensional flow problems
[NASA-TM-102446] 11 p1505 N90-18667
Characterization of fluid flow by digital correlation of scattered light
[NASA-CR-186403] 13 p1799 N90-20324
An evaluation of the two-dimensional Euler and Navier-Stokes calculations based on a flux-vector splitting
[PB90-166778] 14 p1912 N90-20963
PROTEUS two-dimensional Navier-Stokes computer code, version 1.0. Volume 1: Analysis description
[NASA-TM-102551] 14 p1973 N90-21303
Topics in vortex methods for the computation of three- and two-dimensional incompressible unsteady flows
15 p2091 N90-21967
The analysis and simulation of compressible turbulence
[NASA-CR-181997] 16 p2197 N90-22539
Secondary frequencies in the wake of a circular cylinder with vortex shedding
[NASA-CR-181998] 16 p2197 N90-22540
The stability of two-dimensional wakes and shear-layers at high Mach numbers
[NASA-CR-182050] 17 p2401 N90-23678
Local and global resonances in heated 2-D jets
[AD-A221671] 21 p3005 N90-27079
A finite difference treatment of Stokes-type flows: Preliminary report
[NASA-CR-186480] 22 p3168 N90-27970
FINFLO: A finite-volume based computer program for two-dimensional and axisymmetric compressible flow
[PB90-189473] 22 p3169 N90-27974
Calculation of unsteady two dimensional viscous incompressible flows by spectral methods
[ETN-90-97449] 22 p3175 N90-28015
Regular and chaotic motion of uniform elliptical vortices in external linear time dependent velocity fields
23 p3268 N90-28497
Two-dimensional wind tunnel test and comparison with calculations for a 15.2 percent thick airfoil section for wind turbines
[FFA-TN-1990-16] 23 p3269 N90-28501
The effect of rapid spoiler deployment on the transient forces on an aerofoil 23 p3274 N90-28527
Use of liquid crystals for qualitative and quantitative 2-D studies of transition and skin friction
[RAE-TM-AERO-2159] 23 p3325 N90-28800
An investigation of chaotic Kolmogorov flows
[NASA-CR-182079] 23 p3328 N90-28816
A potential-vorticity decomposition for the boundary integral equation analysis of viscous flows
24 p3417 N90-29301
Investigation of ATP blades, part 2. Validation of two-dimensional viscous flow simulation codes around thin airfoils
[NAL-TR-1046] 24 p3421 N90-29326
An investigation of the inviscid spatial instability of compressible mixing layers
[AD-A223776] 24 p3488 N90-29596

TWO DIMENSIONAL JETS
Impingement characteristics of heated plane turbulent jets 09 p1215 N90-17047

TWO DIMENSIONAL MODELS
Two-Dimensional Intercomparison of Stratospheric Models
[NASA-CP-3042] 02 p0248 N90-11405
Report on the 2-D Model Intercomparison Workshop held January 11-16, 1987 in Fort Myers Beach, Florida, chapter 2 02 p0248 N90-11406
Report of the 1988 2-D Intercomparison Workshop, chapter 3 02 p0248 N90-11407
Model documentation, chapter 4
02 p0249 N90-11408
Introduction and data summary, chapter 5
02 p0249 N90-11409
Studying shocks in model astrophysical flows
[DE89-618786] 02 p0295 N90-11677
Coherency properties of strong Langmuir turbulence
[DE89-009290] 03 p0371 N90-12119
Beam dynamics of a liquid metal ion source
[DE89-015856] 03 p0401 N90-12295
DART: A simulation code for charged particle beams, revision 1
[DE89-016697] 03 p0404 N90-12312
Computer simulations of two-dimensional quasiperiodic crystal and random tiling models
[DE89-016909] 03 p0410 N90-12355
Two dimensional conformal supergravity and critical behavior
[DE89-611968] 03 p0420 N90-12414
FLIC (FLame with Implicit Convection): A detailed, two-dimensional flame model
[AD-A212953] 04 p0473 N90-12710
Improved 2D numerical simulation model for strongly coupled heat and fluid flow in a thermal storage
[PB89-218879] 04 p0500 N90-12878
Local mode smoothing analysis of various incomplete factorization iterative methods in two dimensions
[REPT-89-36] 04 p0540 N90-13129
Placing mirrors in grids
[CWI-CS-R8906] 04 p0543 N90-13154
Two-dimensional analysis of two-phase reacting flow in a firing direct-injection diesel engine
[NASA-TM-102069] 05 p0582 N90-13392
Analytical and computer-aided models of InP-based MISFETs and heterojunction devices
[AD-A211861] 05 p0702 N90-14106
Perturbations in high-velocity gas flow
[DE90-000539] 06 p0777 N90-14520
Some edge-enhancing operators and their applications to image enhancement and edge detection
06 p0828 N90-14810
A two dimensional power spectral estimate for some nonstationary processes
[NASA-CR-186100] 06 p0833 N90-14843
Two-dimensional behavior of Megagauss-field-confined solid fiber Z-pinches
[DE90-000684] 06 p0845 N90-14918
Practical aspects of a 2-D edge-plasma model
[DE90-002995] 06 p0848 N90-14932
Further studies on possible coexistence of antiferromagnetism and superconductivity in 2D Heisenberg model
[DE90-601082] 07 p1000 N90-15783
The middle Martian atmosphere
07 p1014 N90-15874
Element-by-element preconditioning techniques for large-scale, vectorized finite element analysis in nonlinear solid and structural mechanics 08 p1087 N90-16291
The development of two-dimensional object identification techniques
[NASA-CR-186203] 08 p1107 N90-16408
Alvey MMI007. Object identification from 2D images: The RSRE contribution
[RSRE-MEMO-4277] 08 p1110 N90-16428
Universe as a topological defect in a higher-dimensional Einstein-Yang-Mills theory
[DE90-719507] 08 p1135 N90-16578
An experimental and analytical examination of stratified thermal storage 09 p1215 N90-17046
Upper semicontinuous global attractors for viscous flow
[NASA-CR-181976] 09 p1217 N90-17056
Test data of flow field of shuttle SRM nozzle joint with bond defects, using unheated air
11 p1470 N90-18464
Heat sink effects on weld bead: VPPA process
12 p1639 N90-19418
Reparametrization BRS cohomology in two-dimensional gravity and non-critical string theories
[DE90-741468] 12 p1725 N90-19911
Finite element models to predict the structural response of 120-mm sabot/rods during launch
[DE90-007497] 13 p1817 N90-20436
Two-dimensional damage models of fiber-reinforced composites 14 p1946 N90-21135
Sensitivity studies in a two-dimensional atmospheric transport model
[DAR-TP-18] 14 p2006 N90-21496
Topics in vortex methods for the computation of three- and two-dimensional incompressible unsteady flows
15 p2091 N90-21967
A 2-D analysis of particle velocity and stress of SH waves from a strip radiator. An experimental verification of both amplitude and phase using EMA transducers
[AERE-R-12600] 16 p2227 N90-22704
Tropical squall lines of the Arizona monsoon
16 p2257 N90-22867
A numerical study of basic coastal upwelling processes 16 p2259 N90-22878
Interdigitated back contact silicon solar cell analysis and design recommendations for space use
[AD-A220414] 17 p2420 N90-23790
PTA en route noise measurements
18 p2608 N90-24855
Heat sink effects on weld bead: VPPA process
[NASA-CR-186723] 19 p2697 N90-25349
Free vibrations of thin-walled semicircular graphite-epoxy composite frames
[NASA-TM-102680] 19 p2701 N90-25365
Perspective transformation for wide-view sky scenes
[AD-A222694] 21 p3007 N90-27093
A two dimensional study of rotor/airfoil interaction in hover
[NASA-CR-183272] 22 p3114 N90-27694
Towards a two dimensional scheme of anisotropic Godunov type. On the calculation of the velocity of the nodes in the multidimensional Lagrangian codes
[ETN-90-97458] 22 p3175 N90-28017
Towards a two dimensional code of anisotropic Godunov type 22 p3175 N90-28018
An influence of solar activity on latitudinal distribution of atmospheric ozone and temperature in 2-D radiative-photochemical model 22 p3206 N90-28187
The instability mechanism of synoptic-scale eddies
22 p3211 N90-28217
Electromagnetic scattering from two-dimensional thick material junctions
[NASA-CR-186468] 23 p3319 N90-28767
Radiative heat transfer
[PB90-247602] 23 p3327 N90-28813
Studies of vortex interactions
[AD-A223864] 23 p3328 N90-28817

Application of the complex variable solution to some problems in linear elastic materials with voids
24 p3478 N90-29658
Trend analysis of total ozone data
24 p3486 N90-29703
A global model of thunderstorm electricity and the prediction of whistler duct formation
24 p3493 N90-29744
Experimental study on two-dimensional free-flying robot satellite model 24 p3519 N90-29896
Computed torque control of a free-flying cooperating-arm robot 24 p3520 N90-29898
Absolute wind measurements in the lower thermosphere of Venus using infrared heterodyne spectroscopy
24 p3561 N90-30146

TWO FLUID MODELS
The generalized drift flux approach: Identification of the void-drift closure law 01 p0067 N90-10386
The role of particle collisions in pneumatic transport
01 p0068 N90-10392

TWO PHASE FLOW
The generalized drift flux approach: Identification of the void-drift closure law 01 p0067 N90-10386
Two-phase potential flow 01 p0067 N90-10387
Interpretation and modeling of the averaged equations for a fluid-solid flow 01 p0068 N90-10388
Effect of particle velocity fluctuations on the inertia coupling in two-phase flow 01 p0068 N90-10391
The role of particle collisions in pneumatic transport
01 p0068 N90-10392
A laser Doppler anemometry investigation of single-phase and particle-laden jet flows
[AD-A210660] 02 p0220 N90-11261
Three-dimensional, two-phase, transonic, canted nozzle flows
[AD-A211528] 03 p0347 N90-11984
Two-phase flow pressure losses in pipeline fittings
[ESDU-89012] 04 p0500 N90-12883
Two-dimensional analysis of two-phase reacting flow in a firing direct-injection diesel engine
[NASA-TM-102069] 05 p0582 N90-13392
Fluid-particle interaction in solid-liquid two-phase grid turbulence 06 p0773 N90-14496
Course A: Numerical modeling of two-phase flows for presentation at Ecole d'Ete d'Analyse Numerique
[DE90-002074] 06 p0778 N90-14526
Interfacial area in two-phase flow
[DE90-002210] 06 p0778 N90-14527
Stability of numerical solutions for stratified two-phase flow
[DE90-701646] 07 p0929 N90-15379
Design manual for microgravity two-phase flow and heat transfer
[AD-A214937] 09 p1201 N90-16957
An engineering approach to two-phase flow modeling in reduced gravity
[DE90-005539] 09 p1202 N90-16967
Boiling inside tubes: Pressure drop in straitht tubes with upward or horizontal flow
[ESDU-89039] 09 p1220 N90-17078
The effect of the virtual mass force term on the stability of transient two-phase flow analysis
[DE90-733142] 10 p1384 N90-18010
Direct and inverse scattering problem associated with the elliptic Sinh-Gordon equation
[AD-A216455] 11 p1551 N90-18931
Study of interfacial behavior in cocurrent gas-liquid flows
[DE90-005988] 12 p1659 N90-19532
Experimental and analytical investigation of adiabatic critical water air two phase flow in small diameter tubes
[TB-88/1] 12 p1660 N90-19540
An experimental investigation of the physical mechanisms controlling the asymmetric flow past slender bodies at large angles of attack
15 p2053 N90-21767
Development and integration of the capillary pumped loop GAS and Hitchhiker flight experiments
[NASA-TM-100756] 15 p2059 N90-21790
Flow boiling with enhancement devices for cold plate coolant channel design
[NASA-CR-186358] 15 p2089 N90-21961
On dual Lagrangian hyperbolic models for one dimensional two phase flow problems
[DE90-007012] 15 p2098 N90-22004
Mathematical modeling of fluid-solid mixtures
[DE90-009152] 15 p2098 N90-22007
Parallel channel flow excursions
[DE90-009129] 16 p2235 N90-22753
Nonstrictly hyperbolic conservation laws
[AD-A218525] 16 p2237 N90-22762
An analytic study of nonsteady two-phase laminar boundary layer around an airfoil
18 p2643 N90-25051
Fingering in 2-D porous media: Experiments, network simulators and statistical models
19 p2691 N90-25308
Particle tracking methods and fractal statistics in groundwater modeling 19 p2691 N90-25309
Numerical analysis of three-dimensional particle-laden flow equations
[IAR-90-2] 20 p2860 N90-26268
Effect of initial conditions on the development of two-phase jets
[AD-A222621] 20 p2864 N90-26293
Two-phase heat transport systems for spacecraft scaling with respect to gravity
[NLR-TP-89127-U] 21 p2965 N90-26857
Velocity interferometry 24 p3420 N90-29316

TWO PHASE SYSTEMS
U BINARY SYSTEMS (MATERIALS)

TWO PHOTON COHERENT STATES
U SQUEEZED STATES (QUANTUM THEORY)

TWO STAGE TURBINES
Heat transfer and pressure measurements for the SSME fuel-side turbopump
[NASA-CR-184928] 17 p2355 N90-23405
Energy Efficient Engine high pressure turbine component test performance report
[NASA-CR-168289] 23 p3278 N90-28553

TYPE 3 BURSTS
Kilometric type III radio bursts and interplanetary transients 06 p0867 N90-15038

TYPEWRITERS
NT TELETYPEWRITERS

TYPHOONS
Forecasting 24 and 48 hour intensity changes, for northwestern Pacific tropical cyclones, using satellite imagery
[AD-A218174] 13 p1846 N90-20597
A description of tropical cyclone recurvature in terms of isentropic potential vorticity
[AD-A218482] 17 p2425 N90-23821
Meteorological Satellite Center Technical Note, no. 17, 1988
[ISSN-0388-9653] 21 p3028 N90-27213
Investigation into position accuracy of typhoon center determined on GMS imagery 21 p3028 N90-27217
Case study on Pre-Typhoon Active Convective Clouds (PTACC) 21 p3029 N90-27220
Behavior of dust clouds from Australian dust storms in 1982-1983 as observed by the GMS
21 p3029 N90-27221

TYROSINE
Pre-treatment with tyrosine reverses hypothermia induced behavioral depression
[AD-A215211] 09 p1252 N90-17265
Strategies to sustain and enhance performance in stressful environments
[AD-A221224] 18 p2583 N90-24711

U

U.S.S.R.
USSR Space Life Sciences Digest, issue 22
[NASA-CR-3922(26)] 03 p0378 N90-12153
USSR Space Life Sciences Digest, issue 23
[NASA-CR-3922(27)] 03 p0378 N90-12154
USSR Space Life Sciences Digest. Index to issues 21-25
[NASA-CR-3922(30)] 06 p0819 N90-14763
COCOM (Coordinating Committee for Multilateral Exports), technology transfer and its impact on national security
[AD-A214569] 09 p1297 N90-17519
Microgravity science and applications bibliography, 1989 revision
[NASA-TM-4192] 14 p1957 N90-21207
JPRS report: Science and technology. USSR: Electronics and electrical engineering
[JPRS-UEE-90-002] 14 p1970 N90-21284
JPRS report. Science and technology. USSR: Earth sciences
[JPRS-UES-88-004] 14 p1995 N90-21431
JPRS report. Science and technology. USSR: Earth sciences
[JPRS-UES-89-002] 14 p1995 N90-21432
JPRS report: Science and technology. USSR: Life sciences
[JPRS-ULS-90-002] 14 p1995 N90-21434
JPRS report: Science and technology. USSR: Physics and mathematics
[JPRS-UPM-90-002] 14 p2022 N90-21593
Opportunities for US-USSR cooperation in the investigation of Arctic stratospheric ozone
15 p2125 N90-22154
USSR Space Life Sciences Digest, issue 25
[NASA-CR-3922(29)] 15 p2135 N90-22203
Brazil, the United States, and the missile technology control regime
[AD-A220551] 17 p2362 N90-23449
USSR space life sciences digest, issue 27
[NASA-CR-3922(32)] 19 p2717 N90-25457
Soviet image pattern recognition research
[DE90-010912] 21 p3059 N90-27396
JPRS report: Science and technology. USSR: Earth sciences
[JPRS-UES-90-004] 24 p3483 N90-29688
JPRS report: Science and technology. USSR: Earth sciences
[JPRS-UES-90-003] 24 p3483 N90-29689
JPRS Report: Science and technology. USSR: Life sciences
[JPRS-ULS-90-007] 24 p3497 N90-29762
JPRS report: Science and technology. USSR: Life sciences
[JPRS-ULS-90-004] 24 p3497 N90-29763
System software for Soviet computers
24 p3523 N90-29921

U.S.S.R. SPACE PROGRAM
JPRS Report: Science and Technology. USSR: Space
[JPRS-USP-89-007] 02 p0158 N90-10900
Meeting of intercosmos space physics group
02 p0158 N90-10902
Soviet Mars program 02 p0158 N90-10903
USSR and international cooperation in space
02 p0158 N90-10905
Sagdeyev discusses space missions, policy, Mars plans 02 p0159 N90-10906
USSR Space Life Sciences Digest, issue 24
[NASA-CR-3922(28)] 03 p0378 N90-12152
Comparison of the space program performance of countries with space programs
[ILR-MITT-222] 05 p0709 N90-14150
JPRS Report: Science and technology. USSR: Space. Soviet space program to the year 2000
[JPRS-USP-89-008] 06 p0728 N90-14248
Glavkosmos U.S.S.R. and the basic objectives of its activity 09 p1174 N90-16788
Glavkosmos operational space transportation systems
09 p1174 N90-16791
Transportation systems for manned space missions
09 p1176 N90-16805
U.S.S.R. space transportation systems
09 p1176 N90-16806
The Magellan Venus explorer's guide
[NASA-CR-186968] 23 p3286 N90-28592

U-2 AIRCRAFT
Global stratospheric change: Requirements for a Very-High-Altitude Aircraft for Atmospheric Research
[NASA-CP-10041] 06 p0723 N90-14220
NASA/USRA high altitude reconnaissance aircraft
[NASA-CR-186885] 18 p2496 N90-24266
Technology development: Future use of NASA's large format camera is uncertain
[GAO/NSIAD-90-142] 20 p2865 N90-26298

UBV SPECTRA
Photometric monitoring of early type emission line stars 15 p2184 N90-22478

UDIMET ALLOYS
Application of high performance metals in gas turbine engines
[PNR90640] 20 p2811 N90-25999

UH-1 HELICOPTER
Using goal programming to determine the optimal engine mix for UH-1 helicopters
[AD-A214893] 09 p1168 N90-16762

UH-60A HELICOPTER
Airworthiness and flight characteristics test of the UH-60A Black Hawk helicopter equipped with the XM-139 multiple mine dispensing system (VOLCANO)
[AD-A210271] 01 p0006 N90-10025
Task analysis of the UH-60 mission and decision rules for developing a UH-60 workload prediction model. Volume 1: Summary report
[AD-A210763] 02 p0255 N90-11446
Preliminary airworthiness evaluation of the Woodward hydromechanical unit installed on T700-GE-700 engines in the UH-60A helicopter
[AD-A216751] 11 p1464 N90-18430
Plan, formulate, and discuss a NASTRAN finite element model of the UH-60A helicopter airframe
[NASA-CR-181975] 13 p1818 N90-20439
Ground shake test of the UH-60A helicopter airframe and comparison with NASTRAN finite element model predictions
[NASA-CR-181993] 19 p2661 N90-25143

ULLAGE
Ignitability of jet-A fuel vapors in aircraft fuel tanks
10 p1313 N90-17594
Prediction of the ullage gas thermal stratification in a NASP vehicle propellant tank experimental simulation using FLOW-3D
[NASA-TM-103217] 20 p2841 N90-26160

ULNA
Experiment K-6-27. Analysis of radiographs and biosamples from primate studies
20 p2897 N90-26478
ULTRA SHORT WAVE RADIO EQUIPMENT
U VERY HIGH FREQUENCY RADIO EQUIPMENT
ULTRAHIGH FREQUENCIES
The effectiveness of adaptive PRF (Pulse Repetition Frequency) selection in minimizing range obscuration in the TDWR (Terminal Doppler Weather Radar) system
[AD-A211267] 02 p0213 N90-11222
Modeling of diffraction reflection and clutter loss in UHF radio wave propagation
[FEL-1988-28] 03 p0340 N90-11938
DSN 70-meter antenna microwave optics design and performance improvements. Part 2: Comparison with measurements 04 p0487 N90-12800
Modelling UHF propagation for frequency assignment in radio relay networks 06 p0764 N90-14445
The Australian experiment with ETS-V
10 p1372 N90-17949
LMSS drive simulator for multipath propagation
10 p1372 N90-17950
Megawatt-klystron amplifiers in L-band
[DE90-004864] 10 p1379 N90-17992
Wideband S band transmitter
[AD-A217620] 13 p1794 N90-20295
Prediction of VHF/UHF mobile reception in urban areas: Comparison with measurements in London
[BBC-RD-1989/11] 14 p1965 N90-21255
Spectral characteristics of low-angle radar ground clutter
[AD-A220817] 17 p2392 N90-23622
An L-band antenna array with integrated phase shifters
[DLR-FB-89-63] 18 p2544 N90-24519
Concept study for UHF T/R modules
[AD-A220281] 18 p2547 N90-24536
Estimation of the impulse response of a broadband mobile radio channel in suburbia at 910 MHz
20 p2846 N90-26187
Wideband characterization of forest propagation channels 20 p2846 N90-26188
A narrowband tactical communication system for the VHF and UHF mobile radio bands
20 p2847 N90-26192
Electric field strength meters for the HF, VHF, and UHF bands
[BBC-RD-1990/3] 20 p2851 N90-26212
Tactical applications of the UHF satellite communications system 21 p3070 N90-27451
Wideband impedance transformer for UHF power transistor time domain waveform measurement system
[PB90-210642] 22 p3167 N90-27962
ULTRAHIGH VACUUM
Thermal stability of the carbon-carbon bond in ethylene adsorbed on Si(100): An isotopic mixing study
[AD-A211591] 04 p0470 N90-12691
Materials for ultra-high vacuum
[DE90-007908] 14 p1959 N90-21217
Surface defects and chemistry on the SnO2(110) surface 18 p2559 N90-24603
Imaging and spectroscopy of small molecules by scanning tunneling microscopy
[AD-A222572] 20 p2924 N90-26641
Impact fracture experiments simulating interstellar grain-grain collisions 21 p3093 N90-27584
An electron spin resonance study of adsorbed gases in ultrahigh vacuum
[ETN-90-97323] 24 p3447 N90-29469
ULTRALIGHT AIRCRAFT
Data of aero acoustic measurements on ultra-light aircraft propellers
[ESA-TT-1147] 19 p2754 N90-25648
ULTRALOW FREQUENCIES
U EXTREMELY LOW RADIO FREQUENCIES
ULTRALOW TEMPERATURE
U CRYOGENIC TEMPERATURE
ULTRASHORT PULSED LASERS
Improvement of ultrashort pulsed laser shadowgraph photography by means of optical filters
[ISL-CO-215/88] 04 p0504 N90-12906
Application of a copper vapour laser to investigation of shock and blade interaction in a shock tube
[PNR90578] 04 p0506 N90-12918
A feasibility study for using CARS in temperature and volumetric measurement as a function of time
[ISL-CO-223/88] 09 p1226 N90-17116
The dynamics of electrons in very intense lasers
[DE90-007246] 11 p1516 N90-18729
ULTRASONIC AGITATION
Cavitation-controlled ultrasonic agitator
[DE90-002773] 06 p0838 N90-14871
ULTRASONIC FLAW DETECTION
Investigation of materials and bonding using the scanning laser acoustic microscope
[KCP-613-4033] 01 p0048 N90-10270
Sensors for nondestructive testing and evaluation of materials
[DE89-014763] 02 p0223 N90-11279
A technique to correlate fractography with NDE (Non-Destructive Evaluation) of small samples
[DE89-016904] 02 p0231 N90-11325
Quantitative non-destructive evaluation using laser generated ultrasonic pulses 05 p0653 N90-13805
Nondestructive evaluation of flaw clusters and thin layer interfaces 06 p0795 N90-14833
Theoretical study on creep damage detection by ultra-sonic wave measurement
[DE90-702472] 08 p1087 N90-16290
Utilization of focused acoustic beams to inspect composite materials
[ETN-90-96084] 09 p1188 N90-16880
The diffraction of ultrasound by cracks: Comparison of experiment with theory
[AERE-R-13334] 13 p1813 N90-20410
Development of ultrasonic nondestructive methods for defect and damage characterization in composite materials 15 p2063 N90-21816
The classification of defects from ultrasonic measurements
[AERE-R-13306] 15 p2108 N90-22056
Ultrasonic detection of critical damage in carbon-epoxy composite materials
[ONERA-RT-5/7256-RY-081-R]
16 p2212 N90-22616
Nondestructive Testing (NDT); Ceramic Matrix Composite Materials (CMCM) --- Nondestructive testing (ndc); ceramic matrix composite materials (CMMC)
[REPT-892-430-123] 16 p2222 N90-22677
Applications of laser ultrasound
[AERE-R-13106] 16 p2239 N90-22777
Development of creep-fatigue damage detection method of rotor steel by ultrasonic wave measurement
[DE90-503792] 20 p2877 N90-26365
A general discussion of the retirement for cause inspection system 21 p2957 N90-26814
Improved transverse crack detection in composites
[NASA-TM-103261] 22 p3153 N90-27875
Development of an automated ultrasonic inspection system for composite structure on in-service aircraft
22 p3186 N90-28079
The application of infrared thermography to the nondestructive testing of composite materials
22 p3187 N90-28084
Advanced NDE techniques for quantitative characterization of aircraft 22 p3188 N90-28088
Inspection system for in-situ inspection of aircraft composite structures 22 p3188 N90-28091
ULTRASONIC RADIATION
Process monitoring using optical ultrasonic wave detection
[DE90-002021] 06 p0838 N90-14870
Cavitation-controlled ultrasonic agitator
[DE90-002773] 06 p0838 N90-14871
Diffraction of light by ultrasonic pulses
15 p2164 N90-22366
High Intensity Electro-Magnetic and Ultrasonic Effects on Inorganic Materials Behavior and Processing Workshop
[AD-A218884] 16 p2215 N90-22640
Superheterodyne three-wave detection of gravitation waves
[DE90-620465] 16 p2255 N90-22856
Investigations of ultrasonic wave interactions at imperfect boundaries separating anisotropic materials
[DE90-010661] 18 p2612 N90-24875
An approach for relating the results of quantitative nondestructive evaluation to intrinsic properties of high-performance materials
[NASA-CR-186484] 19 p2699 N90-25355
Characterization by ultrasonic tests of ceramics submitted to thermal shocks: Influence of several parameters on the crack dimensioning
[ETCA-89-R-060] 22 p3160 N90-27923
Ultrasonic verification of five wave fronts in unidirectional graphite epoxy composite
[NASA-CR-185288] 23 p3337 N90-28858
ULTRASONIC SCANNERS
Investigation of materials and bonding using the scanning laser acoustic microscope
[KCP-613-4033] 01 p0048 N90-10270
ULTRASONIC SOLDERING
Proceedings of the 14th Annual Electronics Manufacturing Seminar
[AD-A224276] 24 p3463 N90-29563
ULTRASONIC SPECTROSCOPY
Collective-mode spectroscopy of textures in superfluid (3)He-B
[PB89-221634] 03 p0413 N90-12370
Ultrasonic evaluation of porosity in aluminum cast materials
[AD-A213548] 07 p0905 N90-15232
Ultrasensitive laser spectroscopy in solids: Single-molecule detection
[AD-A216085] 11 p1514 N90-18716
Ultrasonic detection of critical damage in carbon-epoxy composite materials
[ONERA-RT-5/7256-RY-081-R]
16 p2212 N90-22616
ULTRASONIC TESTS
Generic system components of the Thiokol ultrasonic RSRM case-to-insulation bondline inspection system
[NASA-CR-183738] 01 p0031 N90-10171
Ultrasonic evaluation of porosity in aluminum cast materials
[AD-A213548] 07 p0905 N90-15232
Theoretical study on creep damage detection by ultra-sonic wave measurement
[DE90-702472] 08 p1087 N90-16290
Generalized pulse equations for through-transmission evaluation of arbitrary multilayered structures
[NASA-TM-100752] 09 p1278 N90-17407
Residual stresses: A review of their measurement and interpretation using x ray diffraction
[AERE-R-13005] 13 p1815 N90-20423
Qualification of the RSRM case membrane case-to-insulation bondline inspection using the Thiokol Corporation ultrasonic RSRM bondline inspection system
[NASA-CR-183940] 16 p2209 N90-22602
A 2-D analysis of particle velocity and stress of SH waves from a strip radiator. An experimental verification of both amplitude and phase using EMA transducers
[AERE-R-12600] 16 p2227 N90-22704
Applications of laser ultrasound
[AERE-R-13106] 16 p2239 N90-22777
Qualification of the RSRM field joint CF case-to-insulation bondline inspection using the Thiokol Corporation ultrasonic RSRM bondline inspection system
[NASA-CR-183931] 16 p2242 N90-22788
Recent advances in nondestructive evaluation made possible by novel uses of video systems
[NASA-TM-102491] 16 p2244 N90-22801
Crack detection in silicon nitride by acoustic microscopy
[AERE-R-13196] 16 p2245 N90-22803
Nondestructive measurement of residual stresses in aircraft transparencies
[AD-A218680] 17 p2415 N90-23762
A study on ultrasonic detection and characterization of partially closed fatigue cracks
[DE90-011748] 19 p2702 N90-25371
Laser ultrasonic measurements on ceramic materials with rough surfaces
[DE90-012961] 20 p2838 N90-26141
Characterization by ultrasonic tests of ceramics submitted to thermal shocks: Influence of several parameters on the crack dimensioning
[ETCA-89-R-060] 22 p3160 N90-27923
Input-output characterization of fiber reinforced composites by P waves
[NASA-CR-185287] 22 p3189 N90-28097
ULTRASONIC WAVE TRANSDUCERS
The investigation of the fundamental limits of heterodyne holographic interferometry with the application of imaging laser generated lamb waves
[AD-A211048] 02 p0224 N90-11285
Foundations of millimeter-wave frequency acoustic microscopy 12 p1709 N90-19816
Ultrasonic techniques for aircraft ice accretion measurement 14 p1908 N90-20926
PVDF contact probes
[VTT-RR-623] 20 p2857 N90-26253
ULTRASONIC WAVES
U ULTRASONIC RADIATION
ULTRASONIC WELDING
Application of gallium arsenide solar cell arrays for long duration low earth orbit missions like Columbus
10 p1340 N90-17759
Ultrasonic and parallel gap welding of GaAs solar cells, experimental and simulation results
10 p1341 N90-17766
Development of an aluminium solar cell interconnector technology 10 p1341 N90-17771
ULTRASONICS
Performance of a broadbanded ultrasonic transducer with coaxially mounted, nondirectional receiver
[DE89-015838] 01 p0060 N90-10343
NDE (Non-Destructive Evaluation) publications, 1985
[PB89-229025] 03 p0356 N90-12036

Noncontacting laser ultrasonic generation and detection at the surface of molten metal
[DE90-002020] 06 p0791 N90-14605
Biological effects of hyperthermia and potential risk associated with ultrasonic exposure
[PB89-100702] 06 p0820 N90-14768
Feasibility study of using industrial robot for ultrasound testing
[DE90-002977] 07 p0943 N90-15461
Bulk wave characterization of high T(sub c) superconductors
[AD-A214030] 07 p1004 N90-15813
Apparatus for imaging deep arterial and coronary lesions
[NASA-CASE-NPO-17439-1-CU] 08 p1104 N90-16391
Ultrasonic assisted paint removal method
[AD-D014264] 08 p1119 N90-16479
Subtle porosity variation in the YBa2Cu3O(7-x) high-temperature superconductor revealed by ultrasonic imaging
[NASA-TM-102130] 09 p1235 N90-17167
Method and apparatus for characterizing reflected ultrasonic pulses
[NASA-CASE-LAR-13966-1] 09 p1278 N90-17408
Full field visualization of surface and bulk acoustic waves using heterodyne holographic interferometry
[AD-A214353] 10 p1387 N90-18023
Two dimensional modifications of Gaussian laser light bundles
[AD-A215207] 10 p1389 N90-18033
Improved processes for ultrasonic object recognition in robotics
[ETN-90-95362] 12 p1672 N90-19604
Shaping the insonifying pulse to optimise B-scans obtained in austenite
[AERE-R-13518] 13 p1775 N90-20187
Three-dimensional medical image analysis using local dynamic algorithm selection on a multiple-instruction, multiple-data architecture
[AD-A218024] 13 p1852 N90-20630
Some recent applications of laser ultrasound to the characterisation of materials
[AERE-R-13438] 14 p1985 N90-21374
On-line assessment of weld quality using ultrasonics
[AERE-R-13401] 14 p1989 N90-21398
Institute for Materials Science and Engineering, nondestructive evaluation: Technical activities
[PB90-132739] 15 p2108 N90-22055
Acousto-ultrasonic nondestructive evaluation of materials using laser beam generation and detection
[NASA-CR-186894] 17 p2398 N90-23664
An ultrasonic-switching three phase current source inverter with insulated gate bipolar transistors
[EMV-89-11] 17 p2399 N90-23666
Theory and experimental technique for nondestructive evaluation of ceramic composites
[NASA-TM-102561] 17 p2414 N90-23754
Surface wave characterization of high T(sub c) superconductors
[AD-A221077] 19 p2760 N90-25683
Real-time monitoring of ceramic sintering with laser ultrasonics
[DE90-012960] 20 p2838 N90-26140
Electronics design of the infrared/ultrasonic sensing for a robot gripper
[PB90-160383] 21 p3010 N90-27109
Experimental investigations on the stability and vorticity of the vortex breakdown phenomenon above delta wings, measured by the ultrasonic laser method
[ESA-TT-1079] 23 p3268 N90-28498
Treatment of systematic errors 2: Fusion of ultrasound and visual sensor data
[DE90-014780] 23 p3334 N90-28850
Robots, systems, and flexible automation
[DE90-015802] 24 p3476 N90-29649

ULTRAVIOLET ABSORPTION
Ultraviolet absorption cross-sections of bromoform in the temperature range 295-240 K
[AERONOMICA-ACTA-A-348-1989] 05 p0622 N90-13630

ULTRAVIOLET ASTRONOMY
UVCS: An Ultraviolet Coronagraph Spectrometer for SOHO 04 p0568 N90-13310
Deep detection of hot star populations at balloon ultraviolet wavelengths 05 p0661 N90-13865
The low-ion QSO absorption-line systems 05 p0712 N90-14162
Ultraviolet properties of hot stars in globular clusters 06 p0862 N90-15007
Ultraviolet observations of the atmosphere of Io and the plasma torus 12 p1728 N90-19929
Ultraviolet and infrared studies of Be stars 16 p2329 N90-23275
Galactical ultra wide angle Schmidt system 18 p2536 N90-24468

ULTRAVIOLET DETECTORS
NT TOTAL OZONE MAPPING SPECTROMETER
NT ULTRAVIOLET SPECTROMETERS
Comparison of the LOWTRAN 7 code and S3-4 satellite measurements of UV radiance
[AD-A211356] 03 p0372 N90-12124
UV photo-enhanced MOCVD of cadmium and cadmium telluride
[RSRE-MEMO-4208] 15 p2174 N90-22422

ULTRAVIOLET LASERS
A proposed linac cavity RF drive system for the Los Alamos extreme ultraviolet free-electron laser
[DE89-016814] 03 p0353 N90-12016
Laser detection and discrimination system
[AD-D014301] 07 p0937 N90-15426
CW ultraviolet laser excited with an electron beam
[AD-A214928] 09 p1227 N90-17123
Generation of intensive UV laser radiation and utilization in high resolution spectroscopy of SO2
[ETN-90-95361] 12 p1668 N90-19581
Monitoring of catalyst performance in CO2 lasers using frequency modulation spectroscopy with diode lasers 18 p2561 N90-24614
Research studies on extreme ultraviolet and soft x ray lasers
[AD-A220271] 18 p2562 N90-24621
Raman scattering measurements using UV excimer lasers 21 p2974 N90-26902
Study of a 1-Hz hypocycloidal pinch (HCP) pump for production of ultraviolet lasers
[AD-A224091] 24 p3547 N90-30064

ULTRAVIOLET LIGHT
U ULTRAVIOLET RADIATION

ULTRAVIOLET PHOTOGRAPHY
A long look back: ESA's faint object camera. The story of the faint object camera, one of ESA's contributions to the Hubble space telescope
[ESA-BR-67] 19 p2784 N90-25839

ULTRAVIOLET RADIATION
NT EXTREME ULTRAVIOLET RADIATION
NT FAR ULTRAVIOLET RADIATION
NT LYMAN ALPHA RADIATION
NT NEAR ULTRAVIOLET RADIATION
Silicon dioxide deposition at 100 deg C using vacuum ultraviolet light
[TR-0088(3945-07)-6] 01 p0047 N90-10269
Fuel neutralization by ozone oxidation 02 p0206 N90-11176
Estimated UV clutter levels at 10-100 meter sensor pixel resolution extrapolated from recent polar bear measurements
[AD-A211357] 03 p0372 N90-12125
UV ionospheric remote sensing with the polar BEAR satellite
[AD-A211359] 03 p0372 N90-12127
Energy transfer and non-linear optical properties at near ultraviolet wavelengths: Rare earth 4f(yields)5d transitions in crystals and glasses
[DE90-000065] 03 p0405 N90-12321
Interzodiak 2: Observation of EUV-resonance radiation 05 p0660 N90-13854
Prediction of the 10 cm solar flux index 05 p0662 N90-13872
Measurement of the X-UV emission from the back face of thin foils illuminated by an A4 omega laser 06 p0784 N90-14562
X-UV amplification in a plasma column of five centimeters. Five beams experiment 06 p0786 N90-14574
Potential impact of stratospheric ozone depletion on marine ecosystems
[PB90-112616] 08 p1098 N90-16360
Enhancement of processes for solar photocatalytic detoxification of water
[DE90-003949] 12 p1623 N90-19330
Search for far infrared radiation from optically pumped defect modes
[AD-A216976] 12 p1714 N90-19843
The inter-outburst behavior of cataclysmic variables
[NASA-CR-186374] 13 p1902 N90-20914
UV spectrometer system AFGL 801 A HUP
[AD-A217805] 14 p2026 N90-21619
Atmospheric Propagation in the UV, Visible, IR, and mm-Wave Region and Related Systems Aspects
[AGARD-CP-454] 15 p2079 N90-21907
Minimizing the effects of the atmosphere in the observation of ultraviolet radiation 15 p2080 N90-21911
Modelling UV-visible radiation observed from space 15 p2085 N90-21937
The emission lines in the ultra-violet spectrum of Beta Lyrae 15 p2183 N90-22474
Effects of solar ultraviolet radiation on biogeochemical dynamics in aquatic environments
[AD-A221119] 18 p2578 N90-24687
In vitro photoreactivation of transforming DNA of bacillus subtilis spores after irradiation with UV light
[DLR-FB-89-45] 18 p2583 N90-24710
IUE observations of Cyg X-2 and Sco X-1: Accretion disks and the z-shaped curve 19 p2783 N90-25832
Stratospheric chemistry 20 p2886 N90-26424
The possible presence of interstellar PAHs in meteorites and interplanetary dust particles 21 p3092 N90-27579
Construction of a UV cell for micro-liquid chromatography
[PML-1989-B] 22 p3156 N90-27894
Solar UV variability 22 p3201 N90-28162
Observed solar near UV variability: A contribution to variations of the solar constant 22 p3201 N90-28163
A review of the 11-year solar cycle, the QBO, and the atmosphere relationship 22 p3202 N90-28166
Response of the middle atmosphere to solar UV and dynamical perturbations 22 p3204 N90-28175
Stratospheric effects of solar ultraviolet variations on the solar rotation time scale 22 p3204 N90-28176
Gases of the middle atmosphere and short-term solar radiation variations 22 p3204 N90-28177
Diurnal and temporal variation of UV-flux and its dependence on stratospheric ozone 22 p3205 N90-28184
UV-induced degradation of the Si-SiO2 interface: Applications to the point contact solar cell
[DE90-013843] 23 p3344 N90-28898
DNA damage and repair in human skin: Pathways and questions
[DE90-015126] 23 p3356 N90-28966

ULTRAVIOLET REFLECTION
Reflection indicatrices of natural surfaces for AVHRR channels 1 and 2
[DLR-MITT-89-16] 05 p0664 N90-13882
Reflection indicatrices of natural surfaces for AVHRR channels 1 and 2
[ESA-TT-1192] 19 p2709 N90-25417

ULTRAVIOLET SPECTRA
UV observations of NGC 205
[NASA-CR-185975] 02 p0291 N90-11661
Investigation of atmospheric emissions in ultraviolet, vacuum ultraviolet, and extreme ultraviolet wavelength
[AD-A212169] 03 p0371 N90-12123
Comparison of the LOWTRAN 7 code and S3-4 satellite measurements of UV radiance
[AD-A211356] 03 p0372 N90-12124
The low-ion QSO absorption-line systems 05 p0712 N90-14162
A source of observational constraints on the structure of Wolf-Rayet winds
[DE90-001236] 06 p0864 N90-15023
Eurolaser. High power excimer laser: Optical crystals
[ETN-90-95901] 08 p1132 N90-16558
Ultraviolet observations of the atmosphere of Io and the plasma torus 12 p1728 N90-19929
Nearly simultaneous optical, ultraviolet, and x ray observations of three PG quasars
[NASA-CR-186355] 12 p1728 N90-19932
The development of ultraviolet-ozone cleaning as a production process in the packaging of integrated circuits
[DE90-007960] 14 p1959 N90-21220
UV spectral simulations using LOWTRAN 7 15 p2083 N90-21928
Observations of Cygnus X-2 at x ray, UV, optical and radio frequencies
[MPE-PREPRINT-163] 17 p2481 N90-24191
Observations of Cygnus X-2 with IUE: Ultraviolet results from a multiwavelength campaign 17 p2482 N90-24193
Optical spectroscopy of V1341 Cyg, the optical counterpart of Cyg X-2 17 p2482 N90-24194
Advanced multilayer x ray optics
[DE90-008228] 18 p2616 N90-24902
Emission lines from X ray binaries 19 p2769 N90-25733
Search of the optical counterpart of the X rays source 1H 0521+373 19 p2780 N90-25815
Quantitative spectroscopy of x ray laser plasmas in pulsed power devices
[AD-A221964] 21 p3078 N90-27501
Spectroscopic ellipsometry in vacuum ultraviolet spectral area
[ETN-90-97317] 22 p3249 N90-28426
The ionization structure of planetary nebulae 10: NGC 2392
[NASA-CR-186960] 23 p3411 N90-29274
PW Vul: A classical nova with nearly solar abundances
[NASA-CR-185080] 23 p3411 N90-29275
The impact of IUE on studies of the nova outburst: 1986-1990
[DE90-014915] 24 p3563 N90-30156

ULTRAVIOLET SPECTROGRAPHS
U ULTRAVIOLET SPECTROMETERS
ULTRAVIOLET SPECTROMETERS
NT TOTAL OZONE MAPPING SPECTROMETER
The SMM UV observations of Active Region 5395
03 p0434 N90-12485
Development of the RAIDS (Remote Atmospheric and Ionospheric Detector System) extreme ultraviolet wedge and strip detector
[AD-A213730] 07 p0949 N90-15495
UV spectrometer system AFGL 801 A HUP
[AD-A217805] 14 p2026 N90-21619
The ratio of neutral hydrogen to neutral helium in the local interstellar medium 15 p2189 N90-22499
ULTRAVIOLET SPECTROSCOPY
Shortwavelength coherent radiation: Generation and applications
[AD-A209847] 01 p0074 N90-10427
The effect of degree of aromaticity and alkyl substitution of polyaromatic hydrocarbons on instrumental response factors
[DE89-000761] 02 p0196 N90-11117
High temperature and high resolution UV photoelectron spectroscopy using supersonic molecular beams
[DE90-000176] 03 p0323 N90-11835
Shock layer vacuum UV spectroscopy in an arc-jet wind tunnel
[NASA-TM-102258] 09 p1226 N90-17112
Initiation precursors and initiators in laser-induced copolymerization of styrene and maleic anhydride in acetone
[NASA-TM-4166] 10 p1346 N90-17810
Far-ultraviolet spectroscopy of Comet Halley
12 p1736 N90-19979
Continued investigations of new concepts for improved spectrochemical analysis
[AD-A219403] 16 p2216 N90-22644
UV and VUV spectroscopy and photochemistry of small molecules in a supersonic jet 20 p2947 N90-26771
ULTRAVIOLET TELESCOPES
NT STARLAB
UV ionospheric remote sensing with the polar BEAR satellite
[AD-A211359] 03 p0372 N90-12127
EIT: Solar corona synoptic observations from SOHO with an Extreme-ultraviolet Imaging Telescope
04 p0567 N90-13309
ULYSSES MISSION
The solar flare and cosmic gamma-ray burst experiment aboard the Ulysses spacecraft 03 p0431 N90-12470
Draft Environmental Impact Statement for the Ulysses Mission (Tier 2)
[NASA-TM-102903] 06 p0812 N90-14727
On the development of the power sources for the Ulysses and Galileo missions 10 p1331 N90-17693
Safety Status Report for the Ulysses mission. Book 1: Risk analysis. General purpose heat source radioisotope thermoelectric generator program
[DE90-006826] 12 p1614 N90-19282
Safety status report for the Ulysses mission. Book 2: Risk analysis. General purpose heat source radioisotope thermoelectric generator program
[DE90-006827] 12 p1614 N90-19283
Safety Status Report for the Ulysses mission: Summary. General purpose heat source radioisotope thermoelectric generator program
[DE90-006828] 12 p1614 N90-19284
Safety Status Report for the Ulysses mission. Book 1: Accident analysis. General purpose heat source radioisotope thermoelectric generator program
[DE90-006829] 12 p1614 N90-19285
Safety Status Report for the Ulysses mission. Book 2: Accident analysis-appendices. General purpose heat source radioisotope thermoelectric generator program
[DE90-006830] 12 p1614 N90-19286
Final safety analysis report for the Ulysses Mission. Volume 2: Accident model document-appendices
[DE90-008695] 14 p1940 N90-21104
Final safety analysis report for the Ulysses Mission
[DE90-008690] 14 p1940 N90-21106
Final safety analysis report for the Ulysses mission. Volume 1: Reference design document
[DE90-008693] 14 p1940 N90-21107
Final (Tier 1) environmental impact statement for the Galileo and Ulysses Missions
[NASA-TM-102917] 15 p2056 N90-21779
Draft environmental impact statement for the Galileo Mission (Tier 2)
[NASA-TM-102926] 15 p2124 N90-22148
Final Environmental Impact Statement for the Ulysses Mission (Tier 2)
[NASA-TM-101104] 15 p2126 N90-22162
General purpose heat source radioisotope thermoelectric generator program. Book 1: Accident analysis
[REPT-90SDS4202-BK-1] 15 p2166 N90-22379
General purpose heat source radioisotope thermoelectric generator. Book 2: Accident analysis, appendices
[REPT-90SDS4202-BK-2] 15 p2166 N90-22380
Space exploration: Cost, schedule, and performance of NASA's Ulysses Mission to the Sun. Fact sheet for the Chairman, Subcommittee on Science, Technology, and Space, Committee on Commerce, Science, and Transportation, US Senate
[GAO/NSIAD-88-129FS] 20 p2815 N90-26023
The Ulysses data book: A summary of the technical elements of the Ulysses spacecraft and its scientific payload
[ESA-BR-65] 24 p3440 N90-29427
UMBILICAL CONNECTORS
Independent Orbiter Assessment (IOA): Assessment of the mechanical actuation subsystem, volume 1
[NASA-CR-185527-VOL-1] 02 p0169 N90-10952
Development of a fully automated fluid resupply interface system 18 p2506 N90-24324
UNCAMBERED WINGS
NT RING WINGS
UNCONTROLLED REENTRY (SPACECRAFT)
Galileo: Earth avoidance study report
[NASA-CR-186424] 22 p3123 N90-27730
UNDERGROUND ACOUSTICS
Clutter models for subsurface electromagnetic applications
[PB89-229678] 03 p0338 N90-11925
UNDERGROUND EXPLOSIONS
State-of-the-art of measuring ground shock and cratering phenomena 09 p1235 N90-17170
A linear filtering technique for removal of low-frequency noise
[DE90-006183] 13 p1794 N90-20296
Minutes of the 23rd Explosives Safety Seminar, volume 2
[AD-A218265] 14 p1959 N90-21214
Seismic wave propagation, attenuation and scattering over regional distances
[AD-A219358] 16 p2256 N90-22862
Analysis of regional phases using three-component data
[AD-A219482] 17 p2422 N90-23803
UNDERGROUND STORAGE
Hydrazine fate and transformation in natural waters and soils 02 p0204 N90-11165
Evapotranspiration studies for protective barriers: Experimental plans
[DE90-005206] 10 p1405 N90-18106
Study and analysis of leaking underground storage tank remediation techniques incorporated in states in EPA Region 6
[PB90-214834] 23 p3333 N90-28847
UNDERGROUND STRUCTURES
Greenhouse design for a Martian colony: Structural, solar collection and light distribution systems
[NASA-CR-186818] 20 p2901 N90-26501
UNDERGROUND TRANSMISSION LINES
Heat transfer of buried pipe for heat pump application
[DE90-000580] 06 p0807 N90-14697
Optimal planning method of underground distribution system, part 2. Application to various types of system configurations
[DE89-782323] 11 p1500 N90-18636
UNDERWATER ACOUSTICS
Doppler statistics of ocean velocity variability
[AD-A211687] 03 p0377 N90-12148
ULF/VLF (0.001 to 50 Hz) Seismo-Acoustic Noise in the Ocean
[AD-A212942] 05 p0671 N90-13913
Ring source/force excitation of axisymmetric shell structure
[ARE-TM(UHA)-88519] 05 p0698 N90-14085
A compact acoustic recorder
[AD-A213581] 07 p0933 N90-15403
Wind speed dependence of acoustic ambient vertical directional spectra at high frequency
[AD-A214293] 07 p0989 N90-15712
ZBTAB: Zenith-248 version of BLUGTAB
[AD-A214279] 08 p1108 N90-16415
Underwater acoustic scattering from spherical particulates and bubbles
[AD-A214827] 09 p1279 N90-17414
Generalized Herglotz functions and inverse scattering problem in a finite depth ocean
[PB90-150996] 15 p2134 N90-22197
Proceedings of the 12th Symposium on Signal and Image Processing English-Language Abstracts
[AD-A218806] 17 p2388 N90-23598
ULF/VLF ocean bottom seismo-acoustics
[AD-A218810] 17 p2429 N90-23843
In situ investigation of sea surface noise from a depth of one meter
[AD-A220158] 17 p2432 N90-23857
Analytic parabolic equation solutions
[AD-A218588] 17 p2456 N90-24015
Estimation of noise field directionality: Comparison with Fourier series method
[AD-A220366] 17 p2469 N90-24114
Environmental measurements and analysis: Arctic acoustics experiments in the marginal ice zone
[AD-A220509] 18 p2582 N90-24708
Normal-mode and phase-integral methods for determining phase and group velocities in simple underwater acoustic ducts
[AD-A221393] 18 p2612 N90-24877
Laboratory studies of acoustic scattering from the underside of sea ice
[AD-A221333] 19 p2753 N90-25644
Canonical eigenvalues. Part 1: General theory
[AD-A222812] 20 p2920 N90-26617
An injective far-field pattern operator and inverse scattering problem in a finite depth ocean
[PB90-159294] 22 p3230 N90-28318
Applications of ripple analysis in hydro-acoustics
[ETN-90-97015] 22 p3244 N90-28397
Measuring the vertical directional spectra caused by sea surface sound
[AD-A223883] 23 p3354 N90-28957
UNDERWATER BREATHING APPARATUS
Development of membrane process for carbon dioxide separation from diving atmosphere
[AD-A222606] 20 p2901 N90-26504
UNDERWATER COMMUNICATION
Trends in VLF/LF (Very Low Frequency/Low Frequency) modem performance testing
[AD-A216576] 11 p1497 N90-18614
UNDERWATER ENGINEERING
Long endurance underwater power system
[AD-A211386] 03 p0366 N90-12096
Underwater connect and disconnect plug and receptacle
[AD-D014175] 21 p2998 N90-27039
UNDERWATER OPTICS
All-fiber SFPM (Stimulated Four Photon Mixing) amplifier
[AD-D014358] 12 p1713 N90-19841
UNDERWATER PHOTOGRAPHY
Underwater physiography of the continental shelf of Rio Grande do Norte visible through satellite imagery
[INPE-4964-TDL/392] 13 p1820 N90-20448
UNDERWATER SOUND
U UNDERWATER ACOUSTICS
UNDERWATER TESTS
NT NEUTRAL BUOYANCY SIMULATION
UNDERWATER VEHICLES
NT SUBMARINES
Real time adaptive control of an Autonomous Underwater Vehicle (AUV)
[AD-A219544] 17 p2454 N90-23996
Design and investigation of a dive plane sliding mode compensator for an autonomous underwater vehicle
[AD-A219552] 17 p2454 N90-23997
Guidance and control system for an autonomous underwater vehicle
[AD-A222709] 20 p2873 N90-26343
UNIAXIAL STRAIN
U AXIAL STRAIN
UNIFORM FLOW
NT BLASIUS FLOW
Oblique impact of two cylinders in a uniform flow
[AD-A215933] 10 p1385 N90-18015
Laser Doppler anemometry measurements of a confined turbulent water jet with a uniform background flow
15 p2092 N90-21971
UNIONS (CONNECTORS)
Mechanized fluid connector and assembly tool system
[NASA-CASE-MSC-21434-1] 09 p1230 N90-17138
UNIPHASE FLOW
U SINGLE-PHASE FLOW
UNIPOLAR TRANSISTORS
U FIELD EFFECT TRANSISTORS
UNIQUENESS
A direct two response approach for updating analytical dynamic models of structures with emphasis on uniqueness 02 p0182 N90-11028
Operator product coefficients in non-diagonal conformal field theories
[PB89-216873] 03 p0399 N90-12283
Existence, uniqueness, and approximation of a solution for a K-positive definite operator equation
[DE90-600728] 09 p1272 N90-17373
Uniqueness of closure of the constraint algebra for quantum gravity
[DE90-610476] 12 p1691 N90-19712
Infinite separatrix cycles in the critical case, divergence and uniqueness of limit cycles of a quadratic differential system
[REPT-89-87] 17 p2458 N90-24034

UNIQUENESS THEOREM
A general existence and uniqueness theorem for implicit differential-algebraic equations
[AD-A217965] 13 p1878 N90-20770
UNITED KINGDOM
NT ENGLAND
UK airmisses involving commercial air transport, September to December 1988
[ISSN-0951-6301] 08 p1019 N90-15897
A UK perspective on the uniform engine test programme
[RAE-TM-P-1172] 08 p1025 N90-15922
Tactical UK military satellite ground terminals: A research and development review
[RSRE-MEMO-4262] 08 p1033 N90-15972
A review of UK civil aviation fire and cabin safety research 10 p1312 N90-17587
Frontal structure in a mesoscale model 15 p2132 N90-22187
UNITED STATES
NT ALASKA
NT ARIZONA
NT CALIFORNIA
NT COLORADO
NT FLORIDA
NT HAWAII
NT ILLINOIS
NT LOUISIANA
NT MARYLAND
NT NEW HAMPSHIRE
NT NORTH CAROLINA
NT OHIO
NT OKLAHOMA
NT TEXAS
NT UTAH
NT WISCONSIN
Science and technology resources in US industry: Surveys of science resources series, 1975-1986
[PB90-107194] 06 p0756 N90-14401
Technology transfer and the FSX: Effects on the United States/Japanese relationship
[AD-A216348] 10 p1443 N90-18327
Energy markets in the 1990's and beyond: A comparison of energy intensity in the United States and Japan
[DE90-005535] 11 p1528 N90-18797
Advancing automation and robotics technology for the Space Station Freedom and for the US economy: Submitted to the United States Congress
[NASA-TM-101647] 12 p1613 N90-19279
United States Historical Climatology Network (HCN) serial temperature and precipitation data
[DE90-008029] 13 p1830 N90-20506
Opportunities for US-USSR cooperation in the investigation of Arctic stratospheric ozone 15 p2125 N90-22154
The Department of Defense critical technologies plan for the Committees on Armed Services United States Congress
[AD-A219300] 16 p2227 N90-22702
Brazil, the United States, and the missile technology control regime
[AD-A220551] 17 p2362 N90-23449
Measurements of tropospheric nitric acid over the Western United States and Northeastern Pacific Ocean
[NASA-TM-103470] 20 p2883 N90-26399
National mapping program. Fact sheet: Black and white photographs. NHAP (National High Altitude Photography Program)
[PB90-185042] 21 p3015 N90-27139
Command and control in the age of space-based surveillance 21 p3069 N90-27445
Climate change and America's forests
[PB90-205477] 22 p3199 N90-28155
A preliminary ARM (Atmospheric Radiation Measurements) guide for climatic evaluations
[DE90-015135] 23 p3351 N90-28937
Federal R and D funding by budget function: Fiscal years 1989-1991
[PB90-226879] 23 p3404 N90-29237
UNITS OF MEASUREMENT
NT INTERNATIONAL SYSTEM OF UNITS
UNIVERSAL TIME
Discrete-time control of a spacecraft with retargetable flexible antennas
[AD-A218345] 13 p1764 N90-20125
Diagnosis of auroral dynamics using global auroral imaging with emphasis on large-scale evolutions
[NASA-CR-186623] 17 p2422 N90-23804
Efficient numerical methods for evolution partial differential equations
[AD-A219790] 17 p2457 N90-24020
UNIVERSE
Are there causal vacuum solutions with the symmetries of the Goedel universe in higher-derivative gravity
[DE89-611966] 01 p0134 N90-10770
The origin of the universe from quantum chaos: An introduction to current ideas
[AD-A210441] 01 p0141 N90-10813
Evolution of domain walls in the early universe
[NASA-CR-186076] 04 p0565 N90-13297
Unitarity limits on the mass and radius of dark matter particles
[NASA-CR-186079] 05 p0713 N90-14164
Is the number of photons conserved in an expanding universe
[DE89-618836] 06 p0864 N90-15018
Study of primitive universe in the Bianchi 9 model
[DE89-635903] 08 p1134 N90-16572
Universe as a topological defect in a higher-dimensional Einstein-Yang-Mills theory
[DE90-719507] 08 p1135 N90-16578
The (2+1)-dimensional quantum gravity
[DE90-719556] 08 p1136 N90-16580
Dissipative effects in Friedmann universes
[DE89-618838] 08 p1150 N90-16663
Cosmological observations in an inhomogeneous universe
[DE90-733096] 09 p1299 N90-17528
The Age of the Universe: Concordance
[DE90-004971] 09 p1209 N90-17529
Dimensional transition of the universe
[DE90-741461] 12 p1724 N90-19910
Cosmic string in compactified gauge theory
[DE90-741463] 12 p1738 N90-19988
The dynamics of scalar fields in the early universe 14 p2039 N90-21696
The large scale structure of the universe in pancake models of galaxy formation 14 p2040 N90-21701
Horizon problem in cosmological models with non zero
[DE90-613367] 14 p2042 N90-21708
Big-bang nucleosynthesis revisited
[NASA-CR-186256] 15 p2174 N90-22426
Extraterrestrial life in the universe
[NASA-TM-102363] 15 p2181 N90-22464
The mass of the Coma cluster 15 p2188 N90-22496
Multipole moments in general relativity and dynamical perturbations of black-hole magnetospheres 15 p2190 N90-22509
Skewering the universe with QSO lines of sight: Lyman alpha clouds as probes of large scale structure 16 p2329 N90-23278
A general low-harmonic cosmic string and its self-intersection and fragmentation 16 p2331 N90-23284
Anisotropic inflation 16 p2331 N90-23286
Reconstructing primordial density fluctuations 16 p2333 N90-23293
Gamma ray cosmology: The extra galactic gamma spectrum and methods to detect the underlying source 16 p2337 N90-23321
Dipole analysis on EGRET data of extragalactic gamma ray background radiation 16 p2337 N90-23322
Feasibility for EGRET detection of antimatter concentrations in the universe 16 p2338 N90-23323
Gravitational collapse, Friedman models and cosmological constant: Does the universe oscillate
[DE90-620792] 16 p2338 N90-23324
Cosmological baryon and lepton number in the presence of electroweak fermion-number violation
[NASA-CR-186609] 17 p2470 N90-24123
Evolution of light domain walls interacting with dark matter, part 1
[NASA-CR-181123] 17 p2485 N90-24211
Thermal relics: Do we know their abundances
[NASA-CR-183334] 17 p2485 N90-24213
Identifying decohering paths in closed quantum systems
[NASA-CR-182853] 19 p2761 N90-25690
Nonstandard big bang models
[DE90-625593] 20 p2941 N90-26736
A research program in physics of the early universe
[DE90-013319] 20 p2942 N90-26742
SIRTF: Probing the dark corners of the galaxy 21 p3091 N90-27577
Can the chirality of the ISM be measured 21 p3095 N90-27590
Proceedings of workshop on Dark Matter and the Structure of the Universe
[DE90-791308] 21 p3098 N90-27602
The effect of tidal friction between galaxies on the formation and development of galactic clusters in the expanding universe
[ETN-90-97314] 21 p3098 N90-27603
Biased clustering in a universe with hot dark matter and cosmic string
[FERMILAB-PUB-90/23-A] 22 p3262 N90-28473
Periodicity of redshift distribution in a T-3 universe
[FERMILAB-PUB-90/26-A] 22 p3262 N90-28475
On the infrared behaviour of some non-Minkowskian quantum fields 23 p3410 N90-29273
Relic gravitational waves and extended inflation
[NASA-CR-186469] 24 p3493 N90-29740
UNIVERSITIES
Origins of high-temperature superconductivity in the new copper oxide based ceramic superconductors
[DE89-016543] 02 p0284 N90-11622
Technology transfer to the United States: The MIT (Massachusetts Institute of Technology) Japan Science and Technology Program. A background paper of OTA's (Office of Technology Assessment's) assessment on technology, innovation, and US trade
[PB89-224711] 04 p0564 N90-13291
Summary of research academic departments, 1987-1988
[AD-A213252] 05 p0716 N90-14183
Research Reports: 1989 NASA/ASEE Summer Faculty Fellowship Program
[NASA-CR-183837] 12 p1634 N90-19390
Microgravity Science and Application Program tasks, 1989 revision
[NASA-TM-4191] 13 p1786 N90-20252
Joint University Program for Air Transportation Research, 1988-1989
[NASA-CP-3063] 14 p1905 N90-20921
Preparing technicians for engineering materials technology 18 p2516 N90-24369
The personal computer: An untapped source for the United States Army War College
[AD-A223976] 23 p3379 N90-29087
Federal support to universities, colleges, and selected nonprofit institutions: Fiscal year 1988 (detailed statistical tables)
[PB90-226887] 23 p3404 N90-29236
FEDIX: An on-line information service for universities and other research organizations: User's guide
[DE90-014835] 24 p3559 N90-30137
UNIVERSITY PROGRAM
Investigation of air transportation technology at Princeton University, 1988-1989 14 p1907 N90-20935
Consortium for materials development in space
[NASA-CR-186534] 17 p2383 N90-23575
The Clemson University, university research initiative program in discrete mathematics and computational analysis
[AD-A220103] 17 p2461 N90-24055
NASA/American Society for Engineering Education (ASEE) Summer Faculty Fellowship Program 1989
[NASA-CR-181894] 18 p2639 N90-25034
NASA/USRA university advanced design program at the University of Illinois for the 1989-1990 academic year
[NASA-CR-186829] 20 p2821 N90-26049
NASA/USRA University advanced design program
[NASA-CR-186050] 21 p2965 N90-26855
NASA's educational programs 22 p3258 N90-28447
UNIX (OPERATING SYSTEM)
UNIX internals. Part 1: Intertask communication in UNIX. Part 2: UNIX file system
[CNES-NT-122-PT-1/2] 08 p1107 N90-16405
CPU timing routines for a CONVEX C220 computer system
[NASA-CR-181950] 08 p1110 N90-16424
Implementation of a control system test environment in UNIX
[DE90-007485] 13 p1872 N90-20736
Graphics mini manual
[NASA-TM-87622-REV] 15 p2144 N90-22247
NASTRAN migration to UNIX 18 p2569 N90-24643
UNMANNED SPACECRAFT
NT GALILEO SPACECRAFT
NT GIOTTO MISSION
NT HEAO 1
NT HEAO 2
NT HOTOL LAUNCH VEHICLE
NT JUPITER PROBES
NT MAGELLAN SPACECRAFT (NASA)
NT MARS OBSERVER
NT PIONEER VENUS SPACECRAFT
NT PIONEER VENUS 1 SPACECRAFT
NT PIONEER 10 SPACE PROBE
NT PIONEER 11 SPACE PROBE
NT SOLAR PROBES
NT SPACE PROBES
NT VIKING LANDER SPACECRAFT
NT VOYAGER 1 SPACECRAFT
NT VOYAGER 2 SPACECRAFT
Development of a flight test methodology for a US Navy half-scale unmanned air vehicle
[AD-A210563] 01 p0006 N90-10029
Shuttle C: Heavy-lift vehicle of the 1990's 09 p1178 N90-16830

Statistical techniques for designing a decoupled controller to be robust to model and sensor noise
[AD-A220476] 17 p2412 N90-23745
Fractional state feedback control of undamped and viscoelastically-damped structures
[AD-A220477] 17 p2412 N90-23746
Advanced solar-propelled cargo spacecraft for Mars missions
[NASA-CR-186218] 19 p2665 N90-25164
NASA/USRA university advanced design program at the University of Illinois for the 1989-1990 academic year
[NASA-CR-186829] 20 p2821 N90-26049
Possible applications of tethered systems to Mars exploration missions
[IAF-89-489] 20 p2822 N90-26060

UNSATURATION (CHEMISTRY)
Correlations between surface structure and catalytic activity/selectivity
[DE90-003755] 07 p0896 N90-15181

UNSTEADY AERODYNAMICS
An investigation of counterrotating tip vortex interaction
[NASA-CR-185135] 02 p0271 N90-11549
Prediction of unsteady blade surface pressures on an advanced propeller at an angle of attack
[NASA-TM-102374] 04 p0447 N90-12560
Unsteady forces induced on finite-span cylinders in a cross-flow 05 p0642 N90-13746
Unsteady aerodynamic simulation of multiple bodies in relative motion: A prototype method
[NASA-TM-102181] 06 p0717 N90-14188
Computation of unsteady transonic flow about airfoils in frequency domain using the full-potential equation 06 p0719 N90-14198
An analytical method for the prediction of unsteady rotor/airframe interactions in forward flight 06 p0724 N90-14223
Flight evaluation of a pneumatic system for unsteady pressure measurements using conventional sensors
[NASA-TM-4131] 06 p0724 N90-14225
Temporally and spatially resolved flow in a two-stage axial compressor. Part 2: Computational assessment
[NASA-TM-102273] 06 p0726 N90-14236
Concurrent processing adaptation of aeroplastic analysis of propfans
[NASA-TM-102455] 06 p0799 N90-14656
Canard versus aft-tail ride qualities performance and pilot command response 07 p0871 N90-15053
Unsteady aerodynamics of oscillating and rapidly pitched airfoils 07 p0875 N90-15074
Structural dynamics division research and technology accomplishments for FY 1989 and plans for FY 1990
[NASA-TM-101683] 08 p1019 N90-15894
Test techniques for cryogenic wind tunnels 08 p1030 N90-15952
Numerical solutions of the linearized Euler equations for unsteady vortical flows around lifting airfoils
[NASA-TM-102466] 10 p1307 N90-17562
Aerodynamics of unsteady systems. Numerical study of potential flow/boundary layer coupling
[ETN-90-96257] 11 p1452 N90-18367
Unsteady Aerodynamic Phenomena in Turbomachines
[AGARD-CP-468] 11 p1459 N90-18405
A comparison of flutter calculations based on eigenvalue and energy method 11 p1459 N90-18406
Aerodynamic superposition principle in vibrating turbine cascades 11 p1460 N90-18410
Design guidance to minimize unsteady forces in turbomachines 11 p1460 N90-18411
Unsteady blade loads due to wake influence 11 p1460 N90-18413
Unsteady aerodynamic phenomena in a simulated wake and shock wave passing experiment 11 p1461 N90-18414
Gust response analysis for cascades operating in nonuniform mean flows 11 p1461 N90-18415
Numerical prediction of axial turbine stage aerodynamics 11 p1461 N90-18416
Time-dependent measurements on vibrating annular turbine cascades under various steady state conditions 11 p1463 N90-18424
Methods for making unsteady aerodynamic pressure measurements in a rotating turbine stage 11 p1463 N90-18426
Unsteady aerodynamics of delta wings performing maneuvers to high angle of attack 12 p1598 N90-19196
Conical Euler solution for a highly-swept delta wing undergoing wing-rock motion
[NASA-TM-102609] 12 p1600 N90-19211
Aeroservoelasticity
[NASA-TM-102620] 12 p1603 N90-19227
Unsteady free-wake viscous aerodynamic analysis of helicopter rotors
[AD-A217166] 13 p1750 N90-20048
Aeroelastic characteristics of aircraft with circulation control wings 13 p1754 N90-20070
Numerical simulation methods of incompressible flows and an application to the space shuttle main engine
[NASA-TM-100038] 13 p1800 N90-20333
Development and application of a generalized dynamic wake theory for lifting rotors 15 p2046 N90-21731
Control of flow separation and mixing by aerodynamic excitation
[NASA-TM-103131] 15 p2047 N90-21733
Airloads, wakes, and aeroelasticity
[NASA-CR-177551] 15 p2048 N90-21738
Aeroelastic simulation of higher harmonic control 15 p2054 N90-21768
Forcing function effects on rotor row unsteady aerodynamic response in a multistage compressor 16 p2196 N90-22536
Multi-axis, 3-D, scanning LDA (Laser Doppler Anemometer) system for unsteady aerodynamics
[AD-A218571] 16 p2197 N90-22541
STARS: An integrated general-purpose finite element structural, aeroelastic, and aeroservoelastic analysis computer program
[NASA-TM-101709] 17 p2416 N90-23768
Reduced order models for nonlinear aerodynamics 18 p2492 N90-24244
A time-marching method to calculate unsteady airloads on three-dimensional wings. Part 1: Linearized formulation
[DLR-FB-89-58] 18 p2494 N90-24254
A time-marching method for calculating unsteady airloads on three-dimentional wings. Part 2: Full-potential formulation
[DLR-FB-89-59] 18 p2494 N90-24255
Calculation of the aeroelastic blade stabilization with linearized process
[MITT-87-01] 18 p2497 N90-24272
Studies in non-linear unsteady aerodynamics
[AD-A221228] 19 p2654 N90-25108
Integral-equation methods in steady and unsteady subsonic, transonic and supersonic aerodynamics for interdisciplinary design
[NASA-TM-102677] 19 p2655 N90-25110
Identification of aerodynamic models for maneuvering aircraft
[NASA-CR-186630] 20 p2802 N90-25943
Two-dimensional Euler and Navier-Stokes Time accurate simulations of fan rotor flows
[NASA-TM-102402] 20 p2803 N90-25948
Aerodynamic/dynamic interaction
[AD-A222263] 21 p2954 N90-26798
Adaptation for unsteady flow 21 p2963 N90-26845
Development of a linearized unsteady aerodynamic analysis for cascade gust response predictions
[NASA-CR-4308] 22 p3108 N90-27655
Aerodynamics of a linear oscillating cascade
[NASA-TM-103250] 22 p3108 N90-27657
Unsteady aerodynamics of controls 23 p3273 N90-28525
Turbomachinery rotor forces
[NASA-CR-183779] 23 p3334 N90-28852

UNSTEADY FLOW
NT OSCILLATING FLOW
Basic studies of the unsteady flow past high angle of attack airfoils
[AD-A210252] 01 p0002 N90-10008
Vortex induced characteristics of missiles in unsteady maneuvers 01 p0012 N90-10057
Reheat buzz: An acoustically coupled combustion instability 01 p0036 N90-10200
Numerical simulation of unsteady combustion in a dump combustor 01 p0037 N90-10203
Numerical solution of three-dimensional unsteady flows: Application to instability problems 01 p0065 N90-10375
Numerical simulation of turbulent plane channel flows 01 p0067 N90-10382
Unsteady aerodynamics with applications to flight mechanics
[AD-A211944] 03 p0301 N90-11706
Active control of unsteady and separated flow structures
[AD-A212109] 03 p0301 N90-11707
Steady and unsteady potential flow around thin annular wings and engines with simulation of jet engine flow
[DFVLR-FB-89-18] 03 p0302 N90-11711
Numerical algorithms for steady and unsteady incompressible Navier-Stokes equations
[NASA-CR-186039] 04 p0437 N90-12499
Numerical simulation of unsteady rotational flow over propfan configurations
[NASA-CR-186037] 04 p0438 N90-12500
Unsteady three-dimensional thin-layer Navier Stokes solutions on dynamic blocked grids
[AD-A212377] 04 p0503 N90-12899
Free surface scars and striations
[AD-A212429] 04 p0503 N90-12901
Blunt-nose inviscid airflows with coupled nonequilibrium processes 05 p0573 N90-13336
Low speed hot and cold wire techniques for unsteady flow 05 p0574 N90-13342
Laser applications in supersonic unsteady flow 05 p0574 N90-13344
Application of a two-dimensional unsteady viscous analysis code to a supersonic throughflow fan stage
[NASA-TM-4141] 05 p0581 N90-13387
Numerical Methods for Flows in Turbomachinery, volume 2
[VKI-LS-1989-06-VOL-2] 05 p0641 N90-13741
Numerical methods for unsteady turbomachinery flow 05 p0641 N90-13743
Unsteady hydromagnetic flow of a radiating gas in a vertical channel with axial temperature variation
[DE90-600934] 06 p0778 N90-14525
An alternative derivation for an integral equation for linearized subsonic flow over a wing
[AD-A214140] 07 p0876 N90-15079
Dynamics of a class of vortex rings 07 p0926 N90-15362
Nonlinear viscous waves produced by an impulsively moving plate
[AD-A214014] 07 p0932 N90-15392
Force and moment measurements on delta wings in unsteady flow 08 p1068 N90-16185
Periodically unsteady effects on profiles, induced by separation 08 p1070 N90-16196
Coded trajectories for the investigation of strongly unsteady flow fields 08 p1078 N90-16240
Unsteady heat transfer measurement using thermochromatic liquid crystals as temperature indicators 08 p1081 N90-16254
A computational and experimental study of steady and transient acoustic energy flow from a complex mechanical structure 08 p1119 N90-16478
Wake interaction effects on the transition process on turbine blades
[AD-A214492] 09 p1168 N90-16759
Numerical solutions of the linearized Euler equations for unsteady vortical flows around lifting airfoils
[NASA-TM-102466] 10 p1307 N90-17562
Conditions at the downstream boundary for simulations of viscous incompressible flow
[NASA-TM-102510] 10 p1422 N90-18198
Unsteady Euler analysis of the flow field of a propfan at an angle of attack
[NASA-TM-102426] 10 p1426 N90-18229
Numerical investigation of unsteady flow in oscillating turbine and compressor cascades 11 p1459 N90-18407
Unsteady viscous calculation method for cascades with leading edge induced separation 11 p1459 N90-18408
Calculation of the unsteady two-dimensional, inviscid, compressible flow around a strongly cambered oscillating single blade 11 p1460 N90-18409
Aerodynamic study on forced vibrations on stator rows of axial compressors 11 p1460 N90-18412
Numerical simulation of three-dimensional unsteady flows in turbomachines 11 p1461 N90-18417
High-resolution Euler computations of unsteady transonic flows in cascades 11 p1462 N90-18420
Experiments on the unsteady flow in a supersonic compressor stage 11 p1462 N90-18422
Modelling unsteady transition and its effects on profile loss 11 p1462 N90-18423
Experimental investigation of the influence of rotor wakes on the development of the profile boundary layer and the performance of an annular compressor cascade 11 p1463 N90-18425
Small displacement, long life on-orbit compressor design and fabrication 11 p1475 N90-18489
An investigation of flow structure, mixing and chemical reaction in combusting turbulent flows
[AD-A216739] 11 p1483 N90-18538
Active stabilization of aeromechanical systems
[AD-A216629] 11 p1508 N90-18672
Computation of hypersonic unsteady viscous flow over a cylinder 12 p1597 N90-19194
Spectral simulation of unsteady compressible flow past a circular cylinder
[NASA-CR-182030] 13 p1750 N90-20050
Mass transfer from a sphere in an oscillating flow with zero mean velocity
[NASA-TM-102566] 13 p1801 N90-20338
Experimental investigation of the mechanisms underlying vortex kinematics in unsteady separated flows
[AD-A217889] 13 p1802 N90-20346

Flow visualization studies in a curved rectangular channel with 40 to 1 aspect ratio and a straight channel with bulk flow unsteadiness
[AD-A218020] 13 p1803 N90-20348
A two-dimensional unsteady analysis for transonic and supersonic cascade flows 14 p1911 N90-20955
Measurement of lift development on rapidly-accelerated wings 14 p1911 N90-20956
PROTEUS two-dimensional Navier-Stokes computer code, version 1.0. Volume 1: Analysis description
[NASA-TM-102551] 14 p1973 N90-21303
Notes on the unsteady rectilinear motion of a perfect gas. Part 8: General theory and general waves in a homentropic gas
[PB90-167149] 14 p1974 N90-21309
Extension of a streamwise upwind algorithm to a moving grid system
[NASA-TM-102800] 15 p2048 N90-21739
Topics in vortex methods for the computation of three- and two-dimensional incompressible unsteady flows 15 p2091 N90-21967
An unsteady time asymptotic flow in the square driven cavity
[NASA-TM-103141] 15 p2099 N90-22016
Unsteady separated flows produced by complex harmonic motions: Investigation of wing-flow interactions elicited by a mechanical model simulating dragonfly wing kinematics 15 p2100 N90-22018
Analysis of gamma squared Velorum photometry from the South Pole 15 p2183 N90-22472
Extension of a three-dimensional viscous wing flow analysis user's manual: VISTA 3-D code
[NASA-CR-182024] 16 p2197 N90-22538
Secondary frequencies in the wake of a circular cylinder with vortex shedding
[NASA-CR-181998] 16 p2197 N90-22540
Multi-axis, 3-D, scanning LDA (Laser Doppler Anemometer) system for unsteady aerodynamics
[AD-A218571] 16 p2197 N90-22541
Extension of a three-dimensional viscous wing flow analysis
[NASA-CR-182023] 17 p2344 N90-23348
Unsteady flow phenomena in turbomachines
[AD-A218370] 17 p2402 N90-23680
Numerical study of unsteady flows in large air-driven blast simulators with single and multiple drivers
[UTIAS-334] 17 p2405 N90-23699
A process for the measurement of the unsteady three dimensional stream vectors in turbomachines
[MITT-89-01] 17 p2405 N90-23702
Unsteady potential flow past a propeller blade section
[NASA-CR-4307] 18 p2493 N90-24246
An interactive boundary-layer method for unsteady airfoil flows. Part 1: Quasi-steady-state model
[AD-A221220] 18 p2493 N90-24250
A lifting surface method for the calculation of steady and unsteady, incompressible propeller aerodynamics
[ESA-TT-1151] 19 p2655 N90-25113
LOX manifold tee analysis
[NASA-CR-183994] 19 p2670 N90-25188
Velocity distribution in a gravel-bed flume; for steady and unsteady flow 19 p2687 N90-25283
An unsteady lifting surface method for single rotation propellers
[NASA-CR-4302] 20 p2802 N90-25940
Two-dimensional Euler and Navier-Stokes Time accurate simulations of fan rotor flows
[NASA-TM-102402] 20 p2803 N90-25948
Analysis and mitigation of numerical dissipation in inviscid and viscid computation of vortex-dominated flows
[NASA-CR-186887] 20 p2862 N90-26281
Effects of 2 Hz imposed bulk flow unsteadiness on laminar-turbulent transition in a straight channel
[AD-A223028] 20 p2864 N90-26295
Aerodynamic/dynamic interaction
[AD-A222263] 21 p2954 N90-26798
Fluid Dynamics Panel Working Group 12 on Adaptive Wind Tunnel Walls: Technology and Applications
[AGARD-AR-269] 21 p2961 N90-26838
Adaptation for unsteady flow 21 p2963 N90-26845
Vortex-induced boundary layer separation
[AD-A221564] 21 p3005 N90-27078
Experimental characterization of the effects of pneumatic tubing on unsteady pressure measurements
[NASA-TM-4171] 22 p3116 N90-27703
Experimental study of an unsteady boundary layer on an oscillating plane plate. Optimization and validation of calculation code for the analysis of the potential flow/boundary layer coupling in the neighborhood of a plane plate and an oscillating profile
[ETN-90-97436] 22 p3175 N90-28013
Calculation of unsteady two dimensional viscous incompressible flows by spectral methods
[ETN-90-97449] 22 p3175 N90-28015
Regular and chaotic motion of uniform elliptical vortices in external linear time dependent velocity fields 23 p3268 N90-28497
Development of turbulence models for the analysis of compressible or incompressible unsteady flow
[ETN-90-97486] 23 p3326 N90-28810
Thermal transfers in unsteady compressible inviscid flow
[ETN-90-97557] 24 p3419 N90-29311

UNSTEADY STATE
Unsteady diffusion from a hemispherical pit
[NPL-DMA(A)-190] 04 p0553 N90-13220
The use of piezofoil sensors for the determination of the unsteady pressure distribution at the surface of a gas turbine blade 08 p1080 N90-16250

UNSWEPT WINGS
NT RECTANGULAR WINGS
NT RING WINGS

UP-CONVERTERS
Dynamical model of series-resonant converter with peak capacitor voltage predictor and switching frequency control 10 p1336 N90-17730

UPDRAFTS
U VERTICAL AIR CURRENTS

UPGRADING
US Space Shuttle evolution 09 p1178 N90-16829
Aviation security: Corrective actions underway, but better inspection guidance still needed. Report to the Chairwoman, Government Activities and Transportation Subcommittee, Committee on Government Operations, House of Representatives
[GAO/RCED-88-160] 17 p2347 N90-23367
Further development of the cryogenic Fabry-Perot interchange mechanism for ISO LWS 18 p2539 N90-24492

UPLINKING
Experimental measurements in secondary radar field: Conception and first results
[ETN-90-96074] 12 p1648 N90-19471
Weather data dissemination to aircraft 14 p1907 N90-20934
Preliminary error budget for an optical ranging system: Range, range rate, and differenced range observables 20 p2853 N90-26227

UPPER AIR
U UPPER ATMOSPHERE

UPPER ATMOSPHERE
NT D REGION
NT E REGION
NT EARTH IONOSPHERE
NT EXOSPHERE
NT F REGION
NT F 2 REGION
NT LOWER IONOSPHERE
NT SPORADIC E LAYER
NT THERMOSPHERE
NT UPPER IONOSPHERE
Kiruna geophysical data: Data Summary 88/7-9, July - September 1988
[PB89-210249] 01 p0086 N90-10487
Metal vaporisers: Bicentennial series of five historical monographs
[ISBN-0-642-13584-3] 08 p1052 N90-16081
Upper atmosphere research
[ISBN-0-642-13582-7] 08 p1100 N90-16368
Kiruna geophysical data
[PB90-123985] 09 p1247 N90-17232
Simultaneous observations of the emissions OI (5577), O2A(0.1), NaD(5893) and OH(9.4) and the rotational temperatures TO2 and TOH in the upper atmosphere
[INPE-4851-TDL/366] 10 p1407 N90-18113
An aircraft investigation of a convective boundary layer over Lake Michigan
[AD-A218175] 13 p1846 N90-20598
AFGW's upper air validator system
[AD-A219309] 16 p2258 N90-22876
Proceedings of Workshop on Atmospheric Density and Aerodynamic Drag Models for Air Force Operations, volume 2
[AD-A220382] 17 p2345 N90-23356
A case study of explosive cyclogenesis in the eastern Pacific Ocean 14 to 17 December 1987
[AD-A219543] 17 p2426 N90-23824
Measurements of the methane relaxation times for application to the infrared emission models of the upper atmospheres of outer planets and Titan 20 p2945 N90-26759
Environmental Research Laboratories programs and plans. FY-1989 and FY-1990 plans
[PB90-169988] 22 p3197 N90-28144
Instability bursts associated with Extratropical Cyclone Systems (ECSs) and a forecast index of 3 to 12 hour heavy precipitation
[NOAA-TM-NESDIS-30] 22 p3228 N90-28309
Present state of knowledge of the upper atmosphere 1990: An assessment report
[NASA-RP-1242] 23 p3350 N90-28929
Measurements of the single event upset environment in the upper atmosphere
[RAE-TM-SPACE-373] 23 p3351 N90-28934
Satellite measurements of magnetospheric Poynting flux
[AD-A224391] 24 p3490 N90-29724

UPPER IONOSPHERE
NT F REGION
NT F 2 REGION
Upper ionosphere and magnetospheric-ionospheric coupling
[DE89-619727] 02 p0250 N90-11415

UPPER STAGE ROCKET ENGINES
Ariane-5 upper stage EPS 09 p1176 N90-16809

UPPER SURFACE BLOWN FLAPS
Acoustic-thermal environment for USB flap structure. Report 1: Ground simulation test results
[NAL-TM-567] 03 p0300 N90-11697

UPSTREAM
The role of an upstream cyclone and corresponding synoptic/planetary-scale interactions during the development of a blocking anticyclone 08 p1150 N90-16659
Studies on reactive flows 15 p2066 N90-21831
Three-dimensional structure of plane mixing layers 17 p2344 N90-23347

UPWASH
Aircraft response and pilot behaviour during a wake vortex encounter perpendicular to the vortex axis 07 p0871 N90-15057
Effect of vortex circulation on injectant from a single film-cooling hole and a row of film-cooling holes in a turbulent boundary layer. Part 2: Injection beneath the vortex upwash
[AD-A223894] 23 p3328 N90-28818

UPWELLING
U UPWELLING WATER

UPWELLING WATER
A numerical study of basic coastal upwelling processes 16 p2259 N90-22878
Modeling studies of the LeeUwin current using a high-resolution primitive equation model
[AD-A219595] 17 p2430 N90-23846

URANIUM
NT URANIUM ISOTOPES
Characterization of electron-beam weld processes in uranium by acoustic emission monitoring
[DE89-016044] 01 p0078 N90-10444
Strengthening mechanisms of tungsten powder reinforced uranium
[DE90-009331] 14 p1947 N90-21144
Correlated electron processes in ion-atom collisions
[DE90-009477] 15 p2185 N90-22370
Modeling of combustion processes in a solid fuel particle
[DE90-009140] 16 p2214 N90-22629
The thermal radiative properties of metals at high temperature
[DE90-012468] 21 p2981 N90-26938
Experimental study of the optical constants of metals at high temperatures
[DE90-014732] 23 p3310 N90-28719

URANIUM ALLOYS
Properties of aluminum-uranium alloys
[DE90-003889] 07 p0907 N90-15243
Estimation of thermodynamic properties of alloys from phase diagram and other loose boundary conditions
[DE90-719511] 08 p1135 N90-16579

URANIUM COMPOUNDS
NT URANIUM OXIDES
Studies of novel superconductors
[DE89-016744] 02 p0282 N90-11609

URANIUM ISOTOPES
Low temperature photoluminescence study of uranium implanted into III-V semiconductors and AlGaAs
[AD-A215710] 09 p1291 N90-17484

URANIUM OXIDES
Properties and thermal decomposition of the double salts of uranyl nitrate-ammonium nitrate
[DE89-004909] 07 p0914 N90-15287

URANUS (PLANET)
Auroral ultraviolet darkening on the outer planets 15 p2192 N90-22518
Liquid-vapor equilibrium of multicomponent cryogenic systems 20 p2948 N90-26774
Carbon in the outer solar system 21 p3096 N90-27593
New Voyager radio spectrograms of Uranus
[NASA-CR-180381] 23 p3412 N90-29284

URANUS SATELLITES
NT TITANIA

URBAN AREAS
U CITIES

URBAN DEVELOPMENT
Departments of Veterans Affairs and Housing and Urban Development, and Independent Agencies Appropriations Bill, 1990
[H-REPT-101-150] 04 p0563 N90-13281
Departments of Veterans Affairs and Housing and Urban Development, and Independent Agencies Appropriation Bill, 1990
[S-REPT-101-128] 04 p0563 N90-13284
Department of Veterans Affairs and Housing and Urban Development, and Independent Agencies Appropriations Act, 1990
[HR-2916-PP] 04 p0564 N90-13286
Processes of community development and responses of ecosystems to climate change
[DE90-008640] 13 p1831 N90-20512
URBAN PLANNING
Remote sensing applied to vegetation as subsidized in municipal planning
[INPE-4908-PRE/1509] 11 p1523 N90-18770
URBAN TRANSPORTATION
An approach for testing fuel-cell/battery hybrid power sources for bus applications
[DE90-002090] 08 p1083 N90-16270
UREAS
Modern biofuel cells for waste recycling in life support systems
[NASA-CR-185963] 05 p0638 N90-13718
URETHANES
UV-curable polyurethane-methacrylate co-networks and interpenetrating networks
[AD-A210445] 01 p0050 N90-10285
Synthesis and physical properties of poly(perfluoroalkylether) urethanes
[AD-A210500] 01 p0050 N90-10287
Failure mechanism of urethane elastomer coated fabric collapsible fuel tanks
[AD-A221033] 18 p2530 N90-24435
URINE
Selective removal of organics for water reclamation
[NASA-TM-101890] 17 p2421 N90-23797
Effects of a time zone shift of 9 hours on the circadian rhythms in cockpit aircrew members on longhaul flights
[ESA-TT-1185] 19 p2722 N90-25485
Generation rates and chemical compositions of waste streams in a typical crewed space habitat
[NASA-TM-102799] 22 p3233 N90-28333
USA (UNITED STATES)
U UNITED STATES
USER MANUALS (COMPUTER PROGRAMS)
Composite Blade Structural Analyzer (COBSTRAN) theoretical/programmer's manual
[NASA-TM-101958] 01 p0033 N90-10181
PORFLO-3: A mathematical model for fluid flow, heat, and mass transport in variably saturated geologic media: Users manual, version 1.0
[DE89-013977] 01 p0069 N90-10398
The MHOST finite element program: 3-D inelastic analysis methods for hot section components. Volume 2: User's manual
[NASA-CR-182235-VOL-2] 01 p0079 N90-10450
Satellite Data Processing System (SDPS) users manual V1.0
[NASA-CR-183054] 01 p0082 N90-10468
User's manual for PEPSIG NASA tip vortex version
[NASA-CR-182178] 02 p0146 N90-10835
Experimental database retrieval system DARTS (Handling Manual)
[DE89-906473] 02 p0289 N90-11652
Human Operator Simulator (HOS) 4 user's guide
[AD-A212007] 03 p0310 N90-11763
Manual for Program PSTRESS: Peel stress computation
[NASA-CR-178408] 03 p0321 N90-11822
User's guide for a personal computer model of turbulence at a wind turbine rotor
[DE89-017753] 03 p0366 N90-12095
FEDIX: An on-line information service for universities and other research organizations: User's guide, version 2.0, release 1
[DE89-016695] 03 p0417 N90-12398
CALS (Computer-aided Acquisition and Logistic Support) Test Network information exchange: User's manual
[DE89-016700] 03 p0418 N90-12399
ANDECS-PERLUDE 2.0: A databased, interactive system of control software user's guide
[DFVLR-MITT-89-07] 03 p0418 N90-12404
RAN (Royal Australian Navy) vibration analysis system operator's guide
[AD-A212441] 04 p0453 N90-12596
Batch LCAP2-linear control analysis, version 2.0: User's manual
[AD-A211670] 04 p0461 N90-12643
Spacecraft Orbit Design and Analysis (SODA), version 1.0 user's guide
[NASA-CR-181932] 04 p0529 N90-13050
RTM user's guide
[NASA-CR-186091] 04 p0531 N90-13065
User manual of the force structure model scenario editor SCENE
[FEL-1988-101] 04 p0531 N90-13069
NUMVEC FORTRAN library manual chapter: Simultaneous linear equations
[CWI-NM-R8903] 04 p0541 N90-13135
MOBILE4 oxygenated fuels version user's guide
[PB89-230700] 05 p0629 N90-13674
Image enhancement software for underwater recovery operations: User's manual
[AD-A212943] 05 p0699 N90-14094
Real time image enhancement during underwater recovery operations
[AD-A213139] 05 p0700 N90-14097
User's guide to PMESH: A grid-generation program for single-rotation and counterrotation advanced turboprops
[NASA-CR-185156] 06 p0823 N90-14783
Force user's manual: A portable, parallel FORTRAN
[NASA-CR-4265] 06 p0823 N90-14785
GRAFIN: GRAFIX interactive manual
[PB89-232136] 06 p0827 N90-14809
The development of an Ada programming support environment database: SEAD (Software Engineering and Ada Database), user's manual
[NASA-CR-181219] 06 p0828 N90-14811
Analysis of an elastohydrodynamic lubricated point contact: User's manual
[AD-A214257] 07 p0943 N90-15459
CryoTran user's manual, version 1.0
[NASA-TM-102468] 07 p0973 N90-15622
User's manual for MGMHD: A multigrid three-dimensional computer code for the analysis of magnetohydrodynamic generators and diffusers
[DE90-004453] 08 p1127 N90-16526
Specification for HF Maximum Usable Frequency (MUF) model
[AD-A214996] 09 p1206 N90-16990
One-dimensional single-mode nonlinear FEL amplification code: User's manual
[DE90-719544] 09 p1227 N90-17121
Nimbus 7 solar backscatter ultraviolet (SBUV) ozone products user's guide
[NASA-RP-1234] 09 p1246 N90-17227
AOIPS 3 user's guide. Volume 2: Program descriptions
[NASA-TM-100725] 09 p1247 N90-17236
Subjective Workload Assessment Technique (SWAT): A user's guide
[AD-A215405] 09 p1261 N90-17312
IRUS-II user manual
[AD-A214612] 09 p1265 N90-17334
Interim Design Database (IDDB) CADAM drawing retrieval program user's manual for the IBM 3081
[DE90-004491] 09 p1269 N90-17356
GRASS/GIS (Geographic Resources Analysis Support System/Geographic Information System) implementation guide
[AD-A214623] 09 p1296 N90-17510
Z-grid signal conditioning system user's guide and technical reference
[AD-A215122] 10 p1395 N90-18067
The procedures for easy running of the HULL computer code under VMS
[MRL-GD-0023] 10 p1417 N90-18165
User's guide to OPUS (Optimal Preferential Utility and Strategies)
[AD-A214384] 10 p1424 N90-18217
A user's manual for the method of moments Aircraft Modeling Code (AMC)
[NASA-CR-186371] 11 p1456 N90-18390
ACIRF user's guide: Theory and examples
[AD-A216436] 11 p1496 N90-18613
User manual for NEXT 1.2: NLR engineering X-pert system toolkit
[NLR-TR-87178-U] 11 p1547 N90-18905
Defense Technical Information Center Executive Information System: Documentation and user's manual
[AD-A216235] 11 p1575 N90-19065
Using the K-25 C/TD common file system: A guide to CFSI
[DE90-005815] 11 p1593 N90-19179
The pollution hazard assessment system: Documentation and users manual
[AD-A217108] 12 p1689 N90-19706
ETO (Earth-To-Orbit): A trajectory program for aerospace vehicles
[AD-A218157] 13 p1760 N90-20103
Numerical Arc Segmentation Algorithm for a Radio Conference-NASARC (version 4.0) technical manual
[NASA-TM-101453] 13 p1788 N90-20264
Small and great circle routines
[AD-A217652] 13 p1820 N90-20449
User's guide: Programs for processing altimeter data over inland seas
[NASA-TM-100730] 13 p1841 N90-20572
GRID2D/3D: A computer program for generating grid systems in complex-shaped two- and three-dimensional spatial domains. Part 2: User's manual and program listing
[NASA-TM-102454] 13 p1867 N90-20708
VAPEPS user's reference manual, version 5.0
[NASA-CR-180781] 13 p1868 N90-20713
Optimization of series expressions. Part 1: User's manual for the series macro package
[AD-A218220] 13 p1869 N90-20725
Users manual for the NASA Lewis Ice Accretion Prediction Code (LEWICE)
[NASA-CR-185129] 14 p1909 N90-20943
Numerical Arc Segmentation Algorithm for a Radio Conference (NASARC), version 4.0: User's manual
[NASA-TM-101454] 14 p1964 N90-21250
PROTEUS two-dimensional Navier-Stokes computer code, version 1.0. Volume 2: User's guide
[NASA-TM-102552] 14 p1973 N90-21306
The computational structural mechanics testbed generic structural-element processor manual
[NASA-CR-181728] 14 p1991 N90-21410
User manual for VICONOPT: An exact analysis and optimum design program covering the buckling and vibration of prismatic assemblies of flat in-plane loaded, anisotropic plates, with approximations for discrete supports, and transverse stiffeners
[NASA-CR-181966] 14 p1991 N90-21413
Hypercluster parallel processing library user's manual
[NASA-CR-185231] 14 p2016 N90-21552
OTTER (Organized Techniques for Theorem-proving and Effective Research) 2.0 users guide
[DE90-007978] 14 p2018 N90-21563
Program CICC: Flow and heat transfer in Cable In Conduit Conductors, user's manual
[DE90-007924] 14 p2033 N90-21661
Enhanced Low Level Wind Shear (LLWAS) 6-sensor improvement user's manual for data processing of field data
[DOT/FAA/CT-TN90/8] 15 p2052 N90-21759
Reliability importance measures and their calculation
[DE90-620391] 15 p2108 N90-22057
Extension of a three-dimensional viscous wing flow analysis user's manual: VISTA 3-D code
[NASA-CR-182024] 16 p2197 N90-22538
PLOT3D user's manual
[NASA-TM-101067] 16 p2298 N90-23090
Basic graphics routine technical manual
[AD-A219409] 16 p2302 N90-23117
Codice ETF-3D: Euler transonic flow user manual
[DLC/FLU-INT-TN-006] 17 p2346 N90-23362
NASA Lewis icing research tunnel user manual
[NASA-TM-102319] 17 p2355 N90-23407
Engineer's Refractive Effects Prediction System (EREPS), revision 2.0
[AD-A220742] 17 p2391 N90-23616
SPHC (Smooth Particle Hydrodynamics Code) manual
[AD-A220743] 17 p2444 N90-23928
Flipper user's manual
[AD-A220788] 18 p2590 N90-24734
Users guide for an Airborne Windshear Doppler Radar Simulation (AWDRS) program
[NASA-CR-182025] 19 p2657 N90-25121
PDWAP: A preliminary design and weights analysis program for aerospace vehicles
[AD-A222614] 20 p2808 N90-25979
The NASA/MSFC Global Reference Atmospheric Model, 1990 version (GRAM-90)
[NASA-CR-186717] 20 p2888 N90-26435
Level-2 system: Programmers-users manual
[DE90-013324] 20 p2908 N90-26540
LASER: A Layout Sensitivity Explorer. Report and user's manual
[EUT-89-E-216] 20 p2908 N90-26545
Creating a VAPEPS database: A VAPEPS tutorial
[NASA-CR-186629] 20 p2936 N90-26705
ARLSUPER version 1.0, program users guide
[AD-A222693] 21 p2953 N90-26793
Damage tolerance analysis for manned hypervelocity vehicles. Volume 2: Software user's manual
[AD-A222136] 21 p2959 N90-26826
A user's manual for MCPRAM (Monte Carlo PReprocessor for AMEER) and for the fuze options in AMEER (Aero Mechanical Equation Evaluation Routines)
[DE90-013598] 21 p3051 N90-27345
Zadok user guide
[AD-A222071] 21 p3054 N90-27360
Air Force procedure for predicting aircraft noise around airbases: Airbase operations program (BASEOPS) description
[AD-A223069] 21 p3072 N90-27466
Air Force procedure for predicting aircraft noise around airbases: Noise Exposure Model (NOISEMAP). User's manual
[AD-A223162] 21 p3072 N90-27467

CUIS user's manual
[ESA-TM-03] 22 p3132 N90-27775
Concurrent Image Processing Executive (CIPE). Volume 2: Programmer's guide
[NASA-CR-186854] 22 p3236 N90-28349
Concurrent Image Processing Executive (CIPE). Volume 3: User's guide
[NASA-CR-186848] 22 p3236 N90-28350
User's manual ROBIN: A research and notification system for bird migration
[FEL-1989-103] 23 p3270 N90-28508
Data Base Analyzer and Parameter Estimator (DBAPE) interactive computer program user's manual
[PB90-193053] 23 p3406 N90-29252
Generalized Advanced Propeller Analysis System (GAPAS). Volume 2: Computer program user manual
[NASA-CR-185277] 24 p3434 N90-29394
User's manual for the Trajectory Simulation and Analysis Program (TSAP)
[DE90-014850] 24 p3440 N90-29426
Durra: A task-level description language user's manual
[AD-A223761] 24 p3528 N90-29950
An interactive optimization based, computer graphics software package. Phase 2: Users manual
[AD-A223854] 24 p3529 N90-29954
Automated CADAM data transfer: User's manual
[DE90-014871] 24 p3530 N90-29963

USER REQUIREMENTS
Addressing user display requirements from a large and diverse user community
[DE89-011403] 01 p0103 N90-10582
Feasibility of graphics voice telephones for the post 2000 era
[FEL-1988-26] 03 p0340 N90-11937
Power up modification for video switcher microprocessor interface for sensor system processing system
[AD-A211543] 03 p0344 N90-11962
The design, construction, performance and calibration of pulse generators to fulfil the requirements of specifications defence standard 59-41, FS(F) 510 and FS(S) 457
[RAE-TM-FS(F)-550] 04 p0496 N90-12857
State of the art of human/machine dialog tool prototypes
[TELECOM-PARIS-89-H001] 04 p0527 N90-13038
Telescience Testbed Pilot Program
[NASA-CR-184997] 04 p0528 N90-13047
Cryogenics for LDR 05 p0598 N90-13471
LDR cryogenics 05 p0598 N90-13472
Space Station Engineering Design Issues
[NASA-CR-185978] 05 p0601 N90-13492
Power generation and distribution 05 p0604 N90-13515
User needs, benefits, and integration of robotic systems in a space station laboratory
[NASA-CR-185150] 05 p0651 N90-13794
Esrange 05 p0663 N90-13876
The DOD Gateway Information System: Operational prototype and transition period 1987-1988
[AD-A213044] 05 p0707 N90-14141
A comparative evaluation and analysis of end-user search performance in an academic environment 07 p1009 N90-15845
Columbus: A user's introduction
[ESA-BR-62] 08 p1036 N90-15989
User interaction with self-learning systems
[AD-A214260] 08 p1105 N90-16395
A guide to IRUS-2 application development
[AD-A214758] 09 p1266 N90-17340
Help design software project
[AD-A214883] 09 p1270 N90-17362
Noise and sonic boom impact technology. Initial development of an Assessment System for Aircraft Noise (ASAN). Volume 3: Technical description
[AD-A214455] 09 p1278 N90-17412
An investigation of application development process controls in an end-user setting: A field study 09 p1295 N90-17504
Automated information systems plan
[AD-A214982] 09 p1296 N90-17514
Non-contact temperature measurement requirements 10 p1363 N90-17898
Determination of the underlying task scheduling algorithm for and Ada runtime system
[AD-A215860] 11 p1544 N90-18890
The global positioning system
[AD-A217266] 12 p1602 N90-19222
National Technical Information Service 1989 Users Conference proceedings
[PB90-142563] 12 p1726 N90-19921
Proximity operations concept design study, task 6
[NASA-CR-181971] 13 p1761 N90-20112
ARISTOTELES: A European approach for an Earth gravity field recovery mission 13 p1839 N90-20559
Goes I-M and beyond: Science requirements and technology challenges 14 p1934 N90-21067
A study of mental models through communication between users and advisors solving software manipulation problems 15 p2178 N90-22434
Desk top publishing: What you need to know 15 p2178 N90-22449
Navigation requirements: What they are and where they come from 17 p2358 N90-23422
Comparison of location systems 17 p2360 N90-23437
Distributed user services for supercomputers
[NASA-CR-180370] 17 p2450 N90-23976
Northeast Artificial Intelligence Consortium. Volume 3: The Versatile Maintenance Expert System research project
[AD-A218716] 17 p2453 N90-23993
Integrated controls and health monitoring for chemical transfer propulsion
[NASA-TM-103185] 19 p2668 N90-25178
Land application of imaging spectrometry 19 p2708 N90-25415
Space Station attached payloads 21 p3015 N90-27141
Onboard processor technology review 21 p3017 N90-27152
Applications of ISES for meteorology 21 p3018 N90-27160
Data and analysis center for software
[AD-A221434] 21 p3054 N90-27363
ROBFIT: A code for the analysis of histogram spectra with nonlinear regression and robust estimation
[AD-A221527] 21 p3055 N90-27369
The post-2000 MILSATCOM architecture 21 p3070 N90-27452
The Langley 14- by 22-foot subsonic tunnel: Description, flow characteristics, and guide for users
[NASA-TP-3008] 22 p3107 N90-27649
R and D aspects of the future operational concept of the BFS 22 p3112 N90-27679
Impact of Emerging NDE-NDI Methods on Aircraft Design, Manufacture, and Maintenance
[AGARD-CP-462] 22 p3184 N90-28068
Criteria for device selection: A comparison between a mouse and a touchscreen as an input device for interactive video
[NPL-DITC-158/90] 22 p3235 N90-28344
Liquid Rocket Booster (LRB) for the Space Transportation System (STS) systems study, volume 2
[NASA-CR-183786] 23 p3288 N90-28600
Optical storage technology
[AD-A224028] 23 p3407 N90-29254
GPS integrity requirements for use by civil aviation 24 p3423 N90-29339
Radar receiver procedures
[AD-A224399] 24 p3460 N90-29541
Multi-user facility for high performance optical recording of brain activity (DURIP)
[AD-A223491] 24 p3498 N90-29768
Accessing network databases via SQL transactions in a multi-model database system
[AD-A223946] 24 p3557 N90-30128

USER-COMPUTER INTERFACE
U MAN-COMPUTER INTERFACE

UTAH
An anomalous wind between valleys: Its characteristics and a proposed explanation
[DE90-008965] 15 p2133 N90-22189

UTILITIES
Ozone for trace organic contaminant removal
[PB90-221680] 23 p3347 N90-28916

UTILITY AIRCRAFT
NT C-140 AIRCRAFT
NT U-2 AIRCRAFT
NT UH-1 HELICOPTER
NT UH-60A HELICOPTER

UTILIZATION
NT GEOTHERMAL ENERGY UTILIZATION
NT LASER APPLICATIONS
NT LASER CUTTING
NT LASER FUSION
NT REUSE
NT WASTE ENERGY UTILIZATION
NT WASTE UTILIZATION
NT WINDPOWER UTILIZATION
SPOT after two years in operation: An appraisal of results and a review of selected applications 08 p1093 N90-16326
Independent research and independent exploratory development programs
[AD-A222690] 21 p3101 N90-27612
Establishing viable task domains for telerobot demonstrations 24 p3518 N90-29886

UV CETI STARS
U FLARE STARS

UV LASERS
U ULTRAVIOLET LASERS

V

V BAND
U EXTREMELY HIGH FREQUENCIES

V GROOVES
NT RIBLETS
GaAs solar cells with V-grooved emitters 10 p1339 N90-17754

V/STOL AIRCRAFT
NT AH-1G HELICOPTER
NT AH-64 HELICOPTER
NT CH-47 HELICOPTER
NT FLYING PLATFORMS
NT H-53 HELICOPTER
NT HELICOPTERS
NT LIGHT HELICOPTERS
NT MILITARY HELICOPTERS
NT ROTARY WING AIRCRAFT
NT SHORT TAKEOFF AIRCRAFT
NT TILT ROTOR AIRCRAFT
NT UH-1 HELICOPTER
NT UH-60A HELICOPTER
NT VERTICAL TAKEOFF AIRCRAFT
NT XV-15 AIRCRAFT
Engine inlet distortion in a 9.2 percent scale vectored thrust STOVL model in ground effect
[NASA-TM-102358] 10 p1307 N90-17561
A head up display format for application to V/STOL aircraft approach and landing
[NASA-TM-102216] 10 p1320 N90-17632
Research on a two-dimensional inlet for a supersonic V/STOL propulsion system. Appendix A
[NASA-CR-174945] 11 p1451 N90-18364
The insertion of human dynamics models in the flight control loops of V/STOL research aircraft. Appendix 2: The optimal control model of a pilot in V/STOL aircraft control loops
[NASA-CR-186598] 15 p2055 N90-21776
An adaptive human response mechanism controlling the V/STOL aircraft. Appendix 3: The adaptive control model of a pilot in V/STOL aircraft control loops
[NASA-CR-186599] 15 p2056 N90-21777
A modeling technique for STOVL ejector and volume dynamics
[NASA-TM-103167] 16 p2202 N90-22566
Supersonic flow computations for an ASTOVL aircraft configuration, phase 2, part 2
[NASA-CR-4284] 16 p2234 N90-22746
Preliminary design of a supersonic Short Takeoff and Vertical Landing (STOVL) fighter aircraft
[NASA-CR-186670] 17 p2352 N90-23394
Analysis of internal flow in a ventral nozzle for STOVL aircraft
[NASA-TM-103123] 17 p2355 N90-23404
Rotary-Jet thrust augmentor with jet-flapped blades 18 p2492 N90-24243
Experimental and analytical study of close-coupled ventral nozzles for ASTOVL aircraft
[NASA-TM-103170] 18 p2498 N90-24273
Design of a low cost short takeoff-vertical landing export fighter/attack aircraft
[NASA-CR-186658] 19 p2659 N90-25132
Hot gas ingestion characteristics and flow visualization of a vectored thrust STOVL concept
[NASA-TM-103212] 20 p2813 N90-26009
H-infinity based integrated flight-propulsion control design for a STOVL aircraft in transition flight
[NASA-TM-103198] 20 p2813 N90-26011
Sideslip-induced static pressure errors in flight-test measurements
[NASA-TM-102846] 22 p3116 N90-27702
STOVL fighter propulsion reliability, maintainability, and supportability characterization
[AD-A224221] 23 p3282 N90-28574

VACANCIES (CRYSTAL DEFECTS)
Kinetics and mechanisms of primary and steady state creep in B- and Al-containing alpha silicon carbide
[AD-A210739] 02 p0283 N90-11616
Prospects for wavelength tunable lasers based on vacancy defects in alkaline-earth oxides
[DE90-001078] 06 p0789 N90-14592
The effects of oxygen and strontium vacancies on the superconductivity of single crystals of Bi2Sr(2-x)CuO(6-y)
[DE90-004242] 08 p1133 N90-16561
Photoelectron spectroscopic study of the interaction of thin Fe films with the MoS2(0001) surface
[AD-A214348] 10 p1351 N90-17836
Electron scattering by native defects in uniformly and modulation doped semiconductor structures
[DE90-006084] 10 p1437 N90-18296
Photorefractive damage mechanisms in electro-optic materials
[AD-A219786] 17 p2476 N90-24157
Effects of internal hydrogen on the vacancy loop formation probability in Al
[DE90-011114] 18 p2527 N90-24422

Surface defects and chemistry on the SnO2(110) surface 18 p2559 N90-24603

VACUUM
NT HIGH VACUUM
NT ULTRAHIGH VACUUM
Are there causal vacuum solutions with the symmetries of the Goedel universe in higher-derivative gravity [DE89-611966] 01 p0134 N90-10770
Vacuum ultraviolet backgrounds from space - ten years after [AD-A211353] 03 p0435 N90-12493
Electrical breakdown in vacuum [DE90-001623] 06 p0771 N90-14485
Stable supermembrane vacuum with a discrete spectrum [DE89-635722] 07 p0962 N90-15561
Advanced tribological coatings for high specific strength alloys [AD-A214061] 09 p1196 N90-16930
False vacuum decay in Jordan-Brans-Dicke cosmologies [NASA-CR-186257] 09 p1293 N90-17497
Quantum yield of photocathodes in far and extreme ultraviolet wavelength area [ETN-90-95731] 12 p1654 N90-19505
Plasma centrifuge with vacuum arc discharge applied to the separation of stable isotopes [INPE-4925-TDL/385] 12 p1716 N90-19854
Design and calibration of a vacuum compatible scanning tunneling microscope [NASA-TM-102514] 13 p1804 N90-20353
Numerical investigations of nonlinear behavior in the Einstein equations 15 p2175 N90-22427
Stability of compactification during inflation [NASA-CR-186597] 15 p2189 N90-22502
Measurement of plasma-neutralized super-vacuum currents in a gyrotron configuration [AD-A218505] 16 p2316 N90-23207
The hypersonic vacuum wind tunnels: Status, research, and necessary developments 18 p2490 N90-24231
Technology for low pressure plasma processes, a new approach: The plasma box concept [MBB-UE-0003/89-PUB] 19 p2653 N90-25101
Requirements for long-life operation of inert gas hollow cathodes: Preliminary report [NASA-TM-103242] 22 p3134 N90-27783

VACUUM APPARATUS
NT IONIZATION GAGES
NT VACUUM CHAMBERS
Calculations of soft x ray emission of REB-heated plasma [IPPCZ-287] 03 p0407 N90-12329
Surface cooled, vacuum impregnated superconducting magnet systems: Design, construction, applications [ETN-90-96014] 05 p0696 N90-14072
Role of surface passivation in the integrated processing of MOS structures [AD-A222630] 20 p2859 N90-26264
Vacuum mechatronics 24 p3512 N90-29854

VACUUM CHAMBERS
Onorbit electron beam welding experiment definition [NASA-CR-183847] 07 p0938 N90-15431
Development of a quadrupole-based Secondary-Ion Mass Spectrometry (SIMS) system at Lewis Research Center [NASA-TM-102531] 17 p2367 N90-23476
Rome air development center cryo test facility [AD-A220067] 19 p2662 N90-25147
Vacuum mechatronics 24 p3512 N90-29854

VACUUM DEPOSITION
Silicon dioxide deposition at 100 deg C using vacuum ultraviolet light [TR-0088(3945-07)-6] 01 p0047 N90-10269
The quality of vacuum deposited surface treatments [CETIM-107040] 04 p0476 N90-12729
Method of sensitizing PB-Salt epitaxial films for Schottky diodes [AD-D014244] 06 p0850 N90-14937
Microstructural variations in aluminum oxide coatings deposited using a dual beam ion system [DE90-006040] 11 p1491 N90-18583
Vacuum deposition by pulsed laser radiation: Plasma composition, deposition techniques, and thin film properties [ETN-90-97263] 20 p2931 N90-26677

VACUUM EFFECTS
Requirements for long-life operation of inert gas hollow cathodes: Preliminary report [NASA-TM-103242] 22 p3134 N90-27783

VACUUM GAGES
NT IONIZATION GAGES

VACUUM MELTING
Bearing and gear steels for aerospace applications [NASA-TM-102529] 13 p1809 N90-20391
Realization of equipment for manufacturing titanium alloy electrodes for first step melting [ONERA-RT-15/3578-M] 24 p3453 N90-29498

VACUUM SPECTROSCOPY
Optical spectroscopy of Ti(3+) doped YAlO3 [AD-A219043] 16 p2324 N90-23251
Surface physics instrumentation [AD-A220460] 17 p2373 N90-23512
Spectroscopic ellipsometry in vacuum ultraviolet spectral area [ETN-90-97317] 22 p3249 N90-28426

VACUUM SYSTEMS
Introduction to total- and partial-pressure measurements in vacuum systems [NASA-RP-1219] 01 p0072 N90-10412

VACUUM TESTS
NT THERMAL VACUUM TESTS

VACUUM TUBES
NT BACKWARD WAVE TUBES
NT CARCINOTRONS
NT CATHODE RAY TUBES
NT CYCLOTRON RESONANCE DEVICES
NT KLYSTRONS
NT MAGNETRONS
NT MICROWAVE TUBES
NT TRAVELING WAVE TUBES
Vacuum microelectronics for beam power and rectennas 01 p0028 N90-10146
A progress report on the Livermore Miniature Vacuum Tube Project [DE90-008302] 13 p1794 N90-20299
An assessment of the hardness of miniature vacuum tubes to high-voltage transients [DE90-009541] 15 p2089 N90-21956
Notes on the unsteady rectilinear motion of a perfect gas. 9: The expansion to vacuum of a finite mass of uniform homentropic gas [LR-590-9] 19 p2692 N90-25316

VACUUM ULTRAVIOLET RADIATION
U FAR ULTRAVIOLET RADIATION

VALENCE
Solvent relaxation in electron-transfer reactions: Comparisons between barrier-crossing dynamics in water and polar aprotic media [AD-A210212] 01 p0040 N90-10220
Solvent effects on intervalence electron-transfer energies for biferrocene cations: Comparisons with molecular models of solvent reorganization [AD-A210263] 01 p0120 N90-10691
Superconductivity from valence fluctuations with finite U [DE89-015302] 01 p0129 N90-10742
Strain and density dependent valence-band masses in InGaAs/GaAs and GaAs/GaAsP strained-layer structures [DE89-016882] 02 p0285 N90-11627
Theory of the electronic and optical properties of semiconductor heterostructures [AD-A214132] 08 p1130 N90-16544
Volatile divalent double metal alkoxides [AD-D014355] 10 p1438 N90-18300
Valence-defect chemical equilibria in nonstoichiometric YBa2Cu3O(7-delta) [DE90-010152] 18 p2619 N90-24921

VALIDATION
U PROVING

VALIDITY
Validity domain of the scalar Kirchhoff and Rayleigh-Sommerfeld diffraction theories in the near field of small phase objects: Comparison between calculation models and microwave measure [ETN-90-96963] 20 p2855 N90-26236

VALKYRIE AIRCRAFT
U B-70 AIRCRAFT

VALLEYS
NT IMPERIAL VALLEY (CA)
Image processing of LANDSAT MSS data for buried valley detection in northern Indiana 06 p0802 N90-14668
An anomalous wind between valleys: Its characteristics and a proposed explanation [DE90-008965] 15 p2133 N90-22189
Daytime wind valleys adjacent to the Great Salt Lake [DE90-008991] 15 p2133 N90-22190
The ASCOT 1988 valley/tributary interaction study [DE90-009043] 15 p2133 N90-22191
A study of mesoscale acid deposition in the lower Ohio River Valley 16 p2253 N90-22848

VALUE
NT Q VALUES
Type reconstruction with first-class polymorphic values [AD-A210833] 01 p0106 N90-10605
Procedures for separations within batches of values, 1. The orderly tool kit and some heuristics [AD-A210652] 02 p0268 N90-11531

VALUE ENGINEERING
Designing for reliable and low maintenance cost aero engines [PNR90570] 04 p0455 N90-12604
The joint DOD/NASA Advanced Launch System (ALS) programme 09 p1179 N90-16832
General introduction to location and navigation capabilities 17 p2358 N90-23421
Limits to today's composites: Chances for tomorrow's developments [MBB-Z-0287-89-PUB] 18 p2519 N90-24385
Minimizing sums of addition chains [RUU-CS-89-15] 18 p2635 N90-25013

VALVES
NT ARTIFICIAL HEART VALVES
NT AUTOMATIC CONTROL VALVES
NT BUTTERFLY VALVES
NT CONTROL VALVES
NT DAMPERS (VALVES)
NT GAS VALVES
NT PRESSURE REGULATORS
Advanced actuation systems development, volume 1 [AD-A213334] 04 p0458 N90-12624
Simulation of the control characteristics of an axial piston pump and a flapper-nozzle valve combination 05 p0649 N90-13784
Automatic prestart or post shutoff engine lubricator [AD-D014259] 08 p1084 N90-16273
Low-noise nozzle valve [NASA-CASE-MFS-28383-1] 09 p1216 N90-17051
Construction and characterization of a valve for rapid gas injection [INPE-4789-RPE/583] 12 p1651 N90-19486
Monostable electrovalve [INPE-4928-RPE/595] 12 p1651 N90-19487
A nonintrusive method for measuring the operating temperature of a solenoid-operated valve [DE90-007576] 13 p1804 N90-20355
Analyses of power consumption for two sliding vane type compressors [AD-A218366] 13 p1812 N90-20406
Apparatus for mixing solutions in low gravity environments [NASA-CASE-MFS-26047-1] 14 p1958 N90-21209
Double valve mechanism for an acoustic modulator [AD-D014401] 14 p1987 N90-21386

VAN ALLEN RADIATION BELTS
U RADIATION BELTS

VAN DE GRAAFF ACCELERATORS
Ion bombardment experiments suggesting an origin for organic particles in pre-cometary and cometary ices 08 p1148 N90-16652

VAN DER WAAL FORCES
Infrared spectra of van de Waals complexes of importance in planetary atmospheres 20 p2943 N90-26749
Microwave spectra of van der Waals complexes of importance in planetary atmospheres 20 p2944 N90-26752

VANADIUM
L shell XANES (X ray Absorption Near Edge Structure) for solid metals: Ti, V, Cr, Fe, Ni, Cu [DE90-008043] 13 p1896 N90-20880
Fatigue crack growth investigation of a Ti-6Al-4V forging under complex loading conditions: NATO/AGARD supplemental engine disk program [AD-A220239] 17 p2377 N90-23538
Fabricating vanadium sheet to improve symmetry of drawn parts [DE90-011253] 19 p2682 N90-25257

VANADIUM ALLOYS
Potential difference applied to the measurement of small fatigue crack growth at notches in Ti-6Al-4V [FFA-TN-1989-09] 04 p0512 N90-12952
Threshold for fatigue crack propagation [DLR-FB-89-33] 05 p0655 N90-13815
Heat treatment investigation of 4330 vanadium-modified steel [AD-A214290] 07 p0906 N90-15239
Fusion reactor materials [DE90-000976] 07 p0994 N90-15744
Response of unirradiated and neutron-irradiated vanadium alloys to Charpy-impact loading [DE90-004878] 11 p1486 N90-18551
Vanadium alloys with improved resistance to helium embrittlement [DE90-009811] 17 p2375 N90-23524
Compendium of material test results on HY-130 and Ti-3Al2V metals in support of United States navy programs [DE90-011754] 20 p2833 N90-26112
Formation of Titanium-boron surface alloys by excimer laser mixing [DE90-013172] 20 p2834 N90-26118
Swelling of neutron irradiated vanadium alloys [DE90-015294] 24 p3448 N90-29472

VANADIUM COMPOUNDS
NT VANADIUM OXIDES
A nonlinear-optical method for combining high power laser beams
[AD-A211730] 03 p0354 N90-12022
VANADIUM OXIDES
Lithium polymer electrolyte battery, electrochemical behavior of cathode materials
[AD-A210755] 02 p0216 N90-11235
Vanadium dioxide protective devices
[AD-A212018] 03 p0332 N90-11887
Ceramic epitaxial films and multilayers prepared by MOCVD
[DE90-011090] 18 p2532 N90-24447
VANES
NT GUIDE VANES
NT JET VANES
NT WIND VANES
Study for optimization of redundant vane-type flow-direction sensing systems and numerical analysis for design of the systems
[NAL-TM-571] 02 p0155 N90-10890
Tower wake/blade interaction noise of a wind turbine
[NAL-TR-945] 02 p0236 N90-11344
Fabrication of modulated vanes for a split-coaxial RFQ
[DE88-757235] 03 p0403 N90-12310
Influence of vane sweep on rotor-stator interaction noise 05 p0571 N90-13325
The effectiveness of vane-aileron excitation in the experimental determination of flutter speed by parameter identification
[NASA-TP-2971] 07 p0880 N90-15100
Navier-Stokes analysis of turbine blade heat transfer
[NASA-TM-102496] 14 p1972 N90-21300
Heat transfer and pressure measurements for the SSME fuel-side turbopump
[NASA-CR-184928] 17 p2355 N90-23405
Effect of vane twist on the performance of dome swirlers for gas turbine airblast atomizers
[NASA-TM-103195] 19 p2688 N90-25289
Prediction and measurement of rotor blade/stator vane dynamic characteristics of a modern aero-engine axial compressor
[PNR90667] 20 p2812 N90-26002
The structural dynamics analysis of the main injector LOX inlet tee and its redesign
[NASA-CR-186764] 20 p2875 N90-26358
Validation of the F-18 high alpha research vehicle flight control and avionics systems modifications
[NASA-TM-101723] 23 p3276 N90-28542
Analysis of the T63-A-700 engine used in alcohol turbine fuel extender test
[DOT/FAA/CT-TN90/18] 23 p3278 N90-28549
The effects of a compressor rebuild on gas turbine engine performance: Final results 23 p3306 N90-28701
VANS
U TRUCKS
VAPOR DEPOSITION
NT VACUUM DEPOSITION
Characterization of diamond films by thermogravimetric analysis and infrared spectroscopy
[AD-A210564] 01 p0050 N90-10286
Properties of devices prepared with epitaxial layers on InP
[AD-A210304] 01 p0132 N90-10759
Method of modifying the dielectric properties of an organic polymer film
[AD-D014171] 03 p0330 N90-11879
Application of dimensional analysis to statistical process modeling
[AD-A211881] 03 p0335 N90-11905
Beam assisted fabrication of 3-5/Si monolithic devices
[AD-A212046] 03 p0412 N90-12367
Spectroscopic ellipsometry characterization of CVD deposition and doping of polysilicon multilayer structures
[RSRE-MEMO-4258] 04 p0466 N90-12671
An investigation of diamond film deposition in a premixed oxyacetylene flame
[AD-A212595] 04 p0561 N90-13268
The growth of epitaxial GaAs and GaAlAs on silicon substrates by OMVPE
[AD-A212873] 04 p0561 N90-13269
Wear-resistant coated object
[EP-PATENT-0-289-173-A1] 05 p0624 N90-13643
Novel in situ spectroscopic ellipsometer for real time analysis of CVD diamond films
[AD-A213218] 05 p0644 N90-13762
Study of microcrystalline, silicon-carbon p-layers prepared by photo-CVD and glow discharge
[DE89-009438] 06 p0850 N90-14939
Benefits from combining electroplating and physical vapor deposition technologies
[DE90-002700] 07 p0917 N90-15301
Characterization of MOCVD (Metal Organic Chemical Vapor Deposition) grown epitaxial ceramic oxide thin films
[DE90-003561] 07 p1001 N90-15790
Preparation, structure and properties of VO(sub x) and TiO2 thin films by MOCVD
[DE90-003566] 07 p1001 N90-15793
The substitution of IVD (Ion Vapor Deposition) aluminum for cadmium
[AD-A215633] 09 p1195 N90-16921
Plasma assisted chemical vapor deposition of diamond films
[AD-A214641] 09 p1197 N90-16934
The growth of epitaxial GaAs and GaAlAs on silicon substrates by OMVPE
[AD-A214642] 09 p1288 N90-17469
Investigation of low temperature multilevel dielectrics for application for radiation tolerant, submicron-scaled IC technology
[AD-A216114] 10 p1433 N90-18273
Continuous preparation of a thin refractory carbide deposit on the surface of carbon fibers: Characterization of the C/SiC fiber 11 p1477 N90-18501
Metallaboranes as precursors to metallic glasses
[AD-A216946] 11 p1490 N90-18577
Chemical vapor deposition and photochemical vapor deposition of amorphous silicon photovoltaic devices
[DE89-009510] 11 p1529 N90-18803
Preparation and characterization of alumina films prepared by a novel spray pyrolysis method
[AD-A217570] 12 p1625 N90-19339
Microstructural characterization of multiphase coatings produced by chemical vapor deposition
[DE90-007573] 12 p1632 N90-19379
Light-scattering measurements of CVD (Chemical Vapor Deposition) silicon carbide
[DE90-007885] 12 p1632 N90-19382
Comparison of a 6-layer and a 15-layer version of the Chemical Transfer Model (CTM)
12 p1687 N90-19689
Control of the RADM chemistry mechanism of the gas phase 12 p1687 N90-19690
FWP executive summaries: Basic energy sciences materials sciences programs
[DE90-006373] 12 p1722 N90-19893
Interface science in deformation processing of ceramics
[DE90-008424] 13 p1780 N90-20219
High power semiconductor laser arrays by metalorganic chemical vapor deposition 13 p1805 N90-20363
Electron beam induced damage in PECVD Si3N4 and SiO2 films on InP
[NASA-TM-102544] 13 p1810 N90-20393
Molecular dynamics and spectroscopy at gas-solid interfaces
[AD-A217743] 13 p1885 N90-20813
An ellipsometric measurement of optical properties for InP surfaces
[AD-A217185] 13 p1887 N90-20827
Refractive index profiles of thermally grown and chemically vapor deposited films on silicon
[AD-A217187] 13 p1893 N90-20865
Growth, characterization and device development in monocrystalline diamond films
[AD-A218211] 13 p1898 N90-20895
Extrinsic germanium Blocked Impurity Bank (BIB) detectors 14 p1976 N90-21322
Characterization and comparison of optically transparent conducting films
[DE90-000319] 14 p2033 N90-21660
On the vapour phase deposition mechanism of carbon-boron-nitrogen compounds between 800 and 1000 C
[REPT-892-430-101] 16 p2214 N90-22632
Theoretical studies of silicon chemistry
[AD-A219232] 16 p2225 N90-22690
Indium phosphide planar Gunn diode
[AD-A219337] 16 p2233 N90-22740
Advanced gas phase reactor for growth of Ge sub x Si sub 1-x
[AD-A219012] 16 p2323 N90-23250
Ultrafine microstructure composites prepared by chemical vapor deposition
[AD-A219650] 17 p2369 N90-23484
Reactions of silane in active nitrogen
[AD-A220371] 17 p2373 N90-23511
Photoreflectance for in-situ characterization of MOCVD growth of semiconductors under micro-gravity conditions
[NASA-CR-186600] 17 p2383 N90-23576
Development of high performance beta-SiC field-effect transistors
[AD-A218392] 17 p2394 N90-23637
Mechanical property characterization of fiber-reinforced SiC matrix composites
[DE90-011316] 18 p2520 N90-24390
Ceramic epitaxial films and multilayers prepared by MOCVD
[DE90-011090] 18 p2532 N90-24447
Epitaxy of TiO2 thin film on sapphire by MOCVDVD
[DE90-010054] 18 p2618 N90-24915
Synthesis of large area, monocrystalline TiC as a substrate for heteroepitaxial growth of beta-SiC
[AD-A221392] 18 p2623 N90-24948
Improving the performance of InAs(1-x)Sb(x)/InSb infrared detectors grown by metal organic chemical vapor deposition
[DE90-009743] 18 p2625 N90-24956
Superconducting thin films of YBaCu oxides prepared by MOCVD
[DE90-011109] 18 p2625 N90-24961
Formation of high Tc superconducting films by organometallic chemical vapor deposition
[AD-D014498] 19 p2760 N90-25682
Laser techniques for studying chemical vapor deposition
[DE90-012921] 20 p2867 N90-26311
Dielectric function of InGaAs in the visible
[NASA-TM-103246] 20 p2932 N90-26683
Interfacial studies of Chemical Vapor Infiltrated (CVI) ceramic matrix composites
[AD-A221867] 21 p2972 N90-26893
Laser induced surface chemical epitaxy
[AD-A222082] 21 p2977 N90-26920
Status and applications of diamond and diamond-like materials: An emerging technology
[NASA-CR-186935] 21 p2985 N90-26963
The preparation of ACEL thin films
[AD-A222919] 21 p2999 N90-27048
Self-lubricating surfaces by ion beam processing
[AD-A222489] 21 p3011 N90-27118
Pulsed laser deposition of high (Tc) superconducting thin films: Present and future
[DE90-011950] 21 p3080 N90-27511
A unifying picture of gas-phase formation and growth of PAH (Polycyclic Aromatic Hydrocarbons), soot, diamond and graphite 21 p3091 N90-27575
In-situ integrated processing and characterization of thin films of high temperature superconductors, dielectrics and semiconductors by MOCVD 22 p3148 N90-27851
In Situ deposition of YBCO high-T(sub c) superconducting thin films by MOCVD and PE-MOCVD
22 p3152 N90-27871
Strengthening and toughening mechanisms in ceramic fiber-reinforced glass matrix composites
23 p3300 N90-28666
Mechanical property measurement of polycrystalline diamond films
[AD-A224037] 23 p3402 N90-29222
Investigation of laser diagnostics of PACVO (Plasma Assisted Chemical Vapor Deposition) processes for depositing hard face coatings
[DE90-016209] 24 p3457 N90-29522
VAPOR GENERATORS
U VAPORIZERS
VAPOR LIQUID EQUILIBRIUM
U LIQUID-VAPOR EQUILIBRIUM
VAPOR PHASE EPITAXY
Ordered structures and metastable alloys grown by OMVPE
[DE89-016370] 01 p0129 N90-10744
Ultra high speed compound semiconductors and real time signal processing
[AD-A211394] 03 p0413 N90-12372
The growth of epitaxial GaAs and GaAlAs on silicon substrates by OMVPE
[AD-A214642] 09 p1288 N90-17469
Diffusion and defect characterization studies of mercury cadmium telluride
[AD-A214655] 09 p1289 N90-17470
Structural instabilities, impurities, and defects in electronic materials
[AD-A215384] 09 p1290 N90-17481
Advanced GaAs space solar cells by MOCVD technique 10 p1339 N90-17752
High-efficient solar cells for space application
10 p1342 N90-17777
Peeled film GaAs solar cells for space power
[NASA-TM-103125] 14 p1970 N90-21287
Germanium Blocked Impurity Band (BIB) detectors
14 p1976 N90-21321
Indium phosphide planar Gunn diode
[AD-A219337] 16 p2233 N90-22740
Advanced gas phase reactor for growth of Ge sub x Si sub 1-x
[AD-A219012] 16 p2323 N90-23250
Ultra high-speed compound semiconductors and real time signal processing
[AD-A220721] 17 p2396 N90-23651
Ceramic epitaxial films and multilayers prepared by MOCVD
[DE90-011090] 18 p2532 N90-24447

VAPOR PHASES
An atmospheric pressure flow reactor: Gas phase kinetics and mechanism in tropospheric conditions without wall effects 02 p0203 N90-11160
The behavior of hydrazine vapor in an environmental chamber under simulated atmospheric conditions 02 p0203 N90-11161
Modeling of hydrazine surface interactions in environmental reaction chambers 02 p0203 N90-11162
A matrix-isolation FT-IR study of hydrazine 02 p0204 N90-11168
Transport phenomena and interfacial kinetics in multiphase combustion systems [AD-A212932] 05 p0621 N90-13620
Buoyancy effects on the vapor condensation rate on a horizontal liquid surface [NASA-TM-102437] 05 p0629 N90-13675
Vapor condensation on liquid surface due to laminar jet-induced mixing: The effects of system parameters [NASA-TM-102433] 05 p0643 N90-13751
Heat transfer in condensation of lithium vapors [DE90-002081] 07 p0929 N90-15375
Determination of the minimum energy conformation of alkyl substituted pyrazines [AD-A216974] 11 p1484 N90-18539
Low-energy scattering of electrons and positrons in liquids 11 p1559 N90-18981
Initial results of positron ionization mass spectrometry 11 p1561 N90-18995
Control of the RADM chemistry mechanism of the gas phase 12 p1687 N90-19690
Structure of model gas flames in nitramines [AD-A217578] 13 p1770 N90-20159
Dynamics of electronically excited species in gaseous and condensed phase [AD-A217696] 13 p1884 N90-20812
Determination of rates of reaction in the gas-phase in the troposphere: Theory and practice. 2: Rate of direct photoreaction: Screening-level test guideline-spectroscopic determination of the cross section and the maximum rate of direct photoreaction in sunlight [PB90-146291] 15 p2125 N90-22156
HCl Vapor Characterization and Detection. JANNAF Safety and Environmental Protection Subcommittee Workshop [AD-A216252] 16 p2208 N90-22596
The HCl/aerosol problem 16 p2208 N90-22597
HCl monitor 16 p2209 N90-22599
On the vapour phase deposition mechanism of carbon-boron-nitrogen compounds between 800 and 1000 C [REPT-892-430-101] 16 p2214 N90-22632
Unsteady group behavior of droplet clouds in swirling flows 16 p2233 N90-22743
Chemistry within molecular clusters [AD-A219836] 18 p2520 N90-24392
Observation of a magic number in the ion distribution of ethene clusters [AD-A219837] 18 p2521 N90-24393
A gas-phase high voltage electrical isolator with controlled breakdown [RAE-TR-78030] 19 p2669 N90-25180
Gaseous optical contamination of the spacecraft environment: A review 19 p2730 N90-25519
Carbon chemistry in dense molecular clouds: Theory and observational constraints 21 p3090 N90-27571
CI, CII, and CO as tracers of gas phase carbon 21 p3091 N90-27572
A unifying picture of gas-phase formation and growth of PAH (Polycyclic Aromatic Hydrocarbons), soot, diamond and graphite 21 p3091 N90-27575
The formation and structure of circumstellar and interstellar dust 21 p3091 N90-27576
A study of catalysts and mechanisms in synthesis reactions [DE90-015064] 23 p3304 N90-28691

VAPOR PRESSURE
Vapour pressures and critical points of liquids. Halogenated hydrocarbons [ESDU-89006] 03 p0325 N90-11848
Thermophysical properties of benzene. Part 1: The ideal gas and the saturated liquid and vapour [ESDU-89002-PT-1] 04 p0470 N90-12693
The evaporation of sessile droplets. Part 1: Theoretical factors for a two-component system [AD-A215946] 10 p1353 N90-17848
Vapor pressures of acetylene at low temperatures 20 p2949 N90-26777

VAPOR TRAILS
U CONTRAILS

VAPORIZERS
A vapor generator for transonic flow visualization [NASA-TM-101670] 05 p0584 N90-13403
Metal vaporisers: Bicentennial series of five historical monographs [ISBN-0-642-13584-3] 08 p1052 N90-16081
A composition for the filling of gas-discharge tubes [AD-A222818] 21 p2999 N90-27047

VAPORIZING
NT BOILING
NT EVAPORATION
NT EVAPOTRANSPIRATION
NT FILM BOILING
NT SUBLIMATION
NT TRANSPIRATION
Theory of droplet. Part 1: Renormalized laws of droplet vaporization in non-dilute sprays 01 p0068 N90-10390
Evaporation and combustion of dense sprays with a bimodal droplet size distribution 02 p0192 N90-11094
Experimental measurements of shock-induced vaporization in cadmium and lead [DE89-016877] 02 p0194 N90-11103
Time-dependent free convection in low Prandtl number fluids [DE90-003053] 07 p0929 N90-15377
Aerosol heating and vaporization of high-flux laser beams [DE90-003471] 07 p0937 N90-15428
Externally vaporizing system for turbine combustor [AD-D014284] 08 p1024 N90-15918
Simulation of thermal dynamics of a vaporizing coal-water droplet in a combustor [DE90-005356] 12 p1621 N90-19317
Effects of turbulence mixing, variable properties, and vaporization on spray droplet combustion [NASA-CR-186463] 12 p1623 N90-19326
Atmospheric thermal blooming and beam clearing by aerosol vaporization [DE90-006271] 12 p1690 N90-19711
Unsteady group behavior of droplet clouds in swirling flows 16 p2233 N90-22743
Fuel-rich catalytic combustion: A fuel processor for high-speed propulsion [NASA-TM-103177] 17 p2374 N90-23518
Hypervelocity impact shield [NASA-CASE-MSC-21420-1] 21 p2966 N90-26858
Transient cooling of a hot surface by droplets evaporation [PB90-227968] 23 p3325 N90-28799
Proceedings of a discussion meeting on Thermodynamics of Alloys [AD-A224336] 24 p3449 N90-29476

VAPORS
NT CESIUM VAPOR
NT METAL VAPORS
NT WATER VAPOR
Thermophysical properties of buta-1,3-diene [ESDU-89005] 05 p0620 N90-13619
Gas identification system using graded temperature sensor and neural net interpretation [AD-A213359] 05 p0622 N90-13627
Reflux condensation in vertical tubes [ESDU-89038] 07 p0932 N90-15397
Studies of density distributions in one-dimensional shock-induced debris clouds [DE90-004089] 08 p1085 N90-16282
Ignitability of jet-A fuel vapors in aircraft fuel tanks 10 p1313 N90-17594
Laser-matter interaction at intensities of 10(sup 12) W/cm(sup 2) and below [DE90-007536] 12 p1669 N90-19590
Characterization of ceramic matrix composites fabricated by chemical vapor infiltration [DE90-008409] 13 p1768 N90-20149
Magnetic vapor shield mechanism for protection of material surfaces exposed to high heat load [AD-A217667] 13 p1780 N90-20217
Control of surface melting and ablation in electromagnetic launchers via the magnetic vapor shielding mechanism [AD-A219035] 16 p2204 N90-22578
Diffusion of penetrants in polymers [AD-A223217] 21 p2986 N90-26969
Down-to-earth studies of carbon clusters 21 p3091 N90-27573

VARACTOR DIODES
Design, construction and test of a frequency doubler for 183 GHz [PB89-212591] 03 p0341 N90-11944
High-efficiency Schottky-Varactor frequency multipliers at millimeter waves [PB90-110701] 09 p1209 N90-17007

VARACTORS
U VARACTOR DIODES

VARIABILITY
Tuning of the OSCURS (Ocean Surface Current Simulations) numerical model to ocean surface measurements in the Gulf of Alaska [PB89-103979] 06 p0818 N90-14759
Geosat/ERM altimeter data analysis for the determination of global oceanic mesoscale variability 07 p0949 N90-15492
An analysis of diurnal wind variability in the Santa Barbara Channel from SODAR measurements [AD-A215769] 10 p1408 N90-18121
A study of gravity wave variability, saturation, and turbulence generation in the mesosphere and lower thermosphere [AD-A220018] 17 p2424 N90-23810
Noise variability in Cyg X-1 and Her X-1 17 p2483 N90-24200
Usefulness of heart measures in flight simulation 19 p2734 N90-25542
Spectral variability of LMC X-4 19 p2766 N90-25717
Noise variability in Cyg X-1 and Her X-1 19 p2771 N90-25753
The long-term optical behaviour of X Per = 3U 0352+30 19 p2776 N90-25783
The X ray dip source 4U 1624-49 19 p2776 N90-25786
Long period variations in high mass X ray binaries and their possible relationship with SU UMa stars 19 p2777 N90-25796
A model for 1/f-type variability in active galactic nuclei 19 p2778 N90-25799
Variability in BL Lac objects: A schematic model 19 p2787 N90-25861
Rapid X ray variability in BL Lacertae objects 19 p2787 N90-25862
Long timescale X ray variability in AGN 19 p2788 N90-25868
X ray AGN variability with hour to month timescales 19 p2788 N90-25869
The X ray time variability of NGC 6814 revisited 19 p2790 N90-25882
X ray spectral variability in Seyfert 1 galaxies 19 p2792 N90-25891
Variability of the continuum emission of GQ Comae 19 p2793 N90-25903
X ray spectrum and variability of MRK 509 as observed with EXOSAT and Ginga 19 p2794 N90-25904
A magnetic flare model for X ray variability in AGN 19 p2794 N90-25907
X ray spectral index variability in NGC 4151 19 p2795 N90-25911
X ray variability of active galactic nuclei 19 p2795 N90-25914
Estimating the spatial variability of trace gas deposition velocities [PB90-208570] 23 p3349 N90-28928
Radio outbursts in extragalactic sources 23 p3414 N90-29291
Investigation of x ray variability in highly active cool stars [NASA-CR-183853] 24 p3560 N90-30143

VARIABLE GEOMETRY STRUCTURES
An assessment of robustness of flight control systems based on variable structure techniques 02 p0157 N90-10895
Toward the development of COSMO-LAB 18 p2500 N90-24281

VARIABLE LIFT
U LIFT

VARIABLE MASS SYSTEMS
The spacecraft structure 05 p0604 N90-13512

VARIABLE PITCH PROPELLERS
An approximate model for the performance and acoustic predictions of counterrotating propeller configurations [NASA-CR-180667] 10 p1426 N90-18228
A computer program for the prediction of nozzle-propeller performance [LR-578] 15 p2048 N90-21740

VARIABLE STARS
NT CATACLYSMIC VARIABLES
NT CEPHEID VARIABLES
NT DWARF NOVAE
NT FLARE STARS
NT HERCULES NOVA
NT MIRA VARIABLES
NT NOVAE
NT SUPERNOVA 1987A
NT SUPERNOVAE
NT SYMBIOTIC STARS
NT T TAURI STARS
Variable stars 05 p0608 N90-13541
Equation of state and opacity of dense plasmas [DE90-002223] 06 p0847 N90-14926
Pulsations of delta Scuti stars [DE90-003213] 08 p1139 N90-16598

The infrared spectral signature of star formation
11 p1582 N90-19114
CO infrared bands in atmospheres of long-period variables
11 p1584 N90-19128
Photometry of variable AFGL sources
[AD-A216938] 11 p1594 N90-19185
AFGL ten micron mosaic array spectrometer: Recent results
14 p1978 N90-21333
Activities report of the Institute for Astronomy and Astrophysics
[MITT-10] 18 p2636 N90-25020
Multiwavelength constraints on gamma-ray burst sources
18 p2639 N90-25032
Nonradial instability strips for post-AGB stars
[DE90-014922] 23 p3411 N90-29278

VARIABLE SWEEP WINGS
Design and test of an NLF wing glove for the variable-sweep transition flight experiment
04 p0444 N90-12544
F-14 VSTFE and results of the cleanup flight test program
04 p0445 N90-12547
Variable-Sweep Transition Flight Experiment (VSTFE): Stability code development and clean-up glove data analysis
04 p0445 N90-12548
An aerodynamic tradeoff study of the scissor wing configuration
[NASA-CR-186576] 14 p1913 N90-20965
Flutter clearance of the F-14A variable-sweep transition flight experiment airplane, phase 2
[NASA-TM-101717] 19 p2659 N90-25135

VARIABLE THRUST
The apogee boost motor
05 p0605 N90-13517

VARIANCE
Power spectral estimation algorithms
[NASA-CR-186189] 06 p0828 N90-14812

VARIANCE (STATISTICS)
NT ANALYSIS OF VARIANCE
NT BIVARIATE ANALYSIS
NT COVARIANCE
NT MULTIVARIATE STATISTICAL ANALYSIS
NT REGRESSION ANALYSIS
Improved estimation of the disturbance variance in a linear regression model
[AD-A210272] 01 p0112 N90-10641
Doppler statistics of ocean velocity variability
[AD-A211687] 03 p0377 N90-12148
Multiparameter radar estimation of raindrop size distribution
[AD-A212410] 04 p0521 N90-13007
Statistics of a chi-square random variable obtained from independent Gaussian samples with a non-zero mean and arbitrary variance
[AD-A214477] 09 p1275 N90-17392
Integral and series representation of infinitely divisible processes with applications to their prediction and to their sample path, statistical, and structural properties
[AD-A219625] 17 p2456 N90-24017
Stochastics realization problems
[CWI-BS-R8920] 17 p2467 N90-24097
Ultrasensitive laser spectroscopy in solids: Statistical fine structure and single-molecule detection
[AD-A222391] 21 p3074 N90-27477
Further experiments in variable frame rate analysis for speech recognition
[RSRE-MEMO-4336] 22 p3165 N90-27951
Experiments with grand variance in the ARM continuous speech recognition system
[RSRE-MEMO-4359] 22 p3166 N90-27954

VARIATION METHOD
U CALCULUS OF VARIATIONS

VARIATIONAL PRINCIPLES
A finite element formulation for inelastic plates and shells based on a mixed variational principle
02 p0233 N90-11334
On the extremum electric charge problem of steady electromagnetic equilibria
[TRITA-EPP 89-04] 04 p0489 N90-12809
On the choice of trial function in theoretical calculations of the thermal conductivity
[DE90-001733] 07 p0897 N90-15182
A basic theorem of complementarity for the generalized variational-like inequality problem
[DE90-003102] 07 p0973 N90-15620
A higher-order plate theory with ideal finite element suitability
[AD-A216163] 10 p1397 N90-18075
Finite element approximations of the stokes flow problem based upon various variational principles
[DE90-608612] 12 p1659 N90-19533
The p- and h-p versions of the finite element method: An overview
[AD-A216902] 12 p1705 N90-19789
A 4-node assumed-stress hybrid shell element with rotational degrees of freedom
[NASA-CR-4279] 13 p1815 N90-20422
Generalized quasi-variational inequality and implicit complementarity problems
[AD-A215191] 13 p1875 N90-20755
Termolecular associations of ions in gases, recombination and electron-atom collisions
[AD-A217678] 13 p1883 N90-20805
Direct formulation of a 4-node hybrid shell element with rotational degrees of freedom
[NASA-CR-4282] 14 p1991 N90-21411
Towards a unified analysis methodology for composite rotor blades
15 p2046 N90-21730
Finite element analysis of elastic contact problems with friction
15 p2105 N90-22040
Self-calibration of robot-sensor system
15 p2144 N90-22246
Computations of weight functions in fracture mechanics
16 p2246 N90-22809
A decoupled recursive approach for constrained flexible multibody system dynamics
16 p2289 N90-23042
Variational formulation and finite element implementation of Pagano's theory of laminated plates
24 p3442 N90-29437

VARIATIONS
NT ALTERNATIONS
NT ANNUAL VARIATIONS
NT DIURNAL VARIATIONS
NT GEOMAGNETIC PULSATIONS
NT MAGNETIC VARIATIONS
NT PERIODIC VARIATIONS
NT WIND VARIATIONS
Discrete-time conversion for simulating finite-horizon Markov processes
[AD-A210683] 01 p0116 N90-10666
On the analysis of line profile variations: A statistical approach
03 p0420 N90-12412
Sensitivity of a regional oxidant model to variations in climate parameters, volume 1 and 2
[PB89-224943] 04 p0516 N90-12981
The effects of seasonal and latitudinal earth infrared radiance variations on ERBS attitude control
05 p0586 N90-13414
Fluctuations of the Lyapunov exponent in disordered systems
[PREPRINT-690] 05 p0695 N90-14063
Experimental determination of the fluid velocity by spectral analysis of temperature fluctuations
[DE89-636430] 07 p0928 N90-15372
Global lake-level variations from 18,000 to 0 years ago: A palaeoclimate analysis
[DE90-000998] 07 p0956 N90-15531
Uniform stability for time-varying infinite-dimensional discrete linear systems
[DE89-635712] 08 p1116 N90-16460
Measurement of fluctuations in the tilt of Arctic ice at the CEAREX Oceanography Camp: Experiment review, data catalog, and preliminary results
[AD-A215059] 09 p1249 N90-17249
Finite element analysis of a quartz rotation sensor
[DE90-006959] 12 p1664 N90-19562
Specific heat and critical fluctuations in anisotropic high-T(sub c) oxide superconductors
[DE90-613394] 14 p2031 N90-21651
A mechanism for the formation of knots, kinks and discontinuous events in the plasma tail of comets
[DE90-613285] 14 p2041 N90-21707
Time-varying filter modelling and time-frequency characterisation of nonstationary sound fields due to a moving source
16 p2312 N90-23178
Spatial fluctuations in the diffuse X ray background
19 p2785 N90-25845
X ray spectra of OVV QSOs
19 p2787 N90-25863
Origin of density fluctuations in extended inflation
[NASA-CR-182852] 19 p2795 N90-25915
Spatial cross-correlation of Antarctic Sea ice and seabed topography
[NASA-CR-186815] 20 p2891 N90-26451
Fluctuations in cosmic background radiation
[INPE-4579-PRE/1313] 23 p3415 N90-29294

VARIOMETERS
Improvements of automatic magnetic observatories in Italy
21 p3022 N90-27185
Improvements in fluxgate magnetometers at Danish Meteorological Institute's Magnetic Observatories
21 p3023 N90-27187
About the derivation of geomagnetic indices from digital data
21 p3023 N90-27191

VARISTORS
Energy ratings for metal oxide varistors under repetitively pulsed operation
[DE90-002353] 06 p0770 N90-14480
Sintering studies on high field varistors
[DE90-002626] 07 p0926 N90-15359

VASCULAR SYSTEM
U CARDIOVASCULAR SYSTEM

VASOCONSTRICTION
Field management of accidental hypothermia during diving
[AD-A219560] 17 p2434 N90-23866

VASOMOTOR NERVOUS SYSTEM
U NERVOUS SYSTEM

VAX COMPUTERS
NT VAX-11 SERIES COMPUTERS
Two VAX-PASCAL terminal interface modules for visualizing scanning and parsing
[MEMO-INF-89-17] 02 p0259 N90-11470
Software and hardware description of the helicopter motion equations for VAX computers
[AD-A213248] 05 p0579 N90-13375
The procedures for easy running of the HULL computer code under VMS
[MRL-GD-0023] 10 p1417 N90-18165

VAX-11 SERIES COMPUTERS
NORDA's pattern analysis laboratory: Current contributions to naval mapping, charting, and geodesy
[AD-A212731] 06 p0801 N90-14665

VCO
U VOLTAGE CONTROLLED OSCILLATORS

VECTOR ANALYSIS
NT CURL (VECTORS)
NT VORTICITY
Four vector-matrix primitives
[AD-A211889] 03 p0392 N90-12237
AcSim: Aircraft simulation program with application to flight profile generation
[AD-A212466] 06 p0723 N90-14217
Simulation of radar scattering from rough surfaces
[AD-A217841] 13 p1790 N90-20275
Modeling and classification of acoustic transients by speech recognition techniques
[AD-A218070] 13 p1791 N90-20277
Analysis of heliport environmental data: Indianapolis downtown heliport, Wall Street heliport. Volume 3: Indianapolis downtown heliport data plots
[AD-A217412] 13 p1829 N90-20500
A numerical and theoretical study of seismic wave diffraction in complex geologic structure
[AD-A218209] 14 p2005 N90-21490
Vectors and matrices: Two turbo pascal units for fast program development
[AD-A218917] 16 p2300 N90-23105
Parallel computation of supersonic flows using a three-dimensional, zonal, Navier-Stokes code
[AD-A218824] 17 p2344 N90-23350
Topology of three-dimensional, variable density flows
[NASA-CR-186622] 17 p2402 N90-23683
A vectorization algorithm for the solution of large, sparse triangular systems of equations
[AD-A219850] 17 p2446 N90-23947
DURIP: Improved eye movement monitoring capabilities for studies in visual cognition
[AD-A220355] 18 p2586 N90-24722
A block-LU update for large-scale linear programming
[AD-A219849] 18 p2590 N90-24738
Superconcurrent processing: A dynamic approach to heterogeneous parallelism
[AD-A222798] 20 p2914 N90-26576
Full vector wave calculation of photonic band structures in face-centered cubic dielectric media
[AD-A222616] 20 p2933 N90-26686
Particle simulation of hypersonic flow
[AD-A222704] 21 p2954 N90-26794
Computational methods for problems in aerodynamics using parallel and vector architecture
[AD-A221979] 21 p2954 N90-26795
Parallel numerical simulations of axisymmetric projectile flows using zonal-overlapped grids
[AD-A221711] 21 p3005 N90-27082
Linear algebra on a CRAY X-MP
[AD-A221780] 21 p3056 N90-27374
Applications of gauge theories to enhance numerical solutions of mixed potential integral equations
[AD-A221520] 21 p3065 N90-27424
The existence of smooth densities for the prediction filtering and smoothing problems
[AD-A222108] 21 p3066 N90-27432
Impulse response operators for structural complexes
[AD-A222374] 22 p3191 N90-28107
A vector diagram approach to shaping inputs for vibration reduction
[AD-A223724] 24 p3480 N90-29671
Asymptotic code vector density in topographic vector quantisers
[RSRE-MEMO-4392] 24 p3539 N90-30012

VECTOR CALCULUS
U VECTOR SPACES

VECTOR CONTROL
U DIRECTIONAL CONTROL

VECTOR CURRENTS
Tuning of the OSCURS (Ocean Surface Current Simulations) numerical model to ocean surface measurements in the Gulf of Alaska
[PB89-103979] 06 p0818 N90-14759
VECTOR PROCESSING (COMPUTERS)
Proceedings of the 2nd International Conference on Vector and Parallel Computing
[AD-A209401] 01 p0103 N90-10585
Checking the Goldbach conjecture on a vector computer
[CWI-NM-R8812] 02 p0260 N90-11475
Implementing the discrete Fourier transform on the hypercube FPS T40
[IMAG-RR-773-I] 05 p0684 N90-13983
Solving time harmonic wave problems on vector processors
[DE90-003956] 08 p1119 N90-16480
Raster Metafile and Raster Metafile Translator
[NASA-TM-102588] 10 p1417 N90-18166
Supercomputer environments
[AD-A217682] 13 p1863 N90-20689
(DURIP) Two-Processor Alliant FX/4 System
[AD-A217810] 13 p1864 N90-20692
Stochastic dynamic programming for reservoir optimal control: Dense discretization and inflow correlation assumption made possible by parallel computing
[REPT-89-056] 22 p3238 N90-28360
VECTOR QUANTIZATION
An adaptive vector quantization scheme
15 p2077 N90-21898
Speech coding 21 p2992 N90-27009
VECTOR SPACES
NT ADJOINTS
NT BANACH SPACE
NT CANONICAL FORMS
NT EIGENVALUES
NT EIGENVECTORS
NT HESSIAN MATRICES
NT HILBERT SPACE
NT JORDAN FORM
NT MATRICES (MATHEMATICS)
NT SOBOLEV SPACE
NT STATE VECTORS
NT STIFFNESS MATRIX
NT STOKES THEOREM (VECTOR CALCULUS)
NT VECTORS (MATHEMATICS)
NT VORTICITY
Smooth linearization of hyperbolic fixed points without resonance conditions
[REPT-89-03] 03 p0394 N90-12251
On the approximative normal values of multivalued operators in topological vector space
[DE90-610430] 12 p1707 N90-19800
Classical mechanics on superspace
[DE90-608907] 12 p1724 N90-19906
On induced Hermitian metrics for holomorphic vector bundles
[DE90-612737] 14 p2019 N90-21572
Topological classification of structurally stable quadratic systems without limit cycles
[REPT-89-66] 17 p2457 N90-24025
Gevrey spaces related to Lie algebras of operators
[ETN-90-96892] 17 p2468 N90-24109
Hopf-algebraic structure of combinatorial objects and differential operators
[NASA-CR-186360] 19 p2752 N90-25640
On the infrared behaviour of some non-Minkowskian quantum fields 23 p3410 N90-29273
On equations of motion on complex Grassman manifold
[DE90-628369] 24 p3537 N90-29999
VECTORS (MATHEMATICS)
NT EIGENVECTORS
NT STATE VECTORS
NT VORTICITY
Extended Weyl group for Kac-Moody algebras
[DE89-617525] 01 p0111 N90-10634
Quotient-difference type generalizations of the power method and their analysis
[NASA-TM-102361] 01 p0112 N90-10635
Use of Lanczos vectors in structural dynamics
02 p0179 N90-11011
Calculation of the temperature and velocity vector of the neutral gas using EISCAT CP3-data
02 p0244 N90-11384
LINPACK routines based on the level 2 BLAS
[CWI-NM-R8811] 02 p0261 N90-11483
Solving three dimensional block bidiagonal linear systems on vector computers
[REPT-89-14] 04 p0530 N90-13056
Krylov methods preconditioned with incompletely factored matrices on the CM-2
[NASA-CR-181961] 06 p0822 N90-14779
Parallel projected variable metric algorithms for unconstrained optimization
[NASA-CR-181930] 06 p0833 N90-14842
Vector fields and gravity on the lattice
[DE89-633885] 06 p0836 N90-14860
A vectorized algorithm for 3D dynamics of a tethered satellite 12 p1640 N90-19423
Vector circuit theory for multilayered isotropic and chiral structures: Reflection and transmission
[PB90-122474] 12 p1652 N90-19495
Gradient microphone for measurement of the vectorial sound velocity
[MBB-Z-0259/89-PUB] 19 p2650 N90-25080
Matrix generators for production of equally distributed pseudorandom vectors
[ETN-90-97291] 22 p3243 N90-28390
Superconformal algebra and central extension of meromorphic vector fields with multipoles on super-Riemann sphere
[DE90-627211] 23 p3390 N90-29153
Asymptotic code vector density in topographic vector quantisers
[RSRE-MEMO-4392] 24 p3539 N90-30012
VEGA PROJECT
Organic chemistry of cometary dust as derived from PUMA 1 data 08 p1143 N90-16628
VEGETABLES
Variability of cultivar responses to ozone
[PB89-225460] 07 p0956 N90-15528
A proposal to demonstrate production of salad crops in the space station mockup facility with particular attention to space, energy, and labor constraints
[NASA-CR-186811] 19 p2725 N90-25500
VEGETATION
NT CANOPIES (VEGETATION)
Assessment of the importance of acidic fogwater and cloudwater in affecting terrestrial vegetation: Some important case studies
[DE90-002216] 08 p1098 N90-16361
Spectral responses of soybeans and their relationship with agronomical parameters
[INPE-4832-PRE/1462] 10 p1398 N90-18084
Orbital remote sensing in the decade of the nineties: New approaches and challenges in geology
[INPE-4838-PRE/1467] 11 p1521 N90-18758
Remote sensing applied to vegetation as subsidized in municipal planning
[INPE-4908-PRE/1509] 11 p1523 N90-18770
Physiognomy of vegetation cover in the PNPM identified through the TM/LANDSAT sensor: A multitemporal analysis
[INPE-4834-PRE/1464] 11 p1525 N90-18776
Remote sensing for the classification and quantification of vegetation in Spring staging areas of Brent geese on the Frisian Islands (Netherlands)
[BCRS-89-27] 11 p1527 N90-18790
Definition study of Laser Experimental Active Fluorsensor (LEAF)
[BCRS-88-18] 12 p1668 N90-19582
Proceedings of the 2nd United States/USSR Symposium on Air Pollution Effects on Vegetation Including Forest Ecosystems
[PB90-127119] 12 p1685 N90-19678
Visibility problems in numerical models of terrain
[INPE-4921-TDL/382] 12 p1726 N90-19919
Synthesis and analysis of 25 years (1961-1986) of INPE/SRE activities related to the vegetation/forest area
[INPE-4969-RPE/604] 13 p1819 N90-20446
A split-and-merge method for creating polygonal homogeneous-vegetation regions from digitized terrain data
[AD-A218080] 13 p1821 N90-20453
Wheat yield estimation at the farm level using LANDSAT TM and agrometeorological data
[INPE-5017-RPE/611] 14 p1996 N90-21439
Monitoring of agrocattle-raising projects through visual/digital analysis of LANDSAT-TM imagery south of Para state
[INPE-4982-PRE/1542] 14 p1996 N90-21442
Monitoring vegetation of Brazil: Potentialities of multi-sensors approach
[INPE-4993-PRE/1555] 14 p1998 N90-21451
Evolution of remote sensing applied to vegetation and forest at INPE
[INPE-4970-PRE/1538] 14 p1998 N90-21452
Multitemporal analysis of LANDSAT/TM digital imagery in the detection of areas affected by caterpillar (sibine fusca) attack in the dende (elais guineensis) palm plantation
[INPE-4979-PRE/1544] 14 p1999 N90-21457
Performance evaluation of MSS/LANDSAT data in the estimation of fluvial channel width
[INPE-4906-PRE/1507] 14 p2000 N90-21463
Modeling large-scale vegetation dynamics
[DE90-008883] 14 p2004 N90-21485
The accuracy of the monitoring of pioneer vegetation in the Oostvaardersplassen, Netherlands
[ETN-90-96692] 17 p2419 N90-23783
Multisensor monitoring of deforestation in the Guinea Highlands of West Africa
[NASA-CR-186709] 19 p2706 N90-25396
Applications of ISES for vegetation and land use
21 p3018 N90-27158
Study of anomalies in transition vegetation in Alto Xingo-NT, through remote sensing techniques
[INPE-4601-TDL/334] 23 p3343 N90-28891
VEGETATION GROWTH
NT CROP GROWTH
Effects of microgravity on growth hormone concentration and distribution in plants 05 p0678 N90-13947
Gravitropism in plants: Hydraulics and wall growth properties of responding cells 05 p0678 N90-13950
Carbon dioxide and climate: Summaries of research in FY 1989
[DE90-001791] 06 p0812 N90-14723
The 1988-1989 NASA space/gravitational biology accomplishments
[NASA-TM-4160] 09 p1250 N90-17251
Regulation of nitrogen uptake and assimilation: Effects of nitrogen source, root-zone pH, and aerial CO_2 concentration on growth and productivity of soybeans
[NASA-CR-177546] 10 p1413 N90-18147
The accuracy of the monitoring of pioneer vegetation in the Oostvaardersplassen, Netherlands
[ETN-90-96692] 17 p2419 N90-23783
VEGETATIVE INDEX
Improvement and extension of a radar forest backscattering model
[NASA-CR-186083] 04 p0515 N90-12973
Physically-based parameterization of spatially variable soil and vegetation using satellite multispectral data
[NASA-CR-185957] 05 p0663 N90-13879
Reflection indicatrices of natural surfaces for AVHRR channels 1 and 2
[DLR-MITT-89-16] 05 p0664 N90-13882
Senegalese land surface change analysis and biophysical parameter estimation using NOAA AVHRR spectral data
[NASA-CR-186120] 05 p0664 N90-13883
Quantitative evaluation of object-changes in multitemporal AGRISAR imagery
[FIM-195] 08 p1091 N90-16314
TVI: A mathematical model for global estimation of Brazilian cerrado phytomass
[INPE-4836-PRE/1465] 11 p1521 N90-18759
Relationships between the aerial biomass from ground layers of cerrado and its spectral reflectance
[INPE-4848-PRE/1477] 11 p1521 N90-18760
Areas of aquatic macrophytes classified through vegetative indexes extracted from LANDSAT/TM imagery
[INPE-4860-PRE/1489] 12 p1677 N90-19633
Vegetation stress monitoring by fluorescence
19 p2708 N90-25414
Land application of imaging spectrometry
19 p2708 N90-25415
Reflection indicatrices of natural surfaces for AVHRR channels 1 and 2
[ESA-TT-1192] 19 p2709 N90-25417
Modeling and measurement of tree canopy reflectance
[MITT-86] 21 p3018 N90-27162
VEHICLE WHEELS
NT NOSE WHEELS
Lunar surface mobility studies, past and future
[AD-A216451] 10 p1393 N90-18056
Two wheeled lunar dumptruck
[NASA-CR-182840] 17 p2410 N90-23734
VEHICLES
Practical applications of Loran-C for land mobile use or the possibility to use Loran-C as a vehicle-location or vehicle-navigation system
[ETN-90-96265] 11 p1455 N90-18384
VEHICULAR TRACKS
Lunar construction utility vehicle
[NASA-CR-186231] 07 p0939 N90-15435
Lunar surface mobility studies, past and future
[AD-A216451] 10 p1393 N90-18056
VELOCITY
NT ACOUSTIC VELOCITY
NT AIRSPEED
NT ANGULAR VELOCITY
NT CRITICAL VELOCITY
NT EXHAUST VELOCITY
NT FLOW VELOCITY
NT GROUND SPEED
NT GROUP VELOCITY
NT HIGH SPEED
NT HYPERSONIC SPEED
NT LOW SPEED
NT ORBITAL VELOCITY

NT PHASE VELOCITY
NT PROPAGATION VELOCITY
NT RADIAL VELOCITY
NT ROTOR SPEED
NT SOLAR WIND VELOCITY
NT SUBSONIC SPEED
NT SUPERSONIC SPEED
NT TIP SPEED
NT TRANSONIC SPEED
NT WIND VELOCITY
Interferometry and high speed photography of laser-driven flyer plates
[DE89-016990] 02 p0225 N90-11290
Balance laws and centro velocity in dissipative systems
[MEMO-797] 05 p0639 N90-13726
Solution of the Boltzmann equation using an energy group method
[AD-A213138] 05 p0699 N90-14096
Profile measurements of sulfur dioxide, nitrogen oxides, and nitric acid deposition velocities in California's south coast air basin
[PB90-104001] 06 p0808 N90-14703
Application of the joined wing to tiltrotor aircraft
[NASA-CR-177543] 07 p0879 N90-15093
Effects of parametric variations of complex targets on damage from projectile impact
[DE90-003214] 07 p0941 N90-15450
Cineholography: A relation between the coherence length of the laser and the object velocity
[ISL-CO-234/88] 11 p1515 N90-18724
Visual processing of object velocity and acceleration
[AD-A216509] 11 p1539 N90-18858
Stopping power for protons in Al for the whole range of velocities
[DE90-008558] 13 p1884 N90-20810
Laser velocimeter measurements of multiphase flow of solids
[DE90-007604] 14 p1974 N90-21311
Quasar pairs and quasar's peculiar velocity
[FERMILAB-PUB-90/25-A] 22 p3262 N90-28474
Velocity filtering applied to optical flow calculations
[NASA-TM-102802] 23 p3271 N90-28512
A complete analytical solution for the inverse instantaneous kinematics of a spherical-revolute-spherical (7R) redundant manipulator 23 p3363 N90-29006
Alfven wave solitons and solar intermediate drift bursts
[MPE-PREPRINT-173] 23 p3413 N90-29287

VELOCITY COUPLING
Transient signal distortion and coupling in multilayer multiconductor MIC microstrips
[AD-A222989] 21 p3000 N90-27050
Velocity selection to enable direct measurement of strong single atom-optical cavity coupling
[AD-A223060] 21 p3071 N90-27460

VELOCITY DISTRIBUTION
Frequency domain aerodynamic analysis of interacting rotating systems 02 p0147 N90-10837
Laser anemometer measurements in a transonic axial-flow fan rotor
[NASA-TP-2879] 02 p0218 N90-11245
A laser Doppler anemometry investigation of single-phase and particle-laden jet flows
[AD-A210660] 02 p0220 N90-11261
Air velocity mapping of environmental test chambers
[AD-A212082] 03 p0310 N90-11764
Supersonic boundary-layer transition on the LaRC F-106 and the DFRF F-15 aircraft. Part 2: Aerodynamic predictions 04 p0447 N90-12559
Zonal average cloud characteristics for global atmospheric chemistry modeling
[CM-75] 04 p0518 N90-12992
Practical systems for speckle velocimetry 05 p0574 N90-13341
A wall interference assessment/correction interface measurement system for the NASA/ARC 12-ft PWT
[NASA-CR-185474] 05 p0584 N90-13401
Fluid-particle interaction in solid-liquid two-phase grid turbulence 06 p0773 N90-14496
Characterization of electric vehicle velocity and power profiles using road test data
[DE90-002085] 06 p0795 N90-14630
Two-Dimensional Measuring Techniques
[DGLR-PAPERS-88-04] 08 p1078 N90-16236
Simultaneous determination of temperature and velocity fields in a thermal convection flow with non-enclosed liquid crystal tracers 08 p1078 N90-16239
Experimental study of velocity fields and turbulence in a turbojet engine
[ISL-CO-231/88] 09 p1169 N90-16766
Heterogeneous combustion processes under microgravity conditions 09 p1202 N90-16965
Velocity profile and wall shear stress measurements for a Large Eddy Break-Up (LEBU) device
[AD-A214958] 09 p1217 N90-17059
Theoretical study of instabilities in vortices: Applications to hydrodynamics and magnetohydrodynamics
[ETN-90-96103] 09 p1219 N90-17073
Doppler imagery for the visualisation of velocity fields
[ISL-CO-232/88] 09 p1226 N90-17114
Low speed flowfield characterization by infrared measurements of surface temperatures 10 p1306 N90-17556
Viscous three-dimensional analyses for nozzles for hypersonic propulsion
[NASA-CR-185197] 10 p1321 N90-17635
Gust response analysis for cascades operating in nonuniform mean flows 11 p1461 N90-18415
Measurement of velocity profiles and Reynolds stresses on an oscillating airfoil 11 p1463 N90-18427
Turbulence structure of mixing swirling flows
[AD-A216628] 11 p1506 N90-18671
Effect of a random wind field on thermal blooming instabilities
[DE90-007241] 11 p1532 N90-18823
Study of the turbulent boundary layer on an afterbody
[TM-EA-8901] 12 p1601 N90-19212
Analysis of unsteady heat transfer by natural convection in a two-dimensional square cavity using a high order finite-volume method 12 p1657 N90-19521
Nonintrusive optical measurements of turbulence and mixing in a stably stratified fluid 13 p1799 N90-20322
TiCl4 as a source of TiO2 particles for laser anemometry measurements in hot gas
[NASA-TM-102581] 13 p1805 N90-20358
The optical measurement of acoustic velocity fields 14 p2023 N90-21601
Theoretical and experimental study of flow-control devices for inlets of indraft wind tunnels
[NASA-TM-100050] 15 p2056 N90-21778
A dual potential formulation of the Navier-Stokes equations 15 p2092 N90-21972
Experimental study of vortex ring interaction with a free surface 16 p2233 N90-22742
The 3-D composite velocity solutions for subsonic/transonic flow over forebodies and afterbodies
[AD-A220370] 17 p2345 N90-23354
Determination of the velocity, density, maximum flux, and enthalpy profiles for a very high temperature arc jet nozzle flow
[AD-A218390] 17 p2402 N90-23682
Low Prandtl number convection in a rectangular cavity with longitudinal thermal gradient and transverse g-jitters
[REPT-892-430-109] 17 p2404 N90-23695
Flow studies in impeller passages 18 p2551 N90-24558
Methods of perturbation theory as a means for interactive design from bodies in a flow
[ETN-90-96502] 18 p2553 N90-24573
Review of probabilistic analysis of dynamic response of systems with random parameters
[NASA-CR-186171] 18 p2568 N90-24636
A range-dependent analysis of acoustic transmission across a cold filament in the California current
[AD-A220175] 18 p2583 N90-24709
Computational simulation of transition to turbulence through inverse modeling 18 p2647 N90-25067
An experimental and theoretical investigation of the flow over plane delta wings with supersonic leading edges
[LR-588] 19 p2655 N90-25114
Flow resistance and critical shear stress in steep channels 19 p2687 N90-25282
Velocity distribution in a gravel-bed flume; for steady and unsteady flow 19 p2687 N90-25283
Spatially accelerating flow in smooth open channel 19 p2687 N90-25284
Surface dilation and fluid-dynamical behaviour of Newtonian liquids in an overflowing cylinder. 1: Pure liquids
[LR-601] 19 p2692 N90-25317
Measurement of terms and parameters in turbulent models
[NASA-CR-183993] 20 p2860 N90-26271
Effect of initial conditions on the development of two-phase jets
[AD-A222621] 20 p2864 N90-26293
A search routine for optimization in a wind power system with variable speed
[FOA-C-20779-2.1] 20 p2882 N90-26395
Canonical eigenvalues. Part 1: General theory
[AD-A222812] 20 p2920 N90-26617
Response of a viscous liquid column to pitching- and roll-excitation in zero-gravity environment
[LRT-WE-9-FB-10(1989)] 21 p2991 N90-27000
Response of differently axially excited viscous liquid bridges in zero-gravity
[LRT-WE-9-FB-14(1989)] 21 p2991 N90-27001
Liquid sloshing response in a spinning container due to axial excitation
[LRT-WE-9-FB-9(1989)] 21 p3006 N90-27087
Analytical resolution of the Oseens differential equation of inclined turning cylinder with gliding
[ETN-90-97316] 22 p3171 N90-27988
Regular and chaotic motion of uniform elliptical vortices in external linear time dependent velocity fields 23 p3268 N90-28497
An experimental investigation of a single and multiphase confined coaxial jet 23 p3324 N90-28796
Numerical simulation of the formation of two-dimensional and three-dimensional structures in shear layers and wakes
[ESA-TT-1008] 23 p3325 N90-28802
Extrapolation procedures at outflow boundaries for the Navier-Stokes equations
[FFA-TN-1990-23] 23 p3327 N90-28811
Tropospheric wind profiling using radar interferometry: A feasibility study of a compact mobile system
[PB90-217068] 23 p3351 N90-28939
Velocity Interferometer System for Any Reflector (VISAR): Displacement mode data reduction
[DE90-015027] 23 p3395 N90-29184
A potential-vorticity decomposition for the boundary integral equation analysis of viscous flows 24 p3417 N90-29301
Calculation of turbulent air streams in driver cabs
[ETN-90-97320] 24 p3419 N90-29310
Reynolds stress and the physics of turbulent momentum transport
[AD-A224172] 24 p3467 N90-29588
Structure in the near field of the transverse jet
[AD-A224502] 24 p3467 N90-29591

VELOCITY FIELDS
U VELOCITY DISTRIBUTION

VELOCITY MEASUREMENT
NT WIND VELOCITY MEASUREMENT
Pin switch circuits instrument for microsecond velocity measurements
[AD-A210638] 01 p0074 N90-10426
Development of an adaptive time of flight system for the measurement of fluid flow velocity 02 p0222 N90-11273
Three component laser Doppler measurements in an axisymmetric jet
[NASA-CR-181908] 03 p0300 N90-11702
Observations and modelling of deep equatorial currents in the central Pacific
[PB89-198139] 03 p0377 N90-12145
Measurement Techniques in Aerodynamics
[VKI-LS-1989-05] 05 p0573 N90-13339
Practical systems for speckle velocimetry 05 p0574 N90-13341
Hot and cold wire applications in supersonic flows: Introductory notes 05 p0574 N90-13343
Skin friction measurements with hot elements 05 p0574 N90-13345
The 3D LDA techniques in vortex studies and boundary layer surveys 05 p0574 N90-13346
Laser two focus techniques 05 p0575 N90-13348
The influence of multiple hot-wire probe geometry on the results of measurements in turbulent flows
[DLR-FB-89-26] 05 p0639 N90-13724
Effective utilization of acoustic wave sensor responses: Simultaneous measurement of velocity and attenuation
[DE90-002580] 06 p0838 N90-14872
Solid fuel combustion chamber
[LR-555] 08 p1038 N90-16001
Thickness, velocity, and temperature measurements in falling liquid films
[DE90-004290] 08 p1063 N90-16151
Miniature laser Doppler anemometer with a diode laser
[ISL-CO-224/88] 08 p1077 N90-16232
Analysis of the measuring range and the accuracy of an existing particle image velocimetry system 08 p1080 N90-16247
Further development of the PIV method for use in the large wind tunnel 08 p1080 N90-16248
Development and application of oxygen flow tagging for velocity measurements and flow visualization in turbulent three-dimensional supersonic flows
[AD-A214491] 09 p1160 N90-16715
Development of flow visualization and nonintrusive velocity measurement in turbulent flow
[ETN-90-96077] 09 p1161 N90-16717
Low air speed computation for helicopters: A new approach 09 p1165 N90-16744
Measurement of the speed and temperature of ignition gases
[ISL-CO-246/88] 09 p1192 N90-16908
An experimental study of the effect of streamwise vortices on unsteady turbulent boundary-layer separation 09 p1215 N90-17045
Automation and extension of LDV (Laser-Doppler Velocimetry) measurements of off-design flow in a subsonic cascade wind tunnel
[AD-A216627] 11 p1506 N90-18670

Velocity measurement using interferometry
[ISL-CO-221/88] 11 p1512 N90-18709
An optical white light speckle process in forward dispersion for measurement of the velocity field in free convective currents
[ETN-90-95913] 12 p1661 N90-19546
Nonintrusive optical measurements of turbulence and mixing in a stably stratified fluid
13 p1799 N90-20322
The effect of adverse pressure gradient on turbulent burst structure in low-Reynolds number equilibrium boundary layers
[AD-A217308] 13 p1799 N90-20327
A fiber optic sensor for noncontact measurement of shaft speed, torque, and power
[NASA-TM-102481] 14 p1983 N90-21360
The optical measurement of acoustic velocity fields
14 p2023 N90-21601
Laser Doppler anemometry measurements of a confined turbulent water jet with a uniform background flow
15 p2092 N90-21971
Analysis of velocity and temperature fluctuations in turbulent shear flows 16 p2233 N90-22744
Two-dimensional velocimetry instrumentation
[AD-A218450] 16 p2239 N90-22774
Surface wave characterization of high T(sub c) superconductors
[AD-A221077] 19 p2760 N90-25683
Measurement of velocity and temperature profiles at the exit plane of a tubular gas turbine combustor
[DE90-505519] 20 p2809 N90-25983
An experimental system for measuring the wavenumber-frequency response of Timoshenko beams
[AD-A222569] 20 p2878 N90-26374
Velocity measurements on a lifting rotor/airframe configuration in low speed forward flight
21 p2953 N90-26790
Determination of the ground effect on the characteristics of the A320 aircraft 23 p3275 N90-28534
An investigation of the steady and unsteady near wake and its effect on a laminar boundary layer
23 p3324 N90-28794
Measurement Techniques for Hypersonic Flows
[VKI-LS-1990-05] 24 p3419 N90-29314
Velocity interferometry 24 p3420 N90-29316
Laser velocimetry 24 p3420 N90-29317
Electron beam for velocity determination
24 p3420 N90-29319

VELOCITY PROFILES
U VELOCITY DISTRIBUTION

VENTILATION
High-frequency ventilation in dogs with three gases of different densities
[AD-A212862] 06 p0819 N90-14762
Guidelines for evaluating energy analysis software
[AD-A214171] 07 p0976 N90-15640
Ballast system for maintaining constant pressure in a glove box
[NASA-CASE-NPO-17786-1-CU]
09 p1224 N90-17104
Ignitability of jet-A fuel vapors in aircraft fuel tanks
10 p1313 N90-17594
Fire safety applications for spacecraft
10 p1314 N90-17595
Hot surface ignition studies of aviation fluids
10 p1314 N90-17600
An expert system for the design of heating, ventilating, and air-conditioning systems
[AD-A218287] 13 p1788 N90-20262
Transonic wing charge improvements by passive shock boundary layer interference control: Development status and prospects
[ETN-90-96463] 18 p2496 N90-24267
Toxicological aspects of fire onboard aircrafts: Role of the pressurization and ventilation in the cockpit
[ETN-90-97452] 22 p3233 N90-28335
Calculation of turbulent air streams in driver cabs
[ETN-90-97320] 24 p3419 N90-29310

VENTING
Independent Orbiter Assessment (IOA): Analysis of the purge, vent and drain subsystem
[NASA-CR-185547] 02 p0172 N90-10989
The repair of aircraft integral fuel tanks in the RAF: A user's view of fuel tank technology
08 p1022 N90-15908
Forced and natural venting of aircraft cabin fires: A numerical simulation 10 p1314 N90-17597
Zero-gravity vortex vent and PVT gaging system
11 p1475 N90-18486
Passive venting technique for shallow cavities
[NASA-CASE-LAR-14031-1] 13 p1755 N90-20079
System for venting gas from a liquid storage tank
[NASA-CASE-MSC-21253-1] 13 p1787 N90-20254
Liquid Transfer Cryogenic Test Facility: Initial hydrogen and nitrogen no-vent fill data
[NASA-TM-102572] 14 p1972 N90-21295

VENTS
Independent Orbiter Assessment (IOA): Assessment of the purge, vent and drain subsystem
[NASA-CR-185535] 02 p0168 N90-10949
Independent Orbiter Assessment (IOA): Assessment of the mechanical actuation subsystem, volume 1
[NASA-CR-185527-VOL-1] 02 p0169 N90-10952
Independent Orbiter Assessment (IOA): Assessment of the mechanical actuation subsystem, volume 2
[NASA-CR-185527-VOL-2] 02 p0169 N90-10953
Zero-gravity vortex vent and PVT gaging system
11 p1475 N90-18486

VENUS (PLANET)
Upper ionosphere and magnetospheric-ionospheric coupling
[DE89-619727] 02 p0250 N90-11415
Coronae on Venus observations and models of origin
03 p0427 N90-12449
High resolution imaging of the Venus night side using a Rockwell 128x128 HgCdTe array
14 p1978 N90-21330
Using connected-element interferometer phase-delay data for Magellan navigation in Venus orbit
15 p2075 N90-21885
The Pioneer Venus Orbiter: 11 years of data. A laboratory for atmospheres seminar talk
[NASA-TM-100761] 16 p2328 N90-23273
A numerical investigation of thermal convection in highly viscous spherical shells with applications to mantle dynamics in the Earth and other terrestrial planets
18 p2579 N90-24691
Space exploration: Cost, schedule, and performance of NASA's Magellan Mission to Venus. Fact sheet for the Chairman, Subcommittee on Science, Technology, and Space, Committee on Commerce, Science, and Transportation, US Senate
[GAO/NSIAD-88-130FS] 20 p2815 N90-26022
Absolute wind measurements in the lower thermosphere of Venus using infrared heterodyne spectroscopy
[NASA-CR-4290] 21 p3100 N90-27605
The Magellan Venus explorer's guide
[NASA-CR-186968] 23 p3286 N90-28592
Absolute wind measurements in the lower thermosphere of Venus using infrared heterodyne spectroscopy
24 p3561 N90-30146

VENUS ATMOSPHERE
NT VENUS CLOUDS
Deducing the age of the dense Venus atmosphere
03 p0425 N90-12438
Venus and the Archean Earth: Thermal considerations
03 p0427 N90-12448
Large impact events and atmospheric evolution on the terrestrial planets 12 p1744 N90-20028
High resolution imaging of the Venus night side using a Rockwell 128x128 HgCdTe array
14 p1978 N90-21330
The Pioneer Venus Orbiter: 11 years of data. A laboratory for atmospheres seminar talk
[NASA-TM-100761] 16 p2328 N90-23273
Infrared spectra of van de Waals complexes of importance in planetary atmospheres
20 p2943 N90-26749
Chemical kinetics and modeling of planetary atmospheres 20 p2946 N90-26763
Investigation of plasma density bulge in front of Venus bow shock
[NASA-CR-186937] 22 p3262 N90-28476
Absolute wind measurements in the lower thermosphere of Venus using infrared heterodyne spectroscopy
24 p3561 N90-30146

VENUS CLOUDS
Venus volcanism: Rate estimates from laboratory studies of sulfur gas-solid reactions 03 p0422 N90-12428

VENUS PROBES
NT MAGELLAN SPACECRAFT (NASA)

VENUS RADAR MAPPER
U MAGELLAN SPACECRAFT (NASA)

VENUS RADAR MAPPER PROJECT
U MAGELLAN PROJECT (NASA)

VENUS SURFACE
Abstracts for the Venus Geoscience Tutorial and Venus Geologic Mapping Workshop
[NASA-CR-185432] 03 p0422 N90-12423
Geology of Southern Guinevere Planitia, Venus, based on analyses of Goldstone radar data
03 p0422 N90-12424
Characteristics, distribution and geologic/terrain associations of small dome-like hills on Venus
03 p0422 N90-12425
Tessera terrain: Characteristics and models of origin
03 p0422 N90-12426
Divergent plate boundaries and crustal spreading on Venus: Evidence from Aphrodite Terra
03 p0422 N90-12427
Venus volcanism: Rate estimates from laboratory studies of sulfur gas-solid reactions 03 p0422 N90-12428
Potential for observing and discriminating impact craters and comparable volcanic landforms on Magellan radar images 03 p0423 N90-12429
Venus surface properties deduced from radar and radiometry 03 p0423 N90-12431
A morphologic study of Venus Ridge belts
03 p0423 N90-12432
Evidence for volcanism in NW Ishtar Terra, Venus
03 p0424 N90-12433
Radar scattering mechanisms within the meteor crater ejecta blanket: Geologic implications and relevance to Venus 03 p0424 N90-12435
Aeolian processes on Venus
03 p0425 N90-12436
Architecture of orogenic belts and convergent zones in Western Ishtar Terra, Venus
03 p0425 N90-12437
Clotho Tessera, Venus: A fragment of Fortuna Tessera 03 p0425 N90-12439
Tectonism on Venus: A review
03 p0425 N90-12440
Venus: Mantle convection, hotspots, and tectonics
03 p0426 N90-12442
Lakshmi Planum: A distinctive highland volcanic province 03 p0426 N90-12444
Volcanism on Venus: Large shields and major accumulations of small domes 03 p0426 N90-12445
Impact cratering and the surface age of Venus: The Pre-Magellan controversy 03 p0426 N90-12446
Geology of the Venus equatorial region from Pioneer Venus radar imaging 03 p0427 N90-12447
Crustal deformation: Earth vs Venus
03 p0427 N90-12450
Eastern Ishtar Terra: Tectonic evolution derived from recognized features 03 p0428 N90-12451
Stress distribution and topography of Tellus Regio, Venus 03 p0428 N90-12452
Three ages of Venus 03 p0428 N90-12453
Geology of coronae and domal structures on Venus and models of their origin 15 p2191 N90-22513
The Pioneer Venus Orbiter: 11 years of data. A laboratory for atmospheres seminar talk
[NASA-TM-100761] 16 p2328 N90-23273
Space exploration: Cost, schedule, and performance of NASA's Magellan Mission to Venus. Fact sheet for the Chairman, Subcommittee on Science, Technology, and Space, Committee on Commerce, Science, and Transportation, US Senate
[GAO/NSIAD-88-130FS] 20 p2815 N90-26022
The Magellan Venus explorer's guide
[NASA-CR-186968] 23 p3286 N90-28592

VERBAL COMMUNICATION
NT CONVERSATION
The employment of SITIM-150 as an instructional objective for training in remote sensing
[INPE-4833-PRE/1463] 10 p1440 N90-18310
SHAPA: An interactive software tool for protocol analysis applied to aircrew communications and workload
19 p2734 N90-25541
Mathematical problem-solving transfer: The effects of cognitive load and attention a schema acquisition and rule automation 20 p2917 N90-26594
Instruction dialogues: Teaching new skills to a robot
24 p3517 N90-29884
Interset: A natural language interface for teleoperated robotic assembly of the EASE space structure
24 p3517 N90-29885

VERIFICATION (PROVING)
U PROVING

VERTEBRAE
Radiological investigation of the vertebral column of candidates for military flying training the the Royal Norwegian Air Force 19 p2718 N90-25463
Analysis of the biomechanic and ergonomic aspects of the cervical spine under load 19 p2719 N90-25470
Risk of cervical injury in real and simulated accidents
19 p2721 N90-25475

VERTEBRAL COLUMN
U SPINE

VERTEBRATES
NT AMPHIBIA
NT BIRDS
NT FISHES
NT FROGS
NT HUMAN BEINGS
NT MAMMALS
NT MANATEES
NT MICE
NT MONKEYS
NT PRIMATES
NT RATS
NT RODENTS

VERTICAL AIR CURRENTS
Thermodynamic and dynamic processes in the updraft region of GALE (Genesis of Atlantic Lows Experiment) IOP (Intensive Observation Period) 9
[AD-A208139] 01 p0087 N90-10496
Convective boundary layer and modeling of dispersion 06 p0813 N90-14731
The dynamics of simulated convective storms in hurricane environments 06 p0816 N90-14747
Vertical distribution of pollutants in the presence of convective storms
[DE90-002590] 07 p0960 N90-15549
Spanwise measurements of vertical components of atmospheric turbulence
[NASA-TP-2963] 12 p1692 N90-19718
Distribution and movement of smokes from forest fires that occurred along the boundary of the People's Republic of China and the USSR on April-May 1987 21 p3028 N90-27216
Turbulence structure in clear and cloudy regions of the 7 July 1987 Electra mission 22 p3217 N90-28247
Vertical-velocity skewness in the marine stratus-topped boundary layer 22 p3220 N90-28262
Genesis of bow echoes: A rear-inflow induced meso-convective structure
[PB90-209776] 23 p3349 N90-28926
An investigation of forcing mechanisms during a surprise tornadic thunderstorm
[PB90-216805] 23 p3352 N90-28940
VERTICAL DISTRIBUTION
NT STAR DISTRIBUTION
Vertical distribution of pollutants in the presence of convective storms
[DE90-002590] 07 p0960 N90-15549
Beryllium dispersion near explosive firing tables: A comparison of computed and observed results
[DE90-002635] 07 p0960 N90-15550
Measurements of CH4, N2O, CO, H2O and O3 in the middle atmosphere by the ATMOS experiment on Spacelab 3
[NASA-TM-103476] 20 p2883 N90-26400
Vertical ozone probing with lidar 20 p2885 N90-26416
VISTA (Vertical Integration of Science, Technology, and Applications) user interface software study
[DE90-010003] 20 p2936 N90-26707
The vertical ozone distribution during maximum and minimum solar activity 22 p3205 N90-28182
VERTICAL FINS
U FINS
VERTICAL LANDING
STOVL propulsion system volume dynamics approximations
[NASA-TM-102397] 03 p0306 N90-11740
A head up display format for application to V/STOL aircraft approach and landing
[NASA-TM-102216] 10 p1320 N90-17632
Performance characteristics of a one-third-scale, vectorable ventral nozzle for SSTOVL aircraft
[NASA-TM-103120] 15 p2045 N90-21725
Ground-simulation investigations of VTOL airworthiness criteria for terminal-area operations
[NASA-TM-102810] 19 p2660 N90-25141
VERTICAL MOTION
The interaction and variation of waves and turbulence from MST radar data
[AD-A212849] 05 p0670 N90-13906
Tropopause undulations and the development of extratropical cyclones 15 p2132 N90-22186
Examination of microburst development in Colorado thunderstorm for the 5 August 1982 case
[AD-A218478] 17 p2425 N90-23820
VERTICAL MOTION SIMULATORS
Ground-simulation investigations of VTOL airworthiness criteria for terminal-area operations
[NASA-TM-102810] 19 p2660 N90-25141
VERTICAL ORIENTATION
Demonstration of a dual-lidar method for measuring optical depths in the vertical
[AD-A210598] 01 p0124 N90-10711
The effects of hearing protectors on speech communication and the perception of warning signals
[AD-A212521] 04 p0492 N90-12832
A comparison of two subject-controlled attitude measures during somatogravic illusion exposure
[AD-A212528] 04 p0525 N90-13031
Techniques for studying the effects of microgravity on model particle/cell systems 12 p1640 N90-19424
Critique of the vertical gradient of gravity 13 p1834 N90-20531
High resolution technique and instrument for measuring lattice parameters in single crystals
[AD-D014549] 22 p3177 N90-28029
Measuring the vertical directional spectra caused by sea surface sound
[AD-A223883] 23 p3354 N90-28957
Vestibular responses and motion sickness during pitch, roll, and yaw sinusoidal whole-body oscillation
[AD-A223898] 24 p3497 N90-29767
VERTICAL PERCEPTION
The relationship between subjective and objective measures of simulator-induced ataxia
[AD-A213095] 05 p0673 N90-13922
VERTICAL STABILIZERS
U STABILIZERS (FLUID DYNAMICS)
VERTICAL TAILS
U STABILIZERS (FLUID DYNAMICS)
U TAIL ASSEMBLIES
VERTICAL TAKEOFF
Flowfield effects of launch on a vertically-launched missile
[AD-A214468] 09 p1160 N90-16714
A head up display format for application to V/STOL aircraft approach and landing
[NASA-TM-102216] 10 p1320 N90-17632
Ground-simulation investigations of VTOL airworthiness criteria for terminal-area operations
[NASA-TM-102810] 19 p2660 N90-25141
VERTICAL TAKEOFF AIRCRAFT
NT FLYING PLATFORMS
Powered-lift aircraft technology
[NASA-SP-501] 04 p0452 N90-12589
Aircraft/airport compatibility: Some strategic, tactical, and operational issues
[TT-8902] 05 p0585 N90-13409
A wind tunnel study of a sting-mounted circulation control wing
[AD-A216248] 10 p1310 N90-17577
A study of the technology required for advanced vertical take-off aircraft
[ETN-90-96786] 18 p2497 N90-24268
VERTICAL TAKEOFF AND LANDING
U VERTICAL LANDING
U VERTICAL TAKEOFF
VERTICES
U APEXES
VERTOL MILITARY HELICOPTERS
U BOEING AIRCRAFT
VERY HIGH FREQUENCIES
Joint VHF coherent radar and oblique sounder observations for short term ionosphere forecasting 02 p0247 N90-11399
Petite Amateur Navy Satellite (PANSAT)
[NASA-CR-186049] 03 p0317 N90-11800
Low level range coverage performance prediction for VHF radar 06 p0763 N90-14439
Aspects of VHF radars illustrated by the example of an experimental system
[REPT-1-89] 12 p1647 N90-19488
Prediction of VHF/UHF mobile reception in urban areas: Comparison with measurements in London
[BBC-RD-1989/11] 14 p1965 N90-21255
Evaluation of VHF intercept and direction finding systems
[AD-A219805] 17 p2350 N90-23382
Very high frequency measurements of geometric factors in transmission line lead acid cells
[AD-A219463] 17 p2420 N90-23788
Man-made noise in a military environment 20 p2847 N90-26191
A narrowband tactical communication system for the VHF and UHF mobile radio bands 20 p2847 N90-26192
HF spread spectrum, an audit of the power requirements and LPI vulnerability 20 p2849 N90-26203
Experimentation of a transmission system data processing by meteor bursts 20 p2850 N90-26207
Equipment feasibility study: Very high frequency communication equipment (136-137 megahertz)
[DOT/FAA/CT-TN89/72] 20 p2850 N90-26210
Antennas for portable VHF-FM receivers
[BBC-RD-1990/1] 20 p2850 N90-26211
Electric field strength meters for the HF, VHF, and UHF bands
[BBC-RD-1990/3] 20 p2851 N90-26212
VERY HIGH FREQUENCY RADIO EQUIPMENT
Near real time VHF telemetry of near shore oceanographic data
[AD-A215756] 10 p1327 N90-17668
VERY HIGH SPEED INTEGRATED CIRCUITS
U VHSIC (CIRCUITS)
VERY LARGE ARRAY (VLA)
VLA-Max '91 tests of high energy flare physics 03 p0431 N90-12471
Performance of the image statistics decoder in conjunction with the Goldstone-VLA array 04 p0487 N90-12796
VLA and VLBI observations of core dominated quasars 06 p0860 N90-15002
Automated observation scheduling for the VLT
[NASA-CR-186282] 07 p1012 N90-15861
Validity of the two-level model for Viterbi decoder gap-cycle performance 15 p2077 N90-21896
Herbig-Haro objects and stellar jets 15 p2186 N90-22487
VLA and VLBI angular broadening measurements: The distribution of interstellar scattering at low Galactic latitudes 16 p2330 N90-23279
Spectral measurements of the cosmic microwave background 16 p2340 N90-23334
Sco X-1 the microquasar: New VLA and VLBI results 19 p2775 N90-25780
U. radio emission from quiescent filaments
[NASA-CR-186538] 19 p2797 N90-25922
VERY LARGE SCALE INTEGRATION
The organization of permutation architectures with bussed interconnections
[AD-A210832] 01 p0061 N90-10352
Network of dedicated processors for finding lowest-cost map path
[NASA-CASE-NPO-17716-1-CU] 01 p0107 N90-10608
A distributed pipelined architecture of the recursive Lagrangian equations of motion for robot manipulators with VLSI implementation --- VLSI (very large scale integration)
[RR-353] 03 p0344 N90-11966
An approximate max-flow min-cut theorem for uniform multicommodity flow problems with applications to approximation algorithms
[AD-A211908] 03 p0386 N90-12198
Distributed VLSI architecture for fast Jacobian and inverse Jacobian formulations
[RR-346] 03 p0390 N90-12218
Robot inverse dynamics computation via VLSI distributed architectures
[RR-350] 03 p0390 N90-12223
Algorithmic fault tolerance
[RSRE-MEMO-4214] 04 p0530 N90-13057
Trace theory --- concurrent processing
[MEMO-INF-89-16] 04 p0536 N90-13100
Real-time robot motion: The VLSI implementation via transputers
[RR-364] 04 p0537 N90-13104
The application of artificial intelligence techniques to tracing the interconnections in an integrated circuit
[TELECOM-PARIS-89-E002] 04 p0537 N90-13105
Optical clock distribution to VLSI chips
[AD-A212269] 04 p0560 N90-13264
Resistive fuses: Analog hardware for detecting discontinuities in early vision
[AD-A211891] 05 p0634 N90-13698
An accurate timing model for fault simulation in MOS circuits
[AD-A213153] 05 p0635 N90-13702
VLSI theory and parallel supercomputing
[AD-A214035] 07 p0925 N90-15351
Systolic algorithms for imaging from space
[AD-A213870] 07 p0987 N90-15701
VLSI integrated circuit tests
[IMAG-RR-763-I] 08 p1061 N90-16135
BLITZEN: A highly integrated massively parallel machine 08 p1115 N90-16453
A circuit extraction system and graphical display for VLSI (Very Large Scale Integrated) design
[AD-A215668] 09 p1214 N90-17038
Efficient interconnection schemes for VLSI and parallel computation
[AD-A216405] 10 p1420 N90-18185
Parallel distributed networks for image smoothing and segmentation in analog VSLI
[AD-A216780] 12 p1651 N90-19491
VLSI implementation of moment invariants for automated inspection
[DE90-005318] 12 p1652 N90-19493
Product assurance technology for procuring reliable, radiation-hard, custom LSI/VLSI electronics
[NASA-CR-185954] 13 p1791 N90-20281
ISITE: Automatic circuit synthesis for double-metal CMOS VLSI (Very Large Scale Integrated) circuits
[AD-A217459] 13 p1793 N90-20292
Statistical equipment modeling for VLSI manufacturing
[DE90-008527] 13 p1795 N90-20304
Investigation of tapered multiple microstrip lines for VLSI circuits
[AD-A217855] 13 p1797 N90-20310
Integrated circuits for avionics
[AD-A217964] 13 p1797 N90-20312
VLSI single-chip (255,223) Reed-Solomon encoder with interleaver
[NASA-CASE-NPO-17280-1-CU] 14 p1933 N90-21081
VLSI binary updown counter
[NASA-CASE-NPO-17205-1-CU] 14 p2011 N90-21525
A VLSI decomposition of the deBruijn graph 15 p2077 N90-21895

A VLSI design for a systolic Viterbi decoder
15 p2077 N90-21899
Principles of Very Large Scale Integrated (VLSI) system planning
15 p2088 N90-21950
The WAVE model for advanced knowledge processing
[OUEL-1803/89] 15 p2151 N90-22291
Fault tolerant multiprocessing and development of tools
[AD-A219216] 16 p2301 N90-23110
Statistical design of MOS VLSI (Very Large Scale Integrated) circuits with designed experiments
[AD-A219654] 17 p2396 N90-23647
Circuit recognition of VLSI layouts
[AD-A219806] 17 p2396 N90-23649
VLSI architectures and CAD
[AD-A220736] 17 p2397 N90-23652
UW VLSI chip tester
[AD-A220789] 17 p2397 N90-23653
WireLisp: Combining graphics and procedures in a circuit specification language
[AD-A220740] 17 p2444 N90-23927
Heavy ion tests on programmable VLSI
[ETN-90-97254] 20 p2822 N90-26057
Contribution to CMOS integrated circuit tests: Study of the stuck-on and stuck-open fault tests
[ETN-90-97256] 20 p2859 N90-26261
Contribution to the definition and application of NAUTILE (A new environment for the conception and assembling of integrated circuits)
[ETN-90-97251] 20 p2910 N90-26554
Application of artificial intelligence to the architectural synthesis of VLSI integrated circuits
[ETN-90-97253] 20 p2916 N90-26589
Current methods of digital speech processing
21 p2993 N90-27010
VLSI architecture for a Reed-Solomon decoder
[NASA-CASE-NPO-17897-1-CU]
21 p2998 N90-27040
Finding minimum width for single-layer channel routing in linear time
[AD-A221876] 21 p3002 N90-27062
Neural network with dynamically adaptable neurons
[NASA-CASE-NPO-17803-1-CU]
21 p3057 N90-27385
Cyclic error correcting block codes for reliability increasing of VLSI networks
[ETN-90-97304] 22 p3168 N90-27968
Double sided silicon strip detectors
[MPI-PAE/EXP-EL-217] 22 p3178 N90-28036
Readout of double sided silicon strip detectors with high intensity integrated electronics 22 p3179 N90-28038
New developments in double sided silicon strip detectors 22 p3179 N90-28039
A fast lightstripe rangefinding system with smart VLSI sensor 23 p3366 N90-29019
VLSI design for reliability
[AD-A224264] 24 p3463 N90-29562
Macro cell placement with neural net algorithms
[REPT-90-020] 24 p3466 N90-29585
A comparison of hardware implementations for low-level vision algorithms
[AD-A223699] 24 p3527 N90-29945

VERY LONG BASE INTERFEROMETRY
The Telecommunications and Data Acquisition Report
[NASA-CR-185093] 04 p0485 N90-12786
A statistical study of radio-source structure effects on astrometric very long baseline interferometry observations 04 p0485 N90-12788
MERLIN and VLBI observations of the radio galaxy Virgo A 06 p0860 N90-15001
VLA and VLBI observations of core dominated quasars 06 p0860 N90-15002
Scientific investigations of the Space Research Group
[ISBN-0-642-13252-6] 08 p1138 N90-16595
The determination of maximum deep space station slew rates for a high Earth orbiter 15 p2075 N90-21882
Using connected-element interferometer phase-delay data for Magellan navigation in Venus orbit
15 p2075 N90-21885
A higher density VLBI catalog for navigating Magellan and Galileo 15 p2078 N90-21904
Diffraction-limited imaging on the 200-inch telescope
15 p2183 N90-22475
VLA and VLBI angular broadening measurements: The distribution of interstellar scattering at low Galactic latitudes 16 p2330 N90-23279
The Very Long Baseline Interferometry (VLBI) functional model and the relation with tectonic motions
[ETN-90-96694] 17 p2424 N90-23814
Establishing a GPS-baseline between Seattle, Washington and Monterey, California
[AD-A220069] 18 p2495 N90-24262
Sco X-1 the microquasar: New VLA and VLBI results
19 p2775 N90-25780
Information content of a single pass of phase-delay data from a short baseline connected element interferometer
20 p2852 N90-26220

VERY LOW FREQUENCIES
Omega system performance assessment
[AD-A210342] 01 p0056 N90-10322
TWIRE: A test program for VLF airborne transmissions
[AD-A210516] 01 p0057 N90-10324
A lunar far-side very low frequency array
[NASA-CP-3039] 01 p0139 N90-10805
Direction-of-arrival calculations at VLF/LF (Very Low Frequency/Low Frequency)
[AD-A212620] 04 p0493 N90-12833
Long wave atmospheric noise model, phase 1. Volume 2: Mode parameters
[AD-A212795] 04 p0493 N90-12837
Scientific investigations of the Space Research Group
[ISBN-0-642-13252-6] 08 p1138 N90-16595
Oblique ionospheric heating and effects on radio propagation
[AD-A214756] 09 p1205 N90-16983
Trends in VLF/LF (Very Low Frequency/Low Frequency) modem performance testing
[AD-A216576] 11 p1497 N90-18614
ULF/VLF ocean bottom seismo-acoustics
[AD-A218810] 17 p2429 N90-23843
Spectral structure and generation mechanism of ducted VLF whistler mode sideband waves
24 p3489 N90-29720
A feasibility study for D-region equatorial ionosphere research using VLF radiowaves
[AD-A223685] 24 p3492 N90-29738

VESTIBULAR NYSTAGMUS
The effects of linear acceleration on perception and nystagmus 15 p2136 N90-22209
Voluntary presetting of the vestibular ocular reflex permits gaze stabilization despite perturbation of fast head movements 16 p2274 N90-22960
Influence of gravito-inertial force on vestibular nystagmus in man
[IZF-1989-24] 22 p3231 N90-28325

VESTIBULAR TESTS
Vestibular examination of motion sick student pilots
[IZF-1988-22] 12 p1696 N90-19738
Brain stem evoked responses in altered G environments
[AD-A220097] 17 p2435 N90-23874
Situational awareness and vestibular stimulation: The influence of whole-body rotation upon task performance
[IZF-1989-14] 23 p3361 N90-28994

VESTIBULES
Brain stem evoked responses in altered G environments
[AD-A220097] 17 p2435 N90-23874
Vestibular responses and motion sickness during pitch, roll, and yaw sinusoidal whole-body oscillation
[AD-A223898] 24 p3497 N90-29767

VESTS
Investigation of the effects of external supports on manual lifting
[PB90-103367] 09 p1260 N90-17307

VHSIC (CIRCUITS)
MM and T for VHSIC multichip packages
[AD-A213259] 05 p0635 N90-13703
A distributed kernel for simulation of the VHSIC hardware description language
[AD-A215419] 09 p1213 N90-17032
VHSIC/VHSIC-Like reliability prediction modeling
[AD-A214601] 09 p1288 N90-17468
Direct detection optical intersatellite link at 220 Mbps using AlGaAs laser diode and silicon APD with 4-ary PPM signaling
[NASA-CR-186380] 12 p1646 N90-19460
VHSIC Hardware Description Language (VHDL) benchmark suite
[AD-A217947] 13 p1868 N90-20719
A VHDL interface for Altera design files
[AD-A224476] 24 p3523 N90-29920

VIABILITY
A method for the early detection of instabilities in rotordynamics
[NASA-CR-186307] 09 p1170 N90-16769
Viability study of ionic microthruster tests on MECB satellite
[INPE-4973-RPE/605] 11 p1475 N90-18490
Electronic warfare technology: Trends and visions
[AD-A223034] 20 p2856 N90-26246

VIBRATION
NT BENDING VIBRATION
NT FLUTTER
NT FORCED VIBRATION
NT FREE VIBRATION
NT LATTICE VIBRATIONS
NT LINEAR VIBRATION
NT RANDOM VIBRATION
NT RESONANT VIBRATION
NT STRUCTURAL VIBRATION
NT SUBSONIC FLUTTER
NT TORSIONAL VIBRATION
NT TRANSONIC FLUTTER
Analytical study of mistuning/friction/aerodynamics interaction in a bladed disk assembly
[AD-A211139] 02 p0156 N90-10893
Effects of mistuning and matrix structure on the topology of frequency response curves
[NASA-TM-102290] 03 p0357 N90-12041
The use of Lanczos's method to solve the large generalized symmetric definite eigenvalue problem
[NASA-CR-181914] 03 p0385 N90-12193
Analysis of a system of two weakly nonlinear coupled harmonic oscillators arising from the field of wind-induced vibrations
[REPT-89-22] 03 p0396 N90-12261
Rotational and vibrational nonequilibrium effects in rarefied, hypersonic flow
[NASA-CR-182559] 04 p0437 N90-12498
RAN (Royal Australian Navy) vibration analysis system operator's guide
[AD-A212441] 04 p0453 N90-12596
Vibration isolation technology: Sensitivity of selected classes of space experiments to residual accelerations
[NASA-CR-185443] 04 p0482 N90-12768
Manipulation strategies for massive space payloads
[NASA-CR-186081] 06 p0728 N90-14247
Localized vibrations of nearly periodic structures with irregularities 06 p0798 N90-14648
Control of an experiment to measure acoustic noise in the space shuttle
[NPS62-89-022] 06 p0838 N90-14869
VIBRAFUGE: Combined vibration and centrifuge testing
[DE90-001091] 07 p0884 N90-15114
Characterizing transient vibrations using band limited moments
[DE90-000799] 07 p0945 N90-15473
Pipeline vibrations. Fluid transients in non-rigid, unbranched planar piping systems
[ESDU-89030] 07 p0948 N90-15491
Direct multivariable adaptive controller with application to wing flutter 10 p1322 N90-17642
Gear noise, vibration, and diagnostic studies at NASA Lewis Research Center
[NASA-TM-102435] 10 p1390 N90-18041
Aerodynamic superposition principle in vibrating turbine cascades 11 p1460 N90-18410
Time-dependent measurements on vibrating annular turbine cascades under various steady state conditions
11 p1463 N90-18424
Calculation of flight vibration levels of the AH-1G helicopter and correlation with existing flight vibration measurements
[NASA-CR-181923] 11 p1518 N90-18743
Payload vibration isolation in a microgravity environment
[NASA-CR-186191] 11 p1518 N90-18744
Optimization of the reference parameters in the accompanying solar panel dynamics
[INPE-4795-PRE/1449] 11 p1528 N90-18798
Nonlinear system vibration: The appearance of chaos
[DE90-007546] 12 p1708 N90-19810
Evaluation of thermal and mechanical loading effects on the structural behavior of a SiC/titanium composite
[NASA-TM-102536] 13 p1767 N90-20139
Perturbation solutions in D* for buckling, vibration, and static loading of specially orthotropic plates
13 p1814 N90-20419
Parameter-scheduled trajectory planning for suppression of coupled horizontal and vertical vibrations in a flexible rod
[DE90-002313] 13 p1817 N90-20435
User manual for VICONOPT: An exact analysis and optimum design program covering the buckling and vibration of prismatic assemblies of flat in-plane loaded, anisotropic plates, with approximations for discrete supports, and transverse stiffeners
[NASA-CR-181966] 14 p1991 N90-21413
The Shock and Vibration Digest, volume 22, no. 2
14 p2022 N90-21596
The optical measurement of acoustic velocity fields
14 p2023 N90-21601
Aeroelastic simulation of higher harmonic control
15 p2054 N90-21768
The Shock and Vibration Digest, volume 21, no. 3
15 p2109 N90-22064
Nonlinearity parameters of polymers
15 p2164 N90-22369
Low temperature properties of amorphous solids
15 p2171 N90-22405
Experiments with a laser interferometric gravitational wave antenna 15 p2184 N90-22476

Computational and experimental investigations of rotating stall in compressor cascades
16 p2201 N90-22565
Localization of vibration in disordered nearly cyclic structures 16 p2246 N90-22812
Control of a flexible planar truss using proof mass actuators 16 p2288 N90-23035
A theory of control for infinite dimensional systems with application to large scale space structures
[AD-A219937] 17 p2366 N90-23469
The 18th Informal Conference on Photochemistry
[AD-A219779] 17 p2373 N90-23510
Low Prandtl number convection in a rectangular cavity with longitudinal thermal gradient and transverse g-jitters
[REPT-892-430-109] 17 p2404 N90-23695
Adaptive control of a system with periodic dynamics: Application of an impulse response method to the helicopter vibration problem 17 p2453 N90-23990
Vibrational and optical properties of amorphous metals
[DE90-011427] 18 p2522 N90-24403
Asymptotic analysis of wind-induced vibrations
[ETN-90-96903] 18 p2572 N90-24658
Project TTA-79: Summary project report
[ETN-90-96773] 19 p2661 N90-25146
Space station based Microacceleration Experiment Platform
[NASA-CR-186659] 19 p2666 N90-25167
Out-reach in-space technology experiments program: Control of flexible robot manipulators in zero gravity, experiment definition phase
[NASA-CR-183849] 19 p2696 N90-25343
An unsteady lifting surface method for single rotation propellers
[NASA-CR-4302] 20 p2802 N90-25940
Rotational and translational effects in collisions of electronically excited diatomic hydrides
[NASA-CR-186770] 20 p2829 N90-26093
The use of Lanczo's method to solve the large generalized symmetric Eigenvalue problem in parallel
[NASA-CR-182072] 20 p2907 N90-26533
Asymptotic modal analysis and statistical energy analysis
[NASA-CR-186732] 20 p2923 N90-26634
Suspension mechanism and method
[NASA-CASE-LAR-14142-1] 21 p3011 N90-27116
Theoretical studies of time-of-flight and atom and molecular surface collision
[AD-A221705] 21 p3075 N90-27480
Flight mechanics applications for tethers in space: Cooperative Italian-US programs
22 p3131 N90-27770
Dynamics of multistage gear transmission with effects of gearbox vibrations
[NASA-TM-103109] 22 p3182 N90-28060
Noncontact laser thermomechanical nondestructive evaluation for advanced coatings
22 p3187 N90-28087
Studies in automatic speech recognition and its application in aerospace 23 p3318 N90-28759
Some studies of the vibration welding of thermoplastics 23 p3332 N90-28842
Correlation of AH-1G airframe flight vibration data with a coupled rotor-fuselage analysis
[NASA-CR-181974] 23 p3338 N90-28865
Vibration responses of two house structures during the Edwards Air Force Base phase of the national sonic boom program
[NASA-CR-182089] 23 p3393 N90-29169
Effects and tolerances of injection jitter in the SLC and future linear colliders
[DE90-014805] 23 p3394 N90-29179
An enhanced integrated aerodynamic load/dynamic optimization procedure for helicopter rotor blades
[NASA-CR-4326] 24 p3432 N90-29383
Suspension systems for ground testing large space structures
[NASA-CR-4325] 24 p3439 N90-29424
Activities report of the Institute of Sound and Vibration Research
[ETN-90-97604] 24 p3565 N90-30170

VIBRATION DAMPERS

U VIBRATION ISOLATORS

VIBRATION DAMPING

Flexible structure control experiments using a real-time workstation for computer-aided control engineering
01 p0017 N90-10084
Active vibration mitigation of distributed parameter, smart-type structures using Pseudo-Feedback Optimal Control (PFOC) 01 p0024 N90-10121
Analysis and test of a 16-foot radial rib reflector developmental model
[NASA-TM-101648] 01 p0080 N90-10457
The theory and application of quadratic minimization in the active reduction of sound and vibration
01 p0119 N90-10682
Frequency domain design of robust controllers for space structures
[AD-A211172] 02 p0176 N90-10985
Reduction of dynamic response of spacecraft structures and payloads 02 p0178 N90-11000
The dynamics of circular plates with patch damping: A numerical and experimental study
02 p0232 N90-11329
Controller design for active vibration suppression of a helicopter
[DFVLR-FB-89-20] 03 p0310 N90-11760
Active control of the forced and transient response of a finite beam 03 p0357 N90-12040
The Shock and Vibration Digest, volume 21, no. 10
04 p0483 N90-12771
A survey on nonproportional damping
04 p0483 N90-12773
Pointing control for LDR 05 p0595 N90-13453
PACOSS program 05 p0601 N90-13487
Dynamics and control of flexible spacecraft during and after slewing maneuvers
[NASA-CR-186123] 06 p0733 N90-14270
Measurement of damping of graphite epoxy composite materials and structural joints
[NASA-CR-183802] 06 p0736 N90-14286
Active control system for gust load allevation and structural damping 07 p0871 N90-15056
Vibration damping composition suitable for outer space temperature variations
[AD-D014288] 08 p1088 N90-16296
The 59th Shock and Vibration Symposium, volume 4
[AD-A214581] 09 p1238 N90-17184
Damping loss factor determination of glass and graphite fiber composites
[AD-A214535] 10 p1347 N90-17816
Damping loss factor determination of glass and graphite epoxy laminated composites using vertically oriented cantilever beams
[AD-A216529] 10 p1351 N90-17833
A new approach to active vibration isolation for microgravity space experiments
[NASA-TM-102470] 10 p1368 N90-17929
Adaptive vibration control of vibration isolation mounts, using an LMS-based control algorithm
[AD-A214386] 10 p1394 N90-18061
The 59th Shock and Vibration Symposium, volume 3
[AD-A214580] 10 p1395 N90-18066
Baseline experiment for active control of structural vibrations
[AD-A216194] 10 p1397 N90-18076
Modified independent modal space control of flexible structures 12 p1671 N90-19597
Design and implementation of a flexible robot
[AD-A216453] 12 p1671 N90-19601
An experimental study of the aeroelastic behaviour of two parallel interfering circular cylinders
12 p1673 N90-19609
Constructibility limits of multiflow wind turbines with pivots
[ILR-MITT-215] 12 p1682 N90-19662
Digital-flutter-suppression-system investigations for the active flexible wing wind-tunnel model
[NASA-TM-102618] 13 p1758 N90-20093
Tensile film clamps and mounting block for the rheovibron and autovibron viscoelastometer
[NASA-CASE-LAR-13696-1] 13 p1812 N90-20409
Active control of the forced and transient response of a finite beam
[NASA-CR-181957] 13 p1816 N90-20430
Computational simulation of damping in composite structures
[NASA-TM-102567] 13 p1817 N90-20432
PACOSS program status and results
14 p1933 N90-21065
Vibration isolation versus vibration compensation on multiple payload platforms 14 p1933 N90-21066
Nonlinear and distributed parameter models of the mini-mast truss 14 p1934 N90-21070
LACE flight dynamics experiment
14 p1937 N90-21086
Initial operational capability of the ASTREX large space structures test bed 14 p1938 N90-21091
Multi-objective shape and material optimization of composite structures including damping
[NASA-TM-102579] 14 p1945 N90-21132
A review of gear housing dynamics and acoustics literature
[NASA-CR-185148] 14 p1987 N90-21387
Internal rotor friction instability
[NASA-CR-183942] 14 p1988 N90-21395
The vibro-acoustic mapping of low gravity trajectories on a Learjet aircraft
[NASA-TM-103103] 15 p2045 N90-21723
Development and application of a generalized dynamic wake theory for lifting rotors 15 p2046 N90-21731
Identification of XV-15 aeroelastic modes using frequency-domain methods
[NASA-TM-101021] 15 p2051 N90-21756
Recent advances in structural control
15 p2109 N90-22062
Optimum design of structures under shock and vibration environment 15 p2110 N90-22067
The Shock and Vibration Digest, volume 22, no. 1
15 p2111 N90-22073
Stable response of damped mechanical systems, 4
15 p2111 N90-22074
Dynamics and control of tethered antennas/reflectors in orbit
[AD-A219316] 16 p2207 N90-22594
Elements of active vibration control for rotating machinery
[NASA-TM-102368] 16 p2227 N90-22703
The microstructural basis of damping in high damping alloys
[AD-A219572] 16 p2248 N90-22821
The application of a non-linear least squares method to predicting seat transmissibility
[ISVR-TR-173] 16 p2275 N90-22967
Frequency response modeling and control of flexible structures: Computational methods
16 p2285 N90-23021
Model reduction for flexible spacecraft with clustered natural frequencies 16 p2291 N90-23054
Controlling flexible structures with second order actuator dynamics 16 p2297 N90-23083
Approximation in LQG control of a thermoelastic rod
16 p2297 N90-23084
Modeling and control of flexible space stations (slew maneuvers) 16 p2297 N90-23086
Numerical studies of the active control of sound transmission through double partitions
[ISVR-TR-183] 16 p2313 N90-23181
Experimental evaluation of a tuned electromagnetic damper for vibration control of cryogenic turbopump rotors
[NASA-TP-3005] 17 p2354 N90-23403
Finite element formulations for coupled fluid/structure eigenvalue analysis
[AD-A220793] 17 p2416 N90-23766
Adaptive control of a system with periodic dynamics: Application of an impulse response method to the helicopter vibration problem 17 p2453 N90-23990
Experimental determination of material damping using vibration analyzer 18 p2514 N90-24358
Development of damped metal matrix composites for advanced structural applications
[AD-A219864] 18 p2518 N90-24380
Fabrication of low frequency structureborne vibration isolation mount
[AD-D014532] 19 p2697 N90-25346
Robot vibration control using inertial damping forces
[NASA-CR-186808] 19 p2698 N90-25352
Calculation of flight vibration levels of the AH-1G helicopter and correlation with existing flight vibration measurements
[NASA-CR-182031] 19 p2702 N90-25375
Design and implementation of robust decentralized control laws for the ACES structure at Marshall Space Flight Center
[NASA-CR-4310] 20 p2820 N90-26046
Structural dynamics branch research and accomplishments
[NASA-TM-102488] 20 p2878 N90-26373
Power flow analysis of two coupled plates with arbitrary characteristics
[NASA-CR-182033] 20 p2923 N90-26632
Flow induced nutation instability in spinning solid propellant rockets
[AD-A222504] 21 p2969 N90-26877
Effects of spoiler surfaces on the aeroelastic behavior of a low-aspect-ratio rectangular wing
[NASA-TM-102622] 22 p3115 N90-27700
Reaction-compensation technology for microgravity laboratory robots
[NASA-TM-103271] 22 p3183 N90-28062
The dynamics and control of large flexible space structures - 13
[NASA-CR-186930] 23 p3286 N90-28591
Minimum weight design of a leaf spring tapered in thickness and width for the Hubble Space Telescope-space support equipment
[NASA-TM-4233] 23 p3340 N90-28879
Proceedings of damping '89. Volume 1: Pages AAB-1 through DCD-11
[AD-A223431] 24 p3479 N90-29664
Proceedings of Damping '89. Volume 3: Pages ICA-1 through KDC-15
[AD-A223433] 24 p3479 N90-29666
A vector diagram approach to shaping inputs for vibration reduction
[AD-A223724] 24 p3480 N90-29671

Active vibration damping of flexible structures
[DLR-FB-90-03] 24 p3481 N90-29676
Capture of free-flying payloads with flexible space manipulators 24 p3500 N90-29784

VIBRATION EFFECTS
A contribution to the stability analysis of large space structures 02 p0177 N90-10997
Electron transfer reactions
[AD-A210711] 02 p0271 N90-11545
Non linear vibrations in a drive train when coupled to constant torque and constant power loads
[PNR90593] 04 p0508 N90-12934
Pointing control for LDR 05 p0595 N90-13453
Localized vibrations of nearly periodic structures with irregularities 06 p0798 N90-14648
The response of helicopter rotors to vibratory airload
[AD-A215678] 09 p1167 N90-16756
A study of the vibrational transmission through flanged joints
[ISVR-TR-181] 11 p1520 N90-18755
Ionic disorder in crystals at high temperatures with emphasis on fluorites
[AERE-R-13544] 13 p1893 N90-20862
Transportation monitoring unit qualification
[NASA-CR-183930] 14 p1932 N90-21060
The Shock and Vibration Digest, volume 21, no. 3 15 p2109 N90-22064
Correlation/validation of finite element code analyses for vibration assessment of avionic equipment
[AD-A220393] 17 p2353 N90-23398
Solidification of dilute alloys under fluctuating residual gravity
[REPT-892-430-112] 17 p2377 N90-23535
Control of large space structures
[AD-A221216] 18 p2511 N90-24345
Power flow analysis of two coupled plates with arbitrary characteristics
[NASA-CR-182033] 20 p2923 N90-26632
Static and free-vibrational response of semi-circular graphite-epoxy frames with thin-walled open sections
[NASA-CR-4287] 21 p3012 N90-27122
Criteria for a recommended standard: Occupational exposure to hand-arm vibration
[PB90-168048] 22 p3233 N90-28331
Applications of ripple analysis in hydro-acoustics
[ETN-90-97015] 22 p3244 N90-28397
Rotordynamic properties of high pressure seals: An experimental approach 24 p3475 N90-29640

VIBRATION ISOLATORS
Frequency domain design of robust controllers for space structures
[AD-A211172] 02 p0176 N90-10985
Viscoelastic tuned dampers for control of structural dynamics 02 p0178 N90-10999
Reduction of dynamic response of spacecraft structures and payloads 02 p0178 N90-11000
Controller design for active vibration suppression of a helicopter
[DFVLR-FB-89-20] 03 p0310 N90-11760
Nonintrusive inertial vibration isolation technology for microgravity space experiments
[NASA-TM-102386] 03 p0334 N90-11901
Structural vibration and shock isolator
[AD-D014202] 04 p0509 N90-12940
Structural vibration and shock isolation in a high pressure environment
[AD-D014311] 09 p1238 N90-17186
Astrometric Telescope Facility isolation and pointing study
[NASA-CR-177473] 10 p1328 N90-17675
Damping loss factor determination of glass and graphite fiber composites
[AD-A214535] 10 p1347 N90-17816
A new approach to active vibration isolation for microgravity space experiments
[NASA-TM-102470] 10 p1368 N90-17929
Adaptive vibration control of vibration isolation mounts, using an LMS-based control algorithm
[AD-A214386] 10 p1394 N90-18061
Payload vibration isolation in a microgravity environment
[NASA-CR-186191] 11 p1518 N90-18744
Noise reduction theory acoustic barrier construction
[CRIF-MC-87] 16 p2313 N90-23183
Fabrication of low frequency structureborne vibration isolation mount
[AD-D014532] 19 p2697 N90-25346
Development and approach to low-frequency microgravity isolation systems
[NASA-TP-2984] 23 p3317 N90-28754

VIBRATION MEASUREMENT
Advances in instrumentation for experimental stress and vibration analysis and its applications 02 p0187 N90-11069
Vibration intensity. Evaluation of a remote measuring system
[CETIM-110430] 04 p0504 N90-12907
The 59th Shock and Vibration Symposium, volume 1
[AD-A214578] 09 p1238 N90-17183
Calculation of flight vibration levels of the AH-1G helicopter and correlation with existing flight vibration measurements
[NASA-CR-181923] 11 p1518 N90-18743
Calculating the time domain average of gear vibration data sampled at less than the Nyquist frequency
[OUEL-1768/89] 15 p2107 N90-22052
The Shock and Vibration Digest, volume 21, no. 1 15 p2109 N90-22061
The Shock and Vibration Digest, volume 21, no. 8 15 p2110 N90-22068
Diesel engine condition monitoring: Laser-based diagnostic techniques 17 p2410 N90-23733
Microcomputer-aided ground vibration testing
[DLR-FB-89-57] 18 p2499 N90-24279
Development of damped metal matrix composites for advanced structural applications
[AD-A219864] 18 p2518 N90-24380
Calculation of flight vibration levels of the AH-1G helicopter and correlation with existing flight vibration measurements
[NASA-CR-182031] 19 p2702 N90-25375
Monolithic Optical Programmable Spectrograph (MOPS)
[AD-D014502] 19 p2757 N90-25669
A numerical simulation of the quasi-heterodyne technique for double-pulsed holographic vibration measurements
[PNR90622] 20 p2865 N90-26301
Evaluation of EDR-3 vibration, shock, temperature, and humidity recording unit
[NASA-CR-184006] 22 p3177 N90-28028
Plan, execute, and discuss vibration measurements and correlations to evaluate a NASTRAN finite element model of the AH-64 helicopter airframe
[NASA-CR-181973] 23 p3338 N90-28866
Structural testing and analytical research of turbine components
[AD-A223516] 24 p3434 N90-29396
Noncontact measurement of rotating blade vibrations
[NAL-TR-1033] 24 p3483 N90-29687

VIBRATION METERS
NT SEISMOGRAPHS
Advances in instrumentation for experimental stress and vibration analysis and its applications 02 p0187 N90-11069
Vibration intensity. Evaluation of a remote measuring system
[CETIM-110430] 04 p0504 N90-12907

VIBRATION MODE
Computational aspects of sensitivity calculations in linear transient structural analysis 02 p0231 N90-11327
Problems related to the acquisition, processing and utilization of the modal parameters measured in flight tests in order to obtain the full envelope for flutter
[ETN-89-95210] 03 p0305 N90-11735
Eccentricity effects of square cutouts on the natural frequencies and mode shapes of curved rectangular composite panels
[AD-A216410] 10 p1350 N90-17831
Experimental feasibility of investigating acoustic waves in Couette flow with entropy and pressure gradients
[NASA-TM-102621] 13 p1882 N90-20795
Experimental and theoretical investigation of optimal control methods with model reduction 14 p1928 N90-21039
Integrated modeling and analysis of a space-truss article
[NASA-TM-102615] 14 p1991 N90-21412
Instabilities and subharmonic resonances of subsonic heated round jets, volume 2
[NASA-CR-186058] 15 p2100 N90-22017
A review of approximate methods for determining the vibrational modes of membranes 15 p2109 N90-22063
Natural modes of cracked beams and identification of cracks 15 p2111 N90-22075
The observed properties of the intermediate-degree gravity modes and their relevance to the solar neutrino paradox 15 p2193 N90-22519
An experimental study of tip shape effects on the flutter of aft-swept, flat-plate wings
[NASA-TM-4180] 16 p2199 N90-22555
Flat plate vibration analysis experimental and numerical fillet study
[AD-A218789] 16 p2247 N90-22818
Expansion and orthogonalization of measured modes for structure identification 18 p2647 N90-25068
Dynamic analysis of space-related linear and non-linear structures
[NASA-TM-103490] 19 p2667 N90-25174
Dynamics of multistage gear transmission with effects of gearbox vibrations
[NASA-TM-103109] 22 p3182 N90-28060
Parametrical retiming of vibrational models of structures
[ONERA-RT-9/3313-RY-080-R] 22 p3194 N90-28121

VIBRATION PROTECTION
U VIBRATION ISOLATORS

VIBRATION SIMULATORS
NT VERTICAL MOTION SIMULATORS
Employment of modal survey methodologies in dynamic analysis procedures 02 p0179 N90-11006
Transient vibration testing of spacecraft structures. Experience with multiaxial base motion and combined base motion and point force excitation 02 p0183 N90-11039
Two years experience with the ESTEC multishaker system 02 p0187 N90-11065
Tamaris: A new European facility for low frequency multi-axis vibration simulation 02 p0187 N90-11068
A new European vibration test facility for Ariane 4 class satellites 02 p0187 N90-11070
A comparison of fixed-base and driven-base modal testing of an electronics package
[DE89-016673] 02 p0217 N90-11240

VIBRATION TESTING MACHINES
U VIBRATION SIMULATORS

VIBRATION TESTS
SSME Alternate Turbopump Development Program: Design verification specification for high-pressure fuel turbopump
[NASA-CR-183676] 01 p0008 N90-10033
VIBRAFUGE: A combined environment testing facility-vibration testing on a centrifuge
[DE89-015120] 01 p0080 N90-10458
Modal analysis of space structures with the Ibrahim Time Domain method 02 p0181 N90-11026
Transient vibration testing of spacecraft structures. Experience with multiaxial base motion and combined base motion and point force excitation 02 p0183 N90-11039
Tamaris: A new European facility for low frequency multi-axis vibration simulation 02 p0187 N90-11068
A new European vibration test facility for Ariane 4 class satellites 02 p0187 N90-11070
Investigation of difficult component effects on finite element model vibration prediction for the Bell AH-1G helicopter. Volume 1: Ground vibration test results
[NASA-CR-181916-VOL-1] 03 p0360 N90-12058
Mechanical and thermal testing 05 p0605 N90-13521
Static and free-vibrational response of semi-circular graphite-epoxy frames with thin-walled open sections
[NASA-CR-186097] 05 p0617 N90-13600
Identification of equivalent modulus of a composite beam from nonmodal vibratory tests
[ECL-89-001] 05 p0656 N90-13821
Measurement of damping of graphite epoxy composite materials and structural joints
[NASA-CR-183802] 06 p0736 N90-14286
VIBRAFUGE: Combined vibration and centrifuge testing
[DE90-001091] 07 p0884 N90-15114
Vibrational behavior of a viscous column with a free liquid surface
[LRT-WE-9-FB-1(1989)] 08 p1066 N90-16166
Force determination sensitivities study for full-scale helicopter ground vibration testing
[AD-A215983] 10 p1322 N90-17643
Vibration tests of the ACPB canister flight unit of the RETE experiment, integrated with the tests of the booms from R. Piaggio
[IFSI-89-11] 10 p1328 N90-17670
The 59th Shock and Vibration Symposium, volume 2
[AD-A214579] 10 p1395 N90-18065
Simulation of the dynamic environment for missile component testing: Demonstration
[AD-A216979] 11 p1466 N90-18443
Helicopter flight vibration of large transportation containers: A case for testing tailoring
[DE90-007429] 12 p1601 N90-19215
Complex demodulation for bearing fault detection
[AD-A218367] 13 p1812 N90-20407
The Shock and Vibration Digest, volume 22, no. 2 14 p2022 N90-21596
Flutter investigations on a Transavia PL12/T-400 aircraft
[AD-A219108] 16 p2203 N90-22570
On simplified analytical flutter clearance procedures for light aircraft
[DLR-FB-89-56] 18 p2498 N90-24276
Microcomputer-aided ground vibration testing
[DLR-FB-89-57] 18 p2499 N90-24279

Vibration test procedures for orbiter sidewall-mounted payloads, phase 1
[AD-A220773] 20 p2818 N90-26037
Vibration test procedures for orbiter sidewall-mounted payloads, phase 2
[AD-A220774] 20 p2818 N90-26038
Studies of vortex interactions
[AD-A223864] 23 p3328 N90-26817
Plan, execute, and discuss vibration measurements and correlations to evaluate a NASTRAN finite element model of the AH-64 helicopter airframe
[NASA-CR-181973] 23 p3338 N90-28866
Military aircrew seating: A human factors engineering approach
[AD-A218049] 23 p3362 N90-28999
A human factors engineering approach to the development and dynamic evaluation of a prototype aircrew seat for military aircraft
[AD-A218263] 24 p3500 N90-29779

VIBRATIONAL FREQUENCIES (MOLECULAR)
U VIBRATIONAL SPECTRA

VIBRATIONAL FREQUENCIES (STRUCTURAL)
U RESONANT FREQUENCIES

VIBRATIONAL RELAXATION
U MOLECULAR RELAXATION

VIBRATIONAL SPECTRA
Raman spectroscopic study of the rare earth sesquisulfides
[AD-A210610] 01 p0041 N90-10226
Computer simulations of polymer dynamics in the solid state
[DE89-010337] 01 p0048 N90-10275
A matrix-isolation FT-IR study of hydrazine
02 p0204 N90-11168
Theoretical investigation of gas-surface interactions
[NASA-CR-185492] 02 p0272 N90-11552
Study of disorder and strain in semiconductor heterostructures and superlattices by Raman scattering
02 p0280 N90-11601
Structures and energies for small borane compounds: One and two boron compounds
[AD-A212264] 04 p0471 N90-12701
Propagation of sound in vibrationally excited nitrogen and hydrogen gas mixtures
[AD-A213002] 05 p0696 N90-14073
The production and spectroscopy of molecular ions isolated in solid neon
[AD-A213723] 07 p0895 N90-15174
Dynamics of electron transfer for a nonsuperexchange coherent mechanism, 1
[AD-A213450] 07 p0990 N90-15721
Vibrational behavior of a viscous column with a free liquid surface
[LRT-WE-9-FB-1(1989)] 08 p1066 N90-16166
Conformation, orientation and interaction in molecular monolayers: A surface second harmonic and sum frequency generation study
[DE90-003108] 08 p1128 N90-16536
Combustion of hydrogen and hydrocarbons in fluorine
[AD-A214621] 09 p1190 N90-16896
The 59th Shock and Vibration Symposium, volume 4
[AD-A214581] 09 p1238 N90-17184
Turbulent boundary layer pressure field-induced vibrations in a thin flexible plate under water
10 p1383 N90-18002
Adaptive vibration control of vibration isolation mounts, using an LMS-based control algorithm
[AD-A214386] 10 p1394 N90-18061
VUV (Vacuum Ultraviolet) laser diagnostics of H(-) ion sources
[DE90-006072] 11 p1514 N90-18719
The 2.7/4.3 micron CO2 branching ratio measurement
[AD-A215952] 11 p1534 N90-18830
Toda lattice with transverse degree of freedom
[DE90-002414] 11 p1572 N90-19049
Modal analysis of nonprismatic beams: Uniform segment method
[AD-A216952] 12 p1674 N90-19614
Vibrational spectroscopy of boron nitride at high temperatures and pressures
[DE90-008633] 13 p1772 N90-20172
Laser enhanced chemical reactions
[DE90-008273] 13 p1807 N90-20377
Reactive and anisotropic elastic scattering of highly laser-vibration-excited diatomic molecules
[MPIS-19/1988] 13 p1883 N90-20604
Transverse vibrations of a composite cylindrical tube of circular cross section
[AD-A219227] 16 p2248 N90-22820
Contributions of individual structural modes to the scattered acoustic field
[AD-A219128] 16 p2314 N90-23187
Application of frequency interpolation to acoustic-structure interaction problems
[AD-A219330] 17 p2469 N90-24113
Formation and deactivation of vibrationally excited atmospheric molecules
[AD-A222660] 20 p2889 N90-26442
High resolution spectroscopy in the microwave and far infrared 20 p2943 N90-26746

VIBRATIONAL STRESS
Methodology of developing a combined environmental stress schedule for reliability growth testing
[AD-A211053] 02 p0231 N90-11326
Vibrational behavior of a viscous column with a free liquid surface
[LRT-WE-9-FB-1(1989)] 08 p1066 N90-16166
Turbine blade data acquisition system user's guide
[AD-A214986] 09 p1169 N90-16763
The 59th Shock and Vibration Symposium, volume 4
[AD-A214581] 09 p1238 N90-17184
Damping loss factor determination of glass and graphite epoxy laminated composites using vertically oriented cantilever beams
[AD-A216529] 10 p1351 N90-17833
Complex demodulation for bearing fault detection
[AD-A218367] 13 p1812 N90-20407
VAPEPS user's reference manual, version 5.0
[NASA-CR-180781] 13 p1868 N90-20713
Creating a VAPEPS database: A VAPEPS tutorial
[NASA-CR-186629] 20 p2936 N90-26705
Evaluation of plane-of-light noninterference stress measurement systems for measuring bladed disk vibrations
[AD-A223487] 24 p3479 N90-29667

VIBRATORY LOADS
The 59th Shock and Vibration Symposium, volume 4
[AD-A214581] 09 p1238 N90-17184
Calculation of flight vibration levels of the AH-1G helicopter and correlation with existing flight vibration measurements
[NASA-CR-181923] 11 p1518 N90-18743

VIBROMETERS
U VIBRATION METERS

VIDEO COMMUNICATION
Implementation issues in source coding
[NASA-CR-185327] 05 p0681 N90-13963
Technology assessment of video teleconferencing
[AD-A217318] 13 p1789 N90-20266

VIDEO DATA
Video imaging systems: A survey
[DE89-016920] 03 p0337 N90-11919
Data compression techniques applied to high resolution high frame rate video technology
[NASA-CR-4263] 06 p0765 N90-14452
Scry: A distributed image handling system, version 1.1
[DE90-003105] 07 p0973 N90-15621
Evaluation and analysis of the orbital maneuvering vehicle video system 12 p1638 N90-19411
Spatial constraints of stereopsis in video displays
16 p2267 N90-22920
The interactive digital video interface
16 p2271 N90-22941
Evaluation of the wake effects on plume dispersion using video image analysis
[PB90-186354] 22 p3169 N90-27972
Size, duration, and rate of growth of nocturnal lightning events appearing on space shuttle video tapes
[NASA-CR-4313] 22 p3229 N90-28310
Animated computer-generated video-tape instruction using DIGLIB (Device Independent Graphics Library)
[DE90-015360] 23 p3382 N90-29105

VIDEO DISKS
Use of optical storage devices as shared resources in local area networks
[AD-A219198] 16 p2327 N90-23269

VIDEO EQUIPMENT
NT VIDEO TAPE RECORDERS
Three dimensional object recognition employing combined visual and tactile sensing
[PB89-219489] 03 p0382 N90-12176
Video line processor
[AD-D014198] 04 p0497 N90-12861
A programmable image compression system
08 p1076 N90-16222
Evaluation and analysis of the orbital maneuvering vehicle video system 12 p1638 N90-19411
Contact formation on (Hg,Cd) Te
[AD-A217088] 12 p1723 N90-19900
The design and implementation of a position measuring system for a remotely controlled video camera
[AD-A218077] 13 p1805 N90-20362
Engineering visualization utilizing advanced animation
13 p1859 N90-20664
Multi-tasking computer control of video related equipment 13 p1859 N90-20665
Copyright and home copying: Technology challenges the law
[PB90-151309] 21 p3086 N90-27547
A system for recording physical properties of clouds
22 p3227 N90-28301

VIDEO LANDMARK ACQUISITION AND TRACKING
Position finding and ground target direction finding by an aircraft with a gimballed video camera
[DLR-FB-89-62] 22 p3111 N90-27673

VIDEO SIGNALS
Robot vehicle video image compression, phase 1
[AD-A210974] 01 p0110 N90-10626
Land vehicle teleoperation under conditions of reduced video resolution
[DE89-016925] 02 p0231 N90-11324
Video line processor
[AD-D014198] 04 p0497 N90-12861
Image enhancement software for underwater recovery operations: User's manual
[AD-A212943] 05 p0699 N90-14094
SAND DEVIL: A digital video link for telemetry applications
[DE90-001879] 06 p0730 N90-14259
Focal plane antenna array for millimeter waves
[AD-D014306] 07 p0920 N90-15322
Satellite broadcasting: Requirements for the receiving antenna
[BBC-RD-1989/5] 08 p1055 N90-16098
Eccentricity effects of square cutouts on the natural frequencies and mode shapes of curved rectangular composite panels
[AD-A216410] 10 p1350 N90-17831
A space qualified thermal imaging system using a Pt Si detector array 10 p1367 N90-17921
Issues in visual support to real-time space system simulation solved in the Systems Engineering Simulator
13 p1862 N90-20680
The Orbital Maneuvering Vehicle Training Facility visual system concept 13 p1863 N90-20684
Use of the Xybion ISG-camera in the RETRA-1000 TV-Holography unit
[AD-A219842] 18 p2554 N90-24577
System for shooting of video images in realtime
[MBB-UM-0009/89-PUB] 19 p2653 N90-25097
Video-rate visual servoing for robots
[AD-A218711] 22 p3181 N90-28052

VIDEO TAPE RECORDERS
A digital HDTV recorder using a cluster of four D1 DVTRs
[BBC-RD-1989/13] 12 p1649 N90-19477

VIDEO TAPES
Generation of animation sequences of three dimensional models
[NASA-CASE-MSC-21379-1-SB]
21 p3050 N90-27340
Aerial videotape survey of coastal Louisiana, 1986. Louisiana Barrier Island erosion and land loss study: 1986-1990
[PB90-194648] 22 p3195 N90-28128

VIDICONS
Optical anti-aliasing filters
[AD-A215826] 10 p1430 N90-18251

VIEW EFFECTS
Analysis of radar images of the active volcanic zone at Krafla, Iceland: The effects of look azimuth biasing
03 p0424 N90-12434

VIEWING
NT FIELD OF VIEW
The use of PLAID in the Space Station Freedom viewing analysis 19 p2729 N90-25517

VIKING LANDER SPACECRAFT
Design of a thermal and micrometeorite protection system for an unmanned lunar cargo lander
[NASA-CR-186682] 19 p2664 N90-25161
Lunar polar coring lander
[NASA-CR-186684] 19 p2796 N90-25917
Project Exodus
[NASA-CR-186836] 20 p2816 N90-26026

VIKING MARS PROGRAM
The chemical effects of the Martian environment on power system component materials: A theoretical approach
[NASA-TM-103203] 20 p2825 N90-26074

VIKING SPACECRAFT
NT VIKING LANDER SPACECRAFT

VINYL COPOLYMERS
Rheology of filler rubber: Silica-silicone
[AD-A223600] 24 p3455 N90-29511

VINYL CYANIDE
U ACRYLONITRILES

VINYL ETHYLENE
U BUTADIENE

VINYL POLYMERS
NT POLYVINYL FLUORIDE
NT VINYL COPOLYMERS
The Sandia standard for PVDF (Polyvinylidene Di-Fluoride) shock sensors
[DE89-016530] 02 p0225 N90-11287
Multiplexed robotic tactile sensor fabricated from polyvinylidene fluoride film
[AD-A215354] 09 p1231 N90-17145

Investigation of atomistic simulation of structural and dynamic differences in glassy and liquid states of atactic poly(propylene)
[AD-A218896] 16 p2224 N90-22687
DURIP advanced polymer solid state NMR instrumentation
[AD-A221401] 18 p2531 N90-24440
Radical homopolymerization of a trisubstituted alkene: 1-cyclobutenecarboxylic acid and its polymer
[AD-A223188] 21 p2986 N90-26968
Cell performance of ultra-thin polymer cathode cell systems. Part 2: Cation intercalating composite polymer cathode
[AD-A221919] 21 p3020 N90-27172

VINYLIDENE
Development and polarization of ferroelectric polymer gauges, for dynamical acceleration experiments, as those in ballistics shocks
[ISL-R-119/88] 11 p1511 N90-18703

VIOLENCE
NT ATTACKING (ASSAULTING)

VIRGO GALACTIC CLUSTER
Detection of hard X ray emission from a type 2 Seyfert galaxy 19 p2794 N90-25905

VIRGO STAR CLUSTER
U VIRGO GALACTIC CLUSTER

VIRTUAL MEMORY SYSTEMS
An expert system for VM performance analysis
[REPT-89-30] 04 p0528 N90-13045
PVM (Parallel Virtual Machine): A framework for parallel distributed computing
[DE90-004390] 08 p1106 N90-16403
An investigation of the locality of memory accesses during symbolic program execution
[AD-A218168] 13 p1875 N90-20750

VIRTUAL PROPERTIES
The effects of viewpoint on the virtual space of pictures 16 p2269 N90-22932
The eyes prefer real images 16 p2270 N90-22938

VISCOELASTIC CYLINDERS
Similarity solutions that give rise to hyperbolicity and change of type in steady flow of a viscoelastic fluid
[AD-A210920] 01 p0072 N90-10410
Elastic and viscoelastic analysis of two multiply layered cylinders rolling over each other with Coulomb friction
[REPT-89-50] 15 p2107 N90-22051

VISCOELASTIC DAMPING
Viscoelastic tuned dampers for control of structural dynamics 02 p0178 N90-10999
Free-field response from inclined body waves in viscoelastic random medium
[REPT-88-99] 04 p0499 N90-12876
Improved solution techniques for the eigenstructure of fractional order systems
[AD-A213844] 08 p1088 N90-16295
Energy decay and boundary control for distributed parameter systems with viscoelastic damping
[AD-A216468] 11 p1519 N90-18748
Fractional state feedback control of undamped and viscoelastically-damped structures
[AD-A220477] 17 p2412 N90-23746

VISCOELASTIC FLOW
U VISCOELASTICITY

VISCOELASTICITY
Numerical analysis of nonlinear viscoelastic structures: Application to elastomers and rubber-like materials 02 p0180 N90-11013
The decay of viscoelastic fluid jets
[ETN-89-94667] 02 p0221 N90-11270
Three-dimensional viscoelastic bodies in steady state frictional rolling contact with generalization to Knothe rolling
[REPT-89-23] 03 p0355 N90-12032
Free-field response from inclined body waves in viscoelastic random medium
[REPT-88-99] 04 p0499 N90-12876
Quadratic dynamical systems describing shear flow of non-Newtonian fluids
[AD-A212892] 05 p0638 N90-13720
Investigation of loads generated by temperature transients in pipes
[DE89-636433] 07 p0932 N90-15395
Interdisciplinary research in viscoelasticity and rheology
[AD-A213630] 08 p1063 N90-16145
Traction modeling of military lubricants
[AD-A213866] 09 p1230 N90-17139
The 59th Shock and Vibration Symposium, volume 3
[AD-A214580] 10 p1395 N90-18066
Elastic recovery and polymer-polymer interactions
[AD-A217085] 12 p1633 N90-19384
Viscoelastic adherend effects in adhesively bonded composite-to-composite joints 12 p1670 N90-19594
Calculation of nonlinear viscoelastic processes for plastic layer textile membranes
[ETN-90-95868] 12 p1675 N90-19622
The viscoelasticity of curing thermosets
[DE90-006535] 13 p1781 N90-20221
Tensile film clamps and mounting block for the rheovibron and autovibron viscoelastometer
[NASA-CASE-LAR-13696-1] 13 p1812 N90-20409
Stress analysis of rocket motors with viscoelastic propellant by a mixed finite element model 14 p1941 N90-21112
LaRC TPI 1500 series polymers
[NASA-CR-181899] 14 p1945 N90-21129
Determinations of molecular weight and molecular weight distribution of high polymers by the rheological properties
[NASA-CR-186450] 14 p1953 N90-21180
Computational methods and plasticity
[LR-583] 15 p2119 N90-22120
The analysis of stress relaxation on indentation of a rigid punch into a viscoelastic sheet of finite thickness
[NPL-DMA(A)-193] 15 p2162 N90-22357
A numerical and analytical study of normal stresses and pressure differences in non-Newtonian creeping flows 16 p2234 N90-22749
Axisymmetric and cylindrically orthotropic analysis of filament winding 16 p2246 N90-22811
Rate dependent constitutive models for fiber reinforced polymer composites
[NASA-TM-102665] 17 p2370 N90-23492
Strain softening in viscoelasticity of the rate type
[AD-A219915] 17 p2417 N90-23772
Behaviour in the large of numerical solutions to one-dimensional nonlinear viscoelasticity by continuous time Galerkin methods
[AD-A220197] 17 p2461 N90-24057
Approximations of thermoelastic and viscoelastic control systems
[NASA-CR-182054] 18 p2604 N90-24834
Characterization of the creep compliances J22 and J66 of orthotropic composites with PEEK and epoxy matrices using the nonlinear viscoelastic response of the neat resins
[MBB-Z-0258/89-PUB] 19 p2650 N90-25082
Evolution of structure and viscoelasticity in diethanolamine-cured epoxy
[DE90-011256] 20 p2837 N90-26134
Modeling of free viscoelastic jets and instability mechanisms
[AD-A221672] 21 p3005 N90-27080
A viscoelastic material model for computing stresses in glass
[DE90-014851] 24 p3481 N90-29673

VISCOMETERS
Rheological tests of Rigidite 5245 using the cone-plate and parallel plates method
[DT-310/88] 11 p1485 N90-18544
A modified Ubbelohde viscometer with improved dilution characteristics
[NIAR-90-16] 19 p2693 N90-25326

VISCOPLASTIC FLOW
U VISCOPLASTICITY

VISCOPLASTICITY
An evaluation of the Chaboche and Bodner-Partom viscoplastic constitutive theories for strain rate sensitive materials 02 p0232 N90-11330
Stability conditions for steady shearing. Stability conditions for simple shear under mixed thermal boundary conditions 04 p0499 N90-12873
Viscoplasticity: A thermodynamic formulation
[NASA-TM-102388] 06 p0797 N90-14640
Shear strain localization phenomenon in viscoplastic materials 06 p0798 N90-14649
A new uniformly valid asymptotic integration algorithm for elasto-plastic-creep and unified viscoplastic theories including continuum damage
[NASA-TM-102344] 06 p0799 N90-14655
Ductile failure
[AD-A213864] 07 p0948 N90-15488
Steady-state and transient Zener parameters in viscoplasticity: Drag strength versus yield strength
[NASA-TM-102487] 10 p1395 N90-18064
A micromechanical viscoplastic stress-strain model with grain boundary sliding
[DE90-006013] 10 p1437 N90-18295
Model development in viscoplastic ratchetting
[NASA-TM-102509] 13 p1816 N90-20431
Thermomechanical deformation testing and modeling in the presence of metallurgical instabilities
[NASA-CR-185188] 14 p1993 N90-21420
Computational methods and plasticity
[LR-583] 15 p2119 N90-22120
The mechanics of shear band formation in thermal viscoplastic materials at high rates of loading 15 p2120 N90-22128
NASA-UVA light aerospace alloy and structures technology program
[NASA-CR-182607] 16 p2217 N90-22651
Experimental and computational study of the viscoplastic response of high temperature structures 16 p2220 N90-22663
Rate dependent constitutive models for fiber reinforced polymer composites
[NASA-TM-102665] 17 p2370 N90-23492
HYPUF upgrade
[AD-A218400] 17 p2379 N90-23547
Application of finite-element-based solution technologies for viscoplastic structural analyses
[NASA-CR-185196] 17 p2414 N90-23757
An orthotropic theory of viscoplasticity based on overstress for thermomechanical deformation and its application to laminated metal matrix composites 17 p2415 N90-23759
Effect of constitutive modeling on the dynamic development of shear bands in viscoplastic materials
[AD-A220443] 17 p2416 N90-23765
Finite element analysis of structural components using viscoplastic models with application to a cowl lip problem
[NASA-CR-185189] 17 p2416 N90-23769
A viscoplastic model with application to LiF-22 percent CaF2 hypereutectic salt
[NASA-TM-103181] 17 p2417 N90-23770

VISCOSITY
NT EDDY VISCOSITY
NT GAS VISCOSITY
Shock capturing by the spectral viscosity method
[NASA-CR-181920] 01 p0112 N90-10639
Numerical simulation of leading-edge vortex rollup and bursting 02 p0145 N90-10831
A numerical study of rain-induced surface gravity wave attenuation
[AD-A212762] 04 p0549 N90-13197
Summary physical data tables: Alkanes
[ESDU-PD3] 07 p0893 N90-15162
New transient algorithms for non-Newtonian flows
[AD-A213494] 07 p0930 N90-15385
Nonlinear viscous waves produced by an impulsively moving plate
[AD-A214014] 07 p0932 N90-15392
Thermal analysis of fixed and tilting pad journal bearings including cross-film viscosity variations and deformations 07 p0937 N90-15429
Physical process in MPD plasmas
[AD-A213579] 07 p0996 N90-15761
An improvement of convection fidelity in Euler calculations 09 p1159 N90-16709
Structure and properties of resorcinol-formaldehyde gels
[DE90-005201] 10 p1358 N90-17876
Magnetohydrodynamic liquid-metal flows in a rectangular channel with an axial magnetic field, a moving conducting wall, and free surfaces
[AD-A216276] 10 p1425 N90-18223
A difference scheme with autocontrol artificial viscosity to predict ablated nosetip shape
[AD-A216625] 11 p1468 N90-18452
Hydrodynamic interactions and transport coefficients in a suspension of spherical particles
[DE90-008301] 13 p1801 N90-20336
Measurement of lift development on rapidly-accelerated wings 14 p1911 N90-20956
The effect of viscosity on the resistive tearing mode with the presence of shear flow
[DE90-009340] 14 p1974 N90-21312
Viscosity, density and conductivity of ImCl(HCl) sub 1.3
[AD-A218902] 16 p2216 N90-22641
Rheology of injection mould filling with DMCs
[NPL-DMA(A)-196] 16 p2222 N90-22675
Error cancellation in HPBL derivation of elastic hole-pressure error
[AD-A219854] 17 p2417 N90-23771
New liquid cathode electrolytes in high rate cells
[AD-A219822] 18 p2546 N90-24531
A modified Ubbelohde viscometer with improved dilution characteristics
[NIAR-90-16] 19 p2693 N90-25326
Wear transition surfaces for long-term wear effects
[DE90-011314] 19 p2698 N90-25351
Coronae and winds around accretion discs 19 p2774 N90-25771
On the viscosity in accretion disks 19 p2774 N90-25775
Nonlinear phenomena in accretion disks: Possibility for observational verification 19 p2775 N90-25779
A tough performance simultaneous semi-interpenetrating polymer network
[NASA-CASE-LAR-14339-1] 21 p2984 N90-26955
Approximate natural damped frequencies of a finite viscous floating-zone under zero-gravity condition
[LRT-WE-9-FB-8(1988)] 21 p2990 N90-26995

Thermophysical properties of Helium-4 from 0.8 to 1500 K with pressures to 2000 MPa
[NASA-CR-186992] 23 p3303 N90-28681
Apparatus to determine the complex mass of a viscous fluid contained in a rigid porous solid from acoustic pressure measurements
[AD-A223709] 24 p3472 N90-29619

VISCOUS DAMPING
NT VISCOELASTIC DAMPING
Analytic signals in the damping coefficient estimation 02 p0178 N90-11003
A survey on nonproportional damping 04 p0483 N90-12773
A 17 degree of freedom anthropomorphic manipulator 23 p3362 N90-29001

VISCOUS DRAG
Hypersonic waverider configurations for trans-atmospheric vehicles
[AD-A217925] 13 p1755 N90-20074
Numerical and physical modelling of bubbly flow phenomena
[DE90-009837] 17 p2401 N90-23677

VISCOUS FLOW
NT BOUNDARY LAYER FLOW
NT BOUNDARY LAYER SEPARATION
NT COUETTE FLOW
NT KARMAN-BODEWADT FLOW
NT REATTACHED FLOW
NT SECONDARY FLOW
NT SEPARATED FLOW
NT STOKES FLOW
Iterative performance and an adaptive procedure for viscous flow problems 01 p0069 N90-10397
Two counter-rotating vortices approaching a free surface in a viscous fluid
[AD-A210495] 01 p0070 N90-10404
Analytical and numerical studies in flow development
[DE89-017380] 02 p0221 N90-11269
Hopf bifurcation in the driven cavity
[NASA-TM-102334] 03 p0345 N90-11969
A least-squares finite element method for incompressible Navier-Stokes problems
[NASA-TM-102385] 03 p0392 N90-12231
Numerical algorithms for steady and unsteady incompressible Navier-Stokes equations
[NASA-CR-186039] 04 p0437 N90-12499
Hypersonic boundary layers. Viscous effects within the shock layer
[CERT-RSF-OA-25/5005-AYD] 04 p0438 N90-12502
Multigrid calculations of 3-D turbulent viscous flows
[NASA-CR-185154] 05 p0571 N90-13323
Hypersonic aerodynamics 05 p0573 N90-13335
Application of a two-dimensional unsteady viscous analysis code to a supersonic throughflow fan stage
[NASA-TM-4141] 05 p0581 N90-13387
Gas flows in rocket motors. Volume 2, appendix C: Time iterative solution of viscous supersonic flow
[AD-A213349] 05 p0615 N90-13592
Pressure correction calculation procedures for 3D viscous flow 05 p0641 N90-13736
On the topology of three-dimensional viscous flow structures near a plane wall. A classification and non-hyperbolic singularities on the wall
[LR-541] 05 p0644 N90-13758
Unsteady aerodynamic simulation of multiple bodies in relative motion: A prototype method
[NASA-TM-102181] 06 p0717 N90-14188
Numerical investigations in three-dimensional internal flows
[NASA-CR-186068] 06 p0718 N90-14189
Program VSAERO theory document: A computer program for calculating nonlinear aerodynamic characteristics of arbitrary configurations
[NASA-CR-4023] 06 p0720 N90-14200
An analysis of the viscous flow through a compact radial turbine by the average passage approach
[NASA-TM-102471] 06 p0720 N90-14206
Development of an integrated BEM approach for hot fluid structure interaction
[NASA-CR-186214] 07 p0927 N90-15364
Irreversible processes from reversible mechanics
[DE90-001057] 07 p0927 N90-15368
Using inorganic membranes to separate gases: R and D status review
[DE90-004386] 08 p1042 N90-16019
A numeric analysis of incompressible, viscous flow around a symmetrical body of revolution
[ISL-CO-215/87] 08 p1064 N90-16157
Numerical boundary layer calculations on the DFVLR ellipsoid of revolution 08 p1070 N90-16193
Convergence speeding up in the calculation of the viscous flow about an airfoil 08 p1070 N90-16194
An experimental investigation of viscous aspects of propeller blade flow 09 p1159 N90-16711
Viscous effects on the instability of an axisymmetric jet
[NASA-TM-102396] 09 p1161 N90-16719
An upwind-biased, point-implicit relaxation algorithm for viscous, compressible perfect-gas flows
[NASA-TP-2953] 09 p1214 N90-17042
Upper semicontinuous global attractors for viscous flow
[NASA-CR-181976] 09 p1217 N90-17056
Special Course on Three-Dimensional Supersonic/Hypersonic Flows Including Separation
[AGARD-R-764] 10 p1308 N90-17565
Computation of compressible viscous flows 10 p1308 N90-17567
Viscous three-dimensional analyses for nozzles for hypersonic propulsion
[NASA-CR-185197] 10 p1321 N90-17635
Some Navier-Stokes calculations for the CAST-10 airfoil 10 p1324 N90-17651
Conditions at the downstream boundary for simulations of viscous incompressible flow
[NASA-TM-102510] 10 p1422 N90-18198
Unsteady viscous calculation method for cascades with leading edge induced separation 11 p1459 N90-18408
Semidiscrete Galerkin modelling of compressible viscous flow past a circular cone at incidence
[NASA-CR-186323] 11 p1505 N90-18664
Improved computational fluid dynamics for continuum hypersonic flow
[AD-A216981] 11 p1506 N90-18674
Computation of hypersonic unsteady viscous flow over a cylinder 12 p1597 N90-19194
Three-dimensional viscous rotor flow calculations using a viscous-inviscid interaction approach
[NASA-TM-102235] 12 p1599 N90-19204
Analysis of unsteady heat transfer by natural convection in a two-dimensional square cavity using a high order finite-volume method 12 p1657 N90-19521
Viscous shock profiles and primitive formulations
[NASA-CR-182029] 13 p1750 N90-20049
Analysis of flow-, thermal-, and structural-interaction of hypersonic structures subjected to severe aerodynamic heating
[AD-A217882] 13 p1750 N90-20053
Comparison of 3-D viscous flow computations of Mach 5 inlet with experimental data
[NASA-TM-102518] 13 p1757 N90-20090
Parallel algorithms in the finite element approximation of flow problems
[AD-A217729] 13 p1802 N90-20341
DURIP optical equipment for high-speed viscous-inviscid interaction research
[AD-A217772] 13 p1802 N90-20345
Numerical modeling of airblast
[AD-A217993] 13 p1803 N90-20347
Relating flow between counter-rotating propellers to aerodynamic interaction noise 14 p1909 N90-20944
Comparison of C- and O-grid generation methods using a NACA 0012 airfoil
[AD-A216375] 14 p1910 N90-20948
Effects of nose bluntness and shock-shock interactions on blunt bodies in viscous hypersonic flows
[NASA-CR-186451] 14 p1910 N90-20950
Computation of viscous flow around a propeller-shaft configuration with infinite-pitch rectangular blades 14 p1912 N90-20958
Centrifugal impeller geometry and its influence on secondary flows 14 p1924 N90-21020
Generation and decay of secondary flows and their impact on aerodynamic performance of modern turbomachinery components 14 p1925 N90-21023
PROTEUS two-dimensional Navier-Stokes computer code, version 1.0. Volume 2: User's guide
[NASA-TM-102552] 14 p1973 N90-21306
Plane Stokes flow driven by capillarity on a free surface: Overview and status
[DE90-009186] 15 p2098 N90-22008
Bifurcations in viscous flow fields. On the genesis and development of topologically complicated separated flow structures
[PB90-167156] 15 p2099 N90-22012
European research on viscous flow (EuroVisc)
[NLR-TP-89077-U] 15 p2099 N90-22014
Extension of a three-dimensional viscous wing flow analysis user's manual: VISTA 3-D code
[NASA-CR-182024] 16 p2197 N90-22538
Extension of a three-dimensional viscous wing flow analysis
[NASA-CR-182023] 17 p2344 N90-23348
Large eddy simulation of a fully turbulent plane channel flow
[VKI-TN-171] 17 p2404 N90-23693
Fluid oscillations in an open, flexible container
[REPT-89-69] 17 p2404 N90-23696
Error cancellation in HPBL derivation of elastic hole-pressure error
[AD-A219854] 17 p2417 N90-23771
An interactive boundary-layer method for unsteady airfoil flows. Part 1: Quasi-steady-state model
[AD-A221220] 18 p2493 N90-24250
NSFLEX: An implicit relaxation method for the Navier-Stokes equations for a wide range of Mach numbers
[MBB-FE-122/S/PUB-366] 19 p2651 N90-25086
Integral-equation methods in steady and unsteady subsonic, transonic and supersonic aerodynamics for interdisciplinary design
[NASA-TM-102677] 19 p2655 N90-25110
Viscous fingering in porous media: A discussion of the small length scale cut-off 19 p2691 N90-25311
Three-dimensional viscous flow structures from bifurcation of a degenerate singularity with three zero eigenvalues
[LR-572] 19 p2692 N90-25314
Computation of viscous aerodynamic characteristics of 2-D airfoils for helicopter applications
[NLR-MP-88052-U] 20 p2804 N90-25951
Numerical analysis of three-dimensional particle-laden flow equations
[IAR-90-2] 20 p2860 N90-26268
Do inviscid vortex sheets roll-up
[PD-CF-9010] 23 p3267 N90-28491
A potential-vorticity decomposition for the boundary integral equation analysis of viscous flows 24 p3417 N90-29301
Supersonic/hypersonic aerodynamics and heat transfer for projectile design using viscous-inviscid interaction
[AD-A224354] 24 p3418 N90-29303
Investigation of ATP blades, part 2. Validation of two-dimensional viscous flow simulation codes around thin airfoils
[NAL-TR-1046] 24 p3421 N90-29326
Numerical simulation of hypersonic viscous flow for the design of H-2 orbiting plane (HOPE)
[NAL-TR-1028] 24 p3422 N90-29330

VISCOUS FLUIDS
Two counter-rotating vortices approaching a free surface in a viscous fluid
[AD-A210495] 01 p0070 N90-10404
Analytic theory for the selection of Saffman-Taylor fingers in the presence of thin film effects
[NASA-CR-181910] 01 p0118 N90-10677
Nonlinear acoustics: Reflection and refraction, propagation in a periodic waveguide, scattering of sound by sound and ellipsoidal focusing
[AD-A211224] 02 p0271 N90-11550
Decay estimates for the compressible Navier-Stokes equations in the half-space
[PREPRINT-46] 08 p1065 N90-16163
Vibrational behavior of a viscous column with a free liquid surface
[LRT-WE-9-FB-1(1989)] 08 p1066 N90-16166
Spectral multi-domain approximation of the Navier-Stokes equations in curved complex geometries
[ONERA-NT-1987-2] 11 p1508 N90-18685
Mixing of viscous fluids: Behavior of microstructures and chaos
[DE90-008871] 14 p1973 N90-21304
The minimum drag profile in laminar flow: A numerical way 16 p2196 N90-22535
Rheology and microstructure of concentrated suspensions
[DE90-009976] 18 p2520 N90-24391
Approximate natural damped frequencies of a finite viscous floating-zone under zero-gravity condition
[LRT-WE-9-FB-8(1988)] 21 p2990 N90-26995
Response of a viscous liquid column to pitching- and roll-excitation in zero-gravity environment
[LRT-WE-9-FB-10(1989)] 21 p2991 N90-27000
Response of differently axially excited viscous liquid bridges in zero-gravity
[LRT-WE-9-FB-14(1989)] 21 p2991 N90-27001
Response of a viscous liquid column to various pitch-excitations
[LRT-WE-9-FB-15(1989)] 21 p3006 N90-27090
Viscous causal cosmologies
[DE90-627487] 23 p3412 N90-29282
Apparatus to determine the complex mass of a viscous fluid contained in a rigid porous solid from acoustic pressure measurements
[AD-A223709] 24 p3472 N90-29619

VISIBILITY
NT LOW VISIBILITY
Atmospheric transmissivity update - 1988
[AD-A209130] 01 p0085 N90-10484
US Navy regional climatic study of the United States Atlantic Coast and associated waters
[AD-A210198] 01 p0088 N90-10503

Diagnostic study of atmosphere-terrain interaction leading to the formation of dust clouds and poor visibilities over near east desert areas
[AD-A211243] 02 p0239 N90-11358
Atmospheric horizontal-inhomogeneity effects on the optical depths determined by the double-elevation-angle lidar technique
[AD-A212836] 04 p0493 N90-12839
Design and tests of simple, inexpensive optical beacon for use on small satellites
[AD-A213325] 04 p0555 N90-13238
Measurements of horizontal visibility in the lowest 300 m over Northern Germany 07 p0872 N90-15059
Imaging probabilities, geometry and ergonomics in limited visibility helicopter operations
07 p0872 N90-15060
The assessment of visibility from automatic contrast Measurements 07 p0872 N90-15061
Rule-based systems for visibility forecasts
[AD-A214622] 09 p1248 N90-17239
Automated visibility and cloud cover measurements with a solid-state imaging system
[AD-A216906] 12 p1693 N90-19724
Visibility problems in numerical models of terrain
[INPE-4921-TDL/382] 12 p1726 N90-19919
Modified touchdown zone lighting
[DOT/FAA/CT-TN89/70] 14 p1929 N90-21042
Apparatus and method for locating the axis of symmetry (center of circular cross section) of three dimensional objects
[AD-D014407] 14 p1982 N90-21354
Analysis of distributions of Visual Meteorological Conditions (VMC) heliport data
[DOT/FAA/CT-TN89/67] 14 p2008 N90-21508
A3I visibility modeling project
15 p2140 N90-22230
The visibility diagram: A data structure for visibility and motion planning problems. Part 1: Application to the visibility polygon query problem
[CS-8913-PT-1] 16 p2299 N90-23098
Taxiway sign effectiveness under reduced visibility conditions
[DOT/FAA/CT-TN90/20] 19 p2662 N90-25150
The effects of urban air pollution on solar radiation
[DE89-009455] 19 p2712 N90-25438
Tactical EHF satellite communications for NATO employing non-geostationary orbits
21 p3070 N90-27454
Diffusion in the surface layer of the convective boundary layer
[AD-A224125] 23 p3349 N90-28924

VISIBLE INFRARED SPIN SCAN RADIOMETER
Preliminary report on the demonstration of the VAS CO2 cloud parameters (cover, height, and amount) in support of ASOS
[NOAA-TM-NESDIS-29] 14 p2006 N90-21498

VISIBLE RADIATION
U LIGHT (VISIBLE RADIATION)

VISIBLE SPECTRUM
Computational and visible light experiments for x ray laser holography
[DE90-006774] 11 p1512 N90-18707
Observations of Cygnus X-2 at x ray, UV, optical and radio frequencies
[MPE-PREPRINT-163] 17 p2481 N90-24191
Optical spectroscopy of V1341 Cyg, the optical counterpart of Cyg X-2 17 p2482 N90-24194
Optical motion detector detecting visible and near infrared light
[AD-D014515] 19 p2758 N90-25671
Optical observations of LMXB AC211(M15): Solving the puzzle 19 p2768 N90-25731

VISION
NT BINOCULAR VISION
NT COLOR VISION
NT MONOCULAR VISION
NT NIGHT VISION
NT PERIPHERAL VISION
NT STEREOSCOPIC VISION
Fear-potentiated startle as a model system for analyzing learning and memory
[AD-A212131] 04 p0525 N90-13029
Three stages and two systems of visual processing
[AD-A212670] 04 p0525 N90-13032
Role of retinocortical processing in spatial vision
[AD-A210995] 05 p0672 N90-13918
Effect of contrast on the perception of direction of a moving pattern
[NASA-TM-102234] 07 p0965 N90-15577
Human factors in the naval environment: A review of motion sickness and biodynamic problems
[AD-A214733] 09 p1251 N90-17258
A model for visual attention
[AD-A214505] 09 p1258 N90-17297
Prescribing spectacles for aviators
[AD-A214830] 09 p1260 N90-17310
Parallel distributed networks for image smoothing and segmentation in analog VSLI
[AD-A216780] 12 p1651 N90-19491
Sampling and noise in vision networks
15 p2138 N90-22217
Networks for image acquisition, processing and display 15 p2138 N90-22218
Visions of visualization aids: Design philosophy and experimental results 15 p2138 N90-22220
Human motion perception: Higher-order organization
15 p2140 N90-22226
Filling in the retinal image 15 p2140 N90-22229
Instrumentation and robotic image processing using top-down model control 15 p2142 N90-22239
Pyramid image codes 15 p2143 N90-22243
Field-of-view assessment of low-level flight and an airdrop in the C-130 Weapon System Trainer (WST)
[AD-A218504] 16 p2200 N90-22559
The kinetics of dark adaptation in hypoxic subjects
[AD-A218641] 16 p2260 N90-22885
Laser retinal effects: Electrophysiological determination in visual cortical cells of monkeys and cats
[AD-A218937] 16 p2261 N90-22888
Visual behavior in the F-15 simulator for air-to-air combat
[AD-A218648] 16 p2262 N90-22893
Model for predicting the effects of laser exposures and eye protection on vision
[AD-A219697] 17 p2434 N90-23868
DURIP: Improved eye movement monitoring capabilities for studies in visual cognition
[AD-A220355] 18 p2586 N90-24722
Visualization of three dimensional data
19 p2736 N90-25553
Eye tracking device for the measurement of flight performance in simulators
[AD-A220075] 20 p2898 N90-26484
The integration of complex information from auditory and visual channels under stress
[AD-A222686] 21 p3033 N90-27245
Curvature estimation in orientation selection
[AD-A221481] 21 p3034 N90-27249
Polarization contrast vision
[AD-A221423] 21 p3076 N90-27492
Local spatial frequency analysis for computer vision
[NASA-CR-186990] 22 p3237 N90-28356
Treatment of systematic errors 2: Fusion of ultrasound and visual sensor data
[DE90-014780] 23 p3334 N90-28850

VISORS
Polycarbonate article with chemical resistant coating
[NASA-CASE-MSC-21503-1] 09 p1195 N90-16925

VISUAL ACCOMMODATION
A model of incomplete chromatic adaptation for calculating corresponding colors
[DE90-006905] 11 p1567 N90-19016

VISUAL ACUITY
Visual acuity and stereopsis with night vision goggles
[AD-A211552] 03 p0381 N90-12167
Discriminating rigid from nonrigid motion
[AD-A211794] 03 p0383 N90-12180
A Scheiner-principle pocket optometer for self-evaluation and biofeedback accommodation training
[AD-A213171] 04 p0524 N90-13027
Assessment of visual function in aerospace medicine
[BMVG-FBWM-89-5] 08 p1105 N90-16397
Design principles of the LVT-2 model laser instrument for the measurement of visual characteristics
[AD-A214951] 09 p1228 N90-17124
Attenuating the luminous output of the AN/PVS-5A night vision goggles and its effects on visual acuity
[AD-A214895] 09 p1261 N90-17311
A new method for measuring the transmissivity of aircraft transparencies
[AD-A216953] 12 p1714 N90-19842
Detection acuity in the peripheral retina
[AD-A218183] 13 p1853 N90-20632
Visual sensitivities and discriminations and their role in aviation
[AD-A219319] 16 p2266 N90-22917
Human factors and safety considerations of night vision systems flight using thermal imaging systems
[AD-A223226] 21 p3037 N90-27263
Experimental tests on the minimal visual acuity required for safe air crew and air control personnel performance
23 p3360 N90-28987

VISUAL AIDS
Research in computer vision for autonomous systems
[AD-A212420] 04 p0555 N90-13235
Improved lighting of taxiway/taxiway intersections for Instrument Flight Rules (IFR) operations
[DOT/FAA/CT-TN89/64] 07 p0878 N90-15089
Experimental tests on the minimal visual acuity required for safe air crew and air control personnel performance
23 p3360 N90-28987

VISUAL CONTROL
Synthetic perspective optical flow: Influence on pilot control tasks 16 p2273 N90-22956
Dynamic monocular machine vision and applications of dynamic monocular machine vision
[LRT-WE-13-FB-88-3] 21 p3061 N90-27406

VISUAL DISCRIMINATION
Night sky radiometric measurements during follow-on-evaluation testing of AN/PVS-7 (A, B) at Fort Benning, Georgia
[AD-A211273] 02 p0276 N90-11574
Three dimensional object recognition employing combined visual and tactile sensing
[PB89-219489] 03 p0382 N90-12176
Discriminating rigid from nonrigid motion
[AD-A211794] 03 p0383 N90-12180
Networks for image acquisition, processing and display 15 p2138 N90-22218
Two-dimensional shape recognition using sparse distributed memory 15 p2140 N90-22227
Stanford/NASA-Ames Center of Excellence in model-based human performance
15 p2143 N90-22241
Visual sensitivities and discriminations and their role in aviation
[AD-A219319] 16 p2266 N90-22917
Seeing by exploring 16 p2268 N90-22923
Telepresence for space: The state of the concept
19 p2731 N90-25526
The integrated area measure of visual endogenous ERPs: Relation to cognitive workload and hemisphere
[AD-A223191] 21 p3035 N90-27255

VISUAL DISPLAYS
U DISPLAY DEVICES

VISUAL FIELDS
Spatial tests for aviators
[IZF-1988-15] 04 p0527 N90-13041
The effects of foveal load on peripheral sensitivity in the visual field
[AD-A214872] 09 p1251 N90-17260
Sensitivity of the peripheral vision to simulated aircraft ascent and descent 10 p1413 N90-18145
Filling in the retinal image 15 p2140 N90-22229
Spatial vision within egocentric and exocentric frames of reference 16 p2268 N90-22928
A helmet mounted display to adapt the telerobotic environment to human vision 19 p2737 N90-25555
Cockpit Ocular Recording System (CORS)
[NASA-CR-4281] 21 p3033 N90-27244
Tracking performance and influence of field of view
23 p3360 N90-28988
Effects of short-term weightlessness on roll circularvection 23 p3361 N90-28992

VISUAL FLIGHT
Proximity compatibility and information display: The effects of space and color on the analysis of aircraft stall conditions
[AD-A214488] 09 p1260 N90-17309
Heliport visual approach surface high temperature and high altitude tests
[DOT/FAA/CT-TN89/34] 22 p3112 N90-27675

VISUAL OBSERVATION
Radio and optical observations of nearby active galaxies 06 p0860 N90-15000
A high galactic latitude survey of far ultraviolet excess objects 15 p2183 N90-22473
Fuel-rich catalytic combustion: A fuel processor for high-speed propulsion
[NASA-TM-103177] 17 p2374 N90-23518
Device and method for detecting and displaying crossover pattern in precision winding
[AD-D014539] 19 p2685 N90-25276
Atmospheric environment for space shuttle (STS-28) launch
[NASA-TM-100386] 19 p2715 N90-25452
Intercomparisons of GOES-derived cloud parameters and surface observations over San Nicolas Island
22 p3214 N90-28229

VISUAL PERCEPTION
NT SPACE PERCEPTION
NT VISUAL DISCRIMINATION
Inferences from images
[AD-A210710] 02 p0258 N90-11465
Visual motion perception
[AD-A210994] 03 p0379 N90-12160
Visual acuity and stereopsis with night vision goggles
[AD-A211552] 03 p0381 N90-12167
Eye movements and spatial pattern vision
[AD-A211650] 03 p0381 N90-12169
A Conference on Three-Dimensional Representation held in University of Minnesota on 24-26 May 1989
[AD-A211630] 03 p0406 N90-12324
Electrophysiological studies of visual attention and resource allocation
[AD-A212287] 04 p0525 N90-13030

Pre- and postflight postural control of the D1 Spacelab mission astronauts examined with a tilting room
[IZF-1988-25] 04 p0527 N90-13039
Visual perception processing in a hierarchical control system: Level 1
[PB89-221188] 04 p0536 N90-13101
Computational and psychophysical study of human vision using neural networks
[AD-A213290] 05 p0674 N90-13924
Spatiotemporal characteristics of visual localization, phase 2
[AD-A212934] 05 p0674 N90-13929
Workload induced spatio-temporal distortions and safety of flight
[DE89-016613] 06 p0820 N90-14771
The role of attention in visual processing
[AD-A214158] 07 p0967 N90-15588
Isolating contour information from arbitrary images
08 p1074 N90-16217
Simulator sickness in the UH-60 (Black Hawk) flight simulator
[AD-A214434] 08 p1104 N90-16392
An illustrated guide of optical characteristics of aircraft transparencies
[AD-A214565] 09 p1167 N90-16752
Design principles of the LVT-2 model laser instrument for the measurement of visual characteristics
[AD-A214951] 09 p1228 N90-17124
Measurement of the impulse response of the human visual system using correlation techniques
[AD-A215667] 09 p1254 N90-17274
The perceptual buildup of three-dimensional structure from motion
[AD-A214640] 09 p1259 N90-17300
Development of a performance-based test of gaze capability: A threshold approach
[AD-A214675] 09 p1259 N90-17301
Measures of subjective variables in visual cognition
[AD-A215084] 09 p1259 N90-17303
Stimulus familiarity determines recognition strategy for novel 3-D objects
[AD-A215274] 09 p1260 N90-17305
Visual perception of structure from motion
[AD-A216416] 10 p1412 N90-18141
Visual servoing for autonomous aircraft refueling
[AD-A216042] 11 p1455 N90-18386
Visual processing of object velocity and acceleration
[AD-A216509] 11 p1539 N90-18858
The effects of luminance boundaries on color perception
[AD-A216741] 11 p1539 N90-18860
Recognizing three-dimensional objects without the use of models
[AD-A216766] 11 p1540 N90-18862
Visual target detection and recognition
[DE90-006903] 11 p1567 N90-19015
Visual processing in texture segregation
[AD-A216539] 12 p1696 N90-19737
Multi-dimensional LADAR tracking and adaptive grasping for spaceborne assembly of SDI (Strategic Defense Initiative) platforms
[AD-A218236] 13 p1791 N90-20279
The role of chaos in hemispheric process and attention
[AD-A217674] 13 p1854 N90-20639
The boundaries of hemispheric processing in visual pattern recognition
[AD-A217675] 13 p1854 N90-20640
Lateral asymmetry in pattern recognition: Understanding the effects of familiarity, distinction, and perspective change
[AD-A217739] 13 p1854 N90-20641
Parts of recognition
[AD-A217694] 13 p1868 N90-20714
Filling in the retinal image 15 p2140 N90-22229
Cognitive efficiency considerations for good graphic design
[AD-A218976] 16 p2263 N90-22899
Visual selective attention
[AD-A219204] 16 p2265 N90-22910
A task-analytic approach to the automated design of information graphics
[AD-A219271] 16 p2265 N90-22912
Spatial Displays and Spatial Instruments
[NASA-CP-10032] 16 p2267 N90-22918
Pictorial communication: Pictures and the synthetic universe 16 p2267 N90-22919
Visual slant underestimation 16 p2268 N90-22926
The photo-colorimetric space as a medium for the representation of spatial data 16 p2268 N90-22927
Distortions in memory for visual displays
16 p2268 N90-22929
The effects of viewpoint on the virtual space of pictures 16 p2269 N90-22932
Perceived orientation, spatial layout and the geometry of pictures 16 p2269 N90-22933
On the efficacy of cinema, or what the visual system did not evolve to do 16 p2269 N90-22934
The perception of geometrical structure from congruence 16 p2270 N90-22935
Exocentric direction judgements in computer-generated displays and actual scenes 16 p2270 N90-22936
How to reinforce perception of depth in single two-dimensional pictures 16 p2270 N90-22937
The eyes prefer real images 16 p2270 N90-22938
Displays, instruments, and the multi-dimensional world of cartography 16 p2271 N90-22942
Adapting to variable prismatic displacement
16 p2271 N90-22945
Direction of movement effects under transformed visual/motor mappings 16 p2272 N90-22947
Displays for telemanipulation
16 p2272 N90-22948
Perception-action relationships reconsidered in light of spatial display instruments 16 p2272 N90-22949
A commentary on perception-action relationships in spatial display instruments 16 p2272 N90-22950
Spatial displays as a means to increase pilot situational awareness 16 p2272 N90-22951
Interactive orbital proximity operations planning system 16 p2273 N90-22953
Experiences in teleoperation of land vehicles
16 p2273 N90-22954
Development of a stereo 3-D pictorial primary flight display 16 p2273 N90-22955
Interactions of form and orientation
16 p2274 N90-22958
Optical, gravitational, and kinesthetic determinants of judged eye level 16 p2274 N90-22959
Voluntary presetting of the vestibular ocular reflex permits gaze stabilization despite perturbation of fast head movements 16 p2274 N90-22960
Synesthetic art through 3-D projection: The requirements of a computer-based supermedium
16 p2274 N90-22962
Wide-angle display developments by computer graphics 16 p2275 N90-22963
Volumetric visualization of 3D data
16 p2275 N90-22964
Disparity gradients and depth scaling
[AD-A218612] 17 p2453 N90-23992
Motion sickness, visual displays, and armored vehicle design
[AD-A222678] 20 p2902 N90-26506
Perspective transformation for wide-view sky scenes
[AD-A222694] 21 p3007 N90-27093
Non-linear analysis of visual cortical neurons
[AD-A221543] 21 p3034 N90-27250
The effects of luminance boundaries on color perception
[AD-A221544] 21 p3034 N90-27251
Parallel algorithms for computer vision
[AD-A221871] 21 p3059 N90-27394
The measurement of dark adaptation level in the presence of glare
[PB90-155987] 22 p3231 N90-28323
Categorization and identification of simultaneous targets
[IZF-1989-22] 22 p3234 N90-28337
Time, space and form in vision
[AD-A213889] 23 p3357 N90-28971
The three-dimensional structure of visual attention and its implications for display design
23 p3359 N90-28980
A real time evaluation of the use of a perspective format to promote situational awareness in users of air to air tactical displays 23 p3359 N90-28981
Target acquisition under load factors: Advantages and disadvantages of a helmet mounted sight
23 p3359 N90-28983
The effects of acoustic orientation cues on instrument flight performance in a flight simulator
23 p3359 N90-28985
Maintaining spatial orientation awareness
23 p3361 N90-28993
Attention, imagery, and memory: A neuromagnetic investigation
[AD-A224560] 24 p3499 N90-29775
Head-mounted spatial instruments II: Synthetic reality or impossible dream 24 p3508 N90-29828
Recognition by linear combination of models
[AD-A224268] 24 p3525 N90-29929

VISUAL SIGNALS
An architectural model of visual motion understanding
[AD-A214327] 07 p0967 N90-15589
Determination of depth-viewing volumes for stereo three-dimensional graphic displays
[NASA-TP-2999] 16 p2275 N90-22965
Differential psychological analysis of a computer-based audio-visual test of vigilance
[ESA-TT-1136] 19 p2724 N90-25494

VISUAL STIMULI
Visual motion perception
[AD-A210994] 03 p0379 N90-12160
Electrophysiological studies of visual attention and resource allocation
[AD-A212287] 04 p0525 N90-13030
Three stages and two systems of visual processing
[AD-A212670] 04 p0525 N90-13032
Effects of type of responding on memory/visual search: Responding just yes or just no can lead to inflexible performance
[AD-A212764] 04 p0526 N90-13033
Detection acuity in the peripheral retina
[AD-A218183] 13 p1853 N90-20632
Paradoxical monocular stereopsis and perspective vergence 16 p2267 N90-22922
Visual slant underestimation 16 p2268 N90-22926
Distortions in memory for visual displays
16 p2268 N90-22929
Perception-action relationships reconsidered in light of spatial display instruments 16 p2272 N90-22949
A commentary on perception-action relationships in spatial display instruments 16 p2272 N90-22950
Sensory conflict in motion sickness: An observer theory approach 16 p2273 N90-22957
The making of the mechanical universe
16 p2274 N90-22961
Shape discrimination research using an IBM PC
[AD-A219993] 17 p2447 N90-23953
Categorization and identification of simultaneous targets
[IZF-1989-22] 22 p3234 N90-28337
Terrain visual cue analysis for simulating low-level flight: A multidimensional scaling approach
[AD-A223564] 24 p3436 N90-29407

VISUAL TASKS
Filling or outlining shapes with color: The effects on a visual search task
[AD-A211067] 02 p0255 N90-11444
Spatial tests for aviators
[IZF-1988-15] 04 p0527 N90-13041
Stereoscopic distance perception
16 p2267 N90-22921
Visual slant underestimation 16 p2268 N90-22926
Visual enhancements in pick-and-place tasks: Human operators controlling a simulated cylindrical manipulator
16 p2271 N90-22946
Synthetic perspective optical flow: Influence on pilot control tasks 16 p2273 N90-22956
The making of the mechanical universe
16 p2274 N90-22961

VISUAL TRACKING
U OPTICAL TRACKING

VISUALIZATION OF FLOW
U FLOW VISUALIZATION

VITAMINS
NT NICOTINIC ACID
Motor and cognitive performance do not change during a ten-week submarine patrol
[AD-A218839] 16 p2276 N90-22969

VITERBI DECODERS
Advanced modulation technology development for earth station demodulator applications. Coded modulation system development
[NASA-CR-185149] 13 p1789 N90-20270
On decoding of multi-level MPSK modulation codes
[NASA-CR-186601] 15 p2146 N90-22261

VITON RUBBER (TRADEMARK)
Studies of Aflas fluoroelastomers
[AD-A213046] 05 p0621 N90-13622

VITREOUS MATERIALS
Nucleation kinetics in undercooled, glass-forming metallic melts
[DLR-FB-89-32] 05 p0624 N90-13644

VLASOV EQUATIONS
The free energy of Maxwell-Vlasov equilibria
[DE90-003318] 07 p0988 N90-15705
Vlasov-Maxwell equilibria of solar coronal loops
[DE90-015025] 23 p3414 N90-29289
Propagation of chaos and the McKean-Vlasov equation in duals of nuclear spaces
[AD-A224431] 24 p3543 N90-30039

VLBI
U VERY LONG BASE INTERFEROMETRY

VLSI
U VERY LARGE SCALE INTEGRATION

VOCODERS
Assessment of voice coders for ATC/pilot voice communications via satellite digital communication channels
[CAA-PAPER-89004] 04 p0489 N90-12807
Voice preprocessor for digital voice applications
[AD-A214726] 09 p1205 N90-16982

VOICE
Voice measures of workload in the advanced flight deck: Additional studies
[NASA-CR-4258] 17 p2437 N90-23887
VOICE COMMUNICATION
NT TELEPHONY
Phase 2 testing and evaluation of low data rate voice CODEC equipment
[ACD-330-PHASE-2] 01 p0055 N90-10315
Computer programs for measuring variations in speech
[AD-A211126] 02 p0259 N90-11467
Spoken commands control robot that handles radioactive materials
[DE89-012632] 02 p0262 N90-11488
The effects of hearing protectors on speech communication and the perception of warning signals
[AD-A212521] 04 p0492 N90-12832
Removal of noise from noise-degraded speech signals
[AD-A212876] 04 p0493 N90-12840
The effects of noise on speech and warning signals
[AD-A212520] 04 p0551 N90-13210
Evaluation of speech intelligibility through a bone conduction stimulator
[AD-A212002] 05 p0673 N90-13919
Test procedures for the evaluation of helmet and headset mounted active noise reduction systems
[AD-A212991] 05 p0676 N90-13937
Improved reliability prediction for HF digital voice transmission 06 p0761 N90-14429
Baseband development system implementation
[AD-A213464] 07 p0918 N90-15309
Voice Multiplex System (VMS)
[AD-A213902] 07 p0919 N90-15315
Voice/data integration in mobile radio networks: Overview and future research directions
[AD-A214289] 07 p0919 N90-15319
Dual task performance with LPC (Linear Predictive Coding) degraded speech in a sentence verification task
[AD-A214298] 07 p0920 N90-15320
Voice preprocessor for digital voice applications
[AD-A214726] 09 p1205 N90-16982
Technology assessment of video teleconferencing
[AD-A217318] 13 p1789 N90-20266
Comparison of oculometer and head-fixed reticle with voice or switch and touch panel for data entry on a generic tactical air combat display
[AD-A217231] 13 p1855 N90-20646
Rules and maps in connectionist symbol processing
[AD-A219028] 16 p2264 N90-22903
ISDN in the local environment: The CISLAN project
[MEMO-INF-89-70] 17 p2452 N90-23985
Automatic speech recognition in air-ground data link
18 p2640 N90-25037
A narrowband tactical communication system for the VHF and UHF mobile radio bands
20 p2847 N90-26192
Equipment feasibility study: Very high frequency communication equipment (136-137 megahertz)
[DOT/FAA/CT-TN89/72] 20 p2850 N90-26210
Overview of requirements and networks for voice communications and speech processing
21 p2992 N90-27007
Speech coding 21 p2992 N90-27009
RADC/EEV diagnostic rhyme test system improvements
[AD-A223187] 21 p2995 N90-27025
Comparison of speech intelligibility in cockpit noise using SPH-4 flight helmet with and without active noise reduction
[NASA-CR-177564] 23 p3271 N90-28510
An experimental study of voice communication over a bandlimited channel using variable bit width delta modulation
[AD-A223445] 24 p3461 N90-29548
VOICE CONTROL
Scientific and technical report voice activated gun turrent control
[AD-A210350] 01 p0110 N90-10623
VOICE DATA PROCESSING
NT CEPSTRAL ANALYSIS
Phase 2 testing and evaluation of low data rate voice CODEC equipment
[ACD-330-PHASE-2] 01 p0055 N90-10315
Computer programs for measuring variations in speech
[AD-A211126] 02 p0259 N90-11467
Feasibility of graphics voice telephones for the post 2000 era
[FEL-1988-26] 03 p0340 N90-11937
Simulation of circuits adapted to signal processing
[TELECOM-PARIS-89-E001] 04 p0489 N90-12811
Voice preprocessor for digital voice applications
[AD-A214726] 09 p1205 N90-16982
Research and development in natural language understanding as part of the Strategic Computing Program
[AD-A214586] 09 p1264 N90-17330
Speech synthesis: From segmental synthesis to acoustic rules, using temporal decomposition
[TELECOM-88-E-019] 10 p1375 N90-17972
Unsteady two level models
[TELECOM-89-E-006] 10 p1375 N90-17973
Speech Analysis and Synthesis and Man-Machine Speech Communications for Air Operations
[AGARD-LS-170] 21 p2992 N90-27006
Overview of requirements and networks for voice communications and speech processing
21 p2992 N90-27007
Speech coding 21 p2992 N90-27009
Current methods of digital speech processing
21 p2993 N90-27010
Book of abstracts of the 1st Benelux-Japan Workshop on Information and Communication Theory
[PB90-191446] 24 p3556 N90-30124
VOIDS
Wet spinning of solid polyamic acid fibers
[NASA-CASE-LAR-14162-1] 07 p0910 N90-15259
Statistical model for particle-void deformation kinetics in granular materials during shock wave propagation
[DE89-017729] 07 p0946 N90-15476
Arcjet cathode phenomena 11 p1473 N90-18477
Investigation of methods to produce a uniform cloud of fuel particles in a flame tube
[NASA-TM-102376] 11 p1505 N90-18665
Modeling convective Marangoni flows with void movement in the presence of solid-liquid phase change
[DE90-006474] 11 p1509 N90-18690
Fiber optic void fraction sensor
[DE90-009124] 14 p1983 N90-21366
A casting and imaging technique for determining void geometry and relative permeability behavior of a single fracture specimen
[DE90-009192] 14 p1989 N90-21403
On modeling the effect of pore shapes on ductile fracture
[AD-A221774] 21 p3014 N90-27136
Shock dynamics in the sub-nanometer femtosecond domain
[DE90-014390] 23 p3304 N90-28689
The effect of helium on microstructural evolution in austenitic steels as determined by spectral tailoring experiments
[DE90-016360] 24 p3452 N90-29496
VOLATILITY
Volatile divalent double metal alkoxides
[AD-D014355] 10 p1438 N90-18300
Variations in volatiles in magma bodies based on studies of melt inclusions
[DE90-006272] 11 p1532 N90-18821
Improved Thermo-Oxidative-Deposition screening tests for turbine lubricants
[AD-A217795] 14 p1954 N90-21188
CRC low- and intermediate-temperature driveability program using gasoline-alcohol blends
[AD-A221321] 18 p2533 N90-24453
Formation of high Tc superconducting films by organometallic chemical vapor deposition
[AD-D014498] 19 p2760 N90-25682
Catalytic synthesis of polymethylsilsesquioxanes
[AD-A222643] 22 p3159 N90-27910
VOLATILIZATION
U VAPORIZING
VOLCANICS
U VOLCANOLOGY
VOLCANOES
NT MARS VOLCANOES
Paper 1. Impact of volcanic aerosols on stratospheric chemistry. Paper 2. O2 (1 sigma g +) and O2 (1 delta g) in the H + O2 reaction system. Paper 3. Barotropic instability of zonal jets on Mars, Earth and Venus
01 p0084 N90-10477
Venus volcanism: Rate estimates from laboratory studies of sulfur gas-solid reactions 03 p0422 N90-12428
Potential for observing and discriminating impact craters and comparable volcanic landforms on Magellan radar images 03 p0423 N90-12429
Evidence for volcanism in NW Ishtar Terra, Venus
03 p0424 N90-12433
Analysis of radar images of the active volcanic zone at Krafla, Iceland: The effects of look azimuth biasing
03 p0424 N90-12434
Lakshmi Planum: A distinctive highland volcanic province 03 p0426 N90-12444
Volcanism on Venus: Large shields and major accumulations of small domes 03 p0426 N90-12445
Coronae on Venus observations and models of origin
03 p0427 N90-12449
On the statistics of El Nino occurrences and the relationship of El Nino to volcanic and solar/geomagnetic activity
[NASA-TP-2948] 03 p0429 N90-12456
Mid-term report on-the study and development results of the Sunshine Project in fiscal 1987. Study on the evaluation technology of geothermal sources in Japan
[DE90-710708] 10 p1400 N90-18095
Evolution of midplate hotspot swells: Numerical solutions
[NASA-CR-186462] 12 p1691 N90-19713
Sulphur silicate interactions on the Jovian satellite Io
15 p2192 N90-22515
Proceedings of a workshop on Lunar Volcanic Glasses: Scientific and Resource Potential
[NASA-CR-186631] 20 p2888 N90-26437
VOLCANOLOGY
Evolution of overlapping spreading centers: A Sea Mark 2 investigation
[AD-A214278] 07 p0965 N90-15576
Segmentation of topographic profiles of the seafloor based on a self-affine model
[AD-A215938] 10 p1410 N90-18132
Proceedings of a workshop on Lunar Volcanic Glasses: Scientific and Resource Potential
[NASA-CR-186631] 20 p2888 N90-26437
MEVTV Workshop on Early Tectonic and Volcanic Evolution of Mars
[NASA-CR-186098] 21 p3021 N90-27176
VOLT-AMPERE CHARACTERISTICS
Cyclic voltammetry at a rotating disk, electroreduction of nitrate in acidic nickel solutions, and frequency-response analysis of porous electrodes
[DE90-015317] 24 p3447 N90-29466
VOLTAGE
U ELECTRIC POTENTIAL
VOLTAGE AMPLIFIERS
Null offset voltage compensator for operational amplifier
[AD-D014189] 04 p0496 N90-12859
Analysis of the behaviour of a current-fed multi-stage voltage multiplier with capacitive output
10 p1338 N90-17745
VOLTAGE BREAKDOWN
U ELECTRICAL FAULTS
VOLTAGE CONTROLLED OSCILLATORS
High resolution, wide band Chirp-Z signal analyzer
[AD-D014240] 06 p0768 N90-14465
VOLTAGE CONVERTERS (AC TO AC)
NIST (National Institute of Standards and Technology) measurement services: The ac-dc difference calibrations
[PB89-222616] 04 p0494 N90-12845
State variable modelling for the audiosusceptibility evaluations of current controlled zero ripple structures
10 p1337 N90-17735
Modelling the buck-type converter transient response with pulsating load 10 p1337 N90-17740
VOLTAGE CONVERTERS (DC TO DC)
NIST (National Institute of Standards and Technology) measurement services: The ac-dc difference calibrations
[PB89-222616] 04 p0494 N90-12845
High power density dc/dc converter: Selection of converter topology
[NASA-CR-186129] 06 p0768 N90-14467
European Space Power, volume 1
[ESA-SP-294-VOL-1] 10 p1329 N90-17678
PWM converter topologies 10 p1335 N90-17721
A new vision to model the parallel resonant converter
10 p1336 N90-17727
Design of a power supply system based in two quasi-resonant converters 10 p1336 N90-17728
State variable modelling for the audiosusceptibility evaluations of current controlled zero ripple structures
10 p1337 N90-17735
Comparison of control structures for a bidirectional high-frequency dc-dc converter
10 p1337 N90-17737
Analysis of the CUK converter in delta V mode by charge and flux balances 10 p1337 N90-17738
Modelling the buck-type converter transient response with pulsating load 10 p1337 N90-17740
Lyapunov-based control for switched power converters
[AD-A221974] 21 p3000 N90-27053
VOLTAGE MEASUREMENT
U ELECTRICAL MEASUREMENT
VOLTAGE REGULATORS
Electrical performance characteristics of high power converters for space power applications
[NASA-CR-185947] 06 p0734 N90-14279
Steep front impulse tests on a solid-state relay
[DE90-004243] 08 p1062 N90-16140
Current protections modelisation in a buck cell
10 p1335 N90-17723

Characterization and development report for the SA3274-1 and SA3274-2 transient voltage suppressors
[DE90-005712] 11 p1502 N90-18649
Performance of battery charge controllers
[DE90-011413] 19 p2686 N90-25279

VOLTAGE VARIATION INDICATORS
U VOLTMETERS

VOLTERRA EQUATIONS
Rational expansion for nonlinear input-output maps
[RR-348] 03 p0394 N90-12248
Compression phenomena in hard-saturated microwave amplifiers
[AD-A214546] 09 p1204 N90-16980
Optimization of the intermodulation performance of GaAs MESFET small-signal amplifiers
[AD-A215193] 09 p1212 N90-17026
Modeling the gate I/V characteristic of a GaAs MESFET for Volterra-series analysis
[AD-A215314] 09 p1212 N90-17030
Nonparametric estimation of trends in linear stochastic systems
[AD-A213741] 09 p1272 N90-17374

VOLTMETERS
Personal computer process data acquisition
[DE89-017877] 06 p0828 N90-14816
Solid state voltammetry and sensors in solids and gases
[DE90-003234] 08 p1129 N90-16538

VOLUME
Workshop on Recent Progress in Surface and Volume Scattering
[AD-A212455] 04 p0555 N90-13236
An algorithm for control volume analysis of cryogenic systems
[AD-A213394] 05 p0631 N90-13683
A study of physical properties of ODPA-p-PDA polyimide films
[NASA-TM-102625] 13 p1766 N90-20137

VOLUMETRIC ANALYSIS
Volumetric analysis by spontaneous Raman diffusion in a supersonic wind tunnel
[ISL-R-109/88] 04 p0448 N90-12564
Low-cost volumetric modeling
[CRIF-MC-85] 08 p1111 N90-16435
A feasibility study for using CARS in temperature and volumetric measurement as a function of time
[ISL-CO-223/88] 09 p1226 N90-17116

VOLUMETRIC EFFICIENCY
Study of discharge mechanisms and the stability of transverse electric discharges in the gas mixtures
[ISL-R-114/88] 11 p1516 N90-18733

VON MISES THEORY
U STRESS FUNCTIONS

VORTEX ALLEVIATION
Effective methods of controlling a junction vortex system in an incompressible, three-dimensional, turbulent flow
15 p2047 N90-21732

VORTEX BREAKDOWN
Numerical simulation of leading-edge vortex rollup and bursting 02 p0145 N90-10831
A smoke generator system for aerodynamic flight research
[NASA-TM-4137] 05 p0578 N90-13372
Numerical simulation of a bubble shaped bursting vortex 08 p1069 N90-16187
Velocity profile and wall shear stress measurements for a Large Eddy Break-Up (LEBU) device
[AD-A214958] 09 p1217 N90-17059
Vortex cores and vortex breakdown
[AD-A215266] 09 p1218 N90-17062
Goertler vortices in growing boundary layers: The leading edge receptivity problem, linear growth and the nonlinear breakdown stage
[NASA-CR-181962] 10 p1306 N90-17555
Surface pressure distributions on a delta wing undergoing large amplitude pitching oscillations
[NASA-CR-186326] 10 p1306 N90-17558
Numerical simulation of the vortex breakdown
[ONERA-RSF-4/4368-AY-004A] 11 p1509 N90-18689
Leading edge vortex dynamics on a pitching delta wing
[NASA-CR-186327] 12 p1598 N90-19198
Numerical simulation of vortex breakdown
14 p1970 N90-21288
Three-dimensional simulation of vortex breakdown
[NASA-TM-102664] 15 p2049 N90-21744
Modern developments in shear flow control with swirl
[NASA-CR-186586] 15 p2097 N90-22000
The interaction of a supersonic streamwise vortex and a normal shock wave 16 p2491 N90-24241
Investigation of the vortex flow over a sharp-edged delta wing in the transonic speed regime
[LR-594] 19 p2656 N90-25115
Control of submersible vortex flows
[NASA-TM-102693] 23 p3267 N90-28493
Experimental investigations on the stability and vorticity of the vortex breakdown phenomenon above delta wings, measured by the ultrasonic laser method
[ESA-TT-1079] 23 p3268 N90-28498
In-flight flow visualization with pressure measurements at low speeds on the NASA F-18 high alpha research vehicle
[NASA-TM-101726] 23 p3270 N90-28505

VORTEX COLUMNS
U VORTICES

VORTEX DISTURBANCES
U VORTICES

VORTEX FILAMENTS
A composite numerical procedure for calculating the motion of vortex filaments 06 p0721 N90-14207
Topics in vortex methods for the computation of three- and two-dimensional incompressible unsteady flows
15 p2091 N90-21967

VORTEX FLOW
U VORTICES

VORTEX GENERATION
U VORTEX GENERATORS

VORTEX GENERATORS
Improvements in the formulations and numerical solution of the Euler problem for swept wings
[RAE-TM-AERO-2139] 04 p0447 N90-12562
Laboratory studies of isolated eddies in a rotating fluid
[AD-A213903] 08 p1063 N90-16146
An experimental study of the effect of streamwise vortices on unsteady turbulent boundary-layer separation
09 p1215 N90-17045
Turbulence structure resulting from interaction between an embedded vortex and wall jet
[AD-A215702] 10 p1383 N90-18004
Study of vortex arrays induced artificially and from centrifugal instabilities
[AD-A216499] 11 p1506 N90-18669
Ground evaluation of seeding an in-flight wingtip vortex using infrared imaging flow visualization technique
18 p2639 N90-25035
Effect of vortex generators on the aerodynamic wing characteristics and body of revolution
[AD-A222813] 20 p2804 N90-25955
Jet vortex generators for turbulent flow separation control
[NASA-CR-186959] 22 p3109 N90-27659
Further studies of turbulence structure resulting from interactions between embedded vortices and wall jets at high blowing ratios
[AD-A223296] 24 p3468 N90-29593

VORTEX INJECTORS
United States Air Force research initiation program for 1988, volume 1
[AD-A223123] 21 p3101 N90-27613
Swirl coaxial injector element characterization for booster engines 23 p3294 N90-28632

VORTEX RINGS
A composite numerical procedure for calculating the motion of vortex filaments 06 p0721 N90-14207
Analysis of severe atmospheric disturbances from airline flight records 07 p0869 N90-15045
Dynamics of a class of vortex rings
07 p0926 N90-15382
Dynamics of a class of vortex rings
[NASA-TM-102257] 12 p1657 N90-19524
Rings
[DE90-009035] 14 p2025 N90-21613
Topics in vortex methods for the computation of three- and two-dimensional incompressible unsteady flows
15 p2091 N90-21967
Experimental study of vortex ring interaction with a free surface 16 p2233 N90-22742

VORTEX SHEDDING
The near-wake flow structure of wake-cylinder interaction and surface loading of cylinder
02 p0218 N90-11248
Flow visualization of the effect of pitch rate on the vortex development on the scale model of a F-18 fighter aircraft
[AD-A214244] 07 p0876 N90-15080
A coning motion apparatus for hydrodynamic model testing in a non-planar cross-flow
[AD-A213431] 07 p0930 N90-15383
Low flow vortex shedding flowmeter
08 p1156 N90-16700
Modeling the wake as a continuous vortex sheet in a potential-flow solution using vortex panels
[AD-A216220] 10 p1385 N90-18016
A study on upstream moving pressure waves induced by vortex separation
[ISL-CO-203/88] 12 p1597 N90-19192
Secondary flows and Reynolds stress distributions downstream of a turbine cascade at different expansion ratios 14 p1923 N90-21015
On the direct simulation of vortex shedding
[LR-513] 15 p2048 N90-21743
Secondary frequencies in the wake of a circular cylinder with vortex shedding
[NASA-CR-181998] 16 p2197 N90-22540
Numerical study of the onset of instability in the flow past a sphere 17 p2400 N90-23672
LOX manifold tee analysis
[NASA-CR-183994] 19 p2670 N90-25188
Flow visualization of dynamic stall on an oscillating airfoil
[AD-A222202] 21 p2954 N90-26797
Prediction of subsonic vortex shedding from forebodies with chines
[NASA-CR-4323] 23 p3268 N90-28494
Numerical simulations of flowfields in a central-dump ramjet combustor. 3: Effects of chemistry
[AD-A224145] 23 p3282 N90-28573
Studies of vortex interactions
[AD-A223864] 23 p3328 N90-28817

VORTEX SHEETS
The three-dimensional vortex sheet structure on delta wings 01 p0064 N90-10367
Numerical simulation of leading-edge vortex rollup and bursting 02 p0145 N90-10831
The near-wake flow structure of wake-cylinder interaction and surface loading of cylinder
02 p0218 N90-11248
Free surface scars and striations
[AD-A212429] 04 p0503 N90-12901
An experimental investigation of the interaction between a model rotor and airframe in forward flight
06 p0723 N90-14219
A nonlinear vortex-lattice method for the calculation of interference effects between free vortex sheets and wings 08 p1068 N90-16183
An experimental investigation of viscous aspects of propeller blade flow 09 p1159 N90-16711
Modeling the wake as a continuous vortex sheet in a potential-flow solution using vortex panels
[AD-A216220] 10 p1385 N90-18016
Experiments with unsteady, free surface, three-dimensional vortices in a thermally stable, stratified fluid
[AD-A222088] 21 p2954 N90-26796
Do inviscid vortex sheets roll-up
[PD-CF-9010] 23 p3267 N90-28491
Numerical simulation of the formation of two-dimensional and three-dimensional structures in shear layers and wakes
[ESA-TT-1008] 23 p3325 N90-28802

VORTEX STREETS
NT KARMAN VORTEX STREET

VORTEX TUBES
U VORTICES

VORTEX-BLADE INTERACTION
U BLADE-VORTEX INTERACTION

VORTICES
NT HORSESHOE VORTICES
NT WING TIP VORTICES
On the interaction of stationary crossflow vortices and Tollmien-Schlichting waves in the boundary layer on a rotating disc
[NASA-CR-181859] 01 p0002 N90-10007
Basic studies of the unsteady flow past high angle of attack airfoils
[AD-A210252] 01 p0002 N90-10008
Vortex induced characteristics of missiles in unsteady maneuvers 01 p0012 N90-10057
Acoustic-vortex-chemical interactions in an idealized ramjet 01 p0037 N90-10206
Numerical investigation of the effects of longitudinal vortices on the onset of transition in a flat plate boundary layer 01 p0063 N90-10363
Goertler instability on an airfoil: Comparison of marching solution with experimental observations
01 p0063 N90-10364
Three-dimensional boundary layer transition on a concave surface 01 p0064 N90-10365
Trailing-edge sweep and three-dimensional vortex interactions in jets and mixing layers
01 p0066 N90-10379
A European collaborative investigation of the three-dimensional turbulent shear layers of a swept wing
01 p0066 N90-10380
Convection of a pattern of vorticity through a reacting shock wave
[NASA-CR-181921] 01 p0102 N90-10576
Plasma theory and simulation
[AD-A207952] 01 p0125 N90-10714
Computation of the tip vortex flowfield for advanced aircraft propellers
[NASA-CR-182179] 02 p0146 N90-10836
Method of characteristic studies for rotational flow downstream of a curved shock wave
02 p0219 N90-11252

A computational/experimental study of the flow around a body of revolution at angle of attack
[NASA-TM-88329] 02 p0219 N90-11254
Questions from the Willmarth Workshop on New Directions in Research on Turbulent Wall-Layer Structures
[AD-A211282] 02 p0221 N90-11264
An investigation of counterrotating tip vortex interaction
[NASA-CR-185135] 02 p0271 N90-11549
Near-planar TS waves and longitudinal vortices in channel flow: Nonlinear interaction and focusing
[NASA-CR-181928] 03 p0300 N90-11698
A study of the temporal stability of multiple cell vortices
[NASA-CR-4261] 03 p0345 N90-11968
Hopf bifurcation in the driven cavity
[NASA-TM-102334] 03 p0345 N90-11969
Numerical analysis, scientific computing and fundamental studies of fluid mechanics
[DE89-017554] 03 p0346 N90-11975
An investigation of end-wall vortex cavitation in a high Reynolds number axial-flow pump
[AD-A211426] 03 p0347 N90-11982
Flare-in texture in rotating superfluid (3)He-B
[PB89-218994] 03 p0412 N90-12368
Interaction of Tollmien-Schlichting waves and Goertler vortices 04 p0440 N90-12515
Goertler instability on an airfoil 04 p0440 N90-12517
Experimental studies on Goertler vortices 04 p0442 N90-12529
Development of a VSAERO (Vortex Separation Aerodynamics) model of the F/A-18
[AD-A212442] 04 p0448 N90-12566
Vortex dynamics
[AD-A212119] 04 p0499 N90-12877
Free surface scars and striations
[AD-A212429] 04 p0503 N90-12901
Persistent current, NMR, and ion transmission experiments in rotating He-3 superfluids --- Nuclear Magnetic Resonance (NMR)
[ISBN-952-90056-1-X] 04 p0553 N90-13221
Superfluid phase slippage in (3)He-B flow through a narrow channel
[PB89-218986] 04 p0559 N90-13258
The 3D LDA techniques in vortex studies and boundary layer surveys 05 p0574 N90-13346
A smoke generator system for aerodynamic flight research
[NASA-TM-4137] 05 p0578 N90-13372
Feature modeling: The incorporation of a front and eddy map into optimum interpolation-based thermal analysis
[AD-A213253] 05 p0672 N90-13914
An investigation of the bursting of trailing vortices using numerical simulation 06 p0718 N90-14191
A note concerning the onset of three dimensionality and time dependence in Goertler vortices
[NASA-CR-181956] 06 p0718 N90-14193
A composite numerical procedure for calculating the motion of vortex filaments 06 p0721 N90-14207
An experimental investigation of the interaction between a model rotor and airframe in forward flight 06 p0723 N90-14219
Acoustic-vortical-combustion interaction in a solid fuel ramjet simulator 06 p0726 N90-14234
Comparative study of the vorticity field in turbulent flows: Theory, experiments, and computations
[DE90-001399] 06 p0776 N90-14516
Aircraft response and pilot behaviour during a wake vortex encounter perpendicular to the vortex axis 07 p0871 N90-15057
On strongly nonlinear vortex/wave interactions in boundary-layer transition
[NASA-CR-181963] 07 p0876 N90-15078
Dynamics of a class of vortex rings 07 p0926 N90-15362
Rayleigh-Taylor instability in compressible fluids
[DE90-003027] 07 p0929 N90-15376
An experimental study of the time-dependent behavior of the appendage-body junction vortex
[AD-A213465] 07 p0930 N90-15384
Laboratory studies of isolated eddies in a rotating fluid
[AD-A213903] 08 p1063 N90-16146
Vorticity amplification in nonorthogonal stagnation flow 08 p1064 N90-16152
Wind tunnel investigations on the configuration of the international vortex flow experiment 08 p1068 N90-16181
Flow field visualization study on a 65 deg delta wing at M = 0.85 08 p1068 N90-16182
A nonlinear vortex-lattice method for the calculation of interference effects between free vortex sheets and wings 08 p1068 N90-16183
Research on three different Euler's schemes applied to a delta wing with vortical flows 08 p1068 N90-16184
The determination of vortex separation frequencies by means of laser light sheet images
[DNW-WTI-88.038] 08 p1079 N90-16245
The response of the atmospheric convective boundary layer to surface inhomogeneities 08 p1100 N90-16369
An experimental investigation of viscous aspects of propeller blade flow 09 p1159 N90-16711
Controlled vortical flow on delta wings through unsteady leading edge blowing
[NASA-CR-186267] 09 p1160 N90-16712
Physical models for supersonic turbulent boundary layer structure
[AD-A215284] 09 p1160 N90-16716
An experimental study of the effect of streamwise vortices on unsteady turbulent boundary-layer separation 09 p1215 N90-17045
Vortex cores and vortex breakdown
[AD-A215266] 09 p1218 N90-17062
Effect of vortex circulation on injectant from a single film-cooling hole and a row of film-cooling holes in a turbulent boundary layer. Part 1: Injection beneath the vortex downwash
[AD-A215288] 09 p1218 N90-17063
Theoretical study of instabilities in vortices: Applications to hydrodynamics and magnetohydrodynamics
[ETN-90-96103] 09 p1219 N90-17073
TS - Dean interactions in curved channel flow
[NASA-CR-181983] 10 p1306 N90-17559
Numerical solutions of the linearized Euler equations for unsteady vortical flows around lifting airfoils
[NASA-TM-102466] 10 p1307 N90-17562
Large-eddy interaction model in the turbulent wake of a circular cylinder 10 p1307 N90-17563
Turbulence structure resulting from interaction between an embedded vortex and wall jet
[AD-A215702] 10 p1383 N90-18004
Modeling the wake as a continuous vortex sheet in a potential-flow solution using vortex panels
[AD-A216220] 10 p1385 N90-18016
Numerical simulation of compressible vortices
[AD-A216221] 10 p1385 N90-18017
Nonlinear dynamics of domain walls and vortices in two-dimensional systems
[DE90-004840] 10 p1425 N90-18221
Computational aerodynamics of ordered vortex flows
[ETN-90-96272] 11 p1452 N90-18368
Study of the blade/vortice interaction on a one-blade rotor during forward flight (incompressible, non viscous fluid)
[ISL-R-115/88] 11 p1456 N90-18391
Unsteady Aerodynamic Phenomena in Turbomachines
[AGARD-CP-468] 11 p1459 N90-18405
Gust response analysis for cascades operating in nonuniform mean flows 11 p1461 N90-18415
Zero-gravity vortex vent and PVT gaging system 11 p1475 N90-18486
Numerical simulations of coherent structures in a jet flame with a noncircular cross section
[AD-A216710] 11 p1483 N90-18535
Leading edge vortex dynamics on a pitching delta wing
[NASA-CR-186327] 12 p1598 N90-19198
Water-tunnel investigation of concepts for alleviation of adverse inlet spillage interactions with external stores
[NASA-TM-4181] 12 p1599 N90-19199
A streamwise upwind algorithm applied to vortical flow over a delta wing
[NASA-TM-102225] 12 p1599 N90-19201
Conforming Chebyshev spectral collocation methods for the solution of laminar flow in a constricted channel
[NASA-CR-182011] 12 p1660 N90-19539
Experiments of thermoconvection in a cubic cell
[MPIS-6/1989] 12 p1661 N90-19544
Nucleation of vortices in superfluid helium-4
[DE90-610675] 12 p1720 N90-19880
A video-based experimental investigation of wing rock
[AD-A218244] 13 p1755 N90-20075
Vortex motion phase separator for zero gravity liquid transfer
[NASA-CASE-KSC-11387-1] 13 p1783 N90-20236
Experimental investigation of the mechanisms underlying vortex kinematics in unsteady separated flows
[AD-A217889] 13 p1802 N90-20346
Flow visualization studies in a curved rectangular channel with 40 to 1 aspect ratio and a straight channel with bulk flow unsteadiness
[AD-A218020] 13 p1803 N90-20348
Discrete-vortex model for the symmetric-vortex flow on cones
[NASA-TP-2989] 14 p1909 N90-20946
Measurement of lift development on rapidly-accelerated wings 14 p1911 N90-20956
Experimental and numerical investigation of the vortex flow over a sharp edged delta wing; with and without sideslip
[PB90-167131] 14 p1913 N90-20964
LDV measurements and the flow analysis in the vortex region of a radial inflow turbine 14 p1922 N90-21007
Experimental and numerical study on basic phenomena of secondary flows in turbines 14 p1923 N90-21014
Secondary flows and Reynolds stress distributions downstream of a turbine cascade at different expansion ratios 14 p1923 N90-21015
On the instability of Goertler vortices to nonlinear travelling waves
[NASA-CR-181994] 14 p1970 N90-21289
A time-accurate adaptive grid method and the numerical simulation of a shock-vortex interaction
[NASA-TP-2998] 14 p2011 N90-21524
Instabilities and vortex dynamics in shear flow of magnetized plasmas
[DE90-009448] 14 p2030 N90-21643
Effective methods of controlling a junction vortex system in an incompressible, three-dimensional, turbulent flow 15 p2047 N90-21732
Modeling of vortex-induced oscillations based on indicial response approach
[NASA-CR-186560] 15 p2047 N90-21736
On the direct simulation of vortex shedding
[LR-513] 15 p2048 N90-21743
Analytical study of the origin and behavior of asymmetric vortices
[NASA-TM-102796] 15 p2049 N90-21746
Topics in vortex methods for the computation of three- and two-dimensional incompressible unsteady flows 15 p2091 N90-21967
Instabilities and subharmonic resonances of subsonic heated round jets, volume 2
[NASA-CR-186058] 15 p2100 N90-22017
Semigeostrophic flow over orography in a stratified rotating atmosphere 15 p2127 N90-22163
A new stability criterion in the shallow-water system for two-dimensional coherent eddies in the atmosphere and oceans 15 p2130 N90-22176
Effect of a crystal-melt interface on Taylor-vortex flow
[NASA-CR-186512] 15 p2171 N90-22408
Large-scale advanced propeller blade pressure distributions: Prediction and data
[NASA-TM-102316] 16 p2201 N90-22564
Experimental study of vortex ring interaction with a free surface 16 p2233 N90-22742
A scattering center based numerical simulation of small scale atmospheric turbulence 16 p2312 N90-23179
Three-dimensional structure of plane mixing layers 17 p2344 N90-23347
Numerical simulation of turbulent combustion using vortex methods
[AD-A219624] 17 p2372 N90-23507
Advanced instrumentation for local measurement of gas-solid suspension flows
[DE90-008498] 17 p2400 N90-23671
Unsteady flow phenomena in turbomachines
[AD-A218370] 17 p2402 N90-23680
Center for Analysis of Heterogeneous and Nonlinear Media
[AD-A219627] 17 p2403 N90-23688
Diffraction patterns and vortex rollup
[AD-A219876] 17 p2461 N90-24049
The interaction of a supersonic streamwise vortex and a normal shock wave 18 p2491 N90-24241
Concerning the interaction of non-stationary cross-flow vortices in a three-dimensional boundary layer
[NASA-CR-182037] 18 p2492 N90-24245
Vortex-induced boundary-layer separation 18 p2551 N90-24560
Interaction of the large eddy structure in the inner-half of a turbulent boundary layer 18 p2551 N90-24561
Computational modeling of three-dimensional compressible leading edge vortices
[AD-A221022] 18 p2553 N90-24569
The modeling of drop-containing turbulent eddies
[NASA-CR-186805] 18 p2553 N90-24570
Nonlinear development of Goertler and crossflow vortices and Goertler/Tollmien-Schlichting wave interaction
[AD-A221107] 18 p2553 N90-24571
Ground evaluation of seeding an in-flight wingtip vortex using infrared imaging flow visualization technique 18 p2639 N90-25035
Generation of circumferential velocity contours associated with pulsed point suction on a rotating disk 18 p2646 N90-25065
On the receptivity problem for Goertler vortices: Vortex motions induced by wall roughness
[NASA-CR-182036] 19 p2654 N90-25109

Video photographic considerations for measuring the proximity of a probe aircraft with a smoke seeded trailing vortex
[NASA-TM-102691] 19 p2657 N90-25120
Identification of aerodynamic models for maneuvering aircraft
[NASA-CR-186630] 20 p2802 N90-25943
Euler analysis comparison with LDV data for an advanced counter-rotation propfan at cruise
[NASA-TM-103249] 20 p2803 N90-25946
Experimental study on vortex and shock wave development on a 65 deg delta wing
[NLR-MP-88033-U] 20 p2804 N90-25950
Decay of secondary flow and the associated loss variation downstream of an annular turbine stator cascade
[DE90-505520] 20 p2809 N90-25984
Velocity measurements on a lifting rotor/airframe configuration in low speed forward flight
21 p2953 N90-26790
Experiments with unsteady, free surface, three-dimensional vortices in a thermally stable, stratified fluid
[AD-A222088] 21 p2954 N90-26796
Flow visualization of dynamic stall on an oscillating airfoil
[AD-A222202] 21 p2954 N90-26797
On the linear and nonlinear stability of non-parallel flow 21 p3002 N90-27065
Vortex-induced boundary layer separation
[AD-A221564] 21 p3005 N90-27078
Theoretical and computational aspects of turbulence
[AD-A221795] 21 p3005 N90-27083
A numerical study of the role of meso beta and meso gamma scale vertical exchange processes in the evolution of upper tropospheric frontal systems
[AD-A222057] 21 p3031 N90-27230
Noise from tip vortex and bubble cavitation
[AD-A221962] 21 p3072 N90-27468
Study of the structure of the vortices created by the drag of a natched edge by thermal tracing
[IMFL-89-26] 22 p3109 N90-27660
Experimental study on the vortices generated by the body of a missile during flight. Part 1: Laminar boundary layer
[ONERA-RT-40/1147-AY-130A-PT-1]
22 p3110 N90-27665
Elliptical flux vortices in polycrystalline YBa2Cu3O7
22 p3136 N90-27795
Nonlogarithmic magnetization relaxation at the initial time intervals and magnetic field dependence of the flux creep rate in Bi2Sr2Ca(sub i)Cu2Ox single crystals
22 p3137 N90-27801
Study of the origin of three dimensional structures in shear flows through external forcing
[AD-A221923] 22 p3170 N90-27980
Computation of compressible, vortical flows
22 p3172 N90-27996
Formation of shock waves in a transonic vortex-profile interaction
[MPIS-3/1990] 22 p3174 N90-28010
Experimental study of the Taylor-Goertler instability
[ETN-90-97447] 22 p3175 N90-28014
The instability mechanism of synoptic-scale eddies
22 p3211 N90-28217
Turbulence spectra of the FIRE stratocumulus-topped boundary layers 22 p3217 N90-28246
Modification of the background flow by roll vortices
22 p3219 N90-28258
Control of submersible vortex flows
[NASA-TM-102693] 23 p3267 N90-28493
Prediction of subsonic vortex shedding from forebodies with chines
[NASA-CR-4323] 23 p3268 N90-28494
Aerodynamics of bodies in shear flow
23 p3268 N90-28496
Regular and chaotic motion of uniform elliptical vortices in external linear time dependent velocity fields
23 p3268 N90-28497
Wind tunnel investigation of periodic vortex separation from rough surface circular cylinders by means of acoustic measurements
[ESA-TT-1092] 23 p3268 N90-28499
In-flight flow visualization with pressure measurements at low speeds on the NASA F-18 high alpha research vehicle
[NASA-TM-101726] 23 p3270 N90-28505
Development of non-conventional control methods for high angle of attack flight using vortex manipulation
23 p3273 N90-28522
Control of vortex aerodynamics at high angles of attack 23 p3273 N90-28523
Dynamic ground effects 23 p3275 N90-28531
A flight dynamic model of aircraft spinning
[AR-005-600] 23 p3283 N90-28576
Vortice-propeller interaction
[LIMSI-89-9] 23 p3326 N90-28809
Studies of vortex interactions
[AD-A223864] 23 p3328 N90-28817
Effect of vortex circulation on injectant from a single film-cooling hole and a row of film-cooling holes in a turbulent boundary layer. Part 2: Injection beneath the vortex upwash
[AD-A223894] 23 p3328 N90-28818
Genesis of bow echoes: A rear-inflow induced meso-convective structure
[PB90-209776] 23 p3349 N90-28926
Dynamic separation: Search for the cause of dynamic stall and search for its control
[AD-A223412] 24 p3418 N90-29305
Structure in the near field of the transverse jet
[AD-A224502] 24 p3467 N90-29591
Further studies of turbulence structure resulting from interactions between embedded vortices and wall jets at high blowing ratios
[AD-A223296] 24 p3468 N90-29593
An additive turbulent decomposition of the Navier-Stokes equations implemented on highly parallel computer systems
[AD-A223678] 24 p3468 N90-29595
The experimental investigation of flow in the core of a vortex structure
[BR114893] 24 p3468 N90-29597
Investigation of fluid dynamic performance of LE-7 liquid oxygen pump
[NAL-TR-1020] 24 p3476 N90-29650
The computation and analysis of acoustic waves in transonic airfoil-vortex interactions
24 p3542 N90-30031

VORTICITY
An introduction via vorticity dynamics and statistical theory --- turbulent shear flows
05 p0640 N90-13731
A composite numerical procedure for calculating the motion of vortex filaments 06 p0721 N90-14207
Comparative study of the vorticity field in turbulent flows: Theory, experiments, and computations
[DE90-001399] 06 p0776 N90-14516
Dynamics of a class of vortex rings
07 p0926 N90-15362
Potential vorticity in extratropical cyclones
07 p0962 N90-15564
Assessment of computational prediction of tail buffeting
[NASA-TM-101613] 08 p1018 N90-15886
Vorticity amplification in nonorthogonal stagnation flow
08 p1064 N90-16152
The role of an upstream cyclone and corresponding synoptic/planetary-scale interactions during the development of a blocking anticyclone
08 p1150 N90-16659
Identification and reduction of Wakefield effects in the wiggler region of the Los Alamos free-electron laser
[DE90-004871] 09 p1228 N90-17128
Response of a chemically reacting layer to streamwise vorticity
[NASA-TM-102288] 10 p1383 N90-18005
Analysis of unsteady heat transfer by natural convection in a two-dimensional square cavity using a high order finite-volume method 12 p1657 N90-19521
Dynamics of a class of vortex rings
[NASA-TM-102257] 12 p1657 N90-19524
A sub-cloud layer vorticity budget analysis for two microburst-producing storms from jaws dual-Doppler data
[AD-A218180] 13 p1847 N90-20599
Secondary flow calculations for axial and radial compressors 14 p1925 N90-21024
An experimental investigation of mixing in buoyant flows 15 p2090 N90-21963
Unsteady separated flows produced by complex harmonic motions: Investigation of wing-flow interactions elicited by a mechanical model simulating dragonfly wing kinematics 15 p2100 N90-22018
Semigeostrophic flow over orography in a stratified rotating atmosphere 15 p2127 N90-22163
A theoretical investigation of gravity-wave-generated stress and vorticity in the planetary boundary layer
15 p2191 N90-22512
Three-dimensional structure of plane mixing layers
17 p2344 N90-23347
Nonlinear internal gravity wave critical layers
17 p2422 N90-23801
Initiation and propagation of thunderstorm mesocyclones 17 p2428 N90-23838
On the instability of hypersonic flow past a flat plate
[NASA-CR-182051] 18 p2493 N90-24252
Substitution principle theory for compressible flows
21 p2953 N90-26791
Direct numerical simulation of compressible free shear flows 21 p2974 N90-26901
A finite difference treatment of Stokes-type flows: Preliminary report
[NASA-CR-186480] 22 p3168 N90-27970
Free boundary problems for flow with vorticity
[AD-A218415] 22 p3168 N90-27971
Towards a two dimensional scheme of anisotropic Godunov type. On the calculation of the velocity of the nodes in the multidimensional Lagrangian codes
[ETN-90-97458] 22 p3175 N90-28017
On the calculation of the velocity of the nodes in the multidimensional Lagrangian codes
22 p3175 N90-28019
Regular and chaotic motion of uniform elliptical vortices in external linear time dependent velocity fields
23 p3268 N90-28497
On the use of Lagrangian variables in descriptions of unsteady boundary-layer separation
[NASA-CR-182071] 23 p3323 N90-28789
An investigation of forcing mechanisms during a surprise tornadic thunderstorm
[PB90-216805] 23 p3352 N90-28940
Vorticity balance study for a tropical region, during the Southern Hemisphere summer
[INPE-4634-TDL/336] 23 p3353 N90-28949

VORTICITY EQUATIONS
NT HELMHOLTZ VORTICITY EQUATION
Similarity solutions that give rise to hyperbolicity and change of type in steady flow of a viscoelastic fluid
[AD-A210920] 01 p0072 N90-10410
Connections between the circulation in altitude and convection over South America
[INPE-4923-TDL/383] 11 p1534 N90-18828
Tropical cyclone track predictability and the adjoint method of data assimilation
[AD-A218324] 14 p2007 N90-21505
A potential-vorticity decomposition for the boundary integral equation analysis of viscous flows
24 p3417 N90-29301

VOYAGER PROJECT
NASA Voyager 2 Neptune encounter press kit
[NASA-TM-101851] 01 p0015 N90-10076
The Voyager Neptune travel guide
[NASA-CR-186108] 05 p0585 N90-13412
Parkes radio science system design and testing for Voyager Neptune encounter 12 p1645 N90-19451

VOYAGER 1 SPACECRAFT
Evidence for anomalous cosmic ray hydrogen
06 p0861 N90-15005
Waves in Saturn's rings probed by radio occultation
15 p2191 N90-22511

VOYAGER 2 SPACECRAFT
NASA Voyager 2 Neptune encounter press kit
[NASA-TM-101851] 01 p0015 N90-10076
Evidence for anomalous cosmic ray hydrogen
06 p0861 N90-15005
SHARP: A multi-mission artificial intelligence system for spacecraft telemetry monitoring and diagnosis
[NASA-CR-186285] 11 p1467 N90-18444
Digital Doppler extraction demonstration with the advanced receiver 15 p2076 N90-21893
Carbon in the outer solar system
21 p3096 N90-27593

VTOL
U VERTICAL LANDING
U VERTICAL TAKEOFF

VTOL AIRCRAFT
U VERTICAL TAKEOFF AIRCRAFT

VULCANIZATES
U VULCANIZED ELASTOMERS

VULCANIZED ELASTOMERS
Effect of oxygen on the tear strength of elastomers
[AD-A215845] 10 p1359 N90-17879

VULNERABILITY
Assessing the accuracy of vulnerability models by comparison with vulnerability experiments
[AD-A210871] 01 p0116 N90-10669
HPW (High Power Microwave) testing of electronic components
[DE89-016682] 02 p0217 N90-11241
Fuel tank explosion protection
08 p1023 N90-15914
Validity of empirical studies of information system effectiveness
[AD-A214474] 09 p1295 N90-17507
A paradoxical result in unconditionally secure authentication codes, and an explanation
[DE90-008529] 13 p1867 N90-20710
Pressure rig for repetitive casting
[NASA-CASE-LAR-14050-1] 14 p1959 N90-21216
Aviation security: Corrective actions underway, but better inspection guidance still needed. Report to the Chairwoman, Government Activities and Transportation Subcommittee, Committee on Government Operations, House of Representatives
[GAO/RCED-88-160] 17 p2347 N90-23367

The internet worm
[NASA-CR-181576] 17 p2441 N90-23910
HF spread spectrum, an audit of the power requirements and LPI vulnerability 20 p2849 N90-26203

W

W STARS
U WOLF-RAYET STARS
W WINGS
U VARIABLE SWEEP WINGS
W-R STARS
U WOLF-RAYET STARS
WAFERS
Epitaxial GaAs on SOI wafers
[AD-A209009] 01 p0127 N90-10729
Feedback charge amplifier integrated on the detector wafer
[REPT-89-037] 04 p0496 N90-12852
Defect control and denuded trap zones in the 3-5 semiconductors
[AD-A214099] 07 p1004 N90-15814
Silicon hybrid wafer scale integration interconnect evaluation
[AD-A215353] 09 p1212 N90-17031
Method of producing a thin silicon-on-insulator layer
[AD-D014330] 09 p1290 N90-17478
Fabrication of ultra thin GaAs and Ge substrates for high efficiency solar cells 10 p1339 N90-17753
Preparation and characterization of alumina films prepared by a novel spray pyrolysis method
[AD-A217570] 12 p1625 N90-19339
Radiation-hardened wafer scale integration
[AD-A217332] 13 p1793 N90-20290
Identification of defects in SOI (Silicon-On-Insulator) wafers
[DE90-006020] 13 p1895 N90-20879
Germanium Blocked Impurity Band (BIB) detectors 14 p1976 N90-21321
The investigation of multilayer x ray reflectors as x ray optical elements
[DE90-009044] 14 p2026 N90-21621
Optical shutter switching matrix
[NASA-CASE-KSC-11392-1] 15 p2167 N90-22383
Measurement of localized deep levels and wafer non-uniformities at 3-5 semiconductor heterojunctions
[AD-A218547] 16 p2323 N90-23248
Integrated silicon flow sensors
[ETN-90-96906] 17 p2407 N90-23715
New approach for the thin layer manufacturing: The wafer telemetry system
[MBB-UE-0004/89-PUB] 19 p2653 N90-25102
Development of a multi-purpose, pulsed-laser system for solar cell processing applications
[DE90-012181] 21 p3008 N90-27096
High resolution technique and instrument for measuring lattice parameters in single crystals
[AD-D014549] 22 p3177 N90-28029
Reflection Mass Spectrometry (REMS) during 3/5 MBE
[DE90-014568] 23 p3304 N90-28690
A single wafer bit-sliced convolver: An optimum statistical solution for the implementation of redundancy
[REPT-89-019] 24 p3466 N90-29584
Innovative techniques for the production of low cost 2D laser diode arrays
[AD-A223575] 24 p3474 N90-29632
MUSE: A systolic array for adaptive nulling with 64 degrees of freedom, using Givens transformations and wafer scale integration
[AD-A223812] 24 p3529 N90-29953
WAKES
NT AIRCRAFT WAKES
NT HELICOPTER WAKES
NT LAMINAR WAKES
NT NEAR WAKES
NT PROPELLER SLIPSTREAMS
NT SLIPSTREAMS
NT TURBULENT WAKES
An experimental investigation of the interaction between a model rotor and airframe in forward flight 06 p0723 N90-14219
An analytical method for the prediction of unsteady rotor/airframe interactions in forward flight 06 p0724 N90-14223
Detailed analysis of the wake and free-flow characteristics at the Goodnoe Hills MOD-2 site
[DE90-002725] 06 p0806 N90-14692
An experimental, analytical, and computational investigation of turbomachinery rotor flow fields 07 p0926 N90-15360
Study of flow around a sphere in a hydraulic test tunnel
[CERT-1/2313/MES] 08 p1064 N90-16156
An experimental investigation of viscous aspects of propeller blade flow 09 p1159 N90-16711
Wake interaction effects on the transition process on turbine blades
[AD-A214492] 09 p1168 N90-16759
Large-eddy interaction model in the turbulent wake of a circular cylinder 10 p1307 N90-17563
Modeling the wake as a continuous vortex sheet in a potential-flow solution using vortex panels
[AD-A216220] 10 p1385 N90-18016
Design guidance to minimize unsteady forces in turbomachines 11 p1460 N90-18411
Aerodynamic study on forced vibrations on stator rows of axial compressors 11 p1460 N90-18412
Unsteady blade loads due to wake influence 11 p1460 N90-18413
Unsteady aerodynamic phenomena in a simulated wake and shock wave passing experiment 11 p1461 N90-18414
Modelling unsteady transition and its effects on profile loss 11 p1462 N90-18423
Experimental investigation of the influence of rotor wakes on the development of the profile boundary layer and the performance of an annular compressor cascade 11 p1463 N90-18425
Study of the turbulent boundary layer on an afterbody
[TM-EA-8901] 12 p1601 N90-19212
Unsteady free-wake viscous aerodynamic analysis of helicopter rotors
[AD-A217166] 13 p1750 N90-20048
Spectral simulation of unsteady compressible flow past a circular cylinder
[NASA-CR-182030] 13 p1750 N90-20050
Comparison of C- and O-grid generation methods using a NACA 0012 airfoil
[AD-A216375] 14 p1910 N90-20948
A correlation-spectral method for line detection on noisy data
[DE90-007925] 14 p1967 N90-21266
Development and application of a generalized dynamic wake theory for lifting rotors 15 p2046 N90-21731
Effective methods of controlling a junction vortex system in an incompressible, three-dimensional, turbulent flow 15 p2047 N90-21732
Airloads, wakes, and aeroelasticity
[NASA-CR-177551] 15 p2048 N90-21738
Secondary frequencies in the wake of a circular cylinder with vortex shedding
[NASA-CR-181998] 16 p2197 N90-22540
The stability of two-dimensional wakes and shear-layers at high Mach numbers
[NASA-CR-182050] 17 p2401 N90-23678
The browse file of NASA/JPL quick-look radar images from the Loch Linnhe 1989 experiment
[NASA-CR-186855] 20 p2935 N90-26701
Experiments with unsteady, free surface, three-dimensional vortices in a thermally stable, stratified fluid
[AD-A222088] 21 p2954 N90-26796
Evaluation of the wake effects on plume dispersion using video image analysis
[PB90-186354] 22 p3169 N90-27972
Do inviscid vortex sheets roll-up
[PD-CF-9010] 23 p3267 N90-28491
Numerical simulation of the formation of two-dimensional and three-dimensional structures in shear layers and wakes
[ESA-TT-1008] 23 p3325 N90-28802
An investigation of the inviscid spatial instability of compressible mixing layers
[AD-A223776] 24 p3468 N90-29596
WALKING
The predictability and efficiency of human walking: Metabolic, mechanical, and biophysical considerations 15 p2137 N90-22211
Physiological and perceptual responses to prolonged treadmill load carriage
[AD-A218910] 16 p2260 N90-22886
Physiological and perceptual responses to prolonged treadmill load carriage
[AD-A218809] 17 p2433 N90-23865
Three legged walking mobile platform: Kinematic and dynamic analysis and simulation
[NASA-CR-184929] 18 p2535 N90-24457
Periodic gaits for the CMU ambler 23 p3367 N90-29027
WALKING MACHINES
Expert system control of a six-legged walking telerobot
[DE90-004661] 08 p1086 N90-16285
Power system modeling for a six legged walking vehicle 09 p1221 N90-17083
Monocoque structure for the SKITTER three-legged walker
[NASA-CR-184635] 18 p2534 N90-24454
Three legged walking mobile platform: Kinematic and dynamic analysis and simulation
[NASA-CR-184929] 18 p2535 N90-24457
Man-machine interface for the control of a lunar transport machine
[NASA-CR-184935] 19 p2724 N90-25495
A task control architecture for autonomous robots 19 p2735 N90-25546
University of Maryland walking robot: A design project for undergraduate students
[NASA-CR-186839] 20 p2870 N90-26331
Investigation of maximum achievable body torque for a walking machine with friction cone constraints
[PB90-203175] 23 p3332 N90-28838
First results in terrain mapping for a roving planetary explorer 23 p3375 N90-29066
WALL FLOW
Bifurcations in Poiseuille flow and wall turbulence 01 p0065 N90-10370
Low-Reynolds-number modeling of complex flows with and without density variation 02 p0146 N90-10832
The structure of Reynolds stress in the near wall region of a turbulent pipe flow 02 p0218 N90-11247
On transonic flow over segmented slotted wind tunnel wall with mass transfer 02 p0294 N90-11676
Three-component laser Doppler velocimeter measurements in a juncture flow 04 p0441 N90-12525
Investigation of turbulent flow in highly curved ducts with application to turbomachinery components
[NASA-CR-186060] 04 p0500 N90-12882
Study of the integration of wind tunnel and computational methods for aerodynamic configurations
[NASA-TM-102196] 05 p0572 N90-13332
A two-dimensional adaptive-wall test section with ventilated walls in the Ames 2- by 2-foot transonic wind tunnel
[NASA-TM-102207] 05 p0585 N90-13407
On the topology of three-dimensional viscous flow structures near a plane wall. A classification and non-hyperbolic singularities on the wall
[LR-541] 05 p0644 N90-13758
An experimental investigation of wall-interference effects for parachutes in closed wind tunnels
[DE90-001802] 07 p0875 N90-15076
Direct Monte Carlo calculations on expansion wave structure near a wall
[ISL-CO-249/88] 08 p1064 N90-16154
Grid-independent wall layer turbulence model for complex flow calculations
[DE90-003500] 08 p1071 N90-16200
Velocity profile and wall shear stress measurements for a Large Eddy Break-Up (LEBU) device
[AD-A214958] 09 p1217 N90-17059
Influence of wall strain rate, polymer concentration, and channel height upon drag reduction and turbulent structure
[AD-A215378] 09 p1218 N90-17064
Nonlinear transonic Wall-Interference Assessment/Correction (WIAC) procedures and application to cast-10 airfoil results from the NASA 0.3-m TCT 8- by 24-inch Slotted Wall Test Section (SWTS) 10 p1323 N90-17648
Comparison of conventional and adaptive wall wind tunnel results with regard to Reynolds number effects 10 p1323 N90-17649
Residual interference and wind tunnel wall adaption 10 p1324 N90-17655
Development of a defect stream function, law of the wall/wake method for compressible turbulent boundary layers
[NASA-CR-4286] 11 p1507 N90-18675
A study of low-dimensional models for the wall region of a turbulent boundary layer 13 p1798 N90-20321
Aerodynamic optimization by simultaneously updating flow variables and design parameters 14 p1918 N90-20991
The effects of compressor endwall flow on airfoil incidence and deviation 14 p1922 N90-21011
Development of a defect stream function, law of the wall/wake method for compressible turbulent boundary layers 15 p2100 N90-22019
New transonic test sections for the NAE 5 ft x 5 ft trisonic wind tunnel
[AD-A220933] 18 p2499 N90-24278
A laser-induced fluorescence technique for measurement of slot-injected fluid concentration profiles in a plate turbulent boundary layer
[AD-A221388] 18 p2553 N90-24572
Flow structures around non-hyperbolic singularities on the wall with one vanishing eigenvalue: A discussion of the flow structures and the unfoldings
[LR-586] 19 p2692 N90-25315
A critical evaluation of two-equation models for near wall turbulence
[NASA-CR-182068] 20 p2860 N90-26270

Limits of adaptation, residual interferences
21 p2963 N90-26844
Adaptation for unsteady flow
21 p2963 N90-26845
Near-wall modelling of compressible turbulent flows
[NASA-CR-186961] 22 p3109 N90-27658
Numerical investigation of the thermal stratification in cryogenic tanks subjected to wall heat flux
[NASA-TM-103194] 22 p3171 N90-27984
Modeling of near-wall turbulence
[NASA-TM-103222] 22 p3174 N90-28009
Numerical study of turbulence in the presence of walls
[ONERA-RSF-15/3419-AY-114A]
22 p3176 N90-28024
Three-dimensional model testing in the transonic self-streamlining wind tunnel 23 p3264 N90-28583
A numerical study of the response of the laminar unsteady separated flow about a circular cylinder to changes of boundary conditions
[DLR-FB-90-10] 24 p3471 N90-29613

WALL JETS
An experimental and theoretical study of the aeroacoustics of external-Coanda gas flares
06 p0773 N90-14495
Heat transfer in convective boundary layer and channel flows 06 p0774 N90-14505
Further studies of turbulence structure resulting from interactions between embedded vortices and wall jets at high blowing ratios
[AD-A223296] 24 p3468 N90-29593
Secondary flow in presence of wall jets: Incorporation of compression effects in a quasi-elliptic Navier-Stokes calculation code
[ETN-90-97559] 24 p3469 N90-29602

WALL PRESSURE
Autofrettage-stress distribution under load and retained stresses after depressurization
[AD-A212090] 03 p0358 N90-12048
Fundamental studies of turbulent wall pressure fluctuations with applications to advanced acoustic sensor systems
[AD-A213041] 04 p0552 N90-13212
A wall interference assessment/correction interface measurement system for the NASA/ARC 12-ft PWT
[NASA-CR-185474] 05 p0584 N90-13401
Modifications of the Penn State Boundary Layer Research Facility for boundary layer/structure interaction experimental research
[AD-A213874] 07 p0931 N90-15391
Colinear fluctuating wall shear stress and fluctuating pressure transducer
[AD-D014296] 08 p1076 N90-16226
Turbulent boundary layer pressure field-induced vibrations in a thin flexible plate under water
10 p1383 N90-18002
Vortex-induced boundary layer separation
[AD-A221564] 21 p3005 N90-27078
The dynamics and control of fluctuating pressure loads in the reattachment region of a supersonic free shear layer
[NASA-CR-184943] 22 p3108 N90-27652
Spectral measurements of the wall shear stress and wall pressure in a turbulent boundary layer: Theory
[AD-A224070] 24 p3466 N90-29586

WALL TEMPERATURE
Stream field measurements of a half spheric cylinder by thin hypersonic stream with the electron radiation technique 18 p2490 N90-24232

WALLS
NT POROUS WALLS
NT THICK WALLS
NT THIN WALLS
NT WIND TUNNEL WALLS
Plasma theory and simulation
[AD-A207952] 01 p0125 N90-10714
Questions from the Willmarth Workshop on New Directions in Research on Turbulent Wall-Layer Structures
[AD-A211282] 02 p0221 N90-11264
Gravitropism in plants: Hydraulics and wall growth properties of responding cells 05 p0678 N90-13950
Heat transfer in convective boundary layer and channel flows 06 p0774 N90-14505
Measuring the thickness of austenitic weld deposits on carbon steel walls using a magnetic method
[DE89-635446] 06 p0794 N90-14628
Starlight: A stationary inertial-confinement-fusion reactor with nonvaporizing walls
[DE90-002315] 06 p0847 N90-14927
Enhancement of microchannel plate gain by deposition of CsI on the channel walls
[DE90-003051] 07 p0922 N90-15334
Numerical investigation of transition control of a flat plate boundary layer 07 p0926 N90-15361
Structure properties of confined systems. Hard spheres between ideal walls
[DE90-600818] 07 p0929 N90-15378
Sound attenuation apparatus
[NASA-CASE-LAR-13968-1] 07 p0988 N90-15710
Computation of broadband mixing noise from turbomachinery
[AD-A214448] 07 p0989 N90-15713
Influence of wall strain rate, polymer concentration, and channel height upon drag reduction and turbulent structure
[AD-A215378] 09 p1218 N90-17064
Boundary walls, fences and hoardings: Mean and peak wind loads and overturning moments
[ESDU-89050] 09 p1239 N90-17190
Turbulence structure resulting from interaction between an embedded vortex and wall jet
[AD-A215702] 10 p1383 N90-18004
Magnetohydrodynamic liquid-metal flows in a rectangular channel with an axial magnetic field, a moving conducting wall, and free surfaces
[AD-A216276] 10 p1425 N90-18223
The influence of a wall function on turbine blade heat transfer prediction 12 p1640 N90-19421
Perforation of a reinforced concrete wall by a rigid missile
[AD-A210025] 14 p1986 N90-21381
Transport of gases through concrete
[AERE-G-4977] 16 p2234 N90-22747
On the receptivity problem for Goertler vortices: Vortex motions induced by wall roughness
[NASA-CR-182036] 19 p2654 N90-25109
A critical evaluation of two-equation models for near wall turbulence
[NASA-CR-182068] 20 p2860 N90-26270
Measurement of terms and parameters in turbulent models
[NASA-CR-183993] 20 p2860 N90-26271
Design and construction of a wall-climbing robot
[NIAR-90-20] 20 p2870 N90-26327
Asymptotic analysis of dissipative waves with applications to their numerical simulation
[NASA-TM-103231] 20 p2920 N90-26615
Baryogenesis in extended inflation. 2: Baryogenesis via primordial black holes
[NASA-CR-182843] 20 p2941 N90-26735
Dynamics of fluids in bulk and near a vertical wall: Studied by photoncorrelation spectroscopy
[PB90-200452] 22 p3169 N90-27976
An improved k-epsilon model for near-wall turbulence and comparison with direct numerical simulation
[NASA-TM-103221] 22 p3171 N90-27983
Free shear layer and swirl flow heat transfer enhancement
[PB90-228123] 23 p3325 N90-28798
Further studies of turbulence structure resulting from interactions between embedded vortices and wall jets at high blowing ratios
[AD-A223296] 24 p3468 N90-29593

WARFARE
NT ANTISUBMARINE WARFARE
NT CHEMICAL WARFARE
NT COMBAT
NT ELECTRONIC WARFARE
NT NUCLEAR WARFARE
The importance of environmental data
06 p0757 N90-14406
Propagation-based decision aids in the U.S. Navy
06 p0757 N90-14410
PROPHET and future signal warfare decision aids
06 p0758 N90-14412
Historical review of missile aerodynamic developments
10 p1304 N90-17542
Can the square law be validated
[DE90-007112] 11 p1553 N90-18945
Assessing the morality of using the space environment as a platform for weapons
[AD-A217348] 13 p1879 N90-20780
Space in warfare
[AD-A217527] 13 p1879 N90-20782
Visual behavior in the F-15 simulator for air-to-air combat
[AD-A218648] 16 p2262 N90-22893
Ring laser gyro principles and techniques
24 p3426 N90-29352

WARHEADS
NT PRECISION GUIDED PROJECTILES

WARM FRONTS
Thermodynamic and dynamic processes in the updraft region of GALE (Genesis of Atlantic Lows Experiment) IOP (Intensive Observation Period) 9
[AD-A208139] 01 p0087 N90-10496
A day in the life of a warm front
[AD-A220373] 17 p2426 N90-23826

WARMING
U HEATING

WARNING DEVICES
U WARNING SYSTEMS

WARNING SIGNALS
U WARNING SYSTEMS

WARNING SYSTEMS
NT EARLY WARNING SYSTEMS
Safer skies with TCAS: Traffic Alert and Collision Avoidance System
[PB89-169221] 01 p0004 N90-10016
Data processing in lightning warning systems
[DE89-012495] 01 p0088 N90-10502
See and avoid/cockpit visibility
[DOT/FAA/CT-TN89/18] 02 p0148 N90-10843
Independent Orbiter Assessment (IOA): Analysis of the extravehicular mobility unit
[NASA-CR-185540] 02 p0166 N90-10937
Independent Orbiter Assessment (IOA): Assessment of the displays and controls subsystem
[NASA-CR-185588] 02 p0171 N90-10961
Hydrazine dosimetry 02 p0206 N90-11178
Description of a chemiluminescence detector system specifically designed for monitoring airborne hydrazine and oxidizer propellant vapors 02 p0206 N90-11179
Improved pattern recognition techniques for real time operation
[AD-A211395] 03 p0324 N90-11840
Severe local storm warning verification: 1988
[PB89-226310] 03 p0374 N90-12134
Shape instabilities of plate-like structures. 1: Experimental observations in heavily cold worked in situ composites
[AD-A212251] 04 p0523 N90-13021
Perceived urgency of warning signals determined using a forced choice pair comparison technique
[RAE-TM-MM-12] 04 p0551 N90-13206
An update to the system safety study of TCAS 2
[DOT/FAA/SA-89/3] 05 p0577 N90-13363
Multisensor technologies for low cost methane detection
[PB89-235188] 05 p0645 N90-13766
Field evaluation of a Nissan laser collision avoidance system
[PB90-105602] 06 p0722 N90-14215
How to fly windshear using the fly-by-wire concept
07 p0870 N90-15050
Improved lighting of taxiway/taxiway intersections for Instrument Flight Rules (IFR) operations
[DOT/FAA/CT-TN89/64] 07 p0878 N90-15089
Relative merits of reactive and forward-look detection for wind-shear encounters during landing approach for various microburst escape strategies
[NASA-TM-4158] 07 p0882 N90-15108
The automatic detection of anti-collision lights
[RSRE-MEMO-4272] 08 p1019 N90-15896
Onboard fire- and explosion suppression for fighter aircraft 10 p1315 N90-17602
US Navy aircraft fire protection technology
10 p1315 N90-17603
The signals of an ice warning device in dependence on total water content and normalized icing degree
[DLR-FB-89-52] 11 p1454 N90-18377
Joint University Program for Air Transportation Research, 1988-1989
[NASA-CP-3063] 14 p1905 N90-20921
Cockpit display of hazardous weather information
14 p1906 N90-20929
Selective automatic fire extinguisher for computers (SAFECOMP): Developmental test and evaluation/initial operational test and evaluation
[AD-A217790] 14 p1958 N90-21212
Rapidly quantifying the relative distention of a human bladder
[NASA-CASE-LAR-13901-1-NP]
14 p2010 N90-21519
Maritime safety information in the year 2000: Listen up, Navy, the times they are a changin'
[AD-A220563] 17 p2390 N90-23611
Characteristics of the IAEA correlation monitor material for surveillance programmes
[VTT-RR-639] 19 p2682 N90-25258
Monitoring and control of spacecraft systems using procedural reasoning 19 p2731 N90-25524
Computer access security code system
[NASA-CASE-NPO-17525-1-CU]
19 p2742 N90-25583
Oxygen deficiency monitor system
[DE90-014866] 24 p3523 N90-29917

WARPAGE
Advanced buckling analyses of beams with arbitrary cross sections
[ISBN-90-9002808-0] 18 p2572 N90-24659

WASHING
Coating galvanized steel
[AD-A211775] 03 p0329 N90-11869

WASHOUT (RADIOACTIVITY)
U FALLOUT

WASPALOY
Fatigue life assessment using a short crack growth model
[PNR90663] 20 p2877 N90-26367
Microstructure: Property correlation --- multiaxial fatigue damage evolution in waspaloy
[NASA-CR-180406] 23 p3340 N90-28880
WASTE DISPOSAL
The Third Conference on the Environmental Chemistry of Hydrazine Fuels
[AD-A197632] 02 p0203 N90-11157
The chemistry of the hypochlorite neutralization of hydrazine fuels 02 p0205 N90-11173
Fuel neutralization by ozone oxidation 02 p0206 N90-11176
Evaluation of mid-to-long term basic research for environmental restoration
[DE89-015621] 02 p0238 N90-11355
Proposal for a zero-gravity toilet facility for the space station
[NASA-CR-183151] 04 p0526 N90-13036
Environmental Projects. Volume 9: Construction of hazardous materials storage facilities
[NASA-CR-186296] 09 p1244 N90-17216
Environmental impact statement on the US Antarctic program
[DE90-004940] 09 p1245 N90-17221
Evapotranspiration studies for protective barriers: Experimental plans
[DE90-005206] 10 p1405 N90-18106
Information management systems for integrating the technical data and regulatory requirements of environmental restoration activities
[DE90-008622] 13 p1831 N90-20511
In-situ fracture stiffness determination
[DE90-009202] 15 p2129 N90-22173
Transport of gases through concrete
[AERE-G-4977] 16 p2234 N90-22747
Object-oriented design: Deriving conceptual solutions to large-scale information processing problems
[DE90-011189] 19 p2763 N90-25699
Generation rates and chemical compositions of waste streams in a typical crewed space habitat
[NASA-TM-102799] 22 p3233 N90-28333
WASTE ENERGY UTILIZATION
Conceptual design of liquid droplet radiator shuttle-attached experiment
[NASA-CR-185164] 03 p0318 N90-11805
Conceptual design of liquid droplet radiator shuttle-attached experiment technical requirements document
[NASA-CR-185165] 03 p0318 N90-11806
Field testing of a ceramic heat exchanger for heat recovery application
[DE90-002082] 06 p0778 N90-14523
Design and fabricate a metallic hydride heat pump with a cooling capacity of 9000 BTU/H
[AD-A213756] 07 p0931 N90-15388
Assessment of ground-coupled heat pumps
[DE90-003977] 09 p1220 N90-17079
WASTE HEAT
Design and fabricate a metallic hydride heat pump with a cooling capacity of 9000 BTU/H
[AD-A213756] 07 p0931 N90-15388
Rotary absorption heat pump sensitivity analysis
[DE90-002877] 09 p1216 N90-17053
Hydride heat pumps for upgrading spacecraft waste heat 10 p1385 N90-18013
WASTE TREATMENT
The chemistry of the hypochlorite neutralization of hydrazine fuels 02 p0205 N90-11173
Ozonation of hydrazines and their associated impurities 02 p0205 N90-11174
Modeling the ozonolysis of hydrazines wastewater 02 p0205 N90-11175
Modern biofuel cells for waste recycling in life support systems
[NASA-CR-185963] 05 p0638 N90-13718
Environmental Projects. Volume 8: Modifications of wastewater evaporation ponds
[NASA-CR-186099] 06 p0808 N90-14700
Managing the waste stream: Background information for planning source separation programs
[PB90-100223] 07 p0956 N90-15530
Anode materials for electrochemical waste destruction 18 p2514 N90-24354
Generation rates and chemical compositions of waste streams in a typical crewed space habitat
[NASA-TM-102799] 22 p3233 N90-28333
Electrochemical incineration of wastes
[NASA-CR-187033] 23 p3317 N90-28753
WASTE UTILIZATION
Biofuels program summary. Volume 2: Research summaries
[DE89-009484] 18 p2576 N90-24678
Laboratory tests to determine the chemical and physical characteristics of propellant-solvent-fuel oil mixtures
[AD-A222270] 21 p2990 N90-26991
Production of jet fuels from coal-derived liquids. Volume 13: Evaluation of storage and thermal stability of jet fuels derived from coal liquids
[AD-A224576] 24 p3457 N90-29527
WASTE WATER
Ozonation of hydrazines and their associated impurities 02 p0205 N90-11174
Modeling the ozonolysis of hydrazines wastewater 02 p0205 N90-11175
Modern biofuel cells for waste recycling in life support systems
[NASA-CR-185963] 05 p0638 N90-13718
Environmental Projects. Volume 8: Modifications of wastewater evaporation ponds
[NASA-CR-186099] 06 p0808 N90-14700
Utilization of water hyacinths to upgrade heavily loaded wastewater treatment plant effluents 15 p2073 N90-21873
Selective removal of organics for water reclamation
[NASA-TM-101890] 17 p2421 N90-23797
Contamination of spacecraft by recontact of dumped liquids 19 p2728 N90-25508
WASTES
NT FECES
NT HUMAN WASTES
NT INDUSTRIAL WASTES
NT RADIOACTIVE WASTES
NT SEWAGE
NT SOLID WASTES
NT URINE
NT WASTE WATER
Evaluation of mid-to-long term basic research for environmental restoration
[DE89-015621] 02 p0238 N90-11355
Space station gas compressor technology study program, phase 1
[NASA-CR-183758] 05 p0601 N90-13491
Anode materials for electrochemical waste destruction 18 p2514 N90-24354
Geophysical diffraction tomography: A complementary remote sensing technique for hazardous waste site characterization
[DE90-013025] 23 p3341 N90-28882
WATCHES
U CLOCKS
WATER
NT COASTAL WATER
NT COLD WATER
NT GROUND WATER
NT HEAVY WATER
NT INLAND WATERS
NT POTABLE WATER
NT SEA WATER
NT SHALLOW WATER
NT SURFACE WATER
NT WASTE WATER
Heterogeneous catalysts in water
[AD-A210742] 01 p0041 N90-10228
Independent Orbiter Assessment (IOA): Analysis of the electrical power distribution and control/electrical power generation subsystem
[NASA-CR-185538] 02 p0165 N90-10933
Independent Orbiter Assessment (IOA): Analysis of the hydraulics/water spray boiler subsystem
[NASA-CR-185541] 02 p0165 N90-10934
A new method for the characterization of solutes and solvent phases using solvatochromic parameters
[AD-A211238] 02 p0196 N90-11116
Design of ceramic fabric heat pipe with water working fluid
[DE89-016565] 02 p0221 N90-11265
A high level Ab initio study of the anionic hydrogen-bonded complexes FH-CN-, FH-NC-, H2O-CN- and H2O-NC- 02 p0272 N90-11553
Equation-of-state data of synthetic Uranus
[DE89-016509] 02 p0296 N90-11683
Gas-liquid-liquid equilibria in mixtures of water, light gases, and hydrocarbons
[DE90-003180] 07 p0894 N90-15167
Advanced study in solid transport: Rheological behavior of dense suspension
[DE90-003369] 07 p0947 N90-15483
Conceptual design analysis for hybrid-cycle OTEC plants for co-production of electric power and desalinated water
[DE90-003551] 08 p1097 N90-16350
Evaluating CO, CO2 and H2O concentration by partial integration of absorption band spectra
[ISL-R-110/88] 09 p1244 N90-17219
Aircraft internal fires 10 p1313 N90-17593
The evaporation of sessile droplets. Part 1: Theoretical factors for a two-component system
[AD-A215946] 10 p1353 N90-17848
The size of the alkyl group R is the principal factor determining the wettability of surface-functionalized polyethylenes (PE-CONHR and PE-CO2R) by water
[AD-A216007] 10 p1354 N90-17851
A field study of solid rocket exhaust impacts on the near-field environment
[NASA-TM-4172] 10 p1405 N90-18102
Evapotranspiration studies for protective barriers: Experimental plans
[DE90-005206] 10 p1405 N90-18106
Remote sensing of interior water: Perspectives
[INPE-4875-PRE/1486] 11 p1531 N90-18815
Spectroscopy and physico-chemistry of CO:H2O and CO2:H2O ices 11 p1581 N90-19111
Simulation of thermal dynamics of a vaporizing coal-water droplet in a combustor
[DE90-005356] 12 p1621 N90-19317
Enhancement of processes for solar photocatalytic detoxification of water
[DE90-003949] 12 p1623 N90-19330
Advanced double layer capacitor
[AD-A217110] 12 p1656 N90-19518
Laboratory studies of free radical reactions in cloudwater
[DE90-003961] 12 p1694 N90-19730
Large impact events and atmospheric evolution on the terrestrial planets 12 p1744 N90-20028
Experimental investigation of the thermocapillary migration of water droplets in butylbenzoate
[MPIS-14/1988] 13 p1770 N90-20155
Developments in solar photocatalysis for destruction of organics in water
[DE90-007685] 13 p1771 N90-20162
A technical and economic evaluation of oxygen-enriched combustion in diesel engines using water-emulsified fuels
[DE90-008095] 13 p1810 N90-20394
Depth-averaged equations for turbulent free-surface flow
[PB90-164781] 14 p1974 N90-21308
Digital processing of TM/LANDSAT data in monitoring interior water
[INPE-4956-PRE/1533] 14 p1997 N90-21448
Thermal decay of an initially hot isothermal water body with application to thermal energy storage
[DE90-614742] 14 p2035 N90-21675
WINCOF-I code for prediction of fan compressor unit with water ingestion
[NASA-CR-185157] 15 p2045 N90-21724
Radiometric tests on wet and dry antenna reflector surface panels 15 p2076 N90-21890
Experimental observations on transition to turbulence in confined coaxial jets and other boundary layer flows
[DE90-008939] 15 p2098 N90-22005
Inventory of program packages related to the project SIMONA
[ETN-90-96397] 15 p2148 N90-22270
Theoretical and computer simulation study of the density fluctuations in liquid water
[PREPRINT-697] 16 p2314 N90-23191
Low frequency Raman spectra of liquid water, a molecular dynamics simulation
[PREPRINT-698] 16 p2314 N90-23192
A laboratory comparison of field techniques for measurement of the liquid water fraction of snow
[AD-A219587] 17 p2417 N90-23774
Temperature evolution of single particle correlation functions of TIP4P water
[PREPRINT-694] 17 p2470 N90-24119
The effect of H2O and pretreatment on the activity of a Pt/SnO2 catalyst 18 p2558 N90-24597
Effect of fluid countermeasures of varying osmolarity on cardiovascular responses to orthostatic stress 18 p2628 N90-24978
Electrochemical control of iodine disinfectant for space transportation system and space station potable water 18 p2629 N90-24981
Carbon dioxide and water exchange rates by a wheat crop in NASA's biomass production chamber: Results from an 86-day study (January to April 1989)
[NASA-TM-102788] 19 p2716 N90-25453
Utilization of the water soluable fraction of wheat straw as a plant nutrient source
[NASA-TM-103497] 19 p2716 N90-25455
Evaluation of water cooled supersonic temperature and pressure probes for application to 2000 F flows
[NASA-TM-102612] 19 p2753 N90-25645
Lunar polar coring lander
[NASA-CR-186684] 19 p2796 N90-25917
Transient characteristics of a grooved water heat pipe with variable heat load
[NASA-CR-185280] 20 p2861 N90-26272
Influence of thermal conditioning media on Charpy specimen test temperature
[DE90-012784] 20 p2875 N90-26360

Heat engines
[DE90-000485] 20 p2882 N90-26393
Measurements of CH4, N2O, CO, H2O and O3 in the middle atmosphere by the ATMOS experiment on Spacelab 3
[NASA-TM-103476] 20 p2883 N90-26400
The 27-28 October 1986 FIRE IFO Cirrus case study: Comparison of radiative transfer theory with observations by satellite and aircraft
[NASA-TM-103468] 20 p2890 N90-26446
Isothermal compressibility of SPC/E water
[AD-A222723] 20 p2925 N90-26643
Structure and dynamics of water at the Pt(111) interface: Molecular dynamics study
[AD-A222628] 20 p2933 N90-26687
Photon sputtering of H2O ices: A preliminary report
20 p2949 N90-26783
Carbon in the outer solar system
21 p3096 N90-27593
Scattering of CO2-laser radiation by water droplets
[FOA-C-20776-2.3] 22 p3181 N90-28049
Inhomogeneities of stratocumulus liquid water
22 p3213 N90-28228
Observed cloud reflectivities and liquid water paths: An update 22 p3215 N90-28237
ETO lidar studies of cirrostratus altocumulogenitus: Another role for supercooled liquid water in cirrus cloud formation 22 p3221 N90-28269
Circulation and property distributions in the Central Bering Sea, Spring, 1988
[PB90-155847] 22 p3230 N90-28317
Three functions that model empirically measured unfrozen water content data and predict relative hydraulic conductivity
[AD-A223875] 23 p3343 N90-28892
Shear-resistant drag reduction polymers. Part 1: Molecular investigations of polymer drag reduction and the development of laboratory screening methods
[AD-A223353] 24 p3454 N90-29508

WATER BALANCE
Hypobaric hypoxia (380 torr) decreases intracellular and total body water in goats
[AD-A218192] 13 p1849 N90-20615

WATER CIRCULATION
NT EL NINO
NT GULF STREAM
NT OCEAN CURRENTS
NT WATER CURRENTS
Dynamics of the equatorial undercurrent and its termination
[PB89-198147] 03 p0377 N90-12146
Advanced space power PEM fuel cell systems
10 p1333 N90-17707
MECCA program documentation
[NOAA-TR-NESDIS-46] 14 p2003 N90-21477

WATER COLOR
Effects of heating/cooling on changes in sea surface temperature: Consequences for computation of surface advection from satellite images
[AD-A214125] 10 p1409 N90-18129
Some problems in oceanic radiative transfer
[AD-A215935] 10 p1410 N90-18131
The instrument HOSS (Hydro Optical Sensor System)
[FOA-C-30554-3.1] 22 p3246 N90-28411

WATER CONTENT
U MOISTURE CONTENT

WATER COOLED REACTORS
NT PATHFINDER NUCLEAR REACTOR
NT ZERO POWER REACTORS

WATER COOLING
U LIQUID COOLING

WATER CURRENTS
NT EL NINO
NT GULF STREAM
NT OCEAN CURRENTS
Status of a nonlinear water surge model in February 1988
[KNMI-WR-88-03] 12 p1695 N90-19735
Study of seasonal variation of mixing phenomena in the hypolimnion of Lake Geneva (Switzerland)
19 p2688 N90-25287
On the fine-scale mixing in the metalimnion and the seasonal thermocline of the Leman (Lake Geneva, Switzerland) 19 p2688 N90-25288

WATER CYCLE (HYDROLOGY)
U HYDROLOGICAL CYCLE

WATER DEPRIVATION
Experiment K-6-20. The effect of spaceflight on pituitary oxytocin and vasopressin content of rats
20 p2896 N90-26473

WATER DEPTH
On the applicability of CAESAR for the remote sensing of bottom depth and bottom composition of shallow waters: A model study
[BCRS-89-13] 11 p1526 N90-18783
Analysis of water quality parameters of the Piaui River (SE), Brazil, through field and TM/LANDSAT sensor data
[INPE-4918-PRE/1417] 14 p1998 N90-21453
Modelling bottom stress in depth-averaged flows
[AD-A218605] 17 p2429 N90-23840
Ross Sea oceanographic data, 1983-1987: USCGC GLACIER, January-February 1983; USCGC POLAR SEA, January-February 1984; USCGC POLAR STAR, February 1984; USCGC POLAR SEA, February 1987
[PB90-243932] 23 p3354 N90-28955

WATER FLOW
Measurements of coefficients of discharge for concentric flange-tapped square-edged orifice meters in water over the Reynolds number range 600 to 2,700,000
[PB89-235147] 04 p0502 N90-12892
Flow visualization of water flows using the crystal violet method 08 p1081 N90-16253
Estimating water flow through a hillslope using the massively parallel processor 08 p1114 N90-16449
Influence of wall strain rate, polymer concentration, and channel height upon drag reduction and turbulent structure
[AD-A215378] 09 p1218 N90-17064
Homogeneous dilute turbulent particle-laden water flows 15 p2090 N90-21965
Velocity distribution in a gravel-bed flume; for steady and unsteady flow 19 p2687 N90-25283
A two layer model for the simulation of internal linear and nonlinear waves in Lake Geneva (Switzerland)
19 p2687 N90-25286
Measurement of terms and parameters in turbulent models
[NASA-CR-183993] 20 p2860 N90-26271
Numerical methods for shallow water flow
22 p3172 N90-27992

WATER HEATING
Performance predictions for passive solar water heating systems. Report 1: Performance monitoring to validate site-specific estimates of passive solar water heaters. Report 2: Laboratory report. Passive solar water heater tests
[DE90-002879] 10 p1401 N90-18096
Operational fact-finding report on heat pump systems for industrial use
[DE89-782295] 12 p1658 N90-19527
Extended range tankless water heater
[DE90-014474] 23 p3316 N90-28750

WATER IMMERSION
Effects of serial wet-dry-wet cold exposure: Thermal balance, physical activity, and cognitive performance
[AD-A212704] 04 p0524 N90-13025
Integrated G-suit/immersion suit
[AD-A212989] 06 p0821 N90-14774
Use of self-induced hypnosis to modify thermal balance during cold water immersion
[AD-A216156] 10 p1412 N90-18140
Work enhancement and thermal changes during intermittent work in cool water after carbohydrate loading
[AD-A222877] 21 p3034 N90-27247

WATER JETS
U HYDRAULIC JETS

WATER LANDING
NT DITCHING (LANDING)
Preliminary subsystem designs for the Assured Crew Return Vehicle (ACRV), volume 1
[NASA-CR-186677-VOL-1] 20 p2818 N90-26039

WATER LOSS
Thermal remote sensing in the differentiation of soybean crops (glycine max (L.) merrill) submitted to water deficit
[INPE-4900-PRE/1501] 11 p1522 N90-18762

WATER MANAGEMENT
Water removal studies on high power hydrogen-oxygen fuel cells with alkaline electrolytes
10 p1333 N90-17712

WATER MASERS
New water vapor masers in the Southern Hemisphere
[INPE-4844-PRE/1473] 14 p2037 N90-21689

WATER POLLUTION
Coastal Research Center Woods Hole Oceanographic Institution
[PB89-198238] 01 p0089 N90-10510
Managing human exposure and health risks: An integrated approach and the role of uncertainty
[DE89-008611] 01 p0092 N90-10525
Hydrazine fate and transformation in natural waters and soils 02 p0204 N90-11165
Steady state model to determine lake resources at risk to acid deposition in the Sierra Nevada, California
[PB89-103995] 06 p0809 N90-14705
Enhancement of processes for solar photocatalytic detoxification of water
[DE90-003949] 12 p1623 N90-19330
The pollution hazard assessment system: Documentation and users manual
[AD-A217108] 12 p1689 N90-19706
Development of a laser fluorosensor for the aircraft supported analysis of maritime toxic agents loads: Definition phase
[ETN-90-95320] 13 p1829 N90-20499
The transfer of mercury between the atmosphere and lake or soil surfaces 20 p2886 N90-26419
Mariners Weather Log, volume 33, number 3, Summer 1989
[PB90-146846] 20 p2889 N90-26444
Mariners Weather Log, volume 33, number 4, Fall 1989
[PB90-146853] 20 p2890 N90-26445
Enhanced bioreclamation of jet fuels: A full-scale test at Eglin AFB, Florida
[AD-A222348] 21 p2990 N90-26992
Development of an expert system embedding pattern recognition techniques for pollution source identification
[PB90-185927] 22 p3197 N90-28139
Prediction of episodic acidification in Maryland coastal plain streams
[PB90-194978] 22 p3199 N90-28152
Outer continental shelf environmental assessment program. Volume 66: Principal investigators
[PB90-194747] 22 p3199 N90-28154
Acid deposition in Maryland: Summary of results through 1989
[PB90-229782] 22 p3200 N90-28160
Puerto Rico Workshop on Land-Based Sources of Marine Pollution in the Wider Caribbean Region
[PB90-184094] 23 p3348 N90-28921
SamTrack: A sample tracking system for environmental monitoring
[DE90-016026] 24 p3488 N90-29712

WATER PRESSURE
Remote sensing of atmospheric water vapour by pressure modulation radiometry
06 p0802 N90-14667

WATER PURIFICATION
U WATER TREATMENT

WATER QUALITY
Spatial characterization of acid rain stress in Canadian Shield Lakes
[NASA-CR-183446] 01 p0084 N90-10479
Environmental Projects. Volume 8: Modifications of wastewater evaporation ponds
[NASA-CR-186099] 06 p0808 N90-14700
An evaluation of trend detection techniques for use in water quality monitoring programs
[PB89-100058] 06 p0808 N90-14702
Environmental surveillance data
[DE90-001275] 07 p0956 N90-15532
Eutrophication assessment through remote sensing techniques
[INPE-4932-PRE/1422] 10 p1398 N90-18083
Remote sensing of interior water: Perspectives
[INPE-4875-PRE/1486] 11 p1531 N90-18815
Enhancement of processes for solar photocatalytic detoxification of water
[DE90-003949] 12 p1623 N90-19330
Satellite imagery for water quality assessment in coastal regions
[INPE-4891-PRE/1492] 12 p1678 N90-19636
Possible applications of remote sensing satellite pictures for the water quality management of the Frisian lakes, Netherlands
[BCRS-88-17] 12 p1679 N90-19641
Predicting effects of global climate change on reservoir water quality and fish habitat
[DE90-003674] 12 p1689 N90-19704
Remote sensing applied to sea water quality researches in coastal regions: A review
[INPE-4935-PRE/1425] 14 p1995 N90-21438
Analysis of water quality parameters of the Piaui River (SE), Brazil, through field and TM/LANDSAT sensor data
[INPE-4918-PRE/1417] 14 p1998 N90-21453
The effects of climate change on energy planning and operations in the Pacific Northwest. Volume 2: Technical background
[DE90-009465] 17 p2425 N90-23817
The use of satellite pictures of the Ysselmeer region (Netherlands). Optimization of the use of LANDSAT for water quality applications in the Ysselmeer region
[BCRS-89-31] 18 p2575 N90-24670
The instrument HOSS (Hydro Optical Sensor System)
[FOA-C-30554-3.1] 22 p3246 N90-28411
A computerized data-base system for land-use and land-cover data collected at ground-water sampling sites in the pilot national water-quality assessment program
[PB90-181868] 22 p3258 N90-28453
Puerto Rico Workshop on Land-Based Sources of Marine Pollution in the Wider Caribbean Region
[PB90-184094] 23 p3348 N90-28921

Atmosphere and water quality monitoring on Space Station Freedom
[NASA-CR-186707] 23 p3378 N90-29084
Shear-resistant drag reduction polymers. Part 1: Molecular investigations of polymer drag reduction and the development of laboratory screening methods
[AD-A223353] 24 p3454 N90-29508

WATER RECLAMATION
Selective removal of organics for water reclamation
[NASA-TM-101890] 17 p2421 N90-23797

WATER RECOVERY
U WATER RECLAMATION

WATER RESOURCES
NT AQUIFERS
Activities report of the World Meteorological Organization
[WMO-713] 05 p0671 N90-13912
Steady state model to determine lake resources at risk to acid deposition in the Sierra Nevada, California
[PB89-103995] 06 p0809 N90-14705

WATER SPLITTING
A preliminary investigation of cold fusion by electrolysis of heavy water
[DE90-004383] 09 p1285 N90-17447
IEA (International Energy Agency) implementing agreement for a program of research and development on the production of hydrogen from water. Task 9: Hydrogen production
[DE90-007354] 12 p1625 N90-19337
Photosynthetic water splitting, phase 2
[PB90-132671] 15 p2066 N90-21833
Impact of low gravity on water electrolysis operation
[NASA-CR-185521] 15 p2072 N90-21870

WATER TABLES
Fluctuation history of Great Salt Lake, Utah, during the last 13,000 years, part 2
[NASA-CR-185911] 01 p0082 N90-10466
Use of ground penetrating radar to define recharge areas in the Central Sand Plain
[PB89-224885] 04 p0490 N90-12814

WATER TEMPERATURE
NT OCEAN TEMPERATURE
NT SEA SURFACE TEMPERATURE
Accuracy and precision of GOES data collection platforms for temperature measurements
[AD-A218798] 16 p2250 N90-22832
Integrated radiometric profiler for atmospheric humidity and temperature measurements
[AD-A221931] 21 p3032 N90-27237

WATER TREATMENT
Selective removal of organics for water reclamation
[NASA-CR-185959] 02 p0255 N90-11445
Enhancement of processes for solar photocatalytic detoxification of water
[DE90-003949] 12 p1623 N90-19330
Advanced on-site power plant development technology program
[DE90-000443] 13 p1826 N90-20484
Utilization of water hyacinths to upgrade heavily loaded wastewater treatment plant effluents
15 p2073 N90-21873

WATER TUNNEL TESTS
Turbulent boundary layer pressure field-induced vibrations in a thin flexible plate under water
10 p1383 N90-18002
Water-tunnel investigation of concepts for alleviation of adverse inlet spillage interactions with external stores
[NASA-TM-4181] 12 p1599 N90-19199
A video-based experimental investigation of wing rock
15 p2054 N90-21771
Acoustic confinement in the large hydrodynamic tunnel: Identification of the acoustic charateristics with a one-directional source
[REPT-8228-88] 22 p3244 N90-28399
The experimental investigation of flow in the core of a vortex structure
[BR114893] 24 p3468 N90-29597

WATER TUNNELS
U HYDRAULIC TEST TUNNELS

WATER VAPOR
A study of the impact of simulated 183 GHz water vapor retrievals on numerical weather prediction
[AD-A210431] 01 p0088 N90-10504
Tests of various finite difference algorithms applied to a simple water vapor transport problem on a staggered grid
[AD-A210229] 01 p0105 N90-10596
Progress of research on water vapor lidar
[NASA-CR-185970] 03 p0352 N90-12011
Infrared water vapor continuum absorption: New atmospheric electrical measurements and theory
[AD-A212594] 04 p0519 N90-12994
Remote sensing of atmospheric water vapour by pressure modulation radiometry
06 p0802 N90-14667
Analysis of ambient polar volatile organic compounds using chemical ionization-ion trap detector
[PB90-106451] 07 p0956 N90-15529
Vertical distribution of pollutants in the presence of convective storms
[DE90-002590] 07 p0960 N90-15549
Backscattering effects in DIAL due to water vapor
[SER-WISS-ABHANDL-89] 08 p1082 N90-16265
Assessment of the importance of acidic fogwater and cloudwater in affecting terrestrial vegetation: Some important case studies
[DE90-002216] 08 p1098 N90-16361
Mesoscale analysis by numerical modelling coupled with satellite-based sounding 08 p1100 N90-16370
Continuous gas exchange measurements using individual fascicle cuvettes: The tubule system
[DE90-004932] 10 p1405 N90-18105
On the relationship between water vapor over the oceans and sea surface temperature
[NASA-CR-186199] 10 p1409 N90-18127
Cloud hole-boring with infrared lasers: Theory and experiment
[DE90-006519] 11 p1515 N90-18723
Cloud parameterization in EURAD and its future development 12 p1687 N90-19692
New water vapor masers in the Southern Hemisphere
[INPE-4844-PRE/1473] 14 p2037 N90-21689
The production and spatial distribution of neutral and ionized water vapor in Comet P/Halley
15 p2185 N90-22484
A nonhydrostatic numerical model in sigma-coordinates and simulations of mesoscale phenomena
23 p3350 N90-28932
A study of water vapor, electrical parameters, and radio propagation
[AD-A223582] 24 p3492 N90-29736

WATER VEHICLES
NT AIRCRAFT CARRIERS
NT BOATS
NT SHIPS
NT SUBMARINES
NT UNDERWATER VEHICLES

WATER WAVES
Similarity relations of wind waves in finite depth
[PB89-198113] 03 p0376 N90-12144
A device to extract energy from water waves
[REPT-89-34] 04 p0516 N90-12978
Nonlinear viscous waves produced by an impulsively moving plate
[AD-A214014] 07 p0932 N90-15392
Phase control mechanism for wave energy conversion
[AD-D014354] 12 p1681 N90-19657
A study of the surface layers at an air-water interface
[AD-A219378] 16 p2260 N90-22882
Kinematics under wind waves
[AD-A219541] 17 p2430 N90-23844
Test and evaluation of surf forecasting model
[AD-A219580] 17 p2430 N90-23845
A two layer model for the simulation of internal linear and nonlinear waves in Lake Geneva (Switzerland)
19 p2687 N90-25286
Research in nonlinear water waves
[AD-A224065] 24 p3496 N90-29759

WATERSHEDS
Assessment of the theory and hypotheses of the acidification of watersheds
[DE90-005528] 10 p1406 N90-18111
Hypotheses testing of watershed/landscape dynamics in northern Alaska using digital analysis
[DE90-006721] 13 p1820 N90-20450
Prediction of episodic acidification in Maryland coastal plain streams
[PB90-194978] 22 p3199 N90-28152

WATERWAVE ENERGY CONVERSION
A device to extract energy from water waves
[REPT-89-34] 04 p0516 N90-12978

WATERWAYS
NT CANALS
Inventory of program packages related to the project SIMONA
[ETN-90-96397] 15 p2148 N90-22270
Ice conditions along the Illinois waterway as observed on LANDSAT images, 1972 to 1985
[AD-A219745] 17 p2418 N90-23775

WAVE AMPLIFICATION
Free-field response from inclined body waves in viscoelastic random medium
[REPT-88-99] 04 p0499 N90-12876
All-fiber SFPM (Stimulated Four Photon Mixing) amplifier
[AD-D014358] 12 p1713 N90-19841
Solid state space harmonic amplifier
[AD-D014455] 22 p3166 N90-27955
An investigation of the inviscid spatial instability of compressible mixing layers
[AD-A223776] 24 p3468 N90-29596

WAVE ATTENUATION
NT ACOUSTIC ATTENUATION
NT RADIO ATTENUATION
NT SHOCK WAVE ATTENUATION
Seismic wave attenuation and yield determination at regional distances
[AD-A211548] 03 p0372 N90-12128
A numerical study of rain-induced surface gravity wave attenuation
[AD-A212762] 04 p0549 N90-13197
The influence of gamma-radiation on the bandwidth of optical fibres and the reduction of the induced attenuation by bleaching and hardening the fibre
[FEL-1988-62] 12 p1714 N90-19846
Propagation and attenuation of Lg waves in South America
[AD-A218853] 16 p2255 N90-22859
Seismic wave propagation, attenuation and scattering over regional distances
[AD-A219358] 16 p2256 N90-22862
Analysis of vibrational power transmission through a beam system including a flexible section
[ISVR-TR-176] 23 p3340 N90-28875
Evaluation of a thermistor power measurement system for use on the NPL antenna extrapolation range
[NPL-DES-89] 24 p3466 N90-29583

WAVE DIFFRACTION
Custom diffraction gratings
[AD-A211002] 01 p0124 N90-10712
Modeling of diffraction reflection and clutter loss in UHF radio wave propagation
[FEL-1988-28] 03 p0340 N90-11938
A method to model fuze-performance. Part 3: Diffraction of electromagnetic radiation by an edge
[FEL-1989-22-PT-3] 03 p0340 N90-11940
An investigation of the diffraction of an acoustic plane wave by a curved surface of finite impedance
[NASA-CR-186069] 04 p0550 N90-13204
A new technique for simulating composite material. Task 2: Analytical solutions with Generalized Impedance Boundary Conditions (GIBCs)
[NASA-CR-186249] 07 p0890 N90-15146
Anomalous waves in shock wave - fluid interface collisions
[AD-A213584] 08 p1062 N90-16144
A numerical and theoretical study of seismic wave diffraction in complex geologic structure
[AD-A218209] 14 p2005 N90-21490
Diffraction of light by ultrasonic pulses
15 p2164 N90-22366
Extended optical emission in 3CR radio galaxies
15 p2193 N90-22523
Validity domain of the scalar Kirchhoff and Rayleigh-Sommerfeld diffraction theories in the near field of small phase objects: Comparison between calculation models and microwave measure
[ETN-90-96963] 20 p2855 N90-26236
Electromagnetic scattering from two-dimensional thick material junctions
[NASA-CR-186468] 23 p3319 N90-28767

WAVE DISPERSION
Optical dispersion relations for diamondlike carbon films
[NASA-TM-102356] 01 p0129 N90-10738
Evaluation of dispersive behavior in periodic structures by discrete Fourier transform 02 p0180 N90-11014
On the influence of ionospheric conductivity on dispersion of acoustic gravity waves
02 p0244 N90-11386
Temporal and spatial filtering remedies for dispersion in electromagnetic particle codes
[DE89-017534] 03 p0408 N90-12337
Optical phonon modes in a double heterostructure of polar crystals
[AD-A214208] 07 p1004 N90-15816
A space-time discretization procedure for wave propagation problems
[NASA-TM-102215] 08 p1105 N90-16399
Chromatic dispersion compensation in a Fresnel lens by means of a diffraction grating
[DE90-004030] 08 p1123 N90-16506
One-dimensional single-mode nonlinear FEL amplification code: User's manual
[DE90-719544] 09 p1227 N90-17121
A current disruption mechanism in the neutral sheet for triggering substorm expansions
[NASA-CR-186260] 09 p1298 N90-17525
Magnetoplasma oscillations of the wave-guided type in semiconductor superlattices
[DE90-607260] 10 p1431 N90-18258
Asymptotic boundary conditions for dissipative waves: General theory
[NASA-TM-102497] 11 p1551 N90-18927
Longitudinal traveling waves bifurcating from Vlasov plasma equilibria 12 p1715 N90-19850

Tropospheric monitoring technology for gravity wave experiments 12 p1734 N90-19971
MHD modes driven by anomalous electron viscosity and their role in fast sawtooth crashes
[DE90-009311] 14 p2029 N90-21639
Coupled magnetoplasmon-phonon modes at the surface of a semi-infinite semiconductor superlattice
[DE90-612904] 14 p2031 N90-21647
Topics in vortex methods for the computation of three- and two-dimensional incompressible unsteady flows 15 p2091 N90-21967
Sound waves in weakly ionized gas
[DE90-620704] 16 p2313 N90-23180
Development of a six port network analysis tool for the 1 to 18 GHz bandwidth range
[TELECOM-PARIS-89-D-015] 18 p2545 N90-24527
Surface wave characterization of high T(sub c) superconductors
[AD-A221077] 19 p2760 N90-25683
Theory of biaxial graded-index optical fiber
[NASA-CR-186882] 20 p2927 N90-26652
Linear and nonlinear optical properties of quantum dots
[AD-A223050] 21 p3076 N90-27489
Electron acoustic and magnetoacoustic modes in a magnetized beam plasma system
[DE90-627473] 23 p3398 N90-29199
Magnetostatic wave transducers, resonators and dispersion control
[AD-A223437] 24 p3464 N90-29571
Experimental observations of nonlinear effects in laser-plasma interactions
[DE90-015195] 24 p3549 N90-30079

WAVE DRAG
NT INTERFERENCE DRAG
Optimum shape of a blunt forebody in hypersonic flow
[NASA-CR-181955] 05 p0575 N90-13351

WAVE EQUATIONS
NT DIRAC EQUATION
NT KLEIN-GORDON EQUATION
NT KORTEWEG-DEVRIES EQUATION
NT SCHROEDINGER EQUATION
A straightforward method for finding implicit solitary wave solutions of nonlinear evolution and wave equations
[AD-A210561] 01 p0113 N90-10647
Efficient algorithm for calculation of radar cross section
[AD-A210785] 02 p0213 N90-11217
Non-linear wave-equations for low-frequency acoustic gravity waves 02 p0240 N90-11365
Estimation on nonlinear damping in second order distributed parameter systems
[NASA-CR-181890] 02 p0263 N90-11494
Theory of high-n toroidicity-induced shear Alfven eigenmode in tokamaks
[DE89-016726] 02 p0277 N90-11582
Time-domain analytic and numeric analysis of vertical dipoles in front of dielectric planar interface
[PB89-221642] 03 p0338 N90-11927
Semi-Lagrangian, semi-implicit solutions of the shallow water equations in one dimension
[AD-A212658] 04 p0503 N90-12902
RPE: A parabolic equation radio assessment model 06 p0759 N90-14419
Enhanced resolution concepts in large scale scientific computing
[AD-A214095] 07 p0932 N90-15393
Hidden regularity for a strongly nonlinear wave equation
[DE90-600742] 08 p1116 N90-16465
On scattering by time-dependent potentials: The 2-D case
[DE89-635708] 09 p1275 N90-17390
Two-dimensional calculation of sequential electron layer formation by crossed microwave beams in air at low pressure
[DE90-005254] 09 p1286 N90-17453
Alfven wave stability in D III-D
[DE90-005555] 10 p1437 N90-18291
Theoretical and experimental high energy physics
[DE90-006168] 11 p1565 N90-19006
Linear theory of thermal blooming in turbulence
[DE90-007243] 12 p1667 N90-19579
A linear systems theory approach to the range-independent acoustic channel
[AD-A216551] 12 p1710 N90-19817
Stability of a solitary wave solution to a set of coupled Boussinesq-like equations
[DE90-008927] 14 p2021 N90-21586
On the stability of a certain difference scheme
[PB90-165614] 14 p2021 N90-21588
Propagation of transient acoustic waves in porous media
[ETN-90-96401] 15 p2099 N90-22015
Evidence for self-refraction in a convergence zone: NPE (Nonlinear progressive wave equation) model results
[AD-A218546] 16 p2259 N90-22879
Approximation in LQG control of a thermoelastic rod 16 p2297 N90-23084
Nonlinear waves and inverse scattering
[AD-A218483] 17 p2387 N90-23597
An analysis of propagation in a surface duct over a periodically rough Earth
[AD-A220565] 17 p2390 N90-23612
Diffraction effects in directed radiation beams
[AD-A220785] 17 p2391 N90-23619
An adaptive finite element method for shock developing partial differential equation
[FFI-89/7014] 19 p2751 N90-25632
On traveling wave solutions of a set of coupled Boussinesq-like equations
[DE90-013182] 20 p2917 N90-26597
Asymptotic analysis of dissipative waves with applications to their numerical simulation
[NASA-TM-103231] 20 p2920 N90-26615
Theory of biaxial graded-index optical fiber
[NASA-CR-186882] 20 p2927 N90-26652
Increasing the margin of stability of arbitrarily finite modes of flexible large space structures with damping
[AD-A221742] 21 p2967 N90-26867
Separable coordinate systems for PDE
[AD-A223052] 21 p3063 N90-27415
The validation and application of a rotor acoustic prediction computer program
[NASA-TM-101794] 21 p3072 N90-27465
Numerical methods for shallow water flow 22 p3172 N90-27992
Tailoring explicit time-marching schemes to improve convergence characteristics 22 p3172 N90-27997
Fluctuation splitting for multidimensional convection problems: An alternative to finite volume and finite element methods 22 p3173 N90-28000
Consistency and convergence for numerical radiation conditions
[NASA-TM-103262] 23 p3387 N90-29124

WAVE EXCITATION
NT ACOUSTIC EXCITATION
NT HARMONIC EXCITATION
Applications of frequency and wavenumber nonlinear digital signal processing to nonlinear hydrodynamics research
[AD-A216259] 12 p1658 N90-19530
Full wave computation of electromagnetic wave excitation, propagation, and absorption at the ion cyclotron frequency in fusion experiments
[DE90-009399] 14 p2030 N90-21642
Modern developments in shear flow control with swirl
[NASA-CR-186586] 15 p2097 N90-22000
Convergence of hyperspherical adiabatic expansion for helium-like systems
[DE90-620526] 16 p2214 N90-22631
Destabilization of supersonic free shear layers by parametric excitation using Mach waves generated by a wavy wall
[AD-A219655] 17 p2345 N90-23352

WAVE FRONT DEFORMATION
Adaptive optics correction in real-time for dynamic wavefront errors
[AD-A221588] 21 p3077 N90-27495

WAVE FRONTS
NT SHOCK FRONTS
Wavefront propagation for reaction-diffusion systems of PDE
[AD-A210862] 02 p0265 N90-11510
Wavefront error sensing for LDR 05 p0595 N90-13455
Fast algorithms for calculating laser wavefront phase compensation given noisy measurements of phase gradient
[DE90-006357] 11 p1515 N90-18727
Application of wavefront analysis techniques to restoring of images degraded by atmospheric turbulence
[ONERA-PUBL-1989-1] 11 p1589 N90-19168
Method for holographic correction of beams of coherent light
[AD-D014406] 14 p1981 N90-21353
Frontogenesis in gravity currents: An example with no known applications in oceanography
[MATHS-REPT-A-117] 20 p2863 N90-26284
Optical wavefront computer for stabilizing large space structures
[AD-A221707] 21 p2967 N90-26866
Algorithms to solve nonlinear time dependent problems of engineering and physics
[AD-A221463] 21 p3055 N90-27366
Ultrasonic verification of five wave fronts in unidirectional graphite epoxy composite
[NASA-CR-185288] 23 p3337 N90-28858

WAVE FUNCTIONS
NT MOLECULAR ORBITALS
Markov processes in Hilbert space and continuous spontaneous localization of systems of identical particles
[DE89-618396] 02 p0270 N90-11540
Structure and properties of simple molecular systems at very high density
[DE89-016974] 02 p0273 N90-11557
New theoretical approaches for studying electron collisions with small molecules
[DE89-017543] 02 p0273 N90-11558
Davydov solutions at 300 Kelvin: The final search
[DE89-015248] 03 p0401 N90-12296
Quantum-mechanical derivation of the Davydov equations for multi-quanta states
[DE89-015250] 03 p0401 N90-12297
Calculation of the odd and even integral components of the wave resistance Green's function
[AD-A212384] 04 p0503 N90-12900
A diagnostic for determining the quality of single-reference electron correlation methods
[NASA-TM-101929] 06 p0838 N90-14874
The dissociation energy of N2
[NASA-TM-101930] 07 p0891 N90-15153
Variational quantum Monte Carlo calculation of electronic and structural properties of crystals
[DE90-003265] 07 p0999 N90-15781
General contraction of Gaussian basis sets. Part 2: Atomic natural orbitals and the calculation of atomic and molecular properties
[NASA-CR-186201] 08 p1119 N90-16482
Continuous spontaneous reduction model involving gravity
[DE90-600730] 08 p1135 N90-16573
The (2+1)-dimensional quantum gravity
[DE90-719556] 08 p1136 N90-16580
Study of interfacial behavior in cocurrent gas-liquid flows
[DE90-005988] 12 p1659 N90-19532
The basis spline method and associated techniques
[DE90-008403] 13 p1877 N90-20763
Modified tight-binding approximation and electron-phonon spectral function for transition metals
[DE90-614022] 14 p1950 N90-21166
Large basis space effects in electron scattering form factors of light nuclei
[DE90-613501] 14 p2025 N90-21609
Non-symmetric double well and Euclidean functional integral
[PREPRINT-709] 16 p2305 N90-23133
Anyons and Chern-Simons theory on compact spaces of finite genus
[DE90-627216] 23 p3391 N90-29157
Old and new ideas in the theory of quantum measurement
[DE90-627181] 23 p3403 N90-29229
Effect of retardation on the reflectance properties of the metallic Fibonacci quasi-superlattice
[DE90-627316] 24 p3551 N90-30091
Gaussons and states with gaussian Wigner functions are quasi-free states
[DE90-628370] 24 p3556 N90-30121

WAVE GENERATION
Report from space plasma science 10 p1445 N90-18336
A study of the surface layers at an air-water interface
[AD-A219378] 16 p2260 N90-22682
A study of gravity wave variability, saturation, and turbulence generation in the mesosphere and lower thermosphere
[AD-A220018] 17 p2424 N90-23810
Millimeter-wave generation via plasma three-wave mixing
[AD-A222010] 22 p3247 N90-28415

WAVE INTERACTION
NT SHOCK WAVE INTERACTION
Reheat buzz: An acoustically coupled combustion instability 01 p0036 N90-10200
Acoustic-vortex-chemical interactions in an idealized ramjet 01 p0037 N90-10206
Near-planar TS waves and longitudinal vortices in channel flow: Nonlinear interaction and focusing
[NASA-CR-181928] 03 p0300 N90-11698
Dynamics of baroclinic wave systems 03 p0362 N90-12072
The effect of latent heat release on synoptic-to-planetary wave interactions and its implication for satellite observations: Theoretical modeling 03 p0362 N90-12073
The effect of latent heat release on synoptic-to-planetary scale wave interactions: Observational study 03 p0362 N90-12074
Laboratory and theoretical studies of baroclinic processes 03 p0363 N90-12077
Wave particle interactions
[DE89-017527] 03 p0407 N90-12335
Stability theory applications to laminar-flow control 04 p0439 N90-12513

Interaction of Tollmien-Schlichting waves and Goertler vortices
04 p0440 N90-12515
Surface current and wave modulation measurements over bottom topography: A comparison with theory
[AD-A212469] 04 p0522 N90-13011
Energy exchange of interacting solitons in multidimensions
[PREPRINT-662] 05 p0696 N90-14071
On strongly nonlinear vortex/wave interactions in boundary-layer transition
[NASA-CR-181963] 07 p0876 N90-15078
Excimer emission from alkali diatomic and alkaline-earth-noble-gas molecules
[AD-A214246] 07 p0896 N90-15179
Langmuir wave interaction with ion-sound one. Part 1: Stochastic effects
[DE90-603368] 08 p1118 N90-16474
On condensation driven by electrostatic interactions in macroionic solutions
[DE89-636072] 08 p1120 N90-16487
Studies of optical matrix multiplication and reconfigurable optical interconnect concepts
[AD-A214645] 09 p1281 N90-17427
TS - Dean interactions in curved channel flow
[NASA-CR-181983] 10 p1306 N90-17559
Effects of controlled three-dimensional perturbations on boundary layer transition
[AD-A215080] 10 p1384 N90-18011
Interaction between oblique-angled incident shock wave and turbulent boundary layer on a heated wall. Experimental results
[ONERA-RT-84/7078-AY] 11 p1509 N90-18688
Nonlinear interaction of electrostatic waves at a narrow inhomogeneous layer of a warm magnetoactive plasma
[DE90-610624] 12 p1717 N90-19857
Cell averaging Chebyshev methods for hyperbolic problems
[NASA-CR-182028] 13 p1877 N90-20768
A numerical and theoretical study of seismic wave diffraction in complex geologic structure
[AD-A218209] 14 p2005 N90-21490
Langmuir wave interaction with ion acoustic wave
[DE90-615407] 14 p2027 N90-21624
The interaction between a plane shock wave and a cylindrical afterbody
15 p2046 N90-21728
Diffraction patterns and vortex rollup
[AD-A219876] 17 p2461 N90-24049
Nonlinear development of Goertler and crossflow vortices and Goertler/Tollmien-Schlichting wave interaction
[AD-A221107] 18 p2553 N90-24571
Investigations of ultrasonic wave interactions at imperfect boundaries separating anisotropic materials
[DE90-010661] 18 p2612 N90-24875
Light-millimeter wave interactions in semiconductor devices
[AD-A221214] 18 p2623 N90-24943
Perturbation methods in the theory of waves and bifurcation phenomena
20 p2916 N90-26593
Departures from plane-wave-like coupling to a Maverick missile in the radiating near-field region of a horn antenna
[AD-A222539] 21 p2997 N90-27035
Solid state space harmonic amplifier
[AD-D014455] 22 p3166 N90-27955
Theoretical study of the interaction between an oblique shock wave and a turbulent boundary layer from a heated wall
[ONERA-RSF-87/7078/AY-100-A]
24 p3419 N90-29313
Transonic 3-D Euler analysis of flows around fanjet engine and TPS (Turbine Powered Simulator). Comparison with wind tunnel experiment, evaluation of TPS testing method and 3-D flow
[NAL-TR-1045] 24 p3421 N90-29327

WAVE OSCILLATORS
U OSCILLATORS

WAVE PACKETS
Sound waves in weakly ionized gas
[DE90-620704] 16 p2313 N90-23180

WAVE PROPAGATION
NT ACOUSTIC PROPAGATION
NT DIFFRACTION PROPAGATION
NT GROUND WAVE PROPAGATION
NT HALOS
NT IONOSPHERIC F-SCATTER PROPAGATION
NT IONOSPHERIC PROPAGATION
NT LIGHT SCATTERING
NT SCATTER PROPAGATION
NT SHOCK WAVE PROPAGATION
Observations of spherical-wave scintillation in strong refractive-index turbulence
[PB89-124747] 01 p0062 N90-10355
Stimulated rotational Raman scattering
[DE89-016427] 01 p0075 N90-10430
Kinetic effects in Alfven wave heating. Part 2: Propagation and absorption with a single minority species
[DE89-016619] 01 p0126 N90-10724
Wave-mode coordinate analysis of L junction in LSS
[AD-A211116] 02 p0176 N90-10984
Shock-induced atomic-scale structure in metals
[DE89-016539] 02 p0197 N90-11124
VLF/LF radio wave studies of the structure and variability of the equatorial, mid-latitude and polar ionosphere below 100 km
02 p0242 N90-11373
On the influence of ionospheric conductivity on dispersion of acoustic gravity waves
02 p0244 N90-11386
Ionospheric irregularities and their effects on electromagnetic waves propagating through them
02 p0245 N90-11391
Joint VHF coherent radar and oblique sounder observations for short term ionosphere forecasting
02 p0247 N90-11399
Radio propagation conditions forecast above a low latitude region
02 p0247 N90-11400
Irreversible phase transition and wave propagation in silicate geologic materials
[DE89-016031] 02 p0250 N90-11414
Wavefront propagation for reaction-diffusion systems of PDE
[AD-A210862] 02 p0265 N90-11510
Nonlinear acoustics: Reflection and refraction, propagation in a periodic waveguide, scattering of sound by sound and ellipsoidal focusing
[AD-A211224] 02 p0271 N90-11550
Handbook of radio wave propagation loss (100-20,000 MHz), part 2
[PB89-195473] 03 p0336 N90-11912
Simulation of the EMP (Electromagnetic Pulse) from ESD (Electrostatic Discharge)
[DE89-014484] 03 p0337 N90-11918
Eigensolutions for the reflection problem involving the interface of two chiral half spaces
[PB89-221592] 03 p0338 N90-11926
Modeling of diffraction reflection and clutter loss in UHF radio wave propagation
[FEL-1988-28] 03 p0340 N90-11938
Effects on electromagnetic wave propagation and rocket vapor trails of intense turbulence generated by breaking internal gravity waves
[AD-A211755] 03 p0373 N90-12130
Observations of long Rossby waves in the northern tropical Pacific
[PB89-196331] 03 p0376 N90-12143
Similarity relations of wind waves in finite depth
[PB89-198113] 03 p0376 N90-12144
Wave particle interactions
[DE89-017527] 03 p0407 N90-12335
Tropospheric influences on satellite-Earth paths and their determination by means of radar measurements
[ESA-TT-1143] 04 p0460 N90-12639
Physics of the tropospheric radiopropagation
[DE89-619726] 04 p0485 N90-12783
Digital radio link: Wave propagation investigations on a 13 GHz line-of-sight path
[PB89-213128] 04 p0485 N90-12785
A literature study of wave propagation in the 1-60 GHz range. Application to transportable military communication systems
[FEL-1988-47] 04 p0491 N90-12825
Long wave atmospheric noise model, phase 1. Volume 2: Mode parameters
[AD-A212795] 04 p0493 N90-12837
Electron beam propagation through a magnetic wiggler with random field errors
[AD-A212705] 04 p0498 N90-12867
Analytical control of special numerical calculations of pressure propagation in a fluid
[GRS-70] 04 p0501 N90-12884
Fundamentals of middle atmospheric dynamics
[AD-A211747] 04 p0518 N90-12988
An investigation of the diffraction of an acoustic plane wave by a curved surface of finite impedance
[NASA-CR-186069] 04 p0550 N90-13204
Localization of ultrasound in thick composites
[AD-A212994] 05 p0618 N90-13602
Electromagnetic wave propagation through circular waveguides containing radially inhomogeneous lossy media
[AD-A213062] 05 p0632 N90-13688
Experimental and theoretical study of artificial plasma layers produced by two intersecting beams in a chamber
[NASA-CR-184598] 05 p0701 N90-14102
Operational Decision Aids for Exploiting or Mitigating Electromagnetic Propagation Effects
[AGARD-CP-453] 06 p0757 N90-14405
The importance of environmental data
06 p0757 N90-14406
Propagation assessment and tactical decision aids
06 p0757 N90-14407
Propagation-based decision aids in the U.S. Navy
06 p0757 N90-14410
PROPHET and future signal warfare decision aids
06 p0758 N90-14412
Long wave propagation assessment
06 p0758 N90-14414
Hybrid PE-ray-mode formulation of high frequency propagation in a bilinear tropospheric surface duct
06 p0759 N90-14417
Analysis of propagation in an inhomogeneous atmosphere in the horizontal and vertical direction using the parabolic equation method
06 p0760 N90-14421
Propagation modeling for some horizontally varying tropospheric ducts
06 p0760 N90-14422
Propagation prediction for the North Sea environment
06 p0760 N90-14423
Low level range coverage performance prediction for VHF radar
06 p0763 N90-14439
Detection of a chirping electromagnetic signal
[DE90-002105] 06 p0766 N90-14457
Propagation of detonation waves from an impact region
[DE90-001184] 06 p0776 N90-14515
Nondestructive evaluation of flaw clusters and thin layer interfaces
06 p0795 N90-14633
Effective utilization of acoustic wave sensor responses: Simultaneous measurement of velocity and attenuation
[DE90-002580] 06 p0838 N90-14872
Hamiltonian chaos in a nonlinear polarized optical beam
[DE90-002437] 07 p0934 N90-15408
Laser-supported detonation waves and pulsed laser propulsion
[DE90-002753] 07 p0935 N90-15412
Determination of Q as a function of depth and tectonic province
[AD-A213805] 07 p0960 N90-15554
Bulk wave characterization of high T(sub c) superconductors
[AD-A214030] 07 p1004 N90-15813
A numerical simulation model for the study of magnetohydrodynamic (MHD) waves in a structured medium
07 p1012 N90-15864
Personal computer study of finite-difference methods for the transonic small disturbance equation
[NASA-TM-102582] 08 p1019 N90-15892
An investigation of elastic guided waves for ceramic joint evaluation
[DE90-004400] 08 p1050 N90-16071
Helsinki University of Technology Radio Laboratory
[PB90-110677] 08 p1056 N90-16102
Low-altitude millimeter-wave propagation in the evaporation duct
[AD-A214432] 08 p1057 N90-16108
Direct Monte Carlo calculations on expansion wave structure near a wall
[ISL-CO-249/88] 08 p1064 N90-16154
A space-time discretization procedure for wave propagation problems
[NASA-TM-102215] 08 p1105 N90-16399
Solving time harmonic wave problems on vector processors
[DE90-003956] 08 p1119 N90-16480
Geometrical optics in inhomogeneous chiral media with application to polarization correction in inhomogeneous lens antennas
[PB90-110669] 08 p1122 N90-16497
Scientific investigations of the Space Research Group
[ISBN-0-642-13252-6] 08 p1138 N90-16595
Finite element analysis of propagation in waveguide components with application to ferrite phase shifters
[FOA-C-30529-3.2] 09 p1204 N90-16977
Nonlinear modulational stability and propagation of an electromagnetic pulse in a two-component, neutral plasma
[AD-A215131] 09 p1207 N90-16994
Two-dimensional, long-pulse simulation of microwave-induced electron layer evolution in low-pressure air
[DE90-005180] 09 p1208 N90-17004
Quartz crystal resonator mass loading
[AD-A215199] 09 p1212 N90-17028
A study of a new time-domain method of lines and its application for the characterization of microstrip line and its discontinuities
[AD-A215441] 09 p1213 N90-17034
Phase space and path integral methods applied to direct and inverse ocean seismo-acoustic modeling
[AD-A214777] 09 p1249 N90-17247
Generalized pulse equations for through-transmission evaluation of arbitrary multilayered structures
[NASA-TM-100752] 09 p1278 N90-17407

Two-dimensional calculation of sequential electron layer formation by crossed microwave beams in air at low pressure
[DE90-005254] 09 p1266 N90-17453
Proceedings of the Thirteenth NASA Propagation Experimenters Meeting (NAPEX 13)
[NASA-CR-186062] 10 p1371 N90-17945
NASA Propagation Information Center 10 p1371 N90-17946
Field measurements in MSAT-X 10 p1371 N90-17947
Channel simulator upgrade to use field propagation data 10 p1372 N90-17948
Japanese propagation experiments with ETS-5 10 p1372 N90-17951
Plan of advanced satellite communication experiments using ETS-6 10 p1372 N90-17952
Observations of attenuation at 20.6, 31.65 and 90.0 GHz: Preliminary results from Wallops Island, VA 10 p1373 N90-17957
Recent achievements of OPEX 10 p1373 N90-17961
The ITALSAT experiment 10 p1374 N90-17962
ACTS propagation concerns, issues, and plans 10 p1374 N90-17963
Nonlinear wave propagation
[AD-A215500] 10 p1375 N90-17968
PRPSIM: A FORTRAN code to calculate properties of radio wave propagation in a structured ionized medium. Volume 2: Theory and models
[AD-A216299] 10 p1377 N90-17983
Full field visualization of surface and bulk acoustic waves using heterodyne holographic interferometry
[AD-A214353] 10 p1387 N90-18023
Report from space plasma science 10 p1445 N90-18336
Damage assessment in composites by acousto-ultrasonic technique
[AD-A216590] 11 p1479 N90-18510
Millimeter-wave propagation in the mesosphere
[PB90-119868] 11 p1496 N90-18612
Quick, reliable estimates of high-power microwave fluences: The SNEAKY-2 program
[DE90-006347] 11 p1498 N90-18624
Piezoelectric polymer PVDF shock gauge: State of the research art
[ISL-CO-207/89] 11 p1512 N90-18705
The propagation of time harmonic Rayleigh-Lamb waves in a bimaterial plate
[AD-A216834] 11 p1519 N90-18749
Asymptotic boundary conditions for dissipative waves: General theory
[NASA-TM-102497] 11 p1551 N90-18927
Two-dimensional, long-pulse computer calculation of microwave-induced electron layer formation in low-pressure air
[DE90-005994] 12 p1646 N90-19459
Propagation of electromagnetic waves in multidimensional homogeneous cosmologies
[DE90-610474] 12 p1647 N90-19462
Sparse breakdown and statistical sneakthrough effects in low-altitude microwave propagation
[DE90-007252] 12 p1648 N90-19473
Linear theory of thermal blooming in turbulence
[DE90-007243] 12 p1667 N90-19579
Atmospheric thermal blooming and beam clearing by aerosol vaporization
[DE90-006271] 12 p1690 N90-19711
Nonlinear interaction of electrostatic waves at a narrow inhomogeneous layer of a warm magnetoactive plasma
[DE90-610624] 12 p1717 N90-19857
Nonlinear optics in thin films
[AD-A217336] 13 p1887 N90-20829
Discrete modeling of beds of propellant exposed to strong stimulus
[DE90-008932] 14 p1957 N90-21206
A numerical and theoretical study of seismic wave diffraction in complex geologic structure
[AD-A218209] 14 p2005 N90-21490
On the relativistic Vlasov equation in guiding-center coordinates
[DE90-613241] 14 p2028 N90-21629
Full wave computation of electromagnetic wave excitation, propagation, and absorption at the ion cyclotron frequency in fusion experiments
[DE90-009399] 14 p2030 N90-21642
Precise estimation of tropospheric path delays with GPS techniques 15 p2074 N90-21881
Atmospheric Propagation in the UV, Visible, IR, and mm-Wave Region and Related Systems Aspects
[AGARD-CP-454] 15 p2079 N90-21907
The mm-wave region propagation experiments by satellite 15 p2081 N90-21916
LOWTRAN 7: Status, review, and impact for short-to-long-wavelength infrared applications 15 p2081 N90-21917
Models of aerosols, clouds, and precipitation for atmospheric propagation studies 15 p2081 N90-21919
Modeling millimeter-wave propagation effects in the atmosphere 15 p2082 N90-21922
Atmospheric modelling studies: A modelling comparison between IR and millimetric atmospheric propagation 15 p2086 N90-21941
Theory of a periodic cylindrical waveguide with a nonuniform metal-dielectric filling
[DE90-620099] 15 p2087 N90-21945
Partial acoustic filtering applied to the equations of compressible flow
[DE90-000673] 15 p2097 N90-22001
Beam propagation in direct nuclear pumped laser amplifiers
[DE90-009613] 15 p2104 N90-22035
Free wave propagation in orthogonally stiffened cylinders 15 p2119 N90-22124
A spectral analysis approach to wave propagation in layered solids 15 p2120 N90-22131
Effects of single fractures on seismic wave propagation
[DE90-009191] 15 p2129 N90-22171
A 2-D analysis of particle velocity and stress of SH waves from a strip radiator. An experimental verification of both amplitude and phase using EMA transducers
[AERE-R-12600] 16 p2227 N90-22704
Specification for environmental measurements to assess radar sensors
[AD-A219127] 16 p2250 N90-22833
Propagation and attenuation of Lg waves in South America
[AD-A218853] 16 p2255 N90-22859
Seismic wave propagation, attenuation and scattering over regional distances
[AD-A219358] 16 p2256 N90-22862
Experimental investigations concerning the propagation of second-sound pulses at critical heat flux
[MPIS-12/1989] 16 p2313 N90-23182
New approach to the dynamical diffraction theory in the case of three-dimensional perfect crystal
[DE90-620563] 16 p2322 N90-23240
Critique of nondiffracting beams
[AD-A220722] 17 p2390 N90-23614
Millimeter - wave radar scattering from terrain: Data handbook
[AD-A220770] 17 p2391 N90-23617
Diffraction effects in directed radiation beams
[AD-A220785] 17 p2391 N90-23619
Joint services electronics program: Electronics research at the University of Texas at Austin
[AD-A220834] 17 p2397 N90-23655
Numerical and physical modelling of bubbly flow phenomena
[DE90-009837] 17 p2401 N90-23677
Center for Analysis of Heterogeneous and Nonlinear Media
[AD-A219627] 17 p2403 N90-23688
Tropical-extratropical interaction in a model atmosphere 17 p2422 N90-23800
A study of gravity wave variability, saturation, and turbulence generation in the mesosphere and lower thermosphere
[AD-A220018] 17 p2424 N90-23810
Wave propagation over sea: Tropospheric effects on communication, radar, and ESM systems; proposal for a measuring programme
[FOA-C-30544-8.3] 18 p2543 N90-24517
Utilization of higher frequencies for satellite communications: Determination of atmospheric effects using experiments and models
[DLR-FB-89-46] 18 p2544 N90-24518
Understanding tropscatter propagation
[AD-A220969] 18 p2544 N90-24520
Analysis and applications of the crosstie-overlay slow-wave structure
[AD-A220286] 18 p2547 N90-24537
Transitioning of power flow in beam models with bends 18 p2570 N90-24648
Investigations of ultrasonic wave interactions at imperfect boundaries separating anisotropic materials
[DE90-010661] 18 p2612 N90-24875
Normal-mode and phase-integral methods for determining phase and group velocities in simple underwater acoustic ducts
[AD-A221393] 18 p2612 N90-24877
Finite amplitude surface waves in cooled plasmas with smeared interface
[DE90-611308] 18 p2617 N90-24909
Short range, close to ground, VHF/UHF propagation: A comparison of measured results with a simple ray-based model
[RSRE-MEMO-4335] 19 p2684 N90-25266
On the relationship between energy density and net power (intensity) in coupled one-dimensional dynamic systems
[AD-A221071] 19 p2709 N90-25421
Laser ultrasonic measurements on ceramic materials with rough surfaces
[DE90-012961] 20 p2838 N90-26141
Propagation Effects and Circuit Performance of Modern Military Radio Systems with Particular Emphasis on Those Employing Bandspreading
[AGARD-CP-442] 20 p2844 N90-26178
Experimental analysis of the HF linkage 20 p2845 N90-26181
Progress and remaining issues in the development of a wideband HF channel model and simulation 20 p2845 N90-26182
Wideband characterization of forest propagation channels 20 p2846 N90-26188
System factors to be considered in assessing propagation effects on modern digital satellite communications systems 20 p2850 N90-26208
Theory of circular dielectric waveguide with anisotropic sheet cover
[NASA-CR-186883] 20 p2855 N90-26235
OASIS, LLNL version: Software maintenance manual
[DE90-013522] 20 p2868 N90-26313
Remote sensing of Earth terrain
[NASA-CR-186888] 20 p2880 N90-26382
Asymptotic analysis of dissipative waves with applications to their numerical simulation
[NASA-TM-103231] 20 p2920 N90-26615
Computer modeling wave propagation with a variation of the Helmholtz-Kirchhoff relation
[AD-A222746] 20 p2927 N90-26657
Specification for HF Lowest Usable Frequency (LUF) model
[AD-A222114] 21 p2996 N90-27031
The effects of blast trauma (impulse noise) on hearing: A parametric study source 2
[AD-A221731] 21 p3035 N90-27253
Algorithms to solve nonlinear time dependent problems of engineering and physics
[AD-A221463] 21 p3055 N90-27366
Temporal response of coupled one-dimensional dynamic systems
[AD-A222375] 21 p3073 N90-27470
Input-output characterization of fiber reinforced composites by P waves
[NASA-CR-185287] 22 p3189 N90-28097
Propagation of electromagnetic radiation in a random field of gravitational waves and space radio interferometry
[DE90-627196] 23 p3319 N90-28764
Ultrasonic verification of five wave fronts in unidirectional graphite epoxy composite
[NASA-CR-185288] 23 p3337 N90-28858
Study of the relationships between radar structure and the electrical activity of clouds
[ETN-90-97488] 23 p3352 N90-28946
Detection of ocean inner waves by synthetic aperture radar: Observations at Gibraltar pass
[ETN-90-97477] 23 p3353 N90-28953
Factorization of the characteristic equation for three layer ducts
[AD-A223867] 23 p3354 N90-28956
Consistency and convergence for numerical radiation conditions
[NASA-TM-103262] 23 p3387 N90-29124
Theory of biaxial graded-index optical fiber
[NASA-CR-186977] 23 p3395 N90-29180
Control of a Cossor CSP1250 ionospheric simulator in an automated HF test bed
[AD-A223446] 24 p3461 N90-29549
Specification for a standard electromagnetic propagation model
[AD-A223556] 24 p3461 N90-29551
Research into traveling wave control in flexible structures
[AD-A224504] 24 p3479 N90-29661
Regional phase propagation in three dimensionally heterogeneous media
[AD-A223279] 24 p3491 N90-29731
A feasibility study for D-region equatorial ionosphere research using VLF radiowaves
[AD-A223685] 24 p3492 N90-29738
Elastic interfaces
[REPT-90-003] 24 p3493 N90-29742
The effect of wave data assimilation on the numerical simulation of wave energy advection
[KNMI-TR-121] 24 p3496 N90-29760
The computation and analysis of acoustic waves in transonic airfoil-vortex interactions 24 p3542 N90-30031
Study of the reflection of surface acoustic wave from a material discontinuity boundary using a perturbation method 24 p3542 N90-30032

Numerical pulse propagation studies using two classical ocean waveguide models
[AD-A224118] 24 p3542 N90-30033
Polarization correction of Luneburg lens with chiral medium
[PB90-189127] 24 p3544 N90-30046
Experimental observations of nonlinear effects in laser-plasma interactions
[DE90-015195] 24 p3549 N90-30079

WAVE RADIATION
U ELECTROMAGNETIC RADIATION

WAVE REFLECTION
NT MACH REFLECTION
Nonlinear acoustics: Reflection and refraction, propagation in a periodic waveguide, scattering of sound by sound and ellipsoidal focusing
[AD-A211224] 02 p0271 N90-11550
Modeling of diffraction reflection and clutter loss in UHF radio wave propagation
[FEL-1988-28] 03 p0340 N90-11938
Reflection by defective diffusion bonds
[AD-A212995] 05 p0623 N90-13638
Reflection from layered media with special attention to the microwave region
[ESA-TT-1155] 08 p1057 N90-16111
Vector circuit theory for multilayered isotropic and chiral structures: Reflection and transmission
[PB90-122474] 12 p1652 N90-19495
The classification of defects from ultrasonic measurements
[AERE-R-13306] 15 p2108 N90-22056
Artificial dielectrics
[AD-A219671] 17 p2389 N90-23605
Improved transverse crack detection in composites
[NASA-TM-103261] 22 p3153 N90-27875
Characterization by ultrasonic tests of ceramics submitted to thermal shocks: Influence of several parameters on the crack dimensioning
[ETCA-89-R-060] 22 p3160 N90-27923
Acoustic confinement in the large hydrodynamic tunnel: Identification of the acoustic charateristics with a one-directional source
[REPT-8228-88] 22 p3244 N90-28399
Velocity Interferometer System for Any Reflector (VISAR): Displacement mode data reduction
[DE90-015027] 23 p3395 N90-29184

WAVE RESISTANCE
Calculation of the odd and even integral components of the wave resistance Green's function
[AD-A212384] 04 p0503 N90-12900
Millimeter wave surface resistance of RBa2Cu3O(7-delta) (R=Y,Eu,Dy,Sm,Er) superconductors
[NASA-TM-102571] 13 p1897 N90-20886
Calculation of surface free three dimensional flows
[ONERA-RSF-5/4368-AY-002A] 22 p3176 N90-28022

WAVE SCATTERING
NT ACOUSTIC SCATTERING
NT ATMOSPHERIC SCATTERING
NT ELECTROMAGNETIC SCATTERING
NT HALOS
NT IONOSPHERIC F-SCATTER PROPAGATION
NT LIGHT SCATTERING
NT MICROWAVE SCATTERING
NT MIE SCATTERING
NT RAMAN SPECTRA
NT RAYLEIGH SCATTERING
NT REVERBERATION
NT THOMSON SCATTERING
NT TROPOSPHERIC SCATTERING
NT X RAY SCATTERING
A combined finite element and boundary integral formulation for solution via CGFFT of 2-dimensional scattering problems
[NASA-CR-184781] 01 p0055 N90-10313
Scattering of an ICRF magnetosonic wave by plasma density turbulence
[DE89-015223] 01 p0126 N90-10720
A method to model fuze performance. Part 2: Calculation of target reflections with physical optics
[FEL-1989-21-PT-2] 04 p0491 N90-12822
On scattering by time-dependent potentials: The 2-D case
[DE89-635708] 09 p1275 N90-17390
Magnetostatic wave device characterization by Brillouin light scattering
[AD-A213798] 09 p1281 N90-17426
CW (Continuous Wave) stimulated Brillouin scattering of long-pulse chemical laser beams
[AD-A216409] 10 p1390 N90-18039
Scattering of waves by inclusions in a nonhomogeneous elastic half space solved by boundary element methods
[PB90-145699] 15 p2116 N90-22107
Forced scattering of electromagnetic waves on electron beam in periodically inhomogeneous plasma
[DE90-620705] 16 p2228 N90-22707
Calculation of 3-dimensional synthetic seismograms on the connection machine
[AD-A218472] 16 p2255 N90-22857
Seismic wave propagation, attenuation and scattering over regional distances
[AD-A219358] 16 p2256 N90-22862
Self-consistent Comptonised models for the spectra of low mass X ray binaries 19 p2780 N90-25817
Broadband analysis of ground wave propagation at a50 to 400 MHz 20 p2846 N90-26185
Remote sensing of Earth terrain
[NASA-CR-186888] 20 p2880 N90-26382
Applications of gauge theories to enhance numerical solutions of mixed potential integral equations
[AD-A221520] 21 p3065 N90-27424
Regional phase propagation in three dimensionally heterogeneous media
[AD-A223279] 24 p3491 N90-29731
Elastic interfaces
[REPT-90-003] 24 p3493 N90-29742

WAVEFORMS
NT PULSE AMPLITUDE
NT PULSE DURATION
NT SAWTOOTH WAVEFORMS
Multi-stage noise-reducing system
[AD-D014179] 03 p0341 N90-11942
Similarity relations of wind waves in finite depth
[PB89-198113] 03 p0376 N90-12144
Characteristics of electromagnetic wave forms with lightning in winter season (2): Characteristics in frequency domain
[DE90-734989] 08 p1103 N90-16388
Polarization radar processing technology
[AD-A215242] 10 p1374 N90-17967
Effective waveform recorder evaluation procedures
[DE90-005197] 10 p1387 N90-18027
Waveform methods for ordinary differential equations
[DE90-006593] 11 p1553 N90-18943
A waveform capture and storage unit and its use for investigating disturbances on digital transmission links
[BBC-RD-1989/17] 12 p1649 N90-19478
A linear systems theory approach to the range-independent acoustic channel
[AD-A216551] 12 p1710 N90-19817
The effects of structure and source complexity on waveforms: Crustal structure of Tibet and the recovery of complex seismic sources
[AD-A218202] 13 p1843 N90-20579
Air Force Boom Event Analyzer Recorder (BEAR): Sysstem description
[AD-A218048] 13 p1882 N90-20800
SAR and ISAR imagery of marine targets 14 p1962 N90-21237
Regional studies with broadband data
[AD-A219215] 16 p2256 N90-22861
Wideband impedance transformer for UHF power transistor time domain waveform measurement system
[PB90-210642] 22 p3167 N90-27962
Studies in automatic speech recognition and its application in aerospace 23 p3318 N90-28759

WAVEGUIDE ANTENNAS
NT HORN ANTENNAS
Performance effects of tie-truss modifications for a 70-meter centerline beam waveguide antenna 04 p0486 N90-12791
A closed-cycle refrigerator for cooling maser amplifiers below 4 Kelvin 04 p0487 N90-12797
A design procedure for a slotted waveguide with probe-fed slots radiating into plasma
[DE90-004168] 09 p1284 N90-17446
The 5th Annual Review of Progress in Applied Computational Electromagnetics
[AD-A217994] 14 p1966 N90-21258
Coplanar waveguide fed phased array antenna
[NASA-TM-102522] 14 p1968 N90-21273
Evaluation of a thermistior power measurement system for use on the NPL antenna extrapolation range
[NPL-DES-89] 24 p3466 N90-29583

WAVEGUIDE FILTERS
CdTe buffered GaAs thin-slab IR waveguide modulators and T/R filter
[AD-A215999] 12 p1651 N90-19488

WAVEGUIDE LASERS
Experimental and theoretical study of CO2 staggered hollow-bore array lasers
[AD-A212921] 10 p1389 N90-18032
Gain in waveguide laser at 10.6 micrometer
[FOA-C-30540-3.1] 18 p2563 N90-24624

WAVEGUIDES
NT BEAM WAVEGUIDES
NT CIRCULAR WAVEGUIDES
NT OPTICAL FIBERS
NT OPTICAL WAVEGUIDES
NT PLASMAGUIDES
NT RECTANGULAR WAVEGUIDES
Constitutive parameter measurements of lossy materials
[NASA-CR-183398] 02 p0281 N90-11603
Channelized coplanar waveguide pin-diode switches
[NASA-TM-102289] 03 p0341 N90-11943
Design, construction and test of a frequency doubler for 183 GHz
[PB89-212591] 03 p0341 N90-11944
Optical data transmission systems in radiation environment
[DE90-000174] 03 p0405 N90-12322
Linear (passive) and non-linear guided and studies in glass
[AD-A211693] 03 p0406 N90-12325
Application of the moment method to the design of slotted waveguide array antennas 04 p0484 N90-12780
Analysis of three- and four-sided uniform waveguides with unusual cross-section/boundary conditions
[AD-A212653] 04 p0493 N90-12834
Theoretical and experimental research on a millimeter-wavelength free-electron laser
[AD-A213321] 04 p0507 N90-12925
Effect of the length of the multijunction grill on its lower hybrid current drive efficiency
[IPPCZ-283] 04 p0556 N90-13240
On optimization of the multijunction grill for the lower hybrid current drive
[IPPCZ-280] 04 p0556 N90-13241
An experimental analysis of the waveguide modes in a high-gain free-electron laser amplifier 05 p0648 N90-13779
Long wave propagation assessment 06 p0758 N90-14414
Symmetric waveguide junction combiner
[AD-D014243] 06 p0768 N90-14466
Waveguide effects in superradiant free-electron lasers
[DE90-003605] 07 p0935 N90-15417
Thin films under chemical stress
[DE90-003754] 07 p0947 N90-15484
Method of making carbon dioxide and chlorine free fluoride-based glass
[AD-D014260] 08 p1048 N90-16060
Characterization of B and N implanted fused silica
[DE90-004198] 08 p1050 N90-16069
High-frequency asymptotic methods for analyzing the EM scattering by open-ended waveguide cavities
[NASA-CR-186244] 08 p1056 N90-16103
Finite element analysis of propagation in waveguide components with application to ferrite phase shifters
[FOA-C-30529-3.2] 09 p1204 N90-16977
Universal nondestructive MM-wave integrated circuit test fixture
[NASA-CASE-LEW-14746-1] 09 p1209 N90-17009
A simple method using MAFIA to calculate external Q values of waveguide-loaded cavities
[DE90-741487] 12 p1647 N90-19465
Field theoretical analysis and synthesis of broadband waveguide: Height, plane shunt circulators with multiple layer material insertions
[ETN-90-95360] 12 p1647 N90-19469
Discontinuous-taper directional coupler
[AD-D014324] 12 p1650 N90-19481
Low threshold current implanted-planar-buried-heterostructure, graded-index, separate-confinement-heterostructure GaAs-AlGaAs laser
[DE90-002579] 12 p1666 N90-19572
A linear systems theory approach to the range-independent acoustic channel
[AD-A216551] 12 p1710 N90-19817
Experimental investigations on channelized coplanar waveguide
[NASA-TM-102494] 13 p1792 N90-20286
Computation of coupling elements between waveguides and modes for large launching structures
[IPPCZ-290] 13 p1890 N90-20842
New ferrite-filled waveguiding structures analysed by the averaging method
[PB90-165671] 14 p1967 N90-21269
Coplanar waveguide discontinuities for P-I-N diode switches and filter applications
[NASA-TM-102534] 14 p1969 N90-21278
Low frequency gyrotron amplifier investigation, phase 2
[AD-A217096] 14 p1981 N90-21352
Active control of multi-dimensional random sound in ducts
[NASA-TM-102653] 14 p2024 N90-21603
An 8.4-GHz dual-maser front-end system for Parkes reimplementation 15 p2078 N90-21905

Theory of a periodic cylindrical waveguide with a nonuniform metal-dielectric filling
[DE90-620099] 15 p2087 N90-21945
Stability regimes in a rotating quadrupole focusing accelerator
[AD-A219513] 16 p2317 N90-23209
Radar clutter via waveguide methods
[AD-A220237] 18 p2542 N90-24512
Analysis and applications of the crosstie-overlay slow-wave structure
[AD-A220286] 18 p2547 N90-24537
Analysis and realization of integrated optical polarizers and absorbers on LiNbO3
[ETN-90-96504] 18 p2623 N90-24949
Transmission, reflection, and radiation at junction planes of different open waveguides
[ISBN-90-9002864-1] 20 p2855 N90-26241
Fabrication of microwave guides using high Tc superconductors
[AD-A221560] 21 p3001 N90-27059
Vertical emitting, ring geometry, ultra-low threshold, and ultra-high speed quantum well lasers for optical interconnect
[AD-A222932] 21 p3008 N90-27098
Applications of gauge theories to enhance numerical solutions of mixed potential integral equations
[AD-A221520] 21 p3065 N90-27424
Integrated optics interdigitated-electrode switches
[AD-A223245] 21 p3076 N90-27490
Polarization contrast vision
[AD-A221423] 21 p3076 N90-27492
Optical fiber to waveguide coupling technique
[AD-A221781] 21 p3077 N90-27496
Optical communications system having a wide-core single-mode planar waveguide
[AD-D014485] 22 p3164 N90-27939
Non-contacting printed circuit waveguide elements
[AD-D014489] 22 p3166 N90-27957
Millimeter-wave generation via plasma three-wave mixing
[AD-A222010] 22 p3247 N90-28415
Radar clutter via ray methods
[AD-A223796] 24 p3462 N90-29553
Reliability study of TWT output RF window
[AD-A223688] 24 p3465 N90-29574
Laser physics and laser spectroscopy
[AD-A224379] 24 p3473 N90-29628
Numerical pulse propagation studies using two classical ocean waveguide models
[AD-A224118] 24 p3542 N90-30033
Planar waveguide spectrometer
[DE90-016308] 24 p3546 N90-30057

WAVELENGTH DIVISION MULTIPLEXING
The first year's work of race project 1036 WTDM broadband customer premises network
[BBC-RD-1989/6] 08 p1055 N90-16097
Monochromator configurations for wavelength division multiplexing
[AD-A214833] 09 p1281 N90-17430
High speed all optical networks
[NASA-CR-185311] 20 p2926 N90-26649
Evaluation of a potential Wave Division Multiplexer (WDM) for use in the IRSTD
[AD-A223945] 24 p3463 N90-29560

WAVELENGTHS
Laser Induced Damage in Optical Materials: 1987
[PB89-221162] 04 p0505 N90-12913
Electron theory of long wavelength concentration fluctuations in liquid metal alloys
[DE89-636213] 07 p0904 N90-15225
Non-contact true temperature measurements in the microgravity environment 10 p1364 N90-17906
Stabilized determination of geopotential coefficients by the mixed hom-BLUP approach
13 p1832 N90-20520
Survey of instrumental methods for the determination of the high frequency wave spectrum
[IOS-267] 15 p2135 N90-22200

WAVERIDERS
Hypersonic waverider configurations for trans-atmospheric vehicles
[AD-A217925] 13 p1755 N90-20074
Project Exodus
[NASA-CR-186836] 20 p2816 N90-26026
Terrapin technologies manned Mars mission proposal
[NASA-CR-186838] 20 p2816 N90-26027

WEAK ENERGY INTERACTIONS
NT WEAK INTERACTIONS (FIELD THEORY)
An experiment to search for galactic axions
05 p0710 N90-14158
Few-body collisions in a weakly interacting Bose gas
[ETN-90-96893] 18 p2613 N90-24886
Relativistic effects in low energy nucleon-nucleon scattering
[CEBAF-PR-89-025] 21 p3075 N90-27483

WEAK INTERACTIONS (FIELD THEORY)
Cosmology and the weak interaction
[NASA-CR-186170] 05 p0713 N90-14169
The ultimate structure of matter: The high energy physics program from the 1950s through the 1980s
[DE90-005682] 12 p1713 N90-19836
Experimental constraints on metric and non-metric theories of gravity 12 p1730 N90-19946
Cosmological baryon and lepton number in the presence of electroweak fermion-number violation
[NASA-CR-186609] 17 p2470 N90-24123

WEAPON SYSTEMS
NT GROUND OPERATIONAL SUPPORT SYSTEM
NT LASER WEAPONS
NT MISSILE SYSTEMS
NT SENTINEL SYSTEM
Human health studies of carbon monoxide (CO) under conditions of military weapons systems crewman exposures. Protocol 1: Formation of COHb
[AD-A210344] 01 p0092 N90-10528
Director, Operational Test and Evaluation report FY-88
[AD-A206784] 01 p0135 N90-10778
Development of a marine integrated navigation system
02 p0149 N90-10852
Flight testing a newly-designed stand-off weapon dispenser 02 p0154 N90-10880
Air Combat Environment Test and Evaluation Facility (ACETEF) 02 p0154 N90-10883
HPW (High Power Microwave) testing of electronic components
[DE89-016682] 02 p0217 N90-11241
Human Operator Simulator (HOS) 4 user's guide
[AD-A212007] 03 p0310 N90-11763
Field-of-View variations and stripe-texturing effects on assault landing performance in the C-130 weapon system trainer
[AD-A212763] 04 p0459 N90-12634
Algorithm development for SDI weapons system allocation
[AD-A212973] 04 p0534 N90-13090
Research on heating, instabilities, turbulence and RF emission from electric field dominated plasmas
[AD-A212122] 04 p0557 N90-13243
A new view of weapon system reliability and maintainability
[AD-A213281] 05 p0580 N90-13382
A new view of weapon system reliability and maintainability: Executive summary
[AD-A213282] 05 p0580 N90-13383
Human factors research in aircrew performance and training
[AD-A213285] 05 p0676 N90-13938
Operational Decision Aids for Exploiting or Mitigating Electromagnetic Propagation Effects
[AGARD-CP-453] 06 p0757 N90-14405
The importance of environmental data
06 p0757 N90-14406
The parabolic equation approach to predicting tropospheric propagation effects in operational environments 06 p0759 N90-14418
The United States Air Force approach to all-weather testing 07 p0870 N90-15047
Proposed activities to prepare for testing advanced/stealth weapons systems
[AD-A214453] 07 p0920 N90-15321
China-built airborne synchronous laser ranger the new L-8 jet trainer aircraft
[AD-A213835] 07 p0936 N90-15422
Reusable navigation module 09 p1165 N90-16742
Project management in successful reliability and maintainability improvement programs
[AD-A215424] 09 p1234 N90-17162
The integration of stores on modern tactical aircraft: Where we have been, and what we should do for the future 10 p1305 N90-17552
Limitations of the conventional role of the B-1B in the European theater
[AD-A217285] 12 p1604 N90-19230
Reliability testing of the Hughes temperature controlled 1/4 watt split cycle cryogenic cooler (HD-1045 (V)/UA)
[AD-A216896] 12 p1641 N90-19426
Ejection seat training of jet pilots and weapon system officers at the German Air Force School of Aviation Medicine 13 p1752 N90-20061
Brain activity during tactical decision-making. Part 3: Relationships between probe-evoked potentials, simulation performance, and on-job performance
[AD-A217207] 13 p1854 N90-20638
The Weapons Laboratory technical library: Automating with STILAS 15 p2178 N90-22447
Field-of-view assessment of low-level flight and an airdrop in the C-130 Weapon System Trainer (WST)
[AD-A218504] 16 p2200 N90-22559
The Department of Defense critical technologies plan for the Committees on Armed Services United States Congress
[AD-A219300] 16 p2227 N90-22702
Nonlinear dynamics and control of flexible structures
[AD-A218476] 17 p2386 N90-23589
Proceedings of the 28th Annual US Army Operations Research Symposium (AORS), volume 1
[AD-A219349] 18 p2606 N90-24842
Human performance models
[FFI-90/7002] 20 p2901 N90-26502
Facilities for improving evaluations of electromagnetic susceptibilities of weapon systems and electronic equipment
[PB90-155862] 21 p2961 N90-26837
Tactical Applications of Space Systems
[AGARD-CP-460] 21 p3067 N90-27438
Future applications of GPS to conventional weapons
21 p3069 N90-27447
Integration of externally carried weapon systems with military helicopters
[AGARD-AR-247] 22 p3115 N90-27696
Space Vehicle Flight Mechanics
[AGARD-CP-489] 22 p3126 N90-27741
Thermal analysis of the wearing by removal of melted metal during high speed friction
[ETCA-89-R-139] 22 p3183 N90-28067
How can research and development leadtime be reduced
[AD-A224063] 23 p3404 N90-29240
Extensions to the learning curve: An analysis of factors influence unit cost of weapon systems
[AD-A224119] 23 p3407 N90-29256

WEAPONS
NT ARTILLERY
NT GUNS (ORDNANCE)
NT LASER WEAPONS
NT MINES (ORDNANCE)
NT NUCLEAR WEAPONS
NT PRECISION GUIDED PROJECTILES
NT SPACE WEAPONS
Present and future US and Soviet chemical missiles and chemical rocket projectiles
[AD-A212199] 04 p0461 N90-12644
Summary of research academic departments, 1987-1988
[AD-A213252] 05 p0716 N90-14183
Weapon aerodynamics overview
[RAE-TM-AERO-2150] 08 p1018 N90-15888
The technology challenge of the advanced tactical fighter: A study of the technology transition process
[AD-A216109] 10 p1320 N90-17630
Report of the First Annual Airborne Weapons Training Technology Review
[DE90-007189] 12 p1697 N90-19747

WEAPONS DELIVERY
Development of advanced WTA algorithms for parallel processing
[AD-A214874] 09 p1266 N90-17341

WEAPONS DEVELOPMENT
Measurement of gas leaks between a projectile and the walls of a tube in a ballistic compressor
[ISL-CO-250/88] 11 p1510 N90-18694
Effects produced by pulsed CO2 lasers
[ISL-R-112/88] 11 p1516 N90-18731

WEAPONS INDUSTRY
The use of technology transfer centers by department of defense industrial facilities
[AD-A216863] 10 p1443 N90-18328

WEAR
The response of isotropic brittle materials to abrasive processes
[DE89-016637] 01 p0045 N90-10251
Friction and wear of oxide-ceramic sliding against IN-718 nickel base alloy at 25 to 800 C in atmospheric air
[NASA-TM-102291] 01 p0046 N90-10262
Research on ultra low wear materials for energy conservation
[DE89-015096] 01 p0046 N90-10263
Sliding seal materials for low heat rejection engines
[NASA-CR-182262] 03 p0331 N90-11882
New Fabric Development Program
[AD-A211549] 03 p0332 N90-11891
The limiting friction force
[ECL-89-005] 05 p0652 N90-13801
Mechanisms of wear in structural ceramic materials
06 p0749 N90-14360
Friction and wear of glassy carbon in sliding contact, revision 1
[DE90-000743] 06 p0750 N90-14365
Pipe and bend erosion by pneumatic transport of solids at high temperature
[DE89-015741] 06 p0778 N90-14524
The development of a T53-L11 engine computer model
[AD-A214533] 09 p1168 N90-16760

Investigation into the effect of fibre size on the tribological behaviour of semi-metallic brake material
09 p1185 N90-16864
Scuffing modelling and experiments for heavily loaded elastohydrodynamic lubrication contacts
10 p1391 N90-18047
The mechanism, measurement, and influence of properties on the galling of metals
[DE90-006533] 11 p1487 N90-18558
The joint effect of surface microtopography and near-surface structure on microcontact conditions
[DE90-006494] 11 p1493 N90-18591
In-line wear monitor
[AD-A217799] 13 p1757 N90-20091
Experimentally determined wear behavior of an Al2O3-SiC composite from 25 to 1200 C
[NASA-TM-102549] 13 p1765 N90-20130
Tribological properties of boric acid and boric-acid-forming surfaces. Part 2: Formation and self-lubrication mechanisms of boric acid films on boron- and boric-oxide-containing surfaces
[DE90-005632] 13 p1811 N90-20400
Studies of mechano-chemical interactions in the tribological behavior of materials
[NASA-TM-102545] 14 p1953 N90-21182
Self-lubricating polymer composites and polymer transfer film lubrication for space applications
[NASA-TM-102492] 15 p2071 N90-21862
SPOT 4 space magnetic recorder mechanisms
15 p2112 N90-22082
Positive lubrication system 15 p2115 N90-22097
CVD diamond films for tribological applications
[AD-A220265] 17 p2413 N90-23750
The mechanical properties of Cu/TiB2 multilayer structures
[DE90-010608] 18 p2517 N90-24378
Friction and wear of whisker-reinforced ceramic composite bodies
[DE90-011313] 18 p2519 N90-24389
Wearing of cryomechanisms at 4 K
18 p2537 N90-24476
Wear of gold-plated contacts: Microscopic aspects, role of oxygen 18 p2538 N90-24479
Tribology of MoS2: Effect of film thickness
18 p2541 N90-24505
Wear transition surfaces for long-term wear effects
[DE90-011314] 19 p2698 N90-25351
Wear mechanisms of amorphous carbon and zirconia coatings on rigid disk magnetic recording media
[DE90-011053] 20 p2837 N90-26133
Wear metal analysis in engine oil by microwave digestion and atomic absorption spectroscopy
[AD-A223070] 21 p2985 N90-26964
Self-lubricating-diamond like coatings deposition
[AD-A221756] 21 p2988 N90-26983
Requirements for long-life operation of inert gas hollow cathodes: Preliminary report
[NASA-TM-103242] 22 p3134 N90-27783
Determination of the SSME high pressure oxidizer turbopump bearing temperature
23 p3291 N90-28619
Fretting wear and fretting fatigue at temperatures up to 600 C 23 p3307 N90-28706
Microdamage to ceramic surfaces under sliding conditions 23 p3308 N90-28708
Surface property improvement in titanium alloy gas turbine components through ion implantation
23 p3309 N90-28713
Electrodeposition of wear resistant coatings
[PB90-221839] 23 p3312 N90-28732
Results from the fourth year of operation of the Federal Methanol Fleet at Lawrence Berkeley Laboratory
[DE90-014741] 23 p3315 N90-28743
Use of electron spectroscopies in the tribological evaluation of diamond films
[DE90-014421] 23 p3334 N90-28848
Mechanical properties testing of diamond and diamond-like films by ultra-low load indentation
[DE90-014456] 23 p3337 N90-28861
The friction and wear of lubricated Si3N4/SiC(w) composites
[DE90-015790] 24 p3444 N90-29448
Ion-beam-assisted deposition of silver films on zirconia ceramics for improved tribological behavior
[DE90-009706] 24 p3456 N90-29516
Ion-beam mixing of Fe/B layers for tribological applications
[DE90-010091] 24 p3456 N90-29518
Solid particle erosion in turbulent flows past tube banks
[DE90-015711] 24 p3469 N90-29598
Friction, wear and electric characteristics of slip-ring brush materials for space applications. Part 1: Screening by pin-on-disk friction tests
[NAL-TR-1040] 24 p3478 N90-29657

WEAR RESISTANCE
NT ABRASION RESISTANCE
Friction and wear of oxide-ceramic sliding against IN-718 nickel base alloy at 25 to 800 C in atmospheric air
[NASA-TM-102291] 01 p0046 N90-10262
Coatings in electrical contacts
[DE89-787739] 02 p0216 N90-11234
Thermomechanical contact phenomena and wear of sliding components
[AD-A211290] 03 p0355 N90-12028
Tribological properties of ceramic/Ti3Al-Nb sliding couples for use as candidate seal materials to 700 deg C
[NASA-TM-102401] 04 p0464 N90-12658
The quality of vacuum deposited surface treatments
[CETIM-107040] 04 p0476 N90-12729
Spall resistance of alumina
[AD-A213213] 04 p0477 N90-12735
Wear-resistant coated object
[EP-PATENT-0-289-173-A1] 05 p0624 N90-13643
Structure-property relationships in ion-beam surface-modified ceramics: Theory and applications
[AD-A212785] 08 p1047 N90-16054
Investigation of rough elastohydrodynamic contact
[ISAL-89-0029] 08 p1085 N90-16281
Ion beam modification of metals: Mechanical properties and structure
[AD-A214701] 09 p1194 N90-16915
The experimental evaluation and application of high-temperature solid lubricants
[NASA-TM-102476] 09 p1198 N90-16944
Development of fuel wear tests using the Cameron-Plint high-frequency reciprocating machine
[AD-A216003] 10 p1361 N90-17892
Energy beam treatment for improved adhesion of coatings to surfaces
[AD-D014449] 14 p1954 N90-21190
Ultrafine microstructure composites prepared by chemical vapor deposition
[AD-A219650] 17 p2369 N90-23484
Friction and wear of tungsten carbides with nitrogen ion implants
[ECL-89-19] 17 p2371 N90-23496
The experimental evaluation and application of high temperature solid lubricants 18 p2564 N90-24631
Thermal analysis of the wearing by removal of melted metal during high speed friction
[ETCA-89-R-139] 22 p3183 N90-28067
Pratt and Whitney cryogenic turbopump bearing experience 23 p3292 N90-28624
Rocketdyne LOX bearing tester program
23 p3293 N90-28626
Electrodeposition of wear resistant coatings
[PB90-221839] 23 p3312 N90-28732
Friction, wear and electric characteristics of slip-ring brush materials for space applications. Part 1: Screening by pin-on-disk friction tests
[NAL-TR-1040] 24 p3478 N90-29657

WEAR TESTS
Compatibility of fuel system components with high density fuel
[AD-A210381] 01 p0006 N90-10027
Thermomechanical contact phenomena and wear of sliding components
[AD-A211290] 03 p0355 N90-12028
Tribological properties of PM212: A high-temperature, self-lubricating, powder metallurgy composite
[NASA-TM-102355] 04 p0465 N90-12659
A new test machine for measuring friction and wear in controlled atmospheres to 1200 C
[NASA-TM-102405] 04 p0466 N90-12670
Characterization of self-lubricating surface materials
[CETIM-108060] 04 p0479 N90-12749
Effects of composition and age hardening on precious metal electrical contacts
[DE88-008791] 06 p0769 N90-14476
Solid lubrication of ceramic surfaces by IAD (Ion-Assisted Deposition)-silver coatings for heat engine applications
[DE90-002860] 07 p0909 N90-15253
Development of fuel wear tests using the Cameron-Plint high-frequency reciprocating machine
[AD-A216003] 10 p1361 N90-17892
Characterization of particle impact by quantitative acoustic emission
[AERE-R-13028] 16 p2246 N90-22810
Friction and wear of tungsten carbides with nitrogen ion implants
[ECL-89-19] 17 p2371 N90-23496
Quality evaluation of coatings by automatic scratch testing
[AD-A219331] 17 p2379 N90-23548
Study of ball bearings for space use
18 p2537 N90-24477

WEATHER
NT COLD WEATHER
Mariners Weather Log, volume 32, number 3, Summer 1988
[PB88-248075] 01 p0086 N90-10491
A program to improve performance of AFGL (Air Force Geophysical Laboratory) automated present weather observing sensors
[AD-A207669] 01 p0087 N90-10495
Diagnostic study of atmosphere-terrain interaction leading to the formation of dust clouds and poor visibilities over near east desert areas
[AD-A211243] 02 p0239 N90-11358
World Weather Watch: Implementation
[WMO-714] 03 p0375 N90-12139
The interaction and variation of waves and turbulence from MST radar data
[AD-A212849] 05 p0670 N90-13906
An evaluation of the Smith-Feddes model
[AD-A213237] 05 p0671 N90-13907
Activities report of the World Meteorological Organization
[WMO-713] 05 p0671 N90-13912
Flight in adverse environmental conditions
[AGARD-AR-277] 06 p0723 N90-14218
Airborne FLIR detection of surface targets
06 p0759 N90-14416
The thermal behavior of natural backgrounds and its prediction by means of numerical models
06 p0762 N90-14436
Summary of papers, studies, conference presentations: 1987-1988 (from the National Weather Service, southern region)
[PB90-103896] 06 p0817 N90-14749
Climatology of Lawrence Livermore National Laboratory
[DE90-000905] 06 p0818 N90-14756
Measurements of horizontal visibility in the lowest 300 m over Northern Germany 07 p0872 N90-15059
Effects of lightning on operations of aerospace vehicles 07 p0873 N90-15065
Environmental surveillance data
[DE90-001275] 07 p0956 N90-15532
Winter cloud seeding potential on the Mogollon Rim
[PB89-190540] 07 p0962 N90-15562
Surface observation climatic summaries
[AD-A215786] 10 p1408 N90-18122
Federal methanol fleet update
[DE90-006851] 11 p1517 N90-18741
Colloquium on Synoptic Meteorology
[PB90-121112] 12 p1692 N90-19720
Spectral solar radiation data base documentation, volume 1
[DE89-009447] 13 p1841 N90-20571
Coastal frontogenesis and associated severe weather on 13 March 1986 (GALE IOP 13)
[AD-A217708] 13 p1845 N90-20590
Continental shelf processes affecting the oceanography of the South Atlantic Bight
[DE90-008439] 13 p1848 N90-20606
Investigation of air transportation technology at the Massachusetts Institute of Technology, 1988-1989
14 p1905 N90-20922
Cockpit display of hazardous wind shear information
14 p1905 N90-20924
Cockpit display of hazardous weather information
14 p1906 N90-20929
Weather data dissemination to aircraft
14 p1907 N90-20934
Plan for the FAA air traffic operational evaluation of the Automated Surface Observing System (ASOS)
[DOT/FAA/CT-TN89/56] 14 p1914 N90-20968
Final safety analysis report for the Ulysses Mission. Volume 3 (Book 2): Nuclear risk analysis document-appendices
[DE90-008692] 14 p1939 N90-21102
Meteorologist Weather Processor (MWP) integration test plan
[DOT/FAA/CT-TN89/62] 14 p2007 N90-21500
Analysis of distributions of Visual Meteorological Conditions (VMC) heliport data
[DOT/FAA/CT-TN89/67] 14 p2008 N90-21508
Minimizing the effects of the atmosphere in the observation of ultraviolet radiation
15 p2080 N90-21911
Scintillation of millimeter-wave intensity and phase caused by turbulence and precipitation
15 p2080 N90-21912
Propagation environments, effects, and decision aids
15 p2081 N90-21918
Modelling of optically and IR effective atmospheric turbulence 15 p2082 N90-21923
Calculation of IR propagation statistics in the eastern Atlantic for surveillance system performance assessment 15 p2085 N90-21938
JARE data reports, no. 140 (meteorology 21): Meteorological data at Asuka Camp, Antarctica in 1987
[ISSN-0075-3343] 15 p2132 N90-22188

An anomalous wind between valleys: Its characteristics and a proposed explanation
[DE90-008965] 15 p2133 N90-22189
AFGW's upper air validator system
[AD-A219309] 16 p2258 N90-22876
The effects of climate change on energy planning and operations in the Pacific Northwest. Volume 2: Technical background
[DE90-009465] 17 p2425 N90-23817
Sea breeze: Induced mesoscale systems and severe weather
[NASA-CR-186367] 19 p2715 N90-25450
Annual and interannual variations of Earth-emitted radiation based on a 10-year data set
[NASA-TM-103465] 20 p2887 N90-26432
Mariners Weather Log, volume 33, number 2, Spring 1989
[PB90-146838] 20 p2889 N90-26443
Mariners Weather Log, volume 33, number 3, Summer 1989
[PB90-146846] 20 p2889 N90-26444
Mariners Weather Log, volume 33, number 4, Fall 1989
[PB90-146853] 20 p2890 N90-26445
Analysis and improved design considerations for airborne pulse Doppler radar signal processing in the detection of hazardous windshear
[NASA-CR-186792] 20 p2890 N90-26448
Brief state-of-the-art review on optical communications for the NASA ISES workshop 21 p3017 N90-27153
Dust clouds Kosa from the east Asian dust storms in 1982-1988 as observed by the GMS satellite 21 p3028 N90-27214
A LOWTRAN7 sensitivity study in the 8-12 and 3-5 micron bands: Includes comparison with LOWTRAN6 results
[AD-A222094] 21 p3031 N90-27231
Environmental Research Laboratories programs and plans. FY-1989 and FY-1990 plans
[PB90-169988] 22 p3197 N90-28144
Effects of corpuscular radiation on weather and climate 22 p3201 N90-28164
A search for solar related changes in tropospheric weather 22 p3203 N90-28173
World weather records, 1971-1980. Volume 1: North America
[PB90-182858] 22 p3212 N90-28221
Verification of the naval oceanic vertical aerosol model during FIRE 22 p3219 N90-28257
An investigation of forcing mechanisms during a surprise tornadic thunderstorm
[PB90-216805] 23 p3352 N90-28940
Annual course of precipitation over much of the US: Observed versus GCM simulation
[PB90-221656] 23 p3352 N90-28942
Program on development of basic understanding of severe weather phenomena
[PB90-226564] 23 p3352 N90-28943
A conceptual weather-type classification procedure for the Philadelphia, Pennsylvania area
[PB90-231705] 23 p3352 N90-28944
Meteorological conditions over the North Atlantic Ocean during GCE/CASE/WATOX
[PB90-252032] 24 p3494 N90-29747

WEATHER CHARTS
U METEOROLOGICAL CHARTS

WEATHER CONDITIONS
U WEATHER

WEATHER CONTROL
U WEATHER MODIFICATION

WEATHER DATA RECORDERS
Type-specific dynamic measurements on wind turbines at the test site Schnittlingen (Germany, F.R.)
[DFVLR-MITT-88-31] 03 p0367 N90-12099

WEATHER FORECASTING
NT NUMERICAL WEATHER FORECASTING
NT STATISTICAL WEATHER FORECASTING
Forecasting convection with the AFOS (Automation of Field Operations and Services) data analysis programs. (ADAP-version 2.0) (AFOS data analysis programs-version 2.0)
[PB89-145940] 01 p0086 N90-10492
National Severe Storms Laboratory, fiscal year 1988
[PB89-156145] 01 p0087 N90-10493
Meteorological support: Descriptions of application programs for accessing and displaying data
[PB89-194625] 01 p0088 N90-10500
Research highlights of the NMC (National Meteorological Center) Development Division: 1987-1988
[PB89-206478] 01 p0088 N90-10501
Effects of stress on judgment and decision making in dynamic tasks
[AD-A210605] 01 p0135 N90-10781
Average diurnal and seasonal profiles of ionospheric storms 02 p0241 N90-11371
Hurricane Research Division fiscal year 1988 programs, fiscal year 1989 projections
[PB89-152268] 02 p0250 N90-11418
Composited local area forecast techniques
[AD-A210802] 02 p0253 N90-11432
Low level remote sensing: The Doppler Radar wind profiler 03 p0361 N90-12067
LAWS simulation: Sampling strategies and wind computation algorithms 03 p0364 N90-12081
Satellite-derived rainfall estimates and propagation characteristics associated with the Mesoscale Convective Systems (MCSs)
[PB89-213417] 03 p0365 N90-12086
Contemporary China's meteorological enterprises (selected portions)
[AD-A210697] 03 p0373 N90-12131
Development of high resolution simulations of the atmospheric environment using the MASS model
[NASA-CR-186040] 03 p0374 N90-12133
Severe local storm warning verification: 1988
[PB89-226310] 03 p0374 N90-12134
Investigation of North Atlantic fog and development of a marine fog forecast system
[AD-A211780] 04 p0519 N90-12999
Subjective uses of wind profiler data in warm season analysis and forecasting: Wind profiler training manual number 3
[PB89-223333] 04 p0520 N90-13004
The linear study of zonally asymmetric barotropic flows 05 p0668 N90-13902
A collection of papers related to heavy precipitation forecasting
[PB89-230833] 05 p0671 N90-13910
Three dimensional analysis of the structure of the atmosphere in polar environments by vertical satellite sounding. Interest for the meteorological forecasts at high latitudes
[ETN-90-95506] 05 p0671 N90-13911
An in-flight technique for wind measurement in support of the space shuttle program
[NASA-TM-4154] 06 p0724 N90-14224
Summary of 1989 Atlantic tropical cyclone activity and seasonal forecast verification 06 p0815 N90-14743
Use of operational 0-6 and 3-9 h quantitative precipitation forecasts for predicting heavy rain events
[PB90-103946] 06 p0817 N90-14750
A global ocean wind stress climatology based on ECMWF (European Centre for Medium Range Weather Forecasts) analyses
[PB90-109968] 06 p0817 N90-14752
A dynamic model for forecasting new cloud development
[AD-A213939] 08 p1102 N90-16383
World Weather Watch. Global observing system-satellite sub-system. Information on meteorological and other environmental satellites, second edition
[WMO-411-ED-2] 08 p1103 N90-16386
Analysis of significant weather on meso-alpha scales using conventional and remotely sensed data: Exploratory studies
[AD-A214563] 09 p1248 N90-17238
Rule-based systems for visibility forecasts
[AD-A214622] 09 p1248 N90-17239
Observing systems simulation experiments: Their role in meteorology
[AD-A215705] 09 p1248 N90-17243
The Polar Ice Prediction System: A sea ice forecasting system
[AD-A214600] 09 p1249 N90-17246
An atlas of ECMWF analyses (1980-1987). Part 1: First moment quantities
[NASA-TM-100747-PT-1] 10 p1408 N90-18120
Super-micro computer weather prediction model
[AD-A216329] 10 p1409 N90-18124
ERS-1 European remote sensing satellite: A new tool for global environmental monitoring in the 1990's
[ESA-BR-36] 11 p1526 N90-18782
Forecasters handbook for Central America and adjacent waters
[AD-A216752] 11 p1536 N90-18845
Dynamics of an ERICA (Experiment on Rapidly Intensifying Cyclones over the Atlantic) cyclone
[AD-A216775] 11 p1536 N90-18846
Validation of the EURAD cloud modules 12 p1687 N90-19693
Synoptic-scale forcing of the low-level jet in developing baroclinic waves 12 p1692 N90-19717
Colloquium on Synoptic Meteorology
[PB90-121112] 12 p1692 N90-19720
Analysis of GALE (Genesis of Atlantic Lows Experiment) data
[AD-A217182] 13 p1844 N90-20584
Derivation of kinematic fields using wind profiler data from the 1985 pre-storm experiment
[AD-A217952] 13 p1845 N90-20592
A prototype expert system to forecast severe winds in the western Mediterranean Sea
[AD-A218017] 13 p1845 N90-20593
Forecasting 24 and 48 hour intensity changes, for northwestern Pacific tropical cyclones, using satellite imagery
[AD-A218174] 13 p1846 N90-20597
Forecasting the tornadic intensities of thunderstorms by multivariate techniques
[AD-A218284] 13 p1847 N90-20602
Microwave brightness temperature and its relation to atmospheric general circulation features
[AD-A218312] 13 p1847 N90-20603
The influence of ice accretion physics on the forecasting of aircraft icing conditions 14 p1906 N90-20928
Predictability of weather and climate in a coupled ocean-atmosphere model: A dynamical systems approach
[NASA-CR-186499] 14 p2007 N90-21502
Tropical cyclone track predictability and the adjoint method of data assimilation
[AD-A218324] 14 p2007 N90-21505
Second National Winter Weather Workshop Conducted by the National Weather Service
[PB90-147414] 15 p2131 N90-22183
Impact of marine boundary layer parameterization on a numerical simulation of cyclogenesis during a cold air outbreak event 16 p2256 N90-22864
Predictability of weather and climate in a coupled ocean-atmosphere model: A dynamical systems approach 16 p2256 N90-22865
Next generation weather radar (NEXRAD) initial operational test and evaluation. Phase 2: (IOT and E(2))
[AD-A218770] 16 p2258 N90-22873
Earth observation from the interstellar space
[REPT-44/89] 17 p2418 N90-23781
Seasonal weather forecast verification
[DE90-009467] 17 p2425 N90-23818
A description of tropical cyclone recurvature in terms of isentropic potential vorticity
[AD-A218482] 17 p2425 N90-23821
A case study of explosive cyclogenesis in the eastern Pacific Ocean 14 to 17 December 1987
[AD-A219543] 17 p2426 N90-23824
A Kalman filter with smoothing for hurricane tracking and prediction
[AD-A220413] 17 p2426 N90-23827
A comparison of lightning network data with surface weather observations
[AD-A220003] 17 p2427 N90-23832
Tropical cyclones, 1989: Central north Pacific
[PB90-182536] 17 p2428 N90-23836
Evaluation of Stochastic models for estimating the persistence probability of cloud-free lines-of-sight
[AD-A220283] 18 p2581 N90-24702
Research programs: Meteorological prediction. Oceanic processes. Climate and global change monitoring. Satellite instrumentation and calibration 19 p2714 N90-25447
Advanced mesoscale weather forecasting to support tactical operations on the airland battlefield
[AD-A219421] 19 p2715 N90-25449
An atlas of ECMWF analyses (1980-1987). Part 2: Second moment quantities
[NASA-TM-100762-PT-2] 19 p2715 N90-25451
Applications of ISES for meteorology 21 p3018 N90-27160
Boundary layer parameterization for use in a limited area forecast model 21 p3029 N90-27224
An intercomparison of intraseasonal variability in general circulation models and observations
[NASA-TM-100764] 21 p3030 N90-27228
Wind field derivatives of extratropical cyclones observed by Doppler radar
[AD-A222188] 21 p3031 N90-27232
A regional forecasting model
[AD-A221556] 21 p3031 N90-27235
Gulfcasting: Dynamical forecast experiments for G ulf Stream rings and meanders
[AD-A221482] 21 p3032 N90-27238
Tactical Applications of Space Systems
[AGARD-CP-460] 21 p3067 N90-27438
Tactical applications of Defense Meteorological Satellite Program (DMSP) environmental data 21 p3067 N90-27439
Application of Meteorological Satellite (METSAT) data to support United States forces in the North Atlantic Treaty Organization (NATO) 21 p3068 N90-27440
DMSP's interactive tactical terminal 21 p3068 N90-27441
Space-based wide area surveillance system studies 21 p3068 N90-27444
Global positioning system overview/status 21 p3069 N90-27446

Laboratory experiments on stability and entrainment of oceanic stratocumulus. Part 1: Instability experiment
22 p3220 N90-28263
Instability bursts associated with Extratropical Cyclone Systems (ECSs) and a forecast index of 3 to 12 hour heavy precipitation
[NOAA-TM-NESDIS-30] 22 p3228 N90-28309
Severe thunderstorm cases of July 1988 through June 1989
[PB90-226424] 22 p3229 N90-28311
Severe local storm warning verification: 1989
[PB90-248592] 22 p3229 N90-28313
Proceedings of the 14th Annual Climate Diagnostics Workshop
[PB90-198573] 23 p3351 N90-28938
Program on development of basic understanding of severe weather phenomena
[PB90-226564] 23 p3352 N90-28943
Automated system for meteorological analysis
[INPE-4586-TDL/332] 23 p3352 N90-28945
Severe thunderstorm forecasting: An operational review
[PB90-215484] 23 p3353 N90-28948
The effect of wave data assimilation on the numerical simulation of wave energy advection
[KNMI-TR-121] 24 p3496 N90-29760

WEATHER FRONTS
U FRONTS (METEOROLOGY)

WEATHER MAPS
U METEOROLOGICAL CHARTS

WEATHER MODIFICATION
NT CLOUD DISPERSAL
NT CLOUD SEEDING
NT FOG DISPERSAL
NT LIGHTNING SUPPRESSION
NT STORM SUPPRESSION
Applied atmospheric resources research program in Thailand
[PB89-235402] 05 p0668 N90-13903

WEATHER RADAR
U METEOROLOGICAL RADAR

WEATHER STATIONS
NT AUTOMATIC WEATHER STATIONS
Hanford Meteorological Station computer codes. Volume 10: The ARCHIVE computer code
[DE89-016175] 02 p0252 N90-11429
Contemporary China's meteorological enterprises (selected portions)
[AD-A210697] 03 p0373 N90-12131
Climatic summaries and documentation for the primary meteorological Station, H. J. Andrews Experimental Forest, 1972 to 1984
[PB90-104373] 08 p1102 N90-16382
Handbook of climate of the USSR. Humidity of air, atmospheric precipitations, snow cover
[AD-A220454] 17 p2427 N90-23828
Some results from the precipitation chemistry measurement programme in Sweden
20 p2884 N90-26410
Data Base Analyzer and Parameter Estimator (DBAPE) interactive computer program user's manual
[PB90-193053] 23 p3406 N90-29252

WEATHERING
Development of a semiquantitative corrosion monitor
[AD-A208132] 01 p0072 N90-10414
Coating galvanized steel
[AD-A211775] 03 p0329 N90-11869
Study of alteration covers of part of the Sao Paulo State through remote sensing data
[INPE-4849-TDL/364] 10 p1399 N90-18086
Collapsible fabric tank testing
[AD-A217861] 14 p1987 N90-21388
Quantitative studies of the Martian south polar region using spacecraft images 15 p2191 N90-22514
Erosional development of bedrock spur and gully topography in the Valles Marineris, Mars
[NASA-CR-180655] 17 p2424 N90-23813
The effects of acid fog and dew on materials
[PB90-157496] 19 p2712 N90-25436
Proceedings of a workshop on Differences Between Antarctic and Non-Antarctic Meteorites
[NASA-CR-184918] 20 p2942 N90-26740

WEAVING
The interlaminar fracture toughness of woven graphite/epoxy composites
[NASA-TP-2950] 01 p0033 N90-10179
Three-dimensional stress analysis of plain weave composites
[NASA-TM-101672] 10 p1347 N90-17813
Failure analysis of woven hybrid composite using a finite element method
[OUEL-1791/89] 15 p2065 N90-21828

WEBS (MEMBRANES)
U MEMBRANES

WEBS (SHEETS)
Stick propellant x ray inspection
[AD-A212601] 06 p0753 N90-14380

WEDGE FLOW
Graphs of the state of stress at rounded corners
[MEMT-1] 15 p2119 N90-22122

WEDGES
Experimental investigation of a planar shock wave over a double wedge
[AD-A211366] 03 p0347 N90-11981
Axial flow in corners at supersonic and hypersonic speeds 10 p1308 N90-17570
Prediction of length scales in a Mach reflection flowfield 15 p2089 N90-21959

WEIBULL DENSITY FUNCTIONS
Independent Orbiter Assessment (IOA): Weibull analysis report
[NASA-CR-185534] 02 p0168 N90-10948
Pacific marine radar sea scatter experimental results
[AD-A211593] 03 p0339 N90-11931
Optimum selection procedures in multi-stage screening, reliability, and time
[AD-A216811] 11 p1553 N90-18942
Approximate interval estimation methods for the reliability of systems using component data with exponential and Weibull distributions
[AD-A219857] 17 p2460 N90-24048
Applications of non-parametric density estimation
[AD-A220206] 17 p2466 N90-24094
Probabilistic approach to the certification for fatigue durability of composite structures
[DE90-505521] 20 p2828 N90-26085
Reliability growth modeling analysis of the space shuttle main engines based upon the Weibull process
[NASA-TM-103511] 22 p3189 N90-28098
Reliability analysis of a structural ceramic combustion chamber
[NASA-TM-103264] 22 p3192 N90-28112
Probability models for the failure of fibres and fibrous composite materials 23 p3300 N90-28665

WEIERSTRASS FUNCTIONS
Weierstrass preparation and division theorems for the ring of germs of superanalytic functions
[DE90-612742] 14 p2020 N90-21576

WEIGHT
PDWAP: A preliminary design and weights analysis program for aerospace vehicles
[AD-A222614] 20 p2808 N90-25979

WEIGHT (MASS)
NT ATOMIC WEIGHTS
NT BIOMASS
NT STRUCTURAL WEIGHT

WEIGHT INDICATORS
NT MICROBALANCES
NT STRAIN GAGE BALANCES

WEIGHT REDUCTION
Characterization and cycle tests of lightweight nickel electrodes
[NASA-TM-102399] 04 p0470 N90-12696
Development of an advanced fan blade containment system
[DOT/FAA/CT-89/20] 05 p0581 N90-13386
Aerobraking characteristics for several potential manned Mars entry vehicles
[NASA-TM-101669] 06 p0733 N90-14272
Aluminum-lithium: Application of plate and sheet to fighter aircraft 07 p0900 N90-15202
Advanced composite polar boss
[AD-D014287] 08 p1037 N90-15994
Low risk low power heat pipe/thermoelectric space power supply
[DE89-014817] 08 p1095 N90-16342
Reduction of 50 micron thick solar cell weight by selective back contact silver plating
10 p1342 N90-17778
Structural design of the Telecom 2 solar array
10 p1343 N90-17786
The ITALSAT solar array 10 p1343 N90-17787
Lightweight, low cost, thin silicon cell arrays
10 p1345 N90-17800
Advances in lightweight nickel electrode technology
13 p1825 N90-20476
Multi-objective shape and material optimization of composite structures including damping
[NASA-TM-102579] 14 p1945 N90-21132
Transmission research activities at NASA Lewis Research Center
[NASA-TM-103132] 14 p1988 N90-21394
Advanced tube-bundle rocket thrust chamber
[NASA-TM-103139] 19 p2670 N90-25185
The application of engineering ceramics in gas turbines
[PNR90676] 20 p2812 N90-26005
Design of helicopter components in metal matrix composites
[REPT-100-20-55] 21 p2972 N90-26894
Shuttle to Shuttle 2: Subsystem weight reduction potential (estimated 1992 technology readiness date)
[NASA-TM-89114] 23 p3286 N90-28589

WEIGHTING FUNCTIONS
A polynomial method of approximate weighted centers for linear programming
[REPT-89-13] 03 p0388 N90-12210
Time-weighted accumulations ap(tau) and Kp(tau)
[RAE-TR-88050] 03 p0421 N90-12422
Optimum data weighting and error calibration for estimation of gravitational parameters
[NASA-TM-100737] 04 p0517 N90-12985
Optimum data weighting and error calibration for estimation of gravitational parameters
05 p0591 N90-13437
Study of pressure sensors in hydrodynamic turbulent boundary layer
[ONERA-RF-17/7218-PY] 09 p1218 N90-17067
Initialization of EURAD, part 2
12 p1688 N90-19696
A note on overdispersed exponential families
[AD-A216277] 14 p2018 N90-21565
High order P-G finite elements for convection-dominated problems
[DE90-614743] 15 p2097 N90-21998
Fatigue crack growth in unidirectional metal matrix composite
[NASA-TM-103102] 15 p2118 N90-22117
Probabilistic analysis of the minimum weighted flowtime scheduling problem
[CWI-BS-R8913] 17 p2466 N90-24091
Weight functions and stress intensity factors for mode 1 cracks in arbitrary 2D geometries under general crack surface loading
[FFA-TN-1990-17] 19 p2703 N90-25381
An angular weighting approach for calculating gradients and divergences
[DE90-013164] 20 p2908 N90-26539
Weighted norm inequalities for Riemann-Liouville fractional integral
[DE90-627153] 23 p3388 N90-29132
Recurrence relations and weight functions for approximation by orthonormal polynomials
[DE90-627156] 23 p3388 N90-29134

WEIGHTLESSNESS
Cardiovascular, renal, electrolyte, and hormonal changes in man during gravitational stress, weightlessness, and simulated weightlessness: Lower body positive pressure applied by the antigravity suit
[NASA-TM-102232] 04 p0522 N90-13013
On the wings of a dream: The Space Shuttle
[NASA-EP-269] 05 p0593 N90-13446
Watchfulness and attention during weightlessness simulations: Use of computerized psychometric tests
[REPT-89-TOU-3-1045] 05 p0674 N90-13928
Response of a rotating finite annular liquid layer to axial excitation
[LRT-WE-9-FB-15(1988)] 08 p1053 N90-16090
The 1988-1989 NASA space/gravitational biology accomplishments
[NASA-TM-4160] 09 p1250 N90-17251
Hydrogen/oxygen SPE (trademark) electrochemical devices for zero-g applications 10 p1333 N90-17710
Non-Contact Temperature Requirements (NCTM) for drop and bubble physics 10 p1366 N90-17918
Earth-orbiting resonant-mass gravitational wave detectors 12 p1731 N90-19954
Vortex motion phase separator for zero gravity liquid transfer
[NASA-CASE-KSC-11387-1] 13 p1783 N90-20236
Center of Gravity: Metallic Solidification
[DFVLR-IB-333-89/3] 13 p1784 N90-20238
German microgravity program and flight opportunities
13 p1784 N90-20239
User center and assitance 13 p1784 N90-20240
Microgravity conditions of a space vehicle
13 p1785 N90-20247
A comparison of the mechanisms of cold- and microgravity-induced fluid loss
[AD-A218098] 13 p1852 N90-20631
Space truss zero gravity dynamics
14 p1937 N90-21087
In-house experiments in large space structures at the Air Force Wright Aeronautical Laboratories Flight Dynamics Laboratory 14 p1938 N90-21092
BASG thermomechanical pump helium 2 transfer tests
[NASA-CR-177541] 14 p1939 N90-21097
Zero-G phase detector and separator
[NASA-CASE-LEW-14844-1] 15 p2101 N90-22024
Research in human performance related to space: A compilation of three projects/proposals
18 p2629 N90-24983
The effects of simulated hypogravity on murine bone marrow cells 18 p2631 N90-24989
Early mammalian development and possible involvement of gravity 19 p2680 N90-25242

The first seven minutes of a Zenopus egg fertilised on a sounding rocket in space 19 p2680 N90-25245
The effect of clinostat rotation on plant protoplasts 19 p2681 N90-25247
Experiment K-6-08. Biochemical and histochemical observations of vastus medialis 20 p2893 N90-26462
Experiment K-6-10. Effects of zero gravity on myofibril protein content and isomyosin distribution in rodent skeletal muscle 20 p2894 N90-26464
Experiment K-6-11. Actin mRNA and cytochrome c mRNA concentrations in the triceps brachia muscle of rats 20 p2894 N90-26465
Experiment K-6-14. Hepatic function in rats after spaceflight 20 p2895 N90-26468
Experiment K-6-18. Study of muscarinic and gaba (benzodiazepine) receptors in the sensory-motor cortex, hippcampus and spinal code 20 p2895 N90-26471
Experiment K-6-21. Effect of microgravity on 1) metabolic enzymes of type 1 and type 2 muscle fibers and on 2) metabolic enzymes, neutransmitter amino acids, and neurotransmitter associated enzymes in motor and somatosensory cerebral cortex. Part 1: Metabolic enzymes of individual muscle fibers; part 2: metabolic enzymes of hippocampus and spinal cord 20 p2896 N90-26474
Approximate natural damped frequencies of a finite viscous floating-zone under zero-gravity condition [LRT-WE-9-FB-8(1988)] 21 p2990 N90-26995
Response of a liquid column to one-sided axial excitation in zero-gravity [LRT-WE-9-FB-3(1989)] 21 p2991 N90-26996
Non-linear axial vibrations of a cylindrical liquid column in zero-gravity [LRT-WE-9-FB-4(1989)] 21 p2991 N90-26997
Response of a liquid column to counter-directional excitation under zero-gravity [LRT-WE-9-FB-6(1989)] 21 p2991 N90-26998
Response of a liquid column to unequal counter-directional excitation under zero-gravity [LRT-WE-9-FB-7(1989)] 21 p2991 N90-26999
Response of a viscous liquid column to pitching- and roll-excitation in zero-gravity environment [LRT-WE-9-FB-10(1989)] 21 p2991 N90-27000
Response of differently axially excited viscous liquid bridges in zero-gravity [LRT-WE-9-FB-14(1989)] 21 p2991 N90-27001
Response of a viscous liquid column to various pitch-excitations [LRT-WE-9-FB-15(1989)] 21 p3006 N90-27090
Response of differently axial-excited spinning liquid columns [LRT-WE-9-FB-16(1989)] 21 p3006 N90-27091
Effects of short-term weightlessness on roll circularvection 23 p3361 N90-28992
Formulation of design guidelines for automated robotic assembly in outerspace 23 p3365 N90-29017
Renal response to seven days of lower body positive pressure in the squirrel monkey [NASA-CR-183355] 24 p3497 N90-29761

WEIGHTLESSNESS SIMULATION
NT NEUTRAL BUOYANCY SIMULATION
Cardiovascular, renal, electrolyte, and hormonal changes in man during gravitational stress, weightlessness, and simulated weightlessness: Lower body positive pressure applied by the antigravity suit [NASA-TM-102232] 04 p0522 N90-13013
Small amplitude liquid oscillations in a rectangular container under zero-gravity [LRT-WE-9-FB-2(1989)] 08 p1066 N90-16167
Linear liquid oscillations in cylindrical containers under zero-gravity [LRT-WE-9-FB-5(1989)] 08 p1066 N90-16168
The vibro-acoustic mapping of low gravity trajectories on a Learjet aircraft [NASA-TM-103103] 15 p2045 N90-21723
Noninvasive estimation of fluid shifts between body compartments by measurement of bioelectric characteristics 18 p2628 N90-24976
Cardiovascular deconditioning of cosmonauts: Role, importance and applications of the lower body negative pressure [ETN-90-97507] 23 p3355 N90-28964

WELD STRENGTH
STSA-Space Telescope solar array interconnectors: From simple approaches to complex modeling. A case study of the necessity of complex analysis 02 p0188 N90-11076
A re-evaluation of fatigue threshold test procedures and the simulation and prediction of fatigue crack growth under conditions of low crack closure 02 p0231 N90-11328
Influence of the composition of the metal deposited on carbon manganese welds on the work properties of the melted area depending on the operating mode of the weld [CETIM-104530] 04 p0476 N90-12726
Reflection by defective diffusion bonds [AD-A212995] 05 p0623 N90-13638
On-line assessment of weld quality using ultrasonics [AERE-R-13401] 14 p1989 N90-21398
VAMAS project on variable weld penetration: Surface tension of the steels [NPL-DMA(A)-188] 15 p2070 N90-21856
Robotic and automatic welding development at the Marshall Space Flight Center 23 p3298 N90-28656
Some studies of the vibration welding of therm: /0 astics 23 p3332 N90-28842

WELD TESTS
Influence of the composition of the metal deposited on carbon manganese welds on the work properties of the melted area depending on the operating mode of the weld [CETIM-104530] 04 p0476 N90-12726
Fatigue testing of welded steel assemblies with or without finishing treatments [CETIM-107900] 04 p0513 N90-12961
Metal transfer in gas metal arc welding [AD-A213390] 05 p0624 N90-13642
Reduction of residual stress and distortion in HY100 and HY130 high strength steels during welding [AD-A213532] 07 p0905 N90-15231
Eddy-current inspection of shuttle heat exchanger tube welds [NASA-CR-186302] 07 p0943 N90-15462
Ultrasonic and parallel gap welding of GaAs solar cells, experimental and simulation results 10 p1341 N90-17766
Assembly technology of GaAs solar cell 10 p1341 N90-17772
Fracture toughness and fatigue crack initiation tests of welded precipitation-hardening stainless steel [AD-A218745] 16 p2221 N90-22669
Fatigue crack monitoring from initiation to through cracking in welded thick steel sections [ARE-TM(UHS)-90203] 22 p3194 N90-28122

WELDABILITY
Weldability of ductile nickel aluminides [DE89-017452] 03 p0327 N90-11859
Effects of precipitate distribution on 293 K and 77 K properties of 2090-T81 weldments [DE90-002332] 06 p0747 N90-14349
The feasibility of welding of irradiated materials [DE90-002200] 06 p0795 N90-14631
Welding behavior and welding metallurgy of ductile intermetallic alloys [DE90-008908] 15 p2069 N90-21852
Development and evaluation of advanced austenitic alloys [DE90-011315] 18 p2528 N90-24425
Filler metal development for Hastelloy alloy XR [DE90-791084] 21 p2981 N90-26939
Weldment mechanical properties of aluminum-copper-lithium alloy, 2090, at ambient and cryogenic temperatures [DE90-014178] 21 p2981 N90-26941

WELDED JOINTS
Delayed failure of silver-aided diffusion welds between steel [DE89-016652] 01 p0045 N90-10252
Limit analysis of welded tee end connections for hollow tubes [PB89-191647] 01 p0079 N90-10452
The Meta-Lax method of stress reduction in welds [DE89-016437] 02 p0230 N90-11321
Resistance welding large parts [DE89-010462] 03 p0354 N90-12027
Improvement of rules relating to clamp calculations [CETIM-110610] 04 p0509 N90-12939
Metal transfer in gas metal arc welding [AD-A213390] 05 p0624 N90-13642
Arc current control of a robotic welding system: Modeling and control system design [AD-A213150] 05 p0650 N90-13788
Theoretical evaluation of defects in pressure vessels and pipings [CRIF-MT-174] 05 p0651 N90-13798
Effects of precipitate distribution on 293 K and 77 K properties of 2090-T81 weldments [DE90-002332] 06 p0747 N90-14349
BES welding science contractors summary report, 1988 to 1989 [DE90-001004] 06 p0793 N90-14619
Measuring the thickness of austenitic weld deposits on carbon steel walls using a magnetic method [DE89-635446] 06 p0794 N90-14628
Helium-induced weld cracking in irradiated 304 stainless steel [DE90-001312] 07 p0903 N90-15219
The effect of nitrogen and titanium on the toughness of high strength saw weld deposits [AD-A213400] 07 p0905 N90-15230
Onorbit electron beam welding experiment definition [NASA-CR-183847] 07 p0938 N90-15431
Submerged arc welding consumables for HSLA (High Strength Low Alloy)-100 steel [AD-A213433] 07 p0941 N90-15452
Eddy-current inspection of shuttle heat exchanger tube welds [NASA-CR-186302] 07 p0943 N90-15462
Experience with J testing of 304/308 stainless steel weldment [DE90-002046] 07 p0946 N90-15478
Fatigue behavior of vertical axis wind turbine airfoils with two weld configurations [DE90-002628] 07 p0955 N90-15525
Structural characterization of Spacelab [ETN-90-95214] 08 p1087 N90-16289
A new model for hydrogen absorption in welds [AD-A216951] 12 p1626 N90-19347
Heat sink effects on weld bead: VPPA process 12 p1639 N90-19418
Origin and effect of pores in aluminum welded joints [REPT-87M/43/05720/SCP/GRF] 12 p1675 N90-19620
Evaluation of material homogeneity as a function of thickness of low-alloy ferritic steel [DE90-008069] 13 p1777 N90-20202
Time-dependent failure of silver interlayer welds [DE90-008015] 13 p1818 N90-20440
The effects of a nearby subsequent fusion weld on the properties of an inertia friction weld [DE90-007972] 14 p1988 N90-21396
The effect of aging at 343 C on type 308 stainless steel weldments [DE90-009232] 15 p2069 N90-21853
Characterization of weldments using advanced experimental techniques [DE90-009418] 16 p2242 N90-22792
Ambient-temperature creep failure of silver-aided diffusion bonds between steel [DE90-010687] 18 p2527 N90-24420
The effects of cooling rate XD (trademark) TiAl weld microstructure [DE90-011975] 18 p2528 N90-24427
High-temperature materials. Coating, welding, and service tests [VTT-RR-645] 19 p2675 N90-25214
Heat sink effects on weld bead: VPPA process [NASA-CR-186723] 19 p2697 N90-25349
Inspection of welds with eddy current [TTR-RR-644] 19 p2699 N90-25358
Calculations of welding stresses and deformations by means of finite element method [VTT-RR-648] 19 p2703 N90-25382
The effect of impurity gasses on variable polarity plasma arc welded 2219 aluminum [NASA-CR-183803] 21 p2980 N90-26935
The mathematical modeling of arc welding operation [DE90-013700] 22 p3183 N90-28064
Investigation of weld bead cooling rate during startup of gas metal arc welding [AD-A223567] 24 p3449 N90-29478
The use of automated ball indentation testing to measure flow properties and estimate fracture toughness in metallic materials [DE90-015797] 24 p3452 N90-29493

WELDED STRUCTURES
NT STEEL STRUCTURES
The effect of impurity gasses on variable polarity plasma arc welded 2219 aluminum [NASA-CR-183803] 21 p2980 N90-26935
Issues in expanding the software base management system supporting the Computer Aided Prototyping System (CAPS) [AD-A224344] 24 p3525 N90-29933

WELDING
NT ARC WELDING
NT BRAZING
NT COLD WELDING
NT DIFFUSION WELDING
NT ELECTRIC WELDING
NT ELECTRON BEAM WELDING
NT FRICTION WELDING
NT FUSION WELDING
NT GAS TUNGSTEN ARC WELDING
NT GAS WELDING
NT LASER WELDING
NT PLASMA ARC WELDING
NT ULTRASONIC SOLDERING
NT ULTRASONIC WELDING
Investigation of the pyrometallurgical, physical and mechanical behavior of weld metal [AD-A211114] 01 p0046 N90-10258
Automation of fiber-optic pigtailing process: Laser welding demonstration program [AD-A210351] 01 p0123 N90-10707

Fracture toughness data base for HT9 and modified 9Cr-1Mo irradiated in several reactors up to approximately 100 dpa
[DE90-000111] 03 p0328 N90-11864
Influence of the composition of the metal deposited on carbon manganese welds on the work properties of the melted area depending on the operating mode of the weld
[CETIM-104530] 04 p0476 N90-12726
Activities report of the metallic manufacturing industry
[ISSN-0524-7705] 05 p0625 N90-13649
Temperature measurement during welding of solar cells and calibration of finite element models
10 p1342 N90-17774
Materials for ultra-high vacuum
[DE90-007908] 14 p1959 N90-21217
Attachment of lead wires to thin film thermocouples mounted on high temperature materials using the parallel gap welding process
[NASA-TM-102442] 14 p1983 N90-21361
Welding behavior and welding metallurgy of ductile intermetallic alloys
[DE90-008908] 15 p2069 N90-21852
Institute for Materials Science and Engineering, Fracture and Deformation Division: Technical activities, 1989
[PB90-155359] 15 p2116 N90-22106
Advanced technology in welding, materials processing and evaluation
[DE90-010799] 19 p2697 N90-25347
Filler metal development for Hastelloy alloy XR
[DE90-791084] 21 p2981 N90-26939
Computerization of Welding Data: Proceedings of the conference and workshop
[PB90-219551] 23 p3332 N90-28841
Some studies of the vibration welding of thermoplastics 23 p3332 N90-28842
Investigation of weld bead cooling rate during startup of gas metal arc welding
[AD-A223567] 24 p3449 N90-29478
A welding metallurgy study of Hastelloy Alloys B-2 and W
[DE90-011910] 24 p3449 N90-29481
An effective low-profile thermite torch
[DE90-015746] 24 p3459 N90-29534

WELDING MACHINES
Influence of the composition of the metal deposited on carbon manganese welds on the work properties of the melted area depending on the operating mode of the weld
[CETIM-104530] 04 p0476 N90-12726

WELLS
Use of ground penetrating radar to define recharge areas in the Central Sand Plain
[PB89-224885] 04 p0490 N90-12814

WENTZEL-KRAMER-BRILLOUIN METHOD
Nonparallel stability of boundary layers
04 p0440 N90-12514
Generalized WKB approximation for stratified isotropic chiral structures
[PB90-165689] 14 p1967 N90-21270
Theory of biaxial graded-index optical fiber
[NASA-CR-186882] 20 p2927 N90-26652

WEST GERMANY
The German space science program
05 p0662 N90-13873
Measurements of horizontal visibility in the lowest 300 m over Northern Germany 07 p0872 N90-15059
The German hypersonic technology programme
09 p1174 N90-16790
Progress in Saenger space transportation system definition 09 p1175 N90-16799
Wind conditions near the ground in Federal Republic of Germany
[ISBN-3-88148-248-2] 12 p1694 N90-19727
German microgravity program and flight opportunities
13 p1784 N90-20239
Regional quasigeoid determination in Northern Germany and comparison with GPS 13 p1837 N90-20544

WETLANDS
Global data bases on distribution, characteristics and methane emission of natural wetlands: Documentation of archived data tape
[NASA-TM-4153] 03 p0365 N90-12090
ELF (Extremely Low Frequency) communications systems ecological monitoring program: Wetland studies
[AD-A218632] 16 p2229 N90-22716

WETNESS
U MOISTURE CONTENT

WETTABILITY
Investigations into the infiltration kinetics, wettability, and interfacial bond strength of Al/SiC composites
[AD-A211924] 03 p0320 N90-11815
The size of the alkyl group R is the principal factor determining the wettability of surface-functionalized polyethylenes (PE-CONHR and PE-CO2R) by water
[AD-A216007] 10 p1354 N90-17851

WETTING
Self-assembled organic monolayer films
[AD-A212006] 03 p0323 N90-11838
The size of the alkyl group R is the principal factor determining the wettability of surface-functionalized polyethylenes (PE-CONHR and PE-CO2R) by water
[AD-A216007] 10 p1354 N90-17851
Plasma and ion fluorination for chemical hardening of synthetic rubbers
[AD-A216388] 10 p1360 N90-17885
Wetting of metallic carbides by non-reactive liquid metals
[AERE-M-3759] 13 p1775 N90-20185
Critical point wetting drop tower experiment
[NASA-CR-186513] 14 p1957 N90-21208

WHEAT
Dynamics of carbon dioxide exchange of a wheat community grown in a semi-closed environment
08 p1155 N90-16689
Plant features measurements for robotics
08 p1156 N90-16695
LANDSAT-TM and agrometeorological data in the wheat crop yield estimation at the farm level
[INPE-4842-PRE/1471] 10 p1400 N90-18091
Radiometric study of wheat and bean crops in three types of latossolo
[INPE-4843-PRE/1472] 11 p1523 N90-18767
Relationships between spectral parameters and agronomics of wheat and beam crops
[INPE-4791-RPE/584] 11 p1523 N90-18768
Spectral response of wheat and its relationship with agronomical prameters
[INPE-4950-RPE/599] 11 p1524 N90-18774
Continuous hydroponic wheat production using a recirculating system
[NASA-TM-102784] 11 p1538 N90-18853
Relationship of radiometric field measurements of wheat in the Assis-Safra region, 1988
[INPE-4949-RPE/598] 13 p1819 N90-20443
LANDSAT-5 data in the study of wheat and bean crops
[INPE-4746-RPE/580] 13 p1819 N90-20444
Wheat yield estimation at the farm level using LANDSAT TM and agrometeorological data
[INPE-5017-RPE/611] 14 p1996 N90-21439
Wheat productivity estimate through field radiometry
[INPE-4994-PRE/1556] 14 p2000 N90-21460
Spectral response of wheat and its relationship with agronomic variables in the tropical region
[INPE-5018-RPE/612] 15 p2122 N90-22138
Carbon dioxide and water exchange rates by a wheat crop in NASA's biomass production chamber: Results from an 86-day study (January to April 1989)
[NASA-TM-102788] 19 p2716 N90-25453
Utilization of the water soluable fraction of wheat straw as a plant nutrient source
[NASA-TM-103497] 19 p2716 N90-25455

WHEATSTONE BRIDGES
Design of a custom load cell for a precision assembly application
[DE90-004439] 07 p0923 N90-15340

WHEELS
NT COUNTER-ROTATING WHEELS
NT FLYWHEELS
NT NOSE WHEELS
NT REACTION WHEELS
NT TOROIDAL WHEELS
NT TURBINE WHEELS
NT VEHICLE WHEELS
Design of a digital model following controller of reaction wheel torques
[INPE-4753-PRE/1425] 14 p1938 N90-21093
Proof of principle model for a lunar dumptruck
[NASA-CR-182557] 20 p2869 N90-26323

WHIP ANTENNAS
Design concepts for hardened communications structures
[AD-A221233] 19 p2683 N90-25260

WHIPLASH INJURIES
Data analysis in cervical trauma
19 p2718 N90-25464
Electronystagmographic findings following cervical injuries 19 p2718 N90-25466

WHIRL
U ROTATION

WHIRL INSTABILITY
U ROTARY STABILITY

WHIRLING
U ROTATION

WHIRLING TESTS
U SPIN TESTS

WHISKER COMPOSITES
Friction and wear of oxide-ceramic sliding against IN-718 nickel base alloy at 25 to 800 C in atmospheric air
[NASA-TM-102291] 01 p0046 N90-10262
Ceramic components in machines, Cologne and Aachen, West Germany; Maastricht, The Netherlands and Brussels, Belgium
[DE89-015831] 01 p0047 N90-10264
Zirconia toughened SiC whisker reinforced alumina composites small business innovation research
[NASA-CR-179629] 01 p0052 N90-10294
Deformation behavior of SiC/2014 Al metal-matrix composite
[AD-A212095] 03 p0320 N90-11816
Advances and future directions in superplastic materials 06 p0744 N90-14328
The 7th International Conference on Ceramics
[DE90-002144] 06 p0752 N90-14374
Extrusion of alumina-silicon carbide whisker composites
[DE90-004379] 09 p1186 N90-16869
Analysis of whisker-toughened ceramic components: A design engineer's viewpoint
[NASA-TM-102333] 11 p1478 N90-18504
Mechanical properties and microstructure of Si3N4-whisker-reinforced Si3N4 matrix composite
[DE90-005651] 11 p1480 N90-18518
Identification and development of optimum SiC whiskers for silicon nitride matrix composites
[DE90-006888] 12 p1621 N90-19315
Experimentally determined wear behavior of an Al2O3-SiC composite from 25 to 1200 C
[NASA-TM-102549] 13 p1765 N90-20130
Synthesis of alumina-coated SiC whiskers for production of SiC whisker-reinforced alumina composite materials
[DE90-007778] 13 p1768 N90-20147
Mechanical behavior of whisker reinforced ceramics
[DE90-008758] 13 p1781 N90-20224
Research advances in fine ceramics
[DE90-008983] 14 p1956 N90-21197
Fracture toughness and solid-particle erosion of ceramic-matrix whisker-reinforced composites
[DE90-009713] 18 p2517 N90-24376
Electron microscopy of interfaces in silicon carbide whisker-reinforced alumina composites
[DE90-010439] 18 p2519 N90-24386
Friction and wear of whisker-reinforced ceramic composite bodies
[DE90-011313] 18 p2519 N90-24389
Ceramic technology for advanced heat engines project data base
[DE90-011491] 18 p2532 N90-24448
Investigation of thermo-mechanical effects in silicon carbide Whisker/Al alloy composites
[AD-A222635] 20 p2828 N90-26089
A study of the elastic properties of Al2O3 and Si3N4 matrix composites with SiC whisker reinforcement
[DE90-013674] 21 p2970 N90-26882
High temperature strength of SiC whisker-reinforced silicon nitride composites
[DE90-013822] 21 p2970 N90-26883
Mechanical testing activities related to high-performance structural ceramics
[DE90-014299] 23 p3313 N90-28734
Evaluation of several micromechanics models for discontinuously reinforced metal matrix composites
[NASA-TM-102719] 23 p3339 N90-28872

WHISKERS (CRYSTALS)
Kinetics and mechanisms of primary and steady state creep in B- and Al-containing alpha silicon carbide
[AD-A210739] 02 p0283 N90-11616
Application of artificial intelligence control to the vapor-liquid-solid silicon carbide whisker process
[DE90-007835] 11 p1480 N90-18519

WHISPERING GALLERY MODES
Design considerations in achieving 1 MW CW operation with a whispering-gallery-mode gyrotron
[DE90-007283] 12 p1663 N90-19557
Progress in the CW operation of a 140 GHz gyrotron
[DE90-007382] 12 p1663 N90-19558

WHISTLERS
Producing of an ECR plasma using 2450MHz Whistler wave and the investigating of its parameters
[DE89-618689] 02 p0278 N90-11586
Spectral structure and generation mechanism of ducted VLF whistler mode sideband waves
24 p3489 N90-29720
A global model of thunderstorm electricity and the prediction of whistler duct formation
24 p3493 N90-29744

WHITE BLOOD CELLS
U LEUKOCYTES

WHITE DWARF STARS
Theoretical statistics of zero-age cataclysmic variables
01 p0141 N90-10810
MOXE: An X-ray all-sky monitor for Soviet Spectrum-X-Gamma Mission
[NASA-TM-101266] 02 p0223 N90-11280
Rocket and satellite observations of the local interstellar medium 02 p0292 N90-11668

Nonequilibrium ionization in supernova remnants: The case of Tycho
[MPE-PREPRINT-153] 04 p0565 N90-13295
Pulsars lost and found: The second Princeton-Arecibo millisecond pulsar search 07 p1013 N90-15865
Soft x ray emission from classical novae in outburst
[DE90-006480] 11 p1595 N90-19187
Neon novae, recurrent novae, and type I supernovae
[DE90-003188] 12 p1728 N90-19931
Radiative shock oscillations in AM Her cataclysmic binaries 19 p2783 N90-25834
An analysis of the Palomar-Green subdwarfs and white dwarfs 23 p3409 N90-29263
Nonradial instability strips for post-AGB stars
[DE90-014922] 23 p3411 N90-29278

WHITE LIGHT HOLOGRAPHY
Application of holography to behavior simulators
[ISL-R-111/88] 09 p1226 N90-17115

WHITE NOISE
NT THERMAL NOISE
Discrete filtering techniques applied to sequential GPS range measurements
[NASA-CR-177472] 03 p0305 N90-11730
Performance of the split-symbol moments SNR estimator in the presence of inter-symbol interference 04 p0487 N90-12799
Effect of contralateral masking parameters on difference limen for intensity
[AD-A214169] 10 p1411 N90-18135
Adaptive frequency estimation by MUSIC (Multiple Signal Classification) method
[PB90-166794] 15 p2086 N90-21943
Sampling and noise in vision networks 15 p2138 N90-22217
Parallel and vector computation for stochastic optimal control applications 16 p2282 N90-23007
Integral and series representation of infinitely divisible processes with applications to their prediction and to their sample path, statistical, and structural properties
[AD-A219625] 17 p2456 N90-24017
A white noise theory of infinite dimensional calculus
[AD-A221253] 18 p2607 N90-24850

WICKS
Capillary flow properties of mesh wicks
[AD-A214769] 09 p1217 N90-17057
Wick-type liquid-metal combustion
[AD-A216019] 11 p1482 N90-18530
Measuring flow properties of wicks for heat pipe solar receivers
[DE89-016537] 12 p1683 N90-19664
Ceramic heat pipe wick
[NASA-CASE-GSC-13199-1] 17 p2378 N90-23541
Thermal analysis of heat pipe radiators with a rectangular groove wick structure
[AD-A222952] 21 p3004 N90-27074

WIDE ANGLE LENSES
Theory of wide-angle photometry from standard stars
[NASA-CR-185964] 06 p0860 N90-14999
Analysis and test of a wide angle spectrometer
[AD-A215819] 10 p1388 N90-18030

WIDEBAND
U BROADBAND

WIDEBAND COMMUNICATION
Frequency independent constant beamwidth directional lens antenna for very wideband and multi-channel electromagnetic communications
[AD-D014214] 06 p0765 N90-14449
Supercomputer workstation communication
[AD-A222466] 21 p3039 N90-27272

WIDTH
Adaptive control of an arc welding process
[AD-A223626] 24 p3476 N90-29645

WIENER HOPF EQUATIONS
A new technique for simulating composite material. Task 2: Analytical solutions with Generalized Impedance Boundary Conditions (GIBCs)
[NASA-CR-186249] 07 p0890 N90-15145
Sparse approximations of inverse matrices
[ETN-90-96904] 17 p2464 N90-24074

WIGGLER MAGNETS
Electron beam propagation through a magnetic wiggler with random field errors
[AD-A212705] 04 p0498 N90-12867
Compact RF-linac free-electron lasers
[DE90-002386] 06 p0790 N90-14600
INEX (Integrated Numerical Experiment) simulations of the Los Alamos HIBAF (High-Brightness Accelerator Free-Electron Laser) free-electron laser MOPA (Master Oscillator Power Amplifier) experiment
[DE90-002387] 06 p0790 N90-14601
Microwave Transport Systems for the MTX (Microwave Tokamak Experiment)
[DE90-000821] 06 p0846 N90-14921
A microwiggler Free-Electron Laser at the Brookhaven Accelerator Test Facility
[DE90-003643] 07 p0936 N90-15418
One-dimensional single-mode nonlinear FEL amplification code: User's manual
[DE90-719544] 09 p1227 N90-17121
Identification and reduction of Wakefield effects in the wiggler region of the Los Alamos free-electron laser
[DE90-004871] 09 p1228 N90-17128
INEX (Integrated Numerical Experiment) simulations of the Boeing FEL system
[DE90-004846] 11 p1513 N90-18712
Results of the PALADIN experiment
[DE90-006776] 12 p1667 N90-19578
First direct observation of FEL (Free-Electron Laser) from lambda = 20 to 45 microns
[DE90-007508] 12 p1669 N90-19589
The effects of wiggler errors on free electron laser performance
[AD-A220421] 17 p2409 N90-23725
Microwigglers for submillimeter wavelength free-electron lasers
[AD-A220185] 17 p2409 N90-23730
Microwave generation for magnetic fusion energy applications
[DE90-011042] 18 p2617 N90-24906
Status of the advanced light source
[DE90-015636] 23 p3395 N90-29185

WIGHTMAN THEORY
U FIELD THEORY (PHYSICS)
U QUANTUM THEORY
U RELATIVISTIC THEORY

WIGNER COEFFICIENT
Alias-free Wigner distribution function and complex ambiguity function for discrete-time samples
[AD-A211050] 02 p0269 N90-11533
Gaussons and states with gaussian Wigner functions are quasi-free states
[DE90-628370] 24 p3556 N90-30121

WILDERNESS
Preliminary thoughts on an acoustic metric for the wilderness aircraft overflight study 18 p2609 N90-24862
US Forest Service and National Park Service Wilderness Aircraft Overflight Study: Sociological background and study plans 18 p2609 N90-24863

WIND (METEOROLOGY)
NT GEOSTROPHIC WIND
NT GROUND WIND
NT GUSTS
NT JET STREAMS (METEOROLOGY)
NT MONSOONS
NT SEA BREEZE
NT SQUALLS
NT WINDS ALOFT
A study of the impact of simulated satellite lidar wind observations
[AD-A210430] 01 p0086 N90-10488
National Severe Storms Laboratory, fiscal year 1988
[PB89-156145] 01 p0087 N90-10493
Hurricane Research Division fiscal year 1988 programs, fiscal year 1989 projections
[PB89-152268] 02 p0250 N90-11418
Direct statistical thermal wind estimation procedure
[AD-A211256] 02 p0253 N90-11433
Low level remote sensing: Orographic winds 03 p0361 N90-12066
Aeolian processes on Venus 03 p0425 N90-12436
Project WIND: Experiments with the UK Meteorological Office mesoscale model
[AD-A212291] 04 p0521 N90-13006
Comparison of analytical methods for calculation of wind loads
[NASA-TM-102782] 05 p0654 N90-13813
Airdata calibration of a high-performance aircraft for measuring atmospheric wind profiles
[NASA-TM-101714] 06 p0725 N90-14228
The identification of terrain-induced circulations using principal components
[DE90-001991] 06 p0815 N90-14739
Summary of 1989 Atlantic tropical cyclone activity and seasonal forecast verification 06 p0815 N90-14743
Climatology of Lawrence Livermore National Laboratory
[DE90-000905] 06 p0818 N90-14756
Saltation and suspension of particulate matter in air
[AD-A213618] 07 p0960 N90-15552
The calculation of overground sound propagation in the presence of wind and temperature gradients
[ESDU-89036] 07 p0989 N90-15714
Diagnostic and kinematic fields associated with curved and straight jet streaks using a two-layer primitive equation model 08 p1100 N90-16371
A dynamic model for forecasting new cloud development
[AD-A213939] 08 p1102 N90-16383
A statistical model of the infrared signature of a wind roughened sea
[AD-A214531] 09 p1249 N90-17245
An atlas of ECMWF analyses (1980-1987). Part 1: First moment quantities
[NASA-TM-100747-PT-1] 10 p1408 N90-18120
Doppler lidar working group report
[ESA-SP-1112] 11 p1537 N90-18848
Transport of atmospheric aerosols above the Sierra Nevada slopes
[PB90-120288] 12 p1685 N90-19675
Meteor observations using the 50 MHz MENTOR imaging Doppler interferometer
[AD-A217908] 13 p1790 N90-20276
An improved airborne wind measurement technique for the NAE (National Aeronautical Establishment) Twin Otter
[AD-A217978] 13 p1842 N90-20575
Atmospheric wind measurements using a 50 MHz imaging Doppler interferometer radar
[AD-A218277] 13 p1847 N90-20601
Microwave brightness temperature and its relation to atmospheric general circulation features
[AD-A218312] 13 p1847 N90-20603
The invertibility principle for a simple hurricane model
[AD-A218344] 13 p1848 N90-20605
Regional wind energy assessment
[DE90-009439] 15 p2123 N90-22143
An anomalous wind between valleys: Its characteristics and a proposed explanation
[DE90-008965] 15 p2133 N90-22189
Daytime wind valleys adjacent to the Great Salt Lake
[DE90-008991] 15 p2133 N90-22190
The ASCOT 1988 valley/tributary interaction study
[DE90-009043] 15 p2133 N90-22191
Wind forecasting for utility operations
[DE90-009466] 15 p2133 N90-22193
Climatic handbook of the USSR, issue 27. Kamchatskaya Oblast. Part 3: Wind
[AD-A218720] 16 p2258 N90-22872
Atmospheric transport and dispersion model hierarchy, part 2
[AD-A220136] 17 p2427 N90-23833
The effects of climatological and transient wind forcing on eddy generation in the California current system
[AD-A219858] 17 p2431 N90-23855
A correlation study of wind speed as measured by the special sensor microwave/imager and the GEOSAT altimeter
[AD-A219841] 18 p2581 N90-24701
Derivation of wind fields from Doppler measurements of a single radar and application to a cold front with narrow rainband
[DLR-FB-89-61] 18 p2582 N90-24705
Aeolian removal of dust from radiator surfaces on Mars
[NASA-TM-103205] 20 p2824 N90-26068
Dependence of radar backscatter on the energetics of the air-sea interface
[AD-A221966] 21 p2996 N90-27028
Application of automatic method to estimating high-level cloud motion wind in operational system and the characteristics of the resultant wind vectors 21 p3028 N90-27218
Wind field derivatives of extratropical cyclones observed by Doppler radar
[AD-A222188] 21 p3031 N90-27232
Low-frequency cloud-radiation interactions 22 p3225 N90-28289
The global cycle of reactive nitrogen
[DE90-015041] 23 p3348 N90-28919
On the dynamics of severe thunderstorms
[DE90-627922] 23 p3353 N90-28950
Satellite image atlas of glaciers of the world: Irian Jaya, Indonesia, and New Zealand
[PB90-230095] 24 p3483 N90-29691
Observations of tornadoes and wall clouds with a portable FM-CW Doppler radar: 1989--1990 results
[DE90-013152] 24 p3495 N90-29752

WIND CIRCULATION
U ATMOSPHERIC CIRCULATION

WIND DIRECTION
Pacific marine radar sea scatter experimental results
[AD-A211593] 03 p0339 N90-11931
Analytical and experimental study of runway runoff with wind effects
[PTI-8948] 04 p0458 N90-12627
Observation of wind corners in the middle atmosphere over Andenes (69 N) during winter 1983/84, summer 1987 and summer 1988 05 p0657 N90-13836
Application of a mass-consistent wind model to chinook windstorms
[AD-A213622] 07 p0963 N90-15568
ECC (Electrochemical Concentration Cell) ozonesonde observations at South Pole, Antarctica, during 1988
[PB90-110172] 08 p1098 N90-16355

An analysis of diurnal wind variability in the Santa Barbara Channel from SODAR measurements
[AD-A215769] 10 p1408 N90-18121
Aerodynamics of a full-scale, non rotating wind turbine blade under natural wind conditions
[RISOE-M-2768] 15 p2123 N90-22144
JARE data reports, no. 140 (meteorology 21): Meteorological data at Asuka Camp, Antarctica in 1987
[ISSN-0075-3343] 15 p2132 N90-22188
Cable suspended windmill
[NASA-CASE-LAR-13434-1] 17 p2412 N90-23742
A conceptual weather-type classification procedure for the Philadelphia, Pennsylvania area
[PB90-231705] 23 p3352 N90-28944

WIND EFFECTS
The suitability of diffusion and wind-field techniques for an emergency-response dispersion model
[PB89-190219] 01 p0085 N90-10481
Solar-terrestrial relations: Flare and solar wind effects 02 p0240 N90-11362
Wind/seismic comparisons for upgrading existing structures
[DE89-016055] 03 p0357 N90-12044
Similarity relations of wind waves in finite depth
[PB89-198113] 03 p0376 N90-12144
Equatorial oceanic response to forcing on time scales from days to months
[PB89-206775] 03 p0377 N90-12147
Analysis of a system of two weakly nonlinear coupled harmonic oscillators arising from the field of wind-induced vibrations
[REPT-89-22] 03 p0396 N90-12261
Analytical and experimental study of runway runoff with wind effects
[PTI-8948] 04 p0458 N90-12627
Airborne FLIR detection of surface targets 06 p0759 N90-14416
A global ocean wind stress climatology based on ECMWF (European Centre for Medium Range Weather Forecasts) analyses
[PB90-109968] 06 p0817 N90-14752
Evaluate and characterize mechanisms controlling transport, fate, and effects of army smokes in the aerosol wind tunnel: Transport, transformations, fate, and terrestrial ecological effects of hexachloroethane obscurant smokes
[DE90-002923] 07 p0957 N90-15536
The Shock and Vibration Digest, volume 21, no. 9 09 p1235 N90-17168
Wind-excited behavior of structures, 5 09 p1235 N90-17169
Boundary walls, fences and hoardings: Mean and peak wind loads and overturning moments
[ESDU-89050] 09 p1239 N90-17190
Response of structures to atmospheric turbulence. Response to across-wind turbulence components
[ESDU-89049] 09 p1239 N90-17191
The effects of wind tunnel data uncertainty on aircraft point performance predictions
[AD-A216091] 11 p1456 N90-18387
Aeolian removal of dust from photovoltaic surfaces on Mars
[NASA-TM-102507] 12 p1617 N90-19299
Mechanics of aeolian processes: Soil erosion and dust production 12 p1638 N90-19410
Chemical composition of precipitation and wet/dry deposition of sulfur compounds around the coastal area
[DE89-782324] 12 p1685 N90-19677
Aerodynamic analysis of a US Navy and Marine Corps unmanned air vehicle
[AD-A218282] 13 p1755 N90-20077
Analysis of small-scale rotor hover performance data
[NASA-TM-102271] 13 p1799 N90-20325
Lagrangian model simulation of the turbulent transport of evaporating jet droplets 15 p2128 N90-22168
A study of the surface layers at an air-water interface
[AD-A219378] 16 p2260 N90-22882
The effects of climatological and transient wind forcing on eddy generation in the California current system
[AD-A219858] 17 p2431 N90-23855
Asymptotic analysis of wind-induced vibrations
[ETN-90-98903] 18 p2572 N90-24658
A plasma diagnostic study of two wind-blown shell nebulae: NGC 7635 and NGC 2359 23 p3410 N90-29271
Research in nonlinear water waves
[AD-A224065] 24 p3496 N90-29759

WIND ENERGY
U WINDPOWER UTILIZATION

WIND EROSION
Mechanics of aeolian processes: Soil erosion and dust production 12 p1638 N90-19410

WIND MEASUREMENT
NT WIND VELOCITY MEASUREMENT
An in-flight technique for wind measurement in support of the space shuttle program
[NASA-TM-4154] 06 p0724 N90-14224
Airdata calibration of a high-performance aircraft for measuring atmospheric wind profiles
[NASA-TM-101714] 06 p0725 N90-14228
High resolution Doppler lidar
[NASA-CR-183288] 06 p0781 N90-14542
Systems for airborne wind and turbulence measurement 07 p0869 N90-15046
Fluctuating wind forces measured on a bluff body extending from a cavity
[AD-A216414] 10 p1386 N90-18020
An analysis of diurnal wind variability in the Santa Barbara Channel from SODAR measurements
[AD-A215769] 10 p1408 N90-18121
Atmospheric wind measurements using a 50 MHz imaging Doppler interferometer radar
[AD-A218277] 13 p1847 N90-20601
Editing wind profiler measurements
[PB90-130147] 14 p2007 N90-21503
Kinetic and extraction measurements on 12C18O2
[AD-A220417] 17 p2472 N90-24133
Absolute wind measurements in the lower thermosphere of Venus using infrared heterodyne spectroscopy
[NASA-CR-4290] 21 p3100 N90-27605
A day-to-day comparison study of Seasat scatterometer winds with winds observed from islands in the tropical Pacific
[NASA-CR-186696] 22 p3212 N90-28223
Tropospheric wind profiling using radar interferometry: A feasibility study of a compact mobile system
[PB90-217068] 23 p3351 N90-28939
Observations of tornadoes and wall clouds with a portable FM-CW Doppler radar: 1989--1990 results
[DE90-013152] 24 p3495 N90-29752
Detection and analysis of wind fronts and current shear in digital SAR images
[FFI-89/7016] 24 p3495 N90-29755

WIND PRESSURE
Comparison of analytical methods for calculation of wind loads
[NASA-TM-102782] 05 p0654 N90-13813
Computer simulation of wind/diesel system operation
[DE89-009445] 06 p0805 N90-14688
Inclusion of nonlinear aerodynamics in the FLAP code
[DE89-009507] 07 p0954 N90-15519
Prediction of stochastic blade loads for three-bladed, rigid-hub rotors
[DE89-009508] 07 p0954 N90-15520
Wind loads and local pressure distributions on parabolic dish solar collectors
[DE90-000328] 21 p3019 N90-27166
Methods for detecting low-frequency signals in the presence of strong winds
[AD-A223980] 23 p3320 N90-28769

WIND PROFILES
A study of the impact of simulated satellite lidar wind observations
[AD-A210430] 01 p0086 N90-10488
A scalar/vector potential solution for aerodynamic coefficients in wind shear 02 p0147 N90-10838
Relation of wind field and buoyancy to rainfall inferred from radar
[PB89-208326] 02 p0251 N90-11424
Direct statistical thermal wind estimation procedure
[AD-A211256] 02 p0253 N90-11433
Low level remote sensing: The Doppler Radar wind profiler 03 p0361 N90-12067
Disturbances in the Arizona Monsoon 03 p0362 N90-12071
Evaluation and sensitivity analyses results of the MESOPUFF 2 model with CAPTEX (Cross-Appalachian Tracer Experiment) measurements
[PB89-198253] 03 p0368 N90-12103
Subjective uses of wind profiler data in warm season analysis and forecasting: Wind profiler training manual number 3
[PB89-223333] 04 p0520 N90-13004
A real-time wind model using digital data from aircraft
[RSRE-MEMO-4309] 04 p0521 N90-13005
An in-flight technique for wind measurement in support of the space shuttle program
[NASA-TM-4154] 06 p0724 N90-14224
Airdata calibration of a high-performance aircraft for measuring atmospheric wind profiles
[NASA-TM-101714] 06 p0725 N90-14228
Analysis of significant weather on meso-alpha scales using conventional and remotely sensed data: Exploratory studies
[AD-A214563] 09 p1248 N90-17238
Derivation of kinematic fields using wind profiler data from the 1985 pre-storm experiment
[AD-A217952] 13 p1845 N90-20592
A prototype expert system to forecast severe winds in the western Mediterranean Sea
[AD-A218017] 13 p1845 N90-20593
Editing wind profiler measurements
[PB90-130147] 14 p2007 N90-21503
A linear analysis of monsoon base states associated with banded convection 15 p2130 N90-22179
The emission lines in the ultra-violet spectrum of Beta Lyrae 15 p2183 N90-22474
The role of eddy fluxes of momentum in hurricane formation
[AD-A219417] 18 p2581 N90-24700
Atmospheric environment for space shuttle (STS-28) launch
[NASA-TM-100386] 19 p2715 N90-25452
Atmospheric environment for space shuttle (STS-33) launch
[NASA-TM-100399] 22 p3200 N90-28159
Effects of solar activity in the middle atmosphere dynamical regime over Eastern Siberia, USSR 22 p3207 N90-28195
Modification of the background flow b_y roll vortices 22 p3219 N90-28258
Atmospheric environment for Space Shuttle (STS-32) launch
[NASA-TM-100400] 23 p3346 N90-28912
Atmospheric environment for Space Shuttle (STS-31) launch
[NASA-TM-103508] 23 p3347 N90-28913
Atmospheric environment for space shuttle (STS-36) launch
[NASA-TM-100403] 23 p3347 N90-28914
Atmospheric environment for space shuttle (STS-34) launch
[NASA-TM-100396] 23 p3347 N90-28915
Tropospheric wind profiling using radar interferometry: A feasibility study of a compact mobile system
[PB90-217068] 23 p3351 N90-28939
An investigation of forcing mechanisms during a surprise tornadic thunderstorm
[PB90-216805] 23 p3352 N90-28940
Zonal winds between 25 and 120 km retrieved from solar occultation spectra 24 p3489 N90-29718

WIND SHEAR
A scalar/vector potential solution for aerodynamic coefficients in wind shear 02 p0147 N90-10838
Mesoscale acid deposition modeling studies
[NASA-CR-4262] 04 p0554 N90-13228
A candidate concept for display of forward-looking wind shear information
[NASA-TM-101585] 06 p0725 N90-14232
Adaptive clutter rejection filters for airborne Doppler weather radar applied to the detection of low altitude windshear
[NASA-CR-186211] 06 p0766 N90-14453
Flight in Adverse Environmental Conditions
[AGARD-CP-470] 07 p0869 N90-15041
Wind shear models for aircraft hazard investigation 07 p0869 N90-15044
Analysis of severe atmospheric disturbances from airline flight records 07 p0869 N90-15045
Influence of windshear, downdraft and turbulence on flight safety 07 p0870 N90-15048
Classification of windshear severity 07 p0870 N90-15049
How to fly windshear using the fly-by-wire concept 07 p0870 N90-15050
A pitch control law for compensation of the phugoid mode induced by windshears 07 p0870 N90-15051
Relative merits of reactive and forward-look detection for wind-shear encounters during landing approach for various microburst escape strategies
[NASA-TM-4158] 07 p0882 N90-15108
Analysis of significant weather on meso-alpha scales using conventional and remotely sensed data: Exploratory studies
[AD-A214563] 09 p1248 N90-17238
Report on meteorological assessment of Bald Hills incidents, phase 1
[AD-A216201] 10 p1408 N90-18123
A case study of the 24 August 1986 FLOWS microburst
[AD-A216939] 11 p1537 N90-18847
Structure and dynamics of the Arizona monsoon boundary
[AD-A217378] 13 p1844 N90-20586
A sub-cloud layer vorticity budget analysis for two microburst-producing storms from jaws dual-Doppler data
[AD-A218180] 13 p1847 N90-20599
Joint University Program for Air Transportation Research, 1988-1989
[NASA-CP-3063] 14 p1905 N90-20921
Investigation of air transportation technology at the Massachusetts Institute of Technology, 1988-1989 14 p1905 N90-20922

Cockpit display of hazardous wind shear information
14 p1905 N90-20924
Cockpit display of hazardous weather information
14 p1906 N90-20929
Investigation of air transportation technology at Princeton University, 1988-1989
14 p1907 N90-20935
An expert system for wind shear avoidance
14 p1908 N90-20938
Airborne Doppler radar flight experiments for the detection of microbursts 14 p1963 N90-21243
Windshear case study: Denver, Colorado, July 11, 1988
[DOT/FAA/DS-89/19] 14 p2008 N90-21509
Optimization and guidance of flight trajectories in the presence of windshear
[NASA-CR-186163] 15 p2049 N90-21747
Enhanced Low Level Wind Shear (LLWAS) 6-sensor improvement user's manual for data processing of field data
[DOT/FAA/CT-TN90/8] 15 p2052 N90-21759
Tropical squall lines of the Arizona monsoon
16 p2257 N90-22867
A numerical study of basic coastal upwelling processes 16 p2259 N90-22878
Examination of microburst development in Colorado thunderstorm for the 5 August 1982 case
[AD-A218478] 17 p2425 N90-23820
Use of clutter residue editing maps during the Denver 1988 Terminal Doppler Weather Radar (TDWR) tests
[AD-A218696] 17 p2426 N90-23822
The effects of climatological and transient wind forcing on eddy generation in the California current system
[AD-A219858] 17 p2431 N90-23855
A quantitative technique to estimate microburst wind shear hazard to aircraft 18 p2640 N90-25040
Users guide for an Airborne Windshear Doppler Radar Simulation (AWDRS) program
[NASA-CR-182025] 19 p2657 N90-25121
An analysis of requirements for a P-3 windshear training program
[AD-A222577] 20 p2805 N90-25960
The NASA/MSFC Global Reference Atmospheric Model, 1990 version (GRAM-90)
[NASA-CR-186717] 20 p2888 N90-26435
Analysis and improved design considerations for airborne pulse Doppler radar signal processing in the detection of hazardous windshear
[NASA-CR-186792] 20 p2890 N90-26448
Airborne CO2 Doppler lidar for wind shear detection
22 p3106 N90-27640
Monitoring and controlling flight in windshear
22 p3106 N90-27641
The instability mechanism of synoptic-scale eddies
22 p3211 N90-28217
Genesis of bow echoes: A rear-inflow induced meso-convective structure
[PB90-209776] 23 p3349 N90-28926
Geophysical turbulence research at NCAR
[AD-A223361] 24 p3492 N90-29732
Windshear estimation along the trajectory of an aircraft 24 p3494 N90-29745
Detection and analysis of wind fronts and current shear in digital SAR images
[FFI-89/7016] 24 p3495 N90-29755

WIND TUNNEL APPARATUS
NT WIND TUNNEL NOZZLES
Wind tunnel support system effects on a fighter aircraft model at Mach numbers from 0.6 to 2.0
[AD-A210614] 01 p0002 N90-10010
Hot-film system for transition detection in cryogenic wind tunnels 04 p0441 N90-12522
Basic aerodynamic research facility for comparative studies of flow diagnostic techniques
04 p0441 N90-12526
Recent tests at Langley with a University of Tennessee Space Institute (UTSI) skin friction balance
04 p0441 N90-12527
Development of a multi-component internal strain-gauge balance for model tests in a cryogenic wind tunnel
[NLR-TR-88157-U] 04 p0459 N90-12628
Hermes plasma wind tunnel. Preliminary study, phase A1: Annexes, tables, figures
[DVG-HER-TN-002-PT-2] 04 p0459 N90-12632
The design and development of an acoustic test section for the ARA transonic wind tunnel
[PNR90574] 04 p0550 N90-13202
A vapor generator for transonic flow visualization
[NASA-TM-101670] 05 p0584 N90-13403
High temperature capacitive strain gage
[NASA-CR-4266] 05 p0644 N90-13760
Instrumentation for cryogenic wind tunnels
08 p1030 N90-15950
Design of a high angle of attack robotic sting mount for tests in a low speed wind tunnel
[AD-A218105] 13 p1759 N90-20099
Test and Measurement Technique in Hypersonics
[ILR-MITT-225(1989)] 18 p2489 N90-24225
The wind tunnel of the Ruhr University, Bochum, Federal Republic of Germany for examination of compressible streams until M=6 18 p2489 N90-24226
The Langley 14- by 22-foot subsonic tunnel: Description, flow characteristics, and guide for users
[NASA-TP-3008] 22 p3107 N90-27649

WIND TUNNEL BALANCES
U WIND TUNNEL APPARATUS

WIND TUNNEL CALIBRATION
The design and development of an acoustic test section for the ARA transonic wind tunnel
[PNR90574] 04 p0550 N90-13202
Cryogenic temperature effects on sting-balance deflections in the National Transonic Facility
[NASA-TM-4157] 06 p0727 N90-14244
The US National Transonic Facility, NTF
08 p1028 N90-15942
The Kryo-Kanal Koeln (KKK): Description of the tunnel conversion. Thermal insulation, instrumentation, operational experience, test results and operating costs
08 p1029 N90-15943
The cryogenic Ludwieg tube tunnel at Goettingen
08 p1029 N90-15947
Instrumentation for cryogenic wind tunnels
08 p1030 N90-15950
Half model tests on an ONERA calibration model in the transonic wind tunnel Goettingen, Federal Republic of Germany
[DLR-MITT-89-20] 11 p1452 N90-18370
Flow unsteadiness effects on boundary layers
[NASA-CR-186067] 18 p2550 N90-24557

WIND TUNNEL MODELS
An integrated CFD/experimental analysis of aerodynamic forces and moments
[NASA-TM-102195] 01 p0002 N90-10006
Wind tunnel support system effects on a fighter aircraft model at Mach numbers from 0.6 to 2.0
[AD-A210614] 01 p0002 N90-10010
Wind tunnel tests: The role of the model
01 p0013 N90-10064
Experimental investigation of attachment-line transition in low-speed, high-lift wind-tunnel testing
01 p0062 N90-10358
An experimental investigation of the aerodynamic characteristics of slanted base ogive cylinders using magnetic suspension technology
[NASA-CR-181708] 02 p0146 N90-10834
Wind tunnel test of CAD USB-STOL semi-borne prototype
[NAL-TM-566] 03 p0299 N90-11696
On the application of modified stepwise regression for the estimation of aircraft stability and control parameters
[REPT-8905] 05 p0583 N90-13400
Techniques for extreme attitude suspension of a wind tunnel model in a magnetic suspension and balance system
[NASA-CR-181895] 06 p0728 N90-14245
Fundamental considerations in testing in cryogenic wind tunnels 08 p1030 N90-15951
Test techniques for cryogenic wind tunnels
08 p1030 N90-15952
Flow visualization in the cryogenic wind tunnel
08 p1030 N90-15953
Materials and techniques for model construction
08 p1030 N90-15954
Some recent developments in materials and techniques for model fabrication 08 p1031 N90-15955
Models for cryogenic wind tunnels
08 p1031 N90-15956
Experience with strain-gage balances for cryogenic wind tunnels 08 p1031 N90-15958
The determination of vortex separation frequencies by means of laser light sheet images
[DNW-WTI-88.036] 08 p1079 N90-16245
Quantitative heat transfer measurements using heated liquid crystals 08 p1081 N90-16256
High Reynolds number tests of the CAST-10-2/DOA 2 transonic airfoil at ambient and cryogenic temper ature conditions 10 p1324 N90-17650
Main results of CAST-10 airfoil tested in T2 cryogenic wind tunnel 10 p1324 N90-17652
Comparison of NAE porous wall and NASA adaptive wall test results using the NAE CAST-10 airfoil model
10 p1325 N90-17656
Experience with some repeat tests on the 9 inch chord CAST-10-2/DOA 2 airfoil model in the Langley 0.3-m TCT adaptive wall test section 10 p1325 N90-17657
Comparison of two- and three-dimensional Navier-Stokes solutions with NASA experimental data for CAST-10 airfoil 10 p1325 N90-17658
Supersonic wind tunnel investigation of a tubular projectile
[ISL-CO-306/89] 11 p1452 N90-18366
The DFVLR 3-m x 3-m low speed wind tunnel (NWG) in Goettingen
[ESA-TT-1156] 11 p1465 N90-18436
Contribution to the study of three-dimensional separation in turbulent incompressible flow
[ESA-TT-1169] 11 p1510 N90-18697
Using transonic small disturbance theory for predicting the aeroelastic stability of a flexible wind-tunnel model
[NASA-TM-102617] 13 p1749 N90-20047
Digital-flutter-suppression-system investigations for the active flexible wing wind-tunnel model
[NASA-TM-102618] 13 p1758 N90-20093
Design of a high angle of attack robotic sting mount for tests in a low speed wind tunnel
[AD-A218105] 13 p1759 N90-20099
Slotted-wall research with disk and parachute models in a low-speed wind tunnel
[DE90-002989] 15 p2048 N90-21737
Aerodynamic performance of a 0.27-scale model of an AH-64 helicopter with baseline and alternate rotor blade sets
[NASA-TM-4201] 18 p2491 N90-24237
The low-speed wind tunnel at DFVLR in Brunswick (status 1988)
[ESA-TT-1163] 19 p2662 N90-25152
Wind tunnel study of wake downwash behind A 6 percent scale model B1-B aircraft
[DE90-011783] 20 p2802 N90-25941
Installation and pretest analysis of DARPA suboff model in the DTRC anechoic wind tunnel
[AD-A221497] 21 p2955 N90-26801
Adaptation for unsteady flow
21 p2963 N90-26845
Development and testing of methodology for evaluating the performance of multi-input/multi-output digital control systems
[NASA-TM-102704] 22 p3115 N90-27699
Thermographic phosphor technique
24 p3421 N90-29324

WIND TUNNEL NOZZLES
Design and fabrication requirements for low noise supersonic/hypersonic wind tunnels
04 p0446 N90-12555
The utilization of an infrared imaging system as a cooling slot blockage detector in the inspection of a transpiration cooled nozzle
[NASA-TM-102608] 12 p1663 N90-19555

WIND TUNNEL STABILITY TESTS
Wind tunnel tests of a 20-gore disk-gap-band parachute
[AD-A221326] 18 p2493 N90-24251

WIND TUNNEL TESTS
A study of high-lift airfoils at high Reynolds numbers in the Langley low-turbulence pressure tunnel
[NASA-TM-89125] 01 p0001 N90-10002
An integrated CFD/experimental analysis of aerodynamic forces and moments
[NASA-TM-102195] 01 p0002 N90-10006
Wind tunnel support system effects on a fighter aircraft model at Mach numbers from 0.6 to 2.0
[AD-A210614] 01 p0002 N90-10010
Analysis of results from wind tunnel tests of inlets for an advanced turboprop nacelle installation
[NASA-CR-174937] 01 p0003 N90-10011
Development of a flight test methodology for a US Navy half-scale unmanned air vehicle
[AD-A210563] 01 p0006 N90-10029
Large-scale Advanced Prop-fan (LAP) high speed wind tunnel test report
[NASA-CR-182125] 01 p0010 N90-10045
Wind tunnel tests: The role of the model
01 p0013 N90-10064
Identification of stability and control parameters of a brilliant ammunition 01 p0014 N90-10065
The active flexible wing aeroservoelastic wind-tunnel test program 01 p0024 N90-10119
Experimental investigation of attachment-line transition in low-speed, high-lift wind-tunnel testing
01 p0062 N90-10358
Tower wake/blade interaction noise of a wind turbine
[NAL-TR-945] 02 p0236 N90-11344
Wind tunnel test of CAD USB-STOL semi-borne prototype
[NAL-TM-566] 03 p0299 N90-11696
The determination of the aerodynamic characteristics of an ogive-cylinder body in subsonic, curved, incompressible flow, and an assessment of the effect of flow curvature
[REPT-87-13] 03 p0302 N90-11712
Low-speed wind-tunnel study of reaction control-jet effectiveness for hover and transition of a STOVL fighter concept
[NASA-TM-4147] 03 p0308 N90-11751
The aerodynamic experimental center of Aeritalia: Combat aircraft group
[ETN-89-95213] 03 p0311 N90-11766

Comparison of the results of tests on A300 aircraft in the RAE 5 metre and ONERA F1 wind tunnels
[RAE-TM-AERO-2130] 03 p0311 N90-11768
Research in Natural Laminar Flow and Laminar-Flow Control, part 2
[NASA-CP-2487-PT-2] 04 p0440 N90-12519
Flow quality measurements in compressible subsonic flows 04 p0441 N90-12521
Results of LFC experiment on slotted swept supercritical airfoil in Langley's 8-foot transonic pressure tunnel 04 p0442 N90-12531
Boundary-layer stability analysis of Langley Research Center 8-foot LFC experimental data 04 p0442 N90-12532
Wind tunnel results of the low-speed NLF(1)-0414F airfoil 04 p0444 N90-12541
Wind tunnel results of the high-speed NLF(1)-0213 airfoil 04 p0444 N90-12542
Design and test of a natural laminar flow/large Reynolds number airfoil with a high design cruise lift coefficient 04 p0444 N90-12543
Residual interference assessment in adaptive wall wind tunnels
[NASA-CR-181896] 04 p0458 N90-12625
Development of a multi-component internal strain-gauge balance for model tests in a cryogenic wind tunnel
[NLR-TR-88157-U] 04 p0459 N90-12628
Flow in the neighborhood of an ellipsoid cylinder of revolution model
[ONERA-RT-22/7252-AN-000A] 04 p0502 N90-12895
Analysis of experimental data for CAST 10-2/DOA 2 supercritical airfoil at low Reynolds numbers and application to high Reynolds number flow
[AD-A211654] 05 p0571 N90-13326
Study of the integration of wind tunnel and computational methods for aerodynamic configurations
[NASA-TM-102196] 05 p0572 N90-13332
Pressure measurement techniques in use at the Royal Aerospace Establishment 05 p0574 N90-13347
Reduction of profile drag by modifying the structure next to the wake area
[IMFL-88/35] 05 p0576 N90-13356
A wall interference assessment/correction interface measurement system for the NASA/ARC 12-ft PWT
[NASA-CR-185474] 05 p0584 N90-13401
A two-dimensional adaptive-wall test section with ventilated walls in the Ames 2- by 2-foot transonic wind tunnel
[NASA-TM-102207] 05 p0585 N90-13407
Helicopter rotor test rig (RoTeSt) in DNW: Application and results
[RAE-TRANS-2171] 05 p0585 N90-13408
Measured and predicted aerodynamic coefficients and shock shapes for Aeroassist Flight Experiment (AFE) configuration
[NASA-TP-2956] 06 p0717 N90-14185
Cryogenic temperature effects on sting-balance deflections in the National Transonic Facility
[NASA-TM-4157] 06 p0727 N90-14244
Techniques for extreme attitude suspension of a wind tunnel model in a magnetic suspension and balance system
[NASA-CR-181895] 06 p0728 N90-14245
Saltation thresholds and entrainment of fine particles at Earth and Martian pressures
[NASA-TM-102193] 06 p0860 N90-14997
NASA's program on icing research and technology 07 p0873 N90-15062
Flight and wind tunnel investigation of aerodynamic effects of aircraft ground deicing/antiicing fluids 07 p0873 N90-15064
An experimental investigation of wall-interference effects for parachutes in closed wind tunnels
[DE90-001802] 07 p0875 N90-15076
Wind tunnel tests of the influence of aerofoil thickness on the normal force and pitching moment of two slender wings at transonic and supersonic Mach numbers
[ESA-TT-1129] 08 p1018 N90-15889
Special Course on Advances in Cryogenic Wind Tunnel Technology
[AGARD-R-774] 08 p1028 N90-15939
Introduction to cryogenic wind tunnels 08 p1028 N90-15940
Fundamental considerations in testing in cryogenic wind tunnels 08 p1030 N90-15951
Test techniques for cryogenic wind tunnels 08 p1030 N90-15952
Wind tunnel investigations on the configuration of the international vortex flow experiment 08 p1068 N90-16181
Further development of the PIV method for use in the large wind tunnel 08 p1080 N90-16248
Flowfield effects of launch on a vertically-launched missile
[AD-A214468] 09 p1160 N90-16714
Development of flow visualization and nonintrusive velocity measurement in turbulent flow
[ETN-90-98077] 09 p1161 N90-16717
Measurement of the aerodynamical coefficients related to square section models defined by resemblance to the normalized models AGARD HB1 and HB2 in supersonic flow. Part 2: Incidence up to 25 deg
[ISL-R-108/88-PT-2] 09 p1161 N90-16718
The response of helicopter rotors to vibratory airload
[AD-A215678] 09 p1167 N90-16756
Study of pressure sensors in hydrodynamic turbulent boundary layer
[ONERA-RF-17/7218-PY] 09 p1218 N90-17067
Computational design of low aspect ratio wing-winglet configurations for transonic wind-tunnel tests
[NASA-CR-181939] 10 p1303 N90-17539
A survey of missile aerodynamics 10 p1303 N90-17541
Application of experimental techniques to store release problems 10 p1304 N90-17545
VLA missile development and high angle of attack behavior 10 p1305 N90-17553
Dynamic derivatives of missiles and fighter-type configurations at high angles of attack 10 p1306 N90-17554
Surface pressure distributions on a delta wing undergoing large amplitude pitching oscillations
[NASA-CR-186326] 10 p1306 N90-17558
Supersonic aerodynamic characteristics of a proposed Assured Crew Return Capability (ACRC) lifting-body configuration
[NASA-TM-4136] 10 p1307 N90-17560
A wind tunnel study of a sting-mounted circulation control wing
[AD-A216248] 10 p1310 N90-17577
Stability characteristics of a combat aircraft with control surface failure
[AD-A216196] 10 p1323 N90-17646
CAST-10-2/DOA 2 Airfoil Studies Workshop Results
[NASA-CP-3052] 10 p1323 N90-17647
Nonlinear transonic Wall-Interference Assessment/Correction (WIAC) procedures and application to cast-10 airfoil results from the NASA 0.3-m TCT 8- by 24-inch Slotted Wall Test Section (SWTS) 10 p1323 N90-17648
Comparison of conventional and adaptive wall wind tunnel results with regard to Reynolds number effects 10 p1323 N90-17649
High Reynolds number tests of the CAST-10-2/DOA 2 transonic airfoil at ambient and cryogenic temper ature conditions 10 p1324 N90-17650
Main results of CAST-10 airfoil tested in T2 cryogenic wind tunnel 10 p1324 N90-17652
An experimental AWTS process and comparisons of ONERA T2 and 0.3-m TCT AWTS data for the ONERA CAST-10 aerofoil 10 p1324 N90-17653
Investigation of CAST-10-2/DOA 2 airfoil in NAE high Reynolds number two-dimensional test facility 10 p1324 N90-17654
Residual interference and wind tunnel wall adaption 10 p1324 N90-17655
Comparison of NAE porous wall and NASA adaptive wall test results using the NAE CAST-10 airfoil model 10 p1325 N90-17656
Experience with some repeat tests on the 9 inch chord CAST-10-2/DOA 2 airfoil model in the Langley 0.3-m TCT adaptive wall test section 10 p1325 N90-17657
Comparison of two- and three-dimensional Navier-Stokes solutions with NASA experimental data for CAST-10 airfoil 10 p1325 N90-17658
Aerodynamic testing of a rotating wind turbine blade
[DE90-000312] 11 p1451 N90-18362
Half model tests on an ONERA calibration model in the transonic wind tunnel Goettingen, Federal Republic of Germany
[DLR-MITT-89-20] 11 p1452 N90-18370
The effects of wind tunnel data uncertainty on aircraft point performance predictions
[AD-A216091] 11 p1456 N90-18387
Wind-tunnel investigation of a flush airdata system at Mach numbers from 0.7 to 1.4
[NASA-TM-101697] 11 p1457 N90-18395
The DFVLR 3-m x 3-m low speed wind tunnel (NWG) in Goettingen
[ESA-TT-1156] 11 p1465 N90-18436
Automation and extension of LDV (Laser-Doppler Velocimetry) measurements of off-design flow in a subsonic cascade wind tunnel
[AD-A216627] 11 p1506 N90-18670
Measurements of surface pressures on an operating vertical-axis wind turbine
[DE90-005722] 11 p1529 N90-18805
Heat transfer measurements from a NACA 0012 airfoil in flight and in the NASA Lewis icing research tunnel
[NASA-CR-4278] 12 p1599 N90-19203
Conical Euler solution for a highly-swept delta wing undergoing wing-rock motion
[NASA-TM-102609] 12 p1600 N90-19211
Aeroservoelasticity
[NASA-TM-102620] 12 p1603 N90-19227
Low-speed wind-tunnel investigation of the flight dynamic characteristics of an advanced turboprop business/commuter aircraft configuration
[NASA-TP-2982] 12 p1606 N90-19239
Separation bubbles at high Reynolds number: Measurement and computation
[CUED/A-AERO/15] 12 p1657 N90-19525
An experimental investigation of the flow field around yawed stranded cables
[AD-A215782] 12 p1658 N90-19529
Windblast protection for advanced ejection seats 13 p1752 N90-20063
Aerodynamic analysis of a US Navy and Marine Corps unmanned air vehicle
[AD-A218282] 13 p1755 N90-20077
Digital-flutter-suppression-system investigations for the active flexible wing wind-tunnel model
[NASA-TM-102618] 13 p1758 N90-20093
A data acquisition parallel bus for wind tunnels at ARL (Aeronautical Research Laboratory)
[AD-A218052] 13 p1759 N90-20098
Noise of a simulated installed model counterrotation propeller at angle-of-attack and takeoff/approach conditions
[NASA-TM-102440] 13 p1881 N90-20794
Investigation of air transportation technology at the Massachusetts Institute of Technology, 1988-1989 14 p1905 N90-20922
Laser-velocimeter-measured flow field around an advanced, swept, eight-blade propeller at Mach 0.8
[NASA-TP-2482] 14 p1909 N90-20942
An approximate viscous shock layer method for calculating the hypersonic flow over blunt-nosed bodies 14 p1910 N90-20947
Performance data from a wind-tunnel test of two main-rotor blade designs for a utility-class helicopter
[NASA-TM-4183] 14 p1916 N90-20974
Advanced instrumentation for aircraft icing research
[NASA-CR-185225] 14 p1921 N90-21006
Measurement of the flow field in the blade passage and side-wall region of a plane turbine cascade 14 p1924 N90-21019
Detailed heat transfer measurements in nozzle guide vane passages in linear and annular cascades in the presence of secondary flows 14 p1926 N90-21030
Experimental aeroelasticity history, status and future in brief
[NASA-TM-102651] 14 p1930 N90-21047
Numerical simulation of hypersonic flow around a space plane. Part 2: Application to high angles of attack flow
[NAL-TR-1011T] 15 p2045 N90-21726
Wind tunnel investigation of three sonic anemometers
[PB90-149808] 15 p2046 N90-21729
Slotted-wall research with disk and parachute models in a low-speed wind tunnel
[DE90-002989] 15 p2048 N90-21737
A video-based experimental investigation of wing rock 15 p2054 N90-21771
Analysis of a six-component, flow-through, strain-gage, force balance used for hypersonic wind tunnel models with scramjet exhaust flow simulation
[NASA-CR-186585] 15 p2055 N90-21775
Aerodynamics of a full-scale, non rotating wind turbine blade under natural wind conditions
[RISOE-M-2768] 15 p2123 N90-22144
The aerodynamic characteristics of power-law bodies in continuum and transitional hypersonic flow
[RAE-TM-AERO-2164] 16 p2196 N90-22537
Flowfield measurements in the wake of a missile at high angle of attack
[AD-A219645] 17 p2345 N90-23351
Low speed testing of a laminar flow airfoil in an adaptive wall wind tunnel
[FFA-TN-1989-08] 17 p2346 N90-23363
Pressure measurements on a 5.35 m HAWT in CARDC 12 x 16 m wind tunnel compared to theoretical pressure distributions
[FFA-TN-1989-46] 17 p2347 N90-23365
Experimental performance and acoustic investigation of modern, counterrotating blade concepts
[NASA-CR-185158] 17 p2352 N90-23393
Aerodynamic performance of a 0.27-scale model of an AH-64 helicopter with baseline and alternate rotor blade sets
[NASA-TM-4201] 18 p2491 N90-24237
Static wind-tunnel and radio-controlled flight test investigation of a remotely piloted vehicle having a delta wing planform
[NASA-TM-4200] 18 p2491 N90-24238

Subsonic sting interference on the aerodynamic characteristics of a family of slanted-base ogive-cylinders
[NASA-CR-4299] 18 p2492 N90-24242
Flow unsteadiness effects on boundary layers
[NASA-CR-186067] 18 p2550 N90-24557
Off-design loss measurements in a compressor cascade
[AD-A220094] 18 p2552 N90-24564
The low-speed wind tunnel at DFVLR in Brunswick (status 1988)
[ESA-TT-1163] 19 p2662 N90-25152
Experimental investigation of Tollmien-Schlichting instability and transition in similar boundary layer flow in an adverse pressure gradient (Hartree beta = -0.14)
[LR-604] 19 p2692 N90-25318
Data of aero acoustic measurements on ultra-light aircraft propellers
[ESA-TT-1147] 19 p2754 N90-25648
Wind tunnel study of wake downwash behind A 6 percent scale model B1-B aircraft
[DE90-011783] 20 p2802 N90-25941
Experimental aerothermodynamic research of hypersonic aircraft
[NASA-CR-186903] 20 p2804 N90-25954
Practical developments in holographic interferometry
[PNR90669] 20 p2866 N90-26302
Testing of 3-D models in 2-D adaptive wall test sections 21 p2962 N90-26842
Adaptation for unsteady flow 21 p2963 N90-26845
Advanced recovery systems wind tunnel test report
[NASA-CR-177563] 22 p3108 N90-27653
Study of the flow around the prototype of A300: Results of the third test campaign at F2 and comparison with calculations
[CERT-33/5025-29-DERAT] 22 p3109 N90-27663
Tests of an ultra-light tunnel in the anechoic wind tunnel facility CEPRA 19
[ONERA-RF-20/7294-PH] 22 p3122 N90-27729
Wind tunnel simulation of Antarctic snowdrifting
[PB90-184565] 22 p3212 N90-28222
Two-dimensional wind tunnel test and comparison with calculations for a 15.2 percent thick airfoil section for wind turbines
[FFA-TN-1990-16] 23 p3269 N90-28501
Aerodynamic and propulsive control development of the STOL and maneuver technology demonstrator 23 p3271 N90-28514
Control research in the NASA high-alpha technology program 23 p3272 N90-28516
Aerodynamic control design: Experience and results at Aermacchi 23 p3272 N90-28518
Effects of canard position on the aerodynamic characteristics of a close-coupled canard configuration at low speed 23 p3272 N90-28519
Innovative control concepts and component integration for a generic supercruise fighter 23 p3273 N90-28521
The steady and time-dependent aerodynamic characteristics of a combat aircraft with a delta or swept canard 23 p3274 N90-28526
Determination of the ground effect on the characteristics of the A320 aircraft 23 p3275 N90-28534
Aerodynamic parameters of High-Angle-of attack Research Vehicle (HARV) estimated from flight data
[NASA-TM-102692] 23 p3283 N90-28578
The equipment for mass flow measurements in the low-speed wind tunnel at DFVLR in Brunswick (Federal Republic of Germany)
[ESA-TT-1125] 23 p3285 N90-28585
Comparison of wind tunnel airfoil performance data with wind turbine blade data
[DE90-000343] 24 p3418 N90-29308
Transonic 3-D Euler analysis of flows around fanjet engine and TPS (Turbine Powered Simulator). Comparison with wind tunnel experiment, evaluation of TPS testing method and 3-D flow
[NAL-TR-1045] 24 p3421 N90-29327
Wind tunnel, field, and numerical investigations of plume downwash and dispersion at an arctic industrial site 24 p3489 N90-29721

WIND TUNNEL WALLS

The effects of wall surface defects on boundary-layer transition in quiet and noisy supersonic flow 04 p0446 N90-12556
Residual interference assessment in adaptive wall wind tunnels
[NASA-CR-181896] 04 p0458 N90-12625
Study of the integration of wind tunnel and computational methods for aerodynamic configurations
[NASA-TM-102196] 05 p0572 N90-13332
A wall interference assessment/correction interface measurement system for the NASA/ARC 12-ft PWT
[NASA-CR-185474] 05 p0584 N90-13401
A two-dimensional adaptive-wall test section with ventilated walls in the Ames 2- by 2-foot transonic wind tunnel
[NASA-TM-102207] 05 p0585 N90-13407
An experimental investigation of wall-interference effects for parachutes in closed wind tunnels
[DE90-001802] 07 p0875 N90-15076
Nonlinear transonic Wall-Interference Assessment/Correction (WIAC) procedures and application to cast-10 airfoil results from the NASA 0.3-m TCT 8- by 24-inch Slotted Wall Test Section (SWTS) 10 p1323 N90-17648
Comparison of conventional and adaptive wall wind tunnel results with regard to Reynolds number effects 10 p1323 N90-17649
An experimental AWTS process and comparisons of ONERA T2 and 0.3-m TCT AWTS data for the ONERA CAST-10 aerofoil 10 p1324 N90-17653
Residual interference and wind tunnel wall adaption 10 p1324 N90-17655
Comparison of NAE porous wall and NASA adaptive wall test results using the NAE CAST-10 airfoil model 10 p1325 N90-17656
Experience with some repeat tests on the 9 inch chord CAST-10-2/DOA 2 airfoil model in the Langley 0.3-m TCT adaptive wall test section 10 p1325 N90-17657
Investigation of the development of laminar boundary-layer instabilities along a cooled-wall hollow cylinder at Mach number 8
[AD-A217672] 13 p1800 N90-20331
Slotted-wall research with disk and parachute models in a low-speed wind tunnel
[DE90-002989] 15 p2048 N90-21737
Low speed testing of a laminar flow airfoil in an adaptive wall wind tunnel
[FFA-TN-1989-08] 17 p2346 N90-23363
Experimental validation study of an analytical model of discrete frequency sound propagation in closed-test-section wind tunnels
[NASA-TM-102801] 19 p2754 N90-25647
Fluid Dynamics Panel Working Group 12 on Adaptive Wind Tunnel Walls: Technology and Applications
[AGARD-AR-269] 21 p2961 N90-26838
The aims and history of adaptive wall wind tunnels 21 p2962 N90-26839
Facilities involved in adaptive wall research 21 p2962 N90-26840
Streamlining algorithms for complete adaptation 21 p2962 N90-26841
Testing of 3-D models in 2-D adaptive wall test sections 21 p2962 N90-26842
High productivity testing 21 p2962 N90-26843
Limits of adaptation, residual interferences 21 p2963 N90-26844
Adaptation for unsteady flow 21 p2963 N90-26845
Aerodynamics of a linear oscillating cascade
[NASA-TM-103250] 22 p3108 N90-27657

WIND TUNNELS

NT CRYOGENIC WIND TUNNELS
NT HOTSHOT WIND TUNNELS
NT HYPERSONIC WIND TUNNELS
NT HYPERVELOCITY WIND TUNNELS
NT LOW DENSITY WIND TUNNELS
NT LOW SPEED WIND TUNNELS
NT PLASMA JET WIND TUNNELS
NT SLOTTED WIND TUNNELS
NT SUBSONIC WIND TUNNELS
NT SUPERSONIC WIND TUNNELS
NT TRANSONIC WIND TUNNELS
NT TRISONIC WIND TUNNELS

Wind tunnel support system effects on a fighter aircraft model at Mach numbers from 0.6 to 2.0
[AD-A210614] 01 p0002 N90-10010
Wind effect on sound wave propagation at ground vicinity
[CSTB-2-87-008] 04 p0550 N90-13201
Comparison of two droplet sizing systems in an icing wind tunnel
[NASA-TM-102456] 06 p0793 N90-14617
Evaluate and characterize mechanisms controlling transport, fate, and effects of army smokes in the aerosol wind tunnel: Transport, transformations, fate, and terrestrial ecological effects of hexachloroethane obscurant smokes
[DE90-002923] 07 p0957 N90-15536
Pressure measurement technique in the wind tunnel division of DFVLR
[ESA-TT-1145] 08 p1032 N90-15963
Shock layer vacuum UV spectroscopy in an arc-jet wind tunnel
[NASA-TM-102258] 09 p1226 N90-17112
Comparison of drop size distributions from two droplet sizing systems
[NASA-TM-102520] 09 p1232 N90-17147
Particle resuspension and associated coherent structures in a turbulent boundary layer 09 p1245 N90-17224
Analysis of the National Transonic Facility mishap
[NASA-TM-101686] 10 p1318 N90-17620
Residual interference and wind tunnel wall adaption 10 p1324 N90-17655
Fluctuating wind forces measured on a bluff body extending from a cavity
[AD-A216414] 10 p1386 N90-18020
Wind-tunnel investigation of a flush airdata system at Mach numbers from 0.7 to 1.4
[NASA-TM-101697] 11 p1457 N90-18395
Wind tunnel design of heat island turbulent boundary layer
[IHW-ET/50] 12 p1660 N90-19542
Experimental examination of the development behavior of a gaseous body in a steady state and neutral layer turbulent sheet boundary layer with ground asperity
[ETN-90-96067] 12 p1662 N90-19549
Modeling of surface roughness effects on glaze ice accretion 14 p1905 N90-20925
Theoretical and experimental study of flow-control devices for inlets of indraft wind tunnels
[NASA-TM-100050] 15 p2056 N90-21778
An investigation of turbulence structure in a low Reynolds number incompressible turbulent boundary layer 15 p2091 N90-21966
Thermal/structural analysis of the shaft-disk region of a fan drive system
[NASA-TM-101687] 16 p2245 N90-22807
User's guide to the 1.6 x 2.0 square m high speed wind tunnel HST, part 1
[ETN-90-96772] 17 p2357 N90-23414
Langley aerospace test highlights, 1989
[NASA-TM-102631] 17 p2487 N90-24221
The gun tunnel of the Brunswick Institute for Fluid Mechanics: Current development status 18 p2489 N90-24227
Experimental validation study of an analytical model of discrete frequency sound propagation in closed-test-section wind tunnels
[NASA-TM-102801] 19 p2754 N90-25647
Research at NASA's NFAC wind tunnels
[NASA-TM-102827] 20 p2801 N90-25933
Low-speed wind tunnel investigation of the static stability and control characteristics of an advanced turboprop configuration with the propellers placed over the tail
[NASA-CR-186900] 20 p2814 N90-26017
The effect of a three-dimensional source on the flow through a channel with square cross section
[LR-512] 20 p2863 N90-26289
Installation and pretest analysis of DARPA suboff model in the DTRC anechoic wind tunnel
[AD-A221497] 21 p2955 N90-26801
Fluid Dynamics Panel Working Group 12 on Adaptive Wind Tunnel Walls: Technology and Applications
[AGARD-AR-269] 21 p2961 N90-26838
Facilities involved in adaptive wall research 21 p2962 N90-26840
High productivity testing 21 p2962 N90-26843
Comparison of wind tunnel airfoil performance data with wind turbine blade data
[DE90-000343] 24 p3418 N90-29308
Studies of surface heat transfer in an arc-heated wind tunnel
[NAL-TR-1048] 24 p3437 N90-29410

WIND TURBINES

Some significant results from testing a Remote Multiplexing Unit (RMU) for temperature-induced errors
[DE89-009432] 01 p0073 N90-10421
A comparison of wind turbulence simulation models for stochastic loads analysis for horizontal-axis wind turbines
[DE89-009442] 01 p0083 N90-10473
Model 0A wind turbine generator FMEA
[NASA-TM-102378] 03 p0356 N90-12034
WISPER: A standardized fatigue load sequence for HAWT-blades
[NLR-MP-88029-U] 03 p0359 N90-12055
User's guide for a personal computer model of turbulence at a wind turbine rotor
[DE89-017753] 03 p0366 N90-12095
Type-specific dynamic measurements on wind turbines at the test site Schnittlingen (Germany, F.R.)
[DFVLR-MITT-88-31] 03 p0367 N90-12099
Acoustical effects of a large ridge on low-frequency sound propagation in stationary and moving atmospheres
[NASA-CR-186001] 03 p0400 N90-12290
Control of the variable speed generator on the Sandia 34-metre vertical axis wind turbine
[DE90-000803] 06 p0803 N90-14674

An initial look at the dynamics of the microscale flow field within a large wind farm in response to variations in the natural inflow
[DE89-009501] 06 p0804 N90-14682
Detailed analysis of the wake and free-flow characteristics at the Goodnoe Hills MOD-2 site
[DE90-002725] 06 p0806 N90-14692
Turbulent wind at the equatorial segment of an operating Darrieus wind turbine blade
[DE90-002672] 06 p0807 N90-14698
Inclusion of nonlinear aerodynamics in the FLAP code
[DE89-009507] 07 p0954 N90-15519
Aerodynamic design and initial performance measurements for the SANDIA 34-metre diameter vertical-axis wind turbine
[DE90-002574] 07 p0955 N90-15523
Structural response measurements and predictions for the SANDIA 34-meter test bed
[DE90-002575] 07 p0955 N90-15524
Fatigue behavior of vertical axis wind turbine airfoils with two weld configurations
[DE90-002628] 07 p0955 N90-15525
Performance predictions for an intermediate-sized VAWT based on performance of the 34-m VAWT test bed
[DE90-002635] 08 p1096 N90-16345
Aerodynamic testing of a rotating wind turbine blade
[DE90-000312] 11 p1451 N90-18362
Vertical axis wind turbine turbulent response model. Part 2: Response of Sandia National laboratories' 34-meter VAWT with aeroelastic effects
[DE90-005721] 11 p1529 N90-18804
Measurements of surface pressures on an operating vertical-axis wind turbine
[DE90-005722] 11 p1529 N90-18805
PC-based PCM (Pulse Code Modulation) telemetry data reduction system hardware
[DE90-000316] 12 p1612 N90-19273
Constructibility limits of multiflow wind turbines with pivots
[ILR-MITT-215] 12 p1682 N90-19662
PC-based PCM telemetry data reduction system software
[DE90-000317] 13 p1761 N90-20111
A comparison of two-and three-dimensional S809 airfoil properties for rough and smooth HAWT (Horizontal-Axis Wind Tunnel) rotor operation
[DE89-009512] 13 p1827 N90-20492
Parametric resonance in horizontal axis wind turbines
14 p1912 N90-20962
Regional wind energy assessment
[DE90-009439] 15 p2123 N90-22143
Aerodynamics of a full-scale, non rotating wind turbine blade under natural wind conditions
[RISOE-M-2768] 15 p2123 N90-22144
Rotor loading on a three-bladed wind turbine
15 p2123 N90-22145
Optimization of power output from wind turbines
15 p2124 N90-22146
Pressure measurements on a 5.35 m HAWT in CARDC 12 x 16 m wind tunnel compared to theoretical pressure distributions
[FFA-TN-1989-46] 17 p2347 N90-23365
Aeroelastic and stability behaviour of the WTS 3 Maglarp wind turbine. Calculations and comparisons with tests
[FFA-TN-1989-23] 17 p2420 N90-23792
Analysis of the environmental noise situation around a large Swedish prototype wind turbine
[FFA-TN-1988-16] 17 p2469 N90-24116
Aerodynamic pressure measurements on a rotating wind turbine blade
[DE90-000327] 18 p2494 N90-24256
A preliminary study of the masking of wind turbine noise by ambient sound
[FFA-TN-1990-01] 20 p2923 N90-26636
The production potential of wind power in Finland
[DE90-796157] 22 p3196 N90-28136
An evaluation of three models designed for siting wind turbines in areas of complex terrain
[DE90-013625] 22 p3196 N90-28137
Two-dimensional wind tunnel test and comparison with calculations for a 15.2 percent thick airfoil section for wind turbines
[FFA-TN-1990-16] 23 p3269 N90-28501
Comparison of wind tunnel airfoil performance data with wind turbine blade data
[DE90-000343] 24 p3418 N90-29308

WIND VANES

JARE data reports, no. 140 (meteorology 21): Meteorological data at Asuka Camp, Antarctica in 1987
[ISSN-0075-3343] 15 p2132 N90-22188

WIND VARIATIONS

Laser wave estimation
[AD-A213867] 09 p1227 N90-17119
Analysis of significant weather on meso-alpha scales using conventional and remotely sensed data: Exploratory studies
[AD-A214563] 09 p1248 N90-17238
Measurement of fluctuations in the tilt of Arctic ice at the CEAREX Oceanography Camp: Experiment review, data catalog, and preliminary results
[AD-A215059] 09 p1249 N90-17249
An analysis of diurnal wind variability in the Santa Barbara Channel from SODAR measurements
[AD-A215769] 10 p1408 N90-18121
A comparison of two-and three-dimensional S809 airfoil properties for rough and smooth HAWT (Horizontal-Axis Wind Tunnel) rotor operation
[DE89-009512] 13 p1827 N90-20492
Regional wind energy assessment
[DE90-009380] 15 p2133 N90-22192
Wind forecasting for utility operations
[DE90-009466] 15 p2133 N90-22193
An evaluation of three models designed for siting wind turbines in areas of complex terrain
[DE90-013625] 22 p3196 N90-28137
Satellite measurements of magnetospheric Poynting flux
[AD-A224391] 24 p3490 N90-29724

WIND VELOCITY

NT SOLAR WIND VELOCITY
US Navy regional climatic study of the United States Atlantic Coast and associated waters
[AD-A210198] 01 p0088 N90-10503
Analysis of heliport environmental data: Indianapolis downtown heliport, Wall Street heliport. Volume 2: Wall Street heliport data plots
[DOT/FAA/CT-TN87/54-VOL-2]
03 p0310 N90-11761
Pacific marine radar sea scatter experimental results
[AD-A211593] 03 p0339 N90-11931
Analytical and experimental study of runway runoff with wind effects
[PTI-8948] 04 p0458 N90-12627
Central Sudan surface wind data and climate characteristic
[KNMI-WR-88-01] 04 p0520 N90-13000
Wind effect on sound wave propagation at ground vicinity
[CSTB-2-87-008] 04 p0550 N90-13201
Meteorological atlas of the Northern Hemisphere lower stratosphere for January and February 1989 during the Airborne Arctic Stratospheric Expedition
[NASA-TM-4145] 05 p0671 N90-13908
The winds of high luminosity late-type bright stars
[NASA-CR-182961] 05 p0712 N90-14160
High resolution Doppler lidar
[NASA-CR-183288] 06 p0781 N90-14542
Detailed analysis of the wake and free-flow characteristics at the Goodnoe Hills MOD-2 site
[DE90-002725] 06 p0806 N90-14692
A global ocean wind stress climatology based on ECMWF (European Centre for Medium Range Weather Forecasts) analyses
[PB90-109968] 06 p0817 N90-14752
Application of a mass-consistent wind model to chinook windstorms
[AD-A213622] 07 p0963 N90-15568
Wind speed dependence of acoustic ambient vertical directional spectra at high frequency
[AD-A214293] 07 p0989 N90-15712
ECC (Electrochemical Concentration Cell) ozonesonde observations at South Pole, Antarctica, during 1988
[PB90-110172] 08 p1098 N90-16355
Climatic summaries and documentation for the primary meteorological Station, H. J. Andrews Experimental Forest, 1972 to 1984
[PB90-104373] 08 p1102 N90-16382
Multiparameter scatterometer for remote sensing (RADSER). Project Scatter: State-of-the-art and future applications
[INPE-4871-PRE/1482] 11 p1511 N90-18701
Effect of a random wind field on thermal blooming instabilities
[DE90-007241] 11 p1532 N90-18823
The microchannel plate camera as a detector at high resolution spectrographs: Experiments for velocity distribution in planetary nebulae
[ETN-90-95733] 12 p1664 N90-19560
Spanwise measurements of vertical components of atmospheric turbulence
[NASA-TP-2963] 12 p1692 N90-19718
Wind conditions near the ground in Federal Republic of Germany
[ISBN-3-88148-248-2] 12 p1694 N90-19727
Analysis of heliport environmental data: Indianapolis downtown heliport, Wall Street heliport. Volume 3: Indianapolis downtown heliport data plots
[AD-A217412] 13 p1829 N90-20500
US Navy regional climatic study of the Central East Asian coast and associated waters
[AD-A217448] 13 p1844 N90-20587
Atmospheric wind measurements using a 50 MHz imaging Doppler Interferometer radar
[AD-A218277] 13 p1847 N90-20601
A survey of the maritime-aerosol data collected at South Uist and the implications for the LOWTRAN maritime aerosol model 15 p2079 N90-21908
Aerodynamics of a full-scale, non rotating wind turbine blade under natural wind conditions
[RISOE-M-2768] 15 p2123 N90-22144
Lagrangian model simulation of the turbulent transport of evaporating jet droplets 15 p2128 N90-22168
Wind forecasting for utility operations
[DE90-009466] 15 p2133 N90-22193
Turbulence spectral widths view angle independence as observed by Doppler radar
[AD-A219169] 16 p2199 N90-22550
Characterization of the surfaces of platinum/tin oxide based catalysts by Fourier transform spectroscopy (FTIR) 18 p2643 N90-25054
Analysis and improved design considerations for airborne pulse Doppler radar signal processing in the detection of hazardous windshear
[NASA-CR-186792] 20 p2890 N90-26448
Wind field derivatives of extratropical cyclones observed by Doppler radar
[AD-A222188] 21 p3031 N90-27232
Absolute wind measurements in the lower thermosphere of Venus using infrared heterodyne spectroscopy
[NASA-CR-4290] 21 p3100 N90-27605
The production potential of wind power in Finland
[DE90-796157] 22 p3196 N90-28136
An evaluation of three models designed for siting wind turbines in areas of complex terrain
[DE90-013625] 22 p3196 N90-28137
Diurnal variation in the turbulent structure of the cloudy marine boundary layer during FIRE 1987
22 p3217 N90-28248
Tropospheric wind profiling using radar interferometry: A feasibility study of a compact mobile system
[PB90-217068] 23 p3351 N90-28939
Daily temperature, solar radiation, wind speed, cloud cover, and precipitation data recorded at the meteorological station for calendar years 1957--1988
[DE90-014399] 23 p3352 N90-28941
Absolute wind measurements in the lower thermosphere of Venus using infrared heterodyne spectroscopy
24 p3561 N90-30146

WIND VELOCITY MEASUREMENT

An improved airborne wind measurement technique for the NAE (National Aeronautical Establishment) Twin Otter
[AD-A217978] 13 p1842 N90-20575
Regional wind energy assessment
[DE90-009380] 15 p2133 N90-22192
Derivation of wind fields from Doppler measurements of a single radar and application to a cold front with narrow rainband
[DLR-FB-89-61] 18 p2582 N90-24705
Zonal winds between 25 and 120 km retrieved from solar occultation spectra 24 p3489 N90-29718
Absolute wind measurements in the lower thermosphere of Venus using infrared heterodyne spectroscopy
24 p3561 N90-30146

WINDING

NT FILAMENT WINDING
NT HELICAL WINDINGS
NT WIRE WINDING
AECM3: Acoustic Emission Conditions for failure prediction of winding carbon structures
[REPT-892-430-115] 18 p2517 N90-24374
Device and method for detecting and displaying crossover pattern in precision winding
[AD-D014539] 19 p2685 N90-25276
Improved high power/high frequency inductor
[NASA-CASE-NPO-17830-1-CU]
21 p2998 N90-27042

WINDMILLS (WINDPOWERED MACHINES)

Tower wake/blade interaction noise of a wind turbine
[NAL-TR-945] 02 p0236 N90-11344
Definition, transformation-formulae and measurements of tipvane angles
[IW-R510] 08 p1097 N90-16351
Constructibility limits of multiflow wind turbines with pivots
[ILR-MITT-215] 12 p1682 N90-19662
Rotor loading on a three-bladed wind turbine
15 p2123 N90-22145
Cable suspended windmill
[NASA-CASE-LAR-13434-1] 17 p2412 N90-23742

WINDOWS (APERTURES)

Reflectance modulation with electrochromic Li(sub x)WO(3) films
[DE90-004571] 10 p1435 N90-18279

Reliability study of TWT output RF window
[AD-A223688] 24 p3465 N90-29574
WINDOWS (INTERVALS)
NT LAUNCH WINDOWS
Applications of X windows in astronautics: Status and prospects
[MBB-UO-0082-90-PUB] 22 p3238 N90-28365
WINDPOWER UTILIZATION
Activities report on KEMA R and D
[ST-REPT-VOL-6-NO-12] 03 p0367 N90-12100
Detailed analysis of the wake and free-flow characteristics at the Goodnoe Hills MOD-2 site
[DE90-002725] 06 p0806 N90-14892
Vision for the introduction of the wind power generation system. Survey on the prospective market, part 2
[DE89-910386] 12 p1680 N90-19651
Wind Energy Program summary. Volume 1: Overview
[DE89-009479] 13 p1827 N90-20491
A comparison of two-and three-dimensional S809 airfoil properties for rough and smooth HAWT (Horizontal-Axis Wind Tunnel) rotor operation
[DE89-009512] 13 p1827 N90-20492
Regional wind energy assessment
[DE90-009439] 15 p2123 N90-22143
Optimization of power output from wind turbines
15 p2124 N90-22146
Regional wind energy assessment
[DE90-009380] 15 p2133 N90-22192
Wind energy program summary. Volume 2: Research summaries
[DE89-009480] 19 p2710 N90-25423
Abstracts of 1989 Japan Solar Energy Society and Japan Wind Energy Association Joint Conference
[DE90-503616] 21 p3019 N90-27168
The production potential of wind power in Finland
[DE90-796157] 22 p3196 N90-28136
WINDPOWERED GENERATORS
Computer simulation of wind/diesel system operation
[DE89-009445] 06 p0805 N90-14688
Vision for the introduction of the wind power generation system. Survey on the prospective market, part 2
[DE89-910386] 12 p1680 N90-19651
A search routine for optimization in a wind power system with variable speed
[FOA-C-20779-2.1] 20 p2882 N90-26395
WINDS ALOFT
NT GEOSTROPHIC WIND
NT JET STREAMS (METEOROLOGY)
Airdata calibration of a high-performance aircraft for measuring atmospheric wind profiles
[NASA-TM-101714] 06 p0725 N90-14228
Solar cyclical trend study of the mid-latitude, quiet-time, meridional, neutral winds at winter solstice conditions
[AD-A217398] 13 p1841 N90-20568
Low latitude F-region dynamical processes from atomic oxygen nightglow emissions
[INPE-4999-PRE/1561] 14 p2006 N90-21494
Atmospheric environment for space shuttle (STS-28) launch
[NASA-TM-100386] 19 p2715 N90-25452
WINDSCREENS
U WINDSHIELDS
WINDSHIELDS
Definition and reduction of the F-18 windshield birdstrike hazard
[AD-A210700] 01 p0004 N90-10015
Evaluation of the improved OV-ID anti-icing system, phase 2
[AD-A213928] 07 p0877 N90-15083
An illustrated guide of optical characteristics of aircraft transparencies
[AD-A214565] 09 p1167 N90-16752
A new method for measuring the transmissivity of aircraft transparencies
[AD-A216953] 12 p1714 N90-19842
Full-scale birdstrike testing of in-service aged F-111 ADBIRT windshield transparencies
[AD-A218035] 13 p1754 N90-20069
The effect of windscreen bows and HUD pitch ladder format on pilot performance during simulated flight
[AD-A218139] 14 p2011 N90-21523
Nondestructive measurement of residual stresses in aircraft transparencies
[AD-A218660] 17 p2415 N90-23762
B-1B improved windshield development. Volume 2: Magna analysis: Baseline and parametric
[AD-A221501] 21 p2960 N90-26828
Methods for detecting low-frequency signals in the presence of strong winds
[AD-A223960] 23 p3320 N90-28789
WING CAMBER
Chordwise loading and camber for two-dimensional thin sections
[AD-A213318] 04 p0448 N90-12568
Optimum spanwise camber for minimum induced drag
[BU-403] 11 p1452 N90-18389
Aerodynamic development perspective for traffic aeroplanes
[DGLR-89-141] 18 p2495 N90-24260
WING FLAPS
NT LEADING EDGE FLAPS
WING FLOW METHOD TESTS
Aerodynamics of unsteady systems. Numerical study of potential flow/boundary layer coupling
[ETN-90-96257] 11 p1452 N90-18367
WING LOADING
Advanced actuation systems development, volume 1
[AD-A213334] 04 p0458 N90-12624
A CFD study of tilt rotor flowfields
[NASA-CR-186116] 05 p0575 N90-13349
Advanced actuation systems development, volume 2
[AD-A213378] 05 p0583 N90-13398
Transonic wing charge improvements by passive shock boundary layer interference control: Development status and prospects
[ETN-90-96463] 18 p2496 N90-24267
Model tilt-rotor hover performance and surface pressure measurement
[AD-A222535] 21 p2959 N90-26827
In-flight investigation of shuttle tile pressure orifice installations
[NASA-TM-4219] 23 p3328 N90-28820
WING OSCILLATIONS
Direct multivariable adaptive controller with application to wing flutter 10 p1322 N90-17642
Constructibility limits of multiflow wind turbines with pivots
[ILR-MITT-215] 12 p1682 N90-19662
A video-based experimental investigation of wing rock
15 p2054 N90-21771
An experimental study of tip shape effects on the flutter of aft-swept, flat-plate wings
[NASA-TM-4180] 16 p2199 N90-22555
ARLSUPER version 1.0, program users guide
[AD-A222693] 21 p2953 N90-26793
The steady and time-dependent aerodynamic characteristics of a combat aircraft with a delta or swept canard 23 p3274 N90-28526
Multi-disciplinary optimization of aeroservoelastic systems
[NASA-CR-185931] 24 p3432 N90-29385
WING PANELS
Laminar flow control perforated wing panel development
[NASA-CR-178166] 01 p0034 N90-10187
The INMARSAT-2 solar generator panels
10 p1343 N90-17782
The ITALSAT solar array 10 p1343 N90-17787
Pressure air tightness tests of laminated panels for wing leading edge heat shields
[INFORME-I-377/89] 10 p1358 N90-17873
WING PLANFORMS
NT DELTA WINGS
NT SWEPT FORWARD WINGS
NT SWEPTBACK WINGS
NT VARIABLE SWEEP WINGS
Study of forces and moments on wing-bodies at high incidence, volumes 1 and 2 05 p0575 N90-13350
Application of laminar flow control to supersonic transport configurations
[NASA-CR-181917] 20 p2803 N90-25944
The experimental investigation of flow in the core of a vortex structure
[BR114893] 24 p3468 N90-29597
WING PROFILES
Wind tunnel test of CAD USB-STOL semi-borne prototype
[NAL-TM-566] 03 p0299 N90-11696
Unsteady three-dimensional thin-layer Navier Stokes solutions on dynamic blocked grids
[AD-A212377] 04 p0503 N90-12899
Efficient methods for integrated structural-aerodynamic wing optimum design 05 p0579 N90-13376
A panel process for the calculation of the flow around a wing with front angle damping
[ETN-90-95367] 12 p1600 N90-19207
Static aeroelastic analysis of a three-dimensional generic wing
[NASA-TM-102231] 13 p1757 N90-20087
Measurement of lift development on rapidly-accelerated wings 14 p1911 N90-20956
Study of the ground effects in the CEAT aerohydrodynamic tunnel: Using the results
23 p3274 N90-28530
The aerodynamic design of the oblique flying wing supersonic transport
[NASA-CR-177552] 23 p3276 N90-28540
WING SLOTS
An experimental evaluation of slots versus porous strips for laminar-flow applications 04 p0442 N90-12530
WING TIP VORTICES
Experimental investigations on the stability and vorticity of the vortex breakdown phenomenon above delta wings, measured by the ultrasonic laser method
[ESA-TT-1079] 23 p3268 N90-28498
WING TIPS
Flutter clearance of the F-18 high-angle-of-attack research vehicle with experimental wingtip instrumentation pods
[NASA-TM-4148] 03 p0305 N90-11732
Ground evaluation of seeding an in-flight wingtip vortex using infrared imaging flow visualization technique
18 p2639 N90-25035
Video photographic considerations for measuring the proximity of a probe aircraft with a smoke seeded trailing vortex
[NASA-TM-102691] 19 p2657 N90-25120
WINGLETS
Computational design of low aspect ratio wing-winglet configurations for transonic wind-tunnel tests
[NASA-CR-181939] 10 p1303 N90-17539
WINGS
NT DELTA WINGS
NT FIXED WINGS
NT FLEXIBLE WINGS
NT JOINED WINGS
NT LIFTING ROTORS
NT LOW ASPECT RATIO WINGS
NT OBLIQUE WINGS
NT RECTANGULAR WINGS
NT RIGID ROTORS
NT RIGID WINGS
NT RING WINGS
NT ROTARY WINGS
NT SLENDER WINGS
NT SUPERCRITICAL WINGS
NT SWEPT FORWARD WINGS
NT SWEPT WINGS
NT SWEPTBACK WINGS
NT THIN WINGS
NT TILTING ROTORS
NT VARIABLE SWEEP WINGS
Winged versus wingless airframes
01 p0015 N90-10073
Independent Orbiter Assessment (IOA): Analysis of the elevon subsystem
[NASA-CR-185576] 02 p0166 N90-10935
Development of direct-inverse 3-D methods for applied transonic aerodynamic wing design and analysis
[NASA-CR-186036] 03 p0305 N90-11733
A new test procedure for a wing made with carbon fiber composites
[ETN-89-95220] 03 p0320 N90-11820
Laminar flow: The Cessna perspective
04 p0439 N90-12507
Induced drag for non-planar wings
[LR-521] 05 p0576 N90-13357
Unsteady three-dimensional thin-layer Navier-Stokes solutions on dynamic blocked grids
07 p0874 N90-15069
An alternative derivation for an integral equation for linearized subsonic flow over a wing
[AD-A214140] 07 p0876 N90-15079
The maximum lift coefficient of plain wings at subsonic speeds
[ESDU-89034] 07 p0876 N90-15082
Evaluation of the improved OV-ID anti-icing system, phase 2
[AD-A213928] 07 p0877 N90-15083
Test techniques for cryogenic wind tunnels
08 p1030 N90-15952
Inspection development for T-37 wing spar cap lug
[AD-A214826] 09 p1159 N90-16708
Analysis of indirect effects of lightning on a metallic A 300 wing: Test report
[REPT-E87/645800] 09 p1162 N90-16726
Body effect on wing angle of attack and pitching moment at zero lift at low speeds
[ESDU-89042] 09 p1167 N90-16757
Optimum location of flow conditioners in a 4-inch orifice meter
[PB90-111675] 09 p1216 N90-17049
Heat pipes for wing leading edges of hypersonic vehicles
[NASA-CR-181922] 09 p1216 N90-17055
Opportunities for improved understanding of supersonic and hypersonic flows 10 p1308 N90-17566
A wind tunnel study of a sting-mounted circulation control wing
[AD-A216248] 10 p1310 N90-17577
Direct multivariable adaptive controller with application to wing flutter 10 p1322 N90-17642
Half model tests on an ONERA calibration model in the transonic wind tunnel Goettingen, Federal Republic of Germany
[DLR-MITT-89-20] 11 p1452 N90-18370

Carrier wing profile in nonstationary current
[ETN-90-95368] 12 p1600 N90-19208
Progress in inverse design and optimization in aerodynamics 14 p1916 N90-20977
Aerofoil design techniques 14 p1916 N90-20978
A system for transonic wing design with geometric constraints based on an inverse method 14 p1917 N90-20983
Constrained spanload optimization for minimum drag of multi-lifting-surface configurations 14 p1919 N90-20992
Numerical optimization of wings in transonic flow 14 p1920 N90-20997
Extension of a streamwise upwind algorithm to a moving grid system
[NASA-TM-102800] 15 p2048 N90-21739
Conceptual design optimization study
[NASA-CR-4298] 15 p2051 N90-21755
Unsteady separated flows produced by complex harmonic motions: Investigation of wing-flow interactions elicited by a mechanical model simulating dragonfly wing kinematics 15 p2100 N90-22018
Extension of a three-dimensional viscous wing flow analysis user's manual: VISTA 3-D code
[NASA-CR-182024] 16 p2197 N90-22538
Multilevel decomposition approach to the preliminary sizing of a transport aircraft wing
[NASA-CR-4296] 16 p2200 N90-22557
Application of laminar flow control to supersonic transport configurations
[NASA-CR-181917] 20 p2803 N90-25944
Effect of vortex generators on the aerodynamic wing characteristics and body of revolution
[AD-A222813] 20 p2804 N90-25955
Report of the Fluid Dynamics Panel Working Group 10 on calculation of 3D separate turbulent flows in boundary layer limit
[AGARD-AR-255] 20 p2862 N90-26280
An expert system advisor for damage repair of composite wing skins (repairman) 21 p2956 N90-26810
Advanced recovery systems wind tunnel test report
[NASA-CR-177563] 22 p3108 N90-27653
Do inviscid vortex sheets roll-up
[PD-CF-9010] 23 p3267 N90-28491
Study of the ground effects in the CEAT aerohydrodynamic tunnel: Using the results 23 p3274 N90-28530
System reliability optimization of aircraft wings 23 p3275 N90-28536
Damage tolerance of the fighter aircraft 37 Viggen. Part 1: Analytical assessment
[FFA-TN-1990-12-PT-1] 23 p3276 N90-28538
Damage tolerance of the fighter aircraft 37 Viggen. Part 2: Experimental verification
[FFA-TN-1990-13-PT-2] 23 p3276 N90-28539
In-flight investigation of shuttle tile pressure orifice installations
[NASA-TM-4219] 23 p3328 N90-28820
WingDesign: Program for the structural design of a wing cross-section
[LR-627] 24 p3433 N90-29390

WINTER
Observation of wind corners in the middle atmosphere over Andenes (69 N) during winter 1983/84, summer 1987 and summer 1988 05 p0657 N90-13836
Meteorological atlas of the Northern Hemisphere lower stratosphere for January and February 1989 during the Airborne Arctic Stratospheric Expedition
[NASA-TM-4145] 05 p0671 N90-13908
Winter cloud seeding potential on the Mogollon Rim
[PB89-190540] 07 p0962 N90-15562
Characteristics of electromagnetic wave forms with lightning in winter season
[DE89-901256] 07 p0963 N90-15567
Multiple flow regimes in the Northern Hemisphere winter 08 p1100 N90-16372
Lightning observations on Japan Sea coast in winter
[DE90-702485] 08 p1103 N90-16387
Characteristics of electromagnetic wave forms with lightning in winter season (2): Characteristics in frequency domain
[DE90-734989] 08 p1103 N90-16388
Psychophysiological correlates of human adaptation in antarctica
[AD-A216679] 10 p1412 N90-18142
The sources and chemistry of late winter Arctic tropospheric aerosols
[PB90-131988] 15 p2126 N90-22158
The observed three-dimensional structure of baroclinic waves in the Northern Hemisphere winter as revealed in a linear regression analysis 15 p2128 N90-22167
Coping strategies and mood during cold weather training
[AD-A223915] 24 p3498 N90-29773

WIRE
NT ELECTRIC WIRE
NT EXPLODING WIRES
Composite ceramic superconducting wires for electric motor applications
[AD-A210345] 01 p0060 N90-10346
An algorithm to calculate the beam momentum distribution from flying wire profiles
[DE89-015587] 01 p0073 N90-10418
Analysis of coaxial wire measurement of longitudinal coupling impedance
[DE89-015748] 02 p0215 N90-11230
Battery actuation of NITINOL at sub-zero temperatures
[AD-A211254] 02 p0216 N90-11237
Thermal conduction of SSC (Superconducting Super Collider) wire
[DE89-016710] 03 p0319 N90-11811
Magnetostrictive torque sensor
[AD-D014169] 03 p0349 N90-11996
Wire grid modeling of the linear tapered slot antenna
[AD-A212977] 04 p0494 N90-12842
Development and characterization of PdCr temperature-compensated wire resistance strain gage
[NASA-CR-185153] 05 p0644 N90-13761
Composite ceramic superconducting wires for electric motor applications
[AD-A213742] 07 p0912 N90-15274
Epoxy-resin cable terminations
[AD-A213789] 07 p0942 N90-15454
Processing YBa2Cu3O(x) wires in O3/O2
[DE90-003570] 07 p1001 N90-15794
Method of forming low cost, formable High T(subc) superconducting wire
[NASA-CASE-LEW-14676-2] 09 p1286 N90-17454
HF wire antennas over real ground: Computer simulation and measurement 10 p1370 N90-17937
Proceedings of the 38th International Wire and Cable Symposium
[AD-A216023] 11 p1501 N90-18638
Recent improvements to the electromagnetic surface patch code
[AD-A217479] 13 p1794 N90-20293
Attachment of lead wires to thin film thermocouples mounted on high temperature materials using the parallel gap welding process
[NASA-TM-102442] 14 p1983 N90-21361
Development of shape memory metal as the actuator of a fail safe mechanism 15 p2112 N90-22081
Composite ceramic superconducting wires for electric motor applications
[AD-A219131] 16 p2224 N90-22689
Internal wire guide for GTAW welding
[NASA-CASE-MFS-29489-1] 17 p2385 N90-23586
The effect of magnetic field on the critical current density of bulk superconducting wires
[DE90-010458] 18 p2621 N90-24934
Electrode carrying wire for GTAW welding
[NASA-CASE-MFS-29491-1] 20 p2842 N90-26168
Characterization of NbTi multifilamentary superconducting wires
[DE90-626245] 20 p2930 N90-26672
Improved high power/high frequency inductor
[NASA-CASE-NPO-17830-1-CU] 21 p2998 N90-27042
Composite ceramic superconducting wires for electric motor applications
[AD-A222085] 21 p3001 N90-27055
Fabrication of composite high temperature superconductor wires from Ag/YBa2Cu3O(sub x) powder produced by AgNO3 decomposition
[AD-A221936] 21 p3083 N90-27532
Superconducting film on metallic wire 22 p3146 N90-27840
Composite superconducting wires obtained by high-rate tinning in molten Bi-Pb-Sr-Ca-Cu-O system 22 p3148 N90-27850
Progress in high temperature speckle-shift strain measurement system
[NASA-TM-103255] 22 p3177 N90-28031
Fatigue testing apparatus
[AD-D014544] 22 p3192 N90-28108
Frequency response of a thermocouple wire: Effects of axial conduction
[NASA-CR-180454] 23 p3330 N90-28827

WIRE BRIDGE CIRCUITS
NT WHEATSTONE BRIDGES
Electrothermal response testing more than a quality assurance tool
[DE90-001449] 06 p0780 N90-14536

WIRE CLOTH
Method for fabricating thin film metallic meshes for use as Fabry-Perot interferometer elements, filters and other devices
[AD-D014236] 06 p0779 N90-14529

WIRE GRID LENSES
Transmission micro-grids for shift analysis of x ray frequencies
[MPE-216] 09 p1283 N90-17439

WIRE MESH
U WIRE CLOTH

WIRE WINDING
Mechanical states in wound capacitors. Part 1: Prediction
[DE89-008110] 01 p0059 N90-10337
Mechanical states in wound capacitors. Part 2: Optimization
[DE89-008116] 01 p0059 N90-10338

WIRING
Boeing 727-100 test project (high energy radiated field tests)
[DOT/FAA/CT-88/33] 14 p1964 N90-21247

WIRING SYSTEMS
U WIRING

WISCONSIN
Use of ground penetrating radar to define recharge areas in the Central Sand Plain
[PB89-224885] 04 p0490 N90-12814

WKB APPROXIMATION
U WENTZEL-KRAMER-BRILLOUIN METHOD

WOLF-RAYET STARS
On the analysis of line profile variations: A statistical approach 03 p0420 N90-12412
A source of observational constraints on the structure of Wolf-Rayet winds
[DE90-001236] 06 p0864 N90-15023
Analysis of gamma squared Velorum photometry from the South Pole 15 p2183 N90-22472

WOLFRAM
U TUNGSTEN

WOMEN
U FEMALES

WOOD
NT CORK (MATERIALS)
Method of radiographic inspection of wooden members
[NASA-CASE-LAR-13724-1] 17 p2414 N90-23756
Recycling waste-paper 18 p2514 N90-24359

WOOL
New Fabric Development Program
[AD-A211549] 03 p0332 N90-11891

WORD PROCESSING
Computer programs for measuring variations in speech
[AD-A211126] 02 p0259 N90-11467
Multilayered neural networks: Learning algorithms, implementation on hypercube machines, applications
[ETN-90-97255] 20 p2913 N90-26574
Selective multimode/multiconfigurable data acquisition and reduction processor system
[AD-D014551] 22 p3234 N90-28341

WORDS (LANGUAGE)
Self-organizing semantic maps
[PB89-212609] 04 p0529 N90-13049
A structured connectionist approach to direct inferences and figurative adjective-noun combinations
[AD-A214326] 07 p0978 N90-15649
Research and development in natural language understanding as part of the Strategic Computing Program
[AD-A214587] 09 p1264 N90-17331
Finite word length considerations in high resolution spectral estimation
[AD-A214684] 09 p1273 N90-17377
Schema-based theories of problem solving
[AD-A216717] 11 p1552 N90-18939
The expression of syntagmatic relationships in frame-based indexing 12 p1726 N90-19917
Permuted medical subject headings, 1990
[PB90-100025] 14 p2036 N90-21684
Some remarks on treatment of be in Montague's PTQ --- Proper Treatment of Quantification (PTQ)
[REPT-89-40] 15 p2147 N90-22267
Sentence comprehension: A parallel distributed processing approach
[AD-A218886] 16 p2300 N90-23104
Content effects in mathematics problem solving
[AD-A222436] 21 p3065 N90-27423
A comparison of password techniques for multilevel authentication mechanisms
[AD-A224245] 23 p3379 N90-29089

WORK
NT PHYSICAL WORK
Measurement of mechanical work and energy expenditure in running and bicycling 05 p0675 N90-13935
The predictability and efficiency of human walking: Metabolic, mechanical, and biophysical considerations 15 p2137 N90-22211

Investigation of a heat driven thermoacoustic prime mover
[AD-A223928] 24 p3484 N90-29694

WORK CAPACITY

Exercise countermeasures for bed rest deconditioning
[NASA-TM-101045] 05 p0674 N90-13926
Physiological and perceptual responses to prolonged treadmill load carriage
[AD-A218910] 16 p2260 N90-22886
Overtraining and exercise motivation: A research prospectus 18 p2629 N90-24982

WORK FUNCTIONS

Surface production of ions
[AD-A216470] 11 p1562 N90-19003
Adlayer physics
[AD-A221064] 19 p2673 N90-25203

WORK HARDENING

NT STRAIN HARDENING
Improvement in pre-constraint fatigue resistance of modular ferretic and bainitic steel by shot peening treatments
[CETIM-106370] 04 p0476 N90-12727

WORK-REST CYCLE

Human performance in continuous/sustained operations and the demands of extended work/rest schedules: An annotated bibliography, volume 2
[AD-A210504] 01 p0093 N90-10530
Adjustment and validation of the mathematical prediction model for sweat rate, heart rate, and body temperature under outdoor conditions
[AD-A222599] 20 p2898 N90-26486

WORKING FLUIDS

A thermochemical analysis of proposed working fluids for electrothermal guns
[AD-A210661] 02 p0159 N90-10910
Design of ceramic fabric heat pipe with water working fluid
[DE89-016565] 02 p0221 N90-11265
Superconducting magnets in space
[DE90-002671] 06 p0837 N90-14865
Spacecraft thermal control design data, volume 4
[ESA-PSS-03-108-ISSUE-1-VOL-4] 11 p1469 N90-18458
Ceramic heat pipe wick
[NASA-CASE-GSC-13199-1] 17 p2378 N90-23541
Transient characteristics of a grooved water heat pipe with variable heat load
[NASA-CR-185280] 20 p2861 N90-26272
Two-dimensional model of a Space Station Freedom thermal energy storage canister
[NASA-TM-103124] 20 p2862 N90-26279

WORKLOADS (PSYCHOPHYSIOLOGY)

Computer programs for measuring variations in speech
[AD-A211126] 02 p0259 N90-11467
Forecasting contracting workload
[AD-A211935] 03 p0416 N90-12387
A candidate concept for display of forward-looking wind shear information
[NASA-TM-101585] 06 p0725 N90-14232
Workload induced spatio-temporal distortions and safety of flight
[DE89-016613] 06 p0820 N90-14771
The application of queuing theory to the modelling of CP-140 aircraft communications
[AD-A213479] 07 p0918 N90-15310
Accidents in fighter aircraft caused by human factors. Why do they occur 09 p1254 N90-17278
Training and selecting individuals for high levels of information processing load 09 p1256 N90-17288
Investigation of the effects of external supports on manual lifting
[PB90-103367] 09 p1260 N90-17307
Subjective Workload Assessment Technique (SWAT): A user's guide
[AD-A215405] 09 p1261 N90-17312
Sensitivity of the peripheral vision to simulated aircraft ascent and descent 10 p1413 N90-18145
Assessment of crew workload measurement methods, techniques and procedures. Volume 2: Guidelines for the use of workload assessment techniques in aircraft certification
[AD-A217067] 12 p1697 N90-19748
Assessment of crew workload measurement methods, techniques and procedures. Volume 1: Process, methods and results
[AD-A217699] 13 p1855 N90-20647
Minimum flying qualities. Volume 2: Pilot modeling for flying qualities applications
[AD-A218561] 16 p2201 N90-22561
Helmet-mounted pilot night vision systems: Human factors issues 16 p2269 N90-22930
The physiological cost of wearing the propellant handler's ensemble at the Kennedy Space Center
[NASA-TM-102786] 16 p2275 N90-22966
Voice measures of workload in the advanced flight deck: Additional studies
[NASA-CR-4258] 17 p2437 N90-23887
Effects of monitoring under high and low taskload on detection of flashing and colored radar targets
[AD-A220313] 17 p2439 N90-23895
An empirically derived figure of merit for the quality of overall task performance 18 p2644 N90-25058
Performance-based workload assessment: Allocation strategy and added task sensitivity 19 p2734 N90-25539
Real-time measurement of mental workload: A feasibility study 19 p2734 N90-25540
SHAPA: An interactive software tool for protocol analysis applied to aircrew communications and workload 19 p2734 N90-25541
Usefulness of heart measures in flight simulation 19 p2734 N90-25542
Aviation safety: Conditions within the air traffic control work force. Fact sheet for congressional requesters
[GAO/RCED-89-113FS] 20 p2805 N90-25958
Effects of microgravity on rat muscle 20 p2891 N90-26453
Choosing a pilot subjective workload scale to fit flight operational requirements
[IAR-89-21] 20 p2900 N90-26493
Human performance in cockpit-related systems
[NIAR-90-7] 20 p2900 N90-26495
Psychophysiological assessment of pilot workload in an applied setting
[AD-A222707] 20 p2902 N90-26507
Application of audio/speech recognition for military applications 21 p2993 N90-27014
The integrated area measure of visual endogenous ERPs: Relation to cognitive workload and hemisphere
[AD-A223191] 21 p3035 N90-27255
Real-time measurement of mental workload using psychophysiological measures
[AD-A221462] 21 p3036 N90-27258
Effects of organizational structure on performance: Experimental results
[AD-A222671] 21 p3085 N90-27543
Flight test investigation of flight director and autopilot functions for helicopter decelerating instrument approaches
[DOT/FAA/CT-TN89/54] 22 p3121 N90-27724
Electrocardiogram of military aircraft pilots measured during real flight missions: Study of the variability of the cardiac rhythm in correlation with working stress
[ETN-90-97453] 22 p3231 N90-28324
A methodology for the objective measurement of pilot situation awareness 23 p3357 N90-28974
Situational Awareness Rating Technique (SART): The development of a tool for aircrew systems design 23 p3357 N90-28975
Performance-based measures of merit for tactical situation awareness 23 p3358 N90-28976
Evaluation of the Situational Awareness Rating Technique (SART) as a tool for aircrew systems design 23 p3358 N90-28977
Attention gradients in situation awareness 23 p3358 N90-28978
Workload induced spatio-temporal distortions and safety of flight: An investigation of cognitive intrusions in perceptual processes 23 p3360 N90-28986
Physiological metrics of mental workload: A review of recent progress
[NASA-CR-187290] 24 p3499 N90-29777

WORKSTATIONS

Flexible structure control experiments using a real-time workstation for computer-aided control engineering 01 p0017 N90-10084
An integrated distributed processing interface for supercomputers and workstations
[DE89-016769] 02 p0260 N90-11478
Telescience Testbed Pilot Program
[NASA-CR-184997] 04 p0528 N90-13047
The role of the host in a cooperating mainframe and workstation environment, volumes 1 and 2
[NASA-CR-185463-VOL-1/2] 05 p0602 N90-13496
Advanced Software Development Workstation Project 06 p0827 N90-14807
Continuation of research in software for space operations support
[NASA-CR-186092] 06 p0827 N90-14808
Space station Simulation Computer System (SCS) study for NASA/MSFC. Volume 4: Conceptual design report
[NASA-CR-183843] 13 p1762 N90-20116
Space station Simulation Computer System (SCS) study for NASA/MSFC. Volume 5: Study analysis report
[NASA-CR-183844] 13 p1763 N90-20117
Space station Simulation Computer System (SCS) study for NASA/MSFC. Volume 6: Study issues report
[NASA-CR-183845] 13 p1763 N90-20118
The Real Time Interactive Display Environment (RTIDE), a display building tool developed by Space Shuttle flight controllers 13 p1857 N90-20654
Tools for 3D scientific visualization in computational aerodynamics 13 p1858 N90-20660
Software systems for modeling articulated figures 13 p1861 N90-20677
SES cupola interactive display design environment 13 p1862 N90-20679
Issues in visual support to real-time space system simulation solved in the Systems Engineering Simulator 13 p1862 N90-20680
Real-time graphics for the Space Station Freedom cupola, developed in the Systems Engineering Simulator 13 p1862 N90-20683
Intensity dependent spread processor and workstation 15 p2143 N90-22244
Multimedia system control
[AD-A219392] 16 p2276 N90-22971
Graphics equipment for data analysis
[AD-A218983] 16 p2278 N90-22985
Learning environment for neural networks and transient acoustics
[AD-A219000] 16 p2314 N90-23186
Simulator evaluation of the final approach spacing tool
[NASA-TM-102807] 17 p2348 N90-23374
The Zenith Z-248 as a scientific workstation
[AD-A219991] 17 p2441 N90-23909
NASTRAN migration to UNIX 18 p2569 N90-24643
Applications of an acoustic-emission data-acquisition workstation: 2
[DE90-010941] 18 p2612 N90-24880
Knowledge-based control of an adaptive interface 18 p2630 N90-24987
The implementation of the graphics of program EAGLE: A numerical grid generation code on NASA Langley SNS computer system 18 p2642 N90-25050
Telepresence and Space Station Freedom workstation operations 19 p2731 N90-25527
The human factors of workstation telepresence 19 p2732 N90-25528
An approach to a real-time distribution system 19 p2733 N90-25535
CEBAF control system
[CEBAF-PR-89-013] 19 p2757 N90-25666
Supercomputer workstation communication
[AD-A222466] 21 p3039 N90-27272
A vision-based telerobotic control station 21 p3046 N90-27311
Robot dynamics in reduced gravity environment 21 p3049 N90-27333
The operational feature exchange language
[AD-A222497] 21 p3060 N90-27401
Concurrent Image Processing Executive (CIPE). Volume 1: Design overview
[NASA-CR-186853] 22 p3236 N90-28348
Concurrent Image Processing Executive (CIPE). Volume 2: Programmer's guide
[NASA-CR-186854] 22 p3236 N90-28349
Automated simulation as part of a design workstation
[NASA-TM-102852] 23 p3378 N90-29083
Multi-user facility for high performance optical recording of brain activity (DURIP)
[AD-A223491] 24 p3498 N90-29768
Telerobotic workstation design aid 24 p3504 N90-29805
The telerobot workstation testbed for the shuttle aft flight deck: A project plan for integrating human factors into system design 24 p3518 N90-29887
Supporting large scale applications on networks of workstations
[NASA-CR-186346] 24 p3532 N90-29975

WORLD

U EARTH (PLANET)

WORLD DATA CENTERS

Oceanographic data exchange, 1988
[PB90-232596] 23 p3353 N90-28952
The worldwide ionospheric data base
[NASA-TM-101823] 24 p3488 N90-29714

WORLD METEOROLOGICAL ORGANIZATION

Activities report of the World Meteorological Organization
[WMO-713] 05 p0671 N90-13912
Guide on the global observing system
[WMO-488-REV] 08 p1103 N90-16385
Activities report in meteorological research and associated fields
[ISSN-0349-0068] 18 p2582 N90-24707

WRAPAROUND CONTACT SOLAR CELLS

U SOLAR CELLS

WRIST

Wrist orientation effect on grip strength and endurance
[PB89-200935] 03 p0383 N90-12179

WROUGHT ALLOYS
MATE (Materials for Advanced Turbine Engines) Program, Project 3. Volume 2: Design, fabrication and evaluation of an oxide dispersion strengthened sheet alloy combustor liner
[NASA-CR-180892] 10 p1357 N90-17868
WU-2 AIRCRAFT
U U-2 AIRCRAFT

X

X BAND
U SUPERHIGH FREQUENCIES
X RAY ABSORPTION
Glancing angle x ray studies of oxide films
[DE89-017828] 06 p0852 N90-14953
X ray absorption studies of YBa2Cu3O(6+x), La(2-x)Sr(x)CuO4, and Nd(2-x)Ce(x)CuO4
[DE90-003640] 07 p1002 N90-15797
Auger and x ray absorption studies of solid molecular oxygen
[DE90-003966] 07 p1006 N90-15825
Study of chemical systems in static and time resolved mode by x ray absorption spectroscopy
[AD-A215383] 09 p1191 N90-16904
Nanolayer reactions in aluminum-metal interfaces
[DE90-004955] 12 p1626 N90-19342
Extended x ray absorption fine structure analysis applied to composite materials
[DE90-008575] 13 p1769 N90-20150
L shell XANES (X ray Absorption Near Edge Structure) for solid metals: Ti, V, Cr, Fe, Ni, Cu
[DE90-008043] 13 p1896 N90-20880
Application of x ray absorption edge spectrometry to the non-destructive determination of element concentrations, coating thickness and areal densities
[AERE-R-13030] 16 p2245 N90-22802
The X ray absorption spectra of massive X ray binaries 19 p2766 N90-25716
The X ray dip source 4U 1624-49 19 p2776 N90-25786
Ginga observations of dipping low mass X ray binaries 19 p2781 N90-25821
Fracture-EXAFS: A new method for the study of interfaces in thin films and polycrystalline materials
[DE90-013736] 21 p3081 N90-27521
X RAY ANALYSIS
NT LAUE METHOD
NT X RAY SPECTROSCOPY
A study of progressive cracking damage to carbon-epoxy composites and methods of crack reduction
[REPT-RE-49-324/F] 04 p0467 N90-12676
Soft x ray microscope using Fourier transform holography
[DE90-002291] 06 p0781 N90-14539
X ray microprobe for the microcharacterization of materials
[DE89-006038] 06 p0836 N90-14863
X ray studies of strain, interface, and impurity in semiconductors
[DE90-001525] 06 p0851 N90-14947
Mass loss during x ray microanalysis
[DE90-003954] 08 p1049 N90-16067
Atomic processes in plasmas under ultra-intense laser irradiation
[DE90-003221] 08 p1126 N90-16521
Study of chemical systems in static and time resolved mode by x ray absorption spectroscopy
[AD-A215383] 09 p1191 N90-16904
Damage in a perforated graphite-epoxy composite plate under monotonic and cyclic biaxial loading
[ESA-TT-1117] 11 p1480 N90-18521
Biomedical applications of synchrotron x ray microscopy
[DE90-004957] 11 p1540 N90-18867
X ray specular reflection studies of silicon coated by organic monolayers (alkylsiloxanes)
[AD-A217418] 13 p1779 N90-20213
Structures and mechanical properties of near-beta titanium alloys TiV10Fe2Al3 and TiV10Cu3Al3
[ONERA-NT-1989-3] 20 p2835 N90-26123
Composite materials with improved properties in compression: Synthesis and dimerization 2,3-dimethyl-5-silaspiro(4.4)nona-2,7-diene
[AD-A222552] 22 p3156 N90-27892
High resolution technique and instrument for measuring lattice parameters in single crystals
[AD-D014549] 22 p3177 N90-28029
Development and application of Computed Tomography (CT) for inspection of aerospace components 22 p3187 N90-28083
The application of infrared thermography to the nondestructive testing of composite materials 22 p3187 N90-28084
X RAY ASTRONOMY
The Spartan 1 mission
[NASA-TM-101887] 01 p0015 N90-10077
Solar X-ray Astronomy Sounding Rocket Program
[NASA-CR-183447] 01 p0138 N90-10796
Soft X-ray astronomy using grazing incidence optics 01 p0138 N90-10797
The detection of soft X-rays with charged coupled detectors 01 p0138 N90-10798
The design and evaluation of grazing incidence relay optics 01 p0138 N90-10799
The observation of possible reconnection events in the boundary changes of solar coronal holes 01 p0138 N90-10801
X-ray bright points and He I lambda 10830 dark points 01 p0139 N90-10802
Advances in photographic X-ray imaging for solar astronomy 01 p0139 N90-10803
Correspondence between solar fine-scale structures in the corona, transition region, and lower atmosphere from collaborative observations 01 p0139 N90-10804
Analysis of nearly simultaneous X-ray and optical observations of active galactic nuclei 01 p0139 N90-10806
Nonequilibrium ionization in supernova remnants: The case of Tycho
[MPE-PREPRINT-153] 04 p0565 N90-13295
Project Supernova 1987 05 p0662 N90-13866
The x ray mirror and the PSPC of the supernova-rocket-project 05 p0662 N90-13867
JPRS Report: Science and technology. USSR: Space. Soviet space program to the year 2000
[JPRS-USP-89-008] 06 p0728 N90-14248
The South African Astronomical Observatory
[NASA-CR-186258] 07 p1011 N90-15856
Galactic x ray astronomy with EXOSAT 08 p1139 N90-16597
A low-threshold EAS (Extensive-Air-Shower) array for gamma-ray astronomy at Los Alamos
[DE89-016780] 08 p1139 N90-16600
On the interaction of a pulsar with the ambient medium utilizing x ray images of the Crab nebula
[MPE-215] 08 p1140 N90-16604
Recent and future x ray observations of classical novae during the outburst stage
[MPE-PREPRINT-159] 08 p1140 N90-16606
State of the art in semiconductor detectors
[DE90-005567] 11 p1512 N90-18706
High energy x ray observations on the Crab nebula and the double star source GX 1+4
[ETN-90-95829] 12 p1729 N90-19937
Astronomy and astrophysics
[REPT-33/89] 12 p1729 N90-19938
X ray timing observations and gravitational physics 12 p1732 N90-19956
Contributions of the X Ray Astronomy Group of the Max-Planck-Institut fuer Extraterrestrische Physik
[MPE-PREPRINT-165] 17 p2462 N90-24196
EXOSAT observations of the pulse profile of Her X-1 during intermediate intensity states in a 35-day-cycle in 1985 17 p2483 N90-24201
EXOSAT deep exposure of the LMC X-4 region 17 p2483 N90-24203
Spectral variability of LMC X-4 17 p2483 N90-24204
The role of comptonisation in energy spectra of standard QPO-sources 17 p2484 N90-24205
The 23rd ESLAB Symposium on Two Topics in X Ray Astronomy. Volume 1: X Ray Binaries
[ESA-SP-296-VOL-1] 19 p2765 N90-25711
X ray observations of GS2023+338 by the Kvant module 19 p2771 N90-25747
EXOSAT observations of Cygnus X-1: Study of the soft X ray excess 19 p2771 N90-25750
The soft X ray spectrum of Cygnus X-1 19 p2771 N90-25751
Hard X ray observations of galactic sources 19 p2771 N90-25752
UBVRI-photopolarimetry and the X ray dips of V471 Tau 19 p2775 N90-25781
Spectral signatures of X ray photoionized nebulae 19 p2778 N90-25800
BBXRT observations of X ray binaries 19 p2778 N90-25802
On the nature of the 1980 outburst of the Be/X ray binary A0535+26=HDE 245770 19 p2778 N90-25803
A shell ejection model for optical light variations in Be stars: Application to Be/X ray binaries 19 p2779 N90-25804
Gamma ray bursts from magnetospheric plasma oscillations 19 p2779 N90-25805
Is the hard tail of X rays from GX339-4 a Compton scattering component 19 p2779 N90-25806
High energy X ray observations of GX 1+4 with HEXE 19 p2779 N90-25808
Relativistic light bending near neutron stars 19 p2779 N90-25810
Methods for probing quasi-periodic oscillations on short time scales 19 p2780 N90-25811
Orbitally modulated VHE gamma rays from Cen X-3 19 p2780 N90-25812
Identification of galactic bulge X ray bursts with persistent X ray counterparts 19 p2780 N90-25813
EXOSAT deep exposure of the LMC X-4 region 19 p2780 N90-25814
The pulsed light curve of Vela X-1 19 p2781 N90-25819
Ionization effects in the radiative driving of stellar winds in massive X ray binary systems 19 p2781 N90-25823
The 3A1954+319: A possible supergiant X ray binary 19 p2782 N90-25830
Optical light curves of HZ Her in the model of freely precessing neutron star 19 p2783 N90-25831
IUE observations of Cyg X-2 and Sco X-1: Accretion disks and the z-shaped curve 19 p2783 N90-25832
The 23rd ESLAB Symposium on Two Topics in X Ray Astronomy. Volume 2: AGN and the X Ray Background
[ESA-SP-296-VOL-2] 19 p2784 N90-25841
Signposts to the future 19 p2788 N90-25867
Hard X ray observations of active galaxies 19 p2789 N90-25874
A hard X ray observation of the Coma Cluster 19 p2789 N90-25875
QSO optical counts and constraints on the X ray background 19 p2789 N90-25877
Effect of X ray spectra of Seyfert galaxies on the cosmic X ray background 19 p2792 N90-25896
X RAY ASTROPHYSICS FACILITY
Project Supernova 1987 05 p0662 N90-13866
Long-lived space observatories for astronomy and astrophysics
[NASA-CR-185373] 06 p0731 N90-14261
The charged particle radiation environment for AXAF
[NASA-TM-100405] 20 p2942 N90-26741
X RAY BINARIES
An atlas of aperiodic variability in HMXB
[MPE-PREPRINT-156] 08 p1140 N90-16605
Detecting gravity waves from binary black holes 12 p1730 N90-19943
General relativistic x ray (UV) polarization rotations as a quantitative test for black holes 12 p1732 N90-19957
Underground muons from the direction of Cygnus X-3
[DE90-005646] 12 p1746 N90-20038
Analysis of an observation of the x ray astronomy satellite EXOSAT at the low mass x ray binary star system GX5-1
[ETN-90-95828] 12 p1747 N90-20042
Radiation-driven evolution of low-mass x ray binaries 18 p2637 N90-25022
The 23rd ESLAB Symposium on Two Topics in X Ray Astronomy. Volume 1: X Ray Binaries
[ESA-SP-296-VOL-1] 19 p2765 N90-25711
Black holes in X ray binaries: X ray properties of the galactic black hole candidates 19 p2765 N90-25712
Be/X ray binaries 19 p2766 N90-25715
The X ray absorption spectra of massive X ray binaries 19 p2766 N90-25716
Spectral variability of LMC X-4 19 p2766 N90-25717
Ginga observations of X ray pulsars 19 p2766 N90-25718
The high-energy properties of X ray pulsars 19 p2767 N90-25719
QPOs and preferred time scales in the variability of X ray pulsars 19 p2767 N90-25721
The bright X ray transient GS2023+338 (=V404 Cyg) in optical outburst and decline 19 p2767 N90-25724
Accretion disks in low-mass X ray binaries 19 p2768 N90-25726
Globular cluster X ray binaries 19 p2768 N90-25729
The low mass X ray binaries in the LMC 19 p2768 N90-25730
Optical observations of LMXB AC211(M15): Solving the puzzle 19 p2768 N90-25731
The possible X ray triple 4U2129+47 (=V1727 Cygni) 19 p2768 N90-25732
Emission lines from X ray binaries 19 p2769 N90-25733
Non-thermal radio emission of X ray binaries 19 p2769 N90-25738
Ginga observations of QPO 19 p2769 N90-25739
The Z/atoll classification 19 p2769 N90-25740
QPO from the rapid burster 19 p2770 N90-25741
A unified model of accretion flows and X ray emission in low mass X ray binary systems 19 p2770 N90-25742
QPOs from black-hole candidates 19 p2770 N90-25743

Radiation-driven evolution and statistics of low-mass X ray binaries 19 p2770 N90-25745
Moving out of the galaxy: Future prospects for X Ray binaries studies 19 p2770 N90-25746
M15:AC211/X2127+119: Optical curve, improved ephemeris, and phasing of EXOSAT X ray data 19 p2771 N90-25749
EXOSAT observations of Cygnus X-1: Study of the soft X ray excess 19 p2771 N90-25750
The soft X ray spectrum of Cygnus X-1 19 p2771 N90-25751
Noise variability in Cyg X-1 and Her X-1 19 p2771 N90-25753
X ray nova GS 2000+25 = Nova Vul 1988: X ray and optical light curves, spectra, and model 19 p2772 N90-25757
VHE gamma ray emission from Southern Hemisphere X ray binaries 19 p2772 N90-25758
VHE gamma ray emission from Northern Hemisphere X ray binaries 19 p2772 N90-25760
Unusual counterparts of the soft X ray transients 4U 1543-47 and 4U 2129+47 in quiescence: Interlopers or third stars 19 p2773 N90-25764
XB 1905+00: A very compact low-mass X ray binary viewed at low inclination 19 p2773 N90-25765
Is KO Vel (E1013-477) an intermediate polar 19 p2773 N90-25766
Correlations between X ray luminosity and pulse shape as well as spectral shape in binary X ray pulsars 19 p2773 N90-25767
Variability of the X ray sources in M31 19 p2773 N90-25768
X ray timing and spectral measurements of the X ray pulsar 4U 1538-52 19 p2774 N90-25770
Detection of 2.93 ms pulsations in Sco X-1 19 p2774 N90-25772
HEAO-1 and IR observations of the X ray pulsar 1E2259+586 19 p2774 N90-25773
X rays from the accretion column of compact objects: A Monte Carlo study 19 p2775 N90-25777
A theory of the rapid burster (MXB1730-335) 19 p2775 N90-25782
Accretion onto neutron stars: Radiative transfer in a strong gravitational field 19 p2776 N90-25784
Be/X ray sources 19 p2776 N90-25785
Ginga observations of SS 433 19 p2776 N90-25789
Hard X ray pulses from Vela X-1 19 p2777 N90-25791
The 3S0114+65 and its peculiar companion 19 p2777 N90-25792
Long period variations in high mass X ray binaries and their possible relationship with SU UMa stars 19 p2777 N90-25796
Neutron star formation in low-mass binary systems 19 p2778 N90-25797
The optical light curve of Cygnus X-1 19 p2778 N90-25801
BBXRT observations of X ray binaries 19 p2778 N90-25802
On the nature of the 1980 outburst of the Be/X ray binary A0535+26=HDE 245770 19 p2778 N90-25803
A shell ejection model for optical light variations in Be stars: Application to Be/X ray binaries 19 p2779 N90-25804
High energy X ray observations of GX 1+4 with HEXE 19 p2779 N90-25808
Methods for probing quasi-periodic oscillations on short time scales 19 p2780 N90-25811
On the nature of low-luminosity Be/X ray binaries 19 p2780 N90-25816
Self-consistent Comptonised models for the spectra of low mass X ray binaries 19 p2780 N90-25817
The pulsed light curve of Vela X-1 19 p2781 N90-25819
The role of comptonisation in energy spectra of standard QPO-sources 19 p2781 N90-25820
Ginga observations of dipping low mass X ray binaries 19 p2781 N90-25821
Timing analysis of binary X ray pulsars observed by HEAO 1 19 p2781 N90-25822
Ionization effects in the radiative driving of stellar winds in massive X ray binary systems 19 p2781 N90-25823
New results of numerical simulations of X ray binaries evolution 19 p2782 N90-25828
The 3A1954+319: A possible supergiant X ray binary 19 p2782 N90-25830
Optical light curves of HZ Her in the model of freely precessing neutron star 19 p2783 N90-25831
A multi-wavelength campaign to observe Scorpius X-1: Preliminary results from the X ray data 19 p2783 N90-25835
EXOSAT medium energy observations of binary X ray pulsar 4U1538-52 19 p2783 N90-25837
Constraints on the SS433 system from the Ginga observations 19 p2784 N90-25838

X RAY DENSITY MEASUREMENT

Exploring asymmetric heavy-ion reactions at the KX-ray method: The Ne20 + Tb159 reaction at 15 MeV/unit [KVI-777] 04 p0552 N90-13216
Bone mineral measurement using dual energy x ray densitometry 05 p0680 N90-13958

X RAY DIFFRACTION

Bragg crystal polarimeters [NASA-CR-181331] 01 p0073 N90-10423
Progress report on grain boundaries [DE89-015541] 01 p0130 N90-10749
Use of overlapped reflection for determining the retained austenite by X-ray diffraction [DE89-615450] 02 p0198 N90-11128
Thermal expansion and phase transformation studies on some materials by high temperature X-ray powder diffractometry [DE89-631032] 02 p0198 N90-11130
Report of the Specialists' Workshop on Phase Transition Studies on Hydrogen-Bonded Crystals by Neutron and X-ray Diffractometries [DE89-906638] 02 p0285 N90-11631
Short period multilayers: Interface dominated structures [DE89-017536] 03 p0319 N90-11812
Analysis of carbon fiber's x ray microscopic structure [AD-A212215] 04 p0480 N90-12752
Shock-induced solid state reactions and phase transitions: X ray profile studies on shock-modified Fe3O4 and ZrO2 powders [DE90-000669] 06 p0741 N90-14315
Characterization of nanophase materials by x ray diffraction and computer simulation [DE90-002270] 06 p0752 N90-14378
X ray reflectivity study of SiO2 on Si [DE90-001326] 06 p0851 N90-14943
High-temperature/high-pressure x ray diffraction: Recent developments [DE89-015255] 06 p0851 N90-14949
Synthesis conductivity, and x ray photoelectron spectrum of Bi2Sr2Cu(sub 7+x). A new ternary bismuth-oxide system exhibiting metallic conductivity [DE90-003010] 07 p0999 N90-15778
Flexibility of the zeolite RHO framework: In situ x ray and neutron powder structural characterization of divalent cation-exchanged zeolite RHO [AD-A214573] 09 p1288 N90-17467
Diffraction studies of the structure of glasses and liquids [DE90-007662] 12 p1632 N90-19381
X ray microimaging by diffractive techniques [DE90-008444] 13 p1804 N90-20356
Residual stresses: A review of their measurement and interpretation using x ray diffraction [AERE-R-13005] 13 p1815 N90-20423
Retabulation of space group extinctions for electron diffraction [DE90-612933] 14 p2031 N90-21648
Thermogravimetric analysis of Nd(2-x)Ce(x)CuO(4-delta) [DE90-009184] 14 p2032 N90-21658
Single-crystal diffraction analysis of 2-(trimethylsilylethynyl) 4-nitro-N,N-dimethylaniline [AD-A218955] 16 p2216 N90-22642
Fracture behavior of surface modified ceramics [DE90-011552] 18 p2532 N90-24449
The use of curium as a rare Earth substitute in high T(sub c)-related compounds [DE90-009724] 18 p2620 N90-24928
X ray diffraction analysis of control and test fibers [MTL-TR-89-58] 19 p2678 N90-25233
Analysis of strain relaxation in Au/Ni multilayers by x ray diffraction [IAR-89-25] 20 p2875 N90-26357
Residual stresses measurements by means of x ray diffraction on electron beam welded joints and laser hardened surfaces [ETN-90-97269] 20 p2877 N90-26371
High temperature x ray diffraction and Landau theory investigations of order-disorder transition in defect NaCl-type solids [DE90-011807] 20 p2930 N90-26673
Probing interfacial structure and composition with x ray standing waves [AD-A223071] 21 p2977 N90-28916
Identification of tetragonal and cubic structures of zirconia [AD-A222373] 21 p3083 N90-27535
Characteristics required for thermal barriers of zirconium oxide-yttrium compounds obtained by plasma spraying. Morphological analysis by x ray diffraction [ETCA-89-R-113] 22 p3161 N90-27925
Mechanical property measurement of polycrystalline diamond films [AD-A224037] 23 p3402 N90-28222

X RAY FLUORESCENCE

Compositional analysis of steels by X-ray fluorescence spectrometry [DE89-630803] 02 p0198 N90-11129
Trace element abundance determinations by Synchrotron X Ray Fluorescence (SXRF) on returned comet nucleus mineral grains 08 p1142 N90-16619
Non-destructive trace element microanalysis of as-received cometary nucleus samples using synchrotron x ray fluorescence 08 p1147 N90-16649
Application of x ray fluorescence method to measuring thickness of galvanic coatings and measures of improving sensitivity of such measurings [DE89-633351] 09 p1233 N90-17156
In-line wear monitor [AD-A217799] 13 p1757 N90-20091
Characterization of Monel alloys by x ray fluorescence technique [DE90-617175] 16 p2221 N90-22665
Conference on Instrumental Activation Analysis: IAA 89 [DE90-615661] 19 p2694 N90-25327

X RAY IMAGERY

Advances in photographic X-ray imaging for solar astronomy 01 p0139 N90-10803
Correspondence between solar fine-scale structures in the corona, transition region, and lower atmosphere from collaborative observations 01 p0139 N90-10804
A microchannel plate intensified, subnanosecond, X-ray imaging camera [DE89-017781] 03 p0350 N90-12003
Pre-pulses: Signature of a trigger process in short (less than 60 secs) solar hard x ray flares 03 p0432 N90-12476
Measurement of the X-UV emission from the back face of thin foils illuminated by an A4 omega laser 06 p0784 N90-14562
Tomographic imagery by multislot coding applied to x ray diagnostics of laser plasmas: Implementation of a direct electronic detection camera 06 p0787 N90-14579
X ray microimaging for the life sciences [DE90-002613] 06 p0819 N90-14766
Versatility of the CFR algorithm for limited angle reconstruction [DE90-001421] 06 p0829 N90-14817
Integration of a gated microchannel plate detector into the Nova laser system [DE90-002981] 07 p0935 N90-15413
Necessity and benefit of the X-SAR Space Shuttle experiment [ESA-TT-1164] 08 p1057 N90-16112
End-on soft x ray imaging of Field-Reversed Configurations (FRCs) on the Field-Reversal-C (FRX-C)/Large Scale Modification (LSM) experiment [DE90-004863] 08 p1082 N90-16260
Absolute multilayer characterization at high spatial resolution via real-time soft x ray imaging [DE90-009181] 14 p1984 N90-21371
A study of creep damage using microradiography and continuum damage mechanics 15 p2117 N90-22109
Real-time stereo-microradiography [AD-A218433] 16 p2245 N90-22805
Sea bottom topography with X-band SLAR [BCRS-89-25] 17 p2431 N90-23854
Moving out of the galaxy: Future prospects for X Ray binaries studies 19 p2770 N90-25746
Improvement of the detail reconnaissance in radiographic irradiation images by digital image restoration [ETN-90-97311] 22 p3189 N90-28096
Soft x ray contact imaging of biological specimens using a laser-produced plasma as an x ray source [DE90-016098] 24 p3549 N90-30082

X RAY INSPECTION

Stick propellant x ray inspection [AD-A212601] 06 p0753 N90-14380
Structural characterization of Spacelab [ETN-90-95214] 08 p1087 N90-16289
Inspection of carbon/epoxy and aluminum honeycomb paraboloidal components by HNDT [AD-A216796] 11 p1479 N90-18514
Application of x ray absorption edge spectrometry to the non-destructive determination of element concentrations, coating thickness and areal densities [AERE-R-13030] 16 p2245 N90-22802
Real-time stereo-microradiography [AD-A218433] 16 p2245 N90-22805
On-line x ray inspection of materials and structural components using discrete element x ray detectors for digital radiographic and computed tomographic evaluation [AD-A218911] 16 p2245 N90-22806

Nondestructive x ray methods for characterization of advanced aerospace materials
[DE90-011751] 19 p2999 N90-25356

X RAY IRRADIATION
Use of the NPL linac for x ray dosimetry --- linear accelerator (linac)
[NPL-RSA(EXT)-6] 03 p0404 N90-12314
As observational and theoretical investigation of stellar flares 06 p0862 N90-15012
Polymerization of composites
[REPT-892-430-102] 16 p2213 N90-22621
Polymerization of composite materials: A technique developed by Aerospatiale
[REPT-892-430-107] 16 p2213 N90-22623
A new technique for hardening optically-triggered thyristors
[DE90-006769] 18 p2549 N90-24550
Improvement of the detail reconnaissance in radiographic irradiation images by digital image restoration
[ETN-90-97311] 22 p3189 N90-28096

X RAY LASERS
X-ray lithography studies of polysilane using a laser plasma X-ray source
[DE89-015390] 01 p0047 N90-10266
A compact X-ray free electron laser
[DE89-017236] 02 p0226 N90-11297
Research in X-ray optics with the ultimate aim of constructing a synchrotron radiation pumped soft X-ray lithium laser
[DE89-016788] 02 p0227 N90-11304
Lectures on x ray lasers
[ETN-89-95516] 04 p0506 N90-12917
Activities report in laser matter interactions
[ETN-90-95515] 06 p0782 N90-14544
Study of lithium-like ions for amplifying radiation below 100 angstroms. Experiment at the Rutherford Appleton Laboratory 06 p0786 N90-14572
Single beam interactions for the study of x ray lasers 06 p0786 N90-14573
X-UV amplification in a plasma column of five centimeters. Five beams experiment 06 p0786 N90-14574
Proof-of-principle experiment for a hot electron pumped XUV amplifier
[DE90-000820] 06 p0787 N90-14586
Laboratory x ray lasers
[DE90-000879] 06 p0788 N90-14590
The development of coherent x ray lasers for x ray holography
[DE90-000784] 06 p0789 N90-14595
Ultrahigh-brightness lasers and their applications
[DE90-000877] 06 p0789 N90-14596
Inspection of carbon/epoxy and aluminum honeycomb paraboloidal components by HNDT
[AD-A216796] 11 p1479 N90-18514
Computational and visible light experiments for x ray laser holography
[DE90-006774] 11 p1512 N90-18707
X ray laser with enhanced x ray gain through photodepopulation
[AD-D014448] 14 p1985 N90-21375
Research studies on extreme ultraviolet and soft x ray lasers
[AD-A220271] 18 p2562 N90-24621
X ray laser program report for FY 1989
[AD-A221818] 21 p3009 N90-27107
New resonantly photo-pumped x ray laser scheme
[DE90-015044] 23 p3331 N90-28831

X RAY SCATTERING
Design and optimisation of thin foil x ray telescopes 14 p2038 N90-21690
Gamma ray pulsars: Models and observations 16 p2335 N90-23304
Compression molded polyurethane block copolymers. 3: Evaluation of microphase compositions
[AD-A220160] 17 p2382 N90-23564
X ray scattering studies of non-equilibrium ordering processes
[DE90-015066] 23 p3400 N90-29209

X RAY SOURCES
NT X RAY BINARIES
NT X RAY STARS
X-ray lithography studies of polysilane using a laser plasma X-ray source
[DE89-015390] 01 p0047 N90-10266
X-ray bright points and He I lambda 10830 dark points 01 p0139 N90-10802
X-ray lithography sources: A review
[DE89-017610] 02 p0271 N90-11547
Advanced source development and applications. Laser-produced plasmas: A compact soft x ray source with high peak brightness
[AD-A212677] 04 p0557 N90-13245
The current status of x ray conversion efficiency modeling
[DE90-000931] 06 p0789 N90-14591
Galactic x ray astronomy with EXOSAT 08 p1139 N90-16597
Status of the expansion of the CYGNUS array at Los Alamos
[DE89-016781] 08 p1139 N90-16601
Scaling Z-pinch plasmas with atomic number for a given K-shell emission
[AD-A215703] 09 p1285 N90-17450
Conception of an automatic measurement installation for spatial resolution detectors
[ETN-90-95732] 12 p1729 N90-19935
Examination of the background by High Energy X ray Experiment (HEXE) on the space station MIR
[ETN-90-95735] 12 p1746 N90-20041
The inverse triax x ray diode: An alternate reduced-endpoint-energy bremsstrahlung source
[DE90-006366] 13 p1792 N90-20285
EXOSAT observations of Seyfert type galaxies 13 p1901 N90-20910
Report on the fifth workshop on synchrotron x ray lithography
[DE90-007903] 15 p2172 N90-22411
More data on (possible) gamma ray (point) sources 16 p2335 N90-23309
What can gamma rays tell us about binary x ray sources and SNR's 16 p2336 N90-23310
EXOSAT deep exposure of the LMC X-4 region 17 p2483 N90-24203
Spectral variability of LMC X-4 17 p2483 N90-24204
Activities report of the Institute for Astronomy and Astrophysics
[MITT-10] 18 p2636 N90-25020
X ray observations of GS2023+338 by the Kvant module 19 p2771 N90-25747
Hard X ray observations of galactic sources 19 p2771 N90-25752
A search for radio pulsars in globular clusters and transient X ray sources 19 p2772 N90-25755
Optical observations of GS2000+25 19 p2773 N90-25762
Observations of black hole candidates with the Mir-Kvant HEXE 19 p2774 N90-25774
A theory of the rapid burster (MXB1730-335) 19 p2775 N90-25782
The X ray dip source 4U 1624-49 19 p2776 N90-25786
Einstein SSS and MPC observations of Aql X-1 and 4U1820-30 19 p2777 N90-25790
Is the hard tail of X rays from GX339-4 a Compton scattering component 19 p2779 N90-25806
Identification of galactic bulge X ray bursts with persistent X ray counterparts 19 p2780 N90-25813
EXOSAT deep exposure of the LMC X-4 region 19 p2780 N90-25814
Search of the optical counterpart of the X rays source 1H 0521+373 19 p2780 N90-25815
A new transient X ray burst source near GX 1+4 19 p2782 N90-25826
TTM-Kvant observations of the galactic plane 19 p2783 N90-25836
Theories of the X ray background 19 p2784 N90-25842
Population properties of AGN in the soft X-ray band 19 p2784 N90-25844
Spatial fluctuations in the diffuse X ray background 19 p2785 N90-25845
Contributions of discrete sources to the X ray background 19 p2785 N90-25847
Properties of sources that may contribute the other half of the cosmic X ray background 19 p2788 N90-25866
Fast classification of ROSAT sources on objective prism plates 19 p2788 N90-25871
Hard X ray observations of active galaxies 19 p2789 N90-25874
X ray spectral index variability in NGC 4151 19 p2795 N90-25911
Using the x ray region of the electromagnetic spectrum for alignment: Overview, geometric optics, and design considerations
[DE90-014798] 23 p3317 N90-28752
Some novel sources of x ray beams: Channeling, transition and Cherenkov radiation
[DE90-014442] 23 p3395 N90-29181
An x ray source for lithography
[AD-D014596] 24 p3473 N90-29630
Soft x ray contact imaging of biological specimens using a laser-produced plasma as an x ray source
[DE90-016098] 24 p3549 N90-30082
Detector to study low-flex hard x ray/gamma ray sources
[UT-HE-90/08] 24 p3564 N90-30164

X RAY SPECTRA
The ratio to X-ray spectral shape and variability of blazars 02 p0297 N90-11688
Activities report in laser matter interactions
[ETN-90-95515] 06 p0782 N90-14544
Anisotropy of electron distributions related to the anisotropy and polarization of the continuous emitted x rays 06 p0785 N90-14566
Study of lithium-like ions for amplifying radiation below 100 angstroms. Experiment at the Rutherford Appleton Laboratory 06 p0786 N90-14572
Single beam interactions for the study of x ray lasers 06 p0786 N90-14573
Characteristics of an x ray source created by a laser plasma 06 p0786 N90-14575
Mass loss during x ray microanalysis
[DE90-003954] 08 p1049 N90-16067
X ray spectrophotometric remote sensing of diffuse auroral ionization
[SD-TR-89-09] 08 p1139 N90-16599
Ion-heated thermal Comptonization models and x ray spectral correlations in active galactic nuclei
[DE90-003597] 08 p1151 N90-16667
X ray spectra produced by NaF implosions
[AD-A215803] 10 p1429 N90-18243
Investigations of x ray sensitive PN-CCD's
[MPE-213] 12 p1653 N90-19495
Multifrequency observations of Cyg X-2: X ray observations with Ginga 17 p2482 N90-24192
Mir-Kvant-Hexe hard x ray light curve of SN 1987A 17 p2482 N90-24197
Proof of principle study of thickness measurements using characteristic x ray line ratio techniques
[AD-A221113] 18 p2535 N90-24461
Black holes in X ray binaries: X ray properties of the galactic black hole candidates 19 p2765 N90-25712
The X ray spectrum of Nova Vul 1988. Mir-Kvant data 19 p2766 N90-25713
The X ray absorption spectra of massive X ray binaries 19 p2766 N90-25716
Spectral variability of LMC X-4 19 p2766 N90-25717
Observations of the X ray pulsars from the Kvant module 19 p2767 N90-25720
An X ray pulsar in the dark cloud Lynds 1457 19 p2767 N90-25723
Emission lines from X ray binaries 19 p2769 N90-25733
X ray observations of SS433 and its jets 19 p2769 N90-25734
X ray observations of GS2023+338 by the Kvant module 19 p2771 N90-25747
X ray nova GS 2000+25 = Nova Vul 1988: X ray and optical light curves, spectra, and model 19 p2772 N90-25757
X ray timing and spectral measurements of the X ray pulsar 4U 1538-52 19 p2774 N90-25770
Mir-Kvant-HEXE hard X ray light curve of SN 1987A 19 p2775 N90-25776
X rays from the accretion column of compact objects: A Monte Carlo study 19 p2775 N90-25777
Ginga observations of SS 433 19 p2776 N90-25789
Hard X ray pulses from Vela X-1 19 p2777 N90-25791
Exploration of jet physics with some applications to SS 433 19 p2777 N90-25794
New X ray pulsars discovered with the Ginga satellite 19 p2777 N90-25795
Spectral signatures of X ray photoionized nebulae 19 p2778 N90-25800
On the nature of the 1980 outburst of the Be/X ray binary A0535+26=HDE 245770 19 p2778 N90-25803
Identification of galactic bulge X ray bursts with persistent X ray counterparts 19 p2780 N90-25813
X ray observations of the LMC field by the TTM instrument onboard the Kvant module: November 1988 to June 1989 19 p2782 N90-25825
A new transient X ray burst source near GX 1+4 19 p2782 N90-25826
The 3A1954+319: A possible supergiant X ray binary 19 p2782 N90-25830
A multi-wavelength campaign to observe Scorpius X-1: Preliminary results from the X ray data 19 p2783 N90-25835
The 23rd ESLAB Symposium on Two Topics in X Ray Astronomy. Volume 2: AGN and the X Ray Background
[ESA-SP-296-VOL-2] 19 p2784 N90-25841
The optical characteristics of a sample of soft X ray selected active galactic nuclei 19 p2784 N90-25843
Population properties of AGN in the soft X-ray band 19 p2784 N90-25844
Einstein IPC observations of the 1 to 3 keV X ray background 19 p2785 N90-25846

Contributions of discrete sources to the X ray background 19 p2785 N90-25847
The X ray spectra of emission line AGN 19 p2785 N90-25850
The environmental impact of the X ray flux from active galactic nuclei 19 p2786 N90-25853
Ginga observations of the X ray spectra of AGN 19 p2786 N90-25854
The complex X ray spectra of AGN 19 p2786 N90-25855
AGNs and the spectrum of the X ray background 19 p2787 N90-25858
Complex X ray spectra and thick matter in Seyfert 1 galaxies 19 p2787 N90-25860
Rapid X ray variability in BL Lacertae objects 19 p2787 N90-25862
X ray spectra of OVV QSOs 19 p2787 N90-25863
Ultrasoft components in X ray-selected AGN 19 p2787 N90-25864
Properties of sources that may contribute the other half of the cosmic X ray background 19 p2788 N90-25866
Long timescale X ray variability in AGN 19 p2788 N90-25868
Detailed non-LTE calculations of the iron emission from NGC 1068 19 p2788 N90-25872
Hard X ray observations of active galaxies 19 p2789 N90-25874
A hard X ray observation of the Coma Cluster 19 p2789 N90-25875
The dependence of the soft X ray spectral slope with radio property, luminosity, and redshift, for a large sample of AGN from the Einstein IPC data base 19 p2789 N90-25876
Long term multi-frequency study of 3C 273 19 p2790 N90-25879
Ion-heated thermal comptonization models and X ray spectral correlations in active galactic nuclei 19 p2790 N90-25880
The X ray time variability of NGC 6814 revisited 19 p2790 N90-25882
Pure luminosity evolution and the AGN contribution to the X ray background 19 p2790 N90-25883
Simulations of high-resolution X ray spectra of AGNs 19 p2791 N90-25885
Multiwavelength observations of BL Lacertae 19 p2791 N90-25886
Hard X ray observations of AGN 19 p2791 N90-25889
X ray spectral variability in Seyfert 1 galaxies 19 p2792 N90-25891
X ray polarization of the reprocessed emission from accretion disk in Seyfert galaxies 19 p2792 N90-25892
X ray emission from relativistic jets in AGNs and statistical implications 19 p2792 N90-25893
Effect of X ray spectra of Seyfert galaxies on the cosmic X ray background 19 p2792 N90-25896
The X ray spectrum of MCG-6-30-15 19 p2793 N90-25898
X ray constraints on the beaming hypothesis for BL Lacertae objects 19 p2793 N90-25900
Comparing measurements of AGN X ray spectra with the shape of the diffuse X ray background spectrum 19 p2793 N90-25902
X ray spectrum and variability of MRK 509 as observed with EXOSAT and Ginga 19 p2794 N90-25904
Detection of hard X ray emission from a type 2 Seyfert galaxy 19 p2794 N90-25905
Search for large scale extended diffuse X ray emission from the Coma-A1367 supercluster 19 p2794 N90-25906
Neutral column density and soft excesses in active galactic nuclei 19 p2794 N90-25908
The soft X ray excess in Einstein quasar spectra 19 p2794 N90-25910
The origin of the continuum of AGN and the X ray background 19 p2795 N90-25912
Einstein SSS+MPC observations of Seyfert type galaxies 19 p2795 N90-25913
X ray variability of active galactic nuclei 19 p2795 N90-25914
X ray spectra of cataclysmic variables [NASA-CR-187002] 23 p3412 N90-29280

X RAY SPECTROGRAPHY
U X RAY SPECTROSCOPY

X RAY SPECTROMETRY
U X RAY SPECTROSCOPY

X RAY SPECTROSCOPY
X-ray spectroscopy of the SSME plume [NASA-CR-185308] 01 p0031 N90-10168
Shortwavelength coherent radiation: Generation and applications [AD-A209847] 01 p0074 N90-10427
Dynamics of nucleation at electrochemical interfaces via surface EXAFS and standing wave measurements [AD-A210733] 02 p0195 N90-11109
X-ray and gamma-ray spectroscopy of solids under pressure [DE89-017271] 02 p0196 N90-11118
Compositional analysis of steels by X-ray fluorescence spectrometry [DE89-630803] 02 p0198 N90-11129
A microchannel plate intensified, subnanosecond, X-ray imaging camera [DE89-017781] 03 p0350 N90-12003
High resolution X-ray spectroscopy using germanium microcalorimeters [DE89-017784] 03 p0351 N90-12004
FORTRAN program for x ray photoelectron spectroscopy data reformatting [NASA-TP-2957] 03 p0409 N90-12348
Quantitative AES and XPS: Determination of the electron spectrometer transmission function and the detector sensitivity energy dependencies for the production of true electron emission spectra in AES and XPS [NPL-DMA(A)-194] 05 p0623 N90-13634
Time integrated study of spectral emission in the X-UV domain at the outlet of a laser shock, at the back of single or double foil targets 06 p0784 N90-14561
Measurement of the X-UV emission from the back face of thin foils illuminated by an A4 omega laser 06 p0784 N90-14562
Development of X diagnostics with 1 Gw laser pulses 06 p0786 N90-14578
Development of X diagnostics around the pulse 1 laser 06 p0787 N90-14580
Center for X Ray Optics, 1988 [DE90-003300] 07 p0992 N90-15732
Study of chemical systems in static and time resolved mode by x ray absorption spectroscopy [AD-A215383] 09 p1191 N90-16904
L x ray spectrometry in vivo with a Si(Li)-NaI(Tl) [DE90-005649] 10 p1387 N90-18028
Understanding electronegative effects in core-level electron spectroscopies; application to the high temperature superconductors [AD-A216726] 11 p1570 N90-19037
Infrared and X ray photoelectron spectroscopy studies of the polyimide/metal interface [AD-A218249] 13 p1773 N90-20179
Improved crystal bending techniques applied to the LLNL dual-arm Johann mounting x ray spectrometer [DE90-009528] 15 p2173 N90-22415
Characterization of Monel alloys by x ray fluorescence technique [DE90-617175] 16 p2221 N90-22665
Application of x ray absorption edge spectrometry to the non-destructive determination of element concentrations, coating thickness and areal densities [AERE-R-13030] 16 p2245 N90-22802
XPS studies of doped polypyrrole films [AD-A219424] 17 p2379 N90-23550
Acquisition of an analytical x ray and image analysis system [AD-A221376] 18 p2593 N90-24756
The 3S0114+65 and its peculiar companion 19 p2777 N90-25792
Spectroscopy of AGNs with Xspect/Sodart in 1993 19 p2794 N90-25909
Short-range structure of fluorine-modified phosphate glass [DE90-013494] 20 p2839 N90-26145
XES studies of density of states of high temperature superconductors 22 p3150 N90-27859
Preliminary exposure study to determine the effects of acid deposition on coated steel substrates [PB90-201799] 23 p3309 N90-28715
Relationship between microstructure, spinodal-like decomposition and selective electropolishing of irradiated invar-type alloys [DE90-015293] 24 p3450 N90-29484
Soft x ray emission spectra from laser-irradiated high-Z targets [AD-A223552] 24 p3552 N90-30099

X RAY STARS
NT X RAY BINARIES
An atlas of aperiodic variability in HMXB [MPE-PREPRINT-158] 08 p1140 N90-16605
Observations of Cygnus X-2 at x ray, UV, optical and radio frequencies [MPE-PREPRINT-163] 17 p2481 N90-24191
Multifrequency observations of Cyg X-2: X ray observations with Ginga 17 p2482 N90-24192
Observations of Cygnus X-2 with IUE: Ultraviolet results from a multiwavelength campaign 17 p2482 N90-24193
Optical spectroscopy of V1341 Cyg, the optical counterpart of Cyg X-2 17 p2482 N90-24194
Radio observations of the x ray binary Cygnus X-2 17 p2482 N90-24195
Observations of black hole candidates with the Mir-Kvant HEXE 17 p2483 N90-24198
EXOSAT observations of Cygnus X-1: Study of the soft x ray excess 17 p2483 N90-24199
Noise variability in Cyg X-1 and Her X-1 17 p2483 N90-24200
The pulsed light curve of Vela X-1 17 p2483 N90-24202
Activities report of the Institute for Astronomy and Astrophysics [MITT-10] 18 p2636 N90-25020
Super-critical accretion in Cir X-1 19 p2767 N90-25725
Studies of the possible X ray triple 4U1915-05 19 p2768 N90-25727
The long-term optical behaviour of X Per = 3U 0352+30 19 p2776 N90-25783

X RAY STRESS MEASUREMENT
Residual stresses measurements by means of x ray diffraction on electron beam welded joints and laser hardened surfaces [ETN-90-97269] 20 p2877 N90-26371

X RAY TELESCOPES
NT X RAY ASTROPHYSICS FACILITY
Solar flare gamma-ray and hard x ray imaging with the GRID-on-a-balloon 03 p0432 N90-12474
The soft x ray telescope for Solar-A 03 p0432 N90-12475
The MPI/AIT X ray Imager (MAXI): High speed PN-CCD's for x ray detection [MPE-PREPRINT-154] 08 p1077 N90-16234
Recent and future x ray observations of classical novae during the outburst stage [MPE-PREPRINT-159] 08 p1140 N90-16606
X ray timing observations and gravitational physics 12 p1732 N90-19956
Design and optimisation of thin foil x ray telescopes 14 p2038 N90-21690
Moving out of the galaxy: Future prospects for X Ray binaries studies 19 p2770 N90-25746
Hard X ray observations of galactic sources 19 p2771 N90-25752
Optical observations of GS2000+25 19 p2773 N90-25762
BBXRT observations of X ray binaries 19 p2778 N90-25802
Spectroscopy of AGNs with Xspect/Sodart in 1993 19 p2794 N90-25909
Variable magnification variable dispersion glancing incidence imaging x ray spectroscopic telescope [NASA-CASE-MFS-28013-3] 21 p3096 N90-27594
Multispectral variable magnification glancing incidence x ray telescope [NASA-CASE-MFS-28013-4] 21 p3096 N90-27595
XMM space telescope: Development plan for the lightweight replicated x ray gratings [DE90-015620] 24 p3546 N90-30055

X RAYS
NT COSMIC X RAYS
NT SOLAR X-RAYS
A compact X-ray lithography lattice using superferric magnets [DE89-013947] 01 p0127 N90-10728
The detection of soft X-rays with charged coupled detectors 01 p0138 N90-10798
MOXE: An X-ray all-sky monitor for Soviet Spectrum-X-Gamma Mission [NASA-TM-101266] 02 p0223 N90-11280
Laser production of soft x rays by multiquantum processes and the excitation of atomic inner-shell states [AD-A211372] 03 p0353 N90-12021
Calculations of soft x ray emission of REB-heated plasma [IPPCZ-287] 03 p0407 N90-12329
Heating and acceleration of coronal and chromospheric ions during solar flares 03 p0433 N90-12479
Some of the terrestrial effects of AR 5395 03 p0433 N90-12482
Analysis of high temperature superconductors by means of PIXE and RBS methods [DE89-630241] 04 p0558 N90-13252
Radiation damage and its influence on source requirements for high resolution x ray holography [DE90-002508] 06 p0781 N90-14540
The current status of x ray conversion efficiency modeling [DE90-000931] 06 p0789 N90-14591
X ray microprobe for the microcharacterization of materials [DE89-006038] 06 p0836 N90-14863
Glancing angle x ray studies of oxide films [DE89-017828] 06 p0852 N90-14953

Evaluation of potential cold x ray shield materials tested on Proto II
[DE90-004348] 08 p1039 N90-16003
Material responses to incident x rays
[DE89-015366] 08 p1089 N90-16305
Transmission micro-grids for shift analysis of x ray frequencies
[MPE-216] 09 p1283 N90-17439
Multilayer optical elements for generation and analysis of circularly polarized x rays
[DE90-006103] 10 p1430 N90-18250
Soft x ray emission from classical novae in outburst
[DE90-006480] 11 p1595 N90-19187
Background studies in gas ionizing x ray detectors
12 p1636 N90-19399
Effect of barrier layers in burn-through experiments with 351-nm laser illumination
[DE90-006806] 12 p1667 N90-19577
Nearly simultaneous optical, ultraviolet, and x ray observations of three PG quasars
[NASA-CR-186355] 12 p1728 N90-19932
Studies of the evolution of the x ray emission of clusters of galaxies
[NASA-CR-186471] 13 p1903 N90-20918
The investigation of multilayer x ray reflectors as x ray optical elements
[DE90-009044] 14 p2026 N90-21621
Design and optimisation of thin foil x ray telescopes
14 p2038 N90-21690
Relativistic processes in active galactic nuclei
14 p2040 N90-21698
High energy phenomena during solar flares
[INPE-4961-TDL/390] 14 p2043 N90-21713
Non-random uncertainties in the calibration of protection-level secondary standards
[NPL-RS(EXT)-110] 15 p2166 N90-22378
Derivation of radiation beam non-uniformity corrections for the calibration of large volume ionisation chambers
[NPL-RSA(EXT)-11] 15 p2167 N90-22382
Producing dense plasmas with x rays
[DE90-009539] 15 p2169 N90-22393
An astrophysics data program investigation of cluster evolution
[NASA-CR-181296] 15 p2191 N90-22510
Research and applications of metallic superlattices, high T(sub c) superconductors, x ray optics, and compact synchrotrons 16 p2311 N90-23170
Gamma radiation from the Crab and Vela pulsars
16 p2334 N90-23303
The high energy source 3C 273
16 p2337 N90-23318
COMPTEL observations of active galactic nuclei
16 p2337 N90-23319
OSSE observations of active galactic nuclei
16 p2337 N90-23320
Dose analysis of the model 112A Pulserad pulsed x ray generator by its CYLTRAN
[AD-A220372] 17 p2471 N90-24125
Proof of principle study of thickness measurements using characteristic x ray line ratio techniques
[AD-A221113] 18 p2535 N90-24461
Proof of the feasibility of coherent and incoherent schemes for pumping a gamma-ray laser
[AD-A219972] 18 p2562 N90-24620
X ray optics
[AD-A221218] 18 p2616 N90-24898
Optical emission from the high inclination X ray transient EXO 0748-676 19 p2779 N90-25809
Soft x ray resist characterization: Studies with a laser plasma x ray source
[DE90-013493] 20 p2928 N90-26661
Probing interfacial structure and composition with x ray standing waves
[AD-A223071] 21 p2977 N90-26916
An initial comparison between two 3-D x ray CT algorithms for characterizing
[DE90-013656] 21 p2984 N90-26957
Specification for HF Lowest Usable Frequency (LUF) model
[AD-A222114] 21 p2996 N90-27031
Variable length-scale studies at interfaces with X ray standing waves
[AD-A223043] 21 p3004 N90-27075
Using the x ray region of the electromagnetic spectrum for alignment: Overview, geometric optics, and design considerations
[DE90-014798] 23 p3317 N90-28752
Fifteenth International Conference on X Ray and Inner-Shell Processes
[DE90-013024] 23 p3393 N90-29170
Technical activities 1989, Electron and Optical Physics Division
[PB90-207267] 23 p3415 N90-29296
A tandem system of ionization chambers for effective energy determination of unknown X-radiation fields
[DE90-630463] 24 p3436 N90-29405
Effect of retardation on the reflectance properties of the metallic Fibonacci quasi-superlattice
[DE90-627316] 24 p3551 N90-30091
Soft x ray emission spectra from laser-irradiated high-Z targets
[AD-A223552] 24 p3552 N90-30099
Investigation of x ray variability in highly active cool stars
[NASA-CR-183853] 24 p3560 N90-30143

X-Y PLOTTERS
Rubberlike elasticity experiment
18 p2515 N90-24362
Optical emission from the high inclination X ray transient EXO 0748-676 19 p2779 N90-25809

X-15 AIRCRAFT
Prediction of forces and moments for flight vehicle control effectors. Part 1: Validation of methods for predicting hypersonic vehicle controls forces and moments
[NASA-CR-186571] 15 p2047 N90-21734

X-29 AIRCRAFT
Initial flight qualification and operational maintenance of X-29A flight software
[NASA-TM-101703] 01 p0005 N90-10023
Real-time flight test analysis and display techniques for the X-29A aircraft 02 p0152 N90-10866
A design procedure for the handling qualities optimization of the X-29A aircraft
[NASA-TM-4142] 03 p0308 N90-11753
X-29A aircraft structural loads flight testing
[NASA-TM-101715] 12 p1603 N90-19225
An in-flight interaction of the X-29A canard and flight control system
[NASA-TM-101718] 20 p2807 N90-25973
A look at tomorrow today 23 p3273 N90-28524
An in-flight investigation of ground effect on a forward-swept wing airplane 23 p3275 N90-28533

XANTHINES
NT CAFFEINE

XB-70 AIRCRAFT
U B-70 AIRCRAFT

XENON
A liquid xenon imaging telescope for 1-30 MeV gamma-ray astrophysics
[NASA-CR-185999] 02 p0291 N90-11662
Critical fluid light scattering 09 p1222 N90-17087
State to state kinetics of XeCl*
[AD-A215895] 10 p1353 N90-17847
Performance of large area xenon ion thrusters for orbit transfer missions 11 p1472 N90-18475
Multiple-ionization of xenon atoms by positron impact
11 p1558 N90-18978
Flight model discharge system
[AD-A220261] 18 p2510 N90-24342

XENON CHLORIDE LASERS
Tunable XeCl-laser featuring high spectral luminance
16 p2311 N90-23167
Characterization of a high-intensity, subpicosecond XeCl laser system
[DE90-011970] 20 p2867 N90-26310

XENON FLUORIDE LASERS
Photodissociation of XeF2 (xenon difluoride) at 193 nm
[AD-A211663] 04 p0506 N90-12916
Electron beam pumped XeF(C yields A) laser scaling
[AD-A220022] 17 p2409 N90-23728

XV-15 AIRCRAFT
Ice induced aerodynamic performance degradation of rotorcraft: An overview 07 p0873 N90-15063
Application of the joined wing to tiltrotor aircraft
[NASA-CR-177543] 07 p0879 N90-15093
Identification of XV-15 aeroelastic modes using frequency-domain methods
[NASA-TM-101021] 15 p2051 N90-21756

Y

YAG (GARNET)
U YTTRIUM-ALUMINUM GARNET

YAG LASERS
Efficient nonlinear conversion of laser diode pumped miniature solid state laser sources
[AD-A210708] 01 p0075 N90-10433
Automation of fiber-optic pigtailing process: Laser welding demonstration program
[AD-A210351] 01 p0123 N90-10707
Construction of a picosecond laser system for the investigation of semiconductors using nonlinear optical methods
[ETN-89-94664] 03 p0352 N90-12013
Laser ionization mass spectroscopy
[DE89-008039] 03 p0352 N90-12015
MM and T advanced balancing/machining
[AD-A213103] 05 p0648 N90-13775
Eurolaser definition phase: A comparison of high power lasers available
[ETN-90-96061] 08 p1083 N90-16266
DURIP theoretical/experimental investigations of highly energetic dication species
[AD-A217771] 13 p1808 N90-20383
Injection-seeded Nd:YAG laser linewidth measurement using saturation spectroscopy in iodine
[DE90-009537] 15 p2103 N90-22034
Comparison of solar pumped Nd:YAG and Nd:Cr:GSGG lasers at liquid nitrogen and room temperature
[DLR-FB-89-41] 16 p2240 N90-22781
Measurement and visualization of the shock wave caused by the impact of a pulsed YAG laser in water
[REPT-892-430-113] 16 p2240 N90-22783
MEGALIDAR proof-of-concept demonstration
[AD-A216787] 16 p2255 N90-22856
Models of intracavity frequency doubled lasers
[AD-A221182] 18 p2563 N90-24628
Atmospheric sounding with UV lidar
[FOA-C-30542-3.1] 18 p2579 N90-24692
Development of a large scale Nd:YAG growth process
[DE90-010746] 18 p2624 N90-24954
Characterization of a Ho:Tm:Cr:YAG laser with a Cr:GSAG laser as pumping source
18 p2642 N90-25047
Phase-sensitive optical detection of ballistic phonon pulses using frequency-modulation spectroscopy and persistent spectral holes
[AD-A221521] 21 p2979 N90-26930
Development of a multi-purpose, pulsed-laser system for solar cell processing applications
[DE90-012181] 21 p3008 N90-27096
Intracavity frequency doubling of a Nd:YAG laser with an organic nonlinear optical crystal
[AD-A222392] 21 p3008 N90-27102
Tunable CW single-frequency source for injection seeding 2-micrometer lasers
[AD-A223979] 23 p3331 N90-28834

YAGI ANTENNAS
Planar microstrip Yagi array antenna
[NASA-CASE-NPO-17873-1-CU]
21 p2994 N90-27015

YARNS
Effect of thermal and cyclic loads on silicon carbide yarn reinforced glass matrix composites
[DE89-016554] 02 p0191 N90-11091

YAW
Aircraft modal supression system: Existing design approach and its shortcomings
01 p0023 N90-10115
Development of a three-axis trim program
[AD-A212883] 06 p0726 N90-14237
Explicit and implicit calculations of turbulent cavity flows with and without yaw angle
[NASA-CR-186293] 07 p0929 N90-15381
Yaw rate control of an air bearing vehicle
12 p1639 N90-19420
Actuated forebody strakes
[NASA-CASE-LAR-13983-1] 17 p2352 N90-23390
Aeroelastic and stability behaviour of the WTS 3 Maglarp wind turbine. Calculations and comparisons with tests
[FFA-TN-1989-23] 17 p2420 N90-23792
Yaw fin deployment apparatus for ejection seat
[AD-D014512] 19 p2656 N90-25118

YAWING MOMENTS
Development of non-conventional control methods for high angle of attack flight using vortex manipulation
23 p3273 N90-28522

YAWMETERS
U YAW

YF-17 AIRCRAFT
U F-17 AIRCRAFT

YHU-1 HELICOPTER
U UH-1 HELICOPTER

YIELD POINT
Investigation on sheet material of 8090 and 2091 aluminium-lithium alloy 07 p0898 N90-15192
Densification studies of refractory materials using Hot Isostatic Pressing (HIP) and tantalum containment
[DE90-013481] 20 p2833 N90-26114
Damage tolerance of the fighter aircraft 37 Viggen. Part 1: Analytical assessment
[FFA-TN-1990-12-PT-1] 23 p3276 N90-28538
Damage tolerance of the fighter aircraft 37 Viggen. Part 2: Experimental verification
[FFA-TN-1990-13-PT-2] 23 p3276 N90-28539

YIELD STRENGTH
Fatigue growth and closure of short cracks
[AD-A210824] 01 p0081 N90-10462
The HEL (Hugoniot Elastic Limit) and rate-dependent yield behavior
[DE89-016981] 02 p0199 N90-11134
Elasto-plastic analysis of unidirectional fiber-reinforced composites subjected to transverse normal loading using the finite element method 06 p0737 N90-14292

Spall strength measurements on shockloaded refractory metals
[DE90-000839] 06 p0747 N90-14345
The metallurgical determinants of toughness as cryogenic temperature
[DE90-002331] 06 p0748 N90-14351
The mechanisms of dispersion strengthening and fracture in Al-based XD (TM) alloys
[NASA-CR-4276] 09 p1187 N90-16879
Relationship of fragment size to normalized spall strength for materials
[DE90-004165] 09 p1231 N90-17140
Taylor impact testing
[AD-A215018] 09 p1231 N90-17144
Environmental embrittlement: A major cause for low ductility of ordered intermetallics
[DE90-006161] 10 p1356 N90-17864
Effect of oxygen on the tear strength of elastomers
[AD-A215845] 10 p1359 N90-17879
A computational model of the perforation of multi-layer metallic laminates
[MRL-RR-6-89] 14 p1944 N90-21126
A numerical study of plasticity induced closure in short cracks by the finite element method
[AD-A220471] 18 p2571 N90-24654
Fracture toughness and failure mechanisms in commercial 2091 Al-Li sheet at cryogenic temperatures
[AD-A222803] 20 p2835 N90-26125
Processing and characterization of high strength, high ductility Hadfield steel
[AD-A221769] 21 p2982 N90-26947
Computational investigation of local material strength and toughness on crack growth
[AD-A223189] 21 p3012 N90-27127
Novel side-chain liquid cyrstalline polymers
[AD-A221998] 22 p3159 N90-27911
Comparison of two computer codes for crack growth analysis: NASCRAC versus NASA/FLAGRO
23 p3297 N90-28648
Tensile behavior of borated stainless steels, phase 1
[DE90-014368] 23 p3309 N90-28717
The use of automated ball indentation testing to measure flow properties and estimate fracture toughness in metallic materials
[DE90-015797] 24 p3452 N90-29493

YIG (GARNET)
U YTTRIUM-IRON GARNET

YOUNG MODULUS
U MODULUS OF ELASTICITY

YTTERBIUM
Selective excitation luminescence and photoluminescence investigations of ytterbium doped InP, GaAs and AlGaAs
[AD-A215713] 09 p1291 N90-17485

YTTERBIUM COMPOUNDS
Excited state lifetime measurements of ytterbium in indium phosphide
[AD-A215709] 09 p1291 N90-17483
Photoresponse of YBa2Cu3O(7-delta) granular and epitaxial superconducting thin films
[NASA-TM-103144] 16 p2231 N90-22732
Ellipsometric study of YBa2Cu3O(7-x) laser ablated and co-evaporated films
[NASA-TM-103223] 20 p2932 N90-26682
The effect of temperature cycling typical of low earth orbit satellites on thin films of YBa2Cu3O(7-x)
22 p3140 N90-27812

YTTRIUM
Influence of heat treating on the mechanical values and the stability of heat barrier coatings
[ETN-90-95902] 12 p1631 N90-19375
The NASA high temperature superconductivity program 22 p3145 N90-27836
Microstructures and properties of superconducting Y-Er-BaCu-O thin films obtained from disordered Y-Er-BaF2-Cu films 22 p3147 N90-27848
Synthesis of Y1Ba2Cu3O(sub x) superconducting powders by intermediate phase reaction
22 p3149 N90-27855
Superconductivity in the Sn-Ba-Sr-Y-Cu-O system
22 p3151 N90-27863
A YBCO RF-SQUID magnetometer and its applications 22 p3151 N90-27867
Dynamical information for Fe doped YBa2Cu3O7 superconducting oxides obtained from high temperature Moessbauer studies
[DE90-627871] 23 p3401 N90-29218

YTTRIUM COMPOUNDS
NT YTTRIUM OXIDES
NT YTTRIUM-ALUMINUM GARNET
NT YTTRIUM-IRON GARNET
Y-Si-Al-O-N glass fibers
[AD-A211170] 02 p0190 N90-11088
Thermal barrier coatings for gas turbine and diesel engines
[NASA-TM-102408] 05 p0623 N90-13636
Muon SR investigation of magnetism and superconductivity in (Y(1-x)Pr(x))Ba2Cu3O7
[DE90-000689] 06 p0852 N90-14956
Magnetic and electronic correlations in YBa2Cu3O(sub 6+x)
[DE89-017604] 07 p1000 N90-15785
A ground state depleted laser in neodymium doped yttrium orthosilicate
[DE90-006773] 12 p1668 N90-19586
Performance of Y-TZP materials between 800 C and 1200 C
[AD-A217723] 13 p1897 N90-20890
Low temperature degradation of Y-TZP materials
[AD-A218841] 16 p2223 N90-22684
On the explanation of anomalies in inelastic neutron scattering by high-T(sub c) superconductors
[DE90-620561] 17 p2475 N90-24149
High resolution transmission electron microscopy of partial states of oxygen order in YBa2Cu3O(z)
[DE90-015637] 24 p3554 N90-30108

YTTRIUM OXIDES
Magnetic correlations in high T(sub c) oxides in the superconducting state
[DE89-016421] 01 p0130 N90-10746
A study of the tribological and surface micromechanical properties of YBa2Cu3O7-x
[DE89-015680] 02 p0281 N90-11607
High resolution-angle resolved photoemission studies of high temperature superconductors
[DE89-017691] 06 p0852 N90-14950
Superconducting and microstructural properties of shock-compacted high-T sub c oxide powders
[DE90-000823] 06 p0853 N90-14958
Effects of shock-induced defects on flux pinning in YBa2Cu3O(7-delta)
[DE90-000824] 06 p0853 N90-14959
Shock-induced defects and flux pinning in YBa2Cu3O sub 7-delta + Ag composites
[DE90-000827] 06 p0853 N90-14960
Anisotropy of oxygen tracer diffusion in YBa2Cu3O7-delta single crystals
[DE90-001931] 06 p0856 N90-14979
Linear electron-hole-electron pair model of high-temperature superconductivity in La(2-x)M(x)CuO4 and YBa2Cu3O(7-y): Part 2. Dependence of the superconducting transition temperatures on pressure and on hole concentration
[DE90-003012] 07 p0999 N90-15779
Partial reduction of re-oxidation processing of Y-Ba-Cu-O sputtered thin films
[DE90-003655] 07 p0999 N90-15782
Magnetic flux pinning in YBa2Cu3O7 films
[DE90-003709] 07 p1002 N90-15799
Cu-O chains in YBa2Cu3O(7-delta) and the phonon mechanism of high-Tc superconductivity
[DE90-603502] 07 p1003 N90-15805
Properties of high Tc superconducting oxides
[DE90-003792] 07 p1005 N90-15821
Atomic scale structure of twin boundary in Y-Ba-Cu-O superconductors
[DE90-003955] 07 p1006 N90-15823
ZrO2 sintered compact and method for its production
[DE90-004125] 08 p1039 N90-16006
High modulus coatings
[AD-A215448] 09 p1198 N90-16941
Electrical transport dissipation effects in epitaxial Y1Ba2Cu3O(7-x) thin films
[DE90-004301] 09 p1287 N90-17461
High-temperature deformation of YBa2Cu3O(7-delta) with Ag additions
[DE90-004884] 09 p1292 N90-17491
Effects of O2 ion bombardment of Y-BaCu-oxide during thin film growth
[DE90-005315] 09 p1293 N90-17495
MATE (Materials for Advanced Turbine Engines) Program, Project 3. Volume 2: Design, fabrication and evaluation of an oxide dispersion strengthened sheet alloy combustor liner
[NASA-CR-180892] 10 p1357 N90-17868
Anisotropy and dimensionality in untwinned crystals of YBa2Cu3O(7-delta)
[DE90-004890] 10 p1436 N90-18287
Long laser-pulse method of producing Y-Ba-Cu-O superconducting films
[DE90-005202] 10 p1436 N90-18289
Luminescence from defects and impurity centers in yttrium oxide
[DE90-004842] 11 p1589 N90-19030
Optical studies of dynamical processes in disordered materials
[DE90-007080] 12 p1631 N90-19372
Zirconia-based electrodes for solid oxide fuel cells
[DE90-000462] 12 p1655 N90-19513
Laser surface interactions of high-(Tc) superconductors
[DE90-006894] 12 p1669 N90-19587
Processing, fabrication, characterization and device demonstration of high temperature superconducting ceramics
[AD-A218330] 13 p1782 N90-20231
Y1Ba2Cu3O(7-x) laser-ablation plume dynamics measurement by nanosecond response ion probe: Comparison with optical measurements
[DE90-007658] 13 p1807 N90-20375
High resolution transmission electron microscopy study of defect structures in mixed-phase YBaCuO
[DE90-007767] 13 p1894 N90-20873
Deformation processing of YBa2Cu3O(sub x)
[DE90-007795] 14 p2030 N90-21644
On the substitution of Sr ions at Y sites in YB(suba2)Cu3O(sub7-d)
[DE90-613395] 14 p2031 N90-21652
Superconducting and semiconducting thin films of La(sub 123) and Y(sub 123) and their superlattices
[DE90-009565] 15 p2173 N90-22416
Growth and patterning of laser ablated superconducting YBa2Cu3O7 films on LaAlO3 substrates
[NASA-TM-102436] 15 p2173 N90-22421
Influence of high energy radiation on critical parameters of superconducting ceramics YBa2Cu3O7
[DE90-620562] 16 p2322 N90-23239
Magnetic and resistive measurements of the upper critical field in intwinned single crystals of YBa2Cu3O(7-delta)
[DE90-010083] 18 p2619 N90-24918
The defect structure of ion and neutron irradiated YBa2Cu3O(7-delta) single crystals
[DE90-010100] 18 p2619 N90-24920
Valence-defect chemical equilibria in nonstoichiometric YBa2Cu3O(7-delta)
[DE90-010152] 18 p2619 N90-24921
Thermal and phase analysis of YBa2Cu3O(7-x) powder compacts with organic acid additives
[DE90-010142] 18 p2620 N90-24930
Transverse- and zero-field muon SR investigation of magnetism and superconductivity in (Y(1-x)Pr(x)Ba2Cu3O7)
[DE90-010597] 18 p2624 N90-24953
Practical superconductor development for electrical power applications
[DE90-010262] 18 p2625 N90-24957
Superconducting thin films of YBaCu oxides prepared by MOCVD
[DE90-011109] 18 p2625 N90-24961
Effect of Cu(2+) magnetic moments on the superconductivity of YBa2Cu3O7: The origin of the linear term in the specific heat; the volume fraction of superconductivity
[DE90-011214] 18 p2626 N90-24963
Sequentially evaporated thin film YBa2Cu3O(7-x) superconducting microwave ring resonator
[NASA-TM-103180] 19 p2685 N90-25273
Microstructures of superconducting YBa2Cu3O(7-x) thin films
[DE90-011976] 19 p2761 N90-25688
Large, orientation-dependent enhancements of critical currents in Y1Ba2Cu3O(7-x) epitaxial thin films: Evidence for intrinsic flux pinning
[DE90-009424] 20 p2929 N90-26666
The effect of processing, deformation and annealing on the microstructure of Y1Ba2Cu3O7-(sub delta)
[DE90-011731] 21 p3079 N90-27510
Elliptical flux vortices in polycrystalline YBa2Cu3O7
22 p3136 N90-27795
Microstructure and magnetization of doped Y-Ba-Ca-O materials prepared by melt quench and post annealing method 22 p3138 N90-27803
Effect of shock pressure on the structure and superconducting properties of Y-Ba-Cu-O in explosively fabricated bulk metal-matrix composites
22 p3138 N90-27804
Laser ablated high T(sub c) superconducting thin YBa2Cu3O(7-x) films on substrates suitable for microwave applications 22 p3139 N90-27808
The effects of space radiation on thin films of YBa2Cu3O(sub 7-x) 22 p3147 N90-27845
Superconductivity in 2-2-3 Y2Ba2Cu3O(sub 8+ delta)
22 p3147 N90-27847
Comparative study of flux pinning flux creep and critical currents between YBaCuO crystals with and without Y2BaCuO5 inclusions 22 p3152 N90-27869
Processing of nanocrystalline ceramics
[DE90-015700] 24 p3456 N90-29520
Investigation of YBa2Cu3O(7-sigma) by NMR and construction of an ultra low temperature cryostat
24 p3550 N90-30088
Synthesis and property evaluation of Y-Ba2-Cu3-O(6+x) superconductors
[AD-A223494] 24 p3552 N90-30098
First principles calculation of oxygen ordering in YBa2Cu3O(7-y)
[DE90-015205] 24 p3553 N90-30102

YTTRIUM-ALUMINUM GARNET
Crystallography, spectroscopic analysis, and lasing properties of Nd3+:Y3Sc2Al3O12
[AD-A217792] 13 p1897 N90-20891
YTTRIUM-IRON GARNET
Magnetostatic wave device characterization by Brillouin light scattering
[AD-A213798] 09 p1281 N90-17426
YUH-1 HELICOPTER
U UH-1 HELICOPTER
YUH-60A HELICOPTER
U UH-60A HELICOPTER
YUKAWA POTENTIAL
Exotic Higgs production at e+e- colliders
[PREPRINT-671] 05 p0698 N90-14088

Z

ZAMBIA
MARS (Monitoring Agro-ecological Resources with Remote sensing and Simulation) definition study: Results of the preparatory phase
[REPT-17] 19 p2706 N90-25395
ZEEMAN EFFECT
Zeeman interferometry
[DE89-015296] 03 p0352 N90-12012
Millimeter-wave propagation in the mesosphere
[PB90-119868] 11 p1496 N90-18612
Stark and Zeeman effects on laser cooling of positronium 11 p1560 N90-18986
Modeling millimeter-wave propagation effects in the atmosphere 15 p2082 N90-21922
Excitation of hypersound at boundary between Type-2 superconductor and a concentrated paramagnetic compound 16 p2310 N90-23164
Lectures in plasma diagnostics
[DE90-015825] 24 p3550 N90-30086
Interstellar magnetic fields: An observational perspective 24 p3560 N90-30144
ZENER DIODES
U AVALANCHE DIODES
ZENER EFFECT
Steady-state and transient Zener parameters in viscoplasticity: Drag strength versus yield strength
[NASA-TM-102487] 10 p1395 N90-18064
ZENITH
Atmospheric transmittance determination from a two-angle measurement of radiance change
[AD-A213847] 08 p1101 N90-16375
On airborne measurements of radiation from broken cloud fields
[MITT-67] 21 p3027 N90-27211
ZEOLITES
Applications of NMR spectroscopy to the study of zeolite synthesis
[DE89-015226] 02 p0192 N90-11095
Flexibility of the zeolite RHO framework: In situ x ray and neutron powder structural characterization of divalent cation-exchanged zeolite RHO
[AD-A214573] 09 p1288 N90-17467
Production of high density aviation fuels via novel zeolite catalyst routes
[AD-A216444] 11 p1494 N90-18601
The effect of elevated gravity on the crystallization of the MFI zeolites, ZSM-5, and silicalite 16 p2320 N90-23231
Regenerative Cu La zeolite supported desulfurizing sorbents
[NASA-CASE-NPO-17480-1-CU] 20 p2830 N90-26098
ZERO ANGLE OF ATTACK
The radiation of sound from a propeller at angle of attack
[NASA-CR-4264] 14 p2023 N90-21602
ZERO CROSSINGS
U ROOTS OF EQUATIONS
ZERO GRAVITY
U WEIGHTLESSNESS
ZERO LIFT
Body effect on wing angle of attack and pitching moment at zero lift at low speeds
[ESDU-89042] 09 p1167 N90-16757
ZERO POWER REACTORS
Analysis and evaluation of ZPPR (Zero Power Physics Reactor) critical experiments for a 100 kilowatt-electric space reactor
[DE90-005634] 12 p1713 N90-19835
ZERO SOUND
Construction of the rotating cryostat ROTA2, its use for zero sound experiments in (3)He-B, and calculations of ion mobility in (3)He-A and (3)He-P
[ISBN-952-90091-3-5] 05 p0645 N90-13765
ZETA PINCH
Solid fiber Z-pinches: Cold-start computations
[DE89-016768] 02 p0279 N90-11592
A solvable self-similar model of the sausage instability in a resistive Z-pinch
[AD-A213137] 05 p0688 N90-14006
Two-dimensional behavior of Megagauss-field-confined solid fiber Z-pinches
[DE90-000684] 06 p0845 N90-14918
Scaling Z-pinch plasmas with atomic number for a given K-shell emission
[AD-A215703] 09 p1285 N90-17450
Fusion burn dynamics in Dense Z-Pinch (DZP)
[DE90-007976] 14 p2029 N90-21638
Gas-puff z-pinch experiment
[IPPCZ-286] 15 p2167 N90-22385
Quantitative spectroscopy of x ray laser plasmas in pulsed power devices
[AD-A221964] 21 p3078 N90-27501
ZINC
The secondary slurry-zinc/air battery
[DE90-002600] 06 p0772 N90-14491
Infrared absorption study of zinc-doped silicon
[DE90-007779] 13 p1771 N90-20164
The effects of zinc addition on the environmental stability of Al-Li alloys 16 p2219 N90-22657
Trace metal sources for the atlantic inflow to the Mediterranean Sea
[AD-A218607] 17 p2429 N90-23842
Research on high-specific-heat dielectrics
[AD-A221215] 18 p2623 N90-24944
Synthesis, structure, and properties of Ca2ZnN2
[AD-A222012] 21 p3083 N90-27533
The stability of the martensitic phases in Cu-Zn-Al at an electron concentration of 1.534
[DE90-628628] 23 p3311 N90-28727
ZINC ALLOYS
Cycle-life improvement of Zn/NiOOH cells by the addition of Ca(OH)2 to the zinc electrode
[DE90-004040] 08 p1062 N90-16139
Processing and elevated temperature ductility of aluminum alloy 7475
[AD-A216840] 11 p1486 N90-18554
ZINC COATINGS
Micromechanisms of surface friction in zinc electrogalvanized steel sheets
[DE89-011819] 01 p0077 N90-10440
Coating galvanized steel
[AD-A211775] 03 p0329 N90-11869
Polyelectrolyte-diffused zinc phosphate conversion coatings and polyacid coupling primers for corrosion protection of steel and aluminum, and alkali-catalyzed hydrolysis of polyimide-based materials
[AD-A212240] 04 p0480 N90-12754
Application of x ray fluorescence method to measuring thickness of galvanic coatings and measures of improving sensitivity of such measurings
[DE89-633351] 09 p1233 N90-17156
ZINC COMPOUNDS
NT ZINC OXIDES
NT ZINC SELENIDES
NT ZINC SULFIDES
NT ZINC TELLURIDES
ZINC NICKEL BATTERIES
U NICKEL ZINC BATTERIES
ZINC OXIDES
Growth and characterization of zinc sulfide films by conversion of zinc oxide films with H2S
[AD-A213345] 04 p0561 N90-13271
Energy ratings for metal oxide varistors under repetitively pulsed operation
[DE90-002353] 06 p0770 N90-14480
Processing and properties of nanophase oxides
[DE90-003826] 07 p0895 N90-15171
Sintering studies on high field varistors
[DE90-002626] 07 p0926 N90-15359
Characterization and comparison of optically transparent conducting films
[DE90-000319] 14 p2033 N90-21660
Surface acoustic wave filters in ZnO-SiO2-Si layered structures: Design, technology, and monolithic integration with electronic circuitry
[ETN-90-97218] 20 p2924 N90-26638
ZINC SELENIDES
Chemical beam epitaxy of ZnSe
[AD-A213265] 05 p0621 N90-13625
Passivating layer for III-V semiconductor materials
[AD-D014321] 12 p1719 N90-19872
Chemical beam epitaxy of ZnSe
[AD-A217375] 13 p1893 N90-20866
Preparation and characterization of Cu2ZnGeS(4-y)Se(y)
[AD-A217469] 15 p2171 N90-22407
Optical properties of zinc selenide grown using molecular beam deposition techniques
[RSRE-MEMO-4269] 15 p2174 N90-22423
The II-VI semiconductor superlattices
[AD-A223748] 24 p3553 N90-30101
ZINC SILVER BATTERIES
U SILVER ZINC BATTERIES
ZINC SILVER OXIDE BATTERIES
U SILVER ZINC BATTERIES
ZINC SULFIDES
Preparation, purification and densification of zinc sulfide powder from organometallics
[AD-A210943] 01 p0052 N90-10298
Growth and characterization of zinc sulfide films by conversion of zinc oxide films with H2S
[AD-A213345] 04 p0561 N90-13271
Laser-induced surface ablation and optical damage of ZnS crystals caused by single- and multiple-pulse laser-irradiation
[DE90-003807] 07 p0936 N90-15419
High modulus coatings
[AD-A215448] 09 p1198 N90-16941
ZINC TELLURIDES
Thin film cadmium telluride, zinc telluride, and mercury zinc telluride solar cells
[DE89-009499] 06 p0804 N90-14681
Fundamental and practical studies of metal contacts on mercury zinc telluride
[AD-A218730] 17 p2376 N90-23528
ZINC-BROMIDE BATTERIES
Preparation and evaluation of composite membranes for zinc/bromine storage batteries
[DE89-009931] 01 p0059 N90-10339
Zinc/bromine battery evaluation at SNL (Sandia National Laboratory)
[DE89-015847] 06 p0769 N90-14473
Membrane and durability studies for the zinc/bromine battery
[DE89-016181] 07 p0920 N90-15324
The INEL battery data base
[DE90-010914] 18 p2550 N90-24555
Zinc-bromine battery development
[DE90-014751] 23 p3321 N90-28781
ZIRCONATES
An investigation of the chemistry of silane coupling agents for adhesive bonding of aluminum
[AD-A220797] 17 p2381 N90-23560
ZIRCONIA
U ZIRCONIUM OXIDES
ZIRCONIUM
Exploratory study of niobium, titanium, zirconium and tantalum aluminides
[AD-A210658] 02 p0283 N90-11615
Structural analysis of zirconium-aluminum plasma deposits
[ETCA-89-R-073] 08 p1046 N90-16045
Develop techniques for ion implantation of PLZT for adaptive optics
[AD-A216005] 10 p1431 N90-18253
The improved adhesion of organic polymers to silica and to aluminum metal with zirconium Schiff-base block copolymer coatings
[AD-A216669] 11 p1490 N90-18575
Dehydrogenative polymerization of silanes to polysilanes: A monomeric copper(2) siloxide
[AD-A218550] 16 p2223 N90-22681
ZIRCONIUM ALLOYS
Estimation of thermodynamic properties of alloys from phase diagram and other loose boundary conditions
[DE90-719511] 08 p1135 N90-16579
Studies of the structure and properties of amorphous a-Zr76Fe24Hx
[AD-A214646] 09 p1190 N90-16897
Phase stability in the Al(6-x)Cu(x)Zr2 system for 0 less than x less than 1.0
[DE90-010620] 18 p2620 N90-24925
TEM, positron lifetime, and hardness measurements of irradiated, cold-worked, and annealed Zr-1 percent Nb
[VTT-RR-650] 19 p2676 N90-25216
The roles of strain and reheating interval in continuous recrystallization during the thermomechanical processing by warm rolling of an Al-Mg alloy
[AD-A223673] 24 p3449 N90-29479
ZIRCONIUM COMPOUNDS
NT ZIRCONATES
NT ZIRCONIUM HYDRIDES
NT ZIRCONIUM OXIDES
Thermal barrier coatings for gas turbine and diesel engines
[NASA-TM-102408] 05 p0623 N90-13636
Precipitation on dislocations in Al-Li-Cc-Mg-Zr
[AD-A221124] 18 p2526 N90-24415
ZIRCONIUM HYDRIDES
Reactive flow measurements and calculations for ZrH2-based composite explosives
[DE90-000831] 06 p0755 N90-14393
ZIRCONIUM OXIDES
Structural and surface characterization of dispersed metal catalysts
[DE89-014530] 01 p0038 N90-10208

Shock compression and release in high-strength ceramics
[DE89-013995] 01 p0047 N90-10265
Zirconia toughened SiC whisker reinforced alumina composites small business innovation research
[NASA-CR-179629] 01 p0052 N90-10294
Study of deposition of YBa2Cu3O7-x on cubic zirconia
[NASA-TM-102350] 01 p0128 N90-10737
Influence of core-shell grains on the internal stress state and permittivity response of zirconia modified barium titanate
[AD-A211245] 02 p0202 N90-11153
New mechanism for toughening ceramic materials
[AD-A211651] 03 p0332 N90-11892
Effects of hot corrosion on the room temperature strength of structural ceramics
[AD-A212568] 04 p0481 N90-12762
Thermodynamic properties of some metal oxide-zirconia systems
[NASA-TM-102351] 05 p0628 N90-13666
Perturbed angular correlations in zirconia ceramics
[DE89-017272] 06 p0751 N90-14369
Solid oxide fuel cells electrodes based on In(sub 2)O(sub 3)-PrO(sub 1.83)-ZrO(sub 2)
[DE90-002666] 06 p0806 N90-14691
Potential applications of structural ceramic composites in gas turbines
[DE90-001273] 07 p0908 N90-15248
IEA/Annex 2 powder characterization cooperative program
[AD-A213540] 07 p0911 N90-15271
ZrO2 sintered compact and method for its production
[DE90-004125] 08 p1039 N90-16006
Development of planar geometry solid oxide fuel cells
[PB90-100769] 08 p1095 N90-16341
Zirconia based ceramics
[DE90-606358] 09 p1199 N90-16946
Fundamental aspects of erosion and impact damage
[DE90-006640] 11 p1492 N90-18587
Influence of heat treating on the mechanical values and the stability of heat barrier coatings
[ETN-90-95902] 12 p1631 N90-19375
Zirconia-based electrodes for solid oxide fuel cells
[DE90-000462] 12 p1655 N90-19513
Hydrous metal oxide-supported catalysts. Part 1: Preparation chemistry and physical and chemical properties
[DE90-007607] 13 p1771 N90-20161
Performance of Y-TZP materials between 800 C and 1200 C
[AD-A217723] 13 p1897 N90-20890
Low temperature degradation of Y-TZP materials
[AD-A218841] 16 p2223 N90-22684
Alumina reinforced tetragonal zirconia (TZP) composites
[DE90-011871] 19 p2672 N90-25194
Wear mechanisms of amorphous carbon and zirconia coatings on rigid disk magnetic recording media
[DE90-011053] 20 p2837 N90-26133
Theory of ceramic/zirconia composites: Toughening, strengthening, and synergism
[AD-A222931] 21 p2985 N90-26961
Advanced ceramic armor materials
[AD-A223227] 21 p2986 N90-26970
Identification of tetragonal and cubic structures of zirconia
[AD-A222373] 21 p3083 N90-27535
Scandia-stabilized zirconia coating for composites
[AD-D014550] 22 p3160 N90-27917
Study of the structure of ZrO2-Al2O3 plasma sprayed coatings
[ETCA-89-R-078] 22 p3161 N90-27924
Characteristics required for thermal barriers of zirconium oxide-yttrium compounds obtained by plasma spraying. Morphological analysis by x ray diffraction
[ETCA-89-R-113] 22 p3161 N90-27925
Influence of diesel engine exposure on the rupture strength of silicon nitride and partially stabilized zirconia
[DE90-014759] 23 p3334 N90-28849
Effect of environment upon mechanical behavior of structural ceramics for application in the DOE ceramic technology for advanced heat engines project
[DE90-014770] 24 p3453 N90-29500
Non-destructive evaluation of infiltration-toughened ceramics
[DE90-629716] 24 p3453 N90-29501
Ion-beam-assisted deposition of silver films on zirconia ceramics for improved tribological behavior
[DE90-009706] 24 p3456 N90-29516
Adhesion of silver films to ion-bombarded zirconia
[DE90-010088] 24 p3456 N90-29517
Processing of nanocrystalline ceramics
[DE90-015700] 24 p3456 N90-29520

ZODIACAL DUST
Differentiation of three dimensional models of the zodiacal interplanetary dust cloud for experiments with micrometeoroids decay detectors on the space station
[ETN-90-96488] 18 p2637 N90-25025
ZODIACAL LIGHT
Reexamination of data from the asteroid/meteoroid detector
[NASA-CR-185997] 05 p0714 N90-14175
Image enhancement using the IRAS (Infrared Astronomy Satellite) survey data
[AD-A213811] 07 p0950 N90-15496
ZONAL CIRCULATION
U ZONAL FLOW (METEOROLOGY)
ZONAL FLOW (METEOROLOGY)
Paper 1. Impact of volcanic aerosols on stratospheric chemistry. Paper 2. O2 (1 sigma g +) and O2 (1 delta g) in the H + O2 reaction system. Paper 3. Barotropic instability of zonal jets on Mars, Earth and Venus
01 p0084 N90-10477
Global ionospheric dynamics
02 p0240 N90-11366
Report on the 2-D Model Intercomparison Workshop held January 11-16, 1987 in Fort Myers Beach, Florida, chapter 2
02 p0248 N90-11406
Observational studies of low-frequency oscillations in the Southern Hemisphere 02 p0250 N90-11420
Zonal average cloud characteristics for global atmospheric chemistry modeling
[CM-76] 04 p0518 N90-12992
The linear study of zonally asymmetric barotropic flows 05 p0668 N90-13902
Evolution of atmospheric baroclinic waves
16 p2254 N90-22855
An atlas of ECMWF analyses (1980-1987). Part 2: Second moment quantities
[NASA-TM-100762-PT-2] 19 p2715 N90-25451
The NASA/MSFC Global Reference Atmospheric Model, 1990 version (GRAM-90)
[NASA-CR-186717] 20 p2888 N90-26435
Zonal winds between 25 and 120 km retrieved from solar occultation spectra 24 p3489 N90-29718
ZONAL HARMONICS
On mean elements for satellite orbits perturbed by the zonal harmonics of the geopotential
[AD-A212322] 04 p0461 N90-12642
On mean elements for satellite orbits perturbed by the zonal harmonics of the geopotential
[RAE-TM-SPACE-371] 08 p1033 N90-15971
Satellite motion in an axi-symmetric gravitational field. Part 1: Perturbations due to J2 (second order) and J3
[RAE-TR-88068] 24 p3440 N90-29429
ZONE MELTING
Identification of defects in SOI (Silicon-On-Insulator) wafers
[DE90-006020] 13 p1895 N90-20879
Composite superconducting wires obtained by high-rate tinning in molten Bi-Pb-Sr-Ca-Cu-O system
22 p3148 N90-27850
ZONE REFINING
U ZONE MELTING
ZONES
U REGIONS
ZPR REACTORS
U ZERO POWER REACTORS

VOLUME 28 NUMBERS 1-6

Scientific and Technical Aerospace Reports

Abstracts January—March 1990

TABLE OF CONTENTS

STAR Issue	Page
1	1
2	145
3	299
4	437
5	571
6	717

VOLUME 28 NUMBERS 7-12

Scientific and Technical Aerospace Reports

Abstracts April—June 1990

TABLE OF CONTENTS

STAR Issue	Page
7	869
8	1017
9	1159
10	1303
11	1451
12	1597

VOLUME 28 NUMBERS 13-18

Scientific and Technical Aerospace Reports

Abstracts July—September 1990

TABLE OF CONTENTS

STAR Issue	Page
13	1749
14	1905
15	2045
16	2195
17	2343
18	2489

VOLUME 28 NUMBERS 19-24

Scientific and Technical Aerospace Reports

Abstracts October—December 1990

TABLE OF CONTENTS

STAR Issue	Page
19	2649
20	2801
21	2953
22	3103
23	3267
24	3417

FEDERAL REGIONAL DEPOSITORY LIBRARIES

ALABAMA

AUBURN UNIV. AT MONTGOMERY LIBRARY
Documents Department
Montgomery, AL 36193
(205) 279-9110 ext.253

UNIV. OF ALABAMA LIBRARY
Reference Department/Documents
Box S
Tuscaloosa, AL 35486
(205) 348-6046

ARIZONA

DEPT. OF LIBRARY, ARCHIVES, AND PUBLIC RECORDS
Third Floor State Capitol
1700 West Washington
Phoenix, AZ 85007
(602) 255-4121

ARKANSAS

ARKANSAS STATE LIBRARY
Documents Service Section
One Capitol Mall
Little Rock, AR 72201
(501) 371-2090

CALIFORNIA

CALIFORNIA STATE LIBRARY
Govt. Publications Section
914 Capitol Mall
Sacramento, CA 95814
(916) 322-4572

COLORADO

UNIV. OF COLORADO
Norlin Library
Government Publications Division
Campus Box 184
Boulder, CO 80309
(303) 492-8834

DENVER PUBLIC LIBRARY
Govt. Pub. Department
1357 Broadway
Denver, CO 80203
(303) 571-2346

CONNECTICUT

CONNECTICUT STATE LIBRARY
231 Capitol Avenue
Hartford, CT 06106
(203) 566-4971

FLORIDA

UNIV. OF FLORIDA LIBRARIES
Documents Department
Library West
Gainesville, FL 32611
(904) 392-0367

GEORGIA

UNIV. OF GEORGIA LIBRARIES
Government Documents Dept.
Athens, GA 30602
(404) 542-8949

HAWAII

UNIV. OF HAWAII
Hamilton Library
Government Documents Collection
2550 The Mall
Honolulu, HI 96822
(808) 948-8230

IDAHO

UNIV. OF IDAHO LIBRARY
Documents Section
Moscow, ID 83843
(208) 885-6344

ILLINOIS

ILLINOIS STATE LIBRARY
Federal Documents
Centennial Building
Springfield, IL 62756
(217) 782-5012

INDIANA

INDIANA STATE LIBRARY
Serials Section
140 North Senate Avenue
Indianapolis, IN 46204
(317) 232-3686

IOWA

UNIV. OF IOWA LIBRARIES
Government Publications Dept.
Iowa City, IA 52242
(319) 335-5926

KANSAS

UNIVERSITY OF KANSAS
Spencer Research Library
Government Documents
Lawrence, KS 66045
(913) 864-4662

KENTUCKY

UNIV. OF KENTUCKY LIBRARIES
Government Publications/Maps Dept.
Lexington, KY 40506
(606) 257-8400

LOUISIANA

LOUISIANA STATE UNIVERSITY
Middleton Library
Government Documents Dept.
Baton Rouge, LA 70803
(504) 388-2570

LOUISIANA TECHNICAL UNIV.
Prescott Memorial Library
Government Documents Dept.
Ruston, LA 71272
(318) 257-4962

MAINE

UNIVERSITY OF MAINE
Raymond H. Fogler Library
Govt. Documents & Microforms Dept.
Orono, ME 04469
(207) 581-1680

MARYLAND

UNIVERSITY OF MARYLAND
McKeldin Library
Documents/Maps Room
College Park, MD 20742
(301) 454-3034

MASSACHUSETTS

BOSTON PUBLIC LIBRARY
Government Documents Dept.
666 Boylston Street
Boston, MA 02117
(617) 536-5400 ext.226

MICHIGAN

DETROIT PUBLIC LIBRARY
5201 Woodward Avenue
Detroit, MI 48202
(313) 833-1409

LIBRARY OF MICHIGAN
Government Documents
P.O. Box 30007
735 E. Michigan Avenue
Lansing, MI 48909
(517) 373-1593

MINNESOTA

UNIVERSITY OF MINNESOTA
Wilson Library
Government Publications
309 Nineteenth Avenue South
Minneapolis, MN 55455
(612) 373-7813

MISSISSIPPI

UNIV. OF MISSISSIPPI LIB.
Government Documents Dept.
106 Old Gym Bldg.
University, MS 38677
(601) 232-5857

MISSOURI

University of Missouri at Columbia Library
Government Documents
Columbia, MO 65201
(314) 882-6733

MONTANA

UNIV. OF MONTANA
Mansfield Library
Documents Division
Missoula, MT 59812
(406) 243-6700

NEBRASKA

UNIVERSITY OF NEBRASKA - LINCOLN
Love Memorial Library
Documents Department
Lincoln, NE 68588
(402) 472-2562

NEVADA

UNIV. OF NEVADA-RENO LIB.
Govt. Pub. Department
Reno, NV 89557
(702) 784-6579

NEW JERSEY

NEWARK PUBLIC LIBRARY
U.S. Documents Division
5 Washington Street
P.O. Box 630
Newark, NJ 07101
(201) 733-7812

NEW MEXICO

UNIVERSITY OF NEW MEXICO
General Library
Government Publications/Maps Dept.
Albuquerque, NM 87131
(505) 277-5441

NEW MEXICO STATE LIBRARY
325 Don Gaspar Avenue
Santa Fe, NM 87501
(505) 827-3826

NEW YORK

NEW YORK STATE LIBRARY
Documents Sect. Cultural Educ. Ctr.
Empire State Plaza
Albany, NY 12230
(518) 474-5563

NORTH CAROLINA

UNIVERSITY OF NORTH CAROLINA AT CHAPEL HILL
Davis Library 080A
BA/SS Department Documents
Chapel Hill, NC 27514
(919) 962-1151

NORTH DAKOTA

NORTH DAKOTA STATE UNIVERSITY LIBRARY
Government Documents Dept.
Fargo, ND 58105
(701) 237-8352
In cooperation with Univ. of North Dakota, Chester Fritz Library
Grand Forks

OHIO

STATE LIBRARY OF OHIO
Documents Section
65 South Front Street
Columbus, OH 43266
(614) 644-7051

OKLAHOMA

OKLAHOMA DEPT. OF LIBRARIES
Government Documents
200 NE 18th Street
Oklahoma City, OK 73105
(405) 521-2502, ext. 252

OKLAHOMA STATE UNIV. LIB.
Documents Department
Stillwater, OK 74078
(405) 624-0489

OREGON

PORTLAND STATE UNIV.
Millar Library
934 SW Harrison - P.O. Box 1151
Portland, OR 97207
(503) 229-3673

PENNSYLVANIA

STATE LIBRARY OF PENN.
Government Publications Section
Box 1601
Walnut St. & Commonwealth Ave.
Harrisburg, PA 17105
(717) 787-3752

SOUTH CAROLINA

CLEMSON UNIV. COOPER LIB.
Documents Department
Clemson, SC 29634
(803) 656-5174
In cooperation with Univ. of South Carolina, Thomas Cooper Library, Columbia

TEXAS

TEXAS STATE LIBRARY
Public Services Department
P.O. Box 12927 - 1201 Brazos
Austin, TX 78711
(512) 463-5455

TEXAS TECH. UNIV. LIBRARY
Documents Department
Lubbock, TX 79409
(806) 742-2268

UTAH

UTAH STATE UNIVERSITY
Merrill Library & Learning Resources Center, UMC-30
Documents Department
Logan, UT 84322
(801) 750-2682

VIRGINIA

UNIVERSITY OF VIRGINIA
Alderman Library
Government Documents
Charlottesville, VA 22903
(804) 924-3133

WASHINGTON

WASHINGTON STATE LIBRARY
Document Section
Olympia, WA 98504
(206) 753-4027

WEST VIRGINIA

WEST VIRGINIA UNIV. LIB.
Government Documents Section
P.O. Box 6069
Morgantown, WV 26506
(304) 293-3640

WISCONSIN

ST. HIST SOC. OF WISCONSIN LIB.
Government Pub. Section
816 State Street
Madison, WI 53706
(608) 262-2781
In cooperation with Univ. of Wisconsin-Madison, Memorial Library

MILWAUKEE PUBLIC LIBRARY
Documents Division
814 West Wisconsin Avenue
Milwaukee, WI 53233
(414) 278-3065

WYOMING

WYOMING STATE LIBRARY
Supreme Court & Library Bldg.
Cheyenne, WY 82002
(307) 777-5919

National Aeronautics and
Space Administration
Code NTT
Washington, D.C.
20546
Official Business
Penalty for Private Use, $300

SPECIAL FOURTH-CLASS RATE
POSTAGE & FEES PAID
NASA
PERMIT No. G27



POSTMASTER: If Undeliverable (Section 158 Postal Manual) Do Not Return